

JOURNAL OF HEPATOLOGY

The Home of Liver Research

THE INTERNATIONAL LIVER CONGRESS™

Savour science together again

#ILC2022



22-26
JUNE
2022
LONDON

ABSTRACT

BOOK

easl.eu/ilc2022

JOURNAL OF HEPATOLOGY

The Home of Liver Research

EDITOR IN CHIEF

Paolo Angeli, Italy

DEPUTY EDITOR

Patrizia Burra, Italy

CO-EDITORS

Vlad Ratziu, France | Bruno Sangro, Spain |
Frank Tacke, Germany | Stefan Zeuzem, Germany

ASSOCIATE EDITORS

Alcohol and Drug-Related Liver Diseases

Einar S. Björnsson, Iceland
Alexandre Louvet, France

Cholestasis and Autoimmune Diseases

Tom H. Karlsen, Norway
Ulrich Beuers, Netherlands

Complications of Cirrhosis and Liver Failure

Paolo Caraceni, Italy
Javier Fernández, Spain
Constantine Karvellas, Canada

Disease Burden and Public Health

Gregory Dore, Australia

Genetics

Matias Ávila, Spain

Gut-Liver Axis

Bernd Schnabl, USA
Jonel Trebicka, Germany

Hepatic and Biliary Cancer

Jesper Andersen, Denmark
John Bridgewater, UK
Stephen L. Chan, Hong Kong
Jean-Charles Nault, France
Maria Reig, Spain

Imaging and Non-Invasive Tests

Annalisa Berzigotti, Switzerland
Rita Golfieri, Italy
Maxime Ronot, France

Immunology

Barbara Rehermann, USA

Liver Fibrosis

Massimo Pinzani, UK

Liver Surgery and Transplantation

Pierre-Alain Clavien, Switzerland
Julie K. Heimbach, USA
Francesco P. Russo, Italy

NAFLD

Quentin Anstee, UK
Elisabetta Bugianesi, Italy
Jacob George, Australia
Wajahat Mehal, USA

Pathology

Christine Sempoux, Switzerland

Statistics, A.I. and Modelling Outcomes

Anna Chiara Frigo, Italy
Raphaël Porcher, France

Vascular Liver Diseases

Jordi Gracia-Sancho, Spain

Viral Hepatitis

Thomas Baumert, France
Maria Buti, Spain
Markus Cornberg, Germany
Edward John Gane, New Zealand
Man Fung Yuen, Hong Kong

Consultants

Julius Chapiro, USA
Peter Jepsen, Denmark

SPECIAL SECTION EDITORS

Reviews

Michael Trauner, Austria

Snapshot

Sara Montagnese, Italy
Alexander Ploss, USA

Website/Social Media

Jesus Bañales, Spain
Elliott B. Tapper, USA

EDITORIAL BOARD

Alcohol and Drug-Related Liver Diseases

Raul Andrade, Spain
Michael R. Lucey, USA
Philippe Mathurin, France
Laura E. Nagy, USA
Georges-Philippe Pageaux, France
Mark R. Thursz, UK

Basic Science

Javier Cubero, Spain
José Fernandez-Checa, Spain
Chandrashekar Gandhi, USA
Mathias Heikenwälder, Germany
Irene Ng, China
Cecilia Rodrigues, Portugal
Detlef Schuppan, Germany

Cholestatic and Autoimmune Diseases

Martti Färkkilä, Finland
Michael Heneghan, UK
Gideon Hirschfield, Canada
Pietro Invernizzi, Italy
Verena Keitel, Germany
Ansgar Lohse, Germany
Xiong Ma, China
Aldo J. Montano-Loza, Canada
Atsushi Tanaka, Japan

Complications of Cirrhosis and Liver Failure

Juan G. Abraldes, Canada
Banwari Agarwal, UK
Jasmohan S. Bajaj, USA
William Bernal, UK
Andrés Cárdenas, Spain
Claire Francoz, France
Guadalupe Garcia-Tsao, USA
Pere Ginés, Spain
Thierry Gustot, Belgium
Wim Laleman, Belgium
Mattias Mandorfer, Austria
Sebastian Marciano, Argentina
Salvatore Piano, Italy
Shiv K. Sarin, India

Puneeta Tandon, Canada
Reiner Wiest, Switzerland

Epidemiology/Public Health

Jeffrey Lazarus, Spain
Uwe Siebert, Austria

Genetics

Frank Lammert, Germany
Stefano Romeo, Sweden

Gut-Liver Axis

Sofia Forslund, Germany
Aleksander Krag, Denmark

Hepatic and Biliary Cancer

Ann-Lii Cheng, Taiwan
Laura Dawson, Canada
Peter R. Galle, Germany
Tim Greden, USA
Chiun Hsu, Taiwan
Katie Kelley, USA
Josep Llovet, USA
Tom Luedde, Germany
Tim Meyer, UK
Pierre Nahon, France
Hayato Nakagawa, Japan
Lorenza Rimassa, Italy
Jinsil Seong, Republic of Korea
Beicheng Sun, China
Juan Valle, UK

Immunology

Mala Maini, UK
Elsa Solà, Spain

Liver Fibrosis

Scott Friedman, USA
Tatiana Kisseleva, USA
Isabelle Leclercq, Belgium
Robert E. Schwartz, USA
Thierry Tordjmann, France
Holger Willenbring, USA

Liver Surgery and Transplantation

Martina Gambato, Italy
Giacomo Germani, Italy

Vincenzo Mazzaferro, Italy
Rajender K. Reddy, USA
Alberto Sánchez-Fueyo, UK
Gonzalo Sapisochin, Canada
Christian Toso, Switzerland

NAFLD

Leon Adams, Australia
Guruprasad Aithal, UK
Helena Cortez-Pinto, Portugal
Henning Grønbaek, Denmark
Rohit Loomba, USA
Giulio Marchesini, Italy
Philip N. Newsome, UK
Elizabeth E. Powell, Australia
Manuel Romero-Gómez, Spain
Arun Sanyal, USA
Jörn Schattenberg, Germany
Giovanni Targher, Italy
Luca Valenti, Italy
Grace Wong, Hong Kong
Vincent Wong, Hong Kong
Shira Zelber-Sagi, Israel

Non-invasive Diagnoses and Imaging

Jérôme Boursier, France
Laurent Castera, France
Thierry de Baere, France
Richard (Dick) L. Ehman, USA
Salvatore Petta, Italy
Jordi Rimola, Spain
Riad Salem, USA

Pathology

Karoline Lackner, Austria
Valerie Paradis, France
Peter Schirmacher, Germany
Dina Tiniakos, UK
Achim Weber, Switzerland

Pediatrics

Emmanuel Jacquemin, France
Pietro Vajro, Italy

Statistics, A.I. and Modeling Outcomes

Alex Amoros, Spain
Calogero Camma, Italy

Elisabet García, Spain
Jeremie Guedj, France

Vascular Liver Diseases

Yasuko Iwakiri, USA
Vincenzo La Mura, Italy
Pierre-Emmanuel Rautou, France

Viral Hepatitis

Alessio Aghemo, Italy
Sandra Ciesek, Germany
James Fung, Hong Kong
Jason Grebely, Australia
Ira Jacobson, USA
Patrick Kennedy, UK
Pietro Lampertico, Italy
Darius Moradpour, Switzerland
Jean-Michel Pawlotsky, France
Thomas Pietschmann, Germany
Charles Rice, USA
Jian Sun, China
Robert Thimme, Germany
Stephan Urban, Germany
Heiner Wedemeyer, Germany
Fabien Zoulim, France

EDITORS EMERITUS

Dame Sheila Sherlock†, Founding
Editor, UK (1985-1989)
Jean-Pierre Benhamou†, France (1990-1994)
Gustav Paumgartner, Germany (1995-1999)
Juan Rodés†, Spain (2000-2004)
Massimo Colombo, Italy (2005-2009)
Didier Samuel, France (2010-2014)
Rajiv Jalan, UK (2015-2019)

EDITORIAL OFFICE

Manager

Joël Walicki

Coordinators

Jiyeong Adams
Duncan Anderson

Assistant

Kristina Jajcevic

Scientific Illustrator

Pablo Echeverria

EASL GOVERNING BOARD

SECRETARY GENERAL

Thomas Berg, Germany

VICE SECRETARY

Aleksander A. Krag, Denmark

TREASURER

Francesco Negro, Switzerland

SCIENTIFIC COMMITTEE

Tobias Böttler, Germany
Virginia Hernández-Gea, Spain
Jean-Charles Nault, France
Emmanouil Tsochatzis, UK
Luca Valenti, Italy
Saskia van Mil, Netherlands

EDUCATIONAL COUNCILLOR

Ulrich Beuers, Netherlands

EU POLICY COUNCILLOR

Maria Buti, Spain

EASL Office
Journal of Hepatology Editorial Office
7 rue Daubin
1203 Geneva, Switzerland
Tel.: +41 (0) 22 807 0363
E-mail: jhepatology@easloffice.eu

Application for EASL Membership can be done at <https://easl.eu/community/join-the-community/>

© 2022 European Association for the Study of the Liver. Published by Elsevier B.V. All rights reserved.

This journal and the individual contributions contained in it are protected under copyright, and the following terms and conditions apply to their use in addition to the terms of any Creative Commons or other user license that has been applied by the publisher and the European Association for the Study of the Liver to an individual article:

Photocopying: Single photocopies of single articles may be made for personal use as allowed by national copyright laws. Permission is not required for photocopying of articles published under the CC BY license nor for photocopying for non-commercial purposes in accordance with any other user license applied by the publisher and the European Association for the Study of the Liver. Permission of the publisher and the European Association for the Study of the Liver and payment of a fee is required for all other photocopying, including multiple or systematic copying, copying for advertising or promotional purposes, resale, and all forms of document delivery. Special rates are available for educational institutions that wish to make photocopies for non-profit educational classroom use.

Derivative Works: Users may reproduce tables of contents or prepare lists of articles including abstracts for internal circulation within their institutions or companies. Other than for articles published under the CC BY license, permission of the publisher and the European Association for the Study of the Liver is required for resale or distribution outside the subscribing institution or company. For any subscribed articles or articles published under a CC BY-NC-ND license, permission of the publisher and the European Association for the Study of the Liver is required for all other derivative works, including compilations and translations.

Storage or Usage: Except as outlined above or as set out in the relevant user license, no part of this publication may be reproduced, stored in a retrieval system or transmitted in any form or by any means, electronic, mechanical, photocopying, recording or otherwise, without prior written permission of the publisher and the European Association for the Study of the Liver.

Permissions: For information on how to seek permission visit www.elsevier.com/permissions.

Author rights: Author(s) may have additional rights in their articles as set out in their agreement with the publisher and the European Association for the Study of the Liver (more information at <http://www.elsevier.com/authorsrights>).

Notice: Practitioners and researchers must always rely on their own experience and knowledge in evaluating and using any information, methods, compounds or experiments described herein. Because of rapid advances in the medical sciences, in particular, independent verification of diagnoses and drug dosages should be made. To the fullest extent of the law, no responsibility is assumed by the publisher or the European Association for the Study of the Liver for any injury and/or damage to persons or property as a matter of products liability, negligence or otherwise, or from any use or operation of any methods, products, instructions or ideas contained in the material herein.

Although all advertising material is expected to conform to ethical (medical) standards, inclusion in this publication does not constitute a guarantee or endorsement of the quality or value of such product or of the claims made of it by its manufacturer.

Publication information: *Journal of Hepatology* (ISSN 0168-8278). For 2022, volumes 76 and 77 are scheduled for publication. Subscription prices are available upon request from the Publisher or from the Elsevier Customer Service Department nearest you or from this journal's website (<http://www.elsevier.com/locate/jhep>). Further information is available on this journal and other Elsevier products through Elsevier's website: (<http://www.elsevier.com>). Subscriptions are accepted on a prepaid basis only and are entered on a calendar year basis. Issues are sent by standard mail (surface within Europe, air delivery outside Europe). Priority rates are available upon request. Claims for missing issues should be made within six months of the date of dispatch.

Orders, claims, and journal enquiries: Please visit our Support Hub page <https://service.elsevier.com> for assistance.

Advertising information: Advertising orders and enquiries can be sent to: **USA, Canada and South America:** Elsevier Inc., 360 Park Avenue, Suite 800, New York, NY 10169-0901, USA; phone: (+1) (212) 989 5800. **Europe and ROW:** Robert Bayliss, Pharma Solutions, Elsevier Ltd., 125 London Wall, London EC2Y 5AS, UK; phone: (+44) 207 424 4454; e-mail: r.bayliss@elsevier.com.

Author enquiries: You can track your submitted article at <http://www.elsevier.com/track-submission>. You can track your accepted article at <http://www.elsevier.com/trackarticle>. You are also welcome to contact Customer Support via [http://service.elsevier.com](https://service.elsevier.com).

Funding body agreements and policies: Elsevier has established agreements and developed policies to allow authors whose articles appear in journals published by Elsevier, to comply with potential manuscript archiving requirements as specified as conditions of their grant awards. To learn more about existing agreements and policies please visit <http://www.elsevier.com/fundingbodies>.

Special regulations for authors: Upon acceptance of an article by the journal, the author(s) will be asked to transfer copyright of the article to EASL. Transfer will ensure the widest possible dissemination of information.

USA mailing notice: *Journal of Hepatology*, ISSN 0168-8278 (USPS 11087) is published monthly by Elsevier B.V. Radarweg 29, 1043 NX Amsterdam, the Netherlands. Airfreight and mailing in the USA by agent named World Container Inc, 150-15, 183rd Street, Jamaica, NY 11413, USA. Periodicals postage paid at Brooklyn, NY 11256.

US Postmaster: Send address changes to *Journal of Hepatology*, World Container Inc, 150-15, 183rd Street, Jamaica, NY 11413, USA.

Subscription records are maintained at Elsevier B.V. Radarweg 29, 1043 NX Amsterdam, the Netherlands.

Air Business Ltd is acting as our mailing agent.

© The paper used in this publication meets the requirements of ANSI/NISO Z39.48-1992 (Permanence of Paper).

Printed by Henry Ling Ltd., Dorchester, UK



Join our dynamic & forward-thinking community

- + Best education
- + Journal of Hepatology
- + Best research
- + JHEP Reports
- + Reduced fees for events

JOIN OUR
COMMUNITY



Open-access eLearning anytime, anywhere



2,000+ resources available
21 CME-accredited courses

- 19 CPG slide decks
- 4,100 ePosters
- 20,300 registered users
- 2,200 webcasts





Your weekly hepatology
broadcast news

Every Wednesday
18:00 CET

Topics:

- + JHEP Live**
- + YIs Choice**
- + Nurses & AHPs Focus**
- + and more...**

WATCH
ON DEMAND



JOURNAL OF HEPATOLOGY

VOLUME **77**, SUPPLEMENT **1**, PAGES **S1–S1080**

Abstracts of The International Liver Congress™ 2022
22–26 June 2022, London, United Kingdom

Publication of this Abstract supplement was supported by the European Association for the Study of the Liver (EASL)

ELSEVIER

JOURNAL OF HEPATOLOGY

The Home of Liver Research



- + Premium hepatology journal
- + International Editorial team led by Prof. Paolo Angeli
- + 2020 Impact Factor: 25.1

**Submit your
article now**

SCAN FOR
MORE INFO



JOURNAL OF HEPATOLOGY

VOLUME 77, SUPPLEMENT 1, PAGES S1–S1080

CONTENTS

Oral Presentations

General Session I	S1
General Session II	S5
Late-Breaker	S10
Hepatitis C: Clinical aspects and therapy	S15
Cirrhosis and its complications: Other clinical complications except ACLF and critical illness	S18
Non-invasive assessment of liver disease except NAFLD	S22
Immune-mediated and cholestatic: Experimental and pathophysiology	S26
Non-invasive assessment/treatment and liver related outcomes in NAFLD/ALD	S29
Alcoholic liver disease	S33
Fibrosis	S36
NAFLD: Clinical aspects except therapy	S39
Viral hepatitis elimination	S42
Primary Liver Cancer: Experimental and pathophysiology	S45
Cirrhosis and its complications: ACLF and Critical illness	S48
Liver Immunology	S53
Rare liver diseases (including paediatric and genetic)	S58
Nurses and AHP	S63
Gut microbiota in liver disease and liver regeneration	S65
Hepatitis B emerging therapies	S69
NAFLD: Diagnostics and non-invasive assessment	S73
Liver tumours: Clinical aspects except therapy	S75
Public health	S80
Molecular and cellular biology	S83
NAFLD Therapy	S86
Cirrhosis and its complications: Portal Hypertension	S89
Immune-mediated and cholestatic disease: Clinical aspects	S93
Viral hepatitis basic science	S97

Hepatitis B clinical aspects	S100
Cirrhosis and its complications: Experimental and pathophysiology	S103
Liver tumours: Therapy	S107
NAFLD: Experimental and pathophysiology	S111
Liver transplantation and Acute liver failure: Clinical aspects	S114
Poster Presentations	
Alcoholic liver disease	S119
NAFLD: Clinical aspects except therapy	S144
Gut microbiota and liver disease	S173
Immunology	S183
Public Health	S200
Viral hepatitis A/E: Clinical aspects	S269
Viral hepatitis B/D: Clinical aspects except therapy	S271
Immune-mediated and cholestatic disease: Clinical aspects	S305
Cirrhosis and its complications: ACLF and Critical illness	S339
Cirrhosis and its complications: Experimental and pathophysiology	S358
Liver tumours: Therapy	S372
Acute liver failure and drug induced liver injury	S389
NAFLD: Diagnostics and non-invasive assessment	S409
Fibrosis	S463
Non-invasive assessment of liver disease except NAFLD	S495
Nurses and Allied Health Professionals	S509
Rare liver diseases (including paediatric and genetic)	S513
Viral hepatitis C: Clinical aspects except therapy	S541
Viral Hepatitis C: Post SVR and long term follow up	S561
Viral hepatitis C: Therapy and resistance	S579
Immune-mediated and cholestatic: Experimental and pathophysiology	S599
Cirrhosis and its complications: Portal Hypertension	S608
Liver tumours: Experimental and pathophysiology	S636
NAFLD: Experimental and pathophysiology	S665
NAFLD: Therapy	S713
Liver development, physiology and regeneration	S734
Molecular and cellular biology	S745
Liver transplantation and hepatobiliary surgery: Clinical aspects	S767
Liver transplantation and hepatobiliary surgery: Experimental and pathophysiology	S818
Viral hepatitis B/D: therapy	S823
Cirrhosis and its complications: Other clinical complications except ACLF and critical illness	S882

Liver tumours: Clinical aspects except therapy	S912
Author Index	S940
Disclosures: no commercial relationships	S1021
Disclosures: commercial relationships	S1065
Reviewers list	S1080

Registration of Clinical Trials

The *Journal of Hepatology* endorses the policy of the WHO and the International Committee of Medical Journal Editors (ICMJE) on the registration of clinical trials. Therefore, any trial that starts recruiting on or after July 1, 2005 should be registered in a publicly owned, publicly accessible registry and should satisfy a minimal standard dataset. Trials that started recruiting before that date will be considered for publication if registered before September 13, 2005.

More detailed information regarding clinical trials and registration can be found in *New Engl J Med* 2004; 351:1250–1251 and *New Engl J Med* 2005; 352:2437–2438.

Available online at www.sciencedirect.com

 **ScienceDirect**
for online access via your library

ELSEVIER

JHEP|Reports

Innovation in Hepatology

EASL's first open-access journal

+ **Discoverability**

Indexed by PubMed Central,
Clarivate, and Scopus

+ **Speed**

Time to first decision: 3.6 weeks
Acceptance to online publication: 2.2 weeks

+ **Excellence**

High-quality peer review guaranteed by an
international Editorial team led by Prof. Jessica Zucman-Rossi

First Impact Factor in 2022



**Submit your
article now**

SCAN FOR
MORE INFO





EASL[™]
The Home of Hepatology

THE LANCET



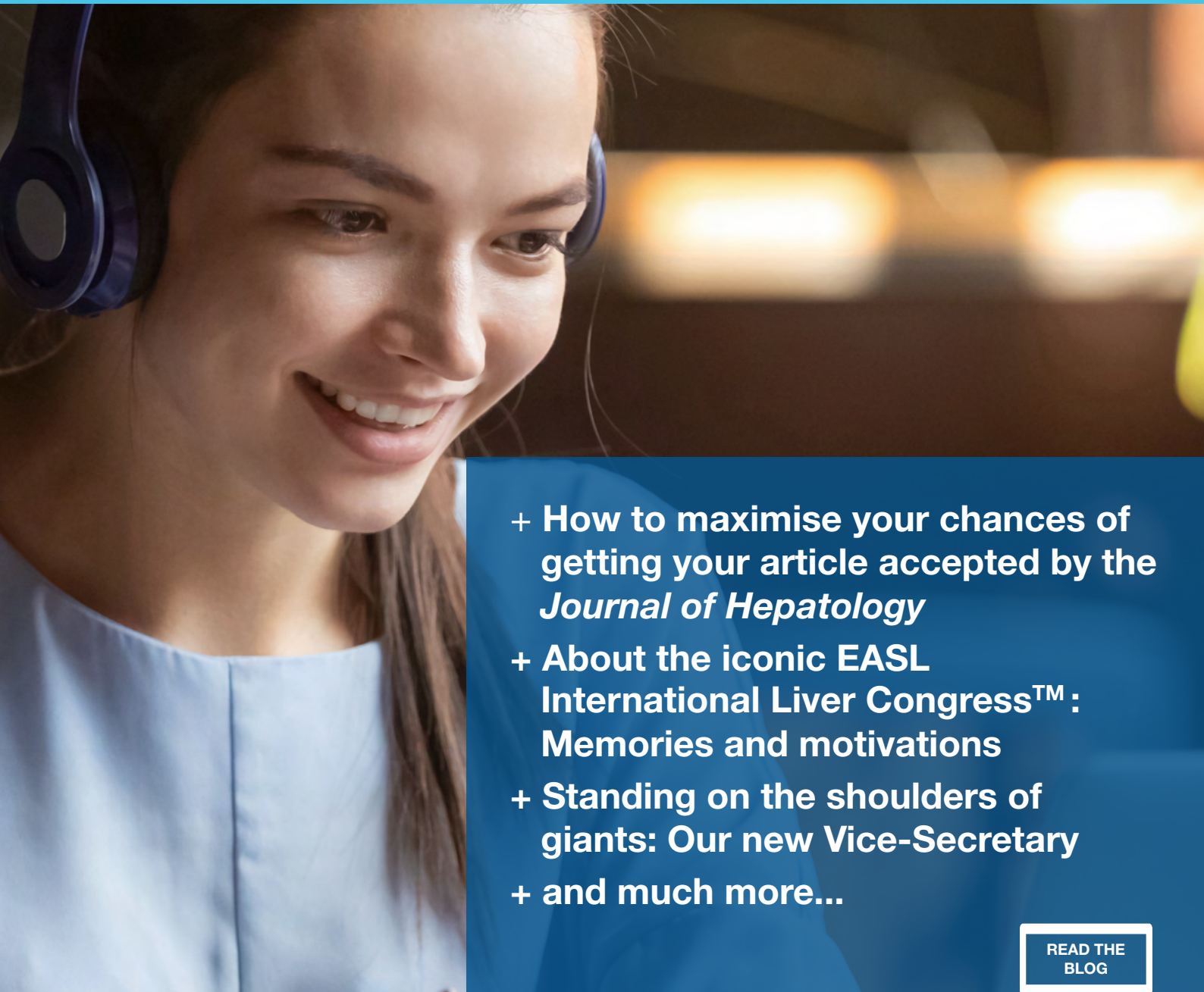
The EASL–*Lancet* Liver Commission

The EASL–*Lancet* Liver Commission
has published a landmark report on
liver diseases in Europe.



Liver Matters

Voices and views from our community



- + **How to maximise your chances of getting your article accepted by the *Journal of Hepatology***
- + **About the iconic EASL International Liver CongressTM: Memories and motivations**
- + **Standing on the shoulders of giants: Our new Vice-Secretary**
- + **and much more...**

READ THE
BLOG



easl.eu/easl-blog



EASL[™]
The Home of Hepatology

FUTURE EVENTS

2022–2023

2022

1–2	July	EASL School	London, UK
1–2	July	EASL School	Freiburg, Germany
15–17	September	EASL NAFLD Summit	Dublin, Ireland
15–17	September	EASL School	London, UK
10–11	December	AASLD-EASL Masterclass	Savannah, USA

2023

20–22	April	EASL Liver Cancer Summit	Estoril, Portugal
12–13	May	Monothematic Biliary Fibrosis	Florence, Italy
TBD	May	AASLD-EASL Endpoints	USA
21–25	June	EASL Congress 2023	Vienna, Austria
Summer		EASL Schools	Europe
7–9	September	EASL NAFLD Summit	Europe
19–21	October	EASL-AASLD Endpoints	Brussels, Belgium
30 Nov. – 2 Dec.		EASL-AASLD Masterclass	Madrid, Spain

SEE OUR
CALENDAR



Young Investigators

The future of hepatology



SCAN FOR
MORE INFO



- + YIs Task Force
- + YIs webinars
- + EASL Schools & Masterclasses
- + Fellowships & Mentorships
- + EASL Emerging Leader Award
- + Abstracts & Bursaries at events
- + YIs newsletter

Nurses & AHPs

On the frontline of hepatology



SCAN FOR
MORE INFO



- + Nurses & AHPs Task Force
- + Nurses & AHPs webinars
- + Nurses & AHPs Forum at ILC
- + Rising Star Award
- + Abstracts & Bursaries at events

Annual Patient Forum: **Making the patient voice heard**

WATCH
ON DEMAND





QUIZ

- + Testing your guidelines knowledge **since June 2020**
- + Sharpening your skills



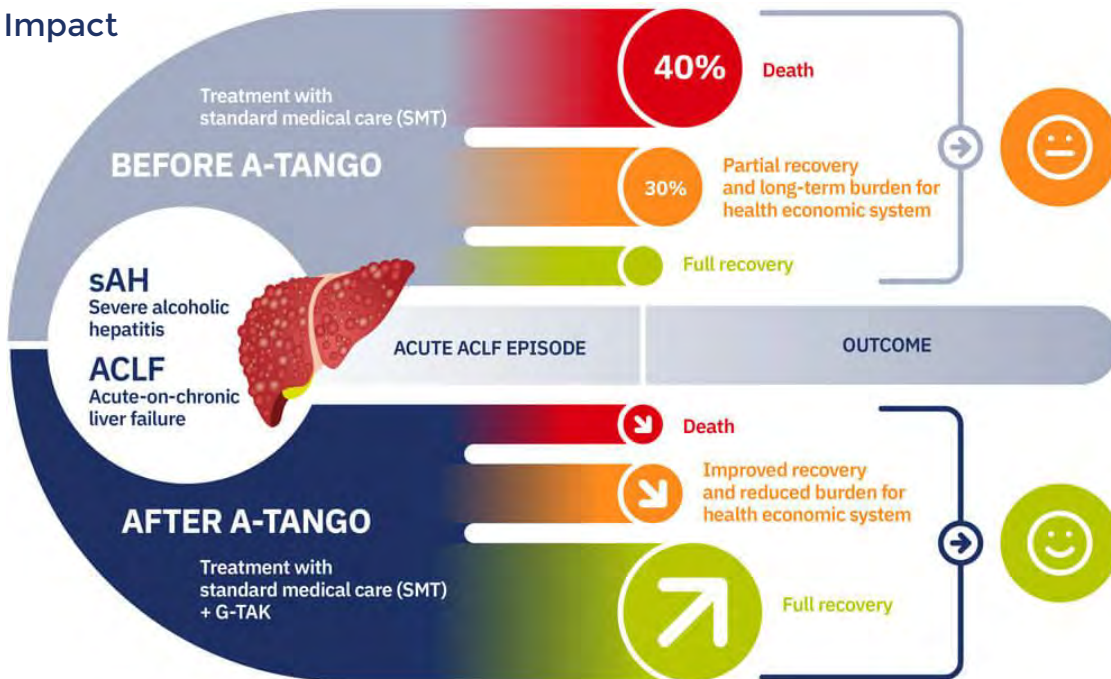
Earn up to two badges
with gamification on
EASL Campus



- + Hear directly from authors and experts in the field
- + Get answers to your questions
- + Take part every month

The A-TANGO project - featuring G-TAK, a novel combinatorial therapy for acute-on-chronic liver failure (ACLF)

Expected Impact

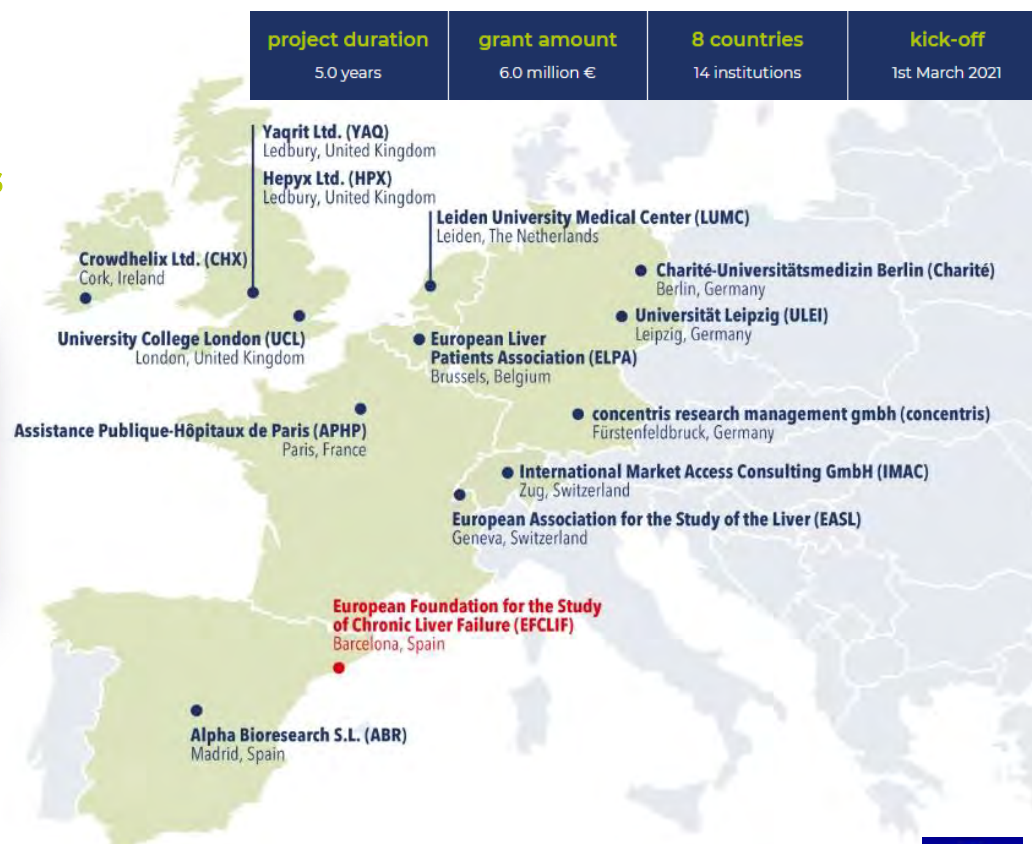


- More than 10 million people suffer from decompensated cirrhosis worldwide.
- Effective treatment of ACLF is an urgent and unmet need.
- A-TANGO performs Phase II clinical studies of G-TAK, a novel and innovative therapeutic strategy that aims to reduce inflammation and improve hepatocyte proliferation.
- A-TANGO also strives to identify reliable biomarkers for better patient stratification and increased survival.

**14 partners, one goal:
Helping cirrhosis patients
in Europe!**

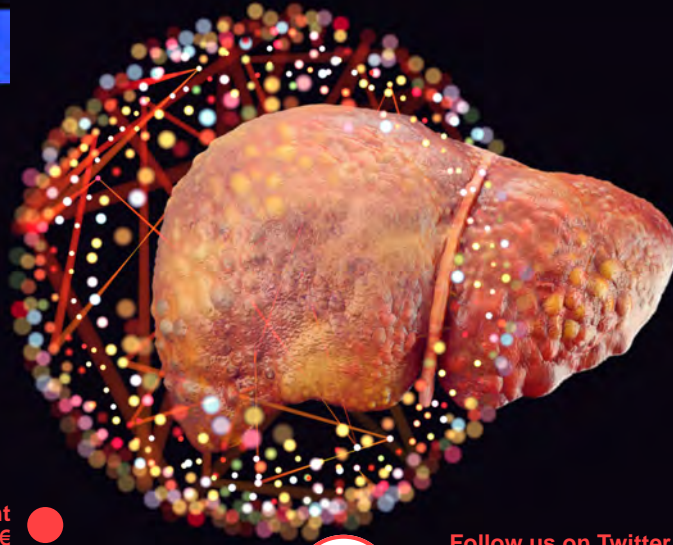


www.a-tango.eu
info@atango.eu



This project has received funding from the European Union's Horizon 2020 research and innovation programme under grant agreement No 945096.





kick-off
1st April 2020

project duration
5 ½ years

10 countries
21 institutions

grant amount
6 million €

www.decision-for-liver.eu



Follow us on Twitter and LinkedIN:



Decision4Liver



decision-project

The objective of **DECISION** is to better understand the pathophysiology of decompensated cirrhosis leading to acute-on-chronic liver failure (ACLF) or death. This consortium will take advantage of already existing large and clinically well-characterised patient cohorts to develop reliable prognostic and response tests and combinatorial therapies tailored to the needs of individual patients to decrease the risk of short-term death.

- Pathophysiologic elucidation of acute decompensated cirrhosis at the systems level (genetics, epigenetics, transcriptomics, metabolomics, lipidomics, miR, and analysis of extracellular vesicles)
- Integration of existing clinical data and new multi-omics data from 2,200 patients with more than 8,600 measurements
- Development of new combinatorial therapies
- Optimization of therapies using existing and new animal models
- Development of novel and robust tests for prediction of outcome following traditional treatment versus response to new therapies
- Phase II clinical trials to test new combination therapies
- Creation of new guidelines for outcome prediction and personalized treatment of acute decompensated cirrhosis to prevent ACLF to death



This project has received funding from the European Union's Horizon 2020 research and innovation programme under grant agreement No 847949.





Liver Investigation: Testing Marker Utility in Steatohepatitis

- 54 partners
- 14 countries for clinical recruitment
- True public-private co-funding model

The overarching aim of LITMUS is to develop, robustly validate and advance towards regulatory qualification biomarkers that diagnose, risk stratify and/or monitor NAFLD/NASH progression and fibrosis stage.

litmus-project.eu
imi.europa.eu



The LITMUS project has received funding from the Innovative Medicines Initiative 2 Joint Undertaking under grant agreement No. 777377. This Joint Undertaking receives support from the European Union's Horizon 2020 research and innovation programme and EFPIA.

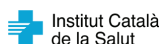
LIVER SCREEN

Screening for liver fibrosis population-based study across European Countries

A project that will change the paradigm
of diagnosis of chronic liver diseases

AIM:

To assess the prevalence of liver fibrosis in the general population
using Transient Elastography, with the objective of establishing
criteria for screening for liver fibrosis in the population.



MICROBiome-based biomarkers to PREDICT decompensation of liver cirrhosis and treatment response



Project duration
6 1/4 years

Start
01 January 2019

Follow-us on Twitter and LinkedIn:



Grant amount
15 million €

10 Countries
22 Partners

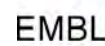
www.microb-predict.eu



will investigate

the human microbiome to identify predictors and mechanisms associated with the development of decompensation of cirrhosis and progression to **acute-on-chronic liver failure (ACLF) and death.**

- New microbiome-based tests for better stratification of cirrhosis patients
- Personalized prediction and prevention of decompensation and ACLF
- Clinical trial to predict response to treatment
- Modern, effective nanobiosensors as clinical tools with improved specificity
- More personalized treatment
- Increased survival times
- Decreased costs for the health systems



This project has received funding from the European Union's Horizon 2020 research and innovation programme under grant agreement No 825694.

Thursday 23 June

General Session I

GS001

Efficacy and safety of ALXN1840 versus standard of care in Wilson disease: primary results from an ongoing phase 3, randomized, controlled, rater-blinded trial

Karl Heinz Weiss¹, Michael Schilsky², Anna Czlonkowska³, Fred Askari⁴, Aftab Ala⁵, Peter Ferenci⁶, Peter Ott⁷, Dzhamal Abdurakhmanov⁸, Ferenc Szalay⁹, Piotr Socha¹⁰, Norikazu Shimizu¹¹, Jeff Bronstein¹², Danny Bega¹³, Sihoun Hahn¹⁴, Eugene Swenson¹⁵, Yi Chen¹⁵, Aurelia Poujois¹⁶. ¹Krankenhaus Salem der Evang. Stadtmission Heidelberg gGmbH, Heidelberg, Germany; ²Yale School of Medicine, New Haven, United States; ³Institute of Psychiatry and Neurology, Warsaw, Poland; ⁴University of Michigan Health System, Ann Arbor, United States; ⁵Royal Surrey County Hospital, Guildford, United Kingdom; ⁶Medical University of Vienna, Vienna, Austria; ⁷Aarhus University Hospital, Aarhus, Denmark; ⁸Sechenov First Moscow State Medical University, Moscow, Russian Federation; ⁹Semmelweis University, Budapest, Hungary; ¹⁰The Children's Memorial Health Institute, Warsaw, Poland; ¹¹Toho University School of Medicine, Tokyo, Japan; ¹²Ronald Reagan UCLA Medical Center, Los Angeles, United States; ¹³Northwestern University Feinberg School of Medicine, Chicago, United States; ¹⁴University of Washington/Seattle Children's Hospital, Seattle, United States; ¹⁵Alexion, AstraZeneca Rare Disease, Boston, United States; ¹⁶Rothschild Foundation Hospital, Paris, France
Email: karlheinz.weiss@stadtmission-hd.de

Abstract GS001 is under embargo until the start of the General Session I on Thursday 23 June 2022, 13:30 BST. It will be made publicly available on the congress website once the embargo has lifted.

Journalists, industry, investigators and/or study sponsors must abide by the embargo times set by EASL.

Violation of the embargo will be taken seriously. Individuals and/or sponsors who violate EASL's embargo policy may face sanctions relating to current and future abstract submissions, presentations and visibility at EASL Congresses. The EASL Governing Board is at liberty to ban attendance and/or retract data.

Copyright for abstracts (both oral and poster) on the website and as made available during The International Liver Congress™ 2022 resides with the respective authors. No reproduction, re-use or transcription for any commercial purpose or use of the content is permitted without the written permission of the authors. Permission for re-use must be obtained directly from the authors.

ORAL PRESENTATIONS

GS002

Anti-fibrotic effect of rifaximin in early alcohol-related liver disease: a double-blind, randomised, placebo-controlled trial

Mads Israelsen¹, Bjørn Stæhr Madsen¹, Nikolaj Torp^{1,2}, Stine Johansen^{1,2}, Camilla Dalby Hansen^{1,2}, Sönke Detlefsen^{1,2}, Peter Andersen¹, Johanne Kragh Hansen^{1,2}, Katrine Prier Lindvig^{1,2}, Ditlev Nytoft Rasmussen¹, Katrine Thorhauge^{1,2}, Maria Kjærgaard^{1,2}, Manimozhiyan Arumugam^{1,3}, Torben Hansen³, Jonel Trebicka^{1,4,5}, Maja Thiele^{1,2}, Aleksander Krag^{1,2}. ¹Odense University Hospital, Odense, Denmark; ²University of Southern Denmark, Faculty of Health Sciences; ³Copenhagen University, CBMR, København, Denmark; ⁴Goethe University Frankfurt, Gastroenterology, Frankfurt, Germany; ⁵European Foundation for the study of chronic liver failure, Barcelona, Spain
Email: mads.egerod.israelsen@rsyd.dk

Abstract GS002 is under embargo until the start of the General Session I on Thursday 23 June 2022, 13:30 BST. It will be made publicly available on the congress website once the embargo has lifted.

Journalists, industry, investigators and/or study sponsors must abide by the embargo times set by EASL.

Violation of the embargo will be taken seriously. Individuals and/or sponsors who violate EASL's embargo policy may face sanctions relating to current and future abstract submissions, presentations and visibility at EASL Congresses. The EASL Governing Board is at liberty to ban attendance and/or retract data.

Copyright for abstracts (both oral and poster) on the website and as made available during The International Liver Congress™ 2022 resides with the respective authors. No reproduction, re-use or transcription for any commercial purpose or use of the content is permitted without the written permission of the authors. Permission for re-use must be obtained directly from the authors.

GS003

The spatial distribution and detailed composition of infiltrating immune cells define autoimmune- and checkpoint-therapy associated hepatitis

Laurenz Krimmel¹, Henrike Salie¹, Saskia Killmer¹, Marilyn Salvat Lago¹, Nisha Rana¹, Peter Bronsert², David Rafei-Shamsabadi³, Frank Meiss³, Ursula Ehmer⁴, Angela Krackhardt⁵, Marius Schwabenland⁶, Marco Prinz^{6,7}, Christoph Neumann-Haefelin¹, Maike Hofmann¹, Michael Schultheiss¹, Robert Thimme¹, Carolin Mogler⁸, Bertram Bengsch^{1,7}. ¹Freiburg University Medical Center, Department of Internal Medicine II (Gastroenterology, Hepatology, Endocrinology und Infectiology), Freiburg, Germany; ²Freiburg University Medical Center, Institute of Pathology, Freiburg, Germany; ³Freiburg University Medical Center, Department of Dermatology, Freiburg, Germany; ⁴Klinikum rechts der Isar Technical University Munich, Department of Internal Medicine II, Munich, Germany; ⁵Klinikum rechts der Isar Technical University Munich, Department of Internal Medicine III, Munich, Germany; ⁶Freiburg University Medical Center, Institute of Neuropathology, Freiburg, Germany; ⁷Signalling Research Centres BIOS and CIBSS, Freiburg, Germany; ⁸Technical University Munich, Institute of Pathology, Munich, Germany
Email: bertram.bensch@uniklinik-freiburg.de

Abstract GS003 is under embargo until the start of the General Session I on Thursday 23 June 2022, 13:30 BST. It will be made publicly available on the congress website once the embargo has lifted.

Journalists, industry, investigators and/or study sponsors must abide by the embargo times set by EASL.

Violation of the embargo will be taken seriously. Individuals and/or sponsors who violate EASL's embargo policy may face sanctions relating to current and future abstract submissions, presentations and visibility at EASL Congresses. The EASL Governing Board is at liberty to ban attendance and/or retract data.

Copyright for abstracts (both oral and poster) on the website and as made available during The International Liver Congress™ 2022 resides with the respective authors. No reproduction, re-use or transcription for any commercial purpose or use of the content is permitted without the written permission of the authors. Permission for re-use must be obtained directly from the authors.

GS004

Prospective randomized controlled trial of biomarkers for early detection of hepatocellular carcinoma

Hooman Farhang Zangneh¹, Orlando Cerocchi¹, Korosh Khalili², Lima Awad El-Karim², Mara Vecchio³, Jeffrey Winick³, Yasuhiro Mori⁴, Hiroyuki Yamada⁴, Harry Janssen¹, Bettina Hansen^{1,5}, Morris Sherman¹, Jordan Feld¹. ¹University Health Network, Toronto General Hospital, Toronto Centre for Liver Disease, Toronto, Canada; ²University Health Network, Joint Department of Medical Imaging, Toronto, Canada; ³Fujifilm Healthcare Americas Corporation, United States; ⁴Fujifilm Wako Pure Chemical Corporation, Osaka, Japan; ⁵University of Toronto, Institute of Health Policy, Management and Evaluation, Toronto, Canada
Email: jordan.feld@uhn.ca

Abstract GS004 is under embargo until the start of the General Session I on Thursday 23 June 2022, 13:30 BST. It will be made publicly available on the congress website once the embargo has lifted.

Journalists, industry, investigators and/or study sponsors must abide by the embargo times set by EASL.

Violation of the embargo will be taken seriously. Individuals and/or sponsors who violate EASL's embargo policy may face sanctions relating to current and future abstract submissions, presentations and visibility at EASL Congresses. The EASL Governing Board is at liberty to ban attendance and/or retract data.

Copyright for abstracts (both oral and poster) on the website and as made available during The International Liver Congress™ 2022 resides with the respective authors. No reproduction, re-use or transcription for any commercial purpose or use of the content is permitted without the written permission of the authors. Permission for re-use must be obtained directly from the authors.

GS005

Development and validation of the gender-equity model for liver allocation (GEMA) to prioritize liver transplant candidates

Manuel Rodríguez-Perálvarez¹, Antonio M. Gómez-Orellana², Avik Majumdar³, Geoff McCaughan³, Paul Gow⁴, David Guijo-Rubio², César Hervás², Michael Bailey⁵, Emmanuel Tsochatzis⁶. ¹Hospital Universitario Reina Sofía, University of Córdoba, IMIBIC, CIBERehd, Department of Hepatology and Liver Transplantation, Córdoba, Spain; ²University of Córdoba, Department of Computer Science and Numerical Analysis, Córdoba, Spain; ³Royal Prince Alfred Hospital, Morrow Gastroenterology and Liver Centre and Australian National Liver Transplant Unit, Sydney, Australia; ⁴The University of Melbourne, Austin Health, Victorian Liver Transplant Unit, Melbourne, Australia; ⁵Australian and New Zealand Intensive Care Research Centre (ANZIC RC), Department of Epidemiology and Preventive Medicine, Melbourne, Australia; ⁶Royal Free Hospital and University College London (UCL), Sheila Sherlock Liver Unit and UCL Institute for Liver and Digestive Health, London, United Kingdom
Email: ropeml@hotmail.com

Abstract GS005 is under embargo until the start of the General Session I on Thursday 23 June 2022, 13:30 BST. It will be made publicly available on the congress website once the embargo has lifted.

Journalists, industry, investigators and/or study sponsors must abide by the embargo times set by EASL.

Violation of the embargo will be taken seriously. Individuals and/or sponsors who violate EASL's embargo policy may face sanctions relating to current and future abstract submissions, presentations and visibility at EASL Congresses. The EASL Governing Board is at liberty to ban attendance and/or retract data.

Copyright for abstracts (both oral and poster) on the website and as made available during The International Liver Congress™ 2022 resides with the respective authors. No reproduction, re-use or transcription for any commercial purpose or use of the content is permitted without the written permission of the authors. Permission for re-use must be obtained directly from the authors.

Policlinico, Division of Gastroenterology and Hepatology, Milan, Italy;
¹⁷CRC “A. M. and A. Migliavacca” Center for Liver Disease, University of Milan, Department of Pathophysiology and Transplantation, Milan, Italy
Email: wedemeyer.heiner@mh-hannover.de

Abstract GS006 is under embargo until the start of the General Session I on Thursday 23 June 2022, 13:30 BST. It will be made publicly available on the congress website once the embargo has lifted.

Journalists, industry, investigators and/or study sponsors must abide by the embargo times set by EASL.

Violation of the embargo will be taken seriously. Individuals and/or sponsors who violate EASL's embargo policy may face sanctions relating to current and future abstract submissions, presentations and visibility at EASL Congresses. The EASL Governing Board is at liberty to ban attendance and/or retract data.

Copyright for abstracts (both oral and poster) on the website and as made available during The International Liver Congress™ 2022 resides with the respective authors. No reproduction, re-use or transcription for any commercial purpose or use of the content is permitted without the written permission of the authors. Permission for re-use must be obtained directly from the authors.

GS006

Efficacy and safety of bulevirtide monotherapy given at 2 mg or 10 mg dose level once daily for treatment of chronic hepatitis delta: week 48 primary end point results from a phase 3 randomized, multicenter, parallel design study

Heiner Wedemeyer¹, Soo Aleman², Maurizia Brunetto^{3,4}, Antje Blank⁵, Pietro Andreone⁶, Pavel Bogomolov⁷, Vladimir Chulanov⁸, Nina Mamonova⁸, Natalia Geyvandova⁹, Morozov Viacheslav¹⁰, Olga Sagalova¹¹, Tatyana Stepanova¹², Dmitry Manuilov¹³, Vithika Suri¹³, Qi An¹³, John F. Flaherty¹³, Anu Osinusi¹³, Julian Schulze zur Wiesch¹⁴, Markus Cornberg¹, Stefan Zeuzem¹⁵, Pietro Lampertico^{16,17}. ¹Medizinische Hochschule Hannover, Klinik für Gastroenterologie, Hepatologie und Endokrinologie, Hannover, Germany; ²Karolinska University Hospital/Karolinska Institutet, Department of Infectious Diseases, Stockholm, Sweden; ³University Hospital of Pisa, Hepatology Unit, Reference Center of the Tuscany Region for Chronic Liver Disease and Cancer, Pisa, Italy; ⁴University of Pisa, Department of Clinical and Experimental Medicine, Pisa, Italy; ⁵Heidelberg University Hospital, Clinical Pharmacology and Pharmacoepidemiology, Heidelberg, Germany; ⁶University of Modena and Reggio Emilia, Internal Medicine, Modena, Italy; ⁷State budgetary institution of health care of Moscow region “Moscow regional research clinical institute after M.F. Vladimirsky”, Moscow, Russian Federation; ⁸FSBI National Research Medical Center for Phthiopulmonology and Infectious Diseases of the Ministry of Health of the Russian Federation, Moscow, Russian Federation; ⁹Stavropol Regional Hospital, Stavropol, Russian Federation; ¹⁰LLC Medical Company “Hepatolog,” Samara, Russian Federation; ¹¹Federal state-funded institution of higher education “Southern Ural State Medical University of Ministry of Health of the Russian Federation”, Chelyabinsk, Russian Federation; ¹²Limited liability company “Clinic of Modern Medicine,” Moscow, Russian Federation; ¹³Gilead Sciences, Foster City, United States; ¹⁴Universitätsklinikum Hamburg-Eppendorf, Medizinische Klinik Studienambulanz Hepatologie, Hamburg, Germany; ¹⁵University Hospital Frankfurt, Department of Medicine, Frankfurt am Main, Germany; ¹⁶Foundation IRCCS Ca' Granda Ospedale Maggiore

Friday 24 June

General Session II

GS007

Transcatheter arterial chemoembolization (TACE) followed by conformal radiotherapy versus TACE alone for hepatocellular carcinoma: a western controlled trial

Cyrille Feray¹, Loic Campion², Isabelle Mabile-Archambeaud³, Philippe Mathurin⁴, Xavier Mirabel⁵, Emmanuel Rio², Jean-Pierre Bronowicki⁶, Yann Toucheffeu³, Jérôme Gournay³, Agnès Rode⁷, Françoise Mornex⁸, Philippe Merle⁹. ¹Centre Hepato Biliaire, Villejuif, France; ²CRLCC, Nantes, France; ³IMAD, Nantes, France; ⁴Hepatology, Lille, France; ⁵CRLCC, Lille, France; ⁶Hepatology, Nancy, France; ⁷Radiology, Lyon, France; ⁸Radiotherapy, Lyon, France; ⁹Hepatology, Lyon, France
Email: cyrille.feray@gmail.com

Abstract GS007 is under embargo until the start of the General Session II on Friday 24 June 2022, 13:40 BST. It will be made publicly available on the congress website once the embargo has lifted.

Journalists, industry, investigators and/or study sponsors must abide by the embargo times set by EASL.

Violation of the embargo will be taken seriously. Individuals and/or sponsors who violate EASL's embargo policy may face sanctions relating to current and future abstract submissions, presentations and visibility at EASL Congresses. The EASL Governing Board is at liberty to ban attendance and/or retract data.

Copyright for abstracts (both oral and poster) on the website and as made available during The International Liver Congress™ 2022 resides with the respective authors. No reproduction, re-use or transcription for any commercial purpose or use of the content is permitted without the written permission of the authors. Permission for re-use must be obtained directly from the authors.

GS008

The global burden of liver cancer (LC) and chronic liver diseases (CLD) is driven by non-alcoholic steatohepatitis (NASH) and alcohol liver disease (ALD)

James Paik^{1,2}, Linda Henry^{1,2,3}, Youssef Younossi³, Janus Ong^{3,4}, Saleh Alqahtani^{3,5,6}, Zobair Younossi^{1,2,7}. ¹Inova Health System, Center for Liver Diseases, Department of Medicine; ²Betty and Guy Beatty Center for Integrated Research, IHS; ³Center for Outcomes Research in Liver Disease; ⁴University of the Philippines, College of Medicine; ⁵Johns Hopkins Medical Center; ⁶King Faisal Specialist Hospital and Research Center; ⁷Inova Health System, Medicine Service Line
Email: zobair.younossi@inova.org

Abstract GS008 is under embargo until the start of the General Session II on Friday 24 June 2022, 13:40 BST. It will be made publicly available on the congress website once the embargo has lifted.

Journalists, industry, investigators and/or study sponsors must abide by the embargo times set by EASL.

Violation of the embargo will be taken seriously. Individuals and/or sponsors who violate EASL's embargo policy may face sanctions relating to current and future abstract submissions, presentations and visibility at EASL Congresses. The EASL Governing Board is at liberty to ban attendance and/or retract data.

Copyright for abstracts (both oral and poster) on the website and as made available during The International Liver Congress™ 2022 resides with the respective authors. No reproduction, re-use or transcription for any commercial purpose or use of the content is permitted without the written permission of the authors. Permission for re-use must be obtained directly from the authors.

ORAL PRESENTATIONS

GS009

Is there a murine model that fully recapitulates human NASH? An unbiased bioinformatics approach to rank pre-clinical models based on proximity to human disease

Michele Vacca^{1,2}, Ioannis Kamzolas^{1,3}, Lea Mørch Harder⁴, Fiona Oakley⁵, Christian Trautwein⁶, Maximilian Hatting⁶, Trenton Ross⁷, Barbara Bernardo⁸, Anouk Oldenburger⁹, Sara Toftegaard Hjuler⁴, Iwona Ksiazek¹⁰, Daniel Linden^{11,12}, Detlef Schuppan¹³, Sergio Rodriguez-Cuenca¹, Maria Manuela Tonini¹⁴, Aimo Kannt^{15,16}, Tamara Rodriguez-Castaneda¹⁵, Cecília M. P. Rodrigues¹⁷, Simon Cockell¹⁸, Olivier Govaere¹⁹, Ann K. Daly¹⁹, Michael Allison²⁰, Kristian Honnens de Lichtenberg⁴, Yong Ook Kim¹³, Anna Lindblom¹¹, Stephanie Oldham²¹, Anne-Christine Andréasson¹¹, Franklin Schlerman²², Jonathon Marionneau²³, Arun Sanyal²⁴, Marta B. Afonso¹⁷, Anthony Rinaldi⁷, Yuichiro Amano²⁵, Valérie Paradis²⁶, Alastair Burt¹⁹, Davies Susan²⁷, Ann Driessen²⁸, Hiroaki Yashiro²⁹, M. Julia Brosnan⁷, Carla Yunis⁷, Pierre Bedossa³⁰, Dina Tiniakos^{31,32}, Quentin Anstee^{31,33}, Evangelia Petsalaki³, Peter Davidsen⁴, Jim Perfield³⁴, Antonio Vidal-Puig¹. ¹University of Cambridge, WT/MRC Institute of Metabolic Science, United Kingdom; ²University of Bari Aldo Moro, Interdisciplinary Department of Medicine, Bari, Italy; ³European Molecular Biology Laboratory, European Bioinformatics Institute (EMBL-EBI), European Molecular Biology Laboratory, European Bioinformatics Institute (EMBL-EBI), Wellcome Genome Campus, Hinxton, UK, Hinxton, Cambridge, United Kingdom; ⁴Novo Nordisk, Research and Early Development, Novo Nordisk A/S, Denmark, Måløv, Copenhagen, Denmark; ⁵Newcastle University, Newcastle Fibrosis Research Group, Biosciences Institute, Faculty of Medical Sciences, Newcastle University, Newcastle upon Tyne, UK, Newcastle, United Kingdom; ⁶Aachen University Hospital, Department of Medicine III, Aachen; ⁷Pfizer IMRU, Internal Medicine Research Unit, Pfizer Worldwide Research and Development, Cambridge Massachusetts, United States; ⁸Pfizer, Internal Medicine, Pfizer Worldwide Research and Development, 558 Eastern Point Road, Groton, CT, 06340, USA, Groton, United States; ⁹Boehringer Ingelheim Pharma GmbH and Co. KG, CardioMetabolic Diseases Research, Boehringer Ingelheim Pharma GmbH and Co. KG, Biberach a.d. Riss, Germany, Biberach an der Riß, Germany; ¹⁰Novartis Pharma AG, Novartis Institutes for BioMedical Research, Novartis Pharma AG, 4056 Basel, Switzerland, Basel, Switzerland; ¹¹AstraZeneca, Bioscience Metabolism, Research and Early Development Cardiovascular, Renal and Metabolism (CVRM), BioPharmaceuticals RandD, AstraZeneca, Gothenburg, Sweden, Gothenburg, Sweden; ¹²University of Gothenburg, Division of Endocrinology, Department of Neuroscience and Physiology, Sahlgrenska Academy, University of Gothenburg, Sweden, Gothenburg, Sweden; ¹³Institute of Translational Immunology and Research Center for Immunotherapy, Johannes Gutenberg University Medical Center, Mainz, Germany; ¹⁴Integrated Biobank of Luxembourg (IBBL), Luxembourg Institute of Health, Translational Medicine Operations Hub, Luxembourg, Dudelange, Luxembourg; ¹⁵Sanofi-Aventis Deutschland GmbH, RandD Diabetes, Sanofi-Aventis Deutschland GmbH, Industriepark Hoechst, 65926 Frankfurt, Germany, Frankfurt am Main, Germany; ¹⁶Fraunhofer Institute for Translational Medicine and

Pharmacology ITMP, Fraunhofer Institute for Translational Medicine and Pharmacology ITMP, Theodor-Stern-Kai 7, 60956 Frankfurt, Germany, Frankfurt am Main, Germany; ¹⁷University of Lisbon, Research Institute for Medicines, Faculty of Pharmacy, Universidade de Lisboa, Lisbon, Portugal, Lisbon, Portugal; ¹⁸Newcastle University, Bioinformatics Support Unit, Faculty of Medical Sciences, Newcastle University, Newcastle upon Tyne, United Kingdom, Newcastle upon Tyne, United Kingdom; ¹⁹Newcastle University, Translational and Clinical Research Institute, Faculty of Medical Sciences, Newcastle University, Newcastle upon Tyne, United Kingdom, Newcastle upon Tyne, United Kingdom; ²⁰Cambridge University Hospitals NHS Foundation Trust, Liver Unit, Cambridge NIHR Biomedical Research Centre, Cambridge, United Kingdom; ²¹AstraZeneca, Bioscience Metabolism, Research and Early Development Cardiovascular, Renal and Metabolism (CVRM), BioPharmaceuticals RandD, AstraZeneca, Gaithersburg, MD, USA, Gaithersburg, MD, United States; ²²Pfizer, Inflammation and Immunology Research Unit, Pfizer Worldwide Research and Development, Cambridge Massachusetts, Cambridge Massachusetts, United States; ²³Sanyal Biotechnology LLC, Sanyal Biotechnology LLC, Norfolk, Virginia, USA, Virginia, United States; ²⁴Virginia commonwealth university, Department of Internal Medicine, Virginia commonwealth university, Richmond, VA, United States; ²⁵Takeda Pharmaceuticals International AG, Takeda Pharmaceuticals International AG, Takeda Pharmaceutical Company Limited, Fujisawa, Japan, Fujisawa, Japan; ²⁶Université Paris-Diderot, Department of Imaging and Pathology, Hôpital Beaujon, Paris, France; ²⁷Cambridge University Hospitals NHS Foundation Trust, Department of Cellular Pathology, Cambridge University Hospitals NHS Foundation Trust, Cambridge, United Kingdom; ²⁸University of Antwerp, Department of Pathology, University of Antwerp, Antwerp, Belgium, Antwerp, Belgium; ²⁹Takeda Pharmaceuticals International AG, Takeda Pharmaceuticals International AG, Takeda Pharmaceutical Company Limited, Cambridge, Massachusetts, Cambridge, Massachusetts, United States; ³⁰Newcastle University, LiverPat, Paris, France and Translational and Clinical Research Institute, Newcastle University, UK, France; ³¹Newcastle University, Translational and Clinical Research Institute, Faculty of Medical Sciences, Newcastle University, Newcastle upon Tyne, UK, Newcastle upon Tyne, United Kingdom; ³²National and Kapodistrian University of Athens, Department of Pathology, Aretaieion Hospital, Medical School, National and Kapodistrian University of Athens, Greece, Athens, Greece; ³³Newcastle University, Newcastle NIHR Biomedical Research Centre, Newcastle upon Tyne Hospitals NHS Trust, Newcastle upon Tyne, United Kingdom, Newcastle upon Tyne, United Kingdom; ³⁴Eli Lilly and Company, Lilly Research Laboratories, Eli Lilly and Company, Indianapolis, Indiana, Indianapolis, Indiana, United States Email: ajv22@medschl.cam.ac.uk

Abstract GS009 is under embargo until the start of the General Session II on Friday 24 June 2022, 13:40 BST. It will be made publicly available on the congress website once the embargo has lifted. Journalists, industry, investigators and/or study sponsors must abide by the embargo times set by EASL. Violation of the embargo will be taken seriously. Individuals and/or sponsors who violate EASL's embargo policy may face sanctions relating to current and future abstract submissions, presentations and visibility at EASL Congresses. The EASL Governing Board is at liberty to ban attendance and/or retract data. Copyright for abstracts (both oral and poster) on the website and as made available during The International Liver Congress™ 2022 resides with the respective authors. No reproduction, re-use or transcription for any commercial purpose or use of the content is permitted without the written permission of the authors. Permission for re-use must be obtained directly from the authors.

GS010

Efficacy and safety of finite 48-week treatment with the siRNA JNJ-3989 and the capsid assembly modulator (CAM-N) JNJ-6379 in HBeAg negative virologically suppressed (VS) chronic hepatitis B (CHB) patients: results from REEF-2 study

Kosh Agarwal¹, Maria Buti², Florian van Bömmel³, Pietro Lampertico⁴, Ewa Janczewska⁵, Marc Bourliere⁶, Thomas Vanwolleghem^{7,8}, Oliver Lenz⁹, Thierry Verbinen⁹, Thomas Kakuda⁹, Cristina Mayer⁹, John Jerzowski⁹, Maria Beumont-Mauviel⁹, Ronald Kalmeijer⁹, Michael Biermer⁹, Isabelle Lonjon-Domanec⁹. ¹Institute of Liver Studies, King's College Hospital; ²Hospital Universitario Valle de Hebrón; ³University Hospital Leipzig; ⁴Fondazione IRCCS Ca' Granda, Ospedale Maggiore Policlinico, University of Milan; ⁵Medical University of Silesia; ⁶Hôpital Saint Joseph; ⁷Antwerp University Hospital (UZA); ⁸Viral Hepatitis Research Group, Laboratory of Experimental Medicine and Pediatrics, University of Antwerp; ⁹Janssen Research and Development
Email: kosh.agarwal@nhs.net

Abstract GS010 is under embargo until the start of the General Session II on Friday 24 June 2022, 13:40 BST. It will be made publicly available on the congress website once the embargo has lifted.

Journalists, industry, investigators and/or study sponsors must abide by the embargo times set by EASL.

Violation of the embargo will be taken seriously. Individuals and/or sponsors who violate EASL's embargo policy may face sanctions relating to current and future abstract submissions, presentations and visibility at EASL Congresses. The EASL Governing Board is at liberty to ban attendance and/or retract data.

Copyright for abstracts (both oral and poster) on the website and as made available during The International Liver Congress™ 2022 resides with the respective authors. No reproduction, re-use or transcription for any commercial purpose or use of the content is permitted without the written permission of the authors. Permission for re-use must be obtained directly from the authors.

GS011

Microbial produced ethanol: an underestimated burden on the liver

Stijn Meijnikman¹, Mark Davids², Hilde Herrema¹, Omrum Aydin¹, Valentina Tremaroli³, Joanne Verheij¹, Maurits De Brauw⁴, Sven Francque⁵, Christophe De Block⁵, Fredrik Backhed³, Victor Gerdes¹, Bert Groen¹, Max Nieuwdorp¹. ¹Amsterdam UMC, locatie AMC, Amsterdam, Netherlands; ²Amsterdam UMC, locatie AMC, Vascular Medicine, Amsterdam, Netherlands; ³Gothenburg University, Gothenburg, Sweden; ⁴Spaarne Hospital Hoofddorp, Hoofddorp, Netherlands; ⁵Antwerp University Hospital, Edegem, Belgium
Email: a.s.meijnikman@amc.uva.nl

Abstract GS011 is under embargo until the start of the General Session II on Friday 24 June 2022, 13:40 BST. It will be made publicly available on the congress website once the embargo has lifted.

Journalists, industry, investigators and/or study sponsors must abide by the embargo times set by EASL.

Violation of the embargo will be taken seriously. Individuals and/or sponsors who violate EASL's embargo policy may face sanctions relating to current and future abstract submissions, presentations and visibility at EASL Congresses. The EASL Governing Board is at liberty to ban attendance and/or retract data.

Copyright for abstracts (both oral and poster) on the website and as made available during The International Liver Congress™ 2022 resides with the respective authors. No reproduction, re-use or transcription for any commercial purpose or use of the content is permitted without the written permission of the authors. Permission for re-use must be obtained directly from the authors.

GS012

A non-calorie restricted low carbohydrate high fat diet improves non-alcoholic fatty liver disease (NAFLD) activity score (NAS) and HbA1c in type 2 diabetes: a six-month randomised controlled trial

Camilla Dalby Hansen^{1,2}, Eva-Marie Gram-Kampmann^{2,3}, Johanne Kragh Hansen^{1,2}, Mie Balle Hugger¹, Bjørn Stæhr Madsen¹, Jane Jensen¹, Sara Olesen², Nikolaj Torp¹, Ditlev Nytoft Rasmussen¹, Maria Kjærgaard^{1,2}, Stine Johansen^{1,2}, Katrine Prier Lindvig^{1,2}, Peter Andersen¹, Katrine Thorhauge^{1,2}, Jan Christian Brønd², Pernille Hermann³, Henning Beck-Nielsen³, Sönke Detlefsen^{2,4}, Torben Hansen⁵, Kurt Højlund³, Maja Thiele^{1,2}, Mads Israelsen¹, Aleksander Krag^{1,2}. ¹Odense University Hospital, Gastroenterology and Hepatology, Odense, Denmark; ²University of Southern Denmark, Clinical Institute, Odense, Denmark; ³Odense University Hospital, Endocrinology, Odense, Denmark; ⁴Odense University Hospital, Pathology, Odense, Denmark; ⁵The Novo Nordisk Foundation Center for Basic Metabolic Research, København, Denmark
Email: aleksander.krag@rsyd.dk

Abstract GS012 is under embargo until the start of the General Session II on Friday 24 June 2022, 13:40 BST. It will be made publicly available on the congress website once the embargo has lifted.

Journalists, industry, investigators and/or study sponsors must abide by the embargo times set by EASL.

Violation of the embargo will be taken seriously. Individuals and/or sponsors who violate EASL's embargo policy may face sanctions relating to current and future abstract submissions, presentations and visibility at EASL Congresses. The EASL Governing Board is at liberty to ban attendance and/or retract data.

Copyright for abstracts (both oral and poster) on the website and as made available during The International Liver Congress™ 2022 resides with the respective authors. No reproduction, re-use or transcription for any commercial purpose or use of the content is permitted without the written permission of the authors. Permission for re-use must be obtained directly from the authors.

Saturday 25 June

Late-Breaker

LB001

Semaglutide 2.4 mg once weekly improved liver and metabolic parameters, and was well tolerated, in patients with non-alcoholic steatohepatitis-related cirrhosis: a randomised, placebo-controlled phase 2 trial

Rohit Loomba¹, Manal F. Abdelmalek², Matthew Armstrong³, Maximilian Jara⁴, Mette Kjaer⁴, Niels Krarup⁴, Eric Lawitz⁵, Vlad Ratziu⁶, Arun Sanyal⁷, Jörn Schattenberg⁸, Philip N. Newsome³.

¹University of California at San Diego, NAFLD Research Center, Division of Gastroenterology, La Jolla, CA, United States; ²Duke University, Durham, United States; ³University of Birmingham and University Hospitals Birmingham NHS Foundation Trust, Birmingham, United Kingdom; ⁴Novo Nordisk A/S, Søborg, Denmark; ⁵Texas Liver Institute, University of Texas Health San Antonio, San Antonio, TX, United States; ⁶Sorbonne Université, Hôpital Pitié-Salpêtrière, Paris, France; ⁷Virginia Commonwealth University School of Medicine, Richmond, VA, United States; ⁸Metabolic Liver Research Program, I. Department of Medicine, University Medical Centre, Mainz, Germany

Email: roloomba@ucsd.edu

The late breaker abstracts are under embargo until the start of the session on Saturday 25 June 2022 at 14:00 BST. They will be made publicly available on the congress website once the embargo has lifted.

Journalists, industry, investigators and/or study sponsors must abide by the embargo times set by EASL.

Violation of the embargo will be taken seriously. Individuals and/or sponsors who violate EASL's embargo policy may face sanctions relating to current and future abstract submissions, presentations and visibility at EASL Congresses. The EASL Governing Board is at liberty to ban attendance and/or retract data.

Copyright for abstracts (both oral and poster) on the website and as made available during The International Liver Congress™ 2022 resides with the respective authors. No reproduction, re-use or transcription for any commercial purpose or use of the content is permitted without the written permission of the authors. Permission for re-use must be obtained directly from the authors.

LB002

Genetic variation in TERT modifies the risk of hepatocellular carcinoma in alcohol-related cirrhosis: results from a genome-wide case-control study

Stephan Buch¹, Hamish Innes², Philipp Lutz³, Hans Dieter Nischalke⁴, Jacob Nattermann⁴, Jens U. Marquardt⁵, Janett Fischer⁶, Karl Heinz Weiss⁷, Jonas Rosendahl⁸, Astrid Marot⁹, Marcin Krawczyk¹⁰, Markus Casper¹⁰, Frank Lammert¹⁰, Florian Eyer¹¹, Arndt Vogel¹², Silke Marhenke¹², Johann von Felden¹³, Rohini Sharma¹⁴, Stephen Atkinson¹⁵, Andrew McQuillin¹⁵, Clemens Schafmayer¹⁶, Christian Strassburg¹⁷, Heidi Altmann¹, Stefan Sulk¹, Veera Raghavan Thangapandi¹, Mario Brosch¹, Carolin Lackner¹⁸, Rudolf E. Stauber¹⁸, Ali Canbay¹⁹, Alexander Link²⁰, Thomas Reiberger²¹, Mattias Mandorfer²¹, Georg Semmler²¹, Bernhard Scheiner²¹, Christian Datz²², Stefano Romeo²³, Stefano Ginanni Corradini²⁴, Luca Valenti²⁵, Sascha Müller²⁶, Marsha Morgan^{15,27}, Jean-Francois Dufour²⁸, Jonel Trebicka²⁹, Thomas Berg³⁰, Pierre Deltenre³¹, Sebastian Mueller³², Jochen Hampe¹, Felix Stickel³³. ¹University Hospital Dresden, TU Dresden, Medical Department 1, Dresden, Germany; ²Glasgow Caledonian University, School of Health and Life Sciences, Glasgow, United Kingdom; ³University of Bonn, Department of Internal Medicine I, Bonn, Germany; ⁴University of Bonn, Department of Internal Medicine I, Bonn, Germany; ⁵University of Luebeck, Department of Medicine, Lübeck, Germany; ⁶Leipzig University Medical Center, Division of Hepatology, Department of Medicine II, Leipzig, Germany; ⁷Salem Medical Center Heidelberg, Department of Internal Medicine, Heidelberg, Germany; ⁸University Hospital Halle/Saale, Department of Gastroenterology, Halle/Saale, Germany; ⁹Université Catholique de Louvain, Department of Gastroenterology and Hepatology, CHU UCL Namur, Belgium; ¹⁰Saarland University, Department of Medicine II, Saarland University Medical Center, Homburg, Germany; ¹¹Technical University of Munich, Department of Clinical Toxicology, Klinikum Rechts der Isar, München, Germany; ¹²Hannover Medical School, Department of Gastroenterology, Hepatology and Endocrinology, Hannover, Germany; ¹³University Medical Center Hamburg-Eppendorf, First Department of Medicine, Hamburg, Germany; ¹⁴Imperial College London, London, United Kingdom; ¹⁵University College London, UCL Institute for Liver and Digestive Health, Division of Medicine, London, United Kingdom; ¹⁶Rostock University Medical Center, Department of General, Visceral, Vascular and Transplant Surgery, Rostock, Germany; ¹⁷Universitätsklinikum Bonn, Medical Department 1, Bonn, Germany; ¹⁸Medical University of Graz, Institute of Pathology, Graz, Austria; ¹⁹University Hospital, Ruhr University Bochum, Department of Medicine, Bochum, Germany; ²⁰Otto-von-Guericke University, Department of Gastroenterology, Hepatology and Infectious Diseases, Magdeburg, Germany; ²¹Medical University of Vienna, Division of Gastroenterology and Hepatology, Department of Internal Medicine III, Vienna, Austria; ²²Teaching Hospital of the Paracelsus Medical University Salzburg, Department of Internal Medicine, General Hospital Oberndorf, Oberndorf, Austria; ²³University of Gothenburg, Department of Molecular and Clinical Medicine, Institute of Medicine, Sahlgrenska Academy, Wallenberg Laboratory, Gothenburg, Sweden; ²⁴Sapienza University of Rome, Division of Gastroenterology, Department of Translational and Precision Medicine, Gastroenterology Unit, Rome, Italy; ²⁵Fondazione IRCCS Ca'Granda Ospedale Maggiore Policlinico, Internal Medicine and Metabolic Diseases, Milan, Italy; ²⁶Clinic Beau-Site, Department of Surgery, Berne, Switzerland; ²⁷UCL Institute for Liver and Digestive Health, Department of Medicine, Royal Free Campus, London, United Kingdom; ²⁸University of Bern, Hepatology, Department of Biomedical Research, Bern, Switzerland; ²⁹Goethe University Frankfurt, Department of Internal Medicine I, Frankfurt, Germany; ³⁰Leipzig University Medical Center, Division of Hepatology, Leipzig, Germany; ³¹Centre Hospitalier Universitaire Vaudois, Division of Gastroenterology and Hepatology, Switzerland; ³²Salem Medical Center, Center for Alcohol Research, University of Heidelberg and Medical Department, Heidelberg, Germany; ³³University Hospital of Zurich,

Department of Gastroenterology and Hepatology, Zurich, Switzerland
Email: stephan.buch@uniklinikum-dresden.de

The late breaker abstracts are under embargo until the start of the session on Saturday 25 June 2022 at 14:00 BST. They will be made publicly available on the congress website once the embargo has lifted.

Journalists, industry, investigators and/or study sponsors must abide by the embargo times set by EASL.

Violation of the embargo will be taken seriously. Individuals and/or sponsors who violate EASL's embargo policy may face sanctions relating to current and future abstract submissions, presentations and visibility at EASL Congresses. The EASL Governing Board is at liberty to ban attendance and/or retract data.

Copyright for abstracts (both oral and poster) on the website and as made available during The International Liver Congress™ 2022 resides with the respective authors. No reproduction, re-use or transcription for any commercial purpose or use of the content is permitted without the written permission of the authors. Permission for re-use must be obtained directly from the authors.

LB003

Reprogramming necroptosis limits immune responses and prevents liver cancer development

Mihael Vucur¹, Ahmed Ghallab², Anne Schneider¹, Jakob Kather³, Olivier Govaere⁴, Augusto Villanueva⁵, Achim Weber⁶, Thomas Longerich⁷, Frank Tacke⁸, Christoph Roderburg¹, Johannes Bode¹, Fabian Geisler⁹, Ulf Neumann¹⁰, Jan G. Hengstler², Mathias Heikenwälder¹¹, Tom Lüdde¹. ¹University Hospital Duesseldorf, Department of Gastroenterology, Hepatology and Infectious Disease, Germany; ²Leibniz Research Centre for Working Environment and Human Factors (IfAdo) at the Technical University Dortmund, Germany; ³Department of Medicine III, University Hospital RWTH Aachen, Germany; ⁴Translational and Clinical Research Institute, Faculty of Medical Sciences, Newcastle University; ⁵Division of Liver Diseases, Department of Medicine, Icahn School of Medicine at Mount Sinai, United States; ⁶Department of Pathology and Molecular Pathology, University Hospital Zurich, Switzerland; ⁷Institute of Pathology, University Hospital Heidelberg, Germany; ⁸Department of Hepatology and Gastroenterology, Charité-Universitätsmedizin, Berlin, Germany; ⁹Second Department of Internal Medicine, Klinikum rechts der Isar, Technische Universität München, Germany; ¹⁰Visceral and

ORAL PRESENTATIONS

Transplant Surgery, University Hospital RWTH Aachen, Germany;

¹¹Department of Chronic Inflammation and Cancer, German Cancer Research Institute (DKFZ), Heidelberg, Germany
Email: mihael.vucur@med.uni-duesseldorf.de

The late breaker abstracts are under embargo until the start of the session on Saturday 25 June 2022 at 14:00 BST. They will be made publicly available on the congress website once the embargo has lifted.

Journalists, industry, investigators and/or study sponsors must abide by the embargo times set by EASL.

Violation of the embargo will be taken seriously. Individuals and/or sponsors who violate EASL's embargo policy may face sanctions relating to current and future abstract submissions, presentations and visibility at EASL Congresses. The EASL Governing Board is at liberty to ban attendance and/or retract data.

Copyright for abstracts (both oral and poster) on the website and as made available during The International Liver Congress™ 2022 resides with the respective authors. No reproduction, re-use or transcription for any commercial purpose or use of the content is permitted without the written permission of the authors. Permission for re-use must be obtained directly from the authors.

LB004A

Efficacy and safety of bepirovirsen in patients with chronic hepatitis B virus infection not on stable nucleos (t)ide analogue therapy: interim results from the randomised phase 2b B-Clear study

Seng Gee Lim¹, Cristina Pojoga^{2,3}, Harry Janssen⁴, Denis Gusev⁵, Robert Plesniak⁶, Keiji Tsuji⁷, Ewa Janczewska⁸, Corneliu Petru Popescu⁹, Pietro Andreone¹⁰, Jinlin Hou¹¹, Manuela Arbune¹², Adrian Gadano¹³, Diana Petrova¹⁴, Jun Inoue¹⁵, Teerha Piratvisuth¹⁶, Young-Suk Lim¹⁷, Apinya Leerapun¹⁸, Masanori Atsukawa¹⁹, Ji-Dong Jia²⁰, Eternity Labio²¹, Jennifer Cremer²², Robert Elston²³, Tamara Lukic²⁴, Geoff Quinn²³, Stuart Kendrick²³, Punam Bharania²³, Fiona Campbell²³, Melanie Paff²², Dickens Theodore²². ¹National University Health System, Singapore; ²Regional Institute of Gastroenterology and Hepatology, Romania; ³Babeş-Bolyai University, Department of Clinical Psychology and Psychotherapy, International Institute for Advanced Study of Psychotherapy and Applied Mental Health, Romania; ⁴Toronto General Hospital, Canada; ⁵Center for Prevention and Control of AIDS and Infectious Diseases, Russian Federation; ⁶University of Rzeszow Centrum Medyczne w Lancucie Sp. z o.o., Poland; ⁷Hiroshima Red Cross Hospital, Japan; ⁸Faculty of Health Sciences in Bytom, Medical University of Silesia, ID Clinic, Poland; ⁹Dr Victor Babes Clinical Hospital of Infectious and Tropical Diseases, Carol Davila University of Medicine and Pharmacy, Romania; ¹⁰Azienda Ospedaliero-Universitaria di Modena, Italy; ¹¹Nanfang Hospital, Southern Medical University, China; ¹²Sf. Cuv. Parascheva Infectious Diseases Clinical Hospital, Romania; ¹³Hospital Italiano de Buenos Aires, Argentina; ¹⁴Diagnostic Consultative Centre Alexandrovska, Bulgaria; ¹⁵Tohoku University Hospital, Japan; ¹⁶NKC Institute of Gastroenterology and Hepatology, Thailand; ¹⁷Asan Medical Center, University of Ulsan College of Medicine, Korea, Rep. of South; ¹⁸Chiang Mai University, Thailand; ¹⁹Department of Internal Medicine, Division of Gastroenterology and Hepatology, Nippon Medical School, Japan; ²⁰Beijing Friendship Hospital, Capital Medical University, China; ²¹Makati Medical Center, Philippines; ²²GlaxoSmithKline, United States; ²³GlaxoSmithKline, United Kingdom; ²⁴GlaxoSmithKline, United Arab Emirates
Email: jennifer.x.cremer@gsk.com

The late breaker abstracts are under embargo until the start of the session on Saturday 25 June 2022 at 14:00 BST. They will be made publicly available on the congress website once the embargo has lifted.

Journalists, industry, investigators and/or study sponsors must abide by the embargo times set by EASL.

Violation of the embargo will be taken seriously. Individuals and/or sponsors who violate EASL's embargo policy may face sanctions relating to current and future abstract submissions, presentations and visibility at EASL Congresses. The EASL Governing Board is at liberty to ban attendance and/or retract data.

Copyright for abstracts (both oral and poster) on the website and as made available during The International Liver Congress™ 2022 resides with the respective authors. No reproduction, re-use or transcription for any commercial purpose or use of the content is permitted without the written permission of the authors. Permission for re-use must be obtained directly from the authors.

publicly available on the congress website once the embargo has lifted.

Journalists, industry, investigators and/or study sponsors must abide by the embargo times set by EASL.

Violation of the embargo will be taken seriously. Individuals and/or sponsors who violate EASL's embargo policy may face sanctions relating to current and future abstract submissions, presentations and visibility at EASL Congresses. The EASL Governing Board is at liberty to ban attendance and/or retract data.

Copyright for abstracts (both oral and poster) on the website and as made available during The International Liver Congress™ 2022 resides with the respective authors. No reproduction, re-use or transcription for any commercial purpose or use of the content is permitted without the written permission of the authors. Permission for re-use must be obtained directly from the authors.

LB004B

Efficacy and safety of bepirovirsen in patients with chronic hepatitis B virus infection on stable nucleos(t)ide analogue therapy: interim results from the randomised phase 2b B-Clear study

Man-Fung Yuen¹, Robert Plesniak², Seng Gee Lim³, Keiji Tsuji⁴, Gheorghe Diaconescu⁵, Adrian Gadano⁶, Ju Hyun Kim⁷, Tarik Asselah⁸, Hyung Joon Yim⁹, Jeong Heo¹⁰, Giuliano Rizzardini¹¹, Harry Janssen¹², Corneliu Petru Popescu¹³, Diana Petrova¹⁴, Alexander Wong¹⁵, Nevin Indriz¹⁶, Cristina Pojoga¹⁷, Yasuhito Tanaka¹⁸, Denis Gusev¹⁹, Ewa Janczewska²⁰, Jennifer Cremer²¹, Robert Elston²², Tamara Lukic²³, Lauren Maynard²², Stuart Kendrick²², Punam Bharania²², Fiona Campbell²², Melanie Paff²², Dickens Theodore²¹. ¹Queen Mary Hospital, China; ²University of Rzeszow, College of Medicine, Centrum Medyczne w Lancucie Sp. z o.o., Poland; ³National University Health System, Singapore; ⁴Hiroshima Red Cross Hospital, Japan; ⁵Spitalul Clinic de Boli Infectioase si Pneumoftiziologie, Romania; ⁶Hospital Italiano de Buenos Aires, Argentina; ⁷Department of Gastroenterology, Gachon University Gil Medical Center, Korea, Rep. of South; ⁸Hôpital Beaujon, France; ⁹Korea University Ansan Hospital, Korea, Rep. of South; ¹⁰College of Medicine, Pusan National University and Biomedical Research Institute, National University Hospital, Korea, Rep. of South; ¹¹Luigi Sacco Hospital, Italy; ¹²Toronto General Hospital, Canada; ¹³Dr Victor Babes Clinical Hospital of Infectious and Tropical Diseases, Carol Davila University of Medicine and Pharmacy, Romania; ¹⁴Alexandrovska, Bulgaria; ¹⁵Department of Medicine, University of Saskatchewan, Canada; ¹⁶UMHAT Sofamed, Bulgaria; ¹⁷Regional Institute of Gastroenterology and Hepatology, Romania; ¹⁸Kumamoto University, Japan; ¹⁹Center for Prevention and Control of AIDS and Infectious Diseases, Russian Federation; ²⁰ID Clinic, Poland; ²¹GlaxoSmithKline, United States; ²²GlaxoSmithKline, United Kingdom; ²³GlaxoSmithKline, United Arab Emirates
Email: jennifer.x.cremer@gsk.com

The late breaker abstracts are under embargo until the start of the session on Saturday 25 June 2022 at 14:00 BST. They will be made

ORAL PRESENTATIONS

LB005

Primary data analyses of MAESTRO-NAFLD-1 a 52 week double-blind placebo-controlled phase 3 clinical trial of resmetirom in patients with NAFLD

Stephen Harrison¹, Rebecca Taub², Guy Neff³, Sam Moussa⁴, Naim Alkhouri⁵, Mustafa Bashir⁶. ¹Pinnacle, Clinical Research, San Antonio, United States; ²Madrigal Pharmaceuticals, RandD, Conshohocken, United States; ³Covenant Research, Sarasota, United States; ⁴Adobe Gastroenterology, Tucson, United States; ⁵Arizona Liver Institute, Phoenix, United States; ⁶Duke University, Radiology, Raleigh, United States

Email: rebeccataub@yahoo.com

The late breaker abstracts are under embargo until the start of the session on Saturday 25 June 2022 at 14:00 BST. They will be made publicly available on the congress website once the embargo has lifted.

Journalists, industry, investigators and/or study sponsors must abide by the embargo times set by EASL.

Violation of the embargo will be taken seriously. Individuals and/or sponsors who violate EASL's embargo policy may face sanctions relating to current and future abstract submissions, presentations and visibility at EASL Congresses. The EASL Governing Board is at liberty to ban attendance and/or retract data.

Copyright for abstracts (both oral and poster) on the website and as made available during The International Liver Congress™ 2022 resides with the respective authors. No reproduction, re-use or transcription for any commercial purpose or use of the content is permitted without the written permission of the authors. Permission for re-use must be obtained directly from the authors.

LB006

Reduction of intra-hepatic Z-AAT synthesis by fazirsiran decreases globule burden and improves histological measures of liver disease in adults with alpha-1 antitrypsin deficiency

Pavel Strnad¹, Mattias Mandorfer², Gourab Choudhury³, Griffiths Bill⁴, Christian Trautwein¹, Rohit Loomba⁵, Romil Saxena⁶, Thomas Schluep⁷, Ting Chang⁷, Min Yi⁷, Bruce Given⁷, James Hamilton⁷, Javier San Martin⁷, Jeffrey Teckman⁸. ¹RWTH University Hospital Aachen, Aachen, Germany; ²Medical University of Vienna, Wien, Austria; ³The University of Edinburgh, United Kingdom; ⁴Cambridge University Hospitals, United Kingdom; ⁵University of California San Diego, La Jolla, United States; ⁶Emory University Hospital, Pathology and Laboratory Medicine, Atlanta, United States; ⁷Arrowhead Pharmaceuticals, Inc., Pasadena, United States; ⁸Saint Louis University, Pediatrics, St. Louis, United States

Email: pstrnad@ukaachen.de

The late breaker abstracts are under embargo until the start of the session on Saturday 25 June 2022 at 14:00 BST. They will be made publicly available on the congress website once the embargo has lifted.

Journalists, industry, investigators and/or study sponsors must abide by the embargo times set by EASL.

Violation of the embargo will be taken seriously. Individuals and/or sponsors who violate EASL's embargo policy may face sanctions relating to current and future abstract submissions, presentations and visibility at EASL Congresses. The EASL Governing Board is at liberty to ban attendance and/or retract data.

Copyright for abstracts (both oral and poster) on the website and as made available during The International Liver Congress™ 2022 resides with the respective authors. No reproduction, re-use or transcription for any commercial purpose or use of the content is permitted without the written permission of the authors. Permission for re-use must be obtained directly from the authors.

Thursday 23 June

Hepatitis C: Clinical aspects and therapy

OS001

Results of a ten year prospective observational study on acute hepatitis C in HCV-mono- and HIV/HCV-coinfected patients

Christiana Graf¹, Lara Fuhrmann^{2,3}, Lutz Thomas⁴, Christoph Stephan⁵, Gaby Knecht⁴, Peter Gute⁴, Markus Bickel⁴, Kai-Henrik Peiffer¹, Fabian Finkelmeier¹, Georg Dultz¹, Nils Wetzstein⁵, Natalie Filmann⁶, Eva Herrmann⁶, Stefan Zeuzem¹, Niko Beerenwinkel^{2,3}, Julia Dietz¹, Christoph Sarrazin^{1,7}. ¹Goethe University Hospital Frankfurt, Department of Internal Medicine I, Frankfurt, Germany; ²ETH Zurich, Department of Biosystems Science and Engineering, Basel, Switzerland; ³SIB Swiss Institute of Bioinformatics, Basel, Switzerland; ⁴Infektiologikum, Frankfurt, Germany; ⁵Goethe University Hospital, Department of Infectious Diseases, Frankfurt, Germany; ⁶Goethe University Frankfurt, Institute of Biostatistics and Mathematical Modeling, Frankfurt, Germany; ⁷St. Josefs-Hospital, Medizinische Klinik II, Wiesbaden, Germany
Email: christiana.graf@kgu.de

Background and aims: Over the last two decades, a persistent epidemic of acute Hepatitis C virus (HCV) infections has been observed in HIV-positive men who have sex with men (MSM) in several metropolitan areas worldwide. In this study, epidemiological and clinical parameters as well as phylogenetic analyses were conducted to characterize HCV transmission among MSM.

Method: This prospective observational study analysed clinical and epidemiological parameters of patients with confirmed acute HCV infection between 2009 and 2019 from 3 centers in Frankfurt. NS5B population-based sequencing was performed at the time of diagnosis to determine HCV genotype (GT) and for phylogenetic analyses.

Results: A total of n=161 patients diagnosed with acute HCV-infection were included in the study, of whom n=140 (87%) were HIV-positive and n=145 (90%) were MSM. We observed a different distribution of HCV genotypes over time. In the first eight years, HCV GT1a was most common (58–100%) but decreased to 30% in 2018. In contrast, the proportion of GT4d cases increased. While no GT4d cases were diagnosed in 2013, the proportion rose to 40% in 2019. There was a slight trend towards more GT3a cases in 2018 and 2019,

while for GT1b and GT2 only individual cases were detected between 2009 and 2014. MSM were mainly infected with HCV GT1a (82%, 115/140) or GT4d (16%, 23/140 with sequencing data available). In contrast, HCV GT were almost equally distributed in non-MSM patients. Here, 36% were infected with HCV GT1a, 21% each with GT1b or GT3a and 16% had GT2. Phylogenetic analyses in NS5B showed a diverse sequence pattern in patients with HCV GT1b and GT3a. In contrast, HCV strains among MSM infected with HCV GT1a and 4d were more closely related. Based on the comparison of HCV GT or NS5B sequences, 24 patients (15%) were diagnosed with an HCV reinfection. The incidence rate in MSM for a first HCV infection declined in the period between 2017 and 2019 (3.6/1000PY) compared to the DAA era between 2013 and 2017 (6.8/1000 PY) and to the interferon era (2008–2013; 10.1/1000 PY). Conversely, the incidence of HCV reinfections among MSM increased slightly from 1.9/100PY to 2.8/100PY over time.

Conclusion: During the last 5 study years the prevalence of GT4 infections increased, while annual acute hepatitis C incidences decreased. HCV reinfection is an issue of major concern in HIV-positive MSM and may have implications for HCV elimination.

OS002

Multicenter prospective study for the use of shortened pre-emptive therapy with Glecaprevir/Pibrentasvir (G/P) and Ezetimibe in hepatitis C (HCV) seronegative non-liver solid organ transplant recipients of HCV viremic grafts

Bashar Aqel¹, Surakit Pungpapong², Adyr Moss¹, Rolland Dickson¹. ¹Mayo Clinic, Gastroenterology, Hepatology and Liver Transplant, Phoenix, United States; ²Mayo Clinic, Jacksonville, United States
Email: aqel.bashar@mayo.edu

This abstract is under embargo until Thursday 23 June 2022, 13:30 BST. This abstract has been selected to be highlighted during official EASL Press Office activities or in official EASL Press Office materials that will be made publicly available on the congress website at 13:30 (BST). Journalists, industry, investigators and/or study sponsors must abide by the embargo times set by EASL.

Violation of the embargo will be taken seriously. Individuals and/or sponsors who violate EASL's embargo policy may face sanctions relating to current and future abstract submissions, presentations and visibility at EASL Congresses. The EASL Governing Board is at liberty to ban attendance and/or retract data.

Copyright for abstracts (both oral and poster) on the website and as made available during The International Liver Congress™ 2022 resides with the respective authors. No reproduction, re-use or transcription for any commercial purpose or use of the content is permitted without the written permission of the authors. Permission for re-use must be obtained directly from the authors.

OS003

Effectiveness of voxilaprevir/velpatasvir/sofosbuvir in hepatitis C patients previously treated with direct-acting antiviral agents (DAA)

Christiana Graf¹, Julia Dietz¹, Beat Müllhaupt², Peter Buggisch³, Jörn Schattenberg⁴, Christoph Antoni⁵, Stefan Mauss⁶, Elena Durmashkina⁷, Claus Niederau⁸, Thomas Discher⁹, Julian Schulze zur Wiesch¹⁰, Tobias Müller¹¹, Thomas Berg¹², Christoph Neumann-Haefelin¹³, Christoph Berg¹⁴, Stefan Zeuzem¹, Christoph Sarrazin^{1,7}. ¹Goethe University Hospital, Department of Internal Medicine I, Frankfurt am Main, Germany; ²University Hospital Zürich, Swiss-Hepato-Pancreato-Biliary Center and Department of Gastroenterology and Hepatology, Zürich, Switzerland; ³Institute of Interdisciplinary Medicine IFI, Hamburg, Germany; ⁴University Medical Center Mainz, I. Department of Medicine, Mainz, Germany; ⁵University Hospital Mannheim, Department of Internal Medicine II, Mannheim, Germany; ⁶Center of HIV and Hepatogastroenterology, Düsseldorf, Germany; ⁷St. Josefs-Hospital, Wiesbaden, Germany; ⁸St. Josefs-Hospital, Katholisches Klinikum Oberhausen, Oberhausen, Germany; ⁹Justus Liebig University Gießen, Department of Medicine, Gießen, Germany; ¹⁰University Medical Center Hamburg-Eppendorf, I. Department of Medicine, Infectious Disease Unit, Hamburg, Germany; ¹¹Charité Universitätsmedizin Berlin, Department of Hepatology and Gastroenterology, Berlin, Germany; ¹²University Hospital Leipzig, Department of Gastroenterology and Rheumatology, Leipzig, Germany; ¹³University Hospital Freiburg, Department of Medicine II, Freiburg, Germany; ¹⁴University Hospital Tübingen, Department of Gastroenterology, Hepatology and Infectiology, Tübingen, Germany
Email: christiana.graf@kgu.de

Background and aims: Voxilaprevir/velpatasvir/sofosbuvir (VOX/VEL/SOF) is approved for HCV retreatment of direct-acting antiviral agents (DAA)-experienced patients. However, real-life data are still limited. The aim of the study was to analyse the effectiveness of VOX/VEL/SOF in a real-world setting.

Method: All consecutive patients with HCV retreated with VOX/VEL/SOF after DAA failure were enrolled in 153 centers in Germany, Austria, Switzerland and Belgium between May 2015 and November 2020. Sustained virological response (SVR) was defined as undetectable HCV RNA 4 (SVR 4) or 12 (SVR12) weeks after the end-of-treatment.

Results: A total of 416 patients were included: median age was 55 (21–84) years, 79% were male, median HCV RNA was 383,000 (10–58,300,000) IU/ml. HCV genotype (GT) was 1 in 54% (1a in 26%, 1b in 28%), 2 in 1%, 3 in 39% and 4 in 6%. Patients received VOX/VEL/SOF for 12 weeks, ribavirin was added in 4% of treatment schedules. Overall, 365/416 (87.7%) patients by intention to treat analysis and 401/416 (96.4%) by per protocol analysis achieved SVR12, respectively. Genotype 3a ($p=0.008$) and hepatocellular carcinoma ($p=0.0034$) were the only predictors of a treatment failure. Treatment effectiveness was not significantly affected by the type of previous DAA regimen, by liver cirrhosis, HCV GT 1a and baseline HCV-RNA viral load. Virologic relapse was observed in 20 patients (10% GT1a, 15% GT1b, 75% in GT3a). The presence of resistance-associated substitutions within NS3, NS5A, and NS5B genes did not impact SVR12 ($p=0.06$).

Conclusion: VOX/VEL/SOF is an effective retreatment for patients with HCV who have failed on a previous DAA course in a real-life setting. We identified HCV GT 3a and HCC as the main predictors of VOX/VEL/SOF failure.

OS004

Glecaprevir/pibrentasvir and sofosbuvir for 16 weeks without ribavirin is safe and highly effective retreatment for patients who have failed an NS5A inhibitor containing antiviral regimen

Edward J. Gane¹, Bridget Faire², Sherine Helmy³, James Freeman⁴. ¹University of Auckland, Grafton Campus, Liver Unit, Auckland, New Zealand; ²New Zealand Liver Transplant Unit-Ward 71, Auckland, New Zealand; ³Pharco Corporation, Cairo, Egypt; ⁴GP2U, Australia
Email: edgane@adhb.govt.nz

Background and aims: Oral DAA therapy has been available in New Zealand since mid-2016 for treatment of chronic hepatitis C. Over the last 5 years, more than 10,000 New Zealanders have been treated with NS5A inhibitor-based DAA therapy, of whom more than 300 have had virologic failure. Retreatment of patients with confirmed antiviral resistance requires a triple DAA combination of a polymerase, a protease and an NS5A inhibitor.

Method: In an open-labelled, ethics-approved study, 100 New Zealanders who had failed DAA therapy with confirmed NS5A resistance will be retreated with glecaprevir/pibrentasvir (GLE/PIB) from Feb 2019) plus sofosbuvir for 16 weeks. Patients with decompensated cirrhosis or hepatocellular carcinoma or post-transplant are excluded.

Results: To-date, 57 patients have been enrolled in the study. Median age was 56 years (38–80), 78% were male and 44% had established cirrhosis. Thirty-five patients had previously failed GLE/PIB, 19 failed ombitasvir, paritaprevir, dasabuvir, and ritonavir (PrOD) and 1 each failed grazoprevir/elbasvir (GRZ/ELB), ledipasvir/sofosbuvir (LDV/SOF) and sofosbuvir/velpatasvir (SOF/VEL). Six patients had failed multiple regimens. Most frequently detected NS5A resistance-associated substitutions (RASs) were Y93H (57%), A30 K (26%), Q30 K/H (26%), M28 T/F/V (11%). Multiple NS5A RASs were detected in 39% patients. Resistance profiles were similar in PrOD and GLE/PIB failures.

One patient died from opioid overdose during treatment. There were no other SAEs or AE-related treatment discontinuations. Two other patients stopped treatment within 4 weeks because of psychosocial issues, one of whom has started retreatment.

45 patients have completed therapy and 37 have reached the SVR12 timepoint, of whom 36 (98%) are cured (complete SVR results will be available in early 2022). The only treatment failure to-date was a 53-year-old noncirrhotic female, previously treated with PrOD.

Conclusion: Glecaprevir/pibrentasvir plus sofosbuvir for 16 weeks is a safe and highly effective retreatment regimen for patients who have previously failed GLE/PIB and other DAA regimens regardless of cirrhosis status, or NS5A RAS profile. There is no indication for adding ribavirin.

OS005

Excess mortality risk among hepatitis C patients after being “cured” in the interferon-free era: results from three population-based cohorts

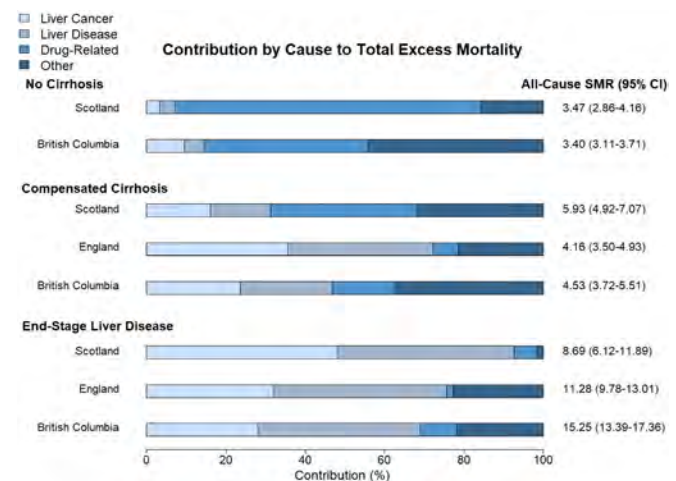
Victoria Hamill^{1,2}, Stanley Wong³, Jennifer Benselin^{4,5}, Mel Krajden^{3,6}, Peter Hayes⁷, David Mutimer⁸, Amanda Yu³, John Dillon⁹, Will Gelson¹⁰, Hector Velasquez^{3,11}, Philip Johnson¹², Stephen Barclay¹³, Maria Alvarez³, Hidenori Toyoda¹⁴, Kosh Agarwal¹⁵, Andrew Fraser^{16,17}, Sofia Bartlett^{3,11}, Mark Aldersley¹⁸, Andrew Bathgate⁷, Mawuena Binka^{3,11}, Paul Richardson¹⁹, Joanne Morling^{4,5,20}, Stephen Ryder⁴, Douglas Macdonald²¹, Sharon Hutchinson^{1,2}, Eleanor Barnes²², Neil Guha^{4,5}, William Irving^{4,5}, Naveed Janjua^{3,11,23}, Hamish Innes^{1,2,20}. ¹Glasgow Caledonian University, School of Health and Life Sciences, Glasgow, United Kingdom; ²Public Health Scotland, Glasgow, United Kingdom; ³British Columbia Centre for Disease Control, Vancouver, British Columbia, Canada; ⁴Nottingham University Hospitals NHS Trust and the University of Nottingham, NIHR Nottingham Biomedical Research Centre, Nottingham, United Kingdom; ⁵University of Nottingham, School of Medicine, Nottingham Digestive Diseases Centre, Nottingham, United Kingdom; ⁶The University of British Columbia, Department of Pathology and Laboratory Medicine, Vancouver, British Columbia, Canada; ⁷Royal Infirmary of Edinburgh, Edinburgh, United Kingdom; ⁸Queen Elizabeth Hospital Birmingham, Liver and Hepatobiliary Unit, Birmingham, United Kingdom; ⁹University of Dundee, School of Medicine, Division of Molecular and Clinical Medicine, Dundee, United Kingdom; ¹⁰Cambridge University Hospitals NHS Foundation Trust, Cambridge Liver Unit, Cambridge, United Kingdom; ¹¹University of British Columbia, School of Population and Public Health, Vancouver, British Columbia, Canada; ¹²University of Liverpool, Department of Molecular and Clinical Cancer Medicine, Liverpool, United Kingdom; ¹³Glasgow Royal Infirmary, Glasgow, United Kingdom; ¹⁴Ogaki Municipal Hospital, Department of Gastroenterology, Ogaki, Japan; ¹⁵King's College Hospital NHS Foundation Trust, Institute of Liver Studies, London, United Kingdom; ¹⁶Aberdeen Royal Infirmary, Aberdeen, United Kingdom; ¹⁷Queen Elizabeth University Hospital, Glasgow, United Kingdom; ¹⁸St James's University Hospital, Leeds Liver Unit, Leeds, United Kingdom; ¹⁹Royal Liverpool and Broadgreen University Hospitals NHS Trust, Liverpool, United Kingdom; ²⁰University of Nottingham, Lifespan and Population Health, Nottingham, United Kingdom; ²¹Royal Free London NHS Foundation Trust, Gastroenterology and Hepatology, London, United Kingdom; ²²University of Oxford, Nuffield Department of Medicine and the Oxford NIHR Biomedical Research Centre, Oxford, United Kingdom; ²³St Paul's Hospital Vancouver, Centre for Health Evaluation and Outcome Sciences, British Columbia, Canada
Email: victoria.hamill@gcu.ac.uk

Background and aims: Although the number of people living with a hepatitis C sustained viral response (SVR) has increased dramatically, mortality rates in this patient group remain poorly understood. Here, our goal was to assess excess mortality after SVR achievement in the interferon (IFN)-free era.

Method: We performed data analysis on patients achieving SVR in the IFN-free era (2014–2018/19) from three population-based cohorts in Scotland (SC), England (EN), and British Columbia (BC). Patients were divided into three disease stage groups: no cirrhosis (SC and BC only); compensated cirrhosis; and end stage liver disease (ESLD). Age-standardised mortality rates were calculated to take account of different age/sex structures between cohorts and disease stage groups. Further, we calculated standardised mortality ratios (SMRs) to compare the frequency of mortality in SVR patients to the general

population (GP). We also quantified the proportion of excess death attributable to: a) death from liver cancer; b) death from liver disease unrelated to cancer; c) and death from drug-related causes. Finally, Poisson regression was used to identify factors associated with excess mortality.

Results: Our analysis included 20,031 patients, of which 1,402 (7%) died during follow-up. Mean follow-up duration was 2.2–3.9 years, and mean age ranged from 46.3 (SC) to 56.7 (BC). Mortality rates varied considerably according to disease stage. For example, the age-standardised mortality rate ranged from 12 to 23, 27–38, and 62–118 deaths per 1000 person-years in non-cirrhosis, compensated cirrhosis and ESLD patients, respectively. SMRs indicated that all-cause mortality was 3.4–3.5 times higher than the GP in non-cirrhosis patients, 4.2–5.9 times higher in compensated cirrhosis patients, and 8.7–15.3 times higher in ESLD patients. For non-cirrhosis patients, drug-related causes were responsible for the greatest proportion of excess death (77% SC; 41% BC). Conversely, for cirrhosis patients, liver-related causes were the key driver, responsible for 30–95% of excess deaths. In the regression analysis, younger age, drug use and comorbidities were associated with greater excess mortality (see Figure).



Conclusion: In the largest study performed to-date, we show that individuals achieving SVR in the interferon-free era have a considerably higher mortality risk than the GP, driven mainly by drug-related mortality (in non-cirrhosis patients) and liver-related causes (in cirrhosis patients).

OS006

Impact of direct-acting antiviral treatment for hepatitis C on cardiovascular diseases and extrahepatic cancers

Laurent Lam¹, Helene Fontaine², Nathanaël Lapidus^{1,2}, Céline Divral¹, Jonathan Bellet¹, Dominique Larrey³, Pierre Nahon^{2,4}, Alpha Diallo⁵, Carole Cagnot⁵, Clovis Lusivka-Nzinga¹, François Teoule¹, Gilles Hejblum¹, Marc Bourliere^{6,7}, Stanislas Pol^{2,8}, Fabrice Carrat^{1,2}. ¹Sorbonne Université, INSERM, Institut Pierre Louis d'Épidémiologie et de Santé Publique, IPLESP, Paris, France; ²Assistance Publique-Hôpitaux de Paris, France; ³Hôpital Saint Eloi and IBR, INSERM, Montpellier, France; ⁴Inserm, UMR-1162, "Génomique fonctionnelle des tumeurs solides", Paris, France; ⁵ANRS, Emerging Infectious Diseases, Paris, France; ⁶Hôpital Saint Joseph, Marseille, France; ⁷INSERM, UMR 1252 IRD SESSTIM, Aix Marseille Université, Marseille, France; ⁸Université de Paris, Paris, France
Email: laurentlam@hotmail.fr

Background and aims: The impact of direct-acting antivirals (DAAs) on extrahepatic complications in chronic hepatitis C (CHC) patients remains poorly described. We estimated the association of DAAs with cardiovascular events and extrahepatic cancers.

Method: The prospective ANRS CO22 HEPATHER cohort was enriched with individual data until December 2018 from the French National Health Insurance Database (SNDS), which contains medical information regarding ambulatory care and hospital admissions. CHC patients were enrolled between August 2012 and December 2015 in 32 French hepatology centers. A total of 8148 CHC adults were selected. Cardiovascular events (stroke, acute coronary syndrome, pulmonary embolism, heart failure, arrhythmias and conduction disorders [ACD], peripheral arterial disease [PAD]) and cancers (colorectal, bladder, prostate, kidney, lung, pancreas, thyroid, head/neck, breast) were derived from the SNDS. Associations between DAAs and extrahepatic events were estimated using marginal structural models, with adjustments for clinical confounders and medications.

Outcomes	Adjusted hazard ratios associated with DAAs (95% Confidence Interval)
Total population (n = 8148)	
Acute stroke	1.30 (0.82, 2.08)
Acute coronary syndrome	1.00 (0.63, 1.60)
Acute pulmonary embolism	2.10 (0.64, 6.85)
Acute heart failure	1.15 (0.74, 1.78)
Arrhythmias and conduction disorders	1.46 (1.04, 2.04)
Peripheral arterial disease	0.54 (0.33, 0.89)
Major cardiovascular events	1.03 (0.81, 1.31)
Any cardiovascular event	1.10 (0.90, 1.36)
Any extrahepatic solid cancer	1.23 (0.50, 3.03)
Patients with advanced fibrosis (n = 3586)	
Acute stroke	0.58 (0.29, 1.18)
Acute coronary syndrome	0.59 (0.29, 1.19)
Acute pulmonary embolism	0.79 (0.16, 3.97)
Acute heart failure	0.47 (0.27, 0.81)
Arrhythmias and conduction disorders	1.02 (0.57, 1.84)
Peripheral arterial disease	0.36 (0.17, 0.73)
Major cardiovascular events	0.50 (0.36, 0.71)
Any cardiovascular events	0.58 (0.42, 0.79)
Any extrahepatic solid cancer ^c	0.39 (0.09, 1.71)

Results: Analyses of 12 905 person-years (PY) of no DAA exposure and 22 326 PY following DAA exposure showed a reduced risk of PAD after DAAs (HR, 0.54; 95% CI, 0.33 to 0.89), a beneficial effect of DAAs on overall cardiovascular outcomes in patients with advanced fibrosis (aHR, 0.58; 95% CI, 0.42 to 0.79), and an increased risk of ACD (hazard ratio [HR], 1.46; 95% CI, 1.04 to 2.04) predominant after the first year following DAA initiation. There was no association between DAAs and extrahepatic cancer (HR, 1.23; 95% CI, 0.50 to 3.03).

Conclusion: DAAs were associated with a decreased risk of cardiovascular outcomes in patients with advanced fibrosis, a decreased risk of PAD regardless of the fibrosis stage, and an increased risk of ACD, supporting long-term cardiac monitoring after DAA therapy. DAAs were not associated with extrahepatic cancer development or reduction.

Cirrhosis and its complications: Other clinical complications except ACLF and critical illness

OS007

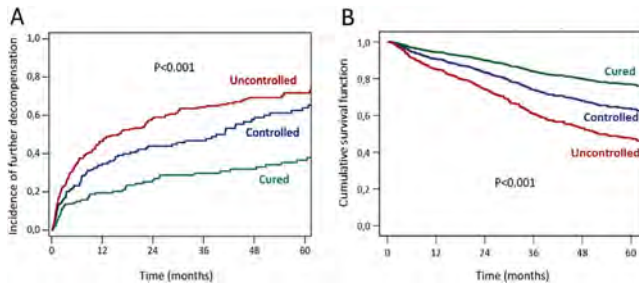
Etiological cure prevents further decompensation and mortality in cirrhotic patients with ascites as the single first decompensating event

Marta Tonon¹, Lorenz Balcar^{2,3}, Georg Semmler^{2,3}, Valeria Calvino¹, Bernhard Scheiner^{2,3}, Simone Incicco¹, Rafael Paternostro^{2,3}, Carmine Gabriele Gambino¹, David JM Bauer^{2,3}, Antonio Accetta¹, Lukas Hartl^{2,3}, Alessandra Brocca¹, Mathias Jachs^{2,3}, Michael Trauner^{2,3}, Mattias Mandorfer^{2,3}, Paolo Angeli¹, Thomas Reiberger^{2,3}, Salvatore Piano¹. ¹University of Padua, Department of Medicine, Padova, Italy; ²Medical University of Vienna, Division of Gastroenterology and Hepatology, Department of Internal Medicine III, Vienna, Austria; ³Medical University of Vienna, Vienna Hepatic Hemodynamic Laboratory, Division of Gastroenterology and Hepatology, Department of Internal Medicine III, Vienna, Austria
Email: salvatorepiano@gmail.com

Background and aims: Etiologic treatment reduces the risk of decompensation and mortality in compensated cirrhosis. However, in the setting of decompensated cirrhosis the impact of etiologic treatment is less predictable, in particular in patients with ascites, who remain at high risk of developing further decompensating events and death. The aim of the study was to evaluate the impact of etiologic treatment in decompensated patients with cirrhosis and ascites as the single index decompensating event. The end points were the occurrence of further decompensation (i.e. refractory ascites, spontaneous bacterial peritonitis [SBP], hepatorenal syndrome [HRS-AKI], variceal bleeding [VB] and hepatic encephalopathy [HE]) and mortality.

Method: Cirrhotic patients with ascites as single first decompensation event at the University Hospital of Padova or the Vienna General Hospital between 2003–2021 were included and followed until death, liver transplantation or September 2021. The etiology was considered as “cured” in case of removal of the primary etiological factor (e.g. HCV: virological cure, HBV: virological suppression, ALD: alcohol abstinence) and as “controlled” in case of partial removal of etiologic factor (e.g. HBV: partial suppression of HBV-DNA, ALD: mostly abstinent but with drinking episodes).

Results: We included 622 patients (mean age: 57 ± 11 years, male 68%, mean MELD 15 ± 6), the most common etiology were ALD (59%) and HCV (23%). Etiology was “cured” in 146 patients (24%), “controlled” in 170 (27%) and uncontrolled in 306 (49%). During a median follow-up of 33 months, 350 patients (56%) developed further decompensation (33% refractory ascites, 29% HE, 17% SBP, 13% HRS-AKI, 9% VB). The incidence of further decompensation at 5 years was significantly lower in patients with “cured” vs “controlled” vs uncontrolled etiology (38% vs 64% vs 72%, respectively; $p < 0.001$; Fig. 1A). In multivariable analysis (adjusted for age, varices, etiology, Child Pugh class, creatinine and sodium), “cured” (aHR = 0.52; $p < 0.001$) and “controlled” etiology (aHR = 0.60; $p < 0.001$) were both independently associated with a lower risk of further decompensation. Considering response to etiologic treatment as time-dependent covariates, 5-year cumulative incidence of survival was significantly higher in patients with cured vs controlled vs uncontrolled etiology (83% vs 58% vs 40%, respectively; $p < 0.001$; Fig. 1B). In multivariable analysis, etiologic cure (aHR = 0.35, $p < 0.001$) and controlled etiology (aHR = 0.61, $p = 0.003$) were independently associated with lower mortality.



Conclusion: In cirrhotic patients with ascites as single first decompensating event, the cure or control of etiology of liver disease reduces the risk of further decompensations and mortality.

OS008

Risk factors for short-term post discharge clinical outcomes in patients hospitalized with decompensated chronic liver disease: interim results from Global CLEARED study

Jasmohan S. Bajaj¹, Patrick S. Kamath², Florence Wong³, Peter Hayes⁴, Ramazan Idilman⁵, Aldo Torre⁶, Mark Topazian⁷, Jacob George⁷, Mario Reis Álvares-da-Silva⁷, Qing Xie⁸, Shiv Kumar Sarin⁹, Abha Nagral¹⁰, Sumeet Asrani¹¹, Mohammad Amin Fallahzadeh¹¹, Somaya Albhaisi¹², CE Eapen¹³, Ashish Goel¹³, Ajay Kumar Duseja¹⁴, Anoop Saraya¹⁵, Jatin Yegurla¹⁶, Mohd. Rela¹⁷, Dinesh Jothimani¹⁸, Marie Jeanne Lohoues¹⁹, Belimi Hibat Allah²⁰, Ricardo Cabello²⁰, Ruveena Bhavani²¹, Nik MA Nik Arsyad²², Sombat Treeprasertsuk²³, Salisa Wejnaruemarn²⁴, Jose Luis Perez Hernandez²⁵, Godolfino Miranda Zazueta²⁶, Neil Rajoriya²⁷, Rosemary Faulkes²⁸, Abdullah Emre Yildirim²⁹, Sezgin Barutcu²⁹, Anand Kulkarni³⁰, Mithun Sharma³⁰, Rajender Reddy³¹, Suditi Rahematpura^{31,32}, Adebayo Danielle³³, James Kennedy³³, Feyza Gunduz³⁴, Rahmi Aslan³⁵, Anil Arora³⁶, Ashish Kumar³⁶, Dalia Allam³⁷, Yashwi Hareesh Kumar Patwa³⁷, Mauricio Castillo³⁸, Hiang Keat Tan³⁹, Liou Wei Lun⁴⁰, Hugo E. Vargas⁴¹, David Bayne⁴¹, Paul J. Thuluvath⁴², Somya Sheshadri⁴², Ajay Haveri⁴³, Andrew Keaveny⁴⁴, Jawaid Shaw⁴⁵, Edith Okeke⁴⁶, David Nyam P⁴⁷, Aloysious Aravinthan⁴⁷, Suresh Vasan Venkatachalapathy⁴⁷, Amey Sonavane⁴⁸, Hailemichael Desalegn⁴⁹, Henok Fisseha⁴⁶, Dominik Bettinger⁵⁰, Michael Schultheiss⁵⁰, Scott Biggins⁵¹, Natalia Filipek⁵¹, Damien Leith⁴⁷, Ewan Forrest⁴⁷, Maria Sarai González-Huezo^{6,52}, René Malé Velazquez⁶, Lilian Torres Made⁷, Diana Yung⁴⁷, Zeki Karasu³⁵, ZhuJun Cao⁵³, Helena Katzman⁵⁴, Liane Rabinowich⁵⁴, Carlos Benitez⁵⁵, Andres Duarte Rojo⁵¹, Sebastián Marciano⁵⁶, Akash Gandotra⁴⁸, Brian Bush⁵¹, Leroy Thacker⁵¹, Ashok Choudhury⁹.
¹Virginia Commonwealth University, Department of Hepatology, United States; ²Mayo Rochester, United States; ³University of Toronto, Toronto, Canada; ⁴Royal Infirmary of Edinburgh, United Kingdom; ⁵Ankara University School of Medicine, Department of Hepatology, Ankara, Turkey; ⁶xx, Mexico; ⁷xx; ⁸Ruijin Hospital, Department of Hepatology, China, China; ⁹Institute of Liver and Biliary Sciences, Department of Hepatology, Delhi, India; ¹⁰Jaslok Mumbai, India; ¹¹Baylor Dallas (Baylor University Medical Center), United States; ¹²Virginia Commonwealth University, Internal Medicine, Richmond, United States; ¹³CMC Vellore, Tamil Nadu, India; ¹⁴PGIMER, India; ¹⁵AIIMS, Deptt. of Gastroenterology and Human Nutrition, New Delhi, India; ¹⁶All India Institute of Medical Sciences New Delhi, Department of Gastroenterology and Human Nutrition Unit, New Delhi, India; ¹⁷Dr. Rela Institute and Medical Centre, Deptt. of Liver Transplant Surgery, Tamil Nadu, India; ¹⁸Dr. Rela Institute and Medical Centre, Tamil Nadu, India; ¹⁹CHU de Cocody, South Africa; ²⁰Mustapha Bacha University Hospital, Algeria; ²¹University of Malaysia; ²²University of Malaysia, Kuala Lumpur, Malaysia; ²³Chulalongkorn University and King Chulalongkorn Memorial Hospital, Bangkok, Thailand; ²⁴Chulalongkorn University and King Chulalongkorn Memorial Hospital, Thailand; ²⁵Hospital General "Gerardo Liceaga", Mexico; ²⁶Instituto Nacional de Ciencias Médicas y Nutrición "Salvador Zubirán, Mexico; ²⁷Queen Elizabeth University Hospitals, Birmingham, United Kingdom; ²⁸Queen Elizabeth University Hospitals, United Kingdom; ²⁹Gaziantep, Turkey; ³⁰Asian Institute of Gastroenterology, Hyderabad, India; ³¹Upenn (University of Pennsylvania), United States; ³²Perelman School of Medicine at the University of Pennsylvania, Gastroenterology and Hepatology, Philadelphia, United States; ³³Royal Berkshire Hospital, United Kingdom; ³⁴Marmara University, Turkey; ³⁵xx, Turkey; ³⁶Sir Ganga Ram Hospital, Delhi, India; ³⁷Ibn. Sina Hospital, Khartoum, Sudan, Sudan; ³⁸Centro Médico la Raza, Mexico; ³⁹Singapore General Hospital, Gastroenterology and Hepatology, Singapore, Singapore; ⁴⁰Singapore General, Singapore; ⁴¹Mayo Scottsdale, United States; ⁴²Mercy Medical Centre, United States; ⁴³Jaslok Hospital, Delhi, India; ⁴⁴Mayo Jacksonville, United States; ⁴⁵VA Richmond, United States; ⁴⁶xx, South Africa; ⁴⁷xx, United Kingdom; ⁴⁸xx, India; ⁴⁹xx, Ethiopia; ⁵⁰xx, Canada; ⁵¹xx, United States; ⁵²Centro Medico Issemym, Gastroenterology, Mexico; ⁵³Department of infectious disease, Ruijin hospital, Shanghai Jiao Tong university school of medicine, Shanghai, China; ⁵⁴xx, Israel; ⁵⁵xx, Chile; ⁵⁶xx, Argentina
 Email: doctor.ashokchoudhury@gmail.com

United Kingdom; ²⁸Queen Elizabeth University Hospitals, United Kingdom; ²⁹Gaziantep, Turkey; ³⁰Asian Institute of Gastroenterology, Hyderabad, India; ³¹Upenn (University of Pennsylvania), United States; ³²Perelman School of Medicine at the University of Pennsylvania, Gastroenterology and Hepatology, Philadelphia, United States; ³³Royal Berkshire Hospital, United Kingdom; ³⁴Marmara University, Turkey; ³⁵xx, Turkey; ³⁶Sir Ganga Ram Hospital, Delhi, India; ³⁷Ibn. Sina Hospital, Khartoum, Sudan, Sudan; ³⁸Centro Médico la Raza, Mexico; ³⁹Singapore General Hospital, Gastroenterology and Hepatology, Singapore, Singapore; ⁴⁰Singapore General, Singapore; ⁴¹Mayo Scottsdale, United States; ⁴²Mercy Medical Centre, United States; ⁴³Jaslok Hospital, Delhi, India; ⁴⁴Mayo Jacksonville, United States; ⁴⁵VA Richmond, United States; ⁴⁶xx, South Africa; ⁴⁷xx, United Kingdom; ⁴⁸xx, India; ⁴⁹xx, Ethiopia; ⁵⁰xx, Canada; ⁵¹xx, United States; ⁵²Centro Medico Issemym, Gastroenterology, Mexico; ⁵³Department of infectious disease, Ruijin hospital, Shanghai Jiao Tong university school of medicine, Shanghai, China; ⁵⁴xx, Israel; ⁵⁵xx, Chile; ⁵⁶xx, Argentina
 Email: doctor.ashokchoudhury@gmail.com

Background and aims: Decompensated chronic liver disease (DCLD) is associated with poor outcomes, but no global study has addressed this after hospitalization. We prospectively evaluated non-elective hospitalized patients with DCLD to determine disease profile, predictors of readmission and 30 days mortality post discharge following index hospital admission under "Chronic Liver disease Evolution And Registry for Events and Decompensation (CLEARED) consortium.

Method: Data were prospectively collected from 49 centres from 6 continents of non-elective admissions in DCLD patients with or without cirrhosis, aged ≥ 18 years. We performed an interim analysis to predict readmission and mortality within 30 days following index hospital discharge. World Bank data were used to stratify countries according to income.

Results: 1383 patients, mean age 54.97 ± 13.55 years; 64% male; diverse ethnicity [White 39%, Asian 30%, Hispanic 10%, Black 9%] were analyzed. Alcohol was the most common etiology (46%), followed by NASH (23%), HBV (13%) and HCV (11%). Admissions were almost exclusively for liver related complications i.e. GI bleed (30%), HE (34%), AKI (33%), and anasarca (24%). Mean admission CTP was 10 (5–14) and MELD-Na 23 (6–40). Only 11% were listed for transplant. 51% had hospitalization in previous six months. 24% were infected at admission and another 13% developed infections subsequently. During hospitalization, organ failures were: AKI 46%; as brain 16%, circulatory 14%, and respiratory 13%; 25% needed ICU admission. Median hospital stay was 7 days (1–140) and 11% lost to follow-up after discharge. 33% were readmitted, 3% were transplanted while 26% of patients died within 30 days. The most significant independent factors predicting readmission within 30 days were being in low/ lower middle income country ($p < 0.0001$), a high discharge MELD-Na ($p = 0.0005$), and hospitalization ≤ 6 M ($p = 0.006$). The most significant independent predictors of 30-day-mortality post index discharge were age, discharge MELD-Na ($p < 0.0001$ for both), and various organ failures during index admission ($p < 0.01$).

Conclusion: The clinical outcomes of patients with DCLD following index hospital admission vary widely around the world. Mortality within 30 days post discharge is largely dependent on patient and disease factors. Readmission post discharge, however, is variable across continents and inversely correlates socio-economic status. Global characterization of patients at high risk of readmission should include further study of socio-economic factors in addition to severity of liver disease.

OS009

Dyserythropoiesis is underrecognized and contributes to severe anemia in liver cirrhosis

Chhagan Bihari¹, Sumit Garg¹, Shiv Kumar Sarin². ¹Institute of Liver and Biliary Sciences, Pathology and Hepatology, Delhi, India; ²Institute of Liver and Biliary Sciences, Hepatology, Delhi, India
Email: shivsarin@gmail.com

Background and aims: Moderate to severe anemia is one of the common complication in liver cirrhosis and is often multifactorial. Contribution of dyserythropoiesis (DE) in cirrhosis related anemia is often neglected and has not been studied. We aimed to investigate the prevalence, severity and mechanisms of dyserythropoiesis in cirrhosis patients.

Method: We studied the bone marrows (BM) of cirrhosis patients (n = 517), who underwent a BM aspiration/biopsy between Jan 2014–Dec 2018, for investigation of anemia, hypersplenism or other clinical indications. Cases of haematological or non-hematological neoplasias, chronic kidney disease, chronic or acute drug injury, acute and chronic hepatitis and granulomatous pathology were excluded. Morphological analysis of BM aspirate, biopsies, erythroid colony assessment were done. A >5% dyserythropoiesis in erythroid lineage was considered and categorized as mild: 5–10%; moderate: 10–15% and marked: >15%.

Results: A 68/517 (13.2%) cirrhosis patients had dyserythropoiesis and none from control group. Of them 44% had mild; 35.4% moderate and 20.6% marked dyserythropoiesis in the BM. Cirrhosis patients with DE had significantly lower hemoglobin than those without DE (7.6 ± 1.4 gm/dl vs 8.9 ± 1.9 gm/dl, $p < 0.001$), but comparable serum iron (83.7 ± 42 vs 90.2 ± 46.6 mcg/dl, $p = 0.997$); total iron binding capacity (243.2 ± 85.1 vs 231 ± 87.2 mcg/dl, $p = 0.291$); and transferrin saturation (50.9 ± 27.9 vs 55.6 ± 30.8 %, $p = 0.206$) and serum folate (16 ± 3.8 vs 15.8 ± 4.4 ng/ml) levels. The former however, had higher vitamin B12 (2339.2 ± 1406 vs 1842 ± 1411.9 pg/ml, $p = 0.010$) levels. Further, other confounding factors for anemia like lactate dehydrogenase ($p = 0.494$), reticulocyte count ($p = 0.808$), thyroid stimulating hormone ($p = 0.208$), hepcidin ($p = 0.16$), erythropoietin ($p = 0.23$), and spleen size ($p = 0.310$) were comparable. Grades of dyserythropoiesis were associated with Child's score ($p = 0.003$) with marked dyserythropoiesis being noted in Child C. Dyserythropoiesis was mainly associated with alcohol and non-alcoholic steatohepatitis (51/68, 75%) as compared to viral, autoimmune and other etiologies. BM examination showed fewer erythroid colonies (8 vs. 10.7, $p < 0.001$)

and proerythroblasts (7 vs. 17.9, $p < 0.001$) in the erythroid colonies of patients with DE. The DE was significantly related with low GATA.1 (7.7 ± 4.3 vs 13.6 ± 7.8 ; $p = 0.001$) non-nuclear localization of HSP70 ($p = 0.04$) and excess erythroferrone (23.4 ± 7 vs 14.2 ± 5.2 , $p < 0.001$) as compared to no-DE.

Conclusion: Approximately 13.2% patients with cirrhosis with severe anemia show dyserythropoiesis. Standard hematological and iron studies fail to identify it and bone marrow examination is merited. Alterations in the erythroid colonies, HSP70 localization and diminished GATA.1 in BM are associated with dyserythropoiesis.

OS010

Effect of recruitment and selection policies on the volume of outcome of patients transplanted with ACLF-3

Baptiste Michard¹, Thierry Artzner¹, Pietro Addeo¹, Philippe Bachellier¹, Camille Besch¹, Vincent Castelain¹, Raphael Clere-Jehl¹, Mathilde Deridder¹, Max Guillot¹, Jean-Étienne Herbrecht¹, Ralf Janssen-Langenstein¹, Maleka Schenck¹, Francis Schneider¹, François Faitot¹. ¹Hopitaux Universitaires de Strasbourg
Email: baptiste.michard@chru-strasbourg.fr

Background and aims: Liver transplantation (LT) for critically ill cirrhotic patients is a debated issue, which raises complex medical, surgical and ethical challenges. In particular, it is crucial to achieve high post-LT survival in order to justify allocating livers to these patients, especially given the current organ shortage. To date, there is no granular data concerning the 3-year post-LT outcome of ACLF-3 patients.

Method: This study describes the three-year post-LT survival of a single center granular cohort of patients with ACLF-3 at the time of LT and compares it to the post-LT survival of all the patients who were transplanted without ACLF-3 in the same center between 2007 and 2018. Over this period of time, two policies were gradually implemented in this center: (i) developing a network of peripheral centers that transferred critically ill cirrhotic patients for LT assessment and (ii) increasing use of the transplantation for ACLF-3 model (TAM) score criteria to identify the optimal transplantability window.

Results: A total of 828 first time single LTs were performed over the study period. 91 patients had ACLF-3 at the time of LT. The overall three-year survival of ACLF-3 patients was 66% vs 82% ($p < 0.001$) for the rest of the cohort. Over the study period, both the number of

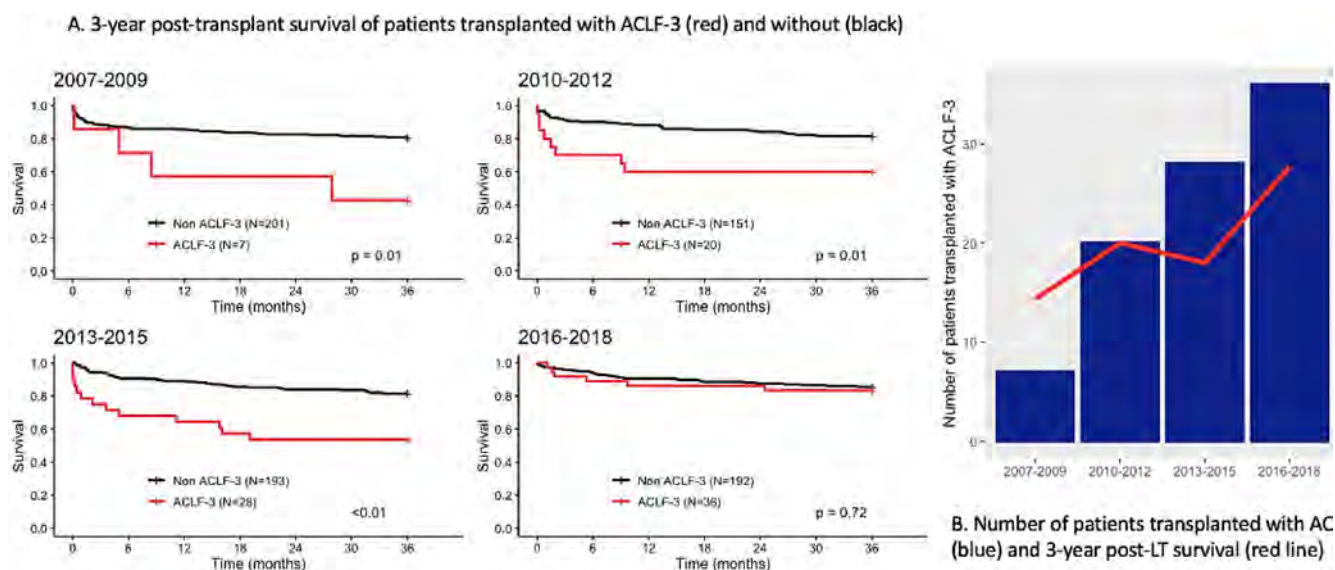


Figure: (abstract: OS010)

patients transplanted with ACLF-3 and their 3-year post-LT survival increased over time: 2007–2009: 7 patients, 43% survival; 2010–2012: 20 patients, 60% survival; 2013–2015: 28 patients, 54% survival; 2016–2018: 36 patients, 83% survival (no significant difference in survival between the ACLF-3 and the non ACLF-3 group in the last period). This increase in the number of patients transplanted and in their post-LT three-year survival was not observed in the general population of patients transplanted without ACLF-3 (cf. Figure). A total of 12 ACLF-3 patients were transplanted with TAM scores >2. However, in the last period (2016–2018), in which both the number of patients transplanted with ACLF-3 and the post-LT survival were the highest, no patient was transplanted with a TAM score >2.

Conclusion: This study, which originates from the largest single center cohort of patients transplanted with ACLF-3, illustrates how gradually building a network of peripheral centers to refer critically ill cirrhotic patients to an expert ICU and LT center can lead to a dramatic increase in the number of patients transplanted with ACLF-3. It also shows that there is a learning curve when transplanting patients with ACLF-3 and that the implementation of the TAM score to help identify the optimal transplantability window at the time of organ proposal contributes to optimizing post-LT outcomes. The combination of these strategies can help centers increase the number of patients transplanted with ACLF-3 while reaching post-LT outcomes for these patients that are similar to those of non ACLF-3 patients.

OS011

Real-world evidence on long-term albumin treatment in patients with decompensated liver cirrhosis in Italy

Wim Laleman¹, Jonel Trebicka², Alastair O'Brien³, Paolo Caraceni⁴, Sandra Santos⁵, Tatiana Vilchez⁶, Kyle Rodney⁷, Sofia Schweiger⁸, Paolo Angeli⁹. ¹University Hospitals Leuven, Department of Gastroenterology and Hepatology, Section of Liver and Biliopancreatic Disorders, Leuven, Belgium; ²Goethe University Hospital Frankfurt, Translational Hepatology Department of Internal Medicine, Frankfurt, Germany; ³University College London, Institute for Liver and Digestive Health, London, United Kingdom; ⁴University of Bologna, Department of Medical and Surgical Science, Bologna, Italy; ⁵CSL Behring, Lisbon, Portugal; ⁶CSL Behring, Barcelona, Spain; ⁷Adivo Associates LLC, California, United States; ⁸Adivo Associates LLC, Buenos Aires, Argentina; ⁹University of Padova, Department of Medicine, Unit of Internal Medicine and Hepatology, Padova, Italy
Email: paolo.angeli54@gmail.com

Background and aims: Human albumin plays an important role in the management of patients with decompensated liver cirrhosis. Guidelines recommend short-term albumin in specific acute conditions, but clinical trial data have also shown benefits of long-term albumin (LTA) treatment. This study aimed to analyse real-world data on LTA treatment in patients with cirrhosis across Italy.

Method: Data from an independent audit platform was collected on patients with cirrhosis and ascites who received non-LTA, defined as standard medical treatment with diuretics and albumin only for acute indications, or LTA, with infusions at weekly intervals for ≥6 months. Audits were performed between 2018 and 2020, using institutional data and callbacks with healthcare professionals in Italy from 43 locations (hospitals, pharmacies and health units). Retrospective analysis was conducted on patient demographics, treatment dose and regimen, complication rates and hospitalisation outcomes.

Results: Data were captured for 6660 patients (non-LTA: 4305; LTA: 2355). Main etiologies of cirrhosis were alcoholic (33%), viral (29%) non-alcoholic steatohepatitis (30%) and other (7%). In LTA patients, the mean (range) treatment duration was 14 (6–36) months and initial dose was 87 (10–280) g/week, followed by 37 (10–60) g/week. The need for paracentesis (3.1 vs 6.2 per patient per year) and the incidence of refractory ascites (0.57 vs 0.71 per patient per year) were lower in LTA than in non-LTA patients. A lower incidence (episodes

per patient per year) of other major complications was also reported in LTA patients: spontaneous bacterial peritonitis (0.19 vs 0.09), hepatorenal syndrome (0.28 vs 0.16) and hepatic encephalopathy (0.40 vs 0.31). Hospitalisations were 2.40 and 2.85 per patient per year in LTA and non-LTA groups, respectively. Differences were maintained when comparing patients within age groups (≤39, 40–59, ≥60 years).

Conclusion: These real-world data captured through an audit methodology indicate that Italian hepatologists consider LTA a valuable approach for the medical management of decompensated cirrhosis, as LTA is currently prescribed in a vast proportion of patients with ascites. Although the present study does not allow the comparison of the two groups, the lower incidence of paracentesis and complications observed in patients receiving LTA is consistent with the benefits documented by the ANSWER trial. Considering this, the cost-effectiveness of LTA and potential for reducing the economic burden upon healthcare systems should be assessed.

OS012

Impact of cirrhotic cardiomyopathy and severity of liver cirrhosis on the development of acute kidney injury

Simona Bota¹, Marcel Razpotnik¹, Philipp Wimmer², Michael Hackl², Gerald Lesnik³, Hannes Alber², Markus Peck-Radosavljevic¹.

¹Klinikum Klagenfurt am Wörthersee, Department of Internal Medicine and Gastroenterology (IMuG) and Emergency Medicine (ZAE), Klagenfurt, Austria; ²Klinikum Klagenfurt am Wörthersee, Department of Internal Medicine and Cardiology (IMuK), Klagenfurt, Austria; ³Klinikum Klagenfurt am Wörthersee, Institut für diagnostic and interventional Radiology, Klagenfurt, Austria
Email: bota_simona1982@yahoo.com

Background and aim: New criteria of cirrhotic cardiomyopathy (CCM) were published from a multidisciplinary consortium (Izzy et al. Hepatology 2019 Nov 11. doi: 10.1002/hep.31034) and define systolic dysfunction of the left ventricle as ejection fraction (EF) ≤50% and/or global longitudinal strain (GLS) <−18%, while the diastolic dysfunction is diagnosed when three of the following conditions are present: average E/e' >14, peak tricuspid regurgitation velocity >2.8 m/s, septal e' <7 cm/s, left atrial volume index >34 ml/m².

Our **aim** was to assess the influence of CCM, severity and etiology of liver cirrhosis on the development of acute kidney injury.

Method: Our prospective study included consecutive patients with liver cirrhosis without structural heart disease, arterial hypertension, HCC outside Milan criteria, portal vein thrombosis, presence of TIPS and with optimal acoustic echocardiography window. The patients were evaluated between 12/2018–11/2021 in our in- and out-patient Department. Conventional and speckle-tracking echocardiography (Vendor GE, EchoPAC PC software) were performed by a single investigator (EACVI TTE certified).

Acute kidney injury (AKIN) was defined according to the International Ascites Club as increase to serum creatinine of 0.3 mg/dL in <48 h or 50% increase in serum creatinine from baseline value within ≤3months.

The follow-up was performed until the patient was last seen or death.

Results: 412 cirrhotic patients were evaluated during the study period and 133 fulfilled the inclusion criteria and were included in the final analysis. The mean age of patients was 57.1 ± 10.2 years (60.1% males), 70.1% with alcoholic etiology and 48.1% with Child-Pugh A liver cirrhosis.

The median follow-up was 21 (0.5–36) months. Acute kidney injury was diagnosed in 26/133 (19.5%) of patients, while CCM (systolic and/or diastolic dysfunction) was present on 15% of patients.

The presence of acute kidney injury was correlated in univariate analysis with presence of CCM, Child-Pugh score, MELD score, alcoholic etiology of liver cirrhosis and prothrombin time (Table).

In multivariate logistic regression analysis only CCM and alcoholic etiology remained significantly associated with AKIN: CCM -OR = 13.6

ORAL PRESENTATIONS

(95% CI: 3.8–54.0), $p = 0.0001$ and alcoholic etiology-OR = 5.3 (95% CI: 1.1–26.3), $p = 0.03$.

	Spearman r correlation coefficient
Age	$r = 0.089$, $p = 0.30$
Male gender	$r = 0.052$, $p = 0.54$
BMI	$r = 0.103$, $p = 0.23$
Alcoholic etiology	$r = 0.186$, $p = 0.03$
Spleen size	$r = 0.082$, $p = 0.34$
Presence of CCM	$r = 0.323$, $p = 0.0001$
Child-Pugh score	$r = 0.259$, $p = 0.002$
MELD score	$r = 0.237$, $p = 0.005$
Presence of portal hypertension	$r = 0.107$, $p = 0.21$
Albumin	$r = -0.169$, $p = 0.06$
Platelet count	$r = 0.037$, $p = 0.67$
Prothrombin time	$r = -0.197$, $p = 0.02$

Conclusion: The presence of CCM is a strong predictor of acute kidney injury development among cirrhotic patients.

Non-invasive assessment of liver disease except NAFLD

OS013

Association of long term methotrexate therapy with liver fibrosis markers: a multi-centre prospective case-control study

Edmond Atallah^{1,2}, Jane Grove^{1,2}, Colin Crooks^{1,2}, Esther Burden-teh³, Ruth Murphy⁴, Sulleman Moreea⁵, Abhishek Abhishek⁶, Kelsey Jordan⁷, Aftab Ala⁸, David Hutchinson⁹, Richard Aspinall¹⁰, Guruprasad Aithal^{1,2}. ¹University of Nottingham, Nottingham Digestive Diseases Centre, School of Medicine, Nottingham, United Kingdom; ²Nottingham University Hospitals NHS Trust and the University of Nottingham, National Institute for Health Research (NIHR) Nottingham Biomedical Research Centre, Nottingham, United Kingdom; ³University of Nottingham, Centre of Evidence Based Dermatology, School of Medicine, Nottingham, United Kingdom; ⁴Sheffield Dermatology Research, University of Sheffield, Sheffield, United Kingdom; ⁵Bradford Teaching Hospitals NHS Foundation Trust, Bradford, United Kingdom; ⁶Nottingham University Hospitals NHS Trust Queen's Medical Centre Campus, United Kingdom; ⁷Brighton and Sussex University Hospitals NHS Trust, Brighton, United Kingdom; ⁸Royal Surrey County Hospital, Surrey, United Kingdom; ⁹Royal Cornwall Hospitals NHS Trust, Cornwall, United Kingdom; ¹⁰Portsmouth Hospitals University NHS Trust, Portsmouth

Email: edmond.atallah@nottingham.ac.uk

Background and aims: Incidence of acute drug-induced liver injury due to methotrexate (MTX) reduces significantly after the first year of treatment. However, decompensated cirrhosis attributed to MTX accounts for 0.07% of patients listed/transplanted in the USA. We evaluated the risk of long-term MTX therapy on liver fibrosis prospectively in a case-control study.

Method: Between 2014–2021, adult patients diagnosed with Rheumatoid Arthritis (RA) or Psoriasis (PS) were recruited prospectively from six UK sites. Patients on MTX for ≥ 6 months were defined as cases, whereas those with RA or PS for ≥ 2 years who never received MTX were controls. All patients underwent full liver profile, enhanced liver fibrosis (ELF) markers, and transient elastography (TE). Multivariate analysis was performed using logistic regression and results were presented as adjusted odds ratio (OR) and 95% confidence interval.

Results: Of 999 patients included (mean age 60.8 ± 12 years, 622 females (62.3%)), 976 had valid TE values; 149 (15.3%) had liver stiffness ≥ 7.9 KPa. Of 892 with available ELF, 262 had ELF score ≥ 9.8 (29.4%). Age and BMI were independently associated with elevated liver stiffness and ELF. Diabetes was associated with significant fibrosis defined by liver stiffness ≥ 7.9 KPa, OR = 3.21 (1.96–5.21), $p < 0.001$. But, neither MTX cumulative dose nor duration of exposure was associated with elevated liver stiffness [OR = 1.02 (0.93–1.12) and 1.00 (0.99–1.0), respectively] and ELF score [OR = 1.06 (1.0–1.12) and 1.00 (0.99–1.0), respectively]. Regular use of non-steroidal anti-inflammatory drugs was associated with ELF score ≥ 9.8 , OR = 1.78 (1.22–2.60), $p = 0.003$.

Conclusion: Lack of association of MTX cumulative dose and duration with liver fibrosis in RA or PS indicates that the risk of liver fibrosis due to MTX itself might have been overestimated. The degree of inflammation in RA and PS may confound ELF as a marker to detect fibrosis.

Table: Demographic and phenotypic features for cases and controls

Characteristics	MTX group (n = 876)	Control group (n = 123)	p
Age (years), mean (SD)	61.6 (11.6)	55.6 (13.5)	<0.001
Female, n (%)	560 (63.9)	62 (50.4)	<0.01
Diagnosis, n (%)		55 (44.7)	<0.001
RA	615 (70.2)	67 (54.5)	
PS	241 (27.5)	1 (0.8)	
Both	20 (2.3)		
Type 2 Diabetes	100 (11.5)	21 (17.1)	NS
Hyperlipidaemia	225 (25.9)	28 (22.8)	NS
BMI (kg/m^2), mean (SD)	29.9 (6.7)	30.9 (7.5)	NS
Alcohol >14 units/week, n (%)	83 (9.5)	25 (20.3)	<0.001
Fibrosis markers			
TE groups, n (%)	731 (85.5)	96 (79.3)	0.08
Low <7.9	124 (14.5)	25 (20.7)	
High ≥ 7.9			
ELF groups, n (%)	562 (71.4)	68 (64.8)	NS
Low risk <9.8	202 (25.7)	34 (32.4)	
Moderate risk (≥ 9.8 to <11.3)	23 (2.9)	3 (2.9)	
High risk ≥ 11.3			

NS: Not significant.

OS014

Development and validation of a machine learning-based model for varices screening in compensated cirrhosis (CHESS2001): an international multicenter study

Yifei Huang¹, Jia Li², Tian-lei Zheng³, Dong Ji⁴, Yu Jun Wong⁵, Hong You⁶, Ye Gu⁷, Musong Li⁸, Lili Zhao², Shuang Li², Shi Geng³, Na Yang³, Guofeng Chen⁴, Yan Wang⁷, Manoj Kumar⁹, Ankur Jindal⁹, Qin Wei⁸, Zhenhuai Chen⁸, Yongning Xin¹⁰, Zicheng Jiang¹¹, Xiaoling Chi¹², Jilin Chen¹³, Mingxin Zhang¹⁴, Huan Liu¹⁴, Ming Lu¹⁵, Li Li¹⁵, Yong Zhang¹⁶, Chunwen Pu¹⁶, Deqiang Ma¹⁷, Qibin He¹⁸, Shanghong Tang¹⁹, Chunyan Wang¹⁹, Shiv Kumar Sarin⁹, Xiaolong Qi¹. ¹The First Hospital of Lanzhou University, CHESS Center, Institute of Portal Hypertension, Lanzhou, China; ²Tianjin Second People's Hospital, Department of Gastroenterology and Hepatology, Tianjin; ³The Affiliated Hospital of Xuzhou Medical University, Artificial Intelligence Unit, Department of Medical Equipment, Xuzhou, China; ⁴The Fifth Medical Center of Chinese PLA General Hospital, Department of Liver Diseases, Beijing, China; ⁵Changi General Hospital, Duke-NUS Academic Clinical Program, SingHealth, Department of Gastroenterology and Hepatology, Singapore; ⁶Beijing Friendship Hospital, Capital Medical University, Liver Research Center, Beijing Key Laboratory of Translational Medicine in Liver Cirrhosis, National Clinical Research Center of Digestive Diseases, Beijing, China; ⁷The Sixth People's Hospital of Shenyang, Portal

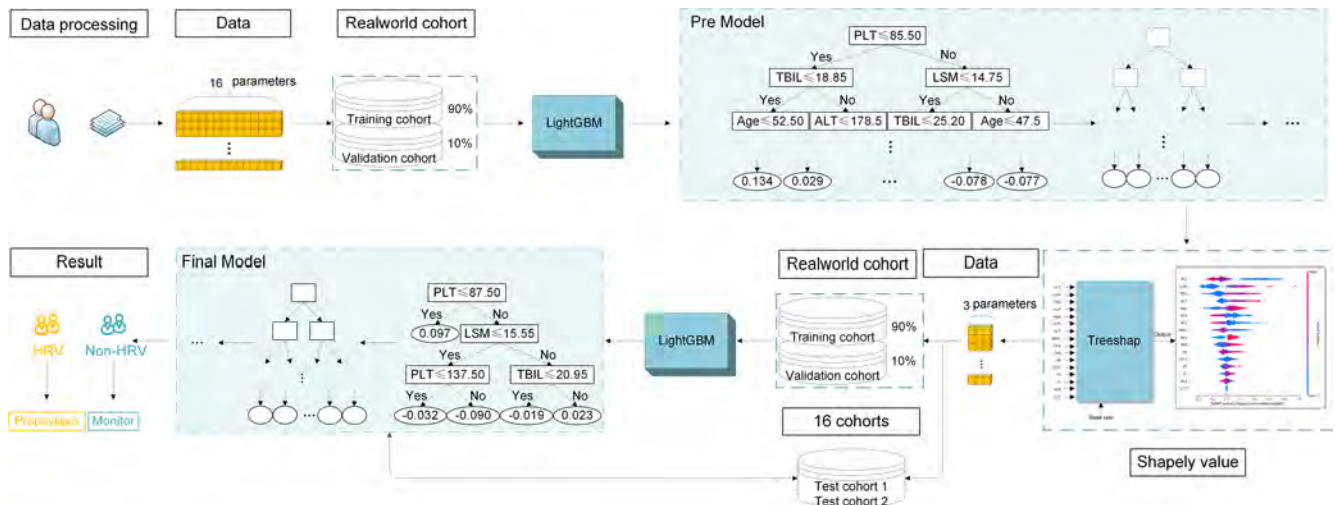


Figure: (abstract: OS014)

Hypertension Center, Shenyang, China; ⁸Baoding people's Hospital, Department of Gastroenterology, Baoding, China; ⁹Institute of Liver and Biliary Sciences (ILBS), Department of Hepatology, New Delhi, India; ¹⁰Qingdao Municipal Hospital, Qingdao University, Department of Infectious Disease, Qingdao, China; ¹¹Ankang Central Hospital, Department of Infectious Diseases, Ankang, China; ¹²Guangdong Provincial Hospital of Chinese Medicine, The Second Affiliated Hospital of Guangzhou University of Chinese Medicine, Department of Hepatology, Guangzhou, China; ¹³Shanghai Public Health Clinical Center affiliated to Fudan University, Department of Gastroenterology and Hepatology, Shanghai, China; ¹⁴The First Affiliated Hospital of Xi'an Medical University, Department of Gastroenterology, Xi'an, China; ¹⁵Mengzi People's Hospital, Department of Gastroenterology, Mengzi, China; ¹⁶Dalian Public Health Clinical Center, Dalian, China; ¹⁷Taihe Hospital, Hubei University of Medicine, Department of Infectious Diseases, Shiyan, China; ¹⁸Second Hospital of Nanjing, Nanjing Hospital of Chinese Medicine, Department of Gastroenterology, Nanjing, China; ¹⁹General Hospital of Western Theater Command PLA, Department of Gastroenterology, Chengdu, China
Email: qixiaolong@vip.163.com

Background and aims: Only a few patients with compensated cirrhosis who underwent esophagogastroduodenoscopy (EGD) screening for varices were found to have varices needing treatment (VNT). Our study aimed to identify a novel machine learning-based model (ML EGD) for ruling out VNT and avoiding unnecessary EGD in patients with compensated cirrhosis.

Method: A total of 2794 patients from China, Singapore and India were enrolled. Of them, 1283 patients in a real-world cohort from one university hospital, 966 in a multicenter cohort (test cohort 1) from 14 university hospitals, and 545 in an international cohort (test cohort 2) from Singapore and India were included, respectively. For the real-world cohort, patients were shuffled and sampled randomly into training and validation cohort with a ratio of 9:1. In the training cohort, a light gradient boosting machine algorithm was used to develop the pre-model to detect VNT based on clinical data. A shapley value method was used to evaluate the importance of included variables according to pre-model. ML EGD was furthermore developed based on the most related variables to detect VNT using light gradient boosting machine algorithm. Then, we validated it in the validation cohort and tested it in the two external test cohorts.

Results: The main etiology of cirrhosis was hepatitis B infection in the training (68.02%), validation cohort (68.99%) and test cohort 1 (79.19%) and the main etiology in test cohort 2 was hepatitis C infection (47.16%). Liver stiffness, platelet count and total bilirubin were evaluated as the most related variables to detect VNT to develop

ML EGD. By receiver operator characteristic curve, the most accurate cut-off to rule out patients with VNT was chosen as a ML EGD below 0.50 with a negative predictive value of 96.4%. In the training cohort, a ML EGD below 0.50 could spare 607 (52.6%) unnecessary EGD with a missed VNT rate of 3.6%. In the validation cohort, test cohort 1 and test cohort 2, a ML EGD score below 0.50 could spare 75 (58.1%), 506 (52.4%), 224 (41.1%) EGD with a missed VNT rate of 1.4%, 2.8%, and 3.1%, respectively. Comparing with Baveno VI criteria, ML EGD improved the proportion of avoided EGD (training cohort, 52.6% vs 29.4%; validation cohort, 58.1% vs 44.2%; test cohort 1, 52.4% vs 26.5%; test cohort 2, 41.1% vs 21.1%).

Conclusion: We developed a robust machine learning-based model, named ML EGD, with excellent performance to exclude VNT in patients with compensated cirrhosis.

OS015

Diagnostic performance of non-invasive liver fibrosis biomarkers: a bayesian individual patient data meta-analysis of hepatitis B cohorts in sub-saharan Africa (HEPSANET)

Alexander Stockdale^{1,2}, Asgeir Johannessen^{3,4}, Marc Henrion^{2,5}, Edith Okeke⁶, Moussa Seydi⁷, Gilles Wandeler⁸, Mark Sonderup⁹, Wendy Spearman⁹, Michael Vinikoor^{10,11}, Edford Sinkala¹⁰, Hailemichael Desalegn¹², Fatou Fall¹³, Nicholas Riches⁵, Davwar Pantong Mark¹⁴, Mary John Duguru¹⁵, Tongai Gibson Maponga¹⁶, Jantjie Taljaard¹⁶, Philippa Matthews¹⁷, Monique Andersson¹⁷, Roger Sombie¹⁸, Yusuke Shimakawa¹⁹, Maud Lemoine²⁰. ¹University of Liverpool, Liverpool, United Kingdom; ²Malawi-Liverpool-Wellcome Trust Clinical Research Programme, Blantyre, Malawi; ³Sykehuset i Vestfold, Norway; ⁴University of Oslo Faculty of Medicine, Norway; ⁵Liverpool School of Tropical Medicine, United Kingdom; ⁶Faculty of Medical Sciences, Jos, Nigeria; ⁷Hospital Center University De Fann, Dakar, Senegal; ⁸Institute of Social and Preventive Medicine (ISPM), Bern, Switzerland; ⁹UCT Faculty of Health Sciences, Cape Town, South Africa; ¹⁰The University of Zambia, Lusaka, Zambia; ¹¹University of Alabama at Birmingham, Birmingham, United States; ¹²St. Paul's Hospital Millennium Medical College, Addis Ababa, Ethiopia; ¹³Hopital Principal de Dakar, Dakar, Senegal; ¹⁴University of Jos, Jos, Nigeria; ¹⁵University of Jos, Jos, Nigeria; ¹⁶Stellenbosch University, Stellenbosch, South Africa; ¹⁷University of Oxford, United Kingdom; ¹⁸Hospital Center Universitaire Yalgado Ouédraogo, Ouagadougou, Burkina Faso; ¹⁹Pasteur Institute, Paris, France; ²⁰Imperial College London, United Kingdom
Email: a.stockdale@liverpool.ac.uk

Background and aims: In sub-Saharan Africa, hepatitis B is the principal cause of liver disease, and associated mortality is rising.

ORAL PRESENTATIONS

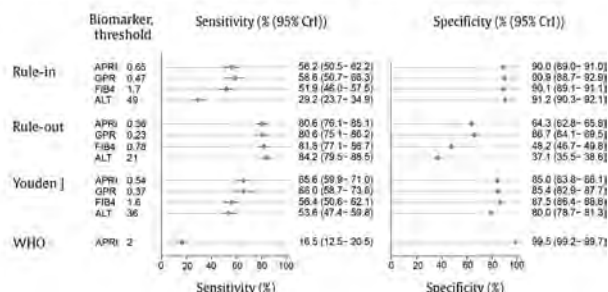
Low-cost non-invasive biomarkers of liver fibrosis are needed to identify patients at risk of HBV-related mortality who therefore require antiviral treatment. We evaluated the performance of the biomarkers APRI (AST to platelet ratio index), FIB-4 and GPR (GGT to platelet ratio) in an individual patient data (IPD) meta-analysis.

Method: We included data from HEPANET, a network comprised of 12 cohorts of HBsAg-positive individuals in 8 sub-Saharan African countries. We used transient elastography as a reference test for cirrhosis (≥ 12.2 kPa) and significant fibrosis (≥ 7.9 kPa). We excluded patients who were pregnant, had hepatitis C, D, or HIV co-infection, were on hepatitis B therapy or had acute hepatitis. Upper limits of normal were 40 U/L for AST/AST and 61 U/L for GGT. We fitted a bivariate Bayesian IPD model with patient-level covariates and study-level random effects.

Results: We included 3549 patients. Median age was 33 years (IQR 28–41) and 60% were male. The prevalence of significant fibrosis and cirrhosis among included cohorts was 18% and 7% respectively. APRI and GPR had the best discriminant performance (area under curve 0.81 and 0.82) relative to FIB-4 (0.77) or ALT alone (0.70) for cirrhosis. The World Health Organization (WHO) threshold of APRI > 2.0 was associated with sensitivity of 16.5% (95% credible interval 12.5–20.5) and specificity of 99.5% (99.2–99.7) for cirrhosis. At rule-in thresholds for cirrhosis APRI (cut-off 0.65) had sensitivity of 56.2% and specificity of 90.0%; GPR (cut-off 0.47) had sensitivity of 58.6% and specificity 90.9%. At rule out-thresholds for cirrhosis APRI (0.33) had sensitivity and specificity of 80.6% and 64.3%; GPR (0.23) had sensitivity 80.6% and specificity of 66.7% (Figure). The subset of asymptomatic patients who were diagnosed with HBV through routine screening had a mean cirrhosis prevalence of 2.5%, and APRI (cut-off 0.65) had a positive predictive value (PPV) of 13.2% and negative predictive value (NPV) of 98.8%. Among patients diagnosed with HBV due to suspected liver disease, cirrhosis prevalence was 27%; with APRI cut-off 0.65, PPV was 59.6% and NPV 84.5%.

Conclusion: APRI at the WHO-recommended threshold of 2.0 has a poor sensitivity for the diagnosis of cirrhosis in sub-Saharan Africa; WHO guidelines should be revised for the WHO African region to reflect these findings. APRI and GPR had equivalent diagnostic performance and performed best at ruling out cirrhosis but were less good at correctly identifying cases. Programs need to be aware of the significant trade-offs between under- and over-diagnosis of liver cirrhosis when implementing low-cost fibrosis markers in hepatitis B programs in sub-Saharan Africa.

Performance of non-invasive biomarkers for the diagnosis of cirrhosis (≥ 12.2 kPa)



OS016

Prediction of ten-year risk of severe liver disease in the general population using commonly available biomarkers

Hannes Hagström¹, Jacinth Yan², Mats Talbäck², Anna Andreasson³, Göran Walldius², Matteo Bottai², Niklas Hammar². ¹Karolinska Institutet; ²Karolinska Institutet, Sweden; ³Stockholm University, Sweden

Email: hannes.hagstrom@ki.se

Background and aims: Estimating risk for severe liver disease, including cirrhosis, in the general population is complicated in part

due to the rarity of this outcome. Existing prediction tools are suboptimal and there is a need for improvement. Here, we aimed to identify subgroups of persons in the general population with high risks for development of severe liver disease using commonly available biomarkers.

Method: We used laboratory and clinical data on 126,925 individuals aged 35–79, in Stockholm, Sweden, with clinical examinations between 1985 and 1996. No individuals had known chronic liver disease, a drug- or alcohol use disorder at baseline. Nationwide registries were used to ascertain ten-year cumulative incidence of severe liver disease, a composite of diagnoses corresponding to cirrhosis or its complications. Candidate biomarkers were selected based on if they meaningfully improved prediction of severe liver disease in addition to the established FIB-4 score. They were then categorized and combined, creating subgroups with different risk profiles.

Results: During a follow-up of average 9.3 years, we ascertained 630 incident cases of severe liver disease (0.5%). On top of the FIB-4 score we identified age, impaired glucose, and gamma-glutamyl transferase (gGT) to meaningfully improve a classification of risk. 24 risk groups were created, with a cumulative incidence of severe liver disease at ten years ranging from 0.2% (age 35–65, low FIB-4, no impaired glucose and normal gGT) to 32.1% (age 35–65, high FIB-4, impaired glucose and high gGT). A heatmap of these risk groups was created (Figure 1).

Cumulative incidence of severe liver disease at ten years					
			FIB-4 Low	FIB-4 Intermediate	FIB-4 High
gGT high	Impaired glucose	age ≥66	13.0	13.7	29.1
		age 35-65	2.6	10.7	32.1
	No Impaired glucose	age ≥66	3.6	0.0	22.7
		age 35-65	2.2	7.4	25.4
gGT normal	Impaired glucose	age ≥66	1.3	2.8	12.5
		age 35-65	0.6	1.0	6.0
	No Impaired glucose	age ≥66	0.6	0.7	2.5
		age 35-65	0.2	0.4	5.5

Figure 1: Heatmap of subgroups with differing risk for severe liver disease at ten years, in percent.

Conclusion: Estimates of risk of severe liver disease in the general population using the FIB-4 score can be substantially improved by adding age and biomarkers commonly available in the primary care setting.

OS017

Gadoxetic acid-enhanced MRI-derived Functional Liver Imaging Score (FLIS) and spleen diameter provide complementary information for risk stratification in ACLD

Nina Bastati¹, Lucian Beer¹, Ahmed Ba-Ssalamah¹, Sarah Poetter-Lang¹, Raphael Ambros¹, Antonia Kristic¹, David Lauber¹, Lorenz Balcar¹, Katharina Pomej², Teresa Binter^{2,3}, Benedikt Simbrunner^{2,3}, Georg Semmler^{2,3}, Yesim Bican¹, Jacqueline C. Hodge¹, Thomas Wrba⁴, Michael Trauner², Thomas Reiberger^{2,3}, Mattias Mandorfer^{2,3}. ¹Department of Biomedical Imaging and Image-Guided Therapy, Medical University of Vienna, Vienna, Austria; ²Division of Gastroenterology and Hepatology, Department of Internal Medicine III, Medical University of Vienna, Vienna, Austria; ³Vienna Hepatic Hemodynamic Lab, Division of Gastroenterology and Hepatology, Department of Internal Medicine III, Medical University of Vienna, Vienna, Austria; ⁴IT-Systems and Communications, Medical University of Vienna, Vienna, Austria
Email: mattias.mandorfer@meduniwien.ac.at

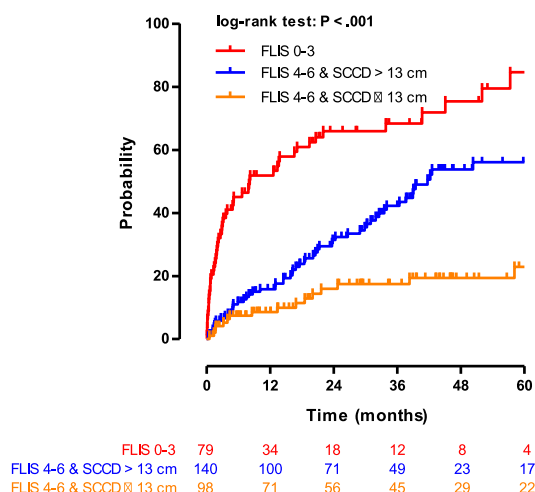
Background and aims: The Functional Liver Imaging Score (FLIS) derived from gadoxetic acid-enhanced MRI (GA-MRI) correlates with hepatic function in chronic liver disease (CLD) patients. Splenic metrics, i.e., volume and craniocaudal diameter (SCCD) are markers of portal hypertension, a key driver of disease progression.

We aimed to investigate the prognostic utility of FLIS and SCCD for hepatic decompensation and transplant-free mortality in CLD.

Method: Three hundred ninety-seven CLD patients undergoing GA-MRI were included. The FLIS was calculated by summing the points (0–2 each) assigned to three hepatobiliary phase features: hepatic enhancement, biliary excretion, and portal vein signal intensity. Patients were stratified into 3 clinical groups according to FIB-4 and presence/history of decompensation: non-advanced CLD (non-ACLD), compensated ACLD (cACLD), and decompensated ACLD (dACLD). The associations between SCCD/FLIS and decompensation/transplant-free mortality were investigated using Cox regression analysis and log-rank test.

Results: We observed a strong correlation between spleen volume and SCCD (Spearman's rho: 0.887; $p < 0.001$), and thus, the simple measure SCCD was used for further analyses. The inter-reader (intraclass coefficient, ICC: 0.982; $n = 241$) and intra-reader (ICC: 0.997; $n = 41$) agreement for the SCCD were excellent. Median SCCD showed stepwise increases from non-ACLD (11.8 cm), cACLD (13.3 cm), to dACLD (15.2 cm; $p < 0.001$).

Since non-ACLD patients are at negligible risk of decompensation/liver-related death, we abstained from analysing direct end points in this subgroup. In patients with cACLD, SCCD predicted decompensation (adjusted-hazard-ratio, [aHR]: 1.1, 95% confidence interval [95% CI]: 1.02–1.18; $p = 0.014$) in an analysis adjusted for MELD and albumin; dichotomizing SCCD resulted in an aHR of 2.51 (95%CI: 1.22–5.21, $p = 0.01$) for those with a SCCD > 13 cm. In patients with ACLD (i.e., cACLD/dACLD combined), FLIS (0–3 vs. 4–6 points) was a risk factor for transplant-free mortality (aHR: 2.64, 95%CI: 1.61–4.01, $p < 0.001$), even after adjusting for age, MELD, and albumin. Of note, FLIS (0–3 vs. 4–6 points; aHR: 1.74, 95%CI: 1.18–2.58, $p = 0.005$) and SCCD (> 13 vs. ≤ 13 cm; aHR: 2.16, 95%CI: 1.44–3.24, $p < 0.001$) were independently predictive of the composite end point of decompensation/transplant-free mortality, even after adjusting for the previously mentioned prognostic indicators. Grouping patients according to FLIS/SCCD accurately stratified the risk of decompensation/transplant-free mortality (Figure).



Conclusion: The FLIS and SCCD are simple GA-MRI-based imaging markers providing complementary information for risk stratification in patients with advanced chronic liver disease.

N.B. and L.B. contributed equally.

OS018

ADAPT, a score incorporating PRO-C3, for the early detection of liver fibrosis in a large population-based study

Ann T. Ma^{1,2,3}, Guillem Pera^{3,4}, Martina Perez^{1,2,3,5}, Mette Juul Nielsen⁶, Morten Karsdal⁶, Diana Leeming⁶, Carmen Expósito⁴, Alba Martínez-Escudé^{4,7}, Isabel Graupera^{1,2,3}, Maja Thiele^{8,9}, Aleksander Krag^{8,9}, Núria Fabrellas^{2,3,5}, Llorenç Caballeria^{3,4}, Pere Ginès^{1,2,3,5}. ¹Liver Unit, Hospital Clínic de Barcelona, Barcelona, Spain; ²Institut d'Investigacions Biomèdiques August Pi i Sunyer (IDIBAPS), Barcelona, Spain; ³Centro de Investigación Biomédica en Red de Enfermedades Hepáticas y Digestivas (CIBEREHD), Madrid, Spain; ⁴Unitat de Suport a la Recerca (USR) Metropolitana Nord, Fundació Institut Universitari d'Investigació en Atenció Primària Jordi Gol i Gurina (IDIAP Jordi Gol), Mataró, Spain; ⁵Facultat de Medicina-Universitat de Barcelona, Barcelona, Spain; ⁶Nordic Bioscience, Herlev, Denmark; ⁷Centre d'Atenció Primària La Llagosta, La Llagosta, Spain; ⁸Department of Gastroenterology and Hepatology, Odense University Hospital, Denmark; ⁹Department of Clinical Research, Faculty of Health Sciences, University of Southern Denmark, Odense, Denmark
Email: pginès@clinic.cat

Background and aims: Non-invasive screening of liver fibrosis in the general population has become an important target in order to identify liver disease early and avoid its progression. Novel biomarkers of extracellular matrix formation, including PRO-C3, a marker of type III collagen formation, have emerged as accurate predictors of advanced fibrosis in NAFLD and alcohol-related liver disease. A composite score known as ADAPT, that includes PRO-C3, age, platelet count, and diabetes, has recently been validated in both these patient populations, but its effectiveness to screen for liver fibrosis in asymptomatic subjects in the general population is unknown.

Method: This study was performed in a large population-based cohort of randomly selected subjects aged 18–75 in the Barcelona metropolitan area without known liver disease (mean age 54, 43% male, 10% with type 2 diabetes, 28% with metabolic syndrome, 9% with at-risk alcohol consumption). Serum PRO-C3 levels were measured by enzyme-linked immunosorbent assay in 2670 subjects. Liver fibrosis was estimated by measuring liver stiffness with transient elastography (TE). Significant fibrosis was defined as a TE ≥ 9.2 kPa based on previous data supporting that this cut-off had the best diagnostic accuracy for fibrosis $\geq F2$ on liver biopsy (Clin. Gastroenterol. Hepatol. 2018 PMID 29452268).

Results: The prevalence of significant fibrosis was 3.1% (83/2670). The median level of PRO-C3 was higher in subjects with significant fibrosis compared to those without (14 vs. 12 ng/ml, $p < 0.001$). The ADAPT score predicted significant fibrosis with moderate accuracy (AUROC 0.76; 95% CI 0.71–0.82), higher than scores frequently used to identify fibrosis in the general population, such as FIB-4 or APRI, and similar to NAFLD Fibrosis Score (NFS). Fatty liver index (FLI) exhibited the highest discriminative ability (AUROC 0.87; 95% CI 0.84–0.91; Figure 1). Amongst subjects with metabolic/alcohol risk factors and a high FLI ≥ 60 , the sequential use of ADAPT using the best cut-off of 6.1 had an excellent negative predictive value for significant fibrosis (Se 51%, Sp 82%, PPV 20%, NPV 95%).

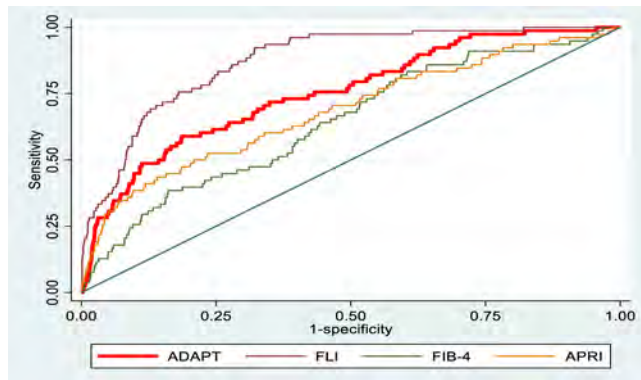


Figure: ROC curves of non-invasive fibrosis scores for prediction of significant fibrosis.

Conclusion: In this population-based study, the ADAPT composite score that includes PRO-C3 offers superior predictive accuracy for the diagnosis of significant liver fibrosis as compared to other recommended screening tools such as FIB-4 and APRI. The individual components of ADAPT are easily accessible clinical parameters and as such could be used as a tool for the early detection of liver fibrosis in the general population, particularly in a sequential-type approach.

Immune-mediated and cholestatic: Experimental and pathophysiology

OS019

Novel anti-cholestatic treatment strategies by combining inhibition of the Apical sodium-dependent bile acid transporter with stimulation of urinary bile salt excretion or lowering bile salt synthesis

Roni Kunst^{1,2}, Esther Vogels¹, Isabelle Bolt¹, Ronald Oude-Elferink^{1,2}, Stan van de Graaf^{1,2}. ¹Tytgat Institute for Liver and Intestinal Research, Department of Gastroenterology and Hepatology; ²Amsterdam Gastroenterology Endocrinology Metabolism, Amsterdam, Netherlands
Email: r.f.kunst@amsterdamumc.nl

Background and aims: The apical sodium-dependent bile acid transporter (ASBT) is primarily expressed in the small intestine and kidney, where it prevents bile salts from being excreted in respectively feces and urine. Intestine-restricted drugs that inhibit ASBT are currently clinically explored to reduce toxic accumulation of bile acids during cholestasis. Intestine-restricted ASBT inhibitors (ASBTi) may be less effective in severe cholestasis and also yield gastrointestinal side-effects in case of high bile salt load in the colon. Here, we test two ASBT-targeting treatment strategies in pre-clinical models with cholestasis-induced liver injury. First, systemic ASBT inhibition, to increase renal bile acid excretion and second a combination treatment with obeticholic acid (OCA) to limit bile salt synthesis and reduce colonic bile acid load.

Method: Systemic ASBT inhibition was tested by performing a bile duct ligation (BDL) in adult ASBT knock-out (KO) mice (129P2/OlaHsd background, Jackson) and wild-type littermates to induce severe cholestasis. In our second strategy, BDL was performed in adult wild-type C57Bl/6 mice after 2 days oral gavage pre-treatment with OCA and ASBTi. In a different model, wild-type C57Bl/6 mice were fed a 0.1% 3, 5-diethoxycarbonyl-1, 4-dihydrocollidine (DDC) diet while receiving daily treatment with either placebo, OCA, ASBTi or both

(OCA + ASBTi). After sacrifice, liver injury was determined by plasma liver enzymes, RT-qPCR and liver histology, while HPLC analysis was used to quantify bile salt concentrations in plasma, liver, small intestine and feces.

Results: ASBT KO mice had reduced liver necrosis, reduced bilirubin and alkaline phosphatase (ALP) levels compared to wild-type mice after BDL. ASBT KO mice also showed a trend to reduced bile salt pool size, and increased urinary bile salt excretion. OCA + ASBTi treatment reduced the total bile salt pool size before cholestasis-onset and resulted in reduced bilirubin, ALP and a ~60% reduction in liver necrosis compared to placebo control in a BDL model. Besides, OCA + ASBTi treatment decreased fecal bile salt excretion compared to monotherapy with ASBTi.

Conclusion: Systemic ASBT inhibition effectively reduces BDL-induced liver damage. Combined OCA + ASBTi treatment lowers the bile salt pool size and improves liver health after BDL-induced cholestasis, while it also shows therapeutic potential by reducing fecal bile salt excretion.

OS020

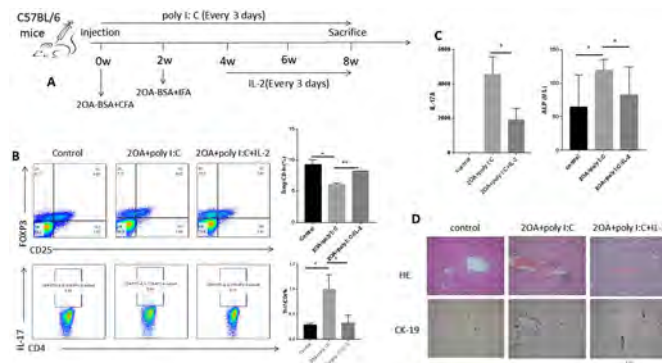
Low-dose IL-2 alleviates drug-induced primary biliary cholangitis in mice by improving Treg and Th17 balance

Zilong Wang¹, Bo Feng¹, Yandi Xie¹, Rui Jin¹, Zhicheng Liu¹. ¹Peking University Hepatology Institute, Beijing, China
Email: fengbo@pkuph.edu.cn

Background and aims: The imbalance of regulatory T (Treg) and Th helper 17 (Th17) cells correlates with increased risk of autoimmune diseases. Their imbalance was also reported in primary biliary cholangitis (PBC) patients. Previous studies have suggested that low-dose IL-2 can alleviate disease severity through modulating CD4⁺T cell subsets in patients with autoimmune diseases. However, the efficacy of low-dose IL-2 in PBC remains unexplored. Hence, the present study aimed to examine effects of low-dose IL-2 in PBC mouse models.

Method: PBC was induced in female C57BL/6 mice by two immunizations with 2-nonynoic acid (2OA-BSA) at two-week intervals. Besides, polyinosinic polycytidylic acid (poly I:C) was injected i.p. every three days. The control group was injected with PBS instead of 2OA-BSA and poly I:C. PBC mice were divided into the treated and untreated groups, and low-dose IL-2 was injected s.c. every three days after four weeks from modeling in the treated group (Fig. A) and the untreated group was replaced with saline. The serum was isolated from blood sampled by eyeball extirpating for biochemical detection. Th17 and Tregs were analyzed by flow cytometry, and the related cytokines were analyzed by ELISA. Liver histopathology was examined by HandE and immunohistochemical staining. The experimental data were analyzed by SPSS 24.0 software. $P < 0.05$ indicated statistical significance.

Results: Eight weeks after modeling, the serum AMA was positive and the ALP was significantly increased in PBC mice compared with control group. The pathology showed lymphocyte infiltration in the portal area, and damage and reactive proliferation of small bile duct, and CD4⁺ and CD8⁺ T cells were infiltrated around the bile duct. Flow cytometric examination of spleen cells revealed recovery of reduced Tregs and increased Th17 after low-dose IL-2 treatment (Treg/CD4%: 9.26 ± 0.50 vs 6.10 ± 0.14 vs 8.24 ± 0.04 ; Th17/CD4%: 0.29 ± 0.20 vs 1.00 ± 0.17 vs 0.33 ± 0.09) ($p < 0.05$) (Fig. B). Low-dose IL-2 treatment inhibited IL-17A levels (0 vs 4549 ± 597.5 vs 1928 ± 387) ($p < 0.05$) and improved serum biochemical index (ALP: 119.1 ± 6.20 vs 82.36 ± 12.6 U/L) (Fig. C). Histopathological examination of liver revealed the improvement of portal area inflammation and reactive bile duct hyperplasia and damage after low-dose IL-2 treatment (Fig. D).



Conclusion: The PBC mouse model was successfully induced by the combination of 20A-BSA and poly I:C and it can model human disease early status. Low-dose IL-2 inhibited PBC by augmenting Treg and decreasing Th17 numbers, which play important role in the pathogenesis of the PBC. The improvement of biochemical indexes and liver histopathology, suggesting that low-dose IL-2 treatment may be considered as novel therapy for PBC in the future.

OS021

Cholangiocytes cleave surface CD100 from biliary infiltrating T cells and mediate pathogenic Th17 differentiation

Xiaojun Jiang^{1,2,3}, Kari Otterdal², Brian K. Chung^{1,2,3}, Christopher Maucourant⁴, Christine Zimmer⁴, Sverre Holm², Daniel Geanon⁴, Annika Bergquist⁵, Tom Hemming Karlsen^{1,3}, Niklas Björkström⁴, Espen Melum^{1,2,3,6,7}. ¹Norwegian PSC Research Center, Oslo University Hospital Rikshospitalet, 0424 Oslo, Norway; ²Research Institute of Internal Medicine, Oslo University Hospital Rikshospitalet, 0424 Oslo, Norway; ³Institute of Clinical Medicine, University of Oslo, 0318 Oslo, Norway; ⁴Center for Infectious Medicine, Department of Medicine Huddinge, Karolinska Institutet, Karolinska University Hospital, 141 52 Stockholm, Sweden; ⁵Department of Gastroenterology and Hepatology, Karolinska University Hospital Huddinge, Karolinska Institutet, 171 77 Stockholm, Sweden; ⁶Section of Gastroenterology, Department of Transplantation Medicine, Division of Surgery, Inflammatory Diseases and Transplantation, Oslo University Hospital Rikshospitalet, 0424 Oslo, Norway; ⁷Hybrid Technology Hub-Centre of Excellence, Institute of Basic Medical Sciences, Faculty of Medicine, University of Oslo, 0317 Oslo, Norway.
Email: espen.melum@medisin.uio.no

Background and aims: Chronic inflammation surrounding bile ducts contributes to the disease pathogenesis of most cholangiopathies, but the mechanism enabling pathogenic immune cells to adapt and survive in the biliary environment remains largely unknown. We have recently reported a variant of CD100 to be the causal mutation for a familial form of primary sclerosing cholangitis (PSC). Herein, we investigate how CD100 participates in the biliary local inflammation and its relevance to the differentiation of pathogenic immune cells.

Method: CD100 expression was assessed by spatial transcriptomics (10x Genomics) and *in situ* immunohistochemistry (IHC) in explanted livers of patients with PSC (n = 4–6) and other cholangiopathies (Ctrl, n = 4–5). Soluble CD100 (sCD100) was measured by ELISA in paired serum, plasma, and bile samples (n = 11–19). Biliary infiltrating immune cells were collected from endoscopic retrograde cholangiopancreatography brush samples (Ctrl, n = 6; PSC, n = 6) and surface expression of CD100 was evaluated by flow cytometry. To model pathogenic interactions between immune cells and cholangiocytes, splenic cells isolated from C57BL/6 wild-type (WT) and CD100 mutated mice were co-cultured with small or large cholangiocytes. Altered gene expression was assessed with RNA sequencing of purified cell subsets after co-culture.

Results: Spatial transcriptomics revealed *SEMA4D*/*CD100* RNA expression in all examined livers and demonstrated the localization

in *KRT19*⁺ bile duct regions (Ctrl, 7–40%; PSC, 11–94%). In contrast, CD100 protein expression measured by IHC was nearly undetectable in diseased periductal areas of the PSC livers. Moreover, surface expression of CD100 on biliary infiltrating immune cells was reduced and accompanied by increased sCD100 in plasma and bile from PSC patients, suggesting that CD100 is cleaved from the surface of immune cells in regions adjacent to the bile ducts. In co-culture experiments, we observed that activated immune cells adhered to cholangiocytes and correlated with the death of large but not small cholangiocytes. T cells were dominant (49.9–64.4%) in the adherent immune population and lost their surface CD100 expression. RNA sequencing data showed increased *Adams4* in co-cultured cholangiocytes which appeared to cleave CD100. Genes involved in anti-apoptosis and T-helper 17 (Th17) differentiation were enriched in adherent T cells and further upregulated in T cells with mutated CD100.

Conclusion: Cholangiocytes induce cleavage of CD100 on biliary infiltrating T cells that facilitates persistent inflammation and local Th17 differentiation. These findings highlight a novel pathway in the liver with cholangiocyte-driven Th17 cell differentiation that is associated with CD100 cytoplasmic signaling. Targeting this pathogenic pathway serves as an attractive target for mitigating bile duct inflammation in PSC.

OS022

Novel approach combining whole liver single-cell RNA sequencing and spatial gene profiling using Nanostring GEOMX enables identification of specific cell sub-populations and pathways regulated by CCL24

Michal Segal-Salto¹, Raanan Greenman¹, Arnon Aharon², Ophir Hay³, Amnon Peled³, Adi Mor⁴. ¹Chemomab Therapeutics Ltd., RandD, Tel Aviv, Israel; ²Chemomab Therapeutics Ltd., Clinical, Tel Aviv, Israel; ³Hadassah Hebrew University Hospital, Genetic Therapy Institute, Jerusalem, Israel; ⁴Chemomab Therapeutics Ltd., Tel-Aviv, Israel
Email: michal@chemomab.com

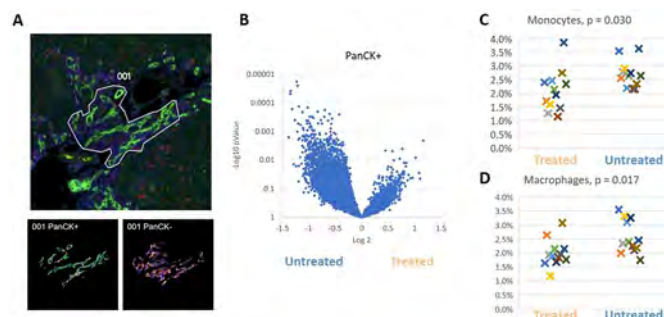
Background and aims: CCL24 (Eotaxin-2) is a chemokine that regulates profibrotic and proinflammatory activities through the CCR3 receptor. We previously demonstrated that CM-101, a CCL24 blocking antibody, improves liver inflammation, fibrosis and cholangitis in the *Mdr2* knockout (*Mdr2*^{-/-}) mouse model. Characterization of CCL24 expression in relation to the different cell populations in *Mdr2*^{-/-} mice and its inhibition effect on cholangiocytes and immune response was studied using two gene expression methods.

Method: Identification of cell population, including immune cells and CCL24 expressing cells in livers of *Mdr2*^{-/-} mice was done by scRNA seq from whole liver. NanoString's technology was utilized for gene expression studies, focusing on the bile-duct injury sites. In this system segmenting of cholangiocytes (PanCK+) and immune cells (Pan-CK-) cells was done in liver sections from *Mdr2*^{-/-} mice non-treated or treated with CM-101.

Results: *Mdr2*^{-/-} mice treated with CM-101 resulted in reductions in: serum ALP, liver inflammation, liver peribiliary collagen deposition and cholangiocytes proliferation. Using whole liver scRNA seq we demonstrated that CCL24 is expressed in macrophage cells. This analysis identified a few specific disease relevant immune sub-populations, however it is missing crucial information that relates to cell localization. To overcome this, we used NanoString to characterize the alternations in peribiliary transcriptome following CM-101 treatment. Spatial profiling separated cholangiocytes (PanCK+) and non-cholangiocytes (PanCK-) peribiliary cells, distinguishing cholestatic, proinflammatory and profibrotic effects. Gene set enrichment analysis showed reduction in proliferation and senescence pathways in PanCK+ cells, whereas PanCK- cells showed reduction in ECM remodeling pathways and increased metabolic pathways. Cell deconvolution of the heterogeneous PanCK- population revealed alternation in the peribiliary immune cells, marked by reduction in macrophages and monocytes following treatment with CM-101.

ORAL PRESENTATIONS

Conclusion: Augmenting whole liver scRNA seq with spatial transcriptome analysis, is a novel approach to identify cell populations and pathways specific to the damaged peribiliary area. Using this approach we demonstrated that CCL24 regulates cholestatic, inflammatory and fibrotic liver damage, and its underlying mechanisms. Understanding the underlying mechanisms of CCL24 blockade and its ability to prevent liver injury in animal supports its role in PSC and its potential beneficial effect for PSC patients.



OS023

T regulatory cells promote bile duct regeneration through modulating ductular reaction in a model of cholestatic liver injury

Naruhiro Kimura^{1,2,3}, Gareth Hardisty¹, Atsunori Tsuchiya³, Shuji Terai³, David Withers², Wei-Yu Lu^{1,2}, ¹University of Edinburgh, Centre for Inflammation Research, Edinburgh, United Kingdom; ²University of Birmingham, Institute of Immunology and Immunotherapy, Birmingham, United Kingdom; ³Niigata University, Division of Gastroenterology and Hepatology, Niigata, Japan
Email: w.y.lu@ed.ac.uk

Background and aims: Reduced regulatory T cells (Tregs) and increased bile duct senescence are observed in primary sclerosing cholangitis (PSC) patients, with the degree of cholangiocyte senescence linking to disease severity and prognosis. Cholangiocytes can act as facultative liver progenitor cells through ductular reaction during extensive liver damage, whether this process is impaired during PSC remains to be investigated. The role of Tregs in modulating tissue resident progenitor cells have been shown in multiple organs, but this remains unclear in the context of liver regeneration. We aim to use transgenic murine models to investigate the cause of reduced Tregs in the liver and whether the lack of Tregs in the liver affect bile duct regeneration and senescence.

Method: Foxp3^{GFP}DTR transgenic mice were used to reduce Tregs number in a dose dependant manner. 50% of Tregs were depleted to avoid triggering systematic autoimmunity whilst cholestatic liver injury was induced by the feeding of 3, 5-diethoxycarbonyl-1, 4-dihydrocollidine (DDC) diet and compared to the control group with intact Tregs population. We generated the Foxp3^{GFP}CreERT²tdTom^{loxSTOPlox} mice to investigate Tregs stability. Tamoxifen was injected intraperitoneally to induce tdTom expression in Foxp3 Tregs and cell fate was investigated after DDC diet to determine Tregs stability. CD4 T-cells were isolated and co-cultured with intrahepatic cholangiocytes organoids to confirm the effect of CD4 T-cells on cholangiocytes.

Results: Mice with reduced Tregs have a lower tolerance to the feeding of DDC diet, with rapid weight loss and two times higher periportal fibrosis than the control group. Histological findings showed that the reduction in Tregs decrease the magnitude of Ck19⁺ ductular reaction by 30%. A two-fold increase in Ck19⁺p21⁺ senescing cholangiocytes was observed in the group with reduced Tregs after DDC induced liver injury. Transcriptional analysis of liver tissue revealed downregulation of *Yap1*, *Sox9* and *Ctgf*, suggesting the Yap pathway is affected following Tregs reduction. This is further

confirmed with immunohistochemistry showing a two-fold reduction in the number of Yap and Sox9 expressing Ck19⁺ cholangiocytes. The Foxp3 fate mapping experiments showed that the labelled Tregs population reduces Foxp3 expression after DDC diet indicating that the stability of Tregs decreases during liver injury.

Conclusion: Our results demonstrated that the role of Tregs in promoting bile duct regeneration by modulating ductular reaction through the Hippo-Yap pathway. Furthermore, the observation that Foxp3 Tregs become unstable in an injured microenvironment in mice may explain the lack of Tregs seen in PSC patients. These show the potential of using Tregs to promote liver regeneration but also highlights the stability of Tregs should be taken into consideration when designing cell based Tregs therapy.

OS024

Deep learning for automatic diagnosis and morphologic characterisation of malignant biliary strictures using digital cholangioscopy: a pilot study

Miguel Mascarenhas¹, João Afonso¹, Tiago Ribeiro¹, Ana Santos¹, Hélder Cardoso¹, João Pedro Sousa Ferreira², Filipe Vilas-Boas¹, Pedro Pereira¹, Guilherme Macedo¹, ¹Centro Hospitalar Universitário de São João, Department of Gastroenterology, Porto, Portugal; ²Faculdade de Engenharia da Universidade do Porto, Department of Mechanical Engineering, Porto, Portugal
Email: miguelmascarenhassaraiva@gmail.com

Background and aims: Patients with indeterminate biliary strictures (BS) pose a significant diagnostic challenge. Digital cholangioscopy (DC) has enabled morphologic characterization as well as the performance of visually guided biopsies. However, the diagnostic yield of DC remains suboptimal, and the visual characterization of these lesions has significant interobserver variability. Recently, the development of artificial intelligence (AI) algorithms, particularly convolutional neural networks (CNNs) for interpretation of endoscopic images has generated intense interest. We aimed to develop a CNN-based system for simultaneous automatic detection of malignant BS in D-SOC images and identification of three morphologic features: nodules (NN), papillary projections (PP) and tumor vessels (TV).

Method: We developed and validated a CNN based on DC images (Spyglass DS II, Boston Scientific, USA). Each frame was labeled as normal/benign finding or as a malignant lesion if definite histologic evidence of biliary malignancy was available. Moreover, we evaluated the performance of the CNN for the detection of morphologic features associated with histology-proved biliary malignancy: NN, PP, and TV. The image dataset was split for constitution of training and validation datasets. The performance of the CNN was measured by calculating the accuracy, area under the curve (AUC), sensitivity, specificity, positive and negative predictive values (PPV and NPV, respectively).

Results: We included 23 595 images from 125 patients (20719 of malignant BS and 2876 of normal or benign findings). The model had a sensitivity of 98.9%, a specificity of 97.7% and an overall accuracy of 98.7%. The AUC was 1.00.

Additionally, the model comprised 2876 images of NN, 1675 images showing PP, and 4153 images of YV. The accuracy for the automatic detection of each of these features was, respectively, 96.9%, 96.1%, and 91.5%.

Conclusion: We developed a combined CNN for automatic detection of malignant BS as well as the automatic identification of morphologic features associated with increased probability of malignancy. The application of AI models to DC may increase its diagnostic yield for patients with indeterminate BS. Furthermore, accurate real-time automatic identification of features associated with increased probability of malignancy may help to guide biopsies, thus increasing their rentability.

Table 1: Performance metrics of the combined convolutional neural network

	Malignant strictures (vs. normal/benign findings)	NN (vs normal/other findings)	PP (vs normal/other findings)	TV (vs normal/other findings)
Sensitivity	98.9%	96.1%	98.2%	85.7%
Specificity	97.7%	98.9%	94.8%	100%
PPV	99.7%	99.5%	91.7%	100%
NPV	92.8%	91.4%	98.9%	82.5%
Accuracy	98.7%	96.9%	96.1%	91.5%
AUC	0.987	1.000	1.000	1.00

Abbreviations; PPV-positive predictive value; NPV-negative predictive value; AUC-area under the curve.

Non-invasive assessment/treatment and liver related outcomes in NAFLD/ALD

OS025

Non-invasive fibrosis scores as prognostic biomarkers of liver events, cardiovascular events and all-cause mortality in people with obesity and/or type 2 diabetes in the UK: a longitudinal cohort study

Quentin Anstee^{1,2}, Tina Landsvig Berentzen³, Louise Nitze³, Maximilian Jara³, Mette Kjaer³, Kamal Kant Mangla³, Jens M. Tarp³, Kamlesh Khunti⁴. ¹Translational and Clinical Research Institute, Faculty of Medical Sciences, Newcastle University, Newcastle Upon Tyne, United Kingdom; ²Newcastle NIHR Biomedical Research Centre, Newcastle Upon Tyne Hospitals NHS Trust, Newcastle Upon Tyne, United Kingdom; ³Novo Nordisk A/S, Søborg, Denmark; ⁴Diabetes Research Centre, University of Leicester, Leicester General Hospital, Leicester, United Kingdom
Email: quentin.anstee@ncl.ac.uk

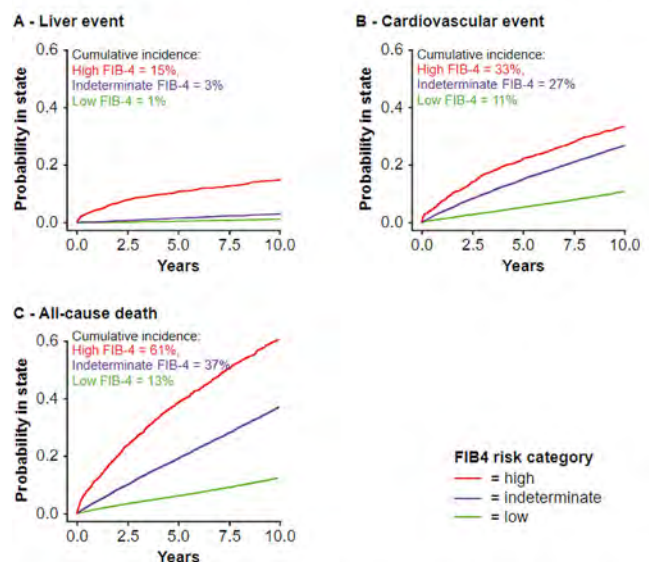
Background and aims: Progression of non-alcoholic steatohepatitis to cirrhosis may lead to life-threatening liver-related complications, increased liver-specific and all-cause mortality and cardiovascular (CV) disease. An important predictor of severe outcomes is biopsy-confirmed liver fibrosis, but biopsies are not scalable outside of specialist practice. This real-world study investigated the prognostic utility of six non-invasive fibrosis scores on clinical outcomes in patients with obesity and/or type 2 diabetes (T2D) seen in routine general practice.

Method: In a longitudinal cohort design, patients ≥ 18 years with obesity and/or T2D, ≥ 1 fibrosis score calculable from the UK Clinical Practice Research Datalink (CPRD) after 1 January 2001, no alcohol-related disorders and/or other chronic liver diseases in Hospital Episodes Statistics (HES) and/or no prescriptions of drugs inducing liver disease in CPRD were included. Patients were followed from inclusion date until time of first clinical outcome event (liver-related

hospitalisation or death [liver event], CV hospitalisation or death [CV event] or all-cause death) recorded in HES or Office for National Statistics Death Registration, database migration, 10 years' follow-up or 1 January 2020, whichever came first. Fibrosis-4 Index (FIB4), the score of focus, was categorised as low (<1.30), indeterminate ($1.30-2.67$) or high (>2.67) risk. Cumulative incidence functions were calculated and hazard ratios (HRs) estimated using Cox proportional hazards models with calendar time as underlying timescale.

Results: In total, 44 481 eligible patients (46% male, median age 58.8 years) had measures available for FIB4 calculation. There were 979 liver events, of which ascites ($n = 412$), cirrhosis ($n = 201$) and gastro-oesophageal varices ($n = 160$) were most common. The risk of an incident liver event was highest in the first years after FIB4 measurement in the high FIB4 group and relatively constant over time in the other two groups (Figure). The incidences of a liver event, CV event and death in the high FIB4 group were 15%, 33% and 61%, respectively. Patients in the indeterminate and high FIB4 groups were at greater risk of liver events vs the low-risk group (HR 2.81 [95% confidence interval 2.43, 3.26] and 18.42 [15.67, 21.65], respectively). An increased risk was also seen for CV events and all-cause mortality in these groups. HRs remained higher for the high vs low FIB4 group after adjustment for sex and age. For the other scores, risk of an outcome event was also elevated for patients with a high vs low score.

Cumulative incidence plots for liver events, cardiovascular events and mortality according to Fibrosis-4 Index (FIB4) in the population with obesity and/or type 2 diabetes



Percentage risks are for 10 years' follow-up. Event risks plotted as Aalen-Johansen cumulative incidence functions, with all-cause mortality included as a competing risk factor in plots of liver and cardiovascular events.

Conclusion: In this real-world population of patients with obesity and/or T2D, and no other clinically recognised liver disease, the risk of a clinical event was significantly higher in patients with high vs low FIB4 score, highlighting the prognostic potential of FIB4 (and other non-invasive fibrosis scores) in this population.

OS026

Liver stiffness predicts incident severe liver disease in patients with chronic liver disease

Hannes Hegmar^{1,2}, Axel Wester², Soo Aleman³, Jens Backman⁴, Erik Degerman⁵, Håkan Ekval⁶, Katarina Lund⁷, Åsa Lundgren⁸, Patrik Nasr^{2,9}, Afshin Shahnava¹⁰, Johan Vessby¹¹, Johan Westin¹², Kristina Önnérhag¹³, Hannes Hagström^{1,2,14}. ¹Division of Hepatology, Department of Upper Gi, Karolinska University Hospital, Huddinge, Sweden; ²Karolinska Institutet, Department of Medicine, Huddinge, Stockholm, Sweden; ³Karolinska Institutet/Karolinska University Hospital, Department of Infectious Diseases, Stockholm, Sweden; ⁴University Hospital of Umeå, Department of Infectious Diseases, Umeå, Sweden; ⁵Falun Hospital, Department of Infectious Diseases, Falun, Sweden; ⁶Sundsvall-Härnösand Regional Hospital, Department of Infectious Diseases, Sundsvall, Sweden; ⁷Northern Älvsborg County Hospital, Department of Infectious Diseases, Trollhättan, Sweden; ⁸Central Hospital Kristianstad, Department of Infectious Diseases, Kristianstad, Sweden; ⁹Linköping University, Department of Gastroenterology and Hepatology, Department of Health, Medicine and Caring Sciences, Linköping, Sweden; ¹⁰Southern Älvsborg Hospital, Department of Infectious Diseases, Borås, Sweden; ¹¹Uppsala University, Department of Medical Sciences, Gastroenterology Research Group, Uppsala, Sweden; ¹²University of Gothenburg and Sahlgrenska University Hospital, Dept of Infectious Diseases, Gothenburg, Sweden; ¹³Skåne University Hospital, Department of Gastroenterology and Hepatology, Malmö, Sweden; ¹⁴Karolinska Institutet, Clinical Epidemiology Unit, Department of Medicine, Solna, Stockholm, Sweden Email: hhegmar@gmail.com

Background and aims: Prognosis in chronic liver disease is heterogenous, and fibrosis stage is the best predictor of liver-related events. Liver stiffness measurement (LSM) by Vibration-Controlled Transient Elastography (VCTE) is a non-invasive biomarker of fibrosis. It is uncertain if LSM can predict risk for future liver-related events. The aim was to investigate the prognostic ability of LSM.

Method: This was a Swedish multi-center cohort study including patients (n = 13,170) with chronic liver disease who underwent LSM by VCTE between 2008 and 2019. Exclusion criteria were an unreliable LSM, congestive heart failure, and decompensated cirrhosis at baseline. Liver-related events were ascertained from Swedish national health registers. In patients without baseline cirrhosis, we investigated progression to "severe liver disease," defined as a diagnosis of cirrhosis, decompensated cirrhosis or hepatocellular carcinoma (HCC). In patients with baseline cirrhosis, we investigated progression to decompensation or HCC. Incidence rates and cumulative incidence at two and five years were calculated. Cox regression was used to evaluate the rate of outcomes for categories of LSM values.

Results: Patients (median age 46 years, 59% men) had a median LSM of 5.9 (interquartile range 4.6–8.0) kPa. Etiologies consisted of hepatitis C (n = 6849, 52.0%), hepatitis B (n = 3497, 26.6%), alcohol-related liver disease (n = 211, 1.6%), autoimmune liver disease (n = 624, 4.7%), non-alcoholic fatty liver disease (n = 699, 5.3%) and other or uncertain etiologies (n = 1290, 9.8%). Patients without baseline cirrhosis (n = 11,883) had 333 (2.8%) events of severe liver disease during a median follow-up time of 2.9 years. Patients with cirrhosis at baseline (n = 1287) had 206 (16.0%) events of decompensation or HCC. In patients without cirrhosis, a LSM of 12–15 kPa was associated with a 42-fold higher rate of severe liver disease than a LSM of <6 kPa (Figure A). In patients with cirrhosis, a LSM >30 kPa was associated with a 5.4-fold higher rate of decompensation compared to a LSM of 15–17 kPa (Figure B). Incidence rates per 1000 person-years in severe liver disease ranged from 2.1 (95%CI 1.6–2.8) to 88.9 (95%CI 73.2–107.9) for LSM <6 kPa and 12–15 kPa, respectively. Incidence rates per 1000 person-years in decompensated cirrhosis ranged from 18.2 (95%CI 10.3–32.0) to 109.6 (95%CI 88.9–135.1) for LSM 15–17 kPa and >30 kPa, respectively. In patients without cirrhosis, the cumulative incidence at two years ranged from 0.4 (0.3–0.6)% to 19.1 (15.1–23.5)%, and at five years from 1.1 (0.8–1.6)% to 32.9 (26.9–38.9)%, respectively.

Conclusion: Increased LSM by VCTE is associated with higher rates of progression to cirrhosis and decompensation in a dose-response manner. The results can be used to guide follow-up and treatment decisions.

OS027

Linear slope of serial FIB-4 measurements predicts liver-related complications and correlates with cirrhosis-associated genetic variants among patients with ALT-based NAFLD phenotype

Craig Teerlink¹, David E. Kaplan², Marijana Vujkovic³, Benjamin Voight⁴, Kyong-Mi Chang³, Julie Lynch⁵, Scott Duvall⁵, Tori Anglin⁵, Timothy Morgan⁶, Linus Schwantes-An Tae-Hwi⁷, Trina Norden-Krichmar⁸, Daniel Dochterman⁹, Poornima Devineni⁹, Philip Tsao¹⁰, Carolin Victoria Schneider¹¹. ¹University of Utah Health, Internal Medicine, Salt Lake City, United States; ²Perelman Center for Advanced Medicine, Gastroenterology, Philadelphia, United States; ³University of Pennsylvania, Medicine, Philadelphia, United States; ⁴University of Pennsylvania, Genetics, Philadelphia, United States; ⁵VA Health Care System, VINCI, Salt Lake City, United States; ⁶University of California Irvine, Medicine, Irvine, United States; ⁷Indiana University, Medicine, Indianapolis, United States; ⁸University of California Irvine, Epidemiology and Biostatistics, Irvine, United States; ⁹VA Health Care System, GenISIS, Boston, United States; ¹⁰Stanford University, Medicine, Palo Alto, United States; ¹¹University of Pennsylvania, Translational

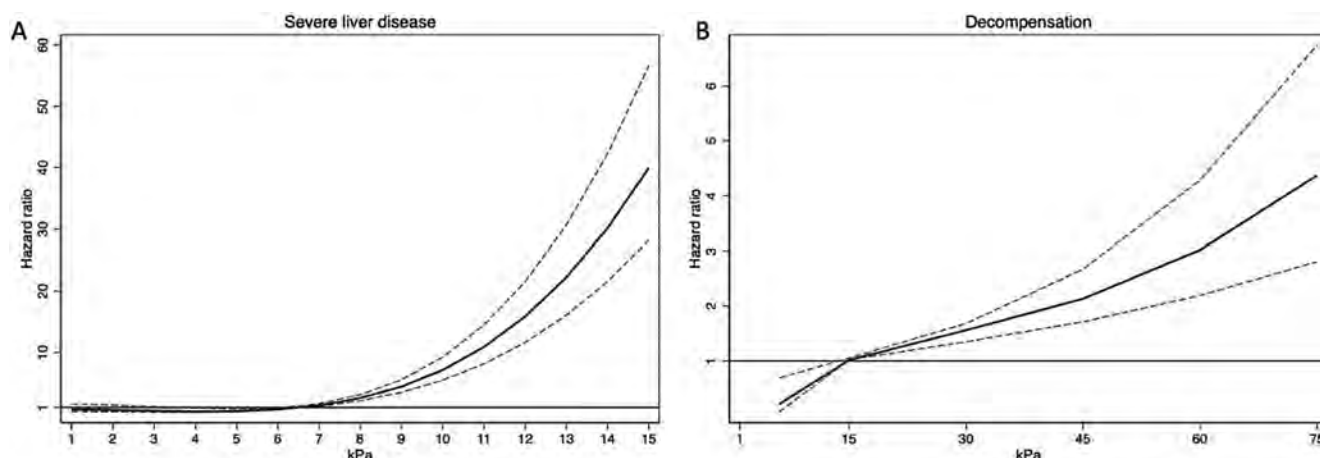


Figure (abstract: OS026): A. Patients without cirrhosis at baseline. B. Patients with cirrhosis at baseline.

Medicine and Human Genetics, Philadelphia, United States
Email: craig.teerlink@va.gov

Background and aims: FIB-4 is a clinically relevant marker to track fibrosis in patients with chronic liver disease including NAFLD/NASH. Here, we first defined Fib-4 trajectory by linear slope of serial FIB-4 measurements as a measure of fibrosis progression, then examined its correlation with liver-related complications and genetic associations with a non-invasive ALT-based proxy NAFLD phenotype recently defined among participants in the VA's Million Veteran Program (MVP) with available clinical and genetic data (Serper et al, PLOS ONE 2020).

Method: Individual FIB-4 slopes were estimated via linear regression for MVP participants with greater than 4 outpatient FIB-4 values who met criteria for proxy NAFLD phenotype based on previously validated algorithm for chronic ALT elevation without other known causes of chronic liver disease. Linear models were constructed excluding outliers at >2 Cook's distances from predicted. Patients whose initial FIB-4 values exceeded the 90th percentile (baseline advanced fibrosis) were assigned slopes equivalent to the 99th percentile of the sample. The AUROCs for the coefficient of FIB-4 slope for predicting development of cirrhosis, hepatocellular carcinoma, ascites and death were generated. MFIB4 was then used as a quantitative phenotype in a genome-wide association analysis using REGENIE software. Variants were restricted to MAF >0.01 and INFO >0.30. Three distinct racial/ethnic groups were defined for the cohort (European, African, and Hispanic ancestry) and analyzed separately; a trans-ancestry meta-analysis was performed with METAL software.

Results: FIB-4 slopes were obtained from 61,689 subjects (10,594 African, 46,137 European, and 4,958 Hispanic ancestry subjects). AUROC of FIB-4 slope for prediction of cirrhosis, hepatocellular carcinoma or ascites were 0.75–0.76. Among European ancestry subjects, FIB-4 slope was associated with 6 genome-wide significant loci (p value $<5 \times 10^{-8}$) including 3 with previously known associations to NAFLD and hepatic fibrosis (GCKR, HSD17B13, and PNPLA3). The GWAS of African and Hispanic ancestry did not return any significant results, however, the trans-ancestry meta-analysis identified an additional signal.

Conclusion: Fibrosis progression based on FIB-4 trajectory correlated with clinically meaningful complications of liver disease progression, as well as known markers of cirrhosis among patients with non-invasive ALT-based NAFLD phenotype. Further work is ongoing to define the use of FIB-4 trajectory and genetic risk factors as predictors for long term outcome of chronic liver disease.

OS028

Machine learned histological fibrosis score empowers characterization of baseline gene signatures associated with fibrosis progression or regression in a NASH F3/F4 clinical trial

Michael D. Berket¹, Francesco Paolo Casale¹, Lorn Kategaya¹, Anna Shcherbina¹, Navpreet Ranu¹, Alicia Lee¹, Kelly Haston¹, Rohit Loomba², Arun Sanyal³, Stephen Harrison⁴, Zobair Younossi⁵, Catherine Jia⁶, David Lopez⁶, Li Li⁶, Robert Myers⁶, David Breckinridge⁶, Andrew Billin⁶, Ellen Berg¹, Santhosh Satapati¹, Eilon Sharon¹, Theofanis Karaletsos¹, Daphne Koller¹, Matthew Albert¹. ¹Insitro, South San Francisco, United States; ²University of California San Diego, La Jolla, United States; ³Virginia Commonwealth University, Richmond, United States; ⁴University of Oxford, United Kingdom; ⁵Inova Fairfax Medical Campus, Fairfax, United States; ⁶Gilead Sciences, Inc., Foster City, United States
Email: research_operations@insitro.com

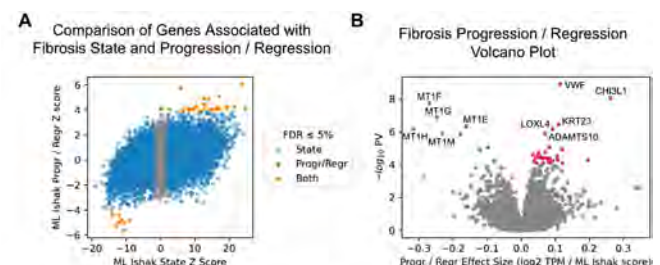
Background and aims: We characterized disease severity with a machine learning (ML) analysis of liver biopsy images, and used it to identify baseline gene signatures that are predictive of fibrosis progression or regression in NASH.

Method: Bulk RNA-seq, HandE stained biopsy images, and pathologist Ishak fibrosis scores are curated from screening and week 48

visits in the STELLAR 3 and STELLAR 4 clinical trials ($n = 1097$ patients with all end points). A continuous score for fibrosis was extracted using convolutional neural networks (CNN) trained to predict pathologist scores from HandE-stained biopsies (Casale et al, EASL 2020). We identify genes associated with fibrosis state by testing for associations between baseline expression and baseline fibrosis scores, controlling for age and sex. Fibrosis progression/regression genes are identified by testing for associations between baseline expression and the difference between baseline and followup fibrosis scores after controlling for both ML and pathologist baseline fibrosis scores, age, sex, and treatment.

Results: The continuous ML fibrosis scores are highly correlated with pathologist Ishak scores (correlation = 0.88). Variation of the ML fibrosis score within Ishak scores exhibits similar transcriptomic associations as variation in Ishak scores (correlation of z scores = 0.88), suggesting that the ML score identifies intra-score variability consistent with pathologist assessed fibrosis. We identify 12,862 genes associated with ML fibrosis state (likely driven in part by changes in cell type composition) and 37 genes associated with ML fibrosis progression/regression (A, B). Using the same covariates, analysis of the ML score identifies a superset of the progression/regression genes identified with the pathologist score (37 vs 3 genes). Notably, the progression/regression-associated genes are not the top state-associated genes. Progression associated genes include expected extracellular matrix and cytoskeletal function-related genes. Lipid metabolism genes identified include the progression associated gene AKR1B10 (involved in hepatic carcinogenesis) and the regression associated gene AKR1D1 (involved in resistance to oxidative stress). Other regression associated genes identified include metallothionein genes, involved in the protection against oxidative stress, and CLEC4M, a liver sinusoidal endothelial cell-specific gene.

Conclusion: ML assessment of liver biopsies and the statistical inference framework introduced herein produced insights on baseline gene expression signatures that are predictive of and potential drivers for NASH fibrosis progression or regression.



Genes associated with fibrosis state and progression / regression. A) Scatter plot of z scores from differential expression analysis of ML fibrosis state and progression / regression. B) ML fibrosis progression / regression differential expression volcano plot.

OS029

Fibrosan-AST (FAST) score predicts liver-related outcomes in 1683 HIV-infected patients at risk for NAFLD

Giada Sebastiani^{1,2}, Jovana Milic³, Dana Kablawi¹, Claudia Gioe⁴, Al Shaima Al Hinai², Bertrand Lebouche⁵, Amine Benmassaoud¹, Marc Deschenes¹, Antonio Cascio⁴, Giovanni Mazzola⁴, Giovanni Guaraldi³. ¹McGill University Health Centre Glen Site (MUHC), Medicine, Montréal, Canada; ²McGill University, Division of Experimental Medicine, Montréal, Canada; ³University of Modena and Reggio Emilia, Modena, Italy; ⁴Università degli Studi di Palermo, Health Promotion Sciences and Mother and Child Care "Giuseppe D'Alessandro", Palermo, Italy; ⁵McGill University Health Centre Glen Site (MUHC), Family Medicine, Montréal, Canada
Email: giada.sebastiani@mcgill.ca

Background and aims: Non-alcoholic fatty liver disease (NAFLD) affects 35% of people living with HIV (PWH) in absence of viral

hepatitis coinfection. About 15% of these PWH have also significant liver fibrosis. Natural history studies employing accurate non-invasive tools are lacking. The FibroScan-AST (FAST) score was developed to identify patients with histologic NASH with advanced fibrosis and elevated NAFLD activity score (NAS) associated with higher risk of end-stage liver disease. We estimated prevalence and evolution of severe NAFLD defined by FAST score in a large multicenter cohort of PWH.

Method: FibroScan was performed in consecutive PWH without viral hepatitis coinfection from three prospective cohorts in Canada and Italy (LIVEHIV in Montreal; liver pathologies in HIV in Palermo; Modena HIV metabolic clinic) as part of a routine screening program for NAFLD. We compared prevalence of FAST>0.35 (90% sensitivity and 50% specificity for NASH with \geq F2 fibrosis and NAS \geq 4) and FAST \geq 0.67 (50% sensitivity, 90% specificity). Incidence of liver-related outcomes (ascites, encephalopathy, variceal bleeding, hepatocellular carcinoma) and extra-hepatic events (cancer, cardiovascular disease) was evaluated by survival analysis.

Results: We included 1683 PWH (mean age 50.1 years, HIV duration 15.5 years, BMI 25.3 Kg/m²; 74.5% male, diabetes prevalence 32%). Prevalence of FAST>0.35 and FAST≥0.67 was 8.1% and 1.5%, respectively. At baseline, on multivariable logistic regression higher BMI (adjusted odds ratio [aOR] 1.15, 95% CI 1.10–1.20), longer duration of HIV infection (aOR 1.05, 95% CI 1.02–1.07), lower CD4 cell count (aOR 0.99, 95% CI 0.99–0.99) and male sex (2.11, 95% CI 1.22–3.65) were associated with FAST >0.35. During a median follow-up period of 3.5 years, incidence of liver-related and extra-hepatic outcomes was 7% and 11.5%, respectively. Incidence of liver-related outcomes significantly increased according to FAST score category (see Figure). There was no difference in extra-hepatic events by FAST score category. On multivariable Cox regression analysis, FAST score >0.35 was an independent predictor of liver-related outcomes (adjusted hazard ratio 4.44, 95% CI 1.66–11.9) after adjusting for sex, BMI, diabetes, duration of HIV infection, protease inhibitors exposure and CD4 cell count.

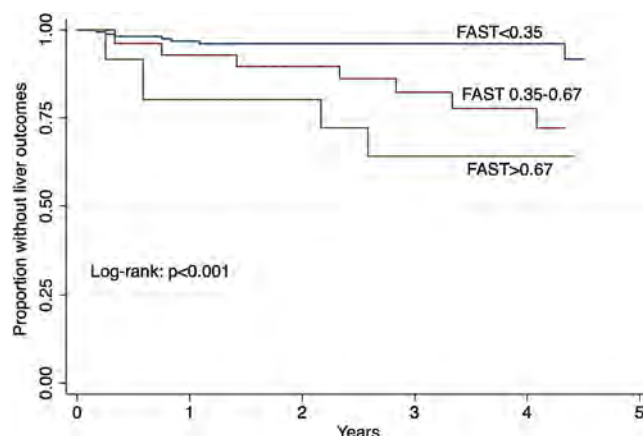


Figure: Survival curves for incidence of liver-related outcomes by FAST score category.

Conclusion: A significant proportion of PWH without viral hepatitis coinfection are at risk for severe NAFLD. FAST score predicts liver-related in this population. Non-invasive testing can help risk stratification and management in this population at risk for NASH and associated liver-fibrosis.

OS030

Impact of resmetirom-mediated reductions in liver volume and steatosis compared with placebo on the quantification of fibrosis using second harmonic generation in a serial liver biopsy study

Dean Tai¹, Mustafa Bashir², Rebecca Taub³, Yayun Ren¹, Elaine Chng⁴,
Stephen Harrison⁵. ¹Histoindex, Research; ²Duke University, Radiology;
³Madrigal Pharmaceuticals, RandD, Conshohocken, United States;

⁴Histoindex, ⁵Pinnacle, Clinical Research

Email: rebeccataub@yahoo.com

Background and aims: Resmetirom (MGL-3196) is a liver-directed, orally active selective thyroid hormone receptor- β agonist that reduces steatosis by MRI-PDFF (-43% (80 mg); -53% (100 mg), Phase 3) and liver volume (IV) -20% (Phase 2 serial liver biopsy).

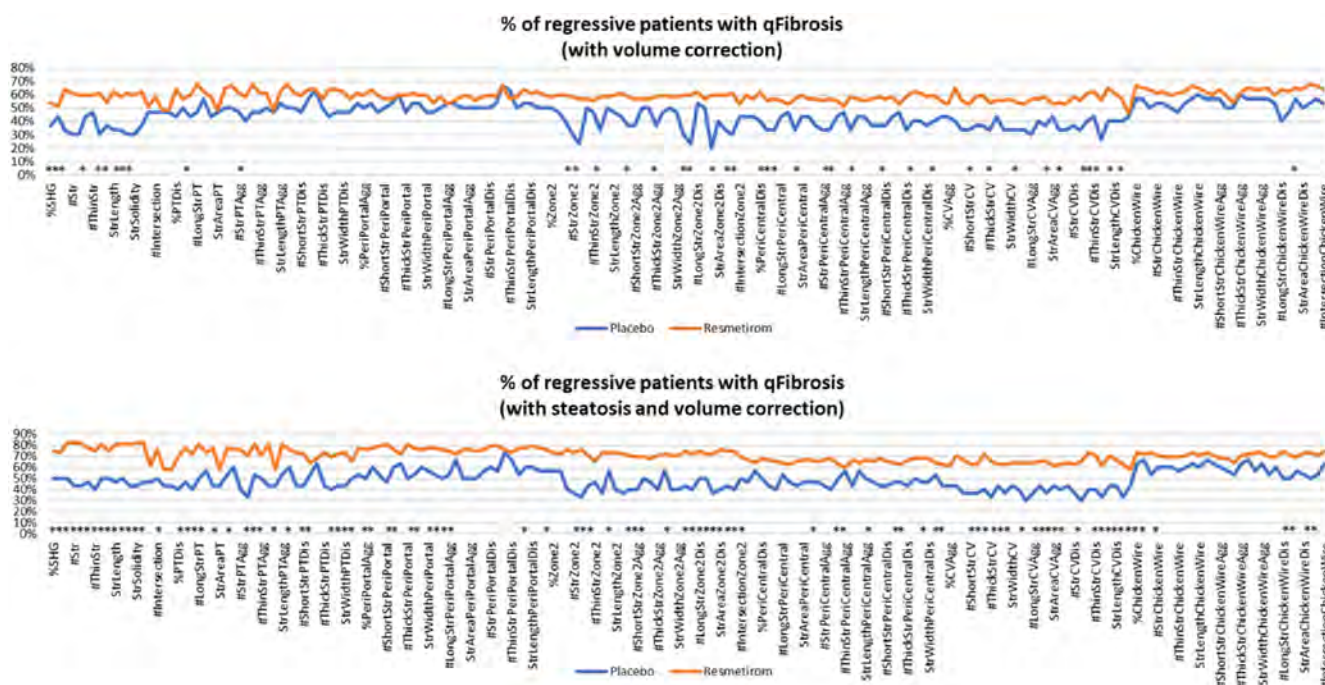


Figure: (abstract: OS030)

study) that were elevated at baseline. Assessment of histological features that stage NASH fibrosis may be impacted in the setting of decreased steatosis and LV following therapeutic intervention. Artificial intelligence (AI)-based algorithms such as qFibrosis can incorporate normalization procedures to account for steatosis area and LV reduction, thereby improving the detection of fibrosis changes. The aim of this analysis is to quantify and correct fibrosis changes related to resmetirom-mediated steatosis and LV changes that are not captured by NASH-CRN scoring system.

Method: Fibrosis was estimated as a continuous variable using second harmonic generation (SHG) (qFibrosis)/two photon excited fluorescence of 102 paired biopsy samples from MGL-3196-05, a 36-week randomized double-blind, placebo-controlled resmetirom phase 2 serial liver biopsy study. qFibrosis (normalized by tissue area) was subsequently corrected for steatosis (tissue area-steatosis area), or LV reduction determined by PDFF (volume/average volume raw parameter based on all samples). In the final model, steatosis and LV were both corrected prior to assessment of qFibrosis. Relative changes in 184 fibrosis parameters were determined as (P) progressing ($\geq 10\%$), (R) regressing ($< 10\%$) or (N) no change.

Results: In normal qFibrosis without correction, resmetirom treatment resulted in a significant reduction in fibrosis (≥ 1 -point reduction) in F3 patients compared to placebo. With LV correction, 45/184 regression parameters demonstrated significant changes after resmetirom treatment (top panel). When steatosis and LV correction factors were combined, 111/184 ($p < 0.05$) regression parameters were reduced significantly with resmetirom (bottom panel). Fibrosis regression was observed in all regions (portal, per-portal, zone 2, peri-central, central). Progression patterns were different from regression and also significantly impacted by correction.

Conclusion: Quantification of changes in NASH fibrosis are impacted by therapeutic interventions that reduce LV. Correcting the AI-based algorithm of qFibrosis for LV and steatosis reveals the significant impact of resmetirom across treated patients in this phase 2 study, regardless of NASH fibrosis stage.

Alcoholic liver disease

OS031

Survival and liver recompensation after declined for early liver transplantation for severe alcohol-associated hepatitis

Christine Hsu¹, Ethan Weinberg², Gene Im³, William Davis¹, Jimin Ko⁴, Stephanie Rutledge³, Matthew Dukewich², Mohamed Shoreibah⁵, Mahmoud Aryan³, Aidan Vosoghi⁶, Michael R. Lucey⁷, John Rice⁷, Norah Terrault⁸, Brian Lee⁶. ¹Medstar Georgetown University Hospital, Medicine, District of Columbia, United States; ²University of Pennsylvania, Medicine, Philadelphia, United States; ³Mount Sinai, Medicine, New York, United States; ⁴Georgetown University School of Medicine, Medicine, District of Columbia, United States; ⁵University of Alabama at Birmingham, Medicine, Birmingham, United States; ⁶University of Southern California, Medicine, Los Angeles, United States; ⁷University of Wisconsin, Medicine, Madison, United States; ⁸University of Southern California, Medicine, Los Angeles, United States
Email: cch87@georgetown.edu

Background and aims: Early liver transplantation (LT) for alcohol-associated hepatitis (AH) is controversial in part because some patients may recover, and obviate the need for LT. We aimed to (i) determine factors associated with survival and liver recompensation among patients with severe AH declined for early LT; (ii) delineate the trajectory of recompensation and MELD recovery among survivors.

Method: In this retrospective, multi-center study among 5 American Consortium of Early Liver Transplantation for Alcohol-Associated Hepatitis (ACCELERATE-AH) sites, we randomly sampled 134 patients

who were evaluated and then declined for early LT for severe AH between 2012 and 2021. All had MELD >20 and less than 6 months of abstinence at LT evaluation. Recompensation was defined as MELD <15 without evidence of variceal bleeding, or ascites requiring diuretics, or overt hepatic encephalopathy requiring medication. Analyses were adjusted for center clustering.

Results: Among 134 patients (median age 49 [IQR 39–57]; 57% male; median abstinence time 36 [IQR 14–70] days; median MELD-Na 33 [IQR 28–38]), the most common reasons for LT decline were: psychosocial (62%), clinical improvement (16%), medical co-morbidities (9%), and financial/insurance (4%). Probability of 3-month, 6-month, and 1-year survival was 58%, 55%, and 48%. Probability of 3-month, 6-month, and 1-year recompensation was 4%, 4%, and 6%. In multivariable analysis, lower MELD-Na (aOR 0.8; $p = 0.01$) and absence of grade 3 or 4 hepatic encephalopathy (aOR 0.02; $p = 0.004$) were associated with 3-month survival. In multivariable analysis, lower MELD-Na (aOR 0.9; $p < 0.001$), married/stable partner (OR 2.0; $p = 0.001$), and private (aOR 3.4; $p = 0.01$) or Medicare (aOR 4.7; $p = 0.002$) vs. Medicaid (reference) insurance were associated with 6-month survival. Among patients declined due to clinical improvement during LT evaluation, 93% were alive at 6 months, but only 15% were recompensated. Among survivors, median MELD at 1-month, 3-months, 6-months, and 1-year were: 28 (IQR 22–38), 26 (IQR 19–33), 15 (IQR 12–23), and 12 (IQR 8–18).

Conclusion: Liver recompensation is very rare among patients with severe AH declined for early LT. Lower MELD was predictive of short- and long-term survival, and marital and insurance status emerged as strong predictors of long-term survival. The distinction between survival and liver recompensation after LT evaluation for severe AH would benefit from further attention.

OS032

Role of macrophage-derived MLKL in alcohol-associated liver disease

Xiaoqin Wu¹, Xiude Fan¹, Megan McMullen¹, Tatsunori Miyata¹, Adam Kim¹, Vai Pathak¹, Jianguo Wu¹, Nicole Welch¹, Jaividhya Dasarathy², Srinivasan Dasarathy¹, Laura Nagy¹. ¹Cleveland Clinic; ²Case Western Reserve University, Department of Family Medicine, Metro Health Medical Center
Email: nagy13@ccf.org

Background and aims: Mixed Lineage Kinase Domain like Pseudokinase (MLKL), a key downstream effector of necroptosis, also has non-necroptotic functions in regulating intracellular and extracellular vesicle trafficking that disrupts the balance between cell death and survival, critical for regulating liver injury and inflammation in alcohol-associated liver disease (ALD). Previously, we observed that *Mlkl*^{-/-} mice were partially protected from ethanol-induced injury. Immunohistochemical staining of liver biopsies from patients with alcohol-associated hepatitis (AH) revealed that phospho-MLKL was localized to both hepatocytes and mononuclear immune cells. Moreover, MLKL co-localized with macrophage marker F4/80 in liver of ethanol-fed mice. Given the important contribution of macrophages to the pathogenesis of ALD, we hypothesized that macrophage-derived MLKL has a potential role in ethanol-induced injury.

Method: Primary mouse Kupffer cells (mKCs) isolated from *Mlkl*^{-/-} and wild type (WT) mice and peripheral monocytes from healthy controls (HC) and patients with AH, treated or not with an inhibitor of MLKL, were used in phagocytosis assays. Bone marrow transplants between *Mlkl*^{-/-} mice and littermates were conducted to distinguish the role of myeloid vs non-myeloid MLKL in the Gao-binge murine model of ALD.

Results: Challenge of macrophages with lipopolysaccharide (LPS) induced STAT1-mediated expression and phosphorylation of MLKL, as well as translocation and oligomerization of MLKL to intracellular compartments including phagosomes and lysosomes, but not the plasma membrane. LPS enhanced uptake and degradation of pHrodo

ORAL PRESENTATIONS

red E.coli bioparticles by mKCs, whilst ethanol impaired this phagocytic process. Pharmacological or genetic inhibition of MLKL suppressed phagocytic capability of mKCs both at baseline or in response to LPS with/without ethanol, as well as peripheral monocytes isolated from both HC and patients with AH. Additionally, *in vivo* study showed that *Mlkl* deficiency in non-myeloid cells (WT→*Mlkl*^{-/-}) had no effect on Gao-binge ethanol-induced injury; in contrast, ethanol-induced hepatic injury, steatosis and inflammation were exacerbated in *Mlkl*^{-/-}→WT chimeric mice. *Mlkl*^{-/-}→WT mice also had elevated numbers of hepatic macrophages, monocytes and neutrophils in response to ethanol. Flow cytometry analysis of non-parenchymal cells demonstrated that *Mlkl* deficiency in myeloid cells suppressed Gao-binge-triggered F4/80⁺ macrophage death via necrosis/necroptosis. Furthermore, *Mlkl* deficiency in myeloid cells exacerbated ethanol-mediated bacterial burden in livers, likely through inhibiting expression of phagocytic receptors.

Conclusion: Together, these data indicate that macrophage-derived MLKL restricts ethanol-induced liver inflammation and injury by regulating hepatic innate cell homeostasis and phagocytosis of macrophage.

OS033

Baseline plasma metabolic phenotype of patients with severe alcoholic hepatitis and its association with outcome

Manisha Yadav¹, Gaurav Tripathi¹, Nupur Sharma¹, Babu Mathew¹, Vasundhara Bindal¹, Jaswinder Maras¹, Shiv Kumar Sarin². ¹Institute of Liver and Biliary Sciences, Molecular and Cellular Medicine, New Delhi, India; ²Institute of Liver and Biliary Sciences, Hepatology, New Delhi, India

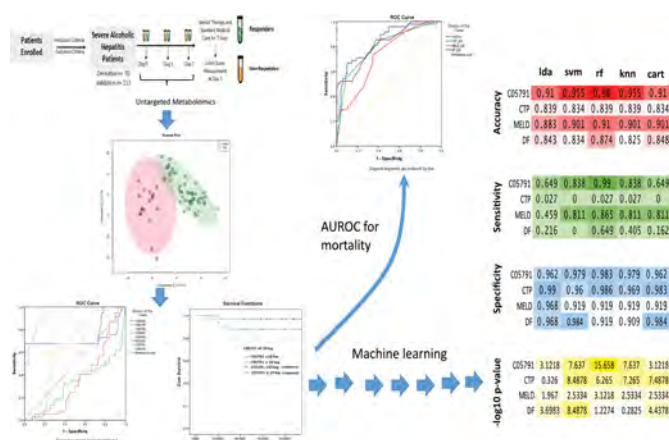
Email: jassi2param@gmail.com

Background and aims: Severe alcoholic hepatitis (SAH) has a high mortality and corticosteroid therapy is effective in reducing 28-day mortality in only about 60% of patients. There are reliable clinical indicators predicting steroid non-response after 7 days of therapy (Lille score >0.45).

Method: Plasma metabolic phenotype was studied using ultra-high-performance liquid chromatography and high-resolution mass spectrometry to identify corticosteroid non-responders at baseline. Altogether, 223 SAH patients were included, 70 in derivative [50 responders (R) and 20 non-responders (NR)] and 153 in validation cohort [136 R, 17 NR]. Temporal change in the metabolic profile and Weighted Metabolome Correlation Network Analysis (WMCNA) were performed and correlated to disease severity.

Results: Of the 713 annotated features (metabolomic/biochemical/spectral databases), 8 plasma metabolites significantly discriminated non-responders; most importantly high urobilinogen (13-fold), cholesterol sulfate (6.9-fold), AMP (4.7-fold), N-Formimino-L-glutamate (4.3-fold), tryptophan (4.7 folds), and low 4-imidazoleacetate (10 fold), urocanic acid (2.2 fold) and thymine (2.4 fold) levels. Additionally, plasma urobilinogen, AMP, and cholesterol sulfate discriminated non-survivors ($p < 0.01$). Temporal change in metabolite expression was higher in responders ($p < 0.05$). WMCNA identified metabolite modules and linked pathways specific to NR and mortality with disease severity ($r > 0.7$; $P < 0.01$). In validation cohort, baseline plasma urobilinogen (C05791) showed high reliability [AUC = 0.94, 0.91–0.97] for predicting non-response with hazard-ratio of 1.5 (1.2–1.6) for mortality prediction. C05791 at 10 log (arbitrary units) cut-off reliably segregated non-survivors (p value <0.01, log-rank test) and showed 98% accuracy, 99% sensitivity and 98% specificity using Random Forest-based Machine-Learning model.

Conclusion: Plasma metabolome signatures can predict pre-therapy steroid response and disease outcome in patients with SAH. Baseline plasma urobilinogen levels should be used for determining corticosteroid response.



OS034

IL-1beta Signal Inhibition in acute alcoholic hepatitis: a multicentre, randomised, double-blind, placebo-controlled phase 2 trial of canakinumab therapy (ISAIAH)

Nikhil Vergis¹, Vishal C. Patel^{2,3,4}, Karolina Bogdanowicz⁵, Justyna Czyzewska-Khan⁵, Rosemary Keshinro⁵, Francesca Fiorentino⁵, Emily Day⁵, Paul Middleton¹, Stephen Atkinson¹, Mary Cross⁵, Daphne Babalis⁵, Neil Foster¹, Alberto Quaglia⁶, Josephine Lloyd¹, Robert D. Goldin¹, William Rosenberg⁷, Richard Parker⁸, Paul Richardson⁹, Steven Masson¹⁰, Gavin Whitehouse¹¹, Cyril Sieberhagen¹², David Patch⁷, Ashwin Dhanda¹³, Emma Lord¹, Ewan Forrest¹⁴, Nikolai Naoumov¹⁵, Mark Thursz¹. ¹Imperial College, Metabolism, Digestion and Reproduction, London, United Kingdom; ²King's College London, School of Immunology and Microbial Sciences, Faculty of Life Sciences and Medicine, United Kingdom; ³King's College Hospital NHS Foundation Trust, Institute of Liver Studies, United Kingdom; ⁴The Roger Williams Foundation for Liver Research, Institute of Hepatology, London, United Kingdom; ⁵Imperial Clinical Trials Unit, United Kingdom; ⁶Royal Free Hospital NHS Foundation Trust; ⁷University College London, United Kingdom; ⁸Leeds Teaching Hospitals NHS Trust, United Kingdom; ⁹Liverpool University Hospitals Foundation NHS Trust, United Kingdom; ¹⁰The Newcastle Upon Tyne Hospitals Foundation NHS Trust, United Kingdom; ¹¹Chelsea and Westminster Hospitals NHS Foundation Trust; ¹²Liverpool University Hospitals Foundation NHS Trust; ¹³University of Plymouth, United Kingdom; ¹⁴Glasgow Royal Infirmary, United Kingdom; ¹⁵London, United Kingdom

Email: nvergis@imperial.ac.uk

Background and aims: Short-term mortality in acute alcohol-related hepatitis (AAH) patients is high and available therapy does not result in durable benefit. A role for IL-1beta has been demonstrated in the pathogenesis of alcohol-induced steatohepatitis in mice. This study explored the safety and potential benefits of canakinumab (CAN), a monoclonal antibody targeting IL-1beta, for patients with AAH in a double-blind placebo (PBO)-controlled randomised trial.

Method: Patients with biopsy-confirmed AAH and discriminant function ≥ 32 but MELD ≤ 27 were randomly allocated 1:1 to receive either CAN 3 mg/kg or PBO once in 4 weeks. Liver biopsies were taken before and 28 days after treatment. The primary end point was histological improvement at 28 days compared to baseline, adjudicated by 3 independent histopathologists who were blinded to treatment allocation. Key secondary end points were the proportions of Lille responders; changes in MELD; and death within 90 days. Adverse events, including infections, were compared between groups.

Results: Fifty-seven patients were randomised: 29 CAN vs 28 PBO. Two patients were withdrawn with negative biopsy results; 1 did not receive allocated intervention due to an adverse event and a further 6 did not attend for second biopsy. Data were therefore available for 48 patients for primary end point analysis. In CAN-treated patients, 14/

24 (58.3%) demonstrated histological improvement compared to 10/24 (41.7%) PBO-treated patients, a difference of 16.7% ($p = 0.248$). Regression models did not identify significant improvement of CAN-therapy on prognostic scores of liver function such as Lille model or MELD. Four of the 55 AAH patients (7.3%) in the intention-to-treat analysis died within 90 days: 2 in each group. There were 20 vs 29 serious adverse events occurring in 10 vs 10 patients (CAN vs PBO). There were no safety signals: of the 49 serious adverse events, 6 were infectious complications of which 1/20 (5%) occurred in CAN-treated and 5/29 (17%) occurred in PBO-treated patients. In exploratory analyses after adjustment for baseline prognostic factors, CAN therapy was associated with overall histological improvement ($p = 0.04$), improvement in mononuclear cell infiltrate ($p = 0.06$), and reduction in serum AST ($p = 0.02$).

Conclusion: CAN therapy in AAH demonstrated a good safety profile but did not alter biochemical or clinical outcomes compared to PBO. After adjustment for baseline prognostic factors, CAN was associated with histological improvements that did not translate into improved prognostic scores of liver function nor survival.

Outcome	Canakinumab	Placebo	P
Histological Improvement (%)	58.3	41.7	0.25
Lille response (% Lille score < 0.45)	22.2	25.0	0.8
Day 28 median MELD change	-5.07	-6.50	0.14
Day 28 median GAHS change	-2	-2	0.69
SAEs (n)	20	29	-
Infection SAEs (n)	1	5	0.38

OS035

Probiotic LGG-derived exosome-like nanoparticles inhibit ALD through intestinal FXR activation in mice: role of miR194 and bile acids

Wenke Feng¹, Mengwei Jiang¹, Fengyuan Li¹, Craig J. McClain¹, Lihua Zhang¹, Jiyeon Lee¹. ¹University of Louisville, Medicine, Louisville, United States

Email: wenke.feng@louisville.edu

Background and aims: Patients with alcohol-associated liver disease (ALD) often exhibit excessive bile acid (BA) accumulation and steatosis. Farnesoid X receptor (FXR)-fibroblast growth factor 15/19 (FGF15/19) signaling plays a critical role in hepatic lipid and BA metabolism. In this study, we aimed to investigate whether alcohol exposure reduced BA-mediated intestinal FXR activation and increased intestinal miR194 expression that suppressed *Fxr* mRNA expression, and whether *Lactobacillus rhamnosus* GG-derived exosome-like nanoparticles (LDNPs) attenuated ALD through regulation of intestinal miR194-FXR-FGF15 signaling in mice.

Method: C57BL/6, global *Fgf15* knockout (*Fgf15*^{-/-}), and intestinal epithelial cell-specific *Fxr* knockout (*Fxr*^{ΔIEC}) mice were administered the NIAAA binge-on-chronic model alcohol exposure protocol. Probiotic strain *Lactobacillus rhamnosus* GG was cultured and LDNPs were isolated from the culture supernatant.

Results: Alcohol feeding increased intestinal miR194 expression, which suppressed intestine *Fxr* and subsequently *Fgf15* expression, resulting in a reduced circulation FGF15 protein level. Gut microbiota-mediated BA transformation was dysregulated by alcohol leading to the decreased ligand-mediated FXR activation. Reduced FXR-FGF15 signaling resulted in an increase in hepatic BA synthesis and lipogenesis and liver injury. Importantly, three-day oral administration of LDNPs suppressed hepatic BA synthesis and lipogenesis and protected the liver from alcohol-induced injury. We further showed that LDNP treatment decreased intestinal miR194 and increased FXR-FGF15 signaling. miR194 suppressing intestinal *Fxr* mRNA expression was further confirmed in Caco-2 cells and mouse enteroid. miR194 mimic decreased, and miR194 inhibitor increased, *Fxr* mRNA expression. Fecal and serum FXR activity was decreased by alcohol

and restored by LDNP treatment. Importantly, the beneficial effects of LDNP were eliminated in intestinal *Fxr*^{ΔIEC} and *Fgf15*^{-/-} mice.

Conclusion: Our results demonstrate that increased intestinal miR194 suppresses *Fxr* expression resulting in a defective FXR-FGF15 gut-liver signaling in ALD. LDNP treatment inhibits alcohol-induced liver injury by suppressing intestinal miR194 and improving BA profile that lead to an activated FXR-FGF15 signaling to suppress BA *de novo* synthesis and lipogenesis during ALD development.

OS036

Does screening for liver fibrosis change alcohol consumption, diet, and exercise? A prospective cohort study on the consequences of screening in 2,764 individuals

Maria Kjærsgaard^{1,2}, Katrine Prier Lindvig^{1,2}, Johanne Kragh Hansen¹, Simon Langkjær Sørensen¹, Stine Johansen^{1,2}, Katrine Thorhauge^{1,2}, Peter Andersen¹, Isabel Graupera³, Pere Ginès³, Aleksander Krag^{1,2}, Maja Thiele^{1,2}. ¹Odense University Hospital, Department of Gastroenterology and Hepatology, Odense, Denmark; ²University of Southern Denmark, Institute of Clinical Research, Odense, Denmark; ³Hospital Clínic de Barcelona, Institut D'investigacions Biomèdiques August Pi I Sunyer (IDIBAPS), Barcelona, Spain
Email: maria.kjaergaard@rsyd.dk

Background and aims: There is a growing interest in screening for liver fibrosis, and a belief that early disease detection will lead to lifestyle changes in screening-positive individuals. However, this assumption is not based in evidence. We therefore evaluated self-reported lifestyle changes after screening for liver fibrosis.

Method: Prospective study of participants from the general population at risk of alcohol related (ALD) or non-alcoholic fatty liver disease (NAFLD). All were screened with transient elastography (TE) and all participants, independently on TE, were given information on recommended lifestyle changes. We considered TE ≥ 8 kPa as screening positive. All participants received an online questionnaire on lifestyle changes one week and six months after the screening visit.

Results: We included 2,764 participants, 1,273 at risk of ALD and 1,491 at risk of NAFLD. Median age was 58 years (52–64), 54% were male, and 268 (10%) had an elevated TE ≥ 8 kPa. Response rate was high, at 89% after one week and 85% after six months. After one week, half of the ALD group (50%) reported abstinence, or a decrease in alcohol consumption, while only 0.8% reported an increase in alcohol consumption. Screening sustained its effect on alcohol consumption after six months (figure), with a reported median alcohol intake decreasing 8 units/week in the ALD group. Screening-positive subjects disclosed more pronounced reductions in alcohol intake than screening negatives (decreased 13 vs 6 units/week), and a positive screening test predicted alcohol abstinence (odds ratio 2.9, 95% CI 1.8–4.7). We observed the same pattern for diet and exercise: After one week, 26% of all respondents reported that they consumed less food and/or more healthy food, increasing to 34% after six months. This was most pronounced in the at-risk of NAFLD group (Figure), where a positive screening test predicted improved diet (OR 1.8, 1.3–2.4). Both groups reported comparable improvements in exercise (figure). In the NAFLD group, 23% reported a weight loss exceeding 3 kg after six months, and a positive screening test predicted a weight loss above 3 kg (OR 3.5, 1.2–10.5).

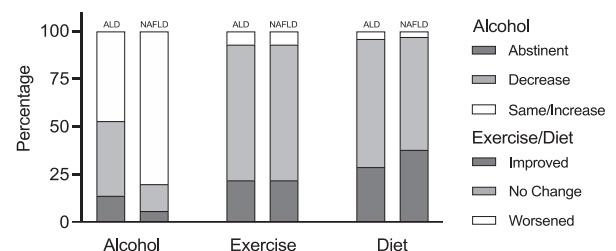


Figure: Lifestyle changes after 6 months.

Conclusion: After being screened for liver fibrosis, participants report improved lifestyle, with both acute and sustained changes in alcohol consumption, diet, exercise, and weight loss. The changes are most pronounced in participants with elevated liver stiffness, but not limited to this.

Fibrosis

OS037

Peroxidasin deficiency re-programs macrophages toward pro-fibrosis function and promotes collagen resolution in liver

Mozhdeh Sojoodi¹, Derek J. Erstad¹, Stephen Barrett¹, Shadi Salloom², Shijia Zhu³, Tongqi Qian³, Eric Gale⁴, Veronica Clavijo Jordan⁴, Yongtao Wang¹, Shen Li¹, Michael Lanuti¹, Peter Caravan⁴, Yujin Hoshida³, Raymond Chung², Gautam Bhav⁵, Georg Lauer², Bryan C. Fuchs¹, Kenneth K. Tanabe¹. ¹Massachusetts General Hospital, Surgery, Boston, United States; ²Massachusetts General Hospital, Gastroenterology, Boston, United States; ³University of Texas Southwestern Medical Center, Internal Medicine, United States; ⁴Massachusetts General Hospital, Radiology, Boston, United States; ⁵Vanderbilt University Medical Center, Division of Nephrology and Hypertension, United States
Email: msojoodi@mgh.harvard.edu

Background and aims: Non-alcoholic liver disease (NAFLD) is stimulated by excessive fat deposition in hepatocytes. During NAFLD, inflammation and activation of tissue repair mechanisms replaces necrotic tissue with extracellular matrix (ECM), which are stabilized into a complex fibrotic scar and creates fibrosis. Peroxidasin (PXDN) is a peroxidase enzyme that is known to stabilize ECM proteins through cross-linking of collagen molecules. In this project, we aim to investigate the expression and function of PXDN during the development of liver fibrosis.

Method: *Pxdn*^{-/-} and *Pxdn*^{+/-} mice were fed with a choline-deficient L-amino acid-defined high-fat diet (CDAHFD) for 16 weeks to create a NAFLD-HCC preclinical model. Liver histology, collagen content, flow cytometry, immunostaining of immune cells, RNA-seq, and liver function tests were analyzed. *In vivo* imaging of liver reactive oxygen species (ROS) was performed using a redox-active iron complex, Fe-PyC3A.

Results: Genome-wide expression analysis of liver tissue and differential gene expression (DGE) combined with Gene Ontology (GO) analysis identified significant upregulation of genes associated with hypoxia and TNF α signaling pathways already in *Pxdn*^{-/-} sham livers (without injury). Using Fe-PyC3A as an MRI contrast agent, we detected a higher content of ROS in *Pxdn*^{-/-} livers (healthy) that could activate hypoxia-related molecular pathways. In addition, we observed an upregulation of genes involved in the innate immune response, leukocyte activation, and chemotaxis. After 16 weeks of CDAHFD, gross analysis of collected liver showed no HCC nodule formation in *Pxdn*^{-/-} mice while 60% of the WT mice had HCC tumors. Collagen staining showed less collagen accumulation in *Pxdn*^{-/-} mice. Flow cytometry of macrophages showed *Pxdn*^{-/-} mice had increased pro-healing M2 macrophages recruitment in early- and mid-stage NAFLD (4 weeks and 8 weeks on CDAHFD) compared to WT controls. In addition, we observed a significant decrease in the number of CD3⁺ T cells and CD8⁺ cytotoxic T cells in the late-stage of NAFLD in *Pxdn*^{-/-} mice. DGE analysis revealed that IL-12 is highly expressed in *Pxdn*^{-/-} injured livers. Additionally, multiple other T cell-related molecules such as IL-10, IL-6, CCL2, IL-7, and CD4 were elevated in *Pxdn*^{-/-}

injured liver. Elevation of these cytokines is an indicator for higher recruitment of pro-healing and anti-HCC macrophage to the site of injury.

Conclusion: Our findings demonstrate that PXDN deficiency is associated with the induction of the hypoxia and TNF α signaling pathways and the recruitment of pro-healing and anti-HCC macrophages to the liver. This results in significantly decreased collagen stabilization during liver fibrosis and accelerates fibrosis reversal. In addition, recruited macrophages-controlled T cell response and inhibited HCC formation in *Pxdn*^{-/-} mice.

OS038

Targeting the liver circadian clock by REV-ERB-alpha activation improves liver fibrosis by circadian gating of TGF-beta signaling

Mayssa Dachraoui¹, Frank Jühling¹, Natascha Roehlen¹, Emilie Crouchet¹, Romain Martin¹, Nicolas Brignon¹, Laurent Mailly¹, Antonio Saviano¹, Sarah Durand¹, Catherine Schuster¹, Emanuele Felli², Patrick Pessaux², Joachim Lupberger¹, Atish Mukherji¹, Thomas Baumert³. ¹Université de Strasbourg, Inserm, Institut de Recherche sur les Maladies Virales et Hépatiques Inserm, UMR_S1110, Strasbourg, France; ²Université de Strasbourg, Inserm, Institut de Recherche sur les Maladies Virales et Hépatiques Inserm, UMR_S1110, Institut Hospitalo-Universitaire, Pôle Hépatodigestif, Nouvel Hôpital Civil, Strasbourg, Strasbourg, France; ³Université de Strasbourg, Inserm, Institut de Recherche sur les Maladies Virales et Hépatiques Inserm, UMR_S1110, Institut Hospitalo-Universitaire, Pôle Hépatodigestif, Nouvel Hôpital Civil, Strasbourg, and Institut Universitaire de France, Paris, Strasbourg, France
Email: mukherji@unistra.fr

Background and aims: Liver fibrosis is the key risk factor for hepatocellular carcinoma, a leading cause of cancer death worldwide. Approved anti-fibrotic therapies are absent and most compounds in clinical development have limited anti-fibrotic efficacy. The circadian clock (CC) is a major regulator of liver metabolism, but its role in the pathogenesis of liver fibrosis and as a potential therapeutic target is unknown.

Method: We utilized liver specific CC-mutant mice to establish the molecular relationship between the CC-oscillator and TGF-beta signaling under physiological conditions. Moreover, we profiled the circadian gene expression pattern in patient-derived models for NASH and fibrotic liver disease including primary human hepatocytes, human myofibroblasts, spheroids and a human liver chimeric mouse model for diet-induced fibrotic liver disease. Furthermore, we performed functional studies using small molecules targeting CC components.

Results: Here we show that the physiological liver CC-oscillator is temporally restricting (gating) TGF-beta signaling and that this regulation is lost in metabolic liver disease progressing to fibrosis. The loss of TGF-beta signaling regulation leads to constitutive expression of genes driving fibrosis in patients. Mechanistic studies in primary human hepatocytes and myofibroblasts revealed a reciprocal relationship between increased TGF-beta-driven fibrotic-signaling and the CC, which we confirmed in patient-derived liver spheroids and in two mouse models for NASH-driven fibrosis. Remarkably, a pharmacological restoration of REV-ERB-alpha activity markedly inhibited fibrosis in a human liver chimeric NASH mouse model in vivo and spheroids generated from patients with liver fibrosis.

Conclusion: We discovered that the perturbation of the liver CC plays a key role in the pathogenesis of liver fibrosis. Furthermore, our in vivo and ex vivo studies in patient-derived models suggest that targeting REV-ERB-alpha is an effective approach for treatment of liver fibrosis-an important and rising global unmet medical need.

OS039

The proteomic analysis of hepatic stellate cell differentiation from iPSCs identifies RORalpha as an antifibrogenic target

Raquel A. Martinez Garcia de la Torre¹, Julia Vallverdú¹, Silvia Ariño Mons¹, Beatriz Aguilar-Bravo¹, Mikel Azkargorta², Felix Elortza², Laura Zanatto¹, Paula Cantallops Vilà¹, Juanjo Lozano³, Benedicte Antoine⁴, Isabel Graupera^{3,5,6}, Pere Ginès^{3,5,6,7}, Pau Sancho-Bru^{1,3,7}. ¹Institut d'Investigacions Biomèdiques August Pi i Sunyer (IDIBAPS), Liver Cell Plasticity and Tissue Repair Group, Barcelona, Spain; ²CIC bioGUNE-Centro de Investigación Cooperativa en Biociencias, Proteomics Platform, Derio, Spain; ³Centro de Investigación Biomédica en Red de Enfermedades Hepáticas y Digestivas (CIBERhd), Barcelona, Spain; ⁴Sorbonne Université, INSERM, Paris, France; ⁵Hospital Clínic de Barcelona, Chronic Liver Diseases Group, Barcelona, Spain; ⁶Institut d'Investigacions Biomèdiques August Pi i Sunyer (IDIBAPS), Barcelona, Spain; ⁷Universitat de Barcelona, Barcelona, Spain
Email: rmartinezg@clinic.cat

Background and aims: Understanding the embryonic development of Hepatic stellate cells (HSCs) and their activation is fundamental to develop new therapeutic strategies. We developed a protocol to differentiate iPSCs to HSCs by sequential addition of growth factors. We hypothesized that the differentiation protocol may be an excellent tool for drug discovery. By performing a time course proteomic characterization, we envision to understand the protein dynamics across differentiation and identify transcription factors involved in the maintenance HSC phenotype and cell activation.

Method: MS proteomics was performed in 4 independent differentiations of iPSC to HSCs and primary human HSCs. Seven staggerer mice (RORA^{-/-}) and their wildtype littermates were treated with CCl₄ during 4 weeks. Fourteen mice were treated with CCl₄ and 7 were treated with the RORA agonist SR1078. qPCR, immunofluorescence and immunohistochemistry assays were used as validation. RORA expression was evaluated in a cohort of 25 patients with alcohol and metabolic associated chronic liver disease.

Results: Proteomic results indicated that iPSC-HSC differentiation occurred in three stages: undifferentiated phase (Day 0 to 4), intermediate fetal stage (Day 6 to 8) and final maturation stage (Day 10 to 12). Developmental markers of fetal HSC, such as VIM, ALCAM, FBLN1 and DCN were sequentially expressed and followed by mature HSC markers, indicating the recapitulation of the embryonic development in vitro. Pathway analysis of iPSC-HSCs and primary HSCs revealed RORA as an important transcription factor in HSC phenotype and commitment. Experimentally, we first evaluated the effect of RORA on HSC development. iPSC-HSC across differentiation were treated with SR1078, which increased the expression of HSC phenotype and quiescence markers such as RELN, PCDH7, LRAT and LHX2. Next, we evaluated the role of RORA on HSC activation by treating iPSC-HSCs, which decreased the expression of ACTA2 and increased the expression of quiescent markers (LRAT and LHX2). *In vivo* studies with the staggerer mice, showed an increased fibrotic content by Sirius Red staining and an increased gene expression of fibrogenic markers such as ACTA2, collagens and MMPs in the mutant group. In addition, SR1078 treatment of CCl₄ mice showed a reduction of collagen deposition and αSMA staining, together with a reduced expression of fibrogenic markers. In patients, expression of RORA correlated negatively with fibrogenic markers and MELD Score. These results suggest that RORA plays a role in the progression of liver fibrosis.

Conclusion: The present study demonstrates that the differentiation protocol is a new and reliable tool for the study of HSC biology and the discovery of new antifibrogenic targets. Moreover, we identify RORA as a targetable transcription factor to mitigate liver fibrosis.

OS040

Stellate cell dynamics in progression and regression of hepatic fibrosis

Laura Almale del Barrio¹, Emma A.H. Scott¹, Frederik Adam Bjerre¹, Mike Terkelsen^{1,2}, Kim Ravnskjaer^{1,2}. ¹University of Southern Denmark, Department of Biochemistry and Molecular Biology, Odense, Denmark; ²University of Southern Denmark, Center for Functional Genomics and Tissue Plasticity (ATLAS), Odense, Denmark
Email: ravnskjaer@bmb.sdu.dk

Background and aims: Non-alcoholic steatohepatitis (NASH) is a metabolic liver disease characterized by hepatic lipid accumulation, chronic inflammation and fibrosis, in which fibrogenic myofibroblasts are central players. These scar-forming cells are derived mainly from activated hepatic stellate cells (HSCs). NASH and cirrhosis were traditionally considered irreversible conditions, but clinical studies have demonstrated that they can be reversed. HSC inactivation seems to be a key mechanism, but the inactivation process is poorly understood. This prompted us to characterize HSC dynamics at single-cell resolution during the induction and regression of NASH-associated fibrosis *in vivo*.

Method: *Lat-cre/mCherry* knock-in mice were fed a western diet (WD) combined with carbon tetrachloride (CCl₄) for eight weeks (treated) or chow diet (untreated). Regression of liver disease was studied four weeks after WD/CCl₄ cessation (reversal). RNA-sequencing, single-cell RNA-sequencing and immunohistochemistry/immunofluorescence were performed to investigate HSC activation and inactivation.

Results: NASH regression led to profound changes at histological, whole-liver transcriptional, and single-cell levels. We annotated 14 discrete hepatic populations including activated and quiescent HSCs in our single-cell data set obtained from treated, reversal, and untreated mice. We next performed gene expression distribution analyses of cells within and across treatment groups to stratify the HSC population. We here identified HSC subpopulations relating to NASH regression; potentially inactivated HSCs and HSCs that had reverted towards a more quiescent state. Additionally, using single-cell gene regulatory network analysis we determined specific gene-regulatory networks for the aforementioned HSC subpopulations.

Conclusion: Our results broaden our understanding of HSC transitions in the liver during induction and regression of NASH, and suggest new molecular mechanisms that could mediate the HSC inactivation and reversion during NASH resolution.

OS041

Machine learning methods for detailed characterization of TGF-beta-induced signatures in a large iPSC-derived hepatic stellate cell cohort

Panagiotis Stanitsas¹, Kara Marie Liu¹, Lorn Kategaya¹, Kelly Haston¹, Alicia Lee¹, Shahin Mohammadi¹, Haoyang Zheng¹, Francesco Paolo Casale¹, Navpreet Ranu¹, Ahmed Sandakli¹, Pooja Prasad¹, Owen Chen¹, Anne Baldwin¹, Albert Kim¹, Eilon Sharon¹, Ajamete Kaykas¹, Daphne Koller¹, Matthew Albert¹. ¹Insitro, South San Francisco, United States
Email: research_operations@insitro.com

Background and aims: Activation of hepatic stellate cells (HSCs) by TGF-beta plays a central role in fibrotic changes related to Non-Alcoholic Steatohepatitis (NASH). We aimed to establish a screenable *in vitro* system for identification of anti-fibrotic targets in activated HSCs. This required the development of a novel machine learning (ML) framework which was used to characterize a large cohort of control and NASH induced pluripotent stem cell-derived HSCs (iHSCs).

Method: We differentiated iHSCs from 56 iPSC lines and characterized them using high content imaging and single cell (sc) RNA-seq analysis. For ML image analysis, we derived a novel deep learning method that was tasked with producing informative featurizations of segmented cell images, followed by covariate correction.

ORAL PRESENTATIONS

Transcriptomic datasets were featurized using a state-of-the-art archetypal analysis based framework. Using each of our transcriptomic and imaging datasets separately, and viewing pHSCs as ground truth, we quantified three quality metrics for iHSCs: (i) predictiveness of TGF-beta response in an ML classifier trained on pHSCs; (ii) separation between TGF-beta and DMSO in an unsupervised ML model; (iii) similarity of the overall cell state distribution between iHSCs and pHSCs.

Results: The established ML framework provided informative featurizations of our cellular assays and allowed for the correction of experimental artifacts. We showed robustness of TGF-beta-induced ML phenotype in pHSCs both in imaging and transcriptomics (mean AUC 0.96 for out-of-line assessment in imaging, Figure 1A; mean AUC 0.98 in transcriptomics, data not shown). Interpretation of learned ML phenotypes revealed insights into the TGF-beta responsiveness of pHSCs. This allowed us to utilize multi-parametric criteria to evaluate the cohort of iHSCs. We observed a strong correlation between transcriptomic and imaging characterizations used for the ranking of iHSC lines (spearman = 0.66, $p = 8.7 \times 10^{-5}$, Figure 1B).

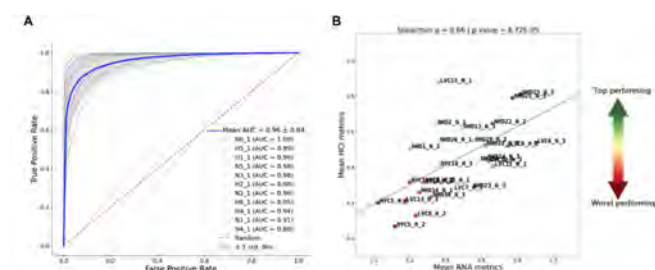


Figure 1 | ML model accurately predicted TGF-beta treatment of HSCs. (A) The ML-learned phenotype was evaluated in an out-of-line setup by reporting area under the curve (AUC) plots for TGF-beta vs PBS using a logistic regression model. Thin lines represent individual pHSC lines; dotted red line indicates random prediction; thick blue line indicates mean AUC; and shaded area indicates ± 1 standard deviation. (B) Correlation for iHSC rankings for transcriptomic-based metrics (x-axis) and image-based metrics (y-axis) are depicted. The naming scheme for lines follows the format: (line ID)_(H=control, N=NASH)_(experiment ID).

Conclusion: We developed a state-of-the-art approach for the characterization of HSC morphological and transcriptional phenotypes. Using the developed framework, we successfully modeled TGF-beta-induced activation signatures in HSCs. These image-based phenotypic assays paired with high-performance ML models present unique opportunities for genetic and chemical screens and the discovery of novel fibrosis targets.

OS042

Biliary epithelial cell-specific RAGE controls ductular reaction-mediated fibrosis during cholestasis

Wai Ling Macrina Lam^{1,2}, Amruta Damle-Vartak¹, Gisela Gabernet³, Doris Schneller¹, Tanja Poth⁴, Simone Jörs⁵, Melanie Sator-Schmitt¹, Auris De Ponti¹, Lena Weiß¹, Mathias Heikenwälder⁶, Nachiket Vartak⁷, Jan G. Hengstler⁷, Fabian Geisler⁵, Sven Nahnsen³, Peter Angel¹. ¹German Cancer Research Center, Division of Signal Transduction and Growth Control, Heidelberg, Germany; ²Ruprecht Karl University of Heidelberg, Faculty of Biosciences, Heidelberg, Germany; ³Eberhard Karls University of Tübingen, Quantitative Biology Center, Tübingen, Germany; ⁴University Hospital Heidelberg, Center for Model System and Comparative Pathology, Heidelberg, Germany; ⁵Technical University of Munich, Clinic and Polyclinic for Internal Medicine II, Germany; ⁶German Cancer Research Center, Division of Chronic Inflammation and Cancer, Heidelberg, Germany; ⁷Leibniz Research Centre for Working Environment and Human Factors at the Technical University Dortmund (IfADO), Systems Toxicology, Germany
Email: m.lam@dkfz-heidelberg.de

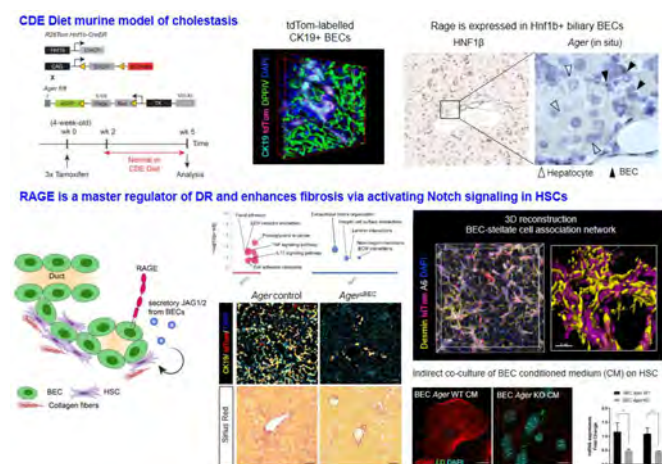
Background and aims: Ductular reaction (DR) is the hallmark of cholestatic diseases characterized by the proliferation of bile ductules lined by biliary epithelial cells (BECs). DR is thought to serve as a reparative and regenerative mechanism in the damaged liver to compensate for the anatomical or functional loss of the biliary

system. Surprisingly, it is also commonly associated with increased risk of fibrosis, cirrhosis and liver cancer. The Receptor for Advanced Glycation End Products (RAGE, encoded by *Ager*) was identified as a critical mediator of DR during chronic injury and carcinogenesis (Pusterla et al. Hepatology. 2013.). Nevertheless, whether DR is reparative or detrimental to the liver during cholestasis remains elusive. Thus, we aimed to delineate the specific function of RAGE on DR and its potential association with fibrosis in the context of cholestasis.

Method: We utilized a biliary tracing reporter murine model (*R26^{Tom}Hnf1bCreER*) and deleted *Ager* conditionally in BECs. Choline-deficient ethionine-supplemented (CDE) diet was fed to the mice for three weeks to induce cholestasis. RNA-seq of FACS-sorted primary BECs from CDE-challenged mice, immunofluorescence (IF) staining and multi-modal 3D architectural staining were employed to investigate the role of BEC-specific RAGE activity in DR and fibrosis. *In vitro* co-culture assays of BECs and hepatic stellate cells (HSCs) combined with flow cytometry and mass spectrometry analysis were utilized to delineate the newly identified RAGE-dependent paracrine crosstalk between BECs and HSCs.

Results: BEC-specific deletion of *Ager* strongly impairs ductular reaction. Remarkably, the number of stellate cell is substantially diminished concomitantly with an attenuation of bridging fibrosis. RNA-seq data revealed a RAGE-dependent mechanistic role of BECs in the modulation of cholestasis-induced fibrosis. Classical fibrotic mediators and ECM genes were differentially expressed between *Ager* wildtype and knockout BECs. Flow cytometry of direct co-culture assay demonstrated that HSCs were activated by BECs in RAGE-dependent manner. Mass spectrometry and indirect co-culture analysis, combined with immunohistochemistry analyses of livers from CDE-treated mice showed that BEC-derived secretory JAG protein activates Notch signalling in HSC *in trans*.

Conclusion: This present study provides a novel insight into the adverse consequence of DR in cholestasis-associated fibrosis. Although hypothesized to provide a regenerative mechanism during cholestasis, it is evident that BEC-specific RAGE activity enhances DR-associated fibrosis via a trans-regulatory mechanism in the current CDE diet model. We demonstrate that Notch signaling in HSCs is activated by BEC in RAGE-dependent manner via paracrine JAG protein, thereby turning HSCs into a myofibroblastic phenotype to establish a profibrotic milieu.



Friday 24 June

NAFLD: Clinical aspects except therapy

OS043

Young-onset diabetes mellitus increases the risk of liver-related events in patients with non-alcoholic fatty liver disease

Xinrong Zhang¹, Grace Lai-Hung Wong¹, Terry Cheuk-Fung Yip¹, Yee-Kit Tse¹, Vicki Wing-Ki Hui¹, Huapeng Lin¹, Che To Lai¹, Henry LY Chan¹, Alice Pik-Shan Kong¹, Vincent Wai-Sun Wong¹. ¹The Chinese University of Hong Kong
Email: wongv@cuhk.edu.hk

Background and aims: The prevalence of type 2 diabetes (T2D) in young people is increasing, but little is known regarding the association between age of onset of T2D and risk of liver-related events. This study aimed to determine the incidence of liver-related events of patients of different ages of onset of T2D.

Method: We conducted a retrospective territory-wide cohort study of adult patients with non-alcoholic fatty liver disease (NAFLD) diagnosed between January 1, 2000 and June 30, 2021. T2D was defined by exposure to any antidiabetic agents, haemoglobin A_{1c} $\geq 6.5\%$, fasting plasma glucose ≥ 7.0 mmol/L in two measurements at least one month apart, and/or ICD-9-CM diagnosis codes. The primary end point was liver-related events, defined as a composite end point of HCC and cirrhotic complications. Fine-Gray model was used to adjust for competing risk of death.

Results: We analysed data from 30,360 NAFLD patients (mean age, 56.4 ± 13.4 years; 46.0% men); a total of 15,430 cases of T2D and 456 cases of liver-related events were recorded over a follow-up of 151,051 person-years. Starting the follow-up at age 60 years, liver-related event rates per 1,000 person-years were 1.05 in patients without T2D at age 60 years, 2.90 for patients with T2D onset ≤ 5 years earlier, 2.77 for 6 to 10 years earlier, and 4.26 for >10 years earlier. In multivariable analysis adjusting for gender, hypertension, dyslipidaemia, cirrhosis, use of metformin, insulin and aspirin, compared with patients without T2D at age 60, the adjusted hazard ratio of liver-related events was 2.58 (95% confidence interval [CI], 1.49–4.45; $p < 0.001$) in patients with T2D onset ≤ 5 years earlier, 2.70 (95% CI, 1.45–5.03; $p = 0.002$) for T2D 6 to 10 years earlier, and 5.00 (95% CI, 2.35–10.60; $p < 0.001$) for diabetes onset >10 years earlier (Figure). Linear trend test ($p < 0.001$) indicated a graded association between age of onset of T2D and risk of liver-related events.

Conclusion: Younger-onset T2D increases the risk of liver-related events. Further studies should determine the role of fibrosis assessment and more aggressive treatment of steatohepatitis in this high-risk group.

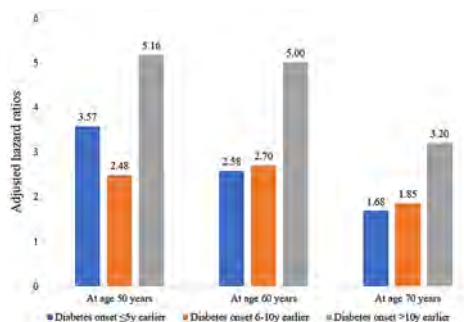


Figure: Association between age of onset of T2D and risk of liver-related events (reference group was patients who did not have T2D at the corresponding ages).

OS044

Non-alcoholic fatty liver disease patients have worse health-related quality of life compared to the general population irrespective of their fibrosis stage: results from a prospective multicenter UK study

Margarita Papatheodoridi¹, Giada Pallini¹, Guruprasad Aithal², Hong Kai Lim³, Jeremy Cobbold⁴, Maria Corina Plaz Torres¹, Marta Guerrero Misas¹, John Ryan¹, Jeremy Tomlinson⁴, Michael Allison³, Louise Longworth⁵, Emmanuel Tsochatzis¹.
¹University College of London, Royal Free Hospital, Institute for Liver and Digestive Health, United Kingdom; ²Nottingham University, Digestive Diseases Centre, United Kingdom; ³Cambridge University Hospital NHS Foundation Trust, Liver Unit, Department of Medicine, NIHR Cambridge Biomedical Research Centre, Cambridge, United Kingdom; ⁴Oxford University Hospitals NHS Foundation Trust, Oxford Liver Unit, Department of Gastroenterology and Hepatology, Oxford, United Kingdom; ⁵PHMR Limited, United Kingdom
Email: margarita.gpap@gmail.com

Background and aims: Health-related quality of life (HRQL) is impaired in patients with chronic liver disease, including those with non-alcoholic fatty liver disease (NAFLD). The primary aim of the study was to assess the HRQL of patients with NAFLD and compare this to the general population. Secondary aims were to examine the associations of fibrosis severity and metabolic comorbidities with impairments in HRQL.

Method: We included 561 consecutive patients with NAFLD prospectively evaluated in 4 UK secondary care centres between 2016 and 2019. Patients completed two HRQL questionnaires: the EQ-5D-5L and the Chronic Liver Disease Questionnaire (CLDQ). Demographic and clinical information, liver stiffness by transient elastography and/or liver biopsy results and history of cirrhosis were recorded. A general population sub-cohort of the Health Survey of England 2018 without alcohol misuse who had completed the EQ-5D-5L was used as a comparator. For the comparison of HRQL in NAFLD patients and the general population, propensity-score (PS) matching was performed, according to age, sex and body mass index (BMI).

Results: The EQ-5D-5L index was significantly lower in 514 NAFLD patients compared to the 514 PS-matched healthy controls (0.762 ± 0.276 vs 0.844 ± 0.200 , $p < 0.001$). The difference was also significant in a subgroup of NAFLD patients without advanced fibrosis ($F < 3$ or $LS < 8$ kPa) compared to the general population (0.781 ± 0.276 vs 0.845 ± 0.200 , $p < 0.001$). Among NAFLD patients, the EQ-5D-5L index, EQ-visual analogue scale (VAS) and CLDQ scores were significantly lower in patients with cirrhosis compared to patients without cirrhosis ($p = 0.021$, $p = 0.011$ and $p = 0.001$ respectively). However, in patients with NASH, there was no difference between patients with and without advanced fibrosis on any of the HRQL measures.

Liver stiffness was the only factor significantly associated with lower scores in all HRQL measures, both in the whole patient population and in non-cirrhotic patients.

In multivariate analysis, the EQ-5D-5L index was negatively associated with type II diabetes, depression and osteoarthritis both in the whole patient population and in patients without cirrhosis. EQ-VAS was associated with age, sex, BMI, depression and osteoarthritis in all patients and non-cirrhotic patients.

Lower CLDQ scores were associated with lower age, male sex, presence of type II diabetes, ischemic heart disease, depression and osteoarthritis in all patients; in the sub-group of non-cirrhotic patients, lower CLDQ was associated with male sex, type II diabetes and depression.

Conclusion: HRQL is similar for NASH patients with or without advanced fibrosis. However, even those without advanced fibrosis ($LS < 8$ kPa or $F < 3$) have worse HRQL compared to the general population, implying that a multi-disciplinary management is required for NAFLD patients, irrespective of their disease severity.

OS045

Genetics of liver fat and volume associate with altered metabolism and whole body magnetic resonance imaging

Shafqat Ahmad¹, Germán Carrasquilla², Taro Langner³, Uwe Menzel³, Filip Malmberg³, Ulf Hammar³, Jenny C. Censin⁴, Sergi Sayols³, Diem Nguyen³, Andrés Martínez Mora³, Jan W. Eriksson³, Robin Strand³, Joel Kullberg³, Håkan Ahlström³, Tove Fall³. ¹Uppsala University, Medical Sciences, Uppsala, Sweden; ²The University of Copenhagen, Faculty of Health and Medical Sciences, København, Denmark; ³Uppsala University, Uppsala, Sweden; ⁴University of Oxford, United Kingdom
Email: shafqat.ahmad@medsci.uu.se

Background and aims: An improved understanding of the underlying biological mechanisms of genetic variation linked to liver fat and volume is pivotal for translational and prevention efforts to tackle liver disease. Here we aim to gain biological insight of liver fat and volume loci using a novel image analysis approach allowing whole-body voxel-wise associations to tissue volume and fat content as well as a large set of other phenotypes.

Method: Liver volume was measured from neck-to-knee water-fat MRI images collected in UK Biobank cohort using a deep learning-based segmentation approach. Liver proton density fat fraction (PDFF) were readily available for 4, 613 subjects. Using deep regression on the above mentioned neck-to-knee MRI images, liver PDFF was inferred for remaining subjects. We conducted a genome-wide association analysis (GWAS) of liver fat (n = 27, 243) and liver volume (n = 24, 752) on non-related European participants of the UK Biobank cohort. We further investigated the associated genetic loci in association with whole body composition in high-resolution anatomical correlation voxel-based maps ("Imiomics"). We also analyzed these loci with various biomarkers and liver disease using independent UK Biobank participants (n = 310, 239).

Results: We confirmed four previously identified liver fat variants *TM6SF2* rs8107974, *TM6SF2* rs188247550, *APOE* rs429358 and *PNPLA3* rs738408. A positive and highly specific relationship was observed between liver fat-associated variants and fat fraction in liver area (*PNPLA3* rs738408 Figure 1). The liver fat-increasing allele of all four genetic variants were positively associated with alanine aminotransferase, conjugated bilirubin while negatively associated with total cholesterol, triglycerides and low-density lipoprotein cholesterol biomarkers. For liver volume, we identified two novel independent variants *CENPW* rs1490384, *ADH4* rs6858148 and confirm eight previously identified variants *SFN* rs75460349, *GCKR* rs1260326, *TNFSF10* rs79287178, *PPP1R3B* rs4240624, *REEP3* rs7896518, *TNKS2* rs10881959, and *PDIA3* rs139974673. We observed a heterogeneous pattern for association with body composition and biomarkers, as for *CENPW* rs1490384, with strong positive association with muscle tissue volume in neck, abdomen, thigh and hip as well as heart and liver volume among both males and females (Figure 1). Two liver fat and three liver volume-associated genetic variants were positively associated with non-alcoholic fatty liver disease and chronic liver disease.

Conclusion: We report two novel liver volume loci and provide specific association with voxel-based maps body composition architecture while confirming previously reported liver fat and volume genetic variants. Liver fat-associated variants were positively associated with liver injury markers and negatively associated with dyslipidemia biomarkers.

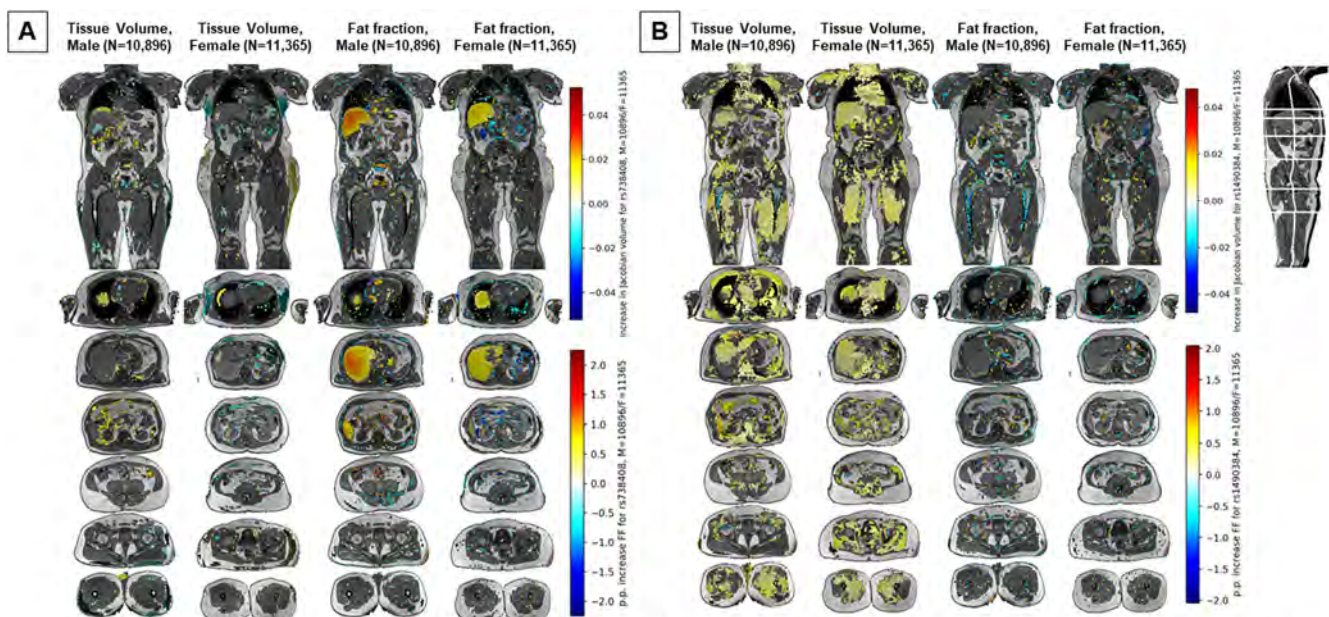


Figure 1. Liver tissue volume and Liver fat associated with *PNPLA3* rs738408 (panel A) and *CENPW* rs1490384 (panel B) variants illustrated with Imiomics maps. Within each panel the top images represent concatenated images from all males or all females in the study from left to right, the volume maps for males, the volume maps for females, the fat fraction maps for males, and the fat fraction maps for females. The colors displayed in the colormaps in the center of the collage, using a common color scale for male and female volume maps (upper color scale), and a common scale for male and female fat fraction maps (lower color scale). Volume map units are relative volume differences (Jacobian determinant of deformation field) per SNP unit, while fat fraction units are p.p. units per SNP unit. Only body regions where the regression computations between voxel data and SNP data are significant ($p < 0.05$) are colored. Non-significant regions are ignored, not colored, and show the water and fat MR images for the chosen male and template subjects. The first row of images represent coronal views of the maps, while the remaining rows represent axial views of those maps in organs of interest (heart, liver, kidneys, abdomen, hip, and thighs). The mid-sagittal slices on the right-hand side of the plots only represent the mixed water and fat images of the male and female templates, with cuts in white color that represent the coronal and axial slices on the left-hand sides of the collage.

Figure: (abstract: OS045)

OS046

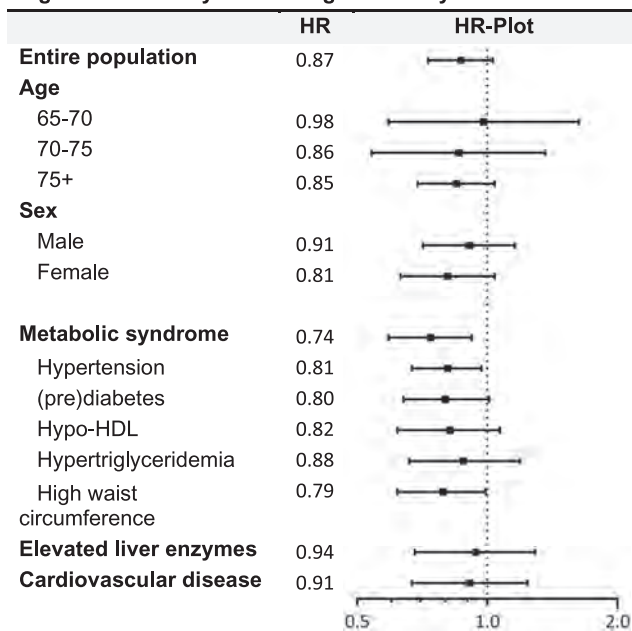
Hepatic steatosis is not associated with increased mortality in the elderly-time for a paradigm shift?

Laurens van Kleef¹, Milan Sonneveld¹, Maryam Kavousi², Arfan Ikram³, Robert De Man¹, Robert De Knecht¹. ¹Erasmus MC, University Medical Center, Gastroenterology and Hepatology, Rotterdam, Netherlands; ²Erasmus MC, University Medical Center, Cardiology, Rotterdam, Netherlands; ³Erasmus MC, University Medical Center, Epidemiology, Rotterdam, Netherlands
Email: l.vankleef@erasmusmc.nl

Background and aims: Fatty liver disease has been associated with excess mortality. Screening for hepatic steatosis in patients with metabolic dysfunction is therefore widely advocated. However, the association between hepatic steatosis and mortality amongst community-dwelling elderly individuals is unclear.

Method: We studied participants of an ongoing prospective cohort: the Rotterdam Study. Individuals aged ≥ 65 years were enrolled from 2009 to 2014 and were followed through 2018. Steatosis was assessed by ultrasound, and liver stiffness by transient elastography. Subsequently, NAFLD was defined as steatosis in the absence of excessive alcohol consumption, viral hepatitis, or steatogenic drug use; and MAFLD was defined as steatosis with either overweight, diabetes, or at least two minor metabolic dysfunction criteria. The association between steatosis and liver stiffness with mortality risk was assessed using Cox regression analysis adjusted for age, sex, education, smoking, the individual components of the metabolic syndrome, heart failure, coronary heart disease, and stroke.

Figure 1: Mortality risk among the elderly with steatosis



Results were obtained with Cox regression analysis. The fully adjusted model was adjusted for age, sex, education, smoking, alcohol, the individual components of the metabolic syndrome (hypertension, (pre)diabetes, hypo-HDL, hypertriglyceridemia, and high waist circumference), heart failure, coronary heart disease and stroke. Abbreviations: CI, confidence interval; HDL, high-density lipoprotein; HR, hazard rate.

Results: We included 4,093 elderly participants (aged 74.4 ± 6.6 ; 42.7% male, BMI 27.6 ± 4.2 kg/m², 44.9% metabolic syndrome), 36.8% had ultrasound-based steatosis and 7.1% had liver stiffness ≥ 8.0 kPa. During the median follow-up of 6.9 years, 793 participants died, resulting in a mortality rate of 29.6 per 1,000 person-years. Among the elderly, steatosis was not associated with impaired survival in multivariable analysis (aHR:0.87, 95%CI:0.73–1.03), similar results were obtained for MAFLD and NAFLD. Furthermore, findings were consistent across a range of clinically relevant subgroups, including age categories, sex, and in participants with metabolic syndrome, elevated liver enzymes, or cardiac disease, as shown in Figure 1. Sensitivity analyses showed similar results for mortality beyond five years of follow-up and for both cancer-related and cerebro-cardiovascular mortality. Furthermore, among participants with steatosis, higher liver stiffness (aHR:1.02 per kPa, 95%CI:0.93–1.12) was not associated with mortality.

Conclusion: The presence of fatty liver disease was not associated with increased mortality risk in this cohort of community-dwelling elderly subjects. Findings were consistent across a range of clinically relevant subgroups. This indicates that screening for fatty liver disease is unlikely to improve outcomes in the elderly.

OS047

Burden of hepatocellular cancer in patients with type-2 diabetes mellitus: a 2011–2020, french, longitudinal, retrospective, national, cohort study

Lucia Parlati¹, Samir Bouam², Michael Schwarzwinger³, Emmanuel Tsochatzis⁴, Philippe Sogni⁵, Stanislas Pol⁵, Vincent Mallet^{2,5}. ¹Institut Cochin, Paris, France; ²Assistance Publique Hôpitaux de Paris, Paris, France; ³Inserm UMR 1219, Bordeaux, France; ⁴UCL Institute for Liver and Digestive Health, Royal Free Hospital and UCL, London, United Kingdom; ⁵Université de Paris, France, France
Email: vincent.mallet@aphp.fr

Background and aims: There are uncertainties on the burden of hepatocellular cancer (HCC) in patients with type-2 diabetes (T2D) in France. We therefore measured national incidences and risks of in-hospital HCC.

Method: The data source was the 2011–2020 National Hospital Discharge database. We selected all T2D patients. HCC and competing death incidences were measured overall and without well-identified risk factors of liver disease progression, including alcoholic liver disease. Risks were computed with multinomial logistic regression models.

Results: The sample comprised 2, 883, 684 adults. Mean (IQR) age was 67 (58, 77) years and 54% were men. HCC incidence (95% CI) was 1.19 (1.17–1.21) per 1000 person-years at risk, totaling 26, 136 (0.9%) cases over 12, 504, 690 patient-years. A history of alcohol use disorders and non-metabolic liver-related risk factors were recorded among 55% and 21% of incident cases, respectively. In patients without well-identified risk factors of liver disease progression, HCC incidence was 0.57 (0.55–0.58) per 1000 person-years at risk. Male sex, age in the 40–70 years category, alcohol use disorders [aOR 20.8 (20.0–21.5)], and obesity [aOR 1.24 (1.2–1.28)] were independently associated with a higher risk of HCC than of competing mortality.

Conclusion: A history of alcohol use disorders was the main driver of liver disease progression to HCC in French patients with T2D. Obesity increased the risk of HCC by ~25%. Patients with T2D should be advised to abstain from alcohol.

Table: Multivariate risks for HCC and competing mortality in 2011–2020 French residents¹ with T2D

Predictors	Hepatocellular carcinoma		Competing mortality	
	aOR ²	P Value	aOR ²	P Value
Age categories at cohort inception ³				
(30, 40]	2.34 (1.25–4.38)	0.008	1.29 (1.17–1.43)	<0.001
(40, 50]	6.29 (3.49–11.37)	<0.001	2.12 (1.94–2.32)	<0.001
(50, 60]	12.69 (7.06–22.83)	<0.001	4.33 (3.97–4.72)	<0.001
(60, 70]	20.02 (11.14–36.00)	<0.001	7.98 (7.33–8.70)	<0.001
(70, 80]	23.47 (13.05–42.20)	<0.001	18.14 (16.65–19.77)	<0.001
(80, Inf]	17.41 (9.66–31.39)	<0.001	37.66 (34.55–41.04)	<0.001
Male sex	3.22 (3.07–3.37)	<0.001	1.38 (1.37–1.39)	<0.001
Alcohol use disorders	20.76 (20.02–21.54)	<0.001	1.72 (1.69–1.74)	<0.001
Obesity	1.24 (1.20–1.28)	<0.001	0.86 (0.86–0.87)	<0.001
Non-liver-related risk factors ⁴	1.05 (1.01–1.10)	0.014	1.79 (1.78–1.80)	<0.001
Smoking	0.71 (0.68–0.74)	<0.001	1.48 (1.46–1.49)	<0.001

¹T2D patients with alcoholic liver disease or non-metabolic liver-related risk factors were excluded from the analysis. HCC cases were recorded after a 2011–2013 (3-year) washout period to reduce the risk of non-incident cases.

²Risks were computed with multinomial logistic regression models.

³Reference was the [18, 30] age category.

⁴Non-liver risk factors were extrahepatic cancer; AIDS; connective tissue disorders; ischemic heart disease; and stage 3–5 chronic kidney disease.

OS048

The impact of non-alcoholic fatty liver disease and liver fibrosis on adverse clinical outcomes and mortality in patients with chronic kidney disease: a prospective study using UK Biobank data

Theresa Hydes¹, Oliver Kennedy², Ryan Buchanan², Daniel Cuthbertson¹, Julie Parkes², Simon Fraser², Paul Roderick².

¹University of Liverpool, Department of Cardiovascular and Metabolic Medicine, Liverpool, United Kingdom; ²University of Southampton, School of Primary Care, Population Sciences and Medical Education, Southampton, United Kingdom

Email: therasa@doctors.org.uk

Background and aims: Chronic kidney disease (CKD) is a well-known extra-hepatic manifestation of non-alcoholic fatty liver disease (NAFLD), independent of common cardio-metabolic risk factors, and the two diseases frequently co-exist. Systematic review data has shown that there is minimal and conflicting data regarding the clinical implications of living concomitantly with these two conditions. We aimed to assess the impact of having of NAFLD and NAFLD fibrosis on adverse clinical outcomes and all-cause mortality for people with CKD.

Method: Data from 26, 074 individuals from the UK Biobank identified to have CKD (eGFR <60 ml/min/1.73 m² or albuminuria >3 mg/mmol) was analysed. Participants completed questionnaires relating to medical history, demographics and lifestyle factors and were prospectively followed-up by electronic linkage to hospital and death records. Cox-regression was used to estimate the hazard ratios (HR) associated with having NAFLD (hepatic steatosis index >36, or ICD-code) and advanced liver fibrosis (elevated fibrosis-4 (FIB-4) score, or NAFLD fibrosis score (NFS) or AST to platelet ratio index (APRI)) on cardiovascular events (CVE), progression to end-stage renal disease (ESRD) and all-cause mortality (ACM).

Results: Overall 54.5% of individuals with CKD had NAFLD at baseline, and 7.0% (NFS ≥0.676), 3.2% (FIB-4 >2.67) and 1.1% (APRI ≥1.0) had evidence of advanced fibrosis. Median follow-up was 10 years. In univariate analysis NAFLD was significantly associated with an increased risk of CVE (HR 1.39 [1.29–1.51], *p* < 0.0001) and ACM (HR 1.10 [1.01–1.19]), but not ESRD (HR 1.22 [0.95–1.56], *p* > 0.05). Following multivariate adjustment for demographics, metabolic factors and baseline renal function, NAFLD was no longer associated

with increased risk of any primary outcomes. In univariate analysis, advanced liver fibrosis identified via all scores was associated with increased ACM (HR 2.34–2.90). NFS and FIB-4 were associated with elevated risk of CVE (HR 2.49 [2.11–2.93], *p* < 0.0001 and 1.94 [1.53–2.45], *p* < 0.0001) and ESRD (HR 6.85 [4.29–10.94], *p* < 0.0001 and 2.35 [1.19–4.67], *p* < 0.05). Following full adjustment FIB-4 was associated with increased incidence of CVE (HR 1.39 [1.06–1.82], *p* < 0.05), notably heart failure (HR 1.65 [1.16–2.33], *p* < 0.01); both FIB-4 and APRI were associated with ACM (HR 1.55 [1.21–2.00], *p* < 0.001 and 2.83 [1.95–4.11], *p* < 0.0001) and NFS ≥1.455 was associated with progression to ESRD (HR 1.89 [1.13–3.17], *p* < 0.05).

Conclusion: In people with CKD and NAFLD, elevated non-invasive markers of liver fibrosis are associated with an increased risk of CVE, ESRD and worse survival.

Viral hepatitis elimination

OS049

Randomized controlled trial of home-based hepatitis C self-testing for key populations in Malaysia

Xiaohui Sem¹, Sonjelle Shilton¹, Huan-Keat Chan², Han Yang Chung³, Anu Karunanithy⁴, Jessica Markby¹, Po-Lin Chan⁵, Niklas Luhmann⁶, Cheryl Johnson⁶, Pamela Nabeta¹, Nazrila Hairizan Binti Nasir⁷, Stefano Ongarello¹, Elena Ivanova¹, Muhammad Radzi Abu Hassan².

¹FIND; ²Clinical Research Centre, Hospital Sultanah Bahiyah; ³Drugs for Neglected Diseases Initiative South-East Asia Regional Office;

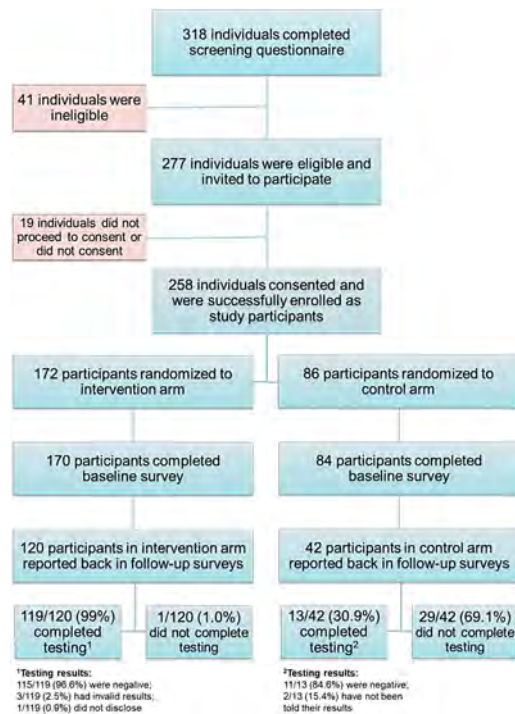
⁴Malaysian AIDS Council; ⁵World Health Organization Regional Office for Western Pacific; ⁶World Health Organization, Global HIV, Hepatitis and STI Programmes; ⁷Ministry of Health

Email: xiaohui.sem@finddx.org

Background and aims: Malaysia is an upper middle-income country and has been expanding and decentralizing HCV care to the community. HCV self-testing (HCVST), recommended by the World Health Organization, provides an additional way to increase access and uptake of HCV testing among key populations who are disproportionately affected by HCV. We integrated HCVST with an existing online HIV self-testing platform to assess the impact of home-based HCVST on the uptake of HCV testing among key populations nationwide.

Method: This is a randomized controlled trial comparing HCVST sent via post (intervention arm, *n* = 500) with standard of care testing at a facility (control arm, *n* = 250). In the intervention arm, participants received either an oral fluid- or blood-based HCVST; in the control arm, participants were provided information about the nearest HCV testing center. All participants also received HCV information and support resources (e.g. access to a call center). We describe preliminary findings for this study reporting on the primary outcome—the uptake of HCV testing. Acceptability, feasibility and attitudes around HCV testing were also evaluated via a series of surveys.

Results: To date, 258 individuals, with a median (IQR) age of 26 (22–30.75) years, were recruited, of whom 88.8% were MSM. Most participants were male (97.6%), completed university (46.9%), and were employed (61.4%). Prior to this study, 60.6% of the participants were not tested for HCV; of these, the top reason why they did not get tested was they did not know how (57.1%). Additionally, acceptability of HCVST was high—71.7% of the participants stated that they preferred to test for HCV by themselves at home; 98.4% were willing to test themselves at home if they had a test kit and instructions on how to do it. After either receiving a HCVST or information about the nearest testing center, 99.0% (119/120) in the intervention arm and 30.9% (13/42) in the control arm reported completing HCV testing (*p* < 0.01) (see Figure).



Conclusion: Preliminary results show that HCVST via an online distribution model, compared with standard testing services, significantly increased the uptake of HCV testing among key populations. The outcomes of this study can further provide critical evidence about testing uptake, linkage to care, acceptability and any social harm due to HCVST. Updated data will be presented at the conference.

OS050

The disease burden of hepatitis B and hepatitis C from 2015 to 2030: the long and winding road

Devin Razavi-Shearer¹, Sarah Blach¹, Ivane Gamkrelidze¹, Chris Estes¹, Ellen Mooneyhan¹, Kathryn Razavi-Shearer¹, Homie Razavi¹. ¹Center for Disease Analysis Foundation, Lafayette, United States
Email: dravishearercdafound.org

Background and aims: This study aims to estimate the future disease burden of HBV and HCV at the global and continental level through 2030. 2015 was used as a baseline in line with the WHO targets to show what progress has been made to date.

Method: The results of a literature review and Delphi expert interviews were integrated into country-specific ProGreSs and Bright Models for the HBV and HCV analyses respectively. Both are

Markov models that utilize country specific inputs to estimate the natural history of the disease and future burden. Where data were unavailable, regional averages were applied to the total population of the country.

Results: 166 country level HBV and 110 HCV models were available. At the current trends, the prevalence of HBV is expected to decrease from 282 million in 2015 to 247 million in 2030, representing an 11% decrease globally with Africa's prevalence to remain relatively constant. The incidence of chronic HBV is expected to decline by 43% from 1,459,000 to 827,000 new cases per year with all continents seeing a decline. Globally, the mortality of HBV is expected to increase by 39% between 2015 and 2030 from 850,300 to 1,109,500 deaths annually. Similarly, the incidence of HCC is expected to increase by 34% from 682,000 to 912,000 cases per year. For both indicators all continents are expected to increase in this time frame. The prevalence of HCV is expected to decrease from 64 million in 2015 to 54 million in 2030, representing a 15% decrease globally. The incidence of chronic HCV is expected to decline by 7% from 1,521,000 to 1,409,000 new cases per year with Asia and North America increasing. Globally the mortality of HCV is expected to increase by 3% between 2015 and 2030 from 284,000 to 293,000 deaths annually. The incidence of HCC is expected to increase by 9% from 202,000 to 220,000 cases per year. Increases are expected in Asia, Oceania, and South America for both indicators.

Conclusion: Progress has been made particularly in regard to prevalence and incidence. However, without additional interventions almost 12 million individuals will die early from preventable deaths. Early gains made by Egypt, high income countries, and other early adopters, for HCV elimination, are offset by raising disease burden in the rest of the world. Innovative guidelines and funding mechanisms are necessary to meet countries where they are to live up to international commitments to elimination.

OS051

The HCV care cascade for children and young people in British Columbia, Canada: a large, linked administrative population-based cohort study

Dahn Jeong¹, Margo Pearce², Amanda Yu², Laura Sauv  ^{3,4}, Richard A. Schreiber^{3,4}, Sofia Bartlett^{2,5}, Muhammad Furqan Waleed^{6,7}, Makuza Jean Damascene¹, Prince Adu^{1,2}, Jane Buxton^{1,2}, Hector Velasquez^{1,2}, Mawuena Binka², Chelsea Elwood^{8,9}, David GoldFarb^{3,5}, Hasina Samji^{2,10}, Stanley Wong², Maria Alvarez², Neora Pick^{8,11}, Naveed Janjua^{1,2,7}. ¹The University of British Columbia, School of Population and Public Health, Vancouver, Canada; ²BC Centre for Disease Control, Vancouver, Canada; ³BC Children's Hospital, Vancouver, Canada; ⁴The University of British Columbia, Department of Pediatrics, Vancouver, Canada; ⁵The University of British Columbia, Department of Pathology and Laboratory Medicine, Vancouver, Canada; ⁶Youthco HIV and Hep C Society, Vancouver, Canada;

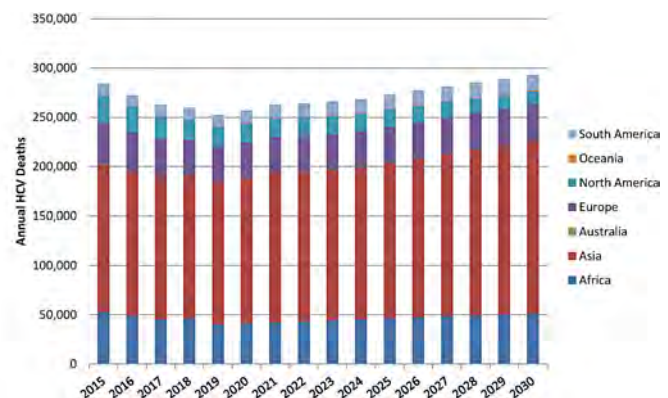
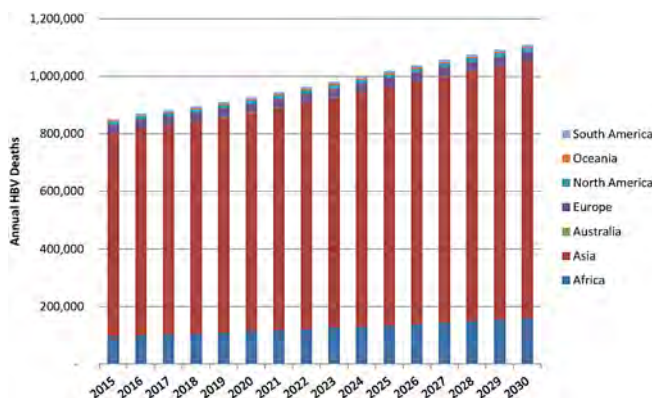


Figure: (abstract: OS050)

⁷The Canadian HIV Trials Network, Vancouver, Canada; ⁸BC Women's Hospital, Vancouver, Canada; ⁹The University of British Columbia, Department of Obstetrics and Gynaecology, Vancouver, Canada; ¹⁰Simon Fraser University, Faculty of Health Sciences, Burnaby, Canada; ¹¹The University of British Columbia, Division of Infectious Diseases, Vancouver, Canada
Email: dahn.jeong@bccdc.ca

Background and aims: In high income countries, new hepatitis C virus (HCV) infections have been occurring at the highest rate among people under 30 years of age, driven by the ongoing opioid crisis and other co-occurring socioeconomic conditions. The clinical experiences of young people living with HCV are underrepresented in research. We aimed to build the HCV care cascade for children and young people under age 30 living with HCV in British Columbia (BC), Canada.

Method: We used data from the BC Hepatitis Testers Cohort, a large population-based administrative dataset linked with data on primary care visits, hospitalizations and medication dispensations. This study includes all BC residents under age 30 who have been diagnosed with HCV by the end of 2019. The HCV care cascade was defined as: 1) HCV antibody (Ab) diagnosed 2) ribonucleic acid (RNA) tested 3) RNA positive 4) genotyped 5) initiated treatment and 6) achieved sustained virologic response (SVR). We estimated the number and proportion of people in each stage.

Results: There were 1,350 children and young people (aged 4 to 29) diagnosed as HCV Ab positive living in BC at the end of 2019. Of these, 82.2% (1,110/1,350) had received an RNA test, and 60.6% (673/1,110) were RNA positive. Among those who were RNA positive, 79.9% (538/673) had their HCV genotyped; however, only 40.3% (217/538) initiated treatment. SVR was achieved by 87.7% (121/138) of individuals for whom data on SVR assessment was available. In 2019, the proportion of HCV RNA positive persons receiving treatment varied by age group: 17.1% (6/35) in 14–19 years, 34.4% (45/131) in 20–24 years, and 34.1% (164/481) in 25–29 years. Treatment initiation increased over time, with the majority of treatments started between 2018 and 2019: 3.7% (8/217) treated between 2009–2011, 7.8% (17/217) between 2012–2014, 25.8% (56/217) between 2015–2017, and 62.7% (136/217) between 2018–2019. Many young people living with HCV were socioeconomically marginalized, had other comorbidities, particularly mood and anxiety disorders, and were accessing harm reduction services such as opioid agonist therapy.

Conclusion: By the end of 2019, more than two-thirds of people under age 30 in BC with chronic HCV remained untreated. The approval of highly effective pangenotypic direct-acting antiviral regimens provides the opportunity for early treatment for young people. Identifying and addressing the barriers that young people experience would be crucial to optimizing access to HCV care and services in this population.

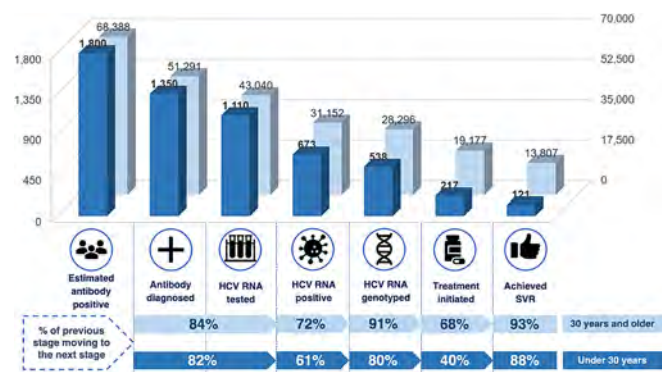


Figure 1: The HCV care cascade for people under 30 years of age and 30 years and older in 2019, British Columbia Hepatitis Testers Cohort.

OS052

Clinical impact and cost-effectiveness of hepatitis C testing in an emergency department in Barcelona, Spain

Jordi Llaneras¹, Ana Barreira^{2,3}, Ariadna Rando-Segura⁴, Raquel Domínguez-Hernández⁵, Francisco Rodríguez-Frías^{3,4}, Magda Campins⁶, Miguel Ángel Casado^{3,5}, Mar Riveiro Barciela^{2,3}, Maria Arranz¹, Rafael Esteban^{2,3}, Maria Buti^{2,3}. ¹Hospital Vall Hebron, Emergency Department, Barcelona, Spain; ²Hospital Vall Hebron, Liver Unit, Barcelona, Spain; ³Centro de investigación biomédica en red de enfermedades hepáticas y digestivas, Madrid, Spain; ⁴Hospital Vall Hebron, Microbiology Department, Barcelona, Spain; ⁵Pharmacoeconomics and Outcomes Research Iberia (PORIB), Madrid, Spain; ⁶Hospital Vall Hebron, Epidemiology Department, Barcelona, Spain
Email: mbuti@vhebron.net

Background and aims: In primary care centers in Spain the prevalence of anti-HCV is approximately 0.8% and HCV-RNA positive 0.22%. In the emergency department (ED) of our hospital, an HCV-RNA+ screening program was initiated with linkage to antiviral treatment assessment, with the aim of increasing HCV detection and safeguarding the hospital from this infection. Results of the HCV screening strategy were analyzed and a cost-effectiveness evaluation performed.

Method: Prospective study conducted in a university hospital ED (FOCUS-A, hospital free of hepatitis C study). All individuals >16 years of age attending the ED and requiring blood extraction underwent anti-HCV screening, HCV-RNA reflex testing, and FIB-4 calculation if anti-HCV+. Individuals with detectable viral load were linked to a specialist for HCV treatment evaluation. A Markov model was developed to analyze the cost-effectiveness of opt-out HCV testing using the data obtained and a National Health Care System perspective. Lifetime liver-related mortality, hepatic complications, and associated costs were assessed.

Results: In total, 13,479 individuals screened (February/20–September/21): 49% male, mean age 70 years. Anti-HCV detected in 553 (4%) cases and HCV-RNA in 100 (0.7%). Risk factors associated with anti-HCV: 58 (10%) HIV co-infection, 98 (18%) injecting drug users, 128 (23%) abusive alcohol consumption, and 205 (37%) diagnosed with a psychiatric disorder. Among viremic patients, 34% (n = 34) were unaware of HCV infection and 48% had an FIB-4 score suggestive of cirrhosis (FIB-4 >3.25). Among HCV-RNA+ cases, 53 (53%) were selected for treatment. Reasons for non-selection were short life expectancy or cognitive impairment (40 cases), and loss to follow-up due to serious social problems (7 cases). Of the 53 candidates linked to a specialist, 27 have received treatment and the 14 who completed treatment have achieved a sustained virological response. This strategy reduced liver-related mortality by 56% and avoided 50%–67% of liver complications with a related cost saving of €247,942.

Conclusion: The prevalence of chronic HCV among in adults in the ED is almost four times higher than in primary care. Almost half the viremic individuals had advanced fibrosis. Screening in the ED is a cost-effective intervention. These findings are of value for informing testing guidelines.

OS053

High Intensity Test and Treat (HITT): an overview of the initiative as part of the hepatitis C elimination programme in England

Beatrice Emmanouil¹, Sean Cox², Rachel Halford², Georgia Threadgold¹, Mark Gillyon-Powell¹, Graham Foster¹. ¹NHS England and NHS Improvement; ²Hepatitis C Trust, United Kingdom
Email: b.emmanouil@nhs.net

This abstract is under embargo until Thursday 23 June 2022, 13:30 BST. This abstract has been selected to be highlighted during official EASL Press Office activities or in official EASL Press Office materials that will be made publicly available on the congress website at 13:30 (BST).

Journalists, industry, investigators and/or study sponsors must abide by the embargo times set by EASL.

Violation of the embargo will be taken seriously. Individuals and/or sponsors who violate EASL's embargo policy may face sanctions relating to current and future abstract submissions, presentations and visibility at EASL Congresses. The EASL Governing Board is at liberty to ban attendance and/or retract data.

Copyright for abstracts (both oral and poster) on the website and as made available during The International Liver Congress™ 2022 resides with the respective authors. No reproduction, re-use or transcription for any commercial purpose or use of the content is permitted without the written permission of the authors. Permission for re-use must be obtained directly from the authors.

Results: By excluding those who were unable to enter the program such as deaths, aging, and mobility, the screening targets total 10,684 people. The HCV antibody screening rate reached 93.4% (9,978 people), with HCV antibody positive rate of 6.1% (608 people), HCV RNA referral rate of 93.4% (568 people), HCV RNA virus checking rate of 92.1% (523 people), detectable HCV RNA rate of 69.6% (364 people), eligible treatment rate was 97.5% (355 people), and final treatment rate was 92.1% (327 people). When compared with the situation before intervention of program, the screening rate and treatment rate have been significantly improved which achieve the goal of HCV elimination. The risk of HCV infection is 1.27 (95%CI: 0.793–2.035), 1.64 (95%CI: 1.057–2.536), 1.90 (95%CI: 1.232–2.937), for patients of 50–59 years, 60–69 years, and over 70 years respectively when compared with patients less than 50 years. Furthermore, the risk of HCV infection is 0.43 (95%CI: 0.253–0.712, $p=0.0012$) in patients of senior high school; and 0.26 (95%CI: 0.108–0.624, $p=0.0026$) in patients of university when compared with patients of illiterate. HCV risk is not associated with other factors such as gender, the duration of diabetes, cigarette smoking, presence of chronic kidney, retinopathy, and foot disease at all. We further evaluated the heterogeneity among townships by using the random effect model, and found that the antibody positive rate was significantly different among townships, but not different on the RNA positive rate and treatment rate.

Conclusion: A novel model was successfully implemented for HCV elimination on diabetic population in the community of Changhua county in Taiwan, by using a series of indicators for caring cascade. This population-based service was provided to the 26 townships with a homogenous quality.

OS054

Hepatitis C elimination in diabetic population from a shared care cascade cohort- under Changhua-Integrated Program to Stop hepatitis C infection (CHIPS-C)

Tsung-Hui Hu¹, Yo-Yu Tsao², Wei-Wen Su³, Chi-Chao Yang⁴, Chi-Chieh Yang⁵, Sam Li-Sheng Chen⁶, Yen-Po Yeh⁷, Hsiu-Hsi Chen⁸.

¹Kaohsiung Chang Gung Memorial Hospital, and Chang Gung University College of Medicine, Kaohsiung, Taiwan, Kaohsiung, Taiwan; ²Changhua County Public Health Bureau, Changhua, Taiwan, Changhua, Taiwan;

³Changhua Christian Hospital, Changhua, Taiwan, Changhua, Taiwan;

⁴Changhua Hospital, Ministry of Health and Welfare, Changhua, Taiwan;

⁵Show Chwan Memorial Hospital, Changhua, Taiwan, Changhua, Taiwan;

⁶School of Oral Hygiene, College of Oral Medicine, Taipei Medical University, Taipei, Taiwan;

⁷Changhua County Public Health Bureau, Changhua, Taiwan;

⁸Graduate Institute of Epidemiology and Preventive Medicine, College of Public Health, National Taiwan University, Taipei, Taiwan, Taipei, Taiwan

Email: dr.hu@msa.hinet.net

Background and aims: Several clinical studies have suggested an association between chronic HCV infection and diabetes mellitus (DM). HCV micro-elimination approach, which focuses treatment on DM population was rarely reported. We aim to conduct HCV elimination for population with diabetes mellitus in a county of Taiwan via 27 local health centers under Changhua-Integrated Program to Stop Hepatitis C Infection (CHIPS-C).

Method: Changhua County, has 26 townships and a total of 1,289,000 residents. In addition to hospitals and local clinics in the county, there are 27 local health centers handled by the Changhua County Public Health Bureau of government. Taking the diabetic cases in the clinics of various township health centers from 2018 to 2020 as the tracking generation, combined with the Changhua County Diabetes Common Care Network since 1996, HCV screening and treatment were implemented and evaluated. The achievement rate of HCV care chain-related indicators, and the difference in HCV positive rate and treatment rate under different influencing factors were analysed.

Primary Liver Cancer: Experimental and pathophysiology

OS055

PMEPA1: an oncogene in hepatocellular carcinoma linked to TGF-beta signaling

Carmen Andreu-Oller^{1,2}, Marta Piqué-Gil², Marina Barcena-Varela¹, Roser Pinyol², Roger Esteban-Fabro^{1,2}, Judit Peix², Katherine E. Lindblad¹, Miguel Torres-Martín², Daniela Sia¹, Amaia Lujambio¹, Josep M. Llovet^{1,2,3,4}, ¹Icahn School of Medicine at Mount Sinai, Division of Liver Diseases, New York, United States; ²Institut d'Investigacions Biomèdiques August Pi i Sunyer (IDIBAPS), Translational Research in Hepatic Oncology, Liver Unit, Barcelona, Spain; ³Universitat de Barcelona, Barcelona, Spain; ⁴Institució Catalana de Recerca i Estudis Avançats (ICREA), Barcelona, Spain

Email: carmenandreuoller@gmail.com

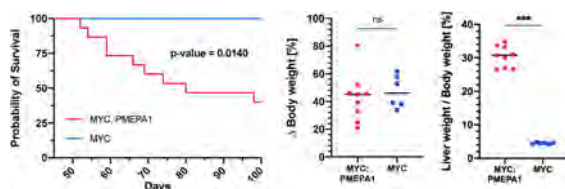
Background and aims: Transforming growth factor beta (TGF-beta) has a dual role in cancer, including hepatocellular carcinoma (HCC). It acts as a tumor suppressor in early stages of hepatocarcinogenesis, but promotes epithelial-to-mesenchymal transition, angiogenesis and immunosuppression in advanced stages. *PMEPA1* (prostate transmembrane protein androgen induced 1), a direct target gene of the TGF-beta pathway that negatively regulates TGF-beta signaling by interacting with SMAD proteins, has been shown to promote TGF-beta oncogenic effects in other cancers. Here, we explored its role in HCC pathogenesis.

Method: We analyzed transcriptomic, genomic, epigenomic and clinicopathological data of a discovery cohort of 228 HCCs and a validation cohort of 361 HCCs. *PMEPA1* levels were quantified by qPCR and IHC in the discovery cohort. *PMEPA1* overexpression was validated in 6 independent cohorts ($n=916$) using microarray and RNAseq data. We evaluated *PMEPA1* expression at the single-cell level using a publicly available scRNAseq dataset from 25 HCCs. Genetically engineered mouse models were generated through hydrodynamic

ORAL PRESENTATIONS

tail-vein injection. Equal amounts of plasmids overexpressing *PMEPA1*, *TGFB1* and *MYC* were injected in mice to evaluate survival. Molecular and histopathological analyses of the murine tumors are currently ongoing.

Results: *PMEPA1* was overexpressed in 18% of human HCCs [FC >2; n = 203/1144], a feature associated with TGF- β signaling ($p < 0.001$). *PMEPA1* was expressed by both malignant and tumor microenvironment (TME) cells including endothelial cells, cancer associated fibroblasts, T cells and B cells. Overexpression of *PMEPA1* was associated with gene body hypermethylation ($p < 0.0001$). HCCs displaying both TGF- β signaling and high *PMEPA1* levels (11% of cases) were significantly enriched in signatures of immune exhaustion, late TGF- β activation, TME response to TGF- β and active stroma ($p < 0.05$), compared to HCCs with TGF- β signaling alone (8% of cases) or *PMEPA1* high levels alone (11% of cases). *In vivo*, overexpression of *MYC*+*PMEPA1* led to HCC development in 9/16 mice and showed a lower survival when compared to the control arm, overexpression of *MYC* alone, ($p = 0.014$) (Figure). On the contrary, only 1/12 mice in the *MYC*+*PMEPA1*+*TGFB1* condition developed HCC and none of the *MYC*+*TGFB1* mice.



Conclusion: *PMEPA1* upregulation is linked to TGF- β activation and an aggressive phenotype in human HCC. Overexpression of *PMEPA1* in combination with *MYC* *in vivo* led to HCC development, showing for the first time the oncogenic role of *PMEPA1* in this cancer.

OS056

Targeting NAE1-mediated protein hyper-NEDDylation halts cholangiocarcinogenesis and impacts on tumour-stroma crosstalk in experimental models

Paula Olaizola¹, Pui-Yuen Lee-Law^{1,2}, Maite G. Fernandez-Barrena^{3,4,5}, Laura Alvarez³, Massimiliano Cadamuro⁶, Mikel Azkargorta^{5,7}, Colm O. Rourke⁸, Francisco J. Caballero¹, Rocio IR Macias^{5,9}, Jose Marin^{5,9}, Marina Serrano-Macia¹⁰, María Luz Martínez-Chantar^{5,10}, Matías A. Avila^{3,4,5}, Patricia Aspichueta^{5,11,12}, Diego Calvisi¹³, Luca Fabris^{6,14}, Felix Elortza^{5,7}, Jesper Andersen⁸, Luis Bujanda^{1,5}, Pedro Miguel Rodríguez^{1,5,15}, María Jesús Perugorria^{1,5,16}, Jesus Maria Banales^{1,5,15,17}. ¹Department of Liver and Gastrointestinal Diseases, Biodonostia Health Research Institute-Donostia University Hospital-, University of the Basque Country (UPV/EHU), San Sebastian, Spain; ²Department of Gastroenterology and Hepatology, Radboud University Nijmegen Medical Center, Nijmegen, Netherlands; ³Hepatology Program, CIMA, University of Navarra, Pamplona, Spain; ⁴Instituto de Investigaciones Sanitarias de Navarra (IdiSNA), Pamplona, Spain; ⁵National Institute for the Study of the Liver and Gastrointestinal Diseases (CIBERehd, "Instituto de Salud Carlos III"), Spain; ⁶Department of Molecular Medicine (DMM), University of Padua, Padua, Italy; ⁷Proteomics Platform, CIC bioGUNE, CIBERehd, ProteoRed-ISCI, Bizkaia Science and Technology Park, Derio, Spain; ⁸Department of Health and Medical Sciences, Biotech Research and Innovation Centre (BRIC), University of Copenhagen, Copenhagen, Denmark; ⁹Experimental Hepatology and Drug Testing (HEVEPHARM) Group, Institute of Biomedical Research of Salamanca (IBSAL), University of Salamanca, Salamanca, Spain; ¹⁰Liver Disease Laboratory, CIC bioGUNE, Basque Research and Technology Alliance (BRTA), Spain; ¹¹Department of Physiology, Faculty of Medicine and Nursing, University of the Basque Country (UPV/EHU), Leioa, Spain; ¹²Biocruces Bizkaia Health Research

Institute, Cruces University Hospital, Barakaldo, Spain; ¹³Institute of Pathology, University of Regensburg, Regensburg, Spain; ¹⁴Department of Internal Medicine, Yale Liver Center (YLC), School of Medicine, Yale University, New Haven, CT, United States; ¹⁵IKERBASQUE, Basque Foundation for Science, Bilbao, Spain; ¹⁶Faculty of Medicine and Nursing, University of the Basque Country (UPV/EHU), Leioa, Spain; ¹⁷Department of Biochemistry and Genetics, School of Sciences, University of Navarra, Pamplona, Spain
Email: jesus.banales@biodonostia.org

Background and aims: Cholangiocarcinoma (CCA) comprises a heterogeneous group of malignant tumors with dismal prognosis. Alterations in post-translational modifications (PTMs), including NEDDylation, result in abnormal protein dynamics, cell disturbances and disease. Here, we investigate the role of NEDDylation in CCA development and progression.

Method: Levels and function of NEDDylation, together with response to pevonedistat (NEDDylation inhibitor) or CRISPR/Cas9 against *NAE1* were evaluated *in vitro*, *in vivo* and/or in patients with CCA. Development of preneoplastic lesions in *Nae1*^{-/-} mice was investigated using an oncogene-driven CCA model. The impact of NEDDylation in CCA cells on tumor-stroma crosstalk was assessed using CCA-derived cancer-associated fibroblasts (CAFs). Proteomic analyses were carried out by mass spectrometry.

Results: NEDDylation machinery was found overexpressed and overactivated in human CCA cells and tumors, correlating with poor prognosis. Most NEDDylated proteins found upregulated in CCA cells, after NEDD8-immunoprecipitation and further proteomics, participate in cell cycle, proliferation or survival. Genetic (CRISPR/Cas9-*NAE1*) and pharmacological (pevonedistat) inhibition of NEDDylation reduced CCA cell proliferation and impeded colony formation *in vitro*. NEDDylation depletion (pevonedistat or *Nae1*^{-/-} mice) halted tumorigenesis in subcutaneous, orthotopic, and oncogene-driven models of CCA *in vivo*. Moreover, pevonedistat potentiated chemotherapy-induced cell death in CCA cells *in vitro*. Mechanistically, impaired NEDDylation triggered the accumulation of cullin RING ligase or NEDD8 substrates, inducing DNA damage and cell cycle arrest. Furthermore, NEDDylation impairment in CCA cells reduced the secretion of proteins involved in fibroblast activation, angiogenesis, and oncogenic pathways, ultimately hampering CAF proliferation and migration.

Conclusion: aberrant protein NEDDylation contributes to cholangiocarcinogenesis by promoting cell survival and proliferation. Moreover, NEDDylation impacts the CCA-stroma crosstalk. Inhibition of NEDDylation with pevonedistat may represent a potential therapeutic strategy for patients with CCA.

OS057

Induction of branching morphogenesis in cholangiocarcinoma organoids *in vitro* improves similarity with the original tumour

Gilles van Tienderen¹, Kathryn Monfils¹, Floris Roos¹, Luc J.W. van der Laan¹, Monique M.A. Verstegen¹. ¹ErasmusMC Transplant Institute, Department of Surgery, Rotterdam, Netherlands
Email: g.vantienderen@erasmusmc.nl

Background and aims: Cholangiocarcinoma (CCA) is an aggressive, heterogeneous cancer with low survival rates. Patient-derived cholangiocarcinoma organoids (CCAOs) hold potential for understanding disease progression and developing novel treatment options, based on their ability to mimic the original tumor. Currently, most organoid expansion protocols focus on stimulation of the canonical WNT/ β -catenin pathway, however there is growing evidence showing that non-canonical WNT pathways also play a crucial role in cancer progression. This project aims to establish a novel *in vitro* model for CCA, better recapitulating the *in vivo* tumor, by stimulating both canonical and non-canonical WNT pathways.

Method: Branching cholangiocarcinoma organoids (BRCCAOs) (n = 3 patients) were established with a two-step protocol. First, CCAOs were initiated and cultured under standard conditions in canonical

WNT stimulating expansion medium. Next, expansion medium was replaced by medium that stimulates canonical WNT-signaling (through R-spondin) and non-canonical WNT-signaling (with Dickkopf-related protein 1) simultaneously, after which a branching-like morphology could be observed. Tumor cell behavior in BRCCAOs and CCAOs was assessed and compared through immunohistochemical stainings, bulk RNA-sequencing, and drug response studies.

Results: BRCCAOs presented a distinct branching morphology, displaying a morphological architecture similar to in vivo tumors, while maintaining tumorigenic potential and expression of cytokeratin-7, with an accompanying lack of defined cellular polarity. Bulk RNA-sequencing of BRCCAOs showed significant upregulation of cancer-associated molecular pathways, including hypoxia, compared to CCAOs and a close correlation (coefficient 0.80 ± 0.05) to the transcriptome of the original tumor tissue. BRCCAOs also exhibited a strong resistant phenotype to a large panel of 166 anti-cancer drugs, including multiple drugs that have previously failed in clinical trials for CCA patients (e.g. docetaxel, palbociclib, and irinotecan). Specifically, compared to CCAOs, BRCCAOs showed an approximately 10,000-fold ($p < 0.0001$) increase in chemo resistance against gemcitabine and cisplatin, first-line chemotherapy drugs for CCA, independent of patient variance.

Conclusion: These results demonstrate that BRCCAOs better resemble in vivo CCA tumor tissue compared to conventional CCAOs, particularly with regards to morphology, transcriptome, and drug responses. Gemcitabine and cisplatin combinational therapy only provides CCA patients with a modest benefit in overall survival, and BRCCAOs appear to mimic this response more closely, thus providing possibilities for personalized medicine applications.

OS058

Cross-talk between MerTK-expressing stromal cells and cholangiocarcinoma

Mirella Pastore¹, Öykü Gönül Geyik^{1,2}, Jesper Andersen³, Monika Lewinska³, Ana Lleo⁴, Paolo Kunderfranco⁴, Chiara Raggi¹, Fabio Marra¹, ¹University of Florence, Firenze, Italy; ²Istinye University, Turkey; ³Copenhagen University, København, Denmark; ⁴Humanitas University, Italy
Email: fabio.marra@unifi.it

Background and aims: A typical feature of cholangiocarcinoma (CCA) is a dense stromal reaction populated by fibrogenic myofibroblasts and immune cells, creating a complex tumor microenvironment where malignant cells survive and proliferate. Cancer stem cells (CSCs) have been proposed as a driving force of tumor initiation, dissemination and drug-resistance in many solid tumors, including cholangiocarcinoma (CCA). Increasing evidence indicates that myeloid-epithelial-reproductive tyrosine kinase (MerTK) is highly expressed by a macrophage subset defined as M2c. The present study aims to investigate whether signals generated by MerTK-expressing macrophages modulate the biology of CCA.

Method: 3D-tumor sphere cultures enriched in CSC were generated from intrahepatic CCA cell lines (HuCC-T1 and CCLP-1). Circulating monocytes were differentiated into M2c macrophages in vitro. Recombinant Gas-6, a MerTK ligand, was used to activate this receptor. MERTK mRNA expression in human CCA tissues was also analyzed.

Results: In CCA cell lines cultured with conditioned medium from Gas-6-stimulated M2c macrophages, cell survival, invasion, sphere-forming efficiency and drug resistance were significantly increased. These effects were reduced following macrophage pre-treatment with the MerTK inhibitor, UNC2025. Analysis of the transcriptome of laser-captured, micro-dissected epithelium and stroma from 23 CCA patients showed that MerTK mRNA expression is significantly higher in intratumoral stroma. Single-cell RNA sequencing of CD45+ sorted cells from paired non-tumoral and tumoral specimens from iCCA patients (n=6) defined eleven clusters characterized by their gene expression profiles. A further reclustering of myeloid cells showed

MerTK expression in Kupffer cells, lipid macrophages, TREM2+ macrophages, and non-classical monocytes.

Conclusion: These data suggest a cross-talk between MerTK-expressing cells in the stroma and CCA cells, to induce increased malignant features.

OS059

Mixed HCC-CCA originates from hepatic progenitor cells, is dependent on IL6 singling and is ablated by senolytic agents

Nofar Rosenberg¹, Matthias Van Haele², Maria Garcia Beccaria³, Mirian Fernández-Vaquero³, Danijela Heide³, Neta Barashi¹, Amnon Peled¹, Yuval Nevo⁴, Shrona Elgavish⁴, Dirk Schmist-Arras⁵, Hanan Edler¹, Alina Simerzin¹, Michal Shoshkes-Carmel⁶, Klaus Kaestner⁶, Hilla Giladi¹, Stefan Rose-John⁵, Tania Roskams², Mathias Heikenwälder³, Eithan Galun¹. ¹The Goldyne Savad Institute of Gene and Cell Therapy, Hadassah Hebrew University, Jerusalem, Israel; ²University of Leuven, Department of Translational Cell and Tissue Research, Leuven, Belgium; ³DKFZ, Department of Translational Cell and Tissue Research, Germany; ⁴Hebrew University of Jerusalem, Hadassah Medical School, Bioinformatics Unit, Israel; ⁵Christian-Albrechts-Universität zu Kiel, Institut für Biochemie, Kiel, Germany; ⁶University of Pennsylvania Perelman School of Medicine, Penn Center for Molecular Studies in Digestive and Liver Diseases, Philadelphia, United States
Email: nofar.ros@gmail.com

Background and aims: Primary liver cancer is the 3rd leading cause of cancer-related death worldwide. Primary liver cancers include: Hepatocellular carcinoma (HCC), intrahepatic cholangiocarcinoma (CCA) and Mixed HCC-CCA tumors. Chronic liver inflammation, which develops to cirrhosis, is a risk for the development of primary liver cancer. It has been suggested that hepatic progenitor cells (HPCs) could contribute to hepatocarcinogenesis. However, this has not yet been proven. HPCs proliferate in response to injury and chronic inflammation. In this study, we aimed to determine whether HPCs contribute to HCC, Mixed HCC-CCA or both types of tumors, in the MDR2 KO mouse model of inflammation-induced cancer.

Method: In order to enable tracing of progenitor cells, we generated a transgenic mouse based on the MDR2 KO that harbours a YFP reporter gene driven by the Foxl1 promoter. Foxl1 is expressed specifically in adult HPCs. These mice (MDR2 KO^{Foxl1CRE}; RosaYFP) develop chronic inflammation by the age of 1 month and develop HCCs by the age of 14–16 months, followed by mixed HCC-CCA tumors at the age of 18 months, as we have first observed, suggesting that the aged mice are a suitable model for mixed HCC-CCA tumors.

Results: In this model, we show that liver progenitor cells are the source of mixed HCC-CCA tumors, but they are not the source of HCC in the chronically inflamed liver. By generating mice with a Diphtheria toxin (DT) receptor in HPCs and administering DT, we ablated the progenitors, and we observed a significant reduction in the development of mixed HCC-CCA tumors but no change in HCCs. RNA-seq analysis revealed enrichment of the IL6 signaling pathway in mixed HCC-CCA tumors in comparison to HCC tumors. A single cell RNA-seq analysis revealed that in the liver, IL6 is expressed from both, immune cells and parenchymal cells which are in senescence, and that IL6 is part of the senescence-associated secretory phenotype (SASP). Upon administration of anti-IL6 antibodies to the MDR2 KO^{Foxl1CRE}; RosaYFP mice, we inhibited the development of the mixed HCC-CCA tumors. Furthermore, by blocking IL6 transsignaling with sgp130, we also decreased mixed HCC-CCA tumors, indicating that mixed HCC-CCA tumors are dependent on IL6 transsignaling. The administration of a senolytic agent to these mice, also inhibited the development of mixed HCC-CCA tumors.

Conclusion: Our results suggest that mixed HCC-CCA but not HCC tumors, originate from HPCs in the inflammation induced liver cancer model, and that the driver of this process involves the IL6 signalling pathway that at least in part, derives from SASP of cells in senescence. These findings could enhance the development of new therapeutic approaches for mixed HCC-CCA liver cancer.

OS060

MAP17 promotes metastasis in hepatocellular carcinoma by modulating the epithelial-mesenchymal-amoeboid transition

Claudia Gil-Pitarch^{1,2,3}, Esther Bertran^{4,5}, Iker Uriarte^{6,7}, Natalia Hermán-Sánchez⁸, José Manuel García-Heredia^{5,9,10}, Naroa Goikoetxea^{1,2,3}, Marina Serrano-Macia^{1,2,3}, Rubén Rodríguez Agudo^{1,2,3}, Sofia Lachiondo-Ortega^{1,2,3}, Maria Mercado-Gómez^{1,2,3}, Miriam Rábano^{2,11}, Teresa Cardoso Delgado^{1,2,3}, Jorge Simón Espinosa^{1,2,3}, Luis Alfonso Martínez-Cruz^{1,2}, Cesar Augusto Martín¹², Maria Vivanco^{2,11}, Matías A. Avila^{6,7,13}, Manuel Gahete Ortiz^{8,14,15,16}, Isabel Fabregat^{4,17,18}, Amancio Carnero^{10,19}, María Luz Martínez-Chantar^{1,2,17}. ¹CIC bioGUNE, Liver disease lab, Derio, Spain; ²Basque Research and Technology Alliance (BRTA), Mendaro, Spain; ³Centro de Investigación Biomédica en Red de Enfermedades Hepáticas y Digestivas (CIBERehd), Derio, Spain; ⁴Bellvitge Biomedical Research Institute (IDIBELL), CIBER Enfermedades hepáticas y digestivas (CIBERehd), Hospitalet de Llobregat, Spain; ⁵Instituto de Biomedicina de Sevilla (IBIS), Sevilla, Spain; ⁶CIMA, University of Navarra, Pamplona, Spain; ⁷CIBERehd, Instituto de Salud Carlos III, Madrid, Spain; ⁸Maimonides Institute for Biomedical Research of Cordoba (IMIBIC), Córdoba, Spain; ⁹Universidad de Sevilla, Departamento de bioquímica vegetal y biología molecular, facultad de biología, Sevilla, Spain; ¹⁰Grupo CIBER de Cáncer, Sevilla, Spain; ¹¹CIC bioGUNE, Basque Research and Technology Alliance, Cancer Heterogeneity Lab, Derio, Spain; ¹²UPV/EHU, CSIC, Department of Molecular Biophysics, Biofisika Institute and Department of Biochemistry and Molecular Biology, Leioa, Spain; ¹³IdiSNA, Navarra Institute for Health Research, Pamplona, Spain; ¹⁴University of Córdoba, Department of Cell Biology, Physiology and Immunology, Córdoba, Spain; ¹⁵Reina Sofía University Hospital, Córdoba, Spain; ¹⁶CIBER Pathophysiology of Obesity and Nutrition (CIBERObn), Córdoba, Spain; ¹⁷CIBER Enfermedades hepáticas y digestivas (CIBERehd), Spain; ¹⁸University of Barcelona, Department of Physiological Sciences II, Barcelona, Spain; ¹⁹Instituto de Biomedicina de Sevilla (IBIS), Hospital Universitario Virgen del Rocío, Universidad de Sevilla, Consejo Superior de Investigaciones Científicas, Sevilla, Spain
Email: mlmartinez@cicbiogune.es

Background and aims: Epithelial-mesenchymal transition (EMT), a key process during embryonic development, promotes cell migration and resistance to apoptosis during tumour invasion and metastasis. In hepatocellular carcinoma (HCC) an amoeboid behaviour tends to increase the aggressiveness and metastatic capacity of epithelial tumours.

MAP17 is a 17 kDa membrane protein expressed during embryogenesis, absent in most adult organs. The presence of MAP17 correlates with an inflammatory environment, hypoxia and increased reactive oxygen species (ROS). MAP17 has been identified in several types of cancer, including HCC. Modulation of EMT and amoeboid behaviour via MAP17 offers an attractive approach to prevent metastasis.

Method: Two separated HCC patient cohorts were used to characterise MAP17 levels. *In vitro*, expression of MAP17 was measured in mesenchymal and epithelial hepatoma cells, and its levels were modulated to study its implication in cell proliferation, drug resistance, mitochondrial dynamics, metabolic rewiring, and proteome homeostasis. *In vivo*, the role of MAP17 in the metastatic capacity was evaluated using orthotopic HCC mice models.

Results: A positive correlation of MAP17 and mesenchymal markers was established in 751 HCC patients *in silico* study and by mRNA expression in 246 HCC patients. Additionally, MAP17 appeared statistically associated with RAC/RHO family genes, markers of amoeboid movement, in the same patient cohort. MAP17 overexpression in 3D epithelial cell experiments led to the formation of rosette invadopodia, proinvasive structures with high metastatic capacity.

MAP17 overexpression *in vitro* produced a reprogramming of energy metabolism in hepatoma cells with epithelial phenotype, increasing

mitochondrial dynamics and Warburg effect-mediated lactic acidosis, which support a tumour microenvironment conducive to cancer cell proliferation. ROS generation was increased as a protective mechanism to avoid apoptotic and senescence processes. Rewiring in the one-carbon metabolic pathway was also identified, proving an accelerated metabolism of the cell. Accordingly, overexpression of MAP17 in PLC/PRF/5 cells in the orthotopic model led to the formation of multiple tumour foci in the liver.

MAP17 silencing in hepatoma mesenchymal cells provided the opposite results, regressing the tumour phenotype and slowing down the cell metabolism and proliferation.

Conclusion: Modulation of MAP17 in epithelial and mesenchymal cells leads to the reprogramming of the transitional genes that define each phenotype. Our findings have identified the metastatic potential of MAP17 in liver cancer, as it triggers the mesenchymal phenotype and amoeboid behaviour in HCC.

Cirrhosis and its complications: ACLF and Critical illness

OS061

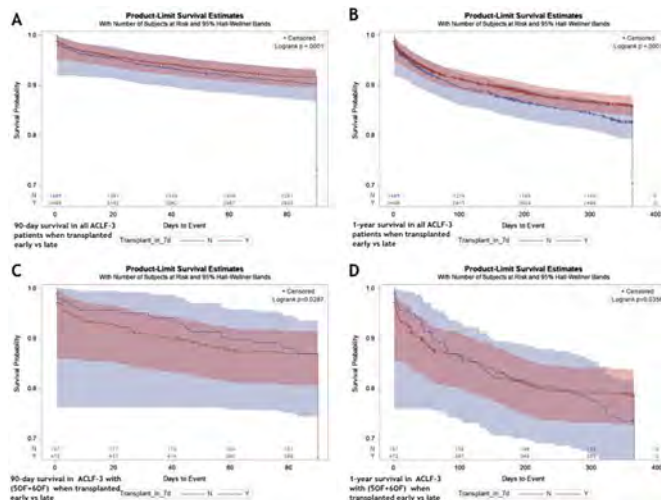
Liver transplantation within 7-days of listing improves survival in ACLF-3

Joseph Alukal¹, Feng Li¹, Paul J. Thuluvath¹. ¹Institute of Digestive Health and Liver Disease, Gastroenterology, Baltimore, United States
Email: jialukal@gmail.com

Background and aims: ACLF-3 is associated with a very high short-term mortality without liver transplantation (LT). The timing of LT, therefore, may be critical for optimal outcomes. The objective of our study was to determine if early LT (<7 days from listing), stratified by the number of organ failures (OF), had an impact on 90-day and 1-year survival in ACLF-3 patients.

Method: United network for organ sharing (UNOS) database was queried to identify adults (>18 years) with ACLF-3 who underwent LT between 2005–2021. We excluded those listed with status 1, 1A, or 1B, multi-organ transplant, living donor transplant and HCC. ACLF patients were identified using EASL-CLIF criteria. Unadjusted Kaplan-Meier (KM) survival curves were used to evaluate patient survival. The Cox proportional hazards (CPH) regression model was used to evaluate the risk factors for survival.

Results: We identified 3,498 patients with ACLF-3 who underwent early LT while 1,485 had transplant >7 days from listing. 90-day and 1-year survival in ACLF-3 patients who underwent early LT were 92% and 87% respectively. KM survival analysis showed that those who were transplanted early (≤7 days) had significantly better 90-day and 1-year survival than who underwent late LT (>7 days) (Figure A and Figure B). This survival benefit was seen across all sub-groups of ACLF-3 including those with 5 and 6 OF (Figure C and Figure D). On multivariable analysis, age (Hazard Ratio [HR] 1.02), body mass index (HR 1.01), donor risk index >1.7 (HR 1.3), respiratory failure (HR 1.9), and etiology of cirrhosis were independent predictors of higher 90-day post-transplant mortality. Similarly, age (HR 1.01), donor risk index >1.7 (HR 1.3), diabetes (HR 1.3), respiratory failure (HR 1.7) and etiology of cirrhosis were independent predictors of higher 1-year mortality while higher albumin (HR 0.87) was associated with a reduced mortality.



Conclusion: Early LT (≤ 7 days from listing) in ACLF-3 after listing is associated with a better 90-day and 1-year survival than those who were transplanted late (> 7 days). This survival benefit was seen even in those with 5 and 6 OF.

OS062

Neutrophil gelatinase-associated lipocalin predicts response to terlipressin and albumin in patients with hepatorenal syndrome

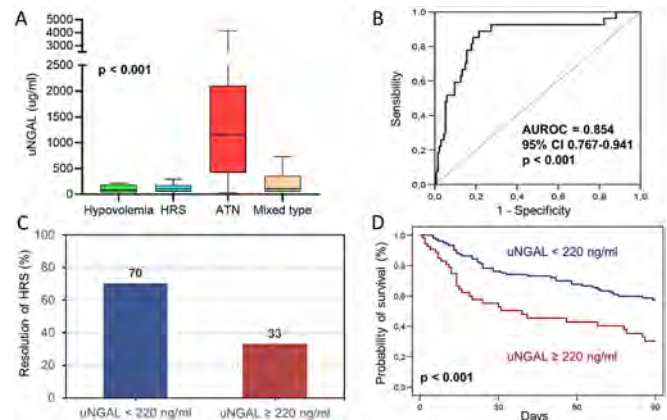
Carmine Gabriele Gambino¹, Matteo Stenico¹, Marta Tonon¹, Alessandra Brocca¹, Valeria Calvino¹, Simone Incicco¹, Chiara Cosma², Martina Zaninotto², Patrizia Burra³, Umberto Cillo⁴, Mario Plebani², Paolo Angeli¹, Salvatore Piano¹. ¹Unit of Internal Medicine and Hepatology, Department of Medicine, University of Padova, Padova, Italy; ²Laboratory Medicine Unit, Department of Medicine, University of Padova, Padova, Italy; ³Multivisceral Transplant Unit, Department of Surgery, Oncology and Gastroenterology, University of Padova, Padova, Italy; ⁴Hepatobiliary Surgery and Liver Transplantation, Department of Surgery, Oncology and Gastroenterology, University of Padova, Padova, Italy

Email: salvatorepiano@gmail.com

Background and aims: Acute Kidney Injury (AKI) commonly occurs in patients with decompensated cirrhosis. Neutrophil Gelatinase-associated Lipocalin (NGAL) is a novel urinary biomarker that could help in discriminating between different etiologies of AKI. The aim of this study was to investigate the ability of urinary NGAL (uNGAL) in: (1) the differential diagnosis of AKI, (2) predicting the response to treatment with terlipressin and albumin in patients with Hepatorenal Syndrome (HRS)-AKI and (3) predicting in-hospital and 90-day mortality.

Method: We included cirrhotic patients with AKI not solved within 48 hours, who were consecutively admitted from 2015 to 2020 at the University Hospital of Padova. uNGAL and standard urinary biomarkers were measured. Data on the type of AKI, AKI treatment, resolution of AKI were collected during the hospitalization and patients were followed up until transplant, death or 90 days.

Results: We enrolled 162 patients (mean age: 62 ± 10 years, male: 77%; alcoholic etiology: 48%; mean MELD: 25 ± 8). Thirty-five patients (22%) had hypovolemic AKI, 64 (39%) HRS-AKI, 27 (17%) acute tubular necrosis (ATN)-AKI and 36 (22%) a mixed form. uNGAL values were significantly higher in patients with ATN-AKI than in patients with other types of AKI (1162 [423–2105] vs 109 [52–192] ng/ml; $p < 0.001$; Fig. A). uNGAL showed a high discrimination ability in predicting ATN-AKI (AUROC = 0.854; [95% CI = 0.767–0.941]; $p < 0.001$; Fig. B) and the best threshold was 220 ng/ml (sensitivity 89%; specificity 78%).



Sixty-two patients with HRS-AKI were treated with terlipressin and albumin. Among them, patients with uNGAL ≥ 220 ng/ml had a significantly lower rate of response to terlipressin and albumin (33 vs 70%; $p = 0.015$; Fig. C). After adjusting for serum creatinine, uNGAL ≥ 220 ng/ml was independently associated with a higher risk of non-response (aOR = 4.55, 95% CI = 1.28–16.67; $p = 0.02$).

In multivariable analysis (adjusted for age, MELD, ACLF, leukocytes and type of AKI) uNGAL was an independent predictor of in-hospital mortality (aOR = 1.74 [95% CI = 1.26–2.38]; $p = 0.001$) and 90-day mortality (aHR = 1.32 [95% CI = 1.13–1.55]; $p = 0.001$). Probability of survival was significantly lower in patients with uNGAL ≥ 220 ng/ml (57% vs 30%; $p < 0.001$; Fig. D).

Conclusion: uNGAL is an excellent biomarker for the differential diagnosis of AKI in cirrhosis, it predicts response to treatment with terlipressin and albumin in patients with HRS-AKI and is an independent predictor of mortality.

OS063

CLEARED Global consortium results highlight regional variation and need for equity in inpatient outcomes in hospitalized patients with Chronic Liver Disease

Jasmohan S. Bajaj¹, Patrick S. Kamath², Florence Wong³, Peter Hayes⁴, Ramazan Idilman⁵, Aldo Torre⁶, Mark Topazian², Jacob George⁷, Mario Reis Álvares-da-Silva⁸, Qing Xie⁹, Shiv Kumar Sarin¹⁰, Abha Nagral¹¹, Ajay Haveri¹¹, Sumeet Asrani¹², Mohammad Amin Fallahzadeh¹³, Somaya Albhaisi¹⁴, Rajender Reddy¹⁵, Suditi Rahematpura¹⁶, Marie Jeanne Lohoues¹⁷, Belimi Hibat Allah¹⁸, Ricardo Cabello¹⁹, Ruveena Bhavani²⁰, Nik MA Nik Arsyad²¹, Sombat Treeprasertsuk²², Salisa Wejnaruemarn²³, Jose Luis Perez Hernandez²⁴, Godolfino Miranda Zazueta²⁵, Neil Rajoriya²⁶, Rosemary Faulkes²⁷, Danielle Adebayo²⁸, James Kennedy²⁹, Abdullah Emre Yildirim³⁰, Sezgin Barutcu³¹, CE Eapen³², Ashish Goel³³, Ajay Kumar Duseja³⁴, Anoop Saraya³⁵, Jatin Yegurla³⁵, Akash Gandotra³⁶, Mohd. Rela³⁷, Dinesh Jothamani³⁸, Anand Kulkarni³⁹, Mithun Sharma³⁹, Amey Sonavane⁴⁰, Hugo E. Vargas⁴¹, David Bayne⁴², Ramazan Idilman⁵, Feyza Gunduz⁴³, Rahmi Aslan⁴⁴, Anil Arora⁴⁵, Ashish Kumar⁴⁶, Andrew Keaveny⁴⁷, Paul J. Thuluvath⁴⁸, Somya Sheshadri⁴⁹, Dalia Allam⁵⁰, Yashwi Haresh Kumar Patwa⁵⁰, Mauricio Castillo⁵¹, Hiang Keat Tan⁵², Liou Wei Lun⁵³, Jawaid Shaw⁵⁴, Edith Okeke⁵⁵, David Nyam P⁵⁵, Diana Yung⁵⁶, Scott Biggins⁵⁷, Natalia Filipek⁵⁸, Andres Duarte Rojo⁵⁹, Carlos Benitez⁶⁰, Sebastián Marciano⁶¹, Hailemichael Desalegn⁶², Henok Fisseha⁶², Helena Katchman⁶³, Liane Rabinowich⁶³, René Malé Velazquez⁶⁴, Lilian Torres Made⁶⁴, Maria Sarai González-Huezo⁶⁵, Aloysius Aravinthan⁶⁶, Suresh Vasan Venkatachalapathy⁶⁷, Damien Leith⁶⁸, Ewan Forrest⁶⁹, Zeki Karasu⁷⁰, Dominik Bettinger⁷¹, Michael Schultheiss⁷¹, Zhujun Cao⁷², Brian Bush⁷³, Leroy Thacker⁷⁴.

ORAL PRESENTATIONS

¹Virginia Commonwealth University and McGuire VA Medical Center; ²Mayo Clinic; ³University of Toronto; ⁴Royal Infirmary of Edinburgh; ⁵Gastroenterology, Ankara University School of Medicine; ⁶Instituto Nacional De Ciencias Médicas y Nutrición Salvador Zubirán; ⁷The University of Sydney; ⁸Hospital de Clínicas de Porto Alegre; ⁹Ruijin Hospital, Shanghai Jiaotong University School of Medicine; ¹⁰Hepatology, Institute of Liver and Biliary Sciences, New Delhi, India; ¹¹Jaslok Hospital, Mumbai, India; ¹²Aaylor Simmons Transplant Institute, Baylor University Medical Center, Baylor Scott & White All Saints Medical Center; ¹³Baylor Dallas (Baylor University Medical Center); ¹⁴Virginia Commonwealth University; ¹⁵Medicine, University of Pennsylvania; ¹⁶GI/Hepatology, University of Pennsylvania; ¹⁷CHU De Cocody; ¹⁸Mustapha University Hospital; ¹⁹University of Pittsburgh; ²⁰University of Malaysia, Kuala Lumpur, Malaysia; ²¹University of Malaya Medical Centre, Malaysia; ²²Chulalongkorn University; ²³Hepatology, King Chulalongkorn Memorial Hospital; ²⁴Hospital General de México "Dr. Eduardo Liceaga"; ²⁵Gastroenterology, Hospital De Nutrición; ²⁶Liver Unit, University Hospitals Birmingham Queen Elizabeth, Birmingham, UK; ²⁷NIHR Birmingham Biomedical Research Centre, Centre for Liver and Gastroenterology Research, University of Birmingham, UK; ²⁸Royal Berkshire Hospital; ²⁹Royal Berkshire NHS Trust; ³⁰Gastroenterology, Gaziantep University School of Medicine; ³¹Gaziantep University Faculty of Medicine Gastroenterology Department; ³²Gastroenterology, Christian Medical College, Vellore; ³³Hepatology, Christian Medical College, Vellore; ³⁴Hepatology, Postgraduate Institute of Medical Education and Research, Chandigarh; ³⁵Gastroenterology and Human Nutrition Unit, All India Institute of Medical Sciences, New Delhi; ³⁶PGIMER Chandigarh India; ³⁷Dr. Rela Institute and Medical Centre; ³⁸Department of Liver Transplant Surgery, Dr. Rela Institute and Medical Centre; ³⁹Asian Institute of Gastroenterology, Hyderabad, India; ⁴⁰Apollo Hospital; ⁴¹Mayo Clinic, Arizona; ⁴²Gastroenterology, Mayo Clinic Arizona; ⁴³Gastroenterology, Marmara University School of Medicine; ⁴⁴Marmara University Pendik Research and Training Hospital; ⁴⁵Gastroenterology & Hepatology, Sir Ganga Ram Hospital; ⁴⁶Gastroenterology, Sir Ganga Ram Hospital, New Delhi; ⁴⁷Transplant, Mayo Clinic; ⁴⁸Mercy Medical Center & University of Maryland School of Medicine, Baltimore, MD; ⁴⁹Mercy Medical Center; ⁵⁰Ibn Sina Center for Gastroenterology & Liver Disease; ⁵¹Hospital De Especialidades Centro Médico Nacional La Raza, México; ⁵²Gastroenterology & Hepatology, Singapore General Hospital; ⁵³Singapore General Hospital; ⁵⁴McGuire VA Medical Center; ⁵⁵Jos University Teaching Hospital; ⁵⁶Royal Infirmary of Edinburgh; ⁵⁷University of Washington, Department of Medicine; ⁵⁸University of Washington; ⁵⁹University of Pittsburgh Medical Center; ⁶⁰Gastroenterology, Pontificia Universidad Católica De Chile; ⁶¹Hepatology and Department of Research, Hospital Italiano De Buenos Aires, Argentina; ⁶²St. Paul's Hospital Millennium Medical College; ⁶³Tel Aviv Sourasky Medical Center; ⁶⁴Instituto De Salud Digestiva y Hepática; ⁶⁵Centro Médico ISSEMYM; ⁶⁶University of Nottingham; ⁶⁷NIHR Nottingham Biomedical Research Centre, Nottingham University Hospitals; ⁶⁸Glasgow Royal Infirmary; ⁶⁹Gastroenterology, NHS Greater Glasgow and Clyde; ⁷⁰Center of Liver Transplantation, Department of Gastroenterology, Ege University; ⁷¹University Medical Center Freiburg; ⁷²Department of Infectious Diseases, Ruijin Hospital, Shanghai Jiao Tong University School of Medicine; ⁷³Virginia Commonwealth University; ⁷⁴Biostatistics, Virginia Commonwealth University; Email: jasmohan.bajaj@vcuhealth.org

Background and aims: A global study with equitable participation for cirrhosis and chronic liver disease (CLD) outcomes is needed. We initiated the Chronic Liver disease Evolution And Registry for Events and Decompensation (CLEARED) study to provide this global

perspective. Aim to evaluate determinants of inpatient mortality and organ dysfunction in a multi-center worldwide study.

Method: We prospectively enrolled pts with CLD/Cirrhosis >18 years without organ transplant or COVID-19 who were admitted non-electively. To maintain equity in outcome analysis, a maximum of 50 pts/site were allowed. Data for admission variables, hospital course, and inpatient outcomes (ICU, death, organ dysfunction [ODF]) were recorded. This was analyzed for death and ODs using significant variables on admission and including World Bank classification of low/middle-income countries (LMIC). A model for in-hospital mortality for all variables during the hospital course, including ODs) was analyzed.

Results: 1383 pts (55 ± 13 yrs, 64% men, 39% White, 30% Asian, 10% Hispanic, 9% Black, 12% other) were enrolled from 49 centers (Fig A). 39% were from high-income while the rest were from LMICs. Admission MELDNa 23 (6–40) with history in past 6 months of hospitalizations 51%, infections 25%, HE 32%, AKI 23%, prior LVP 15%, hydrothorax 8% and HCC 4%. Leading etiologies were Alcohol 46% then NASH 23%, HCV 11% and HBV 13%. Most were on lactulose 52%, diuretics 53%, PPI 49% and statins 11%, SBP prophylaxis 16%, beta-blockers 35% and rifaximin 31%. 90% were admitted for liver-related reasons; GI bleed 30%, HE 34%, AKI 33%, electrolyte issues 30%, anasarca 24% and 25% admission infections. In-hospital course: Median LOS was 7 (1–140) days with 25% needing ICU. 15% died in hospital, 3% were transplanted, 46% developed AKI, 15% grade 3–4 HE, 14% shock, 13% nosocomial infections and 13% needed ventilation.

Logistic Regression: Fig B shows that liver-related/unrelated factors on admission which predicted in-hospital mortality and development of organ dysfunction with MELDNa and Infections being common among all models. Nosocomial infections and organ dysfunctions predicted mortality when all variables were considered. High-income countries had better mortality outcomes likely due to transplant and ICU availability. AUCs were >0.75.



Fig B	AUC(95% CI)	Variables linked with higher risk of Outcome			Variables linked with lower risk of Outcome		
		Variable	OR (95% CI)	P value	Variable	OR (95% CI)	P value
Inpatient mortality	0.81 (0.77-0.84)	Age	1.02 (1.01-1.03)	<0.001	Transplant listing	0.46 (0.26-0.84)	0.01
Inpatient mortality all variables	0.91 (0.89-0.93)	AKI	1.31 (1.09-1.53)	<0.001	SBP prophylaxis	0.44 (0.29-0.74)	<0.001
		Admission infection	2.69 (1.75-4.33)	<0.001			
		Low vs High Income	6.15 (1.35-28.04)	<0.001			
		Nosocomial infections	2.61 (1.54-4.42)	0.0004	Prior LVP	0.48 (0.22-0.96)	0.04
Grade 3-4 HE admission variables	0.77 (0.73-0.81)	MELD-Na	1.05 (1.02-1.09)	0.002	Transplant listing	0.44 (0.29-0.68)	0.04
		In hospital AKI	1.38 (1.04-1.82)	<0.001	SBP prophylaxis	0.45 (0.23-0.88)	0.02
		Grade 3-4 HE	3.27 (1.88-5.60)	<0.001			
		Ventilation	2.37 (1.42-4.24)	0.004			
Ventilation admission variables	0.75 (0.71-0.79)	Shock	1.86 (1.32-2.61)	<0.001			
		ICU transfer	1.89 (1.07-3.34)	0.03			
		Low vs High Income	8.72 (1.38-52.02)	<0.001			
		Prior HE	4.43 (1.25-15.54)	<0.001	Prior variceal bleed	0.56 (0.37-0.85)	0.0017
Shock admission variables	0.78 (0.75-0.82)	Beta-blockers	1.60 (1.08-2.36)	0.02	Prior HCC	0.21 (0.05-0.88)	0.03
		MELD-Na	1.05 (1.02-1.07)	<0.001	Diuretic use	0.67 (0.47-0.97)	0.03
		AKI	1.73 (1.22-2.46)	0.002			
		Low vs High Income	1.70 (1.09-2.72)	0.02			
AKI admission variables	0.85 (0.83-0.88)	Prior HE	1.64 (1.09-2.48)	0.02	Lactulose	0.62 (0.40-0.96)	0.03
		Transplant listing	1.63 (1.09-2.46)	0.02	African/White vs Asian	0.19 (0.04-0.83)	<0.0001
		Infection in 6 mths	1.59 (1.09-2.33)	0.02			
		Statins use	2.04 (1.14-3.67)	0.01			
HE admission variables	0.78 (0.75-0.82)	MELD-Na	1.07 (1.04-1.09)	<0.001			
		AKI	1.64 (1.12-2.23)	0.001			
		Other vs Asian	1.80 (1.12-2.71)	<0.001	Prior hydrothorax	0.38 (0.17-0.87)	0.02
		MELD-Na	1.08 (1.05-1.10)	<0.001	Hospitalized prior 6 mths	0.45 (0.43-0.99)	0.04
AKI admission variables	0.85 (0.83-0.88)	AKI	2.46 (1.47-4.07)	<0.001			
		Age	1.07 (1.02-1.09)	<0.001			
		Others vs Asian	1.67 (1.12-2.49)	0.004			
		MELD-Na	1.15 (1.12-1.17)	<0.001			
HE admission variables	0.85 (0.83-0.88)	AKI	2.45 (1.47-4.07)	<0.001			
		AKI	6.78 (4.48-10.25)	<0.001			
		Prior HE	1.46 (1.06-2.02)	0.02			
		Prior HE	1.46 (1.06-2.02)	0.02			

Conclusion: In this worldwide equitable experience, admission cirrhosis severity and infections are associated with inpatient outcomes, which are greater in low-income settings. Liver-related and unrelated factors and regional variations are important in defining critical care goals and outcome models in inpatients with cirrhosis.

OS064

Maladaptive tubular repair is a harbinger of chronic kidney disease development in critically-ill cirrhosis patients admitted to intensive care unit-a prospective cohort study

Rakhi Maiwall¹, Sama Siva Rao Pasulapati², Archana Rastogi³, Ashini Hidam⁴, Guresh Kumar⁵, Sherin Thomas³, Anupam Kumar⁴, Shiv Kumar Sarin¹. ¹ILBS, Hepatology, India; ²Pachhunga University College, Statistics, Aizawl, India; ³ILBS, Pathology, New Delhi, India; ⁴ILBS, Clinical and Molecular Medicine, New Delhi, India; ⁵ILBS, Statistics, New Delhi, India
Email: shivsarin@gmail.com

Background and aims: Critically ill cirrhosis (CIC) patients with acute kidney injury (AKI), are predisposed to increased CKD risk. Renal tubular epithelial cells (RTECs) initiate repair mechanisms following tubular injury and failure of repair causes renal fibrosis. We evaluated serum Cystatin C (CysC), urinary neutrophil gelatinase-associated lipocalin (u-NGAL) and RTECs as risk factors of progressive AKI (AKI-Pro) and CKD in CIC.

Method: At enrolment we performed CysC, u-NGAL and urine microscopy (repeated at day 7) in all included patients. In a subset of patients (n = 30, 15-AKI-Prog and 15-AKI resolution), a panel of 17 renal biomarkers (in urine), endothelial injury and repair markers and monocyte-chemoattractant-protein-1 (MCP-1) (in plasma), mitochondrial biogenesis markers by QRT-PCR in RTECs was performed. Immunohistochemistry (IHC) for alpha-smooth muscle actin (α -SMA) and collagen (col) 1 and 3 was performed on post-mortem renal biopsies.

Results: Altogether, 369 CIC patients, aged 47.9 ± 11.4 years, 87% males, 84% with AKI at enrolment, sepsis-related AKI in 47%, hepatorenal syndrome in 42%, acute tubular necrosis in 27% were enrolled from august 2016 to September 2020. Of these, 24.9% patients had coarse granular casts, 34.4% had RTECs and 5.7% had albuminuria (>300 mg) at enrolment. At day seven, 58% had AKI-Prog. On median follow-up of 204 days [range 43–365]; 46% developed CKD and 30% died or underwent liver transplant. uNGAL and CysC correlated significantly with AKI cause, severity, presence of sepsis and progression at day 7 ($p < 0.001$). Presence and persistence of granular casts and RTECs, u-NGAL, serum CysC, SOFA scores and AKI-Prog at day seven were independent predictors CKD development in different multivariate competing risk models. Patients with AKI-Prog showed higher MCP-1, increase in renal endothelial injury and markers of fibrosis, a decrease in repair markers of tubular injury [significantly lower osteopontin, calbindin and epidermal growth factor] and failure of mitochondrial biogenesis [figure]. Post-mortem renal biopsies showed a predominance of chronic inflammatory infiltrate comprising of monocyte-macrophages and tubulointerstitial fibrosis, which correlated with uNGAL, CysC, AKI duration and IHC staining for α -SMA, col-1 and 3 [$p < 0.05$].

Conclusion: Almost two-thirds of CICs have AKI, which is often progressive, and associated with sepsis. NGAL and CysC can accurately predict AKI progression and CKD development. Persistence of RTECs in urinalysis at day-7 correlates with AKI progression and CKD development. The RTECs of patients with progressive AKI show loss of renal repair markers and failure of mitochondrial biogenesis. Infiltration with monocyte-macrophages plays a dominant role in renal fibrogenesis in CICs.

OS065

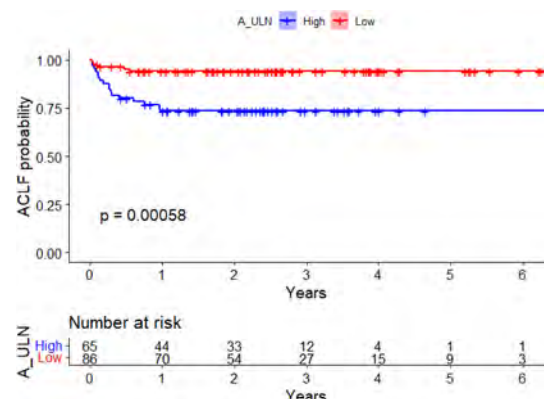
Hyperammonaemia defines the risk of acute-on-chronic liver failure in clinically stable outpatients with cirrhosis

María Pilar Ballester^{1,2}, Thomas H. Tranah³, Juan Antonio Carbonell-Asins², Annarein Kerbert⁴, Gonçalo Alexandrino⁵, Paloma Poyatos-García¹, Andra Caracostea³, Jose Sanchez-Serrano¹, Carmina Montoliu², Karen L. Thomsen⁶, Rajiv Jalan^{4,7}, Debbie L. Shawcross³. ¹Hospital Clínico Universitario de Valencia, Digestive Disease Department, Valencia, Spain; ²INCLIVA Biomedical Research Institute, Valencia, Spain; ³Institute of Liver Studies, School of Immunology and Microbial Sciences, King's College London, London, United Kingdom; ⁴Liver Failure Group, Institute for Liver and Digestive Health, University College London, Royal Free Campus, London, United Kingdom; ⁵Gastroenterology and Hepatology Department, Hospital Prof. Doutor Fernando Fonseca, Amadora, Portugal; ⁶Department of Hepatology and Gastroenterology, Aarhus University Hospital, Denmark; ⁷European Foundation for the Study of Chronic Liver Failure (EF CLIF) and the European Association for the Study of the Liver-Chronic Liver Failure (EASL-CLIF) Consortium
Email: t.tranah@nhs.net

Background and aims: Ammonia level correlates with the severity of hepatic encephalopathy and organ failure and is an independent predictor of mortality in patients with acute decompensation or acute-on-chronic liver failure (ACLF). However, its utility as a prognostic biomarker in patients with cirrhosis remains unclear. We hypothesized that hyperammonaemia predisposes to ACLF in outpatients with cirrhosis. We aimed to determine (i) whether hyperammonaemia is an independent risk factor for ACLF in clinically stable outpatients with cirrhosis, (ii) a threshold value of ammonia that defines this risk of ACLF, and (iii) its association with mortality.

Method: A prospective observational study of clinically stable cirrhotic outpatients followed-up in two tertiary hospitals was performed. Main outcomes were development of ACLF and mortality. Ammonia levels were normalized according to the upper limit of normality (A_{ULN}). Multivariable frailty competing risk modelling was performed with ACLF as event of interest and liver transplantation as a competing risk. Cut-off for A_{ULN} was calculated using maximally selected rank statistics and Kaplan-Meier curves with log-rank test were used to compare ACLF in the high and low risk groups and ACLF as risk factor for mortality.

Results: 603 patients were included (69% males; mean 56 years) with median follow-up of 215 days (range: 2–2453). A total of 68 (11%) patients developed ACLF. A_{ULN} was an independent predictor of ACLF (HR = 2.62; 95CI = 2.34–3.51; $p < 0.001$). Other risk factors were diabetes (HR = 2.6; 95CI = 1.57–4.37; $p < 0.001$), MELD score (HR = 1.1; 95CI = 1.03–1.10; $p < 0.001$) and albumin (HR = 0.5; 95CI = 0.30–0.85; $p = 0.001$). Using 1.48 as cut-off from the training set, statistically differences were found between high and low levels of A_{ULN} for ACLF ($p < 0.001$) in the test set (Figure 1). Overall survival was significantly lower in patients with ACLF (log-rank = 162; $p < 0.001$) and in patients with A_{ULN} >1.48 (log-rank = 19; $p < 0.001$).



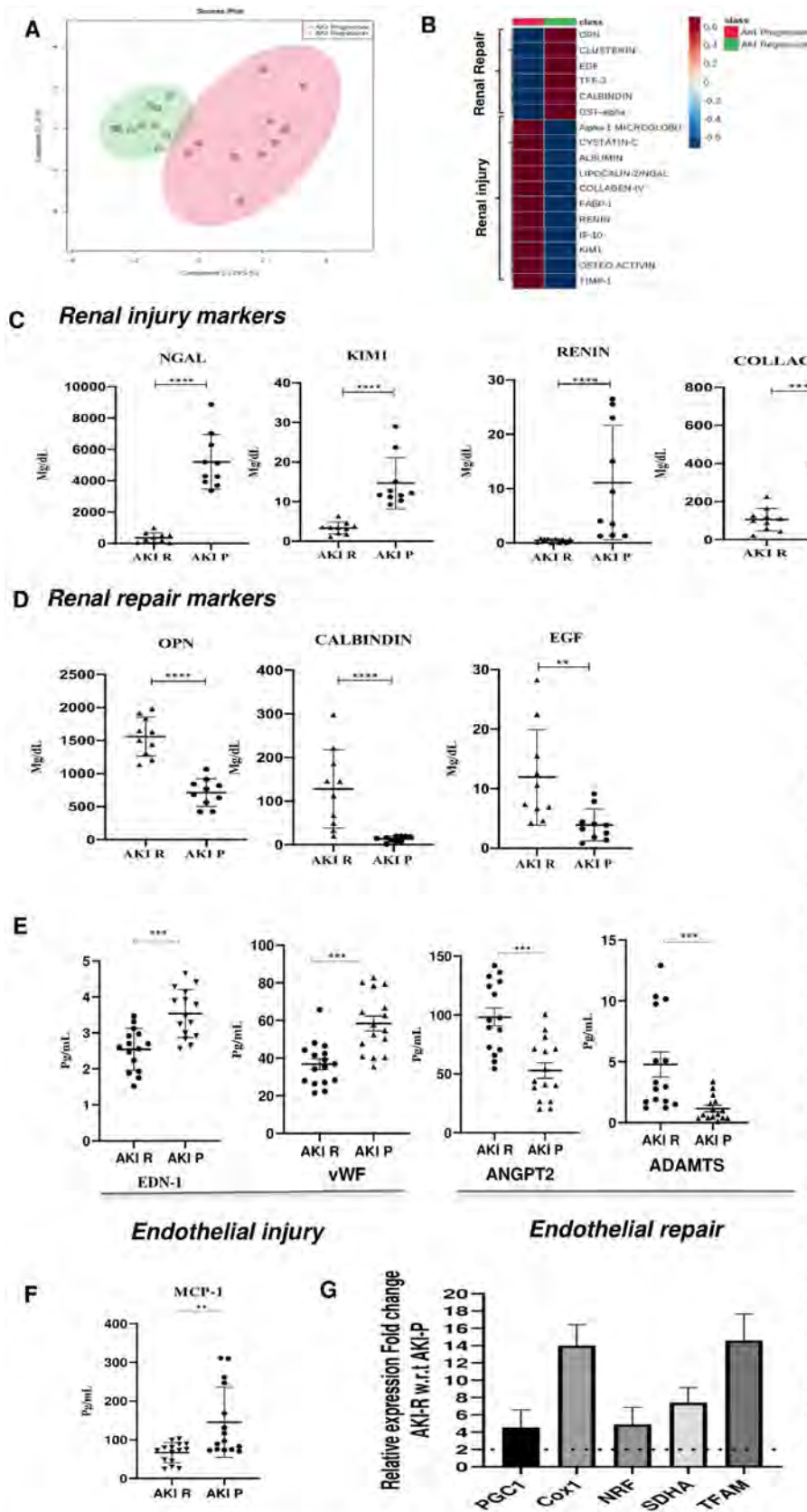


Fig.A&B Principal component analysis and heat map showing differentially expressed urine cytokines in AKI progression (AKI-P) vs. AKI resolution (AKI-R). **C&D**. Elevated renal injury markers such as NGAL (neutrophil gelatinase-associated lipocalin), renin and KIM-1 (kidney injury molecule-1), cystatin C and collagen IV and decreased repair markers osteopontin (OPN), calbindin and epidermal growth factor (EGF) in AKI-P vs. AKI-R. **E**. Endothelial injury endothelin-1 (EDN), von-Willebrand factor (vWF) were increased and protective marker ADAMTS (a disintegrin and metalloproteinase with thrombospondin motifs) and angiopoietin-2 (ANGPT2) were significantly decreased in AKI-P vs. AKI-R. **F**. Increased monocyte-chemoattractant protein-1 in AKI-P. **G**. Fold elevation in expression of various genes related to mitochondrial biogenesis [*peroxisome proliferator-activated receptor-gamma coactivator (PGC1)*, *cyclooxygenase-1 (Cox1)*, *nicotinamide riboside (NR)*, *succinate dehydrogenase (SDHA)*, *transcription factor A mitochondrial (TFAM)*] in exfoliated urine epithelial cells in AKI-R vs. AKI-P.

Monocyte chemoattractant protein-1 **Genes of mitochondrial biogenesis**

Figure: (abstract: OS064)

Conclusion: Ammonia is an independent predictor of ACLF and its associated mortality in clinically stable outpatients with cirrhosis. An ammonia level over 1.48 times the ULN defines the high-risk group for ACLF.

OS066

Predicting prognosis in large cohort of decompensated cirrhosis of liver (DCLD)- a machine learning (ML) approach

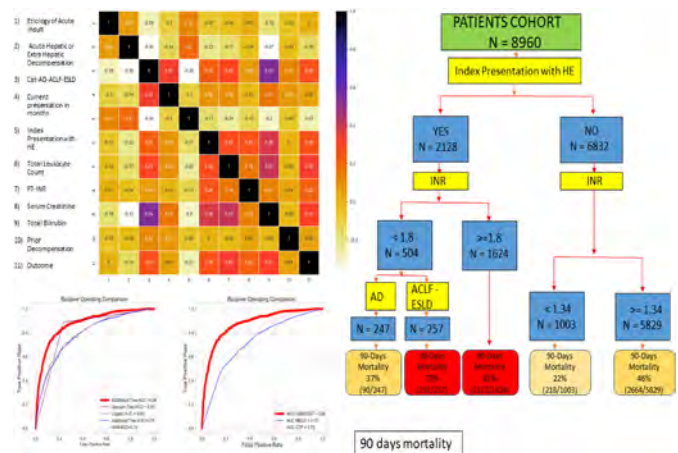
Ashok Choudhury¹, Vinod Arora¹, Kajali Mishra², Harshvardhan Tevethia¹, Vishal Kaushik¹, Babita Prasad¹, Manoj Kumar¹, Shiv Kumar Sarin¹. ¹Institute of Liver and Biliary Sciences, New Delhi, India; ²Henry Ford Hospital, Detroit, United States
Email: doctor.ashokchoudhury@gmail.com

Background and aims: Onset of decompensation in cirrhosis is associated with poor outcome. The current clinico-biochemical tools have limited accuracy in predicting outcomes reliably. Identifying the predictors with precision model on the big data using artificial intelligence may improve predictability. We aimed to develop a machine learning (ML) based prognostic model for predicting 90 day survival in patients of cirrhosis presenting with decompensation.

Method: We analysed electronic medical records retrospectively of hospitalised cirrhosis patients at the ILBS, with a complete 90-day follow-up. Clinical data, laboratory parameters and organ involvement were serially noted. AI-modelling was done after appropriate mining, feature engineering, splitted randomly into train and test-sets (20:80). The class imbalance problem was handled by random over-sampling technique, to make balanced 50:50 ratios. After 10-fold cross validation, 3 repetitions and grid search for optimal hyper parameters, the XGB-CV model was chosen. AUC was the primary selection criteria and confusion matrix was used to compare AUCs between AI-models and existing indices; CTP and MELD-score.

Results: Total of 6326 patients [mean age 48.2 ± 11.5 years, 84% male, Mean CTP 10.4 ± 2.2 and MELD Na- 30.4 ± 11.9 , alcohol 49.4%] were included. Ninety day mortality was 29.2%. Acute insult was identified in 80% cases; of which extra-hepatic 49%, hepatic 46% and unknown 5% cases respectively. The XGB-CV model had the best accuracy for prediction of 90 days event in the train set 0.90 (0.90–0.93), validation set 0.80 (0.79–0.81) and for overall dataset 0.80 (0.79–0.81). The AUC of the XGB-CV model was better than CTP and MELD Na-score by 16% and 15% respectively. The prediction model considered 43 variables; 18 of which predicted the outcome, and 10 maximum contributors are shown in concordance classifier. The most contributors to poor outcome included, index presentation as HE, diagnosis of AD/ACLF/ESLD, PT-INR, serum creatinine, total bilirubin, acute insult etiology, prior decompensation, acute hepatic or extrahepatic insult, leukocyte count and present duration of illness. In the Decision Tree Model, the presence of HE, PT-INR and syndromic diagnosis of AD or ACLF/ESLD was able to stratify the patients into low (22%), intermediate (23–46%) and high risk (>75%) of mortality at 90 days.

Conclusion: The AI based current model developed using a large data base of CLD patients presenting with decompensation immensely adds to the current indices of liver disease severity and can stratify patients at admission. Simple ML algorithms using HE and INR besides syndromic presentation, could help treatment decisions and prognostication.



Liver Immunology

OS067

Differential changes in global and antigen-specific B cell frequencies and function associate with the outcome of HBV nucleos (t)ide analog treatment withdrawal

Sabela Lens^{1,2}, Alice Burton¹, Jessica Davies¹, Mireia García-López², Anna Jeffery-Smith¹, Nikolai Novikov³, Simon Fletcher³, Sofia Pérez-del-Pulgar⁴, Xavier Forn², Mala Maini¹. ¹University College of London, Division of Infection and Immunity, United Kingdom; ²Hospital Clinic, Liver Unit, Barcelona, Spain; ³Gilead Sciences, United States; ⁴Liver Unit, Hospital Clínic, University of Barcelona, IDIBAPS, CIBERehd, Barcelona, Spain
Email: slens@clinic.cat

Background and aims: Despite HBsAg loss and the development of anti-HBs being the hallmark of natural resolution of HBV or achievement of 'functional cure', humoral immunity has not yet been examined in the setting of nucleos (t)ide analog (NA) discontinuation. We analysed HBcAg and HBsAg-specific frequencies and functional potential longitudinally in HBeAg-negative chronic Hepatitis B (CHB) patients stopping NA therapy to assess whether HBsAg loss ± off-treatment viral control associated with a recovery of the defective B cell response characteristic of CHB.

Method: Twenty-one HBeAg- CHB patients with complete viral suppression (>3 years) and without cirrhosis were studied prospectively. 16-colour flow cytometry was used to quantitate and phenotype circulating HBsAg- and HBcAg-specific B cells (dual fluorochrome-labelled antigen baits), global B cells, plasmablasts and Tfh at baseline, 12 and 48 weeks after stopping NA (W12 and W48). Cultured ELISPOTs were used to longitudinally evaluate antibody-secreting cells against HBsAg and HBcAg.

Results: After a median follow-up of 34 months (IQR 26–37), 16 (76%) patients remained off-therapy, with 5 (24% of the total cohort) losing HBsAg, whilst 5 (24%) required NA reintroduction. Frequencies of HBsAg and HBcAg-specific B cells were comparable between groups at baseline and did not correlate with levels of qHBsAg or HBcAg respectively, but did show differential temporal dynamics according to clinical outcome. HBcAg-specific B cells increased at W12 in all groups in association with viral rebound, but decreased to baseline values by W48 only among those achieving HBsAg loss or being re-treated. By contrast, patients remaining off-therapy had a significant increase in HBsAg-specific B cells by W48 compared to re-treated patients. Compared to patients remaining HBsAg+ after NA discontinuation, B cells in patients with HBsAg loss were enriched for the

ORAL PRESENTATIONS

activated memory phenotype and had a marked expansion of plasmablasts by W48. In parallel, ELISPOT data showed an increase in SFU against HBsAg in the 3 patients with HBsAg loss and anti-HBs+ by W48, confirming the recovery of antibody-producing functionality. **Conclusion:** Functional cure (HBsAg loss) and viral control following NA withdrawal associate with recovery of the low frequencies and poor functionality of HBV-specific B cells in CHB. These findings support larger studies to explore the use of B cells as biomarkers of clinical outcome and as targets for further immunotherapeutic boosting.

OS068

Enforced cytotoxic signature of HBV pol455-specific CD8+ T cells in chronic HBV infection

Kathrin Heim^{1,2}, Sagar Sagar¹, Maike Hofmann¹, Robert Thimme¹.

¹University Hospital Freiburg, Freiburg im Breisgau, Germany;

²University of Freiburg Faculty of Biology, Freiburg im Breisgau, Germany

Email: robert.thimme@uniklinik-freiburg.de

Background and aims: T-cell exhaustion represents a distinct T-cell differentiation program associated with chronic viral infections. Several studies have shown that exhausted CD8+ T cells are heterogeneous. In chronic HBV infection, we and others observed major differences in the phenotype and function as well as in the degree of dysfunction of HBV-specific CD8+ T cells targeting different antigens. The aim of this study was to investigate the molecular heterogeneity of HBV-specific CD8+ T cells targeting different antigens. **Method:** To determine the subset diversification of HBV-specific CD8+ T cells targeting different antigens, we performed high-throughput single-cell RNA sequencing using CEL-Seq2 technology. We obtained HBVcore₁₈- and HBVpol₄₅₅-specific CD8+ T cells from HBeAg negative chronically HBV-infected patients who endogenously control the viral infection as well as under NUC treatment. Phenotypic and functional analyses were performed after pMHC tetramer-based enrichment and peptide-specific expansion.

Results: Cluster analysis of single-cell transcriptomes revealed a different subset diversification of HBVcore₁₈- versus HBVpol₄₅₅-specific CD8+ T cells. In particular, HBVcore₁₈-specific CD8+ T cells were mostly comprised of precursor/memory-like exhausted T-cell subsets. Within HBVpol₄₅₅-specific CD8+ T cells, we could identify a cluster of cells that highly expressed cytotoxic genes including *GNLY*, *GZMB* and *PRF1*. Moreover, the cytotoxic regulator *NKG7* was also elevated in this subset. Interestingly, we further observed that the cytotoxic subset is restricted to HBVpol₄₅₅-specific CD8+ T cells obtained from patients who endogenously control the viral infection indicating that the enforced cytotoxic signature may be linked to virological HBV control in these patients. The differential transcriptional profile of HBVpol₄₅₅-specific CD8+ T cells was further confirmed *ex vivo* after pMHC tetramer-based enrichment. Indeed, at the protein level, we detected a terminal effector differentiation and higher cytotoxic effector capacity of HBVpol₄₅₅-specific CD8 T cells obtained from treatment-naïve patients in comparison to patients requiring antiviral therapy.

Conclusion: In sum, our data highlight an enforced cytotoxic signature in HBVpol₄₅₅-specific CD8+ T cells of treatment-naïve patients which may be related to virological control in these patients. This observation might have potential implications for the design of immunotherapeutic approaches in HBV cure.

OS069

Humoral and cellular immune responses to SARS-CoV-2 vaccination across multiple vaccine platforms and liver disease types: an EASL registry multicentre prospective cohort study

Thomas Marjot^{1,2,3}, Sam Murray⁴, Elisa Pose^{5,6}, Zixiang Lim⁷, Maria Carlota Londoño^{5,6}, Melanie Wittner^{8,9}, Marc Luetgehetmann^{8,10}, Virginia Hernandez-Gea^{11,12,13}, Juan Carlos Garcia Pagan^{11,12}, Golda Schaub¹⁴, Paul Duengelhoeft¹⁵, Martina Sterneck¹⁴, Ansgar W. Lohse^{8,13,14,16}, Palak Trivedi¹⁷, Khushpreet Bhandal¹⁸, Benjamin H. Mullish¹⁹, Pinelopi Manousou¹⁹, Patrizia Burra²⁰, Floriana Facchetti²¹, Susan L. Dobson²², Alexandra S. Deeks²³, Lance Turtle²², Paul Klenerman^{4,24}, Susanna Dunachie⁴, Pere Ginès^{5,6}, Massimo Iavarone²⁵, Julian Schulze zur Wiesch^{8,14}, Francesco Paolo Russo²⁰, Eleanor Barnes⁴ and On behalf of the EASL Covid-Hep network, OCTAVE study, and PITCH consortium²⁶. ¹Oxford Liver Unit, Oxford University Hospitals NHS Foundation Trust, Oxford, UK; ²Nuffield Department of Clinical Medicine, University of Oxford, Oxford, UK; ³Oxford Centre for Diabetes, Endocrinology and Metabolism (OCDEM), NIHR Oxford Biomedical Research Centre, Churchill Hospital, University of Oxford, Oxford, UK; ⁴University of Oxford, Nuffield Department of Clinical Medicine, Oxford, United Kingdom; ⁵Centro de Investigación Biomédica en Red de Enfermedades Hepáticas y Digestivas (CIBERehd), Barcelona, Spain; ⁶University of Barcelona, Institut de Recerca Biomèdica August Pi-Sunyer (IDIBAPS), Liver Unit, Hospital Clínic de Barcelona, Barcelona, Spain; ⁷Oxford University Hospitals NHS Foundation Trust, Oxford, UK; ⁸German Center for Infection Research (DZIF), Partner Site Hamburg-Lübeck-Borstel-Riems, Germany; ⁹Department of Internal Medicine, University Medical Center Hamburg-Eppendorf, Hamburg, Germany; ¹⁰Institute of Medical Microbiology, Virology and Hygiene, University Medical Center Hamburg-Eppendorf, Hamburg, Germany; ¹¹Institut d'Investigacions Biomèdiques August Pi i Sunyer (IDIBAPS), University of Barcelona, Barcelona Hepatic Hemodynamic Laboratory, Liver Unit, Hospital Clínic, Barcelona, Spain; ¹²Centro de Investigación Biomédica en Red de Enfermedades Hepáticas y Digestivas (CIBERehd), Barcelona, Spain; ¹³European Reference Network on Hepatological Diseases (ERN RARE-LIVER); ¹⁴University Medical Center Hamburg-Eppendorf, Department of Internal Medicine, Hamburg, Germany; ¹⁵Department of Immunology, University Medical Center Hamburg-Eppendorf, Martinistraße 52, 20249 Hamburg, Germany; ¹⁶Hamburg Center for Translational Immunology (HCTI); ¹⁷National Institute for Health Research Birmingham Biomedical Research Centre, Centre for Liver and Gastroenterology Research, Birmingham, United Kingdom; ¹⁸University Hospitals Birmingham NHS Foundation Trust, Birmingham, United Kingdom; ¹⁹Imperial College London, Department of Metabolism, Digestion and Reproduction, London, United Kingdom; ²⁰University of Padova, Department of Surgery, Oncology and Gastroenterology, Italy; ²¹Division of Gastroenterology and Hepatology, Fondazione IRCCS Ca' Granda Ospedale Maggiore Policlinico, Milan, Italy; ²²NIHR Health Protection Research Unit in Emerging and Zoonotic Infections, Institute of Infection, Veterinary and Ecological Sciences, University of Liverpool, UK; ²³Peter Medawar Building for Pathogen Research, Nuffield Dept. of Clinical Medicine, University of Oxford, UK; ²⁴Translational Gastroenterology Unit, University of Oxford; ²⁵Fondazione IRCCS Ca' Granda Ospedale Maggiore Policlinico, Division of Gastroenterology and Hepatology, Milan, Italy; ²⁶Nuffield Department of Medicine, University of Oxford, Oxford, UK
Email: ellie.barnes@ndm.ox.ac.uk

Abstract OS069 is under embargo until Friday 24 June 2022, 13:40 BST. It will be made publicly available on the congress website once the embargo has lifted.

Journalists, industry, investigators and/or study sponsors must abide by the embargo times set by EASL.

Violation of the embargo will be taken seriously. Individuals and/or sponsors who violate EASL's embargo policy may face sanctions relating to current and future abstract submissions, presentations and

visibility at EASL Congresses. The EASL Governing Board is at liberty to ban attendance and/or retract data.

Copyright for abstracts (both oral and poster) on the website and as made available during The International Liver Congress™ 2022 resides with the respective authors. No reproduction, re-use or transcription for any commercial purpose or use of the content is permitted without the written permission of the authors. Permission for re-use must be obtained directly from the authors.

OS070

CD8+ T cell acquisition of the LPS receptor within the hepatic stroma shapes anti-viral/anti-tumour potential

Laura J. Pallett¹, Mariana Diniz¹, Leo Swadling¹, Jessica Skelton², Alexander Maini³, Jessica Davies¹, Stephanie Kucykowicz¹, Nathalie Schmidt¹, Oliver E. Amin¹, Upkar Gill⁴, Alice Burton¹, Jenifer Sanchez⁵, Giuseppe Fusai⁶, Sabela Lens⁷, Sofia Pérez-del-Pulgar⁸, Patrick Kennedy⁴, Brian R. Davidson⁶, Muzlifah Haniffa⁹, Derek Gilroy³, Marcus Dörner², Anna Schurich⁵, Mala Maini¹. ¹University College London, Division of Infection and Immunity, London, United Kingdom; ²Imperial College London, Department of Medicine, London, United Kingdom; ³University College London, Division of Medicine, London, United Kingdom; ⁴QMUL, Barts and The London School of Medicine and Dentistry, London, United Kingdom; ⁵Kings College London, School of Immunology and Microbial Sciences, London, United Kingdom; ⁶University College London, Division of Surgery, London, United Kingdom; ⁷University of Barcelona, Hospital Clinic, August Pi i Sunyer Biomedical Research Institute, Barcelona, Spain; ⁸Liver Unit, Hospital Clínic, University of Barcelona, IDIBAPS, CIBERehd, Barcelona, Spain; ⁹Newcastle University, Faculty of Medical Sciences

Email: laura.pallett@ucl.ac.uk

Background and aims: Despite being bathed in bacterial products, the liver maintains a state of tolerance, exploited by HBV and tumours. The cellular basis mediating immune tolerance, yet allowing a rapid switch to immunity, needs to be better defined to deliver successful immunotherapy for the treatment of chronic HBV infection.

Method: We analysed the phenotype and function of CD14-expressing CD8 T cells directly *ex vivo* from resected/explanted human liver and explored their derivation, functionality, expansion and LPS-responsiveness in multiple *in vitro* and *in vivo* models.

Results: CD8 T cells expressing CD14 (and other LPS receptor components) were found to be compartmentalised in human liver and to preferentially accumulate amongst donor lymphocytes surviving in liver allografts, within HCC-infiltrating lymphocytes, and in cirrhotic ascites. Moreover, HBV-specific CD8 T cells were significantly enriched for the expression of CD14 compared to the residual, global CD8 T cell pool. CD14⁺CD8 T cells were highly activated and proliferative, with constitutive immunomodulatory features at rest (IL-10, IL-2 production) compared to CD14-CD8 T cells. They selectively expressed receptors (CXCR4/CD49a/CD49b) supporting retention with the stromal cell network to acquire CD14 from neighbouring macrophages. Human CD8 T cells acquire CD14, TLR4 and MD-2 from mononuclear phagocytes by actin cytoskeleton-dependent trogocytosis, promoted by E.coli, stromal cells and CXCL12. CD14 acquisition conferred the capacity to bind LPS and respond with a unique functional profile of chemotactic cytokines. Instead, upon TCR engagement, *ex vivo* and *in vitro*-derived CD14⁺CD8 T cells were poised to mount rapid, potent anti-viral effector function (IFN γ /TNF/MIPI1b). Importantly, CD14 acquisition by HBV-redirected CD8 T cells (HLA-A0201/HBs183-91) could be exploited to induce superior immunotherapeutic efficacy, with enhanced lysis of hepatoma cells expressing HBsAg (HepG2-PreS1-GFP).

Conclusion: A proportion of CD8 T cells compartmentalised in the liver express CD14/TLR4/MD2, recapitulated *in vitro* by trogocytosis from mononuclear phagocytes. CD14⁺CD8 T cells have enhanced TCR-directed effector function and can be induced to target HBV infection. Thus bacterial products in the gut-liver axis can therefore

ORAL PRESENTATIONS

fine tune organ-specific immunity by shaping stromal-interacting CD8 T cells with unique functionality.

OS071

A novel immunophenotyping of hepatocellular carcinoma based on amplified and mutated neoantigens for mRNA vaccine development

He Jing¹, Boqiang Liu¹, Liang Shi¹, Xiujuan Cai¹. ¹Zhejiang University, China

Email: srrsh_cxj@zju.edu.cn

Background and aims: Hepatocellular carcinoma (HCC) is the most common malignancy with poor prognosis. Genetic and phenotypic heterogeneity is a hallmark of HCC and also poses a daunting challenge for treatment. Recently, accumulating evidence suggests that immunotyping can indicate the comprehensive immune microenvironment, which is closely associated with therapeutic response and vaccination potential. In this study, we try to identify potent neoantigens in HCC for tumor immunotherapy, and further distinguish immune subtypes of HCC to construct an immune landscape for predicting the prognosis.

Method: Gene expression profiles, clinical information and simple nucleotide variation data of 328 HCC samples were obtained from TCGA. GEPIA was used to calculate differential expression levels, prognostic indices, and compare genetic alterations. TIMER was used to explore correlation between genes and immune infiltrating cells. Consensus cluster was used for consistency matrix construction and data clustering.

Results: Nineteen novel tumor neoantigens associated with poor prognosis and infiltration of antigen presenting cells were identified in HCC, including CDK1, CCNB1, CDC25C, PTTG1, CHEK1, KPNA2, MKI67, KIF2C, MCM3, EZH2, CDT1, PES1, PRC1, PPM1G, NEK2, TRIP13, TUBG1, AURKA, G6PD (Fig. A–C). Based on these neoantigens, we construct six immune subtypes (IS1-IS6, Fig. D). The immune subtypes showed distinct molecular, cellular and clinical characteristics. Patients with IS1 and IS3 tumors had a superior survival than those with the other subtypes (Fig. E). IS4 and IS6 tumors had immunosuppressive phenotype, and were also associated with higher tumor mutation burden and tumor stage (Fig. F–H). Furthermore, distinct expression of immune checkpoints and immunogenic cell death modulators was observed between different immune subtype tumors (Fig. I).

Conclusion: This study constructed a novel immunophenotyping of HCC for predicting the prognosis of patients. Meanwhile, CDK1, CCNB1, CDC25C, PTTG1, CHEK1, KPNA2, MKI67, KIF2C, MCM3, EZH2, CDT1, PES1, PRC1, PPM1G, NEK2, TRIP13, TUBG1, AURKA, G6PD are potent neoantigens for HCC-mRNA vaccine development, specifically for patients with IS4 and IS6 type.

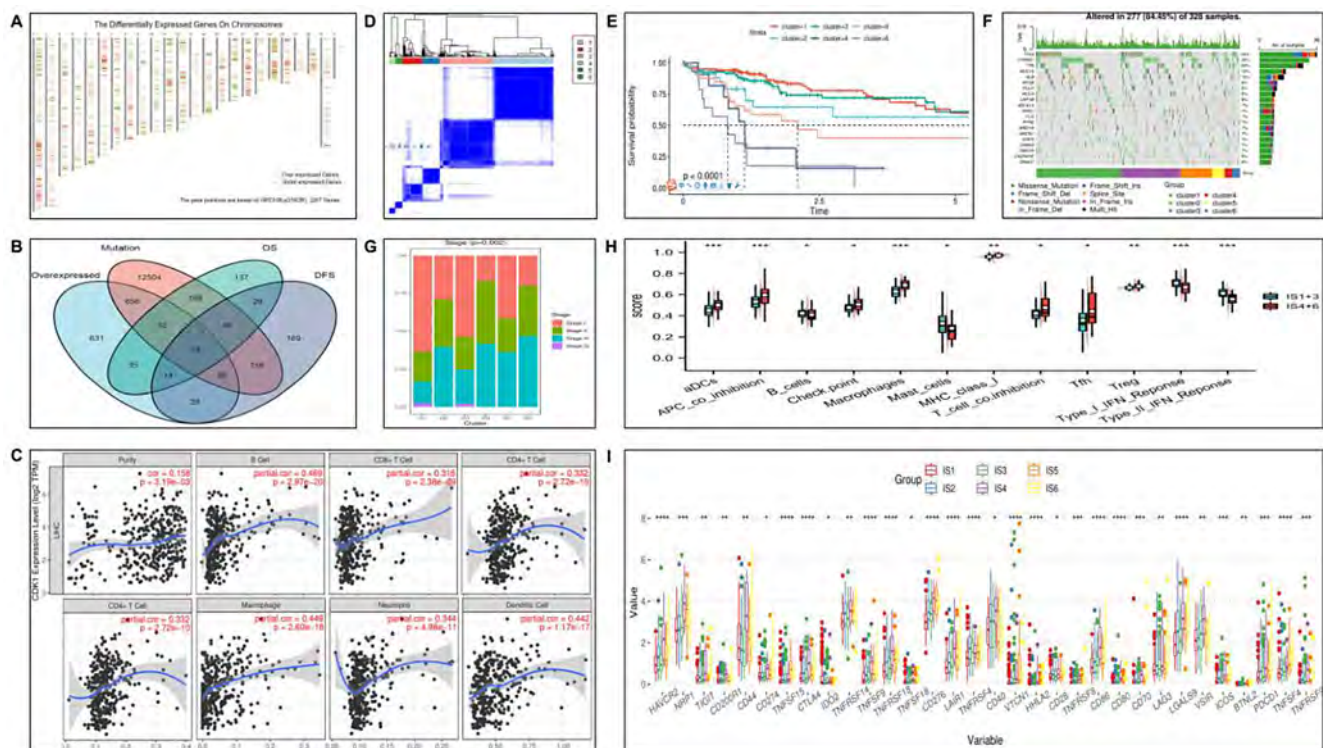


Figure: (abstract: OS071)

OS072A

T cell and humoral immune response to multiple SARS-CoV-2 variants including omicron (B.1.1.529) after two doses of COVID-19 vaccine in patients with cirrhosis and liver diseases requiring immunosuppression: data from the EASL COVID-Hep network

Sam Murray¹, Stephanie Longuet², Tom Tipton², Maria Carlota Londoño³, Elisa Pose³, Stephen Laidlaw², Dung Nguyen², Georgina Meacham¹, Zixiang Lim⁴, Stavros Dimitriadis¹, Sophie Irwin¹, Jonathan Cook⁵, Massimo Iavarone⁶, Pietro Lampertico⁶, Virginia Hernandez-Gea^{7,8,9}, Juan Carlos Garcia Pagan^{7,8,9}, Julian Schulze zur Wiesch^{10,11}, Martina Sterneck¹⁰, Francesco Paolo Russo¹², Jack Satsangi¹³, Susanna Dunachie^{1,14}, Paul Klenerman^{1,13}, Carl Goodyear¹⁵, Iain B. McInnes¹⁵, Pere Ginès⁷, Miles Carroll², Thomas Marjot^{1,16}, Eleanor Barnes^{1,16}. ¹University of Oxford, Nuffield Department of Medicine, United Kingdom; ²University of Oxford, Wellcome Centre for Human Genetics; ³University of Barcelona, Liver Unit, Hospital Clínic de Barcelona; ⁴Oxford University Hospitals NHS Foundation Trust, Department of Gastroenterology; ⁵University of Oxford, Centre for Statistics in Medicine and Surgical Interventions Trials Unit, Nuffield Department of Orthopaedics, Rheumatology and Musculoskeletal Sciences; ⁶Foundation IRCCS Ca' Granda Ospedale Maggiore Policlinico; ⁷University of Barcelona, Liver Unit, Hospital Clinic, Institut d'Investigacions Biomèdiques August Pi i Sunyer (IDIBAPS); ⁸Centro de Investigación Biomédica en Red de Enfermedades Hepáticas y Digestivas (CIBERehd); ⁹Health Care Provider of the European Reference Network on Rare Liver Disorders (ERN-Liver); ¹⁰University Medical Center Hamburg-Eppendorf, Department of Internal Medicine; ¹¹German Center for Infection Research (DZIF), Partner Site Hamburg-Lübeck-Borstel-Riems; ¹²University of Padova, Department of Surgery, Oncology and Gastroenterology DISCOG; ¹³University of Oxford, Translational Gastroenterology Unit, Nuffield Department of Experimental Medicine; ¹⁴University of Oxford, Oxford Centre for Global Health Research, Nuffield Department of Medicine; ¹⁵University of Glasgow, Institute of Infection, Immunity and Inflammation; ¹⁶Oxford University Hospitals NHS Foundation Trust, Oxford Liver Unit
Email: ellie.barnes@ndm.ox.ac.uk

Abstract OS072A is under embargo until Friday 24 June 2022, 13:40

BST. It will be made publicly available on the congress website once the embargo has lifted.

Journalists, industry, investigators and/or study sponsors must abide by the embargo times set by EASL.

Violation of the embargo will be taken seriously. Individuals and/or sponsors who violate EASL's embargo policy may face sanctions relating to current and future abstract submissions, presentations and visibility at EASL Congresses. The EASL Governing Board is at liberty to ban attendance and/or retract data.

Copyright for abstracts (both oral and poster) on the website and as made available during The International Liver Congress™ 2022 resides with the respective authors. No reproduction, re-use or transcription for any commercial purpose or use of the content is permitted without the written permission of the authors. Permission for re-use must be obtained directly from the authors.

ORAL PRESENTATIONS

OS072B

Humoral and cellular immune responses to wild-type and omicron (B.1.1.529) SARS-CoV-2 variants following a fourth COVID-19 vaccination in liver transplant recipients and patients with autoimmune hepatitis

Stavros Dimitriadis¹, Georgina Meacham¹, Sophie Irwin¹, Victoria Walker¹, Sam Murray², Zixiang Lim³, Thomas Marjot^{1,4}, Jack Satsangi⁵, Eleanor Barnes². ¹University of Oxford, Nuffield Department of Medicine, United Kingdom; ²Peter Medawar Building for Pathogen Research, Nuffield Department of Clinical Medicine, United Kingdom; ³Oxford University Hospitals NHS Foundation Trust, Department of Gastroenterology, United Kingdom; ⁴Oxford University Hospitals NHS Foundation Trust, Oxford Liver Unit, Oxford, United Kingdom; ⁵University of Oxford, Translational Gastroenterology Unit, United Kingdom

Email: ellie.barnes@ndm.ox.ac.uk

Abstract OS072B is under embargo until Friday 24 June 2022, 13:40 BST.

It will be made publicly available on the congress website once the embargo has lifted.

Journalists, industry, investigators and/or study sponsors must abide by the embargo times set by EASL.

Violation of the embargo will be taken seriously. Individuals and/or sponsors who violate EASL's embargo policy may face sanctions relating to current and future abstract submissions, presentations and visibility at EASL Congresses. The EASL Governing Board is at liberty to ban attendance and/or retract data.

Copyright for abstracts (both oral and poster) on the website and as made available during The International Liver Congress™ 2022 resides with the respective authors. No reproduction, re-use or transcription for any commercial purpose or use of the content is permitted without the written permission of the authors. Permission for re-use must be obtained directly from the authors.

Rare liver diseases (including paediatric and genetic)

OS073

In vivo CRISPR/Cas9 editing of the TTR gene with NTLA-2001 in patients with transthyretin amyloidosis- dose selection considerations

Edward J. Gane¹, Jörg Täubel², Björn Pilebro³, Marianna Fontana⁴, Justin Kao⁵, Michael Maitland⁶, Mark Stroh⁶, Jessica Seitzer⁶, Jonathan Phillips⁶, Kristy Wood⁶, Yuanxin Xu⁶, Carri Boisselle⁶, Adam Amaral⁶, Adam Boyd⁶, Jeffrey Cehelsky⁶, David Gustin⁷, Odelya Pagovich⁷, Laura Sepp-Lorenzino⁶, Liron Walsh⁶, David Lebowitz⁶, Gillmore Julian⁸. ¹The University of Auckland, New Zealand Liver Transplant Unit, Auckland, New Zealand; ²Richmond Pharmacology Limited, London, United Kingdom; ³Umeå University, Department of Public Health and Clinical Medicine, Sweden; ⁴University College London, National Amyloidosis Centre, Division of Medicine, United Kingdom; ⁵Auckland City Hospital, Department of Neurology, New Zealand; ⁶Intellia Therapeutics, Inc., Cambridge, United States; ⁷Regeneron Pharmaceuticals, Inc., Tarrytown, United States; ⁸University College London, United Kingdom

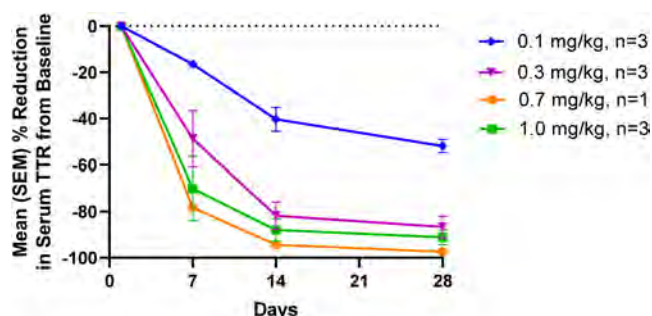
Email: edgane@adhb.govt.nz

Background and aims: The liver produces the toxic precursor protein transthyretin (TTR) in ATTR amyloidosis, a fatal disease of misfolded protein accumulation. Until recently, the only therapeutic

intervention for variant ATTR amyloidosis (ATTRv) was liver transplantation. Gene-silencing agents targeting TTR mRNA prevent disease progression but require lifelong administration. In contrast, gene editing is designed as a single-dose treatment. NTLA-2001 comprises a lipid nanoparticle (LNP) encapsulating mRNA for SpCas9 protein and single guide RNA targeting the transthyretin (TTR) gene. After infusion, LNP uptake into hepatocytes results in precise TTR knockout regardless of disease-causing mutation. This is the first report of the dose, exposure and pharmacodynamic (PD) response relationship in humans for systemically administered liver-directed gene-editing therapy.

Method: The first-in-human phase 1 trial (NCT04601051) enrolls adults with confirmed ATTRv amyloidosis and peripheral neuropathy. Safety, pharmacokinetics (PK), and PD of NTLA-2001 are assessed in 3+3 dose escalation, with a subsequent expansion cohort. Circulating serum TTR was measured in samples collected at baseline, Days 7, 14, and 28, and every 2 months thereafter. Dose selection for the expansion cohort is based on review of safety, PK and PD in the escalation phase.

Results: As of this submission, 14 subjects received NTLA-2001 as single-ascending doses [3 subjects each at 0.1, 0.3, and 0.7 mg/kg, and 5 subjects at 1 mg/kg]. Mild and transient infusion reactions were the most common adverse event with NTLA-2001. Interim pharmacokinetic data suggest that following intravenous (IV) infusion NTLA-2001 ionizable lipid exhibited a rapid decline from peak levels followed by a secondary peak and then a log-linear phase. Serum TTR levels were significantly reduced from baseline in a dose-dependent manner; patients receiving 0.3 mg/kg achieved durable reductions with mean Day 28 TTR reduction of 87% (n = 3) and greater reductions at higher doses (Figure 1, interim data to Day 28 from 10 subjects as of September 13, 2021). Additional data will be available for presentation.



Conclusion: A single IV infusion of the gene editing therapeutic NTLA-2001 resulted in dose-dependent reductions in serum TTR protein with predominately mild adverse events reported. NTLA-2001 represents a potential paradigm shift in the treatment of ATTR amyloidosis.

OS074

ACOX2 deficiency-induced liver fragility (ADILF), a not-so-rare inborn error in bile acid metabolism that responds to ursodeoxycholic acid treatment

Marta Alonso-Peña^{1,2}, Ricardo A. Espinosa-Escudero², Elisa Herraiz^{2,3}, Oscar Briz^{2,3}, María Luisa Cagigal⁴, Jesús González Santiago⁵, Aida Ortega-Alonso⁶, Conrado Manuel Fernández Rodríguez⁷, Luis Bujanda^{3,8}, Marta Calvo⁹, Delia D'Avola¹⁰, María Carlota Londoño^{3,11}, Moises Diago¹², José Fernández-Checa¹³, M. Carmen García-Ruiz¹³, Raul J. Andrade^{3,6}, Frank Lammert¹⁴, Jesus Prieto^{3,10}, Javier Crespo^{1,3,15}, Javier Juampérez Goñi¹⁶, Álvaro Díaz-González^{1,15}, María Monte^{2,3}, Jose Marin^{2,3}. ¹Research Institute Marques de Valdecilla (IDIVAL), Clinical and Translational Research in Digestive Pathology Group, Santander, Spain; ²University of Salamanca, Experimental Hepatology and Drug Targeting (HEVEPHARM), Salamanca, Spain; ³Carlos III National Institute of Health, Center for the Study of Liver and Gastrointestinal Diseases (CIBERehd), Madrid, Spain; ⁴Marques de Valdecilla University Hospital, Pathological Anatomy Service, Santander, Spain; ⁵University Hospital of Salamanca, Department of Gastroenterology and Hepatology, Salamanca, Spain; ⁶Institute of Biomedical Research of Málaga (IBIMA), University Hospital Virgen de la Victoria, Liver Unit, Gastroenterology Service, Málaga, Spain; ⁷Fundación Hospital Alcorcón, Rey Juan Carlos University, Gastroenterology Unit, Madrid, Spain; ⁸Biodonostia Health Research Institute. Donostia University Hospital, University of the Basque Country (UPV/EHU), Department of Liver and Gastrointestinal Diseases, San Sebastian, Spain; ⁹Segovia General Hospital, Segovia, Spain; ¹⁰Clinica Universidad de Navarra and Center for Applied Medical Research (CIMA), University of Navarra, Department of Medicine, Pamplona, Spain; ¹¹Hospital Clínic de Barcelona, University of Barcelona, Liver Unit, Barcelona, Spain; ¹²Valencia General University Hospital, Valencia, Spain; ¹³Institute of Biomedical Research of Barcelona (IIBB), Barcelona, Spain; ¹⁴Saarland University Medical Center, Department of Medicine II, Homburg, Germany; ¹⁵Marques de Valdecilla University Hospital, Gastroenterology and Hepatology Department, Santander, Spain; ¹⁶Vall d'Hebron University Hospital (HVH), Universitat Autònoma de Barcelona, Pediatric Hepatology and Liver Transplantation Unit, Barcelona, Spain

Email: martaalonsop@gmail.com

Background and aims: A variant (p.Arg225Trp) in peroxisomal acyl-CoA oxidase 2 (ACOX2), involved in bile acid (BA) side-chain shortening, has recently been associated with persistent unexplained hypertransaminasemia and accumulation of C27-BAs, mainly trihydroxycholestanic acid (THCA). Our aim was to investigate the prevalence of ACOX2 deficiency-induced liver fragility (ADILF) among patients with hypertransaminasemia of unknown origin and their response to ursodeoxycholic acid (UDCA), to identify other inborn errors that could cause this alteration and to elucidate its pathophysiological mechanisms.

Method: Serum BA profile was determined by HPLC-MS/MS. Genetic analysis of ACOX2 was performed by exon sequencing. In HuH-7 cells exposed to THCA, viability was determined by MTT, reactive oxygen species (ROS) production by flow cytometry and endoplasmic reticulum (ER) stress by analyzing GRP78 and CHOP levels (RT-qPCR and Western Blot), and XBP1-S/XBP1-U ratio (RT-qPCR). The 1000-Genomes database and SIFT and Polyphen scores were used to select ACOX2 variants that were expressed in HuH-7 cells to determine by HPLC-MS/MS its ability to metabolize THCA.

Results: Among 33 patients with suspected ADILF from 11 hospitals and 13 relatives, 7 individuals with abnormally high C27-BA levels (>50% of total BAs) were identified. The p.Arg225Trp variant was found in homozygosity in 2 patients and 3 relatives. Moreover, other 2 non-related patients were heterozygous carriers of different alleles, for c.673C>T (p.Arg225Trp) and c.456_459del (p.Thr154fs). Impaired expression of ACOX2, but not ACOX3 in the liver of these patients was found (immunohistochemistry). Treatment with UDCA normalized

ORAL PRESENTATIONS

transaminases levels. Culture of HuH-7 liver cells with THCA increased ROS production and the ER stress biomarkers GRP78, CHOP and XBP1-S/XBP1-U ratio, whereas decreased cell viability. THCA-induced toxicity was higher than that of major BAs. Among 14 in silico selected genetic variants, in vitro functional tests identified 6 ACOX2 variants as a potential cause of ADILE.

Conclusion: Dysfunctional ACOX2 is found in a substantial proportion of patients with unexplained hypertransaminasemia, suggesting that this disorder of BA metabolism causes enhanced liver fragility, which can be attenuated by UDCA treatment.

OS075

Efficacy and safety of givosiran in patients with acute hepatic porphyria: 36-month results of the phase 3 ENVISION randomised clinical trial

Manish Thapar¹, Herbert L. Bonkovsky², Susana Monroy³, Gayle Ross⁴, Encarna Guillén-Navarro^{5,6}, Maria Domenica Cappellini⁷, Anna-Elisabeth Minder⁸, Shangbin Liu⁹, Marianne T. Sweetser⁹, David Kuter¹⁰. ¹Thomas Jefferson University, Philadelphia, United States;

²Wake Forest University/North Carolina Baptist Medical Center, Winston-Salem, United States; ³Instituto Nacional de Pediatría, Mexico City, Mexico; ⁴Royal Melbourne Hospital, Melbourne, Victoria, Australia; ⁵Medical Genetics Section, Virgen de la Arrixaca University Hospital, IMIB-Arrixaca, Universidad de Murcia, Murcia, Spain; ⁶CIBERER-ISCIII, Madrid, Spain; ⁷University of Milan, Milan, Italy; ⁸Division of Endocrinology, Diabetes and Porphyria, Stadtspital Zürich, Zürich, Switzerland; ⁹Alnylam Pharmaceuticals, Cambridge, United States; ¹⁰Massachusetts General Hospital, Boston, United States
Email: manish.thapar@jefferson.edu

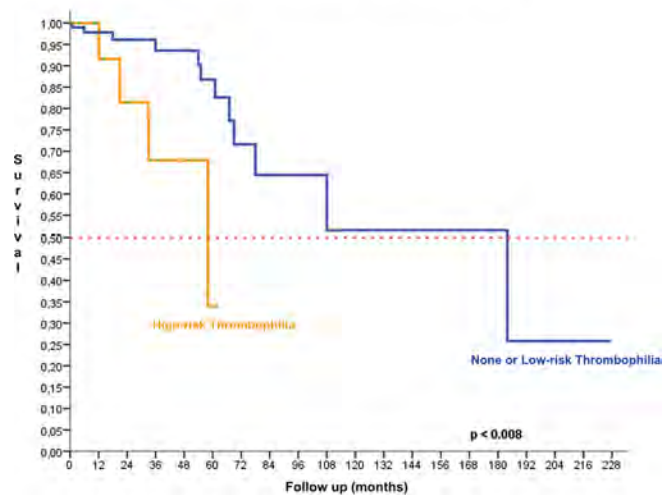
This abstract is under embargo until Thursday 23 June 2022, 13:30 BST. It will be made publicly available on the congress website once the embargo has lifted.

Journalists, industry, investigators and/or study sponsors must abide by the embargo times set by EASL.

Violation of the embargo will be taken seriously. Individuals and/or sponsors who violate EASL's embargo policy may face sanctions relating to current and future abstract submissions, presentations and visibility at EASL Congresses. The EASL Governing Board is at liberty to ban attendance and/or retract data.

Copyright for abstracts (both oral and poster) on the website and as made available during The International Liver Congress™ 2022 resides with the respective authors. No reproduction, re-use or transcription for any commercial purpose or use of the content is permitted without the written permission of the authors. Permission for re-use must be obtained directly from the authors.

Figure 1 - Survival without thrombosis recurrence according to the type of thrombophilia



Results: A thrombophilia was identified in 34/118 (29%) patients, of which 18/118 (15%) were a High-risk Thrombophilia. Thrombosis recurrence incidence rate was 2.94, 95CI = [0.00–6.22] per 100 patient-years (PY) at one year and 4.75, 95CI = [2.46–7.04] per 100 PY after a median follow-up of 19.5 months. The prevalence of thrombophilia did not differ significantly between groups with or without thrombosis recurrence ($p = 0.775$). However, presence of at least a High-risk Thrombophilia was significantly associated with thrombosis recurrence (RR = 4.2, 95CI = [1.18–14.91], $p = 0.026$) (Figure 1). Absence of portal recanalisation was significantly associated with thrombosis recurrence as compared to partial recanalisation (66.7% vs 32.4%, $p = 0.019$). Anticoagulation duration did not appear to be significantly associated with the risk of thrombosis recurrence. However, 91/115 (79%) received long-term anticoagulation (>6 months) while short-term anticoagulation (≤ 6 months) was administered in 24/115 (21%) patients. Thrombosis incidence rate was 5.48, 95CI = [0.00–11.50] per 100 PY in short term anticoagulation group as compared to 4.83, 95CI = [2.16–7.50] per 100 PY in long term anticoagulation group ($p = 0.47$).

Conclusion: In acute non-cirrhotic PVT secondary to local factors, a High-risk Thrombophilia is frequently identified, and increase the risk of thrombosis recurrence. The high number of patients treated by long term anticoagulation in our cohort, does not allow us to draw any conclusion about the potential protective role of anticoagulant.

OS077

Clinical utility of non-ceruloplasmin copper determined by copper speciation for monitoring Wilson disease therapy: comparative data analysis with 24-hour urinary copper excretion from the CHELATE trial

Michael Schilsky¹, Aurelia Poujois², Massimo Giovanni Zuin³, Peter Ott⁴, Karl Heinz Weiss⁵, David Cassiman⁶, Aftab Ala⁷, Anna Czlonkowska⁸, Nicolas Dubois⁹, Naseem Amin¹⁰, C. Omar Kamlin¹¹, ¹Yale University, Departments of Medicine and Surgery, Divisions of Digestive Diseases and Transplant and Immunology, Connecticut, United States; ²Fondation Hopital Rothschild, Paris, France; ³University of Milan, Milan, Italy; ⁴Aarhus University Hospital, Denmark; ⁵Salem Medical Center, Heidelberg, Germany; ⁶University of Leuven, Belgium; ⁷Kings College University Hospital, Institute of Liver Studies, London, United Kingdom; ⁸Institute of Psychiatry and Neurology, Warsaw, Poland; ⁹International Drug Development Institute (IDDI), Belgium; ¹⁰Orphalan SA France, Paris, France; ¹¹Orphalan SA France, France

Email: omarkamlin@doctors.org.uk

Background and aims: Monitoring efficacy of therapy in Wilson disease (WD) is challenging; 24-hour urinary copper excretion (24 hr

OS076

High-risk Thrombophilia predict early thrombosis recurrence in acute non-cirrhotic portal vein thrombosis related to local factors: LOCAPORT

Louise Lebedel¹, Aurélie Plessier², Odile Gorla³, Christophe Bureau⁴, Alexandra Heurgue-Berlot⁵, Pierre-Emmanuel Rautou², Audrey Payance², Kamal Zekrini², Thi Thu Nga Nguyen¹, Thong Dao¹, Rémi Morello¹, Isabelle Ollivier-Hourmand¹. ¹University of Caen Normandie Hospital Center, Caen, France; ²Beaujon Hospital, Clichy, France; ³Hospital Center University De Rouen, Rouen, France; ⁴Hospital Center University De Toulouse, Toulouse, France; ⁵CHU Reims, Department of Hepato-Gastroenterology, Reims, France
Email: louise.lebedel@gmail.com

Background and aims: A local factor is identified in 21% of acute non-cirrhotic portal vein thrombosis (PVT). We aim to determine the risk of thrombosis recurrence in this situation, and risk factors associated with recurrence.

Method: This is a retrospective multicenter study from the French Vascular Liver Diseases cohort between 1992 and 2021. We included acute non-cirrhotic portal vein thrombosis (right or left branch or portal vein extending or not to mesenteric and splenic veins), with at least one local factor (infectious, inflammatory, traumatic, surgical or neoplastic) identified, either concomitantly or in the last 3 months. We screened for prothrombotic factors such as 1st degree unprovoked personal or family history of deep vein thrombosis, High-risk Thrombophilia (myeloproliferative neoplasm, homozygous or composite heterozygous mutation of factor V Leiden and G20210 prothrombin gene, antiphospholipid syndrome, familial antithrombin deficiency), Low-risk Thrombophilia (heterozygous factor V Leiden or prothrombin gene G20210 mutation, hyperhomocysteinemia, protein C or S deficiency, homozygous MTHFR mutation), ongoing oestrogenic or pregnancy up to 6 weeks post-partum, paroxysmal nocturnal haemoglobinuria and Behçet's disease.

ORAL PRESENTATIONS

UCE) is cumbersome, and results show large intra-subject variability. A new non-ceruloplasmin copper assay using liquid chromatography and ICP mass spectroscopy (NCC-Sp) was developed for the CHELATE Trial [trientine tetrahydrochloride (TETA4) vs. d-Penicillamine (DPA)]. We aim to describe the intra-patient variability and compare the clinical utility of UCE and NCC-Sp in monitoring WD therapy.

Method: A multicentre, open label, non-inferiority randomised controlled trial was conducted in which 53 stable adult WD subjects were randomly allocated after a 12-week baseline observation period to either DPA or TETA4 for 24 w with a primary end point (NCC-Sp). An independent adjudication committee blinded to site and treatment allocation assessed clinical stability at randomisation and end of study. Paired samples for NCC-Sp and 24 hr UCE were compared pre- and 24w post-randomisation. Validation studies for NCC-Sp included 50 healthy adults, identifying a range (2.5% to 97.5%) of 40–150 mcg/L. This was used as reference target range for the study population and compared to UCE (recommended therapeutic range of 200–500 mcg/24 hr). Intra-patient (SD) variability was computed for NCC-Sp and UCE measurements during baseline and post-randomisation periods.

Results: The independent adjudication committee unanimously assessed all subjects as clinically stable at randomisation and study end point. NCC-Sp was in the reference range at randomization versus study end in 86% vs. 84% of subjects respectively, while UCE was in the recommended therapeutic range in only 41% vs. 37% respectively (Table). Agreement when both NCC-Sp and UCE were in range at randomization/study end was 17/49 (35%) and 17/51 (33%) respectively. Mean (SD) NCC-Sp and UCE intra-patient variability during baseline (all receiving DPA) was 15.5 (7.8) mcg/L and 196 (125) mcg/24hr respectively. Mean (SD) NCC-Sp intra-patient variability for DPA and TETA4 post randomisation was 17.9 (11.6) and 14.9 (12.1) mcg/L respectively ($p < 0.0001$). Mean (SD) UCE intra-patient variability for DPA and TETA4 post randomisation was 148.9 (127) and 107 (101) mcg/24 hr respectively ($p = 0.74$).

Conclusion: UCE is a test with significant intra-patient variability for WD patients on chelation therapy with either DPA or TETA4. That NCC-Sp had less intra-patient variability than UCE suggests NCC-Sp is a more reliable biomarker for monitoring chelation therapy in WD.

Table: Comparative analysis of “in range” data for NCC-Sp and UCE at randomization and study end point.

	At Randomisation			Primary End point (wk 24 post randomisation)		
	UCE in range**	UCE not in range**	Total	UCE in range**	UCE not in range**	Total
NCC-Sp in range	17	25	42	17	26	43
NCC-Sp not in range	3	4	7	2	6	8

*range for NCC-Sp = 40–150 mcg/L; **range for UCE = 200–500 mcg/24 hr.

OS078

North American evaluation of 2519 patients with primary sclerosing cholangitis: longitudinal patterns of disease activity identify and validate stable and progressive phenotypes

Marwa Ismail¹, John Eaton², Aliya Gulamhusein¹, Morven Cunningham³, Christina Plagiannakos³, Bettina Hansen¹, Gideon Hirschfield¹. ¹Institute of Health Policy Management and Evaluation, Health Services Research, Toronto, Canada; ²Mayo Clinic, Rochester, United States; ³UHN, Toronto Centre for Liver Disease, Toronto, Canada

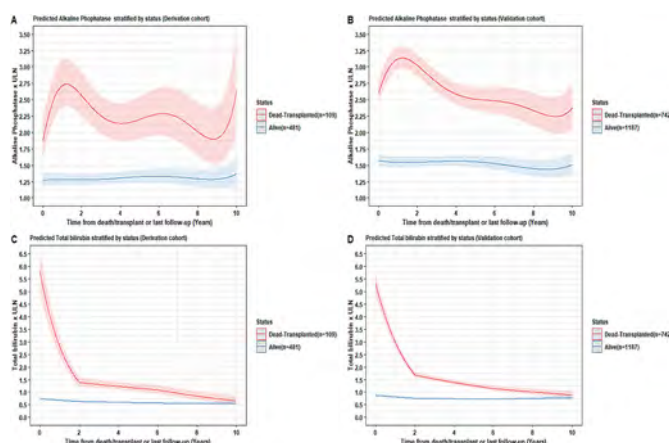
Email: marwa.ismail@uhn.ca

Background and aims: Markers of outcome in patients with primary sclerosing cholangitis fluctuate, reducing utility at single time points.

Longitudinal assessment offers an opportunity to improve surrogate marker utility.

Method: Using retrospectively collected data on 2519 North American patients diagnosed as per AASLD criteria with PSC, a derivation (Toronto: Jan. 2000 to Dec. 2020) and validation cohort (Mayo: Apr. 1978 to Dec. 2017) were evaluated to define progressive and stable disease states (PDS/SDS). Progressive disease was defined as death or transplant. Linear mixed-effects regression with random intercept and random slope was used to study biochemical and transient elastography (fibrosan) trajectories longitudinally over time. Piecewise linear splines and polynomial terms were employed. Time was calculated backwards from death, transplant, or last follow-up (time zero).

Results: Across combined cohorts median follow-up (IQR) was 8.3 (3.6–15) yrs, 63% were male, and mean age at diagnosis 39.5 (SD:16.1) yrs. 88.3% had large duct disease and 78% had IBD at last follow-up. Throughout the 10 yrs prior to death or transplant, patients with PDS in the derivation cohort had estimated ALP means ranging from 1.87–2.64 the upper limit of normal (ULN) with major fluctuations ($p < 0.01$); patients with SDS had lower and stable ALP courses (ALP 1.27–1.37 \times ULN). A similar pattern existed for the validation cohort, where patients with progressive disease had ALP 2.25–3.12 \times ULN, while patients with stable disease had ALP around 1.44–1.57 \times ULN ($p < 0.0001$). The derivation cohort experienced bilirubin (TB) elevation 6 yrs before experiencing death or transplant; similarly for the validation cohort bilirubin elevation was 8 yrs before event. Patients with SDS maintained normal bilirubin values. Both cohorts experienced increases in the 2 yrs prior to death or transplant to reach an estimated mean TB of $\sim 5 \times$ ULN ($p < 0.0001$). ALB and PLT estimated means were lower for patients with progressive disease than those with stable disease in both cohorts; estimated AST and ALT means were notably higher for patients with PDS vs those with SDS (derivation cohort: AST: 1.64–3.34 \times ULN vs 1.21–1.28 \times ULN; ALT: 2–2.83 \times ULN vs 1.56–1.7 \times ULN; validation cohort AST: 1.66–2.88 \times ULN vs 1.09–1.32 \times ULN; ALT 1.65–2.06 \times ULN vs 1.15–1.56 \times ULN) in both derivation and validation cohorts. In the Toronto derivation cohort patients with PDS had progressively increasing estimated transient elastography measurements from 10.8–31.3 kPa between yr 6 and time of death or transplant. Patients with SDS had transient elastography measurements over 6 yrs of study ranging from 7.7–9 kPa.



Conclusion: We evaluate progressive and stable disease phenotypes in >2500 PSC patients. A stable disease course was validated for patients with sustained ALP $< 1.5 \times$ ULN, as well as those with longitudinal transient elastography values < 10 kPa.

Nurses and AHP

OS079

Nurse-led inpatient fibrosis assessment for patients with suspected alcohol related liver disease and previous poor engagement with services

Rebecca Fennell¹, Dianne Backhouse¹, George Abouda¹, Lynsey Corless¹. ¹Hull University Teaching Hospitals NHS Trust, Kingston upon Hull, United Kingdom
Email: lynsey.corless@nhs.net

Background and aims: Identification and staging of fibrosis is a critical part of assessment for people with alcohol related liver disease. For those presenting acutely in hospital, staging tests are frequently deferred until out-patient review. However, engagement with elective services is often poor in those with ongoing alcohol use, leaving investigation incomplete and the need for hepatology follow-up uncertain. To mitigate this, we instituted an in-patient fibrosis assessment service within our Alcohol Care Team (ACT) and evaluated the results.

Method: From February 2020–October 2021, we sought out acutely admitted patients who had been identified as drinking excessively (more than the United Kingdom guidance of 14 units/week) and who had previously not engaged with the ACT for staging of suspected liver disease. All patients were staged by Fibroscan (Echosens). Enhanced Liver Fibrosis (ELF) test was additionally performed when it became available at our facility. Implementation of the pilot was delayed and disrupted due to the impact of Covid-19 on service delivery, with most patients identified from March 2021 onwards.

Results: 70 patients were identified–45 (64%) male, 25 (36%) female, with median age 53 years (range 25–80 yr). Fibroscan results ranged from 3.4 kPa–75 kPa. 40 (57%) were normal (<7.0 kPa), 13 (19%) F1–F3 (7.1 kPa–18.5 kPa) and 17 (24%) F4 (>18.5 kPa). ELF was performed in 32 (46%) patients; 19 (59%) showed severe fibrosis (score 9.8–14.3) and 13 (41%) moderate fibrosis (score 7.9–9.6). ELF and Fibroscan were well matched for identification of cirrhosis, with cirrhotic range Fibroscan results only found in those with severe fibrosis on ELF, suggesting either test could be used to rule out cirrhosis in this group. Following Fibroscan assessment, annual ACT follow-up was arranged for all patients in F1–F3 range, and the 25 patients with a normal Fibroscan who continued to drink excessively. Patients with any results in the cirrhotic range were referred to hepatology for ongoing management.

Conclusion: By performing fibrosis assessment during an inpatient stay, we were able to exclude significant liver disease in many people we had previously been unable to stage, providing important information to the patient and avoiding unnecessary hepatology follow-up. Provision of in-patient non-invasive fibrosis assessment may therefore be a valuable addition to hospital ACT services for capturing patients who poorly engage.

OS080

Natural history of hepatic steatosis associated to metabolic syndrome. Longitudinal study with 5 years of follow-up.

Marta Cervera^{1,2,3,4}, Marta Carol^{1,2,3,4}, Ana Belén Rubio^{1,2,3}, Martina Perez^{1,2,3,4}, Carlota Riba^{1,2,3}, Rosario Hernández⁵, Ann Ma^{1,2,3}, Emma Avitabile^{1,2,3}, Anna Soria^{1,2,3}, Octavi Bassegoda^{1,2,3}, Sara Martínez^{1,2,3}, Jordi Gratacós-Gines^{1,2,3}, Adria Juanola^{1,2,3}, Laura Napoleone^{1,2,3}, Elisa Pose^{1,2,3}, Isabel Graupera^{1,2,3}, Pere Ginès^{1,2,3}, Núria Fabrellas^{1,2,3,4}. ¹Hospital Clinic de Barcelona, Liver Unit, Barcelona, Spain; ²Institut d'Investigacions Biomèdiques August Pi i Sunyer (IDIBAPS) CIF: G59319681, Barcelona, Spain; ³Centro de Investigación Biomédica en Red de Enfermedades Hepáticas y Digestivas (CIBERehd), Madrid, Spain; ⁴University of Barcelona, School of Medicine and Health Sciences, Barcelona, Spain; ⁵Institut Català de la Salut (ICS), Centre d'Assistència Primària La Marina, Barcelona, Spain
Email: mcerverac@clinic.cat

Background and aims: Non-alcoholic fatty liver disease (NAFLD) has a wide range of clinical severity from fatty liver to cirrhosis. Most cases of fatty liver are diagnosed in the community setting. There is lack of information on the evolution of fatty liver in subjects diagnosed in primary care. The objective of this study was to perform a longitudinal analysis of hepatic steatosis, as estimated by controlled attenuation parameter (CAP), in a cohort of patients with fatty liver associated with metabolic syndrome.

Method: Patients with fatty liver with moderate-to-severe steatosis (CAP >280 dB/m) without significant fibrosis (liver stiffness measurement-LSM-<8 kPa) previously included in a population-based cohort randomly selected from primary care (Plos One 2018 PMD 30226889) were again assessed after a median of 5 years of follow-up. Demographic, clinical, and laboratory data, as well as CAP and LSM were assessed at two time points, baseline and 5 years later. Nurse education and counseling about NAFLD was provided at time of first assessment. Improvement of hepatic steatosis was defined as decrease in CAP >10% compared to baseline. Remaining cases were considered as persistent or worsening (CAP increase of >10%).

Results: Seventy-one patients were included (60 ± 11 years; 49% female; BMI 29.9 ± 4.8; 22.5% with diabetes). Baseline CAP and LSM values were 315 ± 32 dB/m and 4.9 ± 1.4 kPa. Twenty-six of the 71 (37%) patients showed improvement in hepatic steatosis (CAP 320 to 231 dB/min; p < 0.001). In 15 of these patients CAP decreased to <240 dB/m, the threshold generally used to define presence of liver fat. Improvement of steatosis was associated with significant decrease in ALT and GGT levels. The remaining 45 patients, showed persistent or worsening of hepatic steatosis (32 and 13 patients, respectively). LSM increased >8 kPa in 3 patients from the latter group (8.1, 11.6 and 12.2) and none from the former. Patients with improvement of hepatic steatosis had significantly lower BMI and ALT at baseline compared to values in patients with persistent/worsening of hepatic steatosis.

Conclusion: In this population-based cohort of patients with fatty liver from primary care, a significant proportion of subjects (37%) show mobilization of liver fat during a 5-yr follow-up period with no intervention other than nurse education and counseling. The remaining two thirds of subjects show persistence/worsening of hepatic steatosis. Reduction of liver fat is associated with improvement in ALT and GGT levels.

OS081

The effort for HCV elimination- dedicated nurse based protocol, single center experience

Assaf Issachar^{1,2}, Evelin Oxtrud¹, Yael Harif¹, Orly Sneh Arbib^{1,2}, Amir Shlomai^{1,2}, Ran Tur-Kaspa^{1,2}, Marius Brown^{1,2}, Michal Cohen-Naftaly^{1,2}. ¹Rabin Medical Center, Beilinson Hospital, Liver Institute, Petah Tikva, Israel; ²Tel Aviv University, Sakler Medical School, Tel Aviv, Israel
Email: assafissa@gmail.com

Background and aims: As part of the global effort for elimination of HCV, Israel, as other countries, adopted a simplified guidelines for HCV treatment.

Our center is a referral center for liver diseases, since the introduction of the first generation of DAA (INF based protocols) we adopted a protocol based on open access for HCV patient, dedicated nurse that communicate with the patients and primary physician before and during treatment, same day fibroscan test for every patient followed by physician recommendation for HCV treatment. Following very good SVR results after this treatment (higher from SVR reported in literature), we implement the dedicated nurse protocol for the INF free protocols.

The aim of our study is to present the result of our experience.

Method: Using our prospective collected database of HCV patients who was treated with DAA in our center, we analyzed SVR rate and some of the patients were asked to complete a questionnaire about the added value of nurse intervention.

Results: During 2011–2013 we treated 105 patients with first generation Peginterferon based DAA with SVR rate of 81%. In the end of 2014, we started to treat with INF free DAA regimens DAA. 831 patients were treated with SVR rate of 98.9%. 33 of the patients were organ transplant patient. 426 patients were diagnosed to have F3–4 fibrosis based on their fibroscan results and these patients continue surveillance post SVR. 74 patients completed the questionnaire about the value of the dedicated nurse intervention. All patients were satisfied with the professionalism of the team. 85% of the patients felt that the explanation provided by the nurse during the appointment contributed to their understanding of their medical situation and the importance of the treatment.

Conclusion: SVR rate of DAA based HCV treatment in our center is very high. The patients pointed the added value of nurse explanations, instruction and follow-up for better understanding of the disease and the importance of treatment and follow-up. Intervention by dedicated nurses improves the communication and compliance.

OS082

Advanced liver disease: master's students' perception. An exercise of introspection

Eva Roman^{1,2}, Montserrat Guillaumet¹, German Soriano², Maria Poca², Edilmar Alvarado-Tapias², Angels Escorsell². ¹School of Nursing, Universitat Autònoma de Barcelona, Spain; ²CIBERehd. Instituto de Salud Carlos III., Madrid
Email: eroman@santpau.cat

Background and aims: Advanced liver disease (ALD) produces physical and mental changes that drastically affect the lived experience of people who suffer from it, affects self-image and self-perception, social and affective relationships, activities and the idea of the future. Empathy allows us to understand each other's experiences, concerns, and perspectives, as well as communicate this understanding (Moser, *Intensive Crit Care Nurs* 2003). To analyze the understanding of the losses and changes experienced by persons with ALD, their experience and transformation, through the narrative based on an exercise of introspection centred on reflection by resident physicians studying a master on digestive diseases.

Method: 3rd year resident doctors of the gastroenterology speciality, students of the master's degree of the Catalan Society of Gastroenterology during the 2019–2020 academic year. Students had to do an introspection exercise and tell in the first person how

they would feel if they were diagnosed with liver cirrhosis: what would change in their life and what would not? Family role, work and social life, economic situation, leisure activities, priorities, future perspective, image (physical and sexual appearance). The writings were analyzed following a semantic interpretive approach (van Manen 1977), and compared with the literature on patients' point of view and perception.

Results: Thirty-three stories were collected of which 30 were written in the first person. Four emerging issues were identified: family, friends and social circles, work situation and self-esteem. The expressed emotions showed higher coincidence with those previously described by patients with ALD. The most recurrent unit of meaning was: "Being diagnosed with cirrhosis would mean a radical change in my life"

Conclusion: The narrative is a useful pedagogical tool in training and provides elements of learning to understand responses to complex situations. In the narratives, issues and emotions coincided with those described by patients with ALD were identified. Observing and analyzing oneself by interpreting the cognitive and emotional processes generated by a disease allows one to identify aspects that contribute to becoming aware of the other's reality and thus fostering empathy.

OS083

Nurse-driven post-discharge intervention reduces risk of readmission and non-attendance in patients with decompensated liver cirrhosis: a randomized controlled study

Malene Barfod O'Connell¹, Lise Hobolth¹, Anne Broedsgaard Madsen^{2,3}, Flemming Bendtsen^{1,4}, Nina Kimer¹. ¹Copenhagen University Hospital, Amager Hvidovre, Gastro Unit, Medical Division, Hvidovre, Denmark; ²Copenhagen University Hospital, Amager Hvidovre, Department of Paediatrics and Adolescent Medicine, Hvidovre, Denmark; ³Aarhus University, Department of Public Health, Research Unit for Nursing and Health Care, Aarhus C, Denmark; ⁴Copenhagen University Hospital, Amager Hvidovre, Department of Clinical Medicine, Hvidovre, Denmark
Email: malene.barfod.oconnell@regionh.dk

Background and aims: Patients with decompensated liver cirrhosis are on average admitted 3 times per year and 20–37% of the patients are readmitted within 30 days from discharge. Repeated admissions have great personal and societal consequences and non-attendance at out-patient visits may impact clinical outcome. In this study we investigated how a post-discharge nurse-driven intervention affected readmissions and outpatient attendance for patients with decompensated liver cirrhosis

Method: This randomized controlled intervention was conducted in the Gastro Unit of a university hospital in the Capital region of Denmark. Patients admitted with decompensated liver cirrhosis were eligible for inclusion. The control group received standard post-discharge care. The intervention group participated in a nurse-driven post-discharge intervention based on concepts from Family Nursing. Before discharge the patient and family received a pamphlet with information on preventive measures. After discharge the participants received three monthly home visits by a nurse specialist in liver diseases comprising: therapeutic conversations; evidence-based information and help to initialize contact to municipal offers. After three months the patients received three monthly follow-up telephone calls, to a total of six months follow-up.

Results: Between December 2019 and October 2021, 111 participants were included. Twenty-four participants were excluded due to cancer, death before intervention or withdrawal of consent, leaving 42 participants in the intervention group and 44 participants in the control group. Fifty-three (62%) were male, mean age was 60.7 years, 81 (94%) had alcohol related cirrhosis, and 43 was classified as Child-Pugh C (Child score ≥ 10), without significant difference between the two groups. Nineteen (45%) participants in the intervention group were readmitted within six months compared to 27 (61%) in the

control group; (HR 0.42; 95% CI: 0.253 to 0.692; stratified log-rank $p = 0.002$). Therefore, the intervention was associated with a 58% reduction in the risk of readmission compared to the control group. Median time to readmission was 42 days in the intervention group as compared to 21 days in the control group ($p = 0.0596$). Five participants in the intervention group did not appear for a total of six outpatient visits during the follow-up period, compared to 17 participants in the control group who did not appear for 29 visits (HR 0.21; 95% CI 0.07 to 0.65; stratified log-rank $p = 0.007$).

Conclusion: In a randomized controlled study, a nurse-driven post-discharge intervention for patients with liver cirrhosis proved a significant reduction in readmissions and in non-attendance for outpatient visits in the intervention group. The period from discharge to first readmission was longer in the intervention group but not statistically significant from the control group.

Gut microbiota in liver disease and liver regeneration

OS084

Monoacylglycerol lipase inhibition specifically in macrophages compromises liver regeneration by inducing interferon type 1 that negatively impacts on hepatocyte proliferation

Manon Allaire¹, Rola Al-Sayegh¹, Morgane Mabire¹, Matthieu Siebert¹, Mathilde Cadoux¹, JingHong Wan¹, Maude Le Gall¹, Catherine Postic², Hervé Guillou³, Pierre de la Grange⁴, Sophie Lotersztajn¹, Hélène Gilgenkrantz¹. ¹Université de Paris, Centre de Recherche sur l'Inflammation (CRI), Paris, France; ²Université de Paris, Institut Cochin, INSERM U1016, CNRS, Paris, France; ³Toxalim (Research centre in Food Toxicology), INRAE, ENVT, INP-Purpan, PS, Université de Toulouse, Toulouse; ⁴GenoSplice, Paris, France
Email: allama5@hotmail.fr

Background and aims: Monoacylglycerol lipase (MAGL) is a proinflammatory enzyme that reprograms lipid metabolism by converting monoacylglycerols into free fatty acids, in particular arachidonic acid. We have previously shown that MAGL displays pro-regenerative properties in the liver by demonstrating the direct contribution of MAGL from hepatocytes and the indirect effects of MAGL from liver macrophages in this impact (Allaire et al, EASL 2021). The aim of this study is to uncover the mechanisms by which MAGL from macrophages modulates liver regeneration.

Method: Mice with genetic invalidation in myeloid cells (MAGL^{Mye-/-}) were submitted to a liver regeneration stimulus induced by an acute intraperitoneal injection of carbon tetrachloride (CCl₄). Gene expression profiling of liver MAGL^{Mye-/-} macrophages was assessed by RNASequencing analysis. The role of identified pathways was confirmed *in vitro* in primary hepatocyte cell culture and *in vivo* by injecting neutralizing antibodies.

Results: Mice with a specific MAGL deletion in myeloid cells showed a regeneration defect compared to their wild type counterparts. RNASeq analysis demonstrated an induction of interferon-stimulated genes in MAGL depleted liver macrophages, suggesting that interferon type I (IFN-I) pathway plays a major role in the delayed

regeneration. The induction of IFN-I was also confirmed in the liver of MAGL^{Mye-/-} mice 24 h after the injury and in bone marrow derived macrophages (BMDM) exposed to the MAGL pharmacological inhibitor MJN110. We cultured primary hepatocytes with IFN- α and/or - β and found that both reduce hepatocyte proliferation *in vitro* with a cumulative effect of IFN- α and IFN- β . The link between IFN pathway and liver regeneration defect was finally demonstrated in an *in vivo* rescue experiment since the injection of IFN type I receptor neutralizing antibodies in MAGL^{Mye-/-} mice before and during the regeneration process restored hepatocyte proliferation to the level of control mice.

Conclusion: Inhibition of MAGL macrophages compromises liver regeneration by inducing IFN-I pathway that negatively impacts on hepatocyte proliferation.

OS085

Complete vascular tree reconstruction in rat decellularized liver scaffolds using differential recellularization pressures

Sandra Melitón Barbancho^{1,2}, Pedro Baptista^{1,3,4,5}, Alba Pueyo Moliner². ¹Aragón Health Research Institute (IIS Aragón), CIBA, Zaragoza, Spain; ²University of Zaragoza, Zaragoza, Spain; ³Centro de investigación biomédica en red, Hepatic Diseases, Madrid, Spain; ⁴Universidad Carlos III de Madrid, Department of Biomedical and Aerospace Engineering, Madrid, Spain; ⁵Fundación ARAID, Zaragoza, Spain
Email: smelitonb01@gmail.com

Background and aims: There are still several challenges slowing the translation of bioengineered livers to the clinic in order to reduce the shortage of organs. One of the most important is to provide the whole organ with a robust vascular network that allows its perfusion and maintenance *in vivo*. Effective revascularization of decellularized liver scaffolds (DLS) is still elusive, so this work focused on the revascularization of DLS, presenting an effective approach for generating functional vasculature that allows us to be closer to the bioengineered liver.

Method: Whitin a bioreactor setup, endothelial cells [unlabelled for *vena cava* and labelled with GFP and tdTomato, for portal vein (PV) and hepatic artery (HA), respectively] (pUVECs), smooth muscle cells (pA-SMCs) and mesenchymal stem cells (pBM-MSCs) were injected through HA, PV, and *vena cava* using distinct seeding pressures to target the different vessel diameters. Next, maturation was enhanced by providing growth factors for vasculogenesis and angiogenesis process keeping constant mechanical-stimulation for 14 days. Microscopic analysis was performed by hematoxylin-eosin (HandE) and immunofluorescence (IF) staining's. Finally, pUVECs function was evaluated by nitric oxide (NO) and prostacyclin (PGI₂) secretion and the contraction of pA-SMC after carbachol inoculation was observed.

Results: HandE analysis confirmed the lining growth of the different kind of cells inside of the decellularized vascular tree. Moreover, IF confirmed the accurate arrangement of pUVECs into vascular-like structures with pBM-MSCs/pA-SMCs arranged around them. Also, pUVEC-TdTomato and pUVECs-GFP differential seeding through HA and PV respectively showed a targeting layout. Secretion of NO and prostacyclin was confirmed upon bradykinin challenge and a pressure increase in the vascular tree was observed because of the contraction of pA-SMC after exposure to carbachol.

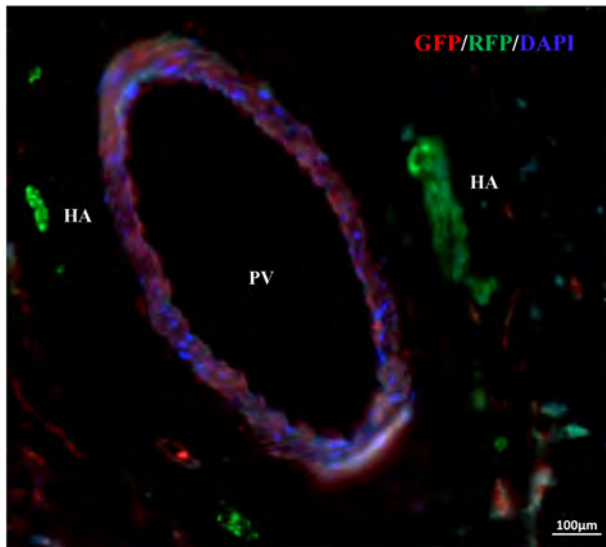


Figure: Recellularized portal vein (red) and hepatic artery (green) with pUVEC-TdTomato and pUVECs-GFP respectively in a bioreactor system after 14 days. GFP: Green fluorescent protein; RFP: Red fluorescent protein and DAPI: 4', 6-diamidino-2-phenylindole.

Conclusion: The generation of a complete and functional vascular tree in DLS using distinct cell types and seeding pressures in a bioreactor system with defined maturation conditions is now possible with the validation of the revascularization method here presented.

OS086

Orthotopic transplantation of the functional bioengineered liver prolonged survival in rats with total hepatectomy

Beibei Guo¹, Li Jiang², Jing Jiang¹, Qian Zhou¹, Jiaxian Chen¹, Jiaojiao Xin¹, Dongyan Shi¹, Keke Ren¹, Xingping Zhou¹, Genren Yang², Jun Li¹. ¹The First Affiliated Hospital, Zhejiang University School of Medicine, State Key Laboratory for Diagnosis and Treatment of Infectious Diseases, National Clinical Research Center for Infectious Diseases, Collaborative Innovation Center for Diagnosis and Treatment of Infectious Diseases, Hangzhou, China; ²The First Affiliated Hospital, Zhejiang University School of Medicine, Hangzhou, China
Email: lijun2009@zju.edu.cn

Background and aims: Functional bioengineered liver (FBL) is a promising alternative to orthotopic liver transplantation. This study aims to determine the therapeutic potency of the FBLs with whole decellularized liver scaffold (DLS) using orthotopic transplantation in rat.

Method: The FBLs were developed using the whole rat DLSs with 1.5×10^7 human umbilical vein endothelial cell lines (HUVECs) implanted through portal vein, 6×10^7 human bone marrow mesenchymal stem cells (hBMSCs) and 3×10^8 mouse hepatocyte cell lines implanted through bile ducts. The FBLs evaluated with endothelial barrier function, bio-synthesis and metabolism were used to orthotopically transplanted into rats for determining survival benefit.

Results: The morphological observation exhibited the well-organized vascular structure lining by HUVECs in vascularized bioengineered liver. Histological and scanning electronic microscopy analysis showed endothelial barrier function with lower leakage of blood cells of the vascularized bioengineered liver. The new developed bioengineered liver displayed that hBMSCs and hepatocytes were, well-aligned, and uniformly distributed over parenchymal space, and HUVECs formed the endothelialized microvascular structure. Significant increases of urea productions and albumin level in culture medium demonstrated that FBLs possessed ammonium translation and albumin synthesis functions. Orthotopic transplantation with FBLs rescued rats with a survival time of up to 100 min,

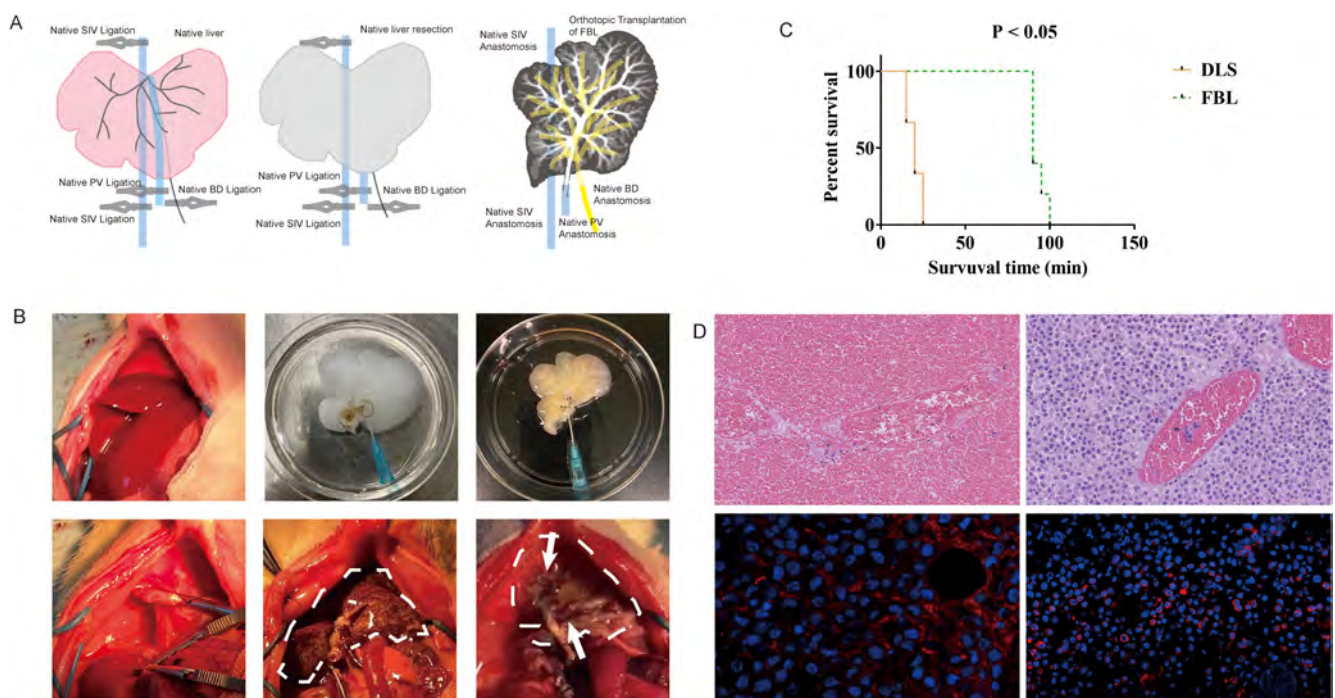


Figure: (abstract: OS086): A. Schematic diagram of orthotopic transplantation of a functional liver-like organ; B. orthotopic transplantation of decellularized liver scaffolds and functional liver-like organs; C. Survival curve after orthotopic transplantation; D. Histological identification after transplantation.

whereas all rats transplanted with DLS died within an average of 25 min. Histological staining showed that most perfused blood cells were limited into vascular lumen and the implanted cells, with positive immunofluorescence staining of CD90 and ALB, evenly distributed into the parenchymal space around vessels in the transplanted FBLs, but the transplanted DLSs became a pool entirely filled with blood cells.

Conclusion: The orthotopically transplanted FBLs effectively prolonged the survival time of rats with total hepatectomy. This study first determined the therapeutic potency of FBLs using orthotopic transplantation, which provides a promising alternative to the liver donor shortage for future clinical therapeutic applications.

OS087

Bacterial infections in cirrhosis are associated with reduction in gut microbial phage-bacterial interactions

Amirhossein Shamsaddini¹, Marcela Peña Rodríguez², Andrew Fagan³, Sara McGeorge³, Masoumeh Sikaroodi¹, Patrick Gillevet¹, Jasmohan S. Bajaj³. ¹George Mason University; ²Universidad de Guadalajara; ³Virginia Commonwealth University
Email: jasmohan.bajaj@vcuhealth.org

Background and aims: The impact of bacterial infections on gut microbiota in cirrhosis is unclear since disease severity and antibiotic use could affect these changes. There is increasing evidence of the role of bacteriophages in the modulation of infection risk and as potential treatment strategies. However, changes in the interaction of the virome with metagenome in infected patients with cirrhosis are unclear. Determine change in the metagenome of pts with cirrhosis

with infection versus uninfected patients and interaction with virome.

Method: Patients with cirrhosis were recruited, including outpatients with/without decompensation and inpatients admitted with/without infections. All pts underwent stool collection for metagenomics for bacterial and phage species. In inpts, stool was collected before antibiotics. DESeq2, PCoA, and correlation network analyses were performed between (a) all uninfected vs. infected patients and (b) inpatients with/without infections matched 1:1 by MELD score, demographics, and medications.

Results: 231 pts with cirrhosis were recruited, of which 30 were infected (20 SBP, 10 UTI). Unmatched comparison showed that infected pts had worse cirrhosis severity. PPI use was similar (Fig A). After matching for MELD score, inpatients with infections had similar disease severity (Ascites, HE) and medication use compared to those without infections (Fig A).

Metagenomics: Unmatched analysis: Pathobionts (*Enterococcus* spp, *C.difficile*) were higher, while short-chain fatty acid producers (*Ruminococcus*, *Alistipes* spp) were lower in infected patients. CrAssphages, *Bifidobacterium*, and *Streptococcus* phages were lower in infected patients. There was also a clear separation on β diversity (PERMANOVA $p < 0.0001$) between groups on bacterial and phage species. Matched analysis: Higher pathobionts (*E.faecalis*, *E.faecium*, *C.difficile*) along with *Lactobacillus* spp and oral-origin taxa (Fig B) persisted even after matching. Phages corresponding to these bacteria were also higher vs. uninfected pts (Fig C). PCoA showed β -diversity changes in bacteria (Fig D) and phages (Fig E) between groups. **Correlation network:** between phages and bacteria showed a collapse between linkages in infected patients centred around

Fig A Variables	Infected (n=30)	Unmatched Uninfected (N=201)	Matched cohort Uninfected (n=30)	P-value Matched uninfected vs infected (n=30)	P-value unmatched uninfected (N=201) vs infected (n=30)
Age	56.5±11.6	58.4±13.9	59.0±13.6	0.45	0.42
Male sex	27	170	23	1.0	0.15
Diabetes	15	92	11	0.65	0.66
MELD score	18.3±8.2	11.5±4.7	17.6±7.2	0.73	<0.0001
PPI	17	112	17	1.0	0.92
Lactulose	20	83	22	0.15	0.009
Rifaximin	15	58	14	0.71	0.06
HE	22	98	23	0.14	0.01
Ascites	24	119	27	1.0	0.06

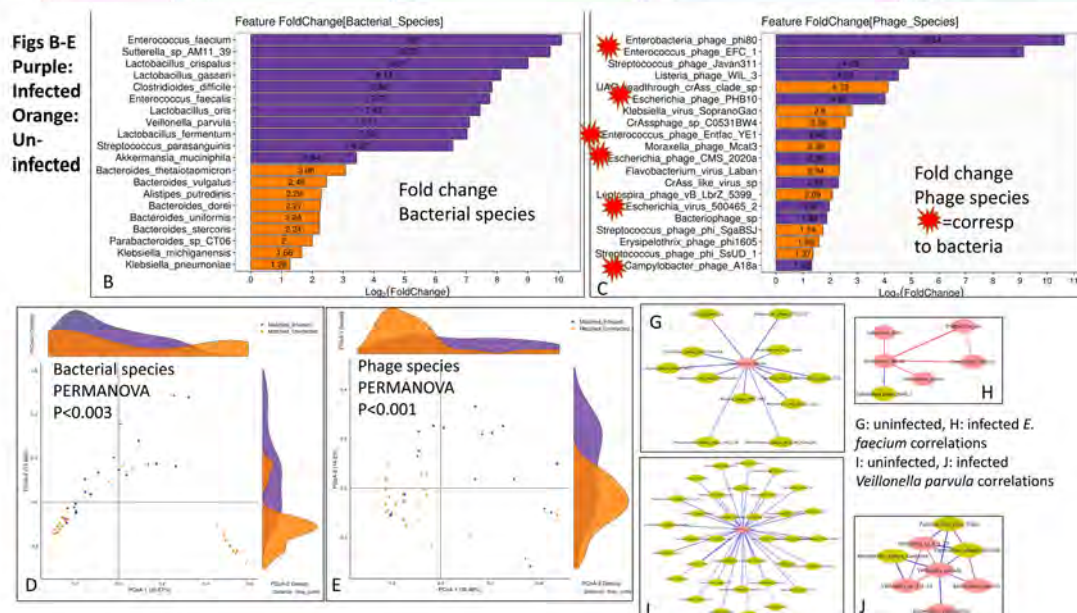


Figure (abstract: OS087): Characteristics and comparisons between infected and uninfected patients.

ORAL PRESENTATIONS

Enterococcus (Fig G/H) and *Veillonella* spp (Fig I/J). Network heterogeneity was higher in infected vs matched uninfected (1.066 vs 1.027) and in unmatched cohorts (1.183 vs 1.025).

Conclusion: Collapse of phage-bacterial interactions centred around *Enterococcus*, Enterobacteriaceae spp and oral-origin taxa are linked with bacterial infections. This pattern persists even when infected pts are compared to disease severity-matched inpatients without infections before antibiotics. Phages directed against pathobionts could be targeted to prevent these infections.

OS088

Altered gut microbiome, metabolome and bile acid composition in sarcopenia in liver cirrhosis

Benard Aliwa^{1,2}, Nicole Feldbacher^{1,3}, Angela Horvath^{1,3}, Julia Traub⁴, Tobias Madl⁵, Günter Fauler⁶, Vanessa Stadlbauer^{1,3}. ¹Medical University of Graz, Department of Gastroenterology and Hepatology, Graz, Austria; ²University of Nairobi, Department of Food Science, Nutrition and Technology, Nairobi, Kenya; ³CBmed Center of Biomarker Research in Medicine, Area Microbiome Research, Graz, Austria; ⁴University Hospital Graz, Dietology Services, Graz, Austria; ⁵Medical University of Graz, Gottfried Schatz Research Center for Cell Signaling, Metabolism and Aging Molecular Biology and Biochemistry, Graz, Austria; ⁶Medical University of Graz, Klinisches Institut für Medizinische und Chemische Labordiagnostik (KIMCL), Graz, Austria
Email: vanessa.stadlbauer@medunigraz.at

Background and aims: 50–70% of liver cirrhotic patients suffer from sarcopenia leading to high mortality risk. The gut microbiome can metabolize bile acids and in turn bile acids can shape the gut microbiome community structure. We aimed to study differences in gut microbiome, bile acids and metabolite composition between sarcopenia and non-sarcopenia in liver cirrhosis and control.

Method: We analyzed 16 s rDNA sequencing of fecal microbiome and measured bile acids and metabolites of cirrhotic patients with and without sarcopenia (n = 78 and n = 38, respectively) as well as control with and without sarcopenia (n = 39 and n = 20, respectively). LEfSe, ANCOM, and LASSO regression, and multivariate logistic regression were applied.

Results: We demonstrated that both in cirrhotic and control patients, sarcopenia associates with a significant reduction in bacteria capable of generating branched-chain amino acids and short-chain fatty acids and a significant increase in bacteria capable of generating secondary bile acid (Sec-BAs). *Sutterella species*, *Vellionella parvula*, *Bacteroides (B.) fragilis*, and *Blautia marseille* were associated with sarcopenia and *B. ovatus*, *Alistipes putredinis*, *Eubacterium*, and *Ruminococcaceae* were associated with non-sarcopenia. In sarcopenic cirrhotic patients, we observed significantly elevated Sec-BAs, including deoxycholic acid (DCA), glycodeoxycholic acid (GDCA), lithocholic acid (LCA), and significantly elevated deoxycholic acid to cholic acid (DCA:CA), lithocholic acid to chenodeoxycholic acid (LCA:CDCA), glycolithocholic acid to chenodeoxycholic acid (GLCA:CDCA) and reduced total ursodeoxycholic acid to total secondary bile acid (T-DCA:T-sec BAs), serum valine, and serum acetate. We further observed that genes coding for 7 α -hydroxysteroid dehydrogenase enzyme (7 α -HSDH) were significantly increased in sarcopenic controls compared to non-sarcopenic controls. Multivariate logistic regression showed that MAMC, BMI, serum valine, serum acetate, GLCA:CDCA, T-DCA:T-sec BAs, and *B. ovatus* were independent predictors for sarcopenia in liver cirrhosis even when corrected for severity of disease and drug use.

Conclusion: *B. ovatus*, serum valine, serum acetate and bile acid profiles are independent predictors for sarcopenia and potential biomarkers for muscle health in liver cirrhosis. Further studies are needed to assess whether increasing *B. ovatus* abundance, serum valine, serum acetate, or altering bile acid composition may affect muscle health.

OS089

In-depth shotgun metagenomic analysis of the oral and gut microbiome identifies striking overlap in microbial community structure, virulence factors and antimicrobial resistance genes based on stage and severity of cirrhosis

Sunjae Lee¹, Bethlehem Arefaine², Neelu Begum¹, Elizabeth Witherden¹, Marilena Stamouli², Azadeh Harzandi¹, Ane Zamalloa³, Eleanor Corcoran⁴, Roger Williams^{2,5}, Shilpa Chokshi^{2,5}, Gordon Proctor¹, Adil Mardinoglu^{1,6}, Mathias Uhlen⁶, Saeed Shoaie^{1,6}, Vishal C. Patel^{2,5,7}. ¹Centre for Host Microbial Interactions, King's College London, London, United Kingdom; ²The Roger Williams Institute of Hepatology, Foundation for Liver Research, London, United Kingdom; ³Institute of Liver Studies and Transplantation, King's College Hospital NHS Foundation Trust, London, United Kingdom; ⁴Department of Critical Care, King's College Hospital NHS Foundation Trust, London, United Kingdom; ⁵School of Immunology and Microbial Sciences, Faculty of Life Sciences and Medicine, King's College London, London, United Kingdom; ⁶SciLifeLab, KTH – Royal Institute of Technology, Sweden, Sweden; ⁷Institute of Liver Studies and Transplantation, King's College Hospital, London, United Kingdom
Email: vishal.patel@nhs.net

Background and aims: Alterations in the gut microbiome in decompensated cirrhosis (DC) and acute on chronic liver failure (ACLF) are recognised as being critical in influencing clinical outcomes (Trebecka *et al.*, Nat Rev Gastro Hepatol, 2020). Knowledge of the oral microbiome is evolving and is increasingly recognised as predisposing to hepatic decompensation (Acharya *et al.*, JCI Insight, 2017). Our aims were to interrogate simultaneously the gut and oral microbiome by shotgun metagenomic sequencing of faecal and saliva samples, respectively, in cirrhosis patients of varying severities, with healthy and positive disease controls.

Method: 18 healthy controls (HC), 20 stable cirrhotics (SC), 50 DC, 18 ACLF and 15 with non-liver sepsis (NLS) i.e. severe infection but without cirrhosis were prospectively recruited. DNA extractions were undertaken from saliva and faecal samples and Illumina sequenced on a NovaSeq 6000 to a minimum depth of 20 million reads. Filtered and trimmed reads were aligned to a human microbiome integrated gene catalogue. Salivatypes and enterotypes were calculated by scaling genus profile abundance and clustering by Dirichlet multinomial mixture models. Comprehensive Antimicrobial Resistance Gene (ARG) and KEGG Orthology databases were used to evaluate ARGs and functional annotations, respectively.

Results: There was a striking decrement in Shannon diversity in the DC and ACLF cohorts vs HC and NLS (Fig A, D). Specific saliva- and enterotypes were identified based on clustering of genera, with a greater proportion of pathobionts and simultaneous reduction in autochthonous genera detected in specific clusters as cirrhosis severity progressed (Fig B, C, E, F). The degree of overlap between oral and gut microbiome communities (independent of antimicrobials, beta-blockers and acid suppressant therapies) and functional changes specific to virulence factor over-expression were significantly higher in DC and ACLF vs SC and HCs. Substantial total numbers of ARGs (1, 218 and 672) were detected in the oral and gut microbiome samples, respectively. 575 of ARGs were common to both sites, but a greater proportion of these were harboured in the gut (>85%) compared to the oral niche (47%), with overall ARG frequency incrementing with worsening cirrhosis (Fig G–I).

Conclusion: Oral and gut microbiome profiles differ significantly according to severity of cirrhosis, with specific saliva- and enterotype clusters reflecting dominance by pathobionts and loss of commensals. The degree of microbial community overlap between the mouth and gut, virulence factor and ARG frequency all increment significantly as cirrhosis worsens. These alterations that predispose to higher infection risk, poorer response to antimicrobial therapy and triggers for hepatic decompensation now form the rationale for non-antibiotic-dependant microbiome-modulating targeted therapies.

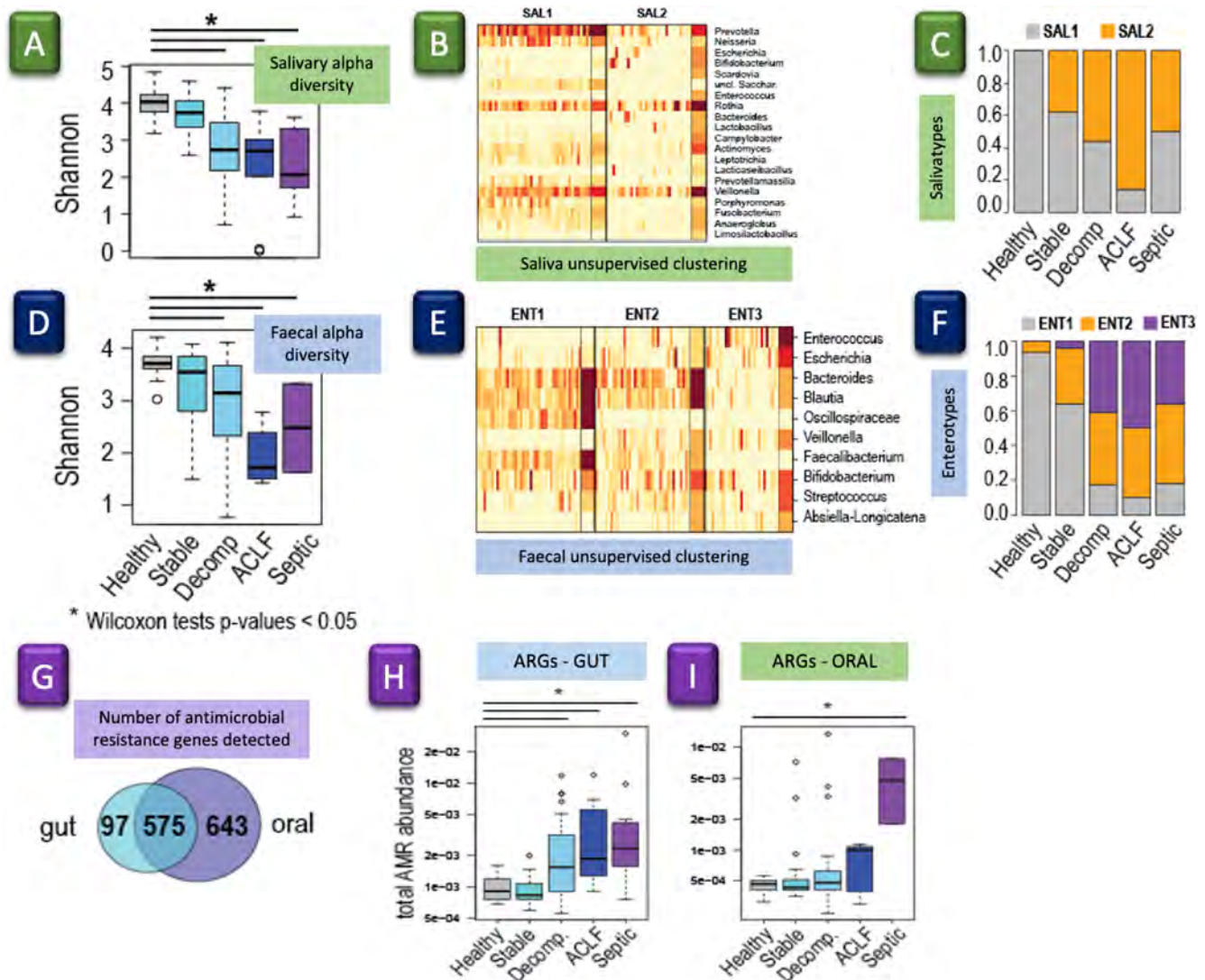


Figure: (abstract: OS089)

Saturday 25 June

Hepatitis B emerging therapies

OS090

Longer treatment duration of monthly VIR-2218 results in deeper and more sustained reductions in hepatitis B surface antigen in participants with chronic hepatitis B infection

Young-Suk Lim¹, Man-Fung Yuen², Daniel Cloutier³, Vaidehi Thanawala³, Ling Shen³, Sneha V. Gupta³, Andre Arizpe³, Andrea Cathcart³, Carey Hwang³, Edward J. Gane⁴. ¹University of Ulsan College of Medicine, Asan Medical Center, Seoul, Korea, Rep. of South; ²The University of Hong Kong, Queen Mary Hospital, Hong Kong, China; ³Vir Biotechnology, Inc., San Francisco, California, United States; ⁴University of Auckland, Faculty of Medicine, Auckland, New Zealand
Email: limys@amc.seoul.kr

Background and aims: Chronic hepatitis B virus (HBV) infection is a substantial global health issue affecting more than 290 million

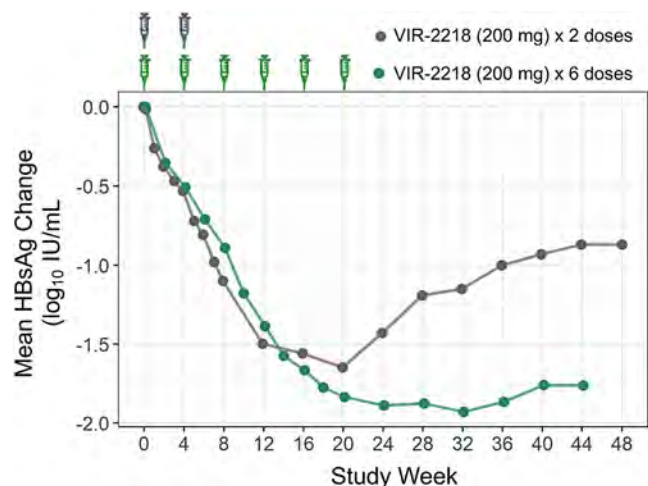
people worldwide. VIR-2218 is a small interfering ribonucleic acid (siRNA) therapeutic targeting the hepatitis B virus X region of the HBV genome currently in development for the treatment of HBV infection. Here, we report preliminary data from an ongoing study evaluating the safety, tolerability, and antiviral activity of 2 dosing regimens of VIR-2218 in participants with HBV infection.

Method: This open-label phase 2 study enrolled adult, virally suppressed, hepatitis B e antigen (HBeAg)-positive or negative participants with chronic HBV infection without cirrhosis. Dosing regimens of 2 doses (n = 6) or 6 doses (n = 15) of VIR-2218 200 mg given subcutaneously every 4 weeks were evaluated. Preliminary data up to the final follow-up visits for the 2-dose (week 48) and 6-dose (week 44) regimens are presented.

Results: Five of 6 participants receiving the 2-dose regimen completed study week 48 and, to date, 7 of 15 participants receiving the 6-dose regimen have completed study week 44. All participants achieved >1-log reduction in hepatitis B surface antigen (HBsAg). The 6-dose regimen was associated with greater mean maximum HBsAg reduction (−1.96 vs −1.61 log₁₀ IU/ml), and more sustained HBsAg reductions (−1.76 vs −0.87 log₁₀ IU/ml at week 44) compared with the 2-dose regimen (Figure). In both cohorts, adverse events (AEs) were generally grade 1 or 2 and no AEs resulted in discontinuation of study drug. Most participants had normal alanine aminotransferase

ORAL PRESENTATIONS

(ALT) levels throughout the study; 2 participants in each regimen had grade 1 ALT elevations. No treatment-related serious AEs were reported.



Conclusion: These preliminary data support that a longer duration of treatment with VIR-2218 results in deeper and more sustained reductions in HBsAg. In both regimens of VIR-2218, no differences in safety or tolerability were observed.

OS091

ALT flares were linked to HBsAg reduction, seroclearance and seroconversion: interim results from a phase IIb study in chronic hepatitis B patients with 24-week treatment of subcutaneous PD-L1 Ab ASC22 (Envafolelimab) plus nucleos (t)ide analogs

Guiqiang Wang¹, Yimin Cui², Yao Xie³, Qianguo Mao⁴, Qing Xie⁵, Ye Gu⁶, Xin-Yue Chen⁷, Guoxin Hu⁸, Yongfeng Yang⁹, Jiajie Lu¹⁰, Guizhou Zou¹¹, Qin Zhang¹², Lei Fu¹³, Yongping Chen¹⁴, Xiaolin Guo¹⁵, Jinlin Hou¹⁶, Yuemei Yan¹⁷, Handan He¹⁷, Jinzi Wu¹⁷. ¹Peking University First Hospital, Infectious Diseases Department, Beijing, China; ²Peking University First Hospital, Clinical Trial Center, Beijing, China; ³Beijing Ditan Hospital Capital Medical University, Beijing, China; ⁴Xiamen Hospital of Traditional Chinese Medicine, Xiamen, China; ⁵Ruijin Hospital of Medical College of Shanghai Jiaotong University, Infectious Diseases Department, Shanghai, China; ⁶Shenyang Sixth People's Hospital, Shenyang, China; ⁷Beijing YouAn Hospital Capital Medical University, Beijing, China; ⁸Peking University Shenzhen Hospital, Shenzhen, China; ⁹Nanjing Second Hospital, Nanjing, China; ¹⁰West China Hospital of Sichuan University, Chengdu, China; ¹¹The Second Affiliated Hospital of Anhui Medical University, Hefei, China; ¹²Shanghai Tongren Hospital, Shanghai, China; ¹³Xiangya Hospital of Central South University, Changsha, China; ¹⁴The First Affiliated Hospital of Wenzhou Medical University, Wenzhou, China; ¹⁵The First Hospital of Jilin University, Changchun, China; ¹⁶Nanfang Hospital of Southern Medical University, Guangzhou, China; ¹⁷Asclepis BioScience Co., Ltd., Hangzhou, China

Email: john131212@sina.com

Background and aims: Blockade of PD-1/PD-L1 pathway can restore T cell functions and lead to a potential cure for chronic hepatitis B (CHB). Hepatitis flares are considered to be mainly immune-mediated and may be linked or mark transitions to HBsAg reduction, even clearance. Previous studies indicated that PegIFN treatment may result in 18–24% of patients with ALT flares since it is an immune modulators. siRNA, a direct antiviral, however, caused as low as 6% of patients with ALT flares. Here we reported characterization of ALT flares and their relationship with HBsAg reduction, seroclearance and seroconversion from the interim analysis of a Phase IIb clinical trial in

CHB patients with 24-week subcutaneous PD-L1 antibody ASC22 (Envafolelimab) plus Nucleos (t)ide analogs (NAs) treatment.

Method: This randomized, single-blind, multi-center Phase IIb trial enrolled a total of 149 CHB patients (negative HBeAg, HBsAg ≤ 10000 IU/ml and HBV DNA < 20 IU/ml) in two cohorts for 24-week treatment of ASC22 (1 or 2.5 mg/kg) and 24-week follow-up (NCT04465890). The relationship between ALT flares and HBsAg reduction/loss was analyzed in patients who completed 24-week treatment of 1 mg/kg ASC22 Q2W (n = 33) or PBO Q2W (n = 11) + NAs. An ALT flare is defined as a transient elevation in serum ALT greater than 3-fold baseline level and more than 2X ULN (upper limit of normal).

Results: The baseline serum levels of HBsAg, ALT and AST were comparable between patients receiving ASC22 or PBO plus NAs. Seven patients had HBsAg reduction > 0.5 log₁₀ IU/ml, and were all with baseline HBsAg ≤ 500 IU/ml. Three patients even experienced HBsAg seroclearance (undetectable, < 0.05 IU/ml). One patient with HBsAg loss had seroconversion of HBsAb 6 weeks after the last dosing of ASC22 (Figure 1A). ALT flares were observed in 5/33 (15%) patients in ASC22 group compared to none in PBO group. Among the patients with HBsAg reduction > 0.5 log₁₀ IU/ml or HBsAg loss, 4/7 (57%) and 2/3 (67%) experienced ALT flares, respectively (Figure 1B). No clinically meaningful changes of total or direct bilirubin were observed in patients with ALT flares. However, more immune-related AEs (irAEs) occurred in ASC22 group. Most common irAEs were Grade 1 ALT/AST elevation and rash.

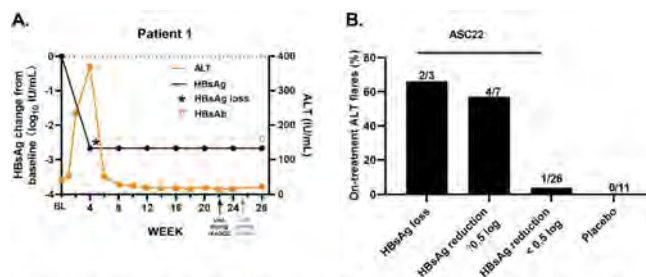


Figure 1: (A) One patient with HBsAg loss had seroconversion of HBsAb 6 weeks after last dosing of ASC22. (B) Percentage of on-treatment ALT flares among patients with different responses or treatments.

Conclusion: ALT flares occurring during ASC22 treatment were shown to be an indicator of a clinically meaningful immune response, resulting in significant HBsAg reduction and subsequent HBsAg loss/HBsAb seroconversion.

OS092

Lonafarnib combination with peginterferon Lambda diminished triphasic HDV kinetic pattern seen under Lambda monotherapy: the LIFT HDV study

Sarah Duehren¹, Christopher Koh², Julian Hercun², Farial Rahman², Pallavi Surana², Anusha Vittal², Walter Lai², Ohad Etzion³, Scott Cotler¹, Jeffrey Glenn⁴, Harel Dahari¹, Theo Heller². ¹Program for Experimental and Theoretical Modeling, Division of Hepatology, Department of Medicine, Stritch School of Medicine, Loyola University Chicago, Maywood, United States; ²Liver Diseases Branch, NIDDK, NIH, Bethesda, United States; ³Soroka University Medical Center, Beer-Sheva, Israel; ⁴Division of Gastroenterology and Hepatology, Stanford University School of Medicine, Stanford, United States

Email: harel.dahari@gmail.com

Background and aims: We recently reported that Lambda Interferon combination Therapy (LIFT) is safe and tolerable for up to 6 months in most patients with HDV. The goal of the current study was to characterize HDV RNA, HBV DNA, HBsAg and ALT kinetics during and after lonafarnib (LNF) and pegylated IFN- λ (Lambda) combination therapy.

Method: Twenty-six chronic HDV infected patients participated in a randomized, open-label Phase 2a clinical study of oral LNF 50 mg plus

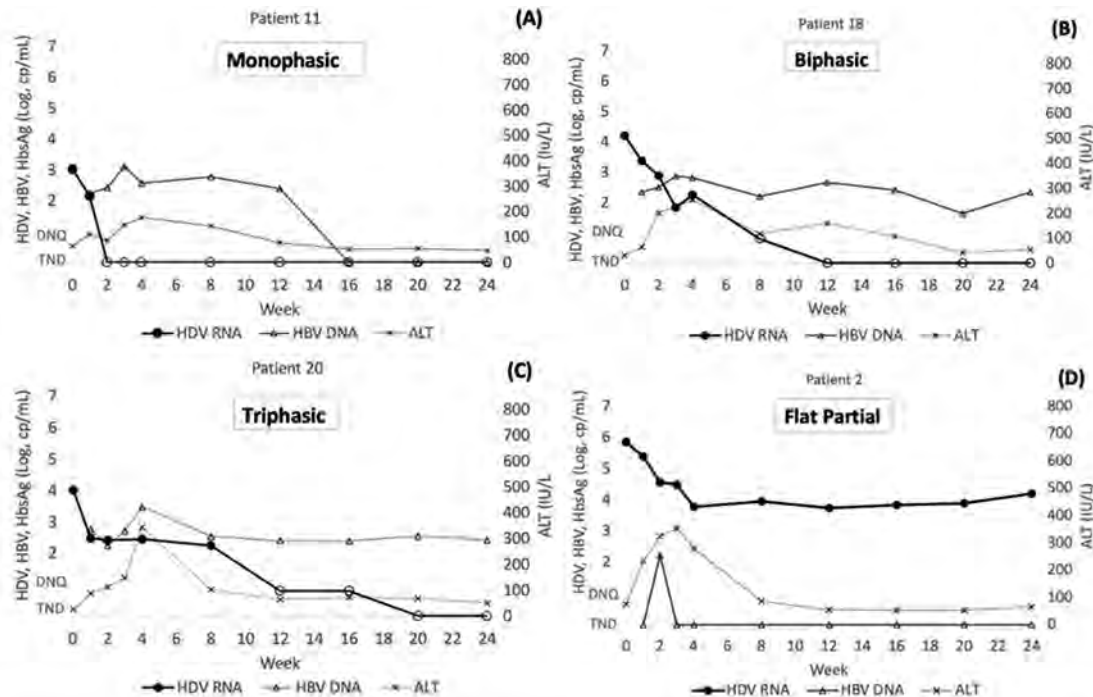


Figure 1. Kinetic characterization categories under Lambda and LNF therapy. (A) Monophasic (n=9) with ALT flare at week 16, and HBV increase at week 12. (B) Biphasic (n=11) with ALT flare at week 4, and HBV fluctuations throughout treatment. (C) Triphasic/Transient (n=2) with ALT flare at week 4 and high HBV viral level maintained throughout treatment. (D) Flat partial response (n=4) with ALT flare at week 3.

Figure: (abstract: OS092)

ritonavir (RTV) 100 mg twice daily and subcutaneous Lambda 180 mcg weekly for 24 weeks, followed by per-protocol post-therapy monitoring for 24 weeks. Three patients completed <24 weeks (12, 16, and 20 weeks). All participants were started on tenofovir or entecavir prior to therapy. Kinetic data were obtained weekly for the first four weeks, and then every four weeks during and post treatment. HDV kinetic phase changes were defined as a 2-fold change in slope. HDV RNA was measured by Robogene 2.0 (limit of quantification, LoQ = 14 cp/ml).

Results: Mean pretreatment HDV RNA, ALT, and HBsAg were 4.9 log IU/ml [IQR 1.6], 80 U/L [IQR 45], and 3.8 log cp/ml [IQR 0.5], respectively. Fourteen (54%) patients had pretreatment HBV DNA target not detected (TND) and 12 patients had mean HBV DNA 2.6 log IU/ml [IQR 0.38]. During therapy, patients fit into 4 HDV kinetic patterns (Fig. 1): monophasic, MP (n=9, Fig. 1A), biphasic, BP (n=11, Fig. 1B), triphasic/transient, TP (n=2, Fig. 1C), and flat-partial response, FPR (n=4, Fig. 1D). HBsAg remained at pretreatment level in all patients (not shown). All patients had a transient ALT increase during therapy (mean 6-fold [IQR 4] from upper limit of normal (40 IU/ml). Six (of 14) patients maintained HBV serum levels at TND, while the other 8 had transient increases or fluctuations from baseline TND. Of the 12 patients with high baseline HBV DNA levels, 8

maintained high levels throughout treatment, and 4 dropped to TND. A 2 log decline (or LoQ, n = 15) from pre-treatment HDV levels at end of therapy (EOT) was seen in 23 (88%) patients: 9/9 MP, 11/11 BP, 2/2 TP, 1/4 FPR. Mean ALT level at EOT was 94 IU/ml [IQR 31], similar to pretreatment levels. At end of follow-up (EFU), 5 (4 MP and 1 BP) out of 15 patients who had HDV LoQ at EOT remained LoQ (Fig. 1A and B), and the remaining had rebound (from EOT) with a mean value of 4.83 log IU/ml [IQR 1.9]. Eleven (42%) patients achieved ALT normalization at EFU.

Conclusion: We previously reported in the LIMT-1 study (The Liver Meeting, AASLD 2019 #LP12) 5 HDV kinetic patterns under Lambda monotherapy: MP (19%), BP (22%), FPR (19%), and triphasic/staircase (40%). Compared to Lambda monotherapy, including LNF significantly (p=0.009) diminished the HDV triphasic/staircase kinetic patterns to 8%, suggesting that LNF reduces intracellular HDV production. The LIMT-1 study saw successful HDV viral decline in only 45% of patients, while the present study showed 88% success in reducing HDV by more than 2 log.

OS093

Real life study of bulevirtide in chronic hepatitis delta: preliminary results of the ANRS HD EP01 BuleDelta prospective cohort

Helene Fontaine¹, Claire Fougerou-Leurent^{2,3}, Emmanuel Gordien⁴, Caroline Scholtes⁵, Sophie Metivier⁶, Victor de Lédighen⁷, Vlad Ratziu⁸, Laurent Alric^{9,10}, Nathalie Ganne-Carrié¹¹, Veronique Loustaud-Ratti¹², Dominique Guyader¹³, Vincent Leroy¹⁴, Jérôme Dumortier¹⁵, Karine Lacombe¹⁶, Georges-Philippe Pageaux¹⁷, Anne Minello Franza¹⁸, Christelle Tual^{2,3}, Alain Renault³, Estelle Le Pabic^{2,3}, Lucie Marchand¹⁹, Dominique Roulot²⁰, Fabien Zoulim²¹. ¹Cochin Hospital-APHP, Pôle Hépatogastroentérologie, Paris, France; ²Rennes University Hospital, Service de Pharmacologie, Rennes, France; ³Inserm, CIC 1414, Rennes, France; ⁴Avicenne Hospital, CNR des hépatites B, C et Delta, Bobigny, France; ⁵Groupement Hospitalier Nord-HCL, Laboratoire de Virologie, Lyon, France; ⁶Rangueil Hospital, Service d'hépatogastroentérologie, Toulouse, France; ⁷Haut-Lévêque Hospital, Service d'hépatogastroentérologie, Bordeaux, France; ⁸La Pitié Salpêtrière Hospital-APHP, Service d'hépatogastroentérologie, Paris, France; ⁹Rangueil Hospital, Service de médecine interne, Toulouse, France; ¹⁰CHU Rangueil, Digestive Department Toulouse 3 University, Toulouse, France; ¹¹Avicenne Hospital, Service d'Hépatologie, Bobigny, France; ¹²Dupuytren Hospital, Service d'hépatogastroentérologie, Limoges, France; ¹³Rennes University Hospital, Service d'hépatogastroentérologie, Rennes, France; ¹⁴Henri Mondor Hospital-APHP, Service d'hépatogastroentérologie, Créteil, France; ¹⁵Edouard Herriot Hospital -HCL, Service d'hépatogastroentérologie, Lyon, France; ¹⁶Saint Antoine Hospital-APHP, Service des Maladies Infectieuses et Tropicales, Paris, France; ¹⁷Saint Eloi Hospital, Service d'hépatogastroentérologie, Montpellier, France; ¹⁸Bocage Hospital, Service d'hépatogastroentérologie, Dijon, France; ¹⁹ANRS MIE, Paris, France; ²⁰Avicenne Hospital, Unité fonctionnelle d'hépatologie, Bobigny; ²¹Croix-Rousse Hospital-HCL, Service d'hépatogastroentérologie, Lyon, France
Email: helene.fontaine@aphp.fr

Background and aims: About 5 % of positive-HBsAg patients are infected with the hepatitis Delta virus (HDV), leading to an increase of 2 to 5-fold of cirrhosis and hepatocellular carcinoma, and a higher mortality in comparison with chronic hepatitis B alone. The management of chronic hepatitis delta (CHD) has improved recently in France, with the availability of bulevirtide (BLV) within an early access program in September 2019 and thanks to a conditional marketing authorization since September 2020.

Method: The aim of the BuleDelta cohort, a French multicenter ANRS |MIE observatory is to analyze the efficacy and the safety of BLV in patients treated since September 2019. This preliminary analysis has been performed in patients treated for at least 24 weeks (W24). The biological response was defined as a normalization of ALT, the virologic response as a decrease of HDV RNA of at least 2 log IU/ml or HDV RNA undetectability, the combined response as the association of both.

Results: as of October 1st, 2021, 138 patients have been included in the BuleDelta cohort: 66% were male, mean \pm SD age of 42 \pm 11 years; 54 % were of European or Asian origin and 44 % from Sub-Saharan Africa, 12 % presented HIV coinfection, 73% were treated with nucleos(t)ides analogs (NUC) and 42% with pegylated interferon- α (Peg-IFN).

At baseline (D0), the mean HDV RNA was 6.1 \pm 1.4 log IU/ml; HBV DNA was above quantification threshold in 38 patients (mean 2.6 \pm 1.6 log IU/ml).

The preliminary analysis included the 98 out of 138 patients with available data at W24 in whom 54 (55%) were treated with BLV only, and 44 (45 %) in association with peg-IFN. Overall 74 (76 %) were concomitantly treated with NUC. The mean decrease of HDV RNA at W24 was of 1.9 \pm 1.4 log IU/ml (2.6 and 1.6 log IU/ml with and without peg-IFN, respectively). The virologic response at W24 was observed in 55 (56%) patients (80% and 37%, with and without peg-IFN, respectively). Among these 55 patients, the virologic response

was observed in 8 (15%) patients at W4, in 26 (47%) at W8 and in 38 (69%) at W12. The biological response was observed in 36 out of 98 (37%) patients at W24 (34% and 40%, with and without peg-IFN, respectively) and the combined response in 25 (26%) patients at W24 (36% and 17%, with and without peg-IFN, respectively).

In the 43 patients without virologic response at W24, Figure 1 presents which therapeutic strategy was adopted. No patient had Peg-IFN add-on.

HDV viral load at W24	Treatment decision		
	Treatment continuation	Increase of BLV from 2 to 10 mg/d	BLV interruption
Quantifiable (n = 34)	26 (76.5%)	6 (17.6%)	2 (5.9%)
Detectable below quantification limit (n = 9)	8 (88.9%)	0 (0%)	1 (11.1%)

Conclusion: In this first real life study, a decrease of HDV viremia greater than 2 log IU/ml after 24 weeks of treatment of BLV was observed in more than half of patients with CHD and was associated with a normalization of ALT in half of them. Updated results will be presented at the meeting.

OS094

Therapeutic vaccine JNJ-0535 induces a strong HBV-specific T-cell response in healthy adults and a modest response in chronic HBV-infected patients

An De Creus¹, Leen Slaets¹, Bart Fevery¹, Ellen Van Gulck¹, Linghua Zhou¹, Tim Van De Parre¹, Celine Van Den Broeke¹, Dessislava Dimitrova², Isabelle Lonjon-Domanec¹, David Blue, Jr³, Pieter Van Remoortere², Stefan Bourgeois⁴, Patrick Kennedy⁵, Sandra De Meyer¹. ¹Janssen Research and Development, Belgium; ²Janssen Research and Development, United States; ³Janssen Biopharma, Inc.; ⁴Hospital Network Antwerp (ZNA), Belgium; ⁵Barts and The London School of Medicine and Dentistry, United Kingdom
Email: adecreus@its.jnj.com

Background and aims: JNJ-0535 is a hepatitis B virus (HBV)-specific therapeutic DNA vaccine administered via electroporation (EP)-mediated intramuscular injection. JNJ-0535 comprises 2 plasmids encoding either HBV core or polymerase (pol) proteins. Induction of functional core and pol-specific T cells was evaluated in healthy and chronic HBV (CHB)-infected individuals.

Method: First in human (FIH) study 64300535HPB1001 evaluated total doses of 0.25 mg (n = 6), 1 mg (n = 7) or 6 mg (n = 10) JNJ-0535 (containing equal quantities of the 2 plasmids) or placebo (n = 7) delivered by intramuscular electroporation with TDS-IM v2.0 in CHB patients who were virologically suppressed, HBeAg- and on stable nucleos(t)ide therapy. Study 64300535HPB1003 evaluates the 6 mg dose of JNJ-0535 in healthy volunteers (HVs) (n = 12). PBMCs collected at baseline, during the vaccination period (10–14 days after the 3 vaccinations, and during follow-up were evaluated for T cell responses against core and pol using ex vivo IFN γ ELISpot and intracellular cytokine staining (ICS). Results of the vaccination period will be presented for both studies comparing the 6 mg dose.

Results: A ≥ 3 -fold increase in ELISpot responses over baseline to core and/or pol was observed in 5/10 CHB patients (50%) and in 11/12 HVs (91.7%) at 6 mg JNJ-0535. Six (50%) HV responded to both antigens whereas no CHB patients responded to both antigens. JNJ-0535 vaccination induced a higher median (interquartile range) maximum fold-increase in T cell responses from baseline in HV (24.4 [10.1–51]) compared to CHB patients (4.8 [4.4–10]). Overall, vaccine-induced core-specific CD4⁺ T cells were polyfunctional in both HV and CHB patients for ELISpot responses ≥ 150 SFU/million PBMC. Polyfunctional core-specific CD8⁺ T cells were only induced in HV. No safety issues have been identified for JNJ-0535 vaccine delivered by intramuscular electroporation.

Conclusion: T cell responses induced in HV were superior to those in CHB patients at a JNJ-0535 dose of 6 mg in terms of the proportion of responders, the magnitude of fold-increase from baseline, the breadth (number of antigens) and CD4+ and CD8+ core-specific T cell polyfunctionality. This supports the hypothesis that CHB infection negatively impacts the ability of patients to induce T cells in response to therapeutic vaccination.

OS095

Sustained 12 week off treatment antiviral efficacy of ATI-2173, a novel active site polymerase inhibitor nucleotide, combined with tenofovir disoproxil fumarate in chronic hepatitis B patients, a phase 2a clinical trial

Myreen Tomas¹, Alina Jucov^{2,3}, Igor Anastasiy⁴, Lauren Ogilvie¹, Karen Fusaro¹, Katherine Squires¹, Douglas Mayers¹. ¹Antios Therapeutics, United States; ²ARENIA Exploratory Medicine, Moldova; ³Nicolae Testemitanu State University of Medicine and Pharmacy, Chisinau, Moldova; ⁴ARENIA Exploratory Medicine, Ukraine
Email: mtomas@antiostherapeutics.com

Background and aims: ATI-2173 is a novel phosphoramidate liver-targeted prodrug of clevudine that functions as an active site polymerase inhibitor nucleotide (ASPIN). In Phase 1, ATI-2173 demonstrated potent hepatitis B virus (HBV) activity with sustained off-treatment responses 4 to 24 weeks after discontinuation. The SAVE-1 Phase 2a trial evaluated the efficacy of ATI-2173 + tenofovir disoproxil fumarate (TDF) in treatment-naïve chronic HBV-infected (CHB) patients.

Method: A randomized, double-blind, placebo-controlled trial (NCT04847440) was conducted at sites in Moldova and Ukraine. Each cohort had 10 CHB patients randomized 8:2 to receive either 25 mg or 50 mg of ATI-2173 + TDF or placebo (PBO) + TDF daily for 90 days. HBV DNA and HBV RNA were measured using a Roche cobas 6800 (lower limit of quantification; LLOQ = 10 IU/ml, and 10 copies/ml respectively). The Roche RNA assay is investigational use only. Hepatitis B surface antigen (HBsAg) was measured using a Roche Elecsys (LLOQ = 0.05 IU/ml).

Results: Most patients were hepatitis B e antigen-negative (90%). Change from baseline virologic responses (HBV DNA) at the end of treatment for TDF alone (N = 4), 25 mg (N = 8) and 50 mg ATI-2173 + TDF (N = 8) were -3.53, -3.72, and -3.54 log₁₀ IU/ml, respectively. No changes in HBsAg were observed. HBV RNA mirrored the HBV DNA responses on treatment. At 12 weeks off treatment, viral load response in the TDF arm was -0.66, while the 25 mg and 50 mg arms had maintained suppression of -3.20 and -3.50 log₁₀ IU/ml, respectively (Figure). 0/4 in the TDF alone, 3/8 in the 25 mg cohort and 3/8 in the 50 mg cohort had HBV DNA below the limit of quantification <10 IU/ml at 12 weeks off treatment. By the week 12 visit, none of the 16 subjects in the ATI-2173 + TDF arms restarted TDF compared to 1 of 4 in the TDF alone arm who restarted TDF at week 8 due to virologic relapse (HBV DNA >2000 IU/ml). An off-treatment alanine aminotransferase (ALT) flare was observed in the TDF arm but not in the ATI-2173 arms.

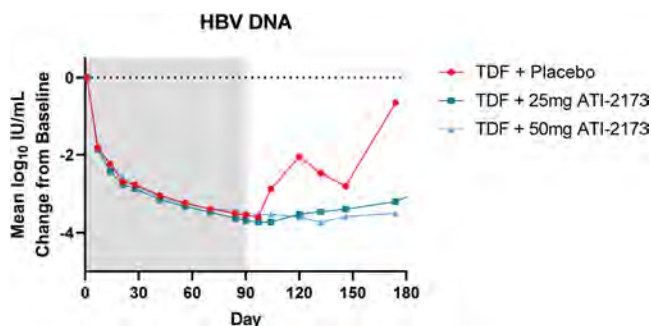


Figure: Mean HBV DNA change from baseline across arms.

Conclusion: Similar on- and off-treatment HBV DNA antiviral activity was observed between 25 mg and 50 mg cohorts of ATI-2173 + TDF. In the off-treatment period, ATI-2173 + TDF provided prolonged HBV DNA suppression, longer time to rebound, and absence of ALT flares compared to TDF alone. 24-week off-treatment data will be presented at the conference.

NAFLD: Diagnostics and non-invasive assessment

OS096

Impact of type 2 diabetes on the accuracy of non-invasive tests of liver fibrosis: a comprehensive analysis of 1,051 biopsy proven NAFLD patients showing clinical implications

Jerome Boursier¹, Clémence M. Canivet¹, Charlotte Costentin², Adrien Lannes³, Adele Delamarre⁴, Nathalie Sturm⁵, Brigitte Le Bail⁶, Sophie Michalak⁷, Frédéric Oberti³, Marie-Noëlle Hilleret², Marie Irlès-Depe⁴, Isabelle Fouchard³, Paul Hermabessière⁴, Justine Barthemon², Bertrand Cariou⁸, Victor de Lédighen⁴, Marine Roux¹. ¹Angers University, HIFIH Laboratory UPRES EA3859; ²Grenoble University Hospital, Hepato-Gastroenterology Department; ³Angers University Hospital, Hepato-Gastroenterology Department; ⁴Bordeaux University Hospital, Hepato-Gastroenterology Department; ⁵Grenoble University Hospital, Pathology Department; ⁶Bordeaux University Hospital, Pathology Department; ⁷Angers University Hospital, Pathology Department; ⁸Nantes University
Email: jeboursier@chu-angers.fr

Background and aims: It has been suggested that non-invasive tests (NITs) of liver fibrosis are less accurate in type 2 diabetes (T2D). We aimed to compare the diagnostic accuracy of six NITs between patients with and without T2D, to explain the observed differences, and to adapt diagnostic algorithms for clinical practice accordingly.

Method: 1,051 patients with non-alcoholic fatty liver disease (NAFLD), liver biopsy, blood fibrosis tests (NAFLD fibrosis score, FIB4, Fibrotest, FibroMeterV2G), vibration controlled transient elastography (VCTE), and the combinatory elasto-blood test FibroMeterVCTE were included. The study end point was advanced fibrosis (NASH CRN staging) on liver biopsy.

Results: The difference in result for NAFLD fibrosis score was highly significant between patients with and without T2D, T2D being included in the test formula. Consequently, only 11% of the patients with T2D were included in the rule-out zone of the NAFLD fibrosis score. AUROCs of the five other NITs were significantly lower in patients with T2D, mostly because of a decrease in specificity. The decrease of FIB4 specificity was explained by the significantly higher age of patients with T2D. After adjustment for age, there was no longer significant difference in FIB4 accuracy between patients with and without T2D. The decrease of specificity observed for Fibrotest, FibroMeterV2G, and FibroMeterVCTE was explained by age but also by higher alpha2macroglobulin level which is known to increase in T2D. Sensitivity of NITs was not affected by T2D but, because of the twofold higher prevalence of advanced fibrosis in this group, it masked a doubled raw number of false negatives in T2D. The sequential algorithm FIB4-VCTE had 90.3% diagnostic accuracy in patients without T2D versus only 79.0% in T2D (p < 0.001). To maintain rates of false-positives and false-negatives in a similar range than obtained with the FIB4-VCTE algorithm in patients without T2D, diagnostic algorithms in patients with T2D required specialized tests (first-line VCTE or FibroMeterV2G, then second-line FibroMeterVCTE).

Conclusion: The diagnostic accuracy of NITs is different between patients with and without T2D because of the different prevalence of advanced fibrosis in these two populations, but also because T2D

ORAL PRESENTATIONS

itself modifies the level of some biomarkers. The diagnosis of advanced liver fibrosis in T2D should use first-line specialized tests.

OS097

Machine learning algorithms identify novel biomarker combinations for NAFLD

Jenny Lee¹, Max Westphal², Yasaman Vali¹, Yu Chen³, Leigh Alexander⁴, Jerome Boursier⁵, Quentin Anstee⁶, Aeilko Zwinderman¹, Patrick Bossuyt¹. ¹Amsterdam UMC, Locatie AMC, Department of Epidemiology and Data Science, Amsterdam, Netherlands; ²Fraunhofer MEVIS, Data Science and Biostatistics, Bremen, Germany; ³Eli Lilly and Company Ltd, Lilly Research Laboratories, Indianapolis, United States; ⁴SomaLogic Inc, Boulder, United States; ⁵Angers University Hospital, Hepatology Department, Angers, France; ⁶Newcastle University, Translational and Clinical Research Institute, Newcastle upon Tyne, United Kingdom
Email: j.a.lee@amsterdamumc.nl

Background and aims: Application of machine learning algorithms for developing diagnostic tests (or NITs) has grown across multiple disciplines, with models achieving promising classification performance levels. For non-alcoholic fatty liver disease (NAFLD), detection of non-alcoholic steatohepatitis (NASH) and advanced fibrosis remains challenging. We aimed to develop classifiers by applying machine learning algorithms to stage NAFLD patients.

Method: Data from the LITMUS Metacohort, which includes adults with biopsy-proven NAFLD were analyzed for NASH (NAS \geq 4) and advanced fibrosis (F \geq 3), staged according to the NASH-CRN scale. Thirty-three predictors (clinical characteristics, serum biomarkers and FibroScan-VCTE) were included in the analysis. Any missing data were handled by multiple imputation. Data were randomly split (75/25) into training and validation sets. Gradient boosting method (GBM) was applied to develop a classifier for each component of NASH (ballooning, inflammation, steatosis) and for advanced fibrosis, with repeated 10-fold cross-validation to tune hyperparameters. Class predictions for each component of NASH were aggregated to obtain a total NASH probability. Area under the receiver operating characteristic (AUC) curve was used to evaluate performance.

Results: Data from 720 NAFLD adults were analyzed (training set: 540, validation set: 180), of which 53% had NASH and 26% advanced fibrosis (including 7% cirrhotics). The AUCs for each component of NASH in the training/validation sets were: steatosis (0.68/0.66), inflammation (0.72/0.80), and ballooning (0.66/0.69). The aggregate GBM model for NASH achieved an AUC of 0.79 in the training and 0.74 in the validation set. For the GBM model for advanced fibrosis, the AUC was 0.90 and 0.84 in the training and validation sets, respectively. Different predictors were selected as most informative for the NASH components and fibrosis models (Table 1).

Table 1: Top five predictors for NASH components and fibrosis models

	Steatosis	Inflammation	Ballooning	Fibrosis
1	Body mass index (BMI)	Hemoglobin	BMI	Liver stiffness measurement-VCTE
2	Cytokeratin-18 (CK-18) M30 antigen	Age	Alkaline phosphatase	CK-18 M30 antigen
3	Age	Hyaluronic acid	Systolic blood pressure	Hyaluronic acid
4	Procollagen III peptide (P3NP)	P3NP	N-terminal type III collagen propeptide (PRO-C3)	PRO-C3
5	Alanine transaminase	Tissue inhibitor matrix metalloproteinase 1 (TIMP1)	Aspartate aminotransferase	Haemoglobin A1c

Conclusion: The GBM algorithm produced a high performing model for detecting advanced fibrosis, performance was less impressive for the NASH models. Better predictors, with understood associations to steatosis, inflammation and ballooning, are needed to develop more

robust models for detecting NASH. Validation of the models in the prospective LITMUS cohort is underway.

OS098

Head to head comparison of MEFIB, MAST, and FAST for detecting candidates with stage 2 fibrosis or higher among patients with NAFLD

Beom Kyung Kim^{1,2}, Nobuharu Tamaki^{1,3}, Jinho Jung¹, Claude Sirlin¹, Atsushi Nakajima⁴, Rohit Loomba¹. ¹University of California San Diego, La Jolla, United States; ²Yonsei University College of Medicine, Korea, Rep. of South; ³Musashino Red Cross Hospital, Tokyo, Japan; ⁴Yokohama City University Graduate School of Medicine, Kanagawa, Japan
Email: roloomba@ucsd.edu

Background and aims: Non-alcoholic fatty liver disease (NAFLD) patients with significant fibrosis (fibrosis stage \geq 2) are candidates for pharmacological trials. Here, we compared head-to-head the diagnostic accuracies of non-invasive models, MEFIB (magnetic resonance elastography [MRE] plus FIB-4), MAST (magnetic resonance imaging-aspartate aminotransferase [AST]), and FAST (FibroScan-AST) for detecting significant fibrosis.

Method: This prospective study included 563 biopsy-proven NAFLD patients undergoing contemporaneous MRE, MRI proton density fat fraction (MRI-PDFF), and FibroScan from two prospective cohorts. Each model was categorized into three classes as rule-in, indeterminate, and rule-out, using rule-in/-out criteria. Diagnostic performances of models were evaluated by area under the receiver operating characteristic (AUROC).

Results: The mean age was 56.5 years and 49% were male. Significant fibrosis was observed in 51.2%. To predict significant fibrosis, MEFIB outperformed both MAST and FAST (both $p < 0.001$); AUROCs (95% confidence interval) for MEFIB, MAST, and FAST as categorical variables were 0.901 (0.875–0.928), 0.770 (0.730–0.810), and 0.725 (0.683–0.767), respectively. Using rule-in criteria, positive predictive value of MEFIB (95.3%) was higher than FAST (83.5%, $p = 0.001$), but similar to MAST (90.0%, $p = 0.056$). Notably, MEFIB's rule-in criteria covered more of the study population than MAST (34.1% vs. 26.6%; $p = 0.006$). Using rule-out criteria, negative predictive value of MEFIB (90.1%) was higher than either MAST (69.6%) or FAST (71.8%) (both $p < 0.001$).

Conclusion: MEFIB showed the reliability of rule-in/-out, with a better predictive performance compared to MAST and FAST. Thus, a two-step strategy by MEFIB (FIB-4 followed by MRE), may be used to identify \geq 2 stage fibrosis.

Key words: NAFLD, significant fibrosis, MEFIB, FAST, MAST, diagnosis, validation

OS099

Validation of the new 2021 EASL algorithm for the non-invasive diagnosis of advanced liver fibrosis in non-alcoholic fatty liver disease

Clémence M. Canivet^{1,2}, Adrien Lannes^{1,2}, Charlotte Costentin³, Adele Delamarre⁴, Nathalie Sturm³, Frédéric Oberti^{1,2}, Thomas Decaens³, Marie Irles-Depe³, Isabelle Fouchard^{1,2}, Paul Hermabessière⁴, Justine Barthemon³, Victor de Lédinghen⁴, Jerome Boursier^{1,2}. ¹Angers University Hospital Center, Angers, France; ²Université d'Angers, HIFIH, UPRES EA3859, Angers, France; ³Centre Hospitalier Universitaire de Grenoble, La Tronche, France; ⁴Chu Haut Leveque, Pessac, France
Email: clemence.canivet@chu-angers.fr

Background and aims: EASL recently proposed in its 2021 guidelines an algorithm for the diagnosis of advanced liver fibrosis (AF) in patients with non-alcoholic fatty liver disease (NAFLD). This original algorithm is based on the sequential use of FIB4, then vibration controlled transient elastography (VCTE) and, innovatively, on the use of patented serum tests as third-line procedure. Our objective was to evaluate the diagnostic accuracy of this algorithm (FIB4/VCTE/patented serum test) in a large cohort of NAFLD patients.

Method: 1,051 NAFLD patients with liver biopsy were included in three tertiary centres. Four non-invasive fibrosis tests were available: FIB4, VCTE, FibroMeter and Fibrotest. The ELF score was available in a subgroup of 396 patients. AF was defined on liver biopsy as fibrosis \geq F3 according to the NASH-CRN classification

Results: The median age was 58.1 years, half of the patients were diabetic, and 60% were male. The prevalence of AF was 39.5%. Agreement between two non-invasive fibrosis tests (FIB4 then VCTE, VCTE then patented serum test) increased specificity and positive predictive value to respectively 83–89% and 79–85%, versus 58–75% and 56–65% with single fibrosis tests. Within the EASL algorithm, the third line testing with a patented serum test allowed to correctly reclassify 29% (FibroMeter), 42% (Fibrotest) and 65% (ELF) of the false positive results following the FIB4 then VCTE sequence. All these results justified the sequential use of NITs proposed by the EASL algorithm. Accuracy of the EASL algorithm for the diagnosis of AF is detailed in the Table. In the whole study population, both FIB4/VCTE/FibroMeter and FIB4/VCTE/Fibrotest algorithms performed similarly. Same results were obtained in the subgroup of 396 patients where the FIB4/VCTE/ELF algorithm was available. In the whole population, 28.7% of F3–F4 patients were false negatives, among whom only 18.5% had cirrhosis. The EASL algorithm provided 85% sensitivity for the diagnosis of cirrhosis.

Conclusion: Our study validates the algorithm proposed by the EASL in its latest 2021 guidelines for the diagnosis of AF in NAFLD.

Figure: Accuracy of the 2021 EASL algorithm for the diagnosis of AF

	Whole study population (n = 1,051)			ELF group (n = 396)		
First line test	FIB4	FIB4	FIB4	FIB4	FIB4	FIB4
Second line test	VCTE	VCTE	VCTE	VCTE	VCTE	VCTE
Third line test	FibroMeter	Fibrotest	FibroMeter	Fibrotest	ELF	
Diagnostic accuracy (%)	81.4	82.8	84.1	85.9	87.4	
Sensitivity (%)	71.3	71.3	73.5	73.5	73.5	
Specificity (%)	88.0	90.2	89.4	92.0	94.3	
Negative predictive value (%)	82.5	82.8	87.1	87.4	87.7	
Positive predictive value (%)	79.6	82.7	77.6	82.2	86.6	
Negative likelihood ratio (%)	0.33	0.32	0.30	0.29	0.28	
Positive likelihood ratio (%)	5.97	7.32	6.93	9.24	12.93	
Odd ratio	18.3	23.0	23.4	32.1	46.0	
Second line test requirement (%)	57.3	57.3	55.1	55.1	55.1	
Third line test requirement (%)	38.3	38.3	35.4	35.4	35.4	
Biopsy rate (%)	6.8	12.7	7.1	14.4	11.9	

OS101

Utility of FIB-4 thresholds to identify patients with at-risk F2–F3 NASH based on screening data from a 2000 patient biopsy confirmed cohort of resmetirom Phase 3 clinical trial, MAESTRO-NASH

Jörn Schattenberg¹, Naim Alkhouri², Rebecca Taub³, Jim Hennen⁴, Mazen Nouredin⁵, Stephen Harrison⁶. ¹Johannes Gutenberg-University Mainz; ²Arizona Liver Institute; ³Madrigal Pharmaceuticals, Conshohocken, United States; ⁴Madrigal Pharmaceuticals; ⁵Cedar Sinai Medical Center; ⁶Pinnacle Research, United States
Email: rebeccataub@yahoo.com

Background and aims: MAESTRO-NASH NCT03900429 is a 52-week Phase 3 registration double blind placebo controlled NASH clinical trial to study the effect of resmetirom in patients with NASH and significant liver fibrosis. Eligibility requires at least three metabolic risk factors, fibroscan VCTE kPa \geq 8.5 and biopsy-proven NASH with fibrosis stage 1B, 2, or 3 (or 1A/C with PRO-C3 \geq 14), and NAFLD activity score (NAS) \geq 4 with at least 1 in each NAS component. FIB-4 of \geq 1.3 is frequently used to identify potential at-risk NASH patients and patients with FIB-4 < 1.3 may be considered low risk.

Method: FIB-4 cutoff values of 1.3 and 1.0 were applied to ~2000 patients who screened for MAESTRO-NASH with screening labs, fibroscan, MRE, MRI-PDFF and a screening liver biopsy. Relationships

between screening FIB-4 \geq 1.0 and \geq 1.3 and liver biopsy NAS and fibrosis stage were assessed.

Results: 56.9% F2, 40.3% F3, 24.4% F4 biopsy confirmed patients had FIB-4 < 1.3 and, 46.4% of patients with active NASH (NAS \geq 4) fibrosis F2/F3 had FIB-4 < 1.3 (Table). 32.6% of F2 and 18.0% of F3 subjects had FIB-4 < 1.0. In patients with active NASH (NAS \geq 4), 41.7% of F2 and 17.3% of F3 subjects had FIB-4 < 1.0. NAS \geq 4 F2–F3 patients with FIB-4 \geq 1.3 had mean age 61.1 while NAS \geq 4 F2–F3 patients with FIB-4 < 1.3 had mean age 52.2 (p < 0.001); those with FIB-4 \geq 1.0 had mean age 59.9; NASH patients with FIB-4 < 1.0, had mean age 47.6 (p < 0.001). More low risk NAFLD patients (F0, F1A/C) had FIB-4 < 1.3 than FIB-4 < 1.0 (F0, 84.3% versus 58.1%, respectively). Absolute values of AST (p < 0.0001), ALT (p < 0.0001), PRO-C3 (p < 0.0001), HbA1c (p = 0.0001), GGT (p < 0.0001) and MRE (p < 0.0001) showed statistically significant differences between low risk (F0) and high risk (F2–F3) NASH patients and could be used to further stratify risk.

Conclusion: Based on a large Phase 3 data set of biopsy confirmed NASH patients, FIB-4 \geq 1.3 lacks the sensitivity to accurately identify patients with at-risk F2–F3 NASH. The influence of age on FIB-4 may require an age adjustment to ensure younger patients are not removed from consideration for therapy.

	FIB-4 (1.3) n < 1.3/total pts.		FIB-4 (1.0) n < 1.0/total pts.	
All Biopsy Subjects		%		%
F0	199/236	84.3	137/236	58.1
F1A/C	212/293	72.4	147/293	50.2
F1B	119/184	64.7	74/184	40.2
F2	253/445	56.9	145/445	32.6
F3	303/752	40.3	135/752	18.0
F4	21/86	24.4	10/86	11.6
All Subjects	1107/1996	55.5	648/1996	32.5
Patients with	FIB-4 (1.3)		FIB-4 (1.0)	
Eligible NAS \geq 4	% < 1.3/NAS eligible pts.		% < 1.0/NAS eligible pts.	
F0	NA		NA	
F1A/C	58.9		28.6	
F1B	63.9		43.6	
F2	55.8		41.7	
F3	39.2		17.3	
F4	NA		NA	
All Subjects	47.9		25.0	

Liver tumours: Clinical aspects except therapy

OS102

Radiomic model based on contrast-enhanced CT imaging to predict early recurrence for patients with hepatocellular carcinoma after radical resection

Liying Ren¹, Dongbo Chen², Tingfeng Xu¹, Pu Chen², Bigeng Zhao¹, Hongsong Chen², Weijia Liao¹. ¹Affiliated Hospital of Guilin Medical University, Laboratory of Hepatobiliary and Pancreatic Surgery; ²Peking University People's Hospital, Peking University Hepatology Institute, Beijing Key Laboratory of Hepatitis C and Immunotherapy for Liver Disease, China
Email: liaoweijia288@163.com

Background and aims: Radical resection remains an effective strategy for patients with hepatocellular carcinoma (HCC), unfortunately, the postoperative early recurrence (recurrence within 2 years) rate is still high. Therefore, we developed a radiomic model based on preoperative contrast-enhanced CT (ce-CT) to evaluate the early recurrence for patients with a single tumor.

Method: We enrolled a total of 422 patients from two centers who were diagnosed with single HCC and received radical resection. At first, the features from venous and arterial phase of ce-CT were extracted based on the region of interest (ROI), and the early recurrence related radiomic features were selected via the Least

ORAL PRESENTATIONS

Absolute Shrinkage and Selection Operator proportional hazards model (LASSO Cox) model and determined radiomic scores for each patient. Then the clinicopathologic data were combined to develop a model to predict early recurrence by Cox regression. Last we evaluated the prediction effect of this model by multiple methods.

Results: A total 1915 radiomic features were extracted from ce-CT images, and 31 of them were used to determine the radiomic scores, which showed significant difference between early recurrence and non-early recurrence groups. Univariate and multivariate Cox regression analyses result showed radiomic scores and serum AFP were independent indicators and were used to develop a combined model to predict early recurrence. The area under the receiver operating characteristic curve (AUC) were 0.77 and 0.74, while C-indexes were 0.712 and 0.674, respectively in the training and validation cohorts. The calibration curves and decision curve analysis showed satisfactory accuracy and clinical utilities, as well. Kaplan-Meier curves based on the recurrence-free survival (RFS) and overall survival (OS) showed significant differences.

Conclusion: The preoperative radiomic model showed value to predict early recurrence for patients with single HCC.

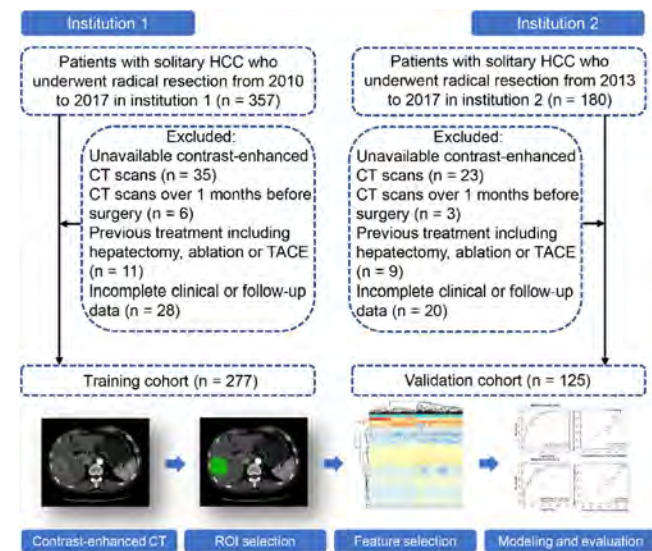


Figure 1:

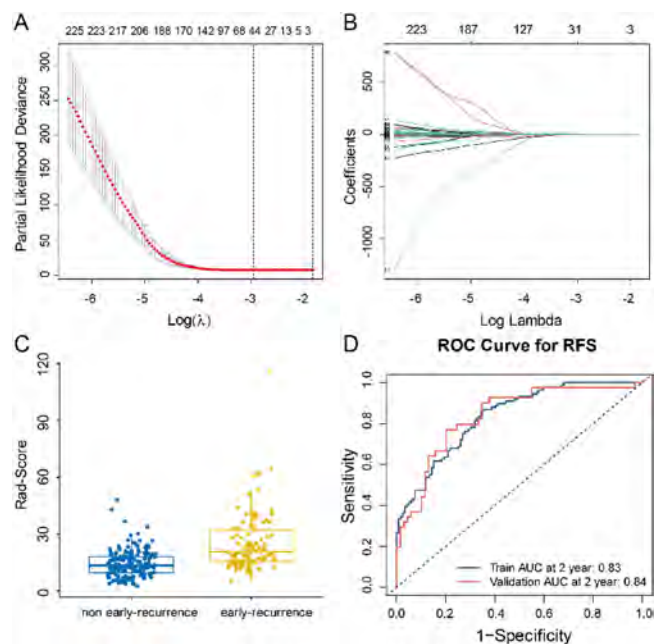


Figure 2:

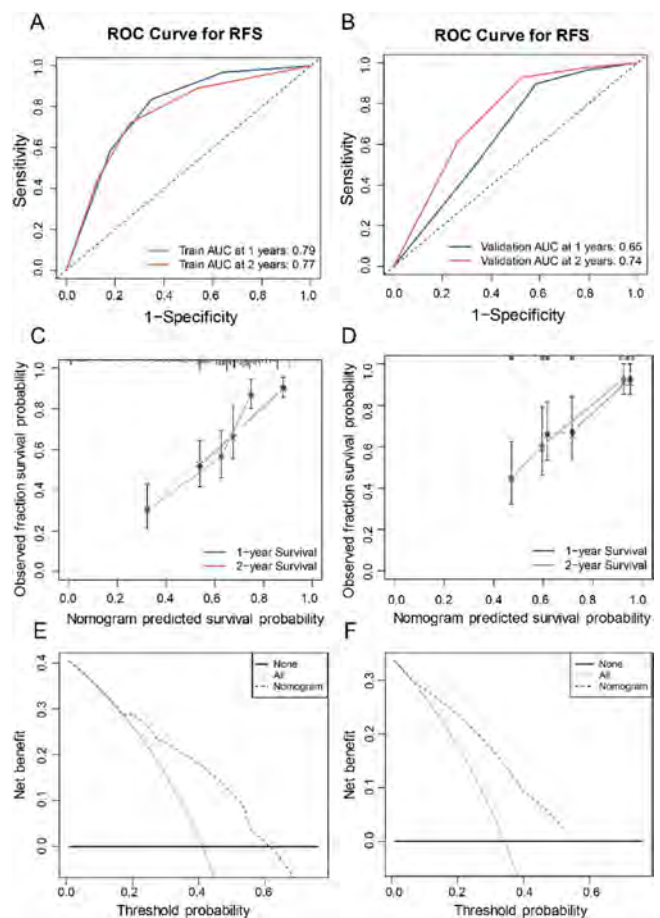


Figure 3:

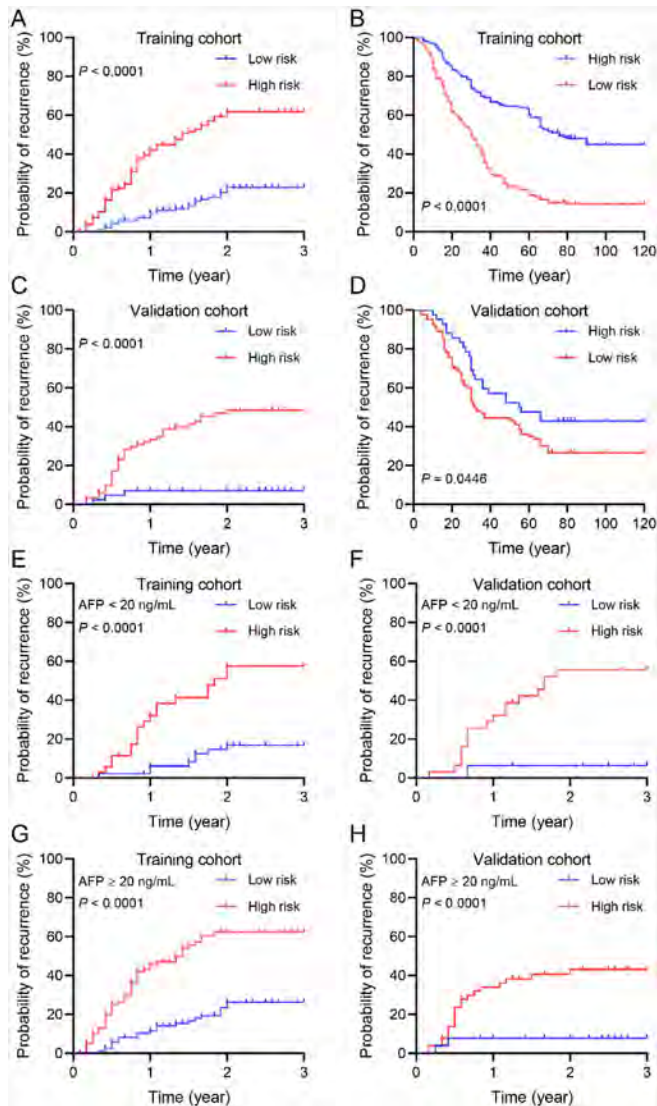


Figure 4:

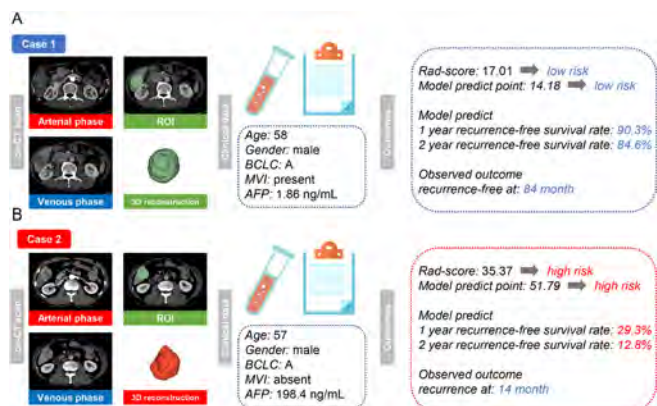


Figure 5:

OS103

Circulating vesicles hold etiology-related protein biomarkers of cholangiocarcinoma risk, early diagnosis and prognosis mirroring tumour cells

Ainhoa Lapitz¹, Mikel Azkargorta^{2,3}, Ekaterina Zhuravleva⁴, Marit M. Grimsrud⁵, Colm O. Rourke⁴, Ander Arbelaiz¹, Adelaida La Casta¹, Mette Vesterhus^{5,6}, Piotr Milkiewicz^{7,8}, Malgorzata Milkiewicz⁸, Raul Jimenez-Aguero¹, Tania Pastor¹, Rocio IR Macias^{1,9}, Ioana Riaño¹, Laura Izquierdo-Sánchez¹, Marcin Krawczyk^{10,11}, Cesar Ibarra¹², Javier Bustamante¹², Felix Elortza^{2,3}, Juan Falcon-Perez^{3,13,14}, María Jesús Perugorria^{1,3}, Jesper Andersen⁴, Luis Bujanda^{1,3}, Tom Hemming Karlsen⁵, Trine Folseraas^{5,15}, Pedro Miguel Rodrigues^{1,3,14}, Jesus Maria Banales^{1,3,14,16}. ¹Biodonostia Health Research Institute, Department of Liver and Gastrointestinal Diseases, San Sebastian, Spain; ²CIC bioGUNE, Proteomics Platform, Derio, Spain; ³National Institute for the Study of Liver and Gastrointestinal Diseases (CIBERehd), ISCIII, Madrid, Spain; ⁴Biotech Research and Innovation Centre, Department of Health and Medical Sciences, Copenhagen, Denmark; ⁵Norwegian PSC Research Center, Department of Transplantation Medicine, Division of Surgery, Inflammatory Medicine and Transplantation, Oslo, Norway; ⁶University of Bergen, Dept. of Clinical Science, Bergen, Norway; ⁷Medical University of Warsaw, Department of General, Transplant and Liver Surgery, Warsaw, Poland; ⁸Pomeranian Medical University, Department of Medical Biology, Szczecin, Poland; ⁹Biomedical Research Institute of Salamanca (IBSAL), Experimental Hepatology and Drug Targeting (HEVEPHARM), Salamanca, Spain; ¹⁰Saarland University Medical Centre, Department of Medicine II, Homburg, Germany; ¹¹Centre for Preclinical Research, Department of General, Transplant and Liver Surgery, Warsaw, Poland; ¹²Hospital of Cruces, Bilbao, Spain; ¹³CIC bioGUNE, Exosomes Laboratory, Derio, Spain; ¹⁴Ikerbasque, Basque Foundation for Science, Bilbao, Spain; ¹⁵Oslo University Hospital, Department of Transplantation Medicine, Oslo, Norway; ¹⁶University of Navarra, Department of Biochemistry and Genetics, Pamplona, Spain. Email: jesus.banales@biodonostia.org

Background and aims: Cholangiocarcinomas (CCAs), heterogeneous biliary tumors with dismal prognosis, lack accurate early-diagnostic methods, especially important for individuals at high-risk (i.e. primary sclerosing cholangitis (PSC)). Here, we aimed to identify precise non-invasive CCA biomarkers.

Method: Serum extracellular vesicles (EVs) from patients with: i) isolated PSC (n = 39); ii) PSC without clinical evidences of malignancy at sampling who developed CCA overtime (PSC to CCA; n = 10); iii) concomitant PSC-CCA (n = 14); iv) CCAs from non-PSC etiology (n = 26); and v) healthy individuals (n = 41) were analyzed by mass-spectrometry. Diagnostic biomarkers of PSC-CCA, non-PSC CCA or CCAs regardless etiology (pan-CCAs) were defined, and their expression evaluated in human multi-organs and within CCA tumors at single-cell level. Prognostic EV-biomarkers for CCA were described.

Results: High-throughput proteomics identified candidate diagnostic biomarkers for PSC-CCA, non-PSC CCA or pan-CCA, independent to sex, age and CCA subtype. Machine learning logit modelling disclosed PLCH1/FGL1 algorithm with diagnostic value of AUC = 0.903 and OR = 27.8 for early-stage PSC-CCA vs isolated PSC, overpowering CA19-9 (AUC = 0.608, OR = 2.0). An algorithm combining SAMP/A1AT allowed the diagnosis of early-stage non-PSC CCAs compared to healthy individuals (AUC = 0.863, OR = 18.5). Noteworthy, the levels of 6 proteins (ALBU;FIBB;FLG1;IGHA1;TLN1;IMA8) showed predictive value for CCA development in patients with PSC before clinical evidences of malignancy. Multi-organ transcriptomic analysis revealed that serum EV-biomarkers were mostly expressed in hepatobiliary tissues and scRNA-seq analysis of CCA tumors indicated that some biomarkers -including PIGR, FGG, SERPINA1, FGL1- were mainly expressed in malignant cholangiocytes. Multivariable analysis revealed EV-prognostic biomarkers independent to clinical features,

ORAL PRESENTATIONS

with FCN2/SDPR/FA9 panel being strongly associated to patients' survival.

Conclusion: Serum EVs contain etiology-specific protein biomarkers for the prediction, early diagnosis and prognosis estimation of CCA, representing a novel tumor cell-derived liquid biopsy for personalized medicine.

OS104

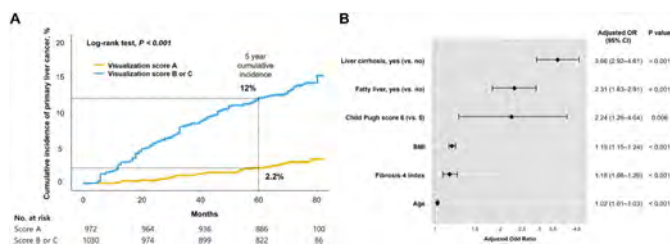
Evaluation of the effectiveness of surveillance according to the ultrasound liver imaging reporting and data system (US LI-RADS) visualization score in patients with chronic hepatitis B

Min Kyung Park¹, Yun Bin Lee¹, Yoon Jun Kim¹, Jung-Hwan Yoon¹, Dong Ho Lee², Jeong-Hoon Lee¹. ¹Seoul National University College of Medicine, Department of Internal Medicine and Liver Research Institute, Seoul, Korea, Rep. of South; ²Seoul National University College of Medicine, Department of Radiology, Seoul, Korea, Rep. of South
Email: pindra@empas.com

Background and aims: Ultrasonography (US) is a standard surveillance tool of hepatocellular carcinoma (HCC) in the high-risk group. This study evaluated the detection power of the US and the occurrence of primary liver cancer (PLC) according to the US Liver Imaging Reporting and Data System (LI-RADS) visualization score.

Method: Consecutive patients with chronic hepatitis B undergoing regular HCC surveillance were included in this cohort study. Outcomes of interest included cumulative incidence of PLC and false-negative rate of US (defined as no HCC on US conducted within 3 months prior to PLC diagnosis) according to baseline LI-RADS visualization scores (A vs B/C). Risk factors associated with poor visualization score were also analyzed.

Results: A total of 2,002 patients were included in this study: 972 were classified as visualization score A and 1,030 as either visualization score B or C (score B, 1,003; score C, 27). During a median follow-up of 75 months (interquartile range, 69–77 months), 166 patients developed PLC (HCC, 158; others, 8). Patients with poor visualization score (visualization score B or C) has significantly higher risk of PLC than those with visualization score A (2.41%/year vs. 0.50%/year; hazard ratio, 4.83; 95% confidence interval, 3.24–7.21; $p < 0.001$ by log-rank test) (Figure 1A). Higher false-negative rate of US was observed in the poor visualization group than visualization score A (43.5% vs. 20.0%). Furthermore, among 51.2% (85 of 166) patients diagnosed as very early-stage PLC, merely 13.9% (10 of 72) of patients with visualization score B/C were detected with US, while in 53.8% (7 of 13) among patients with visualization score A. Poor visualization score was independently associated with the presence of liver cirrhosis (adjusted odds ratio [aOR], 3.66) or fatty liver (aOR, 2.31), high body mass index (aOR, 1.19), high FIB-4 score (aOR, 1.16), and Child-Pugh score 6 (vs score 5: aOR, 2.24) (Figure 1B).



Conclusion: Chronic hepatitis B patients with US LI-RADS visualization score B/C had a higher risk of PLC as well as false-negative rate of US than those with score A. Surveillance using alternative computed tomography or magnetic resonance imaging might be highly recommended for patients with US LI-RADS visualization score B or C.

OS105

Training, validation and testing of a multiscale three-dimensional deep learning algorithm in accurately diagnosing hepatocellular carcinoma on computed tomography

Wai-Kay Seto^{1,2,3}, Keith Wan Hang Chiu^{4,5}, Wenming Cao¹, Gilbert Lui⁶, Jian Zhou⁷, Ho Ming Cheng¹, Juan Wu³, Xinpeng Shen⁸, Lung Yi Loey Mak^{1,2}, Jinhua Huang⁹, Wai Keung Li⁶, Man-Fung Yuen^{1,2}, Philip Yu^{6,10}. ¹The University of Hong Kong, Medicine, Hong Kong; ²The University of Hong Kong, State Key Laboratory of Liver Research, Hong Kong; ³The University of Hong Kong-Shenzhen Hospital, Medicine, Shenzhen, China; ⁴The University of Hong Kong, Diagnostic Radiology, Hong Kong; ⁵Kwong Wah Hospital, Diagnostic and Interventional Radiology, Hong Kong; ⁶The Education University of Hong Kong, Mathematics and Information Technology, Hong Kong; ⁷Sun Yat-sen University Cancer Center, State Key Laboratory of Oncology in South China, Guangzhou, China; ⁸The University of Hong Kong-Shenzhen Hospital, Medical Imaging, China; ⁹Sun Yat-sen University Cancer Center, Department of Minimal Invasive Interventional Therapy, Guangzhou, China; ¹⁰The University of Hong Kong, Computer Science, Hong Kong
Email: wkseto@hku.hk

Background and aims: Liver cancer ranks second globally in cancer death and has a high case-fatality rate. The Liver Imaging Reporting and Data System (LIRADS) categorizes liver observations on cross-sectional imaging based on hepatocellular carcinoma (HCC) risk. Intermediate-risk observations require repeated scans making an early diagnosis of HCC difficult. It remains uncertain if artificial intelligence can improve the diagnostic performance of computed tomography (CT) for HCC.

Method: We retrospectively collected archived thin-cut (<1.25 mm slice thickness) contrast triphasic CT images in raw DICOM format and relevant clinical information. CT observations were contoured and categorized via LIRADS, with ground truth diagnosis of HCC established via AASLD recommendations and validated by a clinical composite reference standard based on subsequent 12-month outcomes. We constructed several deep learning algorithms (NVIDIA Tesla V100 GPUs, Dell Technologies), including the multiscale three-dimensional convolutional network (MS3DCN, Figure 1) model which uniquely considers the multi-phasic nature of CT, and followed the Checklist for AI in Medical Imaging (CLAIM) framework for algorithm training, validation and testing.

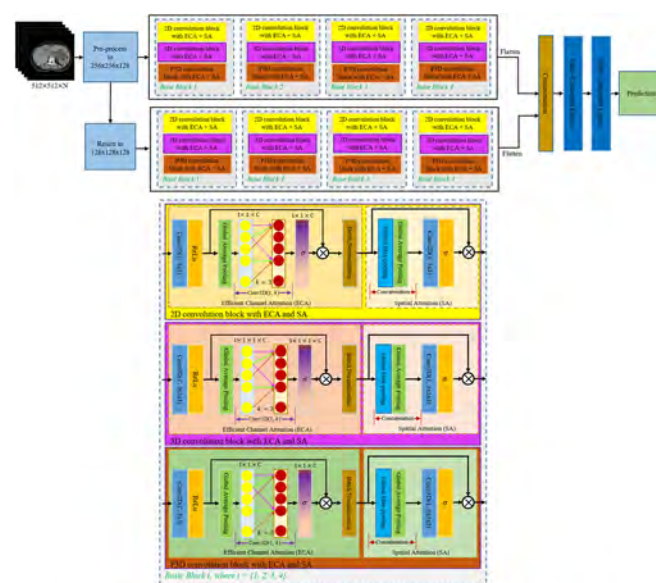


Figure 1. Model architecture of the MS3DCN deep learning algorithm to achieve an accurate diagnosis of HCC

Results: Among 2,796 retrieved scans, 2,281 were included with 3,620 liver observations contoured. The cohort's mean age was 58.4 ± 14.2 years, 61.0% male, with 1,214 (53.2%) at-risk for HCC. Median observation size was 21.0 (IQR 12.6–41.3) mm; 793 (21.9%) had a ground truth diagnosis of HCC. After randomly dividing observations into training and validation sets in a 7:3 ratio, MS3DCN was the best-performing algorithm at observation level for diagnosing HCC, achieving an AUC of 96.9% (95%CI 95.3%–98.2%), sensitivity 95.9%, specificity 98.1%, positive predictive value (PPV) 93.7%, and negative predictive value (NPV) 98.8%; compared to AUC 85.3% (95%CI 82.4%–88.1%), sensitivity 71.3%, specificity 99.3%, PPV 96.7% and NPV 91.9% for LIRADS. Sensitivity analysis found MS3DCN's diagnostic performance to remain robust, achieving an AUC of 96.3% (95%CI 95.8%–97.6%) at patient level and 97.1% (95%CI 95.3%–98.6%) in the at-risk cohort. In external testing of an independent cohort of 551 scans and 780 observations, MS3DCN achieved an AUC of 98.0% (95%CI 96.8%–99.0%) and 97.6% (95%CI 96.0%–98.9%) at observation and patient level respectively.

Conclusion: The MS3DCN deep learning model deployed to triphasic CT was highly and robustly accurate in diagnosing HCC, superior to LIRADS, with performance validated via internal validation and external testing. Artificial intelligence-based technologies can facilitate precise establishment of diagnosis and improve clinical outcomes. Supported by the Innovation and Technology Fund, the Government of the HKSAR; and United Ally Research Limited, a subsidiary of Hong Kong Sanatorium and Hospital Limited.

OS106

Lifestyle factors and population attributable risk of hepatocellular carcinoma in lean vs non-lean populations

Kali Zhou¹, Tiffany Lim¹, Jennifer Dodge¹, Norah Terrault¹, Veronica Setiawan¹. ¹University of Southern California, Los Angeles, United States
Email: kalizhou@usc.edu

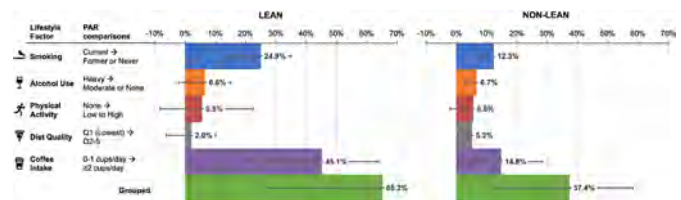
Background and aims: Several lifestyle factors are associated with risk of hepatocellular carcinoma (HCC), but actual impact may differ in individuals with normal (lean) vs elevated (non-lean) body mass index (BMI) due to differential prevalence. We aim to estimate the population attributable risk (PAR) of modifiable lifestyle factors to HCC burden in lean vs non-lean populations to prioritize these factors for patient-level counseling and population-level cancer prevention.

Method: We conducted prospective analysis using data from the Multiethnic Cohort (MEC), a large diverse cohort in Los Angeles County/Hawaii with >20 years of follow-up. Incident HCC was identified via cancer registry linkage. Lifestyle factors were obtained from baseline questionnaire: smoking (never/former/current), alcohol (none/low/heavy), diet quality (alternate Mediterranean diet (aMED) score: Q1 = lowest to Q5 = highest adherence), physical activity (none/low/high), and coffee intake (0, 1, ≥ 2 cups per day). Lean was defined as BMI <23 kg/m² for Asians and <25 kg/m² for non-Asians. BMI-stratified multivariable Cox models examined association of each factor with HCC adjusted for age, sex, race/ethnicity, diabetes, and hypertension, followed by calculation of PAR (%).

Results: Of 181,346 at risk participants, 753 developed HCC during an average follow-up of 19.8 years. 23.1% of cases vs 35.0% of non-cases were lean. At baseline, prevalence of current smoking was higher in lean vs non-lean cases (33.2% vs 21.8%); 23.1% in both groups reported heavy alcohol use. No physical activity was reported in 50.3% of lean vs 45.0% non-lean cases, while 76.4% vs 84.6% had suboptimal adherence to aMED diet (Q1–4). ≥ 2 cups/day of coffee was reported by 14.2% of lean vs 22.0% of non-lean cases. Smoking (former vs. never: HR = 2.08, 95% CI 1.39–3.09; current vs. never: HR = 4.41, 2.85–6.81) and coffee (≥ 2 vs 0 cups/day: HR = 0.47, 0.29–0.77) were associated with developing HCC for lean participants, compared to smoking (former: HR = 1.55, 1.26–1.89; current: HR = 2.62, 2.04–3.35), diet quality (Q5 vs Q1: HR = 0.61, 0.46–0.80), and coffee (≥ 2 vs 0 cups/day: HR = 0.77, 0.60–0.98) for non-lean participants. Alcohol use

approached significance in the non-lean group (heavy vs none: HR 1.22, 0.98–1.53) while physical activity was not significant for either group. Overall, the combined PAR for lifestyle factors was 65.2% in lean compared to 37.4% in non-lean. The lifestyle factor with highest PAR for both was coffee (45.1% lean, 14.8% non-lean), followed by smoking (24.9% lean, 12.3% non-lean). All other lifestyle factors had PAR <10%.

Conclusion: HCC burden can be substantially reduced through modifiable lifestyle factors, more prominently for lean compared to non-lean populations. Drinking ≥ 2 cups of coffee per day could reduce up to 45% of HCC burden among lean individuals. Diet and lifestyle counselling are critical to HCC prevention.



OS107

Validation of the prognostic role of a new distinct assessment of liver function in non surgical HCC patients

Bernardo Stefanini¹, Benedetta Stefanini², Andrea De Sinno³, Francesco Tovoli⁴, Franco Trevisani⁵, Fabio Piscaglia⁴. ¹Division of Internal Medicine, Hepatobiliary and Immunoallergic Diseases, IRCCS Azienda Ospedaliero-Universitaria di Bologna, Bologna, Italy; ²Semeiotica Medica, Azienda Ospedaliero-Universitaria di Bologna, Bologna, Italy; ³Alma Mater Studiorum-University of Bologna, Bologna, Italy; ⁴Division of Internal Medicine, Hepatobiliary and Immunoallergic Diseases, IRCCS Azienda Ospedaliero-Universitaria di Bologna, Department of Medical and Surgical Sciences (DIMEC), University of Bologna, Bologna, Italy; ⁵Semeiotica Medica, Azienda Ospedaliero-Universitaria di Bologna, Department of Medical and Surgical Sciences (DIMEC), University of Bologna, Bologna, Italy
Email: bernardo.stefanini@gmail.com

Background and aims: While the role of distinct HCC tumor burdens is quite consolidated, new insights about the impact of more granular assessment of liver function in the prognosis of HCC patients are emerging.

A very recent review published in Journal of Hepatology described the prognostic relevance of liver functional reserve across the various non-surgical HCC treatments. Based on their experience, the authors proposed a new staging algorithm combining liver functional reserve and tumor bulk separating patients even within the Child-Pugh A and B classes. The present study aims to validate the prognostic role of such system.

Method: We retrospectively evaluated all patients with HCC who were not surgically treated in two large Italian centers between 2010 and 2021. A Kaplan-Meier survival analysis was carried out classifying patients according to the new classification proposed by D'Avola, Piscaglia et al. which identifies four different subclasses considering the liver functional reserve:

LIR 1 (optimal) includes CPT class A patients with CPT score A5 and with no previous hepatic decompensation, no high risk varices, tumor related performance status (PS) ≤ 1 and ALBI grade = 1.

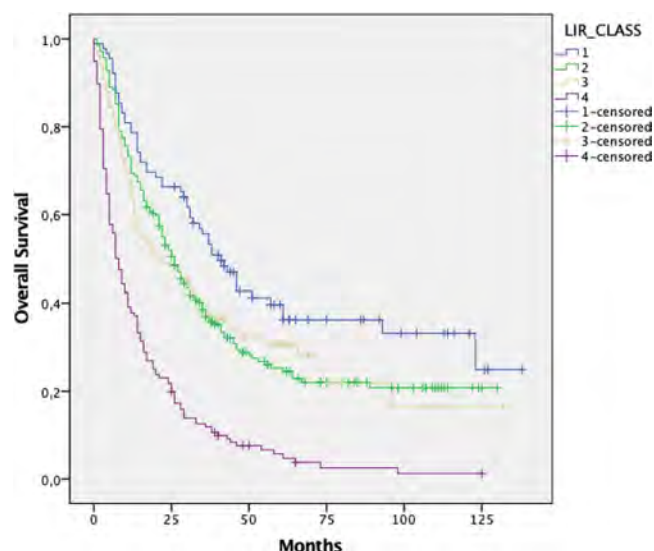
LIR 2 (suboptimal) includes CPT class A patients with ALBI grade ≤ 2 and PS ≤ 1 and either CPT score A5 but with a history of previous hepatic decompensation or score A6 (regardless of previous history of decompensation).

LIR 3 (intermediate) includes CPT class B patients with a CPT score of B7 and PS ≤ 1 regardless of any previous decompensation.

LIR 4 (poor) includes decompensated CPT B or C cirrhotic patients with a PS ≥ 2 .

ORAL PRESENTATIONS

Results: A total of 538 patients were analyzed. Median overall survival was 41 months in LIR 1 (89 pts), 26 months in LIR 2 (209 pts), 20 months in LIR 3 (84 pts) and 16 months in LIR 4 (156 pts). Interestingly, LIR 1 median OS was significantly higher than LIR 2 subgroup ($p < 0.05$), despite both including only CPT class A patients. LIR 2 OS which instead was closer to that of LIR 3 subgroup suggesting an important prognostic role for ALBI grade and past episodes of hepatic decompensation even for patients within the Child-Pugh A class. Additionally within the CPT B/C classes, a current decompensation must be kept separated from CPT B7 patients.



Conclusion: This new classification based on more granular assessment of liver functional reserve confirms its significant prognostic impact with significant differences even within the same Child-Pugh class.

Public health

OS108

Structured early detection of compensated advanced chronic liver disease-results of the SEAL program

Christian Labenz¹, Anita Arslanow¹, Michael Nagel², Marc Nguyen-Tat³, Marcus-Alexander Wörns², Matthias Reichert⁴, Franz Josef Heil⁵, Dagmar Mainz⁵, Gudula Zimmer⁶, Barbara Römer⁷, Johannes Jäger⁸, Erik Farin-Glattacker⁹, Urs Fichtner⁹, Harald Binder⁹, Erika Graf⁹, Dominikus Stelzer⁹, Reyn van Ewijk¹⁰, Julia Ortne¹⁰, Louis Velthuis¹⁰, Frank Lammert^{8,11}, Peter Galle¹. ¹University Medical Center Mainz, Germany; ²Dortmund Hospital; ³Allgäu Hospital Group; ⁴Saarland University Medical Center; ⁵German Gastroenterology Association; ⁶General Practitioners' Association Saarland; ⁷General Practitioners' Association Rhineland-Palatinate; ⁸Saarland University; ⁹University of Freiburg; ¹⁰Johannes Gutenberg University Mainz; ¹¹Hannover Medical School
Email: anita.arslanow@uni-mainz.de

Background and aims: Detection of patients with compensated advanced chronic liver disease (cACLD) is of pivotal importance to prevent the occurrence of complications and improve prognosis. However, a structured screening program to detect patients with cACLD has not been implemented into daily routine. Therefore, it was the aim of the SEAL (structured detection of early liver cirrhosis) program to evaluate the usefulness of a structured screening program to detect cACLD.

Method: SEAL was a prospective cohort study conducted in two states in Germany, Rhineland-Palatinate and Saarland, between 01/2018 and 02/2021. Patients participating in a precautionary program (Check-up 35) with their primary care physician were offered additional testing of liver function tests (AST and ALT). If AST/ALT levels were elevated, the APRI score was calculated, and patients with a score >0.5 were referred to a gastroenterologist/hepatologist for more detailed evaluation of their liver disease. The primary end point of this study was the diagnostic rate of cACLD (F3 and F4) compared to a retrospective cohort (ICD-10 codes) of patients attending check-up 35 in the two states during 2016–2017 ($n = 349, 570$).

Results: In total, 11,859 patients were enrolled into the SEAL program. Slightly more women (54.5%) than men participated in the program, and the mean age of the cohort was 60 years. Elevated LFTs were found in 737 patients (6.1%). The most frequent aetiology of liver disease was non-alcoholic fatty liver disease (59%) followed by chronic alcohol abuse (18%). cACLD was detected in 45 patients. The standardized incidence of cACLD in the SEAL cohort was slightly higher than in controls (3.832‰, 95% CI 2.475, 5.188 vs. 3.358‰, 95% CI 3.136, 3.580). In logistic regression analyses, SEAL was not associated with a higher detection rate of cACLD after adjusting for age and gender (OR 1.141, one-sided 95% CI 0.801, +Inf). When patients with decompensated cirrhosis at diagnosis were excluded from the control cohort, SEAL was associated with a higher detection rate of cACLD on logistic regression analysis (OR 1.586, one-sided 95% CI 1.056, +Inf).

Conclusion: The implementation of a structured screening program may increase the detection rate of cACLD in the general population. In this context, the SEAL program may serve as a feasible concept.

OS109

Abdominal obesity is key when evaluating interactions between alcohol use and obesity for liver disease

Fredrik Åberg¹, Veikko Salomaa², Martti Färkkilä³, Antti Jula², Satu Männistö², Markus Perola², Annamari Lundqvist², Ville Tapio Männistö⁴. ¹Helsinki University Hospital and University of Helsinki, Transplantation and Liver Surgery, Helsinki, Finland; ²Finnish Institute for Health and Welfare, Helsinki, Finland; ³Helsinki University Hospital and University of Helsinki, Department of Gastroenterology, Helsinki, Finland; ⁴University of Eastern Finland and Kuopio University Hospital, Departments of Medicine, Kuopio, Finland
Email: fredrik.berg@helsinki.fi

This abstract is under embargo until Friday 24 June 2022, 13:40 BST. This abstract has been selected to be highlighted during official EASL Press Office activities or in official EASL Press Office materials that will be made publicly available on the congress website at 13:40 (BST).

Journalists, industry, investigators and/or study sponsors must abide by the embargo times set by EASL.

Violation of the embargo will be taken seriously. Individuals and/or sponsors who violate EASL's embargo policy may face sanctions relating to current and future abstract submissions, presentations and visibility at EASL Congresses. The EASL Governing Board is at liberty to ban attendance and/or retract data.

Copyright for abstracts (both oral and poster) on the website and as made available during The International Liver Congress™ 2022 resides with the respective authors. No reproduction, re-use or transcription for any commercial purpose or use of the content is permitted without the written permission of the authors. Permission for re-use must be obtained directly from the authors.

Michigan, Division of Gastroenterology and Hepatology, United States;
¹⁵University of Kansas Medical Center, United States; ¹⁶Mayo Clinic
 Rochester, Division of Gastroenterology and Hepatology, United States;
¹⁷University of South Dakota Sanford School of Medicine, Department of
 Medicine, Division of Gastroenterology, United States; ¹⁸University of
 Pittsburgh Medical Center, Center for Liver Diseases, Division of
 Gastroenterology, Hepatology and Nutrition, United States
 Email: jparab@gmail.com

Background and aims: Harmful alcohol consumption cause a significant burden of disease worldwide. To date, the impact of alcohol-related public health policies (PHP) in alcohol-associated liver disease (ALD) has not been adequately addressed. We aimed to assess the association between alcohol-related PHP and ALD mortality worldwide.

Method: We performed an ecological multi-national study including 193 countries. We recorded socio-demographic data from the World Bank Open Data source. We registered the presence of alcohol-related PHP in each country from the WHO GISAH (in 2016). Data on alcohol consumption measures and their harmful health consequences were collected from the WHO Global Information System of Alcohol and Health (GISAH) and the Global Burden of Disease (GBD) databases (updated to 2019). We constructed generalized linear models (GLM) with a Poisson family distribution, logit link, and a robust variance estimator to assess the association between the number of PHP and disease burden outcomes. The models were adjusted by population size and population structure.

Results: We included 193 countries (7,626,289,120 inhabitants); the median number of PHP was 7 [6–8]. The most developed categories were drink-driving policies and countermeasures (92.2%), tax regulations (87%), limiting drinking age (84.5%), and restrictions to alcohol access (81.9%). Other categories were national license, production, and selling control (81.9%), government monitoring systems and community support (74.1%), control over advertising and promotion (70.5%), and presence of a national plan (50.3%). Importantly, as higher number of PHP was associated with lower mortality due to cirrhosis (all causes) (prevalence ratio [PR]: 0.78 95% CI: 0.67–0.90; $p = 0.001$), mortality due to ALD (RP: 0.81 95% CI: 0.68–0.98; $p = 0.029$), cardiovascular mortality (PR: 0.81 95% CI: 0.67–0.98; $p = 0.029$), and alcohol use disorder (AUD) (PR: 0.80 95% CI: 0.63–0.99; $p = 0.046$) (Figure). The association between PHP on alcohol consumption and burden of disease was significantly higher in Africa, the Americas, and Asia.

OS110

The number of public health policies reduces the burden and mortality of alcohol-associated liver disease worldwide: a call for action

Luis Antonio Diaz¹, Eduardo Fuentes², Francisco Idalsoaga¹, Jorge Arnold¹, Gustavo Ayares¹, Macarena Cannistra³, Danae Vio³, Andrea Márquez⁴, Oscar Corsi¹, Alejandro Villalón¹, Carolina Ramírez⁵, María Paz Medel⁶, Catterina Ferreccio⁷, Mariana Lazo⁸, Juan Pablo Roblero⁹, Anand Kulkarni¹⁰, Won Kim¹¹, Mayur Brahmania¹², Alexandre Louvet¹³, Elliot Tapper¹⁴, Winston Dunn¹⁵, Douglas Simonetto¹⁶, Vijay Shah¹⁶, Patrick S. Kamath¹⁶, Ashwani Singal¹⁷, Ramon Bataller¹⁸, Marco Arrese¹, Juan Pablo Arab¹. ¹Pontificia Universidad Católica de Chile, Departamento de Gastroenterología, Chile; ²Pontificia Universidad Católica de Chile, Departamento de Ciencias de la Salud, Chile; ³Pontificia Universidad Católica de Chile, Escuela de Medicina, Chile; ⁴Universidad Anáhuac Mayab, Escuela de Medicina, Mexico; ⁵Clínica Las Condes, Departamento de Anestesiología, Chile; ⁶Pontificia Universidad Católica de Chile, Departamento de Medicina Familiar, Chile; ⁷Pontificia Universidad Católica de Chile, Public Health Department, Chile; ⁸Drexel University, Department of Community Health and Prevention, Dornsife School of Public Health, United States; ⁹Hospital Clínico Universidad de Chile, Sección Gastroenterología, Chile; ¹⁰Asian Institute of Gastroenterology, Department of Hepatology, India; ¹¹Seoul National University College of Medicine, Division of Gastroenterology and Hepatology, Department of Internal Medicine, Seoul Metropolitan Government Seoul National University Boramae Medical Center, Korea, Rep. of South; ¹²Western University, Department of Medicine, Division of Gastroenterology, Canada; ¹³Hôpital Claude Huriez, Services des Maladies de l'Appareil Digestif, CHRU Lille, France; ¹⁴University of

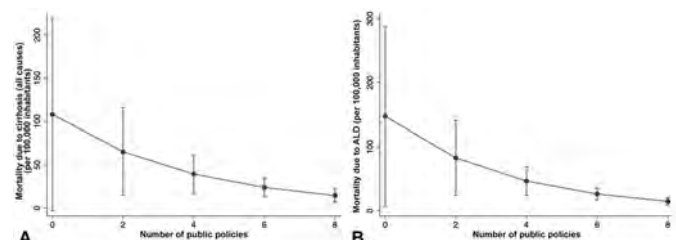


Figure: Relationship between alcohol-related public health policies and (A) deaths due to cirrhosis (all causes), and (B) deaths due to alcohol-associated liver disease (ALD) in 2019.

Conclusion: Those countries with a higher number of PHP had lower mortality due to cirrhosis (all causes), mortality due to ALD, cardiovascular mortality, and AUD. Our results strongly encourage the development and implementation of PHP on alcohol consumption worldwide.

OS111

Smoking, alcohol consumption and combined association risk for developing liver cancer in chronic hepatitis B: a prospective study

Cao Maomao¹, Wanqing Chen¹. ¹National Cancer Center/National Clinical Research Center for Cancer/Cancer Hospital, Chinese Academy of Medical Sciences and Peking Union Medical College, Office of Cancer Screening, Beijing, China
Email: chenwq@cicams.ac.cn

Background and aims: Evidence of liver cancer with tobacco smoking and alcohol consumption remains controversial. We aimed to investigate associations between liver cancer risk and alcohol consumption, smoking, and the combined interaction between these two risk factors in this prospective study.

Method: Baseline smoking and alcohol consumption were collected from all subjects in a population-based prospective cohort. Cox proportional hazard regression models were used to estimate hazard ratios (HRs) and 95% confidence intervals (CIs) adjusting for potential confounders. The population attributable fractions (PAFs) were estimated. The cumulative incidences of liver cancer were generated with the use of Kaplan-Meier methods and compared based on the log-rank test.

Results: A total of 4003 participants were included in this study up to 3 years of follow-up, 72 liver cancer cases were identified. Alcohol consumption was found to increase the risk of liver cancer with a non-significant difference (Adjusted HR = 1.19, 95% CI = 0.66–2.16, PAF = 3.83%). Smoking increased the risk of liver cancer in men (HR = 1.59, 95% CI = 1.22–2.06, PAF = 26.69%). A dose-responsive pattern between the duration and intensity of smoking and the risk of liver cancer was noted. Similar results were also observed in men. Further statistical analysis revealed interactions between the effect of smoking and alcohol consumption on the risk of liver cancer, contributing to 11.12% of liver cancer cases in our cohort.

Conclusion: The findings further support smoking is an independent risk of liver cancer with a clear dose-and duration-dependent relation. We also showed the combined effect of alcohol consumption and smoking on the development of liver cancer.

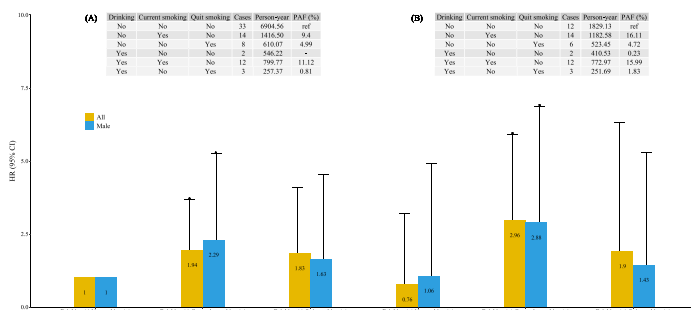


Figure 1: The synergistic effect of smoking and alcohol contributed to liver cancer risk (A. All population; B. Male sex).

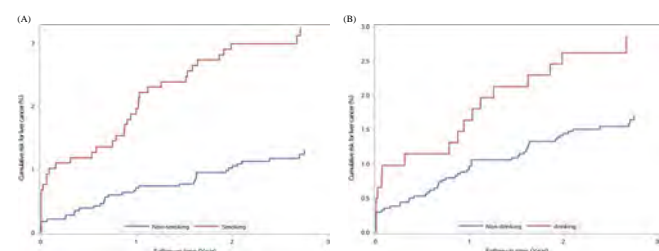


Figure 2: The cumulative incidence of liver cancer by drinking and smoking status (A. Smoking; B. Drinking).

OS112

Incidence, prevalence and mortality of chronic liver diseases in Sweden between 2005 and 2019

Patrik Nasr^{1,2}, Nelson Ndegwa^{3,4,5}, Erik von Seth^{2,6}, Jonas Ludvigsson^{3,7,8,9}, Hannes Hagström^{2,6,10}. ¹Linköping University, Department of Health, Medicine and Caring Sciences, Linköping, Sweden; ²Karolinska Institute, Department of Medicine, Huddinge, Sweden; ³Karolinska Institute, Department of Medical Epidemiology and Biostatistics, Stockholm, Sweden; ⁴Karolinska Institute, Department of Clinical Science, Intervention and Technology, Stockholm, Sweden; ⁵Karolinska University Hospital, Oesophageal and Gastric Cancer Unit, Stockholm, Sweden; ⁶Huddinge Hospital, Division of Hepatology, Department of Upper GI Diseases, Stockholm, Sweden; ⁷Columbia University Irving Medical Center, Division of Digestive Disease and Transplantation, Division of Digestive and Liver Disease, New York, United States; ⁸Örebro University Hospital, Department of Pediatrics, Örebro, Sweden; ⁹University of Nottingham, Division of Epidemiology and Public Health, Nottingham, United Kingdom; ¹⁰Karolinska Institute, Clinical Epidemiology Unit, Department of Medicine, Stockholm, Sweden
Email: patrik.nasr@liu.se

Background and aims: Chronic liver diseases affects approximately 844 million individuals and causes an estimated two million deaths per year. The most common causes are chronic viral hepatitis, alcohol-related liver disease and non-alcoholic fatty liver disease. With the availability of curative treatments and effective vaccines for viral hepatitis and increasing prevalence of metabolic syndrome-the landscape of liver diseases is shifting. In this study, we aimed to describe the incidence and prevalence of a wide range of chronic liver diseases as well as their role in mortality in Sweden.

Method: In this register-based, nationwide cohort study, aggregated statistics, stratified on categories of age, sex and geographical locations, on all adult Swedish inhabitants with a diagnosis of liver disease during 2005 to 2019 were obtained from National registers.

Results: During 2005 to 2019, there were substantial changes in the epidemiology of liver diseases in Sweden. The incidence of alcohol-related cirrhosis increased by 18% annually (incidence rate 13.1/100, 000 in 2019). The incidence rate of non-alcoholic fatty liver disease and cirrhosis with unspecified etiology increased by 14% and 20% annually respectively (incidence rate 15.2 and 18.7/100, 000). Furthermore, incidence rates of chronic hepatitis C steeply declined, while autoimmune hepatitis increased (3.4/100, 000). In parallel with the increasing incidence of liver cirrhosis, liver malignancies have become more common.

The most common causes of liver related mortality were alcohol-related disease without a code for cirrhosis, alcohol-related cirrhosis, and unspecified liver disease with mortality rates of 4.1, 2.9, and 2.8/100, 000. Most liver diseases were more frequent amongst men. Furthermore, varying differences was seen in the incidence rate between regions, with some etiologies (e.g. autoimmune liver diseases) being more common in rural areas.

Conclusion: The incidence rates of non-alcoholic fatty liver disease, alcohol-related cirrhosis, unspecified liver cirrhosis has increased during the last 15 years, in parallel with a decreasing incidence of viral hepatitis. The incidence of AIH and hepatobiliary malignancies is also increasing. Worryingly, mortality in several liver diseases increased, likely reflecting the increasing incidence of cirrhosis. Significant disparities of liver diseases exist across sex and geographical regions, which needs to be considered when allocating healthcare resources.

OS113

Association between liver cirrhosis and cardiovascular events in a large German cohort-a population based study

Kabbani Abdul-Rahman¹, Hannah Schneider¹, Hans Becker^{1,2}, Heiner Wedemeyer^{1,2}, Benjamin Maasoumy¹, Jona T. Stahmeyer^{3,4}.

¹Hannover Medical School, Department of Gastroenterology, Hepatology and Endocrinology, Hannover, Germany; ²German Liver Foundation (Deutsche Leberstiftung), Hannover, Germany; ³AOK Niedersachsen, Health Services Research Unit, Germany; ⁴Hannover Medical School, Institute for Epidemiology, Social Medicine and Health Systems Research, Germany

Email: kabbani.abdul-rahman@mh-hannover.de

Background and aims: Systemic inflammation has been associated with an increased risk for cardiovascular events. Liver cirrhosis is associated with both systemic inflammation and endothelial dysfunction. However, a possible link between liver cirrhosis and cardiovascular diseases remains poorly investigated. We here aimed to analyze the risk of cardiovascular events (myocardial infarction and stroke) in patients with liver cirrhosis compared to non-cirrhotic patients in a population-based study from Northern Germany.

Method: Analysis was based on administrative data from one large German public health insurance fund. All adult individuals continuously insured until death or the end of observation period (2010–2019) were included. We used a pre-observation period (2010–2012) to exclude individuals with cardiovascular events prior to the start of observation in 2013. The presence of liver cirrhosis and cardiovascular risk factors were identified using ICD-10 codes. Myocardial infarction and stroke were analyzed as a composite and as individual end points. To determine the risk of cardiovascular events in patients with liver cirrhosis we used a multivariable Cox regression adjusted for age, gender and selected cardiovascular risk factors (hypertension, heart failure, atherosclerosis, chronic ischemic heart disease, obesity, nicotine abuse, dyslipidemia, diabetes, alcohol abuse and chronic renal failure with dialysis).

Results: A number of 1.29 million patients were included. Liver cirrhosis was present in 6, 517 individuals (0.51%) at the start of the observation in 2013. Individuals with liver cirrhosis were older (62.8 vs. 55.9 yr), more often male (60.4% vs. 44.6%) and had more comorbidities (e.g. alcohol abuse 39.5% vs. 2.3% or atherosclerosis 11.3% vs. 5.4%). Overall incidence of cardiovascular events was significantly higher among patients with cirrhosis (7.7% vs 5.9%, $p < 0.001$). This difference was also documented when limiting the analysis to the incidence of strokes (5.1% vs 3.5%, $p < 0.001$). In contrast, myocardial infarctions occurred with a similar frequency in cirrhotic and non-cirrhotic individuals (2.8% vs 2.6%, $p = 0.327$). After adjusting for potential confounders in the multivariable cox regression analysis liver cirrhosis was associated with a 20.9% and 37.3% higher risk of overall cardiovascular events ($p < 0.001$) and strokes in particular, respectively, while there was no risk difference with regard to myocardial infarction ($p = 0.703$).

Conclusion: Liver cirrhosis is associated with a higher risk of stroke. Importantly, this link is independent from other established cardiovascular risk factors. A correspondingly higher risk of myocardial infarction could not be demonstrated.

Molecular and cellular biology

OS114

MiR-122, the regulator of the immune privileged liver

Maytal Gefen¹, Shanny Layani¹, Emma Klahr¹, Mor Hindi¹, Nofar Rosenberg¹, Rinat Abramovitch^{1,2}, Nathalie Nachmansson^{1,2}, Adi Yehezkel¹, Amnon Peled¹, Jacob Rachmilewitz¹, Michal Abraham¹, Michael Berger³, Daniel Goldenberg¹, Nicola Gagliani⁴, Samuel Huber⁴, Irm Hermans-Borgmeyer⁴, Rebecca Haffner-Krausz⁵, Shifra Ben-Dor⁶, Yuval Nevo⁷, Shrona Elgavish⁷, Hadar Benyamini⁷, Mathias Heikenwälder⁸, Stefan Rose-John⁹, Dirk Schmitt-Arras⁹, Achim Krüger¹⁰, Michael Stürzl¹¹, Elisabeth Naschberger¹¹, Frank Tacke¹², Hilla Giladi¹, Eithan Galun¹. ¹Hadassah Hebrew University Hospital, Goldyne Savad Institute of Gene Therapy, Jerusalem, Israel; ²Hadassah University Medical Center, The Wohl Institute for Translational Medicine, Jerusalem, Israel; ³Israel-Canada Medical Research Institute, Faculty of Medicine, The Hebrew University, The Lautenberg Center for Immunology and Cancer Research, Jerusalem, Israel; ⁴University Medical Center, Hamburg-Eppendorf, Hamburg, Germany; ⁵Weizmann Institute of Science, Dept. of Veterinary Resources, Rehovot, Israel; ⁶Weizmann Institute of Science, Bioinformatics Unit, Rehovot, Israel; ⁷Hadassah Hebrew University Medical Center, Bioinformatics Unit of the I-CORE Computation Center, Jerusalem, Israel; ⁸German Cancer Research Centre Heidelberg (DKFZ), Division of Chronic Inflammation and Cancer, Heidelberg, Germany; ⁹University of Kiel, Biochemical Institute, Germany; ¹⁰Technical University Munich, Institutes of Molecular Immunology and Experimental Oncology, Munich, Germany; ¹¹Universitätsklinikum Erlangen, Friedrich-Alexander University (FAU) of Erlangen-Nürnberg, Division of Molecular and Experimental Surgery, Department of Surgery, Erlangen, Germany; ¹²Charité University Medicine Berlin, Department of Hepatology and Gastroenterology, Berlin, Germany

Email: maytalgefen@gmail.com

Background and aims: The liver, an immune privileged organ, is a sanctuary for acute and chronic infections and a frequent site for metastasis due to its immunosuppressive environment. Chronic liver inflammation is a major risk factor for primary liver cancer. Hepatocellular carcinoma (HCC) is the fourth leading cause of cancer related death, and metastatic liver cancer occurs even more often. Fatty liver is apparent in 30% of the western world due to western diet and lifestyle, increasing the risk of non-alcoholic steatohepatitis (NASH). NASH fuels chronic inflammation which could progress to cirrhosis and HCC.

Method: MicroRNA-122 (miR-122), the liver specific microRNA, plays important roles in regulating several liver-specific processes and was reported to be significantly down-regulated in HCC. Our group has shown that: Inflammatory mediators regulate miR-122 expression and secretion i.e. TNF α (Rivkin M et al Gastroenterology 2016). In NASH, miR-122 is decreased in livers with increased inflammation, steatosis and fibrosis. Upon increasing miR-122 expression the NASH pathologies reverse (Chai C et al Gastroenterology 2020). MiR-122 functions as a hormone, it is produced in hepatocytes and affects remote tissue (Chai C et al Gastroenterology 2017). Concurring with previous studies, we have shown that miR-122 has tumor suppressive effects through numerous mechanisms (Simerzin A et al Hepatology 2016).

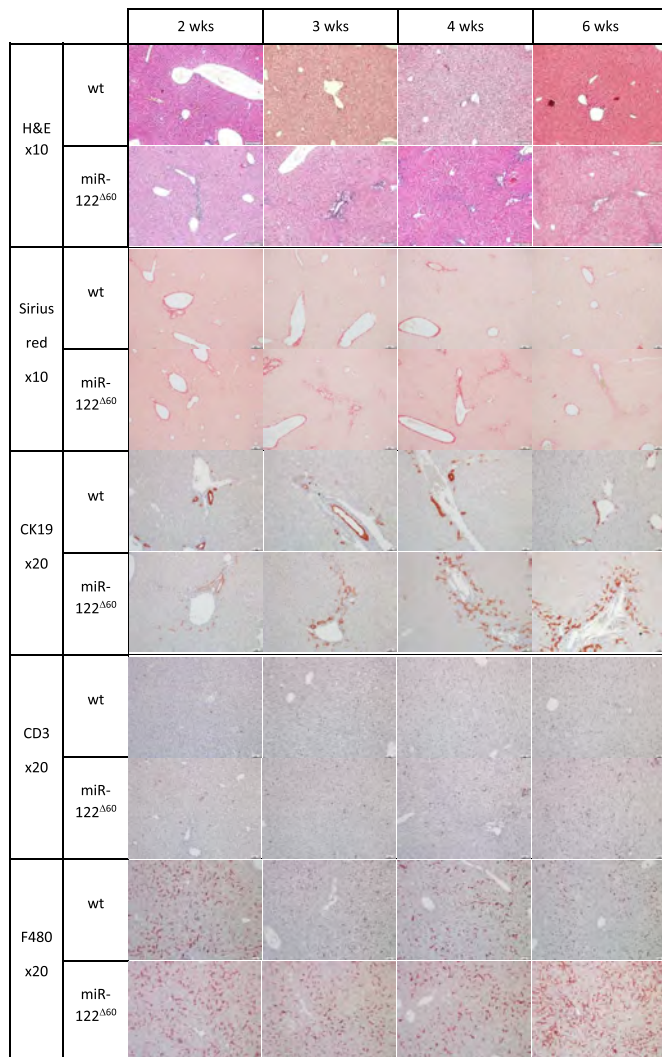


Figure: MiR-122 null mice develop fibrosis and ductular proliferation as well as initiation of an inflammatory response. Liver sections from miR-122 null mice (null) and wild type (WT) controls were obtained at the indicated ages (weeks). Staining for haematoxylin eosin (H&E) and fibrosis (Sirius red). Immunohistochemical staining for cholangiocytes (CK19), T cells (CD3) and Kupffer cells (F480).

Results: We generated a genetically modified mouse model by deleting 60nt of miR-122, (miR-122^{Δ60}). The miR-122^{Δ60} mice develop fibrosis and ductular proliferation as well as initiation of an inflammatory response already by the age of 3 weeks progressing with age. At a later age these mice develop NASH and HCC (age 40–80 weeks old). In a model of metastasis to the liver, miR-122^{Δ60} develop significantly more secondary tumors in the liver with an aggressive phenotype. RNA-seq analysis revealed enhanced epithelial-to-mesenchymal transmission (EMT). This was associated with an increase in ADAM17 expression, a known target of miR-122, which we have collaboratively shown, induces necroptosis of endothelial cells and cause enhanced tumor cell invasion into parenchyma (Bolik J et al, J Exp Med paper in press). All these results teach to the pivotal role of miR-122 in liver tolerance, inflammation and tumorigenesis.

Conclusion: Overall, miR-122 is on the one hand “anti-inflammatory” and on the other hand a “tumor suppressor.” Understanding the regulation of miR-122 and its downstream effects could shed light on mechanisms of the diseased liver and potentially identify disease biomarkers and lead to therapeutic strategies.

OS115

The role of OFD1 and loss of primary cilia in cholangiocarcinoma: a novel promising therapeutic target

Massimiliano Salati¹, Anna Barbato², Francesco Caputo¹, Andrea Spallanzani¹, Fabio Gelsomino¹, Betrice Ricco¹, Gabriele Luppi¹, Luigi Ferrante², Roberta Biondi², Francesco Massaro², Antonella Iuliano², Gennaro Gambardella², Fabiola Piscopo², Pasquale Pisapia³, Antonino Iaccarino³, Maria Salatiello³, Giancarlo Troncone³, Luca Reggiani-Bonetti¹, Massimo Dominici¹, Brunella Franco², Pietro Carotenuto². ¹University of Modena and Reggio Emilia, Modena, Italy; ²Tigem, Pozzuoli, Italy; ³University of Naples Federico II, Napoli, Italy
Email: p.carotenuto@tigem.it

Background and aims: CCA is a highly lethal primary liver cancer with an increasing incidence and limited therapeutic options. The primary cilium has been postulated to have a tumor-suppressor role in the biliary tract being involved in several cancer-related pathways including WNT, Hedgehog and NOTCH. Here, we aimed at identifying and functionally characterizing primary cilium-associated genes with translational relevance for CCA prognostication and treatment.

Method: Whole-transcriptome profiling was performed with RNA-Seq on laser micro-dissected FFPE resected tissue specimens. Knocking-down of OFD1 showed was performed using siRNA interference transfections of CCA cells. Immunofluorescence staining of cilia markers was used to analyze and count cilia.

Results: Overall, 70 CCA patients were included, 51% (36) had intrahepatic and 49% (34) had extrahepatic CCA. Among 3392 and 6315 differentially expressed genes between tumour and normal tissue and tumour and stroma, OFD1 was the top-ranked cilium-associated gene (fold-change \geq 2.5, $p < 0.01$). siRNA-mediated depletion of OFD1 induced ciliogenesis and suppresses tumour growth *in vitro* in normal cholangiocyte and 4 different CCA cell lines. In the Western blot, OFD1 knockdown significantly increase the expression of ciliary proteins such as PCM1, ARL13B and Acetylated Tubulin, while OFD1 overexpression reduced their expression. When assessing the impact of OFD1 on prognosis, higher expression of OFD1 was significantly associated with a worse overall survival in resected CCA patients (10 vs 39 months; HR 2.33, 95%CI 1, 01–5, 31, $p = 0.03$).

Conclusion: We demonstrated that OFD1 acts as an oncogene in CCA and experimentally-induced depletion of OFD1 stimulated ciliogenesis and suppressed tumour growth *in vitro*. Interestingly, higher OFD1 expression adversely impacted survival of CCA patients undergoing curative-intent resection. This work identifies the primary cilium-associated gene OFD1 as a novel promising therapeutic target and prompts ciliotherapy development in CCA.

OS116

Human antigen R (HuR) is a master regulator of hepatic glucose metabolism

Sofía Lachiondo-Ortega¹, Miren Bravo¹, Irene González-Recio¹, María J. González Rellán², Jorge Simón Espinosa^{1,3}, Naroa Goikoetxea¹, Petar Petrov^{1,3}, Rubén Rodríguez Agudo¹, Arantza Sanz-Parra¹, Begoña Rodríguez Iruretagoyena¹, Teresa Cardoso Delgado¹, Dan A. Dixon⁴, Myriam Gorospe⁵, Ruben Nogueiras^{2,6}, María Luz Martínez-Chantar^{1,3}. ¹Center for Cooperative Research in Biosciences (CIC bioGUNE), Liver Disease Lab, Spain; ²Center for Research in Molecular Medicine and Chronic Diseases (CIMUS), Department of Physiology, Spain; ³Centro de Investigación Biomédica en Red de Enfermedades Hepáticas y Digestivas (CIBERehd); ⁴University of Kansas, Department of Molecular Biosciences, United States; ⁵National Institute on Aging (NIA), National Institutes of Health (NIH), Laboratory of Genetics and Genomics, United States; ⁶Centro de Investigación Biomédica en Red de Fisiopatología de la Obesidad y Nutrición (CIBERObn), Spain
Email: mmlmartinez@cicbiogune.es

Background and aims: Human antigen R (HuR) or Embryonic Lethal Abnormal Vision-Like 1 (ELAVL1) is a ubiquitous member of the ELAV/

Hu family of RNA-binding proteins (RBPs). Under normal physiological conditions HuR is primarily nuclear. However, upon specific stimuli, e.g. stress signals, HuR translocates to the cytoplasm where it functions as a potent regulator of the stabilization and translation of target mRNAs. By binding to U/AU-rich elements (AREs) typically present in the 3'-untranslated region (UTR) of mRNAs, HuR post-transcriptionally controls the expression of many proteins and hence governs diverse molecular and cellular functions. Thus, in addition to its implication in disease, HuR is involved in physiological processes, e.g. adipogenesis, myogenesis, senescence, and immune response. However, the role of HuR in hepatic glucose metabolism remains to be addressed and constitutes the main aim of the present work.

Method: HuR expression was modulated in cultured primary mouse hepatocytes and in the THLE-2 human liver cell line stimulated with glucagon, glucose or insulin, as well as in mice fed a high-fat diet (HFD) during 4 days or subjected to glucagon administration for 30 min. Next, changes in glucose levels, RNA and protein expression, HuR localization, fluxomic analysis with ^{13}C -uniformly labelled glucose, RNA and RNA immunoprecipitation (RIP) and sequencing (Seq) assays were performed.

Results: Hepatic HuR expression was increased after intraperitoneal administration of glucagon in mice, while it remained unchanged in the glucagon receptor knockout animal model. Conversely, HuR expression decreased in mice upon insulin injection into the inferior cava vein. Importantly, HuR expression was significantly upregulated in the liver of a cohort of type II diabetes mellitus (T2DM) patients and in the insulin resistance *in vivo* model consisting of mice fed a HFD during 4 days. HuR was mainly located in the nucleus upon glucose and insulin stimuli, whereas it translocated to the cytoplasm after glucagon administration. Silencing the expression of HuR in the HFD mouse model sensitized the liver to insulin-mediated glucose uptake and subsequent glycolysis, while its gluconeogenic capacity was reduced. Importantly, ablating hepatic HuR expression resulted in a two-fold reduction of subcutaneous white adipose tissue weight due to increased lipolysis. Moreover, RNA-Seq analysis revealed different expression signatures of RNAs involved in glucose metabolism upon modulation of HuR expression. Finally, RIP-Seq experiments identified a panel of HuR-interacting mRNAs encoding proteins with molecular functions that helped explain how HuR controls liver glucose homeostasis.

Conclusion: Given that HuR appears to be a master regulator of glucose metabolism, we propose that HuR ought to be considered as a potential pharmacological target for the clinical management of T2DM.

OS117

Primary cilia in biliary regeneration-a potential approach to improve outcomes in liver transplantation

Hannah Esser¹, Sofia Ferreira-Gonzalez¹, Tak Yung Man¹, Alastair Kilpatrick¹, Daniel Rodrigo Torres¹, Rhona E. Aird¹, Candice Ashmore-Harris¹, Kayleigh Thirlwell², Benjamin J. Dwyer³, Gabriel Oniscu⁴, Stefan Schneeberger⁵, Luke Boulter⁶, Stuart Forbes¹.
¹University of Edinburgh, Centre for Regenerative Medicine, Institute for Regeneration and Repair, Edinburgh, United Kingdom; ²Tissues, Cells and Advanced Therapeutics Scottish National Blood and Transfusion Service (SNBTS), Edinburgh, United Kingdom; ³Curtin University, Curtin Medical School, Curtin Health Innovation Research Institute, Perth, Australia; ⁴Transplant Unit, Royal Infirmary of Edinburgh, Edinburgh, United Kingdom; ⁵Innsbruck Medical University, Department of Visceral, Transplant and Thoracic Surgery, Center of Operative Medicine, Innsbruck, Austria; ⁶University of Edinburgh, The Institute of Genetics and Molecular Medicine (IGMM), Edinburgh, United Kingdom
Email: stuart.forbes@ed.ac.uk

Background and aims: Biliary complications (BC) are one of the most common complications after orthotopic liver transplantation. Up to 25% of liver transplant recipients will develop BC, a major factor determining long term patient survival. BC have been associated with

pre-transplant cold storage conditions, hypoxia and insufficient regeneration of biliary epithelial cells (BEC) following transplantation. BEC have primary cilia (PC), a unique organelle that is crucial to sense the extracellular environment and regulate cell proliferation. In this study we investigate the impact of PC and regeneration in the setting of BC arising post liver transplantation.

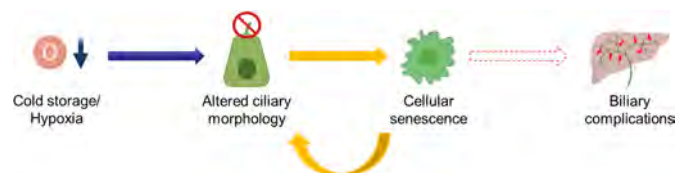
Method: Human biopsies were used to study the structure/function of PC in liver transplant recipients with ($N=7$) and without BC ($N=12$). We developed novel murine models of liver pre-transplantation stages, where we can study the role of PC in BEC, using conditional ablation of PC (K19CreER⁺ KIF3A^{fllox/fllox} mouse model). Lastly, Tubastatin A was used to stabilise PC and promote BEC regeneration, in a combination of *in vitro* and *in vivo* models of cold storage.

Results: BEC's PC are shortened prior to transplantation in livers that later develop BC ($p=0.006$). We identify hypoxia as the main molecular mechanism responsible of this damage during cold storage conditions.

Hypoxia induced shortening/loss of PC triggers the onset of cellular senescence, impairing the regenerative capacity of BEC *in vitro* and *in vivo*. We also explore how hypoxia-independent genetic ablation of PC induces cellular senescence, indicating the presence of a feedback loop that negatively impacts the regenerative response of BEC after liver transplantation.

Inhibition of cellular senescence (using p21^{-/-} mice or by administration of senolytics) preserves PC during cold storage ($p=0.0004$), improving BEC regeneration. We finally show how stabilisation of PC during cold storage improves BEC proliferation *in vitro* ($p=0.0005$).

Conclusion: pre-transplantation hypoxic conditions trigger the loss of PC in BEC, impairing biliary regeneration through cellular senescence. Our results indicate that PC represent a potential novel therapeutic target to improve biliary regeneration and prevent BC development during liver transplantation.



OS118

NFATc1 drives progressive liver inflammation and fibrosis by regulating pro-apoptotic stress responses

Muhammad Umair Latif¹, Geske Schmidt², Sercan Mercan², Kristina Reutlinger², Elisabeth Hessmann², Shiv Kumar Singh², Philipp Ströbel³, Volker Ellenrieder².
¹University Medical center Göttingen, Department of Gastroenterology, Gastrointestinal Oncology and Endocrinology, Göttingen, Germany; ²University Medical center Göttingen, Department of Gastroenterology, Gastrointestinal Oncology and Endocrinology, Göttingen, Germany; ³University Medical center Göttingen, Institute for Pathology, Göttingen, Germany
Email: umair.latif@med.uni-goettingen.de

Background and aims: Chronic liver inflammation lead to fibrosis and cirrhosis, which is the 12th leading cause of death in the world. Many acute and chronic liver disorders including hepatic inflammation originate from stress conditions followed by some complex inter cellular processes. Progression of the disease can progress to distinctive cirrhosis and hepatocellular carcinoma development. Here, we describe a key role of NFATc1 in liver damage, inflammation, and fibrosis. NFATc1, beside its well-established role in inflammatory diseases and inflammation-associated tumors, has not been comprehensively studied in liver diseases. This project aimed to characterize the functional implications of NFATc1 and its therapeutic potential in inflammatory liver diseases.

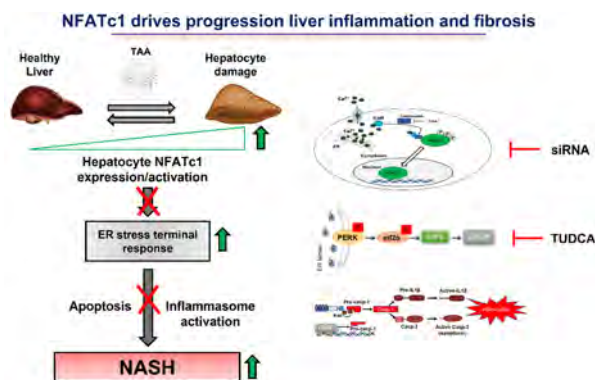
Method: To address this, we analyzed NFATc1 activation in patients with inflammation/fibrosis, cell lines and mice tissues, pretreated

ORAL PRESENTATIONS

with Thioacetamide (TAA), using immunoblot, RT-PCR and immunohistochemistry. Liver tissues from vehicle and TAA treated *NFATc1*^{wt}, *NFATc1*^{c.a.} and *NFATc1*^{fl/fl} mice were examined for NFATc1 dependent morphological changes by analyzing inflammation, and fibrosis. RNA-seq analysis in AML12 cells was performed to identify NFATc1 regulated gene signatures and signaling mechanisms. We further highlighted the therapeutic potential of NFATc1 dependent signaling mechanisms by their inhibition, both *in-vivo* and *in-vitro*.

Results: Liver biopsies from patients with inflammation/fibrosis revealed increased NFATc1 expression and nuclear localization in hepatocytes. Moreover, TAA induced NFATc1 activation resulted in progressive inflammation, fibrosis and cirrhosis whereas hepatocyte-specific depletion of the transcription factor prevented mice from liver damage. Mechanistically, hepatocyte specific NFATc1 activation drives chronic ER stress-responses and promotes apoptosis (cleaved Caspase-3) and pro-inflammatory signaling cascades through PERK-CHOP-mediated NLRP3 inflammasome activation. Finally, TUDCA mediated inhibition of NFATc1-driven signaling prevented hepatocyte damage and subsequent inflammation/fibrosis.

Conclusion: Together, our study successfully established the role of NFATc1 in liver inflammation and fibrosis through terminal ER-stress signalling and subsequent NLRP3 inflammasome activation in hepatocytes. This study also highlighted the therapeutic potential of ER-stress inhibition by TUDCA. In fact, TUDCA application resulted in strikingly lower liver damage and fibrosis in mice.



OS119

The selective PPAR-delta agonist seladelpar suppresses bile acid synthesis by reducing hepatocyte CYP7A1 through the FGF21 pathway

Tetsuya Kouno¹, Xiao Liu², Tatiana Kisseleva², Edward Cable³, Bernd Schnabl¹. ¹University of California San Diego, Department of Medicine, La Jolla, United States; ²University of California San Diego, Department of Surgery, La Jolla, United States; ³CymaBay Therapeutics, Newark, United States

Email: beschnabl@ucsd.edu

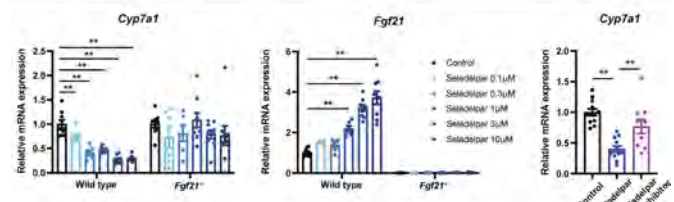
Background and aims: PPAR-delta agonists exert beneficial effects in liver disease and reduce total bile acid levels. Since little is known about the mechanism whereby PPAR-delta agonism reduces bile acid levels, the aim of the current study was to investigate the molecular pathways responsible for reducing bile acid synthesis in hepatocytes following treatment of the selective PPAR-delta agonist, seladelpar.

Method: Wild type C57BL/6 mice were gavaged with vehicle (PBS) or seladelpar (10 mg/kg body weight), and gene expression in the liver and ileum was examined 6 hours later by qPCR. For mechanistic studies, primary mouse hepatocytes isolated from wild type C57BL/6 mice, Ppar-alpha/- mice, or Fgf21/- mice were treated with seladelpar for 48 hours, and gene expression analysis was performed. The effect of seladelpar on bile acid regulation was also investigated in primary human hepatocytes.

Results: Administration of seladelpar to wild type mice repressed the liver expression of cholesterol 7 alpha-hydroxylase (Cyp7a1), a rate limiting enzyme for bile acid synthesis, and decreased plasma 7alpha-hydroxy-4-cholesten-3-one (C4), the freely diffusible metabolite downstream of Cyp7a1, without affecting Farnesoid X receptor pathway in the liver or ileum. In primary mouse hepatocytes, seladelpar significantly reduced the expression of Cyp7a1 and upregulated fibroblast growth factor 21 (Fgf21). The effect of seladelpar on the expression of Cyp7a1 and Fgf21 was observed in the hepatocytes isolated from Ppar-alpha/- mice, confirming the effect of seladelpar is not based on PPAR-alpha activation. Recombinant Fgf21 protein repressed Cyp7a1 gene expression via an activation of the JNK signaling pathway in primary mouse hepatocytes. The suppressive effect of seladelpar on Cyp7a1 expression was blocked by both a JNK inhibitor and in the absence of Fgf21, indicating that Fgf21 plays an indispensable role in PPAR-delta-mediated downregulation of Cyp7a1. Reduction of CYP7A1 expression by seladelpar was confirmed in primary human hepatocytes.

Conclusion: Seladelpar reduces bile acid synthesis via an FGF21-dependent mechanism that signals, at least partially through JNK, to repress Cyp7a1.

Primary mouse hepatocytes



NAFLD Therapy

OS120

Dissecting the effects and mechanism-of-action of statin use on fatty liver disease: a multidimensional study

Ibrahim Ayada^{1,2}, Laurens van Kleef³, Huai Zhang⁴, Pengfei Li³, Kuan Liu¹, Ling Wang³, Marla Lavrijsen³, Mohsen Ghanbari², Luc J.W. Van Der Laan⁵, Maikel Peppelenbosch³, Ming-Hua Zheng⁶, Robert De Knecht³, Qiuwei Pan³. ¹Erasmus MC, Gastroenterology and Hepatology, Rotterdam, Netherlands; ²Erasmus MC, Department of Epidemiology; ³Erasmus MC, Gastroenterology and Hepatology; ⁴Medical Quality Management Office, the First Affiliated Hospital of Wenzhou Medical University, Wenzhou, China, Department of Biostatistics and Records Room; ⁵Erasmus MC, Department of Surgery; ⁶The First Affiliated Hospital of Wenzhou Medical University
Email: ibrahimayada653@hotmail.com

Background and aims: Statins are widely used for the prevention of cardiovascular events and treatment of dyslipidemia. Previous studies have suggested potential beneficial effects of statin use on fatty liver disease, but the evidence is segmented and inconclusive. This study aims to comprehensively investigate the epidemiological and clinical evidence in this respect, and to understand the mechanism-of-action in experimental models.

Method: The association between statin use and fatty liver disease (FLD) was investigated in the Rotterdam Study (a population-based prospective cohort), a biopsy proven FLD cohort and lastly in meta-analysis of published clinical trials and cohort studies. The effect of simvastatin and lovastatin on lipid accumulation was investigated in

3D cultured human liver organoids fed with lactate, pyruvate and octanoic acid to mimic steatosis. Since macrophages are the key drivers of inflammation in FLD, human THP-1 macrophage cell line was used to study inflammatory gene expression.

Results: In the Rotterdam Study cohort (n = 4352 participants), statin use among participants with the metabolic syndrome (n = 1700) was associated with decreased risk for steatosis (OR 0.45, 95%CI 0.33–0.60, p <0.001) and fibrosis (OR 0.51, 95%CI 0.26–0.90, p = 0.031). In the biopsy proven patient cohort (n = 569), statin use in a subpopulation with the metabolic syndrome (n = 266) was associated with decreased risk for non-alcoholic steatohepatitis (OR 0.49, 95%CI 0.25–0.98, p = 0.04). In meta-analysis, lower levels of AST (mean difference: –0.74 U/L) and ALT (mean difference: –0.87 U/L) were observed in fatty liver disease patients using statins. Pooled odds ratio of 0.65 (95%CI 0.35–1.07) was estimated on the association of statin use and FLD development. In liver organoids model of steatosis, we found treatment with statins significantly inhibited the number of formed lipid droplets, although the effect was prominent only at relatively high concentration (10 microM). Our preliminary results suggest that statin inhibits the expression of inflammatory genes, including IL-1beta, IL-6, TNF-alpha and IL-8, but these results require further confirmation.

Conclusion: Our epidemiological and clinical evidence strongly supports the beneficial effects of statin use on multiple stages of fatty liver disease; steatosis, fibrosis and steatohepatitis. This is likely attributed to multiple mechanisms, including inhibition of steatosis and inflammatory response.

OS121

Biomarkers, imaging and safety in a well-compensated NASH cirrhotic cohort treated with resmetromir, a thyroid hormone receptor beta agonist, for 52 weeks

Stephen Harrison¹, Kris Kowdley², Rebecca Taub³, Naim Alkhouri⁴, Guy Neff⁵, ¹Pinnacle Research; ²Liver Institute Northwest, Seattle, United States; ³Madrigal Pharmaceuticals, RandD, Conshohocken, United States; ⁴Arizona Liver Institute, Chandler, United States; ⁵Covenant Research, Sarasota, United States
Email: rebeccataub@yahoo.com

This abstract is under embargo until Friday 24 June 2022, 13:40

BST. This abstract has been selected to be highlighted during official EASL Press Office activities or in official EASL Press Office materials that will be made publicly available on the congress website at 13:40 (BST).

Journalists, industry, investigators and/or study sponsors must abide by the embargo times set by EASL.

Violation of the embargo will be taken seriously. Individuals and/or sponsors who violate EASL's embargo policy may face sanctions relating to current and future abstract submissions, presentations and visibility at EASL Congresses. The EASL Governing Board is at liberty to ban attendance and/or retract data.

Copyright for abstracts (both oral and poster) on the website and as made available during The International Liver Congress™ 2022 resides with the respective authors. No reproduction, re-use or transcription for any commercial purpose or use of the content is permitted without the written permission of the authors. Permission for re-use must be obtained directly from the authors.

OS122

Magnesium modulation by CNNM4 silencing in DIAMOND mice via GalNAC-siRNA therapy: a new and effective therapeutic approach against MAFLD

Rubén Rodríguez Agudo¹, Naroa Goikoetxea¹, Miren Bravo¹, Sofia Lachiondo-Ortega¹, Marina Serrano-Macia¹, Maria Mercado-Gómez¹, Marcos Fernandez Fondevila², Teresa Cardoso Delgado¹, Luis Alfonso Martinez-Cruz¹, Franz Martin-Bermudo³, Ruben Nogueiras², Cesar Augusto Martín⁴, Ute Schaeper^{5,6}, Daniela Buccella⁷, Jorge Simón^{1,8}, María Luz Martínez-Chantar^{1,8}. ¹Liver Disease Laboratory, CIC bioGUNE; ²Molecular Metabolism Lab, CIMUS; ³CABIMER, UPO; ⁴Instituto Biofisika (UPV/EHU); ⁵Silence Therapeutics GmbH; ⁶Silence Therapeutics GmbH, Berlin, Germany; ⁷Department of Chemistry, NYU; ⁸CIBER Enfermedades Hepáticas y Digestivas (CIBERehd)
Email: jsimon@cicbiogune.es

Background and aims: There is mounting evidence that metabolic alterations play an important role in non-alcoholic fatty liver disease (NAFLD), which led to the notion to be renamed metabolic associated fatty liver disease (MAFLD). When extending the focus of the studies to systemic physiology, there are relevant comorbidities that commonly appear with MAFLD such as obesity, insulin resistance or cardiovascular diseases. Magnesium perturbations have been characterized in steatohepatitis and associated comorbidities, together with the role of Cyclin M4 (CNNM4) in modulating magnesium homeostasis. Based on these results, we evaluated the disease-modifying effects of a GalNAC-siRNA therapy targeting CNNM4 in a MAFLD animal model with obesity and insulin resistance.

Method: In vitro: Primary hepatocytes were stimulated with 400 µM oleic acid (OA) for a MAFLD phenotype. In vivo: DIAMONDTM mice were fed a high-fat sugar western diet (HFS-WD) for 25 weeks. Mice were treated twice, at weeks 17 and 21, with either 1 mg/kg or 5 mg/kg CNNM4-targeting GalNAC siRNA. Insulin resistance was characterized by intraperitoneal glucose (IPGTT) and insulin (ITT) tolerance tests and histopathological characterization of NASH was assessed by determining steatosis, inflammation and fibrosis development.

ORAL PRESENTATIONS

Results: Treatment of primary hepatocytes with GalNAc siRNA targeting CNNM4 reduced the lipid accumulation induced by OA stimulation. In the in vivo Diamond mouse model, at 17th week, when GalNAc siRNA treatment was initiated, DIAMONDTM mice had already developed insulin resistance. siRNA treatment did not affect weight gain or food consumption pattern. Hepatomegaly induced by HFS-WD was partially controlled by GalNAc CNNM4-targeting siRNA, while serum transaminases tended to decrease in treated mice. Histopathological characterization showed a significant reduction in steatosis and fibrosis development, together with a tendency of reduced inflammation.

Conclusion: GalNAc CNNM4-targeting siRNA-based treatment appears to reduce steatosis, inflammation and fibrosis in a MAFLD animal model, in which mice develop comorbidities, such as insulin resistance or obesity. Ongoing studies will characterize the effect on systemic alterations in MAFLD such as cardiovascular risk or pancreas and kidney functionality.

OS123

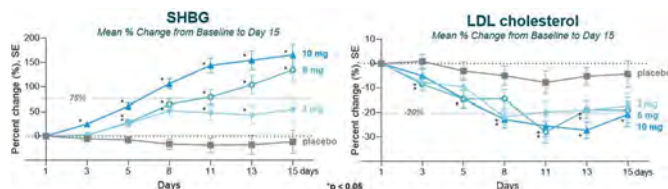
Multiple doses of thyroid hormone receptor-beta agonist TERN-501 were well-tolerated and resulted in significant dose-dependent changes in serum lipids and sex hormone binding globulin in a first-in-human clinical study

Cara H. Nelson¹, Christopher Jones¹, Lois Lee¹, Tonya Marmon¹, Diana Chung¹, Kevin Klucher¹, Yizhao Li¹, Erin Quirk¹, Daria Crittenden¹. ¹Terns Pharmaceuticals, Foster City, United States
Email: cnelson@ternspharma.com

Background and aims: Thyroid hormone receptor-beta (THR-beta) agonists reduce low-density lipoprotein cholesterol (LDL-c), decrease liver fat, and improve liver histology in patients with non-alcoholic steatohepatitis (NASH). TERN-501 is a novel, metabolically stable, highly selective THR-beta agonist. In a first-in-human (FIH) study, single doses of TERN-501 were well-tolerated with significant changes in LDL-c, apolipoprotein B (Apo B), and sex hormone binding globulin (SHBG). Here we describe multiple ascending dose results from the TERN-501 FIH study.

Method: Healthy participants (n=8/cohort) with mildly elevated LDL-c were randomized 3:1 to receive TERN-501 (3, 6, or 10 mg) or placebo once daily for 14 days in 3 cohorts. Intensive PK was assessed on Days 1 and 14, and pharmacodynamic markers were measured pre-dose on Days 1, 3, 5, 8, 11, and 13, and on Days 15, 17, and follow-up. Safety assessments were performed throughout the study.

Results: All 24 subjects completed the study without study drug discontinuations. All adverse events (AEs) were mild (Grade 1); no AEs by preferred term occurred in >1 subject. Vital signs and electrocardiograms remained stable. Transaminase changes in TERN-501 groups compared to placebo were unremarkable. Dose-dependent declines in free thyroxine were observed without clear changes in thyroid stimulating hormone or signs or symptoms of hyper/hypothyroidism. TERN-501 plasma exposures were dose-proportional with low variability. Median half-life was >15 h in all cohorts. SHBG increased dose-dependently with least squares mean (LSM) changes from baseline of 55%, 134%, and 166% on Day 15 in TERN-501 3, 6, and 10 mg groups, respectively (-12% in placebo; see Figure). Statistically significant dose-dependent LSM reductions in Apo B of -18%, -23% and -28% in the 3, 6, and 10 mg groups, respectively, were observed on Day 15 (-6% in placebo). Total cholesterol was reduced in all TERN-501 groups and maximum LSM LDL-c decreases during dosing were -22%, -28%, and -27% for 3, 6, and 10 mg (-8% in placebo; see figure).



Conclusion: Once daily TERN-501 at 3, 6, and 10 mg for 14 days was overall safe and well-tolerated. TERN-501 increased SHBG, a key marker of hepatic THR-beta engagement, in a dose-dependent fashion. Significant reductions in atherogenic serum lipids with favorable PK observed in this study support further investigation of TERN-501 for NASH treatment alone or in combination with other agents.

OS124

Pemvidutide (ALT-801), a novel GLP-1/glucagon dual receptor agonist, achieves rapid and potent reductions in body weight and liver fat: results of a placebo-controlled, double-blind, first-in-human (FIH) clinical trial

Stephen Harrison¹, John Nestor², Sarah Browne³, Jacques Payne⁴, Staci Steele⁵, Robert Casper⁵, Anvar Suyundikov⁶, Vyjayanthi Krishnan⁷, Scot Roberts⁸, Joyce James⁹, M. Scott Harris¹⁰.
¹Pinnacle Research, Research, San Antonio, United States; ²Spitfire Pharma, South San Francisco, United States; ³Altimmune, Inc., Clinical Development, Gaithersburg, United States; ⁴Altimmune, Inc., Clinical Operations, Gaithersburg, United States; ⁵Altimmune, Inc., Clinical Operations, Gaithersburg, United States; ⁶Altimmune, Inc., Biostatistics, Gaithersburg, United States; ⁷Altimmune, Inc., Product Development, Gaithersburg, United States; ⁸Altimmune, Inc., Research, Gaithersburg, United States; ⁹Corvid LLC, Pharmacokinetics, Oakland, United States; ¹⁰Altimmune, Inc., Medical, Gaithersburg, United States
Email: sharris@altimmune.com

This abstract is under embargo until Friday 24 June 2022, 13:40 BST. This abstract has been selected to be highlighted during official EASL Press Office activities or in official EASL Press Office materials that will be made publicly available on the congress website at 13:40 (BST).

Journalists, industry, investigators and/or study sponsors must abide by the embargo times set by EASL.

Violation of the embargo will be taken seriously. Individuals and/or sponsors who violate EASL's embargo policy may face sanctions relating to current and future abstract submissions, presentations and visibility at EASL Congresses. The EASL Governing Board is at liberty to ban attendance and/or retract data.

Copyright for abstracts (both oral and poster) on the website and as made available during The International Liver Congress™ 2022 resides with the respective authors. No reproduction, re-use or transcription for any commercial purpose or use of the content is permitted without the written permission of the authors. Permission for re-use must be obtained directly from the authors.

OS125

Safety, pharmacokinetics and efficacy of the novel pan-phosphodiesterase inhibitor ZSP1601 in 36 NASH patients: a double-blinded, placebo-controlled, multiple-dose escalation phase Ib study

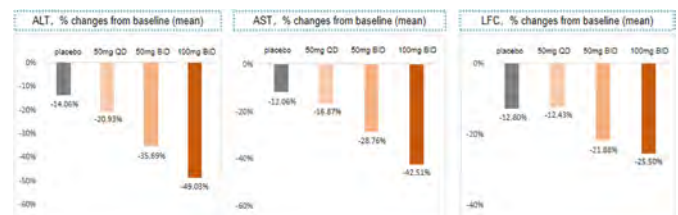
Yue Hu¹, Hai Jun Li², Hong Zhang¹, Jinjun Chen³, Zhongyuan Xu³, Hong You⁴, Ruihua Dong⁴, Xiaoxue Zhu¹, Hong Chen¹, Yun Peng², Jing Li², Xiaojiao Li¹, Lei Zhang⁵, Di Cao⁴, He Jin⁴, Dongdong Qiu⁵, Aruhan Yang¹, Jingrui Liu¹, Haiyan Jia¹, Jinfeng Lou¹, Junqi Niu⁶, Yanhua Ding¹. ¹The First Hospital of Jilin University, Phase I Clinical Research Center, Changchun, China; ²Guangdong Raynovent Biotech Co., Ltd, Guangzhou, China; ³Nanfang Hospital, Nanfang Medical University, Guangzhou, China; ⁴Beijing Friendship Hospital, Capital Medical University, Beijing, China; ⁵The First Hospital of Jilin University, Radiology, Changchun, China; ⁶The First Hospital of Jilin University, Hepatology, Changchun, China
Email: dingyanhua2003@126.com

Background and aims: NASH is a serious healthcare burden. Although there has been steady progress in advancing drug development, no new drug is approved yet for this condition. The primary aim of this clinical trial is to evaluate the safety, pharmacokinetics, and efficacy of ZSP1601 that is a pan-phosphodiesterase (PDE) inhibitor to decrease producing TNF- α to reduce liver inflammation in NASH patients.

Method: This is a double-blind and randomized phase Ib study in 36 NASH patients (aged 18–65 years), the study is consisted of three dose cohorts (50 mg QD, 50 mg BID, 100 mg BID), 12 patients were enrolled for every cohorts of which 9 received ZSP1601 and 3 received placebo orally for 28 days. The patients who were diagnosed by liver biopsy or met clinical features that contains the following two criteria: ALT $\geq 1.5 \times$ ULN (male 75 U/L, female 60 U/L) for two examinations within 28 days with an interval greater than 7 days; BMI ≥ 25 kg/m² and a baseline MRI-PDFF of liver $\geq 10\%$ were enrolled.

Results: A total of 36 NASH patients were enrolled and completed the study. After the consecutive administration of ZSP1601 50 mg QD, 50 mg BID or 100 mg BID for 28 days, the plasma concentration reached steady state on the third day. The AUC increased gradually with increasing dose. There is a relatively lower accumulation of ZSP1601. MRI-PDFF was measured at baseline and day 29. The patients received ZSP1601 50 mg QD or BID or 100 mg BID or placebo had a mean relative reduction from baseline in MRI-PDFF of 12.43%, 21.88%, 25.50% and 12.80%. $\geq 30\%$ reduction in MRI-PDFF relative to baseline was measured in 7 patients received ZSP1601 and 1 patient received placebo. The mean reduction of ALT from baseline were 24.8 U/L, 38.94 U/L, 55.06 U/L and 13.55 U/L. The ALT of 8 patients decrease to normal, including 1 patient in 50 mg QD cohort, 2 patients in 50 mg BID cohort, 4 patients in 100 mg BID cohort and 1 patient in placebo cohort. And the AST of patients in ZSP1601 cohorts also showed obvious change from baseline. In addition, the Cap, HOMA-IR, FIB4, APRI and CK-18 decreased in ZSP1601 cohort. 18 of 36 (50%) patients experienced at least one mild or moderate adverse event (AE), and the incidence rates of AEs were 77.8% and 66.7% in ZSP161 cohorts and placebo cohort, respectively. No serious adverse event. ZSP1601 was well-tolerated in this study. The most frequent AEs were adaptive headaches, creatinine slightly transiently elevated, diarrhoea and indigestion.

Conclusion: The results of this clinical trial showed that a significant reduction in liver fat by MRI-PDFF and ALT level of NASH patients enrolled after 28-days treatment. The phase 1b study suggested that ZSP1601 is safe and effective. The efficacy of 50 mg BID and 100 mg BID cohort were better than the 50 mg QD cohort and placebo cohort. Comparing with the results of other new drugs treating for NASH clinical study, the efficacy of ZSP1601 are inspiring. (This trial registered number is NCT04140123).



Cirrhosis and its complications: Portal Hypertension

OS126

The association between proton pump inhibitor exposure and key liver-related outcomes in patients with cirrhosis: a veterans affairs cohort study

Nadim Mahmud¹, Marina Serper¹, Tamar Taddei², David Kaplan¹. ¹Hospital of the University of Pennsylvania, Gastroenterology, Philadelphia, United States; ²Yale University, New Haven, United States
Email: nadim.mahmud@gmail.com

Background and aims: The impact of proton pump inhibitor (PPI) use on infection, decompensation, and mortality remains a point of controversy in patients with cirrhosis. We aimed to explore these associations in a large U.S. dataset while accounting for complex confounding relationships.

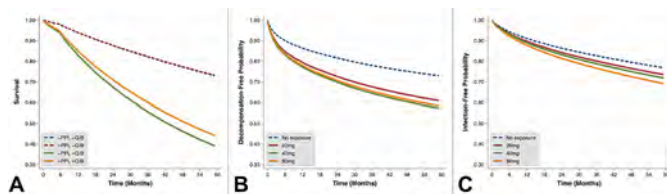
Method: This was a retrospective cohort study of patients with compensated cirrhosis in the Veterans Health Administration (VHA). We identified all PPI prescriptions in the VHA and time-updated PPI exposure every 30 days, including PPI dose which was normalized to omeprazole equivalents. Inverse probability treatment weighting

ORAL PRESENTATIONS

(IPTW) and Cox regression analysis adjusted for time-updated cardiovascular comorbidities, statin medications, antiplatelet medications, and hospitalized gastrointestinal bleed (GIB) were constructed for outcomes of infection, decompensation, and all-cause mortality.

Results: A total 76,251 patients were included, 23,628 (21.0%) of whom were on PPI at baseline. Patients on baseline PPI were more often white (64.4% vs. 60.0%, $p < 0.001$), had higher body mass index (median 29.3 vs. 28.3, $p < 0.001$), and had more cardiovascular and metabolic comorbidities. In IPTW Cox regression, there was a significant interaction between hospitalized GIB and PPI exposure such that there was no association between PPI use and all-cause mortality in patients without hospitalized GIB (hazard ratio [HR] 0.99, 95% confidence interval [CI] 0.97–1.02, $p = 0.58$), but PPIs were associated with reduced hazard of mortality in those who experienced hospitalized GIB (HR 0.88, 95% CI 0.84–0.92, $p < 0.001$). PPI exposure was associated with increased hazard of cirrhosis decompensation (HR 1.64, 95% CI 1.61–1.68, $p < 0.001$) and severe infection (HR 1.21, 95% CI 1.18–1.24, $p < 0.001$), with increased hazard with higher dose exposure (each $p < 0.001$). Among infection types, the strongest observed association was with spontaneous bacterial peritonitis, where PPI exposure conferred a 77% increased hazard (HR 1.77, 95% CI 1.66–1.88, $p < 0.001$).

Conclusion: PPI exposure was associated with an increased risk of severe infection, in particular SBP, as well as cirrhosis decompensation. Regarding all-cause mortality, PPI usage had a protective association in patients with prior hospitalized GIB, but no association with mortality apart from this population. These findings suggest that PPIs should not be avoided in patients with cirrhosis in the setting of an appropriate indication.



OS127

Non-invasive tests for clinically significant portal hypertension after HCV-cure-individual patient data meta-analysis and validation

Georg Semmler^{1,2}, Sabela Lens^{3,4,5}, Elias Laurin Meyer⁶, Anna Baiges^{3,4,5}, Edilmar Alvarado-Tapias^{3,7}, Elba Llop^{3,8}, Javier Martinez^{3,9}, Philipp Schwabl^{1,2}, Ezequiel Mauro¹⁰, Laia Escude^{3,4,5}, Cristina Diez^{11,12}, Luis Ibañez^{3,12,13}, Jose Ignacio Fortea¹⁴, Angela Puente¹⁴, Marta Abadia¹⁵, Ji-Dong Jia^{16,17}, Hitoshi Yoshiji¹⁸, Sven Francque^{19,20,21}, Emmanuel Tsochatzis^{22,23}, Jaime Bosch²⁴, Rafael Bañares^{3,12,13}, Gonzalo Crespo^{3,4,5}, Thomas Reiberger^{1,2}, Cándid Villanueva^{3,7}, Xavier Forns^{3,4,5}, Juan Carlos Garcia Pagan^{3,4,5}, Mattias Mandorfer^{1,2}.

¹Division of Gastroenterology and Hepatology, Department of Internal Medicine III, Medical University of Vienna, Vienna, Austria; ²Vienna Hepatic Hemodynamic Lab, Division of Gastroenterology and Hepatology, Department of Internal Medicine III, Medical University of Vienna, Vienna, Austria; ³Centro de Investigación Biomédica En Red de Enfermedades Hepáticas y Digestivas (CIBERehd), Instituto de Salud Carlos III, Spain; ⁴Liver Unit, Hospital Clínic, Universitat de Barcelona,

Health Care Provider of the European Reference Network on Rare Liver Disorders (ERN-Liver), Barcelona, Spain; ⁵August Pi i Sunyer Biomedical Research Institute (IDIBAPS), Universitat de Barcelona, Barcelona, Spain; ⁶Institute for Medical Statistics, Center for Medical Statistics, Informatics and Intelligent Systems, Medical University Vienna, Vienna, Austria; ⁷Hospital of Santa Creu and Sant Pau, Autonomous University of Barcelona, Hospital Sant Pau Biomedical Research Institute (IIB Sant Pau), Barcelona, Spain; ⁸Liver Unit, Hospital Universitario Puerta De Hierro Majadahonda, Universidad Autónoma de Madrid, Madrid, Spain; ⁹Department of Gastroenterology and Hepatology, Hospital Universitario Ramón y Cajal, IRYCIS, University of Alcalá, Madrid, Spain; ¹⁰Liver Unit, Hospital Italiano, Buenos Aires, Argentina, Buenos Aires, Argentina; ¹¹Unidad de Enfermedades Infecciosas/VIH, Hospital General Universitario Gregorio Marañón, Madrid, Spain; ¹²Instituto de Investigación Sanitaria Gregorio Marañón (IISGM), Madrid, Spain; ¹³Liver Unit, Hospital General Universitario Gregorio Marañón, Madrid, Spain; ¹⁴Aparato Digestivo/Unidad de Hepatología, Hospital Universitario Marqués de Valdecilla, Santander, Spain; ¹⁵Servicio de Aparato Digestivo, Hospital Universitario La Paz, Madrid, Spain; ¹⁶Liver Research Center, Beijing Friendship Hospital, Capital Medical University, Beijing, China; ¹⁷Beijing Key Laboratory of Translational Medicine on Liver Cirrhosis, Beijing, China; ¹⁸Department of Gastroenterology, Nara Medical University, Kashihara, Japan; ¹⁹Department of Gastroenterology and Hepatology, Antwerp University Hospital, Antwerp, Belgium; ²⁰Laboratory of Experimental Medicine and Paediatrics (LEMP), Faculty of Medicine and Health Sciences, University of Antwerp, Antwerp, Belgium; ²¹Translational Sciences in Inflammation and Immunology, University of Antwerp, Antwerp, Belgium; ²²UCL Institute for Liver and Digestive Health, Royal Free Hospital and UCL, London, United Kingdom; ²³Sheila Sherlock Liver Centre, Royal Free Hospital, London, United Kingdom; ²⁴Department of Visceral Surgery and Medicine, Inselspital, University of Bern, Bern, Switzerland

Email: mattias.mandorfer@meduniwien.ac.at

Background and aims: Non-invasive tests (NIT) for clinically significant portal hypertension (CSPH; hepatic venous pressure gradient [HVPG] ≥ 10 mmHg) have predominantly been studied in patients with active HCV-infection, while investigations after HCV-cure are limited and yielded conflicting results. Thus, we conducted an individual patient data meta-analysis.

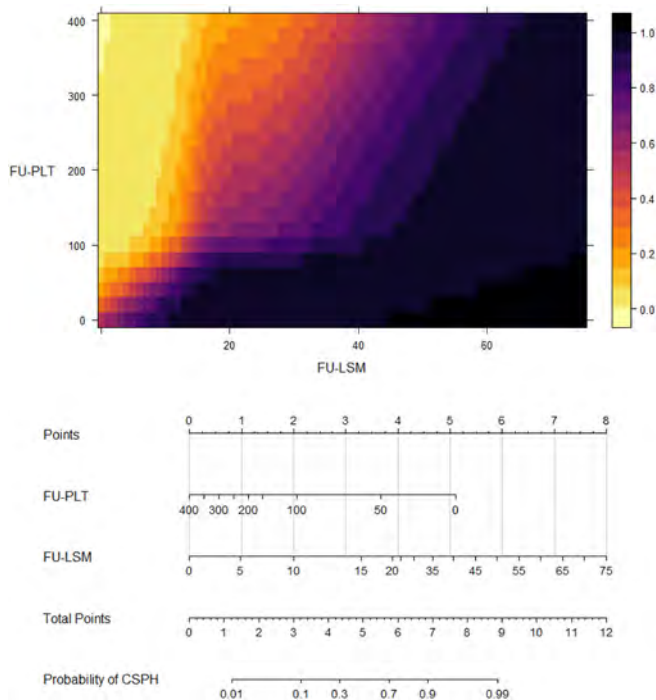
Method: 418 patients with pre-treatment HVPG ≥ 6 mmHg who achieved sustained virological response (SVR) and underwent post-treatment HVPG-measurement. Paired data on pre-/post-treatment liver stiffness-measurement (LSM)/platelet count (PLT) was available in 324 patients.

The derived non-invasive criteria were validated against the direct end point hepatic decompensation in 470 compensated advanced chronic liver disease (cACLD) patients with SVR.

Results: At a median of 28.4 (IQR: 24–44) weeks post-treatment, HVPG decreased in 79.7%, remained unchanged in 5.5%, and increased in 14.8%; median relative difference: -18.8 (IQR: -32.8 – $[-4.8]$ %. Among patients with pre-treatment CSPH (84.4%), HVPG-decreases $\geq 10\%$ were observed in 208 (64.2%).

In cACLD patients with paired NIT, the correlation between LSM/HVPG was significantly stronger post- vs. pre-treatment (Spearman's $\rho = 0.68$ vs. 0.53 ; $P < 0.001$), while that of PLT/HVPG remained unchanged. HVPG tended to be lower post- vs. pre-treatment for any given LSM/PLT-value within the range relevant for clinical decision-making, indicating the need for dedicated algorithms after HCV-cure.

A non-linear model combining post-treatment (FU-)LSM/PLT yielded a high diagnostic accuracy (AUC: 0.89 [95%CI: 0.85 – 0.93]) for post-treatment CSPH in cACLD and can be used to estimate the probability of CSPH in an individual patient (Figure). Post-treatment LSM < 12 kPa and PLT > 150 G/L excluded CSPH (sensitivity: 99.2%), while LSM ≥ 25 kPa was highly specific (93.6%) for CSPH.



The LSM <12 kPa and PLT >150 G/L-criterion was achieved in 185/470 (39.4%) cACLD patients and their 3-year decompensation risk was 0%. In patients with post-treatment LSM ≥ 25 kPa (77/470 [16.4%]), 3-year decompensation risk was 14.2%, while it was 1.3% in those (208/470 [44.3%]) meeting none of the above criteria.

Conclusion: NIT can exclude/rule-in CSH after HCV-cure and predict clinical outcomes. Based on these findings, Baveno VII recommends that patients with LSM <12 kPa and PLT >150 G/L (CSH excluded; no decompensation risk) may be discharged from portal hypertension surveillance (NIT \pm endoscopy), if no co-factors are present, while continuation of carvedilol is warranted in those with LSM ≥ 25 kPa (CSH ruled-in; increased decompensation risk). In patients not meeting these criteria, the presence of post-treatment CSH can be estimated by the provided 3-D plot/nomogram or determined by HVPG-measurement.

G.S. and S.L. contributed equally.

J.C.G-P. and M.M. share corresponding/last authorship.

OS128

Carvedilol plus Simvastatin modulates systemic inflammation in cirrhosis with portal hypertension and non-response to B-blockers: randomised double-blind study

Edilmar Alvarado-Tapias^{1,2}, Rosa Montañés¹, Anna Brujats¹, Berta Cuyas¹, Marta García Guix¹, Claudia Pujol¹, Marianne Murzi-Pulgar¹, Maria Poca^{1,2}, Isabel Graupera^{2,3}, Oana Pavel⁴, Alba Ardevol¹, Xavier Torras^{1,2,5}, Paula Bufi Roig¹, Àngels Escorsell^{1,2}, Silvia Vidal¹, Cándid Villanueva^{1,2}. ¹Hospital de la Santa Creu i Sant Pau. Biomedical Research Institute Sant Pau (IIB Sant Pau). 08025 Barcelona. Universitat Autònoma de Barcelona, Barcelona, Spain; ²Centro de Investigación Biomédica en Red de Enfermedades Hepáticas y Digestivas (CIBERehd), Madrid, Spain; ³IDIBAPS, Hospital Clinic, Barcelona; ⁴Hospital Universitario Sant Joan de Reus Email: cvillanueva@santpau.cat

Background and aims: Carvedilol (Cv) has greater reducing effect on portal hypertension than propranolol and has antioxidant and anti-inflammatory properties. Statins reduce intrahepatic vascular resistance. Some proinflammatory cytokines such as IL-6 have been involved in the progression of cirrhosis. The effect of Cv on systemic inflammation is unclear and whether combination with simvastatin

may modulate this effect in patients with clinically-significant portal-hypertension (CSPH).

Method: Patients with cirrhosis and high-risk varices were consecutively included. The hepatic venous pressure gradient (HVPG) was measured before and after propranolol i.v. and non-responders (i.e. HVPG-decrease $\leq 20\%$) were treated with Cv and randomized to receive simvastatin (Sv) (40 mg/d) or placebo (Pb), under double-blind conditions. One month later, the chronic hemodynamic response was assessed. Plasma was obtained in each hemodynamic study to determine proinflammatory cytokines (IL-6, TNF- α , IL-1 β , MCP-1) and oxidative stress markers (NO, MDA, FvW).

Results: We included 82 patients, 41 treated with Cv + Sv 41 with Cv + Pb. Baseline clinical and hemodynamic characteristics, and cytokine levels were similar. The inflammatory cytokines IL-6, MCP-1, and MDA decreased significantly ($p < 0.05$) in both groups, but such a decrease was greater with Cv + Sv ($p < 0.01$). No significant changes were observed in the other markers. HVPG decreased significantly with both, Cv+Pb (19 ± 3 mmHg to 17 ± 3 mmHg, $p < 0.001$) and Cv + Sv (19 ± 4 mmHg to 16 ± 4 mmHg, $p < 0.001$). The decrease was greater with Cv + Sv ($-17 \pm 12\%$ vs $-11 \pm 8\%$, $p = 0.05$). In patients with chronic decrease in HVPG $> 20\%$, Δ IL-6 was significantly higher with Cv + Sv (-30 ± 6 vs -11 ± 2 , $p = 0.04$). Significant correlation was observed between IL-6 and HVPG at follow-up ($r = 0.52$, $p < 0.001$).

Conclusion: In patients with cirrhosis and CSPH, carvedilol achieves a significant reduction in proinflammatory cytokines and oxidative stress mediators and improves the portal hypertension. All these changes are significantly increased by adding simvastatin. This suggests that the addition of simvastatin to carvedilol may improve clinical efficacy.

OS129

Non-invasive diagnosis of clinically significant portal hypertension and treatment with non-selective beta-blockers: a new paradigm

Elton Dajti¹, Federico Ravaioli¹, Giovanni Marasco², Vanessa Alemanni³, Luigi Colecchia⁴, Alberto Ferrarese⁵, Caterina Cusumano⁵, Stefano Gemini⁵, Amanda Vestito³, Matteo Renzulli³, Rita Golfieri², Davide Festi⁴, Antonio Colecchia⁵. ¹IRCCS S. Orsola Hospital, Bologna, Italy; ²Department of Medical and Surgical Sciences, University of Bologna, Bologna, Italy; ³IRCCS S. Orsola Hospital, Bologna, Italy, University of Bologna, Bologna, Italy; ⁴IRCCS S. Orsola Hospital, Bologna, Italy, Bologna, Italy; ⁵University of Bologna, Bologna, Italy; ⁶Borgo Trento University Hospital of Verona, Verona, Italy Email: e_dajti17@hotmail.com

Background and aims: Non-selective beta-blockers (NSBB) may reduce the risk of decompensation in patients with clinically significant portal hypertension (CSPH). We aimed to improve the available algorithms for the non-invasive diagnosis of CSPH by evaluating spleen stiffness measurement (SSM) in patients with compensated advanced chronic liver disease (cACLD).

Method: This is a retrospective study in patients with liver stiffness measurement (LSM) ≥ 10 kPa, no previous decompensation, and available measurements of hepatic venous pressure gradient (HVPG), LSM and SSM referring to our tertiary center in Bologna. The diagnostic algorithms were adequate if negative (NPV) and positive predictive value (PPV) $> 90\%$ when ruling-out and in CSPH, respectively; these models were validated in a cohort from Verona. The 5-year decompensation rate was reported in each risk group.

Results: One-hundred-ten patients were included in the derivation cohort (CSPH prevalence 58.6%). Available algorithms based on LSM and platelet count (PLT) (LSM > 25 kPa or LSM > 20 kPa and PLT $< 150,000/\text{mm}^3$ for ruling-in CSPH and LSM ≤ 15 kPa or LSM ≤ 20 kPa and PLT $\geq 150,000/\text{mm}^3$ for ruling out-CSPH) were validated. However, a large number of patients (38–59%) remained in the grey zone with indeterminate results for CSPH presence. The application of SSM cut-off 40 kPa and PLT $150,000/\text{mm}^3$ in the “grey zone” patients allowed to significantly reduce the rate of indeterminate

results to 16–23%, maintaining adequate NPV and PPV (above 90%) (Figure 1A). The combined algorithms were validated in an independent (Verona) cohort of eighty-one patients. A nomogram based on LSM, SSM and PLT was developed to predict the individual probability of CSPH presence (AUROC = 0.966) (Figure 1B); the model performed significantly better than the Anticipate model ($p < 0.05$). During follow-up, 21–63% of first decompensation events occurred in the patients within the “grey zone” according to the models based only on LSM and PLT, whereas almost all decompensation events occurred in the “rule-in” zone defined by the models including SSM.

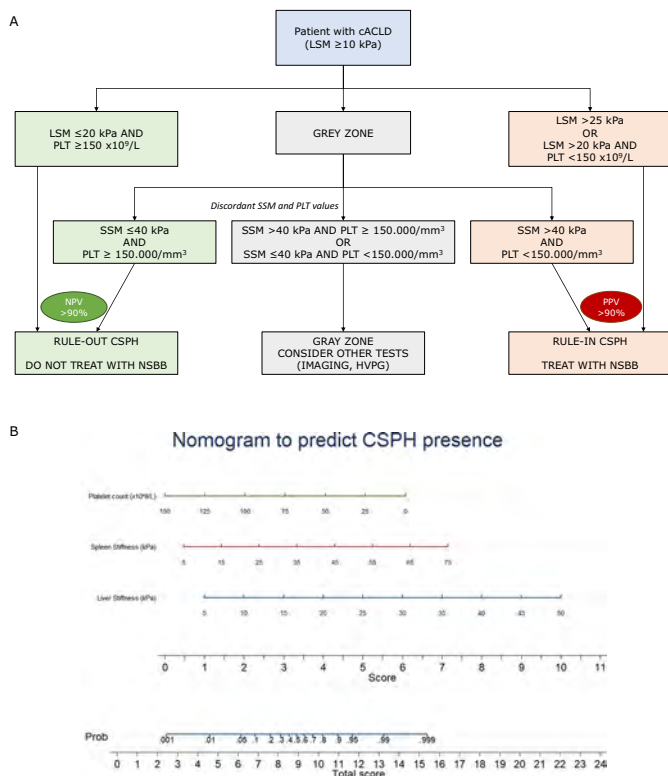


Figure 1 (A) Proposed algorithm based on liver stiffness, platelet count and spleen stiffness for the diagnosis of CSPH in cACLD patients; (B) A newly proposed nomogram based on liver stiffness, platelet count and spleen stiffness to predict the presence of CSPH.

Conclusion: The addition of SSM significantly improves the clinical applicability of the algorithms based on LSM and platelet count for CSPH diagnosis. Our models can be used to non-invasively identify candidates for NSBB treatment and patients at high-risk of decompensation.

OS130

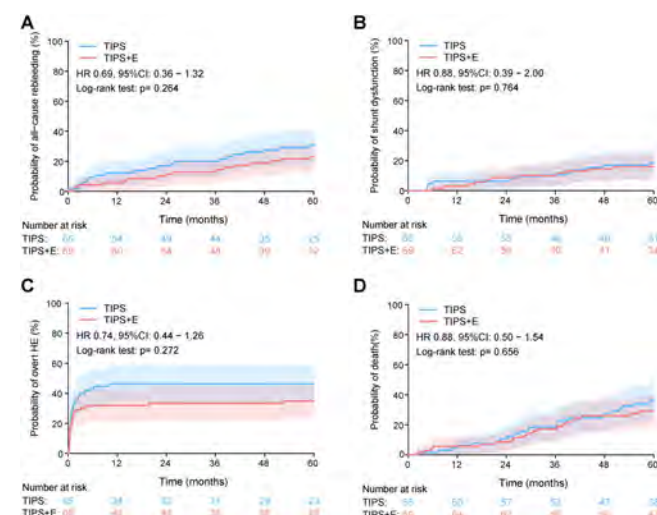
TIPS with versus without variceal embolization for the prevention of variceal rebleeding: a randomized controlled trial

Yong Lv¹, Hui Chen¹, Bohan Luo^{1,2}, Wei Bai^{1,2}, Kai Li¹, Zhengyu Wang^{1,2}, Dongdong Xia^{1,2}, Wengang Guo^{1,2}, Xiaomei Li^{1,2}, Jie Yuan^{1,2}, Zhanxin Yin^{1,2}, Daiming Fan¹, Guohong Han^{1,2}. ¹National Clinical Research Center for Digestive Diseases and Xijing Hospital of Digestive Diseases, Fourth Military Medical University, Department of Liver Diseases and Digestive Interventional Radiology, Xi'an; ²Xi'an International Medical Center Hospital of Digestive Diseases, Department of Liver Diseases and Digestive Interventional Radiology, Xi'an, China Email: 13991969930@126.com

Background and aims: The role of variceal embolization at the time of transjugular intrahepatic portosystemic shunt (TIPS) creation for the prevention of variceal rebleeding remains controversial. This study aimed to evaluate whether adding variceal embolization to TIPS placement could further reduce the incidence of post-TIPS variceal rebleeding in patients with cirrhosis.

Method: From June 2014 to February 2016, 134 consecutive cirrhotic patients who had variceal bleeding in the past 6 weeks were randomly assigned (1:1) to receive TIPS alone (TIPS group, n = 65) or TIPS plus variceal embolization (TIPS + E group, n = 69) to prevent variceal rebleeding. The primary end point was all-cause rebleeding.

Results: TIPS placement and variceal embolization was successful in all patients. During a median follow-up of 63.1 months in the TIPS group and 61.8 months in the TIPS + E group, the primary end point was met in 21 patients (32.3%) in the TIPS group and 16 patients (23.2%) in the TIPS + E group ($p = 0.324$). The 2-year cumulative incidence of all-cause rebleeding was not significantly between the two groups (TIPS + E vs TIPS: 11.6% vs 16.9%; HR: 0.69, 95%CI, 0.36 to 1.32; $p = 0.264$). Neither the incidence of shunt dysfunction (15.9% vs 18.5%, $p = 0.875$), overt hepatic encephalopathy (36.2% vs 46.2%, $p = 0.322$), death (34.8% vs 38.5%, $p = 0.807$) nor other adverse events was significantly different between the two groups.



Conclusion: In patients with cirrhosis, adding variceal embolization to TIPS did not confer further benefit for the prevention of variceal rebleeding. Our study did not support concomitant variceal embolization during TIPS for the prevention of variceal rebleeding.

OS131

Clinical course of cirrhotic patients developing ascites as the single first decompensation

Lorenz Balcar^{1,2}, Marta Tonon³, Georg Semmler^{1,2}, Katharina Pomej^{1,2}, Valeria Calvino³, Bernhard Scheiner^{1,2}, Simone Incicco³, Rafael Paternostro^{1,2}, Carmine Gabriele Gambino³, David JM Bauer^{1,2}, Antonio Accetta³, Lukas Hartl^{1,2}, Alessandra Brocca³, Mathias Jachs^{1,2}, Paolo Angeli³, Michael Trauner¹, Mattias Mandorfer^{1,2,4}, Salvatore Piano^{3,4}, Thomas Reiberger^{1,2,4}. ¹Medical University of Vienna, Division of Gastroenterology and Hepatology, Department of Internal Medicine III, Vienna, Austria; ²Medical University of Vienna, Vienna Hepatic Hemodynamic Lab, Division of Gastroenterology and Hepatology, Department of Internal Medicine III, Vienna, Austria; ³University of Padova, Unit of Internal Medicine and Hepatology, Department of Medicine, Padova, Italy; ⁴Baveno faculty, Baveno cooperation, an EASL consortium, Bologna, Italy Email: thomas.reiberger@meduniwien.ac.at

Background and aims: While ascites is the most frequent first decompensating event in cirrhosis, the clinical course of patients with ascites as the index decompensation is not well defined, in particular regarding the occurrence of further decompensation. The aim of this multicenter study was to investigate (i) the clinical course and (ii) the incidence and type of further decompensation in patients with isolated ascites as the first decompensating event.

Method: 622 patients with cirrhosis presenting with ascites (grade II or III) as the single index decompensating event at the University Hospital of Padova (Italy) or the Vienna General Hospital (Austria) between 2003 and 2021 were included. Patients with concomitant decompensating event (s) were excluded. Death and transplantation were considered as competing risks.

Results: Mean age was 57 ± 11 years and most patients were male ($n = 423$, 68%). 323 (52%) patients presented with grade II and 299 (48%) with grade III ascites. Median Child score was 8 (IQR: 7–10) and mean MELD was 15 ± 6 .

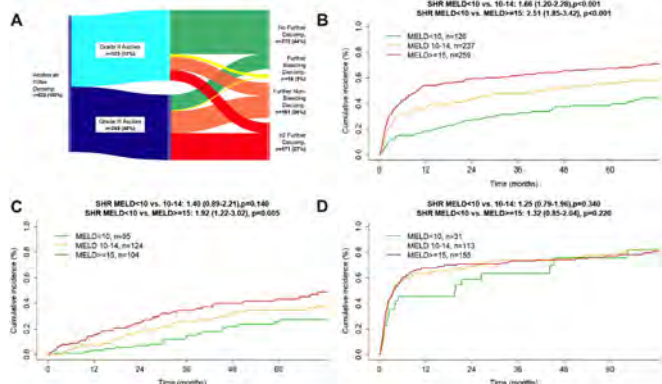
During a median follow-up period of 82 months, 350 (56%) patients progressed to further decompensation: refractory ascites ($n = 204$; 33%), hepatic encephalopathy ($n = 183$; 29%), spontaneous bacterial peritonitis ($n = 105$; 17%), HRS-AKI ($n = 81$; 13%) and variceal bleeding ($n = 54$; 9%). Median time to further decompensation was 27 months. Variceal bleeding as an isolated further decompensation was rare ($n = 18$; 3%), while non-bleeding further decompensation ($n = 161$; 26%) and ≥ 2 further decompensation events ($n = 171$; 27%) were common. Further decompensation occurred more frequently in patients with grade III ascites at index decompensation (75% vs. 33% in grade II ascites; $p < 0.001$; A).

Stratifying patients according to MELD revealed patients with distinct risks of further decompensation after 5 years: <10 : 38% vs. 10–14: 56% vs. ≥ 15 : 67% ($p < 0.001$; B). In patients with grade II ascites, MELD <15 identified patients with intermediate risks (<10 : 27%; 10–14: 34%; $p = 0.510$), whereas MELD ≥ 15 identified patients with high risks for further decompensation after 5 years (53%; $p < 0.001$).

Median transplant-free survival was 65 months. Higher MELD translated into an increased risk of liver-related death. Patients with ascites grade II at index decompensation had increased risk of liver-related mortality in case of impaired liver function (C). In patients with ascites grade III at index decompensation, the incidence of further decompensation and liver-related mortality was similarly high, regardless of liver function (i.e., MELD; D).

Conclusion: Further decompensation is frequent in patients with ascites as a single index decompensation and only rarely due to bleeding. Since further decompensation depends on ascites severity and MELD at index decompensation, risk stratification must consider both initial grade of ascites and hepatic function.

Figure. A Sankey plot for further decompensation. **B** further decompensation according to MELD-strata. **C** liver-related death according to MELD-strata in patients with grade II ascites. **D** further decompensation according to MELD-strata in patients with grade III ascites.



Immune-mediated and cholestatic disease: Clinical aspects

OS132

Incidence and predictors of hepatocellular carcinoma development in patients with autoimmune hepatitis: a multicenter international study

Francesca Colapietro^{1,2}, Patrick Maisonneuve³, Ellina Lytyvak⁴, Ulrich Beuers⁵, Robert Verdonk⁶, Adriaan Van der Meer⁷, Bart Van Hoek⁸, Sjoerd Kuiken⁹, Hans Brouwer¹⁰, Egbert-Jan van der Wouden¹¹, Alessio Aghemo^{1,2}, Aad van den Berg¹², George Dalekos¹³, Mercedes Robles-Díaz¹⁴, Raul J. Andrade¹⁴, Aldo J. Montano-Loza⁴, Floris F. van den Brand¹⁵, Guilherme Macedo¹⁶, Rodrigo Liberal¹⁶, Ynto de Boer¹⁵, Ana Lleo^{1,2}.
¹Humanitas University, Departments of Biomedical Sciences, Pieve Emanuele, Italy; ²Humanitas Research Hospital, Division of Internal Medicine and Hepatology, Department of Gastroenterology, Rozzano, Italy; ³European Institute of Oncology, Division of Epidemiology and Biostatistics, Milan, Italy; ⁴University of Alberta, Department of Medicine, Division of Gastroenterology and Liver Unit, Edmonton, Canada; ⁵Amsterdam UMC, locatie AMC, Department of Gastroenterology and Hepatology, Amsterdam, Netherlands; ⁶St. Antonius Hospital, Department of Gastroenterology and Hepatology, Nieuwegein, Netherlands; ⁷Erasmus MC, Department of Gastroenterology and Hepatology, Rotterdam, Netherlands; ⁸Leiden University Medical Center (LUMC), Department of Gastroenterology and Hepatology, Leiden, Netherlands; ⁹OLVG location East, Department of Gastroenterology and Hepatology, Amsterdam, Netherlands; ¹⁰Reinier de Graaf Gasthuis, Department of Gastroenterology and Hepatology, Delft, Netherlands; ¹¹Isala, Department of Gastroenterology and Hepatology, Zwolle, Netherlands; ¹²University Medical Center Groningen, Department of Gastroenterology and Hepatology, Groningen, Netherlands; ¹³General University Hospital of Larissa, Department of Medicine and Research, Laboratory of Internal Medicine, National Expertise Center of Greece in autoimmune liver diseases, Larissa, Greece; ¹⁴Virgen de Victoria University Hospital- IBIMA, University of Málaga, CIBERehd, Liver Unit, Malaga, Spain; ¹⁵Amsterdam UMC, locatie VUmc, Department of Gastroenterology and Hepatology, Amsterdam, Netherlands; ¹⁶São João University Hospital Center, Department of Gastroenterology and Hepatology, Porto, Portugal
Email: ana.lleo@humanitas.it

Background and aims: Autoimmune Hepatitis (AIH) is a rare disease characterized by circulating autoantibodies, hypergammaglobulinemia and interface hepatitis on histology. Survival is impaired due to the potential evolution to cirrhosis with its complications, including hepatocellular carcinoma (HCC). Risk assessment of HCC in AIH still remains a challenge and available data derive mainly from small cohorts and single-center studies. Our aim was to investigate the risk of HCC across a global AIH cohort and identify predictive factors and potential stratification elements.

Method: We performed a retrospective, observational, and multicenter study of data collected within the International Autoimmune Hepatitis Group Retrospective Registry. The registry is an ongoing, non-interventional, international, and multicenter study. All patients with regular and complete follow-up for AIH were included. Demographic, clinical, biochemical and treatment data were collected both at baseline and during follow-up. Outcomes considered were HCC development, liver transplantation and death.

Results: 1210 patients from 21 centers were included, with a median follow-up of 12.3 years. 74.7 % of them were female (905/1210), with 61.7 % of the cohort being over 40 years of age. 36.2 % of patients were overweight or obese (245/1210 and 196/1210, respectively). Most of the patients did not have a significant alcohol consumption. 21.2 % of patients were already cirrhotic at diagnosis (257/1210), with

ORAL PRESENTATIONS

splenomegaly reported in 116 patients (9.6 %). PBC and PSC overlap syndromes were observed in 9.7 % and 7.5 % of the cohort. Treatment at baseline included the use of prednisone in 83.5 % of patients (1010/1210). 22 patients developed HCC during follow-up (22/1210, 1.8 %). Cumulative incidence of HCC of the whole cohort was 0.7% (0.3–1.4) at 5 and 10-year (95 % CI), 2.6% (1.4–4.4) at 20 years and 5.7 % (2.5–10.9) at 30-years of follow-up. The risk of HCC after cirrhosis development increases proportionally to years from the onset of the disease. Age >40 years (HR 5.99, $p = 0.02$), BMI >30 kg/m² (HR 4.11, $p = 0.02$), splenomegaly (HR 4.03, $p = 0.03$), and PSC overlap syndrome (HR 8.63, $p < 0.001$) resulted independent risk factors for HCC development at multivariate analysis balanced by sex. No association was observed between tumor formation and type of treatment, nor activity on liver histology resulted to have any prognostic value.

Conclusion: The incidence of HCC in AIH is lower than reported to other chronic liver diseases even after cirrhosis development. Age more than 40 years, obesity, splenomegaly and PSC variant syndrome represent risk factors for HCC development, but further studies are needed to identify predictive tools for stratification of the at-risk population.

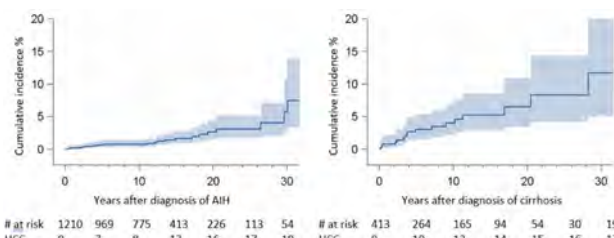


Figure: Development of HCC after diagnosis of AIH and after cirrhosis development in AIH.

OS133

Recurring intrahepatic cholestasis of pregnancy presents with distinct changes in the gut microbiota

Hanns-Ulrich Marschall¹, Peidi Liu², Sara Malcus², Mattias Bergentall², Tanweer Khan², Anita Lövgren-Sandblom³, Peter Malcus⁴, Gun Lindell⁴, Fredrik Backhed¹, Ewa Wiberg-Itzel⁵, Helena Strevens⁴. ¹Gothenburg University, Department of Molecular and Clinical Medicine/Wallenberg Laboratory, Gothenburg, Sweden; ²Metabogen AB, AZ BioVentureHub, HF3, Mölndal, Sweden; ³Karolinska University Hospital Huddinge, Department of Clinical Chemistry C1-62, Stockholm, Sweden; ⁴Skåne University Hospital Lund, Department of Gynaecology and Obstetrics, Lund, Sweden; ⁵Södersjukhuset, Department of Gynaecology and Obstetrics, Stockholm, Sweden
Email: hanns-ulrich.marschall@gu.se

Background and aims: Intrahepatic cholestasis of pregnancy (ICP) is the most common pregnancy-related liver disease with a high recurrence risk (rICP). We aimed to prospectively define distinct metagenomics and metabolite patterns in rICP and non-recurring ICP (n-rICP).

Method: Women with a history of ICP ($n = 50$) were screened at 9–19 weeks of gestation (Visit 1, V1) and 1:1 matched to pregnant women without a history of ICP (controls, C). Visits 2, 3 and 4 were performed at gestational weeks 28 ± 2 and 36 ± 2 , and 6 ± 2 weeks postpartum. ICP was defined as otherwise unexplained pruritus and total BA ≥ 10 mmol/L at any time from V2 to delivery, with normalization at V4. Blood samples were taken at each visit for targeted metabolomics, i.e. bile acid (BA) and sulfated progesterone metabolite (PMxS) profiles and C4, while fecal samples were collected for shot-gun metagenomics.

Results: Out of 50 women with a history of ICP, 17 (34%) developed rICP. Ten of these (59%) were treated with UDCA. Demographics at inclusion were not different between groups. In rICP, BA metabolites and mono- and disulfated PMxS-diols were significantly higher as compared to n-rICP and C. Of note, also in n-rICP, PM2DiS and PM3DiS were significantly increased both at V2 and V3. In rICP, the relative abundance of a specific bacterium with 7-beta-hydroxysteroid dehydrogenase (7 β -HSDH) activity was decreased by 95% at V1 but the abundance became increased at V3 in UDCA-treated rICP. In contrast, at V2 the relative abundance of *Faecalibacterium prausnitzii* was decreased by 40% which was negatively correlated ($p < 0.01$) with PM4S and PM5S.

Conclusion: Recurring ICP presents a distinct metagenome with significant decreases of specific bacteria before the development of the ICP phenotype, which is associated with ICP-predictive increases in sulfated progesterone metabolites and elevated bile acid levels. Bacterial species were identified as potential targets for microbiome-based interventions for the prevention and/or treatment of ICP.

OS134

Quality of life outcomes in patients with primary biliary cholangitis treated with setanaxib: post-hoc results from a phase 2 randomised, placebo-controlled trial

David Jones¹, Marco Carbone^{2,3}, Pietro Invernizzi^{2,3}, Frederik Nevens⁴, Mark G. Swain⁵, Philippe Wiesel⁶, Cynthia Levy⁷. ¹Newcastle University Medical School, Newcastle upon Tyne, United Kingdom; ²University of Milano-Bicocca, Division of Gastroenterology, Centre for Autoimmune Liver Diseases, Department of Medicine and Surgery, Monza, Italy; ³San Gerardo Hospital, European Reference Network on Hepatological Diseases (ERN RARE-LIVER), Monza, Italy; ⁴University Hospital KU Leuven, Department of Gastroenterology and Hepatology, Leuven, Belgium; ⁵University of Calgary, Calgary, Canada; ⁶Genkyotex, Geneva, Switzerland; ⁷University of Miami, Schiff Center for Liver Diseases, United States
Email: david.jones@newcastle.ac.uk

Background and aims: Primary biliary cholangitis (PBC) is an autoimmune cholestatic liver disease.¹ Fatigue substantially impacts quality of life of patients with PBC, and remains an unmet need with currently available treatments.² We present quality of life results from a phase 2, double-blind, randomised trial of setanaxib in patients with PBC.

Method: This trial (NCT03226067) randomised patients with PBC and inadequate response or intolerance to ursodeoxycholic acid (UDCA) at baseline (serum alkaline phosphatase and gamma-glutamyl transferase $\geq 1.5 \times$ upper limit of normal) 1:1 to setanaxib 400 mg once/twice daily (OD/BID) or placebo for 24 weeks.³ Quality of life was assessed using the PBC-40 questionnaire (reported as mean [standard deviation] scores). Patients from the intention-to-treat (ITT) population were stratified post-hoc by baseline fatigue score (mild, moderate or severe) using published PBC-40 fatigue domain cut-offs.⁴ Moderate and severe patients were grouped. Correlations between change in fatigue and quality of life domains from baseline were made.

Results: Of 111 patients (placebo: 37; setanaxib 400 mg OD: 38; setanaxib 400 mg BID: 36), 92 had mild and 19 had moderate-to-severe fatigue at baseline. The ITT group had a baseline fatigue score of 17.2 (11.3) (placebo: 17.4 [12.1]; setanaxib 400 mg OD: 15.7 [10.7]; setanaxib 400 mg BID: 18.5 [11.3]). The moderate-to-severe subgroup had higher PBC-40 social, emotional and cognitive domain scores vs the mild subgroup (social: 30.6 [8.8] vs 19.1 [8.0]; emotional: 11.3 [2.8] vs 6.8 [3.1]; cognitive: 18.3 [6.9] vs 11.3 [5.1]). At Week 24, patients treated with setanaxib 400 mg BID had greater reductions from baseline in mean fatigue scores vs patients treated with placebo or setanaxib 400 mg OD (Figure). Similar observations were made in

social, emotional, cognitive and symptom domains. Patients with moderate-to-severe fatigue had larger changes in mean fatigue scores from baseline at Week 24 vs patients with mild fatigue; these changes were greatest amongst setanaxib 400 mg BID patients (-11.0 [11.5 ; $n = 5$]; vs setanaxib 400 mg OD: -7.5 [5.3 ; $n = 4$], placebo: 0.1 [5.7 ; $n = 7$]). Fewer patients reported “most of the time” or “always” for all PBC-40 fatigue items at Week 24 vs baseline. Improvements in fatigue from baseline at Week 24 in patients with moderate-to-severe fatigue correlated with improved social, emotional, symptom (all $r = 0.5$) and cognitive ($r = 0.4$) measures.

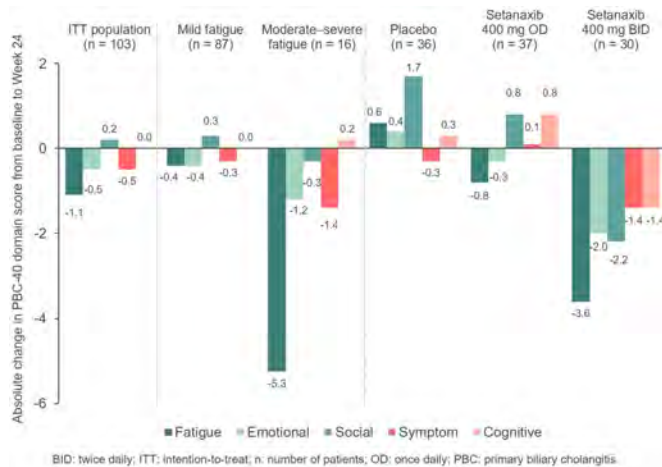


Figure: Summary of absolute score changes from baseline to Week 24 of the PBC-40 domains.

Conclusion: Setanaxib 400 mg BID, in addition to UDCA, is a promising treatment for reducing fatigue in patients with PBC and enhancing quality of life by improving social, emotional and cognitive function.

References

1. Lleo A *Semin Liver Dis* 2020;40:34–48.
2. Mells GF *Hepatology* 2013;58:273–83.
3. Huang JC *Hepatology* 2019;70:777–9.
4. Newton JL *Hepatology* 2007;45:1496–505.

OS135

Quantitative magnetic resonance cholangiopancreatography outperforms Mayo risk score in predicting clinical outcomes in primary sclerosing cholangitis

Raj Vuppalanchi¹, Vijay Are¹, Sofia Mouchti², Carla Kettler¹, Mark Gromski¹, Sarah Finnegan², Fatih Akisik¹. ¹Indiana University School of Medicine, Indianapolis; ²Perspectum Ltd, Oxford, United Kingdom

Email: sarah.finnegan@perspectum.com

Background and aims: Magnetic resonance cholangiopancreatography (MRCP) is a non-invasive imaging technique commonly used to evaluate biliary diseases. Despite its widespread use, MRCP relies on subjective assessments, lacks quantitative metrics and cannot predict the onset of liver-related events. Quantitative MRCP (MRCP+™) is a novel technique that automatically segments biliary anatomy and provides quantitative biliary tree metrics. This study sought to understand the utility of MRCP+ in predicting clinical outcomes for primary sclerosing cholangitis (PSC).

Method: Patients with PSC underwent standardized MRCP imaging post-processed with MRCP+ software, which, via artificial intelligence (AI) driven pathfinding algorithms, enhanced tubular biliary structures to quantify biliary tree volume and dilated and strictured regions of the biliary tree. The duration (in years) between the MRCP scan and clinical event (liver transplantation or death) was calculated. Survival analysis was performed, and a stepwise Cox regression was used to investigate the optimal combination of MRCP+ metrics for predicting clinical outcomes. The resulting risk score was compared to the Mayo risk score using the Akaike Information Criterion (AIC) and expressed as a hazard ratio (HR).

Results: In this retrospective study of 149 PSC patients [32% male; 83% Caucasian; median age 47 years (31.0–61.2)], 29 patients reached clinical outcomes over the course of the study (18 underwent liver transplantation and 11 died). Eight quantitative MRCP+ metrics (M) and total bilirubin (B) were associated with the probability of a clinical event. When combined as a risk score, the overall discriminative performance of the MRCP+ composite biomarker (M+B) was excellent for predicting clinical outcomes with at AUC of 0.87 (95% 0.81, 0.94) and a hazard ratio (HR) of 21.1. (95% 6.4, 70.1) This was superior to the Mayo risk score with AUC of 79 (95% 0.69, 0.89) and HR of 7.2 (95% 3.24, 16.17).

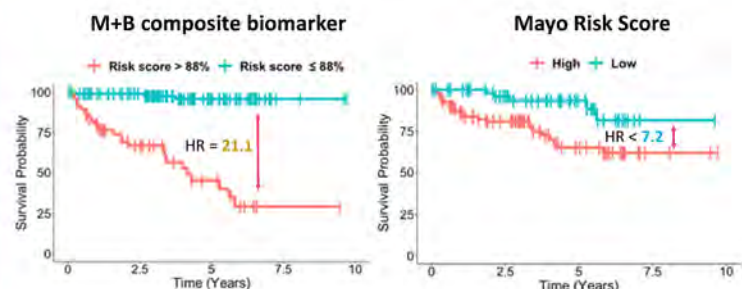
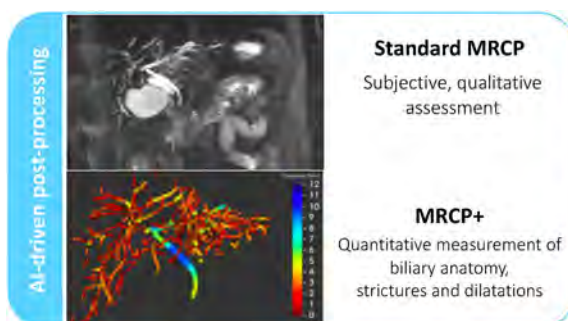


Figure 1: A standard MRCP image (top left), novel MRCP+ quantitative image (bottom left), Kaplan-Meier curves when adjusting for the composite biomarker M+B risk classifier (middle) binary Mayo risk score classified with “intermediate” is redefined as “low” (right) to predict a clinical event within 3-years of entering the study.

Figure: (abstract: OS135)

ORAL PRESENTATIONS

Conclusion: A composite score of MRCP+ metrics and total bilirubin outperformed Mayo risk score for identifying patients with PSC who were at the highest risk of liver failure and death.

OS136

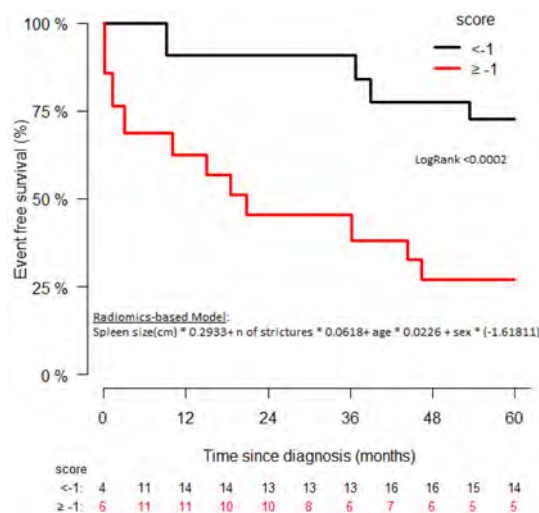
Radiomics-based model for outcome prediction in primary sclerosing cholangitis

Laura Cristofori^{1,2,3}, Marco Porta⁴, Davide Bernasconi³, Leonardi Filippo⁵, Giacomo Mulinacci^{1,2}, Andrea Palermo^{1,2}, Alessio Gerussi^{1,2}, Miki Scaravaglio^{1,2}, Camilla Gallo^{1,2}, Eliana Stucchi^{1,2}, Cesare Maino⁴, Davide Ippolito⁴, Daphne D'Amato⁶, Carlos Ferreira⁷, Marija Mavar-Haramija⁷, Rajarshi Banerjee⁷, Laura Antolini³, Maria Grazia Valsecchi³, Stefano Fagioli⁵, Pietro Invernizzi^{1,2}, Marco Carbone^{1,2}. ¹Division of Gastroenterology, Center for Autoimmune Liver Disease, Department of Medicine and Surgery-University of Milano Bicocca, Monza, Italy; ²European Reference Network on Hepatological Diseases (ERN RARE-LIVER), San Gerardo Hospital, ASST Monza, Monza, Italy; ³Bicocca Bioinformatics Biostatistics and Bioimaging Centre, Department of Medicine and Surgery-University of Milano Bicocca, Monza, Italy; ⁴Diagnostic Radiology, San Gerardo Hospital, ASST Monza, Monza, Italy; ⁵Gastroenterology Hepatology and Transplantation Unit, ASST Papa Giovanni XXIII, Bergamo, Italy; ⁶Gastroenterology Unit, Città della Salute e della Scienza, Turin, Italy; ⁷Perspectum Ltd., Oxford, United Kingdom
Email: l.cristofori@campus.unimib.it

Background and aims: Magnetic resonance cholangiopancreatography (MRCP) is the gold standard for diagnosis and follow-up of patients with primary sclerosing cholangitis (PSC). The semi-quantitative MRCP-derived ANALI score, while performant in risk stratification, has poor-to-moderate inter-reader agreement. We aimed to evaluate the prognostic performance of novel quantitative MRCP in PSC.

Method: This is a retrospective study of PSC patients with at least one MRCP available from 2012 to 2019. Images have been analysed using MRCP+ software (Perspectum Ltd, Oxford) which, using AI-driven pathfinding algorithms to enhance biliary structures, provides quantitative metrics of the bile ducts (number, length and severity of strictures and dilations, and biliary tree volume). The prognostic value of radiomic biomarkers has been assessed towards both soft (hepatic decompensation, variceal bleeding, bacterial cholangitis, and hepatobiliary cancer) and hard end points (death or liver transplantation [LT]). Left truncated Cox regression model was used to account for MRCPs performed later than PSC diagnosis. The multivariate model was internally validated using k-fold cross-validation.

Results: 115 PSC patients with MRCP were evaluated; 90 MRCP passed the quality control. Median age was 41 (IQR 26–51) years, 61% were male, with a follow-up from MRCP to event/censoring of 242 patient-years. An adverse outcome occurred in 28 (25%) patients (8 LT, 3 liver-related death, 5 liver decompensation, 10 bacterial cholangitis, 2 cholangiocarcinoma). Univariate analysis showed a good prognostic performance of all radiomics features evaluated. At multivariable analysis, adjusted for age and sex, the number of strictures and the spleen length were independently associated with the occurrence of adverse event with a HR of 1.06 (per unit, CI 95% 1.03–1.09, $p < 0.0001$) and 1.34 (per cm, CI 95% 1.11–1.6, $p = 0.002$), respectively and a C-statistic of 0.81. The model was internally validated and outperformed the ANALI score in our cohort (C-statistic of 0.72 vs 0.6). The radiomics-based model, using the mean value as cut-off (-1), enabled risk-stratification of PSC patients (Fig).



Conclusion: A radiomics-based model, which includes the number of strictures and the spleen length, can identify PSC patients at higher risk of adverse outcome and outperforms the available radiological scores. MRCP+ features represent a novel biomarker for disease monitoring and a potential surrogate end point for clinical trials.

OS137

Critical shortfalls in the management of PBC: results of the first nationwide, population-based study of care delivery across the U.K.

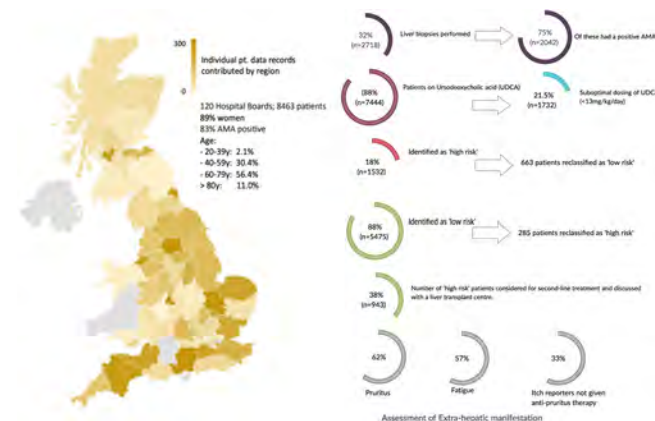
Nadir Abbas^{1,2}, Rachel Smith³, Steve Flack⁴, Richard Aspinall⁵, Rebecca L. Jones⁶, Joanna Leithead⁷, Douglas Thorburn⁸, Conor Braniff⁹, Michael Heneghan¹⁰, Andrew Yeoman¹¹, Collette Thain¹², Chris Mitchell¹², Robert Mitchell-Thain¹², David Jones¹³, Palak Trivedi^{1,2,14}, George Mells³, Laith Al-Rubaay^{15,16} and UK-PBC Consortium¹⁷. ¹University of Birmingham, Institute of Immunology and Immunotherapy, Birmingham, United Kingdom; ²University of Birmingham, United Kingdom; ³Cambridge University Hospitals NHS Foundation Trust, United Kingdom; ⁴University of Cambridge, United Kingdom; ⁵Portsmouth Hospitals NHS Trust, United Kingdom; ⁶Leeds Teaching Hospitals NHS Trust, United Kingdom; ⁷Forth Valley Royal Hospital, United Kingdom; ⁸Royal Free Hospital, United Kingdom; ⁹Belfast Health and Social Care Trust, Northern Ireland; ¹⁰Institute of Liver Studies, King's College Hospital, United Kingdom; ¹¹Aneurin Bevan University Health Board, United Kingdom; ¹²PBC Foundation, United Kingdom; ¹³Newcastle University, United Kingdom; ¹⁴University of Birmingham, Institute of Biomedical Research, United Kingdom; ¹⁵St Mark's Hospital and Academic Institute, United Kingdom; ¹⁶Imperial College School of Medicine, United Kingdom; ¹⁷UK-PBC Consortium, United Kingdom
Email: nadir.abbas@uhb.nhs.uk

Background and aims: Herein, we present the first population-based, nationwide evaluation of healthcare delivery in primary biliary cholangitis (PBC) since publication of the European (EASL) and British guidelines (BSG). Our aim was to assess adherence to guideline recommendations and identify gaps in service provision.

Method: This was a cross-sectional study conducted between 01/21 and 01/22. All 154 hospital boards across England, Scotland, Wales, and Northern Ireland were invited to participate. Data was accrued through the REDcapTM platform, accumulating parameters relating diagnosis, treatment pathways, symptoms, risk stratification and clinical end points.

Results: In entirety, data was returned from 120 hospital boards, with data capture from 8461 pts across the UK. The majority ($n = 7084$; 83%) tested positive for anti-mitochondrial antibodies (AMA, Figure), with 2718 (32%) of the latter subgroup also undergoing liver biopsies. Ursodeoxycholic acid (UDCA) was used as first-line treatment in 7444

patients (88%) but sub-optimally dosed (<13 mg/kg/day) in 1732 (21.5%). Only 197 pts who were under-dosed were documented to have intolerance to higher dosing. Of individuals who were not taking UDCA, only 214 (23%) were referred for alternative/second-line therapy. Of pts taking UDCA for >12 months (n = 7007), 5475 (78%) and 1532 (22%) were classified as low-risk and high risk, respectively, by the contributing hospital. However, on applying the POISE criteria, 663 and 285 patients could be reclassified as 'low-risk and high risk' respectively. Among all who were deemed high-risk with regards disease progression (n = 2476; 29%), 1228 (49.5%) commenced second-line therapy (inc. 551 obeticholic acid; 468 bezafibrate; 68 fenofibrate; 76 combination therapy) and 35 referred directly to a transplant centre. In all, 1831 pts were identified as having cirrhosis (22%), of which 1304 (71%) participated in hepatocellular carcinoma surveillance. Features of decompensated liver disease were identified in 272 pts, of which only 46% (n=67) were discussed with a transplant centre. With regards symptoms/extrahepatic manifestations, n=3237 and 3690 pts did not undergo any assessment of pruritus (38%) or fatigue (44%) in the 24 months prior to data collection. 1803 pts reported ongoing pruritus at the time of assessment, of whom only 1205 (67%) were receiving anti-pruritus therapy.



Conclusion: Our study of real-world practice identifies significant gaps in clinical care across the UK PBC population. Potential future strategies to maximise adherence to guideline standards include the implementation of an integrated care pathway, along with key performance indicators, and development of a centralised referral network, allowing equitable and virtual access to specialists for all those living with PBC.

Viral hepatitis basic science

OS138

A genome-wide CRISPR/Cas9 screen identifies Rab5A as host factor of the hepatitis E virus life cycle

Noémie Oechslin¹, Nathalie Da Silva¹, Maliki Ankavay¹, Darius Moradpour¹, Jérôme Gouttenoire¹. ¹Service of Gastroenterology and Hepatology, Lausanne, Switzerland
Email: noemie.oechslin@chuv.ch

Background and aims: Hepatitis E virus (HEV) is a major cause of acute hepatitis worldwide. Current understanding of the molecular mechanisms allowing for productive HEV infection is limited, especially with respect to host factors required for the viral life cycle. Hence, our study aims at identifying host factors required for HEV replication.

Method: A genome-wide CRISPR/Cas9 screen was performed in permissive human cell lines harboring newly developed subgenomic HEV replicons allowing for positive and negative selection, followed by next-generation sequencing and bioinformatic analyses. Candidates were validated by siRNA-mediated gene silencing and CRISPR/Cas9-mediated gene knockout in cells transfected with subgenomic HEV replicons or infected with cell culture-derived HEV. **Results:** The newly developed replicons and a library of 120,000 unique guide RNAs were employed in two separate screens, identifying 20 top host factor candidates. Validation yielded five host factors, including GBF1, which had been identified previously by a directed approach, and the Ras-related early endosomal protein Rab5A. The expression level and functional activity of Rab5A and of well-characterized mutants thereof were found to modulate HEV RNA replication. Colocalization studies revealed close proximity to the HEV replicase of Rab5A and other endosomal components. **Conclusion:** We describe an innovative approach exploiting CRISPR/Cas9 to identify host factors of a noncytolytic virus. Future studies shall address the mechanisms by which Rab5A modulates HEV RNA replication and define the role of early endosomes in the establishment of a functional replication complex. Altogether, this work yields new insights into the HEV life cycle and the virus-host interactions required for productive infection.

OS139

Novel ultra-potent capsid assembly modulators prevent abnormal accumulation of empty capsids and associated T-cell mediated liver injury in a mouse model of hepatitis B virus infection

Romano Di Fabio^{1,2}, Matteo Iannaccone^{3,4,5}, Leda Bencheva¹, Matteo Conti⁶, Katherine Squires⁷, Mark Lockwood⁷, Raffaele De Francesco^{8,9}, Luca Guidotti^{3,10}. ¹Promidis, Italy; ²IRBM Science Park, Pomezia, Rome, Italy; ³IRCCS San Raffaele Scientific Institute, Division of Immunology, Transplantation and Infectious Diseases, Milan, Italy; ⁴IRCCS San Raffaele Scientific Institute, Experimental Imaging Center, Milan, Italy; ⁵Vita-Salute San Raffaele University, Milan, Italy; ⁶INGM, National Institute of Molecular Genetics "Romeo ed Enrica Invernizzi," Milan, Italy; ⁷Antios Therapeutics, United States; ⁸INGM, National Institute of Molecular Genetics, Italy; ⁹Università degli Studi di Milano, Department of Pharmacological and Biomolecular Sciences, Milan, Italy; ¹⁰Vita-Salute San Raffaele University, Milano, Italy
Email: guidotti.luca@hsr.it

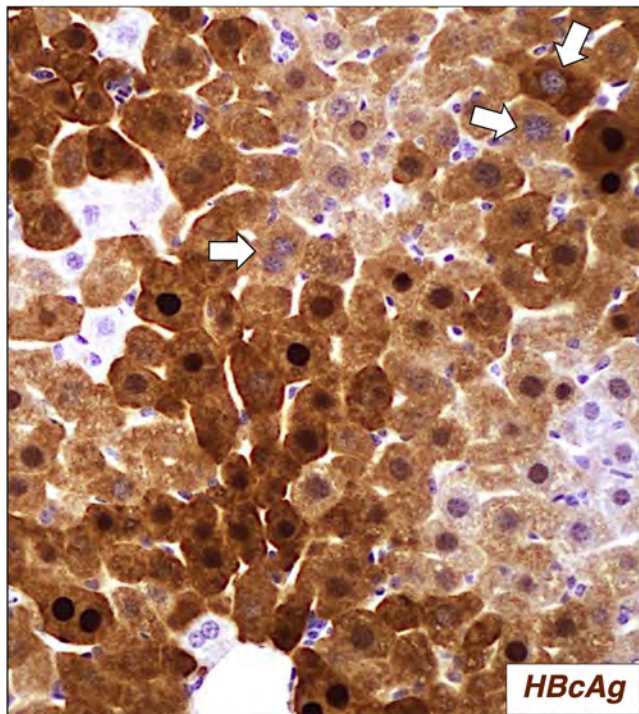
Background and aims: ATI-1428 is a sub-nM active class II capsid assembly modulator (CAM) that safely and durably blocks hepatitis B virus (HBV) replication in immunocompetent transgenic (HBV Tg) mice. Different from other CAMs, ATI-1428 induced no *in vivo* abnormal accumulation of hepatitis B core antigen (HBcAg)-expressing empty capsids (EC) in the hepatocellular cytoplasm. Herein, we extend our understanding of the functional consequences of EC accumulation in the presence of HBcAg-specific CD8⁺ T cells and identify another 4th-generation class II CAM (ATI-1645) that may foster EC degradation.

Method: HBV Tg mice were treated with ATI-1428 or ATI-1112 (a class II CAM causing abnormal EC accumulation) at 50 mg/kg every day (QD) for 16 days. Antiviral potency, drug- or T cell-induced liver injury and HBcAg distribution in hepatocytes (HCs) that, divided or not, were assessed at autopsy (d7 after T cell transfer). ATI-1645 was profiled in HepAD38 cells, HBV-infected HepG2-NTCP cells, and HBV Tg mice.

Results: While inhibiting HBV replication, neither ATI-1428 nor ATI-1112 caused liver injury. T cell transfer in ATI-1112-treated mice induced higher serum alanine aminotransferase peak levels and failed to eliminate ECs, even from post-mitotic HCs becoming nuclear HBcAg-negative (see Figure and PMID: 8057429). By contrast, ECs disappeared from the liver of ATI-1428- and T cell-treated animals. ATI-1645 showed sub-nM EC₅₀/EC₉₀ potency profiles with low nM activity against covalently closed circular DNA establishment.

ORAL PRESENTATIONS

Pharmacokinetic (PK)/pharmacodynamic analyses and safety/efficacy studies in HBV Tg mice indicated that 1645 possesses excellent PK and anti-HBV activity. 28-day ATI-1645 treatment (50 mg/kg QD) cleared ECs from the cytoplasm of most HCs in the absence of any drug- or immune-mediated liver injury.



Conclusion: ATI-1112-related abnormal accumulation of cytoplasmic ECs sensitized HCs to T cell-mediated killing and allowed these particles to survive in resting and post-mitotic HCs no longer replicating HBV. This suggests that CAMs fostering an EC-accumulating phenotype may generate targets of inadequate immunopathology. Conversely, the lack of cytoplasmic EC accumulation that typifies the *in vivo* behavior of ATI-1428 or ATI-1645 should not interfere with productive T cell-mediated viral clearance. The subsequent

characterization of 1645 as an ultra-potent HBV inhibitor that may induce cytoplasmic EC degradation makes it a promising candidate for clinical development.

OS140

Identification of cyclin L1 as a hepatitis B virus host factor regulating viral transcription

Collins Oduor Owino¹, Yi Lin Gian², Pauline AW Poh Kim¹, Nivriti Ganesh¹, Balakrishnan Chakrapani Narmada², Giridharan Periyasamy², Pablo Bifani³, Ramanuj Dasgupta¹. ¹Genome Institute of Singapore (GIS), Singapore, Singapore; ²Experimental Drug Development Centre, Singapore, Singapore; ³Department of Microbiology and Immunology (MD4), Singapore, Singapore
Email: dasguptar@gis.a-star.edu.sg

Background and aims: HBV remains a global public health threat, with over 250 million people chronically infected and about 800,000 deaths reported annually. Even though much work has been done to understand HBV pathogenesis, how the virus manipulates the host cell machinery remains underexplored. In this study we aimed to identify novel host factors that affect HBV replication and gene expression. We describe the role of cyclin L1 (*CCNL1*), a non-canonical cyclin with transcriptional regulatory functions as a novel host cell factor in the control of HBV transcription.

Method: We employed whole transcriptome analysis of HBV infected primary human hepatocytes (PHH), as well as reverse genetics to identify and validate the role of *CCNL1* during HBV replication. Using RNAi and ectopic expression models, we studied the function of cyclin L1 on HBV replication in hepatoma cells and PHH. We also analyzed the effect of *CCNL1* knockdown on the production and stability of HBV RNAs. Using RNA immunoprecipitation (RIP), chromatin immunoprecipitation (ChIP), and immunoprecipitation (IP) techniques, we evaluated the interaction between cyclin L1 and HBV RNAs as well as HBx and HBc. Lastly, we explored the expression profiles of cyclin L1 in chronic HBV patient cohorts and publicly available microarray datasets GSE83148 and GSE52752.

Results: Knockdown of cyclin L1 resulted in a remarkable reduction of HBV gene expression in both hepatoma cells (HepAD38.7 and HepG2-NTCP) and PHH. We observed a remarkable reduction in the levels of HBV surface and e antigens, pre-genomic RNA, and extracellular HBV DNA. Interestingly, overexpression of *CCNL1* resulted in enhanced HBV gene expression with a significant increase in the viral transcripts, thus, corroborating its pro-viral effect. Furthermore, loss of function of cyclin L1 resulted in reduced levels

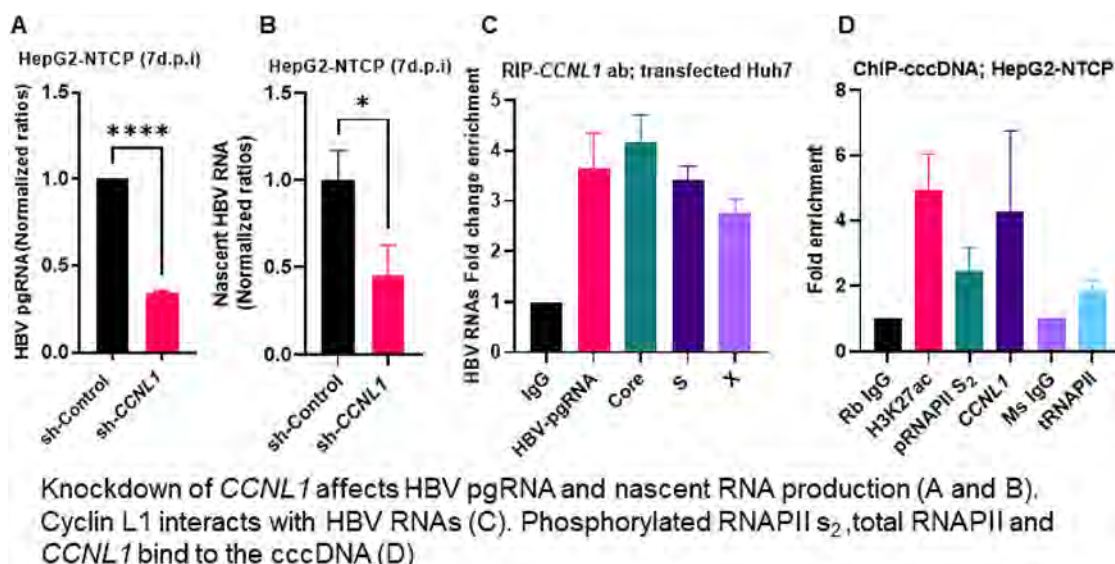


Figure: (abstract: OS140)

of HBV nascent RNA, highlighting its role during HBV transcription. RIP data showed that *CCNL1* might be modulating HBV RNA production through direct interaction with viral RNAs. Lastly, we observed enhanced expression of cyclin L1 in CHB from our patient cohort data and publicly available data sets underscoring its putative function in HBV replication and virus-induced liver disease.

Conclusion: Here, we report that cyclin L1 is a novel HBV host factor modulating the production and stability of viral RNAs. Our data contributes towards the understanding of HBV infection biology and provide a new perspective towards developing host-directed anti-HBV therapies.

OS141

Liver-resident T cell PD-1 correlates with intrahepatic HBV-DNA and is reduced following prolonged antiviral therapy

Mireia García-López¹, Laura J. Pallett², Sergio Rodríguez-Tajes¹, Ernest Belmonte³, Thais Leonel¹, Ester García-Pras¹, Sabela Lens¹, Zoe Mariño¹, Concepció Bartres¹, Ariadna Rando-Segura⁴, Francisco Rodríguez-Frías⁴, Xavier Forns¹, Mala Maini², Sofia Pérez-del-Pulgar¹. ¹Liver Unit, Hospital Clínic, University of Barcelona, IDIBAPS, CIBEREHD, Barcelona, Spain; ²Division of Infection and Immunity, Institute of Immunity and Transplantation, University College London, London, United Kingdom; ³Radiology Department, Centro de Diagnóstico por la Imagen (CDI), Hospital Clínic, University of Barcelona, Barcelona, Spain; ⁴Liver Pathology Unit, Department of Biochemistry and Microbiology, Hospital Universitari Vall d'Hebron, Universitat Autònoma de Barcelona, CIBEREhd, Barcelona, Spain
Email: sofiaapp@clinic.cat

Background and aims: PD-1 is known to be upregulated on global and virus-specific T cells in the HBV-infected liver and is a major target of current immunotherapies in chronic hepatitis B (CHB). However, factors driving its expression in the liver compartment, and potential modulation by antivirals have not been well-defined. Here we therefore investigated the relationship between intrahepatic HBV load and liver-resident T cell PD-1 and whether this could be reduced by prolonged NUC suppression.

Method: This study included 22 CHB patients who underwent hepatic fine needle aspiration (FNA) and biopsy, 9 of whom were treated with NUCs for at least 4 years; a subset had a repeat FNA following treatment withdrawal. Multiparameter flow cytometry was used for immunophenotyping PBMCs and intrahepatic leukocytes extracted from FNAs. Liver biopsies were used to determine total intrahepatic HBV-DNA (iHBV-DNA) and cccDNA levels.

Results: T cells with a tissue-resident memory (T_{RM}) phenotype were excluded from PBMC but detectable in all FNAs whether treated with antivirals or not, confirming reliable sampling of the intrahepatic compartment ($CD103^+CD69^+$: 3%, IQR 2–7%, $CD103^-CD69^{hi}$: 17%, IQR 10–23%). PD-1 expression was strikingly higher on intrahepatic than circulating CD8 T cells, particularly the tissue-resident fraction ($CD103^-CD69^+$ and T_{RM} , $p < 0.0001$) as described previously (Fisicaro et al. 2010, Pallett et al. 2017). Measurement of liver viral parameters showed that CD8 T cell PD-1 expression correlated with both iHBV-DNA ($r = 0.6$, $p = 0.007$) and cccDNA ($r = 0.7$, $p = 0.002$) but not with ALT. Supporting a role for HBV in driving PD-1 expression, FNAs from the cohort with prolonged viral suppression on NUCs had significantly lower proportions of PD-1-expressing T cells and lower expression levels. By contrast, no significant changes in CD8 T cell PD-1 between NUC-treated and naïve patients were detectable in the periphery. Therefore, although CD8 T cell PD-1 in PBMC and intrahepatic lymphocytes showed an overall correlation, blood sampling cannot fully predict the impact of NUCs on this immune target in the liver compartment. In a small subset of patients re-sampled by FNA 6 months after NUC discontinuation, preliminary data suggested the withdrawal of viral suppression had the potential to drive re-expression of high levels of PD-1 on intrahepatic T cells.

Conclusion: Our results reveal a close association between intrahepatic HBV-DNA and global liver-resident T cell PD-1 expression

within the liver, with a reduction on prolonged NUC therapy and the potential for re-expression following treatment withdrawal. The mechanism by which HBV load associates with global (rather than just HBV-specific) T cell PD-1 remains to be explored. These findings underscore the need for further consideration of NUC-induced changes in global liver T cell PD-1 when targeting this axis in HBV functional cure.

OS142

Phospho-proteomic analysis of HBV infection revealed novel mechanisms for the regulation of viral transcription and pro-fibrotic stellate cell activation

Alessia Virzi^{1,2}, Zakaria Boulahtouf^{2,3}, Sarah Durand^{1,2,4}, Emanuele Felli^{2,3,4}, Patrick Pessaux^{2,3,4}, Oliver Popp^{5,6}, Evelyn Ramberger^{5,6}, Philipp Mertins^{5,6}, Eloi Verrier^{2,3}, Catherine Schuster^{1,2,4}, Thomas Baumert^{2,3,4,7}, Joachim Lupberger^{2,3}. ¹Inserm U1110, Strasbourg, France; ²Université de Strasbourg, Strasbourg, France; ³Inserm U1110, Strasbourg, France; ⁴Institut Hospitalo-Universitaire, Pôle Hépatodigestif, Nouvel Hôpital Civil, Strasbourg, France; ⁵Max Delbrück Center for Molecular Medicine, Berlin, Germany; ⁶Berlin Institute of Health, Berlin, Germany; ⁷Institut universitaire de France (IUF), Paris, France
Email: joachim.lupberger@unistra.fr

Background and aims: Chronic hepatitis B virus (HBV) pathological course are characterized by the dysregulation of fibrogenic and oncogenic signalling. Considering the lack of efficient anti-fibrotic therapies and treatment to eradicate cccDNA, the understanding of regulatory pathways is urgently needed. To identify the potential drivers of this dysregulation, we studied HBV-induced signalling in HBV infection models.

Method: Proteomic and phospho-proteomic analysis of HBV-infected HepG2-NTCP were performed using liquid chromatography-mass spectrometry. The deregulated signalling pathways were examined by gene set enrichment analysis and validated in primary human hepatocytes. Perturbation studies, trans-dominant phospho-dead/mimetic mutagenesis and ex vivo experiment were performed to validate the results.

Results: Our data revealed a strong HBV-induced dysregulation of signalling involved in extra-cellular matrix (ECM) and cell cycle. ECM-associated leading-edge genes comprised collagen VI, which was upregulated in HBV-infected hepatocytes. Interestingly, silencing of *COL6A1* impairs viral transcription suggesting a pro-viral role of collagen VI. Myofibroblasts account for the majority of collagen I deposited into the ECM. We found that treatment of hepatic stellate cells (HSCs) with collagen VI significantly induced an expression of HSCs activation markers, revealing a role of collagen VI in promotion of liver fibrosis. In addition, our phospho-proteomics provides new insight on viral life cycle regulation. Although HBV predominantly replicates in G1/G2 phase, we found linker histones H1.4 among the top hits of the HBV phospho-proteomic analysis. Linker histones are generally phosphorylated during S/M phase and associated to chromatin relaxation. We found that mimicking H1.4 detachment by RNAi augmented viral transcription, while a trans-dominant phospho-dead mutation S104A in H1.4 inhibited HBV RNA transcription. This suggests that HBV requires H1.4 phosphorylation to maintain cccDNA transcription. Chip experiments with the H1.4 mutants are under way.

Conclusion: We identified the phospho-proteomic landscape of HBV-host interaction which serves as a resource for the identification of novel drivers regulating viral life cycle and pathogenesis. We revealed a previously unrecognized role of collagen VI and linker histones in HBV replication with potential impact on liver fibrosis progression and cccDNA transcription, respectively.

ORAL PRESENTATIONS

OS143

CD4 T cell immunity to HEV-infection is characterized by sustained capsid-specific responses that correlate with neutralizing antibodies

Benedikt Csernalabics¹, Stefan Marinescu¹, Lars Maurer², Katharina Wild¹, Katharina Zoldan¹, Marcus Panning³, Philipp Reuken⁴, Tony Bruns⁵, Christoph Neumann-Haefelin¹, Bertram Bengsch¹, Maike Hofmann¹, Robert Thimme¹, Viet Loan Dao Thi², Tobias Böttler¹. ¹University Hospital Freiburg, Department of Medicine II, Freiburg, Germany; ²Heidelberg University Hospital, Department of Infectious Diseases and Virology, Heidelberg, Germany; ³University Hospital Freiburg, Institute of Virology, Freiburg, Germany; ⁴Jena University Hospital, Department of Medicine IV, Jena; ⁵University Hospital RWTH Aachen, Department of Medicine III, Aachen, Germany
Email: benedikt.csernalabics@uniklinik-freiburg.de

Background and aims: CD4 T cells are key protagonists in shaping an antiviral immune response. However, there are only limited insights into their specificity and distinction in the context of a hepatitis E Virus (HEV) infection. Therefore, we aim to characterize the specificity, phenotype and differentiation of CD4 T cells targeting different epitopes of the HEV polyprotein and their correlation with neutralizing antibodies targeting hepatitis E virions.

Method: HEV-specific CD4 T cells targeting different HEV-specific CD4 T cell epitopes from the viral polyprotein were identified by intracellular cytokine staining in 7 acutely infected and 33 resolved patients. Surface markers, relevant costimulatory receptors and transcription factors were analysed by using HEV-specific HLA-DRB1*01:01 and *04:01 tetramers. Additionally, neutralizing antibodies targeting naked (nHEV) and quasi-enveloped (eHEV) virions were determined (n = 72).

Results: Robust and multi-specific CD4 T cell responses were identified against the viral capsid and non-structural polyprotein (NSP). In contrast, only few phosphoprotein-specific responses were detectable. Overall, the virus-specific CD4+ T cell response was stronger and broader in acutely infected versus resolved patients. Moreover, a switch from a highly activated Th1 and Tfh cell phenotype towards a heterogeneous memory population was observed after viral elimination. Noteworthy, the presence of a capsid-specific IFN- γ - or IL-21-producing CD4 T cell response positively correlated with IgG- and neutralizing antibody titers against nHEV.

Conclusion: Collectively, our results reveal important novel insights into the HEV-specific CD4 T cell response by demonstrating a solid maintenance of capsid- and NSP-specific CD4 T cell responses with the formation of a robust HEV-specific memory compartment. They also reveal a clear immunodominance with phosphoprotein being less immunogenic.

Sunday 26 June

Hepatitis B clinical aspects

OS144

Metabolic dysfunction-associated fatty liver disease subgroups and risk of hepatocellular carcinoma and mortality in patients with chronic viral hepatitis

Mi Na Kim¹, Kyungdo Han², Juhwan Yoo³, Seong Gyu Hwang¹, Sang Hoon Ahn⁴. ¹CHA Bundang Medical Center, CHA University School

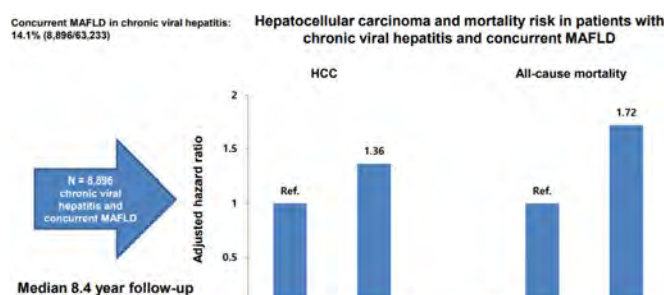
of Medicine, Department of Internal Medicine, Seongnam, Korea, Rep. of South; ²Soongsil University, Department of Statistics and Actuarial Science, Seoul, Korea, Rep. of South; ³the Catholic University of Korea, Department of Biomedicine and Health Science, Seoul, Korea, Rep. of South; ⁴Yonsei University College of Medicine, Department of Internal Medicine, Seoul, Korea, Rep. of South
Email: ahnsh@yuhs.ac

Background and aims: Metabolic dysfunction-associated fatty liver disease (MAFLD) is a recently proposed concept for fatty liver disease. However, heterogeneous disease severity and prognosis might exist even among patients with the same disease category of MAFLD. We investigated the risk stratification of long-term outcomes according to MAFLD subgroups based on diagnostic criteria in patients with chronic viral hepatitis using a nationwide cohort.

Method: We included 63, 233 chronic hepatitis B and chronic hepatitis C patients who underwent health examinations in 2009. Hepatic steatosis was defined as a fatty liver index ≥ 60 . MAFLD was defined as the presence of hepatic steatosis with any one of the following three conditions, overweight/obesity (body mass index ≥ 23 kg/m²), diabetes, two or more metabolic dysregulation. The primary end points of this study were incident hepatocellular carcinoma (HCC) and all-cause mortality.

Results: The prevalence of MAFLD was 14.1% (n = 8, 896). During a median 8.4-year follow-up, we documented 3, 732 HCC cases and 4, 778 deaths. Compared to patients with no MAFLD (n = 54, 377), the risk of HCC and mortality was significantly higher in patients with MAFLD (adjusted hazard ratio [aHR] = 1.34, 95% confidence interval [CI] = 1.23–1.46) for HCC; aHR = 1.26, 95% CI = 1.17–1.36 for mortality). Among patients with MAFLD, 687 HCCs and 861 deaths were documented. The prevalence of diabetes among patients with MAFLD was 25.9% (n = 2, 303). The risk of HCC and mortality was significantly higher in patients with diabetes (aHR = 1.36, 95% CI = 1.16–1.59 for HCC; aHR = 1.72, 95% CI = 1.50–1.97 for mortality) compared to patients with no diabetes, among patients with MAFLD. When we stratified patients with MAFLD according to the other criteria (overweight/obesity or metabolic dysregulations), risk of HCC and mortality was not different across the groups (all p > 0.05).

Conclusion: Concurrent MAFLD was associated with higher risk of HCC and mortality in patients with chronic viral hepatitis. Our results suggest that diabetes can stratify the risk of HCC and mortality in patients with chronic viral hepatitis and concurrent MAFLD.



OS145

Long term persistence of anti-HBs antibodies after vaccination with a 3-antigen HBV vaccine compared to a single-antigen HBV vaccine

Timo Vesikari¹, Aino Forstén¹, Vlad Popovic², Johanna Spaans², Francisco Diaz-Mitoma². ¹Nordic Research Network Oy, Tampere, Finland; ²VBI Vaccines Inc., Canada
Email: timo.vesikari@nrnetwork.fi

Background and aims: Hepatitis B virus (HBV) infection is a serious public health problem that can be effectively prevented with

hepatitis B vaccination. The magnitude of the immune response to HBV vaccination can be measured by serum levels of anti-HBs, persistence and durability, which is believed to be dependent upon the induced peak levels. PROTECT was a double-blind, randomized, Phase 3 study to evaluate immunogenicity and safety of a 3-antigen HBV vaccine (3A-HBV, manufactured by VBI Vaccines) and a single-antigen HBV vaccine (1A-HBV, Engerix-B®). Three doses of vaccine were administered IM at Days 1, 28, and 168. Seroprotection rate (SPR-% of subjects achieving anti-HBs ≥ 10 mIU/ml) and geometric mean concentration (GMC) of anti-HBs were evaluated for 12 months. Following the completion of PROTECT, this follow-up investigator-initiated study of PROTECT aimed to assess the long-term persistence of anti-HBs titers 2–3 years after the 3rd dose in participants enrolled in Finland.

Method: Subjects were eligible for the follow-up study if they had been enrolled in PROTECT study in Finland and had achieved seroprotection (anti-HBs ≥ 10 mIU/ml). Between February 2021 and June 2021, subjects were contacted to participate in the follow-up study. Serum samples were tested for Anti-HBs titers at the central laboratory (LabConnect, USA) using the same validated anti-HBs quantitative assay [VITROS, Ortho 3600 NJ, USA] as used in the PROTECT study.

Results: Of the 528 subjects contacted, 465 agreed to participate in the follow-up study, including 244 [52.5%] vaccinated with 3A-HBV and 221 [47.5%] vaccinated with 1A-HBV. Baseline characteristics were well balanced between the groups and consistent with the PROTECT study population, the mean age for both vaccine groups was 59 years. Data from the PROTECT study demonstrated a peak GMC of anti-HBs of 8021.9 mIU/ml for 3A-HBV and 3787.3 mIU/ml for 1A-HBV in study participants one month after the third dose (Day 196). Data from this follow-up study showed that approximately 2.5 years following Day 196 in the PROTECT study, the mean concentration of anti-HBs was 1382.9 mIU/ml for 3A-HBV participants and 251.4 mIU/ml for 1A-HBV participants. Additionally, more than 2x the number of subjects vaccinated with 3A-HBV retained anti-HBs ≥ 100 mIU/ml compared to 1A-HBV (72.9% vs. 32.6%). After approximately 2.5 years, 27.6% in the 1A-HBV group and 11.9% in the 3A-HBV group no longer had seroprotective levels of anti-HBs (titers < 10 mIU/ml).

Conclusion: 2.5 years after achieving peak seroprotection in the PROTECT study, the mean anti-HBs titers were five times higher in the 3A-HBV group than in the 1A-HBV group. Additionally, the percentage of participants who no longer had seroprotective levels of anti-HBs (titers < 10 mIU/ml) was more than double in the 1A-HBV group compared to the 3A-HBV group.

OS146

Fatty liver index as a risk factor for all-cause and liver related mortality in patients under therapy for chronic hepatitis B (ANRS CO22 Hepathier cohort study)

Paul Hermabessiere¹, Mathieu Chalouni², Marc Bourliere³, Pierre Nahon⁴, François Teoule⁵, Clovis Lusivka-Nzinga⁵, Helene Fontaine⁶, Stanislas Pol⁶, Fabrice Carrat⁵, Victor de Ledinghen¹, Linda Wittkop². ¹Hôpital Haut-Lévêque Magellan, Pessac, France; ²ISPED, Bordeaux, France; ³Hospital Paris Saint-Joseph, Paris, France; ⁴Jean-Verdier Hospital Ap-Hp, Bondy, France; ⁵Hospital Saint-Antoine Ap-Hp, Paris, France; ⁶Cochin Hospital, Paris, France
Email: hermabessierepaul@gmail.com

Background and aims: A quarter of patients with chronic hepatitis B (CHB) have associated fatty liver disease and the prognosis of these patients has been poorly investigated. In the general population, Fatty Liver Index (FLI) is a recommended alternative to ultrasonography for the diagnosis of steatosis (EASL 2016) and predict clinical outcomes related to non-alcoholic fatty liver disease (NAFLD). The aim was to evaluate the association between FLI and all-cause and liver-related mortality in treated CHB participants from the ANRS CO22 HEPATHER cohort.

Method: All patients under CHB therapy at entry in the ANRS CO22 HEPATHER cohort were selected. Patients with history of liver transplantation or hepatitis D virus co-infection were excluded. Multiple imputations of GGT, triglycerides, waist circumference and BMI were realized. Outcomes were first, the occurrence of death from any cause, then death from liver complication (primary liver cancer, decompensated cirrhosis, and liver transplantation). Proportional hazard adjusted on age, gender and diabetes status. Cox models were performed. Potential non-linear relationships were examined using fractional polynomial models.

Results: 2877 treated CHB patients were included. Median age was 48.9 years [Interquartile range (IQR): 38.1; 59.8] and 2044 (71.0%) were men. Almost all patients were treated by nucleos (t)idic analogues (98%) for a median time of 2.9 years (IQR [0.4; 5.2]) and 92.0% had an HBV DNA level $< 2,000$ UI/ml at entry. After a median follow-up of 7.0 years (IQR [6.2; 7.6]), incidence of all-cause mortality was 7.7/1000 person-years (95% Confidence Interval (CI) 6.6–9.1), and 4.0/1000 person-years (95% CI 3.2–5.0) for liver-related mortality. After adjustment, an increase of ten points of FLI was significantly associated with an increased risk of all-cause mortality (Hazard Ratio (HR): 1.09 [1.02–1.16]) and tended to be associated with liver-related mortality (HR: 1.08 [0.99–1.19]).

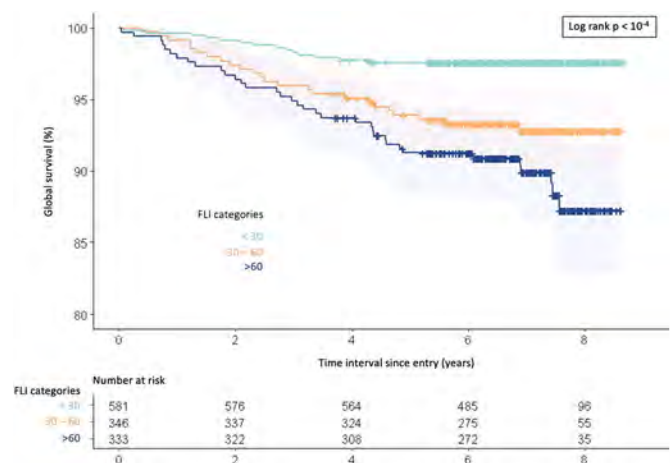


Figure: Kaplan-Meier survival estimates according FLI categories. ANRS CO22 HEPATHER cohort, treated CHB participants.

Conclusion: In this first large prospective cohort of French patients with treated chronic HBV infection, FLI was independently associated with all cause and liver-related mortality.

OS147

The discriminatory power of risk scores for hepatocellular carcinoma in treated chronic hepatitis B patients with and without diabetes: a territory-wide study of 48,706 subjects

Terry Cheuk-Fung Yip¹, Mandy Sze-Man Lai¹, Vincent Wai-Sun Wong¹, Yee-Kit Tse¹, Yan Liang², Vicki Wing-Ki Hui², Henry LY Chan^{3,4}, Grace Lai-Hung Wong¹. ¹The Chinese University of Hong Kong, Medical Data Analytics Centre (MDAC), Department of Medicine and Therapeutics, Institute of Digestive Disease, Faculty of Medicine, Hong Kong; ²The Chinese University of Hong Kong, Medical Data Analytics Centre (MDAC), Department of Medicine and Therapeutics, Faculty of Medicine, Hong Kong; ³Union Hospital, Department of Internal Medicine, Hong Kong; ⁴The Chinese University of Hong Kong, Medical Data Analytics Centre (MDAC), Faculty of Medicine, Hong Kong
Email: wonglaihung@cuhk.edu.hk

Background and aims: Patients with chronic hepatitis B (CHB) are aging with a rising prevalence of diabetes mellitus (DM) to over 20% in recent years. While DM is associated with a doubled risk of hepatocellular carcinoma (HCC) in CHB patients, few HCC risk scores

include DM as a factor. We aimed to compare the performance of HCC risk scores among DM and non-DM patients on nucleos (t)ide analogue (NA) treatment.

Method: Adult CHB patients on at least 6 months of entecavir or tenofovir treatment from January 2005 to March 2020 were identified using a territory-wide database in Hong Kong. DM was defined by any use of non-insulin antidiabetic agents, continuous use of insulin for ≥ 28 days, haemoglobin A_{1c} $\geq 6.5\%$, fasting glucose ≥ 7 mmol/L, and/or diagnosis codes. Two HCC risk scores with DM as a factor for treated CHB patients (i.e., cirrhosis, age, male sex, and DM [CAMD] score and Real-world Effectiveness from the Asia Pacific Rim Liver Consortium for hepatitis B virus [REAL-B] score) were studied; 2 other HCC risk scores without DM as a factor (i.e., PAGE-B and modified PAGE-B [mPAGE-B] scores) were also examined. The discriminatory power of the scores was assessed by area under the time-dependent receiver operating characteristic curves (AUROCs) with death as a competing event. Comparisons were done based on 1,000 bootstrap samples.

Results: Of 48,706 patients included, the mean age was 54.3 ± 13.6 years; 62.1% were male and 12.7% had cirrhosis. The prevalence of DM rose steadily from 15.5% to 24.3% in those who started NA treatment in 2005–08 and 2017–20 respectively. At a median (25th percentile–75th percentile) follow-up of 4.4 (2.2–5.0) years, 2,157 (4.4%) patients developed HCC. All the 4 HCC scores were less predictive in DM patients than non-DM patients (all $p < 0.001$; Figure). DM was an independent risk factor for HCC on top of the risk groups of PAGE-B score (adjusted hazard ratio [aHR] 3.85, 95% CI 2.06–7.18, $p < 0.001$), and had an interaction with PAGE-B risk groups (aHR [95% CI]: 0.40 [0.21–0.77] for intermediate-risk group and 0.27 [0.14–0.51] for high-risk group as compared to non-DM patients in low-risk group). DM was however found to be not associated with HCC after adjusting for mPAGE-B score (aHR 1.04, 95% CI 0.95–1.14, $p = 0.423$).

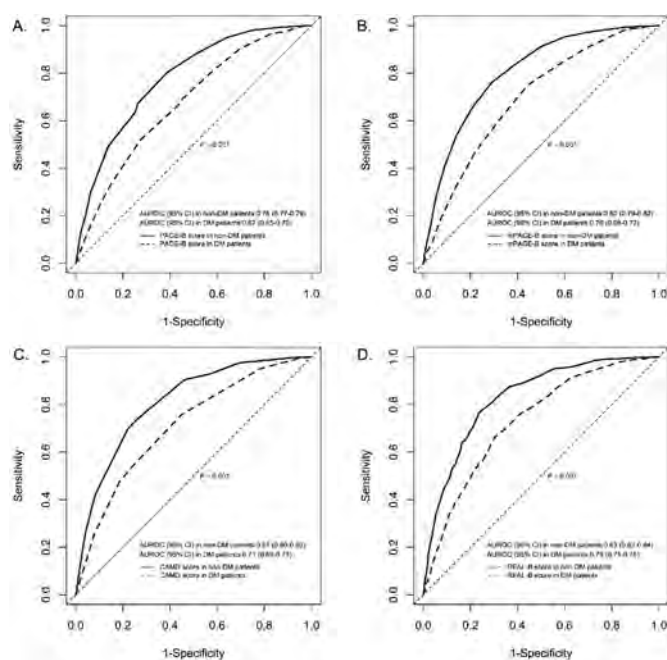


Figure: The area under the time-dependent receiver operating characteristic curves (AUROCs) of A. PAGE-B score; B. mPAGE-B score; C. CAMD score; and D. REAL-B score for predicting the development of hepatocellular carcinoma in nucleos (t)ide analogue-treated chronic hepatitis B patients with and without diabetes mellitus (DM).

Conclusion: HCC risk scores are less accurate in NA-treated diabetic CHB patients than their non-diabetic counterparts, with a drop of AUROCs from around 0.8 to 0.7 regardless of whether DM is a component in the risk scores or not.

OS148

Hepatocellular carcinoma incidence is reduced in cirrhotic chronic hepatitis B patients with HBsAg seroclearance comparing to those with viral suppression

Rachel Wen-Juei Jeng^{1,2,3}, Chien-Hung Chen^{1,4}, Hwai-I Yang⁵, Yi-Cheng Chen^{1,2,3}, Yen-Chun Liu^{1,2,3}, Chia-Ying Wu^{2,3}, Rong-Nan Chien^{1,2,3}, Yun-Fan Liaw^{1,2}. ¹Chang Gung University, College of Medicine, Taiwan; ²Linkou Chang Gung Memorial Hospital, Liver Research Unit, Taiwan; ³Linkou Chang Gung Memorial Hospital, Department of Gastroenterology and Hepatology, Taiwan; ⁴Kaohsiung Chang Gung Memorial Hospital, Division of Hepatogastroenterology, Department of Internal Medicine, Taiwan; ⁵Academia Sinica, Genomic Research Center, Taiwan
Email: rachel.jeng@gmail.com

Background and aims: Cirrhosis is a major risk factor for hepatocellular carcinoma (HCC) development in chronic hepatitis B patients. It remains unknown whether HBsAg seroclearance in cirrhotic patients reduces the risk of HCC compared to those under long-term Nuc treatment. This study aims to investigate the HCC incidence between these two groups.

Method: The study recruited chronic hepatitis B patients with cirrhosis undergoing Nuc therapy with viral suppression (Nuc arm, N = 805) and cirrhotic CHB patients with HBsAg seroclearance (S-loss arm, N = 165, 65 untreated, 90 off-therapy, 10 on-treatment HBsAg loss) from two medical centers and REVEAL-HBV cohort. The baseline in the Nuc arm was set since HBV DNA being undetectable (complete viral suppression) while in the S-loss arm was set since HBsAg loss. Those with HCC occurred prior to the baseline or within 6 months after the baseline were excluded from this analysis. Kaplan Meier analysis and log rank test were done for the cumulative HCC incidence comparison.

Results: Comparing the baseline features between Nuc arm and S-loss arm, the mean age (55.5 vs. 56.8, $P = 0.14$), gender (male: 74.5% vs. 81.2%, $P = 0.07$) and HBV genotype ($p = 0.27$) were comparable. The median ALT (29 vs. 20 U/L, $P < 0.001$) and AFP (4.16 vs. 3.0 mg/dL, $P < 0.001$) level were higher in the Nuc arm while follow-up duration was longer in the S-loss arm (median: 7.9 vs. 4.3 years, $P < 0.001$). In univariate analysis, older age [crude HR (cHR): 1.04, $P < 0.0001$], higher FIB-4 level [cHR: 1.1, $P = 0.0004$], higher AFP level [cHR: 1.02, $P < 0.001$] were positively associated with HCC occurrence while HBsAg loss is a protective factor for HCC [cHR: 0.502, $P = 0.0314$]. In multivariate analysis, older age [adjusted HR (aHR): 1.04 (1.02–1.06), $P < 0.0001$] and HBsAg loss [aHR: 0.19 (0.05–0.76), $P = 0.0193$] are the two independent predictor for HCC. The annual incidence and 8-year cumulative HCC incidence in cirrhotic patients in Nuc arm versus S-loss arm were 2.43% and 16% versus 1.16% and 8%, respectively (Log rank test, $P = 0.0282$). After propensity score matching with age, gender and FIB-4 at 1 to 1 ratio with 77 patients at each arm, HBsAg loss arm still had much lower HCC incidence than those under Nuc arm (annual incidence: 0.46% vs. 3.2%, log rank test, $P = 0.0035$).

Conclusion: This is the first study proved the HBsAg seroclearance, reflecting the inactive transcriptional activity of cccDNA, is a protective factor for HCC in cirrhotic chronic hepatitis B patients.

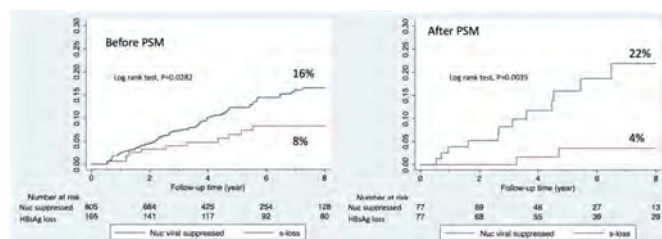


Figure: Cumulative HCC incidence between cirrhotic CHB patients with Nuc viral suppressed (blue line) and HBsAg loss (red line) before and after propensity score matching.

OS149

Treatment with bulevirtide improves patient-reported outcomes in patients with chronic hepatitis delta: An exploratory analysis of a Phase 3 trial at 48 weeks

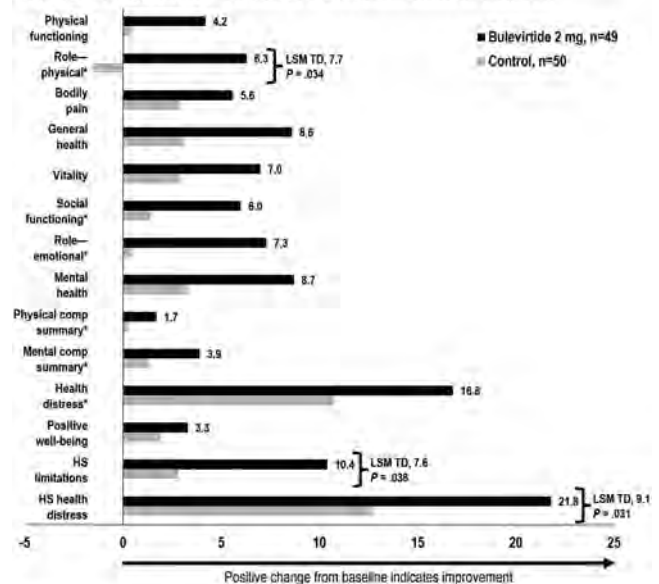
Maria Buti¹, Heiner Wedemeyer², Soo Aleman³, Vladimir Chulanov⁴, Morozov Viacheslav⁵, Olga Sagalova⁶, Tatyana Stepanova⁷, Robert G. Gish⁸, Andrew Lloyd⁹, Ankita Kaushik¹⁰, Vithika Suri¹⁰, Dmitry Manuilov¹⁰, Anu Osinusi¹⁰, John F. Flaherty¹⁰, Pietro Lampertico¹¹. ¹Hospital Universitario Valle Hebrón, Barcelona, Spain; ²Medizinische Hochschule Hannover, Hannover, Germany; ³Karolinska Universitetssjukhuset, Karolinska Institutet, Stockholm, Sweden; ⁴Central Research Institute of Epidemiology, Moscow, Russian Federation; ⁵Hepatolog, LLC, Samara, Russian Federation; ⁶Southern Ural State Medical University, Chelyabinsk, Russian Federation; ⁷Clinic of Modern Medicine, Moscow, Russian Federation; ⁸Robert G. Gish Consultants, LLC, San Diego, United States; ⁹Acaster Lloyd Consulting Ltd, London, United Kingdom; ¹⁰Gilead Sciences, Inc., Foster City, United States; ¹¹Foundation IRCCS Ca' Granda Ospedale Maggiore Policlinico, CRC "A.M. and A. Migliavacca" Center for Liver Disease, University of Milan, Milan, Italy
Email: mbuti@vhebron.net

Background and aims: Chronic hepatitis delta (CHD) infection is caused by a defective RNA virus that requires the presence of the hepatitis B virus (HBV) surface antigen for replication and transmission. Compared with HBV mono-infection, patients with CHD have a greater risk of cirrhosis, hepatocellular carcinoma, liver transplant, and liver-related mortality. In 2020, the European Medicines Agency granted conditional marketing authorisation to bulevirtide (BLV) 2 mg, a novel NTCP entry inhibitor, as the first treatment approved for CHD. We report an exploratory analysis of health-related quality-of-life outcomes in patients with CHD after 48 weeks of treatment with BLV 2 mg in an ongoing Phase 3 trial.

Method: MYR301 (NCT03852719; EudraCT 2019-001213-17) is a randomised, open-label, parallel-group, multicentre trial that assigned 150 CHD patients (1:1:1) to 3 exploratory arms (BLV 2 or 10 mg or control) for up to 3 years. (As BLV 10 mg is not an approved dosage, we do not report that treatment arm.) Control patients received no active anti-HDV treatment until Week (W)48. Patients completed the Hepatitis Quality of Life Questionnaire (HQLQ), including the SF-36 and 15 supplemental items, at study baseline (BL), W24, and W48. Higher scores on the HQLQ (range 0–100) indicate better health. Interim results collected at W24 were reported previously.¹

Results: BL characteristics were well balanced between BLV 2 mg (n = 49) and controls (n = 51). For BLV 2 mg, mean age was 44 years, BMI was 24 kg/m², 61% were male, 83% were White, and 47% had compensated cirrhosis. Across groups, patients reported varying scores of HQLQ. From BL to W48, BLV 2 mg was associated with improvements in all HQLQ domains; notably, >5-point improvements in mean values were observed for 10 of the 14 items (Figure). Treatment differences vs controls in least-squares mean changes from BL to W48 were statistically significant (p < 0.05) for role-physical, hepatitis-specific (HS) limitations, and HS health distress. Improvements with BLV 2 mg seen at W24 were largely maintained or increased at W48.

Figure. LSM change from baseline to Week 48 in HQLQ domain-scores, full analysis set



Patients in the control group received no active treatment until Week 48.

n=49 for control group.

Comp. component: HQLQ, Hepatitis Quality of Life Questionnaire; HS, hepatitis-specific; LSM, least-squares mean; TD, treatment difference.

Conclusion: CHD patients treated with BLV 2 mg showed an improvement at W48 in all domains of the HQLQ, while patients in the control group remained largely unchanged, apart from substantial improvements in health distress and HS health distress. Patients receiving BLV 2 mg reported significant improvements in quality-of-life domains, including role-physical, HS limitations, and HS health distress, compared with controls.

Medical writing support was provided by Ellie Manca, AlphaScientia, LLC, and was funded by Gilead Sciences, Inc.

1. Wedemeyer H *et al.* Treatment with bulevirtide improves patient-reported outcomes in patients with chronic hepatitis delta (CHD): an interim exploratory analysis at week 24. Presented at AASLD Nov 12–15, 2021. Poster 680.

Cirrhosis and its complications: Experimental and pathophysiology

OS150

Extracellular vesicles from mesenchymal stem cells reduce neuroinflammation in hippocampus and restore cognitive function in hyperammonemic rats

Paula Izquierdo-Altarejos¹, Carlos Sanchez-Huertas², Victoria Moreno-Manzano³, Vicente Felipo^{1,4}. ¹Centro de Investigación Príncipe Felipe, Neurobiology, Valencia, Spain; ²Instituto de Neurociencias CSIC-UMH, Laboratory of Bilateral Neural Circuits, Alicante, Spain; ³Centro de Investigación Príncipe Felipe, Neuronal and Tissue Regeneration Lab, València, Spain; ⁴CIPF Centro de Investigación Príncipe Felipe, Valencia, Spain
Email: vfelipo@cipf.es

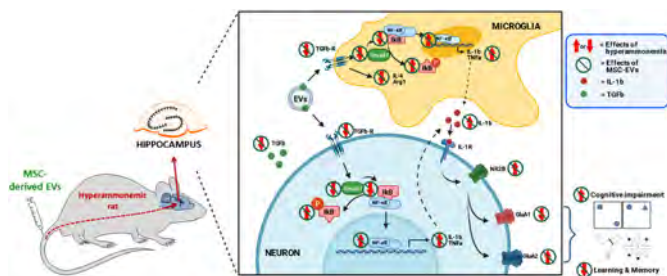
Background and aims: Chronic hyperammonemia, a main contributor to hepatic encephalopathy, leads to neuroinflammation which alters neurotransmission leading to cognitive impairment. Currently there are no specific treatments for the neurological alterations in hepatic encephalopathy. Extracellular vesicles (EVs) from mesenchymal stem cells (MSCs) reduce neuroinflammation in some pathological conditions. The aim of this work was to assess if treatment of

ORAL PRESENTATIONS

hyperammonemic rats with EVs from MSCs reduces neuroinflammation, improves neurotransmission in hippocampus and restores cognitive function and to analyze the mechanisms involved.

Method: Treatment with EVs from MSCs was performed in vivo by intravenous injection and ex vivo in hippocampal slices in hyperammonemic and control rats. Effects on neuroinflammation (microglia and astrocytes activation and content of inflammatory markers in hippocampus) were assessed by immunohistochemistry, immunofluorescence and western blot. Learning and memory were assessed using the following tests: object location, object recognition, Y maze and radial maze.

Results: The EVs injected reached the hippocampus. Hyperammonemia induced neuroinflammation in hippocampus and impaired learning and memory in the tests performed. Treatment with EVs reduced microglia and astrocytes activation, the content of IL-1 β and NF- κ B activation and restored performance of hyperammonemic rats in all the behavioral tests. Studies adding EVs to hippocampal slices ex vivo showed that these beneficial effects were dependent on TGF β present in the EVs, which reduced NF- κ B activation and the subsequent neuroinflammation.



Conclusion: Extracellular vesicles from mesenchymal stem cells reduce neuroinflammation in hippocampus and restore cognitive function in hyperammonemic rats. EVs from MSCs may be useful to improve cognitive function in patients with Minimal Hepatic Encephalopathy.

OS151

Lipidomics analyses of ATTIRE trial patients' plasma at day 1 demonstrates that reduced cholesterol esterification predicts development of hospital acquired infection

Harriett Fuller¹, Thais Tittanegro², Alex Maini², Louise China², James Thorne³, J. Bernadette Moore¹, Alastair O'Brien². ¹University of Leeds School of Food Science and Nutrition, Leeds, United Kingdom; ²UCL Institute for Liver and Digestive Health Upper 3rd Floor, University College London Division of Medicine, London, United Kingdom; ³School of Food Science and Nutrition @ Parkinson (p2.32), Faculty of Environment University of Leeds, Leeds, United Kingdom
Email: fshf@leeds.ac.uk

Background and aims: Hospital acquired infections (HAIs) are common in acute decompensation (AD) patients and studies support an anti-inflammatory role for statins. We investigated the role of lipid metabolism pathways in AD patients that developed HAIs.

Method: Plasma from 56 ATTIRE trial patients (31 male, 25 female) at day 1 (pre-albumin infusions or standard care) were analysed using Lipotype Shotgun Lipidomics platform. Patients were not diagnosed with infection nor taking antibiotics at sampling, with 26 subsequently developing HAI and 30 not. Lipidomic profiles predicting HAI status were analysed via multivariate statistical techniques (principal component analysis (PCA), partial least squares discriminatory analyses (PLSDA) and sparse PLSDA (sPLSDA)) on 245 lipids with <25% missing data prior to imputation. In non-ATTIRE patients without infection and not on antibiotics, we performed whole blood bulk RNA sequencing (RNA-seq) comparing healthy volunteers (HV,

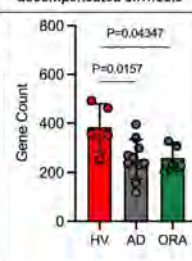
n = 5), outpatients with refractory ascites (ORA, n = 5) and hospitalised AD patients (n = 10). Finally, we examined HAI incidence in the 47 ATTIRE patients on statins at baseline.

Results: Median time to HAI was 6 days. PLSDA models including clinical covariates significantly predicted HAI development, with Bilirubin at baseline having a variable importance in projection (VIP) score of 2.5. Within each metabolite class, only PCAs of Cholesterol Esters (CEs) and Sphingomyelin (SM) class resulted in separation by HAI status, driven by CE 18.16.0, CE 18.2.1, CE 18.2.2 and SM 42.2.2. When included in PLSDA models, CE 18.1.0 and CE 18.2.0 were both important in predicting HAI (VIP >1) (table). RNA-seq showed reduced blood Sterol O-acyltransferase 1 (SOAT1) expression compared to HV (mean \pm SD gene count: 384.0 \pm 94.9) in ADs (254.9 \pm 81.0; P = 0.02) and ORA patients (260.0 \pm 55.1; P = 0.04, figure). There was no difference in HAI according to baseline statin use, which occurred in 9/47 statin (19.1%) and 141/730 non-statin (19.3%) patients.

Table: PLSDA Models to predict HAI in ATTIRE AD Patients

Model output	Model 1	Model 2	Model 3	Model 4
Outcome variance explained (R ² Y)	0.19	0.20	0.20	0.21
Outcome variance explained cross validation (Q ² Y)	0.13	0.13	0.14	0.14
p value - R ² Y	0.05	0.05	0.05	0.05
p value - Q ² Y	0.05	0.05	0.05	0.05
Included variables	VIPs			
Bilirubin D1	2.51	2.75	2.19	2.27
CE 18.2.0	-	-	2.19	2.29
CE 18.1.0	-	-	1.11	1.15
CE 16.0.0	-	-	0.71	0.73
Baseline creatinine	0.70	0.83	0.47	0.49
Age	-	0.68	0.57	0.59
MELD Score	0.42	0.46	0.35	0.36
SM 42.2.2	-	-	-	0.18
CRP D1	0.18	0.23	0.09	0.09
WCC D1	0.13	0.15	0.10	0.11
Baseline albumin	0.03	0.08	0.09	0.10
Sex	-	0.08	0.03	0.03
Statin use	0.03	0.04	0.02	0.02

Fig: SOAT1 mRNA expression in healthy volunteers and decompensated cirrhosis



Conclusion: Data are consistent with a downregulation of blood cholesterol esterification via SOAT1 in AD patients predicting development of HAI. Statins do not affect cholesterol esterification and were non-predictive of HAI status within PLSDA models and had no effect clinically, although small numbers were analysed. CE may be novel and functional biomarkers that predict HAI in AD, providing mechanistic insight.

OS152

Integrating single-cell RNA and spatial transcriptomic data defines altered cell state in human liver fibrosis

Nigel Hammond¹, Sokratia Georgaka¹, Syed Murtuza-Baker¹, Ali Al-Anbaki¹, Elliot Joki¹, Harry Spiers^{2,3}, Ajith Siriwardena¹, Varinder Athwal¹, Neil Hanley¹, Magnus Rattray¹, Karen Piper Hanley¹.

¹The University of Manchester, United Kingdom; ²University of Cambridge, Department of Surgery, Cambridge, United Kingdom;

³Addenbrooke's Hospital, Department of Hepato-pancreato-biliary Surgery, Cambridge, United Kingdom

Email: karen.piperhanley@manchester.ac.uk

Background and aims: Advances in single cell technology have revolutionised our understanding of the liver, enabling genome-wide RNA-profiling of thousands of transcriptomes at single cell resolution. Recent studies utilising single cell RNA sequencing (scRNA-seq) have characterised progenitor cell populations, uncovered gene expression zonation of multiple cell types, and revealed their contribution to disease pathogenesis. However, scRNA-seq does not capture the spatial distribution of transcripts in cells and dissociated tissue can cause transcriptomic changes. In contrast, the recent explosion of spatial transcriptomics (ST) technologies has enabled genome-wide characterisation of cellular heterogeneity at near single-cell resolution, while preserving spatial information.

Method: In this study, we have utilised ST to profile the fibrotic niche in human cirrhotic liver. Using 10X Genomics Visium, we

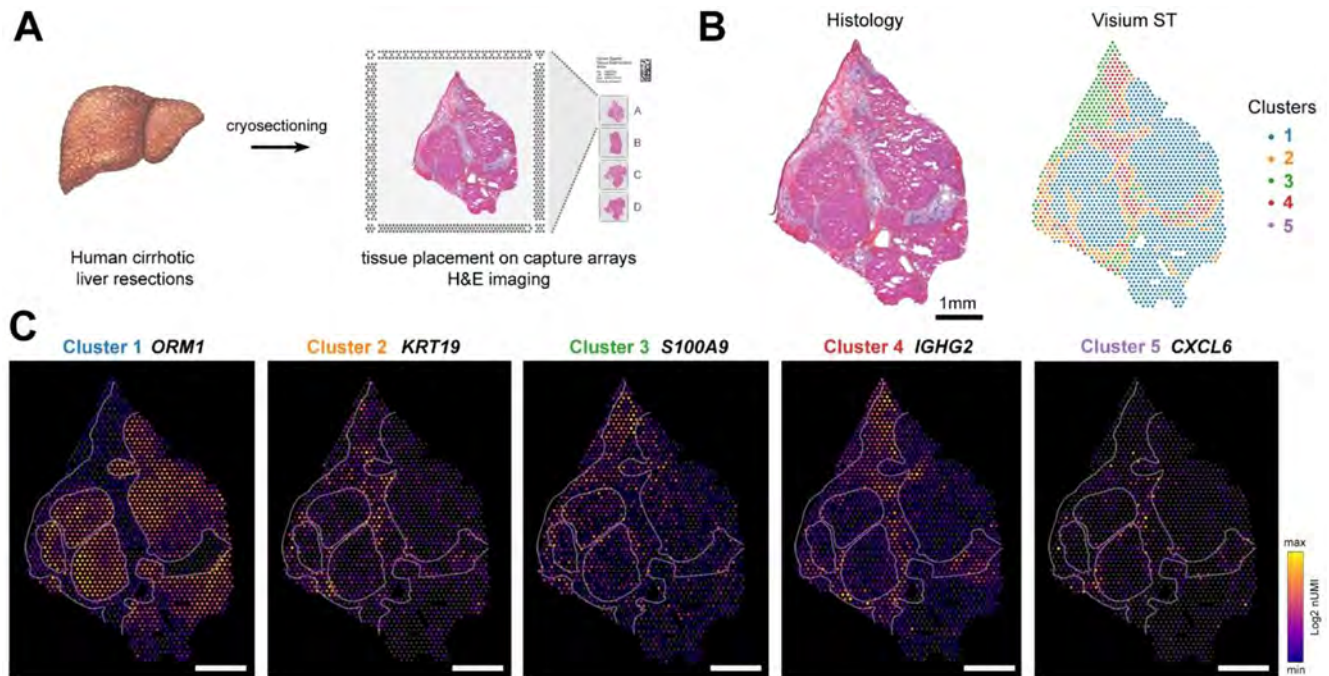


Figure 1: (abstract: OS152): Spatial transcriptomics of human cirrhotic liver. (A) Human cirrhotic liver resections are fresh frozen, cryo-sectioned and placed onto Visium ST capture slides. Tissue permeabilisation enables mRNA to be captured, ST libraries constructed, sequenced and mapped back to Visium spots. (B) Spatially-significant gene clusters were identified by performing dimensionality reduction followed by unsupervised clustering and projecting clusters back onto the tissue. (C) Gene expression of significant targets representing spatial clusters. Scalebars 1 mm.

demonstrate ST can resolve diseased liver tissue into discrete gene expression clusters which correlate with histological landmarks, revealing spatial expression profiles of the fibrotic scar and interface with regenerative nodules (Figure 1). To increase the resolution of ST data, we generated a complementary human cirrhotic liver scRNA-seq dataset. Through Cell2location computational approaches, we defined cell type clusters and deconvoluted multi-cell ST data to reveal spatial molecular signatures of several scar-associated cell subpopulations.

Results: Furthermore, our data spatially located impaired extracellular matrix (ECM) signalling associated with the pathogenesis of progressive liver disease and provided insight into mechanoadaptive mechanisms during myofibroblast activation.

Conclusion: This study demonstrates how comprehensive ST aligned to computational approaches can be used to delineate spatial gene expression patterns during liver disease. Our data highlights the future of ST in studies to understand mechanisms underlying progressive liver disease as well as its potential in clinical pathology.

OS153

Vascular endothelial growth factor C mediated restoration of mesenteric lymphatic vessels permeability and drainage improves gut immunity surveillance in experimental cirrhosis

Pinky Juneja¹, Dinesh Mani Tripathi¹, Impreet Kaur¹, Sumati Rohilla¹, Sukriti Sukriti¹, Subham Banerjee², Shiv Kumar Sarin³, Savneet Kaur¹.

¹Institute of Liver and Biliary Sciences, Department of Molecular and Cellular Medicine, New Delhi, India; ²NIPER Guwahati, Department of Pharmaceuticals, Guwahati, India; ³Institute of Liver and Biliary Sciences, Department of Hepatology, New Delhi, India

Email: savykaur@gmail.com

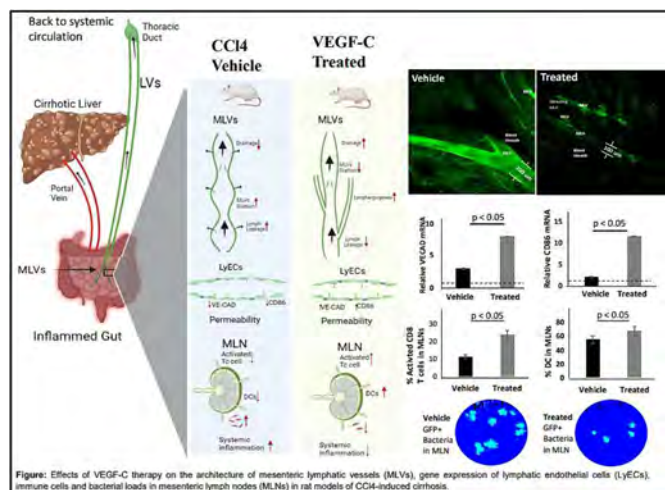
Background and aims: Mesenteric lymphatic vessels (MLVs) are functionally impaired in cirrhosis. We explored therapeutic effects of a human recombinant pro-lymphangiogenic factor, vascular endothelial growth factor C (rhVEGF-C, Cys156Ser) on MLVs and the draining lymph nodes (LNs) in experimental cirrhosis.

Method: CCl₄-induced rat models of cirrhosis were prepared. Molecular and histological studies of the MLVs were performed. rhVEGF-C (10 ug/kg), which binds to VEGF-receptor 3 (VEGFR3) on lymphatic endothelial cells (LyECs), was injected intraperitoneally in 5 doses on alternate days in cirrhotic models. CCl₄ rats were given saline as vehicle. The sprouting and drainage of MLVs was analyzed using histology and whole-mount BODIPY of mesentery. To gain mechanistic insights, gene expression profiling of isolated and sorted mesenteric LyECs was performed by RT-PCRs. Dendritic Cell (DCs) and T cell subsets were quantified in LNs, portal and peripheral circulation by flow cytometry. Systemic inflammatory cytokines were examined. Gut bacterial translocation to mesenteric lymph nodes, liver, and systemic circulation was studied using orally administered GFP labelled *Salmonella typhimurium*.

Results: An increased gene and protein expression of VEGF-C was observed in the mesenteric tissues of treated rats in comparison to the vehicle. Histology displayed a significant increase in area per field of the MLVs in treated versus vehicle rats (1.8 vs 3.9, $p < 0.001$). Drainage of mesenteric lymph was increased in treated as compared to vehicle (30 a.u. vs 60 a.u., $p < 0.001$) with decreased lymph leakage (50 a.u. vs 20 a.u., $p < 0.001$) in comparison to vehicle. Sprouting of MLVs from pre-existing vessels was observed in treated rats with significantly reduced dilation wrt vehicle (200 μ m vs 100 μ m, $p < 0.001$). Sorted LyECs showed increased expression of LyVE1 (7.4 fc, $p < 0.01$) and Prox1 (7.7 fc, $p < 0.05$) in treated rats wrt vehicle. Enhanced expression of adhesion molecules such as VE-CAD (5 fc, $p < 0.05$) in LyECs correlated with decreased lymph leakage and permeability of MLVs in treated rats. Expression of CCL21 (2.04 fc, $p < 0.05$), a chemoattractant for DCs and T cells, and CD86 (9.36 fc, $p < 0.05$), an antigen presentation molecule was increased in LyECs of treated wrt vehicle rats. Among all immune cells, LNs showed an increased percentage of activated CD8 T cells (24.07 vs 11.37, $p < 0.05$) and DCs (67.03 vs 55.52, $p < 0.05$) in treated versus vehicle. Treated rats also exhibited increased clearance in LNs as compared to vehicle ($p < 0.05$).

ORAL PRESENTATIONS

Conclusion: In cirrhosis, treatment with VEGF-C ameliorates mesenteric lymph drainage and permeability owing to the increased expression of adhesion molecule, VE-CAD in the LyECs. VEGF-C modulates gut immunity and bacterial clearance and thus may serve as an emerging therapy for combating gut infection and inflammation in cirrhosis.



OS154

Effect of engineered poly (beta-amino ester) nanoparticles containing a nitric oxide donor on systemic and portal hemodynamics

Meritxell Perramón¹, María Navalón², Guillermo Fernández Varo¹, Belén González¹, Alazne Moreno-Lanceta¹, Cristina Fornaguera², Pedro Melgar-Lesmes^{1,3,4}, Salvador Borrós^{2,5}, Wladimiro Jiménez^{1,3}.
¹Biochemistry and Molecular Genetics Service of Hospital Clínic Universitari, Institut d'Investigacions Biomèdiques August Pi i Sunyer (IDIBAPS), Centro de Investigación Biomédica en Red de Enfermedades Hepáticas y Digestivas (CIBERehd), Barcelona, Spain; ²Grup d'Enginyeria de Materials (Gemat), Institut Químic de Sarrià (IQS), Ramon Llull University (URL), Barcelona, Spain; ³University of Barcelona, Medicine Faculty, Department of Biomedicine, Barcelona, Spain; ⁴Institute for Medical Engineering and Science, Massachusetts Institute of Technology, Cambridge, United States; ⁵Centro de Investigación Biomédica en Red en Bioingeniería (CIBER-BBN), Barcelona, Spain
 Email: wjimenez@clinic.cat

Background and aims: Decompensated liver cirrhosis results from the worsening of the liver function and is characterized by the appearance of a clinical phenotype, frequently ascites and portal hypertension. The primary cause of portal hypertension is an increase in the resistance to portal blood flow. Architectural distortion, hepatic stellate cell contraction, and endothelial dysfunction with increased vasoconstrictor and deficient nitric oxide (NO) production are major factors governing this process. Here, we assessed the potential therapeutic effect of engineered poly (beta-amino esters) nanoparticles (PBAE NPs) containing an NO donor in experimental decompensated cirrhosis.

Method: NO donor pGFP PBAE NPs with retinol moiety were synthesized and characterized by dynamic light scattering. Next, liver cirrhosis was induced in male Wistar rats by repetitive carbon tetrachloride inhalation (1 g/l) twice a week until the appearance of ascites. Cirrhotic rat precision cut liver slices (PCLS) were treated with PBAE NPs and ex vivo transfection was evaluated by fluorescence microscopy. In order to assess organ biodistribution, the NPs were also administered intravenously. Finally, another group of cirrhotic rats received functionalized control or NO donor PBAE NPs (30 mg/kg

body weight) and subsequently an hemodynamic study was performed.

Results: Engineered NO donor PBAE NPs had an average hydrodynamic size of 170 nm and were positively charged; remaining stable for at least 24 h. After 48 h treatment, the NPs were successfully internalized by cirrhotic PCLS. Besides, when administered intravenously, engineered PBAE NPs targeted the liver, spleen and kidney of already after 24 h, although the signal of the two latter was significantly of lower intensity. Notably, they did not reach the brain, heart or lung. Finally, the treatment with functionalized NO donor PBAE NPs resulted in a significant ($p < 0.05$) decrease of portal hypertension (9.6 ± 0.6 mmHg) in comparison to control NPs (13.2 ± 0.9 mmHg) in rats with decompensated cirrhosis. Remarkably, the treatment did not affect mean arterial pressure, being 96.7 ± 1.1 and 92.3 ± 4.2 mmHg, in cirrhotic rats treated with control or NO donor NPs, respectively. Likewise, the cardiac output was not affected (390.7 ± 80.8 L/min vs 301.3 ± 48.9 L/min).

Conclusion: Engineered NO donor PBAE NPs effectively target the liver, and could be therapeutically useful to mitigate portal hypertension.

OS155

Neurometabolic and gliovascular changes in murine hepatic encephalopathy

Wouter Claeys^{1,2,3}, Lien Van Hoecke^{1,2}, Anja Geerts³, Hans Van Vlierberghe³, Xavier Verhelst³, Sander Lefere^{3,4}, Helena Degroote³, Griet Van Imschoot^{1,2}, Elien Van Wouterghem^{1,2}, Roosmarijn Vandenbroucke^{1,2}, Christophe Van Steenkiste^{5,6}.
¹VIB Center for Inflammation Research, Barriers in Inflammation, Ghent, Belgium; ²Ghent University, Department of Biomedical Molecular Biology, Ghent, Belgium; ³Ghent University, Department of Gastroenterology and Hepatology, Hepatology Research Unit, Ghent, Belgium; ⁴Ghent University, Basic and Applied Medical Sciences, Gut-Liver Immunopharmacology Unit, Ghent; ⁵Antwerp University, Department of Gastroenterology and Hepatology, Antwerp, Belgium; ⁶Maria Middelaers Hospital, Department of Gastroenterology and Hepatology, Ghent, Belgium
 Email: wouter.claeys@ugent.be

Background and aims: Type C hepatic encephalopathy (HE) develops on the background of cirrhosis. Both hyperammonemia and inflammation contribute to disease development. Murine models of type C HE are either not available or poorly characterized, hampering translational research. This project aims to validate and characterize murine bile duct ligation (BDL) as a model for type C HE. **Method:** Male C57BL/6j mice ($n = 15$ /timepoint/group) were subjected to BDL or sham surgery. Animals were sacrificed on day 7, 14, 21 or 28. Standardized motor function tests were performed. Plasma samples were isolated for ammonia and cytokine measurement. Targeted metabolomics (LC-MS/MS) for amino acids, bile acids, energy metabolites and redox markers was performed on cerebrospinal fluid (CSF). Brain samples were taken for immunostainings and cytokine profiling. In a separate experiment, mice were injected with 4 kDa FITC-Dextran 15 min before sacrifice to assess blood-brain barrier (BBB) permeability changes.

Results: BDL induces motor dysfunction, demonstrated by increased beam traversal time (+60%, $p = 0.0056$ on day 7) and reduced travelling in the open field (-71%, $p < 0.0001$ on day 14). Concomitantly, plasma ammonia increases progressively in BDL mice ($p = 0.0012$ on day 21). CSF metabolomics reveal a significant glutamine increase from 14 days on ($p = 0.0029$). Additionally, a glutamate decrease is observed. Other osmolytes taurine and creatine transiently decrease. Interestingly, plasma ammonia correlates significantly with CSF glutamine ($r = 0.5076$, $p = 0.0113$). AMP is depleted at 14 days ($p = 0.0021$), but other energy markers are not altered in BDL mice. Remarkably, tauro-conjugated bile acids ($p = 0.0016$), but also tryptophan ($p = 0.0084$) accumulate in CSF after 7 days.

Systemic inflammation is evident from 7 days onward with increased plasma IL-6 levels ($p = 0.0002$). From 14 days on, 3D reconstructed cortical microglial cells reveal activated morphology, indicating neuroinflammation (Figure 1). CCL2 levels are significantly increased in the cortex 28 days after BDL ($p = 0.0418$), coinciding with increased BBB permeability ($p = 0.0031$).

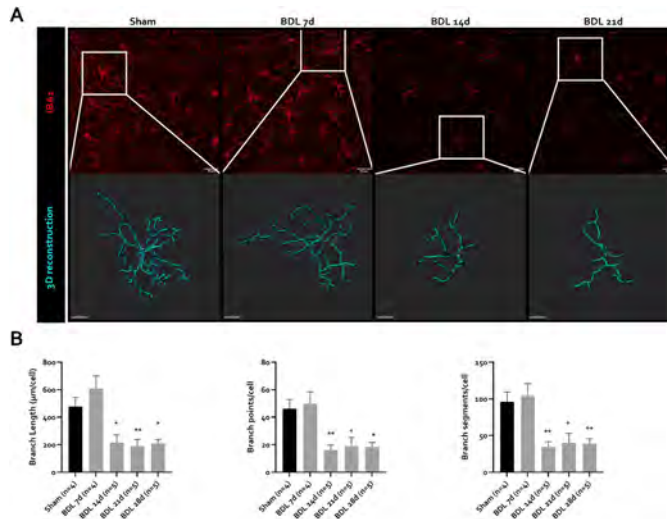


Figure 1. Microglial ramification at different timepoints after BDL. **A.** Representative confocal maximum intensity positive microglia and magnified 3D reconstructed microglia in prefrontal cortex at different timepoints after BDL. **B.** Reconstructed microglia, showing branch length, number of branch points, branch segments and endpoints per cell. $n = 4$. Statistical differences between sham and BDL at different time points using one-way ANOVA and Dunnett post-hoc test data are represented as mean + SEM. Scale bar IBA1 = 20 µm. Scale bar 3D reconstruction = 10 µm. BDL, bile duct ligation.

Conclusion: Murine BDL reproduces clinical, metabolic and gliovascular features of type C HE. Early behavioural changes are obvious before plasma ammonia and brain glutamine accumulate, and potentially reflect the effect of systemic inflammation and cerebral bile acid/tryptophan accumulation on behaviour. Altogether, these data support the clinical relevance of this HE model, which can now be used for further neurobiological and intervention studies.

Liver tumours: Therapy

OS156

Yttrium-90 radioembolization versus drug-eluting beads chemoembolization for unresectable hepatocellular carcinoma: results from the TRACE phase 2 randomized controlled trial

Elisabeth Dhondt¹, Bieke Lambert^{2,3}, Laurens Hermie¹, Lynn Huyck¹, Peter Vanlangenhove¹, Anja Geerts⁴, Xavier Verhelst⁴, Maridi Aerts⁵, Aude Vanlander⁶, Frederik Berrevoet⁶, Roberto Ivan Troisi^{2,7}, Hans Van Vlierberghe⁴, Luc Defreyne¹. ¹Ghent University Hospital, Vascular and Interventional Radiology, Ghent, Belgium; ²Ghent University, Faculty of Medicine and Health Sciences, Belgium; ³AZ Jan Palfijn and AZ Maria Middelaers, Nuclear Medicine, Belgium; ⁴Ghent University Hospital, Gastroenterology and Hepatology, Ghent, Belgium; ⁵University Hospital Brussels, Gastroenterology, Belgium; ⁶Ghent University Hospital, General and HPB Surgery and Liver Transplantation, Ghent, Belgium; ⁷Frederico II University Hospital, Hepatobiliary and Minimally Invasive and Robotic Surgery, Naples, Italy
Email: elisabeth.dhondt@ugzgent.be

Background and aims: Transarterial chemoembolization (TACE) is the recommended treatment for intermediate hepatocellular carcinoma (HCC) in the Barcelona Clinic Liver Cancer guidelines. Prospective uncontrolled studies suggest that Yttrium-90

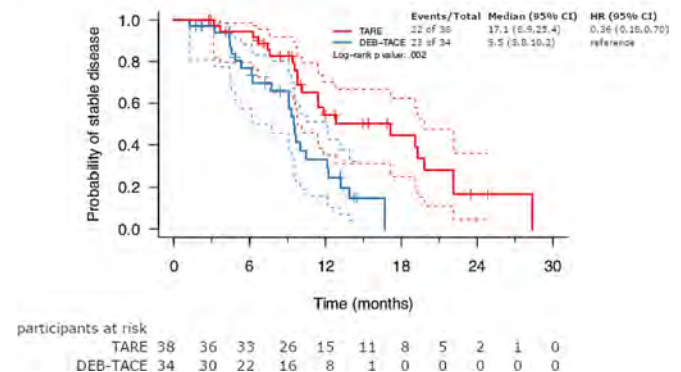
transarterial radioembolization (TARE) is a safe and effective alternative. The aim of the study was to compare the efficacy and safety of TARE to TACE for unresectable HCC.

Method: In this single-center prospective randomized controlled trial (TRACE), Yttrium-90 glass TARE was compared with doxorubicin-eluting beads TACE (DEB-TACE) in patients with intermediate stage HCC extended to Eastern Cooperative Oncology Group performance status 1 and early-stage HCC patients not eligible for surgery or thermoablation. Participants were recruited between September 2011 and March 2018. Primary end point was time to progression (TTP_{overall}; Kaplan-Meier analysis) in the intention-to-treat (ITT) and per protocol (PP) population.

Results: Ad interim analysis, 38 participants (median age, 67 years; IQR 63–72; 33 men) were randomized to the TARE arm and 34 (median age, 68 years; IQR 64–74; 30 men) to the DEB-TACE arm (ITT population). Median TTP_{overall} was 17.1 months in the TARE arm versus 9.5 months in the DEB-TACE arm (ITT: HR 0.36; 95% CI: 0.18, 0.70; $p = 0.002$) (PP: 32 and 34 participants respectively: HR 0.29; 0.14, 0.60; $p < 0.001$). Median overall survival was 30.2 months after TARE and 15.6 months after DEB-TACE (ITT: HR 0.48; 0.28, 0.82; $p = 0.006$). Serious adverse events grade ≥ 3 (13 of 33 (39%) versus 19 of 36 (53%) after TARE and DEB-TACE respectively, $p = 0.47$) and 30-day mortality (0 of 33 (0%) versus 3 of 36 (8%), $p = 0.24$) were similar in the safety populations. Ad interim the HR for the primary end point TTP_{overall} was <0.39 , indicative to halt the study.

Conclusion: With similar safety profile, Yttrium-90 radioembolization conferred superior tumor control and survival compared to drug-eluting beads chemoembolization in selected participants with early and intermediate HCC.

Time to progression (TTP_{overall}) in the intention to treat (ITT) population



OS157

Cholangiocarcinoma landscape in Europe: diagnostic, prognostic and therapeutic insights from the ENSCCA Registry

Laura Izquierdo-Sánchez^{1,2}, Angela Lamarca^{3,4}, Adelaida La Casta^{1,5}, Stefan Buettner⁶, Kirsten Utpatel⁷, Heinz-Josef Klumpen⁸, Jorge Adeva⁹, Arndt Vogel¹⁰, Ana Lleo¹¹, Luca Fabris^{12,13}, Mariano Ponz-Sarvisé¹⁴, Brustia Raffaele¹⁵, Vincenzo Cardinale¹⁶, Chiara Braconi^{17,18}, Gianpaolo Vidili¹⁹, Nigel B. Jamieson^{17,20}, Rocio IR Macias²¹, Philipp Jonas^{22,23}, Marco Marzoni²⁴, Wacław Hołówo²⁵, Trine Folseraas^{26,27}, Juozas Kupcinskas²⁸, Zeno Sparchez²⁹, Marcin Krawczyk^{25,30}, Łukasz Krupa³¹, Viorel Scripcariu³², Gianluca Grazi³³, Ana Landa-Magdalena^{1,5}, Jan Ijzermans⁶, Katja Evert⁷, Joris Erdmann⁸, Flora López-López⁹, Anna Saborowski¹⁰, Alexander Scheiter⁷, Alvaro Santos-Laso¹, Guido Carpino³⁴, Jesper Andersen³⁵, Jose Marin²¹, Domenico Alvaro³⁶, Luis Bujanda^{1,2,37}, Alejandro Forner³⁸, Juan Valle^{3,4}, Bas Groot Koerkamp⁶, Jesus Maria Banales^{1,2,39,40}. ¹IIS

ORAL PRESENTATIONS

Biodonostia, Liver and Gastrointestinal Diseases, San Sebastián, Spain; ²CIBER-Center for Biomedical Research Network, Liver and Gastrointestinal Diseases, Madrid, Spain; ³The Christie NHS Foundation Trust, Department of Medical Oncology, United Kingdom; ⁴The University of Manchester, United Kingdom; ⁵Donostia Unibertsitate Ospitalea, Department of Medical Oncology, Donostia, Spain; ⁶Erasmus University Medical Center, Department of Surgery, Rotterdam, Netherlands; ⁷University of Regensburg, Institute of Pathology, Regensburg, Germany; ⁸Amsterdam UMC, locatie AMC, Department of Medical Oncology, Amsterdam, Netherlands; ⁹University Hospital October 12, Department of Medical Oncology, Madrid, Spain; ¹⁰Hannover Medical School, Department of Gastroenterology, Hepatology and Endocrinology, Hannover, Germany; ¹¹IRCCS Istituto Clinico Humanitas Humanitas Cancer Center, Division of Internal Medicine and Hepatology, Milan, Italy; ¹²University of Padua School of Medicine and Surgery, Department of Molecular Medicine, Padova, Italy; ¹³Yale University School of Medicine, Digestive Disease Section, New Haven, United States; ¹⁴Clinica Universidad de Navarra, Program in Solid Tumors, Pamplona, Spain; ¹⁵University Hospitals Pitié Salpêtrière-Charles Foix, Department of Hepatobiliary and Liver Transplantation Surgery, Paris, France; ¹⁶Sapienza University of Rome, Department of Medico-Surgical Sciences and Biotechnologies, Roma, Italy; ¹⁷Institute of Cancer Sciences, University of Glasgow, Bearsden, United Kingdom; ¹⁸Royal Marsden Hospital-Sutton, London, United Kingdom; ¹⁹Azienda Ospedaliero Universitaria di Sassari, Department of Medical, Surgical and Experimental Sciences, Sassari, Italy; ²⁰Glasgow Royal Infirmary, West of Scotland Pancreatic Unit, United Kingdom; ²¹Instituto de Investigación Biomédica de Salamanca, Experimental Hepatology and Drug Targeting (HEVEPHARM), Salamanca, Spain; ²²University Hospital of Zürich, Department of Visceral- and Transplant Surgery, Zürich, Switzerland; ²³Klinik Favoriten, Department for Surgery, Wien, Austria; ²⁴Marche Polytechnic University, Department of Gastroenterology, Ancona, Italy; ²⁵Medical University of Warsaw, Department of General, Transplant and Liver Surgery, Warszawa, Poland; ²⁶Oslo universitetssykehus Rikshospitalet, Department of Transplantation Medicine, Norway; ²⁷Institute of Clinical Medicine University of Oslo, Division of Surgery, Inflammatory Diseases and Transplantation, Oslo, Norway; ²⁸Lithuanian University of Health Sciences, Department of Gastroenterology and Institute for Digestive Research, Kaunas, Lithuania; ²⁹Iuliu Hațieganu University of Medicine and Pharmacy, 3rd Medical Department, Institute for Gastroenterology and Hepatology, Cluj-Napoca, Romania; ³⁰Saarland University Hospital, Department of Internal Medicine II-Gastroenterology, Hepatology, Endocrinology, Diabetology, and Nutritional Medicine, Homburg, Germany; ³¹Kliniczny Szpital Wojewódzki Nr 1 im. Fryderyka Chopina w Rzeszowie, Department of Gastroenterology and Hepatology with General Medicine, Rzeszów, Poland; ³²Universitatea de Medicină și Farmacie "Grigore T. Popa", Department of Morpho-Functional Sciences I, Department of Surgery II, Iași, Romania; ³³Regina Elena National Cancer Institute, Rome, Italy; ³⁴University of Rome "Foro Italico", Department of Movement, Human and Health Sciences, Roma, Italy; ³⁵Biotech Research and Innovation Centre, Department of Health and Medical Sciences, København, Denmark; ³⁶Sapienza University of Rome, Department of Translational and Precision Medicine, Roma, Italy; ³⁷Donostia Unibertsitate Ospitalea, Department of Digestive System, Donostia, Spain; ³⁸Institut d'Investigacions Biomèdiques August Pi i Sunyer (IDIBAPS), Liver Unit, Barcelona Clinic Liver Cancer (BCLC) group, Barcelona, Spain; ³⁹University of Navarra, Department of Biochemistry and Genetics, School of Sciences, Pamplona, Spain; ⁴⁰Ikerbasque Basque Foundation For Science, Donostia, Spain
Email: jesus.banales@biodonostia.org

Background and aims: Cholangiocarcinoma (CCA) is a rare and heterogeneous biliary cancer, with increasing incidence and related mortality. This study investigates the clinical course of CCA and subtypes (intrahepatic (iCCA), perihilar (pCCA), and distal (dCCA)) in a pan-European cohort.

Method: The ENSCCA Registry is a multicenter observational study. Patients with histologically-proven CCA diagnosis between 2010–2019 were included. Demographic, histomorphological, biochemical, and clinical studies were performed.

Results: Overall, 2,234 patients were enrolled (male:female = 1.29). iCCA (n = 1,243) was associated with overweight/obesity (58.5%) and chronic liver diseases involving cirrhosis (12.6%) and/or viral hepatitis (10.4%); pCCA (n = 592) with primary sclerosing cholangitis (8.8%); and dCCA (n = 399) with choledocholithiasis (10.3%). At diagnosis, 42.2% of patients had local disease, 29.4% locally-advanced disease (LAD), and 28.4% metastatic disease (MD). Serum CEA and CA19–9 showed low diagnostic sensitivity (69.1% and 40.9% below cutoff, respectively), but their concomitant elevation was associated with increased risk of presenting with LAD [OR = 2.16; 95%CI: 1.43–3.27] or MD [OR = 5.88; 95%CI: 3.69–9.25]. Patients undergoing resection (50.3%) showed the best outcome, particularly with negative-resection margin (R0) [median overall survival (mOS) = 45.1 months]; however, margin involvement (R1) [HR = 1.92; 95%CI: 1.53–2.41; mOS = 24.7 months] and lymph node invasion [HR = 2.13; 95%CI: 1.55–2.94; mOS = 23.3 months] compromised prognosis. Among patients with unresectable disease (49.6%), the mOS was 10.6 months for those receiving active palliative therapies, mostly chemotherapy (26.2%). Patients receiving best supportive care (20.6%) had mOS of 4.0 months, with iCCAs showing worst outcome compared to p/dCCAs. ECOG performance status [HR = 1.52; 95%CI: 1.01–2.31], MD [HR = 4.03; 95%CI: 1.82–8.92] and CA19–9 [HR = 2.79; 95%CI: 1.46–5.33] were independently prognostic for OS.

Conclusion: CCA is still diagnosed at advanced stage, a proportion of patients fail to receive cancer-specific therapies, and prognosis is dismal. Identification of preventable risk factors and implementation of surveillance in high-risk populations are required to decrease cancer-related mortality.

OS158

PRIME-HCC: phase Ib study of neoadjuvant ipilimumab and nivolumab prior to liver resection for hepatocellular carcinoma

Antonio D'Alessio^{1,2}, Madhava Pai³, Duncan Spalding³, Poyyamozhi Rajagopal³, Thomas Talbot¹, Robert Goldin⁴, Claudia Angela Maria Fulgenzi^{1,5}, Caroline Ward¹, Vincent Yip⁶, Tony Dhillon⁷, Sarah Slater⁸, Mikael Sodergren³, Paul Tait⁹, Nagy Habib³, Robert Thomas⁹, Alessio Cortellini¹, Rohini Sharma¹, David J. Pinato^{1,10}. ¹Imperial College London, Division of Cancer, Department of Surgery and Cancer, London, United Kingdom; ²Humanitas University, Department of Biomedical Sciences, Pieve Emanuele, Milan, Italy; ³Imperial College London, Division of Surgery, Department of Surgery and Cancer, London, United Kingdom; ⁴Centre for Pathology, Imperial College London, Charing Cross Hospital, Fulham Palace Road, London, UK; ⁵Division of Medical Oncology, Policlinico Universitario Campus Bio-Medico, Rome, Italy; ⁶Barts and The London HPB Centre, The Royal London Hospital, Barts Health NHS Trust, London, UK; ⁷Faculty of Health and Medical Sciences, University of Surrey and Department of Oncology, Royal Surrey County Hospital, Egerton Rd, Guildford GU2 7XX; ⁸Department of Medical Oncology, Barts Health NHS Trust, London, United Kingdom; ⁹Department of Radiology, Imperial College NHS Trust, Hammersmith Hospital, Du Cane Road, W120HS London, United Kingdom; ¹⁰Department of Translational Medicine, Università del Piemonte Orientale "A. Avogadro", Via Paolo Solaroli, 17, 28100, Novara, NO, Italy
Email: a.dalessio@imperial.ac.uk

Background and aims: Up to 70% of patients with early-stage hepatocellular carcinoma (HCC) treated with liver resection (LR) relapse within two years after surgery. Immune checkpoint inhibitors (ICPI) are an established treatment for unresectable HCC, but ICPI combinations have not been explored in the peri-operative setting.

Method: PRIME-HCC is a phase Ib study investigating safety and bioactivity of the nivolumab (3 mg/kg, day 1 and day 22) plus ipilimumab (1 mg/kg, day 1 only) combination prior to LR in

early-stage HCC. The primary safety analysis assessed treatment-related adverse events (trAE) and delays to surgery. Secondary end point included overall response rates (ORR) by RECIST v1.1 and pathologic responses on resection specimens.

Results: At data censoring on the 4th of November 2021, 12 patients were enrolled, of whom 83% (n = 10) were male, with a median age of 65 years (range 47–70). Liver cirrhosis was found in 75% (n = 9) of the patients, and the most frequent aetiology was viral hepatitis (50%, n = 4 with HCV and n = 2 with HBV infection). All patients were Child-Pugh A, with 58% classified as albumin-bilirubin (ALBI) grade 1. Median tumour diameter was 3.4 cm (interquartile range [IQR] 1.4, range 1.1–7.3), and the median number of liver nodules was 1 (IQR 1, range 1–3). Median baseline AFP was 6 mcg/L (IQR 115, range 2–11'777). Any-grade trAEs were reported by 75% of the patients (n = 9). Four patients (33%) reported grade 2 trAEs including hypothyroidism (n = 2), diarrhoea (n = 1), and fatigue (n = 1), and one (8%) grade 3 ALT/AST elevation. After a median follow-up of 9.1 months (IQR 19.1, range 2.5–24.9), no deaths had occurred, and one disease relapse was recorded 20.8 months after treatment commencement. Median time to LR from screening was 2.5 months (IQR 0.9, range 2.2–3.6). One patient had a surgery delay due to liver function worsening (ICPI-unrelated) and remained progression-free by RECIST 9.6 months post-screening. In another patient LR was switched to radiofrequency ablation by the treating surgeon due to surgical risk independent of ICPI exposure. One patient was found to have cholangiocarcinoma (CCA) on LR specimen and was excluded from efficacy analyses. ORR was 18%, with two partial responses. Disease control rate was 91%, and one patient with mixed HCC/CCA histology showed primary progression. Of the nine pathologically evaluable patients, seven (78%) achieved a pathological response, including two (22%) complete responses.

Conclusion: Neoadjuvant immunotherapy with nivolumab plus ipilimumab is tolerable and is characterised by evidence of anti-tumour efficacy in early-stage HCC.

OS159

Liver transplantation for patients with fibrolamellar hepatocellular carcinoma: a comprehensive multicenter analysis to support future decision making

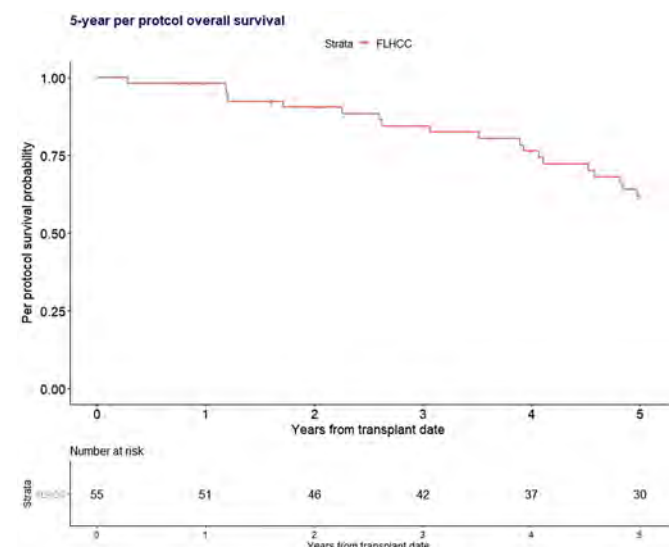
Marco Claasen^{1,2}, Tommy Ivanics¹, Wojciech Polak², Jan Ijzermans², Gonzalo Sapisochin¹. ¹University Health Network, Multi-Organ Transplant Program, Toronto, Canada; ²Erasmus MC Transplant Institute, University Medical Centre Rotterdam, Department of Surgery, Division of HPB and Transplant Surgery, Rotterdam, Netherlands
Email: marco.claasen@uhnresearch.ca

Background and aims: Fibrolamellar hepatocellular carcinoma (FL-HCC) is a rare tumour accounting for ~1% of all primary liver cancers. Due to its rarity, there is a shortage of data on liver transplantation (LT) for patients with FL-HCC. Previously post-LT outcomes have been evaluated based on patients transplanted a decade ago, however contemporary and intention-to-treat (ITT) and recurrence outcomes are lacking. Therefore, to gain more insight on the management of these patients, we conducted a comprehensive multicenter analysis of FL-HCC patients looking at both post-listing and post-LT outcomes.

Method: All patients with a diagnosis of FL-HCC and listed for LT or transplanted between 1987–2019 were extracted from the UNOS registry. Re-LT and multi-organ transplants were excluded. Outcomes of interest were waitlist (WL) dropout and ITT overall survival (OS), derived from all patients with a FL-HCC diagnosis at listing, and post-transplant OS, recurrence-free survival (RFS), cumulative incidence of recurrence, and 30-/90-day post-transplant mortality, for all patients with a confirmed diagnosis of FL-HCC at explant pathology. WL dropout was defined as dropping out of the WL due to death, clinical deterioration, or medical unsuitability. Recurrence and death were the events for predicting RFS. For the cumulative incidence of recurrence, death was a competing event. For all other outcomes, death was the only event. Median follow-up times were 4.5 years

(interquartile range [IQR] 1.2–8.2) from listing and 5.0 years (IQR 2.6–9.8) post-LT.

Results: A total of 96 unique patients with a diagnosis of FL-HCC at listing or post-LT were extracted. Of these, 53% were female and 76% adult, with a median age of 25.5 years (range 10–66). Cirrhosis was present in 10 patients (10%) and 8 patients had an underlying disease (8%): hepatitis C virus (5), non-alcoholic steatohepatitis (2), glycogen storage disease (1). Of all FL-HCC patients, 72 were diagnosed at listing (75%), 10 post-LT (10.5%), and of 14 the moment of diagnosis was unknown (14.6%). Sixty-nine patients received a LT, of which 55 were post-operatively confirmed of having FL-HCC. Eight patients received a living donor LT. WL dropout at 1- and 2-years post-listing was 15.3% and 19.4%. ITT OS at 1, 3, 5 years was 86.5%, 67.9%, 55.5%, where post-LT OS was 98.2%, 84.4%, 61.9% at 1, 3, 5 years. No patients died within 90 days post-LT. RFS was 85.3%, 69.9%, and 47.5% at 1, 3, and 5 years. The cumulative incidence of recurrence at 1, 3, 5 years was 12.8%, 24.4%, and 44.7%. There was no statistical difference in all outcomes between adult and pediatric patients.



Conclusion: LT for patients with FL-HCC offers acceptable long-term survival outcomes despite a substantial risk of tumour recurrence. Further research is needed to determine which patients with FL-HCC would benefit most from LT and potential adjuvant therapies to reduce the risk of recurrence.

OS160

A preferable signature of gut microbiota and bile acids predicted better outcomes of unresectable hepatocellular carcinoma to immune checkpoint inhibitors

Pei-Chang Lee¹, Chijung Wu¹, Ya-Wen Hung¹, Chieh-Ju Lee¹, Chen-Ta Chi¹, I-Cheng Lee¹, Jiing-Chyuan Luo¹, Ming-Chih Hou¹, Yi-Hsiang Huang¹. ¹Taipei Veterans General Hospital, Division of Gastroenterology and Hepatology, Department of Medicine, Taipei, Taiwan

Email: yhhuang@vghtpe.gov.tw

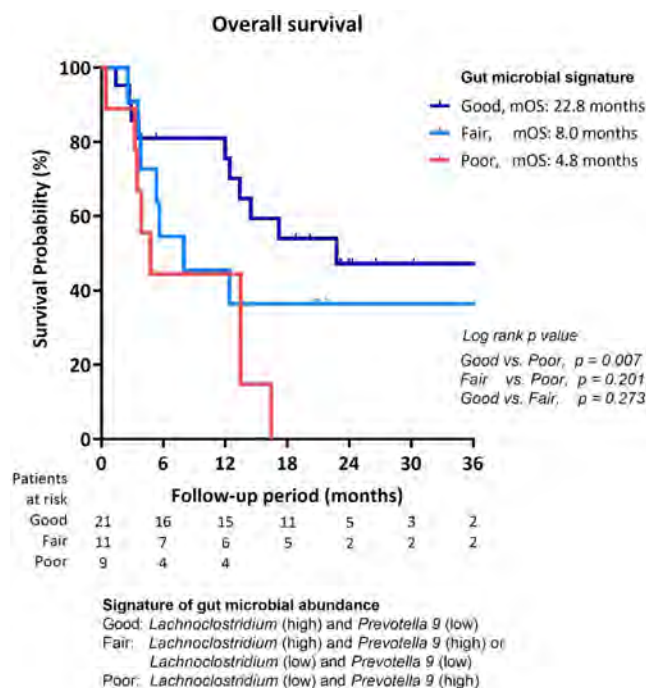
Background and aims: Immune checkpoint inhibitors (ICI) are newly emerged, promising therapeutic agents for unresectable hepatocellular carcinoma (uHCC). However, no effective biomarker has been found to predict treatment response. Gut microbiota could modulate outcomes of melanoma to immunotherapy. In this study, we aimed to investigate the effects of gut microbiota and metabolites on ICI-treated uHCC.

Method: From May 2018 to February 2020, patients who received ICI therapy for uHCC in Taipei Veterans General hospital were prospectively enrolled. Of them, fecal samples collected before treatment from

ORAL PRESENTATIONS

twenty objective responders and 21 non-responders (proved by radiology) were taken into analyses of microbiota and metabolites. Since March 2020, 33 consecutive Child-Pugh A, ICI-treated patients were investigated for validation. Besides, fecal samples from 17 healthy volunteers were also analyzed as control.

Results: A significant bacterial dissimilarity was observed between responders and non-responders before ICI treatment ($p = 0.016$ and 0.019 by Anosim and Adonis tests). *Lachnospiraceae*, *Veillonella* were predominant faecal microbiota of responders; whereas, *Prevotella 9* was predominant in non-responders. Ursodeoxycholic acid and ursocholic acid were found significantly enriched in the feces of responders, and were strongly correlated with the abundance of *Lachnospiraceae*. A fecal signature of enriched *Lachnospiraceae* and depleted *Prevotella 9* could significantly predict better overall survival (OS) in these patients. In the validation cohort, the best objective response rate (52.6%) was noted in patients with a preferable microbial signature. Besides, the progression-free survival (PFS) and OS were better in patients with a preferable microbial signature as compared with the counter-group. (PFS: 8.8 vs. 1.8 months; OS: not reached vs. 6.5 months, both $p < 0.001$).



Conclusion: Pre-treatment fecal microbiota and bile acids are associated with treatment outcomes of ICIs for uHCC. These findings provided a potential strategy to enhance the efficacy of immunotherapy by modifying gut microbiota and metabolites in patients with uHCC.

OS161

The impact of treatment and treatment status on health state utility in patients with unresectable hepatocellular carcinoma: an EQ-5D analysis from Himalaya

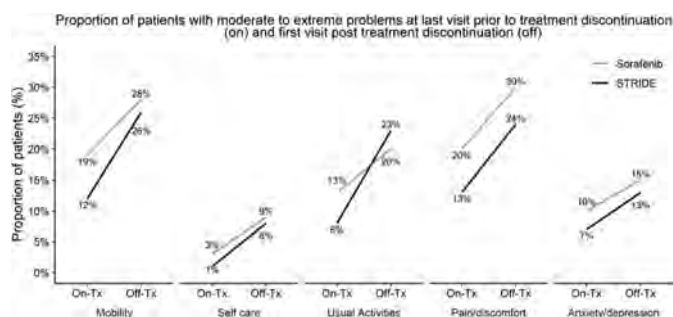
Lei Qin¹, Miguel Miranda², Cal Shephard³, Abdul-Azeez Ganiyu², Vincent Tam⁴, ¹AstraZeneca, Gaithersburg, United States; ²AstraZeneca, Cambridge, United Kingdom; ³AstraZeneca Canada, Mississauga, Canada; ⁴Tom Baker Cancer Centre, Calgary, Canada
Email: lei.qin@astrazeneca.com

Background and aims: The HIMALAYA trial (NCT03298451) showed that tremelimumab 300 mg added to durvalumab (STRIDE regimen) significantly improved survival compared to sorafenib for the

treatment of patients with unresectable hepatocellular carcinoma (uHCC). This study also assessed predictors of health-related quality of life (HRQoL) using EuroQoL 5-Dimension, 5-Level health state utility (HSU) index (EQ-5D-5L) and visual analogue scale (VAS).

Method: EQ-5D-5L data were collected at baseline, every 8 weeks for 48 weeks, then every 12 weeks until treatment discontinuation, and additional assessments up to 12 weeks for patients with confirmed progression. Impact of treatment and treatment status on domain score and proportion of patients reporting any problem by domain at first off-treatment visit were assessed using last on-treatment visit as baseline. Impact on HSU was assessed by mixed models for repeated measures (MMRM). Univariate and multivariate analyses were conducted using treatment as base fixed effect and treatment status (on/off treatment), progression (progression-free/progressed) and baseline Child Pugh score as covariates. Interactions between covariates and treatment were considered. A random intercept model assuming independent within-subject errors was fitted to account for subject variability. Model performance was compared using AIC/BIC score. Analysis used algorithms reflecting societal preferences of UK, US and Canadian populations and validation analysis was conducted using VAS.

Results: Treatment and treatment status models were consistently the best fitting. Mean HSU for STRIDE was 0.815 (95% CI: 0.802, 0.827, $p < 0.0001$) and 0.785 (95% CI: 0.766, 0.804, $p < 0.0001$) for sorafenib, using a mapping algorithm reflecting Canadian preferences. Sorafenib treatment was associated with a utility decrement of -0.030 (95% CI: -0.046 , -0.014 , $p = 0.0002$) and a utility increment of 0.055 (95% CI: 0.046 , 0.063 , $p < 0.0001$) for those with a status of remaining on treatment. Results with UK and US algorithms, and when assessed by VAS, were consistent. Interaction of treatment and treatment status was non-significant in all models. The proportion of patients experiencing any problems on each domain of EQ-5D-5L increased between the last visit prior to- and first visit post-discontinuation for both regimens. The proportion of patients experiencing moderate to extreme problems was lower on all domains with STRIDE vs sorafenib for both on- and off-treatment, except usual activities (Figure 1).



Conclusion: The best predictors of HRQoL in patients with uHCC were treatment received and treatment status, where treatment with STRIDE and being on-treatment were associated with better HSUs compared to sorafenib treatment and being off-treatment. Results highlight there are notable HRQoL benefits for maintaining uHCC patients on treatment with STRIDE.

NAFLD: Experimental and pathophysiology

OS162

Heterogeneity of phosphatidylcholine metabolism in non-alcoholic fatty liver disease

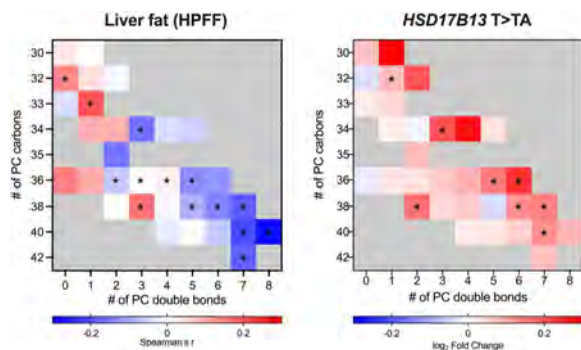
Sami Qadri^{1,2}, Sami Blom³, Kari Pitkänen³, Noora Ahlholm^{1,2}, Kimmo Porthan^{1,2}, Panu K. Luukkonen^{1,2,4}, Anne Juuti⁵, Henna Sammalkorpi⁵, Anne Penttilä⁵, Johanna Arola⁶, Matej Orešič^{7,8}, Tuulia Hyötyläinen⁹, Hannele Yki-Järvinen^{1,2}. ¹University of Helsinki and Helsinki University Hospital, Department of Medicine, Helsinki, Finland; ²Minerva Foundation Institute for Medical Research, Helsinki, Finland; ³Aiforia Technologies Oy, Helsinki, Finland; ⁴Yale University, Department of Internal Medicine, New Haven, United States; ⁵University of Helsinki and Helsinki University Hospital, Department of Gastrointestinal Surgery, Abdominal Center, Helsinki, Finland; ⁶University of Helsinki and Helsinki University Hospital, Department of Pathology, Helsinki, Finland; ⁷Örebro University, School of Medical Sciences, Örebro, Sweden; ⁸University of Turku and Åbo Akademi University, Turku Bioscience Centre, Turku, Finland; ⁹Örebro University, School of Science and Technology, Örebro, Sweden
Email: hannele.yki-jarvinen@helsinki.fi

Background and aims: In murine models of non-alcoholic fatty liver disease (NAFLD), liver damage associates with a deficiency of phosphatidylcholines (PCs), particularly polyunsaturated PCs (PUFA-PCs). We studied whether human PC metabolism is altered by NAFLD or by the protective genetic variant in *HSD17B13* (rs72613567 T>TA).

Method: In 143 obese patients with a liver biopsy and genotyping for *HSD17B13* rs72613567, we analysed the hepatic lipidome (UPLC-MS). As the hepatic parenchymal fat fraction (HPFF) affects apparent concentrations of amphiphilic lipids, we normalised hepatic phospholipid concentrations to fat-free liver mass. To this end, we employed a state-of-the-art deep learning image analysis method (Aiforia Technologies) to accurately quantify HPFF in liver biopsies.

Results: Total unadjusted hepatic PCs correlated negatively with HPFF ($r_s = -0.26$, $P < 0.01$), but this association disappeared after normalising to fat-free liver mass ($r_s = 0.02$, $P = 0.81$). With increasing HPFF, concentrations of especially saturated and monounsaturated PCs significantly increased, whereas concentrations of PUFA-PCs decreased. Accordingly, the hepatic triacylglycerol composition significantly correlated with that of hepatic PCs. In carriers of the protective variant in *HSD17B13*, as compared to non-carriers, the hepatic lipidome was enriched in especially PUFA-PCs.

Conclusion: Patients with NAFLD have a deficiency of PUFA-PCs. The protective *HSD17B13* rs72613567 variant opposes these changes, increasing intrahepatic PC concentrations.



OS163

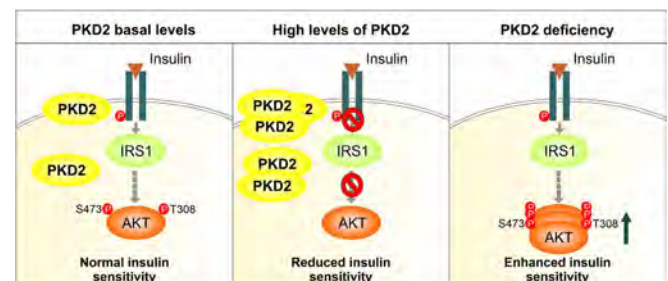
Unravelling the role of Protein Kinase D2 in the control of hepatic insulin sensitivity

Patricia Rada^{1,2}, Ana B. Hitos^{1,2}, Esther Rey^{3,4}, Elena Carceller-Lopez¹, Julia Pose-Utrilla^{1,5}, Carmelo Garcia-Monzon⁴, Guadalupe Sabio⁶, Teresa Iglesias^{1,5}, Águeda González^{3,4}, Angela Martinez Valverde^{1,2}. ¹Instituto de Investigaciones Biomédicas "Alberto Sols" (CSIC-UAM), Madrid, Spain; ²Centro de Investigación Biomédica en Red de Diabetes y Enfermedades Metabólicas Asociadas (CIBERDEM), Madrid, Spain; ³Centro de Investigación Biomédica en Red de Enfermedades Hepáticas y Digestivas (CIBEREHD), Spain; ⁴Liver Research Unit, Instituto de Investigación Sanitaria Princesa, University Hospital Santa Cristina, Spain; ⁵Centro de Investigación Biomédica en Red sobre Enfermedades Neurodegenerativas (CIBERNED), Spain; ⁶Centro Nacional de Investigaciones Cardiovasculares Carlos III (CNIC), Spain
Email: prada@iib.uam.es

Background and aims: Protein kinase D2 (PKD2) is a Ser/Thr kinase of the Ca^{2+} -Calmodulin kinase superfamily. Growing evidences support that PKD2 participates in the control of glucose homeostasis. Two previous studies, one conducted in global PKD2-deficient mice, and the other in mice lacking PKD2 in intestine, reported opposite results with metabolic dysfunction or protection against HFD-induced obesity, respectively. However, the role of PKD2 in the liver in the context of obesity-related insulin resistance has not been addressed and it is the aim of this study.

Method: PKD inhibition by pharmacological and genetic approaches was analyzed in primary hepatocytes and in Huh7 cells. To over-express PKD2, Huh7 cells were transfected with EGFP-PKD2-CA, a constitutively active PKD2 fused to EGFP. Insulin signaling cascade was examined by treating hepatocytes with insulin (10 nM, 5–15 min). As an *in vivo* model of hepatic insulin resistance, mice with a liver-specific PKD2 depletion ($\text{PKD2}^{\Delta\text{Hep}}$) were fed high fat diet (HFD, 20 weeks). Parameters assessing glucose homeostasis and hepatic insulin sensitivity were analyzed. PKD2 was overexpressed in liver by an injection of AAV bearing EGFP-PKD2-CA and insulin sensitivity was evaluated. PKD signature was analyzed in liver biopsies from NAFLD patients.

Results: PKD pharmacological inhibition resulted in an increased insulin sensitivity showed by a higher AKT phosphorylation after insulin stimulation in both primary mouse hepatocytes and Huh7 cells. Moreover, PKD2 knocking down by siRNA or shRNA-lentiviral particles enhanced the insulin response. Alternatively, EGFP-PKD2-CA overexpression in Huh7 cells reduced AKT phosphorylation upon insulin stimulation compared to EGFP-transfected cells. In this line, *in vivo* injection of AAV bearing EGFP-PKD2-CA resulted in a moderate impairment of glucose homeostasis and reduced IR and AKT phosphorylation in the liver. Importantly, HFD-fed $\text{PKD2}^{\Delta\text{Hep}}$ mice displayed a tendency to improve glucose tolerance and insulin sensitivity compared to control mice. These results were confirmed by analysis of AKT phosphorylation in liver extracts. Moreover, PKD immunostaining revealed that PKD2 was increased in NAFLD patients.



Conclusion: Our results strongly suggest that PKD2 is involved in the control of hepatic insulin signaling and point PKD2 as a new

ORAL PRESENTATIONS

therapeutic target in the progression of hepatic insulin resistance-related pathologies.

OS164

Metabolomic changes in NASH phenotype liver-on-a-chip caused by INI-678, a small molecule HSD17B13 inhibitor, supports a role for HSD17B13 in inflammation and fibrosis

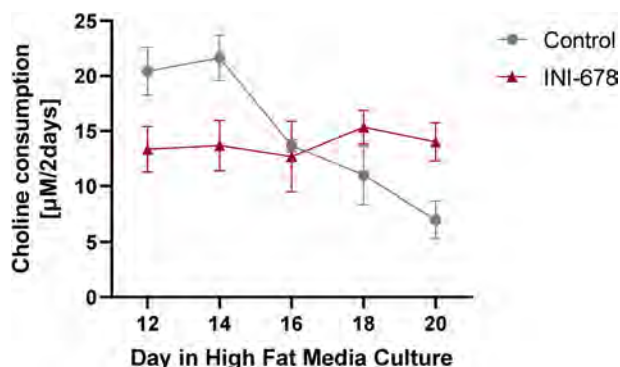
Heather Hsu¹, Michael Carleton¹. ¹Inipharm, Bellevue, United States
Email: hhsu@inipharm.com

Background and aims: Polymorphisms producing catalytically inactive HSD17B13 protect against non-alcoholic steatohepatitis (NASH), cirrhosis, and liver cancer and are associated with reduced hepatic inflammation and fibrosis. Preliminary results demonstrated that INI-678, a novel selective inhibitor of HSD17B13, decreased fibrotic markers in response to high fat media in liver-on-chip (LOC) co-cultures. The aim of this study was to determine the impact of inhibiting HSD17B13 with a well characterized inhibitor on metabolism in a NASH phenotype LOC.

Method: NASH LOC co-cultures containing primary human hepatocytes, homozygous for the active HSD17B13 allele; Kupffer cells, and stellate cells were cultured in a high fat containing media to induce a NASH phenotype. LOC were exposed to INI-678 or a DMSO vehicle control for Days 4–20. LOC co-cultures were analyzed for fibrotic markers by immunohistochemistry and media samples were analyzed for cell health markers, albumin and lactate dehydrogenase, by ELISA and activity, respectively. Metabolites were quantified in media samples using electrospray ionization by tandem mass spectrometry.

Results: Treatment of NASH LOC with INI-678 and related analog inhibitors of HSD17B13 decreased fibrotic marker proteins, alpha smooth muscle actin and collagen type 1, compared to vehicle control in LOC co-cultures. Choline consumption remained stable in INI-678-treated LOC throughout high fat media exposure. Choline consumption in the vehicle control was initially elevated and decreased throughout high fat media treatment ultimately lower than INI-678-treated LOC co-cultures. INI-678 treatment resulted in lower primary bile acids compared to vehicle control. INI-678 treatment significantly reduced hexose and increased lactate in the media.

Conclusion: The decrease in fibrotic markers in NASH LOC with INI-678 treatment was accompanied by changes in the metabolome. The metabolic changes include stabilization of choline, decreases in bile acids and decreased hexose. The inhibition of HSD17B13 significantly altered metabolism consistent with the hepatoprotective effect and anti-fibrotic effects observed in LOC. The direct effects of small molecule inhibitors of HSD17B13 are consistent with decreased fibrosis in NASH subjects carrying inactive HSD17B13 alleles. These results suggest a potential precision medicine approach to treating NASH.



OS165

The inhibition of the epigenetic effectors DNMT1 and G9a as a potential therapeutic strategy against the non-alcoholic fatty liver development

José María Herranz¹, Alex Claveria-Cabello², Leticia Colyn², María U. Latasa², Maite Perez-Araluce², Bruno Sangro^{1,3,4}, Julen Oyarzabal⁵, Antonio A. Pineda⁵, Maria Arechederra^{2,4}, Carmen Berasain^{1,2,4}, Matías A. Avila^{1,2,4}, Maite G. Fernandez-Barrena^{1,2,4}. ¹CIBERehd, Madrid, Spain; ²CIMA-University of Navarra, Hepatology Program, Pamplona, Spain; ³Clínica Universidad de Navarra, Hepatology Unit, Pamplona, Spain; ⁴Instituto de Investigación Sanitaria de Navarra, IdiSNA, Pamplona, Spain; ⁵CIMA-University of Navarra, Molecular Therapies Program, Pamplona, Spain
Email: magarfer@unav.es

Background and aims: Non-alcoholic fatty liver disease (NAFLD) encompasses a spectrum of histological changes ranging from simple steatosis to inflammation and ballooning, which define non-alcoholic steatohepatitis (NASH). NASH can lead to cirrhosis and hepatocellular carcinoma. Currently, no drugs have proven efficacy for NAFLD treatment. Understanding the mechanisms leading to NAFLD progression is essential for the identification of effective therapies. Epigenetic mechanisms are fundamental for gene expression regulation and functional homeostasis, and their impairment is recognized to participate in disease. Here we have performed a systematic transcriptomic analysis of epigenetic genes in human liver tissues from patients with different stages of NAFLD. We identified marked alterations in a significant number of epigenetic effectors, including DNA methyltransferase 1 (DNMT1) and its epigenetic cofactor UHRF1. DNMT1 and UHRF1 work in concert with the histone methyltransferase G9a in DNA methylation and gene expression regulation. We evaluated the potential relevance of the DNMT1/G9a/UHRF1 complex in vitro and in vivo models of NAFLD.

Method: We analyzed four publicly available liver transcriptome datasets integrating more than 520 patients. In vitro studies were performed in HepG2 cells challenged with a NASH cocktail. Cells were treated with the DNMT1/G9a/UHRF1 complex small molecule inhibitor CM272. In vivo studies were performed in C57BL6 mice fed with normal chow diet (ND) or high-fat diet (HFD, 45% fat) for 4 or 9 months and different regimes of CM272 treatment (one month and one week, respectively). Transcriptomic profiling, biochemistry and histological analyses were performed.

Results: Inhibition of DNMT1 and G9a with CM272 significantly reduced serum triglyceride and free fatty acids, and hepatic lipids accumulation in the two HFD models. Liver tissues transcriptomic analyses revealed that CM272 modulated metabolic pathways fundamentally involved in fatty acids and cholesterol metabolism and, intriguingly also the expression of genes involved in immune pathways, such as antigen presentation and processing. DNMT1 and G9a inhibition also caused significant changes in the expression of genes involved in energy expenditure and lipid metabolism in brown and white adipose tissue. In vitro studies confirmed most of the in vivo findings, including a robust induction by CM272 of carboxylesterase 1 (CES1), a key enzyme in the liver triglyceride metabolism.

Conclusion: A profound dysregulation in the expression of epigenetic effectors characterizes human NAFLD progression. We show that the pharmacological modulation of the epigenetic complex DNMT1/G9a/UHRF1 markedly affects the course of this disease in its early stages. Our findings suggest that characterization of epigenetic pathways in NAFLD may help to understand the disease and to expose new targets.

OS166

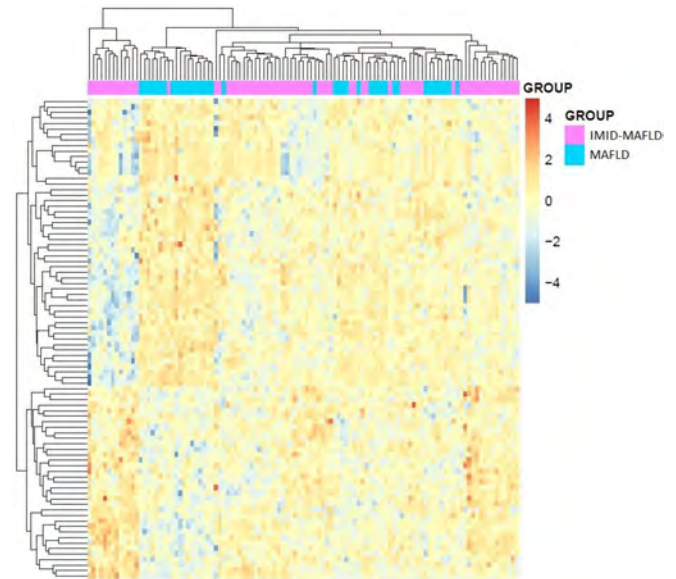
Molecular characterization of metabolic associated fatty liver disease as an immune-mediated inflammatory disease: IMID associated fatty liver disease

Enrique García-Nieto¹, Juan Carlos Rodríguez-Duque^{1,2}, Paula Iruzubieta^{1,2}, Agustín García-Blanco¹, Coral Rivas^{1,2}, María Luisa Cagigal³, Javier Rueda-Gotor⁴, Montserrat Rivero^{1,2}, Susana Armesto⁵, Marcos Antonio Gonzalez-Lopez⁵, Carlos Duran-Vian⁵, Anna Esteve Codina⁶, Marta Gut⁶, Jose Pedro Vaqué^{1,7}, Javier Crespo^{1,2}, María Teresa Arias Loste^{1,2}.
¹Research institute Marqués de Valdecilla (IDIVAL), Group of Clinical and Translational Research in Digestive Diseases Infection, Immunity and Digestive Pathology Group, Santander, Spain; ²University Hospital Marqués de Valdecilla, Gastroenterology and Hepatology Department, Santander, Spain; ³University Hospital Marqués de Valdecilla, Pathological Anatomy Service, Santander, Spain; ⁴University Hospital Marqués de Valdecilla, Division of Rheumatology, Santander, Spain; ⁵University Hospital Marqués de Valdecilla, Dermatology Department, Santander, Spain; ⁶CNAG-CRG, Centre for Genomic Regulation (CRG), Barcelona Institute of Science and Technology (BIST), Universitat Pompeu Fabra (UPF), Barcelona, Spain; ⁷University of Cantabria, Molecular Biology Department, Santander, Spain
 Email: javiercrespo1991@gmail.com

Background and aims: Growing evidence support an increased prevalence of metabolic associated fatty liver disease (MAFLD) in the context of immune-mediated inflammatory diseases (IMIDs) that can occur independently of classic metabolic risk factors. We aimed to characterize clinically and mechanistically a prospective cohort of IMID-MAFLD patients compared to regular MAFLD patients.

Method: Cross-sectional, case-control study including a subset of IMID patients (inflammatory bowel disease, psoriasis, hidradenitis, and spondyloarthritis). Controls from a random sample drawn from the general population were age, gender, type 2 diabetes, and BMI matched in a 1:2 ratio. MAFLD was established by the controlled attenuation parameter. Liver biopsies were collected when MAFLD with significant liver fibrosis was suspected. Total RNA was obtained from freshly frozen cases and analyzed by RNA-seq. Differential gene expression was performed with 'limma-voom' adjusting for BMI, sex and fibrosis severity. Gene set enrichment analysis (GSEA) was performed with fgsea R package with a pre-ranked "limma t-statistic" gene list. Serum protein concentrations were obtained using 'Quantikine ELISA Kit' in same patients analyzed by mRNA-seq.

Results: 1435 IMID patients and 2918 controls were included. MAFLD prevalence was significantly higher among IMID patients than controls, as well as the prevalence of advanced-MAFLD (LSM >9.7 kPa). In multivariate analysis, concomitant IMID was an independent and the strongest predictor of advanced-MAFLD. We compared transcriptomic data from 69 liver biopsies from IMID-MAFLD and 40 from MAFLD patients adjusted for BMI, sex, and fibrosis severity. We observed 87 highly significant genes differentially expressed between the two groups. Whereas genes like *IGFBP2* or *GPX2* showed an upregulated expression in IMID-MAFLD, others like *DGCR5* or the Metallothioneins *MT1M*, *MT1G* and *MT1F* were downregulated. Normalized expression values of significantly expressed genes and specific clustering of IMID-MAFLD and MAFLD cases are shown in Figure. A GSEA analysis detected the most relevant cellular activities in IMID-MAFLD vs. MAFLD. IMID-MAFLD cases displayed an enriched expression of genes implicated in pro-tumoral activities like signaling by Rho-GTPases or the control of the Cell Cycle concomitant with a negative expression of genes related to the metabolism. IGFBP-2 protein levels in serum samples from IMID-MAFLD and MAFLD validated the transcriptional data.



Conclusion: MAFLD has a disproportionately high tendency to occur in IMID populations, which may be explained by its distinctive chronic inflammatory burden. Supporting this, we provide a functional explanation to distinguish between MAFLD groups, and show that IMIDs can trigger a pro-tumoral liver condition that can lead to an aggressive form of MAFLD independently of classic metabolic pathways.

OS167

EphB2 is a novel signaling receptor in non-alcoholic steatohepatitis liver fibrosis

Patrice Mimche¹, Severin Donald Kamdem¹, Erika Egal¹, Quinian Johanson¹, Tuan Pham², Kimberley Evason³, Sihem Boudina⁴, Michael Ortiz⁵, Francis Sprouse⁵, Chinthaka Mahesh Udamulle Gedara⁵, Karina Cortez⁵, Mahmoud Ahmed⁶, Hesham Sadek⁶, Mark Henkemeyer⁵.
¹University of Utah, Department of Pathology, Salt Lake City, United States; ²University of Utah, Department of Internal Medicine, Division of Gastroenterology, Hepatology and Nutrition, Salt Lake City, United States; ³University of Utah and Huntsman Cancer Institute, Department of Pathology, Salt Lake City, United States; ⁴University of Utah, Department of Nutrition and Integrated Physiology, Salt Lake City, United States; ⁵UT Southwestern Medical Center, Department of Neuroscience, Dallas, United States; ⁶UT Southwestern Medical Center, Department of Internal Medicine and Molecular Biology, Dallas, United States
 Email: patrice.mimche@path.utah.edu

Background and aims: Emerging evidence suggests that the EphB2 receptor tyrosine kinase regulates tissue inflammation and fibrosis. However, its role in diet-induced non-alcoholic steatohepatitis (NASH) fibrosis has not been explored. We aimed to decipher the contribution of EphB2 to non-alcoholic steatohepatitis (NASH) development in mouse NASH models and in patients at various stages of non-alcoholic fatty liver disease progression.

Method: In NASH patients, hepatic EphB2 and serum sEphrinB2 ligand were evaluated. Disease phenotyping was performed in male and female wild type (WT), *EphB2*^{-/-}, EphB2-kinase-dead (*EphB2*^{K661R}), EphB2-kinase-overactive (*EphB2*^{F620D}) mice, and in hepatic stellate cell (HSC) specific *EphB2*^{-/-} mice fed the obesogenic Gubra-Amylin NASH (GAN) diet for 22–28 weeks and the Choline Deficient Amino-acid improved (CDA) high-fat diet for 10–12 weeks. The crosstalk between EphB2 and TGFβ signaling in primary human HSC was investigated *in vitro*. Pharmacological inhibition of EphB2 for the treatment of NASH was also evaluated *in vivo*.

ORAL PRESENTATIONS

Histology, flow cytometry, qPCR, biochemical assays, bulk RNA sequencing, and single cell RNA-sequencing were used to dissect the molecular mechanism underlying EphB2 function in NASH.

Results: Hepatic EphB2 was strongly upregulated in NASH patients and correlated with NASH fibrosis score. Serum sEphrinB2 was also elevated in NASH patients. In mouse models of NASH, *EphB2*^{-/-} knockout mice showed a significant reduction in liver steatosis, inflammation, and fibrosis compared to WT mice. This is supported by a significant reduction of liver fat content, pro-inflammatory and fibrotic genes in *EphB2*^{-/-} compared to WT mice. EphB2 forward signaling is likely the main driver of NASH progression as depicted by the significant increase in steatosis, inflammation, and fibrosis observed in *EphB2*^{F620D} kinase-overactive mice compared to WT and *EphB2*^{K661R} kinase-dead mice. Flow cytometry and single-cell RNA-sequencing reveal that macrophages and mesenchymal populations are reduced in *EphB2*^{-/-} mice compared to WT mice. Consistent with the above results and upregulated expression in NASH, HSC-specific knockout of *EphB2*^{-/-} also resulted in reduced NASH fibrosis. *In vitro*, rhTGFβ1, 2, and 3 upregulate EphB2 in human HSC and its silencing with *EphB2*-siRNA abrogates TGFβ-mediated HSC trans-differentiation into myofibroblasts-producing collagen. Finally, pharmacological inhibition of EphB2 reduced NASH fibrosis in mice. **Conclusion:** We have identified EphB2 as a key player in the pathogenesis of diet-induced fatty liver disease in human and mouse and showed that therapeutic targeting of this receptor mitigates NASH fibrosis.

Liver transplantation and Acute liver failure: Clinical aspects

OS168

Cumulative exposure to tacrolimus and incidence of cancer after liver transplantation

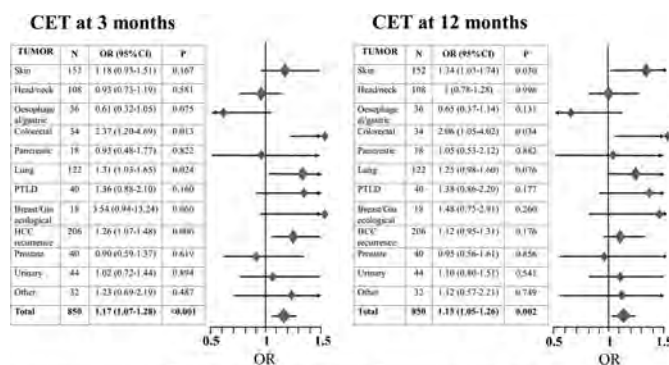
Manuel Rodríguez-Perálvarez¹, Gonzalo Crespo², Jesús Rivera², Antonio González Rodríguez³, Estefanía Berge Garrido³, Mikel Gastaca⁴, Patricia Ruiz⁴, Anna Curell⁵, Cristina Dopazo⁵, Ainhoa Fernández-Yunquera⁶, Fernando Diaz⁶, Ana Sánchez Martínez⁷, María Luisa Ortiz⁷, Marina Berenguer⁸, Tommaso Di Maira⁸, Jose Ignacio Herrero⁹, Mercedes Iñarrairaegui⁹, Carolina Almohalla¹⁰, Esteban Fuentes Valenzuela¹⁰, Sara Lorente Perez¹¹, Cristina Borao¹¹, Fernando Casafont¹², Emilio Fabrega¹², Sonia Pascual¹³, Patricio Más-Serrano¹³, Maria Angeles Lopez Garrido¹⁴, Flor Noguera López¹⁴, Rocio González-Grande¹⁵, Javier Zamora¹, Rafael Alejandro¹, Antonio M. Gómez-Orellana¹⁶, Carmen Bernal¹⁷, Miguel Ángel Gómez Bravo¹⁷. ¹Hospital Universitario Reina Sofía, University of Córdoba, IMIBIC, CIBERehd, Department of Hepatology and Liver Transplantation, Córdoba, Spain; ²Hospital Clínic Barcelona, IDIBAPS, CIBERehd, Univ. of Barcelona, Spain; ³Hospital Universitario Ntra. Sra. de Candelaria, Spain; ⁴Hospital Universitario Cruces, Biocruces Bizkaia Health Research Institute, Spain; ⁵Hospital Universitario Vall d'Hebron, Spain; ⁶Hospital General Universitario Gregorio Marañón, CIBERehd, Spain; ⁷Hospital Universitario Virgen de la Arrixaca, IMIB, Spain; ⁸Hospital Universitario I Politécnico La Fe, CIBERehd, Spain; ⁹Clínica Universidad de Navarra, CIBERehd, IdSNa, Spain; ¹⁰Hospital Universitario Río Hortega, Spain; ¹¹Hospital Lozano Blesa, Spain; ¹²Marqués de Valdecilla University Hospital, Idival, Spain; ¹³Hospital General Universitario Alicante, CIBERehd, Spain; ¹⁴Hospital Universitario Virgen de las Nieves, Spain; ¹⁵Hospital Regional Universitario de Málaga, Spain; ¹⁶University of Córdoba, Department of Computer Science and Numerical Analysis, Spain; ¹⁷Hosp. Univ Virgen del Rocío, Spain
Email: ropeml@hotmail.com

Background and aims: Cancer, either de novo or recurrent, is the leading cause of death after liver transplantation (LT). We aimed to evaluate the effect of maintenance immunosuppression on post-LT malignancy.

Method: Multicentre case-control nested study involving 16 LT institutions. The eligible cohort included adult patients undergoing LT (2010–2015) who received tacrolimus-based immunosuppression. Patients developing malignancy after LT, either de novo or recurrent, formed the group of cases. Controls were selected among patients without cancer after an identical follow-up period. Cases and controls were matched by propensity score based on age, gender, smoking habit, aetiology of liver disease and hepatocellular carcinoma (HCC) before LT. The exposure to immunosuppressive drugs within the first year after LT was recorded. Cumulative exposure to tacrolimus (CET) was calculated by the area under curve of trough levels (PMID: 31107827). The relationship between the immunosuppression protocol and the risk of post-LT malignancy was evaluated using multivariate logistic and Cox's regression.

Results: The eligible cohort included 2,495 patients. The study cohort comprised 425 patients who developed post-LT malignancy and 425 matched controls. The most frequent types of malignancy were: HCC recurrence (24%), non-melanoma skin cancer (16.1%), lung cancer (13.7%) and head and neck tumors (12.6%). Cases and controls were comparable in terms of age, gender, smoking habit, aetiology of liver disease and presence of HCC before LT. The immunosuppression protocol was similar in cases and controls ($p = 0.51$), and there were no differences in terms of individual drugs. Patients with post-LT malignancy had increased CET as compared with matched controls, both within the first 3 months ($p = 0.002$) and within the first 12 months ($p = 0.009$). An increased CET was the only independent predictor of post-LT malignancy after controlling for clinical features and concomitant immunosuppressive drugs: the hazard ratio (HR) of post-LT malignancy for a 20% increase of CET was 1.11 (95%CI 1.05–1.19; $p = 0.001$) at 3 months, and 1.10 (95%CI 1.03–1.17; $p = 0.004$) at 12 months. These results were consistent when considering exclusively de novo malignancy (CET at 3 months HR = 1.09; $p = 0.020$ and CET at 12 months HR = 1.10; $p = 0.016$).

Conclusion: CET is the most important immunosuppression-related risk factor of cancer after LT, thus highlighting the relevance of tacrolimus minimization.



OS169

Multidrug resistant bacterial infections after liver transplantation: prevalence, impact and associated risk factors

Rosa Martín-Mateos^{1,2}, Laura Martínez-Arenas³, Ángela Carvalho-Gomes^{3,4}, Laia Aceituno^{5,6}, Valle Cadahía-Rodrigo⁷, María Magdalena Salcedo^{8,9}, Ana Arias¹⁰, Sara Lorente Perez¹¹, Aitor Odriozola^{12,13}, Javier Zamora^{14,15}, Marino Blanes¹⁶, Óscar Len^{17,18}, Laura Benítez¹⁰, Isabel Campos-Varela^{5,19}, María Luisa Gonzalez Dieguez⁷, Diego Rojo Lázaro¹, Jesús Fortún²⁰, Antonio Cuadrado^{12,13}, Natalia Marcos Carrasco²¹

Manuel Rodríguez-Perálvarez^{22,23}, Emilio Fabrega^{12,13}, Trinidad Serrano¹¹, Valentín Cuervas Mons^{10,24}, Manuel Rodríguez⁷, Lluís Castells^{5,19}, Marina Berenguer^{25,26}, Javier Graus^{1,27}, Agustín Albillos^{1,2}. ¹Hospital Ramón y Cajal, Gastroenterology, Madrid, Spain; ²IRYCIS, CiberEHD, Alcalá University, Spain; ³IIS La Fe Valencia, Hepatology and Liver Transplantation Unit, Spain; ⁴CiberEHD; ⁵Vall d'Hebron Hospital, Liver Unit, Spain; ⁶VHIR, Spain; ⁷Hospital Universitario Central de Asturias, Gastroenterology, Asturias, Spain; ⁸Hospital Universitario Gregorio Marañón, Hepatology, Madrid, Spain; ⁹CiberEHD, Universidad Complutense, Madrid; ¹⁰Hospital Universitario Puerta de Hierro, Internal Medicine, Transplant Unit, Majadahonda, Spain; ¹¹Hospital Clínico Universitario Lozano Blesa, Gastroenterology, Zaragoza, Spain; ¹²Hospital Universitario Marqués de Valdecilla, Gastroenterology; ¹³IDIVAL; ¹⁴Reina Sofía University Hospital, Hepatology and Liver Transplantation, Cordoba, Spain; ¹⁵IMIBIC, CiberEHD; ¹⁶Hospital La Fe, Infectious Diseases; ¹⁷Vall d'Hebron Hospital, Infectious Diseases, Spain; ¹⁸VHIR, Autònoma University Barcelona, Spain; ¹⁹VHIR, Autònoma University Barcelona, Ciber EHD; ²⁰Hospital Ramón y Cajal, Infectious Diseases, Spain; ²¹Hospital Príncipe de Asturias, Alcalá de Henares; ²²Reina Sofía University Hospital, Hepatology and Liver Transplantation, Cordoba; ²³Hospital Universitario Reina Sofía, University of Córdoba, IMIBIC, CIBERehd, Department of Hepatology and Liver Transplantation, Córdoba, Spain; ²⁴Universidad Autónoma Madrid, Medicina, Madrid, Spain; ²⁵Hospital La Fe, Hepatology and Liver Transplantation Unit, Spain; ²⁶IIS La Fe Valencia, CiberEHD, University of Valencia; ²⁷Alcalá University
Email: agustin.albillos@uah.es

Background and aims: Infections caused by bacteria resistant to 3 or more antibiotic families (multidrug-resistant bacterial infections or MDRBIs) are an increasing healthcare issue. Our aim was to analyze the prevalence, burden, and risk factors associated with MDRBIs after liver transplantation (LT).

Method: Retrospective multi-center cohort study including adult patients who underwent LT from January 2017 to December 2019. Risk factors related to pre-LT liver disease, surgical procedure, and post-operative stay were recorded. A multivariate logistic regression analysis was performed to identify independent predictors of MDRBIs within the first 90-days after LT.

Results: We included 1,089 LT (1,004 patients) performed in 9 tertiary Spanish hospitals. Mean age was 56.83 ± 9.31 years, 72.5% (784) were male, and alcoholic liver disease was the most prevalent underlying etiology (42.5% (452)). Bacterial infections occurred in 442 LT (40.6%), that presented a total of 706 infections (respiratory 19.6%, urinary 17.9%, bacteremia 12.7%, cholangitis 10.7% and surgical wound infections 9.3%, among others). MDR were isolated in 230 LT (21.1%) (358 infections, 50.7%). *E. faecium* 88 (24.6%), *E. Coli* 77 (21.5%) and *Klebsiella pneumoniae* 48 (13.4%) were the most frequent isolated bacteria. In the multivariate analysis, previous intensive care unit admission (0–3 months before the LT), previous MDRBIs (0–3 months before the LT), renal-replacement therapy after LT and the number of packed red blood cells units transfused during surgery were identified as independent predictors of MDRBIs (table 1). Mortality at 30, 90, 180 and 365 days was significantly higher in patients with MDRBIs.

Conclusion: MDRBIs are highly prevalent after LT and have a significant impact on prognosis. *E. faecium* is the most frequently isolated MDR microorganism. New pharmacologic or surveillance strategies aimed at preventing MDRBIs after LT should be considered for patients with high-risk factors.

	Univariate (p)	Multivariate (p)
Body mass index	0.83	-
Number of packed red blood cells	0.00	0.04
Number of platelet pools	0.31	-
Plasma (cc)	0.93	-
MELD score (biochemical) pre-LT	0.01	0.41
Age	0.92	-
Biliary-enteric anastomosis	0.14	-
Renal replacement therapy	0.00	0.02
Rifaximin	0.17	-
Carriers of MDRB	0.00	0.21
Diabetes	0.48	-
Prophylaxis with norfloxacin	0.33	-
HIV	0.31	-
Fulminant etiology	0.44	-
CEP	0.44	-
Retransplantation	0.77	-
MDRBIs (0–3 months before LT)	0.00	0.03
ICU admission (0–3 months before LT)	0.00	0.04
Hospitalization (0–3 months before LT)	0.01	0.74

OS170

Modeling ischemic cholangiopathy in human cholangiocyte organoid for screening of novel cholangio-protective agents

Shaojun Shi¹, Henk P. Roest¹, Marcel Bijvelds², Jeroen de Jonge¹, Hugo de Jonge², Jan Ijzermans¹, Monique M.A. Verstegen¹, Luc J.W. van der Laan¹. ¹Erasmus MC Transplant Institute, University Medical Center, Department of Surgery, Rotterdam, Netherlands; ²Erasmus MC-University Medical Center, Department of Gastroenterology and Hepatology, Rotterdam, Netherlands
Email: l.vanderlaan@erasmusmc.nl

Background and aims: Ischemic cholangiopathy refers to biliary damage caused by disruption of blood supply in the peribiliary plexus. Detailed knowledge of ischemic cholangiopathy pathogenesis remains scarce due to the lack of appropriate *in vitro* models. We aimed to recapitulate ischemia-evoked biliary damage using human intrahepatic cholangiocyte organoids (ICOs) *in vitro* for the study of ischemic cholangiopathy and preclinical drug discovery.

Method: Human ICOs (n=5) were initiated from liver biopsies. Cultures were exposed to hypoxia (~1% O₂) for 72 hours and reoxygenated for 6 (H/R6 h) or 24 hours (H/R24 h). To enable immediate tracking of hypoxia, ICOs were transduced with a hypoxia-inducible factor 1α (HIF-1α) reporter. The effect of hypoxia on cell proliferation, apoptosis, and necroptosis was determined by immunostaining with Ki67, active caspase 3, and phosphorylated mixed lineage kinase domain-like protein, respectively, and ATP content.

Results: Extensive activation of the HIF-1α reporter was observed in ICOs at 72 h of hypoxia. This signal was partially reduced after H/R24 h. Hypoxia- and H/R6h-exposed ICOs were significantly smaller in size (p < 0.001) than untreated ICOs. Also, the disintegration of the cytoskeleton and disrupted epithelial integrity were observed. Cell viability of ICOs undergoing hypoxia or H/R6 h was drastically lower (p < 0.05) than under normoxia and was restored after H/R24 h (p < 0.05). Transcriptional and morphological analysis indicated a clear decrease of Ki67 expression after hypoxia or H/R6 h, which recovered after H/R24 h to normal levels. Immunostaining revealed that extensive apoptosis, but not necroptosis, was induced by hypoxia and H/R6 h. Exposure of the ICOs to Emricasan, a caspase inhibitor, failed to attenuate apoptosis but switched it into necroptosis. We further identified clinical-grade alpha-1 antitrypsin (AAT) as a potent inhibitor of hypoxia-induced apoptosis without necroptotic switch (p < 0.05). Treatment of ICOs with AAT in hypoxia exposed ICOs increased the cell viability (p < 0.05) and partially restored the Ki67 expression.

Conclusion: ICOs recapitulate ischemic cholangiopathy *in vitro*, featured by extensive apoptosis and reduced cell proliferation,

ORAL PRESENTATIONS

which could be partially restored by reoxygenation. AAT is identified as a novel cholangiocellular protective agent by restoring proliferation and preventing apoptosis.

OS171

The prognostic role of lysophosphatidylcholines and their immunomodulatory potential in acute liver failure

Francesca Maria Trovato¹, Salma Mujib¹, Florent Artru¹, Anna Cavazza¹, Ellen Jerome¹, Evangelos Triantafyllou², Mark J. W. McPhail¹. ¹Institute of Liver Studies, Inflammation Biology, London, United Kingdom; ²St Mary's Hospital, Liver Unit, United Kingdom
Email: trovatofrancesca@gmail.com

Background and aims: Acute liver failure (ALF) is a life-threatening disease in people without previous liver disease. It is characterised by inflammation and parallel immunoparesis with a high incidence of death from sepsis and multiorgan failure. In this context, immune cell function is often suppressed by multiple mechanisms, including inhibitory signalling via immune checkpoint pathways. The aim of this research was to modulate systemic immune responses through the immunometabolic Lysophosphatidylcholine (LPC)-Autotaxin (ATX)-Lysophosphatidylcholine acid (LPA) pathway.

Method: 43 ALF, 21 cirrhotics, 24 HC, and 31 septic (as proinflammatory control) patients were included. The pathway of interest was identified on the basis of multivariate analysis of a 180 metabolite targeted metabolomics panel (Biocrates p180). Autotaxin and LPA levels were measured by ELISA. Plasma cytokines were analysed with an MSD V-PLEX kit. PBMCs were cultured with LPA 16:0, 18:0, 18:1, and their immune checkpoint surface expression (CTLA-4, TIGIT/CD155, PD-1/PDL-1, Tim-3) was assessed by flow cytometry.

Results: LPC 16.0 was identified as highly discriminant between ALF and HC (principal component analysis (PCA) and Orthogonal partial least squares discriminant analysis (OPLS-DA): R2X 0.592; R2Y 0.666, Q2 0.613, AUROC 0.969961). There was an increase in ATX (Kruskal-Wallis test, ALF vs HC $p < 0.001$) and its product LPA in ALF comparing to HC and Sepsis (Kruskal-Wallis test, ALF vs HC $p < 0.01$). LPC 16.6, 18.0 and 18.1 were reduced in ALF patient with poor prognosis (dead at 90 days or transplanted) (for LPC 16.0 and LPC 18.1 $p < 0.05$). Despite increased proinflammatory cytokines in plasma, PBMCs from ALF patients produced less IL-6 when stimulated with LPS ($p < 0.05$), and the addition of LPAs failed to reverse this. However, in monocytes LPA 16.0 increased and restored PDL-1 expression (% of positive cells, $p < 0.05$), usually reduced comparing to HC ($p < 0.05$), and reduced CD155 expression (% of positive cells and MFI, $p < 0.05$), without effect on the CD4⁺ counterparts PD1 and TIGIT.

Conclusion: Reduced lysophosphatidylcholines (LPC16.0, LPC 18.0 and LPC 18.1) are biomarkers of poor prognosis in patients with ALF. The LPC-ATX-LPA axis appears to modulate innate immune response in ALF and requires further investigation to identify novel therapeutic agents.

OS172

Prescription event monitoring of checkpoint inhibitor-induced liver injury and outcomes of rechallenge: a 10-year experience

Edmond Atallah^{1,2}, Ana Oshaughnessy³, Dolapo Igboin³, Yvette Moore³, Joyce Ntata³, Ankit Rao³, Hester Franks⁴, Poulam Patel⁴, Guruprasad Aithal^{1,2}. ¹University of Nottingham, Nottingham Digestive Diseases Centre, School of Medicine, Nottingham, United Kingdom; ²Nottingham University Hospitals NHS Trust and the University of Nottingham, National Institute for Health Research (NIHR) Nottingham Biomedical Research Centre, Nottingham, United Kingdom; ³Nottingham University Hospitals NHS Trust, Nottingham, United Kingdom; ⁴BioDiscovery Institute, University of Nottingham, Centre for Cancer Sciences, Translational Medical Sciences, Nottingham, United Kingdom
Email: edmond.atallah@nottingham.ac.uk

Background and aims: Among cancer patients on checkpoint inhibitors (CPI), 1–16% develop checkpoint inhibitor-induced liver injury (ChILI). However, there are limited accurate reports of the incidence rate of ChILI as assessed by time on treatment. Using a prospective database and review of patient records, we estimated the risk and incident rate of ChILI in all melanoma and renal cancer patients who received CPI at Nottingham University Hospitals (NUH) from 2011–2021.

Method: Using 'ChemoCare', a prospective oncology prescribing database, we identified all adult patients who received CPI for adjuvant or metastatic melanoma or metastatic renal cell carcinoma (RCC) since 2011. Prescription event monitoring was performed using patient-related records and digital records; ChILI, other immune-related adverse events (irAE) and response to rechallenge were recorded. International Expert Working Group (EWG) for drug-induced liver injury case definitions were used to define ChILI cases and grade severity. Causality was assessed using Roussel Uclaf Causality Assessment Method (RUCAM).

Results: Out of 432 patients, ChILI occurred in 38 (8.8%). RUCAM was 'possible' in 9, 'probable' in 22 and 'highly probable' in 7 cases. The incidence rate of ChILI was 10.93 (95% CI 5.66–18.75) per 1000 patient-months of CPI exposure, with most cases occurring in patients treated with dual checkpoint inhibition. ChILI severity was 'mild' in 11 and 'moderate' in 27 (based on EWG grading); 36 of 38 (94.7%) received corticosteroids. Mean time to resolution of ChILI was 77 days ± 59 following steroid therapy compared to 49 days ± 21 in those untreated. Of 38 ChILI cases, 15 (39.5%) were re-treated with a single CPI, and only one patient developed recurrent ChILI. However, three developed colitis, one each developed hypophysitis and severe neuropathy.

Table: Risk and incidence rate of ChILI per CPI regime.

Cancer	CPI Regime	Number of Patients	Mean number of cycles	Person-Time at risk (months)	ChILI cases	Risk	Incidence rate per 1000 patient-months
Melanoma	Ipilimumab	88	3	210.53	2	2.27%	9.50
	Ipilimumab + Nivolumab followed by Nivolumab maintenance	102	3 combination 8 Nivolumab	949.23	29	28.43%	30.55
	Nivolumab	22	12	281.20	0	0%	0.00
	Pembrolizumab	108	9	1035.37	3	2.78%	2.90
	Adjuvant Pembrolizumab	39	7	316.70	1	2.56%	3.16
RCC	Ipilimumab + Nivolumab followed by Nivolumab maintenance	19	3 combination 6 Nivolumab	160.10	2	10.53%	12.49
	Nivolumab	54	12	524.70	1	1.85%	1.91
Total		432		3477.83	38	8.8% (95% CI 6.2–11.8)	10.93 (95% CI 5.66–18.75)

Conclusion: Prescription event monitoring provides an accurate estimate of the risk of ChILI as well as its outcomes. Rechallenge with single-agent CPI is feasible, with most patients not having a recurrence of ChILI. However, there is a risk of developing other irAE, especially colitis. The benefits and risks of corticosteroid therapy should be evaluated in a larger cohort of ChILI patients.

OS173

Impact of increasing MELD 3.0 beyond 40 on liver transplant outcomes

W. Ray Kim¹, Ajitha Mannalithara¹, Branden Tarlow¹, Allison Kwong¹. ¹Stanford University School of Medicine, Stanford, United States
Email: allison.kwong@gmail.com

Background and aims: MELD 3.0 improves upon MELD-Na by incorporating sex and albumin alongside bilirubin, creatinine, INR, and sodium, updating the existing coefficients, adding relevant

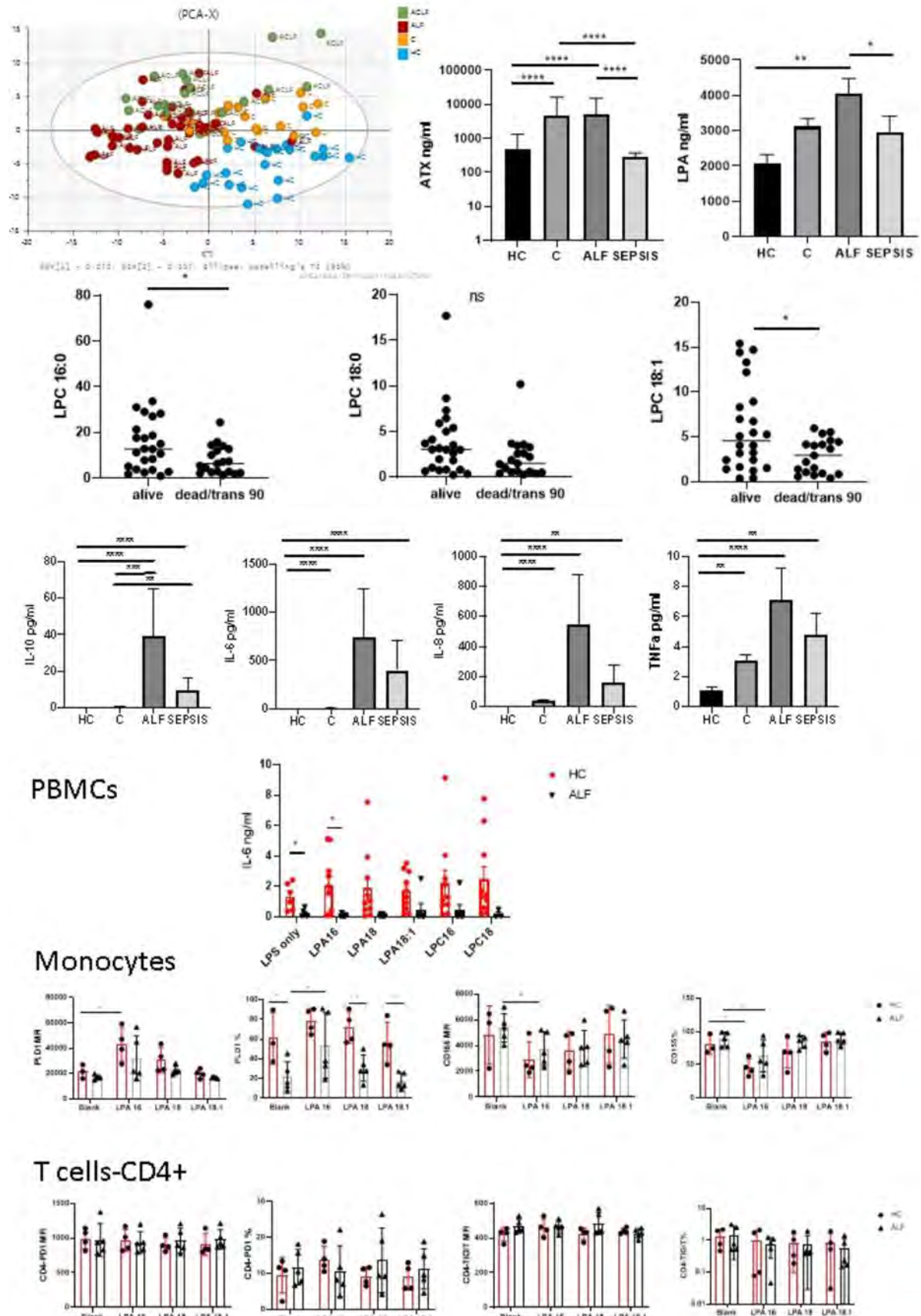


Figure: (abstract: OS171)

interactions, and resetting the upper bound of serum creatinine to 3.0 from 4.0 mg/dL. In the US liver allocation system, previous versions of MELD including MELD-Na have been capped at 40. We study the impact of increasing MELD score beyond this threshold on liver transplant outcomes.

Method: Adult waitlist registrations for liver transplantation from 15 Jan 2016 to 30 Jun 2021 were identified using OPTN data. MELD 3.0 = $1.33 \text{ (if female)} + 4.56 \cdot \log_e(\text{bilirubin}) + 0.82 \cdot (137 - \text{Na}) - 0.24 \cdot (137 - \text{Na}) \cdot \log_e(\text{bilirubin}) + 9.09 \cdot \log_e(\text{INR}) + 11.14 \cdot \log_e(\text{creatinine}) + 1.85 \cdot (3.5 - \text{albumin}) - 1.83 \cdot (3.5 - \text{albumin}) \cdot \log_e(\text{creatinine}) + 6$. Survival analysis evaluated the effect of increasing MELD 3.0 beyond 40 on 30-day waitlist mortality. Individual follow-up time started from the first qualifying MELD score ≥ 40 ; patients were censored after 30 days of follow-up, at the time of an approved exception, death, or liver transplant, whichever occurred first. In a sensitivity analysis, the Cox regression model was performed to consider MELD 3.0 as a time-dependent covariate if MELD remained ≥ 40 . 2-year posttransplant outcomes were also assessed.

Results: There were 54,060 new waitlist registrations during the study period, 2476 (4.6%) with MELD-Na ≥ 40 and 2820 (5.2%) with MELD 3.0 ≥ 40 at listing. 23.9% of candidates with MELD ≥ 40 met clinical criteria for acute-on-chronic liver failure. An additional 3,254 candidates recorded MELD 3.0 ≥ 40 during their waiting time. 30-day waitlist mortality was higher for each point increase in MELD 3.0 (HR 1.13, 95% CI 1.12–1.15), with a linear relationship from MELD 3.0 of 40 up to 55. 30-term waitlist mortality was higher for each increasing MELD stratum, from 65.6% to 88.7% for those with MELD 40–44 compared to MELD 50+ (Figure). Results were similar when MELD 3.0 considered as a time-dependent covariate. Posttransplant outcomes were comparable across MELD strata including MELD 35–39.

Conclusion: MELD 3.0 is anticipated to increase the proportion of patients reaching or surpassing the maximum allocation score of 40. Patients with MELD >40 may derive greater survival benefit from LT compared to MELD 40 without necessarily worse post-transplant outcome. Increasing the maximum score for MELD 3.0 may improve risk stratification of waitlist mortality and better represent liver transplant urgency for the sickest patients, including those with acute-on-chronic liver failure.

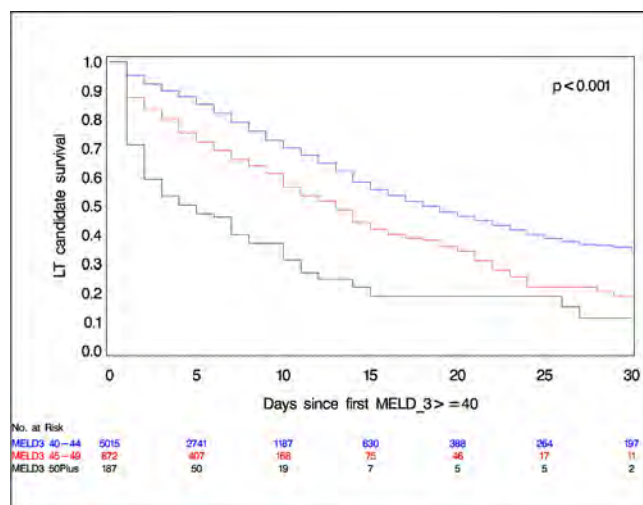


Figure: Kaplan-Meier curves: 30-day survival of patients with MELD 3.0 ≥ 40 at any time on waitlist.

MELD 3.0	n	Within 30 days since first MELD 3.0 ≥ 40			Median survival time in days (95% CI)
		# Transplanted	# of deaths	30-day mortality	
40-44	5015	3463	1304	65.6%	18 (17-20)
45-49	872	525	327	81.2%	13 (11-14)
50+	187	74	109	88.7%	5 (3-7)

OS174

Bile duct on a chip: engineering a microfluidic platform for studying biliary epithelium in a dish

Jorke Willemse¹, Mees N.S. de Graaf², Gilles van Tienderen¹, Luc J.W. van der Laan¹, Valeria Orlova², Jeroen de Jonge¹, Monique M.A. Verstege¹. ¹Erasmus MC Transplant Institute University Medical Center, Department of surgery, Rotterdam, Netherlands; ²Leiden University Medical Center, Department of Anatomy and Embryology, Netherlands
Email: j.willemse@erasmusmc.nl

Background and aims: Biliary complications that may arise after liver transplantation, such as non-anastomotic strictures and diffuse bile leakage, are challenging and complex. Ischemia-related cell death and impaired regeneration of damaged biliary epithelium is known to be involved in causing these complications. Intrahepatic cholangiocyte organoids (ICO) allow for the expansion and study of cholangiocyte-like cells, but access to the lumen of the organoids is limited and can only be studied after disrupting the 3D structure. There are currently no *in vitro* models mimicking the circumstances as exposure of bile ducts to warm ischemia time or cold storage, and therefore we aimed to establish a microfluidic bile-duct-on-chip (BDOC) platform for studying the effect of these conditions on biliary epithelium *in vitro*.

Method: ICO were initiated from human liver biopsies (N=5) obtained during liver transplant procedures. Three-channel BDOC (dimensions; length 1 cm, width and height 500 μm) were prepared by casting polydimethylsiloxane (PDMS) into a mold. Subsequently, plasma treated PDMS chips were bonded to glass slides. The BDOC channels were filled with collagen type I pre-gel and viscous finger patterning procedures were used to create channels inside these collagen hydrogels. ICO-derived cells ($25 \cdot 10^3$ cells/channel) were introduced into the channels and ICO expansion medium was added to the reservoirs. The BDOC were incubated for up to 21 days. Growth of epithelial cells was monitored using confocal microscopy and histology.

Results: ICO-derived cells populated the entire surface of the channels with a single layer of cells within 7 days after seeding. Whole mount confocal imaging revealed that cells were columnar in shape and morphologically looked like biliary epithelium. Zonula Occludens-1 (ZO-1) staining showed cholangiocyte-like polarization of cells in honey comb patterns. The cells express the cholangiocyte markers cytokeratin 7 and 19 on gene and protein level.

Conclusion: The results show that microfluidic approaches combined with cholangiocyte-like (KRT 7 and 19-positive) cells from ICO can be used to create healthy small diameter intrahepatic bile duct structures *in vitro*. This model allows for detailed analysis of epithelial damage and regeneration during warm and cold ischemic conditions that are known to cause post transplantation complications to the biliary system, and also to study onset and progression of biliary diseases.

Thursday 23 June

Alcoholic liver disease

THU001

Heavy alcohol intake along with ALDH2 polymorphism increases the risk of hepatocellular carcinoma and mortality in hepatitis B virus-related cirrhosis

Chih-Wen Lin¹, Ming Chao Tsai², Sien-Sing Yang³, Chih-Che Lin², Wen-Lung Wang², Yao-Chun Hsu², Yaw-Sen Chen², Ming-Lung Yu⁴, Jui-Ting Hu³. ¹E-Da Hospital, Medicine, Kaohsiung, Taiwan; ²Kaohsiung Chang Gung Memorial Hospital, Kaohsiung, Taiwan; ³Cathay General Hospital, Taipei, Taiwan; ⁴Kaohsiung Medical University Chung-Ho Memorial Hospital, Kaohsiung, Taiwan
Email: lincw66@gmail.com

Background and aims: Hepatitis B virus (HBV) infection and alcoholism are risk factors for hepatocellular carcinoma (HCC) and mortality. We investigated the effect of heavy alcohol intake, ALDH2 polymorphism, and HBV infection on clinical outcomes and risk factors in cirrhotic patients.

Method: We enrolled 1515 cirrhotic patients (342 patients with HBV infection and alcoholism, 796 patients with HBV infection, and 373 patients with alcoholism) from three tertiary hospitals in Taiwan between 2005 and 2020.

Results: Of patients with concomitant HBV infection and alcoholism, HBV infection alone, and alcoholism alone, 81 (23.7%), 134 (16.8%), and 55 (14.6%) patients developed HCC and 151 (45.3%), 322 (40.5%), and 150 (39.8%) patients experienced mortality, respectively. The 15-year cumulative incidences of HCC (66.4% vs. 46.8% vs. 54.8%, $P < 0.001$) and mortality (88.9% vs. 81.9% vs. 90%, $P < 0.001$) were significantly higher in cirrhotic patients with HBV infection and alcoholism than in those with HBV infection alone or alcoholism alone before and after propensity score matching. The ALDH2 polymorphism (allele GA/AA) with heavy alcohol intake significantly increased the risk of HCC and mortality in HBV-related cirrhotic patients. Risk factors for HCC were baseline serum HBV DNA (HR = 4.08), antiviral therapy (HR = 0.13), alcohol intake (HR = 1.77 and 1.49), abstinence (HR = 0.41), and ALDH2 polymorphism (HR = 5.09). Risk factors for mortality were abstinence (HR = 0.22), ALDH2 polymorphism (HR = 1.49), Child-Pugh class (HR = 1.43 and 1.98), serum albumin (HR = 0.62), and HCC development (HR = 1.57) in cirrhotic patients with HBV infection and alcoholism.

Conclusion: Heavy alcohol intake along with the ALDH2 polymorphism significantly increased the risk of HCC and mortality in HBV-related cirrhotic patients.

THU002

Biomarkers for prediction of alcohol-related liver cirrhosis in the Swedish general population

Gustav Jakobsson^{1,2}, Mats Talbäck³, Göran Walldius³, Niklas Hammar³, Ying Shang⁴, Hannes Hagström^{1,4,5}. ¹Division of Hepatology, Department of Upper GI, Karolinska University Hospital, Stockholm, Stockholm, Sweden; ²Department of Medicine Capho St Göran's hospital, Stockholm, Sweden; ³Unit of Epidemiology, Institute of Environmental Medicine, Karolinska Institutet, Stockholm, Sweden; ⁴Department of Medicine, Huddinge, Karolinska Institutet, Stockholm, Sweden; ⁵Clinical Epidemiology Unit, Department of Medicine, Solna, Karolinska Institutet, Stockholm, Sweden
Email: gustav.jakobsson@ki.se

Background and aims: Alcohol-related liver cirrhosis (ARLC) is a severe and well-known complication to chronic alcohol overconsumption. There are several known biomarkers associated with increased intake of alcohol and liver damage. There is limited knowledge on which biomarkers that have the best predictive capabilities for future ARLC, especially in a general population setting. Here, we investigated this in a large, population-based Swedish cohort.

Method: We used data from the AMORIS cohort, a general population cohort with blood samples from routine health care and outpatient visits in primary or occupational care collected from 1985 through 1996. The cohort consists of 812 073 individuals, approximately 35% of the total population in Stockholm county, Sweden, during this period. We included all persons above 18 years old, with a baseline blood sample of Alanine transaminase (ALT) and Aspartate transaminase (AST). We excluded subjects with known liver cirrhosis at baseline.

We ascertained incident cases of ARLC by linking the AMORIS cohort to Swedish national health registers. All subjects were followed until a first event of ARLC, death, emigration or end of the study period, December 31, 2011. Biomarkers were standardized to increase comparability. Associations between biomarkers and incident ARLC were analyzed with Cox regression models and discrimination was assessed using C-statistics.

Results: We identified 537 479 individuals with a mean follow-up time of 19.0 years. The biomarkers with the best predictive capabilities in both unadjusted and adjusted analyses were gamma-glutamyl transferase (GGT) and mean corpuscular volume (MCV), with an adjusted C-index of 0.81 and 0.85 respectively. The AST/ALT-ratio showed a lower predictive value, with a C-index of 0.70 (Table 1).

Table 1: Hazard ratios (HR) reflect an increase of one standard deviation for each parameter. *Unadjusted; **Adjusted for sex and age; ^h Harrell's C-index.

	Number	HR*	95 % CI	C-Index ^h	HR**	95 % CI	C-Index ^h
ALT	537 479	1.05	1.05 1.05	0.81	1.05	1.04 1.05	0.75
AST	537 479	1.04	1.03 1.04	0.85	1.03	1.03 1.04	0.76
GGT	515 958	1.14	1.14 1.15	0.90	1.14	1.13 1.14	0.81
Bilirubin	121 260	0.71	0.68 0.74	0.58	0.70	0.66 0.73	0.72
Albumin	470 915	1.19	1.17 1.21	0.62	1.18	1.16 1.20	0.71
MCV	172 891	2.14	2.07 2.21	0.80	2.10	2.03 2.17	0.85
AST/ALT ratio	537 479	0.97	0.93 1.02	0.52	1.08	1.05 1.11	0.70



POSTER PRESENTATIONS

Conclusion: The best predictive biomarkers for ARLC in the general population were MCV and GGT, whereas the commonly used AST/ALT ratio had a lower predictive capability.

THU003

A history of bariatric surgery is independently associated with a younger age at onset of severe alcoholic hepatitis

Lukas Van Melkebeke^{1,2}, Annelotte Broekhoven³, Tessa Ostyn⁴, Minneke Coenraad³, Hannelie Korf¹, Tania Roskams⁴, Schalk van der Merwe^{1,2}, Frederik Nevens^{1,2}, Jef Verbeek^{1,2}. ¹KU Leuven, Laboratory of Hepatology, Belgium; ²University Hospitals Leuven, Department of Gastroenterology and Hepatology, Belgium; ³Leiden University Medical Center, Department of Gastroenterology and Hepatology, Netherlands; ⁴KU Leuven, Department of Imaging and Pathology, Translational Cell and Tissue Research, Belgium
Email: lukas.vanmelkebeke@kuleuven.be

Background and aims: Patients with prior bariatric surgery (BS) are at risk to develop an alcohol use disorder (AUD). We assessed the effect of prior BS on disease profile and outcome of patients with severe alcoholic hepatitis (sAH).

Method: From 01/2008 to 04/2021, consecutive patients admitted to our tertiary referral center with biopsy-proven sAH were included in a prospective database. Student's t-test, Wilcoxon rank sum test and Fisher's exact test were used. A p value <0.05 after multiple testing correction was considered significant.

Results: sAH patients (n = 158) were identified with a median follow-up of 366 (68–1656) days. Out of this cohort, 28 (18%) patients had a history of BS (BS-group): 27 (96%) underwent bypass surgery and 1 patient gastric banding. No patient underwent sleeve gastrectomy. The proportion of patients with BS increased significantly over time reaching a number of 4 (8%) within the first 5 years, 11 (19%) within the following 5 years and 13 (28%) during the last 4 years (p = 0.02) of the follow-up period. An important finding from our analysis was that patients in the BS-group were significantly younger at diagnosis of sAH, were more frequently female, featured an elevated body mass index (BMI) and advanced steatosis upon histological evaluation of the liver biopsy (Table 1). Furthermore, there were no differences in sAH disease severity (histological and Maddrey) or corticosteroid response (Lille score) (Table 1). Importantly, the correlation between BS and a younger age at diagnosis remained significant after correction for sex, steatosis and BMI in a multivariate regression analysis (p <0.001). Notably, survival determined after 28 or 90 days following the onset of sAH remained unchanged (Table 1).

		BS-group (n = 28)	Other (n = 130)	p value
Age*		44.3 ± 8.1	52.4 ± 10.3	0.0005
Sex (male)		8 (30%)	80 (62%)	0.02
BMI*		29.7 ± 4.9	26.6 ± 5.0	0.02
Steatosis	<33% 33–66% >66%	5 (18%) 4 (14%) 19 (68%)	48 (37%) 36 (28%) 45 (35%)	0.03
Polymorphonuclear infiltration	No or mild Severe	2 (7%) 26 (93%)	17 (13%) 113 (87%)	NS
Mallory bodies		28 (100%)	130 (100%)	NS
Ballooning	Occasional Marked	1 (4%) 27 (96%)	13 (10%) 116 (90%)	NS
Maddrey score [§]		56.3 (37.8–75.2)	53.6 (40.6–70.9)	NS
MELD score [§]		23.3 (20.7–29.9)	24.0 (21.1–27.6)	NS
Lille response		14 (74%)	56 (66%)	NS
Survival 28 days		27 (96%)	118 (91%)	NS
Survival 90 days		24 (86%)	91 (70%)	NS

* Mean ± standard deviation; § Median ± interquartile range

Conclusion: The proportion of sAH patients with prior BS has increased 3-fold over the last 15 years. Bypass surgery is independently associated with younger age of sAH onset but not with corticosteroid response or short-term survival. These novel findings indicate the need for early and effective prevention of AUD and sAH in patients who underwent bypass surgery.

THU004

Cyclophilin inhibitor CRV431 as a potential therapy for alcohol-related liver disease

Elena Palma^{1,2}, Sara Campinoti^{1,2}, Una Rastovic^{1,2}, Nicola Harris^{1,2}, Tsing Shue Koay^{1,2}, Lola Ajayi^{1,2}, Bruna Almeida^{1,2}, Sandra Phillips^{1,2}, Daren Ure³, Melissa Preziosi⁴, Marjorie Yumol⁴, Rosa Miquel⁴, Yoh Zen⁴, Andreas Prachalias⁴, Krishna Menon⁴, Nigel Heaton⁴, Luca Urbani^{1,2}, Shilpa Chokshi^{1,2}. ¹The Roger Williams Institute of Hepatology, London, United Kingdom; ²King's College London, Faculty of Life Sciences and Medicine, London, United Kingdom; ³Hepion Pharmaceuticals, United States; ⁴Institute of Liver Studies, King's College London, United Kingdom
Email: e.palma@researchinliver.org.uk

Background and aims: Cyclophilins are peptidyl-prolyl isomerases that facilitate protein folding and regulate several biological processes with isoforms A, B, D being best characterised. Cyclophilin inactivation via therapeutic inhibition or genetic manipulation has been shown beneficial at various stages of liver disease, including steatosis, fibrosis, inflammation, cell injury and in hepatocellular carcinoma. CRV431 is a pan-cyclophilin inhibitor (non-immunosuppressant cyclosporin derivative) that is currently in clinical development for NASH (Phase 2A). Our study aims to evaluate the effects of CRV431 in human experimental models of Alcohol-related Liver Disease (ALD) and on fibrosis in primary hepatic stellate cell (HSC) cultures.

Method: Patient-matched Precision Cut Liver Slices (PCLS) and primary HSCs were prepared from human liver specimens (different fibrotic stages, n = 8). PCLS were exposed to hepatotoxic insults including ethanol 250 mM, fatty acids 0.1 mM, LPS 10 µg/ml individually and/or combined for up to 5 days and HSCs activated with TGF-β1 for up to 10 days, in the presence/absence of 5 µM CRV431. Tissue functionality was evaluated by histology, cytotokeratin-18 release and mitochondrial assays. In PCLS and HSCs, fibrosis/HSC activation status was assessed by gene expression, immunofluorescence and secretion of fibrotic markers. Pro-inflammatory cytokines were quantified by Luminex.

Results: Features of alcoholic steatohepatitis were observed in human PCLS exposed to the insults, and CRV431 profoundly reduced the expression and secretion of pro-fibrogenic markers and restored a balanced cytokine profile. CRV431 alone was not hepatotoxic and did not induce cell death. In HSCs, CRV431 reduced αSMA and collagen deposition/expression when added simultaneously or after TGF-β1 activation. In addition, alignment of collagen fibers deposited by HSCs was significantly affected by the drug treatment.

Conclusion: Our results confirm the role of cyclophilins in liver fibrosis, including HSC activation, collagen deposition and orientation. These data reveal for the first time the potential for the cyclophilin inhibitor CRV431 to reduce ALD-induced fibrosis and suggest the possibility of using this drug as a therapy in ALD patients.

THU005

UK national service evaluation of transplant assessments for patients with alcohol related liver disease

Christopher Oldroyd¹, Varuna Aluvihare², Yun Chew³, Andrew Holt⁴, Steven Masson⁵, Richard Parker³, Neil Rajoriya⁴, Jennifer Ryan⁶, Liz Shepherd⁶, Kenneth J. Simpson⁷, Clare Wai¹, Ian Webzelli², Michael Allison¹. ¹Cambridge Liver Unit, Addenbrooke's Hospital, Cambridge, United Kingdom; ²Institute of Liver Studies, King's College Hospital NHS Foundation Trust, London, United Kingdom; ³The Liver Unit, St James's University Hospital, Leeds, United Kingdom; ⁴The Liver Unit, Queen Elizabeth Hospital, Birmingham, United Kingdom; ⁵The Liver Unit, Freeman Hospital, Newcastle, United Kingdom; ⁶The Sheila Sherlock Liver Unit, Royal Free Hospital, London, United Kingdom; ⁷Scottish Liver Transplant Unit, Royal Infirmary of Edinburgh, Edinburgh, United Kingdom
Email: christopher.oldroyd@nhs.net

Background and aims: Alcohol-related liver disease (ArLD) is responsible for 60% of all liver disease and 84% of liver related

death in the UK. Although we know how many patients with ArLD are registered for a liver transplant, it is not known how many people with ArLD are being assessed for liver transplantation.

Method: Prospective data was collected for all patients with a diagnosis of ArLD assessed at the seven UK liver transplant centres from 1st Aug 2020 to 31st July 2021. This included: gender, age category, indication for transplant, United Kingdom Model for End-Stage Liver Disease Score (UKELD), co-factors for liver disease, duration of abstinence from alcohol at assessment, listing decision and reasons for decline or deferral.

Results: 568 patients were included. Median UKELD was 54 (range 41–76). 144 patients (25%) were female. Median duration of abstinence was 12 months (range 0–240), with 18.4% of assessments having ≤ 6 months abstinence. 329 (58%) were listed for liver transplantation, with 204 (36%) not listed, and 35 (6%) deferred. Indications for assessment were: UKELD ≥ 49 (90%), ascites (32%), hepatic encephalopathy (19%), hepatocellular carcinoma (16%) and other (11%) with most patients having multiple indications. The most common co-factor was non-alcoholic steatohepatitis ($n=57$) with hepatitis C virus infection second most common ($n=24$). Most common reasons for not listing were: medical co-morbidities (29%), potential recoverability (20%), too early to need transplant (19%), active or recent alcohol use (12%), concern about return to harmful drinking (11%) and surgical risk (5%).

Comparing patients listed for transplant with those not listed we noted higher UKELD (Mean 55.66 vs 53.77 $p < 0.001$), longer duration of abstinence (Median 12 vs 11 months $U = 35751$, $p = 0.018$) and no significant differences between gender (Chi Sq $p = 0.258$) or age distribution (Chi Sq $p = 0.53$).

	Patients	Median UKELD (range)	Median months of abstinence (range)	Female
Listed	329	55 (41-74)	12 (3-204)	76 (23.1%)
Not Listed	204	53 (43-76)	11 (0-240)	56 (27.5%)
Deferred	35	54 (45-67)	10 (0-150)	11 (31.4%)
Totals	568	54 (41-76)	12 (0-240)	143 (25.2%)

Conclusion: This study provides a complete representation of all patients with ArLD assessed for liver transplantation over a 12-month period in the UK. Future work is planned to investigate outcomes of patients not listed for transplant and better understand reasons for patients being declined transplantation.

THU006

Fibroblast growth factor 21 is the main alcohol responsive peptide hormone in humans and individuals with alcohol use disorder exhibit increased plasma concentrations after alcohol intake

Amalie Lannig¹, Lærke Gasbjerg^{1,2}, Andrea Sucksdorff¹, Jens Svenningsen³, Samuel Trammell², Tina Vilsbøll^{1,4,5}, Matthew Gillum³, Filip Krag Knop^{1,3,4,5}. ¹Gentofte Hospital, Center for Clinical Metabolic Research, Hellerup, Denmark; ²University of Copenhagen, Department of Biomedical Sciences, Faculty of Health and Medical Sciences, Copenhagen N, Denmark; ³University of Copenhagen, Novo Nordisk Foundation Center for Basic Metabolic Research, Faculty of Health and Medical Sciences, Copenhagen N, Denmark; ⁴Steno Diabetes Center Copenhagen, Herlev, Denmark; ⁵University of Copenhagen, Department of Clinical Medicine, Faculty of Health and Medical Sciences, Copenhagen N, Denmark
Email: amalie.rasmussen.lannig@region.hk

Background and aims: Alcohol use disorder (AUD) is responsible for 5.3% of worldwide deaths annually. The pathophysiology of AUD

remains obscure. Fibroblast growth factor 21 (FGF21) is a liver-derived hormone secreted after alcohol intake. Several lines of evidence suggest that FGF21 inhibits preference for alcohol and reduces alcohol intake. Using plasma proteomics via proximity extension assay technology, we here establish FGF21 as the main alcohol responsive peptide hormone in healthy humans and, further, compare the plasma FGF21 response after an acute alcohol challenge in males diagnosed with AUD, healthy males with paternal AUD, and healthy males without any predisposition to AUD.

Method: Proteomics was evaluated in plasma sampled before and after alcohol intake (0.7 g per kg body weight) in 12 individuals. Subsequently, plasma FGF21 concentrations were evaluated before, during and for 10 hours after alcohol exposure (0.5 g per kg body weight ingested over 10 minutes) in 15 males diagnosed with AUD (Group A), 15 males with paternal AUD (Group B), and 15 males without any predisposition to AUD (Group C). The desire for alcohol was assessed by visual analogue scale.

Results: Out of 1,472 proteins, only 11 changed after alcohol exposure in the 12 individuals, with FGF21 increasing the most (10-fold, $p < 0.0001$) (Fig. 1A). The three groups were similar with regards to age and body mass index, and all participants had normal plasma concentrations of transaminases and bilirubin. Baseline plasma FGF21 concentrations did not differ between groups ($p = 0.10$). Peak plasma concentration of FGF21 was significantly higher in Group A (mean \pm standard deviation: 4.0 ± 0.8 ng/ml) compared to Group C (1.8 ± 0.4 ng/ml) ($p = 0.03$) but not compared to Group B (2.2 ± 0.5 ng/ml) ($p = 0.08$) (Fig. 1B). Area under the curve for FGF21 was greatest in Group A (763 ± 150 ng/ml \times min) followed by Group B (488 ± 120 ng/ml \times min) and Group C (356 ± 77 ng/ml \times min) with borderline statistical significant difference between Group A and C ($p = 0.05$) (Fig. 1B). Group A exhibited a greater desire to drink alcohol than seen in Group B ($p = 0.02$) and C ($p = 0.01$).

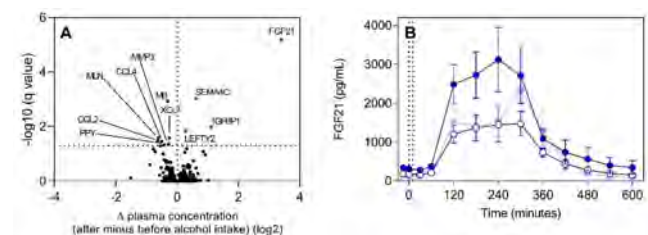


Figure 1. Volcano plot of differences in plasma proteomics before and after alcohol intake in healthy individuals (A). Horizontal dotted line indicates limit of statistical significance, red dots indicate peptides/proteins significantly upregulated by alcohol intake and blue dots indicate peptides/proteins significantly downregulated by alcohol intake. Plasma fibroblast growth factor 21 (FGF21) concentrations after alcohol intake (marked with dotted lines) (B) in individuals with alcohol use disorder (AUD) (Group A, dark blue), healthy individuals with paternal AUD (Group B, light blue) and healthy individuals without predisposition to AUD (Group C, white circles), respectively. CCL2, C-C motif chemokine ligand; IGFBP1, insulin-like growth factor binding protein 1; LEFTY2, left-right determinant factor 2; MB, myoglobin; MLN, motilin; MMP3, matrix metalloproteinase 3; PYY, pancreatic polypeptide; SEMA4C, semaphorin 4C; XCL1, X-C motif chemokine ligand 1. Data and mean \pm standard error of the mean.

Conclusion: We show that FGF21 is the main alcohol responsive peptide hormone in healthy humans and we show greater plasma FGF21 concentrations after alcohol intake in individuals suffering from AUD compared to healthy individuals and individuals predisposed to AUD, respectively, implicating FGF21 in the pathophysiology of AUD.

THU007

Tight junction damage and increased gut permeability in alcohol-related liver disease may be mediated by gut proteases

Charlotte Skinner¹, Julian Marchesi¹, Benjamin H. Mullish¹, Hiromi Kudo¹, Lauren Roberts¹, Haoyu Sun¹, Roberta Forlano¹, Emma Lord¹, Mark Thursz¹, Nikhil Vergis¹. ¹Imperial College London, United Kingdom
Email: cskinner@doctors.org.uk

Background and aims: Recent data have implicated gut-derived virulence factors in the pathogenesis of ArLD. However, it is not clear how virulence factors gain access to portal circulation. We investigated if gut-derived proteases enable bacterial translocation in

POSTER PRESENTATIONS

patients with ArLD including patients with severe alcohol-related hepatitis (sAH).

Method: Protease activity of faecal water (FW) was assayed using fluorescently-labelled casein. Madin Darby Canine Kidney (MDCK) cells grown to confluent monolayers on Transwell plate inserts were used to create a model of gut barrier function validated against CACO-2 cells. FW was applied to the apical surface of the insert and the transepithelial electrical resistance (TEER), a marker of monolayer integrity, was measured at 120 min. *Enterococcus faecalis* (GelE⁺) supernatant served as a high-protease positive control while phosphate buffered solution (PBS) was a negative control. Zymography allowed differentiation of proteases in FW by substrate protein and molecular weight. Next, MDCK cells were grown to confluence on histology slides. FW was applied and the slides fixed and stained for the tight junction protein zonulin-1 (ZO-1). Finally, patient FW aliquots were plated on to protease-indicator agar and the bacterial isolates showing a protease phenotype were taxonomically characterised.

Results: FW samples were obtained from 38 subjects: sAH n = 14, decompensated ArLD n = 11 and control subjects n = 13. Protease activity in FW correlated with change in TEER (Δ TEER) for all subjects ($r = -0.5888$, $p < 0.001$) (Fig. 1). Interestingly, Δ TEER correlated with liver function ($r = -0.472$, $p = 0.0036$ for MELD) with the greatest change in TEER seen in sAH FW samples. Strikingly, a broad-spectrum protease inhibitor added to the FW abolished the correlation between Δ TEER and protease activity ($r = 0.0897$, $p = 0.644$) (Fig. 1) and MELD score ($r = -0.0645$, $p = 0.754$). ZO-1 staining was markedly decreased in slides treated with sAH FW samples vs controls (Fig. 1b+c). Zymography showed the altered pattern of proteases within the FW of sAH patients. Protease-differential agar culture identified *E. faecium*, *S. epidermidis* and *E. coli* as the putative source of proteases responsible for tight junction damage.

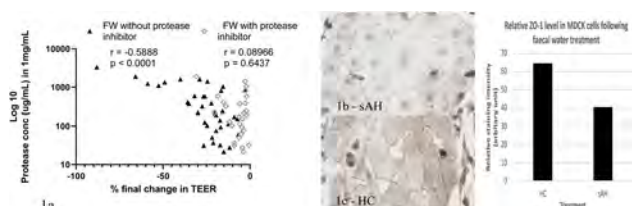


Figure 1: A: TEER change across MDCK monolayers vs protease activity of FW samples with and without a protease inhibitor. B: ZO-1 staining in sAH FW samples. C: ZO-1 staining in control FW samples.

Conclusion: Protease activity in patient FW can cause tight junction damage and increased gut permeability *in vitro* and correlates strongly with liver function. This points to a potential mechanism for gut derived virulence factors to reach the liver in ArLD, and particularly in sAH.

THU008

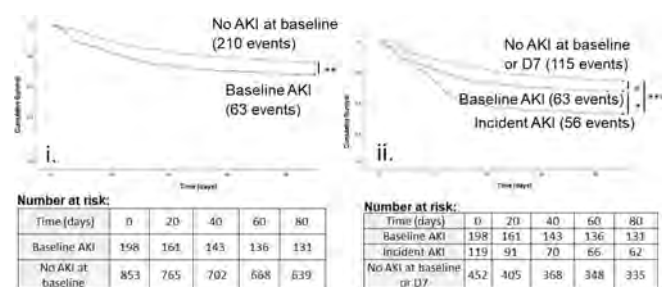
Incident acute kidney injury in severe alcohol-related hepatitis is strongly associated with mortality and can be predicted using micro-RNAs and markers of systemic inflammation

Luke D. Tyson^{1,2}, Stephen Atkinson^{1,2}, Michael Allison³, Andrew Austin⁴, Lily Cross⁵, James Dear⁵, Ewan Forrest⁶, Tong Liu¹, Emma Lord¹, Steven Masson⁷, Joao Nunes⁸, Paul Richardson⁹, Stephen Ryder¹⁰, Mark Wright¹¹, Mark Thursz^{1,2}, Nikhil Vergis^{1,2}.
¹Imperial College London, Department of Metabolism, Digestion and Reproduction, London, United Kingdom; ²St Mary's Hospital, The Liver Unit, London, United Kingdom; ³Addenbrooke's Hospital, Cambridge, United Kingdom; ⁴Royal Derby Hospital, United Kingdom; ⁵University of Edinburgh, United Kingdom; ⁶Glasgow Royal Infirmary, United Kingdom; ⁷Newcastle Freeman Hospital, High Heaton, United Kingdom; ⁸Meso Scale Diagnostics, Gaithersburg, United States; ⁹The Royal Liverpool University Hospital, Liverpool, United Kingdom; ¹⁰Queens Medical Centre, Nottingham, United Kingdom; ¹¹University Hospital Southampton NHS Foundation Trust, United Kingdom
 Email: luke.tyson@nhs.net

Background and aims: Acute kidney injury (AKI) can complicate severe alcohol-related hepatitis (sAH) and has been associated with increased mortality. However, the relative impact of AKI at baseline compared to AKI that develops on treatment has not been evaluated. Moreover, treatments that may modulate the risk of AKI are poorly defined. A range of biomarkers have shown promise to predict the development of AKI, but few have been independently validated in sAH.

Method: Data was available from 1051 sAH patients recruited to the STOPAH trial. AKI was defined by an adapted International Club of Ascites definition as either: an increase in creatinine >26.5 micromol/L above or $1.5\times$ the lowest recorded; creatinine >133 micromol/L; or new renal replacement therapy. Incident AKI was defined as AKI at day 7 without baseline AKI. We compared baseline and incident AKI to 90-day mortality using Kaplan-Meier survival analysis and binary logistic regression. Further, we identified factors associated with baseline and incident AKI by multivariable models. Finally, we tested previously published and novel serum biomarkers and a micro-RNA panel measured by PCR array to predict incident AKI using AUROC analyses.

Results: Baseline AKI was present in 198/1051 (19%) patients and associated with increased D90 mortality (OR 1.42, 95% confidence interval 1.02–2.00, $p = 0.038$). Excluding 282 patients alive at D7 without D7 creatinine available, incident AKI developed in 119/769 (15%) patients and was associated with higher D90 mortality (OR 2.61, 1.72–3.96, $p < 0.001$) and remained associated after adjustment for age and MELD. After adjustment for MELD score, prednisolone was associated with reduction in incident AKI (OR 0.57; 0.37–0.88, $p = 0.011$) but pentoxifylline was not (OR 1.10, 0.72–1.67, $p = 0.656$). Use of beta-blockers at baseline showed a trend to increased incident AKI after propensity-score matching for MELD and systolic blood pressure ($p = 0.063$). Baseline Cystatin C, NGAL, Beta-2 microglobulin and IL-18 were not predictive of incident AKI but TGF- β 2 and IL-8 were strongly associated ($p < 0.001$) and a combination of bilirubin and IL-8 showed AUROC 0.72 ($p < 0.001$) for incident AKI. Several micro-RNAs had AUROC >0.75 , the highest of which was miR-4505 at AUROC 0.78 ($p < 0.006$).



Kaplan-Meier survival curves for patients with severe alcohol-related hepatitis with a baseline acute kidney injury and without (i) and for baseline and incident acute kidney injury and without, excluding those alive at day 7 without creatinine available (ii)
 *Beslov (Generalised Wilcoxon) $P < 0.05$; ** $P < 0.01$; *** $P < 0.001$

Conclusion: Incident AKI is associated with higher 90-day mortality compared to AKI present at baseline in patients with sAH. IL-8 and several micro RNAs, including 4505, show promise as biomarkers and should be validated in independent cohorts.

THU009

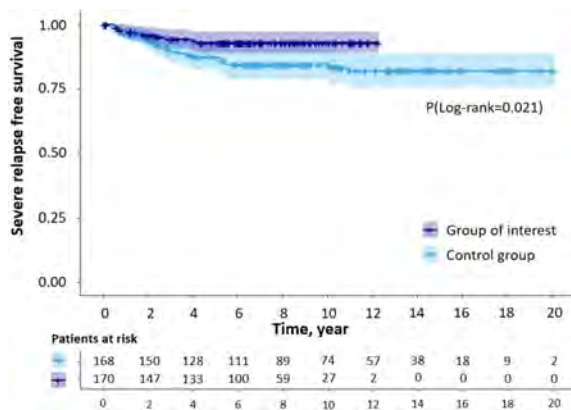
The impact of addiction team integration into the management of patients transplanted for alcohol-related liver disease: results from a multicenter comparative study

Jules Daniel¹, Jérôme Dumortier², Arnaud Del Bello³, Lucie Gamon⁴, Nicolas Molinari⁴, José Ursic-Bedoya¹, Magdalena Meszaros¹, Georges-Philippe Pageaux¹, Hélène Donnadieu-Rigole¹.
¹University Hospital Center Saint Eloi Hospital, Montpellier, France; ²University Hospital Center Édouard Herriot Hospital, Lyon, France; ³University Hospital Center Rangueil Hospital, Toulouse, France; ⁴University Hospital Center La Colombière Hospital, Montpellier, France
 Email: jules.daniel@gmail.com

Background and aims: Alcohol-related liver disease (ALD) is the commonest indication for liver transplantation (LT) in Western Europe. Up to 40% of patients resume alcohol consumption after LT. Severe relapse is associated with a poor prognosis. Specific management of alcohol use disorder could reduce the rate of severe relapse after LT. The aim of this study was to evaluate the effect on prognosis of the integration of an addiction team into an LT center.

Method: This retrospective multicenter study included all adult patients transplanted for "pure" ALD, excluding mixed cirrhosis, between 2000 and 2015 at the three participating centers. Patients transplanted between 2008 and 2015 were managed by an addiction team embedded in the LT team at one of the centers (the interest group), unlike those at the other centers (control group). Propensity score matching (PSM) was performed to minimize differences between groups. The primary outcome was the rate of severe alcohol relapse defined as four or more standard drinks per day for at least 100 consecutive days.

Results: 616 patients were included, 195 of whom received specific addiction follow-up (entire cohort). 79.4% were men, with a mean age of 55.4 years. 58.3% had Child-Pugh C cirrhosis, their median MELD score was 19, and 32.7% had HCC. The median follow-up was 9 years, 6.6 years in the interest group and 11.1 years in the control group. The survival rate of the entire cohort was 97.4%, 83.8%, and 70.1% at 1, 5, and 10 years, respectively. After 1:1 PSM, 170 pairs were created (matched cohort) comparable for age, gender, smoking history, duration of pre-LT abstinence ± 6 months, cardiovascular risk factors, and MELD and Child-Pugh scores. Addiction follow-up was significantly associated with a reduced risk of severe alcohol relapse (6.5% vs. 15.5%; HR = 0.33, 95% CI 0.16–0.69; $p = 0.0033$) and the occurrence of severe cardiovascular events (10.0% vs. 20.0%; OR = 0.39, 95% CI 0.20–0.79; $p < 0.001$). There were no significant differences in terms of mortality (HR = 1.00; $p = 0.99$), occurrence of *de novo* cancer (21.7% vs. 24.7%; OR = 0.86; $p = 0.17$), HCC recurrence (15.7% vs. 10.7%; OR = 1.67; $p = 0.32$), or alcohol-related graft cirrhosis (5.1% vs. 3.5%; OR = 1.60; $p = 0.41$) between the two groups.



Conclusion: In this multicenter study of a large cohort of patients transplanted for ALD, addiction follow-up was associated with a decrease in severe alcohol relapse.

THU010

Risk of fractures and subsequent mortality in alcohol-related cirrhosis: a nationwide population-based cohort study

Axel Wester¹, Nelson Ndegwa², Hannes Hagström¹. ¹Karolinska Institutet, Department of medicine Huddinge, Stockholm, Sweden;

²Karolinska Institutet, Department of medical epidemiology and biostatistics

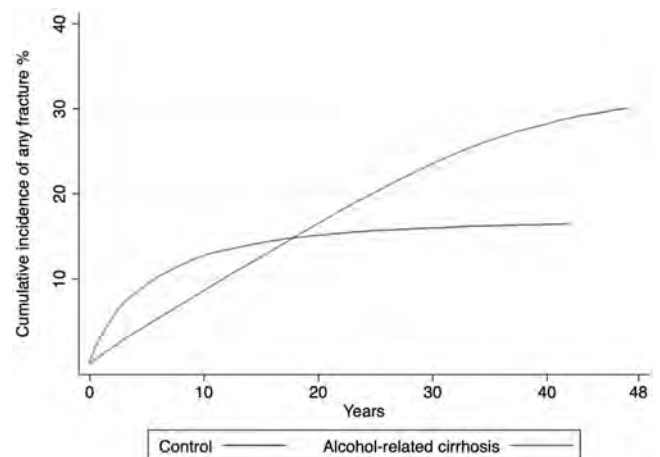
Email: axel.wester@ki.se

Background and aims: Alcohol-related cirrhosis is linked to an increased risk of fractures. However, fracture risk assessments on a

national level for this population are scarce. The aim was to evaluate the risk of fractures and post-fracture mortality in patients with alcohol-related cirrhosis compared to individuals from the general population.

Method: In this nationwide population-based cohort study, data were retrieved from the Swedish National Patient Registry on 23, 847 patients with alcohol-related cirrhosis from 1969 to 2016. Patients were matched for sex, age, and municipality with 229, 907 controls from the Swedish Total Population Registry. Cox regression models were fitted to investigate the risk of any fracture and post-fracture mortality in patients with a fracture during follow-up. The cumulative incidence of fractures was calculated while accounting for the competing risks of death or liver transplantation.

Results: A total of 47, 375 fractures occurred during 3, 410, 949 person-years of follow-up. Patients with alcohol-related cirrhosis had a higher incidence of fractures (35.9 per 1000 person-years) than matched controls (13.3 per 1000 person-years; adjusted hazard ratio [aHR] 3.6, 95% confidence interval [CI] 3.5–3.8). Results were consistent for osteoporotic fractures, fractures due to high-energy trauma, and all fracture sites. The cumulative incidence of fractures was higher for patients the first 18 years of follow-up, with a 5-year risk of 9.4% compared to 4.5% for controls. The post-fracture mortality rate was elevated in patients with alcohol-related cirrhosis compared to controls who also experienced a fracture at both 30 days (aHR 1.5, 95% CI 1.3–1.8) and 1 year (aHR 1.6, 95% CI 1.5–1.8).



Conclusion: Alcohol-related cirrhosis is associated with a more than threefold increased fracture rate, resulting in a higher cumulative incidence of fractures the first two decades after initial diagnosis. In addition, alcohol-related cirrhosis is associated with a higher post-fracture mortality rate. Preventive interventions to reduce modifiable fracture risk factors in this population are justified.

THU011

Use of statins among patients with cirrhosis due to alcohol-related liver disease-a danish nationwide cohort study

Anna Marine Sølling Ramsing¹, Frederik Kraglund¹, Peter Jepsen¹.

¹Aarhus University Hospital, Department of Hepatology and Gastroenterology, Aarhus N, Denmark

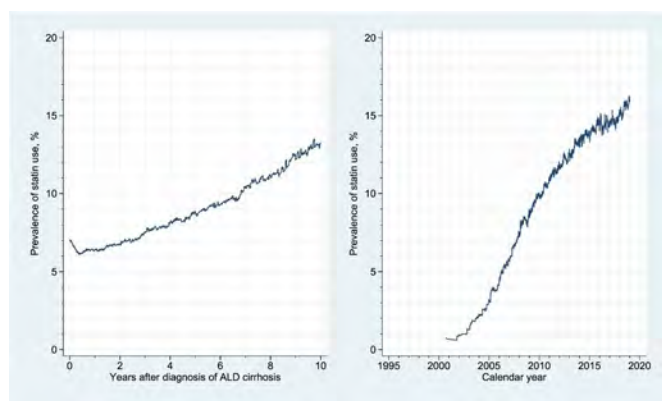
Email: marine.ramsing@me.com

Background and aims: Statins reportedly increase the survival of patients with cirrhosis due to alcohol-related liver disease (ALD cirrhosis) but may be underutilized due to fear of hepatotoxicity. It remains unclear how many patients with ALD cirrhosis use statins, and which factors predict statin initiation. We aimed to examine time-trends in prevalence of statin use and predictors of statin initiation among patients with ALD cirrhosis.

POSTER PRESENTATIONS

Method: Using data from the Danish healthcare registries, we conducted a nationwide cohort study, including all Danish citizens receiving their first diagnosis of ALD cirrhosis (ICD-10: K703 and K704) between 1995 and 2018. We examined how the prevalence of statin use has changed during this period and used Cox regression to identify predictors of statin initiation.

Results: During the 1995 to 2018 period, we identified 30723 patients, of whom 7% used statins at the time of cirrhosis diagnosis, and 4% became first-time statin users within 5 years after cirrhosis diagnosis. The prevalence of statin use rose sharply during the 1995–2018 period, reaching more than 15% in late 2018 (Figure). Factors predicting a higher probability of initiating statin use after diagnosis of ALD cirrhosis included diabetes (hazard ratio [HR] = 2.21, 95% CI: 1.85–2.65) and cardiovascular disease (HR = 2.97, 95% CI: 2.19–4.03), and compensated cirrhosis (HR = 1.40, 95% CI: 1.25–1.55). Socio-economic predictors included living with a partner (HR = 1.17, 95% CI: 1.06–1.30) as opposed to living alone, low educational attainment, i.e., primary school (HR = 1.22, 95% CI: 1.04–1.43) or secondary school (HR = 1.23, 95% CI: 1.05–1.44) as opposed to higher education, and older age (HR = 1.18 for every ten-year increase in age, 95% CI 1.11–1.24). Employment status and sex were not statistically significant predictors.



Conclusion: Use of statins has become common practice among patients with ALD cirrhosis in Denmark. Predictors of initiating statin use were diabetes, cardiovascular disease, compensated cirrhosis, living with a partner, low educational attainment, and older age.

THU012

Antibody response to gut microbiome bacteria in human alcoholic liver disease

Antonella Putignano^{1,2}, Shilpee Sharma², Anaïs Thiriard², Dalila Lakhoulfi³, Yiwei Jiang², Anne Botteaux³, Eric Trépo¹, Delphine Degré¹, Christophe Moreno¹, Thierry Gustot¹, Arnaud Marchant². ¹CUB Erasme Hospital, Dept of Gastroenterology, Hepato-Pancreatology and Digestive Oncology, Bruxelles, Belgium; ²Institute for Medical Immunology, ULB-Campus Erasme, Brussels, Belgium; ³Molecular Bacteriology Laboratory, ULB-Campus Erasme, Brussels, Belgium
Email: antonella.putignano@erasme.ulb.ac.be

Background and aims: Hypergammaglobulinemia (H-IgG) is a feature of chronic liver disease (CLD) but its origin remains poorly understood. Translocation of microbiome components could trigger B cells to produce microbiome-specific (M)-IgG and thereby stimulate the formation of immune complexes that could contribute to cirrhosis-associated immune dysfunction (CAID). Systems serology (SS) provides a global approach to profile antigen specific antibodies and their relationship with clinical outcomes. The aims of the study were to investigate the contribution of M-IgG to the H-IgG of CLD and

to characterize their biophysical and functional features using a SS approach.

Method: A cohort of patients affected by alcoholic liver disease (ALD), including steato-fibrosis (n = 49), compensated cirrhosis (n = 54), decompensated cirrhosis (n = 64) and severe alcoholic hepatitis (n = 45) was studied. Fifty healthy adults were included as controls. Biophysical (titers, isotype, subclass, IgG Fc fragment glycosylation) and functional-antibody-dependent complement deposition (ADCD), macrophage phagocytosis (ADCP) and neutrophil phagocytosis (ADNP) and NK cell activation (ADCA)-features of M-IgG (*E.Coli*, *S.Aureus*, *St.Salivarius*, *E.Foecalis*) were investigated, and compared to vaccine (Diphtheria Toxoid, Tetanus Toxoid) antigen-specific (V)-IgG as control of passed antigen-exposure.

Results: Patients with ALD showed increased titers of M-IgG, M-IgG1 and M-IgG2 as compared to healthy controls. M-specific antibody titers correlated with H-IgG. Patients with ALD also had higher M-specific ADCD than healthy controls and levels of ADCD correlated with titers of M-IgG. The highest M-IgG titers and ADCD levels were observed in patients with decompensated cirrhosis or with severe alcoholic hepatitis. In contrast, similar levels of M-specific ADCP, ADNP and ADCA were detected amongst the ALD groups, suggesting an altered functional profile. The increased titers of M-specific antibodies in ALD patients were not associated with increased titers of V-specific antibodies and V-IgG did not correlate with H-IgG. Patients with ALD also had higher proportions of fucosylated and agalactosylated total IgG Fc as compared to healthy controls.

Conclusion: These results indicate that the H-IgG observed in ALD patients involves an increased production of antibodies directed against microbiome antigens. The biophysical features (subclass, Fc glycans) of M-IgG and their potent complement activation potential could promote inflammation and thereby contribute to the pathogenesis of ALD.

THU013

Socio-economic factors and healthcare setting are independently associated with medium and long-term outcomes from alcohol-related hepatitis

Joshua Lambert¹, Nikhil Vergis², Michael Allison², Andrew Austin², Ewan Forrest², Emma Lord², Steven Masson², Paul Richardson², Stephen Ryder², Mark Wright², Mark Thursz², Stephen Atkinson². ¹Imperial College School of Medicine, London, United Kingdom; ²Imperial College London, London, United Kingdom
Email: joshua.lambert17@imperial.ac.uk

Background and aims: Socio-economic factors are known to influence outcomes in liver disease but the impact in severe alcohol-related hepatitis (sAH) is unknown. Similarly, the healthcare setting where a patient is treated can modify outcomes in various diseases but its impact in sAH has not been studied. Here, we investigate the impact of these two factors on medium and long-term outcomes in sAH.

Method: Data was available from 1092 sAH patients enrolled in the STOPAH trial. Variables measured comprised education, housing, employment, relationship status, Index of Multiple Deprivation (IMD) and treating hospital setting. The latter was categorised as transplant, tertiary and secondary care centres using the British Society of Gastroenterology National Liver Disease Survey 2011. Multivariable logistic regression models were fitted for two distinct time periods: medium-term mortality between hospital admission to 90 days; and long-term mortality from 90 to 365 days (806 patients). Statistical adjustments were made for age, MELD and drinking status. Models were fitted using all available data plus data generated by multiple imputation for missing MELD scores and drinking status.

Results: In the medium-term, there was no association between IMD and 90-day mortality on univariate analysis; however adjustment for age and MELD revealed a significant independent association (OR, 1.16; 95% CI: 1.01–1.34). In the medium-term, treatment at a transplant centre was associated with a reduction in 90-day mortality

in univariate (OR, 0.61; 95% CI: 0.38–0.95) and adjusted models (OR, 0.47; 95% CI: 0.28–0.78). In the long-term, leaving education at 19 or older was the only factor associated with a reduced risk of death at 365 days compared to leaving education at 16 or younger in univariate (OR, 0.55; 95% CI: 0.30–0.94) and adjusted models (OR, 0.56; 95% CI: 0.30–0.97).

Logistic regression analysis for Index of Multiple Deprivation and healthcare settings for 90-day mortality.

Variable	Univariate Analysis OR 95% CI p	Adjusted Model OR 95% CI p
Index of Multiple Deprivation*	1.0357 0.9132-1.1782 0.5886	1.1601 1.0064-1.3433 0.0435
Service		
Secondary centre	1.0000 (Reference)	1.0000 (Reference)
Tertiary centre	0.7212 0.5318-0.9724 0.0336	0.7531 0.5378-1.0487 0.0958
Transplant centre	0.6075 0.3753-0.9534 0.0355	0.4731 0.2768-0.7829 0.0047

Associations are expressed as odds ratios (ORs) with 95% confidence intervals (CI) and p values (p) before (Univariate) and after adjustment for age and MELD (Adjusted).

*ORs are quoted per quintile change in Index of Multiple Deprivation, ranging from five (most deprived) to one (least deprived).

Conclusion: Socio-economic factors and type of healthcare facility in which an AH patient is treated are associated with medium and long-term survival outcomes. These findings reinforce the need to reduce health inequalities in alcohol-related liver disease.

THU014

Sex-related differences in outcomes in alcohol-related cirrhosis following an episode of hepatic decompensation do not explain subsequent management inequalities

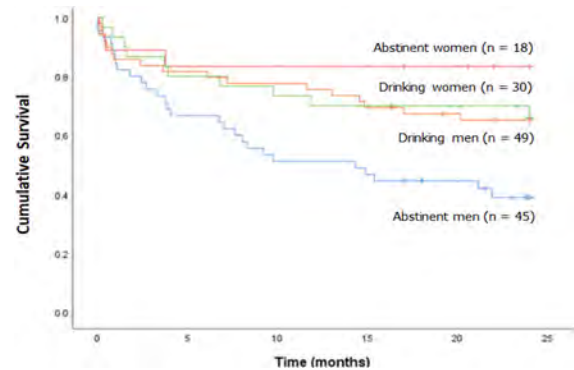
Aaminah Mohammed¹, Nora Khattab¹, Clive Jackson², Jennifer Ryan³, Marsha Morgan¹. ¹UCL Institute for Liver and Digestive Health, Division of Medicine, Royal Free Campus, University College London, London, United Kingdom; ²Department of Clinical Neurophysiology, Royal Free Hospital, Royal Free NHS Foundation Trust, London, United Kingdom; ³Department of Gastrointestinal and Liver Services, Royal Free Hospital, Royal Free NHS Foundation Trust, London, United Kingdom
Email: marsha.morgan@ucl.ac.uk

Background and aims: There is evidence of sex-differences in the management of patients with alcohol-related cirrhosis to the detriment of the 30% who are female. Thus, women are less likely to be selected for liver transplantation; are 10% more likely to be delisted and have higher wait-list mortality rates (Cullaro *et al*, Am J Transplant 2018;18:1214). Erroneous assumptions about the natural history of alcohol-related cirrhosis in women may underlie these observed management inequalities. The aims of this study were to: (i) determine resolution and survival rates following an episode of hepatic decompensation, by sex; and, (ii) identify possible predictors of outcome.

Method: All patients with a primary diagnosis of alcohol-related cirrhosis admitted to the Royal Free Hospital in 2016 and 2018 with an episode of hepatic decompensation were reviewed. Patients who survived the index admission were followed for 24-months post discharge specifically in relation to their drinking behaviour, rates of hepatic recompensation and survival. Rates of recompensation were assessed using Box plots to map out the changes in MELD and Child Pugh scores by sex and drinking behaviour. Kaplan Meier curves were plotted to measure differences in survival by sex and drinking behaviour; data were censored at death, transplantation or end of follow-up; the Mantel-Cox test was used to determine significance. Cox regression analyses were used to identify variables which were significant predictors of survival.

Results: The study cohort comprised of 142 patients with cirrhosis (median [range] age: 54 [30–87] years; 66% men). During the follow-up period 79 (56%) people continued to drink excessively while 63 remained abstinent or else consumed alcohol at low risk levels. There was no significant difference in the proportions of men and women who continued to misuse alcohol (62.5% vs. 52.1%). There were no significance differences in the rates of recompensation, determined by changes in the MELD and Child Pugh scores, by sex or drinking behaviour. Fifty-one of the 142 (35.9%) patients died during a median

follow-up of 23.5 (0–24) mo. The overall mean survival in women was significantly longer than in men (18.9 mo vs. 15.7 mo; $p=0.034$). There was no difference in survival between the men and women who continued to drink (18.1 mo vs. 18.0 mo) but women who drank little or nothing survived significantly longer than their male counterparts (20.2 mo vs. 13.4 mo; $p=0.002$) (Figure). Age and the Child-Pugh score were the only independent predictors of survival.



Conclusion: Women with decompensated cirrhosis have similar recovery rates to their male counterparts but significantly better survival rates. Thus, the sex-related inequalities in disease management likely reflect undue bias and need to be urgently addressed.

THU015

Influence of comorbidities and lifestyle factors on health-related quality of life in alcohol-related liver disease: a population-based survey

Karen Dombestein Elde¹, Natasja Von Wövern², Matilde Winther-Jensen³, Cathrine Lau³, Lone Madsen², Peter Jepsen⁴, Gro Askgaard^{2,3,4}. ¹Førde Central Hospital, Department of Internal Medicine, Førde, Norway; ²Zealand University Hospital, Section of Gastroenterology and Hepatology, Medical Department, Køge, Denmark; ³Bispebjerg and Frederiksberg Hospital, Center for Clinical Research and Prevention, Copenhagen, Denmark; ⁴Aarhus University Hospital, Department of Hepatology and Gastroenterology, Aarhus, Denmark
Email: karen_d_e@hotmail.com

Background and aims: Health-related quality of life (HRQoL) is impaired in alcohol-related liver disease (ALD). We examined the effects of extra-hepatic comorbidities, alcohol, and smoking on HRQoL in ALD and whether low HRQoL influenced survival.

Method: We used health registers to identify patients with ALD and comparators without ALD among the participants in the Danish National Health Surveys 2010–2017. Survey data on HRQoL (12-item Short Form), comorbidities, alcohol consumption, alcohol use disorder (CAGE score ≥ 2), and smoking was linked with vital statistics through 2020. Associations of comorbidities, alcohol, and smoking with poor HRQoL (Z-score <1.5) in ALD were studied with multivariable logistic regression adjusting for liver disease severity, age and sex. We calculated adjusted hazard ratios (HR) of mortality until 2020 according to stated HRQoL.

Results: Poor physical and mental HRQoL were found in 37% and 22% of 772 ALD patients compared to 10% and 9% of 4319 comparators. Asthma/COPD, cancer, disc herniation, and osteoarthritis were associated with poor physical QoL in ALD, whereas diabetes and cardiovascular diseases were not (Figure 1). Osteoarthritis, alcohol use disorder, and smoking >20 cigarettes/day were associated with poor mental HRQoL. Both poor physical and poor mental QoL were associated with higher mortality rates [HR 1.6 (95% CI: 1.3–2.0) and HR 1.4 (95% CI: 1.1–1.8)] in ALD.

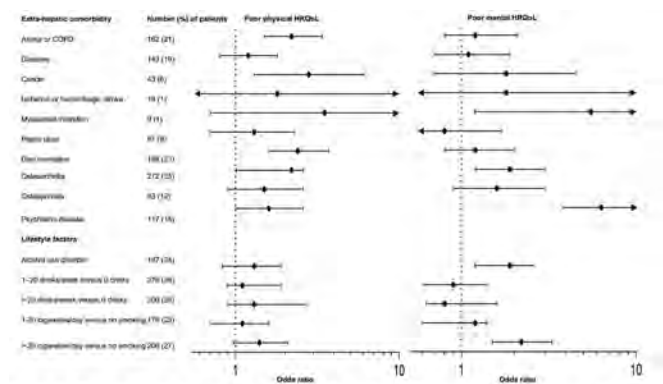


Figure 1. Odds ratios for poor health-related quality of life (HRQoL) scores according to comorbidities and lifestyle factors in patients with alcohol-related liver disease participating in the National Health Survey 2010, 2013, and 2017. Analyses are mutually adjusted and further adjusted for severity of liver disease, age and sex. N = 772

Conclusion: Respiratory and musculoskeletal diseases, cancer, alcohol use disorder, and smoking are associated with poor HRQoL in ALD. Poor HRQoL decrease survival in ALD. These findings should raise physicians' awareness on potentially modifiable factors affecting quality of life and survival in ALD patients.

THU016

Patient and system-level factors underline offering and acceptance of alcohol use disorder therapy in veterans with cirrhosis

Rahul Chaudhari¹, Nikki Duong¹, Shreesh Shrestha¹, Neerav Dharia¹, Bryan Badal¹, James Wade¹, Linda Chia², Patrick Spoutz², Ernesto Robalino Gonzaga², Shari Rogal², Jasmohan S Bajaj¹. ¹Virginia Commonwealth University and Richmond VAMC; ²Pittsburgh VA Medical Center

Email: jasmohan.bajaj@vcuhealth.org

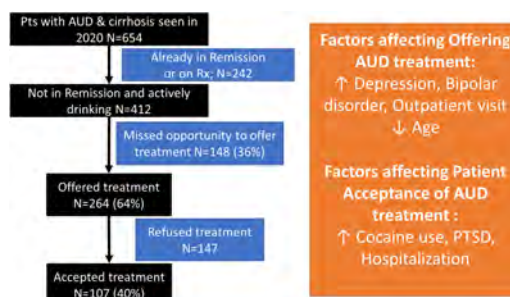
Background and aims: Cirrhosis with continued alcohol use disorder (AUD) is linked with poor outcomes. AUD Rx is efficacious, but a recent study showed only 12% of Veterans with AUD and cirrhosis received it. The reasons behind this are unclear.

Aim: Define patient, and system-level factors associated with AUD Rx.

Method: Veterans seen in 2020 with 2 ICD codes for cirrhosis/complications+AUD at 3 large VA centers were evaluated. Data regarding demographics, mental health comorbidities, and cirrhosis severity were collected, and an in-depth chart review performed to collect AUD Rx settings and details. Determinants of lack of uptake were examined using logistic regression.

Results: We included 654 pts with AUD and cirrhosis (95% men, 64.3 yrs, 56% white, 8% Hispanic). Common mental health conditions on chart review were depression 47%, PTSD 24%, anxiety 17%, cocaine use 25%, bipolar 5% and cannabis use disorder 19%. Cirrhosis decompensation was seen in 19%. **AUD Rx history:** 5% had received prior AUD medications, 24% got behavioral therapy, and 11% both. The remaining 60% were not on prior AUD Rx. At baseline, 24% (n = 174) were noted in the chart to be in AUD remission, while the remaining 76% had ongoing alcohol use (Figure). **Course:** Most pts were seen by primary care, hepatology, or both (48%, 5%, 35%); 28% were hospitalized in 2020. **AUD Rx discussion:** Of the 412 patients not on Rx or in remission at baseline, AUD Rx offered to 264 (64%). Most Rx offers were made in the outpatient setting (n = 207) then in inpatients (n = 30). This was most often offered by primary care (n = 162), hepatology (n = 45), or both (n = 41); fewer were offered Rx through mental health (n = 19). The factors significantly associated with AUD treatment offer in the regression model included depression (OR 1.58 95% CI 1.01–2.48, p = 0.05), bipolar disorder (3.0, 1.1–8.4, p = 0.03), seen as outpts (6.8, 3.3–14.3, p < 0.0001), and younger age (OR/yr 0.96, 0.94–0.99, p = 0.003). Decompensation, gender, race, ethnicity, hospitalizations, or decompensation were not significantly associated with Rx offer. **Patient acceptance:** Of the 264 pts offered AUD Rx, 40%

agreed. Most Rx initiated was behavioral (n = 78), medication (N = 13) or both (n = 39). On regression, patients who were offered and accepted, were more likely to have PTSD (OR 2.1, 1.1–4.0, p = 0.03), cocaine disorder (2.3, 1.3–4.1, p = 0.004) and were offered Rx as inpatients (2.6, 1.5–4.7, p = 0.001).



Conclusion: Most Veterans with cirrhosis and AUD with opportunities to engage were offered AUD Rx but missed opportunities remain. Younger outpatients with co-occurring psychiatric disorders were more likely to be offered AUD Rx. When offered, Rx was accepted by only 40% of Veterans, especially inpatients and those with concomitant PTSD/cocaine abuse disorder. While system and patient-related factors are linked with Rx offers and initiation, in these three centers most eligible Veterans with cirrhosis were offered AUD Rx.

THU017

24-Norursodeoxycholic acid ameliorates experimental alcoholic liver disease in both preventive and therapeutic settings

Christoph Grander¹, Moritz Meyer¹, Daniel Steinacher², Thierry Claudel², Felix Grabherr¹, Julian Schwärzler¹, Timon Adolph¹, Michael Trauner², Herbert Tilg¹. ¹Medical University Innsbruck, Department Internal Medicine I; ²Medical University of Vienna, Department of Medicine III

Email: christoph.grander@i-med.ac.at

Background and aims: Alcoholic liver disease (ALD) is the hepatic manifestation of alcohol overconsumption. Ethanol toxicity, systemic pro-inflammatory cytokines as well as the intestinal microbiota contribute to the progression of ALD. 24-Norursodeoxycholic acid (norUDCA) is a side chain shortened UDCA with potent choleretic properties and therapeutic effects in non-alcoholic liver disease and primary sclerosing cholangitis. Therefore, we hypothesized that norUDCA could ameliorate experimental ALD.

Method: Female *wildtype* mice were fed an ethanol-containing diet (Lieber-DeCarli diet) or pair-diet for 15 days. Two different settings of experiments were performed: First, the diet was supplemented with 1 mg/ml norUDCA starting from day one. In a second experiment, mice received norUDCA (1 mg/ml) starting from day ten, mimicking a therapeutic approach.

Results: Ethanol-feeding resulted in hepatic injury, displayed by elevated ALT concentration, increased number of TUNEL⁺ hepatic cells, indicating augmented apoptosis and hepatic steatosis. NorUDCA treatment diminished ALT levels (p < 0.001), reduced the number of TUNEL⁺ cells (p < 0.05) and decreased hepatic steatosis compared to ethanol-fed controls. Moreover, the hepatic mRNA expression of pro-inflammatory cytokines like *Tnf-alpha* (p < 0.001), *Il-1beta* (p < 0.01), *Il-6* (p < 0.001) and *Il-10* (p < 0.01) was significantly reduced by norUDCA treatment in ethanol-fed mice. Important to note, systemic ethanol concentration was not altered by norUDCA administration. NorUDCA treatment enhanced bile acid metabolism in ethanol-fed mice, displayed by increased gall bladder weight (p < 0.001), circulating bile acids (p < 0.001) and the mRNA expression of hepatic *Sult2a1* (p < 0.001), *Mrp4* (p < 0.001) and *Cyp7a1* (p < 0.001), important regulators in bile acid metabolism. Interestingly,

norUDCA induced hepatic Ppar-gamma in ethanol-fed mice, which could mechanistically explain the observed protective effects. In a second experiment we tested the efficacy of norUDCA in a therapeutic setting. In ethanol-fed mice the administration of norUDCA for 5 days resulted in a 45% reduction of ALT concentration. Furthermore, the hepatic mRNA expression of *Tnf-alpha* ($p < 0.05$) and *Il-6* ($p < 0.05$) was significantly decreased in ethanol-fed norUDCA treated mice compared to ethanol-fed mice.

Conclusion: NorUDCA ameliorates hepatic inflammation and steatosis in experimental ALD and could serve as a therapeutic agent for ALD in the future.

THU018

Impact of sex and recurrence in the prognosis of alcoholic hepatitis

Jordi Gratacós-Gines¹, Manuel Rodríguez², Alvaro Giráldez-Gallego³, Joaquín Cabezas⁴, Inmaculada Fernández Vázquez⁵, Meritxell Ventura Cots⁶, Diana Horta⁷, Jordi Sánchez-Delgado⁸, Silvia Acosta-López⁹, Tomás Artaza Varasa¹⁰, David Martí-Aguado¹¹, Vanesa Bernal Monterde¹², Rosa Martín-Mateos¹³, Ana Clemente¹⁴, Javier Tejedor-Tejada¹⁵, Jose Pinazo Bandera¹⁶, Margarita Sala¹⁷, Esther Badia-Aranda¹⁸, Victoria Aguilera Sancho¹⁹, Santiago Tomé²⁰, Conrado Fernández-Rodríguez²¹, Joan Caballería¹, Elisa Pose¹.

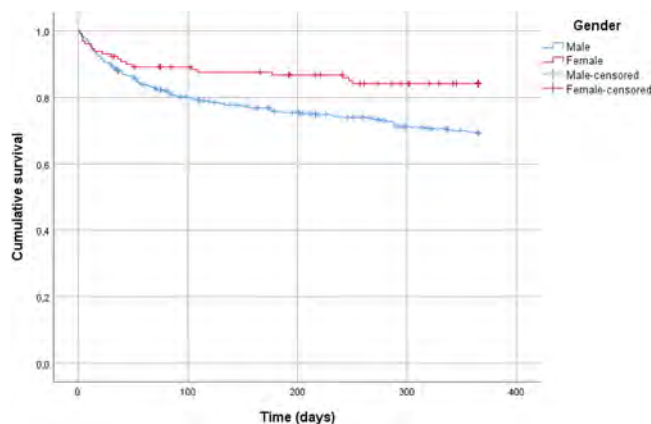
¹Hospital Clínic de Barcelona, Liver Unit, Barcelona, Spain; ²Central University Hospital of Asturias, Oviedo, Spain; ³Virgen del Rocío University Hospital, Sevilla, Spain; ⁴Marqués de Valdecilla University Hospital, Santander, Spain; ⁵University Hospital October 12, Madrid, Spain; ⁶Hospital Universitari Vall d'Hebron, Barcelona, Spain; ⁷Hospital Universitari MútuaTerrassa, Terrassa, Spain; ⁸Hospital Parc Taulí de Sabadell, Sabadell, Spain; ⁹Our Lady of Candelaria University Hospital, Santa Cruz de Tenerife, Spain; ¹⁰Virgin Health Hospital, Toledo, Spain; ¹¹Hospital Clínic Universitari, València, Spain; ¹²Hospital Universitario Miguel Servet, Zaragoza, Spain; ¹³Hospital Ramón y Cajal, Madrid, Spain; ¹⁴Gregorio Marañón Hospital, Madrid, Spain; ¹⁵Hospital Universitario de Cabueñes, Department of Gastroenterology, Gijón, Spain; ¹⁶Hospital Universitario Virgen de la Victoria, Málaga, Spain; ¹⁷Hospital Universitari de Girona Doctor Josep Trueta, Girona, Spain; ¹⁸Burgos University Hospital, Burgos, Spain; ¹⁹La Fe University and Polytechnic Hospital, Valencia, Spain; ²⁰Santiago Clinic Hospital CHUS, Santiago de Compostela, Spain; ²¹Hospital Universitario Fundación Alcorcón, Alcorcón, Spain
Email: EPOSE@clinic.cat

Background and aims: alcoholic hepatitis (AH) is a clinical syndrome characterized by recent onset of jaundice in the context of heavy alcohol use that bears a high mortality. Current studies on AH point female sex as associated with poorer prognosis. Also, information on prognosis and clinical features of recurrent AH is scarce. The aims of this registry were to gain knowledge on the epidemiology, clinical presentation and mortality of AH in Spain, with special focus on the influence of sex and recurrent AH.

Method: retrospective multicentric Spanish registry of hospitalized cases of AH from 2014 to 2020 including 20 centers. Criterion for inclusion was to meet the defined criteria for "probable HA" of the National Institute of Alcohol Abuse and Alcoholism (NIAAA). Clinical, alcoholological, demographic and prognostic data of the cohort were recorded.

Results: Five hundred twenty-five patients were included. The majority were men (72%) with a median age of 51 and about half of them had no previous history of liver disease (51%). Most cases presented with hepatic decompensation of established cirrhosis (61%), mainly ascites and encephalopathy, and had important impairment in liver function (median MELD score 21). As for diagnosis of AH, liver biopsy was performed in 124 cases (21%); pathology was consistent with the clinical diagnosis in most of them (79%). There were 351 cases of severe AH (63%). Corticosteroids were prescribed in 229 patients (65%); enteral nutrition and pentoxifylline were also used (20% and 9%), while 23% of patients remained without

specific treatment. Regarding mortality, 134 patients (26%) had died after one year, 51% of them during the index hospitalization. In the multivariate analysis, only male sex, older age, MELD score and failure to withdraw alcohol remained independently associated with mortality. Interestingly, women had significantly higher survival at one year (85% vs 71%, $p < 0.05$). These differences were more pronounced in the subset of severe AH (79% vs 62%, $p < 0.05$). No differences between men and women were found regarding liver function, alcohol withdrawal or corticosteroid treatment. Twenty-nine patients (5.5%) presented recurrent episodes of AH. Compared to patients with no recurrence, patients with recurrent AH were more frequently men (93% vs 72%, $p < 0.05$) and there was a trend to lower survival (83% vs 92%, $p = 0.091$).



Conclusion: AH in a large European cohort typically features young men, presenting with acute decompensation. Recurrent AH was not exceptional, especially in men, and was associated with a trend to higher mortality, which highlights the relevance of alcohol withdrawal and clinical follow-up in this population. In our series, women had higher survival rate; this finding questions the latest studies suggesting poorer prognosis in this group and deserves further investigation.

THU019

Hepatocyte-derived biomarkers concentrations predict liver-related events within 2 years in patients with Child-Pugh class A alcohol-related cirrhosis

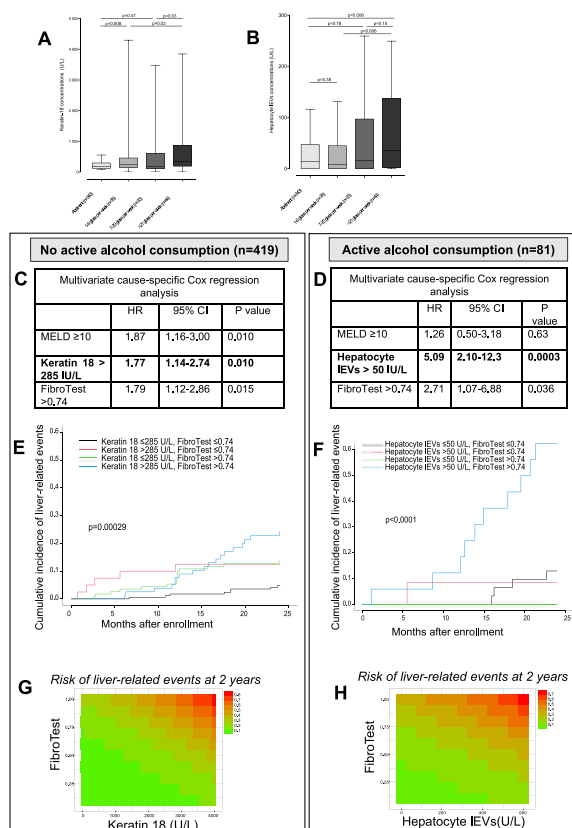
Laure Elkrief¹, Nathalie Ganne-Carrié², Hana Manceau³, Marion Tanguy⁴, Nathalie Barget⁵, Cendrine Chaffaut⁶, Shantha Valainathan⁷, Alix Riescher⁷, Katell Peoch³, Thierry Poynard⁸, Sylvie Chevret⁶, Pierre-Emmanuel Rautou⁷. ¹Tours University Hospitals, Hepatogastroenterology, France; ²Hôpital Avicenne, Liver Unit, France; ³Hôpital Beaujon, Service de Biochimie, France; ⁴Inserm, Centre de recherche sur l'inflammation, France; ⁵Hôpital Avicenne, Centre de ressources biologiques, France; ⁶APHP Hôpital saint Louis, Service de Biostatistique et Information médicale, France; ⁷Hôpital Beaujon, Liver Unit, France; ⁸Université Sorbonne Paris, France
Email: laure_elkrief@yahoo.fr

Background and aims: Keratin-18 and hepatocyte derived large extracellular vesicles (IEVs) concentrations reflect disease activity in patients with liver disease, and are therefore attractive biomarkers. Their ability to predict liver-related events in patients with alcohol-related cirrhosis is unknown. The aim of the present study was to evaluate the usefulness of hepatocyte-derived biomarkers, alone or combined with MELD and FibroTest, to predict liver-related events in patients with Child-Pugh class A alcohol-related cirrhosis, taking into account the reported alcohol consumption status.

Method: We measured plasma keratin-18 and hepatocyte IEVs concentrations in 500 patients with Child-Pugh class A alcohol-related cirrhosis, from the prospective multicenter CIRRAL cohort

study. Primary end point was liver-related events at 2 years. Since the course of liver disease is largely influenced by alcohol consumption, patients were separated according to reported active alcohol consumption at enrollment (i.e. ≥ 7 glasses/week) or not. Cumulative incidence of liver-related events was estimated using the nonparametric cumulative incidence function, considering hepatocellular carcinoma and liver-unrelated deaths as competing events; in patients without active alcohol consumption at enrollment, alcohol relapse was considered as an additional competing event.

Results: Both keratin-18 and hepatocyte IEVs concentrations increased with alcohol consumption (Fig A and B). In patients without active alcohol consumption at enrollment (n = 419), keratin-18 concentration predicted liver-related events at 2 years, independently of FibroTest and MELD (Fig C). Patients with both keratin-18 concentration >285 U/L and FibroTest >0.74 had a 24% cumulative incidence of liver-related events at 2 years, versus 5% to 14% in patients with other combinations of these two markers (Fig E, G). Similar results were obtained when combining keratin-18 concentration >285 U/L with MELD ≥ 10 (not shown). In patients with active alcohol consumption at enrollment (n = 81), hepatocyte IEVs concentrations predicted liver-related events at 2 years, independently of FibroTest and MELD (Fig D). Patients with both hepatocyte IEVs concentration >50 U/L and FibroTest >0.74 had a 62% cumulative incidence of liver-related events at 2 years, versus 8% to 13% for patients with other combinations of these two markers (Fig F, H). Combining hepatocyte IEVs concentration >50 U/L with MELD >10 had a lower discrimination ability (not shown).



Conclusion: In patients with Child-Pugh class A alcohol-related cirrhosis, combining hepatocyte-derived biomarkers with FibroTest or MELD score identifies patients at high-risk of liver-related events, and could be used for risk stratification and patient selection in clinical trials.

THU020

Dynamic multiomics analysis characterizes circulating molecular determinants associated with poor outcome in patients with severe alcoholic hepatitis

Jaswinder Maras¹, Adil Bhat^{1,2}, Nupur Sharma¹, Manisha Yadav¹, Gaurav Tripathi¹, Babu Mathew¹, Vasundhara Bindal¹, Shvetank Sharma¹, Rakhi Maiwall³, Shiv Kumar Sarin³. ¹Institute of liver and biliary sciences, Molecular and Cellular Medicine, New Delhi, India; ²University of California, Los Angeles, Pathology and Lab Medicine, Los Angeles, United States; ³Institute of liver and biliary science, Hepatology, New Delhi, India
Email: jassi2param@gmail.com

Background and aims: Severe alcoholic hepatitis (SAH) has high morbidity, with steroid therapy providing 65% 28-day survival. Steroid non-responders (NR) have higher incidence of infections and mortality. Faecal microbiota transplant (FMT) is another emerging therapy for SAH patients. We investigated whether multi-omic studies and machine learning (ML) approaches could identify non-responders to corticosteroid or FMT at baseline.

Method: Thirty SAH patients who were randomized in an on-going steroid vs. FMT protocol (Gov-no.NCT03091010) received either prednisolone (40 mg/day- 7 days, responders for 4weeks, n = 13) or FMT (daily through nasoduodenal tube for 7 days, n = 17). Multi-omic analysis was performed on blinded serial plasma samples collected at baseline, day-7 and day-28. Molecular determinants linked with non-response (NR) to steroid or FMT therapies were identified and validated for survival outcomes in a separate set of 70 SAH (NR = 21) patients using artificial neural networking (ANN) and ML.

Results: Baseline characteristics of derivative and validation cohorts were comparable. FMT treatment temporally increased amino-acid metabolism, primary bile-acid biosynthesis, energy metabolism and cori cycle metabolites (p < 0.05). Steroid therapy temporally induced vitamin and fat metabolism (p < 0.05). Circulating meta-proteome alpha/beta diversity was temporally increased by FMT with increase in bacterial species; orientia, geobacter and streptococci. Steroid therapy added (p < 0.05) desulfovibrio, clostridiales and other species at day 28. Compared with steroid therapy, FMT significantly reduced inflammatory metabolic pathways [arachidonic acid and tryptophan metabolism, TLR and immune-cell activation, complement cascade and prostaglandin synthesis (p < 0.05)] and increased antioxidant, vitamins, neurotransmitters signalling and energy metabolism (p < 0.05). Multi-omics profile of non-survivors was distinct, FMT non-survivors compared to survivors, showed highest alpha-diversity with increase in actinobacteria and firmicutes (p < 0.05). Using multi-omics integration along with ANN and ML, specific molecular clusters were identified in non-survivors. Cluster-1 specific to complement, coagulation and leukotriene biosynthesis, cluster-3 (P38-MAPK) in the FMT arm and cluster-7 (complement, TLR activation) in the steroid arm significantly predicted mortality (Norm Imp > 95%, AUC>0.90, log-rank<0.01). Of these clusters;>3Fold increase in molecules; CD44, 3-Oxosteroid and Proteobacteria; Ecoli for FMT and protoporphyrinogen-IX, MYCBP2, Proteobacteria; rhizobium for steroid arm were associated to higher mortality (AUC>0.95; log-rank<0.01).

Conclusion: Baseline levels of panel; CD44, 3-Oxosteroid, proteobacteria; E.coli, rhizobium protoporphyrinogen-IX and MYCBP2 can predict NR and non-survival in SAH patients.

Paradigm for multi-omics integration and biomarker identification in SAH

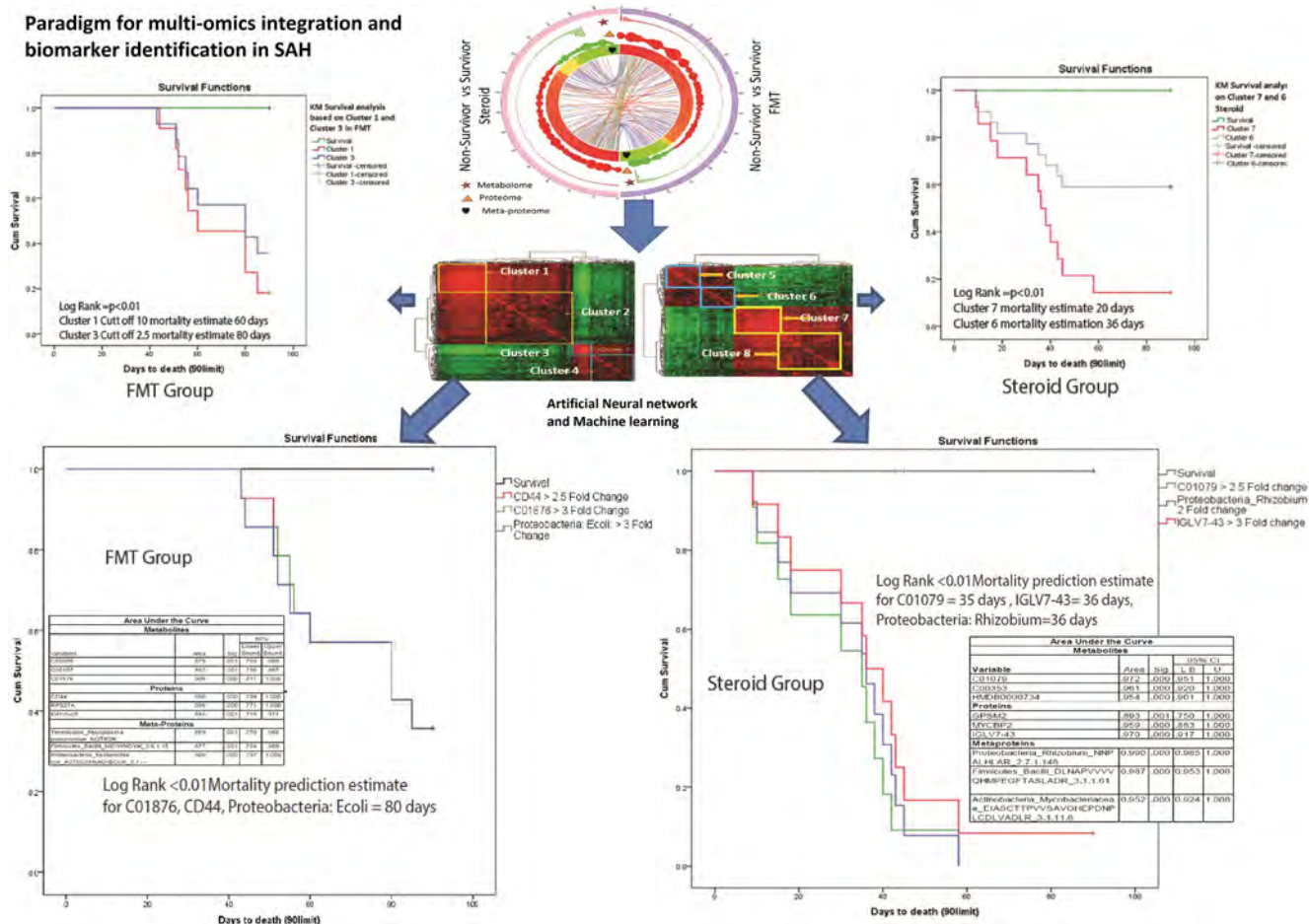


Figure (abstract: THU020)

THU021

Alcohol-induced changes of inflammatory markers in hepatic and systemic venous blood in early alcohol-related and non-alcoholic fatty liver disease

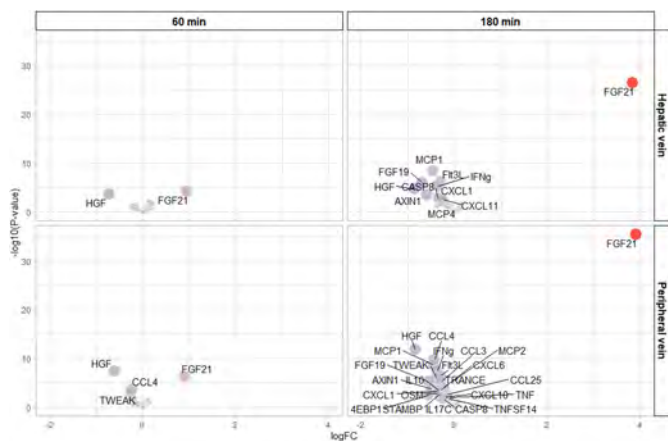
Evelina Stankevici¹, Mads Israelsen^{2,3}, Helene Bæk Juel¹, Anne Lundager Madsen¹, Nikolaj Torp^{2,3}, Stine Johansen^{2,3}, Camilla Dalby Hansen^{2,3}, Katrine Prier Lindvig^{2,3}, Bjørn Stæhr Madsen^{2,3}, Maja Thiele^{2,3}, Aleksander Krag^{2,3}, Torben Hansen¹. ¹The Novo Nordisk Foundation Center for Basic Metabolic Research, København, Denmark; ²Odense University Hospital, Department of Gastroenterology and Hepatology, Odense C, Denmark; ³University of Southern Denmark, Department of Clinical Research, Faculty of Health Sciences, Odense C, Denmark
Email: evelina@sund.ku.dk

Background and aims: Alcohol consumption is believed to increase intestinal permeability, leading to inflow of pathogens and other immune-activating compounds to the liver. Further, alcohol intake is known to suppress the immune system, and is related to an increased risk of systemic infections. Taken together, these factors could play a central role in the initiation of hepatic inflammation, an important step in the development and progression of alcohol-related liver disease (ALD). We aimed to investigate the effects of alcohol consumption on inflammatory markers in hepatic and systemic venous blood in people with ALD, non-alcoholic fatty liver disease (NAFLD) and healthy controls.

Method: We included 40 participants with three distinct hepatic phenotypes: 15 with ALD, 15 with NAFLD and 10 healthy controls. All participants received 2.5 ml of 40% ethanol per kg body weight,

infused over 30 minutes via a nasogastric tube. Ninety-two circulating inflammatory cytokines were quantified using the Target-96 'Inflammation' panel from Olink Proteomics, in plasma samples obtained from two sites (hepatic and systemic vein), at three time points (0, 60 and 180 min). Linear (mixed) models were used and significant results ($p < 0.05$) reported after correcting for False Discovery Rate (FDR).

Results: At baseline, 31 cytokines were differentially expressed in the ALD group and 16 in the NAFLD group, when compared to the healthy group. Alcohol induced changes for 2 cytokines at 60 min and 11 cytokines at 180 min in hepatic venous blood, and for 4 cytokines at 60 min and 24 cytokines at 180 min in systemic venous blood, in all three groups combined. Fibroblast growth factor 21 (FGF-21) was the only cytokine that increased during the observation period. Hepatocyte growth factor (HGF) was the first cytokine (after 60 min) to decrease in hepatic venous blood, while the concentration of 8 additional cytokines dropped within three hours (Figure showing volcano plots (upregulated (red) and downregulated (blue) cytokines in hepatic and systemic circulation after 60 and 180 min. The X axis-log fold change and Y axis-log₁₀ p value from a linear mixed model. Cytokines, significantly different after alcohol intoxication at FDR 5% are labeled)). Moreover, the concentration of 19 cytokines was different in hepatic vein, when compared to systemic vein.



Conclusion: Our findings indicate that while ALD and NAFLD are associated with an increased concentration of inflammatory cytokines at baseline, acute alcohol consumption dampens the hepatic and systemic inflammatory response, which might affect the ability of the liver to deal with pathogens arriving from the portal vein. Differences in cytokine concentrations between hepatic and systemic vein suggests direct hepatic production or sequestration of these cytokines, respectively, further highlighting the central role of the liver in systemic inflammation.

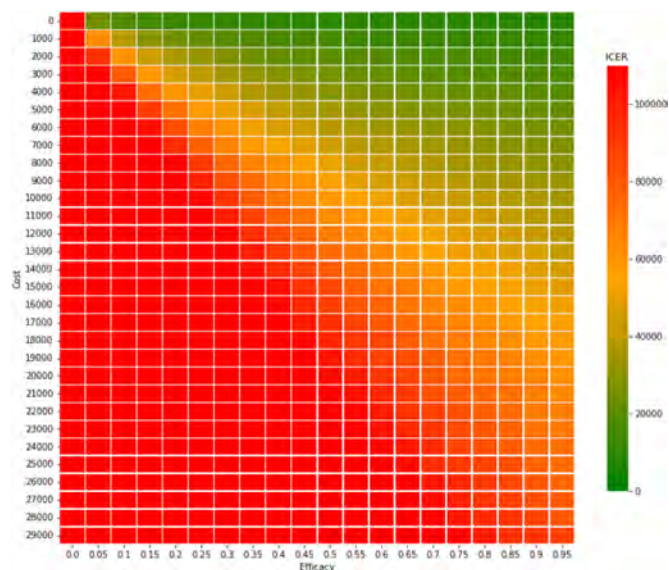
THU022

New treatment for alcohol-related liver disease: combinations of efficacy and treatment cost required for cost-effectiveness

Maja Thiele¹, Davit Khlgatyan², Lars Asphaug³, Stine Johansen⁴, Hans Olav Melberg². ¹Odense University Hospital, University of Southern Denmark; ²University of Oslo, Department of Health Management and Health Economics; ³University of Oslo, Department of Health Management and Health Economics, Oslo, Norway; ⁴Odense University Hospital, University of Southern Denmark, Department of Gastroenterology and Hepatology
Email: maja.thiele@rsyd.dk

Background and aims: Alcohol-related liver disease (ALD) has a poor prognosis, with a 5-year survival rate below 50%, and substantial costs for the healthcare system with no effective treatment currently available. Recently, accurate diagnostic tools have allowed for early detection of ALD, further enabling the development of targeted interventions. Without an idea of future value, and by extension the likelihood of eventual reimbursement, producers and research funders may have less incentive to focus on this opportunity. We, therefore, aimed to identify the relationship between required efficacy and the cost of a potential new treatment for early ALD needed to achieve uptake into clinical practice.

Method: We simulated excessive drinkers with advanced fibrosis over their lifetime using a mathematical computer model. Two scenarios were applied: 1) no treatment (current standard) and 2) a progression-halting treatment modelled on a possible novel treatment in an ongoing trial. Model input data was in the no-treatment scenario sourced from the literature and a prospective Danish natural history study and the currently unknown treatment efficacy (reduced risk of progression)-and cost (USD) was simulated over a vast range of possible values. The simulation allowed the identification of pairs of treatment efficacies and costs resulting different ratios of incremental costs to incremental effectiveness (ICERs) compared to current management (Figure).



Results: In countries with a willingness-to-pay threshold of \$ 50, 000, treatments halting progression in ALD at the fibrosis stage is cost-effective upon reaching 30% efficacy contingent on annual treatment costs not exceeding \$ 5, 000, or 60% efficacy if costs are less than \$ 10, 000 per annum. In the UK, where willingness to pay per quality-adjusted life-year is between 20 and 30 000 £, progression-halting treatments should reach an efficacy of 60% at an annual cost between £ 3000 and £ 5000 to be considered cost-effective.

Conclusion: Our results are useful for research funders and producers of new treatments for ALD in determining to reimburse or develop a new treatment for advanced liver fibrosis in patients with alcohol-related liver disease. The calculated ICERs can be interpreted across different healthcare systems with varying levels of cost-effectiveness thresholds.

THU023

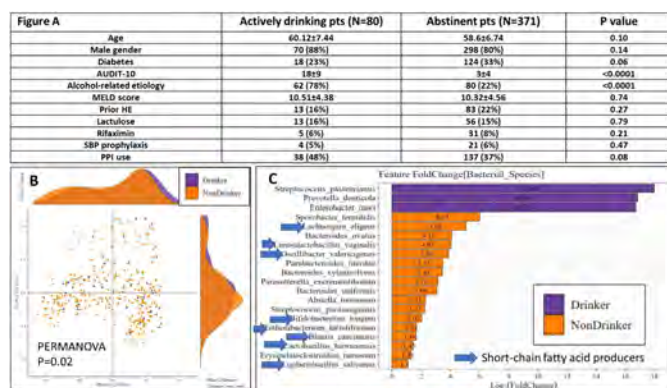
Active alcohol misuse is linked with lower short-chain fatty acid producing microbiota in a matched study of 450 patients with cirrhosis

Jasmohan S Bajaj¹, Amirhossein Shamsaddini², Masoumeh Sikaroodi², Brian Davis¹, Puneet Puri¹, Michael Fuchs¹, Andrew Fagan¹, Sara McGeorge¹, Patrick Gillevet². ¹Virginia Commonwealth University and Richmond VAMC; ²George Mason University
Email: jasmohan.bajaj@vcuhealth.org

Background and aims: Alcohol use disorder (AUD) alters gut microbiota and can lead to cirrhosis development. However, cirrhosis, regardless of etiology is also linked with microbial change. Several AUD pts continue to drink despite the development of cirrhosis but the interaction between active alcohol misuse and cirrhosis is unclear. Bacterial products such as short-chain fatty acids (SCFAs) can strengthen the intestinal barrier and promote abstinence in a small FMT trial. Aim: Determine the impact of active alcohol misuse on gut microbial structure and function in the background of cirrhosis.

Method: Outpts with cirrhosis diagnosed on biopsy, fibroscan or prior decompensation underwent stool collection while drinking habits (AUDIT-10), demographics, cirrhosis severity and medication use were collected. Active drinkers were matched with non-drinkers with respect to cirrhosis details and demographics. Non-drinkers had to be abstinent for ≥6 mths before stool collection. Microbiota structure was analyzed using 16SrRNA sequencing and predicted function using PiCRUST between actively drinking and non-drinking pts.

Results: We enrolled 451 patients with cirrhosis (MELD 10.3 ± 4.5 , Age 58.8 ± 6.8 , 80 actively drinking pts). They were matched 1:4 with at least 320 non-drinkers (Fig A). Groups were similar on demographics, cirrhosis details and medications apart from AUDIT-10 and alcohol-related etiology, which were higher in actively drinking patients. **Alcohol use:** Actively drinking subjects had constant drinking habits without binges. Abstinent pts had been abstinent for 15 ± 8 years before enrollment. **Microbiota composition:** β -diversity was different between groups (Fig B) but Shannon diversity was statistically similar. Prevotella, Enterobacter and Streptococcus spp were higher while potentially beneficial taxa belonging to Eubacterium, Bifidobacterium, Blautia, Roseburia, Alistipes, and Lactobacillus were lower in active drinkers. Short-chain fatty acid producing taxa specifically propionate and butyrate were lower in active drinkers (Fig C). **Microbiota predicted function:** Propanoate metabolism-related enzymes, which are also associated with branched amino acid degradation were higher in patients who were drinking (3-hydroxyisobutyrylCoA hydrolase and methylmalonylCoA carboxytransferase).



Conclusion: SCFA producing microbiota, especially butyrate and propionate metabolism, were significantly lower in actively drinking patients with cirrhosis compared to abstinent patients despite matching for demographics, cirrhosis severity and medication use. SCFAs could have a link with continued alcohol intake in this advanced population.

THU024

Infections are common in patients with early alcohol-related liver disease and increases the risk of death

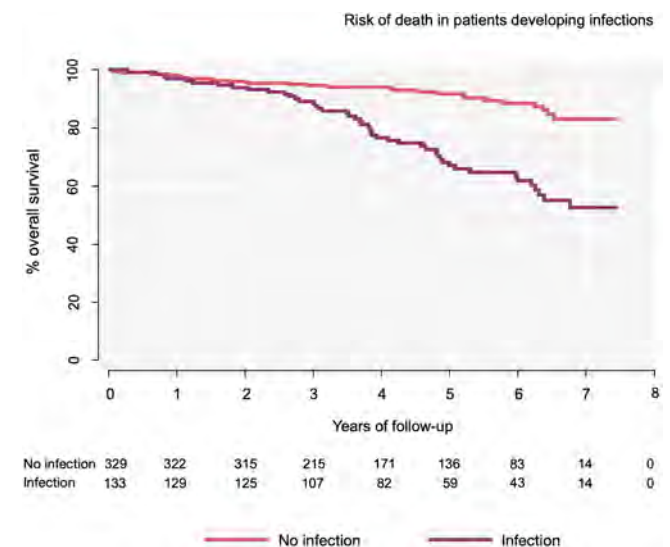
Stine Johansen^{1,2}, Simon Langkjær Sørensen^{1,2}, Ditlev Nytoft Rasmussen^{1,2}, Mads Israelsen^{1,2}, Katrine Prier Lindvig^{1,2}, Maria Kjærgaard^{1,2}, Johanne Kragh Hansen^{1,2}, Camilla Dalby Hansen^{1,2}, Katrine Thorhauge^{1,2}, Nikolaj Torp^{1,2}, Peter Andersen^{1,2}, Sönke Detlefsen^{2,3}, Helene Bæk Juel⁴, Torben Hansen⁴, Aleksander Krag^{1,2}, Maja Thiele^{1,2}. ¹Odense University Hospital, Department of Gastroenterology and Hepatology, Denmark; ²University of Southern Denmark, Department of Clinical Research, Denmark; ³Odense University Hospital, Department of Pathology, Denmark; ⁴University of Copenhagen, Novo Nordisk Foundation Center for Basic Metabolic Research, Denmark
Email: stine.johansen@rsyd.dk

Background and aims: Infections are frequent in patients with alcohol-related liver cirrhosis and worsen prognosis. We hypothesized that this also applies in earlier stages of alcohol-related liver disease (ALD). We therefore aimed to examine 1) the incidence of infections in patients with early ALD, 2) risk factors associated with developing infections, and 3) the impact of infections on the risk of liver-related events and all-cause mortality.

Method: We performed a prospective cohort study of patients from primary and secondary care with a history of excess alcohol intake,

excluding patients with decompensation or competing aetiologies for liver disease. At baseline, we performed liver biopsies along with clinical investigations. During follow-up, we reviewed patients' electronic healthcare records for infections, liver-related events, all-cause mortality, and alcohol intake.

Results: We included 462 patients with a mean age of 57 ± 10 years, 76% males, with fibrosis stage F0-1/F2/F3-4 = 259/107/96. During a median follow-up of 54 months (IQR 35–76), 133 patients (29%) developed a total of 307 infections with a median of two infections each (range 1–3). Seventy-six % of infections were treated during hospitalization, most frequently pneumonia (103/307, 34%) and urinary tract infections (56/307, 18%). In approximately half of all infections cultures were obtained, and the most common isolated bacterium was *Escherichia coli*. Liver stiffness measured by transient elastography was a stronger predictor of infections than fibrosis stage, consequently excessive drinking during follow-up and transient elastography were the only independent predictors of infections in multivariable regression (hazard ratio (HR) 2.08; 95%CI 1.33–3.27, and HR 1.87; 1.54–2.28). Eighty-seven patients (19%) developed a liver-related event during follow-up and 60 of these patients had 147 infections in total. Patients who developed at least one infection had a significantly increased risk of death (HR 3.36; 95%CI 2.12–5.33, $p < 0.001$), but not of developing a liver-related event (HR 1.35; 95% CI 0.84–2.15, $p = 0.22$). Infections increased the risk of death independent of baseline fibrosis stage and liver stiffness.



Conclusion: In patients with early alcohol-related liver disease, infections are frequent and worsen prognosis. Risk of infections increases with liver disease severity and ongoing harmful use of alcohol.

THU025

Abstinence is associated with better outcome in patients with hepatocellular carcinoma

Adeline Donati¹, Jean Henrion², Maxime Regnier³, Pierre Deltenre^{1,4,5}, Astrid Marot¹. ¹CHU UCL Namur, Department of Gastroenterology and Hepatology, Yvoir, Belgium; ²Hôpital de Jolimont, Department of Gastroenterology and Hepatology, Haine St Paul, Belgium; ³CHU UCL Namur, Department of biostatistics, Yvoir, Belgium; ⁴Clinique St Luc Bouge, Department of Gastroenterology and Hepatology, Namur, Belgium; ⁵CUB Hopital Erasme Université Libre de Bruxelles, Department of Gastroenterology, Hepatopancreatology and Digestive Oncology, Bruxelles, Belgium
Email: astridmarot@gmail.com

Background and aims: Data suggest that patients with alcohol-related hepatocellular carcinoma (HCC) have a reduced survival as

POSTER PRESENTATIONS

compared to those with nonalcohol-related HCC. The role of abstinence in this setting is unknown. We aimed to compare access to treatment and prognosis of patients with alcohol-related HCC and nonalcohol-related HCC and to evaluate the impact of abstinence.

Method: All patients with HCC were retrospectively included in a single center during a 23-year period. Abstinence was defined as discontinuation of alcohol consumption at least 3 months before HCC diagnosis in patients with alcohol-related cirrhosis. Treatment by resection, ablation, and transplantation were considered curative. Multivariate Fine and Gray proportional hazards models were used to identify factors associated with 5-year overall mortality after adjustment for the lead-time bias. A logistic regression model was used to identify factors associated with access to curative treatment.

Results: 200 patients were included, 114 (57%) with nonalcohol-related HCC and 86 (43%) with alcohol-related HCC of whom 35 were abstainers and 51 were consumers. All of them had a cirrhosis. During a median follow-up of 14 months (95%CI: 11–16), 12 patients were transplanted and 156 died. At HCC diagnosis, consumers were younger as compared to abstainers and non-alcoholic patients (59 vs. 63 vs. 68 years, $p = 0.001$), had a worse liver function (MELD score: 11 vs. 10 vs. 8, $p = 0.01$, Child-Pugh score: 6 vs. 5 vs. 5, $p = 0.02$), were less likely to be screened for HCC (33% vs. 74% vs. 51%, $p < 0.001$) and had more frequently a metastatic disease (16% vs. 0% vs. 6%, $p = 0.02$). After adjustment for the lead-time bias, the 5-year cumulative incidence rates of overall death were significantly lower in abstainers than in consumers and in non-alcoholic patients (51.5% vs. 78.4% vs. 80.5%, respectively, $p = 0.04$). In multivariate analyses, while abstainers were significantly associated with lower overall mortality as compared to consumers (HR: 0.47, 95% CI 0.28–0.80, $p = 0.005$), patients with nonalcohol-related cirrhosis and consumers had similar overall mortality (HR: 0.86, 95% CI 0.60–1.24, $p = 0.4$). The proportion of patients who received a curative treatment was 65% in abstainers, 44% in consumers and 57% in non-alcoholic patients ($p = 0.1$). In multivariate analyses, preserved liver function (Child A vs. B/C, OR: 3.10 95% CI 1.58–6.26, $p = 0.001$) and adherence to a screening program (OR: 4.96, 95% CI 2.50–10.15, $p < 0.001$) were the only two factors associated with a better accessibility to curative treatment.

Conclusion: Abstinence improves the outcome of patients with alcohol-related HCC because of better liver function, less advanced tumour disease and better adherence to screening.

THU026

In severe alcohol-related hepatitis, hepatocyte ballooning correlates with expression of p16 and components of a secretory phenotype that has been associated with cellular senescence

Nikhil Vergis¹, Isabelle Hall¹, Callum Arthurs¹, Hiromi Kudo¹, Stephen Atkinson¹, David Shapiro², Michael Lutz², Birgit Jung², Markus Weissbach², Wolfgang Albrecht², Luke D. Tyson¹, Tong Liu¹, Emma Lord¹, Lars Zender³, Mark Thursz¹, Robert D. Goldin¹. ¹Imperial College, United Kingdom; ²HepaRegeniX GmbH, Tuebingen, Germany; ³University Hospital Tuebingen, Klinik für Medizinische Onkologie and Pneumologie, Germany
Email: nvergis@imperial.ac.uk

Background and aims: Poor outcome in severe alcohol-related hepatitis (sAH) is frequently attributed to failure of hepatic regeneration. This may be due to lack of trophic factors, inability of hepatocytes to proliferate and/or the induction of stable cell cycle arrest known as senescence. Senescent cells undergo morphological changes that may be consistent with the hepatocyte ballooning found in steatohepatitis. Here, we investigate the potential causes of regenerative failure in sAH and seek evidence for markers of senescence in ballooned hepatocytes.

Method: Data was available from 731 AH patients with sAH recruited to the STOPAH trial, 37 compensated cirrhotic patients (CLD) and 64 healthy controls (HC). We evaluated serum levels of the senescence associated secretory phenotype (SASP) for a range of trophic factors (HGF, EGF, IGF, VEGF, TWEAK) plus inflammatory and/or pro-

regenerative cytokines (IL1b, IL6, IL8, IL10, IL22, and TNFa). Immunohistochemistry was used to identify cell proliferation (Ki67) and senescence (p16) in liver biopsy sections ($n = 29$). HandE stains were used to differentiate occasional from marked ballooning of hepatocytes. Digital image analysis was used to quantify staining and a nuclear morphology algorithm attributed stains to individual cell types.

Results: p16⁺ hepatocytes were more frequent in sAH compared to control tissue without steatohepatitis ($p < 0.05$). Moreover, in sAH tissue expression of p16 on hepatocytes strongly associated and co-localized with ballooned hepatocytes ($p = 0.005$, Figure 1). In contrast, no correlations were seen in cholangiocyte p16 expression nor with Ki67 expression in any cell type. Components of a secretory phenotype consistent with the SASP (serum IL1, IL6, IL8, TNFa, HGF, EGF, TWEAK) were associated with hepatocyte ballooning ($p < 0.05$ for all). Serum bilirubin was higher in patients with marked ballooning ($p = 0.0003$) but prothrombin time was not ($p = 0.24$). Strikingly, HGF levels were >7-fold higher in sAH vs HC and CLD ($p < 0.001$) and correlated with both baseline MELD ($r = 0.21$, $p < 0.001$) and Lille score ($r = 0.16$, $p < 0.001$). Conversely, EGF was lower in sAH vs HC vs CLD ($p < 0.001$) and in sAH patients who died within 28 ($p = 0.01$) and 90 days ($p = 0.003$) compared to sAH patients who survived.

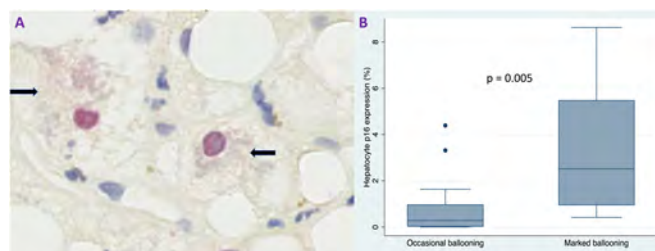


Figure: **A.** representative immunohistochemistry of two ballooned (black arrows) p16⁺ (red) hepatocytes. **B:** Comparison of hepatocyte p16 expression in sAH liver biopsy samples with marked vs occasional hepatocyte ballooning

Conclusion: Serum proteins implicated in hepatocyte regeneration and senescence are associated with clinical outcome in sAH. p16⁺ hepatocytes are prevalent and are strongly associated with hepatocyte ballooning in sAH liver biopsies. Further characterization of the senescent properties of p16⁺ cells may stimulate senolytic or SASP-modulating therapies in sAH.

THU027

Targeting cyclin M4 as a new therapeutical approach to treat alcoholic liver disease

Irene González-Recio¹, Naroa Goikoetxea¹, Rubén Rodríguez Agudo¹, Jorge Simón Espinosa¹, Marina Serrano-Macia¹, Mikel Azkargorta², Felix Elortza², Irene Diaz-Moreno³, Antonio Diaz-Quintana³, Ute Schaeper⁴, Ramon Bataller⁵, Matías A Avila⁶, Luis Alfonso Martínez-Cruz¹, María Luz Martínez-Chantar¹. ¹CIC bioGUNE, Liver Disease Lab, Derio, Spain; ²CIC bioGUNE, Proteomics platform, Derio, Spain; ³Instituto de Investigaciones Químicas (IIQ), Sevilla, Spain; ⁴Silence Therapeutics GmbH, Berlin, Germany; ⁵University of Pittsburgh, Department of medicine, Pittsburgh, United States; ⁶CIMA, Hepatology program
Email: mlmartinez@cicbiogune.es

Background and aims: An excessive alcohol consumption is a main reason of chronic liver disease and liver-related deaths in Western countries and causes alcoholic liver disease (ALD), featured by fatty liver, alcoholic hepatitis (AH), cirrhosis and liver cancer. Approximately 50% of liver cirrhosis cases caused by alcohol abuse, result in 3.3 million deaths. Today, there are no effective treatments other than abstinence or liver transplantation for end-stage ALD. Acute and chronic alcohol consumption are associated with a decrease in liver Mg²⁺ content. The underlying mechanisms remain

unknown. The alteration of Mg^{2+} levels in ALD and the key role of Mg^{2+} transporters in enabling the flux of Mg^{2+} across cell membranes, have prompted us to investigate the role of cyclin M4 in ALD. In this context, the inhibition of CNM4 by RNA interference emerge as a new therapeutic approach for ALD.

Method: The expression of CNNM4 was studied in ALD patients, in primary hepatocytes under ethanol exposure and in mice under chronic and binge ethanol feeding (the NIAAA model). Primary hepatocytes were treated with a GalNAc siRNA targeting *Cnnm4* to evaluate the effect of silencing *Cnnm4* in hepatocytes exposed to 50 mM EtOH for 12 h, 24 h and 36 h. NIAAA model mice were divided into 2 groups after day 5 of the diet and treated with a control molecule or GalNAc siRNA that specifically silences *Cnnm4* in hepatocytes.

Results: The expression of *Cnnm4* was upregulated in the liver of patients with ALD and correlated with the stages of the disease: early AH, non-severe AH, severe AH, compensated HCV-related cirrhosis, AH explants and cirrhosis hepatitis C virus. Hepatic CNNM4 levels were overexpressed in the NIAAA model. Silencing *Cnnm4* exhibited a reduction in transaminases. Importantly, the absence of *cnnm4* resulted in a significant decrease in mitochondrial ROS and ER stress in hepatocytes. High-throughput proteomic analysis performed in liver tissue from NIAAA models revealed a significant representation of the following processes in the absence of CNNM4; oxidation-reduction, lipid metabolism, cellular response to oxidative stress, endoplasmic reticulum stress or protein folding families. The machinery for repairing damaged proteins, represented by the enzyme protein-L-isoaspartate (D-aspartate) O-methyltransferase

(PIMT), was significantly overexpressed in the absence of CNNM4. Further experiments will investigate whether Mg^{2+} homeostasis mediated by silencing of CNNM4 modulates PIMT activity, which has been shown to be impaired during excessive ethanol consumption.

Conclusion: CNNM4 magnesium transport appears to be dysregulated in patients with AH and in NIAAA model. Targeting *Cnnm4* with GalNAc siRNA has emerged as a novel therapeutic approach for ALD that ameliorates AH in the NIAAA model. Further experiments will address the role of CNNM4 in the protein repair machinery mediated by PIMT activity.

THU028

Hepatic transcriptional signature of alcohol on genes involved in canonical retinoid metabolism

Marta Melis¹, Xia-Han Tang¹, Nabeel Attarwala¹, Qiuying Chen¹,
Carlos Prishker¹, Lihui Qin², Steve Gross¹, Lorraine Gudas¹,
Steven Trasino^{1,3}. ¹Weill Cornell Medical College, Pharmacology,
New York, United States; ²Weill Cornell Medical College, Pathology and
Laboratory Medicine; ³Hunter College, CUNY, Urban Public Health and
Nutrition, New York, United States
Email: st1647@hunter.cuny.edu

Background and aims: A large body of data show that alcohol abuse leads to reductions to hepatic vitamin A (retinoids) levels beginning in early stages of chronic alcohol abuse (<2–3 weeks), which is associated with progression of liver damage, and early stages of alcohol liver disease (ALD). However, to date, there remains little understanding of the genes involved in alcohol-driven hepatic retinoids depletions during early stages of ALD.

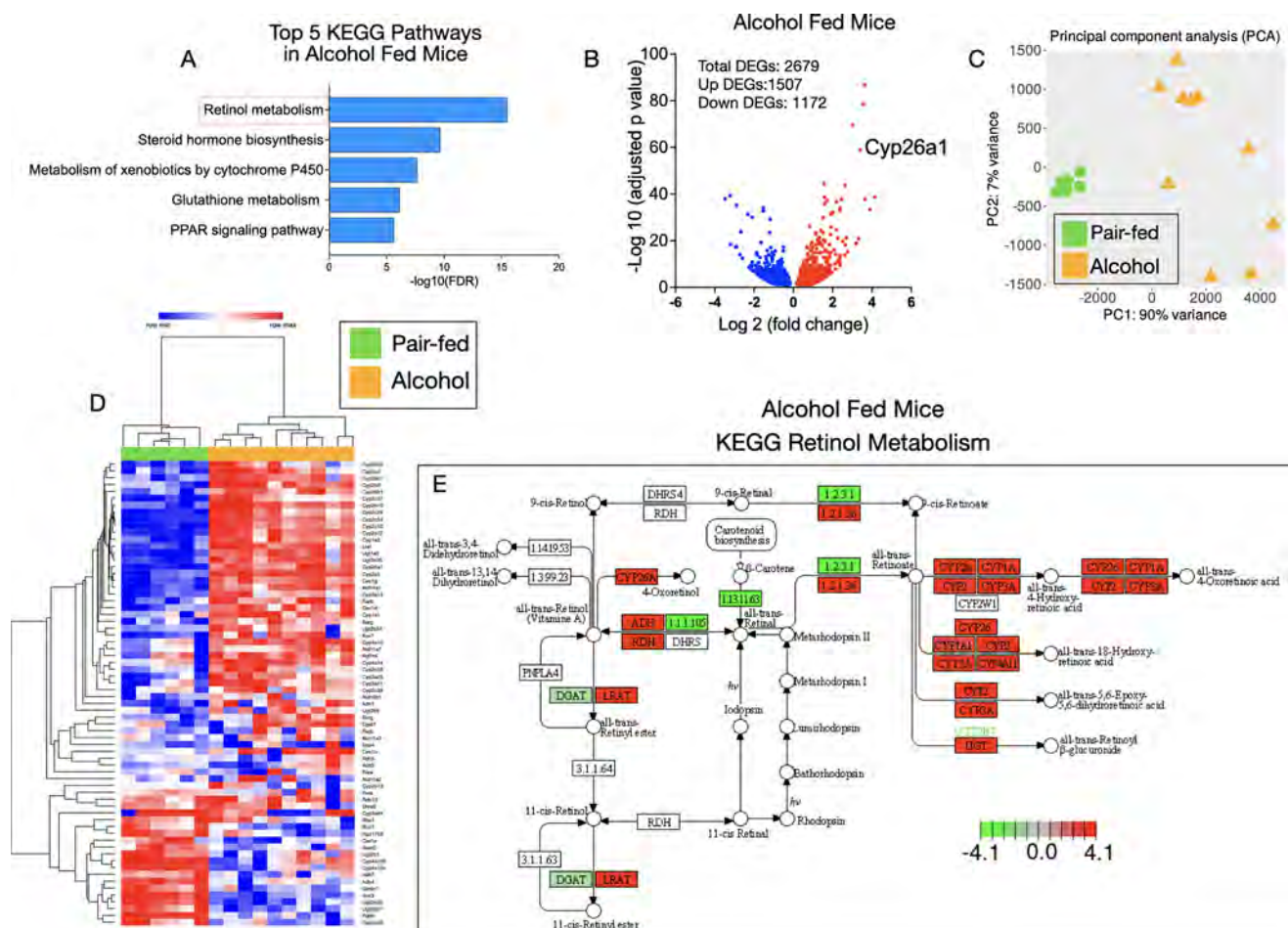


Figure 1: (abstract: THU028)

POSTER PRESENTATIONS

Method: Using a 3-week murine model of chronic alcohol intake and RNA sequencing technology, we determined the hepatic transcriptional signature of alcohol on genes involved in canonical retinoid metabolism.

Results: Our results show that 3 weeks of alcohol intake led to increases in serum retinol levels, but reductions to hepatic retinoids (retinol, and retinyl-esters), and concomitant increases in plasma AST, ALT, and macro and microvesicular steatosis. By RNA sequencing technology, we found that 3 weeks of chronic alcohol intake led to modulation of 68 transcripts involved in canonical retinoid metabolism. These transcripts include the genes *Ces1d*, *Ces1g*, *Rbp1*, *LRAT*, *Rdh10*, *Aldh1a1*, *Cyp26a1*. Interestingly, among the 2679 significant differentially expressed genes (DEGs) in livers of alcohol-fed mice, *Cyp26a1*, the major retinoic acid catabolizing enzyme was the 6th top significantly upregulated DEG. We also detected broad hepatic increases in transcripts of families of *Cyp1a*, *Cyp2a-c*, *Cyp3a-c* xenobiotic enzymes, capable of retinoid catabolism. Using western blotting we confirmed that compared to untreated mice, hepatic protein expression of the retinyl-ester hydrolases CES1D, CES1G, and a rate-limiting enzyme in retinoic acid synthesis, ALDH1A1, were significantly increased in livers of alcohol-fed mice. However, protein levels of RBP1, which is critical to hepatic retinol transport and homeostasis, was markedly decreased in livers of alcohol-fed mice. Moreover, we detected specific reductions to RBP1 in hepatic stellate cells (HSC) and portal hepatocytes.

Conclusion: These data show for the first time that reductions to hepatic retinoid in early stages of ALD may be due to pleiotropic effects, involving impaired retinoid transport and metabolism in portal hepatocyte and HSCs, but also concurrent increases in hepatic retinyl-ester hydrolysis, and oxidative metabolism of retinol to retinoic acid, and CYP-mediated retinoid catabolism. Given that *Cyp26a1* was the 6th top DEG in alcohol-fed mice, our data also strongly suggest that retinoid metabolism is among the key micronutrient pathways negatively impacted in early stages of ALD. These data may help develop future therapies aimed at mitigating hepatic retinoid losses in individuals that struggle with alcohol cessation.

THU029

COVID-19 pandemic impact on alcoholic hepatitis healthcare utilisation

Leya Nedumanni¹, Sukhdeep Steven Cheema¹, Karl Vaz¹, Ronald Ma², Daryl Jones³, Stephen Warrillow³, Josephine Grace^{1,4}, Darren Wong¹, Matthew Choy^{1,4}. ¹Austin Hospital, Gastroenterology, Heidelberg, Australia; ²Austin Hospital, Clinical Costings, Heidelberg, Australia; ³Austin Hospital, Intensive Care, Heidelberg, Australia; ⁴University of Melbourne, Department of Medicine, Austin Academic Centre, Heidelberg, Australia
Email: leya.nedumanni2@austin.org.au

Background and aims: Alcoholic hepatitis (AH) is associated with significant morbidity, mortality and healthcare expenditure. The global SARS-CoV-2 (COVID-19) pandemic and related lockdown measures have potentially contributed to an increase in alcohol misuse. This study examines frequency and patient outcomes of AH admissions to an Australian quaternary liver transplant referral centre. We aimed to ascertain the change in AH severity, ICU admission rates and healthcare utilisation costs over the last 5 years to identify temporal associations with the COVID-19 pandemic.

Method: A retrospective analysis of patients aged 18 years and older fulfilling National Institute on Alcohol Abuse and Alcoholism diagnostic criteria for AH between January 2016 and March 2021 was conducted. Data were collected from electronic medical records and analysed. Primary end points were the frequency of AH admissions, ICU admission rates and healthcare costs, which were evaluated with a divergence at the beginning of lockdown restrictions (March 2020-March 2021 "COVID cohort") versus the "historical cohort" (January 2016-February 2020).

Results: In total, 105 eligible AH admissions were identified. Overall, 90 day mortality was 18% (19/105). AH admission rate for the COVID cohort was significantly higher at 3.38 cases/month (n = 44) compared to the historical cohort at 1.22 cases/month (n = 61), p < 0.001. The COVID cohort had greater disease severity with a higher Glasgow Alcoholic Hepatitis Score during admission [8.5 (IQR 7–10) vs 7 (IQR 6–9), p = 0.04]. The AH COVID cohort trended towards a greater proportion requiring ICU admission, inotropic support and longer ICU length of stay. Whilst per-episode adjusted healthcare costs were similar across the study, monthly costs of the COVID cohort were higher compared to the historical cohort due to increased admission frequencies [mean (SD) \$137,549 (54,058) vs \$38,000 (27,448), p = 0.02 (Figure 1)]. No patients in this study were diagnosed with COVID-19.

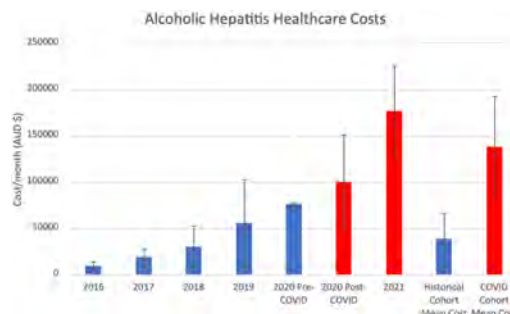


Figure 1: Alcoholic Hepatitis Healthcare Costs

Conclusion: In this study, alcoholic hepatitis admission frequency and healthcare costs were found to have increased since the COVID-19 pandemic. These observations provide the impetus for future studies to understand how the COVID-19 pandemic has led to increased AH presentations and develop preventative strategies that reduce alcohol related admissions and associated costs.

THU030

The role of integrated alcohol liver care in the management of patients with alcohol related liver disease in an acute hospital setting

Khin Han¹, Phyto Wah Wah¹, Ian Webzell¹, Joshua Stapleton², Huyen Adams¹, Abid Suddle¹, Michael Heneghan¹, Nicola Kalk², Naina Shah¹. ¹Kings College Hospital, Hepatology, London, United Kingdom; ²South London and Maudsley, Psychological Medicine, London, United Kingdom
Email: nkshah26@yahoo.com

Background and aims: Acute on Chronic Liver failure (ACLF)/Acute decompensation (AD) following Alcohol use disorder (AUD) is a common presentation to the Hospital. The office of national statistics in the UK reported 7,423 deaths in 2020. 80% of these were attributed to Alcohol related Liver Disease. Alcohol related admissions and deaths costs the National health service (NHS) over 3.5 billion/year. As a part of the NHS long term plan, Alcohol care team comprising of Consultants: Hepatologist, Addiction Psychiatrist and clinical nurse specialists was established at Kings College Hospital in 2018, to manage AUD and prevent recurrent Hospital presentation. Integrated outpatient treatment providing medical treatment and alcohol interventions has been previously shown to improve abstinence in medically ill patients. Explore the utility of an integrated Alcohol Liver clinic led by Consultants: Hepatologist and Addiction Psychiatrist in facilitating abstinence in patients with ArLD.

Method: 159 patients with Alcohol related cirrhosis were reviewed in the clinic, male: n = 95 with a median age of 58 (36 ± 83), female, n = 64 with a median age of 54 (32 ± 77). 29/159 presented with ACLF.

Results: Abstinence led to a Liver recovery in patients with ACLF (table 1). 61/159 (38%) presented to the Hospital with decompensation. 51/61 (83%) recompensated following abstinence. Unfortunately 18/159 patients who died had AUD prior to presentation. The overall

abstinence rate was 104/159 (65%) (table 1). Number of patients achieving abstinence has increased following the implementation of integrated care service as shown in figure 1.

Table 1: Alcohol use disorder in patients with Alcohol related Liver disease

	Abstinent	Drinking	Harm reduction
ACLF grade 1 (n = 7)	5	2	0
ACLF grade 2 (n = 15)	6	5	4
ACLF grade 3 (n=7)	6	1	0
Decompensated ArLD (n = 61)	51	6	4
recompensated (n = 51) 83%			
Cirrhosis compensated (n = 69)	36	18	15
mortality (n = 22)	4	18	0

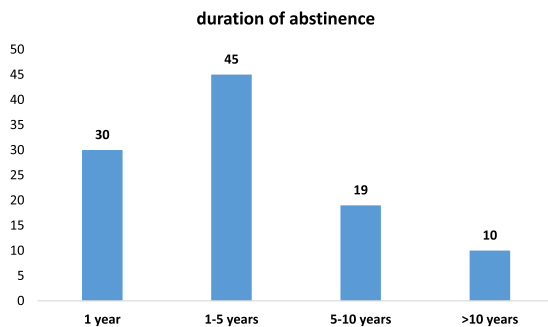


Figure 1: Number of patients achieving abstinence

Regular Liver health education, motivational intervention including engagement with the community and Hospital Addictions team has helped patients maintain abstinence. Sustained sobriety led to Liver recovery and prevention of Hospital presentation with complications related to portal hypertension/ACLF. This has led to a reduction in monthly readmission rate to 6–8%. In addition to being cost-effective, it has improved the long term prognosis of patients with ArLD.

Conclusion: Sustained abstinence leads to Liver recovery, reduced Hospital presentation and readmission. Facilitating abstinence is vital in improving the long term prognosis in patients presenting with ArLD. Integrated care approach should be considered as a standard of care in managing AUD.

There is an unmet clinical need in exploring pharmacological and psycho-social intervention tailored towards treating AUD in patients with ArLD thus preventing the development of ACLF/AD.

THU031

Untargeted lipidomics unveils a specific plasma signature of severe alcoholic hepatitis

Florent Artru^{1,2}, Stephen Atkinson², Francesca Trovato¹, Nikhil Vergis², Vishal C Patel^{3,4,5}, Salma Mujib¹, Anna Cavazza¹, Alexandros Pechlivanis², Ellen Jerome¹, Marc Zentar¹, Evangelos Triantafyllou², Elaine Holmes², Mark J W McPhail^{1,2}, Mark Thursz². ¹Institute of Liver Studies, King's College London, London, United Kingdom; ²Imperial College London, London, United Kingdom; ³The Roger Williams Foundation for Liver Research, Institute of Hepatology, London, United Kingdom; ⁴King's College Hospital, Institute of Liver Studies, London, United Kingdom; ⁵King's College London, School of Immunology and Microbial Sciences, London, United Kingdom
Email: m.thursz@imperial.ac.uk

Background and aims: Severe alcoholic hepatitis (SAH) is associated with systemic inflammation and immune dysfunction. Lipids are involved in inflammatory and immune responses; however, lipidomics is understudied in the setting of SAH. We evaluated whether specific changes in the blood lipidome are observed in patients with SAH.

Method: Untargeted serum lipidomics was performed using reversed phase ultra-performance liquid chromatography coupled

to mass spectrometry in patients with SAH participating in the STOPAH trial (n = 159), with cirrhosis (n = 81-including compensated and decompensated cirrhosis) and healthy controls (HC, n = 35). Serum lipidome changes between SAH and cirrhosis were evaluated in a derivation set (n = 160) and a validation set (n = 80) by principal component analysis (PCA) and orthogonal partial least squares discriminant analysis (OPLS-DA).

Results: Patients with SAH and cirrhosis had a similar age (51 vs. 51-year-old, p = 0.9) but different MELD scores (21.8 vs. 15.3, p < 0.0001). According to Lille score, 44.8% of SAH patients were responders to medical treatment with a 29.1% 90-day survival. The derivation and validation sets were well matched for clinical and biological variables. In the derivation cohort, PCA accurately discriminated between patients with SAH, cirrhosis and HC. In OPLS-DA both ionisation modes accurately discriminated SAH vs. cirrhosis (in positive mode: R²Y = 0.55 Q² = 0.49 CV-ANOVA p < 0.0001 AUROC = 0.92; in negative mode: R²Y = 0.54 Q² = 0.36 p < 0.0001 AUROC = 0.96). The 20 metabolites showing the greatest variable importance projection in positive and negative mode were included in multivariate analysis adjusting for age, sex and MELD score. Three lipids in positive mode (PC 34:2, PC 36:3 and PE 39:2) and five in negative mode (PC-0-19:0, PS 41:4, PG 41:0, LPC 16:0, ST 21:4;O2) disclosed independent associations with SAH. Using these lipids, we derived 2 scores relating to positive and negative ionisation modes; both accurately discriminated SAH from cirrhosis with an AUROC of 0.90 and 0.86 in the derivation set and 0.89 and 0.92 in the validation sets, respectively.

Conclusion: Untargeted lipidomic profiling by MS indicates a lipidomic signature-mainly composed by glycerophospholipids species-in patients with SAH distinct from cirrhosis. Since these lipids are involved liver repair, some immune-modulatory functions and are associated with organ failure in sepsis they urgently require further exploration in the SAH setting.

THU032

Toll-like receptor 2 activation in monocytes of alcohol use disorder patients contributes to systemic inflammation and alcohol-associated liver disease

Luca Maccioni¹, Joyce Kasavuli¹, Sophie Leclercq^{2,3}, Boris Pirlot¹, Géraldine Laloux⁴, Yves Horsmans⁵, Isabelle Leclercq¹, Bernd Schnabl^{6,7}, Peter Stärkel^{1,5}. ¹UCLouvain, Université Catholique de Louvain, Institute of Experimental and Clinical Research, Laboratory of Hepato-gastroenterology, Brussels, Belgium; ²UCLouvain, Université Catholique de Louvain, Louvain Drug Research Institute, Metabolism and Nutrition Research Group, Brussels, Belgium; ³UCLouvain, Université Catholique de Louvain, Institute of Neuroscience, Brussels, Belgium; ⁴UCLouvain, Université Catholique de Louvain, de Duve Institute, Brussels, Belgium; ⁵Cliniques Universitaires Saint-Luc, Department of Hepato-gastroenterology, Brussels, Belgium; ⁶University of California San Diego, Department of Medicine, La Jolla, United States; ⁷University of California San Diego, Department of Medicine, VA San Diego Healthcare System, San Diego, United States
Email: luca.maccioni@uclouvain.be

Background and aims: A minority of alcohol use disorder (AUD) patients develops progressive alcohol-associated liver disease (ALD) potentially linked to gut barrier dysfunction, microbial translocation and activation of systemic immune responses. Activation of circulating monocytes by microbial products might contribute to systemic and liver inflammation leading to ALD progression. Human data linking monocytes to early stages of ALD are lacking. We explored the links between changes in monocytes, microbial translocation, systemic inflammation and monocyte-derived macrophages in early human ALD.

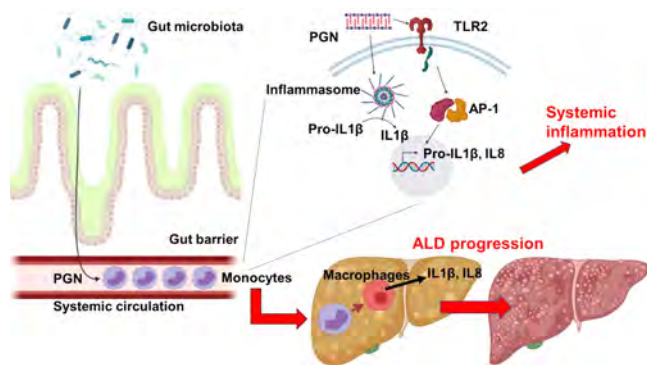
Method: We included n = 123 AUD patients following a highly-standardized rehabilitation program and n = 26 healthy controls. We determined the total number of monocytes and proportion of monocytes subsets by FACS. Serum microbial translocation markers and cytokines were measured by ELISA and multiplex assay,

POSTER PRESENTATIONS

respectively. Cytokines reflecting activation of monocytes were assessed by qPCR. Toll-like receptor (TLR) expression in monocytes and activation as well as phagocytosis were assessed *in vitro*. ALD severity and liver inflammatory responses were analyzed in liver biopsies by histology, qPCR, immunohistochemistry and ELISA.

Results: In AUD patients, the number of blood monocytes increased ($p < 0.0001$). Among the 3 monocyte subpopulations, intermediate and non-classical increased while classical monocytes decreased compared to controls. Monocytes from AUD patients up-regulated IL1 β and IL8 together with TLR2, down-stream AP-1 and inflammasome NLRP3. IL1 β and IL8 were actively secreted by those monocytes upon stimulation *in vitro* with the TLR2 ligand Peptidoglycan. Stimulation with *E. coli* confirmed preserved bacterial phagocytic activity. Systemic levels of cytokines and alterations in monocytes correlated with microbial translocation markers.

In parallel, IL1 β and IL8 were increased in ALD livers together with activation of intrahepatic macrophages (CD163+, iNOS+, TREM1+). Liver chemokines (MCP1, CX3CL1) involved in monocytes attraction were induced in liver tissue. IL1 β and IL8 correlated with liver chemokines, iNOS+ up-regulation in macrophages and ALD severity markers (e.g. fibrosis, AST/ALT, CK18-M65 and M30).



Conclusion: Our results point to a contribution of activated monocytes to systemic and liver inflammation. Monocytes likely infiltrate the liver, transform into monocyte-derived macrophages and release IL1 β and IL8 in response to Peptidoglycan and TLR2 activation, ultimately leading to ALD progression.

THU033

Improving NIAAA criteria for the diagnosis of alcoholic hepatitis, role of systemic inflammation

Elisa Pose^{1,2,3}, Emma Avitabile⁴, Alba Díaz⁵, Carla Montironi⁶, Martina Perez^{1,7}, Jordi Gratacós-Gines^{1,7}, Helena Hernández Evole^{1,7}, Tejasav Sehrawat⁸, Harmeet Malhi⁸, Pol Olivas^{7,9}, Virginia Hernández-Gea^{1,3,7}, Vijay Shah⁸, Patrick S. Kamath⁸, Pere Ginès^{1,3,7,10}. ¹Hospital Clínic of Barcelona, Liver Unit, Barcelona, Spain; ²Institut d'Investigacions Biomèdiques August Pi i Sunyer (IDIBAPS), Chronic liver disease, Barcelona; ³Centro de Investigación Biomédica en Red, Chronic liver disease, Madrid, Spain; ⁴Institut d'Investigacions Biomèdiques August Pi i Sunyer (IDIBAPS), CIF: Q5856414G, Chronic liver disease, Barcelona, Spain; ⁵Hospital Clínic of Barcelona, Pathological Department, Barcelona, Spain; ⁶Hospital Clínic of Barcelona, Pathology Department and Molecular Biology CORE, Barcelona, Spain; ⁷Institut d'Investigacions Biomèdiques August Pi i Sunyer (IDIBAPS), Chronic liver disease, Barcelona, Spain; ⁸Mayo Clinic, Division of Gastroenterology and Hepatology, Rochester, United States; ⁹Hospital Clínic of Barcelona, Psychiatry, Barcelona, Spain; ¹⁰University of Barcelona, Barcelona, Spain
Email: EPOSE@clinic.cat

Background and aims: The National Institute of Alcohol Abuse and Alcoholism (NIAAA) clinical criteria for the diagnosis of probable alcoholic hepatitis (AH) are commonly used to select subjects for

clinical studies and to diagnose AH in clinical practice. The objectives of this study were to assess the sensitivity and specificity and to improve the diagnostic accuracy of NIAAA clinical criteria for AH.

Method: 268 consecutive patients with Alcohol-related liver disease (ArLD) that underwent liver biopsy were prospectively included: 210 and 58 in the derivation and validation cohorts. NIAAA criteria and histological diagnosis of AH were independently reviewed by clinical investigators and pathologists from Hospital Clínic and Mayo Clinic. Using liver biopsy as gold standard we determined specificity, sensitivity and accuracy of the NIAAA clinical criteria. To improve the diagnostic accuracy of NIAAA criteria the threshold of quantitative variables was optimized and combinations with categorical variables were tested. Factors associated with 1-year transplant-free survival were evaluated.

Results: In the study cohort, NIAAA criteria showed a sensitivity of 63% (95% CI, 52–73) a specificity of 78% (95% CI, 69–84) and an accuracy of 72% (95% CI, 65–78). A significant percentage (37%) of patients with histological-proven AH did not meet NIAAA criteria. These patients had higher MELD score values, higher frequency of cirrhosis decompensation, higher inflammation in terms of C-reactive protein (CRP) levels and lower 1-yr survival compared to subjects without histological AH (63% vs 91%, $p = 0.000$). A new version of the NIAAA criteria, NIAAAs-CRP criteria, was generated by simplifying the current NIAAA criteria and adding a new parameter as follows: bilirubin ≥ 2.5 mg/dl instead of ≥ 3 mg/dl; AST ≥ 50 UI/L and AST > ALT, instead of AST ≥ 50 UI/L, AST/ALT ratio ≥ 1.5 mg/dl and AST < 400 UI/L; active alcohol consumption or alcohol abstinence less than 120 days instead of 60 days before the inclusion; not considering the presence of confounding factors and adding C reactive protein ≥ 1 mg/dl. These modified criteria showed a good combination of sensitivity, specificity and accuracy among all the combinations tested (70%, 83%, 78%, respectively). Factors associated with survival in the study cohort were histological AH, decompensated cirrhosis, MELD score and NIAAAs-PCR criteria, but not NIAAA original criteria. Similar findings were observed in the validation cohort where NIAAA original criteria showed 52% sensitivity, 82% specificity and 69% accuracy, while NIAAAs-PCR showed 56% sensitivity, 91% specificity and 76% accuracy for the clinical diagnosis of AH.

Statistic	NIAAA original (95% CI)	NIAAAs-PCR (95% CI)
Sensitivity	63 % (52-73)	70 % (59-80)
Specificity	78 % (69-84)	83% (75-90)
Disease prevalence (*)	39 % (32-46)	39% (32-46)
Positive Predictive Value (*)	64 % (55-72)	72% (63-80)
Negative Predictive Value (*)	77 % (71-81)	82% (76-86)
Accuracy (*)	71.90 % (65.30-77.90)	78.10 (71.88-83.49)

(*) These values are dependent on disease prevalence

Conclusion: A modified version of NIAAA criteria, NIAAAs-CRP criteria, with higher sensitivity, specificity and accuracy, improves non-invasive diagnosis of AH in patients with ArLD and adds prognostic value to NIAAA criteria.

THU034

Alcohol associated hepatitis in Latin America: results from the AH-LATIN study

Jorge Arnold¹, Luis Antonio Diaz¹, Francisco Idalsoaga¹, Gustavo Ayares¹, Eduardo Fuentes², Carolina Ramirez³, María Paz Medel⁴, Catterina Ferreccio⁵, Mariana Lazo⁶, Juan Pablo Roblero⁷, Mayur Brahmanian⁸, Rodolfo Carbonetti⁹, Sebastián Marciano¹⁰, Manuel Mendizabal¹¹, Fernando Bessone¹², Gustavo Romero¹³, Ana Palazzo¹⁴, Estela Florencia Manero¹⁵, Melisa Dirchwolf¹⁶, Diego Piombino¹⁷, María Ayala Valverde¹⁸, Fernando Cairo¹⁹, María Alejandra Gracia Villamil²⁰, María Mercedes Rodríguez Gazari^{21,21}, Patricia Gallardo²², Geraldine Ramos^{23,23}, Patricia Guerra²⁴, Fabio Silveira²⁵, Roberta Chaves²⁶, Giovanni Silva²⁷, Cirley Lobato²⁸, Jozelda Lemos²⁹, Rogério Alves³⁰, Gustavo Pereira³¹, Rita de Cássia Martins Alves da Silva³², Liliana Sampaio Costa Mendes³³, Cláudia Alves Couto³⁴, Cristina Melo Rocha³⁵, Raul Lazarte³⁶, Pamela Yaquich³⁷, Blanca Norero³⁸, Camila Jure³⁹, Alejandra Dominguez⁴⁰, Marta Mac Vicar⁴¹, Violeta Rivas⁴², Juan Pablo Arancibia⁴³, Armando Sierralta⁴⁴, Jose Valera⁴⁵, Sebastian Diaz⁴⁶, Carlos Sanchez⁴⁷, Luis Toro⁴⁸, Adrian Varon⁴⁹, Elizabeth Correa⁵⁰, Juan Carlos Restrepo⁵¹, Monica Tapias⁵², Ricardo Aguilera Rosales⁵³, Mirtha Infante⁵⁴, Galo Pazmiño⁵⁵, Xiimena Armijos⁵⁶, Enrique Carrera⁵⁷, Regina Ligoría⁵⁸, Gerson Avila⁵⁹, Abel Sanchez⁶⁰, Marco Sánchez⁶¹, Scherezada Mejia⁶², Jacqueline Cordova⁶³, Maria De Fatima Higuera de La Tijera⁶⁴, Raul Contreras⁶⁵, Francisco Solis⁶⁶, Jesus Varela⁶⁷, Janett Jacobo⁶⁸, Jose Antonio Velarde-Ruiz Velasco⁶⁹, Julissa Lombardo Quezada⁷⁰, Esther Veramendi⁷¹, Victor Vela⁷², Claudia Pamo⁷³, Donny Puma⁷⁴, Julio Marcelo⁷⁵, Laura Tenorio⁷⁶, Maria Cabrera⁷⁷, Jose Rivera⁷⁸, Pedro Montes⁷⁹, Ramon Bataller⁸⁰, Alexandre Louvet⁸¹, Vijay Shah⁸², Patrick S. Kamath⁸², Ashwani Singal⁸³, Marco Arrese⁵, Juan Pablo Arab⁸⁴. ¹Pontificia Universidad Católica de Chile, Gastroenterología, Chile; ²Pontificia Universidad Católica de Chile, Ciencias de la Salud, Chile; ³Clinica Las Condes, Anestesiología, Chile; ⁴Pontificia Universidad Católica de Chile, Medicina Familiar, Chile; ⁵Pontificia Universidad Católica de Chile; ⁶Johns Hopkins University School of Medicine, Chile; ⁷Hospital Clínico Universidad de Chile, Gastroenterología, Chile; ⁸Western University, London Health Sciences Center, Gastroenterology; ⁹Hospital de Clínicas D. N. Avellaneda; ¹⁰Hospital Italiano Buenos Aires; ¹¹Hospital Universitario Austral; ¹²Hospital Provincial del Centenario; ¹³Hospital de Gastroenterología Dr. Carlos Bonorino Udaondo; ¹⁴Hospital Padilla. Tucuman; ¹⁵Hospital Pablo Soria; ¹⁶Hospital Privado de Rosario; ¹⁷Hospital de Emergencia Clemente Alvarez; ¹⁸Hospital el Pino, Medicina Interna, Chile; ¹⁹Hospital el Cruce, Argentina; ²⁰Centro Medico Talar y Grupo Medico Santa Clara; ²¹Hospital Británico, Argentina; ²²Fundación Sayani; ²³Instituto de Gastroenterología Boliviano Japonés; ²⁴Instituto de Gastroenterología Boliviano-Japonés; ²⁵Hospital do Rocio; ²⁶Hospital das Clínicas da Faculdade de Medicina de Ribeirão Preto-USP; ²⁷Universidade Estadual Paulista (UNESP)-Botucatu/São Paulo; ²⁸FUNDHACRE-, Serviço de Assistência Especializada-, Acre; ²⁹Hospital Getúlio Vargas-Teresina/Piauí; ³⁰Hospital do Servidor Público Estadual-São Paulo/São Paulo; ³¹Hospital Federal de Bonsucesso; ³²Unidade de Transplante de Fígado e do Hospital de Base da Faculdade de Medicina de São Jose do Rio Preto/SP; ³³Universidade de Brasília-Distrito Federal; ³⁴Hospital das Clínicas-Universidade Federal de Minas Gerais; ³⁵Fundação Hospital Adriano Jorge; ³⁶Hospital Clínico Universidad de Chile; ³⁷Hospital San Juan de Dios; ³⁸Hospital Sotero del Rio; ³⁹Hospital de Coquimbo; ⁴⁰Hospital Padre Hurtado; ⁴¹Hospital de Concepción; ⁴²Hospital de Concepción; ⁴³Hospital Clínico Universidad de Chile; ⁴⁴Hospital Hernán Henríquez Aravena; ⁴⁵Hospital de la Serena; ⁴⁶Fundación Valle del Lili; ⁴⁷Clinica

Universitaria Colombia; ⁴⁸Hospital San Vicente Fundación Rionegro; ⁴⁹Fundación Cardioinfantil; ⁵⁰Hospital San Vicente Fundación Medellín; ⁵¹Hospital Pablo Tobon Uribe. Univ. De Antioquia; ⁵²Hospital Universitario Fundación Santa Fe de Bogotá; ⁵³Hospital Clínico Quirúrgico Carlos Font; ⁵⁴Instituto Nacional de Gastroenterología; ⁵⁵Pontificia Universidad Católica de Ecuador; ⁵⁶Hospital Carlos Andrade Marín; ⁵⁷Hospital Eugenio Espejo; ⁵⁸Hospital General San Juan de Dios; ⁵⁹Hospital Roosevelt; ⁶⁰Hospital Roosevelt; ⁶¹Hospital Escuela; ⁶²Hospital Juárez de México; ⁶³Hospital Juarez de Mexico; ⁶⁴ISSSTE; ⁶⁵Centro de Investigación en Enfermedades Hepáticas y Gastroenterología; ⁶⁶Hospital Angeles Torreón; ⁶⁷Hospital Dublan; ⁶⁸Hospital General 450, Secretaría de Salud de Durango; ⁶⁹Hospital Civil de Guadalajara; ⁷⁰Private Clinic; ⁷¹Hospital Nacional Hipólito Unanue; ⁷²HBCASE; ⁷³Hospital Goyoneche Arequipa; ⁷⁴Hospital Regional Honorio Delgado; ⁷⁵Hospital de Emergencias de Villa el Salvador; ⁷⁶Hospital Edgardo Rebagliati Martins; ⁷⁷Guillermo Almenara Hospital; ⁷⁸JRA Gastroenterology; ⁷⁹Hospital Nacional Daniel Alcides Carrión-Callao; ⁸⁰University of Pittsburgh; ⁸¹Service des maladies de l'appareil digestif; ⁸²Mayo Clinic; ⁸³University of South Dakota; ⁸⁴Pontificia Universidad Católica de Chile, Gastroenterología
Email: jparab@gmail.com

Background and aims: Severe alcohol-associated hepatitis (HA) has a high morbidity and mortality, however, the information in Latin America is limited. We aimed to characterize patients hospitalized for AH in a multinational cohort in Latin America.

Method: Multicenter prospective cohort study. We included patients admitted with severe AH between 2015–2021. Sociodemographic and clinical information was recorded. The analysis included survival analysis using Kaplan-Meier curves. This study was approved by the institutional ethics committee.

Results: 319 patients from 24 centers (8 countries: Argentina, Bolivia, Brazil, Chile, Colombia, Ecuador, Mexico, Peru) were included. Age 49.9 ± 10.3 years, 84.6% men and 54.1% had a previous diagnosis of cirrhosis. Median MELD at admission 27 [21–32] points. 25.6% met SIRS criteria and 47.6% had acute renal failure on admission. 36.11% were treated with corticosteroids. Survival at 30 days was 77.6% (95% CI: 69.7–83.7%) and at 90 days 71.6% (95% CI: 62.5–78.9%). 39.6% presented infections. The most frequent locations were urinary (34.1%), respiratory (30.7%), spontaneous bacterial peritonitis (17.1%) and skin (11.4%). The most frequent pathogens were Escherichia coli (55.6%), Klebsiella pneumoniae (11.1%) and Enterococcus (7.4%). In the long term, only 2.9% of patients have been transplanted.

Conclusion: This multicenter study shows high morbidity and mortality in patients with severe HA, which is comparable to other centers in the world.

THU035

Prophylaxis of withdrawal syndrome decreases mortality in patients with alcohol-associated hepatitis

David Marti-Aguado¹, Concepción Gómez¹, Amir Gougol², Dalia Morales Arraez³, Alejandro Jiménez Sosa³, Anjara Hernandez³, Claudia Pujol⁴, Edimar Alvarado-Tapias⁴, Ares Villagrasa⁵, Meritxell Ventura Cots⁵, Ana Clemente², Abo Zed Abdelrhman², Keith Burns², Aditi Bawa², Haritha Gandicheruvu², Vikrant Rachakonda², Ramon Bataller². ¹Clinic University Hospital, Department of Gastroenterology and Hepatology, Valencia, Spain; ²University of Pittsburgh Medical Center, Hepatology Department, Pittsburgh, Spain; ³Hospital Universitario de Canarias, Liver Unit, Tenerife, Spain; ⁴Hospital de la Santa Creu i Sant Pau, Hepatology Department, Barcelona, Spain; ⁵Hospital Vall d'Hebron, Barcelona, Spain
Email: davidmmaa@gmail.com

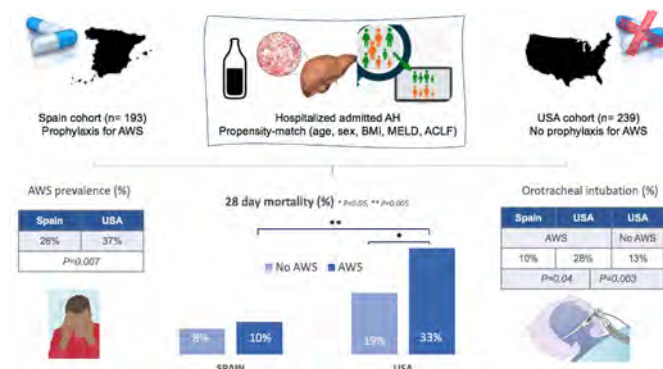
Background and aims: Alcohol withdrawal syndrome (AWS) is a serious medical condition that often complicates hospitalized patients with advanced alcohol-related liver disease including alcoholic hepatitis (AH). There are no studies evaluating the prevalence, impact, and effect of AWS prophylaxis in the setting of AH. We aimed at evaluating the incidence and outcomes of AWS in

POSTER PRESENTATIONS

patients hospitalized with AH from two countries with different AWS management strategies.

Method: A multicenter, international, retrospective, case-control study was performed evaluating consecutive patients hospitalized with AH in Spain (four participating centers) and USA (one center). In Spain, clomethiazole is used as prophylactic therapy for AWS while in USA a symptom-triggered approach is followed. Electronic medical history of all patients hospitalized with the diagnosis code of AH since 2015 were revised. Diagnosis of AWS was based on the clinician criteria and the need for treatment with benzodiazepines to control symptoms. Primary outcome was 28-days mortality. Prescribed benzodiazepine dose expressed in diazepam-equivalent was compared between groups who developed AWS. A propensity score (match by age, sex, BMI, MELD and ACLF score) was performed to compare clinical outcomes between patients who developed WDS in Spain vs. USA, using stratified logistic regression for matched pairs.

Results: Study population included 432 patients (n = 193 from Spain and n = 239 from USA), of whom 63% were women with mean age 48 ± 10 years, median BMI $28 (24-32)$ kg/m² and mean MELD score at admission of 23.7 ± 7.9 . Overall prevalence of AWS and mortality was 32% (n = 140) and 17% (n = 74), respectively. Presence of AWS was lower in patients receiving prophylaxis (Spain) than in patients who did not receive it (USA) (26% vs. 37% $P < 0.007$). In patients receiving prophylaxis, the development of AWS was not associated with worse clinical outcomes, including mortality (10% vs. 8%, $P = 0.52$). In patients not receiving prophylaxis in the USA, the development of AWS was associated with higher mortality (33% vs. 19%, $P = 0.009$) [Figure 1]. After propensity matching, a higher mortality was seen among patients presenting AWS in USA vs. Spain ($p = 0.003$). Importantly, patient with AWS in Spain had similar mortality that those who did not developed AWS in USA ($p = 0.35$). There were marked differences in several key parameters in patients with AWD with and without prophylaxis, respectively: the diazepam equivalent dose used (87 ± 119 vs. 136 ± 190 mg), ICU admission (16% vs. 48%, $P = 0.02$) and orotracheal intubation rate (10% vs. 28%, $P = 0.04$).



Conclusion: In AH setting, prophylactic therapy for AWS is associated with lower prevalence of both withdrawal symptoms and short-term mortality. This data supports that prophylactic therapy is a better approach than symptom-triggered therapy in patients hospitalized with AH.

THU036

The use of pharmacotherapy in the treatment of alcohol use disorder

Kathryn Allen¹, Tobias Maharaj¹, John Ryan¹. ¹Beaumont Hospital, Hepatology, Dublin, Ireland
Email: kathrynallen123@hotmail.com

Background and aims: Alcohol use disorder (AUD) is an important cause of preventable morbidity and mortality. The prevalence of AUD and alcohol related liver disease is increasing in Ireland. Several medications have been demonstrated to be effective for the

treatment of AUD. We wanted to ascertain the current attitude of gastroenterology physicians in Ireland towards pharmacotherapy as a treatment option for AUD.

Method: An anonymous, questionnaire-based survey was sent to gastroenterology physicians nationwide. This survey collected demographic information and assessed prescribing habits towards medications which have been approved to treat AUD (Naltrexone, Disulfiram, Baclofen, Librium, Nalmefene and Acamprosate). Where pharmacotherapy was not routinely utilised, we examined factors which may have led to their avoidance.

Results: We received 60 responses, 56% (n = 32) consultant gastroenterologists, and 40% (n = 23) GI specialist registrars (SpRs). 80% (n = 48) report being frequently (daily/weekly) involved in the management of AUD. 95% (n = 57) of prescribers believe that there is a role for pharmacotherapy in treating AUD, but only 22% (n = 13) routinely use these in clinical practice. Librium was commonly used by 88% (n = 53), while <10% regularly prescribed Naltrexone, Baclofen, or Acamprosate. Prohibitive factors identified were lack of hospital alcohol services (61%) [48% of respondents reported no alcohol service or support in their hospital], side effect profile for patients (26%), lack of compliance (26%), lack of adjuvant psychosocial support in community (47%), and unfamiliarity with medications (61%).

Conclusion: Despite the burden of alcohol on our acute hospitals, there is a clear and significant lack of support for alcohol related conditions. Emanating from this is the underutilisation of pharmacotherapy as a treatment for AUD, despite its evidence base. This survey highlights an urgent need to develop alcohol support services, in conjunction with physician education about the role of pharmacotherapy in treating AUD.

THU037

Application of machine learning algorithms to classify steatohepatitis on liver biopsy

Resham Ramkissoon¹, Joseph Ahn¹, Yung-Kyun Noh², Yubin Yeon³, Chady Meroueh¹, Priya Thanneer¹, Amit Das¹, Jason Hipp¹, Alina Allen¹, Douglas Simonetto¹, Patrick S. Kamath¹, Vijay Shah¹.
¹Mayo Clinic, Rochester, United States; ²Hanyang Univ., Department of Computer Science, Korea, Rep. of South; ³Hanyang Univ., Department of Artificial Intelligence, Korea, Rep. of South
Email: ramkissoon.resham@mayo.edu

Background and aims: Currently, it is very challenging to distinguish alcoholic steatohepatitis (ASH) and non-alcoholic steatohepatitis (NASH) on liver biopsy alone as they share many of the same histological characteristics. Artificial intelligence (AI) models utilizing deep learning have demonstrated superhuman degrees of accuracy in interpretation of digitized liver histology. The aim of our study was to develop a deep learning algorithm in the form of a convolutional neural network (CNN) to classify ASH and NASH on liver biopsy.

Method: We obtained liver biopsy slides from 38 patients with ASH and 59 patients with NASH. ASH was determined based on the clinical diagnosis of alcohol-associated hepatitis, and patients with NASH were identified from a cohort of morbidly obese patients undergoing bariatric surgery. The slides were digitized into an electronic database with whole-slide diagnosis labels. Each whole-slide image was rescaled and randomly cropped to generate 256 patches of 256×256 pixels. Each cropped patch retained the diagnosis label from the original whole-slide image (0 = NASH, 1 = ASH). The patches were randomly split into training and testing sets in an 8:2 ratio. Patches in the training set were used to train a 50-layer CNN (ResNet50), and the CNN's performance as a binary classifier was tested on the patches in the testing set. Gradient-weighted Class Activation Mapping (Grad-CAM) was used as a method to understand the CNN's decisions.

Results: The CNN had an outstanding performance in distinguishing ASH versus NASH with an AUC of 0.962. Using an optimal threshold of 0.504, the CNN had an accuracy of 90.4%, sensitivity of 79.5%, and specificity of 96.3%. The positive predictive value is 92.1% and

negative predictive is 89.7%. Grad-CAM highlighted distinct regions within each patch that the algorithm used to make its decisions.

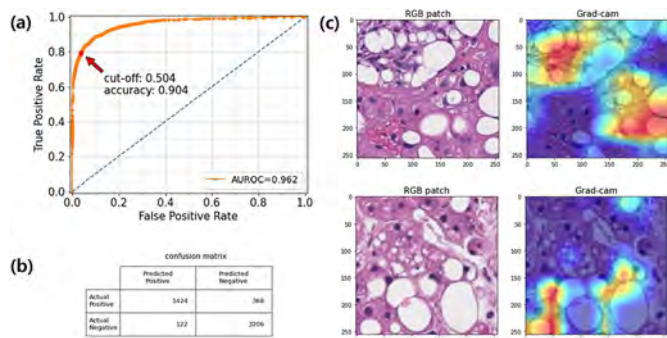


Figure: (a) Receiver operating characteristic (ROC) curve for the CNN's classification of ASH versus NASH. (b) Confusion matrix for the CNN; a diagnosis of ASH is indicated by "Positive" and a diagnosis of NASH is indicated by "Negative." (c) Activation map for classification of ASH patch (top row) and NASH patch (bottom row).

Conclusion: Our deep learning-based AI algorithm had an outstanding performance for patch-level classification of liver biopsy images from patients with ASH and NASH. After further validation on a larger set of liver biopsy images and evaluation of model performance at the level of whole slides, our AI algorithm may prove to be a novel way to distinguish ASH versus NASH histologically.

THU038

Calorie-protein deficit and body mass index are the independent predictors of mortality in severe alcoholic hepatitis

Harshita Tripathi¹, Jaya Benjamin², Puja Bhatia¹, Rakhi Maiwall³, Guresh Kumar⁴, Yogendrakumar Joshi⁵, Shiv Kumar Sarin³. ¹Institute of Liver and Biliary Sciences, Clinical Nutrition, DELHI, India; ²Institute of Liver and Biliary Sciences, Clinical Nutrition, New Delhi, India; ³Institute of Liver and Biliary Sciences, Hepatology, DELHI, India; ⁴Institute of Liver and Biliary Sciences, Biostatistics, DELHI, India; ⁵Institute of Liver and Biliary Sciences, Clinical Nutrition and Hepatology, DELHI, India
Email: jayabenjaminilbs@gmail.com

Background and aims: Short term mortality is high in severe alcoholic hepatitis (SAH), which is influenced by multiple factors. We planned to assess the independent predictors of 60 day mortality for optimizing management.

Method: SAH patients with Maddrey's discriminant function (mDF) 32–100 were enrolled; excluding sepsis, AKI and malignancy. Baseline clinical, biochemical parameters, disease severity [MELD, CTP, MDF, FIB-4], BMI, fat free mass index (FFMI), hand grip strength, usual diet [calorie (C) and protein (P) intake] and 60 day mortality were assessed. C and P deficit was the difference of ideal requirement [C (35kcal) and P (1.2 g) per kg ideal body weight] and actual intake. Logistic regression analysis was done.

Table 1: Predictors of Mortality in SAH

Parameter	Death (n = 16)	Alive (n = 44)	P value	Multivariate
Demographic Details				
Age (yrs)	40.6 ± 8.4	39.5 ± 6.2	0.314	
Height (cm)	171 ± 4.7	169 ± 8.9	0.511	
Dry BMI (kg/m ²)	19.7 ± 2.7	22 ± 4.1	0.051	0.048
Weight reduced (kg)	9.47 ± 7.0	8.9 ± 6.3	0.785	
Duration of weight loss (mo)	4.87 ± 1.6	8.3 ± 1.29	0.257	
Clinical details				
Ascites	32 (53.3%)	12 (20%)	0.676	
Duration of alcohol intake (yrs)	14.47 ± 5.7	13.08 ± 7.3	0.113	
Alcohol Quantity (gm)	571 ± 153	478 ± 194	0.468	
Last intake (days)	24 ± 9.45	36.4 ± 15.7	0.001	
Biochemical Parameters				
Total Bil (mg/dl)	21.3 ± 8.9	15.5 ± 7.2	0.041	0.022
AST (IU/L)	116 ± 54	157 ± 73	0.040	
ALT (IU/L)	127 ± 63	162 ± 56	0.031	
ALP (IU/L)	91.9 ± 27	157 ± 91	0.001	
Total protein (g/dl)	6.28 ± 0.93	6.99 ± 1.09	0.028	
Albumin (g/dl)	2.8 ± 0.66	2.8 ± 0.54	0.978	
INR	2.01 ± 0.34	1.96 ± 0.55	0.716	
Urea (mg/dl)	38.5 ± 16	28 ± 06	0.089	
Creatinine (mg/dl)	0.80 ± 0.4	0.73 ± 0.2	0.581	
Sodium (mmol/L)	129.5 ± 4.2	132.3 ± 3.3	0.039	
Potassium (mmol/L)	4.07 ± 0.68	4.08 ± 0.68	0.963	
Severity Scores				
MELD	28.3 ± 2.9	28.3 ± 10.8	0.317	
MDF	63.05 ± 18.4	63.05 ± 23.1	0.203	
CTP	10.4 ± 1.06	10.7 ± 1.5	0.115	
FIB-4	8.4 ± 3.6	6.95 ± 1.08	0.028	
Body composition parameters				
Fat mass (kg)	18.6 ± 4.8	22.6 ± 5.6	0.118	
Fat free mass (kg)	49.36 ± 13	51.2 ± 13.3	0.720	
FFMI kg/m ²	16.8 ± 4.2	18.02 ± 4.6	0.501	
Hand grip (kg)	22.1 ± 6.17	23.3 ± 6.2	0.986	
Diet				
Energy requirement (kcal)	2289 ± 738	2358 ± 523	0.730	
Protein requirement (g)	85.6 ± 5.7	83.8 ± 10.7	0.511	
Energy intake (kcal)	598.8 ± 231	737.3 ± 278.4	0.643	
Protein intake (g)	26.65 ± 10.6	20.3 ± 9.9	0.06	0.022
Calorie deficit (kcal)	2035 ± 214	1813 ± 508	0.05	0.045
Protein deficit (g)	70.7 ± 7.5	60.9 ± 19.2	0.02	0.051

Data expressed as mean ± SD, n (%). P value ≤0.05 is significant.

Conclusion: High calorie and protein diet with maintained body weight improves survival in SAH.

Results: In 60 patients with SAH [age 40 ± 7.37 yrs; ascites 47 (84%); BMI- 21.3 ± 3.8 kg/m²; mDF-62.4 ± 21.4, MELD 28 ± 9.3, CTP 10.6 ± 1.4, on steroids 14 (25%)] there was significantly low calorie intake despite >3 weeks of abstinence (Table 1). Those 16 (26.6%) patients who died at 2 mo had significantly lower BMI, higher P and C deficit and total bilirubin compared to survivors; that predicted mortality.

THU039

Alcoholic foamy degeneration: a unique variant of ALD that shows a characteristic pattern of gene expression with upregulation of lipid metabolism and mitochondrial genes and downregulation of fibrosis genes

Jordi Gratacós-Gines¹, Delia Blaya², Helena Hernández Evole¹, Carla Montironi³, Emma Avitabile¹, Martina Perez¹, Marta Cervera¹, Marta Carol¹, Ana Belén Rubio¹, Núria Fabrellas¹, Anna Soria¹, Octavi Bassegoda¹, Laura Napoleone¹, Ann Ma¹, Adria Juanola¹, Isabel Graupera¹, Alba Díaz⁴, Juan Jose Lozano⁵, Pere Ginès¹, Elisa Pose¹. ¹Hospital Clínic de Barcelona, Liver Unit, Barcelona, Spain; ²Institut d'Investigacions Biomèdiques August Pi i Sunyer (IDIBAPS), Barcelona, Spain; ³Hospital Clínic de Barcelona, Pathology Department and Molecular Biology CORE, Barcelona, Spain; ⁴Hospital Clínic de Barcelona, Pathology Unit, Barcelona, Spain; ⁵centro de investigación biomédica en red de enfermedades hepáticas y digestivas (CIBERehd), Barcelona, Spain
Email: EPOSE@clinic.cat

Background and aims: alcoholic foamy degeneration (AFD) is a variant of alcoholic liver disease that is diagnosed based on histology, with a pattern of microvesicular steatosis in the liver biopsy. Recently, in one of the largest series reported to date, we described AFD as an entity with similar clinical presentation to alcoholic hepatitis (AH), but faster improvement of liver function and markedly better long-

POSTER PRESENTATIONS

term prognosis. Molecular mechanisms underlying AFD are unknown and histological pattern has been scarcely studied. Our aim was to unveil the histological and transcriptional characteristics of AFD in this series.

Method: liver biopsies from 16 patients with AFD and 20 patients with AH diagnosed in the same period, were obtained. Results from RNA sequencing were analyzed with IPA, GO and RA platforms. Moreover, liver biopsies were reviewed by two pathologists to describe steatosis, steatohepatitis, degree of inflammation and fibrosis.

Results: compared to patients with AH, patients with AFD presented with a lower proportion of ascites and had higher levels of transaminases, cholesterol and triglycerides. Bilirubin levels were similar but MELD score was lower in patients with AFD. RNA sequencing analysis revealed that patients with AFD and AH have a differential gene expression pattern. On PCA analysis using gene expression, AFD patients clustered apart from AH patients. Moreover, the analysis of the deregulated gene expression showed that AFD patients have a significant upregulation of pathways associated with lipid metabolism, such as cholesterol and triglycerides biosynthesis, stearate and retinol biosynthesis, mitochondrial function and cell cycle, and a downregulation of pathways related to hepatic fibrosis such as wound healing signaling, integrin signaling and extracellular matrix deposition. Genes involved in senescence, autophagy and inflammation are also downregulated. Half of the cases (n=8) had predominant microvesicular steatosis, six (37.5%) had a mixed pattern of micro and macrovesicular steatosis and the remaining two cases (12.5%) showed macrovesicular steatosis ($\geq 40\%$) with focally associated steatohepatitis. Fibrosis was uncommon, especially in the cases of predominant microvesicular steatosis.

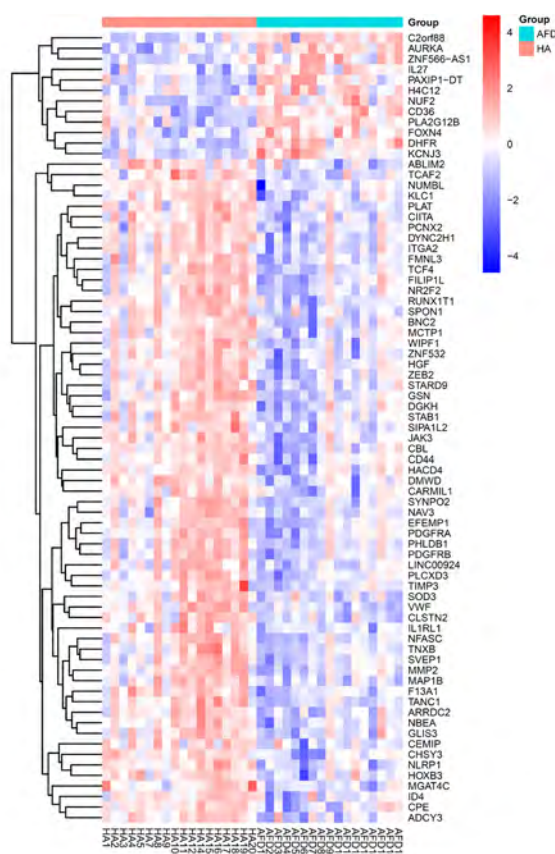


Figure: heatmap of the top upregulated (red) and downregulated (blue) genes in liver biopsies with AFD (green bar) and AH (orange bar).

Conclusion: AFD displays a specific gene signature differentiated from that of AH. Genetic functional pathways associated with lipid metabolism and mitochondrial function are upregulated in patients with AFD. In contrast, there is a downregulation of pathways associated with inflammation, fibrosis and senescence. Histological findings are consistent with genetic profile, with a predominant pattern of steatosis, with scarce fibrosis and steatohepatitis.

THU040

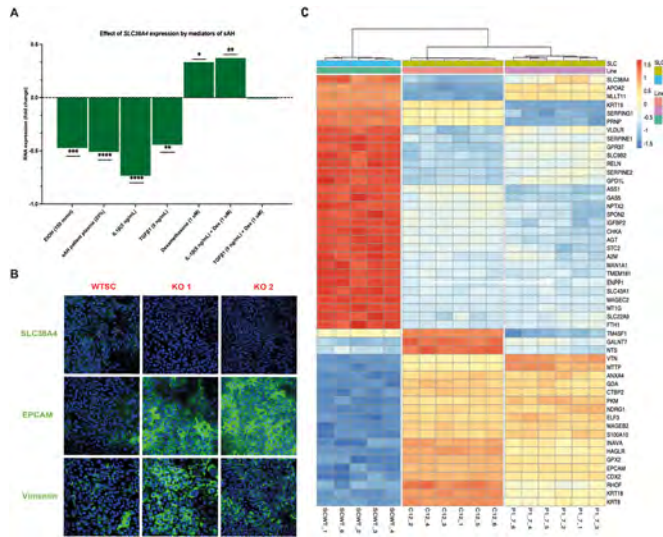
Loss of solute carrier family 38 member 4 (SLC38A4) as a driver for the pathogenesis of severe alcoholic hepatitis

Nchimunya Nelisa Tebeka¹, Stephen Atkinson¹, Luke D. Tyson¹, Josepmaria Argemi², Adam Syanda¹, Ramon Bataller², Tamir Rashid¹, Mark Thursz¹. ¹Imperial College London, Department of Metabolism, Digestion and Reproduction, London, United Kingdom; ²University of Pittsburgh, Medical Center, Pittsburgh, United States
Email: n.tebeka@imperial.ac.uk

Background and aims: Severe alcohol-related hepatitis (sAH) is a florid presentation of alcohol-related liver disease with very high short-term mortality. A genome-wide association study identified solute carrier family 38 member 4 (SLC38A4) as a potential risk locus for the development of sAH. SLC38A4 is characterised as an amino acid transporter and is predominantly hepatically expressed under the regulation of HNF4a. The aim of this project was to investigate how changes in SLC38A4 expression may contribute to the pathogenesis of sAH.

Method: SLC38A4 expression was determined by RNA-seq in whole liver biopsies obtained from patients with alcohol related liver disease, including sAH, from a published study. *In vitro* experiments were conducted to investigate the effects of known disease mediators on SLC38A4 expression in Huh7.5 cells. SLC38A4 knock-out lines (aliases P1.7 and C12 SLC38A4-KO) were generated by CRISPR/Cas9 editing in Huh7.5 cell lines; a control cell line (SCWT) was generated using a non-targeted scramble guide RNA. The functional impact of SLC38A4 knock-out was then characterised using gene expression analysis (RT-qPCR and RNA-seq) and protein expression by immunofluorescence (IF). Assays were performed to assess the impact of knock out on cell morphology and proliferation in addition to CYP3A4 activity and ureagenesis.

Results: SLC38A4 expression was reduced in whole liver tissue from cohorts of patients with sAH compared to their early alcoholic steatohepatitis controls (p < 0.0001). *In vitro* SLC38A4 expression was downregulated by mediators of alcoholic hepatitis i.e., IL-1b, TGFb1, TNFa and sAH patient plasma but upregulated by dexamethasone (Figure 1A). SLC38A4-KO lines demonstrated upregulation in the epithelial-mesenchymal transition markers, EPCAM and Vimentin (p < 0.0001 and p < 0.01 respectively) (Figure 1B). SLC38A4-KO resulted in reduced cell proliferation, ureagenesis, and downregulation of bile acid transporters, BSEP (p < 0.0001) and MRP2 (p < 0.01). The cell morphology of knock-out cells exhibited stemness like features and the upregulation of the foetal isoform of HNF4a, P2 (p < 0.001). CYP3A4 expression and activity were reduced (p < 0.001). RNA-seq confirmed the increase of EPCAM and Vimentin and the reduction of CYP3A4 across the SLC38A4-KO lines. Additionally, SLC38A4-KO resulted in differential expression of other SLC genes and cell growth/differentiation regulating genes (Figure 1C). Pathway analysis indicated changes in amino acid metabolism and cytokine signalling pathways.



Conclusion: *SLC38A4*, a gene identified as a potential risk locus in sAH through genetic studies, demonstrates reduced hepatic expression in patients with disease. This expression is downregulated *In vitro* by recognised disease drivers. *SLC38A4* knock out in cell lines recapitulates several features considered important in disease pathogenesis.

THU041

Refining the natural history of alcohol related liver disease: a competing risk analysis

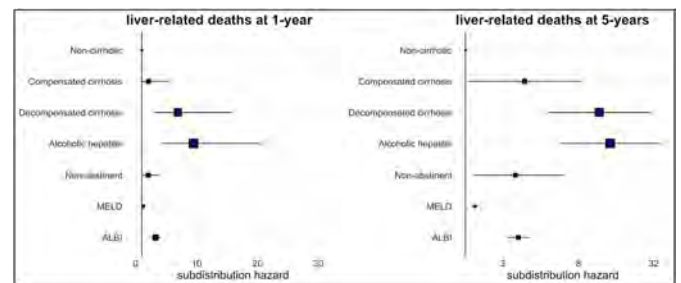
Richard Parker¹, Guruprasad Aithal², Michael Allison³, Juan Pablo Arab⁴, Mayur Brahmanian⁵, Ewan Forrest⁶, Hannes Hagström⁷, Alisa Likhitsup⁸, Steven Masson⁹, Anne McCune¹⁰, Neil Rajoriya¹¹, Ian Rowe¹². ¹Leeds Teaching Hospital Trust, Leeds Liver Unit, Leeds, United Kingdom; ²NIHR Nottingham BRC, Nottingham, United Kingdom; ³Addenbrooke's Hospital, Hepatology, Cambridge, United Kingdom; ⁴Pontificia Universidad Católica de Chile, Departamento de Gastroenterología, Santiago, Chile; ⁵Western University, Department of Gastroenterology and Multiorgan Transplant, London, Canada; ⁶Queen Elizabeth Hospital, Hepatology, Glasgow, United Kingdom; ⁷Karolinska University Hospital, Centre for Digestive Diseases, Stockholm, Sweden; ⁸St Luke's Hospital Kansas City, Kansas City, United States; ⁹Newcastle Upon Tyne Hospitals NHS Foundation Trust, Liver Unit, Newcastle Upon Tyne, United Kingdom; ¹⁰University Hospitals Bristol NHS Foundation Trust, Department of Liver Medicine, Bristol, United Kingdom; ¹¹University Hospitals Birmingham NHS Foundation Trust, Liver and Hepatobiliary Unit, Birmingham, United Kingdom; ¹²University of Leeds, Leeds Institute for Medical Research, Leeds, United Kingdom
Email: richardparker@nhs.net

Background and aims: Alcohol-related liver disease (ALD) is common throughout the world and is a frequent cause of ill-health and death. Alcohol consumption affects multiple organs and systems, therefore, increasing the risk of a wide range of conditions. Previous systematic review demonstrated that both liver and non-liver related mortality increased depending on the stages of liver disease. We have analysed a cohort of patients with biopsy-proven liver disease using competing risk analysis to accurately describe the risks of liver and non-liver related outcomes in ALD.

Method: WALDO is an international, retrospective cohort of patients with biopsy-proven liver disease followed up through health records to capture outcome data regarding mortality and morbidity. Competing risk analysis was used to estimate cumulative incidence functions (CIF) of mortality (liver-related or non-liver related deaths), and morbidity. Morbidity was classed as liver-associated clinical

events (LACE) and major adverse medical events included cancer, cardiovascular disease or diabetes. Subdistribution hazards were calculated with univariable and multivariable analyses to understand factors affecting outcomes. These analyses were used to describe the cumulative incidence of liver-specific mortality for given MELD scores.

Results: The WALDO cohort includes 710 patients of whom 423 had cirrhosis. Alcoholic hepatitis was present in 184 patients at the time of biopsy, and 216 patients were not cirrhotic and without alcoholic hepatitis. During a median follow-up of 4.6 years (IQR 1.1–9.5 years, totalling over 4 thousand patient-years) there were 381 deaths (54% of the total cohort) and 47 patients (7%) underwent liver transplantation. Deaths were liver related in 144 cases (39% of all deaths). New LACE occurred in 87 patients during follow-up and new medical morbidity occurred in 133 patients (19%). When compared to patients without cirrhosis CIF for liver-related death was significantly higher in patients with cirrhosis (1.87, 1.56–2.18, $p = 0.042$), decompensated cirrhosis (5.88, 5.60–6.165, $p < 0.001$) and alcoholic hepatitis (6.40, 6.12–6.68, $p < 0.001$), whereas the CIF of non-liver related deaths was not significantly different. The strongest baseline predictors of outcomes were stage of disease, MELD or ALBI scores, and abstinence. The cumulative incidence of liver-related deaths at sample baseline MELD scores of 6, 12, and 20 was 8%, 18% and 49% respectively with significant differences between patients who were abstinent or non-abstinent.



Conclusion: Patients with ALD are at risk of multiple causes of ill health. Competing risk analysis takes these into account to give a more accurate analysis of the probability of outcomes. The risk of liver-related mortality increases significantly above that of non-liver related mortality only in decompensated cirrhosis and alcoholic hepatitis.

THU042

Potential biomarkers for differentiating alcoholic hepatitis from decompensated cirrhosis by serum metabolomic analysis

Adelina Horhat^{1,2}, Fischer Petra¹, Mina Ignat², Bogdan Procopet^{1,2}, Carmen Socaciu³, Stefanescu Horia². ¹Iuliu Hațieganu University of Medicine and Pharmacy, Cluj-Napoca, Romania; ²Regional Institute of Gastroenterology and Hepatology "Prof. Dr. O. Fodor", Cluj-Napoca, Romania; ³RTD Center for Applied Biotechnology BIODIATECH SC Proplanta, Cluj-Napoca, Romania
Email: adelinahorhat25@gmail.com

Background and aims: Patients with alcoholic hepatitis (AH) have a high risk of short-term mortality. The diagnosis of AH relies on clinical and biochemical parameters, but it is impossible to differentiate from alcoholic related decompensated cirrhosis (ArDC) without liver biopsy. The main objective of this study was to assess the metabolomic fingerprint of AH; Secondary objective was to identify potential biomarkers to differentiate between the AH and ArDC.

Method: We performed an untargeted metabolomic profiling of blood serum from 36 patients with biopsy proven AH and 36 patients with ArDC, using high performance liquid chromatography and mass spectrometry. More than 300 metabolites were identified; Eighty-

POSTER PRESENTATIONS

three molecules were selected for further analysis and the most significant biomolecules were selected to discriminate the AH versus ArDC phenotype and infection status.

Results: Seventy-two percent of patients were male and 97% of them had cirrhosis. The main molecules that showed increased levels in AH group comparative to ArDC group were C16 Sphinganine-1-phosphate (S1P), Prostaglandin F1a/b (PGF1a/b), Cerotic acid and arachidic acid while Prostaglandin D2/E2 (PGD2/E2), Prostaglandin E2-ethanolamide (PGE2-EA), dinor cholic acid, 12-ketodeoxycholic acid 2-hydroxy stearic acid, D-Sphingosine decreased (1a).

In the multivariate analysis, PLS-DA score plot showed a co-variance of 19.4%, with a good discrimination between AH and ArDC groups (figure 1b)

In the subgroup analysis, (infected AH and ArDC and non-infected AH and ArDC), a good discrimination was showed by S1P, with a p value = 1.49E-15, Mean Decrease Accuracy (MDA) >0.035 and an area value under ROC curve (AUC) of 0.984 (0.943–1) and PGD2/E2, which had a decreased level (p = 2.56E-1, MDA >0.025 and AUC 0.958 (0.898–0.994)) (Figure 1c, d). The semiquantitative analysis of the combination between S1P and PGD2 showed increased (95%) diagnostic accuracy to discriminate AH from ArDC, with 100% NPV and 100% Se.

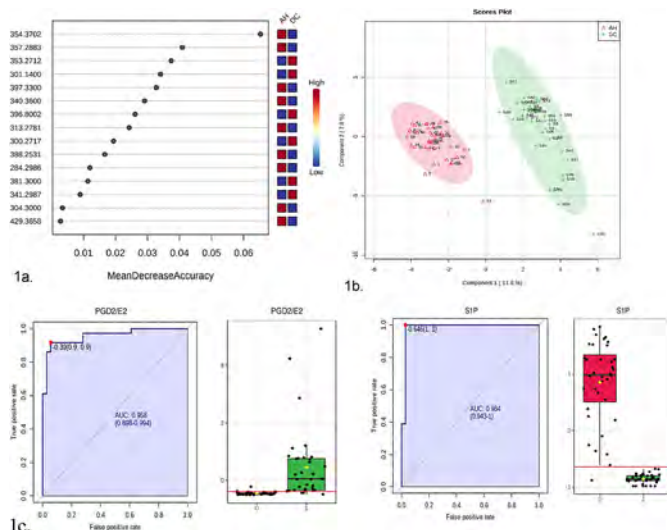


Figure 1: (a) Main molecules that showed good discrimination between AH and ArDC (red - increased, blue -decreased). (b) PLSDA score plot showed a co-variance of 19.4%, with a good discrimination between AH and ArDC groups. (c) AUC curves for S1P 0.984; (0.943-1) and PGD2/E2 0.958 (0.898-0.994).

Conclusion: Sphingolipids are now known to regulate important physiological cellular processes (1). Especially, S1P has an anti-necrotic and anti-inflammatory effects via TNF- α signaling pathway; In an ischemia/reperfusion (I/R) model, plasma S1P levels were noted to be decreased after hepatic I/R injury (2). Prostaglandins have protective effects by inhibiting the generation of reactive oxygen species and regulating the production of inflammatory cytokines. In

this study, the prostaglandin levels were decreased in patients with AH showing that beta-oxidation could be a valuable target pathway.

THU043

A phase II, multicenter, open-label, randomized trial of pegfilgrastim for patients with alcohol-associated hepatitis

**Timothy Morgan¹, Aliya Asghar¹, John Tayek², Danh Nguyen³,
M. Wayne Fleischman², John Donovan⁴, Joseph Alcorn⁵, Daniel Chao⁶,
Andrew Stolz⁴.** ¹VA Medical Healthcare System, Medicine, Long Beach,
United States; ²Harbor-UCLA Medical Center, Torrance, United States;
³University of California-Irvine, Irvine, United States; ⁴LAC-USC Medical
Center, Los Angeles, United States; ⁵VA Healthcare System, Albuquerque,
United States; ⁶VA Healthcare System, Loma Linda, United States
Email: timothy.morgan@va.gov

Background and aims: In trials conducted in India, recombinant granulocyte colony stimulating factor (GCSF) improved survival in alcohol-associated hepatitis (AH). The aim of this trial was to determine the safety and efficacy of pegfilgrastim, a long-acting recombinant GCSF, in patients with AH in the United States.

Method: This prospective, open label trial randomized patients with a clinical diagnosis of AH and a Maddrey discriminant function score ≥ 32 to standard of care (SOC) or SOC+pegfilgrastim (0.6 mg subcutaneously) on Day 1 and Day 8. SOC was 28 days of either pentoxifylline or prednisolone, as determined by the patient's primary physician. The second injection of pegfilgrastim was not administered if the white blood cell count exceeded 30,000/mm³ on Day 8. Primary outcome was survival at Day 90. Secondary outcomes included the incidence of acute kidney injury (AKI), hepatorenal syndrome (HRS), hepatic encephalopathy, or infections.

Results: The study was terminated early due to COVID19 pandemic. Eighteen patients were randomized to SOC and 16 to SOC+pegfilgrastim. All patients received prednisolone as SOC. Nine patients failed to receive a second dose of pegfilgrastin due to WBC>30, 000/mm³ on Day 8. Survival at 90 days was similar in both groups (SOC: 0.83 [95% confidence interval {CI}: 0.57–0.94] vs. pegfilgrastim: 0.73 [95% CI: 0.44–0.89]; *p* > 0.05). The incidences of AKI, HRS, hepatic encephalopathy, and infections were similar in both treatment arms and there were no serious adverse events attributed to pegfilgrastim.

Conclusion: This phase II trial found no survival benefit at 90 days among subjects with AH who received pegfilgrastim+prednisolone compared with subjects receiving prednisolone alone.

THU044

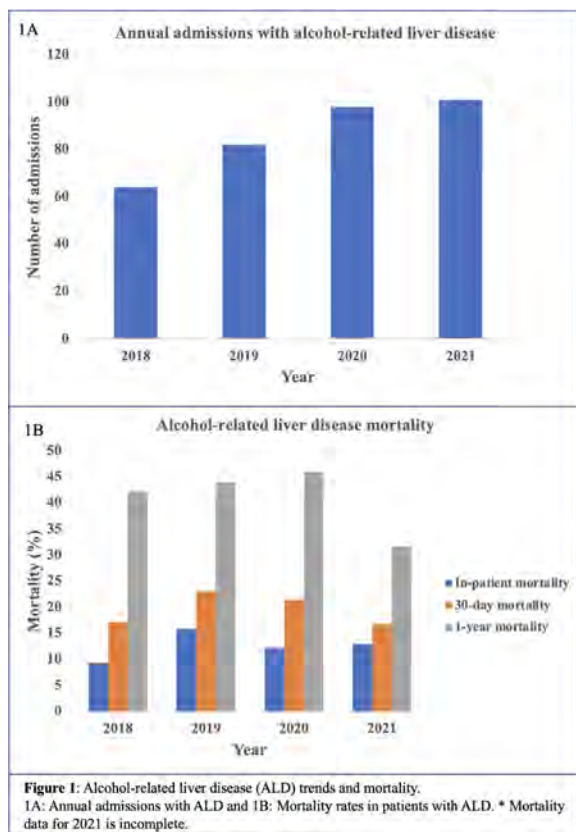
Trends of alcohol-related liver disease hospitalisation during the COVID-19 pandemic

Oyekoya Ayonrinde^{1,2,3}, Richard Goodheart¹. ¹Fiona Stanley Hospital, Gastroenterology and Hepatology, Murdoch, Australia; ²The University of Western Australia, Medical School, Crawley, Australia; ³Curtin University, Faculty of Health Sciences, Bentley, Australia
Email: oyekoya.ayonrinde@uwa.edu.au

Background and aims: Alcohol-related liver disease (ALD) is a common and potentially serious liver disorder associated with substantial morbidity and mortality. Recent reports have described increased alcohol since the onset of the COVID-19 pandemic. Therefore, the primary aim of this study was to examine trends in ALD hospital admissions prior to and during the Covid-19 pandemic. The secondary aim was to assess patient demographic and clinical characteristics associated with short and medium-term mortality.

Method: We retrospectively analysed data on patients who were admitted with ALD to a quaternary care hospital in Australia. The study population comprised adults hospitalised with International Classification of Diseases, Tenth Revision (ICD-10) principal diagnosis code K70.1 (alcoholic hepatitis), 70.3 (alcoholic cirrhosis), and 70.4 (alcoholic hepatic failure) between January 2018 and December 2021. Data recorded included patient demographics, alcohol history, clinical and laboratory characteristics. The Model for End Stage Liver Disease (MELD) score was calculated.

Results: Amongst 345 hospitalisations with ALD, there was a non-statistically significant rise in cases comparing the two years preceding and during the first two years of the COVID-19 pandemic (Figure 1). There were 104 (30.1%) ARH and 69.9% with decompensated ARC or alcoholic liver failure (ALF). Those with ARH, compared with those with ARC and ALF, had a higher mean [standard deviation] MELD score (22.6 [9.3] vs. 20.3 [7.8], $p = 0.02$), were younger (47.6 [11.7] vs 54.6 [10.6] years, $p < 0.001$), had longer median [interquartile range] length of hospital stays (7.7 [4.0–13.0] vs. 6.0 [2.0–9.0] days, $p = 0.008$), and were predominantly male (58.7%). The in-hospital mortality was 12.8% overall, comprising 17.3% with ARH, 10.8% with ARC/ALF, and 5/47 (10.6%) aged under 40 years. Patients aged <40 years, compared with those ≥ 40 years had a similar 30-day mortality (14.9% vs. 20.5%, $p = 0.37$) but lower one-year mortality (25.5% vs. 43.0%, $p = 0.02$). Using multivariable logistic regression analysis, predictors of 30-day mortality were male sex (odds ratio [OR] 2.89, 95% confidence interval [CI] 1.29–6.46, $p = 0.02$), age (OR 1.06, 95% CI 1.02–1.10, $p = 0.004$), serum bilirubin (OR 1.006, 95% CI 1.003–1.008, $p < 0.001$), respiratory failure (OR 3.64, 95% CI 1.62–8.21, $p = 0.002$), hepatic encephalopathy (OR 6.43, 95% CI 2.91–14.21, $p < 0.001$), and type 2 hepatorenal syndrome (OR 3.27, 95% CI 1.55–6.87, $p = 0.002$).



Conclusion: Admissions with ALD have risen during the COVID-19 period. Young adults with severe ALD requiring hospitalisation, have a high mortality that is identical to mortality after a fractured neck of

femur in older people. Multi-organ involvement and male sex predict mortality.

THU045

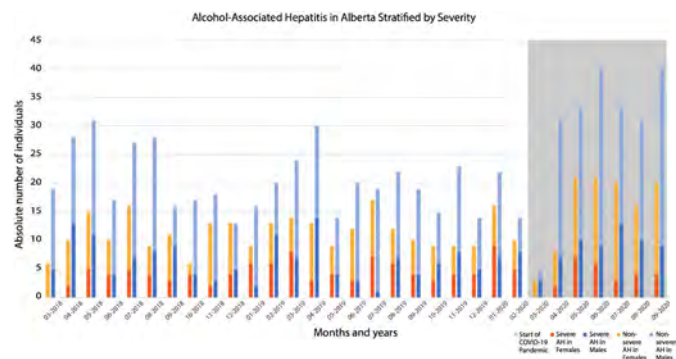
Increased hospital admissions for alcohol-associated hepatitis during the COVID-19 pandemic in Alberta, Canada: a retrospective cohort study

Alexandra Frolkis¹, Meredith Borman¹, Matthew Sadler¹, Stephen Congly¹, Henry Nguyen¹, Samuel Lee¹, Mark G Swain¹, Kelly Burak¹, Carla Coffin¹, Alexander Aspinall¹, Laura Stanton¹, Abdel Aziz Shaheen¹. ¹University of Calgary, Calgary Liver Unit
Email: adfrolki@ucalgary.ca

Background and aims: Alcohol-associated hepatitis (AH) is the most severe and fulminant form of alcohol-related liver disease with females at greater risk of liver injury from alcohol use. Alcohol consumption increased during the COVID pandemic. The aim of our study was to assess the changing epidemiology of hospitalizations for AH by sex before and during the COVID-19 pandemic.

Method: We identified all hospitalizations for adults >18 -years-old in Alberta, Canada using a validated algorithm of international classification of disease-10 codes and lab values for AH between March 2018 and September 2020. Severe AH was defined as Model for End-Stage Liver Disease (MELD) >20 . Onset of the pandemic was defined as March 2020. Logistic regression was used to identify factors associated with AH severity, and separately mortality, adjusted for age, sex, and pandemic onset. Binomial regression was used to assess changes in frequency of admission for AH with the denominator as all cirrhosis-related admissions over the same time-period.

Results: There were 991 hospitalizations for AH prior to the pandemic ($n = 381$, 38.5% female) and 417 during the pandemic ($n = 144$, 34.5% female). Hospitalizations for AH significantly increased during the pandemic ($p = 0.04$) (Figure 1). Overall, a higher percentage of females (34.5%) had severe AH compared to males (31.0%) however this difference was not statistically significant ($p = 0.25$) (Figure 1). Though the total number of hospitalizations for AH increased during the pandemic, the odds of severe AH was higher pre-pandemic (odds ratio [OR] 0.73; 95% confidence interval [CI] 0.55–0.98) after adjusting for age and sex. For every year increase in age, the adjusted odds of severe AH increased by 1.02 (95% CI 1.01–1.03). Prior to the pandemic, more females (38.6%) than males (32.2%) had severe AH; during the pandemic, more males (28.4%) than females (24.0%) had severe AH though these differences were not statistically significant ($p = 0.1$). Median age at admission was significantly lower for both male and female during the pandemic (age 44 and 41, respectively) as compared to prior (age 47 and 45, respectively) $p < 0.05$. There was no significant difference in mortality between sexes before (10.4% in female, 11.5% in male, $p = 0.22$) and after the pandemic (9.2% in female, 9.9% in male, $p = 0.67$).



Conclusion: Hospitalizations for AH rose during the pandemic and occurred at younger ages in both sexes with less severe presentations.

POSTER PRESENTATIONS

There was no significant difference in mortality by sex before and during the first wave of the pandemic. Advanced age was associated with more severe AH. Public health efforts should continue to educate about the harms of alcohol excess and offer community support.

THU046

The lysosomal enzyme cathepsin D as a new marker for alcoholic liver disease

Mengying Li¹, Tom Houben¹, Mads Israelsen², Maria Kjærgaard², Marit Westertorp³, Aleksander Krag², Maja Thiele², Ronit Shiri-Sverdllov¹. ¹School of Nutrition and Translational Research in Metabolism, Maastricht University, Department of Genetics and Cell Biology, Netherlands; ²Center for Liver Research, Odense University Hospital and University of Southern Denmark, Odense, Denmark; ³University Medical Center Groningen, University of Groningen, Department of Pediatrics, Groningen, Netherlands
Email: r.sverdllov@maastrichtuniversity.nl

Background and aims: Alcohol is the seventh leading cause of premature death worldwide, many of whom die from alcohol-related liver disease (ALD). However, the underlying pathological mechanisms that cause the early stages of ALD are currently under-investigated. Lysosomal cathepsin D (CTSD) was previously shown to be useful in detecting NASH, and circulating CTSD is elevated in advanced liver disease. We therefore investigated plasma CTSD in relation to different histological stages of early ALD.

Method: We conducted a cross-sectional study of 305 asymptomatic ALD patients with a liver biopsy scored according to the NAS CRN system, and compared their plasma CTSD levels with 40 healthy controls, matched for age, gender and BMI. We excluded patients with decompensation at baseline. Next, we determined the correlations between plasma CTSD levels and histology scored for fibrosis, ballooning, lobular inflammation and steatosis. Areas under the receiver operating characteristic curve (AUC) were generated to investigate the accuracy of plasma CTSD levels alone or in combination with known non-invasive markers of fibrosis to predict ALD.

Results: Plasma CTSD levels were significantly higher in ALD patients compared to matched healthy controls (37.7 vs 22.9 ng/ml; AUC 0.84). The highest CTSD levels was measured in ALD patients with no ballooning and lobular inflammation, and a slightly lower CTSD levels were observed in patients with more severe inflammatory activity. Further, plasma CTSD levels exhibited a weak negative correlation with the ELF test and transient elastography, and did not correlate with fibrosis stage. Moreover, transient elastography, ELF, GGT, AST/ALT, and AST independently correlated with plasma CTSD levels. Furthermore, combining plasma CTSD levels with transient elastography and AST/ALT resulted in a high diagnostic accuracy (ROC-AUC: 0.908) for predicting ALD.

Conclusion: Lysosomal leakage of CTSD into the circulation may be a sensitive marker of early stages of ALD.

THU047

Ductular bilirubinostasis is a diagnostic biomarker for acute-on-chronic liver failure: results from a well-defined cohort of patients with alcoholic steatohepatitis

Annelotte Broekhoven¹, Tessa Ostin², Lukas Van Melkebeke³, H.W. Verspaget¹, Schalk van der Merwe³, Jef Verbeek¹, Minneke Coenraad¹, Tania Roskams², Frederik Nevens³. ¹Leiden University Medical Center, Gastroenterology and Hepatology, Leiden, Netherlands; ²Translational Cell and Tissue Research, KU Leuven, Imaging and Pathology, Leuven, Belgium; ³University Hospitals KU Leuven, Gastroenterology and Hepatology, Leuven, Belgium
Email: a.g.c.broekhoven@lumc.nl

Background and aims: Alcoholic steatohepatitis (ASH) is one of the main precipitating events for the development of acute-on-chronic liver failure (ACLF). Ductular bilirubinostasis (DB) is identified as a

marker of ACLF in alcoholic cirrhosis, but overall, the histological features of ACLF are not well characterized. We assessed the diagnostic and prognostic value of DB and other histological features in addition to clinical features for the presence and development of ACLF in a well-defined cohort of ASH patients.

Method: Prospective study in consecutive patients admitted with a diagnosis of ASH to a tertiary referral center between 03-2008 and 04-2021. Diagnosis of ASH was based on clinical presentation and confirmed by transjugular liver biopsy. All biopsies were assessed by a dedicated liver pathologist who was blinded for clinical data and outcome. Clinical and histological data were collected from time of biopsy until 1 year follow-up. Diagnosis of ACLF was based on EASL-CLIF criteria. Differences between patients with and without ACLF at baseline were assessed using chi-square test. Predictors for development of ACLF within 28 days were assessed using Cox regression.

Results: 184 patients with biopsy-confirmed ASH were enrolled, with a median follow-up time of 365 days (IQR 83.5-365). At baseline, ACLF was present in 73 patients (39.7%). Another 30 (16.3%) patients developed ACLF within 28 days (median 7.5 days, IQR 2-20). At baseline, DB was significantly more present in patients with ACLF compared to patients without ACLF (50.7% vs. 30.6%, $p=0.007$). Presence of DB was not correlated with level of c-reactive protein, level of white blood cell count, presence of infection or positive blood culture (all $p>0.05$). None of the other histological features, including the histological severity of ASH, was associated with presence of ACLF. The CLIF-C AD score predicted the development of ACLF at 28-days (HR_{cs} 1.09, $p<0.001$). However, no association between histological features and development of ACLF could be found.

Conclusion: In this well-defined cohort of patients with biopsy-proven ASH, we show that DB is a histological feature of the presence of ACLF. Presence of DB was independent of presence of clinical features of sepsis within this group. The CLIF-C AD score had a high performance in predicting the development of ACLF, while the additional role of histology seems limited.

NAFLD: Clinical aspects except therapy

THU048

The most recent and in-depth meta-analytic assessment of the global epidemiology of non-alcoholic fatty liver disease (NAFLD)

Zobair Younossi^{1,2,3}, Pegah Golabi^{1,2,3}, James Paik^{1,2,3}, Austin Henry², Catherine Van Dongen², Linda Henry^{3,4}. ¹Inova Fairfax Medical Campus, Center for Liver Disease, Department of Medicine, Falls Church, United States; ²Inova Health System, Betty and Guy Beatty Center for Integrated Research, Falls Church, United States; ³Inova Health System, Inova Medicine, Falls Church, United States; ⁴Center for Outcomes Research in Liver Disease, Washington, DC, United States
Email: zobair.younossi@inova.org

Background and aims: NAFLD is a leading cause of liver-related morbidity and mortality. We assessed the global and regional prevalence and incidence of NAFLD using an in-depth meta-analytic approach.

Method: We systematically searched PubMed and Ovid MEDLINE® for population-based studies of NAFLD published 2015-2021 (data collected: 1988-2020). Two reviewers extracted data according to age, sex, race, diagnostic methods, sample size, data collection year, comorbidities, and other study characteristics. Adjustments were applied using prevalence of viral hepatitis and ALD from the Global Burden of Disease study 2019 to approximate prevalence and incidence of NAFLD in general population. The meta-analysis was conducted using a random-effects model. Assessment of bias risk used the Joanna Briggs Institute Critical Appraisal Instrument for studies reporting prevalence data.

Results: Of 1,857 studies included, 132 studies (N=9,945,423) met the eligibility criteria [106 NAFLD prevalence and 26 NAFLD incidence, high-income North America (H-NA, 19.8%), high-income Asia Pacific (27.4%), East Asia (23.6%), and Western Europe (WE, 11.3%)]. The pooled global prevalence of NAFLD based on a random-effects model was 29.1% (95% confidence interval: 26.8–31.5%). The highest prevalence was reported in Latin America (n=3, 44.4% [30.7–59.0%]), followed by Middle East and North Africa (MENA) (n=9, 39.9% [32.6–47.6%]), H-NA (n=21, 32.9% [27.4–38.9%]) and WE (n=12, 24.6% [19.1–31.0%]). The prevalence of NAFLD increased over time: 1991–2006 (n=10, 24.4% [19.6–30.0%]), 2007–2010 (n=28, 25.7% [22.1–29.7%]), 2011–2015 (n=38, 27.9% [24.1–32.0%]) and 2016–2020 (n=30, 36.0% [31.6–40.7%]). The global prevalence rate of NAFLD varied between 11.23%–48.61% depending on the diagnostic modality (Table). The incidence of NAFLD ranged from 19.0–99.0 per 1,000 person-years. Meta-regression showed that diagnostic method/criteria ($p < .001$), data collection year ($p = 0.004$) and geographic location ($p = 0.015$) jointly accounted for 72.1% of the heterogeneity between studies.

Diagnostic Modality	N. of study	Prevalence % (95% CI)	I ²
Ultrasound: mild to severe steatosis	54	32.61 (30.30 to 35.01)	99.74
Ultrasound: moderate to severe steatosis	14	15.36 (13.33 to 17.63)	99.07
Controlled Attenuation Parameter	9	40.78 (32.22 to 49.93)	99.47
CAP of ≥ 248 dB/m	3	46.76 (37.12 to 56.65)	98.50
CAP of ≥ 260 dB/m	3	48.61 (43.16 to 54.08)	95.29
CAP of ≥ 274 dB/m	3	27.71 (16.41 to 42.80)	99.20
Computerized Tomography	3	11.23 (8.37 to 14.89)	93.43
Non-invasive Biomarkers (FLI, US-FLI, HIS)	22	31.11 (26.37 to 36.28)	99.95
Other (ICD-9 or 10)	4	25.23 (23.37 to 27.18)	81.36

Conclusion: The global prevalence of NAFLD is high and growing. Given its impact on the heterogeneity of the reported studies, it is critical to use standardized diagnostic criteria to provide accurate and consistent epidemiologic data across the world.

THU049

Comorbidities and malignancy among NAFLD patients compared to general population

Naim Abu-Freha¹, Bracha Cohen², Michal Gordon³, Alexander Fich², Daneila Munteanu⁴, David Yardeni⁴, Ohad Etzion⁵. ¹Soroka University Medical Center, Department of Gastroenterology and liver diseases, Beer Sheva, Israel; ²Soroka University Medical Center, Beer-Sheva, Israel; ³Soroka University Medical Center, Beer-Sheva, Israel; ⁴Soroka University Medical Center, Beer Sheva, Israel; ⁵Soroka University Medical Center, Beer Sheva, Israel
Email: abufreha@yahoo.de

Background and aims: Non-alcoholic fatty liver disease (NAFLD) is a common liver disease; we aimed to investigate the frequency of comorbidities and malignancy among NAFLD patients compared to general population.

Method: Retrospective study included all patients older than 18 years with NAFLD diagnosis. A control group was matched in gender and age. The data were extracted using the MDClone platform of the largest health maintenance organization "Clalit" in Israel. Demographics, comorbidities, malignancy and mortality were collected and compared.

Results: 211,955 NAFLD patients (mean age 42.2 ± 15 years, 47.2% males) were analyzed in comparison to 452,012 matched general population controls (mean age 42.4 ± 14.8 years, 48.5% males). Significant higher rate of diabetes mellitus (23.2% vs 13.3%), obesity (58.8% vs 27.8%), Hypertension (57.2% vs 39.9%), chronic ischemic

heart disease (24.7% vs 17.3%), CVA (3.2% vs 2.8%) and chronic obstructive lung disease (10.1% vs 8.3%) was found among NAFLD patients. Patients with NAFLD have significant higher rate of the following malignancy: prostate (1.6% vs 1.2%) breast cancer (2.6% vs 1.9%), colorectal cancer (1.8% vs 1.4%), uterus (0.4 vs 0.2%) kidney (0.8% vs 0.5%), melanoma (1.6% vs 1.2%), basal cell carcinoma (11.6% vs 8.6%) thyroid (0.7% vs 0.5%) cancer, non-Hodgkin lymphoma (0.7% vs 0.6%) and lower rate of lung cancer (0.9% vs 1.2%), stomach (0.3% vs 0.4%). The all-cause mortality among NAFLD patients was significantly lower in comparison to general population (10.8% vs 14.7%, $p < 0.001$)

Conclusion: Higher rate of comorbidities and malignancy among NAFLD patients was observed, but lower rate of all-cause mortality was found.

Keywords: Fatty liver, comorbidities, malignancy, Israel

THU050

The prevalence of non-alcoholic fatty liver disease in the United Kingdom: a systematic review and meta-analysis

Yusef Alenezi¹, Timothy Card^{1,2}, Joanne Morling^{1,2}, Rebecca Harris². ¹University of Nottingham, Lifespan and Population Health, Nottingham, United Kingdom; ²University of Nottingham, NIHR Nottingham Biomedical Research Centre (BRC), United Kingdom
Email: msxya10@nottingham.ac.uk

Background and aims: Non-alcoholic fatty liver disease (NAFLD) is a growing cause of cirrhosis and indication for a liver transplant. Since this growth is putting pressure on hepatology services and healthcare systems, up-to-date measures of the size of the problem are needed to plan future services. We have therefore conducted a systematic review of studies in the UK to estimate the prevalence of NAFLD.

Method: We identified studies that investigate NAFLD prevalence among the UK population through a systematic search of electronic databases (PubMed, EMBASE via OVID, CINAHL, Web of Science, and Google). A random-effects meta-analysis was performed on subsets of studies limited to populations with specific conditions and those not so restricted.

Results: Our study included a total of 25,439 participants from 9 studies. Our results indicate a pooled prevalence of 23.7% in non-disease restricted populations (95% CI 20.6%–26.8%). Of the disease restricted populations, a single study of HIV patients reported a prevalence of 71.2% (CI: 59.7%–82.7%). Two studies of liver-related hospital referral yielded a prevalence of 37.90% (CI: 15.3%–60.5%), a single study of BMI ≥ 25 (29.6%) (CI: 27.9%–31.3%), and type-1 diabetic patients (1.8%) (CI: 0.0%–3.6%). Our results also included three studies of type-2 diabetic patients with an overall prevalence of 38.6% (CI: 25.5%–51.7%).

Conclusion: Our major finding is that the prevalence of NAFLD within the UK general population is similar to the average global estimate. There is good evidence that adults with T2DM have a higher prevalence of NAFLD. We were unable to determine time trends in prevalence and so updates to this data will be essential to allow ongoing appropriate service planning.

THU051

Health-related quality of life is impaired in people living with HIV and hepatic steatosis

Maurice Michel^{1,2}, Christian Labenz^{1,2}, Malena Anders^{1,2}, Alisha Wahl^{1,2}, Lisann Girolstein^{1,2}, Leonard Kaps^{1,2}, Wolfgang Maximilian Kremer^{1,2}, Yvonne Huber^{1,2}, Peter Galle^{1,2}, Martin Sprinzi^{1,2}, Jörn Schattenberg^{1,2}. ¹Metabolic Liver Disease Research Program, I. Department of Medicine, University Medical Centre Mainz, Mainz, Germany; ²I. Department of Medicine, University Medical Centre Mainz, Mainz, Germany
Email: joern.schattenberg@unimedizin-mainz.de

Background and aims: People living with HIV (PLWH) show a high prevalence of hepatic steatosis and non-alcoholic fatty liver disease (NAFLD). NAFLD has been linked to impaired health-related quality of

POSTER PRESENTATIONS

life (HRQL) and therefore could be an aggravating factor in PLWH. The aim of this study was to determine differences in HRQL between PLWH presenting with and without hepatic steatosis and to identify predictors associated with impaired HRQL.

Method: A total of 245 PLWH were prospectively enrolled at an outpatient clinic. Hepatic steatosis was assessed using vibration controlled transient elastography (VCTE) and defined as a controlled attenuation parameter (CAP) of >275 dB/m. The cohort was then divided into two groups: no steatosis and steatosis. The generic EQ-5D-5L questionnaire was used to determine differences in the HRQL. It consists of an overall value (UI-value) and five dimensions, each addressing different aspects of an individual HRQL. Univariable and multivariable linear regression models were applied to identify predictors with impaired HRQL in both groups.

Results: In this cohort of PLWH, the prevalence of hepatic steatosis was 35% ($n=85$) of whom 76.5% ($n=65$) had NAFLD and 16.5% ($n=14$) alcoholic liver disease. The median age was 52 years (IQR 42; 58) and the majority of PLWH were male ($n=174$, 71%). Metabolic risk factors were more prevalent in the steatosis group. The mean UI-value in the total cohort was $0.90 (\pm 0.15)$. The HRQL (UI-value) was significantly lower in PLWH and steatosis in comparison to no steatosis ($p=0.013$). The most strongly affected dimensions were mobility ($p=0.016$) and pain/discomfort ($p=0.012$) in the steatosis group, and the dimension anxiety/depression was equally impaired in both groups ($p=0.629$) (Figure 1). Unemployment ($\beta=-0.270$, $p=0.025$) and waist circumference ($\beta=-0.289$, $p=0.017$) remained independent predictors of a poor HRQL in the steatosis subgroup. In turn, age ($\beta=-0.168$, $p=0.045$), female sex ($\beta=-0.173$, $p=0.030$), BMI ($\beta=-0.214$, $p=0.010$) and arterial hypertension ($\beta=-0.194$, $p=0.025$) were independent predictors of a low HRQL in the subgroup without steatosis.

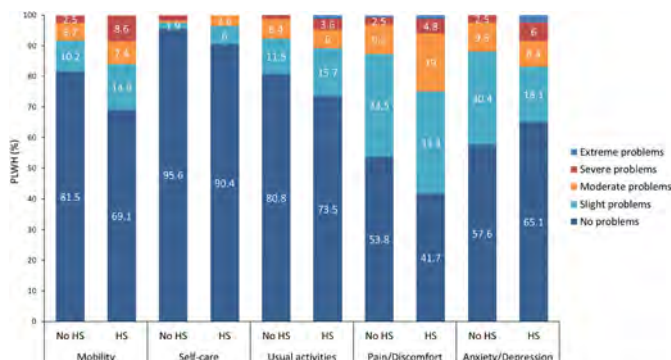


Figure 1: Distribution (%) of the EQ-5D-5L dimensions in PLWH and without hepatic steatosis (no HS) or with hepatic steatosis (HS).

Conclusion: Hepatic steatosis and metabolic comorbidities negatively affect HRQL. Addressing these factors may improve patient reported and liver related outcomes in PLWH.

Funding: This analysis was in parts supported by a research grant from Gilead Sciences.

THU052

Moderate alcohol consumption is associated with significant fibrosis progression in non-alcoholic fatty liver disease-a cohort study with over 17 years of follow-up

Julia Blomdahl¹, Patrik Nasr¹, Mattias Ekstedt¹, Stergios Kechagias¹.

¹Linköping University, Department of Gastroenterology and Hepatology, Department of Health, Medicine, and Caring Sciences, Linköping, Sweden

Email: julia.blomdahl@liu.se

Background and aims: Non-alcoholic fatty liver disease (NAFLD) affects approximately 25% of the adult population worldwide. The effect of moderate alcohol consumption on NAFLD histology is disputed. Assessment of alcohol consumption is commonly

performed with interview or questionnaires. A highly sensitive and specific alcohol biomarker is phosphatidylethanol in blood (PEth), which only forms in the presence of ethanol. PEth has hitherto not been evaluated in longitudinal NAFLD studies. This study aimed to examine the impact of moderate alcohol consumption on histologic progression and to evaluate the utility of PEth in NAFLD.

Method: A cohort of NAFLD patients with serial biopsies were reviewed for inclusion in the study. Baseline alcohol consumption was <140 g/week in all patients. Anthropometric and biochemical measurements were performed at baseline and follow-up. Alcohol consumption was measured at follow-up, using three different methods (clinical interview, Alcohol Use Disorder Identification Test-Concise [AUDIT-C], and analysis of PEth). Patients were reviewed for progression of steatosis, ballooning, lobular inflammation, and significant fibrosis progression, defined as progression of fibrosis stage ≥ 2 stages or development of end-stage liver disease (ESLD).

Results: Eighty-two patients were included. Mean follow-up time was 17.2 years ($SD \pm 6.0$). Twenty-two patients were considered to have fibrosis progression or developed ESLD. Patients with significant fibrosis progression reported higher alcohol consumption and had significantly higher PEth. Progression of other histological parameters (i.e., steatosis, ballooning and lobular inflammation) was unaffected during follow-up and showed no significant associations with alcohol consumption. Consumption $>66-96$ grams per week (i.e., moderate alcohol consumption) was associated with increased risk for significant fibrosis progression compared with no or low consumption. PEth ≥ 50 ng/ml and binge drinking showed the highest risk for significant fibrosis progression (aOR 5.2 [95% CI 1.4–19.6], $p<0.05$, and aOR 5.1 [95% CI 1.4–18.1], $p<0.05$, respectively).

Conclusion: NAFLD patients consuming moderate amounts of alcohol are at increased risk for significant fibrosis progression and development of ESLD. PEth can be used as a reliable biochemical alcohol marker in NAFLD. Patients reporting moderate consumption or exhibiting PEth ≥ 50 ng/ml should be advised to reduce alcohol consumption.

THU053

Prevalence trends of non-alcoholic fatty liver disease among young men in Korea: Korean military population-based cross-sectional study

Jaejun Lee^{1,2}, Hyun Yang¹, Si Hyun Bae². ¹Eunpyeong St. Mary hospital, Department of Internal Medicine, Seoul, Korea, Rep. of South; ²College of Medicine, Eunpyeong St. Mary's Hospital, The Catholic University of Korea, Department of Internal Medicine, Seoul, Korea, Rep. of South

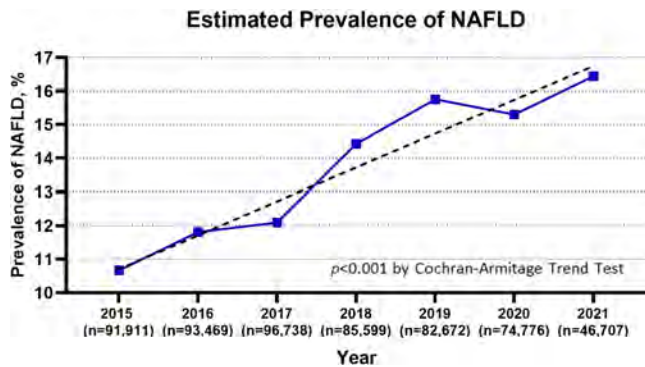
Email: baesh@catholic.ac.kr

Background and aims: Non-alcoholic fatty liver disease (NAFLD) has become a major concern in Korea since its emergence as a dominant cause of chronic liver disease. However, no study has explored its prevalence in adults under 30 years of age. Therefore, we performed a cross-sectional study to investigate the prevalence of NAFLD in Korean men in their early twenties.

Method: We collected data on 596, 359 Korean soldiers who participated in a health examination between January 2015 and July 2021. A total of 571, 872 individuals were analyzed after excluding those with missing data and hepatitis B antigen positivity. Hepatic steatosis was determined using the hepatic steatosis index (HSI). Participants with an HSI >36 were considered to have NAFLD. The BARD score was used to determine the presence of advanced fibrosis.

Results: All participants were men, and the mean age was 20.9 ± 1.3 years. Of the 571, 872 participants screened, 77, 020 (13.47%) were classified as having NAFLD. The prevalence of NAFLD consistently increased from 2015 to 2021 (10.66% vs. 16.44%, $P<0.001$). Increases from 2015 to 2021 were also noted in the prevalence of hypercholesterolemia (1.78% vs. 2.56%, $P<0.001$), dysglycemia (10.17% vs. 11.68%, $P<0.001$), and hypertension (2.87% vs. 3.51%, $P<0.001$). The mean body mass index (BMI) also increased from 23.3 ± 3.0 kg/m² to

23.9 ± 3.1 kg/m² between 2015 and 2021 (p < 0.001). Finally, 24, 092 out of 77, 020 (31.2%) participants with NAFLD had a BARD score of 2 or greater, which was indicative of advanced fibrosis.



Conclusion: The prevalence of NAFLD and of other metabolic dysfunctions (hypercholesterolemia, dysglycemia, and hypertension) in Korean men in their early twenties increased from 2015 to 2021. The Korean society should be alert for an increase in the disease prevalence and continue making efforts to reduce the associated complications.

THU054

Hepatocellular and extrahepatic cancers in non-alcoholic fatty liver disease: a systematic review and meta-analysis

James Thomas^{1,2}, Bradley Kendall^{1,2}, Christine Dalais², Graeme Macdonald^{1,2}, Aaron Thrift³. ¹Princess Alexandra Hospital, Woolloongabba, Australia; ²The University of Queensland, Saint Lucia, Australia; ³Baylor College of Medicine, Houston, United States
Email: aaron.thrift@bcm.edu

Background and aims: Non-alcoholic fatty liver disease (NAFLD) affects approximately one-quarter of the global adult population. Its prevalence is expected to continue to increase with rising rates of obesity and its associated metabolic disorders. Hepatocellular (HCC) and extrahepatic cancers have been associated with NAFLD however the extent and nature of this relationship remain to be clarified. We aimed to estimate the absolute incidence rates of these cancers in adults with NAFLD with respect to key clinical factors.

Method: This systematic review and meta-analysis of published studies reporting the incidence rates of any cancer in adults with NAFLD was registered with PROSPERO (CRD42020164725). The literature search of 4 databases (PubMed, Embase, Cochrane Library and Web of Science) was from inception to 31 August 2020. Teams of independent reviewers assessed each record for inclusion with subsequent extraction of reported data. The main outcomes were pooled incidences of cancers in NAFLD using a random-effects model with subgroup analyses to examine the effects of NAFLD disease stage.

Results: The systematic review returned 10, 042 unique records from which 64 studies including 625, 984 and 41, 027 patients were eligible for analysis of HCC and extrahepatic cancer incidence respectively. The pooled HCC incidence rate was 1.25 per 1000 person-years (95%CI 1.01–1.49; I² = 94.8%). In NAFLD patients with advanced liver fibrosis or cirrhosis, the HCC incidence rate was 14.46 per 1000 person-years (95%CI 10.89–18.04; I² = 91.3%). The pooled extrahepatic cancer incidence rate was 10.58 per 1000 person-years (95%CI 8.14–13.02; I² = 97.1%). The most frequently occurring extrahepatic cancer sites were uterine, breast, prostate, colorectal and lung. Extrahepatic cancer incidence rates were not higher in NAFLD patients with advanced liver fibrosis or cirrhosis.

Conclusion: The rate of HCC development in NAFLD patients who have progressed to advanced liver fibrosis or cirrhosis supports current HCC surveillance recommendations targeted for this group.

The pooled incidence rate of extrahepatic cancers in NAFLD is over eight-fold higher than HCC. Extrahepatic cancer rates are not related to liver fibrosis stage thereby implicating the metabolic dysfunction associated with NAFLD as a risk factor for these malignancies. Given the high and increasing prevalence of NAFLD, these findings support a public health focus on its prevention and the early detection of cancer in adults with NAFLD.

THU055

Association of non-alcoholic fatty liver disease and fibrosis with incident dementia and cognitive function: the Rotterdam Study

Tian Xiao¹, Laurens van Kleef², Kamran Ikram¹, Robert De Knegt², Arfan Ikram¹. ¹Erasmus MC, University Medical Center, Epidemiology, Rotterdam, Netherlands; ²Erasmus MC, University Medical Center, Gastroenterology and Hepatology, Rotterdam, Netherlands
Email: l.vankleef@erasmusmc.nl

Background and aims: Non-alcoholic fatty liver disease (NAFLD) might affect brain health, via the so-called liver-brain axis. Whether this results in increased risk for dementia remains unclear. Therefore, we investigated the association of NAFLD and fibrosis with incident dementia and cognition among the elderly.

Method: We performed longitudinal and cross-sectional analyses within The Rotterdam Study, an ongoing prospective cohort. Participants visiting between 1997 and 2002 with available fatty liver index (FLI) (set 1; n = 3, 975; FU = 15.5 years) or participants visiting between 2009 and 2014 with abdominal ultrasound (set 2; n = 4, 577; FU = 5.7 years) and liver stiffness (set 3, n = 3, 300; FU = 5.6 years) were included. Exclusion criteria were secondary causes for steatosis, prevalent dementia and missing alcohol data. NAFLD was defined as FLI ≥ 60 or steatosis on ultrasound and fibrosis as liver stiffness ≥ 8.0 kPa. Dementia was defined according to the DSM-III-R. Cox-regression was used to quantify associations for NAFLD, fibrosis, or liver stiffness with incident-dementia and logistic regression for NAFLD and cognitive function.

Results: NAFLD and fibrosis were consistently not associated with increased risk for dementia (NAFLD based on ultrasound, HR:0.84, 95%CI:0.61–1.16; NAFLD based on FLI, HR:0.92, 95%CI:0.69–1.22; fibrosis, HR:1.07, 95%CI:0.58–1.99) in fully adjusted models. Interestingly, NAFLD was associated with a significantly decreased risk for incident dementia until five years after FLI-assessment (HR:0.48; 95%CI:0.24–0.94). Moreover, NAFLD was not associated with worse cognitive function (G-factor, mean difference:0.032; 95% CI:-0.029–0.092).

Table 1: Risk of incident dementia for NAFLD and liver stiffness

	cases	FU (year)	Fully adjusted models	
			HR	95% CI
NAFLD (FLI ≥ 60)	753/3975	15.5	0.92	0.69–1.22
NAFLD (Ultrasound)	262/4557	5.7	0.84	0.61–1.16
Fibrosis	127/3300	5.6	1.07	0.58–1.99
Liver stiffness (kPa)	127/3300	5.6	1.01	0.92–1.10

Results are given as HR and 95% CI for incident dementia as outcome. NAFLD was either based on FLI ≥ 60 or on hepatic steatosis assessed with abdominal ultrasound and was compared to participants with FLI < 30 or participants without hepatic steatosis.

Conclusion: In conclusion, individuals with NAFLD were not at increased risk of dementia among this general elderly population, nor could an association with fibrosis and dementia be demonstrated. Moreover, NAFLD was associated with a reduced risk of dementia for the first five years after the assessment, suggesting that NAFLD regression is likely before dementia onset, which could be driven by weight loss before dementia onset. As yet, NAFLD may have no clinical implications for dementia awareness. Further studies should focus on NAFLD exposure duration and risk of dementia with longer follow-up durations.

THU056

High meat consumption is prospectively associated with non-alcoholic fatty liver disease and liver fibrosis markers

Dana Ivancovsky Wajcman¹, Naomi Fliss-Isakov², Laura Sol Grinshpan¹, Muriel Webb², Oren Shibolet², Revital Kariv², Shira Zelber-Sagi^{1,2}. ¹University of Haifa, School of Public Health, Haifa, Israel; ²Tel Aviv Medical center, Gastroenterology, Tel Aviv, Israel
Email: danaivanc@gmail.com

Background and aims: Non-alcoholic fatty liver disease (NAFLD) is a chronic disease related to lifestyle. The association of meat consumption with NAFLD has been tested. However, the prospective association between meat consumption and steatosis incidence and remission and liver fibrosis is yet to be tested. Therefore, this study aims to prospectively test the association of meat types consumption with incidence and remission of NAFLD and liver fibrosis markers.

Method: A prospective cohort study among subjects 40–70 years old, participating in two screening days, at least five years apart. NAFLD was determined by ultrasonography or CAP \geq 294 dB/m. Liver fibrosis was evaluated by Fibrotest (significant fibrosis \geq F2 was defined as a result of \geq 0.48) or Fibroscan (significant fibrosis \geq F2 was defined as a result of \geq 8.2 Kp). Meat consumption was assessed by a detailed food frequency questionnaire (FFQ), the trajectories of consumption were calculated as the percent of change from baseline (gr/d).

Results: A total of 320 subjects had completed two screening days and had valid FFQ. Mean follow-up of 6.65 \pm 0.73 years. In multivariate-adjusted analyses, high consumption of red and/or processed meat (gr/d above the baseline consumption median) was associated with higher risk for NAFLD with elevated ALT incidence (OR = 5.97, 1.84–19.37, P = 0.003). Unprocessed red meat consumption was associated with NAFLD with elevated ALT incidence, lower odds for NAFLD remission, and greater odds for new or persistent significant fibrosis, evaluated by Fibroscan (OR = 3.52, 1.22–10.17, P = 0.020; OR = 0.33, 0.14–0.78, P = 0.012; OR = 4.69, 1.43–15.40, P = 0.011, respectively). Regarding meat consumption trajectories, 10% daily increments in total or processed meat consumption were significantly associated with greater risk for new or persistent NAFLD (OR = 2.09, 1.20–3.65, P = 0.010; OR = 1.90, 1.04–3.46, P = 0.037, respectively).

Conclusion: High consumption of red meat or processed meat is associated with NAFLD and significant fibrosis in a prospective study

THU057

Relevance of diabetes medication on recruitment criteria for clinical studies in patients with non-alcoholic fatty disease and type 2 diabetes mellitus

Michael Holzhey¹, David Petroff², Valentin Blank¹, Florian Gerhardt³, Albrecht Boehlig³, Toni Herta³, Florian van Bömmel³, Thomas Berg³, Thomas Karlas¹, Johannes Wiegand³. ¹University of Leipzig, Division of Gastroenterology, Germany; ²University of Leipzig, Clinical Trial Center, Germany; ³University of Leipzig, Division of Hepatology, Leipzig, Germany
Email: johannes.wiegand@medizin.uni-leipzig.de

Background and aims: Guidelines for patients with diabetes mellitus increasingly recommend the use of sodium-glucose cotransporter 2 (SGLT-2) inhibitors and glucagon-like peptide 1 (GLP-1) agonists to prevent cardiovascular end points. Both drugs are promising candidates for treatment of non-alcoholic fatty liver disease (NAFLD). However, pre-existing therapies with SGLT-2 inhibitors or GLP-1 agonists are often an exclusion criterion for clinical trials. Thus, we analyzed use of diabetes medications and their adjustment.

Method: Patients with type 2 diabetes mellitus and NAFLD were prospectively recruited from 2011 to 2018 and followed up in 2021. They were characterized non-invasively by transient elastography (TE) including liver stiffness measurement (LSM), controlled attenuation parameter (CAP) and Fibroscan-AST-score (FAST). Diabetes

medication was recorded from patient charts. Data were compared to the time point of the first available TE measurement.

Results: 90 patients were recruited (57% female, age 63.9 \pm 9.6 years, BMI 31.3 \pm 5.0 kg/m², LSM 7.4 kPa [5.3, 14.1], CAP 315 \pm 57 dB/m, FAST 0.38 [0.18, 0.65]). After 4.2 [3.7, 7.9] years, follow-up data were available from 78 cases, the remaining 12 individuals had died.

At follow-up, patients received the following diabetes medication:

SGLT-2 inhibitors: 17/78 (22%)

GLP-1 agonists: 13/78 (17%)

Metformin: 42/78 (54%)

Dipeptidyl-Peptidase-4 (DPP-4) inhibitors: 15/78 (19%)

Insulin: 42/78 (54%).

From these five drug classes, patients took a mean of 1.38 substances at baseline compared to 1.65 at follow-up (difference 0.27, 95% CI 0.01 to 0.53, p = 0.046).

The net change compared to baseline was an additional 14 (18%), 10 (13%), and 7 (9%) patients on SGLT-2 inhibitors, GLP-1 agonists, and insulin, whereas metformin and DPP-4 were used in 9 (12%) and one (1%) fewer individuals.

The geometric mean of LSM changed from 8.3 to 7.8 kPa for a relative change by a factor of 0.94 (95% CI 0.85 to 1.03, p = 0.18).

Mean CAP changed from 313 to 306 dB/m for a change of – 7.4 dB/m (95% CI – 22.8 to 7.9, p = 0.34)

The mean of FAST score changed from 0.38 to 0.31 implying an odds ratio of 0.74 (95% CI 0.56 to 0.96, p = 0.027).

Conclusion: A relevant and increasing proportion of NAFLD patients with diabetes mellitus is treated with SGLT-2 inhibitors and GLP-1 agonists in clinical routine. These treatments affect recruitment for clinical studies and should be considered as confounders in case they are continued during the study period.

THU058

Comorbidity severity scores and cardiovascular comorbidities in patients with non-alcoholic steatohepatitis (NASH), with and without cirrhosis, in a real-world setting

Jeffrey Lazarus¹, Abhishek Shankar Chandramouli², Kamal Kant Mangla³, Zobair Younossi⁴. ¹Barcelona Institute for Global Health (ISGlobal), Hospital Clínic, University of Barcelona, Barcelona, Spain; ²Novo Nordisk Service Centre India Pvt Ltd, Bangalore, India; ³Novo Nordisk A/S, Søborg, Denmark; ⁴Center for Liver Disease, Inova Medicine, Falls Church, VA, United States
Email: Jeffrey.Lazarus@isglobal.org

Background and aims: NASH is estimated to be present in 3–6% of the US population and has been linked to end-stage liver disease, type 2 diabetes (T2D), and cardiovascular disease (CVD). The AWARE study aimed to describe the association of NASH with comorbidity severity scores and CVD comorbidities, which has not been well studied previously.

Method: Data were collected from a large US healthcare dataset covering 1 October 2015 to 31 December 2020. Records were included for adult patients diagnosed with NASH (using ICD-10 CM), with no evidence of hepatitis B or C, excessive alcohol use, or liver transplant prior to NASH diagnosis, and with no evidence of pregnancy or cancer in the study period. ICD CM coding was used to identify all diagnoses. Statistical significance of differences in comorbidities and severity scores between cirrhotic patients (CPs) and non-cirrhotic patients (NCPs) was assessed.

Results: Of 4,989 patients identified, 489 had evidence of cirrhosis prior to NASH diagnosis. CPs were older and more progressed in terms of NASH-relevant biomarkers, glycated haemoglobin (HbA_{1c}), and comorbidities (Table). CVD comorbidities were significantly higher in CPs at baseline, including atherosclerotic CVD, as were severity scores for T2D and comorbidities overall.

Table: Selected baseline characteristics

	NCPs (n = 4, 500)	CPs (n = 489)
Age, years	52.2 (11.0)	59.6 (9.4)
Female, %	55.2	62.4
NAFLD, %	56.5	67.4
Provider,	20: 17: 16	28: 11: 7
Gastroenterologist:		
Internist: GP, %		
Aspartate transaminase:	586; 0.62 (0.96)	86; 1.09 (1.57)
platelet ratio index*		
Fib-4*	493; 1.56 (1.42)	71; 4.68 (5.28)
NAFLD fibrosis score*	454; - 1.13 (1.63)	66; 1.74 (2.04)
Quan-Charlson	1.9 (1.5)	4.4 (1.9)
Comorbidity Index*		
Adaptive Diabetes	0.1 (0.4)	0.4 (1.0)
Complexity Severity Index*		
BMI (kg/m ²)	1, 957; 35.0 (5.7)	243; 35.1 (6.1)
Predicted waist circumference, cm	1, 957; 110.4 (15.0)	243; 109.4 (15.9)
HbA _{1c} (%)	485; 6.9 (1.7)	64; 7.1 (1.5)
T2D* %	40.6	73.4
Chronic kidney disease* %	5.9	17.8
Diabetic neuropathy* %	6.8	22.1
CVD* %	29.8	73.0
Atherosclerotic CVD*†	13.1	25.8
Heart failure*	2.2	13.3
Oesophageal varices*	1.2	33.3
Hypertensive disease* %	64.8	81.8

Data are mean (SD) or n; mean (SD) unless stated

BMI, body mass index; NAFLD, non-alcoholic fatty liver disease.

*Assessed by univariate analysis for statistical significance: p < 0.001 for NCPs vs CPs.

†Multivariate logistic regression analysis for atherosclerotic CVD, adjusted for demographic factors: odds ratio 1.34 (1.02, 1.78); p < 0.05 for CPs vs NCPs.

Conclusion: This study found that patients with NASH are often not diagnosed until an advanced stage, suggesting the need for greater disease awareness to avoid diagnostic inertia and to better assess the burden associated with NASH. These data also suggest that NASH correlates with a higher risk of developing comorbidities, especially CVD and T2D, particularly as patients progress to cirrhosis.

THU059

NAFLD association with renal impairment in type 2 diabetes patients

Jesús Rivera¹, Monica Pons¹, Alejandra Planas², Rafael Simo Canonge², Jordi Bañeras³, Ignacio Ferreira³, María José Soler⁴, Daniel Seron⁴, Joan Genesca¹, Juan Manuel Pericàs¹. ¹Vall d'Hebron Hospital Universitari, Liver Unit, Spain; ²Vall d'Hebron Hospital Universitari, Diabetes and Metabolism Research Unit, Spain; ³Vall d'Hebron Hospital Universitari, Cardiology Department, Spain; ⁴Vall d'Hebron Hospital Universitari, Nephrology Department
Email: jesusriveraest@gmail.com

Background and aims: Non-alcoholic fatty liver disease (NAFLD) and type 2 diabetes (T2DM) frequently coexists in high-risk metabolic patients. NAFLD and T2DM share a multisystemic involvement and the coexistence of both may increase the organ damage, worsening the patient prognosis. The aim of this study was to evaluate the role of NAFLD in the development and severity of extrahepatic conditions in a well-characterized T2DM cohort.

Method: Prospective cohort with case-control analysis comprising 200 T2DM subjects with 60 non-diabetic subjects matched by age with available transient elastography data. Patients were selected from the Outpatient Diabetes Clinic of Vall d'Hebron Hospital and the Primary Healthcare centres within its catchment area. Diabetic nephropathy (DN) was defined as the presence of microalbuminuria >30 mg/dl. According KDIGO guidelines, we defined renal impairment (RI) as a urine albumin:creatinine ratio >30 mg/g and chronic

kidney disease (CKD) as an estimated glomerular filtrate rate (eGFR) 60 ml/min per 1.73m². NAFLD was defined as Controlled Attenuation Parameter (CAP) ≥275 dB/m and/or Fatty liver index (FLI) ≥60 after exclusion of the other liver diseases and alcohol consumption over 30 gr/day in males and over 20 gr/day in females. Multivariate regression analysis was performed to identify predictors of extrahepatic diseases.

Results: Patients with T2DM with NAFLD (n = 134) presented higher rates of arterial hypertension (76.1% vs 61.5%, p 0.047) and obesity-BMI ≥30 kg/m² (61.2% vs 23.1%, p < 0.001) than T2DM-nonNAFLD (n = 52). Distribution for gender, age and presence of dyslipidemia were similar between groups. Respect to T2DM complications, 38.6% of T2DM-NAFLD patients showed DN compared to 19.6% T2DM-nonNAFLD subjects (p 0.014). No statistical differences were found for diabetic retinopathy (25.4% vs 30.8%, p 0.45) or peripheral neuropathy (19.4% vs 17.3%, p 0.74). Of note, T2DM-NAFLD patients showed worse median creatinine and eGFR values (0.85 ± 0.26 vs 0.74 ± 0.14, p 0.001 and 80.1 ± 17.4 vs 86.1 ± 10.1, p 0.004, respectively), and also presented a higher proportion of RI (71.6% vs 49.0%; p 0.004) and CKD (14.2% vs 3.9%, p 0.049) respect to T2DM subjects without NAFLD. Median liver stiffness did not differ among patients with and without RI or CKD. In multivariate analysis the presence of NAFLD (HR = 2.48; 95%CI 1.61–5.32, p 0.019) was associated with the development of RI, independently of well-known risk factors, such as arterial hypertension (HR = 3.23; 95%CI 1.58–6.58, p 0.001) or advanced age (HR = 2.79; 95%CI 1.40–5.56, p 0.003).

Multivariate logistic regression analysis			
	Hazard Ratio	95% CI	p
NAFLD	2.48	1.61-5.32	0.019
Age ≥ 65y	2.79	1.40-5.56	0.003
Arterial hypertension	3.23	1.58-6.58	0.001
Obesity (BMI ≥ 30 kg/m ²)	1.37	0.66-2.73	0.40

Conclusion: Our results suggest that NAFLD poses an increased risk of extrahepatic diseases in T2DM patients, including other metabolic conditions and specially kidney disease. Renal function in diabetic patients with NAFLD should be screened and monitored closely, since NAFLD may lead to further worsening of kidney disease.

THU060

The impact of liver fibrosis on the immune response to SARS-CoV-2 vaccination in metabolic associated fatty liver disease patients

Marta Freitas^{1,2,3}, Tiago Capela^{1,2,3}, Vítor Macedo Silva^{1,2,3}, Sofia Xavier^{1,2,3}, Joana Teixeira Magalhães^{1,2,3}, Carla Maria Moura Marinho^{1,2,3}, José Cotter^{1,2,3}. ¹Hospital da Senhora da Oliveira, Guimarães, Portugal, Gastroenterology Department; ²School of Medicine, University of Minho, Braga, Portugal, Life and Health Sciences Research Institute (ICVS); ³PT Government Associate Laboratory, Braga/Guimarães, Portugal, ICVS/3B's
Email: martasfreitas@gmail.com

Background and aims: There has been growing concern about the response to severe acute respiratory syndrome coronavirus 2 (SARS-CoV-2) vaccination in patients with chronic liver disease, as it may confer an immunosuppression state, potentially being associated with a lower response to vaccination. However, this issue in metabolic associated fatty liver disease (MAFLD) patients remains unestablished. We aimed to assess the impact of liver fibrosis on the immune response to SARS-CoV-2 vaccination in patients with MAFLD.

Method: Prospective cohort study that included MAFLD patients with complete SARS-CoV-2 vaccination. Patients with previous SARS-CoV-2 infection were excluded. Serum SARS-CoV-2 immunoglobulins (Ig), laboratory and transient elastography (TE) data were assessed 1 month after complete vaccination. Significant fibrosis was defined as

POSTER PRESENTATIONS

liver stiffness measurement (LSM) ≥ 8.2 kPa, NAFLD fibrosis score ≥ -1.455 , FIB-4 score ≥ 1.45 , or FAST score > 0.35 .

Results: Thirty-seven patients were included, 62.2% of male gender, with a mean age of 55 ± 9 years. The mean LSM was 6.9 ± 2.9 kPa and 32.4% of patients had significant fibrosis in TE. The mean SARS-CoV-2 IgG levels were 10048 ± 9395 U/ml and all patients had response to vaccination (IgG ≥ 50 U/ml). There were no differences in SARS-CoV-2 IgG levels regarding gender ($p = 0.93$), presence of obesity ($p = 0.20$), metabolic syndrome ($p = 0.26$), diabetes ($p = 0.70$), hypertension ($p = 0.52$), dyslipidemia ($p = 0.96$), and tobacco use ($p = 0.99$). There were no differences in SARS-CoV-2 IgG levels between patients with or without significant fibrosis ($p = 0.13$) in TE, NAFLD fibrosis score ($p = 0.18$), FIB-4 score ($p = 0.56$), or FAST score ($p = 0.24$).

Conclusion: In our cohort, all MAFLD patients had Ig response to vaccination. Significant liver fibrosis did not compromised response of MAFLD patients to SARS-CoV-2 vaccination. SARS-CoV-2 vaccination is serologically effective in MAFLD patients, regardless of fibrosis.

THU061

Non-alcoholic steatohepatitis is also becoming a major liver transplant indication in Spain, a historically low risk area

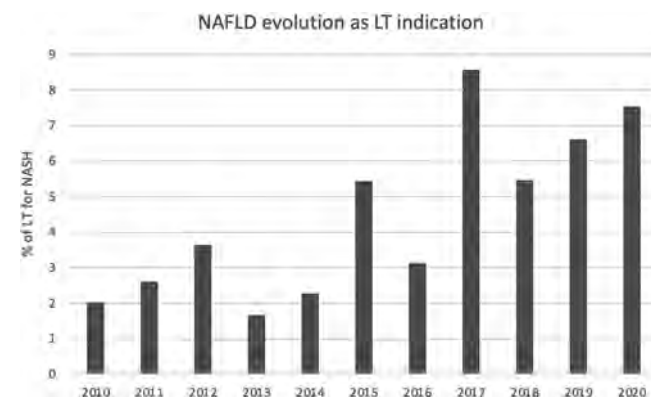
Laura Martínez-Arenas¹, Ângela Carvalho-Gomes², Fernando Díaz Fontela³, Sara Lorente Perez⁴, Marta Guerrero⁵, Jose Ignacio Herrero⁶, Marina Berenguer⁷. ¹Instituto de Investigación Sanitaria La Fe, Hepatology, Hepatobiliopancreatic Surgery and Transplant, Valencia, Spain; ²Instituto de Investigación Sanitaria La Fe, CIBERehd, Hepatology, Hepatobiliopancreatic Surgery and Transplant, Valencia, Spain; ³Hospital General Universitario Gregorio Marañón, Liver Unit and Digestive Department, Madrid, Spain; ⁴Hospital Clínico Universitario Lozano Blesa, Hepatology and Liver Transplantation Unit, Zaragoza, Spain; ⁵Hospital Universitario Reina Sofía, Instituto Maimónides de Investigación Biomédica de Córdoba, CIBERehd, Department of Hepatology and Liver Transplantation, Córdoba, Spain; ⁶Clínica Universidad de Navarra, Instituto de Investigación Sanitaria de Navarra, CIBERehd, Department of Internal Medicine, Pamplona, Spain; ⁷Hospital Universitario y Politécnico La Fe, Instituto de Investigación Sanitaria La Fe, Universidad de Valencia, CIBERehd, Hepatology and Liver Transplantation Unit, Valencia, Spain
Email: laura_munera15@hotmail.com

Background and aims: Non-alcoholic fatty liver disease (NAFLD) is becoming one of the most common chronic liver diseases in Spain, particularly in individuals with features of metabolic syndrome, yet its exact prevalence and incidence are not completely known. In fact, non-alcoholic steatohepatitis (NASH) is a growing indication for liver transplantation (LT) in our setting. Our aim was to describe NAFLD evolution as a LT indication and the most frequently found features associated with this indication.

Method: Patients undergoing LT for NASH-related cirrhosis from 2010 to 2020 in five reference LT centers in Spain were included. The medical records of all these patients were reviewed for determining NASH-associated comorbidities. Survival analyses were performed with SPSS to determine survival rates at different follow-up points after LT.

Results: NASH-related cirrhosis was the LT indication in 118 patients from 2010 to 2020. Taking into account the five centers, the percentage of LT for NASH increased 3.8-fold between 2010–2020, from 2.0% to 7.5% (Figure 1). The highest percentage (25.0%) was registered in 2020 in one of the centers. While there were no transplants performed for NASH in some centers in some of the years, mainly in the first years of the study, the number has progressively increased since 2015. Comorbid conditions were found in most patients; 77.1% had obesity, 59.3% type 2 diabetes mellitus (T2DM), 61.9% hypertension (HTN), 37.3% dyslipidemia (DL) and 22.0% a history of prior cardiovascular disease (CVD). While posttransplant complications were frequent, survival was similar to that of other indications with a cumulative proportion surviving of 0.92 and 0.8 at

1- and 5-year post-LT and only 2 cases of graft loss due to recurrence of primary disease. The greatest number of deaths occurred within the first year after transplantation ($n = 10$), none of them related to primary liver disease.



Conclusion: NAFLD is an increasingly common indication for LT in our country. However, the incidence is still far from that described in countries like the US. As reported, most of these transplant candidates have significant comorbid conditions associated with posttransplant complications and poorer long-term outcome such as obesity, T2DM, HTN, DL and CVD. Yet, in the short-midterm transplant survival is similar to that reported by the Spanish Liver Transplantation Registry, with a survival rate of 87% and 75% at 1- and 5- year post-LT, respectively.

THU062

Total healthcare cost and characteristics associated with higher change in cost in patients with non-alcoholic steatohepatitis

Zobair Younossi¹, Kamal Kant Mangla², Abhishek Shankar Chandramouli³, Jeffrey Lazarus⁴. ¹Center for Liver Disease, Inova Medicine, Falls Church, VA, United States; ²Novo Nordisk A/S, Søborg, Denmark; ³Novo Nordisk Service Centre India Pvt Ltd, Bangalore, India; ⁴Barcelona Institute for Global Health (ISGlobal), Hospital Clínic, University of Barcelona, Barcelona, Spain
Email: zobair.younossi@inova.org

Background and aims: The economic burden in patients with non-alcoholic steatohepatitis (NASH) is often underestimated. The AWARE study collected baseline data on patients with NASH to determine the associated healthcare cost burden.

Method: Data were collected from a large US healthcare dataset (electronic health records linked with claims) from 1 October 2015 to 31 December 2020. Adult patients diagnosed with NASH, with no evidence of hepatitis B or C, excessive alcohol use, or liver transplant prior to NASH diagnosis, and with no evidence of pregnancy or cancer in the study period, were included. All diagnoses were made using ICD CM. Total healthcare follow-up costs and change in total healthcare cost post-NASH are reported as mean (standard deviation). The effect on change in cost by baseline characteristics was assessed using a multivariate generalised linear model.

Results: Of 4, 989 adult patients diagnosed with NASH, 489 had evidence of cirrhosis at baseline. Mean follow-up was 22 months for non-cirrhotic patients (NCPs) and 21 months for cirrhotic patients (CPs). Annualised follow-up costs (US\$) were \$28, 707 (\$140, 814) for NCPs and \$84, 582 (\$204, 552) for CPs. Among NCPs, approximately 70% had a high annual cost burden ($> \$5,000$) and 38% had a very high cost burden ($> \$15,000$) (Figure). Increases in costs following onset of NASH were \$13, 202 (\$141, 095) for NCPs and \$44, 509 (\$177, 055) for CPs. For NCPs, the change in costs post-NASH diagnosis significantly increased (in %) with increasing Quan-Charlson Comorbidity Index score (21% per unit increase) and adaptive Diabetes Complexity Severity Index score (36% per unit increase), increasing use of

cardiovascular (CV) drug classes (8%) and anti-diabetes medication classes (12%), and presence (vs absence) of CV disease (71%) and osteoarthritis (51%) at baseline. Female (vs male) patients had higher follow-up costs and a larger change in costs.

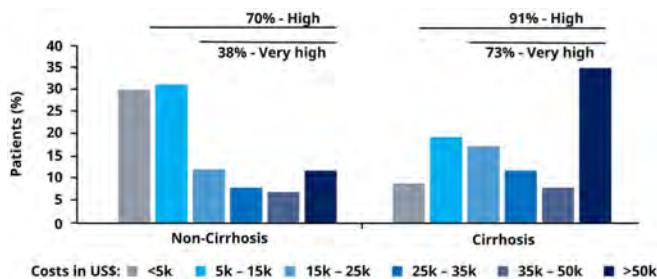


Figure: Annualised follow-up total healthcare cost (US\$) for patients with NASH

Conclusion: NASH correlates with noticeable total healthcare cost and increases in costs following onset of NASH for all patients. The costs reported here are reflective of short-term burden. This analysis did not include indirect costs or costs associated with loss of work productivity. Due to the unavailability of approved treatments for patients with NASH, the cost burden is expected to increase with the presence and increasing severity of comorbidities. Therefore, the aim of managing NASH through pharmacotherapy should be to stop progression to cirrhosis and to manage NASH-related comorbidities.

THU063

Non-alcoholic fatty liver disease (NAFLD)/non-alcoholic steatohepatitis (NASH) is associated with worse outcomes in patients hospitalised for COVID-19: a real-world analysis of a large population from the premier healthcare database

Frank Tacke¹, Fady Tanios², Lin Xie², Deepa Malhotra², Simon Dagenais², Nino Katchiuri², Birol Emir². ¹Charité University Medical Center, Berlin, ²Pfizer Inc, New York, United States
Email: frank.tacke@charite.de

Background and aims: NAFLD and NASH contribute to the global burden of liver disease. Previous studies suggest an association between NAFLD/NASH and the severity of COVID-19 illness. This analysis aimed to characterise the impact of NAFLD/NASH on hospitalisation-related outcomes for patients with COVID-19 using hospital administrative data from the United States (US) Premier Healthcare Database Special Release (PHD-SR).

Method: Adults with COVID-19 (primary or secondary International Classification of Diseases [ICD]-10 diagnosis code U07.1) hospitalised for the first time (index event) and discharged between 1 Apr 2020 and 31 Mar 2021 were examined. Pregnant patients and those with human immunodeficiency virus, alcohol dependence/abuse, viral hepatitis, biliary cirrhosis or sclerosing cholangitis were excluded. Cases with NAFLD/NASH (ICD-10: K75.81, K76.0) at index or 3 months pre-index (in- or outpatient) hospitalisation were matched to controls without NAFLD/NASH using exact matching for age; propensity scores were calculated for sex, race and other variables. Outcomes included length of stay (LOS), invasive mechanical ventilator (IMV) use, in-hospital mortality and all-cause network-hospital readmission within 30 days of index event discharge. Linear and logistic regression with inverse probability treatment weight (IPTW) compared outcomes in cases and controls.

Results: The PHD-SR dataset included 513, 623 eligible patients; 14, 672 (2.9%) with a NAFLD/NASH diagnosis. Among 29, 334 patients analysed (14, 667 cases with NAFLD/NASH and 14, 667 matched controls), mean (standard deviation) age was 57.5 (15.0) years, 51.0% were female and 43.8% were white non-Hispanic. Baseline characteristics (eg, age, sex, race) were similar (standard difference <0.10) in cases and controls, except for cirrhosis (9.7% cases vs 0.5% controls) and malignancy (13.6% cases vs 10.2% controls). Regression analysis

with IPTW adjusted for cirrhosis and malignancy revealed that patients without NAFLD/NASH had a significantly shorter mean LOS and reduced odds of IMV use with no difference in in-hospital mortality and readmission vs patients with NAFLD/NASH (Table), controlled for age, sex, race and other NAFLD-related comorbidities (eg, diabetes, obesity).

Table: Hospitalisation-related outcomes in matched controls without NAFLD / NASH versus cases with NAFLD / NASH hospitalised with COVID-19

Outcome	Adjusted differences and OR (95% CI) between controls and cases
LOS at index hospitalisation, days	LSM: -1.02 (-1.26, -0.78)
IMV use including ECMO	OR: 0.93 (0.88, 0.99)
In-hospital mortality at index hospitalisation	OR: 1.02 (0.95, 1.10)
Readmission, all-cause within 30 days	OR: 1.06 (0.97, 1.16)

LSM difference for LOS based on linear regression with IPTW adjusted for cirrhosis and malignancy. OR based on logistic regression with IPTW adjusted for cirrhosis and malignancy.

CI, confidence interval; ECMO, extracorporeal membrane oxygenation; IMV, invasive mechanical ventilator; IPTW, inverse probability treatment weight; LOS, length of stay; LSM, least squares mean; NAFLD, nonalcoholic fatty liver disease; NASH, nonalcoholic steatohepatitis; OR, odds ratio.

Conclusion: Real-world US hospital data suggests that patients hospitalised with COVID-19 who also have NAFLD/NASH have worse hospitalisation-related outcomes than those without NAFLD/NASH.

THU064

Estimating the prevalence of advanced fibrosis due to non-alcoholic fatty liver disease in the United States population

Naim Alkhouri¹, Julia Yang Payne², Pankaj Aggarwal¹, Prido Polanco¹, Phillip Leff¹, Mazen Nouredin³, Phuc Le². ¹Arizona Liver Health, United States; ²Cleveland Clinic, United States; ³Cedars-Sinai Medical Center, United States
Email: naim.alkhouri@gmail.com

Background and aims: Previous estimates of the prevalence of advanced fibrosis (AF) due to NAFLD in the general US population utilized non-invasive tests that have relatively low positive predictive value leading to potentially overestimating the true prevalence. The AGILE 3+ score was developed by combining routine clinical variables and vibration-controlled transient elastography parameters to specifically increase the PPV of predicting AF. Our aim was to estimate the prevalence of AF due to NAFLD using the AGILE3+ score in the general US adult population.

Method: Our study population included participants aged ≥18 years old who had a complete VCTE exam in the national health and nutrition examination survey (NHANES) 2017–2018 cycle. We excluded pregnant women, patients with excessive alcohol consumption defined as >2 drinks/day for males and >1 drink/day for females, hepatitis B or C, and ALT or AST >500 IU/L.

NHANES used FibroScan model 502 V2 Touch equipped with medium and extra-large probes. The presence of NAFLD was based on having a CAP score >248 dB/m. NAFLD subjects with AGILE3+ score of ≥0.68 were considered to have AF (rule-in), 0.45–0.67 were to be the grey zone, and <0.45 were considered low risk for AF (rule-out).

Results: Our cohort consisted of 1244 subjects with evidence of NAFLD and complete data to calculate the AGILE3+ score. The Median age was 52.5 (50.7–54.2) years, 54.9% were male, median BMI was 32.7 kg/m² and 36.2% had type 2 diabetes. Based on AGILE3+ score <0.45, 80.3% (95%CI: 77.1–83.2) of the NAFLD population were at low risk for AF. 11.5 (9.2–14.5) of patients were in the grey zone and would have needed another test to determine the presence of AF. The overall prevalence of AF due to NAFLD was 8.1 (6.2–10.6) corresponding to 4.5 million Americans. Patients with AF were older, more likely to be obese and have type 2 diabetes.

Conclusion: Using NHANES 2017–2018, our results suggest that approximately 4.5 million people in the US have AF due to NAFLD based on the AGILE3+ score. Evaluating the cost-effectiveness of using AGILE3+ as a screening tool in high-risk populations is needed before implementing in clinical practice.

THU065

Non-alcoholic fatty liver disease associated liver fibrosis is linked with the severity of coronary artery disease mediated by systemic inflammation

Xianbin Cai¹, Lingzi Chen¹. ¹The First Affiliated Hospital of Shantou University Medical College, Department of Gastroenterology, Shantou, China
Email: cxbin1@qq.com

Background and aims: Non-alcoholic fatty liver disease (NAFLD) is an independent risk factor of cardiovascular disease. Hepatic fibrosis is the most significant determinant of all cause- and liver -related mortality in NAFLD. However, the relationship between NAFLD fibrosis and severe coronary artery disease (CAD) remains unclear.

Method: We conducted a retrospective study of 531 patients with ultrasonogram-confirmed NAFLD who underwent percutaneous coronary intervention (PCI). Then all patients were separated into four categories by Gensini score (0, 0–9, 9–48, ≥48) for use in ordinal logistic regression analysis to determine whether NAFLD fibrosis was associated with increased Gensini scores. Mediation analysis was used to investigate whether systemic inflammation is a mediating factor in the association between NAFLD fibrosis and CAD severity.

Results: FIB-4 >2.67 (OR = 5.67, 95%CI 2.59–12.38) and APRI >1.5 (OR = 14.8, 95%CI 3.24–67.60) remained to be independent risk factors for the severity of CAD after adjusting for conventional risk factors, whereas among the inflammation markers, only neutrophils and neutrophil-to-lymphocyte ratio (NLR) were independently associated with CAD. Multivariable ordinal regression analysis suggested that increasing Gensini score (0, 0–9, 9–48, ≥48) was associated with advanced NAFLD fibrosis. ROC curve showed that either fibrosis markers or inflammation markers, integrating with traditional risk factors, could increase the predictive capacity for determining CAD (Figure 1). Inflammation markers, especially neutrophils and NLR, were mediators of the relationship between NAFLD fibrosis and CAD severity (Figure 2).

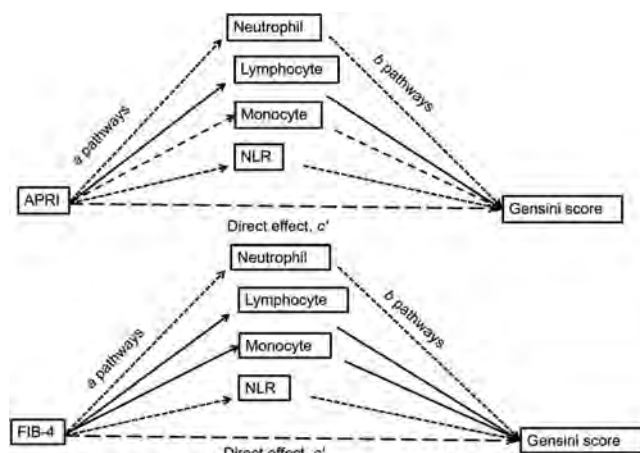


Figure 2: Mediated Model of Fibrosis Markers with Gensini Score.

(1) The coefficient a is the effect of fibrosis markers on the inflammation markers; (2) the coefficient b is the effect of inflammation markers on Gensini score after controlling the influence of fibrosis markers; (3) the coefficient c' is the direct effect of fibrosis markers on Gensini score after controlling the influence of inflammation markers. Dash line means the pathway is statistically significant.

Conclusion: NAFLD patients with advanced fibrosis are at a high risk of severe coronary artery stenosis, and inflammation might mediate the association between NAFLD fibrosis and CAD severity.

THU066

Prevalence of portal vein thrombosis in non-alcoholic fatty liver disease related cirrhosis: a meta-analysis of observational studies

Roberta Stupia¹, Filippo Cattazzo¹, Alessandro Mantovani², David Sacerdoti¹, Andrea Dalbeni¹. ¹Azienda Ospedaliera Universitaria Integrata Verona, General Medicine, Hypertension and Liver Unit, Verona, Italy; ²Azienda Ospedaliera Universitaria Integrata Verona, Endocrinology, Diabetes and Metabolism, Verona, Italy
Email: robertastupia1@gmail.com

Background and aims: Portal vein thrombosis (PVT) is a common complication of cirrhosis because of modification in hemodynamics and hemostatic balance, especially in decompensated stage1. Furthermore, patients with non-alcoholic fatty liver disease

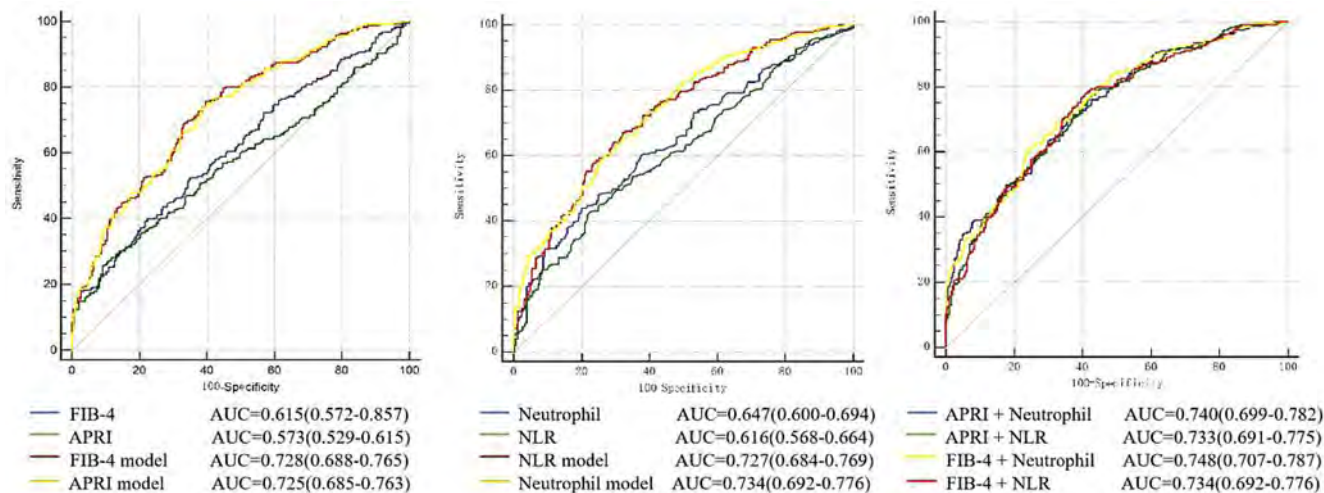


Figure 1: (abstract: THU065): Receiver Operating Characteristics (ROC) Curve Analysis of the Predictive Power of Fibrosis markers, NLR and Neutrophil for CAD.

APRI model, FIB-4 model, NLR model, Neutrophil model, APRI + Neutrophil, FIB-4 + Neutrophil: new models integrating non-invasive markers and recognized risk factors for CAD (gender, age, smoking, hypertension, DM, triglyceride, HDL, LDL).

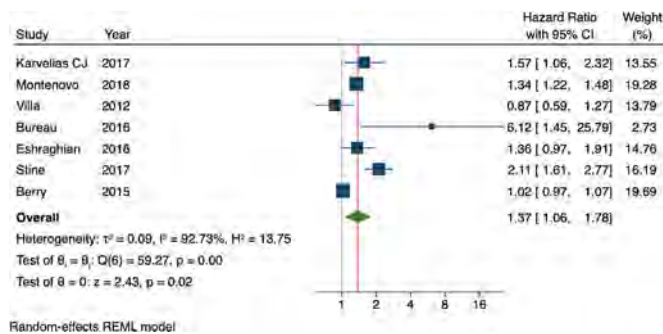
(NAFLD) related cirrhosis seem to be at higher risk of PVT development than patients with cirrhosis due to other causes². Nevertheless, definitive data in favor of an increased rate of PVT in NAFLD are missing. This meta-analysis attempted to estimate the prevalence of PVT in patients with NAFLD related cirrhosis.

Method: We systematically searched PubMed, Scopus and Web of Science databases from the inception date to November 1st 2021 using predefined keywords to identify observational cohort studies. Meta-analysis was performed using random-effects modelling.

Results: We included seven articles published over the past 10-year period reporting a total of 231,399 cirrhotic patients from five different countries. NAFLD-cirrhosis patients were 26,853 (11, 6%), with a PVT incidence of 6.5% (n = 1,748). Meta-analysis demonstrated a significant positive association between NAFLD and PVT (OR 1.37, 95% CI 1.06–1.78 p < 0.001). The between-study heterogeneity was substantial (I² = 92, 73%).

After stratifying the eligible cohort studies by country, we observed that, compared to other regions, in European patients the incidence of PVT in NAFLD-cirrhosis was higher (OR: 2.03, 95% CI 0.30–13.53) than in North-American patients (OR: 1.42, 95% CI 1.05–1.94) and Arabian patients (OR: 1.36, 95% CI 0.97–1.91).

By a meta regression analysis, neither age nor diabetes seemed to impact on the relationship between NAFLD and PVT.



Conclusion: This meta-analysis suggests that NAFLD-cirrhosis is associated with an increased risk of developing PVT. Further research is required to understand the complex link between NAFLD and PVT development.

References

- Englesbe MJ, Kubus J, Muhammad W, Sonnenday CJ, Welling T, Punch JD, Lynch RJ, Marrero JA, Pelletier SJ. Portal vein thrombosis and survival in patients with cirrhosis. *Liver Transpl* 2010; 16: 83–90 [PMID: 20035521 DOI: 10.1002/lt.21941]
- Lin H, Bai Z, Guo X, Qi X. Association between non-alcoholic fatty liver disease and portal vein thrombosis: a systematic review and meta-analysis. *Eur J Gastroenterol Hepatol*. 2020 Oct;32 (10):1405–1406. doi: 10.1097/MEG.0000000000001689. PMID: 32858662.

THU067

Real-world prevalence of metabolic associated fatty liver disease (MAFLD) and fibrotic-non-alcoholic steatohepatitis (NASH) in patients with obesity (PwO) in an outpatient specialist clinic in Italy

Federico Ravaioli¹, Maria Letizia Petroni¹, Francesca Marchignoli¹, Laura Leoni¹, Giulia Bocedi¹, Federica Sacilotto¹, Valentino Osti¹, Dorina Mita¹, Francesca Barbanti¹, Lucia Brodosi¹, Giulio Marchesini Reggiani¹, Loris Pironi¹. ¹IRCCS Azienda Ospedaliero-Universitaria di Bologna, Dipartimento di Scienze Mediche e Chirurgiche (DIMEC)
 Email: f.ravaioli@unibo.it

Background and aims: Obesity is a major player of "metabolic dysfunction associated fatty liver disease" (MAFLD); however, scanty data is available on the prevalence of MAFLD and non-alcoholic steatohepatitis (NASH) in patients presenting with obesity to a

specialist outpatient clinic; to date, data being available from bariatric surgery patient series only. For this purpose, we aimed to evaluate the prevalence of MAFLD and the applicability of non-invasive tests (NITs) for fatty liver and liver fibrosis identification in an outpatient specialist clinic in Italy.

Method: We consecutively screened patients with obesity (PwO) who attended our outpatient obesity clinic from January 2020 to June 2021. Diagnosis of MAFLD was based on results from abdominal ultrasound (US); the anthropometric and laboratory data of the patients were collected, and the Fatty Liver Index (FLI), Fibrosis-4 (FIB4) and NAFLD (NFS) scores were calculated. Liver fibrosis was assessed within one month of the first visit using liver stiffness measurements (LSM) by transient elastography (FibroScan); Probe-specific LSM cut-offs were used to detect significant (F_{≥2}) and advanced (F_{≥3}) fibrosis and NASH cirrhosis. In a subgroup, hepatic fat was also evaluated through controlled attenuation parameters (CAP) with the FibroScan Expert 630 apparatus; all patients underwent oral glucose tolerance test (OGTT).

Results: Among 249 PwO, according to the WHO obesity classification, obesity I^o, II^o, III^o was classified in 144 (57.8%), 56 (22.5%), 49 (19.6%), respectively. In addition, about half of the PwO had type 2 diabetes (T2DM) or impaired glucose tolerance (IGT) with a median HOMA index of 3.6 (IQR 2.44–4.94). According to US or FLI definitions, the prevalence of MAFLD was 90.4% and 91.6% and did not differ significantly in the different WHO categories of obesity (p value 0.264). The distribution of hepatic steatosis classification on ultrasound was 25.8%, 38.7%, 35.6% for mild, moderate, and severe steatosis, respectively. The median CAP values were 287 dB/m (IQR 262–337). According to LSM values, 29%, 18% and 9.8% had significant fibrosis, advanced fibrosis, and NASH cirrhosis, respectively. The median LSM value was 5.4 kPa (IQR 4.3–7.5). The liver fibrosis prevalence significantly increased according to WHO categories of obesity (p value < 0.0001). Applying the screening with NITs, 10% and 9% of patients are wrongly classified, and this leads to misclassify about 50% and 11.4% of patients with advanced fibrosis using FIB-4 or NFS, respectively; moreover, 34.1% and 54.5% of patients with advanced fibrosis result in the grey area of the two tests respectively.

Patients (n=249)	Absence of Fibrosis (71%)		Advanced Fibrosis (15%)		Cirrhosis-NASH (14%)
	F0/F1 (LSM <7)	F2 (LSM 7 & <8.7)	F3 (LSM 8.7 & 10.3)	F4 (LSM >10.3)	
Obesity I ^o (n=144)	117 (81.3%)	13 (9%)	8 (5.6%)	5 (3.4%)	
Obesity II ^o (n=56)	39 (69.6%)	8 (14.3%)	3 (5.4%)	6 (10.7%)	
Obesity III ^o (n=49)	21 (42.9%)	7 (14.3%)	8 (16.3%)	13 (26.5%)	
DMT2-IGT (yes) (n=113)	63 (55.8%)	10 (8.9%)	12 (10.6%)	17 (15%)	

Conclusion: The results from the present study in a real-world setting strongly advocate for routine screening for MAFLD and NASH by LSM in PwO, regardless of WHO category, attending the outpatient specialist clinic for obesity.

THU068

Postprandial dysfunction in metabolic associated fatty liver disease (MAFLD)

Josephine Grandt^{1,2}, Anne Sofie Jensen^{1,2}, Mikkel Werge¹, Elias Rashu¹, Anders Junker¹, Lise Hobolth¹, Christian Mortensen¹, Maria Kristiansen², Mogens Vyberg^{3,4}, Reza Serizawa⁴, Søren Møller⁵, Lise Lotte Gluud¹, Nicolai J. Wewer Albrechtsen^{2,6,7}. ¹Gastro Unit, Copenhagen University Hospital Hvidovre, Denmark, Hvidovre, Denmark; ²Novo Nordisk Foundation Center for Protein Research, Faculty of Health and Medical Sciences, University of Copenhagen, Copenhagen, Denmark, København, Denmark; ³Center for RNA Medicine, Department of Clinical Medicine, Aalborg University, Copenhagen, Aalborg, Denmark; ⁴Department of Pathology, Copenhagen University Hospital Hvidovre, Denmark, Hvidovre, Denmark; ⁵Department of Clinical Physiology and Nuclear Medicine, Center for Functional and Diagnostic Imaging and Research, Copenhagen University Hospital Hvidovre, Denmark, Denmark; ⁶Department of Clinical Biochemistry, Rigshospitalet, Copenhagen, Denmark, Denmark; ⁷Department of Biomedical Sciences, Faculty of Health and Medical Sciences, University of Copenhagen, Copenhagen, Denmark, Denmark Email: nicolai.albrechtsen@sund.ku.dk

Background and aims: Fatty liver disease has been associated with metabolic disturbances. MAFLD is defined as hepatic steatosis with either overweight, type 2 diabetes (T2D), or at least two metabolic comorbidities. We hypothesized that metabolic disturbances associated with liver disease are pronounced in the postprandial phase and may be identified by a standardized meal. We therefore aimed to study the fasting and postprandial state in biopsy-proven healthy, MAFLD and cirrhosis.

Method: We included 29 participants, 10 healthy controls (age 23 ± 0 years, BMI 25 ± 1 kg/m²), 9 patients with non-alcoholic fatty liver disease (NAFLD) (age 50 ± 5 years, BMI 35 ± 2 kg/m², no/mild fibrosis) and 10 patients with cirrhosis (age 62 ± 3 years, BMI 32 ± 2 kg/m², Child A/B). None of the included participants had T2D. The participants were randomized 1:1 to "fasting" or "postprandial" (Nutridrink, Nutricia, 300 kcal). Blood samples were obtained at baseline and 15, 45, 60, 90 and 120 minutes. At time point 60, blood from the liver vein was collected and a transjugular liver biopsy was performed. Levels of glucose, insulin, C-peptide, glucagon, and fibroblast growth factor 21 (FGF21) were measured in peripheral blood, and glucagon and FGF21 as well in liver vein blood. Results are presented as ± SEM. Peak concentrations were calculated as mean ± SEM of individual peaks. The analyses compared controls versus NAFLD and cirrhosis.

Results: 8/9 patients with NAFLD and 9/10 patients with cirrhosis were classified as MAFLD. Postprandial increase in glucose and C-peptide was significantly greater in NAFLD and cirrhosis compared to controls, with peak glucose of 7 and 10 mmol/L (p = .006), and peak C-peptide of 2675 ± 273 and 3340 ± 1048 pM versus 1689 ± 190 pM. Postprandial iAUC for insulin was greatest in patients with NAFLD (p = .037). Patients with NAFLD and cirrhosis had hyperglucagonemia, a phenotype causally related to prediabetes. FGF21 was significantly increased in NAFLD and cirrhosis and correlated to age (r = .61, p = .001) and fasting glucose (r = .54, p = .006). Glucagon was higher in liver vein compared to peripheral blood while FGF21 levels were similar in liver and peripheral blood.

Conclusion: We found significant metabolic dysfunction after a test meal in patients with MAFLD without diabetes compared to healthy controls and that finding that was pronounced in cirrhosis. Patients with MAFLD had impaired glucose tolerance, hyperinsulinemia and hyperglucagonemia, suggesting MAFLD to be a condition of prediabetes.

THU069

Lean non-alcoholic fatty liver disease patients from the global NASH registry

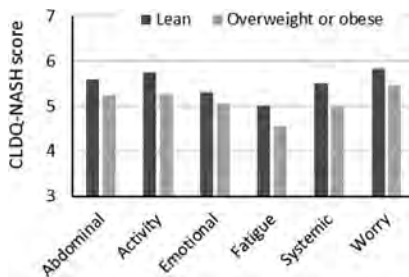
Zobair Younossi^{1,2,3}, Yusuf Yilmaz⁴, Ming-Lung Yu⁵, Vincent Wai-Sun Wong⁶, Marlen Castellanos-Fernandez⁷, Vasily Isakov⁸, Ajay Kumar Duseja⁹, Nahum Méndez-Sánchez¹⁰, Yuichiro Eguchi¹¹, Elisabetta Bugianesi¹², Patrizia Burra¹³, Jacob George¹⁴, Jian-Gao Fan¹⁵, George Papatheodoridis¹⁶, Wah-Kheong Chan¹⁷, Khalid Alswat¹⁸, Saeed Sadiq Hamid¹⁹, Ashwani Singal²⁰, Manuel Romero Gomez²¹, Stuart C Gordon²², Stuart Roberts²³, Mohamed El Kassas²⁴, Marcelo Kugelman²⁵, Janus Ong²⁶, Saleh Alqahtani²⁷, Mariam Ziaee², Brian Lam^{1,2}, Issah Younossi²⁸, Andrei Racila^{1,2}, Linda Henry²⁸, Maria Stepanova²⁸. ¹Center for Liver Disease, Inova Medicine; ²Beatty Liver and Obesity Research Program, Inova Health System; ³Inova Medicine, Inova Health System; ⁴Marmara Üniversitesi Tıp Fakültesi; ⁵Kaohsiung Medical University Chung-Ho Memorial Hospital; ⁶The Chinese University of Hong Kong; ⁷Instituto Nacional de Gastroenterología, La Habana, Cuba; ⁸Federal Research Center of Nutrition and Biotechnology; ⁹PGIMER; ¹⁰Medica Sur Clinic and Foundation; ¹¹Saga University; ¹²University of Torino; ¹³Padova University Hospital; ¹⁴Westmead Hosp/Westmead Institute; ¹⁵Shanghai Jiaotong University School of Medicine; ¹⁶Laiko General Hospital; ¹⁷University of Malaysia, Department of Medicine; ¹⁸Liver Disease Research Center, Department of Medicine, College of Medicine, King Saud University; ¹⁹Department of Medicine, Aga Khan University; ²⁰University of South Dakota and Avera Transplant Institute; ²¹Digestive Diseases Department, Virgen del Rocío University Hospital, Institute of Biomedicine of Seville, University of Seville; ²²Henry Ford Hospital, Department of Hepatology and Gastroenterology; ²³The Alfred, Department of Hepatology and Gastroenterology; ²⁴Endemic Medicine Department, Faculty of Medicine, Helwan University; ²⁵South Denver Gastroenterology, PC; ²⁶University of the Philippines, College of Medicine; ²⁷King Faisal Specialist Hospital and Research Center; ²⁸Center for Outcomes Research in Liver Disease Email: zobair.younossi@inova.org

Background and aims: Although vast majority of patients with NAFLD are overweight and obese, NAFLD can be seen among lean individuals. The aim was to assess prevalence of lean NAFLD in different regions of the world.

Method: The Global NASH Registry enrolled patients with an established diagnosis of NAFLD from real-world practices in 18 countries (Australia, China, Cuba, Egypt, Greece, Hong Kong, India, Italy, Japan, Saudi Arabia, Malaysia, Mexico, Pakistan, Russia, Spain, Taiwan, Turkey, USA) in 6 out of 7 Global Burden of Disease (GBD) super-regions. Clinical and patient-reported outcomes (PRO) data (CLDQ-NASH, FACIT-F, WPAI) were collected. Lean NAFLD was defined as NAFLD in patients with BMI <25 kg/m², or 23 kg/m² for patients of East Asian origin.

Results: There were 6096 NAFLD patients included (as of November 10, 2021): 48% from High-Income super-region, 24% Middle East and North Africa (MENA), 12% Southeast Asia, 7% Latin America, 6% from Eastern Europe and Central Asia, and 3% South Asia super-region. Of these, 7.3% were lean. The rates of lean NAFLD were the highest in Southeast Asia (12%) and South Asia (31%), the lowest in Eastern Europe and Central Asia (<2%) and MENA (4%) (p < 0.0001). In comparison to overweight/obese patients, lean NAFLD patients were older (mean age 53 vs. 51 years) and predominantly of Asian race (48% vs. 18%) (p < 0.01). Furthermore, lean patients had lower rates of diabetes (28% vs. 41%), hypertension (35% vs. 52%), hyperlipidemia (40% vs. 50%), sleep apnea (8% vs. 33%), clinically overt fatigue (25% vs. 36%), and histologic cirrhosis (10% vs. 15%), but more abdominal pain (25% vs. 18%) and higher FIB-4 scores (mean 1.8 vs. 1.3) (all p ≤ 0.02). In multivariate analysis, having lean NAFLD (as opposed to overweight/obese NAFLD) was independently associated with older age (OR = 1.019 (1.008–1.030) per year), enrollment outside of MENA region (OR = 0.43 (0.31–0.58)) and from South Asia (OR = 5.01 (3.42–7.45)) sites (reference: High-Income), absence of type 2 diabetes

(OR = 0.61 (0.46–0.80)) and hypertension (OR = 0.46 (0.35–0.60)), and presence of regular exercise (OR = 1.55 (1.21–2.00)) (all $p < 0.01$). Lean NAFLD also had higher PRO scores than overweight/obese NAFLD (all domains of CLDQ-NASH and FACIT-F) (all $p < 0.01$) (Figure). In multivariate analysis, lower total CLDQ-NASH scores (range 1–7) in lean NAFLD patients were independently associated with enrollment from MENA region, history of anxiety, depression, fatigue, and abdominal pain (beta from – 0.40 to – 0.67 for each condition) ($p < 0.01$).



Conclusion: Lean NAFLD patients seen in real-world practices across the world have different clinical and PRO profiles in comparison to NAFLD patients who are overweight or obese.

THU070

Automated FIB-4 calculator and targeted provider education improved referral of at-risk fibrotic NAFLD patients

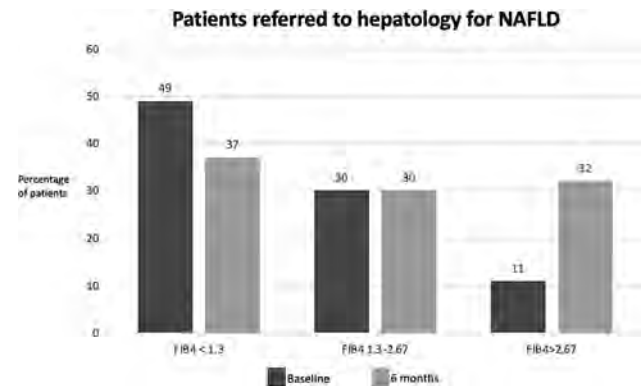
Cindy Piao¹, Elvis Arteaga², Connor Reilly², Jesse Simpson², Ryan Peck², Trevor Pratt², Troy Peterson², Mopelola Adeyemo³, Shuai Chen², Aili Guo², Scott MacDonald², Souvik Sarkar¹. ¹UC Davis Health-Gastroenterology, Sacramento, United States; ²UC Davis Medical Center, Sacramento, United States; ³University of California, Los Angeles, Los Angeles, United States
Email: ssarkar@ucdavis.edu

Background and aims: Non-alcoholic fatty liver disease (NAFLD) is the leading cause of chronic liver disease with increasing rates globally. Patients with a higher degree of liver fibrosis in NAFLD are at an increased risk for liver-related mortality but get missed easily during the referral process, based on our¹ and other prior data². Our project aims to improve early detection and linkage-to-care of fibrotic NAFLD patients using a combination of automated electronic health record (EHR)-based FIB-4 score and directed provider education within our tertiary care center, serving a large population of Northern California.

Method: We implemented a health-system wide FIB-4 score calculator, embedded in the EHR that providers can easily add to their workflow for NAFLD patient triaging. Subsequently we provided targeted education to all relevant providers taking care of NAFLD patients. All referrals for NAFLD (defined by specific ICD 9/10 codes), to the hepatology from February 2020–August 2021, were retrieved. Patient characteristics were determined with FIB-4 score being essential for determination of fibrotic NAFLD and comparative analysis with prior data¹.

Results: A total of 303 referrals were placed for NAFLD, of which 62% (n = 188) patients had FIB-4 score at the time of referral. Of the 188 patients, 62 patients with diabetes mellitus and 44% of them had FIB-4 ≥ 1.3 . Compared to prior referrals of 49% with FIB-4 score < 1.3 , in current referrals after a 6-month post-FIB-4 triage implementation, 37% had FIB-4 < 1.3 (Fig 1). This suggested a decrease in unnecessary referrals to hepatology. Primary care doctors referred 73% while

endocrinology referred 1% of all patients. We noted higher rates of fibrotic NAFLD patients with FIB-4 ≥ 1.3 in current referrals compared to prior (63% vs 41%). Furthermore, 32% of current referrals were with severe fibrotic disease defined by FIB-4 > 2.67 vs 11% previously (Fig 1). This suggested an increase in appropriate referrals for specialty care. Secondary fibrotic testing using imaging modalities such as ultrasound or magnetic resonance elastography was done in 36% of those with FIB-4 ≥ 1.3 , suggesting room for further refinement.



Conclusion: Automated FIB-4 score in EHR can improve appropriate linkage-to-care for at-risk fibrotic NAFLD, especially when coupled with targeted provider education. The durability of such improvement is essential to study along with the need to increase broad acceptance across health systems.

References

Leung *et al.*, PMID: 3227318
Srivastava *et al.*, PMID: 30965069

THU071

Long term outcomes of non-alcoholic fatty liver disease (NAFLD) and metabolic associated fatty liver disease (MAFLD)

Zobair Younossi^{1,2,3}, James Paik^{2,3}, Issah Younossi⁴, Pegah Golabi^{1,2,3}, Michael Harring¹, Linda Henry^{1,2,4}. ¹Inova Health System, Inova Medicine; ²Beatty Liver and Obesity Research Program, Inova Health System; ³Center for Liver Disease, Inova Medicine; ⁴Center for Outcomes Research in Liver Disease
Email: zobair.younossi@inova.org

Background and aims: NAFLD and MAFLD are part of the spectrum of fatty liver disease (FLD). Our aim was to compare the outcomes of patients with NAFLD or MAFLD.

Method: Using data from NHANES III and NHANES 2017–2018, FLD was defined as moderate to severe hepatic steatosis by ultrasound (NHANES III) or controlled attenuation parameter (CAP) of ≥ 285 dB/m (NHANES 2017–2018). Death data were obtained from National Death Index (NDI). NAFLD was defined as FLD without other liver diseases and excessive alcohol consumption (EAC). MAFLD was defined as FLD with metabolic dysfunction—one of the following three criteria, overweight/obesity, presence of type 2 diabetes mellitus or metabolic dysregulation (at least two metabolic risk abnormalities).

POSTER PRESENTATIONS

Table 1. Hazard ratios of risk factors for All-Cause Mortality among Adults with MAFLD and NAFLD: NHANES III

Risk factors	MAFLD		NAFLD	
	HR* (95% CI)	P	HR* (95% CI)	P
Metabolic risk abnormalities				
Central obesity	1.37 (1.05 - 1.78)	0.0217	1.30 (1.05 - 1.63)	0.0192
High Triglycerides	1.42 (1.16 - 1.73)	0.0009	1.47 (1.17 - 1.87)	0.0017
Low HDL	1.30 (1.04 - 1.64)	0.0224	1.43 (1.18 - 1.74)	0.0005
Insulin resistance	1.31 (1.02 - 1.70)	0.0353	1.35 (1.03 - 1.77)	0.0294
T2DM	1.88 (1.53 - 2.31)	<.0001	1.89 (1.52 - 2.34)	<.0001
CKD	1.96 (1.50 - 2.55)	<.0001	1.90 (1.40 - 2.58)	0.0001
History of Cancer	1.36 (1.08 - 1.70)	0.0096	1.41 (1.08 - 1.85)	0.0121
History of CVD	1.92 (1.52 - 2.41)	<.0001	2.05 (1.55 - 2.71)	<.0001
Risk for fibrosis**	1.30 (1.08 - 1.57)	0.0062	1.28 (1.07 - 1.53)	0.0073
Excess Alcohol Use	1.34 (0.97 - 1.84)	0.073		
ALD	1.37 (1.01 - 1.88)	0.0469		

Abbreviations: Metabolic Associated Fatty Liver Disease; MAFLD, Non-alcoholic Fatty Liver Disease; T2DM, Type 2 Diabetes Mellitus; CKD, Chronic Kidney Disease; CVD, Cardiovascular disease; SE, standard error.
* HRs and 95% CI were weighted to U.S. population and adjusted for age, sex, race, education, income, marital status, smoking status, and physical activity.
** defined as FIB-4 ≥ 1.30

Results: In NHANES III, 12, 878 adults (age 43.1 years; 49.5% male; 20.3% FLD, 16.5% NAFLD; 18.1% MAFLD, EAC 15.0%) were included. In NHANES 2017–2018, 4, 328 adults (age 48.0 years; 49.1% male; 36.8% FLD; 34.2% NAFLD; 36.3% MAFLD). In both cohorts, there was excellent concordance between diagnosis of MAFLD and NAFLD [Cohen's kappa coefficient of 0.83 (95% CI: 0.82–0.85) in NHANES III and 0.94 (95% CI: 0.93–0.95) in NHANES 2017–2018]. There were no statistical differences in the characteristics of MAFLD as compared to NAFLD except for presence of obesity and EAC. After 19.2 years of follow-up for NHANES III cohort, there were no significant differences in cumulative mortality between MAFLD and NAFLD: all-causes (45.0% [95% Confidence interval, 41.6–48.3] vs 41.5% [38.3–44.8]); cardiovascular disease (15.5% [13.4–17.6] vs 13.9 [11.8–15.9]); extra-hepatic cancer (9.2% [7.5–10.8] vs. 8.6% [6.6–10.5]); liver (3.0% [2.0–4.0] vs. 1.8% [1.0–2.7]) and diabetes (1.4% [1.4–3.5] vs. 2.5% [1.3–3.8]). Furthermore, except for diagnosis of ALD among MAFLD, there were no discernable differences in mortality risk factors between NAFLD and MAFLD. In fact, independent predictors of mortality for both included presence of central obesity, insulin resistance/T2DM, CKD, CVD as well as high triglycerides and low HDL cholesterol ($p < 0.05$). Of 75 liver deaths among MAFLD patients, 66.7% were also classified as NAFLD and 33.3% as ALD. Among MAFLD, the strongest predictor of liver deaths was diagnosis of ALD (HR = 4.50 [1.89–10.75]).

Conclusion: MAFLD and NAFLD diagnostic classifications have excellent concordance. Furthermore, there are similar cause-specific or overall mortality. The strongest predictor of liver mortality among MAFLD is presence of ALD.

THU072

MARC1 and HSD17B13 variants have protective effects on liver injury in the obese: results from a prospective cohort of patients undergoing bariatric surgery

Piotr Kalinowski¹, Wiktor Smyk², Małgorzata Nowosad¹, Rafał Paluszkiwicz¹, Łukasz Michałowski³, Bogna Ziarkiewicz-Wróblewska³, Susanne N Weber², Frank Lammert^{2,4}, Krzysztof Zieniewicz¹, Marcin Krawczyk^{2,5}.

¹Department of General, Transplant and Liver Surgery, Medical University of Warsaw, Warsaw, Poland; ²Department of Medicine II, Saarland University Medical Center, Saarland University, Homburg, Germany; ³Department of Pathology, University Clinical Center of Medical University of Warsaw, Warsaw, Poland; ⁴Hannover Health Science, Hannover Medical School, Hannover, Germany; ⁵Laboratory of Metabolic Liver Diseases, Department of General, Transplant and Liver Surgery, Centre for Preclinical Research, Warsaw, Poland
Email: marcin.krawczyk@uks.eu

Background and aims: Hepatic steatosis is modulated by genetic variants like *PNPLA3* (p.I148M), *TM6SF2* (rs58542926), and *MBOAT7* (rs641738). Recently, *MARC1* (rs2642438) and *HSD17B13* (rs72613567) polymorphisms were shown to have protective effects

in patients with chronic liver diseases. Here, we analyse these fatty liver-related genes in patients undergoing bariatric surgery.

Method: The study cohort was composed of 165 prospectively recruited obese individuals (BMI 43.8 ± 5.7 kg/m², 66% women, 48 with diabetes mellitus) who underwent laparoscopic sleeve gastrectomy. The *PNPLA3*, *TM6SF2*, *MBOAT7*, *MARC1* and *HSD17B13* polymorphisms were genotyped performed using TaqMan assays. Liver biopsies were performed intraoperatively in all patients.

Results: In total, 70.3% of operated patients presented with hepatic steatosis, whereas NASH was detected in 28.5% of them; none had cirrhosis. Patients carrying the *MARC1* minor allele displayed a lower risk of developing fibrosis stage 1a (OR = 0.54, $p = 0.03$), 1b (OR = 0.47, $p = 0.01$), 1c (OR = 0.46, $p = 0.01$), and 2 (OR = 0.42, $p = 0.03$). The *PNPLA3* risk allele was associated with increased odds of hepatic steatosis (S2 and S3), fibrosis (1b to 2), and NASH (OR = 2.22, $p = 0.04$ in multivariate model). This variant was also significantly ($p < 0.01$) associated with increased fasting glucose ($p = 0.03$) and glycated haemoglobin (HbA1c) levels. Analysis restricted to 48 carriers of the *PNPLA3* risk alleles (29.1%) showed that the *MARC1* polymorphism decreases the odds of developing fibrosis. Furthermore, *MARC1* was an independent protective factor against fibrosis in multivariate analysis (OR = 0.51, 95% CI 0.28–0.92, $p = 0.04$). Carriers of the *HSD17B13* variant presented, in turn, with lower serum ALT ($p = 0.03$) and AST ($p = 0.04$) activities. The *TM6SF2* polymorphism was associated with the risk for S3 steatosis (OR = 17.52, $p < 0.01$) and increased ALT ($p = 0.04$).

Conclusion: Fatty liver is a frequent condition in patients scheduled for bariatric surgery, but the *MARC1* and *HSD17B13* gene variants diminish hepatic injury in these individuals. Variant *MARC1* might reduce the harmful effects of the major genetic risk factor for fatty liver, namely, *PNPLA3* p.I148M.

THU073

The impact of fatigue on mortality of patients with non-alcoholic fatty liver disease (NAFLD): data from national health and nutrition examination survey (NHANES) 2005–2018

Zobair Younossi^{1,2,3}, James Paik^{1,2,3}, Pegah Golabi^{1,2,3}, Youssef Younossi⁴, Linda Henry^{1,3,4}, Fatema Nader⁴. ¹Inova Health System, Medicine Service Line; ²Center for Liver Disease, Inova Medicine; ³Betty and Guy Beatty Center for Liver and Obesity, Inova Health System; ⁴Center for Outcomes Research in Liver Disease
Email: zobair.younossi@inova.org

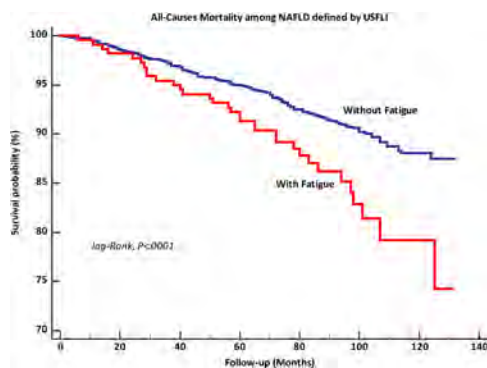
Background and aims: Fatigue is common among patients with NAFLD. Fatigue can negatively impact patient reported outcomes and clinical outcomes.

Aim: To determine the prevalence of fatigue and its association with all-cause mortality for patients with NAFLD.

Method: Data for adults (≥ 18 years) collected as part of the National Health and Nutrition Examination Survey (NHANES 2005–2010 and 2017–2018) with mortality data via linkage to the National Death Index (through 2015) were used for this study. For NHANES 2005–2010, NAFLD was defined by Fatty Liver Index adjusted for the multiethnic U.S. population (US-FLI). Additionally, transient elastography (TE) with a controlled attenuation parameter (CAP) of ≥ 285 dB/m was used to define NAFLD for NHANES 2017–2018. Excluded were patients with other liver diseases and excessive alcohol use. Fatigue was assessed through the Patient Health Questionnaire (PHQ-9) question, “Over the last 2 weeks, how often have you been bothered by feeling tired or having little energy?” Significant fatigue was defined as a response of “nearly every day” to the question.

Results: Of the NHANES 2005–2010 study cohort ($n = 5,429$, mean age 47.1 years, 49.7% male, 69.9% white), 37.6% had NAFLD. Compared to non-NAFLD group, fatigue was more common in individuals with NAFLD (8.35% vs 6.0%, $P = 0.002$). Among the NHANES 2017–2018 study cohort ($n = 3,830$, mean age 48.3 years, 48.6% male, 62.3% white), 36.9% had NAFLD and 7.2% had fatigue. Compared to non-

NAFLD subjects, those with NAFLD were older (51.4 vs 46.4 years), more likely to be male (55.6% vs 44.6%), and more likely to report fatigue (8.7% vs 6.2%), sleep trouble (ST) (34.0% vs 26.7%), metabolic abnormalities (90.4% vs. 58.4%), asthma (17.3% vs 12.7%), Chronic Obstructive Pulmonary Disease (COPD) (7.7% vs 6.1%), arthritis (34.3% vs 24.1%), thyroid disease (13.0% vs 9.9%), cardiovascular disease (CVD) (10.4% vs. 6.3%), significant fibrosis (liver stiffness >8.0 kPa, 17.9% vs 3.5%), and advanced fibrosis (>13.1 kPa, 5.4% vs 0.9%) (all $p < .003$). Among NAFLD, multivariate logistic regression analysis showed that presence of depression (Odds Ratio = 16.2, 95% Confidence interval, 6.02–43.6), ST (3.34, 1.85–6.05), arthritis (2.25, 1.29–3.92), COPD (2.91, 1.47–5.77), CVD (3.64, 2.04–6.51) and sleep quantity (+7 hours) (0.52, 0.31–0.88) were associated with presence of fatigue. Multivariable cox model demonstrated that NAFLD patients with fatigue had a 2.3-fold higher mortality than NAFLD without fatigue (HR: 2.31, 95%CI: 1.37–3.89, $P = 0.0024$).



Conclusion: Fatigue is more common among NAFLD and is driven mainly by depression, sleep trouble, and CVD. Among NAFLD, presence of fatigue is associated increased risk for mortality.

THU074

Metabolic dysfunction-associated fatty liver disease increases cardiovascular risk regardless of classical risk factors

María Del Barrio Azaceta¹, Paula Iruzubieta¹, Rocio Aller De La Fuente², Jesus Maria Banales³, Álvaro Santos-Laso¹, José Luis Calleja Panero⁴, Luis Ibañez⁵, María Teresa Arias Loste¹, Manuel Romero Gomez⁶, Carmelo García-Monzón⁷, Judith Gómez-Camarero⁸, Pere Ginès⁹, Rosa M Morillas¹⁰, Juan Manuel Pericàs¹¹, Patricia Aspichueta¹², Rosa Martín-Mateos¹³, Rocío Gallego-Durán¹⁴, Mercedes De La Torre Sanchez¹⁵, Desamparados Escudero-García¹⁶, Vanesa Bernal Monterde¹⁷, Salvador Benlloch¹⁸, Juan Turnes¹⁹, Javier Crespo¹. ¹Gastroenterology and Hepatology Department, Marqués de Valdecilla University Hospital, Clinical and Translational Digestive Research Group, IDIVAL, Santander, Spain; ²Center of Investigation of Endocrinology and Nutrition, School of Medicine, and Unit of Investigation, Hospital Clínico Universitario de Valladolid, Valladolid, Spain; ³Department of Liver and Gastrointestinal Diseases, Biodonostia Health Research Institute-Donostia University Hospital, University of the Basque Country (UPV/EHU), San Sebastian, Spain; ⁴Gastroenterology Department, Hepatology Unit, Hospital Universitario Puerta de Hierro, IDIPHSA, Madrid, Spain; ⁵Gastroenterology and Hepatology Department Hospital Universitario Gregorio Marañón Instituto de Investigación Sanitaria Gregorio Marañón (IISGM) Universidad Complutense de Madrid, Madrid, Spain; ⁶UCM Digestive Diseases, Virgen del Rocío University Hospital, SeLiver group at the Institute of Biomedicine of Seville (IBIS), The University of Seville, Seville, Spain; ⁷Liver Research Unit, Hospital Universitario Santa Cristina Instituto de Investigación Sanitaria Princesa, Madrid, Spain; ⁸Department of Gastroenterology and Hepatology, Complejo Asistencial Universitario de Burgos, Burgos, Spain; ⁹Liver Unit, Hospital Clínic,

IDIBAPS, University of Barcelona, Barcelona, Spain; ¹⁰Gastroenterology and Hepatology Department, Hospital Universitari Germans Trias i Pujol, Badalona, Spain; ¹¹Liver Unit, Vall d'Hebron University Hospital, Vall d'Hebron Institute of Research (VHIR), Barcelona, Spain; ¹²Department of Physiology, Faculty of Medicine and Nursing, Biocruces Research Institute, University of the Basque Country UPV/EHU, Leioa, Spain; ¹³Department of Gastroenterology and Hepatology, Hospital Universitario Ramón y Cajal, Instituto Ramón y Cajal de Investigación Sanitaria (IRYCIS), Madrid, Spain; ¹⁴Unit for the Clinical Management of Digestive Diseases, Hospital Universitario de Valme, Sevilla, Spain; ¹⁵Hepatology Unit, Consorcio Hospital General Universitario de Valencia, Valencia, Spain; ¹⁶Hospital Clínico Universitario de Valencia, Universitat de València, Valencia, Spain; ¹⁷Hospital Universitario Miguel Servet, Zaragoza, Spain; ¹⁸Department of Hepatology, Hospital Universitario y Politécnico La Fe, Valencia, Spain; ¹⁹Service of Digestive Diseases, Complejo Hospitalario Universitario de Pontevedra, IIS Galicia Sur, Pontevedra, Spain
Email: javiercrespo1991@gmail.com

Background and aims: Cardiovascular disease (CVD) is the main cause of mortality among patients with Metabolic dysfunction-Associated Fatty Liver Disease (MAFLD). Currently, clinical evidence shows that MAFLD could be a precursor for future development of metabolic syndrome (MS) components, linked to higher cardiovascular risk (CVR), regardless of classical risk factors. For this reason, our main aim was to determine if patients with MAFLD have a higher CVR as a consequence of liver disease activity.

Method: Cross-sectional study that includes 1, 587 patients with MAFLD, diagnosed by liver biopsy from the HEPamet Registry, and 1, 587 from the general population (ETHON cohort), age- and sex-matched. The CVR was evaluated with the Systematic Coronary Risk Evaluation (SCORE) model. In addition, the presence of carotid plaques and carotid intima-media thickness were analysed by ultrasound, in a subgroup of MAFLD patients without previous CVD, to establish their use in reclassification of CVR determined by SCORE. Multivariate regression analysis, adjusted for classical CVR factors, was used to evaluate whether CVR is influenced by liver disease activity.

Results: An increased prevalence of cardiovascular events was observed among patients with MAFLD compared to general population (10.3% vs 7.9%; $p = 0.02$), finding significant differences ($p < 0.001$) in CVR regarding SCORE categories (low CVR: 32.5% vs 37.3%; very high CVR: 36.9% vs 14.6%). NASH presence (OR 1.490 [IC 95%: 1.037–2.141]) and advanced fibrosis (OR 1.442 [IC 95%: 1.001–2.076]) were independent risk factors associated with high/very high SCORE category, after adjusted by classical CVR factors. The Fibrosis-4 (FIB-4) index was associated with high/very high SCORE category, maintaining as an independent and significant risk factor after adjusting by classical factors (OR 1.423 [IC 95%: 1.238–1.634]; $p < 0.001$), and showing statistically significant discrimination of high/very high CVR category (AUC: 0.655 [IC 95%: 0.628–0.682], $p < 0.001$). Using carotid ultrasound, it was observed that 20% of patients with low/moderate CVR were reclassified into high-risk category due to the presence of atheromatosis.

Conclusion: The presence of NASH, advanced fibrosis and a higher FIB-4 index were associated with a high/very high CVR in patients with MAFLD, even after considering classical risk factors. The ability of the SCORE model to predict CVD in MAFLD patients may not be as powerful as in the general population.

POSTER PRESENTATIONS

THU075

Changes in hepatic fat fraction as assessed by MRI-PDFF are correlated with changes in markers of hepatic inflammation, disease activity and fibrosis in biopsy-proven non-cirrhotic NASH with fibrosis

Samuel Daniels¹, Darren Robertson¹, Jose Sanchez², Janeli Sarv², Antonio Manzur¹, Lutz Jermutus³, Arun Sanyal⁴, Benjamin Challis⁵, Sudha Shankar⁶. ¹Early CVRM, Biopharmaceuticals RandD, Early Clinical Development, Cambridge, United Kingdom; ²Data Science and Artificial Intelligence, RandD, Early Biometrics and Statistical Innovation, Gothenburg, Sweden; ³Early CVRM, Biopharmaceuticals RandD, Cambridge, United Kingdom; ⁴Virginia Commonwealth University, Division of Gastroenterology, Hepatology and Nutrition, Richmond, United States; ⁵Early CVRM, Biopharmaceuticals RandD, Translational Science and Experimental Medicine, Research and Early Development, Cambridge, United Kingdom; ⁶Early CVRM, Biopharmaceuticals RandD, Early Clinical Development, Gaithersburg, United States
Email: samuel.daniels@astrazeneca.com

Background and aims: MRI-PDFF is the gold standard for non-invasive assessment of hepatic fat fraction (HFF) in non-alcoholic steatohepatitis (NASH) and is commonly used within early clinical trials to determine treatment efficacy on steatosis. HFF reduction has been associated with an increased likelihood of NASH resolution. However it is unclear whether reductions in hepatic steatosis bear a relationship with changes in markers of hepatic inflammation, disease activity and fibrosis.

Method: PROXYMO was a 19 week multi-centre phase 2 trial to investigate the safety and efficacy of cotadutide in 74 participants with biopsy confirmed non-cirrhotic NASH with fibrosis (NCT04019561). Post-hoc analysis was performed to investigate whether changes in HFF in the study population were associated with changes in non-invasive markers of hepatic fibrosis, NASH disease activity and inflammation within participants who had baseline and week 19 values. Participants were pooled (active and placebo) and the relative changes in HFF after 19 weeks were assessed against percentage change in non-invasive markers.

Results: Within pooled participants, relative change in HFF was significantly correlated with markers of hepatic inflammation (ALT R=0.52 (p<0.0001)), NASH disease activity (NIS-4 R=0.63 (p<0.0001)) and hepatic fibrosis (PRO-C3 R=0.44 (p=0.0012)). Changes in fibrosis biomarkers were correlated with changes in liver enzymes. Change in body weight was significantly correlated with change in HFF. Relative HFF change was divided into quartiles; those in the quartile of greatest relative HFF reduction had significantly greater reductions in ALT, AST, NIS-4 and PRO-C3.

Spearman Correlation Statistics					
Variable correlated to HFF	N	R	95% Confidence Limits	p Value	
PRO-C3	49	0.44	0.19 0.64	0.0012	
NIS-4	38	0.63	0.39 0.79	<.0001	
ALT	51	0.52	0.29 0.70	<.0001	

Conclusion: Reductions in HFF as assessed by MRI-PDFF were associated with reductions in non-invasive markers of hepatic inflammation, NASH disease activity and fibrosis. Furthermore, subjects with improvements in HFF had significantly greater reductions in ALT, AST, NIS-4 and PRO-C3.

THU076

The metabolic dysfunction-associated fatty liver disease definition, regardless of its clinical subclassification, identifies patients at high risk for liver disease progression

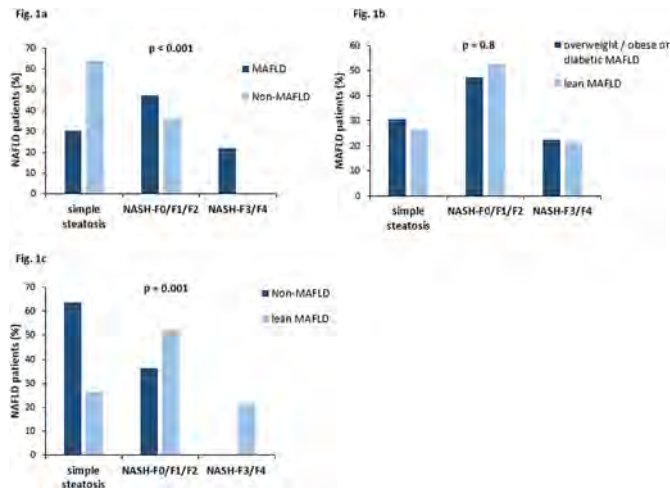
María Del Barrio Azaceta¹, Paula Iruzueta¹, Rocio Aller de la Fuente², Jesus María Banales³, Álvaro Santos-Laso¹, José Luis Calleja Panero⁴, Luis Ibañez⁵, María Teresa Arias Loste¹, Manuel Romero Gomez⁶, Carmelo García-Monzón⁷, Judith Gómez-Camarero⁸, Pere Ginès⁹, Rosa M Morillas¹⁰, Juan Manuel Pericàs¹¹, Patricia Aspichueta¹², Rosa Martín-Mateos¹³, Rocío Gallego-Durán¹⁴, Mercedes De La Torre Sanchez¹⁵, Desamparados Escudero-García¹⁶, Vanesa Bernal Monterde¹⁷, Salvador Benlloch¹⁸, Juan Turnes¹⁹, Javier Crespo¹. ¹Gastroenterology and Hepatology Department, Marqués de Valdecilla University Hospital, Clinical and Translational Digestive Research Group, IDIVAL, Santander, Spain; ²Center of Investigation of Endocrinology and Nutrition, School of Medicine, and Unit of Investigación, Hospital Clínico Universitario de Valladolid, Valladolid, Spain; ³Department of Liver and Gastrointestinal Diseases, Biodonostia Health Research Institute-Donostia University Hospital, University of the Basque Country (UPV/EHU), San Sebastian, Spain; ⁴Gastroenterology Department, Hepatology Unit, Hospital Universitario Puerta de Hierro, IDIPHSA, Madrid, Spain; ⁵Gastroenterology and Hepatology Department Hospital Universitario Gregorio Marañón Instituto de Investigación Sanitaria Gregorio Marañón (IiSGM) Universidad Complutense de Madrid, Madrid, Spain; ⁶UCM Digestive Diseases, Virgen del Rocío University Hospital, SeLiver group at the Institute of Biomedicine of Seville (IBIS), The University of Seville. Seville, Spain; ⁷Liver Research Unit, Hospital Universitario Santa Cristina Instituto de Investigación Sanitaria Princesa, Madrid, Spain; ⁸Department of Gastroenterology and Hepatology, Complejo Asistencial Universitario de Burgos, Burgos, Spain; ⁹Liver Unit, Hospital Clínic, IDIBAPS, University of Barcelona, Barcelona, Spain; ¹⁰Gastroenterology and Hepatology Department, Hospital Universitari Germans Trias i Pujol, Badalona, Spain; ¹¹Liver Unit, Vall d'Hebron University Hospital, Vall d'Hebron Institute of Research (VHIR), Barcelona, Spain; ¹²Department of Physiology, Faculty of Medicine and Nursing, Biocruces Research Institute, University of the Basque Country UPV/EHU, Leioa, Spain; ¹³Department of Gastroenterology and Hepatology, Hospital Universitario Ramón y Cajal, Instituto Ramón y Cajal de Investigación Sanitaria (IRYCIS), Madrid, Spain; ¹⁴Unit for the Clinical Management of Digestive Diseases, Hospital Universitario de Valme. Sevilla, Spain; ¹⁵Hepatology Unit, Consorcio Hospital General Universitario de Valencia, Valencia, Spain; ¹⁶Hospital Clínico Universitario de Valencia, Universitat de València, Valencia, Spain; ¹⁷Hospital Universitario Miguel Servet, Zaragoza, Spain; ¹⁸Department of Hepatology, Hospital Universitario y Politécnico La Fe, Valencia, Valencia, Spain; ¹⁹Service of Digestive Diseases, Complejo Hospitalario Universitario de Pontevedra, IIS Galicia Sur, Pontevedra, Spain
Email: javiercrespo1991@gmail.com

Background and aims: Several population studies indicate that Metabolic dysfunction-Associated Fatty Liver Disease (MAFLD) diagnostic criteria better identify which patients are at high risk for liver disease progression. However, the impact of this new definition on specialized clinical practice is still unknown. Here, our aim was to compare, MAFLD vs non-MAFLD patients, from a cohort of Non-Alcoholic Fatty Liver Disease (NAFLD) patients with liver biopsy.

Method: A cross-sectional multicenter study with 2, 148 NAFLD patients from the HEPamet Registry with liver biopsy, with no other causes of chronic liver disease and with the necessary clinical data to reach MAFLD diagnosis. Clinical, analytical and elastographic data, close to liver biopsy date, were collected. The Non-Alcoholic Steatohepatitis (NASH) diagnosis was based on the presence at once of steatosis, ballooning and lobular inflammation.

Results: Only 1.5% of patients did not fulfill MAFLD diagnostic criteria. Compared to non-MAFLD, MAFLD patients showed a higher mean value of Fibroscan (12.5±9 vs 6.5±2.3; p=0.002) and had more ballooning, lobular inflammation and significant/advanced fibrosis

(38.6% vs 9.1%; $p = 0.001$); as well as, NASH (Fig. 1a). Among MAFLD patients, there were no differences in histological diagnosis between lean MAFLD and the remaining of patients (Fig. 1b). Differences in liver affection between lean MAFLD and non-MAFLD maintained significant (Fig. 1c). The most powerful independent risk factors for advanced fibrosis in MAFLD patients were Type 2 Diabetes Mellitus (OR 2.37; IC 95% 1.79–3.15; $p < 0.001$) and Arterial Hypertension (OR 1.47; IC 95% 1.09–1.99; $p = 0.01$). Alcohol consumption (10–30 g/d) was the only factor associated with the presence of advanced fibrosis in lean MAFLD (OR 8.44; IC 95% 1.57–45.39; $p = 0.01$).



Conclusion: The metabolic dysfunction that defines MAFLD better identifies patients at risk for advanced liver disease, regardless of whether they are overweight/obese or diabetic.

THU077

Assessment of the prevalence of non-alcoholic fatty liver disease, its severity, and comorbidities in lean Americans: national health and nutrition examination surveys (NHANES) with transient elastography assessment from 2017 to 2018

Emily Truong¹, Galen Cook-Wiens², Naim Alkhouri³, Mazen Noureddin⁴. ¹Cedars Sinai Medical Center, Internal Medicine, Los Angeles, United States; ²Cedars Sinai Medical Center, Los Angeles, United States; ³Arizona Liver Health, Phoenix, United States; ⁴Cedars Sinai Medical Center, Karsh Division of Gastroenterology and Hepatology, Comprehensive Transplant Center, Los Angeles, United States
Email: emily.truong@cshs.org

Background and aims: Previous studies examined lean non-alcoholic fatty liver disease (NAFLD), which affects 10–20% of non-obese or lean Americans and is associated with lower rates of hyperlipidemia, hypertension, diabetes, and cirrhosis. We described characteristics and NAFLD prevalence and severity in the lean population in National Health and Nutrition Examination Surveys (NHANES) from 2017 to 2018 by using Fibroscan to directly assess steatosis and fibrosis.

Method: We analyzed NHANES data from 2017–2018. Inclusion criteria were age ≥ 18 years and completion of interview, laboratory testing, and FibroScan[®]. Exclusion criteria were excessive alcohol use (≥ 7 or 14 drinks/week for females or males, respectively) or viral hepatitis. Non-lean NAFLD was defined as body mass index (BMI) ≥ 25 kg/m², and lean NAFLD was defined as BMI < 25 kg/m². NAFLD was defined as controlled attenuation parameter > 274 dB/m.

Results: Of 3899, 120 (3.1%) respondents were lean NAFLD, and 1453 (37.3%) respondents were non-lean NAFLD. Overall NAFLD prevalence was 40.34% (non-lean 37.27% vs lean 3.08%). Compared to non-lean NAFLD, lean NAFLD had significantly lower prevalence of prediabetes,

though not significantly different prevalence of diabetes or hypertension. Lean NAFLD had lower mean CAP, FAST score, and median stiffness than that of non-lean NAFLD. Lean NAFLD had lower prevalence of fibrosis stage 2 or 3 and higher ($\geq F2$ or $\geq F3$) and Fibroscan-AST (FAST) score compared to non-lean NAFLD. Neither fibrosis stage 4 (F4) nor FAST score ≥ 0.67 were significantly different between lean and non-lean NAFLD.

	CAP ≥ 274		
	Non-lean NAFLD (unweighted n = 1453, weighted n = 66070260)	Lean NAFLD (unweighted n = 120, weighted n = 3807897)	p value
Mean or percent (95% CI)			
Severity of steatosis			
Mean CAP	324.17* (321.27 ; 327.07)	304.11* (299.32 ; 308.91)	<0.0001
Prevalence of fibrosis			
$\geq F2$	15.72* (11.75 ; 20.32)	6.03* (2.21 ; 12.5)	0.0137
$\geq F3$	10.31* (7.86 ; 13.16)	3.49* (1.07 ; 8.04)	0.0061
F4	5.08 (3.48 ; 7.09)	1.57 (0.1 ; 6.59)	0.1364
FAST ≥ 0.67	3.06 (2.27 ; 4.01)	1.04 (0.04 ; 5.06)	0.2496
Severity of fibrosis			
Mean FAST score	0.17* (0.16 ; 0.18)	0.11* (0.08 ; 0.13)	0.0002
Median stiffness (kPa)	6.88* (6.39 ; 7.38)	5.4* (4.27 ; 6.52)	0.0095

*Statistically significant. $\geq F2$, $\geq F3$, and F4 were defined by median stiffness ≥ 8.2 , ≥ 9.7 , and ≥ 13.6 kPa. F2/F3/F4 = fibrosis stage 2/3/4.

Conclusion: Compared with non-lean NAFLD, lean NAFLD had significantly higher prevalence of prediabetes and severity of hyperlipidemia. Although lean NAFLD had significantly decreased prevalence of $\geq F2$ and $\geq F3$ and lower FAST score compared to non-lean NAFLD, neither fibrotic non-alcoholic steatohepatitis nor cirrhosis prevalence were significantly different between lean and non-lean NAFLD. The largest to date to examine this subpopulation, this study highlights important implications for monitoring disease progression in the lean NAFLD population.

THU078

Coagulation imbalance is associated with hepatic fibrosis and vascular complications in patients with type2 diabetes and NAFLD

Francesca Alletto^{1,2}, Paolo Francione^{1,2}, Gabriele Maffi^{1,2}, Giordano Sigon^{1,2}, Annalisa Cespiati^{1,2}, Daniela Bignamini¹, Mariagrazia Clerici³, Veena Chantarangkul³, Armando Tripodi³, Flora Peyvandi^{2,4}, Silvia Fargion^{1,2}, Anna Ludovica Fracanzani^{1,2}, Rosa Lombardi^{1,2}. ¹Fondazione Ca' Granda IRCCS, Policlinico Hospital of Milan, Unit of Internal Medicine and Metabolic Diseases, Milan, Italy; ²University of Milan, Department of Pathophysiology and Transplantation, Milan, Italy; ³Fondazione Ca' Granda IRCCS, Policlinico Hospital of Milan, Angelo Bianchi Bonomi Hemophilia and Thrombosis Center and Fondazione Luigi Villa, Milan, Italy; ⁴Fondazione Ca' Granda IRCCS, Policlinico Hospital of Milan, Unit of Internal Medicine Hemostasis and Thrombosis, Milan, Italy
Email: rosa.lombardi@unimi.it

Background and aims: Both non-alcoholic fatty liver disease (NAFLD) and type 2 diabetes mellitus (T2DM) are characterized by a pro-coagulant state and expose patients to vascular complications. The interaction between pro-coagulant state, vascular complications and advanced liver disease has not been defined yet. Aim: to evaluate in a cohort of patients with T2DM and NAFLD if alterations in coagulation tests are associated with high prevalence of hepatic fibrosis and vascular complications.

Method: 96 consecutive outpatients with T2DM and ultrasound fatty liver and an age and sex matched control group of 156 healthy individuals were enrolled. For all subjects, determination of serum pro- (i.e factor II-FII, factor VIII-FVIII) and anti-coagulant factors (i.e protein C-PC, antithrombin-AT) and test of thrombin generation (ETP ratio, peak ratio, FVIII/PC) were obtained. In the T2DM cohort, significant liver fibrosis ($\geq F2$) was diagnosed by Fibroscan (i.e liver stiffness measurement-LSM $> 7.0/6.2$ kPa M/XL probe). Evaluation of microvascular (i.e retinopathy, nephropathy and neuropathy) and macrovascular complications (i.e carotid plaques and history of cardiovascular (CV) events) was assessed.

POSTER PRESENTATIONS

Results: In the T2DM group mean age was 65 ± 7 years, 66% male. Mean FII was 95.9 ± 12.8 , FVIII 130.3 ± 33.2 , PC 112.8 ± 20.8 , AT 106 ± 14.4 , ETP ratio 0.64 ± 0.09 , peak ratio 0.93 ± 0.05 , FVIII/PC 1.2 ± 0.3 . Despite only 5% of the cohort had increased transaminases, significant hepatic fibrosis was present in 14% by LSM. Microvascular complications were present in 29 (30%) patients (retinopathy in 8%, nephropathy in 23% and neuropathy in 4%) whereas plaques in 70 (73%) and CV events in 23 (24%). Compared to the control group, T2DM patients presented a pro-coagulant imbalance (ETP ratio 0.64 ± 0.09 vs 0.59 ± 0.18 , $p = .012$; FVIII/PC 1.2 ± 0.3 vs 1.02 ± 0.3 , $p = 0.03$). In the T2DM cohort, indexes of procoagulant imbalance as AT and FVIII/PC were independently associated with significant fibrosis by LSM $>7.0/6.2$ kPa with M/XL probe (multivariate analysis for AT corrected for age, sex, T2DM duration, HbA1c, overweight, hypertension: OR 0.89; CI 95% 0.80–0.98) and microvascular complications (multivariate analysis corrected for age, sex, smoking, T2DM duration, HbA1c, overweight, hypertension, use of statins, uric acid for AT: OR 0.93; CI 95% 0.88–0.98; and for FVIII/PC ratio: OR 8.0; CI 95% 1.00–65.8).

Conclusion: In patients with T2DM and NAFLD a pro-coagulant imbalance was found compared to healthy controls and it was associated with both hepatic and vascular complications, speculating on a possible common pathogenetic pattern. Further studies and a wider cohort are warranted to define the clinical application of these coagulation alterations. However, our results point on the need of a careful evaluation also of hepatic complications in diabetics.

THU079

Presence of two or more metabolic risks regardless of fatty liver is a risk factor for significant hepatic fibrosis

Huiyul Park¹, Dae Won Jun², Eileen Yoon², Sang Bong Ahn³, Hyo Young Lee⁴, Hyunwoo Oh⁴, Bo-Kyeong Kang⁵, Mi Mi Kim⁵, Chul-min Lee⁵, Joo Hyun Sohn⁶. ¹Uijeongbu Eulji Medical Center, Department of Family medicine, Gyeonggi-do, Korea, Rep. of South; ²Hanyang University College of Medicine, Department of Medicine, Seoul, Korea, Rep. of South; ³Nowon Eulji Medical Center, Eulji University School of Medicine, Department of Medicine, Seoul, Korea, Rep. of South; ⁴Uijeongbu Eulji Medical Center, Department of Medicine, Gyeonggi-do, Korea, Rep. of South; ⁵Hanyang University College of Medicine, Department of Radiology, Seoul, Korea, Rep. of South; ⁶Hanyang University Guri Hospital, Hanyang University College of Medicine, Department of Medicine, Gyeonggi-do, Korea, Rep. of South
Email: mseileen80@gmail.com

Background and aims: Metabolic syndrome and diabetes are well-known risk factors for hepatic fibrosis. However, hepatic fibrosis screening strategies for subjects with these risks have not yet been established. We aimed to identify the high-risk group for hepatic fibrosis screening, according to the type and number of metabolic risk factors.

Method: This was a retrospective cross-sectional cohort study using data from 13 nationwide centres. A total of 5,111 subjects who underwent both magnetic resonance elastography and abdominal ultrasound as part of their health check-up were included. Subjects with viral hepatitis and/or a history of significant alcohol consumption were excluded.

Results: The prevalence of significant hepatic fibrosis was 7.3%. Among subjects with significant hepatic fibrosis, 41.3% did not have fatty liver. Hepatic fibrosis burden increased according to the number of metabolic abnormalities. Nearly 70% of subjects with significant hepatic fibrosis also had two or more metabolic risks and/or diabetes. However, significant fibrosis prevalence did not differ between the groups with and without fatty liver among those with healthy metabolic conditions. The presence of two or more metabolic abnormalities was an independent risk factor for significant hepatic fibrosis, even when the presence of fatty liver was corrected.

Conclusion: Health check-up examinees who have two or more metabolic risks and/or diabetes are at risk of hepatic fibrosis, regardless of fatty liver status. Thus, active screening for hepatic

fibrosis in the setting of health check-up centres should be extended to subjects with two or more metabolic risks and/or diabetes, beyond those with fatty liver.

THU080

Pregnancy as a unique opportunity to identify NAFLD in women: a prospective assessment

Tatyana Kushner¹, Shaelyn O'Hara¹, Marcia Lange¹, Carin Carroll², Emma Rosenbluth¹, Pamela Argiriadi¹, Rachel Meislin¹, Joanne Stone¹, Keith Sigel¹, Rhoda Sperling¹, Scott Friedman¹, Norah Terrault³. ¹Icahn School of Medicine at Mount Sinai; ²University of Miami School of Medicine; ³University of Southern California Keck School of Medicine
Email: tatyana.kushner@mssm.edu

Background and aims: Non-alcoholic fatty liver disease (NAFLD) in U.S. women of reproductive age is rising and recent administrative claims-based data suggest a significant association of NAFLD with adverse pregnancy outcomes. We evaluated the prevalence and associated risk factors of NAFLD at a high-volume obstetrics center.

Method: In this prospective study, a liver ultrasound at time of routine pregnancy anatomy scan at 18–22 weeks' gestation was performed to assess for presence of NAFLD. Obstetric sonographers were trained to obtain liver images that were subsequently graded for hepatic steatosis by a radiologist blinded to clinical status. The proportion having elevated hepatic steatosis index (HSI) and meeting recently defined metabolic associated fatty liver disease (MAFLD) criteria was evaluated. A multivariable logistic regression model assessed independent predictors of NAFLD among pregnant women.

Results: Among 749 women approached for participation, satisfactory liver ultrasounds were obtained on 560 (75%) pregnant individuals; median age 28, 58% Hispanic ethnicity, 65% with pre-pregnancy BMI ≥ 25 , 22% nulliparous. Seventy-eight (14.3%) had steatosis on ultrasound; 83% grade 1, 14% grade 2 and 3% grade 3. Overall, 36% had HSI ≥ 36 ; 11% satisfied MAFLD criteria. Only 4 of 560 (0.71%) carried a previous diagnosis of NAFLD. Women with steatosis were more likely to be of Hispanic ethnicity, have diagnoses of chronic hypertension and diabetes and have a pregnancy history of gestational diabetes ($p < 0.05$; see Table). Women with grade 2/3 steatosis were more likely to have a history of preeclampsia (30% vs 10%, $p = 0.05$). In multivariable analyses, Hispanic ethnicity (OR 2.57; 95% CI 1.30–5.09) and BMI (OR 1.06; 95% CI 1.01–1.11) were independently associated with NAFLD.

Conclusion: In this first time U.S. based prospective study of pregnant women, integration of ultrasound into obstetric care was feasible and effective in identifying women with NAFLD. NAFLD prevalence was 14%, similar to reports in non-pregnant women of reproductive age with Hispanic and elevated pre-pregnancy BMI women being at highest risk of NAFLD. Most had no prior diagnosis of NAFLD, highlighting a unique opportunity to identify and link women to specialized care.

	No NAFLD n = 469 (85.7%)	NAFLD n = 78 (14.3%)	p value
Age (median, IQR)	28 (24, 33)	28 (24, 33)	0.666
Hispanic ethnicity, n (%)	254 (56%)	60 (77%)	0.002
Pre-pregnancy BMI (kg/m ²), median	26 (23, 31)	29 (25, 34)	0.001
Chronic HTN, n (%)	31 (7%)	11 (14%)	0.022
Type II DM, n (%)	9 (2%)	7 (9%)	0.001
Autoimmune disease, n (%)	23 (5%)	8 (11%)	0.055
Prior Pregnancy History			
Gestational Diabetes	17 (5%)	7 (13%)	0.023
Preeclampsia	34 (10%)	10 (18%)	0.065
Cholestasis of Pregnancy	7 (1%)	0 (0%)	0.291
Preterm birth	53 (15%)	6 (11%)	0.395
NAFLD Clinical scores			
Mean HSI (SD) (n = 368)	37.88 (8.44)	40.84 (8.97)	0.013
No. Satisfying any MAFLD Criteria (%) (n = 549)	4 (0.85)	58 (74.36)	0.001

THU081

N-terminal propeptide of type III collagen (PRO-C3) based risk for liver fibrosis predict cardiovascular events in non-alcoholic fatty liver disease

Francesco Baratta¹, Giulia Tozzi², Daniele Pastori¹, Alessandra Colanoni¹, Nicholas Cocomello¹, Stefano Cecchi², Mattia Coronati¹, Francesco Angelico¹, Maria Del Ben¹. ¹Sapienza-University of Rome; ²Children's Hospital Bambino Gesù
Email: francesco.baratta@uniroma1.it

Background and aims: N-terminal propeptide of type III collagen (PRO-C3) is cleaved off during the process of collagen III deposition. Serum levels of PRO-C3 properly correlate to biopsy-proven liver fibrosis stage and PRO-C3 was included in some risk scores, namely ADAPT, FIB-C3 and ABC3D to predict advanced liver fibrosis. While the association between other liver fibrosis risk scores (FIB4 and NAFLD fibrosis score) and cardiovascular events (CVEs) has been demonstrated, the association between PRO-C3 derived scores and CVEs has never been investigated. Aim of the study was to investigate the association between scores including PRO-C3, and CVEs incidence in a large prospective cohort of NAFLD patients.

Method: The present study is a post hoc analysis of the Plinio Study (ClinicalTrials.gov: NCT04036357). PRO-C3 detection was performed in plasma using ELISA commercial kit (Novus Biological). ADAPT, FIB-C3 and ABC3D were calculated. Data on CVEs were prospectively collected with periodical phone calls (every six months) and visits (every 12 months).

Results: The median follow-up was 47.8 [25.3–72.8] months yielding 2786.5 person-years of observation. During the follow-up, 41 patients (1.5% year) experienced CVEs. Patients who experienced CVEs were more frequently males ($p=0.010$) and had higher prevalence of type 2 diabetes ($p=0.006$), metabolic syndrome ($p=0.002$) and of prior CVE event ($p<0.001$). The prevalence of impaired ADAPT ($p=0.038$), FIB-C3 ($p=0.015$) and ABC3D ($p<0.001$) were higher in patients with CVEs. At multivariate Cox regression analyses, the association with CVEs was confirmed for ABC3D >3 (HR: 2.29 [1.17–4.47]) in the whole population and for FIB-C3 (HR: 1.40 [1.06–1.85]) and ABC3D (HR: 1.40 [1.06–1.84]) only in patients who did not experience a CV event before enrollment (in primary prevention) (Table 1). In all the analyses performed in the whole cohort, prior-CVE was the strongest predictor of new onset CVEs during the follow-up (data not shown).

Table 1. Multivariate cox regression analysis in the whole population (Panel A) and in patients in primary prevention (Panel B).

	CVEs		CHD	
	aHR (95% C.I. for aHR)	aHR (95% C.I. for aHR)	aHR (95% C.I. for aHR)	aHR (95% C.I. for aHR)
Panel A.				
ADAPT ²	1.24 [0.93-1.64]	1.19 [0.83-1.69]		
ADAPT $>6.3287^2$	1.23 [0.42-3.63]	0.50 [0.07-2.93]		
FIB-C3 ³	1.22 [0.97-1.55]	1.21 [0.90-1.61]		
FIB-C3 $>0.4^3$	1.40 [0.66-2.98]	1.04 [0.38-2.86]		
ABC3D ³	1.24 [0.98-1.57]	1.27 [0.95-1.70]		
ABC3D $>3^1$	2.29 [1.17-4.47]*	2.38 [1.04-5.43]*		
Panel B.				
ADAPT ²	1.34 [0.91-1.99]	1.39 [0.87-2.21]		
ADAPT $>6.3287^2$	1.98 [0.46-8.54]	1.35 [0.18-10.15]		
FIB-C3 ³	1.40 [1.06-1.85]*	1.43 [1.01-1.95]*		
FIB-C3 $>0.4^3$	1.23 [0.44-3.39]	1.07 [0.30-3.85]		
ABC3D ³	1.40 [1.06-1.84]*	1.27 [0.95-1.70]		
ABC3D $>3^1$	1.69 [0.69-4.18]	1.27 [0.89-1.83]		

¹Adjusted for age, sex, prior CVEs, smoking habits, BMI, diabetes, platelets; ²Adjusted for sex, prior CVEs, smoking habits, and BMI; ³Adjusted for sex, prior CVEs, smoking habits; * $p<0.05$. CVEs: cardiovascular and cerebrovascular events; composite; CVEs + new onset atrial fibrillation; CHD: coronary heart disease; HR: Hazard ratio; aHR: adjusted HR; C.I.: confidence interval. PRO-C3: N-terminal propeptide of type III collagen; ADAPT: age, of diabetes, PRO-C3, and platelet algorithm; FIB-C3: FIB-C3 diagnostic panel; ABC3D: age, BMI, platelet count, PRO-C3, diabetes derived score.

Conclusion: This from the Plinio cohort study is the first evidence of an association between ADAPT, FIB-C3, ABC3D and cardiovascular events in NAFLD. These scores detect high-risk patients for both liver and cardiovascular complications, may contribute to better identify a sub-population of NAFLD patients who deserve a more holistic approach.

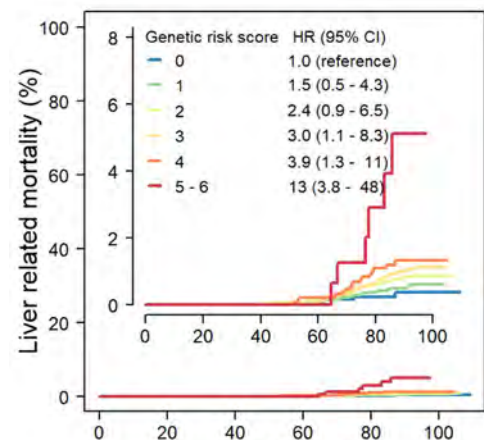
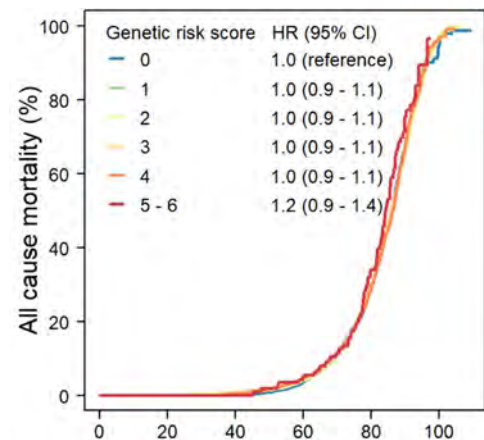
THU082

Genetic risk of fatty liver disease and mortality in the general population

Helene Gellert-Kristensen¹, Børge Nordestgaard², Anne Tybjaerg Hansen¹, Stefan Stender¹. ¹Rigshospitalet, Clinical Biochemistry, Copenhagen, Denmark; ²Herlev Hospital, Clinical Biochemistry, Herlev, Denmark
Email: stefan.stender@regionh.dk

Background and aims: Fatty liver disease associates with increased mortality due to extrahepatic causes, as well as increased all-cause mortality. However, it remains unclear if these associations reflect a causal effect of fatty liver disease rather than confounding due to coexisting comorbidities. The aim of this study was to use genetic variants (which are less susceptible to confounding) to assess if fatty liver disease *per se* is likely to causally influence mortality.

Method: We included participants from two prospective studies of the general Danish population, the Copenhagen City Heart Study and the Copenhagen General Population Study, totaling 110,913 persons. All participants were genotyped for six variants with known effects on fatty liver disease: *PNPLA3* rs738409, *TM6SF2* rs58542926, *HSD17B13* rs72613567, *MBOAT7* rs641738, *MTARC1* rs2642438, and *GCKR* rs1260326.



Number at risk

0	44	289	1208	730	9
1	219	1498	6714	3752	19
2	326	2357	11110	6386	40
3	234	1342	6115	3433	22
4	97	320	1449	779	6
5-6	11	36	152	66	0

POSTER PRESENTATIONS

Results: During a median of 9.5 years of follow-up, 16, 119 individuals died, hereof 201 due to liver-related causes, 1, 736 to ischemic heart disease, and 4, 973 to extrahepatic cancer. The variants at *PNPLA3*, *HSD17B13*, *TM6SF2*, and *MBOAT7* (but not those at *MTARC1* and *GCKR*) were individually associated with liver-related mortality, with per-allele hazard ratios of 1.3 to 1.6 (*p* values <0.06). The strongest effect was seen for the *PNPLA3* variant, for which homozygous carriers had a three-fold higher risk of liver-related death compared to non-carriers. A previously developed genetic risk score comprised of the variants at *PNPLA3*, *TM6SF2* and *HSD17B13* was robustly associated with stepwise increased liver-related mortality, with a maximum hazard ratio of 13 (95% CI: 3.8 to 48) for those with 5 or 6 versus 0 risk-increasing alleles (*p* for trend = 9×10^{-7} , see Figure, bottom panel). The fatty liver disease variants, individually or combined into risk scores, did not associate with ischemic heart disease-related, extrahepatic cancer-related, or all-cause mortality (Figure, top panel).

Conclusion: High genetic risk of fatty liver disease increased liver-related mortality but did not influence the risk of death due to ischemic heart disease or extrahepatic cancer, nor all-cause mortality in the general population. These data support that fatty liver disease is causally associated with liver-related mortality, but not with mortality due to other causes.

THU083

Role of NAFLD-associated genetic variants on renal function in patients with non-alcoholic fatty liver disease

Laura D'Erasmo¹, Francesco Baratta¹, Alessia Di Costanzo¹, Ilaria Umbro¹, Alessandra Colantoni¹, Nicholas Cocomello¹, Daniele Pastori¹, Marcello Arca¹, Francesco Angelico¹, Maria Del Ben¹.
¹Sapienza, University of Rome
 Email: laura.derasso@uniroma1.it

Background and aims Previous studies demonstrated the association between non-alcoholic fatty liver disease (NAFLD) and chronic kidney disease (CKD). Recent studies focused the attention on the role of Patatin-like Phospholipase domain-containing 3 (*PNPLA3*) rs738409 polymorphism in the association between NAFLD and CKD in non-metabolic adults and children, but the genetic impact on NAFLD-CKD association is still matter of debate. Aim of the study was to investigate the impact of *PNPLA3*, Transmembrane 6 Superfamily Member 2 (*TM6SF2*), Membrane Bound O-Acyltransferase Domain Containing 7 (*MBOAT7*) and Glucokinase Regulatory Protein (*GCKR*) genes on renal function in a large population of NAFLD patients.

Method: The present study is a post hoc analysis of the Plinio Study (ClinicalTrials.gov: NCT04036357). *PNPLA3*, *TM6SF2*, *MBOAT7* and *GCKR* genes were analyzed by using Real Time PCR with TaqMan probes. Glomerular filtration rate (GFR) was estimated with CKD-epi formula. The effect of the NAFLD genetic background on eGFR was estimated both including each gene individually and considering the NAFLD genetic risk score (wGRS). The effect of NAFLD on renal function was assessed by analyzing two end points: 1) eGFR <90 ml/min (rGFR) or 2) eGFR <60 ml/min (moderate-to-severe CKD).

Results: This analysis was conducted on 564 NAFLD patients with available renal function data. Among these, the 48.0% had an eGFR below 90 ml/min while only 6.6% had moderate-to-severe CKD. The distribution of genotypes was superimposable if considering the entire group of patients with eGFR <90 ml/min or only those with eGFR <60 ml/min. At multivariate regression analyses (table 1), we did not observe any correlation between genotypes and renal function. Conversely, we found that metabolic syndrome was highly associated with rGFR (Odds ratio (OR): 1.52 (1.07–2.18)), whereas prior Atherosclerotic Cardiovascular Disease (ASCVD) with moderate-to-severe CKD (OR: 3.54 (1.22–10.24)). When introduced in the model, arterial hypertension emerged as the strongest risk factor for eGFR decline (OR: 1.45 (1.02–2.06) and OR: 2.85 (1.20–6.79) respectively for rGFR and moderate-to-severe CKD) (table 1).

Table 1. Multivariate regression analyses

Panel A. Factors Associated with eGFR < 90 ml/min				
	Model A OR (95% C.I.)	Model B OR (95% C.I.)	Model C OR (95% C.I.)	Model D OR (95% C.I.)
Metabolic Syndrome ^a	1.52* (1.07-2.18)	-	-	1.53* (1.07-2.18)
Arterial Hypertension	-	-	1.45* (1.02-2.06)	-
Panel B. Factors Associated with moderate-to-severe CKD				
	Model A OR (95% C.I.)	Model B OR (95% C.I.)	Model C OR (95% C.I.)	Model D OR (95% C.I.)
Prior ASCVD	3.54* (1.22-10.24)	3.55* (1.19-10.55)	-	3.44* (1.19-9.90)
Arterial Hypertension	-	-	2.85* (1.20-6.79)	-

^aAccording to ATP III modified criteria; **p*<0.05

Model A: including BMI, metabolic syndrome, prior ASCVD, *PNPLA3* GG/CG and FIB4 -.
 Model B: including component of the metabolic syndrome (namely high blood glucose, high waist circumference, high blood pressure, low HDL cholesterol, high triglycerides) instead of the composite score, prior ASCVD, *PNPLA3* GG/CG genotype and FIB4 -.

Model C: including arterial hypertension instead of high blood pressure, diabetes instead of high blood glucose, high waist circumference, low HDL cholesterol, triglycerides, prior ASCVD, *PNPLA3* GG/CG genotype and FIB4 -.

Model D: including BMI metabolic syndrome, prior ASCVD, weighted GRS and FIB4 -.

Conclusion: In our cohort of adult patients with NAFLD, we found no association between CKD and *PNPLA3*, *TM6SF2*, *MBOAT7* and *GCKR* gene variants. Hypertension was the stronger predictor of eGFR impairment. Based on these findings, the association between NAFLD and CKD might be due to the shared metabolic risk factors rather than the genetic NAFLD background.

THU084

The association between non-alcoholic fatty liver disease and insulin resistance within normal glucose level population

Chun-Yi Wang¹, Kuan-Yu Lai¹, Wen-Yuan Lin¹, Tsung Po Chen¹.
¹China Medical University Hospital, Department of Community and Family Medicine, Taichung, Taiwan
 Email: tsungpo88@gmail.com

Background and aims: The study of non-alcoholic fatty liver disease (NAFLD) with association of type 2 diabetes (T2DM) reveals rapid growth of prevalence and incidence in recent years. The mechanism of NAFLD shows connection between insulin resistance (IR) and T2DM. The aim of this study was to investigate the association between NAFLD and IR in normal glucose level population.

Method: We recruited participants from community and outpatient department in a hospital from central and northern Taiwan. Those with impaired fasting glucose or with diagnosis of T2DM were excluded from our study. We screened the items of body mass index (BMI), systolic/diastolic blood pressure (SBP/DBP), body fat ratio (%) and social factors. We performed serum test after 8 hours overnight fasting. NAFLD was diagnosed based on an abdominal ultrasonography measurement. The calculation of IR used HOMA-IR formula and was shown by tertile (T1, T2, and T3). The method of statistics counted through analysis of variance (ANOVA) and multivariate logistic regression.

Results: A total of 485 subjects (mean age 42.0 ± 11.4 years) were involved. The prevalence of NAFLD increased significantly among increasing level of IR (34.1%, 40.1%, 47.8%, *p* <0.001). Although fasting plasma glucose were within normal range among three groups, higher level of IR presented higher glucose value (81.9 ± 7.4 mg/dL, 85.1 ± 7.6 mg/dL, 87.3 ± 6.5 mg/dL, *p* < 0.0001). After adjusting for age, sex, BMI, exercise, alcohol consumption and cigarette smoking, the risk of NAFLD was increased with the increment of IR (T3 v.s. T1: Odd ratio [OR] 3.87, 95% confidence interval [CI], 2.08 to 7.21; T2 v.s. T1: OR 1.83, 95% CI, 1.11 to 3.00) after adjusting for confounding factors.

Conclusion: This study shows that in normal sugar level groups, the significant increasing risk of NAFLD if IR presented even in normal glucose level groups. The mechanism of NAFLD influenced hepatic enzymes production and further IR involved. We should take early intervention if abnormal IR present.

THU085

Chronic pruritus represents a major burden in non-cholestatic hepatobiliary disorders

M. Düll^{1,2}, Vanessa Karlen^{1,2}, Marcel Vetter^{1,2}, Peter Dietrich^{1,2,3}, Jörg Kupfer⁴, Markus F. Neurath^{1,2}, Andreas E Kremer^{1,2,5}. ¹Deutsches Zentrum Immuntherapie (DZI), Erlangen, Germany; ²Friedrich-Alexander-University Erlangen-Nürnberg, Department of Medicine 1, Erlangen, Germany; ³Friedrich-Alexander-University Erlangen-Nürnberg, Institute of Biochemistry, Emil-Fischer-Zentrum, Erlangen, Germany; ⁴Justus-Liebig-University Giessen, Institute of Medical Psychology, Giessen, Germany; ⁵University Hospital Zürich, Department of Gastroenterology and Hepatology, Germany
Email: andreas.kremer@usz.ch

Background and aims: While previous data indicated a high prevalence of pruritus in patients with immune-mediated liver disorders, there is only limited data on pruritus in hepatobiliary diseases in general. This study therefore aimed at further investigating epidemiology, clinical features, and influence on quality of life (QoL) in a large cohort of patients with different liver diseases.

Method: We performed a prospective, cross-sectional study in a large Hepatology outpatient clinic from August 2020-May 2021. We collected extended clinical data including characteristics of pruritus (e.g. mean/worst itch intensity on a numeric rating scale, NRS) and questionnaires containing validated scores such as ItchyQoL and SF12. Statistical analyses were performed using Mann-Whitney-U-test and Spearman's rank correlation. Data are given as mean ± SEM.

Results: In total, 609 patients participated in this study of whom 27.3% (N = 166) presented with liver cirrhosis. 24.1% (N = 147) of all patients reported on pruritus with 61.9% (N = 91) being female. In the pruritus group 52.7% (N = 79) of all patients suffered from non-cholestatic liver diseases such as (non)alcoholic fatty liver disease, (non)alcoholic steatohepatitis (N)ASH, viral hepatitis, and associated liver cirrhosis. Immune-mediated and cholestatic liver diseases such as primary biliary cholangitis, primary and secondary sclerosing cholangitis, and genetic disorders represented 46.3% (N = 68). The majority of all pruritic patients reported on chronic itch with a duration >6 weeks (80.9%; N = 119). Only 17.7% (N = 26) received oral anti-pruritic therapy with fibrates being most commonly prescribed (30.5%, N = 8). Mean and worst itch intensity during the last week were rated at moderate intensities of 3.7 ± 0.2 and 4.2 ± 0.3 on a NRS, respectively. The QoL of affected patients quantified by ItchyQoL correlated with the mean and worst itch intensities ($r_s = 0.34$; $p < 0.001$; $r = 0.40$; $p < 0.0001$). SF-12 analyses exhibited significantly lower median physical ($p < 0.0001$) and mental scores ($p < 0.01$, Mann-Whitney-U-test) in the pruritus group.

Conclusion: Pruritus affected almost every fourth patient with hepatobiliary diseases and reduced their QoL. A significant number of patients remain treated insufficiently. Our findings underscore the need to increase awareness of chronic itch in hepatobiliary disorders and to study this symptom in clinical trials beyond the classical cholestatic liver disorders.

THU086

Mortality prediction in non-alcoholic fatty liver disease using SteatoSITE: an integrated gene-to-patient data commons for high-definition non-alcoholic fatty liver disease research

Maria Jimenez Ramos¹, Frances Turner², Prakash Ramachandran¹, Donald R. Dunbar², Lynn McMahon³, Marian McNeil³, Tim Kendall^{1,4}, Jonathan Fallowfield¹. ¹The Queen's Medical Research Institute, Centre for Inflammation Research, Edinburgh, United Kingdom; ²Edinburgh Genomics, Edinburgh, United Kingdom; ³Precision Medicine

Scotland-Innovation Centre (PMS-IC), Glasgow, United Kingdom; ⁴Edinburgh Pathology, Edinburgh, United Kingdom
Email: jonathan.fallowfield@ed.ac.uk

Background and aims: Studies have correlated liver gene expression to pathological and clinical features of NAFLD cross-sectionally, but there is a paucity of longitudinal data using molecular features to predict patient outcomes. Such data is critical for accurate risk stratification and identification of novel treatments for specific subphenotypes of NAFLD. Using SteatoSITE (<https://steatosite.com/>), a resource containing integrated genetic, clinical and pathological data, we studied hepatic RNA-sequencing (RNA-seq) and linked electronic health record (EHR) data to identify gene expression patterns across the full histological NAFLD spectrum and to determine transcriptomic signatures that are associated with adverse clinical outcomes. Bulk tissue cell-type deconvolution was also performed using published single-cell RNA-seq (scRNA-seq) data to elucidate changes in cellular composition to inform rational biomarker and drug development.

Method: Bulk RNA-seq data was analysed from 692 liver samples (normal liver controls (n = 28), isolated steatosis (n = 43), steatosis with inflammation and/or hepatocyte ballooning (n = 621), including samples from all fibrosis stages). Time until death or censoring was retrieved for each patient. Differentially expressed genes (DEGs) between alive and dead patients at 1, 2, 3 and 5 years were used to generate a transcriptional signature predictive of mortality. Multi-subject Single-cell Deconvolution (MuSiC) was used to compare counts from each bulk RNA-seq sample with scRNA-seq data from healthy and cirrhotic livers to estimate proportions of liver macrophage, mesenchyme, endothelial, B- and T-cell subtypes across discrete NAFLD stages.

Results: RNA-seq identified 45 DEGs in early NAFLD (i.e., isolated steatosis) and 9826 DEGs in advanced NAFLD (i.e., fibrosis stage F4), compared with controls. KEGG analysis showed enrichment of inflammatory pathways in early-stage disease (e.g., cytokine-cytokine receptor interactions; $q < 0.01$), whilst pathways linked to extracellular matrix were only enriched in advanced disease ($q < 0.0001$). Linkage of RNA-seq with EHR data identified DEGs associated with mortality including potential biomarkers such as growth/differentiation factor 15 (GDF15) and fibroblast growth factor 21 (FGF21). Deconvolution analysis revealed statistically significant correlations between histological fibrosis scores and expanded populations of scar-associated macrophages, myofibroblasts, endothelial cells and B-cells.

Conclusion: Using SteatoSITE, the world's first data commons for NAFLD, we defined hepatic gene signatures across the full disease severity spectrum. Linkage to EHR-derived outcomes enables identification of liver transcriptional features associated with increased mortality. This work will underpin future studies aimed at developing a stratified medicine approach for NAFLD.

THU087

Different effects of low muscle mass on the risk of non-alcoholic fatty liver disease and liver cirrhosis in a prospective cohort

Hun Jee Choe^{1,2}, Hyunsuk Lee^{1,2}, DongHo Lee^{1,2}, Soo-Heon Kwak^{1,2}, Bo Kyung Koo^{2,3}. ¹Seoul National University Hospital, Internal Medicine, Seoul, Korea, Rep. of South; ²Seoul National University College of Medicine, Internal Medicine, Seoul, Korea, Rep. of South; ³Seoul, Boramae Medical Center, Seoul, Korea, Rep. of South
Email: bokyungkoomd@gmail.com

Background and aims: As non-alcoholic fatty liver disease (NAFLD) and sarcopenia share insulin resistance as a common pathophysiology and have overlapping clinical manifestation of metabolic derangement, it is hard to differentiate the independent effect of sarcopenia on the development of NAFLD from concomitant metabolic disorders. Using a community-based prospective cohort study, the contributions of low muscle mass and genetic risk factors,

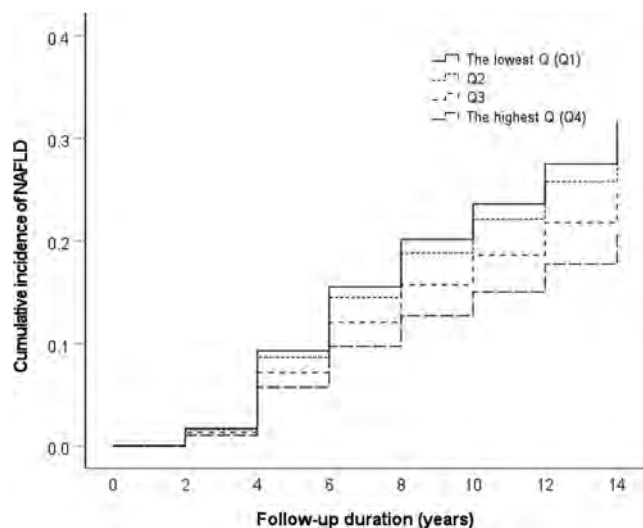
POSTER PRESENTATIONS

to the development of NAFLD and NAFLD-related liver cirrhosis were investigated in the Korean population.

Method: This prospective community-based cohort study included 40–70-year-old adults, followed-up biennially from 2001–2002 to 2017–2018. NAFLD was defined as a hepatic steatosis index of 36 or higher, and liver cirrhosis was defined based on the fibrosis-4 index. Sex-specific quartiles of body mass index (BMI)-adjusted muscle mass were calculated, and low muscle mass was defined as the lowest quartile (Q1). Cox proportional hazard models for incident NAFLD or liver cirrhosis incorporating age, sex, BMI of 25 kg/m² or higher, metabolic syndrome, and *PNPLA3* and *TM6SF2* risk alleles were used to assess the independent determinants for incident NAFLD and liver cirrhosis among individuals with NAFLD at baseline.

Results: Among the 4,038 participants without NAFLD at baseline (mean age, 51.5 ± 8.8 years), 920 (22.8%) developed NAFLD during the follow-up period of 12 years. As muscle mass decreased, the risk of NAFLD increased even after adjustment for age, sex, obesity, metabolic syndrome, and *PNPLA3* and *TM6SF2* risk alleles (hazard ratio [HR] per quartile, 1.18, 95% confidence interval (CI), 1.11–1.27, *p* < 0.001). *TM6SF2* also affected the risk of NAFLD (HR 1.19, [95% CI, 1.00–1.40]).

Of the 1,176 patients with NAFLD but without hepatic fibrosis at baseline, incident liver cirrhosis was found in 51.8%, 44.7%, 42.6%, and 41.0% in Q1, Q2, Q3, and Q4 of BMI-adjusted muscle mass, respectively, during the follow-up period (*p* for trend = 0.006). However, this trend lost its statistical significance when adjusted for confounders. The *PNPLA3* risk variant and not the *TM6SF2* genotype, was an independent risk factor for developing liver cirrhosis among NAFLD patients (HR 1.17, 95% CI 1.04–1.32, *p* = 0.010).



Conclusion: Both lower muscle mass index and genetic risk variants are important contributors to the development of NAFLD. In patients already diagnosed with NAFLD, however, *PNPLA3* conferred a greater risk for progression to liver cirrhosis than did lower muscle mass.

THU088

Age and the relative importance of liver-related deaths in non-alcoholic fatty liver disease

Huapeng Lin¹, Terry Cheuk-Fung Yip¹, Xinrong Zhang¹, Guanlin Li¹, Yee-Kit Tse¹, Vicki Wing-Ki Hui¹, Yan Liang¹, Che To Lai¹, Stephen Chan¹, Henry LY Chan¹, Grace Wong¹, Vincent Wai-Sun Wong¹. ¹The Chinese University of Hong Kong, Hong Kong

Email: linhuapeng5@163.com

Background and aims: It is unclear if the leading causes of death in patients with non-alcoholic fatty liver disease (NAFLD) differ by age.

In particular, we aim to investigate if the relative importance of liver-related deaths is lower in the elderly population such that screening is no longer meaningful.

Method: We conducted a territory-wide retrospective cohort study of adult NAFLD patients between 2000 and 2021 in Hong Kong. The outcomes of interest were all-cause and cause-specific mortality. Age at time of death were studied by subgroups of 10-year intervals.

Results: During 662,471 person-years of follow-up of 30,943 NAFLD patients, there were 2,097 deaths. The top 3 causes of death were pneumonia, extrahepatic cancer and cardiovascular diseases. Extrahepatic cancer was the leading cause of death, followed by pneumonia and cardiovascular diseases before the age of 80. Pneumonia became the leading cause of death after the age of 80. Liver disease was the sixth leading cause of death in patients aged 70–79 and 80–89 years, accounting for 5.1% and 5.9% of deaths, respectively, but only accounted for about 3% or less of the deaths in the other age groups. The incidence of liver-related death was higher in men before the age of 70 but higher in women afterwards. The incidence of liver-related death in women increased from 0.62 to 7.14 per 10,000 person-years from age 60–69 to 70–79 years.

Conclusion: The relative importance of liver-related death increases with age in NAFLD patients, especially among women. Thus, detection of NAFLD and advanced liver disease should be continued in the elderly population so far if they remain candidates for treatment.

Key words: non-alcoholic fatty liver disease, liver-related deaths, age

THU089

Hepatic fat as a novel marker for high-risk coronary atherosclerosis in familial hypercholesterolaemia: a CT-based study

Gavin Huangfu¹, Biyanka Jaltotage¹, Jing Pang², Nick Lan¹, Arun Abraham¹, Jacobus Otto³, Abdul Ildayhid^{1,4}, Jamie Rankin¹, Benjamin Chow⁵, Gerald Watts^{2,6}, Girish Dwivedi^{1,2,4}, Oyekoya Ayonrinde^{2,7}. ¹Department of Cardiology, Fiona Stanley Hospital, Murdoch, Western Australia, Australia; ²School of Medicine, Faculty of Health and Medical Sciences, University of Western Australia, Australia; ³Department of Radiology, Fiona Stanley Hospital, Murdoch, Western Australia, Australia; ⁴Harry Perkins Institute of Medical Research, Murdoch, Western Australia, Australia; ⁵Department of Medicine (Cardiology), University of Ottawa Heart Institute, Ottawa, Ontario, Canada; ⁶Lipid Disorders Clinic, Department of Cardiology, Royal Perth Hospital, Perth, Western Australia, Australia; ⁷Department of Gastroenterology and Hepatology, Fiona Stanley Hospital, Murdoch, Western Australia, Australia
Email: oyekoya.ayonrinde@uwa.edu.au

Background and aims: The liver is a transducer of cardiovascular risk factors through central regulation of lipid and glucose metabolism, insulin signalling and the production of inflammatory and thrombotic factors. Individuals with heterozygous familial hypercholesterolaemia (FH) have accelerated but variable progression of coronary artery disease (CAD). We investigated the association between hepatic steatosis (HS) and coronary atherosclerosis, including plaque burden, composition, and morphology in adults with FH.

Method: High-risk plaque (HRP) features (low attenuation, positive remodelling, spotty calcification), plaque volume (PV) and pericoronary adipose tissue (PCAT) attenuation were assessed using coronary computed tomography angiography (CCTA). From concurrently captured upper abdominal images, severity of HS was computed, as liver minus spleen computed tomography attenuation (HU_{L-S}) and stratified into quartiles. Associations were assessed using logistic regression, adjusting for cardiometabolic and conventional risk factors, lipid-lowering treatment use, coronary artery calcium (CAC) and obstructive CAD (≥50% stenosis).

Results: Of 213 patients with FH (median age 54.0 [46.0–59.5] years, 58.7% female), median HU_{L-S} was 13.17 [6.58–18.33], 59% had CAC score >0, 36% obstructive CAD and 77% HRP features. Increasing HS

was associated with higher CAC score ($p=0.008$), number of HRP features ($p=0.007$) and presence of obstructive CAD ($p=0.01$) and CAC ($p=0.02$) as demonstrated in Figure 1. HS was associated with the presence of both HRP (odds ratio [OR]: 1.48; 95% confidence interval [CI]: 1.09–2.00; $p=0.01$) and proximal HRP features (OR: 1.52; 95% CI: 1.18–1.96; $p=0.001$). Associations persisted when controlling for cardiovascular risk factors, features of metabolic syndrome, lipid-lowering treatment use, presence of obstructive CAD and CAC score. HS was associated with a higher PV (Q4: 499 mm³ vs Q1: 414 mm³, $p=0.02$), driven by low attenuation ($p=0.03$) and non-calcified ($p=0.03$) plaques. No differences in PCAT were observed.

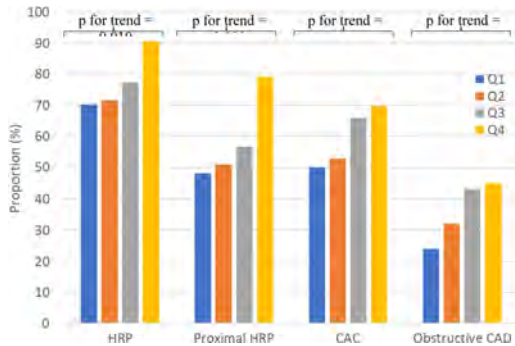


Figure 1: Coronary Artery Disease Characteristics, Stratified by HU-L-s Quartile

Conclusion: HS is associated with multiple indices of coronary atherosclerosis, particularly HRP features, in patients with FH. This appears to be independent of conventionally measured risk factors and may involve additional mechanisms related to HS.

THU090

Non-alcoholic fatty liver disease impact on cardiovascular disease death: a population-based study

Chaonan Jin¹, Sheng Bi¹, Mei Deng^{2,3,4}, Jifang Sheng¹. ¹The First Affiliated Hospital, College of Medicine, Zhejiang University, State Key Laboratory for Diagnosis and Treatment of Infectious Diseases, National Clinical Research Center for Infectious Diseases, Collaborative Innovation Center for Diagnosis and Treatment of Infectious Diseases, Hangzhou, Zhejiang Province, China; ²Guangxi Key Laboratory of Molecular Medicine in Liver Injury and Repair, Affiliated Hospital of Guilin Medical University, Guilin, Guangxi, China; ³Department of Radiation Oncology, Affiliated Hospital of Guilin Medical University, Guilin, Guangxi, China; ⁴Guangxi Health Commission Key Laboratory of Basic Research in Sphingolipid Metabolism Related Diseases, Affiliated Hospital of Guilin Medical University, Guilin, Guangxi, China
Email: jifang.sheng@zju.edu.cn

Background and aims: Non-alcoholic fatty liver disease (NAFLD) represents a common risk factor for cardiovascular disease (CVD). However, the impact of NAFLD on CVD mortality remains to be defined. We aimed to investigate whether NAFLD has a negative influence on CVD mortality.

Method: 11035 participants who were aged 20–74 years, completed both interview and examination in mobile examination centers, with 'confident or absolute confident' reports from clear and gradable ultrasound images, from US Third National Health and Nutrition Examination Survey (NHANES III: 1988–94) with follow-up of mortality to 2015 were included.

NAFLD was defined as moderate or severe steatosis grade. Mortality and follow-up data were obtained from NHANES III public-use linked mortality file with underlying cause of death ICD-10 (U001, 001 or 005 as CVD) recorded. Weighted demographic and clinical

characteristics from non-NAFLD and NAFLD participants were compared. Weighted survival was analyzed using univariate and multivariate Cox proportional hazards model.

Results: A total of 2299 (weighted 2*10⁷ subjects) NAFLD and 8736 (weighted 108 subjects) subjects without NAFLD were included. NAFLD individuals were older (age 20–39 years 34.8% (standard error (SE) (1.9) vs 52.5% (1.1), $p<0.001$), male dominant (54.0% (SE (1.5) vs 45.3% (0.7), $p<0.001$), had more often a lower education level (<9 years 15.6% (1.2) vs 9.6% (0.7), $p<0.001$), hypertension (33.0% (1.8) vs 18.3% (0.7), $p<0.001$), type 2 diabetes (10.8% (0.8) vs 3.4% (0.3), $p<0.001$) and CVD history (7.3% (0.7) vs 3.5% (0.3), $p<0.001$) comparing to no-NAFLD participants.

Multivariate analysis showed that after adjusting age and gender, NAFLD was not associated independently with CVD mortality (adjusted hazard ratio (aHR) 1.079, 95% confidence interval (CI) 0.911–1.279, $p=0.369$). This did not differ (aHR 1.109 95% CI 0.892–1.378, $p=0.345$) after adjustment for putative risk factors including age, gender, race, education, poverty income ratio, hypertension, diabetes, smoking status and CVD history.

Conclusion: This prospective cohort suggests that the presence of NAFLD is not associated with CVD mortality among US adults.

THU091

Sarcopenia is associated with the severity of metabolic associated fatty liver disease in elderly residents

Xiaohui Liu¹, Jingjing Song¹, Shuang Zhang¹, Shan Liang¹, Zhang Jing¹. ¹Beijing Youan Hospital, Capital Medical University, The Third Unit, The Department of Hepatology, Beijing, China
Email: zjyouan@ccmu.edu.cn

Background and aims: It has been proved that sarcopenia was associated with the metabolic associated fatty liver disease (MAFLD), but their relationship in elderly patients has not been studied in which sarcopenia is more prevalent.

Method: A cross-sectional survey was conducted among 1353 elderly residents over 65 years old in a community in Beijing. Demographic data, medical history, physical examination and laboratory examination results were collected for all subjects. Fatty liver was detected by B type ultrasound. Body composition was detected by Inbody720 (Bios pace, Korea). Liver fat content and liver stiffness was examined by Fibro Scan. Sarcopenia index (SI) was calculated as total ASM (kg)/BMI (kg/m²). Sarcopenia was defined as SI<0.789 for men and <0.521 for women.

Results: Among the 1353 elderly residents, the mean age is 70.5 ± 5.0 years old and women account for 66.0%. There were 755 (55.8%) patients were diagnosed as MAFLD. The BMI, waist circumference, hip circumference, waist-to-hip ratio, upper arm circumference, body fat percentage and visceral fat area in MAFLD group were significantly higher than those in the non-MAFLD group (all $p<0.05$). The proportion of patients with sarcopenia (20.3%) was significantly higher than in non-MAFLD group (15.6%, $p=0.026$). MAFLD patients with sarcopenia had higher BMI, waist circumference, hip circumference, waist-to-hip ratio, upper arm circumference, body fat rate, visceral fat area, glucose and lipid metabolism indexes than those without sarcopenia (all $p<0.05$). They also had higher liver fat content [300.6 ± 43.5] vs. [295.1 ± 40.3], $p<0.001$] and liver stiffness scores [5.3 (4.3, 7.0) vs. 5.0 (4.1, 6.3), $p<0.001$] when compared to non-sarcopenia group. According to quartile stratification, Serum creatinine, HbA1c, HOMA-IR, hs-CRP, CAP and LSM increased significantly from subjects with non-MAFLD to subjects with non-sarcopenia in MAFLD group and subjects with sarcopenia in MAFLD group (all p for trend <0.001).

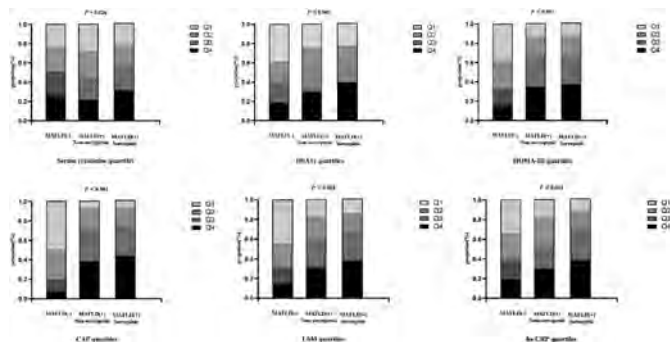


Figure 1: Association between the status of metabolic dysfunction-associated fatty liver disease (MAFLD)/sarcopenia and SCr, HbA1c, HOMA-IR, CAP, LSM, hs-CRP by quartile stratification.

Conclusion: We found that in elderly MAFLD patients, sarcopenia is closely correlated with liver fat content and fibrosis. We should pay more attention to the system metabolic abnormal in elderly population.

THU092

NAFLD patients scheduled for bariatric surgery present with a milder disease phenotype as compared to not morbidly obese NAFLD patients: analysis of a large real-world cohort

Monika Rau¹, Sarah Kaps¹, Hans Benno Leicht¹, Florian P Reiter¹, Marcin Krawczyk², Andreas Geier¹. ¹University Hospital Würzburg, Department of Internal Medicine II, Würzburg, Germany; ²Saarland University Medical Center, Department of Medicine II, Homburg, Germany

Email: rau_m@ukw.de

Background and aims: Non-alcoholic fatty liver disease (NAFLD) is the leading chronic liver disease worldwide associated with the metabolic syndrome. Based on recent findings, one can speculate that patients with morbid obesity might present have a milder NAFLD than those without. Aim of this study is to analyze the clinical phenotype of NAFLD in patients with and without (w/o) bariatric surgery (BarSur).

Method: In total, 814 patients were prospectively included (10/12–04/21) in a single-center study at a tertiary hospital. NAFLD was diagnosed either clinically by Fibroscan/CAP (n = 413) or histologically (n = 348). Routine laboratory parameters were available for all patients and 351 patients were genotyped for PNPLA3 p.I148M variant.

Results: 761 NAFLD patients were included (n = 512 with and n = 249 w/o BarSur) in this cohort. A case-control matching for age, sex, and diabetes mellitus (T2DM) was performed to analyse different disease phenotypes (n = 202 with and n = 201 w/o BarSur). Patients with BarSur had more often arterial hypertension (82% vs. 52%; p < 0.001), hypertriglyceridemia (16% vs. 9%; p < 0.01) and coronary heart disease (9% vs. 3%; p < 0.01) compared to NAFLD patients w/o BarSur. However, BarSur NAFLD patients were characterized by significantly lower disease specific serum profile including ALT (32 vs. 55U/l; p < 0.001), AST (28 vs. 39U/l; p < 0.001), gGT, ferritin and FIB-4 (1, 00 vs. 1, 17; p < 0, 001). Although higher frequency of PNPLA3 p. I148M genotype was observed in NAFLD patients w/o BarSur compared to BarSur NAFLD patients (CC: 46% vs. 58%; CG: 39% vs. 38%; GG: 15% vs. 4%; p < 0.01), an additional matching for the PNPLA3 genotype showed the same significantly lower serum ALT, AST, GGT and ferritin in BarSur NAFLD patients. Differences in histology were analysed by case-control matching for age, sex and T2DM only in patients with available histology (n = 74 for each patient group). NAFLD patients w/o BarSur had significantly higher frequency of NASH (74% vs. 49%; p < 0.01), steatosis, ballooning and fibrosis (F2-F4 46% vs. 8%; p < 0.001). Non-invasive liver stiffness assessment by Fibroscan was also significantly higher in NAFLD patients w/o BarSur (8.4 vs. 6.6kPa; p < 0.01).

Conclusion: NAFLD Patients with BarSur present a clinically milder disease phenotype in terms of serum profile and histology in our large cohort of NAFLD patients after case-control matching and independently of PNPLA3 genotype. Our observation warrants further pathophysiological studies in this special subpopulation of NAFLD.

THU093

Effects of SARS-CoV2 pandemic in a cohort of italian NAFLD patients

Bernardo Stefanini^{1,2}, Simona Leoni¹, Roberta Capelli^{1,2}, Alice Secomandi^{1,2}, Luca Muratori^{1,2}, Fabio Piscaglia^{1,2}, Silvia Ferri¹. ¹IRCCS Azienda Ospedaliero-Universitaria di Bologna, Division of Internal Medicine, Hepatobiliary and Immunoallergic Diseases, Bologna, Italy; ²University of Bologna, Department of Medical and Surgical Sciences (DIMEC)

Email: silvia.ferri@aosp.bo.it

Background and aims: SARS-Cov2 wide and uncontrolled spread in Italy in winter 2020 forced the authorities to declare an emergency status characterized by a complete lock-down and a massive temporary conversion of medical resources into COVID-positive patients care. Some of the consequences were a great limitation to physical activity and a reduced possibility to regularly follow outpatients in hospital.

Aim of our study was to evaluate the effect of COVID pandemic on subjects with stable NAFLD followed in our outpatient liver clinic.

Method: we enrolled 43 patients (58% females, median age 59 years, mean BMI 29) with defined NAFLD in charge to our liver outpatient unit with these characteristics: a first visit in 2017–2018, a pre-pandemic visit in 2019, a programmed visit between March and June 2020 not performed due to the pandemic condition and a post-pandemic visit after September 2020.

At first visit all patients were given dietary advice following the Mediterranean approach and encouraged to increase physical activity up to 150 minutes/week of aerobic and/or anaerobic activity of moderate intensity. Medications were prescribed when needed. At the three time points a complete anamnestic, physical, laboratory and ultrasound evaluation was performed.

Patients with advanced disease (decompensated cirrhosis and/or hepatocellular carcinoma) were excluded from the study as they were seen in outpatient clinic also during the lock-down period.

Results: compared to first visit, post-pandemic evaluation in our cohort of patients revealed stable BMI, HOMA index, transaminases, lipid profile, NAFLD fibrosis score (NFS), FIB-4, B-mode hepatorenal ratio (BMHRR) and liver stiffness (2D:SWE:SSI), whereas a reduction was detected in gammaGT levels (p = 0.02).

We then considered separately patients that at pre-pandemic visit had lost >5% of their basal weight (10 patients, mean weight -7.2%, mean BMI 27, 0) and those who had not (33 patients, mean weight +1.4%, mean BMI 29, 4). At post-pandemic control, patients in both groups maintained their weight trend (mean BMI 27, 3 and 29, 6 respectively; weight change compared to first visit -6.0% and +2, 1% respectively, p < 0.0001). Weight variations were associated to NFS (but not FIB-4, BMHRR and liver stiffness) modifications (in weight losers: -19.4%, in weight maintainers +55.9%, p = 0.034).

Surprisingly, all patients, especially those in the latter group, reported an increase in their physical activity after the first visit that was maintained also during the pandemic phase (from scarce-moderate to moderate-good p = 0.004).

Conclusion: in patients with NAFLD, when the behavioral approach (in which physical activity may exert an independent protective role) had been well consolidated in the pre-pandemic phase, it was maintained also during COVID pandemic even without a strict medical follow-up, thus allowing a preservation of the results obtained.

THU094

A higher Fibrosis-4 (FIB-4) score is associated with higher healthcare costs and hospitalizations in patients with non-alcoholic steatohepatitis (NASH)

Elliot Tapper¹, Jesse Fishman², Stephen Dodge², Keith Miller², Ni Zeng², Alina Bogdanov³, Machaon Bonafede³. ¹University of Michigan, United States; ²Madrigal Pharmaceuticals, United States; ³Veradigm

Email: alina.bogdanov@gmail.com

Background and aims: The cost and complexity of care for patients with Non-alcoholic Steatohepatitis (NASH) increases with disease stage. we aimed to study the Fibrosis-4 (FIB-4) score as a proxy for disease severity and test its association with increased disease burden.

Method: The Veradigm Health Insights Electronic Health Record Database and linked Komodo administrative claims data were used to identify adult patients with coded NASH with aspartate aminotransferase (AST), alanine aminotransferase (ALT) and platelet results and age to compute a FIB-4. The index date was the first coded NASH encounter between 2016 and 2020 with at least 6 months of database activity pre- and post-encounter and a FIB-4 score. We excluded patients coded with viral hepatitis, alcoholism, or alcoholic liver disease. Inpatient hospital admissions and log-transformed costs for pharmacy, hospital inpatient, emergency department, and outpatient services were measured in the 12-month period surrounding index. Multivariate logistic regression for any hospitalization and linear regression for log total cost was performed, controlling for patient demographics (age, race, sex, and geography), smoking status, Charlson comorbidity index (CCI), and diabetes complications severity index (DCSI).

Results: 6, 743 patients met the study criteria; mean age was 56.1 ± 13.3, patients were 62.9% female and 53.6% of patients were diagnosed with Type 2 Diabetes. Mean FIB-4 at index was 1.79 ± 1.88. A 1 unit increase FIB-4 at index was associated with a 4.2% increase in mean total annual cost (p < 0.0001 CI 2.2% to 6.3%) and with an odds ratio of 1.12 (p < 0.0001 CI 1.08 to 1.15) for hospitalization. CCI and DCSI were also significantly associated with higher odds ratios for hospitalization (OR 1.27, p < 0.001 CI 1.23 to 1.31 and OR 1.27, p < 0.001 CI 1.22 to 1.33).

Figure 1. Summary of Modeling results for log total cost and hospital admissions

Item	Log Total Cost			Hospital Admission		
	e ^B	e ^{Lower CI}	e ^{Upper CI}	Odds Ratio	Lower CI	Upper CI
FIB-4 at Index	1.042*	1.022	1.063	1.116*	1.080	1.153
Demographic Variables						
Age	0.997*	0.994	0.999	0.989*	0.983	0.994
Male	0.711*	0.662	0.763	0.891	0.784	1.013
White	0.905*	0.839	0.976	0.897	0.783	1.028
Hispanic	0.817*	0.732	0.912	0.876	0.715	1.073
Region: Northeast	1.384*	1.263	1.516	0.988	0.839	1.164
Region: Midwest	1.326*	1.185	1.484	1.072	0.881	1.305
Region: West	1.046	0.951	1.151	0.887	0.745	1.056
Region: Other	1.211*	1.046	1.402	1.181	0.921	1.515
Smoking Status						
Current Smoker	1.144*	1.029	1.272	1.089	0.902	1.315
Former Smoker	1.133*	1.018	1.262	1.093	0.903	1.323
Never Smoker	0.996	0.912	1.088	1.027	0.874	1.208
Health Status						
Charlson Comorbidity Index	1.276*	1.251	1.302	1.267*	1.225	1.310
Diabetes Complications Severity Index	1.232*	1.199	1.266	1.273*	1.219	1.329

* p < 0.05

Conclusion: Higher FIB-4 score across a variety of ranges is associated with increased costs and hospitalizations in the NASH population.

THU095

Comparison of hepatic and cardiovascular damage between HIV patients with steatosis and NAFLD: role of metabolic alterations and low visceral adiposity

Felice Cinque^{1,2}, Rosa Lombardi^{1,2}, Annalisa Cespiati^{1,2}, Paolo Francione², Erika Fatta², Cristina Bertelli², Giuseppina Pisano², Giovanna Oberti^{1,2}, Lucia Colavolpe^{1,2}, Francesca Alletto^{1,2}, Paola Dongiovanni², Marica Meroni², Giorgio Bozzi³, Alessandra Bandera^{1,3}, Anna Ludovica Fracanzani^{1,2}. ¹University of Milan, Department of Pathophysiology and Transplantation, Milan, Italy; ²Fondazione Ca' Granda IRCCS Ospedale Maggiore Policlinico, Unit of Internal Medicine and Metabolic Disease, Milan, Italy; ³Fondazione Ca' Granda IRCCS Ospedale Maggiore Policlinico, Infectious Diseases Unit, Milan, Italy

Email: rosa.lombardi@unimi.it

Background and aims: People living with HIV (PLWH) develop metabolic alterations and hepatic steatosis (HS), exposing them to increased cardiovascular (CV) risk. However, if presentation of HS in this category of patients is different from that of non-alcoholic fatty liver disease (NAFLD) is unknown. Aim: to evaluate metabolic, hepatic and CV alterations in PLWH and to compare them with those observed in primary NAFLD subjects.

Method: forty-two HIV mono-infected patients (mean age 46 ± 12 ys, male 81%; 90% with viral suppression) were enrolled. The cohort of PLWH underwent hepatic ultrasound (US) and those with evidence of HS were compared to a sex and age matched NAFLD control group (1:2). For all enrolled subjects, anthropometric parameters (BMI, waist circumference-WC), metabolic comorbidities, CV damage by carotid ultrasound (plaques, arterial stiffness by radiofrequency as pulse wave velocity-pWv) and heart ultrasound (systolic and diastolic function and epicardial adipose tissue-EAT) were assessed. All patients underwent transaminases determination, Fibroscan to detect advanced fibrosis (LSM >8.9/7.2 kPa M/XL probe) and bioimpedance (BIA) to quantify sarcopenia (SMI ≤10.75/6.75 kg/m² male/females) and fat mass. CV risk was assessed according to ESC guidelines. Genotyping for PNPLA3 was determined by Taqman assay.

Results: Thirty (63%) PLWH presenting HS were compared with 60 NAFLD patients. PLWH with HS presented no difference in the prevalence of metabolic alterations (type 2 diabetes 13% vs 13%, p = 1.0; hypertension 47% vs 42%, p = 0.82; dyslipidemia 83% vs 85%, p = 1.0) and sarcopenia (40% vs 52%, p = 0.81) compared to NAFLD, despite lower BMI (27.1 ± 4 vs 29.1 ± 4.3 kg/m², p = 0.04), WC (98 ± 9 vs 103.1 ± 10.3 cm, p = 0.03) and trunk fat mass (9.8 ± 3.3 vs 12.4 ± 4.7 kg, p = 0.02). No difference in the prevalence of increased transaminases (17% vs 20%, p = 0.78) and advanced fibrosis (17% vs 12%, p = 0.53) was found, as well of high CV risk (84% vs 83%, p = 0.86), pWv (7.4 ± 2 vs 6.9 ± 1.4 m/s, p = 0.18), carotid plaques (39% vs 28%, p = 0.33), increased EAT (20% vs 17%, p = 0.77) and systolic (6% vs 5%, p = 1.0) and diastolic dysfunction (7% vs 6%, p = 1.0). PNPLA3 distribution was not significantly different between groups (p = 0.16).

Conclusion: Hepatic steatosis and fibrosis are highly prevalent in patients with HIV. Interestingly, in PLWH metabolic alterations, liver and cardiovascular damage are superimposable with those observed in a primary NAFLD cohort, although in presence of lower visceral adiposity. Therefore, screening for liver disease in HIV patients is mandatory independently of obesity, as the increased risk of metabolic and CV complications.

THU096

Impact of intermittent fasting on anthropometric and clinical outcomes in non-alcoholic fatty liver disease: systematic review and meta-analysis

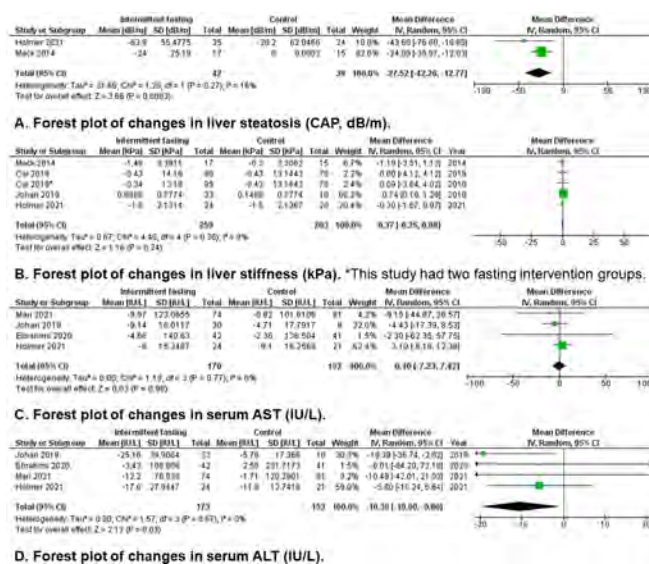
Marcia Lange¹, Devika Nadkarni¹, Lily Martin¹, Carolyn Newberry², Sonal Kumar², Tatyana Kushner³. ¹Icahn School of Medicine at Mount Sinai, New York, United States; ²Weill Cornell Medicine, Division of Gastroenterology and Hepatology, New York, United States; ³Icahn School of Medicine at Mount Sinai, Division of Liver Medicine, New York, United States

Email: marcia.lange@icahn.mssm.edu

Background and aims: Currently, weight loss through caloric restriction is the cornerstone of initial non-alcoholic fatty liver disease (NAFLD) management. However, there remains a lack of evidence-based guidelines on the benefits of intermittent fasting (IF) for NAFLD. In this systematic review with meta-analysis, we evaluated the effect of IF on anthropometric and clinical markers of NAFLD.

Method: We conducted a comprehensive search of MEDLINE, EMBASE, and Cochrane Central databases as well as trial registries and conference abstracts up to January 31, 2022. The search strategy included all appropriate controlled vocabulary and keywords for NAFLD and fasting. No date, language, or article type restrictions were included in the search strategy. Studies of adults with NAFLD or non-alcoholic steatohepatitis (NASH) undergoing an intermittent fasting intervention reporting at least one anthropometric or clinical outcome were included in our review. A random effects model was used for meta-analysis to estimate mean differences between intervention and control group for various outcomes.

Results: Initial literature search yielded 16 294 studies, of which 10 772 were duplicates, leaving 5517 studies to screen for title/abstract. An additional 5367 studies were excluded after title/abstract review with moderate concordance ($k=0.53$). The remaining 150 studies were assessed for full text review with fair concordance ($k=0.24$). Twelve studies were included in the systemic review and meta-analysis, totaling 908 participants with NAFLD, combined mean age of 42.50 years (SD 14.54), 50% male. Meta-analysis of anthropometric outcomes showed that the effect of IF on BMI and body weight was statistically significant (Mean difference (MD) -0.69 kg/m², 95% CI -1.29 to -0.09 , $p<0.05$; MD -2.51 kg, 95% CI -4.44 to -0.58 , $p<0.05$) with moderate though statistically significant heterogeneity for both ($I^2=47\%$, $p=0.07$; $I^2=62\%$, $p=0.02$). Clinical outcome analysis showed that the effect of IF on liver steatosis (CAP, dB/m) and ALT levels was also statistically significant (MD -27.52 dB/m, 95% CI -42.26 to -12.77 , $p<0.01$; MD -10.35 IU/L, 95% CI -19.9 to -0.8 , $p<0.05$) with zero to low heterogeneity for both outcomes ($I^2=16\%$, $p<0.01$; $I^2=0\%$, $p<0.05$). IF did not have a significant effect on AST levels or liver stiffness (kPa).



Conclusion: Intermittent fasting interventions may improve BMI and body weight as well as reduce both liver steatosis and serum ALT levels in adults with NAFLD. Studies with varying types of IF interventions and varying intervention durations likely contributed to meta-analysis heterogeneity. This data suggests that IF likely provides a benefit in NAFLD, but future randomized controlled studies are needed to validate the use of IF for NAFLD treatment.

THU097

The burden of liver fibrosis in the obese population

Gres Karim¹, Dewan Giri¹, Andrea Delgado Nieves¹, Caileen Sennett¹, Andre Khazak¹, Bo Hyung Yoon², Amreen Dinani³. ¹Icahn School of Medicine at Mount Sinai Beth Israel, Department of Medicine, New York, United States; ²Icahn School of Medicine at Mount Sinai Beth Israel, Mount Sinai Morningside, and Mount Sinai West (MSBIMW), Department of Gastroenterology, New York, United States; ³Icahn School of Medicine, Division of Liver Diseases, New York, United States

Email: gres.karim@mountsinai.org

Background and aims: The impact of obesity extends beyond non-alcoholic fatty liver disease (NAFLD). It is an independent risk factor for hepatocellular carcinoma (HCC), cirrhosis and liver decompensation. Liver fibrosis (LF) is linked to overall and liver-related mortality. The impact of obesity and LF is not as well established. Identifying LF in a high risk population with obesity is crucial to prevent disease progression and implement early intervention. We aim to describe the burden of LF in a population with obesity (BMI ≥ 30 kg/m²) and understand the variables that contribute to the development of LF.

Method: Patients with a body mass index (BMI) ≥ 30 kg/m² and no chronic liver diseases (CLD) were identified using electronic medical records from a tertiary care clinic between 01/2019 to 01/2020. Demographic information, markers of liver inflammation and synthetic function, medical conditions, imaging and histology were recorded. The Fibrosis Index 4 (FIB-4) was calculated to determine the stage of liver fibrosis; FIB-4 ≥ 1.3 indicated significant fibrosis. A univariate and multivariate logistic regression analysis was performed to identify factors contributing to the stage of fibrosis. Other outcomes of interest were complications of cirrhosis, development of HCC and mortality.

Demographic and laboratory characteristics of Patients			
Patient Characteristics	All patients [N (%)]	FIB-4 ≤ 1.3 [N (%)]	FIB-4 > 1.3 [N (%)]
Sex			
Male :	361	218 (20%)	361(13%)
Female :	720	478 (44%)	720(22%)
BMI (kg/m ²)	34.5	34.9	33.9
Ethnicity			
Hispanic	185 (17%)	107 (10%)	78 (7%)
Non-Hispanic	520 (48%)	350 (32%)	170 (16%)
Race:			
White	322 (30%)	212 (20%)	110 (10%)
Black	236 (22%)	158 (15%)	78 (7%)
Other	293 (27%)	186 (17%)	107 (10%)
Hypertension	518 (48%)	287 (27%)	231 (21%)
CAD	123 (11%)	52 (5%)	71 (7%)
DM2	264 (24%)	158 (15%)	106 (10%)
AST			
Mean	23	21	27
≤ 30 IU/L	955 (88%)	647 (60%)	308 (28%)
> 30 IU/L	127 (12%)	50 (5%)	77 (7%)
ALT			
Mean	24	23	26
≤ 30 IU/L	886 (82%)	571 (53%)	315 (29%)
> 30 IU/L	196 (18%)	126 (12%)	70 (6%)
GFR			
≥ 60 mL/min	895 (84%)	604 (57%)	291 (27%)
< 60 mL/min	165 (16%)	76 (7%)	89 (8%)
Outcomes			
Cirrhosis	7	0	7 (100%)
HCC	62	40 (6%)	22 (35%)
Death	3	1 (33%)	2 (67%)

Results: A total of 2999 patients with BMI ≥ 30 kg/m² were identified, of which 1082 patients had no documentation of CLD during the study period. Majority were female (66%), mean age 57 years (SD 13), and mean BMI 35 kg/m² (SD 4.9). One third were white and 17% Hispanic. Mean ALT and AST were 23 IU/L (3–671). Approximately 40% (385/1082) had a FIB-4 ≥ 1.3 , of which 80% had normal aminotransferases (≤ 30 IU/ml). Those with FIB-4 ≥ 1.3 were likely to be female, Hispanic or black. Coronary artery disease (2.8[1.9, 4.1]), hypertension (2.1[1.6, 2.7]), impaired renal function (GFR < 60) (2.4 [1.7, 3.4]), elevated low density lipoprotein (0.99[0.98, 0.99]) and total cholesterol (0.993 [0.990, 0.997]), were associated with liver fibrosis in univariate analysis, $p < 0.001$. No association was seen with diabetes. An inverse association was found between BMI and liver fibrosis (0.96[0.93, 0.99], $p = 0.03$) in univariate analysis, but not statistically significant in the multivariate analysis (0.96[0.92, 1.00], $p = 0.08$). In the multivariate model, female, older age, black, elevated AST and low platelet count were found to be associated with significant LF.

Conclusion: In our analysis of an obese population we found a high 40% degree of significant liver fibrosis in those without known CLD. The presence of CAD, HTN, and GFR < 60 appear to be significantly associated with liver fibrosis. Sex, ethnicity may have a role in development of LF in obesity. Majority of these patients would not have been assessed for liver disease due to normal liver enzymes. People with obesity should be pro-actively assessed for CLD and NAFLD.

THU098

Impact of screening and treatment of obstructive sleep apnea in non-alcoholic fatty liver disease

Kelsey Collins¹, Amreen Dinani¹, Horacio Romero Castillo¹, Brooke Wyatt¹, Indu Ayappa¹, Anne Mooney¹. ¹Mount Sinai Medical Center, New York, United States

Email: kelsey.collins@mountsinai.org

Background and aims: Obstructive sleep apnea (OSA) has been recognized as a risk factor for non-alcoholic fatty liver disease (NAFLD). Oxidative stress and chronic intermittent nocturnal low oxygen state promotes liver injury, inflammation, and liver fibrogenesis. It is estimated that persons with OSA are 2–3 times likely to have NAFLD. Treatment of NAFLD is based around managing co-morbidities and weight loss. The aim of our study is to prospectively screen patients with NAFLD for OSA and evaluate the impact of OSA treatment on NAFLD.

Method: Patients with NAFLD (defined by presence of hepatic steatosis on imaging, controlled attenuated parameter [CAP] ≥ 240 dB/m, or histology) were prospectively screened for OSA using STOP-BANG (SB) and Epworth Sleepiness Score (ESS) in an outpatient liver clinic. SB ≥ 3 or ESS ≥ 10 were characterized as ‘high risk’ for OSA and referred to Sleep Medicine for home sleep testing with a WatchPAT device. Patients confirmed with OSA were followed in Sleep Medicine and Hepatology. Baseline characteristics, demographics and severity of liver disease were collected and students t test as well as logistic regressions were used to assess differences. Patients with NAFLD and OSA were followed over time to determine the impact of OSA treatment on NAFLD.

Results: Sixty-eight patients with NAFLD from a tertiary hospital system were screened for OSA from; 41% were male, mean age 49 years, 21% were White Non-Hispanic, 32% Hispanic, 26% Other/Unknown. The median BMI was 32.8 kg/m² with 68% ≥ 30 kg/m² consistent with obesity. At baseline, 53% had ALT above the upper limit of normal (ALT ≥ 30 IU/L). Forty patients (59%) screened positive for OSA (mean SB=5 and ESS=7). There were no differences observed in BMI, ALT, AST, liver stiffness (LF), or CAP scores for patients that screened positive and negative for OSA, however, the group that screened negative for OSA, on average had higher high-density lipoprotein (HDL) (44.1 mg/dL vs 52.4 mg/dL, $p = 0.01$), low-density lipoprotein (LDL) (99.1 mg/dL vs 116.9 mg/dL, $p = 0.03$), and cholesterol (176.4 mg/dL vs 200.7 mg/dL, $p = 0.01$). Compared to patients with no diabetes (DM) ($p = 0.015$), preDM and DM showed statistically significant increased odds of screening OSA positive (OR = 5.3 [CI: 1.535–18.15]; OR = 4.6 [CI: 1.12–18.80]). Of those referred for formal OSA testing, $n = 20$ (55%) complied, and $n = 17$ (85%) patients were subsequently diagnosed with OSA and underwent treatment (mean AHI4 = 19.6/hr). Due to lack of OSA treatment acceptance/adherence, overall impact could not be assessed.

Conclusion: Screening for high risk OSA with a combination of STOP-BANG and ESS was reliable for identifying subjects with OSA confirmed by sleep test. Closer attention to lipid profile and insulin resistance (preDM and DM) were risk factors identified contributing to the diagnosis of OSA. Impact of treatment for OSA needs further evaluation.

POSTER PRESENTATIONS

THU099

Undiagnosed NAFLD in the obese population: in sight, out of mind

Dewan Giri¹, Gres Karim², Andrea Delgado Nieves², Andre Khazak², Cailleen Sennett², Bo Hyung Yoon³, Ilan Weisberg⁴, Amreen Dinani⁵.
¹Icahn School of Medicine at Mount Sinai Beth Israel, Department of Medicine, New York, United States; ²Mount Sinai Beth Israel, Internal Medicine, New York; ³Mount Sinai Beth Israel, Morningside and West, Department of Gastroenterology, New York, United States; ⁴New York Presbyterian-, Brooklyn Methodist, Department of Gastroenterology and Hepatology; ⁵Icahn School of Medicine, Division of Liver Diseases, New York, United States
 Email: gres.karim@mountsinai.org

Background and aims: Obesity is a leading risk factor for non-alcoholic fatty liver disease (NAFLD), with estimated prevalence rates as high as 50–90%. There is a strong correlation between obesity and hepatocellular carcinoma (HCC), cirrhosis and advanced liver disease. Despite the rising burden of NAFLD in obesity, no concrete guidance exists for screening in this high-risk population. Early detection can facilitate early intervention and development of pathways to specialty care. Herein, we describe the burden of NAFLD in an obese population and affirm the need to proactively assess patients that would otherwise be undiagnosed.

Method: Patients with a diagnosis of obesity (body mass index [BMI] >30 kg/m²) and no documented chronic liver diseases (CLD) were identified using electronic medical record (EMR) from a tertiary care clinic between 01/2019 to 01/2020. Patients who met the criteria for NAFLD (as per AASLD guidelines) were also identified from the same cohort with attention to those who had documentation of NAFLD diagnosis in EMR (ICD-10 codes and review of notes) and those who did not. Demographic information, markers of liver inflammation and synthetic function, medical conditions, imaging and histology were recorded. Fibrosis Index 4 (FIB4) was calculated to determine the stage of liver fibrosis. We reviewed the reason for referrals, differences in the two groups of patients with NAFLD who were and were not diagnosed.

Results: A total of 2999 patients with BMI >30 kg/m² were identified, 586 (20%) had a diagnosis of NAFLD (D-NAFLD) and 1350 had no diagnosis of CLD. One-fifth (268/1350, 20%) of patients without diagnosis of CLD met diagnostic criteria for NAFLD (UD-NAFLD). Baseline characteristics of D-NAFLD and UD-NAFLD were comparable. Majority of UD-NAFLD had normal (<30IU/L) alanine transaminase (ALT) and aspartate transaminase (AST), 65% and 69% compared to 48% and 60% in D-NAFLD, respectively. Mean AST and ALT were higher in D-NAFLD (38 IU/L and 46 IU/L, respectively) versus UD-NAFLD (33 IU/L and 33 IU/L, respectively). Mean FIB4 was similar, 1.62 and 1.64. FIB4 in the UD-NAFLD group with normal ALT and AST was 1.17 compared to 1.34 in D-NAFLD. Hypertension (55%), coronary artery disease (15%) and diabetes mellitus (30%) were more common in patients in the undiagnosed cohort. Presence of CAD or DM in both groups was associated with a higher FIB4. Majority of patients in D-NAFLD were referred to the specialty clinic for either elevated liver tests (24%), radiographic evidence of steatosis (26%) or both (19%).

Patient Characteristics	Undiagnosed NAFLD (UD-NAFLD) (N=268) Mean or N(%)	Diagnosed NAFLD (D-NAFLD) (N=586)
Sex		
Male	90 (34%)	243 (41%)
Female	178 (66%)	343 (59%)
Mean Age (SD)	57 (12.6)	56 (12.7)
BMI (kg/m ²) (SD)	35.5 (5.5)	35.6 (5.5)
Ethnicity		
Hispanic	73 (27%)	137 (23%)
Non-Hispanic	112 (42%)	279 (48%)
Race		
White	64 (31%)	225 (38%)
Black	46 (18%)	85 (14%)
Other	91 (34%)	153 (26%)
Comorbidities		
Hypertension	148 (55%)	294 (27%)
CAD	39 (15%)	64 (6%)
DM	81 (30%)	211 (20%)
FIB-4		
Mean	1.62	1.64
FIB-4 ≤ 1.3	147 (55%)	321 (55%)
FIB-4 > 1.3	131 (45%)	247 (45%)
AST		
Mean	33	38
≤30 IU/L	184 (69%)	347 (60%)
>30 IU/L	84 (31%)	239 (40%)
ALT		
Mean	33	46
≤30 IU/L	174 (65%)	283 (48%)
>30 IU/L	94 (35%)	303 (52%)
GFR		
≥60 mL/min	223 (83%)	507 (89%)
<60 mL/min	38 (14%)	61 (9%)
Outcomes		
Cirrhosis	18 (7%)	71 (12%)
HCC	3 (1%)	3 (0.5%)
Death	2 (0.7%)	5 (0.9%)
Lifestyle Changes recommended	112 (42%)	478 (44%)

Conclusion: We have demonstrated that obesity continues to be an underrecognized risk factor for NAFLD. In our cohort, 20% of patients with obesity had missed diagnosis of NAFLD. Based on current guidelines, 70% of these patients would not have been worked up for NAFLD with normal liver enzymes. NAFLD should be considered as a comorbidity when evaluating patients with obesity.

THU100

Prevalence of non-alcoholic steatohepatitis in patients undergoing laparoscopic cholecystectomy for gallstone with non-alcoholic fatty liver disease

Utpal Anand^{1,1}, Aaron John¹, Ramesh Kumar¹, Rajeev Priyadarshi². ¹All India Institute of Medical Sciences, Patna, Surgical Gastroenterology, Patna, India; ²All India Institute of Medical Sciences, Patna, Radiodiagnosis, Patna, India
 Email: utpalanand2@gmail.com

Background and aims: Gallstone disease (GSD) and non-alcoholic fatty liver disease (NAFLD) shares common risk factors. Non-alcoholic steatohepatitis (NASH) is a more progressive form of NAFLD and is among the most frequent causes of cirrhosis. There is a lack of prospective studies utilizing liver biopsy during laparoscopic cholecystectomy in patients of gallstones and NAFLD for assessing the prevalence of NASH and factors associated with it. The aim of the study was to assess the usefulness of liver biopsy for patients with gallstones and NAFLD who underwent laparoscopic cholecystectomy. **Method:** Among the 250 patients with symptomatic GSD, 55 had associated NAFLD diagnosed by ultrasound. These patients underwent liver biopsy during laparoscopic cholecystectomy between June 2021 to Feb 2022.

Results: The mean age of patients was 41.6 ± 11.69 years and 60% of patients were female. The mean BMI of subjects was 26.43 ± 3.84 kg/m². Eight patients had hypothyroidism, 7 patients had diabetes mellitus, and 6 patients had hypertension as comorbidities. The histopathology of NAFLD patients revealed no significant steatosis in 7 patients, NAFLD in 38 patients and NASH in 10/55 (18.1%). Higher AST (44 ± 22.15 vs 31.5 ± 13.0 ; $p = 0.02$) and controlled attenuation parameter (CAP) (294 ± 58.5 vs 202.9 ± 69.6 ; $p < 0.001$) were significantly associated with NASH in GSD patients with NAFLD

Table: Clinical characteristics of NASH and non-NASH patients

	Non-NASH	NASH	P value
Age (years)	40.9 ± 10.6	44.8 ± 12.0	0.34
Female	31 (68%)	8 (80%)	0.48
Body mass index (kg/m ²)	26.46 ± 3.96	26.33 ± 3.46	0.92
Laboratory parameters			
INR	0.97 ± 0.10	0.94 ± 0.07	0.49
ALT (U/L)	31.3 ± 17.9	40.8 ± 24.67	0.18
AST (U/L)	31.5 ± 13.0	44 ± 22.15	0.02*
ALP (U/L)	$88 (72.5-102)$	$76.5 (74-84.5)$	0.23
Total bilirubin (mg/dL)	$0.61 (0.45-0.8)$	$0.75 (0.48-0.94)$	0.23
Albumin (g/dL)	4.09 ± 0.37	4.10 ± 0.32	0.93
Cholesterol (mg/dL)	164.9 ± 36.64	169.22 ± 33.89	0.73
Triglyceride (mg/dL)	137.24 ± 60.9	161.37 ± 53.7	0.25
HDL (mg/dL)	39.08 ± 11.08	42.78 ± 6.53	0.31
CAP	202.9 ± 69.6	294 ± 58.5	<0.001*
LSM (kPa)	5.3 ± 1.8	6.1 ± 1.8	0.19

ALP: Alkaline phosphatase; ALT: Alanine aminotransferase; AST: Aspartate aminotransferase; INR: International normalized ratio; HDL: high-density lipoprotein; LSM: Liver stiffness measurement; CAP: controlled attenuation parameter

Conclusion: The high prevalence of NASH in patients of GSD with NAFLD may justify the need of routine liver biopsy during laparoscopic cholecystectomy in these patients.

THU101

Lack of awareness of a NAFLD pandemic in a high risk group. Is it time to act in primary care?

Maria Guerra Veloz¹, Kosh Agarwal¹, Marck Chamley², Saima Ajaz¹.

¹Institute of Liver Studies, King's College Hospital, London, United Kingdom; ²Partner, North Wood Group Practice, Lambeth Diabetes Intermediate Care Team, United Kingdom

Email: maria.guerraveloz@nhs.net

Background and aims: Non-alcoholic fatty liver disease (NAFLD) includes a wide spectrum of conditions and is currently the leading cause of chronic liver disease. NAFLD is intrinsically associated with obesity and is particularly common in people with type 2 diabetes (T2D) with a prevalence ranging from 70 to 80%. As NAFLD is mostly a silent disease, early diagnosis and the accurate staging of fibrosis is crucial for patients who are at risk. The complex relationship between NAFLD and T2D, the risk of cardiovascular disease, raises the question of the cost effectiveness of screening for NAFLD in the general population. With current guidelines discouraging screening in the general population, early recognition and intervention are important in high-risk groups in order to improve clinical outcomes.

The aim of our project was to evaluate the awareness of NAFLD knowledge, the prevalence of NAFLD, and the prevalence of advanced fibrosis in patients with T2D who regularly attend a secondary diabetes clinic.

Method: Patients with T2D that have a regular follow-up at the Lambeth Diabetes Intermediate Care Centre were invited to participate in the NAFLD screening using a Fibroscan. A structured diet, exercise activity and NAFLD knowledge **questionnaires** were provided by a liver doctor to all patients that agreed to participate in this project. Anthropometric measures, medical history, LSM and CAP

were recorded for each patient. The presence of steatosis was defined with a CAP cut off ≥ 275 dB/m and advanced fibrosis ≥ 8 kpa.

Results: We screened 90, 47.3% were male with a median age of 59 years (IQR 52 – 66), most were of black African descent 55.6% (50) with a median BMI of 31.8 kg/m² (26 – 37). Comorbidities, such as hypertension, coexisted in 61.1% and 58.9% had dyslipidaemia. (Baseline characteristics Figure 1)

The Fibroscan data was valid in 96.7% (87), 56.3% (49/87) had steatosis and 27.6% (24/87) had advanced fibrosis.

14.4% (13) were aware of NAFLD/NASH, 33.3% were aware that they were overweight or obese and 88.9% stated that they had received guidance about having a healthy lifestyle. Of the patients who were not aware of NAFLD (85.6%), 58% of these had steatosis and those who were not aware of being overweight/obese (66.7%), 40.6% of these were overweight and 25% were obese.

38% of patients who had steatosis and 47.8% who had advanced fibrosis were on GLP-1 analogue (24.4% of all patients).

Demographic variables	n=90
Males n (%)	43 (47.8)
Age (years), median (IQR)	59 (52–66)
Race n (%)	
White	18 (20)
Black African/Caribbean	50 (55.6)
Asian	1 (1.1)
Mediterranean	9 (10)
Hispanic	5 (5.6)
Weight Kg median (range)	89.5 (74 – 104)
BMI kg/m ² median (range)	31.8 (26.7–37.2)
Normal weight	14 (15.6)
Overweight	19 (21.1)
Obese	49 (54.4)
Comorbidities (%)	
Hypertension	55 (61.1)
Dyslipidaemia	53 (58.9)
OH consumption (yes %)	2 (2.3)
Active smokers (yes %)	30 (33.3)
GLP-1 treatment (yes %)	22 (24.4)
Diet evaluation (yes %)	
Daily vegetables/fruits	48 (53.3)
Daily olive oil/nuts	17 (18.9)
Ultra-processed food weekly	19 (21.1)
Daily carbohydrates	40 (44.4)
Exercise n (%)	
No	44 (48.9)
Low activities	18 (20)
Moderate activities	28 (31.1)
Fibroscan (n=87)	
Median Kpa (range)	5.4 (4 – 8.1)
Advanced Fibrosis (%)	24 (27.6)
*Median Kpa (range)	12 (9–14)
CAP	
Median dB/m (range)	295 (235–338)
Steatosis (%)	49 (56.3)

Conclusion: T2D patients are mostly unaware of this silent epidemic, and so do not recognise themselves as being overweight/obese, which is intrinsically linked with NAFLD. Preliminary data suggests that the screening of NAFLD in patients with T2D can yield important information regarding the prevalence of advanced fibrosis and factors affecting the progression of NAFLD in this *multi-ethnic high-risk group*. It is particularly important to screen the patients who are already in our healthcare system due to other pre-existing conditions.

THU102

Non-alcoholic fatty liver disease and type 2 diabetes: low referral rate of patients at increased risk of progressive liver disease

Lucy Gracen^{1,2}, Kelly Hayward^{1,2}, Melanie Aikebuse^{1,2}, Anthony Russell^{3,4}, James O'Beirne⁵, Katharine Irvine⁶, Suzanne Williams⁷, Patricia Valery⁸, Elizabeth Powell^{1,2}. ¹Princess Alexandra Hospital, Gastroenterology and Hepatology, Woolloongabba, Australia; ²Translational Research Institute, The University of Queensland, Centre for Liver Disease Research, Faculty of Medicine, Woolloongabba, Australia; ³Princess Alexandra Hospital, Department of Endocrinology, Woolloongabba, Australia; ⁴The University of Queensland, Centre for Health Services Research, Faculty of Medicine, Saint Lucia, Australia; ⁵Sunshine Coast University Hospital, Gastroenterology and Hepatology, Birtinya, Australia; ⁶Translational Research Institute, Mater Research, Woolloongabba, Australia; ⁷Inala Primary Care, Inala, Australia; ⁸QIMR Berghofer Medical Research Institute, Herston, Australia
Email: lucy.gracen@hotmail.com

Background and aims: Routine assessment of liver fibrosis in people with non-alcoholic fatty liver disease (NAFLD) is recommended. The aim of this study was to determine whether a community-based NAFLD diagnosis, risk-stratification and referral pathway for people with type 2 diabetes (T2D) provides targeted detection of advanced fibrosis and appropriate referral to liver clinics.

Method: People with T2D were screened for NAFLD when they attended a diabetes clinic appointment in the community, using FibroScan (VCTE) as a point-of-care test to assess steatosis (CAP score ≥ 248) and fibrosis (liver stiffness measurement, LSM). A letter to participants' general practitioners (GPs) provided the LSM result and guidance on appropriate management/follow-up of their patients in primary care, as well as investigation of abnormal liver enzymes. Referral to a liver clinic was advised if LSM ≥ 8.0 kPa. Patients were advised to discuss their liver health and FibroScan result with their GP. A monthly audit of GP referrals to liver clinics was provided by the central referral hub to assess whether GPs pursued the recommended referral.

Results: To date, 129 people with T2D (61.9% male, 58.8 ± 9.7 years) were assessed and VCTE met quality criteria in 126 (97.7%). Referral to a liver clinic for further assessment was advised for 28 (22.2%) patients with LSM ≥ 8.0 kPa and 8 patients with other indications (Figure). 68 (54.0%) of 126 patients had abnormal liver function tests and 13 (10.3%) had LSM ≥ 12.0 kPa suggestive of advanced chronic liver disease (CLD). 34 (27.0%) of 126 patients had a prior liver ultrasound (US) of which two-thirds ($n=23$) showed steatosis and 2 had clear signs of CLD. None of these patients had been referred for fibrosis assessment reflecting the need to embed this in routine clinical pathways. A greater proportion of people with LSM ≥ 8 kPa had a prior US compared to those with LSM <8 kPa (46.4% vs. 21.4%, $p=0.009$), suggesting GPs are identifying patients that need investigation but not pursuing further management. A GP referral was received for 13 (36.1%) of the 36 patients with a recommendation for referral.

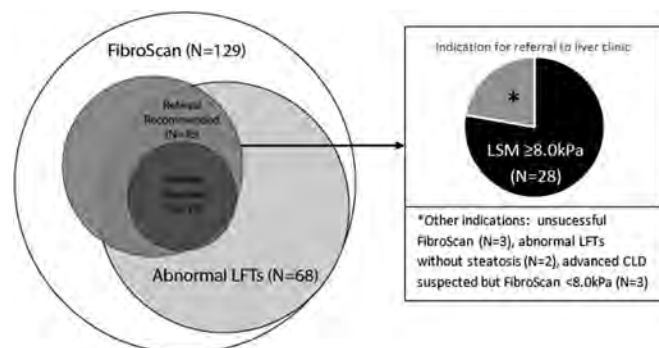


Figure: Proportion of patients with type 2 diabetes recommended for referral to liver clinic following FibroScan assessment. Circles proportionate to group size; liver function tests (LFTs).

Conclusion: VCTE as a point-of-care test provides a well-validated real-time assessment of liver fibrosis as well as steatosis and allows for timely delivery of the diagnosis and fibrosis risk category (low or increased risk) to the patient's healthcare team. The high detection rate of people requiring specialist assessment supports this screening approach. However the low GP referral rate in a cohort at increased risk of progressive liver disease calls attention to the need for improved education, guidelines and referral pathways for NAFLD to embed fibrosis assessment in the patient workflow.

THU103

Hypertension and diabetes mellitus are associated with high FIB-4 index in a health checkup examination cohort without known liver disease

Shunsuke Sato¹, Hidehiko Kawai², Sho Sato¹, Hirohiko Iwasaki², Yuji Kita¹, Yuji Ikeda¹, Ayato Murata¹, Yuji Shimada¹, Takuya Genda¹. ¹Juntendo University Shizuoka Hospital, Gastroenterology and Hepatology, Shizuoka, Japan; ²Fuji Town Medical Center, Shizuoka, Japan
Email: syusato@juntendo.ac.jp

Background and aims: Non-alcoholic fatty liver disease (NAFLD) is usually asymptomatic and lacks a specific biomarker; therefore, many individuals might remain undiagnosed even with advanced liver fibrosis. The aim of this study was to clarify the prevalence and clinical features of subjects with a high risk of advanced liver fibrosis in the general population, using the Fibrosis-4 (FIB-4) index.

Method: We retrospectively investigated 6,183 subjects without known liver disease who had participated annual health checkup examination. We analyzed the factors associated with high FIB-4 index (≥ 2.67) using a logistic regression analysis.

Results: Among 6,183 subjects, 76 (1.2%) had high FIB-4 index. Multivariate analysis identified hypertension (odds ratio [OR] = 8.926; 95% confidence interval [CI] 4.031–19.768; $P < 0.001$) and diabetes mellitus (OR = 4.045; 95% CI 1.694–9.660; $P = 0.002$) as important risk factors for high FIB-4 index. The rates of hypertension and diabetes mellitus in subjects with high FIB-4 index were 78.9% and 23.7%, respectively. No significant association was observed between obesity or large waist circumference and a high FIB-4 index. A history of cardiovascular disease was significantly more common in subjects with high FIB-4 index. These results were also observed in the subjects with normal aminotransferase (ALT) levels.

Conclusion: The present study revealed that approximately 1% of the general Japanese population has a high risk of advanced liver fibrosis. Many of these patients had hypertension and/or diabetes mellitus. The findings suggest that there are many undiagnosed NAFLD patients with risk of advanced liver fibrosis in the general population.

THU104

Statins, but not aspirin, reduce the risk of hepatocellular carcinoma and mortality in Danish patients with cirrhosis due to alcohol-related liver disease: a nationwide causal study

Frederik Kraglund¹, Diana Hedevang Christensen², Peter Jepsen¹. ¹Aarhus University Hospital, Department of Hepatology and Gastroenterology, Aarhus N, Denmark; ²Aarhus University Hospital, Department of Clinical Epidemiology, Aarhus N, Denmark
Email: frekra@clin.au.dk

Background and aims: Observational studies have shown a strong association between use of statins or aspirin and a lower risk of hepatocellular carcinoma (HCC). We emulated a trial assessing the causal link between statin and aspirin use and HCC development and mortality in Danish patients with cirrhosis due to alcohol-related liver disease (ALD cirrhosis).

Method: Using nationwide Danish healthcare registries, we identified all patients diagnosed with ALD cirrhosis, 2000–2018. We determined their statin and aspirin use through reimbursed prescriptions. A target trial was designed in which patients were randomised to initiate and adhere to statins (and, in a separate analysis, aspirin) or to not initiate treatment. The primary end point

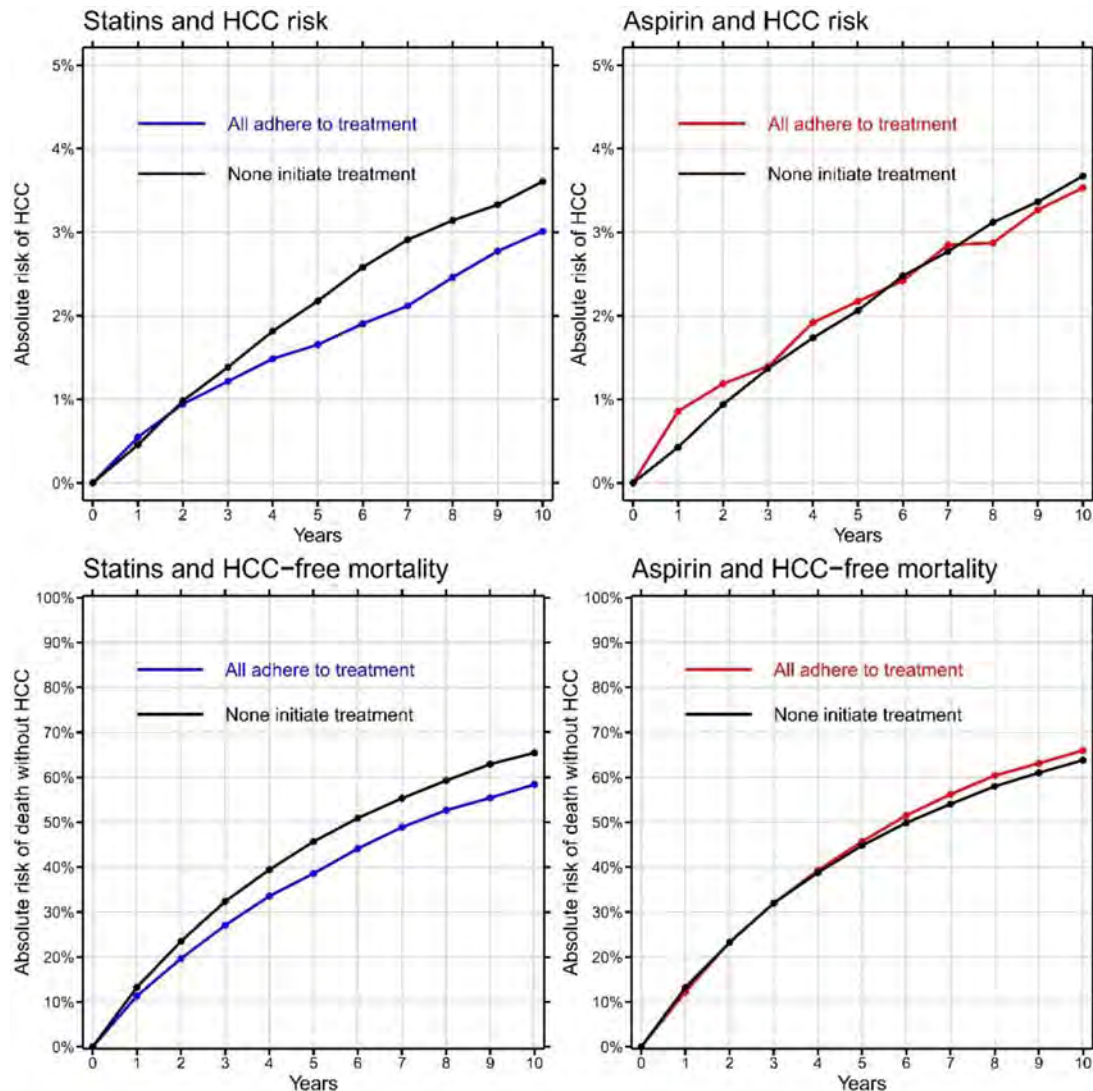


Figure: (abstract: THU104)

was HCC development, and the secondary end point was death without HCC. The target trial was emulated using inverse probability of treatment and censoring weights to create a marginal structural model adjusted for comorbid diseases, prescription drugs, procedures, hospital contacts, and prior use of statins among other covariates. Based on this model we estimated the average treatment effect (ATE) of statin use (and aspirin use) on the cumulative risk of HCC and of death without HCC.

Results: Of 16,811 patients with ALD cirrhosis, 4,540 used statins at some point during follow-up, 4,647 used aspirin, and 899 were diagnosed with HCC. The ATE of statin use was 0.74 (95% confidence interval [CI] 0.47 to 1.02) for HCC and 0.77 (95% CI 0.70 to 0.83) for death without HCC. The ATE of aspirin use was 1.08 (95% CI 0.73 to 1.44) for HCC and 1.10 (95% CI 1.02 to 1.19) for death without HCC. The cumulative HCC incidence functions and corresponding relative risk estimates reflected the ATEs (Figure).

Conclusion: Statin use reduces the risk of HCC and death without HCC in patients with ALD cirrhosis. Conversely, aspirin use does not reduce the risk of either HCC or death without HCC in patients with ALD cirrhosis. Thus, statins, but not aspirin, likely have a chemopreventive effect in patients with ALD cirrhosis. While we wait for truly randomized studies, studies such as ours provide the strongest possible evidence in favour of statins.

Gut microbiota and liver disease

THU151

Altered fecal microbiome and metabolome in hepatitis B related chronic liver diseases

Wei Jiang¹, Yue Shen¹, Wu ShengDi¹, Jian Wu^{2,2,2}, ¹Zhongshan Hospital, Fudan University, Shanghai Institute of Liver Diseases, Department of Gastroenterology and Hepatology, Xuhui District, Shanghai, China; ²Fudan University Shanghai Medical College, Dept. of Medical Microbiology and Parasitology, MOE/NHC/CAMS Key Laboratory of Medical Molecular Virology, School of Basic Medical Sciences, Shanghai, China
Email: jiang.wei@zs-hospital.sh.cn

Background and aims: It is well accepted that microbiota is a major modulator of liver diseases and is associated with severe clinical outcomes. However, the influence of gut dysbiosis on chronic hepatitis B (CHB) progression as well as the interplay between microbiota shift and antiviral treatment remains to be clarified. The present study aims to provide a comprehensive profile of gut microbiome and metabolomics in CHB patients at different disease stages. Taking advantage of a cohort of CHB patients with entecavir

POSTER PRESENTATIONS

therapy for five years, influence of antiviral treatment on the characteristics of microbial composition and function in CHB patients was investigated.

Method: Fecal samples from subjects with CHB (n = 64) and healthy controls (n = 17) were sequenced with 16 s rRNA analysis. Fecal metabolomics was measured via untargeted LC-MS in subgroups of 58 subjects (Fig. 1A).

Results: Compared to healthy controls, community richness, diversity and evenness of gut microbiota were decreased during CHB progression (Fig. 1B and 1C). Overall gut microbial community was shifted (Fig. 1D). Four genera: Faecalibacterium, Streptococcus, Sutterella and Ruminiclostridium_9 were enriched in CHB patients. Eight genera including Blautia, Escherichia-Shigella, Klebsiella, Bifidobacterium, Parasutterella, Eubacterium hallii group,

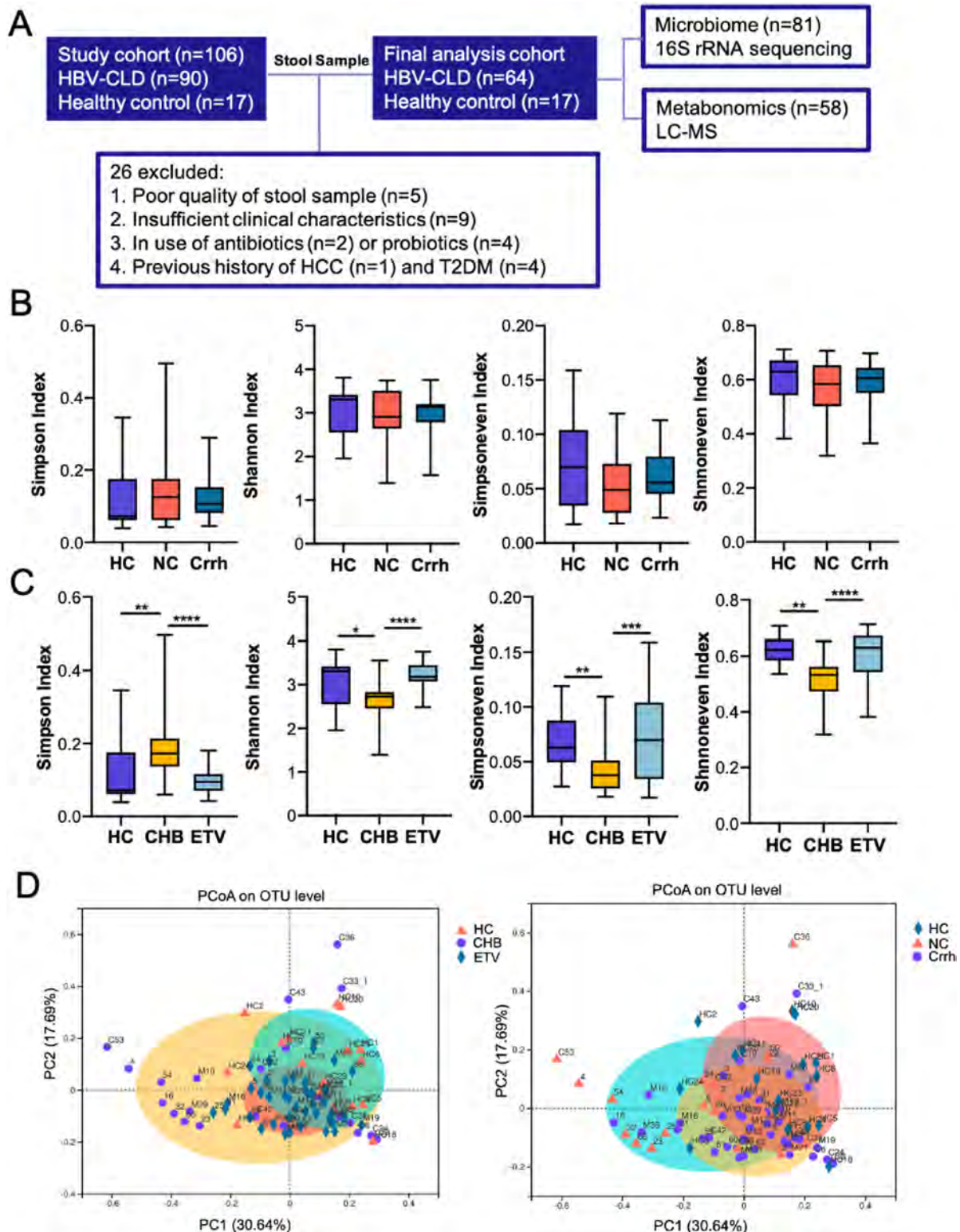


Figure 1: (abstract: THU151)

Collinsella and Lactococcus were found to decrease, accompanying with 206 metabolites statistically different in abundance. Importantly, distinct patterns of microbiota composition and metabolic activity were identified in subgroup analysis based on disease stages and the presence of antiviral treatment (Fig. 2 and 3). It was demonstrated that there was a potential association between microbial or metabolic signatures and clinical characteristics (Fig. 4). Notably, disease-enriched genera Streptococcus and metabolite 20-hydroxy-leukotriene E4 were negatively correlated with albumin (ALB) and positively with direct bilirubin (DB). Concordant depletion of Turicibacter and Adlercreutzia accompanying with 4-hydroxyretinoic acid tended to correlate with elevated AST and DB in CHB patients. Potential links between clinical parameters and restored genera or metabolites in CHB patients receiving antiviral treatment were detected. In particular, concordant increase of Ruminococcaceae_UCG-013 and sebacinic acid was positively correlated with ALB, suggesting that novel host-microbial interplay was involved in the antiviral treatment of CHB patients.

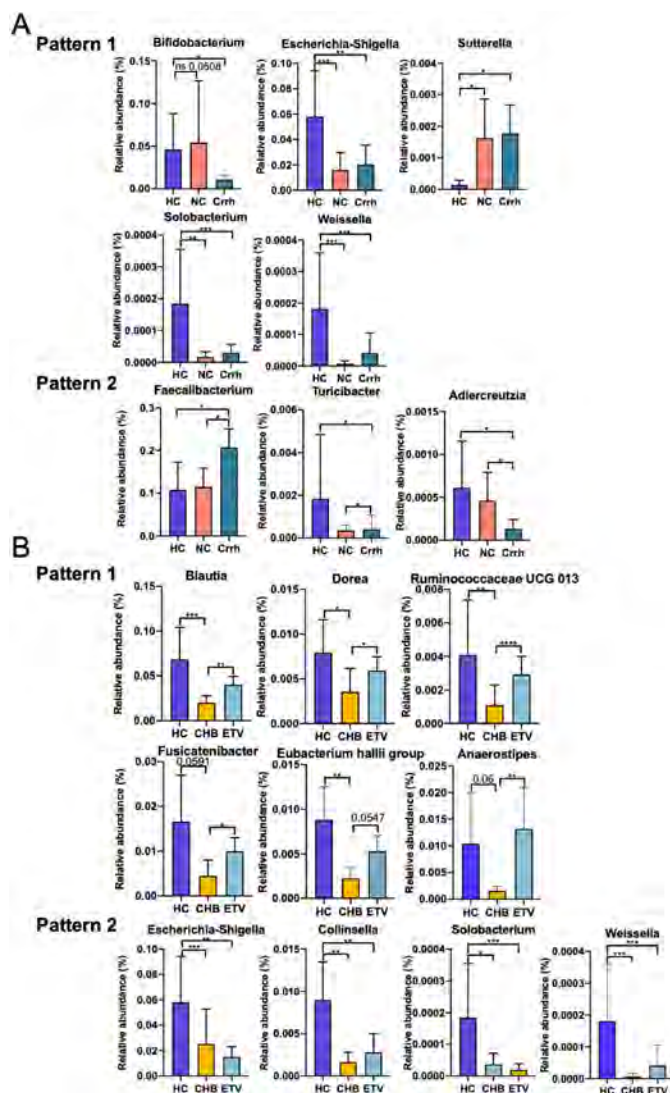


Figure 2:

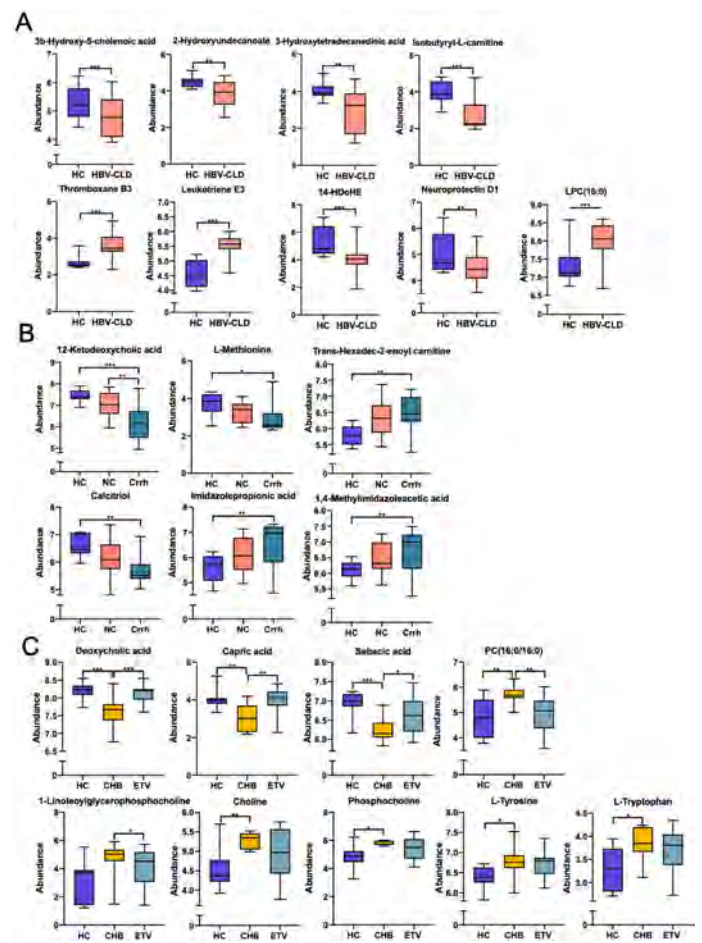
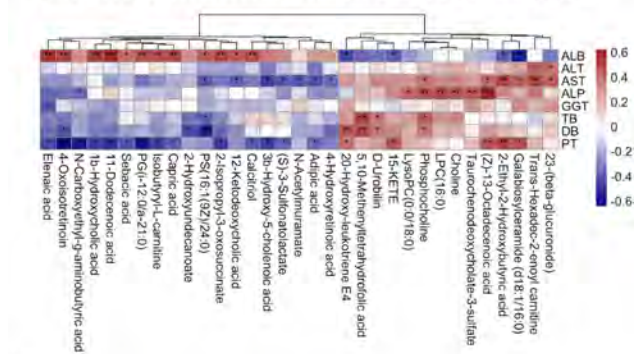


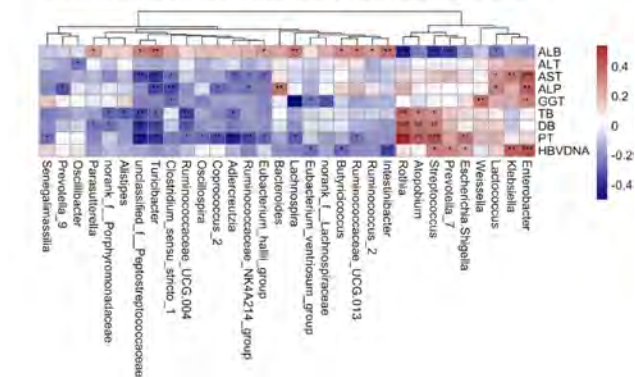
Figure 3:

Conclusion: Microbiome and metabolomics analysis was integrated to provide a comprehensive profile of gut dysbiosis characterized by microbial and metabolic alterations in CHB patients. CHB progression and antiviral treatment significantly contributed to the imbalance of gut microbial community and metabolomics profiles in this study.

A Associations of disease-related metabolites and clinical characteristics



B Associations of disease-related taxa and clinical characteristics

**THU152**

The therapeutic effect of *Lactobacillus plantarum* on metabolic phenotypes in non-alcoholic fatty liver disease mice model

DongYun Kim^{1,2}, Jun Yong Park^{3,4}, Heon Yung Gee². ¹*Yonsei University Graduate School of Medicine, Department of Medicine, Physician-Scientist Program;* ²*Yonsei University College of Medicine, Department of Pharmacology, Graduate School of Medical Science, Brain Korea 21 Project;* ³*Yonsei University College of Medicine, Department of Internal Medicine, Institute of Gastroenterology;* ⁴*Yonsei University College of Medicine, Yonsei Liver Center*
Email: drpjy@yuhs.ac

Background and aims: *Lactobacillus* is considered a potential probiotic and has shown therapeutic potential for several liver diseases including non-alcoholic fatty liver disease (NAFLD). However, it is not known how dietary supplementation of *L. plantarum* has favoring effect on liver. Therefore, we investigated the therapeutic potential of *L. plantarum* supplementation on NAFLD in a mouse model and aimed to elucidate its mechanism.

Method: We used the choline-deficient high fat diet (CD-HFD)-induced murine model that recapitulates key features of human metabolic syndrome. To induce NASH status, C57BL/6N mice were fed a CD-HFD for 30 weeks. Then these mice were divided into three groups: vehicle, *L. plantarum* (10⁹ CFU/day), and empagliflozin, selective SGLT2 inhibitor (10 mg/kg/day). After 12 weeks of treatment, mice were sacrificed and subjected to blood measurements, and liver tissue for RNA isolation, lipid measurements, histology, and stool for microbiome analysis.

Results: *L. plantarum* and empagliflozin treatment significantly improved several metabolic phenotypes such as insulin tolerance, and hepatic lipid contents compared to vehicle group, respectively. However, the histological NAFLD activity score (NAS) was more improved in the *L. plantarum* group (3.0, $p=0.0286$) than in the empagliflozin group (4.0, $p=0.0591$) compared to vehicle group (5.5).

RNA-sequencing analysis revealed that administration of *L. plantarum* downregulated genes related to inflammation such as T cell differentiation and leukocyte activation in liver. In the microbial analysis of stool samples, the elevated Firmicutes-to-Bacteroidetes ratio in the vehicle group (21.97) was decreased in the *L. plantarum* group (0.86). Furthermore, disrupted intestinal epithelial barrier function was restored in *L. plantarum* group and elevated serum endotoxin level was significantly reduced in *L. plantarum* group compared to vehicle group.

Conclusion: Our data demonstrated that administration of *L. plantarum* can improve NAFLD associated phenotypes by altering gut microbiome composition and decreasing serum endotoxin levels.

THU153

Stool microbiota, compared to salivary microbiota, show more extensive correlations with plasma metabolites in decompensated cirrhosis in a multinational cirrhosis cohort

I. Jane Cox^{1,2}, Marcela Peña Rodríguez³, Andrew Fagan⁴,
Mayra Rojas Lara⁵, Adrien Le Guenneq⁶, Fatima Rodriguez-Alvarez⁷,
Sara McGeorge⁴, Ivonne Escalona Nandez⁵, Aldo Torre⁵,
Jasmohan S Bajaj⁴. ¹The Roger Williams Institute of Hepatology, London,
United Kingdom; ²King's College London, United Kingdom; ³Laboratory
for the Diagnosis of Emerging and Reemerging Diseases (LaDEER),
Mexico; ⁴Virginia Commonwealth University and McGuire VA Medical
Center, United States; ⁵Instituto Nacional de Ciencias Médicas y
Nutrición Salvador Zubirán; ⁶King's College London, Randall Centre for
Cell and Molecular Biophysics, United Kingdom; ⁷Instituto Nacional de
de Ciencias Médicas y Nutrición Salvador Zubirán, Mexico
Email: j.cox@researchinliver.org.uk

Background and aims: Cirrhosis is associated with changes in gut microbiota in both saliva and stool. However, the relative linkage patterns of stool vs saliva microbiota with systemic metabolomics are unclear. Moreover, these may differ across countries. We hypothesized that stool has a greater linkage with plasma metabolites than saliva, which is unique depending on country of origin. Aim: Correlation analyses of plasma metabolomics with stool and saliva microbiota in healthy and cirrhotic subjects from USA vs Mexico (MX).

Method: Age-balanced outpt cirrhotics, compensated (Comp) and decompensated (Decomp), and controls from USA and MX underwent plasma collection and dietary recall. Plasma metabolomics were analyzed using NMR spectroscopy. Microbiota in stool and saliva samples were analyzed using 16S rRNA community analyses. Correlation network differences between both saliva and stool gut microbiota and plasma metabolites were compared in controls, Comp and Decomp pts within/between countries.

Results: 313 age-balanced subjects; 135 USA (47 control, 48 Comp, 40 Decomp) and 178 MX (71 control, 56 Comp, 51 Decomp) were enrolled. MELD/cirrhosis severity including lactulose and rifaximin use was comparable (Fig A). Correlation networks demonstrated more microbiome-metabolite linkages in stool compared to saliva in both populations, while there were no salivary correlations with microbiota across MX and decomp USA (Fig B).

***Lactobacillus* correlations:** Network differences of plasma lactate showed a positive correlation to stool *Lactobacillus* in MX Decomp. For USA Decomp, plasma lactate showed a positive correlation to stool *Bifidobacterium* but no correlation with stool *Lactobacillus*. Stool *Lactobacillus* in USA showed a negative correlation with *Faecalibacterium*. Stool *Lactobacillus* correlations with microbiota in stool (pink) vs saliva (blue) vs metabolites (orange) are shown for USA (Fig C) and MX (Fig D) Decomp.

Fig A Clinical Metadata *p<0.05 US vs MX, †p<0.05 within USA, ‡p<0.05 within MX						
	USA (n=133)			Mexico (n=142)		
	Control (n=40)	Comp (n=50)	Decomp (n=43)	Control (n=41)	Comp (n=49)	Decomp (n=52)
Age	57.8±10.1	61.2±6.9	60.4±6.6	57.9±7.1	59.0±9.2	58.1±9.7
Male*	35%	80%	80%	30%	50%	50%
MELD score††	-	8.8±3.1	14.5±5.5	-	9.2±2.5	16.0±7.9
NASH etiology	-	16%	7%	-	17%	12%
Alcohol etiology	-	22%	34%	-	2%	33%
Diabetes	-	26%	30%	-	15%	20%
PPI use*†	20%	34%	47%	10%	20%	25%
Lactulose use	-	-	81%	-	-	76%
Rifaximin use	-	-	46%	-	-	35%
Ascites ††	-	-	67%	-	-	76%
Prior HE ††	-	-	81%	-	-	76%
S. albumin (g/dl) ††	-	3.75±0.49	3.01±0.98	-	3.80±0.53	2.89±0.73

Fig B Correlation between metabolites and sample type (r<-0.6 or 0.6 & p<0.05)						
	USA			Mexico		
Any significant correlations?	Control	Comp	Decomp	Control	Comp	Decomp
Stool	Yes	Yes	Yes	No	No	Yes
Saliva	Yes	Yes	No	No	No	No

Fig C USA Decomp

Fig D MX Decomp

Conclusion: Stool microbiota are more extensively linked with systemic metabolites than saliva microbiota, irrespective of cirrhosis severity and country. These changes are more prominent in Decomp and are centered around plasma lactate, which might be related to interaction of diet and lactulose therapy. Stool microbiota have a greater functional footprint associated with the systemic milieu compared to salivary microbiota.

THU154

The gut virome in non-alcoholic fatty liver disease: distinct changes in Phaeococcovirus composition in a human microbiota associated animal model

Hau-Tak Chau¹, Hein Tun², Saisai Zhang¹, Dengwei Zhang², Fung Yu Huang¹, Lung Yi Loey Mak^{1,3}, Man-Fung Yuen^{1,3}, Wai-Kay Seto^{1,3}. ¹The University of Hong Kong, Hong Kong, Department of Medicine, Hong Kong; ²The University of Hong Kong, Hong Kong, School of Public Health, Hong Kong; ³The University of Hong Kong, Hong Kong, State Key Laboratory of Liver Research, Hong Kong
Email: wkseto@hku.hk

Background and aims: There is increasing knowledge on the role of the gut microbiome in the development of non-alcoholic fatty liver disease (NAFLD), but the role of the gut viral community in disease development remains poorly understood. We aimed to discover gut virome related to NAFLD development via a human-microbiota-associated (HMA) rodent model of NAFLD.

Method: Human fecal donors were recruited and classified into obese NAFLD, non-obese NAFLD and non-obese healthy controls. Liver steatosis was assessed by vibration-controlled transient elastography (Fibroscan, Echosens, Paris). The HMA-NAFLD rodent model was established by high-fat diet and transplantation of human fecal microbiota (FMT) for 12 weeks. The profile of the gut virome of both human donors and rodents was assessed by shotgun metagenomic sequencing (Illumina NovaSeq 6000, US).

Results: Human donors with NAFLD had a significantly higher controlled attenuation parameter measurement when compared to healthy controls (median 324 [IQR 305.5–355.75] vs. 182.5 [179.25–199.25] dB/m, $p < 0.001$). Based on Bray-Curtis distance and PERMANOVA testing, human NAFLD donors had a distinct gut DNA virome compared with healthy controls ($p = 0.04$). Analysis via linear

discriminate analysis (LDA) effect size method identified the Phaeococcovirus genus as a potential biomarker (LDA score 3.80), indicating a lower median relative abundance of Phaeococcovirus in NAFLD donors when compared to healthy donors (3.54% [IQR 2.93%–3.98%] vs. 4.15% [3.94%–4.94%], $p = 0.038$). As a putative host for Phaeococcovirus, the abundance of *Escherichia coli* was negatively associated with Phaeococcovirus ($\rho = -0.51$, $p = 0.012$). In the animal model, mice receiving FMT from obese NAFLD (FMT-ON) displayed a more severe NAFLD phenotype than those receiving FMT from healthy control (FMT-HC) (liver triglyceride: median 65.35 [IQR 62.32–73.33] vs. 48.7 [38.61–54.44] mg/g liver tissue, $p = 0.015$; blood triglyceride: 207.89 [187.87–216.94] vs. 110.05 [102.16–120.76] mg/dL, $p < 0.001$). Phaeococcovirus genus was similarly identified as a potential fecal biomarker when comparing FMT-ON vs. FMT-HC (LDA score 3.19). It was the only viral genus that distinguished NAFLD from control in both human donors and mouse recipients. FMT-ON mice with more severe NAFLD had a significantly lower level of fecal Phaeococcovirus than FMT-HC mice (median 2.47% [IQR 2.39%–2.75%] vs. 2.82% [2.6%–3.14%], $p = 0.038$).

Conclusion: We reported the association of reduced fecal Phaeococcovirus with NAFLD in both human donors and HMA-mice recipients. Further interventional studies in animal and human are warranted to determine its potential causality and function in NAFLD.

THU155

Mitochondrial hyperactivation determines a transferable protective gut microbiota profile in metabolic-associated fatty liver disease development

María Juárez-Fernández¹, Naroa Goikoetxea², David Porras¹, María-Victoria García-Mediavilla^{1,3}, Héctor Rodríguez⁴, Esther Nistal^{1,3}, Susana Martínez-Flórez¹, Mercedes Rincón⁵, Marta Varela-Rey², Javier González-Gállego^{1,3}, Leticia Abecia^{4,5}, Juan Anguita^{4,6}, María Luz Martínez-Chantar^{2,3}, Sonia Sánchez-Campos^{1,3}. ¹Institute of Biomedicine (IBIOMED) University of León, Spain; ²Liver Disease laboratory, CIC bioGUNE, Centro de Investigación Biomédica en Red de Enfermedades Hepáticas y Digestivas (CIBERehd), Spain; ³Centro de Investigación Biomédica en Red de Enfermedades Hepáticas y Digestivas (CIBERehd), ISCIII, Spain; ⁴Inflammation and Macrophage Plasticity laboratory, CIC bioGUNE, Spain; ⁵University of Vermont, Department of Medicine and Immunobiology, College of Medicine, Burlington, United States; ⁶Ikerbasque, Spain
Email: ssanc@unileon.es

Background and aims: Mitochondrial dysfunction plays a key role in metabolic-associated fatty liver disease (MAFLD). Methylation-controlled J protein (MCJ) is a negative regulator of mitochondrial complex I. Its deletion increases mitochondrial activity and reduces diet or hepatotoxic drug-induced lipid accumulation and hepatic damage. The study aims to determine the microbiome signature associated to MCJ deficiency and its capacity to transfer its hepatoprotective phenotype to germ-free (GF) mice through caecal microbiota transplantation.

Method: Wild type (WT) and MCJ-KO C57BL/6J mice were fed with a control or a choline-deficient high fat diet (CDA-HFD) for 6 weeks. Then, a donor mouse from each experimental group was selected based on MAFLD development parameters. GFm were colonized with caecal microbiota from donors and subjected to dietary intervention (C or CDA-HFD) for 3 weeks. After that, samples were collected and processed for assessment of liver disease and gut microbiota composition.

Results: CDA-HFD during 6 weeks induced an inflammatory and fibrotic state compatible with steatohepatitis development. MCJ-KO mice showed a lower liver expression of inflammatory and fibrotic markers. This effect was reproduced in GFm colonized with microbiota from MCJ-KO donors and fed with CDA-HFD. Metagenomic analysis revealed a profound reshaping of gut microbiota due to the diet, but also changes in specific bacterial

POSTER PRESENTATIONS

taxa attributed to MCJ-KO genotype. *Dorea* and *Oscillospira* genera were increased, while *AF12*, *Allobaculum* and *Ruminococcus* were decreased. This microbiota profile was also observed in GFm following microbiota transplantation, highlighting an increase in the abundance of the genus *Dorea* in all groups colonized with microbiota of MCJ-KO mice. Finally, MCJ-KO mice fed with CDA-HFD showed a higher hepatic and intestinal production of nicotinamide-adenine dinucleotide (NAD), likewise a higher expression of its synthesis enzymes. These results were reproduced in GFm transplanted with MCJ-KO microbiota.

Conclusion: The protective effect of MCJ deficiency on MAFLD progression implies a mitochondrial hyperactivation mechanism associated to a higher NAD production capacity, that determines a gut microbiota profile, which is transferred by transplantation to GFm. Supported by BFU2017-87960-R, PID2020-120363RB-I0, GRS2126/A/2020, LE017-P20. CIBERehd is funded by ISCIII.

THU156

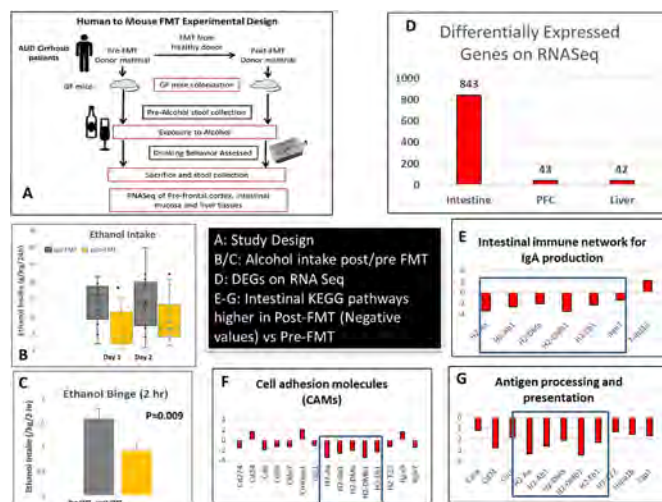
Fecal transplant-related reductions in Alcohol intake from human to mice are associated with alterations in the intestinal but not liver or prefrontal cortex transcriptome

Jennifer Wolstenholme¹, Maren Smith¹, Ryan Balfour Sartor², Javier Maeso-Gonzalez¹, Derrick Zhao¹, Huiping Zhou¹, Jason Kang¹, Phillip Hylemon¹, Jasmohan S Bajaj¹. ¹Virginia Commonwealth University and Richmond VA Medical Center; ²UNC Chapel Hill
Email: jasmohan.bajaj@vcuhealth.org

Background and aims: In a recent randomized placebo-controlled trial in men with cirrhosis, we found that fecal microbiota transplant (FMT) reduced alcohol craving and consumption compared to placebo. We found that transmitting stool post-FMT but not pre-FMT to germ-free mice (GF) reduces alcohol drinking but the metabolic pathways associated with this reduction are unclear. Aim: determine the genes activated along the gut-liver-brain axis after stool transfer into mice.

Method: To test whether FMT can act as a therapy to reduce craving, mice were gavaged with fecal microbiota material from the same patients described above (Fig A). 30 GF male C57BL/6 mice received combined stool from pts prior to FMT (pre-FMT) or stools from the same pts after FMT (post-FMT). Initial ethanol acceptance, intake and preference were measured using a 2-bottle choice ethanol drinking assay. A bottle of ethanol (20% v/v) and water were placed on each mouse's cage and readings were taken at 2 (binge), 24 and 48 hours. Intestinal mucosa, liver and prefrontal cortex (PFC) were harvested 18 hours post-alcohol. RNASeq was run on 6 mice that drank the most in the pre-FMT and the least in the post-FMT group for all 3 sites. Differentially expressed genes (DEG) were further analyzed using GO and KEGG pathway analyses with DAVID and Revigo. Finally, Ingenuity Pathway Analysis was also performed.

Results: Alcohol preference/intake: Exposure to post-FMT stool significantly reduced initial ethanol acceptance, and 24-hour ethanol intake and preference compared to those who got pre-FMT material (Fig B/C). RNASeq Results: The overwhelming majority of DEGs were in the intestine (Fig D) with only 1/20th of genes differentially expressed in the liver and PFC pre- vs. post-FMT. Overrepresented KEGG pathways were focused on IgA production, antigen processing and presentation, and cell adhesion molecules most of which were significantly higher in post-FMT vs. pre-FMT mice (Fig E-G). Specifically, these were related to immune regulators such as transforming growth factor beta 1 (*Tgfb1*), interleukin receptor 10 alpha and 1 beta (*Il10ra*, *Il1b*), interferon γ (*Infg*), and tumor necrosis factor (*Tnf*). Sphingosine synthesis was lowered post-FMT.



Conclusion: FMT from humans, through a successful trial, leads to lower alcohol intake in GF mice colonized with post-FMT stools through significant changes in intestinal genes rather than liver or prefrontal cortex. Changes in gut immune-inflammatory response after FMT could strengthen the gut barrier and reduce gut-liver-brain signaling and underlines the role of the gut in the modulation of behavior that is transmissible from humans.

THU157

New insights from mapping of the mucosal gut microbiota in primary sclerosing cholangitis before and after liver transplantation

Mikal Jacob Hole¹, Kristin Jorgensen^{1,2}, Kristian Holm¹, Malin Holm Meyer-Myklestad³, Asle Wilhelm Medhus⁴, Dag Henrik Reikvam³, Alexandra Götz¹, Krzysztof Grzyb⁵, Kirsten Muri Boberg¹, Tom Hemming Karlsen¹, Martin Kummén¹, Johannes R. Hov¹. ¹Oslo University Hospital and University of Oslo, Norwegian PSC Research Center, Department of Transplantation Medicine; ²Akershus University Hospital, Department of gastroenterology; ³Oslo University Hospital and University of Oslo, Department of infectious diseases; ⁴Oslo University Hospital, Department of gastroenterology; ⁵Oslo University Hospital, Division of pathology
Email: m.j.hole@studmed.uio.no

Background and aims: The fecal microbiota in primary sclerosing cholangitis (PSC) is characterized by low diversity and increased relative abundance of *Veillonella*, while data on the mucosal microbiota are inconsistent. No particular microbiota features have been linked to the presence of PSC-IBD, and little is known about the impact of recurrent PSC (rPSC-LT) after liver transplantation (LT). We aimed to investigate the mucosal microbiota in PSC and utilize rPSC to define consistent microbiota features associated with PSC irrespective of transplantation.

Method: We included 84 PSC and 51 PSC-LT patients (of which 25/51 [49%] had or developed rPSC median 5.0 years after LT) with biopsies available from at least two ileocolonic segments. 19 healthy controls (HC) were included for comparison. Biopsy DNA was subjected to 16S rRNA sequencing (V3-V4) and analyzed using QIIME2.

Results: Mucosal gut expansion of Proteobacteria was more pronounced in PSC-LT (up to 19%) than in PSC (up to 11%), compared to only ~5% in HCs ($Q_{FDR} < 0.05$). A limited set of genera was significantly associated with PSC both before (PSC compared with HCs) and after LT (rPSC-LT compared with PSC-LT). This set consisted of *Bifidobacteria*, *Eubacterium hallii* and two different *Lachnospiraceae*, which had reduced relative abundance in PSC, and *Enterococcus*, *Streptococcus*, *Eisenbergiella* and *Hungatella*, which had increased abundance in PSC.

Alpha diversity was reduced ($p < 0.05$) and *Veillonella* was significantly increased in PSC and PSC-LT compared to HCs, but did not separate rPSC-LT from PSC-LT. Concomitant IBD was associated with significantly reduced relative abundance of *Akkermansia*, irrespective of LT, ranging from 0.8–1.0% to 4.5–5.6% mean relative abundance. The potential pathobiont *Klebsiella* was detected in the mucosa in at least one segment in 18% of the patients before and 41% after LT ($p < 0.05$) and associated with significantly reduced transplantation- and recurrence-free survival.

Conclusion: Liver transplantation does not normalize potentially disease-related microbiota features. Multiple bacterial genera associated with both PSC and rPSC-LT, and *Akkermansia* associated with PSC-IBD irrespective of transplantation status. Furthermore, *Klebsiella* associated with poor outcome both before and after liver transplantation.

THU158

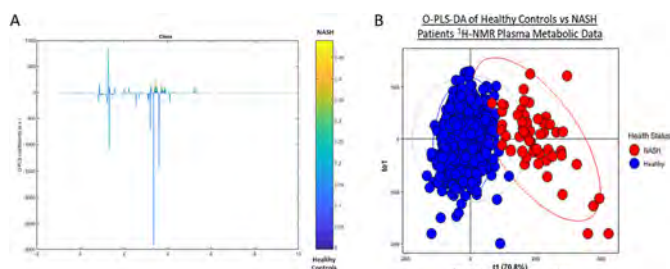
Designing a polymetabolic risk score for non-alcoholic steatohepatitis patients by differentiating their metabolic profiles from healthy controls

Nadeen Habboub^{1,1}, Pinelopi Manousou¹, Roberta Forlano¹, Benjamin H. Mullish¹, Gary Frost¹, Benjamin Challis², Mark Thursz¹, Marc-Emmanuel Dumas^{1,3}. ¹Imperial College London, Metabolism, Digestion and Reproduction, London, United Kingdom; ²AstraZeneca, Biopharmaceuticals Research and Early Development, Translational Science and Experimental Medicine, Cambridge, United Kingdom; ³Imperial College London, Heart and Lung Institute, London, United Kingdom
Email: nh819@ic.ac.uk

Background and aims: The gut microbiome plays a role in the pathogenesis of non-alcoholic fatty liver disease (NAFLD) and its progression to non-alcoholic steatohepatitis (NASH). Studies have shown that changes in gut microbiota result in increased intestinal permeability, facilitating the translocation of bacteria and gut microbiome-modulated metabolites to the liver, inciting NASH. Our aim is to investigate the differences in metabolic profiles of NASH patients in comparison to healthy controls. We designed a metabolic profile scoring model based on plasma ¹H-NMR metabolic data which could distinguish NASH/NAFLD patients from healthy individuals.

Method: Biopsy-proven NASH patients ($n = 55$) were recruited from St Mary's Hospital and were compared to controls ($n = 677$), selected from the AIRWAVE population study by excluding the clinical characteristics of metabolic syndrome. Metabolic profiling of non-fasted plasma and urine samples were carried out by ¹H-NMR spectroscopy and UPLC-MS using HILIC and C18 reverse-phase columns. Untargeted and targeted ¹H-NMR metabolic profiles of plasma samples from both cohorts were examined by multivariate analysis for signature variation and scoring.

Results: We have demonstrated distinct differences in the plasma ¹H-NMR metabolic profiles of NASH patients and healthy controls. Multivariate models of the ¹H-NMR data showed a significant separation between the controls and NASH patients' clusters ($R^2 > 0.6$, $Q^2 > 0.6$, $pR^2Y < 0.001$, $pQ^2 < 0.001$). The polymetabolic based risk score was computed using the O-PLS-DA model of the untargeted ¹H-NMR metabolic profiles of the controls and NASH patients.



Conclusion: We have shown that the ¹H-NMR plasma metabolic profiles of NASH patients and healthy controls are significantly distinctive, which allowed for the construction of a polymetabolic risk-score to separate and distinguish these groups, demonstrating potential for interventions based on the metabolome.

THU159

Intestinal hyperpermeability in cirrhosis is predictive for survival and associated with distinct microbiome changes

Rosa Haller¹, Benard Aliwa^{1,2}, Angela Horvath¹, Vanessa Stadlbauer^{1,3}. ¹Medical University of Graz, Department of Gastroenterology and Hepatology, Graz, Austria; ²University of Nairobi, Department of Food Science, Nutrition and Technology, Nairobi, Kenya; ³CBmed Center of Biomarker Research in Medicine, Area Microbiome Research, Graz, Austria
Email: vanessa.stadlbauer@medunigraz.at

Background and aims: Liver cirrhosis, the 10th most common cause of death in the western world is associated with increased intestinal permeability and alterations of gut microbiome composition. It is however not fully understood how intestinal permeability and the microbiome are interrelated in cirrhosis. We aim to investigate the potential of gut permeability biomarkers to predict mortality and their relation to microbiome composition.

Method: Stool, serum and urine samples from 78 cirrhotic patients (56 ± 9 years, 22 female) were obtained at baseline and after six months; survival was assessed after 24 months. Intestinal permeability was assessed by zonulin in stool and diamine oxidase (DAO) in serum. Kaplan-Mayer survival analysis, group comparisons and correlation analysis (Spearman) were performed. Gut microbiome 16s rRNA sequencing data were analyzed by diversity metrics, ANCOM and LefSe.

Results: Neither DAO nor zonulin at baseline were able to predict mortality, but when assessing the dynamics over 6 months, patients whose zonulin levels worsened or did not change (ZWOR, $n = 45$) had a higher mortality than those whose zonulin levels improved (ZIMP, $n = 33$) (log rank Mantel-Cox $p = 0.048$). ZWOR patients did not differ in etiology from ZIMP patients but had significantly worse international normalized ratio ($p = 0.021$) levels, and MELD score at baseline ($p = 0.032$). Microbiome composition (alpha- and beta diversity) did not differ between ZWOR and ZIMP patients. The genus *Phascolarctobacterium* was more abundant in ZIMP patients with both ANCOM and LefSe. The relative abundance of *Phascolarctobacterium* correlated negatively with calprotectin in stool and sCD14 in serum as biomarker for intestinal inflammation and bacterial translocation.

Conclusion: Worsening of zonulin levels in over 6 months predicted mortality in patients with liver cirrhosis, indicating that serial assessments of this biomarker improve predictive power in cirrhosis. The genus *Phascolarctobacterium* was more abundant in ZIMP patients and correlated negatively with markers for intestinal inflammation and bacterial translocation. *Phascolarctobacterium* can produce short-chain fatty acids and upregulate the mRNA expression of claudin-1, a tight junction protein, indicating a possible link between the microbiome and intestinal hyperpermeability.

THU160

Novel multi-technology meta-analysis identifies gut microbiome strains associated with clinical fibrosis in NAFLD patients

Nicole Narayan¹, Erica Rutherford¹, Karim Dabbagh¹, Arun Sanyal², Todd Z. DeSantis¹. ¹Second Genome, Brisbane, United States; ²Virginia Commonwealth University, Richmond, United States
Email: nicole@secondgenome.com

Background and aims: While NAFLD consists of two subtypes (NAFL and NASH), patients within both subtypes lie on spectrums of multiple axes of disease severity including fibrosis. NASH diagnosis typically relies on liver biopsy. However, liver biopsies are not only invasive but carry substantial risk of complications rendering them

POSTER PRESENTATIONS

impractical for tracking disease progression in patients. Therefore, there is a substantial need for non-invasive diagnostic tools to identify patients with advancing stages of NASH, including clinical fibrosis (fibrosis scores 2–4). While many studies have associated members of the gut microbiota with NAFLD and NASH, these studies either do not discriminate by fibrosis score or they focus on advanced disease (fibrosis score 4). Here we integrated samples from multiple datasets to find strains specifically associated with clinical fibrosis compared to controls and low fibrotic score NAFLD patients using multi-technology meta-analysis (MTMA). We hypothesized that patients with clinical fibrosis would display a different microbial signature and this could constitute the basis of a diagnostic method to non-invasively diagnose clinical fibrosis.

Method: We incorporated data from 189 patients across three studies (two public datasets and one collaboration between Arun Sanyal and Second Genome). Across this meta-cohort, 42 patients had clinical fibrosis (fibrosis score 2–4) and 147 patients were either controls or NAFL with low fibrosis (fibrosis score 0–1). All studies were processed using Second Genome's sg-4sight platform to harmonize 16S amplicon and shotgun metagenomic sequencing, mapping all data against our proprietary StrainSelect reference database. We developed a novel multi-technology meta-analysis (MTMA) procedure to identify the strains which are consistently associated with clinical fibrosis in NAFL patients.

Results: A total of 996 strains were found common across at least two of the three datasets used for analysis. After adjusting for false discovery, MTMA found seven strains from families Lachnospiraceae, Erysipelatoclostridiaceae, and Ruminococcaceae were associated with clinical fibrosis, with four reduced and three enriched in clinical fibrosis. Two of these strains are within provisionally-named taxa not identified with existing open access tools, and therefore would not have been found without leveraging Second Genome's StrainSelect database. This demonstrates the utility of using reference databases which organize both well-documented and emerging taxa.

Conclusion: Second Genome's proprietary technology (including sg-4sight, StranSelect, and MTMA) was able to leverage multiple datasets and find a robust signature of strains associated with clinical fibrosis.

THU161

A nine-strain bacterial consortium improves portal hypertension and insulin signaling and delays non-alcoholic fatty liver disease progression in vivo

Iris Pinheiro¹, Aurora Barbera², Imma Raurell^{2,3}, Federico Estrella², Marcel de Leeuw¹, Selin Bolca¹, Davide Gottardi¹, Nigel Horscroft¹, Sam Possemiers¹, Maria Teresa Salcedo⁴, Joan Genesca^{2,3}, María Martell^{2,3}, Salvador Augustin^{2,3}. ¹MRM Health NV, Ghent, Belgium; ²Hospital Universitari Vall d'Hebron, Institut de Recerca Vall d'Hebron, Universitat Autònoma de Barcelona, Liver Unit, Department of Internal Medicine, Barcelona, Spain; ³Centro de Investigación Biomédica en Red de Enfermedades Hepáticas y Digestivas (CIBERehd), Madrid, Spain; ⁴Pathology Department, Hospital Universitari Vall d'Hebron, Universitat Autònoma de Barcelona, Barcelona, Spain
Email: salva.augustin@gmail.com

Background and aims: The current lack of approved therapies encourages to search for new treatments that allow reversing the progression of non-alcoholic steatohepatitis (NASH). Stool transplantation has been shown to improve NASH features and portal hypertension. However, more patient-friendly treatments are required. Here, we aimed testing the effect of a defined bacterial consortium of nine gut commensal strains on two *in vivo* rodent models of NASH (a rat dietary model of NASH and portal hypertension (PHT), and the STAM™ mouse model).

Method: The bacterial consortium was administered orally *qd* after disease induction in 2 NASH models. In the NASH PHT rats, the consortium was administered for 2 weeks and compared to stool transplant, and effects on PHT and endothelial dysfunction were

evaluated. Liver transcriptomics and predictive functional metagenomic studies were then carried out. In the STAM™ study administration was performed for 4 weeks, and effects on NASH activity and fibrosis were compared to vehicle or Telmisartan at the stage of early fibrosis. A second group of animals was followed for another 3 weeks to assess later-stage fibrosis.

Results: In the NASH rats, the bacterial consortium showed a protective effect on body weight, a trend to improve fasting blood insulin levels and HOMA-IR, and a marked protective effect on PHT, namely a significant reduction in portal pressure (10.32 vs. 9.58 mmHg, $p < 0.05$) and intrahepatic vascular resistance (7.58 vs. 4.20 mmHg/ml*min*100 g, $p < 0.05$). An improvement in all features of endothelial function (p-eNOS, p-Akt and Klf2) and fibrotic markers (*alpha-Sma* and *Col1a1*) was also observed. Gut microbial compositional changes revealed that the consortium achieved a more defined and richer replacement of the gut microbiome than stool transplantation. Moreover, liver transcriptomics suggested a beneficial modulation of pro-fibrogenic pathways. An improvement in histological liver fibrosis was then confirmed in the STAM™ study, significantly reducing collagen- and fibronectin-positive areas in liver sections at 12 weeks. The consortium also improved the NASH activity score, consistent with a decrease in steatosis and ballooning. In addition, consortium-treated animals displayed reduced inflammation (as measured through macrophage F4/80 positive area) and apoptosis (reduction in serum cytokeratin 18 levels), suggesting an overall beneficial effect on all key aspects of NASH biology.

Conclusion: Administration of a specific bacterial consortium of defined composition can ameliorate NASH, PHT and fibrosis and delay disease progression.

Funded by Instituto de Salud Carlos III [PI18/00947, PI21/00691] and International Flavors and Fragrances Inc.

THU162

Duodenal permeability is associated with mucosal microbiota in compensated cirrhosis

Patricia Bloom¹, Krishna Rao¹, Shi-Yi Zhou¹, Christine Bassis¹, Borko Nojkov¹, Chung Owyang¹, Vincent B. Young¹, Anna Lok¹.

¹University of Michigan, Ann Arbor, United States

Email: ppbloom@med.umich.edu

Background and aims: Several complications of cirrhosis result from the translocation of bacteria or their products across the intestinal epithelium. However, little is known regarding the precise relationship between mucosal bacteria and epithelial permeability in cirrhosis. We aimed to assess epithelial permeability and associations with mucosal bacteria in patients with compensated cirrhosis.

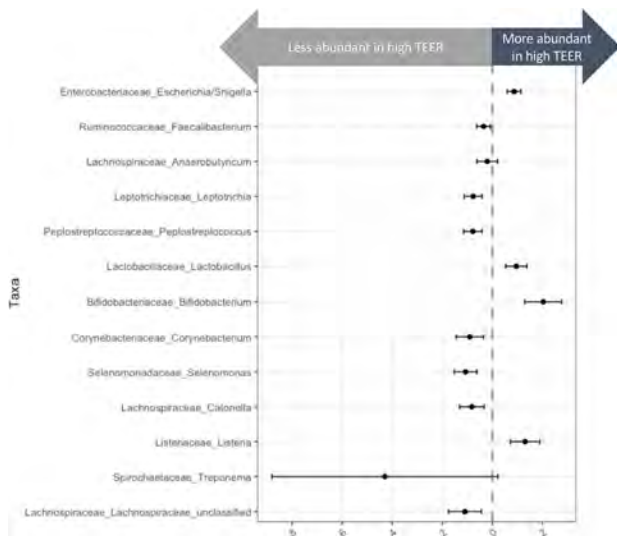
Method: We obtained duodenal tissue biopsies from patients with compensated cirrhosis and controls without liver disease. Patients were excluded if they used antibiotics or immunosuppression. The composition of the mucosal microbiota was determined via 16S rRNA gene sequencing and epithelial permeability assessed by measuring transepithelial electrical resistance (TEER) and tight junction protein expression. Associations between microbiota relative abundance and markers of epithelial permeability were assessed in a beta binomial model.

Results: We studied 24 patients with compensated cirrhosis and 20 controls. Patients with cirrhosis were older than controls (61 vs. 51 years, $p = 0.02$), but had a similar number of extra-hepatic comorbidities (Charlson Comorbidity Index without points for liver disease: 2.2 vs. 1.4, $p = 0.13$). Patients with compensated cirrhosis had median MELD 7 (IQR 7, 10); 62% were male.

Patients with compensated cirrhosis had lower duodenal TEER (i.e. increased epithelial permeability; $13.3 \Omega/\text{cm}^2 \pm 3.4$ vs. $18.9 \Omega/\text{cm}^2 \pm 7.1$; $p = 0.004$) and trended towards diminished expression of tight junction proteins: claudin-1 ($p = 0.18$), occludin ($p = 0.19$), and zonulin-1 ($p = 0.09$).

Patients with compensated cirrhosis had lower microbial burden in the duodenal mucosa (median: 34, 962 copies vs. 20, 982 copies,

$p = 0.08$), as well as lower alpha diversity (median Inverse Simpson: 13.1 vs. 4.6, $p = 0.14$). Furthermore, patients with compensated cirrhosis had a distinct mucosal microbiota community structure relative to controls based on analysis of molecular variance of the Yue and Clayton dissimilarity index ($p = 0.09$). The beta binomial model found that 13 microbes associated with TEER, when using a false discovery rate of 0.05 (Figure). Relative abundance of a *Lactobacillus* and a *Bifidobacterium* bacteria positively associated with TEER, indicating that these two microbes are associated with a less permeable epithelial layer.



Conclusion: Compensated cirrhosis is characterized by increased duodenal epithelial permeability, with a distinct mucosal microbial community. Intriguingly, bacteria previously associated with health, *Lactobacillus* and *Bifidobacterium*, were protective of duodenal permeability. Future research will be required to extend and validate these findings in larger cohorts, to investigate if these microbes have a mechanistic role in epithelial barrier function, and to assess whether these trends persist or progress in decompensated cirrhosis.

THU163

Impact of phenylacetic acid, a microbiota derived-metabolite, on hepatic endoplasmic reticulum-mitochondria interactions and steatosis

Rémy Lefebvre¹, Cyrielle Caussy^{1,2}, Jennifer Rieusset¹. ¹CarMeN Laboratory, UMR INSERM U1060/INRA U1393, 69495 Pierre-Bénite, France; ²Hospices civils de Lyon, département endocrinologie, diabète et nutrition, 69495 Pierre-Bénite, France
Email: remy.lefebvre@univ-lyon1.fr

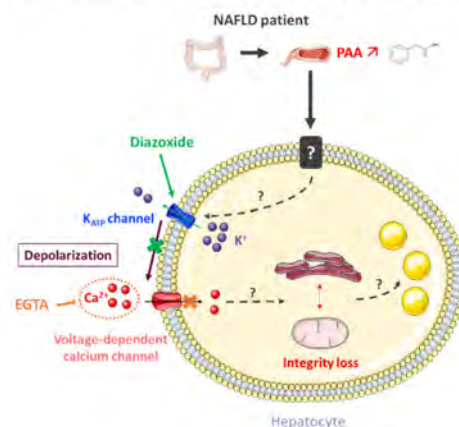
Background and aims: The gut-liver axis has emerged as an important factor in the development of non-alcoholic fatty liver diseases (NAFLD). Microbiota-derived metabolites such as phenylacetic acid (PAA) have been shown to trigger hepatic steatosis in human primary hepatocytes but the molecular mechanism involved is not elucidated. Moreover, mitochondrial dysfunction is also a key component of NAFLD and oxidative capacities of mitochondria are regulated by the communication of this organelle with endoplasmic reticulum at contact points named mitochondria-associated membranes (MAMs). Hence, MAMs are nutrient sensitive controlling mitochondrial oxidative metabolism and ER-mitochondria miscommunication was associated with hepatic insulin resistance and steatosis. We hypothesized that PAA may induce hepatic steatosis through a disruption of MAMs integrity (Figure 1).

Method: We investigated the impact of PAA (500 μ M) on MAMs integrity and steatosis in Huh7 cell line and primary mouse hepatocytes (PMH) incubated for 16 hours in normal (BSA) and

lipotoxic (palmitate 200 μ M) conditions. Co-treatments with diazoxide (100 μ M) or EGTA (10 mM) allowed to investigate the involvement of electrogenic effects of PAA in Huh7 cells. ER-mitochondria interactions were measured by *in situ* proximity ligation assay (PLA) targeting VDAC1 (mitochondrial protein) and IP3R1 (reticular protein) proximity and BODIPY labelling was used to evaluate hepatocyte lipid accumulation. Fixed cells were analyzed by fluorescent microscopy and images analyses were performed using either blobfinder (PLA) or ImageJ (BODIPY) to quantify mitochondria-endoplasmic reticulum contacts and lipid droplets size respectively. All experiments were performed in a single time triplicate.

Results: Treatment with PAA reduced MAMs in Huh7 ($n = 30$ photos, fold change = $-72 \pm 0.025\%$, $p = 0.0001$) and PMH ($n = 30$ photos, fold change = $-23 \pm 0.064\%$, $p < 0.0001$), it also induced lipid accumulation in Huh7 ($n = 30$ photos, fold change = $+20 \pm 0.035\%$, $p = 0.0001$) and PMH ($n = 20$ photos, fold change = $+35 \pm 0.047\%$, $p = 0.0001$). The effect of PAA on MAM integrity is observed as soon as one hour of treatment ($n = 30$ photos, fold change = $-39 \pm 0.029\%$, $p < 0.0001$) in Huh7. This effect is fully prevented by diazoxide which inhibits membrane depolarization ($n = 30$ photos, fold change = $+9 \pm 0.066\%$ with diazoxide versus $-30 \pm 0.042\%$ without it, $p < 0.0001$) and partially by EGTA treatment, a Ca^{2+} chelation agent, ($n = 30$ photos, fold change = $-29 \pm 0.044\%$ with EGTA versus $-50 \pm 0.022\%$ without it, $p < 0.0007$). Altogether, these results suggest an electrogenic mechanism of PAA action on MAMs.

Figure 1: Potential electrogenic effect of PAA leading to MAMs disruption and hepatic steatosis



Conclusion: PAA, a gut-microbiome derived metabolite, induces MAM disruption and hepatocyte lipid accumulation. The effect of PAA on MAMs is mediated through an electrogenic mechanism. Whether preventing the electrogenic effect of PAA impacts hepatic steatosis is under investigation.

THU164

Dynamics of the gut-liver axis in rats with varying fibrosis severity

Hongyan Xiang¹, Zongyi Liu¹, Huanyu Xiang¹, Dejuan Xiang¹, Shuang Xiao¹, Jing Xiao¹, Wei Shen¹, Peng Hu¹, Hong Ren¹, Ming-Li Peng¹. ¹The Second Affiliated Hospital, Chongqing Medical University, Key Laboratory of Molecular Biology for Infectious Diseases (Ministry of Education), Institute for Viral Hepatitis, Department of Infectious Diseases, Chongqing, China
Email: peng_mingli@hospital.cqmu.edu.cn

Background and aims: The classic carbon tetrachloride (CCl₄)-induced liver injury model is widely used to study the pathogenesis of fibrosis and evaluate anti-fibrotic drugs. However, the alterations of gut-liver axis in this model itself remain unclear. Here, this study aimed to explore the dynamic changes of gut microbiota, bile acid and gut barrier over fibrosis severity in CCl₄-induced rats.

Method: Hepatic fibrosis was induced by intraperitoneal injection of CCl₄ with 50% CCl₄ 1 ml/kg body weight, twice weekly for 12 weeks.

POSTER PRESENTATIONS

Fecal samples lengthways collected at 1, 4, 8 and 12 weeks after modeling were used for gut microbiota 16S rDNA sequencing. Bile acid profiles in feces and serum were measured by ultra-performance liquid chromatography-tandem mass spectrometry (UPLC-MS/MS). Intestinal barrier integrity was assessed by measuring ileal permeability to FITC-dextran 4 kDa and Lipopolysaccharide.

Results: Different fibrosis stages from inflammation, mild, moderate to advanced fibrosis were successfully induced by CCL₄ administration for 1, 4, 8, 12 weeks respectively. 16S rDNA sequencing revealed that gut dysbiosis mainly occurred in the early and advanced stages of fibrosis, while the composition of the gut microbiota was close to normal in the moderate stage of fibrosis. Only the relative abundances of Lactobacillus at different phylogenetic levels were underrepresented in the four fibrosis stages. As fibrosis progressed, total bile acids in feces gradually decreased, mainly manifested as a decrease in unconjugated bile acids such as lithocholic acid (LCA) and Deoxycholic acid (DCA). Conversely, serum total bile acids increased, with marked increase in conjugated bile acids such as glycocholic acid hydrate (GCA) and tauro- α -murocholic acid (T- α -MCA). The hepatic FXR-SHP and intestinal FXR-FGF15 pathways, the master regulators of BA biosynthesis in the enterohepatic circulation, were significantly inhibited with increasing fibrosis. Interestingly, in our experimental settings, ileal pathology and permeability tests showed that the intestinal barrier remained relatively intact even in the cirrhotic stage.

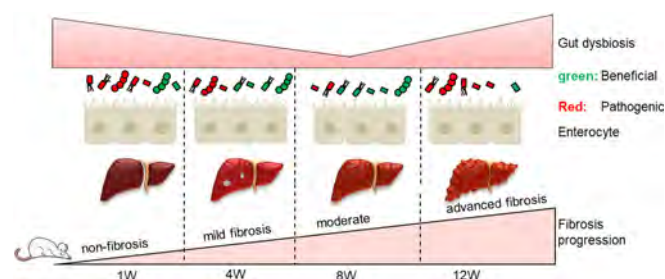


Figure 1: Dynamics of the gut microbiota in rats with varying fibrosis severity

Conclusion: The advances in knowledge of the gut-liver axis of this model provide useful supplements for us to apply it for research and drug evaluation.

THU165

Association between gut microbiome and variceal bleeding risk in compensated cirrhosis: a prospective multicenter study

Hongwei Zhou^{1,2}, Xiaojiao Chen¹, Zewen Li¹, Xiang Huiling³, Tinghong Li³, Ping Zhu³, Dengxiang Liu⁴, Qingge Zhang⁵, Jitao Wang⁶, Xiaoling Zhao⁷, Xiaorong Mao⁸, Junfeng Li⁸, Yongwu Mao⁸, Jia Li⁹, Yu-Pei Liu⁹, Ying Ma⁹, Liting Zhang¹⁰, Shiyang Yang¹⁰, Xiaoqin Gao¹⁰, Guo Huan¹¹, Chao Liu¹¹, Qingli Tu¹¹, Nanping Xiao¹², Zheng Zeng¹², Hui Zhang¹³, Wenjuan Wang¹³, Yulin Yuan¹³, Ye Gu¹⁴, Tiejing Song¹⁵, Liangyu Pan¹⁶, Xiqiao Zhou¹⁷, Mengyu Li¹⁷, Chengwen Fang¹⁷, Tong Dang¹⁸, Xianmei Meng¹⁸, Yi Zhou¹⁸, Qin Wei¹⁹, Zhenhui Chen¹⁹, Musong Li¹⁹, Xiaolong Qi²⁰. ¹Microbiome Medicine Center, Division of Laboratory Medicine, Zhujiang Hospital, Southern Medical University, Guangzhou, China; ²State Key Laboratory of Organ Failure Research, Southern Medical University, Guangzhou, China; ³Department of Hepatology and Gastroenterology of The Third Central Hospital of Tianjin, Tianjin, China; ⁴Personnel Section, Xingtai people's Hospital, Xingtai, China; ⁵Hepatology Department of integrated traditional Chinese and Western Medicine, Xingtai people's Hospital, Xingtai, China; ⁶Hepatobiliary surgery, Xingtai people's Hospital, Xingtai, China; ⁷Cancer Laboratory, Xingtai people's Hospital, Xingtai, China; ⁸Department of infectious diseases, the First Hospital of Lanzhou University, Lanzhou, China; ⁹Tianjin Second People's Hospital, Tianjin,

China; ¹⁰Department of Infectious Diseases, The First Hospital of Lanzhou University, Lanzhou, China; ¹¹Department of Gastroenterology, Hospital of Chengdu Office of People's Government of Tibetan autonomous Region, Chengdu, China; ¹²Department of Gastroenterology and Hepatology, Guangyuan First People's Hospital, Guangyuan, China; ¹³The People's Hospital of Guangxi Zhuang Autonomous Region, 530021, Nanning, China; ¹⁴Gastroenterology clinic, The Sixth People's Hospital of Shenyang, No.85, South Heping Street, Heping District, Shenyang, Liaoning 110006, P.R.China; ¹⁵Department of Gastroenterology, The Sixth People's Hospital of Shenyang, No.85, South Heping Street, Heping District, Shenyang, Liaoning 110006, P.R.China; ¹⁶Department of Gastroenterology, The Sixth People's Hospital of Shenyang, No.85, South Heping Street, Heping District, Shenyang, Liaoning 110006, P.R.China; ¹⁷Department of Gastroenterology, the First Affiliated Hospital of Nanjing Medical University, Nanjing, Jiangsu 210029, People's Republic of China; ¹⁸Department of Gastroenterology and Hepatology, The Second Affiliated Hospital of Baotou Medical College, Baotou, China; ¹⁹Department of Gastroenterology, Baoding people's Hospital, Baoding, China; ²⁰CHESS Center, Institute of Portal Hypertension, The First Hospital of Lanzhou University, Lanzhou, China
Email: qixiaolong@vip.163.com

Background and aims: Gut microbial dysbiosis is associated with the progression of cirrhosis, but the relationship to the risk of variceal bleeding (EVB) remain unknown. Our study aims to evaluate the diagnostic value of gut microbiome for EVB in compensated cirrhosis.

Method: A total of 270 compensated cirrhotic patients from 13 centers in China were prospectively recruited between July 2019 and April 2021. Stool samples and results of endoscopy was collected following a standard detailed protocol. The total bacterial DNA in each stool sample was extracted and profiled by sequencing the 16S rRNA gene V4 region. Then the role of gut microbiome in EVB was explored and compared with endoscopy, which was considered as the gold standard for evaluating the risk of EVB.

Results: In this prospective multicenter study (NCT03990753, CHESS1901), the median age was 53 years (range 20–75 years), and 69.6% (n = 188) were male. 95 patients were assessed as high risk of EVB, and 175 patients were estimated at low risk. Firstly, patients from Lanzhou (LZ, n = 30), Tianjin (TJ, n = 131), Xingtai (XT, n = 74) and Chengdu (CD, n = 20) cities were picked out to explore whether regional variation could affect the composition of gut microbiota. Although alpha diversity was similar in four regions (Fig. A), the relative abundances at the phylum and genus levels of all samples were quite different (Fig. B, C). At the phylum level, the relative abundance of Firmicutes was higher in XT than in other cities; conversely, Bacteroidetes were relatively less abundant in XT. Furthermore, the genus level further reflected the relative differences in the abundance of microbial composition. Principal coordinate analysis (PCoA) based on unweighted UniFrac distance showed that the spatial distributions of patients for four regions were significantly different from each other overall (p = 0.001, Fig. D). However, we did not observe significant differences between high risk and low risk of EVB groups for alpha diversity, beta diversity or the relative abundances of the predominant bacterial taxa (Fig. E-H). In addition, no significant difference was obtained between the groups of high and low risk of EVB for the single center in TJ and XT, respectively (Fig. J, K).

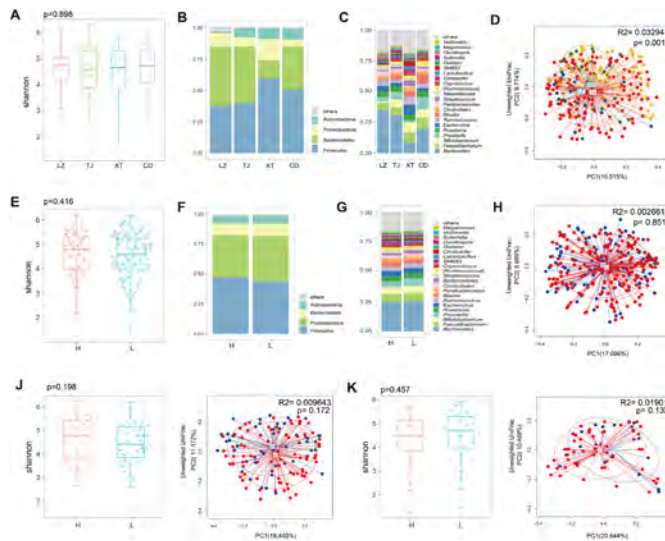


Figure: Gut microbiota composition for four major cities and groups of EVB risk. Composition of Alpha diversity (A, E). Average relative abundances of the predominant bacterial taxa at the phylum (B, F) and genus (C, G) levels. Scatter plots of PCoA based on Unweighted UniFrac for gut microbiota composition to show beta diversity (D, H). Alpha diversity and PCoA plots for the single center in TJ (J) and XT (K).

Conclusion: The multicenter study suggested that gut microbiome varies from region to region, but both alpha and beta diversity weren't associated to risk of EVB in compensated cirrhosis. Further studies exploring specific differential bacteria correlated with the risk of EVB are needed.

Immunology

THU167

Increased expression of programmed cell death ligand 1 and galectin 9 in transplant recipients who achieved tolerance after immunosuppression withdrawal

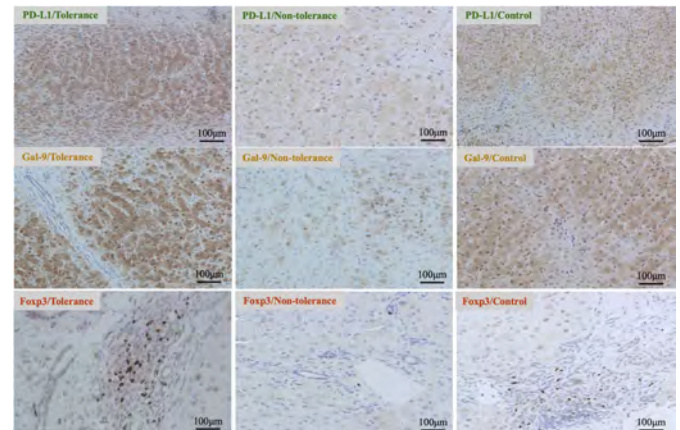
Nguyen Hai Nam¹, Kojiro Taura¹, Yukinori Koyama¹, Takahiro Nishio¹, Gen Yamamoto¹, Yusuke Uemoto¹, Yusuke Kimura¹, Li Xuefeng¹, Daichi Nakamura¹, Kenji Yoshino², Eri Ogawa³, Tatsuya Okamoto³, Atsushi Yoshizawa⁴, Satoru Seo¹, Keiko Iwaisako⁵, Tomoaki Yoh¹, Koichiro Hata¹, Toshihiko Masui¹, Hideaki Okajima⁶, Hironori Haga⁷, Shinji Uemoto⁸, Etsuro Hatano¹. ¹Graduate School of Medicine, Kyoto University, Kyoto, Japan, Division of Hepato Biliary Pancreatic Surgery and Transplantation, Department of Surgery, Kyoto, Japan; ²Nagahama City Hospital, Nagahama, Shiga, Japan, Department of Surgery, Japan; ³Kyoto University Hospital, Kyoto, Japan, Department of Pediatric Surgery, Japan; ⁴Kansai Electric Power Hospital, Osaka, Japan, Department of Surgery, Japan; ⁵Faculty of Life and Medical Sciences, Doshisha University, Kyotanabe, Japan, Department of Medical Life Systems, Japan; ⁶Kanazawa Medical University, Ishikawa, Japan, Department of Pediatric Surgery, Japan; ⁷Kyoto University, Kyoto, Japan, Department of Diagnostic Pathology, Japan; ⁸Shiga University of Medical Science, Otsu, Shiga, Japan
Email: ktaura@kuhp.kyoto-u.ac.jp

Background and aims: Programmed cell death protein 1 (PD-1)/its ligand PD-L1, concomitant with T cell immunoglobulin and mucin domain-containing protein 3 (TIM-3)/its ligand galectin 9 (Gal-9) and the forkhead box protein P3 (Foxp3) might be involved in tolerance after liver transplantation (LT).

Method: Liver biopsies from 38 tolerant, 19 nontolerant (including 16 samples that triggered reintroduction of immunosuppression (IS)

and 19 samples after IS reintroduction) and 38 control LT patients were studied. The expressions of PD-1, PD-L1, Gal-9, and Foxp3 were determined by immunohistochemical and immunofluorescence (IF) staining. The success period of IS withdrawal was calculated using Kaplan-Meier analysis.

Results: Tolerant and control patients exhibited higher PD-L1, higher Gal-9, and higher Foxp3 levels than nontolerant patients at the moment of triggering IS reintroduction. High expression of PD-L1 and Gal-9 was associated with prolonged success of tolerance (83.3% vs. 36.7%, $p < 0.01$; 73.1% vs. 42.9%, $p = 0.03$). A strong correlation between PD-L1 and Gal-9 expression levels was detected (Spearman $r = 0.73$, $p < 0.0001$) and IF demonstrated colocalization of PD-L1 and Gal-9 in the cytoplasm of hepatocytes.



Conclusion: The present study demonstrated that an increased expression of PD-L1 and Gal-9 was associated with sustained tolerance after IS withdrawal in pediatric liver transplantation.

THU168

Acidic microenvironment aggravates the severity of hepatic ischemia/reperfusion injury by modulating PPAR- γ signal

Wei Ding¹, Yunfei Duan¹, Zhen Qu¹, Donglin Sun¹, Yunjie Lu¹. ¹The Third Affiliated Hospital of Soochow University, Hepatopancreatobiliary Surgery Department, Changzhou, China
Email: slddoctor@163.com

Background and aims: Hepatic injury induced by ischemia and reperfusion (HIRI) is a major clinical problem after liver resection or transplantation. The polarization of macrophages plays an important role in regulating the severity of hepatic ischemia/reperfusion injury. Recent evidence had indicated that the ischemia induces an acidic microenvironment by causing increased anaerobic glycolysis and accumulation of lactic acid.

Method: We hypothesize that the acidic microenvironment might cause the imbalance of intrahepatic immunity which aggravated HIRI. The hepatic ischemia/reperfusion injury model was established to investigate the effect of the acidic microenvironment to liver injury. Liposomes were used to deplete macrophages in vivo. Macrophages were cultured under low pH conditions to analyze the polarization of macrophages in vitro. Activation of the PPAR- γ signal was determined by Western Blot. PPAR- γ agonist GW1929 was administrated to functionally test the role of PPAR- γ in regulating macrophage-mediated effects in the acidic microenvironment during HIRI.

Results: We demonstrate that acidic microenvironment aggravated HIRI while NaHCO₃ reduced liver injury through neutralizing the acid, besides, liposome abolished the protective ability of NaHCO₃ through depleting the macrophages. In vivo and vitro experiment showed that acidic microenvironment markedly promoted M1 polarization but inhibited M2 polarization of macrophage. Furthermore, the

POSTER PRESENTATIONS

mechanistic study proved that the PPAR- γ signal was suppressed during the polarization of macrophages under pH=6.5 culture media. The addition of PPAR- γ agonist GW1929 inhibited M1 polarization under acidic environment and reduced HIRI.

Conclusion: Our results indicate that acidic microenvironment is a key regulator in HIRI which promoted M1 polarization of macrophages through regulating PPAR- γ . Conversely, PPAR- γ activation reduced liver injury, which provides a novel therapeutic concept to prevent HIRI.

THU169

Toll-like receptor 3 polymorphisms rs5743305 and rs3775291 affect innate immune responses in whole blood analyses

Sophia Barkow¹, Madlen Matz-Soja¹, Thomas Berg¹, Janett Fischer¹.

¹Division of Hepatology, Department of Medicine II, Leipzig University Medical Center, Laboratory for Clinical and Experimental Hepatology, Leipzig, Germany

Email: janett.fischer@medizin.uni-leipzig.de

Background and aims: As a part of the innate immunity, the Toll-like receptors (TLR) 3 signaling has been linked to the outcome of hepatitis B virus (HBV) infection. Polymorphisms (SNPs) in the *TLR3* gene were associated with an increased risk of developing chronic hepatitis B. This research aimed to assess the impact of the two *TLR3* SNPs rs5743305 and rs3775291 on the immune responses in a whole blood assay.

Method: The study included 30 healthy volunteers matched according to the two functionally relevant *TLR3* SNPs (10 TT/10 TA/10 AA for rs5743305 and 11 CC/12 CT/7 TT for rs3775291), and in age and gender. Heparinized whole blood was treated with 5 μ g/ml polyinosinic-polycytidylic acid (PolyI:C) for 3 and 6 hours. The relative gene expression (rGE) of *TLR3*, *IL1 β* , *IL6*, *IL10*, *IL12*, *IFN β* , *IFN α* and *TNF α* was analyzed by quantitative real-time polymerase chain reaction. Normalization ($2^{-\Delta\Delta C_t}$) was performed in relation to the housekeeping gene *TBP* and untreated blood. The plasma protein levels (PPL) of all cytokines were measured after 6 h of stimulation by performing a bead-based sandwich-immunoassay.

Results: The rs5743305 minor allele A showed significantly lower rGE of *IL10* (A: 8.97, TT: 14.82, $p=0.022$) and absolute PPL (A: 6.99 pg/ml, TT: 15.6 pg/ml, $p=0.025$) after 6 h compared to the wild type (WT) TT. Additionally, *IL1 β* PPLs were reduced for the minor allele A compared to the WT (A: 43.5 pg/ml, TT: 75.95 pg/ml, $p=0.011$) as depicted in figure A. The rs3775291 risk allele T showed increased rGE of *IFN β* after 6 h (T: 4.32, CC: 2.08, $p=0.017$). Interestingly, the relative PPL of *IFN β* was significantly lower for the T allele than for the WT CC (T: 2.6, CC: 8.52, $p=0.014$). Furthermore, the risk allele significantly reduced the relative PPL of *IFN α* (T: 1.4, CC: 1.9, $p=0.004$) (figure B).

Conclusion: This study showed significant effects of the two *TLR3* SNPs on cytokine expression in the complex whole blood system. The minor allele A of rs5743305 decreased pro- and anti-inflammatory cytokine expression. As expected, the rs3775291 risk allele T reduced the synthesis of inflammatory type 1 interferons. This may lead to a dysbalanced immune system and therefore to a less functional defense against virus infections. Further research in larger cohorts and in cell culture systems are required to enlighten the impact of the SNPs on immune responses, especially during HBV infection.

THU170

IL-15 boots HBV-specific CD8⁺ cell response by activated progenitor pool mitochondrial remodelling in on treatment e-Ag negative chronic hepatitis B

Julia Peña Asensio^{1,2}, Henar Calvo¹, Joaquin Miquel¹,

Eduardo Sanz de Villalobos¹, Alejandro González Praetorius¹,

Miguel Torralba^{1,3}, Juan Ramón Larrubia^{1,3}. ¹Guadalajara University

Hospital, Translational Hepatology Unit, Guadalajara, Spain; ²University

of Alcalá, Department of Biology of Systems, Alcalá de Henares, Spain;

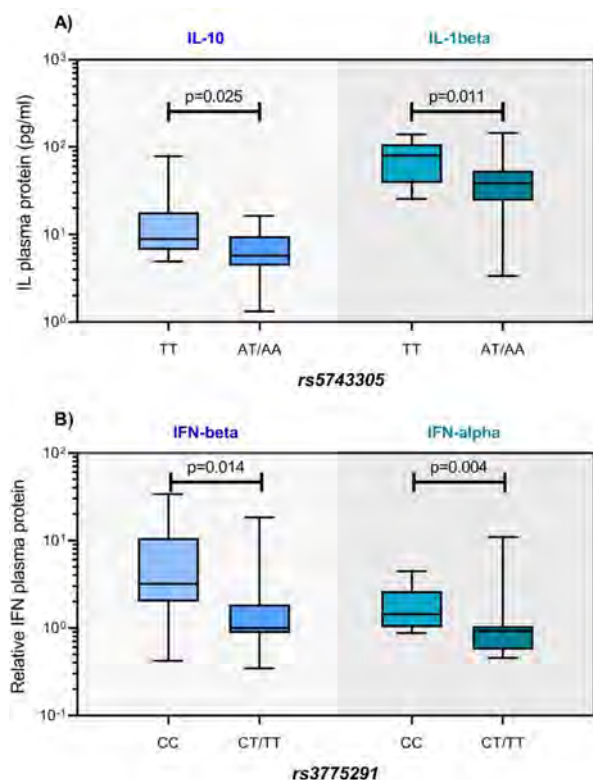
³University of Alcalá, Department of Medicine and clinical specialties, Alcalá de Henares, Spain

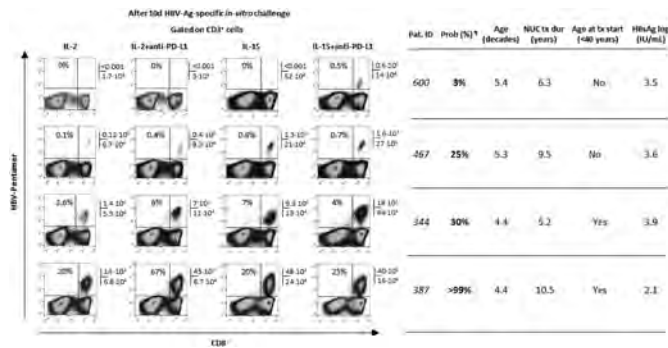
Email: hlnd.julia@gmail.com

Background and aims: In the HBV-specific-CD8⁺ progenitor pool (PP), mitochondrial remodelling could re-establish the functionality of the effector proliferative progeny (EPP) in nucleos (t)ide analogue (NUC) treated eAg (-) chronic hepatitis B (CHBe (-)). We analysed the role of IL-15 in the metabolic profile of the HBV-specific CD8⁺ PP after Ag encounter in CHBe (-) with low probability of T cell restoration during NUC treatment.

Method: According to clinical variables, level of HBV-specific-CD8⁺ cell exhaustion was estimated in NUC treated CHBe (-). HBV-specific-CD8⁺ cells were visualized by pentameric technology. After Ag-specific stimulation, activated PP (APP) was detected by TCF1 staining and FSC level. Metabolic profile, memory-like phenotype and mTORC1 activation in PP were analysed by Glut1, PGC1 α , CPT1, PD-1, CD127 and prS6-P expression. The effector abilities in the effector proliferative progeny (EPP) were tested by proliferation ability, interferon- (γ), Tumour necrosis factor (TNF) α and CD107a expression. The role of IL-15 \pm anti-PD-L1 in remodelling metabolic profile and improving effector function was assessed.

Results: During CHBe (-), quiescent PP expresses a memory-like phenotype (PD-1⁺/CD127⁺). After Ag-encounter, APP gives rise to the EPP. In comparison with IL2, IL-15 decreases the initial boost of mTORC1 in APP, but maintains its activation longer, which translates into an inflation of EPP, and improvement in metabolic profile (Glut1^{low}, PGC1 α ^{high}, CPT1^{high}). IL-15 induced metabolic changes correlate with an enhancement in EPP effector abilities (IFN γ ^{high}, TNF α ^{high}, CD107a^{high}). In those cases with low probability of HBV-specific-CD8⁺ cell restoration during NUC treatment, IL-15 plus anti-PD-L1 restored the proliferation ability of these cells after Ag-specific in-vitro challenge.





Conclusion: IL-15 induces an intermediate but sustained mTORC1 activation in HBV-specific CD8⁺ APP that translates into a catabolic mitochondrial profile and enhancement in EPP of effector abilities. In those CHBe (-) cases with low probability of achieving a functional response during NUC treatment, IL-15+anti-PD-L1 in-vitro treatment restores their reactivity.

THU171

Mucosal-associated invariant T cells are rendered functionally exhausted within the tumour microenvironment in HCC in a cell-contact dependent manner

Junika Pohl¹, Alexandra Georgieva¹, Anna-Marie Pedde², Anna Hirschberger², Sebastian Deschler¹, Melanie Laschinger³, Daniel Hartmann³, Jan Boettcher², Norbert Hüser³, Roland M. Schmid¹, Percy A. Knolle², Katrin Böttcher¹. ¹University Hospital Rechts der Isar, School of Medicine, Technical University of Munich (TUM), Department of Internal Medicine II, München, Germany; ²University Hospital Rechts der Isar, School of Medicine, Technical University of Munich (TUM), Institute of Molecular Immunology and Experimental Oncology; ³University Hospital Rechts der Isar, School of Medicine, Technical University of Munich (TUM), Department of Surgery
Email: katrin.boettcher@mri.tum.de

Background and aims: Hepatocellular carcinoma (HCC) is still one of the major causes of cancer death worldwide. Immunotherapy has recently become the first-line treatment for advanced HCC, although response rates remain low. MAIT cells, innate-like T cells particularly enriched in the liver, express pro-inflammatory cytokines as well as cytolytic molecules and have therefore been attributed anti-tumour properties. In this study, we aim to decipher direct interactions between MAIT cells and HCC cells in order to unravel mechanisms of immune cell exhaustion within the tumour microenvironment in HCC.

Method: MAIT cells were isolated from tumour tissue, adjacent liver tissue and peripheral blood of human patients with HCC or other liver tumours and healthy controls. Primary MAIT cells were co-cultured with various HCC cell lines *in vitro* and MAIT cell phenotype and function was analysed by multi-colour flow cytometry.

Results: We show that MAIT cells frequency is significantly reduced in peripheral blood of HCC patients compared to healthy controls, as well as in HCC tumour tissue compared to the adjacent liver tissue. Such MAIT cell loss was specific, since frequency of conventional T cell subsets was unaffected in HCC and MAIT cell frequency was unchanged in other liver tumours. Whereas MAIT cells from peripheral blood of HCC patients remained functional, tumour-educated liver-derived MAIT cells showed increased exhaustion marker expression and significantly impaired effector function, suggesting MAIT cell exhaustion within the tumour microenvironment in HCC. Interestingly, such MAIT cell dysfunction could be induced by co-culture of MAIT cells with different HCC cell lines, while the hepatocyte-like cell line HepG2 was unable to induce MAIT cell exhaustion. Mechanistically, induction of MAIT cell exhaustion by HCC cells was dependent on direct cell-cell contact.

Conclusion: Taken together, we show that MAIT cells, innate-like T cells with anti-cancer potential, are rendered dysfunctional within

the HCC microenvironment, suggesting MAIT cells as a potential target for anti-cancer therapy in HCC. Understanding mechanisms of local MAIT cell exhaustion in HCC may facilitate the development of novel immunotherapeutic strategies against HCC.

THU172

Preclinical model for the study of immune responses specific for a hepatic-self-antigen

Anais Cardon^{1,2}, Jean-Paul Judor^{1,2}, Arnaud Nicot^{1,3}, Sophie Conchon^{1,3}, Amédée Renand^{1,3}. ¹INSERM UMR 1064 Centre de Recherche en Transplantation et Immunologie, Nantes, France; ²Université de Nantes, Nantes, France; ³INSERM, France
Email: anais.cardon@univ-nantes.fr

Background and aims: Despite a bias toward immune tolerance in the liver, autoimmune liver diseases such as autoimmune hepatitis (AIH) can occur. The etiology of this disease is still not well characterised, and little is known about the emergence process and dynamics of self-antigen-specific immune responses. Thus, to better understand AIH initiation mechanisms, we developed preclinical murine models allowing the study of specific immune responses (CD4⁺ and CD8⁺ T cells and antibody) against a liver antigen.

Method: The expression of the antigen hemagglutinin (HA) was induced with a CRE/LoxP system (cross-breeding of ROSA HA floxed mice with TTR-CREind mice). An adenovirus encoding for the CRE recombinase (AdCRE) was injected intramuscularly (i.m.) to induce a peripheral immunization or intravenously (i.v.) to induce hepatic HA expression and inflammation. Feeding mice with tamoxifen dry food induced HA expression only in the liver. In the different settings, HA-specific CD4⁺ and CD8⁺ T cells in the spleen and the liver were detected and characterized using tetramers, and antibody class switch was assessed by ELISA tests.

Results: Peripheral HA immunization (AdCRE i.m.) leads to a strong HA immune response, marked by the emergence of anti-HA responses (CD4⁺ T cells and antibodies) and linked to HA expression in the muscle (but not in the liver). When HA expression is specifically induced in the liver (tamoxifen), no HA-specific adaptive response is detected, confirming the tolerogenic environment of the liver. However, after a peripheral immunization (AdCRE i.m.), tamoxifen-induced liver-specific HA expression leads to a massive recruitment of HA-specific PD-1⁺ CD25⁺ CD4⁺ T cells in the liver. Finally, AdCRE i.v. causes concomitant hepatic HA expression and inflammation leading to the generation of HA-specific PD-1⁺ CD25⁺ CD4⁺ T cells in the spleen and liver for over 12 weeks, and anti-HA IgG1 antibodies reflecting a chronic reaction against HA.

Conclusion: Our study shows that the conditions of expression of the antigen in the liver (e.g. inflammatory environment, peripheral immunisation) modulate hepatic self-antigen-specific responses. Taken together, this could depict a key element in the initiation of autoreactive responses toward a hepatic antigen. A long-term analysis of antigen-specific responses (CD4⁺ T cells and antibody) in our models will provide a better understanding of responses dynamics during AIH development.

THU173

Proximity labelling reveals potential cis interactions of CD52 glycoprotein counter-receptors on circulating CD4⁺HLA-G⁺ regulatory T cells in acute decompensation of cirrhosis

Tong Liu¹, Gang Wu², Cathrin Gudd¹, Thomas Barbera¹, Rooshi Nathwani¹, Francesca Trovato³, Yan Liu¹, Mark J W McPhail³, Mark Thursz¹, Wafa Khamri¹. ¹Imperial College London, Department of Metabolism, Digestion and Reproduction, London, United Kingdom; ²Imperial College London, Department of Life Sciences, London, United Kingdom; ³King's College London, Institute of Liver Studies, London, United Kingdom
Email: tong.liu15@imperial.ac.uk

Background and aims: We have recently described the expansion of a non-classical regulatory CD4⁺HLA-G⁺ T cell population and its

POSTER PRESENTATIONS

potential contribution to defective peripheral immune responses in patients with acute decompensation (AD) of cirrhosis. Gene profiling of this cell subset revealed an up-regulation of gene encoding for CD52: a sialylated glycosylphosphatidylinositol-anchored glycoprotein known to be involved in lymphocyte functions by ligating its released soluble form and the sialic acid-binding immunoglobulin-like lectin 10 (Siglec-10) receptor. However, the impact of cell surface CD52 is not fully understood. In this study, we aim to investigate the role of membrane-bound CD52 in CD4⁺HLA-G⁺ T cells.

Method: First, we examined the cell surface protein expression of CD52 and Siglec-10 in CD4⁺HLA-G⁺ versus CD4⁺HLA-G⁻ T cells of AD patients (n = 17) using flow cytometry. Endogenous CD52 N-glycan was digested with sialidase and binding affinity of CD52 to Siglec-10 was measured by flow cytometry using fluorochrome-labelled recombinant Siglec-10. Proximity labelling was used to identify potential membrane counter-receptors of CD52 on CD4⁺HLA-G⁺ T cells. Cells were probed with horseradish peroxidase (HRP) conjugated anti-CD52 antibody, biotinyl tyramide was used to biotinylate membrane proteins within 100 nm radius of the HRP complex. Biotinylated proteins in proximity of CD52 were then enriched by streptavidin beads and identified via mass spectrometry.

Results: CD52 cell surface expression was significantly increased in CD4⁺HLA-G⁺ compared to HLA-G⁻ cells (mean fluorescence intensity (MFI) median 25052 IQR [22989–26755] vs. 11529 [9459–14081], p < 0.0001). Siglec-10 expression was also significantly increased in the same subset (MFI 26987 [23892–28533] vs. 16765 [14534–17983], p < 0.0001). The membrane CD52 on CD4⁺ T cells showed high binding affinity towards Siglec-10, and this affinity could be reversed by digestion of the sialylated N-glycan of CD52. Proximity labelling revealed the T cell receptor (TCR) complex namely CD3 epsilon, CD3 gamma, and TCR beta were in the immediate vicinity of CD52 on CD4⁺HLA-G⁺ T cells from patients with AD. Moreover, the results imply that Siglec-10 interacting with CD52 could depend on TCR stimulation.

Conclusion: CD52 and its counter-receptor Siglec-10 are co-expressed on the CD4⁺HLA-G⁺ T cells of AD patients. Proximity labelling identified potential *cis*-ligands recruited to the proximity of the membrane-bound CD52 likely to have implications on CD4⁺HLA-G⁺ T cells responsiveness to TCR stimulation.

THU174

Humoral and cellular immunity after vaccination against SARS-CoV-2 is reduced in patients with chronic liver disease

Al-Dury Samer¹, Johan Waern¹, Anna Martner², Hevar Hamah Saed¹, Marko Alavanja¹, Johan Ringlander³, Andreas Törnelli², Mohammad Arabpour², Jesper Waldenström⁴, Hanna Grauers Wiktorin², Gisela Ringström¹, Martin Lagging⁴.

¹Sahlgrenska University Hospital, Department of Medicine, Gastroenterology and Hepatology Unit, Gothenburg, Sweden;

²Gothenburg University, Institute of Biomedicine, Sahlgrenska Academy, Gothenburg, Sweden; ³Sahlgrenska University Hospital, Department of Clinical Microbiology, Gothenburg, Sweden; ⁴Sahlgrenska University Hospital, Department of Infectious Diseases, Gothenburg, Sweden
Email: samer.al-dury@wlab.gu.se

Background and aims: Patients with chronic liver disease are at a higher risk of morbidity and mortality in COVID-19 and professional societies have recommended the vaccination despite the scarce data from registration trials regarding their efficacy and safety in this vulnerable population.

Method: In a prospective study, we compared the rate of humoral (antibody response to spike protein) and cellular (interferon- γ production) immunity before, after the 1st and 2nd dose of mRNA vaccines in patients with chronic liver disease (CLD) with and without liver cirrhosis and healthy volunteers. We also investigated whether the degree of immune response correlates with liver fibrosis stage using transient elastography.

Results: 64 patients with CLD and 39 healthy volunteers were included. Both serological and T-cell responses were significantly lower in patients with CLD compared to healthy volunteers after the 1st and 2nd vaccine dose. 79% and 15% of CLD patients had inadequate antibody response after the 1st and 2nd vaccine dose respectively. Additionally, 79% and 38% of CLD patients had inadequate interferon- γ production after the 1st and 2nd vaccine dose, respectively. The potency of immune response did not correlate to liver fibrosis grade. Nevertheless, patients with higher Child-Pugh (CP) scores had a worse response to the vaccine. There were no differences in the occurrence of side effects to the vaccine between the groups.

Conclusion: Patients with CLD have a poorer response to vaccination against SARS-CoV-2 compared to healthy volunteers regardless of their fibrosis stage and many continue to be inadequately protected despite full vaccination.

THU175

Efficacy of branched-chain amino acid granules to restore innate immunity in cirrhosis-associated immune dysfunction: a randomized controlled trial

Natthapat Rujeerapaiboon^{1,2}, Teerha Piratvisuth¹, Naichaya Chamroonkul¹, Pimsiri Sripongpun¹, Apichat Kaewdech¹.

¹Songklanagarind Hospital, Internal Medicine, Tambon Kho Hong, Thailand; ²Ramathibodi Hospital, Internal Medicine, Thailand
Email: teerha.p@psu.ac.th

Background and aims: Cirrhosis-associated immune dysfunction (CAID) has been proposed as one of the significant complications in cirrhotic patients, demonstrated by an impairment of innate immunity. Previous studies showed that reduction of phagocytic activity, as a part of innate immunity, might predict infection occurrence and 90-day survival in cirrhosis. However, there are still limited data on immunotherapeutic approaches to modulate the dysfunctional immune response. Our study aims to determine the effect of branched-chain amino acid (BCAA) granules on phagocytic activity in cirrhotic patients.

Method: A double-blinded, randomized-controlled trial was conducted at a single-centre tertiary care hospital. Thirty-seven cirrhotic patients were randomly assigned in a 1:1 ratio stratified by Child-Pugh status to receive either BCAA granules at a dose of 4.15 grams thrice daily or placebo. All patients received a multidisciplinary approach from hepatology and nutrition specialists. They were also assigned to record the adherence to study drug, seven-day food recall, and side effects, if occurred, in an interventional diary. At baseline, the 3rd and 6th months of the study, the phagocytic activity was assessed by a biochemist using pHrodo Red *E. coli* BioParticles Phagocytosis Kit and Image Stream II Imaging Flow Cytometer. The primary end point was the restoration of innate immunity at the sixth month, define by phagocytic activity $\geq 75\%$. Key secondary end points were the accretion of phagocytic activity and number of hospitalizations due to infection.

Results: Of all 37 eligible patients, the patients in Child-Pugh A/B/C were 26/8/3, respectively. Eighteen patients were in placebo, and nineteen were in BCAA group, the baseline characteristics and phagocytic activity were comparable between groups. At 6th month, a significantly higher phagocytic activity restoration was demonstrated in the BCAA group compared with placebo (68.4% vs 5.6%, p < 0.001). The mean phagocytic activity in the BCAA and placebo group were 75.4% and 63.4%, respectively (p < 0.001). The progressive accretion of phagocytic activity was observed during the 3rd and 6th months, as shown in Figure. There were no differences in serum albumin and other inflammatory markers. Despite a higher phagocytic restoration rate in the BCAA group, there was no difference in hospitalization due to infectious events in comparison to the placebo group (2 VS 3 events, p = 0.487).

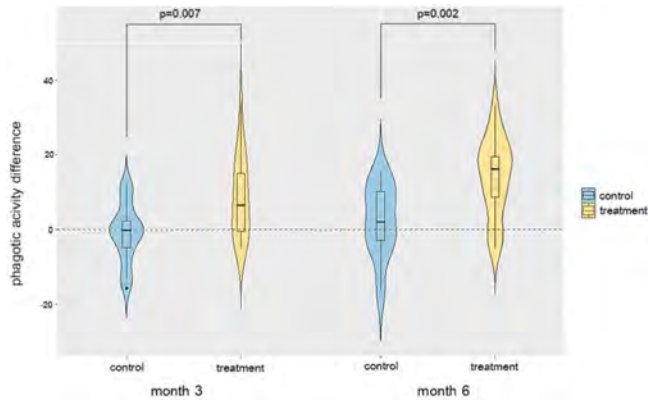


Figure: Phagocytic activity change from baseline at the 3rd month and 6th month of the study.

Conclusion: BCAA can significantly improve phagocytic activity in cirrhotic patients across all Child-Pugh stages. This may be an option for immunotherapeutic intervention of CAID. However, whether the improvement in phagocytic activity would correlate with a better outcome especially infectious complications may need longer follow-up studies.

THU176

The close correlation between sarcopenia and the phagocytic dysfunction in respond to bacterial pathogen *E. coli* in cirrhotic patients

Naichaya Chamroonkul¹, Natthapat Rujeerapaiboon^{1,2}, Pimsiri Sripongpun¹, Apichat Kaewdech¹, Teerha Piratvisuth¹.
¹Songklanagarind Hospital, Tambon Kho Hong, Thailand; ²Ramathibodi Hospital, Thailand
 Email: naichaya@gmail.com

Background and aims: Sarcopenia and phagocytic dysfunction were demonstrated to be associated with poorer clinical outcomes in cirrhotic patients. Branched-chain amino acid (BCAA) is a pivotal factor that activates the mammalian target of rapamycin (mTOR) complex, a central node that controls immunity and muscle synthesis. In cirrhosis with sarcopenia, the BCAA is depleted, which may associate with phagocytic dysfunction. However, there is a

paucity of studies that established the effect of sarcopenia on phagocytic activity. Therefore, our study aims to determine the correlation between sarcopenia and the phagocytic activity in cirrhotic patients.

Method: We conducted a randomized controlled trial (RCT) evaluating the role of BCAA on phagocytic activity. In this study, we used the baseline data in patients enrolled in the RCT to study the correlation and factor affecting phagocytic activity. Thirty-seven cirrhotic patients with sarcopenia were included in this study (defined with skeletal muscle index [SMI] according to the JSH criteria). The SMI was measured at L3 vertebra by a cross-sectional CT scan and calculated by DICOM software. The phagocytic activity assessment was performed by a biochemist, using the pHrodo Red *E. coli* BioParticles Phagocytosis Kit for flow cytometry and Image Stream Mk II Imaging Flow Cytometer. The correlations between SMI and phagocytic activity was analysed using spearman test and adjusted with other covariates by multivariable linear regression

Results: Thirty-seven patients were included, the patients in Child-Turcotte-Pugh (CTP) A/B/C were 26/8/3, respectively. The baseline characteristics were difference as cirrhotic stage progressed from CTP-A to C. Our study demonstrated a trend towards lower phagocytic activity in the more severity of cirrhosis, but not statistically significant, as 62.3%, 60.5%, and 54.3% in CTP A, B, C, respectively ($p = 0.12$). In a multivariable linear regression analysis, CTP-C and SMI (cm^2/m^2) are independent factors associated with the prediction of phagocytic activity, with adjusted beta-coefficients of -14.4% ($p = 0.001$), and $+0.75\%$ ($p < 0.001$), respectively. The strong correlation between SMI and phagocytic activity was demonstrated in the CTP-A cirrhosis, $r = 0.84$ ($p < 0.001$) whereas there was no significant correlation in CTP-B/C cirrhosis, $r = -0.068$ ($p = 0.84$) as shown in the figure.

Conclusion: In cirrhosis with sarcopenia, our study demonstrated that both CTP-C and lower SMI were associated with phagocytic dysfunction. Emerging data had shown a strong correlation between sarcopenic status and phagocytic dysfunction, especially in CTP-A. Therefore, sarcopenic assessment is essential for all stages of cirrhosis despite compensated CTP-A status, to initiate the treatment and prevent further decompensation.

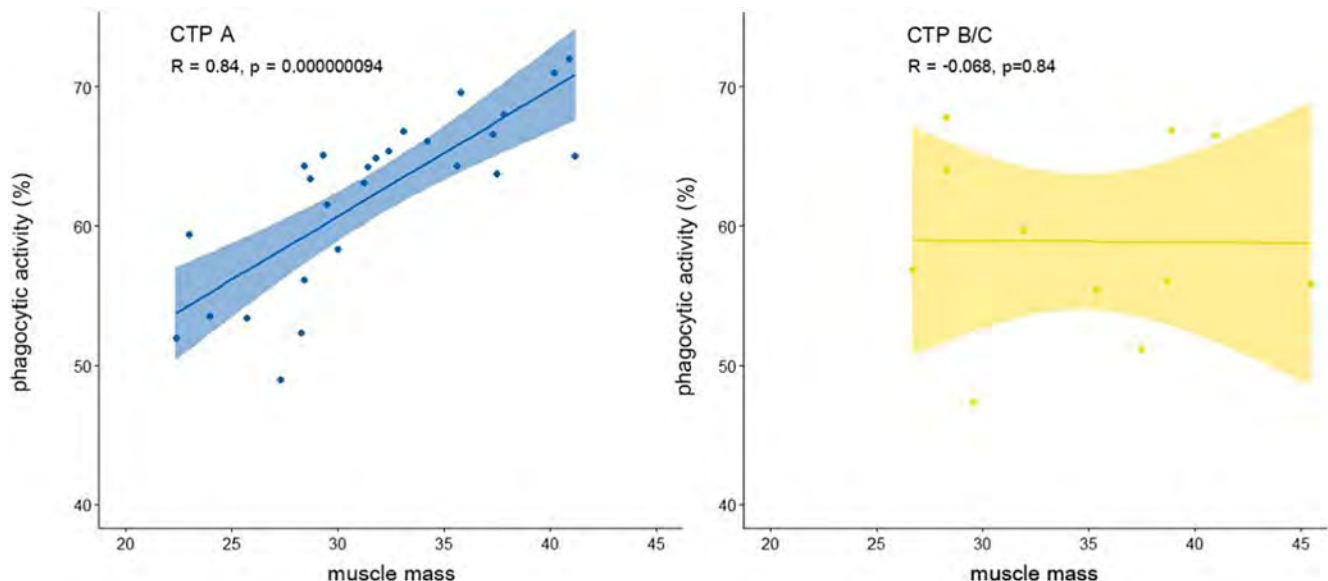


Figure: (abstract: THU176): The correlation between phagocytic activity and muscle mass in various stages of cirrhosis.

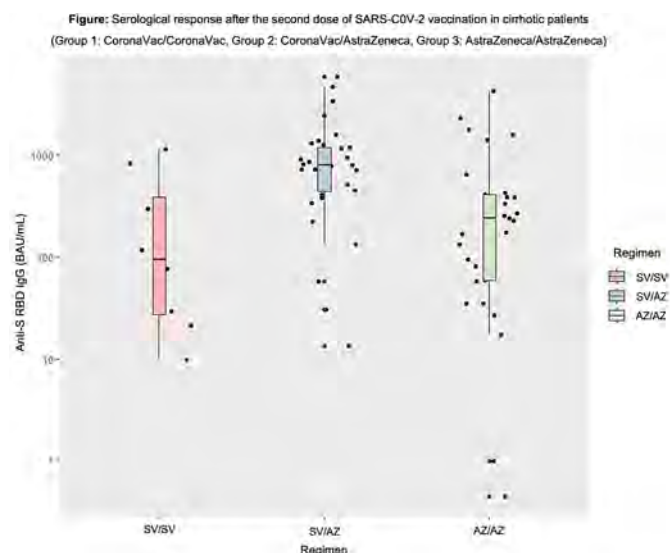
THU177

Heterologous SARS-CoV-2 vaccine triggers more humoral immune responses among patients with liver cirrhosis

Apichat Kaewdech¹, Nawamin Pinpathomrat², Naichaya Chamroonkul¹, Teerha Piratvisuth^{1,3}, Pimsiri Sripongpun¹.
¹Prince of Songkla University, Gastroenterology and Hepatology Unit, Department of Internal Medicine, Faculty of Medicine, Hatyai, Thailand;
²Prince of Songkla University, Department of Biomedical Sciences, Faculty of Medicine, Hatyai, Thailand; ³Prince of Songkla University, NKC Institute of Gastroenterology and Hepatology, Songklanagarind Hospital, Faculty of Medicine, Hatyai, Thailand
 Email: pim072@hotmail.com

Background and aims: To control the COVID-19 pandemic, vaccination is the principal for general population globally. In patients suffered from SARS-Cov-2 infection, having cirrhosis has been associated with a higher risk of poor outcomes, and those with cirrhosis were strongly advised affirmatively by international hepatology societies to receive the SARS-Cov-2 vaccine. However, cirrhosis-associated immune dysfunction might contribute to hyporesponsive to the vaccine. Moreover, data of immune responses in those who received the different types of vaccines, especially heterologous vaccines are lacking. We studied whether different regimens of COVID-19 vaccines affect the humoral immune response in patients with cirrhosis.

Method: We conducted a prospective observational study, collecting blood samples from patients with cirrhosis who were regularly followed up at our centre, a tertiary care hospital in Thailand, and received 2 doses of SARS-Cov-2 vaccine. This is a preliminary report of patients enrolled between June and October 2021. Those who were on immunosuppressive agent were excluded. The SARS-Cov-2 vaccination in Thailand is provided by the government; there were 3 major vaccination regimens: inactivated vaccine (CoronaVac; SV/SV), viral vector vaccine (ChAdOx1 nCoV-19 vaccine; AZ/AZ), and heterologous vaccine (SV/AZ), and neither patients nor investigators had involved in the decision of the regimens given. The antibody (Ab) levels were measured at two-time points, before and at 4-week after receiving the 2nd dose vaccination. The anti-spike receptor-binding domain protein (RBD) IgG was measured using the Abbott SARS-CoV-2 IgG II Quant assay to determine Ab response. The Ab level of <50 AU/ml (7.15 BAU/ml) is considered to be inadequate immune response.



Results: A total of 61 patients completed their 2nd dose vaccine and had Ab level data available, 61% were male, the major cause of cirrhosis was chronic hepatitis B (42%), and 51/9/1 patients were in child A/B/C, respectively. Of those, 8 (13.1%) received SV/SV, 28

(45.9%) got heterologous SV/AZ, and 25 (40.9%) received AZ/AZ. The mean age was 53, 62, and 69 years in SV/SV, SV/AZ, and AZ/AZ, respectively ($p < 0.001$). Two patients in AZ/AZ had inadequate immune response while all patients in SV/SV and SV/AZ had Ab level >7.15 BAU/ml. Among 3 different vaccine regimens, the heterologous SV/AZ had the highest anti-spike RBD IgG level at the median level of 801.8 (IQR: 615.1, 1195.6) BAU/ml, significantly higher than SV/SV (median 95.8 (IQR: 27.3, 427.6) BAU/ml, $p = 0.01$) and AZ/AZ (median 238.3 (IQR: 57.7, 387.2) BAU/ml).

Conclusion: Heterologous COVID-19 vaccine with the inactivated vaccine followed by viral vector vaccine had a significant humoral immune response among patients with cirrhosis. This result highlighted the prime-boost effect of the vaccine to alleviate the shortage of vaccines in the situation of COVID-19 pandemic.

THU178

Predictive immune biomarkers to safely discontinue nucleos (t)ide analogue treatment in HBeAg negative chronic hepatitis B (NUC-B study)

Sandra Phillips^{1,2}, Sameer Mistry^{1,2}, Nicola Harris^{1,2}, Celia Moore³, Gareth Hahn³, Michelle Rosario³, Camilla Carr-Smith⁴, Maria Cortes Carrillo⁴, Lavanya Elangovan⁴, Kosh Agarwal⁴, James Hand⁵, Chris Sivell⁵, Patrick Kennedy⁵, Susan Congreave⁶, Mathew Barnes⁶, Stephen Ryder⁶, Mariam Habib³, Mark Thursz³, Shilpa Chokshi^{1,2}. ¹The Roger Williams Institute of Hepatology Foundation for Liver Research, London, United Kingdom; ²School of Immunology and Microbial Sciences King's College London, United Kingdom; ³St Mary Hospital Faculty of Life Sciences and Medicine Digestive Diseases Division Imperial College London, United Kingdom; ⁴Kings college hospital NHS foundation trust; ⁵Barts Health NHS trust Royal London hospital; ⁶Nottingham University Hospitals NHS trust London
 Email: s.phillips@researchinliver.org.uk

Background and aims: Discontinuation of long-term nucleos (t)ides analogue (NA) treatment can lead to clinical relapse and increased risk of hepatic decompensation in patients with HBeAg negative chronic hepatitis B. In others, NA cessation can result in functional cure. It is widely believed that restoration of antiviral immunity underpins this favourable outcome.

Method: Patients virally suppressed for >3 years were randomised to either stop-NA or discontinue NA for 4 weeks followed by 16 weeks of PEG-IFN-alpha before stopping both treatments (NA/IFN) (see Figure). Patients with exaggerated flares (ALT>20xULN) were retreated with NAs (RTx). Longitudinal peripheral blood mononuclear cells (PBMCs) ($n = 459$) were collected from 23 Stop-NA and 18 NA/IFN patients during a 3-year follow-up. Additional samples were collected during moderate (ALT>2xULN) and exaggerated flares. PBMCs were stimulated with 15 overlapping genotype-specific peptide pools (OPP), HBV core, surface (HBcAg/HBsAg) and recall antigens. Ex-vivo frequency of HBV-specific IFN-gamma (IFN-g) producing T-cells was assessed by ELISpot assays, validated and standardised at GCLP. Virological and clinical parameters were correlated with immunological assessments.

Results: At week 130, 74% Stop-NA and 94% NA/IFN patients remained off treatment while 26% and 6% needed RTx respectively. A lower frequency of IFN-g-specific T-cells at BL, which persisted during follow-up, was associated with RTx ($p = 0.04$). Conversely, one HBcAg OPP-specific T-cell subset was associated with RTx and detected at higher frequency at BL ($p = 0.019$). PEG-IFN treatment was associated with a broad loss of T-cell response and epitope recognition contraction. Whilst this T-cell response recovered after PEG-IFN cessation, a high proportion of patients experienced viral rebound (>2000 IU/ml) (63% vs 18%). In the Stop-NA group, NA withdrawal was associated with moderate flares (52%), accompanied by a peak in T-cell response in sharp contrast to NA/IFN group with flares (62%) occurring when T-cell response was diminished. Finally, the frequency of 3 OPP-specific T-cells subsets at BL was associated with flares in both groups ($p = 0.007$; $p = 0.005$; $p = 0.035$).

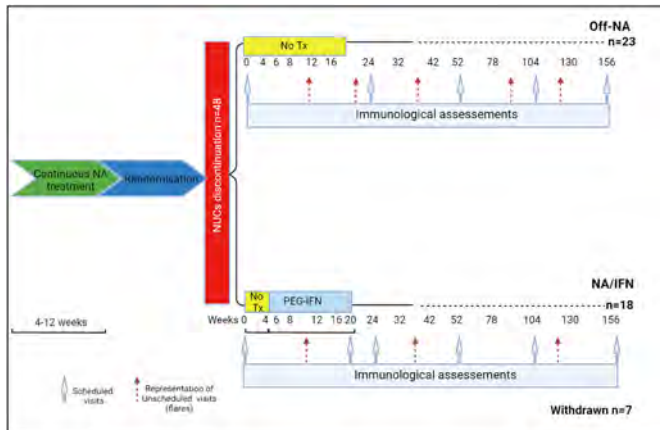


Figure: Created with BioRender.com

Conclusion: This is the first study to systematically characterise the HBV-specific T-cell responses during NA withdrawal and assess the impact of IFN therapy post-NA cessation on antiviral immunity. The findings reveal that epitope-specific T-cells may effectively predict CHB patients that can safely discontinue NA treatment.

THU179

MAIT-cells in blood are associated with a higher risk of infection in patients with cirrhosis

Bonnie Bengtsson^{1,2}, Christopher Maucourant³, Ying Shang¹, Johan K. Sandberg³, Niklas Björkström³, Hannes Hagström^{1,2,4}.
¹Karolinska Institute, Huddinge Hospital, Unit of Gastroenterology and Rheumatology, Department of Medicine, Stockholm, Sweden; ²Karolinska University Hospital, Huddinge, Division of Hepatology, Department of Upper GI diseases, Stockholm; ³Karolinska Institute, Huddinge Hospital, Center for Infectious Medicine, Department of Medicine, Stockholm; ⁴Karolinska Institutet, Solna, Clinical Epidemiology Unit, Department of Medicine, Stockholm
 Email: bonnie.bengtsson@ki.se

Background and aims: Bacterial infection is a common and serious complication in patients with liver cirrhosis. Previous research has found that mucosa-associated invariant T cells (MAIT cells), anti-bacterial T cells, are reduced in numbers in patients with cirrhosis, both in liver and in peripheral blood. Little is known if MAIT cell levels might predict incident clinically relevant outcomes including infections. The aim of this study was to evaluate if MAIT cell levels in peripheral blood can serve as a novel biomarker to cirrhotic patients with a higher risk for adverse outcomes.

Method: Patients with liver cirrhosis attending the Hepatology department at the Karolinska University Hospital between 2016 and 2019 were included. Levels of peripheral MAIT cells in blood were determined using flow cytometry. Baseline characteristics and incident outcomes (bacterial infections, hepatic decompensation and death) were ascertained by manual chart review during a mean follow-up of 2.6 years. A competing risk regression was performed to assess the risk of bacterial infection and hepatic decompensation, with death and liver transplant as competing events. Cox regression was performed to evaluate mortality rates. Both models were adjusted for age, sex and severity of liver disease.

Results: We included 106 patients with cirrhosis, median age was 63 years and 64% were men. Median MAIT-cell percentage was 0.8% MAIT cells out of T cells. We found an association of higher MAIT cell percentages with the risk of bacterial infections (adjusted sub-distribution hazard ratio (aSHR) 1.20 (95%CI = 1.05–1.38)). Higher MAIT cell percentages were also associated with a higher risk of hepatic decompensation (aSHR 1.24 (95%CI = 1.08–1.42)) but not with a higher risk of death (adjusted hazard ratio 1.08 (95%CI = 0.96–1.23)).

Conclusion: In contrast to our hypothesis, higher MAIT cell percentage were associated with a higher risk of bacterial infections

and decompensation. These findings need to be further validated but identify MAIT cells as an interesting biomarker for adverse outcomes in patients with cirrhosis.

THU180

Fatty acids directly limit mucosal-associated invariant T cell effector function in non-alcoholic fatty liver disease

Sebastian Deschler¹, Percy A. Knolle², Katrin Böttcher¹, Ulrike Bauer¹, Marc Ringelhan¹, Jan Boettcher², Lukas Ramsauer², Alexandra Georgieva¹, Fabian Geisler¹, Roland M. Schmid¹, Junika Pohl¹.
¹University Hospital rechts der Isar, School of Medicine, Technical University of Munich (TUM), Department of Internal Medicine II, München, Germany; ²University Hospital Rechts der Isar, School of Medicine, Technical University of Munich, Institute of Molecular Immunology and Experimental Oncology, München, Germany
 Email: katrin.boettcher@mri.tum.de

Background and aims: Non-alcoholic fatty liver disease (NAFLD) driven by lipotoxicity and inflammation is becoming the most common chronic liver disease worldwide. Besides promoting pathogenesis, the unique liver microenvironment allows for the development of hepatocellular carcinoma in NAFLD. Here, we aim to decipher novel mechanisms of hepatic immune regulation in NAFLD that could be exploited for therapy. To this end, we analysed how metabolic changes in NAFLD affect the phenotype and effector function of mucosal-associated invariant T (MAIT) cells, innate-like T cells with antimicrobial and anti-cancer potential enriched in the liver.

Method: MAIT cells were isolated from peripheral blood of NAFLD patients or healthy controls and re-stimulated *in vitro* in presence of free fatty acids. MAIT cell phenotype and function was analysed by multi-colour flow cytometry. MAIT cell metabolism was investigated by metabolic flux analysis.

Results: We show that MAIT cell frequency is significantly decreased in peripheral blood of NAFLD patients and that NAFLD MAIT cells express significantly higher levels of activation markers and effector cytokines *ex vivo*, suggesting MAIT cell activation in NAFLD *in vivo*. However, upon *in vitro* restimulation, these activated MAIT cells are dysfunctional and fail to produce effector cytokines, such as IFN gamma, Granzyme B and TNF alpha. Metabolically, MAIT cell effector function was dependent on glycolysis and oxidative phosphorylation, which was unaffected in NAFLD MAIT cells. Culture with distinct fatty acid species characteristic of the NAFLD microenvironment, however, impaired expression of effector cytokines by MAIT cells and induced MAIT cell death. Mechanistically, these effects were mediated by corrupted mitochondrial function and aberrant lipid metabolism.

Conclusion: These results show that MAIT cells are highly activated but dysfunctional in NAFLD and suggest that impairment of MAIT cell effector function is mediated by metabolic signals in the NAFLD microenvironment. Our data unravel a connection between lipotoxicity and immune cell dysfunction in NAFLD which may facilitate the development of therapeutic strategies.

THU181

Multimodal single cell analysis reveals the basis for butyrate induction of TNF α -secreting regulatory T cells

Mo Atif^{1,2,3}, Mustapha Cherai¹, Clara Cretet¹, Melissa Saichi⁴, Lynda Aoudjehane⁵, Baptiste Fouquet¹, Robert Balderas⁶, Filomena Conti^{1,2}, Olivier Scatton^{1,2}, Ye Htun Oo^{3,7}, Guy Gorochoy^{1,2}, Makoto Miyara^{1,2}.
¹University Hospitals Pitié Salpêtrière-Charles Foix, Paris, France; ²Sorbonne Université, Paris, France; ³University of Birmingham, United Kingdom; ⁴Institut Curie Hospital, Paris, France; ⁵Hospital Saint-Antoine Ap-Hp, Paris, France; ⁶BD Biosciences, San Jose, United States; ⁷University Hospitals Birmingham NHS Trust, United Kingdom
 Email: muhammadatif2@gmail.com

Background and aims: Short-chain fatty acids (SCFAs) such as butyrate are increasingly implicated in modulating T cells in the gut and liver. This is particularly relevant for regulatory T (Treg) cells as

POSTER PRESENTATIONS

they play an important role in maintaining homeostasis. However, Treg cells are phenotypically and functionally heterogeneous. In this study, we used multimodal single-cell profiling to delineate the mechanistic basis for the effects of butyrate on Treg cell heterogeneity.

Method: We studied the whole transcriptome and several surface protein markers of approximately 6000 Treg cells. This was combined with experimental studies for biological validation.

Results: We found that butyrate polarised naïve Treg cells into heterogeneous subpopulations with both immunosuppressive and pro-inflammatory subsets. Upon reconstructing the gene regulatory networks, we found an upregulation of the hypoxia, NF- κ B, JAK-STAT, TNF α , and MAPK signalling pathways. We also identified the individual regulons driving them. These findings were subsequently validated experimentally. Strikingly, butyrate increased the secretion of TNF α , IL-2, and IL-17A from the activated Treg cells whilst maintaining their immunosuppressive capacity. We also uncovered the novel capacity of butyrate to acutely inhibit STAT5 and p38.

Conclusion: Collectively, our work demonstrates the basis by which butyrate promotes diverse regulatory and effector cell subpopulations. These mechanisms could be therapeutically targeted to modulate the effects of SCFAs on Treg cells in the gut and liver.

THU182

COVID-19 vaccination in liver cirrhosis: safety and immune and clinical responses

Maria Ines Canha¹, Mario Jorge Silva¹, Maria Azevedo Silva², Mara Costa³, Rita Catarina Saraiva¹, André Ruge², Mariana Machado⁴, Catarina Félix⁵, Bárbara Morão⁶, Pedro Narra Figueiredo³, Milena Mendes¹, Carina Leal², Filipe Calinas¹. ¹Centro Hospitalar Universitário de Lisboa Central, Gastroenterology; ²Centro Hospitalar de Leiria, Gastroenterology; ³Centro Hospitalar Universitário de Coimbra, Gastroenterology; ⁴Hospital de Vila Franca de Xira, Gastroenterology; ⁵Centro Hospitalar de Lisboa Ocidental, Gastroenterology; ⁶Hospital Beatriz Ângelo, Gastroenterology
Email: m.inescanha@gmail.com

Background and aims: Available data regarding safety and efficacy of COVID-19 vaccination in liver cirrhosis patients is lacking. Their dysregulated immune system makes them susceptible to serious disease and to an attenuated response to certain vaccines. Our goal was to study safety, immunological and clinical responses of cirrhotic patients to COVID-19 vaccination and assess their relation to demographic, clinical and vaccine-related factors.

Method: Interim analysis of an ongoing multicentric prospective study in patients with liver cirrhosis eligible for COVID-19 vaccination without prior infection. Demographic data, liver disease severity, comorbidities, medication and adverse events were registered. Patients were requested to assess IgG antibody titers (AbT) for SARS-CoV-2 at 2 weeks (W2), 3 months (M3) and 6 months after completing vaccination. During follow-up, post-vaccination infection and severity were registered. We analyzed the patients who completed the M3 assessment, using Stata[®] 15 and a p < 0.05.

Results: We included 121 patients, 82% males, mean aged 61 years. Alcohol is the most common (61%) cause of cirrhosis. Twenty percent have a Child Pugh score (CPS) of B/C; 42% had at least one decompensation and 68% have portal hypertension (PHT) signs. Seventeen percent of the patients reported adverse reactions after vaccination, none of them serious. Median [Q1; Q3] AbT were 1115 [291; 2080] BAU/ml at W2 and 293 [88; 1190] BAU/ml at M3. Group differences in AbT (using 33.8 and 200 BAU/ml as cut-offs) were assessed in a multivariable logistic regression considering the patients' age, gender, cause of cirrhosis, immunosuppressant drugs, severity of cirrhosis (Table 1), type of vaccine and adverse reactions. Only older age and type of vaccine proved to be associated with lower AbT at W2 and M3. None of the patients was diagnosed with COVID-19 infection during a mean follow-up of 137 days.

	AbT at W2			AbT at M3		
	Median (BAU/ml)	<33.8 BAU/ml* (%)	<200 BAU/ml (%)	Median (BAU/ml)	<33.8 BAU/ml* (%)	<200 BAU/ml (%)
Clinical features						
CPS A	1090	7.7	23.1	265	16.7	40.0
CPS B/C	1600	5.9	17.6	675	7.7	30.7
No PHT	1115	6.7	23.3	279	16.7	43.3
PHT	1135	7.7	21.2	304	14.0	34.8
Compensated disease	1585	8.0	24.0	304	12.7	38.3
Previous decompensation	1085	6.3	18.8	265	19.2	38.5

*Reference laboratory value for negative result.

Conclusion: COVID-19 vaccines in cirrhotics were safe and their clinical and humoral response seem not different from the observed in the general population assessed in clinical trials.

THU183

Building a case for pancreas and liver targeted interleukin-22 therapy in fatty liver disease

Haresh Saji¹, Kuan Yau Wong¹, Alexandra Mueller¹, Sahar Keshvari², Ran Wang¹, Percival Wiid¹, Grant Ramm³, Graeme Macdonald⁴, John Prins⁵, Michael McGuckin⁵, Sumaira Hasnain^{1,6}. ¹Mater Research Institute-The University of Queensland, Immunopathology group, Brisbane, Australia; ²Mater Research Institute-The University of Queensland, Brisbane, Australia; ³QIMR Berghofer Medical Research Institute, Brisbane, Australia; ⁴Princess Alexandra Hospital, Brisbane, Australia; ⁵The University of Melbourne, Melbourne, Australia; ⁶Australian Infectious Diseases Research Centre, Brisbane, Australia
Email: sumaira.hasnain@mater.uq.edu.au

Background and aims: We discovered that the cytokine interleukin-22 (IL-22) is an efficient natural inhibitor of cellular stress and improved insulin quality in pancreatic beta-cells in preclinical models of Type 2 diabetes. Importantly, IL-22 completely restored glucose tolerance, suppressed fasting hyperinsulinaemia/hyperproinsulinaemia, and restored insulin sensitivity in obese animals. Treatment of obese animals with IL-22 also showed significant improvements in circulating triglycerides, liver function (AST:ALT ratio) and a reduction in hepatic lipid accumulation. IL-22 has also been shown to be protective in other models of liver disease including alcoholic hepatitis, acute-on-chronic liver failure, hepatic fibrosis and paracetamol induced liver injury, and there are 3 versions of IL-22 based therapeutics in clinical trials for such pathologies. Interestingly, the IL-22 receptor, IL-22Ra1 is highly expressed in the pancreas and liver. Our study aimed to define the role of endogenous IL-22 in the liver and pancreas to provide additional support for IL-22-therapy in non-alcoholic fatty liver disease (NAFLD).

Method: To study the role of endogenous IL-22 in the pancreas and liver, we generated tissue specific IL-22Ra1 knockout mice lacking the receptor in pancreatic beta-cells (IL-22Ra1^{b-cell} ^{-/-}) and hepatocytes (IL-22Ra1^{Hep} ^{-/-}). We then challenged them with a high fat diet, and measured their glycaemic control, hepatic lipid accumulation, and hepatic markers of cellular stress, lipid, and glucose metabolism.

Results: We found that IL-22Ra1^{Hep} ^{-/-} animals had increased hepatic markers of inflammation and cellular stress. Interestingly, we also observed this phenomenon in IL-22Ra1^{b-cell} ^{-/-} mice. Additionally, IL-22Ra1^{b-cell} ^{-/-} animals also had defective glycaemic control and insulin secretion compared to littermate control animals, which worsened on a high-fat diet. We also found that whilst female animals did not gain as much weight as male animals on a high-fat diet, female IL-22Ra1^{b-cell} ^{-/-} mice had a worsened phenotype compared to males.

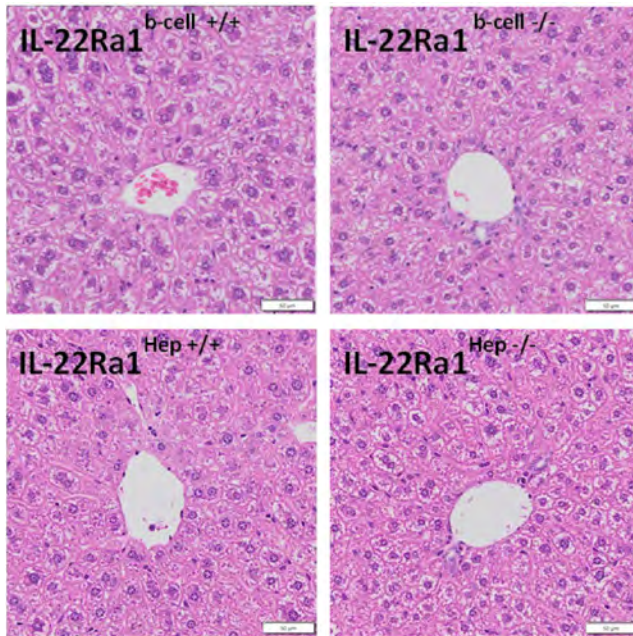


Figure: HandE sections of animal livers at 20 weeks of age

Conclusion: We confirmed the role of endogenous IL-22 in maintaining insulin quality control and healthy hepatic function. We also discovered a novel role for endogenous IL-22 in the pancreatic-beta cell-liver axis and demonstrated the importance of targeting IL-22 to both pancreatic beta-cells and hepatocytes to treat NAFLD.

THU184

Patients with decompensated cirrhosis and liver transplant recipients demonstrate poor humoral and cellular immune response against COVID-19 vaccine

Anand Kulkarni¹, Sasikala Mitnala¹, Sowmya Iyengar¹, Shashidhar Jaggaiahgari¹, Baqar Gora¹, Hardik Rugwani¹, Mithun Sharma¹, Nagaraja Rao Padaki¹, Nageshwar Reddy¹. ¹AIG Hospitals, Hyderabad, India
Email: anandvk90@gmail.com

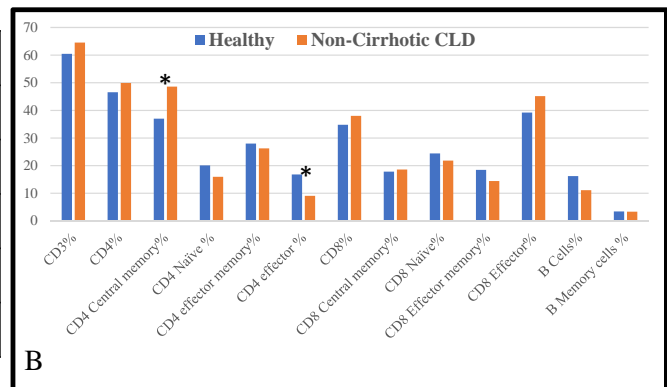
Background and aims: Coronavirus disease-2019 (COVID-19) vaccination is recommended for all patients with chronic liver disease (CLD) and liver transplant recipients (LTR). However, the immunogenicity of COVID-19 vaccines such as ChAdOx1 (vector-based) and BBV152 (inactivated virus) in these immunocompromised patients is unknown. Therefore, we aimed to compare the humoral and cellular immune responses of CLD patients, LTR, and healthy individuals against the available COVID-19 vaccines.

Method: Completely vaccinated (either with ChAdOx1 or BBV152) non-cirrhotic CLD patients (NCCLD), cirrhotic patients, and LTR were compared against age-matched healthy controls (HC) for anti-spike antibody response (by chemiluminescence immunoassay [CLIA] method) and immune profiling of the T and B cells (by flow cytometry). Also, we assessed the number of patients developing breakthrough infections post-vaccination. We excluded patients with renal failure, active sepsis, patients <2 weeks from the last vaccination dose. An individual with antibody levels <15 AU/ml was considered as a non-responder.

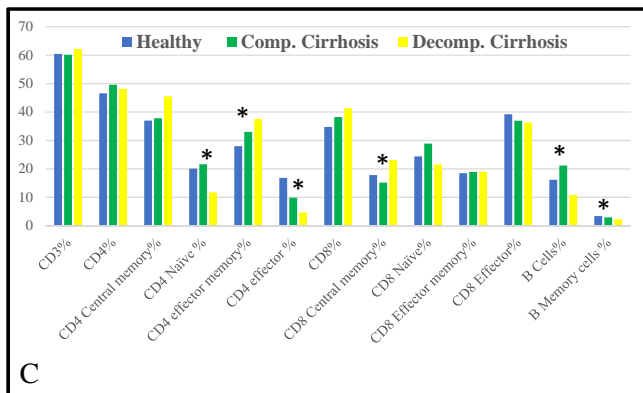
Results: Fifty NCCLD patients, 63 compensated cirrhosis (CC), 50 decompensated cirrhosis (DC) patients, 60 HC, and 17 LTR consented for the study (Fig. A). A similar proportion of patients in NCCLD (16%) and HC (8.3%) were non-responders ($p = 0.21$). CD4 central memory

Groups	Responders
Healthy controls (n = 60)	91.7%
Non-cirrhotic CLD (n = 50)	84%
Compensated cirrhosis (n = 63)	82.5%
Decompensated Cirrhosis (n = 50)	66%
LT recipients (n = 17)	41.2%

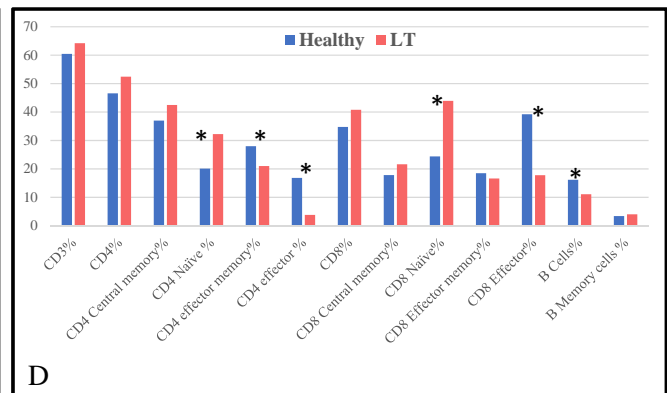
A



B



C



D

* $P < 0.05$

Figure: (abstract: THU184)

POSTER PRESENTATIONS

cells and CD4 effector cells were lower in the NCCLD patients, while the other immune cells were similar in both groups (Fig. B). Non-response was similar between CC (17.5%) and healthy individuals (8.3%; $p = 0.18$). Only CD4 effector cells were lower in CC patients than healthy individuals, while the other immune cells were similar in both groups. A higher proportion of patients in DC group (34%) were non-responders than CC (17.5%; $p = 0.04$) and HC group (8.3%; $p = 0.001$). CD4 naïve cells, CD4 effector cells, B cells, and B memory cells were lower in the DC group. Though the central memory cells were higher in the DC group, they could not differentiate into effector cells (Fig. C). Fifty-nine percent in LT group were non-responders compared to 8.3% in HC group ($p < 0.001$). On immune profiling, CD4 and CD8 naïve cells were higher in the marrow in the LT group, while the CD4 effector memory cells and CD4 and CD8 effector cells were lower in the LT group. Furthermore, B cells were lower in the LT group, suggesting poor antibody response (Fig. D). Breakthrough infections were slightly higher in CC and DC group but non-significant (healthy-3.3%; NCCLD-2%; CC-8%; DC-8%; LTR-5.88%). Except for two patients in the DC group, all breakthrough infections were mild.

Conclusion: Patients with decompensated cirrhosis and liver transplant recipients demonstrate poor humoral and cellular immune response against COVID-19 vaccines. Therefore, decompensated cirrhosis patients and liver transplant recipients require a booster dose of COVID-19 vaccination.

THU185

Presence of cirrhosis in chronic liver disease patients associates with a lower immune response to COVID-19 vaccines-a multicenter european study

André L. Simão¹, Carolina Santos Palma¹, Laura Izquierdo-Sánchez², Antonella Putignano³, Ângela Carvalho-Gomes⁴, Andreas Posch⁵, Paola Zanaga⁶, Irina Girleanu⁷, Carlos Araújo¹, Degré Delphine⁸, Thierry Gustot⁸, Iván Sahuco⁴, Elia Spagnolo⁶, Sofia Carvalhana⁹, Miguel Moura⁹, Mariana Moura Henrique¹, Diogo A. E. Fernandes¹, Francisco Marques¹, Jesus Maria Banales^{2,10,11,12}, Manuel Romero Gomez¹³, Anca Trifan⁷, Francesco Paolo Russo⁶, Rudolf E. Stauber⁵, Marina Berenguer⁴, Christophe Moreno³, João Gonçalves¹, Helena Cortez-Pinto^{9,14}, Rui Castro¹. ¹Research Institute for Medicines (iMed.Ulisboa), Faculty of Pharmacy, Universidade de Lisboa, Lisbon, Portugal; ²Department of Liver and Gastrointestinal Diseases, Biodonostia Health Research Institute, Donostia University Hospital, University of the Basque Country (UPV/EHU), San Sebastian, Spain; ³Department of Gastroenterology, Hepatopancreatology and Digestive Oncology, C.U.B. Hôpital Erasme, Université Libre de Bruxelles, Brussels, Belgium; ⁴Hepatology and Liver Transplantation Unit, La Fe University Hospital, University of Valencia, CIBER-EHD and IIS La Fe, Valencia, Spain; ⁵Department of Internal Medicine, Medical University of Graz, Graz, Austria; ⁶Gastroenterology and Multivisceral Transplant Unit, Department of Surgery, Oncology and Gastroenterology, Azienda Ospedale-Università Padova, Padova, Italy; ⁷"Grigore T. Popa" University of Medicine and Pharmacy, "St. Spiridon" Emergency Hospital, Institute of Gastroenterology and Hepatology, Iasi, Romania; ⁸Institute for Medical Immunology, Erasme Campus, Brussels, Belgium; ⁹Departamento de Gastreenterologia, Centro Hospitalar Universitário Lisboa Norte, Lisbon, Portugal; ¹⁰National Institute for the Study of Liver and Gastrointestinal Diseases, CIBERehd, "Instituto de Salud Carlos III" (ISCIII), Madrid, Spain; ¹¹Department of Biochemistry and Genetics, School of Sciences, University of Navarra, Pamplona, Spain; ¹²Ikerbasque, Basque Foundation for Science, Bilbao, Spain; ¹³Digestive Diseases Department, Virgen del Rocío University Hospital, Institute of Biomedicine of Seville, University of Seville, Seville, Spain; ¹⁴Clínica Universitária de Gastreenterologia, Faculdade de Medicina, Universidade de Lisboa, Lisbon, Portugal
Email: adlsimao@ff.ulisboa.pt

Background and aims: Vaccines in the European Union (EU) to prevent COVID-19 have been shown to be safe and effective in

immunocompetent subjects. Nonetheless, studies in patients with chronic liver disease (CLD) are lacking. Our aim was to assess the humoral immune response of two-dose COVID-19 vaccines among CLD patients of different etiologies and identify predictors of "low" versus "high" humoral response.

Method: Patients were recruited from clinical centers in 6 EU countries, as part of a large consortium study. Serum levels of IgG, IgM (nM) and neutralizing antibodies (NA, %) against the SARS-CoV-2 spike S1 protein were determined in samples collected prior to vaccination (T0) and at least 14 days after the second vaccination dose (T2). Patients (n = 195) were divided into "low" (51.4%) or "high" (48.6%) responders according to their IgG antibodies at T2, using 419 nM (median) as the cut-off value. Logistic regression analysis was used to explore features associated with the vaccine-induced IgG levels.

Results: All patients were fully vaccinated with either BNT162b2 (68%), mRNA-1273 (21.5%) or ChAdOx1 (10.5%). Their median age was 58 (range 21–85); 57.4% were male. Underlying liver disease etiology included alcohol (28.7%), NAFLD (21%), HCV (29.2%) and HBV (16.9%), among others. 61.5% presented with cirrhosis. At T0, spike S1 IgG, IgM and NA levels were 0.76 (95% confidence interval (CI), 0.42–1.10), 0.37 (95% CI, 0.30–0.45) and 22.99 (95% CI, 21.39–24.58), respectively, increasing to 446.07 (95% CI, 400.60–491.53), 3.91 (95% CI, 2.20–5.62) and 78.88 (95% CI, 74.91–82.85) at T2 ($p < 0.0001$ for all). In addition, IgG and NA levels showed a high positive correlation. Age [odds ratio (OR) 1.06 (1.03–1.10)], alcohol [OR 2.25 (1.15–4.41)], metabolic drugs [OR 2.30 (1.20–4.43)], hepatocellular carcinoma [OR 5.41 (1.15–25.52)] and evidence of cirrhosis [OR 3.85 (1.95–7.61)], as well as type of vaccine, predicted "low" response. In multivariable analysis, cirrhosis and type of vaccine (ChAdOx1 >BNT162b2 >mRNA-1273) remained the only independent predictors of "low" response.

Conclusion: CLD patients with cirrhosis exhibit lower immune responses to COVID-19 vaccination, irrespective of disease etiology. Further, the type of administered vaccine appears to predict levels of humoral response, although this needs validation in larger cohorts with a more balanced representation of all vaccines.

THU186

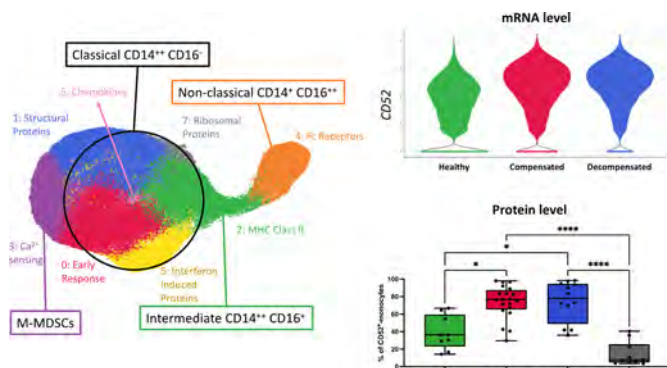
Heterogeneity of peripheral blood monocytes in patients with cirrhosis

Anne Geng¹, Robert G Brenig^{1,2}, Mechthild Lütge³, Julien Roux⁴, Hung-Wei Cheng³, Patrizia Kuenzler⁵, David Semela², Markus Heim^{6,7}, Burkhard Ludewig³, Christine Bernsmeier^{1,7}. ¹University Hospital of Basel, Department of Biomedicine, Translational Hepatology, Basel, Switzerland; ²Division of Gastroenterology and Hepatology, Cantonal Hospital St. Gallen, Liver Biology Laboratory, St. Gallen, Switzerland; ³Cantonal Hospital St. Gallen, Institute of Immunobiology, St. Gallen, Switzerland; ⁴University Hospital Basel, Department of Biomedicine, Bioinformatics Core Facility, Basel, Switzerland; ⁵Cantonal Hospital St. Gallen, Division Gastroenterology and Hepatology, St. Gallen, Switzerland; ⁶University Hospital of Basel, Department of Biomedicine, Hepatology, Basel, Switzerland; ⁷Clarunis, University Center for Gastrointestinal and Liver Disease, Basel, Switzerland
Email: anne.geng@unibas.ch

Background and aims: In patients with cirrhosis, we recently discovered dysfunctional monocytes (M-MDSC, CD14⁺HLA-DR⁺AXL⁺, CD14⁺MERTK⁺) prevailing over regular monocytes, which were associated with reduced capacity to repel microbial challenge and infection susceptibility. Transcriptome wide single cell RNA sequencing (scRNA-seq) is expected to further enhance the understanding of the plasticity of immune cell differentiation processes in disease conditions. We aimed to systematically dissect the stage specific heterogeneity of circulating monocytes using scRNA-seq in cirrhosis with the intention to identify potential future immunotherapeutic targets.

Method: Monocytes (20.000 cells/sample) from compensated (CC, n=5), decompensated (DC, n=5) cirrhosis patients and healthy controls (HC, n=5) were prepared for scRNA-seq (10x Genomics) and analysed (>4000 cells/sample) using R/Bioconductor. Flow cytometric analyses were used to confirm transcriptional findings on a translational level and to further evaluate the function of distinct monocytes.

Results: Our scRNA-seq data was grouped into eight monocyte clusters, based on the expression of specific genes, of which five clusters were annotated to classical (CD14⁺CD16⁻), one cluster to intermediate (CD14⁺CD16⁺) and one cluster to non-classical (CD14⁺CD16⁺) monocyte subsets. One cluster showed a M-MDSC-like gene expression. CD14⁺CD16⁺-like monocytes were reduced in CC and DC patients, while M-MDSC-like monocytes were increased and gene expression of MHC class II members was downregulated compared to healthy controls. Differentially expressed (DE) gene analysis revealed upregulation of *Cd52*, a T cell suppressor and inhibitor of TLR-signaling, in monocytes from CC/DC compared to HC. Upregulation of *CD52* on monocytes was confirmed on translational level in CC/DC patients, but not detected on monocytes of patients with acute decompensation (AD) or acute-on-chronic liver failure (ACLF). *CD52*-expressing monocytes exhibited higher levels of *CD16*, *HLA-DR*, *AXL* and *CD206*, showed higher phagocytosis capacity and increased cytokine production (TNF- α , IL-6 and IL-10) upon microbial challenge (TLR4/TLR2 agonism). T cells co-cultured with monocytes with high proportion of *CD52* expression (>60%) from cirrhosis patients showed reduced proliferation activity compared to T cells co-cultured with monocytes from healthy donors with lower *CD52* expression (<40% of monocytes).



Conclusion: Using scRNA Seq we have identified eight circulating monocyte clusters with distinct prevalence between HC and CC/DC. DE gene analysis highlighted plasticity of *CD52* expression on monocytes during disease evolution of cirrhosis.

THU187

JAM-A is a multifaceted regulator in hepatic fibrogenesis, supporting LSEC integrity and stellate cell quiescence

Jonathan Frederik Brozat¹, Elisa Brandt¹, Myriam Stark¹, Petra Fischer¹, Theresa Hildegard Wirtz¹, Alexander Flašhove¹, Aaron Nikolai Rodenhausen¹, Tanja Vajen², Alexandra C.A. Heinzmann³, Sophia M. Schmitz⁴, Samira Abu Jhaisha¹, Anjali A. Röth⁴, Rory R. Koenen³, Hacer Sahin¹, Christian Trautwein¹, Marie-Luise Berres¹. ¹University Hospital RWTH Aachen, Department of Gastroenterology, Digestive Diseases and Medical Intensive Care, Internal Medicine III, Aachen, Germany; ²Heinrich-Heine-University, Cardiovascular Research Laboratory, Division of Cardiology, Pulmonology and Vascular Medicine, Medical Faculty, Düsseldorf, Germany; ³Maastricht University, Department of Biochemistry, Cardiovascular Research Institute Maastricht, Maastricht, Netherlands; ⁴University Hospital RWTH Aachen, Department of

General, Visceral and Transplantation Surgery, Aachen, Germany
Email: jbrozat@ukaachen.de

Background and aims: Leukocyte extravasation is a hallmark of hepatic inflammation. Reduced shear stress within hepatic sinusoids and the specific phenotype of liver sinusoidal endothelial cells (LSEC) cumulate in differing adhesion characteristics during liver fibrosis. The Junctional Adhesion Molecule A (JAM-A) is a crucial regulator of leukocyte extravasation and upregulated in human viral fibrosis. The aim of this study was to define the functional role of cell-specific surface JAM-A during hepatic fibrogenesis, applying distinct knock-out strategies in a murine model.

Method: Complete, conditional intestinal epithelial, conditional endothelial and bone marrow chimeric *Jam-a* knockout animals (C57Bl/6) were treated with carbon tetrachloride (CCl₄, 6 weeks). Livers were investigated by qRT-PCR, Western blotting, immunohistochemistry, immunofluorescent stainings and flow cytometry. The functional relevance of JAM-A was assessed using co-culture models and flow-based adhesion assays.

Results: Complete and bone-marrow derived *Jam-a* knockout animals showed aggravated fibrosis with increased non-sinusoidal, perivascular accumulation of CD11b⁺F4/80⁺ monocyte-derived macrophages in contrast to wild type mice. Despite being associated with disturbed epithelial barrier function, an intestinal epithelial *Jam-a* knockout did not affect fibrogenesis. In endothelial-specific *Jam-a* knockout animals, liver fibrosis was aggravated alongside CD31-sinusoid capillarization and hepatic stellate cell (HSC) activation. Here, leukocyte infiltration and adhesion to LSECs remained unaffected.

Conclusion: Our models decipher cell-specific JAM-A to exert crucial functions during hepatic fibrogenesis. JAM-A on bone marrow-derived cells regulates non-sinusoidal vascular immune cell adhesion and recruitment, while endothelial JAM-A controls liver sinusoid capillarization and LSEC-linked HSC quiescence.

THU188

Diminished function of cytotoxic T- and NK- cells in severe alcohol-associated hepatitis

Adam Kim¹, Christina Cajigas-Du Ross¹, David Streem², Nicole Welch¹, Jaividhya Dasarathy³, Srinivasan Dasarathy¹, Laura Nagy⁴. ¹Cleveland Clinic, Inflammation and Immunity, Cleveland, United States; ²Cleveland Clinic, Lutheran Hospital, United States; ³MetroHealth; ⁴Cleveland Clinic, Inflammation and Immunity, Cleveland, United States
Email: kima7@ccf.org

Background and aims: Severe Alcohol-associated Hepatitis (sAH) is characterized by inflammation and infiltration of immune cells into the liver. Peripheral monocytes are a major infiltrating cell type that can exacerbate inflammation and damage to the liver. sAH patients have a higher peripheral leukocyte count and an increased proportion of inflammatory monocytes. Even though there are more monocytes, sAH patients are often extremely susceptible to infections. Cytotoxic NK-cells and CD8 T-cells play an important immunological role in triggering apoptosis in infected cells, particularly monocytes. Cytotoxic cells secrete cytotoxic granules containing granzymes, perforin, and in humans, granulysin, to kill cells. We hypothesize that in sAH, cytotoxic cells are dysfunctional and unable to trigger cell death in target cells.

Method: We performed single-cell RNA-seq (scRNA-seq) in PBMCs collected from patients with sAH (n=4) and healthy controls (HC, n=4). Multi-panel intracellular flow cytometry was conducted to understand changes in cell proportion, correlated gene expression, and cytotoxic granule contents in NK-cells and CD8 T-cells in PBMCs from patients with sAH (n=9) and HC (n=7), as well as patients with moderate AH (mAH, n=6), heavy drinkers (HD, n=8), alcohol-associated cirrhosis (AC, n=8), and non-alcohol-associated steatohepatitis (NASH, n=8).

Results: scRNA-seq revealed receptors required for cytotoxic cell recognition of activated monocytes were downregulated in all

POSTER PRESENTATIONS

peripheral immune cells in patients with sAH. Additionally, granulysin was the most downregulated gene in both NK cells and effector CD8 T-cells. In cells from HC, expression of granulysin, perforin, and granzymes A and B was highly correlated, but in sAH these genes lost coordination, indicative of dysfunctional cytotoxic granule formation. Using flow cytometry, we observed a severe decrease in perforin and granzyme B expression in sAH patients. Interestingly, NK cells from patients with mAH, HD, AC, and NASH were not deficient in cytotoxic granules, but perforin and granzyme B were lower in CD8 T-cells from HD and AC.

Conclusion: Cytotoxic cells from sAH patients are deficient in cytotoxic granules, likely impairing their ability to kill target cells. While sAH patients had both dysfunctional NK-cells and CD8 T-cells, patients with HD and AC also had dysfunctional CD8 T-cells. Loss of cell-cell recognition receptors in both cytotoxic cells and monocytes is indicative of a loss of cell-cell communication and a possible mechanism for increased inflammatory monocytes in sAH. Together, these results indicate a loss of cytotoxic cell function in sAH, which might contribute to increased numbers of inflammatory monocytes and a decreased ability to kill infected cells.

THU189

Multi-omics analysis of human livers reveals variation in intrahepatic inflammation across chronic hepatitis B infection phases

Noé Axel Montanari¹, Ricardo Ramirez², Abhishek Aggarwal², Nicholas Van Buuren², Michael Doukas¹, Christina Moon², Scott Turner², Lauri Diehl², Li Li², Jose Debes¹, Becket Feierbach², Andre Boonstra¹. ¹Erasmus MC; ²Gilead Sciences
Email: boonstra.andre@gmail.com

Background and aims: Chronic HBV is clinically defined in 4 phases by a combination of serum HBV DNA levels, HBeAg status and ALT: immunotolerant (IT), immune-active (IA), inactive carrier (IC) and HBeAg-negative hepatitis (ENEG). Immune and virological differences between phases, as detected in blood, have proven useful but do not fully explain the interrelation between the clinical phenotype and the immunological mechanism in the liver. We aimed to study the intrahepatic immune profile across the clinical phases in order to better understand the immunological mechanism of HBV.

Method: Immunological composition and transcriptional profiles of FFPE core needle liver biopsies in chronic HBV phases vs healthy were evaluated by multiplex immunofluorescence and RNA-Seq (n = 37 and 78, respectively).

Results: Irrespective of the phase-specific serological profiles, increased intrahepatic immune-gene expression and frequency were observed in chronic HBV compared to healthy control livers. Greater transcriptomic de-regulation was seen in IA and ENEG (172 vs 243 DEGs) than in IT and IC (13 vs 35 DEGs) livers. ISG, immune-activation and exhaustion genes (ICOS, CTLA4, PDCD1) together with chemokine genes (CXCL10, CXCL9) were significantly induced in IA and ENEG livers. Moreover, distinct immune profiles associated with ALT elevation, and a more accentuated immune-exhaustion profile (CTLA4, TOX, SLAMF6, FOXP3) found in ENEG and set it apart from IA phase (LGALS9, PDCD1). Interestingly, all HBV phases showed downregulation of metabolic pathways vs healthy livers (fatty acid and bile acid metabolism). Finally, we found increased leukocyte infiltrate correlated with serum ALT, but not with HBV DNA or viral proteins.

Conclusion: Our comprehensive multi-omics analysis of human livers revealed distinct inflammatory profiles and pronounced differences in intrahepatic gene profiles across all chronic HBV phases in comparison to healthy liver.

THU190

Liver cirrhosis and cirrhosis etiology impacts the circulating immune mediators of early stage hepatocellular carcinoma

Boris Beudeker¹, Anthony Grooshuismink¹, Annemiek Van der Eijk², Jose Debes¹, Andre Boonstra¹. ¹Erasmus MC, Gastroenterology and hepatology, Rotterdam, Netherlands; ²Erasmus MC, Viroscience, Rotterdam, Netherlands
Email: borisbeudeker@live.nl

Background and aims: Novel blood biomarkers to predict and detect curable, early stage hepatocellular carcinoma (HCC) is the most effective strategy to improve survival of HCC patients. Others and we have recently published on the applicability of serum immune proteins as early HCC biomarkers, but these studies had limited reproducibility. We now study in detail the contribution of the cirrhotic stage and disease etiology on the circulating immune response, in order to increase the diagnostic robustness of an early HCC immune signature.

Method: A retrospective cohort of 1585 patients with pathology- or radiology-proven HCC was established of patients diagnosed at our large tertiary HCC referral center, among them were 522 (33%) with BCLC 0/A stage HCC. Immune profiles of a balanced cohort of 188 cirrhotic patients, and 195 early HCC patients with hepatitis B (HBV), hepatitis C (HCV), ALD alcoholic liver disease (ALD) or non-alcoholic liver disease (NAFLD) were determined through serum multiplex profiling.

Results: We show that liver cirrhosis had a profound effect on the levels of circulating immune proteins with significant dysregulation of 24 out of 59 serum immune mediators. Stratification of cirrhosis patients in groups with distinct etiologies identified 45 significant immune mediators and heat map revealed obviously distinct immune profiles in each etiology. HBV-cirrhosis was characterized by high levels of circulating TRAIL and IFN-gamma, HCV-cirrhosis by high levels of IP-10 and the immune profiles of ALD-cirrhosis; NAFLD-cirrhosis were more comparable with higher levels of IL-8, IL-6, CCL25 and LIF.

Eight immunological mediators were significant independent predictors of early stage HCC and displayed specificity for one of the four cirrhosis etiologies. These immune mediators improved existing tumors marker efficacy and when combined with AFP detected early stage HCC with an AUC of 0.80.

Conclusion: HCC develops in an inflammatory heterogenous background. In our search for predictive HCC markers, we found that liver cirrhosis and cirrhosis etiology had a profound impact on the circulating immune response and associated with a wide repertoire of pro-inflammatory and HCC promoting immune mediators. Moreover, we identified Immunological markers that differentiated early stage HCC from cirrhosis. Strict stratification resulted in a set of immune mediators with good sensitivity for early stage HCC of different etiologies.

THU191

Ebola virus infection promotes reduced gene expression of antigen presentation molecules in hepatic CD68+ macrophages in cynomolgus macaques

Timothy Wanninger^{1,2}, Omar Saldarriaga¹, Daniel Millian¹, Jason Comer², Kamil Khanipov³, George Golovko³, Slobodan Paessler¹, Heather Stevenson¹. ¹University of Texas medical branch, Pathology, United States; ²University of Texas medical branch, Microbiology and immunology, United States; ³University of Texas medical branch, Pharmacology and toxicology, United States
Email: tiwannin@utmb.edu

Background and aims: Ebola virus (EBOV) is an emerging infectious disease found in West Africa, with the potential for case importation to other countries. Antigen presenting cells, including macrophages, are among the first cells infected following EBOV exposure. As a result, the liver, a macrophage-laden organ, is a key participant in EBOV infection. While the inflammatory contributions of

macrophages have been characterized *in vitro* or *ex vivo*, studying these cells within their tissue context is essential for understanding disease progression.

Method: We compared formalin-fixed, paraffin-embedded liver tissue from uninfected control and terminal EBOV-infected cynomolgus macaques. We characterized region-specific whole transcriptome expression in these tissues using GeoMx Digital Spatial Profiling (NanoString). Biological processes enriched or depleted in infection were identified using gene set analysis (Global Test) and Ingenuity Pathway Analysis (Qiagen). Macrophage (CD68+) accumulation in liver tissue was quantified by immunofluorescence image analysis using QuPath digital pathology software.

Results: Ebola virus infection was associated with increased CD68+ macrophage accumulation in the liver. Gene set analysis revealed altered immune, coagulation, metabolism, apoptosis, and tissue remodeling processes. Within the altered immune processes, key down-regulated genes included multiple MHC-II alleles (HLA-DPA1, HLA-DQB1, HLA-DRA, HLA-DRB1), CD74, and LGMN. In CD68+ macrophages, these down-regulations were associated with antigen presentation, monocyte/macrophage differentiation, as well as T cell differentiation, activation, and cytotoxicity gene sets.

Conclusion: Down-regulated MHC-II-related gene expression by hepatic CD68+ macrophages may reduce T cell activation in EBOV-infected cynomolgus macaques. Such impairment, identified by *in situ* regional transcriptomic analysis, may synergize with the known disruption of dendritic cell-mediated antigen presentation in this disease, further compromising the adaptive immune response to EBOV infection.

THU192

Plasmalemma vesicle-associated protein expression is driven by senescent cell-endothelial crosstalk and shapes the immune landscape in chronic liver disease

Alex Wilkinson¹, Daniel Patten¹, Sam Hulme¹, Matthew Hoare², Shishir Shetty¹. ¹University of Birmingham, Institute of Immunology and Immunotherapy, United Kingdom; ²University of Cambridge, Department of Medicine, United Kingdom
Email: axw717@student.bham.ac.uk

Background and aims: Chronic liver diseases (CLDs) are driven by leukocyte recruitment and persistent inflammation. Cellular senescence is a key feature of CLD, yet its contribution to liver inflammation is poorly understood. Senescent cells release a secretome (senescence-associated secretory phenotype or SASP) which facilitates their clearance through leukocyte recruitment. This process is mediated by hepatic sinusoidal endothelial cells (HSEC) which undergo phenotypic and functional changes in response to SASP treatment. Plasmalemma vesicle-associated protein (PLVAP) is highly expressed by foetal liver endothelium, playing an important developmental role, yet human single-cell studies have highlighted its re-emergence in liver cirrhosis and hepatocellular carcinoma (HCC). Whilst PLVAP has previously been proposed as a leukocyte trafficking molecule, its specific role in hepatic leukocyte recruitment is not known. We hypothesised that PLVAP expression is driven by the senescent tissue microenvironment in CLD and sought to investigate its potential role in SASP-mediated leukocyte recruitment.

Method: PLVAP expression was characterised, in human liver samples by qPCR and immunohistochemistry, and in primary human HSEC by immunocytochemistry. SASP was obtained using a model of oncogene-induced senescence (conditioned media from RAS-senescent IMR90 fibroblasts-RAS-CM), and the effects of SASP treatment on primary HSEC were determined by qPCR and confocal microscopy. To investigate the molecular mechanisms of SASP-mediated

leukocyte recruitment, flow-adhesion assays were performed with SASP-stimulated HSEC (following siRNA or antibody treatment) and peripheral blood lymphocytes or monocytes.

Results: PLVAP was significantly upregulated in liver endothelium of CLD and HCC patients compared to healthy controls, correlating with increased expression of senescent markers, p21 and p16. Treatment of primary HSEC with RAS-CM significantly increased PLVAP expression and stimulated recruitment of both lymphocytes and monocytes under physiologically low shear stress. However, these processes were morphologically and molecularly distinct. Lymphocytes predominantly (~60%) transmigrate via the transcellular pathway which was selectively inhibited by ICAM-1 blockade. In contrast, >90% monocytes transmigrate paracellularly in a CD31-dependent manner. Furthermore, genetic or antibody-mediated inhibition of PLVAP selectively impaired SASP-mediated monocyte transmigration whilst having no effect on lymphocyte recruitment.

Conclusion: These data highlight a previously unreported link between PLVAP and senescence, in which PLVAP expression is driven in HSEC by the senescent secretome to facilitate monocyte recruitment. PLVAP could therefore be a novel target for perturbing aberrant monocyte recruitment in liver disease.

THU193

Dysfunctional liver-resident CXCR6+ CD8 T cells during persistent viral liver infection

Miriam Bosch¹, Nina Kallin¹, Donakonda Sainitin¹, Hannah Wintersteller¹, Ulrike Protzer^{2,3}, Dirk Wöhleber¹, Percy A. Knolle^{1,4}. ¹Institute of Molecular Immunology, Technical University of Munich, Munich, Germany; ²Institute of Virology, Technical University of Munich; ³Institute of Virology, Helmholtz Center for Environment and Health; ⁴German Center for Infection Research, Munich
Email: percy.knolle@tum.de

Background and aims: CD8 T cell-mediated immunity is key for the clearance of hepatitis B virus infection and other hepatotropic viral infections. Persistent viral liver infections, however, are characterized by a lack of a robust anti-viral CD8 T cell response. We aimed at determining the mechanism causing the lack of CD8 T cell functionality during persistent viral liver infection.

Method: We used Adenovirus-based models (coding for ovalbumin or the HBV genome) to investigate persistent or acute-resolved infection. For virus-specific T cell analysis, we transferred naïve (CD44^{neg}CD62L^{hi}) virus-specific CD8 T cells bearing a congenic marker before infection. T cells were analyzed at different time points for phenotypic and functional characterization and RNAseq.

Results: After acute-resolved viral infection, we identified two distinct virus-specific CD8 T cell populations in the liver, i.e. CX₃CR1⁺ and CXCR6⁺CD69⁺ CD8 T cells. Contrastingly, virus-specific CD8 T cells during persistent infection were mainly CXCR6⁺CD69⁺ liver-resident CD8 T cells. Independent of infection outcome, liver CXCR6⁺CD69⁺ CD8 T cells expressed a tissue-residency gene signature. However, virus-specific CXCR6⁺CD69⁺ CD8 T cells during persistent infection did not produce cytokines, lacked cytotoxicity, and were hence termed dysfunctional liver-resident T cells. Transcriptome analysis enabled us to define a single pathway marking these dysfunctional CXCR6⁺CD69⁺ T cells in persistent infection when compared to cytotoxic liver-resident memory T cells after resolved infection.

Conclusion: The identification of a single transcription factor distinguishing effector liver-resident memory T cells from dysfunctional tolerized virus-specific liver-resident CD8 T cells in preclinical models of persistent expression of ovalbumin and HBV points towards a liver-specific mechanism mediating immune tolerance during persistent hepatocyte infection.

POSTER PRESENTATIONS

THU194

Fate of HDV-specific CD8⁺ T cells during bulevirtide monotherapy in patients with chronic hepatitis delta

Valerie Oberhardt¹, Elisabetta Degasperi², Marta Borghi², Kathrin Heim¹, Roberta Soffredini², Alessandro Loglio², Özlem Sogukpinar¹, Frances Winkler¹, Bertram Bengsch¹, Maike Hofmann¹, Robert Thimme¹, Pietro Lampertico^{2,3}, Christoph Neumann-Haefelin¹. ¹Medical Center-University of Freiburg, Department of Medicine II, Freiburg, Germany; ²Foundation IRCCS Ca' Granda Ospedale Maggiore Policlinico, Milan, Italy; ³CRC "A. M. and A. Migliavacca" Center for Liver Disease, Department of Pathophysiology and Transplantation, Milan, Italy
Email: valerie.oberhardt@uniklinik-freiburg.de

Background and aims: The viral entry-inhibitor bulevirtide (BLV) leads to a decline of HDV viremia in chronic HDV infection, however, treatment for several years is likely required to prevent relapse. Sustained treatment response may be fostered by therapy-induced restoration of HDV-specific CD8⁺ T cell responses that are exhausted due to high viremia and antigen loads during chronic HDV infection. We thus studied the effect of BLV monotherapy on HDV-specific CD8⁺ T cell repertoire, phenotype, and functionality.

Method: HDV-specific CD8⁺ T cell responses were studied in 35 HDV infected patients, of whom 14 cirrhotic patients started treatment with BLV. Samples were collected from baseline up to 40 weeks on-treatment. HDV-specific CD8⁺ T cells were analyzed either upon stimulation with overlapping peptides (olp), spanning the entire L-HDAg (51 olps, 15mers) or upon stimulation with optimal epitopes in HLA-matched patients, following 14 days of *in vitro* culture. *Ex vivo* high-dimensional flow cytometry analysis of peptide-loaded MHC class I-specific CD8⁺ T cells in selected patients throughout therapy is currently ongoing.

Results: In two-thirds of patients, an HDV-specific CD8⁺ T cell response was detectable at baseline. This was characterized by interferon (IFN) γ and tumor necrosis factor (TNF) co-secretion, without additional interleukin (IL)-2 production in response to optimal epitope stimulation in HLA matched patients. Targeted epitopes were restricted by HLA-B alleles only, predominantly by HLA-B*35 and HLA-B*18. Direct comparison of patient samples from an early time point during therapy (week 4) with a later time point during treatment (week 36–40) did not indicate a restoration or boosting of HDV-specific CD8⁺ T cell functionality coinciding with decreasing HDV viremia. Using the comprehensive olps approach, half of the patients displayed an HDV-specific CD8⁺ T cell response at the late time point during treatment (median of 2 olps recognized per patient), which is comparable with the response-rate in untreated patients.

Conclusion: During the first 40 weeks of BLV treatment, no obvious increase in HDV-specific CD8⁺ T cell response breadth and magnitude was observed. This might be due to the slow decline of HDV viremia, the fact that all patients treated with BLV had liver cirrhosis, and mostly unchanged HBsAg levels during BLV monotherapy that may continue to mediate HDV-specific CD8⁺ T cell exhaustion. In addition, some of the HDV-specific CD8⁺ T cell responses target epitopes affected by viral escape mutations and these responses are unlikely to benefit from reduction of viremia. Longer follow-up during continued BLV therapy, high-dimensional analysis of CD8⁺ T cell phenotype and function, as well as analysis of patients with BLV/pegIFN combination therapy will expand our understanding of HDV-specific CD8⁺ T cell restoration during BLV therapy.

THU195

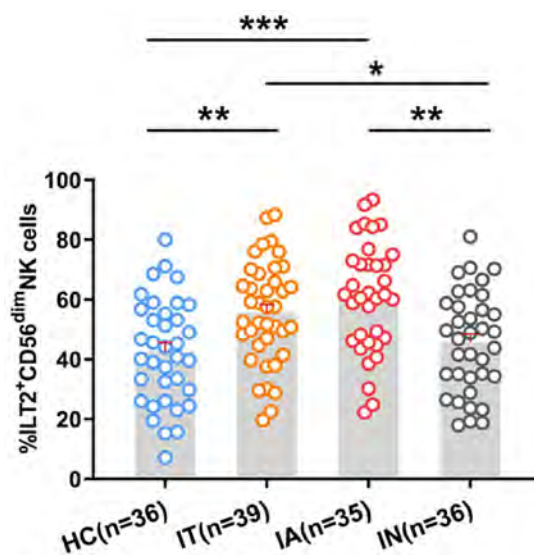
Increased ILT2 expression contributes to dysfunction of CD56^{dim}CD16⁺NK cells in chronic hepatitis B virus infection

Wenwei Yin¹, Yingzhi Zhang¹, Hong Ren¹. ¹Institute for Viral Hepatitis, Department of Infectious Diseases, Chongqing, China
Email: yww@cqmu.edu.cn

Background and aims: Natural killer (NK) cells play a crucial role in the control of human viral infections but their activity is significantly impaired in patients infected with chronic hepatitis B (CHB). The mechanism that contributes to NK cell dysfunction in CHB needs further elucidation.

Method: In this study, we analyzed the expression and function of the novel inhibitory receptor immunoglobulin-like transcript-2 (ILT2) on NK cells from 110 CHB patients and 36 healthy controls.

Results: We observed ILT2 expression on circulating CD56^{dim}CD16⁺NK cells was increased in immune-tolerant and active CHB patients compared with inactive carriers and controls. The frequency of ILT2⁺CD56^{dim}NK cells was positively correlated with serum viral load in immune-tolerant patients. The percentage of ILT2⁺CD56^{dim}NK cells decreased along with HBV load in active CHB patients that received antiviral therapy. Functional analysis showed that ILT2⁺CD56^{dim}NK cells in CHB patients had significantly reduced degranulation and IFN- γ production. Up-regulation of ILT2 was associated with high levels of apoptosis in CD56^{dim}CD16⁺NK cells from CHB patients. ILT2 blockade was shown to increase CD107a expression and cytotoxicity of CD56^{dim}NK cells in CHB patients. Finally, ILT2 was found to be up-regulated by TGF- β 1, which was increased in immune-tolerant and active CHB patients.



Conclusion: Our findings imply that high ILT2 expression would facilitate HBV viral persistence by tempering NK cells into silence and blockade of ILT2 can enhance NK cell function as an alternative approach to treat CHB.

THU196

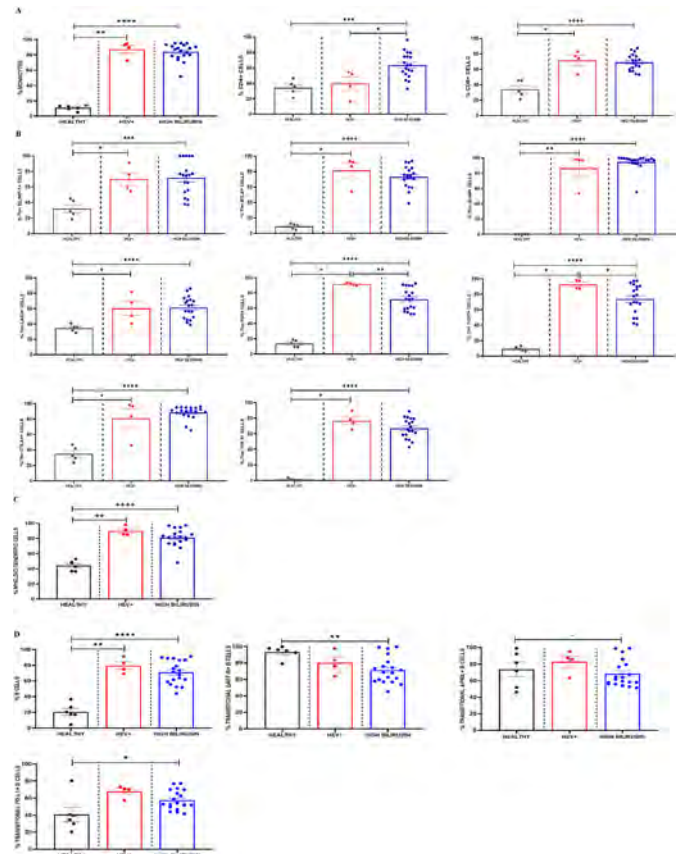
Elevated serum bilirubin levels and aminotransferases are associated with immuno-modulatory and suppressive subsets in pregnant females with intrahepatic cholestasis and hepatitis E virus infection

Anoushka Saxena¹, Minal Kashyap², Prabhjyoti Pahwa¹, Fatima Ali¹, Hamda Siddiqui¹, E. Preedia Babu¹, Y.M. Mala², Shakun Tyagi², Nirupma Trehanpati¹. ¹Institute of Liver and Biliary Sciences, New Delhi, India, Department of Molecular and Cellular Medicine, New Delhi, India; ²Maulana Azad Medical College, New Delhi, India, Department of Obstetrics and Gynaecology, New Delhi, India
Email: trehanpati@gmail.com

Background and aims: Elevated serum bilirubin levels and liver functions are well-recognized markers of hepatic damage and inflammation. Viral hepatitis, intrahepatic cholestasis of pregnancy, gallstones and pre-eclampsia are the most common causes of jaundice in pregnant women, inducing significant morbidity and mortality in both pregnant women and their infants. Therefore, we aimed to investigate the relationship between deranged liver function, high bilirubin and the immune dysfunction during pregnancy.

Method: An observational prospective study was carried out at a tertiary care hospital on antenatal patients with clinical and biochemical jaundice over a period of one year. Peripheral immune cell subsets were analyzed in pregnant women with serum bilirubin >2.0 mg/dl (Gr.1, n=20, 25.8±2), positive for IgM/IgG Hepatitis E virus (AVH-E) (Gr.2, n=5, 24±2) and healthy pregnant women (Gr.3, n=7, 24.5±2) by flow cytometry.

Results: Females with high bilirubin levels; 2–5 mg/dl (64%), 5–10 mg/dl (16%), >10 mg/dl (12%) had deranged LFT (28%), asymptomatic (12%), jaundice (31%), k/c/o liver disease (3%), k/c/o hepatitis-E (3%) and 6% presented with other complaints. Pregnant females with high bilirubin levels showed an overall increased percentage of Monocytes (p=0.0012), CD4+ (p=0.0009) and CD8+ T-cells (p<0.0001), compared to healthy (Fig. A). However, an increased expression of inhibitory markers (Fig. B); PD-1 (p<0.0001), CTLA-4 (p<0.0001), BTLA (p<0.0001), BLIMP-1 (p=0.0008), SLAMF1 (p<0.0001), LAG-3 (p<0.0001), TIGIT (p<0.0001), TIM-3 (p<0.0001) on Transitional memory subset and PD-1 (p<0.0001), CTLA-4 (p<0.0001), BTLA (p<0.0001), BLIMP-1 (p=0.0006), SLAMF1 (p<0.0001), LAG-3 (p<0.0001), TIGIT (p<0.0001), TIM-3 (p<0.0001) on effector memory subset of T-cells was evident. Compared to healthy, myeloid dendritic cell population was significantly higher (Fig. C) in females with high bilirubin (p<0.0001) and infected with HEV (p=0.0095), as compared to healthy females, indicating immune suppression. An elevated frequency of B-cell subsets (p<0.0001) was observed in all females with high bilirubin. Yet, a defect in activation and proliferation as suggested by diminished expression of BAFF-R (p=0.04) and APRIL (p=0.02) and rise in PDL1 (p=0.0025) was determined (Fig. D).



Conclusion: Our results clearly indicate that pregnant females with high bilirubin, including those infected with HEV exhibit increased suppressive T and B cells with diminished BAFFR/APRIL expressing B cells.

THU197

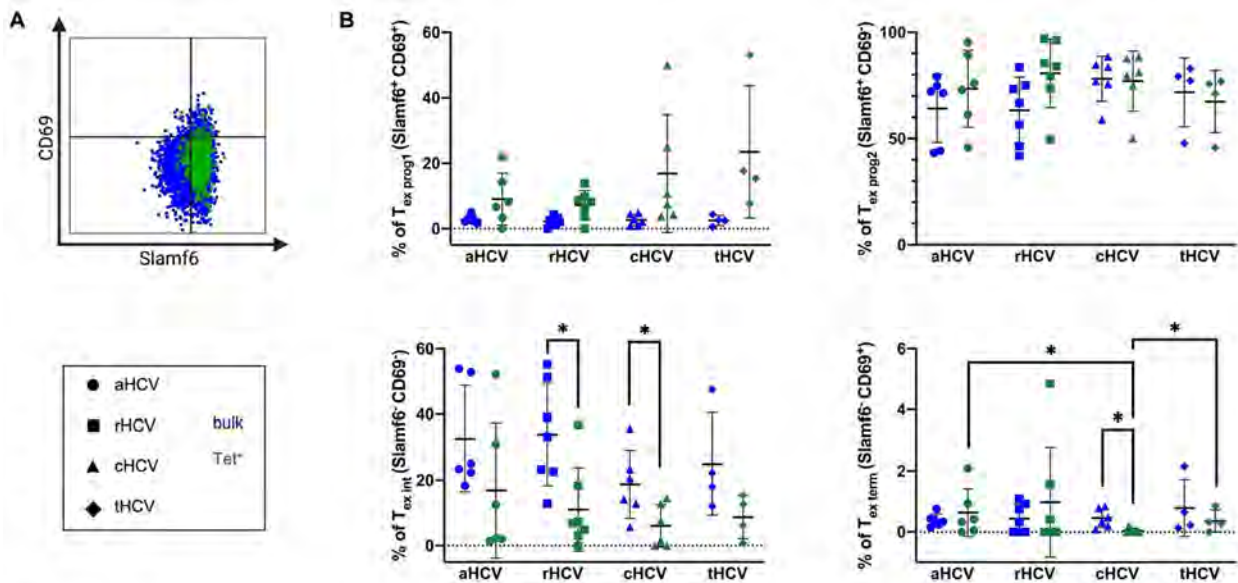
Classification of HCV-specific CD8+ T cells by the differential expression pattern of Slamf6 and CD69 predicts that the majority of cells are rather preterminally versus terminally exhausted regardless of disease stage

Maximilian Knapp¹, Christin Ackermann¹, Claudia Beisel¹, Vanessa Ditt², Melanie Wittner¹, Julian Schulze Zur Wiesch¹.

¹University Medical Center Hamburg-Eppendorf, I. Department of Medicine, Infectious Diseases Unit, Hamburg, Germany; ²University Medical Center Hamburg-Eppendorf, Center for Diagnostics, Institute of Transfusion Medicine, Hamburg, Germany
Email: julianszw@googlemail.com

Background and aims: Exhausted T effector cells, commonly described in chronic viral infections and cancer, are phenotypically and functionally heterogeneous cell populations whose development, maintenance, and response to immunotherapies are incompletely understood. Today, many differentiations into progenitors, intermediates and terminal stages of exhausted T cells are already known based on numerous markers. A better description regarding different subsets of exhausted T cells will allow a better understanding for future cancer therapy and viral cure approaches. Acute and chronic hepatitis C (HCV) infection are ideal models to examine the development of T-cell exhaustion and its potential reversibility at cellular and molecular levels. To assess the molecular fingerprint of potential populations, we aimed to investigate the interaction of different immunomodulatory targets.

Method: HCV-specific CD8+ T cells from HLA-A*01:01, HLA-A*02:01 and HLA-A*24:02 positive patients were analyzed with a 21-color



Distribution of T_{ex} subsets and on total and HCV-specific CD8⁺ T cells.

HCV-specific CD8⁺ T cells from human PBMC of patients with acute (aHCV), resolved (rHCV), chronic (cHCV) and treated (tHCV) HCV infection were enriched and analysed due to MHC class I tetramers. The distribution of T_{ex} subsets as well as novel immunomodulatory molecules were analysed using flow cytometry. (A) Representative overlay of bulk (blue) and Tet⁺ (green) CD8⁺ T cells gating Slamf6 vs. CD69 for differentiation between the T_{ex} subsets. (B) Frequencies of the different exhausted subtypes: progenitor 1 ($T_{ex\ prog1}$: Slamf6⁺ CD69⁻), progenitor 2 ($T_{ex\ prog2}$: Slamf6⁺ CD69⁺), intermediate ($T_{ex\ int}$: Slamf6⁻ CD69⁻) and terminally exhausted ($T_{ex\ term}$: Slamf6⁻ CD69⁺). For all tests, two-tailed p values were generated and results with a p-value ≤ 0.05 were considered statistically significant. Levels of significance are translated to asterisks as follows: * p ≤ 0.05; ** p ≤ 0.01; *** p ≤ 0.001; **** p ≤ 0.0001.

Figure: (abstract: THU197)

FACS-panel evaluating the surface expression of lineage markers (CD3, CD4, CD8), ectoenzymes (CD38, CD39, CD73), markers of differentiation (CD62L, CD127), and markers of exhaustion and activation (CD96, TIGIT, PD-1, CD69, Slamf6, CD28) and transcription factors (T-bet, TCF1, NR2F6, TOX, IRF4).

Results: Analyzing the TIGIT-CD96-axis, the majority of HCV-specific Tet⁺ CD8⁺ T cells of all patient groups was TIGIT⁺ and CD96⁺. The frequencies of CD96⁺ cells in the Tet⁺ T cells were significantly higher than in bulk CD8⁺ T cells for acute, resolved and chronic infection. Furthermore, HCV-specific CD8⁺ T cells were stratified into four novel subsets of exhausted T cells based on expression of the transmembrane protein Slamf6 and the early activation antigen CD69 as currently described by Beltra et. al. (2020, Immunity 52, 825–841) in the LCMV mouse model describing progenitor 1 ($T_{ex\ prog1}$: Slamf6⁺ CD69⁻), progenitor 2 ($T_{ex\ prog2}$: Slamf6⁺ CD69⁺), intermediate ($T_{ex\ int}$: Slamf6⁻ CD69⁻) and terminally exhausted ($T_{ex\ term}$: Slamf6⁻ CD69⁺) T cells. The majority of HCV-specific Tet⁺ cells in peripheral blood are in the $T_{ex\ prog2}$ state and less than 6% of the Tet⁺ T cells were at the $T_{ex\ term}$ state.

Conclusion: We identified four exhausted T cell subsets defined by Slamf6 and CD69 in patients with different clinical status of HCV infection. The frequencies detected in PBMC of our patients are similar to those described in the LCMV mouse model by Beltra et al. They could also show that the majority of the $T_{ex\ term}$ subset is localized in the liver. To investigate the $T_{ex\ term}$ population in human, analyses from liver biopsies are required. In this context, it will be of interest whether the responsiveness of the $T_{ex\ int}$ subset to PD-1 blockade described in mice can also be confirmed in human. Co-inhibitory receptors like CD96 in the TIGIT-CD155 signaling pathway also shaped the HCV-specific T cells.

THU198

TAPBPR shapes the hepatitis B immunopeptidome presented on HLA class I molecules

Ricky Sinharay^{1,2}, Andreas Neerincx¹, Arwen Altenburg¹, Jens Bauer^{3,4,5}, Mark R. Wills⁶, Juliane S. Walz^{3,4,5,7}, Will Gelson⁸, Louise H. Boyle¹. ¹University of Cambridge, Department of Pathology, Cambridge, United Kingdom; ²Cambridge University Hospitals NHS Foundation Trust, Cambridge Liver Unit, Addenbrooke's Hospital, Cambridge, United Kingdom; ³University Hospital Tübingen, Clinical Collaboration Unit Translational Immunology, German Cancer Consortium (DKTK), Department of Internal Medicine, Tübingen, Germany; ⁴University of Tübingen, Institute for Cell Biology, Department of Immunology, Tübingen, Germany; ⁵University of Tübingen, Cluster of Excellence iFIT (EXC2180) "Image-Guided and Functionally Instructed Tumor Therapies", Tübingen, Germany; ⁶University of Cambridge, Department of Medicine, Addenbrookes Hospital, Cambridge, United Kingdom; ⁷Margarete Fischer-Bosch Institute of Clinical Pharmacology and Robert Bosch Center for Tumor Diseases (RBCT), Stuttgart, Germany; ⁸Cambridge University Hospitals NHS Foundation Trust, Cambridge Liver Unit, Addenbrooke's Hospital, Cambridge, United Kingdom
Email: rickysinharay@doctors.org.uk

Background and aims: The presentation of virus derived peptides on HLA class I molecules is crucial for mounting antiviral immune responses. TAPBPR is a recently identified peptide editor involved in optimizing antigen selection on MHC class I molecules. Here, we present novel data on the impact of TAPBPR on the hepatitis B (HBV) immunopeptidome presented on HLA class I by using a mass spectrometry approach.

Method: HeLa cells (HLA-A*68:02, -B*15:03 and -Cw12) and TAPBPR knock-out HeLa cells (TAPBPR^{KO}) overexpressing individual HBV proteins HBsAg, Pol, HBCAg and HBx were generated. These cells were expanded to 5 × 10⁸ cells, lysed and peptides were eluted using a pan HLA class I antibody (W6/32). Analysis was performed by liquid

chromatography coupled to tandem mass spectrometry (LC-MS/MS). Mass spectra data were then searched against a database of possible peptides that could be derived from the host and/or pathogen proteomes, to identify HBV derived peptides presented on HLA class I. The HBV immunopeptidome in TAPBPR depleted cells was compared to HeLa cells expressing wild type TAPBPR and individual HBV proteins.

Results: A greater number of HBV peptides were presented in TAPBPR^{KO} cell lines compared to wild type cell lines, which was consistently observed between cells expressing different HBV proteins. This was despite the fact that no substantial change in the total cellular peptide count was observed between wild type and TAPBPR^{KO} cells. Amino acids positions 2 and 9 were clearly preferred for binding in both wild type and TAPBPR^{KO} cells, and a greater number of peptides were assigned to HLA-B*15:03 than HLA-A*68:02. Furthermore, semi quantitative analysis revealed that depletion of TAPBPR resulted in up-modulation of almost all HBV-derived peptides identified. In addition, changes in the hierarchy of the abundance of HBV peptides presented were observed in TAPBPR^{KO} cells. Of the up-modulated peptides, only four have been identified previously and are catalogued on IEDB. A total of 26 HBV-derived peptides were identified, 22 (84.62%) of which were novel. Of the novel peptides 7 were only identified in the TAPBPR^{KO} cell lines.

Conclusion: These findings strongly support a role of TAPBPR in HBV-derived peptide selection for presentation on HLA class I. However, it is still unclear whether this is advantageous for individuals with HBV expressing HLA alleles where TAPBPR mediates peptide exchange.

THU199

Phenotypes of NK cells and the activation profile of T cells in the early stages of alcohol liver diseases

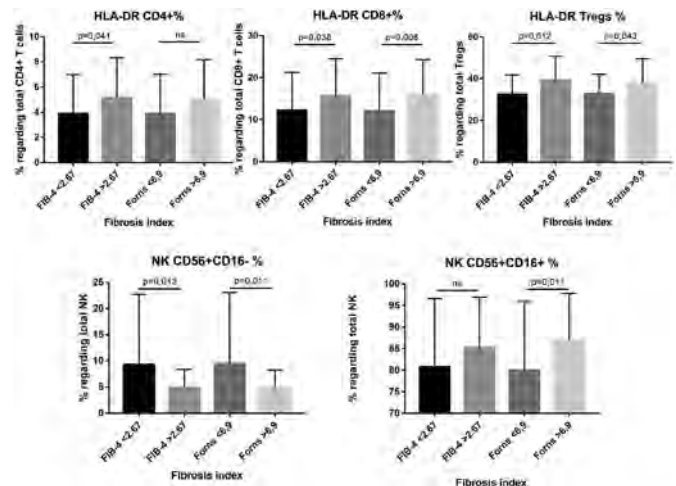
Coral Zurera^{1,2}, Anna Hernandez³, Aina Teniente¹, Daniel Fuster³, Eva Martínez-Cáceres¹, Robert Muga³, Paola Zuluaga^{1,3}. ¹investigation institute germans trias i pujol, immunology, badalona, Spain; ²Universitat Autònoma de Barcelona, Bellaterra, Spain; ³university hospital germans trias i pujol, internal medicine, badalona, Spain Email: ypzuluaga.germanstrias@gencat.cat

Background and aims: The role of cellular immunity in alcohol-related liver diseases (ARLD) is currently being characterized. While CD8 T cell activation is known to be detrimental, enhancing liver damage, the decrease of naïve T cells is associated with advanced liver fibrosis (ALF) in patients with alcohol use disorder (AUD). Natural Killer (NK) cells and NKT cells play an important role in the development of ARLD having subsets with opposing roles in the development of liver fibrosis. We aimed to evaluate the phenotype of NK and NKT cells and the activation profile of T cells in patients with AUD according to the presence of ALF.

Method: Patients were admitted to treatment of AUD between 2019 and 2021 in Germans Trias I Pujol Hospital, Spain. ALF was defined if the FIB-4 score was >2.67 (n = 19) or Forns score was >6.9 (n = 21). Patients with HCV infection, HIV infection and history of liver cirrhosis were excluded. Immunophenotyping of NK cells (CD3-CD56+CD16+, CD3-CD56+, CD3-CD16+), NKT cells (CD3+CD56+), and the activation status of CD4+, CD8+ and regulatory T cells (Tregs) was evaluated according to the presence of HLA-DR.

Results: 79 patients (51 years, 71% males) were included. Patients had a mean AUD duration of 18 ± 11 years with a daily alcohol consumption of 155 ± 77 gr/day. Regarding the immunophenotype in peripheral blood, the mean ± SD absolute values were: 2.1 ± 0.9 cells/L for total lymphocytes, 1054.5 ± 501.7 cells/μL for CD4+, 540 ± 335.7 cells/μL for CD8+, 49.3 ± 24.8 cells/μL for Tregs, 150.3 ± 97.5 cells/μL for NK cells and 69.8 ± 78.3 cells/μL for NKT cells. The percentage of CD3-CD56+ NK cells of patients with ALF was significantly lower (4.8 ± 3.3 and 4.9 ± 3.4) than in patients without ALF (7.8 ± 6.2 and 7.7 ± 6.2) according to Forns and FIB-4, respectively. The percentage of CD3-CD16+CD56+ NK cells was significantly higher in patients with ALF (87 ± 11) compared to patients without ALF (80 ±

16) according to Forns. No significant differences were observed in the percentage of CD3-CD16+ NK cells and NKT cells among groups. ALF patients also presented an increased percentage of HLA-DR+ expressing Tregs (38 ± 11.6 and 39.2 ± 11.5) and CD8+ (16 ± 8.3 and 15.6 ± 8.8) compared to Tregs (32.7 ± 9.4 and 32.5 ± 9.3) and CD8+ (12 ± 9.1 and 12.2 ± 9) in patients without ALF according to Forns and FIB-4, respectively. The percentage of HLA-DR+ CD4+ was higher in patients with ALF (5.1 ± 3.1) than in patients without ALF (3.9 ± 3) according to FIB-4. Figure 1 depicts the aforementioned significant differences (p < 0.05).



Conclusion: Severe AUD patients with ALF presented an increased NK cytotoxic phenotype concomitant with a decreased immunoregulatory and cytokine-secreting phenotype, possibly as a compensating mechanism of liver fibrosis. Meanwhile, the increased activation pattern observed in T cell subsets of patients with ALF could be a mechanism that favors the development and maintenance of liver fibrosis.

THU200

A spatio-temporal map of malaria infected mouse liver

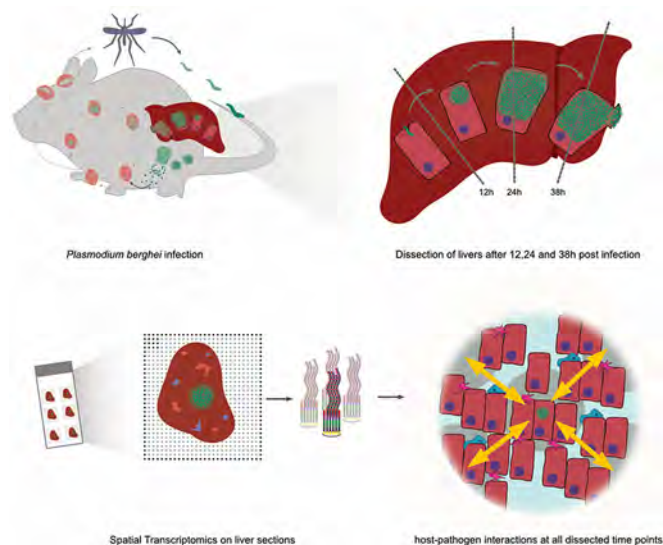
Franziska Hildebrandt¹, Johan Ankarklev¹. ¹Stockholm University, Department of Molecular Biosciences, Stockholm, Sweden Email: franziska.hildebrandt@su.se

Background and aims: The liver is crucial for malaria parasite development in the vertebrate host. Once transmitted by a female mosquito, the malaria parasites start their development in the liver, before entering the symptomatic blood stage. Since the liver has high potential for an effective immune response towards invading parasites and other intruders, choosing the liver as a developmental niche is paradoxical. Thus, we aim to delineate host-pathogen interactions during the time course of an ongoing liver infection *in vivo*, with the main aim of studying the host's response in a spatial context.

Method: To this end we are using Spatial Transcriptomics to describe the spatial organization of transcriptomic response in the mouse liver to an ongoing infection, using mosquito salivary gland lysate as a control.

Results: Our preliminary data suggests a differential onset of inflammation between infected and control mice, due to the presence of parasites in the tissue. We further investigated gene expression as a function of the distance to the site of infection for multiple time points and cell type compositions in specific areas of infection but also in the larger tissue context.

POSTER PRESENTATIONS



Conclusion: Our data indicates patterns of differential expression due to the influence of malaria parasites both locally and across tissues in challenged mice. Our preliminary data further suggests that the immune response towards a *Plasmodium* infection shows spatio-temporal patterns on the transcriptional level, providing a promising outlook for more detailed studies on the influence of the parasite on the surrounding liver environment.

Public Health

THU217

Reducing the risk of liver cirrhosis and hepatocellular carcinoma after treatment for smoking cessation in patients with chronic hepatitis B or C infection: a 12-year follow-up study

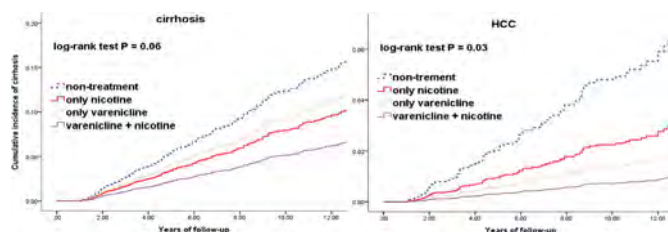
Ruey-Chang Lin¹, Chun Hsiang Wang^{1,2}, Kuo-Kuan Chang¹, Lien-Juei Mou¹, Yuan Tsung Tseng³, ¹Tainan Municipal Hospital (Managed by Show Chwan Medical Care Corporation), Tainan, Taiwan, Department of Hepatogastroenterology; ²Chung Hwa Medical University, Tainan, Taiwan, Department of Optometry; ³Tainan Municipal Hospital (Managed by Show Chwan Medical Care Corporation), Tainan, Taiwan, Committee of Medical Research
Email: b891040733@yahoo.com.tw

Background and aims: The possible hepatotoxic effect of cigarette smoking in patients with chronic hepatitis B virus (CHB) or chronic hepatitis C (CHC) virus infection has been proposed in numerous epidemiological and experimental studies. Varenicline and nicotine replacement therapy (NRT) are the current first-line treatment for smoking cessation. The present study compared the effects of different standard treatments for smoking cessation and of receiving no treatment for smoking cessation on the risk of liver cirrhosis and hepatocellular carcinoma (HCC) among patients with CHB or CHC infection.

Method: We identified patients with CHB or CHC infection who smoked regularly and whose data were input into Taiwan's National Health Insurance Research Database between January 1, 2007, and December 31, 2018. The patients' demographic data, medical history (including smoking habits), and paraclinical information were collected. The patients were classified into 4 groups—the no smoking cessation treatment, NRT only, varenicline only, and varenicline + NRT groups—according to the smoking cessation

treatment they had received. Cox proportional hazards models were used to analyze the patients' risks of liver cirrhosis and HCC, with adjustment for age, sex, comorbidities, and Charlson Comorbidity Index.

Results: A total of 4210 patients with CHB or CHC infection were recruited; 2535, 568, 427, and 680 were assigned to the NRT only, varenicline only, varenicline + NRT, and comparison (no treatment) groups, respectively. The mean follow-up duration was 7.2 ± 4.8 years. The outcomes were significantly different among the four groups. The NRT only, varenicline only, and varenicline + NRT groups had a lower prevalence of liver cirrhosis ($p = .06$) and HCC ($p = .03$) than did the no-treatment group in the cumulative incidence analysis (liver cirrhosis: prevalence = 8.5%, 3.9%, and 2.1% vs 11.3%, respectively; HR = 0.74[95%CI: 0.33–1.63], 0.63[0.34–1.15], and 0.40[0.19–0.84], respectively; HCC: prevalence = 15.0%, 11.6%, and 11.5% vs 23.1%, respectively; HR = 0.62[0.31–1.25], 0.32[0.10–1.00], and 0.26[0.10–0.69], respectively).



Conclusion: This study evaluated the effect of one month of NRT, varenicline, both, or no treatment on the risk of liver cirrhosis and HCC in smokers with CHB or CHC infection undergoing a smoking cessation program. All 3 smoking cessation treatments appeared to be effective in minimizing the risk of liver cirrhosis and HCC; a low prevalence of both conditions was observed in each of the 3 treatment groups.

Cumulative incidence rates of liver cirrhosis and HCC over time among patients with CHB or CHC infection in the no smoking cessation treatment, NRT only, varenicline only, and varenicline + NRT groups.

THU218

Testing coverage and strategy required to sustain Hepatitis C elimination in an injecting network of people who inject drugs: a network-based model

Chloe Siegle-Brown¹, Martin Siegle-Brown², Charlotte Cook³, Mark Wright¹, Julie Parkes³, Salim Khakoo³, Ryan Buchanan³.

¹University Hospital Southampton NHS Foundation Trust, United Kingdom; ²University of Sussex, United Kingdom; ³University of Southampton, United Kingdom

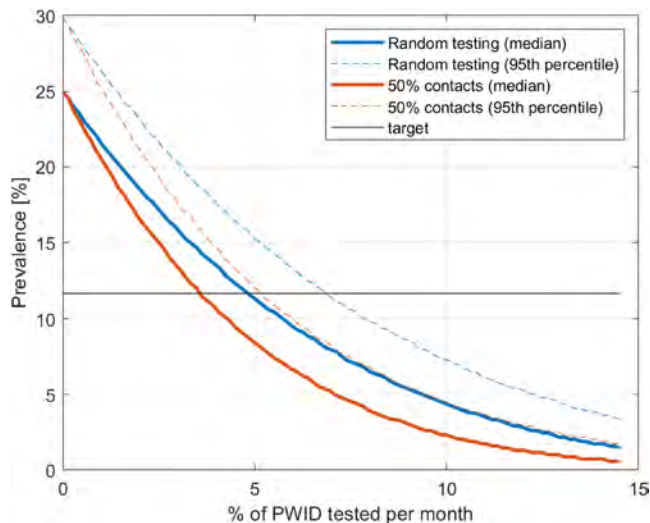
Email: chloe.brown@doctors.org.uk

Background and aims: The World Health Organisation has set a target for the global elimination of Hepatitis B (HBV) and C (HCV) by 2030. To achieve the elimination target, a widespread scale-up of testing and treatment services is required. However, little is known about the level of testing required to sustain the low-prevalence state of elimination. In this study we model the testing coverage required to maintain HCV elimination in an injecting network of people who inject drugs (PWID). We also test the hypothesis that a 'bring your friends' testing strategy will be more efficient.

Method: We create a dynamic injecting network structure connecting 689 PWID based on empirical data. A burn-in period, where PWID are randomly treated according to empirical parameters until the elimination target is achieved, is followed by the 5-year simulation period. The primary outcome is the testing coverage required per month to maintain prevalence at the elimination threshold over 5 years. We compare two treatment scenarios: 1) random testing, and 2) 'bring your friends' testing, where 50% of tests are random and 50% of tests in injecting partners of randomly selected individuals.

Results: After 5 years, without any testing or treatment provision, the prevalence of HCV increased from the elimination threshold (11.68%) to a mean of 25.0% (SD 3.0%). To maintain elimination with random testing, on average 4.92% (SD 0.84%) of the injecting network needs to be tested per month. However, with a 'bring your friends' strategy, 3.69% (SD 0.63%) of the network needs to be tested per month ($p < 0.000001$).

The superiority of the 'bring your friends' approach was maintained in a sensitivity analysis that adjusted for changes in needle and syringe provision and the rate of engagement with treatment following a positive test.



Conclusion: If HCV testing and treatment does not continue after elimination targets are met, the prevalence of HCV in an actively injecting network of PWID will increase. A 'bring your friends' approach to treatment is a more efficient approach to maintaining elimination.

Line graph showing change in prevalence at 5 years (y axis) with increasing testing coverage in two testing scenarios. The elimination threshold (prevalence <11.68%) is indicated. Results are from 100 simulations in 100 generated networks.

THU219

Hepatocellular carcinoma screening trends in individuals with cirrhosis in North Carolina

Christine Hsu¹, Jennifer Lund¹, Andrew Moon², Louise Henderson².

¹University of North Carolina at Chapel Hill, Chapel Hill, United States;

²UNC School of Medicine, Chapel Hill, United States

Email: cdhsu@live.unc.edu

Background and aims: The epidemiology of cirrhosis has shifted but little is known about how these shifts impact hepatocellular carcinoma (HCC) screening. We characterized patterns of HCC screening over time and by cirrhosis aetiology among a privately insured population in North Carolina.

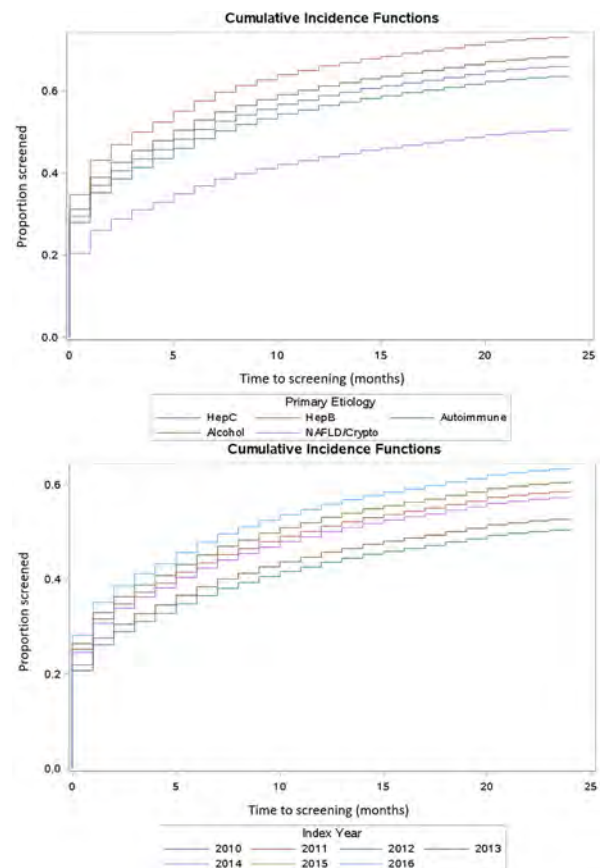
Method: We conducted a retrospective cohort study of individuals with a diagnosis of cirrhosis using insurance claims data from a large private insurer in North Carolina that covers 3.5 million people annually, or 35% of the state's population. We included individuals ≥ 18 years with an ICD-9/10 code for cirrhosis between 1 January 2010 and 30 June 2018 with continuous enrolment one year before their cirrhosis diagnosis and no prior HCC or liver transplant. Cirrhosis aetiology was defined using a validated claims-based algorithm. The main outcome was HCC screening by abdominal ultrasound, CT, or

MRI. We determined 1-year and 2-year cumulative incidences for HCC screening overall, by aetiology, and by calendar year of cirrhosis diagnosis.

Results: Among the 7,739 individuals in the cohort, 56.9% were male, 75.2% lived in an urban area, and the mean age was 53 years. Most individuals had NAFLD/cryptogenic aetiology (43.4%), followed by alcohol-related liver disease (25.1%), hepatitis C virus (21.4%), autoimmune hepatitis (8.5%), and hepatitis B virus (1.6%). Nearly half of individuals had decompensated cirrhosis (47%). Most individuals (68.9%) received care from a gastroenterologist/hepatologist during their follow-up time, while 22.4% received care from a general practitioner alone.

The 1-year and 2-year cumulative incidences were 43.5% and 49.8%, respectively, for receiving screening by abdominal ultrasound. The 1- and 2-year cumulative incidences were 53.0% and 60.0%, respectively, for receiving any HCC screening. Individuals with hepatitis B virus had the highest 2-year cumulative incidence (73.2%) while those with NAFLD/cryptogenic aetiology had the lowest 2-year cumulative incidence (50.6%).

The 2-year cumulative incidence was 66.1% for hepatitis C virus, 63.7% for autoimmune hepatitis, and 68.4% for alcohol-related liver disease aetiologies. The 2-year cumulative incidence of HCC screening by calendar year of cirrhosis diagnosis ranged from 52.5% in 2012 to 63.4% in 2016.



Conclusion: We observed that HCC screening was underutilized among privately insured individuals with cirrhosis in North Carolina, indicating a need for targeted interventions to increase HCC screening rates.

POSTER PRESENTATIONS

THU220

Cost-effectiveness evaluation of the hepatitis C elimination strategy in Cyprus in the era of affordable direct-acting antivirals

Ilias Gountas¹, Petros Katsioloudes², Ioanna Yiasemi³, Evi Kyprianou³, Christos Mina³, Chrysanthos Georgiou⁴, Antri Kouroufexi⁵, Anna Demetriou⁶, Eleni Xenofontos⁷, Georgios Nikolopoulos¹.

¹University of Cyprus, Medical School; ²Evangelistria Medical Centre;

³Cyprus National Addictions Authority, Cyprus Monitoring Centre;

⁴Nicosia General Hospital; ⁵Pharmaceutical Services, Ministry of Health;

⁶Health Monitoring Unit, Ministry of Health; ⁷Limassol General Hospital, Department of Internal Medicine

Email: eliagoun@gmail.com

Background and aims: In the Republic of Cyprus, the prevalence of chronic Hepatitis C virus (CHC) among the general population is estimated at 0.6%, while the CHC prevalence among people who inject drugs (PWID) is estimated at 43%. A previous mathematical modeling study highlighted that to achieve Hepatitis C virus (HCV) elimination, 3080 (95% Credible intervals (CrI): 3000, 3200) patients need to be diagnosed and treated by 2034 (2680 from the general population and 400 from PWID)¹. For the optimal use of available resources, it is essential to evaluate the cost-effectiveness of any proposed strategy. This study aims to undertake a cost-effectiveness analysis of the proposed HCV elimination strategy in Cyprus.

Method: A previously published, dynamic, stochastic, individual-based model of HCV transmission, disease progression, and cascade of care was calibrated to data from Cyprus (1). The model stratifies the population into the infected general population and the PWID population. We assumed that the ongoing HCV transmission is limited to the PWID group. The incremental cost-effectiveness ratio (ICER) per disability-adjusted life year (DALY) averted for HCV elimination versus the status quo scenario was computed. Cost-effectiveness was determined using Cyprus' willingness-to-pay (WTP) threshold of €26623 per DALYs averted.

Results: Compared to the status quo, the elimination strategy would prevent 195 (95% CrI: 115, 220) and 2070 (95% CrI: 1600, 2640) new infections and DALYs by 2034, respectively. The additional required investment to meet the HCV elimination goals would be €20.4M (95% CrI: €19.4M, €21.4M). The cost per averted DALY is estimated at €9915 (95% CrI: €7600, €13100) indicating that the elimination strategy is very cost-effective. In the probabilistic sensitivity analysis, 100% of simulations were below the WTP threshold (Figure).

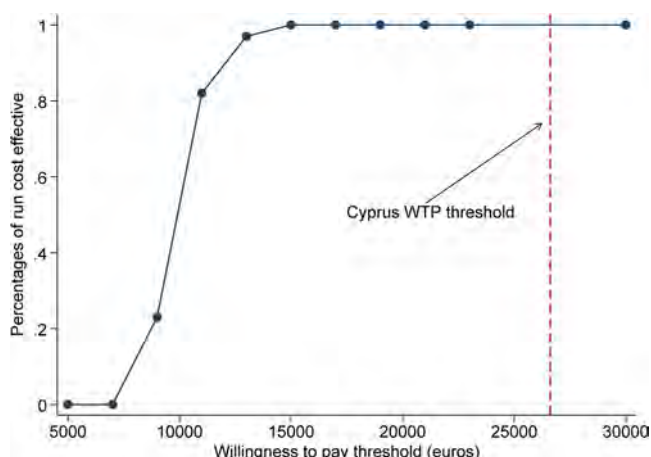


Figure: Cost-effectiveness acceptability curve

Conclusion: Scaling-up HCV testing and treatment in Cyprus to reach the elimination targets is estimated to generate significant health and economic benefits.

Reference: Gountas et al. WJG 2021.

THU221

Rethinking the management of chronic hepatitis B in the context of rural sub-saharan Africa: results from a social justice mixed methods study in rural Senegal (the AmbASS-PeCSen study)

Marion Coste^{1,2}, Cilor Ndong³, Aldiouma Diallo⁴, Assane Diouf⁴, Sylvie Boyer², Jennifer Prah⁵.

¹Aix Marseille University, CNRS, AMSE, Aix-Marseille School of Economics, Marseille, France; ²Aix Marseille Univ, INSERM, IRD, SESSTIM, Sciences Économiques and Sociales de la Santé and Traitement de l'Information Médicale, Marseille, France;

³Cheikh Anta Diop University, Anthropology, Dakar, Senegal; ⁴Campus International IRD-UCAD de l'IRD, UMR VITROME, IRD-Université Aix

Marseille, AP-HM, SSA, IHU-Méditerranée Infection, Dakar, Senegal;

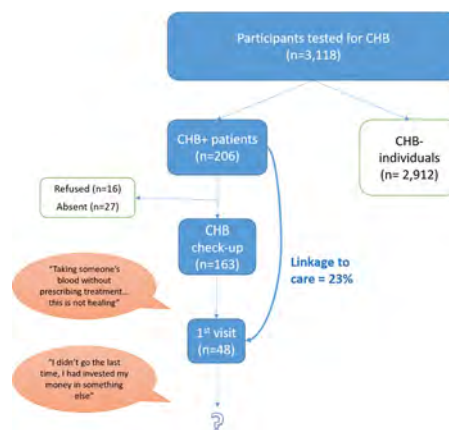
⁵University of Pennsylvania, School of Social Policy and Practice and

Perelman School of Medicine, Philadelphia, United States
Email: marion.coste@univ-amu.fr

Background and aims: Worldwide, the burden of chronic hepatitis B (CHB) infection is estimated to reach 800,000 deaths annually, with highest CHB prevalence found in Western Pacific and Africa. In Senegal, where up to 10% of the adult population lives with CHB, the government aims to treat 30,000 patients by 2023. In this context, the Ministry of Health is piloting the decentralization of CHB care to rural populations in the Fatick region drawing from the 2017 EASL Clinical Practice Guidelines on the management of CHB. This study documents the CHB cascade of care in rural Senegal after community-based testing.

Method: All residents of households randomly selected in the rural area of Niakhar (Senegal) were offered at-home hepatitis B testing using dried blood sampling and administered socio-economic questionnaires (ANRS12356 AmbASS survey). Following a free CHB initial check-up, patients were referred to local healthcare facilities or invited to join a cohort in Dakar if eligible for CHB management as per the Senegalese national recommendations adapted from the 2017 EASL guidelines. A few months after referral, purposeful sampling of one-on-one qualitative interviews based on an adaptation of the health capability profile were conducted to document perceptions, obstacles and levers in CHB participants linked to care and those who were not (A*Midex PeCSen study).

Results: In 2018–2019, 3,118 participants representative of the Niakhar area's population undertook hepatitis B testing. 206 participants tested positive, and among them, 163 patients (79%) performed the initial CHB check-up. By September 30 2021, 48 patients had gone to at least one visit for CHB management—a 23% linkage to care. Interviews (n = 34) revealed complex CHB-related health capability profiles, starting high health-related motivation, skills, and self-efficacy despite low CHB-related knowledge. Gendered social norms, shared decision-making, reluctance towards blood sampling in the absence of treatment prescription, and limited ability to pay are among the main obstacles to linkage to care, and retention in CHB follow-up.



Conclusion: As the first mixed-methods study of the cascade of CHB care in rural Sub-Saharan Africa, our results call for action in rethinking CHB management to make it acceptable, accessible, and affordable to rural populations.

THU222

Global survey of healthcare workers' attitudes to treatment of chronic hepatitis C infection in children and adolescents

Fariyah Malik¹, Philippa Easterbrook², Giuseppe Indolfi³, Claire Thorne¹. ¹UCL Great Ormond Street Institute of Child Health, London, United Kingdom; ²World Health Organization, Genève, Switzerland; ³University Hospital Meyer, Firenze, Italy
Email: fariyah.malik.18@ucl.ac.uk

Background and aims: Direct acting antivirals (DAAs) are now approved for treatment of adolescents and children >3 years living with chronic hepatitis C (HCV) however, there is limited understanding of the attitudes of health care workers (HCWs) on expanding treatment, especially to younger age groups. We undertook the first global survey of HCWs managing HCV infection regarding treatment of children and adolescents, and on key challenges to implementation, to inform updated World Health Organization (WHO) HCV guidelines.

Method: A cross-sectional online survey was conducted during September 2021, distributed to networks providing care to children and adolescents living with HCV infection, and other key stakeholders. Survey questions were developed to reflect two key questions: which age groups to treat and prioritise, and which DAA regimens to use.

Results: There were 142 survey respondents, of whom 94 (66%) had cared for children or adolescents with HCV over the past 3 years. Every WHO region was represented, with highest proportion of respondents from the Western Pacific (43%) and the Americas (19%). There was a trend towards higher preference for treating older age groups: 60% of respondents reported a strong preference for treating (i.e., stating they were very likely or likely to treat) children aged 3 to <6 years, increasing to 81% and 94% for those aged 6 to <12 years and 12 to <18 years respectively. The main reasons reported for preferring not treating younger age groups were the chance of spontaneous clearance, lack of drug approvals and registration for treatment of younger age groups, slow disease progression and asymptomatic nature of disease in early childhood, difficulties with administering medication to young children and lack of clinical trial data.

The most commonly preferred and used DAA regimens for treatment across all paediatric age groups were: sofosbuvir/velpatasvir, sofosbuvir/ledipasvir and glecaprevir/pibrentasvir. The most frequent reasons for these regimen preferences were safety, guideline recommendations, drug availability, suitability to treat prevalent HCV genotypes (including pangenotypic) and efficacy.

Conclusion: This survey demonstrates strong HCW support for treatment of children and adolescents with HCV infection, especially those 6 years or older. Future priorities include updating national policies to incorporate case-finding strategies and treatment for children and adolescents, and access to paediatric DAA formulations.

THU223

Impact of community-based campaign in United States to increase hepatitis B virus screening and linkage to care among Asian immigrants from high endemic countries

Sung Kwon^{1,2}, Aziza Win³, Gregory Wu⁴. ¹Holy Name Medical Center, Teaneck, United States; ²Columbia University Irving Medical Center, New York, United States; ³Ross University School of Medicine-Academic Campus, Bridgetown, Barbados; ⁴Geisinger Commonwealth School of Medicine, Scranton, United States
Email: steve-kwonmd@holynamc.org

Background and aims: With the ongoing population movements of migrants from high (>8%) to low (<2%) endemic regions, the prevalence and incidence of chronic Hepatitis B virus surface

antigen (HBsAg) carriers are changing in low endemic countries like the United States. To address this, in the efforts for hepatitis B virus (HBV) eradication, the American Association for the Study of Liver Disease has established guidelines pushing for HBV screening in immigrants from high endemic regions including many Asian countries. Yet, many Asian immigrants remain unscreened and those with chronic hepatitis B (CHB) are often not linked to care citing multiple barriers. We sought to determine the impact of community-based HBV campaigns on screening and linkage to care (LTC) efforts through a large-scale community screening initiative.

Method: Asian immigrants from the New Jersey and New York metropolitan areas were screened for HBV using surveys and serological testing from 2009 to 2019. Those participants found to be positive were followed up by telephone, mail or email. We started to collect LTC data starting in 2015. In 2017, because of low LTC rates, nurse navigators whose role was to help participants navigate through individual barriers to care were hired to aid in the LTC process. Those excluded from the LTC data included those who were already linked to care, those who declined to be linked to care and those who had moved or passed away.

Results: 13,566 participants were screened from 2009 to 2019, of which, the results for 13,466 were available. Of these, 372 (2.7%) were found to have positive HBV status. Approximately 49.3% were female and 50.1% were male, and the rest were of unknown gender. A total of 1,191 (10.0%) participants were found to be HBV negative but required vaccination. When we started to track LTC, we found 195 participants that were eligible for LTC between 2015 through 2017 after the exclusion criteria were applied. It was found that only 33.8% were successfully linked to care in that time period. After hiring nurse navigators, we saw LTC rates increase to 85.7% in 2018 and to 89.7% in 2019.

	Number of HBV Infected	Percentage (%)
Successful LTC		
Up to 2017	56 (out of 195)	33.8%
2018	12 (out of 14)	85.7%
2019	26 (out of 29)	89.7%

Figure: Successful linkage to care rates 2009 to 2019. A nurse navigator was hired in 2017 to focus on linkage to care.

Conclusion: HBV community screening initiatives are imperative to increase screening rates in the Asian immigrant population. We were also able to demonstrate that nurse navigators can successfully help increase LTC rates. Our HBV community screening model can address issues with barriers to care including lack of access in comparable populations.

THU224

The prognostic implications of liver function test abnormalities in patients admitted to hospital with COVID-19

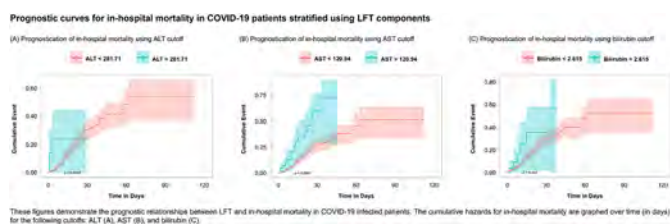
Jason Cohen¹, David Uihwan Lee², Gregory Fan¹, David Hastie¹, Akaash Mittal¹, Khanh Le¹, Yeeun Jang¹, Sarav Daid¹, Raffi Karagozian¹, Raza Malik¹. ¹Tufts Medical Center, Gastroenterology/Hepatology, Boston, United States; ²University of Maryland Medical Center, Gastroenterology/Hepatology, Baltimore, United States
Email: jcohen1353@gmail.com

Background and aims: Prior studies have indicated the presence of hepatic inflammation (as signified by elevated liver function test (LFT) values), as conferring an escalated risk toward adverse outcomes in patients admitted with COVID-19. In line with this hypothesis, we study the various thresholds of LFTs and its associated prognostic risks toward COVID-19 related hospital deaths.

Method: This was a single-center retrospective study involving patients admitted with COVID-19. Univariate Cox regression analysis identified the LFT variables significantly associated with our primary end point, in-hospital death. Subsequently, 500 iterations of thresholds were generated for each biomarker to estimate the prognostic

POSTER PRESENTATIONS

relationship between biomarker and end point. Multivariate Cox regression and event-analyses were performed for each threshold to identify the minimal cutoffs at which the prognostic relationship was significant. Event curves were drawn for each significant relationship. **Results:** A total of 858 patients with COVID-19 were included with a median follow-up time of 5 days from admission. From the total, 90 patients passed away during admission (10.5%). Upon univariate Cox analysis, the following LFT parameters were associated with in-hospital death: Bilirubin ($p < 0.001$), AST ($p < 0.001$), ALT ($p < 0.001$). However, alkaline phosphatase ($p = 0.449$) was not associated with the primary end point. The iterations of event regression analyses using 500 sequences of LFT thresholds showed the following cutoffs to be significantly associated with in-hospital death (minimally significant values): ALT (281.71 IU/L), AST (120.94 IU/L), bilirubin (2.615 mg/dL). On the multivariate analysis, while controlling for demographics and cardiopulmonary/medical comorbidities, the following adjusted hazard ratios were derived for each cutoff: ALT (aHR: 6.43 95%CI 1.85–22.40), AST (aHR: 3.35 95%CI 1.84–6.11), and bilirubin (aHR: 2.77 95%CI 1.15–6.65).



Conclusion: The delineated cutoffs for AST, ALT, and bilirubin levels can serve as clinical benchmarks to help determine when a COVID-19 infection poses significant risk. Given this finding, the cutoffs can be used as part of a risk assessment for patients to support early preventative therapies and medical management.

THU225

A novel prognostic model including liver function parameters accurately predicts 30-day mortality in patients admitted with COVID-19

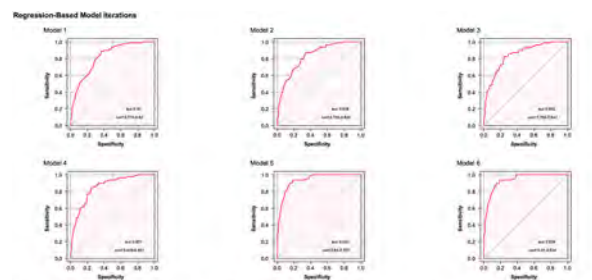
David Uihwan Lee¹, Jason Cohen², Gregory Fan², David Hastie², Akaash Mittal², Khanh Le², Yeeun Jang², Sarav Daid², Raffi Karagozian², Raza Malik². ¹University of Maryland Medical Center, Gastroenterology/Hepatology, Baltimore, United States; ²Tufts Medical Center, Gastroenterology/Hepatology, Boston, United States
Email: jcohen1353@gmail.com

Background and aims: While the relationship between elevated liver enzymes and COVID-19 related adverse events is well-established, a liver-dependent prognostic model that predicts the risk of death is helpful to accurately stratify admitted patients. In this study, we use a bootstrapping-enhanced method of regression modeling to predict COVID-19 related deaths in admitted patients.

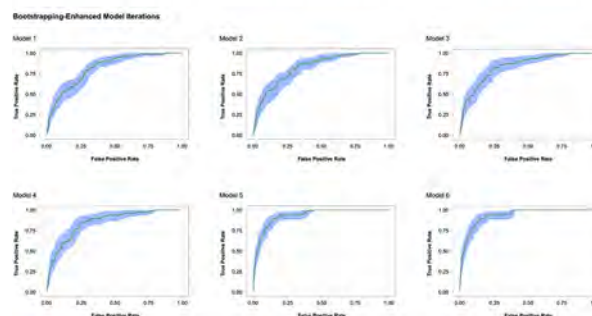
Method: This was a single-center, retrospective study. Univariate and multivariate Cox regression analyses were performed using 30-day mortality as the primary end point to establish associated hepatic risk factors. Regression-based prediction models were constructed using a series of modeling iterations with an escalating number of categorical terms. Model performance was evaluated using receiver operating characteristic (ROC) curves. Model accuracy was internally validated using bootstrapping-enhanced iterations.

Results: 858 patients admitted to hospital with COVID-19 were included. 78 were deceased by 30 days (9.09%). Cox regression (greater than 20 variables) showed the following core variables to be significant: INR (aHR 1.26 95%CI 1.06–1.49), AST (aHR 1.00 95%CI 1.00–1.00), age (aHR 1.05 95%CI 1.02–1.08), WBC (aHR 1.07 95%CI 1.03–1.11), lung cancer (aHR 3.38 95%CI 1.15–9.90), COPD (aHR 2.26 95%CI 1.21–4.22). Using these core variables and additional

categorical terms, the following model iterations were constructed with their respective AUC; model 1 (core only): 0.82 95%CI 0.776–0.82, model 2 (core + demographics): 0.828 95%CI 0.785–0.828, model 3 (prior terms + additional biomarkers): 0.842 95%CI 0.799–0.842, model 4 (prior terms + comorbidities): 0.851 95%CI 0.809–0.851, model 5 (prior terms + life-sustaining therapies): 0.933 95%CI 0.91–0.933, model 6 (prior terms + COVID-19 medications): 0.934 95%CI 0.91–0.934. Model 1 demonstrated the following parameters at 0.91 TPR: 0.54 specificity, 0.17 PPV, 0.98 NPV. Bootstrapped iterations showed the following AUC for the respective models: model 1: 0.82 95%CI 0.765–0.882, model 2 0.828 95%CI 0.764–0.885, model 3 0.842 95%CI 0.779–0.883, model 4: 0.851 95%CI 0.808–0.914, model 5: 0.933 95%CI 0.901–0.957, model 6: 0.934 95%CI 0.901–0.961.



This figure demonstrates the regression-based model iterations that used an escalating number of variables categorized for each consecutive model configuration. The following variables were included: For Model 1: AGE, AST, INR, WBC, Lung Cancer, COPD, COVID-19 prior variables configuration; For Model 2: prior variables configuration + DEMOGRAPHICS; For Model 3: prior variables configuration + COMORBIDITIES; For Model 4: prior variables configuration + LIFE-SUSTAINING THERAPIES; For Model 5: prior variables configuration + COVID-19 MEDICATIONS; For Model 6: prior variables configuration + COVID-19 MEDICATIONS.



This figure demonstrates the bootstrapping-enhanced model iterations that used an escalating number of variables categorized for each consecutive model configuration. The following variables were included: For Model 1: AGE, AST, INR, WBC, Lung Cancer, COPD, COVID-19 prior variables configuration; For Model 2: prior variables configuration + DEMOGRAPHICS; For Model 3: prior variables configuration + COMORBIDITIES; For Model 4: prior variables configuration + LIFE-SUSTAINING THERAPIES; For Model 5: prior variables configuration + COVID-19 MEDICATIONS; For Model 6: prior variables configuration + COVID-19 MEDICATIONS.

Conclusion: Model 1 displays high prediction performance (AUC >0.8) in both regression-based and bootstrapping-enhanced modeling iterations. Therefore, this model can be adopted for clinical use as a calculator to evaluate the risk of 30-day mortality in patients admitted with COVID-19.

THU226

Low health literacy is associated with higher healthcare service utilisation and costs among patients with cirrhosis

Patricia Valery¹, Christina Bernardes¹, Kelly Hayward^{2,3}, Gunter Harte¹, Katelin Haynes⁴, Louisa Gordon¹, Amy Johnson^{2,3}, Elizabeth Powell^{2,3}. ¹QIMR Berghofer Medical Research Institute, Herston, Australia; ²Princess Alexandra Hospital, Woolloongabba, Australia; ³The University of Queensland, Centre for Liver Disease Research, Faculty of Medicine, Woolloongabba, Australia; ⁴Hepatitis Queensland, Coorparoo, Australia
Email: patricia.valery@qimrberghofer.edu.au

Background and aims: Optimal management of cirrhosis is complex, and patients often lack knowledge and skills which can affect self-management. We assessed patient knowledge about cirrhosis and examined whether knowledge was associated with clinical outcomes, healthcare service utilisation, and healthcare costs.

Method: A cross-sectional 'knowledge survey' was conducted between Jun-2018 and Aug-2020 with 123 cirrhosis patients with cirrhosis (44.4% of 277 invited and eligible). The 'knowledge survey' questions were derived from prior studies, and an expert panel

unanimously deemed eight items to be “key knowledge” about cirrhosis. The proportion of correct answers were calculated (“key knowledge” score) and patients were categorized as having ‘good knowledge’ vs ‘poor knowledge’ (cut-off based on median score). Detailed clinical data (extracted from medical records and through linkage to hospital admissions, emergency department presentations), healthcare costs, and self-reported health-related quality of life (SF-36) were available. Cumulative overall survival (Kaplan-Meier), rates of hospital admissions, emergency presentations and costs were assessed according to “key knowledge.” Incidence rate ratios (IRR; Poisson regression) were reported.

Results: Patients were aged 60.7 ± 10.8 years, 65.9% were male, 47.2% had formal education to Junior High School level or less, 43.9% lived in ‘most disadvantaged’ areas, alcohol was a cofactor for 65.9%, NAFLD was a cofactor for 50.4%, and 29.3% had decompensated cirrhosis. 58.5% of patients had ‘good knowledge’ about cirrhosis. In multi-variable analysis, higher level of education was associated with over 5-fold odds of having ‘good knowledge’ about liver disease (adj-OR = 5.61, 95%CI 2.47–12.75). Patients with ‘good knowledge’ had a higher health status in the SF-36 domain related to physical functioning ($p = 0.036$) compared to those with ‘poor knowledge’. Patients with ‘good knowledge’ had 73% fewer all-cause admissions (IRR = 0.27, 95%CI 0.23–0.33), 57% fewer emergency presentations for cirrhosis (IRR = 0.43, 95%CI 0.21–0.89), and more planned one-day cirrhosis admissions (IRR = 4.47, 95%CI 1.61–12.37; see Table). The total cost of cirrhosis admissions was 45% lower for patients with ‘good knowledge’ (IRR = 0.55, 95%CI 0.54–0.56) during the follow-up period.

Table: Incidence rate ratios and cost ratios by knowledge score

	IRR (95%CI)*	p-value
Data source: Queensland Hospital Admitted Patient Data Collection		
All-cause admission	0.27 (0.23–0.33)	<0.001
Cirrhosis admission	0.72 (0.44–1.19)	0.206
Planned one-day admission (cirrhosis admission)	4.47 (1.61–12.37)	0.004
Admitted via the emergency department (any admission)	0.59 (0.40–0.86)	0.007
Admitted via the emergency department (cirrhosis admission)	0.67 (0.39–1.17)	0.157
Data source: Emergency Data Collection		
Emergency presentation (any reason)	0.65 (0.50–0.84)	0.018
Cirrhosis-related emergency presentation	0.43 (0.21–0.89)	0.022
Data source: National Hospital Cost Data Collection		
Total cost for any admission	Cost ratio (95%CI)**	p-value
	0.68 (0.68–0.69)	<0.001
Total cost for cirrhosis admissions	0.55 (0.54–0.56)	<0.001

Conclusion: Low health literacy is associated with increased use of healthcare services and increased total cost of health care. This may reflect poorer health status and quality of life. Improving the health literacy of patients with cirrhosis may be an effective strategy to promote a more cost-effective use of healthcare services with fewer preventable emergency department visits and greater use of planned admissions.

THU227

A modelling approach to estimate alcohol-related liver morbidity and mortality in France

Claire Delacôte¹, Line Carolle Ntandja Wandji^{1,2}, Alexandre Louvet^{1,2}, Pierre Bauvin¹, Guillaume Lassailly^{1,2}, Massih Ningarhari^{1,2}, Sebastien Dharancy^{1,2}, Guillaume Clement³, Amelie Bruandet³, Xavier Lenne³, Philippe Mathurin^{1,2}, Sylvie Deuffic-Burban^{1,4}.
¹INSERM U1286-INFINITE, Lille, France; ²CHU de Lille, Service des maladies de l'appareil digestif, Lille, France; ³Lille University Hospital, Medical Information Department, Lille, France; ⁴INSERM U1137-IAME, Paris, France
 Email: claire.delacote@inserm.fr

Background and aims: Harmful alcohol use leads to the development of alcohol-related liver disease (ALD). In-depth knowledge of the natural history of ALD according to patterns of alcohol consumption is required to predict the future burden of ALD morbidity and mortality. This would allow to implement health policies targeting at-risk drinkers. Our aim was to integrate the relevant natural history data of ALD in a mathematical model. This

model includes estimates of the incidence of at-risk drinking in order to predict morbidity and mortality related to ALD in France.

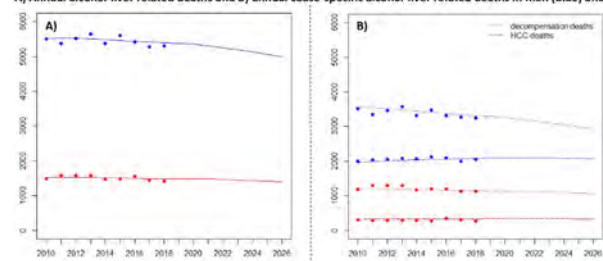
Method: First, we developed a Markov model simulating the trajectory of cohorts starting at-risk alcohol consumption until they die. It integrates the common risk factors associated with the progression of ALD (sex, age, amount of alcohol, genetic polymorphism). Unknown parameters of progression were back-calculated on the 2010–2018 alcohol-related decompensated cirrhosis and HCC mortality data provided by the French National Hospital Discharge database. Second, morbidity and mortality were predicted up to 2026.

Results: The developed model fits the observed mortality data: 63, 016 deaths were predicted over 2010–2018 for 62, 934 observed in database (Fig. A). Prediction of deaths fits the observed mortality according to cause of death and sex (Fig. B), as well as age. Between 2010 and 2021, annual ALD deaths decreased by 4%, from 7, 100 to 6, 700. However, while deaths by decompensation decreased from 4800 to 4, 300 (–10%), deaths by HCC rose from 2, 300 to 2, 400 (+4%) (Fig. B). Most of the ALD deaths occurred in men: 3 out 4 deaths by decompensation and 9 out 10 deaths by HCC.

In addition, the model estimated that, in 2021, 80, 000 French individuals have alcohol-related cirrhosis with 7, 900 incident cases. Decompensated cirrhosis and HCC are observed in around 33, 000 and 6, 000 cases, respectively. Women represent 30% of the cirrhotic individuals.

The decline of French per capita consumption would lead in 2026 to decrease in cirrhosis (~70, 000) and liver related deaths (6, 400) compared to currently (Fig. B).

A) Annual alcohol-liver related deaths and B) annual cause-specific alcohol-liver related deaths in men (blue) and women (red)



Conclusion: The present model predicts future burden of ALD in the general French population, based on robust epidemiological data. This model allows to predict not only liver-related mortality but also burdens of cirrhosis and liver-related complications. It may help to propose new health policies targeting patients most at-risk in order to obtain further reductions in the burden of ALD.

THU228

A model to predict drinking population at-risk of liver disease in France: a tool for decision-making public health policies

Claire Delacôte¹, Line Carolle Ntandja Wandji^{1,2}, Alexandre Louvet^{1,2}, Pierre Bauvin¹, Guillaume Lassailly^{1,2}, Massih Ningarhari^{1,2}, Sebastien Dharancy^{1,2}, Philippe Mathurin^{1,2}, Sylvie Deuffic-Burban^{1,3}.
¹INSERM U1286-INFINITE, Lille, France; ²CHU de Lille, Service des maladies de l'appareil digestif, Lille, France; ³INSERM U1137-IAME, Paris, France
 Email: claire.delacote@inserm.fr

Background and aims: In France, daily alcohol intake is decreasing among 15–64 y-o whereas consumption of ≥ 6 drinks per occasion (binge drinking) is becoming more common, especially among 15–35 y-o. Estimating the proportions of individuals with alcohol use with intermediate (20–50 g/d) or high (≥ 50 g/d) risks of alcohol-related liver disease (ALD) would allow to predict the incident cases of cirrhosis and provide new tool for decision-making public health policies. Our aim was to predict the incidence of French people having an alcohol intake ≥ 20 g/d.

Method: Daily alcohol intake was calculated from individual data from national surveys (ESPS), conducted on a representative sample

POSTER PRESENTATIONS

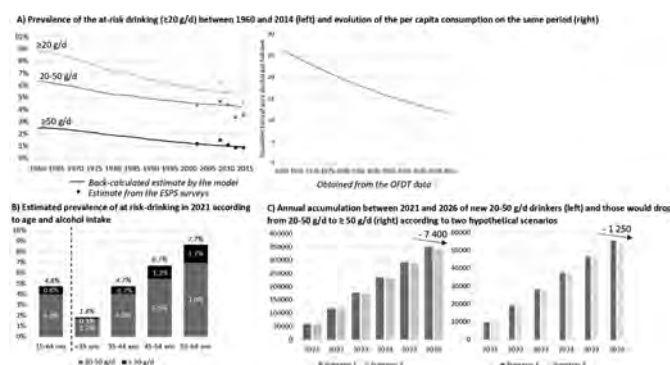
of 15–64 y-o French people. A Markov model was fitted to this data to estimate entry into risky drinking, according to the history of binge drinking or not. Incidences were back-calculated by sex, age and annual per capita consumption from ESPS 2002 to 2014 ($n = 45,054$). The adequacy of the model was assessed by comparing the predicted alcohol patterns and prevalence to those estimated from ESPS. Entries into at liver-risk drinking were simulated between 1910 and 2014 considering competitive mortality. At liver-risk drinking incidences and prevalence were predicted until 2026 under 2 scenarios.

Annual distributions of predicted and observed prevalence were closed according to daily alcohol intake (Fig. A), sex and age.

Results: While per capita consumption dropped from 26L to 12L (–54%) over 1960–2014, prevalence of at liver-risk drinking among 15–64 y-o decreased from 8.8% to 5.1% (–42%) (Fig. A). The number of new intermediate and high at liver-risk drinkers had respectively decreased by 35% and 65%.

In 2021, ~5% of French people have an alcohol intake ≥ 20 g/d (8/10 are men). This prevalence increases with age (Fig. B). Each year, 60,000 individuals become intermediate at liver-risk drinkers and 9,500 switch from intermediate to high at-risk consumption.

If the current decrease in per capita consumption continues (scenario 1), it will be 10.6L in 2026 (–4.5% over 5 years) and there will be 350,000 new at liver-risk drinkers over 2021–2026. If the per capita consumption significantly drops to 10L in 2026 (–10%, scenario 2), 7,400 intermediate at liver-risk drinkers would be avoided and ~1,200 intermediate at liver-risk drinkers will not switch into high at liver-risk drinking (Fig. C).



Conclusion: Although these 2 scenarios will allow differences in terms of incident cases, the expected prevalence will be little changed and 4.5% of the 15–64 y-o would be at-liver risk drinkers. 1/1000 French initiates an alcohol intake ≥ 20 g/d each year. In 2021, 1.9 million of French people have an alcohol consumption associated with a risk of cirrhosis and 310,000 of them have a high risk (≥ 50 g/d). By quantifying for the 1st time the incidence of French people drinking ≥ 20 g/d, this model could help developing new public health strategies targeting the reduction of ALD morbidity and mortality.

THU229

Blood donors in Europe have substantially higher risk of exposure to HEV than in North America: results from a systematic review and meta-analysis

Annika Wolski¹, Ann-Kathrin Ozga², Marylyn Addo¹, Samuel Huber¹, Ansgar W. Lohse¹, Sven Pischke¹, Thomas Horvatits¹. ¹University Medical Center Hamburg-Eppendorf, Center for Internal Medicine I, Medical Clinic and Polyclinic, Hamburg, Germany; ²University Medical Center Hamburg-Eppendorf, Medicine Institute of Medical Biometry and Epidemiology, Hamburg, Germany
Email: annika@wolski.at

Background and aims: The increasing number of diagnosed hepatitis E virus (HEV) infections in Europe, as well as the potentially

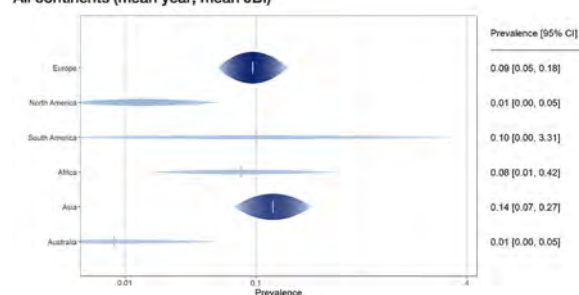
fatal consequences in vulnerable patients resulting from this disease, led to the implementation of blood product-testing in various countries. However, many nations, including the U.S. have not yet implemented such screening efforts. To assess the need for HEV-screening in blood products worldwide, we conducted a systematic review and meta-analysis comparing the rate of HEV RNA positivity and anti-HEV seroprevalence in blood donors.

Method: Studies reporting the anti-HEV IgG and/or HEV-RNA positivity rates among blood donors worldwide were identified via predefined search terms ("Hepatitis e" OR "HEV") AND ("blood donors" OR "transfusion" OR "blood donation" OR "blood testing") in Pubmed and Scopus. Data were stratified by year of publication, country/continent, diagnostic assay and methodological quality (according to PRISMA). Estimates were calculated by pooling study data (separately for each country/continent) via multivariable linear mixed effects meta regression analysis.

Results: Out of 1,103 studies, 151 (14%) were included in the final analysis. Estimated HEV viremia rate ranged from 0.01% to 0.14% worldwide (56 studies, 3,438,276 blood donors). Highest estimated HEV viremia rates were seen in Asia (0.14%), followed by South America (0.10%), Europe (0.09%), Africa (0.08%), Australia and North America (each 0.01%). In Europe highest rates could be found in Serbia (0.31%), closely followed by Germany (0.28%) and France (0.18%). Rate of HEV viremia as well as anti HEV seroprevalence were significantly lower in North America in comparison to Europe (OR = 0.14 [95% CI 0.03–0.58]; OR = 0.62 [95% CI 0.35–1.10]), independently of year of publication and methodological quality.

Prediction

All continents (mean year; mean JBI)



Conclusion: Our data demonstrate large regional differences regarding the risk of exposure to HEV. Considering the cost-benefit ratio, this supports blood-product screening programs in areas of high endemicity, such as Europe or Asia, in contrast to low-endemic regions, such as the U.S.

THU230

A population based-study of rates and trends of hepatitis C in immigrants and the Canadian-born in Quebec, Canada, 1998–2018

Ana Maria Passos-Castilho^{1,2}, Marina B. Klein^{2,3}, Julie Bruneau^{4,5}, Dimitra Panagiotoglou⁶, Karine Blouin⁷, Donald Murphy⁸, Christina Greenaway^{1,2,9}. ¹Lady Davis Institute, Jewish General Hospital, Centre for Clinical Epidemiology, Montreal, Canada; ²McGill University, Department of Medicine, Montreal, Canada; ³McGill University Health Center, Division of Infectious Diseases, Montreal, Canada; ⁴Centre Hospitalier de l'Université de Montréal, CHUM Research Centre, Montreal, Canada; ⁵Université de Montréal, Department of Family and Emergency Medicine, Faculty of Medicine, Montreal, Canada; ⁶McGill University, Department of Epidemiology, Biostatistics and Occupational Health, Montreal, Canada; ⁷Institut National de Santé Publique du Québec, Unité des infections transmissibles sexuellement et par le sang, Québec, Canada; ⁸Institut National de Santé Publique du Québec,

Laboratoire de Santé Publique du Québec, Sainte-Anne-de-Bellevue, Canada; ³Jewish General Hospital, Division of Infectious Diseases, Montreal, Canada
Email: anampassos@gmail.com

Background and aims: Immigrants bear a disproportionate hepatitis C (HCV) burden in Canada. They account for 30% of HCV cases and are at increased risk of end stage liver disease and liver cancer at the time of diagnosis. Determining sub-groups of immigrants at highest HCV risk will be essential to supporting micro-elimination efforts in this population. We estimated annual reported rates and trends of HCV over a 20-year period in Quebec.

Method: A population-based cohort of all HCV cases in Quebec from 1998 to 2018 reported to public health and the provincial reference laboratory were linked to the provincial health registry and the landed immigrant database. Immigrant status and country of birth were assigned through linkage to the immigrant database. Region of birth was classified by World Bank regions; East Asia/Pacific (SEA), South Asia (SA), Middle East/North Africa (MENA), Sub-Saharan Africa (SSA), Latin America/Caribbean (LAC), Western Europe (EUS), Other Europe/Central Asia (OECA) and North America/Australia/New Zealand (NAANZ). Annual reported crude cumulative incidence rates of HCV among immigrants and the Canadian-born were estimated using Quebec population census data during the study period. Comparative rate ratios (RR) with 95% confidence intervals (CI) and the trend of HCV rates over the study period stratified by immigrant status were estimated using Poisson regression.

Results: Among 34,881 HCV cases identified, 13.5% (n = 4,720) were immigrants. Immigrants were older (median 46.8 vs. 44.1 years; p < 0.001) and diagnosed a median of 9.3 (IQR 2.8–17.2) years after arrival in Quebec. Comparing immigrants with Canadian-born: the HCV average annual rate/100,000 population was 33.1 vs. 30.8 and 18.4 vs. 12.3 during the periods 1998–2008 and 2009–2018, respectively; and the RR was 1.08 (1.03–1.12) in 1998–2008, and 1.50 (1.42–1.57) in 2009–2018. Between 2009 and 2018, subgroups of immigrants with higher HCV rates compared to the Canadian-born were those from OECA [rate; RR (95% CI); 45.6; 3.7 (2.0–7.0)], SSA [44.7; 3.6 (1.9–6.8)], and SA [28.8; 2.3 (1.2–4.6)]. Rates decreased more slowly over the study period among immigrants vs. Canadian-born [–4.84% (–6.17–3.49%) vs. –7.74% (–9.22–6.24%)] per year.

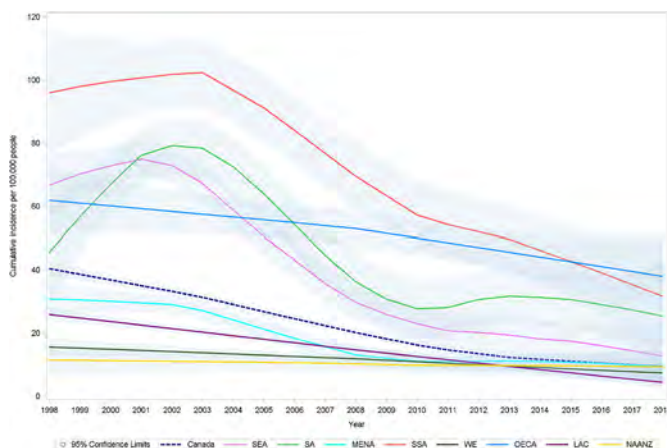


Figure: Reported rates of HCV cases per 100,000 people by region of origin (1998–2018). Smoothed (loess) reported crude cumulative incidence with 95% confidence bounds.

Conclusion: High rates of HCV among immigrants and long delays to HCV diagnosis after arrival in Canada highlight important gaps in HCV screening among immigrants. These data can be used to inform micro elimination efforts among the immigrant population in Quebec and Canada.

THU231

HBV screening in west african migrant community and faith-based organizations increases HBV vaccination among this high-risk population in greater Barcelona, Spain

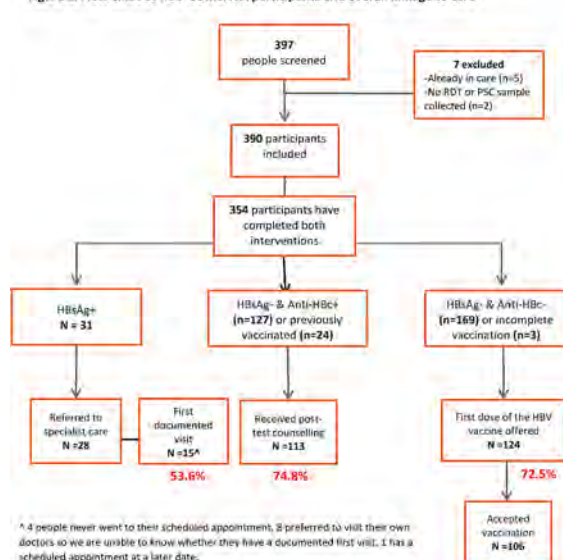
Camila Picchio¹, Ariadna Rando-Segura², Emma Fernandez¹, Nélida López¹, Silvia Gómez Araujo¹, Daniel Kwakye Nomah³, Omar Diatta^{1,4}, Sergio Rodríguez-Tajes^{5,6}, Sabela Lens^{5,6}, Xavier Forn^{5,6}, Francisco Rodríguez-Frías², Maria Buti^{6,7}, Jeffrey Lazarus¹. ¹Barcelona Institute for Global Health (ISGlobal), Hospital Clínic, University of Barcelona, Barcelona, Spain; ²Liver Pathology Unit, Biochemistry and Microbiology Service, Hospital Universitari Vall d'Hebron, Barcelona, Spain; ³Center for Epidemiological Studies on HIV/AIDS and STIs in Catalonia (CEEISCAT), Badalona, Spain; ⁴Community and Public Health Unit, Department of International Health Drassanes-Hospital Universitari Vall d'Hebrón. Programa de Salut Internacional de l'Institut Català de la Salut (PROSICS), Spain; ⁵Liver Unit, Hospital Clínic, IDIBAPS, University of Barcelona, Barcelona, Spain; ⁶CIBER Hepatic and Digestive Diseases (CIBERehd), Instituto Carlos III, Madrid, Spain; ⁷Liver Unit, Hospital Universitari Vall d'Hebron, Barcelona, Spain
Email: camila.picchio@isglobal.org

Background and aims: African migrant populations living in Europe are disproportionately affected by HBV infection and oftentimes use health services at lower rates due to structural and/or cultural/linguistic barriers. Efforts to scale up prevention, testing, and treatment are needed to reach the 2030 hepatitis elimination targets set by the WHO. The HBV-COMSAVA study aims to use point-of-care testing with simplified diagnostic tools in community settings to identify and link to care or vaccinate west African migrants in the greater Barcelona area.

Method: 393 study participants were offered HBV screening in a “pop-up” clinic in a community setting from 21/11/20–13/11/21. Rapid tests to screen for the presence of HBsAg were used and a blood sample was collected using plasma separation cards and analyzed in a laboratory. The interactive tool, *HeparJoc*, was used to increase HBV knowledge, which was co-created by migrant populations. HBsAg+ patients were given a referral to a specialist on the spot. Remaining patients received their results during a second pre-programmed visit and were offered: post-test counselling (PTC) or vaccination of the first dose of the HBV vaccine *in situ*. Vaccination cards and referrals to their primary care center for subsequent doses were provided to all who received first doses. Sociodemographic and linkage to care data were collected and basic standard descriptive statistics were utilized using STATA software.

Results: 354 were included for analysis. 75.1% returned to receive their results and were linked to care or offered PTC with 44.6% (n = 158) showing evidence of past or current HBV infection. The overall HBsAg prevalence was 8.8% (n = 31). Of those who were HBsAg+, anti-HBc positivity was detected in 35.9% (n = 127). The majority (n = 172) required vaccination against HBV, followed by post-test counselling (n = 151) and referral to a specialist (n = 31) (Figure 1). The HBV vaccination acceptance rate was 85.4% and the main reason for not accepting included having results picked up by a family member and not being physically present (38, 9%, n = 7).

Figure 1. Flow chart of HBV-COMSAVA participants and overall linkage to care



Conclusion: Despite the COVID-19 pandemic, by employing a community-based model of care utilizing novel simplified diagnostic tools, the HBV-COMSAVA study demonstrated the possibility to screen and vaccinate African migrants who may otherwise not have received care, reducing the possible pool of new infections among this high-risk group.

THU232

Community-based HBV testing among west african migrants in greater Barcelona, Spain increases linkage to specialist care and vaccination: the HBV-COMSAVA model

Camila Picchio¹, Daniel Kwakye Nomah², Ariadna Rando-Segura³, Silvia Gómez Araujo¹, Emma Fernandez¹, Omar Diatta^{1,4}, Maria Buti^{5,6}, Sergio Rodríguez-Tajes^{6,7}, Sabela Lens^{6,7}, Xavier Forn^{6,7}, Nélida López¹, Francisco Rodríguez-Frías³, Jeffrey Lazarus¹. ¹Barcelona Institute for Global Health (ISGlobal), Hospital Clínic, University of Barcelona, Barcelona, Spain; ²Center for Epidemiological Studies on HIV/AIDS and STIs in Catalonia (CEEISCAT), Badalona, Spain; ³Liver Pathology Unit, Biochemistry and Microbiology Service, Hospital Universitari Vall d'Hebron, Barcelona, Spain; ⁴Community and Public Health Unit, Department of International Health Drassanes-Hospital Universitari Vall d'Hebrón. Programa de Salut Internacional de l'Institut Català de la Salut (PROSICS), Barcelona, Spain; ⁵Liver Unit, Hospital Universitari Vall d'Hebron, Barcelona, Spain; ⁶CIBER Hepatic and Digestive Diseases (CIBERehd), Instituto Carlos III, Madrid, Spain; ⁷Liver Unit, Hospital Clínic, IDIBAPS, University of Barcelona, Barcelona, Spain
Email: camila.picchio@isglobal.org

Background and aims: Hepatitis B virus (HBV) infection affects an estimated 250 million people worldwide. Sub-Saharan Africa is disproportionately affected, particularly west and central African countries. Migrants arriving to Europe from these high-endemic areas may be unaware of their HBV status due to the unreliable testing and vaccination strategies in their home countries and underutilization of the host country health services, delaying timely diagnosis and linkage to care. The HBV-COMSAVA study aims to use point-of-care testing with simplified diagnostic tools in community settings to identify and link to care or vaccinate west African migrants in the greater Barcelona area. We report the HBV prevalence, associated risk factors, and the continuum of care.

Method: From 21/11/20–13/11/21, 397 people were offered HBV testing in community settings in greater Barcelona. Participants were first tested with an HBsAg rapid detection test (DETERMINE™ HBsAg 2, Abbott Inc.). Then a whole blood sample (140 µl per spot) was

collected utilizing a plasma separation card (PSC) (cobas® PSC, Roche Diagnostics) which was air-dried and transported to the laboratory. Those who tested positive for HBsAg were provided an instant referral to one of two collaborating tertiary hospitals where a full work-up was done, including liver function tests and liver fibrosis assessment (Fibroscan®). The proportion of participants with different HBV-serological status analyzed as of November 16, 2021 are reported using descriptive stats (STATA 16.0).

Results: 379 participants are included; 314 (82.8%) were Ghanaian with a mean age of 41.1 years (SD = 10.0), and 41.9% (n = 159) were female. The overall HBsAg prevalence was 9.0% (n = 34) of which 14 (41.2%) had detectable HBV-DNA and two (5.9%) had anti-HDV antibodies, none were HBeAg+. The mean HBV-DNA and HBsAg levels among patients attending a first specialist visit (n = 17) was 125, 834 UI/ml and 8, 190 UI/ml, respectively. Evidence of past resolved infection (anti-HBc+) was seen in 35.6% (n = 135) of those who were HBsAg- (Table 1).

Table 1. Description of participants who were HBsAg+, HBsAg-/anti-HBc+, and HBsAg-/anti-HBc-.

	HBsAg+ (n=34)	HBsAg-/ Anti-HBc+ (n=135)	HBsAg-/ anti-HBc- (n=204)
Age, SD	39.9 (9.0)	41.8 (9.5)	40.8 (10.5)
Female, n (%)	10 (29.4)	62 (45.9)	84 (41.2)
Years in Spain			
0-5	7 (20.6)	34 (25.2)	55 (27.1)
6-12	11 (32.3)	28 (20.7)	41 (20.2)
13-20	12 (35.3)	61 (45.2)	87 (42.9)
21+	2 (5.9)	10 (7.4)	18 (8.9)
Missing values	2 (5.9)	2 (1.5)	2 (1.0)
Education level			
No education	3 (8.8)	13 (9.6)	13 (6.4)
Primary school completed	9 (26.5)	22 (16.3)	41 (20.2)
Secondary school completed	17 (50.0)	91 (67.4)	112 (55.2)
Undergraduate/trade school of greater completed	5 (9.6)	9 (6.7)	38 (18.6)
Country of origin			
Ghana	30 (88.2)	115 (85.2)	165 (81.3)
Senegal	3 (8.8)	19 (14.1)	32 (15.8)
Liberia	1 (2.9)		
Mali	0 (0)	0 (0)	1 (0.5)
Nigeria	0 (0)	0 (0)	2 (1.0)
Niger	0 (0)	0 (0)	1 (0.5)
Cameroon	0 (0)	0 (0)	2 (1.0)
Benin	0 (0)	1 (0.7)	0 (0)
Traditional tattoo or scarring	0 (0)	5 (3.7)	2 (1.0)
HIV or STI diagnosis	1 (2.9)	2 (1.5)	2 (1.0)
Ever been in jail	0 (0)	2 (1.5)	5 (2.5)
Ever received surgery outside of Spain	3 (8.8)	16 (11.8)	20 (9.8)
Family member living with HBV	4 (11.8)	14 (10.4)	14 (6.9)
Self-reported HBV vaccination status			
Complete	4 (11.8)	14 (10.4)	19 (9.4)
1 or 2 doses	0 (0)	3 (2.2)	4 (1.9)
Don't know/Not sure	3 (8.8)	26 (19.3)	38 (18.7)
HBV-DNA (mean, UI/mL)*	125,834	-	-
qHBsAg (mean, UI/mL)*	8,190	-	-
HBeAg+ (n,%)	0 (0)		

* Only patients who had a first documented visit with one of the participating hospitals are included here (n = 17) ^b Fibrosis stage determined by Fibroscan® Missing values are not reported

Conclusion: This ongoing community-based HBV screening program provides an effective model of identifying and providing care to migrant populations at high risk of HBV infection in the greater

Barcelona area, who otherwise may not have been previously engaged in care. Community screening initiatives can increase testing, vaccination, and linkage to care, helping to reach the 2030 WHO HBV elimination targets.

THU233

The impact of COVID-19 pandemic control measures on HCV treatment initiation in British Columbia, Canada

Naveed Janjua^{1,2}, Stanley Wong¹, Dahn Jeong^{1,2}, Mawuena Binka¹, Terri Buller-Taylor¹, Sofia Bartlett¹, Prince Adu¹, Hector Velasquez¹, Makuza Jean Damascene², Amanda Yu¹, Maria Alvarez¹, Jason Wong¹, Mel Krajden¹. ¹BC Centre for Disease Control, Vancouver, Canada; ²The University of British Columbia, School of Population and Public Health, Vancouver, Canada
Email: naveed.janjua@bccdc.ca

Background and aims: Coronavirus disease 2019 (COVID-19) and measures taken to limit the transmission of severe acute respiratory syndrome coronavirus 2 (SARS-CoV-2) have directly and indirectly restricted access to healthcare services worldwide. We assessed the impact of these measures, first introduced in British Columbia (BC), Canada in March 2020, on hepatitis C (HCV) treatment initiation.

Method: We used data from the BC Hepatitis Testers Cohort, a large population-based cohort integrating data on HCV testing, primary care visits, hospitalizations, and medication dispensations. We compared the monthly HCV treatment initiations during 2020 with those in 2018 and 2019. We compared the sociodemographic and clinical characteristics of people initiating HCV treatment during pre-pandemic time period (Jan 2018-Feb 2020) to those initiating treatment during pandemic time period (Apr-Aug 2020).

Results: There was a declining trend in HCV treatment initiations pre-pandemic from 3, 172 in 2018 to 2, 331 in 2019 (26% reduction). However, there was a higher decline in 2020 to 1, 475 treatment initiations (37% reduction from 2019). HCV treatment initiations decreased immediately following the imposition of pandemic control measures; monthly pre-pandemic average treatment initiations fell from 172 to 106 during the pandemic (38% change).

There were slight decreases in treatment initiations for the 1945–64 birth cohort (56% to 45%) and for people with HIV coinfection (5.9% to 4.3%) or HBV co-infection (5% to 4.3%). However, there was a slight increase in treatment initiation among the ≥1975 birth cohort (19% to 29%), people who inject drugs (44% to 49%), and people with problematic alcohol use (32% to 37%) between pre-pandemic and pandemic time periods, respectively.

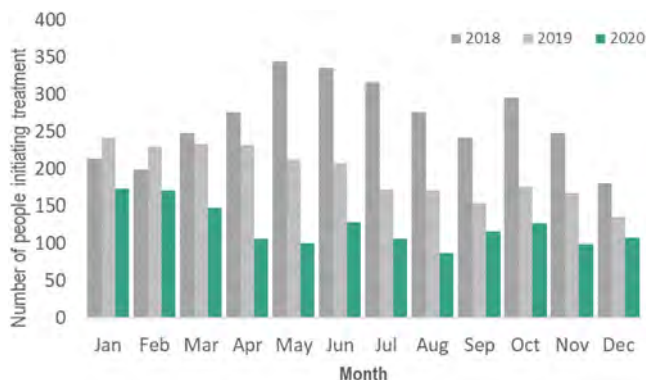


Figure: Monthly HCV treatment initiations 2018–2020, British Columbia, Canada

Conclusion: Similar to other healthcare services and HCV testing, there was a reduction in HCV treatment initiation following the introduction of control measures. Pandemic-related disruptions and the overall decline of treatment initiations could have a negative impact on progress towards HCV elimination goals.

THU234

Negative impact of COVID-19 infection related to life disruption events and health scores on patients with chronic liver disease

Zobair Younossi^{1,2,3}, Yusuf Yilmaz⁴, Mohamed El Kassas⁵, Ajay Kumar Duseja⁶, Saeed Sadiq Hamid⁷, Gamal Esmat⁸, Nahum Méndez-Sánchez⁹, Wah-Kheong Chan¹⁰, Ashwani Singal¹¹, Janus Ong¹², Brian Lam^{1,2}, Sean Felix¹, Elena Younossi¹, Manisha Verma^{1,2}, Jillian Price¹, Fatema Nader¹³, Issah Younossi¹³, Andrei Racila^{1,2,3}, Maria Stepanova². ¹Betty and Guy Beatty Center for Integrated Research, IHS; ²Center for Liver Disease, Inova Medicine; ³Inova Health System, Medicine Service Line; ⁴Department of Gastroenterology, Marmara University, Turkey; ⁵Helwan University; ⁶Postgraduate Institute of Medical Education and Research; ⁷Department of Medicine, Aga Khan University; ⁸Endemic Medicine and Hepatogastroenterology Department, Cairo University; ⁹Medica Sur Clinic and Foundation; ¹⁰University of Malaysia, Gastroenterology and Hepatology Unit; ¹¹University of South Dakota and Avera Transplant Institute; ¹²University of the Philippines, College of Medicine; ¹³Center for Outcomes Research in Liver Disease
Email: zobair.younossi@inova.org

Background and aims: Patients with chronic liver disease (CLD) may experience a substantial burden from COVID-19 infection as well as disruption of life and routine healthcare associated with the pandemic. We assessed the impact of COVID-19 pandemic on patients with CLD.

Method: Patients with CLD enrolled in our Global Liver Registry since 2018 completed a specifically designed 23-item COVID-19 survey between March 2020–November 2021. Questions included patients' COVID-19 infection status and, if infected, characteristics of the illness, along with various aspects of pandemic-related life disruptions for everyone regardless of the infection.

Results: As of November 2021, from 11, 200 historic enrollees, 2635 from 7 countries completed the survey: 21% chronic hepatitis B, 14% chronic hepatitis C, and 66% non-alcoholic fatty liver disease; mean (SD) age 49 ± 13 years, 53% male. Of all survey completers, 10.3% reported having had COVID-19. Of those infected, 87% reported being diagnosed by a laboratory test, 94% had at least one symptom, and 73% received treatment for their symptoms. The mean (SD) duration of their illness was 12.5 ± 10.7 days, 66% reported receiving antiviral treatment, 19% were hospitalized, 13% needed oxygen support but no one was put on mechanical ventilation. Of all included CLD patients regardless of COVID-19 infection, 11.4% reported that the pandemic had an impact on their liver disease ($p = 0.45$ between those who were and were not infected); the majority of those (75%) reported delays in follow-up care. The Life Disruption Event Perception (LDEP) questionnaire confirmed that 80% of COVID-19-infected patients vs. 69% patients without history of COVID-19 infection ($p = 0.0001$) experienced worsening in at least one aspect of their life (food/nutrition, exercise, social life, vocation/education, financial situation, housing, or healthcare). The most substantial worsening was observed for social life (73% in infected vs. 61% in not infected), exercise (49% vs. 42%), and financial situation (36% vs. 30%) (all $p < 0.05$). Self-assessed health scores were lower in patients with history of COVID-19 than in those not infected: 6.8 ± 2.1 vs. 7.4 ± 2.2 (on a 1–10 scale with 10 indicating perfect health) ($p < 0.0001$) despite similar scores reported before the pandemic (8.5 ± 1.4 vs. 8.4 ± 1.6 , $p = 0.77$). In multivariate regression analysis, after adjustment for country of enrollment, liver disease etiology and severity (assessed by FIB-4 score), age, sex, BMI, diabetes, and history of psychiatric comorbidities, having had COVID was found to be independently associated with lower self-assessed health scores ($\beta = -0.62 \pm 0.13$, $p < 0.0001$).

Conclusion: Patients with CLD experienced a substantial burden of COVID-19 pandemic on their daily lives regardless of actual infection history. Self-reported health scores were lower in patients with history of COVID-19 infection.

POSTER PRESENTATIONS

THU235

Associations of food insecurity and fast-food consumption with diet quality in adults with non-alcoholic fatty liver disease in a large population-based U.S. cohort

Ani Kardashian¹, Jennifer Dodge^{1,2}, Norah Terrault¹. ¹University of Southern California, Division of Gastrointestinal and Liver Diseases, Los Angeles, United States; ²University of Southern California, Department of Population and Public Health Sciences, Los Angeles
Email: ani.kardashian@med.usc.edu

Background and aims: Food insecurity (FIS) impacts the quality of foods consumed and is associated with greater risk of non-alcoholic fatty liver disease (NAFLD). While racial-ethnic disparities in NAFLD risk have been reported, the interplay between FIS, diet quality (DQ) and fast food (FF) consumption in different racial-ethnic groups with NAFLD has not been explored.

Method: A cross-sectional analysis of adults (≥ 20 years) in the U.S. National Health and Nutrition Examination Survey 2017–2018 with valid transient elastography and food security (FS) measurements using the U.S. Department of Agriculture Food Security Survey Module was performed. NAFLD was defined as controlled attenuated parameter score ≥ 280 decibels/meter without other known liver disease. Diet quality (DQ) was assessed by the healthy eating index (HEI)-2015 (score range 0–100), with poor DQ defined as $< 25^{\text{th}}$ percentile of possible scores. We used multivariable linear and logistic regression to examine associations of FIS, FF consumption, and race/ethnicity with DQ and its individual components.

Results: In total, 1,420 adults had NAFLD, of whom 520 (37%) were food insecure. Food insecure compared to food secure adults were more likely to be non-Hispanic (NH) black (11% vs 7%), Hispanic (33% vs 13%), foreign born (28% vs 15%), live in poverty (31% vs 4%), or have public/no insurance (59% vs 27%). Mean (standard error) DQ score was 49.1 (0.9) and 46.7 (1.2) for food secure and insecure groups, respectively. Controlling for age, gender, race/ethnicity, poverty, education, and alcohol use, FIS was associated with a 2.5-unit lower DQ score, though did not reach statistical significance (95%CI: -5.7 to 0.7). However, FF consumption was associated with a -0.7 unit lower DQ score (per additional FF meal consumed weekly; 95%CI: -1.0 to -0.4). NH blacks (+2.9 units, 95%CI[0.3–5.4]), NH Asians (+9.3[5.1–13.6]), and Hispanics (+5.2[1.1–9.2]) all had significantly better overall mean DQ than NH whites. Odds ratios of poor DQ for individual components are shown in the table. NH blacks, Asians, and Hispanics had lower odds of saturated fat consumption compared to NH whites, but differences between groups were also seen for total vegetables, whole fruits, whole grains, and total protein. The largest differences in individual DQ components by FS were seen among NH whites; in this group, food insecure (vs secure) adults had a greater proportion of poorer scores for seafood/plant proteins (60% vs 46%) and added sugars (29% vs 11%).

Table. Multivariable logistic regression* evaluating the association of race/ethnicity with odds of poorer diet quality components compared to NH Whites

Race/ethnicity	Total vegetables	Whole fruits	Whole grains	Total protein	Saturated fats	Added sugars
	OR (95% CI)	OR (95% CI)	OR (95% CI)	OR (95% CI)	OR (95% CI)	OR (95% CI)
NH white	reference	reference	reference	reference	reference	reference
NH black	1.06 (0.76–1.48)	0.94 (0.51–1.73)	1.04 (0.55–1.97)	1.07 (0.56–2.07)	0.37 (0.25–0.56)	1.13 (0.68–1.87)
NH Asian	0.80 (0.40–1.60)	0.44 (0.22–0.89)	0.50 (0.27–0.94)	2.74 (1.03–7.29)	0.41 (0.18–0.91)	0.64 (0.27–1.56)
Hispanic	0.59 (0.36–0.94)	0.40 (0.22–0.73)	0.99 (0.60–1.63)	0.67 (0.20–2.22)	0.40 (0.26–0.62)	0.66 (0.37–1.17)

*model also controlled for food security status, poverty, age, gender, education level, alcohol use

Conclusion: There was a trend towards worse DQ in food insecure adults with NAFLD. Fast-food consumption was also associated with lower DQ in NAFLD. NH whites had the lowest DQ with food insecurity potentiating poor DQ. Exploration of the sociocultural factors contributing to the observed differences in DQ by race/ethnicity may offer the potential opportunity to mitigate NAFLD disparities and reduce disease burden.

THU236

Implementation of HCV screening in the 1969–1989 birth-cohort undergoing COVID-19 vaccination: a pivotal study in Italy

Roberta D'Ambrosio¹, Giuliano Rizzardini², Massimo Puoti³, Stefano Fagioli⁴, Maria Paola Anolli¹, Claudia Gabiati⁵, Federico D'Amico³, Luisa Pasulo⁴, Massimo Colombo⁶, Pietro Lampertico^{1,7}. ¹Foundation IRCCS Ca' Granda Ospedale Maggiore Policlinico, Gastroenterology and Hepatology, Milan, Italy; ²ASST Fatebenefratelli-Sacco, First Division of Infectious Diseases, Milan, Italy; ³ASST Grande Ospedale Metropolitano Niguarda, Division of Infectious Diseases, Milan, Italy; ⁴AASST Papa Giovanni XXIII, Gastroenterology, Hepatology and Transplantation, Bergamo, Italy; ⁵ASST Fatebenefratelli-Sacco, Internal Medicine, Italy; ⁶Ospedale San Raffaele, Liver Center, Milan, Italy; ⁷University of Milan, CRC "A. M. and A. Migliavacca" Center for Liver Disease, Department of Pathophysiology and Transplantation
Email: roberta.dambrosio@policlinico.mi.it

Background and aims: The World Health Organization (WHO) goal of hepatitis C virus (HCV) elimination by 2030 relies on the scaling-up of policies of both identification and treatment of the infected population, worldwide. In Italy, it has been estimated that at least 200,000 people are unaware of their HCV infection thus reinforcing the need for broadening population access to effective screening programs.

Method: A pivotal screening program targeting subjects born between 1969 and 1989 has been conducted in Lombardy, Northern Italy, where point-of-care (POC) testing was offered for free concomitantly to COVID-19 vaccination.

Result: Overall, 7,219 subjects underwent HCV screening in 4 vaccination hubs. Characteristics of the screened cohort and pivotal strategies are reported in Table. Seven (0.1%) subjects tested anti-HCV positive and 5 (0.07%) were HCV-RNA positive by standard confirmation tests. Patients with HCV infection were all males, aged 41–46 years; only one of them came from Italy. Clinical data were available for 3 patients: all of them have altered transaminases, without HBV or HIV co-infection; HCV genotypes were 1b, 3 and 4, and liver stiffness ranged between 4.5 and 10.3 kPa. All patients underwent DAA therapies.

Table: Pivotal screening strategies according to each participating Center

	Milan Policlinico (N = 4,000)	Milan FBF-Sacco (N = 1,222)	Milan Niguarda (N = 1,000)	Bergamo (N = 997)
Time spent for screening program, hours	53	25	128	16
Daily vaccinations [§]				
Any birth-cohort	7,081 (5,833–9,440)	1,803 (427–1,978)	694 (260–894)	2,365 (2,080–2,650)
1969–1989 birth-cohort	2,726 (2,077–3,447)	766 (183–923)	336 (80–605)	1,355 (1,325–1,385)
Proposed anti-HCV POC	4,721	1,629	NA	1,575
Accepted anti-HCV POC	4,000 (85%)	1,222 (75%)	1,000 (NA%)	997 (63%)
Age, years	42 (32–52)	44 (32–52)	44 (32–52)	43 (32–52)
Males	1,840 (46%)	745 (61%)	432 (43%)	NA
Screening Team (per day)	9–12	5–6	2–3	9–11
Physicians	3–4	2	1	2
Nurses	3–4	2–3	0–1	3–4
Others	3–4	1 Auxiliary Nurse	0–1	4–5
Research Assistants			Research Assistant	Volunteers
Anti-HCV positive by POC test	6 (0.15%)	0	0	1 (0.10%)
Lost to follow-up after POC test	1 (0.01%)	–	–	0
Anti-HCV positive by confirmatory test	4 (0.10%)	–	–	1 (0.10%)
HCV-RNA positive	3 (0.08%)	–	–	1 (0.10%)

Results are reported as number (n) and percentages (%) or median (range).

HCV: Hepatitis C Virus; POC: Point-of-Care; NA: Not Available

[§]refers only to screening days, in each vaccination hub;

*all from patients' alliance

Conclusion: This pivotal study demonstrated the feasibility of a POC-based anti-HCV screening program in young adults undergoing

COVID-19 vaccination. The prevalence of HCV infection in subjects born in the 1969–1989 cohort in Italy seems to be lower than previously estimated, thus raising the question whether more HCV carriers can be identified if screening is moved up to embrace subjects born before 1969.

THU237

Real life pooling of plasma samples for hepatitis C RNA detection as a screening strategy of hepatitis C active chronic infection

A. Aguilera^{1,2,3}, M. Cea^{1,2,3}, A. Fuentes^{4,5}, S. Pereira^{1,2,3}, L. Vinuela^{4,5}, Federico Garcia Garcia^{4,5,6}. ¹University Hospital of Santiago de Compostela, Microbiology, Santiago de Compostela, Spain; ²University of Santiago de Compostela, Microbiology, Santiago de Compostela, Spain; ³Instituto de Investigación Sanitaria de Santiago, Santiago de Compostela, Spain; ⁴University Hospital Cinic San Cecilio, Microbiology, Granada, Spain; ⁵Instituto de Investigación Biosanitario Ibs. Granada, Granada, Spain; ⁶Ciber Enfermedades Infecciosas ISCIII, Granada Email: antonio.aguilera.guirao@sergas.es

Background and aims: The diagnosis of active hepatitis C virus (HCV) infection is the necessary first step for its elimination. In most countries, universal population screening and/or screening by age groups have not been adopted due to cost and cost-effectiveness considerations. Here we show a real-life sample pooling diagnosis strategy to overcome this challenge, and to contribute to increase the diagnostic capacity of clinical laboratories and expand access to massive screening of hepatitis C.

Method: we have analyzed consecutive samples submitted to microbiology services of CHUS (Santiago de Compostela, Spain) and HUCSC (Granada, Spain) for hepatitis C diagnosis during the first three weeks of November 2022. Samples were tested for HCV antibodies and, in parallel and in a blinded way, were pooled into 100 samples with the following strategy: first, 10 pools of 10 samples were built (a); second, two pools comprising five of the previous were made (b); finally, these two were pooled together and tested for HCV-RNA using Cobas® HCV 6800 (Roche Diagnostics) at CHUS and both Xpert HCV Viral load (Cepheid) and Cobas® HCV 6800 at HUCSC. When positive, the previous two pools (b) were tested and after, a strategy to unmask the positive (s) sample (s) that needed up to 15 total HCV-RNA tests was used.

Results: A total of 1700 samples (17 pools) were analyzed, 800 at CHUS and 900 at HUCSC. The overall anti HCV and HCV-RNA prevalence was 0, 24% (4/1700). After our pooling strategy, we could detect all samples previously detected by standard diagnosis (anti-HCV followed by reflex HCV-RNA testing). While 13 master pools were negative, we needed to unmask 4 master pools, resulting in 60 total HCV-RNA tests to finally unmask the positive sample for each master pool. Specificity and sensitivity of the pooling strategy were 100%. Given median current prices on the market in Spain for anti-HCV (3€) and HCV-RNA (30€), testing with the pooling strategy would have resulted in 3420 € save (5220 € by traditional testing vs 1800 € by the pooling strategy), and a cost of 1, 05€ per patient screened.

Conclusion: The strategy of pooling samples for the diagnosis of active HCV infection has advantages that should be exploited with the aim of eliminating HCV as a public health threat. Here we demonstrate that in settings with a low prevalence of chronic infection, by substantially improving cost-effectiveness, this strategy enables and provides the necessary sustainability for use in large-scale diagnosis of HCV.

THU238

Epidemiology of hepatocellular carcinoma in Portugal

Mario Jorge Silva^{1,2}, Guilherme Simões¹, Rita Catarina Saraiva¹, Filipe Calinas¹, Paulo Nogueira^{3,4,5,6}. ¹Centro Hospitalar Universitário Lisboa Central, Gastroenterology, Lisboa, Portugal; ²NOVA Medical School, Lisboa, Portugal; ³Faculdade de Medicina da Universidade de Lisboa, Instituto de Medicina Preventiva e Saúde Pública, Lisboa, Portugal; ⁴Faculdade de Medicina da Universidade de Lisboa, Instituto de Saúde Ambiental, Lisboa, Portugal; ⁵Faculdade de Medicina da Universidade de Lisboa, Área Disciplinar Autónoma de Bioestatística; ⁶Universidade NOVA de Lisboa, NOVA National School of Public Health, Comprehensive Health Research Center Email: mariojorgesilva01@gmail.com

Background and aims: There is scarce data on the burden of hepatocellular carcinoma (HCC) in Portugal. We aim to characterize the recent epidemiology of HCC in Portugal.

Method: We evaluated HCC-related hospital admissions and mortality in Portugal between 2010 and 2017. We analyzed all hospital admissions from patients with HCC in public hospitals (data from Portuguese Health System's Central Administration) and mortality due to HCC (data from National Statistics Institute)-coded with 155.0 (International Classification of Diseases-ICD-9-CM) or C22.0 (ICD-10). Additional analyses were performed to evaluate longitudinal trends and regional differences.

Results: Between 2010 and 2017, there were 20, 704 hospital admissions of patients with HCC, ranging annually from 2, 086 in 2010 to 2, 989 in 2015. In-hospital mortality rate during admission was 16.7%.

Considering individual patients admitted with HCC, the number of patients admitted annually varied from 1, 046 in 2010 to 1, 560 in 2017. 7, 739 individual patients were admitted during the 8-year period: 80.1% males and with mean age 66 ± 12.2 years.

In the whole country, both in-hospital and ambulatory, the annual number of deaths ranged from 471 in 2010 to 620 in 2017 (4, 316 deaths during the 8 years). Potential years of life lost ranged annually from 2477 in 2010 to 3838 in 2017.

Annual number of admissions, admitted patients, mortality and potential years of life lost are detailed in the table.

The mean annual mortality rate due to HCC, considering the 8-year period, was 5.2/100, 000 inhabitants (9.0/100, 000 inhabitants among males and 1.8/100, 000 inhabitants among females). The highest regional mortality rate was observed in the Lisbon metropolitan area (6.3/100, 000 inhabitants overall, 11.2/100, 000 inhabitants among males and 2.0/100, 000 inhabitants among females).

	2010	2011	2012	2013	2014	2015	2016	2017	Longitudinal trend 2010–2017 (p value)
Hospital admissions (n)	2086	2600	2425	2641	2694	2989	2793	2476	(p = 0.125)
Admitted patients (n)	1046	1205	1220	1376	1371	1511	1560	1410	Increasing (p = 0.003)
Deaths (n)	461	557	558	496	535	536	553	620	(p = 0.073)
Potential years of life lost (n)	2477	3215	3340	2955	3228	3005	3013	3838	(p = 0.126)

Conclusion: The burden of HCC in Portugal is high and had an increasing trend between 2010 and 2017.

THU239

“Zero C” hospital project: an innovative screening and referral model in hospitalized patients at different divisions

Valerio Rosato¹, Loreta Kondili², Riccardo Nevola¹, Alessio Aghemo³, Pasquale Perillo¹, Ruben Napolitano⁴, Antonio Sciambra⁵, Davide Mastrocinque¹, Ernesto Claar¹. ¹Ospedale Evangelico Betania, Liver Unit, Naples, Italy; ²Istituto Superiore di Sanità, Center for Global Health, Roma, Italy; ³Humanitas Clinical and Research Center IRCCS, Division of Internal Medicine and Hepatology, Department of Gastroenterology, Rozzano, Italy; ⁴Ospedale Evangelico Betania, Laboratory Medicine Unit, Naples, Italy; ⁵Ospedale Evangelico Betania, Health Management, Naples, Italy
Email: valeriososato@gmail.com

Background and aims: Chronic hepatitis C is a major public health problem in Southern Italy. Screening strategies in key populations and birth cohort 1969–1989 has been addressed for free of charge screening in Italy. However, larger birth population cohorts need to be screened due to expected high HCV prevalence. We conducted a hospital-based mass screening in order to assess the HCV active infection prevalence and address the feasibility of the opportunistic screening in the linkage to care of the infected patients.

Method: From January 2020 to May 2021 all consecutive in-patients were screened for HCV antibody (HCV Ab) at hospital admission throughout all divisions in the Evangelic Hospital Betania of Naples. HCV Ab positive patients were evaluated for previous HCV treatment. HCV RNA testing was required for those not previously treated. In patients with active infection the linkage to care and treatment start were planned within the hospital admission.

Results: Of 12.665 inpatients consecutively screened, 510 (4%) were HCV Ab positive. The HCV Ab positivity increased with age with the highest prevalence in those born before 1947 (9, 49%). In each birth cohort, 20–30% of patients have been previously treated whereas 30–45% were discharged and not tested for HCV RNA. 194 (38% of HCV +) patients were tested for HCV RNA and 91 (46.2%) had active HCV infection. 87 patients were treated during hospital admission, while 4 were not evaluated for treatment due to severe comorbidities. All patients treated achieved sustained virological response at week 12 (SVR 12). Among HCV RNA tested patients, 47% of 1969–1989 birth cohort, 35% of 1948–1968 birth cohort and 53% of those born before 1947 had active infection. Among 91 HCV RNA positive patients, 33 (36%) were admitted to liver unit for known liver damage without being HCV diagnosed or linked to care (all, except one, were born before 1968). The remaining 58 patients were admitted for comorbidities in cardiology, internal medicine, ophthalmology, surgery, orthopedics, senology and intensive care unit. Among them, 49 (54%) belonged to patients born before 1968 and 9 (10%) to 1969–1989 cohort. All available patients underwent linkage to care and treatment start during hospital admission. (Figure 1)

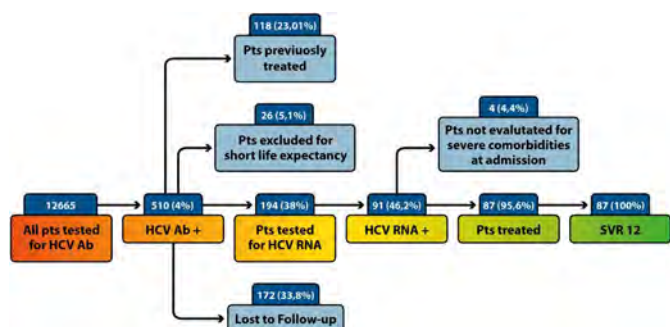


Figure 1: A care cascade during the opportunistic screening in Evangelic Hospital Betania of Naples (Italy) 2010–2020.

Conclusion: A high prevalence of active infection is observed in patients with comorbidities in Southern Italy. The possibility of active infection testing in less than 50% of HCV Ab positive patients

underline the importance of reflex testing for identifying active infection. HCV elimination requires increase of screening in patients who are unaware of the HCV status, but also of the screening and linkage to care in those with known liver damage yet unaddressed.

THU240

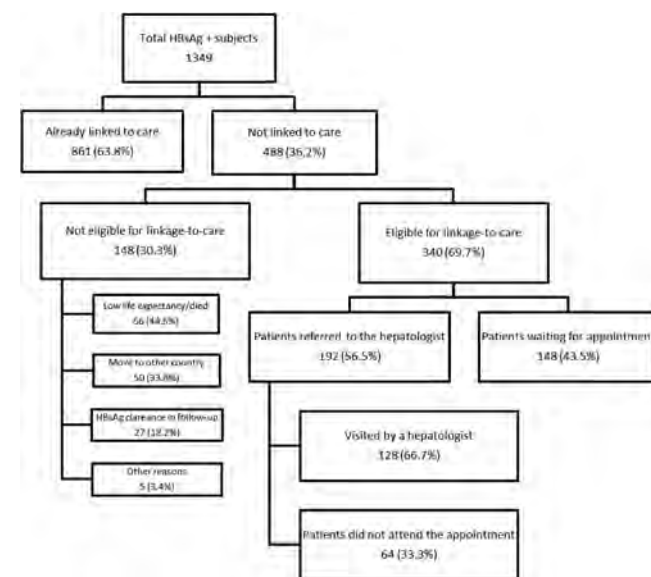
LINK-B: a hepatitis B program to test and link to care patients lost of follow-up

Ana Barreira^{1,2}, Ariadna Rando-Segura³, Anna Feliu-Prius¹, Francisco Rodríguez-Frías^{2,3}, Elena Vargas Accarino¹, Judit Vico-Romero¹, Mar Riveiro Barciela^{1,2}, Adriana Palom¹, Rafael Esteban^{1,2}, Maria Buti^{1,2}. ¹Hospital Universitario Vall de Hebrón, Liver Unit; ²Instituto de Salud Carlos III, Centro de Investigación Biomédica en Red de Enfermedades Hepáticas y Digestivas (CIBERehd); ³Hospital Universitario Vall de Hebrón, Microbiology Department
Email: mbuti@vhebron.net

Background and aims: Hepatitis B affects more than 250 million people worldwide. In Spain an estimated 320, 000 people are living with hepatitis B. Most HBsAg-positive individuals are not linked to care in our setting, and this is an obstacle to receiving treatment and controlling hepatitis B in the population. The primary aim of this research was to promote adequate linkage-to-care and treatment of HBsAg-positive individuals lost to follow-up.

Method: This is a single-center retrospective and prospective search of all HBsAg-positive cases in the microbiology database of the Northern Health Area of Barcelona (450, 000 inhabitants). The retrospective phase included all HBsAg cases seen between 2018 and 2020 and the prospective phase covered January 2021 to end 2022. Medical records were reviewed to identify and retrieve HbsAg-positive cases not linked to care. Candidates for contacting were called to offer disease assessment.

Results: Here, we present the data from January 2018 to end April 2019 (retrospective), and the first month of 2021 (prospective). In total, 1349 HBsAg-positive individuals were detected by the laboratory. The flowchart of patients is summarized in the Figure. After the initial assessment, 192 patients were referred to a hepatologist: 128 (66.7%) attended the visit and 33.3% did not. Overall baseline characteristics: mainly males (57.8%), median age 45 (± 14) years. Overall, 82.3% (152) were inactive carriers, 6 HBeAg-positive chronic hepatitis, 4 immune-tolerant and 12 (6.3%) could not be classified in a single determination. Baseline characteristics were similar between patients who attended the visit and those who did not.



Conclusion: The link B strategy showed that more than one-third of known HBsAg-positive individuals had not been linked to care, and enabled the retrieval of a large number of patients.

THU241

Testing for liver disease in primary care: fibrosis first

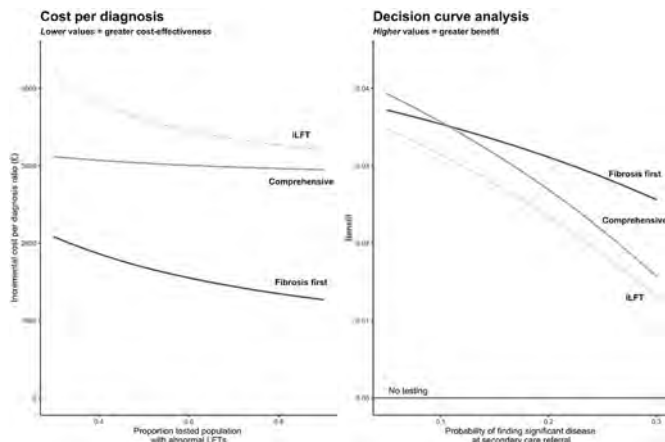
Ian Rowe^{1,2}, Richard Parker². ¹University of Leeds, Leeds Institute for Medical Research, United Kingdom; ²St James's Hospital, Leeds Liver Unit, United Kingdom

Email: i.a.c.rowe@leeds.ac.uk

Background and aims: The optimal method to identify persons with liver disease in primary care is unknown. Approaches to diagnose all persons with abnormal liver blood tests, e.g. intelligent liver function tests (iLFT), or screening all those with specific risk factors have been proposed but each incompletely identifies the population being tested in primary care. The aim of this study was to define testing strategies to identify persons with treatable liver disease and/or advanced fibrosis in primary care using unified pathways.

Method: A decision model was developed to assess 3 approaches to testing in comparison to the current practice of limited testing for liver disease and liver fibrosis in primary care. The outcomes considered were the incremental cost per diagnosis ratio and the net benefit of each pathway. Diagnosis was defined by treatable liver disease (viral hepatitis, metabolic liver disease, or autoimmune liver disease) and advanced fibrosis (in the case of alcohol-related liver disease or non-alcoholic fatty liver disease). The tested approaches were: 1. "iLFT" (full aetiology testing of persons with abnormal LFTs); 2. "Comprehensive" (full aetiology testing for abnormal LFTs and non-invasive fibrosis tests for all persons tested); 3. "Fibrosis first" (abbreviated aetiology testing [HBV, HCV, iron studies] and non-invasive fibrosis testing for all). These approaches were compared with current practice patterns where 20% of persons with newly abnormal LFTs undergo downstream testing. Parameters were estimated from literature data and costs were derived from the UK NHS.

Results: All tested approaches identified more persons with treatable liver disease ± advanced liver fibrosis than the current standard of care. In the base case scenario, where 80% of the tested population had abnormal LFTs, the fibrosis first approach made a diagnosis of treatable disease/advanced fibrosis in 3.9% of the total population compared with 3.8% for iLFT and 4.3% in the comprehensive approach. Fibrosis first had the lowest incremental cost per diagnosis ratio: fibrosis first, £1349 (€1590); iLFT £3247 (€3828); and comprehensive, £2964 (€3494). The number of secondary care referrals was increased in all approaches above current testing, greatest in the comprehensive strategy. Considering these trade-offs the net benefit was greatest for the fibrosis first approach (Figure).



Conclusion: Current testing for liver disease is inadequate. Pathways that streamline testing, including testing of persons with normal liver blood tests but that are at risk of significant liver disease, will increase the yield of testing for liver disease in primary care. A "fibrosis first" pathway, taking a fast and frugal approach to identify persons with prognostically significant liver disease, warrants testing in comparison to comprehensive evaluation in primary care.

THU242

Hepatitis C care cascade analysis among adult women in Georgia

Ketevan Stvilia¹, Shaun Shadaker², Amiran Gamkrelidze³, Irma Khonelidze³, Maia Tsereteli³, Vladimer Getia³, Paige A Armstrong². ¹National Center for Disease Control and Public Health, Tbilisi, Georgia; ²Centers for Disease Control, Department of Viral hepatitis, United States; ³National Center for Disease Control and Public Health, Tbilisi, Georgia

Email: stviliak@gmail.com

Background and aims: According to the National HCV seroprevalence study of 2015, 3.8% of women in Georgia are positive for hepatitis C virus (HCV) antibodies; however, female-targeted interventions to promote HCV testing and treatment have been lacking. Further, women of reproductive age can transmit HCV during pregnancy, making outreach to this population particularly important. We constructed the HCV care cascade for women age ≥18 years, screened for anti-HCV within the National Hepatitis C Elimination Program during January 2015–October 2021 to compare progress in care and treatment and to assess gaps in the cascade of HCV care and treatment.

Method: The seven stages of HCV care recommend by WHO were assessed for women who tested positive for anti-HCV: (1) HCV antibody positive; (2) tested for viremia; (3) confirmed active infection; (4) initiated HCV treatment; (5) eligible for test for sustained virologic response (SVR), (6) tested for SVR and (7) achieved SVR. HCV care cascade results were assessed for women by age group to define gaps, and proportion retained at each step in the care cascade.

Results: As of October 2021, 2.1 million adults with known sex were screened for anti-HCV, including 1.1 million women. Among them, 38,881 (3.4%) were positive for anti-HCV, and the majority (65.0%) were aged ≥50 years. Overall, 77.3% of women who screened anti-HCV positive were tested for viremia. The positivity rate for active HCV infection was 73.2% (21,978) among all females, ranging from 62.7% among those aged 18–29 years to 75.8% among those aged 40–49 years. Overall, 76.1% (16,729) of women with HCV viremia initiated treatment, including 63.0% of women aged ≥60 years, and ≥84.0% of women in all other age groups. Of women enrolled in treatment, 95.6% (15,986) completed the regimen, and 98.2% of those women were eligible for an SVR test. Women have demonstrated high uptake of SVR testing; 82.0% were tested for SVR across all age groups with an overall cure rate of 99.4%.

Conclusion: To reach elimination of hepatitis C by 2025 it is important to improve access to and support uptake of viremia testing and enrollment in treatment among anti-HCV positive women in Georgia, with special attention to ensuring the large proportion of anti-HCV positive women over 50 years complete viremia testing. Once enrolled in treatment, Georgian women with active HCV infection show high rates of compliance resulting in more than 99% of cases cured.

POSTER PRESENTATIONS

THU243

Progress in HCV screening in the national hepatitis C elimination program in Georgia during the COVID-19 pandemic, 2019–2021

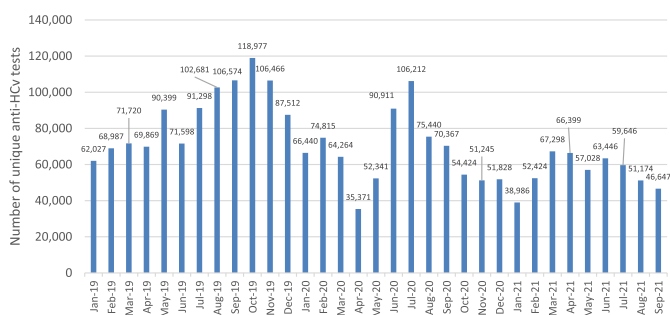
Amiran Gamkrelidze¹, Alexander Turdziladze¹, Maia Tsreteli¹, Vladimir Getia¹, Ana Aslanikashvili¹, Tinatin Kuchuloria², Irina Tskhomelidze², Sophia Surguladze², Lia Gvinjilia³, Senad Handanagic⁴, Shaun Shadaker⁴, Paige A Armstrong⁴. ¹National Center for Disease Control and Public Health Georgia, Tbilisi, Georgia; ²The Task Force for Global Health, Tbilisi, Georgia; ³Eastern Europe and Central Asia (EECA) Regional Office, Centers for Disease Control and Prevention, Tbilisi, Georgia; ⁴Division of Viral Hepatitis, Centers for Disease Control and Prevention, Atlanta, United States
Email: a.gamkrelidze@ncdc.ge

Background and aims: Georgia, with a population of 3.7 million, had an estimated 150,000 adults living with chronic hepatitis C virus (HCV) infection based on a serosurvey conducted in 2015. The same year, the country initiated the world's first national HCV elimination program, with free screening and treatment available to all citizens. Despite great progress, the COVID-19 pandemic has created new challenges for the program. This analysis describes the progress made in HCV screening since program initiation and the impact of the COVID-19 pandemic on HCV screening.

Method: The Hepatitis C Elimination Program tracks testing and treatment data using two databases, the national HCV Screening Registry, and the HCV treatment database. These databases are linked by the national ID. This analysis uses data from both databases and the 2014 general population census.

Results: As of September 30th, 2021, 2,081,548 adults have been screened for antibody to HCV (anti-HCV) (75% of the adult population), of whom 144,857 (6.9%) were anti-HCV positive. Overall, 118,398 (81.7%) anti-HCV positive individuals received follow-up viremia testing, and 94,315 (79.7%) were found to have active HCV infection. The number of anti-HCV tests performed among adult persons dropped as restrictions were imposed in March of 2020 from 74,815 tests in February 2020 to just 35,371 in April of the same year. Screening increased in the summer, with 106,212 tests performed in July, due in part to relaxed restrictions and intensified integrated screening programs (HCV, tuberculosis, and HIV). Compared to 2019, the number of tests performed in 2020 decreased by 24% (1,048,108 vs. 793,658). As the pandemic progresses, the number of tests performed for HCV during January–September 2021 remained lower than in the same period in 2020 (503,048 vs. 636,161).

Anti-HCV Screening in Georgian Adults, January 2019–September 2021:



Conclusion: Although the program has made significant progress towards HCV elimination, the ongoing pandemic has led to a decline

in screening for HCV infection, with numbers continuing to decline in 2021. In response, Georgia intends to increase integrated screening, and seek active approaches to link patients to HCV care and treatment. The impact of the pandemic on the HCV elimination program demonstrates how a pandemic can be challenging for different public health programs and highlights the need to employ innovative strategies to avoid slowing of progress towards HCV elimination.

THU244

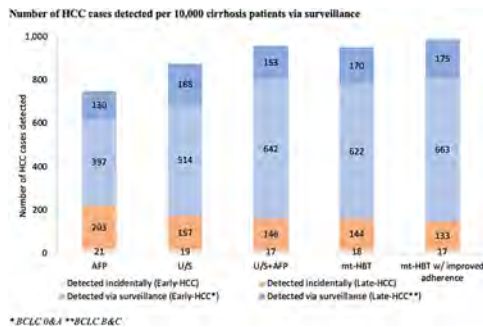
Could a multi-target blood test make hepatocellular carcinoma surveillance programs more effective? A modelling-based virtual trial

Jagpreet Chhatwal^{1,2,3}, Sumeyye Samur⁴, Ju Dong Yang⁵, Lewis Roberts⁶, Mindie Nguyen⁷, A. Burak Ozbay⁸, Turgay Ayer^{9,10}, Neehar D. Parikh¹¹, Amit Singal¹². ¹Harvard Medical School, Boston, United States; ²Mass General Hospital, Boston, United States; ³Harvard Medical School, Boston, United States; ⁴Value Analytics Labs, Boston, United States; ⁵Cedars-Sinai Medical Center, Los Angeles, United States; ⁶Mayo Clinic, Rochester, United States; ⁷Stanford University School of Medicine, Stanford, United States; ⁸Exact Sciences Corporation, Madison, United States; ⁹Georgia Institute of Technology, Atlanta, United States; ¹⁰Emory University-School of Medicine, Atlanta, United States; ¹¹University of Michigan Medical School, Ann Arbor, United States; ¹²UT Southwestern, Dallas, United States
Email: jagchhatwal@mgh.harvard.edu

Background and aims: Hepatocellular carcinoma (HCC) is among the fastest rising causes of cancer mortality in the Western world. Although guidelines recommend biannual ultrasound (U/S)-based HCC surveillance in at-risk patients, utilization in practice remains poor in practice. A recently validated, multi-target HCC blood test (mt-HBT), may potentially improve adherence to surveillance by forgoing the need for U/S. Our objective was to evaluate the comparative effectiveness of mt-HBT with the current surveillance strategy in cirrhosis patients.

Method: We simulated a virtual trial by developing a clinically valid microsimulation model of HCC natural history in compensated cirrhosis patients. Model parameters, including tumor progression, competing risks of mortality, and real-world adherence, were estimated from the literature. Test performance characteristics of U/S, AFP, and mt-HBT were informed from a network meta-analysis. We simulated the life course of cirrhosis patients and compared biannual surveillance using (1) AFP only, (2) U/S only, (3) U/S+AFP, and (4) mt-HBT only. We also simulated a scenario where mt-HBT would improve adherence by 10% (~4% absolute improvement) compared to current utilization.

Results: Per 10,000 cirrhosis patients simulated in each arm, mt-HBT detected 225 (+57%) more early-stage HCC cases compared with AFP, 108 (+21%) more early-stage HCC compared with U/S, and 20 (~3%) less early-stage HCC compared with U/S+AFP. In contrast, mt-HBT with improved adherence detected 21 (+3%) more early-stage HCC compared with U/S+AFP (Figure). The remaining HCC cases were either symptomatically identified or patients died from competing causes prior to detection. mt-HBT increased life years by 709 per 10,000 patients screened compared with AFP, 360 compared with U/S, but decreased life years by 19 compared with U/S+AFP. Of note, mt-HBT with improved adherence increased life years by 52 compared with U/S+AFP.



Conclusion: mt-HBT as a single blood test offers similar diagnostic efficacy for early HCC detection compared with the combination of U/S+AFP. Potential improved adherence with use of blood-based biomarkers, such as mt-HBT, would likely further increase real-world effectiveness of HCC surveillance.

THU245

Evaluation of immune response and disease flares in metabolic-associated fatty liver disease patients following SARS-CoV-2 vaccination: a prospective cohort study

Junping Shi¹, Qianru Zhu^{2,3}, Jin Gao⁴, Jiaping Gu⁵, Lu Shen⁵, Jing Liu⁶, Yu Song⁷, Xiyong Gong⁷, Yutong Chen⁵, Jie Liao⁷, Yining He⁵, Siyi Zhang⁵, Li Shao^{3,5}, Yee Hui Yeo⁸, Jie Li^{9,10}. ¹The Affiliated Hospital of Hangzhou Normal University, Department of Hepatology and infectious Disease, Hangzhou, China; ²Macau University of Science and Technology, Faculty of Chinese Medicine, Macau, China; ³The Affiliated Hospital of Hangzhou Normal University, Department of Translation Medicine Platform, Hangzhou, China; ⁴The Affiliated Hospital of Hangzhou Normal University, Department of Clinical Laboratory, Hangzhou, China; ⁵Hangzhou Normal University, Medical college, Hangzhou, China; ⁶The Affiliated Hospital of Hangzhou Normal University, Department of Hepatology and infectious Disease, Hangzhou, China; ⁷Zhejiang Chinese Medical University, The Fourth School of Clinical Medicine, Hangzhou, China; ⁸Cedars-Sinai Medical Center, Division of General Internal Medicine, United States; ⁹Nanjing University, Institute of Viruses and Infectious Diseases, Nanjing, China; ¹⁰The Affiliated Hospital of Nanjing University Medical School, Department of Infectious Diseases, Nanjing, China
Email: 20131004@hznu.edu.cn

Background and aims: The safety and efficacy profile of Covid-19 vaccines in patients with MAFLD (metabolic associated fatty liver disease) remains unclear. We aimed to determine the safety and immunogenicity of an inactivated vaccine in MAFLD.

Method: In this prospective cohort, 50 participants with MAFLD and 114 healthy controls received two doses of CoronaVac with a 28-day interval between doses and underwent blood sample collection on days 0, 28, 57, and 180. Baseline vibration-controlled transient elastography as well as the level of neutralizing antibody against the SARS-CoV-2 spike receptor-binding domain, fasting metabolic markers, and liver function test on four assessment dates were assessed. Repeated measures ANCOVA was used to estimate the magnitude of change of these markers throughout study period.

Results: No significant difference in proportion of patients with neutralizing antibody was observed between two groups. The proportions of adverse event and liver injury was similar between both groups. There was no difference between the two groups in the change of most biomarkers throughout study period. On multivariable analysis, age and waist circumference were negatively associated with seropositivity of neutralizing antibody on day 57 while RBC and lymphocyte count were independent positive predictors on day 180 (Table).

Table: Factors associated with seropositive of neutralizing antibody on days 57 and 180, respectively.

Characteristics	D57			Multivariable analysis*			D180			Multivariable analysis**		
	OR	95% CI	p	aOR	95% CI	p	OR	95% CI	p	aOR	95% CI	p
Age	0.938	0.159-1.054	0.008	0.039	0.900-0.997	0.039	0.984	0.951-1.019	0.364			
Male (vs female)	0.409	0.159-1.054	0.064				2.045	0.981-4.265	0.056			
Waist	0.943	0.904-0.984	0.006	0.949	0.906-0.994	0.027	0.995	0.963-1.028	0.760			
CAP	0.998	0.989-1.006	0.589				1.006	0.999-1.013	0.074			
LSM	0.882	0.664-1.170	0.383				1.299	1.019-1.656	0.035			
BMI	0.887	0.791-0.993	0.038				0.981	0.891-1.081	0.703			
ALT	1.010	0.977-1.043	0.568				1.024	1.003-1.045	0.025			
AST	1.009	0.952-1.069	0.769				1.051	1.007-1.096	0.022			
ALP	0.996	0.974-1.019	0.737				1.010	0.992-1.027	0.275			
CRP	1.145	0.938-1.399	0.183				1.151	0.989-1.340	0.068			
Fasting glucose	1.065	0.663-1.710	0.795				0.867	0.595-1.264	0.459			
HOMA-IR	0.903	0.746-1.093	0.295				1.117	0.931-1.339	0.233			
WBC	0.921	0.671-1.265	0.613				1.324	1.025-1.710	0.032			
RBC	0.733	0.309-1.736	0.480				3.461	1.634-7.332	0.001	2.746	1.212-6.223	0.016
Lymphocyte	0.931	0.421-2.059	0.861				2.758	1.397-5.442	0.003	2.377	1.150-4.914	0.019
Hemoglobin	0.996	0.971-1.021	0.751				1.025	1.003-1.048	0.028			

*Adjusted for age,sex,waist,CAP,LSM,BMI,ALT,AST,Glu,HOMA-IR,ALP;

**Adjusted for age,sex,CAP,LSM,WBC,RBC,lymphocytes,hemoglobin,ALT,AST.

Conclusion: CoronaVac vaccination in MAFLD patients was safe and well tolerated. MAFLD patients showed a similar immune response to health controls.

THU246

A model, screen test and treat hepatitis C elimination project among under-served communities in Islamabad-the federal capital of Pakistan

Huma Qureshi¹, Hassan Mahmood², Nabil Ahmed³, Lillian Lou⁴, Francisco Averhoff⁵, Ameer Abutaleb⁶, Shyamashundaran Kottitil⁶. ¹Integral Global (IG), Pakistan; ²Integral Global (IG), Public Health, Islamabad, Pakistan; ³Integral Global (IG), Atlanta, United States; ⁴John C. Martin Foundation, United States; ⁵Abbott Diagnostics, United States; ⁶University of Maryland, United States
Email: drhumapmrc@gmail.com

Background and aims: Pakistan has a large burden of hepatitis C virus (HCV) infection, and access to care and treatment is limited. In order to increase access for underserved populations, a same-day testing and treatment initiation model program for adults in marginalized communities (i.e. slums) in Islamabad was launched on March 02, 2019. We describe the results of the program.

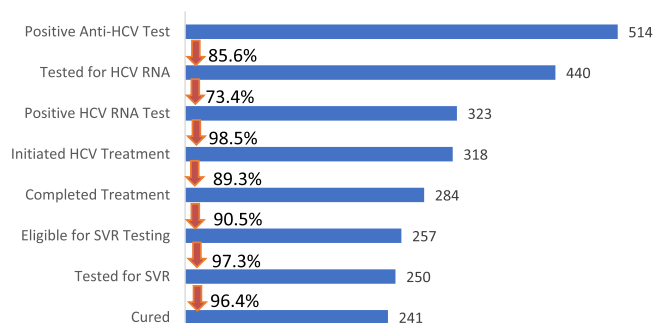
Method: A total of 17 slums with an estimated total population of 50, 000 in Islamabad have been selected by the Ministry of National Health Services, Regulations and Coordination for the project. This project includes free hepatitis C testing and treatment and utilizes trained community health workers (CHWs). The CHWs visit every dwelling in the slum and offer household members aged ≥18 years screening for hepatitis C by a rapid hepatitis C antibody (anti-HCV) test. Those that test positive are referred to an established clinic for diagnosis of active HCV infection (RNA) by GeneXpert. RNA results are made available to patients within two hours. If found to be HCV RNA Positive, the Aspartate to Aminotransferase (AST) to Platelet Ratio Index (APRI) is calculated, subjects receive counseling, and their first 4-week supply of sofosbuvir plus daclatasvir and the first of three doses of hepatitis B vaccine during the initial clinic visit. A treatment regimen of 12 weeks for non-cirrhotic (APRI<1.5) patients is prescribed. Patients with an APRI ≥1.5 are referred to specialists.

POSTER PRESENTATIONS

Patients are seen every 4 weeks at the clinic and given refills on their medications and queried about adverse reactions, until the end of treatment. RNA testing is conducted at 12 weeks following completion of treatment to determine viral clearance (cure). The CHWs ensure referral and follow-up of HCV infected persons.

Results: As of November 15, 2021; a total of 24,216 participants have been screened from seventeen slums, 514 (2.12%) tested positive for anti-HCV and were referred to receive testing for HCV RNA. Of those, 440 (85.6%) got tested for HCV RNA and 323 (73.4%) had detected RNA. Three hundred and eighteen individuals (98.5%) had initiated treatment, of which 284 (89.3%) had completed treatment. To date, 257 (90.5%) patients are eligible to test for Sustained Virologic Response (SVR), out of which 250 (97.3%) were tested; 241 (96.4%) were HCV RNA negative, four (1.6%) were loss to follow-up and five patients were (2%) HCV RNA positive. Those five patients were given Sofosbuvir and Velpatasvir and are on treatment.

Care Cascade of Hepatitis C Elimination Project in Islamabad (March 02, 2019 - November 15, 2021)



Conclusion: Same day hepatitis C testing and treatment initiation is feasible among underserved communities in urban slums in Pakistan. CHWs can be effective in reaching “hard-to-reach” populations with limited access to health services and achieving high rates of linkage to care and adherence with treatment for hepatitis C.

THU247

Hepatitis B and hepatitis C testing practices and seroconversions among dialysis facilities in Georgia

Maia Butsashvili¹, George Kanchelashvili¹, Ana Aslanikashvili², Tinatin Kuchuloria³, Shaun Shadaker⁴, Irina Tskhomelidze³, Maia Tsereteli², George Kamkamidze¹, Priti Patel⁴, Paige A Armstrong⁴. ¹Health Research Union, Tbilisi, Georgia; ²National Center for Disease Control and Public Health, Tbilisi, Georgia; ³The Task Force for Global Health, Tbilisi, Georgia; ⁴Centers for Disease Control and Prevention, Atlanta, United States
Email: maibutsashvili@gmail.com

Background and aims: Hemodialysis can facilitate transmission of hepatitis C and hepatitis B as a result of a large number of patients receiving treatment in a shared space. Strict adherence to infection prevention and control practices is essential to prevent transmission through contaminated equipment and surfaces. Despite a comprehensive hepatitis C Elimination Program in Georgia, there is currently no system in place to adequately capture the prevalence of chronic HBV infection or chronic HCV infection and to promptly identify cases of HCV and HBV seroconversion among persons receiving dialysis. This study evaluates HCV and HBV testing practices among patients receiving dialysis and estimates the number of seroconversion cases in dialysis units in Georgia.

Method: All 27 dialysis centers in the country were invited to participate. Facility questionnaires were completed by the infection control representatives at each center from April to June, 2021. Respondents were asked about HBV and HCV screening practices, and the number of seroconversions among facility patients in the preceding year. Data entry, management and analyses were conducted using the statistical package SPSS v.22.0.

Results: A total of 22 (81.5%) dialysis centers participated in the survey. HBV screening is routinely performed upon admission at 21 facilities (95.5%). Susceptible patients are routinely vaccinated with the hepatitis B vaccine at about half (13; 59.1%) of facilities. Anti-HCV screening is performed at 15 institutions (68.2%) upon admission to the center, and anti-HCV screening is performed once every 6 months in 12 (54.5%) clinics for patients who were previously anti-HCV negative.

Ten (45.5%) of the dialysis facilities included in the study reported HBV and HCV seroconversions in the prior year. A total of 31 HBV seroconversions from 8 facilities and 39 HCV seroconversions from 7 facilities occurred. The largest number in a single facility was 25 total seroconversions of HBV or HCV infection.

Conclusion: The high seroconversion rate of HBV and HCV infections at dialysis units suggests opportunities for improved infection prevention practices and need for increased hepatitis B vaccination efforts. Surveillance could help identify cases and clusters early and contribute to preventing infection in this high-risk population.

THU248

Innovative linkage model to re-engage loss-to-follow-up individuals in the national hepatitis C elimination program of Georgia

Amiran Gamkrelidze¹, Alexander Turdziladze¹, Maia Tsereteli¹, Vladimer Getia¹, Ana Aslanikashvili¹, Sophia Surguladze², Irina Tskhomelidze², Shaun Shadaker³, Paige A Armstrong³. ¹National Center for Disease Control and Public Health Georgia, Tbilisi, Georgia; ²The Task Force for Global Health, Tbilisi, Georgia; ³Division of Viral Hepatitis, National Center for HIV, Viral Hepatitis, STD and TB Prevention, CDC, Atlanta, United States
Email: a.gamkrelidze@ncdc.ge

Background and aims: The National Hepatitis C Elimination Program has made notable progress in Georgia. However, in the setting of COVID-19 related limitations, the number of individuals registering in the treatment program has declined over time, from an average of 996 per month in 2019 to 339 per month in 2021. As of September 30, 2021, 75% (n = 2,081,548) of the adult population of Georgia has been screened for hepatitis C virus (HCV), but among antibody positive adults, 20,913 (15%) had not completed a viremia test.

In 2019, the National Center for Disease Control and Public Health Georgia piloted a project to link to care those individuals who screened positive for anti-HCV but had not completed a viremia test. After success of the initial pilot, the model will be scaled up across Georgia.

Method: All anti-HCV positive adults (aged ≥18 years) who did not have record of viremia testing in the national HCV electronic database 3 months from the date of a positive result, and who were not registered in the HIV/AIDS program or with a correctional facility, were eligible for follow-up.

Using the phone number listed in the database, individuals were contacted by phone or home visit by patient navigators (trained epidemiologists and primary healthcare physicians) and referred to HCV care and treatment. If the first attempt was unsuccessful, one repeat attempt was made to contact the individual. Incentives were

provided to regional health personnel for each patient that was successfully linked to care, defined as presenting for viremia testing. **Results:** As of October 1, 2020, 18, 030 persons were not linked to care; patient navigators attempted to reach 8, 907 (49%) with phone numbers in the database; 6, 718 (75%) were reached. The remaining 2, 189 could not be reached, had moved, or emigrated. Of those contacted, 1, 546 (23%) presented for viremia testing, and 811 (52%) were positive for HCV RNA or core antigen. Overall, 419 (52%) persons with chronic HCV infection were enrolled in the HCV treatment program as a result of this effort.

Conclusion: Program-wide implementation of the piloted model showed that this can be scaled up and is effective for re-engaging people in care. The main challenge in Georgia remains linkage-to-care, which is essential to meet elimination goals. Innovative approaches are necessary to reinforce linkage to care. This is especially important during the COVID-19 pandemic when there is an increased need for programs that can re-engage people in HCV care.

THU249

Combined COVID-19 vaccination and HIV and hepatitis C virus screening intervention for high-risk populations at a mobile testing unit in Madrid, Spain

Jorge Valencia¹, Pablo Ryan¹, Guillermo Cuevas¹, Julieta Domingorena², Álvaro Vicario², Marcela Villota-Rivas³, Jeffrey Lazarus^{3,4}. ¹Hospital Universitario Infanta Leonor, Department of Internal Medicine, Madrid, Spain; ²SMASD, Harm reduction Unit, Madrid, Spain; ³Barcelona Institute for Global Health (ISGlobal), Hospital Clínic, University of Barcelona, Barcelona, Spain; ⁴University of Barcelona, Faculty of Medicine, Barcelona, Spain
Email: Jeffrey.Lazarus@isglobal.org

Background and aims: The COVID-19 pandemic has hindered efforts to address HIV and hepatitis c virus (HCV) by reducing testing, particularly in marginalised groups, who have some of the highest rates of HIV and HCV and lowest rates of COVID-19 vaccination. This study aimed to explore the acceptability of combining HIV and HCV testing with COVID-19 vaccination in a mobile testing unit (MTU) in Madrid, Spain.

Method: From 9/28/2021 to 10/26/2021, 101 individuals from high-risk populations (e.g., homeless people, those with substance use and/or mental disorders, sex workers, refugees, undocumented migrants) were invited to get the COVID-19 vaccine at the MTU. If HCV antibody (Ab) positive, they were offered HCV-RNA point-of-care testing to confirm active infection. HIV and HCV-RNA-positive patients were offered linkage to care.

Results: All 101 participants accepted the combined intervention of which 69.3% were male, 30.7% of Spanish origin, most reported a precarious living situation or being homeless (59.4%) and being unemployed (70.3%), and 28.7% a history of incarceration. The mean age was 35.6 (SD: 11.9). Of the total, 11.9% reported a previous COVID-19 diagnosis, none had been vaccinated for COVID-19 and all subsequently received the Janssen vaccine without any adverse events (Figure). All individuals were tested for HIV and HCV Ab and 8.9% (n = 9) and 14.9% (n = 15) tested positive, respectively. Of those HIV positive, none were new diagnoses, and most (55.6%, n = 5) had abandoned antiretroviral therapy. Of those HCV Ab positive, all were tested for HCV-RNA and 60.0% (n = 9) tested positive, of which most (55.6%, n = 5) reported that the most likely route of transmission was injecting drug use, 44.4% (n = 4) were reinfection cases and 33.3% (n = 3) were HIV co-infected. Everyone with an active infection was offered linkage to care and to date 44.4% (n = 4) have started treatment for HCV. The average intervention duration was 20 minutes (minimum: 7; maximum: 60).

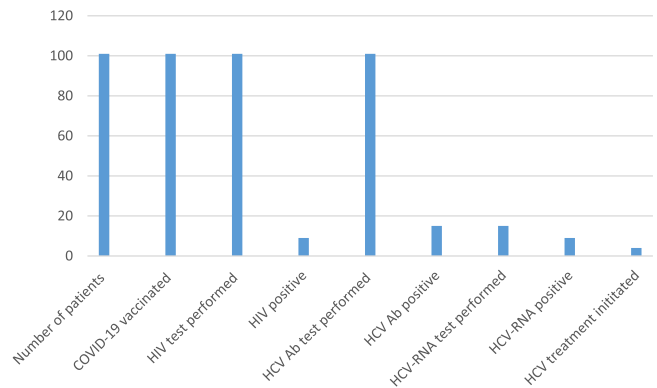


Figure: Analysis of the combined COVID-19 vaccination and HIV and HCV screening intervention at the MTU in Madrid

Abbreviations: Ab, antibody; HCV, hepatitis C virus; MTU, mobile testing unit.

Conclusion: Combining HIV and HCV testing with COVID-19 vaccination in high-risk individuals at the MTU was effective, with an acceptability rate of 100%, and safe since there were no adverse events. The process was also efficient, since it maximised the use of time that participants would have spent waiting for HIV and/or HCV test results or post-vaccine administration. This intervention can serve as an example of a novel model of care to increase HIV and HCV screening and linkage to care as well as COVID-19 vaccination in high-risk populations.

THU250

A model to eradicate HCV in undocumented migrants and low-income refugees in Italy

Mariantonietta Pisaturo¹, Margherita Macera², Loredana Alessio², Stefania de Pascalis², Lorenzo Onorato¹, Maria Stanzone², Gianfranca Stornaiuolo², Vincenzo Messina³, Nicola Coppola¹. ¹University of Campania L.vanvitelli, mental health and preventive medicine, Naples, Italy; ²Vanvitelli hospital, Naples, Italy; ³Caserta Hospital, Caserta, Italy
Email: mariantonietta.pisaturo@unicampania.it

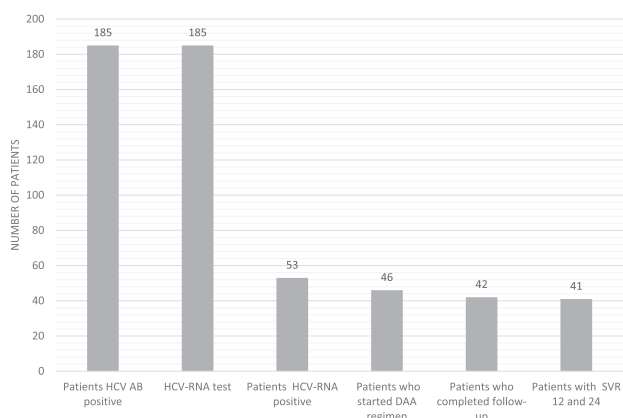
Background and aims: To validate an innovative eradication model for HCV infection in undocumented migrants and low-income refugees living Southern Italy.

Method: a prospective, multicenter, collaborative study was started in June 2018 with The study was stopped in February 2020 due to the outbreak of SARS-CoV-2 infection in Italy and was resumed in February 2021. At the six 1st level centers participating to the study volunteer associations that deal with the first needs of disadvantaged people performed the enrolment and the screening for anti-HCV, HBsAg and anti-HIV; epidemiological data were collected in an electronic database. Anti-HCV-positive subjects were sent to two 3rd level centers for the clinical, virological and therapeutic evaluation. For the HCV-RNA-positive subjects HCV genotyping and a clinical, biochemical and ultrasound staging was performed. The HCV RNA-positive subjects have been treated with sofosbuvir-velpatasvir for 12 weeks and followed for 12 months from the end of therapy.

Results: Of the 3, 991 migrants observed in the study period, 3, 897 (97.6%) accepted to be screened. They were young (median age 26 years), predominantly male (85.9%) and came from North Africa (3.8%), from Sub-Saharan Africa (68.4%), from Eastern Europe (8.1%), from Indo-Pakistan (17%) and from other countries (2.7%). Of the 3, 897 enrolled subjects, 185 (4.7%) resulted anti-HCV positive. The Figure shows the HCV-cure cascade. All the 185 anti-HCV-positive subjects were linked to care at 3rdID and tested for HCV RNA and 53 (28.6%) resulted HCV-RNA positive. Of these, 46 (86.8%) started DAA regimen with sofosbuvir plus velpatasvir (15 with GT 1b, 10 with 1a, 16 with 3, 3 with 4 and 2 with 2). Forty-two completed the follow-up and 4 was still pending. Of these 42 subjects, 41 (97.6%) showed a

POSTER PRESENTATIONS

SVR12 and SVR 24, and one dropped-out in follow-up after the stop of DAA treatment. No subject had adverse event.



Conclusion: This model seems to be effective to eradicate HCV infection among a difficult-to-manage population, such as undocumented migrants and low-income refugees

THU251

Enhancing the cascade of hepatitis C care in community-recruited high-risk people who inject drugs during the COVID-19 pandemic: the Alexandros program

Vana Sypsa¹, Sotiris Roussos², Efrossini Tsirogianni^{3,4}, Despina Trafali⁵, Dimitra Tsiagka⁵, Athena Gavalaki⁵, Zafiris Papanikolaou⁵, Ioanna Papagiouvanni^{3,5}, Athena Tampaki⁵, Dimitrios Paraskevis², George Kalamitsis⁶, Ioannis Goulis⁷, Angelos Hatzakis^{1,5}. ¹Medical School of National and Kapodistrian University of Athens, Department of Hygiene, Epidemiology and Medical Statistics, Athens, Greece; ²Medical School of National and Kapodistrian University of Athens, Department of Hygiene, Epidemiology and Medical Statistics, Athens, Greece; ³Fourth Department of Internal Medicine, Hippokratia Hospital, Aristotle University of Thessaloniki; ⁴Greek Organisation Against Drugs; ⁵Hellenic Scientific Society for the Study of AIDS and Sexually Transmitted Diseases and Emerging Diseases, Athens, Greece; ⁶Hellenic Liver Patients Association "Prometheus"; ⁷Fourth Department of Internal Medicine, Hippokratia Hospital, Aristotle University of Thessaloniki, Thessaloniki, Greece
Email: vsipsa@med.uoa.gr

Background and aims: Despite the availability of effective treatment for chronic hepatitis C, treatment initiation rates remain low among People Who Inject Drugs (PWID) worldwide, especially among those not linked to opioid substitution treatment programs (OST). A community-based program was implemented in Thessaloniki (the second largest city in Greece) during September 2019–August 2021 with the aim to screen for HCV/HIV and improve access to care among high-risk PWID. We aim to provide data on the cascade of HCV care in this population.

Method: ALEXANDROS was a “seek-test-treat” community-based program where PWID were recruited using peer-driven chain referral with monetary incentives (Respondent-Driven Sampling). The program was implemented in five consecutive rounds during September 2019–August 2021 and PWID could participate in multiple rounds but only once in each round. Participation included interviewing, counselling, rapid HCV/HIV test and blood sample collection for testing of anti-HCV (+) participants (HCV genotype/biochemical evaluation). PWID eligible for DAAs with available social security number were entered to the national HCV treatment registry

and visited the program site for their prescriptions and assessment of sustained virological response. The personnel of the program, including a peer-navigator, assisted patients through all stages.

Results: In total, 1,101 unique PWID were recruited. The majority of participants were current PWID (54.0% with injection in the past 30 days), 15.0% were homeless and 79.7% were not linked to OST. Anti-HCV prevalence was 62.9% and 6.9% were HCV/HIV coinfecting. Only 9.7% of anti-HCV (+) PWID reported previous treatment with DAAs. Chronic HCV prevalence in anti-HCV (+) PWID was 67.6%. Among PWID with chronic HCV mono-infection, it was possible to identify the social security number for 97.4% of them, 96.9% were entered to the national HCV treatment registry to apply for free treatment with DAAs, 61.8% were linked to HCV care and 53.6% initiated treatment by September 2021.

Conclusion: Despite the disruptions due to the COVID-19 pandemic, ALEXANDROS was successful in reaching rapidly a population of PWID most in need (current injectors, homeless, low OST coverage) and in offering HCV testing, linkage to care as well as in encouraging HCV treatment initiation.

THU252

SVR4 and SVR12 monitoring by using dried blood spot test: is it the best alternative for people who use drugs?

Andrea Herranz¹, María Victoria Fernández-Baca², Maria Dolores Macia Romero³, María Paz Díaz², Maria Carmen Gallegos Alvarez², Ricardo M Arcay³, Francisco Salvà³, Adoración Hurtado⁴, Maria Buti^{5,6}, Àngels Vilella⁷, Jeffrey Lazarus^{1,8}. ¹Barcelona Institute for Global Health (ISGlobal), Hospital Clínic, University of Barcelona, Barcelona, Spain; ²Hospital Universitari Son Llàtzer, Microbiology Service, Palma, Spain; ³Hospital Universitari Son Espases, Microbiology Service, Palma, Spain; ⁴Hospital Can Misses, Microbiology Service, Eivissa, Spain; ⁵Universitari Vall d'Hebron, Liver Unit, Barcelona, Spain; ⁶Instituto Carlos III, CIBER Hepatic and Digestive Diseases (CIBERehd), Madrid, Spain; ⁷Hospital Universitari Son Llàtzer, Department of Gastroenterology, Palma, Spain; ⁸University of Barcelona, Faculty of Medicine, Barcelona, Spain
Email: Jeffrey.Lazarus@isglobal.org

Background and aims: People who use drugs (PWUD) are one of the key at-risk population groups for hepatitis C virus (HCV) infection and typically have difficulties in being linked to care and are often lost to follow-up. The *Hepatitis C Free Balears* project carries out micro-elimination strategies to facilitate the screening, treatment and follow-up of this population.

Method: This project has been implemented in 13 of 17 addiction service centres in the Balearic Islands and consists of four phases: 1) recruitment and HCV screening onsite via a point-of-care anti-HCV antibody test (Oraquick®) and a dried blood spot (DBS) test or blood analysis to confirm viremia (HCV-RNA) and detect HBsAg and HIV antigen/antibody; 2) linkage to care; 3) treatment prescription via telemedicine; and 4) monitoring onsite via DBS test of sustained virological response (SVR) at 4 and 12 weeks after treatment and for reinfection monitoring after a year. DBS samples are analyzed in the microbiology laboratories of the two major Balearic hospitals with chemiluminescent technology for the serological determinations and reverse transcription-polymerase chain reaction assay for the HCV viral load quantification.

Results: Out of 395 recruited patients, 150 (38%) were anti-HCV+, 1 (0.3%) was HBV-Ag+, 25 (6%) were anti-HIV+ and 60 (15%) had an active HCV infection. Of these 60, 43 (73%) initiated treatment, 17 (28%) are pending and 21 (35%) have already finished it. SVR4 and SVR12 monitoring were performed in 15 (75%) and 5 (25%) of those patients who completed treatment, respectively. Three (14%) SVR4 and three (14%) SVR12 tests were not performed, as the patients did

not show up at the settled appointments, and 3 (14%) SVR4 tests and 13 (62%) SVR12 tests are pending. The 93% (n = 14) SVR4 monitoring tests and the 100% (n = 5) SVR12 monitoring tests showed undetectable HCV-RNA. At the moment, only four patients performed both SVR4 and SVR12 tests, and all of them had concordant results.

Conclusion: DBS testing has been proven to be an alternative for HCV screening in PWUD by the *Hepatitis C Free Balears* team, since it is performed onsite and facilitates screening of drug users who otherwise would have not either reached or received care. It is also useful as a follow-up control method, since it simplifies circuits and reduces difficulties faced by PWUD. Although the SVR4 and SVR12 control tests results were concordant, more data are needed to know if the SVR4 control performed with DBS test is an alternative to lost to follow-up of this vulnerable population.

THU253

Collateral benefit of Georgia national hepatitis C elimination program-improving blood transfusion safety in the country of Georgia

Maia Alkhazashvili¹, Evan Bloch², Shaun Shadaker³, Tinatin Kuchuloria⁴, Tamar Samadashvili¹, Vladimir Getia¹, Alexander Turdziladze¹, Jan Drobeniuc³, Paige A Armstrong³, Amiran Gamkrelidze¹. ¹National Center for Disease Control and Public Health of Georgia, Tbilisi, Georgia; ²Johns Hopkins School of Medicine, Baltimore, United States; ³Centers for Disease Control and Prevention, Atlanta, United States; ⁴The Task Force for Global Health, Tbilisi, Georgia
Email: doctormailko@gmail.com

Background and aims: In 2015, a national seroprevalence survey identified blood transfusion as a risk factor for transmission of hepatitis C virus (HCV) and hepatitis B virus (HBV) in Georgia. Based on recommendations from the HCV elimination program's Technical Advisory Group, the EU-funded Technical Assistance and Information Exchange (TAIEX) with the support of the Global Fund, centralized nucleic acid testing (NAT) was implemented at the Richard Lugar Center for Public Health Research at the National Center for Disease Control and Public Health, Tbilisi, Georgia.

Method: One year of blood donor screening data (January-December, 2020) was analysed from the Unified Electronic Donor Database. Two samples were collected from all donors, one for primary serological testing by blood centers, and a second for NAT using the Procleix[®] Ultrio Elite Assay (multiplex for HCV, HBV, and HIV). In the event of a discordant result between NAT and serology (NAT positive, serology negative), additional discriminatory testing was performed. A subset of the discordant samples was retested using ARCHITECT i2000SR immunoassay for HBV surface antigen, HBV core antibody, HCV antibody, and HIV 1/2 Ab/Ag.

Results: A total of 54, 116 donations representing 39, 164 unique donors were evaluated. Overall, 671 donors (1.7%) tested positive for at least one infectious marker by serology or NAT. Sixty donations were serology/NAT discordant (serology-/NAT+). Discordance was more likely among females vs. males (adjusted odds ratio [aOR] 2.06; 95% confidence interval [95%CI]: 1.05–4.05), paid (aOR 10.15; 95%CI: 2.80–36.86) or voluntary (aOR 4.30; 95%CI: 1.27–14.56) vs. replacement donors, and repeat vs. first time (aOR 13.98; 95%CI: 4.06–48.12) donors. After repeat serologic testing was performed to confirm blood center reported results, a total of 12 donations (6 HBV+ donations, 5 HCV+ donations and 1 HIV+) were deemed NAT yield and would not have been detected with serology. Out of the total 54, 116 donations, the final NAT yield rate was 1 in 9, 019 for HBV, 1 in 10, 823 for HCV, and 1 in 54, 116 for HIV.

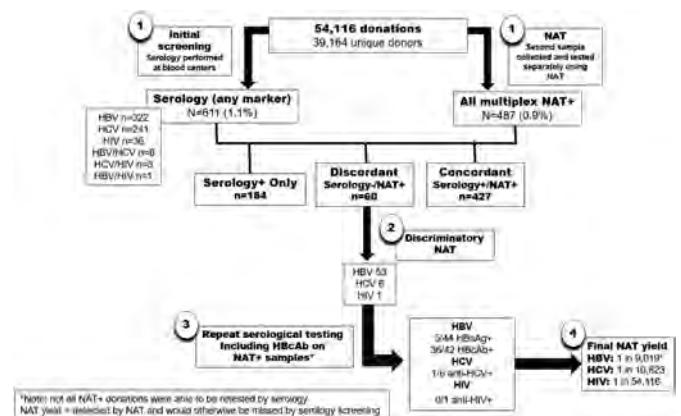


Figure: Study overview of testing and composition and results

Conclusion: This project offers a regional model for NAT implementation, demonstrating the feasibility and clinical utility in a nationwide blood screening program. NAT is resource intensive and expensive to implement system-wide, and may not be feasible in all settings. Balancing cost and yield is important, and countries with high prevalence may benefit more from NAT testing implementation.

THU254

Outcomes of a community led comprehensive HCV and HBV care provision model, including same-day "test and treat" to facilitate micro-elimination of HCV among people who inject drugs in Manipur, India

Khumukcham Lokeshwar Singh¹, Thangjam Dhabali², Rajkumari Rosie³, Rajkumar Nalinikanta⁴, Samurailatpam Rajesh Sharma¹, Sanjay Sarin⁵, Giten Khwairakpam⁶, Sonjelle Shilton⁵. ¹Jawaharlal Nehru Institute of Medical Sciences, Manipur, India; ²Babina Diagnostics, Manipur, India; ³Department of Health Services, Government of Manipur, India; ⁴CoNE, Manipur, India; ⁵FIND, the global alliance for diagnostics, Geneva, Switzerland; ⁶TREAT Asia/amfAR, Thailand
Email: sonjelle.shilton@finddx.org

Background and aims: The prevalence of hepatitis C virus (HCV) infection among people who inject drugs (PWID) in the state capital of Manipur, India, is 65%; however, access to and uptake of HCV care is poor, largely due to lengthy pre-treatment processes. We piloted a community-led, comprehensive, simplified hepatitis care model that includes same-day HCV testing and treatment initiation ("test and treat") at drug rehabilitation centres in Manipur, to expand access to care for chronic hepatitis.

Method: Participants were screened using HCV antibody (Ab) and hepatitis B virus (HBV) surface antigen (HBsAg) rapid diagnostic tests. Positive HCV Ab samples were tested using a point of care platform for HCV RNA (Molbio TrueNat). HCV RNA-positive participants eligible for treatment under national guidelines were initiated on sofosbuvir and daclatasvir on the same day and are followed until tests of cure (SVR). Participants who were HBsAg negative received HBV vaccine per the WHO rapid regimen. Positive HBsAg samples were sent to a referral lab for HBV DNA tests; and will be referred for treatment per national guidelines.

Results: Between 12–22 November 2021, 133 individuals were approached, of whom 103 (77%) were eligible and all consented to participate. To date, 98 (95%) participants have been screened; all were male and identified as PWID and had a median age of 27 (IQR 22–32) years. A total of 39 (40%) were HCV Ab positive; all were tested for HCV RNA, of whom 24 (61.5%) were HCV RNA positive. Of those with viremia, 23 (96%) were initiated on treatment on the same day,

POSTER PRESENTATIONS

with 1 awaiting HBV DNA results to be initiated on treatment. The median time from screening to HCV treatment initiation was 8 hours and 12 minutes (range 6:03–9:58). First SVR tests for sustained virologic response are due in April 2022. A total of 6 (6.1%) were HBsAg-positive. Of the 92 participants with negative HBsAg tests, 89 (97%) had not previously been vaccinated and all have completed at least 1 dose of the HBV vaccine.

Conclusion: Preliminary results show that community led comprehensive hepatitis care which incorporates same day “test and treat” for HCV is feasible and effective in this context. HBV screening identified a large proportion who had not been vaccinated. Additional follow-up and implementation research would inform how this model could be replicable in other settings to increase equity in access to HCV and HBV screening, treatment, and prevention.

THU255

A novel hepatitis C intervention in Denmark to test and treat people who inject drugs

Jeffrey Lazarus^{1,2}, Anne Øvrehus³, Jonas Demant⁴, Louise Krohn-Hehli⁵, Jannet van der Veen⁴, Nina Weis^{5,6}. ¹Barcelona Institute for Global Health (ISGlobal), Hospital Clínic, University of Barcelona, Barcelona, Spain; ²University of Barcelona, Faculty of Medicine, Barcelona, Spain; ³Odense University Hospital, Odense, Denmark; ⁴Users Academy, Copenhagen, Denmark; ⁵Copenhagen University Hospital, Department of Infectious Diseases, Hvidovre, Denmark; ⁶University of Copenhagen, Department of Clinical Medicine, Faculty of Health and Medical Sciences, Copenhagen, Denmark
Email: Jeffrey.Lazarus@isglobal.org

Background and aims: Providing testing and treatment for hepatitis C (HCV) for people who inject drugs (PWID) is critical in eliminating HCV, but reaching this population with traditional healthcare services can be challenging. Combining point-of-care (PoC) testing with peer support and counselling is a model of care (MoC) that can be effective for PWID. This study aims to investigate if a peer-led mobile van equipped with rapid PoC tests for HCV antibodies (Ab) and RNA could simplify testing and link PWID to care and treatment.

Method: In Copenhagen, Denmark, a peer-led mobile service providing counselling, Ab testing (In-Tec™) and linkage to standard of care was equipped with a PoC HCV-RNA finger-prick test (Xpert HCV Viral Load Finger-Stick Point-of-Care Assay, Cepheid). Eligible HCV-RNA+ individuals were offered assisted referral to a fast-track hospital clinic for evaluation and treatment, with peer support available if needed.

Results: From 1 May 2019 to 25 October 2021, 1013 people were tested for HCV-RNA and 10.2% (n = 103) were positive. Nine additional individuals with HCV infection contacted the service to be linked to care. Of the 112 individuals with chronic HCV infection, 72.3% (n = 81) were evaluated for treatment at the hospital clinic, of whom 86.4% (n = 70) initiated direct-acting antiviral therapy and 3.7% (n = 3) are waiting to initiate treatment. Major reasons for not being evaluated for treatment included being undocumented (38.7%; n = 12) and being lost to follow-up (32.3%; n = 10). Among those who initiated treatment, 20.0% (n = 14) were connected to drug addiction treatment services. The peer-led service assisted all treated with communication with the hospital nurse, collection of treatment medicine and accompaniment to follow-up visits.

Conclusion: We found that a peer-led mobile PoC service is an MoC that can engage PWID in HCV testing and link them to treatment, even during the COVID-19 pandemic. We identified being an undocumented migrant as a major cause for not accessing care. This poses a challenge for HCV elimination in Denmark due to the risk of onward transmission. Next steps include engaging with health authorities to provide care for these migrants.

THU256

Peer-led hepatitis C services reach poorly served populations at scale: a model for tackling health inequalities

Leila Reid¹, Rachel Halford^{1,2}, Stuart Smith¹, Sean Cox¹. ¹The Hepatitis C Trust, London, United Kingdom; ²World Hepatitis Alliance, Geneva, Switzerland

Email: leila.reid@hepcctrust.org.uk

Background and aims: England's approach to HCV elimination includes significant involvement-including leadership-from people with lived experience of hepatitis C. This is unique worldwide, and is proving very effective, in particular in engaging, diagnosing and treating groups typically excluded from health services. This large-scale, national programme bears out emerging evidence on peer-based models for tackling health inequalities.

Method: England's elimination programme tasked drug companies to not only treat but find people with HCV. This responds to a key challenge in the UK and many other countries: most people with HCV are hard to engage and undiagnosed.

Led by The Hepatitis C Trust, a national charity led by people with lived experience, England's HCV peers work together nationally as well as forming part of local NHS HCV delivery networks to engage marginalised populations. Launched in 2019, the model has three core components:

Peer Support: at its core, HCT provide patient support from another person (a peer) with lived experience of HCV, drug use and/or prison. The Peer provides a bespoke approach, support from testing to diagnosis to treatment and with other conditions.

Partnership: collaboration is paramount to improving systems. Working closely with services and clinicians, HCT's peer workers shorten pathways, ensure accessible clinics, improve patient understanding, and move services ever closer to those who need them most.

Patient-centred innovation: developed from patient feedback, HCT places the needs of people with HCV at the centre, regularly seeking feedback, adapting and innovating to reach new populations.

Results: Since 2019 HCT's peer teams have: engaged almost 75,000 people at risk of HCV: 33,324 through outreach and 39,333 in prisons.

Trained 15,401 health, care and prison staff tested 18,467 people in the community, and 17,691 in prison. 15% of community tests find markers for current/past HCV (prison data is being collated).

Received 6,517 referrals for support 62% have started treatment, and 94% for whom an SVR has been obtained (n = 1018) are cured

Feedback is consistently positive; patients highlight one to one relationships, shared experience and trust as pivotal to engagement.

Conclusion: HCT's highly assertive outreach, partnership-based model has seen peers embedded in NHS and prison systems. Links across the peers-who work as part of regional teams and as a national body-generates innovation, rapid sharing of good practice and excellent reach.

People experiencing marginalisation and often very complex needs engage with the peer model, often their first experience of sustained service engagement.

This is an effective, transferable and likely cost-effective approach (a study is planned), which stimulates both system-level and individual-level change, both positively impacting health inequalities.

THU257

Cost-effectiveness of integrated treatment for hepatitis C virus among people who inject drugs in Norway: an economic evaluation of the INTRO-HCV trial

Aaron G. Lim¹, Christer F. Aas^{2,3}, Ege Su Çağlar^{2,3}, Jørn-Henrik Vold^{2,3}, Lars Thore Fadnes^{2,3}, Kjell Arne Johansson^{2,3}, Peter Vickerman¹.

¹University of Bristol, Population Health Sciences, Bristol Medical School, United Kingdom; ²Haukeland University Hospital, Norway; ³University of Bergen, Norway

Email: aaron.lim@bristol.ac.uk

Background and aims: People who inject drugs (PWID) have the highest burden of hepatitis C virus (HCV) globally, but are often undertreated due to stigma and lack of access to services. Implementing efficient treatment algorithms for PWID is required to reach this population. The INTRO-HCV randomised control trial conducted in Norway over 2017–2019 found that integrating HCV treatment, using direct-acting antivirals (DAAs), into community settings improved treatment outcomes, but did not compare the longer-term health economic benefits. This study analyses the cost-effectiveness of integrated treatment compared to the standard referral pathway of care.

Method: A health state transition Markov model of HCV disease progression and treatment was developed based on the INTRO-HCV trial. Treatment cost and outcome data were analysed from the trial. Parameters related to disease progression came from published literature. The incremental cost-effectiveness ratio (ICER) was calculated in terms of cost per quality-adjusted life year (QALY) gained from the health provider's perspective over a lifetime horizon and compared against a conventional (NOK 500,000) willingness-to-pay (WTP) threshold for Norway. Probabilistic and univariate sensitivity analyses were undertaken.

Results: Preliminary results suggest that compared to the standard treatment pathway, integrated treatment resulted in an ICER of NOK 305,000 per QALY gained, with an 80.7% probability of being cost-effective against the conventional WTP threshold. Sensitivity analyses suggest that the cost of DAA medications strongly affected the ICER, with a 30% lower DAA price resulting in integrated treatment having an ICER of NOK 176,000 per QALY gained and a 95.8% probability of being cost-effective. A 60% lower DAA price led to an ICER of NOK 10,400 per QALY gained, with a 99.8% probability of being cost-effective and a 42.4% probability of being cost-saving.

Conclusion: Integrating HCV treatment for PWID in community settings is likely to be highly cost-effective and may become cost-saving even with moderate reductions in DAA price.

THU258

Characterization of HCV recent infections and re-infections among high-risk population from Georgia using global hepatitis outbreak and surveillance technology

Adam Kotorashvili¹, Amiran Gamkrelidze¹, Nato Kotaria¹, Maia Tsereteli¹, Ana Papkauri¹, Ketevan Galdavadze¹, Maia Alkhazashvili¹, Paata Imnadze¹, Tinatin Kuchuloria², Lilia Ganova-Raeva³, Sumathi Ramachandran³, Saleem Kamili³, Shaun Shadaker³, Paige A. Armstrong³, Yuri Khudyakov³. ¹National Center for Disease Control and Public Health (NCDC), Tbilisi Georgia, Georgia; ²The Task Force for Global Health, Tbilisi, Georgia; ³Centers for Disease Control and Prevention (CDC), Atlanta, GA, United States

Email: adam.kotorashvili@gmail.com

Background and aims: Global Hepatitis Outbreak and Surveillance Technology (GHOST), is a novel technology that identifies transmission links between specimens, creating a graphic display. GHOST was developed by the Centers for Disease Control and Prevention, and the National Center for Disease Control and Public Health of Georgia became the first GHOST center outside of the United States. The study aimed to gain insight into the variability of the hepatitis C virus (HCV) and potential transmission networks using GHOST in

recently seroconverted and reinfect cases in persons who inject drugs (PWID) in selected Georgian harm reduction (HR) sites.

Method: GHOST uses next-generation deep sequencing of Hyper Variable Region 1 (HVR1) of HCV. Genotypes of the HCV strains were determined by HVR1 sequence data analysis. Two HR sites in the cities of Tbilisi and Zugdidi were selected. Samples were collected from HR beneficiaries with documented reinfection or seroconversion. All participants provided written informed consent for participation and completed a questionnaire on the relevant epidemiological information.

Overall, 58 people with a history of injecting drugs were invited to participate, including 33 (57%) in Tbilisi and 25 (43%) in Zugdidi; 52% agreed to participate (n = 30/58).

Results: Among the 30 enrolled participants, 17 (57%) had HCV reinfection and 13 (43%) seroconverted during the observation. In the 6 months prior to the study, 27 participants (90%) reported injecting drugs and 3 (10%) reported needle sharing. Among reinfect participants (n = 17), one (6%) received a blood transfusion, 13 (76.4%) had an invasive medical procedure, and 4 (23.5%) were incarcerated. Among participants with new infection, 5 (38.4%) received blood transfusion, 8 (62%) had an invasive medical procedure more than 1 year ago, and 5 (38%) were incarcerated prior to seroconversion.

Genotype 1a was predominant (n = 8, 44%), followed by 2k/1b recombinant (n = 4, 22%), 2a (n = 3, 17%), 2c (n = 2, 11%), and 1b (n = 1, 6%). Using GHOST transmission detection module, a transmission cluster consisting of 2 participants reinfect with HCV genotype 2c was identified in Tbilisi. Although no cluster was found in Zugdidi alone, a reinfect participant from Zugdidi and seroconverted participant from Tbilisi formed another small transmission cluster. The Tbilisi participant carried mixed HCV genotype infection. Additionally, we found two mixed infections, one in each city, indicating a very high rate of exposure.

Conclusion: This is the first molecular epidemiological report among the high risk PWID population of Georgia using GHOST. The detected transmission clusters and mixed genotype infections indicate a very high rate of exposure in studied communities. GHOST can be utilized for surveillance for early intervention on networks as well as successfully applied to other infectious diseases including HBV, HAV, and HIV.

THU259

Prevalence and predictors of significant liver fibrosis : a population-based cross-sectional study

Aayushi Rastogi¹, Manya Prasad¹, Umesh Kapil¹, Ekta Gupta², Sherin Sarah Thomas³, Chhagan Bihari⁴, Shiv Kumar Sarin⁵. ¹Institute of Liver and Biliary Sciences, Epidemiology, Delhi, India; ²Institute of Liver and Biliary Sciences, Virology, Delhi, India; ³Institute of Liver and Biliary Sciences, Biochemistry, Delhi, India; ⁴Institute of Liver and Biliary Sciences, Pathology, Delhi, India; ⁵Institute of Liver and Biliary Sciences, Hepatology, Delhi, India

Email: rastogiaayushi6@gmail.com

Background and aims: Liver fibrosis is one of the most common chronic liver diseases worldwide caused due to alcohol consumptions, viruses, diabetes and other metabolic disorders. Steatosis is a common feature of several liver diseases resulting from different etiologies. Early detection of liver fibrosis can help timely interventions to reduce progression to cirrhosis and hepatocellular carcinoma. Aim: The present study was aimed at assessing the prevalence and predictors of significant liver fibrosis among asymptomatic adults in general population.

Method: A cross-sectional study was undertaken between 26 June 2021 to 15 November 2021 in the randomly selected primary health clinics of Delhi; the Mohalla Clinics. A mobile screening unit with trained research staff screened the population in the catchment areas of the clinics. A brief questionnaire was administered which assessed the medical and family history, information on life style factors such

POSTER PRESENTATIONS

as physical activity and alcohol consumption of the participants. In addition, anthropometric measurements, transient elastography and blood samples were collected for biochemical tests such as ALT, AST, total bilirubin, cholesterol, triglycerides and fasting blood sugar in participants who volunteered for screening. Liver stiffness measurement (LSM) of ≥ 8 kPa was used to define significant liver fibrosis. Univariable and multivariable analysis was done to determine the factors associated with liver fibrosis.

Results: A total of 2863 participants were screened with mean age of 43 ± 13.6 years, with 56% being males. Mean fasting blood sugar was 114.5 ± 49.78 mg/dl whereas median triglyceride was found to be 130.2 mg/dl (IQR: 95.4–181.2). The prevalence of significant liver fibrosis in the general population was 7.6% (95%CI: 6.65%–8.64%). The following factors were found to have a statistically significant ($p < 0.001$) association with significant liver fibrosis after adjusting for other factors: age (aOR: 1.03; 95%CI: 1.01–1.04), male gender (aOR: 1.73; 95%CI: 1.22–2.43), diabetes (aOR: 3.15; 95%CI: 2.23–4.44), morbid obesity (aOR: 7.53; 95%CI: 2.28–24.8) as seen in Table 1.

Table 1: Univariate and multi-variate analysis for predictors of liver fibrosis

Predictors	OR (95%CI)	p-values	aOR (95%CI)	p-values
Diabetes				
No	1		1	
Yes	4.56 (3.37 – 6.18)	<0.001	3.15 (2.23 – 4.44)	<0.001
Hypertension				
No	1		1	
Yes	2.51 (1.83 – 3.44)	<0.001	1.11 (0.77 – 1.60)	0.554
BMI Category				
Underweight (<18.5)	1		1	
Normal (18.5–23.9)	1.79 (0.52 – 6.09)	<0.001	1.27 (0.37 – 4.4)	0.698
Overweight (24–24.9)	2.3 (0.88 – 7.76)		1.39 (0.40 – 4.82)	0.601
Obese 1 (25–29.9)	4.9 (1.5 – 15.7)		2.93 (0.89 – 9.57)	0.075
Obese 2 (≥ 30.0)	11.5 (3.6 – 36.9)		7.53 (2.26 – 24.81)	0.001
Physical Activity				
Low	1		1	
Moderate	0.7 (0.49 – 0.93)	0.024	0.72 (0.51 – 1.01)	0.060
High	0.7 (0.46 – 0.99)		0.79 (0.52 – 1.21)	0.282
Gender				
Female	1		1	
Male	1.19 (0.89 – 1.58)	0.22	1.73 (1.23 – 2.43)	0.002
Alcohol consumption				
No	1		1	
Yes	1.51 (0.97 – 2.35)	0.066	1.59 (0.96 – 2.62)	0.068
Age				
			1.03 (1.01 – 1.04)	<0.001

OR: Odds ratio

aOR: Adjusted Odds ratio

Conclusion: There is high prevalence of fibrosis in the general population screened for the present study. There is a need for large scale public health interventions with high-risk approach to detect and treat liver fibrosis and prevent its complications.

THU261

Prognostic value of liver function test for COVID-19 hospitalized patients with respiratory disease

Carlos Alventosa Mateu¹, Elena Guillen Botaya¹, Cecilia Albert-Antequera², Irene Perez Alvarez¹, Alejandro Fernandez Soro¹, Eva Sanchez Ramos¹, Salvador Benlloch², Juan Jose Urquijo Ponce¹, Francesc Puchades Gimeno³, Francisco Sanz Herrero⁴, Miguel García Deltoro⁵, Mercedes Latorre Sánchez¹, Inmaculada Castelló Miralles¹, Dolores Ocete Mochon⁶, Concepcion Gimeno Cardona⁶, Moises Diago¹. ¹Consorcio Hospital General Universitario Valencia, Digestive Diseases, Valencia, Spain; ²Hospital Arnau de Vilanova, Digestive Diseases, Valencia, Spain; ³Consorcio Hospital General Universitario Valencia, Internal Medicine, Valencia, Spain; ⁴Consorcio Hospital General Universitario Valencia, Respiratory Diseases, Valencia, Spain; ⁵Consorcio Hospital General Universitario Valencia, Infectious Diseases, Valencia, Spain; ⁶Consorcio Hospital General Universitario Valencia, Microbiology, Valencia, Spain
Email: almacar84@hotmail.com

Background and aims: Abnormal liver function tests (ALFT) have been associated with worse evolution in COVID-19 hospitalized

patients with respiratory disease, but it is unclear if it is an independent prognostic factor. Our aim is to determine whether ALFT have a direct impact on the prognosis of these patients.

Method: A single-center, retrospective study of COVID-19 hospitalized patients with respiratory disease from February 15th, 2020, to February 28th, 2021. Patients with already known liver diseases were excluded. ALFT were defined as elevated total bilirubin (TBIL), aspartate transferase (AST), alanine transferase (ALT), alkaline phosphatase (ALP) and/or gamma-glutamyltransferase (GGT) above the upper limit of normality (ULN) in our laboratory. COVID-19 respiratory disease was classified as mild (no pneumonia), moderate (pneumonia) and severe (pneumonia with respiratory failure). Worsening of respiratory disease was defined as mild/moderate to severe respiratory disease progression or death. An association of ALFT with moderate/severe disease, worsening of respiratory disease, hospital stay, need for intensive care unit (ICU) admission and mortality was assessed. Statistical analysis was based on T-test and logistic regression. They included an adjusted multivariate model for age, sex, Charlson Comorbidities Index (CCI) and liver steatosis and fibrosis prior to hospital admission (defined by Hepatic Steatosis Index and FIB-4 scores respectively). Significance was set at $p < 0.05$.

Results: The data of 2075 patients (51.5% males), average age 66.5 (SD 17.8) years, were analyzed. Despite excluding patients with already known liver diseases, the overall prevalence of liver steatosis was 57.8% and that of fibrosis was 18.4%. 1225 patients (51.9%) presented ALFT at hospital admission and 1572 (75.8%) during hospital stay. ALFT were significantly associated with moderate/severe disease, likelihood of worsening of respiratory disease, longer hospital stay (8 vs 11.9 days, $p < 0.001$) and higher rate of ICU admission, but not with higher mortality. Higher FIB-4 was also significantly associated with worsening of respiratory disease (OR = 1.98, $p < 0.001$). Age and CCI were associated with higher mortality. Female sex was a protective factor against unfavorable events. Among ALFT, TBIL was the most associated with worsening of respiratory disease (OR = 2.4, $p < 0.001$) and ALT with ICU admission (OR = 1.42, $p < 0.001$) and mortality (OR = 1.03, $p = 0.04$). The exclusion of patients with elevated ALT/AST prior to admission did not change the results.

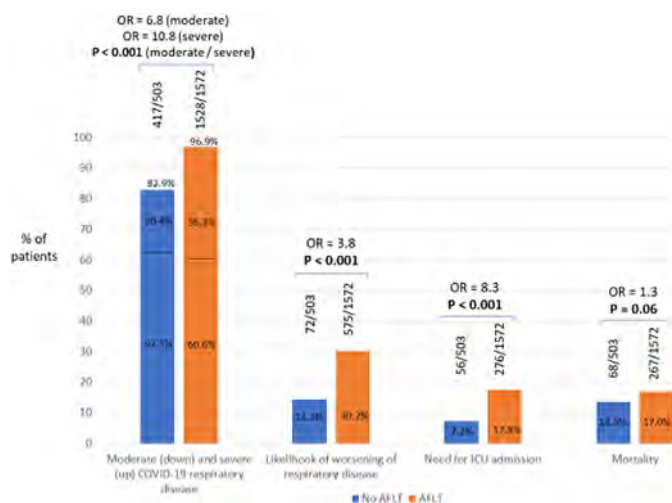


Figure: Association of ALFT with the different clinical events.

Conclusion: According to our study, ALFT can be considered as an independent risk factor for worse evolution in COVID-19 hospitalized patients with respiratory disease. Liver fibrosis had only influence in worsening of respiratory disease.

THU262

Effectiveness of COVID-19 viral vector vaccine Ad.26.COV2.S vaccine and comparison with mRNA vaccines in patients with cirrhosis

Binu John^{1,2}, Akash Doshi³, Yangyang Deng⁴, Natalie Mansour², A. Sidney Barritt⁵, Andrew Moon⁵, George Ioannou⁶, Paul Martin¹, Hann-Hsiang Chao⁷, Tamar H Taddei⁸, David Kaplan⁹, Bassam Dahman⁴. ¹University of Miami Hospital And Clinics | UHealth Tower, Miami, United States; ²Miami VA Medical Center, Miami, United States; ³University of Miami, Coral Gables, United States; ⁴Virginia Commonwealth University Health, Richmond, United States; ⁵University of North Carolina at Chapel Hill, Chapel Hill, United States; ⁶University of Washington, Seattle, United States; ⁷Hunter Holmes McGuire VA Medical Center, Richmond, United States; ⁸Yale University, New Haven, United States; ⁹University of Pennsylvania, Philadelphia, United States
Email: binu.john@gmail.com

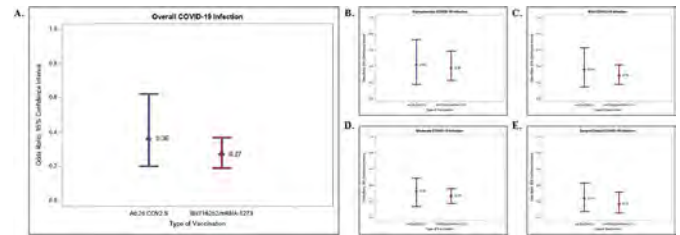
Background and aims: Viral vector COVID-19 vaccines have been administered more commonly worldwide but their effectiveness in participants with cirrhosis is unknown. We explored the effectiveness of vaccination with the Janssen Ad.26.COV2.S compared to the mRNA Pfizer BNT162b2 or Moderna 1273-mRNA vaccine in participants with cirrhosis.

Method: This was a test-negative case control study among participants with cirrhosis. This study design is widely used in evaluations of vaccine effectiveness and has the advantage of minimizing biases associated with access to vaccination or health care. Cases were those who were SARS CoV2 PCR positive, controls were those who tested negative during the study period between March 15, 2021 and October 3, 2021. Participants who did not undergo SARS CoV2 PCR testing, who had COVID-19 before the study period, or received a liver transplant, were excluded. COVID-19 was classified based on individual chart review using the National Institute of Health (NIH) COVID-19 severity scale as asymptomatic, mild, moderate, severe or critical illness.

Propensity score matching was used to match test positive cases and test negative controls. The propensity score of having COVID-19 were derived from a logistic regression that adjusted for the participant's sex, age, date of testing, race/ethnicity, location, alcohol as the etiology of liver disease, body mass index (BMI), diabetes mellitus, current tobacco use, current alcohol use, co-morbidities, and the Child Turcotte Pugh score. Multinomial logistic regression models were fit for COVID-19, to assess the adjusted effect from vaccination with either the Ad.26.COV2.S or the mRNA-1273 or BNT162b2 vaccines.

Results: A total of 955 cases and 955 matched controls were included in the study population. The two groups were well matched to all baseline characteristics.

The Ad.26.COV2.S vaccine had an effectiveness of 64% against COVID-19 (adjusted Odds Ratio [aOR] 0.36, 95% CI 0.20–0.62, $p = 0.005$). Effectiveness was lowest with asymptomatic illness (aOR 0.42, 0.18–0.73, $p = 0.03$), and higher against mild (aOR 0.36, 0.15–0.63, $p = 0.006$), moderate (aOR 0.33, 0.14–0.49, $p = 0.002$) and severe/critical (aOR 0.24, 0.08–0.83, $p = 0.04$) COVID-19. In the same period, mRNA vaccines had a 73% effectiveness against overall COVID-19 (aOR 0.27, 0.19–0.37, $p < 0.0001$), progressively higher from asymptomatic (aOR 0.38, 0.23–0.59, $p = 0.0004$) to mild (aOR 0.29, 0.18–0.42, $p < 0.0001$), moderate (aOR 0.27, 0.18–0.36, $p < 0.0001$), and severe or critical illness (aOR 0.17, 0.06–0.32, $p < 0.0001$). There were no statistically significant differences between the viral vector and mRNA vaccines.



Conclusion: In participants with cirrhosis, the Ad.26.COV2.S demonstrated a 64% effectiveness against COVID-19, and a 74% effectiveness against severe or critical COVID-19, similar to that associated with mRNA vaccines.

THU263

Humoral, cellular, clinical responses and safety to SARS-CoV-2 messenger RNA vaccines in patients with compensated and decompensated cirrhosis: a long-term single center prospective study

Massimo Iavarone¹, Giulia Tosetti¹, Floriana Facchetti¹, Matilde Topa¹, Andrea Lombardi², Roberta D'Ambrosio¹, Elisabetta Degasperi¹, Alessandro Loglio¹, Chiara Oggioni³, Alessandra Bandera², Andrea Gori², Ferruccio Ceriotti⁴, Luigia Scudeller⁵, Antonio Bertoletti⁶, Pietro Lampertico¹. ¹Foundation IRCCS Ca' Granda Ospedale Maggiore Policlinico, Division of Gastroenterology and Hepatology, MILANO, Italy; ²Foundation IRCCS Ca' Granda Ospedale Maggiore Policlinico, Division of Infectious Disease; ³IRCCS Humanitas Research Hospital, Quality and Patient Safety Unit, Rozzano, Italy; ⁴Foundation IRCCS Ca' Granda Ospedale Maggiore Policlinico, Clinical Laboratory, MILANO, Italy; ⁵IRCCS Azienda Ospedaliero-Universitaria di Bologna, Research and Innovation Unit, Bologna, Italy; ⁶Duke-NUS Medical School, Programme in Emerging Infectious Diseases, Singapore, Singapore
Email: massimo.iavarone@gmail.com

Background and aims: SARS-CoV-2 mRNA vaccines have been approved to prevent COVID-19 in the general population but little is known in patients with cirrhosis. We assessed immunogenicity, effectiveness and safety of vaccines in patients with compensated and decompensated cirrhosis with different aetiologies.

Method: This is a prospective single center study assessing humoral and cellular response, incidence post-vaccination SARS-CoV-2 infections and adverse events to mRNA vaccines in cirrhotics compared to healthy controls, according to previous SARS-CoV-2 infection. Antibodies against the spike- and nucleocapside-protein (anti-S and anti-N) of SARS-CoV-2 were tested at baseline, 21 days after the first and 21 days after the second doses and during follow-up in both patients and healthy controls. Longitudinal assessment of quantity of spike-specific T-cells was conducted by a test based on the stimulation of whole blood with peptides covering the SARS-CoV-2 spike protein, followed by cytokine (IFN- γ , IL-2) measurement. Side effects after vaccination were recorded.

Results: 182 cirrhotics (61 years, 75% males, 45% viral-related, 74% Child-Pugh A, 31% HCC) and 38 healthy unmatched subjects were enrolled. 15% cirrhotics and 32% controls had previously SARS-CoV-2 infection. In both groups, individuals with previous SARS-CoV-2 infection showed higher anti-S titres at all time points after vaccination. Among COVID-19 naïve subjects, patients with cirrhosis showed significantly lower anti-S titres compared to controls [998.5 (0.4–12, 500) vs 1,520 (259–12, 500) U/ml, $p = 0.048$]. In COVID-19 naïve cirrhotics, anti-S titres significantly decreased after a median of 133 (70–182) days [536 (0.4–8, 777) U/ml, $p < 0.0001$]. Decompensated cirrhotics showed lower anti-S titres compared to compensated ones [632 (0.4–12, 500) vs 1,377 (0.4–12, 500) U/ml, $p = 0.028$]. By multivariable analysis in COVID-19 naïve cirrhotics, independent predictors of lower anti-S titres after second dose, were: active HCC, immunocompromised conditions, Pfizer vaccine and

POSTER PRESENTATIONS

lower anti-S after first dose. The spike-specific T cell response was evaluated in 14 cirrhotics, showing a heterogeneous magnitude of response, but on average the quantity and kinetics of decline of the spike-specific cellular responses diverged in cirrhotics compared to controls, with lower concentrations of both IFN- γ and IL-2, at all time-points. During follow-up, 4/133 (3%) COVID-19 naïve cirrhotics tested positive for anti-N: all asymptomatic, no hospitalization required. Neither unexpected nor severe adverse events emerged in our patients.

Conclusion: In COVID-19 naïve patients with cirrhosis undergoing SARS-CoV-2 mRNA vaccine, humoral and cellular responses appeared suboptimal compared to healthy controls, but the rates of post vaccination infection remained low. The response after the third dose will be also presented.

THU264

The protective role of dairy protein on sarcopenic obesity in middle-aged and older women: a community-based, 12-year, prospective cohort study

Jun-Hyuk Lee¹, Joo Hyun Oh², Sang Bong Ahn², Huiyul Park³, Joo Hyun Sohn⁴, Bo-Kyeong Kang⁵, Mi Mi Kim⁵, Chul-min Lee⁵, Dae Won Jun⁶, Eileen Yoon⁶, Hyo Young Lee⁷, Hyunwoo Oh⁷. ¹Nowon Eulji Medical Center, Eulji University School of Medicine, Department of Family medicine, Seoul, Korea, Rep. of South; ²Nowon Eulji Medical Center, Eulji University School of Medicine, Department of Medicine, Seoul, Korea, Rep. of South; ³Uijeongbu Eulji Medical Center, Department of Family medicine, Gyeonggi-do, Korea, Rep. of South; ⁴Hanyang University Guri Hospital, Hanyang University College of Medicine, Department of Medicine, Gyeonggi-do, Korea, Rep. of South; ⁵Hanyang University College of Medicine, Department of Radiology, Seoul, Korea, Rep. of South; ⁶Hanyang University College of Medicine, Department of Medicine, Seoul, Korea, Rep. of South; ⁷Uijeongbu Eulji Medical Center, Department of Medicine, Gyeonggi-do, Korea, Rep. of South
Email: dr486@eulji.ac.kr

Background and aims: Changes in body composition during aging include decreased muscle mass and increased fat mass, especially in women. Individuals with sarcopenic obesity (SO) could be at higher risk of morbidities and mortality than those with either sarcopenia or obesity alone. Dairy products, which contain whey protein and all essential amino acids, could have a beneficial role in preserving muscle mass and reducing obesity. We aimed to analyze the effect of dairy protein on the development of SO in women using a large-scale, community-based prospective cohort.

Method: Our analysis included 4251 women from the Korean Genome and Epidemiology Study. Participants were categorized into three groups by the tertile of dairy protein intake, which was assessed using a semi-quantitative 103-food item food frequency questionnaire. Appendicular skeletal muscle mass was estimated using the anthropometric equation. Obesity was defined as a body mass index of 25 kg/m² or greater. Multiple Cox hazard regression analysis was conducted to examine associations between dairy protein intake and incident SO.

Results: During follow-up (mean, 9.6 years), 280 women newly developed SO. Using Cox proportional regression models, the hazard ratios (95% confidence interval) for incident SO of the middle and highest tertiles were 0.93 (0.70–1.24) and 0.72 (0.52–0.98) compared with lowest tertile after adjusting for confounding variables.

Conclusion: These findings indicate high dairy protein intake is inversely related to SO development in Korean women. Dairy protein intake could be an effective strategy to prevent incident SO.

Keywords: dairy protein; sarcopenia; obesity; sarcopenic obesity; women

THU265

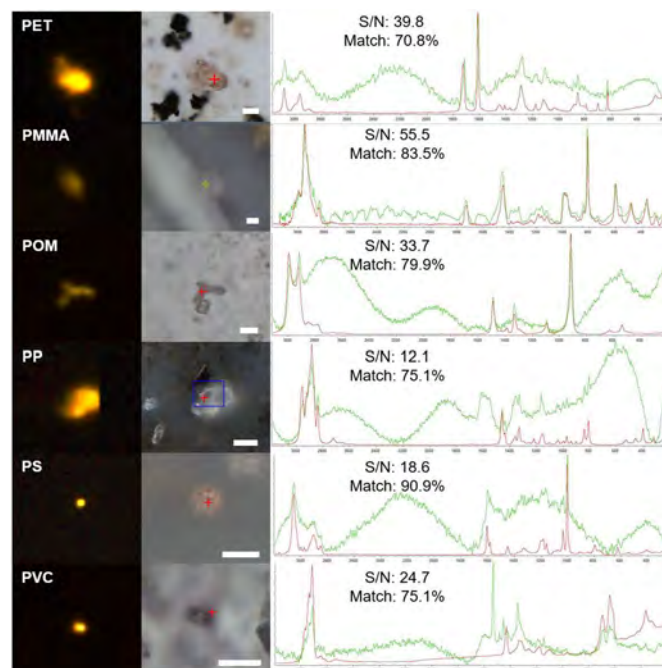
Detection of microplastics in cirrhotic liver tissue

Thomas Horvatits¹, Matthias Tamminga², Beibei Liu¹, Marcial Sebode¹, Klaus Püschel³, Ansgar Lohse¹, Samuel Huber¹, Elke Fischer². ¹University Medical Center Hamburg-Eppendorf, I. Department of Medicine, Gastroenterology and Hepatology, Hamburg, Germany; ²University of Hamburg, Center for Earth System Research and Sustainability (CEN), Hamburg, Germany; ³University Medical Centre Hamburg-Eppendorf, Institute of Legal Medicine, Hamburg, Germany
Email: t.horvatits@uke.de

Background and aims: The contamination of ecosystem compartments by microplastics (MPs) is an ubiquitous problem. Tissue accumulation of MPs has been observed in mice, and recently MPs have been observed in human stool and placenta. However, whether MPs accumulate in human tissues, and the resulting consequences are still unclear. Aim of this study was to examine various human tissue samples for the presence of MPs, and to determine whether MPs may deposit in the liver, kidney or spleen.

Method: This proof-of-concept case series was conducted in Hamburg, northern Germany, Europe. Tissue samples from 6 patients with liver cirrhosis and portal hypertension and from 7 individuals without underlying liver disease were assessed. A reliable method for detection of MP particles in human tissue was developed. A total of 17 samples (11 human liver, 3 kidney and 3 spleen samples) were analysed according to the final protocol. Chemical digestion of the tissue samples, staining with Nile red, subsequent fluorescent microscopy and Raman spectroscopy were performed. Procedural blanks were processed and analysed during each series of analyses. Shape, size and types of MP polymers were assessed in all tissue samples.

Results: Considering the limit of detection, all samples (liver, spleen, kidney) from patients without liver disease tested negative for MPs (n = n.s.), whereas MPs in liver samples from patients with cirrhosis tested positive and MP concentrations (5 to 12 particles per g tissue) were significantly higher than those from blank samples (n = 6, p = 0.009, α = 0.05). Six different microplastic polymers (polystyrene (PS), polyvinyl chloride (PVC), polyethylene terephthalate (PET), polymethyl methacrylate (PMMA), polyoxymethylene (POM), and polypropylene (PP)) ranging from 4 to 30 μ m in size have been detected, see figure 1.



Conclusion: This is the first study, assessing MPs in different types of human tissues. MPs were found only in liver tissues from patients with cirrhosis. Hepatic deposition may be the consequence of impaired intestinal barrier function due to portal hypertension and portal enteropathy. Future studies on the possible effects on human health are urgently needed.

Examples of MP particles found in human tissue samples displayed as fluorescence images (left column) and true colour microscope images (mid column) as well as related Raman-spectra. White scale bar indicates 10 µm, library reference spectra are displayed in red, particle spectra are given in green. S/N: signal to noise ratio

THU266

Patient Navigators: an innovative approach to improve hepatitis c case finding leveraging existing human immunodeficiency virus service delivery models to reach last mile patients in Nasarawa State, Nigeria

Chukwuemeka Agwuocha^{1,2}, Olayinka Adisa¹, Onyeka Nwobi¹, Muhammad-Mujtaba Akanmu¹, Caroline Boeke³, Magdalena Witschi³, Amy Azania³, Jibrin Kama¹, Folu Lufadeju¹, Owens Wiwa¹. ¹Clinton health access initiative, Abuja, Nigeria; ²Clinton Health Access Initiative, Abuja, Nigeria; ³Clinton health access initiative, United States

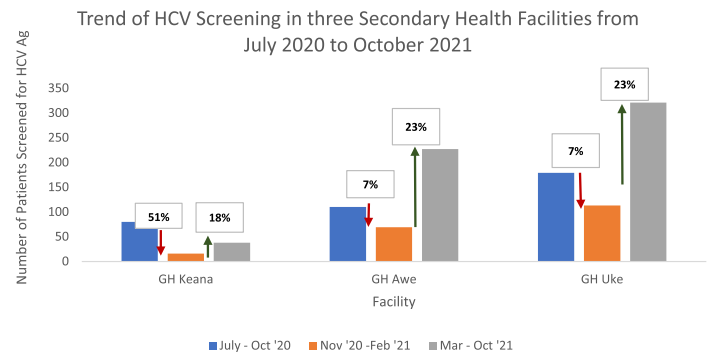
Email: cagwuocha@clintonhealthaccess.org

Background and aims: The natural history of Hepatitis C Virus (HCV) demonstrates an asymptomatic disease that often leads to liver degeneration in approximately three decades. In HIV/HCV coinfection, liver degeneration is accelerated with decompensated cirrhosis occurring in less than two decades resulting in higher mortality rates. The asymptomatic nature of HCV, increased rate of disease progression in HIV, low awareness, and poor care seeking behaviour emphasizes the need to improve HCV case finding in People Living with HIV (PLHIV).

In Nigeria, the Nasarawa State Government has committed to HCV elimination, with an initial focus on PLHIV, necessitating integration of services to screen ART patients for HCV. However, due to the COVID pandemic and the resultant scale-up of Differentiated Service Delivery (DSD) models within the HIV program, screening yield from facility-based case finding reduced significantly. To ensure last mile linkage to HCV screening, the Patient Navigator pilot was conducted from March-October 2021. This analysis aims to assess screening coverage before and during this pilot period.

Method: One healthcare worker across three secondary facilities i.e., General Hospitals Keana, Awe, and Uke, labelled patient navigator (PN) was charged with the responsibility of identifying unscreened PLHIV using facility screening records and enrolment data. These PNs were HIV program defaulter trackers, consequently integrating this service within the HIV program. The PN employed strategic patient tracking approaches like phone calls, community engagements and peer group meetings. Using laboratory screening registers, screening progress was compared pre-intervention (July 2020 to February 2021) versus during the intervention (March to October 2021).

Results: A total of 125, 560, and 923 were active on ART care as of January 2020 in General Hospitals Keana, Awe, and Uke respectively. Across sites, the first 4 months of the pre-intervention phase saw high screening numbers as all available patients presenting to facilities were screened. Subsequently, a decline in screening numbers across all facilities. However, the intervention phase demonstrated extended coverage, reaching the last mile patients leading to an increase in case finding by 18% in GH Keana, and 23% in GH Awe and GH Uke respectively.



Conclusion: The use of patient navigators demonstrates the feasibility and cost-effectiveness of increasing case-finding through HCV/HIV program integration.

THU267

The Community Pop-Up Clinic (CPC): a unique strategy to achieve HCV elimination in the inner city

Brian Conway^{1,2}, Shawn Sharma¹, Leo Yamamoto¹, Rossitta Yung¹, David Truong¹. ¹Vancouver Infectious Diseases Centre, Vancouver, Canada; ²Simon Fraser University, Burnaby, Canada
Email: bconway5538@gmail.com

Background and aims: A number of strategies have been proposed to help identify HCV-infected inner-city residents, engage them in care, provide them with Hepatitis C Virus (HCV) therapy, and achieve and measure cure. While many programs have successfully identified large numbers of subjects eligible for treatment, the rate of successful completion and cure is highly variable. The most relevant outcome measure for such programs may be the number of HCV cures achieved over time, and programmatic changes should be implemented and evaluated according to this metric. We have evaluated our Community Pop-Up (CPC) program in terms of this outcome measure, as a function of the resources required for its implementation.

Method: On a weekly basis, a team consisting of a physician, nurse and three support staff interact with up to 30 individuals over 4 hours in the inner city of Vancouver, at a community centre or single room occupancy dwelling to provide point-of-care HCV testing or ascertainment of previously identified HCV infection status. Treatment for HCV infection is offered in the context of a low-barrier treatment program, with medications delivered daily/weekly, at the place of residence, local pharmacy or at our community clinic. Strategies are in place to limit loss to follow-up and maximize engagement in care throughout treatment and thereafter, to ascertain if cure has been achieved.

Results: From 07/20–09/21 (15 months), we conducted 55 community pop-up clinics and screened a total of 774 individuals for their HCV status. Of 280 HCV-infected individuals by antibody test, 99 (35.4%) had documented HCV viral load result. Key demographic characteristics include: median age 43 (28–86) years, 77.5% male, F0/F1 (22, 55%), opioid antagonist therapy 26 (65%), HIV co-infected 2 (5%), fentanyl/cocaine/amphetamine use (24/12/18, 60%/30%/45%). Of 40 individuals on treatment, none have been lost to follow-up, 26 have demonstrated cure, with outcome results pending in the other 14 subjects. Strategies are in place to engage the remaining 49 viremic individuals in HCV treatment

POSTER PRESENTATIONS

Conclusion: In the context of an established, multidisciplinary clinic serving the inner city, a 4 hour/week initiative staffed with 2 health care providers and 3 support staff led to successful HCV treatment of 40 individuals, with none lost to follow-up once treatment has been initiated and the possibility of 40–50 additional treatment starts in the short term. This represents a very cost effective and productive initiative to address HCV infection in similar populations.

THU268

Age, gender and region-specific HBsAg and anti-HCV seroprevalence in Ghana: a nationwide hospital based cross-sectional study

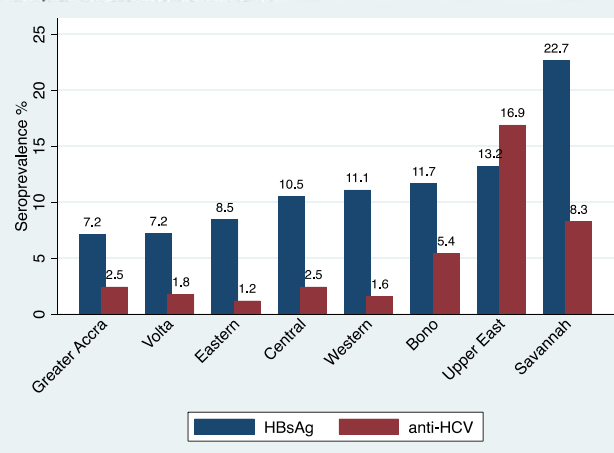
Yvonne Narthey^{1,2}, ¹Cape Coast Teaching Hospital, Internal Medicine, Cape Coast, Ghana; ²Karolinska Institute, Medical Epidemiology and Biostatistics, Stockholm, Sweden
Email: yvonne.narthey@ki.se

Background and aims: Hepatitis B (HBV) and Hepatitis C (HCV) viral infection continue to pose a significant global health burden and are responsible for high morbidity and mortality worldwide due to sequelae of end stage liver disease. Previous estimates in Ghana report a seroprevalence of anti-HCV of 3.3% and HBsAg of roughly 9%. These estimates fall short of describing age and gender-specific rates and have relied on small sample sizes in few centers. Particularly for HCV, there is a paucity of data from several regions in Ghana. Numerous challenges, including lack of focused and definitive testing and treatment strategies and policies limit the impact of current elimination efforts. Providing a robust programmatic foundation requires a scale-up of hepatitis testing nationwide, and this in turn requires up-to-date epidemiologic data to understand the burden of disease in all parts of the country and across all age groups. This study aimed to perform an epidemiological assessment of HBV and HCV infection in Ghana to determine age, gender, and region specific seroprevalence. Additionally, it aimed to convene a coalition of local stakeholders for policy development in Ghana.

Method: A nationwide cross-sectional study using de-identified data was collated from January 1st to October 30th 2021. Data from health information management systems for 2017–2021 was reviewed from 20 centers including teaching, regional, and district hospitals in 11 regions in Ghana. Sixty thousand labour ward, 54, 000 blood bank, and 48, 000 laboratory-based records were reviewed and analyzed for age and gender-specific HBV and HCV prevalence. Regional differences in seroprevalence were also determined.

Results: A stakeholder meeting was held in Accra, Ghana bringing together key players from the public and private sector involved in viral hepatitis elimination for policy planning. Crude prevalence among pregnant women was 6.36% (95% CI 5.70–7.02) for HBsAg; among blood donors was 5.09% (95% CI 4.91–5.28) for HBsAg and 3.22% (95% CI 3.08–3.38) for anti-HCV. From laboratory-based registers, overall seroprevalence was 8.90 (95% CI 8.65–9.16%) for HBsAg and 3.39 (95% CI 3.17–3.63) for anti-HCV. Prevalence of both HBV and HCV were significantly higher in the northern Ghana. HBsAg prevalence was higher in males (9.70%) than females (8.20%) $p < 0.05$, but there was no difference in gender-specific seroprevalence for anti-HCV. The highest age preponderance was among 40–49 (13.53%) year olds for HBsAg and 60+ year olds (7.59%) for anti-HCV. Seroprevalence in children <5 years was 1.87% for HBsAg and 1.53% for anti-HCV.

Figure 1. Region specific crude HBsAg and anti-HCV seroprevalence among hospital lab attendants in Ghana



Conclusion: Ghana remains a region of high endemicity for HBV and moderate-high endemicity for HCV. Northern Ghana consistently demonstrates a higher disease burden than the rest of the country. Focused and targeted policies are essential to reach elimination targets.

THU269

The elimination of hepatitis C in the Cherokee Nation: the impact of harm reduction

Jorge Mera¹, Whitney Essex¹, Molly Feder², Homie Razavi³, Devin Razavi-Shearer³, ¹Cherokee Nation Outpatient Health Center, Tahlequah, United States; ²Cardea Services, Seattle, United States; ³Center for Disease Analysis Foundation, Lafayette, United States
Email: drazavishearer@cdafound.org

Background and aims: In the United States, American Indians/Alaskan Natives have the highest rates of HCV incidence, liver cancer and mortality compared to all other racial/ethnic groups.

The Cherokee Nation (CN) a sovereign tribal nation, began a hepatitis C (HCV) elimination program in 2015 with a 6-fold increase in treatment in 2016. The primary aim of this study is to estimate what would need to be done to meet the World Health Organization's (WHO) 2030 targets by 2025. In addition to examining increase in treatment, the implementation and lack of syringe service programs (SSP) were considered in the analysis.

Method: CN specific input data populated a dynamic Markov model. Three scenarios were considered. The Base scenario examined the impact of maintaining the current treatment and diagnosis levels into the future. The 2025 w/o SSP scenario examined how much treatment would need to be increased to attempt to meet the 2030 targets in 2025 without access to SSP. The 2025 w/SSP scenario examined the accompanying treatment uptake necessary to meet the 2030 goals in 2025 with a robust SSP program.

Results: In the Base scenario, it was estimated that the 90% diagnosis and 80% treatment targets would be met prior to 2025. By 2030, there is estimated to be an 84% reduction in mortality and a 50% reduction in incidence when compared to 2015 (Figure 1). 2025 w/o SSP required a large increase in treatment, from 162 to 400 annually. This scenario resulted in an 89% reduction in mortality by 2025 but only a 50% reduction in incidence by 2025. The 2025 w/SSP scenario required a modest increase in treatment to 255 individuals annually. This resulted in a 65% reduction in mortality and an 86% reduction in incidence by 2025 thus meeting all targets.

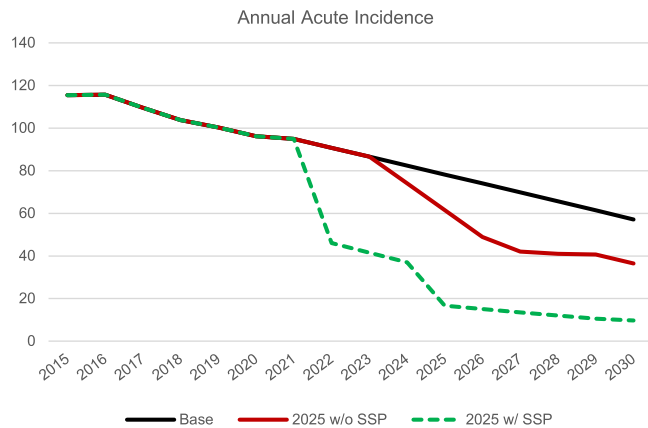


Figure: Annual Acute Incidence of HCV on The Cherokee Nation, 2015–2030

Conclusion: The current HCV elimination program would meet almost all of the WHO targets prior to 2030. However, in the absence of SSP that provide access to all of those that need it, it is estimated that the incidence would not drop substantially enough by 2030. With the CN approving SSP an opportunity has opened for the CN to meet all targets by 2025. In the first year of the elimination program 222 individuals were treated thus increasing treatment to 255 for three years would be within the capacity of the program. To achieve this goal the CN should have a swift broad rollout of SSP. This combined with a slight increase in treatment will lead to early elimination and a positive impact on the population health of the CN.

THU270

Effectiveness of mRNA vaccines in patients with cirrhosis with rising prevalence of SARS-CoV-2 delta variant

Binu John^{1,2}, Raphaella Ferreira¹, Dustin Bastaich³, Akash Doshi⁴, Tamar H Taddei⁵, David Kaplan⁶, Seth Spector^{1,4}, Bassam Dahman³.
¹Miami VA Medical Center, Miami, United States; ²University of Miami Hospital And Clinics | UHealth Tower, Miami, United States; ³Virginia Commonwealth University, Graduate School, Richmond, United States; ⁴University of Miami, Coral Gables, United States; ⁵Yale University, New Haven, United States; ⁶University of Pennsylvania, Philadelphia, United States

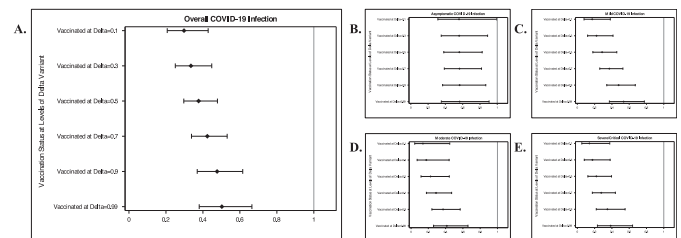
Email: binu.john@gmail.com

Background and aims: The effectiveness of COVID-19 vaccines with the increasing prevalence of SARS CoV2 B.1.617.2 delta variant among patients with cirrhosis is unknown. The aim of the study was to investigate the effectiveness of COVID-19 vaccination at varying community prevalence of the B.1.617.2 variant among patients with cirrhosis.

Method: This study used was a test-negative case control design, where adults with cirrhosis who had a diagnosis of COVID-19 as documented by a positive SARS-CoV-2 Polymerase Chain Reaction (PCR) were considered as cases, and those with a negative SARS CoV2 PCR were considered controls. This study design is widely used in evaluations of vaccine effectiveness and has the advantage of minimizing biases associated with access to vaccination or health care. Participants who did not undergo SARS CoV2 PCR testing, who had COVID-19 before the study period, received a vaccine other than an mRNA vaccine, or received a liver transplant, were excluded. Patients were considered fully vaccinated 14 days after receipt of either the Pfizer BNT162b2 or the Moderna 1273-mRNA vaccine. COVID-19 was classified based on individual chart review using the National Institute of Health (NIH) COVID-19 severity scale as asymptomatic, mild, moderate, severe or critical illness. The weekly proportion of the delta variant in the United States was obtained using data from the Center for Disease Control COVID-19 genomic surveillance data.

Propensity score matching was used to match test positive cases and test negative controls. The propensity score of having COVID-19 were derived from a logistic regression that adjusted for the participant's baseline variables.

Results: The study sample included 1,720 participants, including 860 cases and 860 controls. The effectiveness of mRNA vaccines against COVID-19 was inversely related to the community prevalence of the B.1.617.2 variant. For every 10% increase in the community prevalence of delta, the likelihood of COVID-19 after full vaccination increased by 5% (aOR 1.05, 1.02–1.07, $p = 0.0001$). At community delta prevalence of 10%, mRNA vaccines were 70% effective (aOR 0.30, 0.21–0.43, $p < 0.0001$). Vaccine effectiveness dropped to 62% (aOR 0.38, 0.30–0.48, $p < 0.0001$) when the community prevalence of the delta variant increased to 50%, to 52% (aOR 0.50, 0.38–0.67, $p < 0.0001$) at a community delta prevalence of 90% and to 50% (aOR 0.38–0.67, $p < 0.0001$) with a community delta prevalence of 99%.



Conclusion: Vaccine effectiveness is inversely associated with community prevalence of the delta variant, with effectiveness dropping from 30% at delta prevalence of 10%, down to 50% with a community delta prevalence of 99%. Further studies are needed to understand if booster doses are able to overcome the drop in vaccine effectiveness with increasing prevalence of delta variant, among patients with cirrhosis.

THU271

Epidemiology and management of hepatitis B and C in primary care in the Netherlands-data from the Rijnmond primary care database

Sylvia Brakenhoff¹, Robert De Man¹, Robert De Knecht¹, Patrick Bindels², Evelien de Schepper².
¹Erasmus MC, University Medical Center, Gastroenterology and Hepatology, Rotterdam, Netherlands; ²Erasmus MC, University Medical Center, General Practice, Rotterdam, Netherlands

Email: s.brakenhoff@erasmusmc.nl

Background and aims: The Dutch guideline for general practitioners (GPs) advises biannual surveillance of hepatitis B (HBV) patients and referral of every hepatitis C (HCV) patient. We aimed to study the prevalence, incidence and the management of hepatitis B and C in primary care.

Method: This is a retrospective cohort study using the Rijnmond Primary Care database (RPCD), including healthcare data of medical records of GPs of approximately 200,000 patients in the area of Rotterdam, the Netherlands. Patient records were selected based on laboratory results, International Classification of Primary Care (ICPC) codes and free text words.

Results: In total, 977 patients were included; 717 HBV, 252 HCV, and 8 HBV/HCV co-infected patients. Between 2013 and 2019, the prevalence of HBV and HCV declined from 5.21 to 2.99/1,000 person years (PYs; -43%) and 1.50 to 0.70/1,000 PYs (-53%) respectively. We observed that the majority of the patients had been referred to a medical specialist at least once (71% HBV and 89% HCV patients). However, among the 406 chronic hepatitis B patients, we observed that 36.2% of the patients did not receive adequate surveillance by their GP (≥ 2 ALT checks within 3 years) or by a medical specialist. In addition, among the 153 chronic hepatitis C patients, 113 (73.9%)

POSTER PRESENTATIONS

received antiviral therapy. However, 68 patients (44.4%) had no record about successful antiviral treatment and might still be chronically infected on 31.12.2019.

Conclusion: This study demonstrated a declining prevalence in viral hepatitis B and C in primary care in the Netherlands. However, a substantial of the patients did not receive adequate surveillance or antiviral therapy. It is therefore crucial to involve GPs in the road to elimination.

THU272

Point of care testing for hepatitis C in the priority settings of mental health, prisons and drug and alcohol facilities

Catherine Ferguson¹, Lucy Ralton¹, Erin McCartney¹, Joshua Dawe², Jacqui Richmond², Edmund Tse³, Alan Wigg⁴, Victoria Cock⁵, Tom Rees⁶, David Shaw¹. ¹Royal Adelaide Hospital, Infectious Diseases, Adelaide, Australia; ²Burnet Institute, Melbourne, Australia; ³Royal Adelaide Hospital, Hepatology, Adelaide, Australia; ⁴Flinders Medical Center, Gastroenterology and Hepatology, Adelaide, Australia; ⁵Drug and Alcohol Services South Australia, Adelaide, Australia; ⁶Communicable Disease Control Branch, SA Health, Adelaide, Australia
Email: erin.mccartney@sa.gov.au

Background and aims: A key barrier to hepatitis C (HCV) diagnosis and treatment is the multi-stage process of conventional testing that requires multiple visits to pathology services and healthcare providers to obtain a HCV antibody (Ab) test, HCV RNA test, diagnosis, and linkage into care to commence treatment. Point of care testing for hepatitis C in the priority settings of mental health, prisons and drug and alcohol facilities (PROMPt) aims to overcome critical roadblocks to HCV treatment in the community by providing HCV point-of-care testing (POCT) and direct referral into treatment. Over a 12 month period PROMPt aims to evaluate the effect of POCT on HCV testing rates, linkage to care and explore the acceptability of HCV POCT in facilities and services for individuals at high risk of HCV infection. Primary end points: 1. Number/proportion of participants who receive rapid POCT HCV Ab plus POC RNA. HCV Ab/RNA positivity at each site 2. Number/proportion of HCV RNA positive participants who are linked to care. Secondary end points: 1. Acceptability of HCV POCT to participants in each setting.

Method: Participants are offered POC HCV diagnostic testing using SD Bioline fingerstick Ab assay and those returning a positive HCV Ab result are offered a Cepheid finger stick HCV RNA Xpert assay. Project staff, including peer support workers, provide HCV education, pre- and post-test counselling, and linkage to care at the time of diagnosis.

Results: Interim analysis at 6 months reports 707 participants recruited across all 3 priority settings. 125/707 (18%) positive HCV Ab participants were reflexed to HCV RNA testing, resulting in 35 positive RNA participants 35/125 (28%). To date 27/35 (77%) RNA positive participants have commenced treatment.

The complete 12 months of recruitment and final analysis of end points will be presented.

	HCV Ab Test	% Ab Positive	% RNA Test	% RNA Positive	RNA Positivity
Remand Prison	409	76/409 (19%)	76/409 (19%)	25/409 (6%)	25/76 (33%)
Inpatient AOD	207	36/207 (17%)	36/207 (17%)	4/207 (2%)	4/36 (11%)
Inpatient Mental Health Service	91	13/91 (14%)	13/91 (14%)	6/91 (7%)	6/13 (46%)
Overall	707	125/707 (18%)	125/707 (18%)	35/707 (5%)	35/125 (28%)

Conclusion: PROMPt has demonstrated high rates of HCV POC testing and acceptability in 3 high priority settings. The hepatitis C infection rates have been lower than anticipated and the combined HCV Ab and RNA POCT approach to testing has allowed for efficient and economical testing scale up in each site.

THU273

Association of novel lifestyle- and whole foods base inflammation scores with metabolic dysfunction-associated fatty liver disease: a population-based study among Iranian adults

Ehsaneh Taheri¹, Roberd M Bostick², Behzad Hatami¹, Mohammadamin Pourhoseingholi¹, Hamid Asadzadeh Aghdaei¹, Alireza Moslem³, Alireza MosusaviJarahi⁴, Mohammadreza Zali¹. ¹Shahid beheshti university of medical sciences, Research institute for gastroenterology and liver disease center, Tehran, Iran; ²Emory University, Epidemiology, Atlanta, United States; ³Sabzevar university of medical sciences, Cellular and molecular research center, Sabzevar, Iran; ⁴Shahid beheshti university of medical sciences, Department of community medicine, Tehran, Iran
Email: ehsaneh_taheri@yahoo.com

Background and aims: Chronic inflammation, associated with lifestyle and dietary patterns, may contribute to metabolic dysfunction-associated fatty liver disease (MAFLD) risk. Recently, a novel dietary inflammatory score based on weighted inflammatory scores of 19 components (whole foods) from food frequency questionnaire (FFQ) and lifestyle inflammatory score based on weighted inflammatory scores of 4 components of lifestyle (physical activity, adiposity, alcohol, and smoking) were proposed. The main aim of this study was to evaluate the associations of these novel inflammatory scores with MAFLD risk. The secondary aim of our study was to compare novel dietary- and lifestyle inflammatory scores-MAFLD associations with previous dietary inflammatory scores.

Method: We investigated associations of 19-component dietary and 4-component lifestyle inflammatory separately and jointly with MAFLD risk among Iranian adults aged 35–70 years of age at baseline phase of PERSIAN cohort study in Sabzevar city. MAFLD was defined as having a fatty liver index (FLI) ≥ 60 , plus one of the following: being overweight or obese (body mass index [BMI] ≥ 25 kg/m²), a Type II diabetes mellitus (T2DM) diagnosis, or having any evidence of metabolic dysregulation. We also calculated previous well-known diet-related inflammatory markers such as dietary inflammatory index (DII) and empirical dietary inflammatory pattern (EDIP) using information from 115-item FFQ. Higher score were considered more inflammatory status. We assessed inflammatory scores-MAFLD associations using multivariable unconditional logistic regression.

Results: Of 4241 participants of Persian Sabzevar Cohort study, 968 patients with MAFLD and 964 age- and gender adjusted controls were recruited in this nested case-control study. Among participants in the highest relative to the lowest dietary- and lifestyle inflammatory score tertiles, the adjusted odds ratios (OR) and their 95% confidence intervals (CI) were 1.84 (1.61–2.07; p-trend <0.001) and 1.96 (1.69–2.21; p-trend <0.001), respectively. Among those in the highest relative to the lowest joint dietary- and lifestyle inflammatory score tertiles, the adjusted OR (95% CI) was 2.56 (95% CI: 2.19–2.93; p-interaction <0.001). The third tertile ORs (95% CI) for the DII- and EDIP-MAFLD associations were 1.63 (1.05–5.62) and 1.71 (1.17–4.62), respectively.

Conclusion: More pro-inflammatory diets and lifestyles, separately and particularly jointly, are associated with higher risk of having MAFLD among adults. The associations of novel dietary- and lifestyle inflammatory with MAFLD were stronger than DII- or EDIP- MAFLD associations.

THU274

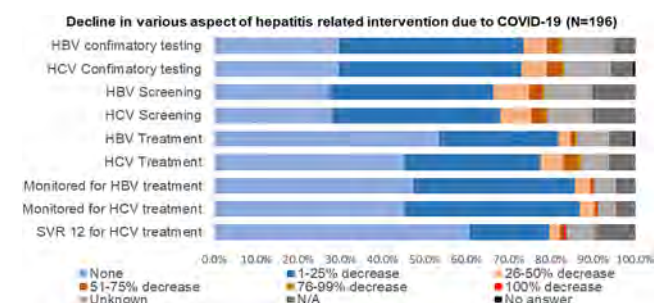
Assessment of COVID-19 impact and response on hepatitis B virus and hepatitis C virus prevention and treatment from nationwide survey in Japan

Md Razeen Ashraf Hussain¹, Aya Sugiyama¹, Lindsey Hiebert^{1,2}, Serge Ouoba^{1,3}, Bunthen E^{1,4}, Ko Ko¹, Tomoyuki Akita¹, Shuichi Kaneko⁵, Tatsuya Kanto⁶, John Ward², Junko Tanaka¹.
¹Hiroshima University, Department of Epidemiology: Infectious Disease Control and Prevention, Graduate School of Biomedical and Health Sciences, Hiroshima, Japan; ²The Task Force for Global Health, Coalition for Global Hepatitis Elimination, Georgia, United States; ³Institut de Recherche en Science de la Santé (IRSS), Unité de Recherche Clinique de Nanoro (URCN), Nanoro, Burkina Faso; ⁴Ministry of Health, Payment Certification Agency, Cambodia; ⁵Kanazawa University, Department of Gastroenterology, Graduate School of Medical Science, Japan; ⁶National Center for Global Health and Medicine, The Research Center for Hepatitis and Immunology, Tokyo, Japan
 Email: jun-tanaka@hiroshima-u.ac.jp

Background and aims: Elimination of Hepatitis B Virus (HBV) and Hepatitis C Virus (HCV) requires continuous diagnosis and treatment. Ongoing pandemic COVID-19 has been affecting on health care system including on preventive care and testing of HBV and HCV. This study aimed to assess the impact of COVID-19 on hepatitis prevention and treatment in Japan. This international joint research conducted by three research groups of Ministry of Health, Labour and Welfare of Japan with the Task Force for Global Health and in cooperation with Japan Society of Hepatology (JSH).

Method: We conducted this cross-sectional study by a questionnaire survey in Japanese and English language on online Microsoft forms platform from 24 August to 03 October 2021. The electronic version of the questionnaire was disseminated by e-mail to all the members of JSH. The questionnaire was designed to address the impact of COVID-19 on hepatitis testing, screening, treatment; mitigation strategies; response to COVID-19; and perceived benefits of COVID-19.

Results: Total 196 medical doctors participated from 35 prefectures of whom 49.5% are in administrative positions. 55.6% of participants responded about no interruption while 11.7% reported supply chain disruptions during the survey period. 1–25% decrease in HBV screening and confirmatory testing was reported by 38.8% and 43.9% participants, respectively. Decrease of 1–25% in HCV screening and confirmatory testing was reported by 39.8% and 43.4% participants, respectively. However, no decline to initiate HBV and HCV treatment were reported by 53.6% and 45.4%, respectively, but extension of hospital visits was reported by 65.3%. The response illustrated the decrease in patients' imaging (65.8%), laboratory testing (68.4%), hepatocellular carcinoma screening (55.1%), gastro-intestinal endoscopy (87.2%) and liver biopsy (43.4%). Patient anxiety and fear (67.4%), loss of staff to COVID-19 response (49.0%) and limited availability of staff (46.4%) were responded as challenges to resume services to pre-COVID-19 level. About COVID-19 response, engagement in COVID-19 testing and vaccination were reported by 51.5% and 61.2%, respectively. For Perceived benefits of COVID-19 response were strengthening general health care system (45.9%), demonstration of hepatitis infrastructure for COVID-19 response (44.4%) and improved training of infectious disease testing and management (35.7%)



Conclusion: In Japan, a greater decrease was noticed on HBV and HCV confirmatory testing, screening than treatment initiation. However, anxiety and fear of patients, lack of staff and facilities are major challenges to overcome such situation. Perceived benefits of COVID-19 on hepatitis were strengthened health care system, demonstration of hepatitis infrastructure and improved training in infectious disease testing and management.

THU275

Knowledge, attitude and practice regarding COVID-19 vaccination among HCV infected patients in Georgia

Lasha Gulbiani¹, Tiko Kamkamidze¹, Ana Gamezardashvili¹, George Kamkamidze², Maia Butsashvili¹. ¹Health Research Union, Tbilisi, Georgia; ²Clinic Neolab, Tbilisi, Georgia
 Email: lashagulbiani7@gmail.com

Background and aims: COVID Vaccination coverage is low in Georgia (24.7%). There are different vaccine-related misconceptions, particularly among people with different chronic diseases, who are at greatest risk of COVID related health complications and death. The aim of this study was to assess the COVID vaccine knowledge, attitude and practice among HCV infected patients enrolled in HCV elimination program in Georgia

Method: The interviewer administered questionnaire was used to survey the random sample of patients at one of the outpatient clinics providing HCV treatment services within HCV elimination program in Tbilisi, capital of Georgia. The sample included patients at different types of visits at the clinic-having diagnostic tests before the treatment, receiving the treatment and having sustained viral load (SVR) test at 12–24 weeks after treatment. Patients with and without liver cirrhosis were enrolled in the survey.

Results: 230 patients were interviewed in total. Only 42 (18.2%) reported to receive two doses and 12 (5.2%)-1 dose of COVID vaccine. Out of 176 not vaccinated patients 45 (25.5%) declared that they do not wish to get vaccinated because of their disease (HCV infection); 32 (18.1%) plan to get the vaccine; 29 (16.4%) patients think they are not at risk of COVID related health problems, 12 (6.8%) did not get the vaccine because they had COVID in the past and consider themselves defended against the disease, 25 (14.2%) are afraid of side effects and 33 (18.7%) do not trust the vaccine. Among not vaccinated patients 38 (21.5%) had liver cirrhosis.

Conclusion: COVID vaccination coverage is very low among patients enrolled in HCV elimination program, including patients with liver cirrhosis. Targeted educational campaigns for people with chronic diseases are needed to fight vaccine misconceptions among this high-risk population.

THU276

CRIVALVIR-FOCUS: low HIV and chronic Hepatitis B and C infection prevalence among women in reproductive and sexual health services in Valencia, Spain

Miguel Garcia-Deltoro¹, Pilar Obon¹, Caterina Canapele², Jose Maria Mari², Adela Vidal², Maria Martinez-Roma³, Maria Dolores Ocete⁴, Concepción Gimeno Cardona⁴, Moisés Diago⁵, Neus Gomez-Muñoz³, Alba Carrodegua⁶, Diogo Medina⁶, Enrique Ortega González³. ¹Consorcio Hospital General Universitario de Valencia, Enfermedades Infecciosas, Valencia, Spain; ²Consorcio Hospital General Universitario de Valencia, Ginecología y Obstetricia, Valencia; ³Fundacion de Investigacion HGV, Valencia, Spain; ⁴Consorcio Hospital General Universitario de Valencia, Microbiología, Valencia, Spain; ⁵Consorcio Hospital General Universitario de Valencia, Hepatología, Valencia, Spain; ⁶Gilead Science, Madrid, Spain
 Email: gdelromomiguel@gmail.com

Background and Aims: In Spain, HIV, HBV, and HCV prevalence are lower in females. A 2017–2018 Ministry of Health serosurvey in 7,675 primary care patients found 0.35% and 0.08% chronic HCV infection in men and women. A previous opportunistic, population-based screening program in 11,449 primary care patients seen in our

POSTER PRESENTATIONS

health department found 0.18% and 0.06% HIV infection prevalence, 1.11% and 0.56% chronic HBV infection prevalence, and 0.73% and 0.25% chronic HCV infection prevalence in men and women from February to December 2019.

We aimed to assess HIV, HBV, and HCV prevalence among women seeking care in our health department's 5 Sexual and Reproductive Health Units (SRHU), in the Human Reproduction Unit (HRU), and the Obstetrics and Gynecology Service (OGS).

Method: We implemented opportunistic HIV, HBV, and HCV screening from March to October 2021, despite challenges related to a fifth wave of the SARS-CoV-2 pandemic. We used existing infrastructure and staff, aided by electronic health record system modifications, to identify screening eligibility and request serologies.

Patients were eligible for testing upon verbal consent if they were between 18 and 80, and had no record of testing in the previous year, and required blood tests in their current health care visit. Follow-up or discharge was given, regardless of test results. A case manager contacted positive patients to ensure and monitor linkage to specialist medical care.

Herein we analyze data from patients aged 18 to 45 – the maximum age of patients seen in the HRU.

Results: We screened 934 women, of whom 48.1% (449) in SRHUs, 26.0% (243) in the HRU, and 25.9% (242) in the OGS (26%). Regarding age and nationality, 14.6% (136) were aged 18 to 25, 45.5% (425) were 26 to 35, 39.9% (373) were 36 to 45, and 20.6% (192) were foreigners. We found 1 (0.1%) HIV antibody positive patient (a 45-year-old from the Dominican Republic), 1 (0.1%) HBV surface antigen positive patient (a 36-year-old from China), 1 (0.1%) HCV antibody positive patient, and no HCV RNA positive patients.

Conclusion: HIV prevalence among Valencian women in reproductive and sexual health services was similar to the general population in primary health care in the area. In contrast, chronic HBV infection prevalence was low, and chronic HCV infection was not found.

Our data suggest that opportunistic HBV and HCV screening of women aged 18 to 45 out of populations at increased risk is an inefficient public health strategy in our area.

THU277

mRNA COVID-19 vaccine effectiveness in liver transplant patients

Muhammad Khan¹, Kamran Mushtaq¹, Deema AlSoub¹, Hussam Almasri¹, Bisher Sawaf¹, Saad AlKaabi¹, Yasser Kamel¹.

¹Hamad Medical Corporation, Doha, Qatar

Email: mumair86@gmail.com

Background and aims: There is poor antibody response in up to 61% of the liver transplant patients after mRNA COVID-19 vaccination, and almost 20% of liver transplant recipients have undetectable antibody levels. However, antibodies are surrogate markers of disease protection and absence of seroconversion does not mean complete susceptibility to the disease. We hypothesized that COVID-19 vaccines are effective in liver transplant patients despite low seroconversion rates.

Method: We designed a test-negative case-control study to assess the vaccine effectiveness (VE) of COVID-19 vaccination in liver transplant recipients followed at our center in Hamad Medical Corporation. All liver transplant patients who were tested for SARS-CoV-2 infection between 1st of February till 30th of July in Qatar were included in the study. Case patients were identified as patients who had positive SARS-CoV-2 test on nasopharyngeal and throat swab while control patients were identified as patients who were tested negative during the same period. Information regarding demographic and clinical characteristics, transplant history, current immunosuppressive treatment was obtained from the medical records. Also, we recorded the type of COVID-19 vaccination, number of vaccine doses (one or two), COVID-19 complications, hospitalizations, and ICU admissions.

VE was estimated by a test-negative case-control design in which symptomatic liver transplant patients who were tested negative for COVID-19 were recorded as controls, while patients who tested

positive were considered cases. VE was defined as “1- OR (odds ratio).”

Results: A total of 136 liver transplant patients were included in the study. 13 (9.6%) patients were diagnosed with COVID-19 during the study period, out of which 7 (5.2%) needed hospitalization and 5 (3.7%) were admitted to the ICU. None of the patients died. The baseline characteristics, transplant history, comorbid conditions, and current immunosuppressive treatment for the participants is summarized in the table.

Among the vaccinated patients, 86 (83.5%) had received **Pfizer** vaccine, and 92 (89.3%) of the patients had received both the doses, three weeks apart.

VE of mRNA based vaccines against any COVID-19 infection, hospitalization and ICU admission is shown. In liver transplant patients VE was 84.1% (38.2%-96.2%, p=0.002) for any documented infection. VE was 88.9% (26.4%- 98.9%, p=0.003), and 92.8% (22.8%-99.8%, p=0.003) for COVID-19 related hospitalizations and ICU admissions respectively.

	Overall (N=136)	Vaccinated (n=103)	Unvaccinated (n=33)	p-value
Age	55.1 ± 14.5	55.9 ± 13.9	52.5 ± 16.1	0.12
Gender, male	103 (75.7%)	74 (71.8%)	15 (45.5%)	0.006
BMI	26.8 ± 5.4	28.0 ± 5.1	26.9 ± 6.4	0.098
Smoking	7 (5.2%)	3 (2.9%)	4 (12.1%)	0.037
Years since Tx	6 (3-11)	6 (3-11)	5 (3-12)	0.638
Reason of Tx				0.535
HCV	30 (22.1%)	25 (24.3%)	5 (15.2%)	
HBV	7 (5.2%)	4 (3.9%)	3 (9.1%)	
HCC	38 (27.9%)	30 (29.1%)	8 (24.2%)	
Alcohol	9 (6.6%)	8 (7.8%)	1 (3.0%)	
NAFLD	23 (16.9%)	16 (15.3%)	7 (21.2%)	
AIH	9 (6.6%)	7 (6.8%)	2 (6.1%)	
Misc.	20 (14.7%)	13 (12.6%)	7 (21.2%)	
Type of Tx				0.646
DDC	58 (42.7%)	46 (44.7%)	12 (36.4%)	
DBD	38 (27.9%)	27 (26.2%)	11 (33.3%)	
LRT	40 (29.4%)	30 (29.1%)	10 (30.3%)	
DM	82 (60.3%)	61 (59.2%)	21 (63.6%)	0.652
HTN	56 (41.2%)	45 (43.7%)	11 (33.3%)	0.293
CAD	9 (6.6%)	8 (7.8%)	1 (3.0%)	0.341
CKD	40 (29.4%)	32 (31.1%)	8 (24.2%)	0.798
Active malignancy	2 (1.5%)	1 (0.97%)	1 (3.0%)	0.094
Chronic resp. disorder	5 (3.7%)	3 (2.9%)	2 (6.1%)	
Charlson comorbidity index				0.507
1	29 (21.3%)	23 (22.3%)	6 (18.2%)	
2	69 (50.7%)	49 (46.8%)	21 (63.6%)	
3-4	33 (24.3%)	29 (27.2%)	5 (15.2%)	
5-6	5 (3.7%)	4 (3.9%)	1 (3.0%)	
Immunosuppressive Tx				
Steroids	12 (8.8%)	7 (6.8%)	5 (15.2%)	0.141
Tacrolimus	128 (94.1%)	98 (95.2%)	30 (90.9%)	0.368
Mycophenolate	53 (38.9%)	42 (40.8%)	11 (33.3%)	0.445
Cyclosporin	3 (2.21%)	3 (2.91%)	0 (0.00%)	0.321
Everolimus	2 (1.47%)	1 (0.97%)	1 (3.03%)	0.392
AZA/6-MP	11 (8.1%)	5 (4.9%)	6 (18.2%)	0.015
Sirolimus	6 (4.4%)	3 (2.9%)	3 (9.1%)	0.133
Median F-up	11 (7.5-14)	11 (7-15)	12 (8-14)	
Type of vaccine				
Pfizer	86 (83.5%)			
Moderna	17 (16.5%)			
Both doses	92 (89.3%)			
Outcomes				
Any COVID-19 Infection	13 (9.6%)	5 (4.85%)	8 (24.2%)	0.002
Hospitalization	7 (5.2%)	2 (1.9%)	5 (15.2%)	0.003
ICU	5 (3.7%)	1 (0.97%)	4 (12.1%)	0.003
Vaccine Effectiveness for different outcomes				
OR		VE (1-OR)		
Any COVID-19 Infection	0.16 (0.04 - 0.46)	84.1% (38.2% - 96.2%)		0.002
Hospitalization	0.11 (0.01 - 0.74)	88.9% (26.4% - 99.9%)		0.003
ICU Admission	0.07 (0.001 - 0.78)	92.8% (22.8% - 99.8%)		0.003

Conclusion: In liver transplant patients, two doses of mRNA based SARS-CoV-2 vaccines is effective against any documented infection. The protection is higher against hospitalization and ICU admissions. Combined analysis of cellular and humoral response is needed to identify vaccine responders

THU278

Evaluation of global progress towards HBV and HCV elimination

Sarah Blach¹, Devin Razavi-Shearer¹, Ellen Mooneyhan¹, Chris Estes¹, Kathryn Razavi-Shearer¹, Ivane Gamkrelidze¹, Homie Razavi¹. ¹Center for Disease Analysis Foundation, Lafayette, United States
Email: sblach@cdafound.org

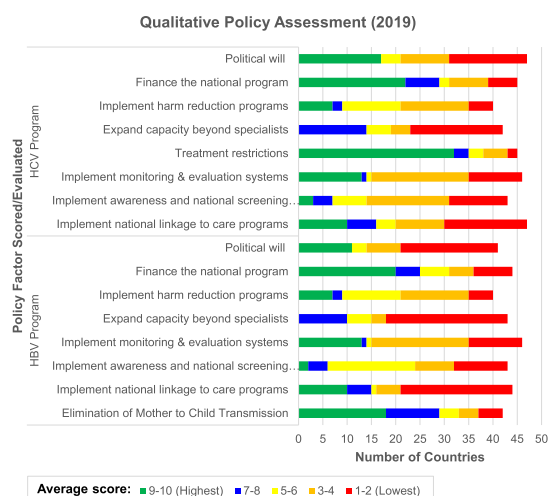
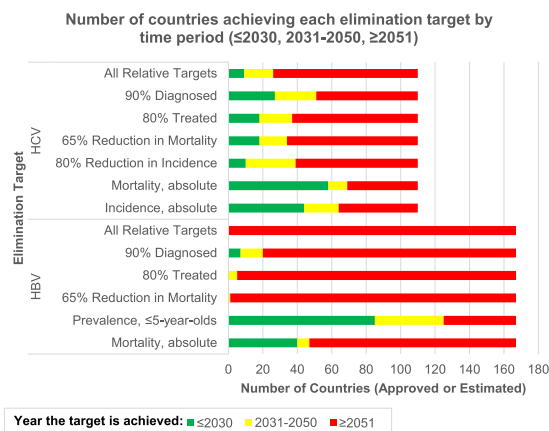
Background and aims: The Polaris Observatory maintains mathematical models for hepatitis B (HBV) and hepatitis C (HCV) viruses which are updated annually and used to monitor progress towards elimination. The outcomes of this work, including country/territory progress reports are publicly available online. The objective of this

analysis was to evaluate progress towards elimination (by elimination target) among the countries with approved or estimated models, and to report on policy assessment surveys returned by country experts.

Method: The year of elimination (by target) was extracted from 110 HCV and 167 HBV models available on the Polaris Observatory website (data from 2020). Results were summarized across countries by disease area and time period of elimination (target achieved before 2030, target achieved between 2031 and 2050, target achieved after 2050). Additionally, average country-level results from a qualitative policy assessment survey (administered in 2020 by the CDA Foundation, with responses from 47 countries) were used to score national viral hepatitis elimination policies.

Results: Based on 2020 data, no countries were on track to achieve all HBV elimination targets by 2030; however, 85 countries were expected to achieve the target for prevalence among 5-year-olds, 40 countries were on track to achieve absolute mortality targets, and 7 were on track to achieve the diagnosis target. Based on 41 survey responses, only 11 countries (26%) received the highest score of 10 for political will ("Government is fully committed to the elimination in any population who tests positive for the virus").

Nine countries were on track to achieve all relative HCV elimination targets by 2030, with 27 expected to achieve the diagnosis target and 18 expected to achieve the treatment target. When absolute targets were considered, 58 countries would achieve the mortality target and 44 would achieve the incidence target. Relative mortality and incidence targets would only be met by 18 and 10 countries, respectively. Based on 47 survey responses, 17 countries (36%) received a score of 10 for political will. Political will was found to be the strongest predictor of country achieving viral hepatitis elimination. Unfortunately, across the board, countries reported a lower political will score for HBV elimination as compared to HCV.



Conclusion: Nuanced country reports on viral hepatitis elimination progress and policies are vital feedback mechanisms for policy makers. Although most countries were not on track to achieve all HBV or HCV targets, substantial progress has been made by countries with regards to individual targets. Substantial work is needed to increase political will for HBV and HCV elimination.

THU279

The impact of vaccination on the global and regional pediatric prevalence of hepatitis B from 1985 to 2022

Devin Razavi-Shearer¹, Ivane Gamkrelidze¹, Sarah Blach¹, Chris Estes¹, Ellen Mooneyhan¹, Kathryn Razavi-Shearer¹, Homie Razavi¹. ¹Center for Disease Analysis Foundation, Lafayette, United States
Email: drazavishearer@cdafound.org

Background and aims: The first vaccine to prevent the hepatitis B virus (HBV) was available in 1981. The rollout and coverage of the vaccine varied by country, but three dose coverage became widespread in 2001 when Gavi, the vaccine alliance, began to support these programs. This study aims to examine the impact of prophylaxis measures on the pediatric, under 18 years of age, prevalence of HBV between 1985 and 2022.

Method: The Polaris Observatory maintains 166 country specific ProGreSs Models. These models consider the impact of prophylaxis measures (timely birth dose, three dose, hepatitis B immunoglobulin, and anti-viral treatment of pregnant women) and treatment on the incidence and disease burden of HBV. These models were utilized to estimate the historical and current prevalence among the pediatric population at the country and regional level. For countries in which models were not available, a regional prevalence was applied to the population of said missing country.

Results: Modeled countries represented 99.6% and 99.7% of all estimated pediatric cases in 1985 and 2022 respectively. Globally it was estimated that in 1985 the pediatric HBV prevalence was 5.23%, representing 101.9 million infections, this dropped to 1.0%, 23.8 million infections, by 2022 (Figure 1). This represents an 81% reduction in prevalence. High income and upper middle-income countries saw the largest drop, 96%, whereas lower middle- and low-income countries only saw a reduction of 74–75%. Discrepancies in regional reductions were also observed of 95% in Europe, 91% in the Americas, 88% in Asia, 77% in Oceania and 72% in Africa.

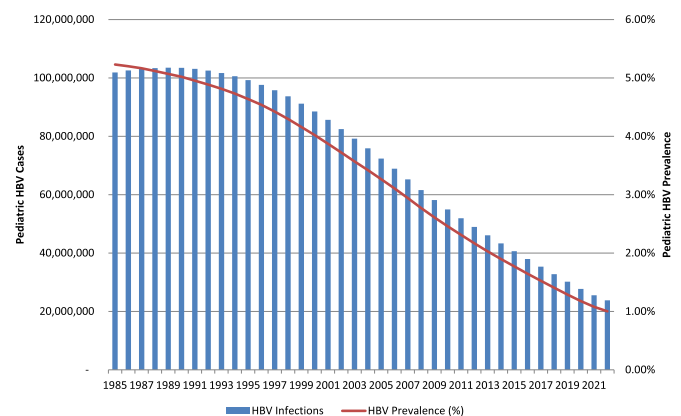


Figure 1: The Global HBV Pediatric Prevalence, 1985–2022.

Conclusion: Countries and regions that historically provided timely birth-dose as well as additional mother to child transmission prophylaxis measures have greatly reduced the burden of HBV in their pediatric population. While all regions have reduced the pediatric prevalence, the reductions have been highly inequitable with lower-middle- and low-income countries continuing to bear the brunt of the disease. Without additional assistance to provide timely birth dose and other prevention measures these inequities will continue well into the future.

POSTER PRESENTATIONS

THU280

Feasibility and effectiveness of hepatitis C micro-elimination among 19 prisons of northern India

Kanudeep Kaur¹, Gagandeep Singh Grover², Praveen Kumar Boora³, V K Bansal³, Veena Singh³, S Suman⁴, Virendra Singh⁵, Arka De⁵, Rajashree Sen¹, Sanjay Sarin⁶, Sonjelle Shilton⁶. ¹FIND India, Public Health, Delhi, India; ²Directorate of Health Services, Public Health, Punjab, India; ³Directorate of Health Services, Public Health, Panchkula, India; ⁴Directorate of Health Services, Public Health, Chandigarh, India; ⁵Post Graduate Institute of Medical Education and Research, PGIMER, Hepatology, Chandigarh, India; ⁶FIND, Public Health, Geneva, Switzerland

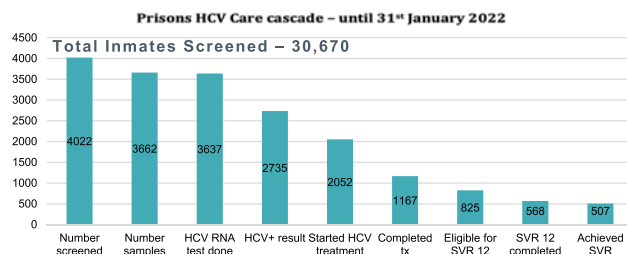
Email: kanudeep.kaur@finddx.org

Background and aims: The estimated prevalence of hepatitis C virus (HCV) infection in India is 0.32%, which comprises a considerable proportion of the global HCV burden. The incarcerated population is disproportionately affected by HCV and significant scale-up of access to testing and treatment is needed in order to achieve the 2030 global targets for the elimination of HCV. The objective of this intervention was to provide early diagnosis and management of HCV and evaluate the feasibility and efficacy of a decentralised HCV micro-elimination care model in 19 prisons across states of Punjab, Haryana and Union Territory of Chandigarh in the northern part of India.

Method: Anti-HCV antibody rapid diagnostic test (RDT) was performed for the inmates at time of admission or via screening camps. Inmates with positive HCV RDT results received reflex blood draw for HCV RNA testing and pre-treatment investigations. Liver staging was determined by APRI and FIB-4 scores (non-cirrhotic is APRI <2 and FIB-4 <3.5 and cirrhotic as APRI >2 and FIB-4 >3.5). Non-cirrhotic patients were initiated on treatment by the prison medical officer trained by the health department of the respective states. The cirrhotic cases were referred to specialist care at the model treatment centers set up by the states. Test of cure (SVR12) was assessed with an HCV RNA test done 12 weeks after completion of treatment.

Results: A total of 30,670 inmates, which represent 100% of the prison population in the 19 prisons at the time the intervention started, were screened from November 2019 to January 2022. Of the 13.11% (n = 4022) HCV antibody-positive, 90.42% (n = 3637) received a confirmatory viral load test, of which, 75.19% (n = 2735) were HCV RNA-positive, 74.04% (n = 2052) of those testing HCV RNA positive were initiated on treatment, and 56.87% (n = 1167) had completed treatment as of January 2022. Of those who completed treatment, 48.67% (n = 568) were assessed for SVR cure assessment, with SVR achieved in 89.26% (n = 507) inmates.

The median days and IQR for the turnaround time from RDT screening to viral load result completion was 6 days, IQR 4–12 days (n = 2553); between viral load results and treatment initiation was 6 days, IQR 0–15 days (n = 1622) and total median time between RDT screening and treatment initiation was 16 days with an IQR of 10–30 day (n = 1597).



Conclusion: This simple decentralised HCV testing and treatment model in prison settings has shown to be feasible, effective, and replicable in the Indian context. As this care model is fully transitioned to government partners, additional efforts are being

made to re-engage individuals released from incarceration that had not completed all steps in the HCV care cascade.

THU281

The impact of treatment and health policies for Hepatitis C Virus on hospitalizations in the last decade: data analysis of records of hospital discharge (SDO) at Italian national level

Francesco Saverio Mennini^{1,2}, Paolo Sciatella³, Claudia Simonelli¹, Andrea Marcellusi¹, Loreta Kondili⁴. ¹Economic Evaluation and HTA (EEHTA-CEIS), Centre for Economic and International Studies, Faculty of Economics, University of Rome "Tor Vergata", Rome, Italy; ²Institute of Leadership and Management in Health, Kingston Business School, Kingston University, London, United Kingdom; ³Economic Evaluation and HTA (EEHTA-CEIS), Centre for Economic and International Studies, Faculty of Economics, University of Rome "Tor Vergata"; ⁴Center for Global Health, Istituto Superiore di Sanità, Rome, Italy

Email: claudia.simonelli1996@gmail.com

Background and aims: In the last decade, innovative treatments and health policies for Hepatitis C Virus (HCV) are leading to the reduction of the burden of HCV-related diseases. Direct-Acting Antiviral (DAA) therapy has shown a high rate of viral eradication, and there is evidence that HCV cure reduces HCV complications and is cost-saving in most western countries in the long term. The aim of this analysis is to evaluate the trend of hospitalizations in patients with HCV chronic infection and HCV-related liver complications in Italy and to discuss the impact of the introduction of DAAs in 2015.

Method: The analysis was based on records of hospital discharge (SDO) at national level from 2012 to 2019. SDO collect information related to all discharges from public and private hospitals in Italy. Data was extracted based on primary and secondary diagnosis for HCV, cirrhosis and hepatocellular carcinoma (HCC). We calculated the annual incident hospitalizations with diagnosis of HCV and HCV-related complications. Analyses were stratified by age cohort (40–59, 60–79 and 80+ years) and divided into two distinct periods: (1) 2012–2015, in which DAAs were not available or had just been approved, and (2) 2016–2019, in which DAAs were available initially with prioritized access and later with universal access. The trend of alcoholic liver complications was also evaluated with the same methodology as comparison.

Results: Annual incident hospitalizations for cirrhosis reduced from 73 new cases per 100,000 inhabitants in 2012 to 44 in 2019 (-39%). Each year, patients with age ≥80 years represent around 20% of new hospitalizations. For alcoholic liver related complications, a reduction of only 9% was observed, and patients with age ≥80 years only represent around 5% of new hospitalizations. From 2012 to 2019, incident cases of HCC also reduced from 52 to 45 per 100,000 inhabitants (-14%) and incident cases of HCV reduced from 113 to 49 per 100,000 inhabitants (-57%). For cirrhosis, HCC, and HCV the reduction was more marked in the second period (2016–2019) than in the first period (2012–2015).

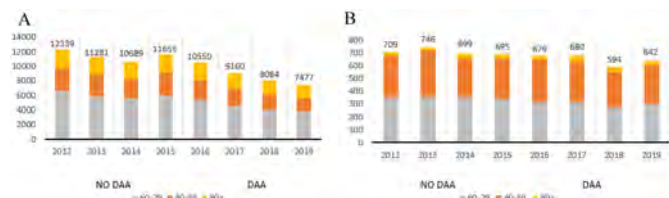


Figure: Annual incident hospitalizations for cirrhosis (A) without and (B) with mention of alcohol, by age cohort

Conclusion: From 2012 in Italy there has been a decreasing trend of hospitalizations for chronic HCV infection, cirrhosis complications and HCC. This reduction is becoming more evident in recent years. Alcoholic liver related complications are decreasing at a slower rate and affect younger patients on average. Overall, these data confirm

the clinical benefit of viral eradication by DAA and the long-term economic benefit of reduced expenses for severe liver complications.

THU282

Hepatitis B birth dose coverage remains dramatically low in The Gambia and has been disrupted by the COVID-19 pandemic

Gibril Ndow¹, Esu Ezeani¹, Cecile de Bezenac^{2,3}, Julien Randon-Furling⁴, Umberto D'Alessandro¹, Yusuke Shimakawa⁵, Maud Lemoine⁶. ¹MRC Unit The Gambia at LSHTM, Fajara, Gambia; ²Turing Institution, LONDON, United Kingdom; ³The Alan Turing Institute, LONDON, United Kingdom; ⁴Sorbonne University, Paris, France; ⁵Pasteur Institution, Paris, France; ⁶Imperial College London, Hepatology, LONDON, United Kingdom
Email: m.lemoine@imperial.ac.uk

Background and aims: Africa has the lowest coverage of hepatitis B birth dose (HepB-BD) vaccination (11%) worldwide and lags far behind the 90% coverage target recommended by the WHO for viral hepatitis elimination by 2030. We aimed to assess i. the coverage and limiting factors of HepB-BD vaccination and ii. the impact of the COVID-19 pandemic on HepB-BD coverage in The Gambia, the first African country to introduce in 1990 hepatitis B vaccination at birth. **Method:** we analysed data from the Health and Demographic Surveillance system (HDSS) in four areas in The Gambia. HepB-BD coverage was calculated at birth (0–1 day), day 7 and day 28 in children born between 2015 and 2021. We also performed multiple comparisons tests and a logistic regression to identify factors associated with lack of timely delivery.

Results: between 1 January 2015 and 31 July 2021, 77,913 births were recorded; of them 77,515 live births with complete information were analysed. 3,494/77,515 babies (4.5%) received a timely HepB-BD (D0–1). The median age at first dose was 20 days (IQR: 12–31 days). HepB-BD was administered at D7 and D28, in 7,308/77,515 (9.4%) and 38,239/77,515 (49.3%) babies, respectively. Whilst timely HepB-BD coverage steadily increased over time (Figure 1), a major disruption was observed between March and August 2020, corresponding to the first wave of COVID-19 outbreak in The Gambia. Between March and August 2020, the HepB-BD coverage dropped from 9% (July 2019 to Feb 2020) to 5%.

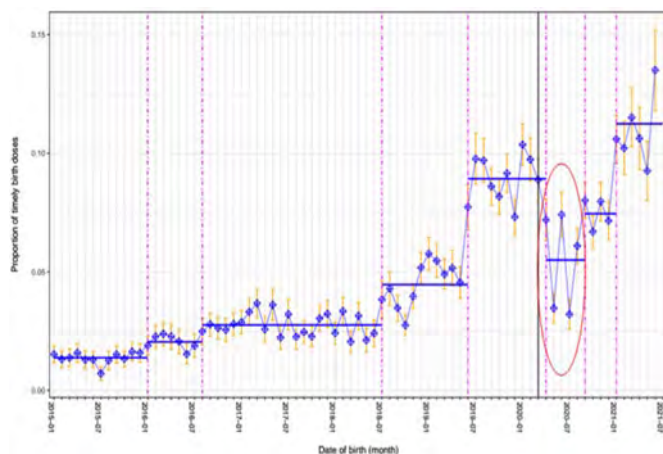


Figure: Monthly proportion of timely HepB-BD from 1st Jan. 2015 to 31st July 2021. Circled in red is the disruption observed in the immediate wake of the first CoViD 19 outbreak (the black vertical line shows the date of the 1st case, 17 March 2020). Magenta dashed vertical lines are change points detected using general fluctuations tests (Bai-Perron). Blue horizontal segments show the mean timely BD rate for each period between change points.

Factors associated with lack of timely HepB-BD were: births on Friday or Saturday (OR:3.2 (95% CI: 2.0 to 3.5), p value $<10^{-15}$), high maternal age (OR:1.5 (1.4 to 1.6), $p <10^{-12}$ for mothers older than 20 with respect to (wrt) mothers younger than 20, and OR: 1.8 (1.6 to 2.1), p

$<10^{-15}$) for older than 25 wrt younger than 25), delivery outside the hospitals (OR: 4.6 (3.7 to 5.8), $p <10^{-15}$) especially home delivery (OR:2.1 (95% CI: 1.9 to 2.3), $p <10^{-15}$), born to a primiparous mother (OR: 1.8 (1.6 to 2.2), $p <10^{-12}$) and delivery during the first COVID-19 outbreak (17 March 2020–1st August 2020) (OR:1.7 (1.4 to 1.9, $p <10^{-11}$, among all babies born after June 2019).

Conclusion: more than 30 years after adoption of the HepB-BD vaccination, only minor progress has been made in HepB-BD coverage in The Gambia, putting at risk the HBV elimination goals.

THU283

Hepatitis B prevalence and the impact of vaccination in Georgia: results from a nationwide serosurvey

Nino Khetsuriani¹, Amiran Gamkrelidze², Shaun Shadaker³, Maia Tsreteli², Maia Alkhazashvili², Nazibrola Chitadze², Irina Tskhomelidze⁴, Lia Gvinjilia⁵, Francisco Averhoff⁶, Gavin Cloherty⁶, Qian An¹, Giorgi Chakhunashvili², Jan Drobeniuc³, Paata Imnadze², Khatuna Zakhazashvili², Paige A Armstrong³. ¹Centers for Disease Control and Prevention, Global Immunization Division, Atlanta, United States; ²National Center for Disease Control and Public Health, Tbilisi, Georgia; ³Centers for Disease Control and Prevention, Division of Viral Hepatitis, Atlanta, United States; ⁴The Task Force for Global Health, Tbilisi, Georgia; ⁵Centers for Disease Control and Prevention, Eastern Europe and Central Asia Regional Office, Tbilisi, Georgia; ⁶Abbott Diagnostics, Abbott Park, United States
Email: nck7@cdc.gov

Background and aims: Georgia introduced routine infant hepatitis B (HepB) vaccination in 2001 with >90% coverage over the last decade. In 2015, a nationwide serosurvey demonstrated an anti-hepatitis B core antibody (anti-HBc) prevalence of 25.9% and hepatitis B surface antigen (HBsAg) prevalence of 2.9% among adults ≥ 18 years. No prevalence data were available for children. In 2021, we assessed hepatitis B virus (HBV) infection prevalence among children and updated estimates for adults in a combined COVID-19, hepatitis C and hepatitis B serosurvey of persons aged ≥ 5 years.

Method: We used a stratified, multi-stage cluster design. We collected data on demographics, medical and exposure history; we tested blood samples for anti-HBc and, if positive, for HBsAg. Nationally representative weighted proportions and 95% confidence intervals (CI) for anti-HBc and HBsAg were calculated. Participants aged 5–20 years had been eligible for routine HepB vaccination as infants.

Results: Among children aged 5–17 years, 0.7% were anti-HBc+ and 0.03% were HBsAg+ (Table). Among adults ≥ 18 years, 21.7% were anti-HBc+ and 2.7% were HBsAg+. Anti-HBc prevalence increased with age from 1.3% among 18–23-year-olds to 28.6% among ≥ 60 years. HBsAg prevalence was lowest (0.2%) among 18–23-year-olds and highest (8.6%) among 35–39-year-olds. Males had higher HBsAg prevalence than females (3.6% versus 2.0%; $p = 0.003$). Anti-HBc prevalence was highest in Samegrelo-Zemo Svaneti, Adjara, and Imereti regions. Higher education and income were associated with lower anti-HBc, and unemployment-with higher HBsAg prevalence.

Table. National anti-HBc and HBsAg prevalence by age and sex, Georgia, 2021

Age, years/sex	No. tested	Anti-HBc+, weighted % (95% CI)	HBsAg+, weighted % (95% CI)
All ages ≥ 5	8,710	17.9 (16.7–19.1)	2.2 (1.8–2.8)
Children 5–17	1,473	0.7 (0.3–1.6)	0.03 (0.0–0.19)
Adults ≥ 18	7,237	21.7 (20.4–23.2)	2.7 (2.2–3.4)
18–23	322	1.3 (0.6–3.1)	0.2 (0.0–1.5)
24–29	430	3.8 (2.0–7.1)	0.9 (0.2–4.8)
30–34	565	11.7 (8.2–16.5)	2.9 (1.2–7.0)
35–39	684	27.8 (23.4–32.6)	8.6 (6.1–12.1)
40–49	1,233	27.4 (23.9–31.3)	3.0 (2.0–4.5)
50–59	1,517	28.2 (25.0–31.7)	3.0 (1.6–5.7)
≥ 60	2,476	28.6 (26.1–31.2)	1.7 (1.2–2.6)
Sex (adults)			
Male	2,409	23.1 (20.9–25.5)	3.6 (2.8–4.7)
Female	4,828	20.5 (19.1–22.1)	2.0 (1.4–2.7)

POSTER PRESENTATIONS

Conclusion: The impact of HepB vaccination in Georgia is demonstrated by a low HBsAg prevalence among children that is below the 0.5% European regional hepatitis B control target and meets the $\leq 0.1\%$ seroprevalence target for elimination of mother-to-child transmission of HBV. Chronic HBV infection remains a problem among adults born before routine infant HepB vaccination. Focusing efforts on screening, treatment, and preventive interventions among adults, along with sustaining high immunization coverage among children, can help Georgia achieve elimination of hepatitis B as public health threat by 2030.

THU284

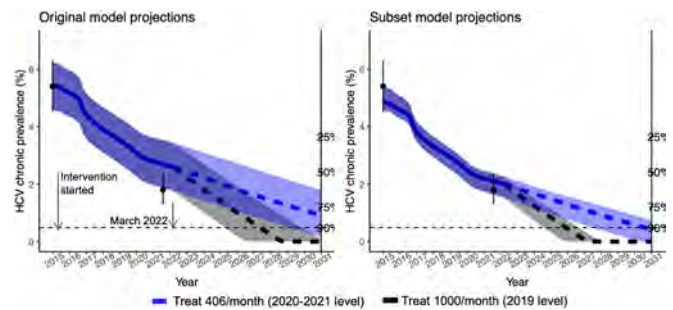
Progress towards HCV elimination in the country of Georgia: insights from modelling and national survey

Josephine Walker¹, Irina Tskhomelidze², Shaun Shadaker³, Maia Tsreteli⁴, Senad Handanagic³, Paige A Armstrong³, Amiran Gamkrelidze⁴, Peter Vickerman¹. ¹University of Bristol, Population Health Sciences, Bristol, United Kingdom; ²Task Force for Global Health, Tbilisi, Georgia; ³Centers for Disease Control and Prevention, Division of Viral Hepatitis, Atlanta, United States; ⁴National Center for Disease Control and Public Health, Tbilisi, Georgia
Email: jogwalker@gmail.com

Background and aims: A national serosurvey in 2015 found the country of Georgia had high hepatitis C virus (HCV) prevalence, with 5.4% of adults (~150,000 people) chronically infected. In April 2015, Georgia launched a national program to eliminate HCV infection (reduce prevalence by 90%). We developed an HCV transmission model to capture current and historical dynamics of HCV infection in Georgia, and project long-term impact of the elimination program. A follow-up serosurvey in 2021 provided data which was used to validate the model and update impact projections.

Method: The original model was calibrated to the 2015 serosurvey and surveys among people who inject drugs (PWID), accounting for age, sex, PWID status, and liver disease state. We compare model projected prevalence overall and by age group, sex, and among ever injected drugs to 2021 serosurvey prevalence, and filter the original 532 parameter sets to match the serosurvey results. We used logistic regression to assess which input parameters or model characteristics affect fit. We used program data on 77,168 persons treated May 2015–February 2022 to estimate current incidence of HCV infection, cases and deaths averted. We project the impact of reductions in treatment rates that occurred during the COVID-19 epidemic.

Results: The original modelled adult hepatitis C prevalence for 2021 (2.7%, 1.9–3.5%) was higher than the observed serosurvey prevalence (1.8%, 1.3–2.4%); across all groups uncertainty bounds overlap. Only 14% of 532 model runs fit within the 95% confidence interval of all hepatitis C prevalence estimates; 32% fit overall, 28% fit in females, 43% fit in males, 85% fit in ever-injected drugs. Runs that fit the 2021 serosurvey data tend to have lower total population and lower general population hepatitis C incidence, suggesting the model overestimated the initial burden of infection. After filtering, modelled hepatitis C adult prevalence is slightly higher than the observed prevalence (2.1%, 1.6–2.4%). Hepatitis C incidence in March 2022 is estimated to be 0.05 (95% credible interval (CrI) 0.03–0.11) per 100 person-years in general population, and 1.14 (0.08–6.4) per 100 person-years in PWID, a 60% decrease since 2015. As of March 2022, 9,186 (5,396–16,720) infections and 842 (489–1324) deaths have been averted, with benefit accumulating to 26,154 (15,850–47,627) infections and 3,971 (2,516–5,536) deaths averted if tracked to 2030. Treatment numbers went from 996/month in 2019 to 406/month March 2020–March 2022 during the COVID-19 pandemic, resulting in 14,127 fewer treatments, 471 (242–817) fewer infections averted by March 2022. At 406 treatments/month, elimination can be reached in 2031.



Conclusion: HCV prevalence reduction due to treatment and prevention interventions was greater than originally projected, but treatment numbers must still increase in order to reach HCV elimination by 2030.

THU285

Measuring the alcohol related hospital burden in Ireland and the impact of Minimum Unit Pricing (MUP)

Tobias Maharaj^{1,2}, Olufemi Aoko^{1,2}, Elizabeth Gilligan³, Siobhan MacHale^{1,3}, John Ryan^{1,2}. ¹Royal College of Surgeons in Ireland (RCSI), Ireland; ²Beaumont Hospital, Hepatology Unit, Dublin, Ireland; ³Beaumont Hospital, Liaison Psychiatry, Dublin, Ireland
Email: maharaj@tcd.ie

Background and aims: Alcohol harms are a significant burden on healthcare services and in Ireland alcohol related hospital admissions account for approximately 7% of state health expenditure. Minimum Unit Pricing (MUP) sets a legally required floor price per alcohol unit. On 4 January 2022, MUP was introduced in Ireland at €1.00 per unit (10 grams of alcohol). Accurately determining the hospital burden of alcohol in Ireland is a challenge due to inadequate clinical documentation and hospital coding of alcohol harms. Previously published MUP studies have suggested immediate reductions in admissions for acute alcohol-related conditions. The objective of this study was to accurately determine the alcohol-related hospital burden, as well as to measure any immediate impact from the introduction of MUP.

Method: All patients presenting to the emergency department of a major hospital in Dublin city were interviewed by a research clinician from 22:00 to 04:00, over seven consecutive nights before and after the introduction of MUP (total of 84 hours). Data collection included a brief clinical history of presenting complaint, time of last alcohol consumption, AUDIT-C alcohol screening score, and type of alcoholic beverage preference. Each hospital attendance was determined to be either alcohol-related or non-alcohol-related using published ICD codes of alcohol-related conditions from MUP modelling data in Ireland. Alcohol presentations were further categorized into acute or chronic conditions, and directly related or partially related to alcohol.

Results: Excluding missing data (n = 43), there were 245 presentations to hospital: 114 pre-MUP and 131 post-MUP. The median age of attendances was 49 years old with 50% females pre-MUP and 51.2% females post-MUP. High risk alcohol consumption (AUDIT-C score ≥ 5) was similar pre-MUP (43%) and post-MUP (42.0%). Beer was the most preferred beverage pre-MUP (45.5%) and post-MUP (48.8%) compared to all other beverage types. Since the introduction of MUP, there was no immediate difference in alcohol-related hospital attendances (31.6% versus 27.5%; p = 0.48) and no difference in alcohol-related admissions (8.8% versus 7.6%; p = 0.75). Acute alcohol-related admissions signaled a 40% reduction (95% CI = 3.9%, 76.1%; p = 0.03) with MUP. Alcohol admissions for 'partially related', 'directly related', and 'chronic conditions', as well as beverage preferences did not show any significant difference with MUP (p > 0.05).

Conclusion: Almost a third of all hospital attendances and almost a tenth of all hospital admissions are alcohol related, representing a

significant burden on healthcare resources. Alcohol is a modifiable risk factor and interventions such as €1.00 MUP may have an immediate impact on reducing admissions for acute alcohol conditions. Larger sample sizes and longitudinal data are awaited.

THU286

Is hepatic steatosis individually a risk factor for colorectal adenoma?

Yuvaraj Singh¹, Maya Gogtay¹, Anuroop Yekula¹, Kartikeya Tripathi², George Abraham^{1,3,4}. ¹Saint Vincent Hospital, Internal Medicine, Worcester, United States; ²University of Massachusetts Medical School, Baystate campus, Department of Gastroenterology, Springfield, United States; ³UMass Chan Medical School, Internal Medicine, Worcester, United States; ⁴American College of Physicians, Philadelphia, United States

Email: yuvaraj.singh@stvincenthospital.com

Background and aims: Most colorectal cancers (CRC) originate from adenomatous lesions. Data suggests that obesity, insulin resistance, and metabolic syndrome are risk factors for CRC. Non-alcoholic fatty liver disease (NAFLD) is one of the manifestations of metabolic syndrome. Many studies have correlated metabolic syndrome with a risk of CRC but there is a paucity of evidence on NAFLD and its association with CRC. We aim to study the association between moderate to severe hepatic steatosis detected on vibration-controlled transient elastography (VCTE) and colorectal adenomas.

Method: This retrospective cohort study was approved by the institutional review board (IRB). We included adult patients who underwent VCTE and colonoscopy. Other causes of liver diseases, such as autoimmune hepatitis, alcohol use disorder, viral hepatitis, and primary biliary cirrhosis were excluded. Steatosis was categorized as S0-S1 (mild) and S2-S3 (moderate/severe) based on the controlled attenuation parameter (CAP) grade of VCTE. Colonoscopy findings were stratified on the biopsy results i.e., hyperplastic, adenoma, CRC, inflammatory or normal mucosa. Continuous variables were assessed using the Mann Whitney U test and categorical variables using chi-square with $p < 0.05$ considered statistically significant. A multinomial logistic regression analysis (MLRA) was done between colorectal adenoma and significant covariates.

Results: Out of the 415 patients analyzed, 206 patients met inclusion criteria. 124 had moderate/severe steatosis and 82 had no/mild steatosis. Descriptive analysis showed that BMI ($p = 0.001$), aspirin ($p = 0.011$), smoking ($p = 0.004$), and adenoma ($p = 0.02$) were significantly different between both groups. In the MLRA model; aspirin had an odds ratio (OR) = 0.39 [0.25–0.84] ($p = 0.01$), moderate/severe steatosis OR = 3.5 [2.39–10.45] ($p = 0.03$) and obesity OR = 2.9 [1.07–6.78] ($p = 0.02$) in association with colorectal adenoma.

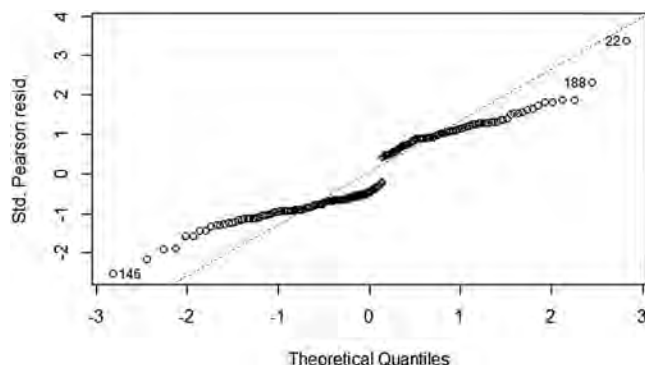


Figure: Q-Q plot for MLRA

Conclusion: Our study indicated that moderate/severe hepatic steatosis is associated with an increased risk of colorectal adenoma detection on colonoscopy. Several patients were excluded due to the non-availability of colonoscopy reports, many of whom were less than 45 years of age. Current guidelines do not recommend earlier

screening for CRC after detection of hepatic steatosis for patients. We recommend prospective studies to understand this positive association better. Further studies would be needed to determine if the increase in adenoma detection lowers the risk for the detection of CRC.

THU287

No effect of HBsAg positivity on antibody response after COVID-19 vaccine

Ganbolor Jargalsaikhan^{1,2}, Enkhtuul Batbold^{1,2}, Delgersaikhan Zulkhuu^{1,2}, Oyungerel Lkhagva-Ochir^{1,2}, Uurtsaikh Baatarsuren^{1,2}, Myagmarjav Budeebazar^{1,2}, Khatanzul Ganbold^{1,2}, Sumiya Byambabaatar^{1,2}, Byambasuren Ochirsum^{1,2}, Munkhaya Munkhbaatar^{1,2}, Purevjargal Bat-Ulzii^{1,2}, Bishguurmaa Renchindorj^{1,2}, Andreas Bungert^{1,2}, Naranbaatar Dashdorj^{1,2}, Katy Shaw-Saliba³, Irini Sereti³, Sally Hunsberger³, Renee Ridzon³, Naranjargal Dashdorj^{1,2}. ¹Onom Foundation, Ulaanbaatar, Mongolia; ²The Liver Center, Ulaanbaatar, Mongolia; ³National Institute of Health, Bethesda, Maryland, United States

Email: dashdorj@onomfoundation.org

Background and aims: Immune responses to vaccines may vary based on nutritional status, underlying comorbidities and/or concomitant infections. Despite the high burden of chronic HBV infection worldwide it is not known if this affects the immune response following COVID-19 vaccination. We aimed to evaluate antibody levels in people with chronic Hepatitis B virus (HBV) infection, compared to control group among those receiving either their third or fourth COVID-19 vaccination.

Method: Samples from a subset of participants in the InVITE study (ClinicalTrials.gov Identifier: NCT05096091) were assessed for SARS-CoV-2 IgG level (MINIVIDAS 3.0, BIOMERIEUX, France) and HBsAg (HISCL-5000, Sysmex, Japan). Chronic HBV infection was defined as HBsAg > 0.03 mIU/ml. T-tests were used to compare mean IgG levels and a regression analysis was performed to control for age, sex, history of COVID-19, number of vaccines received, obesity, and time since previous vaccine.

Results: Participants received BBIP CorV ($n = 377$), ChAdOx1 nCov-19 ($n = 196$), BNT162b2 (23), Sputnik V ($n = 17$) vaccines as their initial two-dose COVID-19 vaccine regimen. Of the 613 participants included in this analysis, 104 with chronic HBV and 504 controls. Overall characteristics included: 6.5% older than 60 years, 62% female, 20% with history of COVID-19, 17% receiving a fourth dose of vaccine, 20% obese, and 48% had greater than 6 months since previous vaccine; these were well balanced between groups. The IgG levels between groups were not significantly different ($p = 0.265$), with mean (std) of control 32.3 (13.6) BAU/ml, chronic HBV, 34.0 BAU/ml (14.4). Only history of COVID-19 was significantly associated with increased antibody levels in the regression model ($p = 3.0 \times 10^{-3}$).

Conclusion: This study showed no difference in SARS-CoV-2 IgG levels between control and HBsAg positive groups. SARS-CoV-2 IgG level was higher in participants with previous COVID-19 infection than those without COVID-19 infection.

THU288

Prevalence of hepatitis B and C virus in the Uzbekistan Hepatitis Elimination Program (UHEP) patients

Erkin Musabaev¹, Chris Estes², Shakhlo Sadirova³, Shokhista Bakieva¹, Krestina Brigida¹, Kathryn Razavi-Shearer², Bakhodir Yusupaliyev⁴, Homie Razavi². ¹Research Institute of Virology, Tashkent, Uzbekistan; ²Center for Disease Analysis Foundation, Lafayette, United States; ³Center for Disease Analysis Foundation, Tashkent, Uzbekistan; ⁴Ministry of Health, Tashkent, Uzbekistan

Email: homie.razavi@centerforda.com

Background and aims: Chronic infection with hepatitis B and C viruses (HBV and HCV) is a major contributor to liver disease and liver-related mortality in Uzbekistan. There is a need to better

POSTER PRESENTATIONS

quantify the number of undiagnosed cases, the characteristics of infected patients, and the risk factors associated with disease.

Method: In the capital city of Tashkent, 13 clinics were established to diagnosed and treat chronic HBV and HCV infection among the general adult population. Patients underwent testing for HBV and HCV infection, along with follow-up biochemical measures and questionnaire items. Nurses were trained to use rapid HCV and HBV tests to screen large number of people and an electronic medical system was put in place to record the test and questionnaire results. The prevalence of previously undiagnosed HBV and HCV was estimated and adjusted to the Uzbekistan population. Regression analyses quantified risk of infection based on demographic factors.

Results: HBV and HCV screening was conducted on 62, 000 people over a 12-month period that included a 6-month shutdown due to the COVID-19 pandemic. Before the shutdown, 30, 000 people were screened while another 32, 000 were screened in conjunction with COVID-19 testing. Complete dataset was available for 53, 841 HBV

patients and 54, 396 HCV patients. Age-adjusted adult prevalence of previously undiagnosed chronic HBV and HCV infection were estimated at 3.23% (3.00–3.37%) and 3.02% (2.80–3.16%), respectively. Prevalence was significantly higher in males for both HBV and HCV, while increasing age was significantly associated with higher HCV prevalence. The most commonly reported risk factors among HCV+ patients were dental procedures and medical injections, and 2.5% of HCV+ patients had APRI score >2.5. Among HBV+ patients 1.2% had eFGR <30 while for HCV+ patients the portion was 3.3%.

Conclusion: This program represent the first of its kind in terms of scope (HBV and HCV testing) and size providing a detailed estimate of viral hepatitis infection. A large population of patients chronically infected with HBV and HCV remains undiagnosed in Uzbekistan. There should be further efforts to screen, diagnose and treat these patients in the general population to achieve the WHO 2030 elimination targets.

HBV	HBV Positive	Total	Crude Prevalence (%)	Adjusted Prevalence (%)	Univariate	Multivariate
Total	1,509	53,841	2.80 [2.60–2.94]	3.23 [3.00–3.37]		
Sex	HBV Positive	Total	Crude Prevalence (%)	Adjusted Prevalence (%)	aPR	a
Male	714	16,761	4.26 [3.90–4.57]	4.39 [4.10–4.64]	2.09 [1.90–2.32]	<.001
Female	795	37,080	2.14 [2.00–2.29]	2.10 [1.90–2.27]	Ref	1.92 [1.74–2.10]
Age Group	HBV Positive	Total	Crude Prevalence (%)	Adjusted Prevalence (%)	aPR	a
18–29	347	14,320	2.42 [2.10–2.69]	2.56 [2.30–2.81]	Ref	Ref
30–39	533	13,112	4.06 [3.70–4.42]	4.75 [4.30–5.12]	1.86 [1.64–2.10]	<.001
40–49	347	10,290	3.37 [3.00–3.74]	4.11 [3.70–4.53]	1.61 [1.40–1.84]	<.001
50–59	183	8,913	2.05 [1.70–2.37]	2.43 [2.00–2.80]	0.95 [0.79–1.13]	<.001
60–69	71	5,145	1.38 [1.00–1.74]	1.49 [1.10–1.88]	0.58 [0.45–0.74]	<.001
70–99	28	2,061	1.36 [0.90–1.90]	1.38 [0.90–2.00]	0.54 [0.36–0.78]	<.01
Birthplace - Region	HBV Positive	Total	Crude Prevalence (%)	Adjusted Prevalence (%)	aPR	a
Tashkent	1,061	44,415	2.39 [2.20–2.53]	2.71 [2.50–2.86]	Ref	Ref
Andizhan	25	504	4.96 [3.30–7.33]	6.17 [4.30–8.65]	2.28 [1.58–3.16]	<.001
Bukhara	27	644	4.19 [2.80–6.12]	4.54 [3.10–6.45]	1.67 [1.15–2.35]	<.05
Fergana	37	683	5.42 [3.80–7.46]	6.54 [4.80–8.72]	2.41 [1.77–3.21]	<.001
Dzhizak	27	447	6.04 [4.00–8.77]	6.37 [4.40–8.97]	2.35 [1.62–3.28]	<.001
Namangan	26	452	5.75 [3.80–8.42]	6.81 [4.70–9.56]	2.51 [1.74–3.50]	<.001
Navoi	15	304	4.93 [2.80–8.17]	5.15 [3.00–8.33]	1.90 [1.12–2.98]	<.05
Kashkadarya	89	1,218	7.31 [5.90–8.95]	8.69 [7.20–10.39]	3.21 [2.63–3.87]	<.001
Samarkand	52	1,172	4.44 [3.30–5.81]	5.29 [4.10–6.75]	1.95 [1.50–2.49]	<.001
Syrdarya	21	396	5.30 [3.30–8.11]	6.16 [4.00–9.14]	2.27 [1.48–3.32]	<.001
Surkhandarya	49	694	7.06 [5.30–9.29]	7.95 [6.10–10.19]	2.93 [2.24–3.77]	<.001
Khorezm	27	510	5.29 [3.50–7.70]	5.34 [3.60–7.75]	1.97 [1.32–2.82]	<.01
Republic of Karakalpakstan	16	342	4.68 [2.70–7.63]	5.48 [3.40–8.61]	2.02 [1.23–3.10]	<.01
Outside Uzbekistan	37	2,060	1.80 [1.20–2.49]	2.20 [1.60–2.98]	0.81 [0.59–1.09]	0.87 [0.63–1.19]
HCV	HCV Positive	Total	Crude Prevalence (%)	Adjusted Prevalence (%)	Univariate	Multivariate
Total	1,610	54,396	2.96 [2.80–3.10]	3.02 [2.80–3.16]		
Sex	HCV Positive	Total	Crude Prevalence (%)	Adjusted Prevalence (%)	aPR	a
Male	603	17,084	3.53 [3.20–3.81]	3.50 [3.20–3.73]	1.38 [1.25–1.52]	<.001
Female	1,007	37,312	2.70 [2.50–2.86]	2.54 [2.30–2.73]	Ref	1.45 [1.32–1.58]
Age Group	HCV Positive	Total	Crude Prevalence (%)	Adjusted Prevalence (%)	aPR	a
18–29	168	14,464	1.16 [0.90–1.30]	1.20 [1.00–1.37]	Ref	Ref
30–39	260	13,471	1.93 [1.70–2.18]	1.99 [1.70–2.24]	1.66 [1.39–2.00]	<.001
40–49	422	10,448	4.04 [3.60–4.43]	4.70 [4.20–5.14]	3.92 [3.33–4.63]	<.001
50–59	395	8,902	4.44 [4.00–4.89]	4.89 [4.40–5.40]	4.08 [3.44–4.85]	<.001
60–69	274	5,089	5.38 [4.70–6.04]	5.46 [4.80–6.15]	4.56 [3.79–5.48]	<.001
70–99	91	2,022	4.50 [3.60–5.52]	4.49 [3.60–5.51]	3.75 [2.91–4.78]	<.001
Birthplace - Region	HCV Positive	Total	Crude Prevalence (%)	Adjusted Prevalence (%)	aPR	a
Tashkent	1,287	44,802	2.89 [2.70–3.04]	2.97 [2.80–3.12]	Ref	Ref
Andizhan	26	514	5.06 [3.30–7.42]	5.32 [3.60–7.64]	1.79 [1.21–2.54]	<.01
Bukhara	21	661	3.18 [2.00–4.89]	2.78 [1.70–4.36]	0.94 [0.58–1.42]	0.90 [0.55–1.45]
Fergana	20	731	2.74 [1.70–4.27]	2.27 [1.30–3.70]	0.77 [0.45–1.20]	0.74 [0.44–1.25]
Dzhizak	9	494	1.82 [0.80–3.50]	1.50 [0.70–3.00]	0.51 [0.23–0.93]	0.60 [0.28–1.25]
Namangan	19	468	4.06 [2.50–6.38]	3.70 [2.20–5.88]	1.25 [0.75–1.92]	1.33 [0.80–2.10]
Navoi	9	315	2.86 [1.40–5.54]	2.54 [1.20–5.04]	0.86 [0.40–1.57]	1.00 [0.47–2.10]
Kashkadarya	38	1,297	2.93 [2.10–4.03]	2.95 [2.10–4.01]	0.99 [0.72–1.34]	1.05 [0.75–1.45]
Samarkand	28	1,198	2.34 [1.50–3.40]	2.64 [1.80–3.74]	0.89 [0.62–1.24]	0.83 [0.57–1.19]
Syrdarya	19	411	4.62 [2.80–7.25]	5.14 [3.20–7.89]	1.73 [1.09–2.60]	<.05
Surkhandarya	28	737	3.80 [2.50–5.51]	3.14 [2.00–4.67]	1.06 [0.69–1.54]	1.05 [0.68–1.61]
Khorezm	24	514	4.67 [3.00–6.96]	4.89 [3.20–7.21]	1.65 [1.08–2.39]	<.05
Republic of Karakalpakstan	5	364	1.37 [0.50–3.30]	1.76 [0.70–3.86]	0.59 [0.24–1.18]	0.52 [0.21–1.25]
Outside Uzbekistan	77	2,090	3.68 [2.90–4.60]	3.72 [2.90–4.68]	1.26 [0.98–1.58]	0.93 [0.73–1.19]

Figure: (abstract: THU288): aPR = Adjusted prevalence ratio.

THU289

Evaluation of the clinical and economic value of sofosbuvir/velpatasvir (SOF/VEL) in patients with chronic hepatitis C in Spain during the last 5 years

Rafael Esteban¹, Raquel Domínguez-Hernández², Helena Cantero³, Miguel Ángel Casado². ¹Hospital Universitari Vall d'Hebron, Barcelona, Spain; ²Pharmacoeconomics and Outcomes Research Iberia (PORIB), Pozuelo de Alarcón, Spain; ³Gilead Sciences, Madrid, Spain
Email: rdominguez@porib.com

Background and aims: The introduction of direct-acting antivirals in the therapeutic arsenal for the treatment of hepatitis C virus (HCV) infection represented a paradigm shift. Sofosbuvir/velpatasvir (SOF/VEL; Epclusa®) has added value to HCV treatments, achieving high response rates that lead to a cure in most HCV chronic patients. The aim of this analysis was to evaluate the long-term impact on health and economic outcomes of patients with chronic hepatitis C treated with SOF/VEL during the first 5 years after its approval in Spain (2017–2022).

Method: A previously developed lifetime Markov model was adapted to estimate HCV morbidity and mortality comparing two treatment alternatives: SOF/VEL versus previous therapies (peginterferon and ribavirin in double/triple therapy with telaprevir or boceprevir). The target population (30,488 patients) entered the model during the first 5 years (22% 1st year, 26% 2nd, 22% 3rd, 13% 4th, 17% 5th) and were distributed among the fibrosis states in treated or untreated. In SOF/VEL, all patients (100%) were treated regardless of fibrosis states (F0–F4) with an average weighted sustained viral rate (SVR) of 98.9% from real-world data. In previous therapies, only 49% of ≥F2 states HCV patients were treated, with 61% SVR. All parameters required for the analysis were obtained from real-world data and the literature. Only direct healthcare costs associated with disease management were included. A discount rate (3%) was applied to costs and healthcare outcomes. The results were measured as the number of cases of decompensated cirrhosis (DC), hepatocellular carcinoma (HCC), and liver transplant as well as their costs associated, in addition to liver-related deaths, comparing both alternatives. An alternative analysis was performed with a reduction in the SVR rate of SOF/VEL to 95%.

Results: In the analysis of SVR rate (98.9%), the lifetime results showed that SOF/VEL decreased liver-related mortality by 85% (4,017 cases avoided) as well as avoided cases of liver complications: 3,467 DC (-92%), 2,536 HCC (-80%) and 474 LT (-87%), having the greatest impact on DC. In economic terms, the costs associated with SOF/VEL in the management of liver complications generated a total saving of 197 million euros. In the alternative analysis, a variation in the SVR rate (95%) decreased the impact on the reduction of avoided liver-related events between 75 and 86%.

Mortality and liver complications	Number of cases with each alternative treatment	
	Previous therapies	Sofosbuvir/Velpatasvir
Liver-related death	4,727	710
Decompensated cirrhosis	3,757	291
Hepatocellular carcinoma	3,151	615
Liver transplant	547	73

Conclusion: SOF/VEL significantly decreases HCV morbidity and mortality adding value to the management of patients with chronic hepatitis C reducing the clinical and economic burden of the disease and contributing to the goal of disease elimination in Spain.

THU290

The value of increased HCV testing and treatment strategies in Spain to achieve elimination goals

José Luis Calleja Panero¹, Jaime Espin², Ankita Kaushik³, Manuel Hernández Guerra⁴, Rob Blissett⁵, Adam Igloi-Nagy⁵, Alon Yehoshua³. ¹Universidad Autónoma de Madrid, Hospital Universitario Puerta de Hierro, Madrid, Spain; ²Escuela Andaluza de Salud Pública, Granada, Spain; ³Gilead Sciences, Inc., Foster City, United States; ⁴Hospital Universitario de Canarias, Tenerife, Spain; ⁵Maple Health Group, LLC, New York City, United States
Email: alon.yehoshua@gilead.com

Background and aims: In 2015, Spain launched a national eradication strategy for Hepatitis C virus (HCV) through prevention, screening, diagnosis, and link-to-care, resulting in the highest HCV treatment rate of any European country and substantial reductions in HCV prevalence. To achieve the goal of HCV elimination, it is necessary to scale up the diagnosis, treatment, and management of HCV infection in the general population, migrants and people who inject drugs (PWID). Our aim was to assess the prevalence, incidence, and cost effectiveness of scaling up compared to status quo scenarios.

Method: A compartmental dynamic transmission model was developed in visual basic for applications (VBA). The model comprises two modules: the first represents the cascade of HCV care and the second represents the progression of liver disease. Direct and indirect costs, as well as utilities to estimate quality of life were considered as model inputs. Outcomes included the prevalence and incidence of HCV infection as well as the incremental cost per quality-adjusted life year (QALY) and per life year (LY). Outcomes for a hypothetical elimination strategy were compared to those expected with the status quo staying in place. Costs and effects were discounted at 3.0%; the model time horizon is until the year 2030 in the base case and extended to 2040 in scenario analysis.

Results: The base case analysis found that scaling up testing and treatment reduced both the prevalence and incidence of HCV over time resulting in incremental costs per QALY and LY of €13,291 and €12,285 respectively, compared to the status quo. Excluding indirect costs from the analysis brought the incremental costs per QALY and LY to €13,761 and €12,720, respectively. Main drivers of the cost-effectiveness results included cost of diagnosis, cost of treatment, proportion of people who are unaware, percentage of population of people who inject drugs, and various calibration parameters related to HCV infection prevalence. Scenario analyses found that reducing the screening intervals decreased the prevalence of HCV infection over time; extending screening to include migrants upon arrival in Spain also decreased the prevalence over time with the same or better cost effectiveness metrics.

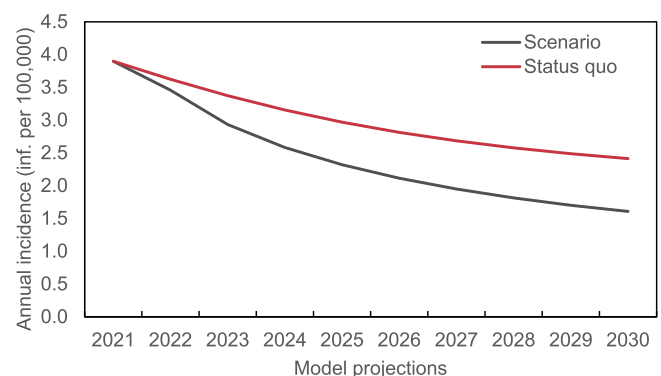


Figure 1: Annual incidence of HCV in Spain over time in the increased testing scenario compared to status quo.

Conclusion: This analysis demonstrated that scaling up testing and treatment with direct acting antivirals (DAAs) is an efficient strategy for reducing the incidence and prevalence of HCV infection among

POSTER PRESENTATIONS

key populations of interest in Spain. Given the global burden of HCV infection, and its associated liver-related morbidity and mortality, increasing access to testing and treatment among key populations of interest may be a successful strategy to achieve HCV elimination goals in Spain.

THU291

National hepatitis elimination profiles: progress towards HBV and HCV elimination in five European countries

Lindsey Hiebert¹, Isabelle Nassar¹, Vanessa Nunez¹, Loreta Kondili², Sema Mandal³, Graham Foster⁴, Francisco Javier Garcia-Samaniego Rey^{5,6}, Philip Bruggmann^{7,8}, Paolo Bonanni⁹, Camila Picchio¹⁰, Rui Marinho¹¹, Jeffrey Lazarus¹⁰, John Ward¹. ¹Task Force for Global Health, Coalition for Global Hepatitis Elimination, Decatur, United States; ²Istituto Superiore di Sanità, Italy; ³UK Health Security Agency, United Kingdom; ⁴Queen Mary University of London, United Kingdom; ⁵Alianza para la Eliminación de las Hepatitis Víricas en España, Spain; ⁶Hospital Universitario La Paz, Spain; ⁷Swiss Hepatitis, Switzerland; ⁸Arud Centre for Addiction Medicine, Switzerland; ⁹University of Florence, Italy; ¹⁰University of Barcelona, Institute of Global Health (ISGlobal); ¹¹University of Lisbon (FMUL)
Email: lhiebert@taskforce.org

Background and aims: To achieve WHO goals for hepatitis elimination, Member States (MS) are in various stages of national planning and policy development. To track country-level progress and identify feasible next steps, CGHE is developing National Hepatitis Elimination Profiles (NHEPs). The status of hepatitis elimination in European countries are described.

Method: Together with local partners, profiles were prepared for England (EG), Italy (IT), Portugal (PT), Spain (ES) and Switzerland (CH). For comparison, key indicators include policies for prevention, testing, and treatment. Country-specific data were collected from peer-reviewed reports, ministries of health (MoH), ECDC, WHO and other credible sources. Partners in MoH, clinical practice, and civil society organizations (CSO) validated data.

Results: All MS have an HCV action plan; ES, IT, and CH have HBV action plans. EG, ES, and CH have set HBV and HCV elimination goals, while PT has goals for HCV. For CH and ES, the hepatitis AP and goals were prepared by clinical associations and CSO. All MS have >95% coverage of infant 3-dose HepB vaccination. All MS have policies for routine HBV screening of pregnant women; IT recommends maternal HCV screening. All countries recommend HepB birth dose vaccination (Hep-BD-V) for newborns of HBsAg+ mothers. PT recommends universal HepB-BD- V <24 hours of birth; PT has >50% coverage, the WHO 2020 target. The 4 countries with data distribute 27–139 needle-syringes per person who injects drugs (PWID) per year, 14%–70% of the WHO 2020 target. At least two MS have safe injection programs for persons who are incarcerated. All countries have risk-based HBV and HCV screening; IT recommends HCV testing for persons born 1969–1989. All have removed most restrictions to HCV treatment. However, some MS require HCV genotyping (CH, IT, PT) and specialty care (ES, IT, PT) (figure). Data suggest 3 countries have reduced HCV mortality rates approaching or exceeding the 2030 WHO target ($\leq 2/100,000$). As feasible next steps, local partners prioritize community awareness of hepatitis, expanded adult testing, and micro-elimination programs for key populations (PWID, INC).

	CH	EG	ES	IT	PT
Simplified care algorithm					
<2 visits required during treatment	Partial (Optional)	Partial (Varies across country)	No	No	✓
Non-specialists can prescribe treatment	✓	✓	No	No	No
No mandatory genotyping	No	✓	✓	Partial (for key populations)	No
No co-payments	✓	✓	✓	✓	✓
Removal of restrictions Based on fibrosis	✓	✓	✓	✓	✓
Based on sobriety	✓	✓	✓	✓	✓

Conclusion: NHEPs reveal advances and challenges to hepatitis prevention and care and lessons learned for overcoming barriers. With NHEPs, local coalitions (CSO, MoH, clinical) can advocate for policies expanding HBV and HCV services, accelerating progress toward hepatitis elimination.

THU292

Economic investment and strategies to eliminate hepatitis C in Mexico

Ellen Mooneyhan¹, Alethse De la Torre Rosas², Daniel Bernal Serrano², David Kershenovich³, Maria Jesus Sanchez⁴, Leandro Soares Sereno⁵, Ivane Gamkrelidze¹, Sarah Blach¹, Homie Razavi¹. ¹Center for Disease Analysis Foundation, Lafayette, United States; ²National Center for the Prevention and Control of HIV (CENSIDA), Mexico City, Mexico; ³The National Institute of Health Sciences and Nutrition Salvador Zubirán (INCMNSZ), Tlalpan, Mexico; ⁴Pan American Health Organization, Mexico City, Mexico; ⁵Pan American Health Organization, Washington DC, United States
Email: emooneyhan@cdafound.org

Background and aims: In July 2020, the Mexican Government initiated the National Program for Elimination of Hepatitis C (HCV) under a procurement strategy that secured universal, free access to HCV screening, diagnosis, and treatment for 2020–22. This analysis quantifies the clinical and economic burden of HCV under a continuation (or an end) to this agreement.

Method: A modeling and Delphi approach was used to evaluate the current and future disease burden (from 2020 to 30) and economic impact (from 2020 to 35) of the historical paradigm (Historical Base) compared to HCV elimination (Elimination). The elimination cost analysis was stratified assuming the agreement continues (Elimination-Agreement to 2035) or terminates (Elimination-Agreement to 2022). We also analyzed the price of HCV treatment needed to achieve net-zero cost (defined as the difference in cumulative direct costs between the scenario and the Historical Base), starting at a base price of 77,838 MXN per person per treatment. Elimination is defined by the World Health Organization as a 90% reduction in new infections, 80% diagnosis coverage, 80% treatment coverage, and 65% reduction in mortality, by 2030.

Results: A viremic prevalence of 0.55% (0.38–0.60) was estimated in Mexico on January 1, 2021, corresponding to 745,000 (677,000–812,000) viremic infections. In the Historical Base, cases of advanced liver disease and liver-related deaths are projected to rise 75%–80% and annual direct costs are projected to remain at 2.4–2.5 billion MXN, with cumulative direct costs reaching 39.7 billion MXN. Elimination could save 23,500 lives and divert 6.5 billion MXN in healthcare costs. Under Elimination-Agreement to 2035, annual direct costs are projected to peak at 2.6 billion MXN, with cumulative direct costs

of 31.2 billion MXN. Under the Elimination- Agreement to 2022, annual direct costs would peak at 8.1 billion MXN, estimating 74.2 billion MXN in cumulative direct costs. The price of HCV treatment must decrease to 11, 000 MXN per patient to achieve net-zero cost by 2035.

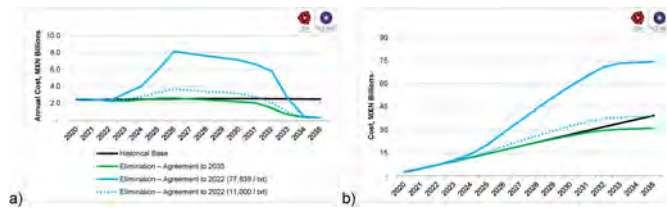


Figure 2: Direct Medical Costs, 2020–2035 annual direct medical costs, b) cumulative direct medical cost

Conclusion: To achieve HCV elimination at net-zero cost or below, the Mexican Government could either extend the procurement agreement through 2035 or reduce the cost of HCV treatment from 77, 838 MXN to 11, 000 MXN per person per treatment, starting in 2023. Otherwise, the Mexican Government must increase national budget allocation to the elimination program in order to achieve elimination by 2030.

THU293

Assessing the cost-effectiveness of integrated screening of viral hepatitis C, HIV, and tuberculosis

Ketevan Goginashvili¹, Ekaterine Adamia¹. ¹Ministry of Internally Displaced Persons from the Occupied Territories, Labour, Health and Social Affairs of Georgia, Policy Department, Tbilisi, Georgia
Email: kgoginashvili@moh.gov.ge

Background and aims: Georgia has made significant progress in reducing the burden of communicable diseases, which is due to effective measures taken to manage these diseases. The aim of the study was to evaluate the cost-effectiveness of integrated screening for the early detection of hepatitis C, HIV/AIDS, and tuberculosis, introduced at the level of primary health care since 2018.

Method: A pre and post-intervention study focused on comparing of two different methods of hepatitis screening using the cost-effectiveness evaluation. For the purpose of the study: the costs, screening coverage, and prevalence rates were compared for two different screening methods 1) integrated screening for hepatitis C, tuberculosis, and HIV/AIDS; 2) Separate screening of all three diseases in Samegrelo region.

Method: In Samegrelo region, primary health physicians conducted an average of 0.68 integrated screenings per adult person for hepatitis C, tuberculosis, and HIV/AIDS in 2019–2020, the mean screening cost was 9.4 GEL per person and the hepatitis C prevalence rate was 6.5% ($p < 0.05$). While in 2017–2018, Separate screening of all three diseases per adult person in the same region was 0.35, expenditure on hepatitis screening was GEL 17.4 and the prevalence rate was 6.9% ($p < 0.05$). The Cost-effectiveness coefficient was 13.8 and 49.7 for integrated screening and for hepatitis screening respectively ($p = 0.01$).

Results: In Samegrelo region, primary health physicians conducted an average of 0.68 integrated screenings per adult person for hepatitis C, tuberculosis, and HIV/AIDS in 2019–2020, the mean screening cost was 9.4 GEL per person and the hepatitis C prevalence rate was 6.5% ($p < 0.05$). While in 2017–2018, Separate screening of all three diseases per adult person in the same region was 0.35, expenditure on hepatitis screening was GEL 17.4 and the prevalence rate was 6.9% ($p < 0.05$). The Cost-effectiveness coefficient was 13.8 and 49.7 for integrated screening and for hepatitis screening respectively ($p = 0.01$).

	Integrated screening of three diseases	Hepatitis C screening	P value
Screening per person	0.68	0.35	<0.05
Screening mean cost per adult person, GEL	9.4	17.4	<0.05
Hep. C prevalence rate	6.5%	6.9%	<0.05
Cost-effectiveness coefficient	13.8	49.7	0.01

Table: Clinical and economic outcomes for integrated screening of three diseases and hepatitis C screening

Conclusion: This study provides evidence that adherence to the integrated screening of Hepatitis C, HIV/AIDS, and tuberculosis is more cost-effective and increases the rate of screening coverage compared to single hepatitis C screening alone.

THU294

Eliminating chronic hepatitis B in the northern territory of Australia through a holistic care package delivered in partnership with the community

Jane Davies¹, Joshua Saul Davis¹, Kelly Hosking², Paula Binks¹, Catherine Gargan², Belinda Greenwood-Smith², Sarah Bukulatjipi³, Terese Ngurruwuthun³, Amanda Dhagapan³, Phillip Wilson², Teresa De Santis², Karen Fuller⁴, Melita McKinnon¹, Mikaela Mobsby², Emily Vintour-Cesar¹. ¹Menzies School of Health Research; ²Northern Territory Government, Department of Health, Darwin City, Australia; ³Miwatj Health Aboriginal Corporation; ⁴Katherine West Health Board Aboriginal Corporation

Email: jane.davies@menzies.edu.au

Background and aims: Hep B PAST is a partnership project developed to eliminate chronic hepatitis B (CHB) from the Aboriginal population of the Northern Territory (NT) in Australia. Preliminary results from the project demonstrate significant improvements in the cascade of care for those living with CHB. The project aims to:

Improve hepatitis B related health literacy

Improve the cascade of care for people living with CHB

Method: Aim 1: Using a participatory action approach (PAR) the “Hep B Story” educational app was designed, translated (forward and back translation) launched in pilot language Yolŋu matha, and evaluated, with the process then repeated for the seven next most widely spoken NT Aboriginal languages.

Aim 2: Reviewing existing pathology and vaccination data from electronic health record systems, individuals in consenting health services were allocated to one of six hepatitis B sero-status codes (Hep B: Fully vaccinated, Hep B: Immune by Exposure, Hep B: Infected ON Treatment, Hep B: Infected NOT ON Treatment, Hep B: Non-Immune, No data) triggering an appropriate follow-up response for all clients. To support primary care to manage recalls and follow-ups as appropriate, we delivered hepatitis B education to remote doctors, nurses, and Aboriginal Health Workers (AHWs). Using a PAR, a hepatitis B management education course for AHWs was developed, delivered, and evaluated.

Results: The Hep B Story App is now available in English and eight Aboriginal languages spoken in the NT and roll out and evaluation is underway. All client files in participating health services have been reviewed, with approximately 30, 000 Aboriginal clients allocated a hepatitis B serocode and appropriate care pathway. Hepatitis B education has been delivered to over 150 general practitioners and nurses in the NT, and to approximately 100 AHWs. The cascade of care for those living with hepatitis B in the NT has significantly improved, now exceeding National Hepatitis B Strategy Targets, with 90% allocated a serocode (national target = 80%), 61% engaged in care (national target = 50%), and 21% receiving antiviral treatment (national target = 20%).

Conclusion: This project is demonstrating the effectiveness of a partnership approach with communities, with AHWs at the centre of the care model, and creating a community led, culturally acceptable, in-language health promotion tool in improving client outcomes for CHB. The preliminary findings from the project demonstrate

POSTER PRESENTATIONS

improvements in clinical care whilst preserving Aboriginal languages and empowering community through increased health literacy.

THU295

Hepatitis C prevalence and elimination in Pakistan; a bottom-up approach accounting for provincial variation

Ellen Mooneyhan¹, Huma Qureshi², Hassan Mahmood², Samra Mazhar², Muhammad Tariq³, Nabeel Ahmed Maqbool³, Ambreen Khan³, Masood Anwar³, Sarah Blach¹, Homie Razavi⁴, Sabeen Shah⁵, Saeed Sadiq Hamid⁶, Tanweer Hussain³, Saira Khawaja⁵, Uzma Khan⁷, Syeda Zahida Sarwar³, Khalid Mahmood^{8,9}, Gul Sabeen Azam Ghoreza¹⁰, Farooq Azam¹¹, Ayub Rose¹², Mohammad Khalil Akhter¹³, Aamir Ghaffoor Khan¹³, Mujahid Aslam¹⁴, Ahmad Nawaz^{13,14}. ¹Center for Disease Analysis Foundation, United States; ²Ministry of National Health Services, Regulations and Coordination, Islamabad, Pakistan; ³Chemonics International, Pakistan; ⁴Center for Disease Analysis Foundation, Lafayette, United States; ⁵Indus Hospital and Health Network, Karachi, Pakistan; ⁶Aga Khan University and Hospitals, Karachi, Pakistan; ⁷IRD Pakistan, IRD Global, Karachi, Pakistan; ⁸Singapore, Singapore, Pakistan; ⁹Punjab Hepatitis Control Programme, Lahore, Pakistan; ¹⁰Punjab Hepatitis Control Programme, Lahore, Pakistan; ¹¹Balochistan Hepatitis Control Programme, Quetta, Pakistan; ¹²Chemonics International/USAID, Quetta, Pakistan; ¹³Chemonics International/USAID, Peshwar, Pakistan; ¹⁴Health Department Khyber Pakhtunkhwa, Peshawar, Pakistan; ¹⁵Lady Reading Hospital, Peshwar, Pakistan
Email: emooneyhan@cdafound.org

Background and aims: In Pakistan, substantial changes to hepatitis C virus (HCV) programming and treatment have occurred since the 2008 national serosurvey estimated a 4.8% anti-HCV prevalence. However, a recent national serosurvey is unavailable. This analysis estimates a national prevalence using a bottom-up approach to account for provincial variation, coupled with screening, treatment, and prevention targets needed to achieve elimination by 2030.

Method: Using a Delphi method, epidemiologic HCV data for the four provinces of Pakistan (accounting for 97% of the country's population) were reviewed with 21 provincial and national subject-matter experts over 10 virtual meetings. Province-level estimates were then aggregated and inputted into a mathematical model to estimate the national HCV disease burden in the absence of intervention (Base), and if the World Health Organization (WHO) elimination targets of a 90% reduction in new infections, 80% diagnosis coverage, 80% treatment coverage, and 65% reduction in mortality, are achieved by 2030 (WHO Elimination).

Results: An estimated 9, 746, 000 (7, 573, 000–10, 006, 000) Pakistanis are living with viraemic HCV as of January 1, 2021, corresponding to a viraemic prevalence of 4.3% (3.3–4.4). Under the Base, it is estimated that 21% (2, 010, 000) of the infected Pakistani population has been diagnosed with HCV and only 2% (215, 000) of those infected received treatment in 2021. WHO Elimination would require an annual average of 18.8 million people screened, 1.1 million treated, and 46, 700 new infections prevented between 2021–2030. WHO Elimination would reduce total infections by 7, 040, 000, save 152, 000 lives and prevent 104, 000 incidence cases of hepatocellular carcinoma between 2015 and 2030.

Conclusion: Recent blood surveys, programmatic data, and expert panel input from the four provinces of Pakistan uncovered a higher number of HCV infections and lower number of patients treated than has been estimated using national extrapolations, which demonstrates the benefits of a bottom-up approach. Screening and treatment must increase 20-fold and 5-fold, respectively, from current levels, to curb the HCV epidemic in Pakistan and achieve elimination by 2030.

THU296

Association between immunosuppressants and poor antibody responses to inactivated SARS-CoV-2 vaccines in patients with autoimmune liver diseases

Hu Li¹, Yuting Wang¹, Ling Ao¹, Mingxia Ke¹, Zhi-wei Chen¹, Min Chen¹, Ming-Li Peng¹, Ning Ling¹, Peng Hu¹, Dachuan Cai¹, Dazhi Zhang¹, Hong Ren¹. ¹Key Laboratory of Molecular Biology for Infectious Diseases (Ministry of Education), Institute for Viral Hepatitis, Department of Infectious Diseases, the Second Affiliated Hospital of Chongqing Medical University
Email: renhong0531@vip.sina.com

Background and aims: To evaluate the safety, antibody responses and explore the impact of immunosuppressants on inactivated SARS-CoV-2 vaccines in patients with autoimmune liver diseases (AILD).

Method: In this prospective study, 76 adult patients with AILD and 136 healthy subjects were enrolled at least 21 days since the second dose of vaccines (BBIBP-CorV or CoronaVac). All adverse events (AEs) after the COVID-19 vaccination were recorded and graded. The anti-RBD-IgG and neutralizing antibodies (NAbs) were determined. In addition, SARS-CoV-2 specific B cells were also analyzed.

Results: All AEs were mild and self-limiting, and the incidence was similar between AILD patients and controls within 7 days and 30 days after COVID-19 vaccination. The anti-RBD-IgG and NAbs were detectable in 74 (97.4%, 100% in healthy controls, $p=0.13$) and 48 (63.2%, 84.6% in healthy controls, $p<0.001$) patients. The titers of anti-RBD-IgG ($p=0.02$) and NAbs ($p<0.001$) were both significantly lower in AILD patients than healthy controls. In multiple regression analysis, immunosuppressive therapy was an independent risk factor for the low-level anti-RBD-IgG responses (AOR: 4.7; 95% CI, 1.5–15.2; $p=0.01$) and reduced probability of NAbs seropositivity (AOR, 3.0; 95% CI, 1.0–8.9; $p=0.04$) in AILD patients. However, regardless of with or without immunosuppressants, the RBD-specific MBCs responses were comparable between patients with AILD and healthy controls.

Conclusion: The COVID-19 inactivated vaccine is safe and achieves efficient antibody responses in patients with AILD. In addition, immunosuppressants are significantly associated with poor antibody responses to the SARS-CoV-2 vaccine.

THU297

“Like what? You think I have that?”-Impact of stigma on pharmacy-based identification and treatment of hepatitis C in Victoria, British Columbia

Marion Selfridge^{1,2}, Tamara Barnett¹, Kellie Guarasci¹, Karen Lundgren¹, Anne Drost¹, Chris Fraser^{1,3}. ¹Cool Aid Community Health Centre, Victoria, Canada; ²University of Victoria, Canadian Institute of Substance Use Research, Victoria, Canada; ³University of British Columbia, Department of Family Medicine, Vancouver, Canada
Email: mselfridge@coolaid.org

Background and aims: Canada is currently on target to reach the 2030 WHO goal of HCV elimination. Continued high rates of treatment initiation are required to meet this goal. Novel models have proven successful to engage populations who use drugs (PWUD) in HCV therapy with a simplified, task-shifted cascade of care: Tayside, Scotland pharmacy-based HCV screening and treatment has demonstrated excellent outcomes and progress towards local HCV elimination. The EPIC Study seeks to determine whether pharmacy-based treatment successes can be replicated at community pharmacies in Victoria BC.

Method: Four community pharmacies known to work with PWUD and provide opioid agonist therapy (OAT) were provided training sessions to equip staff with a standardized tool kit of resources. In fall 2020, pharmacy staff were trained to provide verbal informed consent and perform point of care HCV OraQuick antibody screening. Pharmacies were supported by a study nurse to link to HCV RNA testing when antibody positive patients were identified, with initiation of HCV treatment offered to those found to be RNA positive.

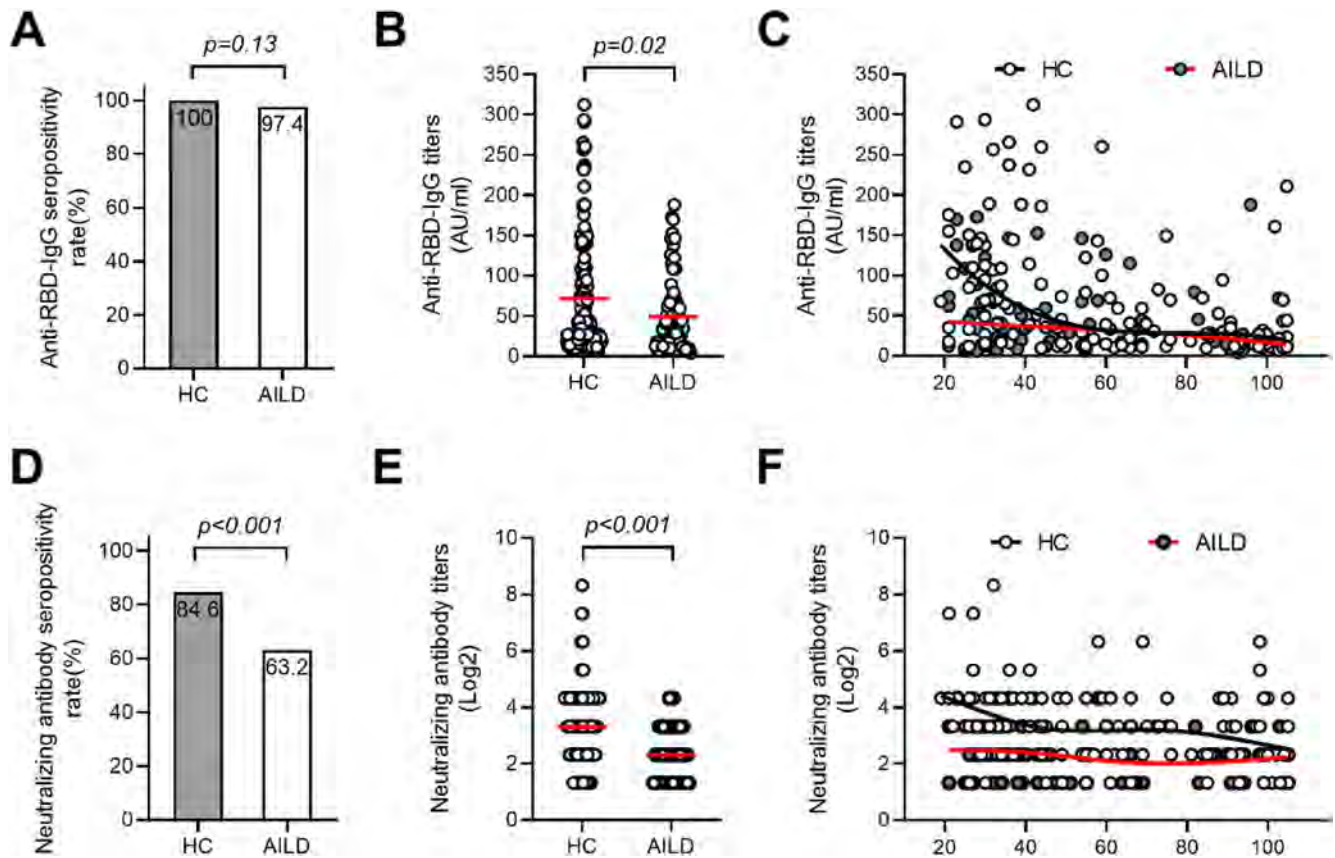


Figure: (abstract: THU296): Antibody responses after the COVID-19 vaccination in patients with AILD and healthy controls. (A-B) The seropositivity rate (A) and titers (B) of anti-RBD-IgG in patients with AILD and healthy controls. (D-E) The seropositivity rate (D) and titers (E) of NAbs in patients with AILD and healthy controls. The distribution of anti-RBD-IgG (C) and NAbs (F) antibody titers over time in patients with AILD and healthy controls. AILD, autoimmune liver disease; anti-RBD-IgG, spike receptor-binding domain IgG antibody; NAbs, neutralizing antibodies.

The study nurse worked with pharmacy staff to strategize adherence and support as needed by study subjects. Qualitative interviews have been conducted with five pharmacy staff to explore their experiences with testing and monitoring HCV treatment and the feasibility of involving pharmacists in the HCV care cascade.

Results: To date pharmacy staff completed 171 HCV OraQuick tests finding 53 tested positive for HCV antibodies: 23 people were HCV RNA negative, (20 previously treated and 2 self-cleared), 8 unk/LTF. Of the 22 RNA positive participants, 1 is pending treatment start, 21 people have started treatment, with 8 achieving SVR. While great success has been achieved in treating identified people, less than half of projected OraQuick tests have been completed. Although the onset of the Covid 19 pandemic was a fundamental barrier incorporating HCV testing at pharmacies, stigma related to HCV and illicit drug use continues to impact this process. Pharmacists described feeling hesitant about approaching participants, especially after receiving negative responses from clients about HCV testing. Some worried their relationship would change with clients as asking about HCV implied risky drug use.

Conclusion: This innovative and novel approach to HCV therapy in PWUD attempted to use a pharmacy-based approach to find people with limited connection to primary health care to test and treat HCV. Increased training of pharmacy staff related to stigma around drug use and HCV is required both before and ongoing for successful integration of pharmacy-led HCV testing and treatment in Canada.

THU298

Improved clinical and economic outcomes in an intensive care unit with a focus on hepatology through interprofessional cooperation between physicians, staff nurses, and pharmacists

Schmid Stephan¹, Schlosser Sophie¹, Karsten Guelow¹, Vlad Pavel¹, Alexander Mehrl¹, Martina Mueller-Schilling¹, Alexander Kratzer².

¹University Hospital Regensburg, Department of Internal Medicine I, Gastroenterology, Hepatology, Endocrinology, Rheumatology, and Infectious Diseases, Regensburg, Germany; ²University Hospital Regensburg, Hospital Pharmacy, Regensburg, Germany

Email: stephan.schmid@ukr.de

Background and aims: Since 2015, the medical intensive care unit (ICU) with a focus on hepatology of the Department of Internal Medicine 1 at the University Hospital Regensburg, Germany, has a particular emphasis on interprofessional collaboration with staff nurses and hospital pharmacists. The hospital pharmacists have access to the hospital information system and the electronic charting program. Consultations take place on daily basis. Furthermore, weekly joint rounds within the antibiotic stewardship program are performed. Furthermore, there is a joint training and teaching of medical, nursing and pharmacy students within the intensive care training ward Regensburg (I'M A-STAR project). The study aims to investigate to what extent the newly introduced structural changes affect clinical and economic outcomes.

Method: We examined clinical performance data and consumption figures for antibiotics and other drugs over a 10-year period from

POSTER PRESENTATIONS

2011 to 2021. Data from the hospital pharmacy, hospital administration, electronic charting, and hospital information systems were included in the analyses. An electronic platform was developed specifically to improve documentation. The years 2020 and 2021 were considered separately due to the COVID-19 pandemic and the care of numerous COVID-19 patients in the ICU.

Results: It could be shown that the pharmacist's recommendations regarding drug administration were mainly related to indication (43.6%), dosage (27.6%), interactions (9.4%), and side effects (4.1%). Antibiotic consumption was reduced by 12.2% from 2015 to 2019. Encouragingly, this included a 23.4% reduction in carbapenem use. Antibiotic spending was reduced by 24.9% overall.

An analysis of the intensive care G-DRGs showed that the case-mix points increased significantly by 31.6% during the period under review. Similarly, patient severity of illness as measured by the SAPS II score increased by 21.4%. The proportion of mechanically ventilated patients exceeded 50%.

In another analysis, antibiotic spending per case-mix point was calculated. While spending was EUR 60.22 per case-mix point in 2015, this could be reduced by 42.9% to EUR 34.37 per case-mix point by 2019.

Conclusion: Through close interprofessional collaboration between physicians, staff nurses, and pharmacists, the consumption of antibiotics and other drugs (e.g., albumin) was significantly reduced, thus improving patient care. There was also a positive economic effect-with a simultaneous increase in case-mix points, expenditure on antibiotics was significantly reduced.

Responsible use of resources and high-performance medicine are not contradictory. In our view, a close interprofessional collaboration between physicians, staff nurses, and pharmacists will be of outstanding importance in the future, particularly in intensive care medicine.

THU299

Need to implement the screening strategy to advance HCV elimination in Italy: a cost-consequences analysis

Andrea Marcellusi¹, Kristi Tata², Francesco Mennini¹, Massimo Andreoni³, Loretta Kondili⁴. ¹Tor Vergata University, CEIS, Rome, Italy; ²University Hospital Center of Tirana, Tirana, Albania; ³Tor Vergata University, Rome, Italy; ⁴Istituto Superiore di Sanità, Center for Global Health, Rome, Italy
Email: loreta.kondili@iss.it

Background and aims: In Italy, the HCV disease burden is the highest of western Europe. A graduated screening strategy that covers the birth cohort population from 1948-to 1988 is cost-effective to achieve HCV elimination in Italy. A dedicated fund for HCV screening could permit free of charge testing of the population from 1969-to 1989, but if the screening is not implemented to other birth cohorts the HCV elimination targets could not be achieved. Based on the HCV infection burden, by a cohort of age and fibrosis stage previously estimated, we evaluated the cost-consequences of a delay of HCV diagnosis in the next 5 years in Italy.

Method: We used a previously designed and validated probabilistic model to estimate the clinical, and economic outcomes of different screening coverage uptakes, considering the HCV disease costs by the fibrosis stage as reported by the PITER cohort real-life data. The model starts with a decision probabilistic tree that simulates 5 years of HCV testing in the general population cohort born between the years 1948–1967 (15, 485, 565 individuals to be tested) with different coverage rates lower in the lack of active screening and higher in case of screening implementation. The first part of the model identified and categorized HCV chronic patients by the fibrosis stage. A Markov model was considered for 10 years horizon time. The simulations consider two alternative coverage rates and timing during the five years simulated scenarios: 1) Incremental approach (coverage rates equal to 10%, 20%, 25%, 30% respectively at years 1, 2, 3, and 4) and 2)

Fast approach (50% of the target population each year at years 1, 2, 3 and 4).

Results: The overall estimated number of HCV active infections to be diagnosed in the target population was 106, 200. The incremental approach scenario estimated 62% of the target population diagnosed vs 94% diagnosed in the fast approach scenario. An increase in overall costs was observed in the fast approach scenario up to year 5, but at year 6 the cost starts to decrease due to a higher number of diagnosed patients versus the incremental approach in which the disease costs continue to increase. (Figure 1). At ten years' time-horizon, the model estimated a cumulative not mutually exclusive reduction of 5, 406 persons living in the HCC health state, 4, 614 in decompensated cirrhosis and 11, 081 liver-related deaths. A cost reduction of € 74 million was estimated if a fast approach was adopted versus the incremental one.

Conclusion: A delay in HCV diagnosis in the general population from 1968-to 1948, yet not addressed for the HCV free of charge screening, will have important clinical and economic consequences in Italy.

THU300

Evaluation of access to treatment for hepatitis C: a large retrospective cohort from a tertiary care hospital in Turkey

Merve Eren Durmus^{1,2}, Gökhan Köker³, Yeşim Çekin⁴, Serkan Ocal⁵, Ayhan Çekin³. ¹Antalya Education and Research Hospital, Gastroenterology, Antalya, Turkey; ²Antalya Education and Research Hospital, Gastroenterology, Turkey; ³Antalya Education and Research Hospital, Internal Medicine, Antalya, Turkey; ⁴Antalya Education and Research Hospital, Medical Microbiology, Turkey; ⁵Antalya Education and Research Hospital, Gastroenterology, Turkey
Email: drmerveeren@gmail.com

Background and aims: Hepatitis C virus (HCV) infection is a major public health issue. According to 2015 data, approximately 71 million people have chronic HCV viremia in the world. It is one of the leading causes of liver-related morbidity and mortality globally. The seroprevalence of anti-HCV in our country has been detected 0.5–1%. Due to its silent progress many patients may be unaware of the situation. In our study, we aimed to determine the rate of the anti-HCV positive patients who were able to access to treatment.

Method: Subjects who had anti-HCV positivity between 2014–2019 have been reviewed retrospectively. The data of the patients were recorded and patients referred for further evaluation and accessed to treatment were identified.

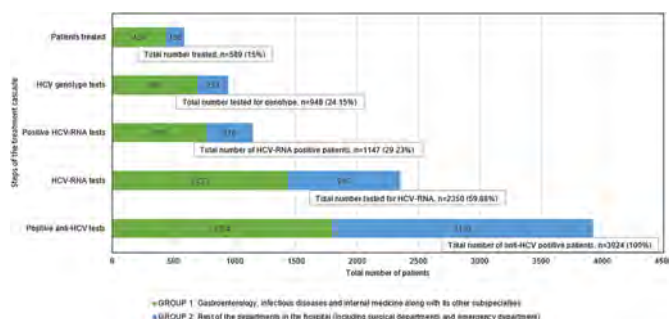


Figure: Disparity between the number of anti-HCV positive individuals, those who were tested for HCV-RNA viremia, HCV genotypes and the ones who could access to the treatment and comparison of two groups contributions on each stage.

Results: The clinics that requested anti-HCV tests were divided in to two groups. Group 1 included gastroenterology, infectious diseases and internal medicine along with its other subspecialties; and the rest of the clinics are defined as Group 2. There were 3924 anti-HCV positive patients in 5-years period. 2350 of them were tested for HCV viremia (59.9%). HCV-RNA were positive in 1147 of them (29.2%), corresponding to 48.8% of the patients who have been tested. Among the patients with HCV-RNA positivity, 948 of them were tested for

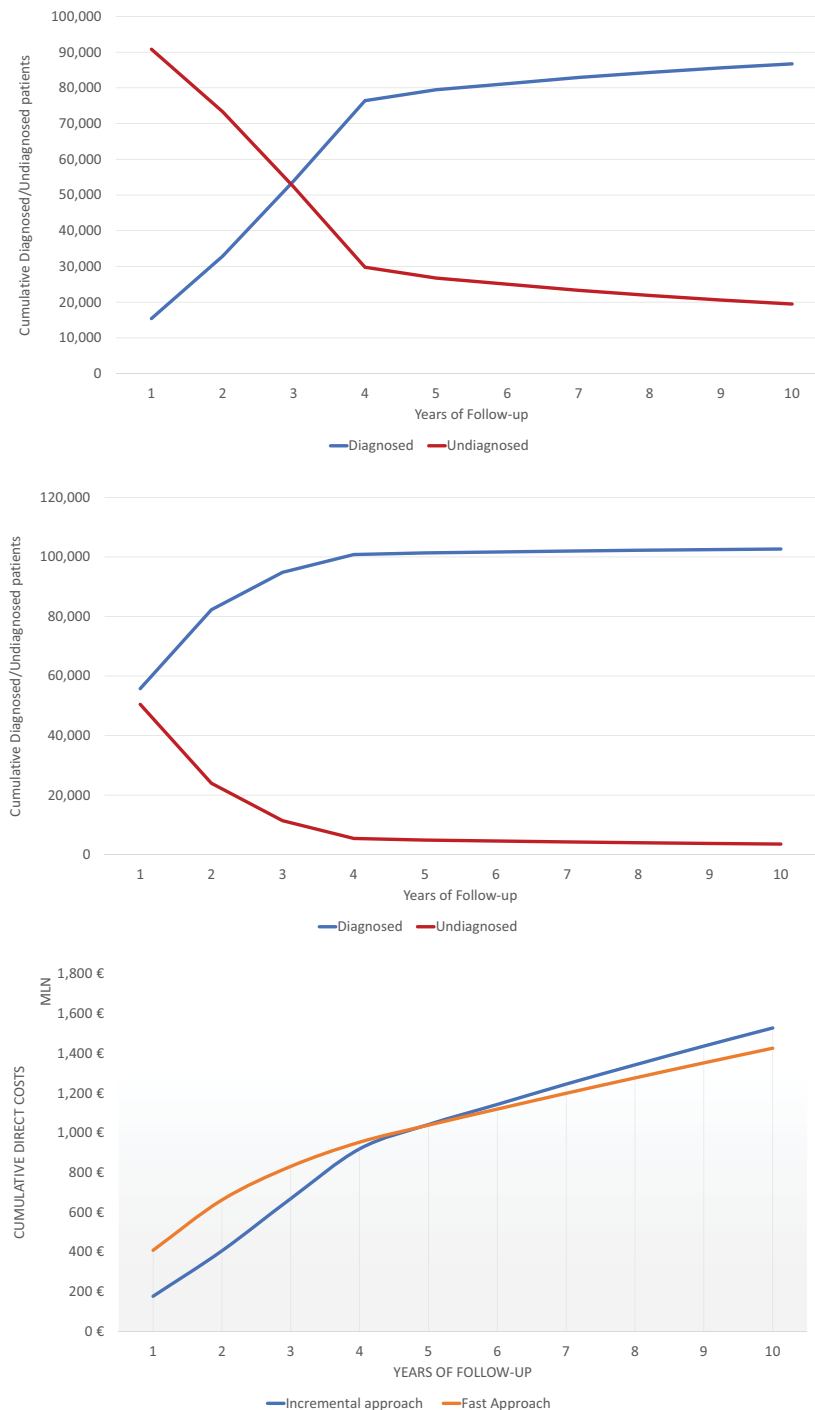


Figure: (abstract: THU299) Cumulative diagnosed patients at each year of simulation- Incremental Scenario (Panel A) Fast Scenario (Panel B) and the respective Costs (Panel C)

HCV genotype (%24.1). Of these patients, 251 were genotype 1A, 438 were genotype 1B, 26 were genotype 2, 193 were genotype 3, 39 were genotype 4 and one patient was genotype 5. Only 589 of them could access to treatment (%15). Numbers of patients in each step of the treatment cascade are presented in Figure 1. Although the departments in Group 2 detected more anti-HCV positivity, the number of the ones that could access treatment were lower.

Conclusion: World Health Organization has been set international targets for the elimination of HCV infection by 2030, which is a public

health threat. According to our study, there are significant deficiencies in several stages of the treatment cascade, which is consistent with world data. The rate HCV- RNA testing was low among all clinics. However, Group 2 has lower referral rates according to Group 1 indicating a lower level of awareness. Knowledge of all physicians should be improved to prevent losses and delays in the diagnosis and treatment of HCV infection independent of their departments.

POSTER PRESENTATIONS

THU301

Hepatitis E Virus Capsid Antigen (HEV-Ag): a practical diagnostic biomarker in the HEV outbreak scenario

Simon Lytton¹, Rakibul Hassan Bulbul², Mamunur Rashid².

¹SeraDialogistics; ²Bangladesh Institute Of Tropical And Infectious Diseases Hospital, Chittagong, Bangladesh

Email: simon.lytton@t-online.de

Background and aims: The increased global incidence of hepatitis E virus (HEV) infections, warrants accurate and affordable diagnostics across different geographical regions. The soluble and highly conserved HEV open reading frame 2 (ORF2) capsid antigen (HEV-Ag) is detectable in self-limited acute enteric hepatitis by HEV-Ag ELISA which is a promising serological assay in settings where HEV-RNA testing is not feasible. Our aim was to assess the HEV-Ag biomarker in an HEV outbreak in a low income country.

Method: A prospective single center longitudinal study during HEV outbreaks in the Chittagong, Bangladesh region between October 2018 and October 2019 was conducted based on recruitment of acute jaundice cases with clinical signs and symptoms of suspect HEV infections. Acute HEV infection was defined as a positive test result for anti-HEV IgM antibodies.

Results: Forty four of the 51 enrolled enteric hepatitis cases (86%) were confirmed HEV by anti-HEV IgM ELISA at day 0 hospital entry. The anti-HEV-IgM and IgG were positive in all patients and did not reveal significant differences; neither between the time points day 0 and follow-up hospitalization on day 2–6 or day 7–10 nor between RNA-positive (n = 36) versus RNA-negative (n = 8) HEV groups. The HEV-Ag positivity was higher in viral RNA-positive (29/36, 81%) than the viral RNA-negative (1/8, 12%) group, p < 0.001 and the HEV-Ag levels positively correlated with viremia, r = 0.77, p < 0.0001. All non-HEV cases; n = 7 tested negative anti-HEV IgM and HEV-Ag and 5 of 7 (71%) tested anti-HAV IgM positive.

Conclusion: The HEV-Ag ELISA is a reliable and practical diagnostic tool in this acute HEV outbreak.

THU302

Bulevirtide is broadly active against all HDV genotypes expressing envelopes from HBV genotypes A-H and a large panel of clinical isolates

Savrina Manhas¹, Bin Han¹, Simin Xu¹, Lindsey May¹, Dong Han¹, Tahmineh Yazdi¹, Silvia Chang¹, Thomas Aeschbacher¹, Rishi Aryal¹, Ross Martin¹, Yang Liu¹, Roberto Mateo¹, Vithika Suri¹, Dmitry Manuilov¹, John F. Flaherty¹, Julius Hollnberger^{2,3}, Stephan Urban⁴, Tomas Cihlar¹, Evguenia S Svarovskaia¹, Hongmei Mo¹. ¹Gilead Sciences, Inc., Foster City, United States;

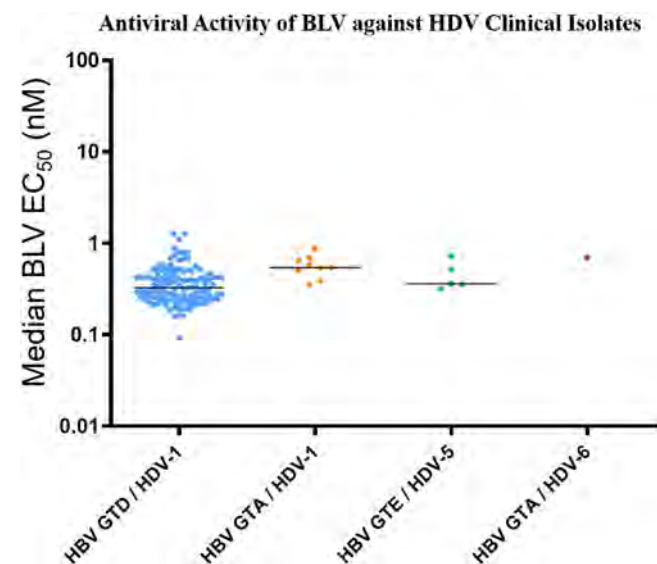
²University Hospital Heidelberg, Department of Molecular Virology, Heidelberg, Germany; ³German Center for Infection Research (DZIF), Heidelberg; ⁴University Hospital Heidelberg, Heidelberg, Germany

Email: savrina.manhas1@gilead.com

Background and aims: Bulevirtide (BLV) is a 47-amino acid lipopeptide derived from the HBV large envelope protein (LHBsAg). BLV binds to the HDV/HBV host entry receptor sodium taurocholate cotransporting polypeptide and acts as a potent HDV entry inhibitor. BLV has been approved for treatment of HDV in the European Union and is under late stage clinical evaluation in the United States. Based on sequence divergence, there are eight HDV genotypes (HDV-1 to HDV-8) and eight HBV genotypes (GTA to GTH). To determine the activity of BLV against diverse HDV/HBV variants sequences, the antiviral activity of BLV against HDV-1 to HDV-8 enveloped with HBV GTA-H and against 137 clinical isolates from study participants with HDV infection was assessed.

Method: HDV viruses were produced by co-transfection of Huh7 cells with HDV genome and HBV envelope plasmids. Subsequently, virus containing supernatant was collected, titrated and used to infect primary human hepatocytes (PHHs). For the HDV phenotyping assay, PHHs were pre-treated with BLV and then infected with clinical plasma or a lab strain of HDV. After five days, immunofluorescence staining was performed to determine cells that were positive for HDV antigen (HDAG). The concentration of BLV decreasing the HDV HDAG positive cells by 50% was expressed as a mean EC₅₀ value from at least two independent experiments.

Results: For HDV lab strains, the median EC₅₀ of BLV against HDV-1 to HDV-8 pseudotyped with HBV GTA-D envelopes ranged from 0.35 nM to 0.64 nM. Similarly, for HDV-1 to HDV-8 lab strains pseudotyped with HBV GTE-H envelopes, the median EC₅₀ of BLV ranged from 0.21 nM to 0.61 nM. Across HDV-1 to HDV-8 lab strains enveloped with HBV GTA-H envelopes, the median EC₅₀ of BLV ranged from 0.26 nM to 0.64 nM. Additionally, the median EC₅₀ of BLV against HDV-1 with envelopes carrying common polymorphisms in the LHBsAg PreS1 region that corresponds to the BLV sequence region for HBV GTA, GTB, GTC and GTD were 0.57, 0.59, 0.43 and 0.33 nM, respectively. The activity of BLV was also evaluated against 165 clinical isolates with a total of 137 out of 165 clinical isolates having sufficient infectivity to be tested for BLV activity. Most clinical isolates tested (n = 122) belonged to HBV genotype D/HDV genotype 1 (D/1) and had a median EC₅₀ value of 0.33 nM. Similarly, the median EC₅₀ values for clinical isolates of A/1 (n = 9), E/5 (n = 5) and A/6 (n = 1) were 0.54, 0.36, and 0.70 nM, respectively (Figure).



Conclusion: BLV demonstrated potent broad spectrum antiviral activity against HDV-1 to HDV-8 enveloped with HBV GTA to GTH and against a larger panel of HDV clinical isolates showing similar EC₅₀ values across different HBV/HDV genotypes irrespective of the presence of polymorphisms. These results support that BLV has broad genotype coverage potential for the treatment of patients with chronic HDV infection.

THU303

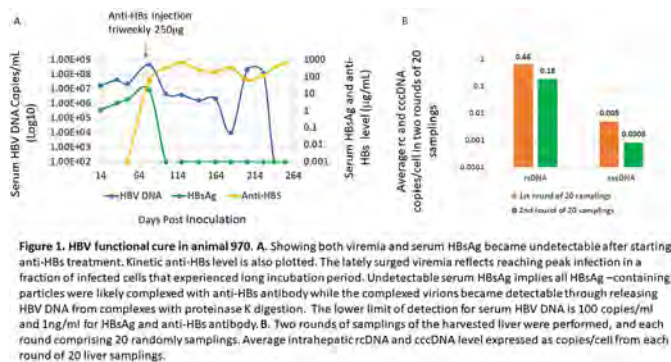
A persistent HBV infection features spontaneous cccDNA loss and new rounds of infection

Bai-Hua Zhang¹, Yuanping Zhou², Stephen Horrigan³, Fabien Zoulim⁴, David Baltimore⁵, Yong-Yuan Zhang¹. ¹HBVtech, Virology, Frederick, United States; ²Nanfang Hospital, Southern Medical University, Dept. of Gastroenterology and Hepatology Unit, Guangzhou, China; ³Noble Life Sciences, Preclinical Studies, Sykesville, United States; ⁴Cancer Research Center of Lyon, Hepatology, Lyon, France; ⁵California Institute of Technology, Biology, Pasadena, United States
Email: yongyuanzhang50@gmail.com

Background and aims: Clinical evidence shows frequent replacement of serum wild type viral population with mutants in chronic HBV infection, which indicates cccDNA turnover and new rounds of infection. We hypothesized that HBV infection is maintained by new rounds of infection. This hypothesis can be tested in HBV infected uPA/SCID chimeric mice by blocking new rounds of infection using anti-HBs antibody. Since anti-HBs Ab mainly functions extracellularly, its administration in HBV infected chimeric mice is expected to have a therapeutic impact on HBV infection level only if it is sustained with new rounds of infection.

Method: An optimized AAV vector that carries human anti-HBs Ab genes was used to express sustained high level of anti-HBs antibody. HBV infected uPA/SCID chimeric mice were treated with AAV vector expressing malaria antibody or anti-HBs antibody day 49 post infection. Serum HBV DNA and HBsAg level were monitored until day 183 and liver HBV DNA was determined through 20 random samplings of each autopsied liver.

Results: Two key findings were observed: I. Dynamic cccDNA status and spontaneous cccDNA loss: average cccDNA level ≤ 1 copy/cell was detected in 260 (46%) of 566 cccDNA samplings of 18 HBV infected human livers from chimeric mice, suggesting cccDNA was already lost spontaneously in a fraction of infected cells. II. Anti-HBs treatment profoundly impacts HBV infection level: i) Viremia was significantly lowered by up to >100-fold; ii). Intrahepatic rcDNA level was significantly lowered by 4, 000 to 10, 000 copies/cell; iii). The number of cccDNA samplings with cccDNA level ≤ 1 copy/cell was significantly expanded (50.2%, 244/486) in anti-HBs treated animals compared to malaria antibody animals (20%, 16/80); and iv) HBV functional cure with nearly complete cccDNA elimination was achieved in one animal with baseline viremia of 4.6E HBV DNA copies/ml (Figure 1).



Conclusion: cccDNA level is dynamic with spontaneous cccDNA loss, which mediates spontaneous HBV clearance and but can be replenished by new rounds of infection in infected human livers of chimeric mice. New rounds of infection prolong HBV persistent infection. Therapeutic blocking of new rounds of infection profoundly impacts both rcDNA and cccDNA level including a nearly complete cccDNA elimination in one animal with HBV functional cure. Our study identifies an opportunity to durably terminate persistent HBV infection through blocking new rounds of infection.

THU304

Functional and mitochondrial dynamics alterations in patients with chronic hepatitis B and advanced fibrosis

Dimitri Loureiro^{1,2}, Issam Tout^{1,2}, Cheikh Mohamed Bed^{1,2}, Morganer Roinard^{1,2}, Ahmad Sleiman^{1,2}, Boyer Nathalie^{1,2}, Stephanie Narguet^{1,2}, Nathalie Pons-Kerjean^{2,3}, Corinne Castelnau^{1,2}, Nathalie Giuly^{1,2}, Vassili Soumelis⁴, Jamel El Benna², Patrick Soussan⁵, Richard Moreau², Valérie Paradis^{1,2}, Abdel Mansouri^{1,2}, Tarik Asselah^{1,2}. ¹Hospital Beaujon AP-HP, Hepatology, Clichy, France; ²Center Recherche Sur l'Inflammation, U1149, Paris, France; ³Hospital Beaujon AP-HP, Pharmacy, Clichy, France; ⁴Hospital Saint-Louis, Laboratoire d'Immunologie et Histocompatibilit, Paris, France; ⁵Paris Diderot University, U1135, Paris, France
Email: dimitri.loureiro@inserm.fr

Background and aims: Patients with chronic hepatitis B (CHB) have an increased risk of advanced fibrosis and hepatocellular carcinoma (HCC). In experimental models, hepatitis B virus (HBV) infection causes oxidative stress and alters hepatic mitochondria. The aim of the study is to investigate the role of mitochondrial stress in the progression of fibrosis in CHB.

Method: 132 treatment-naïve CHB mono-infected patients with available liver biopsies specimen were included in this study. Patient demographics and laboratory parameters were recorded at the time of the biopsy. Liver mitochondrial DNA (mtDNA) damage was screened by long PCR and sequencing and levels by Slot blot. The expression of the main genes of cytochrome c oxidase subunits, mitophagy, mitochondrial peptidases and chaperonins, TNF α and IL6, inducible NO synthase and MnSOD were investigated by RT-qPCR and Western-blotting. Patients with CHB and advanced fibrosis (F3-F4 Metavir score; n=43) were compared to patients with no-mild-moderate fibrosis (F0-F2; n=89). In vitro, HBV and HBx were transiently expressed in HepG2 cells and the superoxide anion formation, peroxynitrite, nitration of mitochondrial chain complexes, iNOS, MnSOD protein levels and mtDNA depletion were assessed.

Results: Whereas 100% of patients with F3-F4 exhibited multiple mtDNA deletions, 50% of those with F0-F2 ($\kappa^2 = 6.8$; $p < .001$) carried a single mtDNA deletion. Significant decreases were observed in patients with F3-F4 compared to those with F0-F2 for the mRNAs of MT-CO1 (0.55 ± 0.36 and 1.20 ± 0.75 , $p < .001$), HSPA9 (0.70 ± 0.28 and 1.06 ± 0.37 , $p < .001$), HSPD1 (0.83 ± 0.36 and 1.10 ± 0.44 , $p < .05$), Lon Peptidase 1, LONP1 (0.83 ± 0.22 and 1.06 ± 0.33 , $p < .05$), PRKN (0.45 ± 0.26 and 1.12 ± 0.57 , $p < .0001$), PINK1 (0.59 ± 0.17 and 1.06 ± 0.26 , $p < .0001$), Liver TNF α (1.72 ± 0.2 and 0.99 ± 0.2 ; $p < .05$), IL6 (7.82 ± 0.90 and 1.14 ± 0.26 ; $p < .05$). Protein levels significantly decreased in F3-F4 for MT-CO1 (2.55 ± 0.88 and 3.44 ± 0.80 , $p < .01$), LONP1 (0.67 ± 0.31 and 0.87 ± 0.51 , $p < .05$), HSPA9 (0.67 ± 0.31 and 1.20 ± 0.77 , $p < .05$) MT-ATP8 (0.14 ± 0.03 and 0.30 ± 0.06 , $p < .05$). iNOS and MnSOD proteins are significantly increased in patients with F3-F4 with MnSOD activity decreased in these patients ($p < .05$).

In HepG2 cells, HBV or HBx expression increase mitochondrial superoxide formation at 24 and 48 h ($p < .05$), increase iNOS protein levels, but only HBV increase MnSOD protein expression by 2-fold ($p < .05$). Then, an increase of peroxynitrite as well as mtDNA depletion ($p < .01$) and nitration of the mitochondrial respiratory chain complexes were observed.

Table: Patients characteristics

Number (n)	Patients
132	
Sex (M/F)	84/48
Age (ans)	44 ± 3.47
(mean ± SEM)	
BMI (Kg/m ²)	24.55 ± 3.34
(mean ± SEM)	
ALT (UI/L)	109.22 ± 12.79
(mean ± SEM)	
AST (UI/L)	70.86 ± 13.72
(mean ± SEM)	
γ-GT (UI/L)	78.51 ± 18.53
(mean ± SEM)	
Cholesterol (mmol/L)	4.38 (2.9-6.5)
Triglycerides (mmole/L)	1.13 (0.38-3.69)
Glucose (mmole/L)	5.05 ± 0.56
HBeAg positive, n (%)	41 (37.48)
HBeAg (log ₁₀ IU/mL)	3.72
(moyenne)	
HBV DNA (log ₁₀ IU/mL)	5.12 (2.17-8.04)
Hepatic histology	
Metavir	
Activity A0	33
A1	65
A2	24
A3	10
Fibrosis (Metavir)	
F0-F2 (n=89)	
F0	26
F1	32
F2	31
F3-F4 (n=43)	
F3	27
F4	16

Conclusion: Diverse mtDNA damages and alterations of mitochondrial function and dynamic seems to be involved in the progression of fibrosis in patients with CHB. Our results emphasized the importance on modulating mitochondrial function, and therefore could be an attractive therapeutic strategy to block the progression of fibrosis in CHB.

THU305

Dual antiviral activity of farnesyl transferase inhibitor on hepatitis D virus infection revealed by RT-ddPCR

Eloi Verrier¹, Anna Salvetti², Caroline Pons², Michelet Maud³, Thomas Baumert^{1,4}, David Duranton², Julie Lucifora². ¹Université de Strasbourg, Inserm, Institut de Recherche sur les Maladies Virales et Hépatiques UMR_S1110, Strasbourg, France; ²CIRI-Centre International de Recherche en Infectiologie, Univ Lyon, Université Claude Bernard Lyon 1, Inserm, U1111, CNRS, UMR5308, ENS Lyon, Lyon, France; ³Inserm, U1052, Cancer Research Center of Lyon (CRCL), Université de Lyon (UCBL1), CNRS UMR5286, Centre Léon Bérard, Lyon, France; ⁴Institut Hospitalo-Universitaire, Pôle Hépatodigestif, Nouvel Hôpital Civil, Strasbourg, France
Email: e.verrier@unistra.fr

Background and aims: Chronic hepatitis D is the most severe form of chronic viral hepatitis and to date, efficient therapeutic approaches against hepatitis D virus (HDV) are absent. Among the antiviral molecules currently tested in clinical trials, the farnesyl transferase inhibitor (FTI) Lonafarnib inhibits the prenylation of the large delta antigen (L-HDAg), blocking virus assembly. Given the importance of L-HDAg in the virus life cycle, We hypothesized that Lonafarnib treatment may have side effects on virus replication.

Method: Here, we setup an innovative method based on reverse transcription digital droplet PCR (RT-ddPCR) for the quantification of HDV RNA allowing the independent quantification of edited and non-edited versions of the HDV genome upon infection.

Results: We demonstrated that FTI treatment of HBV-HDV co-infected cells leads to an accumulation of intracellular HDV RNAs and a marked increase in the levels of edited HDV RNAs not only within the infected cells but also in the viral particles that are secreted. Interestingly, these viral particles were less infectious, probably due to an enrichment in edited genomes that are packaged, leading to unproductive infection given the absence of S-HDAg synthesis after viral entry.

Conclusion: Taken together, we setup an innovative quantification method allowing the investigation of HDV RNAs editing during HDV infection in a simple, fast, clinically-relevant assay and demonstrated for the first time the dual antiviral activity of FTI on HDV infection.

THU306

Characterization of circulating hepatitis B Virus RNAs in vitro and chronic hepatitis B patients

Doohyun Kim¹, Delphine Bousquet^{1,2}, Marie-Laure Plissonnier¹, Hyoseon Tak¹, Xavier Grand¹, Chloe Goldsmith³, Françoise Berby¹, Bordes Isabelle¹, Alexia Paturel^{1,2}, Aaron Hamilton⁴, Marantha Heil⁴, Massimo Levvero^{1,2,5}, Barbara Testoni¹, Fabien Zoulim^{1,2,6}. ¹Cancer Research Center of Lyon, Chronic Viral Hepatitis: virus/host interactions, pathogenesis and novel antiviral strategies, Lyon, France; ²Université de Lyon, Lyon, France; ³University of Canberra, Bruce, Australia; ⁴Roche Diagnostics, Pleasanton, United States; ⁵Sapienza University of Rome, Roma, Italy; ⁶La Croix-Rousse Hospital, Lyon, France
Email: fabien.zoulim@inserm.fr

Background and aims: Circulating HBV RNA (CirB-RNA) is a promising non-invasive biomarker for cccDNA transcriptional activity. However, the molecular characteristics and circulating particles containing cirB-RNA in vitro and in vivo remain to be fully defined.

Method: Supernatants from cultured hepatocytes infected by HBV and treated or not with lamivudine, and sera from 9 untreated [4 HBeAg (+) and 5 HBeAg (-)] and 1 HBeAg (+) ETV-treated chronic hepatitis B (CHB) patients were subjected to Iodixanol/Sucrose ultracentrifugation for buoyant density. Each density fraction was analyzed for HBV DNA/RNA by specific qPCR and droplet digital (dd) PCR. Viral and extracellular vesicles (EVs)-associated proteins were detected by ELISA and Western Blotting. 5' RACE PCR followed by ONT MinION sequencing was used to identify CirB-RNA species. Longitudinal serum samples before and at two time points after NUC therapy initiation were obtained from two additional patients [HBeAg (+) TDF-treated CHB and HBeAg (-) ETV-treated CHB].

Results: After ultracentrifugation, CirB-RNA was mainly detected in core-associated virion-like particles, in 2 log₁₀ less amount than HBV DNA. However, CirB-RNA was the predominant species in lighter density fractions (1.17–1.18 g/ml) deprived of viral proteins, both in cell supernatant and in serum. The enrichment for EVs in these fractions was confirmed by detection of CD9 and CD81 by Western Blotting, immunoprecipitation assay, Nanoparticle tracking analysis and Transmission Electron Microscopy. Distribution of CirB-RNA did not differ significantly according to HBeAg status, while in a patient with low HBsAg level, CirB-RNA was mainly detected in the EVs-enriched fractions. Lastly, CirB-RNA profiling by 5' RACE and ONT MinION sequencing identified different proportions of pgRNA-derived transcripts according to HBeAg status and HBsAg level.

Conclusion: Our results indicate that EVs-enriched compartment also contributes to the circulation of HBV-RNAs. Moreover, different HBV-RNA transcripts in addition to pgRNA can be detected *in vivo*. Altogether, these data could significantly contribute to the characterization of cirB-RNAs as new viral biomarker.

THU307

Identification of shuttle protein hnRNPA1 as a modulating factor of circulating hepatitis B Virus RNAs release in chronic hepatitis B patients

Hyoseon Tak¹, Doohyun Kim¹, Delphine Bousquet^{1,2}, Marie-Laure Plissonnier¹, Françoise Berby¹, Bordes Isabelle¹, Aaron Hamilton³, Marantha Heil³, Massimo Levrero^{1,2,4}, Barbara Testoni¹, Fabien Zoulim^{1,2,5}. ¹Cancer Research Center of Lyon, Lyon, France; ²Université de Lyon, Lyon, France; ³Roche Diagnostics, Plesanton, United States; ⁴Sapienza University of Rome, Roma, Italy; ⁵Croix Rousse hospital, Lyon, France
Email: fabien.zoulim@inserm.fr

Background and aims: Circulating HBV RNA (CirB-RNA) reflects the transcriptional activity of the intrahepatic cccDNA, thus representing a promising non-invasive serum biomarker for the reduction or inactivation of cccDNA pool. Although several studies have suggested that cellular releasing pathways may determine the fate of these RNAs, the specific regulators of the shuttle machinery involved remain largely unknown.

Method: Expression of candidate shuttle proteins were analyzed by Western Blotting and RT-qPCR in cell lysate and supernatant from HBV-infected HepG2-NTCP cells and Primary human hepatocytes (PHHs). Shuttle protein interaction with CirB-RNAs was investigated by RNP-IP (Ribonucleoprotein-Immunoprecipitation) and Biotin pull down assay. Adapted Iodixanol/Sucrose density ultracentrifugation allowed to isolate exosome-enriched fractions from sera of 5 untreated [2 HBeAg (+) and 3 HBeAg (-)], 2 HBeAg (-) chronic infection and 2 NUC-treated chronic hepatitis B (CHB) patients.

Results: Among the RNA-binding proteins analyzed, heterogeneous nuclear ribonucleoprotein A1 (hnRNPA1) expression was increased in both cell lysates and supernatants of HepG2-NTCP cells and PHHs upon HBV infection. hnRNPA1 was also detected in the serum of CHB patients and, after density ultracentrifugation of serum samples, hnRNPA1 was mostly detected in the exosome-enriched fractions. Loss-of-function studies in HepG2-NTCP cells indicated that hnRNPA1 downregulation was associated to reduced expression of exosome markers CD9 and CD81 in cell supernatant, as well as a decreased secretion of CirB-RNA in exosome fractions. Anti-CD81 IP confirmed the association between hnRNPA1 and exosomes. RNP-IP experiments revealed that hnRNPA1 was able to bind to 5' region of 3.5Kb RNA and to the 3' region common to all HBV transcripts. Specific binding sites for hnRNPA1 on HBV RNAs were mapped by Biotin pull-down assays.

Conclusion: Altogether, our data suggest that hnRNPA1 directly binds to HBV RNAs and can function as a novel shuttling mechanism for the export of HBV RNAs in vivo.

THU308

Long-read sequencing of HCC samples reveals complete architecture of HBV integrations and chimeric mRNA isoforms associated with oncogenes

Cameron Soulette¹, Lindsey May¹, Atefeh Khakpoor², Dong Han¹, Ricardo Ramirez¹, Narmada Balakrishnan³, Nicholas Van Buuren¹, Ramanuj Dasgupta³, Vithika Suri¹, Li Li¹, Hongmei Mo¹, Becket Feierbach¹, Jeffrey Wallin¹, Seng Gee Lim². ¹Gilead Sciences, Inc., Foster City, United States; ²Yong Loo Lin School of Medicine, Singapore, Singapore; ³Genome Institute of Singapore (GIS), Singapore, Singapore
Email: cameron.soulette@gilead.com

Background and aims: Hepatitis B virus (HBV) integrations are associated with large-scale genomic rearrangements that dysregulate gene expression and are implicated in hepatocellular carcinoma (HCC). Our work is aimed towards understanding the development of oncogenesis mediated by HBV integrations by characterizing integrations in HCC patients. We use a long-read DNA and mRNA sequencing approach to characterize complete HBV integrations and their expression from paired tumor and adjacent tissue.

Method: HCC liver resections were collected from 20 patients, 15% were HBeAg-, 10% were treatment naïve, and 75% on nucleos (tide) analogue treatment. DNA and RNA were sequenced from tumor/tumor adjacent tissue. We enriched for HBV sequences using a pan-genotypic panel of biotinylated oligos from sheared genomic DNA (~7 kb) and polyA+ reverse transcribed cDNA. Samples were sequenced on the PacBio long-read platform and analyzed with a bioinformatic method for identification of VirAL Integrations AND Translocations (VALIANT). cDNA was also sequenced using standard Illumina RNA-Seq. We used Catalogue of Somatic Mutations in Cancer (COSMIC) to identify integrations near cancer-associated genes.

Results: We found that nearly all HBV DNA reads (avg. ~95%) from tumor and adjacent tissue were derived from integrated HBV. We found integration sites common to paired tumor and adjacent tissue in nearly half of samples. We found >20 COSMIC genes with nearby integrations, including *HLF*, *LRP1B*, *ERBB4*, and *TERT*. Moreover, we found numerous HBV-associated translocations, including a chromosome 1 to 3 translocation in *NAALADL2*, a known HBV integration hotspot. We further quantified the frequency of translocations and insertions in our HCC cohort and a cohort of chronic hepatitis B patients and found a higher translocation frequency in HCC samples (~30% vs 15%). Finally, our long-read RNA-seq data captured HBV transcripts chimeric with various genes, including HBV-TERT isoforms which coincided with elevated TERT expression measured by short-read RNA-seq.

Conclusion: We find a substantial amount of HBV integrations in tumors. Increased translocation frequency in tumors supports the hypothesis that HBV integrations may promote oncogenesis through genomic instability and highlights the importance of treatments that prevent HBV integration. Moreover, our observation of HBV-TERT chimeric isoforms and TERT upregulation strengthens the view that HBV integrations are a direct driver of HCC.

THU309

Polymorphic analysis of bulevirtide sequence in PreS1 of large HBsAg across HBV genotypes A-H

Roberto Mateo¹, Thomas Aeschbacher¹, Yang Liu¹, Simin Xu¹, Bin Han¹, Tahmineh Yazdi¹, Savrina Manhas¹, Lindsey May¹, Dong Han¹, Silvia Chang¹, Rishi Aryal¹, Ross Martin¹, Evguenia S Svarovskaia¹, Hongmei Mo¹. ¹Gilead Sciences, Inc., Foster City, United States
Email: roberto.mateo@gilead.com

Background and aims: Bulevirtide (BLV) is a novel 47-amino acid, N-terminally myristoylated lipopeptide that binds specifically to the sodium taurocholate cotransporting polypeptide (NTCP) and acts as a potent, highly selective entry inhibitor of HDV into hepatocytes. The BLV sequence was designed based on the consensus sequence of the preS1 domain of the large HBsAg (LHBsAg) of eight different genotypes of HBV (A-H). The aim of this study was to investigate the impact of polymorphisms found in the LHBsAg PreS1 region from HBV clinical isolates of eight HBV genotypes on susceptibility to BLV. **Method:** The polymorphic residues in BLV sequence region of Pre-S1 were identified using an alignment of 7427 PreS1 sequences of HBV genotypes A-H obtained from clinical isolates and public databases. HDV genotype 1 viruses containing these polymorphisms were generated by transient transfection and analyzed phenotypically for their susceptibility to BLV in an infectious assay using primary human hepatocytes.

Results: Polymorphic analyses of HBV sequences from genotypes A-H revealed a high degree of conservation of the 47aa long peptide, with a remarkable conservation of the sequence from positions 9-NPGLFFP-15, which is crucial for binding. Only one amino acid residue was found to be variable with a frequency above 5% for genotype A; genotypes B, C and D had 2, 5 and 2 amino acids above the 5% cut-off value, respectively. Within representative sequences for the most common genotypes A-D, genotype C was the closest to the BLV sequence with only one amino acid change (K57Q).

POSTER PRESENTATIONS

Genotypes A and B had 4 to 6 amino acid changes, respectively, and genotype D had 8. Despite their sequence differences, HDV genotype 1 viruses containing HBV genotype A-H preS1 representative sequences and the most prevalent HBV genotype A-D polymorphisms were fully susceptible to BLV with EC₅₀ values that ranged from 0.28 nM to 0.85 nM.

Conclusion: BLV demonstrated potent activity against HDV harboring the polymorphisms in the PreS1 region corresponding to the BLV sequence across HBV genotypes A-D, indicating the broad-spectrum antiviral activity of BLV for the treatment of patients infected with HDV viruses.

THU310

RIPK1 plays a survival role in the liver of mice with active HDV replication

Gracian Camps¹, Sheila Maestro², Carla Usai³, Mirja Hommel¹, Cristina Olague Micheltorena¹, África Vales Aranguren¹, Rafael Aldabe¹, Gloria González-Aseguinolaza¹. ¹CIMA Universidad de Navarra, Gene therapy and regulation of gene expression, Pamplona, Spain; ²Viralgene; ³Blizard Institute
Email: ggasegui@unav.es

Background and aims: Hepatitis delta virus (HDV) infection represents the most severe form of viral hepatitis; however, the molecular mechanisms involved in the severity of the disease remain unknown. The absence of mouse models in which HDV-induced liver damage occurs has prevented the study of this important aspect of the disease. We developed an adeno-associated virus (AAV)-mediated HDV/HBV co-infection model in which, for the first time, liver damage associated with HDV was detected in mice that was, at least partially, associated with TNF- α production. The aim of the present study is to elucidate the mechanisms involve in HDV-mediated liver damage.

Method: Replication competent HBV and HDV genomes were delivered to mouse hepatocytes using AAVs as shuttle vector to establish an active replication of both viruses. Using blocking agents, KO mice, and CRISPR Cas9 system to delete the expression of key molecules we evaluate the role of different players involve in hepatocytes death.

Results: Here, we report that TNF- α was mainly produced by liver macrophages and that the death of HDV-hepatocytes occurs predominantly by caspase-8 induced-apoptosis.

Upon AAV-HBV/HDV co-injection, RIPK1-edited mice presented with a significantly higher liver damage than mice receiving control CRISPR/Cas9, reflected by higher transaminase serum levels and an increased percentage of apoptotic hepatocytes, indicating that RIPK1 plays a significant role in hepatocytes survival in an HDV infected liver. The elimination of both caspase 8 and RIPK1 from hepatocytes resulted in the almost complete absence of hepatocytes death after AAV-HBV/HDV injection, which further corroborated caspase 8-induced apoptosis as the main cell death mechanism in RIPK1-edited mice. Surprisingly, the absence of TNF- α or the depletion of macrophages had no effect on the exacerbation of liver disease associated with the RIPK1 downregulation in hepatocytes. Interestingly depletion of macrophages had a significant detrimental effect, indicating that these cells play a protective role.

Conclusion: Our investigations demonstrate the protective role of RIPK1 in HDV-induced liver pathology and strongly suggest that the RIPK1-caspase-8 axis influences the pathogenesis of HDV infection. More experiments are needed for a better understating of the mechanism involved.

THU311

Limited value of HBV-RNA levels for the prediction of relapse after discontinuation of nucleos (t)ide analogue therapy in HBe antigen negative chronic hepatitis B patients

Valerie Ohlendorf¹, Maximilian Wübbolding¹, Christoph Hoener zu Siederdisen¹, Birgit Bremer¹, Katja Deterding¹, Heiner Wedemeyer¹, Markus Cornberg¹, Benjamin Maasoumy¹.

¹Hannover Medical School, Clinic of Gastroenterology, Hepatology and Endocrinology, Hannover, Germany

Email: ohlendorf.valerie@mh-hannover.de

Background and aims: EASL guidelines suggest that treatment with nucleos (t)ide analogue (NA) can be stopped in HBeAg negative patients after three years of viral suppression. Recently, the combination of HBsAg and HBV-RNA level at the time of NA cessation has been linked to a better prediction of off-treatment response compared to HBsAg alone in mixed cohorts of HBeAg negative and positive patients. In this study we investigated the association of relapse after NA cessation with baseline serum HBV-RNA level in a large cohort of HBeAg negative patients.

Method: Serum level of HBV-RNA, HBsAg and HBcrAg were determined in 154 HBeAg negative patients, participating in a prospective, multicenter therapeutic vaccination trial (ABX-203, NCT02249988) or in an observational register trial (Terminator 2), before stop of NA therapy. Importantly, vaccination showed no impact on relapse. HBV DNA >2,000 IU/ml 24 weeks after NA cessation was defined as virological relapse, while clinical relapse comprised attendant ALT levels $\geq 2 \times$ ULN. The lower limit for the quantification of HBV-RNA was 10 copies/ml. For the comparison of continuous and categorical variables the Mann-Whitney U and the Fisher's exact test were used. Kaplan-Meier analysis with the log-rank test was used for the calculation of cumulative relapse rates.

Results: The majority of patients were male (n = 115/154; 75%) with a median age of 53 years. Two thirds of patients were treated with entecavir (n = 94/154; 61%), while the rest received tenofovir. Median HBV-RNA, HBsAg and HBcrAg BL level was 0 copies/ml, 950 IU/ml and 1585 kU/ml, respectively. No significant correlation was found between HBV-RNA and HBsAg (r = -0.253, p = 0.055) or HBV-RNA and HBcrAg (r = 0.044, p = 0.73), respectively. Virological relapse occurred in 53% of patients (N = 82/154), including 8 patients (10%) developing an ALT flare. BL HBV-RNA level did not differ significantly between relapsers and off-treatment responders (p = 0.86) or between virological relapsers and clinical relapsers (p = 0.36), respectively. Further, no significant difference occurred in proportions of detectable HBV-RNA BL level between off-treatment responders (N = 10/72; 14%) and relapsers (N = 13/82; 16%) (p = 0.68). Relapse prediction could not be improved by combining predefined HBsAg cut-offs (100 IU/ml, p = 0.0016) or HBcrAg cut-offs (3 log U/ml, p = 0.07) with a HBV-RNA cut-off of ≤ 10 copies/ml (p = 0.0031) (figure).

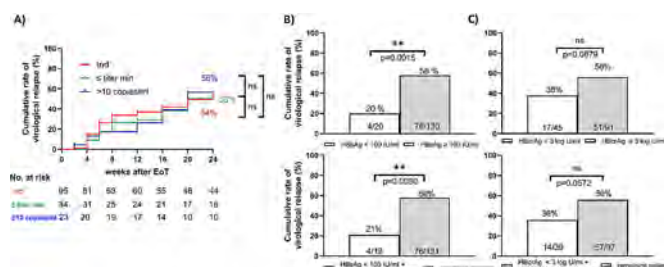


Figure: A) Cumulative relapse rates after NA cessation according to end of treatment (EoT) grouped by serum RNA baseline levels and proportion of patients with virological relapse grouped by B) BL HBsAg level \pm HBV-RNA level or C) BL HBcrAg level \pm HBV-RNA level.

Conclusion: In a cohort of exclusively HBeAg negative patients no improvement in relapse prediction was achieved by considering HBV-RNA BL levels.

THU312

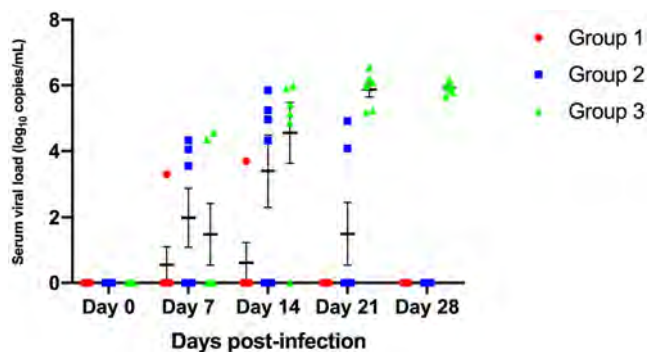
A versatile small animal immunocompromised model for chronic hepatitis E

Siddharth Sridhar¹, Shusheng Wu², Jianwen Situ². ¹The University of Hong Kong, Microbiology; ²The University of Hong Kong, Microbiology
Email: sid8998@hku.hk

Background and aims: Hepatitis E virus (HEV) is an important cause of chronic hepatitis in immunocompromised persons. We aimed to develop a small animal model of chronic hepatitis E using immunocompromised rats infected with *Orthohepevirus* species C (HEV-C; rat hepatitis E virus), which is an emerging cause of human hepatitis.

Method: Female 6–8 week old Sprague-Dawley rats were divided into 3 groups (6 rats per group): immunocompetent (group 1), low-dose immunosuppressed (group 2) and high-dose immunosuppressed (group 3). Rats in groups 2 and 3 were immunosuppressed using a combination of tacrolimus (5 mg/kg vs 7.5 mg/kg respectively), mycophenolate mofetil (25 mg/kg vs 30 mg/kg respectively), and prednisolone (10 mg/kg vs 4 mg/kg respectively). Drugs were administered 10 days prior to infection and continued thereafter. Filtered stool supernatants containing 2.5×10^5 copies/ml of HEV-C were administered to rats intravenously. Stool supernatants were either from infected humans (3 rats per group) or rats (3 rats per group). Stool and serum viral loads in infected rats were monitored. Antibody responses and liver tissue histology were assessed. Ethics approval was obtained.

Results: HEV-C infections in group 1 rats were fleeting with transient viremia (figure). Group 2 and 3 rats developed higher viral loads in both stool and serum (figure). No differences in viral loads between human or rat-derived HEV-C strains were observed. Most group 1 and 2 rats cleared virus from stool or serum by day 28, but group 3 rats maintained high viral loads in stool and serum throughout. Mean viral loads in liver tissue at day 28 were markedly higher in group 3 ($8.89 \log_{10}$ copies/ml) compared to group 1 ($3.76 \log_{10}$ copies/ml) and 2 ($4.35 \log_{10}$ copies/ml) rats; this was reflected by strongly positive immunohistochemical staining in liver tissue of group 3 rats. Western blot antibody responses to HEV-C were weaker in group 3 rats than group 1 rats. Alanine aminotransferase was similar in all 3 groups. The immunosuppressive regimen was tolerated well by rats in groups 2 and 3. A couple of rats in group 3 were monitored beyond day 28 and they supported viral infection for up to 3 months without any drop in viral loads.



Conclusion: We designed a versatile gradable immunocompromised rat model of chronic hepatitis E infection using immunosuppressants commonly taken by transplant recipients. This model will enable convenient investigation of pathogenicity and antivirals for HEV infections. This work establishes capacity to perform chronic HEV

research without using large animal models or genetically modified rats. Further evaluation of this model for studying antivirals is required.

THU313

Acquisition of positively charged amino acids in HBsAg C-terminus correlates with HBV-induced liver cancer, hampers HBsAg stability and secretion and promotes cell survival

Lorenzo Piermatteo¹, Luca Carioti¹, Gianluca Leoni¹, Leonardo Duca¹, Patrizia Saccomandi¹, Daniele Stella¹, Eleonora Andreassi¹, Ada Bertoli^{1,2}, Giuseppina Cappiello³, Hervé Fleury⁴, Pascale Trimoulet⁴, Simona Francioso⁵, Ilaria Lenci⁵, Massimo Andreoni⁵, Mario Angelico⁶, Sandro Grelli^{1,2}, Antonella Minutolo¹, Loredana Sarmati⁶, Claudia Matteucci¹, Francesca Ceccherini Silberstein¹, Valentina Svicher^{1,7}, Romina Salpini¹. ¹University of Rome "Tor Vergata", Experimental medicine, Rome, Italy; ²Tor Vergata University Hospital, Microbiology and Virology Unit, Rome, Italy; ³Sandro Pertini Hospital, Microbiology and Virology Unit, Rome, Italy; ⁴Hôpital Pellegrin tripode, Laboratoire de Virologie, Bordeaux, France; ⁵Tor Vergata University Hospital, Hepatology Unit, Rome, Italy; ⁶Tor Vergata University Hospital, Infectious Diseases Unit, Rome, Italy; ⁷University of Rome "Tor Vergata", Biology, Rome, Italy
Email: lorenzo.piermatteo@uniroma2.it

Background and aims: HBsAg C-terminus is a hydrophobic transmembrane domain, crucial for HBsAg secretion. Gain of charged amino acids (aa) in this domain can alter HBsAg folding, and in turn its secretion, a mechanism known to favor HBV-induced hepatocellular carcinoma (HCC). Here, we assess the role of HBsAg C-terminus mutations, associated with gain of charged aa, on HCC onset.

Method: We analyze HBsAg sequences from 807 CHB patients: 28 with HCC (78.6%D; 21.4%A) and 779 without HCC (79.8%D; 20.2%A). Impact of mutations on HBsAg-secretion is analyzed by transfecting Huh7 cells with plasmids encoding wt- and mutated-HBsAg. Extra- and intra-cellular HBsAg is quantified by Liaison immunoassay (DiaSorin) and used to define HBsAg secretion factor (extracellular/intracellular HBsAg). Cell viability after treatment with etoposide (a cell death inducer) was evaluated by MTS assay. HBsAg structure and stability was assessed by I-Tasser ($\Delta\Delta G[\text{wt-mutated}] < 0$ indicates decreased stability vs wt, Quan, 2016).

Results: The acquisition of ≥ 1 positively charged aa at HBsAg C-terminus positions 204, 207 and 210 strongly correlates with HCC (71.4% with HCC vs 30.2% without HCC, $P < 0.001$). Result confirmed by multivariable analysis ($\text{OR}[95\% \text{CI}]: 6.3[2.6-15.3]$, $P < 0.001$). These positively charged aa derive from S204R, S207R and S210R, found in 14.3%, 28.6% and 28.6% of HCCs, respectively.

In vitro, all these mutations determine a significant decrease in extracellular HBsAg compared to wt (42% for S204R, 39% for S207R and 32% for S210R, $P < 0.0001$ for all). Moreover, S204R and S210R cause a 58% and 28% reduction in HBsAg secretion factor respect to wt ($p < 0.0001$ and $P = 0.009$), reinforcing their detrimental role in HBsAg release.

Notably, despite etoposide treatment at 25 and 50 μM , S204R determines a 50% and 30% increase in cell viability respect to wt ($p < 0.001$ for both), supporting its ability to promote cell survival. Finally, in silico, S204R, S207R and S210R decrease HBsAg stability ($\Delta\Delta G[\text{S204R-wt}] = -0.27$; $\Delta\Delta G[\text{S207R-wt}] = -0.11$; $\Delta\Delta G[\text{S210R-wt}] = -0.14$) and determine a shortening of transmembrane motif (predicted length: aa209–224 for S204R, S207R and S210R vs 205–225 for wt).

Conclusion: Gain of positively charged aa in HBsAg C-terminus tightly correlates with HCC, hampers HBsAg release and promotes cell survival, thus potentially predisposing to HBV-related HCC. The detection of these mutations may help identifying patients at higher HCC-risk, deserving more intense liver monitoring.

THU314

PAGE-B and FIB-4 predict the occurrence of hepatocellular carcinoma in HBV patients: a french nationwide cohort study

Gautier Boillet¹, Mathieu Chalouni², Clovis Lusivka-Nzinga³, François Teoule³, Helene Fontaine⁴, Pierre Nahon⁵, Marc Bourliere⁶, Fabrice Carrat³, Stanislas Pol⁴, Victor de Ledinghen¹, Linda Wittkop².
¹Maison Du Haut-Lévêque-Haut-Lévêque Hospital Group Sud-Chu De Bordeaux, Pessac, France; ²ISPED, Bordeaux, France; ³Hospital Saint-Antoine Ap-Hp, UMR-S 1136, Paris, France; ⁴Gh Cochin-St Vincent De Paul, Hepatology, Paris, France; ⁵Hospital Jean-Verdier, UMR-1162, Bondy, France; ⁶Hôpital Saint Joseph, Hepatology, Marseille, France
 Email: boillet.gautier@yahoo.fr

Background and aims: Hepatocellular Carcinoma (HCC) is the first cause of death among chronic hepatitis B (CHB) patients. PAGE-B and FIB-4 may predict the occurrence of HCC among all CHB patients. We aimed to compare the predictive capacity of PAGE-B and FIB-4 for the occurrence of HCC in CHB patients at 1, 3 and 5 years of follow-up in the ANRS CO22 HEPATHER cohort.

Method: CHB patients included in the ANRS CO22 HEPATHER cohort between August 6, 2012 and December 31, 2015 were eligible. Exclusion criteria were chronic HCV, HDV co-infection, liver-transplantation, or history of HCC. Primary outcome was the time between inclusion and occurrence of HCC. Predictive performances were compared by the AUROC at year 1, 3 and 5. Two cutoffs were determined for each score, maximizing respectively sensitivity then specificity, to establish three different risk groups.

Results: Among 5, 214 patients, with a median follow-up of 5.6 years (IQR: 4.3–6.9), 69 experienced HCC. Median scores values were of 10 (IQR: 6–14) for PAGE-B and 1.0 (IQR: 0.7–1.5) for FIB-4. Corrected AUROCs of PAGE-B and FIB-4 at year 1, 3 and 5, were 0.91 (0.8–0.97), 0.85 (0.81–0.97) and 0.81 (0.76–0.86) and 0.85 (0.70–0.97), 0, 83 (0.77–0.89) and 0.80 (0.75–0.86), respectively. No significant difference between the AUROCs of the two scores was estimated at any time. Best cut-offs to identify patients at lower and higher risk of HCC were 10 and 18 for PAGE-B score, and 1.0 and 2.2 for FIB-4, respectively. Cumulative probability of HCC according to these new risk groups are depicted on the figure above.

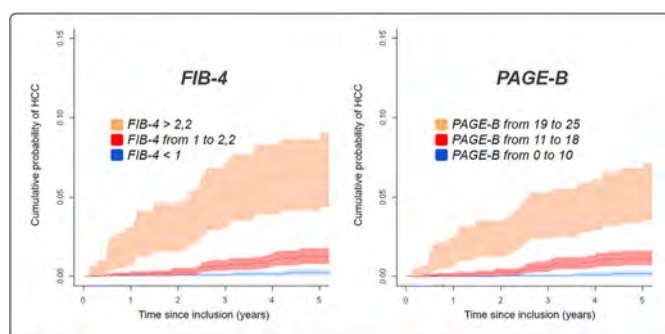


Figure: Incidence curves of HCC among low-risk groups (blue curves), intermediate risk groups (red curves) and high risk groups (orange curves) for PAGE-B and FIB-4, according to the new thresholds founded in the study.

Conclusion: PAGE-B and FIB-4 scores showed good and equivalent predictive performances for HCC in chronic hepatitis B patients in a French nationwide cohort, and could be used in clinical practice.

THU315

High tolerance of hepatitis E virus towards alcohol-based disinfectants

Patrick Behrendt^{1,2,3}, Martina Friesland², Jan-Erik Wissmann⁴, Volker Kinast⁴, Yannick Stahl², Dimas Praditya⁴, Lucas Hueffner², Pia Maria Nörenberg², Birgit Bremer¹, Benjamin Maasoumy^{1,3,5}, Jochen Steinmann⁶, Britta Becker⁶, Dajana Paulmann⁶, Florian H. H. Brill⁶, Joerg Steinmann^{7,8}, Rainer Ulrich⁹, Yannick Brueggemann⁴, Heiner Wedemeyer^{1,3}, Daniel Todt⁴, Eike Steinmann^{3,4}.
¹Hannover Medical School, Department of Gastroenterology, Hepatology and Endocrinology, Hannover, Germany; ²TWINCORE, Institute for Experimental Virology, Hannover, Germany; ³German Centre for Infection Research (DZIF), Germany; ⁴Ruhr University Bochum, Department of Molecular and Medical Virology, Bochum, Germany; ⁵Centre for Individualised Infection Medicine (CIIM), Hannover, Germany; ⁶Dr. Brill + Partner GmbH, Institute for Hygiene and Microbiology, Bremen, Germany; ⁷Paracelsus Medical University, Institute for Clinical Hygiene, Medical Microbiology and Infectiology, Nuernberg, Germany; ⁸University Hospital Essen, University of Duisburg-Essen, Institute of Medical Microbiology, Germany; ⁹Friedrich-Loeffler-Institut, Federal Research Institute for Animal Health, Institute of Novel and Emerging Infectious Diseases, Greifswald-Insel Riems, Germany
 Email: behrendt.patrick@mh-hannover.de

Background and aims: The Hepatitis E virus (HEV) is the most common cause of acute viral hepatitis worldwide and mainly transmitted via the fecal-oral route or consumption of contaminated food products. Due to the lack of efficient cell culture systems for the propagation of HEV, limited data regarding HEV sensitivity to chemical disinfectants are available. Consequently, preventive and evidence-based hygienic guidelines on HEV disinfection are lacking. In this study we evaluated different principal components of hand disinfectants as well as commercial hand disinfectants for their virucidal activity against HEV using a recently described high titer cell culture HEV model.

Method: We used a robust HEV genotype 3 cell culture model which allows quantification of viral infection of quasi-enveloped and naked HEV particles. For HEV genotype 1 infections the primary isolate Sar55 in a faecal suspension was applied. Standardized quantitative suspension tests using end point dilution and large-volume-plating were performed for the determination of virucidal activity of alcohols (1-propanol, 2-propanol, ethanol), WHO disinfectant formulations and five different commercial hand disinfectants against HEV. Iodixanol gradients were conducted to elucidate the influence of ethanol on quasi-enveloped viral particles.

Results: Naked and quasi-enveloped HEV was resistant to alcohols as well as alcohol-based formulations recommended by WHO. Of the tested commercial hand disinfectants only one product displayed a virucidal activity against HEV. This activity could be linked to phosphoric acid as essential ingredient. Finally, we observed that ethanol and possibly non-active alcohol-based disinfectants disrupted the quasi-envelope structure of HEV particles, while leaving the highly transmissible and infectious naked virions intact.

Conclusion: Different alcohols and alcohol-based hand disinfectants were insufficient to eliminate HEV infectivity with the exception of one commercially ethanol-based product which including phosphoric acid. These findings have strong implications for the efficient prevention measures to reduce viral transmission in clinical practice.

THU316

Multicentre performance evaluation of the Elecsys HCV Duo immunoassay

Mario Majchrzak¹, Korbinian Bronner², Syria Laperche³, Elena Riester², Ralf Bollhagen⁴, Markus Klinkicht⁴, Christian Voitenleitner⁵, Marion Vermeulen⁶, Michael Schmidt⁷.

¹German Red Cross Blood Donor Service West GmbH, Hagen, Germany;

²Labor Augsburg MVZ GmbH, Augsburg, Germany; ³National Institute of

Blood Transfusion, Paris, France; ⁴Roche Diagnostics GmbH, Penzberg,

Germany; ⁵Roche Diagnostics International Ltd, Rotkreuz, Switzerland;

⁶South African National Blood Service, Roodepoort, South Africa;

⁷German Red Cross Blood Donor Service, Frankfurt am Main, Germany
Email: m.schmidt@blutspende.de

Background and aims: This study evaluated the diagnostic accuracy of the Elecsys[®] HCV Duo immunoassay on the cobas e 801 analyser (Roche Diagnostics International Ltd) for the detection of hepatitis C virus (HCV) infection vs commercially available comparators.

Method: This international, multicentre study was conducted at seven sites (August 2020-March 2021). Blood donor samples and clinical laboratory samples (from routine diagnostic testing, pregnant women and patients on haemodialysis) were used for specificity analyses, while confirmed HCV-positive samples and seroconversion panels were used for sensitivity analyses. All samples were pseudonymised or fully anonymised residual serum or ethylenediaminetetraacetic acid-plasma. The Elecsys HCV Duo immunoassay was compared with two registered antigen-antibody (Ag-Ab) combination assays: the Monolisa HCV Ag-Ab ULTRA V2 and Murex HCV Ag/Ab Combination. The Elecsys HCV Duo immunoassay provides parallel, but separate, read-out of HCV Ag and Ab results (while other combination assays show a combined result only). We compared the HCV Ab (anti-HCV) module with the Elecsys Anti-HCV II and Alinity s Anti-HCV assays; no neutralisation method was available to test the HCV Ag module singularly.

Results: In all blood donor samples (n = 20634), the specificity of the Elecsys HCV Duo immunoassay was 99.94% (95% confidence interval [CI], 99.89–99.97). In all clinical laboratory samples (n = 2531), the specificity of both the Elecsys HCV Duo immunoassay and the Elecsys HCV Duo anti-HCV module was 99.92% (95% CI, 99.71–99.99), vs 99.84% (95% CI, 99.59–99.96) for the Monolisa HCV Ag-Ab ULTRA V2 and 99.76% (95% CI, 99.48–99.91) for the Elecsys Anti-HCV II assays, respectively. The sensitivity of the Elecsys HCV Duo immunoassay in confirmed HCV-positive samples (n = 257) was 99.6% vs 96.1% for the Monolisa HCV Ag-Ab ULTRA V2 assay. The Murex HCV Ag/Ab Combination assay could not detect 19% of the seroconversion panels and the Elecsys Anti-HCV II assay could not detect 20%. The former found HCV infections 2 days later (58 panels; 11 undetected) and the latter 18 days later (40 panels; 8 undetected) vs the Elecsys HCV Duo immunoassay.

Conclusion: The Elecsys HCV Duo immunoassay had comparable specificity and better sensitivity vs the comparator assays, including anti-HCV tests. The Elecsys HCV Duo immunoassay may be an alternative diagnostic tool in countries where nucleic acid testing is not possible.

THU317

Intrahepatic transcriptional profiling demonstrates preclinical models of chronic hepatitis B resemble different stages of natural history in humans

Ricardo Ramirez¹, Anastasia Hyrina², Rudolf Beran², Stephane Daffis², Sarah Gilmore², Don Kang², Noé Axel Montanari³, Nicholas Van Buuren², Li Li², Dara Burdette², Becket Feierbach², Andre Boonstra³, Simon Fletcher². ¹Gilead Sciences, Inc., Foster City, United States; ²Gilead Sciences, Inc., Foster City, United States; ³Erasmus MC, Rotterdam, Netherlands

Email: ricardo.ramirez@gilead.com

Background and aims: The woodchuck and adeno-associated virus HBV (AAV-HBV) models are commonly used to evaluate novel agents

for the treatment of chronic hepatitis B (CHB). However, the translational relevance of these models is not well understood. In this study, we compared the intrahepatic transcriptional profiles of the woodchuck and AAV-HBV models with a diverse group of CHB patients to determine which stage (s) of natural history they most closely resemble.

Method: Whole transcriptome profiling (RNA-Seq) was performed on liver biopsies from mice transduced with AAV-HBV (n = 8) or empty AAV (n = 8), as well as from woodchucks chronically infected with WHV (woodchuck hepatitis virus, n = 49) and from uninfected woodchucks (n = 9). These data was compared to a collection of human liver biopsies from healthy (n = 9), immune tolerant (IT, n = 15), immune active (IA, n = 15), inactive carrier (IC, n = 23), and HBeAg negative (ENEG, n = 16) donors. Pathway analysis was performed using gene set variation analysis (GSVA). Cell type deconvolution was performed using EPIC. Mouse livers were also analyzed by immunohistochemistry (IHC).

Results: Like most IT patients, AAV-HBV transduction only modestly altered the liver transcriptome, despite high intrahepatic expression of HBV RNAs. IHC confirmed there was little-to-no intrahepatic CD3⁺ T cell infiltration in this model. Consistent with previous studies, chronic WHV infection was associated with up-regulation of intrahepatic B cell, T cell and neutrophil gene signatures in woodchucks, as well as interferon and inflammatory response pathways. Globally, the intrahepatic transcriptional signature of chronically infected woodchucks was similar to IA and ENEG patients, although there were some important differences. Most notably, an intrahepatic neutrophil signature was present in chronically infected woodchucks but neither IA or ENEG patients.

Conclusion: Comparative intrahepatic transcriptional analysis revealed that the woodchuck and AAV-HBV models of CHB most closely resemble the IA/ENEG and IT stages of human disease, respectively. These fundamental differences in intrahepatic immune environment may impact the response to immune modulatory therapies.

THU318

Hepatitis B virus splice variants are associated with reduced likelihood of functional cure and differ across phases of chronic hepatitis B infection

Olivia Maslac¹, Josef Wagner², Vitina Sozzi², Hugh Mason², Evguenia S Svarovskaia³, Susanna Tan³, Anuj Gaggai³, Stephen Locarnini², Lilly Yuen¹, Margaret Littlejohn¹, Peter Revill¹.

¹The Peter Doherty Institute for Infection and Immunity, Victorian Infectious Diseases Reference Laboratory, Australia; ²The Peter Doherty Institute for Infection and Immunity, Victorian Infectious Diseases Reference Laboratory; ³Gilead Sciences, Inc., Foster City, United States
Email: peter.revill@mh.org.au

Background and aims: Chronic hepatitis B (CHB) is characterized by progression through different phases of hepatitis B virus (HBV) infection and disease. Although not necessary for HBV replication, there is increasing evidence that HBV splice variants are associated with liver disease progression and pathogenesis.

Method: Next generation sequencing data from 404 patient samples of HBV genotype A, B, C, or D in Phase I, Phase II or Phase IV of CHB was analysed for HBV splice variants. Sp1 may include minor splice variants Sp2 and Sp4 = Sp1*, Sp13 may include minor splice variants Sp7 and Sp8 = Sp13*, and Sp9 may include minor splice variants Sp 10 and Sp12 = Sp9*.

Results: HBV splice variants differed in frequency and type by genotype and phase of natural history. Splice variant Sp1 was the most frequently detected (206/404 51% of patients), followed by Sp13 (151/404 37% of patients). These splice variants were detected in all HBV genotypes, in all three CHB phases except in phase I for genotype A in contrast to Sp5 and Sp9*, which were detected only in genotypes B and C. The diversity of splice variants was greatest amongst genotypes B and C, with all splice variants identified, and lowest in

POSTER PRESENTATIONS

genotype D with only 2 splice variants identified (Sp1* and Sp13*). The frequency of variants was generally highest in Phase II (123/165 75% of patients), a phase typically associated with enhanced immune activation, followed by Phase I (69/99 70% of patients). In Phase II there was significantly higher number of patients with splice variants across all genotypes A to D compare to the number of patients without splice variants ($p = 0.0004$). Splice variants were associated with reduced hepatitis B e antigen (HBeAg) levels and statistically reduced likelihood of achieving HBsAg loss (functional cure) in Phase II patients for Sp1 and Sp13 ($p = 0.0014$ and 0.0156 , respectively, Figure 1 A and B).

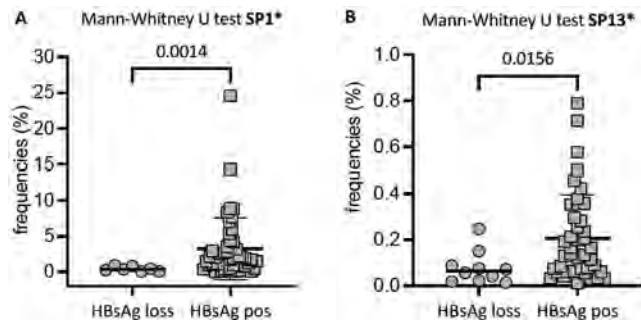


Figure 1: Sp1* and Sp13* found at statistically lower frequencies in HBsAg loss patients

Conclusion: HBV splice variants detected in patient serum are not merely a by-product of HBV replication, differing markedly by HBV genotype and phase of CHB natural history. Their frequency was generally highest in Phase II, the “immune clearance” phase of CHB natural history, suggesting an immune escape phenotype. The contribution of splice variants to the likelihood of achieving functional cure on therapy requires further investigation.

THU319

Understanding acute HCV infection kinetics in humanized mice via an agent-based modeling approach

Zhenzhen Shi¹, Yuji Ishida^{2,3}, Nicholson Collier^{4,5}, Michio Imamura^{3,6}, Chise Tateno^{2,6}, Jonathan Ozik^{4,5}, Jordan Feld⁷, Harel Dahari¹, Kazuaki Chayama^{3,8,9}. ¹Program for Experimental and Theoretical Modeling, Division of Hepatology, Department of Medicine, Stritch School of Medicine, Loyola University Chicago, Maywood, United States; ²PhoenixBio Co., Ltd., Higashi-Hiroshima, Japan; ³Research Center for Hepatology and Gastroenterology, Graduate School of Biomedical and Health Sciences, Hiroshima University, Hiroshima, Japan; ⁴Consortium for Advanced Science and Engineering, University of Chicago, Chicago, United States; ⁵Decision and Infrastructure Sciences, Argonne National Laboratory, Argonne, United States; ⁶Department of Gastroenterology and Metabolism, Applied Life Sciences, Institute of Biomedical and Health Sciences, Hiroshima University, Hiroshima, Japan; ⁷Toronto Centre for Liver Disease, Toronto, Canada; ⁸Collaborative Research Laboratory of Medical Innovation, Graduate School of Biomedical and Health Sciences, Hiroshima University, Hiroshima, Japan; ⁹RIKEN Center for Integrative Medical Sciences, Yokohama, Japan
Email: harel.dahari@gmail.com

Background and aims: uPA-SCID chimeric mice with humanized livers (SCID-MhL) are a useful tool for studying HCV infection in the absence of an adaptive immune response. Here we sought to analyse and model the HCV kinetics from inoculation to steady state in the uPA-SCID mouse model, using an agent-based modelling (ABM) approach.

Method: Ten male mice (5 PXB SCID-MhL with hepatocyte donor: JFC [1 year, male Caucasian] and human albumin >9 mg/ml, and 5 SCID mice without humanized livers, SCID-M) were inoculated intravenously with HCV (genotype 1a)-infected serum of 1×10^6 copies/animal. Viral levels were frequently measured from blood samples up

to 35 days post infection (p.i.). HCV RNA was measured using quantitative real-time PCR (qRT-PCR) as previously reported (BBRC. 2006; 346 (1):67–73). We developed an ABM that accounts for two types of agents: hepatocytes and virus in the blood, attempting to recapitulate the stochastic process of HCV infection of hepatocytes in mice. The ABM simulates a series of infection stages including initial infection of uninfected cells, infected cells in a non-productive viral eclipse phase, and infected cells in a productive infection phase releasing HCV virion, which then proceed to infect additional hepatocytes. Several model parameters (e.g., virion production cycle) were calculated based on the in vivo experimental design. Model parameter fitting was done using a Genetic Algorithm (GA) with the EMEWS framework on the Midway2 high-performance computing cluster at the University of Chicago.

Results: While in SCID-M HCV was rapidly cleared (Fig. 1a, dashed lines), a productive infection was established in SCID-MhL (Fig. 1a, solid lines). After an initial viral decline, the virus resurged, followed by a transient decline (in 4 mice) that eventually stabilized at high steady state levels (Fig. 1). To account for a transient decline, a decrease in viral production was assumed reminiscent of our previous observation of such transient HCV decline seen in chimpanzees (Gastroenterology; 128 (4):1056–66). The ABM quantitatively reproduces the multi-phasic HCV kinetic patterns observed (Fig. 1b and c). The ABM predicts that: (1) the viral eclipse phase lasts between 1 and 20 h; (2) Once the infected cell passes the eclipse phase, the viral production rate is not constant, but rather increases over time. Initially all mice started with a long production cycle of 1 virion per 9–15 h but gradually reaching 1 virion per hour after 12 hr; (3) Within 5 days, the virion production reaches a steady state production rate of 1–3 virions per hour in each infected cell; and (4) a viral production drop of 83%–98% starting between 2–5 days p.i. in 4 mice.

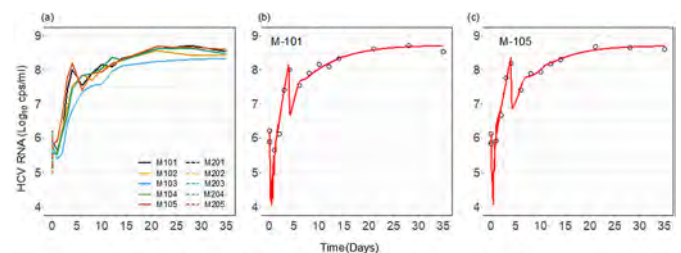


Fig 1: Kinetic and modeling of acute HCV infection in SCID mice. (a) HCV kinetics in SCID-M (dashed lines) and SCID-MhL (solid lines). (b and c) ABM calibration using GA approach (solid lines) with measured HCV kinetics (circles) in two representative SCID-MhL mice.

Conclusion: The ABM provides novel insights into the HCV life cycle in vivo. The model suggests a partial block of virion production possibly due to an early stage of innate immune response.

THU320

Presence of sodium taurocholate co-transporting polypeptide and hepatitis B replication markers on placenta: another home for the virus?

Garima Garg¹, Meenu Mn¹, Kajal Patel^{1,2}, Shashank Purwar¹, Sramana Mukhopadhyay³, Nitu Mishra⁴, Sumit Rawat⁵, Shashwati Nema², Debasis Biswas¹, Anirudh Kumar Singh¹, Ashish Kumar Vyas¹. ¹All India Institute of Medical Sciences Bhopal, Microbiology, India; ²All India Institute of Medical Sciences Bhopal, Pathology, India; ³All India Institute of Medical Sciences Bhopal, Pathology; ⁴Gandhi Medical College Bhopal, India; ⁵Bundelkhand Medical College Sagar, India
Email: a88_ashish@yahoo.co.in

Background and aims: The role of sodium taurocholate co-transporting polypeptide (NTCP), in facilitating the binding of the virus on surface of hepatocytes is well documented. Expression of NTCP in extra hepatic cells may make these cells susceptible to HBV

infection and support cellular proliferation akin to hepatocytes. *Placental replication of HBV is not well explored/studied.* In this study we have assessed the expression of NTCP and HBV replication markers (HBeAg, HBcAg, and HBV DNA) in placental cells, to investigate if these cells act as host/reservoir for HBV.

Method: Twenty HBsAg+ve pregnant women along with 10 healthy controls were enrolled after obtaining informed consent. The HBV DNA in placenta was detected by qPCR using primers for X and core ORF. Expression of NTCP in placenta was analyzed by qRT-PCR and was further investigated by immunohistochemistry (IHC) along with HBV replication biomarkers, HBsAg, HBeAg, and HBcAg.

Results: HBV infected females showed increased expression of NTCP in trophoblasts of placenta compared to control group (3.62 ± 0.96 Vs 1.44 ± 0.81). Furthermore, significant difference in NTCP expression was also observed between HVL and LVL group (3.62 ± 0.96 Vs 2.06 ± 1.3) and it was correlated with the maternal HBV DNA load. Membranous and/or Cytoplasmic immunostaining of NTCP, and cytoplasmic staining of HBeAg and HBcAg in trophoblasts along with presence of HBV DNA indicated that trophoblasts are not only susceptible to HBV infection but may also be a probable site for viral replication.

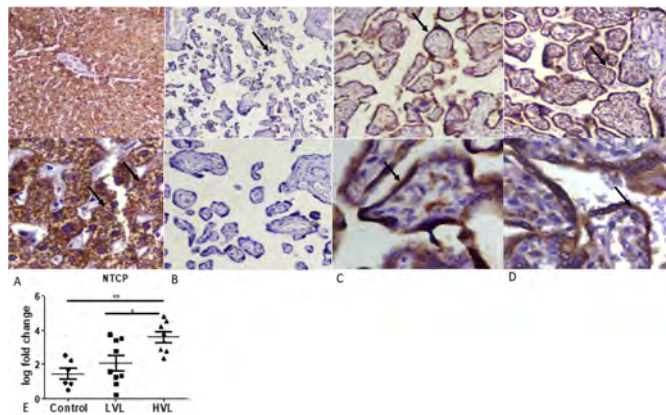


Figure: Fig. (A-D) NTCP Expression at 100X and 400X. A. NTCP expression in liver. B. NTCP expression in placenta of control. C. NTCP expression in placenta of Group B. D. NTCP expression in placenta of Group A. E. NTCP mRNA fold change among groups.

Conclusion: This is the pioneer study, which demonstrates expression of NTCP on placenta which may facilitate the entry of HBV. Furthermore, the study establishes the presence of HBeAg in trophoblasts indicating these cells may act as replication host/reservoir. Correlation of NTCP expression with maternal viral load and presence of HBeAg in placenta indicates its probable role in vertical transmission of HBV. Our preliminary finding suggest that NTCP blocking strategy may be used for therapeutic intervention of vertical transmission.

Disclosure-Conflict of interest: There are no conflict of interest among the authors.

THU321

Exploring dynamic changes in HBcAg and HBV RNA in e-Antigen negative HBV/HIV patients on antiretroviral therapy: still evidence of integrated activity after 5 years of treatment

Ruth Byrne¹, Mark Anderson², Gavin Cloherty², Kate Childs³, Ivana Carey³, Mark Nelson¹, Kosh Agarwal³. ¹Chelsea and Westminster Hospital, London, United Kingdom; ²Abbott Diagnostics, Department of Infectious Diseases, Chicago, United States; ³Kings College Hospital, Institute of Liver Studies, London, United Kingdom
Email: ruthbyrne@nhs.net

Background and aims: Hepatitis B core-related antigen (HBcAg) and pre-genomic (pg) HBV RNA are surrogates of covalently closed circular (ccc) DNA and have emerged as new HBV biomarkers. There

is growing evidence for their role in predicting treatment durability and successful cessation of nucleos(t)ide analogue therapy in chronic HBV. Limited data exist on their utility predicting outcomes in HBV/HIV co-infection. We aimed to evaluate the value of longitudinal measurement of HBcAg and HBV RNA in two cohorts of HBV/HIV co-infected patients.

Method: Two cohorts of e-antigen negative HBV/HIV co-infected patients were retrospectively studied. Patients were classified into 2 groups: those who started tenofovir (TDF) based antiretroviral therapy (ART) at baseline (Cohort A, n=30) and those already established on TDF based ART with suppressed HBV DNA for 5 years at baseline (Cohort B, n=37). HBcAg and HBV RNA were tested at baseline, year 3 and year 5. HBcAg was measured by automated CLEIA-method (Lumipulse G 1200 HBcAg, Fujirebio). HBV RNA was measured by real-time PCR research assay Abbott Diagnostic with LLQ 1.65 log₁₀ U/ml.

Results: Cohort A: at baseline 11 patients (37%) had undetectable HBcAg and 10 (33%) had HBV RNA below the limit of detection. After 3 years of ART all patients had completely suppressed HBV DNA, 40% still had detectable HBcAg and 43% had detectable HBV RNA. After 5 years of therapy there were still 10 patients (33%) with detectable HBcAg (median 4.4 log₁₀ U/ml; range 3.3–4.1) and 10 patients (33%) with detectable HBV RNA (median 1.96 (log₁₀ U/ml; range 1.78–3.6). Cohort B: at baseline all patients had been on TDF based ART for 5 years and had undetectable HBV DNA, 17 patients (46%) had undetectable HBcAg and 20 (54%) had HBV RNA below the limit of detection. After 3 years 45% still had detectable HBcAg and 32% had detectable HBV RNA. After 5 years, there were still 15 patients (41%) with detectable HBcAg (median 3.7 log₁₀ U/ml; range 3.0–5.4) and 11 (30%) with detectable HBV RNA (median 2.19 (log₁₀ U/ml; range 1.78–3.6). The impact of HBV genotype, pre therapy HIV viral load and nadir CD4 count on HBV markers in both cohorts was analysed and no significant effect found.

Conclusion: HBcAg and HBV RNA are sensitive biomarkers for continued transcription of cccDNA in HBeAg negative HBV/HIV co-infected patients despite long term suppression of HBV DNA by TDF based ART. TDF withdrawal studies are needed in HBV/HIV cohorts but as ART moves into a new era of TDF-sparing two drug regimens, these biomarkers may have clinical utility identifying those who can stop TDF safely with minimal risk of HBV reactivation.

THU322

Next-generation sequencing of Swiss HEV isolates allows for reconstitution of functional clones

Jérôme Gouttenoire¹, Roland Sahli², Daniela Müllhaupt¹, Montserrat Fraga Christinet¹, Darius Moradpour¹. ¹Lausanne University Hospital (CHUV) and University of Lausanne, Division of Gastroenterology and Hepatology, Lausanne, Switzerland; ²Lausanne University Hospital (CHUV) and University of Lausanne, Institute of Microbiology, Lausanne, Switzerland
Email: jerome.gouttenoire@chuv.ch

Background and aims: Hepatitis E acquired in Switzerland is caused primarily by a specific hepatitis E virus (HEV) subtype which has been provisionally designated as 3 s and recently assigned as a distinct group to 3 h (3 s[p]/h). Here, we analyzed HEV from patients with severe outcomes of hepatitis E by a newly developed next-generation sequencing (NGS) protocol and assembled subgenomic replicons as well as full-length clones.

Method: Illumina RNA sequencing coupled with HEV-specific sequence enrichment was carried out on plasma samples from 24 patients with hepatitis E acquired in Switzerland and severe outcomes (severe acute hepatitis, acute-on-chronic liver failure and neurologic complications). Viral genomes reconstituted by DNA synthesis and molecular cloning were functionally characterized in cell culture.

Results: The entire HEV genomes from plasma of 24 patients could be sequenced successfully, confirming the predominance of subtype 3 s

Conclusion: We were able to recapitulate, in cell culture models, the improved anti-HBV effect of combining Vonavexor and peg-IFN α . We also observed that the effect is achieved without inducing toxicity. This study provides support for the existence of a mechanism of action underlying the antiviral activity in combining Vonavexor and peg-IFN α , details of which should be explored further to eventually assist in identifying efficacy predictive factors in clinical trials.

THU325

Hepatitis Delta virus quasispecies conservation and variability in ribozyme region

Beatriz Pacín Ruiz^{1,2,3}, Maria Francesca Cortese^{1,2,3}, Sara Sopena Santistevé³, Josep Gregori¹, Selene Garcia-Garcia^{1,2,3}, David Tabernero^{2,3}, Rosario Casillas^{1,3}, Marta Vila^{1,3}, Ariadna Rando-Segura³, Adriana Palom⁴, Mar Riveiro Barciela⁴, Francisco Rodríguez-Frías^{1,2,3}, Maria Buti⁴. ¹Vall D'hebron Research Institute, Barcelona, Spain, Liver Unit, Barcelona, Spain; ²Instituto De Salud Carlos III, Madrid, Spain, Centro De Investigación Biomédica En Red, Enfermedades Hepáticas y Digestivas (CIBERehd), Madrid, Spain; ³Vall D'hebron University Hospital, Biochemistry and Microbiology/Liver Pathology Unit, Barcelona, Spain; ⁴Vall D'hebron University Hospital, Liver Unit, Internal Medicine Department., Barcelona, Spain
Email: beatriz.pacin@vhir.org

Background and aims: Around the 5% of hepatitis B virus (HBV) infected patients are co-infected with Hepatitis D virus (HDV). HDV genome is characterized by an 85 nucleotides-length domain with autocatalytic activity called ribozyme, which covers a key role in HDV replication. Of note, HDV presents a high rate of evolution and circulates as a mixture of variants forming a quasispecies (QS). Here, we analyzed by Next Generation sequencing (NGS) the ribozyme QS in longitudinal samples to study its conservation and identify possible mutations that could potentially affect HDV replication.

Method: Thirty-two patients with chronic hepatitis delta (CHD) were selected and two serum samples were collected per patient with a mean follow-up of 2.25 years. Viral genotype was determined by analyzing HDV delta antigen sequence. The HDV RNA region between nt 663 and 899, corresponding to ribozyme, was analyzed by NGS (MiSeq Illumina, San Diego, USA). Conservation was studied by calculating QS information content. Nucleotide substitutions were identified by aligning sample QS with its genotype consensus sequence.

Results: All patients were infected by genotype 1 HDV. A median of 5040 reads/sample was obtained. The ribozyme was overall highly conserved. A hyper-conserved region was identified between nt 715–745, whereas the more variable portion was between nt 739–769, although more the 90% of nt showed a maximum of conservation. When looking QS evolution between the two follow-up samples, limited distance was observed. Eleven mutations were observed. Of them, 3 mutations (T23C, T64del, and T69C) presented a high

frequency (respectively 5.51, 98.60, and 8.20%) in viral QS and were selected in the two patients' sample.

Conclusion: As expected and considering its role in viral replication, the ribozyme QS was highly conserved without changes between the two samples. The mutations observed interested domains involved in ribozyme excision activity (L3) and structural stabilization (P4), and they could potentially interfere with viral replication. Thanks to its high rate of conservation, the ribozyme could be a valuable target of gene therapy. Further *in vitro* studies are required to evaluate the effects of the mutations in HDV expression. Funding: Instituto de Salud Carlos III (grant PI17/02233), co-financed by the European Regional Development Fund (ERDF).

THU326

Exosomal cargo as a key player of the immune response after direct-acting antiviral treatment in chronic hepatitis C patients

Eirini Karamichali¹, Pelagia Foka¹, Vaia Valiakou¹, Petros Eiliadis², Domniki Loukaki-Gkountara¹, Konstantina Andresaki¹, Georgia Papadopoulou¹, Urania Georgopoulou¹, Ioannis-Georgios Koskinas³. ¹Hellenic Pasteur Institute, Molecular Virology, Athens, Greece; ²Hellenic Pasteur Institute, Laboratory of Molecular Biology and Immunobiotechnology, Athens, Greece; ³Medical School of Athens, Greece, 2nd Department of Internal Medicine, Hippokration General Hospital, Athens, Greece
Email: koskinasj@yahoo.gr

Background and aims: HCV infection causes severe liver disease. Direct-acting antivirals (DAAs) eradicate HCV but host immunity fails to fully recover. Exosomes are extracellular vesicles secreted by all cell types. They are masters of intercellular communication in health and disease. It has been demonstrated that HCV infection can be transmitted by exosomes between hepatocyte-like cells establishing a productive infection. Viruses exploit exosomes to establish persistent infection and escape the immune response. Exosomal cargo promotes disease progression possibly by "dampening down" host immune responses.

We aimed to elucidate the role of exosomes in the immune response of chronic HCV patients at various stages of liver fibrosis, before and after DAAs treatment.

Method: Whole blood from 40 chronic HCV patients with characterized fibrosis was collected before and after DAAs administration and used for isolation of exosomes and peripheral blood mononuclear cells. The existence of specific T-cell subpopulations was assessed by FACS. Exosomal cargo was analyzed for immunosuppressive factors by immunoblotting, FACS and ELISA.

Results: The (%) ratio of cytotoxic (CTL) over total T-lymphocytes (CD3/CD8) remained unaffected by DAAs treatment and fibrosis stage. Conversely, the Tregs (CD4/CD25/FOXP3) subpopulation post-DAAs treatment was statistically decreased in mild fibrosis (stages F0-F1-F2), but remained stable in advanced fibrosis and cirrhosis

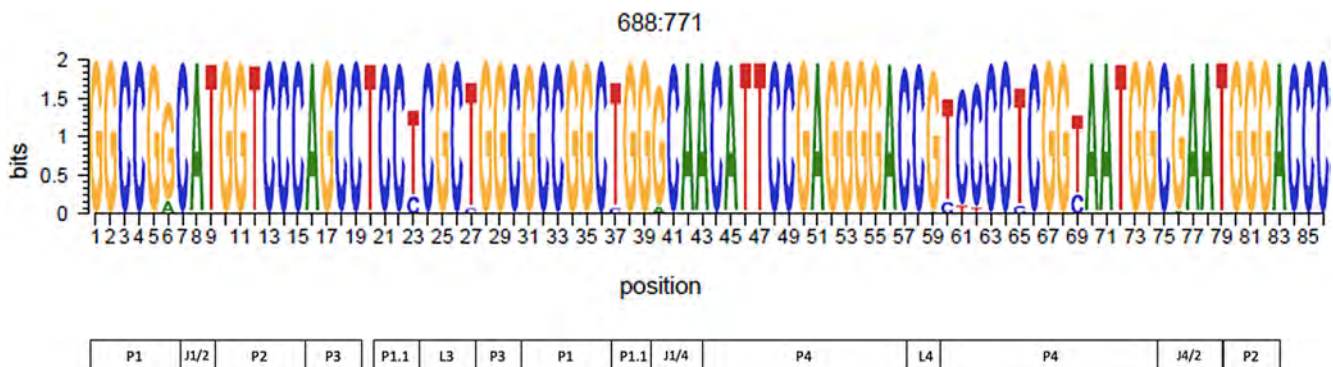


Figure: (abstract: THU325): Logo representation of the nucleotide sequence corresponding to the ribozyme region in the genomic sense (nt 688-771). At the bottom are indicated the different regions of the ribozyme and to which of them each nucleotide group corresponds

POSTER PRESENTATIONS

(stages F3–F4). Importantly, the active form of the immunosuppressive cytokine TGF- β was detected in the exosomal cargo and matching serum, albeit varying between fibrosis stages. We observed that the TGF- β levels of both sera and exosomes before DAAs treatment were statically increased in advanced fibrosis (F3). Treatment with DAAs statistically reduced serum TGF- β levels by 50% in the advanced stages of fibrosis and cirrhosis, whereas it did not alter TGF- β levels in exosomes in the different stages of fibrosis. Finally, we confirmed the presence of the immunosuppressive PD-L1 molecule in exosomes isolated from the same samples both before and after treatment.

Conclusion: HCV-manipulated exosomes may confer continuing immune suppression in the otherwise cured HCV patients bearing advanced liver disease. Despite DAA-mediated HCV eradication, the presence of immunosuppressive factors in the exosomal cargo supports the notion of a remaining “viral fingerprint” that could promote liver disease in susceptible individuals.

THU327

Therapeutic suppression of HBV transcripts promotes reappearance of the SMC5/6 complex and cccDNA silencing in vivo without affecting posttranslational modifications of cccDNA-bound histones

Lena Allweiss^{1,2}, Moritz Calaminus¹, Katja Giersch³, Tassilo Volz¹, Andrea Piroso⁴, Marc Luetgehetmann^{2,3}, Maura Dandri^{1,2}. ¹University Medical Center Hamburg-Eppendorf, I. Department of Internal Medicine, Hamburg, Germany; ²German Center for Infection Research (DZIF), Hamburg-Lübeck-Borstel-Riems, Germany; ³University Medical Center Hamburg-Eppendorf, Department of Medical Microbiology, Virology and Hygiene, Germany; ⁴Leibniz Institute for Experimental Virology, Department of Viral Immunology, Hamburg, Germany
Email: l.allweiss@uke.de

Background and aims: There is a strong need to explore interventions able to suppress the hepatitis B virus (HBV) reservoir, the cccDNA, since its silencing may promote a functional cure of chronic hepatitis B (CHB). We previously showed that treatments with siRNA targeting all HBV transcripts or pegylated interferon α (peg-IFN α) strongly reduce all HBV markers, including HBx, thus enabling reappearance of the host restriction factor “structural maintenance of chromosome 5/6” (SMC5/6) complex and cccDNA suppression in vivo (Allweiss/Giersch, Gut 2021). The aim of this study was to investigate the epigenetic landscape of cccDNA-bound histones in HBV-infected humanized mice after siRNA or peg-IFN α treatment.

Method: HBV-infected human liver chimeric mice received siRNA or peg-IFN α for 4 or 6 weeks, respectively, or were left untreated. RNA in situ hybridisation demonstrated suppression of HBV transcripts in human hepatocytes. Active and repressive posttranslational modifications (PTMs) of cccDNA-bound histones and SMC5/6 occupancy were analysed by chromatin immunoprecipitation-qPCR (ChIP-qPCR) and compared with PTMs on host genes.

Results: In untreated mice with high HBV replicative activity, canonical transcriptionally active PTMs (H3K27ac, H3K4me3) were highly enriched on the cccDNA minichromosome while the repressive mark H3K27me3 was undetectable. This pattern was consistent with active transcription and similar to the active host gene promoter GAPDH. Remarkably, neither siRNA nor peg-IFN α provoked significant PTM changes on the cccDNA despite strong reduction of HBV transcription. Consistent with previous results, only NSE4 occupancy, a subunit of the SMC5/6 complex, became detectable on the cccDNA after siRNA and peg-IFN α treatment.

Conclusion: Despite shutting down cccDNA transcription in a great proportion of human hepatocytes, siRNA or peg-IFN α treatment did not alter the pattern of the analysed cccDNA-bound histone PTMs. In line with the function of SMC5/6 as a DNA micro-compaction machine (Serrano, Molecular Cell 2020), the data suggest that SMC5/6 could mediate silencing through physical cccDNA compaction rather than through epigenetic changes.

THU328

Updated national prevalence estimates of chronic hepatitis B virus infection in countries within the European (EU) and European Economic Area (EEA): a systematic review

Sandra Bivegute^{1,2}, Adam Trickey¹, Zak Thornton¹, Becky Scanlan¹, Anna McNaughton¹, Aaron G. Lim¹, Lina Nerlander³, Hannah Fraser¹, Josephine Walker¹, Matthew Hickman^{1,2}, Peter Vickerman^{1,2}, Helen Johnson³, Erika Duffell³, Ellen Brooks-Pollock¹, Hannah Christensen¹. ¹University of Bristol, Population Health Science, Bristol Medical School, Bristol, United Kingdom; ²University of Bristol, NIHR HPRU in Behavioural Science and Evaluation, Bristol, United Kingdom; ³European Centre for Disease Control, Stockholm, Sweden
Email: hannah.christensen@bristol.ac.uk

Background and aims: Hepatitis B virus (HBV) is a leading public health problem globally. In Europe, the burden of HBV disproportionately affects at-risk groups, including men who have sex with men (MSM), migrants and prisoners. There are no recent population-level estimates of HBV prevalence in Europe.

Method: We undertook a systematic review to update estimates of chronic HBV (CHB) prevalence for the EU/EEA and UK in key sentinel and at-risk population groups. Databases were searched for original research articles in English published between 1/1/2018 to 24/2/2021. Titles and abstracts were screened to identify articles containing relevant information on CHB prevalence in Europe as measured by HBsAg status, with full text screening undertaken to confirm inclusion. Sentinel groups included first-time blood donors (FTB), general population (GP) and pregnant women; at-risk groups included MSM, migrants and prisoners. The updated estimates were incorporated into an existing HBV prevalence database (spanning 2005–2017) developed by the European Centre for Disease Control using the same inclusion/exclusion criteria. External grey literature data were obtained from country experts.

Results: A total of 5678 articles were title and abstract screened, of which 307 were full-text screened. A total of 41 published studies were included in the review, consisting of studies in GP (n = 12), migrants (n = 17), pregnant women (n = 5), MSM (n = 3) and prisoners (n = 4). Additional estimates from grey literature were also included (n = 109), comprising of GP (n = 11), migrants (n = 7), pregnant women (n = 16), MSM (n = 6), prisoners (n = 8) and FTB (n = 61). Weighted CHB prevalence estimates from the existing and updated database indicated a low HBV prevalence ($\leq 2\%$) among sentinel populations in all regions with exceptions in Romania, Bulgaria, Italy and Greece (reported prevalences 3.4–7.6%). Prevalence among prisoners varied considerably across all regions (range 2.1–25.2%) and 56% countries lacked data. Studies among migrants recorded some of the highest HBV prevalences, and estimates in this sub-population were typically higher in Southern European regions (range 5.0–12.2%). Reported HBV prevalence among MSM was low ($\leq 2\%$), except in Belgium and Estonia (range 2.3–3.4%). Studies on MSM and migrants were absent in Eastern Europe.

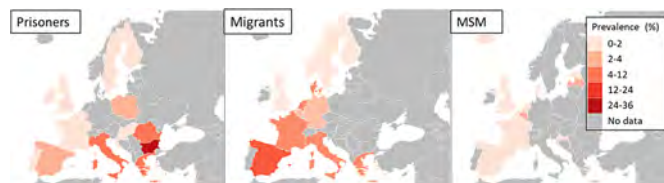


Figure: Updated HBsAg prevalence estimates in high-risk groups in the EU/EEA and UK. Maps show the weighted average prevalence in each country.

Conclusion: This review builds on previous estimates in the EU/EEA and UK, providing an additional 150 prevalence estimates across the region (updated total; n = 582). HBV prevalence was higher in Southern and south-Eastern Europe compared to other regions. Furthermore, CHB prevalence remains high among high-risk groups,

indicating that further interventions targeting these groups are required to reduce the burden of HBV in Europe.

THU329

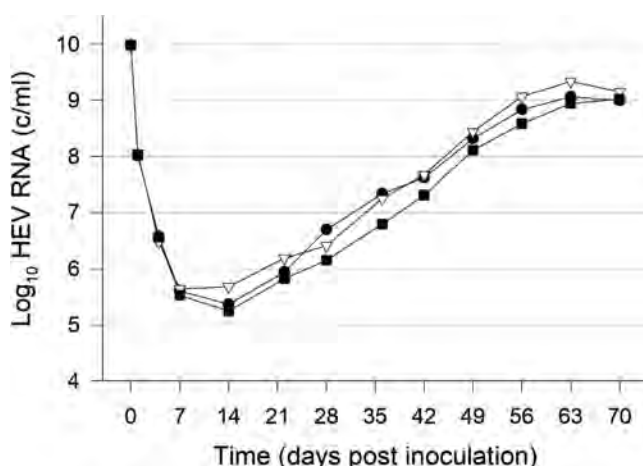
Relevance of HEV detection in ejaculate of chronically infected patients

Mathias Schemmerer¹, Marc Luetgehetmann², Hans Bock³, Jörn Schattenberg⁴, Samuel Huber⁵, Susanne Polywka², M Mader⁵, Ansgar Lohse⁵, Daniel Todt^{6,7}, Eike Steinmann⁶, Jürgen Wenzel¹, Thomas Horvatits⁵, Sven Pischke⁵. ¹University Medical Center Regensburg, Institute of Clinical Microbiology and Hygiene, National Consultant Laboratory for HAV and HEV, Regensburg, Germany; ²University Hospital Hamburg-Eppendorf, Microbiology, Germany; ³University Hospital Düsseldorf, Gastroenterology, Germany; ⁴University Medical Center Mainz, Gastroenterology, Germany; ⁵University Medical Center Hamburg-Eppendorf, Department of Medicine, Germany; ⁶Ruhr-University Bochum, Department of Molecular and Medical Virology, Germany; ⁷European Virus Bioinformatics Center (EVBC), Jena, Germany Email: mathias.schemmerer@ukr.de

Background and aims: Recently, HEV particles have been detected in the ejaculate of 2 out of 3 chronically infected patients. HEV RNA in the ejaculate can be significantly higher than in serum or plasma. However, it was unclear whether these viral particles in the ejaculate are infectious, and how often HEV generally occurs in the ejaculate of chronically infected individuals.

Method: After a previous cell culture model failed to demonstrate the infectivity of HEV particles from the ejaculate of two chronically infected patients (Horvatits et al. Journal of Hepatology 2021), we now used an alternative cell culture model based on overconfluent PLC/PRF/5 cells (Schemmerer et al. Viruses 2019) to study these particles for infectivity. Furthermore, we monitored HEV viral load in blood, urine, stool and ejaculate in 9 chronically HEV infected patients.

Results: For the first time, HEV particles from ejaculate were shown to be infectious in overconfluent PLC/PRF/5 cells (figure). HEV replicated to high viral loads of 10e9 HEV RNA copies per ml. Moreover, HEV was detected in the ejaculate of 7 out of 9 chronically infected patients (age 36–67 years, median 56 years). In 5 of the patients the viral loads were significantly higher (more than 2 log) compared to their serum, while in 2 patients, viral loads were lower than in their serum (more than 1 log).



Conclusion: In the context of chronic HEV infection, HEV particles can be detected in the ejaculate of 78% (7/9) of infected men, usually with significantly higher viral loads than in serum. In this regard, it should be noted that the gap between high viral load in ejaculate compared to viral load in blood may even be much higher than previously suspected. After the infectivity of HEV particles from

ejaculate could not be demonstrated so far, it could now be shown that they are infectious in PLC/PRF/5 cells. While there is probably no danger from this ejaculate for immunocompetent sexual partners, safer sex practice should be followed if the sexual partners are immunocompromised.

THU330

HDV-mediated inhibition of HBV in superinfection mouse model: the role of type I Interferon

Beatriz Pacín Ruiz^{1,2,3}, Gracián Camps⁴, Maria Francesca Cortese^{1,2,3}, Josep Gregori^{1,2}, David Tabernero^{1,3}, Selene Garcia-Garcia^{1,2,3}, África Vales Aranguren⁴, Cristina Olague Micheltorena⁴, Ariadna Rando-Segura¹, Josep Quer^{2,3}, Rafael Esteban^{3,5}, Mar Riveiro Barciela^{3,5}, Maria Buti^{3,5}, Gloria González-Aseguinolaza⁴, Francisco Rodríguez-Frías^{1,2,3}. ¹Vall D'Hebron University Hospital, Biochemistry and Microbiology/Liver Pathology Unit, Barcelona, Spain; ²Vall D'Hebron Research Institute, Liver Unit, Barcelona, Spain; ³Instituto De Salud Carlos III, Centro De Investigación Biomédica En Red, Enfermedades Hepáticas Digestivas (CIBERehd), Madrid, Spain; ⁴University of Navarra, Center for Applied Medical Research (CIMA), Pamplona, Spain; ⁵Vall D'Hebron University Hospital, Liver Unit, Department of Internal Medicine, Barcelona, Spain Email: beatriz.pacin@vhir.org

Background and aims: While Hepatitis B virus (HBV) replication does not significantly activate the innate immune response, it has been observed that in the presence of Hepatitis Delta virus (HDV) there is an increased type I interferon (INF) response. The aim of this study is to analyze the potential role of the INF response on the HBV inhibition upon HDV super-infection in a novel HBV-expressing transgenic (HBVtg) mouse model knock out for the INF alpha-receptor (IFNαR KO).

Method: Wild type (WT) and IFNαR KO HBVtg mice were intravenously administered with 5×10^{10} viral genomes of adeno-associated vector (AAV) expressing luciferase (LUC) or HDV. While Hepatitis B viremia was weekly monitored during the experiment, liver HBcAg expression and HBV-DNA levels were analyzed at 21 days after AAV injection. At this timepoint, the complexity of the HBV quasispecies (QS) at the 5' (nt 1255–1611) and 3' (nt 1596–1912) ends of the X gene of intrahepatic RNA was analyzed by next-generation sequencing (NGS) (MiSeq Illumina, San Diego, USA). Nucleotide substitutions were identified by aligning sample QS with its genotype master sequence and QS complexity was calculated using Rare Haplotype Load (RHL) index (threshold 1%).

Results: Both liver HBcAg expression and viremia was higher in HBVtg × IFNαR KO than in WT HBVtg mice under steady state conditions. AAV-HDV injection induced the decrease of hepatic HBcAg expression and HBV-DNA levels in HBVtg mice. This effect disappeared in HBVtg × IFNαR KO mice. Likewise, viremia was reduced from day 7, reaching the lowest levels at day 21 after vector administration in HBVtg mice, while HBV serum levels in HBVtg × IFNαR KO animals remained constant until the end of the experiment. Similar ALT serum levels presented by HBVtg and HBVtg × IFNαR KO mice excluded differential liver damage as the reason for the HBV repression observed in HBVtg animals. An average higher number of changes was observed in 5'HBX region than in 3'HBX region (42.72 vs. 15.61). In 5'HBX the RHL index was higher in presence of HDV. This index was even more pronounced in wt HBVtg than IFNαR KO.

Conclusion: The limited inhibition of HBV expression in presence of HDV in IFNαR KO mice suggested that IFN type I is essential for HDV-mediated HBV inhibition. The higher QS variability in presence of HDV might contribute to the inhibition of HBV replication. This variability is more pronounced in wt mice, thus suggesting a possible role of IFN-dependent activation of mutagenic enzymes. Further studies are required to better characterize the molecular mechanisms involved in HBV inhibition and variability, and to identify novel therapeutic strategies for HDV-infected patients. Funding: Instituto

POSTER PRESENTATIONS

de Salud Carlos III (grant PI18/01436), co-financed by the European Regional Development Fund (ERDF).

THU331

Assessment of Myrcludex or heparin antiviral activity on HBV infection using a 3-dimensional primary human hepatocyte culture system

Juliette Besombes¹, Charlotte Pronier¹, Jeremy Bomo¹, Philippe Gripon¹, Vincent Thibault¹. ¹CHU Rennes-Pontchaillou Hospital, Virology, Rennes, France
Email: vincent.thibault@chu-rennes.fr

Background and aims: Despite effective vaccination, Hepatitis B Virus (HBV) infection remains responsible for significant morbidity and mortality worldwide. Robust *in vitro* models mimicking the complex liver architecture are still lacking and culture of differentiated primary human hepatocytes (PHH) remains fastidious. Three dimensional (3D) culture models of PHH have been developed offering a microenvironment closer to *in vivo* conditions. Here, we describe the characterization of a 3D cell culture model based on the formation of PHH spheroids supporting HBV infection. We focus on the effect of Heparin and Myrcludex B (MyrB) on HBV infection.

Method: PHH (freshly collected or cryopreserved) were first incubated overnight in ultra-low-attachment plates to make them aggregate in spheroids before being embedded in a collagen matrix. HBV infection was performed 2 days after seeding using a 50-fold concentrated culture supernatant of HepG.2.2.15 cells or HBV purified from chronically infected patients' plasmas using different multiplicity of infection (MOI). Susceptibility to infection was monitored by HBe antigen (HBeAg) secretion in the supernatant. HBV infection under different concentrations of Heparin (4 and 133 µg/ml) or MyrB (50 to 800 nM) was evaluated.

Results: After defining the optimal MOI of 400 HBV genome equivalents (GE)/cell, long-term HBV infections for at least 38 days were obtained with this model. The dose-response study showed that infections at a low MOI of 10 GE/cell, similar to the one used *in vivo* in animal models, were possible even though HBeAg secretion remains weak. We confirmed that high concentration of heparin (133 µg/ml) blocked HBV infection leading to 85% inhibition of HBeAg secretion ($p < 0.05$) at 14 days post infection (dpi). Conversely, heparin at therapeutic concentration (4 µg/ml) in the culture medium promoted infection with a 130% increase in HBeAg secretion ($p < 0.05$). In this model, 50 nM MyrB efficiently blocked HBV infection with an average inhibition of HBeAg secretion of 63%, at 7 dpi. An increase of MyrB concentration from 50 to 800 nM did not improve the inhibition of infection. The level of HBeAg secretion was comparable when MyrB (100nM) was present only at the time of infection or maintained throughout the culture duration with an inhibition of HBeAg secretion of 84% at 14 dpi, whatever the condition. Adjunction of MyrB in the culture medium at 4 and 8 dpi resulted in a decrease in HBeAg secretion of 61% and 25%, respectively, at 14 dpi ($p < 0.05$ compared to without MyrB).

Conclusion: This 3D PHH culture system supports long-term HBV infection. Activity of MyrB even when added at distance from infection suggests late or secondary infections. Heparin activity on HBV infection depended on its concentration in the medium, yet the mechanism underlying this effect remains partially unexplained. Optimization and characterization of this model are warranted.

THU332

Concordance of the Xpert hepatitis B viral load test and conventional quantitative PCR in detecting and quantifying viremia using stored plasma and dried blood spot samples in West Africa

Gibril Ndow¹, Amie Ceesay¹, Yusuke Shimakawa², Alpha Omar Jallow¹, Haddy Nyang¹, Baboucarr Bittaye¹, Francis Mendy¹, Ousman Secka¹, Umberto D'Alessandro¹, Mark Thursz³, Isabelle Chemin⁴, Maud Lemoine³. ¹MRC Unit The Gambia at LSHTM, Disease Control and Elimination, Fajara, Gambia; ²Institut Pasteur, Unité d'épidémiologie des maladies émergentes, Paris, France; ³Imperial College London, Metabolism, Digestion and Reproduction, London, United Kingdom; ⁴INSERM U1052, Center de Recherche en Cancérologie, CNRS UMR5286, Lyon, France
Email: gibril.ndow@lshtm.ac.uk

Background and aims: The new Xpert hepatitis B virus (HBV) viral load test (Cepheid, USA) provides an opportunity to scale up and decentralise hepatitis B diagnosis, treatment and monitoring in resource-limited settings where HBV is endemic and molecular diagnostics to quantify HBV DNA are scarce. We assessed the concordance between the new Xpert HBV viral load test and the conventional quantitative PCR (Abbott, USA) in quantifying HBV viremia using stored plasma and dried blood spot (DBS) samples.

Method: Paired plasma and DBS (Whatman 903 Protein Saver cards) samples were collected from adults with chronic HBV infection followed up in the PROLIFICA (Prevention of Liver Fibrosis and Cancer in Africa) programme in The Gambia. Samples were stored in – 80°C for at least 12 months before analysis.

For each plasma sample, HBV DNA was quantified using both realtime qPCR (Abbott, detection limit 26 IU/ml in plasma) and Xpert (detection limit 3.2 IU/ml in plasma). For DBS, HBV DNA was quantified using Xpert.

Concordance of the Xpert HBV test and the conventional qPCR in detecting and quantifying HBV viremia in plasma was assessed by kappa statistics, and the agreement between the two assays was assessed using the Bland-Altman plot. The concordance of HBV viremia between paired plasma and DBS samples was also assessed by kappa statistics.

Results: We analysed 266 stored plasma samples from patients at various hepatitis B disease stages. Of these, HBV viral load results were concordant between the Xpert and the conventional qPCR: 130 (48.9%) and 63 (23.7%) were detectable and undetectable by both assays, respectively. The results were discordant in 71 (26.7%) samples that were detectable by Xpert but not qPCR, and 2 (0.8%) samples that were detectable by qPCR but not Xpert. In 110 samples with quantified viral load results from both assays, the mean difference between the two assays was 0.316 log IU/ml (95% limits of agreement – 1.189, 1.820) with only 6/110 results (5.45%) being outside the limits of agreement (figure 1), indicating good agreement.

From 91 paired plasma and DBS samples analysed by Xpert assay, the mean bias between plasma and DBS was statistically significant at +1.831 log IU/ml (95% limits of agreement: 0.660–3.001). Bias was smaller at lower viral loads. The kappa statistic was 0.10 indicating very poor agreement between results. After excluding samples with error or invalid result by either sample type ($n = 40$), kappa statistic was 0.34 indicating a poor agreement.

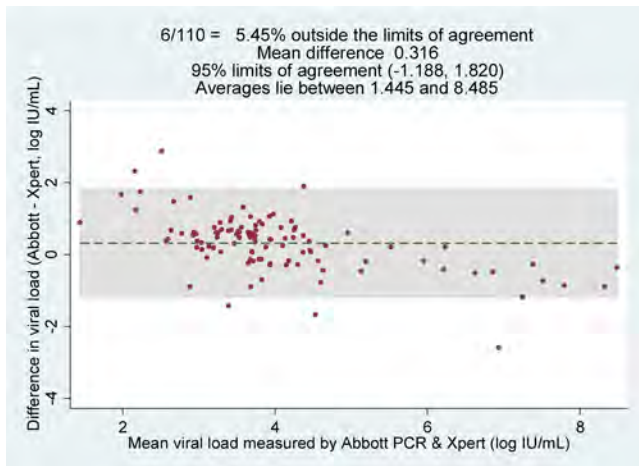


Figure 1: Bland-Altman plot of Xpert HBV minus Abbott qPCR (vertical axis) against mean of Xpert HBV and Abbott qPCR (horizontal axis) for samples with detectable viral load ($n = 110$).

Conclusion: The Xpert HBV DNA test provides a reliable alternative for detecting and quantifying HBV DNA viral load using stored plasma samples. However, the assay is not reliable for detecting viremia from DBS samples.

THU333

A high-throughput viral integration sequencing method reveals that mitochondrial DNA is frequently targeted by HBV integration

Domenico Giosa¹, Daniele Lombardo¹, Cristina Musolino², Valeria Chines¹, Giuseppina Raffa¹, Deborah D'aliberti³, Francesca Casuscelli di Tocco¹, Carlo Saitta¹, Riccardo Aiese Cigliano⁴, Orazio Romeo⁵, Angela Alibrandi⁶, Giuseppe Navarra², Giovanni Raimondo¹, Teresa Pollicino². ¹University Hospital of Messina, Clinical and Experimental Medicine, Messina, Italy; ²University Hospital of Messina, Human Pathology, Messina, Italy; ³University of Milano Bicocca, DIPARTIMENTO DI MEDICINA E CHIRURGIA (SCHOOL OF MEDICINE AND SURGERY), Milan, Italy; ⁴Sequentia Biotech SL, Barcelona; ⁵University of Messina, Dipartimento di Scienze chimiche, biologiche, farmaceutiche e ambientali, Messina, Italy; ⁶University of Messina, Dipartimento di Economia, Messina, Italy
Email: tpollicino@unime.it

Background and aims: Although research on HBV DNA integration has made relevant progress, important aspects remain unclear. Development of new integration detection methods may help in improving knowledge in the field and in better understanding HBV-related tumorigenesis. Our aim was to conduct a high-throughput integration detection on tumor (T) and non-tumor tissues (NT) from HBsAg-positive patients using a highly sensitive method for assaying HBV integration.

Method: We studied T from 7 patients with HBV-related HCC and paired NT from 6 of the 7 cases. HBV integration sites were recovered by semi-nested ligation-mediated PCR from host DNA (fragmented by sonication and ligated to asymmetric DNA linkers) and the use of forward or reverse HBV-specific primers. Targeted sequences were further enriched by nested-PCR with forward or reverse MiSeq HBV primers and forward or reverse MiSeq plinkers. PCR products were subjected to paired-end sequencing, and reads were aligned to a hybrid genome including human genome (GRCh38.p10) and HBV genome (NC_003977).

Results: A total of 3,339 unique HBV integration sites were detected in the 7 patients: 2,913 integrations in T and 426 in NT. The average number of integration sites in T and NT was 416 and 71, respectively. All patients had HBV integrations, with an average of 256.8 integrations per individual patients. The detected integration sites were randomly distributed across the whole genome and no hotspot was detected. Compared to individual chromosomes, a significant

enrichment of virus integration sites was observed in mitochondrial DNA (mtDNA) both in T ($p < 0.0001$) and NT ($p < 0.0001$), after normalization of the number of integrations to chromosome length. We found a total of 20 unique HBV integrations in mtDNA from the tissue samples obtained from 4/7 patients (17 breakpoints in T from 4/4 patients and 3 breakpoints in NT from 2/4 patients). HBV integration in mtDNA was associated with HBV DNA ($p = 0.01$) and pgRNA amounts ($p = 0.02$). In mtDNA, the integration breakpoints were preferentially located in mitochondrial genes in T (17/17 vs 0/3; $P < 0.0001$) and in the D-loop region in NT (2/17 vs 3/3; $P = 0.001$). *RNR2*, *ATP6*, *ND4*, and *ND5* mitochondrial genes were identified as recurrent sites of integration in T. Moreover, in T of individual patients, HBV integrations were detected in *CYTB*, *COX1*, *ND1*, and *ND2* genes. Furthermore, we found that HBV RNAs are imported into mitochondria.

Conclusion: The new HBV integration sequencing method importantly increased the detection efficiency of HBV integration breakpoints. We detected a significant enrichment of virus integrations in mtDNA from both T and NT. HBV integrations in mtDNA preferentially involved OXPHOS mitochondrial genes in T, suggesting that there is selection for mitochondria harboring HBV integration in these genes or for cells containing these mitochondria during hepatocarcinogenesis.

THU334

Enhanced T cell responses in patients and mouse model of hepatitis B and comorbid non-alcoholic fatty liver disease

Nishi Patel¹, Dan Boghici², Micol Rava³, Matteo Iannacone³, Konstantin Koro⁴, Craig Jenne², Carla Osiowy⁵, Carla Coffin². ¹University of Calgary, Cumming School of Medicine, Calgary, Canada; ²University of Calgary, Cumming School of Medicine, Calgary, Canada; ³San Raffaele Hospital, Division of Immunology, Transplantation and Infectious Diseases, Milano, Italy; ⁴Alberta Precision Laboratories, Calgary, Canada; ⁵Public Health Agency of Canada, National Microbiology Laboratory, Winnipeg, Canada
Email: nishi.patel@ucalgary.ca

Background and aims: Individuals living with hepatitis B and comorbid non-alcoholic fatty liver disease (NAFLD) are at an increased risk for hepatocellular carcinoma. Large cohort studies show a positive association between hepatic steatosis and reduced hepatitis B virus (HBV) replication. The objective of this study is to determine the viral and immune factors and mechanisms that contribute towards lower HBV replication in patients and mouse model of hepatitis B and NAFLD.

Method: 55 patients with hepatitis B and NAFLD were recruited from 3 Canadian liver clinics. Plasma, sera, and peripheral blood mononuclear cells (PBMCs) were isolated from blood. A parallel mouse model study of HBV and NAFLD was performed using 1.3.32DH transgenic mice that included healthy, NAFLD, and HBV control groups ($N = 10/\text{group}$). The mice were followed for 8 weeks and then sacrificed to obtain plasma, sera, PBMCs, and liver tissue (for histopathological scoring and viral antigen staining). HBV biomarkers were quantified using in-house and/or standard clinic assays in both patient and mice samples. Next-generation sequencing of HBV surface and core genes was performed using the Illumina MiSeq platform. A panel of 13 pro-and-anti-inflammatory cytokines was measured using multiplex Luminex assay. PBMCs phenotypic profile and *ex vivo* HBV-specific T cell responses were characterized through flow cytometry and IFN-gamma ELISPOT, respectively.

Results: In 55 patients with hepatitis B and NAFLD (35% female, mean age of 45 ± 10.6 years), 52 (95%) were HBeAg negative. The mean HBV DNA, qHBsAg, and HBV pgRNA levels were $3.2 \pm 1.8 \log_{10} \text{ IU/mL}$, $2.9 \pm 1.2 \log_{10} \text{ pg/mL}$, and $2.1 \pm 1.3 \log_{10} \text{ copies/mL}$, respectively. Hepatitis B patients with NAFLD clinical factors (i.e., dyslipidemia, hypertension, and metabolic syndrome) had lower levels of qHBsAg ($p < 0.001$). Similarly, mice with HBV and NAFLD had lower levels of HBV DNA ($p = 0.022$) and nucleic acid related antigen ($p = 0.044$) at 8 weeks. Greater frequency of immune escape mutations in HBV surface gene

POSTER PRESENTATIONS

(i.e., 1277L/T, M133L/I/T, and E164D/G) was detected in hepatitis B patients with severe steatosis ($p < 0.05$). Elevated levels of Th1 cytokines like IL-8 ($p = 0.002$), TNF- α ($p = 0.004$), IFN- γ ($p = 0.021$), and IL-10 ($p = 0.007$) were observed in hepatitis B patients with NAFLD clinical factors (figure 1). Hepatitis B and NAFLD patients with mild steatosis had higher levels of IL-2 ($p = 0.031$). In mice with HBV and NAFLD, IL-2 levels declined with HBV DNA at 8 weeks ($p = 0.04$). Increased frequency of functional HBV-specific T cells was observed in hepatitis B and NAFLD patients compared to control groups ($p < 0.05$).

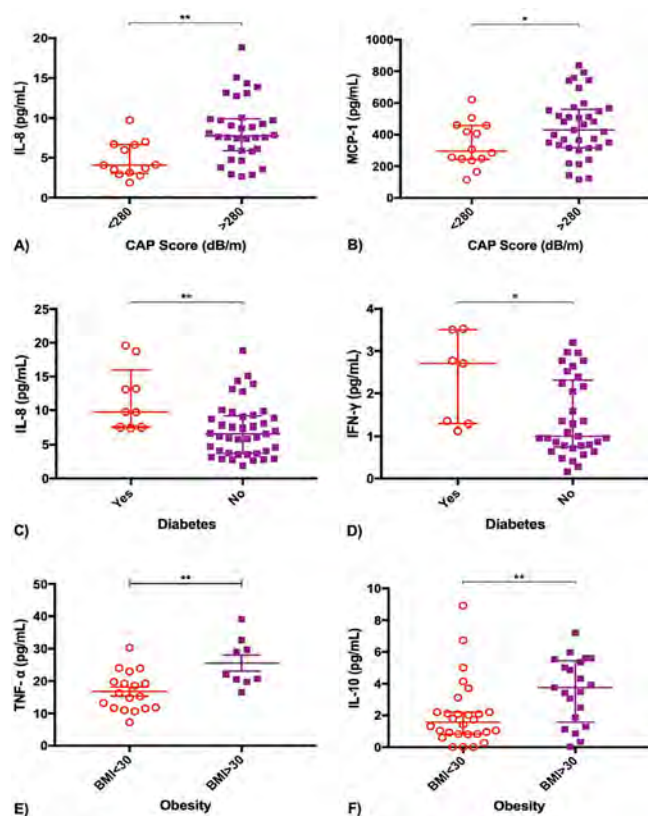


Figure 1: Cytokine levels based on NAFLD clinical factors in hepatitis B patients (Mann-Whitney U test). * $p < 0.05$. ** $p < 0.01$.

Conclusion: Heightened T cell responses observed in patients and mouse model of hepatitis B and NAFLD contribute towards suppression of HBV replication.

THU335

Hepatitis B virus sero-prevalence and genotype distribution among pregnant women in Siem Reap, Cambodia

Bunthen E^{1,2}, Ko Ko¹, Shintaro Nagashima¹, Serge Ouoba^{1,3}, Kanon Abe¹, Aya Sugiyama¹, Kazuki Takahashi¹, Rattana Kim⁴, Vichit Ork⁵, Md. Shafiqul Hossain⁶, Junko Tanaka¹. ¹Hiroshima University, Department of Epidemiology, Infectious Disease Control and Prevention, Graduate School of Biomedical and Health Sciences, Hiroshima, Japan; ²Ministry of Health, Payment Certification Agency, Phnom Penh, Cambodia; ³Institut de Recherche en Science de la Santé (IRSS), Unité de Recherche Clinique de Nanoro (URCN), Nanoro, Burkina Faso; ⁴Ministry of Health, National Maternal and Child Health Center, Phnom Penh, Cambodia; ⁵Ministry of Health, National Immunization Program (NIP), Phnom Penh, Cambodia; ⁶World Health Organization Country Office, Expanded Program on Immunization, Phnom Penh, Cambodia

Email: jun-tanaka@hiroshima-u.ac.jp

Background and aims: The latest report hepatitis B virus (HBV) infection prevalence in Cambodia was 4.4% among mothers and 0.56%

among their 5–7 years old. High infection prevalence in women of childbearing age showed potential of vertical transmission, threatening WHO target of eliminating hepatitis virus infection by 2030. This study aimed to estimate HBsAg prevalence among pregnant women, and then to examine their genomic structure and the mutation pattern. **Method:** Hospital based cross-sectional study was performed in a total of 1565 pregnant women who visited three hospitals in Siem Reap for their antenatal care from Feb-Sep 2020. The sero-markers such as HBsAg, HBsAb, HBeAg and HBeAb were detected from their blood samples using chemiluminescent enzyme linked. Viral titer was measured by real-time PCR. Full HBV genomes were amplified by direct sequencing. The study has been approved by ethical committees of Hiroshima University and Cambodia.

Results: The age of pregnant women participated in this study ranged from 15 to 47 years old with the mean age of 28.3 ± 5.6 years old. The prevalence of HBsAg, HBsAb, and HBeAb were 4.28%, 38.53%, 23.13%, respectively. Among the HBsAg positives, the prevalence of HBeAg and HBeAb were 41.79% and 55.22%, respectively. The overall mean viral titer was 2.22×10^6 copies/ml, where 5.30×10^6 copy/ml for HBeAg+ and 5.58×10^3 copy/ml for HBeAb+. Thirty-seven samples were able to perform full-genome sequencing. HBV genotype C1 was predominant (70.27%), followed by B4 (16.22%) and B2 (13.51%). All HBV genotype B were found to be recombinant B/C. By full genome analysis on 37 HBV isolates, mutation at a determinant region of surface protein was 24.32%. Additionally, the combination mutation was found in 2.70% and double mutation in 29.73% and V149I mutation at core region in 2.70%, all of which were highly associated to hepatocellular carcinoma occurrence.

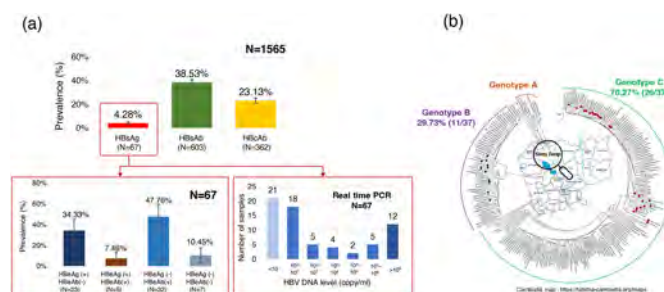


Figure: (a) prevalence of HBV sero-markers and (b) genotype distribution among pregnant women in Siem Reap, Cambodia

Conclusion: The findings from our study demonstrated the intermediate level of HBV infection endemicity, genotype distribution and mutation pattern among pregnant women in Siem Reap. These findings contribute to the establishment of HBV screening program and the management of HBsAg positive for pregnant women in Cambodia.

THU336

Genotype distribution and mutations associated with hepatocellular carcinoma risk among hepatitis B carriers in Goto Islands, Japan

Serge Ouoba^{1,2}, Ko Ko¹, Shintaro Nagashima¹, Bunthen E^{1,3}, Kazumi Yamasaki⁴, Kazuki Takahashi¹, Junko Tanaka¹. ¹Hiroshima University, Department of Epidemiology, Infectious Disease Control and Prevention, Graduate School of Biomedical and Health Sciences, Hiroshima, Japan; ²Institut de Recherche en Science de la Santé (IRSS), Unité de Recherche Clinique de Nanoro (URCN), Nanoro, Burkina Faso; ³Ministry of Health, Payment Certification Agency (PCA), Phnom Penh, Cambodia; ⁴National Hospital Organization Nagasaki Medical Center, Clinical Research Center, Nagasaki, Japan

Email: jun-tanaka@hiroshima-u.ac.jp

Background and aims: Hepatitis B virus (HBV) genotype and specific mutations are associated with the risk of hepatocellular carcinoma (HCC). Using stored serum of a cohort of HBsAg-positive patients in

Goto Islands, we studied the genotype distribution and the mutations related to the progression of liver disease.

Method: A total of 910 samples from a cohort of Hepatitis B surface Antigen-positive patients between 1980 and 2017 underwent genomic analyses. Partial and full HBV genomes were amplified by direct sequencing using an in-house developed primer set to identify HBV genotype and mutations related to HCC risk. Phylogenetic tree was performed by the neighbor-joining method.

Results: Men represented 57.4% of the cohort and the mean age at the start of the cohort was 45.5 ± 17.3 years. The median follow-up duration was 14.6 years. At entry, 61% were asymptomatic carriers but a 172% increment of hepatocellular carcinoma was found at the end of follow-up. The mean viral load was 2.0×10^4 copies/ml, and the prevalence of HBeAg and HBeAb were 26.5% and 71.2%, respectively. The predominant circulating genotype was genotype C2 (96.2%), followed by genotype B (3.4%) and A (0.6%). Three main clusters of cases were found having 95.61%-99% homology and were closely

related to HBV isolates from China and Japan. A total of 92 isolates underwent full genome analysis and mutations related to HCC occurrence were observed. Double mutation (A1762T/G1764A) was found in 73.5%, combination mutation (C1653 T and A1762T/G1764A or T1753C and A1762T/G1764A) in 29.4%, and V149I mutation in the core region in 26.9% of the isolates.

Conclusion: Genotype C, which is known to be associated with HCC risk, is the predominant circulating genotype in Goto islands, suggesting a large influence from East Asia. Mutations related to hepatocellular carcinoma occurrence were also found. In addition to the improvement of countermeasures against HBV infection in Goto Islands, genomic surveillance of HBV is essential to reduce the burden of the infection.

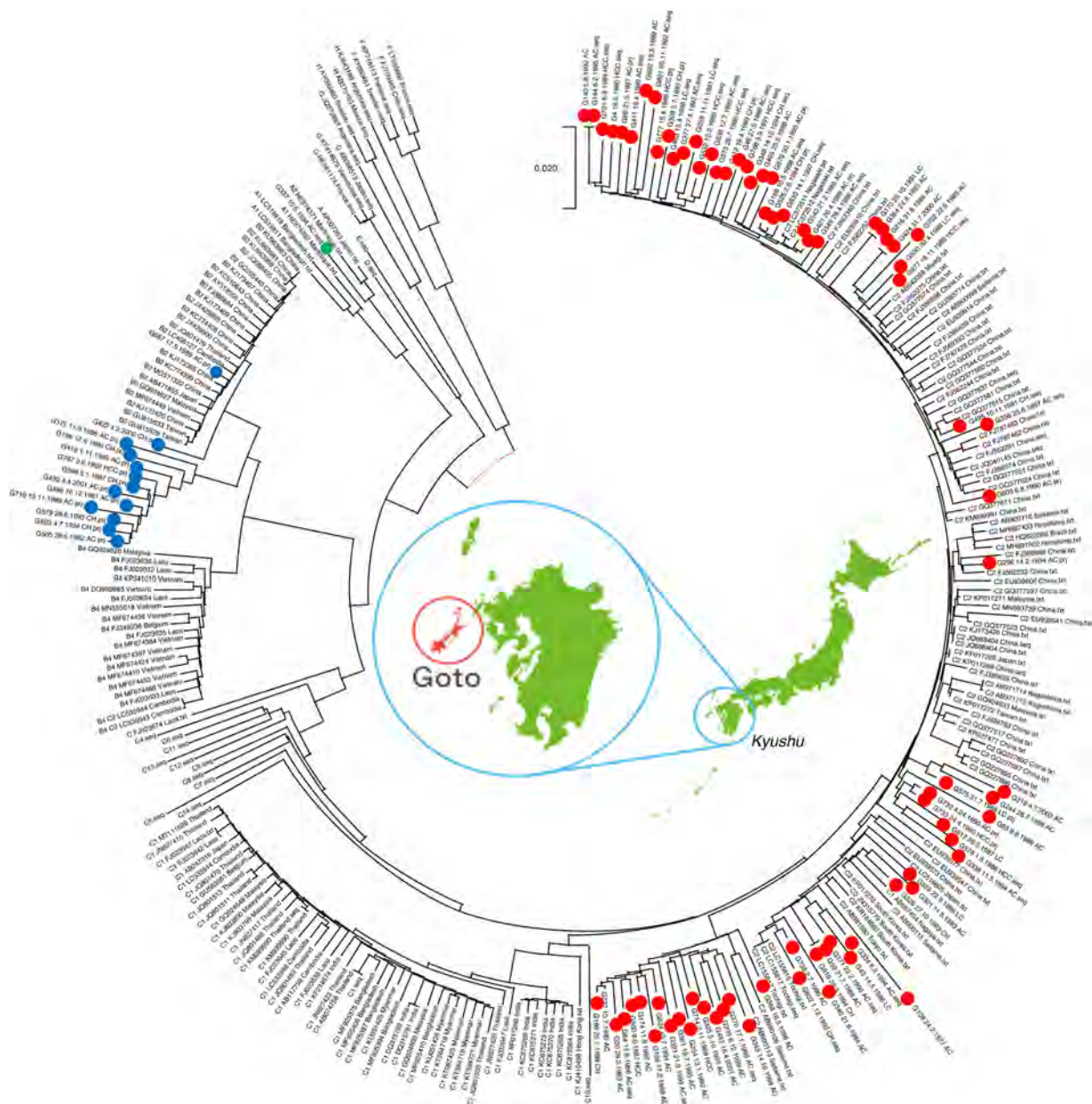


Figure: (abstract: THU336)

THU337

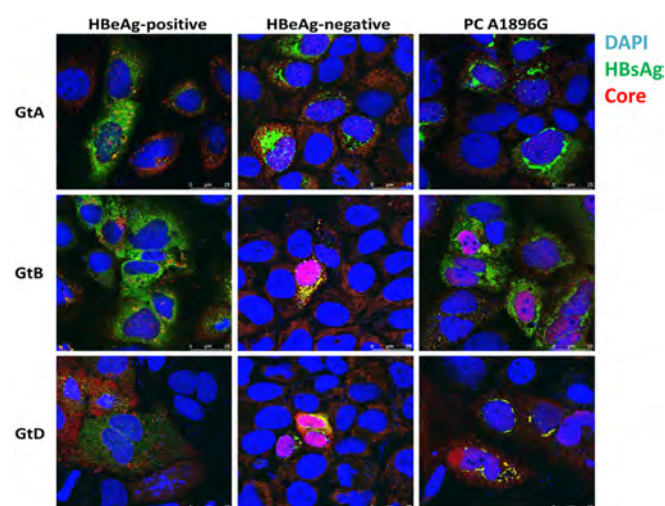
Comprehensive analysis of the different phases of chronic hepatitis B virus infection

Michael Basic^{1,2}, Qingyan Wu², Anja Schollmeier², Christoph Sarrazin^{1,3}, Stefan Zeuzem¹, Eberhard Hildt^{2,4}, Kai-Henrik Peiffer^{1,2}. ¹University Hospital Frankfurt, Frankfurt am Main, Germany; ²Paul Ehrlich Institute, Langen (Hessen), Germany; ³St. Joseph's Hospital in Wiesbaden, Wiesbaden, Germany; ⁴German Center for Infection Research, Braunschweig
Email: basic.michael@gmail.com

Background and aims: Chronic Hepatitis B virus (HBV) infection was classified into four active phases by the EASL: 1. HBeAg-positive chronic infection, 2. HBeAg-positive chronic hepatitis, 3. HBeAg-negative chronic infection and 4. HBeAg-negative chronic hepatitis. Recently, it was observed that released HBsAg amounts, ratios of L-, M- and S-proteins and morphology of subviral particles varied by viral genotype (Gt). Further, HBsAg composition was described to be distinct during the different phases of infection. Here, we characterized different phases of chronic HBV infection regarding HBsAg, core and particle assembly *in vivo* and *in vitro*.

Method: Sera of patients infected with GtA or GtD of different disease phases according to the EASL classification were analyzed by HBsAg-specific Western Blot (WB) and density gradient centrifugation. For *in vitro* studies, HBV genomes of GtA, GtB, and GtD of patients with HBeAg-negative chronic infection and presence of precore mutation G1896A were cloned into pUC-18 and expressed in Hepatoma cells. Corresponding HBeAg-positive wildtype genomes were used for comparison. Expression and localization of HBsAg and core protein, replication, particle morphology and infectivity as well as subcellular localization were analyzed.

Results: In the sera of patients, the ratio of HBsAg proteins differed among genotypes but not among the different disease phases. Density of HBsAg-particles varied among genotypes but not between the stage of infection. *In vitro*, the HBeAg-negative genomes showed a reduction in HBsAg expression in comparison to the corresponding HBeAg-positive genomes. By WB analyses, intracellular accumulation of LHBs and core protein was found. Further, perinuclear accumulation of LHBs and core protein was observed in HBeAg-negative genomes by immunofluorescence analyses (see fig.). Reintroduction of precore G1896A mutation did not restore HBsAg expression and did not affect intracellular distribution of HBsAg. Furthermore, immunofluorescence microscopy analyses and subcellular fractionation showed a strong intranuclear localization of assembled core protein.



Conclusion: In contrast to other studies, consistent ratios of HBsAg and similar particle densities were observed among the four different phases of active HBV infection. In comparison to HBeAg-positive genomes, HBeAg-negative genomes are characterized by an enhanced intranuclear localization of assembled core protein and a perinuclear accumulation of HBsAg *in vitro*. This is further reflected by an impaired release of HBsAg. Interestingly, neither HBeAg nor presence of precore G1896A mutation seem to be causative for the observed characteristics in HBsAg and core virology in genomes derived from patients with HBeAg-negative chronic infection. Further analyses of the underlying mechanisms might also affect novel antiviral strategies.

THU338

Human stem cell-derived hepatic and intestinal culture systems to study HEV transmission along the gut-liver axis

Viet Loan Dao Thi^{1,2}, Michael Dill^{3,4}, Sarah Prallet¹, Ann-Kathrin Mehnert¹, Sabrina Schweiggert³. ¹Center for Integrative Infectious Disease Research (CIID) University Hospital Heidelberg, Department of Infectious Diseases, Virology, Heidelberg, Germany; ²German Centre for Infection Research (DZIF), Heidelberg, Germany; ³University Hospital Heidelberg, Division of Gastroenterology, Heidelberg, Germany; ⁴German Cancer Research Center (DKFZ), Experimental Hepatology, Inflammation and Cancer (F240) Deutsches Krebsforschungszentrum, Heidelberg, Germany
Email: vietloan.daothi@med.uni-heidelberg.de

Background and aims: The intestine and the liver are anatomically and functionally linked, often referred to as the gut-liver axis. They cooperate in nutrient uptake and metabolism, as well as provide immunity to pathogens, due to their organization as barrier tissues. Enterically transmitted hepatitis E virus (HEV), the most common cause of acute hepatitis in the world, is dependent on this axis: Once in the gastrointestinal tract, HEV passes the intestinal epithelium to gain access to the blood stream from where it reaches the liver and infects hepatocytes. Conventional cell culture systems fail to recapitulate the intricacy of this axis. Human induced pluripotent and adult tissue stem cell-derived organoid culture systems that reflect *in vivo*-like organ complexity, allow for better and authentic recapitulation of these human epithelial tissues, including polarization and cellular differentiation.

Method: The human induced pluripotent stem cell line iPSC.C3A was differentiated to hepatocyte-like cells (HLCs), which were embedded into Matrigel domes to initiate the formation of hepatic organoids. iPSC.C3A cells were also differentiated to small intestinal organoids using a commercially available kit. In addition, we differentiated human LGR5-positive bipotent cholangiocyte organoids to mature hepatic organoids.

Results: Following organoid formation of iPSC-derived HLCs and further differentiation of both, HLCs-derived and cholangiocyte organoids into mature hepatic organoids, we observed a strong increase in albumin expression, by qRT-PCR analysis and, partially, by IF staining. Both intestinal and hepatic organoid culture systems supported authentic HEV infection using the HEV GT3 Kernow-C1 p6 strain, as evidenced by an increase in HEV viral genomes and the upregulation of interferon-stimulated genes. Interestingly, even immature, bipotent cholangiocyte organoid progenitors were readily permissive for HEV infection.

Conclusion: We have established novel hepatic and intestinal culture systems supporting authentic HEV infection. We will use these systems to study tissue-specific determinants of HEV infection, including the analysis of an HEV-induced innate immune response. In the future, we will combine both systems to study HEV transmission along the gut-liver axis.

Keywords: Hepatitis E virus, induced pluripotent stem cells, hepatic organoids, intestinal organoids, cholangiocyte organoids, gut-liver axis.

Disclosure-Conflict of interest: On behalf of all authors, I hereby confirm that there are no conflicts of interest.

THU339

A novel class of glycan-specific human monoclonal antibodies neutralizing the hepatitis E virus

Katja Dinkelborg^{1,2}, George Ssebyatika³, Elina Muriel Guzmán³, Prossie Lindah Nankya³, Luisa J Ströh⁴, Lucas Hueffner¹, Volker Kinast^{5,6}, Toni Luise Meister⁶, Heiner Wedemeyer^{2,7}, Eike Steinmann^{6,7}, Thomas Pietschmann^{1,7}, Thomas Krey^{3,4,7,8,9}, Patrick Behrendt^{1,2,7}. ¹TWINCORE, Centre for Experimental and Clinical Infection Research, a Joint Venture between the Medical School Hannover (MHH) and the Helmholtz Centre for Infection Research (HZI), Experimental Virology; ²Hannover Medical School, Department of Gastroenterology, Hepatology and Endocrinology; ³Institute of Biochemistry, University of Lübeck, Center of Structural and Cell Biology in Medicine, Germany; ⁴Hannover Medical School, Department of Medical Microbiology and Virology; ⁵Carl von Ossietzky University Oldenburg, Department of Medical Microbiology and Virology; ⁶Ruhr University Bochum, Department of Molecular and Medical Virology; ⁷German Center for Infectious Disease Research (DZIF); ⁸Hannover Medical School, Excellence Cluster 2155 RESIST; ⁹Centre for Structural Systems Biology (CSSB)
Email: behrendt.patrick@mh-hannover.de

Background and aims: Acute viral hepatitis is most commonly caused by infection with the hepatitis E virus (HEV). It can lead to chronic infection in immunocompromised hosts, as well as severe hepatitis with the risk of liver failure in certain cases. Four main human pathogenic genotypes (gt 1–4) have been described. They differ in their worldwide distribution and route of infection. HEV infected cells secrete glycosylated isoforms of the viral capsid protein (open reading frame 2, pORF2) that are hypothesized to help the virus evade the humoral immune response of infected individuals. However, a gt1 protein-based vaccine has been developed in China and large cohort studies showed that the generated antibody titre correlated with protection from infection. Here, we aimed to generate human monoclonal antibodies neutralising HEV.

Method: Memory B cells of two acutely infected individuals were selected by recognizing the protruding domain (pdomain) of pORF2. Heavy and light chain of the B cell receptor were sequenced and single chain variable fragments (scFv) or monoclonal antibodies (mAb) were expressed in Expi293F cells. To analyse binding, Enzyme-linked Immunosorbent Assays (ELISA) and Biacore experiments were performed. Neutralisation assays were performed using three different HEV strains (gt3: Kernow C1 p6 G1634R and HEV-83–2–27; gt1: Sar55). Additionally, selected scFvs in complex with HEV gt3 pdomain were crystallised and structures were analysed.

Results: *In vitro* neutralization assays led to the identification of 16 hit candidates. ELISA confirmed the identification of at least four mAbs specifically recognizing the non-glycosylated, infectious form of pORF2. Further experiments confirmed neutralisation of genotype 1 and 3 viral strains by selected mAbs. Titration of identified mAbs determined the half-maximal inhibitory concentration of the best neutralizers at ≤ 0.01 μ g/ml. ELISA using patient sera over the course of acute or chronic infection with HEV confirmed the specificity of a subgroup of identified mAbs to infectious viral particles. Additionally, the specific mAbs but not the non-specific mAbs were unaffected in their ability to neutralize HEV by glycosylated pORF2 isoforms. Structure analysis confirmed that specific mAbs directly bind the

glycosylation site, which is highly conserved between different HEV genotypes.

Conclusion: Here, we identified a novel subgroup of human mAbs neutralising different genotypes of HEV. They specifically bind to infectious viral particles and neutralisation is not disrupted by the presence of secreted isoforms of pORF2. These antibodies may serve as a novel therapeutic option for severe and chronic HEV infection, for which effective and specific treatment is currently lacking in the clinic. Furthermore, we offer new insights for the development of cross-genotype effective vaccines against HEV in the future.

THU340

Increased lymphocyte trafficking and myeloid activation in patients with chronic hepatitis delta

Ester García-Pras¹, Thais Leonel¹, Sergio Rodríguez-Tajes¹, Mireia García-López¹, Sabela Lens¹, Zoe Mariño¹, Alba Díaz², Yilliam Fundora³, Xavier Fornis¹, Sofia Pérez-del-Pulgar¹. ¹Liver Unit, Hospital Clínic, University of Barcelona, IDIBAPS, CIBERehd, Barcelona, Spain; ²(2) Pathology Department, Biomedical Diagnostic Center, Hospital Clínic, CIBERehd, Barcelona, Spain; ³(3) Hepatobiliopancreatic and Liver Transplant Department, Hospital Clínic, Barcelona, Spain
Email: egrpras@clinic.cat

Background and aims: Hepatitis Delta virus (HDV) is a satellite virus of hepatitis B virus (HBV), as it requires the HBV envelope proteins (HBsAg) to form viral particles. Compared to HBV monoinfection, chronic hepatitis delta (CHD) represents the most aggressive form of viral hepatitis leading to a faster progression towards cirrhosis, liver decompensation and hepatocellular carcinoma. Immune-mediated liver damage upon HDV infection is an important factor of HDV pathogenesis. The aim of the study was to analyze intrahepatic gene expression in CHD patients compared to HBV-infected patients and healthy controls.

Method: Formalin fixed paraffin embedded (FFPE) liver biopsies from 21 anti-HDV positive patients were included in the study. Patients were classified as HDV+ and HDV- based on whether or not they had detectable HDV-RNA in serum. Untreated HBV monoinfected patients and healthy donors were used as control groups. Gene expression analysis of immune-regulatory pathways was performed by using the nCounter[®] Host Response Panel of Nanostring. Differential expression between groups was considered if log2 fold-change > 1 and p < 0.05, FDR adjusted by Benjamin-Yekutieli.

Results: The median age of the patients was 51 years; 62% were male, 62% had liver cirrhosis and 43% were on nucleos(t)ide analog (NA) treatment. Gene expression analysis revealed 223 genes significantly upregulated in HDV+ patients compared to healthy donors and 198 compared to HDV- patients. Chemokines were the molecules with the highest differential expression between groups, being CXCL9, CXCL10, CXCL11 (and its cognate receptor CXCR3) the most relevant. Consequently, genes involved in trafficking and activation pathways of myeloid cells (CCR2, CCR5, CCL18) and lymphocytes (CD2, ICOS, CD40L, CD20, CD79A) were significantly upregulated in HDV+ compared to healthy donors and HDV- patients. Consistent with increased immunopathogenesis associated with HDV infection, apoptotic (BCL-2, TNF), cytotoxic (GZMH, GZMA and PRF-1) and inflammasome (NLRP1, PYCARD y AIM2) pathways were enriched in CHD patients. Immune activation and liver damage pathways were also increased in untreated HBV patients, but significantly less pronounced compared to HDV+ patients. Remarkably, some innate (IFIT1, IFIT2 and IFIT3) and adaptive (CD2, CCL5 and IL17RE) response molecules persisted upregulated after HDV clearance.

Conclusion: HDV infection induces innate and adaptive responses that contribute to aggravating the progression of liver disease. A strong recruitment and activation of myeloid cells and lymphocytes elicits inflammation and cell death processes in CHD. The resolution of HDV infection might not be able to completely reverse altered signaling pathways, due to molecule sequelae or the persistence of HBV.

THU341

Discordant serum HBV DNA and RNA correlation with quantitative HBsAg and high levels of intrahepatic integrated HBV DNA in HBeAg negative chronic hepatitis B

Daryl Lau¹, Elena Kim², Chosha Bai³, Wendy C King⁴, Yixiao Cui³, David E Kleiner⁵, Marc Ghany⁶, Thi Thuy Tu Nguyen³, Amanda S Hinerman⁴, Zhili Wang⁷, Raymond Chung⁸, Richard Sterling⁹, Gavin Cloherty¹⁰, Ying-Hsiu Su³, Haitao Guo². ¹Beth Israel Deaconess Medical Center, Harvard Medical School, Gastroenterology and Hepatology, Boston, United States; ²University of Pittsburgh School of Medicine, Department of Microbiology and Molecular Genetics, Pittsburgh, United States; ³The Baruch S. Blumberg Institute, Translational Medical Science, Doylestown, United States; ⁴School of Public Health, University of Pittsburgh, Epidemiology, Pittsburgh, United States; ⁵National Cancer Institute, National Institutes of Health, Laboratory of Pathology, Bethesda, United States; ⁶National Institutes of Health, Liver Diseases Branch, NIDDK, Bethesda, United States; ⁷JBS Science Inc, Doylestown, United States; ⁸Massachusetts General Hospital, Harvard Medical School, GI Division, Boston, United States; ⁹Virginia Commonwealth University, Gastroenterology and Hepatology, Richmond, United States; ¹⁰Abbott Laboratories, Infectious Disease Research, Abbott Park, United States
Email: dlau@bidmc.harvard.edu

Background and aims: Circulating HBsAg can be derived from both intrahepatic cccDNA and integrated HBV DNA. Functional cure may be dependent on the origins of the HBsAg. We sought to correlate cccDNA and integrated DNA from liver tissues of HBeAg (+) and (-) CHB participants with serum virological parameters and intrahepatic HBcAg and HBsAg immunostaining patterns.

Method: Liver tissues from untreated CHB participants of the North American Hepatitis B Research Network (HBRN) were evaluated. For cccDNA analysis, DNA prep was heat denatured and digested by plasmid-safe ATP-dependent DNase (PSAD) to remove rcDNA and integrated DNA prior to qPCR quantification. Mitochondrial DNA COX3 gene qPCR was used for cccDNA normalization. For integrated DNA detection, 100 ng of total DNA was subjected to HBV-enriched next generation sequencing (NGS) assay. Enriched DNA library was sequenced by Illumina MiniSeq. The resulting HBV-host junction sequences were identified by ChimericSeq. Integrated DNA quantity was estimated based on percent of HBV-host junction reads per HBV reads and HBV sequence distribution. Serum HBV RNA was measured by Abbott research assay, HBcrAg by Fujirebio Europe, and qHBsAg by Roche Diagnostics' Elecsys platform.

Results: The cohort [24 HBeAg (+), 32 HBeAg (-)] was predominantly Asian (75%) with mean age of 44 years. The intrahepatic cccDNA, serum HBV DNA, RNA, HBcrAg and qHBsAg were higher among the HBeAg (+) participants (Table). HBeAg (-) vs. (+) participants had larger proportion of integrated HBV DNA in liver (Figure). There were significant Pearson's correlations between cccDNA and serum RNA [$r = .53$, $p < .001$] and HBcrAg [$r = .41$, $p = .002$]. The correlations between serum DNA and RNA were strong among both HBeAg (+) and (-) CHB (Table). Correlations between serum qHBsAg levels with serum DNA or RNA were moderate for HBeAg (+) but very weak for HBeAg (-) participants (Table). The majority [88%] of HBeAg (+) samples had positive intrahepatic HBcAg stain compared to 13% of HBeAg (-) samples. In contrast, 96% of HBeAg (+) and 88% of HBeAg (-) livers had positive HBsAg stain. Granular cytoplasmic HBsAg staining was noted in 57% and 64% of HBeAg (+) and (-) livers respectively. Membranous HBsAg stain pattern was noted in only 14% of HBeAg (-) compared to 78% of HBeAg (+) samples. There was a significant inverse relationship between HBV RNA and integrated HBV DNA that may explain the low level of membranous HBsAg stain in HBeAg (-) livers.

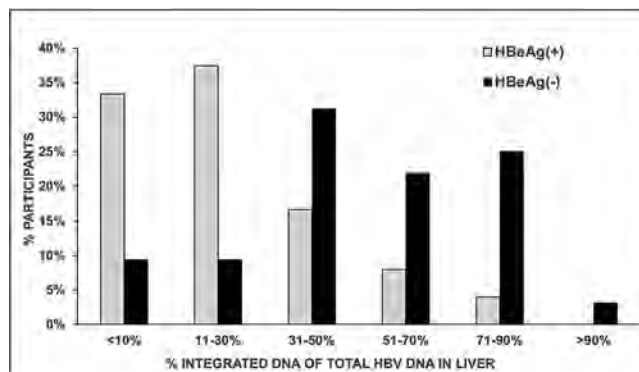


Figure:

Mean (range)	HBeAg(+) n=24	HBeAg(-) n=32	P value
Liver cccDNA (log ₁₀ copies/1 million cells)	4.97 (3.55 - 5.74)	3.86 (2.86 - 5.24)	0.00001
Serum HBV DNA (log ₁₀ IU/ml)	7.5 (3.2 - 9.2)	4.5 (2.6 - 7.7)	<0.00001
Serum HBV RNA (log ₁₀ U/ml)	6.59 (3.11 - 7.97)	2.88 (<1.69 - 6.53)	<0.00001
Serum HBcrAg (log ₁₀ U/ml)	8.4 (5.8 - 10.3)	3.6 (<3 - 10.3)	<0.00001
Serum qHBsAg (log ₁₀ IU/ml)	4.25 (1.94 - 5.35)	2.96 (0.01 - 4.15)	<0.00001
Pearson's correlations between			
Serum RNA and serum DNA	$r = .93$ $P = .00001$	$r = .87$ $P = .000001$	
Serum RNA and serum qHBsAg	$r = .45$ $P = .03$	$r = .27$ $P = .14$	
Serum DNA and serum qHBsAg	$r = .55$ $P = .005$	$r = .33$ $P = .06$	

Table:

Conclusion: Serum RNA and HBcrAg reflect the intrahepatic cccDNA concentrations. Participants with HBeAg (-) CHB had high levels of integrated HBV DNA in the liver. The HBsAg derived from the integrated DNA likely contributed to the discordant serum DNA and RNA correlations to qHBsAg and the HBsAg immunostaining patterns in HBeAg (-) participants. These findings are important for the design and monitoring of therapies aiming for HBV functional cure.

THU342

Hepatitis B virus-replicating transgenic mice exhibit a functional but restricted responsiveness to exogenous Tlr3 and Rig-I stimuli

Stefan Schefczyk¹, Xufeng Luo², Yaojie Liang¹, Mike Hasenberg³, Bernd Walkenfort³, Martin Trippel¹, Mengji Lu⁴, Heiner Wedemeyer⁵, Hartmut Schmidt¹, Ruth Broering¹. ¹University Hospital Essen, Department of Gastroenterology, Hepatology and Transplant Medicine, Essen, Germany; ²Affiliated Cancer Hospital of Zhengzhou University, Institute for Lymphoma Research, China; ³University Hospital Essen, Institute for Experimental Immunology and Imaging, Essen, Germany; ⁴University Hospital Essen, Institute for Virology, Essen, Germany; ⁵Medizinische Hochschule Hannover, Klinik für Gastroenterologie, Hepatologie und Endokrinologie, Hannover, Germany

Email: stefan.schefczyk@uni-due.de

Background and aims: Pathogenesis of Hepatitis B virus (HBV) infection is driven by innate and adaptive immune responses. Although HBV is suggested to be a stealth virus, recent findings indicate that HBV particles activate a Tlr2 response in murine and human hepatocytes. Furthermore, in HBV-transgenic mice lacking the surface antigen (HBsAg) a Tlr3-mediated response in non-parenchymal liver cells has been described. Aim of this study was to investigate how HBsAg influence hepatic innate immune responses in different HBV-transgenic mouse models.

Method: Liver tissue from C57/Bl6 and HBV-transgenic mouse strains (tg[Alb1HBV]44Bri [Alb/HBs], tg1.4HBV-s-mut and tg1.4HBV-s-rec [F1 generation Alb/HBs × tg1.4HBV-s-mut]) was analysed using transmission electron microscopy (TEM). HBV replication was characterized on RNA and protein level. All-in-one liver cell preparation enabled extraction of primary murine hepatocytes, liver sinusoidal endothelial cells and Kupffer cells and remaining non-parenchymal cells (rNPC). Responsiveness to poly (I:C) treatment (Tlr3) and transfection (Rig-I) was determined using quantitative RT-PCR and multiplex-based cytokine assay.

Results: TEM visualised viral particles (tg1.4HBV-s-rec), nuclear spot formations (tg1.4HBV-s-mut and tg1.4HBV-s-rec) and malformation of the endoplasmic reticulum (Alb/HBs). Viral replication did not differ comparing tg1.4HBV-s-rec and tg1.4HBV-s-mut, except HBsAg levels. A distinct cell type-dependent and mouse strain-dependent gene expression pattern for interferon (Ifnb, Ifit1), cytokine (Tnf, Il1b, Il10) and chemokine (Ccl2, Ccl5) was observed by quantitative RT-PCR and validated using a multiplex-based cytokine assay. Emphasizing that tg1.4HBV-s-rec-derived liver cells responded to poly (I:C) with significantly suppressed expression levels, compared to the other mouse strains. Contrary, rNPC of tg1.4HBVs-rec mice showed the highest induction for Il10, Tnf, Il1b and Ccl5 in response to poly (I:C). In all HBV-transgenic mice, the induction of Ccl2 was significant lower in PMH but increased in rNPC.

Conclusion: Production of HBV particles and release of HBsAg in tg1.4HBV-s-rec mice led to suppressed hepatic Tlr3 and Rig-I signaling. However, rNPC seemed to be more potent in producing poly (I:C)-induced inflammatory cytokines.

THU343

Profiling at single hepatocyte level indicates variance in viral replication associated with HBeAg status in chronic hepatitis B patients

Alfonso Blázquez-Moreno¹, Nadia Neto¹, Hinrich Göhlmann¹, Cheng-Yuan Peng^{2,3}, Jeroen Aerssens¹, Marianne Tuefferd¹. ¹Janssen Research and Development, Beerse, Belgium; ²CMUH (China Medical University Hospital), Taichung, Taiwan, China; ³China Medical University, School of Medicine, Taiwan
Email: mtueffe1@its.jnj.com

Background and aims: Chronic infection with hepatitis B virus (CHB) is characterized by heterogeneity of viral replication across hepatocytes. Here we report on an approach that assesses multiple viral parameters at single hepatocyte level: status of hepatitis B virus (HBV) surface antigen (HBsAg) and core antigen (HBcAg), presence of covalently closed circular DNA (cccDNA) and quantification of HBV RNA. We applied this method to liver biopsy samples collected from 7 treatment-naïve male patients covering for HBV e-antigen (HBeAg) positive (n = 4) and negative (n = 3) CHB phases.

Method: Cryosections from the liver core biopsies were fluorescently stained for 4', 6-diamidino-2-phenylindole (DAPI), cytokeratin 18 (CK18), HBsAg and adjacent HBcAg. For each patient, up to 96 (range 60–96, average 85) individual hepatocytes (DAPI and CK18 positive) were randomly collected using a RareCyte Finder II, separately deposited into tubes and subjected to simultaneous DNA and RNA extraction using DNA/RNA Zymo columns. HBV RNA and cccDNA, together with mitochondrial RNA and DNA as positive controls, were measured using the Bio-Rad digital droplet polymerase chain reaction system.

Results: HBeAg (+) vs HBeAg (-) patients showed contrasted expression of viral markers, with higher percentages of individual hepatocytes positive for HBsAg (median: 88% vs 16%), HBcAg (median: 82% vs <1%), HBV RNA (94% vs 21%) and cccDNA (37% vs 17%). The percentage of infected hepatocytes (positive hepatocytes for either cccDNA, RNA or HBsAg) was higher in HBeAg (+) vs HBeAg (-) patients (median: 99% vs 53%). Quantitative assessment of HBV RNA demonstrated that expression levels within individual hepatocytes was higher in HBeAg (+) vs HBeAg (-) patients (median: 84 vs 0

HBV RNA counts/cell). Within HBeAg (+) subjects, cccDNA-positive hepatocytes showed higher transcriptomic activity (median: 87 vs 72 RNA counts/cell) than cccDNA-negative hepatocytes, compared to HBeAg (-) subjects (median: 0 vs 0 RNA counts/cell). Interestingly, CHB patients with lower (<300 IU/ml) peripheral HBsAg levels had also the lowest proportion of HBsAg (+) hepatocytes (<32%), whereas patients with peripheral HBsAg levels >1000 IU/ml showed large variation in percentage of HBsAg (+) (range 31–100%). Peripheral levels of HBV DNA or alanine aminotransferase were not associated with any of the hepatocyte-derived readouts.

% of hepatocytes that are:	HBeAg (+) patients (n = 4)		HBeAg (-) patients (n = 3)	
	Range	Median	Range	Median
HBsAg positive	55 - 100	82	< 1	< 1
HBcAg positive	31 - 100	88	0 - 32	16
HBV RNA positive	88 - 99	94	19 - 25	21
cccDNA positive	13 - 76	37	14 - 27	17
HBV RNA counts	0 - 9620	84	0 - 876	0

Conclusion: We demonstrated that CHB patients at different stages of disease show diverse profiles of viral markers measured at single hepatocyte level.

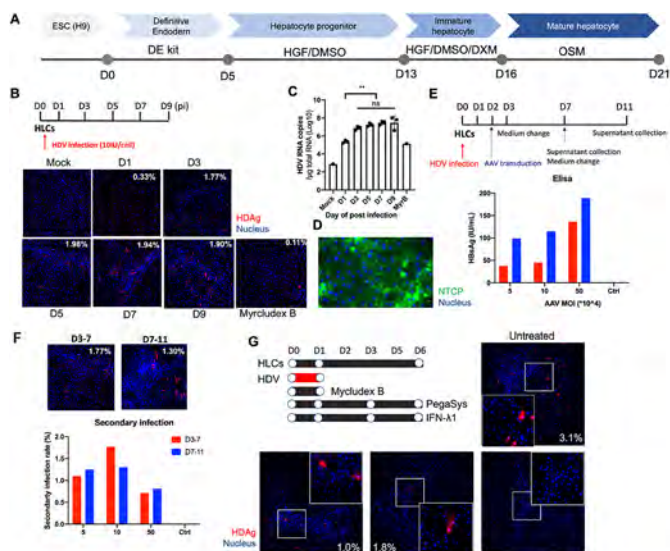
THU344

Human stem cell-derived hepatocytes as a model for hepatitis D virus infection

Huanting Chi^{1,2}, Bingqian Qu¹, Angga Prawira¹, Lars Maurer¹, Rebecca Fu¹, Florian Lempp¹, Charlotte Decker¹, Zhenfeng Zhang¹, Dirk Grimm^{1,2,3}, Viet Loan Dao Thi^{1,2}, Stephan Urban^{1,2}. ¹University Hospital Heidelberg, Department of Infectious Diseases; ²German Centre for Infection Research (DZIF); ³German Center for Cardiovascular Research (DZHK), Partner Site Heidelberg
Email: chihuanting@gmail.com

Background and aims: An estimated 12~15 million people worldwide are suffering from chronic hepatitis D virus (HDV) infection without a curative therapeutic regimen so far. Primary human hepatocytes represent the most physiological model for HDV research, but their application is restricted. Hepatoma cells can also support the entire HDV life cycle via gene editing techniques, but they only partially resemble hepatocytes due to their aberrant nature. Recently, human pluripotent stem-cell derived hepatocyte-like cells (HLCs) have been proposed as an attractive cell culture system for hepatitis B, C, and E viruses. Here, we show that HLCs support the entire HDV life cycle and propose this model as a new platform for the study of HDV biology and the evaluation of antiviral treatments.

Method: We optimized a stem cell-based differentiation protocol which yields HDV-permissive HLCs (Fig A). Mature HLCs were inoculated with HDV in the presence of 4% Polyethylene Glycol 8000 (PEG8000) and 1.5% dimethyl sulfoxide (DMSO), with samples being harvested for immunofluorescence and quantitative RT-PCR analysis. Adeno-associated viruses (AAVs) encoding hepatitis B virus S antigen (HBsAg) were transduced to HDV infected HLCs for viral assembly and secretion. The supernatant was taken to subsequently infect Huh7 cells to determine infectivity of secreted HDV particles.



(A) Stem cell differentiation protocol to generate HLCs. (B&C) HLCs were infected with HDV and harvested every 2 days for IF and qRT-PCR. (D) NTCP was stained with Atto565-NHS-ester-coupled Mycludex B. (E&F) AAV encoding HBsAg were transduced to HDV infected HLCs. The supernatant was collected for Elisa and secondary infection. (G) HDV infected HLCs were treated with antivirals respectively.

Results: HDV infection of HLCs was assessed by measuring HDV RNA by quantitative RT-PCR and immunofluorescence staining of delta antigen (HDAg) (Fig B and C). HDV infection could be completely blocked by Mycludex B, suggesting entry in HLCs. In agreement, staining with Atto565-NHS-ester-coupled Mycludex B showed that HLCs express NTCP on their plasma membrane (Fig D), albeit at lower levels than NTCP overexpressing hepatoma cells. Upon Adeno-associated virus transduction with the HBsAg, HDV-infected HLCs assembled and released infectious HDV progeny particles, showing that HLCs can recapitulate the entire HDV life cycle (Fig E and F). We further found that HLCs could be infected with HDV genotypes 1 from Ethiopia, 2 and 4 from Japan, and 3 from Peru. Finally, HDV infection of HLCs could be inhibited by IFN- α and IFN- λ treatment (Fig G). Further testing of other antivirals is currently being performed.

Conclusion: HLCs provide an attractive, genetically tractable, and physiologically relevant platform for studying pan-genotype HDV life cycle and evaluating antiviral treatments.

THU345

Hepatitis B viral load variation between the first and third trimesters of pregnancy

Stuart Gallacher¹, Alan Yeung^{2,3}, Megan Glancy^{2,3}, Ewan Forrest⁴, Stephen Barclay⁴. ¹NHS Greater Glasgow and Clyde, Department of Infectious Diseases, Brownlee Centre, Glasgow, United Kingdom; ²Glasgow Caledonian University, School of Health and Life Sciences, Glasgow, United Kingdom; ³Public Health Scotland, Glasgow, United Kingdom; ⁴NHS Greater Glasgow and Clyde, Department of Gastroenterology, Glasgow Royal Infirmary, Glasgow, United Kingdom
Email: stuart.gallacher3@nhs.scot

Background and aims: Hepatitis B virus (HBV) infection may be transmitted vertically, with maternal HBV viral load (VL) >5.3 log₁₀ IU/ml an indication for prophylactic antiviral therapy in the third trimester. However, no consensus exists on the optimal time to check HBV VL in pregnancy. We sought to identify if VL varied between early pregnancy and week 26, when VL is currently checked according to our local protocol.

Method: HBV screening samples taken at antenatal booking appointments in our health board Jan '10 to Jun '19 were identified from a virology database. Locally, first detection of HBV surface antigen in a patient triggers reflex VL testing (hereafter booking viral load (BVL)). Patients with a BVL and repeat VL 12–20 weeks after

booking (hereafter follow-up VL (FVL)), were identified for inclusion. Case note review was performed, and patients were excluded for: inappropriate testing chronology, acute HBV, antiviral therapy started prior to BVL/FVL, or incomplete clinical records. Changes between BVL and FVL were analysed using paired Wilcoxon tests.

Results: 306 pregnancies with both BVL and FVL (median of 14.6 weeks later) were identified. After application of exclusion criteria, 241 pregnancies were included for analysis. Median BVL was 2.61 (1.60–3.59) log₁₀ IU/ml, and median FVL 2.47 (1.78–3.30) log₁₀ IU/ml, with a median reduction from BVL to FVL of –0.19 log₁₀ IU/ml, 95% CI –0.33, –0.09 (p < 0.001). Changes according to BVL and e-Antigen (HBeAg) status are shown below. Of 36 patients with a BVL >5.3 log₁₀ IU/ml, 10 (27.8%) had a FVL <5.3 log₁₀ IU/ml.

	Number of Pregnancy-Episodes*	Median (IQR) log ₁₀ Viral Load at Baseline	Median (IQR) log ₁₀ Viral Load at Follow-Up	Median (95% CI**) Change in log ₁₀ Viral Load	p value for Change in Viral Load***
Total	241	2.61 (1.60, 3.59)	2.47 (1.78, 3.30)	–0.19 (–0.33, –0.09)	<0.001
Baseline Viral Load					
<5.3 log ₁₀ IU/ml	205	2.48 (1.78, 3.03)	2.22 (1.71, 2.92)	–0.12 (–0.26, –0.01)	<0.001
>5.3 log ₁₀ IU/ml	36	7.78 (7.22, 8.46)	7.23 (5.10, 7.95)	–0.57 (–1.70, –0.33)	<0.001
HBeAg Status					
Negative	202	2.53 (1.84, 3.05)	2.27 (1.74, 2.95)	–0.14 (–0.30, –0.03)	<0.001
Positive	39	7.69 (6.50, 8.39)	6.70 (4.08, 7.92)	–0.39 (–0.94, –0.13)	<0.001

*34 patients had two pregnancy-episodes and 1 patient had three pregnancy-episodes.

**95% bootstrap confidence interval generated using 10,000 random resamplings of the change in viral load data.

***Paired Wilcoxon test with alternative hypothesis as change in median not equal to zero.

Conclusion: Median HBV VL falls during pregnancy regardless of baseline factors. No patients with a BVL <5.3 log₁₀ IU/ml required treatment based on FVL. Falls from above to below treatment threshold were noted in some patients. A BVL rules out the need for treatment in the majority of pregnancies with a BVL <5.3 log₁₀ IU/ml. Repeat sampling at 26–28 weeks gestation for those with a BVL >5.3 log₁₀ IU/ml may prevent unnecessary treatment.

THU346

Greater sequence diversity during early hepatitis B virus decline on vebicorvir plus entecavir is associated with a lower level of virus rebound following switch to entecavir monotherapy

Lewyn Li¹, Peter Revill², Ran Yan¹, Calvin Chan¹, Hua Tian¹, Julie Ma¹, Luisa M Stamm¹, Man-Fung Yuen³, Alexander Thompson⁴, Kathryn M Kitrinos¹. ¹Assembly Biosciences, South San Francisco, United States; ²Victorian Infectious Diseases Reference Laboratory, Melbourne, Australia; ³The University of Hong Kong, Department of Medicine, Hong Kong, China; ⁴St Vincent's Health Australia, Fitzroy, VIC, Australia
Email: lewynli@assemblybio.com

Background and aims: Vebicorvir (VBR) is a first-generation core inhibitor being developed for the treatment of chronic hepatitis B virus infection (CHBV). In Study 202 (NCT03577171), treatment-naïve HBeAg positive CHBV patients were randomized to VBR+entecavir (ETV) or placebo+ETV for 24 weeks. Eligible patients then received open label VBR+ETV in Study 211 (NCT03780543) for ≥52 weeks. In Study 211, 19 patients discontinued (DCed) VBR and remained on ETV at end of study. Following VBR DC, a mean HBV DNA increase of 1.0 log₁₀ IU/ml was observed, with 11/19 patients having a maximal increase of >1 log₁₀ IU/ml. Here we further characterize the patients who DCed VBR and remained on ETV and describe the results of next

generation sequencing (NGS) analyses to characterize viral quasi-species during treatment.

Method: Viral nucleic acids were purified from Study 202 baseline (BL), Week (Wk) 4, and rebound (if possible) patient plasma and whole genome NGS (Illumina MiSeq) was conducted. 18/19 patients had NGS data available: 11 with $\geq 1 \log_{10}$ IU/ml HBV DNA maximal increase and 7 with $< 1 \log_{10}$ IU/ml HBV DNA maximal increase after VBR DC. To determine sequence diversity, Shannon entropy was calculated from demultiplexed FASTQ read files using an in-house pipeline with genotype-specific reference sequences. The pipeline includes data quality control, read trimming and alignment, variant calling, and annotation in a workflow orchestrated by Nextflow.

Results: Patients with $< 1 \log_{10}$ IU/ml HBV DNA increase had significantly lower HBeAg and HBcrAg ($p < 0.05$) and trended lower for HBV DNA and pregenomic RNA with most having ALT $> \text{ULN}$ at BL compared to patients with $\geq 1 \log_{10}$ IU/ml HBV DNA increase. At BL, similar diversity levels were observed across the viral genome in both groups. At Wk 4, diversity remained stable for patients with $< 1 \log_{10}$ IU/ml HBV DNA increases, while diversity declined at Wk 4 for patients with $\geq 1 \log_{10}$ IU/ml HBV DNA increases ($p < 0.01$) (Figure). For patients with a $\geq 1 \log_{10}$ IU/ml HBV DNA increase, diversity returned towards BL levels at rebound following VBR DC.

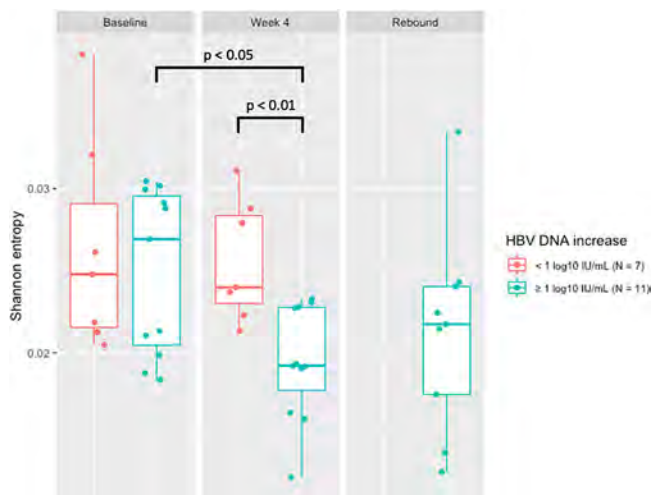


Figure: The dynamic changes of HBV nucleotide sequence diversity along with HBV DNA increase after VBR discontinuation.

Conclusion: Greater sequence diversity was observed during initial HBV DNA decline during HBV treatment among patients with lower rebound when VBR was DCed and ETV continued. The early differences in sequence diversity may reflect differences in HBV specific immune responses (also reflected in ALT levels) and viral load set points between these 2 groups, although the mechanism needs to be further defined.

THU347

Results from a nationwide hepatitis C serosurvey and progress towards HCV elimination in the country of Georgia

Amiran Gamkrelidze¹, Shaun Shadaker², Maia Tsereteli¹, Maia Alkhazashvili¹, Nazibrola Chitadze¹, Irina Tskhomelidze³, Lia Gvinjilia⁴, Nino Khetsuriani⁵, Francisco Averhoff⁶, Gavin Cloherty⁶, Giorgi Chakhunashvili¹, Jan Drobeniuc², Paata Imnadze¹, Khatuna Zakhashvili¹, Paige A Armstrong². ¹National Center for Disease Control and Public Health, Tbilisi, Georgia; ²Centers for Disease Control and Prevention, Division of Viral Hepatitis, Atlanta, United States; ³The Task Force for Global Health, Tbilisi, Georgia; ⁴Eastern Europe and Central Asia (EECA) Regional Office, Centers for Disease Control and Prevention (CDC); ⁵Global Immunization Division, CDC, Atlanta, United States; ⁶Abbott Diagnostics, Abbott Park, United States

Email: gamkrelidze@gmail.com

Background and aims: The country of Georgia launched its national Hepatitis C Virus (HCV) Elimination Program in 2015, and a serosurvey the same year showed prevalence of HCV antibody (anti-HCV) and HCV RNA among adults aged ≥ 18 years was 7.7%, and 5.4%, respectively. Since then, over 76,000 people with chronic HCV have been treated, with a cure rate of 98.9%. To monitor progress, a second serosurvey was conducted in 2021 to estimate the prevalence of hepatitis C, hepatitis B, and anti-SARS-CoV-2. This analysis reports hepatitis C results of the serosurvey and progress towards elimination.

Method: The serosurvey used a stratified, multi-stage cluster design with systematic sampling. Adults and children ≥ 5 years consenting (or assenting with parental consent) to the interview and blood draw were eligible to participate. All blood samples were tested for anti-HCV and if positive, HCV RNA. Nationally representative weighted proportions and 95% confidence intervals (CI) were calculated and compared with 2015 age-adjusted estimates for adults.

Results: A total of 7,237 adults and 1,473 children participated in the survey. For adults, the median age was 46 years (interquartile range: 32–60), and 53.3% (95% CI: 51.3–55.2) were female. The prevalence of anti-HCV was 6.8% (95% CI: 5.9–7.7), which was not significantly different from 2015 (7.7% [95% CI: 6.6–8.8]; $p = 0.20$). The HCV RNA prevalence was 1.8% (95% CI: 1.3–2.4), compared to 5.4% [95% CI: 4.5–6.3] in 2015 ($p < 0.001$). This represents a 67% reduction in persons with chronic HCV infection, despite the program having treated 51% of the estimated 150,000 infected. HCV RNA prevalence decreased among all age groups, most notably among those aged 40–59 years (9.3% in 2015 to 2.2% in 2021; $p < 0.001$). Substantial decreases were also observed among both males (9.0% to 3.1%; $p < 0.001$) and females (2.2% to 0.6%; $p < 0.001$). HCV RNA prevalence also decreased from 51.1% to 17.8% among persons who ever injected drugs, and 13.1% to 3.8% among those who received a blood transfusion (both $p < 0.001$). No children tested positive for anti-HCV or HCV RNA.

Conclusion: These results demonstrate the substantial progress made since Georgia launched its HCV Elimination Program in 2015. The 67% reduction in chronic HCV infections during 2015–2021 also supports treatment as a means for prevention, as the reduction is larger than would be expected based on those treated alone. These findings can inform strategies to meet HCV elimination targets.

THU348

Clinical impact of drug interaction in the use of antipsychotics by HCV patients treated with pangenotypic direct-acting antivirals

Juan Turnes¹, Antonio Garcia Herola², Ramón Morillo Verdugo³, Marinela Mendez Pertuz⁴, Cristina De Alvaro⁵, Candido Hernández⁵, Antoni Sicras-Mainar⁶. ¹CHU, Pontevedra, Gastroenterology and Hepatology Department, Spain; ²Hospital Marina Baixa de Villajoyosa, Villajoyosa, Alicante, Spain; ³Hospital de Valme, AGS Sur de Sevilla, Sevilla, Spain; ⁴Gilead Sciences S.L., Madrid, Spain, Medical Affairs, Madrid, Spain; ⁵Gilead Sciences S.L., Madrid, Spain, Medical Affairs, Madrid, Spain; ⁶Atrys Health, Health Economics and Outcomes Research, Barcelona, Spain

Email: ansicras@atryshealth.com

Background and aims: Previous analysis showed that central nervous system drugs were the most prescribed in patients with hepatitis C. This sub-analysis describes the use, drug-drug interactions (DDIs), and clinical impact of antipsychotic use in real-world patients treated with Pangenotypic Direct Action Antivirals (DAAp).

Method: Retrospective observational study, using the BIG-PAC database (Atrys Health), in HCV patients treated from 2017 to 2020 with DAAs. Potential DDIs between concomitant medication and the DAAs, Sofosbuvir/Velpatasvir [SOF/VEL] and Glecaprevir/Pibrentasvir [GLE/PIB], were evaluated using the University of Liverpool Hepatitis Interactions database. The risk of DDIs, the report of related adverse effects (AEs), and the clinical actions linked to the management of DDIs with antipsychotics (dose reduction; change of antipsychotic or DAAp; electrocardiogram-ECG and discontinuation) were analyzed.

Results: 187 patients prescribed antipsychotics were included, 150 treated with SOF/VEL [median age: 53 years; men: 59%; F3/4: 44%] and 37 with GLE/PIB [median age 48 years; men: 60%; F3/4: 46%]. The mean pill number was 5.0 and 5.9 tablets/patient, respectively. Accounting for all comedication, GLE/PIB was associated with a higher risk of single and multiple DDIs (≥ 2 comedications with DDIs with pDAAs) compared to SOF/VEL, [73% vs 43% of patients ($p < 0.001$)] and [24% vs 15% ($p = 0.002$)], respectively.

Regarding antipsychotics, there was a higher number of active ingredients with potential DDIs for GLE/PIB vs SOF/VEL (6 vs 2, respectively), linked to a higher percentage of patients at risk of DDIs (51% vs 23%, $p < 0.001$, respectively). Two AE were reported with GLE/PIB for quetiapine and paliperidone, and none with SOF/VEL. The AE reported with quetiapine and GLE/PIB (extrapyramidal symptoms) occurred at a dose of < 300 mg/day.

Quetiapine was the most prescribed antipsychotic (SOF/VEL, 42 and GLE/PIB, 7). Regarding clinical actions reported for patients prescribed quetiapine, a higher percentage of actions were reported for GLE/PIB (86%; 6/7 patients) vs SOF/VEL group (5%; 2/42 patients), $p < 0.001$. These clinical actions were ECG monitoring (1 vs 0), dose reduction (2 vs 1), change of DAA/antipsychotic (2 vs 1), and comedication discontinuation (1 vs 0) for GLE/PIB vs SOF/VEL, respectively.

Conclusion: This analysis confirms that the greater use of SOF/VEL in patients with antipsychotic treatment may be due to its favorable DDI profile, which implies a lower number of adverse effects and required clinical actions.

THU349

Occult hepatitis C infection detection in people who use drugs with or without direct antiviral agents therapy

Eliane Silva^{1,2}, Sara Marques¹, Sofia Salta³, José Pedro Sequeira³, João Madaleno⁴, Adelia Simão⁴, Armando Carvalho⁴. ¹Research Center in Biodiversity and Genetic Resources (CIBIO/InBIO), University of Porto, Vairão, Portugal; ²Institute of Biomedical Sciences Abel Salazar (ICBAS) of the University of Porto, Porto, Portugal; ³Portuguese Oncology Institute of Porto (IPO Porto), Porto, Portugal; ⁴Coimbra Hospital and University Center (CHUC), Coimbra, Portugal

Email: up412743@up.pt

Background and aims: Occult hepatitis C infection (OCI) can occur in anti-HCV (hepatitis C virus) and HCV-RNA peripheral blood mononuclear cells (PBMCs) positive subjects with normal or abnormal values of liver enzymes (LE) without serum HCV-RNA. The goal of HCV therapy is to cure the infection, i.e. achieve a sustained virological response (SVR) after therapy with direct acting antiviral agents (DAAs). Here, we evaluate OCI in people who are injection drug users (IDUs) with or without DAAs therapy.

Method: This study includes 4 patients study groups: AVP-14 patients (SVR 12 with DAAs therapy); SEP-2 patients (spontaneously elimination of HCV after acute infection); CNP-4 patients; CPP-10 patients (HCV positive patients), all anti-HCV positive (Table). HCV-RNA detection from serum at baseline was performed by Real-Time PCR (RT-PCR). After, was performed from serum, plasma, PBMCs and red blood cells (RBCs) by droplet digital PCR (ddPCR).

Table: Characteristics of IDUs patients (%), except sex and age.

Total, male	30
Age, mean	42
CNP	75
SEP	50
CPP	100
AVP	86
*AST/ALT U/ml	
+/+	60
±	3
Normal	30
N.D.	7
*GGT/**ALP U/ml	
+/+	10
±	30
Normal	57
N.D.	3
***Stage of liver disease	
Mild (F1)	67
Moderate (F2)	11
Advanced (F3)	11
Cirrhosis (F4)	11
HCV genotype	
1a	40
3a	20
4a/4c/4d	13
1b	3
N.D.	23
OCI	
CNP	50
SEP	50
CPP	10
AVP	29

*Normal values: AST (aspartate aminotransferase) < 35 U/L, ALT (alanine aminotransferase) < 45 U/L, GTT (gamma glutamyl transpeptidase) < 55 U/L

**Reference values: ALP (alkaline phosphatase) 30–120 U/L

***Reference values Fibrosis/Fibroscan: F0/F1: < 7 kPa; F2: 7–9, 5 kPa; F3: 9, 6–12, 5; F3/F4: 12, 5–14, 5 kPa; F4: > 14 , 5 kPa

N.D.- Not determined.

Results: At baseline HCV-RNA was detected in the CPP and AVP (both 100%) groups and was negative for AVP-SVR8 or 12 by RT-PCR. Although, OCI was shown in 50% of the CNP and SEP groups, 10% in the CPP group and 29% in the AVP group by ddPCR (Table). Two

patients-CNP, with normal values of LE; 1-SEP, with abnormal values of LE; 1 patient-CPP with normal values of LE, HCV-1a, DAAs therapy; 4-AVP (1 with abnormal values of LE, HCV-1a, DAAs therapy; 1 with abnormal values of LE and advanced fibrosis, HCV-3a, DAAs therapy; and 2-HCV-4a/4c/4d, one with normal values of LE, DAAs therapy, and the other with abnormal values of LE and cirrhosis, DAAs therapy). Positive results were shown in serum (71%), plasma (13%), PBMCs (79%) and RBCs (83%) analyzed samples in the CPP and AVP groups by ddPCR.

Conclusion: A total of 80% HCV-cure with DAAs was shown in the CPP and AVP groups, but 10% and 29% of OCI was shown in these groups, respectively, by ddPCR. HCV/OCI positive results were shown in patients with HCV 1a, 1b, 3a, or 4a/4c/4d genotypes, with normal or abnormal values of LE, and/or advanced fibrosis, and/or cirrhosis. Droplet ddPCR was more sensitive than RT-PCR for OCI detection. OCI and HCV positive patients should be newly evaluated for a reinfection or relapse possibility and avoid HCV transmission.

THU350

Strong correlation between HBsAg, ALT and HDV-RNA levels in patients with chronic hepatitis D. Results of phase 3 D-LIVR study.

Maria Buti^{1,2}, Ohad Etzion^{3,4}, Adriana Palom¹, David Yardeni^{3,4}, Anat Nevo-Shor^{3,4}, Daniela Munteanu^{3,4}, Ingrid Choong⁵, Lisa Weissfeld⁶, Mar Riveiro Barciela^{1,2}, Naim Abu-Freha^{3,4}, Ana Barreira^{1,2}, Rob Howard⁷, Tarik Asselah⁸, Pietro Lampertico^{9,10}.
¹Hospital Vall Hebron, Liver Unit, Barcelona, Spain; ²Centro de investigación biomédica en red de enfermedades hepáticas y digestivas, Madrid, Spain; ³Faculty of Health Sciences, Ben-Gurion University of the Negev, Beer-Sheva, Israel; ⁴Soroka University Medical Center, Gastroenterology and Liver Diseases, Beer-Sheva, Israel; ⁵Eiger BioPharmaceuticals, Palo Alto, California, United States; ⁶Statistics Collaborative Inc, Washington DC, United States; ⁷Veridical Solutions, Del Mar, California, United States; ⁸Hôpital Beaujon, Liver Unit, Clichy, France; ⁹CRC "A. M. and A. Migliavacca" Center for Liver Disease, University of Milan, Pathophysiology and Transplantation, Milan, Italy; ¹⁰Foundation IRCCS Ca' Granda Ospedale Maggiore Policlinico, Gastroenterology and Hepatology, Milan, Italy
 Email: mbuti@vhebron.net

Background and aims: Several new treatments for chronic hepatitis B are focused in achieving a decline in HBsAg levels. Some of these new molecules are evaluated in patients with chronic hepatitis D (CHD). The aim of this study is to evaluate whether ALT, HBsAg and HDV-RNA levels correlate in untreated patients with CHD.

Method: In this study, hepatitis delta virus (HDV)-RNA, hepatitis B surface antigen (HBsAg) and hepatitis B virus (HBV)-DNA were prospectively quantified in 407 patients with compensated liver disease who enrolled in the on-going Phase 3 HDV D-LIVR trial (NCT03719313). At baseline, demographic data, clinical and biochemical characteristics were collected. HBV and HDV serological and virological markers were measured. Descriptive statistics were used to summarize demographic and clinical baseline characteristics. Pearson correlation coefficients were computed for ALT, HBsAg and HDV-RNA in the full population of 407 subjects, the population of 146 subjects over 45, and the population of 261 subjects younger than 45 years old. Significance levels are provided for the test of the null hypotheses when the correlation is 0.

Results: 407 patients were included, mainly male (69%), with a mean age of 45 years old, Caucasians (73%) and with liver cirrhosis (26.5%). At baseline in the entire cohort, mean HDV-RNA levels were 4.98 ± 1.17 logIU/ml, HBsAg levels 10079 IU/ml and mean ALT 100.05 ± 67.7 IU/ml. HDV-RNA and HBsAg levels showed positive correlation (0.154) with strong statistical significance (0.0018) (Table 1). In patients older than 45, HDV-RNA and HBsAg levels did not show a statistically significant correlation. However, in patients younger than 45, HDV-RNA and HBsAg levels showed positive correlation (0.162) with strong statistical significance (0.0089). HBsAg levels and ALT showed a negative correlation, meaning that ALT levels tend to

decline when HBsAg levels are high. This correlation showed statistical significance across all groups.

Table 1. Correlation of ALT, HBsAg, and HDV RNA in the full population, subjects over 45, and subjects 45 years and younger in the D-LIVR study

	Correlation coefficient	Significance level
All subjects N = 407		
HDV RNA - ALT	0.097	0.0499
HBsAg - ALT	-0.248	<0.0001
HDV RNA - HBsAg	0.154	0.0018
Subjects ≥ 45 years N = 146		
HDV RNA - ALT	0.095	0.2552
HBsAg - ALT	-0.248	0.0026
HDV RNA - HBsAg	0.100	0.2288
Subjects < 45 years N = 261		
HDV RNA - ALT	0.106	0.0862
HBsAg - ALT	-0.242	<0.0001
HDV RNA - HBsAg	0.162	0.0089

Conclusion: In untreated chronic hepatitis D, HDV-RNA and HBsAg levels show positive correlation mostly in younger people. Normal ALT levels are associated with significantly increased HBsAg levels. Monitoring of HDV-RNA and HBsAg serum levels in patients with chronic hepatitis D provides insight in the design of new therapeutic strategies.

Viral hepatitis A/E: Clinical aspects

THU351

Detection of highly variable RNA-containing viral particles on CNT-based electrochemical impedimetric DNA-nanosensors

Andrei Babenka¹, Victor Hryharovich¹, Halina Grushevskaya², Igor Lipnevich², Nina Krylova², Elena Lebedeva³, Uladzimir Davydau¹, Svetlana Marchuk¹, Dmitry Borisovets⁴, Sergei Zhavoronok¹.
¹Belarusian State Medical University, Minsk, Belarus; ²Belarusian State University, Minsk, Belarus; ³Vitebsk State Medical University, Viciebsk, Belarus; ⁴Institute of Experimental Veterinary Medicine named after S.N. Vysheslesky, Minsk, Belarus
 Email: labmdbt@gmail.com

Background and aims: Due to the high variability of RNA-containing viruses genome, neither PCR nor ELISA methods give a 100% guarantee. For example, in the case of infection with the hepatitis E virus (HEV), the likelihood of a false negative diagnosis is considered very high. One of the possible ways to overcome this problem in general and for the diagnosis of HEV in particular, may be the use of alternative, non-PCR technologies. CNT-based electrochemical impedimetric DNA-nanosensors make it possible to recognize HEV RNA/cDNA using short probes (less than 20 bp), which sharply increases the likelihood of capturing variable genomes. This ensures high specificity of recognition. We offer a novel highly-performed and selective impedimetric DNA sensor with redox-active nanoporous transducer based on bundles of carbon nanotubes (CNTs) for diagnosing of HEV RNA in clinical samples.

Method: A target double-stranded (ds) cDNA was synthesized by reverse transcription of the total RNA isolated by standard commercial spin-column based kits from the whole blood, serum, feces and urine of patients with confirmed acute HEV diagnosis. A non faradaic impedimetric DNA-sensor is fabricated by depositing the two monomolecular layer of carboxylated multiwalled CNTs with probe single-stranded (ss) DNA molecules. A short (24 bp) DNA oligonucleotide was used as a probe, which was complementary to the most conserved region of the HEV genome and, according to preliminary estimates, is able to recognize about 99% of all sequences

POSTER PRESENTATIONS

of the HEV genome presented in the GeneBank database (more than 500) and sequenced in Belarus (more than 100). DNA-nanosensors are interdigital electrode structures with the sensitive coating. The electron-dense layers of the probe oligonucleotide and CNTs were fabricated by Langmuir-Blodgett technique. The impedance DNA-nanosensors are utilized as measured capacitance C entering a resistor (R)-capacitor (C)-oscillator. Impedance measurements are performed using the non faradaic impedance spectroscopy at quasi-resonance frequencies of the RC-oscillator.

Results: The capacitive characteristics of the DNA sensors in the frequency range from 100 kHz to 1 MHz after hybridization with targeted DNA at various concentrations have been investigated. It was found that the addition of molten target DNA at low concentrations leads to a significant decrease in capacity over the entire frequency range. Interacting the probe ss-DNA and target ss-cDNA molecules form homoduplexes on the sensor surface that leads to increasing the electron density of the nucleotide CNT-cover, providing capacity reduction due to an emerging screening surface effect.

Conclusion: The novel highly-performed and high-sensitive electrochemical method reliably detects the presence or absence of HEV in a sample in dose-dependent manner and does not demand expensive consumable materials.

THU352

Hepatitis B Delta: assesment of knowledge and practices of French non academic hepato-gastroenterologists

Jean-François David Cadranel¹, Honore Zougmore¹, Bertrand Hanslik², Jean-René Ngele¹, Xavier Causse³, Denis Ouzan⁴, Thierry Thévenot⁵, Philippe Halfon⁶, Dominique Roulot⁷, Veronique Loustaud-Ratti⁸, Tristan Lemagoarou⁹. ¹GHPSO DE CREIL, liver and diseases department, Creil, France; ²cabinet gastroenterologie, liver and diseases department, MONTPELLIER, France; ³Hospital Center Régional D'orléans Hospital La Source, liver and diseases department, Orléans, France; ⁴Arnault Institute Tzanck, liver and diseases department, Saint-Laurent-du-Var, France; ⁵Centre hospitalier régional universitaire de Besançon, liver and diseases department, Besançon, France; ⁶liver and INFECTIOUS diseases department, MARSEILLE, France; ⁷liver and DIGESTIVE diseases department, bobigny, France; ⁸liver and ANDF DIGESTIVE diseases department, limoges, France; ⁹GHPSO DE CREIL, DIM, Creil, France
Email: jcadranel5@gmail.com

Background and aims: Hepatitis B-Delta (BD) is uncommon or underestimated in France; there are no data from hepato-gastroenterologists (HG) practicing in non-university hospitals or in private practice on the management of BD hepatitis in France. The aim of this study was to evaluate the knowledge and practices concerning the diagnosis and treatment of BD hepatitis among HGs practicing in non-academic settings.

Method: A Google form questionnaire was sent to senior or junior non-academic from May to September. The following were evaluated: demographic data, predominant specialty, status, modality of virological diagnosis and screening for hepatitis BD according to HBs status, evaluation of hepatic fibrosis, modalities of treatment (Pegylated interferon, Bulevirtide, combination).

Results: 129 HGs (H 58, 1%) of age :44, 8 (13, 4) answered this survey. The number of patients (pts) followed by HG was: : 1 (0–30). The search for delta infection in all HBs antigen positive pts was performed by 89.1% of HGs and not by 10%: juniors 77.8%, seniors 84.4%, $p=0.009$; in any pts carrying HBs antigen with anti HBe: juniors 67%, seniors 92%, $p=0.002$, in any pts infected with HIV (juniors 83.8%, seniors 95.4%, $p=0.064$. Concerning fibrosis assessment, among the non-invasive markers of fibrosis: the fibrotest was never used by 47% of the respondents, the fibrometer was never used by 55% of the respondents. APRI and FIB 4 were not used; the delta fibrosis score adapted to hepatitis Delta was used by 13% of the HGE. Fibrosis assessment was mainly done by Fibroscan® in 77% of cases and liver biopsy in 81% of cases. Treatment was proposed for patients

>F2 in 49% of cases, whatever the transaminase level, and for all patients by 39% of the Gs. The HGE proposed treatment with pegylated interferon in 48.4% of cases, Bulevirtide in 43% of cases, and a combination of the two in 42% of cases. Half of the HGs referred their patients to an academic colleague. Among the criteria for treatment efficacy, a decrease or normalization of transaminases was retained by 84% of the HGs; 60% of the HGs defined VR by a cancellation or a 2-log decrease of viral replication; and a PVR by a disappearance of RNA after 12 (45.4%) or 24 months (16%) with normal transaminase activity. Discussion: The number of respondents to this survey is low despite the number of reminders, reflecting the rarity of the disease or its lack of awareness in non-academic settings, HGs often refer their patients to another colleague, the search for BD infection is not systematically performed, elastometry and liver biopsy are most often used to assess fibrosis.

Conclusion: The results of this survey show a certain degree of ignorance of BD hepatitis by non-academic HGs; the modalities of diagnosis and the need for systematic screening of BD infection in any HBsAg patient should be recalled by the learned societies.

THU353

Hepatitis E seroprevalence in solid organ transplant recipients in Croatia

Petra Dinjar Kujundžić¹, Tatjana Vilibic-Cavlek^{2,3}, Alan Ayoub², Adriana Vince^{2,4}, Anna Mrzljak^{2,5}. ¹Merkur Clinical Hospital, Zagreb, Croatia; ²School of Medicine, University of Zagreb, Zagreb, Croatia; ³Croatian Institute for Public Health, Zagreb, Croatia; ⁴University Hospital for Infectious Diseases Dr. Fran Mihaljevic, Zagreb, Croatia; ⁵University Hospital Centre Zagreb, Zagreb, Croatia
Email: petra.dinjar@gmail.com

Background and aims: Hepatitis E virus (HEV) is an emerging infectious disease and growing concern in Europe. After solid organ transplantation (SOT), patients are at greater risk of developing acute and chronic graft hepatitis with progression to cirrhosis. The consumption of undercooked or raw pig meat is the main route of HEV infection in developed countries. However, risk factors for the acquisition of HEV among SOT recipients are incompletely understood. This study aimed to determine the exposure of HEV in the SOT cohort.

Method: In this cross-sectional study, 639 SOT recipients were screened during routine post-transplant outpatient visits during 2002–2017 for anti-HEV IgG seroprevalence; 420 after liver transplantation (LT) and 219 after kidney transplantation (KT). Serum samples were tested for anti-HEV IgG using an enzyme immunoassay (Mikrogen, Neuried, Germany). All participants completed a risk factor assessment questionnaire.

Results: Anti-HEV IgG seroprevalence in LT recipients was 21%, and in KT recipients was 16.4%. The majority of the recipients were male (68.4%), median age 58 years (18–80). Anti-HEV IgG positive recipients were older ($p=0.029$) and lived more often in a rural area ($p=0.045$) than anti-HEV negative recipients. There was no significant difference in HEV seroprevalence regarding the type of transplanted organ, gender, level of education, number of household members, having a farm within a household, type of sewage system, or type of drinking water. Contrary to initial assumptions, production and/or consumption of cured meat and occupational exposure had no statistically significant strength of association with anti-HEV IgG seropositivity.

Conclusion: Our results show that anti-HEV IgG seroprevalence is high among SOT recipients (19, 4%). Socio-demographic factors for exposure to HEV are the basis for further research of sources and routes of transmission and clinical significance of HEV infection after SOT.

THU354

Microarray analysis of virus-specific IgM and IgG antibodies significantly improves the serological diagnosis of hepatitis E virus infection

David Springer¹, Christian Borsodi¹, Stephan Aberle¹, Lukas Weseslindtner¹. ¹Medical University of Vienna, Center for Virology, Vienna, Austria
Email: lukas.weseslindtner@meduniwien.ac.at

Background and aims: Due to the limited availability of PCR, the rapid decrease of viral RNA in the blood, and the possibility of unspecific reactivity in serological assays, the laboratory diagnosis of hepatitis E virus (HEV) infection remains challenging. Therefore, we evaluated a commercial microarray for HEV-specific IgM and IgG antibodies featuring nine target antigens (HEV Virachip[®], Viramed). **Method:** The evaluation panel comprised 408 serum samples first characterized by HEV-PCR (in-house) and Anti-HEV-IgM- and IgG-ELISAs (Wantai-HEV-IgG/IgM ELISA[®], Wantai Biological Pharmacy Ent). Based on these results and additional IgG avidity testing, samples were staged as early viremic (serum PCR+, IgM ±, IgG ±; n = 94), progressed non-viremic (serum PCR-, IgM+, IgG+; n = 80) and past HEV infection (PCR-, IgM-, IgG+; n = 117). Additional 117 samples negative for all HEV parameters served as controls.

Results: Microarray results significantly concurred with the ELISAs in 94.8% of IgM positive and 97.7% of IgG positive samples, indicating a high concordance of the applied serological assays. However, IgM and IgG antibodies against specific antigens included in the microarray (e.g., IgM and IgG against O2-1C4 and O2-1N, respectively) were earlier detectable in 14.9% of still ELISA-IgM negative and 35.3% of ELISA-IgG negative samples. In addition, samples with negative PCR but positive IgM ELISA results (progressed HEV infection) were reliably identified as HEV infection by the microarray and constituted a specific infection stage based on the serological microarray profile. Finally, we calculated an algorithm to identify HEV infection (with PCR positivity as reference) with the highest accuracy using all serological parameters provided by the microarray (ROC-AUC 0.90, p < 0.005).

Conclusion: Microarray analysis of HEV-specific IgM and IgG antibodies displays high sensitivity to diagnose HEV infection, especially in the early phase of the infection, and identifies the progressed infection stage when PCR from serum already tests negative.

Viral hepatitis B/D: Clinical aspects except therapy

THU355

Hepatitis delta virus reflex testing in patients with hepatitis B improves the HDV screening cascade: 10 years of real-world experience from Avicenne University Hospital, France

Segolene Brichler^{1,2,3}, Dominique Roulot^{2,3,4}, Samira Dziri^{1,3}, Athenais Gerber^{1,3}, Frédéric Le Gal^{1,3}, Heloise Delagereverie^{1,2}, Chakib Alloui^{1,3}, Emmanuel Gordien^{1,2,3}. ¹Avicenne Hospital, AP-HP, Virology Unit, Bobigny, France; ²Paris Nord University, Bobigny, France; ³INSERM U955, Creteil, France; ⁴Avicenne Hospital, AP-HP, Hepatology Unit, Bobigny, France
Email: segolene.brichler@aphp.fr

Background and aims: Chronic infection with Hepatitis delta virus (HDV) leads to the most severe form of chronic viral hepatitis, with higher rates of cirrhosis and hepatocellular carcinoma than with Hepatitis B virus (HBV) mono-infection. EASL international guidelines recommend systematic HDV screening for all HBsAg positive patients. However, it is not performed in most areas. In our university hospital, hepatologists and virologists have implemented a "HDV

reflex testing" protocol, consisting of the systematic addition of a serological HDV test on all samples with a first diagnosis of hepatitis B (HBsAg+). We report the effectiveness of this strategy over a 10-year period.

Method: This is a single-centre retrospective survey in Avicenne University Hospital (Assistance Publique-Hôpitaux de Paris, France). The hospital is set in a suburban area, home to many patients originating from countries with a high burden of viral hepatitis. Our laboratory database was screened for all HDV tests performed in HBsAg positive patients from June 2012 to February 2022. Duplicates were excluded based on name, sex and date of birth. Patient serum samples were assayed for HBsAg using the Abbott Architect HBsAg qualitative II and quantitative HBsAg kits, and for total HDV antibodies (HDV-Abs) using the ETI-DELTA[®] or the Diasorin Liaison XL Murex anti-HDV kits. HDV viral loads were obtained first by in-house RT-qPCR, then by using the EurobioPlex HDV kit since 2016.

Results: A total of 84, 671 patients were screened at least once for HBV during the evaluation period. Among the 3198 HBsAg positive patients (3.8%, median age 39.0, sex ratio 2.04), 2886 (90.2%) were screened for HDV-Abs, 172 of them being positive (6.0%, median age 39.5, sex ratio 1.92). At least one HDV-RNA assay was available for 149 of them (86.6%) and was found positive for 91 patients (61.1%). HDV screening rate steadily improved with time, from 85–87% in the initial 2012–2015 period to 95–98% in the 2019–2022 years, while the annual frequency of HDV-Abs positivity among tested HBsAg+ samples remained stable (range: 4.4–7.7%).

Conclusion: HDV reflex testing in our centre was effective, allowing earlier identification of most HBV-HDV infected patients and a fast referral to hepatologists for adequate clinical management. The prevalence of HDV co-infection in HBsAg positive patients is twice higher than that initially reported in France among HBsAg positive blood donors. Active HDV replication was present in more than 60% of co-infected patients identified through our systematic screening. In the future, further molecular HDV reflex testing in HDV-Ab positive patients may improve the complete HDV screening cascade in our centre.

THU356

T cell epitope mapping of hepatitis B virus in chronic infection

Marie Viuff¹, Marianne Tuefferd², Christina Heeke¹, Kamilla Kjærgaard Munk¹, Mohammad Kadivar¹, Georg Lauer³, Jacques Bollekens², Sine Reker Hadrup¹. ¹Technical University of Denmark, Department of Health Technology, Kgs. Lyngby, Denmark; ²Janssen Pharmaceuticals, Infectious Diseases and Vaccines, Beerse, Belgium; ³Massachusetts General Hospital, Department of Medicine, Boston, United States
Email: macviu@dtu.dk

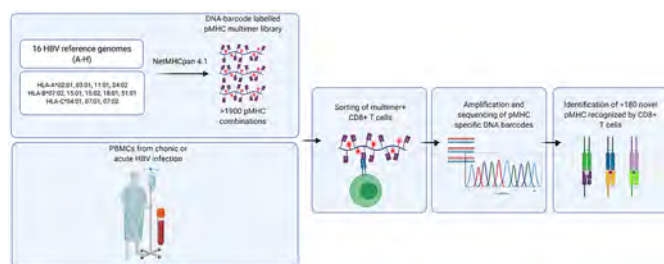
Background and aims: Affecting more than 250 million patients worldwide, chronic hepatitis B virus (HBV) infection still poses a substantial global health threat, without available curative therapy. CD8 T cells are known to be crucial for the elimination of the virus, however, in chronically infected patients, the cellular immune response proves inefficient. Thus, uncovering the full repertoire of HBV epitopes and functionality of the HBV-specific CD8 T cells is highly relevant for understanding the immune response. Identification of HBV epitopes recognized by T cells has historically been limited to few HLA types and selected viral proteins. Here, we have performed a large-scale screening covering HBV genotypes A-H to identify T cell recognition restricted by 12 different HLA molecules, in patients with acute and chronic hepatitis. This data is substantially extending the present knowledge about the T cell recognition of HBV.

Method: A library of >1, 900 peptide-MHC combinations was used to generate DNA-barcode labelled multimers to screen CD8 T cells from peripheral blood for recognition of hepatitis B epitopes in HLA-matching patients with either acute, chronic, or resolved chronic hepatitis (n=40). The peptide-MHC library was generated by

POSTER PRESENTATIONS

selecting specific 8–11mers from HBV genotypes A–H, predicted to bind to 12 different HLA types.

Results: Performing the large-scale multimer screening we found a total of 212 unique peptide-MHC, which were recognized by CD8 T cells across all patient groups. Out of these, 189 peptide-MHC have not previously been described. Furthermore, 45% of the peptide-MHCs were recognized in multiple patients. T cell recognition was detected in both acute and chronic patients, with no significant difference observed between chronic and HBsAg loss patients. Interestingly, T cells recognizing the identified peptides display different level of functional responses upon peptide stimulation, which will be further investigated.



Conclusion: In this study, we were able to fully map the CD8 T cell recognition towards HBV genomes A–H and identify >180 novel CD8 T cell epitopes of potential relevance for viral control and clearance.

THU357

The Comparison of tenofovir alafenamide fumarate with tenofovir disoproxil fumarate in preventing hepatitis B transmission in mothers with high viral load: a retrospective cohort study

Yunxia Zhu¹, Jinhua Wang², Ming Wang², Xin Zhou¹, Shuangxia Zhang¹, Shujie Zhang¹, Bo Yang¹, Ping Yang¹, Zhongjie Hu³.
¹Beijing Youan Hospital, Capital Medical University, Obstetrics and Gynecology, Beijing, China; ²Beijing Obstetrics and Gynecology Hospital, Capital Medical University, Department of Gynecologic Oncology, Beijing, China; ³Beijing Youan Hospital, Capital Medical University, Hepatology, Beijing, China
 Email: zyxno7@163.com

Background and aims: Tenofovir disoproxil fumarate (TDF) is most commonly utilized in the prevention of maternal-to-child transmission of the hepatitis B virus. The previous studies show antiviral prophylaxis with tenofovir alafenamide fumarate (TAF) was also generally safe for both mothers and infants and reduced the mother-to-child transmission (MTCT) rate to 0%. However, few safety and effectiveness results have been published regarding the comparison of two drugs during pregnancy for the prevention of MTCT of HBV, especially for the early markers of bone metabolism like alkaline phosphatase (ALP) and Z value for bone mineral density (BMD) of infants.

Method: We performed a prospective cohort study involving women who had HBV DNA $\geq 2 \times 10^5$ IU/ml and initiated TAF or TDF for preventing MTCT during gestational weeks 24–28 weeks. All enrolled patients had normal liver function and had not received antiviral therapy before pregnancy. We collected the name, ID, age, and drug duration of the maternal, monitoring HBV viral load and ALP at the same time besides infants' HBV marks and their Z value for BMD. The primary outcomes were the decrease in virus load and the rates for MTCT, which was defined as the proportion of infants who had a serum HBV DNA level of more than 20 IU per milliliter (i.e. above the lower limit of detection) or who were positive for hepatitis B surface antigen (HBsAg). The secondary outcomes were the changes in serum ALP expression of the mother and the BMD of newborns.

Results: A total of 61 patients received TAF treatment and 73 patients received TDF. 51 pairs of patients were matched by Propensity Score Match (PSM). The levels of HBV-DNA decline in TDF-treated mothers were compared to TAF treated mothers (3.70 ± 0.91 log10IU/ml vs 3.43 ± 1.30 log10IU/ml, $P > 0.05$) before delivery. The rates of MTCT in the TAF group were similar to the TDF group (with the transmission of 0.00% [0 of 39] vs 0.00% [0 of 29], $p > 0.05$) in the per-protocol analysis. As for BMD, no significant difference in the Z value of newborns was found between the two groups. However, the expression level of ALP was significantly higher in the TDF group than TAF group.

Variables	TDF Treated (n = 51)	TAF Treated (n = 51)	t/X2	p
Age (years)	30.75 \pm 2.95	30.43 \pm 3.70	0.473	0.637
Drug Duration (weeks)	12.52 \pm 4.54	12.74 \pm 4.86	0.229	0.819
HBV DNA before Drug Use (log10IU/ml)	8.06 \pm 8.13	8.07 \pm 8.10	0.023	0.982
Decline of HBV DNA (log10IU/ml)	3.43 \pm 1.20	3.70 \pm 0.91	1.244	0.216
ALP (U/L)	162.06 \pm 42.30	144.67 \pm 45.71	1.995	0.049
Z for BMD	0.69 \pm 0.46	0.66 \pm 0.41	0.259	0.797

Conclusion: TDF and TAF use in MTCT for highly viremic mothers was equally effective and the study showed both two drugs have no statistically different effect on neonatal BMD. However, TAF has less influence on serum ALP in pregnant women than TDF.

THU358

Detection of notable hepatitis B virus serologic activity after hepatitis B surface antigen seroclearance

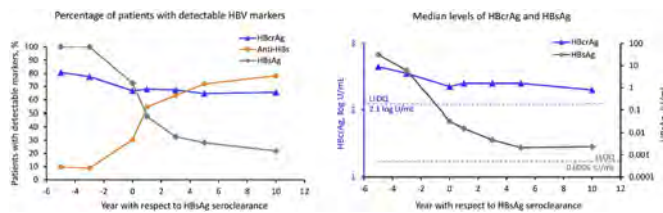
Danny Ka-Ho Wong^{1,2}, Takako Inoue³, Lung Yi Loey Mak^{1,2}, Yan Yue James Fung^{1,2}, Ka-Shing Cheung¹, Wai-Kay Seto^{1,2}, Yasuhito Tanaka⁴, Man-Fung Yuen^{1,2}.
¹The University of Hong Kong, Medicine, Hong Kong; ²The University of Hong Kong, State Key Laboratory of Liver Research, Hong Kong; ³Nagoya City University Hospital, Clinical Laboratory Medicine, Nagoya, Japan; ⁴Kumamoto University, Gastroenterology and Hepatology, Kumamoto, Japan
 Email: dannykh Wong@gmail.com

Background and aims: Undetectable serum hepatitis B surface antigen (HBsAg) measured by conventional assays (lower limit of detection ~ 0.05 IU/ml) is regarded as functional cure to chronic hepatitis B (CHB). It has been demonstrated that some HBV proteins are detectable in patients after HBsAg seroclearance (SC). We evaluated the use of two novel investigational assays to detect hepatitis B core-related antigen (HBcrAg) and HBsAg in serial patient samples collected before and after SC.

Method: Serum samples were collected from 98 CHB patients (72 males and 26 females) with SC at the following 7 time-points: 5 years and 3 years before SC, at the time of SC, and 1 year, 3 years, 5 years and 10 years after SC. HBsAg and HBcrAg were measured using the iTACT- (stands for Immunoassay for Total Antigen including Complex via pre-Treatment)-HBsAg and iTACT-HBcrAg assays (Fujirebio, Tokyo, Japan) respectively. The lower limit of quantitation (LLOQ) of the iTACT-HBsAg and iTACT-HBcrAg assays are 0.0005 IU/ml and 2.1 log U/ml respectively, which are 100 times and approximately 10 times more sensitive than the current HBsAg and HBcrAg assays (LLOQ 3 log U/ml). Anti-HBs was measured by the Lumipulse Presto anti-HBs assay (LLOQ 10 mIU/ml).

Results: The median age of SC was 52 years (IQR: 45–57). A total of 572 samples (142 collected before SC and 430 collected after SC) were tested. HBsAg was detectable by iTACT-HBsAg in all the 142 samples collected before SC (median level: 10.9 IU/ml) and in 165/430 (38.4%) samples collected after SC (median level for those with detectable HBsAg: 0.0082 IU/ml). 61.6% of samples collected after SC had detectable anti-HBs. Of these anti-HBs positive samples, 70 (26.4%) had detectable HBsAg. HBcrAg was detectable in 78.9% of samples collected before SC and 66.4% after SC. There was a positive correlation between HBsAg and HBcrAg levels ($r = 0.330$, $P <$

0.00001). The detectability rate and median levels of both HBsAg and HBcrAg progressively decreased over time from before to after SC, while the detectability rate of anti-HBs increased after SC (Figure 1). Of the 98 patients, 9 (9.2%) had detectable HBsAg and HBcrAg at all time points after SC, and 11 (11.2%) patients had undetectable HBsAg and HBcrAg at all time points after SC. 87 (88.8%) patients had detectable HBsAg and/or HBcrAg at least one time point after SC. Of note, at 10 years after SC, 21.9% and 65.6% of the patients still had detectable HBsAg and HBcrAg, respectively.



Conclusion: The iTACT-HBsAg assay could detect a low level of HBsAg in >20% patients even at 10 years after SC. A relatively stable expression of HBcrAg was also detected in >60% patients after SC. The findings suggested that the threshold of SC may be raised using an ultrasensitive HBsAg assay and that expression of HBV proteins could still be detected after SC. The association between the expression levels of these proteins and disease progression deserves further studies.

THU359

Comparison of on-treatment ALT or FIB-4 as an on-treatment biomarker of hepatitis B treatment for liver cirrhosis patients

Joo Hyun Oh¹, Dong Hyun Sinn², Sang Bong Ahn¹, Wonseok Kang², Geum-Yon Gwak², Yong-Han Paik², Moon Seok Choi², Joon Hyeok Lee², Kwang Cheol Koh², Seung Woon Paik². ¹Nowon Eulji Medical Center, Department of Medicine, Korea, Rep. of South; ²Samsung Medical Center, Department of Medicine, Korea, Rep. of South
Email: dh.sinn@samsung.com

Background and aims: Alanine aminotransferase (ALT) levels are usually mildly elevated in patients with cirrhosis. Therefore, it is unclear whether 'normalization of ALT' with antiviral therapy is associated with a lower risk of hepatic events in hepatitis B virus (HBV)-related cirrhosis patients. We tested on-treatment ALT and several other potential on-treatment biomarkers that can be clinical surrogate or end point of antiviral therapy.

Method: A total of 911 hepatitis B virus-related liver cirrhosis patients who started entecavir or tenofovir were analyzed. We tested 'ALT normalization', 'undetectable serum HBV DNA', 'fibrosis-4 (FIB-4) index improvement', and 'serum HBeAg loss or seroconversion' at 1 year as a potential on-treatment biomarker for future HCC risk.

Results: During 6.6 (3.8–10.2) years of follow-up, 222 patients (24.4%) newly developed HCC. Among 747 patients with elevated ALT levels, ALT normalization was observed in 49.5% at one year. HCC incidence rate was not different between those with and without ALT normalization (17.6% vs. 16.8% at 5-years, $p=0.39$). Undetectable HBV DNA level was observed in 73.2% at one year, and HCC incidence rate was significantly different between those with and without undetectable HBV DNA levels (16.6% vs. 20.9% at 5-years, $p=0.004$). FIB-4 improvement (FIB-4 <3.25) was observed in 163 patients (34.1%) among 478 patients with elevated FIB-4 index (FIB-4 ≥3.25). HCC incidence rate was lower for those with FIB-4 improvement than those without (14.9% vs. 25.6% at 5-years, $p=0.006$), and was associated with lower risk of HCC (adjusted hazard ratio 0.59, 95% CI 0.55–0.82). HBeAg loss or seroconversion was observed in 55 patients (15.0%) at one year among 367 HBeAg positive patients, and the HCC incidence rate was not different between those with and without HBeAg seroconversion (19.7% vs. 20.1% at 5-years, $p=0.55$).

Conclusion: Among HBV-related liver cirrhosis patients who started antiviral therapy, complete virological response and improvement of FIB-4 index at one-year was independently associated with future HCC risk, while ALT normalization and serological biomarkers were not. This indicate HBV DNA and FIB-4 index can be better on-treatment clinical end points of antiviral therapy for cirrhotic patients.

THU360

Liver fibrosis burden determines risk of hepatocellular carcinoma among patients with hepatitis B surface antigen seroclearance

Lung Yi Loey Mak^{1,2}, Ka-Shing Cheung¹, Rex Wan-Hin Hui¹, Danny Ka-Ho Wong^{1,2}, Yan Yue James Fung^{1,2}, Man-Fung Yuen^{1,2}, Wai-Kay Seto^{1,2,3}. ¹The University of Hong Kong, Medicine, Hong Kong, Hong Kong; ²State Key Laboratory for Liver Research, The University of Hong Kong, State Key Laboratory for Liver Research, Hong Kong, Hong Kong; ³The University of Hong Kong-Shenzhen Hospital, Medicine, Shenzhen, China
Email: loeymak@gmail.com

Background and aims: Hepatitis B surface antigen (HBsAg) seroclearance is regarded as functional cure in chronic hepatitis B infection (CHB). We investigated the risk of hepatocellular carcinoma (HCC) in CHB patients after achievement of HBsAg seroclearance.

Method: 337 Asian CHB patients (69.1% male) who developed spontaneous HBsAg seroclearance between April 1996 to October 2012 with retrievable blood samples before HBsAg seroclearance were recruited and prospectively followed up for a median duration of 12.7 (interquartile range [IQR] 9.5–16.2) years. Blood levels of Enhanced Liver Fibrosis (ELF) were determined. Variables of interest included gender, age of HBsAg seroclearance (ageSC), presence of diabetes mellitus (DM), ELF score, and antibody to HBsAg (anti-HBs). Independent risk factors of HCC were determined by univariate then multivariate Cox regression and Kaplan Meier survival analysis.

Results: The median ageSC was 51.6 (IQR 42.6–58.1) years old, and 24.6% patients had DM. ELF at a median interval of 3.4 (IQR 0.4–4.9) years before HBsAg seroclearance was 9.5 (IQR 9.0–10.1). 216/337 (64.1%) developed anti-HBs at a median time of 2.3 (IQR 0–4.0) years after HBsAg seroclearance with median level of 42 (IQR 18–138) mIU/ml. Nine cases of HCC were diagnosed at a median time of 6.6 (IQR 2.6–7.9) years after HBsAg seroclearance. At Cox regression analysis, ageSC (hazard ratio [HR] univariate: 1.118, multivariate: 1.096, both $p < 0.01$) and ELF (HR univariate: 3.282, multivariate: 3.090, both $p < 0.001$) were significant variables associated with HCC, while DM (HR 2.490, $p=0.273$), anti-HBs (HR 1.17, $p=0.876$) and gender (HR 1.695, $p=0.514$) were not significant variables. The area under receiver-operating characteristic curve value for ELF was 0.856 (95% confidence interval [CI] 0.714–0.997, $p < 0.001$). By maximizing the Youden's index, ELF <10.8 was associated with lower risk of HCC with 77.8% sensitivity and 90.2% specificity. Among patients with ageSC ≥50 (known to be associated with residual risk of HCC; $n=190$), ELF <10.8 before HBsAg seroclearance was associated with >97% reduction in risk of HCC development [Figure 1].

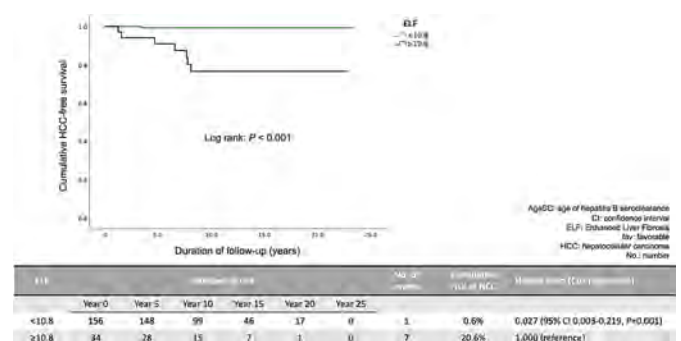


Figure: Cumulative HCC-free survival in Asian CHB patients who achieved HBsAg seroclearance at or after age of 50 years-old

POSTER PRESENTATIONS

Conclusion: ELF <10.8 was associated with markedly reduced risk of HCC development upon long-term follow-up among CHB patients with ageSC ≥ 50 . Ongoing HCC surveillance is required for patients who achieved HBsAg seroclearance at an older age and had advanced liver fibrosis before HBsAg seroclearance. [Supported by SK Yee Medical Foundation (reference number: 2171213)]

THU361

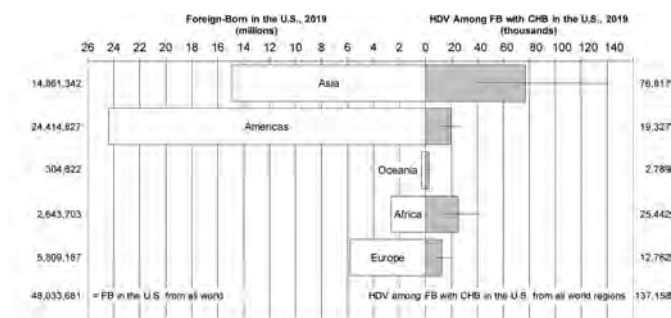
Estimating the prevalence of hepatitis delta infection among foreign-born adults with chronic hepatitis B in the United States

Robert Wong¹, Carol Brosgart², Steven Wong³, Jordan Feld⁴, Jeffrey Glenn⁵, Saeed Sadiq Hamid⁶, Kate Moraras⁷, John Ward⁸, Heiner Wedemeyer⁹, Cihan Yurdaydin¹⁰, Robert G. Gish⁷. ¹Stanford University School of Medicine, Veterans Affairs Palo Alto Healthcare System, Palo Alto, United States; ²University of California San Francisco Parnassus Campus, San Francisco, United States; ³S Wong Consulting, LLC, United States; ⁴University Health Network, Toronto, Canada; ⁵Stanford University School of Medicine, Stanford, United States; ⁶Aga Khan University Hospital, Karachi, Pakistan; ⁷Hepatitis B Foundation, Doylestown, United States; ⁸The Task Force for Global Health, Decatur, United States; ⁹Hannover Medical School, Department of Gastroenterology, Hepatology and Endocrinology, Germany; ¹⁰Koç University School of Medicine, Department of Gastroenterology and Hepatology
Email: rwong123@stanford.edu

Background and aims: Suboptimal awareness and testing for hepatitis delta virus (HDV) infection among adults with chronic hepatitis B (CHB) contributes to the poor understanding of the true prevalence of HDV and appropriate policy development. Our recent study estimated 1.47 million (M) foreign-born (FB) persons with CHB were living in the United States (US) in 2018. FB persons with CHB contribute to the majority of the burden of HDV infection in the U.S., given the high burden of HDV in many world regions from which CHB patients emigrate from. This study aims to provide an estimate of HDV prevalence among FB adults with CHB in the US.

Method: We updated analyses of CHB prevalence among FB adults in the US by performing systematic reviews and meta-analyses (surveys published from 1980 to 2019) that combined country-specific CHB prevalence rates with number of FB living in the US in 2019 by country of birth from the US Census Bureau. To estimate HDV prevalence among FB adults with CHB, we combined country-specific HDV prevalence rates (anti-HDV or HDV RNA positive) for persons with CHB from meta-analyses and applied these estimates to the number of FB with CHB in the US in 2019 by country of birth to estimate the number of FB CHB patients with combined HDV infection.

Results: In 2019, the overall FB population in the US was 48.0M, among which the estimated prevalence of CHB was 3.10% (95% CI 2.55–3.65), resulting in 1.49M (95% CI 1.22–1.75) FB adults with CHB, which accounts for nearly 80% of all adults with CHB in the US. Among FB adults with CHB, overall estimated pooled prevalence of HDV infection was 9.22% (95% CI 4.90–15.73), resulting in 137,158 FB adults with HDV (95% CI 72,936–233,984). World region-specific estimates of HDV infection among adults with CHB were 8.73% in Asia, 6.98% in the Americas, 22.52% in Oceania, 11.18% in Africa, and 14.08% in Europe, representing 76,817 (Asia), 19,327 (Americas), 2,789 (Oceania), 25,442 (Africa), and 12,782 (Europe), FB CHB adults with HDV infection in the US.



Abbreviations: CHB, chronic hepatitis B; HDV, hepatitis delta virus; FB, foreign-born.

Figure: FB Populations Living in the U.S. and Number of HDV among FB with CHB Living in the U.S. by World Region of Origin, 2019.

Conclusion: This analysis provides an estimate of the number of FB adults with CHB living in the US who are also infected with HDV, which is expected to further grow with patterns of increased immigration into the US. The burden of HDV will be even greater when factoring in US-born CHB patients who have combined HDV infection acquired primarily through high-risk activities.

THU362

Secular trend of the accuracy of hepatocellular carcinoma risk scores in treated chronic hepatitis B patients in 2005–2020: a territory-wide study of 48,706 subjects

Terry Cheuk-Fung Yip¹, Mandy Sze-Man Lai¹, Vincent Wai-Sun Wong¹, Yee-Kit Tse¹, Yan Liang², Vicki Wing-Ki Hui², Henry LY Chan^{3,4}, Grace Lai-Hung Wong¹. ¹The Chinese University of Hong Kong, Medical Data Analytics Centre (MDAC), Department of Medicine and Therapeutics, Institute of Digestive Disease, Faculty of Medicine, Hong Kong; ²The Chinese University of Hong Kong, Medical Data Analytics Centre (MDAC), Department of Medicine and Therapeutics, Faculty of Medicine, Hong Kong; ³Union Hospital, Department of Internal Medicine, Hong Kong; ⁴The Chinese University of Hong Kong, Medical Data Analytics Centre (MDAC), Faculty of Medicine, Hong Kong
Email: wonglaihung@cuhk.edu.hk

Background and aims: Patients with chronic hepatitis B (CHB) are aging with more comorbidities such as diabetes mellitus (DM). In contrast, the reimbursement of antiviral treatment has been less restrictive over time, leading to better coverage. We aimed to examine whether the resulting change in patients' clinical characteristics over time affects the accuracy of risk scores for hepatocellular carcinoma (HCC).

Method: Adult CHB patients who received entecavir or tenofovir for at least 6 months between January 2005 and March 2020 were identified using a territory-wide electronic healthcare database in Hong Kong. DM was defined by any use of non-insulin antidiabetic agents, continuous use of insulin for ≥ 28 days, haemoglobin A_{1c} $\geq 6.5\%$, fasting glucose ≥ 7 mmol/L, and/or diagnosis codes. Four HCC risk scores for treated CHB patients including PAGE-B and modified PAGE-B (mPAGE-B) scores; cirrhosis, age, male sex, and DM (CAMD) score; and Real-world Effectiveness from the Asia Pacific Rim Liver Consortium for hepatitis B virus (REAL-B) score were studied. The accuracy of scores was assessed by area under the time-dependent receiver operating characteristic curves (AUROCs) with death as a competing risk. Comparisons were done based on 1,000 bootstrap samples.

Results: Of 48,706 patients included, 2,792, 11,563, 15,471, and 18,880 patients started antiviral treatment in 2005–08, 2009–12, 2013–16, and 2017–20 respectively; their mean age at treatment initiation were 50, 52, 54, and 57 years respectively. DM prevalence rose from 16% in 2005–08 to 19% in 2009–12, 21% in 2013–16, and 24% in 2017–20, whereas the prevalence of cirrhosis dropped from 21% to 17%, 9%, and 5% respectively through the 4 periods. The median follow-up time was 5, 5, 5, and 2 years in 2005–08, 2009–12, 2013–16, and

2017–20 respectively; 7.4%, 6.8%, 5.2%, and 1.9% of patients developed HCC respectively. PAGE-B and modified PAGE-B scores performed well across the 4 periods with comparable AUROCs ranged from 0.75–0.77 for PAGE-B score ($p = 0.726$) and 0.76–0.80 for mPAGE-B score ($p = 0.150$). For the other two scores with DM as a predictor, CAMD score was less predictive in the most recent period ($p = 0.025$). REAL-B score tended to be less predictive in the most recent period ($p = 0.085$) (Figure).

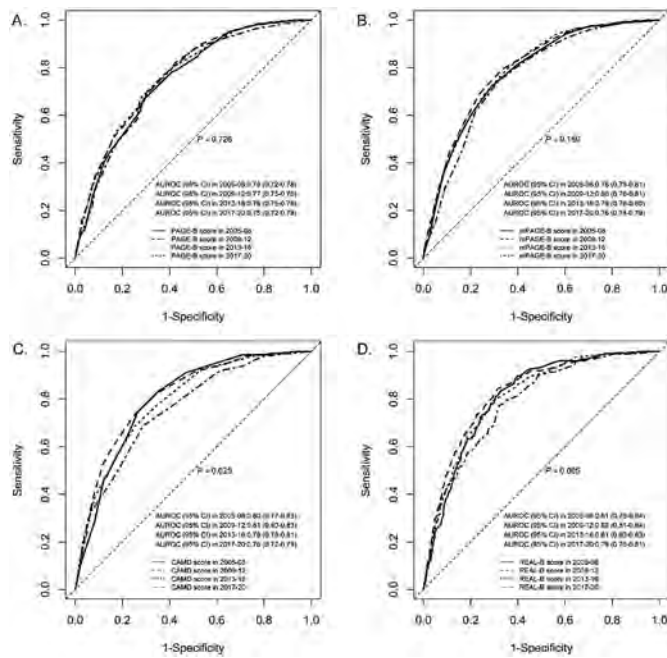


Figure: The area under the time-dependent receiver operating characteristic curves (AUROCs) of A. PAGE-B score; B. mPAGE-B score; C. CAMD score; and D. REAL-B score for predicting the development of hepatocellular carcinoma among chronic hepatitis B patients who started nucleos(t)ide analogue treatment in the 4 periods.

Conclusion: Two PAGE-B scores performed well regardless of the change in clinical characteristics of CHB patients over time. HCC risk scores that have DM as a predictor may however be less predictive in recent years.

THU363

Risk prediction of hepatocellular carcinoma in chronic hepatitis B patients outside current treatment criteria

Gi-Ae Kim¹, Seungbong Han², Young-Suk Lim³, Gwang Hyeon Choi⁴, Jonggi Choi⁵, Dong Hyun Sinn⁵, Yong Han Paik⁵, Jeong-Hoon Lee⁶, Ju-Yeon Cho⁷. ¹Kyung Hee University School of Medicine, Department of Internal Medicine, Korea, Rep. of South; ²Korea University, Department of Biostatistics; ³Asan Medical Center, Department of Gastroenterology, Liver Center; ⁴Seoul National University Bundang Hospital, Department of Internal Medicine, Seongnam-si, Korea, Rep. of South; ⁵Samsung Medical Center, Department of Medicine, Korea, Rep. of South; ⁶Seoul National University College of Medicine, Department of Internal Medicine and Liver Research Institute, Korea, Rep. of South; ⁷Chosun University, Department of Internal Medicine, Korea, Rep. of South. Email: limys@amc.seoul.kr

Background and aims: A considerable number of chronic hepatitis B (CHB) patients outside the current treatment criteria develop hepatocellular carcinoma (HCC), suggesting many patients at high risk are left untreated and risk prediction for this population is called for. Thus, we aimed to investigate the risk of HCC in CHB patients who are not indicated for antiviral treatment including a broader range of HBV DNA levels and develop a risk prediction model for them.

Method: This multi-center study recruited 9,058 treatment-naïve, non-cirrhotic CHB patients with ALT <2 × upper limit of normal: 6,949 for training cohort from Asan Medical Center and 2,109 for validation cohort from two tertiary hospitals in Korea. A risk prediction model for HCC was developed using predictors based on multivariable cox models, and bootstrapping was performed for validation.

Results: In the training cohort, 363 patients (5.2%) developed HCC during 8.0 years of median follow-up. By multivariable cox regression analysis, HCC risk was the highest with HBV DNA levels of 6–7 log₁₀ IU/ml (adjusted hazard ratio [aHR] 4.98; $P < 0.001$), and lowest with >8 log₁₀ IU/ml (aHR 0.90; $P = 0.71$) and ≤4 log₁₀ IU/ml (aHR 1.00; reference). HBV DNA levels, male sex, older age, and lower platelet counts were independent predictors of HCC but ALT levels did not predict HCC risk ($p = 0.33$). An ALT-independent 24-point risk prediction model (“ABC model 1”) was developed including the 4 independent predictors: sex, age, platelet counts, and HBV DNA levels combined with HBeAg status. HCC risk was calculated to range widely (0.19%–72.46%) at 10 years. The model showed good prediction performance with a concordance index (c-index) of 0.845. The area under receiver operating curves in the validation cohort was 0.79 (CI, 0.71–0.88) and 0.85 (CI, 0.72–0.99) at 5 and 10 years. A calibration plot showed a satisfactory calibration function. The model excluding HBeAg status (“ABC model 2”) showed a c-index of 0.843.

Conclusion: Incorporating the parabolic association between HBV DNA levels and HCC risk with the risk prediction models for untreated non-cirrhotic CHB patients is reliable for risk estimation. Our novel risk prediction model may help identify patients at high risk but left untreated and serve as a steppingstone to extend treatment indication.

Funding: Patient Centered Clinical Research Project (grant number: HC20C0062) and the National R&D Program for Cancer Control through the National Cancer Center (grant number: HA21C0110), funded by the Ministry of Health and Welfare, Republic of Korea.

THU364

Suboptimal glycemic control is associated with adverse clinical outcomes in patients with chronic hepatitis B and diabetes mellitus

Lung Yi Loey Mak^{1,2}, Rex Wan-Hin Hui¹, Ka-Shing Cheung¹, Danny Ka-Ho Wong^{1,2}, Yan Yue James Fung^{1,2}, Man-Fung Yuen^{1,2}, Wai-Kay Seto^{1,2,3}. ¹The University of Hong Kong, Medicine, Hong Kong, Hong Kong; ²The University of Hong Kong, State Key Laboratory of Liver Research, Hong Kong, Hong Kong; ³The University of Hong Kong-Shenzhen Hospital, Shenzhen, China, Medicine, Shenzhen, China. Email: loeymak@gmail.com

Background and aims: Diabetes mellitus (DM) is common among patients with chronic hepatitis B infection (CHB) and has been associated with increased risk hepatocellular carcinoma (HCC) and liver decompensation. We investigated the factors associated with adverse clinical outcomes among CHB patients with DM.

Method: 624 Asian CHB patients (64.4% male, 65.1% antiviral-treated for median duration of 5.5 years) who had concomitant DM (median duration of 8.0 years) were prospectively recruited for transient elastography and followed-up (FU) for a median of 3.2 (interquartile range [IQR] 2.9–5.3) years. Adverse clinical outcome was defined as any liver decompensation event including ascites, variceal bleeding, hepatic encephalopathy (HE), HCC, liver transplantation (LT) or death. Variables of interest included age, cigarette smoking, antiviral therapy, liver stiffness (LS), controlled attenuation parameter (CAP), liver function, renal function, and glycemic control as reflected by individual mean glycated hemoglobin (HbA1c) during FU period. Good glycemic control was defined as mean HbA1c 6.5–7.0%. Advanced fibrosis and cirrhosis were defined by LS ≥9.0 and ≥12.0 kPa, respectively for normal alanine aminotransferase (ALT) or ≥12.0 and 13.5 kPa, respectively for raised ALT.

POSTER PRESENTATIONS

Results: The median age was 62.1 (IQR 56.0–67.9) years old, and 25.2% were smokers or ex-smokers. 17.5% had cirrhosis at recruitment. Mean HbA1c was 6.9%, with 24.0% and 46.3% patients having levels of <6.5% and >7.0% (both are defined as suboptimal glycemic control), respectively. A total of 45 events (HCC, n = 29; ascites, n = 10; variceal bleeding, n = 7; HE, n = 7; death, n = 13; LT, n = 0) were observed during FU. Using multivariate Cox regression analysis, age (hazard ratio [HR] 1.038), smoking history (HR 2.814), LS (HR 1.037), suboptimal glycemic control (HR 3.362) [Figure 1] and albumin (HR 0.921; all $p < 0.05$) were independently associated with adverse clinical outcomes, while CAP (HR 0.995, univariate $p = 0.082$), antiviral therapy (HR 2.311, multivariate $p = 0.088$) and HBV DNA (HR 1.000, univariate $p = 0.65$) were not significant variables. For the specific outcome of HCC, multivariate Cox regression showed that smoking history (HR 2.706), LS (HR 1.032) and mean HbA1c >7.0% (HR 2.252; all $p < 0.05$) were independent variables.

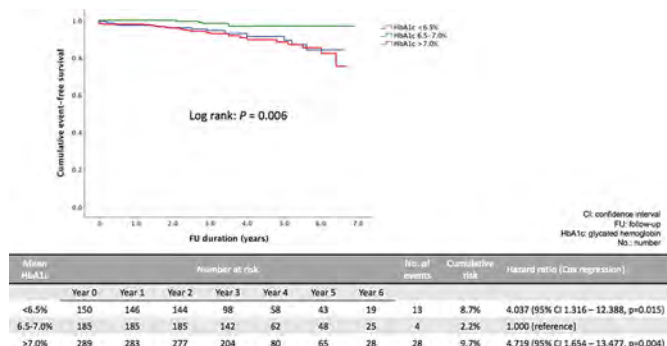


Figure: Cumulative event-free survival in Asian CHB patients with DM, stratified by mean HbA1c level. Event was defined as any adverse clinical outcome including ascites, variceal bleeding, hepatic encephalopathy (HE), HCC, liver transplantation (LT) or death.

Conclusion: Suboptimal glycemic control (<6.5% or >7%) and history of cigarette smoking are associated with liver decompensation and HCC in CHB patients with DM.

THU365

Statin use and surface antigen loss in patients with chronic hepatitis B

Shahed Iqbal¹, Ruidong Li², Silpa Suthram², Jeffrey Wallin¹, James Trevaskis³, Anastasia Hyrina⁴, Simon Fletcher⁴, Meghan Holdorf⁴. ¹Gilead Sciences, Inc., Biomarker Sciences, FOSTER CITY, United States; ²Gilead Sciences, Inc., Research Data Science, FOSTER CITY, United States; ³Gilead Sciences, Inc., Fibrosis Biology, FOSTER CITY, United States; ⁴Gilead Sciences, Inc., Discovery Virology, FOSTER CITY, United States
Email: shahed.iqbal1@gilead.com

Background and aims: Statin use has been associated with reduced risk of liver outcomes (e.g., cirrhosis, liver cancer). One explanation is that the lipid composition of hepatitis B surface antigen (HBsAg) contains cellular cholesterol that is modified by statin use. We explored the association between statin use and sAg loss in patients with chronic hepatitis B (CHB).

Method: Adults (≥ 18 years) with CHB were identified from the IQVIA Ambulatory EMR database using International Classification of Disease (ICD) codes (ICD 9: 070.22–23, 070.32–33, ICD 10: B18.0, B18.1) or by HBsAg positive test. sAg loss was defined by having a negative HBsAg or positive hepatitis B surface antibody test. HIV disease, cancer, long-term steroid use, chronic liver disease, other hepatitis, or pregnancy were exclusion criteria. Statin use was measured using WHO recommended defined daily dose for statin. Multivariate (age, race, sex, statin use) logistic regression was used to determine association between statin use and sAg loss. Due to limited data, virologic measures (e.g., HBV DNA) were not included in the model.

Results: Patients with CHB (N = 12, 314) diagnosed between 2001–2020 were included (mean age: 49.5 years, 47% men). The study comprised Caucasian (39%), Asian (27%), African American (10%) and other races (2%). Mean BMI was 26.1; 17% (n = 2054) of patients had any antiviral use and 4% (n = 505) had sAg loss (median time to sAg loss = 820 [121–4516] days). Current statin use (>28 days during follow-up) was recorded for 11.5% (n = 1421) of patients (2.4% used statin for 1–2 years and 2.2% for >2 years). Compared to no statin use, current statin use of >28–365 days (odds ratio[OR], 95% confidence interval [95% CI] = 1.9, 1.5–2.5), and 1–2 years (OR, 95% CI = 2.3, 1.4–3.4) were associated with sAg loss, but >2 years was not (OR, 95% CI = 1.2, 0.6–2.0). Current statin use was also associated with sAg loss (OR, 95% CI = 1.5, 1.2–2.0) after adjusting for age, sex, and race. In a stratified analysis, statin use was associated with sAg loss among patients who did not use antiviral (OR, 95% CI = 2.1, 1.6–2.7) but not among those who did (OR, 95% CI = 0.7, 0.2–1.5).

Table: Statin use and sAg loss in patients with chronic hepatitis B (N = 12, 314)

Variable	Odds Ratio	95% Confidence interval	p-Value
Statin use (yes vs. no)	1.5	(1.2, 2.0)	0.002
Age ≥ 45 to 65 vs. 18–44 yrs	1.6	(1.3, 2.1)	<0.001
Age ≥ 65 vs. 18–44 yrs	1.5	(1.1, 2.1)	0.013
Male vs. Female	1.3	(1.0, 1.5)	0.027
African American vs. Caucasians	1.7	(1.3, 2.2)	<0.001
Asian vs. Caucasians	1.1	(0.9, 1.4)	0.317
Other race vs. Caucasians	0.9	(0.4, 1.6)	0.683

Conclusion: In this large cohort of CHB patients, while statin use was associated with spontaneous sAg loss with dose response correlation up to two years of statin use, the interplay between age, virologic parameters, antiviral use, and statins need further research. These findings provide impetus for exploring the therapeutic role of statins in patients with CHB.

THU366

Patient engagement in hepatitis B clinical trials: 'HBV cure' is a motivation for participation in all ethnically diverse patients

Almuthana Mohamed¹, Akudo Nwaogu¹, Dusan Jovovic¹, James Lok¹, Maria Guerra Veloz¹, Khin Aye Wint Han¹, Jeya Anice Sundararaj¹, Andrew Ayers¹, Ivana Carey¹, Kosh Agarwal¹. ¹King's College Hospital, Institute of Liver Studies, London, United Kingdom
Email: almuthana700@gmail.com

Background and aims: Despite advances in treatment, chronic hepatitis B (CHB) remains a global health challenge. Clinical trials are key to the development of novel therapies for 'HBV cure'. Patient enrolment can be challenging, especially in ethnic minorities, with reported participation rates of less than 20%. This study aimed to explore the experiences of patients enrolled in phase I or II CHB clinical trials at our hospital, and their motivation for participation.

Method: In this study, a constructivist research paradigm was implemented with the use of questionnaires as the primary modality of data collection. The questionnaire was carefully designed to contain a mixture of question styles, including open and Likert style questions. Baseline patient characteristics, including age and ethnicity, were also collected. The questionnaire was sent to all individuals enrolled in phase I or II CHB clinical trials at King's College Hospital between 2019 and 2021. Open space answers underwent emergent coding and thematic analysis, whilst the results of the Likert scale questions were expressed as median (\pm IQR). Quantitative data analysis was performed using SPSS.

Results: Online questionnaires were sent to 83 CHB patients who had recently participated in clinical trials at our hospital and a total of 50 patients responded to our survey (60.3%). The ethnic distribution of

our cohort was representative of our local CHB population spread and the global burden of CHB. As shown in figure 1, the majority of our cohort resided within the Greater London region (80.7%). Most responders to the survey had undergone higher levels of education (86%). However, those from Sub-Saharan Africa were less likely to respond compared to other ethnicities ($p=0.0048$). Thematic analysis of the qualitative data found that the concept of finite therapy and curative options are key drivers that encourage patients to participate in clinical trials. Whilst most responders to the survey (78%) would participate in future clinical trials, a significant proportion ($n=12$, 24%) expressed difficulty in attending the extra clinic appointments.

Figure 1: Patient characteristics of all subjects included in analysis

Characteristics	Total Cohort	Responders	Non-responders	P-value
Age (Years)	83	50	33	
18-40	26	17	9	
41-60	41	23	18	
61-65	16	10	6	0.604
Gender				
Male	58	36	22	
Female	25	14	11	0.604
Ethnicity				
Caucasian	18	13	5	
Sub-Saharan African	33	16	17	
Asian	13	12	1	
South Asian	7	1	6	
Other/Mixed	12	8	4	0.0048
Level of Education				
Primary School	-	1	-	
Secondary school	-	7	-	
College Degree	-	10	-	
Undergraduate Degree	-	19	-	
Postgraduate Degree	-	14	-	
Geographic Distribution				
Within Greater London	67	37	30	
Outskirts of London	16	13	3	0.0559

Conclusion: 'HBV cure' is a motivation for patients' participation in early phase clinical trials. Whilst most patients are happy to be re-involved in clinical trials, provisions must be taken to minimise the potential disruption of extra clinic appointments. Further work needs to be done in wider education for CHB patients to optimise participation in clinical trials.

THU367

Anti-HDV reflex testing increases the number of hepatitis D cases diagnosed in both academic and community centers

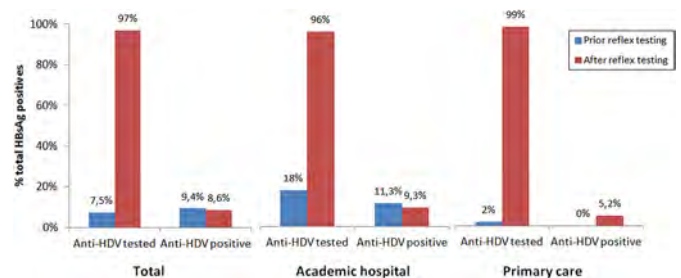
Adriana Palom¹, Ariadna Rando-Segura², Francisco Rodríguez-Frías^{2,3}, Ana Barreira^{1,3}, Jordi Llaneras¹, Mar Riveiro Barciela^{2,3}, Rafael Esteban^{1,3}, Maria Buti^{1,3}. ¹Hospital Vall Hebron, Liver Unit, Barcelona; ²Hospital Vall Hebron, Department of Microbiology, Barcelona; ³Centro de investigación biomédica en red de enfermedades hepáticas y digestivas, Madrid
Email: mbuti@vhebron.net

Background and aims: Although EASL guidelines recommend anti-HDV testing in all HBsAg-positive individuals, HDV still remains underdiagnosed. In a study in Barcelona (Spain) in a catchment population of 400, 000 inhabitants, only 9.4% of HBsAg-positive (HBsAg+) patients were tested for anti-HDV (Palom *et al.* AASLD 2021). We describe the initial results of a nontargeted HDV screening program using anti-HDV reflex testing of all HBsAg+ individuals and compare the results with those obtained before implementation of this strategy.

Method: We reviewed 2144 consecutive HBsAg+ samples sent to a central laboratory (January 2018–October 2021). Before reflex testing, we determined the rate of anti-HDV testing in 1553 HBsAg+ samples (January 2018–December 2020). Prospective anti-HDV reflex testing was done in all HBsAg+ serum samples (January to October 2021).

Demographics and clinical characteristics were recorded in patients testing anti-HDV, including HDV-RNA.

Results: Before implementation of anti-HDV reflex testing, anti-HDV had been tested in 7.5% (117/1553) of HBsAg+ individuals: 18% (97/532) of those attending an academic hospital and only 2% (20/1021) of those in primary care centers. After starting reflex testing, 97% (572/591) were tested for anti-HDV: 96% (475/493) attending an academic hospital and in 99% (97/98) in primary care. (Figure 1).



The overall prevalence of anti-HDV+ among those tested was similar before and after reflex implementation: 9.4% (11/117) and 8.6% (49/572), respectively. However, the absolute number of patients diagnosed with HDV increased from 3 cases in 2018, 2 cases in 2019 and 6 cases in 2020, to 49 cases in 10 months of 2021. Among 56 anti-HDV+ patients, HDV-RNA was detectable in 33 (66%) of 50 tested. HDV-RNA positive patients were more likely to be young, white, and HBeAg-negative, 69% had undetectable HBV-DNA and 58% elevated ALT.

Conclusion: In summary, anti-HDV reflex testing in all HBsAg+ individuals led to 5-fold increase in chronic hepatitis D diagnoses. Before reflex testing, a large percentage of HBsAg+ individuals were not tested for anti-HDV, particularly in primary care centers. The cost-effectiveness of anti-HDV reflex testing should be evaluated to inform testing guidelines.

THU368

HBVoice: a framework to enhance advocacy for patients and communities affected by hepatitis B virus infection

Philippa Matthews¹, Kathryn Jack², Su Wang³, Jane Abbott⁴, Kathleen Bryce⁵, Benny Cheng⁶, Indrajit Ghosh⁷, Alistair Story⁸, Jacki Chen⁹, Chris Munoz¹⁰, John Bell¹¹, Steven Riddell¹¹, Amanda Goldring¹¹, Chun Goddard¹², Kate Moraras¹³, Chari Cohen¹³, Kenneth Brown¹¹, Ahmed Elsharkawy¹⁴, Jeffrey Lazarus¹⁵. ¹The Francis Crick Institute, London, United Kingdom; ²Nottingham University Hospitals NHS Trust Queen's Medical Centre Campus, United Kingdom; ³World Hepatitis Alliance, United Kingdom; ⁴Barts Health NHS Trust, United Kingdom; ⁵Royal Free London NHS Foundation Trust, United Kingdom; ⁶Waverley Care Milestone, United Kingdom; ⁷Mortimer Market Centre, United Kingdom; ⁸Find and Treat, University College Hospitals, London, United Kingdom; ⁹Rutgers Robert Wood Johnson Medical School, New Brunswick, United States; ¹⁰Yellow Warriors Society of the Philippines, Inc.; ¹¹British Liver Trust, United Kingdom; ¹²Sheffield Children's NHS Foundation Trust, United Kingdom; ¹³Hepatitis B Foundation, Doylestown, United States; ¹⁴University Hospitals Birmingham, United Kingdom; ¹⁵Global Health-Trasplante Capilar en Turquia-1.960 €, Barcelona, Spain
Email: philippa.matthews@crick.ac.uk

Background and aims: Hepatitis B virus (HBV) is hidden from public view, with a long history of stigma and neglect, despite an estimated 300 million individuals being chronically infected worldwide. To make progress towards WHO elimination targets, it is essential to improve awareness of HBV among patients, the public, healthcare workers, funders, industry, academia and policy makers. As new HBV drugs enter clinical trials, the engagement of a diverse community is urgently required to deliver studies that engage and represent real-world populations. We present the rationale and groundwork for a

POSTER PRESENTATIONS

new network, 'HBVoice', to increase HBV patient representation. Our aim is to develop this activity by promoting dialogue, connecting to a wider community and relevant stakeholders, and stimulating engagement between sectors.

Method: We have drawn on the published literature and data, and personal testimony in the public domain, alongside dialogue with patients, The British Liver Trust, Hepatitis B Foundation and the World Hepatitis Alliance. Context is also provided by the first externally led patient forum focused on HBV, convened by the Hepatitis B Foundation in partnership with the U.S. Food and Drug Administration (FDA) in 2020.

Results: We have established an expanding interdisciplinary group, representing healthcare workers, academia, non-governmental organisations, and people living with HBV. We are expanding to increase reach into diverse communities and sectors, and to identify and promote HBV champions. Our developing portfolio of activities includes hosting webinars, sharing lived experience of HBV infection, linking the HBV community to opportunities for involvement in clinical research, production of educational materials, political advocacy, and developing plans for industry funding to support a sustainable platform for patient engagement.

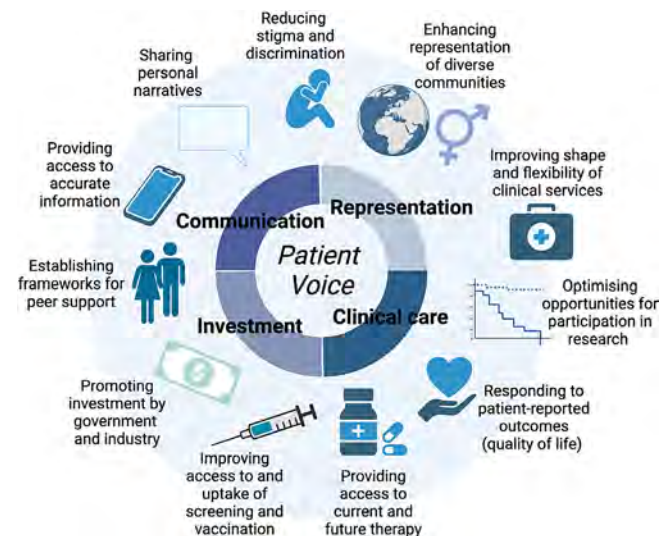


Figure: Aims of 'HBVoice' network

Conclusion: We highlight the urgent need for patient voice to represent HBV infection, supported by interdisciplinary professionals. Sharing experiences of HBV infection will inform awareness and education, and build partnerships to support enhanced clinical care, public health initiatives, policy and funding, and patient-centric research. We will provide a platform through which the substantial physical, emotional and psychosocial impacts of HBV infection can be

better addressed, supporting advances towards 2030 elimination goals.

THU369

HBsAg-positive patients with HBsAg < 135 IU/ml or HBcrAg < 3.6 logU/ml have more chance to be HBsAg loss after nucleos (t)ide analogue cessation

Yandi Xie¹, Minghui Li², Xiaojuan Ou³, Sujun Zheng⁴, Yinjie Gao⁵, Xiaoyuan Xu⁶, Ying Yang⁷, Anlin Ma⁸, Jia Li⁹, Lai Wei¹⁰, Yuemin Nan¹¹, Huanwei Zheng¹², Bo Feng¹. ¹Peking University People's Hospital, Peking University Hepatology Institute, Beijing, China; ²Beijing Ditan Hospital, Capital Medical University, Department of Hepatology Division, Beijing, China; ³Beijing Friendship Hospital, Capital Medical University, Liver Research Center, Beijing, China; ⁴Beijing Youan Hospital, Capital Medical University, Complicated Liver Diseases and Artificial Liver Treatment and Training Center, Beijing, China; ⁵The Fifth Medical Center, General Hospital of PLA, Department of Infectious Diseases, Beijing, China; ⁶Peking University First Hospital, Department of Infectious Diseases, Beijing, China; ⁷The Second Hospital of Xingtai, Department of Infectious Diseases, Xingtai, China; ⁸China-Japan Friendship Hospital, Department of Infectious Diseases, Beijing, China; ⁹Tianjin Second People's Hospital, Department of Liver Disease, Tianjin, China; ¹⁰Beijing Tsinghua Changgung Hospital, School of Clinical Medicine, Tsinghua University, Department of Hepatopancreatobiliary Disease, Beijing, China; ¹¹The Third Hospital of Hebei Medical University, Department of Traditional and Western Medical Hepatology, Shijiazhuang, China; ¹²Shijiazhuang Fifth Hospital, Department of Liver Disease, Shijiazhuang, China
Email: xyfyfb_1@sina.com

Background and aims: Cessation of nucleos (t)ide analogue (NAs) may increase hepatitis B virus (HBV) surface antigen (HBsAg) loss rate in chronic hepatitis B (CHB) patients. We aimed to identify predictor of HBsAg loss using serum quantitative HBsAg, HBV RNA and hepatitis B core-related antigen (HBcrAg) in CHB patients who stopped NAs treatment.

Method: Initially HBV e antigen (HBeAg)-positive CHB patients without cirrhosis who met the stopping criteria were included in 12 hospitals in China. Enrolled patients ceased NAs and were followed up with clinical and laboratory assessments every 3 months for 24 months after NAs cessation or until clinical relapse (CR).

Results: This is a multicenter prospective cohort study, in which 158 patients were included. Patients were divided into two groups according to the HBsAg status when NAs cessation. Group A included patients with HBsAg positive when NAs cessation (n = 139) and Group B included patients with HBsAg negative when NAs cessation (n = 19). In Group A, the 12-month and 24-month cumulative rates of HBsAg loss were 4.3% and 9.4%, respectively. End of treatment (EOT) HBsAg (hazard ratio (HR) = 0.152, p < 0.001), EOT HBcrAg (HR = 0.257, p = 0.001) were found to independently predict possibility of HBsAg loss. To predict HBsAg loss, the area under the receiver operating characteristic (AUROC) value of the EOT HBsAg and HBcrAg were

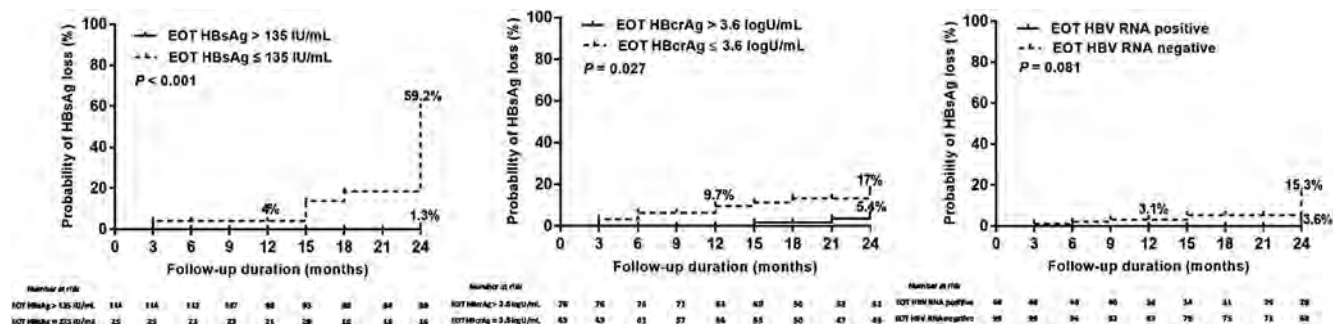


Figure 1: (abstract: THU369): Cumulative incidences of hepatitis B surface antigen (HBsAg) loss stratified by end of treatment (EOT) HBsAg, hepatitis B core-related antigen (HBcrAg) and hepatitis B virus (HBV) RNA in Group A patients.

0.952 ($p < 0.001$) and 0.765 ($p < 0.001$), respectively. Cumulative rates of HBsAg loss stratified by EOT HBsAg, HBV RNA or HBcrAg levels, results showed that patients with EOT HBsAg ≤ 135 IU/ml (59.2% vs 1.3%, $P < 0.001$) or HBcrAg ≤ 3.6 logU/ml (17% vs 5.4%, $P = 0.027$) had higher 24-month cumulative HBsAg loss rate. In Group B, none of the patients had virological relapse (VR) or CR after NAs cessation. Only 1 (5.3%) patient had HBsAg reversion with HBV DNA detectable but less than 2000 IU/ml and without ALT elevation.

Conclusion: Some patients may get HBsAg loss after NAs cessation. An EOT HBsAg ≤ 135 IU/ml or HBcrAg ≤ 3.6 logU/ml, identified a patient with more chance to be HBsAg loss after NAs cessation. Patients with HBsAg negative when NAs cessation had a low risk of HBsAg reversion after NAs discontinuation.

THU370

Serum markers of cccDNA transcriptional activity (HBcrAg and pre-genomic HBV RNA) and large HBsAg (LHBs) protein are predicting response to pegylated interferon in HDV infection

Ivana Carey¹, Mark Anderson², Christiana Moigboi¹, Gavin Cloherty², Geoffrey Dusheiko¹, Kosh Agarwal¹. ¹King's College Hospital, Institute of Liver Studies, London, United Kingdom; ²Abbott Diagnostics, Department of Infectious Diseases, North Chicago, United States
Email: ivana.kraslova@kcl.ac.uk

Background and aims: Hepatitis delta virus (HDV) requires HBsAg envelope for propagation. The large, (LHBs), containing preS1+preS2 +S mediates HBV attachment to the NTCP receptor. A response to pegylated-interferon (Peg-IFN) treatment is achieved in less than 50% of patients, and unless HBsAg loss is achieved, patients are at a risk of late relapse. We aimed to compare baseline and post treatment virological serum biomarkers (total HBsAg and LHBs levels, HBcrAg and pgRNA concentrations, HDV genotypes and HDV RNA viral load) in HDV-positive responders versus non-responders (NR) to Peg-IFN. **Method:** Serum samples of 33 HDV RNA-positive patients (median age 38 yrs, 21 (63%) males, 2 (6%) HBeAg+, 12 (36%) with compensated cirrhosis) were tested at the start and 3 years after completing therapy for the following markers: total HBsAg levels by Abbott Architect [IU/ml], LHBs levels by in-house ELISA [ng/ml and % of total HBsAg], HBcrAg by CLEIA Fujirebio [log₁₀U/ml] and pgRNA by real-time PCR Abbott Molecular Diagnostic RUO assay (LLQD = 1.65 log₁₀U/ml), HDV RNA by in-house real-time PCR assay (LLQD = 640 IU/ml) and HDV genotypes by direct sequencing. The outcome was correlated with the concentrations of these biomarkers. All results are shown as medians.

Results: 3 years post Peg-IFN therapy, 15 (45%) patients were HDV RNA negative (responders), (2 patients with HBsAg loss), whereas 18 patients had persistent HDV RNA (NR). Age and total HBsAg levels (6801 vs. 8326 IU/ml, $p = 0.16$) at baseline were similar in responders and NR. Responders were less likely to have cirrhosis (13% vs. 55%, $p = 0.03$) and were infected with HDV genotype 5 (93% vs. 27%, $p < 0.01$). Peg-IFN responders had significantly lower baseline levels of LHBs (20607 vs. 81106; 7.6% vs. 19%, $p < 0.01$), HBcrAg (3.1 vs. 4.3, $p < 0.01$), pgRNA (1.7 vs. 2.3, $p = 0.04$) and HDV RNA (23, 300 vs. 671, 000, $p = 0.016$) levels than NR. Total HBsAg (6801 to 452, $p < 0.01$), as well as LHBs (20806 to. 4316, 7.6% to 2.4%, $p < 0.01$), HBcrAg (3.1 to 2.2, $p < 0.01$) and pgRNA (1.7 vs. undetectable, $p < 0.01$) reduced significantly in responders. In NR, although we observed a decline in LHBs levels (81106 to 39506; 19% to 11.5%, $p < 0.05$), HBcrAg (4.3 to 3.4, $p < 0.01$) and pgRNA (2.3 to 1.72, $p < 0.01$) these did not reach median baseline levels seen in responders. Total HBsAg and HDV RNA did not change significantly from the start of treatment in NR.

Conclusion: Lower baseline levels of LHBs, HDV RNA, HDV genotype 5 and lower concentrations of markers of cccDNA transcriptional activity were associated with response to Peg-IFN. Transcriptional changes induced by Peg-IFN may reduce LHBs and HDV assembly and thus spreading of hepatitis D. Measurement of cccDNA transcriptional activity and the LHBs isoform may be of greater

utility than total HBsAg in predicting a response to Peg-IFN in HDV infection and could be considered before Peg-IFN therapy for HDV.

THU371

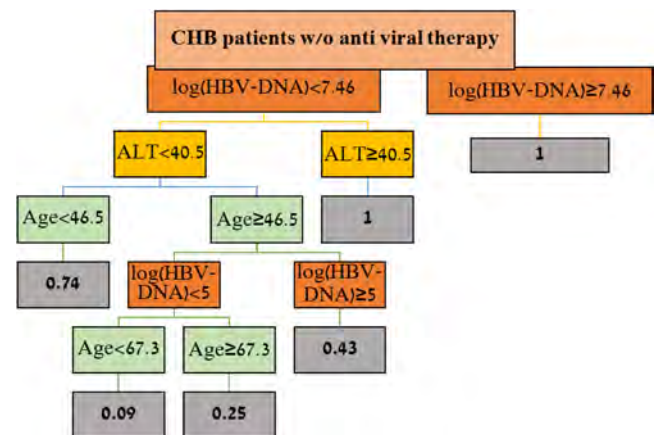
A decision-making model for prediction of a stable disease course in chronic hepatitis B patients

Imri Ofri^{1,2}, Noam Peleg³, Moshe Leshno⁴, Amir Shlomai^{1,2}. ¹Rabin Medical Center, Beilinson Hospital, Department of Medicine D, Petah Tikva, Israel; ²Tel Aviv University, The Sackler Faculty of Medicine, Tel Aviv, Israel; ³Rabin Medical Center, Beilinson Hospital, The Institute of Gastroenterology, Petah Tikva, Israel; ⁴Tel Aviv University, The Collier Faculty of Management, Tel Aviv, Israel
Email: ofriimri@gmail.com

Background and aims: Patients with chronic Hepatitis B (CHB) infection are regularly monitored for HBV DNA and liver enzyme levels in order to assess disease progression and the need for antiviral therapy. Identifying patients with a stable course of disease (i.e long-lasting low HBV DNA and normal liver enzymes) can potentially prolong the intervals between visits, withhold unnecessary tests, resulting in reduced expenses. Accordingly, we aimed to find predictors for a stable disease course in patients with CHB.

Method: An inception cohort of 579 patients with CHB, who were followed in a tertiary referral center between January 2004 to December 2018, was retrospectively analyzed. Patients with low and steady viral load titer (< 2000 IU/ml) and normal ALT levels (< 40 IU/ml) in 6 consecutive clinic encounters were considered to have a stable course of CHB. A stepwise multivariate logistic regression analysis and a random forest decision tree model were used to identify predictors of a stable disease course.

Results: Following exclusion for various reasons, a total of 220 patients, with no active anti-viral treatment, were included in the final analysis. 64 had a stable disease course, whereas 156 had an unstable course. Patients with a stable disease were older and had lower baseline levels of AST, ALT and HBV DNA. In a multivariate analysis, age (OR 0.95, 95% CI 0.928–0.986), baseline ALT (OR 1.083, 95% CI 1.041–1.127) and Log HBV-DNA (OR 1.056 95% CI 1.032–1.08), were significantly associated with a stable disease. In a decision tree model, patients between 46–67 years old, with Log HBV-DNA below 5 IU/ML and ALT below 40.5 IU/ML had the best probability (0.91) for a stable disease course.



Conclusion: Integrating baseline viral DNA, ALT levels and patients' age can predict the disease course in patients with CHB. Thus, stratification of CHB patients according to these simple parameters can determine the required intervals between scheduled clinic visits and may economize patients' management.

THU372

Healthcare resource utilization and costs of hepatitis delta in the United States: an analysis of all-payer claims database

Joseph Lim¹, Vinod Rustgi², Robert G. Gish^{3,4}, Ira M Jacobson⁵, Ankita Kaushik⁶, Yan Liu⁶, Emily Acter⁷, Robert Wong⁸. ¹Yale School of Medicine, New Haven, United States; ²Rutgers Robert Wood Johnson Medical School, New Brunswick, United States; ³University of Nevada, Reno School of Medicine, Kirk Kerkorian School of Medicine at UNLV, Las Vegas, United States; ⁴UC San Diego Skaggs School of Pharmacy and Pharmaceutical Sciences, Hepatitis B Foundation, La Jolla, United States; ⁵NYU Grossman School of Medicine, New York, United States; ⁶Gilead Sciences, Inc., Foster City, United States; ⁷STATinMED, Plano, United States; ⁸Stanford University School of Medicine, Stanford and VA Palo Alto Healthcare System, Palo Alto, United States
Email: joseph.lim@yale.edu

Background and aims: Hepatitis delta is the most severe form of viral hepatitis, causing rapid progression to advanced liver disease. Hepatitis delta is caused by the hepatitis D virus (HDV), a defective RNA virus that requires the presence of the hepatitis B surface antigen (HBsAg) for its complete replication and transmission. This study assesses the healthcare resource utilization and costs associated with HDV infection among adults with chronic HBV infection in the United States (US).

Method: Using the All-Payer Claims Database (APCD), adult patients (≥ 18 years) with ≥ 1 inpatient claim or ≥ 2 outpatient claims spaced ≥ 30 days apart for HDV infection based on ICD-9/10-CM diagnosis codes were identified from 01/01/2015 to 12/31/2019. Patients were required to have ≥ 12 months continuous enrolment before and after their first date of HDV infection diagnosis in the study period. All-cause healthcare-related resource utilization and costs were assessed in the 12 months pre- and post-HDV diagnosis period.

Results: Among 6,719 adults with HDV who met inclusion criteria, mean total number of all-cause healthcare utilization claims were significantly greater in the postdiagnosis than pre-diagnosis period (20.3 vs 15.9, $p < 0.0001$). Patients had more inpatient admissions (mean, 1.6 vs 1.3, $p < 0.0001$), emergency department visits (mean, 1.1 vs 0.9, $p < 0.0001$), outpatient visits (mean, 10.6 vs 7.9, $p < 0.0001$), and pharmaceutical claims (mean, 8.2 vs 6.7, $p < 0.0001$) postdiagnosis compared to prediagnosis. Furthermore, the mean total annual cost of healthcare services (Figure 1) was significantly greater postdiagnosis than prediagnosis (mean, \$20,230 vs \$16,056, $p < 0.0001$), including inpatient admissions (mean, \$8,748 vs \$6,876, $p < 0.0001$), outpatient visits (mean, \$5,272 vs \$4,176, $p < 0.0001$), and pharmaceutical claims (mean, \$6,210 vs \$5,004, $p < 0.0001$). Mean emergency department costs were \$657 vs \$552 ($p = 0.4346$).

Figure 1: Annual Healthcare Costs Pre- and Post-index Diagnosis Among HDV-infected Adults by Cost Category (n = 6,719)



NOTE: ED: Emergency department; An asterisk indicates a statistically significant difference ($p < 0.05$)

Conclusion: In a large national US healthcare claims database, representing ~80% of the US insured population, patients experienced significantly greater overall healthcare resource utilization and costs following diagnosis of HDV infection. These findings underscore

a need for more effective strategies for the screening, diagnosis, and treatment of HDV, which may translate into cost savings for the healthcare system.

THU373

Validation of an internal hepatitis D virus DNA quantitative assay: developing assay suitable for global clinical application and clinical trials assessment

Natalie Bolton¹, Dazhuang Shang¹, Kosh Agarwal¹, Ivana Carey¹. ¹King's College Hospital, Institute of Liver Studies, London, United Kingdom
Email: natalie.bolton@nhs.net

Background and aims: Patients co-infected with both hepatitis B virus (HBV) and hepatitis D virus (HDV) have an increased risk of developing severe liver disease. HDV displays high genetic diversity, with previous studies identifying eight distinct genotypes. Robust, standardised assays for quantifying HDV viral load are needed to assess treatment impact, including standardisation of viral load reported units; two units currently used are copies/ml and international units (IU)/ml, with differing correction factors between these. This retrospective study aimed to assess the quality of an existing internal, pan-genotypic HDV RNA quantitative nucleic acid amplification test (NAAT), utilising the World Health Organisation (WHO) HDV international standard (WHO-HDV-IS), in a diverse South London population.

Method: Data was collected on 163 specimens taken from 89 HBV and HDV co-infected patients between January 2020 and October 2021, with HDV infection confirmed by a positive result on DIA.PRO Delta Ab (Total) assay. HDV viral load was quantified using an internal HDV RNA quantitative assay (Cobas® TaqMan® 48). Assay quality was assessed each run by inclusion of one negative internal control, two positive internal controls (low and high viral load dilutions of the same patient specimen), and the WHO-HDV-IS (genotype 1). Results for the WHO-HDV-IS were analysed using a previously described calculation to determine the correction factor for the assay. HDV genotyping was performed by direct sequencing and phylogenetic tree analysis using neighbor-joining distances analyses software.

Results: 84 (52%) of samples had a viral load below the limit of detection of the HDV RNA quantitative assay (6.40×10^2 copies/ml) whilst 5 (3%) did not have viral load analysed. Within the remaining 74 (45%) samples with quantifiable viral load the median HDV RNA level was 1.31×10^5 copies/ml. 40 (45%) and 36 (40%) of the patients were infected with genotype 1 and genotype 5 HDV, respectively. The internal low and high positive controls were found to be genotype 5. The correction factor calculation determined that the correction factor for the in-house HDV RNA quantitative assay was 1.06, meaning the limit of detection can be recalculated from 6.40×10^2 copies/ml to 6.76×10^2 IU/ml.

Conclusion: The correction factor of 1.06 shows that our internal HDV RNA quantitative NAAT calibrates extremely well in comparison with the WHO-HDV-IS. Despite the WHO standard derivation from genotype 1 HDV (the most prevalent genotype worldwide), our assay accurately quantitates HDV RNA in genotype 5 patients. More work is needed in the future to improve sensitivity and further standardize pan-genotypic HDV RNA quantification, in particular the introduction of a panel of standards across genotypes 1–8. Developing standardized assays suitable for HDV RNA quantitation in clinical trials of new therapeutic agents is an urgent need.

THU374

Early increase in HBcrAg levels after peginterferon withdrawal predicts subsequent ALT flares

Sylvia Brakenhoff¹, Andre Boonstra¹, Robert De Man¹, Bettina Hansen², Robert De Knecht¹, Harry Janssen^{1,2}, Milan Sonneveld¹. ¹Erasmus MC, Gastroenterology and Hepatology, Rotterdam, Netherlands; ²Toronto Western and General Hospital, Toronto Center for Liver Disease
Email: s.brakenhoff@erasmusmc.nl

Background and aims: Chronic hepatitis B (CHB) patients are at risk for ALT flares after antiviral therapy withdrawal. Since serum levels of hepatitis B core-related antigen (HBcrAg) and HBsAg may reflect intrahepatic transcriptional activity, we hypothesized that early post-treatment kinetics could predict off-treatment ALT flares.

Method: We included HBeAg-positive CHB patients who achieved HBeAg loss after one year of peginterferon (\pm lamivudine) treatment. Serum HBV DNA, HBcrAg and HBsAg were quantified at end of treatment (EOT) and at weeks 8 and 12 post-treatment; the peak value was used for analysis. An ALT flare was defined as ALT $\geq 5 \times$ ULN during the first 6 months after EOT.

Results: A total of 67 patients were included, the majority of whom were Caucasian (78%) and had HBV genotype A/D (52/27%). ALT flares occurred in 18%, after a median of 20 weeks (IQR 20–24). Patients who experienced flares had a median post-treatment HBcrAg increase of 0.71 log, compared to a decline of 0.19 log in patients without a flare ($p = 0.003$). Among patients with an HBcrAg increase of >0.5 log, 53% experienced a flare, versus 8% of the patients without an HBcrAg increase ($p < 0.001$). In contrast, HBsAg kinetics were not associated with ALT flares ($p = 0.313$). As expected, patients with flares also experienced a more prominent HBV DNA rebound; we observed a median HBV DNA increase of 4.79 log vs 0.66 log in patients with and without flares ($p = 0.005$). Among patients with an HBV DNA increase of >3 log, 60% experienced a flare, versus 8% of the patients with <3 log HBV DNA increase. Patients with both HBcrAg and HBV DNA increase experienced a flare in 86% versus 8% in patients without a concomitant increase ($p < 0.001$). Consistent results were observed in the subset of patients with HBV DNA <200 IU/ml at EOT ($n = 36$), 67% of the patients with an HBcrAg increase >0.5 log experienced a flare, compared to 4% of patients without an HBcrAg increase ($p < 0.001$).

Conclusion: Early increase in HBcrAg levels after therapy withdrawal predicts subsequent ALT flares, and a combined increase of HBcrAg and HBV DNA identifies patients at very high risk of flares. These findings suggest that HBcrAg could be used to guide off-treatment follow-up. Our findings warrant further confirmation among patients treated with other finite treatment regimens.

THU375

Hepatitis B pre-genomic RNA differentiates HBeAg-negative disease from infection: time to refine disease stages with new biomarkers?

Bo Wang¹, Mark Anderson², Natalie Bolton¹, Christiana Moigboi¹, James Lok¹, Gavin Cloherty², Ivana Carey¹, Geoffrey Dusheiko¹, Kosh Agarwal¹. ¹King's College Hospital, Institute of Liver Studies, United Kingdom; ²Abbott Laboratories, Lake Bluff, United States
Email: bo.wang@nhs.net

Background and aims: Hepatitis B core-related antigen (HBcrAg) and hepatitis B pre-genomic RNA (HBV RNA) are serological biomarkers of cccDNA transcription in patients with hepatitis B virus (HBV) infection. We examined the potential of these markers to differentiate HBeAg-negative disease from HBeAg-negative infection.

Method: In this single-centre retrospective case-control study, HBeAg-negative patients followed for 5 years from 2014 were grouped by whether they started treatment with a nucleos(t)ide analogue. Baseline characteristics including patient demographics, ALT, liver disease stage, and virological data (HBV DNA, quantitative HBsAg, HBcrAg and HBV RNA) were collated. Statistical analysis was

performed to examine differences between the groups and assessed the predictive value of viral markers.

Results: 199 patients were included in the study, with a mean age of 40 years and infected with a range of HBV genotypes (A-11%, B-5%, C-7%, D-17%, E-51%). 62% were male. 111 patients remained untreated for 5 years and were defined as having HBeAg-negative infection, whereas 88 patients started treatment for ostensible HBeAg-negative disease. Our analysis showed significant differences at baseline between the groups (table). A logistic regression analysis showed only HBV DNA and HBV RNA to be significant separators of these HBeAg-negative states. However, the odds ratio for HBV DNA was 2.0 ($p = 0.006$) and for HBV RNA was 10.1 ($p < 0.001$). ROC curve analysis showed these variables to be a good model for prediction, with AUROC of 0.90 (95% CI 0.85–0.95). HBV RNA concentration <1.65 U/ml (i.e. below lower limit of quantification) when HBV DNA was between 2000–20,000 IU/ml (so called “grey zone”) had 92.3% sensitivity for identifying inactive HBeAg-negative infection.

Table: Baseline characteristics, median (range).

	HBeAg-negative infection (n = 111)	HBeAg-negative disease (n = 88)	P
ALT IU/L	23 (5–121)	40 (10–253)	<0.001
Mean liver stiffness kPa	4.5 (2.5–8.7)	6.2 (3.7–21.3)	0.001
HBV DNA logIU/ml	2.62 (0.00–5.59)	4.01 (1.37–6.85)	<0.001
qHBsAg logIU/ml	3.51 (0.15–4.59)	3.54 (1.89–4.99)	0.296
HBcrAg logIU/ml	2.80 (2.00–5.60)	3.90 (2.00–6.20)	<0.001
HBV RNA logU/ml	0.00 (0.00–1.99)	2.12 (0.00–4.84)	<0.001

Conclusion: Serum HBV RNA in addition to HBV DNA provides an excellent discriminator between HBeAg-negative phases. This study demonstrates the potential of a single-point HBV RNA measurement to unequivocally define an indication to start treatment reducing uncertainty. As HBV RNA measurement at current levels of sensitivity reflects ongoing cccDNA transcription, the biomarker provides an additional tool to refine disease status and aid treatment decisions.

THU376

Evaluating hepatitis delta virus disease prevalence and patient characteristics among adults in the United States: an analysis of all-payer claims database

Robert G. Gish^{1,2}, Ira M Jacobson³, Joseph Lim⁴, Ankita Kaushik⁵, Yan Liu⁵, Anissa Cyhaniuk⁶, Robert Wong⁷. ¹University of Nevada, Reno School of Medicine, Kirk Kerkorian School of Medicine at UNLV, Las Vegas, United States; ²UC San Diego Skaggs School of Pharmacy and Pharmaceutical Sciences, Hepatitis B Foundation, La Jolla, United States; ³NYU Grossman School of Medicine, New York, United States; ⁴Yale School of Medicine, New Haven, United States; ⁵Gilead Sciences, Inc., Foster City, United States; ⁶STATinMED, Plano, United States; ⁷Stanford University School of Medicine, Stanford and VA Palo Alto Healthcare System, Palo Alto, United States
Email: rgish@robertgish.com

Background and aims: Hepatitis delta virus (HDV) infection leads to the most severe form of viral hepatitis and is always associated with hepatitis B virus (HBV) infection. This study estimates the prevalence and describes patient characteristics for HDV-infected adults in the US using real-world insurance claims data.

Method: Adults (≥ 18 years) with ≥ 1 inpatient claim or ≥ 2 outpatient claims (ICD-9/10-CM diagnosis codes) ≥ 30 days apart for HDV infection or HBV monoinfection in the All-Payer Claims Database from 1/1/2014 to 12/31/2020 (study period) were identified. Prevalence was the proportion of HDV-infected among HBV-infected patients. Patient characteristics were reported for a subcohort of patients with HDV. The HDV index date was defined as the first HDV diagnosis from 1/1/2015 to 12/31/2019 with ≥ 12 months pre- and post-diagnosis continuous enrolment. Patient characteristics included age, gender, race, geographic region, and payer type. Socioeconomic status data captured annual household income and

POSTER PRESENTATIONS

education. Comorbidities were assessed over the 12-months pre-index (baseline) period.

Results: Among 194, 573 adults with HBV, 9, 376 (4.8%) were coinfecting with HDV. Among 6, 719 adults in the HDV subcohort, mean age was 51.9 ± 15.1 years, mean Charlson Comorbidity score was 1.7 ± 2.3 , 50.5% were female; 44.9% lived in the north-central and 23.7% in the northeast region of US. Among those with available data on race and socioeconomic status, the majority were white (48.8%), followed by black (36.6%) and Asian (13.7%); mean annual household income was \$41, 515 (\pm \$44, 697); 64.0% had high school as the highest education category. Patients most commonly had commercial insurance (42.7%), followed by Medicaid (34.2%), or Medicare (19.9%). At Baseline, 16.3% of patients had compensated cirrhosis, 10.4% had decompensated cirrhosis, 2.8% had liver cancer, and 2.2% had liver transplant. Diabetes (50.5%), hypertension (49.8%), HIV infection (30.9%), substance abuse (28.7%), and smoking history (28.1%) were the top five comorbidities.

Conclusion: Among a large database capturing approximately 80% of the US insured population, HDV infection prevalence was 4.8% among HBV-infected adults. HDV-infected patients had high rates of baseline comorbidities and liver complications. Earlier identification of HDV infection among HBV-infected patients may provide opportunities to reduce the risk of liver-related morbidity and mortality.

THU377

Hepatitis delta in Northern Portugal-a long-term follow-up study

Isabel Garrido¹, Rodrigo Liberal¹, Sofia Teixeira¹, Carmo Koch¹, Guilherme Macedo¹. ¹São João University Hospital Center, Porto, Portugal

Email: isabelmng@hotmail.com

Background and aims: Hepatitis delta virus (HDV) occurs worldwide but prevalence data are limited due to inaccurate reporting and delayed detection. In fact, no data are available on the epidemiologic status of HDV infection in Portugal. In addition, long-term data on clinical follow-up is limited. This study aimed to investigate the prevalence, clinical features and long-term outcomes of a cohort of Portuguese patients with HDV infection.

Method: All adult patients diagnosed with hepatitis B virus (HBV) infection in the past 10 years at Centro Hospitalar Universitário de São João were retrospectively evaluated. Demographic and laboratory data of those with HDV infection were assessed.

Results: Five hundred and eighty individuals tested positive for hepatitis B surface antigen HBsAg (HBsAg) between January 2010 and December 2020. Twenty patients (3.4%) had also positive anti-HDV antibodies. Of these, most were male (80%), former injection drug users (55%) and native Portuguese (70%). The median age was 42 years old (IQR 33–47). Positive serum hepatitis B e-antigen was present in 3 (15%) patients and 6 (30%) had undetectable HBV-DNA. Tenofovir was prescribed as antiviral therapy in 40% of individuals and entecavir in 15%. Coinfection with human immunodeficiency virus was found in 9 (45%) patients, and 6 (30%) had hepatitis C virus antibodies. It is noteworthy that since year 2011 the rate of HDV diagnosis significantly decreased. Although 7 (35%) patients had cirrhosis at the time of diagnosis, only one of them had hepatic decompensation during follow-up, and eventually died. Patients were followed for a period of 5 years (IQR 2–10). They were periodically screened for hepatocellular carcinoma and none of them developed it. The majority of individuals (95%) had stable disease or improved outcomes during follow-up. Interestingly, 4 (20%) patients have cured HBV infection. The overall survival rate of this cohort was 90%.

Conclusion: The prevalence of chronic hepatitis delta is currently very low (<5%) among positive HBsAg carriers in Portugal, with lower rates in recent years. We show that HDV infection has favorable outcomes, assuming adherence to therapy and lack of other insults to their liver, and an adequate quality of life can be achieved, resulting in

longer overall survival. Therefore, HDV co-infection does not seem to have a significant clinical impact in Portuguese patients.

THU378

Impact of hepatitis B virus infection on liver-related death among people tested for HBV in British Columbia: results from a large longitudinal population-based cohort study

Makuza Jean Damascene^{1,2,3}, Dahn Jeong^{1,2}, Mawuena Binka², Prince Adu², Sofia Bartlett², Amanda Yu², Stanley Wong², Georgine Cua^{1,2}, Hector Velasquez^{1,2}, Maria Alvarez², Mel Krajden², Mohammad Ehsanul Karim¹, Naveed Janjua^{1,2}. ¹The University of British Columbia, School of Population and Public Health, Vancouver, Canada; ²BC Centre for Disease Control, BC HTC, Vancouver, Canada; ³Rwanda Biomedical Center (RBC), IHDPC, Kigali, Rwanda
Email: makorofr@gmail.com

Background and aims: A substantial number of people are living with hepatitis B virus (HBV) infection in Canada, which may result in higher morbidity and mortality among them. However, data on the contribution of HBV infection to liver-related mortality in Canada is limited. We assessed the impact of HBV infection on liver-related deaths in British Columbia (BC), Canada.

Method: We used data from the BC Hepatitis Testers Cohort (BC-HTC), a large population-based cohort that integrates data on HCV, HBV testing and diagnoses with data on primary care visits, hospitalizations, deaths and medication dispensations. Individuals who tested for HBV in the BC-HTC were followed from the first test date among HBV positive individuals and last test date among HBV negative individuals until the end of the study period (2020/06/30) or liver-related death. Liver-related mortality rates were computed for HBV positive and negative individuals. Multivariable Cox proportional hazards model was used to assess the impact while adjusting for confounders. Propensity scores (PS) pair matching analysis was conducted as a sensitivity analysis to assess the robustness of the main findings.

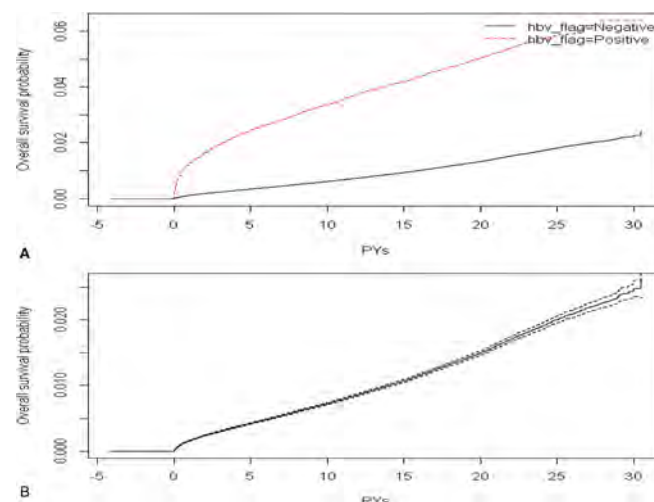


Figure 1: The 30 PYs Cumulative incidence rate for people HBV tested positive vs. those HBV tested negative in BC from 1990–2015. (A) Cumulative incidence of liver-related mortality in individuals with and without HBV infection, over 30 PYs of follow-up. Solid lines: cumulative incidence of liver-related mortality; dashed lines: 95% confidence intervals. (B) Cumulative incidence of liver-related mortality in all individuals, over 30 years of follow-up. Solid lines: cumulative incidence of liver-related mortality; dashed lines: 95% confidence intervals. PYs, Person years; CI, confidence interval; HBV, hepatitis B virus.

Results: During the study duration, 40, 704 people tested positive for HBV. Among them, 38, 847 HBV-positive individuals were matched to HBV-negative individuals. The mean follow-up time for the study sample was 13.46 (standard deviation 6.53) years. A higher

proportion of those testing positive compared to negative were males (54% vs 43%), born in 1945–64 (46% vs 30%) and of East Asian ethnicity (63% vs 14%). The liver-related mortality rate was higher among people with HBV infection than those without [2.76 per 1,000 PYs (95%CI: 2.64, 2.89) vs. 0.66 per 1,000 PYs (95%CI: 0.65, 0.68), respectively]. In multivariable analysis, HBV infection was associated with increased liver-related mortality [adjusted hazard ratio (aHR): 3.35; 95%CI: 3.02, 3.71]. We found similar results in the PS-matched analysis (aHR: 3.36; 95%CI: 3.17, 3.57).

Conclusion: HBV infection is associated with a higher risk of liver-related mortality. Findings highlight an urgent need for HBV screening and diagnosis and continued monitoring for liver-related diseases to prevent mortality.

THU379

Comparable risk of hepatocellular carcinoma between immune-tolerant and active phase in hepatitis B e antigen-positive patients

Han Ah Lee¹, Seung Up Kim², Yeon Seok Seo³, Chai Hong Kim⁴. ¹Inje University College of Medicine, Internal Medicine, Seoul, Korea, Rep. of South; ²Yonsei University College of Medicine, Internal Medicine, Seoul, Korea, Rep. of South; ³Korea University College of Medicine, Internal Medicine, Seoul, Korea, Rep. of South; ⁴Korea University College of Medicine, Radiation Oncology, Seoul, Korea, Rep. of South
Email: crusion3@naver.com

Background and aims: Antiviral therapy is not indicated for patients with chronic hepatitis B (CHB) in the immune-tolerant (IT) phase. We compared the treatment outcomes between untreated IT-phase and treated immune-active (IA) phase in patients with CHB.

Method: We systematically searched four databases including Pubmed, Medline, Embase, and Cochrane database until August, 2021. The cumulative incidence of hepatocellular carcinoma (HCC) and mortality in IT and IA cohorts and that of CHB phase change in IT cohort was investigated. Studies regarding patients who have

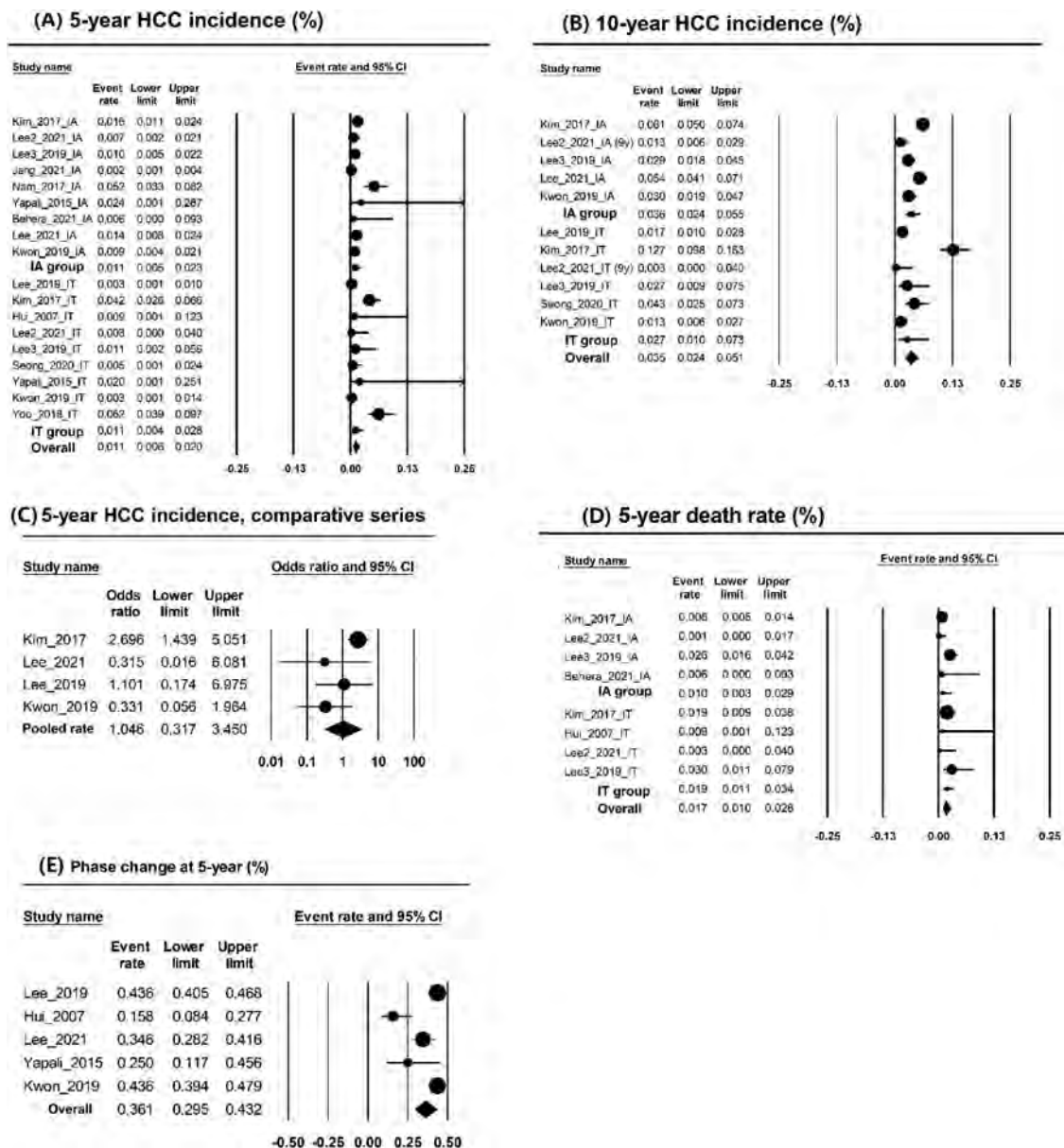


Figure: (abstract: THU379)

POSTER PRESENTATIONS

clinically or pathologically diagnosed liver cirrhosis were excluded. Random effects model was used for pooled analyses. The study adhered PRISMA and referenced Cochrane handbook v6.2 for methodologic regards.

Results: A total of 13 studies involving 19 cohorts, including 11, 903 patients were included. Quantitative quality assessment was performed and five and eight studies were regarded to have high and moderate quality; therefore none of 13 studies were dropped from formal analysis for quality issue. The overall median of median follow-up period was 62.4 months, (range: 51–103 months). The overall median value of median age was 40 (range: 29–53.5), and proportion of male was 59.6% (31.8–68.9). Possible publication bias was noted in pooled analyses of 5- (Egger's test $p = 0.082$) and 10-year HCC incidence (Egger's test $p = 0.019$).

The pooled HCC incidence rate at 5-years was 1.1% (95% confidence interval [CI]: 0.6–2.0%) in all cohorts. No statistical difference in HCC incidence rate at 5-years was observed between IT [1.1% (95% CI, 0.4–2.8%)] and IA cohorts [1.1% (95% CI, 0.5–2.3%)] ($p = 0.976$). The pooled odds ratio of comparative series between IT and IA cohorts was 1.05 (95% CI, 0.32–3.45; $p = 0.941$). Pooled HCC incidence rate at 10-years was 3.5% (95% CI, 2.4–5.1%) in all cohorts. No statistical difference in HCC incidence rate at 10-years was observed between IT [2.7% (95% CI, 1.0–7.3%)] and IA cohorts [3.6% (95% CI, 2.4–5.5%)] ($p = 0.587$). No statistical difference in pooled mortality rates at 5-years was observed between IT [1.9% (95% CI, 1.1–3.4%)] and IA cohorts [1.0% (95% CI, 0.3–2.9%)] ($p = 0.285$). Finally, pooled incidence rate of CHB phase change in IT cohort was 36.1% at 5 years (95% CI, 29.5–43.2%).

Conclusion: The long-term risks of HCC and mortality were similar between the IT and IA phase. However, various definitions of CHB phase in different studies have to be considered.

THU380

Evidence of extensive transcriptionally active HBV integrations involving genetic regions crucial for cell proliferation in the setting of HBeAg positive infection

Romina Salpini¹, Luca Carloti¹, Arianna Battisti^{1,2}, Lorenzo Piermatteo¹, Livia Benedetti¹, Francesca Ceccherini Silberstein¹, Upkar Gill², Valentina Svicher¹, Patrick Kennedy². ¹University of Rome Tor Vergata, Department of Experimental Medicine, Rome, Italy; ²Blizard Institute, Barts and The London SMD, QMUL, London, United Kingdom, Barts Liver Centre, United Kingdom
Email: rsalpini@yahoo.it

Background and aims: HBV integration into the human genome can mediate oncogenic activity. Limited information is available about initial HBV integration events, particularly in the early phases of infection. Here, we characterize chimeric HBV-human RNAs reflecting transcriptionally active HBV integrations in the setting of eAg positive phases of HBV infection.

Method: Liver tissues from 42 eAg+ chronically infected patients (27 with eAg+ hepatitis [eAg + CH] and 15 with eAg+ infection [eAg + CI]) were studied to perform total RNA-seq by NGS [Illumina, median (IQR) RNA reads per sample: 22 (18–27) millions]. An ad-hoc bioinformatic pipeline was applied to recognize chimeric HBV-human transcripts (present in >2 reads), resulting from HBV integration. Role of genes involved in HBV integration was assessed by GeneCards and Protein Atlas.

Results: Patients with eAg+CI were significantly younger than eAg+CH [27 (22–29) vs 29 (25–35) years, $p < 0.001$]. Median (IQR) serum HBV DNA and HBeAg were 8.0 (5.7–8.6) logIU/ml and 4.4 (4.1–4.8) logIU/ml respectively, with no significant difference according to HBV infection status. Overall, >1 chimeric HBV-human RNA was revealed in almost all patients (98%, 41/42) for a total number of 1048 unique HBV-human transcripts, reflecting an abundance of transcriptionally active HBV integration events. The number of unique chimeric transcripts in each patient did not differ in eAg+CH and eAg+CI groups [median (IQR): 13 (11–22) and 14 (10–39); $P = 0.46$],

highlighting an early occurrence of HBV integration in young patients with no or limited fibrosis. 69.6% of integration events originated from HBx/Core, indicating double stranded linear DNA as a major source of HBV integration. Moreover, 20.7% of chimeric transcripts involved HBsAg coding region, posing the basis to produce truncated/aberrant HBsAg forms.

Notably, by gene ontology, 18% (189/1048) of HBV-human chimeric transcripts involved human exons and splicing signals, crucial for gene expression. Among them, 35.4% corresponds to genes playing a pivotal role in modulating cell survival/proliferation, including genes (BIRC6, SYF2, EVI5, BTG1) known to be dysregulated in HCC.

Conclusion: Transcriptionally active HBV integrations occur frequently in the eAg-positive phases of HBV infection, even in young patients with no or limited liver fibrosis. These events result in the production of chimeric HBV-human aberrant transcripts, that mostly involve genes regulating crucial intracellular pathways, that could confer a proliferative advantage to the hepatocytes. This is further evidence to support early treatment initiation in eAg positive chronic infection.

THU381

In the setting of HIV-infection, HBV-reactivation is revealed by highly sensitive assays in a conspicuous fraction of anti-HBc-positive/HBsAg-negative patients switching to Tenofovir-sparing therapy

Romina Salpini¹, Stefano D'Anna¹, Mohammad Alkhatib¹, Lorenzo Piermatteo¹, Alessandro Tavelli², Eugenia Quiros-Roldan³, Antonella Cingolani⁴, Chiara Papalini⁵, Stefania Carrara⁶, Massimo Puoti⁷, Loredana Sarmati⁸, Antonella d'Arminio Monforte^{9,10}, Francesca Ceccherini Silberstein¹, Carlo Federico Perno¹¹, Valentina Svicher¹. ¹University of Rome "Tor Vergata", Department of Experimental Medicine, Rome, Italy; ²ICONA Foundation, Milan, Italy; ³Spedali Civili di Brescia, Division of Infectious and Tropical Diseases, Brescia, Italy; ⁴Fondazione Policlinico Universitario A. Gemelli, Unit of Infectious Diseases, Rome, Italy; ⁵University of Perugia, Department of Medicine, Perugia, Italy; ⁶National Institute of Infectious Diseases Lazzaro Spallanzani, Microbiology Biobank and Cell Factory Unit, Roma, Italy; ⁷ASST Great Metropolitan Niguarda, Unit of Infectious Diseases, Milano, Italy; ⁸Hospital Tor Vergata Roma, Unit of Infectious Diseases, Roma, Italy; ⁹ASST Santi Paolo e Carlo, Clinic of Infectious Diseases, Milano, Italy; ¹⁰University of Milan, Department of Health Sciences, Milano, Italy; ¹¹Bambino Gesù Children's Hospital, Roma, Italy
Email: stefanodanna26@gmail.com

Background and aims: Tenofovir-sparing antiretroviral therapy (ART) is increasingly used in the setting of HIV-infection, raising the issue to properly identify those anti-HBc-positive/HBsAg-negative patients (pts) who can safely suspend this drug. Here, we aim at unravelling HBV replication kinetics after tenofovir withdrawal in HIV-infected anti-HBc-positive/HBsAg-negative pts.

Method: This study includes 101 HIV-infected anti-HBc-positive/HBsAg-negative pts from ICoNA cohort, treated with TDF/TAF-containing ART for >12 months and switching to TDF/TAF-sparing ART: 73 with LAM and 28 with no active HBV drugs. At switching (T0) 98% of pts has undetectable HIV-RNA.

For each pt, a plasma sample is analyzed at T0 and during the first 12 months of TDF/TAF-sparing ART (T1). HBV-reactivation (HBV-R) during TDF/TAF-sparing ART is defined as HBV-DNA>1IU/ml in pts with negative HBV-DNA at T0 or a >2-fold increase in HBV-DNA from T0 to T1. HBV-DNA and -RNA are quantified by highly sensitive droplet digital PCR (HS-ddPCR, LLOD:1IU/ml) and anti-HBc by Fujirebio (anti-HBc>15COI indicating active HBV reservoir based on Salpini, 2020).

Results: At T0, despite TDF/TAF therapy, 34 (33.7%) pts have detectable HBV-DNA by HS-ddPCR (median[IQR]: 2[1–5]IU/ml). Among the remaining 67 pts, 9% has detectable HBV-RNA (median [IQR]:6[5–7]IU/ml) and anti-HBc>15COI, indicating a transcriptionally active cccDNA.

At T1, after TDF/TAF withdrawal, HBV-R occurs in 40 (39.6%) pts (median[IQR] HBV-DNA: 4[2–13]IU/ml) with no difference between LAM- vs no LAM-group (42.5% vs 32.1%, $P=0.34$). Among HBV-R cases, 32.5% has HBV-DNA>10IU/ml (median[IQR]:31[15–73]IU/ml) and 25% has ALT>40U/L.

Notably, HBV-R is confirmed in 77.3% of pts with an additional sample available during TDF/TAF-sparing ART (median [IQR] HBV-DNA:24 [13–31]IU/ml), supporting persistent HBV replication.

Finally, pts with a nadir CD4+T cell count <100cells/ul have a higher risk to develop HBV-R (15/27[55.6%] with vs 25/74[33.8%] without nadir <100cells/ul, $P=0.04$), suggesting a role of immunocompromise in promoting reuptake of HBV replication under suboptimal/absent drug pressure.

Conclusion: A conspicuous fraction of HIV-infected anti-HBc-positive/HBsAg-negative pts has a transcriptionally active intrahepatic reservoir that can predispose to HBV-reactivation under suboptimal/absent drug pressure. The status of HIV-driven immunocompromise can exacerbate this phenomenon. Highly sensitive and accurate assays to measure HBV replicative activity are crucial for a proper management of HIV-infected anti-HBc-positive/HBsAg-negative pts candidate to TDF/TAF-sparing regimen.

THU382

Absence of hepatitis B virus (HBV) in at-risk infants receiving early antiretroviral therapy in a cohort of HIV-transmitting mothers in KwaZulu-Natal, South Africa

Jane Millar¹, Gabriela Cromhout², Noxolo Mchunu², Philip Goulder¹, Philippa Matthews^{3,4}, Anna McNaughton^{3,5}, ¹University of Oxford, Department of Paediatrics, Oxford, United Kingdom; ²University of KwaZulu-Natal, HIV Pathogenesis Programme, South Africa; ³University of Oxford, Nuffield Department of Medicine, Oxford, United Kingdom; ⁴Department of Infectious Diseases and Microbiology, Oxford University Hospitals NHS Foundation Trust, Oxford, United Kingdom; ⁵University of Bristol, Population Health Science, Bristol Medical School, Bristol, United Kingdom

Email: anna.mcnaughton@bristol.ac.uk

Background and aims: Both HIV and hepatitis B virus (HBV) prevalence are high in KwaZulu-Natal (KZN), South Africa (ZA). HIV co-infection can negatively impact HBV prognosis, and is associated with an increased likelihood of HBV mother-to-child-transmission (MTCT) in the absence of appropriate treatment/prophylaxis. This study worked with an established cohort of HIV-transmitting mother-child pairs in KZN, in which HIV-positive infants were treated with antiretrovirals (ART) within 48hrs of life. We generated a detailed characterisation of HBV serological markers in the maternal cohort, and tested the infants at-risk of HBV MTCT.

Method: Maternal serum samples ($n=175$) were screened for active HBV infection (HBsAg), exposure to HBV (anti-HBc) and vaccination responses (anti-HBs-positive in the absence of other HBV markers). HBV vaccination has been part of the routine ZA infant immunization schedule since 1995, with the first dose given at age 6 weeks. HBV infections in HBsAg-positive mothers were further characterised with HBeAg and HBV DNA testing. Infants of HBV infected mothers were screened for HBsAg.

Results: Evidence of HBV exposure was present in 31.4% (55/175) mothers and HBV infection was present in 8.6% (15/175). Anti-HBc responses were absent in 53.3% (8/15) HBV-positive cases, suggesting it may be a poor biomarker in HIV-positive cohorts. A lone anti-HBs profile, indicating HBV vaccination, was present in 8.0% (14/175) mothers. HBV DNA was detectable in 46.7% (7/15) HBsAg-positive mothers, with 26.7% (4/15) also HBeAg-positive. Where HBV-DNA was detected, median viral load was $3.8 \log_{10}$ IU/ml (range 1.9–8.2 \log_{10} IU/ml). Among HBV-infected mothers, CD4+ counts were lower in those also testing HBV DNA positive (mean 264 vs 643; $p=0.003$). Using a threshold of $>5.3 \log_{10}$ IU/ml, 20% (3/15) HBV-positive mothers were defined as high risk of MTCT. Screening of infants found no cases (0/15) of HBV MTCT.

Conclusion: Within this vulnerable cohort of HIV-transmitting mothers, we found evidence of a high HBV prevalence, and indications that 20% of the HBV-positive mothers are also high-risk for HBV MTCT. ART regimens prescribed to the infants early in life contained agents active against HBV (lamivudine), and this may have prevented MTCT in high-risk cases. Larger studies, incorporating long-term follow-up would be informative. Prevention of HBV MTCT at a population level requires consistent antenatal HBV screening and birth-dose immunisation of infants, together with specific antiviral prophylaxis.

THU383

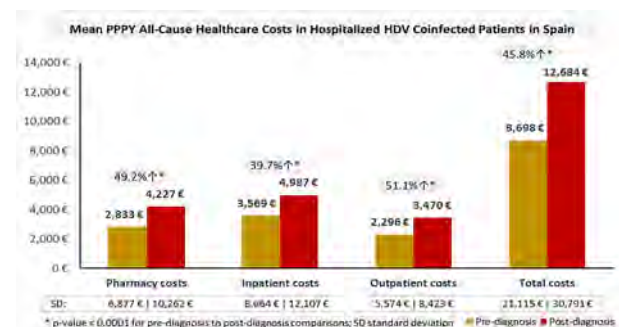
Rising clinical and economic burden among hepatitis D patients who attended Spanish hospitals

Maria Buti¹, Ankita Kaushik², Mertixell Ascanio³, Josep Darba³, Nandita Kachru⁴, ¹Hospital Universitario Valle Hebrón, Barcelona, Spain; ²Gilead Sciences, Inc., Foster City, United States; ³BCN Health Economics and Outcomes Research SL, Barcelona, Spain; ⁴Gilead Sciences, HEOR-Global Value and Access, Foster City, United States
Email: mbuti@vhebron.net

Background and aims: Hepatitis D virus (HDV) coinfects with hepatitis B virus (HBV) causing the most severe form of viral hepatitis. This study examined the epidemiology, baseline characteristics and healthcare resource use (HRU) and costs among hospitalized HDV coinfecting patients in Spain.

Method: Adult patients with ≥ 1 HDV or HBV diagnosis (ICD-9/10-CM) were identified retrospectively from Jan 2000 to Dec 2019 (study period) using the Spain hospitalization database that covers 192 private and 313 public hospitals, with >40 million patients. HDV patients were identified from Jan 2001 to Dec 2018 (identification period) with their first diagnosis defined as the diagnosis date, having ≥ 12 months of continuous enrollment (CE) before and after the diagnosis date. Prevalence was measured as the proportion of HDV patients among HBV. Baseline characteristics were assessed over the entire duration prior to diagnosis date. Mean per patient per year (PPPY) all-cause HRU and costs (pharmacy, inpatient, outpatient, total) were obtained over 12 months before and after the diagnosis date.

Results: The study included 12,317 patients diagnosed with HDV or HBV, of which only 597 had HDV diagnosis, and 536 had a new diagnosis (no evidence of HDV during 1 year prior to diagnosis date)-5% prevalence and 4.7% incidence over the study duration. After applying CE criteria, the analytical cohort included only 159 HDV patients (mean age 42.7 ± 14.4 years; 73.6% males). High rates of liver disease severity were reported-26.4% compensated cirrhosis, 49.7% decompensated cirrhosis, 5.7% hepatocellular carcinoma and 5% liver transplant. Other comorbidities included smoking 23.9%, alcohol abuse 19.5%, substance abuse 18.9%, HIV 13.8%, HCV 8.8%. Mean PPPY number of admissions, readmissions and length of stay increased significantly from pre- to post-diagnosis. Mean PPPY all-cause healthcare costs among incident patients totaled to €8,698 (pre-diagnosis) and €12,684 (post-diagnosis), representing 45.8% increase ($p<0.001$). Inpatient costs were the major contributors of total pre-diagnosis (41%) and post-diagnosis costs (39%), at €3,569 and €4,987, respectively.



POSTER PRESENTATIONS

Conclusion: Hospitalized HDV patients in Spain have a high comorbidity burden. Total healthcare costs are high, with inpatient costs as the primary driver, posing a high economic burden. Novel treatment strategies are needed to improve patient outcomes and reduce the economic burden among HDV coinfecting patients in Spain.

THU384

Analysis from national hospital discharge records database in Spain : increased baseline comorbidity burden including liver severity among HDV coinfection versus HBV mono-infection patients

Maria Buti¹, Ankita Kaushik², Mertixell Ascanio³, Josep Darba⁴, Nandita Kachru². ¹Hospital Universitario Valle Hebrón, Liver Unit, Barcelona, Spain; ²Gilead Sciences, HEOR-Global Value and Access, California, United States; ³BCN Health Economics and Outcomes Research SL, Barcelona, Spain; ⁴University of Barcelona, Department of Economics, Barcelona, Spain
Email: mbuti@vhebron.net

Background and aims: Hepatitis D virus (HDV) is considered as the most severe form of chronic viral hepatitis, given its relatively rapid progression to cirrhosis and liver-related complications. This retrospective study compares baseline characteristics of adult patients with HDV coinfection versus (vs.) hepatitis B virus (HBV) mono-infection in a national hospital database in Spain.

Method: The study population included subjects ≥ 18 years having ≥ 1 ICD-9/10-CM diagnosis code for HDV or HBV in the Spanish National Health System's Hospital Discharge Records Database (Conjunto Mínimo Básico de Datos) from 01/01/2000 to 12/31/2019 (study period). HDV and HBV cohorts were identified from 01/01/2001 to 12/31/2018 (identification period) with their first diagnosis defined as the diagnosis date, having ≥ 12 months of continuous enrollment before and after the diagnosis date. Baseline characteristics were assessed over the entire duration prior to diagnosis date. Descriptive statistics were summarized, and comparisons were made via chi-square tests.

Results: The study reported 12,317 patients diagnosed with HDV or HBV, of which 3,079 met the inclusion criteria-159 HDV and 2,920 HBV patients. HDV patients [mean age 42.7 ± 14.4 | Charlson Comorbidity Index (CCI) score 0.92] were significantly younger than HBV patients [mean age 46.6 ± 15.9 ; $p = 0.0034$ | CCI score 0.77]. The male to female ratio (roughly 3:1) was similar across the two cohorts. Both the cohorts were largely covered by public insurance (93.7% HDV vs. 95.4% HBV; $p = 0.3311$) and roughly half were seen by gastroenterologists (44.7% HDV vs. 50.3% HBV; $p = 0.1673$) followed by other specialists (36.5% HDV vs. 29.8% HBV; $p = 0.0763$). HDV patients were significantly more likely to have decompensated cirrhosis (49.7% vs. 29%; $p < 0.0001$), compensated cirrhosis (26.4% vs. 9.8%; $p < 0.0001$) and liver transplant (5% vs. 1.8%; $p = 0.0109$) than HBV patients, whereas hepatocellular carcinoma rates were at 5.7% and 3%, respectively. Further, HDV patients reported significantly higher rates of HCV (8.8% vs. 3.6%; $p = 0.0043$), HIV (13.8% vs. 3.3%, $p < 0.0001$) and substance abuse (18.9% vs. 7%; $p < 0.0001$) than HBV patients.

Conclusion: In a national hospital Spanish database, HDV coinfecting patients had greater comorbidities and significantly higher liver disease severity than HBV mono-infected patients. These findings underscore the need for early screening and diagnosis, and eventual treatment of HDV to mitigate future disease progression.

THU385

Value of intrahepatic HBV markers in virologically suppressed HBV and HDV infected patients

Ester García-Pras¹, Thais Leonel¹, Yabetse Girma¹, Sergio Rodríguez-Tajes¹, Alba Díaz², Sabela Lens¹, Mireia García-López¹, Maria Saez-Palma¹, Yilliam Fundora³, Xavier Forns¹, Sofia Pérez-del-Pulgar¹. ¹Liver Unit, Hospital Clínic, University of Barcelona, IDIBAPS, CIBERehd, Barcelona, Spain; ²Department of Pathology, Centre of Biomedical Diagnosis, CIBERehd, Hospital Clínic; ³HBP and Liver Transplant Surgery, IDIBAPS, Hospital Clínic de Barcelona
Email: sofiaapp@clinic.cat

Background and aims: The utility of measuring HBV and HDV markers in liver biopsies (including cccDNA levels) to assess clinical outcomes is currently under evaluation. A recent study has shown high variability in cccDNA and HBV-RNA levels in multiple pieces of explant liver tissue in patients with different viral loads (Rydell GE et al. 2021). The aim of our study was to investigate whether the liver biopsy is representative for the detection of cccDNA in patients with low levels of HBV replication, either induced by NUCs or in the context of HDV coinfection.

Method: We included 10 patients undergoing liver transplantation due to end-stage liver disease related to HBV ($n = 5$) or HDV ($n = 5$) infection. From each liver explant, we obtained 9–10 fresh-frozen tissue pieces and we quantified total intrahepatic HBV-DNA (iHBV-DNA), cccDNA and HDV-RNA by Taqman real-time PCR. The presence of HBsAg and HDAg was assessed by IHC in FFPE liver samples.

Results: HBV replication was suppressed in all patients (undetectable serum HBV-DNA, $n = 4$; ≤ 27 IU/ml, $n = 6$) either because of NUC therapy, HDV coinfection or both. iHBV-DNA was detectable in all HBV and HDV liver samples ($n = 98$). In contrast, detection of cccDNA in HBV patients was very heterogeneous, ranging from 10% to 80% of liver samples. Remarkably, no cccDNA was detected in any of the pieces from 4 out of 5 HDV-infected patients despite having higher iHBV-DNA levels than HBV mono-infected patients (median 1.342 vs 0.004 copies/cell, $p = 0.03$). Interestingly, HBsAg immunostaining in liver tissue samples showed a higher proportion of HBsAg-positive hepatocytes in HDV-infected patients compared to HBV-mono-infected patients ($>80\%$ vs 5–60%), suggesting greater HBsAg expression from HBV integrants in HDV-infected patients. HDV-RNA was detected in all the liver pieces ($n = 49$) from the HDV-infected patients, showing higher variability in patients with low serum HDV-RNA levels (2–4 Log IU/ml).

Conclusion: Based on our data, cccDNA detection is highly variable in virologically suppressed HBV-infected patients, and frequently undetectable in HDV-infected patients. The variability of intrahepatic viral markers, along with the potential interference of HBV integrants, should be considered when defining end points for drug development studies.

THU386

Hepatitis Delta virus infection in patients with chronic hepatitis B is associated with greater risk of liver disease progression and liver-related mortality: a systematic review and meta-analysis

Robert G. Gish¹, Robert Wong², Gian Luca Di Tanna³, Ankita Kaushik⁴, Nate Smith⁵, Patrick Kennedy⁶. ¹University of Nevada, Reno School of Medicine, Las Vegas, United States; ²Veterans Affairs Palo Alto Healthcare System, Division of Gastroenterology and Hepatology, California, United States; ³University of New South Wales, The George Institute for Global Health, Sydney, Australia; ⁴Gilead Sciences Inc, Foster City, United States; ⁵Maple Health Group, LLC, New York, United States; ⁶Blizard Institute, Department of Hepatology, Centre for Immunobiology, London, United Kingdom
Email: rgish@robertgish.com

Background and aims: Previous studies have suggested more aggressive liver disease progression in chronic hepatitis B (CHB) patients with hepatitis delta virus (HDV) infection. We conducted a

systematic literature review and meta-analysis to examine whether HDV RNA positivity (HDV RNA+) vs. RNA negativity (HDV RNA-) is associated with increased risk of advanced liver disease events (ALDEs), including compensated cirrhosis (CC), decompensated cirrhosis (DCC), hepatocellular carcinoma (HCC), liver transplant (LT), and liver-related mortality (LRM).

Method: PubMed, Embase and Cochrane Central were searched in August 2021. Observational, case-control, and cross-sectional studies along with clinical trials reports addressing the clinical question of the review were included. Data extraction focused on data related to the relative rate of progression to advanced liver disease events for HDV RNA+/detectable versus HDV RNA-/undetectable patients and quality evaluation was based on the modified Risk of Bias in Non-randomised Studies-of Interventions (mROBINS-I) checklist. Data were pooled using the Hartung-Knapp-Sidik-Jonkman method for random-effects models for both risk (RR) and hazard ratios (HRs). We assessed the proportion of variability due to between-study heterogeneity with the I^2 statistics.

Results: Among a total of 2,034 studies identified, 34 met analysis inclusion criteria. After meta-analysis, presence of HDV RNA+ was associated with a significant increased risk of any ALDE (mean effect [95% CI]: RR: 1.85 [1.11, 3.09]; HR: 2.39 [1.56, 3.68]). When compared to HDV RNA- patients, HDV RNA+ was associated with a significantly higher risk of progressing to CC (RR 2.19 [1.60, 2.99]), DCC (RR 2.07 [1.45, 2.96]; HR 3.82 [1.94, 7.49]), HCC (RR: 1.59 [1.02, 2.50]; HR 2.91 [1.98–4.29]), LT (HR 7.07 [1.61, 31.00]), and LRM (RR 1.92 [1.02, 3.63]; HR 4.58 [2.72, 7.70]).

Conclusion: This comprehensive systematic review and meta-analysis demonstrates that HDV RNA+ patients have significantly greater risk of liver disease progression compared to HDV RNA- patients. These findings highlight the need for improved HDV screening in patients with chronic HBV, leading to early detection of HBV/HDV, linkage to care, and timely initiation of appropriate antiviral therapies to reduce the risk of liver-related morbidity and mortality.

THU387

The serum markers of cccDNA transcriptional activity have a role in predicting long-term outcomes in children with perinatally acquired HBV infection

Christiana Moigboi¹, Mark Anderson², Gavin Cloherty², Kosh Agarwal¹, Ivana Carey¹. ¹King's College Hospital, Institute of Liver Studies, London, United Kingdom; ²Abbott Diagnostics, Department of Infectious Diseases, North Chicago, United States
Email: christiana.moigboi@nhs.net

Background and aims: Perinatally acquired chronic hepatitis B (CHB) has often indolent course in childhood, but persistent viral infection leads to progressive liver disease in 40% of patients in adulthood. The combination of non-invasive serological (HBeAg, HBsAg levels) and virological (HBV DNA) markers together with liver enzyme activity (ALT) and liver damage scores (APRI or FIB-4) aids in monitoring disease stages and progression. Novel serological markers of cccDNA transcriptional activity-HBV core-related antigen (HBcrAg) and pre-genomic HBV RNA (pgRNA) might add more insight and were not studied in paediatric populations. We aimed to investigate whether markers of cccDNA transcriptional activity in serum: HBcrAg and pgRNA can help to predict future disease progression (need for therapy) in patients with perinatally acquired chronic hepatitis B infection.

Method: A retrospective study was carried out with samples from 29 chronic hepatitis B (CHB) paediatric patients diagnosed in childhood (median age 12 years, 48% males, 52% HBeAg positive) with long-term follow-up in the same centre (median follow-up duration 6.5 years, range 3–16 years) with available serum samples at the time of diagnosis. HBV DNA viral load was tested by TaqMan PCR [IU/ml], HBeAg status and HBsAg plasma levels by Abbott Architect® [log₁₀IU/ml], HBcrAg concentrations by CLEIA Fujirebio [log₁₀U/ml] and pgRNA concentrations by real-time PCR Abbott Molecular Diagnostic RUO assay (LLQD=1.65 log₁₀U/ml). Only 5 patients required to be started on antiviral therapy during follow-up.

Results: At diagnosis 79% patients had detected HBV pgRNA and HBcrAg was detected in all patients. There were strong positive correlations between serum pgRNA and HBV DNA levels ($r=0.82$, $p<0.01$), pgRNA and HBsAg levels ($r=0.74$, $p<0.01$) and pgRNA and HBcrAg concentrations ($r=0.859$, $p<0.01$). When compared untreated vs. patients who required therapy-pgRNA was detected in 100% of untreated patients vs. 80% of patients needing therapy, but patients who needed therapy had higher pgRNA levels than untreated cohort (median: 3.02 log₁₀U/ml vs. 1.94 log₁₀U/ml, $p<0.05$). In contrast, HBcrAg was detected in all patients irrespective of therapy status, but patients who required therapy had lower HBcrAg concentrations than untreated patients (median: 3.84 log₁₀U/ml vs. 5.15 log₁₀U/ml, $p<0.05$) likely reflecting higher proportion of HBeAg negative patients in patients needing therapy (80% vs. 29%, $p<0.05$).

Conclusion: The markers of cccDNA transcriptional activity-pgRNA and HBcrAg-combined with the traditional serological/virological markers (HBeAg, HBsAg and HBV DNA levels) were helpful to predict at diagnosis patients who might require antiviral therapy in future and represent a valuable tool to be applied in regular diagnostics. Studies in larger paediatric cohorts to further assess this are needed.

THU388

Presence of liver inflammation and fibrosis in Asian patients with chronic hepatitis B in the grey zone

Jiacheng Liu¹, Jian Wang², Yiguang Li³, Li Zhu⁴, Weimao Ding⁵, Chuanwu Zhu⁴, Yuanwang Qiu³, Jie Li², Rui Huang², Chao Wu². ¹Nanjing Drum Tower Hospital Clinical College of Traditional Chinese and Western Medicine, Nanjing University of Chinese Medicine, Department of Infectious Diseases, Nanjing, China; ²Nanjing Drum Tower Hospital, The Affiliated Hospital of Nanjing University Medical School, Department of Infectious Diseases, Nanjing, China; ³The Fifth People's Hospital of Wuxi, Department of Infectious Diseases, Wuxi, China; ⁴The Affiliated Infectious Diseases Hospital of Soochow University, Department of Infectious Diseases, Suzhou, China; ⁵Huai'an No. 4 People's Hospital, Department of Hepatology, Huai'an, China
Email: dr.wu@nju.edu.cn

Background and aims: Over a quarter of chronic hepatitis B (CHB) patients did not meet criteria of the traditional natural phases and hence classified as grey zone (GZ). However, few studies reported the liver inflammation and fibrosis of Asian CHB patients in the GZ.

Method: This multicenter, retrospective study included 1,064 CHB patients underwent liver biopsy (LB). Phases of natural history were determined according the AASLD 2018 Guidance. GZ patients were divided into four categories: HBeAg-positive, normal ALT and HBV-DNA $\leq 10^6$ IU/ml (GZ-A); HBeAg-positive, elevated ALT and HBV-DNA $< 2 \times 10^4$ IU/ml (GZ-B); HBeAg-negative, normal ALT and HBV-DNA $\geq 2 \times 10^3$ IU/ml (GZ-C); HBeAg-negative, elevated ALT and HBV-DNA $< 2 \times 10^3$ IU/ml (GZ-D).

Results: 263 (24.7%) patients were in the GZ with the median age of 41.5 years and male of 67.2%. Among the GZ patients, GZ-D (44.1%) was the dominate category, followed by GZ-C (37.6%), GZ-A (9.9%) and GZ-B (8.4%). Surprisingly, as high as 60.4% of GZ patients had significant inflammation ($\geq G2$) and 89.7% GZ patients had significant fibrosis ($\geq S2$), which were higher than that of patients with immune-tolerant and inactive phases. Over half of patients had significant inflammation or fibrosis in each GZ category. GZ-B patients had the highest proportions of significant inflammation (95.5%) and fibrosis (81.9%) compared to other GZ categories (GZ-A: 76.9% and 69.3%; GZ-C: 53.5% and 52.5%; GZ-D: 56.1% and 60.4%, respectively).

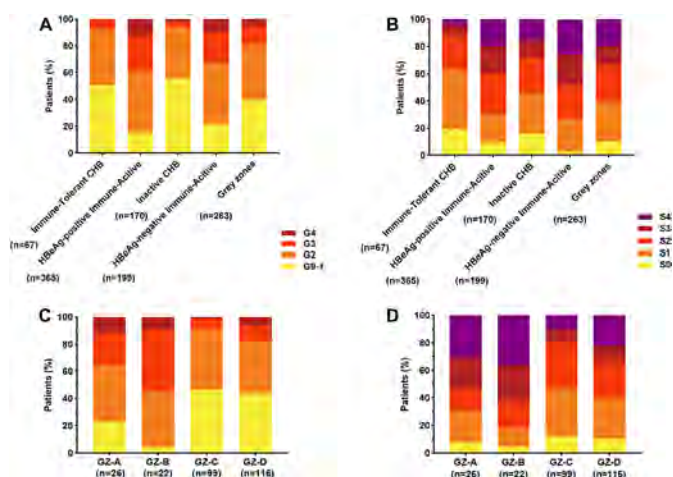


Figure: Liver inflammation and fibrosis in chronic hepatitis B with different phases of natural history and grey zones.

Conclusion: A substantial GZ patients had significant liver inflammation or fibrosis, especially for CHB patients with GZ-B. Using liver biopsy to assess the liver histological activity should be encouraged in GZ patients.

THU389

Characteristics and renal function in patients with chronic hepatitis B virus infection: baseline data from the phase 2b B-Clear study

Seng Gee Lim¹, Robert Plesniak², Keiji Tsuji³, Harry Janssen⁴, Cristina Pojoga^{5,6}, Adrian Gadano⁷, Corneliu Petru Popescu⁸, Tarik Asselah⁹, Diana Petrova¹⁰, Hyung Joon Yim¹¹, Gheorghe Diaconescu¹², Jeong Heo¹³, Alexander Wong¹⁴, Ewa Janczewska¹⁵, Man-Fung Yuen¹⁶, Jennifer Cremer¹⁷, Tamara Lukic¹⁸, Stuart Kendrick¹⁹, Robert Elston¹⁹, Geoff Quinn¹⁹, Punam Bharania¹⁹, Fiona Campbell¹⁹, Melanie Paff¹⁷, Dickens Theodore¹⁷. ¹National University Health System, Singapore; ²University of Rzeszow Centrum Medyczne w Lancucie Sp. z o.o., Poland; ³Hiroshima Red Cross Hospital, Japan; ⁴Toronto General Hospital, Canada; ⁵Institutul Regional de Gastroenterologie si Hepatologie prof dr O Fodor, Romania; ⁶Babeş-Bolyai University, International Institute for Advanced Study of Psychotherapy and Applied Mental Health, Romania; ⁷Hospital Italiano de Buenos Aires, Argentina; ⁸Dr Victor Babes Clinical Hospital of Infectious and Tropical Diseases, Carol Davila University of Medicine and Pharmacy, Romania; ⁹Hôpital Beaujon, Université de Paris, France; ¹⁰Diagnostic Consultative Centre Alexandrovsk, Bulgaria; ¹¹Korea University Ansan Hospital, Korea, Rep. of South; ¹²Spitalul Clinic de Boli Infectioase si Pneumoftiziologie, Romania; ¹³College of Medicine, Pusan National University and Biomedical Research Institute, Pusan National University Hospital, Korea, Rep. of South; ¹⁴University of Saskatchewan, Department of Medicine, Canada; ¹⁵ID Clinic, Poland; ¹⁶Queen Mary Hospital, The University of Hong Kong, China; ¹⁷GlaxoSmithKline, United States; ¹⁸GlaxoSmithKline, United Arab Emirates; ¹⁹GlaxoSmithKline, United Kingdom
Email: mdclimg@nus.edu.sg

Background and aims: Chronic hepatitis B (CHB) infection has been associated with the development of chronic kidney disease. Bepirovirsen (BPV; GSK3228836) is an antisense oligonucleotide known to distribute into the kidneys and liver. Here, we aim to characterise the baseline renal parameters in patients (pts) enrolled in B-Clear and to understand any associations between renal parameters (estimated glomerular filtration rate [eGFR]), nucleos (t) ide analogue (NA) treatment status and other baseline laboratory/clinical characteristics.

Method: B-Clear is an ongoing trial (NCT04449029) to assess the efficacy and safety of BPV in pts with CHB infection on stable NA treatment (+NA) or not on NA (-NA) at study start. Pts were grouped

based on eGFR (in ml/min/1.73m²): low (60-<90), normal (90-<120) and high (≥120). Frequency counts, descriptive statistics and 95% confidence intervals (CI) were used for comparison.

Results: A total of 455 pts were enrolled: 225 +NA and 230 -NA (Table). Mean age and length of diagnosis was inversely related to eGFR status for both those +NA and -NA. For both +NA and -NA pts, the highest proportion of pts with low eGFR were Asian (74% and 70%, respectively), and within race groups, Asians had the highest proportion of pts with low eGFR. +NA pts in the high eGFR group had higher HBsAg (mean [95% CI]: 10, 939.4 [6264.0, 15614.8]) vs pts in the low eGFR group (2723.5 [1545.9, 3901.1] IU/ml); this was not observed in -NA pts. In the -NA group, mean eGFR was lower in HBeAg negative pts (mean [95% CI]: 107.1 [105.0, 109.2]) vs HBeAg positive pts (114.4 [110.2, 118.6]). The number of pts with baseline non-steroidal anti-inflammatory drug (NSAID) or angiotensin-converting enzyme inhibitor/angiotensin receptor blocker use, or pts with diabetes or hypertension were low, but mean eGFR tended to be lower in these pt groups than in those without concomitant medication use or comorbidities, except for -NA pts with baseline NSAID use or diabetes. The most common NA used at baseline was entecavir (reported by 41% of those on NA).

Conclusion: Preliminary assessment of pts enrolled in B-Clear indicates that renal function may be associated with characteristics such as age, length of CHB diagnosis, race, HBsAg level, HBeAg status, and concomitant medications/comorbidities. [on behalf of the B-Clear study group].

Funding: GSK (209668).

THU390

Characterisation of baseline complement values in patients with chronic hepatitis B virus infection in the phase IIb B-clear study

Jennifer Cremer¹, Anna Richards², Tamara Lukic³, Seng Gee Lim⁴, Robert Plesniak⁵, Keiji Tsuji⁶, Harry Janssen⁷, Cristina Pojoga^{8,9}, Corneliu Petru Popescu¹⁰, Tarik Asselah¹¹, Diana Petrova¹², Hyung Joon Yim¹³, Gheorghe Diaconescu¹⁴, Jeong Heo¹⁵, Alexander Wong¹⁶, Ewa Janczewska¹⁷, Giuliano Rizzardini¹⁸, Man-Fung Yuen¹⁹, Geoff Quinn², Punam Bharania², Melanie Paff¹, Dickens Theodore¹. ¹GlaxoSmithKline, United States; ²GlaxoSmithKline, United Kingdom; ³GlaxoSmithKline, United Arab Emirates; ⁴National University Health System, Singapore; ⁵University of Rzeszow Centrum Medyczne w Lancucie Sp. z o.o., Poland; ⁶Hiroshima Red Cross Hospital, Japan; ⁷Toronto General Hospital, Canada; ⁸Institutul Regional de Gastroenterologie si Hepatologie prof dr O Fodor, Romania; ⁹Babeş-Bolyai University, International Institute for Advanced Study of Psychotherapy and Applied Mental Health, Romania; ¹⁰Dr Victor Babes Clinical Hospital of Infectious and Tropical Diseases, Carol Davila University of Medicine and Pharmacy, Romania; ¹¹Hôpital Beaujon, Université de Paris, France; ¹²Diagnostic Consultative Centre Alexandrovsk, Bulgaria; ¹³Korea University Ansan Hospital, Korea, Rep. of South; ¹⁴Spitalul Clinic de Boli Infectioase si Pneumoftiziologie, Romania; ¹⁵College of Medicine, Pusan National University and Biomedical Research Institute, Pusan National University Hospital, Korea, Rep. of South; ¹⁶University of Saskatchewan, Department of Medicine, Canada; ¹⁷ID Clinic, Poland; ¹⁸Fatebenefratelli Sacco Hospital, Italy; ¹⁹Queen Mary Hospital, The University of Hong Kong, China
Email: jennifer.x.cremer@gsk.com

Background and aims: The immune system plays an important role in disease pathogenesis and viral clearance of hepatitis B virus (HBV) infection, but the impact of HBV on the complement system, the inflammatory/immune state of patients (pts) and implications for disease and treatment are poorly understood. Here we present associations between baseline complement factors, other laboratory and clinical characteristics, and nucleot (s)ide analogue (NA) treatment status in pts screened in the B-Clear trial.

Method: B-Clear is an ongoing phase IIb trial (NCT04449029) to assess the efficacy and safety of bepirovirsen (BPV, GSK3228836), an antisense oligonucleotide, in pts with chronic HBV. Pts on either

Table: Summary of demographic and baseline characteristics for +NA and -NA treatment groups

Characteristic	eGFR 60–<90	eGFR 90–<120	eGFR ≥120	Total
+NA, N (%)	43 (19.1)	159 (70.7)	23 (10.2)	225 (100)
Age, years				
Mean	56.1	45.9	32.3	46.4
Median	55.0	44.0	28.0	45.0
95% CI	53.1, 59.2	44.3, 47.4	26.9, 37.7	44.9, 48.0
Hepatitis B e antigen, n (%)				
Positive	14 (33)	45 (28)	10 (43)	69 (31)
Negative	29 (67)	114 (72)	13 (57)	156 (69)
HBsAg, IU/mL				
Mean	2723.5	4356.6	10939.4	4717.4
Median	1740.0	1864.0	8792.0	2085.0
95% CI	1545.9, 3901.1	3284.2, 5429.1	6264.0, 15614.8	3768.9, 5665.9
HBV DNA level, IU/mL				
Mean (95% CI)	7.2 (2.9, 11.5)	8.0 (6.4, 9.5)	10.9 (6.7, 15.0)	8.1 (6.7, 9.5)
Length of diagnosis, years				
Mean (95% CI)	18.6 (15.0, 22.1)	15.3 (13.7, 16.9)	12.4 (7.9, 17.0)	15.6 (14.3, 17.0)
Race, n (%)				
Asian	32 (74)	77 (48)	9 (39)	118 (52)
White	10 (23)	77 (48)	12 (52)	99 (44)
Black or African American	1 (2)	4 (3)	2 (9)	7 (3)
American Indian or Alaska Native	0	1 (<1)	0	1 (<1)
Mixed race	0	0	0	0
-NA, N (%)	23 (10.0)	156 (67.8)	51 (22.2)	230 (100)
Age, years				
Mean	49.4	43.7	33.2	42.0
Median	48.0	43.0	33.0	41.5
95% CI	45.2, 53.7	42.1, 45.4	30.9, 35.4	40.6, 43.4
Hepatitis B e antigen, n (%)				
Positive	4 (17)	35 (23)	21 (42)	60 (27)
Negative	19 (83)	117 (77)	29 (58)	165 (73)
HBsAg, IU/mL				
Mean	21680.1	15495.4	22556.1	17679.5
Median	5426.0	3795.5	8820.0	4784.5
95% CI	3813.1, 39547.1	8138.6, 22852.2	13083.6, 32028.6	12036.7, 23322.3
HBV DNA level, IU/mL				
Mean (95% CI)	5687821 (330085, 11045556)	6043339 (3474703, 8611974)	15193241 (6204777, 24181705)	8045383 (5343721, 10747044)
Length of diagnosis, years				
Mean (95% CI)	15.9 (9.9, 21.9)	15.0 (13.1, 16.9)	8.9 (6.8, 11.0)	13.7 (12.2, 15.3)
Race, n (%)				
Asian	16 (70)	86 (55)	28 (55)	130 (57)
White	7 (30)	57 (37)	15 (29)	79 (34)
Black or African American	0	12 (8)	8 (16)	20 (9)
Mixed race	0	1 (<1)	0	1 (<1)

CI, confidence interval; HBsAg, hepatitis B surface antigen; HBV, hepatitis B virus; NA, nucleos(t)ide analogue

Table: (abstract: THU389)

Table.

Assessment	Patients on NA (n=286)			Patients not on NA (n=432)		
	Low C3 (N = 25)	Normal C3 (N = 258)	High C3 (N = 3)	Low C3 (N = 58)	Normal C3 (N = 371)	High C3 (N = 3)
Age, n (%)						
< 50 years	12 (48)	159 (62)	2 (67)	46 (79)	267 (72)	3 (100)
≥ 50 years	13 (52)	99 (38)	1 (33)	12 (21)	104 (28)	0 (0)
Sex, n (%)						
Female (F)	7 (28) [9 % of female +NA population]	71 (28)	0 (0)	33 (57) [18 % of female -NA population]	151 (41)	2 (67)
Male (M)	18 (72) [9 % of male +NA population]	187 (72)	3 (100)	25 (43) [10 % of male -NA population]	220 (59)	1 (33)
Race, n (%)						
Asian	17 (68) [12 % of Asian +NA population]	129 (50)	0 (0)	42 (72) [21 % of Asian -NA population]	161 (43)	0 (0)
Black	0 (0)	10 (4)	1 (33)	5 (9)	39 (11)	1 (33)
White	8 (32) [6 % of White +NA population]	118 (46)	2 (67)	11 (19) [6 % of White -NA population]	168 (45)	2 (67)
Others	0 (0)	1 (< 1)	0 (0)	0 (0)	2 (< 1)	0 (0)
Complement C3						
Mean (SD) C3, g/L	0.81 (0.08)	1.16 (0.17)	1.89 (0.09)	0.80 (0.08)	1.19 (0.18)	1.88 (0.06)
95% CI	(0.8, 0.8)	(1.1, 1.2)	(1.7, 2.1)	(0.8, 0.8)	(1.2, 1.2)	(1.7, 2.0)
Low, n (%)	25 (100)	0 (0)	0 (0)	58 (100)	0 (0)	0 (0)
Normal, n (%)	0 (0)	258 (100)	0 (0)	0 (0)	371 (100)	0 (0)
High, n (%)	0 (0)	0 (0)	3 (100)	0 (0)	0 (0)	3 (100)
Complement C4						
Mean (SD) C4, g/L	0.15 (0.04)	0.21 (0.06)	0.51 (0.14)	0.13 (0.05)	0.21 (0.06)	0.30 (0.04)
95% CI	(0.1, 0.2)	(0.2, 0.2)	(0.2, 0.9)	(0.1, 0.1)	(0.2, 0.2)	(0.2, 0.4)
Low, n (%)	2 (8)	2 (< 1)	0 (0)	15 (26)	4 (1)	0 (0)
Normal, n (%)	23 (92)	254 (98)	1 (33)	43 (74)	362 (98)	3 (100)
High, n (%)	0 (0)	2 (< 1)	2 (67)	0 (0)	5 (1)	0 (0)
Complement Bb, n	19	205	1	34	195	1
Mean (SD) Bb, mg/L	0.90 (0.16)	1.0 (0.45)	0.99 (NA)	1.09 (0.36)	1.07 (0.45)	1.28 (NA)
95% CI	(0.8, 1.0)	(0.9, 1.1)	NA	(1.0, 1.2)	(1.0, 1.1)	NA
Low (< 0.45), n (%)	0 (0)	1 (< 1)	0 (0)	0 (0)	1 (< 1)	0 (0)
Normal (0.49–1.42), n (%)	19 (100)	188 (92)	1 (100)	29 (85)	175 (90)	1 (100)
High (> 1.42), n (%)	0 (0)	16 (8)	0 (0)	5 (15)	19 (10)	0 (0)
Complement C5a, n	19	205	1	34	195	1
Mean (SD) C5a, µg/mL	5.11 (3.00)	7.11 (4.74)	12.3 (NA)	6.52 (2.86)	7.01 (4.82)	9.63 (NA)
95% CI	(3.7, 6.6)	(6.5, 7.8)	NA	(5.5, 7.5)	(6.3, 7.7)	NA
Normal (0.37–74.3), n (%)	19 (100)	205 (100)	1 (100)	34 (100)	195 (100)	1 (100)
Hepatitis B virus surface antigen, n	19	205	1	34	195	1
Mean (SD), IU/mL	5911 (11359)	4624 (8756)	1118 (NA)	15735 (20943)	18048 (46380)	11930 (NA)
95% CI	(436, 11386)	(3694, 5555)	NA	(8428, 23042)	(11498, 24599)	NA
Low (≤ 3 log10 IU/mL), n (%)	6 (32) [9 % of low HBsAg]	58 (28)	0 (0)	4 (12) [10 % of low HBsAg]	38 (19)	0 (0)
High (> 3 log10 IU/mL), n (%)	13 (68) [8 % of high HBsAg]	147 (72)	1 (100)	30 (88) [16 % of high HBsAg]	157 (81)	1 (100)
Hepatitis B virus e-antigen, n	19	205	1	33	191	1
Mean (SD), IU/mL	41.5 (178.9)	11.9 (80.9)	0.53 (NA)	473 (1008)	249 (752)	0.05 (NA)
95% CI	(-44.8, 127.7)	(0.1, 23.1)	NA	(116, 831)	(142, 357)	NA
Positive, n (%)	5 (26)	63 (31)	1 (100)	14 (42)	46 (24)	0 (0)
Negative, n (%)	14 (74)	142 (69)	0 (0)	19 (58)	145 (76)	1 (100)
Hepatitis B Virus DNA, n	19	204	1	34	194	1
Mean (SD), IU/mL	4.98 (7.92)	8.30 (10.79)	19.90	12,276,923 (21,759,141)	7,345,220 (20,582,504)	4516
95% CI	(1.2, 8.8)	(6.8, 9.8)	NA	(4,684,799, 19,869,046)	(4,430,632, 10,259,809)	NA

CI, confidence interval; NA, not applicable; SD, standard deviation.

Table: (abstract: THU390)

stable NA therapy (+NA), or not receiving NA therapy (-NA) were enrolled. All pts screened for B-Clear were included in this analysis; pts were grouped based on baseline values of complement C3 ([in g/L] low <0.9; normal 0.9–1.8; high >1.8) and C4 ([in g/L] low <0.1; normal 0.1–0.4; high >0.4) at screening. Descriptive statistics and 95% confidence intervals were used for comparison.

Results: Of the 725 screened pts with data (N = 718 [+NA: n = 286; -NA: n = 432]): 83 had low C3 (+NA: n = 25; -NA: n = 58), 23 had low C4 (+NA: n = 4; -NA: n = 19), and 17 had both low C3 and C4 (+NA: n = 2; -NA: n = 15) (Table). A greater proportion of females had low C3 in the -NA group versus the +NA group (18%, versus 9%, respectively). Most pts with low C3 were Asian (+NA: 68%; -NA: 72%). In the +NA low C3 group, the mean hepatitis B virus surface antigen (HBsAg; 5911 IU/mL) and hepatitis B virus e-antigen (HBeAg; 41.5 U/mL) was higher vs the normal C3 mean HBsAg (4624 IU/mL) and HBeAg (11.9 U/mL). In the -NA low C3 group, the mean HBV DNA (12, 276, 923 IU/mL) and HBeAg (473 U/mL) was higher vs the normal C3 group (HBV DNA 7, 345, 220 IU/mL; HBeAg 249 U/mL), while HBsAg was lower (low C3 group 15735 IU/mL; high C3 group 18048 IU/mL).

The complement split product C5a and factor Bb were similar, and mostly in the normal range, in pts with low, normal or high C3 in both the +NA and -NA groups.

Conclusion: Preliminary findings indicate that gender, race, HBsAg, HBV DNA, and HBeAg level may all contribute to low C3 among pts with HBV. Observed differences may be due to different stages of disease or level of immune status for pts +NA, versus -NA. Due to low numbers of pts with low C4, no conclusions could be made regarding associations with baseline characteristics. [on behalf of the B-Clear study group].

Funding: GSK (209668).

THU391

Estimations of the global prevalence and clinical burden of occult hepatitis B infection (OBI): a systematic review and meta-analysis

Yu Ri Im¹, Rukmini Jagdish¹, Damien Leith², Jin Un Kim¹, Gibril Ndow³, Kyoko Yoshida¹, Amir Majid⁴, Yueqi Ge⁵, Yusuke Shimakawa⁶, Maud Lemoine¹. ¹Imperial College London, Section of Hepatology, Division of Digestive Diseases, Department of Metabolism, Digestion and Reproduction, London, United Kingdom; ²Glasgow Royal Infirmary, Department of Gastroenterology, Glasgow, United Kingdom; ³London School of Hygiene and Tropical Medicine, MRC Unit The Gambia, Fajara, Gambia; ⁴West Middlesex University Hospital, Department of Anaesthetics, Isleworth, United Kingdom; ⁵Chelsea and Westminster Hospital, Department of Gastroenterology, London, United Kingdom; ⁶Institut Pasteur, Unité d'Épidémiologie des Maladies Émergentes, Paris, France

Email: yuri.im@doctors.org.uk

Background and aims: Occult hepatitis B infection (OBI) is defined as the presence of replication-competent hepatitis B virus (HBV) DNA in the blood or liver tissue of individuals who test negative for the hepatitis B surface antigen (HBsAg). Previous studies have suggested that individuals with OBI could transmit the virus and may be at higher risk of hepatocellular carcinoma (HCC). Despite possible implications for both affected individuals and global HBV elimination goals, the prevalence of OBI is not known. Therefore, we performed a meta-analysis to estimate the global prevalence of OBI.

Method: We systematically searched the MEDLINE, Embase, Global Health and Web of Science databases for articles published between Jan 1, 2010, and August 14, 2019. We included studies on adult populations from which the prevalence of OBI could be calculated, regardless of anti-hepatitis B core (anti-HBc) status or viral load. We excluded studies on individuals <18 years of age and those on antiviral therapy active against HBV. The prevalence was pooled to

determine effect estimates and 95%CI weighted by study size for blood donors, low-risk populations, high-risk populations due to increased HBV exposure risk, and patients with advanced liver disease. We also assessed the effects of study design, HBV serology, HBV endemicity and presence of advanced liver disease on OBI prevalence.

Results: Our meta-analysis included 400 studies and 143, 980, 492 individuals. Amongst anti-HBc-positive individuals (n = 7, 863), OBI prevalence was 7.9% (5.3–10.8) in blood samples (n = 7, 345) and 55.2% (42.9–67.3) in liver samples (n = 367). Amongst anti-HBc-negative individuals (n = 45, 853), OBI prevalence was 1.1% (0.6–1.8) in blood samples (n = 44, 637) and 17.9% (5.1–35.2) in liver samples (n = 302). When assessing studies that included all individuals negative for HBsAg regardless of anti-HBc status and tested OBI in the blood, OBI prevalence was lowest in blood donors (0.2% [0.2–0.4]), followed by low-risk populations (2.5% [1.0–4.5]), high-risk populations due to increased HBV exposure risk (6.4% [4.2–9.0]) and patients with advanced liver disease (15.8% [8.1–25.2]). Endemicity of the country of study was predictive of OBI prevalence in blood donors. The presence of advanced liver disease was associated with an increased prevalence of OBI across case-control studies of patients with cirrhosis or HCC compared to healthy controls (p < 0.001).

Conclusion: OBI is common, clinically significant, and underestimated. Our study reports a consistently high prevalence of OBI in HBV-endemic areas and, globally, across high-risk groups. Screening of blood products with both nucleic acid testing (NAT) and anti-HBc might be necessary to eradicate this reservoir of HBV infection globally. OBI should no longer be overlooked in regional and global hepatitis B screening, prevention, and elimination programmes.

THU392

Time for universal screening for hepatitis D? A study describing screening patterns, characteristics and outcomes of hepatitis D virus infection

Rohit Nathani¹, Bo Hyung Yoon², Carolina Villarroel³, Sidra Salman¹, Dewan Giri³, Amreen Dinani⁴, Ilan Weisberg⁴. ¹Icahn School of Medicine at Mount Sinai Morningside-West, Department of Medicine, New York, United States; ²Icahn School of Medicine at Mount Sinai Beth Israel-Morningside-West, Division of Gastroenterology, Department of Medicine, New York, United States; ³Icahn School of Medicine at Mount Sinai Beth Israel, Department of Medicine, New York, United States; ⁴Icahn School of Medicine at Mount Sinai Beth Israel, Division of gastroenterology, Department of Medicine, New York, United States
Email: rohit.nathani@mountsinai.org

Background and aims: The prevalence of hepatitis D virus (HDV) is as high as 10% in patients with hepatitis B virus (HBV) infection. Asian and European guidelines recommend universal testing for HDV in all HBV surface antigen positive persons. However, the AASLD guidelines recommend testing only those at increased 'risk.' The aim of our study was to identify patterns of screening for HDV and to understand the characteristics and outcomes of those infected with HDV.

Method: A retrospective cohort of patients with chronic hepatitis B (CHB) infection was identified using electronic medical record data in a tertiary health system from 01/2016 to 10/2021. We also identified those who were screened with an HDV antibody test. For this submission, detailed chart review of patients with a confirmed diagnosis of HDV infection was performed. Baseline demographic data, comorbidities, and markers of severity of liver disease (determined by FIB 4 score) and cirrhosis status (based on imaging and clinical criteria) at the time of diagnosis was recorded. We also recorded the type of screening test and the type of clinician performing the screening. Primary outcome was mortality and secondary outcomes included liver decompensation (LD), development of hepatocellular carcinoma (HCC), and need for liver transplant (LT).

Results: Over 6 years 11, 110 patients were diagnosed with CHB and 1390 (12.5%) of them had been screened for HDV infection. A detailed

chart review was performed of 86/1390 patients (6.1%) who were positive for HDV infection and had complete data. More than half (58.14%) were male, mean body mass index was 27.88 (SD ± 5.5) units. After CHB, most common co-existing condition was hepatitis C virus (HCV) infection (11.62%). Median FIB-4 score was 1.8 (1.1–4.2) and 53.48% had cirrhosis at the time of HDV diagnosis. Majority (81.4%) of screening tests were ordered at attending clinics by gastroenterologists (90.7%). Among patients with cirrhosis 17 (37%) developed LD with ascites and esophageal varices (82% each) being the most common decompensating events. 12 (13.95%) patients developed HCC and 16 (18.6%) patients needed LT. No patients died during follow-up.

Conclusion: Our study demonstrates that people with HBV who are infected with HDV have high morbidity and increased risk for HCC, LD, and LT. A small proportion of HBV infected persons are screened for HDV and many of them develop liver cirrhosis by the time of diagnosis. Contrary to AASLD guidelines, we found a sizable number of HDV-positive people who do not have co-existing high-risk conditions like Human Immunodeficiency Virus and HCV. Most of the screening for HDV occurred in attending clinics vs trainee/mid-level provider clinics, identifying an area for improving knowledge around HDV. We describe a significant liver-related disease burden in those with HDV and thus universal screening for HDV in people with HBV infection may be reasonable.

THU393

Distribution of patients by guideline-defined disease phase and/or grey zones in B-Clear, an international multicentre clinical trial

Seng Gee Lim¹, Cristina Pojoga^{2,3}, Harry Janssen⁴, Michio Imamura⁵, Ewa Janczewska⁶, Robert Plesniak⁷, Keiji Tsuji⁸, Corneliu Petru Popescu⁹, Diana Petrova¹⁰, Adrian Gadano¹¹, Alexander Wong¹², Tarik Asselah¹³, Hyung Joon Yim¹⁴, Jeong Heo¹⁵, Man-Fung Yuen¹⁶, Gheorghe Diaconescu¹⁷, Giuliano Rizzardini¹⁸, Jennifer Cremer¹⁹, Robert Elston²⁰, Stuart Kendrick²⁰, Geoff Quinn²⁰, Fiona Campbell²⁰, Melanie Paff²¹, Dickens Theodore¹⁹. ¹National University Health System, Singapore, Singapore; ²Institutul Regional de Gastroenterologie si Hepatologie prof dr O Fodor, Cluj-Napoca, Romania; ³Babeş-Bolyai University, International Institute for Advanced Study of Psychotherapy and Applied Mental Health, Cluj-Napoca, Romania; ⁴Toronto General Hospital, Toronto, Canada; ⁵Hiroshima University Hospital, Hiroshima, Japan; ⁶ID Clinic, Myslowice, Poland; ⁷University of Rzeszow Centrum Medyczne w Lancucie Sp. z o.o., Lancut, Poland; ⁸Hiroshima Red Cross Hospital, Hiroshima, Japan; ⁹Dr Victor Babes Clinical Hospital of Infectious and Tropical Diseases, Carol Davila University of Medicine and Pharmacy, Bucharest, Romania; ¹⁰Diagnostic Consultative Centre, Varna, Bulgaria; ¹¹Hospital Italiano de Buenos Aires, Buenos Aires, Argentina; ¹²University of Saskatchewan, Regina, Canada; ¹³Hôpital Beaujon, Clichy, France; ¹⁴Korea University Ansan Hospital, Ansan, Korea, Rep. of South; ¹⁵Pusan National University Hospital, Busan, Korea, Rep. of South; ¹⁶Queen Mary Hospital, Hong Kong, China; ¹⁷Spitalul Clinic de Boli Infectioase si Pneumoftiziologie, Craiova, Romania; ¹⁸Luigi Sacco Hospital, Milan, Italy; ¹⁹GlaxoSmithKline, Durham, United States; ²⁰GlaxoSmithKline, Stevenage, United Kingdom; ²¹GlaxoSmithKline, Collegeville, United States
Email: jennifer.x.cremer@gsk.com

Background and aims: Many patients (pts) with chronic hepatitis B virus (CHB) lie in a grey zone (GZ) (i.e. they do not fit into a guideline-defined disease phase). We evaluated the distribution and characteristics of CHB pts enrolled in B-Clear, who were not on nucleos (t)ide analog (NA) therapy, by guideline-defined disease phase and GZ.

Method: B-Clear is an ongoing trial (NCT04449029) to assess the efficacy and safety of bepirovirsen (GSK3228836, BPV)-an antisense oligonucleotide- in pts with CHB. Pts not on NA (N = 230) were categorised as HBeAg positive (eAg+) chronic infection, eAg+ chronic hepatitis, HBeAg negative (eAg-) chronic infection, and eAg- chronic hepatitis, based on HBV DNA, alanine aminotransferase (ALT) and eAg status at baseline as per EASL 2017, AASLD 2018 and APASL 2015 CHB

POSTER PRESENTATIONS

guidelines. In addition, 'Strict' or 'Common' criteria were applied based upon eAg status and ALT cut-offs of 35/25 IU/ml [males/females] or 40/33 IU/ml [males/females], respectively. Pts in the GZ were categorised into four groups: A (eAg+, normal ALT), B (eAg+, high ALT), C (eAg-, normal ALT), D (eAg-, high ALT).

Results: Of the four guideline-defined disease phases, the highest proportion of pts were eAg+ chronic hepatitis (EASL 16.2%; AASLD 18.8%) or eAg- chronic hepatitis (EASL 16.2%; APASL 8.7%) (Figure); however, the majority of patients (55.5%, 65.9% and 81.2%) fell in the GZ using EASL, AASLD and APASL guidelines, respectively. Most pts in the GZ were eAg-. GZ C was the most common GZ group: 48.5% (EASL), 36.2% (AASLD) and 48.5% (APASL); however, the proportion of pts in other GZ groups differed by guideline. The EASL guidelines had the lowest proportion of pts in the GZ for Asian (48.8%), Black (75%) and White (60.8%) pts. The APASL guidelines had the highest proportion in the GZ for Asian (86%) and Black (95%) pts, while AASLD guidelines had the highest proportion of pts in the GZ for White pts (74.7%). When the criterion for HBV DNA was removed, the highest proportion of GZ pts fell into the eAg-, normal ALT category (52.2% 'Common'; 40.4% 'Strict') and eAg-, high ALT category (21.7% 'Common'; 33.5% 'Strict').

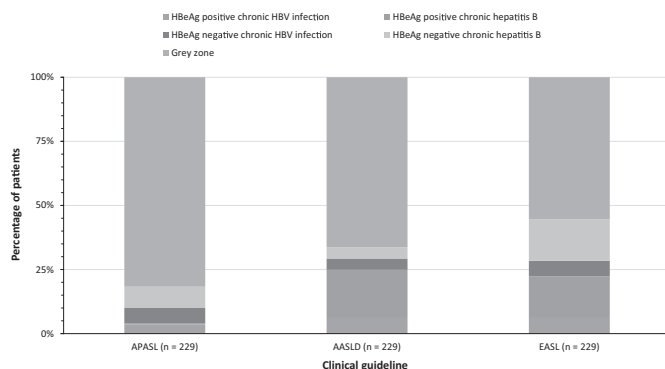


Figure: Percentage of patients in each disease phase by clinical guideline.

Conclusion: Most pts enrolled in B-Clear lie in the GZ. There is a need to understand how best to categorise pts with CHB to improve their overall management. Observations may be limited by the inclusion criteria of the study. [on behalf of the B-Clear study group].

Funding: GSK (209668).

THU394

Benign course of HBV reactivations during DAAs in untreated ENI with HBV-HCV co-infections correlates with different HBsAg kinetics compared to NAs treated CHB patients

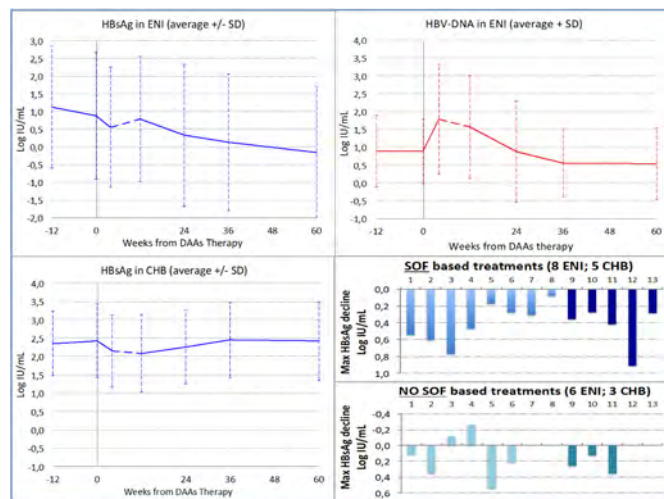
Piero Colombatto¹, Elena Palmisano², Gabriele Ricco¹, Daniela Cavallone¹, Filippo Oliveri¹, Barbara Coco¹, Antonio Salvati¹, Veronica Romagnoli¹, Lidia Surace¹, Maria Linda Vatteroni², Mauro Pistello², Agostino Virdis³, Ferruccio Bonino⁴, Maurizia Brunetto^{1,5}. ¹University Hospital of Pisa, Hepatology Unit, Pisa, Italy; ²University of Pisa, Virology Unit, Pisa, Italy; ³University of Pisa, Internal Medicine Unit; ⁴National Research Council; ⁵University of Pisa Email: p.colombatto@ao-pisa.toscana.it

Background and aims: Direct-acting antivirals (DAA) carry a potential risk of inducing hepatitis B virus (HBV) reactivations in HBV-HCV co-infected patients (pts). However, dynamics and outcomes may be different according to the phase of HBV infection. Our aim was to investigate HBsAg and HBV-DNA kinetics across DAAs therapy in untreated carriers with HBeAg Negative Infection (ENI) and in HBeAg negative Chronic Hepatitis B (CHB) pts receiving Nucleos (t)ide Analogs (NA).

Method: We prospectively enrolled 15 (F/M: 4/11, median age: 62.1y) ENI with HBV-DNA persistently 2,000 IU/ml, and 8 CHB (F/M: 3/6, median age: 54.8y) pts under NA (entecavir: 6; tenofovir: 3) with

concomitant HCV infection (genotype 1a:4; 1b:7; 2a:c:3; 3a:7; 4d:2) who received DAAs with Sofosbuvir (SOF:13) or without (NO-SOF:10) for 8 (4), 12 (12) or 24 (7) weeks (w). HBsAg (Abbott) and HBV-DNA (Roche) were measured at: -12w, DAAs baseline (BL), 4w, End of Therapy (EOT), EOT + 12w (24w), EOT + 24w (36w) and EOT + 48w (60w).

Results: No significant difference between ENI and CHB were observed in BL Liver Stiffness (10.5 vs 15.7 kPa; p=0.495), ALT (51 vs 44 U/L; p=0.495) and HCV-RNA (6.2 vs 6, 0 Log IU/ml, p=0.561), whereas HBsAg levels were lower in ENI than in CHB (0.88 vs 2.42 Log IU/ml, p=0.035). At BL HBV-DNA was undetectable or <10 IU/ml in 5 and 3 ENI; it was undetectable in all NA treated CHB and remained so thereafter. All pts achieved SVR for HCV and normalized ALT. During DAAs, HBV-DNA increased >1 Log or became detectable >100 IU/ml in 5 and 2 ENI, respectively (overall: 46.7%), showing a trend for higher mean Log values at 4w (p=0.100) and at EOT (p=0.104) as compared to BL (Figure). Mean Log HBsAg levels significantly decreased in ENI from -12w to BL (p=0.002), but not in CHB (p=0.564). During DAAs a significant decline occurred at 4w in both ENI (p=0.020) and CHB (0.015), followed by a rebound at EOT in ENI only. After DAAs, HBsAg returned progressively to pre-DAAs levels in CHB, whereas continued to decline in ENI (6 cleared HBsAg). Among factors associated to a greater HBsAg decline during DAAs, there was a trend for SOF in the schedule (p=0.083).



Conclusion: In ENI co-infected with HCV, reactivations of HBV during DAAs led to moderate increases of HBV-DNA, without clinically relevant events. DAAs caused a significant HBsAg decline during therapy, however, such effect did not appear able to modify the pre-treatment individual profile, which was more favorable in untreated ENI than in CHB under NAs.

THU395

Predictors of advanced liver fibrosis in chronic hepatitis B patients in the daily clinical practice

Fadi Abu Baker¹, Saif Mahmud Abu Mouch², Yael Kopelman², Yana Davidov³, Ziv Ben Ari³. ¹Hillel Yaffe Medical Center, Gastroenterology and Hepatology, Hadera, Israel; ²Hillel Yaffe Medical Center, Gastroenterology and Hepatology, Israel; ³Sheba Medical Center, Center of liver diseases, Israel Email: Fa_fd@hotmail.com

Background and aims: Staging liver disease severity using liver biopsy or, more recently, non-invasive tests such as elastography are important in guiding surveillance and assisting with treatment decisions in chronic hepatitis B (CHB) patients. The use of these tests, however, is not widely implemented as they are costly, used in limited centers, and not always covered by health insurances. Thus,

we aimed to elucidate simple clinical predictors of advanced liver fibrosis in patients with CHB in daily practice.

Method: We conducted a two-center, prospective study, recruiting CHB patients presenting to regular clinic visits in our hepatology units. A detailed medical history, including age, gender, ethnicity, BMI, medical background and medications, HBV infection status and treatment, as well as smoking and alcohol drinking habits were documented. Laboratory results performed within 1 month before or after the clinic visit were documented. During the clinic visit, all patients were referred for abdominal ultrasounds and all of them underwent two-dimensional shear wave elastography (2D SWE) to assess hepatic fibrosis. Univariate and multivariable logistic regression analyses were used to determine predictors of advanced fibrosis ($F2 \leq 7.2 \text{ KPa}$).

Results: Of the 173 patients included in the final analysis, 40 (22%) had evidence of advanced fibrosis on 2D SWE. Age > 50 (OR 3.88, CI 1.49–9.73; $p = 0.005$), ALT > 40 (OR 7.41, CI 2.44–22.4; $p = 0.001$), HBV DNA > 2000 (OR 11.44, CI 3.19–41.02; $P < 0.001$), moderate to severe steatosis on US (OR 5.35, CI 1.82–15.8; $P = 0.002$) as well as moderate-excessive alcohol consumption and heavy smoking (>20 pack-years) were all independent predictors of advanced fibrosis.

Conclusion: We outlined clinical and laboratory variables that may effectively identify CHB patients at high risk of advanced liver fibrosis. These variables, alone or in combination, may guide the use of invasive or non-invasive tests for liver fibrosis assessment in daily clinical practice, especially in low-resource settings.

THU396

Metabolic associated fatty liver disease is associated with appendicular lean soft tissue abnormalities in patients with chronic hepatitis B

Cecy Maria de Lima Santos^{1,2}, Matheus Duarte Brito^{2,3}, Olívio Brito Malheiro^{2,4}, Tatiana Bering Bering⁵, Maria Isabel Toulson Davidson Correia⁶, Rosangela Teixeira², Rodrigo Cambraia², Gifone Aguiar Rocha⁷, Luciana Diniz Silva^{1,2,8}.
¹UFMG Faculty of Medicine, Sciences Applied to Adult Health Care Post-Graduate Programme, Brazil; ²UFMG Faculty of Medicine, Outpatient Clinic of Viral Hepatitis, Instituto Alfa de Gastroenterologia, Brazil; ³UFMG Faculty of Medicine, Medical undergraduate student, Brazil; ⁴UFMG Faculty of Medicine, Locomotor System Department, Brazil; ⁵UFMT-Universidade Federal de Mato Grosso, Department of Food and Nutrition, Brazil; ⁶UFMG Faculty of Medicine, Department of Surgery, Brazil; ⁷UFMG Faculty of Medicine, Laboratory of Research in Bacteriology, Brazil; ⁸UFMG Faculty of Medicine, Department of Internal Medicine, Brazil
 Email: lucianadinizsilva@gmail.com

Background and aims: The clinical impact of Metabolic Associated Fatty Liver Disease (MAFLD) in patients with chronic hepatitis B (CHB) has not been completely clarified. Particularly, the crosstalk between sarcopenia and metabolic derangements in CHB is scarcely investigated. Thus, the aims of this study were to assess the prevalence as well as the risk factors associated with sarcopenia and its components, appendicular lean soft tissue index (ALSTI) and handgrip strength (HGS) in HBV-chronically infected patients.

Method: Sarcopenia was assessed by measurements of appendicular lean soft tissue index [ALSTI; ASLT adjusted for body mass index (BMI)] and handgrip strength adjusted for BMI (HGS_{BMI}) using dual-energy-X-ray and dynamometer, respectively. Sarcopenia severity was assessed by gait speed, using the get-up-and-go timed test. Sarcopenia was defined as the lowest quintile for sex specific ALSTI and HGS_{BMI} cut-off values (<0.759 for men and <0.503 for women) and (<1.2 for men and <0.65 for women), respectively, modified from the Foundation for the National Institutes of Health Biomarkers Consortium Sarcopenia Project consensus. Sarcopenic obesity (SO) was defined as the presence of both sarcopenia and body fat percentage >27, 0% and >38, 0% for men and women, respectively. MAFLD was defined according to an international expert consensus

statement. A Body Shape Index (ABSI) was used to the assessment of abdominal obesity. The International Physical Activity Questionnaire was used to determine the physical activity level. Associations were investigated by logistic regression models.

Results: Among the 105 outpatients with CHB (mean age, 48.5 ± 12.0 yrs.; 58.1% males; 76.2% without cirrhosis; 23.8% with compensated cirrhosis), SO, low ALSTI and low HGS were found in 4.8%, 21.9% and 10.5% patients, respectively. All SO patients had MAFLD and sedentary life. In the multivariate analysis, low ALSTI were positively associated with MAFLD, sedentarism and high ABSI. Low HGS_{BMI} was associated with MAFLD and high ABSI. After adjusting for confounders, in male patients, cirrhosis was independently associated with age >50 yrs., high ABSI and hepatic steatosis.

Conclusion: ASLT abnormalities were associated with MAFLD and abdominal obesity in HBV-chronically infected patients. These findings may contribute to the development of effective strategies to screen the ASLT and metabolic abnormalities in CHB patients, independently of the stage of the liver disease.

THU397

The course of COVID-19 infection in patients with chronic hepatitis B and Delta

Yavuz Emre Parlar¹, Onur Keskin¹, Beril Kirmizigül², Genco Gencdal³, Mujdat Zeybel³, Mesut Gumussoy⁴, Ramazan Idilman⁴, Cihan Yurdaydin³. ¹Hacettepe University School of Medicine, Gastroenterology, Turkey; ²Hacettepe University School of Medicine, Internal Medicine, Turkey; ³Koc University School of Medicine, Turkey; ⁴Ankara University School of Medicine, Gastroenterology, Turkey
 Email: onurkeskin81@gmail.com

Background and aims: SARS CoV-2-induced COVID-19 disease has caused as of November 2021 more than 5 Million deaths. Older age and co-morbidities such as liver cirrhosis have been associated with mortality (Bajaj et al, Hepatology 2020, Hamid et al JCG 2021). Among etiologies of liver disease only alcoholic liver disease was associated with mortality by multivariate analysis. Chronic hepatitis delta (CHD) had not been studied in this context. In the current study the course of COVID-19 disease in chronic hepatitis B (CHB) and CHD patients was explored in 2 academic hospitals.

Method: CHB and CHD patients followed in the gastroenterology departments of Hacettepe and Koç University Medical School Hospitals in Ankara and Istanbul were included in the study (n:551; 302M/249F). Median age was 47. While 479 of the patients had CHB, 77 patients had CHD. 372 of 479 CHB patients were receiving nucleos (t)ide analogs (NAs (TDF:221, ETV:107, LMV-TAF:37), 107 patients were being followed without treatment. 52 patients had cirrhosis. 52 of 77 CHD patients were receiving NAs. Diagnosis of COVID-19 was made by PCR detection of SARS CoV-2 RNA in nasopharyngeal swap specimens.

Results: In the CHB group (n:479), 43 patients (5 of them had cirrhosis) were diagnosed with COVID-19 infection. CHB patients with and without COVID-19 infection did not differ in terms of age, gender and laboratory parameters. No patient had a COVID-related death. ALT-AST reactivation, defined as an increase of ALT to more than 3x ULN, occurred in 3 patients (6.9%) including hepatic decompensation in 1 cirrhotic patient after COVID-19. None of the patients were followed up in the intensive care unit. In CHD patients (n:77; 37 cirrhotic), 8 patients developed COVID-19 infection and 4 had documented hepatic reactivation. None were receiving treatment for CHD. COVID-19 infection developed in 3 cirrhotic patients, of whom one died and one developed hepatic decompensation.

Conclusion: The course of COVID-19 infection is not severe in CHB patients but maybe so in CHD. This may be due to effective antiviral treatment in CHB but lack of it in CHD.

POSTER PRESENTATIONS

THU398

Serum soluble program cell death-1 is predictive of hepatocellular carcinoma in untreated chronic hepatitis B patients

Rachel Wen-Juei Jeng^{1,2}, Yu-Ju Chu³, Mei-Hung Pan³, Hui-Han Hu³, Wun-Sheng Luo³, Chien-Yu Su³, Chen-Tse Chiang³, Chin-Lan Jen³, Sheng-Nan Lu^{2,4}, Li-Yu Wang⁵, Chien-Jen Chen³, Hwai-I Yang³.

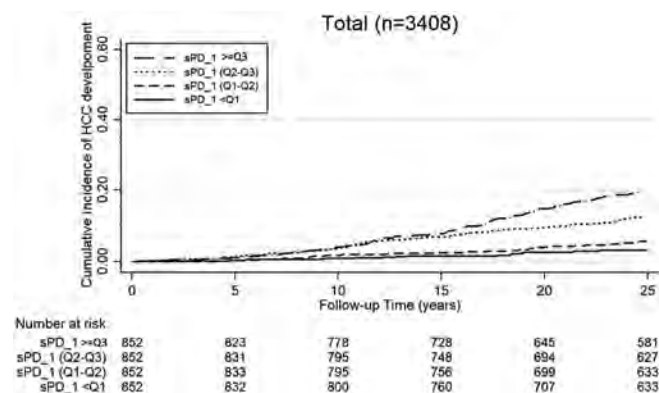
¹Linkou Chang Gung Memorial Hospital, Department of Gastroenterology and Hepatology, Taiwan; ²Chang Gung University, College of Medicine, Taiwan; ³Academia Sinica, Genomic Research Center; ⁴Kaohsiung Chang Gung Memorial Hospital, Division of Hepatogastroenterology, Department of Internal Medicine; ⁵Mackay Medical College, Taiwan

Email: rachel.jeng@gmail.com

Background and aims: Soluble programmed cell death 1 (sPD-1) is a novel immunological marker which has been reported to be correlated to hepatocellular carcinoma in chronic hepatitis B in a case-cohort study. Although it has strong correlations with some viral markers such as qHBsAg, whether it is a predictor of HCC independent of other known host and viral risk factors remains to be explored. We aimed to investigate the association between sPD-1 levels and HCC development.

Method: Baseline serum samples from 3408 chronic hepatitis B subjects in the REVEAL-HBV cohort were assayed for sPD-1 level. Among them, 2934 with available follow-up serum samples were longitudinally analyzed. The ascertainment of HCC was done through the data linkage with the Taiwan Cancer Registry. Multivariate Cox regression analysis was used to estimate the adjusted hazard ratio (aHR) and 95% confidence interval (CI), adjusted for host and viral factors.

Results: By end of 2017, 344 HCC cases were newly developed. Both the baseline and follow-up sPD-1 level were higher in the HCC versus non-HCC patients. Despite there exists linear correlation between sPD-1 and HBsAg level ($r = 0.92$, $P < 0.001$) or HBV DNA level ($r = 0.59$, $P < 0.001$), a dose-dependent increase of adjusted hazard ratio for HCC along with higher sPD-1 level was observed [sPD-1 <Q1 as referent, aHR (95% CI) for Q1-Q2, Q2-Q3, \geq Q3: 1.6 (0.9–2.9), $P = 0.092$; 2.9 (1.5–5.5), $P = 0.001$; and 3.9 (2–7.6), $P < 0.001$] after adjusting age, gender, alcohol drinking, cirrhosis, family history, HBeAg serostatus, HBV DNA and qHBsAg at baseline. This association was even more marked when limited to subjects with low HBV DNA levels (<2000 IU/ml). By repeat measurement, those with sPD-1 level <944 pg/ml (Q1) at baseline or subsequent follow-up had minimal or decreased risk of HCC.



Conclusion: sPD-1 is another useful immunological marker in addition to the current markers used to predict HCC development in untreated CHB patients.

THU399

Parameters related to ALT elevation in patients with HBeAg negative chronic infection

Ulus Akarca¹, Merve Gur², Galip Ersoz¹, Zeki Karasu¹, Ilker Turan¹, Fulya Günsar¹. ¹Ege University, Gastroenterology, Izmir, Turkey; ²Ege University, Internal Medicine, Izmir, Turkey

Email: ulusakarca@gmail.com

Background and aims: The majority of patients with chronic hepatitis B virus infection are in the HBeAg negative chronic infection phase. Elevated transaminase levels and exacerbation of hepatitis can be seen in a small number of these patients. Criteria that can predict which patients will have an exacerbation have not yet been clearly established. If ALT elevation can be predicted in the follow-up of patients, recommendations can be made for close follow-up of these patients. In this study, in patients with HBeAg negative chronic infection who had normal ALT for at least three years, relationships of basal parameters at their first admission with subsequent ALT elevations were investigated.

Method: The files of all hepatitis B carrier patients who applied to the Hepatology Clinic since 2005 were reviewed retrospectively. Patients who had at least 4 years of follow-up, had no evidence of advanced fibrosis, and had not received antiviral therapy were included in the study. Those who had other liver disease, who used more than 2 units of alcohol per day for men and 1 unit for women, who had HCC and who had systemic disease were excluded from the study. After 3 years of normal ALT values, ALT elevation was investigated in patients who were followed for at least 1 more year.

Results: A total of 223 patients were included in the analysis. 106 (47.5%) were male and 117 (52.5%) were female. The mean age was 45.1 ± 11.8 . The mean follow-up period was 7.98 ± 2.91 years. The number of patients whose ALT value exceeded the upper limit of normal was 26 (11.7%), and the number of patients with ALT increased more than twice the normal value was 6 (2.7%). While AST, ALP, total protein, albumin, urea, creatinine, prothrombin time, cholesterol and HBV DNA levels were significantly different between those with and without ALT elevations, age and gender were not significant. After three years of follow-up, the parameters associated with ALT elevation were found to be ALT > 26 U/L and albumin < 4.3 g/dL, the highest HBV DNA level, according to the results of multivariate analysis; It was found that ALT > 26 U/L and albumin < 4.3 g/dL, the lowest albumin level, and the lowest leukocyte count were found to be significant in those who exceeded ALT $2 \times$ ULN. In our study, prognostic indices were obtained according to multivariate analysis in patients with ALT exceeding the upper limit of normal and ALT $> 2 \times$ ULN. The prognostic index obtained in those whose ALT rises more than twice the normal value is $-40.05 + 2.71$ (if ALT > 26 and Alb < 4.3) $+ 6.12 \times$ Albumin $+ 0.00111 \times$ WBC. The predictive value of ALT elevation of this index was investigated by ROC analysis. When cut-off > 0.13 was taken, AUC = 0.93, sensitivity 83%, specificity 97% specificity in predicting ALT $> 2 \times$ ULN.

Conclusion: A prognostic index derived from ALT, albumin, and WBC can predict an ALT elevation of $> 2 \times$ ULN in patients with HBeAg negative chronic infection who remained with normal ALT for at least 3 years.

THU400

Clinical evidence for unconventional hepatitis delta virus infections in endemic countries

Mary Rodgers¹, Ana Olivo¹, Christopher Lark¹, Abbas Hadji¹, Pham Duong², Nguyen TT Dung², Acana Susan Elaborot³, Dora Mbanya⁴, Mia Biondi⁵, Jordan Feld⁵, Gavin Cloherty¹. ¹Abbott Laboratories, Lake Bluff, United States; ²National Institute of Hematology and Blood Transfusion, Hanoi, Viet Nam; ³Uganda Blood Transfusion Service, Kampala, Uganda; ⁴University of Yaounde I, Yaounde, Cameroon; ⁵Toronto Centre for Liver Disease, University of Toronto, Medicine, Toronto, Canada

Email: jordan.feld@uhn.ca

Background and aims: Although cell culture and mouse studies have demonstrated that hepatitis delta virus (HDV) replication can occur in

the absence of hepatitis B virus (HBV) when other co-infecting viruses are present, such as hepatitis C virus (HCV), clinical evidence for such unconventional HDV infections has not yet confirmed they occur naturally in patients. As conventional HDV infection affects the severity and progression of liver disease, it may also have the same effects in a potential unconventional co-infection.

Method: To determine the prevalence of HDV unconventional HDV/HCV infections, a series of HBV surface antigen negative (HBsAg-), anti-HCV positive specimen panels from Cameroon (N = 87), Vietnam (N = 100), and Uganda (N = 368) were screened for HDV antibodies using two prototype assays on the automated high throughput ARCHITECT instrument.

Results: 23 specimens were positive with both anti-HDV assays and 1 with 1 anti-HDV assay, indicating that the prevalence of potential unconventional HDV infections is 3% (11/368) in Uganda, 13.8% (12/87) in Cameroon, and 2% (2/100) in Vietnam, consistent with the higher prevalence of conventional HDV infections in Cameroon and Uganda compared to Vietnam. Notably, the reported dual anti-HDV positives identified were also negative for HBV core antigen antibodies (anti-HBc-), evidence that these individuals had not had a past history of HBV infection. However, HDV RNA was not detectable in these specimens, confirming that active HDV viremia had been cleared in these patients despite detection of active HCV viremia (HCV RNA+).

Conclusion: These data serve as the first clinical evidence of unconventional HDV infections and indicate that unconventional infections can be cleared even in the continued presence of chronic HCV infection. This study also highlights the need for additional screening for unconventional HDV infections to evaluate their potential impact to patient health.

THU401

Rapid point-of-care test for hepatitis B core-related antigen (HBcrAg) to identify HBV-infected patients eligible for antiviral therapy.

Yusuke Shimakawa^{1,2}, Gibril Ndow^{3,4}, Théo Cerceau¹, Amie Ceesay³, Akira Hasegawa⁵, Atsushi Kaneko⁵, Katsumi Aoyagi⁵, Jeanne Perpétue Vincent¹, Takehisa Watanabe⁶, Masaya Baba², Bakary Sanneh⁷, Ignatius Baldeh⁷, Ramou Njie^{8,9}, Umberto D'Alessandro³, Maimuna Mendy¹⁰, Isabelle Chemin¹¹, Mark Thursz⁴, Maud Lemoine⁴, Yasuhito Tanaka⁶. ¹Institut Pasteur; ²International Research Center for Medical Sciences (IRCMS), Kumamoto University; ³Medical Research Council (MRC) Unit The Gambia at the London School of Hygiene and Tropical Medicine; ⁴Department of Metabolism, Digestion and Reproduction, Imperial College London; ⁵Fujirebio Inc.; ⁶Kumamoto University; ⁷National Public Health Laboratories, Ministry of Health, The Gambia; ⁸Edward Francis Small Teaching Hospital, Banjul, The Gambia; ⁹School of Medicine and Allied Health Sciences, University of The Gambia; ¹⁰International Agency for Research on Cancer (IARC), Lyon, France; ¹¹Centre de Recherche en Cancérologie, Université Claude Bernard, Lyon, France
Email: yusuke.shimakawa@pasteur.fr

Background and aims: To eliminate hepatitis B virus (HBV) infection, it is vital to scale up testing services. However, conventional tools to evaluate treatment eligibility, particularly real-time polymerase chain reaction assays (RT-PCR) to quantify HBV DNA, are hardly available and affordable in resource-limited settings. We developed a simple, low-cost, lateral flow rapid diagnostic test to detect hepatitis B core-related antigen (HBcrAg-RDT) and evaluated its performance to diagnose clinically important HBV DNA thresholds ($\geq 2,000$; $\geq 20,000$;

and $\geq 200,000$ IU/ml) and select patients for antiviral therapy in African patients.

Method: Analytical validation was performed using chemiluminescent enzyme immunoassay (CLEIA, LUMIPULSE G1200, Fujirebio, Japan) as a reference. Clinical validation was conducted using sera from 284 treatment-naïve patients with chronic HBV infection and 75 control participants negative for HBV surface antigen (HBsAg) participated in the PROLIFICA (Prevention of Liver Fibrosis and Cancer in Africa) programme in The Gambia.

Results: Using HBcrAg-CLEIA as a reference, the limit of detection of HBcrAg-RDT was 4.3 log U/ml for serum and plasma, and 4.9 log U/ml for whole blood. None (0/75) of HBsAg-negative samples was detected by HBcrAg-RDT. In 284 treatment-naïve HBsAg-positive patients (median age 36 years, interquartile range: 30–45, 66% were men), hepatitis B e antigen (HBeAg), HBcrAg-RDT, HBcrAg-CLEIA, and HBV DNA were positive in 13%, 23%, 53%, and 58% of the participants, respectively. HBV genotypes were E in 84% and A in 16%. The clinical sensitivity and specificity of HBcrAg-RDT to identify highly viraemic individuals were: 72.7% and 91.7% to diagnose HBV DNA levels of $\geq 2,000$ IU/ml; 86.7% and 88.7% for $\geq 20,000$ IU/ml, and 91.4% and 86.3% for $\geq 200,000$ IU/ml, respectively. A simplified HBV DNA-free treatment algorithm using HBcrAg-RDT had a sensitivity of 96.6% and specificity of 83.2% to identify HBV-infected patients eligible for antiviral therapy by the European Association for the Study of the Liver (EASL) criteria using the reference tests.

Table: Performance of HBcrAg-RDT, HBcrAg-CLEIA, and HBeAg-EIA to discriminate clinically important HBV DNA levels in HBsAg-positive patients (n = 284).

	HBV DNA levels								
	≥ 2000 IU/ml			$\geq 20,000$ IU/ml			$\geq 200,000$ IU/ml		
	HBcrAg RDT	HBcrAg CLEIA	HBeAg EIA	HBcrAg RDT	HBcrAg CLEIA	HBeAg EIA	HBcrAg RDT	HBcrAg CLEIA	HBeAg EIA
Cut-off values	Positive ≥ 3.6 log U/ml	Positive ≥ 3.6 log U/ml	Positive ≥ 4.5 log U/ml	Positive ≥ 4.5 log U/ml	Positive ≥ 4.5 log U/ml	Positive ≥ 5.3 log U/ml	Positive ≥ 5.3 log U/ml	Positive ≥ 5.3 log U/ml	Positive ≥ 5.3 log U/ml
Sensitivity (%)	72.7	83.3	47.7	86.7	88.9	61.4	91.4	91.4	70.6
Specificity (%)	91.7	83.9	97.6	88.7	90.4	96.0	86.3	93.2	94.9

Conclusion: HBcrAg-RDT is a rapid (45 minutes), robust (operating temperature up to 39 °C), and inexpensive alternative to HBV DNA quantification potentially allowing the decentralisation of hepatitis care in areas with limited access to laboratory services.

THU402

Prevalence of HBV infection and receiving antiviral treatment for eligible patients in blood relatives from clustering families of HBV infection with unfavorable prognoses and cascading of care linked to treatment in West China

Yuan Yang¹. ¹The First Affiliated Hospital of Xi'an Jiaotong University, Department of Infectious Disease, Xi'an, China
Email: xayangyuan@mail.xjtu.edu.cn

Background and aims: Accumulating evidence had shown that HBV infection had the characteristic of family clustering, and higher risk of progression to cirrhosis or HCC. Although many of the professional organizations provide guidelines related to the prevention and treatment of HBV infection, the cascade of care is still poor.

Method: First- and second-blood relatives from clustering families of HBV infection with unfavorable prognoses, which were defined as those families in which HBV infection patients occurred in three successive generations, and there was more than one patient with HBV-associated cirrhosis of liver or HCC in two generations, were enrolled in the study, and general information and serum samples were collected. Biochemical examinations were performed by the

POSTER PRESENTATIONS

Department of Laboratory, the First Affiliated of Hospital, Xi'an Jiaotong University. Virologic assessments included, HBV DNA (Roche), HBsAg, anti-HBs, HBeAg, anti-HBe, anti-HBc (Abbott Architect quantitative).

Results: Collected the liver function and virological features of the 1,568 participants from families with clusters of HBV infection and unfavorable prognoses included in this study. The patients with positive of HBsAg were 1033, and there were 351 (33.98%) patients receiving antiviral therapies. There were 451 (43.66%) patients with HBsAg-positive have not received antiviral treatment who should receive the antiviral treatment according to the 2019 Chronic hepatitis B Guideline of China, with age over 30 years with family with cirrhosis or HCC, or less than 30 years and ALT were elevated over upper limit normal (ULN). Patients were lack of awareness of screening before suggesting by the cascading of care linked to treatment for the blood relatives from clustering families of HBV infection with unfavorable prognoses. There were 535 participants with negative of HBsAg, and there were 278 (51.96%) participants with positive anti-HBc and 160 (29.91%) participants with only anti-HBs positive.

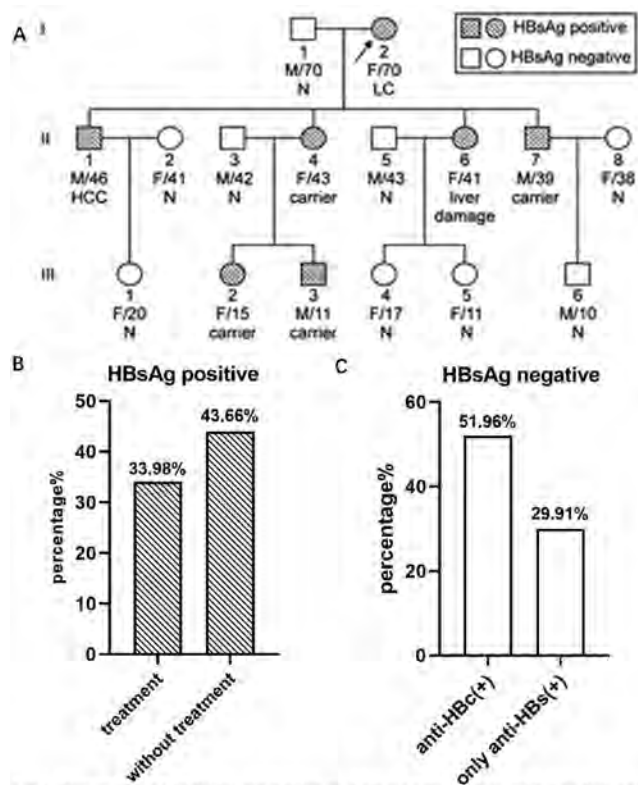


Fig 1 prevalence of antiviral treatment in participants with HBsAg positive and biomarker of HBV in participants with HBsAg negative in blood relatives from clustering families of HBV infection with unfavorable prognoses

A: proband (I-2) was diagnosed at first; first-blood relatives (II-1, II-4, II-5, II-7) and second-blood relatives (III-1, III-2, III-3, III-4, III-5, III-6) were suggested to screen for biomarker of hepatitis B virus, liver function and ultrasound for cascading of care linked to treatment.
B: treatment: patients received antiviral treatment before enrolled this study; without treatment: patients should receive antiviral treatment according to the 2019 Chronic hepatitis B Guideline of China with age over 30 years from family with cirrhosis or HCC, or less than 30 years and elevated ALT.

Conclusion: There were high prevalence of HBV infection in the families with clusters of HBV infection and unfavorable prognoses, and low prevalence of receiving antiviral therapies for patients eligible for treatment by professional practice guidelines. Cascading of care linked to treatment in families with clusters of HBV infection, could improve the treatment initiation rate.

THU403

Liver inflammation in asian chronic hepatitis B patients with detectable HBV-DNA and normal alanine aminotransferase according to diverse upper limits of normal

Jiacheng Liu¹, Jian Wang², Li Zhu³, Yiguang Li⁴, Ming Li⁵, Zhonghua Lu⁴, Yuanwang Qiu⁴, Chuanwu Zhu³, Weimao Ding⁶, Jie Li², Rui Huang², Chao Wu². ¹Nanjing Drum Tower Hospital Clinical College of Traditional Chinese and Western Medicine, Nanjing University of Chinese Medicine, Department of Infectious Diseases, Nanjing, China; ²Nanjing Drum Tower Hospital, The Affiliated Hospital of Nanjing University Medical School, Department of Infectious Diseases, Nanjing, China; ³The Affiliated Infectious Diseases Hospital of Soochow University, Department of Infectious Diseases, Suzhou, China; ⁴The Fifth People's Hospital of Wuxi, Department of Infectious Diseases, Wuxi, China; ⁵The Affiliated Infectious Diseases Hospital of Soochow University, Department of Hepatology, Suzhou, China; ⁶Huai'an No. 4 People's Hospital, Department of Hepatology, Huai'an, China
Email: dr.wu@nju.edu.cn

Background and aims: Upper limits of normal (ULN) for alanine aminotransferase (ALT) are different among international guidelines or recommendations for chronic hepatitis B (CHB). We investigated the proportion of significant inflammation in Asian CHB patients with detectable HBV-DNA under diverse ALT ULNs.

Method: CHB patients with detectable HBV-DNA underwent liver biopsy were included from four hospitals. Liver inflammation and fibrosis were assessed by Scheuer's classification. ULN was defined as 40 U/L in EASL 2017 and APASL 2015, 35/25 U/L (male/female) in AASLD 2018, and 30/19 U/L (male/female) in East Asia recommendations 2020. The definitions of significant inflammation and fibrosis were $G \geq 2$ and $S \geq 2$, respectively.

Results: Of 921 patients included, 640 (69.5%) patients had significant inflammation, while 577 (62.6%) had significant fibrosis. 85.6% of patients with significant fibrosis and 42.4% of patients without significant fibrosis had significant inflammation. Among CHB patients with detectable HBV-DNA and normal ALT, the proportions of those with significant inflammation was 43.8% according to the ALT ULN of 30/19 U/L (male/female), while the corresponding proportions were 53.1% and 48.1% according to the ULNs of 40U/L and 35/25 U/L (male/female), respectively. In patients with detectable HBV-DNA and normal ALT levels in absence of significant fibrosis, the proportions of significant inflammation were comparable among different ULNs of ALT by 40 U/L (30.7%), 35/25U/L (27.3%) and 30/19 U/L (25.0%).

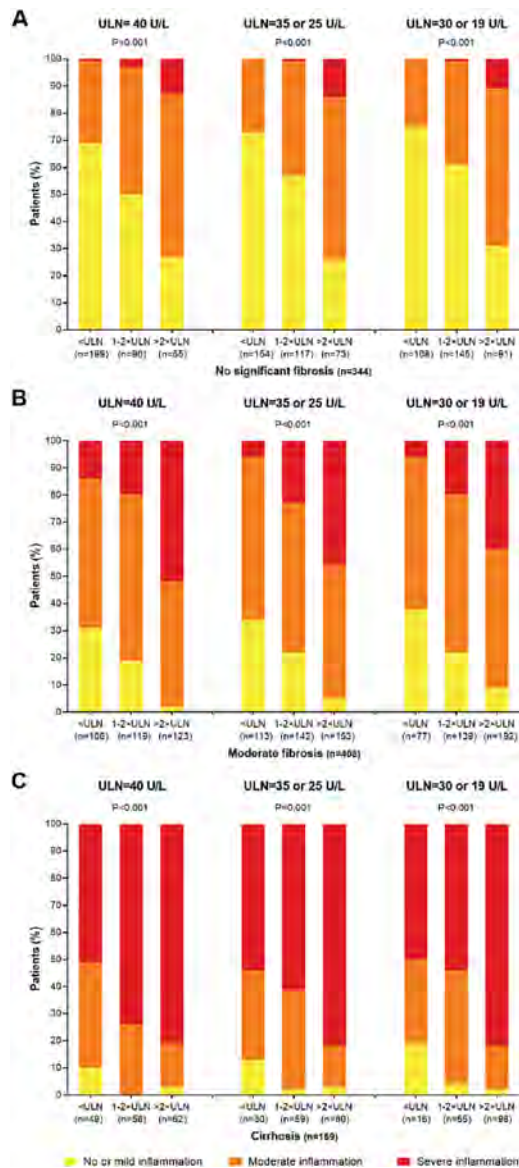


Figure: Liver inflammatory activity in CHB patients with detectable HBV with different fibrosis stages and ALT levels according to diverse criteria of ALT ULN

Conclusion: A quarter of CHB patients with detectable HBV-DNA and normal ALT without significant fibrosis had significant inflammation irrespective of the ALT ULNs. The optimal ULNs of ALT for CHB patients deserve further investigation and novel biomarkers for liver inflammation are urgently needed.

THU404

Diversity of circulating HBV genomes and impact on viral infection

Jules Sotty¹, Aurélie Schnuriger¹, Pierre Bablon¹, Bouchra Lekbaby¹, Jeremy Augustin¹, Morgane Girier-Dufournier¹, Lucas Langlois¹, Céline Dorival², Fabrice Carrat², Stanislas Pol³, Helene Fontaine³, Nazim Sarica⁴, Christine Neuveut⁴, Chantal Housset¹, Dina Kremsdorf¹, Patrick Soussan¹. ¹Inserm Sorbonne Université, CRSA Inserm U938, Paris, France; ²Inserm Sorbonne Université; ³Cochin, France; ⁴Institut de génétique humaine, Montpellier, UMR 9002, France Email: patrick.soussan@inserm.fr

Background and aim: Besides the prototype of HBV infectious particle containing a 3.2 kb partially double-stranded DNA (wtDNA), additional circulating virus-like particles containing pregenomic RNA (pgRNA), spliced-RNA (spRNA) or spliced-derived DNA (defDNA) genomes have been described. Independently, detection of these circulating viral genomes may contribute to the clinical management of HBV infection and/or as a predictive marker of therapy response. Here, the diversity of circulating viral genomes was investigated in chronic infected patients then, its impact on viral lifecycle was explored.

Method: 335 chronic HBV infected patients treated (n = 158) or not (n = 177) were selected from the Hepather French Cohort. Pangenomic qPCRs were set up to quantify the four forms of circulating viral genomes from the same nucleic extract. Principal component analysis and hierarchical clustering were performed to characterize the circulating HBV genome diversity. Viral infection of differentiated HepG2-NTCP cells using blood samples from untreated patients was achieved to study its impacts on viral replication.

Results: Hierarchical clustering of circulating viral genome diversity in bloodstream divided untreated patients in 2 clusters. The cluster 1 (C1) was defined by the predominance (>50% of circulating genomes) of wtDNA while the cluster 2 (C2) contained various amount of the four viral genomes with a majority of pgRNA, wtDNA and defDNA in 77%, 18% and 5% of cases, respectively. Genomic diversity in C2 was associated with a higher level of viral load ($7.1 \pm 7.3 \text{ Log}_{10} \text{ copies/ml}$ of wtDNA), compared with C1 ($6.6 \pm 7.1 \text{ Log}_{10} \text{ copies/ml}$ of wtDNA; $p < 0.001$). The greatest proportion of circulating pgRNA forms was preferentially observed in high replicative patients in C1 and unexpectedly, in low replicative patients in C2. Analysis of treated patients reinforced the contribution of HBV replication in the genome diversity occurrence. *In vitro* infection with untreated patient samples from both clusters showed that viral diversity in inoculum modulated the intracellular viral cycle. Before infection, inoculum enrichment with pgRNA particles demonstrated their ability to interfere on viral cycle.

Conclusion: Our data provide evidences for the main role of viral replication in circulating HBV genomes diversity. Novel biomarker of HBV infection, circulating pgRNA genomes may also contribute to modulate the viral cycle in an unconventional process.

THU405

Chronic hepatitis delta with normal ALT and hepatitis D viremia

Sena Arici¹, Adriana Palom², Mesut Gumussoy³, Ramazan Idilman³, Genco Gencdal⁴, Rafael Esteban⁵, Mujdat Zeybel⁴, Maria Buti², Cihan Yurdaydin⁴. ¹Gulhane Training and Research Hospital, Internal Medicine, ANKARA, Turkey; ²Hospital Universitario Valle Hebron, Department of Gastroenterology, Barcelona, Spain; ³Ankara University, School of Medicine, Department of Gastroenterology, Ankara, Turkey; ⁴Koç University, School of Medicine, Department of Gastroenterology, Zeytinburnu, Turkey; ⁵Universitat Autònoma de Barcelona (UAB), Department of Gastroenterology, Barcelona, Spain Email: gencogencdal@yahoo.co.uk

Background and aims: Chronic hepatitis delta (CHD) represents the most severe form of chronic viral hepatitis and the main cause of liver-related mortality due to suboptimal therapy. However, there is data to suggest that CHD runs a less severe course than in the past

POSTER PRESENTATIONS

(Rosina et al, Gastro 1999, Wranke et al, JVH 2021). Patients with persistent normal ALT and hepatitis D viremia (PNAV) have been described for chronic hepatitis C and B but not for CHD.

Method: PNAV were arbitrarily defined as patients with normal ALT and hepatitis D viremia on at least four determinations, 3 to 6 months apart within a duration of 2 years among patients who had never received interferon based treatment for CHD. Such patients have been collected between January 2005 to 2021 in 2 academic hospitals in Turkey and one in Spain. A total of 19 patients were found out of a cohort comprising around 420 patients. The 19 patients with PNAV were compared with sex and age-matched control patients with CHD at a 1 to 1.5 ratio. Follow-up of patients ranged from 18 months to 12 years.

Results: ALT, AST and GGT levels were lower and platelets were higher in PNAVs vs control CHD patients (29 IU/L [18–39] vs. 45 [23–178], 30 IU/L [24–43] vs. 52 [21–99] and 18 IU/L [13–48] vs. 57 [14–328], $240 \times 10^9/L$ [88–420] vs. 114 [52–309], respectively, $p < 0.05$ for all comparisons). HDV RNA levels were similar (3.60 ± 1.11 vs 4.23 ± 1.43 IU/ml). Liver biopsy was available in 10 patients. Histologic activity index and fibrosis stage were lower in PNAVs vs controls (8 [3–13] vs 10 [8–14] and 2 [0–4] vs 3 [2–6], $p = 0.05$ and $p = 0.014$, respectively). In the PNAV group, 2 patients had fibrosis stage 3 and 4 according to Ishak et al and one patient had cirrhosis on biopsy. Three additional patients had clinical or radiologic evidence of cirrhosis. On long-term follow-up patients normal ALT persisted. HDV RNA became undetectable in one patient.

Conclusion: This study suggests that a small subgroup of CHD patients may present with normal ALT and HD viremia and milder liver disease. However, underestimation due to referral bias is also likely. PNAV patients had compared to CHD patients lower ALT and GGT and higher platelet counts indicative of milder liver disease. Liver biopsy data confirm the latter. However, 3 out of 19 PNAV had clinical or histologic cirrhosis and 2 patients had moderate to severe fibrosis (Ishak score 3 to 4), suggesting that these patients may also need to be considered for treatment. Thus CHD patients with PNAV represent a heterogeneous group and need careful assessment.

THU406

Hepatitis B core related antigen, not as good as it seems: a critique and systematic review

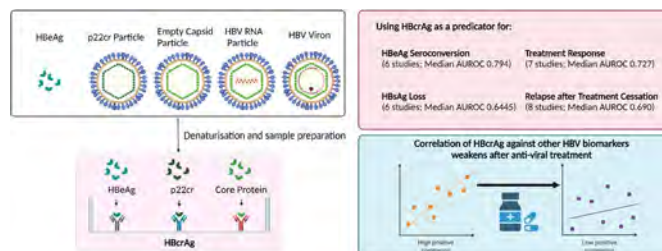
Yong Chuan Tan^{1,2}, Celina Adraneda¹, Ee Jin Yeo¹, Guan Sen Kew², Atefeh Khakpoor¹, Seng Gee Lim^{1,2}. ¹Yong Loo Lin School of Medicine, National University of Singapore, Department of Medicine, Singapore; ²National University Hospital, Division of Gastroenterology and Hepatology, Singapore
Email: mdcv341@nus.edu.sg

Background and aims: Hepatitis B core-related antigen (HBcrAg) is a new biomarker for Chronic Hepatitis B (CHB) but its performance has not been critically or systematically appraised.

Method: We reviewed the biological pathway of HBcrAg. We also performed a systematic review of PubMed for studies that evaluated the role of HBcrAg in predicting important HBV specific clinical events and/or examined the strength of correlation of HBcrAg against other HBV biomarkers. Area under the receiver operating characteristic (AUROC) curve values and correlational coefficients were consolidated to appraise the predictive accuracy and correlational strength of HBcrAg. Median values from the pooled data were used as estimates and reported.

Results: HBcrAg consists of Hepatitis B core antigen (HBcAg), e antigen (HBeAg), and 22 kDa precore protein (p22cr). Individual contribution of HBeAg, HBcAg, and p22cr to HBcrAg in HBeAg positive CHB patients is $72 \pm 10\%$, $17 \pm 8\%$, and $15 \pm 9\%$ respectively. The constituent contribution to HBcrAg in HBeAg negative CHB patients is unknown. HBcrAg has a false positive rate of 9.3% and false negative rate of 12–35%. The new iTACT-HBcrAg assay is more sensitive but does not solve the false positive performance. PubMed search found 58 of 248 papers on HBcrAg suitable for analysis.

Median AUROC for use of HBcrAg in predicting HBeAg seroconversion, HBsAg loss, treatment response, and relapse after stopping therapy is 0.794, 0.6445, 0.706 and 0.688 respectively. Median correlation coefficient (r) of HBcrAg with HBV DNA, qHBsAg, HBV RNA and cccDNA is 0.660, 0.4755, 0.698, and 0.590 respectively. Strength of correlation weakens after antiviral therapy.



Conclusion: HBcrAg is a suboptimal biomarker and performs best as predictor of HBeAg seroconversion. Otherwise, its performance is moderate at best, and has poor correlation with HBsAg loss and antiviral therapy.

THU407

Utilizing phenotyping algorithms as tools for increasing linkage to guideline-concordant care in patients at risk for hepatitis B

Brooke Wyatt¹, Anna Mageras^{1,2}, Stephanie Zhang¹, Mark Miller¹, Douglas T Dieterich¹, Andrea Branch¹. ¹Icahn School of Medicine at Mount Sinai, New York, United States; ²Icahn School of Medicine at Mount Sinai, Liver Diseases, New York, United States
Email: brooke.wyatt@mssm.edu

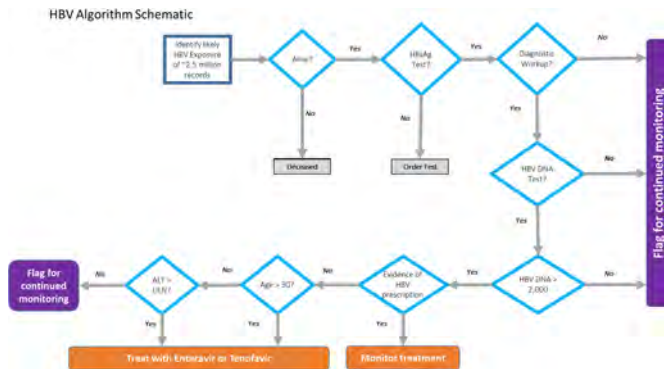
Background and aims: An estimated 241, 000 (2.9%) NYC residents are living with chronic hepatitis B virus (HBV) infection. Management of HBV with antiviral drugs can slow disease progression and increase longevity. However, in the United States, only ~40–60% of patients with chronic HBV receive guideline-concordant care, and only ~3% of Americans with HBV receive antiviral treatment.

There is a significant need to improve methods for identifying treatment-eligible patients and linking them to care. The Mount Sinai Health System (MSHS) serves the greater NYC area. Through this study, we aim to develop and validate an HBV case-finding algorithm that identifies diagnosed HBV-infected MSHS patients who are not receiving guideline-concordant antiviral treatment or monitoring, as defined by EASL or AASLD. This project builds on our previous success developing an algorithm to identify HCV treatment candidates performing with a sensitivity of 90.0%, specificity of 97.1%, positive predictive value of 85.7%, and negative predictive value of 98.1%.

Method: We will develop an algorithm to search ~2.5 million EPIC electronic medical records (EMRs; data entered 1/2003 to 12/2021). Death record data will be utilized to identify deceased patients. To enhance impact and portability, the algorithm will be written in SQL a versatile, widely used programming language. The algorithm will automate the interpretation of HBV serological data, ALT values, demographic information, and data about antiviral medications; and it will estimate fibrosis stage by calculating the FIB-4 score. It will categorize patients as a) receiving AASLD/EASL guideline-concordant treatment, b) not receiving guideline-concordant treatment and in need of follow-up, c) HBV negative, or d) deceased. Results will be stratified by treatment site. The algorithm is being developed iteratively, assessing each iteration by performing manual chart review at planned stages.

Results: The first iteration of the algorithm identified approximately 1, 000 MSHS patients with an HBV DNA viral load $> 2, 000$ IU/ml and no record of a prescription for any HBV medication. Manual review of a random selection of 100 of these patients' charts revealed that three patients had died, two were children, and four cleared HBV

spontaneously; of the remaining 91 patients, only five were on treatment.



Conclusion: Our preliminary results are highly promising. Once refined and validated, the algorithm will allow us to identify patients in need of HBV outreach and care leading to evaluation for hepatitis D as well. It will also help to highlight clinical settings with suboptimal HBV care in our healthcare system. Applicable to other health systems utilizing EPIC EMR, our algorithm will be vital in streamlining case finding, freeing up resources for patient engagement and care, and advancing viral hepatitis elimination.

THU408

Hepatitis B virus antigen reduction effect of RO7049389 plus NUC with/without Peg-IFN in chronic hepatitis B patients

Jinlin Hou¹, Edward J Gane², Wenhong Zhang³, Jiming Zhang³, Man-Fung Yuen⁴, Tien Huey Lim⁵, Rozalina Balabanska⁶, Qing Xie⁷, Piyawat Komolmit⁸, Xieer Liang¹, Wen Zhang⁹, Xue Zhou⁹, Zenghui Xue¹⁰, Miriam Triyatni¹¹, Ethan Chen¹⁰, Yuchen Zhang⁹, Qingyan Bo¹⁰. ¹Nanfeng Hospital, Southern Medical University, Guangzhou, China; ²New Zealand Liver Transplant Unit, The University of Auckland, Auckland, New Zealand; ³Huashan Hospital, Fudan University, Shanghai, China; ⁴Queen Mary Hospital, The University of Hong Kong, Hong Kong, China; ⁵Middlemore Hospital, Auckland, New Zealand; ⁶Acibadem City Clinic Tokuda Hospital EAD, Sofia, Bulgaria; ⁷Ruijin Hospital, Shanghai Jiaotong University School of Medicine, Shanghai, China; ⁸King Chulalongkorn Memorial Hospital, Bangkok, Thailand; ⁹Roche Pharma Research and Early Development, Roche Innovation Centre Shanghai, Shanghai, China; ¹⁰Roche (China) Holding, Shanghai, China; ¹¹F. Hoffmann-La Roche, Basel, Switzerland
Email: qingyan.bo@roche.com

Background and aims: RO7049389 is a Class I HBV core protein allosteric modulator. In addition to potent suppression of HBV replication, in mouse model studies, RO7049389 also induced HBsAg and HBeAg reduction alongside transient and controlled immune responses. Here we report on HBV antigens reduction with RO7049389+NUC±Peg-IFN in chronic hepatitis B patients (NCT02952924).

Method: NUC-suppressed patients received RO7049389+NUC (Cohort A, n = 32); treatment-naïve patients received RO7049389+NUC without (Cohort B, n = 10) or with (Cohort C, n = 30) Peg-IFN-alpha for 48 weeks. At Week 48, all patients except those who met NUC stopping criteria (HBV DNA <LLOQ and HBsAg <100 IU/ml) entered a 24-week NUC-alone follow-up period.

Results: In Cohort A, 30 NUC-suppressed patients completed the study; no obvious changes in HBsAg, HBeAg or HBcrAg were observed. In treatment naïve patients, no HBsAg loss occurred among 10 Cohort B and 27 Cohort C patients who completed the study. In Cohort B, at Week 48, HBsAg, HBeAg and HBcrAg showed mean changes from baseline of +0.1, -1.5 log₁₀IU/ml, and -1.2 log₁₀U/ml, respectively; 2/6 HBeAg+ patients achieved HBeAg loss without anti-HBe seroconversion. Two HBeAg+ patients had maximal HBsAg

declines of 0.4–0.45 log₁₀IU/ml, both occurring after Grade 3 ALT flare. In Cohort C, at Week 48, HBsAg declined by mean 1.4 log₁₀IU/ml (from mean baseline 4.0 log₁₀IU/ml); 15/18 HBeAg+ vs. 5/10 HBeAg- patients achieved >1 log₁₀IU/ml HBsAg decline. Larger mean HBsAg declines were observed in patients with baseline HBsAg >4 log₁₀IU/ml. Genotype C patients (n = 11) achieved the largest mean HBsAg decline (1.7 log₁₀IU/ml at Week 48) compared to other genotypes. At Week 48, 6/28 and 19/28 patients achieved HBsAg <100 IU/ml and <1000 IU/ml, respectively. At Week 48, HBeAg declined by mean 2.1 log₁₀IU/ml with loss in 7/18 and anti-HBe seroconversion in 6/18. HBcrAg declined by mean 1.8 log₁₀U/ml. RO7049389+NUC ± Peg-IFN was safe and well tolerated up to 72 weeks. Two early terminations in each cohort of A and C were due to non-safety reasons. Grade 2–4 treatment-emergent ALT flares (TEAFs) occurred in 55% of treatment naïve patients, mainly with concurrent HBsAg declines. Spearman's rank correlation analysis showed a significant positive correlation between Grade 2–4 TEAFs and categorical maximal HBsAg declines (Cohort B: p = 0.025, rho 0.697; Cohort C: p = 0.017, rho 0.432).

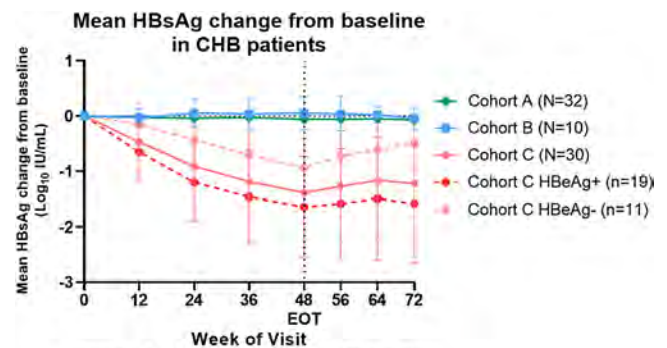


Figure. HBsAg kinetics over 72 weeks.

Conclusion: RO7049389 did not induce obvious HBV antigen reduction in NUC-suppressed patients. RO7049389+Peg-IFN+NUC led to larger HBsAg declines, especially in difficult-to-treat Genotype C patients. HBeAg positivity and high HBsAg baseline levels seemed to positively modulate the ability of RO7049389+Peg-IFN+NUC to reduce HBsAg. Positive correlation between graded TEAFs and categorical maximal HBsAg declines may be consistent with the concept of a “good” ALT flare during RO7049389 ± Peg-IFN treatment.

THU409

Presence of HbeAg, HBV DNA in cord blood and down regulation of TLR9 may act as predictive marker for HBV mother to child transmission

Simanta Kalita¹, Manash Jyoti Kalita¹, Gautam Hazarika¹, Partha Pratim Das², Sangit Dutta², Anjan Jyoti Talukdar², Panchanan Das², Subhash Medhi³. ¹Gauhati University, Bioengineering and Technology, Guwahati, India; ²Gauhati Medical College and Hospital, Guwahati, India; ³Gauhati University, Guwahati, India
Email: subhashmedhi@gauhati.ac.in

Background and aims: Hepatitis B virus infection is a global health problem which needs special attention mainly due to mother to child transmission of HBV. Expression pattern of TLR 9 were analysed in venous cum cord blood samples collected from 25 HBsAg+ve mother during delivery from Gauhati Medical College and Hospital, Guwahati, Assam.

Method: HbsAg, HbeAg and HbeAb were detected using ELISA and TLR9 mRNA expression is performed by Real time PCR.

Results: Serological analysis of the venous blood (N = 25) showed the presence of HbeAg in 10 (40%) samples and HBV DNA+ve in 9 (36%) samples. Further, in cord blood samples (N = 25) HbsAg was positive in 17 (68%) and HbeAg was positive in 13 (52%) of the sample. HBV DNA was found to be positive in 13 (52%) of the sample. Among 25 samples, 10 samples (40%) with HbeAg positive status exhibit

POSTER PRESENTATIONS

downregulation of TLR-9 with mean fold change of 0.55 ± 0.16 ($p = 0.001$). Similarly 13 (52%) HbsAg positive cord blood samples (mean fold change 0.65 ± 0.18 , $p = 0.007$). 14 (56%) venous HBV DNA positive samples and 12 (48%) cord blood HBV DNA positive samples showed (mean fold change of 0.53 ± 0.18 , $p = 0.001$; mean fold change 0.58 ± 0.16 , $p = 0.095$) significant alteration in favour of downregulation of TLR-9 among the study cohort.

Conclusion: In the study, presence of HbeAg and HBV DNA in cord blood and down regulation of TLR9 may be an indication of vertical transmission of HBV.

Acknowledgements: The presenting author acknowledges Department of Science and Technology, Govt. of India, Ministry of Science and Technology, New Delhi- 110016, for providing DST INSPIRE Fellowship vide sanction number: No. DST/INSPIRE Fellowship/2019/IF190163.

THU410

Patients with CHD coinfection have greater comorbidities, higher healthcare resource use and costs than CHB monoinfection- results from a Spanish national hospital database

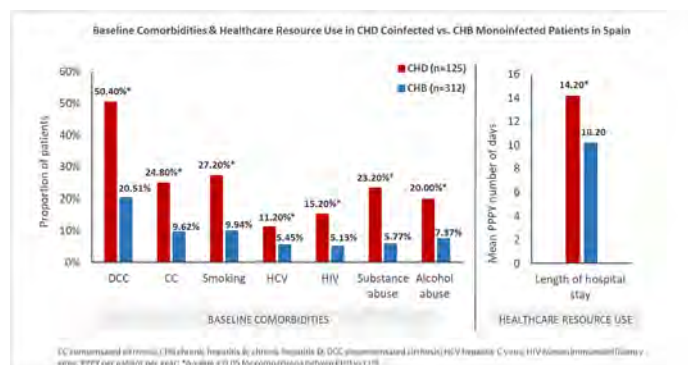
Maria Buti¹, Ankita Kaushik², Mertixell Ascanio³, Josep Darba⁴, Nandita Kachru². ¹Hospital Universitario Valle Hebrón; ²Gilead Sciences, Inc.; ³BCN Health Economics and Outcomes Research SL; ⁴University of Barcelona

Email: Nandita.Kachru@gilead.com

Background and aims: Chronic hepatitis delta (CHD) coinfection among chronic hepatitis B (CHB) patients is associated with higher morbidity and mortality, given its relatively rapid progression to cirrhosis and liver-related complications. This retrospective study aims to compare baseline comorbidities, healthcare resource use (HRU) and costs in a matched cohort of adult patients with CHD coinfection versus (vs.) CHB monoinfection in a national hospital database in Spain.

Method: The study included subjects ≥ 18 years having ≥ 1 ICD-9/10-CM diagnosis code for CHD or CHB in the Spanish National Health System's Hospital Discharge Records Database that covers 192 private and 313 public hospitals, with >40 million patients during the study period (Jan 1, 2000 to Dec 31, 2019). CHD and CHB cohorts were identified from Jan 1, 2001 to Dec 31, 2018 (identification period) with their first diagnosis defined as the diagnosis date, having ≥ 12 months of continuous enrollment before and after the diagnosis date. CHD and CHB patients were age- and gender-matched (1:3) to evaluate incremental differences in HRU and costs.

Results: The study reported 12,317 patients diagnosed with CHD or CHB, of which 3,079 (159 CHD; 2,920 CHB) met the inclusion criteria; matching yielded 125 CHD and 312 CHB patients. The male to female ratio was significantly higher in CHB vs CHD (roughly 10:1 vs. 5:1; $p = 0.0281$). CHD patients were significantly more likely to have decompensated (50.40% vs. 20.51%; $p < 0.0001$) and compensated cirrhosis (24.80% vs. 9.62%; $p < 0.0001$) than CHB patients; hepatocellular carcinoma and liver transplant rates were at 6.40% vs. 2.56% and 5.60% vs. 1.92%, respectively. Charlson Comorbidity Index score was significantly higher for CHD than CHB (0.84 vs. 0.36; $p < 0.0001$). CHD patients also reported significantly higher rates of smoking (27.20% vs. 9.94%; $p < 0.0001$), HCV (11.20% vs. 5.45%; $p = 0.0403$), HIV (15.20% vs. 5.13%, $p = 0.0013$), substance abuse (23.20% vs. 5.77%; $p < 0.0001$) and alcohol abuse (20% vs. 7.37%; $p = 0.0003$) than CHB patients. Mean per patient per year (PPPY) all-cause healthcare costs totaled to €13,716 in CHD vs. €7,177 in CHB, representing 91% higher cost in CHD than CHB patients ($p = 0.0002$). Consequently, pharmacy, inpatient and outpatient costs were significantly higher for CHD vs. CHB patients; all $p < 0.05$. Mean PPPY length of stay was significantly higher for CHD than CHB patients (14.20 vs. 10.20; $p < 0.0001$). Further, mean PPPY number of admissions and readmissions for CHD vs. CHB were at 2.10 vs. 1.80 and 1.30 vs. 0.90, respectively.



Conclusion: CHD coinfection patients had significantly greater comorbidities, HRU and costs than CHB monoinfection patients within an age- and gender-matched cohort of Spanish patients from a hospital database study over 19 years of duration. These findings further confirm the need for early linkage to care to alleviate future disease progression.

THU411

Clinical features predictive of cirrhosis in a large cohort of patients with chronic hepatitis delta infection- Insights from the D-LIVR trial

Ohad Etzion¹, Maria Buti², David Yardeni³, Anat Nevo-Shor⁴, Daneila Munteanu⁴, Ingrid Choong⁵, Lisa Weissfeld⁶, Naim Abu-Freha⁷, Rob Howard⁸, Tarik Asselah⁹, Pietro Lampertico^{10,11}. ¹Soroka University Medical Center, Department of Gastroenterology and Liver Diseases, Beer-Sheva, Israel; ²Hospital Universitario Valle Hebrón and CIBEREHD del Instituto Carlos III, Liver Unit, Barcelona, Spain; ³National Institutes of Health, Liver Disease Branch, Bethesda, United States; ⁴Soroka University Medical Center, Department of Gastroenterology and Liver Diseases, Beer Sheva, Israel; ⁵Eiger Biopharmaceuticals, Palo Alto, United States; ⁶Statistics Collaborative Inc, Washington, DC, United States; ⁷Soroka University Medical Center, Department of Gastroenterology and Liver Diseases, Beer Sheva, Israel; ⁸Veridical Solutions, Del Mar, CA, United States; ⁹AP-HP, Hôpital Beaujon, Department of Hepatology, Clichy, France; ¹⁰Foundation IRCCS Ca' Granda Ospedale Maggiore Policlinico, Division of Gastroenterology and Hepatology, Milan, Italy; ¹¹CRC "A. M. and A. Migliavacca" Center for Liver Disease, Department of Pathophysiology and Transplantation, University of Milan, Milan, Italy

Email: ohadet34@yahoo.com

Background and aims: Chronic hepatitis delta (CHD) infection is the most rapidly progressive form of chronic viral hepatitis. Data regarding predictors of cirrhosis in chronic HDV is fairly limited especially in those of younger age. The aim of the current analysis was to assess the predictive value of demographic and laboratory variables as well as non-invasive test scores of liver fibrosis for diagnosis of biopsy proven cirrhosis in a large cohort of patients CHD.

Method: We prospectively evaluated 407 patients with compensated liver disease who enrolled in the on-going Phase 3 HDV D-LIVR trial (NCT03719313). At baseline, demographic data and anthropometric measurements were collected. Liver stiffness measurement (LSM) and/or Fibrotest were performed, and blood tests were obtained for complete blood count, biochemical panel, and HBV and HDV serologic and viral markers. All patients underwent liver biopsy within 45 days from non-invasive testing. Descriptive statistics were used to summarize demographic and clinical baseline patient characteristics, and chi-square test was used for univariate and multivariate analysis. A series of logistic regression models was fit to the data including cirrhosis status as the outcome, and LSM results, AST, ALT, platelets, albumin, bilirubin, Fibrotest score, HbsAg, and BMI as potential covariates.

Results: Of the 407 patients enrolled to the study, median age of 42.7 (SE 0.55), 69.4% male, with 108 (26.5%) patients showing biopsy confirmed cirrhosis. Of those, 48 (44.4%) were ≤ 45 years of age. In patients ≥ 45 years of age (146), 60 (41%) were cirrhotic at baseline. In univariate analysis, the following variables were statistically significantly associated with cirrhosis: older age ($p < 0.001$), BMI ($p = 0.02$), AST ($p < 0.001$), but not ALT, platelet count ($p < 0.001$), albumin ($p = 0.002$), INR ($p = 0.006$), HBsAg levels ($p = 0.03$) by both LSM and Fibrotest ($p < 0.001$ for both). In multivariate logistic regression, the model that best fit the data included age, platelets, and Fibrotest result as covariates ($p = 0.04$, 0.007 and 0.008, for age, platelets and Fibrotest, respectively). Odds ratio was 1.032 (CI 1.001–1.064) for age, 0.98 (CI 0.98–0.99) for platelet count and 7.168 (CI 1.647–31.191) for Fibrotest. In the subgroup of patients ≤ 45 years of age, the model that best fit the data included LSM results, platelets, and INR ($p = 0.04$ for all). Odds ratio was 1.079 (CI 1.002–1.162) for LSM, 0.99 (CI 0.98–1.0) for platelet count and 66.9 (CI 1.176–999.999) for INR.

Conclusion: In a large cohort of patients with CHD, alarmingly high rates of cirrhosis were seen among younger patients with compensated liver disease. A high index of suspicion for cirrhosis should be maintained in this population especially as it ages, and in those showing subtle changes in markers of synthetic liver function and portal hypertension.

THU412

Establishment of a new diagnostic model for significant liver tissue damage in patients with chronic hepatitis B virus infection in the immune tolerance phase

Airong Hu¹, Suwen Jiang¹, Xiaojun Shi², Dedong Zhu³, Zheyun He², Chenqian Zhu⁴, Lukan Zhang⁴. ¹HwaMei Hospital, University of Chinese Academy of Sciences, Ningbo Institute of Liver Diseases, Ningbo, China; ²HwaMei Hospital, University of Chinese Academy of Sciences, Liver Disease Department, Ningbo, China; ³HwaMei Hospital, University of Chinese Academy of Sciences, Liver Oncology Department, Ningbo, China; ⁴Medical School of Ningbo University, Graduate School, Ningbo, China

Email: huairong@ucas.edu.cn

Background and aims: To establish a new diagnostic model for judging significant liver tissue damage in patients with chronic hepatitis B virus (HBV) infection in the immune tolerance (IT) phase.

Method: The clinicopathological data of 275 patients in the IT phase who underwent liver biopsy from January 2015 to November 2020 were included. According to the liver pathological changes, patients were divided into $<G2$ group and $\geq G2$ group, $<S2$ group and $\geq S2$ group, non-significant liver pathological damage group (GS0 group, $<G2 + <S2$) and significant liver pathological damage group (GS1 group, $\geq G2$ and/or $\geq S2$). The liver pathological changes and clinical features, the diagnostic models and their evaluation values for significant liver pathological damage were analyzed.

Results: Among 275 patients, 43 cases (15.64%) with liver histologic activity $\geq G2$, 30 cases (10.91%) with liver fibrosis $\geq S2$, and 55 cases (20.00%) met the liver pathological damage (GS1, $\geq G2$ and/or $\geq S2$). The correlated independent risk factors affecting significant liver pathological damage were age, levels of hepatitis B e antigen, γ -glutamyltransferase, platelet, alkaline phosphatase and alanine aminotransferase ($p < 0.05$). The established diagnostic models included Y_G ($\geq G2$), Y_S ($\geq S2$), and $Y_{G/S}$ (GS1). The diagnostic values of $Y_{G/S}$ were the highest for $\geq G2$ and GS1, the diagnostic values of Y_G and Y_S were the highest for $\geq S2$. The threshold of $Y_{G/S}$ was 0.18, the sensitivity, specificity and negative predictive value were 78.18%, 73.64% and 93.10%, respectively. When $Y_{G/S} < 0.05$, the sensitivity, negative predictive value and negative likelihood ratio were 98.18%, 97.96% and 0.08, respectively. When $Y_{G/S} \geq 0.25$, the specificity and positive likelihood ratio were 90.45% and 5.14, respectively. When $Y_{G/S} \geq 0.30$, the specificity and positive likelihood ratio were 95.91% and 9.33, respectively.

Conclusion: Approximately 20% of patients with chronic HBV infection in IT phase have significant liver pathological damage. The diagnostic model of $Y_{G/S}$ (< 0.05 or ≥ 0.30) has certain evaluation value for significant liver pathological damage and can avoid liver biopsy to a certain extent.

THU413

Provider factors shaping hepatitis delta screening

Dewan Giri¹, Rohit Nathani², Randy Leibowitz², Carolina Villarroel³, Sidra Salman², Gres Karim³, Bo Hyung Yoon⁴, Amreen Dinani⁵, Ilan Weisberg⁶. ¹Icahn School of Medicine at Mount Sinai Beth Israel, Department of Medicine, New York, United States; ²Mount Sinai Morningside/West, Medicine; ³Mount Sinai Beth Israel, New York, United States; ⁴Mount Sinai Beth Israel/Morningside/West; ⁵Icahn School of Medicine at Mount Sinai; ⁶New York Presbyterian Brooklyn Methodist Hospital, United States

Email: dewan.giri@mountsinai.org

Background and aims: Hepatitis Delta is a defective RNA Virus that requires Hepatitis B Virus to propagate. Infection results in the most severe form of viral hepatitis and is associated with a high risk of cirrhosis and hepatocellular carcinoma. The global burden remains undefined despite its discovery almost 40 years ago. Increased public health measures saw a decrease in the incidence of HDV in the 1990s leading to under-testing and a complacent view of the HDV public health problem. Despite the resurgence of interest seen in the last few years, it continues to remain unrecognized, especially in the primary care setting. The objective of our study is to assess physician knowledge, attitudes, and behaviors toward hepatitis delta screening.

Method: An anonymous 6-question internet-based survey assessing knowledge, attitudes, and behavior around HDV was sent to internal medicine residents, primary care providers (PCP), gastroenterologists, and Gastroenterology Fellows at tertiary care hospital systems, New York, USA from 2/1/2022 through 03/20/2022.

Results: Approximately 200 surveys were sent, and a total of 121 (60%) responses were completed. There were 75 responses from PCP and 46 responses from Specialty Care Providers. Gastroenterologists and fellows were more likely to order HDV antibody than HDV RNA as a screening test than PCP (66% and 61% vs 18% and 22%). A substantial portion of PCPs (50%) and residents (33%) were unsure about appropriate screening tests for HDV. Less than one-third of PCPs (26%), residents (24%), and fellows (28%) identified chronic hepatitis B (CHB) in combination with additional risk factors (CHB + RF) as a criterion for HDV screening. Gastroenterologists were evenly divided between all CHB and CHB + RF patients (48% vs 44%) for screening. Majority (97%) of the participants acknowledged that HDV infection contributed to disease progression, 78% agreed that patients who have cleared HDV are at risk for re-infection and 63% agreed with the statement that the majority of the patients with HDV cleared the infection with treatment. Lack of knowledge of screening guidelines and lack of comfort interpreting results were the two most commonly cited barriers to HDV screening.

<p>In your opinion which is the best screening test for hepatitis delta?</p> <p><input type="radio"/> Anti-HDV</p> <p><input type="radio"/> HDV RNA</p> <p><input type="radio"/> Don't know</p>	<p>Patients who have cleared HDV but who remain hepatitis B surface antigen (HBsAg) positive are still at risk of reinfection with HDV.</p> <p><input type="radio"/> Agree</p> <p><input type="radio"/> Disagree</p>
<p>According to AASLD guidelines, who should be screened for Hepatitis Delta?</p> <p><input type="radio"/> All Patients</p> <p><input type="radio"/> All Patients with Chronic Hepatitis B</p> <p><input type="radio"/> Chronic Hep B patient with additional risk factors</p> <p><input type="radio"/> Universal Screening is not recommended</p>	<p>Majority of patients treated for Hepatitis Delta clear the infection.</p> <p><input type="radio"/> Agree</p> <p><input type="radio"/> Disagree</p>
<p>In your opinion, the presence of Co-infection or Super-infection of HDV can accelerate disease progression to cirrhosis and HCC.</p> <p><input type="radio"/> Agree</p> <p><input type="radio"/> Disagree</p>	<p>From your perspective, what do you think are the biggest barriers to Hepatitis Delta screening in your practice?</p> <p>Please select all that apply</p> <p><input type="checkbox"/> Lack of knowledge of screening guidelines</p> <p><input type="checkbox"/> Limited consultation time</p> <p><input type="checkbox"/> Lack of laboratory services</p> <p><input type="checkbox"/> Lack of comfort interpreting results</p>

POSTER PRESENTATIONS

Conclusion: There are significant gaps in knowledge among providers regarding HDV. Our quest to eliminate HDV should start with disease awareness, develop familiarity with guidelines and testing.

THU414

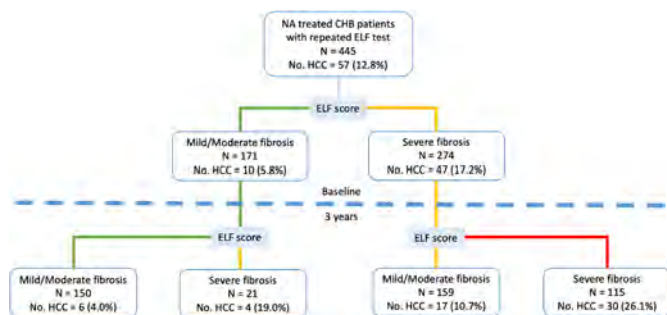
Changes of enhanced liver fibrosis score predict hepatocellular carcinoma in chronic hepatitis B patients receiving antiviral treatment

Yan Liang¹, Terry Cheuk-Fung Yip¹, Che To Lai¹, Shuk Man Lam¹, Yee-Kit Tse¹, Vicki Wing-Ki Hui¹, Henry LY Chan², Vincent Wai-Sun Wong¹, Grace Wong¹. ¹Department of Medicine and Therapeutics, the Chinese University of Hong Kong, Hong Kong; ²Union Hospital, Hong Kong
Email: wonglaihung@gmail.com

Background and aims: Enhanced liver fibrosis (ELF) score is a widely used non-invasive assessment for liver fibrosis. We aimed to derive and evaluate an algorithm based on ELF score changes at three years apart to predict hepatocellular carcinoma (HCC).

Method: Antiviral treated chronic hepatitis B (CHB) patients who had two stored serum samples at about three years apart were included. ELF score was assessed by retrieving the two stored serum samples. Baseline was defined as the date of the first ELF results. The primary end point was the cumulative incidence of HCC.

Results: There were 445 CHB patients (mean age: 51.6 ± 10.3 years; male: 73.9%) included, among whom 57 (12.8%) patients developed HCC during the mean follow-up of 158 months. At baseline, 171 (38.4%) and 274 (61.6%) patients had mild/moderate and severe fibrosis respectively by ELF score (cutoff: 9.8). About three years later, 35.7%, 59.6% and 4.7% of patients had ELF score improved, stable and deteriorated, respectively. 150 patients with continuous low ELF score had lowest risk of HCC (4.0%). 21 patients with deteriorated ELF score had HCC risk increased from 5.8% to 19.0%. 159 patients with ELF score improved had HCC incidence reduced from 17.2% to 10.7%. 115 patients with continuous high ELF score had highest HCC risk (26.1%). (Figure) The cumulative incidence of HCC was significantly different between these four groups ($p < 0.001$).



Conclusion: The algorithm based on ELF score changes at three years apart is a good predictor of HCC in CHB patients receiving antiviral treatment.

THU415

Trends in decompensated cirrhosis and hepatocellular carcinoma diagnosis among people with a hepatitis B notification in New South Wales: a population-based data linkage study

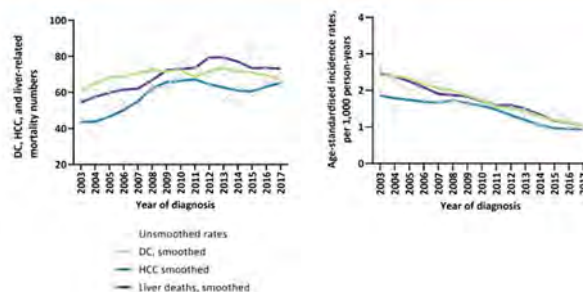
Syed Hassan Bin Usman Shah¹, Maryam Alavi², Behzad Hajarizadeh¹, Gail Matthews², Marianne Martinello¹, Mark Danta³, Janaki Amin⁴, Matthew Law⁵, Jacob George⁶, Gregory Dore¹. ¹The Kirby Institute, UNSW Sydney, Viral Hepatitis Clinical Research Program, Sydney, Australia; ²The Kirby Institute, UNSW Sydney, Viral Hepatitis Clinical Research Program, Sydney, Australia; ³St Vincent's Hospital Sydney, Darlinghurst, Australia; ⁴Macquarie University, Department of Health Systems and Populations, Macquarie Park, Australia; ⁵Kirby Institute, Kensington, Australia; ⁶Westmead Hospital, Westmead, Australia
Email: hbinusman@kirby.unsw.edu.au

Background and aims: Population-level trends and factors associated with hepatitis B virus (HBV)-related decompensated cirrhosis (DC), hepatocellular carcinoma (HCC), and liver mortality are crucial to evaluate therapeutic intervention impacts.

Method: Trends in HBV-DC and -HCC diagnoses and liver-related mortality in New South Wales, Australia, were determined through linkage of HBV notifications (1993–2017) to hospital admissions (2001–2018), mortality (1993–2018), and cancer registry (1994–2014) databases. Late HBV notification was defined as notification at or within two years of DC and HCC diagnosis. Cox proportional hazards regression and multivariable logistic regression analyses were performed to evaluate factors associated.

Results: Among 59,911 people with HBV notification, 1,196 (2.0%) DC and 1,001 (1.7%) HCC diagnoses, and 1,158 (1.9%) liver-related deaths were documented. Since early 2000s, DC and HCC diagnoses numbers increased; however, age-standardised incidence decreased from 2.58 and 1.99 in 2003 to 0.96 and 0.95 per 1,000 person-years (PYs) in 2017. Similarly, age-standardised liver mortality decreased from 2.64 in 2003 to 0.97 per 1,000 PYs in 2017. Among people with DC and HCC diagnoses, late HBV notification declined from 41% and 40% during 2001–2009 to 28% and 26% in 2010–2018, respectively. Predictors of DC diagnosis included older age (birth <1944, adjusted hazard ratio [aHR] 8.15, 95% CI 6.26, 10.61), alcohol-use disorder (aHR 7.19, 95% CI 5.83, 8.86) and HCV co-infection (aHR 2.17, 95% CI 1.74, 2.70). Predictors of HCC diagnosis included older age (birth <1944, aHR 11.61, 95% CI 8.63, 15.61) and male gender (aHR 3.65, 95% CI 2.90, 4.59).

Temporal trends in the numbers and age-standardised rates of decompensated cirrhosis, HCC, and liver mortality, 2003–2017



Conclusion: In an era of improved antiviral therapies, HBV liver morbidity and mortality risk has declined. HCV co-infection and alcohol-use disorder are key modifiable risk factors to HBV disease burden.

THU416

Point of care screening tests for hepatitis B and commitment of a dedicated nurse lead to succesful linkage to care of ethnic minorities

Axelle Vanderlinden^{1,2}, Erwin Ho^{2,3}, Liesbeth Govaerts², Bo De Fooz², Pierre Van Damme⁴, Peter Michiels^{2,3}, Thomas Vanwolleghem^{2,3}.

¹University of Antwerp, Viral Hepatitis Research Group, Laboratory of Experimental Medicine and Pediatrics, Antwerpen, Belgium; ²Antwerp University Hospital, Department of Gastroenterology and Hepatology, Edegem, Belgium; ³University of Antwerp, Viral Hepatitis Research Group, Laboratory of Experimental Medicine and Pediatrics, Antwerpen, Belgium; ⁴University of Antwerp, Vaxinfectio, Antwerpen, Belgium
Email: axelle.vanderlinden@uza.be

Background and aims: In low endemic countries, screening for hepatitis B surface antigen (HBsAg) in migrants is cost-effective to reduce the disease burden of hepatitis B virus (HBV) infections, but linkage to care (LTC) remains a challenge. We previously found outreach screenings for HBV using point of care tests (POCT) to result in a 2.5 times higher LTC compared to venepunctures in an Asian migrant population. In the current study we compared LTC between different ethnic groups screened for HBsAg with POCT in an outreach setting. A secondary objective, was to compare the estimated HBsAg seroprevalence for ethnic minorities to the established prevalence in the general population in order to guide future screening initiatives.

Method: Opportunistic outreach screenings using finger prick Vikia HBsAg tests were performed at municipal integration classes between 11/2017 and 03/2021. If tested positive, an appointment was given immediately at the outpatient hepatology clinic for follow-up and confirmation of HBsAg positivity in blood. A dedicated nurse contacted identified patients via phone, social media or home visits to motivate them for further linkage to care. The latter was defined as having received medical care from a hepatologist, a blood test and an abdominal ultrasound.

Results: A total of 521 persons with different ethnicities (Asia, Middle-East and Africa) were serologically screened using POCT tests. The seroprevalence for HBsAg was 3.45% (18/521) and was significantly higher compared to that of the general population (i.e. 0.66% in 2003 ($p < 0.0001$)). All HBsAg-positive patients were linked to care and assessed by a hepatologist. LTC for all ethnicities combined ($p < 0.0001$), for Sub-Saharan African patients ($p = 0.023$) and Middle-Eastern patients ($p < 0.0001$) was significantly higher compared to the previously observed rate of 34.38% (11/32 patients) using venepunctures as a screening method, but without the commitment of dedicated nurse. Among the HBV infected patients, 22.22% (4/18), 83.33% (15/18) and 22.22% (4/18) met criteria for treatment indication, intrafamilial transmission risk and HCC surveillance respectively. Despite COVID-19 pandemic, linkage to care remains high using POCT and through the commitment of a dedicated nurse. However, the time frame between screening and the first hospital visit is significantly higher ($p = 0.0049$) during the COVID-19 pandemic than in the pre-pandemic period.

Conclusion: HBsAg seroprevalence in ethnic minorities is higher than the general population and warrants targeted screening. Most of the identified patients meet the indication for treatment, counseling to prevent intrafamilial transmission or HCC surveillance. In addition, the use of POCT and commitment of a dedicated nurse can overcome previously identified barriers for linkage to care.

THU417

Prediction of comprehensive prognosis through computed tomography analysis using deep learning algorithm in patients with chronic hepatitis B

Jeongin Yoo¹, Heejin Cho², Dong Ho Lee^{1,3}, Eun Ju Cho². ¹Department of Radiology, Seoul National University Hospital, Seoul, Korea, Rep. of South; ²Department of Internal Medicine and Liver Research Institute, Seoul National University College of Medicine, Seoul, Korea, Rep. of South; ³Institute of Radiation Medicine, Seoul National University Medical Research Center, Seoul, Korea, Rep. of South
Email: creatioex@gmail.com

Background and aims: Computed tomography (CT)-based metrics, such as spleen, liver volume or body fat area, has been reported to be associated with liver-related or metabolic outcomes; however, the prognostic value of artificial intelligence-based CT metric analysis has not been much studied yet. We aimed to evaluate the comprehensive prognosis through CT analysis using deep learning algorithm in patients with chronic hepatitis B (CHB).

Method: Consecutive patients without hepatic decompensation events who underwent contrast-enhanced abdomen CT for hepatocellular carcinoma (HCC) surveillance between January 2005 and June 2016 were included. CT images were processed in an automated analysis software program using convolutional neural network (DeepCatch and MEDIP, MedicalIP, Seoul, Korea). We assessed the cumulative incidence (CI) of the occurrence of HCC, hepatic decompensation, and diabetes mellitus (DM), and identified the significant predictors of each outcome. The optimal cutoff values related to each outcome was obtained using the minimal p value approach method.

Results: A total of 3041 patients were included and retrospectively reviewed. During the median follow-up period of 10.3 years, HCC occurred in 141 patients, and a larger spleen volume was significantly correlated with HCC development ($p < 0.001$). 103 patients experienced hepatic decompensation, and spleen volume was also significantly associated with decompensation ($p < 0.001$). DM developed in 127 patients, and only the abdominal visceral fat area (VFA) showed a significant association with DM development ($p = 0.002$). The optimal cutoff spleen volume was estimated to be 197 ml for HCC development and 259 ml for the occurrence of decompensation. In addition, the optimal cutoff of abdominal VFA for DM development was predicted to be 7604 mm². The estimated 5-year, 10-year, and 15-year CI of HCC occurrence with spleen volume >197 ml were 4.2%, 7.5%, and 9.5%, respectively, and were approximately two times higher than in those of 1.7%, 2.8%, and 4.3% with spleen volume ≤197 ml ($p < 0.001$). For hepatic decompensation, the estimated 5-

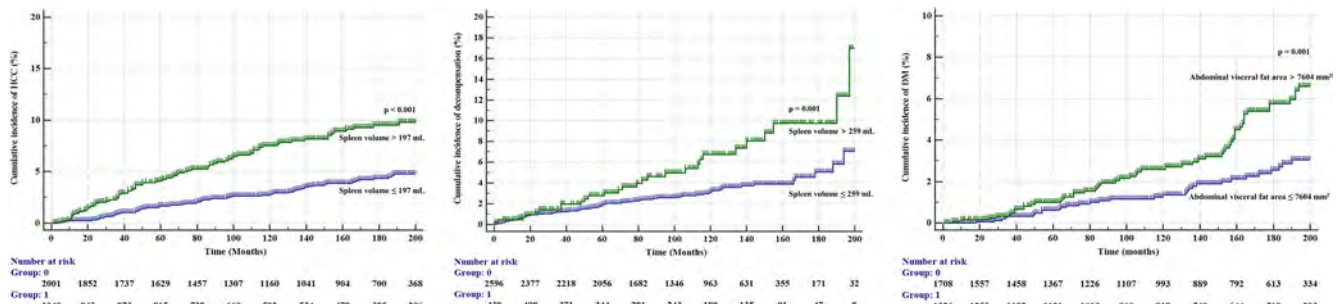


Figure: (abstract: THU417)

POSTER PRESENTATIONS

year, 10-year, and 15-year CI were 2.8%, 6.7%, and 9.7%, respectively, with greater than 259 ml in spleen volume, compared with 1.9%, 3.2%, and 5.0% with less than 259 ml of spleen volume ($p = 0.001$). In DM development, the estimated 5-year, 10-year, and 15-year CI were 1.0%, 2.6%, and 5.8% with more than 7604 mm² in abdominal VFA, significantly different from 0.6%, 1.4%, and 2.5% respectively below 7604 mm² of abdominal VFA ($p = 0.001$).

Conclusion: A larger spleen volume was significantly associated with HCC occurrence and hepatic decompensation, and a higher abdominal VFA was strongly correlated with DM development in patients with CHB. Automatically measured spleen volume and abdominal VFA might be used as relevant prognostic biomarkers in CHB patients.

THU418

Analysis on the normal threshold of alanine aminotransferase level based on liver pathology in patients with chronic hepatitis B

Airong Hu¹, Suwen Jiang¹, Xiaojun Shi¹, Dedong Zhu², Zheyun He³, Lukan Zhang⁴, Chenqian Zhu⁴. ¹HwaMei Hospital, University of Chinese Academy of Sciences, Ningbo Institute of Liver Diseases, Ningbo, China; ²HwaMei Hospital, University of Chinese Academy of Sciences, Liver Oncology Department, Ningbo, China; ³HwaMei Hospital, University of Chinese Academy of Sciences, Liver Disease Department, Ningbo, China; ⁴Medical School of Ningbo University, Graduate School, Ningbo, China
Email: huairong@ucas.edu.cn

Background and aims: To comparatively analyze the liver pathology and clinical characteristics in chronic hepatitis B virus (HBV) infected patients with normal alanine aminotransferase (ALT) of different upper limits of normal (ULN), and to explore the normal threshold of ALT for initiating treatment.

Method: The clinical data of 667 chronic HBV infected patients who underwent liver biopsy from January 2014 to December 2020 were included in this study. The inclusion criteria were ALT <ULN and HBV DNA positive (>30 IU/ml). According to the ULNs of ALT, the enrolled patients were divided into ALT I group (male for <30 IU/L, female for <19 IU/L), ALT II group (30 IU/L ≤ male <35 IU/L, 19 IU/L ≤ female <25 IU/L) and ALT III group (35 IU/L ≤ male <40 IU/L, 25 IU/L ≤ female <40 IU/L). The clinicopathological characteristics and their correlation, and the ALT cut-off value for significant liver pathological damage were analyzed.

Results: The constituent ratios of GS II ($G \geq 2$ and/or $S \geq 2$) in the three groups were 26.05% (99/380), 32.03% (41/128) and 46.54% (74/159), respectively. And there were significant differences in the mean Ridi values of G and S and the constituent ratios of G II ($\geq G2$), S II ($\geq S2$) and GS II among the three groups ($p < 0.001$). There were significant differences in the constituent ratios of gender and HBsAg staining positivity, and the levels of ALT, aspartate aminotransferase (AST), APRI, LIF-5 among the three groups ($p < 0.01$). The positively correlated factor that affect the liver tissue damage was γ -glutamyl-transferase level, and the negatively correlated factors were PLT, albumin/globulin and HBV DNA levels. The ALT thresholds for G I (<G2) and G II, S I (<S2) and S II, GS I (<G2 + <S2) and GS II in total patients were 21.5 IU/L, 22.5 IU/L, and 25.6 IU/L, respectively. And those of male patients were 25.6 IU/L, 23.5 IU/L and 25.6 IU/L, respectively. Those of female patients were 17.5 IU/L, 22.5 IU/L and 25.5 IU/L, respectively.

Conclusion: There are statistically significant differences in the significant liver pathological damage in chronic HBV infected patients with normal ALT of different ULN. The normal threshold (diagnostic cut-off value) of ALT for judging significant liver pathological damage is recommended to be adjusted to 25 IU/L.

THU419

Prevalence rates and eligibility for antiviral treatment against hepatitis B in Casamance, Senegal

Victor Arendt¹, Mame Aisse Thioubou², Kalilou Diallo², Henri Goedertz³, Daouda Diouf⁴, Benjamin Sambou⁴, Chabi Bindia⁴, Ousseynou Cisse⁵, Salimata Camara⁴, Noel Manga², Esther CalvoLassoDelaVeiga¹, Boubacar Diouf⁴. ¹Centre Hospitalier de Luxembourg, Infectious Diseases, Luxembourg, Luxembourg; ²Hôpital de la Paix, Gastroenterology, Ziguinchor, Senegal; ³SANACCESS, Psychology, Luxembourg, Luxembourg; ⁴Enda Santé, Epidemiology, Ziguinchor, Senegal; ⁵Centre de Sante Silence, Medicine, Ziguinchor, Senegal
Email: vicarendt@yahoo.fr

Background and aims: HBV infection is a major public health problem in Casamance, southern Senegal. A cohort of HBV carriers has been set up within the framework of the CARES program. The objective of this study was to assess the prevalence of HBV in the region and the antiviral treatment needs of patients in this cohort based on current recommendations.

Method: Descriptive multicenter cohort study of patients followed in four health facilities in the region (Bignona and Ziguinchor health centers, Regional and La Paix hospitals), carried out as part of the CARES program from January 01, 2019 to December 31, 2021. Screening for HBsAg was performed with kits from Rapid Signal TM HBsAg Serum/Plasma Dipstrip (Organics Ltd Israel). Treatment eligibility was assessed based on age, family history of severe HBV-related disease, degree of fibrosis, HBe antigen, viral load and transaminase levels according to WHO, EASL and the TREAT-B score.

Results: HBV prevalence rates were: 8, 8% in blood donors, 9, 7% in bus drivers, 7, 7% in fishermen; 8, 5% in health care workers, 6% in women living with HIV (WLHIV), 5, 5% in pregnant women, 0% (0/88) in children born to WLHIV. We included 1449 HBsAg positive patients. The mean age was 35.6 years with a sex ratio (M/F) of 1, 37. The predominant circumstances of screening were: blood donation (368 cases), symptoms or medical consultation (306 cases), antenatal screening (167 cases), routine or occupational health visit (148 cases) and a screening campaign (151 cases). To assess the need for treatment we analyzed the available results of the following tests: viral load (969/1449); transaminases and GGT (1153/1449); HBe antigen assay (846/1449), Fibroscan (830/1449), AST-platelet ratio index (609/1449), Fib-4 score (608/1449), history of cirrhosis or hepatocellular carcinoma in first degree relatives (8/463). The complete panel of parameters was available in only 315 patients.

The proportion of eligible patients according to the different recommendations was 6, 3% (WHO 2015), 8, 9% (WHO simplified), 7, 6% (EASL 2017), 8% (TREAT-B).

Conclusion: The prevalence of HBV in Casamance remains high. The proportion of HBV patients eligible for antiviral treatment ranges from 6, 3 to 8, 9% with only small differences according to the different consensus recommendations (WHO 2015, EASL 2017, TREAT-B).

THU420

Comorbidities, and not viral load, are predictors of cirrhosis in AgHBe-negative chronic infection

Sara Archer¹, Luís Maia¹, Catarina Afonso^{2,3}, Jose Manuel Ferreira¹, Teresa Moreira¹, Marta Rocha¹, Tiago Pereira Guedes¹, Isabel Pedrote¹. ¹Centro Hospitalar Universitário do Porto, Portugal; ²Instituto de Ciências Biomédicas Abel Salazar, Portugal; ³Instituto de Ciências Biomédicas Abel Salazar, Porto, Portugal
Email: u13418@chporto.min-saude.pt

Background and aims: There is an ongoing debate about the heterogeneity of the definition of HBeAg-negative chronic HBV infection (formerly inactive carriers, IC), which patients to treat, and how comorbidities can influence its natural course. The aim of our study is to assess risk factors, including higher viral load (VL) and increased ALT, for cirrhosis.

Method: This is a retrospective cohort of chronic HBV hepatitis patients with at least 2 consultations between 2010–2020 in a western center mediterranean tertiary centre. Demographic and clinical data were retrieved. Individuals with less than 1 year of follow-up, HCV or HIV co-infection and with insufficient data were excluded. Statistical analysis was performed using SPSS. As per EASL guidelines, upper limit of normal (ULN) of 40U/L for ALT was considered.

Results: 635 patients were included, of which 340 as IC. From these, 53.5% were men with mean current age 56.16 ± 13.4 years, mean follow-up of 10.14 ± 8 years, during which 4.1% developed cirrhosis. Liver-related mortality was 0.9%. 14.5% patients had excessive alcohol consumption; 12.4% diabetes, 15.9% arterial hypertension and 18.2% dyslipidemia.

Risk factors for cirrhosis: diabetes (OR 4.8, $p=0.002$), arterial hypertension (OR 7.3, $p=0.000$), dyslipidemia (OR 4.46, $p=0.004$), alcohol (OR 4.91, $p=0.002$), ALT > ULN or VL > 2000 IU/ml (OR 5.32, $p=0.005$). On multivariate analysis including age and follow-up time, none was an independent predictor.

When analysed separately, alcohol (OR 18.31, $p=0.031$) predicted cirrhosis in patients with both ALT < ULN and VL < 2000 IU/ml, while in the others diabetes (OR 4.4, $p=0.028$) and arterial hypertension (OR 5.4, $p=0.012$) were the main predictors. This may be justified as alcohol abuse has less influence in ALT values.

The cut-off of 2000 IU/ml for VL did not predict development of cirrhosis in any group of patients.

Conclusion: In our cohort, comorbidities, and not VL, are predictors of cirrhosis in IC. Treating HBV in these patients may not be as relevant as controlling comorbidities. Our results support EASL current guidelines.

THU421

A systematic literature review and meta-analysis of primary sources reporting health state preference values in chronic hepatitis B, C, and D

Ankita Kaushik¹, Sarah Hofmann², Mariajão Janeiro², Geoffrey Dusheiko^{3,4}, Andrew Lloyd⁵, Filipa Aragão^{2,6}. ¹Gilead Sciences, Inc., Foster City, California, United States; ²Maple Health Group, New York, United States; ³University College London, Medical School, London, United Kingdom; ⁴King's College Hospital, London, United Kingdom; ⁵Acaster Lloyd Consulting Ltd, London, United Kingdom; ⁶Universidade NOVA de Lisboa, NOVA National School of Public Health, Public Health Research Centre, Lisbon, Portugal
Email: ankita.kaushik@gilead.com

Background and aims: Chronic viral hepatitis is associated with severe patient impairment and reduction in health-related quality of life (HRQoL). This is also reflected in low patient health state preference values (utilities) for severe health states. Utilities for health states are essential variables for cost effectiveness analyses for treatments. This study aimed to derive utilities for health states in chronic hepatitis B (cHBV), C (cHCV) and D (cHDV) through a systematic literature review (SLR) and meta-analyses (MA).

Method: Electronic literature databases (EMBASE and MEDLINE) were searched for primary articles that reported health state utilities for cHBV, cHCV or cHDV. Health states evaluated include Metavir fibrosis stages F0 to F4, decompensated cirrhosis (DC), hepatocellular carcinoma (HCC), post-liver transplant (LT), post-LT in year (Y1), and post-LT in year 2 and beyond (Y2+). MAs were performed with utilities based on EQ-5D-3L and based on a combination of instruments, also including EQ-5D-5L, HUI3, HUI2, SF-6D, SF-36, and standard gamble (SG), time trade-off (TTO) or visual analogue scale (VAS) techniques.

Results: The SLR identified 22 studies that derived utilities for cHBV and/or cHCV but none for cHDV. There was considerable heterogeneity in the methods adopted for utility elicitation and in the health states evaluated. Non-cirrhotic (NC; F0 to F3) and compensated cirrhosis (CC; F4) were the most evaluated health states. Mean

utilities were higher in cHBV patients than in cHCV patients (except for advanced liver disease) and higher when determined based on the EQ-5D-3L than when derived from a combination of all instruments. Utility estimates decreased with disease progression, with the development of cirrhosis having the largest impact while LT seems to allow for some recovery.

Health state	cHCV			cHBV		
	Mean utility	95 % CI	n	Mean utility	95 % CI	n
EQ-5D-3L						
NC (F0-F3)	0.85	0.80-0.90	4	0.90	0.86-0.93	3
CC (F4)	0.72	0.65-0.79	2			
DC	0.70	0.61-0.79	3			
HCC	0.69	0.59-0.78	2			
PLT						
PLT (Y1)						
PLT (Y2)						
Combined instruments						
NC (F0-F3)	0.79	0.75-0.82	13	0.85	0.78-0.91	7
CC (F4)	0.66	0.61-0.71	11	0.76	0.65-0.87	3
DC	0.63	0.58-0.69	8	0.46	0.20-0.73	3
HCC	0.70	0.63-0.77	3	0.52	0.22-0.82	3
PLT	0.74	0.70-0.79	3			
PLT (Y1)				0.57	0.51-0.62	2
PLT (Y2)				0.67	0.62-0.72	2

Figure: Results of the MAs by utility instrument and health state

Conclusion: There is a large body of available literature reporting on utilities of patients living with cHCV, less in cHBV, but a paucity of studies in cHDV. The results show a large heterogeneity in reported health state utilities, likely due to the variation in the methods used and health states considered. The most comprehensive set of health state utility estimates were derived using EQ-5D for cHCV and from a combination of instruments for cHBV. This is the first meta-analysis of utilities in chronic viral hepatitis which could be used in future economic evaluations.

Immune-mediated and cholestatic disease: Clinical aspects

THU422

Hepatitis B transmission in early life in very remote Aboriginal communities in northern Australia

Richard Sullivan^{1,2,3}, Jane Davies^{1,2}, Paula Binks¹, Melita McKinnon¹, Roslyn Dhurrkay¹, Kelly Hosking^{1,4}, Sarah Bukulatjpi⁵, Stephen Locarnini⁶, Margaret Littlejohn⁶, Steven YC Tong^{1,7}, Joshua Saul Davis^{1,8}. ¹Menzies School of Health Research, Charles Darwin University, Darwin, Australia; ²Department of Infectious Diseases, Royal Darwin Hospital, Darwin, Australia; ³Department of Infectious Diseases, Immunology and Sexual Health, St George and Sutherland Clinical School UNSW, Kogarah, Australia; ⁴Population and Primary Health Care, Top End Health Service Northern Territory, Darwin, Australia; ⁵Miwatj Health Aboriginal Corporation, Northern Territory, Australia; ⁶Victorian Infectious Diseases Reference Laboratory, Peter Doherty Institute for Infection and Immunity, Royal Melbourne Hospital and University of Melbourne, Melbourne, Australia; ⁷Victorian Infectious Disease Service, The Royal Melbourne Hospital and Doherty Department University of Melbourne at the Peter Doherty Institute for Infection and Immunity, Melbourne, Australia; ⁸John Hunter Hospital, New Lambton Heights, Australia
Email: richie.sullivan@menzies.edu.au

Background and aims: Chronic hepatitis B is a public health concern in Aboriginal communities of northern Australia with prevalence almost four times the non-Aboriginal population in the Northern Territory. Infection is suspected to occur in early life, however, the mode of transmission and vaccine effectiveness is not known in this population. WHO has set a target for hepatitis B elimination by 2030; elimination in this disproportionately affected population will require understanding of transmission and vaccine effectiveness.

POSTER PRESENTATIONS

Method: We conducted the study at four very remote communities. We approached mothers who were Hepatitis B surface antigen (HBsAg) positive and gave birth between 1988 and 2013. We obtained hepatitis B serology, immunisation and birth details. If both mother and child had hepatitis B viral DNA detected, we performed viral whole genome sequencing.

Results: We included 20 mothers and 38 of their children. The median age of the children was 8.8 years (IQR 5.7–13.0). Of 33 children with results available, 8 (24.2%, 95%CI 11.1–42.3) were anti-hepatitis B core (anti-HBc) positive, 3 (9.1%, 95%CI 1.9–24.3) of whom were also HBsAg positive. Hepatitis B immunoglobulin (HBIG) had been given at birth in 29 (76.3%, 95%CI 59.8 – 88.6) children and 26 children (68.4%, 95%CI 51.3–82.5) were fully vaccinated. Of the 3 children who were HBsAg positive, all had received HBIG at birth and two were fully vaccinated. Of the 5 who were anti-HBc positive and HBsAg negative, 4 had received HBIG at birth and one was fully vaccinated. Whole genome sequencing revealed one episode of mother to child transmission.

Conclusion: Although uncommon, there is ongoing transmission of hepatitis B in Aboriginal communities of northern Australia despite vaccination, and is likely occurring by both vertical and horizontal routes. Prevention will require ongoing investment to overcome the many barriers experienced by this population in accessing care.

THU423

the changing scenario of HBV chronic related disease in the transplant setting

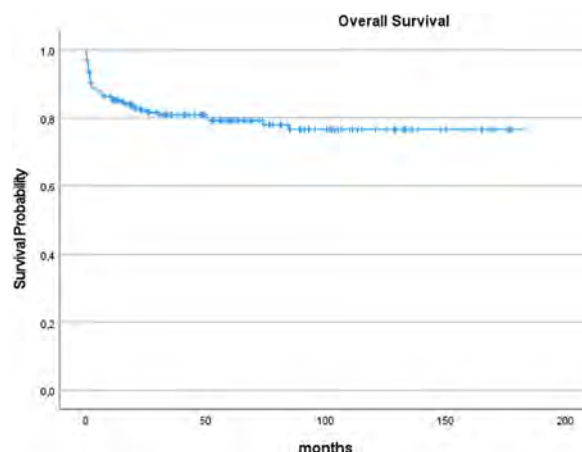
Sara Battistella¹, Martina Gambato¹, Umberto Cillo¹, Alberto Zanetto¹, Alessandro Vitale¹, Enrico Gringeri¹, Marco Senzolo¹, Patrizia Burra¹, Francesco Paolo Russo¹. ¹University of Padova, Department of Surgery, Oncology and Gastroenterology, Italy
Email: sarabattistella93@gmail.com

Background and aims: Hepatitis B virus (HBV) related chronic liver disease is one of the most common indication for liver transplantation (LT), for both decompensated cirrhosis and hepatocellular carcinoma (HCC). Introduction of nucleos (t)ide analogues (NA) significantly modified the natural history of the disease in the pre- and post- transplant setting, preventing decompensation of liver disease, disease recurrence and increasing post-LT patient and graft survival. This study aimed to assess the evolution of admission and management of patients affected by HBV-related liver disease in the WL for LT relatively to the introduction and spreading of high barrier NA and to evaluate overall long-term graft and patient survival after LT.

Method: All adults with HBV listed for LT at Padua University Hospital between 01.2006 to 12.2020 were retrospectively evaluated. Patients were divided in two groups according to their indication to inclusion in the WL (decompensated cirrhosis group: patients listed with MELD >15 with or without HCC; HCC group: patients with MELD <15 and presence of HCC). Patients were further divided according to the time of inclusion in the WL (2006–2013 and 2014–2020). For each patient we evaluated the antiviral treatment and HBV DNA at the time of inclusion in WL and the type of prophylaxis after LT. Patient survival were calculated using Kaplan Meier curves and comparison between different groups were performed using Log-Rank test.

Results: From 01.2006 to 12.2020 a total of 1502 patients included in the WL for LT, among them 186 patients were HBV infected. One fourth of patients had HBV DNA detectable at the time of inclusion in the WL and 86% were on antiviral treatment. Almost 60% of patients were wait-listed for decompensated disease, 30% of them had HCC as well. Eventually 31 patients were excluded from the waiting list: 17 for HCC progression, 3 for not liver related causes and 11 for stability of the disease, principally after the introduction of high barrier NA treatment. A total of 29 patients died in the waiting list, mainly during the first period of the study, and 126 patients underwent LT with a median waiting time of 6 months. The overall survival after LT was 90% at 1 year and 80% at 5 years. No significative difference in survival

were observed between HBV patients transplanted for decompensated cirrhosis and those for HCC. Almost all HBV patients were treated with a combination therapy of HBIG and NA after LT and we recorded only 2 cases of transitory HBV reactivation, with no consequences on liver function.



Conclusion: HBV still remains one of the most common indication to LT, both for end stage liver disease and hepatocellular carcinoma. Thanks to high barrier NAs the mortality in the waiting list is decreased during the last years.

THU431

Outcomes of pregnancy in patients with autoimmune hepatitis in the Netherlands

Susan Fischer¹, Elsemieke de Vries¹, Ynto de Boer², Adriaan Van der Meer³, Robert De Man³, Johan Kuyvenhoven⁴, Michael Klemt-Kropp⁵, Tom Gevers⁶, E.T.T.L. Tjwa⁷, Edith Kuiper⁸, Marc A.M.T. Verhagen⁹, Philip W. Friederich¹⁰, Bart Van Hoek¹. ¹Leiden University Medical Center (LUMC), Gastroenterology and Hepatology, Leiden, Netherlands; ²Amsterdam UMC, locatie VUmc, Gastroenterology and Hepatology, Amsterdam, Netherlands; ³Erasmus MC, Gastroenterology and Hepatology, Rotterdam, Netherlands; ⁴Spaarne Hospital Hoofddorp, Gastroenterology and Hepatology, Hoofddorp, Netherlands; ⁵Noordwest Ziekenhuisgroep locatie Alkmaar, Gastroenterology and Hepatology, Alkmaar, Netherlands; ⁶Academic Hospital Maastricht, Gastroenterology and Hepatology, Maastricht, Netherlands; ⁷Radboud University Medical Center, Gastroenterology and Hepatology, Nijmegen, Netherlands; ⁸Maasstad Hospital, Gastroenterology and Hepatology, Rotterdam, Netherlands; ⁹Diakonessenhuis Utrecht, Gastroenterology and Hepatology, Utrecht, Netherlands; ¹⁰Meander Medical Center, Gastroenterology and Hepatology, Amersfoort, Netherlands
Email: s.e.fischer@lumc.nl

Background and aims: Data regarding the outcomes of pregnancy in patients with autoimmune hepatitis (AIH) are limited. This study focuses on the effects of pregnancy in AIH patients and neonatal outcomes.

Method: A retrospective multicenter cohort study was performed at the Leiden University Medical Centre (LUMC) in collaboration with nine participating hospitals from the Dutch Autoimmune Hepatitis Study Group in the Netherlands. Data concerning maternal and neonatal outcomes during and after pregnancy were collected from medical records in AIH patients with pregnancy. Risk factors were identified using logistic regression analysis to examine the association of defined risk variables with adverse maternal and neonatal outcomes.

Results: 93 pregnancies in 47 women resulted in 66 deliveries (71%) with a live birth rate of 98.5%. Preterm birth was mentioned in 20% and 19% of the children were born dysmature. 34% of the neonates were admitted to the hospital after birth. Flares of disease activity occurred in

4.5% during pregnancy, and in 26% of the postpartum episodes. The absence of biochemical remission at conception was identified as risk factor for the occurrence of postpartum flares (Odds ratio (OR) 6.8, 95% Confidence Interval (CI) 1.6–7.65). Flares in the year before conception were identified as a risk factor for the occurrence of gestational flares (OR 21.6, CI 1.7–282.0) and were associated with the occurrence of postpartum flares ($p = 0.01$). Maternal hypertensive disorders during pregnancy occurred in 15%. Women who were partially in remission were at higher risk for loss of biochemical remission after delivery (OR 10.0, CI 1.5–67.0) and to develop hypertensive disorders during pregnancy (OR 10.3, CI 1.5–68.6). No risk factors were found for the occurrence of adverse neonatal outcomes. Cirrhosis was found a risk factor for miscarriages (OR 3.4, CI 1.1–10.8). No other correlations between the presence of cirrhosis and adverse outcomes for both mother and child were observed.

Conclusion: Pregnancy in women with AIH ended in childbirth in 71%. There was a high incidence of spontaneous abortion, prematurity, dysmaturity compared to the general population. The rate of postpartum flares of AIH was similar to previous literature. Absence of biochemical remission at conception and a flare in the year prior to conception increases the risk of maternal complications during and after pregnancy. Lastly, cirrhosis was found a risk factor for miscarriages.

THU432

Cholangiopathy after severe COVID-19: what do we know so far?

Valéria Ferreira de Almeida e Borges¹, Helma Pinchemel Cotrim², Marcelo Simão Ferreira³, José Humberto Caetano Marins¹, Haroldo Luis Oliva Gomes Rocha¹, Leonardo Augusto Dias Nascimento¹, Mayra Machado Fleury Guedes¹, Julia Esteves Guerra¹. ¹Universidade Federal de Uberlândia, Uberlândia, Brazil; ²Universidade Federal da Bahia, Medicine School, Brazil; ³Universidade Federal de Uberlândia, Medicine School, Brazil
Email: valeriafaborges@gmail.com

Background and aims: From 2001 to 2018, before the Covid-19 pandemic, at least 16 studies described a type of secondary sclerosing cholangitis (SSC) in critically ill patients. During the pandemic, similar cases of cholangiopathy were observed in patients with severe Covid-19. The hypotheses suggested to explain this disease will be a liver ischemia related to micro thrombosis associated with SARS-CoV-2 or direct biliary epithelial infection. To describe the clinical characteristics of cholangiopathy in patients who survived the ICU period with severe Covid-19.

Method: Adult patients diagnosed with Covid-19, who presented severe cholestasis were included. All of them had prolonged stay in the ICU, needed for mechanical ventilation, high doses of vasopressors, ketamine use, and prone positioning. Criteria for SSC were elevated levels of alkaline phosphatase (ALP) and bilirubin; no previous history of liver disease; magnetic resonance cholangiopancreatography (MRCP) or endoscopic retrograde cholangiopancreatography (ERCP), and or liver biopsy, which showed the biliary tract alterations. The diagnosis of Covid-19 was with a positive PCR test in all cases.

Results: A total of 24 patients were include. Mean age was 57 ± 10 years and 66% were male. All developed cholestasis, after a mean of 20 days. The peak mean level of ALP was 1541 U/L, gamma-glutamyl transferase 2366 U/L, aspartate aminotransferase 248, alanine aminotransferase was 276 U/L, and total bilirubin 10 mg/dL. MRCP were performed in 75% of cases, ERCP in 37% and cholangioscopy in one. The most relevant finding was rarefaction of the intrahepatic bile ducts in all, and bacterial cholangitis in two cases. Biliary casts were removed in seven of nine cases who underwent ERCP. All patients presented elevated levels of ALP, GGT and bilirubin after discharge, regardless of the ursodiol used. During the mean follow-up of 205 days, 6 patients progressed to cirrhosis and 7 (29%) to death. At follow-up, the most recent bilirubin dosage was on average 19 mg/dL in the group that died and 3.7 mg/dL in the group that survived ($p < 0.001$).

Conclusion: In this simple of 24 cases, patients with Covid-19 presented a severe cholestatic disease and with rapid progression to

cirrhosis or obit. The role of SARS-CoV-2 seems relevant, however other factors associated should be considered: mechanical ventilation for a long time; high doses of vasopressors and possible severe hemodynamic instability; prolonged stay in the intensive care unit and the ketamine used.

THU433

Enhanced liver fibrosis score correlates with transient elastography in patients with treated autoimmune hepatitis

Anna Stoelting¹, Elsemieke de Vries¹, Maarten Tushuizen¹, Albert Stättermayer², Xavier Verhelst³, Bart Van Hoek¹. ¹Leiden University Medical Center (LUMC), Gastroenterology and Hepatology, Leiden, Netherlands; ²Medical University of Vienna, Wien, Austria; ³Ghent University Hospital, Gent, Belgium
Email: b.van_hoek@lumc.nl

Background and aims: Cirrhosis is an important prognostic factor for long-term survival of patients with autoimmune hepatitis (AIH). Little is known about progression of fibrosis during adequate therapy. The Enhanced Liver Fibrosis score (ELF-score) has not been validated in patients with AIH. The aim of this study is to evaluate the diagnostic accuracy of the ELF test for fibrosis compared to transient elastography (TE).

Method: Patients with AIH or AIH-variant syndrome, treated for a minimum of 6 months at baseline (BL) were eligible for inclusion. Serum samples of all patients were taken and TE was done simultaneously at BL and after one year. Patients were divided into two groups: complete biochemical remission (CR) (group 1) and incomplete remission (group 2) at BL. ELF-scores and its components were calculated from the collected serum. We investigated if there is a correlation between the ELF score and liver elastography for severe fibrosis. Cut-off for cirrhosis (=F4 fibrosis) at TE was >16 kPa. A cut-off for the ELF score was determined for cirrhosis in a receiver operator characteristics (ROC) curve analysis.

Results: A total of 66 patients in three academic hospitals in the Netherlands, Belgium and Austria were included. 68.2% were female, mean age at inclusion was 51.20 years (± 17.24), median treatment duration at inclusion was 6.50 years (IQR: 2.00–11.00). During follow-up, two patients died (3%), two patients were lost-to-follow-up (3%). Group 1 consisted of 35 patients (53.0%), of whom 16 (45.7%) had moderate-severe fibrosis. Group 2 consisted of 31 patients (47.0%). 24 patients (77.4%) had none-mild fibrosis. ELF-score (9.46 vs 9.27, $p = 0.58$) and liver stiffness (8.70 vs 7.10 kPa, $p = 0.078$) at BL did not differ significantly between the groups. Liver stiffness did not change after one year irrespective of remission status.

There was a positive correlation between ELF-score and liver stiffness ($\rho = 0.48$, $p < 0.001$). For F4 fibrosis, the area under the curve was calculated as 0.83. The cut-off value was determined at 9.68. sensitivity, specificity, positive and negative predictive value were 86.4%, 71.7%, 40.4% and 95.9%, respectively.

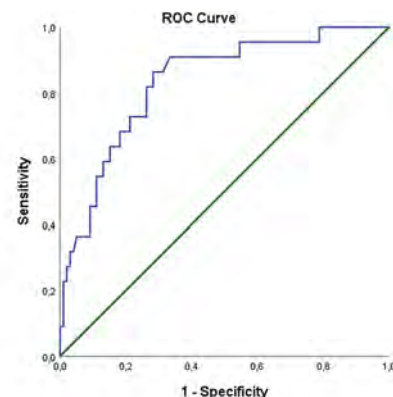


Figure 2: ROC analysis: ELF score. Diagnostic value of ELF score.

POSTER PRESENTATIONS

Conclusion: ELF-score shows good diagnostic accuracy in patients with AIH under immunosuppressive treatment irrespective of remission status. A cut-off at 9.68 can rule out severe fibrosis in patients with AIH. Change in remission status did not significantly change fibrosis with ELF-score or TE results.

THU434

Rationale for evaluation of PLN-74809 treatment in participants with primary sclerosing cholangitis in Phase 2a study INTEGRIS-PSC

Eric Lefebvre¹, Greg Cosgrove¹, Simon Wong¹, Erica Park², Fiona Cilli¹, Theresa Thuener¹, Marzena Jurek¹, Scott Turner¹, Martin Decaris¹, Johanna Schaub¹. ¹Pliant Therapeutics, Inc., South San Francisco, United States; ²Pliant Therapeutics, Inc. (at time of study), South San Francisco, United States

Email: elefebvre@pliantrx.com

Background and aims: Transforming growth factor beta (TGF-beta) signalling is a key driver of liver fibrosis. In primary sclerosing cholangitis (PSC), integrins over-expressed on injured cholangiocytes (alpha-v/beta-6) and myofibroblasts (alpha-v/beta-1) regulate TGF-beta activity. PLN-74809 is an oral, once-daily, dual-selective inhibitor of integrins alpha-v/beta-6 and alpha-v/beta-1 in development for the treatment of PSC and idiopathic pulmonary fibrosis. It has shown favourable tolerability in over 280 healthy participants, reduced TGF-beta signalling and achieved high target engagement in human lungs. Pre-clinical evaluation of antifibrotic activity resulting from dual integrin inhibition was performed to support clinical evaluation.

Method: PLN-74809 was administered orally for 6 weeks in BALBc.Mdr2^{-/-} mice with established fibrosis. A tool alpha-v/beta-6 and alpha-v/beta-1 inhibitor compound, PLN-75068, was tested therapeutically in a diet-induced mouse model of biliary fibrosis using 3, 5-diethoxycarbonyl-1, 4-dihydrocollidine (DDC). Hepatic collagen was quantified by hydroxyproline (OHP) and collagen proportionate area (CPA) and TGF-beta signalling by phosphorylated SMAD3 (pSMAD3) levels. An *ex vivo* study evaluated the effects of 2-day treatment with PLN-74809 on the expression of profibrotic genes, COL1A1 and COL1A2, in precision-cut liver slices (PCLivS) from tissue explants of participants with biliary fibrosis (n = 2 PSC; n = 2 primary biliary cholangitis [PBC]). A review of available blinded safety data from the enrolling Phase 2a study in participants with PSC was performed (NCT04480840).

Results: PLN-74809 dose-dependently reduced OHP (up to ~30%, p < 0.05), CPA (up to ~50%, p < 0.05) and pSMAD3 (up to ~40%, p < 0.001) in the BALBc.Mdr2^{-/-} mouse model, as well as COL1A1 and COL1A2 gene expression (up to ~30%, p = 0.0789) in PCLivS from tissue explants of participants with PSC and PBC. PLN-75068 reduced OHP (up to ~20%, p < 0.05) in DDC-injured mice in a dose-dependent manner. PLN-74809 was well tolerated in participants with PSC. Most adverse events (AEs) were mild; none were severe. The most common AE was mild headache. One participant experienced serious AEs at least 20 days after the last dose of study drug, deemed not related by the investigator. One participant prematurely discontinued due to COVID-19. PLN-74809 pharmacokinetics in participants with PSC were consistent with those of healthy participants.

Conclusion: Pharmacological inhibition of integrins alpha-v/beta-6 and alpha-v/beta-1 demonstrated antifibrotic activity in two models of biliary fibrosis and in PCLivS from participants with PSC or PBC. Available safety findings from participants with PSC enrolled in the ongoing Phase 2a INTEGRIS-PSC study, continue to support the favourable tolerability profile of PLN-74809.

THU435

Acute hepatitis after COVID-19 vaccine: case series by the International autoimmune hepatitis group (IAIHG) and the European reference network on hepatological diseases (ERN RARE-LIVER)

Greta Codoni³, Maria Alejandra Gracia Villamil⁴, Albert Stättermayer⁵, Agustin Castiella⁶, Christoph Schramm^{7,8}, Jan-Philipp Weltzsch⁷, Marcial Sebode⁷, Christine Bernsmeier⁹, Wikrom Karnsakul¹⁰, Ana Lleo¹¹, Tom Gevers¹², Limas Kupcinskas^{8,13}, Nélia Hernandez¹⁴, Andreas Cerny², Michele Ghielmetti¹⁵, Diego Vergani¹⁶, Giorgia Mieli-Vergani¹⁶, Jose Pinazo Bandera^{17,18,19}, Maria Isabel Lucena^{20,21,22}, Raul J. Andrade^{20,21,22}, Yoh Zen¹⁶, Richard Taubert^{8,23}. ¹USI Università della Svizzera italiana, Lugano, Switzerland; ²Epatocentro Ticino, Lugano, Switzerland; ³Università della Svizzera Italiana, Facoltà di Scienze Biomediche, Lugano, Switzerland; ⁴Hospital Italiano de Buenos Aires, Argentina; ⁵Medical University of Vienna, Wien, Austria; ⁶Donostia Unibertsitate Ospitalea, Donostia, Spain; ⁷University Medical Center Hamburg-Eppendorf, Hamburg, Germany; ⁸European Reference Network on Hepatological Diseases (ERN RARE-LIVER); ⁹Centre for Gastrointestinal and Liver Diseases, Basel, Switzerland; ¹⁰The Johns Hopkins University School of Medicine, Baltimore, United States; ¹¹IRCCS Humanitas Research Hospital Milan, Milano, Italy; ¹²Maastricht University Medical Center, Maastricht, Netherlands; ¹³Lithuania University of Health Sciences, Kaunas, Lithuania; ¹⁴Hospital de Clínicas, Facultad de Medicina, Montevideo, Uruguay; ¹⁵Medical Practice, Mendrisio, Switzerland; ¹⁶King's College Hospital, United Kingdom; ¹⁷University Hospital, Málaga, Spain; ¹⁸IBIMA, Málaga, Spain; ¹⁹UMA, Málaga, Spain; ²⁰Virgen de la Victoria University Hospital-IBIMA, Málaga, Spain; ²¹University of Malaga, Málaga, Spain; ²²CIBERehd, Málaga, Spain; ²³Medizinische Hochschule Hannover, Hannover, Germany

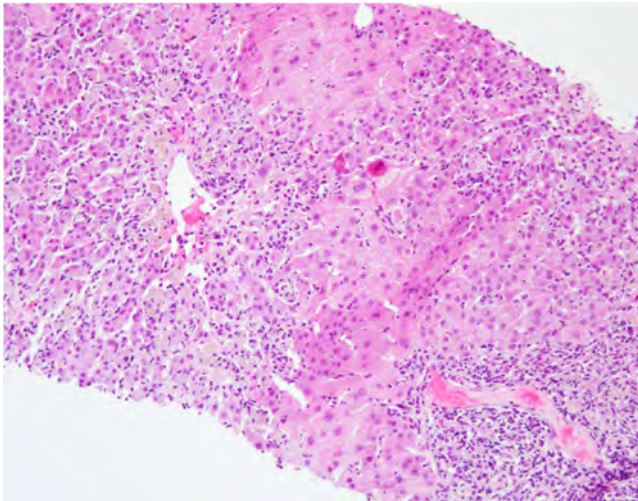
Email: greta.codoni@usi.ch

Background and aims: Autoimmune phenomena and clinically apparent autoimmune diseases, including autoimmune-like hepatitis, have increasingly been reported after SARS-CoV-2 infection, and after vaccination against it. It has been suggested that post-COVID19 vaccine hepatitis may be a novel clinical entity, urgently requiring investigation of well characterized cases. Our international case collection aims at investigating in a standardized way, clinical, serological and pathological features of a large number of patients with acute hepatitis after COVID-19 vaccination.

Method: Patients with acute hepatitis within 2 months from last vaccine dose and available liver biopsy, but without a history of autoimmune hepatitis, are included. Clinical data at diagnosis and outcome after a follow-up of 6 months are collected. Histology and autoimmune serology are centrally reviewed/tested.

Results: 42 patients included so far; 27 (65%) females; median age 59 years (range 16–78). Vaccine type: 16 BNT162b2; 9 ChAdOx1 nCov-19; 6 mRNA-1273; 5 Gam-COVID-Vac; 1 BBIBP-CorV; 2 ChAdOx1 nCov-19 + BNT162b2; 2 Gam-COVID-Vac + ChAdOx1 nCov-19; 1 Gam-COVID-Vac + mRNA-1273. Locally tested serology was positive for anti-nuclear antibody (ANA) in 31 cases; anti-smooth muscle antibody (ASMA) in 14, anti-mitochondrial antibody (AMA) in 3; 12 were ANA and ASMA-positive; none was anti-soluble liver antigen or anti-liver kidney microsomal antibody positive; 11 were seronegative. Mean IgG was 16.8 g/l (range: 6.6–34.4). Median time from vaccination to hepatitis diagnosis: 24.6 days (IQR 10.7–38). 12 had pre-existing extrahepatic autoimmune conditions.

Central histological review of the first 7 cases showed isolated central perivenulitis (n = 2) or mixed portal and lobular hepatitis with interface injury and confluent necrosis (n = 5; Figure). Aggregates of plasma cells and eosinophils (>5 cells/hpf) were observed in 4 and 3 cases, respectively.



35/42 patients were treated with immunosuppressive drugs; 33 steroids, 1 azathioprine, 1 azathioprine + steroids; all but one being still on treatment. Mean follow-up is 5 months; one patient died of extrahepatic cause 7 months after the diagnosis of hepatitis. All treated patients responded satisfactorily.

Conclusion: acute hepatitis arising after COVID-19 appears to be a heterogeneous condition: long-term follow-up will help understanding if in some cases the vaccine triggers autoimmune hepatitis or if it is a novel drug-induced nosological entity.

THU436

Scheduled endoscopic program for patients with primary sclerosing cholangitis improves transplant-free survival and enables early risk stratification

Burcin Özdirik¹, Wilfried Veltzke-Schlieker¹, Jule-Marie Nicklas¹, Hilmar Berger¹, Daniel Schmidt¹, Silke Leonhardt¹, Andreas Adler¹, Tobias Müller¹, Alexander Wree¹, Frank Tacke¹, Michael Sigal¹.

¹Charité Universitätsmedizin Berlin, Department of Hepatology and Gastroenterology, Campus Virchow Klinikum (CVK) and Campus Charité Mitte (CCM), Berlin, Germany

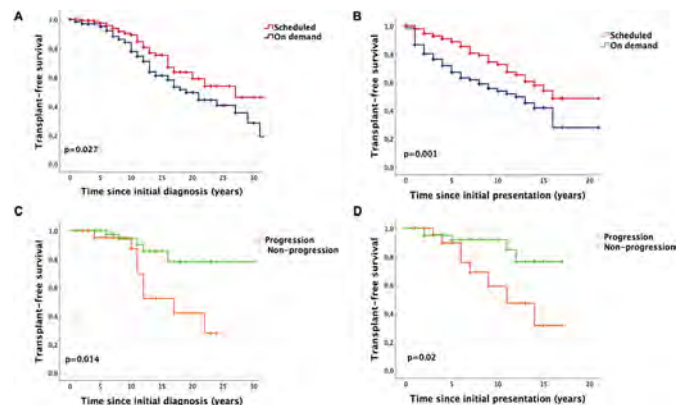
Email: michael.sigal@charite.de

Background and aims: Primary sclerosing cholangitis (PSC) is associated with biliary obstructions that can require endoscopic retrograde cholangiopancreatography (ERCP). While beneficial short-term effects of ERCP are well documented, follow-up interventional strategies are less defined and their long-term impact is debated. Here, we evaluated the outcome of a scheduled program that has been implemented at our tertiary liver center for over more than 20 years.

Method: Within our program, ERCPs were performed at regular and pre-defined intervals to follow-up or treat previously detected biliary stenosis and/or to remove concretions. In this retrospective cohort study, we evaluated the outcomes of this scheduled programmed ERCP approach in comparison to patients, who received endoscopic interventions only on clinical demand. The primary end point was transplantation-free survival. The secondary end points were occurrence of hepatic decompensation, recurrent cholangitis episodes, development of hepatobiliary malignancies and endoscopy-related adverse events.

Results: We included 268 consecutive patients with diagnosed PSC, 135 receiving scheduled ERCP and 133 receiving on demand ERCP. The rates of transplant-free survival since initial diagnosis (median 27 vs. 19 years; $p=0.027$) and initial presentation (median 16 vs. 12 years; $p=0.001$) were significantly higher in patients receiving scheduled vs. on demand ERCP. Subgroup analysis revealed that progression in cholangiographic findings between the 1st and 2nd ERCP (progression cohort) was associated with a poorer outcome

compared to patients without progression (non-progression cohort) (median transplant-free survival: 17 years vs. undefined; $p=0.021$).



Conclusion: Our data indicate that implementation of a scheduled ERCP program with interventions performed in predefined intervals improves transplant-free survival in patients with PSC. Furthermore, we reveal that a progression in cholangiographic findings after the first ERCP procedure enables a prediction of the future disease activity and outcome.

THU437

Immune response and safety in standard and third dose SARS-CoV-2 vaccination in patients with autoimmune hepatitis on immunosuppressive therapy, a prospective cohort study

Kristin Jorgensen^{1,2}, Adity Chopra³, Joseph Sexton⁴, Anne T Tveter⁴, Johannes R. Hov^{2,5,6,7}, Ingrid Jysum^{4,7}, Lise Sofie H. Nissen-Meyer³, John T Vaage^{3,7}, Silje W Syversen⁴, Guro L Goll⁴, Fridtjof Lund-Johansen^{3,8}, Jørgen Jahnsen^{1,7}. ¹Akershus University Hospital, Dept. of Gastroenterology, Norway; ²Oslo University Hospital, Norwegian PSC Research Centre; ³Oslo University Hospital, Department of Immunology, Norway; ⁴Diakonhjemmet Hospital, Division of Rheumatology and Research, Norway; ⁵Oslo University Hospital, Research Institute of Internal Medicine, Norway; ⁶Oslo University Hospital, Section of Gastroenterology, Department of Transplantation Medicine; ⁷University of Oslo, Institute of Clinical Medicine, Norway; ⁸University of Oslo, ImmunoLingo Convergence Center

Email: kristin.kaasen.jorgensen@outlook.com

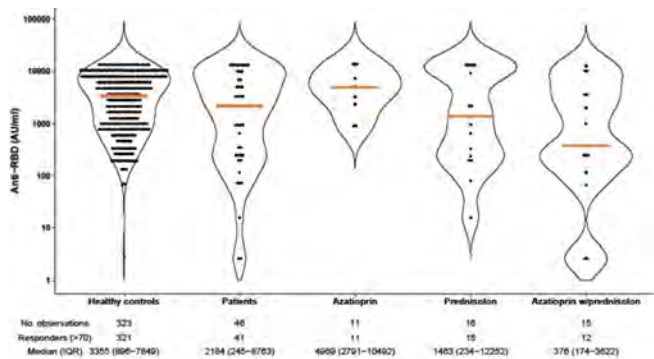
Background and aims: vaccines against SARS-CoV-2 are proven efficacious and safe in the general population. Data on vaccine response in patients with autoimmune hepatitis (AIH) are currently lacking. The aim of this study was to evaluate immunogenicity and safety following standard and three dose SARS-CoV-2 vaccination in patients with AIH on immunosuppressive therapy.

Method: this prospective, observational study included adult AIH patients and healthy controls, both groups receiving standard two dose SARS-CoV-2 vaccination. The patients were voluntarily allotted a third vaccine dose according to the national vaccine strategy. Antibodies to the receptor-binding domain (RBD) of SARS-CoV-2 spike proteins were analyzed in serum samples collected prior to, and after vaccination, and serologic response was defined as >70 AU/ml.

Results: a total of 46 patients (median age 56 years [IQR 47–63], 32 [70%] women), and 1114 healthy controls (median age 43 years [IQR 32–55], 854 [77%] women) were included in the study. All patients had compensated liver disease (Child Pugh A), the median disease duration was 6.2 years (IQR 4.2–9) and 80% received BNT 162b2 as standard two-dose vaccine. After standard vaccination, 89% of patients compared to 99% of healthy controls were serologic responders, $p=0.005$. Anti-RBD levels were significantly lower in patients (median 2184 AU/ml [IQR 245–8763]) than controls (3355 AU/ml [IQR 896–7849]), $p=0.005$. Prednisolone and

POSTER PRESENTATIONS

azathioprine combination therapy demonstrated the lowest response rate (80%), compared to azathioprine (94%) and prednisolone (100%) monotherapy (figure). The patients received the third vaccine dose median 112 days (IQR 88–133) after the second dose. The serologic response rate increased from 81% at time of receiving the third dose, to 91%, measured 3–5 weeks post third vaccination. Likewise, the overall anti-RBD levels increased from median 264 AU/ml [IQR 115–6485] to 6383 AU/ml [IQR 1480–9412]. After standard vaccination, adverse events (AE) were reported in 30 (71%) of patients and in 191 (78%) of 244 healthy controls with a comparable safety profile. Following the third dose, 74% of patients reported AEs, without new safety issues emerging. No serious AEs were reported.



Anti-SARS-CoV-2 IgG antibodies following standard two dose SARS-CoV-2 vaccination according to medication group, compared to healthy controls. Violin plot showing the probability density of the data at different values, smoothed by a kernel density estimator. Each data point is a participant, and the solid orange line show the group median.

Conclusion: response rates as well as anti-RBD levels were lower in AIH patients than healthy controls following standard vaccination, with an attenuated serologic response in particular in patients on combination therapy with azathioprine and prednisolone. Third dose vaccination was safe without new safety issues emerging and resulted in an overall increased serologic response.

THU438

Analyses of obeticholic acid treatment retention in UK patients based on medicine delivery data

Carl Gibbons¹, Subash Srinivasan¹, Jaysal Bodhani², Jing Li³, Li Chen³, Palak Trivedi⁴. ¹Intercept Pharmaceuticals, United Kingdom; ²Intercept Pharmaceuticals, Level 6, United Kingdom; ³Intercept Pharmaceuticals Inc, New York, United States; ⁴University of Birmingham, NIHR Birmingham Biomedical Research Centre, Birmingham, United Kingdom
Email: carl.gibbons@interceptpharma.com

Background and aims: Between 30–40% of patients with primary biliary cholangitis (PBC) inadequately respond to Ursodeoxycholic acid (UDCA) and are candidates for second-line therapy. Obeticholic acid (OCA) is the only licensed second-line treatment in the UK, however, compliance, treatment adherence and rates of drug discontinuation have not been quantified at scale.

Method: 6, 857 orders for OCA were examined, which were delivered to 744 patients with PBC between 1 May 2017 and 1 Sept 2021. We constructed longitudinal datasets allowing study of patient dose order histories. Dropped-out status was assigned to patients against which there had been no new orders for ≥ 6 months after the date covered by their most recent medicine delivery. Kaplan-Meier estimates were then generated based on the cohort of 744 patients. Additionally, to examine potential relationships between drop-out and dose order history, patients were classified into one of 4 categories: 1) 5 mg doses ordered only; 2) up-titrated to and remained on 10 mg doses; 3) up-titrated to 10 mg but later returned to 5 mg doses; and 4) mixed 5 mg and 10 mg dosing patterns.

Separate Kaplan-Meier curves were generated for each of these categories and analysed using Cox regression.

Results: 744 patient order histories yielded 1138 person-years of ordering data and 204 drop-out events, with an estimated 87%, 78% and 69% of patients who continued to receive OCA deliveries at 6, 12 and 24 months respectively after their first Homecare order. Only 51% of patients had order histories indicating successful titration to 10 mg OCA daily, with 43% never increasing beyond 5 mg. The remaining 6% had orders suggesting either mixed dosing, or 10 mg dosing for a period before returning to 5 mg doses. We observed marked separation between some dose order groups in terms of drop-out, with the 5 mg only group most likely to drop out (69%, 56%, and 49% remaining on treatment at 6, 12 and 24 months respectively). By contrast, those who received 10 mg dosing (at any point) remained on OCA at a rate of 99%, 93%, and 82% at 6, 12 and 24 months respectively. The difference in retention was statistically significant (hazard ratio of 10 mg vs 5 mg only dosing: 0.22, 95% CI 0.17, 0.30, $p < 0.001$). See Figure. Moreover, these differences in retention rate remained statistically significant on restricted analysis of those receiving OCA for ≥ 6 months.

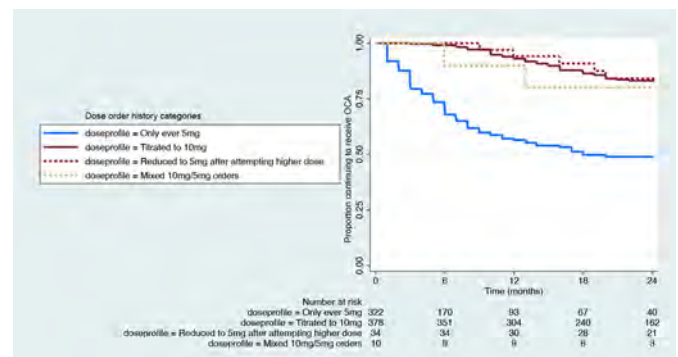


Figure: Proportion of patients continuing to receive OCA orders by time since first Homecare order, separated by dose order history categories

Conclusion: Our findings suggest an association between dose order history category and retention on treatment, prompting further study into optimal systems of management and support for patients on OCA. Conclusions about drop-out should be made with caution, as the analyses only consider product orders, disconnected from clinical characteristics.

THU439

Real-world prevalence of pruritus with obeticholic acid: a systematic literature review and meta-analysis

Patrick Horne¹, Christina Hanson², Tracy Mayne³, Leighland Feinman³. ¹University of Florida, Gainesville, United States; ²South Denver Gastroenterology, Englewood, United States; ³Intercept Pharmaceuticals Inc, New York, United States
Email: patrick.horne@medicine.ufl.edu

Background and aims: Obeticholic acid (OCA) is the only approved 2nd line therapy for patients with primary biliary cholangitis (PBC) with an inadequate response or intolerant to ursodeoxycholic acid (UDCA). High rates of pruritus observed in OCA trials have not been observed in real-world studies. We performed a systematic review and meta-analysis to estimate real-world prevalence of pruritus and associated OCA discontinuation compared to the POISE phase 3 clinical trial.

Method: Systematic review and meta-analysis. We searched Embase and MEDLINE for English-language publications and conference abstracts from real-world settings in patients with PBC treated with OCA monotherapy or combined with UDCA. A fixed- or random-effects pooled estimate was performed based on heterogeneity. POISE. We analyzed data from 209 patients with 1 year follow-up on OCA in the double-blind and open-label phase of POISE. Patients were

censored if they exceeded the approved 10 mg dose. Pruritus was assessed via visual-analogue scale, 5-D pruritus scale, Itch domain of the PBC-40 scale, and standard adverse event assessment. We compared prevalence of pruritus and discontinuations due to pruritus in POISE to the real-world meta-analysis estimates via a chi-square goodness of fit test.

Results: Eleven studies were included in the meta-analysis (total patients = 1192). The random-effects pooled estimate of pruritus prevalence was 29% (95% CI, 24%–33%; Figure 1A); the fixed-effects pooled estimate of treatment discontinuation due to pruritus was 9% (95% CI, 8%–11%; Figure 1B). Real-world pruritus prevalence was significantly lower than in POISE (29% vs 62% in POISE; $\chi^2 = 108.69$; $p < 0.001$); real-world treatment discontinuation was significantly higher than in POISE (9% vs. 4%; $\chi^2 = 5.62$; $p < 0.02$).

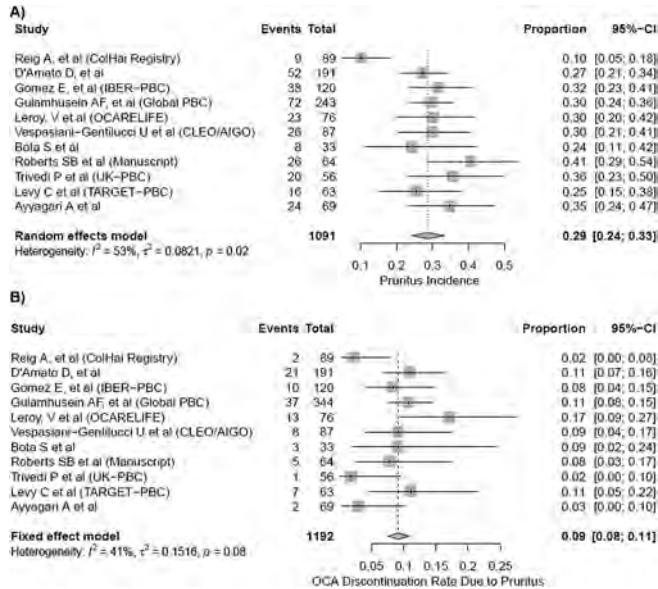


Figure: Forest Plot of Pooled Real-world Prevalence of (A) Pruritus and (B) Treatment Discontinuation due to Pruritus

Conclusion: The prevalence of pruritus in real-world data was significantly lower than observed in POISE. Data collection in POISE, with extensive repeated questions on itch, may have primed subjects to report greater pruritus. The real-world discontinuation estimate of 9% was higher than reported in POISE, though still low. Experience with other drugs indicates discontinuation can be higher in real-world settings, in the absence of mechanisms and motivation in clinical trials to maintain patients on therapy. Our observation of significantly lower pruritus prevalence in the real-world vs clinical trial setting may help providers calibrate treatment expectations when considering OCA treatment.

THU440

Cognitive symptoms in non-cirrhotic primary biliary cholangitis

Naw April Phaw¹, Aaron Wetten^{2,3}, David Jones^{4,5}, Jessica Dyson³, Amardeep Khanna⁶. ¹Newcastle University, Translational and Clinical Research Institute, Newcastle upon Tyne, United Kingdom; ²Newcastle University, Translational and Clinical Research Institute; ³Freeman Hospital, The Newcastle upon Tyne Hospitals NHS Foundation Trust, Hepatology, Newcastle upon Tyne, United Kingdom; ⁴Newcastle University, Liver Immunology, Newcastle upon Tyne, United Kingdom; ⁵The Newcastle upon Tyne Hospitals NHS Foundation Trust, Hepatology, Newcastle upon Tyne, United Kingdom; ⁶Nottingham University Hospitals NHS TRUST, Hepatology Department, Nottingham, United Kingdom
Email: mail2april@gmail.com

Background and aims: There is emerging evidence of cognitive symptoms, such as memory loss and poor concentration even in early

stage Primary Biliary Cholangitis (PBC), with functional imaging studies demonstrating abnormalities of the central nervous system. The aim of this study was to objectively assess performance in cognitive tasks, using CANTAB Neuropsychological Battery in PBC patients and the differences between those with and without cognitive symptoms.

Method: Non-cirrhotic PBC patients were recruited from a single tertiary hospital; those with significant additional medical conditions were excluded. Participants completed PBC-40 questionnaires and CANTAB tasks (PAL, OTS, MTT, SWM, ERT, RTI, RVP) assessing working memory, executive function, emotional cognition, attention and psychomotor speed. Analysis was performed against a normal population, with a z score of <-1.5 standard deviations considered a significant deficit

Results: 38 PBC patients were recruited. Nearly a third of PBC patients demonstrated significant cognitive deficits in memory tasks (PAL) with more errors and fewer correct first attempt responses along with reduced correct hits and slower response times in the emotional cognition domain (ERT). PBC patients underperformed in 2 out of 3 executive function tasks (OTS; $p = 0.00$, SWM; $p = 0.00$, MTT; $p = 0.42$), with fewer correct responses in the attention domain (RVP) and slower responses to stimuli however they outperformed the normative population in psychomotor speed domain (RTI). There was, however, no significant difference in CANTAB performance between cognitively symptomatic ($n = 16$) and asymptomatic ($n = 22$) PBC patients when stratified by the PBC-40 cognitive domain. (Table)

Table: CANTAB test scores of different groups in the study						
Test		Normative population (NP)	Total PBC (TP) (n=38)	CS PBC (n=16) mean±SD	CAS PBC (n=22) mean±SD	P value
PAL	PALFAMs (+)	13.32±4.0	9.9±3.9	9.1±4	10.4±3.8	NP vs TP (p<0.00)** CS vs CAS (p=0.26)*
	PALTEA (-)	13.89±12.2	25.2±14.2	26.1±13.5	24.5±14.9	NP vs TP (p<0.00)** CS vs CAS (p=0.72)*
OTS (+)		10.82±2.7	8.8±3.6	9.8±2.4	8.1±4.2	NP vs TP (p<0.00)** CS vs CAS (p=0.29)*
SWM	SWMDE (-)	9.9±9.2	17.8±8.9	17.8±6.5	17.5±10.4	NP vs TP (p<0.00)** CS vs CAS (p=0.93)*
	SWMIS (-)	7.0±2.8	9±2.5	9.3±1.7	8.8±2.9	NP vs TP (p<0.00)** CS vs CAS (p=0.98)*
ERT	ERTMOORT (-)	1267±195.3	1579.8±347.5	1674.2±385.1	1511.2±308.4	NP vs TP (p<0.00)** CS vs CAS (p=0.28)*
	ERTTH (+)	56.8±6.8	50.5±7.6	51.5±7.95	49±7.2	NP vs TP (p<0.00)** CS vs CAS (p=0.24)*
RVP (-)		0.9±0.1	0.8±0.1	0.8±0.1	0.8±0.1	NP vs TP (p<0.00)** CS vs CAS (p=0.19)*

NP = normative population; TP = total PBC population; CS = cognitively symptomatic; CAS = cognitively asymptomatic; PAL = Perceptual Association Test; PALFAM = PAL first attempt memory score; PALTEA = PAL final attempt memory score; OTS = One-trial set-back test of Cambridge; SWM = spatial working memory; SWMDE = SWM between events; SWMIS = SWM in strings; ERT = Error Recognition Test; ERTMOORT = ERT overall median reaction time; ERTTH = ERT trial hits; RVP = rapid visual processing.

(+) = higher scores indicate better performance; (-) = lower scores indicate better performance.

** = the mean between the group different significantly; * = the mean between the group did not differ significantly.

Conclusion: Objective cognitive dysfunction was frequent in PBC patients, with pronounced deficits observed in memory and emotional domains. No significant differences in CANTAB performance was observed between cognitive symptomatic and non-symptomatic patients suggesting behavioral adaption/variation may influence the symptoms exhibited in PBC patients. The patterns of abnormality integrated with functional imaging may shed light on the anatomical abnormality.

THU441

Screening and surveillance of biliary neoplasia based on brush cytology in primary sclerosing cholangitis (PSC): prevalence and outcomes

**Martti Färkkilä¹, Sonja Boyd², Kalle Jokelainen¹, Andrea Tenca¹,
Lauri Puustinen¹, Hannu Kautiainen³, Johanna Arola⁴,
Helena Isoniemi⁵.** ¹*Helsinki University Hospital, Clinic of
Gastroenterology, Helsinki, Finland;* ²*Helsinki University Hospital, Clinic
of Gastroenterology, Helsinki, Finland;* ³*University of Eastern Finland,
Institute of Public Health and Clinical Nutrition, Kuopio, Finland;*
⁴*Helsinki University Hospital, Pathology, Helsinki, Finland;* ⁵*Helsinki
University Hospital, Transplantation and Liver Surgery, Helsinki, Finland*
Email: martti.farkkila@hus.fi

Background and aims: PSC is characterised with chronic inflammation of biliary epithelium leading to strictures in bile ducts and secondarily to cirrhosis. Chronic inflammation is associated with the increased risk for biliary dysplasia (BD) and cholangiocarcinoma (CCA), with lifetime risk 10%. CCA is the most common cause of death among PSC patients and up to half of CCAs are detected at the time of dg or within one year after. The current guidelines for surveillance for CCA in PSC are contradictory and the evidence for efficacy of surveillance is scarce. AGA guidelines recommend US, CT or MRI, with or without Ca19-9 for surveillance of CCA, none of which are suitable for early detection of biliary neoplasia.

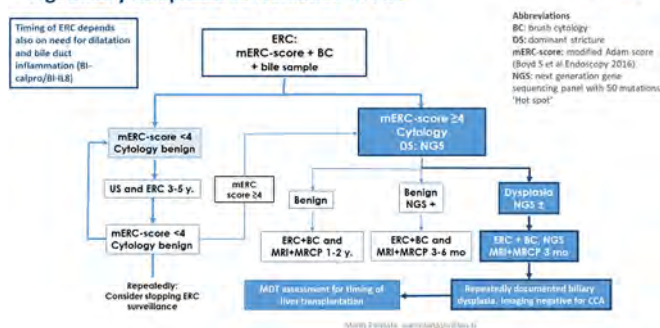
We aimed to evaluate the role ERC with brush cytology (BC) in screening and surveillance of BD and to assess its prevalence and its impact on patient outcome.

Method: In total 989 patients were retrieved from Helsinki University PSC registry referred for ERC: documentation of dg, MRCP/liver histology suggestive for PSC or surveillance of PSC progression and/or BD. We excluded 98 patients: age <18 years (n = 69) or >65 y (n = 19), CCA detected at time of diagnosis or within one year (n = 7), serious concomitant disease or malignancy, liver transplantation (LTx) before f/u, n = 3. BC was systematically collected from intra- and extrahepatic bile ducts, regardless of the presence of dominant strictures for detection of BD. Cytological evaluation from cytospin and cell-block slides was performed, using three-tiered criteria as benign, suspicious, or malignant (CCA). Suspicious cytology: any of the following: biphasic cell population, lack of polarity, nuclear moulding, nuclear membrane irregularities, high nuclear-cytoplasm ratio, hyper/hypochromacy and lack of cohesion. The screening and surveillance strategy is presented in fig.

Results: Prevalence of BD and risk for CCA: Suspicion of dysplasia was detected ≥ 1 times in 91 patients (10%) during median f/u of 10 years, CCA in 25. If dysplasia was documented ≥ 3 times, the patient was referred for evaluation for LTx.

LiverTx: 22 patients were transplanted for suspicion of malignancy, 58 for other indications. Out of the 58 patients with suspicion of dysplasia (≤ 2 times), but not transplanted, 11 (19%) developed CCA. 800 patients without dysplasia, only 7 (0.9%) were diagnosed with CCA. In patients transplanted for dysplasia, 91% were found to have dysplasia in explant, in 3 CCA was detected at LTx. The sensitivity of BC with suspicion of malignancy at least once to detect histologically confirmed biliary neoplasia (transplantation/surgery) was 65% (52–76%) and specificity 94% (93–96%) with OR 30. If patient had BC with suspicion of malignancy ≥ 3 times the sensitivity to detect histologically confirmed CCA was 100% (48% to 100%) and specificity 98% (97–99%).

Fig. Biliary neoplasia surveillance in PSC



Conclusion: ERC with brush cytology is an accurate method to screen and detect biliary neoplasia in PSC.

THU442

Impact of pruritus in primary sclerosing cholangitis (PSC): a multinational survey

Kris Kowdley^{1,2}, Ricky Safer³, Rachel Gomel³, Joanne Hatchett³,
Martine Walmsley⁴, Julio Burman⁵, Sindee Weinbaum⁵,
Kerrie Goldsmith⁶, Meej Kim⁷, Will Garner⁷, Andrew McKibben⁷,
Elaine Chien⁷. ¹Liver Institute Northwest, Seattle, WA, United States;
²Elson. S. Floyd College of Medicine, Washington State University,
Spokane, WA, United States; ³PSC Partners Seeking a Cure, Greenwood
Village, CO, United States; ⁴PSC Support, Oxford, United Kingdom; ⁵Hetz:
The Israeli Association for the Health of the Liver, Ramat Gan, Israel; ⁶PSC
Support Australia Inc, Melbourne, Australia; ⁷Mirum Pharmaceuticals
Inc, Foster City, CA, United States
Email: mkim@mirumpharma.com

Background and aims: Intense pruritus (itch) can be a debilitating complication of cholestatic liver diseases, including primary sclerosing cholangitis (PSC), and in some cases can be an indication for liver transplantation. Currently there are no clinically effective or approved pharmacological therapies to treat cholestatic itch associated with PSC. The aim of this survey was to provide information about the presentation and severity of cholestatic itch in PSC and its broader burden from the patient perspective.

Method: A multinational survey of patients with self-reported PSC was conducted. The 39-question web-based survey was focused on the impact of itch in patients with PSC, how itch severity affected quality of life (QoL), and therapeutic interventions used to address itch. Severity of itch was quantified using a numerical rating scale (0 for no itch, 10 for worst itch you can possibly imagine). The survey was distributed to participants via Hetz, PSC Australia, PSC Partners, and PSC Support. Responses were collected from June 2020 to Feb 2021.

Results: Of the 482 patients who responded, 91% had experienced itch due to PSC and 34% (164/482) were currently experiencing itch, with the median worst itch reported as a 6/10; 45% (74/164) reported the itch episode was at least 1 month in duration. Itch severity was associated with a higher degree of reported sleep disturbance and worsening fatigue, with 63% of respondents indicating that evening and night-time were the worst times of the day for itching. 50% (197/392) reported that itch led to disruption of day-to-day responsibilities and lasted >30 days in 32% (62/197). 22% (88/392) reported missing school or work. Itch was also associated with mood changes, including but not limited to anxiety, irritability, and feelings of hopelessness in more than half of patients (58%; 228/392). The most commonly used medicines to treat itch were antihistamines (46%), UDCA (39%), Cholestyramine (39%), topical creams/ointments (28%), and Rifampicin (19%). Half of the respondents (235/482) reported using ≥ 2 medications but 75% (177/235) described only partial or no relief with these interventions (Table).

Table. Anti-Pruritic Medications Utilized By Respondents (N = 482)

	N (%) Taking Medication	N (%) with Full Resolution	N (%) with Partial Resolution	N (%) with No Impact
Antihistamines	224 (46%)	5 (2%)	117 (52%)	85 (38%)
UDCA	188 (39%)	19 (10%)	48 (26%)	86 (46%)
Cholestyramine	188 (39%)	18 (10%)	110 (59%)	50 (27%)
Topical creams/ointments	134 (28%)	6 (4%)	77 (57%)	44 (33%)
Rifampicin	91 (19%)	22 (24%)	43 (47%)	22 (24%)
Taking 2+ Medications*	235 (49%)	51 (22%)	149 (63%)	28 (12%)

*Outcome is the best response outcome across all medications taken, sorted by "Full Resolution", then "Partial Resolution", then "No Impact". Percentages do not add to 100% due to missing outcomes.

Conclusion: Itch related to PSC has a major adverse impact on QoL (eg, sleep, mood, fatigue), interferes with daily activities in a substantial proportion of patients but remains inadequately treated in most patients. These data highlight a major unmet need for the development of safe and effective therapies for treatment of cholestatic itch in patients with PSC.

THU443

A dynamic approach to modelling baseline disease status and ALT elevation over follow-up on clinical-event free survival in autoimmune hepatitis: a canadian multicentre cohort

Christina Plagiannakos^{1,2}, Gideon Hirschfield^{1,2}, Ellina Lytvyak³, Surain Roberts⁴, Marwa Ismail^{1,2}, Kattleya Tirona¹, Andrew L. Mason³, Harry Janssen^{1,5}, Aliya Gulamhusein^{1,2}, Aldo J Montano-Loza³, Bettina Hansen^{1,2}. ¹University Health Network, Toronto Centre for Liver Disease, Toronto Western and General Hospital, Toronto, Canada; ²University of Toronto, Institute of Health Policy, Management and Evaluation, Toronto, Canada; ³University of Alberta, Department of Medicine-Division of Gastroenterology and Liver, Edmonton, Canada; ⁴Unity Health Toronto, St. Michael's Hospital, Toronto, Canada; ⁵University of Toronto-St. George Campus, Department of Medicine, Toronto, Canada
Email: christina.plagiannakos@uhn.ca

Background and aims: Current and future treatments for autoimmune hepatitis (AIH) target ALT as a biomarker of efficacy. In patients with AIH, we sought to model ALT response dynamically over long-term follow-up, to understand clinical associations with clinical-event free survival (CEFS).

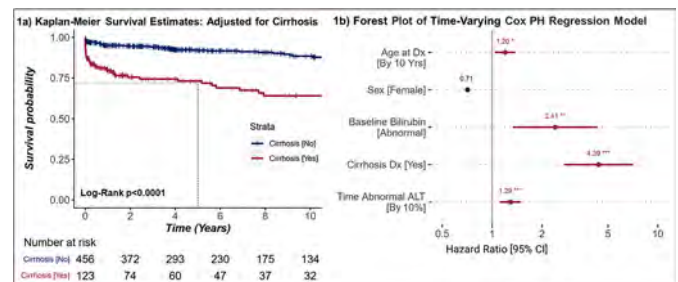
Method: Patients diagnosed with AIH (simplified score ≥ 6) who initiated treatment were included from the Canadian Network for Autoimmune Liver Disease. AASLD sex-specific upper limits of normal (ULN) defined ALT normalization and site-specific ULN were used for other biochemical markers. CEFS included the absence of a decompensation event, liver transplant, or death. Kaplan-Meier estimates and Cox proportional hazards dynamic time-varying models adjusted for age at diagnosis, sex, cirrhosis at diagnosis, baseline total bilirubin, and stratified by site were used; alpha = 0.05.

Results: 579 patients with AIH initiated treatment between November 1987 and June 2020, with a median follow-up time of 6.54 years [IQR 2.70–11.6] and an average of 9 visits [4.0–21]. Median age at diagnosis was 48 years [31.0–59.4], 75.5% of patients were female (n = 437) and 71.2% reported white ethnicity (n = 412). Median baseline ALT was 15.7xULN [5.84–34.2], AST 10.5xULN [3.36–23.8], IgG 1.48xULN [1.12–1.93], total bilirubin 1.8xULN [0.68–6.25] and INR 1.17 [1.05–1.34].

Among the 21.2% (n = 123) of patients with cirrhosis at diagnosis, 40 had an event during follow-up, and of the 456 (78.7%) without cirrhosis, 48 had an event. At 5-years of follow-up, the CEFS estimate was 73% (CI 0.66–0.82) for patients with, and 92% (CI 0.90–0.95) for those without, cirrhosis (Figure 1a). The survival probability at 5 years for patients with elevated and normal bilirubin values were 83% (CI

0.78–0.87) and 94% (CI 0.91–0.98), respectively. In univariate analysis AST (HR 1.58, CI 1.02–2.45), and IgG (HR 3.05, CI 1.1–8.4) were significantly related to long-term outcomes in patients without cirrhosis. In the multivariable model, cirrhosis at diagnosis (HR 4.39, CI 2.73–7.07), baseline bilirubin (HR 2.41, CI 1.34–4.33), and older age (HR 1.20, CI 1.04–1.38, unit = 10 years) were all independently associated with poorer outcomes.

The predicted cumulative impact of time spent with elevated ALT during follow-up was significant (HR 1.29, CI 1.11–1.50, unit = 10% of time with elevated ALT values had an increased risk of experiencing an event, and this was most marked in patients with cirrhosis.



Conclusion: Patients with AIH are at increased risk of a clinical event as the time spent with abnormal ALT values increases, especially those with cirrhosis at baseline. Persistent improvement in ALT values is a logical treatment goal in AIH.

THU444

Secondary sclerosing cholangitis following COVID-19 disease: a multicenter retrospective study

Peter Hunyady¹, Lea Streller², Darius Ruether³, Sara Reinartz Groba⁴, Dominik Bettinger⁵, Daniel Fitting⁶, Karim Hamesch⁷, Jens Marquardt⁸, Victoria Mücke¹, Fabian Finkelmeier¹, Asieb Sekandarzad⁵, Tobias Wengenmayer⁵, Ayoub Bounidane¹, Felicitas Weiss⁷, Kai-Henrick Peiffer¹, Bernhard Schlevogt⁴, Stefan Zeuzem¹, Oliver Waidmann¹, Marcus Hollenbach⁹, Martha M Kirstein⁸, Johannes Kluwe³, Fabian Kütting², Marcus Mücke¹. ¹University Hospital Frankfurt; ²University Hospital Cologne; ³University Hospital Hamburg Eppendorf; ⁴University Hospital Münster; ⁵University Hospital Freiburg; ⁶University Hospital Würzburg; ⁷University Hospital Aachen; ⁸University Hospital Schleswig-Holstein Campus Lübeck; ⁹University Hospital Leipzig
Email: marcus.m.muecke@gmail.com

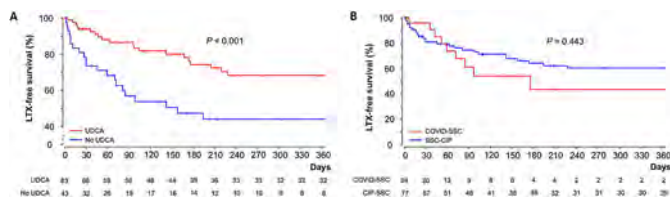
Background and aims: Secondary sclerosing cholangitis (SSC) is a rare disease with poor prognosis. Cases of SSC have been reported following coronavirus disease 2019 (COVID-19), COVID-SSC. Aim of this study was to compare COVID-SSC to SSC in critically ill patients (SSC-CIP) and to assess factors influencing transplant-free survival.

Method: In this retrospective, multicenter study involving 127 patients with SSC from 9 tertiary care centers in Germany, COVID-SSC was compared to SSC-CIP and logistic regression analyses were performed investigating factors impacting transplant-free survival.

Results: Twenty-four patients had COVID-SSC, 77 patients SSC-CIP and 26 patients had other forms of SSC. COVID-SSC developed after a median of 91 days following COVID-19 diagnosis. All patients had received extensive intensive care treatment (median days of mechanical ventilation 48). Patients with COVID-SSC and SSC-CIP were comparable in most of the clinical parameters and transplant-free survival was not different from other forms of SSC (p = 0.443 in log-rank test). In the overall cohort, the use of ursodeoxycholic acid (UDCA, OR 0.36, 95%-CI 0.16–0.80, P = 0.013; P < 0.001 in log-rank test) and high serum albumin levels (OR 0.40, 95%-CI 0.17–0.96, P = 0.040) were independently associated with an increased transplant-free survival, while the presence of liver cirrhosis (OR 2.52, 95%-CI

POSTER PRESENTATIONS

1.01–6.25, $P=0.047$) was associated with worse outcome. MDRO colonization or infection did not impact patients' survival.



Conclusion: COVID-SSC and CIP-SSC share the same clinical phenotype, course of the disease and risk factors for its development. UDCA may be a promising therapeutic option in SSC, though future prospective trials need to confirm our findings.

THU445

The efficacy of combined treatment of bezafibrate and ursodeoxycholic acid was reduced in patients with primary cholangitis at advanced stage

Kosuke Matsumoto¹, Junko Hirohara², Toshiaki Nakano², Atsushi Tanaka¹. ¹Teikyo University School of Medicine, Department of Medicine, Tokyo, Japan; ²Kansai Medical University, The Third Department of Internal Medicine, Osaka, Japan
Email: m-kosuke0716@med.teikyo-u.ac.jp

Background and aims: Bezafibrate (BZF) is a dual PPARs/PXR agonist with potent anti-cholestatic efficacy. Previously, we took advantage of a large-scale retrospective cohort of patients with primary biliary cholangitis (PBC) in Japan and demonstrated that a combination of BZF and ursodeoxycholic acid (UDCA) was significantly associated with an improved liver transplantation (LT)-free survival in patients with PBC. Nevertheless, we found patients who deceased or underwent LT in this cohort even with a combination treatment of UDCA and BZF. In the current study, we explored baseline covariates which were significantly associated with poor outcome, death or LT, in patients treated with UDCA and BZF.

Method: The Japanese PBC cohort is established by the nation-wide surveys, initiated in 1980 and updated every 3 years by the Intractable Hepato-Biliary Diseases Study Group (Japan PBC Study Group). To date, 9,919 patients with PBC have been registered. Baseline covariates included age, sex, presence of symptoms, serum levels of bilirubin, alkaline phosphatase (ALP), and albumin. Primary outcome (liver-related death or LT) was assessed using multivariable adjusted Cox proportional hazard models.

Results: 1,739 patients were excluded from the analysis due to missing data in terms of outcome and final follow-up date. Among the remaining 8,180 patients, 889 patients (mean age at diagnosis 54.8yrs, 139 males (15.6%)) were treated with a combination of UDCA and BZF and enrolled in the current study. During 9.9 ± 6.8 yrs of mean observational period, 16 out of 889 (1.8%) reached primary end point (death in 15, LT in 1). By the Cox proportional hazard model, low albumin (<3.5 mg/dL) and high bilirubin (>1.5 mg/dL) at baseline were significantly associated with death or LT; adjusted hazard ratio (aHR) of low albumin was 5.511 (95% confidential interval 1.754–17.315, $p=0.003$), and aHR of high bilirubin was 9.986 (95% CI 3.097–32.199, $p<0.001$).

Conclusion: In patients with PBC at advanced stage who had low albumin or high bilirubin at baseline, the risk for death or LT was significantly increased compared to those with normal albumin or bilirubin even with a combination treatment of UDCA and BZF.

THU446

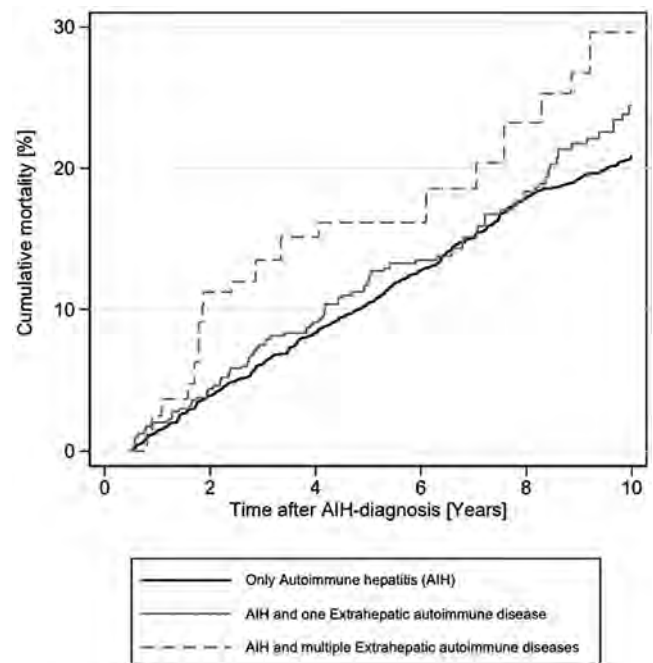
Extrahepatic autoimmune diseases in autoimmune hepatitis: effect on mortality

Rasmine Birn-Rydder¹, Morten Daniel Jensen¹, Peter Jepsen¹, Lisbet Groenbaek^{1,2}. ¹Aarhus University Hospital, Department of Hepatology and Gastroenterology, Aarhus, Denmark; ²Regional Hospital Horsens, Department of Medicine, Horsens, Denmark
Email: rasmine_br@live.dk

Background and aims: Autoimmune hepatitis (AIH) is a chronic inflammatory liver disease associated with an increased prevalence of extrahepatic autoimmune diseases and an increased mortality compared with the general population. The contribution of extrahepatic autoimmune diseases to the increased mortality has not yet been clarified. Our aim was to determine the effect of extrahepatic autoimmune diseases on mortality in patients with AIH.

Method: This nationwide register-based cohort study included all Danish patients diagnosed with AIH between 1995 and 2019. We examined the presence of extrahepatic autoimmune diseases concurrent with AIH in all included patients. We followed the patients until 30 April 2021 and calculated the cumulative mortality using the Kaplan-Meier estimator comparing AIH-patients with and without extrahepatic autoimmune diseases. We estimated the effect of extrahepatic autoimmune diseases on mortality using Cox regression adjusted for age at AIH-diagnosis, calendar year of AIH-diagnosis, sex, cirrhosis, and other comorbidities (cancer, chronic obstructive pulmonary disease, and ischemic heart disease).

Results: Our study included 2479 patients with AIH of whom 23.1% had one or more extrahepatic autoimmune diseases. The adjusted 10-year cumulative mortality was 27.3% (95% confidence interval [CI]: 25.3–29.4) in patients with extrahepatic autoimmune diseases and 21.6% (95% CI: 19.9–23.6) in patients without. The adjusted mortality hazard ratio was 1.28 (95% CI: 1.10–1.49) in AIH patients with vs. without concurrent extrahepatic autoimmune diseases; it was 1.22 (95% CI: 1.03–1.44) for patients with one extrahepatic autoimmune disease, and 1.59 (95% CI: 1.19–2.12) for those with more than one.



Conclusion: Extrahepatic autoimmune diseases increased the mortality in patients with AIH. Moreover, patients with multiple extrahepatic autoimmune diseases had higher mortality than patients with just one extrahepatic autoimmune disease.

THU447

Confidence in treatment is contributing to quality of life in patients with autoimmune liver diseases. The results of ERN-RARE Liver online survey

Ewa Wunsch¹, Linda Krause², Tom Gevers^{3,4}, Christoph Schramm^{4,5,6}, Maciej K. Janik^{4,7}, Marcin Krawczyk^{4,8,9}, Natalie Uhlenbusch^{4,10}, Bernd Löwe^{4,10}, Ansgar W. Lohse^{4,11}, Piotr Milkiewicz^{1,4,7}

¹Pomeranian Medical University in Szczecin, Translational Medicine Group, Szczecin, Poland; ²University Medical Centre Hamburg-Eppendorf, Institute of Medical Biometry and Epidemiology, Hamburg, Germany; ³Maastricht University Medical Center, Department of Internal Medicine, Maastricht, Netherlands; ⁴RARE-LIVER European Reference Network; ⁵University Medical Centre Hamburg-Eppendorf, Department of Medicine and Martin Zeitz Centre for Rare Diseases, Hamburg, Germany; ⁶Hamburg Center for Translational Immunology (HCTI), Hamburg, Germany; ⁷Medical University of Warsaw, Liver and Internal Medicine Unit, Warsaw, Poland; ⁸Saarland University Medical Center, Department of Medicine II, Homburg, Germany; ⁹Medical University of Warsaw, Laboratory of Metabolic Liver Diseases, Warsaw, Poland; ¹⁰University Medical Centre Hamburg-Eppendorf, Department of Psychosomatic Medicine and Psychotherapy, Hamburg, Germany; ¹¹University Medical Centre Hamburg-Eppendorf, Department of Medicine, Hamburg, Germany
Email: ewa.wunsch@gmail.com

Background and aims: Patients with autoimmune liver diseases (AILDs) have been reported to have an impaired health-related quality of life (HrQoL) in studies based on small sample sizes. The aim of this project was to investigate HrQoL in a large transnational cohort of patients with AILDs and to identify potentially modifiable factors in the context of impaired HrQoL.

Method: A cross-sectional online survey was conducted in patients with a diagnosis of autoimmune hepatitis (AIH), primary biliary cholangitis (PBC) or primary sclerosing cholangitis (PSC) from 15 European countries. HrQoL was measured with EQ-5D-5L and EQ visual analogue scale (EQ VAS) and analysed in relationship to demographic, psychosocial, disease- and treatment-related factors. A PHQ-2 score larger than two indicated clinically relevant depression. Multivariable linear regression analyses were used to identify potentially modifiable factors associated with HrQoL and confidence in treatment while adjusting for known confounders.

Results: A group of 1,178 European patients (470 with AIH, 368 with PBC and 317 with PSC, 79% female, mean age 48 ± 14 years) participated in the study. HrQoL was markedly impaired in all three liver diseases (mean EQ-5D-5L = 0.75, mean EQ VAS = 68.9), particularly in patients with PBC (mean EQ-5D-5L = 0.73, mean EQ VAS = 66.2). Clinically relevant depression was reported in 17% of the total sample. Depression, gender, age and advanced disease stage were expectedly associated with HrQoL. Confidence in treatment was identified as a modifiable factor strongly contributing to EQ-5D-5L in the entire cohort (reg. coef.: 0.12, 95%CI: 0.07 to 0.18, p < 0.001). PSC or PBC diagnosis, advanced disease stage, treatment in non-transplant center and depression were negatively associated with patients' confidence in their treatment (Figure).

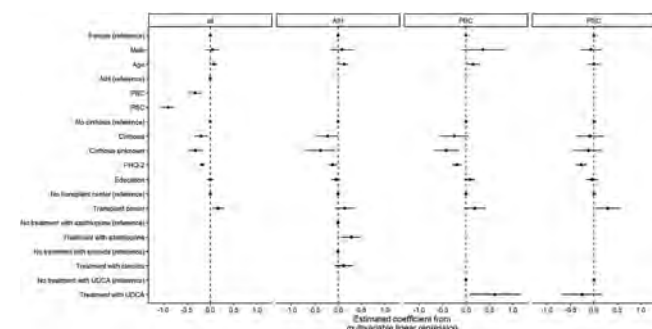


Figure: Factors associated with treatment confidence

Conclusion: Our analysis detects confidence in treatment as a novel central determinant of HrQoL in patients with AILDs. This modifiable and so far undepreciated factor should be further investigated in order to improve care for patients with AILDs.

THU448

A pilot study of PBC symptom management with melatonin and fenofibrate: the PIMBLE study

Beverly Rodrigues¹, Steven Nicolaides¹, Rohit Sawhney^{1,2}, Amanda Nicoll^{1,2}, Stephen Bloom^{1,2}, ¹Eastern Health, Gastroenterology; ²Eastern Health Clinical School, Monash University, Australia
Email: beverly.rodrigues91@gmail.com

Background and aims: Primary biliary cholangitis (PBC) disease progression is usually well controlled with ursodeoxycholic or obeticholic acid. Bezafibrate has shown benefits in refractory disease but is not available in Australia, and it is unknown if fenofibrate is similarly effective. Despite good biochemical response, the symptoms of pruritus, fatigue and altered sleep often remain. Melatonin may improve fatigue as demonstrated in animal models. We studied the short-term symptomatic and biochemical responses of PBC patients to melatonin and fenofibrate therapy.

Method: A randomised, cross-over 12-week intervention study examining symptoms and biochemistry in response to melatonin and fenofibrate between 20th July 2020–15th November 2021 inclusive.

Results: The interim results of 10 patients are shown in Table 1. Six out of 10 patients completed both trial arms, patient 10 optionally completed the melatonin arm only, and the remaining 3 are soon to complete arm 2 (n = 1 fenofibrate, n = 2 melatonin). Both agents were well tolerated overall; 3 patients had a mild rise in transaminases (<5x upper limit of normal) post commencement of fenofibrate. ALP improvement was seen in 6/8 on fenofibrate and 3/8 on melatonin, with degree of improvement meeting Paris II criteria in all trialled arms. Symptom improvement was seen in 6/8 on fenofibrate and 6/8 on melatonin.

Table 1: Descriptive analyses of clinical and biochemical responses to each trial arm

Patient	Age (years)	Gender	Abnormal ALP (baseline)	Fenofibrate arm						Melatonin arm							
				Improved ALP (Y/N)	Improved symptoms Y/N MFIS: SF36: VAS (itch)						Improved ALP (Y/N)	Improved symptoms Y/N MFIS: SF36: VAS (itch)					
					MFIS	SF36	VAS	MFIS	SF36	VAS		MFIS	SF36	VAS			
1	54.6	F	N	Y	N/A	Y	N	N	N/A	Y	Y	N					
2	68.8	F	N	Y	N/A	N/A	N/A	Y	N/A	N/A	N/A						
3	65.8	F	N	Y	Y	N	Y	Y	Y	N	Y						
4	57.8	F	N	N	Y	N	Y	N	Y	Y	Y						
5	72.7	F	N	N	Y	N	N	N	Y	N	N						
6	60.6	F	N	P	P	P	P	Y	N/A	N	N						
7	61.3	F	Y	Y	Y	N	N	P	P	P	P						
8	55.1	M	N	Y	P	P	P	N	N	N	Y						
9	52.9	M	N	Y	Y	N	N	P	P	P	P						
10	45.2	F	Y	N/A	N/A	N/A	N/A	N	Y	N	N						

Y = (Yes); N = (No); N/A = (not applicable or available); p = (pending)

Conclusion: This pilot study suggests that there is potential benefit in these therapies for PBC and further studies evaluating their efficacy is required.

THU449

Portal hypertension-associated clinical features in patients with primary biliary cholangitis are of distinct prognostic value

Lukas Burghart¹, Emina Halilbasic¹, Philipp Schwabl¹, Benedikt Simbrunner¹, Albert Stättermayer¹, Oleksandr Petrenko¹, Bernhard Scheiner¹, David JM Bauer¹, Matthias Pinter¹, Kaan Boztug¹, Mattias Mandorfer¹, Michael Trauner¹, Thomas Reiberger¹, ¹Medical University of Vienna, Austria
Email: burghartlukas@gmail.com

Background and aims: Primary biliary cholangitis (PBC) may progress to cirrhosis and clinically significant portal hypertension

POSTER PRESENTATIONS

(CSPH). This study assesses different features of CSPH and their distinct prognostic impact regarding decompensation and LTX-free survival in patients with PBC.

Method: Patients with PBC were identified during a database query of our digital patient reporting system.

Results: A total of 333 PBC patients (mean age: 54.3 years, 86.8% female, median follow-up: 5.8 years) were retrospectively assessed. Overall, 127 (38.1%) showed features of CSPH: 63 (18.9%) developed varices, 98 (29.4%) splenomegaly, 62 (18.6%) ascites and 20 (15.7%) experienced acute variceal bleeding.

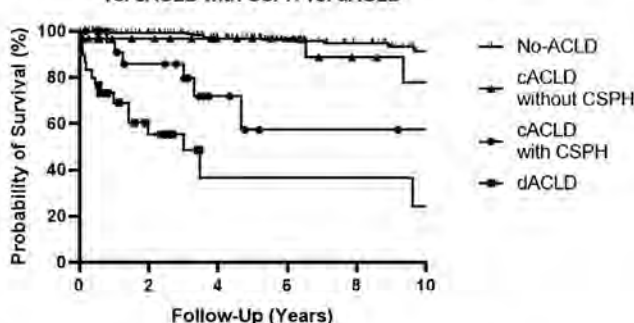
Splenomegaly, portosystemic collaterals and esophageal varices were associated with an increased 5-year (5Y) risk of decompensation (15.0%, 17.8% and 20.9%, respectively).

Patients without advanced chronic liver disease (ACLD) had a similar 5Y-transplant free survival (TFS) (96.6%) compared to patients with compensated ACLD (cACLD) but without CSPH (96.9%). On the contrary, PBC patients with cACLD and CSPH (57.4%) or decompensated ACLD (dACLD) (36.4%) had significantly decreased 5Y survival rates.

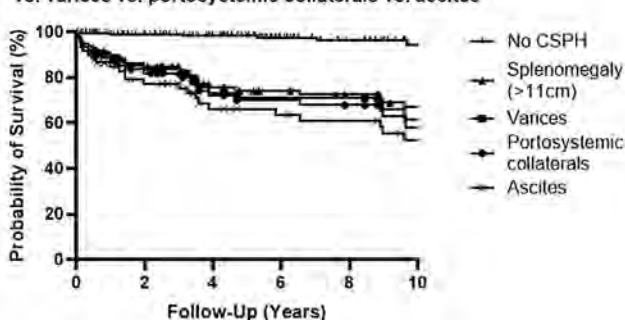
During a subanalysis, the combination of LSM <15 kPa and platelets ≥ 150 G/L indicated a negligible risk for decompensation (5Y 0.0%) and for mortality (5Y 0.0%).

Overall, 44 (13.2%) patients died, with 18 (40.9%) deaths attributed to CSPH-related complications.

(A) Survival with non-ACLD vs. cACLD without CSPH vs. cACLD with CSPH vs. dACLD



(B) Survival in patients without CSPH vs. splenomegaly vs. varices vs. portosystemic collaterals vs. ascites



Conclusion: In PBC, features of CSPH may occur early and indicate an increased risk for subsequent decompensation and mortality. Hence, regular screening and on-time treatment for CSPH is crucial. Combining LSM and platelets serves as a valuable preliminary assessment, as LSM <15 kPa and platelets ≥ 150 G/L indicate an excellent long-term outcome.

THU450

The low incidence of HBV reactivation among anti-HBc+ subjects on immunotherapy reduces the impact of suboptimal screening rate

Laia Aceituno¹, Juan Bañares¹, Lourdes Ruiz¹, Ana Callejo-Pérez², Eva Muñoz-Couselo², Carolina Ortiz-Velez², Nely Díaz-Mejía², Ana Barreira^{1,3}, Maria-Josep Carreras⁴, Anna Farriols⁴, Maria Buti^{1,3}, Mar Riveiro Barciela^{1,3}. ¹Hospital Vall Hebron, Liver Unit, Barcelona, Spain; ²Instituto de Oncología Vall d'Hebron (VHIO), Hospital Universitari Vall d'Hebron, Oncology Department, Barcelona; ³Centro de investigación biomédica en red de enfermedades hepáticas y digestivas, Madrid; ⁴Hospital Vall Hebron, Pharmacy Department, Barcelona
Email: mar.riveiro@gmail.com

Background and aims: Immunotherapy with check-point inhibitors (CPIs) has become the pillar of treatment of many advanced cancers. CPIs can reactivate Hepatitis B (HBV) in patients with chronic infection. However, there is scarce data on their possible impact on subjects with chronic hepatitis C or resolved HBV infection. To date, there is no evidence on awareness of Oncologists about the risk of prescribing CPIs for patients with viral hepatitis.

Method: Retrospective-prospective study of all patients who began Oncological immunotherapy between January 2019 and December 2020 in a University Hospital. Data on viral hepatitis screening prior to the beginning of CPIs were collected retrospectively. In subjects lacking information, serological tests were requested prospectively. HBV reactivation was defined as the increase of 2 log of HBV-DNA compared to baseline (HBsAg+ subjects) or reversed seroconversion to HBsAg+ or detectable HBV-DNA (isolated antiHBc+).

Results: 595 subjects received CPIs: 364 (61.2%) male, mean age 64 years (IQR 57–72). Most prevalent cancers: lung (34.8%), urinary (13.1%), melanoma (12.1%), gastrointestinal (11.6%), gynecological (9.2%). CPIs: anti-PD1 (64.2%), anti-PD-L1 (19.2%), combined therapy with anti-PD1 + anti-CTLA-4 (13.8%), anti-CTLA-4 alone (0.8%), others (2.0%). Time between cancer diagnosis and CPI beginning was 13 months (IQR 3–33). Forty-three (7.2%) patients had underlying liver disease, 15 (2.5%) of them cirrhosis and 16 (2.7%) hepatocellular carcinoma. In 460 (77.3%) subjects anti-HCV was requested prior to the beginning of immunotherapy, HBsAg in 459 (77.1%) and anti-HBc in 325 (55.8%), complete screening (anti-HCV, HBsAg and anti-HBc) in 325 (54.6%). In the remaining cases, serological tests were completed prospectively in those alive, leading to diagnosis of 1 case of HCV, 1 HBsAg+ and 22 antiHBc+. Overall hepatitis prevalence was: anti-HCV 3.6% (19/528), HBsAg 1.3% (7/528), anti-HBc 15.6% (74/473). All anti-HCV positive subjects presented undetectable viral load except two patients with hepatocellular carcinoma. Five out of the 7 HBsAg carriers received antiviral prophylaxis, leading to HBV reactivation in 1 case with previously unknown infection without prophylaxis. Only 1 anti-HBc+ subject received antiviral prophylaxis (HIV infection). Among the remaining anti-HBc+ individuals, just one isolated case of HBV reactivation was observed (1.4%).

Conclusion: HBV and HCV screening prior to Oncological immunotherapy is suboptimal, especially regarding anti-HBc+. Though the rate of HBV reactivation among anti-HBc+ subjects is very low, efforts should be done to optimize viral hepatitis screening prior to immunotherapy for selection of candidates to either antiviral prophylaxis or periodical check-up.

THU451

The ABCB4 variant c.711 increases liver injury in PBC but not in PSC: prospective analysis with a median follow-up of 7 years in 331 patients

Beata Kruk¹, Malgorzata Milkiewicz², Piotr Milkiewicz^{3,4}, Marcin Krawczyk^{1,5}. ¹Laboratory of Metabolic Liver Diseases, Department of General, Transplant and Liver Surgery, Medical University of Warsaw, Warsaw, Poland; ²Department of Medical Biology, Pomeranian Medical University in Szczecin, Szczecin, Poland; ³Liver and Internal Medicine Unit, Medical University of Warsaw, Warsaw, Poland; ⁴Translational Medicine Group, Pomeranian Medical University in Szczecin, Szczecin, Poland; ⁵Department of Medicine II, Saarland University Medical Center, Saarland University, Homburg, Germany
Email: marcin.krawczyk@uks.eu

Background and aims: Primary biliary cholangitis (PBC) and primary sclerosing cholangitis (PSC) are two progressive chronic cholestatic liver diseases. The ABCB4 gene encodes the hepatobiliary phospholipid transporter. Defects in the ABCB4 gene cause several cholestatic diseases (Stättermayer et al., J Hepatol. 2020). Here we aim to investigate role of the ABCB4 genetic variant in patients with PBC and PSC.

Method: We genotyped the ABCB4 c.711 polymorphism in a total of 331 patients with PBC and PSC who were prospectively recruited in our center from year 2005. The PBC cohort was composed 196 patients (173 females, median age 59 years, 49% with cirrhosis). The PSC cohort was composed of 135 patients (96 males, median age 35 years, 39% with cirrhosis). Clinical data were collected at least at two time points: The follow-up ranged from 2 to 20 years (median: 7 years) The PBC-40 and Short Form (SF-36) questionnaires were used for assessment health related quality of life.

Results: Allele and genotype distributions of the ABCB4 variant in patients with PBC and PSC cohort were consistent with Hardy-Weinberg equilibrium ($p > 0.05$). At baseline, the ABCB4 c.711 variant was associated with an increased cirrhosis risk ($OR = 1.84$, $p = 0.02$) in the PBC cohort, the risk of cirrhosis was also modulated by patients gender ($p < 0.01$). Carriers of heterozygote genotype showed significantly increased serum AST ($p = 0.02$), GGTP ($p < 0.01$) and ALP ($p < 0.01$). Although we detected significant improvements in laboratory findings (i.e., AST, ALT, ALP and GGTP) during the follow-up, a total of 22 patients developed new cirrhosis and this risk was significantly modulated by the ABCB4 polymorphism ($OR = 5.65$, $p = 0.04$). On the other hand, the ABCB4 genotype did not affect life quality in either of the cohorts, did not modulate liver injury in patients with PSC did not increase the odds of requiring transplantation (all $p > 0.05$).

Conclusion: The ABCB4 c.711 polymorphism might represent a common risk genetic factors for progressive liver injury in PBC. Carriers of the c.711 ABCB4 might require more aggressive therapy to lower the progression of liver scarring.

THU452

A multicentric study to estimate mortality and graft loss risk after liver transplantation (LT) in patients with recurrent primary biliary cholangitis (PBC)

Aldo J Montano-Loza¹, Thierry Berney², Christian Toso², Giulia Magini², Gideon Hirschfield³, Bettina Hansen³, Andrew L. Mason¹, Maryam Ebadi¹, Frederik Nevens⁴, Natalie Van den Ende⁴, Debora Raquel Terrabuio⁵, Albert Parés⁶, Pablo Ruiz⁷, Alan Bonder⁸, Ellina Lytyak¹, Adriaan Van der Meer⁹, Rozanne de Veer⁹, Annarosa Floreani¹⁰, Nora Cazzagon¹⁰, Stefania Casu¹¹, Francesco Paolo Russo¹⁰, Mark Pedersen¹², Marlyn J. Mayo¹², Michael P. Manns¹³, Richard Taubert¹⁴, Theresa Kirchner¹³, Thomas Schiano¹⁵, Brandy Haydel¹⁵, Xavier Verhelst¹⁶, Mercedes Robles-Díaz¹⁷, Miguel Jiménez-Pérez¹⁸, Jérôme Dumortier¹⁹, Ansgar Lohse²⁰, Christoph Schramm²⁰, Darius Ruether²⁰, Benedetta Terziroli Beretta-Piccoli²¹, Maria Francesca Donato²², Christophe Corpechot²³. ¹University of Alberta, Canada; ²Geneva University Hospitals, Switzerland; ³Toronto Center for Liver Disease, Canada; ⁴Division Liver and Biliopancreatic Disorders, Belgium; ⁵University of São Paulo School of Medicine, Brazil; ⁶University of Barcelona, Spain; ⁷Liver Unit, Hospital Clínic, Spain; ⁸Beth Israel Deaconess Medical Center, United States; ⁹Erasmus MC, Netherlands; ¹⁰University of Padova, Italy; ¹¹Universitätsspital Bern, Switzerland; ¹²Southwestern University, United States; ¹³Hannover Medical School, Germany; ¹⁴Dept. Gastroenterology, Hepatology and Endocrinology, Hannover Medical School, Germany; ¹⁵Mount Sinai Medical Center, United States; ¹⁶Ghent University Hospital, Belgium; ¹⁷University Hospital Virgen de la Victoria, Spain; ¹⁸Málaga Regional Hospital, Spain; ¹⁹Croix Rousse Hospital and Edward Herriot Hospital, France; ²⁰University Medical Center Hamburg-Eppendorf, Germany; ²¹Epatocentro Ticino, Switzerland; ²²Fondazione IRCCS Maggiore Hospital Policlinico Milan, Italy; ²³Saint-Antoine Hospital, France
Email: montanol@ualberta.ca

Background and aims: Recurrent PBC (rPBC) developed in approximately 30% of patients, and negatively impacts graft and patient survival after LT. Liver function tests and scores to evaluate response to ursodeoxycholic acid (UDCA) have been developed to monitor disease progression and evaluate the addition of second-line treatments before LT. We aimed to evaluate the utility of serum liver function tests and the GLOBE and UK-PBC scores to predict graft and overall survival after LT in patients with rPBC.

Method: A total of 231 patients who had a liver biopsy-proven diagnosis of rPBC after LT from 18 centers across Europe, North and South America, were evaluated. The mean age at the time of rPBC was 58 ± 10 years, and 206 patients (89%) were women. At the time of rPBC, 145 patients (63%) were receiving tacrolimus, and 78 (34%) with cyclosporine. The biochemical response was measured with alkaline phosphatase (ALP) and bilirubin, and continuous prognostic (GLOBE and UK-PBC scores) at 1-year after UDCA was started. Graft loss was defined using a death-censored definition of graft failure and therefore, graft loss did not include patients who died with a functioning graft. Cox regression analysis was performed to determine associations between biochemical markers, scores and graft loss and mortality.

Results: A total of 219 patients (95%) received treatment with UDCA after rPBC diagnosis. During a median follow-up 9.16 ± 5.47 years, 47 patients (20%) had lost graft and 76 (33%) died. Graft survival after rPBC was 92% and 85%, and overall survival was 87% and 76%, at 5-, and 10-years, respectively. Use of tacrolimus or cyclosporine was not associated with graft or overall survival. Serum ALP (HR 1.002, 95% CI 1.001–1.004, $p = 0.01$), and bilirubin (HR 1.009, 95% CI 1.004–1.015, $p = 0.001$) at 1-year after UDCA were associated with graft survival. The GLOBE (HR 2.45, 95% CI 1.45–4.16, $p < 0.001$) and UK-score 5-year formula (2.99, 95% CI 0.48–18.77, $p < 0.001$) at 1-year after UDCA initiation were associated with graft survival. In addition, serum ALP (HR 1.31, 95% CI 1.10–1.55, $p = 0.002$), and bilirubin (HR 1.008, 95% CI 1.004–1.012, $p < 0.001$) at 1-year after UDCA initiation were

POSTER PRESENTATIONS

associated with overall survival. The GLOBE (HR 2.04, 95% CI 1.38–3.01, $p < 0.001$) and UK-score 5-year formula (1.94, 95% CI 0.37–10.05, $p < 0.001$) at 1-year after UDCA were associated with overall survival. Patients with an ALP $> 2 \times$ ULN (Figures 1a–b) and bilirubin $> 1 \times$ ULN (Figures 1c–d) at 1-year of UDCA treatment had worse graft and overall survival. Only two (1%) and 10 patients (4%) started second-line treatment with obeticholic acid and fibrates, respectively.

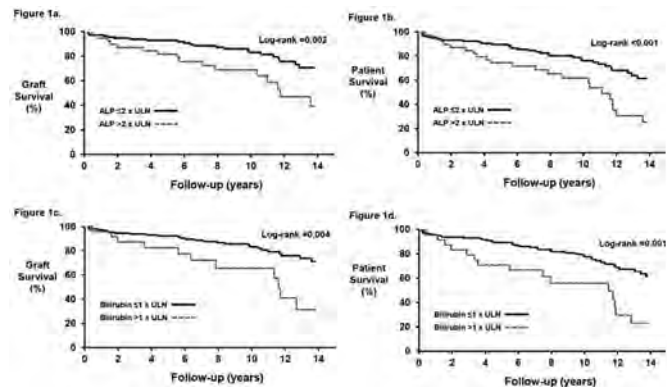


Figure: Graft and patient survival according to ALP and bilirubin at 1-year of UDCA.

Conclusion: Patients with rPBC and disease activity as indicated by standard PBC risk scores have impaired outcomes, supporting efforts to treat recurrent disease in similar ways to pre-transplant PBC.

THU453

Associations between novel serum biomarkers chitinase-2-like protein (YKL-40), type IV collagen, and thrombospondin-2 (TSP-2) with fibrosis stage and clinical outcomes in patients with primary sclerosing cholangitis (PSC)

Michael Trauner¹, Andrew Muir², Jun Xu³, Mina Khoshdeli³, Bryan Downie³, Andrew Billin³, Chuhan Chung³, Robert Myers³, Zachary Goodman⁴, Mitchell Shiffman⁵, Harry Janssen⁵, Aldo J Montano-Loza⁶, Stephen Caldwell⁷, Velimir Luketic⁸, Michael P. Manns⁹, Cynthia Levy¹⁰, Christopher Bowlus¹¹. ¹Medical University of Vienna, Vienna, Austria; ²Duke Clinical Research Institute, Durham, United States; ³Gilead Sciences, Inc., Foster City, United States; ⁴Inova Fairfax Hospital, Falls Church, United States; ⁵Bon Secours Mercy Health, Liver Institute of Virginia, United States; ⁶University of Alberta, Edmonton, Canada; ⁷University of Virginia, Charlottesville, United States; ⁸VCU Medical Center, Richmond, United States; ⁹University of Miami, Hannover, Germany; ¹⁰University of Miami, Miami, United States; ¹¹University of California Davis, Davis, United States
Email: jun.xu@gilead.com

Background and aims: Primary sclerosing cholangitis (PSC) is a chronic and progressive fibrotic liver disease associated with an increased risk of liver-related complications and mortality. Non-invasive biomarkers of fibrosis are needed for risk stratification and monitoring of PSC patients. YKL-40, TSP-2, and type IV collagens (α -subunit) are biomarkers of liver injury, inflammation, or extracellular matrix turnover during hepatic fibrogenesis. Our study aimed to evaluate associations between these biomarkers with fibrosis stage and PSC-related clinical events in a longitudinal study.

Method: Serum biomarkers YKL-40, TSP-2, and COL4A1 were measured via ELISA at baseline (BL) and Week 96 (W96) in PSC patients enrolled in a 96-week, phase 2 trial of simtuzumab (NCT01672853). Since simtuzumab was ineffective in this trial, data from the treatment and placebo groups were combined. Fibrosis was staged according to the Ishak classification and biomarker values were log-transformed. Odds ratios (OR) for associations between BL biomarker values with progression to cirrhosis (Ishak 5–6) at W96 among non-cirrhotic patients (Ishak 0–4) at BL were calculated using logistic regression models.

Results: At BL, serum COL4A1 and TSP-2 were moderately correlated with other serum markers, including ELF score, AST, ALP, and GGT (Spearman correlations $\rho = 0.38$ – 0.74 , all $p < 0.001$). YKL-40 demonstrated weaker but significant correlations to ALP, AST and ELF score ($\rho = 0.24$ – 0.54 , $p < 0.05$). TSP-2 and COL4A1 were increased with fibrosis stage in PSC patients (both $p < 0.001$), but YKL-40 was increased mainly in patients with cirrhosis (Figure). By W96, 44 patients (20%) developed a PSC-related clinical event (hepatic decompensation, cholangiocarcinoma, ascending cholangitis, or jaundice). Compared with patients without events ($n = 175$), those with events had higher YKL-40 (median 42.5 vs 29.0 ng/ml, $p = 0.001$), COL4A1 (168.4 vs 121.1 ng/ml, $p < 0.001$) and TSP-2 (85.0 vs 50.4 pg/ml, $p < 0.001$) at BL. Among 176 non-cirrhotic patients at BL, 27 progressed to cirrhosis at W96. Compared with patients without progression to cirrhosis ($n = 149$), those with progression had higher BL levels of YKL-40 (OR = 1.91, $p = 0.002$), TSP-2 (OR = 4.24, $p < 0.001$), and COL4A1 (OR = 8.24, $p < 0.001$). In addition, patients with progression to cirrhosis had greater relative increases from BL to W96 in YKL-40 (median 45.8% vs 11.8%, $p < 0.001$), COL4A1 (34.9% vs 3.4%, $p = 0.0025$) and TSP-2 (24.7% vs 0.1%, $p < 0.001$).

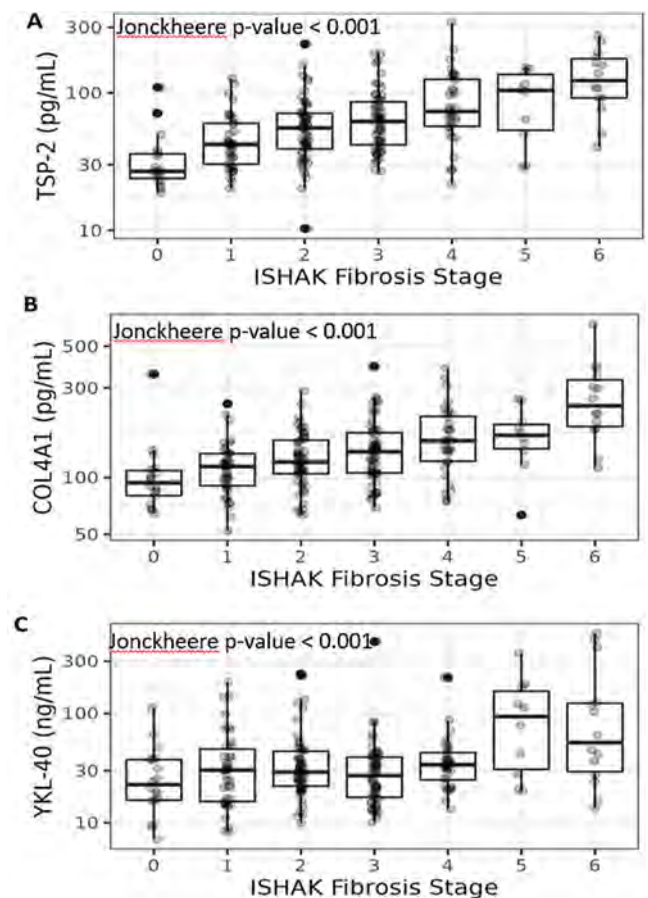


Figure: Associations between serum COL4A1, TSP-2, and YKL-40 and Ishak fibrosis stage

Conclusion: Serum levels of the novel fibrosis markers YKL-40, TSP-2, and COL4A1 are associated with fibrosis stage, progression to cirrhosis, and liver-related clinical events in patients with PSC. The utility of these biomarkers for the staging of fibrosis, risk stratification, and disease monitoring in PSC will be explored in additional studies.

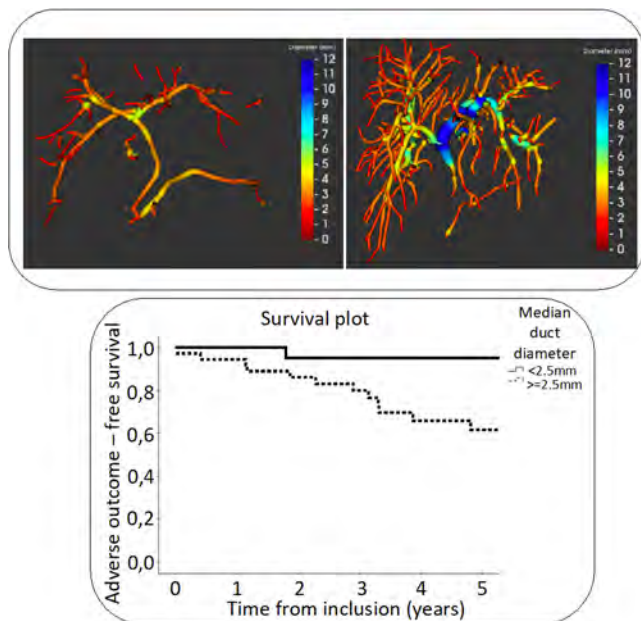
THU454

MRCP+TM-derived biliary metrics are associated with disease severity and clinical outcomes in patients with primary sclerosing cholangitis

Nora Cazzagon^{1,2}, Sanaa El Mouhadi³, Quentin Vanderbecq³, Carlos Ferreira⁴, Sara Lemoine¹, Christophe Corpechot¹, Olivier Chazouillères¹, Lionel Arrivè³. ¹Assistance Publique-Hôpitaux de Paris, Sorbonne University, INSERM, Reference Center for Inflammatory Biliary Diseases and Autoimmune Hepatitis and Saint-Antoine Research Center (CRM MIVB-H, ERN RARE-LIVER), Saint-Antoine Hospital, Paris, France, Paris, France; ²Department of Surgery, Oncology and Gastroenterology, University of Padova, European Reference Network on Hepatological Diseases (ERN RARE-LIVER), Azienda Ospedale-Università Padova, Padova, Italy, Padova, Italy; ³Assistance Publique-Hôpitaux de Paris, Sorbonne University, Department of Radiology, Saint-Antoine Hospital, Paris, France, Paris, France; ⁴Perspectum Ltd, Oxford UK, Oxford, United Kingdom
Email: nora.cazzagon@gmail.com

Background and aims: Patients with primary sclerosing cholangitis (PSC) have a variable, and often progressive disease course which is associated with biliary and parenchymal changes. These changes are typically assessed by magnetic resonance imaging (MRI), including magnetic resonance cholangiopancreatography (MRCP). Our aim was to study the association of novel quantitative MRCP metrics with prognostic scores and patient outcomes.

Method: We performed a retrospective study including 77 large-duct PSC patients with baseline MRCP images, which were post-processed to obtain quantitative measures of bile ducts and biliary volume using MRCP+™ (Perspectum Ltd, Oxford). The participants' ANALI scores, liver stiffness (measured by vibration controlled transient elastography) and biochemical indices were collected at baseline. Adverse outcome-free survival was measured as the absence of decompensated cirrhosis and liver transplantation. The prognostic value of MRCP+™ derived metrics was assessed by univariate analysis and multivariate Cox regression modelling.



Results: During a total 386 patients-years, we recorded 16 cases of decompensated cirrhosis, 2 liver transplantations and 5 liver-related deaths. At baseline, ~50% of the patients were classified as being at risk of developing disease complications based on radiological, elastographic, and biochemical prognostic scores. MRCP+™ metrics, particularly those describing the severity of bile duct dilatations,

were correlated with all prognostic factors. Univariate analysis showed that MRCP+ metrics representing duct diameter, dilatations, and the percentage of ducts with strictures and/or dilatations were associated with survival. According to the multivariate Cox regression model, the median duct diameter was independently associated with adverse outcome-free survival over 5 years (HR 10.9, 95% CI 1.3–90.3, $p = 0.027$) (Figure). Biliary tree volume was significantly higher in patients with advanced disease as defined by the ANALI scores.

Conclusion: MRCP+™ metrics demonstrated a significant correlation with biochemical, elastographic and radiological prognostic scores and were predictive of patients' outcomes highlighting its prognostic utility in PSC.

THU455

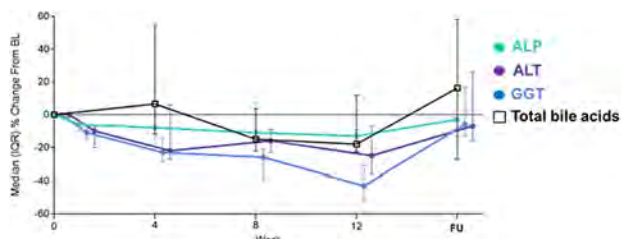
Safety and efficacy of the farnesoid X receptor (FXR) agonist cilofexor in a proof-of-concept study in patients with compensated cirrhosis due to primary sclerosing cholangitis (PSC)

Cynthia Levy¹, Stephen Caldwell², Parvez Mantry³, Velimir Luketic⁴, Charles Landis⁵, Jonathan Huang⁶, Edward Mena⁷, Rahul Maheshwari⁸, Kevin Rank⁹, Jun Xu¹⁰, Xiangyu Lu¹⁰, Xiaomin Lu¹⁰, Chuhan Chung¹⁰, Robert Myers¹⁰, Kris Kowdley¹¹. ¹University of Miami Miller School, Miami, United States; ²University of Virginia School of Medicine, Charlottesville, United States; ³The Liver Institute At Methodist Dallas, Dallas, United States; ⁴VCU School of Medicine, Richmond, United States; ⁵University of Washington School of Medicine, Seattle, United States; ⁶University of Rochester School of Medicine and Dentistry, Rochester, United States; ⁷Pasadena Liver Center, Pasadena, United States; ⁸Piedmont Transplant Institute, Atlanta, United States; ⁹MNGI Digestive Health-Northeast Minneapolis Clinic, Minneapolis, United States; ¹⁰Gilead Sciences, Inc., Foster City, United States; ¹¹Liver Institute Northwest, Seattle, United States
Email: clevery@med.miami.edu

Background and aims: Cilofexor (CILO) is a nonsteroidal FXR agonist being evaluated in the phase 3 PRIMIS trial of non-cirrhotic patients with PSC. The safety and efficacy of CILO in patients with cirrhosis is unknown. This proof-of-concept, open-label study evaluated the safety and efficacy of escalating doses of CILO in patients with PSC and cirrhosis.

Method: Subjects with PSC and compensated cirrhosis were treated with escalating doses of CILO for 12 weeks (30, 60, and 100 mg daily for 4-week intervals). Safety, liver biochemistry, and serum markers of fibrosis, cellular injury, and pharmacodynamic effects of CILO (bile acids [BAs]) were evaluated.

Results: Among 19 subjects screened, 11 were enrolled and 10 (91%) completed the study. The median age was 48 years, 55% were male, 55% had IBD, and 46% were on ursodeoxycholic acid. At baseline (BL), median (IQR) laboratory parameters were: total bilirubin 1.1 mg/dL (0.8, 1.5), albumin 4.0 g/dL (3.9, 4.6), INR 1.0 (0.9, 1.1), platelets $201 \times 10^3/\mu\text{L}$ (113, 218), ALP 510 U/L (269, 592), and GGT 344 U/L (208, 455). BL ELF and liver stiffness by transient elastography were 10.4 (9.5, 12.6) and 18.0 kPa (8.5, 67.6), respectively. At week 12 (W12), liver biochemistry tests improved relative to BL values including serum ALP (median: -13% [IQR: -22, -9]; $p = 0.006$), GGT (-43% [-52, -31]; $p = 0.002$), ALT (-25% [-36, -7]; $p = 0.012$), and AST (-12% [-29, 7]; $p = 0.32$), and rebounded after 4 weeks of untreated follow-up (Figure). Total bilirubin decreased at W12 relative to BL (-13% [-25, 0], $p = 0.13$), while albumin and INR remained stable. Among 10 subjects with detectable serum BAs at baseline (26.1 $\mu\text{M/L}$ [19.7, 52.9]), median change in BAs at W12 was -18% (-23, 12; $p = 0.73$). One patient discontinued treatment prematurely (subject decision). While no treatment-emergent (TE) serious adverse events (AEs) or deaths occurred in the study, Grade 2 or higher TEAEs occurred in 5 subjects (45%). Pruritus was reported by 8 subjects (73%), the majority (7 of 8) being Grade 1 or 2.



ALP, $p=0.006$; GGT, $p=0.002$; ALT, $p=0.012$; total bile acids, $p=NS$ at W12 versus baseline. 4-week dose escalation regimen, 30 mg at BL, 60 mg at W4, and 100 mg at W8.

Conclusion: In this proof-of-concept study of patients with compensated cirrhosis due to PSC, escalating doses of CIO over 12 weeks were well tolerated and improved markers of cholestasis and liver biochemistry.

THU456

Association between patient-reported outcome measures and surrogate markers of liver fibrosis in large-duct primary sclerosing cholangitis

Emmanuel Selvaraj^{1,2,3}, Jane D. Collier², Emma Culver², J Michael Brady^{4,5}, Adam Bailey^{2,3}, Michael Pavlides^{1,2,3}. ¹University of Oxford, Oxford Centre for Clinical Magnetic Resonance Research, Radcliffe Department of Medicine, Oxford, United Kingdom; ²University of Oxford, Translational Gastroenterology Unit, Nuffield Department of Medicine, Oxford, United Kingdom; ³NIHR Oxford Biomedical Research Centre, Oxford University Hospitals NHS Foundation Trust, Oxford, United Kingdom; ⁴University of Oxford, Department of Oncology, Oxford, United Kingdom; ⁵Perspectum Ltd., Oxford, United Kingdom
Email: emmanuel.selvaraj@cardiov.ox.ac.uk

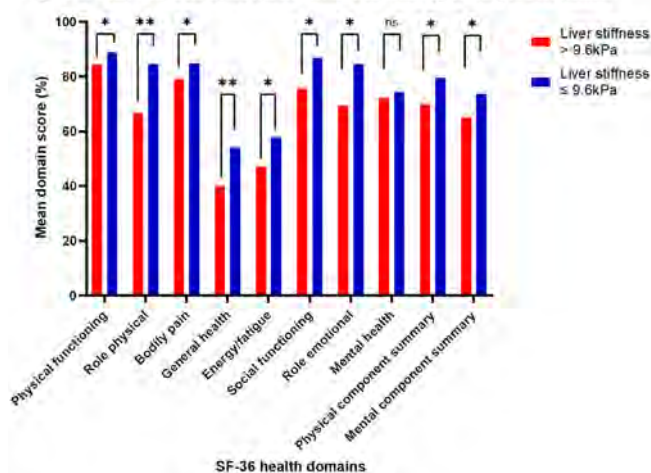
Background and aims: Liver fibrosis is the main driver of disease progression in primary sclerosing cholangitis (PSC). Patient-reported outcome measures (PROMs) are increasingly used as exploratory end points in clinical trials. The aim of this study was to investigate the impact of liver fibrosis on health-related quality of life (HrQoL) using generic (SF-36) and disease-specific (PSC-PRO) tools.

Method: Patients with large-duct PSC were invited to complete HrQoL questionnaires in an outpatient setting. SF-36 and PSC-PRO domains were scored out of a maximum of 100% and 5, respectively. Mean scores were calculated for each health domain with lower SF-36 and higher PSC-PRO scores representing poorer quality of life. Transient elastography liver stiffness (LS; Echosens, France), enhanced liver fibrosis (ELF; Siemens Healthineers, Germany) and LiverMultiScan-derived iron-corrected T1 (cT1; Perspectum, Oxford, UK) were obtained on the same day. Advanced fibrosis was defined as LS >9.6 kPa and ELF >9.8 according to published cut-offs in PSC.

Results: Eighty patients (68% male) with median age 42 years (range: 18–76) and median PSC duration 8 years (range: 1–25) completed both HrQoL questionnaires. Median cT1 was 760ms (range: 640–1053), median LS was 6.9 kPa (range: 3.7–45.5) and median ELF was 9.4 (range: 8.0–13.7). For the SF-36, median cT1 correlated with all health domains. Mental health ($\rho = -0.37$, $p < 0.01$), bodily pain ($\rho = -0.31$, $p < 0.01$) and physical functioning ($\rho = -0.31$, $p < 0.01$) showed the strongest correlations. LS also correlated with all domains of SF-36 with bodily pain ($\rho = -0.28$, $p = 0.02$), social functioning ($\rho = -0.27$, $p = 0.02$) and physical functioning ($\rho = -0.25$, $p = 0.03$) showing the strongest correlations, albeit weaker than median cT1. ELF did not correlate with any of the SF-36 domains. SF-36 scores were lower in patients with advanced fibrosis defined by LS cut-off, particularly for role physical (67% vs 85%, $p < 0.01$) and general health (40% vs 54%, $p < 0.01$) domains (Figure 1). For the PSC-PRO, median cT1 did not correlate with any of the domains. Physical function correlated with LS ($\rho = 0.30$, $p < 0.01$) and ELF ($\rho = 0.26$, $p = 0.02$) with higher scores in those with advanced fibrosis (LS: 1.5 vs 1.2,

$p = 0.01$; ELF: 1.5 vs 1.2, $p = 0.02$). Activities of daily living correlated with LS ($\rho = 0.26$, $p = 0.02$) and ELF ($\rho = 0.25$, $p = 0.03$) with higher scores in those with advanced fibrosis (LS: 1.5 vs 1.2, $p = 0.01$; ELF: 1.5 vs 1.3, $p = 0.03$).

Figure 1: Mean scores for SF-36 health domains stratified by severity of liver fibrosis



Conclusion: SF-36 and PSC-PRO health domains showed significant correlations with surrogate markers of liver fibrosis. Advanced fibrosis appears to have a greater impact on the physical than mental components of both PROMs. Future antifibrotic drug trials in PSC should consider assessing the impact of drug on physical well-being as one of the secondary end points.

THU457

Association between patient-reported outcome measures and severity of cholangiopathy in large-duct primary sclerosing cholangitis

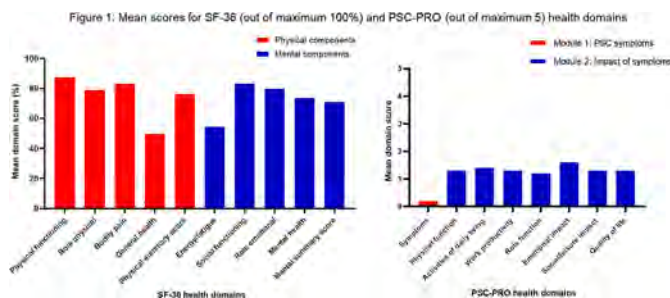
Emmanuel Selvaraj^{1,2,3}, Ahmed Ba-Ssalamah⁴, Sarah Poetter-Lang⁴, Jane D. Collier², Emma Culver², J Michael Brady^{5,6}, Adam Bailey^{2,3}, Michael Pavlides^{1,2,3}. ¹University of Oxford, Oxford Centre for Clinical Magnetic Resonance Research, Radcliffe Department of Medicine, Oxford, United Kingdom; ²University of Oxford, Translational Gastroenterology Unit, Nuffield Department of Medicine, Oxford, United Kingdom; ³NIHR Oxford Biomedical Research Centre, Oxford University Hospitals NHS Foundation Trust, Oxford, United Kingdom; ⁴Medical University of Vienna, Department of Biomedical Imaging and Image-Guided Therapy, Vienna, Austria; ⁵University of Oxford, Department of Oncology, Oxford, United Kingdom; ⁶Perspectum Ltd., Oxford, United Kingdom
Email: emmanuel.selvaraj@cardiov.ox.ac.uk

Background and aims: Magnetic resonance cholangiopancreatography (MRCP) is used alongside serum alkaline phosphatase (ALP) to assess the severity of cholangiopathy in primary sclerosing cholangitis (PSC). Patient-reported outcome measures (PROMs) are increasingly used as exploratory end points in clinical trials. The aim of this study was to investigate the impact of ALP and the severity of cholangiopathy on MRCP on health-related quality of life (HrQoL) using generic (SF-36) and disease-specific (PSC-PRO) tools.

Method: Patients with large-duct PSC were invited to complete HrQoL questionnaires in an outpatient setting. SF-36 and PSC-PRO domains were scored out of a maximum of 100% and 5, respectively. Mean scores were calculated for each health domain with lower SF-36 and higher PSC-PRO scores representing poorer quality of life. 3D MRCP and serum ALP were acquired on the same day. Two radiologists reviewed MRCP images for the presence of dominant stricture (DS) and measured the maximum intrahepatic bile duct dilatation (IHBD) for Anali score. Images were analysed using a quantitative biliary tool, MRCP+ (Perspectum, Oxford, UK) to compute

the intrahepatic sum of relative severity of dilatations (SumRelSevDilat). Patients were classified into high or low risk group for disease progression using ALP cut-off 1.5x upper limit normal (ULN) and the presence of DS.

Results: Eighty patients (68% male) with median age 42 years (range: 18–76) and median PSC duration 8 years (range: 1–25) completed both questionnaires. Median ALP was 150 IU/ml (range: 48–1180). DS was reported in 25 (31%) patients. Maximum IHBD was ≤ 3 mm in 26 (33%), 4 mm in 19 (23%) and ≥ 5 mm in 35 (44%) patients. Median MRCP+–derived SumRelSevDilat was 7.0mm^{-1} (range: 0.0–19.8). The mean score for each health domain is shown in Figure 1 below. DS correlated with SF-36 bodily pain ($\rho = -0.28$, $p = 0.02$). Maximum IHBD correlated with PSC-PRO physical function domain ($\rho = 0.36$, $p < 0.01$). SumRelSevDilat correlated with physical functioning ($\rho = -0.25$, $p = 0.04$) and bodily pain ($\rho = -0.26$, $p = 0.03$) domains of SF-36, and the physical function ($\rho = 0.26$, $p = 0.03$) and activities of daily living ($\rho = 0.29$, $p = 0.01$) domains of PSC-PRO. ALP correlated with bodily pain ($\rho = -0.37$, $p < 0.01$), general health ($\rho = -0.26$, $p = 0.03$), and energy/fatigue ($\rho = -0.29$, $p = 0.01$) domains of SF-36, and the physical function ($\rho = 0.30$, $p < 0.01$) and emotional impact ($\rho = 0.38$, $p < 0.01$) domains of PSC-PRO. Bodily pain score was lower in those with DS compared to those without (74% vs 87%, $p = 0.02$). Both physical functioning (80% vs 92%, $p = 0.04$) and bodily pain (78% vs 85%, $p = 0.03$) scores were lower in patients with ALP greater than 1.5x ULN.



Conclusion: The presence of DS, severity of intrahepatic biliary dilatations, and ALP $>1.5\times$ ULN have a significant impact on both physical and mental health of patients with large-duct PSC.

THU458

Ultrasound for the diagnosis of gallbladder polyps in PSC: polyps greater than 8 mm indicate malignancy

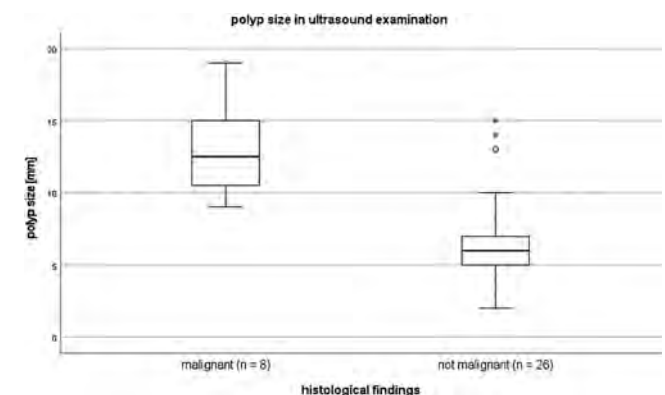
Johannes Altenmüller¹, Marcial Sebode^{2,3}, Christina Weiler-Normann^{2,4}, Christiane Wiegand², Ansgar Lohse^{2,3,5}, Christoph Schramm^{2,3,4,5}. ¹University Medical Center Hamburg-Eppendorf, Hamburg, Germany; ²University Medical Center Hamburg-Eppendorf, 1st Department of Medicine, Hamburg, Germany; ³European Reference Network on Hepatological Diseases (ERN RARE-LIVER); ⁴University Medical Center Hamburg-Eppendorf, Martin Zeitz Centre for Rare Diseases, Hamburg, Germany; ⁵University Medical Center Hamburg-Eppendorf, Hamburg Center for Translational Immunology, Hamburg, Germany
Email: 6817657@stud.uke.uni-hamburg.de

Background and aims: The risk of gallbladder carcinoma is increased in primary sclerosing cholangitis (PSC). Surveillance imaging every 6–12 months is used for early diagnosis. The aim of the study is to assess the reliability of ultrasound and MRI in detecting gallbladder polyps in people with PSC.

Method: All patients with PSC and a history of cholecystectomy were included for the evaluation and comparison of the two imaging methods, ultrasound and MRI for the detection of gallbladder polyps. Data including gallbladder histology were gathered retrospectively from the electronic medical records. Polyps with high-grade

dysplasia were assigned to the malignancy group. We determined a cut-off for detecting malignant polyps in ultrasound using a receiver operating characteristics curve.

Results: From a cohort of 596 people with PSC at the University Medical Center Hamburg-Eppendorf, 139 patients underwent cholecystectomy. 77 patients underwent cholecystectomy for a suspected underlying gallbladder pathology. In 37 of those patients (21 m, 16 f) the detection of a polyp on imaging was the indication for surgery. Additionally, 62 patients had their gallbladder removed in the context of other interventions such as liver transplantation. Looking at all 139 cholecystectomy patients, ultrasound (sensitivity = 100%) was significantly more sensitive than MRI in detecting gallbladder polyps (sensitivity = 35%) ($p < 0.001$). MRI missed 3 of the 8 polyps with malignant histology. In ultrasound, malignant polyps ($n = 8$, median size = 13 mm) were found to be significantly larger than non-malignant polyps ($n = 26$, median size = 6.6 mm) ($p < 0.001$). Ultrasound was able to reliably detect a malignant polyp (area under the curve = 0.92, $p < 0.001$). At a cut-off value of 8 mm, sensitivity was 100% and specificity was 81%.



Conclusion: In people with PSC, ultrasound is more sensitive in the detection of gallbladder polyps than MRI. Based on the size of polyps, a reliable distinction can be made between malignant and benign findings: no malignant polyp was smaller than 8 mm. This validates previously published data from the Mayo Clinic. Cholecystectomy needs to be offered if a polyp of 8 mm or more is detected. Therefore, ultrasound and MRI may be complementary methods for hepatobiliary malignancy surveillance in people with PSC. A multicentre validation of the data is ongoing.

THU459

Temporal changes in patient-reported outcome measures stratified by liver fibrosis severity in large-duct primary sclerosing cholangitis

Emmanuel Selvaraj^{1,2,3}, Jane D. Collier², Emma Culver², J Michael Brady^{4,5}, Adam Bailey^{2,3}, Michael Pavlides^{1,2,3}. ¹University of Oxford, Oxford Centre for Clinical Magnetic Resonance Research, Radcliffe Department of Medicine, Oxford, United Kingdom; ²University of Oxford, Translational Gastroenterology Unit, Nuffield Department of Medicine, Oxford, United Kingdom; ³NIHR Oxford Biomedical Research Centre, Oxford University Hospitals NHS Foundation Trust, Oxford, United Kingdom; ⁴University of Oxford, Department of Oncology, Oxford, United Kingdom; ⁵Perspectum Ltd., Oxford, United Kingdom
Email: emmanuel.selvaraj@cardiov.ox.ac.uk

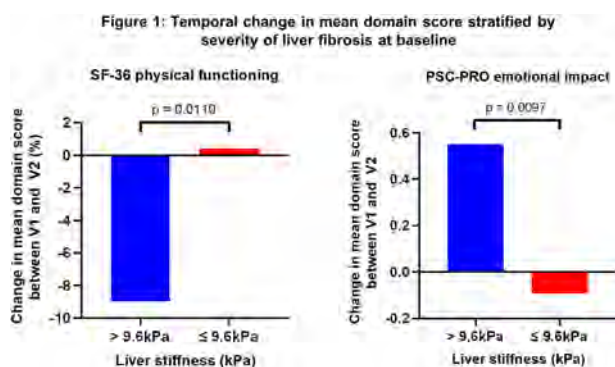
Background and aims: Patient-reported outcome measures (PROMs) are increasingly used as exploratory end points in clinical trials. The aim of this study was to evaluate the temporal relationship between health-related quality of life (HrQoL) and liver fibrosis using generic (SF-36) and disease-specific (PSC-PRO) tools.

Method: Patients with large-duct PSC were invited to complete HrQoL questionnaires in an outpatient setting at baseline (V1) and

POSTER PRESENTATIONS

follow-up (V2) visits at least 12 months apart. Transient elastography liver stiffness (LS; Echosens, France) measurements were recorded on the same day. SF-36 and PSC-PRO health domains were scored out of a maximum of 100% and 5, respectively. Mean scores were calculated for each domain with lower SF-36 and higher PSC-PRO scores representing poorer quality of life. Advanced fibrosis (F3-6) was defined based on published cutoff of LS >9.6kPa in PSC.

Results: Fifty-five patients (64% male) with median age 45 years (range: 20–77) and median PSC duration 11 years (range: 2–26) attended both study visits. The median time between visits was 417 days (range: 362–582). The mean scores were numerically lower at V2 than V1 in all the SF-36 domains but only three domains showed statistically significant difference: bodily pain (74% vs 83%, $p < 0.01$), energy/fatigue (47% vs 57%, $p < 0.0001$), and mental summary score (66% vs 71%, $p < 0.001$). There were no differences in any of the PSC-PRO domains between the visits. When stratified by baseline LS >9.6 kPa threshold (Figure 1), SF-36 physical functioning mean score dropped in the F3-6 group but increased slightly in the F0-2 group ($-9.0 \pm 17\%$ vs $0.4 \pm 21\%$, $p = 0.01$). In the PSC-PRO, the emotional impact mean score increased in the F3-6 group but decreased in the F0-2 group (0.6 ± 0.7 vs -0.1 ± 0.5 , $p < 0.01$). There were no significant differences in mean scores in the other domains between the visits.



Conclusion: There was worsening of bodily pain, levels of energy and mental health even within a year in patients with large-duct PSC. Patients with advanced fibrosis reported lower physical functioning and higher emotional impact of their disease compared to those without advanced fibrosis. Changes in PROMs are related to liver fibrosis and need to be considered in future antifibrotic drug trials. These findings, however, need to be interpreted in the context of imposed restrictions during the Covid-19 pandemic which may have had a significant psycho-social impact on patients.

THU460

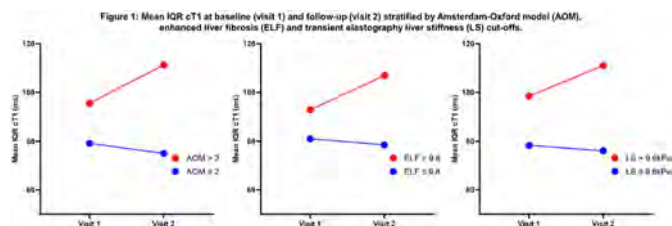
Temporal increase in interquartile range iron-corrected T1 in high-risk patients with large-duct primary sclerosing cholangitis

Emmanuel Selvaraj^{1,2,3}, Jane D. Collier², Emma Culver², J Michael Brady^{4,5}, Adam Bailey^{2,3}, Michael Pavlides^{1,2,3}. ¹University of Oxford, Oxford Centre for Clinical Magnetic Resonance Research, Radcliffe Department of Medicine, Oxford, United Kingdom; ²University of Oxford, Translational Gastroenterology Unit, Nuffield Department of Medicine, Oxford, United Kingdom; ³NIHR Oxford Biomedical Research Centre, Oxford University Hospitals NHS Foundation Trust, Oxford, United Kingdom; ⁴University of Oxford, Department of Oncology, Oxford, United Kingdom; ⁵Perspectum Ltd., Oxford, United Kingdom
Email: emmanuel.selvaraj@cardiov.ox.ac.uk

Background and aims: Median iron-corrected T1 (cT1) derived from LiverMultiScan (Perspectum, Oxford, UK) correlates well with histological liver fibrosis. Interquartile range (IQR) cT1 has been proposed to better reflect the patchy liver fibrosis in primary sclerosing cholangitis (PSC). The aim of this study was to investigate the temporal changes in IQR cT1 in large-duct PSC.

Method: Patients with large-duct PSC attended study visits at baseline (V1) and follow-up (V2). Standardised liver T1 and T2* maps, transient elastography liver stiffness (LS; Echosens, France), enhanced liver fibrosis (ELF; Siemens Healthineers, Germany), and blood tests were performed on the same day at each visit. MRI data were analysed using LiverMultiScan to derive liver IQR cT1. The Amsterdam-Oxford model (AOM) score was also calculated. Patients were classified into high-risk or low-risk groups for disease progression using baseline data according to published cut-offs in PSC: AOM >2, ELF >9.8 and LS >9.6 kPa. Mixed ANOVA models were used to examine the within-subject effect (time), between-subject effect (high-risk or low-risk), and interaction between the two on changes in IQR cT1. The magnitude of effects (partial-ETA squared) was defined as: 0.01 (small), 0.06 (medium), and 0.14 (large). Receiver operating characteristic curve (ROC) analyses were conducted to assess the diagnostic performance of V1 and delta V1–V2 measurements to identify the high-risk groups.

Results: Fifty-five patients (64% male) with median age 45 years (range: 20–77) and median PSC duration 11 years (range: 2–26) attended both study visits. The median time between visits was 417 days (range: 362–582). IQR cT1 was higher in the high-risk groups compared to low-risk groups at either time points (AOM: $p < 0.001$; ELF: $p = 0.001$; LS: $p < 0.001$). IQR cT1 increased over time in the high-risk group and not in the low-risk group (AOM: $p = 0.03$; ELF: $p = 0.04$; LS: $p = 0.07$). There was a significant interaction between time and risk grouping on IQR cT1 when stratified by AOM ($F = 15.3$, $p < 0.001$; partial-ETA squared = 0.23), ELF ($F = 9.1$, $p < 0.01$; partial-ETA squared = 0.15) and LS ($F = 7.2$, $p = 0.01$; partial-ETA squared = 0.12). Delta V1–V2 (AUC = 0.78, 95% CI: 0.61–0.95) numerically had a higher diagnostic performance than V1 IQR cT1 (AUC = 0.75, 95% CI 0.61–0.89; $p < 0.001$) to detect the AOM >2 group but was no better when stratified by ELF and LS.



Conclusion: Patients who are at higher risk of death and/or liver transplantation (AOM >2) or with advanced fibrosis (ELF >9.8, LS >9.6 kPa) are likely to have a progressively higher IQR cT1 over time. Single baseline measurements alone outperformed dynamic measurements over two time points in detecting the high-risk group. Further follow-up data points with repeated-measures analysis and correlation with clinical outcomes are needed.

THU461

Seladelpar treatment of patients with primary biliary cholangitis (PBC) for 2 years improves the GLOBE PBC score and predicts improved transplant-free survival

Bettina Hansen^{1,2}, Elaine Watkins³, Ke Yang³, Yun-Jung Choi³, Charles McWherter³, Gideon Hirschfield⁴. ¹Toronto Centre for Liver Disease, Toronto General Hospital, University Health Network, Toronto, Canada; ²Institute of Health Policy, Management and Evaluation (IHPE), University of Toronto, Toronto, Canada; ³CymaBay Therapeutics, Inc, Newark, United States; ⁴Toronto Centre for Liver Disease, University of Toronto, Toronto, Canada
Email: bettina.hansen@utoronto.ca

Background and aims: The GLOBE score is a validated risk assessment tool providing an estimate of transplant-free survival for patients with PBC. Seladelpar is a PPAR-delta agonist with anti-cholestatic, anti-inflammatory and anti-pruritic activity in PBC

patients. Our aim was to evaluate change in GLOBE score in patients with PBC treated with seladelpar for 2 years.

Method: Eligible patients with PBC and an inadequate response or intolerance to UDCA (alkaline phosphatase (ALP) $\geq 1.67 \times \text{ULN}$) were enrolled into an open-label one-year phase 2 study (EudraCT: 2016-002996-91) receiving daily oral 5 or 10 mg seladelpar. After 1 year, patients were eligible for an open label long-term study (EudraCT: 2017-003910-16). The change in GLOBE score following seladelpar treatment over 2 years and the resulting predictions of transplant-free survival were assessed. The contributions of alkaline phosphatase, total bilirubin, albumin, and platelets to changes in GLOBE score were examined.

Results: 101 patients entered the long-term study with available GLOBE score and were evaluated: 94% female, mean (SD) age 57 (9.0) years, duration of PBC 10 (6.6) years, and UDCA dose of 15 (3.7) mg/kg/day. Mean baseline values were ALP 321 (165) U/L, bilirubin 0.8 (0.3) mg/dL, albumin 4.1 (0.3) mg/dL, platelets $237 (82) \times 10^3/\mu\text{L}$ and GLOBE score 0.390 (0.656). After treatment with seladelpar for 3 months, 1 year and 2 years the mean (SD) change from baseline in GLOBE score was $-0.330 (0.321)$, $-0.324 (0.281)$, and $-0.417 (0.269)$, respectively. The observed early fall of GLOBE score within 3 months was followed by a gradual decline through 2 years (Fig. 1A). The improvements in GLOBE score for all patients and those completing two years were comparable. The greatest changes in GLOBE score were attributable to changes in alkaline phosphatase values followed by those of total bilirubin (Fig. 1B). Seladelpar treatment led to predicted changes in survival (Fig. 1C) at 3 months, 1 year and 2 years with hazard ratios of 0.72, 0.72 and 0.66 compared to baseline, respectively. The improvements in GLOBE score were observed for nearly all patients completing 2 years treatment (47 of 50, Fig. 1D).

Figure 1A. Change in GLOBE Score During 2 Years of Seladelpar Treatment

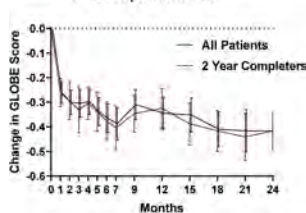


Figure 1B. Change in Individual Components of GLOBE Score

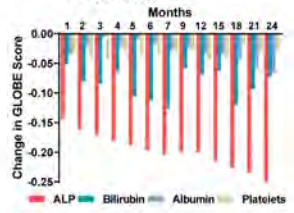


Figure 1C. Predicted Transplant-Free Survival

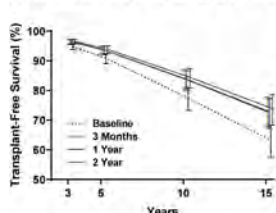
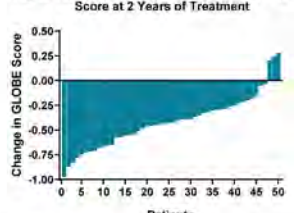


Figure 1D. Change in Individual Patient GLOBE Score at 2 Years of Treatment



Months	0	1	2	3	4	5	6	7	9	12	15	18	21	24
All Patients (N)	101	96	100	95	98	99	97	95	98	95	93	77	61	50
2-Yr Completers (N)	50	48	49	47	49	48	47	47	49	49	47	50	48	50

Conclusion: Seladelpar treatment over 2 years resulted in a sustained decrease in GLOBE score for patients with PBC that is associated with a predicted improvement in transplant-free survival.

THU462

Validation of a novel method of identifying patients with Primary Sclerosing Cholangitis (PSC) in a Canadian population

Harshil Patel¹, Fengjuan Yang¹, Mark G Swain¹, Gideon Hirschfield², Gilaad Kaplan¹, Bettina Hansen², Abdel-Aziz Shaheen¹. ¹University of Calgary, Calgary, Canada; ²University Health Network, Toronto, Canada
Email: az.shaheen@ucalgary.ca

Background and aims: Studies describing the epidemiology of primary sclerosing cholangitis (PSC) have been limited due to

suboptimal case-finding and case-ascertainment. Using administrative databases to identify PSC in the population is not reliable. Guidelines recommend PSC patients should undergo a colonoscopy to rule out inflammatory bowel disease (IBD). Therefore, we aimed to evaluate the role of using an endoscopy database to improve PSC patient identification.

Method: We used the Pentax medical endoscopy endoPRO iQ[®] database to identify adult (≥ 18 years) patients who had undergone a colonoscopy in the Calgary Health Zone [(CHZ) population ~ 1.5 million]. We searched the endoscopy report database for one of the following predefined texts: *primary sclerosing cholangitis*, *PSC*, *sclerosing cholangitis*, between 2005 and 2019. The CHZ is a one-payer system providing medical care to all residents in the zone. All endoscopies performed in the CHZ are captured within a secure Pentax medical database. We used the International Classifications of Diseases (ICD) codes to identify patients with PSC in the following administrative databases: inpatient, ambulatory, and physician claims. Finally, for case-ascertainment, we conducted a validation study using medical charts on all PSC patients identified in the endoscopy database and a systematic random sample of patients identified by the administrative databases but not by the endoscopy database (sample size = 207). In our validation study, we identified patients with ulcerative colitis (UC), Crohn's disease (CD), and indeterminate colitis.

Results: During our study period, we identified 535 patients using the endoscopy database and 4,544 patients in administrative databases with a potential PSC diagnosis. Within the endoscopy database, we identified 406 PSC patients (male sex 59.4%) who had a confirmed PSC diagnosis using radiological modalities and/or a liver biopsy. In this cohort, 1.5% (n = 6) patients were not identified in the administrative databases. IBD was prevalent at 81.5% (n = 331) in our cohort (UC 149 [36.7%], CD 146 [36.0%], and 36 [8.9%] indeterminate colitis). In our validation study (n = 742 charts), 412 patients had a confirmed PSC diagnosis. Using the endoscopy database alone to identify PSC patients had sensitivity 98.5% (406/412), specificity 60.9% (201/330), positive predictive value (PPV) 75.9% (406/535), and negative predictive value (NPV) 97.1% (201/207). Using multiple previously recommended algorithms in the administrative databases to identify PSC patients had a maximum PPV of 62% and sensitivity of 54%.

Conclusion: Using endoscopy databases to identify PSC patients is a reliable, accurate and feasible method compared to using administrative databases. Our proposed method would lead to better case-ascertainment and should improve the quality of future studies evaluating the natural history of PSC.

THU463

The prevalence of primary biliary cholangitis (PBC) is on the rise: a Canadian population-based study

Bryce Tkachuk¹, Fengjuan Yang², Gideon Hirschfield³, Mark G Swain², Abdel-Aziz Shaheen². ¹University of Calgary, Medicine, Calgary, Canada; ²University of Calgary, Calgary, Canada; ³University Health Network, Toronto, Canada
Email: az.shaheen@ucalgary.ca

Background and aims: Canada has one of the highest rates of primary biliary cholangitis (PBC) incidence and prevalence worldwide. Our group reported the natural history of PBC in Calgary (population ~ 1.5 million) more than a decade ago. Significant awareness and recent advancement of PBC management were reported. Therefore, we aimed to study the impact of these factors on the natural history of PBC in a well-defined Canadian population and evaluate the temporal trends of PBC incidence and prevalence.

Method: We used population-based administrative data (inpatient, ambulatory care, and physician claims) and a previously validated International Classification of Diseases coding algorithm to identify PBC patients in the Calgary Health Zone between 2003 and 2018. We applied the same validated methods that we implemented in our

POSTER PRESENTATIONS

original study (Myers *et al.*, 2009, study period: 1996–2002). We conducted a validation study on incident cases to confirm the performance of the used algorithm in order to identify definite PBC patients (those who had at least two of the following criteria: positive anti-mitochondrial antibody, cholestatic liver enzymes, and a compatible liver biopsy). The positive predictive value (PPV) was 78.2%, while PPV of the original algorithm was 73.1%. We used a washout period of 2 years (2003–2004) to identify incident PBC cases. We chose March 31st of each year as point prevalence. Temporal trends were evaluated using generalized linear models assuming a Poisson distribution or a negative binomial distribution if over-dispersion is present. Rates were adjusted to the Canadian population census of 2016.

Results: Between 2005 and 2018, the overall age/sex annual incidence of PBC was 39.4 cases per million. Age-adjusted incidence rates were 60.7 per million in women versus 16.7 per million in men (incidence rate ratio [IRR] 3.68; 95% CI 2.98–4.54). The highest adjusted incidence was observed among the age group 60–79 years (74.0 case per million). Age/sex-adjusted point prevalence rates of PBC increased from 295.8 to 500.0 per million between 2005 and 2018, $p < 0.001$. As expected, adjusted point prevalence rates were much higher among women than men (799.8 versus 169.0 per million). We identified 520 incident cases during our study time (female 78.7% [$n = 409$]). After a median follow-up of 6.8 years (IQR 3.9–10.6), 29 patients underwent transplantation (5.6%) and 81 patients died (15.6%). The annual mortality rate was 8.1% (95% CI 9.8%–14.0%). The estimated 5- and 10-year survival rates were 90.7% (87.5%–93.0%) and 77.4% (72.2%–81.7%), respectively. Survival was not significantly different between men and women, $p = 0.50$.

Conclusion: In this well-defined cohort, we reported a significant increase in the prevalence of PBC in a Canadian population. Prevalence of PBC is higher among the older age group which could reflect better case-identification and management.

THU464

Rituximab is a safe and effective treatment for patients with autoimmune hepatitis: results from the Spanish registry for cholestatic and autoimmune hepatitis

Ana Barreira^{1,2}, Maria Carlota Londoño^{2,3}, Carmen Álvarez-Navascués⁴, Carlos Ferre Aracil⁵, Indhira Perez Medrano⁶, Juan Turnes^{2,6}, Diana Horta⁷, Álvaro Díaz-González⁸, Fernando Díaz Fontela⁹, Magdalena Salcedo^{2,9}, Mar Riveiro Barciela^{2,10}. ¹Hospital Vall Hebron, Liver Unit, Barcelona; ²Centro de investigación biomédica en red de enfermedades hepáticas y digestivas; ³Hospital Clínic, Liver Unit, Barcelona; ⁴Hospital Universitario Central de Asturias, Digestive Department, Oviedo; ⁵Hospital Universitario Puerta de Hierro Majadahonda, Digestive Department, Madrid; ⁶Complejo Hospitalario Universitario de Pontevedra, Digestive Department, Pontevedra; ⁷Hospital Universitari Mutua de Terrassa, Digestive Department, Barcelona; ⁸Hospital Universitario Marqués de Valdecilla. Instituto de Investigación Sanitaria Valdecilla., Digestive Department, Santander; ⁹Hospital General Universitario Gregorio Marañón, Digestive Department, Madrid; ¹⁰Hospital Vall Hebron, Liver Unit, Barcelona
Email: mar.riveiro@gmail.com

Background and aims: The evidence of second-line therapy for autoimmune hepatitis (AIH) is relatively scarce, especially concerning biological agents such as rituximab. This study aims to evaluate the efficacy and safety of rituximab in patients with autoimmune hepatitis (AIH).

Method: multicenter retrospective study of all patients with AIH from the ColHai registry who received rituximab from January 2015 to September 2021. Efficacy was assessed by improvement in transaminases and Immunoglobulin (Ig) G or normalization (biochemical response) and later development of flares; safety in terms of adverse reactions, infectious and tumoral complications.

Results: 2763 AIH patients were included in the ColHai registry (Spanish registry for cholestatic and autoimmune disorders). Out of them, 13 patients with type 1-AIH were treated with rituximab in 8 different hospitals. The majority were women (10/13), median age 43 years. At diagnosis 1 presented an acute severe hepatitis and 2 had liver cirrhosis. Time from diagnosis to beginning of rituximab was 20 months and to last follow-up 5 years. The reasons for biological therapy were: 4 difficult-to-manage AIH and 9 due to indication for other concomitant autoimmune disorder (4 multiple sclerosis, 3 vasculitis and 2 rheumatoid arthritis). The majority (11/13) received a 2-dose induction course followed by a new dose every 6 months. After rituximab, at the 1-month follow-up an improvement of IgG levels was observed ($p = 0.018$) and a tendency towards decrease of AST/ALT. At month 6, the reduction in AST/ALT was statistically significant ($p = 0.012$ and $p = 0.008$). Eight out of 13 presented increased transaminases and IgG levels at the start of rituximab, and 5/8 achieved biochemical response after rituximab therapy. Treatment was well tolerated, without infusion reactions, though 3 patients developed non-severe infectious complications. All patients but one were on corticoids at the beginning of rituximab and in 8/12 they could be tapered or discontinued. Moreover, in five of these patients other immunosuppressants could be stopped due to the positive impact of rituximab as shown in the figure. Despite initial improvement, four patients presented flares of AIH during follow-up that were successfully managed with new doses of rituximab.

	Corticoids	Azathioprine	MMF	Tacrolimus	Everolimus
Patient 1					
Patient 2					
Patient 3					
Patient 4					
Patient 5					
Patient 6					
Patient 7					
Patient 8					
Patient 9					
Patient 10					
Patient 11					
Patient 12					
Patient 13					

Figure: Individual therapy at the beginning of rituximab (grey squares) and drugs that were reduced or discontinued during follow-up (striped squares).

Conclusion: Rituximab is a safe and effective treatment for AIH, leading to reduction of immunosuppression in a high proportion of patients and improvement of transaminases and IgG levels.

THU465

Autoimmune hepatitis diagnosed after COVID-19 vaccination. Results from the Spanish registry for autoimmune and cholestatic hepatitis

Ana Barreira^{1,2}, Mar Riveiro Barciela^{1,2}, Agustín Castiella³, Álvaro Díaz-González⁴, María Carlota Londoño^{2,5}, Indhira Pérez Medrano⁶, Judith Gómez-Camarero⁷, Marta Casado⁸, Carmen Del Pozo-Calzada⁹, María Dolores Antón Conejero^{2,10}, Magdalena Salcedo^{2,11}. ¹Hospital Universitario Vall de Hebrón, Liver Unit; ²Instituto de Salud Carlos III, Centro de Investigación Biomédica en Red de Enfermedades Hepáticas y Digestivas (CIBERehd); ³Hospital Universitario de Donostia, Liver Unit; ⁴Hospital Universitario Marqués de Valdecilla. Instituto de Investigación Sanitaria Valdecilla (IDIVAL), Servicio de Aparato Digestivo; ⁵Hospital Clínic Barcelona, Liver Unit; ⁶Complejo Hospitalario Universitario de Pontevedra, Servicio de Aparato Digestivo; ⁷Hospital Universitario de Burgos, Servicio de Aparato Digestivo; ⁸Hospital Universitario de Torrecárdenas, Servicio de Aparato Digestivo; ⁹Hospital Clínico Universitario de Valladolid, Servicio de Aparato Digestivo; ¹⁰Hospital Universitario Dr. Peset, Valencia, Servicio de Aparato Digestivo; ¹¹Hospital General Universitario Gregorio Marañón, Madrid, Hepatology and Liver Transplantation Unit
Email: magdalena.salcedo@salud.madrid.org

Background and aims: Universal vaccination has become the main strategy against the COVID-19 pandemic. The SARS-CoV-2 spike protein used in the vaccines is believed to be responsible for stimulating the immune system, thus suggesting a possible association between COVID-19 vaccines and the development of autoimmune diseases. To date, different events of probable autoimmune origin have been reported in association with the COVID-19 vaccine, including few cases of autoimmune hepatitis (AIH). The aim of this study was to describe the clinical and epidemiological characteristics of a number of patients with AIH debut or reactivation after COVID-19 vaccination.

Method: Multicenter, retrospective-prospective study, that included subjects who have received one or two doses of any of the approved COVID-19 vaccines and later presented increased transaminases values due to AIH within the 90 days after vaccination.

Results: 23 patients from 9 Spanish academic hospitals were included. 17/23 were female, mean age 51 (± 15) years. 19/23 patients were biopsied and four were not, 3 of them had a previous diagnosis of AIH. Seven patients had another prior autoimmune disorder. COVID-19 vaccines: 12/23 Pfizer, 4 Moderna, 5 Astrazeneca and 2 Janssen. In 14/23 patients the AIH episode happened after the second dose and in 9 after the first dose. Median time from the last dose of vaccine to AIH was 21 (11–36) days. Table 1 summarizes the analytical data of patients at the time of hepatitis. Antinuclear antibodies (ANA) $\geq 1/80$ was observed in 18/23 patients. Regarding the severity of hepatitis, it was mild in the majority of patients (20/23), two patients presented with fulminant hepatitis and in one subject it was severe. All but one of the biopsied patients showed histological findings compatible with AIH. The RUCAM to assess causality showed at least possible association (≥ 4 points) in 11 patients. Simplified AIH Score showed at least probable AIH (≥ 6 points) in 16/23 patients. All patients received treatment with corticosteroids and in 19 patients immunosuppressive treatment with azathioprine was initiated.

	Median (IQR)
Aspartate aminotransferase (AST), IU/L	915 (622-1448)
Alanine aminotransferase (ALT), IU/L	966 (704-1498)
Alkaline phosphatase (AP), IU/L	135 (131-239)
Gamma-glutamyl transferase (GGT), IU/L	183 (120-266)
Total bilirubin, mg/dL	2.96 (1.8-10.3)
Direct bilirubin, mg/dL	2.3 (1.3-11)
International Normalized Ratio (INR)	1.09 (0.98-1.28)
Immunoglobulin G (IgG), mg/d	1684 (1252-2240)
Total proteins, mg/dL	7.4 (6.6-7.9)

Figure: Analytical data of the patients at the time of hepatitis

Conclusion: An increase in transaminase values after administration of COVID-19 vaccine should be evaluated given the possibility of diagnosing autoimmune hepatitis.

THU466

A prospective trial of a gluten free diet in primary sclerosing cholangitis with associated colitis

Timur Liwinski¹, Sina Hübener¹, Lara Henze¹, Peter Huebener¹, Melina Heinemann¹, Bettina Jagemann¹, Marcus Tetzlaff¹, Guido Schachschal¹, Thomas Rösch¹, Erika Monguzzi², Corinna Bang³, Andre Franke³, Ansgar W. Lohse¹, Detlef Schuppan², Christoph Schramm¹. ¹University Medical Center Hamburg-Eppendorf, Hamburg, Germany; ²Universitätsmedizin der Johannes Gutenberg-Universität Mainz, Mainz, Germany; ³University of Kiel, Kiel, Germany
Email: liwinski@gmail.com

Background and aims: Primary sclerosing cholangitis (PSC) is a progressive autoimmune disease of the bile ducts associated with inflammatory bowel disease. Several studies indicated that gluten restriction might ameliorate autoimmune liver disease and inflammatory bowel disease (IBD) symptoms. We investigated whether patients with PSC with associated IBD can benefit from a diet free of wheat and gluten (GFD) using a prospective multi-omics approach.

Method: We performed a prospective clinical pilot study administering an eight-week GFD to PSC patients with non-advanced liver disease and associated colitis without overt clinical activity. A clinical dietitian trained patients and controlled adherence to the intervention by validated questionnaires and measuring gluten peptides in urine. The patients were evaluated at several time points, including endoscopy before and after the GFD period. We recorded multiple clinical parameters, dietary information, and biologically relevant parameters, including intestinal mucosal cytokine levels, intestinal bulk RNA-Seq transcriptomics. The enteric fecal and mucosal microbiota were analyzed by sequencing the variable region V1/V2 of the 16S rRNA gene and shotgun metagenomics.

Results: In total, fifteen patients were enrolled and completed the study. A decreased expression of proinflammatory mucosal cytokines and chemokines such as IL6 ($p < 0.001$), IL8 ($p < 0.001$), CCL2 ($p = 0.042$), and TNF-alpha ($p < 0.001$) was observed after GFD. Moreover, the intestinal transcriptome indicated improvement of the gut barrier, with an increase of pathways related to “adherens junction” ($p = 0.0471$), “cell-substrate junction” ($p = 0.0262$), “cell-substrate adherens junction” ($p = 0.0233$), and “focal junction” ($p = 0.0217$). We found mild to moderate changes in luminal microbiota composition after GFD, including a decrease of Romboutsia ilealis ($FC = -9.02$, $FDR < 0.001$). As expected from the short intervention period and the low disease activities, no statistically significant response was observed regarding clinical parameters such as the endoscopic score ($p = 0.398$) and patient-reported outcome measures. According to the food frequency questionnaire, the macronutrient composition (other than gluten) did not change during eight weeks of diet.

Conclusion: This is the first study to demonstrate that GFD may improve intestinal inflammation and barrier function in patients with PSC-IBD. This effect was linked to changes in the enteric microbiota composition. This pilot study justifies subsequent studies in patients with more severe disease activity.

THU467

The international autoimmune hepatitis group retrospective registry: quality assessment and analysis of clinical characteristics and liver-related outcome

Charlotte Slooter¹, Floris van den Brand¹, Ana Lleo², Francesca Colapietro², Marco Lenzi³, Paolo Muratori³, Nanda Kerkar⁴, George Dalekos⁵, Kalliopi Zachou⁵, Maria Isabel Lucena⁶, Mercedes Robles-Díaz⁶, Daniel E. Di Zeo-Sánchez⁶, Raul J. Andrade⁶, Aldo J Montano-Loza⁷, Ellina Lytvyak⁷, Guilherme Macedo⁸, Gerd Bouma¹, Rodrigo Liberal^{8,9}, Ynto de Boer¹. ¹Amsterdam University Medical Center, Netherlands; ²Humanitas University, Italy; ³University of Bologna, Italy; ⁴Golisano Children's Hospital, University of Rochester Medical Center, Rochester, United States; ⁵University Hospital of Larissa, Greece; ⁶Virgen de Victoria University Hospital, University of Málaga, Spain; ⁷University of Alberta Hospital, Edmonton, Canada; ⁸Centro Hospitalar Sao Joao, Porto, Portugal; ⁹King's College, United Kingdom
Email: y.deboer1@amsterdamumc.nl

Background and aims: The International Autoimmune hepatitis (AIH) Group retrospective registry (IAIHG-RR) is a web-based platform for large scale aetiological and therapeutic studies in paediatric and adult subjects enrolled with a diagnosis of AIH. This study aimed to ascertain data quality and describe the clinical characteristics and outcomes of this cohort.

Method: This retrospective analysis included all patients with a clinical diagnosis of AIH (n = 2278) from the IAIHG-RR entered between December 2018 and September 2021. This registry contains data on clinical characteristics and liver-related outcomes from 37 centers in 7 countries. Quality assessment included cohort completeness for 31 pre-defined variables, consistency and data was externally validated.

Results: Completeness of individual data was 75.8% (range 3.0–100). Per center, completeness varied between 69.5% and 99.9%. Consistency of inclusion criteria and outlier analysis was nearly 100%. Among patients for whom a simplified AIH score was available, diagnosis was classified as possible in 27.5%, probable in 25.0% and in 47.5% as definite. At diagnosis, 21.9% showed signs of cirrhosis and median Model for End-Stage Liver Disease (MELD) score was 11 [range 6–40]. Primary biliary cholangitis and primary sclerosing cholangitis were reported in 10.0% and 7.0%, respectively. Other associated diseases were reported in 26.3%. For 1191 patients follow-up and outcome data was available. With a median follow-up period of 12 [range 0–49] years 36.8% demonstrated signs of cirrhosis, 2.2% were diagnosed with hepatocellular carcinoma and 10.6% underwent liver transplantation. 172 patients died during the follow-up period at a median age of 65 (range 15–94). In 49.7%, the cause of death was reported liver-related. Liver transplantation and liver related death were both associated with signs of cirrhosis at baseline (hazard ratio [HR] 1.90; p < 0.001), the MELD score at baseline (HR 1.09; p < 0.001) and with persistence of elevated aminotransferases at 6 months (HR 2.75; p < 0.001).

Conclusion: The IAIHG-RR represents world's largest patient cohort with moderate-to-good quality of baseline and follow-up data with relevant number of liver-related adverse events. This study showed that cirrhosis and MELD score at baseline and persistence of elevated aminotransferases at 6 months are associated with liver transplantation and liver-related death. This registry is a suitable platform, which allows for patient selection for future therapeutic and aetiological studies.

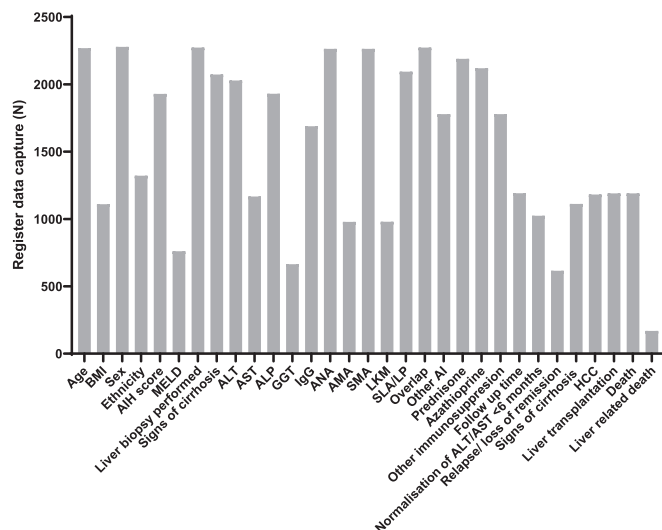


Figure: Data captured in absolute numbers for a pre-defined set of 31 variables in the IAIHG-RR (n = 2278).

THU468

Liver inflammation activity in autoimmune hepatitis patients with normal ALT and IgG levels

Chuanwu Zhu¹, Jiacheng Liu², Jian Wang³, Huali Wang⁴, Yilin Liu², Yiguang Li⁵, Li Zhu¹, Weimao Ding⁶, Yuanwang Qiu⁵, Yongfeng Yang⁴, Jie Li³, Rui Huang³, Chao Wu³. ¹The Affiliated Infectious Diseases Hospital of Soochow University, Department of Infectious Diseases, Suzhou, China; ²Nanjing Drum Tower Hospital Clinical College of Traditional Chinese and Western Medicine, Nanjing University of Chinese Medicine, Department of Infectious Diseases, Nanjing, China; ³Nanjing Drum Tower Hospital, The Affiliated Hospital of Nanjing University Medical School, Department of Infectious Diseases, Nanjing, China; ⁴Nanjing Second Hospital, Nanjing University of Chinese Medicine, Department of Hepatology, Nanjing, China; ⁵The Fifth People's Hospital of Wuxi, Department of Infectious Diseases, Wuxi, China; ⁶Huai'an No. 4 People's Hospital, Department of Hepatology, Huai'an, China
Email: dr.wu@nju.edu.cn

Background and aims: Serum alanine transaminase (ALT) and IgG levels are considered as surrogate markers for histological activity in autoimmune hepatitis (AIH). We assessed the inflammatory activity in AIH patients with normal ALT and IgG levels.

Method: 257 AIH patients underwent liver biopsy (LB) were retrospectively included from four medical centers. Liver inflammation and fibrosis were estimated by Scheuer scores. The definitions of advanced inflammation and fibrosis were G ≥ 3 and S ≥ 3, respectively.

Results: 163 (63.3%) AIH patients had advanced inflammation, while 125 (48.6%) patients had advanced fibrosis. The proportion of advanced inflammation was 62.1% in patients with normal ALT and 55.6% in patients despite normal ALT and IgG. The proportion of advanced inflammation was 44.0% in patients without advanced fibrosis and was 81.8% in those with advanced fibrosis. Of patients with advanced fibrosis, 78.6% (33/42) of patients with normal ALT presented advanced inflammation, which was 75.0% in patients with normal ALT and IgG. Among patients without advanced fibrosis, the proportion of advanced inflammation was as high as 33.3% in those with normal ALT and 31.3% in those despite normal ALT and IgG. Red cell distribution width was independently associated with advanced inflammation (OR: 1.521, 95%CI: 1.193–1.938, P = 0.001) in entire patients.

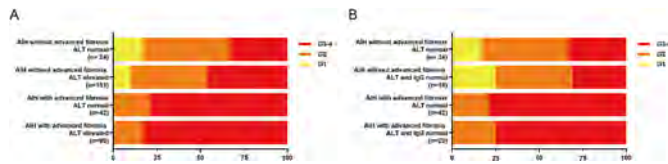


Figure: Histological activity in relation to ALT and IgG levels in AIH patients with or without advanced fibrosis

Conclusion: High proportion of advanced inflammation was found in AIH patients despite normal ALT and IgG levels even for those without advanced fibrosis. Though fibrosis can be ruled out by non-invasive methods in AIH patients with normal ALT and IgG, LB is encouraged to assess inflammatory activity.

THU469

Novel screening test for primary sclerosing cholangitis: the role of serology, liver function tests, histology and radiology

Nina Barner-Rasmussen¹, Nelli Sjöblom², Hannu Kautiainen³, Johanna Arola², Martti Färkkilä¹. ¹University of Helsinki and Helsinki University Hospital, Department of Gastroenterology, Helsinki, Finland; ²University of Helsinki and Helsinki University Hospital, Department of Pathology, Helsinki, Finland; ³University of Eastern Finland, Institute of Public Health and Clinical Nutrition, Kuopio, Finland
Email: nina.barner-rasmussen@hus.fi

Background and aims: Primary sclerosing cholangitis (PSC) is a chronic cholestatic liver disease. There is no specific laboratory test for surveillance or screening in PSC unlike in primary biliary cholangitis. At present, the screening of PSC is mainly based on elevated alkaline phosphatase (ALP) in patients with inflammatory bowel disease (IBD). However, ALP and gamma-glutamyl transferase (GT) may be normal, even in advanced bile duct disease. The diagnosis is made by magnetic resonance cholangiopancreatography (MRCP) or by endoscopic retrograde cholangiography (ERC). The latest guidelines from Europe and America do not recommend liver biopsy, apart from small-duct PSC or a suspicion of an overlap syndrome. We aim to produce a screening system to predict the likelihood of PSC evaluating the role of laboratory tests, liver histology and MRCP.

Method: We retrieved 395 PSC patients from the PSC registry of Helsinki University Hospital who came for their 1st ERC to confirm the diagnosis. 69 patients with suspicion of PSC who underwent ERC, liver biopsy and MRCP excluding PSC, served as controls (non-PSC patients). Liver histology was scored according to the Nakanuma classification from Herovici stained core needle biopsy specimens. MRCP before diagnosis was scored from the existing radiology report as negative for PSC, finding suggestive for PSC, and clear findings for PSC. We included demographics and eleven different laboratory tests in the analysis. Area under the curve (AUC), positive prediction value, likelihood ratio, sensitivity, specificity, and odds ratio (OR) were calculated. Variables with highest OR were selected for multivariate logistic regression, which was used to create the novel scoring system.

Results: IBD, perinuclear anti-neutrophil cytoplasmic antibodies (P-ANCA) and ALP had the best predictive value. A score was assigned to each statistically significant predictor. Presence of IBD and P-ANCA gives 2 points each and ALP > UNL 1 point. The optimal cut-off point for the score was ≥ 3 , with AUC of 0.83 (95%CI 0.78–0.88). If a patient got a score of 3 or higher, the probability of a true PSC diagnosis was >90%. Adding liver histology or MRCP to the score did not add predictive value.

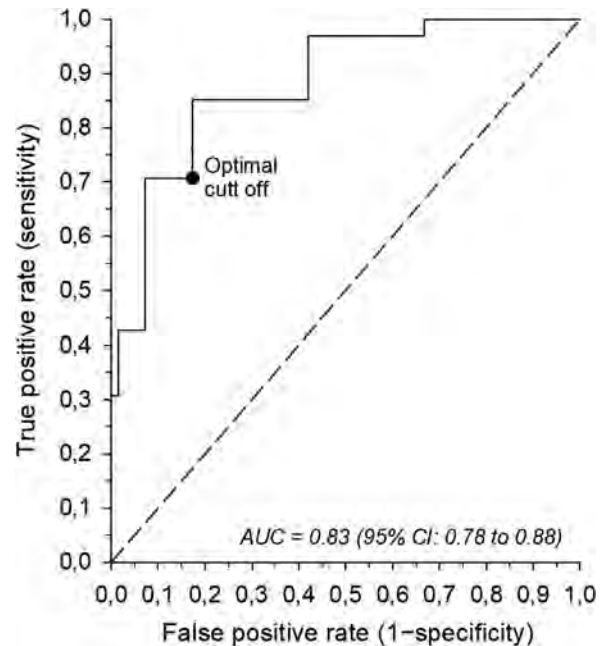


Figure: Prognostic performance of HelpScreening-score

Conclusion: We have created a novel scoring system to screen the probability of PSC using non-invasive tests. The HelpScreening-score may help target further investigations in patients with suspicion of PSC.

THU470

More than just an itch: impact of cholestatic pruritus in primary biliary cholangitis (PBC) on health-related quality of life (HRQoL)

Helen Smith¹, James Fettiplace¹, Robyn von Maltzahn¹, Sugato Das², Megan McLaughlin³, David Jones⁴. ¹GlaxoSmithKline, United Kingdom; ²GlaxoSmithKline, India; ³GlaxoSmithKline, United States; ⁴Newcastle University, United Kingdom
Email: helen.t.smith@gsk.com

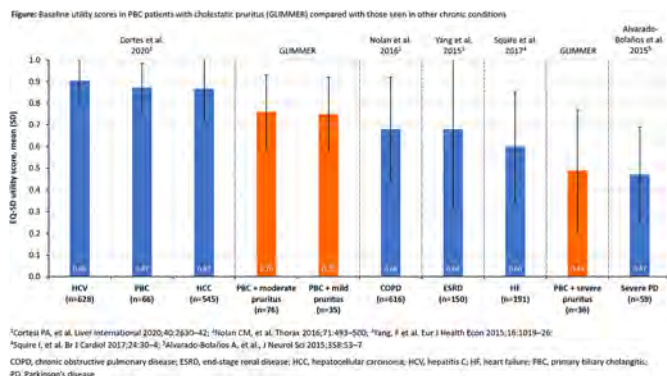
Background and aims: Pruritus associated with PBC affects sleep and social and emotional wellbeing. Limited data exist on the impact of pruritus on health utility (a single value between 0 [death] and 1 [perfect health]), commonly used in health technology assessments to calculate quality-adjusted life years and compare different conditions. A recent UK study explored EQ-5D utilities in a broad PBC population (Rice et al. *Clin Gastroenterol Hepatol* 2021;19:769–76). Here, using data from the Phase 2b GLIMMER study (post hoc) investigating linaclixibat for the treatment of pruritus in PBC (NCT02966834), the impact of itch severity on health utility in PBC is explored and quantified for the first time.

Method: Patients in GLIMMER recorded itch twice daily on a 0–10 numeric rating scale (NRS) and completed the EQ-5D-5L at study entry, baseline (BL) and end of treatment. BL followed a 4-week single-blind placebo run-in. Patients were classed as having mild (<4), moderate (≥ 4 to <7) or severe pruritus (≥ 7 to 10) based on mean Worst Daily Itch NRS score in the 7 days prior to BL.

Results: The GLIMMER population (N = 147) was 94% female with a mean (SD) age at BL of 55.8 (11.04) years. Most patients had moderate pruritus (n = 76), with similar numbers with mild (n = 35) and severe (n = 36) pruritus. At BL, alkaline phosphatase levels were higher with greater itch severity: mean (SD) 177 (115.4) and 249 (190.8) IU/L in patients with mild and severe itch, respectively. Overall, mean (SD) BL utility was 0.69 (0.23), lower than the general PBC population (Figure) and with a clear and notable impact of pruritus severity on health utility. Thus, patients with mild or moderate pruritus at BL had similar utilities (0.75 [0.17] and 0.76 [0.17], respectively), marginally lower than the general UK population

POSTER PRESENTATIONS

(mean at age 55–64 years: 0.804). Patients with severe pruritus at BL had notably worse utility (0.49 [0.28]), similar to patients with severe Parkinson's disease (0.47 [0.22]; Figure). Over the course of the study health utility declined in the placebo group (–0.01) and increased across all linerixibat arms (0.04–0.05). Although improvements were small (confidence intervals crossed zero), the directional change supports a treatment effect of linerixibat.



Conclusion: Pruritus (particularly severe pruritus) has a significant negative impact on HRQoL and health utility. Presence and severity of itch should be evaluated in PBC and prioritised in treatment plans.

Funding: GSK (201000).

THU471

Isolated IgG elevation is not associated with worse outcome in patients with autoimmune hepatitis

Alvaro Diaz Gonzalez¹, Lorena Carballo-Folgoso², Carmen Álvarez-Navascués², Judith Gómez-Camarero³, Diana Horta⁴, Beatriz Mateos Muñoz⁵, María Del Barrio¹, Marina Cobreros¹, Sergio Rodríguez-Tajes⁶, Olivas Ignasi⁶, Indhira Perez Medrano⁷, Inmaculada Castello⁸, Alberto Gómez⁹, Manuel Rodríguez-Perálvarez^{9,10}, Javier Crespo¹, Magdalena Salcedo¹¹, Ana Barreira¹², Mar Riveiro Barciela¹², Maria Carlota Londoño⁶. ¹Marqués de Valdecilla University Hospital, Digestivo, Santander, Spain; ²Central University Hospital of Asturias, Oviedo, Spain; ³Burgos University Hospital, Burgos, Spain; ⁴Hospital Universitari MútuaTerrassa, Terrassa, Spain; ⁵Hospital Ramón y Cajal, Madrid, Spain; ⁶Hospital Clínic de Barcelona, Barcelona, Spain; ⁷Complejo Hospitalario Universitario de Pontevedra, Digestivo, Pontevedra, Spain; ⁸Consorci Hospital General Universitari de València, València, Spain; ⁹Hospital Universitario Reina Sofia, Córdoba, Spain; ¹⁰University of Córdoba, IMIBIC, CIBERehd, Department of Hepatology and Liver Transplantation, Córdoba, Spain; ¹¹Gregorio Marañón Hospital, Madrid, Spain; ¹²Hospital Universitari Vall d'Hebron, Barcelona, Spain

Email: mlondono@clinic.cat

Background and aims: The goal of treatment in patients with autoimmune hepatitis (AIH) is biochemical remission, (normalization of transaminases and IgG). However, the clinical impact and the management of isolated IgG elevation is unknown. We aimed to describe the outcome of AIH patients with persistently normal transaminases attending to evolutionary changes in IgG levels.

Method: Multicenter retrospective study of patients with AIH diagnosed at 10 referral centres in Spain. Only patients with persistently normal transaminases after induction treatment were included in the study. Patients were divided according to IgG levels during the follow-up as: a) persistently normal (IgGn); b) persistently elevated (IgGe); c) IgG flares (IgGf).

Results: Out of 1253 patients with AIH, 266 (21%) presented persistently normal transaminases during the follow-up. Baseline characteristics are shown in table 1. IgG was persistently elevated in

78 (29%) patients and flared in 28 (11%). The median time to transaminases normalization was 15 months (IQR 7–27). Patients with IgGn were more frequently diagnosed with non-severe acute AIH (NS-AIH; $p = 0.001$) and those with IgGe had lower prevalence of positive anti-smooth muscle antibody (SMA, $p = 0.001$). Immunosuppression was intensified in 13 (12%) patients with abnormal IgG, leading to normalization in 7 patients. 95 patients had at least two liver stiffness measurements (LSM) available. After a median follow-up of 4.5 years (IQR 3–8), LSM worsen in 12 (13%) patients, improved in 23 (24%), and remained stable in 60 (63%). IgG levels did not impact the evolution of LSM. 17 patients (6%) developed cirrhosis, without differences between groups. The risk of cirrhosis was higher in patients who normalized transaminases beyond month 15 after induction treatment (OR 3.42; CI95% 1.1–10.8) and in those with LSM higher than 10.5 kPa at the time of transaminases normalization (OR 6.13; CI95% 1.18–31.8).

Age	Total (n = 266). 64 (52–73)	IgGe (n = 78). 63 (52–72)	IgGn (n = 160). 63 (52–73)	IgGf (n = 28). 67.1 (59–75)
AIH at diagnosis				
Acute liver failure	3 (1)	2 (23)	0	1 (4)
Acute severe-AIH	43 (16)	18 (23)	20 (12)	5 (18)
Chronic AIH	80 (30)	26 (33)	43 (27)	11 (39)
NS-AIH	137 (52)	32 (41)	97 (61)	11 (39)
Cirrhosis at diagnosis (n, %)	32 (12)	8 (10)	22 (14)	2 (7)
ALT (U/L)	584 (230–1204)	580 (390–1141)	622 (229–1264)	426 (161–1094)
Bilirubin (mg/dL)	2.2 (0.8–8)	2.1 (0.6–8)	2.4 (0.8–8)	1.3 (0.7–8.1)
INR	1.1 (1–1.3)	1.2 (1.03–1.44)	1.1 (1–1.24)	1.18 (1–1.24)
ANA (n, %)	209 (80)	56 (75)	126 (80)	27 (100)
ASMA (n, %)	121 (46)	24 (32)	77 (49)	20 (71)
Anti-SLA (n, %)	5 (2)	1 (1)	2 (1)	1 (3)
IgG (mg/dL)	1954 (1405–2560)	2033 (1462–2520)	1740 (1300–2290)	2800 (2200–3330)
Cirrhosis follow-up (n, %)	17 (6)	4 (5)	10 (6)	3 (11)

Continuous variables are presented as median and IQR.

Conclusion: Isolated IgG elevation in patients with persistently normal transaminase levels, did not impact the outcome of patients with AIH.

THU472

Linerixibat dose-response analysis of C4 concentrations as a quantitative approach to predict gastrointestinal tolerability

Fernando Carreño¹, Rashmi Mehta², Andrea Ribeiro³, Jon Collins², Brandon Swift². ¹GlaxoSmithKline, Upper Providence, PA, United States; ²GlaxoSmithKline, Research Triangle Park, NC, United States; ³GlaxoSmithKline, Madrid, Spain

Email: fernando.o.carreno@gsk.com

Background and aims: Linerixibat is an ileal bile acid transporter (IBAT) inhibitor in Phase 3 development for the treatment of cholestatic pruritus in primary biliary cholangitis (PBC). IBAT inhibition reduces bile acid (BA) reabsorption from the intestine, reducing circulating systemic BA concentrations and pruritus but leading to excess BA in the colon with potential to cause diarrhoea. Linerixibat increases concentrations of 7-alpha-hydroxy-4-cholesten-3-one (C4), a prognostic biomarker for BA-induced diarrhoea. Here we evaluate the relationships between (1) linerixibat and serum C4 concentrations; and (2) effect of C4 on probability of diarrhoea using the gastrointestinal symptoms rating scale (GSRS).

Method: Serum C4 data were included from healthy subjects in three Phase 1 studies (114985, 116511, 205808) and from patients with PBC in two Phase 2 studies (177213, 201000 [GLIMMER]).

C4 concentrations over time were described by a k-PD indirect-response model with a stimulatory effect of linerixibat on C4 production. Weekly GSRS data were collected in GLIMMER, which evaluated the impact of five linerixibat treatment regimens in patients with PBC.

Results: The k-PD model showed a saturable dose-response relationship with C4 concentrations. The two BID linerixibat

regimens led to a 24% increase in C4 compared with the change from baseline for a similar daily QD dose (i.e. 90 mg BID vs 180 mg QD). Increased C4 concentrations trended with increased diarrhoea scores in the GSRS tool. C4 concentrations ≥ 52 ng/ml were associated with a 62% increased probability of moderate-to-severe diarrhoea scores compared with C4 concentrations < 14 ng/ml, as observed in participants in the placebo arm. Simulations showed increases of 9%, 17%, 20%, 19% and 23% in moderate-to-severe diarrhoea scores for the 20 mg, 90 mg and 180 mg QD, and 40 mg and 90 mg BID doses, respectively, after the first week of linerixibat dosing. This was consistent with the rate of on-treatment diarrhoea adverse events by treatment arm in GLIMMER (placebo: 11%; 20 mg QD: 38%; 90 mg QD: 65%; 180 mg QD: 67%; 40 mg BID: 52%; 90 mg BID: 68%).

Conclusion: Linerixibat led to dose-dependent increases in serum C4 concentrations that predicted an increased probability of moderate-to-severe diarrhoea. The increase in diarrhoea scores highlights the trade-off between maximising the pharmacodynamic effect of linerixibat on pruritus and increase in GSRS scores, which guided dose selection for Phase 3.

Funding: GSK (114985, 116511, 205808, 177213, 201000)

THU473

Urinary sulfated progesterone metabolites are diagnostic markers for cholestatic pregnancy and markers of treatment response to ursodeoxycholic acid

Luiza Borges Manna¹, Caroline Ovadia¹, Jenna Sajous¹, Anita Lövgren-Sandblom², Hanns-Ulrich Marschall³, Catherine Williamson¹. ¹King's College London, Women and Children's Health, London, United Kingdom; ²Karolinska University Hospital Huddinge, Stockholm, Sweden; ³University of Gothenburg, Department of Molecular and Clinical Medicine, Gothenburg, Sweden
Email: blmanna@hotmail.com

Background and aims: Serum concentrations of sulfated metabolites of progesterone are elevated in intrahepatic cholestasis of pregnancy (ICP), and have been proposed as predictive and diagnostic biomarkers. Ursodeoxycholic acid (UDCA) treatment can alter urinary excretion of progesterone sulfates. We aimed to determine whether urinary progesterone sulfate excretion is predictive or diagnostic of ICP, and whether their levels are associated with UDCA treatment response.

Method: Urine was obtained from women with cholestatic and uncomplicated pregnancies throughout pregnancy and postpartum, including matched samples before and 1–2 weeks after commencing UDCA treatment. Urinary progesterone sulfates were measured by ultra performance liquid chromatography-mass spectrometry, and normalised according to creatinine levels (measured by colorimetric assay). Results were compared in Graphpad Prism by multiple t tests with Benjamini-Hochberg correction for multiple testing, Fisher's exact test and logistic regression.

Results: Urinary 5 α -pregnan-3 α , -20 α -diol-3, 20-disulfate (PM2DiS), 5 β -pregnan-3 α , 20 α -diol-3, 20-disulfate (PM3DiS), 5 β -pregnan-3 α , -20 α -diol-3-sulfate (PM3S), 5 α -pregnan-3 α -S, 20-one (PM4S) and 5 α -pregnan-3 β , 20 β -diol-3-sulfate (PM8S) were higher in women with cholestatic than uncomplicated pregnancies; PM8S differentiated well between the two groups (AUC 0.86, figure 1). UDCA treatment was associated with significantly reduced PM2DiS and PM3DiS (from 19.10 to 12.22, $p = 0.032$). Symptomatic response (pruritus improvement) with UDCA was predicted by the total disulfated progesterone metabolites (area under curve (AUC) = 0.80), whilst biochemical response (fall in total serum bile acid concentration) was predicted by urinary 5 α -pregnan-3 β -ol-20-one-sulfate (PM5S) and 5 β -pregnan-3 β -ol-20-one-sulfate (PM7S) (AUC = 0.81).

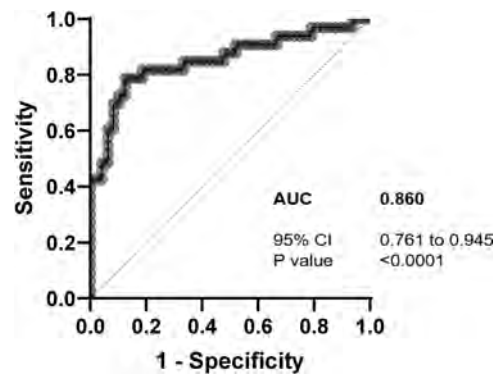


Figure: Receiver operating characteristic curve demonstrating the ability of urinary PM8S to diagnose ICP at disease onset

Conclusion: Urinary progesterone sulfate excretion appears useful diagnostically for ICP, which obviates the need for blood sampling. Similarly, using the individual profile of urinary PMS may be helpful to identify the subgroup of women for whom UDCA treatment is beneficial, and may contribute to the variable clinical response to UDCA treatment that complicates trials of its use in ICP.

THU474

COVID-19 vaccine induced autoimmune hepatitis-a first case series from India

Sowmya Iyengar¹, Anand Kulkarni¹, Goutham Reddy Katukuri², Mithun Sharma¹, Nageshwar Reddy², Nagaraja Rao Padaki¹. ¹AIG Hospital, Hepatology, Hyderabad, India; ²AIG Hospital, Gastroenterology, Hyderabad, India
Email: sowmyaiyengar.18@gmail.com

Background and aims: Liver injury is common in patients with coronavirus disease-2019 (COVID-19) infection. Recently, few studies have reported the development of autoimmune hepatitis (AIH) following COVID-19 vaccination. However, there is a lack of studies reporting the outcomes of AIH following ChAdOx1 (vector-based) and BBV152 (inactivated virus) from India. Here we aimed to describe the clinical profile of patients who developed AIH following COVID-19 vaccination. The causal association is attributed based on the temporal relationship in patients with no prior liver diseases.

Method: Patients presenting with deranged liver functions following COVID-19 vaccination to hepatology clinic were included. Virus infections were ruled out in all patients either by serology or viral quantification methods. We aimed to assess the demographics, clinical profile, and outcome of patients with vaccine-induced AIH (V-AIH) in the absence of known liver disease.

Results: A total of 31 patients presented with altered liver chemistries following vaccination. Seventeen patients were diagnosed with V-AIH (age-39.8 \pm 11.4 years; males-70.4%). None of the patient had history of alcohol overconsumption. Seventy six percent of patients had received ChAdOx1 and 23.53% had received BBV152 vaccine (Table). Seventy six percent of patients following first dose of vaccine and 23.5% following second dose of vaccine were diagnosed as V-AIH. Mean duration for development of symptoms after first dose was 25.7 days. Common symptom at presentation was jaundice in 82.3% of patients. Antinuclear antibody was positive in 71% of patients and 17% patients were negative for all serological markers of autoimmune hepatitis but had elevated IgG levels. Fifty-nine percent of patients required immunosuppression of which 41% percent of patients received oral steroids, 17% patients received intravenous steroids for 3 days followed by oral steroid, 12% patients received azathioprine. One patient succumbed to pneumonia with multiorgan failure by day 30. At 3 months, it was observed that only 17% patients needed prolonged immunosuppression and had deranged liver functions until last follow-up. Mean duration of recovery amongst rest of 76.4% patients was 5.15 \pm 3.1 weeks.

POSTER PRESENTATIONS

Table: Clinical characteristics and outcome of V-AIH

Characteristics	Number of patients (Total=17 patients)
Gender	
Male	12(70.6%)
Female	5(29.4%)
AGE(Mean±SD)	39.8±11.4 years
Vaccine type	
COVID-19	13(76.5%)
COVID-19	4(23.5%)
Symptoms onset	
After first dose	13(76.5%)
After second dose	4(23.5%)
Mean duration for symptoms onset	25.7±6.8 days
After first dose	24.2±5.1 days
After second dose	24.2±5.1 days
Mean BMI	24.23±3.1 kg/m ²
Comorbidities	
Hypothyroidism	4(23.5%)
Type 2 diabetes	4(23.5%)
Rheumatoid arthritis	1(5.9%)
CKD	1(5.9%)
Hypertension	1(5.9%)
NAFLD	1(5.9%)
Alternative medicine intake	3(17.6%)
Symptoms	
Jaundice	14(82.3%)
Nausea	7(41.2%)
Fatigue	9(52.9%)
Fever	4(23.5%)
Pain abdomen	4(23.5%)
Liver function tests	
Peak total bilirubin (Mean±SD)	8.3±7.06
Peak ALT(Mean±SD)	696±630
Peak AST(Mean±SD)	695±740
Peak ALP(Mean±SD)	1780±74
Peak serum IgG(Mean±SD)	2357±1171
Peak INR(Mean±SD)	1.73±0.24
AH1 serology	
ANA	12(70.6%)
ASMA	11(64.7%)
Anti-LKM1	5(29.4%)
AMA	4(23.5%)
Anti-SLA	0
Seronegative biopsy proven	2(11.8%)
Liver biopsy	
Typical features of AH1	10(58.8%)
Interface hepatitis	10(100%)
Mild	2(20%)
Moderate	5(50%)
Severe	3(30%)
Fibrosis	Mild in all cases (Metavir score 0-2)
BILI pattern and severity	
Hepatocellular pattern	16(94.1%)
Cholestatic pattern	3(17.6%)
Mild	5(29.4%)
Moderate	8(47.1%)
Severe	4(23.5%)
Treatment	
Conservative	7(41.2%)
Steroids	10(58.8%)
Oral steroids alone	7(41.2%)
IV followed by oral steroids	3(17.6%)
Outcome	
Alive	14(82.3%)
Dead	3(17.6%)
Mean duration for recovery	5.1±3.1 weeks

SD-standard deviation, CKD- chronic kidney disease, NAFLD- Non-alcoholic fatty liver disease, ALT- alanine amino transferase, AST- aspartate amino transferase, ALP- alkaline phosphatase, ANA-anti-nuclear antibody, ASMA- anti smooth muscle antibody, Anti-LKM1- liver-kidney microsomal antibody type 1, AMA-Anti mitochondrial antibody.

Conclusion: COVID-19 vaccine can trigger autoimmune hepatitis. Males are affected more often than females. Treatment with steroids has high success rate and significant proportion of patients have self-limiting disease and may not require long term immunosuppression.

THU475

Lymphoma in IgG4-related disease: should we be concerned?

Arif Hussienbux^{1,2}, Rory Peters^{1,2}, Charis Manganis¹, Eve Fryer³, Helen Bungay⁴, Joel David⁵, Emma Culver¹. ¹John Radcliffe Hospital, Gastroenterology, Oxford, United Kingdom; ²Authors contributed equally; ³John Radcliffe Hospital, Histopathology, Oxford, United Kingdom; ⁴John Radcliffe Hospital, Radiology, Oxford, United Kingdom; ⁵John Radcliffe Hospital, Rheumatology, Oxford, United Kingdom
Email: arif.hussienbux@hotmail.co.uk

Background and aims: Immunoglobulin G4-Related Disease (IgG4-RD) is a systemic fibroinflammatory disorder, with a predilection for the pancreas and biliary tree. We have reported an association of malignancy in our cohort of IgG4-related pancreato-biliary disease¹. We sought to assess the frequency and type of malignancy in our prospective cohort of IgG4-RD patients with radiological and histological evaluation through our monthly IgG4-RD multi-disciplinary meeting (MDM).

Method: Patients diagnosed with IgG4-RD and discussed at the MDM between November 2016 and September 2021 were included, with diagnosis based on established HISORT, CDC or Boston

histopathological consensus criteria. Retrospective evaluation of presence and timing of malignancy confirmed radiologically and histologically through the MDM. UK national cancer registry data² was used to determine the age and gender standardised incidence ratios (SIR) for malignancy and non-hodgkin's lymphoma (NHL) for comparison.

Results: Of 105 IgG4-RD patients (median age 67; IQR 56–76 years, male:female ratio 2.4:1), 21 (20%) developed malignancy (table 1), with an SIR of 12.3 (95%CI 7.6–18.8).

Table 1:

Primary Cancer	Observed Cases
Lymphoma	7
Renal	2
Gastric	1
Biliary	2
Breast	1
Oesophagus	1
Thyroid	1
Pancreas	1
Prostate	2
Colon	2
Ovarian	1

One-third (7/21) had lymphoma. Most (6/7) were NHL B cell lymphomas, SIR 93.6 (95%CI 34.2–203.7). 3 patients with lymphoma had IgG4-related pancreato-biliary disease, 3 had IgG4-related head and neck disease and 1 had IgG4-related renal disease. 3 lymphomas were diagnosed prior, and 4 subsequent, to their IgG4-RD diagnosis. The median time between lymphoma and IgG4-RD diagnosis was 4.4 years; (range –10.5–11.8 years). Of these, 1 had been exposed to an immunomodulator, azathioprine, prior to lymphoma. Lymphoma was successfully treated with R-CHOP chemotherapy in all cases.

Conclusion: We demonstrate an increased incidence of malignancy in our IgG4-RD cohort with a striking incidence of NHL, which otherwise accounts for <4% of annual UK new cancer diagnoses. There are currently no cancer surveillance guidelines in IgG4-RD, and the frequency of lymphoma makes us question the use of off-label azathioprine as relapse prevention in this older male cohort.

References

- Huggett MT, *et al.* Type 1 Autoimmune Pancreatitis and IgG4-Related Sclerosing Cholangitis Is Associated With Extrapancreatic Organ Failure, Malignancy, and Mortality in a Prospective UK Cohort. *Am. J. Gastroenterology*. 2014;109
- Cancer Research UK-All cancer and Non-Hodgkin's lymphoma incidence statistics comprising data from the National Cancer Registration and Analysis Service, ISD Scotland, Welsh and the Northern Ireland Cancer Registry-Accessed 22/11/2021 <https://www.cancerresearchuk.org/health-professional/cancer-statistics/statistics-by-cancer-type/non-hodgkin-lymphoma>

THU476

Measurement properties of the PBC-10 in a dutch population

Maria van Hooff¹, Rozanne de Veer¹, Maren Harms¹, Geraldine Da Silva¹, José Willemse², Herold Metselaar¹, Elaine Utomo³, Adriaan Van der Meer¹. ¹Erasmus University Medical Center, Department of Gastroenterology and Hepatology, Rotterdam, Netherlands; ²Dutch Liver Patients Association, Hoogland, Netherlands; ³Independent Researcher, Berkel en Rodenrijs, Netherlands
Email: m.vanhooff@erasmusmc.nl

Background and aims: Practice guidelines advice to evaluate the Health Related Quality of life (HRQoL) of all patients with primary biliary cholangitis (PBC). The PBC-40 has proven to be an adequate PBC-specific HRQoL measure. However, as this measure can be time consuming and thus less practical, the UK-PBC group developed the PBC-10 as a shorter version for screening HRQoL in clinical practice. The aim of this study was to assess the measurement properties of the items selected for the PBC-10 in a Dutch PBC population.

Method: Our study group previously translated the PBC-40 into Dutch and validated it in a Dutch population. Existing data of the Dutch PBC-40 questionnaire was used to assess patients responses on the PBC-10 items. Internal consistency of the PBC-10 was assessed by Cronbach's alpha. A value between 0.70 and 0.95 is considered as adequate. Content validity was assessed by determination of floor and ceiling effects (i.e. >15%). Each PBC-10 item was correlated with the total score of the corresponding original PBC-40 domain.

Results: In total, 177 patients with PBC were included. The mean (SD) age was 61.1 (9.9) years and the majority of patients was female (n = 164; 92.7%). Of the total 1770 items, 81 items (4.6%) were missing. The PBC-10 showed a Cronbach's alpha of 0.895. Floor and ceiling effects were observed in 7 and 3 items, respectively. Floor effects ranged from 13.6% to 61.0%. All PBC-10 items were significantly correlated with the corresponding domains of the PBC-40 (Pearson correlations ranged from 0.711 to 0.912, $p < 0.001$ for all) (Table).

PBC-10 items	n	Floor (%)	Ceiling (%)	Pearson correlation with PBC-40 domains $p < 0.001$ for all				
				Symptoms (7 items)	Itch (3 items)	Fatigue (11 items)	Cognition (6 items)	Social (10 items)
1 Embarrassed because of itching	105	61.0	1.9	0.854				
2 Bloating after small amounts of intake	177	36.8	2.3	0.711				
3 Very dry mouth	176	21.6	11.9	0.730				
4 Fatigue interfered with daily routine	177	13.6	12.4			0.894		
5 Need to force myself to be active	177	14.7	6.2			0.885		
6 Need extra day to recover	176	15.9	23.9			0.850		
7 Difficult to concentrate	175	28.0	1.7				0.912	
8 Guilt regarding impact PBC on activity	175	54.3	8.0					0.772
9 Social life almost stopped	175	44.0	3.4					0.833
10 PBC reduces quality of life	176	17.0	18.2					0.893

Conclusion: In a Dutch population, the PBC-10 showed an adequate internal consistency and reflects the content of corresponding PBC-40 domains. There were, however, substantial floor effects. The PBC-10 may be considered in clinical practice as a screening tool for patients with a profound impact of PBC on their HRQoL. However, the Dutch PBC-10 may be less suitable to identify PBC patients with less severe HRQoL impairment or to detect further improvement of their HRQoL following intervention.

THU477

Gluco-regulatory disturbances in primary biliary cholangitis and non-alcoholic fatty liver disease compared with healthy individuals

Anne-Sofie Houlberg Jensen^{1,2}, Henriette Ytting^{1,3}, Josephine Grandt^{1,2}, Andreas Møller¹, Mikkel Werge¹, Elias Rashu¹, Liv Hetland¹, Mira Thing¹, Anders Junker¹, Lise Hobolth¹, Christian Mortensen¹, Flemming Bendtsen^{1,4}, Flemming Tofte¹, Mogens Vyberg^{5,6}, Reza Serizawa⁵, Lise Lotte Gluud¹, Nicolai J Wewer Albrechtsen^{2,7,8}. ¹Hvidovre Hospital, Gastro Unit, Hvidovre, Denmark; ²Novo Nordisk Foundation Center for Protein Research, København, Denmark; ³Rigshospitalet, European Reference Network on Hepatological Diseases (ERN-RARE-LIVER), København, Denmark; ⁴The University of Copenhagen, Faculty of Health and Medical Sciences, København, Denmark; ⁵Hvidovre Hospital, Department of Pathology, Hvidovre, Denmark; ⁶Center for RNA Medicine, Aalborg, Denmark; ⁷Rigshospitalet, Department of Clinical Biochemistry, København, Denmark; ⁸The University of Copenhagen, Faculty of Health and Medical Sciences, Department of Biomedical Sciences, København, Denmark

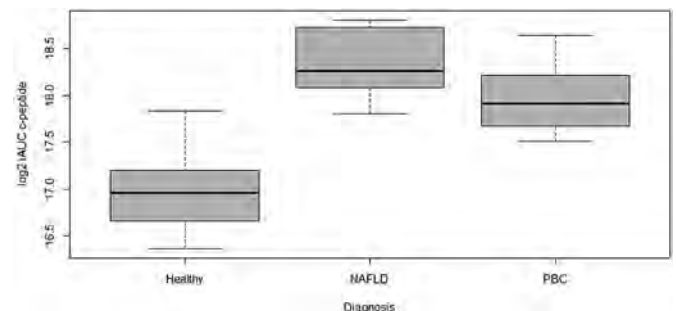
Email: nicolai.albrechtsen@sund.ku.dk

Background and aims: Gluco-regulatory disturbances such as hepatic insulin resistance, hyperinsulinemia and pre-diabetes are observed in individuals with non-alcoholic fatty liver disease (NAFLD). Whether autoimmune liver diseases-herein primary

biliary cholangitis (PBC)-also carry gluco-regulatory disturbances is unknown. We therefore investigated glucose and hormonal responses to an oral glucose tolerance test (OGTT) in patients with biopsy-verified non-cirrhotic PBC and NAFLD and healthy controls. The data presented are early results from FALL, a prospective cohort study.

Method: 23 participants have been included hereof 8 healthy controls (mean age 23, mean BMI 23 kg/m²), 9 patients with PBC (mean age 55, mean BMI 31 kg/m²) and 6 patients with NAFLD (mean age 38, mean BMI 31 kg/m²). None of the included patients had diabetes. In the PBC group, 3 had NAFLD. Blood samples were obtained at baseline (fasting) and 15, 30, 45, 60, 90 and 120 minutes during the OGTT. Glucose, c-peptide and insulin concentrations were measured. A validated marker for hepatic insulin resistance (the homeostasis model assessment of insulin resistance (HOMA-IR)) and the incremental area under curve (iAUC) for glucose, c-peptide and insulin responses were calculated. Results are presented as means (95% CI).

Results: Fasting glucose, c-peptide and insulin levels were significantly increased in both PBC (glucose 5.6 mM (4.7–6.7), c-peptide 993 pM (556–1773), insulin 98 pM (33–298)) and NAFLD (glucose 5.7 mM (5.2–6.1), c-peptide 1334 pM (1036–1719), insulin 166 pM (103–267)) compared with healthy (glucose 4.7 mM (3.9–5.6), c-peptide 483 pM (268–869), insulin 43 pM (14–136)). Hepatic insulin resistance (reflected by fasting HOMA-IR) was present in PBC (4.0 (1.2–13.9)) and NAFLD (7.0 (4.1–11.9)) but not in healthy individuals (1.5 (0.4–5.4)). No significant difference in glucose levels was observed between the groups ($p = 0.106$). Beta-cell secretion (c-peptide) was significantly increased in PBC ($p < 0.001$) and NAFLD ($p < 0.001$) suggesting that peripheral insulin resistance was present in patients with PBC and NAFLD. Insulin responses (reflecting both beta-cell secretion and hepatic insulin extraction) were numerically higher in both PBC and NAFLD compared with healthy but only reached statistical significance in NAFLD ($p = 0.002$).



Conclusion: Our data suggest that patients with PBC may have gluco-regulatory disturbances including both hepatic insulin resistance and altered pancreatic endocrine function. Whether these impairments reflect an obesity prone phenotype in PBC and NAFLD patients cannot be concluded from the current data. Metabolic dysfunction of PBC may be underestimated and warrant further investigation.

THU478

Proportion of time and degree to which liver biochemistries are out-of-range predicts time to first occurrence of negative hepatic outcomes in people with primary biliary cholangitis

Timothy Ritter¹, Christina Hanson², Christopher C. Fernandes³, Joanna MacEwan⁴, Xin Zhao⁴, Craig Parzynski⁴, Erik Ness⁵, Gail Cawkwell⁵, Darren Wheeler⁵, Tracy Mayne⁵. ¹GI Alliance, United States; ²South Denver Gastroenterology, United States; ³TCU and UNTHSC School of Medicine, United States; ⁴Genesis Research, United States; ⁵Intercept Pharmaceuticals Inc, United States
Email: tim.ritter@gialliance.com

Background and aims: Previous research has demonstrated a significant association between abnormal liver biochemistries at one time point and the risk of death and liver transplant in patients with primary biliary cholangitis (PBC). We hypothesized that both the proportion of time and degree to which liver biochemistries are out-of-range, including normal values associated with adverse liver health, predict time to first occurrence of negative hepatic outcomes.

Method: Patients in the Optum Clinformatics database between July 1, 2016 and December 31, 2020 were included if they were diagnosed with PBC by either ≥ 1 inpatient discharge claim with a PBC diagnosis or ≥ 2 outpatient claims with a primary PBC diagnosis on separate days and had >1 of each liver biochemistry available (ALP, TB, AST, ALT, and ALB). Patients with autoimmune hepatitis, HIV, gastric bypass, liver disease, hepatic decompensation, or use of second line (2L) treatment (obeticholic acid or fibrates) prior to PBC diagnosis were excluded. Survival analysis with the proportion of time spent out-of-range as a time-dependent variable and a composite end point of hepatic decompensation, liver transplant, or death was conducted. Biochemistry values were carried forward until the next recorded value. Patients were censored at end of follow-up or initiation of 2L treatment.

Results: 2, 379 patients (85.3% female) were included. At baseline, mean age was 63 years; 11% had cirrhosis; 7% had NASH. During the follow-up period (mean 2.5 yrs), 73.8% received ursodeoxycholic acid and 3.6% (N=86) were censored at start of 2L treatment. Mean number of measures per biochemistry ranged from 7.2–8.4. On average patients spent 52.5%, 8.5%, 37.5%, and 20.7% of the follow-up period over ULN for ALP, TB, AST, and/or ALT, respectively, and 19.1% under LLN for ALB. For each individual biochemistry the risk of negative hepatic events increased significantly with greater proportion of time out-of-range and greater divergence from desired values (Figure). For example, for a patient with all 5 years follow-up (i.e., 100% time) with ALB $\leq 0.9 \times$ LLN, the risk of an event was 271% higher than that of a patient with ALB $>0.9 \times$ LLN all 5 years (i.e., 0% time); 104% higher for ALP $>1.5 \times$ ULN; 124% for ALT $>2 \times$ ULN; 145% higher for AST $>1.5 \times$ ULN; and 157% higher for TB $>1 \times$ ULN.

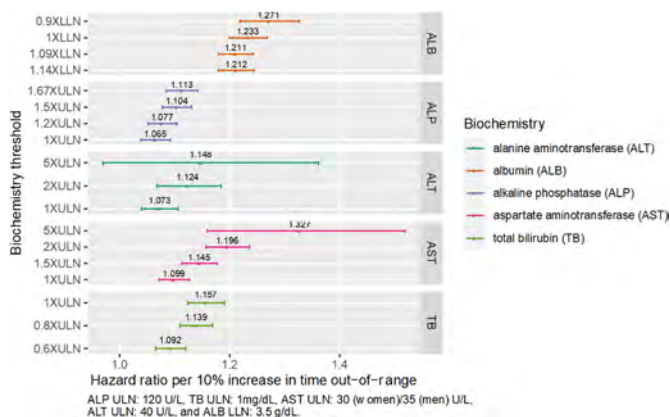


Figure: Hazard ratio of decompensation, transplant, or death for each additional 10% of time out-of-range by biochemistry threshold

Conclusion: Greater proportion of time spent out-of-range and greater divergence from normality on each liver biochemistry was associated with significantly increased risk of hepatic decompensation, liver transplant, or death in patients with PBC. These results suggest that avoiding substantial time with out-of-range liver biochemistries, potentially through greater utilization of effective first line and 2L therapies, may improve hepatic outcomes for patients with PBC.

THU479

Outcomes following immune checkpoint inhibitor re-challenge in patients who developed grade 3 and 4 hepatotoxicity

Amy Hicks¹, Ramu Chimakurthi¹. ¹Leeds Teaching Hospitals NHS Trust, Hepatology, Leeds, United Kingdom
Email: amy.hicks@nhs.net

Background and aims: Immune checkpoint inhibitors (ICI) are used to treat a variety of cancers. Immune-related adverse events (irAEs) are not uncommon, with Grade 3 hepatitis in 1–2% of those treated with single agents and ~15% in those treated with Ipilimumab and Nivolumab combination (ESMO guidelines 2017). European and American society guidelines recommend discontinuation of ICI after development of Grade 3 or 4 hepatitis. Re-challenge with single ICI can be considered in those who developed Grade 3 hepatitis on combination therapy. We reviewed our outcomes following re-challenge in those who developed Grade 3 and 4 hepatitis in our regional oncology centre.

Method: Patients who received ICI from January 2018 to January 2022 were reviewed. Those who developed Grade 3 and 4 hepatotoxicity were identified by accessing their electronic health record. We assessed the following outcomes in these patients: a) those who had re-challenge with ICI b) choice of ICI in re-challenged c) whether they developed further hepatitis d) outcomes in those who were not re-challenged.

Results: 1045 patients received ICIs over a 4-year period (807 single agent and 238 Ipilimumab-Nivolumab combination). 54 patients developed Grade 3 or 4 hepatitis. Of these, 22 (40.7%) were re-challenged and their outcomes are shown in Table 1. All patients were off immunosuppression at the time of re-challenge. Contrary to existing guideline recommendations, 3 patients with Grade 4 hepatitis and 7 patients with Grade 3 hepatitis on single agent were re-challenged with ICIs. 4 out of 11 (36%) developed further hepatitis (Grade ≥ 3) on re-challenge. Of note, all patients with recurrent hepatotoxicity developed this after only 1 cycle of re-treatment. ICI were discontinued permanently in the remaining 32 patients. 15 had complete response to treatment, 8 had disease progression and were switched to an alternative treatment, 6 patients deteriorated and died (1 from irAE and 5 from disease progression), 1 is due for re-challenge soon, and 2 patients changed to an alternative regimen due to the hepatitis.

Table 1: ICI re-challenge outcomes.

Initial hepatitis grade (n = no. patients)	Initial ICI	Re-challenge ICI	Recurrence of hepatitis and cycle number (Cx)
Gr 3 = 19	Ipi and Nivo = 12	Nivo = 12	- 2 pts (17%): - Gr 2 (C2) - Gr 4 (C1)
	Nivo = 3	Nivo = 3	- 1 pt (33%): - Gr 4 (C1)
	Pembro = 4	Pembro = 3 Ipi = 1	None - 1 pt (100%): - Gr 3 (C1)
Gr 4 = 3	Pembro = 2	Pembro = 2	- 2 pts (100%): - Gr 3 (C1) - Gr 3 (C1)
	Ipi and Nivo = 1	Nivo = 1	None (Stopped due to colitis after C2)

Conclusion: Re-challenge with ICI following Grade 4 hepatitis resulted in early irAE recurrence in our group. However, the vast majority (>70%) re-challenged with ICIs after Grade 3 hepatitis on

single agent did not develop hepatitis recurrence. Nearly 50% of patients are in remission and alive to this day despite cessation of ICI following Grade 3 and 4 hepatitis. Our numbers are small but will add to a growing body of evidence in this field.

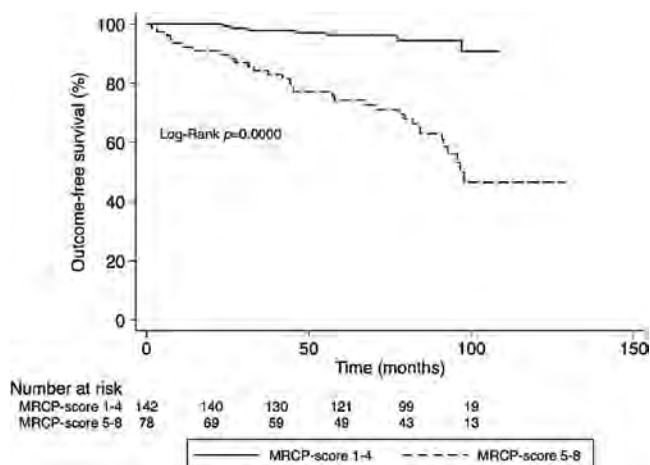
THU480

Development of a novel MRCP-score for patients with primary sclerosing cholangitis, and assessment of agreement and prognostic value

Aristeidis Grigoriadis^{1,2}, Kristina Ringe³, Johan Bengtsson^{4,5}, Erik Fridh Baubeta⁶, Cecilia Forsman⁷, Nafsika Korsavidou-Hult⁸, Fredrik Rorsman⁹, Emma Nilsson¹⁰, Nikolaos Kartalis^{2,11}, Annika Bergquist^{1,12}. ¹Karolinska Institutet, Medicine, Stockholm, Sweden; ²Karolinska University Hospital, Radiology, Stockholm, Sweden; ³Hannover Medical School, Diagnostic and Interventional Radiology, Hannover, Germany; ⁴Lund University, Department of Clinical Sciences/Division of Radiology, Lund, Sweden; ⁵Skåne University Hospital, Center for Medical Imaging and Physiology, Lund, Sweden; ⁶Skåne University Hospital, Diagnostic Radiology, Department of Translational Medicine, Lund, Sweden; ⁷Uppsala University Hospital, Medical Imaging Centre, Sweden; ⁸Uppsala University, Radiology and Nuclear Medicine, Sweden; ⁹Uppsala University Hospital, Gastroenterology and Hepatology, Sweden; ¹⁰Skåne University Hospital, Department of Clinical Sciences, Lund, Sweden; ¹¹Karolinska Institutet, Department of Clinical Science, Intervention and Technology (CLINTEC), Stockholm, Sweden; ¹²Karolinska University Hospital, Hepatology, Stockholm, Sweden
Email: aristeidis.grigoriadis@ki.se

Background and aims: MRCP is used for diagnosis and follow-up of patients with primary sclerosing cholangitis (PSC). Interest in the prognostic value of MRCP is increasing. Aim of our study is to develop an MRCP-score based on cholangiographic findings previously associated to outcomes and assess its reproducibility and prognostic value in PSC.

Method: The MRCP-score was developed based on the extent and severity of cholangiographic changes of intrahepatic and extrahepatic bile ducts (range 0–8) in coronal 3D-MRCP. In this ethics review-board approved retrospective, multicenter study, three pairs of radiologists (2 pairs of experienced, one pair of experienced and less experienced) from three tertiary centers, applied the score independently on MRCP-examinations of 220 consecutive PSC patients (103, 52, and 65, respectively) from a prospectively collected PSC-cohort, with median follow-up of 7.4 years. Interreader and intrareader agreements were assessed with intraclass correlation coefficient (ICC). After consensus reading, the prognostic value of the score was assessed with Cox-regression and outcome-free survival rates with Kaplan-Meier estimates. Area under the curve (AUC) was calculated and 10-fold cross-validation was performed.



Results: 40 patients developed outcomes (liver transplantation or liver-related death). Interreader agreement between experienced radiologists was good (ICC = 0.82; 95%CI:0.74–0.87, and ICC = 0.81; 95%CI:0.70–0.87, respectively) and better than agreement for the pair of experienced/less experienced radiologist (ICC = 0.48; 95%CI:0.05–0.72). Agreement between radiologists from the three centers was good (ICC = 0.76; 95%CI:0.57–0.89). Intrareader agreement was good to excellent (ICC = 0.85–0.93). AUC for the MRCP-score was 0.83. Patients with MRCP-score 5–8 had 8.4 times higher risk (HR = 8.4; 95%CI:3.9–18.3) for developing outcomes, and significantly worse survival ($p < 0.000$), compared to those with MRCP-score 0–4.

Conclusion: This novel MRCP-score is reproducible and strongly associated to outcomes which indicates its value for the prognosis of PSC-patients in clinical practice.

THU481

Right and left lobe biopsies by mini-laparoscopy reveals clinically significant sampling error in staging and grading in AIH

Johannes Hartl¹, Marcial Sebode¹, Malte Wehmeyer¹, Sören Weidmann¹, Christoph Schramm¹, Ansgar Lohse¹, Till Krech¹, Jörg Schrader¹. ¹University Hospital Hamburg-Eppendorf (UKE), First Department of Medicine, Hamburg, Germany
Email: j.hartl@uke.de

Background and aims: Liver diseases may affect the liver heterogeneously. Thus, not only diagnosis but also grading and staging of inflammatory activity and fibrosis may largely depend on the area of liver biopsy. Hence, the aim of this study was to assess the added benefit of double biopsy of both liver lobes during minilaparoscopy in patients with autoimmune liver disease.

Method: We identified all patients with autoimmune hepatitis (AIH), primary biliary cholangitis (PBC), primary sclerosing cholangitis (PSC) or variant syndromes (AIH/PBC and AIH/PSC), who underwent a double biopsy of both liver lobes via minilaparoscopy between 01/2016–12/2020 in our prospectively maintained database. Differences in fibrosis stage and disease activity between liver lobes were assessed by an experienced hepato-pathologist.

Results: A total of 111 patients with AIH received a biopsy of both liver lobes (AIH: N = 83, AIH/PBC: N = 24, AIH/PSC: N = 4). Differences in inflammatory activity as assessed by Ishak's modified activity index (mHAI) were observed in 69 (62%) patients. In 41 (38%) patients the difference was ≥ 2 points, in 12 patients (11%) ≥ 3 points. According to current EASL guidelines, starting/intensification of immunosuppression should be discussed in patients with a mHAI of 4–5, as it was reported to be associated with excess mortality, a mHAI ≥ 6 prompts intensified immunosuppression in most cases. Thus, a mHAI 4–6 represents a most relevant range for guiding treatment decisions. 48% of the AIH patients had a mHAI within this range. Importantly, in 21 patients (20%) a mHAI ≥ 4 was only observed in one liver lobe. Also, 17 (15%) patients demonstrated a mHAI ≥ 6 in only in one liver lobe. Based on these observations, the number needed to double-biopsy to identify clinically relevant differences in inflammatory activity was only 5 patients. Differences of fibrosis stage were identified in 31/111 (28%) AIH patients. In 3/18 (17%) cirrhotic patients, histological changes consistent with cirrhosis were only observed in one liver lobe.

A biopsy of both liver lobes was performed in 16 PSC and 13 PBC patients. Differences of fibrosis stage were observed in 1/16 and 3/13 patients, and differences in mHAI in 8/16 and 5/13 patients, respectively. However, no treatment relevant difference was identified.

No major adverse event occurred.

Conclusion: Obtaining a biopsy of the right and left liver lobe is a safe procedure during minilaparoscopy that results in more accurate staging and grading with direct therapeutic consequences in patients with AIH.

THU482

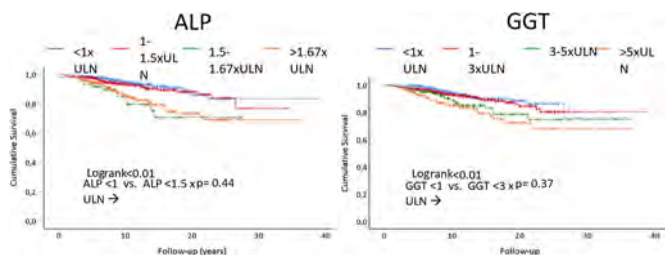
Should we seek complete liver tests normalization in primary biliary cholangitis? Data from ColHai registry

Álvaro Díaz-González¹, Sergio Rodríguez-Tajes², Mercedes Vergara Gómez³, Emilio Fabrega¹, Manuel Romero Gomez⁴, Agustín Albillos⁵, Judith Gómez-Camarero⁶, Diana Horta⁷, Adolfo Gallego⁸, Montserrat García-Retortillo⁹, Raul J. Andrade¹⁰, Moisés Diago¹¹, Rosa M Morillas¹², Manuel Hernández Guerra¹³, Carlos Ferré Aracil¹⁴, Margarita Sala¹⁵, Elena Gómez Domínguez¹⁶, Marina Berenguer¹⁷, María Carlota Londoño¹⁸, Grupo del Registro Col-Hai Enfermedades Autoinmunes y colestásicas¹⁹. ¹Hospital Marqués de Valdecilla; ²Hospital Clínic Barcelona; ³Hospital Universitario Parc Taulí; ⁴Hospital Universitario Virgen Del Rocío; ⁵Hospital Universitario Ramón y Cajal; ⁶Hospital Universitario de Burgos; ⁷Hospital Mutua de Terrassa; ⁸Hospital de la Santa Creu i Sant Pau; ⁹Hospital del Mar; ¹⁰Universidad de Málaga; ¹¹Hospital Universitario General de Valencia; ¹²Hospital Germans Trias i Pujol; ¹³Hospital Universitario de Canarias; ¹⁴Hospital Universitario Puerta del Hierro; ¹⁵Hospital Josep Trueta; ¹⁶Hospital Universitario Doce de Octubre; ¹⁷Hospital La Fe; ¹⁸Hospital Clínic Barcelona, Liver Unit, Barcelona, Spain; ¹⁹AEEH, CIBEREHD
Email: mlondono@clinic.cat

Background and aims: Response criteria to ursodeoxycholic acid (UDCA) treatment in patients with primary biliary cholangitis (PBC) are based on the reduction of alkaline phosphatase (ALP), total bilirubin (TB), and aspartate aminotransferase (AST). However, recent studies suggest that complete normalization of these tests result in better clinical outcomes. More studies are necessary to validate these data and to determine the need for increasing the strictness of UDCA treatment-response criteria. Therefore, we sought to investigate the impact of TB, AST, ALP and gamma-glutamyl transferase (GGT) normalization after 12 months of UDCA treatment on patients' survival.

Method: Retrospective analysis of 1154 patients with PBC patients included in the ColHai registry (Spanish registry for patients with autoimmune and cholestatic liver disease). Liver tests were categorized according to the upper limit of normal (ULN) for each center: 1) AST: <1, 1–1.5, >1.5; 2) ALP: <1, 1–1.5, 1.5–1.67, >1.67; 3) GGT: <1, 1–3, 3–5, >5; 4) TB: <0.6, 0.6–1.2, >1.2.

Results: Most of the patients were female (90%), with a median age of 55 years (range 46–63). 116 (10%) died during a median follow-up period of 10 years (range 6.7–15.7). In the univariate analysis AST < ULN (HR 0.45; 95CI% 0.35–0.65), ALP < ULN (HR 0.51; 95CI% 0.34–0.78), GGT < ULN (HR 0.60; 95CI% 0.38–0.94) and TB < 0.6 × ULN (HR 0.35; 95CI% 0.24–0.52) were associated with a significantly lower mortality rate. There were no significant differences in survival between patients with ALP < ULN vs. <1.5 × ULN or those with GGT < ULN vs. <3 × ULN (Figure). In the multivariate analysis, only TB < 0.6 × ULN and ALP < 1.5 × ULN were independently associated with lower mortality (HR 0.42; p < 0.01 and HR 0.57; p = 0.01, respectively).



Conclusion: ALP normalization was not better than the usual cut-off of 1.5 × ULN to predict survival but decreasing TB to better than normal levels (0.6 × ULN) significantly improved patients' survival.

THU483

Home-based exercise in patients with refractory fatigue associated primary biliary cholangitis: final results from the EXerCise Intervention in choleStatic LivEr Disease (EXCITED) clinical trial

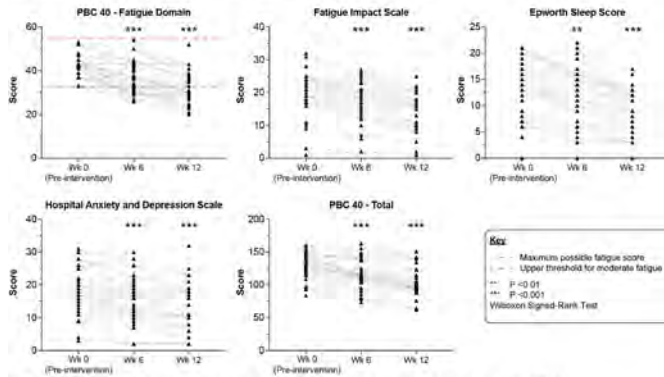
Alice Freer¹, Felicity Williams^{1,2}, Simon Durman¹, Jennifer Hayden¹, Matthew Armstrong¹, Palak Trivedi^{1,3}. ¹University Hospital Birmingham NHS Foundation Trust, Liver Department, Birmingham, United Kingdom; ²University of Birmingham, Institute of Inflammation and Ageing, Birmingham; ³University of Birmingham, NIHR Birmingham Centre for Liver and Gastrointestinal Research, Birmingham, United Kingdom
Email: freerae218@yahoo.com

Background and aims: Debilitating, refractory fatigue is the most commonly reported symptom of primary biliary cholangitis (PBC), affecting 40–80% of patients (pts). The pathogenesis is unknown, but muscle bioenergetic abnormalities are proposed to contribute. Herein, we present the results of a single-arm, open-label clinic trial, to assess the efficacy and safety of a novel home-based exercise program (HBEP) in pts with PBC and severe fatigue (NCT04265235). **Method:** A remotely-monitored, 12-week (wk) HBEP was delivered to patients with PBC and moderate-severe fatigue (PBC40 fatigue score >33; other causes excluded). This consisted of individualised body weight resistance exercises completed at moderate intensity and weekly telephone health calls (first 6 wks only). Adherence was monitored using GeneActiv wrist monitors. The primary efficacy outcome measure was the proportion of individuals attaining at least a >5-point reduction in the PBC40 fatigue domain at wk 12. Key secondary outcomes included assessment of the Fatigue Impact Scale (FIS), other domains of the PBC-40, the Chronic Liver Disease Questionnaire (CLDQ), the Epworth Sleep Score (ESS), the Hospital Anxiety and Depression Scale (HADS), aerobic exercise capacity (incremental shuttle walk test [ISWT]; Duke Activity Status Index [DASI]; metabolic equivalent of task [MET]), and functional capacity (short physical performance battery [SPPB]) at 6 and 12wks. Full study protocol is available at BMJ Open Gastro (PMID33707216).

Results: In all, 31 pts were recruited. One individual withdrew prior to wk12 due to unforeseen personal issues. The remaining thirty participants (29 women, 1 man) completed the 12-wk HBEP: median age 53yrs, ALP 1.9xULN, bilirubin 17 µmol/L, MELD 7, and baseline PBC40 fatigue score 41. The primary outcome was met by 26 pts (87%); the median reduction in PBC40 fatigue score at wk12 was 11 points (interquartile range –9 to –13 (Fig)). Significant reductions were also observed in the FIS, score, ESS, HADS and the composite PBC40 score (Fig), alongside individual symptom, cognition, emotion and social domains, and the CLDQ (data not shown). Significant changes were seen in METs (+0.46, p < 0.001) and SPPB (+1 point, p < 0.001), with 28 pts (93%) achieving the maximum SPPB score at 12 wks (vs. 43% at baseline; p < 0.001). No significant differences in ALP values or MELD score were observed from baseline to 12wks. No significant adverse events were observed during the course of the study.

Conclusion: A 12-wk individualised HBEP, incorporating resistance and aerobic exercise, is safe, feasible, and significantly improves fatigue, quality of life, and exercise/functional capacity in patients with refractory fatigue associated with PBC. These findings warrant validation through a longer duration randomised control trial.

Figure: Efficacy of HBEP on PBC-associated fatigue and quality of life



Dot plots indicating changes from baseline to 6 and 12wks, following introduction of HBEP.

THU484

Long-term obeticholic acid (OCA) for primary biliary cholangitis (PBC) in a clinical trial improved event free survival (death, liver transplant and hepatic decompensation) compared to external controls from the GLOBAL PBC real-world database

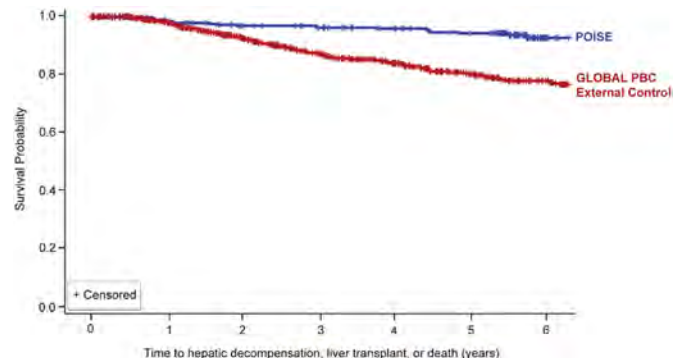
Carla Fiorella Murillo Perez¹, Femi Adekunle², Tracy Mayne², Elizabeth Malecha², Erik Ness², Adriaan Van der Meer³, Willem Lammers³, Palak Trivedi⁴, Pier Maria Battezzati⁵, Frederik Nevens⁶, Kris Kowdley⁷, Tony Bruns⁸, Nora Cazzagon⁹, Annarosa Floreani⁹, Andrew L. Mason¹⁰, Albert Pares¹¹, Maria Carlota Londoño¹¹, Pietro Invernizzi¹², Marco Carbone¹², Ana Lleo¹³, Marlyn J. Mayo¹⁴, George Dalekos¹⁵, Nikolaos Gatselis¹⁵, Douglas Thorburn¹⁶, Xavier Verhelst¹⁷, Aliya Gulamhusein¹, Harry LA Janssen¹⁸, Michael Trauner¹⁹, Christopher Bowlus²⁰, Keith D. Lindor²¹, Christophe Corpechot²², Gideon Hirschfield²³, Bettina Hansen¹⁸. ¹Toronto Centre for Liver Disease, Division of Gastroenterology and Hepatology, Toronto General Hospital, Toronto, Canada; ²Intercept Pharmaceuticals Inc; ³Erasmus MC University Medical Center Rotterdam; ⁴University of Birmingham, United Kingdom; ⁵Università degli Studi di Milano, Italy; ⁶University Hospital KU Leuven, Belgium; ⁷Liver Institute Northwest, United States; ⁸University Hospital RWTH Aachen, Germany; ⁹University of Padua, Italy; ¹⁰University of Alberta, Canada; ¹¹Liver Unit, Hospital Clinic Barcelona, Spain; ¹²University of Milano-Bicocca, Italy; ¹³Humanitas University, Italy; ¹⁴UT Southwestern, United States; ¹⁵University Hospital of Larissa, Greece; ¹⁶The Royal Free Hospital, United Kingdom; ¹⁷Ghent University Hospital, Belgium; ¹⁸Erasmus MC University Medical Center Rotterdam, Netherlands; ¹⁹Medical University of Vienna, Austria; ²⁰University of California Davis, United States; ²¹Arizona State University, United States; ²²Saint-Antoine Hospital, Assistance Publique-Hôpitaux de Paris, Sorbonne University, France; ²³Toronto Centre for Liver Disease, University Health Network, University of Toronto, Canada
Email: fiorella.murillo@uhn.ca

Background and aims: The POISE randomized double-blind (DB) placebo-controlled trial and open label extension (OLE) demonstrated that obeticholic acid (OCA) reduced biomarkers associated with adverse clinical outcomes in patients with primary biliary cholangitis (PBC). The objective of this analysis was to evaluate event-free survival in OCA-treated patients in POISE (DB + OLE) compared to non-OCA treated external controls.

Method: The treatment arm included patients in the POISE study. External controls were OCA-naïve patients from the GLOBAL PBC registry who were diagnosed with PBC, treated or untreated with ursodeoxycholic acid (UDCA), with >1 year of follow-up. Study end point was time to first occurrence of hepatic decompensation, liver transplant (LT) or death. As treatment was not assigned randomly, baseline variables could influence both the chances of a clinical event and of receiving treatment. To ensure a fair and balanced comparison,

inverse probability of treatment weighting (IPTW) was used to balance groups. Logistic regression model was used to create weights for the following key baseline confounders: age, sex, calendar year of diagnosis, PBC duration, UDCA use, ALP, bilirubin and AST or ALT. Weights were assigned to each patient. Cox-proportional hazards models were run to establish the hazard ratio (HR) and 95% confidence. A secondary analysis examined the impact of adding cirrhosis to the model.

Results: Over the 6.3 years of follow-up, there were 16 events of hepatic decompensation, liver transplant or death in 209 subjects in the POISE arm (Incidence rate (IR) 18.0 per 1,000 person-years; 95% CI 10.7–28.6) and 212 events in 1381 patients (IR 35.5 per 1,000 person-years; 95% CI 31.0–40.5) in the GLOBAL PBC external control group. The IPTW HR = 0.42 (95% CI 0.21, 0.85; p = 0.02), indicating that patients treated with OCA in a trial setting had significantly greater event-free survival than patients in the Global PBC control group. The Kaplan-Meier curve is shown in Figure. When cirrhosis was added to the model, it was a significant predictor (HR = 0.26; 95% CI 0.21–0.43, p < 0.01), and increased the effect size of treatment (HR = 0.35; 95% CI 0.17–0.71, p < 0.01). For patients with cirrhosis, HR = 0.38 (95% CI 0.12, 1.20) versus Global PBC controls; for patients without cirrhosis, HR = 0.34 (95% CI 0.14, 0.82). With widely overlapping confidence intervals, while cirrhosis significantly predicts time to events, it does not significantly affect treatment response.



FIRST EVENT	POISE (n=16)	Global PBC (n=212)
Decompensation	12	126
Liver Transplant*	1	23
Death	3	63

Conclusion: Patients treated with OCA in a trial setting demonstrated a statistically significant and clinically meaningful 58% reduction in relative risk of hepatic decompensation, LT or death compared to non-OCA treated patients in the GLOBAL PBC registry. Reduction in risk was independent of cirrhosis. These results support the continued use of long-term OCA therapy to optimize prognosis of patients with PBC.

THU485

Investigation of linerixibat 40mg BID for cholestatic pruritus of primary biliary cholangitis (PBC); further data from the phase 2b GLIMMER study to support the phase 3 GLISTEN study

James Fettiplace¹, Brandon Swift², Shu Zhang², Robyn von Maltzahn¹, Megan McLaughlin². ¹GlaxoSmithKline, United Kingdom; ²GlaxoSmithKline, United States
Email: jamesfettiplace@hotmail.com

Background and aims: Reduction of pruritic bile acids in circulation is under investigation for the treatment of cholestatic pruritus in PBC. Due to lack of previously approved therapies, what constitutes a meaningful within-patient change in itch has not been determined. The phase 2b GLIMMER study was a randomized, double-blind, placebo-controlled, dose response study of linerixibat, a minimally

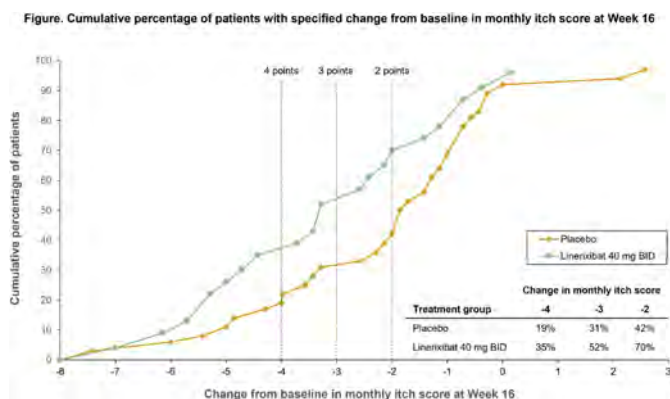
POSTER PRESENTATIONS

absorbed ileal bile acid transporter inhibitor, in PBC patients with moderate to severe pruritus; 12 weeks of treatment followed a 4-week placebo run-in (N = 147). Data from GLIMMER was reanalyzed to look at multiple potential itch responder definitions for the linerixibat 40mg BID group, the phase 3 dose. Consistent with the mechanism of action, changes in total serum bile acids (TSBA) are also reported.

Method: Participants assessed itch daily using a 0–10 numeric rating scale. Proportion of responders were assessed using reductions in monthly itch scores (MIS) at week 16 compared to baseline. An empirical cumulative distribution function (eCDF) graph was generated for the percentage of participants with change from baseline in MIS for the linerixibat 40mg BID (N = 23) and placebo (N = 36) groups. Bile acid samples from GLIMMER were reanalyzed using an enzymatic assay that quantifies TSBA consistent with the Phase 2a study method (the original analysis summed specific bile acids utilizing a liquid chromatography tandem mass spectrometry method). Change from baseline in TSBA were analyzed using a mixed model repeated measures analysis (MMRM).

Results: The eCDF curves showed clear separation of linerixibat 40 mg BID and placebo groups. The percentages of participants with an improvement from baseline in MIS at week 16 were greater in linerixibat group than placebo group for a wide range of responder threshold values. The largest differences between the curves were observed between thresholds of –3 to –2, where the cumulative percentages were more than 20% greater in the linerixibat group than the placebo group.

Linerixibat 40mg BID (n = 22) reduced mean TSBA from a baseline of 18.6 μ M (21.8) by –6.94 μ M (17.5) [Mean (SD)] on average after 12-weeks of treatment. A MMRM analysis resulted in a significant decrease of 39% (p = 0.0001) from baseline and 37% (p = 0.0030) from placebo (n = 36) over the 12-week double-blind treatment period.



Conclusion: Consistent with inhibition of reuptake of bile acids, 40 mg BID linerixibat resulted in significant reductions in total serum bile acids. The proportion of participants with change from baseline in MIS at week 16 was greater in the linerixibat 40mg BID group than placebo over a range of responder threshold values. Linerixibat 40 mg BID is being studied in the ongoing confirmatory phase 3 GLISTEN study (NCT04950127). Responder thresholds of 2, 3 and 4-point improvements in MIS compared to baseline are key secondary end points of this phase 3 study.

Funding: GSK (study 201000)

THU487

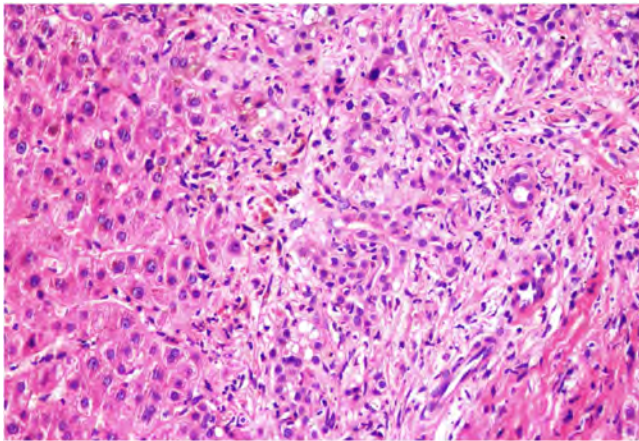
Post-COVID-19 cholangiopathy: does SARS-CoV-2 play a relevant role in histopathological findings?

Valéria Ferreira de Almeida e Borges^{1,2}, Helma Pinchemel Cotrim³, Marcelo Costa Silva⁴, Lílana Sampaio Costa Mendes⁵, Francisco Guilherme Cancela Penna^{6,7}, Antônio Ricardo Cardia Ferraz de Andrade³, Frederico Chaves Salomão⁸, Juliana Daud², Luiz Antônio Rodrigues de Freitas^{3,9,10}. ¹Federal University of Bahia, Postgraduate Program in Medicine and Health, Brazil; ²Federal University of Uberlândia, Brazil; ³Federal University of Bahia, Medicine School, Brazil; ⁴Hospital e Clínica São Roque, Ipiaú, Brazil; ⁵Hospital de Base do Distrito Federal, Brasília-DF, Brazil; ⁶Federal University of Minas Gerais, Instituto Alfa de Gastroenterologia, Belo Horizonte, Brazil; ⁷IPSEMG Hospital Governador Israel Pinheiro HGIP, Belo Horizonte, Brazil; ⁸Centro Diagnóstico de Patologia, Uberlândia, Brazil; ⁹FIOCRUZ Fundação Oswaldo Cruz, Pathology, Salvador, Brazil; ¹⁰Imagepat Laboratory of Pathology, Salvador, Brazil
Email: valeriafaborges@gmail.com

Background and aims: Cholangiopathy (CHP) occurs in critically ill patients (CIP) after prolonged therapy in intensive care unit. Findings akin to those described in CIP were deemed a novel entity in patients with severe Covid-19. This study evaluates liver histopathological findings in patients with post Covid-19 cholangiopathy.

Method: Liver sections from 10 patients with post-Covid-19 CHP were stained with hematoxylin and eosin and sirius red for fibrosis. Immunostaining for cytokeratin-7 was done in 7 cases to evaluate ductular proliferation and biliary metaplasia of hepatocytes. Semiquantitative analysis included portal changes (fibrosis, inflammation, and biliary tree changes), and parenchymal alterations (cholestasis, inflammation, hepatocellular lesions, and fibrosis).

Results: All 10 patients, 5 women and 5 men, mean age: 54 ± 11.29 years, were RT-PCR positive for Sars-CoV-2 infection, with respiratory distress requiring mechanical ventilation, pronation, sedation and vasoactive drugs. Median of liver enzymes closely before the biopsy procedure were serum gamma-glutamyl transferase 925 U/L, alkaline phosphatase 605 U/L, alanine aminotransferase 91 U/L, aspartate aminotransferase 90 U/L and bilirubin 3 mg/dL. Imaging studies revealed irregularities in the intrahepatic bile ducts. Biliary casts were seen in 6 cases. Biopsies were performed 190 ± 16 days after the molecular diagnosis of the infection. The median number of portal tracts was 25 (15–32). Portal and periportal fibrosis were evidenced in all cases, and septal fibrosis in 7. A mild to moderate inflammatory infiltrate (mononuclear and neutrophilic with rare eosinophils) was seen in all without interface activity. Moderate to severe ductular proliferation was found in all, as well as bile duct dystrophy (irregular contours, cytoplasmic vacuolization, loss of nuclear polarization, nuclear pyknosis and cellular drop-out). Bile plugs were found in the ductules in 6 cases. Mild swelling of endothelial cells of arterioles was observed in 5 cases. In one case, a thrombus was found in a small portal vein branch and in another a mild periductal fibrosis was present. Ductopenia was not seen. Mild to severe parenchymal cholestasis was evidenced in 9 cases. One case had multiple small biliary infarcts. Hepatocyte biliary metaplasia (CK7+ cells) was found in all seven tested cases. Acinar inflammation, as well as hepatocyte necrosis and apoptosis, were minimal and focal. One case showed multiple small biliary infarcts.



Case 4: an enlarged portal tract with ductular proliferation, dystrophic bile ducts, and mild inflammatory infiltrate. Cholestasis is present at the periportal hepatic parenchyma (hematoxylin-eosin; original magnification $\times 100$).

Conclusion: The present findings are akin to those described in the CHP of CIP. Only Covid-19 patients requiring intensive care develop CHP. This suggests that the virus does not have a direct role in the CHP. It is more likely that, as with CIP, hypoxemia due to arterial hypotension and lung damage associated with vasoconstrictor and other drugs cause damage to the biliary tree.

THU488

Examining the role of thiopurine metabolite testing in the management of patients with autoimmune hepatitis

Andrew Roberts¹, Declan Connolly¹, Ryan Hirsch¹, Gauri Mishra¹, Marcus Robertson¹, Sally Bell¹, Dilip Ratnam¹. ¹Monash Health, Department of Gastroenterology and Hepatology, Clayton, Australia
Email: atr444@gmail.com

Background and aims: Thiopurines (TP) are widely used to maintain steroid-free remission in autoimmune hepatitis (AIH), however there is a lack of data examining the role of metabolite testing in the management of AIH. We evaluated whether metabolite monitoring affected steroid-free remission and TP-attributed adverse event (AE) rates in our AIH patients.

Method: We conducted a retrospective cohort study of adult patients with AIH treated with TPs at a metropolitan health network over a 10-year period (2011–2021). Baseline demographic and clinical data were recorded. Patients were stratified by metabolite testing status. Time of censor was last clinical review. The primary outcome was steroid-free remission status in patients who received metabolite testing compared to those who had not. Secondary outcomes included mean reduction in ALT and IgG levels from diagnosis, rates of AIH flares (defined as an increase in steroid dose or reintroduction of steroids in response to clinical or biochemical change), and TP-related AE rates.

Results: 109 AIH patients treated with TPs were included. Mean follow-up time was 5.7 ± 6.6 years. Mean age was 54.5 ± 19.4 years, 71.6% were female and 74.3% were Caucasian. 43 (39.4%) were anti-smooth muscle antibody, 79 (72.4%) had typical AIH findings on biopsy and 30 (27.5%) were cirrhotic. At time of diagnosis, the median ALT was 666 (IQR 134–1148) U/L. At time of censor, 62 (56.9%) patients remained on TPs with a mean azathioprine dose of 88.5 mg and 6-mercaptopurine dose 32.1 mg in the metabolite tested group vs. 78.8 mg ($p = 0.38$) and 50 mg ($p = 0.08$) in the non-metabolite tested group respectively.

Metabolite testing was performed in 44 (40.4%) patients. No difference in steroid-free remission rate was detected between patients who received TM testing compared to those who did not (59.1% vs. 61.5%, $p = 0.80$). In these patients, achieving a therapeutic 6-thioguanine level (defined as $225\text{--}450\text{ pmol}/8 \times 10^8$ erythrocytes)

did not impact steroid-free remission rates (52.4% vs. 66.7%, $p = 0.47$) or low-dose steroid (prednisolone 5mg or less) maintenance rates (90% vs. 100%, $p = 0.57$). An AIH flare was documented in 29.4% of patients over the study period, which did not differ by testing status (40.0% vs 38.1%, $p = 0.86$). No significant differences in mean ALT, IgG or TE were noted between groups from time of diagnosis to time of censor. When stratified by testing status, no differences in TP-related AEs were detected (16% vs. 25%, $p = 0.30$).

Conclusion: TP metabolite testing was not associated with improved steroid-free remission, improvements in AIH disease activity, reduction in AIH flares or reduction in thiopurine-related adverse events. Aiming for therapeutic metabolite levels did not improve steroid-free remission rates. Metabolite testing may provide little utility in the management of AIH patients on TPs and may result in increased patient testing and healthcare resource burden.

THU489

Patient reported symptom burden in primary biliary cholangitis and how to inform trial design

Aaron Wetten^{1,2}, Claire Johnstone-hume², Kathryn Houghton¹, Chris Mitchell³, David Jones^{1,2}, Jessica Dyson^{1,2}. ¹Newcastle Freeman Hospital, Liver unit, High Heaton, United Kingdom; ²Newcastle University, Translational and Clinical Research Institute, United Kingdom; ³PBC Foundation, United Kingdom
Email: aaron.wetten@nhs.net

Background and aims: Primary Biliary Cholangitis (PBC) is a chronic, cholestatic autoimmune liver disease. Symptoms of pruritus, fatigue and 'brain fog' are common, and significantly impact quality of life. Current pruritus treatments are effective for some patients, but no therapies address fatigue or cognitive symptoms. This remains an area of significant unmet need, reflected by the recent increase in clinical trials to identify new agents. This study explored the prevalence of PBC symptoms, patients' priorities for their management, what they consider a meaningful improvement in their symptoms and how we should collect symptom data. These are crucial questions to inform trial design in this area where patient-reported outcomes are key metrics for success.

Method: An electronic survey was sent to members of the PBC Foundation (an international patient support group) in February 2022 with responses collected over 6 weeks. The survey comprised 9 questions regarding: current/past symptom burden; nature/degree of symptom (fatigue, itch and brain fog) management that they would consider a meaningful improvement, and their views on digital symptom assessment.

Results: 599 surveys were completed. Symptom prevalence was high: 64% reporting current/past itch, 93% fatigue and 78% brain fog. 'Any improvement being significant' was the commonest category for each symptom: brain fog 54%, fatigue 53% and itch 48% (Figure 1). When asked how a treatment should help reduce symptoms, 'a treatment that made all day every day a little better' was the most frequent response for brain fog (51%) and fatigue (47%), whilst 56% of respondents with itch preferred a treatment that could be taken when 'needed on really bad days'. 71% preferred symptom collection using an electronic device, 7% did not have a smartphone to use and 3% would decline to participate.

POSTER PRESENTATIONS

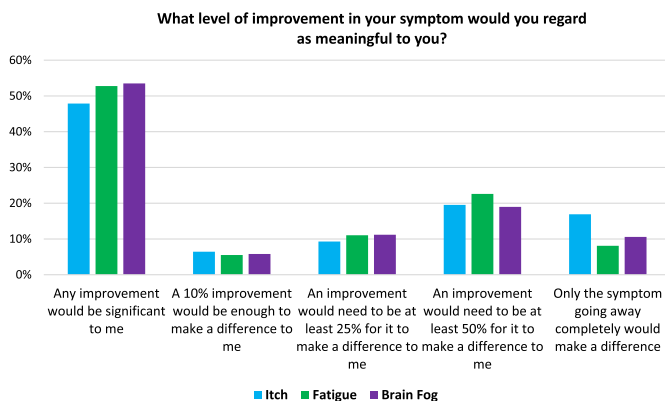


Figure: What level of improvement in symptoms (itch, fatigue and brain fog) are meaningful to patients

Conclusion: The prevalence of fatigue and brain fog were even higher than classically reported, demonstrating the unmet need. The majority of respondents felt that any symptom improvement would be significant, with daily treatment for brain fog and fatigue being preferable. A 'pill in the pocket' approach to treating pruritus is not currently utilised and is an interesting concept. Electronic symptom reporting was preferred by most patients and would standardise data collection and facilitate care delivery. This cross-sectional data helps us understand patient priorities' when designing clinically relevant outcomes from drug trials and how to assess symptom burden and treatment efficacy in clinical practice.

THU490

A randomized control trial evaluating the impact of a web-based mind-body wellness intervention for patients with primary biliary cholangitis

Makayla Watt¹, Ashley Hyde¹, John Spence¹, Gail Wright², Shauna Vander Well², Emily Johnson¹, Andrew L. Mason¹, Hin Hin Ko³, Edward Tam⁴, Puneeta Tandon¹. ¹University of Alberta, Edmonton, Canada; ²Canadian PBC Society, North York, Canada; ³The University of British Columbia, Vancouver, Canada; ⁴Dr. Edward Tam, Vancouver, Canada
Email: mewatt@ualberta.ca

Background and aims: People with primary biliary cholangitis (PBC) experience significantly higher rates of mental distress, fatigue and impaired health related quality of life (HrQoL) as compared to the general population. Online mind-body wellness programming has improved mental wellness and decreased fatigue in a variety of chronic disease populations, but limited data is available in PBC. We previously conducted a pilot study of a novel online mind-body wellness intervention in PBC that demonstrated high feasibility and acceptability, as well as promising exploratory efficacy. After refining the intervention using feedback from the pilot study, the current study aimed to assess the efficacy of the online intervention.

Method: This was a sequential mixed-methods randomized control trial (RCT). Adult participants with PBC were randomized to receive either standard of care (SOC) or SOC alongside a 12-week online mind-body intervention involving mindful movement, breathwork, meditation, an acceptance and commitment therapy chronic disease skills program, and tips from PBC physicians. The primary outcome was changes in the Hospital Anxiety and Depression Scale (HADS). Secondary outcomes evaluated fatigue, perceived stress, resilience, HrQoL through the PBC-40, and physical functioning. ANCOVA was used to determine between group differences. A qualitative descriptive approach with semi-structured interviews was used to evaluate study experiences.

Results: Of the 123 patients screened for the study, 87 were randomized to the control (n = 44) and intervention (n = 43) groups (mean age 59.8 ± 10.6 years; 98% female). The between-group HADS total score improved by 20.0% (95% CI 4.7, 35.2, p = 0.011) and the

HADS depression score improved by 25.8% (95% CI 4.8, 46.8, p = 0.017). Significant improvements were seen in the PSS (15.2%), and two PBC-40 domains (emotional symptoms by 16.3%, and social symptoms by 11.8%) with a mean satisfaction score of 82/100. While no significant improvements were observed in fatigue, interviews revealed improved ability to cope with fatigue. In the 36/43 participants who completed the intervention, 25 (69%) adhered to the program goal of completing the program at least 3x per week. Enhancing group support was highlighted as a way to improve adherence.

Conclusion: This 12-week intervention improved measures of mental wellness and quality of life. High satisfaction and adherence rates were observed. Future online mind-body online wellness studies could explore strategies to optimize adherence and increase the physical activity intervention, which may in turn result in a greater impact on fatigue.

THU491

Health-related quality of life in patients with primary sclerosing cholangitis: a longitudinal population-based cohort study

Bregje Mol¹, Kim van Munster¹, Johannes Bogaards², Rinse Weersma³, Akin Inderson⁴, Joline de Groof¹, Noortje Rossen¹, Willemijn Ponsioen¹, Maud Turkenburg¹, Karel J. van Erpecum⁵, Alexander Poen⁶, B.W. Marcel Spanier⁷, Ulrich Beuers¹, Cyriel Ponsioen¹. ¹Amsterdam UMC, Locatie AMC, Gastroenterology and Hepatology, Amsterdam, Netherlands; ²Amsterdam UMC, Locatie AMC, Epidemiology and Data Science, Amsterdam, Netherlands; ³University Medical Center Groningen, Gastroenterology and Hepatology, Groningen, Netherlands; ⁴Leiden University Medical Center (LUMC), Gastroenterology and Hepatology, Leiden, Netherlands; ⁵UMC Utrecht, Gastroenterology and Hepatology, Utrecht, Netherlands; ⁶Isala Zwillle, Gastroenterology and Hepatology, Zwillle, Netherlands; ⁷Rijnstate, Gastroenterology and Hepatology, Arnhem, Netherlands
Email: c.y.ponsioen@amsterdamumc.nl

Background and aims: Data regarding health-related quality of life (HRQoL) in primary sclerosing cholangitis (PSC) is sparse and has only been studied cross-sectionally in a disease which runs a fluctuating and unpredictable course. In this study we aim to describe HRQoL longitudinally by using repeated measurements in a population-based cohort.

Method: Every three months from May 2017 up to August 2020 patients received a digital questionnaire at home. These included the Short Form-36, EuroQol-5D-5L, 5-Dimension Itch, patient-based Simple Clinical Colitis Activity Index, and patient-based Harvey-Bradshaw Index. Data were compared with Dutch reference data and a matched IBD disease-control from the population-based POBASIC cohort. Mixed-effects modelling was performed to identify factors associated with HRQoL.

Results: 328 patients completed 2576 questionnaires. A significant reduction compared to the Dutch reference population of both the physical component summary (46.4 versus 48.0, p = 0.018) and mental component summary (47.5 versus 50.5, p = 0.004) scores measured by the SF-36 was found. HRQoL outcomes were significantly negatively associated with a coexisting active IBD which was not the case in case of quiescent IBD. Decreasing HRQoL scores were also negatively associated with increasing age, female sex, diagnosis of AIH overlap, end-stage liver disease, and the presence of itch. The odds of reporting a clinically relevant reduction in EQ-5D score showed seasonal variation, being lowest in summer (OR 0.48 (0.31–0.74), p < 0.001). In patients with a liver transplant, HRQoL outcomes were comparable to the Dutch general population.

	PCS			MCS		
	Estimate	95% CI		Estimate	95% CI	
Intercept	50.6	48.2		53.0	48.9	50.7
Female	-2.8	-5.0	-	-0.7		
Age per 10 years (reference 40y)	-0.1	-0.2	-	-0.0		
End-stage liver disease	-4.3	-7.8	-	-0.9	3.5	-0.0
AIH Overlap	-3.7	-7.4	-	0.1		6.7
IBD						
None	(reference)			(reference)		
Ulcerative Colitis	2.3	-0.1	-	4.8	2.5	-0.0
Crohn's Disease	3.3	0.2	-	6.4	-0.3	-3.8
IBD activity*	-12.2	-16.7	-	-7.6	-12.0	-18.9
Itch*	-9.2	-12.2	-	-6.2	-3.1	-6.9

Table linear mixed-effects model SF-36. The intercept indicates the reference value of the physical component summary (PCS) and mental component summary (MCS) score for all patients without or before LT conditional on the reference value of the other variables included. The estimate of the listed factors indicates the particular effect of each factor.

*Itch and IBD activity are transformed to a 0 to 1 scale. 1 equals most severe complaints.

Conclusion: PSC patients report impaired HRQoL compared to the general population. After liver transplantation, HRQoL scores of PSC patients are at comparable levels as in the general population. HRQoL scores are associated with potentially modifiable factors such as itch and IBD activity, emphasizing the importance of adequate treatment.

Cirrhosis and its complications: ACLF and Critical illness

THU493

COVID-19 in patients with cirrhosis: insights from the multinational LEOSS registry

Jonathan Frederik Brozat¹, Frank Hanses², Martina Haselberger³, Melanie Stecher⁴, Michael Dreher⁵, Lukas Tometten⁶, Maria Madeleine Rührich⁷, Janne Vehreschild⁸, Christian Trautwein¹, Stefan Borgmann⁹, Maria Vehreschild¹⁰, Carolin E. M. Jakob⁴, Andreas Stallmach¹¹, Kai Wille¹², Kerstin Hellwig¹³, Nora Isberner¹⁴, Philipp Reuken¹¹, Fabian Geisler¹⁵, Jacob Nattermann¹⁶, Tony Bruns¹.

¹University Hospital RWTH Aachen, Department of Gastroenterology, Digestive Diseases and Medical Intensive Care, Internal Medicine III, Aachen, Germany; ²University Hospital Regensburg, Emergency Department, Regensburg, Germany; ³Klinikum Passau, Department of Internal Medicine I, Passau, Germany; ⁴University of Cologne, Department I of Internal Medicine, Faculty of Medicine and University Hospital Cologne, Cologne, Germany; ⁵University Hospital RWTH Aachen, Department of Pneumology and Intensive Care Medicine, Internal Medicine V, Aachen, Germany; ⁶Hospital Ernst von Bergmann, Potsdam, Germany; ⁷Jena University Hospital, Department of Internal Medicine II, Jena, Germany; ⁸Goethe University Frankfurt, Department II of Internal Medicine, Hematology/Oncology, Frankfurt, Germany; ⁹Hospital Ingolstadt, Department of Infectious Diseases and Infection Control, Ingolstadt, Germany; ¹⁰Goethe University Frankfurt, Department of Internal Medicine, Infectious Diseases, Frankfurt, Germany; ¹¹Jena University Hospital, Department of Internal Medicine IV, Jena, Germany; ¹²Johannes Wesling Hospital Minden, Ruhr University Bochum, University Clinic for Haematology, Oncology, Haemostaseology and Palliative Care, Minden, Germany; ¹³Catholic Hospital Bochum (St. Josef Hospital), Ruhr University Bochum, Department of Neurology, Bochum, Germany; ¹⁴University Hospital Würzburg, Department of Internal Medicine II, Würzburg, Germany; ¹⁵Klinikum rechts der Isar der Technischen Universität München, Department of Internal Medicine II, München, Germany; ¹⁶UKB University of Bonn, Department of Internal Medicine I, Bonn, Germany
Email: jbrozat@ukaachen.de

Background and aims: International registries have reported high mortality rates in patients with liver disease and coronavirus disease 2019 (COVID-19). However, the paucity and heterogeneity of data leaves the extent to which comorbidities contribute to excess COVID-19 mortality in cirrhosis as controversial. This study thus aimed to control the influence of comorbidities through propensity score matching, enabling a controlled comparison of symptomatic presentation, disease progression and mortality of patients with COVID-19 and underlying cirrhosis to those without chronic liver disease.

Method: We used the multinational Lean European Open Survey on SARS-CoV-2-infected patients (LEOSS) to identify patients with cirrhosis. We compared symptoms, disease progression and mortality after propensity score matching (PSM) for age, sex, obesity, smoking status, and concomitant diseases. Mortality was further compared with that of patients with another significant precipitator of acute-on-chronic liver failure, spontaneous bacterial peritonitis (SBP).

Results: Among 7096 patients with SARS-CoV-2 infection eligible for analysis, 70 (0.99%) had cirrhosis, and all were hospitalized. Risk factors for severe COVID-19, such as diabetes, renal disease and cardiovascular disease were more frequent in patients with cirrhosis. Case fatality rate in patients with cirrhosis was 31.4% with the highest odds of death in patients older than 65 years (43.6% mortality; odds ratio [OR] 4.02; $p = 0.018$), Child-Pugh class C (57.1%; OR 4.00; $p = 0.026$), and failure of two or more organs (81.8%; OR 19.93; $p = 0.001$). After PSM for demographics and comorbidity, the COVID-19 case fatality of patients with cirrhosis was comparable to that of patients without (28.8% vs. 26.1%, $p = 0.644$) and similar to 28-day mortality in a comparison group of patients with cirrhosis and SBP (33.3% vs. 31.5%; $p = 1.000$). In contrast, the number of patients that initially reported no symptoms of COVID-19 was significantly higher in patients with cirrhosis (37.5% vs. 10.5%; $p < 0.001$), yet more than half progressed into complicated or critical disease phases.

Conclusion: Although patients with cirrhosis and SARS-CoV-2 infection regularly present without any specific symptoms, the mortality in hospitalized SARS-CoV-2-infected patients with cirrhosis is high. Propensity score matching suggests this can be largely attributed to pre-existing comorbid conditions and extrahepatic organ failure.

THU494

Serum metabolites on admission associate with the development of nosocomial infections in inpatients with cirrhosis

Jasmohan S Bajaj¹, Jacqueline O'Leary², Puneeta Tandon³, Guadalupe Garcia-Tsao⁴, Patrick S. Kamath⁵, Paul J. Thuluvath⁶, Ram Subramanian⁷, Hugo E. Vargas⁸, Sara McGeorge¹, Andrew Fagan¹, Florence Wong⁹, Jennifer Lai¹⁰, Leroy Thacker¹, Rajender Reddy¹¹.
¹Virginia Commonwealth University and Richmond VAMC, GI, Richmond, United States; ²Dallas VAMC; ³University of Alberta; ⁴Yale University; ⁵Mayo Clinic, Rochester; ⁶Mercy Medical Center; ⁷Emory university; ⁸Mayo Clinic, Arizona; ⁹University of Toronto; ¹⁰UCSF; ¹¹University of Pennsylvania
Email: jasmohan.bajaj@vcuhealth.org

Background and aims: The inpatient course of patients with cirrhosis is complicated by a high rate of nosocomial infections (NI). These infections increase the need for intensive care, often lead to acute on chronic liver failure (ACLF), and death and are challenging to predict using clinical biomarkers. Better determination of a group that develops NI on admission could prevent one of the leading causes of ACLF and death in cirrhosis. Aim: Determine predictors of NI using serum metabolomics on admission in large cohort of inpatients with cirrhosis

invasive tool for assessing the cardiocirculatory effects of terlipressin; however, additional studies with larger sample sizes are needed to confirm these results.

THU497

SARS-CoV-2 infection in patients with underlying chronic liver disease is associated with significantly greater risks of inpatient hospitalization, intensive care unit admission, and overall mortality

Robert Wong¹, Yi Zhang², Mae Thamer². ¹Stanford University School of Medicine, United States; ²Medical Technology and Practice Patterns Institute, Bethesda, United States
Email: rwong123@stanford.edu

Background and aims: Patients with chronic liver disease (CLD) are hypothesized to have greater risk of developing liver decompensation following COVID-19. However, it is unclear whether the increased risks of liver decompensation result in higher overall mortality in CLD patients with COVID-19 (CLD+COVID-19). We aim to evaluate whether CLD+COVID-19 patients have higher rates of inpatient hospitalization, intensive care unit (ICU) admission, and overall mortality compared to CLD patients without COVID-19 among one of the largest U.S. cohorts evaluating COVID-19 outcomes.

Method: Using the Common Data Schema from COVID-19 Research Database, a large U.S. database containing over 72 million linked patients with both electronic health records and claims data, we identified patients with CLD (hepatitis C, hepatitis B, alcoholic liver disease, and non-alcoholic fatty liver disease/steatohepatitis) with COVID-19 (CLD+COVID-19) and without COVID-19. Patients were followed for at least 6 months until a censoring event (i.e. death) or end of the study period (August 31, 2021). Outcomes assessed included need for inpatient hospitalization, ICU admission, and overall mortality, and outcomes were compared between groups with chi-square testing. Multivariate regression models evaluated whether COVID-19 was independently associated with greater risk of hospitalization, ICU admission, and overall mortality in CLD patients.

Results: Among 973, 634 adult patients with CLD (55.2% men, 44.8% women, 28.9% age >65y, 40.4% age 45–64y, 30.7% age 18–44, 12.0% with cirrhosis), 3.5% had CLD+COVID-19 and 96.5% had CLD without COVID-19. Compared to CLD without COVID-19, CLD+COVID-19 patients had significantly higher rates of hospitalization (25.7% vs. 9.2%, $p < 0.01$), ICU admission (15.5% vs. 4.9%, $p < 0.01$), and overall mortality (5.6% vs. 3.8%, $p < 0.01$). On adjusted multivariate regression, when compared to CLD patients without COVID-19, patients with CLD+COVID-19 had significantly greater risk of hospitalization (OR 3.27, 95% CI 3.19–3.35, $p < 0.01$), ICU admission (OR 3.36, 95% CI 3.26–3.47), and overall mortality (OR 1.36, 95% CI 1.29–1.42). These findings were likely mediated by increased risks liver decompensation (HR 1.23, 95% CI 1.15–1.32, $p < 0.01$) and acute on chronic liver failure (ACLF) (HR 7.32, 95% CI 6.40–8.38, $p < 0.01$) due to acute SARS-CoV-2 infection observed in CLD+COVID-19 compared to CLD without COVID-19 patients.

Conclusion: Among one of the largest cohorts evaluating COVID-19 outcomes in patients with underlying CLD, we observed that SARS-CoV-2 infection was associated with significantly greater risks of inpatient hospitalization, ICU admission, and overall mortality in patients with CLD. The increased mortality observed in CLD patients with COVID-19 is likely a result of the increased risks of liver decompensation and ACLF due to COVID-19.

THU498

Low FT3 levels are associated with acute decompensation and acute-on-chronic liver failure

Mona-May Langer^{1,2}, Alina Bauschen¹, Sabrina Guckenbiehl¹, G. Sebastian Hönes³, Denise Zwanziger³, Lars Christian Möller³, Christian M. Lange^{1,2}. ¹University Hospital Essen, Department for Gastroenterology and Hepatology, Essen, Germany; ²Hospital of the Ludwig Maximilian University (LMU), Medical Clinic and Polyclinic II, Munich, Germany; ³University Hospital Essen, Department of Endocrinology, Diabetes and Metabolism and Division of Laboratory Research, Essen, Germany
Email: monamay.langer@med.uni-muenchen.de

Background and aims: Thyroid hormones (TH) are important for regulation of hepatic lipolysis, gluconeogenesis, and immune-metabolism, and may thereby impact the pathogenesis and severity of liver cirrhosis and acute-on-chronic liver failure (ACLF). Therefore, we determined associations between TH, clinical stages of liver cirrhosis including ACLF and TH targets in immune cells.

Method: From a prospective cohort study, patients with compensated liver cirrhosis ($n = 163$) or acute decompensation ($n = 169$) or ACLF ($n = 36$) were recruited. Thyroid-stimulating hormone (TSH), free T3 (FT3) and free T4 (FT4) levels were determined by immunoassays. Associations between TH and clinical parameters were assessed by regression analyses. T cells of healthy donors and patients were isolated from peripheral blood and characterized for expression of TH target genes by RT-PCR.

Results: TSH concentration in patients with acute decompensation (2.81 ± 0.2 mU/l) was increased compared to patients with compensated liver cirrhosis (2.01 ± 0.1 mU/l, $P = 0.03$) and ACLF (2.18 ± 0.34 mU/l, $P = 0.42$). Contrariwise FT3 levels were significantly lower already in patients with acute decompensation (3.80 ± 0.06 pmol/l) compared to compensated liver cirrhosis (4.79 ± 0.06 pmol/l, $P < 0.0001$), and even lower in those with ACLF (3.24 ± 0.15 pmol/l; compensated vs. ACLF $P < 0.0001$; acute decompensation vs. ACLF $P < 0.01$). Decreased FT3 concentrations were associated with infections in acute decompensated patients (3.45 ± 0.10 pmol/l with vs. 3.90 ± 0.07 pmol/l without infection, $P = 0.0009$), while FT3 concentrations were not different in ACLF with (3.23 ± 0.24 pmol/l) or without infections (3.25 ± 0.16 pmol/l, $P = 0.8$). FT3 concentrations correlated inversely with CLIF-OF-, CLIF-C-AD/ACLF- and MELD-scores ($p < 0.0001$). Furthermore, low FT3 levels ($p < 0.0001$) as well as a low FT3/FT4 ratio ($p < 0.001$) were associated with mortality of liver cirrhosis patients. RT-PCR showed that T cells derived from healthy donors and patients with liver cirrhosis or ACLF did not express TH receptor β , but TH receptor α . Compared to T cells of healthy donors, expression of TH receptor α was significantly decreased in T cells derived from patients with compensated liver cirrhosis ($p = 0.02$) and even more in T cells of patients with acute decompensation ($p = 0.001$) or ACLF ($p = 0.009$).

Conclusion: Acute decompensation complicated with infections as well as ACLF with or without infections is associated with profound alterations in the TH balance resembling low T3 syndrome. Strikingly, low FT3 level and decreased FT3/FT4 ratio are associated with elevated mortality in patients with liver cirrhosis. Reduced TH receptor α expression suggests impaired TH signaling in T cells of patients with liver cirrhosis possibly contributing to reduced survival. Mechanism and functional consequences of these findings will be further explored in the new SFB-CRC/TR 296.

POSTER PRESENTATIONS

THU499

Post hoc analyses of the ATTIRE trial suggest potential gender differences in response to albumin

Margaret Hook¹, Thais Tittanegro@gmail.com¹, Louise China¹, Alastair O'Brien¹. ¹UCL Institute for Liver and Digestive Health Upper 3rd Floor, University College London Division of Medicine, London, United Kingdom
Email: rmhaajo@ucl.ac.uk

Background and aims: Acute decompensation (AD) and acute-on-chronic Liver failure (ACLF) are characterised by increased systemic inflammation and immunosuppression. There are data supporting gender differences in the inflammatory response in health and differences in outcomes between genders in AD/ACLF. Post-hoc subgroup analyses of the neutral ATTIRE trial (Albumin To Prevent Infection in Chronic Liver Failure) suggested a differential effect of targeted albumin infusions according to gender and so we investigated this in greater detail.

Method: ATTIRE was a randomized, multicenter, open-label trial involving 777 patients including 227 women, hospitalized with decompensated cirrhosis and serum albumin <30 g/L. Patients received standard of care or targeted albumin therapy (aiming for serum albumin >30 g/L) for up to 14 days or discharge. Baseline clinical characteristics and patient outcomes were analysed using appropriate statistical tests in RStudio software.

Results: Baseline characteristics, including MELD (Model for End-Stage Liver Disease) score, age and cirrhosis aetiology were similar between genders apart from an elevated creatinine in men (70 (57–94) vs 60 (48–77) $\mu\text{mol/L}$, $p < 0.001$). The volume of albumin infused did not differ between genders but resulting serum albumin values in the targeted albumin group were higher in women throughout the trial treatment period ($p < 0.001$). Women also had higher white cell counts (WCC) throughout the trial independent of treatment group ($p < 0.001$) but not C-reactive protein values. Overall outcomes did not differ between genders, although fewer events of renal dysfunction were seen in women (but not men) in the albumin treatment group compared to standard care (Chi-squared test ($X^2(1) = 6.85$, $p = 0.009$). The incidence of serious adverse events with pulmonary oedema or fluid overload was similar between treatment groups in women, in contrast to men in which these were four times as common in the albumin group.

Table: Outcomes and serious adverse events in ATTIRE according to gender and treatment group

Treatment group (n)	MALE		FEMALE	
	Albumin (257)	Standard care (293)	Albumin (123)	Standard care (104)
Outcome – n (%)				
New infection	55 (21.4)	48 (16.3)	24 (19.5)	23 (22.1)
Renal dysfunction	30 (11.7)	35 (11.9)	10 (8.1)	22 (21.1)
Death during trial	20 (7.8)	23 (7.8)	10 (8.1)	10 (9.6)
Death at 28 days	37 (14.4)	47 (16)	16 (13)	15 (14.4)
Death at 90 days	65 (25.3)	70 (23.9)	27 (22)	23 (22.1)
Death at 180 days	94 (36.6)	87 (29.7)	38 (30.9)	32 (30.8)
Severe adverse events - n	63	52	24	20
Pulmonary oedema/ Fluid overload	19	4	4	4
GI Bleed	8	9	3	4

Conclusion: Higher WCC levels in women irrespective of treatment group might suggest a difference in the inflammatory response but infection rates and overall outcomes were similar. The improved renal function in albumin-treated women without evidence of increased adverse events may relate to their increased rate of serum albumin increment, however, there was no mortality benefit according to gender. These findings may warrant further investigation.

THU500

Can machines predict liver decompensation? Analysis of 1, 415 patients with liver cirrhosis recruited at three German referral centers

Sophie Elisabeth Müller¹, Cristina Ripoll², Alexander Zipprich², Tony Bruns³, Paul Horn⁴, Marcin Krawczyk¹, Frank Lammert¹, Matthias Reichert¹. ¹Saarland University Medical Center, Saarland University, Department of Medicine II, Homburg, Germany; ²University Hospital Jena, Clinic for Internal Medicine IV, Jena, Germany; ³Aachen University Hospital, Department of Medicine III, Aachen, Germany; ⁴University of Birmingham, Centre for Liver and Gastrointestinal Research, Institute of Immunology and Immunotherapy, Birmingham, United Kingdom
Email: mueller.sophie.elisabeth@t-online.de

Background and aims: Since decompensation of cirrhosis significantly increases mortality, early detection of patients at risk of worsening liver function is of paramount importance. Hence, we applied machine learning techniques to identify parameters predicting hepatic decompensation.

Method: Using Python, Keras, and Scikit-Learn, several machine learning techniques including Decision Trees, Random Forests, Neural Networks, and Support Vector Machines (SVM) were applied to the INCA trial database containing both pro- and retrospective data from 1, 415 patients with cirrhosis from three German university hospitals (Homburg, Halle, Jena). In addition to laboratory values and medical history, genetic data (including nucleotide-binding oligomerization domain-containing protein 2 [NOD2] genotypes) were analyzed. The models were trained and tested with an 85:15 split. After performing hierarchical clustering on the numerical variables based on Spearman rank-order correlation using Ward's minimum variance method, we applied Permutation Feature Importance (PFI) to evaluate the impact of features on the prediction of decompensation.

Results: At the index date, 313 patients were permanently compensated, 354 patients had been decompensated before, and 748 patients were currently decompensated. Overall, 825 patients could be followed up (median duration: 12 months, maximum: 55 months), of whom 46.5% decompensated during follow-up. SVM showed the best performance in predicting decompensation, achieving an accuracy of 84.1% for the training and 77.7% for the test data set in retrospective assessment, and 78.4% and 73.8% in prospective analysis. PFI revealed baseline levels of albumin and bilirubin as well as minimum serum sodium concentrations as highest-ranking parameters associated with former decompensation. The maximum level of bilirubin and baseline levels of sodium and albumin were the most accurate variables for prospective data. In addition to the parameters of established scores such as MELD and Child-Pugh, NOD2 genotype and parameters related to infections (e.g. inflammatory markers and intake of antibiotics) were highly ranked.

Conclusion: Among tested machine learning models, SVM seems to have the highest accuracy in predicting liver decompensation. In addition to classical laboratory parameters, genetic factors and infections were critical parameters for individual predictions by SVM.

THU501

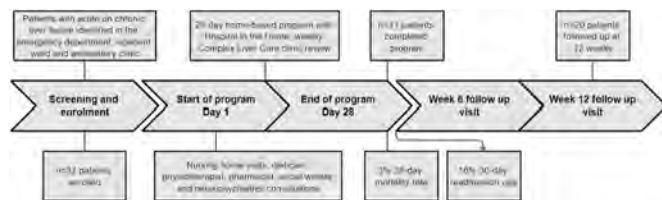
LivR Well: a feasibility study for a home-based, multidisciplinary liver optimization program for the first 28 days after an admission for acute-on-chronic liver failure

Natalie Ngu^{1,2}, Edward Saxby¹, Patricia Anderson¹, Lisa Stothers¹, Anita Figredo³, Thomas Worland¹, Stephen Pianko^{1,2}, William Sievert¹, Benjamin Rogers^{2,3}, Sally Bell^{1,2}, Danny Liew², Suong Le^{1,2}. ¹Monash Health, Gastroenterology and Hepatology, Melbourne, Australia; ²Monash University Clayton Campus, Faculty of Medicine, Nursing and Health Sciences, Clayton, Australia; ³Monash Health, Hospital in the Home, Australia
Email: natalielyn@gmail.com

Background and aims: Acute on chronic liver failure (ACLF) has a 28-day mortality of 33.9% (1) and 30-day re-admission rate of 30% (2).

LivR Well is a multidisciplinary intervention aimed at reducing mortality and readmission through a home-based, liver optimisation program after an ACLF episode. We assessed feasibility, safety, patient acceptability and clinical impact.

Method: A prospective, feasibility study was conducted at an Australian tertiary hospital from March to October 2021. ACLF was defined as an acute hepatic insult with serum bilirubin ≥ 50 $\mu\text{mol/L}$ and International Normalized Ratio ≥ 1.5 , complicated within 4 weeks by ascites and/or encephalopathy. Exclusions included end-of-life care, heart failure management and aged care residents. Participants received weekly medical review and oral nutritional supplementation. Home nursing, dietitian, physiotherapist, pharmacist, social worker, and neuropsychiatrist consultations were provided (Fig 1). The primary outcomes were adverse events/death. Secondary outcomes were attrition, liver disease severity, healthcare utilization, and patient-reported outcomes.



Results: We enrolled 32 patients; 31 patients completed the program. The median age was 53 years (Interquartile range (IQR) 49–60); 75% were male. The median Charlson Co-Morbidity Index score was 4 (IQR 3–5.5). Excess alcohol was the most common etiology (72%). Baseline median Model for End-Stage Liver Disease (MELD) score was 17 (IQR 13–21). Baseline handgrip strength in 11/27 (41%) patients met sex-specific criteria for sarcopenia. Two patients died at 16 and 148 days from enrolment. The 28-day mortality was 3% and the 30-day readmission rate was 16%. LivR Well cost \$4, 947 AUD compared to \$16, 197 AUD for an inpatient ACLF admission. Median MELD score improved at 28 days (17 vs. 15, $p=0.31$). The Chronic Liver Disease Questionnaire showed improvement in 'fatigue' ($p=0.03$) and 'worry' ($p=0.05$), at 28 days compared to baseline. Qualitative interviews were undertaken in 24 participants with all reporting positive experience pertaining to interactions with clinicians. The importance of health literacy (22/24) and patient autonomy (20/24) were emphasized in >80% of interviews.

Conclusion: LivR Well was safe, feasible, acceptable, and cost-efficient with a reduction in 28-day mortality and 30-day readmission rates. We plan to conduct a randomized controlled trial of LivR Well compared to standard care to evaluate cost-effectiveness and clinical impact on re-admission and mortality.

- Hernaez R, Kramer JR *et al*. Prevalence and short-term mortality of acute-on-chronic liver failure: A national cohort study from the USA. *J Hepatol*. 2019;70 (4):639–47.
- Moreau R, Jalan R *et al*. Acute-on-chronic liver failure is a distinct syndrome that develops in patients with acute decompensation of cirrhosis. *Gastroenterology*. 2013;144 (7):1426–37, e1–9.

THU502

Alcohol-associated hepatitis with acute-on-chronic liver failure in a diverse cohort: lung and circulatory organ failures along with MELD 35 are predictive of mortality

Stephanie Rutledge¹, Rohit Nathani², Erin Eschbach³, Lily Chu⁴, Parth Trivedi³, Thomas Schiano⁵, Leona Kim-Schluger⁵, Sander Florman⁵, Scott Friedman⁴, Gene Im⁵. ¹Icahn School of Medicine at Mount Sinai, Division of Gastroenterology, Department of Medicine, New York, United States; ²Icahn School of Medicine at Mount Sinai Morningside-West, Department of Medicine, New York, United States; ³Icahn School of Medicine at Mount Sinai, Department of Medicine, New York, United States; ⁴Icahn School of Medicine at Mount Sinai, Division of Liver Diseases, Department of Medicine, New York, United States; ⁵Icahn School of Medicine at Mount Sinai, Recanati/Miller Transplantation Institute, Division of Liver Diseases, Department of Medicine, New York, United States
Email: stephaniemrutledge@gmail.com

Background and aims: Severe alcohol-associated hepatitis (sAH) without response to medical therapy is associated with unacceptably high mortality, particularly with concomitant acute-on-chronic liver failure (ACLF). Only a minority of these sAH-ACLF patients are eligible for early liver transplantation (eLT) and the outcomes of declined candidates are unknown. The aim of our study was to determine the outcomes of declined eLT for sAH candidates and to examine variables associated with outcomes in sAH-ACLF.

Method: We analysed a prospectively maintained database of sAH patients (probable or definite per NIAAA guidelines, MELD >20) hospitalized at a LT centre from 1/2012–7/2021. All non-responders to corticosteroids were presented at our transplant selection meeting. Patients declined for eLT for sAH and those accepted who died prior to eLT were identified. The U.S. centralised National Death Index (NDI) was used to determine outcomes of patients lacking follow-up at our centre.

Results: Over 9.5 years, a total of 234 sAH patients were either declined for eLT ($n=207$) or accepted and died prior to eLT ($n=27$). Median time to eLT decision was 5 days (3–11). The cohort was young and diverse: median age 44 years (35–53), nearly half were women (108/234, 46%) with significant racial minority representation: 55% White, 26% Hispanic, 8% Black, 7% Asian, 3% unknown. Most of the cohort met EASL-CLIF criteria for ACLF (62%); 71% had ACLF grade 2 or 3. Mean MELD score at the time of waitlisting decision was 33 (± 8), mean Maddrey's discriminant function was 96 (± 79), median CLIF-C Organ Failure score (CLIF-C OFs) was 10 (9–12) and median CLIF-C ACLF score was 49 (43–55). Over a median follow-up of 494 days (17–1291), 145/234 died (62%) Of patients with ACLF-3, 38/45 (84%) died and median time to death was 8 days (3–18) versus 17 days (9–59) in ACLF-2, 78.5 days (22.5–228) in ACLF-1 and 71 days (19.5–210) in patients without ACLF ($p=0.001$) (figure).

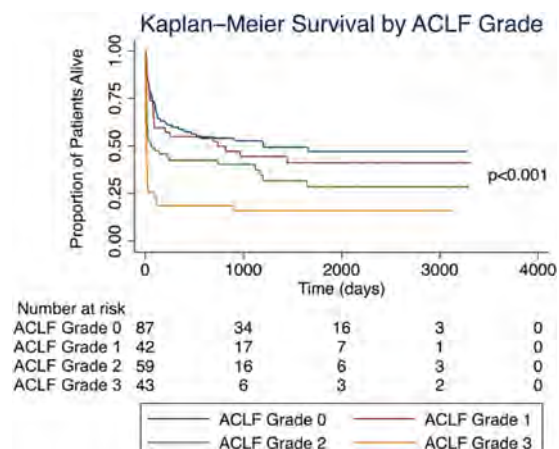


Figure: Kaplan-Meier survival by ACLF grade

POSTER PRESENTATIONS

Of the components of CLIF-C OFs, lung (HR 3.9, 95% CI 1.4–11.3) and circulatory scores (HR 3.13, 95% CI 1.6–6.2) were most predictive of mortality. Liver (HR 2.5, 95% CI 1.4–4.6), brain (HR 2.4, 95% CI 1.5–3.8), kidney (HR 1.6, 95% CI 1.2–2.2) and coagulation scores (HR 1.4, 95% CI 1.03–1.97) were also significantly associated. MELD >35 was determined as the optimal threshold for predicting mortality (HR 3.1, 95% CI 1.7–5.6). Compared with a "static" bilirubin during admission, a 10% bilirubin decrease had 66% lower mortality risk ($p = 0.01$) and a 20% increase was associated with 200% higher mortality ($p = 0.05$).

Conclusion: In a diverse, real-world cohort of patients with sAH declined for eLT, we identified a high prevalence of ACLF with very high short-term mortality. Lung and circulatory components of CLIF-C OFs and MELD >35 at the time of waitlisting decision were most predictive of mortality and may help guide clinical decision-making.

THU503

Bilirubin and its dynamics are independently associated with mortality in patients with acute decompensation of cirrhosis

Konstantin Kazankov^{1,2}, Peter Holland-Fischer^{1,3}, Karen Louise Thomsen^{1,2}, Rajiv Jalan¹, Raj Mookerjee¹. ¹University College London (UCL), Institute for Liver and Digestive Health, UCL Medical School, Royal Free Hospital, Liver Failure Group, United Kingdom; ²Aarhus University Hospital, Department of Hepatology and Gastroenterology, Denmark; ³Aalborg University Hospital, Department of Medical Gastroenterology, Denmark
Email: konskaza@rm.dk

Background and aims: Patients with acute decompensation of cirrhosis (AD) are at high risk of mortality, and current practice is still devoid of accurate parameters indicating poor outcome. In our AD cohort, we assessed the value of bilirubin alone and its dynamic changes to predict mortality.

Method: We included patients with AD cirrhosis from a prospective database in which clinical and biochemical data were registered. Multivariate logistic regression and Kaplan-Meier analysis were used for statistical analysis. Odds ratios (OR) were based on bilirubin increments of 1.45 mg/dL (25 μ mol/L).

Results: 519 patients were included, with alcohol (68%) as the predominant etiology. Main precipitants for AD were: harmful drinking (35%), infection (17%) and unknown (24%). 137 patients had alcoholic hepatitis. 354 patients (67%) did not have ACLF on admission or develop ACLF pre-discharge, whereas 24% had ACLF on admission, and 9% developed ACLF during hospitalization. Fifty-nine patients (11%) died within 4 weeks, and 118 (23%) within 12 weeks, with the highest mortality in patients with ACLF on admission or during hospitalization.

In multivariate analysis, admission bilirubin was associated with both 4- (OR 1.09 [CI 1.03–1.15]) and 12-week mortality (OR 1.08 [CI 1.03–1.13]) adjusted for age, sodium, creatinine, INR, white cell count, CRP and presence of alcoholic hepatitis and infection. Bilirubin levels beyond 12 mg/dL, the liver failure threshold according to the CLIF-Consortium ACLF-score, showed increasing 12-week mortality (Figure, log-rank test $p < 0.001$).

During admission (median 11 [IQR 7–20] days), 328 (63%) patients decreased their bilirubin, whereas it increased or was unchanged in 190 (37%) patients. Lack of reduction in bilirubin was strongly associated with death after 4 (OR 4.12 [CI 2.13–7.99]) and 12 weeks (OR 2.77 [CI 1.65–4.64]) in multivariate analysis. Accordingly, 18% of patients with a decrease in bilirubin died after 12 weeks vs. 35% in those with an increase or no change.

In patients with AD without ACLF, admission bilirubin lost its association with death at 4 weeks (OR 0.96 [CI 0.75–1.24]) but remained associated with 12-week mortality (OR 1.09 [CI 0.997–1.20]) in multivariate analysis, especially for levels >17.5 mg/dL. In patients without ACLF at admission, bilirubin was independently associated with ACLF development during hospitalization (OR 1.16 [CI 1.07–1.26]).

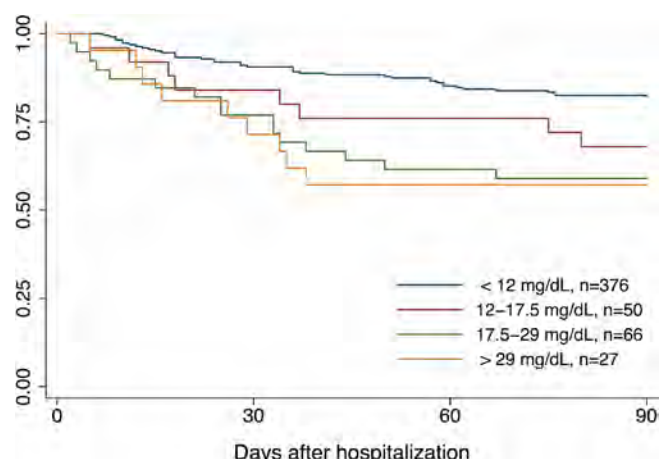


Figure: Kaplan-Meier 12-week survival estimates according to bilirubin at admission.

Conclusion: In AD cirrhosis patients, bilirubin at admission is a strong independent predictor of mortality. A step-wise increase in mortality arises from bilirubin levels >12 mg/dL. Failure to improve bilirubin during admission is an even stronger predictor of death. We propose a more detailed analysis of bilirubin and its dynamics in future studies, to generate new models for prognostication in AD cirrhosis.

THU504

Impact of predisposition and precipitants on the short-term prognosis among inpatients with chronic liver disease

Yan Zhang¹, Guohong Deng², Xian-Bo Wang³, Xin Zheng⁴, Yan Huang⁵, Jinjun Chen⁶, Zhong-Ji Meng⁷, Yanhang Gao⁸, Zhiping Qian⁹, Feng Liu¹⁰, Xiao-Bo Lu^{11,11}, Yu Shi¹², Yan Huadong¹³, Zheng Yubao¹⁴, Hai Li^{1,1}. ¹Ren Ji Hospital, School of Medicine, Shanghai Jiao Tong University, Department of Gastroenterology, Shanghai, China; ²Southwest Hospital, Third Military Medical University (Army Medical University), Department of Infectious Diseases, Chongqing, China; ³Beijing Ditan Hospital, Capital Medical University, Center of Integrative Medicine, Beijing, China; ⁴Institute of Infection and Immunology, Union Hospital, Tongji Medical College, Huazhong University of Science and Technology, Department of Infectious Diseases, Wuhan, China; ⁵Hunan Key Laboratory of Viral Hepatitis, Xiangya Hospital, Central South University, Department of Infectious Diseases, Changsha, China; ⁶Nanfang Hospital, Southern Medical University, Hepatology Unit, Department of Infectious Diseases, Guangzhou, China; ⁷Taihe Hospital, Hubei University of Medicine, Department of Infectious Disease, Shiyan, China; ⁸The First Hospital of Jilin University, Department of Hepatology, Changchun, China; ⁹Department of Liver Intensive Care Unit, Shanghai Public Health Clinical Centre, Fudan University, Shanghai, China; ¹⁰Tianjin Institute of Hepatology, Nankai University Second People's Hospital, Tianjin, China; ¹¹Infectious Disease Center, The First Affiliated Hospital of Xinjiang Medical University, Urumqi, China; ¹²The State Key Laboratory for Diagnosis and Treatment of Infectious Diseases, The First Affiliated Hospital of School of Medicine, Zhejiang University, Hangzhou, China; ¹³Department of Infectious Diseases, Hwamei Hospital, Ningbo, China; ¹⁴Department of Infectious Diseases, The Third Affiliated Hospital of Sun Yat-sen University, Guangzhou
Email: haili_17@126.com

Background and aims: Little is known about the impact of predisposition, especially the severity of liver fibrosis, and the type of precipitants on the short-term prognosis in hospitalized patients with chronic liver disease. We aimed to evaluate the risk of predisposition and precipitants on the short-term prognosis in hospitalized patients with chronic liver disease.

Method: This study was performed in 3970 cirrhosis and other chronic liver disease patients hospitalized for acute decompensation

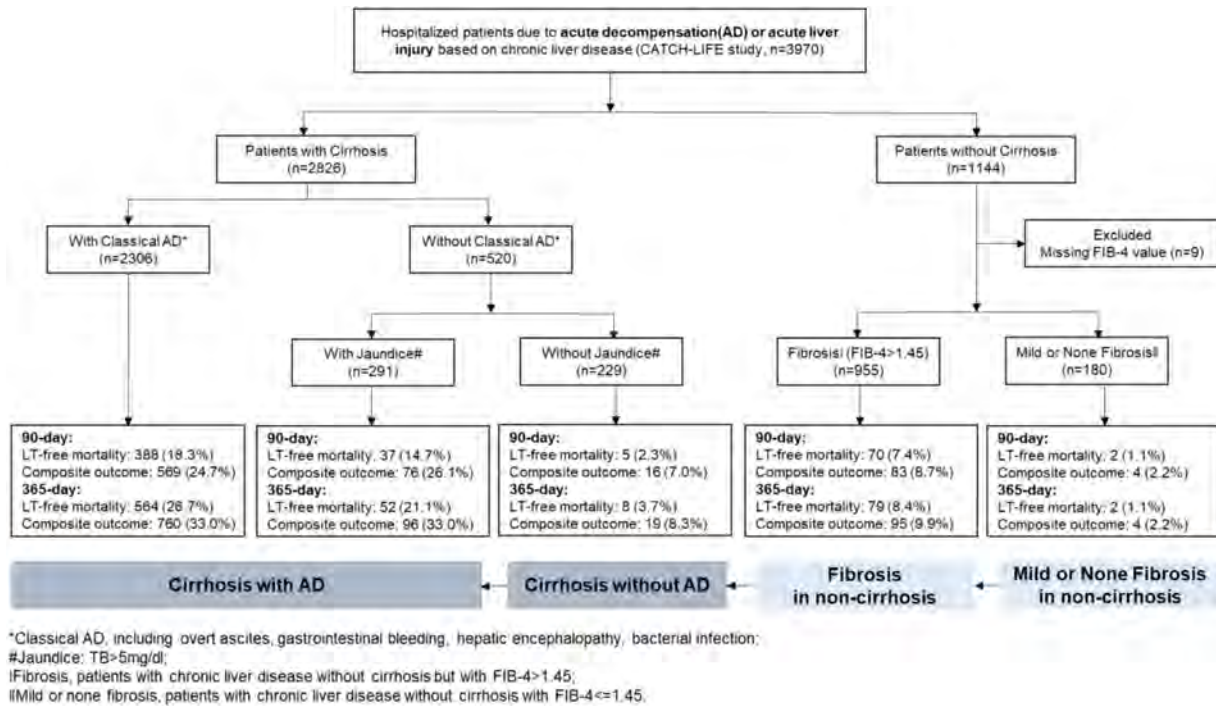


Figure: (abstract: THU504)

or acute liver injury from two prospective large multicenter studies in high-endemic HBV areas (NCT02457637 and NCT03641872). The primary end point was a composite outcome comprised of death and liver transplantation. We investigated the natural history of composite outcome within 1 year and assessed the risk of predisposition, precipitants for 90-day or 365-day composite outcome.

Results: In 2826 patients with cirrhosis, 2306 admitted for classical AD (including overt ascites, hepatic encephalopathy, gastrointestinal bleeding and bacterial infection) burdened with high 90-day and 365-day composite outcome rate (24.7%, 33.0%), while 291 admitted without classical AD but with jaundice (TB > 5 mg/dl) showed comparable high 90-day and 365-day composite outcome rate (26.1%, 33.0%). In 1144 patients without cirrhosis, 955 patients with advanced fibrosis (FIB-4 > 1.45) burdened with relatively high 90-day and 365-day composite outcome rate (8.7%, 9.9%) when compared to those with mild or none fibrosis (2.2%, 2.2%). After adjusting age, gender, TB, INR, Creatine and sodium, the severity of liver fibrosis in non-cirrhosis had no impact of 90-day ($p=0.222$) and 365-day composite outcome ($p=0.581$). But the occurrence of cirrhosis significantly increased the risk for 90-day ($p<0.001$, OR = 2.45) and 365-day ($p<0.001$, OR = 3.09) composite outcome when compared to non-cirrhosis. Moreover, in patients with cirrhosis and AD, previous decompensation independently increased the risk of 365-day adverse outcomes by 1.39-fold ($p=0.005$) and 365-day composite outcome by 1.85-fold ($p<0.001$), and the risk of 90-day and 365-day adverse outcomes in patients with extrahepatic precipitants was significantly higher than that in patients with intrahepatic precipitants.

Conclusion: The severity of liver fibrosis did not impact the 90-day and 365-day composite outcome in patients without cirrhosis, but the occurrence of cirrhosis significantly increased the risk for 90-day and 365-day composite outcome. In cirrhosis, jaundice should be also recognized as a kind of AD owing to its contribution to the comparable high 90-day mortality. Moreover, in patients with cirrhosis and AD, long-term surveillance monitoring in patients with previous decompensation and intensive therapy targeting

extrahepatic precipitants are suggested which could enhance disease management and decrease the mortality.

THU505

A study evaluating outcomes of a virtual specialist liver cirrhosis clinic

Claudia Moore-Gillon¹, Alex Cole¹, Maria Bashyam¹, Mathew Vithayathil¹, Rooshi Nathwani^{1,2}, David Koeckerling², Sujit Mukherjee^{1,2}, Benjamin H. Mullish^{1,2}, Maud Lemoine^{1,2}, Lucia Possamai^{1,2}, Heather Lewis^{1,2}, Nowlan Selvapatt^{1,2}, Ameet Dhar^{1,2}. ¹Imperial College Healthcare NHS Trust, United Kingdom; ²Imperial College London, United Kingdom
Email: c.moore-gillon@nhs.net

Background and aims: Managing patients in a specialist cirrhosis clinic improves survival. The COVID-19 pandemic necessitated the transition to virtual clinics (VC). We aimed to evaluate the clinical impact of VC on survival, admission and decompensation rates in cirrhotic patients managed in a specialist service.

Method: We retrospectively analysed cirrhotic patients who had a specialised VC from March to June 2020. Clinical parameters were collected at baseline and 6 months and compared with a cohort of patients reviewed face to face (F2F) in the same specialist cirrhosis clinics from March to June 2019. Patients with COVID-19 were excluded.

Results: 143 patients attended for VC, 129 for F2F review. Groups were matched for age, sex, aetiology, and Child Pugh grade (CP). There was no difference at 6 months in survival, change in MELD/UKELD, decompensation or need for ambulatory review in all cirrhosis grades combined or CP BandC subgroup alone ($p>0.05$) (Table 1). Fewer patients were admitted in the VC vs the F2F group ($p=0.01$) but this was not validated in CP BandC subgroup ($p=0.28$). Fewer blood tests were ordered for the VC group ($p=0.0001$). The VC group had longer delays for ultrasound HCC surveillance (<0.0001) without an increase in new HCC cases.

POSTER PRESENTATIONS

Table: Baseline Patient Demographics and 6 months' outcome (*p < 0.05, **p < 0.01)

	VC (n = 143)	F2F (n = 129)
Age-yrs (range)	61 (30–85)	60 (32–84)
Gender-no (%)		
Male	98/143 (69%)	93/129 (72%)
Main Aetiology-no (%)		
Alcoholic Liver Disease	90/143 (63%)	72/129 (56%)
Baseline Disease Severity		
CP A-no (%)	72/143 (50%)	59/129 (46%)
CP BandC-no (%)	71/143 (50%)	70/129 (54%)
MELD	10	11*
UKELD	50	51
Outcomes at 6 months:		
Survival (all)-no (%)	138/143 (97%)	125/129 (97%)
CP BandC	67/71 (94%)	66/70 (94%)
UKELD change (median)	0	0
CP BandC	–1	0
New decomp (all)-no (%)	30/143 (21%)	25/129 (19.4%)
CP BandC	25/71 (35%)	23/70 (44%)
Admissions (all)-no (%)	38/143 (27%)	53/129 (41%)
		**
CP BandC	29/71 (41%)	35/70 (50%)
Ambulatory Review (all)-no (%)	15/143 (11%)	12/129 (9%)
CP BandC	11/71 (16%)	11/70 (16%)
Blood tests ordered-no (%)	110/143 (77%)	124/129 (96%)
		**
CP BandC	54/71 (76%)	66/70 (94%) **
Delay in HCC surveillance –months	3.0 ± 2.4	1.7 ± 2.7 **
CP BandC	2.2 ± 2.0	1.2 ± 1.8 **
New HCC cases (all)- no (%)	2/143 (1%)	2/129 (2%)
CP BandC	1/71 (1%)	1/70 (1%)

Conclusion: VC have not resulted in poorer clinical outcomes, even in patients with decompensated cirrhosis. Access to ambulatory care was still required. Fewer blood tests ordered and completed in the VC group did not result in adverse outcomes and this raises the possibility of cost-saving. Further studies need to confirm the long-term clinical impact and cost-effectiveness of specialist VC in management of cirrhotic patients.

THU506

A novel metabolomics-based prognostic model shows superior diagnostic accuracy than MELD in chronic liver failure

Tobias Madl^{1,2}, Jakob Kerbl-Knapp¹, Florian Rainer³, Philipp Douschan³, Vanessa Stadlbauer³, Alexander Avian⁴, Gunther Marsche⁵, Joan Claria⁶, Rudolf E. Stauber³. ¹Medical University of Graz, Molecular Biology and Biochemistry, Graz, Austria; ²BioTechMed-Graz, Graz, Austria; ³Medical University of Graz, Department of Internal Medicine, Graz, Austria; ⁴Medical University of Graz, Institute for Medical Informatics, Statistics and Documentation, Graz, Austria; ⁵Medical University of Graz, Division of Pharmacology, Graz, Austria; ⁶European Foundation for the study of chronic liver failure, Barcelona, Spain
Email: rudolf.stauber@medunigraz.at

Background and aims: Chronic liver failure is associated with multiple metabolomic alterations that are related to its severity and pronounced in acute decompensation (AD) and more so in acute-on-chronic liver failure (ACLF). We previously showed that high-density lipoprotein cholesterol (HDL-C) levels are reduced in patients with chronic liver failure, showing similar prognostic information as the model for end-stage liver disease (MELD). In the present study we aimed to determine whether a combination of metabolite parameters

altered in chronic liver failure can yield superior prognostic accuracy for short- and intermediate-term survival.

Method: We studied a multinational cohort of patients with chronic liver failure of varying severity, including compensated cirrhosis (CC), AD and ACLF. Metabolomics analysis was performed by NMR spectroscopy and revealed several metabolites that were significantly associated with survival in univariate analyses. After checking intercorrelation of prognostic parameters by variance inflation factors (VIF), multivariable competing risk analysis was performed with death as the event and liver transplantation as a competing risk to identify independent predictors of survival. The performance of the new prognostic model was compared to that of MELD using ROC analysis (DeLong test) for 3-month, 1-year and 2-year survival.

Results: We included 423 patients (median age 58 years; 70% male; CC 54%/AD 35%/ACLF 11%; etiology alcohol 55%). Thirty-nine patients received liver transplantation, 160 patients died and 224 were censored. The risk of death (HR, 95%CI) increased with age (1.03, 1.00–1.07), ln (creatinine) (1.88, 1.13–3.13), ln (bilirubin) (1.75, 1.31–2.35), ornithine (0 vs. >0) (1.69, 1.06–2.69) and lower HDL-C (0.98, 0.97–1.00). While the performance of this multivariable model was similar to that of MELD in the prediction of 3-month survival, it was superior to that of MELD for 1-year and 2-year survival (Table).

	90-day survival	1-year survival	2-year survival
	AUROC (95%CI)		
Metabolomics-based model	0.88 (0.82–0.94)	0.90 (0.86–0.95)	0.87 (0.82–0.92)
MELD	0.87 (0.82–0.93)	0.85 (0.80–0.90)	0.81 (0.76–0.87)
p value (DeLong test)	0.934	0.006	0.004

Conclusion: A metabolomics-based prognostic model including age, creatinine, bilirubin, ornithine and HDL-C showed superior accuracy for prediction of 1-year and 2-year survival as compared to MELD. External validation is warranted to confirm our findings.

THU507

Uncovering monocyte transcription, functional and metabolic signatures in recovery and non-recovery ACLF patients

Rita Furtado Feio de Azevedo¹, Hannelie Korff¹, Markus Boesch¹, Silvia Radenkovic^{1,2,3}, Marie Wallays¹, Lena Smets¹, Lukas Van Melkebeke^{1,4}, Bart Ghesquiere^{2,3}, David Cassiman^{1,4}, Philippe Meersseman⁵, Hannah Van Malenstein^{1,4}, Frederik Nevens^{1,4}, Wim Laleman^{1,4}, Jef Verbeek^{1,4}, Schalk van der Merwe^{1,4}. ¹Laboratory Hepatology, KU Leuven, CHROMETA Department, Leuven, Belgium; ²VIB Center for Cancer Biology, Metabolomics Expertise Center, Center for Cancer Biology, Leuven, Belgium; ³KU Leuven, Metabolomics Expertise Center, Department of Oncology, Leuven, Belgium; ⁴UZ Leuven, Department of Gastroenterology and Hepatology, Leuven, Belgium; ⁵UZ Leuven, Department of Internal Medicine, Leuven, Belgium
Email: rita.azevedo@kuleuven.be

Background and aims: Cirrhosis is the end-result of a progressive chronic liver disease that may progress to the development of ascites, variceal hemorrhage, encephalopathy and hepatic decompensation. A precipitating event such as an infection can trigger a rapid deterioration of liver function and result in organ failure: acute-on-chronic liver failure (ACLF). It is a devastating clinical entity with a mortality exceeding 70% within a 28-day period in its most severe form. It is not known if these patients have infections due to a failure

of monocytes in dampening the production of pro-inflammatory mediators, or whether they trigger a prolonged anti-inflammatory response making these patients incapable to respond to a secondary infection. Likewise, the functional and metabolic defects in ACLF are incompletely understood, and this information may be the key to restoring immune dysfunction. We aim to study the dynamics of monocyte function during the course of ACLF progression and how this associates with disease outcome.

Method: We performed paired transcriptional, functional and metabolic analysis of CD14⁺CD16⁻ monocytes at day 0 and 7 from ACLF patients to compare profiles in recovery vs non-recovery. ACLF patients with a CLIF-SOFA score of 2/3 with underlying chronic alcoholic liver disease and no corticoid therapy were included in the study and were followed for 28 days after admission.

Results: Transcriptomic analysis unraveled a distinct pattern between ACLF non-recovery and recovery at baseline together with expression differences between day 0 and 7 in each group. Non-recovery monocytes showed an impaired phagocytic capacity, oxidative response and incapability of inducing CD4⁺T cell proliferation and low capacity to trigger Tcell activation. Conversely, ACLF patients that recovered showed an improvement in phagocytic and oxidative burst capacity from day 0 to 7, and despite being inefficient in triggering Tcell proliferation they featured an intact ability to induce T cell activation. In addition, monocyte metabolic profile of recovery patients clustered separately from non-recovery ACLF patients at day 0. And, the monocyte metabolic profile clustered separately day 0 from 7 on both groups.

Conclusion: The immune phenotype seen in monocytes from ACLF patients that recover can effectively respond to an infectious challenge. In stark contrast monocytes from non-recovery ACLF patients showed a functional impairment, which renders these patients susceptible to new infections.

THU508

Early initiation of continuous renal replacement therapy improves renal outcomes and survival in patients with acute on chronic liver failure-a prospective cohort study

Rakhi Maiwall¹, Ashini Hidam², Sonia Kadyan¹, Mansi Singh¹, Anupam Kumar², Rajendra Mathur³, Harshvardhan Tevethia¹, Hitesh Singh³, Siva Tez Pv³, Shiv Kumar Sarin¹. ¹ILBS, Hepatology, New Delhi, India; ²ILBS, Clinical and Molecular Medicine, New Delhi, India; ³ILBS, Nephrology, New Delhi, India
Email: shivsarin@gmail.com

Background and aims: Systemic inflammatory response syndrome (SIRS) is a driver of acute kidney injury (AKI) in patients with acute-on-chronic liver failure (ACLF). Early initiation of continuous renal replacement therapy (CRRT) improves outcomes in patients with acute liver failure, however there are no studies in patients with ACLF. We aimed to investigate the impact of initiation strategy of CRRT on AKI outcomes in patients with ACLF. Our primary outcome was to evaluate predictors of renal recovery. Our secondary outcomes included lactate and ammonia clearance, impact of CRRT on systemic inflammation, endothelial function and adverse effects. Early initiation group (EG) was defined as initiation of CRRT within 24 hours of initiation of vasopressors (norepinephrine or terlipressin)

Method: Prospective cohort of ACLF patients admitted to the intensive care unit. In all patients, urine and plasma samples were collected at baseline and 24 hours for analysing the impact of CRRT on markers of inflammation, endothelial function, renal injury and repair. Clinical, hemodynamic and lung parameters (VolumeView

system, Edwards Lifesciences) and blood gas parameters were recorded.

Results: Thirty patients with ACLF [early group (EG, n = 15) and late group (LG, n = 15)], aged 43.33 ± 10.1; 87% males, 70% alcoholics with mean MELD 37 ± 5, AARC 10 ± 1.61 and SOFA 14 ± 2.55 score were enrolled. The median time to CRRT after onset of AKI was [44 ± 7.1 vs. 113.6 ± 40] hours and after initiation of vasopressors was [(14.3 ± 7.56) vs. (49.7 ± 17.8)] hours in EG vs. LG respectively (p < 0.001). Only 36.7% had renal recovery and shock at day 7 (dialysis responders-DR), majority in the EG [60% vs. 13.3%; p = 0.008]. A significant improvement in SIRS, extravascular lung water (EVLW), pulmonary vascular permeability index, arterial lactate and ammonia was noted in dialysis-responders (DR) compared to non-responders (p < 0.05). A significant decrease in the renal injury markers and increase in renal repair markers [Figure] was noted in DR compared to non-responders. Responders had lower 15-day mortality [18% vs. 58%; HR 0.21, 0.05–0.96; P = 0.045]. Time to CRRT after initiation of vasopressors [OR 0.93, 0.88–0.99] and SOFA score [OR 0.54, 0.32–0.93] were independently associated with dialysis response. Each hour delay in CRRT initiation was associated with 7% decreased chances of renal recovery. The most frequent adverse event was bleeding (40%) followed by hypotension (30%).

Conclusion: Only one in three patients of ACLF achieve renal recovery with CRRT. Response to CRRT is associated with improvement in hemodynamics, systemic inflammation, endothelial and renal function. Each hour delay in CRRT after onset of shock and higher SOFA score are associated with decreased chances of renal recovery and worse outcomes in patients with ACLF.

THU509

Different clinical courses of acutely decompensated cirrhosis in hepatitis B virus high-endemic area: data from Chinese Acute-on-Chronic Liver Failure (CATCH-LIFE) study

Tongyu Wang¹, Yu Shi², Hai Li¹. ¹Shanghai, China; ²Hangzhou, China
Email: haili_17@126.com

Background and aims: Cirrhotic patients with acute decompensation (AD) have different clinical course and pathophysiology base on the PREDICT study in a predominately alcohol-related etiologic population: pre-ACLF (acute-on-chronic liver failure), UDC (unstable decompensated cirrhosis) and SDC (stable decompensated cirrhosis) patients with different pathophysiology and prognosis. However, in hepatitis B virus (HBV) high-endemic area, the characteristics of these three subtypes are not well characterized. The aims of this study were to explore the characteristics and outcomes of different clinical courses within 1 year.

Method: We identified 2597 cirrhotic patients with AD from a prospective multi-center cohort with 66.85% HBV-related etiology and explored the disease dynamics and prognosis within 1 year. Clinical and biological parameters during hospitalization, 3-month re-admission and outcomes during follow-up were collected. Pre-ACLF was defined as patients developed ACLF within hospitalization. Subgroup analysis was conducted based on etiology, prognostic scores were recorded to predict outcomes in ACLF, UDC and SDC patients, respectively.

Results: Totally, 2188 AD without ACLF at baseline were identified. There are 184 (8.41%) pre-ACLF patients with 3-month and 1-year LT-free mortality rates of 60.49% and 70.93%, respectively. 663 UDC (27.38%) patients had at least one readmission within 3 month and had no ACLF development during hospitalization, with 22.05% and

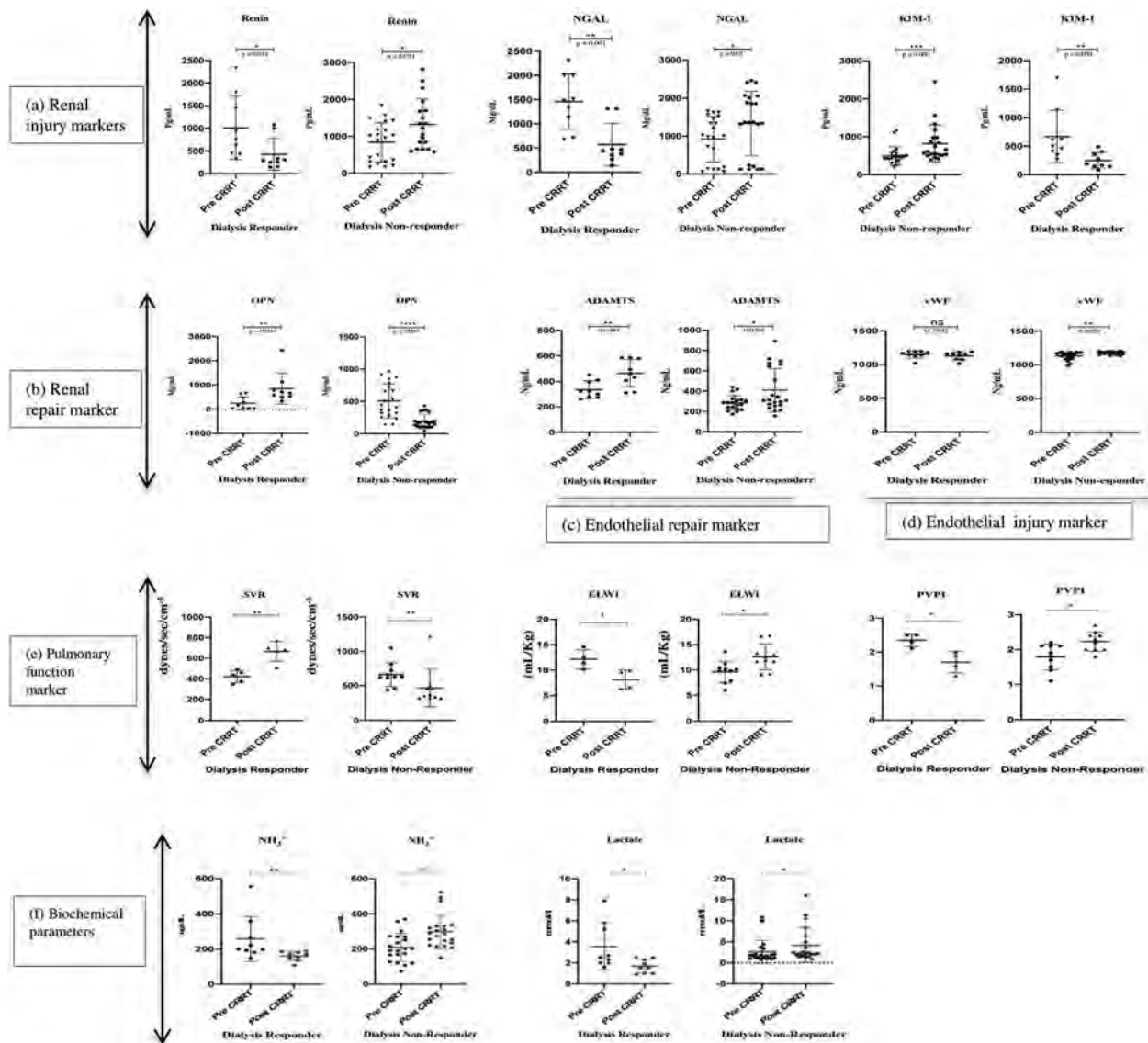


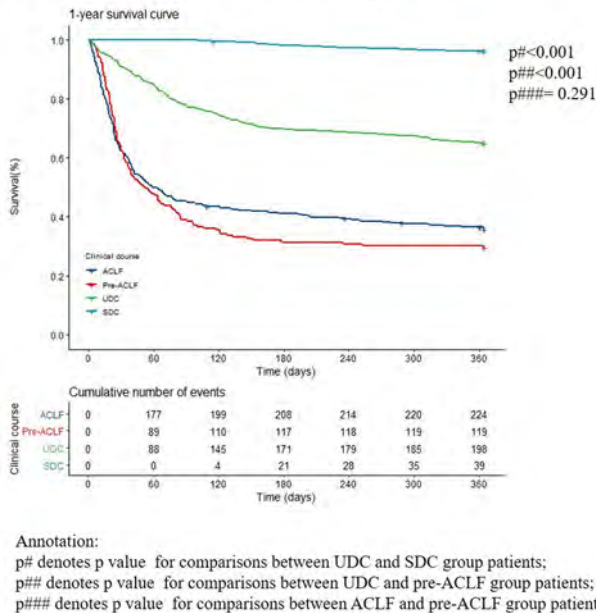
Fig. (a) In urine marker analysis, renal injury markers such as NGAL (neutrophil gelatinase-associated lipocalin), renin and KIM-1 (kidney injury molecule-1) were significantly elevated after post RRT (renal replacement therapy) in dialysis non-responder (D-NR) ACLF patients, while these markers were declined after post therapy in case of dialysis responders (DR). Also, the renal repair marker OPN (osteopontin) was significantly increased after post therapy in DR as compared to D-NR. In vascular functional analysis, vascular protective marker ADAMTS (a disintegrin and metalloproteinase with thrombospondin motifs) was significantly elevated after RRT in DR as compared to D-NR. On the other hand, vascular injury marker vWF (Von Willebrand factor) was significantly increased after therapy in D-NR in comparison to DR. Further, patients with DR showed improvement in (e) pulmonary functions [extravascular lung water (ELWI) (mL/kg), pulmonary vascular permeability index (PVPI) and systemic vascular resistance (SVR) dynes·sec·cm⁻⁵], and (f) reduction of arterial lactate and serum ammonia (umol/L).

Figure: (abstract: THU508)

35.27% mortality rates. 1232 (49.36%) SDC patients had neither readmission within 3 months nor ACLF development, with 3.42% 1-year mortality. Systemic inflammation parameters including WBC, CRP and PCT increased markedly in pre-ACLF group, while had no

significant differences between UDC and SDC group. Portal hypertension related complications including variceal haemorrhage and portal vein thrombosis proportion were significantly higher in UDC group than those in SDC group.

Figure Comparison of 1-year survival between different clinical courses of hospitalized patients with cirrhosis (LT-free mortality).



Conclusion: The recently proposed different courses of hospitalized decompensated cirrhosis with AD are validated in a multi-center large cohort. The systemic inflammation marked ACLF development in cirrhotic AD patients during hospitalization, whereas severe portal hypertension related complications are related to unstable episode of decompensation exclusively, without apparent variation of systemic inflammation. Developing a 90-day readmission prediction model for the rational management of patients with decompensated cirrhosis is necessary.

THU510

Characterization of energy and substrate metabolism in patients with spontaneously breathing and mechanically ventilated patients with liver cirrhosis: an indirect calorimeter based study
Varsha Shasthry¹, Jaya Benjamin¹, Rakhi Maiwall², Vandana Saluja³, Prashant Mohan Agarwal³, Guresh Kumar⁴, Yogendrakumar Joshi¹, Shiv Kumar Sarin². ¹Institute of liver and biliary sciences, Clinical Nutrition, New Delhi, India; ²Institute of liver and biliary sciences, Hepatology, New Delhi, India; ³Institute of liver and biliary sciences, Critical care anesthesia, New Delhi, India; ⁴Institute of liver and biliary sciences, Biostatistics, New Delhi, India
Email: jayabennaminilbs@gmail.com

Background and aims: Energy and substrate metabolism is anomalous in liver cirrhosis (LC), which may be affected by critical illness. Indirect calorimetry (IC) provides a precise insight into the same.

Aim: To compare the resting energy expenditure (REE- Kcal/day), volumes (ml/min) of oxygen consumed (VO₂) and carbon dioxide released (VCO₂), respiratory quotient (RQ-VCO₂/VO₂), percentage oxidation of carbohydrate (CHO), fat (FO) and protein (PO), between spontaneously breathing LC (sLC), ventilated LC (vLC), ventilated acute on chronic liver failure (vACLF) patients and healthy controls (HC).

Method: In 20 HC and 129 patients with LC [sLC: vLC: vACLF (%)-36:38:26; all males], 24 hour urinary urea nitrogen (UN- g/day) and IC (Quark RMR) was performed after 6 hrs of fasting; within 24 hrs of intubation, following calibration and steady state attainment.

Metabolic state [measured REE (IC)/predicted REE (Harris-Benedict equation)*100] was defined as hyper (>110%), hypo (<90%) and normometabolic (90–110%).

Results: The clinical and metabolic characteristics are shown in table 1. Compared to HC, all 129 LC patients had increased REE and a state of accelerated starvation (AS) [low RQ; low CHO; high FO]. Among LC, vACLF had highest REE. Critical illness (sLC vs. vLC) worsens AS (RQ: 0.81vs.0.74) commensurate to incomplete macronutrient oxidation (VCO₂:185 vs.164) with a comparable REE. The prevalence of hypermetabolism was higher in vACLF (38%); hypometabolism was higher in vLC (45%). UN excretion and PO remained comparable.

Table 1: Age and BMI adjusted comparison of clinical and metabolic characteristics

Parameter	1 (HC) (n=20)	2 (sLC) (n=46)	3 (vLC) (n=49)	4 (vACLF) (n=34)	Overall p	Intergroup- p
Age	28 ± 7.3	46.7 ± 9.3	47.1 ± 10.9	42.6 ± 9.6	<0.001	-
BMI	24.4 ± 3.3	24.5 ± 4.8	26.1 ± 4.6	26.1 ± 5.6	0.01	-
Etiology:n (%)					-	-
Ethanol		29 (63)	33 (67.3)	28 (82.4)		
NASH		7 (15.2)	6 (12.2)	3 (8.8)		
others		10 (21.7)	10 (20.4)	3 (8.8)		
CTP		8.6 ± 1.2	12.8 ± 1.4	13.8 ± 1.9	-	-
MELD		15.3 ± 5.8	29 ± 8.8	34.1 ± 5.8	-	-
CLIF SOFA		-	12.9 ± 3	15.2 ± 1.8	-	-
REE	1393 ± 82	1581 ± 47	1528 ± 46	1760 ± 54	0.001	4 vs all<0.005 1 vs 2-0.05 1 vs 3-0.01 2 vs 3-0.01 2 vs 3-0.01 3 vs 4-0.04 1 vs all ; 4 vs all <0.005 1 vs all 0.001 2vs 3-0.04 1 vs all 0.001
VO ₂	198.2 ± 13	229.3 ± 7.5	226 ± 7.3	263.2 ± 8.5	0.001	
VCO ₂	180.8 ± 9.6	185.5 ± 5.6	164.3 ± 5.4	181.2 ± 6.4	0.039	
RQ	0.95 ± 0.03	0.81 ± 0.02	0.74 ± 0.02	0.71 ± 0.02	0.001	
CHO	59.3 ± 7.9	27.7 ± 4.1	14.4 ± 5.2	18.9 ± 6.4	0.001	
FO	27.4 ± 8.3	62.4 ± 4.3	71.3 ± 5.5	69.8 ± 6.8	0.001	
PO	13.4 ± 3.4	11.5 ± 1.9	14.3 ± 2.2	11.2 ± 2.8	0.72	
UN	7.7 ± 2.1	8.5 ± 1.1	9.6 ± 1.3	7.9 ± 1.9	0.82	
Metabolic state (%)						
Normo		48	37	47	0.03	3 vs.4-0.01
Hypo		30	45	15		
Hyper		22	18	38		

Data expressed in mean ± SE

Conclusion: Accelerated starvation is the hallmark in LC, that worsens with critically illness. vACLF have highest energy expenditure. Critical illness does not augment energy demands in vLC patients. This characterisation may help to redefine nutritional targets in critically ill LC.

THU511

Extracorporeal membrane oxygenation, a valuable life-saving treatment in liver transplanted patients

Benjamin Buchard^{1,2}, Sophie-Caroline Sacleux^{2,3}, Samir Jaber⁴, François Stéphan⁵, Alain Combes⁶, Elise Lemaître², Marc Boudon^{2,3,7}, Audrey Coilly^{2,3,7}, Faouzi Saliba^{2,3,7}, Didier Samuel^{2,3,7}, Armand Abergel¹, Philippe Ichai^{2,3}. ¹Chu Estaing, Medecine digestive et hépatobiliaire, Clermont-Ferrand, France; ²Chb-Centre Hépatobiliaire, Liver Intensive Care Unit, Villejuif, France; ³DHU Hepatov, Villejuif, France; ⁴University Hospital Center Saint Eloi Hospital, Department of Anesthesiology and Intensive Care, Montpellier, France; ⁵Hospital Marie Lannelongue, Département de réanimation adulte, Le Plessis-Robinson, France; ⁶University Hospitals Pitié Salpêtrière-Charles Foix, Département de réanimation médicale, Paris, France; ⁷Université Paris-Saclay, INSERM Unité 1193, Villejuif
Email: benjamin.buchard@gmail.com

Background and aims: Despite a great improvement in post-liver transplantation (LTx) survival over the last years, multiple organ failure still accounts for 5% of deaths following surgery. ExtraCorporeal Membrane Oxygenation (ECMO) is a salvage therapy providing circulatory and/or ventilatory assistance. Outcomes following ECMO initiation remain uncertain. The procedure itself can lead to bleeding and sepsis, especially in immunocompromised patients. Data on outcome and safety of ECMO after LTx are

POSTER PRESENTATIONS

scarce. The aim of this retrospective study was to assess both survival and safety under ECMO in post-LTx.

Method: We retrospectively reviewed all LTx patients undergoing veno-venous (VV) or arterio-venous (AV) ECMO between 2010 and 2020 in three LTx centers. We collected data about liver disease before transplantation, indication for ECMO, number of organ failure including Sequential Organ Failure Assessment (SOFA) score, outcomes and complications under ECMO.

Results: Twenty six transplanted patients were referred to an ECMO centre. Five were contraindicated for ECMO as they were considered as too critically ill. ECMO was initiated in 21 out of 26 transplanted patients (80%). 13/21 (62%) had VA ECMO and 8/21 (38%) a VV ECMO. Five patients underwent VA ECMO following cardiac arrest (n = 5). Others developed cardiogenic shock due to: Takotsubo syndrome (n = 2), infectious myocarditis (n = 2), refractory sepsis (n = 1), severe ischemia-reperfusion syndrome (n = 1), right ventricular failure secondary to pulmonary hypertension (n = 1) and unknown biventricular failure (n = 1). The main indication for VV ECMO was septic acute respiratory distress syndrome (ARDS) (n = 7). The other patient developed refractory transfusion-related acute lung injury. Median delay between LTx and ECMO was 10 days. Median duration of VA ECMO and VV ECMO until patient's death or ECMO withdrawal was respectively 2 and 10 days. The survival rates at day 30, in patient treated with VA ECMO and VV ECMO, were 38.5% (5/13) and 37.5% (3/8) respectively (figure). In total, 11/13 (84.7%) patients died from multiorgan failure and 2 from brain death. One third of patients (7/21) presented bleeding during ECMO, mainly at the insertion site of cannulas (n = 5). Sepsis occurred in 4/21 patients. No liver graft dysfunction was observed in these patients treated with ECMO. The 30-days post-ECMO survival was significantly associated with SOFA score at the initiation (14 in survivors vs. 16 in non-surviving patients, $p = 0.03$) and 24 hours after initiation of ECMO (12 in survivors vs. 18 in non-surviving patients $p = 0.04$).

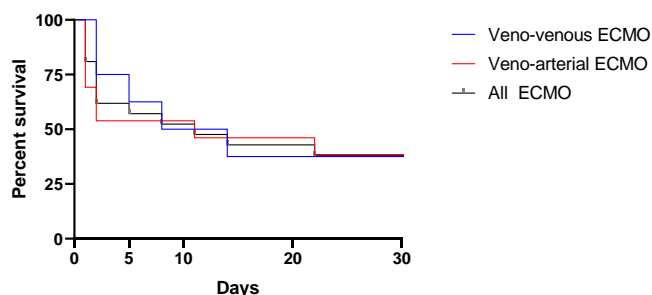


Figure: Survival of transplanted patients during the first 30 days following ECMO initiation

Conclusion: ECMO in liver transplanted patients should be considered as a salvage treatment for refractory respiratory and/or circulatory failure. Our work reveals similar survival under ECMO compared to the general population.

THU512

Prevalence, profile and predictors of invasive fungal infections in acute on chronic liver failure (ACLF): analysis of APASL-ACLF research consortium database

Pratibha Ramchandra Kale¹, Ashok Choudhury², Vikas Khillan¹, Niharika Patel², Sarin Shiv Kumar². ¹Institute of Liver and Biliary Sciences, Clinical Microbiology, New Delhi, India; ²Institute of Liver and Biliary Sciences, Hepatology, New Delhi, India
Email: drpratibhapgi@gmail.com

Background and aims: Acute-on-chronic liver failure (ACLF) causes immune dysregulation and increased susceptibility to fungal infections. We studied the epidemiology and risk factors associated with invasive fungal infections (IFI) in ACLF. We correlated the timing of

occurrence, predictors of development, diagnostic potential of biomarkers, antifungal prophylaxis with the outcome of IFI.

Method: The demographic, clinical and laboratory characteristics of ACLF patients, admitted to ILBS, developing IFI were studied retrospectively based on the APASL ACLF Research Consortium (AARC) data base. The diagnosis of IFI was based on revised definitions of invasive fungal disease from the European organization for research and treatment of cancer/Invasive fungal infections cooperative group and the national institute of allergy and infectious diseases mycoses study group (EORTC/MSG) consensus group. We also measured the biomarkers in bronchoalveolar lavage (BAL) and serum Galactomannan index (GMI).

Results: Amongst 1670 ALCLF patients, 320 (19.16%) had recent history of neutropenia, prolonged use of corticosteroids or immunosuppressive therapy, and sufficient clinical evidence consistent with IFD but no mycological evidence were classified as possible IFI. Sixty (3.6%) patients who had host factors, clinical features, and mycological evidence consisting of direct test (cytology, direct microscopy, or culture) and indirect test, positive Galactomannan assay, were classified as probable IFI. Amongst the probable IFI group, the most common site of infection was urinary tract (n = 42/60, 70%) followed by respiratory (n = 12/60, 20%) and blood (n = 6/60, 10%). On univariate analysis, prior antibiotic use, high total leucocyte count (TLC), acute renal failure, hemodialysis, diabetes mellitus, multiorgan failures, were predictors for development of IFI ($p < 0.05$). On multivariate analysis, $TLC > 14.3 \times 10^3/\text{ml}^3$, multiorgan failure, hemodialysis and prior antibiotics use predicted the development of IFI ($p < 0.05$). IFI occurrence was associated with significantly high 30 and 90 day mortality ($p < 0.001$). 68.4% patients with IFI in the first 7 days of enrolment died as compared to 47.9% in control group ($p = 0.002$). BAL GMI (cut-off > 1) was positive in 38/60 (63.33%) and serum GMI was positive in 11/60, (18.33%). BAL GMI above 3.25 was a better predictor of IFI (sensitivity 72.7%, specificity 51.5%).

Conclusion: Invasive fungal infections cause high mortality in ACLF patients. High TLC at admission, multiorgan failure, hemodialysis, prior antibiotics usage and high BAL GMI predict the development of IFI. High vigilance, early diagnosis and initiation of anti-fungal therapy is essential to prevent mortality due to IFI in ACLF.

THU513

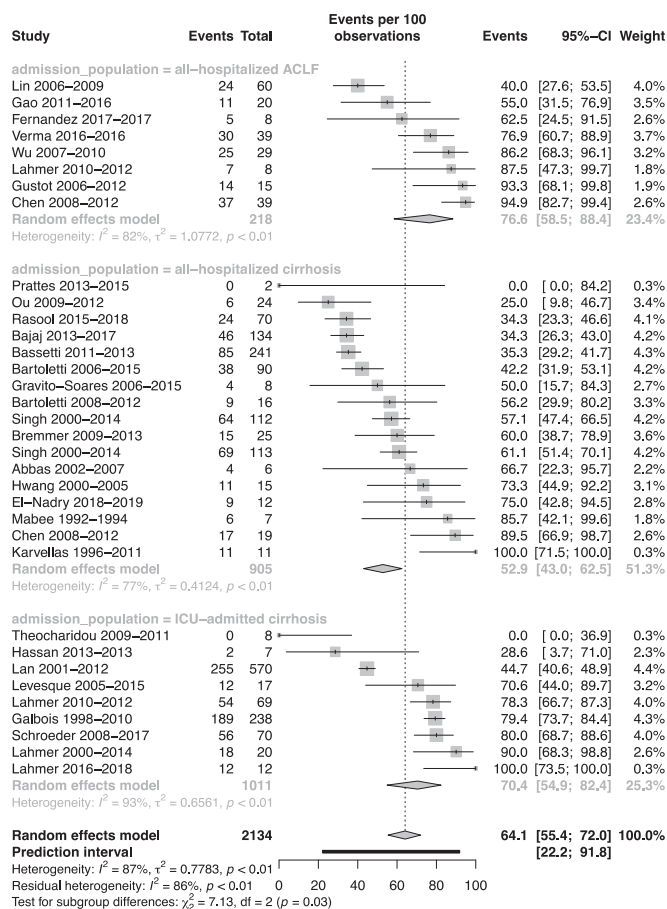
Outcomes in patients with cirrhosis and fungal infections: a systematic review and meta-analysis with machine learning

Nipun Verma¹, Shreya Singh², Akash Roy³, Arun Valsan¹, Pratibha Garh¹, Pranita Pradhan⁴, Meenu Singh⁵. ¹Postgraduate Institute of Medical Education and Research, Hepatology, Chandigarh, India; ²Postgraduate Institute of Medical Education and Research, Microbiology, Chandigarh, India; ³Sanjay Gandhi Postgraduate Institute of Medical Sciences, Hepatology, Lucknow, India; ⁴Postgraduate Institute of Medical Education and Research, Pediatrics, Chandigarh, India; ⁵Postgraduate Institute of Medical Education and Research, Pediatrics, Chandigarh, India
Email: nipun29j@gmail.com

Background and aims: Fungal infections (FIs) are an emerging threat in patients with cirrhosis. Due to the lack of systematic data, we performed a comprehensive literature search to systematically evaluate the impact of FIs on mortality and contributory factors in cirrhosis patients.

Method: PubMed, Embase, Ovid, and Web of Science were searched since their inception till Oct 30, 2020, for full-text articles describing mortality in cirrhosis patients with FIs. Point and relative-risk estimates of mortality were pooled on random-effects meta-analysis, and their variation (I^2) was explored on subgroups, meta-regression, and machine learning (ML). Quality of studies was evaluated with the New-castle Ottawa scale and estimate's asymmetry with a funnel plot and Eggers regression. (CRD42019142782)

Results: Of 4345, 34 studies (2134 patients) were included (good/fair/poor quality: 12/21/1). The pooled mortality of patients with FIs was 64.1% (95% CI: 55.4–72.0, I^2 : 87%, $p < 0.01$). Patients with proven, probable, and proven + probable FIs had a mortality of 61.4%, 73.6%, and 63.8%, respectively. Patients with acute-on-chronic liver failure (ACLF: 76.6%) and intensive care unit admission (ICU: 70.4%) had a higher mortality than all-hospitalized patients (52.9%), $p = 0.03$ (Figure 1). Significant variation in mortality estimates was identified on geographic dimensions and site of infection. The highest mortality was noted in pulmonary-FIs (79.4%), followed by peritoneal-FIs (68.3%) and fungemia (55%). On meta-regression, MELD of cases was identified as a predictor of mortality; adjusted estimate: 64.5% (54.5–83.9). The mortality among patients with FIs was 1.7 (1.4–2.1) and 2.9 (1.8–4.9) times higher than bacterial infections and non-infected controls. The relative risk persisted above 1.5 times in ICU-admitted and ACLF patients as well. After adjusting for the proportion of bacterial infection in controls, the relative risk was 2.16 (1.85–2.53). Asymmetry was evident in point-estimate and relative-risk estimates of FIs. Three k-means clusters, 2 DBSCAN clusters, 8 GMM clusters, and 5 outlier studies were detected on ML. On excluding these, the estimate's heterogeneity was abolished (I^2 :0%, $p = 0.68$). Estimates did not vary as per the quality of the study.



Conclusion: About 2/3rd cirrhosis patients with FIs die with the highest risk of death among ACLF and ICU patients. FIs are more serious than bacterial infections and warrant dedicated efforts in the cirrhosis patients.

THU514

Impact of de presence of acute on chronic liver failure on morbi-mortality after liver transplantation

Carlos Benitez¹, Verónica Cambindo Santana¹, Jorge Arnold^{1,2}.

¹Pontificia Universidad Católica, Hepatología, Santiago, Chile; ²Pontificia Universidad Católica de Chile, Gastroenterología

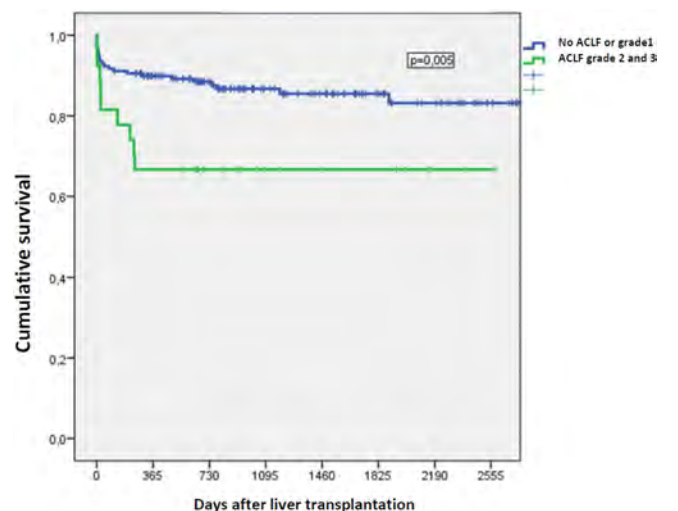
Email: vcambindo@gmail.com

Background and aims: Acute over chronic liver failure (ACLF) implies high short-term mortality. The impact of its presence at the time of liver transplantation (LT) has been less studied.

Objectives: To evaluate the impact of ACLF on post-LT survival.

Method: A retrospective registry of 263 liver recipients between 2013 and 2020 was evaluated; 197 patients met the inclusion criteria and their survival and complications were recorded at one year of follow-up.

Results: The average age was 57.1 ± 10.5 , men 55.3%, MELD Na 23.15 ± 9.76 . The main etiologies were MAFLD (35.5%), alcohol (12.7%), autoimmune hepatitis (9.6%), PBC (9.1%) and HCV (7.6%). 22.5% of the patients developed ACLF. One year survival of those transplanted without ACLF, ACLF grade 1, grade 2, and grade 3 were 89.8%, 91.7%, 66.7%, and 66.7%, respectively ($p = 0.042$). Survival of those without ACLF and grade 1 vs grade 2 and 3 were 90% vs 66.7% ($p = 0.005$) (figure). Transplant patients with grade 2–3 ACLF had more post-LT bacterial infections 59.3% vs 36.5% ($p = 0.024$), a higher frequency of mechanical ventilation 46.2% vs 19.4% ($p = 0.003$) and renal replacement therapy (RRT) (42.3% vs 11.6% ($p < 0.001$)). In the multivariate analysis, the variables independently related to survival were the requirement for mechanical ventilation before LT (OR 4.3, $p = 0.026$, CI (1.19–15.62) and RRT post LT (OR 2.95, $p = 0.39$, CI (1.05–8.2).



Conclusion: The presence of ACLF grade 2 and 3 at the time of LT is associated with marked reduction of one year patient survival. 1530/1600 (with space)

THU516

Untargeted lipidomics differentiate ACLF precipitated by severe alcoholic hepatitis

Florent Artru^{1,2}, Stephen Atkinson¹, Ewan Forrest³, Francesca Trovato², Nikhil Vergis¹, Vishal C Patel^{2,4,5}, Salma Mujib², Anna Cavazza², Alexandros Pechlivanis¹, Ellen Jerome², Marc Zentar², Evangelos Triantafyllou¹, Elaine Holmes¹, Mark J W McPhail^{1,2}, Mark Thursz¹. ¹Imperial College London, London, United Kingdom; ²Institute of Liver Studies, King's College Hospital, London, United Kingdom; ³University of Glasgow, Glasgow, United Kingdom; ⁴The Roger Williams Institute of Hepatology London, Foundation For Liver Research, London, United Kingdom; ⁵Institute of Liver Sciences, King's College London, Department of Inflammation Biology, School of Immunology and Microbial Sciences, FoLSM, London, United Kingdom
Email: florent.артру@kcl.ac.uk

Background and aims: Severe alcoholic hepatitis (SAH) is a common cause of acute on chronic liver failure (ACLF). Patients with SAH-ACLF present intense systemic inflammation and immune dysfunction. While lipids are involved in inflammatory and immune responses, lipidomics is understudied in the setting of SAH-ACLF. We evaluated whether specific changes in the blood lipidome are observed in ACLF precipitated by SAH.

Method: Untargeted serum lipidomics was performed using reversed phase ultra-performance liquid chromatography coupled to mass spectrometry in patients with SAH participating in the STOPAH trial (n = 154–46 with ACLF labelled SAH-ACLF) and with cirrhosis (n = 74–21 with ACLF labelled Cirrh-ACLF). Serum lipidome changes between patients with and without ACLF in SAH and cirrhosis groups were evaluated by principal component analysis (PCA) and orthogonal partial least squares discriminant analysis (OPLS-DA).

Results: MELD score was higher in patients with SAH without ACLF vs. cirrhotics without ACLF (20.7 vs. 11.3, p < 0.0001) but matched between patients with SAH-ACLF vs. Cirrh-ACLF (26.1 vs. 24.7, p = 0.4). PCA and OPLS-DA analyses were not able to accurately discriminate between SAH with or without ACLF (OPLS-DA in positive mode R²Y = 0.14 Q² = 0.06 CV-ANOVA p = 0.01 AUROC = 0.71 and negative mode R²Y = 0.18 Q² = 0.04 p = 0.22 AUROC = 0.62). Importantly, PCA and OPLS-DA did accurately discriminate between SAH-ACLF and Cirrh-ACLF (OPLS-DA in positive mode: R²Y = 0.78 Q² = 0.49 CV-ANOVA < 0.0001 AUROC = 0.91; in negative mode: R²Y = 0.66 Q² = 0.4 p < 0.0001 AUROC = 0.88) (Figure 1). The 10 metabolites showing the greatest variable importance projection were included in multivariate analyses adjusting for age, sex and MELD score. Two lipids in positive mode (PE P-38:4, PE P-36:3) and negative mode (PC 41:5, LPC 14:0) disclosed independent associations with SAH-ACLF (Figure 1). Using these lipids, we derived 2 scores relating to positive and negative ionisation modes; both accurately discriminated SAH-ACLF from Cirrh-ACLF with an AUROC of 0.86 (CI95% 0.73–0.93, p < 0.0001, sensitivity 76% specificity 88%) and 0.82 (CI95% 0.68–0.90, p < 0.0001, sensitivity 71% specificity 84%).

Abstract withdrawn

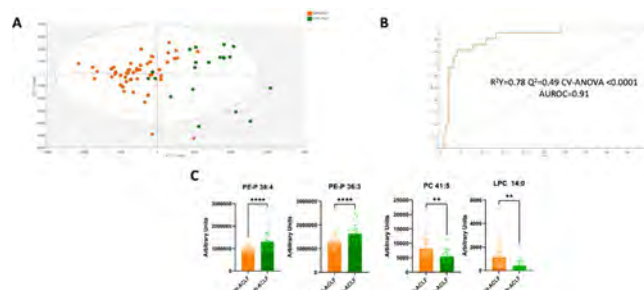


Figure: A. OPLS-DA in positive mode. B. ROC curve of OPLS-DA model in positive mode. C. Univariate analyses of the lipids included in the 2-lipids models in positive (PE-P38:4, PE-P36:3) and negative modes (PC41:5, LPC14:0).

Conclusion: This lipidomic analysis of the STOPAH cohort demonstrates a specific lipidomic signature- mainly composed of species that are known to be involved in immune-modulatory functions and liver repair-in patients with SAH-ACLF. These pathways require further exploration on their diagnostic and mechanistic role in the development of SAH-ACLF compared to other cause of ACLF.

THU517

Metabolomic analysis of organ failure marker compounds in blood samples of patients with decompensated liver cirrhosis after administration of the novel drug VS-01

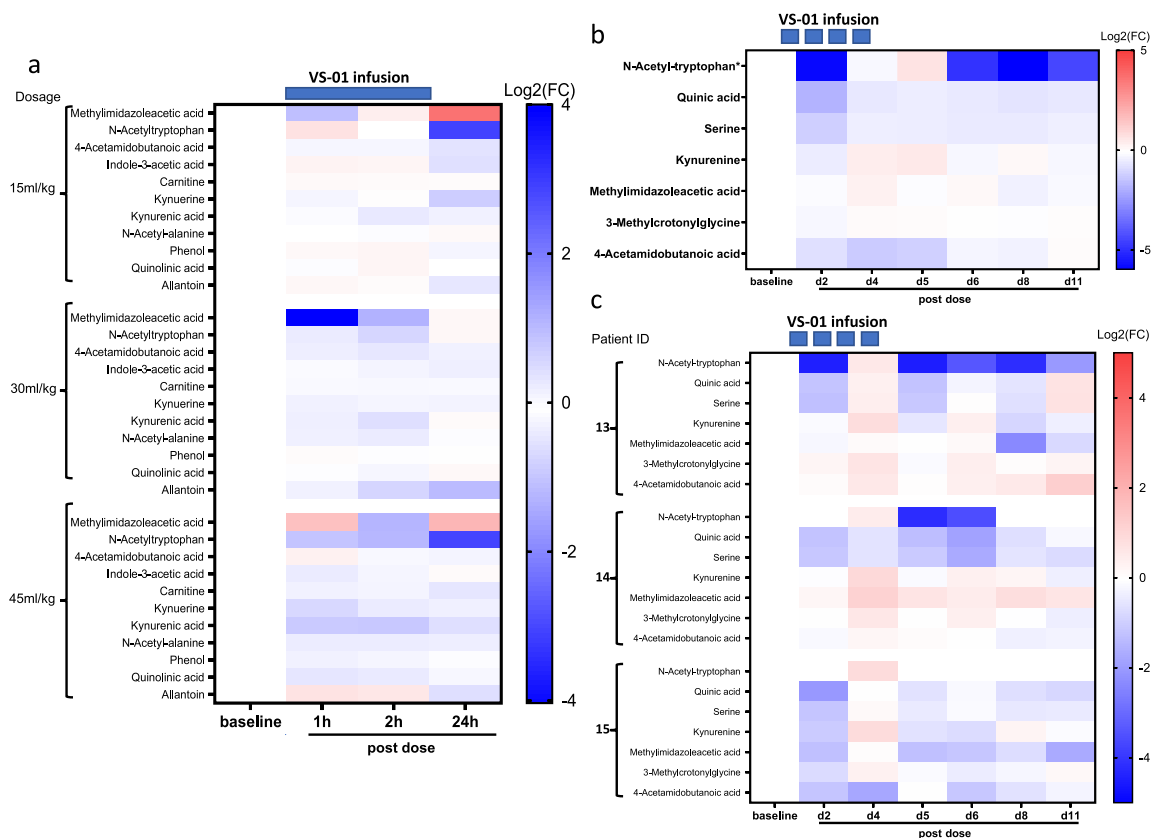
Frank Uschner¹, Wenyi Gu¹, Olaf Tyc¹, Martin Schulz¹, Philip Ferstl¹, Katharina Katharina Stauer², Stoffers Philipp¹, Hans-Peter Erasmus¹, Johannes Masseli¹, Kai-Henrik Peiffer¹, Fabian Finkelmeier¹, Anita Pathil-Warth¹, Jörg Bojunga¹, Stefan Zeuzem¹, Meriam Kabbaj², Jonel Trebicka^{1,3}. ¹Department of Internal Medicine I, University Hospital Frankfurt, Frankfurt, Germany; ²Versantis AG, Zurich, Switzerland; ³European Foundation for the Study of Chronic Liver Failure, Barcelona, Spain
Email: jonel.trebicka@kgu.de

Background and aims: Acute-on-chronic liver failure (ACLF) is defined by the presence of organ dysfunctions and failures in decompensated cirrhosis and is associated with high short-term mortality. VS-01 is a novel intraperitoneal (i.p.) pH-gradient liposomal infusion drug that enhances the clearance of ammonia and other potentially harmful metabolites. This study analyzed metabolite clusters already described to be involved in organ failure (OF) of liver, brain and kidney in patients with liver cirrhosis (Moreau et al. 2019) in the phase 1b clinical trial of VS-01 (Eudra no.: 2018-004606-25).

Method: VS-01 was infused in the peritoneal cavity of the patients and removed by paracentesis after two (part A) or three hours (part B). Patients received a single dose of 15, 30 or 45 ml/kg VS-01 (Part A; n = 9) or four consecutive doses of 34–42 ml/kg VS-01 (Part B; n = 3). Metabolomic analysis was performed on plasma samples of patients with ascites and covert hepatic encephalopathy (HE) using an untargeted LC/MS analysis approach. Peak areas were extracted and peak lists containing the mass features and identified compounds were exported to MetaboAnalyst 5.0 for statistical analysis.

Results: In the whole dataset, 24 out of 65 highly upregulated OF metabolites were detected. In part A of the study, we were able to detect 19 OF metabolites in plasma samples, of which 11 showed a decreasing trend in the plasma samples of the patients up to 24 hours after infusion of VS-01. In part B of the study, we could detect 10 OF metabolites in plasma samples of which 7 metabolites showed a decreasing trend during the infusion of VS-01 (Figure 1).

Conclusion: VS-01 is a novel drug, which is able to reduce metabolites that are associated with organ failures e.g. brain, liver and kidney failure. The current metabolic results support the future development of VS-01 in patients with ACLF and organ failure.



THU518

Metabolomic analysis of bacterial infection markers in blood samples of patients with decompensated liver cirrhosis infused with the novel drug VS-01

Frank Uschner¹, Olaf Tyc¹, Wenyi Gu¹, Martin Schulz¹, Philip Ferstl¹, Katharina Stauffer², Philipp Stoffers¹, Hans-Peter Erasmus¹, Johannes Masseli¹, Kai-Henrik Peiffer¹, Fabian Finkelmeier¹, Anita Pathil-Warth¹, Jörg Bojunga¹, Stefan Zeuzem¹, Meriam Kabbaj², Jonel Trebicka^{1,3}. ¹Department of Internal Medicine I, University Hospital Frankfurt, Frankfurt, Germany; ²Versantis AG, Zurich, Switzerland; ³European Foundation for the Study of Chronic Liver Failure, Barcelona, Barcelona, Spain
Email: jonel.trebicka@kgu.de

Background and aims: Bacterial infections are known as one frequent precipitant event for the development of acute decompensation (AD) and its maximal-form acute-on-chronic liver failure (ACLF) (PREDICT study). VS-01 is a novel intraperitoneal (i.p.) pH-gradient liposomal infusion drug that enhances the clearance of ammonia and other metabolites associated to bacterial infection in patients with ACLF. This study analyzed metabolites described to be associated with bacterial infection in patients with liver cirrhosis (Moreau *et al.* 2019) in the phase 1b clinical trial of VS-01 (Eudra no.: 2018-004606-25).

Method: The novel drug VS-01 was infused in the peritoneal cavity and removed by paracentesis after two (part A) or three hours (part B). Patients received either a single dose (15, 30 or 45 ml/kg) VS-01 (Part A; n = 9) or four consecutive doses of 34–42 ml/kg VS-01 (Part B; n = 3). Metabolomic analysis was performed on blood samples of cirrhotic patients with ascites and covert hepatic encephalopathy (HE) using untargeted LC/MS analysis. Peak areas were extracted and peak lists containing the mass features and identified compounds were exported to MetaboAnalyst 5.0 for statistical analysis.

Results: Overall, 10 out of 31 metabolites included in the metabolite cluster of infection-related ACLF were identified in plasma samples of

the patients. The infusion of VS-01 resulted in a decrease of several markers for bacterial infection in the blood of the patients (Figure 1). In part A of the study, 6 metabolites related to bacterial infection showed a decreasing trend in plasma up to 24 hours after infusion of VS-01. In part B of the study, 7 metabolites related to the infection-related ACLF cluster were detected in plasma samples, from which 4 showed a decreasing trend over time after infusion of VS-01 (Figure 1).

Conclusion: Single and repeated i.p. administrations of the novel drug VS-01 was able to reduce the concentration of several metabolites that are associated with the sepsis-related ACLF metabolite cluster. These results support the future investigation of VS-01 in patients with ACLF and bacterial infection.

THU519

Disturbances in sodium and chloride hemostasis predict outcome in stable and critically-ill patients with cirrhosis-not two sides of the same coin

Georg Semmler^{1,2}, Bernhard Scheiner^{1,2}, Rafael Paternostro^{1,2}, Benedikt Simbrunner^{1,2}, Lorenz Balcar^{1,2}, Matthias Pinter^{1,2}, Michael Trauner¹, Mattias Mandorfer^{1,2}, Christian Zauner¹, Thomas Reiberger^{1,2}, Georg-Christian Funk^{3,4}. ¹Medical University of Vienna, Division of Gastroenterology and Hepatology, Department of Internal Medicine III, Wien, Austria; ²Medical University of Vienna, Vienna Hepatic Hemodynamic Lab, Division of Gastroenterology and Hepatology, Department of Internal Medicine III, Wien, Austria; ³Klinik Ottakring, Department of Internal and Respiratory Medicine, Vienna, Austria; ⁴Karl-Landsteiner-Institute for Lung Research and Pulmonary Oncology, Vienna, Austria
Email: georg.semmler@meduniwien.ac.at

Background and aims: Serum electrolyte disturbances are common in patients with cirrhosis. Hyponatremia has profound prognostic implications, and thus, has been incorporated in the 2016 update of

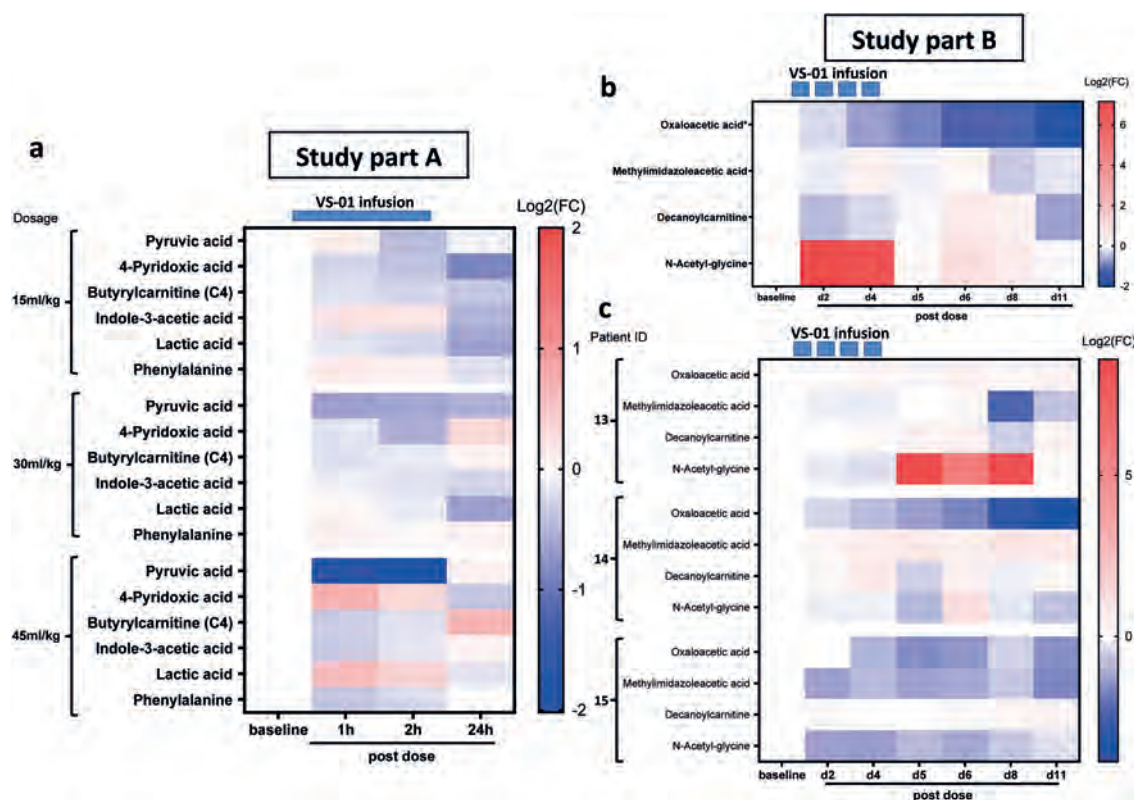


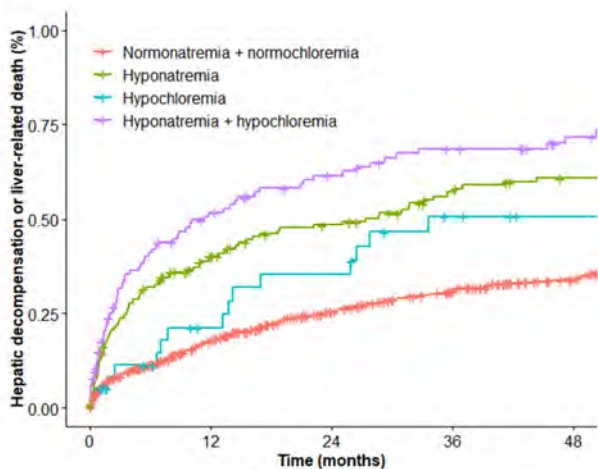
Figure: (abstract: THU518): Heatmap of log₂ (fold-change) reduced bacterial infection markers in plasma samples of study A shown per dosage (a) and study B shown per marker compound (b) and per patient (c) after administration of VS-01 (red = high/Blue = low). *, FDR < 0.05.

the UNOS MELD. Changes in serum chloride (Cl) are thought to be interrelated, however, are less well studied in the context of cirrhosis. We investigated the prognostic utility of Na- and Cl-changes on hepatic decompensation/liver-related death in patients with stable advanced chronic liver disease (ACLD) as well as on ICU-mortality in critically-ill patients with cirrhosis.

Method: 1256 patients with stable ACLD (defined by hepatic venous pressure gradient (HVPG) ≥ 6 mmHg) undergoing HVPG measurement at the Vienna Hepatic Hemodynamic Lab between 2003–2020 were included in *cohort I*. 181 critically-ill patients with cirrhosis admitted to our ICU between 1993–2003 were recruited for *cohort II*. Hypo-/hyper-Na (normal: 136–145 mmol/L) and hypo-/hyper-Cl (normal: 98–107 mmol/L) were assessed.

Results: *Cohort I:* 68% male patients with a mean UNOS MELD (i.e., excluding Na) of 12 ± 4 were included (CPS-A/B/C: 53%/35%/12%). Na and Cl levels were significantly interrelated (Spearman's $\rho = 0.54$, $p < 0.001$). Hypo-/hyper-Na was present in 25%/0% and hypo-/hyper-Cl in 15%/8%. Patients with hypo-Na (HR: 2.44 [95%CI:2.05–2.90], $p < 0.001$) and hypo-Cl (HR: 2.19 [95%CI: 1.74–2.77], $p < 0.001$) had an increased risk for hepatic decompensation/liver-related death. When incorporating both variables in a model adjusting for age, HVPG, albumin levels, and MELD score, hypo-Cl (aHR: 1.77 [95%CI:1.37–2.29], $p < 0.001$) but not hypo-Na (aHR:1.10 (95%CI:0.88–1.38), $p = 0.40$) remained independently associated with the outcome of interest. As depicted in the Figure, the presence of hypo-Na, hypo-Cl, none, or both identified patient groups with a distinct prognosis.

Figure: Kaplan-Meier curve comparing the incidence of hepatic decompensation/liver-related death in stable ACLD patients according to the presence of hypo-Na and/or hypo-Cl.



Cohort II: 70% male patients had a mean UNOS MELD of 27 ± 9 at ICU admission (92% with Child-Pugh-stage [CPS] C). Again, Na and Cl levels were strongly correlated (Spearman's $\rho = 0.81$, $p < 0.001$). Hypo-/hyper-Na was present in 47%/7% and hypo-/hyper-Cl in 30%/25%. ICU-mortality was 50% after a median of 6 (IQR:5–7) days. While the effect of Na on ICU mortality was U-shaped in restricted cubic spline analyses, it seemed to be rather linear for chloride with a worse prognosis in patients with hypo-Cl as well as hypo- and hyper-Na. In univariable logistic regression analyses, patients with hypo-Cl (OR: 2.65 [95%CI:1.30–5.53], $p = 0.008$), but not hypo-Na had a significantly worse ICU survival, which was confirmed after adjusting for hypo-Na and MELD (aOR CI: 3.24 [95%CI: 1.31–8.23], $p = 0.012$).

Conclusion: Even though Na and Cl levels are strongly interrelated in patients with stable ACLD/cirrhosis and critical illness, hypo-Cl rather than hypo-Na is associated with a worse outcome.

THU520

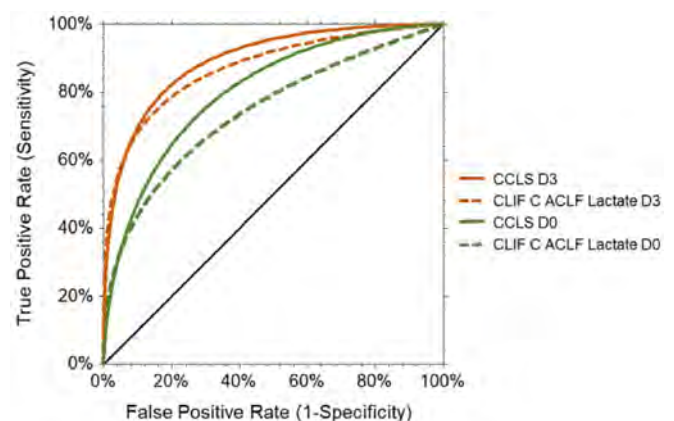
Sarcopenia assessed via computed tomography is associated with short-term outcomes and improves prognostic scores' performance in critically ill patients with acute on chronic liver failure

Thomas Mangana Del Rio¹, Fabio Becce¹, Julien Vionnet¹, Alban Denys¹, Antoine Schneider¹, Alexandre Wetzel¹, Darius Moradpour¹, Jean-Daniel Chiche¹, Florent Artru^{1,2}. ¹Lausanne University Hospital, Lausanne, Switzerland; ²King's College Hospital, Institute of Liver Studies, London, United Kingdom
Email: florent.artu@kcl.ac.uk

Background and aims: Prognostication of patients with cirrhosis and acute-on-chronic liver failure (ACLF) relies on organ failure scores. Sarcopenia is associated with poor outcomes in patients with cirrhosis but has not been investigated in critically ill patients with ACLF. We aimed to evaluate whether sarcopenia was associated with short-term outcome in this population.

Method: We retrospectively included all patients with cirrhosis and ACLF (as defined by EASL criteria) admitted to the intensive care unit (ICU) of Lausanne University Hospital between January 2010 and December 2019, who had a recent CT (within 15 days from admission to the ICU). L3 skeletal muscle index (L3SMI) was quantified by using a deep learning-based method from a single axial CT image at the level of lumbar vertebra 3. Sarcopenia was defined by previously published sex-specific cut-offs: 50 cm²/m² in men and 39 cm²/m² in women.

Results: A total of 194 patients fulfilled the inclusion criteria. Their characteristics at admission were the following: 26% were female, median age was 62 years (IQR, 54–70 years), MELD 21 (13–28), CLIF-C ACLF 79 (74–85), CLIF-C ACLF-lactate 83 (76–92). Sixty percent of patients had ACLF grade 3, 34% grade 2 and 6% grade 1. Median 28-day transplant-free survival (TFS) was 58% (95% CI, 51–65%). Median L3SMI was 43 (37–51), with 59% of patients being sarcopenic. In multivariate Cox-regression analyses at day 0 (D0), the three independent variables associated with 28-day TFS were CLIF-C ACLF-lactate (HR 1.06, 1.04–1.09, $p < 0.0001$), MELD score (HR 1.03, 1.01–1.07, $p = 0.03$) and sarcopenia (HR 2.1, 1.3–3.5, $p = 0.003$). At day 3 (D3), the two independent variables associated with 28-day TFS were CLIF-C ACLF-lactate on day 3 (HR 1.08, 1.07–1.11, $p < 0.0001$) and sarcopenia (HR 1.9, 1.2–3.1, $p = 0.01$). Based on the results of multivariate analyses, we derived two scores (CLIF-C ACLF-lactate-sarcopenia at D0 and D3, CCLS-D0 and CCLS-D3) with the aim of improving prognostic stratification. For the prediction of 28-day TFS, CCLS-D0 had an AUROC of 0.80 and outperformed CLIF-C ACLF-lactate on day 0 (0.74, $p = 0.004$). Similarly, CCLS-D3 had an AUROC of 0.89 and outperformed CLIF-C ACLF-lactate on day 3 (0.86, $p = 0.04$) (Figure 1).



POSTER PRESENTATIONS

Conclusion: Sarcopenia, as assessed by CT-Scan is independently associated with 28-day TFS in critically ill patients with cirrhosis and ACLF. Adding sarcopenia to CLIF-C-ACLF-lactate score at D0 and D3 improved the performance of the scores. Sarcopenia is an important parameter related to outcomes and should be evaluated in this population.

THU521

Use of Tocilizumab in patients with stable chronic liver disease and severe COVID-19 for prevention of decompensated cirrhosis, a prospective, open-label, randomized controlled trial.

Luis Alejandro Rosales Renteria^{1,2}, Hiram Jaramillo-Ramírez³, Francisco Calderón-Mendieta³, Jesús Camacho-Escobedo¹, José Manuel Avendaño-Reyes², Diana Laura López-Rubio¹, Adrián Sáenz Araiza¹, Gisel Estefanía Reyes-Higuera¹, Dulce Renée Soto-González¹, Erikc Jesús Arzola-Renteria¹. ¹Mexicali General Hospital, Internal Medicine, Mexicali, Mexico; ²Faculty Of Medicine UABC, Mexicali, Mexico; ³Mexicali General Hospital, Mexicali, Mexico

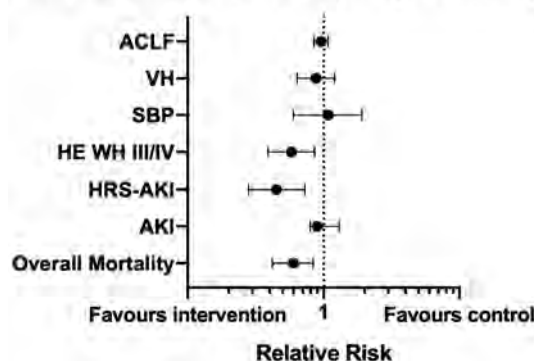
Email: luis.alejandro.rosales.renteria@uabc.edu.mx

Background and aims: Interleukin-6 (IL-6) is involved both in the pathogenesis of severe COVID-19 (SC) and decompensated Chronic Liver Disease (CLD). Tocilizumab, a monoclonal antibody used to block the IL-6 signal transduction pathway, has been proved to have beneficial effects in the prognosis of patients with SC. However, evidence of its effect on patients with CLD that develop SC is scarce. We aimed to evaluate the efficacy of Tocilizumab on patients with CLD and SC in a tertiary care hospital from Mexico.

Method: A single center, prospective, open-label, randomized controlled trial, which included patients with CLD with either compensated cirrhosis or stable decompensated cirrhosis (according to EASL definition) that developed SC, and were admitted to our hospital in Mexicali, Mexico, from March 1, 2020, to December 31, 2021. General characteristics were obtained. The Primary Outcome was overall mortality according to the absence or presence of Tocilizumab administration (administered in the first 12 hours of arrival according to hospital availability at an 8mg/kg single IV dose), secondary outcomes were mortality according to each stage of CTP, and development of acute decompensation (AD), defined as one or more of the following : Acute Kidney Injury (AKI), Hepatorenal syndrome-AKI (HRS-AKI), Variceal Hemorrhage (VH), West Haven (WH) grade III or IV Hepatic Encephalopathy (HE), Spontaneous Bacterial Peritonitis (SBP) or Acute on Chronic Liver Failure (ACLF). A value of $p < 0.05$ was significant. Exclusion criteria were age younger than 18 years and patients with unstable decompensated cirrhosis at baseline.

Results: A total of 361 patients were included. They were classified according to the Child-Turcotte-Pugh (CTP) classification, and the Model for end-stage Liver Disease-Sodium (MELD-Na). Most patients were classified as CTP B (216 patients, 59.8%). Median MELD-Na in the intervention group was 22 vs 19 in control. 77 patients were randomized to Tocilizumab, and 284 patients were not. With regards to the primary outcome, 32.4% patients in the intervention group died vs 53.8% patients in the control group, this difference was significant with a relative risk (RR) of 0.6, a 95% confidence interval (CI) of (0.4–0.8), $p < 0.001$, and a number needed to treat (NNT) of 4.6 with a NNT 95% CI of (2.9–11.3). Secondary outcomes were significant for mortality reduction in the CTP subgroup for all grades of severity and showed a lower risk of developing HRS- AKI (RR = 0.4, 95% CI [0.2–0.7], NNT 4.3, 95% NNT CI [2.8–9.1], $p < 0.001$) and WH III/IV HE (RR = 0.5, 95% CI [0.3–0.8], NNT 5.2, 95% NNT CI [3.1–14.7], $p = 0.003$).

Tocilizumab use in CLD and SC, both primary and secondary outcomes



Conclusion: Tocilizumab reduced mortality in CLD patients with SC, overall, in each stage of CTP classification, and reduced the risk of developing both HRS-AKI and severe HE, but not other events. Whether these results can be reproduced in patients without SC warrants further research.

THU522

Comprehensive immunophenotyping reveals profound alterations of T cell subsets in acute decompensation of liver cirrhosis

Yasmina Chouik^{1,2}, Fabienne Venet^{3,4}, Morgane Gossez^{3,4}, Thibault Andrieu², Marie-Laure Plissonnier², Bordes Isabelle², Teresa Antonini¹, Domitille Erard¹, Miroslava Subic-Levrero¹, Francois Villeret^{1,2}, Wafa Khamri⁵, Fabien Zoulim^{1,2}, Massimo Levrero^{1,2}, Fanny Lebosse^{1,2}. ¹Hospices Civils of Lyon, Hepatology Unit, Lyon, France; ²Cancer Research Center of Lyon INSERM U1052, Lyon, France; ³Hospices Civils of Lyon, Immunology Laboratory, Lyon, France; ⁴International Center for Infectology Research, Lyon, France; ⁵Imperial College London, Liver Immunology Laboratory, London, United Kingdom

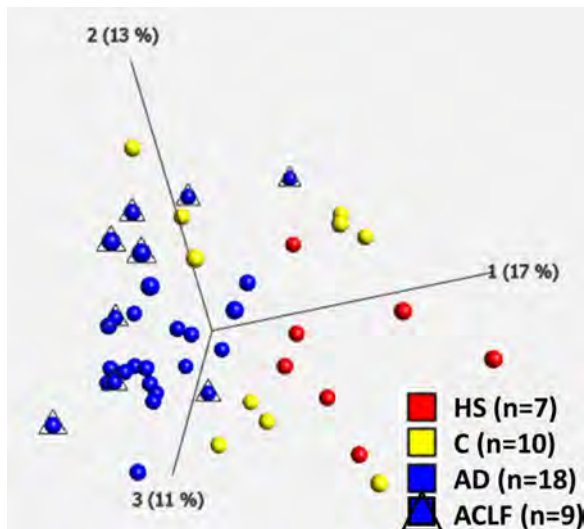
Email: fanny.lebosse@inserm.fr

Background and aims: Bacterial infection is a frequent and life threatening event in acute decompensation (AD) of cirrhosis, with a 1-month mortality rate of 20–30%. Septic risk is notably underpinned by cirrhosis-associated immune dysfunction. Recent data suggest the potential involvement of adaptive immune responses in cirrhosis-related immune dysfunction. We conducted a detailed analysis of circulating T cells in patients with AD compared to patients with compensated cirrhosis (C) and healthy subjects (HS) in order to gain insights in circulating adaptive immune cells alterations in cirrhosis.

Method: Thirty seven patients from a monocentric prospective study (EmiC cohort, n = 97 patients) were selected for T cells phenotyping. Clinical and biological samples were collected at hospital admission and up to 6 months after inclusion. PBMC from HS were obtained from the French Blood Bank. Phenotyping of circulating T cells was conducted on frozen PBMC by spectral cytometry (26-color panel). This panel enables the analysis of effector, memory and naïve T cells, regulatory T cells (Treg), T-helper (Th)1, Th2, Th17, Th17+1, Th22 CD4+ T cells, Tc1, Tc2, Tc17, Tc22 CD8+ T cells, gamma delta T cells and NKT cells. Activation, inhibition and death markers were also studied (CD38, HLA-DR, PD1, CD95). Unsupervised analysis was performed using Qlucore™ and Cytobank™. Plasma cytokines were measured by Simple Plex™ immunoassays on a microfluidic ProteinSimple® ELA analyzer.

Results: Spectral cytometry analysis was performed in 7 HS, 10 C and 27 AD patients including 9 patients with Acute on Chronic Liver Failure. Principal component analysis showed clear distinct T cells features between HS, C and AD patients (Figure 1). T cell phenotyping revealed progressive imbalance between type 1 and type 2 T cell responses with a decrease of the Th1/Th2 and Th1/Treg ratios

throughout cirrhosis progression. T cells of patients with decompensated cirrhosis displayed increased surface expression of both activation and death markers. In addition, circulating Th17 cells significantly decreased in patients with bacterial infection (n = 12) and correlated with C-reactive protein and albumin levels. Increased Th1/Th2 ratio was associated with the occurrence of nosocomial infection (n = 6), while proportion of Th17 could significantly predict 6-month survival in AD patients.



Conclusion: Alterations of circulating T cells subsets are associated with cirrhosis severity and clinical outcomes. These results underlie the role of T cells in cirrhosis-associated immune dysfunction.

THU523

Low hemoglobin level predicts early hospital readmission in patients with cirrhosis and acute decompensation

Enrico Pompili¹, Maurizio Baldassarre^{1,2}, Giacomo Zaccherini¹, Manuel Tufoni³, Giulia Iannone¹, Dario Pratelli¹, Clara De Venuto¹, Marco Domenicali^{1,4}, Paolo Caraceni^{1,2,3}. ¹University of Bologna, Department of Medical and Surgical Sciences, Bologna, Italy; ²University of Bologna, Center for Applied Biomedical Research, Bologna, Italy; ³IRCSS Azienda Ospedaliero-Universitaria di Bologna, Division of Medical Semiotics, Bologna, Italy; ⁴S. Maria delle Croci Hospital, AUSL della Romagna, Department of Internal Medicine, Ravenna, Italy
Email: paolo.caraceni@unibo.it

Background and aims: Patients with decompensated cirrhosis are at high risk of emergent hospitalizations leading to a very economic and social burden. This study aimed to determine the incidence of readmission up to 1 year after discharge from an index hospitalization and to identify predictors of liver-related early readmission (within 30 days).

Method: We performed a secondary analysis in a prospectively collected cohort of patients admitted to hospital for acute decompensation (AD) complicated or not by acute-on-chronic-liver-failure (ACLF). After discharge, patients were prospectively followed until death, liver transplantation or up to a maximum of 1 year for recording any emergent hospitalization and related cause. Laboratory and clinical data at admission and discharge of the index hospitalization and the occurrence of nosocomial bacterial infection and ACLF were also collected.

Results: Of the 329 patients included in the analysis, 182 patients were hospitalized during the 1-year follow-up (26% once, 15% twice, 10% three times and 6% four or more times, leading to a total of 369 readmissions). The most frequent causes of readmission were hepatic encephalopathy (36%), ascites (22%) and bacterial infection (21%).

Cumulative incidence of all-cause readmission was 19% at 30 days, 36% at 90 days and 56% at 1 year. Fifty-four patients were readmitted for emergent liver-related causes within 30 days after discharge. Early readmission was associated to a higher 1-year mortality (47 vs 32%, $p = 0.037$). Data collected both at admission (MELD-Na score, diabetes), during hospitalization (development of ACLF, days spent in hospital) and at discharge (hemoglobin (Hb) value, MELD-Na score) were significantly associated with early readmission. Multivariable competing risk regression analysis showed that Hb lower than 8.75 mg/dL (sHR 2.38 [95%CI 1.22–4.64], $p = 0.011$), MELD-Na > 16 at discharge (sHR 2.25 [95%CI 1.27–3.99], $p = 0.005$), and diabetes (sHR 1.74 [95%CI 1.02–2.99], $p = 0.044$) were independent predictors of early readmission. Cumulative incidence of early readmission was 8% (95% CI 4–14) in patients without risk factors, 16% (95% CI 11–22) in those presenting one risk factor and 35% (95% CI 23–47) in those presenting 2 or more risk factors ($p < 0.001$). For instance, in patients with MELD-Na > 16 at discharge, the presence of Hb < 8.75 g/dl doubles the risk of early re-hospitalization (42% vs 21%, $p = 0.031$).

Conclusion: Besides the already documented MELD-Na and diabetes, this study identifies a level of Hb < 8.75 g/dl at discharge as a new independent risk factor for liver-related early readmission, thus contributing to identify the subgroup of high-risk patients to be included in programs of transitional care after discharge.

THU524

Thrombospondin 1: an emerging key-role in the acute-on-chronic liver failure pathogenesis

Hozeifa Mohamed Hassan¹, Xi Liang¹, Jiaojiao Xin^{1,2}, Dongyan Shi^{1,2}, Keke Ren², Qi Chen¹, Jiang Li², Peng Li², Hui Yang², Jinjin Luo², Jing Jiang^{1,2}, Jun Li^{1,2}. ¹Taizhou Central Hospital (Taizhou University Hospital), Precision Medicine Center, Taizhou, China; ²The First Affiliated Hospital, Zhejiang University School of Medicine, State Key Laboratory for Diagnosis and Treatment of Infectious Diseases, National Clinical Research Center for Infectious Diseases, Collaborative Innovation Center for Diagnosis and Treatment of Infectious Diseases, Hangzhou, China
Email: lijun2009@zju.edu.cn

Background and aims: Acute-on-chronic liver failure (ACLF) is a clinical syndrome that develops in patients with chronic liver diseases following a precipitating event and associated with a high mortality rate due to systemic multiorgan failure. In China, the most common precipitating disorder is hepatic insult due to hepatitis B virus (HBV) reactivation. Although HBV-ACLF disease progress rapidly with limited treatment options, the pathogenesis still unclear and there is a lack of effective biomarkers for early diagnosis and prognosis of HBV-ACLF. Thrombospondin 1 (THBS1) was recognized among the top significantly differentially expressed potential key molecular biomarkers associated with HBV-ACLF disease progression, but the THBS1 key-role participation in ACLF is not clear. This study aimed to evaluate the biomarker probabilities of THBS1 in ACLF pathogenesis.

Method: The biobanked peripheral blood mononuclear cells (PBMCs) from 330 subjects with HBV-related etiologies, including HBV-ACLF, liver cirrhosis (LC), chronic hepatitis B (CHB) and normal controls (NC) from the Chinese Group on the Study of Severe Hepatitis B (COSSH) prospective multicenter cohort were subjected to transcriptome analyses (ACLF = 20; LC = 10; CHB = 10; NC = 15), and the findings were validated in humans and ACLF preclinical rat model. Substantially, a THBS1 knockout mice model was developed to validate the liver protection capabilities following drugs intoxication.

Results: THBS1 was identified as the top significantly differentially expressed genes (DEGs) in PBMCs transcriptome, with most significant upregulation in ACLF, and qPCR (ACLF = 110; LC = 60; CHB = 60; NC = 45) verified the consistency of THBS1 expression with the ACLF disease severity. Moreover, the precision of THBS1 prediction abilities for ACLF short-term mortality were 0.8438 and 0.7778 at 28 and 90 days, respectively ($p < 0.05$). THBS1 expression patterns were significantly positively correlated with inflammatory-

POSTER PRESENTATIONS

related cytokine gene (CCL2, IL-6, IL-1 α , CXCL2, ...etc.), and apoptosis-related genes (Bcl2 and Caspase-9). External validation in ACLF rat serum and liver tissues fortified the functional association between THBS1, immune response and cellular apoptosis. THBS1 knockout improves mice survival, showed significant repressions of major inflammatory cytokines (CCL2, IFN γ , IL-1 β , ...etc.), enhances expression ($p < 0.01$) of several anti-inflammatory mediators (IL-10, IL-4, IL-13, ...etc.) and impedes hepatocellular apoptosis.

Conclusion: THBS1 might be considered as a new key-molecule in severity prediction of ACLF, being a disease development-related biomarker, promoting inflammatory responses and hepatocellular apoptosis, thus facilitating timely intensive clinical interventions by providing clinicians with potential new targets to improve the diagnostic and therapeutic strategies for ACLF management.

THU525

Beta-blockers can reduce mortality in patients with acute-on-chronic liver failure-a multi-center study

Anand Kulkarni¹, Madhumita Premkumar², Karan Kumar³, Juned Khan⁴, Baqar Gora¹, Sowmya Iyengar¹, Mithun Sharma¹, Nageshwar Reddy¹, Nagaraja Rao Padaki¹. ¹Asian Institute of Gastroenterology, Hyderabad, India; ²Post Graduate Institute of Medical Education and Research, Chandigarh, Chandigarh, India; ³Mahatma Gandhi Hospital, Jaipur, Jaipur, India; ⁴Hopewell Hospital, Lucknow, India

Email: anandvk90@gmail.com

Background and aims: Beta-blockers (BBs) can reduce the incidence of complications in patients with cirrhosis and prolong survival. The safety and efficacy of BBs in real-world settings in patients with ACLF identified by the Asian Pacific Association for the Study of Liver (APASL) criteria is unknown. Therefore, we aimed to assess the safety and efficacy of BB in patients with APASL defined ACLF.

Method: In this retrospective, multi-center study, patients with ACLF with complete 30 days follow-up were included. The primary objective was to compare day 30, 90, and 1-year mortality among standard of care (SOC) and BB (+SOC) groups. The secondary objectives were: to compare the incidence of infection and variceal bleed on days 30, 90, and one year among both the groups. We also assessed the time to resolution of ACLF (recompensation).

Results: A total of 346 patients were included. Only 26% ($n = 89$) received BBs, while 74% ($n = 257$) received only SOC. Age and severity scores (MELD NA-SOC: 28.4 ± 5.21 vs. 27.88 ± 4.9 in BB; $p = 0.3$) were similar in both groups. Alcohol was the most common cause of ACLF. Heart rate was higher and mean arterial pressure (MAP) lower in the SOC group than in the BB group. The indication for BB was large high-risk varices in 48.3% (43/89), history of acute variceal bleed in 40.4% (36/89), and 11.2% (10/89) were prophylactically started on BB to prevent further decompensation. Fifteen percent in SOC group and 12.35% in BB group were ACLF grade III patients. Though 9% of patients had a history of AVB in the SOC group, BB could not be added either due to sepsis, low MAP, or kidney injury. The incidence of mortality was 21% (54/257) in SOC group compared to only 8% (7/89) in BB group at day 30 ($p = 0.005$). Similarly, at day 90, mortality was 37.2% (84/226) in SOC group compared to 17% (15/88) in BB group ($p = 0.001$). Mortality at one year was 48% (88/183) in SOC group compared to 27% (18/66) in BB group ($p = 0.003$). BB therapy could not reduce the incidence of infections or variceal bleed (Table). Complete resolution of ACLF (recompensation) was noted in 47% (121/257) of patients in SOC group and 73% (65/89) patients in BB group ($p < 0.001$). The mean time to recompensation was 2.66 ± 1.42 months in the SOC group compared to 2.3 ± 1.15 months in the BB group ($p = 0.07$). Four percent in SOC group and 1% in BB group underwent liver transplantation. Carvedilol was prescribed in 77.5% and propranolol in 22.5% of patients. Eight patients discontinued BB. On subgroup analysis, BB reduced mortality in ACLF grades I and II but not in grade III. Recompensation was significantly better in those with

ACLF I and II but not in grade III. Furthermore, there was a significant reduction in the incidence of infection in the BB group in ACLF grade I.

Outcomes in standard of care of care group and beta-blocker group among the whole cohort.

Outcome	SOC	SOC + Beta blocker	P
Mortality at			
30 days	21% (54/257)	8% (7/89)	0.005
90 days	37.2% (84/226)	17% (15/88)	0.001
one year	48% (88/183)	27% (18/66)	0.003
Infection at			
30 days	20.2% (52/257)	17% (15/89)	0.48
90 days	42% (94/226)	31% (27/88)	0.07
one year	53.55% (98/183)	47% (31/66)	0.35
AVB at			
30 days	4.3% (11/257)	5.6% (5/89)	0.6
90 days	5.75% (13/226)	9% (8/88)	0.28
one year	8.2% (15/183)	13.64% (9/66)	0.19

SOC, standard of care; AVB, acute variceal bleed.

Conclusion: Only 1 in 4 ACLF patients are suitable for beta-blocker therapy. Beta-blocker therapy can reduce mortality and lead to early recompensation, especially in early grades of ACLF.

Cirrhosis and its complications: Experimental and pathophysiology.

THU526

Increased platelet aggregation in decompensated cirrhosis indicates higher risk of further decompensation and liver-related mortality

Alberto Zanetto¹, Elena Campello², Cristiana Bulato², Sabrina Gavasso², Fabio Farinati¹, Patrizia Burra¹, Francesco Paolo Russo¹, Paolo Simioni², Marco Senzolo¹.

¹Gastroenterology and Multivisceral Transplant Unit, Surgery, Oncology, and Gastroenterology, Padova, Italy; ²Thrombotic and Hemorrhagic Diseases Unit, General Internal Medicine, Medicine, Padova, Italy

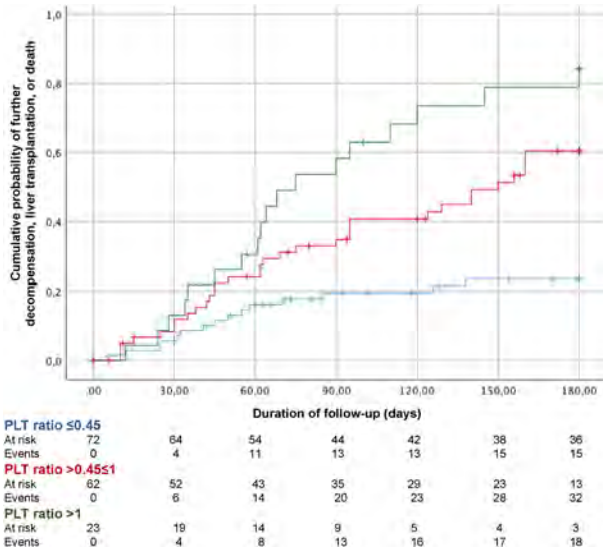
Email: alberto.zanetto@yahoo.it

Background and aims: Studies on platelet aggregation in cirrhosis are controversial because interpretation of platelet function is challenged by thrombocytopenia. In this two-part study, we investigated platelet aggregation in cirrhosis and its correlation with development of liver-related events.

Method: Platelet aggregation was assessed by whole blood aggregometry. To overcome the influence of platelet count, we calculated a "platelet aggregation/platelet count ratio" (PLT ratio) to compare cirrhosis with thrombocytopenia and controls (60 chronic hepatitis and 45 healthy subjects) with normal platelet count (study part #1). Then, we prospectively followed patients with cirrhosis and investigated predictors of hepatic decompensation, transplantation, and death (study part #2).

Results: 203 cirrhosis patients were prospectively recruited (77% decompensated; median MELD 14). PLT ratio was significantly higher in cirrhosis than in chronic hepatitis and healthy subjects (0.44 vs. 0.25 and 0.26, respectively; $p < 0.0001$). Among patients with

cirrhosis, the ratio increased with disease severity (Child C > B > A) and was particularly elevated in decompensated patients with severe thrombocytopenia. During a 6-month follow-up, among decompensated patients, 65 had further decompensation, transplantation, or died. As shown in the Figure, the relative risk of such events was 4-fold higher in patients with a baseline PLT ratio >1 than in those with a PLT ratio ≤0.45 (RR: 3.8, 95%CI: 2.3–6.2; $p < 0.0001$). On multivariate analysis, PLT ratio (OR: 22.17, CI95%: 5.88–83.61; $p < 0.0001$) and MELD score (OR: 1.07, CI95%: 1.01–1.13; $p = 0.03$) were independently predictive of outcome.



Conclusion: Patients with cirrhosis, particularly when decompensated, have increased platelet aggregation. Among decompensated patients, those with PLT ratio >1 have an 80% probability of progressing towards further decompensation, transplantation, or liver-related death within 6 months.

THU527

Renin/angiotensin system-coagulation-inflammation axis abnormalities: a possible explanation for susceptibility to severe COVID-19 in cirrhosis

Lukas Hartl^{1,2}, Mathias Jachs^{1,2}, Benedikt Simbrunner^{1,2,3}, David JM Bauer^{1,2}, Georg Semmler^{1,2}, Daniela Gompelmann⁴, Thomas Szekeres⁵, Peter Quehenberger⁵, Michael Trauner¹, Mattias Mandorfer^{1,2}, Bernhard Scheiner^{1,2}, Thomas Reiberger^{1,2,3}.

¹Medical University of Vienna, Division of Gastroenterology and Hepatology, Department of Medicine III, Vienna, Austria; ²Medical University of Vienna, Vienna Hepatic Hemodynamic Lab, Division of Gastroenterology and Hepatology, Department of Medicine III, Vienna, Austria; ³Medical University of Vienna, Christian Doppler Lab for Portal Hypertension and Liver Fibrosis, Vienna, Austria; ⁴Medical University of Vienna, Division of Pulmonology, Department of Internal Medicine II, Vienna, Austria; ⁵Medical University of Vienna, Department of Laboratory Medicine, Vienna, Austria

Email: thomas.reiberger@meduniwien.ac.at

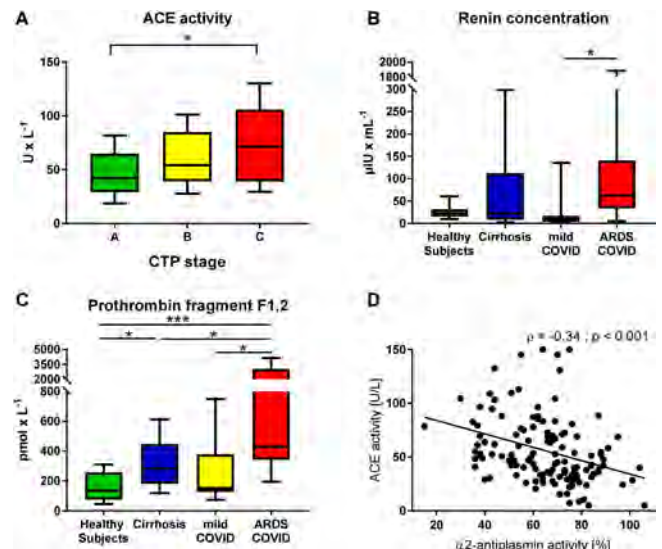
Background and aims: Risk for severe coronavirus disease of 2019 (COVID-19) is increased among cirrhotic patients. Plasmin may aggravate COVID-19 by facilitation of cell entry of the virus. We investigated parameters of the renin/angiotensin system (RAS), endothelial dysfunction, coagulation/fibrinolysis and inflammation in both cirrhotic patients and COVID-19 patients.

Method: 127 prospectively characterized cirrhotic patients (CIR), as well as 9 patients with mild COVID-19 (mCOV), 11 patients with COVID-19 ARDS (aCOV) and 10 healthy subjects (HS) were included in

the study. In cirrhotic patients, portal hypertension was assessed by hepatic venous pressure gradient (HVPG).

Results: With increasing liver disease severity (Child-Pugh stage A vs. B vs. C) and compared to HS, CIR patients displayed higher RAS activity (renin, angiotensin-converting enzyme [ACE], aldosterone), endothelial dysfunction (von Willebrand-factor [VWF] antigen) and inflammation (C-reactive protein [CRP], interleukin-6 [IL-6]), along with a dysregulated coagulation/fibrinolysis profile (D-dimer, prothrombin fragment F1, 2, plasminogen activity, antiplasmin activity). Renin (i.e. RAS activity), VWF antigen (i.e. endothelial dysfunction), coagulation parameters (D-dimer, prothrombin fragment F1, 2) and parameters of inflammation (CRP, IL-6) were significantly elevated in COVID-19 patients and increased from mCOV to aCOV.

In CIR patients, ACE activity was associated with IL-6 ($p = 0.26$; $p = 0.003$), independently linked to VWF antigen (aB: 0.10; $p = 0.001$) and was inversely correlated with prothrombin fragment F1, 2 (aB: -0.03; $p = 0.023$) and antiplasmin activity (aB: -0.58; $p = 0.006$).



Conclusion: RAS activity is considerably upregulated in Child-Pugh B/C cirrhosis and linked to endothelial dysfunction, abnormal coagulation profile and systemic inflammation. The cirrhosis-associated abnormalities of ACE (i.e. RAS activation), VWF antigen (i.e. endothelial dysfunction), antiplasmin (i.e. coagulation dysregulation and increased plasmin) and IL-6 (i.e. increased inflammation) may explain the susceptibility for severe COVID-19.

THU528

Improvement of hepatic and extrahepatic functions and anti-inflammatory effects of nitazoxanide in disease models of LPS-induced systemic inflammation and acute-on-chronic liver failure

Vanessa Legry¹, Philippe Delataille¹, Maryse Malysiak¹, Valérie Daix¹, Simon Debaecker¹, Bart Staels², Remy Hanf¹, Dean Hum¹. ¹GENFIT SA, Loos, France; ²Univ. Lille, Inserm, CHU Lille and Institut Pasteur de Lille, U1011-EGID, Lille, France

Email: vanessa.legry@genfit.com

Background and aims: Systemic inflammation (SI) is a hallmark of multiple organ failures in Acute on Chronic Liver failure (ACLF). Therefore, anti-inflammatory compounds may have the potential to alleviate ACLF, especially if they have immediate effects on the inflammatory state. The FDA approved anti-parasitic drug, nitazoxanide (NTZ), is suspected to exert direct anti-inflammatory actions. Our aim was to assess the efficacy of NTZ to rapidly counteract SI and improve hepatic and extra-hepatic functions after LPS challenge in healthy and fibrotic rats.

POSTER PRESENTATIONS

Method: Direct effects of NTZ on LPS-induced activation of human differentiated THP1 macrophages were assessed *in vitro*. Single ip LPS injection (1 mg/kg) was applied to healthy rats to induce a transient increase in circulating cytokines at 1–3 hours. A single oral dose of NTZ (100 mg/kg) was administered just before LPS injection and blood samples were collected 3 h later before sacrifice.

To assess NTZ's effects in an ACLF-model, a single ip LPS injection (0.03 mg/kg-adapted dose to limit mortality) was administered to rats with liver fibrosis induced by oral CCl₄ administration for 15 weeks followed by 1-week CCl₄ washout. Before the LPS challenge, the rats received NTZ (50 mg/kg BID) or vehicle for 3 days. Plasma samples were collected 24 h post-LPS.

Results: In THP1 macrophages, the active NTZ metabolite tizoxanide blunted LPS-induced TNF α secretion (IC₅₀ = 6 μ M, E_{max} = 88%). In healthy rats, NTZ reduced the LPS-induced rise in circulating cytokines (619 vs 1782 pg/ml TNF α , p = 0.01; 17.5 vs 24.8 ng/ml IL6, p = 0.06; 633 vs 834 pg/ml IL1 β , p = 0.10; 4740 vs 6760 pg/ml IFN γ , p = 0.09) within 3 hours of treatment. In rats with CCl₄-induced fibrosis (F3-F4), NTZ treatment before LPS-induced ACLF reduced ALT (214 vs 919 U/l, p = 0.007), AST (355 vs 2072 U/l, p = 0.005) and total bilirubin (3.7 vs 13.3 μ mol/l, p = 0.02), resulting in hepatoprotective effects. Moreover, NTZ treatment also prevented LPS-induced increases in creatinine (48 vs 83 μ mol/l, p = 0.009), urea (46 vs 140 mg/dl, p = 0.002) and cystatin C (1471 vs 2869 ng/ml, p = 0.02).

Conclusion: These results suggest that the rapid anti-inflammatory effects of NTZ may participate in beneficial effects on hepatic and extrahepatic functions in a disease model of ACLF.

THU529

In silico characterization of the interactome of hepatic nonparenchymal cells reveals promising targets for antifibrotic therapy

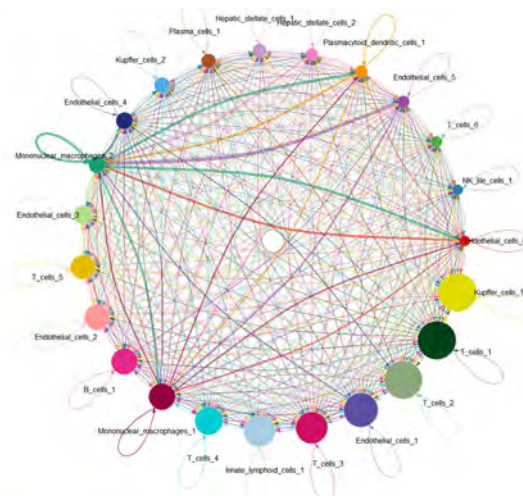
Oleksandr Petrenko^{1,2,3,4}, Ksenia Brusilovskaya^{1,2,3,4}, Benedikt Hofer^{1,2,3,4}, Philipp Königshofer^{1,2,3,4}, Benedikt Simbrunner^{1,2,3,4}, Kaan Boztug^{1,2}, Michael Trauner^{3,4}, Philipp Schwabl^{1,2,3,4}, Thomas Reiberger^{1,2,3,4}. ¹Ludwig Boltzmann Institute for Rare and Undiagnosed Diseases (LBI-RUD), Vienna, Austria; ²CeMM Research Center for Molecular Medicine of the Austrian Academy of Sciences, Vienna, Austria; ³Vienna Hepatic Hemodynamic Lab (HEPEX), Division of Gastroenterology and Hepatology, Department of Internal Medicine III, Medical University of Vienna, Vienna, Austria; ⁴Christian Doppler Laboratory for Portal Hypertension and Liver Fibrosis, Medical University of Vienna, Vienna, Austria
Email: thomas.reiberger@meduniwien.ac.at

Background and aims: Advances in tissue dissociation and sequencing methodology allow functional characterization of non-parenchymal liver cells (NPCs) on a single-cell resolution. Based on the cellular expression of ligand-receptor pairs, the predicted molecular crosstalk in distinct cell populations can identify potential therapeutic targets.

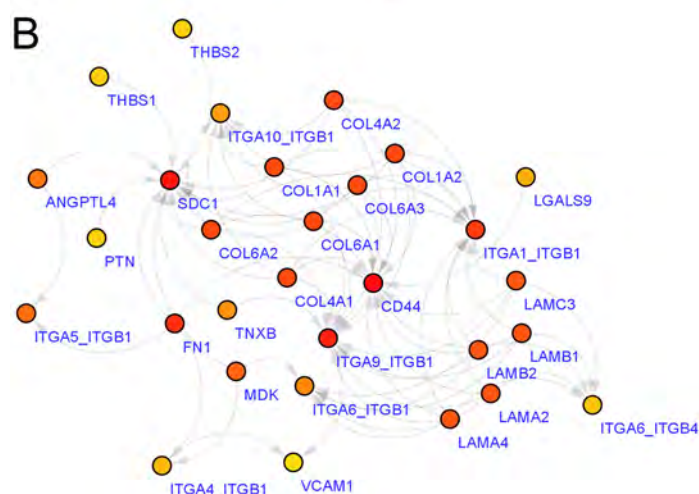
Method: We used published single-cell RNA sequencing (scRNA-seq; MacParland-Nature Communications 2018; Ramachandran-Nature 2019) to predict *in silico* the interactome of hepatic non-parenchymal cells (NPCs) from patients with healthy and fibrotic livers. After filtering, integrating, and annotating the scRNA-seq datasets, CellChat algorithms were used to build an interaction network among both healthy and cirrhotic NPCs. Subsequently, Reactome pathway analysis using predicted ligand-receptor pairs revealed key pathways associated with cirrhosis. The PanDrugs platform was used to identify drug-gene associations.

Results: We computed the cellular interactome among NPCs based on both healthy and cirrhotic scRNA-seq datasets (Figure-A). In cirrhosis (vs. healthy), the outgoing interactome of macrophages primarily addressed endothelial and dendritic cells, and hepatic stellate cells (HSCs) had significantly increased interactions, mainly with endothelial and infiltrating immune cells.

A



B



Specifically, in cirrhosis, the endothelial cell-selective adhesion molecule (ESAM) and thrombospondin 1 (THBS) pathways were over-represented. Cirrhotic HSCs became a major source of ESAM, especially directed towards endothelial cells. In healthy livers, THBS participated in the cellular crosstalk between macrophages and other immune cells. However, in cirrhosis, HSCs were linked to this THBS-based interaction with immune cells.

Top drug-gene associations were identified based on the elements of the cirrhotic NPC interactome with the highest network centrality score. The latter were represented mainly by extracellular matrix and immunovascular signaling transcripts, such as collagens, laminins, and integrins (Figure-B, red vs. yellow indicating higher network centrality score).

We identified 59 drug candidates (8 approved drugs, 16 in clinical trials, and 35 compounds with experimental evidence) with predicted ESAM and THBS pathways activity.

Conclusion: Prediction of the cellular and cell-matrix interactions based on NPC scRNA-seq data represents a new bioinformatics approach to identify potential therapeutic targets for liver fibrosis, such as ESAM and the THBS. An increased number of high-quality scRNA-seq datasets with clinical annotations will aid in the search for new anti-fibrotic agents.

THU530

Long-chain acylcarnitines promote leukocyte mitochondrial dysfunction: role in patients with acutely decompensated cirrhosis

Ingrid Wei Zhang^{1,2}, Cristina López-Vicario^{1,2,3}, Mireia Casulleras^{1,2}, Marta Duran-Güell^{1,2}, Roger Flores-Costa^{1,2}, Paula Segalés^{3,4}, M. Carmen Garcia-Ruiz^{3,4,5}, José Fernandez-Checa^{3,4,5}, Joan Clària^{1,2,3,6}. ¹Institut d'Investigacions Biomèdiques August Pi i Sunyer (IDIBAPS), Barcelona, Spain; ²European Foundation for the study of chronic liver failure, Barcelona, Spain; ³CIBER-Center for Biomedical Research Network, Madrid, Spain; ⁴Institut d'Investigacions Biomèdiques de Barcelona (IIBB-CSIC), Barcelona, Spain; ⁵Keck School of Medicine of USC, Research center for ALPD, Los Angeles, United States; ⁶Universitat de Barcelona, Department of Biomedical Sciences, Barcelona, Spain
Email: ingrid-wei.zhang@charite.de

Background and aims: Acute-on-chronic liver failure (ACLF) is characterized by acute decompensation (AD) of cirrhosis, organ failure (s) and high short-term mortality. The cytokinome of these patients revealed that exaggerated systemic inflammatory response is an important driver of disease progression. Recently, it has been demonstrated that the elevated circulating levels of acylcarnitines predict mortality in patients with AD and ACLF. Therefore, inflammation-associated mitochondrial dysfunction can be regarded as another major contributor to disease progression. Here, we hypothesize that acylcarnitines not only function as biomarkers of mitochondrial dysfunction but also exert biological effects on mitochondria of circulating immune cells. In addition, as organ donors are scarce, we explore whether existing treatments such as human serum albumin (HSA) might modulate the effect of acylcarnitines on mitochondrial function.

Method: Peripheral blood mononuclear leukocytes from healthy subjects were isolated by Ficoll gradient and *in vitro* experiments were performed to assess mitochondrial function under treatment with long- and medium-chain acylcarnitines, in the presence or absence of HSA. We assessed mitochondrial membrane potential (MMP) with the cationic dye JC-1 and mitochondrial respiration using Agilent Seahorse XF technology. This was complemented by electron microscopic evaluation of mitochondrial ultrastructure of immune cells treated with acylcarnitines and expression analysis of genes involved in mitochondrial function and biogenesis.

Results: Palmitoyl- and hexanoylcarnitine were increased in blood of patients with AD cirrhosis. In contrast to hexanoylcarnitine, the long-chain palmitoylcarnitine impaired maximal respiration of leukocyte mitochondria and reduced MMP in peripheral mononuclear leukocytes without affecting cell viability. Palmitoylcarnitine also down-regulated *HMOX-1* gene expression in a concentration-dependent manner, indicating impairment of cell antioxidant responses. The effect of palmitoylcarnitine on *HMOX-1* expression was reversed by etomoxir, an inhibitor of the carnitine palmitoyltransferase 1A located at the outer mitochondrial membrane. Finally, HSA partially reversed the MMP-reducing effect, without being physically localized to mitochondria.

Conclusion: Our results indicate that elevated circulating long-chain acylcarnitines in patients with AD are not only an epiphenomenon but have the potential to actively promote mitochondrial dysfunction in immune cells, thereby contributing to immune dysbalance in these patients.

THU531

Reduced plasma extracellular vesicle CD5L content in patients with acute-on-chronic liver failure: interplay with specialized pro-resolving lipid mediators

M. Belén Sánchez-Rodríguez¹, Érica Téllez², Mireia Casulleras¹, Francesc Borrás³, Vicente Arroyo⁴, Joan Clària^{1,4,5}, Maria-Rosa Sarrias^{2,6}. ¹Hospital Clínic-IDIBAPS, Biochemistry and Molecular Genetics Service, Spain; ²Innate Immunity Lab, IGTP, Spain; ³IVECAT, IGTP, Spain; ⁴European Foundation for the Study of Chronic Liver Failure, Spain; ⁵Universitat de Barcelona, Department of Biomedical Sciences, Spain; ⁶CIBERehd, Spain
Email: jclaria@clinic.cat

Background and aims: Acute-on chronic liver failure (ACLF) is a syndrome that develops in patients with acutely decompensated cirrhosis (AD). It is characterized by a systemic hyperinflammatory state, leading to multiple organ failure. Our objective was to analyze macrophage anti-inflammatory protein CD5L in plasma extracellular vesicles (EVs) and assess its as yet unknown relationship with lipid mediators in ACLF.

Method: EVs, isolated by size exclusion chromatography from the plasma of healthy subjects (HS) (n=9) and patients with compensated cirrhosis (CC) (n=8), AD (n=13) and ACLF (n=14), were defined as positive for CD9, CD5L and CD63 and their size, number, morphology and lipid mediator content were characterized by nanoparticle tracking analysis, electron microscopy and liquid chromatography with tandem mass spectrometry, respectively. Plasma CD5L was quantified by enzyme-linked immunosorbent assay in 10 HS, 20 CC and 149 AD patients (69 with ACLF). Macrophage CD5L expression and the biosynthesis of specialized pro-resolving lipid mediators (SPMs) were characterized *in vitro* in primary cells.

Results: Circulating EVs were significantly suppressed in cirrhosis, regardless of severity, and showed considerable alterations in CD5L and lipid mediator content as the disease progressed. In AD patients, levels of EV CD5L correlated best with those of the SPM resolvin E1 (RvE1). Analysis of total plasma supported these data and showed that, in ACLF, low CD5L levels were associated with circulatory (p < 0.001), brain (p < 0.008) and respiratory (p < 0.05) failure (Mann-Whitney test). Functional studies in macrophages indicated a positive feedback loop between CD5L and RvE1 biosynthesis.

Conclusion: We have determined a significant alteration of circulating EV contents in ACLF, with a loss of anti-inflammatory and pro-resolving molecules involved in the control of acute inflammation in this condition.

THU532

Peptidylglycine alpha-amidating monooxygenase and adrenomedullin measurements suggest cardio-circulatory dysfunction in advanced cirrhosis

Søren Møller¹, Andrei Voiosu¹, Signe Wiese², Janun Schulte³, Paul Kaufmann³, Andreas Bergmann³, Emil Bartels⁴, Jens Peter Goetze⁴. ¹Hvidovre Hospital, Center of Functional and Diagnostic Imaging and Research, Department of Clinical Physiology and Nuclear Medicine 260, Hvidovre, Denmark; ²Hvidovre Hospital, Gastro Unit, Hvidovre, Denmark; ³SpingoTec GmbH, Berlin, Germany; ⁴Rigshospitalet, Department of Clinical Biochemistry, Copenhagen, Denmark
Email: soeren.moeller@regionh.dk

Background and aims: Peptidylglycine α -amidating monooxygenase (PAM) is a processing enzyme involved in maturation of a plethora of regulatory peptides. One product of PAM activity is adrenomedullin (bio-ADM), which regulates vascular tone and endothelial integrity. In this study, we aimed to examine PAM activity and bio-ADM concentrations in patients with cirrhosis and explore the role of the liver in net release of the two markers.

Method: We enrolled 48 patients with cirrhosis and 16 control subjects. The patients were evenly distributed according to the Child-

POSTER PRESENTATIONS

Turcotte class (16 patients in class A, 16 patients in class B, and 16 patients in class C). All underwent a complete hemodynamic examination with catheterization of the liver, renal, and femoral veins and corresponding arteries, from where blood was simultaneously collected. PAM activity was determined in heparin plasma with a new assay from PAM Theragnostics GmbH (Hennigsdorf, Germany). Bio-ADM was measured in heparin plasma at a research laboratory at SphingoTec GmbH (Hennigsdorf, Germany).

Results: Patients with Child C cirrhosis displayed increased circulating PAM activity. PAM activity was similar across tissues and there were no significant associations to ascites, esophageal varices, or portal hypertension. We found associations of PAM activity to alanine aminotransferase ($r = 0.30$, $p = 0.04$), bilirubin ($r = 0.47$, $p = 0.001$) and INR ($r = 0.42$, $p = 0.004$). With respect to bio-ADM concentrations, there was a marked difference within the Child classes ($p < 0.0001$) and significant associations of circulating bio-ADM concentrations and prothrombin time and serum albumin, ($p < 0.0001$). We also found a net release of bio-ADM across the liver (hepatic artery: 13.0 (8.7–21.0) vs. hepatic vein: 19.7 (12.7–29.6) pg/ml, $n = 48$, $p < 0.001$). There was a release of bio-ADM across the lower limb (femoral artery: 12.6 (7.6–22.0) vs. femoral vein: 21.8 (13.5–29.2) pg/ml, $n = 48$, $p < 0.001$). Bio-ADM concentrations were increased in patients with ascites ($n = 26$) compared to patients without ($n = 22$).

Conclusion: PAM activity is progressively increased in cirrhosis, but without a net release across the studied organs. In contrast, bio-ADM is released by the liver and relates to the severity of the disease. Given the major expression of PAM in the heart, we propose that increased PAM activity in cirrhosis may reflect a cardio-circulatory dysfunction in advanced cirrhosis.

THU533

Combination of CCL4-induced decompensated cirrhosis with acute polymicrobial peritonitis as an optimized experimental model mimicking extrahepatic organ failures defined in ACLF

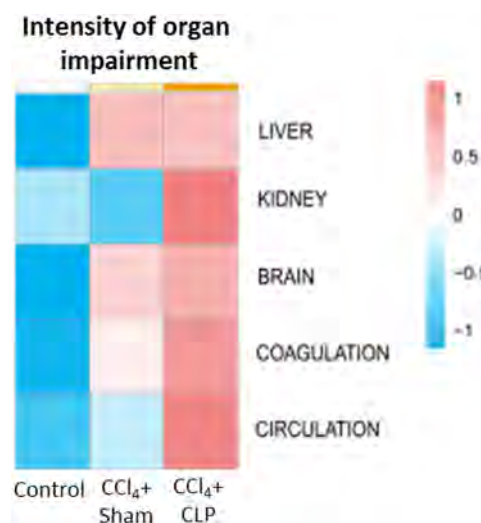
Roger Flores-Costa^{1,2}, Albert Salvatella¹, Bryan J Contreras^{1,2}, Marta Duran-Güell^{1,2}, Mireia Casulleras^{1,2}, Nico Kraus³, Sabine Klein³, Cristina López-Vicario^{1,2}, Ingrid Wei Zhang^{1,2}, Pierre-Emmanuel Rautou⁴, Javier Fernández^{2,5}, Jonel Trebicka^{2,3}, Vicente Arroyo², Joan Clària^{1,2,6}. ¹Hospital Clínic-IDIBAPS and CIBERehd, Biochemistry and Molecular Genetics Service, Barcelona, Spain; ²European Foundation for the study of Chronic Liver Failure (EF-CLIF) and Grifols Chair, Barcelona, Spain; ³Goethe University Frankfurt, Department of Internal Medicine I, Frankfurt, Germany; ⁴Hôpital Beaujon and INSERM, Centre de Recherche sur l'Inflammation, Paris, France; ⁵Hospital Clínic-IDIBAPS and CIBERehd, Liver ICU, Liver Unit, Barcelona, Spain; ⁶University of Barcelona, Department of Biomedical Sciences, Barcelona, Spain
Email: jclaria@clinic.cat

Background and aims: Acute-on-chronic liver failure (ACLF), which develops in patients with acutely decompensated cirrhosis, is characterized by multiple extrahepatic organ failures leading to high 28-day mortality. The investigation of ACLF pathophysiology is hampered by the lack of a proper animal model that reproduces the full spectra of extra-hepatic organ failures characteristic of this disease. Since there is an unmet need for an animal model of ACLF, the current investigation explored the value of combining the well-established model of chronic liver cirrhosis induced by carbon tetrachloride (CCl₄) with the acute model of polymicrobial septic peritonitis induced by cecal ligation and puncture (CLP) as novel experimental model of ACLF.

Method: The study was performed in Sprague-Dawley rats induced to cirrhosis ($n = 12$) by CCl₄ (i.p., 1 µL/g, 2 times/week). After developing ascites, rats underwent CLP surgery (CCl₄ + CLP group). The study also included control ($n = 6$) and sham operated CCl₄-treated (CCl₄-sham group) ($n = 6$) rats. Forty-eight hours after CLP or sham surgery, functional tests and collection of blood and tissue samples were performed to assess tissue injury and organ

impairments by measuring biochemical and histological parameters (hematoxylin-eosin and sirius red), gene expression of inflammatory genes (qPCR) and serum cytokine levels (Luminex technology).

Results: As compared to CCl₄-sham, CCl₄ + CLP rats exhibited more severe hypoalbuminemia and significantly higher serum levels of AST, GGT and bilirubin accompanied by increased liver expression of inflammatory genes. CCl₄ + CLP rats also showed increased serum creatinine and BUN levels and higher inflammatory gene expression. Of note, 33% of animals of this study group manifested acute tubular necrosis. Compared to CCl₄-sham, CCl₄ + CLP rats showed circulatory (higher plasma renin activity), coagulation (higher INR) and brain (impaired neurological behavior test score) failures. Moreover, CCl₄ + CLP rats exhibited up-regulated expression of lung injury markers and more exuberant systemic inflammation (higher levels of serum cytokines). Importantly, CCl₄ + CLP rats had 25% mortality at 48 hours whilst CCl₄-sham rats showed 100% survival.



Conclusion: The CCl₄ + CLP model in rats reproduces the spectra of extra-hepatic organ impairments present in patients with ACLF and thus appears as an optimized experimental model to explore the pathophysiology of this disease.

THU534

Thrombin-induced platelet activation across distinct stages of portal hypertension and cirrhosis

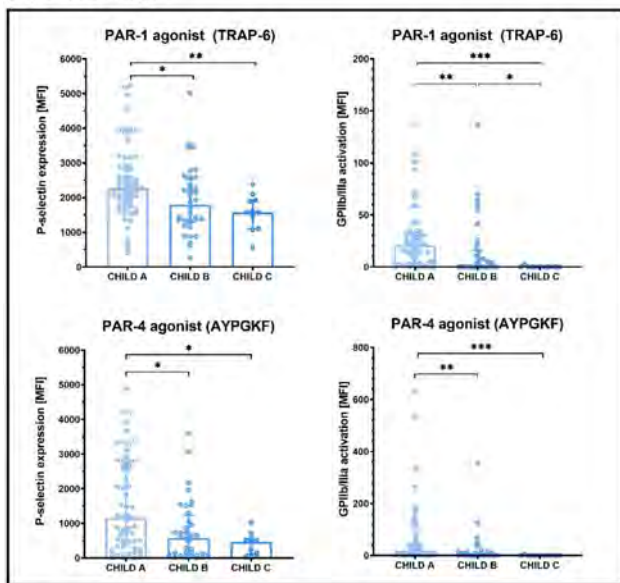
Ksenia Brusilovskaya^{1,2,3}, Benedikt Hofer^{1,2,3}, Beate Eichelberger⁴, Simon Panzer⁴, Benedikt Simbrunner^{1,2,3}, Mattias Mandorfer^{1,2}, Thomas Gremmel^{5,6,7}, Thomas Reiberger^{1,2,3}. ¹Medical University of Vienna, Division of Gastroenterology and Hepatology, Department of Medicine III, Vienna, Austria; ²Medical University of Vienna, Vienna Hepatic Hemodynamic Lab (HEPEX), Division of Gastroenterology and Hepatology, Department of Medicine III, Vienna, Austria; ³Medical University of Vienna, Christian-Doppler laboratory for portal hypertension and liver fibrosis, Vienna, Austria; ⁴Medical University of Vienna, Department of blood group serology and transfusion medicine, Vienna, Austria; ⁵Medical University of Vienna, Department of Internal Medicine II, Vienna, Austria; ⁶Landesklinikum Mistelbach-Gänserndorf, Department of Internal Medicine I, Cardiology and Intensive Care Medicine, Mistelbach, Austria; ⁷Karl Landsteiner society, Institute of antithrombotic therapy in cardiovascular disease, St. Poelten, Austria
Email: thomas.reiberger@meduniwien.ac.at

Background and aims: Patients with advanced chronic liver disease (ACLD) often show thrombocytopenia; however, primary hemostasis seems re-balanced by higher levels of von Willebrand factor (VWF). Still, alterations in thrombin-induced platelet activation may put ACLD patients at increased risk for both bleeding and

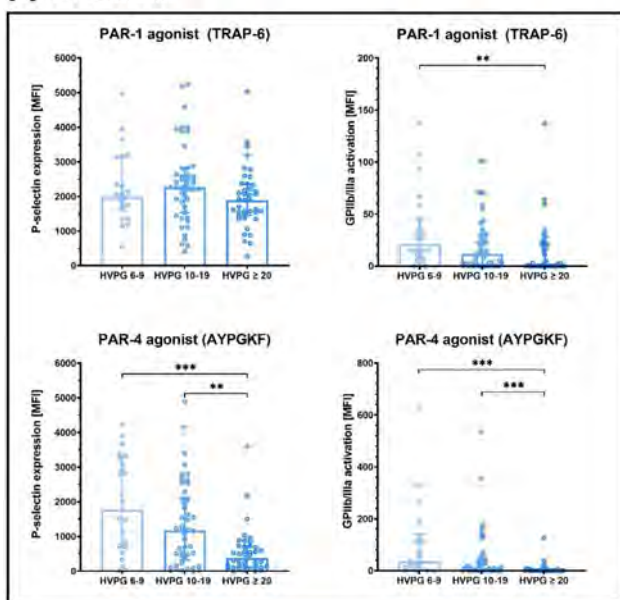
thromboembolic events. Therefore, we aimed to characterize platelet function in a thoroughly characterized ACLD patient cohort.

Method: 110 ALCD patients with portal hypertension (PH), i.e., a hepatic venous pressure gradient (HVPG) ≥ 6 mmHg, were prospectively included and stratified by Child-Pugh stage (CPS) and HVPG. Platelet surface P-selectin and activated glycoprotein IIb/IIIa (GPIIb/IIIa) (mean fluorescent intensity, MFI) were assessed with flow cytometry as sensitive parameters of platelet activation in unstimulated and stimulated (agonists of the protease-activated receptors, PAR-1 and PAR-4) conditions.

[A] CHILD stage:



[B] HVPG strata:



Results: The level of “baseline” platelet activation was similar across CPS stages A, B, and C (unstimulated P-selectin expression: 0.0 MFI vs. 0.0 MFI vs. 0.0 MFI, $p = ns$; unstimulated GPIIb/IIIa expression: 0.0 MFI vs. 0.0 MFI vs. 0.0 MFI, $p = ns$). PAR-1 mediated platelet activation was significantly impaired in CPS-B and C patients (P-selectin: CPS-A: 2261.0 MFI [1815.0–2942.0] vs. B: 1793.0 MFI [1299.0–2523.0], $p = 0.02$ vs. C: 1577.0 MFI [1101.0–1926], $p < 0.01$; GPIIb/IIIa: CPS-A: 20.6

MFI [3.4–32.8] vs. B: 1.8 MFI [0.0–16.2], $p < 0.01$ vs. C: 0.0 MFI [0.0–0.0], $p < 0.001$). Similarly, a decreased response to PAR-4 mediated platelet activation was observed with increasing CPS stages (P-selectin: CPS A: 1159.0 MFI [332.8–2721.0] vs. B: 582.3 MFI [101.3–1236.0], $p = 0.03$ vs. C: 464.0 MFI [107.1–547.1], $p = 0.02$; GPIIb/IIIa: CPS-A: 18.1 MFI [2.1–93.8] vs. B: 0.0 MFI [0.0–13.7], $p < 0.01$ vs. C: 0.0 MFI [0.0–0.0], $p < 0.001$). The severity of PH had no impact on “baseline” activation (all $p = ns$). PAR-1 mediated platelet surface expression of P-selectin was comparable across the HVPG strata 6–9 vs. 10–19 vs. ≥ 20 mmHg ($p = ns$), while activated GPIIb/IIIa was significantly reduced in HVPG ≥ 20 group (HVPG 6–9: 20.8 MFI [7.5–46.4] vs. HVPG ≥ 20 : 0.5 MFI [0.0–20.8], $p < 0.01$). PAR-4 mediated platelet activation was also reduced in the HVPG ≥ 20 mmHg group (P-selectin: HVPG 6–9: 1775.0 MFI [668.6–3287.0] vs. HVPG ≥ 20 mmHg: 383.9 MFI [112.6–721.6], $p < 0.001$; GPIIb/IIIa: HVPG 6–9: 36.1 MFI [8.0–141.1] vs. HVPG ≥ 20 : 0.0 MFI [0.0–6.8], $p < 0.001$).

Conclusion: ACLD patients exhibit decreased thrombin-inducible platelet activation when progressing to Child stages B and C. Moreover, high risk PH (HVPG ≥ 20 mmHg) is associated with impaired platelet activation upon stimulation. The impact of these alterations on the risk of bleeding or thrombotic events remains to be studied.

THU535

Exploring metabolic space of advanced chronic liver disease regression

Yuly Mendoza¹, Sofia Tsouka², Jaime Bosch¹, Annalisa Berzigotti¹, Mojgan Masoodi³. ¹University Hospital Bern, Visceral Surgery and Medicine; ²University hospital Bern, Institute of Clinical chemistry; ³University hospital Bern, Institute of Clinical chemistry, Bern, Switzerland

Email: mojgan.masoodi@insel.ch

Background and aims: Liver fibrosis is the main determinant of clinical outcomes in advanced chronic liver disease (ACLD) of any etiology. Regression of bridging fibrosis and cirrhosis can take place after effective etiological treatment, but not in all cases, suggesting that factors other than the etiology play a role in the modulation of this important outcome. In patients achieving regression of ACLD, liver function markedly improves, suggesting that several metabolic pathways are influenced by regression of fibrosis. However, the metabolic pathways associated with fibrosis regression in ACLD have not been characterized. We hypothesize that thorough assessment of liver metabolism could provide evidence-based data for better characterization of cirrhosis patients with regression following effective etiological treatment, thus providing a rational basis for personalized interventions.

Method: We performed a case-control pilot study of 60 patients with ACLD of different etiologies, 30 with histological and/or clinical evidence of regression of ACLD (Regressors) and 30 without any improvement (Non-regressors) after a minimum of 24 months of successful etiological therapy. We used the combination of metabolic modelling and metabolic profiling to define metabolic pathways and associated signature that differentiate Regressors from Non-regressors. We have developed a transcriptomics-driven metabolic modelling approach to assess the regression of ACLD. We further investigated the associated metabolic signature using mass spectrometry-based metabolomics.

Results: Although Regressors and Non-regressors showed similar profiles at baseline, our observation is pointing to fatty acid β -oxidation and arachidonic acid metabolism (associated to inflammation and oxidative stress) as key metabolic pathways differentiating Regressors from Non-regressors after therapy, suggesting that lipid metabolism plays a central role in the modulation of the extracellular matrix in ACLD. In addition, Using Least Absolute Shrinkage and Selection Operator (LASSO) analyses, the Regressor phenotype was predicted with 80% accuracy based on the levels of identified lipid markers after etiologic therapy.

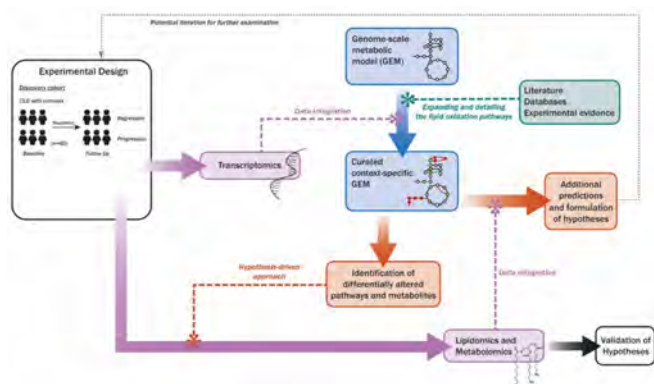


Figure: Workflow for metabolic phenotyping.

Conclusion: Our preliminary observations suggest several metabolic pathways that were associated with persistence or regression of ACLD after successful etiological therapy. These results allow proposing a metabolic signature of regression of fibrosis in ACLD.

THU536

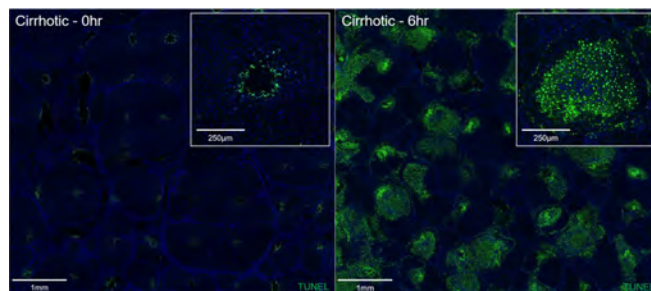
Exacerbated response to patterned injury in the cirrhotic liver: potential susceptibility to ischemia

Benjamin Leaker^{1,2}, Mozhdeh Sojoodi³, Kenneth K. Tanabe³, R. Rox Anderson^{2,4}, Joshua Tam^{2,4}. ¹Massachusetts Institute of Technology, Harvard-MIT Health Sciences and Technology, Cambridge, United States; ²Massachusetts General Hospital, Wellman Center for Photomedicine, Boston, United States; ³Mass General Cancer Center, Division of Surgical Oncology, Boston, United States; ⁴Harvard Medical School, Department of Dermatology, Boston, United States
Email: leakerb@mit.edu

Background and aims: The response to injury in the cirrhotic liver is an important factor in both the pathogenesis of cirrhosis and the treatment of patients living with end stage liver disease. This study aimed to investigate the differences in the short-term tissue response to a controlled injury between the healthy and cirrhotic liver.

Method: Healthy and cirrhotic rats underwent a laparotomy to expose the liver followed by treatment with a tunable ablative laser to create a pattern of micro-injuries in the left lobe. The roughly 1cm² treatment area contains over 100 uniformly spaced micro-injuries, each approximately 300um in diameter and 2 mm deep. Animals were euthanized 0hr, 2hr, 4hr, 6hr, 3d, 7d, and 14d after laser treatment. RNA samples from the 4hr timepoint were used for RNAseq transcriptome analysis. With DESeq2, a difference-in-differences statistical model was used to identify genes that respond differently between the laser-treated cirrhotic and laser-treated non-cirrhotic liver while controlling for the differences between the untreated samples. Over-representation analysis and gene set enrichment analysis were then used to identify biological processes associated with the differential expression results.

Results: In both cirrhotic and non-cirrhotic liver, the laser produced a regular and uniform array of micro-injuries. These injuries completely healed within 7 days in the non-cirrhotic liver. In the cirrhotic liver, TUNEL staining showed expanding zones of cell death between the 4hr and 6hr timepoints, resulting in enlarged and haphazard injuries (see figure). Histology showed cells near blood vessels are spared, particularly near the vascularized fibrous septa encapsulating nodules. Evidence of these injuries could still be found at 14d. Functional analysis of the differential expression data returned enrichment of gene sets related to hypoxia, starvation, and angiogenesis, as well as revealing suppression of a variety of metabolic processes.



Conclusion: Our histology and transcriptomics data show that the cirrhotic liver has an exacerbated response to injury, possibly due to an increased susceptibility to ischemia which can compound with other injuries to cause far greater damage. This could be a result of the changes in the hepatic microvasculature that occur in cirrhosis, most notably capillarization of sinusoids and the formation of intrahepatic vascular shunts.

THU537

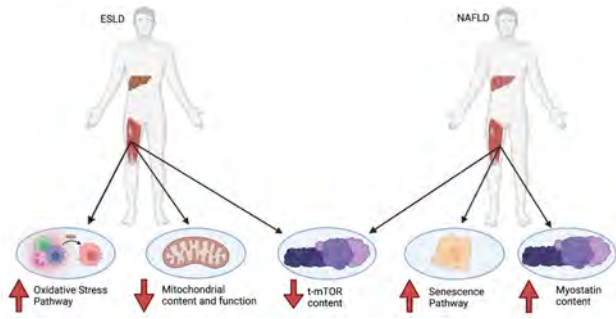
The regulatory protein and gene expression profile of skeletal muscle in chronic liver disease patients

Sophie Allen¹, Jonathan Quinlan¹, Amritpal Dhaliwal², Thomas Nicholson², Felicity Williams², Matthew Armstrong³, Ahmed Elsharkawy³, Simon Jones², Carolyn Greig¹, Janet Lord², Gareth Lavery⁴, Leigh Breen¹. ¹University of Birmingham, School of Sport, Exercise and Rehabilitation Sciences, Birmingham, United Kingdom; ²University of Birmingham, Institute of Inflammation and Ageing, Birmingham, United Kingdom; ³University Hospitals Birmingham, Liver Unit, Birmingham, United Kingdom; ⁴Nottingham Trent University, Department of Biosciences, Nottingham, United Kingdom
Email: s.l.allen@bham.ac.uk

Background and aims: The molecular pathways which may underpin sarcopenia in Chronic Liver Disease (CLD) are largely unclear. The aim of this study was to characterize the intracellular signaling pathways that may underscore sarcopenia in CLD patients of different etiologies and disease stages.

Method: Muscle biopsy and blood samples were obtained from 9 non-cirrhotic non-alcoholic fatty liver disease patients (NAFLD; aged 61.1±9.0), 12 decompensated alcoholic related end-stage liver disease patients (ESLD;55.7±5.7) and 12 healthy, age-matched healthy controls (CON;55.7±8.7). The protein content of skeletal muscle anabolic, catabolic and mitochondrial signaling intermediates was determined via western blot. The muscle transcriptome was analyzed using RNA-sequencing.

Results: Citrate synthase activity (~43%) and the protein content of OXPHOS complex I was significantly lower (~26%) in ESLD vs. CON (p < 0.01 for both), whereas OXPHOS complex IV was significantly lower in ESLD vs. CON (71%; p < 0.01) and NAFLD (61%; p = 0.04). Total-mTOR protein was significantly lower in NAFLD (62%, p = 0.01) and ESLD (52%, p = 0.03) vs. CON. Myostatin protein content was significantly greater in NAFLD vs. CON (77%; p < 0.01) and ESLD (70%; p < 0.01). Gene pathway analysis revealed a significant enrichment in pathways related to oxidative stress in ESLD vs. CON. A significant enrichment in genes related to senescence was evident in NAFLD vs. CON.



Conclusion: Collectively these findings highlight some similar but largely distinct signaling pathways that may underscore sarcopenia in CLD patients across different etiologies and disease stages.

THU538

Proteomic analysis of dysfunctional liver sinusoidal endothelial cells reveals substantial differences in the most common experimental models of chronic liver disease

Mar Gil¹, Carla Fuster¹, Mikel Azkargorta^{2,3}, Imma Raurell^{1,3}, Aurora Barbera¹, Felix Elortza^{2,3}, Joan Genesca^{1,3}, Diana Hide^{1,3}, María Martell^{1,3}. ¹Liver Diseases, Vall d'Hebron Institut de Recerca (VHIR), Liver Unit, Hospital Universitari Vall d'Hebron (HUVH), Vall d'Hebron Barcelona Hospital Campus, Universitat Autònoma de Barcelona (UAB), Barcelona, Spain; ²Proteomics Platform, CIC bioGUNE, BRTA (Basque Research and Technology Alliance), ProteoRed-ISCIII, Bizkaia Science and Technology Park, Derio, Spain; ³Centro de Investigación Biomédica en Red de Enfermedades Hepáticas y Digestivas (CIBERehd), Madrid, Spain
Email: diana.hide@vhir.org

Background and aims: Therapies specifically aimed at liver sinusoidal endothelial cells (LSEC), first inducers of liver damage, could help to slow down the entire pathological process. Although

physiological markers of LSEC have been described, there is lack of information regarding dysfunctional LSEC in chronic liver diseases (CLD). Here, we aimed to decipher the molecular profile of dysfunctional LSEC in different pathological situations to improve the effectiveness of potential therapeutic agents.

Method: LSEC from three experimental rat models (bile duct ligation-BDL, inhaled carbon tetrachloride-CCl₄ and high fat glucose/fructose diet-HFGFD) and their controls were isolated and sorted by flow cytometry using cd11b to eliminate macrophages and cd32b to sort dysfunctional (CD32⁻) LSEC. Full proteomic profile was performed applying label free proteomics by nano-scale liquid chromatography tandem mass spectrometry on an EvoSep ONE (EVOSEP) coupled on-line to a TIMS ToF Pro (Bruker). Obtained data was processed and analyzed with PEAKS software.

Results: The percentage of CD32⁻ LSEC was different between groups. Of relevance is the comparison between HFGFD (early stage of CLD) with 16.9% CD32⁻ LSEC and CCl₄ (advanced stage) with only 6.0%, suggesting differences in the capillarization process.

Principal component analysis (PCA) revealed that CD32⁺ LSEC are more similar between models and to healthy controls than to CD32⁻ LSEC of their respective model (Fig A). Accordingly, the number of differentially expressed proteins vs. control LSEC is lower in CD32⁺ than in CD32⁻ LSEC. Nevertheless, further PCA also clusters CD32⁺ LSEC in separate groups by models (Fig B) representing protein expression differences between them.

Looking for similarities in the capillarization process, we found 51 common proteins differentially expressed compared to controls in CD32⁻ LSEC from the 3 models and 354 shared by at least 2 models. Finally, heatmap representation of significantly differentially expressed proteins between models, both for CD32⁺ and CD32⁻ LSEC, evidenced specific patterns for each model being CCl₄ and HFGFD more similar to each other than BDL (Fig C).

Conclusion: Substantial differences in dysfunctional LSEC from the three most common models of CLD were found, supporting the idea that in different etiologies/disease stages, LSEC may harbor different protein expression profiles. In deep analysis of deregulated proteins

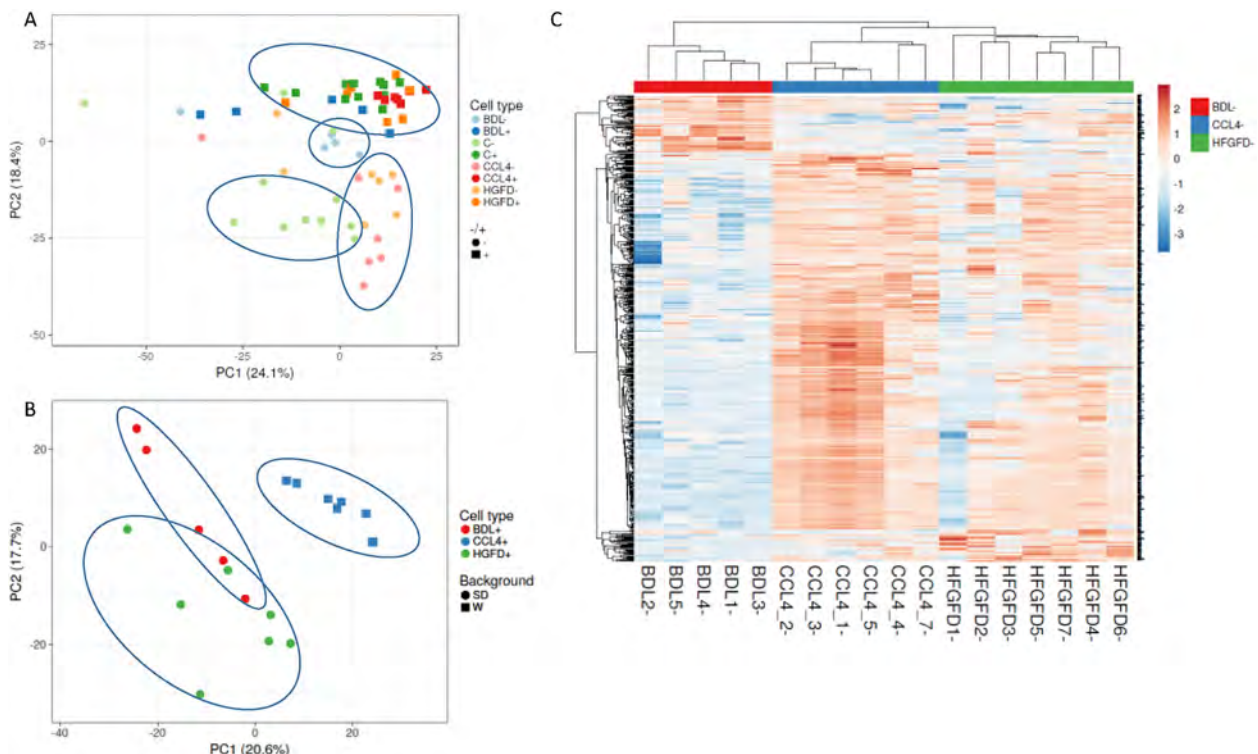


Figure: (abstract: THU538)

POSTER PRESENTATIONS

and pathways in each model will allow to better understand and use the preclinical models in translational research and will facilitate the specific targeting of experimental drugs.

Funded by Instituto de Salud Carlos III and European Union EuroNanoMed III [AC18/00033].

THU539

Long-term albumin administration improves survival, reduces TLR4 mediated hepatic inflammation and reduces gut translocation in models of cirrhosis

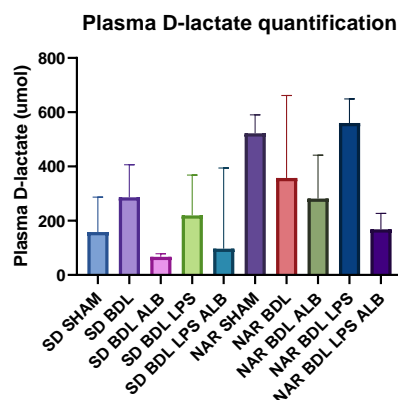
Alexandra Phillips¹, Qianwen Zhao², Abeba Habtesion¹, Fausto Andreola¹, Nathan Davies¹, Lindsey A Edwards³, Jane Macnaughtan¹, Rajiv Jalan¹. ¹University College London, Institute of liver and digestive health, United Kingdom; ²Sichuan University, Department of Gastroenterology and Hepatology, West China Hospital, Chengdu Shi, China; ³Institute of Hepatology, King's College Hospital, United Kingdom

Email: alexandra.phillips5@nhs.net

Background and aims: Long-term albumin administration reduces mortality in patients with decompensated cirrhosis. The underlying mechanisms are unknown. The aims of this study were to investigate how the absence of endogenous albumin and albumin administration impacts liver injury, toll-like receptor 4 (TLR4) signalling and gut translocation.

Method: 10 rodent groups: Naïve, cirrhosis (4-wk; bile-duct ligation (BDL)) and acute-on-chronic liver failure (ACLF) models (induced by lipopolysaccharide (LPS) 0.025 mg/kg intraperitoneal (i.p.) to BDL) ± albumin infusion (1.5 g/kg ip; 2-wk) of analbuminaemic (NAR) and wild-type (SD) rats. Plasma biochemistry and hepatic TUNEL staining. *Hepatic TLR4 expression and pathways (hTLR4):* qPCR and RT² PCR profiler. *Gut permeability:* d-lactate and zonulin in plasma. *Ileal integrity:* western blot of tight junction proteins.

Results: ALT levels showed significant improvement after albumin administration in SD BDL LPS group ($p = 0.01$), and non-significant improvement in SD BDL and NAR BDL LPS. Significant reduction in the liver of TUNEL positive areas in LPS groups with albumin administration ($p < 0.001$). Coma-free survival increased from 62.5% to 80% between NAR and SD animals exposed to LPS respectively, with 100% survival in NAR animals exposed to LPS after albumin administration. *hTLR4:* NAR animals had greater hTLR4 expression, with all treatment groups showing a reduction of hTLR4 expression after albumin administration. hTLR4 gene array confirmed the activation of TLR4 dependent pathways in the cirrhotic NAR animals, which was abrogated by albumin infusion. *Markers of gut permeability:* Plasma D-lactate showed a reduction in all treatment groups with albumin (see figure). Plasma zonulin decreased after albumin in NAR BDL animals with and without LPS administration. *Tight junction:* ZO-1, claudin-4 and occludin in ileum showed a reduction in NAR diseased animals compared to SD groups with albumin administration increasing tight junction protein abundance in all disease groups.



Conclusion: The results of this study show for the first time that that analbuminaemic animals have increased mortality, significantly increased liver injury and increased sensitivity to LPS. Chronic albumin administration partially reversed this, as well as reduces gut translocation resulting in decreased TLR4 pathway activation and improving the integrity of tight junctions. The data provide mechanistic insight into the biological effect on albumin on gut-liver interactions.

THU540

The prevalence and prognostic significance of vitamin C deficiency in patients with cirrhosis: a prospective observational cohort study

Declan Connoley¹, Phil Ha¹, Joseph Nim¹, Elaine Koh¹, Ryan Hirsch¹, Marcus Robertson¹. ¹Monash Health, Department of Gastroenterology, Melbourne, Australia

Email: declan.connoley@gmail.com

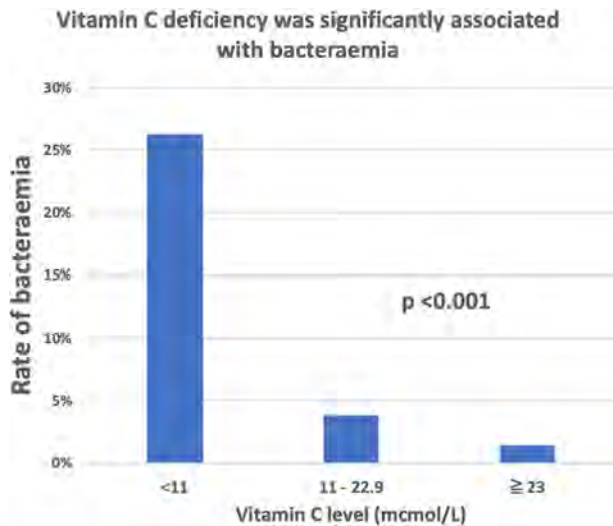
Background and aims: Malnutrition is a common comorbidity in cirrhotic patients and confers a poorer prognosis. Vitamin C (VC) is a micronutrient essential for human health. Vitamin C deficiency (VCD) can lead to scurvy and may impair immune and liver functions. Although previously thought to be rare in developed countries, VCD is now well described in patients with pneumonia, COVID19 and upper gastrointestinal bleeding (UGIB). The prevalence and clinical significance of VCD in cirrhosis remains poorly studied.

Method: Patients with cirrhosis admitted to 3 metropolitan tertiary centres in Australia were prospectively included over a 10-month period in 2021. Fasting VC levels were collected on admission and we recorded demographic data and clinical outcomes. The primary outcomes were the prevalence of VCD (defined as VC level < 23 $\mu\text{mol/L}$) and severe VCD (SVCD), defined as < 11 $\mu\text{mol/L}$. Secondary outcomes included mortality, intensive care admission, length of stay (LOS) and rate of infection.

Results: 117 patients were included. Mean age was 57.1 ± 13.9 years, 59.0% were male and 23.9% belonged to the lowest socioeconomic decile. The most common aetiologies of cirrhosis were alcohol (62.4%), viral hepatitis (24.0%) and non-alcoholic fatty liver disease (18.8%). Median MELD score was 29 (IQR 22–36) and Child Pugh (CP) grades were 12.8% A, 46.2% B and 41.0% C. Most patients (74.4%) were hospitalised with complications of decompensated cirrhosis, including ascites (59.0%), encephalopathy (31.6%) and variceal bleeding (11.1%).

Median VC level was 34 $\mu\text{mol/L}$ (IQR 16–55) and did not differ with age, gender, or aetiology of cirrhosis. Increasing CP grade correlated with significantly lower median VC levels (CP-A 46.0 $\mu\text{mol/L}$ vs. CP-B 36.5 $\mu\text{mol/L}$ and CP-C 20.5 $\mu\text{mol/L}$, $p = 0.026$). The prevalence of VCD and SVCD were 39.3% and 17.1% respectively. SVCD was more prevalent in patients with a body mass index < 25 (28.3% vs 13.0%, $p = 0.036$).

In-hospital mortality was 12.8% and did not differ by VCD status, however in the subgroup of patients presenting with UGIB, SVCD correlated with significantly higher mortality (50% vs 4.1%, $p = 0.045$). Bacteraemia was more frequent in patients with VCD (13.3% vs. 1.4%, $p = 0.014$) and SVCD (26.3% vs 2.1%, $p < 0.001$), which remained significant at multivariate analysis (OR for every 1 $\mu\text{mol/L}$ increase in VC, 0.91 (95% CI: 0.83–0.99), $p = 0.037$). Overall infection rates were higher in patients with SVCD (40.0% vs. 27.8%) although this was non-significant ($p = 0.279$). Median hospital LOS was 10 (IQR 6–18) days and did not differ by VCD status.



Conclusion: VCD is common in hospitalised cirrhotic patients and prevalence increases with severity of liver disease. VCD increases the risk of infective complications and higher mortality was observed in patients with UGIB and SVCD. Further studies are required to assess the significance of VCD in cirrhosis and the impacts of VC replacement.

THU541

Wnt as activator of regeneration in cirrhosis of human liver: tissue collapse brings the Wnt source in hepatic veins to the site of the progenitor cell niche

IanR Wanless¹, Ashley Stueck¹. ¹Dalhousie University, Anatomic Pathology, Halifax, Canada
Email: ian2460@gmail.com

Background and aims: Recent studies show that Wnt is secreted by hepatic vein endothelial cells (HV-EC). Glutamine synthetase (GS) activation in peri-venular hepatocytes (HC) of normal livers is considered a downstream event initiated by Wnt. Thus, we consider GS activation a surrogate histologic marker for Wnt and call it Wnt-GS. Hepatic regeneration is also activated by the Wnt/beta-catenin pathway. We previously showed that human cirrhotic liver is repopulated by buds of new hepatocytes derived from distal bile ducts. GS expression was a prominent feature in ducts forming buds, which is consistent with a response to local exposure to secreted Wnt. However, in normal livers, Wnt secreted from HV-EC affects a thin rim of perivenular/zone 3 hepatocytes and is then washed toward the cava. In order to reach portal tracts and activate the bud sequence in cirrhosis, we hypothesize that some Wnt is distributed to the distal bile ducts by altered circulation. The aim is to identify the anatomic basis of this pathway in human cirrhosis.

Method: Resected liver samples with chronic disease (n = 38) or normal (2) were serially sectioned and stained with GS, CD34, and CK19. Wnt-GS was semi-quantitated by location.

Results: Perivenular Wnt-GS generally decreased with advancing stage, associated with decreased HV number but also decreased Wnt-GS per HV, likely because of damage to HV-EC and arterialization with washout. Stage 4A and 4B livers usually had occasional nodules with focal increase in Wnt-GS, likely because of retrograde flow. Active budding correlated with Wnt-GS, mostly in septal ducts and associated new hepatocytes, usually in stage 4A and 4B. Wnt-GS in HC at nodular periphery were often seen to connect with intranodular HVs but also appeared to be a response to Wnt-secreting HV remnants that were deeply embedded in adjacent septa (see fig); these HVs appear to be the main conduits allowing HV-derived Wnt to be transported to small duct regions.

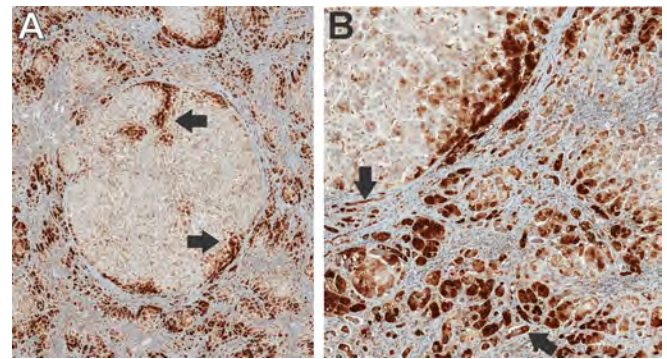


Figure: Cirrhosis (GS stain). A. Nodule showing HVs (arrows) draining into septa with adjacent active GS+ buds. B. High mag. showing Wnt-GS in ducts (arrows) and in new bud HC.

Conclusion: In cirrhotic livers, Wnt appears to migrate in intact HV remnants to distal ductal regions, either by veno-portal approximation in collapsed tissue (PELs) or, where sinusoidal connections are intact, by reversed sinusoidal blood flow aided by focal shunt-related blood flow, as seen in other liver conditions. This explains how Wnt can be delivered from hepatic veins to the progenitor cell niche and activate regeneration.

Wnt-GS is a useful surrogate marker for the location of Wnt, although confirmation with direct techniques is required. The patchy anatomic distribution of Wnt-GS suggests that Wnt concentration is focally suboptimal to support regeneration, justifying therapeutic trial options.

THU542

The portal vein in patients with cirrhosis is not an extensively inflammatory or hypercoagulable vascular bed

Ellen Driever¹, Marta Magaz², Jelle Adelmeijer¹, Fanny Turon², Anna Baiges², Pol Olivas², Virginia Hernandez-Gea², Annabel Blasi³, Juan Carlos Garcia Pagan², Ton Lisman¹. ¹University Medical Center Groningen, Department of Surgery, Groningen, Netherlands; ²Barcelona Hepatic Hemodynamic Laboratory, Liver Unit, Hospital Clínic, Institut de Investigacions Biomèdiques August Pi i Sunyer (IDIBAPS); ³Hospital Clínic, Department of Anesthesiology, Barcelona, Spain
Email: e.g.driever@umcg.nl

Background and aims: Portal vein thrombosis (PVT) is a common complication in patients with cirrhosis. Although we previously demonstrated that hypercoagulability is a reflection of severity of liver disease rather than a causal factor for PVT, other groups demonstrated elevated levels of markers of inflammation and activation of haemostasis in the portal vein (PV) compared to post-hepatic veins. However, many studies did not take clearance of these markers by the liver into account. We aimed to determine whether the PV in cirrhotic patients has particular proinflammatory or hypercoagulable characteristics by comparing blood sampled in the PV, in the hepatic vein (HV), and in the peripheral circulation.

Method: Plasma samples from 52 cirrhotic patients with clinically significant portal hypertension receiving transjugular intrahepatic portosystemic shunt, were taken from the PV, HV, and jugular vein (JV). Plasma levels of markers of inflammation, endothelial damage and haemostasis were determined and compared between the three vascular beds.

Results: Inflammatory markers LPS and IL-6 were slightly, but significantly higher in the PV than in the HV and JV. The neutrophil extracellular trap markers cfDNA and MPO-DNA were similar between the vascular beds. Endothelial marker VWF and markers of haemostasis were modestly elevated in the PV. Levels of multiple markers are lower in the HV compared to the PV and JV.

POSTER PRESENTATIONS

Table 1: Levels of markers of inflammation, endothelial damage and haemostasis, measured in plasma sampled from different vascular beds.

	Portal vein	Hepatic vein	Jugular vein
LPS (pg/ml)	162 [96–259]*	125 [68–233] ^{‡‡}	156 [66–251] ^{§§}
TNF- α (pg/ml)	12 [6–22.5]	11.7 [5.1–23.9]	11.9 [5.2–21.5]
IL-6 (ng/ml)	16.5 [7–35.1]*	8.5 [5.5–32.5] ^{‡‡}	10.3 [5.4–34.7] [§]
cfDNA (μ g/ml)	1 [0.9–1.2]	1 [0.8–1.2]	1 [0.8–1.2]
MPO-DNA (AU)	0.2 [0.1–0.4]	0.1 [0.1–0.4]	0.2 [0.1–0.4]
VWF (%)	339 [229–449]*	309 [218–456]	301 [216–425]
TAT (μ g/ml)	47.9 [29.8–47.9]	19.5 [7.2–35.6] [‡]	43.8 [12–117] ^{§§}
PAP (ng/ml)	1091 [556–4845]*	796 [535–1581] [‡]	867 [533–2146] [§]
D-dimers (ng/ml)	3670 [2237–7205]*	2720 [1700–3662] ^{‡‡‡}	3040 [1827–5330]

* Comparison between portal vein and peripheral vein; [‡] comparison between portal vein and hepatic vein; and [§] comparison between hepatic vein and jugular vein. *: $p < 0.05$; **: $p < 0.001$; ***: $p < 0.0001$.

Conclusion: In contrast to published studies, we found only a slight prothrombotic environment in the PV. In previous studies, comparison of levels of markers in PV with an immediate post-hepatic vascular bed may have erroneously led to the conclusion that the portal circulation is hypercoagulable. Here we demonstrate that many markers are lowest in the HV compared to the PV and the systemic circulation, indicating that the low level of these markers in the HV, at least in part, reflect clearance of those markers in the liver.

THU543

Effect of liver stiffness on hepatocellular carcinoma phenotype in a biometric 3D model

Carlemi Calitz¹, Jaafar Khaled¹, Jenny Rosenquist², Maria Kopsida¹, Oliver Degerstedt³, Hans Lennernas³, Mårten Fryknäs⁴, Ayan Samanta², Femke Heindryckx¹. ¹Uppsala University, Medical Cell Biology, Uppsala, Sweden; ²Uppsala University, Department of Chemistry-Ångström Laboratory, Polymer Chemistry, Uppsala, Sweden; ³Uppsala University, Department of Pharmaceutical Biosciences, Uppsala, Sweden; ⁴Uppsala University, Department of Medical Sciences, Cancer Pharmacology and Computational Medicine, Uppsala, Sweden
Email: c.calitz@amsterdamumc.nl

Background and aims: Hepatocellular carcinoma (HCC) usually occur in patients with an underlying chronic liver disease. The tumor micro-environment (TME) is therefore characterized by an increased deposition of extracellular matrix proteins (ECM). The abundance of ECM results in physical and biomechanical changes in the TME, which could influence tumor behavior. The aim of our study was to determine how liver stiffness affects the HCC phenotype in a novel biomimetic 3D model to study tumor-stroma interactions.

Method: HepG2 and Huh7 cells were grown in a 3D biomimetic hydrogel model with tuneable biomechanical properties for 21 days. Matrix stiffness, epithelial-to-mesenchymal transitions (EMT), metastatic potential, drug sensitivity and overall survival was assessed and compared to current two-dimensional (2D) models, an *in vivo* HCC mouse model and clinical data. Tumour nodules were collected from the culture medium and cells were extracted from the gels for subsequent RT-qPCR analyses.

Results: Cells were embedded in hydrogels mimicking the onset of a fibrotic and cirrhotic TME, as determined by patient-derived data. HepG2 and Huh7 cells grown in a stiffer matrix (resembling a cirrhotic liver) increased proliferation and protein content, compared to those grown in a less stiff matrix (resembling a fibrotic liver). HepG2 cells significantly decreased albumin synthesis in the cirrhotic TME compared to the fibrotic TME, while Huh7 cells increased albumin synthesis. While urea production in HepG2 cells decreased over time, it increased in Huh7 cells in both conditions. Tumor nodules started to form spontaneously outside the 3D gels after 11 days. The HepG2 tumour nodules appeared earlier in the medium outside the cirrhotic gels and were significantly larger in size when compared to those found in the medium outside a fibrotic gel. Cells derived from these tumor nodules showed an increased mRNA expression of α SMA and SNAI1 and decrease in E-cadherin when

comparing cirrhotic to fibrotic environment, thus suggesting that increased stiffness could induce EMT in HCC cells. HepG2 cells grown in the 3D cirrhotic group were also more resistant to doxorubicin treatment compared with those grown in the 3D fibrotic group or grown in 2D. No differences were seen in drug distribution and penetrations between the two different gel compositions, thus further confirming that stiffness induced changes in the HCC phenotype that could explain a reduced response to chemotherapeutics. This was then confirmed by an increased expression of the drug resistance gene MDR1 in HepG2 cells grown in a cirrhotic gel, compared to those grown in a fibrotic gel.

Conclusion: Increasing the stiffness of the liver markedly increases the formation of metastatic nodules, induces several markers of EMT and reduces response to chemotherapeutics in a biomimetic 3D model of HCC.

THU545

Ascites reduction and anti-inflammatory effects after albumin infusion for the management of cirrhosis: evidence from an animal model

Raquel Horrillo¹, Anna Mestre¹, Estefania Alcaraz¹, Guillermo Fernández Varo², Wladimiro Jiménez^{2,3}, Ricardo Gonzalo¹, Jordi Vidal¹, Vicente Arroyo⁴, Joan Clària^{2,3,4}, Todd Willis¹, Montserrat Costa¹. ¹Grifols, Bioscience Research Group, Barcelona, Spain; ²Hospital Clinic, IDIBAPS and CIBERehd, Barcelona, Spain; ³University of Barcelona Medical School, Department of Biomedical Sciences, Barcelona, Spain; ⁴EF Clif, EASL-CLIF Consortium and Grifols Chair, Barcelona, Spain
Email: montse.costa@grifols.com

Background and aims: The prevention of mortality by long-term albumin treatment in decompensated cirrhotic patients with ascites is currently under investigation (PRECIOSA phase 3 trial, NCT03451292). Albumin has non-oncotic functions such as binding, antioxidant and immunomodulatory capacities which have been postulated to be related to beneficial effects of albumin administration in cirrhotic patients. However, the specific mechanisms of action associated with albumin in liver cirrhosis are still under research. The present study was aimed at evaluating the effect of therapeutic albumin infusion in cirrhotic rats with ascites. Assessments included were albumin binding capacity, inflammation biomarkers, and a transcriptomic analysis.

Method: Male Wistar rats underwent chronic exposure to carbon tetrachloride to induce cirrhosis. Two weeks after ascites development, rats were randomized to receive intravenously therapeutic human albumin 1.5 g/Kg (Albumin[®], Grifols; $n = 20$) or vehicle (0.9% saline; $n = 16$) on days 1 and 3. At day 4, ascites volume was assessed and serum and tissue samples were collected for biochemical and inflammatory markers determination (total protein, albumin, IL-2, IL-18, TNF- α), albumin binding capacity (using a specific fluorescent marker) and transcriptomic analysis (oxidative stress panel in liver and Toll-Like Receptors (TLR) panel in liver, heart and kidney). Results were expressed as median [IQR].

Results: Therapeutic albumin infusion increased total protein and albumin levels (32 [27–34] g/L), compared to vehicle (22 [18–26] g/L; $p < 0.0001$), 72 h after the initial administration. Human albumin represented 41% of total albumin. Ascites volume was significantly reduced after albumin infusion (2.0 [2.0–3.0] ml vs vehicle infused rats 13.5 [6.5–25.0] ml; $p < 0.01$). These changes were accompanied by an increase of albumin binding capacity (treated 49.2 [43.3–55.8] % vs vehicle 35.7 [33.3–43.4] %; $p < 0.01$) and a decrease of serum proinflammatory cytokines IL-2 ($p < 0.01$), IL-18 ($p < 0.01$) and TNF- α ($p < 0.05$) in treated rats compared to vehicle. Furthermore, transcriptomic analysis in albumin-treated rats revealed an increase in albumin gene expression in the liver, and an attenuation of transcriptomic changes associated with TLR signaling pathways previously altered by cirrhosis induction in liver, heart and kidney.

Conclusion: Albumin infusion resulted in increased albumin binding capacity that was accompanied by ascites mobilization and reduced systemic inflammation as observed by a decrease of cytokine levels and attenuation of transcriptomic changes in TLR signaling pathways. These results using an animal model are in agreement with the role of albumin ameliorating liver disease complications.

THU546

Presence of NOD2 mutations is not associated with hepatic or systemic hemodynamic abnormalities of cirrhosis

Robin Greinert¹, Alexander Zipprich², Anna Hauptmann³, Markus Casper³, Frank Lammert³, Cristina Ripoll². ¹Martin-Luther University Halle Wittenberg, Internal Medicine I, Halle, Germany; ²University Hospital Jena, Internal Medicine IV, Jena, Germany; ³Saarland University Medical Center, Internal Medicine II, Homburg, Germany
Email: robin.greinert@uk-halle.de

Background and aims: Presence of NOD2 Mutation has been associated to infections in cirrhosis. This association is more evident in compensated patients (pts) (PMID: 30702490). According to the systemic inflammation hypothesis, bacterial translocation is one of the main drivers of complications of end-stage liver disease. The **aim** was to evaluate the association of NOD2 mutations with hepatic and systemic hemodynamics.

Method: The presence of NOD2 risk variants (p.N289S, p.R702W, p.G908R, c.3020insC, rs72796367) were evaluated in 825 pts (screening in context of INCA trial: EudraCT 2013-001626-26). From these, 215 pts received a hepatic hemodynamic study and right heart catheterization. This cross-sectional study compared hepatic hemodynamic and systemic hemodynamics according to NOD2 status. Variables are described with median (IQR) or proportions. Mann Whitney U or Chi-square test were applied.

Results: Two-hundred-fifteen pts were included [median age 59 (IQR 53–66); male 67%; 76% alcohol associated cirrhosis]. Most pts were Child Pugh stage B (A 25%, B 64%, C 11%). Sixty-six pts (31%) carried a NOD2 risk variant, of which 64 were heterozygous pts. Although there was an increase in the proportion of NOD2 risk variants among Child Pugh stage C (p = 0.05), no differences were observed in MELD score [wild-type: 13 (10–16); NOD2 variants 13 (10–18)]. No significant differences in hepatic and systemic hemodynamics were observed when comparing patients with and without NOD2 risk variants (table 1). Analyses were repeated excluding patients who were on prophylactic or therapeutic antibiotics, and again no association between hepatic or systemic hemodynamic parameters and NOD2 risk variants could be observed.

	NOD2 wild-type	NOD2 Variants	p value
HR (bpm)	74 (65–83)	78 (65–87)	0.405
MAP (mmHg)	83 (76–89)	83 (75–91)	0.961
CO (l/min)	5.56 (4.67–7.08)	5.97 (4.98–7.64)	0.183
CI (l/min/m ²)	2.93 (2.47–3.52)	3.31 (2.59–3.95)	0.075
SVR (dyn-sec-cm ⁻⁵)	1069 (840–1376)	1042 (747–1273)	0.219
SVRI (dyn-sec/cm ⁵ /m ²)	2016 (1641–2490)	1814 (1473–2399)	0.315
PAP (mmHg)	16 (13–20)	17 (14–20)	0.285
PCWP (mmHg)	11 (7–15)	12 (8–15)	0.237
PVR (dyn-sec-cm ⁻⁵)	75 (43–112)	65 (32–112)	0.542
VCI (mmHg)	8 (6–12)	8 (5–11)	0.395
WHVP (mmHg)	29 (23–32)	28 (23–35)	0.483
FHVP (mmHg)	12 (8–15)	12 (7–15)	0.982
HVPG (mmHg)	19 (15–22)	19 (15–23)	0.994

Conclusion: The presence of NOD2 mutations is not associated with hepatic or systemic hemodynamic abnormalities in patients with cirrhosis, suggesting that other mechanisms leading to bacterial translocation predominate.

THU547

Demonstration of gut-barrier dysfunction and endotoxemia in patients with cirrhosis presenting with acute variceal bleeding: a proof of concept

Rajat Bansal¹, Samagra Agarwal¹, Sanchit Sharma^{1,2}, Kanav Kaushal^{1,2}, Srikanth Gopi¹, Deepak Gunjan¹, Anoop Saraya¹. ¹All India Institute of Medical Sciences, Gastroenterology and Human Nutrition Unit, New Delhi, India; ²John Radcliffe Hospital, Translational Gastroenterology Unit, Oxford, United Kingdom
Email: ansaraya@yahoo.com

Background and aims: Limited data exist on the demonstration of gut-barrier dysfunction and factors predisposing to this in patients with chronic liver disease (CLD) presenting with acute variceal bleeding (AVB). We studied the presence of this dysfunction in a prospectively

recruited cohort of patients with AVB.

Method: Consecutive patients with CLD presenting with AVB were prospectively included, who underwent duodenal biopsy at the time of upper GI endoscopy. Gut-barrier dysfunction was demonstrated by semi-quantitative immunohistochemical (IHC) expression of tight junction proteins like claudin-2, claudin-4, zonulin-1, occludin and junctional adhesion molecule-A (JAM-A) in both villi and crypt of duodenal biopsies. Endotoxemia was estimated indirectly using serum IgM anti-endotoxin assay and systemic inflammation was evaluated using serum interleukin-1 (IL-1) and tumor necrosis factor alpha (TNF-alpha) levels. The expression was compared across different Child-Pugh strata of liver disease and with a control group of cirrhosis without AVB.

Results: Patients with CLD presenting with AVB (n = 71) (Child A/B/C: 25/30/16) and controls (n = 84) were recruited. Zonulin-1 protein expression was elevated [H score at crypt: AVB: 9 (9–9) vs controls: 2 (1–6), p < 0.001; H score at villi: AVB: 6 (6–9) vs controls: 2 (2–6), p < 0.001] in patients with AVB. IgM endotoxin levels (AVB: 28.5 ± 9.9 MMU/ml vs controls: 87.4 ± 20.2 MMU/ml; p < 0.001) were lower while IL-1 (AVB: 1005 ± 82 pg/ml vs controls: 49 ± 14.4 pg/ml; p < 0.001) were elevated in AVB cohort. No difference was seen in the IHC expression of any tight junction barrier proteins, IgM endotoxin, IL-1 and TNF-alpha levels across different strata of liver disease. No association was seen between the studied proteins expression with the aetiology, active alcohol consumption, hypotension at presentation, hepatic venous pressure gradient and presence of active bleeding on endoscopy.

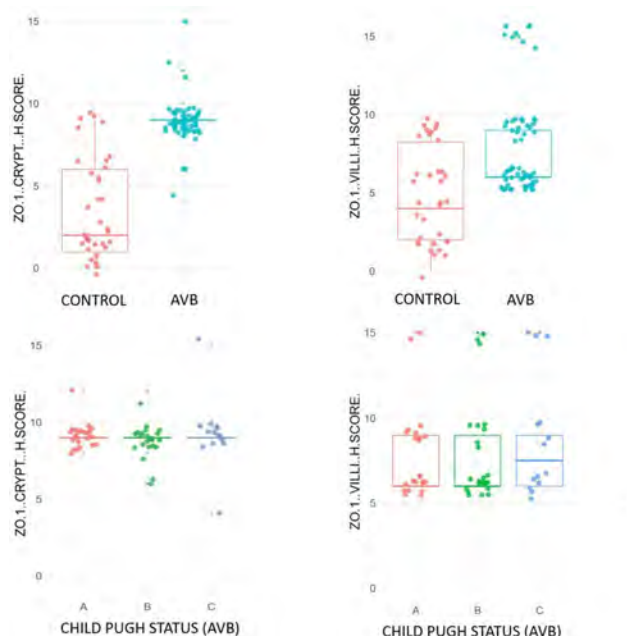


Figure: Scattered boxplots showing Zonulin-1 expression in crypt and villi between controls and AVB and different Child Pugh strata of AVB

Conclusion: While the gut-barrier dysfunction, endotoxemia and systemic inflammation are upregulated in patients with cirrhosis with AVB, the extent of these changes may be independent of aetiology and severity of liver disease, degree of portal hypertension and severity of bleeding episode.

THU548

Worsening of low-grade systemic inflammation heralds decompensation in patients with compensated cirrhosis

Rubén Sánchez-Aldehuelo¹, Cándid Villanueva^{2,3}, Joan Genesca^{3,4}, Juan Carlos García Pagan^{3,5}, Ana Brujats², José Luis Calleja Panero^{3,6}, Carlos Aracil⁷, Rafael Bañares^{3,8}, Rosa M Morillas^{3,9}, Maria Poca^{2,3}, Beatriz Peñas^{1,3}, Salvador Augustin^{3,10}, Juan Abalde^{3,5,11}, Edilmar Alvarado-Tapias^{2,3}, Ferran Torres^{12,13}, Jaime Bosch^{3,5,14}, Agustin Albillos^{1,3}. ¹Ramon y Cajal University Hospital, Ramon y Cajal Institute of Health Research (IRYCIS), University of Alcalá, Madrid, Spain, Spain; ²Hospital of Santa Creu and Sant Pau, Autonomous University of Barcelona, Hospital Sant Pau Biomedical Research Institute (IIB Sant Pau) Barcelona, Spain; ³Centre for Biomedical Research in Liver and Digestive Diseases Network (CIBERehd); ⁴Liver Unit, Vall d'Hebron University Hospital, Vall d'Hebron Research Institute (VHRI), Autonomous University of Barcelona, Barcelona, Spain; ⁵Barcelona Hepatic Haemodynamic Laboratory, Liver Unit, Institute of Digestive and Metabolic Diseases, August Pi i Sunyer Institute of Biomedical Research, Hospital Clinic, Barcelona, Spain; ⁶Puerta de Hierro University Hospital, Puerta de Hierro Hospital Research Institute, Autonomous University of Madrid, Madrid, Spain; ⁷Institute of Biomedical Research, Arnau de Vilanova University Hospital (IRBLleida), Lleida, Spain; ⁸Gregorio Marañón University General Hospital, Gregorio Marañón Sanitary Research Institute, Faculty of Medicine, Complutense University of Madrid, Spain; ⁹University Hospital Germans Trias i Pujol, Badalona, Spain; ¹⁰Liver Unit, Vall d'Hebron University Hospital, Vall d'Hebron Research Institute (VHRI), Autonomous University of Barcelona, Barcelona, Spain; ¹¹University of Alberta, Edmonton, Canada; ¹²Medical Statistics Core Facility, August Pi i Sunyer Biomedical Research Institute, Hospital Clinic, Barcelona; ¹³Biostatistics Unit, Faculty of Medicine, Autonomous University of Barcelona, Barcelona, Spain; ¹⁴Inselspital, Bern University, Switzerland
Email: ruben.sanchez.aldehuelo@gmail.com

Background and aims: Portal hypertension is a major driver of progression and decompensation in cirrhosis. Systemic inflammation

has been recognized in decompensated cirrhosis, where it contributes to accelerate the disease course. However, less information is available regarding inflammation in patients with compensated cirrhosis. Our aims were to investigate i) whether systemic inflammation is present in patients with compensated cirrhosis, and if so, ii) whether its worsening associates with the development of complications.

Method: This is a nested cohort study within the PREDESCI trial, a double blind multicentre, RCT to evaluate the efficacy of beta-blockers to prevent decompensation in patients with compensated cirrhosis and clinically significant portal hypertension (HVPG ≥ 10 mmHg). Biomarkers were measured in blood at baseline and at 1-year follow-up. Development of complications of portal hypertension was registered during the study. A group of 35 healthy controls was included for the specific purposes of this study.

Results: We included 201 patients with compensated cirrhosis, most (56.2%) by chronic hepatitis C, that were followed-up for a median of 37 months (27–47). Decompensation occurred in 17.4% at a median of 24 months (13.6–31.4), being ascites the main cause of decompensation (14.4%). Low-grade systemic inflammation was present at baseline and at 1-year as shown by greater serum levels of IL-6, von Willebrand factor (vWF) and CD163 at both time points in patients compared to controls (Table). Compared to baseline, IL-6 increased ($p < 0.05$) at 1-year in those patients that decompensated on follow-up. Fatty acid binding protein (FABP), used as marker of intestinal barrier function, was greater in patients compared to controls. Values of TNF α , IL1 β , IL8 LBP and CD14 were similar in patients and controls at all points. The macrophage activation marker, CD163, correlated ($p < 0.01$) with HVPG at baseline ($r = 0.27$) and at 1-yr ($r = 0.46$).

		Baseline			1-yr			P intra
		Median	IQR	P	Median	IQR	P	
IL-6 (pg/ml)	Controls (n = 30)	1.6	1.01–2.6	<0.05				0.001
	Cirrhosis (n = 116)	2.3	1.3–3.6		Cirrhosis (n = 97)	2.93	1.29–5.16	
CD163 (ng/ml)	Controls (n = 34)	258.74	210.7–362.4	<0.001				<0.001
	Cirrhosis (n = 157)	857.72	605.5–1117		Cirrhosis (n = 101)	820.35	524.2–1087.1	
vWF (ng/ml)	Controls (n = 20)	2.95	1.46–5.13	<0.001				0.005
	Cirrhosis (n = 160)	6	3.61–9.81		Cirrhosis (n = 108)	4.79	2.78–9.18	
FABP (ng/ml)	Controls (n = 30)	0.31	0.19–0.50	<0.001				<0.001
	Cirrhosis (n = 149)	0.72	0.52–1.04		Cirrhosis (n = 103)	0.73	0.419–1.01	

P: controls vs cirrhosis. P intra: baseline vs 1-yr.

Conclusion: Low-grade systemic inflammation is present in patients with compensated cirrhosis. In this setting, worsening of systemic inflammation herald cirrhosis decompensation.

THU549

Patients with acutely decompensated cirrhosis present a distorted blood lipid landscape that affects the ability of albumin to promote inflammation resolution

Mireia Casulleras^{1,2}, Roger Flores-Costa^{1,2}, Marta Duran-Güell^{1,2}, Ingrid W. Zhang^{1,2}, Cristina López-Vicario^{1,2}, Anna Curto², Javier Fernandez^{2,3}, Vicente Arroyo², Joan Clària^{1,2,4}. ¹Hospital Clínic-IDIBAPS, Biochemistry and Molecular Genetics Service, Barcelona, Spain; ²EF-Clif, European Foundation for the Study of Chronic Liver Failure, Barcelona, Spain; ³Hospital Clínic, Liver ICU, Liver Unit, Barcelona, Spain; ⁴University of Barcelona, Department of Biomedical Sciences, Barcelona, Spain
Email: jclaria@clinic.cat

Background and aims: Lipids, especially lipid mediators derived from polyunsaturated fatty acids (PUFA), play a critical role in the regulation of inflammatory and immune responses. In this investigation, we characterized the blood lipid profile in patients with

acutely decompensated (AD) cirrhosis and explored how changes in this profile might affect the composition of circulating albumin. In addition, we investigated the effects of albumin on the release of PUFA-derived lipid mediators by peripheral leukocytes.

Method: Lipids and lipid mediators were measured by liquid chromatography-tandem.

mass spectrometry in leukocyte incubations, plasma and albumin-enriched and albumin-depleted plasma fractions from 18 patients with AD and 10 healthy subjects. Lipid mediators were also measured in 41 patients with AD included in an albumin therapy trial.

Results: The plasma lipidome associated with AD cirrhosis was characterized by generalized suppression of all lipid classes except FAs. The lipid profile of circulating albumin in AD patients was dominated by reduced content of docosahexaenoic acid (DHA) (omega-3-PUFA) and anti-inflammatory/pro-resolving lipid mediators (i.e. 15-hydroxyicosatetraenoic (15-HETE) and 17-hydroxydocosahexaenoic (17-HDHA)). In addition, albumin from AD patients was depleted in prostaglandins (PGs) (PGE₂, PGD₂ and PGF_{2α}), implying dysregulated degradation and higher circulatory content of these pro-inflammatory lipid mediators. Incubation of leukocytes with exogenous albumin reduced PG production while inducing 15-lipoxygenase expression and 15-HETE and 17-HDHA release. Finally, PGE₂ and PGD₂ levels were lower in AD patients receiving albumin therapy whereas 15-HETE was increased after albumin treatment compared to baseline.

Conclusion: Our findings indicate that both blood and albumin lipid landscape is severely disorganized in AD cirrhosis and that exogenous albumin has potential to redirect leukocyte biosynthesis from pro-inflammatory to pro-resolving lipid mediators.

THU550

miRNA associated with systemic inflammation may have prognostic utility in predicting decompensation in patients with chronic liver disease

Oliver Tavabie¹, Vishal C Patel^{2,3,4}, Siamak Salehi¹, Marilena Stamouli¹, Francesca Trovato¹, Savannah Rivera¹, Salma Mujib¹, Ane Zamalloa¹, Eleanor Corcoran¹, Krishna Menon¹, Andreas Prachalias¹, Michael Heneghan¹, Kosh Agarwal¹, Mark J W McPhail¹, Varuna Aluvihare¹. ¹King's College Hospital, United Kingdom; ²King's College Hospital, Institute of Liver Studies and Transplantation, London, United Kingdom; ³Foundation For Liver Research, The Roger Williams Institute of Hepatology, London, United Kingdom; ⁴Institute of Liver Sciences, King's College London, Department of Inflammation Biology, School of Immunology and Microbial Sciences, FoLSM, London, United Kingdom

Email: oliver.tavabie@nhs.net

Background and aims: Chronic liver disease (CLD) is associated with significant mortality and encompasses; acute-on-chronic liver failure (ACLF), acute decompensation (AD), chronic decompensation (dCLD) and compensated CLD (cCLD). Transition between these states impacts on patient (Pt) survival. Here we investigate miRNA expression across the spectrum of CLD to evaluate their prognostic utility.

Method: Plasma samples were provided by Pts and healthy controls (HC). Pts sampled included ACLF, AD, cCLD, HC (each groups n = 20) and dCLD (n = 94). ACLF and AD Pts were sampled within 72 hours of admission. 90-day transplant-free survival (TxFS) across Pts with CLD was 68.8%. 6 Pts in the cCLD group decompensated in the year post-sampling. A panel of 21 miRNA developed from our previous studies were analysed. Univariate and multivariate analyses were utilized to identify miRNA associated with decompensated CLD states and 90-day TxFS.

Results: Figure 1 demonstrates significant correlations of miRNA with clinical and laboratory parameters across CLD groups. Notably, miR-24 correlated with markers of systemic inflammation (CRP), liver failure (bilirubin, INR, lactate and ascites) and CLD prognostic models (Child-Pugh $r_{(s)} = 0.25$ (95%CI 0.09–0.40), MELD $r_{(s)} = 0.25$ (95%CI

0.09–0.40)). miRNA expression was compared between ACLF/AD/dCLD cohorts and HC/cCLD cohorts. Downregulation of miR-122, -24 and -30a and upregulation of miR-223, -27a and -29b was associated with decompensated CLD states. MetaCore™ pathway analysis demonstrated an association between these miRNA and systemic inflammation ($z = 188.35$, $p < 0.0001^*$). A model including miR-24 and -27a discriminated Pts with ACLF/AD/dCLD from cCLD/HC Pts (AUC 0.77 (95%CI 0.69–0.85)). Sensitivity analyses were performed excluding each group individually. Excluding the HC cohort reduced model performance (AUC 0.69 (95%CI 0.56–0.81)). However, subsequently excluding the 6 cCLD Pts who decompensated the following year improved this (AUC 0.74 (95%CI 0.60–0.88)). Only the detection of miR-200b discriminated 90-day TxFS across CLD groups but did not remain significant when adjusted for MELD. Subgroup analysis of Pts with; dCLD, alcohol related CLD (ARLD) and ascites Pts demonstrated different miRNAs associated with 90-day TxFS (miR-24 in dCLD, miR-220b in ARLD and no miRNA in ascites Pts). Only the detection miR-200b in ARLD Pts remained significant when adjusted for MELD (aOR 0.23 (95%CI 0.06–0.82).

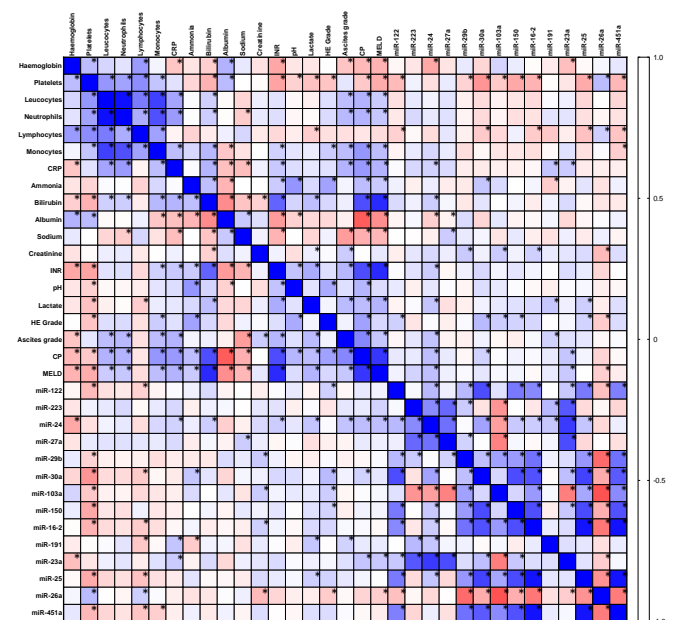


Figure: Correlation matrix of clinical and laboratory parameters with miRNA expression in CLD Pts

Conclusion: miRNA associated with systemic inflammation discriminate Pts with and without decompensated CLD states. Whilst miRNA have limited prognostic value in predicting 90-day TxFS likely reflecting the impact of aetiology, disease phase and decompensation manifestation, they may have prognostic utility in predicting future decompensation.

Liver tumours: Therapy

THU566

Systemic treatments with tyrosine kinase inhibitors and platinum-based chemotherapy in patients with unresectable or metastatic hepato-cholangiocarcinoma

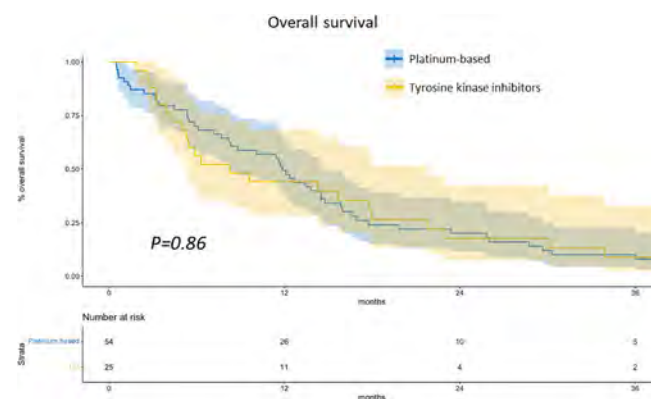
Elia Gigante^{1,2}, Christian Hobeika³, Brigitte Le Bail⁴, Valérie Paradis⁵, David Tougeron⁶, Marie Lequoy⁷, Mohamed Bouattour⁸, Jean-Frédéric Blanc⁹, Nathalie Ganne-Carrié¹, Henri Tran¹, Clemence Hollande¹⁰, Manon Allaire¹¹, Giuliana Amadeo¹², Helene Regnault¹², Paul Vigneron¹², Maxime Ronot¹³, Laure Elkrief¹⁴, Gontran Verset¹⁵, Eric Treppe¹⁵, Aziz Zaanani¹⁶, Marianne Zioli¹⁷, Massih Ningharhari¹⁸, Julien Calderaro¹⁹, Julien Edeline²⁰, Jean Charles Nault¹. ¹Hôpital Avicenne, Service d'hépatologie, Bobigny, France; ²Centre de recherche sur l'inflammation, Inserm, Université de Paris, INSERM UMR 1149 « De l'inflammation au cancer », Paris, France, Clichy, France; ³Hôpital de la Pitié Salpêtrière, Service de Chirurgie Digestive, Hépatobilio-pancréatique et Transplantation Hépatique, France; ⁴Hôpital Pellegrin-CHU Bordeaux, Service d'Anatomo-Pathologie; ⁵Hôpital Beaujon, AP-HP, Service d'Anatomo-Pathologie, France; ⁶CHU de Poitiers et Université de Poitiers, Service d'Hépatogastroentérologie; ⁷Hôpital Saint-Antoine, AP-HP, Service d'hépatologie; ⁸Hôpital Beaujon, AP-HP, Service d'hépatologie; ⁹Hôpital Haut-Lévêque, CHU Bordeaux, Pessac and INSERM U1053, Université de Bordeaux, Service d'hépatogastroentérologie et d'oncologie digestive; ¹⁰Hôpital Cochin, AP-HP, Paris, France, Service d'hépatologie; ¹¹Hôpital de la Pitié Salpêtrière, AP-HP, Service d'hépatologie; ¹²Hôpital Mondor, AP-HP, Paris, Service d'hépatologie; ¹³Hôpital Beaujon, AP-HP, Service de radiologie; ¹⁴HC-UMUH 1, CHRU Tours, Service d'hépatologie; ¹⁵Erasmus Hospital, Brussels, Department of Gastroenterology and Digestive Oncology; ¹⁶Hôpital Européen Georges-Pompidou HEGP, AP-HP, Service Hépatogastro-entérologie et oncologie digestive; ¹⁷Hôpital Avicenne, AP-HP, Service d'Anatomo-Pathologie; ¹⁸CHU Lille-Hôpital Huriez, Maladies de l'appareil digestif; ¹⁹Hôpital Mondor, AP-HP, Paris, Service d'Anatomo-Pathologie; ²⁰Centre Eugène Marquis, Service d'oncologie Email: elia.gigante@hotmail.it

Background and aims: Although there is currently no validated systemic therapy for unresectable hepato-cholangiocarcinoma (cHCC-CCA), tyrosine kinase inhibitors and platinum-based chemotherapy are frequently used in clinical practice. Our study has aim to describe the effectiveness of first-line systemic treatments in patients with cHCC-CCA.

Method: Patients with histological diagnosis of unresectable or metastatic cHCC-CCA confirmed by a centralized review (WHO classification 2019) who received systemic treatment from 2009 to 2020 were included retrospectively in 11 centers. The outcomes of patients with cHCC-CCA were compared with patients with hepatocellular carcinoma (HCC) treated by sorafenib (n=225) and with intrahepatic cholangiocarcinoma (iCCA, n=94) treated mainly by platinum using a frailty Cox model. The efficacy of tyrosine kinase inhibitors and platinum-based chemotherapies in patients with cHCC-CCA was assessed using a doubly robust estimator.

Results: A total of 83 patients with cHCC-CCA were included and were predominantly male (72%), 67% of patients had extrahepatic metastases and 31% macrovascular tumor invasion. Compared with iCCA (n=94) and HCC (n=225), cHCC-CCA were more often developed on cirrhosis (55%) than iCCA (27%) but less frequently than HCC (88%) (p<0.001). cHCC-CCA (66%) and HCC (30%) had extrahepatic metastases less frequently than iCCA (81%) (p<0.001). Unadjusted overall survival was better in CCA (13 months) compared to cHCC-CCA (12 months) and HCC (9 months) (p=0.017). In multivariate analysis after adjustment by a Cox frailty model, patients with cHCC-CCA had the same survival than HCC and iCCA (HR = 1.5; 95% CI = 0.98, 2.3; p = 0.063). ALBI score (HR = 2.15; CI05%: 1.23, 3.76;

p = 0.09), ascites (HR = 3.45, CI95%: 1.31, 9.03; p = 0.013) and tobacco (HR = 2.29; CI95%: 1.08, 4.87; p = 0.032) were independently associated with OS in patients with cHCC-CCA. Among patients with cHCC-CCA, 25 patients treated with tyrosine kinase inhibitors were compared with 54 patients with platinum-based chemotherapies. Patients treated by tyrosine kinase inhibitors had a median overall survival of 7.28 months versus 12.1 months for patients treated with platinum-based chemotherapies (p=0.86) (Figure). After a robust double adjustment on tumor number and size, vascular invasion, ALBI, MELD and cirrhosis, treatment's regimen had no influence on overall survival (HR = 0.92, 95%CI = 0.27–3.15, P = 0.88) and progression-free survival (HR = 1.24, 95%CI = 0.44–3.49, P = 0.67).



Conclusion: Systemic treatments with tyrosine kinase inhibitors or platinum-based chemotherapies have similar efficacy in first line of patients with unresectable/metastatic cHCC-CCA. The ALBI score predicts overall survival.

THU567

The systemic inflammatory response identifies patients with adverse clinical outcome from immunotherapy in hepatocellular carcinoma

Claudia Fulgenzi^{1,2}, Ambreen Muhammed², Sirish Dharmapuri³, Matthias Pinter⁴, Lorenz Balcar⁴, Bernhard Scheiner⁴, Thomas U. Marron³, Tomi Jun³, Anwaar Saeed⁵, Hannah Hildebrand⁵, Mahvish Muzaffar⁶, Musharraf Navaid⁶, Abdul Rafef Naqash⁶, Anuhya Gampa⁷, Umut Ozbek⁸, Jung-Yi Lin⁸, Ylenia Perone², Bruno Vincenzi¹, Marianna Siletta¹, Anjana Pillai⁷, Yinghong Wang⁹, Uqba Khan¹⁰, Yi-Hsiang Huang¹¹, Dominik Bettinger¹², Yehia Abugabal¹³, Ahmed Kaseb¹³, Tiziana Pressiani¹⁴, Nicola Personeni^{14,15}, Lorenza Rimassa^{14,15}, Naoshi Nishida¹⁶, Luca Di Tommaso¹⁷, Masatoshi Kudo¹⁶, Arndt Vogel¹⁸, Francesco Mauri², Alessio Cortellini², Rohini Sharma², Antonio D'Alessio^{19,20}, Celina Ang³, David J. Pinato². ¹Campus Biomedico, Medical Oncology, Roma, Italy; ²Imperial College London, Hammersmith Hospital, Surgery and Cancer, London, United Kingdom; ³The Mount Sinai Hospital, Department of Medicine, Division of Hematology/Oncology, New York, United States; ⁴Medical University of Vienna, Department of Internal Medicine III, Division of Gastroenterology and Hepatology, Wien, Austria; ⁵University of Kansas, Division of Medical Oncology, Department of Medicine, Westwood, United States; ⁶East Carolina University, Division of Hematology/Oncology, Greenville, United States; ⁷UChicago Medicine, Section of Gastroenterology, Hepatology and Nutrition, Chicago, United States; ⁸Icahn School of Medicine at Mount Sinai, Department of Population Health Science and Policy, New York, United States; ⁹The University of Texas MD Anderson Cancer Center, Department of Gastroenterology, Hepatology and Nutrition, Houston, United States; ¹⁰NY-Presbyterian Hospital, Division of Hematology and Oncology, New York, United States; ¹¹Veterans General Hospital, Division of Gastroenterology and Hepatology, Institute of Clinical Medicine, National Yang Ming Chiao

Tung University School of Medicine, Taiwan; ¹²University of Freiburg, Department of Medicine II, Faculty of Medicine, Medical Center University of Freiburg, Freiburg im Breisgau, Germany; ¹³The University of Texas MD Anderson Cancer Center, Department of Gastrointestinal Medical Oncology, Houston, United States; ¹⁴IRCCS Humanitas Research Hospital, Medical Oncology and Hematology Unit, Humanitas Cancer Center, Cascina Perseghetto, Italy; ¹⁵Humanitas University, Department of Biomedical Sciences, Milan, Italy; ¹⁶Kindai University Hospital, Department of Gastroenterology and Hepatology, Osakasayama, Japan; ¹⁷IRCCS, Humanitas Research Hospital, Pathology Unit, Cascina Perseghetto, Italy; ¹⁸Hannover Medical Center, Department of Gastroenterology, Hepatology and Endocrinology, Sharjah, United Arab Emirates; ¹⁹Humanitas University, Department of Biomedical Sciences, Italy; ²⁰Imperial College London, Department of Surgery and Cancer, London, United Kingdom
Email: fulgeclaud@gmail.com

Background and aims: Systemic inflammation is a hallmark of cancer, and it has a pivotal role in HCC development and progression. The role of systemic inflammation in influencing outcomes of patients treated with immunotherapy for HCC has not been fully elucidated.

Method: We conducted a retrospective study including 362 patients receiving immune-checkpoint inhibitors (ICIs) across 3 continents, evaluating the influence of neutrophils to lymphocytes ratio (NLR), platelet to lymphocytes ratio (PLR) and prognostic nutritional index (PNI) on overall (OS), progression free survival (PFS) and radiologic responses.

Results: In our 362 patients treated with immunotherapy, median OS and PFS were 9 and 3.5 months respectively. Amongst tested inflammatory biomarkers, patients with NLR ≥ 5 had shorter OS (7.7 vs 17.6 months, $p < 0.0001$), PFS (2.1 vs 3.8 months, $p = 0.025$) and lower ORR (12% vs 22%, $p = 0.034$), similarly, patients with PLR ≥ 300 reported shorter OS (6.4 vs 16.5 months, $p < 0.0001$) and PFS (1.8 vs 3.7 months, $p = 0.0006$). NLR emerged as independent prognostic factors for OS in univariate and multivariate analysis (HR 1.95, 95%CI 1.45–2.64, $p < 0.001$; HR 1.73, 95%CI 1.23–2.42, $p = 0.002$) and PLR remained an independent prognostic factor for both OS and PFS in multivariate analysis (HR 1.60, 95%CI 1.6–2.40, $p = 0.020$; HR 1.99, 95%CI 1.11–3.49, $p = 0.021$).

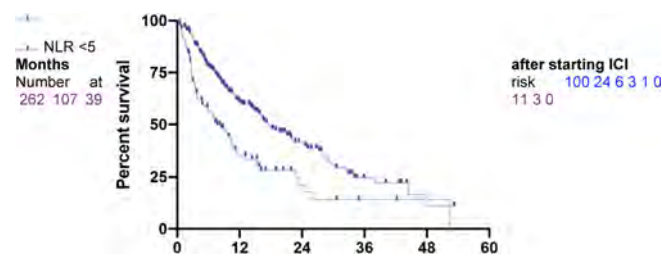


Figure: OS by pre-treatment NLR

Conclusion: Systemic inflammation measured by NLR and PLR is an independent negative prognostic factor in HCC patients undergoing ICI therapy. Further studies are required to understand the biological mechanisms underlying this association and to investigate the predictive significance of circulating inflammatory biomarkers in HCC patients treated with ICIs.

THU568

Combination of crafity score with alpha-fetoprotein response predicts a favorable outcome of atezolizumab plus bevacizumab for unresectable hepatocellular carcinoma

Wei Teng¹, Chen-Chun Lin¹, Po-Ting Lin¹, Yi-Chung Hsieh¹, Ming-Mo Ho², Chia-Hsun Hsieh³, Chun-yen Lin¹, Shi-Ming Lin¹.

¹Linkou Chang Gung Memorial Hospital, Gastroenterology and Hepatology, Taoyuan, Taiwan; ²Linkou Chang Gung Memorial Hospital, Medical Oncology, Taoyuan, Taiwan; ³Tucheng Hospital, Medical Oncology, New Taipei City, Taiwan
Email: chunyenlin@gmail.com

Background and aims: Immune checkpoint inhibitors (ICIs) with atezolizumab plus bevacizumab are promising agents for unresectable hepatocellular carcinoma (HCC). Recently, the CRAFTY score composed of baseline alpha-fetoprotein (AFP) and CRP level is associated with survival and radiological response in patients with ICIs treatment. Therefore, we tried to propose an algorithm based on CRAFTY score combining with on-treatment AFP response to guide treatment.

Method: Seventy-two patients who received atezolizumab plus bevacizumab regardless of as a first- or more than a second-line therapy for unresectable HCC in Chang Gung Memorial Hospital, Linkou Medical center were enrolled for analyses. Radiologic evaluation was based on modified Response Evaluation Criteria in Solid Tumors (mRECIST).

Results: Of 72 patients, the objective response rate (ORR) and disease control rate (DCR) were 23.4% and 57.8%, respectively. Twenty-five patients (34.7%) died during median 7.0 months follow-up duration. Multivariate analysis showed that low CRAFTY score (AFP < 100 ng/ml or CRP < 10 mg/l) and satisfactory AFP response at 6 weeks ($\geq 75\%$ decrease or $\leq 10\%$ increase from baseline) were independent factors associated with good OS (hazard ratio [HR] = 0.263, $p = 0.041$ and HR = 0.102, $p = 0.004$), PFS (HR = 0.681, $p = 0.046$ and HR = 0.326, $p = 0.008$) and good responder (odds ratio [OR] = 4.354, $p = 0.044$ and OR = 6.406, $p = 0.017$). Patients were further divided into three classes: low CRAFTY score (0–1 points) with satisfactory AFP response at 6 weeks (class I), either high CRAFTY score (2 points) or unsatisfactory AFP response at 6 weeks (class II) and neither low CRAFTY score nor satisfactory AFP response at 6 weeks (class III). ORR was 41.7%, 15.4%, and 0% in class I, II and III patients, respectively (overall $p = 0.033$). Patients in the class I had the longest overall survival (OS) and progression-free survival (PFS), followed by class II and class III (median OS: not reached vs. 8.6 vs. 4.3 months, log-rank $p < 0.001$; median PFS: 5.9 vs. 4.7 vs. 2.7 months, log-rank $p = 0.014$). Combination CRAFTY score and AFP response at 6 weeks with AUROC predicts OS and tumor response to be 0.809 and 0.816, respectively, superior to either CRAFTY score (0.771 and 0.767) or AFP response at 6 weeks (0.725 and 0.729) alone.

Conclusion: The CAR (CRAFTY score and AFP-Response) classification which combining CRAFTY score and AFP response at 6 weeks provides a practical guidance for atezolizumab plus bevacizumab therapy in unresectable HCC patients.

THU569

Survival of patients with advanced hepatocellular carcinoma treated with sorafenib in France during 2009–2018: analysis of the French hospital and claim database

Jean-Pierre Bronowicki¹, Julien Dupin², Alexandre Pissewoewoe Tanang², Anika Gilbert-Marceau², Jean-Frédéric Blanc³, Pierre Nahon⁴, Caroline Laurendeau⁵, Stéphane Bouée⁵, Mélina Gilbert⁶. ¹CHRU Nancy, Hépatogastroentérologie, VANDOEUVRE LES NANCY, France; ²Roche, Boulogne-Billancourt; ³CHU Bordeaux, Hépatogastroentérologie, Bordeaux; ⁴APHP Hôpital Avicenne, Hépatologie, Bobigny; ⁵CEMKA, Bourg La Reine, France; ⁶Roche, Boulogne-Billancourt, France
Email: jp.bronowicki@chu-nancy.fr

Background and aims: Hepatocellular carcinoma (HCC) is often diagnosed at an advanced stage of the disease. Until 2017, sorafenib

POSTER PRESENTATIONS

was the only systemic therapy indicated in advanced HCC as first-line therapy. This analysis describes the profile, overall survival (OS) and proxy of progression free survival (PFS) in patients with advanced HCC treated with sorafenib in France.

Method: This study was conducted using the French administrative healthcare claims database. All patients treated with sorafenib for HCC (identified by the ICD-10 code for hepatocellular carcinoma) as long-term illnesses or diagnosis-related group during hospitalization were included in the study between 2009 and 2018. The cause of the underlying chronic liver disease (CLD) was identified from ICD-10 codes and ATC codes of specific treatments. OS from sorafenib initiation was measured. PFS was defined on the proxy of the time from sorafenib initiation until treatment discontinuation or death. The Kaplan-Meier method was used to estimate survival rates.

Results: 17,680 newly treated HCC patients were identified. Their mean age was 66.9 years (SD:10.3) and 87.6% were male. The most frequent causes of underlying CLD were alcohol liver disease (54.8%) and viral hepatitis (24.4%). The median OS from sorafenib initiation was 8.4 months (95% CI = [8.2; 8.7]).

OS differed according to HCC etiologies:

Alcohol + (HCV or HBV) (1,749 patients, 9.9%), 8.9 months [8.4;9.4]

Alcohol without viral hepatitis (7,933 patients, 44.9%), 8.8 months [8.4;9.1]

NASH/NAFLD without viral or alcohol hepatitis (403, 2.3%), 9.8 months [8.9;11.8]

Hepatitis B without alcohol hepatitis (655 patients, 3.7%), 5.9 months [5.3;6.9]

Co-infection VHB/VHC without alcohol hepatitis (268 patients, 1.5%), 9.7 months [8.2;11.7]

Hepatitis C without alcohol hepatitis (1,646 patients, 9.3%), 9.0 months [8.2;9.7]

No identified etiology (5,026 patients, 28.4%), 7.7 months [7.3;8.1]

The median survival decreased over the years: from 10.0 months in 2009 to 7.3 months in 2018.

The median proxy PFS was 3.5 months [3.3; 3.7]. Probability of sorafenib discontinuation or death before 12 months was 85%.

Conclusion: These results confirmed the high clinical burden of treated HCC regardless of the cause of CLD.

OS in this real-world setting study is lower than in clinical trials and consistent according to all etiologies.

Earlier management adapted as well as the arrival of new treatments such as immunotherapy, will improve the prognosis of patients.

THU570

Textbook outcome after major hepatectomy for perihilar cholangiocarcinoma—definitions and influencing factors

Christian Benzing¹, Lena Haiden¹, Felix Krenzien¹, Alexa Mieg¹, Annika Wolfsberger², Cecilia Atik¹, Nora Nevermann¹, Uli Fehrenbach², Wenzel Schöning¹, Moritz Schmelzle¹, Johann Pratschke¹. ¹Charité University Medicine Berlin, Department of Surgery | Campus Charité Mitte and Campus Virchow Klinikum, Berlin, Germany; ²Charité University Medicine Berlin, Department of Diagnostic and Interventional Radiology, Berlin, Germany
Email: christian.benzning@charite.de

Background and aims: The concept of “textbook outcome” (TO) as composite quality measure depicting the ideal surgical outcome has not yet been defined for patients undergoing major hepatectomy (MH) which remains the only curative therapy option for perihilar cholangiocarcinoma (PHC). This study aimed to propose a uniform definition through a systematic literature review as well as to identify patient- or procedure-related factors influencing TO.

Method: In this retrospective study, we analyzed all patients undergoing MH for PHC at our department between January 2005 and August 2019. After conducting a systematic literature search, we defined TO as the absence of 90-day mortality and major complications, no hospital readmission within 90 days after discharge, and no

prolonged hospital stay (<75. percentile). A multivariate logistic regression analysis was performed to identify factors influencing TO. **Results:** Of 283 patients, TO was achieved in 67 (24%) patients. Multivariate analysis revealed that preoperative biliary drainage was associated with a decreased (OR = 0.405, 95% CI: 0.194–0.845, $p = 0.016$) and left-sided-resection (OR = 1.899, 95% CI: 1.048–3.440, $p = 0.035$) with increased odds for TO. Overall survival (OS) and DFS (disease-free survival) did not differ significantly between the outcome groups (OS: $p = 0.280$, DFS: $p = 0.735$). However, there was a trend towards better overall survival, especially in the late course with TO. The differences in OS between the TO and no TO groups were statistically significant when analyzing patients with survival of at least 30 months ($p = 0.039$, Figure 1).

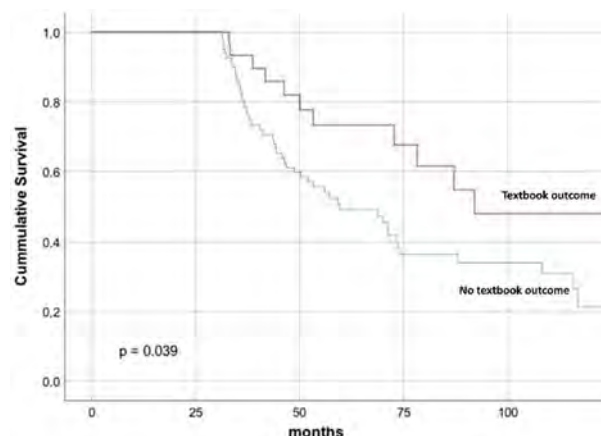


Figure: Long-term survival of patients after major hepatectomy for perihilar cholangiocarcinoma according to textbook outcome groups excluding patients surviving less than 30 months.

Conclusion: Our analysis proposed a uniform definition of TO after MH for PHC. We identified left hepatectomy as an independent factor positively influencing TO. In patients where both right- and left-sided resections are feasible, this underlines the importance of a careful selection of patients who are scheduled for right hepatectomy.

THU571

Impact of body mass index in patients receiving atezolizumab plus bevacizumab for hepatocellular carcinoma

Mathew Vithayathil¹, Antonio D'Alessio^{1,2}, Arndt Weinmann³, Peter Galle³, Claudia Angela Maria Fulgenzi^{1,4}, Petros Fessas¹, Dominik Bettinger⁵, Bertram Bengsch⁵, Arndt Vogel⁶, Lorenz Balcar⁷, Bernhard Scheiner⁷, Mahvish Muzaffar⁸, Suneetha Amara⁸, Ambreen Muhammed¹, Abdul Rafeh Naqash⁸, Nicola Personeni^{2,9}, Tiziana Pressiani⁹, Antonella Cammarota^{2,9}, Matthias Pinter⁷, Alessio Cortellini^{1,10}, Lorenza Rimassa^{2,9}, David J. Pinato^{1,11}, Rohini Sharma¹. ¹Imperial College London, United Kingdom; ²Humanitas University, Italy; ³Universitätsmedizin der Johannes Gutenberg-Universität Mainz, Mainz, Germany; ⁴Bio-Medico Campus University Hospital, Roma, Italy; ⁵University of Freiburg, Freiburg University Medical Center, Freiburg im Breisgau, Germany; ⁶Hannover Medical School, Hannover, Germany; ⁷Medical University of Vienna, Wien, Austria; ⁸East Carolina University, Greenville, United States; ⁹Humanitas Research Hospital, Cascina Perseghetto, Italy; ¹⁰University of L'Aquila, L'Aquila, Italy; ¹¹University of Eastern Piedmont, Vercelli, Italy
Email: mathew.vithayathil@doctors.org.uk

Background and aims: Atezolizumab plus bevacizumab is the new first line-treatment for unresectable hepatocellular carcinoma (HCC). Body mass index (BMI) has demonstrated predictive value for response to immunotherapy in non-HCC cancer types. Our study investigated the effect of BMI on safety and efficacy of real-life use of atezolizumab plus bevacizumab.

Method: Sixty-four consecutive patients from seven centres receiving atezolizumab plus bevacizumab were included in the retrospective study. Overall survival (OS), progression-free survival (PFS), overall response rate (ORR) and disease control rate (DCR) defined by RECIST v1.1 were measured in overweight (BMI ≥ 25) and non-overweight (BMI < 25) patients. Treatment-related adverse events (trAEs) were evaluated for each BMI cohort.

Results: Baseline Child-Pugh class, Eastern Cooperative Oncology Group performance status and Barcelona Clinic Liver Cancer stage was similar between overweight (n=36) and non-overweight patients (n=28). Underlying non-alcoholic fatty liver disease was more prevalent in overweight patients (27.8 vs. 7.1%; $p=0.04$). Overweight patients had a longer OS compared to non-overweight (median OS 11.6 vs. 7.5 months; $p=0.045$) (Figure 1). BMI did not influence median PFS (6.9 vs. 3.0 months; $p=0.34$), ORR (26.7% vs. 25.0%; $p=0.90$) and DCR (63.3% vs. 60.0%; $p=0.81$). trAEs were comparable between the two groups (atezolizumab-related 44.4% vs. 53.6%; $p=0.47$ and bevacizumab-related 18.8% vs. 12.5%; $p=0.68$).

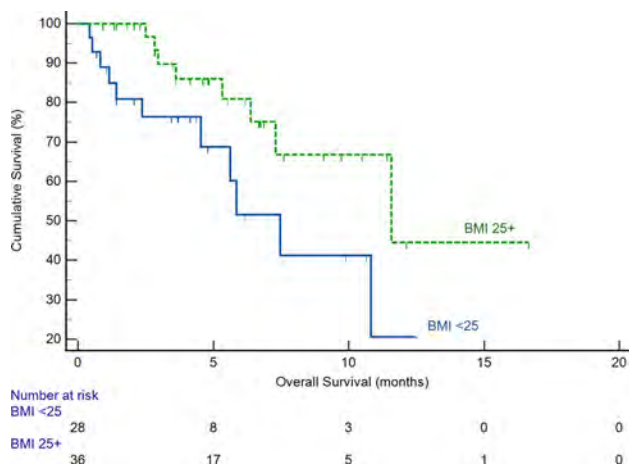


Figure: Kaplan-Meier curve showing increased overall survival (months) for overweight patients compared to non-overweight unresectable hepatocellular carcinoma patients after atezolizumab plus bevacizumab administration.

Conclusion: Higher BMI is associated with increased OS in HCC patients receiving atezolizumab plus bevacizumab for unresectable HCC, without an increase in trAEs. BMI may have a predictive role in immunotherapy treatment response in HCC.

THU572

Outcome predictors of gemcitabine-based or fluoropyrimidine-based chemotherapy for unresectable intrahepatic cholangiocarcinoma

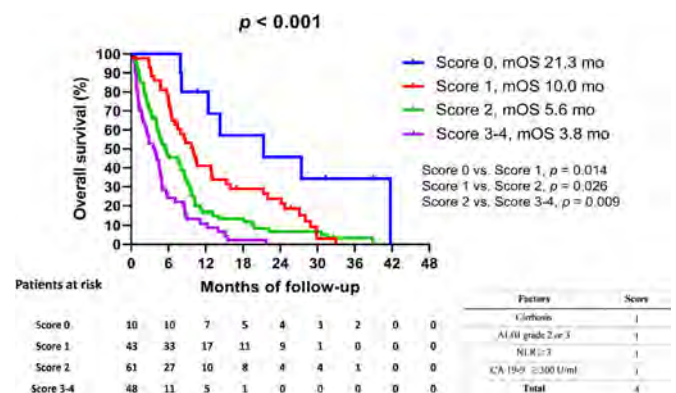
Chen-Ta Chi^{1,2}, I-Cheng Lee¹, Ming-Huang Chen³, Pei-Chang Lee¹, Yi-Ping Hung³, Ming-Chih Hou¹, Yee Chao³, Yi-Hsiang Huang^{1,2}.

¹Taipei Veterans General Hospital, Taipei, Taiwan, Division of Gastroenterology and Hepatology, Department of Medicine; ²National Yang Ming Chiao Tung University, Taipei, Taiwan, Institute of Clinical Medicine, School of Medicine; ³Taipei Veterans General Hospital, Taipei, Taiwan, Department of Oncology
Email: yhhuang@vghtpe.gov.tw

Background and aims: Intrahepatic cholangiocarcinoma (ICC) is a highly aggressive malignancy, and the resectability rate for curative surgical resection is low. Gemcitabine-based and fluoropyrimidine-based chemotherapy are the mainstay treatments for Unresectable ICC, even though the survival is still far from satisfaction in real-world experience. This study aimed to assess outcomes and identify the prognostic factors for patients with unresectable ICC patients receiving gemcitabine-based or fluoropyrimidine-based chemotherapy.

Method: From December 2006 to January 2020, consecutive 309 unresectable ICC patients were enrolled. Of them, 162 ICC patients received chemotherapy as first-line treatment were retrospectively reviewed, and 123 patients had evaluable images for tumour response evaluation. Objective response rate (ORR) and overall survival (OS) were assessed and factors associated with ORR and OS were analysed.

Results: Of the 162 ICC patients received chemotherapy as first-line therapy, the mean age was 62 years old. Most patients were within Child-Pugh class A (61.7%) and Albumin-bilirubin (ALBI) grade 2/3 (67.3%). Of them, 106 (65.4%) received gemcitabine-based regimen, while 56 (34.6%) patients received fluoropyrimidine-based regimen. The ORR was 26.0% and disease control rate (DCR) was 48.0% in the whole 123 ICC patients with evaluable images (including 32 partial responses, 27 stable diseases, and 64 progressive disease). HBV infection (OR, 3.223; $p=0.032$), gemcitabine-based regimen (OR, 4.714; $p=0.008$) were the independent predictors of ORR. In general, the median OS of the 162 ICC patients was 6.1 months. Presence of cirrhosis, Albumin ≤ 3.5 g/dl, Child-Pugh B/C, ALBI grade 2/3, NLR ≥ 3 , and CA 19-9 ≥ 300 U/ml were independent risk factors associated with OS. A novel ALBI-based scoring system to predict OS was created, the patients could be classified into 4 groups. Kaplan-Meier analysis showed that the new ALBI-based model could significantly discriminate OS between contiguous groups ($p<0.001$, Figure). Noteworthy, patients without any risk factors had a promising overall survival of 21.3 months.



Conclusion: Albumin-bilirubin grade is an important factor associated with survival in unresectable ICC patients receiving chemotherapy. The new ALBI-based model can be applied to select patients who can get the best benefit from chemotherapy.

Conflict of interest: The authors declared no conflicts of interest.

Funding: The work was partly supported by the Taipei Veterans General Hospital, Taipei, Taiwan (grant numbers V110A-004).

THU573

Transarterial radioembolisation in non resectable hepatocellular carcinoma in curative strategies: a single centre experience

Helene Regnault¹, Clara Perrin², Giuliana Amaddeo¹, Sebastien Mulé¹, Hicham Kobeiter¹, Edouard Reizine¹, Emmanuel Itti¹, Christophe Duvoux¹, Alexis Laurent¹, Vincent Leroy¹, Raffaele Brustia¹, Daniele Sommacale¹, Françoise Roudot-Thoraval¹, Lerman Lionel¹, Alain Luciani¹, Julien Calderaro¹, Julia Chalaye¹, Vania Tacher¹, Athena Galletto³. ¹Henri Mondor University Hospital, Hepatology, Créteil, France; ²Antoine Beclere University Hospital, Hepatology, Clamart, France; ³Henri Mondor University Hospital, Medical Imaging, Creteil, France
Email: helene.regnault@aphp.fr

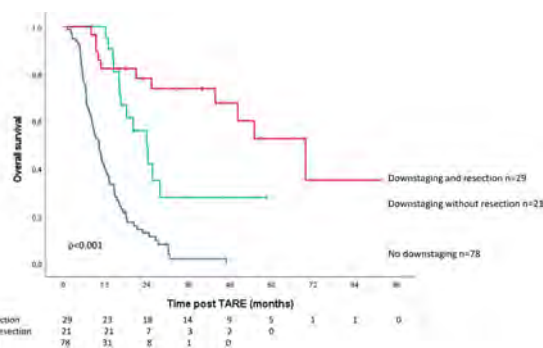
Background and aims: Transarterial radioembolisation (TARE) has the potential to be curative either directly (radiation segmentectomy) or as neoadjuvant strategy before resection or transplantation.

POSTER PRESENTATIONS

However, its place remains largely debated. The aim of our study was to evaluate the outcome of initially non-operative patients after TARE in a single tertiary centre.

Method: This retrospective, observational study included all consecutive patients treated by TARE in our centre between October 2013 and June 2020. Clinical, biological and imaging data were collected at baseline and every 3 months during follow-up. Tumour response was evaluated at 6 months according to Response Evaluation Criteria in Solid Tumors (RECIST) 1.1 and modified RECIST (mRECIST). The suitability of surgical treatment after downstaging was systematically discussed in a weekly tumour board.

Results: 128 patients (male = 90%, mean age 64 years) were included. The majority (n = 88%) had cirrhosis (CPT A: 84%, CPT B: 16%) mainly due to viral hepatitis (21%), non-alcoholic steatohepatitis (18%) and alcohol (18%). HCC was classified as BCLC A: n = 14 (11%), BCLC B: n = 50 (39%) and BCLC C: n = 64 (50%). The majority of patients had an imaging infiltrative pattern: n = 52 (41%), a median diameter of 50 mm and portal vein invasion (n = 62, 49%) classified as VP1: n = 3, VP 2: n = 22, VP3: n = 28 and VP4: n = 9. Median AFP was 115. TARE was the first-line therapy in 77 patients. TARE could be successfully applied in all patients. At 6 months, the rates of complete and partial responses were 4 and 40% respectively, according to RECIST and 23 and 28% according to mRECIST. A downstaging was obtained in 50 (39%) patients, whom 29 (23%) had access to a curative treatment (transplantation: n = 17 (13%), resection: n = 11 (9%) and ablation: n = 1) in a median time of 4.3 months. Absence of access to surgery was due to general contra-indication (n = 10), progression (n = 5), refusal (n = 4) and presence on waiting list (n = 2). Median overall survival of patients with or without downstaging were 50.1 months [8.6–78.8] and 10.2 months [8.1–12.4] ($p < 0.001$) respectively. Progression free survival (PFS) of patients with or without downstaging were 20.8 months [14.8–26.8] and 5.4 months [4.7–6.1] ($p < 0.001$) respectively. In patients who achieved downstaging, PFS was higher in patients who had surgery (median not achieved). Two variables were independently associated to downstaging: BCLC score ($p = 0.049$) and ALBI score ($p = 0.042$).



Conclusion: These results suggest that TARE could be an effective treatment leading to downstaging of 40% patients with unresectable HCC, and allowed curative treatment in 57% of them. Combination of TARE followed by curative treatment is associated with a 2 year-survival of 70% vs 0% in patients with no downstaging.

THU574

Preliminary evidence of safety and tolerability of atezolizumab plus bevacizumab in patients with hepatocellular carcinoma and Child-Pugh A and B cirrhosis: a real-world study

Antonio D'Alessio^{1,2}, Arndt Weinmann³, Peter Galle³, Vincent Gaillard⁴, Claudia Angela Maria Fulgenzi^{1,5}, Dominik Bettinger⁶, Bertram Bengsch⁶, Arndt Vogel⁷, Lorenz Balcar⁸, Bernhard Scheiner⁸, Suneetha Amara⁹, Mahvish Muzaffar⁹, Abdul Rafeh Naqash^{9,10}, Nicola Personeni^{2,11}, Tiziana Pressiani¹¹, Rohini Sharma¹, Matthias Pinter⁸, Alessio Cortellini¹, Lorenza Rimassa^{2,11}, David J. Pinato^{1,12}. ¹Imperial College London, Department of Surgery and Cancer, London, United Kingdom; ²Humanitas University, Department of Biomedical Sciences, Italy; ³Johannes Gutenberg University of Mainz, Mainz, Germany; ⁴F. Hoffmann-La Roche Ltd., Basel, Switzerland; ⁵Policlinico Universitario Campus Bio-Medico, Division of Medical Oncology, Roma, Italy; ⁶Department of Medicine II (Gastroenterology, Hepatology, Endocrinology and Infectious Diseases), Freiburg University Medical Center, Faculty of Medicine, University of Freiburg, Freiburg, Germany; ⁷Hannover Medical School, Hannover, Germany; ⁸Division of Gastroenterology and Hepatology, Department of Internal Medicine III, Medical University of Vienna, Vienna, Austria; ⁹Division of Hematology/Oncology, East Carolina University, 600 Moye Boulevard, Greenville, NC, 27834, USA; ¹⁰Medical Oncology/TSET Phase 1 program, Stephenson Cancer Center, University of Oklahoma USA; ¹¹IRCCS Humanitas Research Hospital, Humanitas Cancer Center, Cascina Perseghetto, Italy; ¹²Division of Oncology, Department of Translational Medicine, University of Piemonte Orientale, Novara, Italy
Email: a.dalessio@imperial.ac.uk

Background and aims: Atezolizumab plus bevacizumab (A+B) is new standard of care for first-line treatment of unresectable hepatocellular carcinoma (HCC). No evidence exists as to its use in routine clinical practice in patients with impaired liver function.

Method: This retrospective, multi-centre observational study was conducted across 7 tertiary centres and collected 64 HCC patients consecutively treated with A+B. Safety outcomes included treatment-related adverse events (trAEs) graded according to CTCAE v5.0. We also assessed overall survival (OS), progression-free survival (PFS), overall response (ORR) and disease control rates (DCR) defined by RECIST v1.1 in patients treated according to label.

Results: Fifty-four patients had Barcelona Clinic Liver Cancer (BCLC)-C stage HCC (84%), mostly secondary to non-viral aetiology (n = 30; 47%) and Hepatitis C virus (n = 24; 37%). Forty-three patients (67%) suffered from any trAE, of which 11 (17%) were G3 and 1 (2%) G4. Compared to Child-Pugh A (n = 46, 72%), Child-Pugh B patients showed comparable distribution of trAEs, with similar rates of bevacizumab-related bleedings and atezolizumab-related AEs. In the 44 patients (69%) with a pre-treatment esophagogastroduodenoscopy, presence and grade of varices did not correlate with gastrointestinal bleeding events. Median OS of patients treated in first line was 12.7 months (95% CI, 7.6–12.7), while median PFS was 6.97 months (95% CI, 2.8–11.3). ORR and DCR were respectively 29% and 67%, with no difference between patients with Child-Pugh A and B cirrhosis.

Conclusion: This study confirms reproducible efficacy and safety of A + B in routine practice. Child-Pugh B patients had similar tolerability and radiologic response compared to Child-Pugh A patients, warranting prospective evaluation of atezolizumab plus bevacizumab in this treatment-deprived population.

THU575

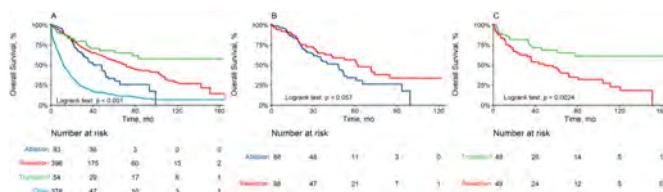
Comparative effectiveness of treatment for early-stage intrahepatic cholangiocarcinoma

Yi-Te Lee¹, Amit Singal², Marie Lauzon³, Michael Luu³, Vatche Agopian¹, Mazen Nouredin³, Tsuyoshi Todo³, Irene Kim³, Kambiz Kosari³, Nicholas Nissen³, Gregory Gores⁴, Ju Dong Yang³.
¹University of California, Los Angeles, Los Angeles, United States;
²University of Texas Southwestern Medical Center, United States;
³Cedars-Sinai Medical Center, Los Angeles, United States; ⁴Mayo Clinic Rochester MN, Rochester, United States
 Email: judong.yang@cshs.org

Background and aims: Incidence rates of intrahepatic cholangiocarcinoma (iCCA) continue to increase in western countries. Despite increases in the detection of early-stage iCCA, comparative effectiveness of treatment for early-stage iCCA remains unknown.

Method: We performed a retrospective cohort study using the National Cancer Database (NCDB), which represents more than 70 percent of newly diagnosed cancer cases nationwide. Patients diagnosed with single iCCA less than 3 cm in size without lymph node or extrahepatic involvement between 2004 and 2018 were analyzed. Multivariable cox regression was used to compare the efficacy of treatments. Propensity score matched analyses were performed to compare the outcome between resection, liver transplant, and local ablation.

Results: 1093 patients received the following treatments: 464 (42%) resection, 113 (10%) ablation, 62 (6%) transplant, and 454 (42%) other noncurative treatments including best supportive care. Overall median survival was 71.1 months (95% confidence interval [CI]: 60.5–93.7), 48.0 months (95% CI: 33.1–52.1), 11.7 months (95% CI: 10.4–14.3) for resection, ablation, and other treatments, respectively. Median survival was not reached in patients who received liver transplant (95% CI: 77.4–nonestimable). One, three, and five year survival were 89% (95% CI: 86%–92%), 68% (95% CI: 63%–73%), 56% (95% CI: 51%–62%) for resection, 89% (95% CI: 83%–96%), 54% (95% CI: 45%–66%), 33% (95% CI: 23%–47%) for ablation, 89% (95% CI: 81%–98%), 73% (95% CI: 62%–86%), 68% (95% CI: 56%–83%) for liver transplant, 49% (95% CI: 44%–55%), 20% (95% CI: 16%–25%), 13% (95% CI: 10%–17%) for other treatments ($p < 0.001$) (Figure 1A). With surgical resection as a reference group, patients receiving liver transplant had improved overall survival (adjusted hazard ratio [aHR]: 0.61, 95% CI: 0.38–1.00) while those who underwent ablation (aHR: 1.32, 95% CI: 0.96–1.82) or other noncurative treatments (aHR: 3.95, 95% CI: 3.24–4.82) had worse overall survival. Propensity score matched analyses showed a trend toward higher mortality with ablation than resection (aHR: 1.46, 95% CI: 0.91–2.36) (Figure B) and reduced mortality with liver transplant compared to resection (aHR: 0.37, 95% CI: 0.18–0.78) (Figure C).



Conclusion: In early-stage iCCA patients, curative treatments are associated with improved survival. Surgical resection and liver transplantation are associated with improved survival compared to ablation.

THU576

Twenty-year trends in radiofrequency ablation for treatment-naïve hepatocellular carcinoma within the Milan criteria

Se Young Jang¹, Soo Young Park¹, Yu Rim Lee¹, Young Oh Kweon¹, Won Young Tak¹, Won Kee Lee², Sungmin Kim³. ¹School of Medicine, Kyungpook National University, Kyungpook National University Hospital, Internal Medicine, Daegu, Korea, Rep. of South; ²School of Medicine, Kyungpook National University, Medical Informatics; ³University of Ulsan, Biomedical Engineering, Korea, Rep. of South
 Email: wytak@knu.ac.kr

Background and aims: Radiofrequency ablation (RFA) is widely used to treat hepatocellular carcinoma (HCC) because of its safety, cost effectiveness, and liver function conservation. We examined temporal trends in the long-term results of percutaneous RFA for treatment-naïve HCC within the Milan criteria and analysed factors affecting treatment outcomes.

Method: We retrospectively analysed 1,099 HCC cases within the Milan criteria treated with percutaneous RFA from January 2000 to December 2019 at a single tertiary hospital. The follow-up period ranged from 0.3 to 247.9 months (median: 53.2 months). Overall survival, recurrence-free survival, and factors affecting survival and progression were analysed. A trend test was performed to analyse the changing trends of subject characteristics and treatment outcome.

Results: The overall and recurrence-free survival rates of patients improved in the later period. Viral hepatitis-related HCC decreased, while alcohol- or non-alcoholic fatty liver disease-related HCC increased from the earlier to the later period (P for trend < 0.001). Tumour size and alpha-fetoprotein levels decreased. Older age ($p < 0.001$), Child-Pugh class B ($p < 0.001$), the presence of cirrhosis ($p < 0.001$), non-viral aetiology ($p < 0.001$), and large tumour size ($p = 0.001$) were independent prognostic factors that predicted poor overall survival. Only large tumour size predicted local tumour progression ($p < 0.001$). Tumour location, such as subcapsular, subphrenic, or perivascular, was not a significant factor in survival or local tumour progression.

Conclusion: Twenty-year outcomes of RFA showed excellent results in treating early-stage HCC within the Milan criteria. Both subject characteristics and treatment outcomes of have changed over time. Advances in technology and antiviral therapy have improved treatment outcomes.

THU577

Incidence of hepatocellular carcinoma reduced in chronic hepatitis B patients treated with entecavir plus Biejia-Ruangan: extended follow-up of a multicenter, randomised, double-blinded, placebo-controlled trial

Dong Ji¹, Yan Chen¹, Zheng Dong¹, Xiao-he Xiao¹, Yongping Yang¹.
¹Fifth Medical Center of Chinese PLA General Hospital, Senior Department of Hepatology, Beijing, China
 Email: jidg302@126.com

Background and aims: Chronic hepatitis B virus (HBV) infection and liver cirrhosis have been proven to be high-risk factors for hepatocellular carcinoma (HCC), which is the fifth most common tumour worldwide and the second most common cause of cancer-related death in China. Over the past two decades, progress has been made in treating fibrosis with traditional Chinese medicine due to their multi-targeted molecular mechanism. In the present study, we aimed to compare incidence of HCC in chronic hepatitis B (CHB) patients treated with entecavir (ETV) plus Biejia-Ruangan (BJRG) versus entecavir (ETV) plus placebo.

Method: In this study, we extended to followed up the participants of a multicenter, randomised, double-blinded, placebo-controlled trial (NCT01965418) after the end of the original trial. Originally, we had randomised 1000 CHB patients in equal numbers (1:1) to receive either ETV plus BJRG or ETV plus placebo treatment. The eligible patients underwent paired biopsies at treatment baseline and week 72. Afterward, patients entered a long-term prospective

POSTER PRESENTATIONS

observational open-label study, and were monitored at least every 12 weeks. Surveillance for HCC was performed by ultrasonography and alpha-fetoprotein (AFP) at each visit. HCC was diagnosed by multi-phase dynamic contrast-enhanced MRI. Intention-to-treat analysis was performed with the use of Kaplan-Meier curves and log-rank test. The incidence of HCC was estimated with Cox proportional hazards regression models.

Results: Totally 1000 patients who received randomised treatment, 946 (94.6%) patients entered the open-label phase, and 872 (87.2%) completed 84-month follow-up. Overall (during a median follow-up of 89.0 months), 23 (4.6%) in ETV plus BJRG group and 43 (8.6%) patients in ETV plus placebo group developed HCC, cumulative HCC incidence was notably lower for ETV plus BJRG group than ETV plus placebo group (HR 0.52, 95%CI 0.32–0.87, $P=0.001$). one (0.2%) patient in the ETV plus BJRG group and 13 (2.6%) patients in the placebo group died. While there was no significant difference in non-HCC events (e.g., colorectal, thyroid or pancreatic cancer, upper gastrointestinal bleeding, ascites, etc.) between the two groups (HR 0.47, 95%CI 0.12–1.89, $P=0.280$).

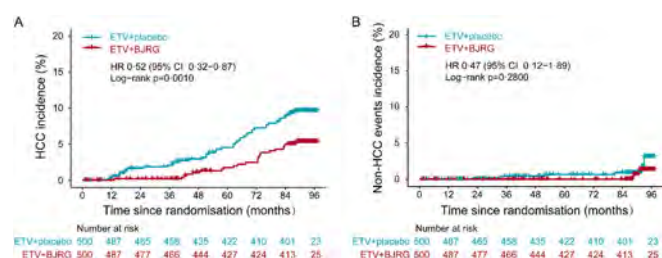


Figure: Cumulative incidence of HCC and Non-HCC events in ETV plus BJRG or ETV plus placebo groups

Conclusion: Comparing to ETV plus placebo treatment, ETV plus BJRG could further markedly reduce the incidence of HCC in chronic hepatitis B patients.

THU578

In vitro and in vivo preclinical efficacy of PD-L1-targeted liposomal doxorubicin as a combined therapy for the treatment of hepatocellular carcinoma

Daniela Gabbia¹, Antonella Grigoletto², Luana Cannella¹, Ilaria Zanutto¹, Veronica Mazzucco¹, Gianfranco Pasut², Sara De Martin¹. ¹University of Padova, Dept. of pharmaceutical and pharmacological sciences, Padova, Italy; ²University of Padova, Dept of pharmaceutical and pharmacological sciences, Padova, Italy
Email: sara.demartin@unipd.it

Background and aims: Hepatocellular carcinoma (HCC), the primary malignancy of the liver and the outcome of chronic liver diseases of different etiologies, remains a global health challenge, due to the lack of effective therapeutic options. The aim of this study is to evaluate a novel liposomal doxorubicin (DXR) formulation targeted with the PD-L1 checkpoint inhibitor atezolizumab, for the selective delivery of

DXR to cancer cells, with the double aim of enhancing its activity and decreasing its off-target toxicity.

Method: Two liposomal formulations were evaluated, i.e. atezolizumab-targeted liposomal DXR (Stealth Immunoliposomes, SIL_atezolizumab) and untargeted liposomal DXR (Stealth Liposomes, SL). The in vitro cytotoxicity of liposomal doxorubicin was evaluated after 72 h of treatment by means of the ATP assay on the three PD-L1 expressing HCC cell lines Hu7, HepG2 and Hepa1-6 (Figure). In vivo efficacy was evaluated in a syngeneic HCC mouse model, obtained by injecting the murine HCC cells Hepa1-6 in C57BL/6J immunocompetent mice. SIL_atezolizumab and SL were administered e.v. once a week for 4 weeks. Tumor volumes were measured by an electronic caliper and collected and weighed at sacrifice for further analyses.

Results: Atezolizumab targeting increased the *in vitro* cytotoxic effect of liposomal DXR in HepG2 and Hepa1-6 cells, showing significant lower IC50 values with respect to SL ($p<0.01$ and $p<0.05$, respectively). Both SL and SIL_atezolizumab decreased tumor growth *in vivo* since tumor volumes measured at sacrifice were significantly lower in treated mice compared to controls ($p<0.05$). A slight increase of survival was observed in SIL_atezolizumab treated mice.

Conclusion: PD-L1-targeted liposomal doxorubicin is effective in limiting HCC cells growth in vitro and in vivo. This approach could open new avenues for HCC therapy, using two already approved two drugs, joined in a novel combined formulation.

THU579

LiMax facilitates patient selection prior radioembolization for patients with hepatocellular carcinoma in liver cirrhosis

Catherine Leyh¹, Niklas Heucke², Clemens Schotten¹, Matthias Buechter¹, Lars Bechmann³, Marc Wichert⁴, Alexander Dechene⁵, Ken Hermann⁶, Antonios Katsounas⁷, Mustafa Özcürümez⁷, Dominik Heider⁸, Svenja Sydor^{7,9}, Johannes M. Ludwig⁶, Jens Theysohn⁶, Robert Damm¹⁰, Maciej Powerski¹⁰, Maciej Pech¹⁰, Ali Canbay⁷, Jochen Weigt², Verena Keitel-Anselmino¹, Christian Lange¹, Jan Best⁷, Paul Manka⁷. ¹University Hospital Essen, Department of Gastroenterology and Hepatology, Essen, Germany; ²Otto-von-Guericke University Hospital Magdeburg, Department of Gastroenterology, Hepatology and Infectious Diseases, Magdeburg, Germany; ³University Hospital Knappschaftskrankenhaus Bochum, Department of Internal Medicine, Bochum, Germany; ⁴University Hospital Essen, Central Laboratory, Essen, Germany; ⁵University Hospital Nürnberg, Nürnberg, Germany; ⁶University Hospital Essen, Radiology, Essen, Germany; ⁷University Hospital Knappschaftskrankenhaus Bochum, Department of Internal Medicine, Bochum, Germany; ⁸University Margurg, Marburg, Germany; ⁹University Hospital Knappschaftskrankenhaus Bochum, Department of Internal Medicine, Bochum, Germany; ¹⁰Otto-von-Guericke University Hospital Magdeburg, Radiology, Magdeburg, Germany
Email: svenja.sydor@rub.de

Background and aims: LiMax is a non-invasive test for liver function, measuring the maximum metabolic capacity for ¹³C-Methacetin by

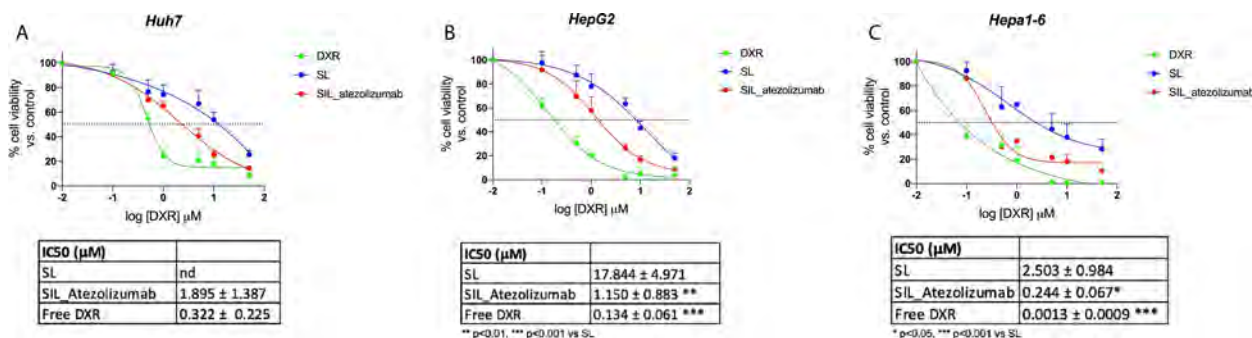


Figure: (abstract: THU578): Anti-proliferative effect of liposomal doxorubicin and IC50 values after 72 h-treatment.

the liver-specific enzyme CYP 450 1A2. Recently, radioembolization (RE) has demonstrated a non-inferior survival outcome compared to systemic therapy for advanced hepatocellular carcinoma (HCC). Therefore, current guidelines recommend RE for patients with advanced HCC and preserved liver function who are unsuitable for transarterial chemoembolization (TACE) or systemic therapy. However, despite the excellent safety profile of RE, post-therapeutic hepatic decompensation remains a serious complication that is difficult to be predicted by standard laboratory liver function parameters or imaging modalities. Our study investigates the potential of LiMAX for predicting post-interventional.

Method: In total, 50 patients with HCC with or without liver cirrhosis and not amenable to conventional locoregional or systemic treatments were included in the study. The study was carried out in a two-step fashion, including a retrospective and a prospective cohort. In both cohorts, LiMAX was carried out one day before RE (baseline). Standard liver function parameters were assessed at baseline, day 28, and day 90 after RE. First, the relationship between baseline LiMAX and pre- and post-interventional liver function parameters was analyzed in the retrospective cohort and subsequently validated in the prospective cohort. Subsequently, the ideal cutoff for LiMAX to predict post-interventional hepatic decompensation has been determined in the prospective part of the study.

Results: We observed a significant correlation between baseline LiMAX and Bilirubin, Albumin, ALBI-Grade, and MELD Score, especially at day 28 in the prospective cohort. Patients presenting with Child-Pugh B Score 28 days after RE had a significantly lower baseline LiMAX than those with a Child-Pugh A Score ($223.5 \mu\text{g/kg/h}$ vs. $309 \mu\text{g/kg/h}$, $p=0.0263$). Using the ROC curve analysis, the potential of LiMAX for predicting hepatic decompensation after RE was determined and compared to MELD Score and ALBI Grade. LiMAX achieved an AUC of 0.8117. Patients with LiMAX values $<238 \mu\text{g/kg/h}$ had a significantly higher risk of suffering hepatic decompensation after RE.

Conclusion: Patients with low LiMAX values ($<238 \mu\text{g/kg/h}$) despite Child-Pugh A situation at baseline have a significantly increased risk of hepatic decompensation after RE. Therefore, LiMAX can be used as an additional tool to identify patients at high risk of post-interventional hepatic failure.

THU580

The efficacy of molecular targeted therapies after atezolizumab plus bevacizumab in patients with unresectable hepatocellular carcinoma (HCC) in Japan

Kaoru Tsuchiya¹, Yuka Hayakawa¹, Yutaka Yasui¹, Tatsuya Kakegawa¹, Mayu Higuchi¹, Kenta Takaura¹, Shohei Tanaka¹, Chiaki Maeyashiki¹, Shun Kaneko¹, Nobuharu Tamaki¹, Hiroyuki Nakanishi¹, Masayuki Kurosaki¹, Namiki Izumi¹. ¹Musashino Red Cross Hospital, Department of Gastroenterology and Hepatology, Japan
Email: tsuchiyaakaoru5@gmail.com

Background and aims: In systemic therapy for unresectable HCC, 6 regimens (sorafenib, regorafenib, lenvatinib, ramucirumab, atezolizumab plus bevacizumab, and cabozantinib) have been approved in Japan. Atezolizumab plus bevacizumab (atez+bev) is recommended as 1st-line, and there is no established regimen after atez+bev. We investigated the efficacy of the other 5 regimens after atez+bev.

Method: A total of 76 patients who received atez+bev at our institution between Oct 2020 and Sep 2021 was enrolled.

Tumor assessments in accordance with RECIST v1.1 were done using dynamic CT or MRI every 6–12 weeks. Clinical course, including the efficacy of molecular targeted therapies after atez+bev was investigated retrospectively.

Results: The median age of the patients was 73 years. The median ALBI score was -2.19 , and 58% of the patients were modified ALBI grade 2b. Line of treatment was 1st ($n=41$), 2nd ($n=19$), 3rd ($n=7$), 4th ($n=5$), 5th ($n=3$), and 6th-line ($n=1$). Forty-eight (63%) of the patients were BCLC stage B, and 28 patients were BCLC stage

C. Median overall survival (OS) was not reached, and the 6-months survival rate was 83.0%. The median follow-up duration was 6.4 months, and the median time to progression (TTP) was 6.8 months. Overall response rate (ORR) in 1st-line and later-line were 30.5 and 13.5%. Disease control rate (DCR) in 1st-line and later-line were 86.1% and 66.7%. Discontinuation of atez+bev due to disease progression was observed in 33 patients, while discontinuation due to adverse events was reported in 12 patients. In the 12 patients, lenvatinib ($n=4$), sorafenib-regorafenib ($n=1$), cabozantinib ($n=3$), and TACE ($n=3$) were performed after atez+bev. Three patients received multiple therapies. Four of 12 (33%) patients received only supportive therapy. In the 33 patients with disease progression, 5 patients (15%) received only supportive therapy, and all 5 patients were pretreatment PS 1 or modified ALBI 2b. Of the 33 patients, 2 were treated with HAIC, and 26 received other molecular targeted therapies after atez+bev. Sorafenib was administered after atez+bev in 5 patients, and 2 patients showed SD. Regorafenib was started in 4 patients, and 2 patients showed SD. Lenvatinib was started in 12 patients, and ORR and DCR were 22% and 67%. Ramucirumab was administered in 3 patients, and 1 patient showed SD. Cabozantinib was started in 14 patients, and ORR and DCR were 14% and 80%. In total, 33 of 45 (73%) patients who discontinued atez+bev received molecular targeted therapy.

Conclusion: Discontinuation of atez+bev due to adverse events in real-world practice was similar to the clinical trial, and all patients with pretreatment PS 0 and modified ALBI 1 or 2a could receive post-atez+bev therapies after disease progression. The efficacy of molecular targeted agents after atez+bev would be different from the results of the past clinical trials without immunotherapy.

THU581

The LiMAX level before transarterial chemoembolization or radioembolization is a predictor for short-time survival in patients with early stage HCC

Janett Fischer¹, Stella Wellhöner¹, Sebastian Ebel², Bettina Maiwald^{2,3}, Steffen Strocka^{2,3}, Tim-Ole Petersen^{2,3}, Albrecht Boehlig¹, Florian Gerhardt¹, Rhea Veelken¹, Timm Denecke², Thomas Berg¹, Florian van Bömmel¹. ¹Division of Hepatology, Department of Medicine II, University Hospital Leipzig, Leipzig, Germany; ²Department of Diagnostic and Interventional Radiology, University Hospital Leipzig, Leipzig, Germany; ³Clinic for Diagnostic and Interventional Radiology, St. Elisabeth and St. Barbara Hospital Halle, Halle (Saale), Germany
Email: janett.fischer@medizin.uni-leipzig.de

Background and aims: Transarterial chemoembolization (TACE) and transarterial radioembolization (TARE) are standard treatment strategies for patients with hepatocellular carcinoma (HCC). The liver maximum capacity test (LiMAX) is a potential monitoring tool for post-interventional liver failure. The study aimed to investigate the correlation of LiMAX with patients' response to TACE or TARE treatment and the severity of adverse events after therapy as well as short-term and overall survival.

Method: In this study, 69 patients with TACE ($n=57$) or TARE ($n=12$) treatment were enrolled. Liver function was assessed on the day before as well as at 4 weeks after TACE or TARE using the LiMAX test and the well-established biochemical markers as well as MELD, CHILD Pugh and ALBI scores. Adverse events were each recorded over 4 weeks after the intervention. Survival was followed up until 3 years.

Results: A complete response to TACE/TARE and stable disease were observed in 10.3% and 51.5% of patients, respectively, and progressive disease in 38.2%. Mild adverse events developed in 48.5% of patients whereas 14.7% suffered from severe complications such as ascites and hepatic encephalopathy. LiMAX levels did not show a significant association with the occurrence of adverse events, laboratory parameters, liver function-associated scores and tumor response. However, survival analysis showed significant lower 30-day and 60-day survival rates for patients with LiMAX $\leq 150 \mu\text{g/kg/h}$ before

POSTER PRESENTATIONS

treatment compared to patients with LiMAX >150 µg/kg/h levels (30-day: 86.7% ± 8.8% vs. 100%, $p = 0.006$; 60-days: 86.7% ± 8.8% vs. 98.1% ± 1.8%, $p = 0.048$). When the patients were divided into groups according to the BCLC stage (BCLC A: $n = 32$, BCLC B: $n = 29$), significant differences in survival rates were detected for early but not for intermediate disease stage. The survival rates of patients with BCLC A stage with LiMAX ≤150 µg/kg/h were significantly lower after 30 days (75.0% ± 15.3% vs. 100%, $p = 0.011$) and 90 days (62.5% ± 17.7% vs. 95.8% ± 4.1%, $p = 0.011$) compared to those of patients with higher LiMAX levels. This was even more pronounced after 180 days with 50.0% ± 17.7% vs. 95.8% ± 4.1%, ($p = 0.001$) survival.

Conclusion: The LiMAX test identifies patients with early stage HCC and reduced short-time survival after transarterial treatment.

THU582

Implementation of a new prognostic scoring system after major hepatectomy in curative intent for perihilar cholangiocarcinoma

Christian Benzing¹, Thea-Charlotte Fritsch¹, Lena Haiden¹, Felix Krenzien¹, Alexa Mieg¹, Annika Wolfsberger¹, Cecilia Atik¹, Nora Nevermann¹, Uli Fehrenbach², Wenzel Schöning¹, Moritz Schmelzle¹, Johann Pratschke¹. ¹Charité University Medicine Berlin, Department of Surgery | Campus Charité Mitte and Campus Virchow Klinikum, Berlin, Germany; ²Charité University Medicine Berlin, Department of Diagnostic and Interventional Radiology, Berlin, Germany
Email: christian.benzing@charite.de

Background and aims: Major hepatectomy (MH) is the only curative therapy option for patients with perihilar cholangiocarcinoma (PHC). Despite recent advancements in adjuvant treatments and perioperative management, recurrence rates are still high and overall prognosis is poor. Current staging systems such as the American Joint Committee on Cancer (AJCC)/the Union for International Cancer Control (UICC) or the Bismuth staging system fail to adequately depict the patients' risk profile in terms of tumor recurrence. The present study seeks to establish a reliable scoring system that allows to classify the risk of tumor recurrence for individual patients in order to improve surveillance and adjuvant treatment programs.

Method: In this retrospective study, all patients undergoing MH for PHC at our department between January 2005 and August 2018 were retrospectively reviewed and analyzed. Demographic variables as well as perioperative, histopathological data and information on recurrence and overall survival were collected. After excluding postoperative 90-day mortality ($n = 38$, 14%), a uni- and multivariate logistic cox regression analysis was performed to identify factors associated with tumor recurrence. Subsequently, a score was assigned to each independent risk factor, which was summed up to a prognostic score ranging from 0 to 3 was created.

Results: We included 232 patients in the analysis. Median age was 64 years (33–86). The majority of patients had Bismuth-Corlette IV tumors (42%, $n = 97$) and UICC stage IIIb (41%, $n = 93$). Tumor-free resection margins (R0) were achieved in 160 patients (70%), 131 patients were lymph node negative (N0, 57%). The 1–3- and 5-year disease-free survival (DFS) and overall survival (OS) rates were 77%, 36% and 20% vs. 82%, 45% and 24%, respectively. Multivariate cox regression showed that R1-status (Hazard Ratio, HR = 1.525, 95% Confidence interval, CI: 1.021–2.277, $p = 0.039$), V1 status (HR = 2.187, 95% CI: 1.378–3.470, $p = 0.001$), and N+ status (HR = 1.856, 95% CI = 1.272–2.709, $p = 0.001$) were independently associated with tumor recurrence. When calculating the prognostic score, 82 patients (35%) had a score of 0 points, 72 patients (31%) had a score of 1 point, 32 patients (14%) had a score of 2, and 13 patients (6%) had a score of 3 points. Kaplan Meier analysis showed highly significant correlation of disease-free survival (DFS) and overall survival (OS) with the scoring system ($p < 0.001$).

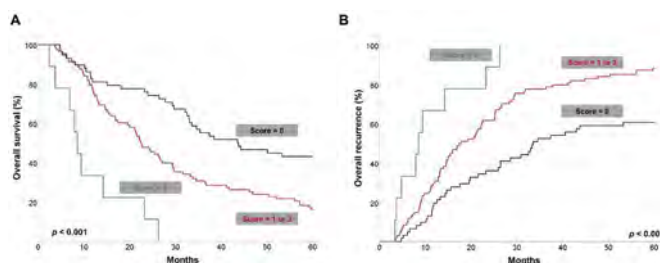


Figure 1: Overall (A) and Disease-free survival (B) after curative resection for perihilar cholangiocarcinoma according to the proposed prognostic score.

Conclusion: We proposed a simple scoring system that showed highly significant correlations with the clinical outcome (DFS and OS). This is of particular clinical significance since it allows a better risk stratification when compared to conventional scoring systems such as UICC and Bismuth stages.

THU583

The effect of discordance between preoperative imaging and postoperative pathology on the prognosis of hepatocellular carcinoma

Woo Sun Rou¹, Byung Seok Lee², Hyuk Soo Eun², Seok Hyun Kim², Hong Jae Jeon², In Sun Kwon³. ¹Chungnam National University Sejong Hospital, Gastroenterology and Hepatology, Sejong-si, Korea, Rep. of South; ²Chungnam National University Hospital, Gastroenterology and Hepatology, Daejeon city, Korea, Rep. of South; ³Chungnam National University Hospital, Clinical Trial Center, Statistics Office, Biomedical Research Institute, Daejeon city, Korea, Rep. of South
Email: gie001@cnuh.co.kr

Background and aims: In patients who have undergone surgical resection, the discordance between preoperative imaging and postoperative pathological findings may be found. There was a report that the mismatch of the Milan criteria before and after liver transplantation (LT) was reported to be 22.0–27.2% and had an effect on the survival rate. However, there is no studies about impact of this discordance in patients who have undergone surgical resection. In this study, preoperative imaging and postoperative pathologic findings were compared for tumor size, number, vascular or biliary tract invasion, and lymph node (LN) metastasis. In addition, the survival rate according to the discrepancy for each factor is compared, and according to the number of discrepancies, the impact on HCC prognosis is investigated.

Method: Among the 13,838 patients with HCC extracted randomly from the 2008–2016 national cohort of the Korean Central Cancer Registry, we selected the 2,781 patients who had undergone surgical resection or LT. And we evaluated the concordance of tumor maximal diameter, tumor number, bile duct invasion, LN metastasis, and vascular invasion including portal vein (PV), hepatic vein (HV), hepatic artery (HA) by comparing preoperative imaging findings with postoperative pathologic findings. In addition, the survival rate was compared by Kaplan-Meier according to the number of discrepancies, and further analyzed by Cox proportional hazards regression analysis.

Results: Vascular invasion including HA, HV and PV invasion had a poorer prognosis than the both negative group when either of the imaging findings or pathological findings were positive ($p = 0.001$ and $p < 0.001$, respectively). In particular, PV invasion, when both findings were positive, was significantly worse prognosis ($p < 0.001$). Bile duct invasion had a poorer prognosis when pathological findings were positive than those that were not ($p = 0.001$), and there was no difference in survival rate when pathologic findings were negative even if bile duct invasion was suspected on imaging findings ($p = 0.911$). When analyzing according to the number of mismatched factors among seven factors, as the number of mismatched factors increased, the prognosis of HCC patients was poor ($p < 0.001$). Multivariate analysis also showed that the number of discrepancies

(for all concordance, vs. 1 discrepancy HR 1.529, $p=0.001$ or vs. 2 discrepancy, HR 2.889, $p<0.001$ or vs. 3 discrepancy, HR 3.986, $p<0.001$, respectively), discrepancy in tumor diameter (HR 0.683, $p=0.003$), and discrepancy in LN metastasis (HR 2.399, $p=0.001$) were independent factors for the HCC prognosis.

Conclusion: This study revealed for the first time that the more factors that did not match the preoperative imaging findings and the postoperative pathological findings is associated with the poorer survival rate in patients undergoing surgical resection as independent predictive factor.

THU584

Early Nivolumab addition to Regorafenib in patients with hepatocellular carcinoma progressing under 1st line therapy (GOING trial). Interim analysis and safety profile

Marco Sanduzzi Zamparelli¹, Ana M Matilla², Jose Luis Lledó³, Sergio Muñoz Martínez¹, Maria Varela⁴, Mercedes Iñarrairaegui⁵, Christie Perelló⁶, Beatriz Minguez⁷, Neus Llarch¹, Laura Marquez Perez⁸, Antonio Guerrero³, Gemma Iserte¹, Andrés Castano-García⁴, Laura Carrión⁸, Jordi Rimola⁹, Maria Ángeles García-Criado⁹, Gema Domenech¹⁰, Loreto Boix¹, Jordi Bruix¹, María Reig¹. ¹Hospital Clinic of Barcelona, IDIBAPS, CIBERhd, University of Barcelona, BCLC group. Liver Unit., Barcelona, Spain; ²Hospital General Universitario Gregorio Marañón, CIBERhd, Gastroenterology Department, Madrid, Spain; ³Hospital Universitario Ramón y Cajal, IRYCIS, CIBERhd, University of Alcalá, Gastroenterology and Hepatology Department, Madrid, Spain; ⁴Hospital Universitario Central de Asturias, IUOPA, ISPA, Universidad de Oviedo., Liver Unit, Gastroenterology Department, Oviedo, Spain; ⁵Clinica Universidad de Navarra, IDISNA and CIBEREHD, Liver Unit and HPB Oncology Area, Pamplona, Spain; ⁶Hospital Universitario Puerta de Hierro, IDIPHISA, CIBERhd, Gastroenterology Department. Hepatology Unit, Madrid, Spain; ⁷Vall d'Hebron Institute of Research (VHIR), Vall d'Hebron Barcelona Hospital Campus, CIBERhd, Universitat Autònoma de Barcelona, Liver Unit, Hospital Universitari Vall d'Hebron, Liver Diseases Research Group, Barcelona, Spain; ⁸Hospital General Universitario Gregorio Marañón, Gastroenterology Department, Madrid, Spain; ⁹Hospital Clínic de Barcelona, IDIBAPS, University of Barcelona, BCLC Group, Radiology Department, Barcelona, Spain; ¹⁰Medical Statistics Core Facility, IDIBAPS-Hospital Clínic, Barcelona, Spain
Email: mreig1@clinic.cat

Background and aims: Regorafenib (Rego) improves survival in patients with hepatocellular carcinoma (HCC) (RESORCE trial) while Nivolumab (Nivo) is also safe and active in terms of radiologic response (15–20% objective response) in second-line. The GOING trial (NCT04170556) is an investigator-initiated phase I/IIa study assessing the safety of Rego plus Nivo in HCC patients who progress and tolerate sorafenib (Cohort A) or who discontinue atezolizumab plus bevacizumab (Cohort B).

Method: Patients from cohort A receive Rego as monotherapy for the first 2 cycles (starting dose 160 mg/day, 3 weeks on/1 week off and adjusted for adverse events [AEs]) and Nivo is added at day 1 of cycle 3 (the first 10 patients at 3 mg/kg; since they did not present serious-AE (SAE), the final dose is 240 mg every two weeks). Treatment continues until unacceptable AEs, symptomatic tumor progression, patient decision or death. Safety is measured by the rate of AEs, rate of treatment related-AEs (Tr-AE), rate of AEs leading to treatment discontinuation and rate of death. Severity of AEs are evaluated according to CTCAE v5.0. A futility analysis using the non-binding Lan and DeMets beta-spending functions with a boundary of $p=0.814$ is mandated when 32.8% of cohort A has data of tumor assessment at least at week 16 by RECIST 1.1.

Results: Fifty-one patients have been enrolled in cohort A as of May 15, 2021. The first 30 (BCLC-C 73%) were considered in this safety analysis. All patients developed at least one AE, 29 (96.7%) had Tr-AEs of any grade and 10 (33.3%) had grade 3 (no grades 4 or 5 have been reported). Ten (33.3%) patients had a Rego-related AE, 4 (13.3%) Nivo-

related, and 4 (13.3%) Tr-AE grade 3 of special interest. Table 1 describes the profile Tr-AE occurring in >10% of patients. Only 4 (13.3%) patients developed Tr-SAE, 3 (10%) Rego-related and 3 (10%) Nivo-related. Four patients discontinued the study due to physician decision, 2 for progression, and 2 for AEs (one related to study treatment). One patient had surgical resection after treatment discontinuation and a complete necrosis was observed at pathology.

Table 1. Profile of Tr-AE occurring in >10% in the first 30 included patients.

Adverse Events	Any Grade		Grade 3	
	Patients, n	Patients, %	Patients, n	Patients, %
Hand-foot-skin reaction	17	56.6	3	10.0
Asthenia	13	43.3	-	-
Diarrhea	11	36.7	1	3.3
Decreased Appetite	9	30.0	-	-
Arterial Hypertension	9	30.0	2	6.7
Hypertransaminasaemia	9	30.0	1	3.3
Hyperbilirubinaemia	6	20.0	1	3.3
Aspartate Aminotransferase Increased	6	20.0	1	3.3
Abdominal Pain	6	20.0	-	-
Dysphonia	5	16.7	-	-
Alanine Aminotransferase Increased	4	13.3	-	-

* None of these Tr-AE was grade 4-5

Conclusion: The sequential combination of Rego-Nivo has a manageable safety profile. Less than one third of the patients developed grade 3/4 Tr-AE and there was no treatment-related death. Futility analysis allowed to continuing recruitment.

THU585

Impact of endobiliary radiofrequency ablation on survival of patients with advanced extrahepatic cholangiocarcinoma under systemic chemotherapy

Christian Möhring¹, Maria Angeles Gonzalez-Carmona¹, Robert Mahr¹, Taotao Zhou¹, Alexandra Bartels¹, Farsaneh Sadeghlar¹, Maximilian Bolch¹, Annabelle Vogt¹, Dominik Kaczmarek¹, Dominik Heling¹, Leona Dold¹, Jacob Nattermann¹, Vittorio Branchi², Hanno Matthaei², Steffen Manekeller², Jörg Kalff², Christian Strassburg¹, Raphael Mohr¹, Tobias Weismüller¹. ¹University Hospital of Bonn, Germany, Internal Medicine I, Bonn, Germany; ²University Hospital of Bonn, Germany, Department of Surgery, Bonn, Germany
Email: mariangelesgc@gmx.net

Background and aims: Prognosis of patients with advanced extrahepatic cholangiocarcinoma is still poor. The current standard first-line treatment is systemic chemotherapy with gemcitabine and a platinum derivate. Additionally, endobiliary radiofrequency ablation (eRFA) can be applied to treat biliary obstructions. The aim of this study was to evaluate the additional benefit of scheduled regular eRFA in a real-life patient cohort with advanced extrahepatic cholangiocarcinoma under standard systemic chemotherapy.

Method: This is a single center retrospective analysis. All patients with irresectable extrahepatic cholangiocarcinoma treated at University Hospital Bonn between 2010 and 2020 were eligible for inclusion. Patients were stratified according to treatment: standard systemic chemotherapy (n=26) vs. combination of eRFA with standard chemotherapy (n=40). Overall survival (OS), progression free survival (PFS), feasibility and toxicity were analyzed using univariate and multivariate approaches.

Results: Combined eRFA and chemotherapy resulted in significantly longer median OS (17.3 vs. 8.6 months, $p=0.004$) and PFS (12.9 vs. 5.7 months, $p=0.045$) compared to the chemotherapy only group. While groups did not differ regarding age, sex, tumor stage and chemotherapy treatment regimen, mean MELD was even higher (10.1 vs. 6.7, $p=0.015$) in the eRFA+CT group. The survival benefit of concomitant eRFA was more evident in the subgroup with locally advanced tumors. Severe hematological toxicities (CTCAE grades 3–5) did not

POSTER PRESENTATIONS

differ significantly between the groups. However, therapy-related cholangitis occurred more often in the combined treatment group ($p = 0.031$).

Conclusion: Combination of eRFA and systemic chemotherapy was feasible, well-tolerated and could significantly prolong survival compared to standard chemotherapy alone. Thus, eRFA should be considered during therapeutic decision making in advanced extra-hepatic cholangiocarcinoma.

THU586

Interleukin 10 and Interferon Gamma levels are elevated in patients with hepatocellular carcinoma showing response to treatment with atezolizumab and bevacizumab

Sabine Lieb², Aaron Schindler², Johannes Niemeyer², Rhea Veelken², Janett Fischer², Rami Al-Sayegh², Thomas Berg², Florian van Bömmel².

¹Leipzig University Medical Center, Division of Hepatology, Department of Medicine II, Leipzig, Germany; ²Leipzig University Medical Center, Division of Hepatology, Department of Medicine II, Leipzig, Germany
Email: florian.vanboemmel@medizin.uni-leipzig.de

Background and aims: The combination treatment of the PD-L1 inhibitor atezolizumab plus bevacizumab (atezo/bev) has become standard of care in first line therapy in advanced hepatocellular carcinoma (HCC). However, prediction of treatment response is not well defined. Effector cytokines signalling (e.g. interferon gamma (IFN-g) is supposed to drive clinical response to immune checkpoint blockade. We have analysed circulating cytokine pattern in patients treated with atezo/bev.

Method: Thirty-three patients (31 male, mean age of 65 ± 11 (range 29–80) years) with advanced HCC (7 BCLC B, 26 BCLC C) treated at the University Cancer Center of Leipzig were retrospectively analysed. Twenty-eight patients had liver cirrhosis (23 Child-Pugh A, 5 Child-Pugh B), two underwent liver transplantation, two showed no hepatic disease and one had fatty liver disease. All together 136 cycles (mean 4.12, range 1–16 cycles) atezo/bev were applied to the patients. Tomography imaging was performed after 3 to 4 cycles of atezo/bev and evaluated according to mRECIST criteria. A cytokine panel including interleukin (IL)-1beta, interferon (IFN) alpha2, IFN-g, TNF alpha, IL-6, IL-8, IL-10, IL-12p70, Monocyte chemotactic protein 1 (MCP-1), IL-17A, IL-18, IL-23 and IL-33 was measured at baseline and correlated with treatment outcomes.

Results: The mean overall survival was 7 ± 5.3 (range 0–17) months. At the end of observation, 13 Patient showed stable disease (SD), 2 partial response (PR), 1 patient complete response (CR), 2 progressive disease (PD) and 15 patients died. Patients showing either CR, PR or SD at month 3 of treatment had higher mean baseline levels of IFN-g and IL-10 in comparison to patients with PD (IFN-g: 8.0 ± 5.48 (range 4.18–18.96) vs. 4.6 ± 0.87 (range 4.18–6.79), $p < 0.001$) and IL-10 (11.19 ± 9.6 (range 4.07–33.64) vs. 5.74 ± 2.05 (range 4.07–11.04), $p < 0.001$). At month six of treatment, patients with either CR, PR or SD still presented higher mean baseline levels of IFN-g in comparison to patients with PD (8.74 ± 6.01 (range 4.18–18.96) vs. 4.18 ± 0.0 , $p = 0.026$). There was no association of other cytokine levels measured with response to atezo/bev.

Conclusion: Response to atezo/bev in the treatment of HCC may depend on IFN gamma and IL-10 signalling. The value of these cytokines as response predictors needs to be evaluated in a larger cohort.

THU587

Potential feasibility of atezolizumab-bevacizumab therapy in patients with hepatocellular carcinoma: a real-world analysis

Benedetta Stefanini^{1,2}, Laura Bucci¹, Valentina Santi¹, Nicola Reggiori¹, Davide Rampoldi¹, Lorenzo Lani¹, Franco Trevisani¹.

¹S. Orsola-Malpighi Polyclinic, Division of Medical Semeiotics, Bologna, Italy; ²Bologna, Semeiotica Medica, Bologna, Italy
Email: benedetta.stefanini@studio.unibo.it

Background and aims: Option treatments for patients with unresectable hepatocellular carcinoma (HCC) not amenable/

responding to locoregional treatments is represented by systemic therapy, and sorafenib and lenvatinib, two tyrosine-kinase inhibitors (TKIs) are currently the standard of care, providing modest but significant benefit on survival. Recently, the IMBrave-150 trial has demonstrated that the combination of with atezolizumab plus bevacizumab (Atezo-Beva) is the best first-line systemic therapy for HCC patients, showing a clear superiority compared to sorafenib.

This study aimed at assessing the real-world potential feasibility of the Atezo-Beva therapy in a large cohort of HCC patients treated with TKIs.

Method: We retrospectively analysed 1448 patients diagnosed with unresectable HCC not amenable/not responding to locoregional treatments, treated with TKIs (sorafenib 98%, lenvatinib 2%) and followed-up from January 2010 to December 2020 by 24 Italian centres. The percentage of patients potentially amenable to Atezo-Beva treatment (according to IMBrave-150 trial criteria) and the overall survival (OS) of eligible/non-eligible patients were assessed.

Results: 423 (29.2%) of patients treated with TKIs were found to be qualified for the Atezo-Beva therapy. Their median OS was 17.3 months (95% CI 19.7–14.9) while that of non-eligible patients was 13.1 months (95% CI 14.5–11.6) ($p = 0.038$), likely due to better baseline clinical characteristics (Table 1). The main exclusion causes were a Child-Pugh class >A (399 cases) and a performance status >1 (187 cases). The proportion of eligible cases considering, as selection criterion, PLT >50000 mmc (instead of >75000 mmc requested by the IMBrave trial) increased by 43 cases (+2.9%), while including Child-Pugh Class B7 it increased by 85 patients (+5.9%).

	Eligible population n. 423	Non eligible population n. 1025	p
Age (years) N, (%) Median (range)	423 (100%) 69 (33-90)	1025 (100%) 69 (21-92)	0.198
Sex N, % M F	423 (100%) 344 (81%) 79 (19%)	1025 (100%) 843 (82%) 182 (18%)	0.679
Child-Pugh Class N (%) A B ¹ C	423 (100%) 423 (100%) 0 (0%) 0 (0%)	916 (89%) 478 (52%) 417 (46%) 21 (2%)	<0.001
BCLC N (%) 0 A B C D	423 (100%) 4 (1%) 56 (13%) 80 (19%) 283 (67%) 0 (0%)	966 (94%) 1 (0%) 117 (12%) 153 (16%) 663 (69%) 32 (3%)	0.007
MELD Score N (%) Median (range)	423 (100%) 8 (6-23)	900 (88%) 9 (6-31)	<0.001
Alpha-fetoprotein N (%) ≤10 ng/ml 11-200 ng/ml >200 ng/ml	391 (92%) 131 (31%) 125 (30%) 135 (32%)	828 (81%) 218 (26%) 293 (35%) 316 (38%)	0.036
ECOG (Performance Status) N (%) 0-1 >1	423 (100%) 423 (100%) 0 (0%)	959 (93.6%) 832 (87%) 127 (13%)	<0.001

¹ In Child-Pugh class B 258 (62%) patients showed a score of 7 (B7)
Figure 1. Characteristic of eligible population and not eligible population

Conclusion: Real world data indicate that no more than one-third of HCC patients treated with TKIs are potentially eligible for Atezo-Beva therapy. These patients have a better OS than non-eligible ones, owing to a better baseline clinical profile. Therefore, TKIs will remain the front-line approach for most of the HCC patients qualified for systemic therapy, due to the stringent selection criteria dictated by immunotherapy trials and the use of TKIs currently extended to Child-Pugh B patients. However, further prospective studies in real life may broaden Atezo-Beva indications.

THU588

Progression patterns and therapeutic sequencing following immune checkpoint inhibition for HCC: an observational study

Thomas Talbot¹, Antonio D'Alessio^{1,2}, Matthias Pinter³, Lorenz Balcar³, Bernhard Scheiner³, Thomas Marron⁴, Tomi Jun⁵, Sirish Dharmapuri⁴, Celina Ang⁴, Anwaar Saeed⁶, Hannah Hildebrand⁶, Mahvish Muzaffar⁷, Claudia Angela Maria Fulgenzi^{1,8}, Suneetha Amara⁷, Abdul Rafeh Naqash^{7,9}, Anuhya Gampa¹⁰, Anjana Pillai¹⁰, Yinghong Wang¹¹, Uqba Khan¹², Pei-Chang Lee¹³, Yi-Hsiang Huang^{13,14}, Bertram Bengsch¹⁵, Dominik Bettinger¹⁵, Yehia Abugabal¹⁶, Ahmed Kaseb¹⁶, Tiziana Pressiani¹⁷, Nicola Personeni^{2,17}, Lorenza Rimassa^{2,17}, Naoshi Nishida¹⁸, Masatoshi Kudo¹⁸, Arndt Weinmann¹⁹, Peter Galle¹⁹, Ambreen Muhammed¹, Alessio Cortellini¹, Arndt Vogel²⁰, David J. Pinato^{1,21}. ¹Imperial College London, Department of Surgery and Cancer; ²Humanitas University, Department of Biomedical Sciences; ³Medical University of Vienna, Department of Internal Medicine III; ⁴Tisch Cancer Institute, Mount Sinai Hospital, Department of Medicine, United States; ⁵Sema4, Stamford, CT, United States; ⁶Kansas University Cancer Center, Division of Medical Oncology, United States; ⁷East Carolina University, Division of Hematology/Oncology, United States; ⁸University Campus Bio-Medico, Department of Medical Oncology, Italy; ⁹National Cancer Institute, Division of Cancer Treatment and Diagnosis, Bethesda, Maryland, United States; ¹⁰The University of Chicago Medicine, Section of Gastroenterology, Hepatology and Nutrition, Chicago, United States; ¹¹The University of Texas MD Anderson Cancer, Department of Gastroenterology, Hepatology and Nutrition, United States; ¹²Weill Cornell Medicine/New York Presbyterian Hospital, Division of Hematology and Oncology, United States; ¹³Taipei Veterans General Hospital, Division of Gastroenterology and Hepatology, Department of Medicine, Taiwan; ¹⁴National Yang Ming Chiao Tung University School of Medicine, Institute of Clinical Medicine, Taiwan; ¹⁵Medical Center University of Freiburg, Department of Medicine II, Faculty of Medicine, Germany; ¹⁶The University of Texas MD Anderson Cancer Center, Dept of Gastrointestinal Medical Oncology, United States; ¹⁷Humanitas Cancer Center, IRCCS Humanitas Research Hospital, Medical Oncology and Hematology Unit, Italy; ¹⁸Kindai University Faculty of Medicine, Department of Gastroenterology and Hepatology, Osaka, Japan; ¹⁹University Medical Center of the Johannes Gutenberg-University Mainz, 1st Department of Internal Medicine, Gastroenterology and Hepatology, Germany; ²⁰Hannover Medical School, Department of Gastroenterology, Hepatology and Endocrinology, Germany; ²¹University of Piemonte Orientale "A. Avogadro," Division of Oncology, Department of Translational Medicine, Italy
Email: twt18@ic.ac.uk

Background and aims: Different approaches are available after progression of disease (PD) while on treatment with immune checkpoint inhibitors (ICI) for hepatocellular carcinoma (HCC), including continuation of ICI, switching to tyrosine kinase inhibitors (TKIs) and cessation of therapy. Little is known about progression patterns and their relationship with optimal sequencing and survival outcomes post-ICI.

Method: From an international consortium of 13 tertiary-care referral centres, we screened 604 HCC patients treated with ICIs, including only those who experienced PD by data cut-off. We evaluated post-progression survival (PPS) according to treatment strategy at PD and verified its relationship with radiologic patterns of progression: intrahepatic growth (IHG), new intrahepatic lesion (NIH), extrahepatic growth (EHG), new extrahepatic lesion (NEH) and new vascular invasion (nVI).

Results: 364 (60.3%) patients had PD during observation, mostly following PD-1/PD-L1 monotherapy (80%). Median PPS was 5.3 months (95%CI: 4.4–6.9; 271 events). At data cut-off, 165 patients (45%) received no post-progression anticancer therapy. Both IHG (HR 1.64 [95%CI: 1.21–2.22]; $p = 0.0013$) and nVI (HR 2.15 [95%CI: 1.38–3.35]; $p = 0.0007$) at PD were significantly associated with shorter PPS. Continuation of ICI therapy beyond PD occurred in 64 patients (17.6%). Multivariate models adjusted for progression patterns, treatment line, and ALBI grade and ECOG-PS at PD confirmed receipt of ICI beyond PD with (HR 0.17, 95%CI 0.09–0.32; $p < 0.0001$), or without subsequent TKI (HR 0.39, 95%CI 0.26–0.58; $p < 0.0001$) as predictors of prolonged PPS compared to no anticancer therapy.

Conclusion: ICI-TKI sequencing is a consolidated option in advanced HCC, with poorer prognosis predicted by nVI and IHG. Despite lack of recommendation, continuation of ICI beyond progression in HCC is adopted in clinical practice: efforts should be made to identify patients who benefit from this approach.

THU590

GALAD score correlates with therapy response for transarterial and systemic therapies in patients with hepatocellular carcinoma

Anne Olbrich¹, Johannes Niemeyer¹, Hendrik Seifert¹, Olga Gros², Florian Lordick³, Dirk Forstmeier³, Daniel Seehofer⁴, Robert Sucher⁴, Sebastian Rademacher⁴, Timm Denecke⁵, Sebastian Ebel⁵, Nicolas Linder⁵, Madlen Matz-Soja^{1,6}, Thomas Berg¹, Florian van Bömmel¹. ¹Leipzig University Medical Center, Department of Medicine II, Division of Hepatology, Leipzig, Germany; ²Helios Clinic Köthen, Department of Anesthesia and Intensive Care, Köthen, Germany; ³Leipzig University Medical Center, University Cancer Center Leipzig (UCC), Leipzig, Germany; ⁴Leipzig University Medical Center, Department of Visceral, Vascular, Thoracic and Transplant Surgery, Leipzig, Germany; ⁵Leipzig University Medical Center, Department of Diagnostic and Interventional Radiology, Leipzig, Germany; ⁶University of Leipzig, Rudolf-Schönheimer-Institute for Biochemistry, Leipzig, Germany
Email: anne.olbrich@medizin.uni-leipzig.de

Background and aims: The GALAD score is a biomarker-based scoring system used for prediction of early hepatocellular carcinoma (HCC) in patients with chronic liver disease. It consists of the two risk factors gender (G) and age (A) and levels of AFP-L3 (L), AFP (A), and DCP (D). So far, a possible association of baseline GALAD score and therapy response was not investigated. For patients with advanced HCC, loco-regional treatment approaches, such as transarterial chemoembolization (TACE) and transarterial radioembolization (TARE) as well as systemic therapies are available, but response to these therapies is highly variable. The study aim is to assess the value of the GALAD model as a response marker to these treatment approaches.

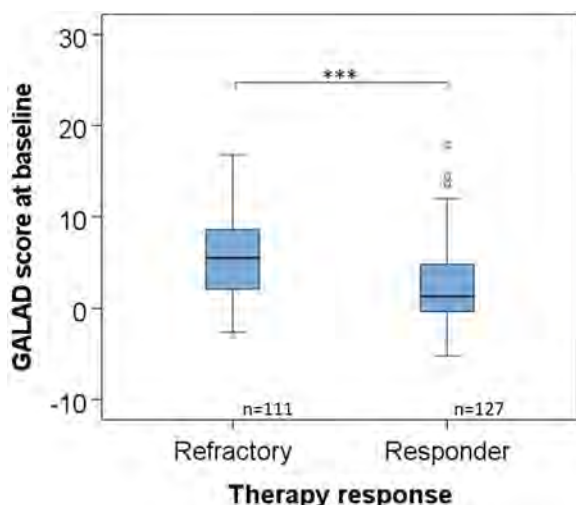
Method: In a retrospective German single-center study, 238 patients with HCC treated with either TARE or TACE or systemic drugs were enrolled. Serum samples at baseline were analyzed to evaluate the prognostic performance of the GALAD score. Treatment efficacy was evaluated by mRECIST criteria based on magnet resonance imaging (MRI) three months (10–14 weeks) after intervention.

Results: In our patient cohort ($n = 238$) the mean GALAD score at baseline was 3.96 [range, –5.19–17.89]. Baseline GALAD scores were

POSTER PRESENTATIONS

significantly higher in patients in BCLC stage B or C/D as compared to stages A.

At baseline, mean GALAD scores were significantly higher in the refractory group compared to response group (5.66 versus 2.49; $p < 0.001$; Fig.). Regarding the different therapy options, the GALAD score showed a significant discrimination between the refractory and responder in the transarterial therapy group ($p < 0.001$) as well as in the systemic treatment group ($p = 0.01$).



Using ROC analyses the GALAD score for response of transarterial or systemic treatment showed higher AUC (AUC = 0.704; $p < 0.001$) than the individual biomarkers AFP, AFP-L3, and DCP in the overall cohort (AUC = 0.685, 0.629 and 0.645, respectively).

Conclusion: The GALAD model is a potent predictor of tumor response to transarterial and systemic treatment in HCC at baseline.

THU591

Antiviral and antitumor activity of SCG101, an autologous HBV-specific T cell receptor engineered T cell (TCR-T) therapy in HBV-related advanced hepatocellular carcinoma (HCC) patients after receiving ≥ 2 prior lines of systemic therapies

Shunda Du¹, Yuhong Zhou², Xiujuan Qu³, Wei Wu⁴, Ke Zhang⁵, Xueshuai Wan¹, Wei Li², Dongmei Quan⁴, Karin Wisskirchen^{6,7}, Ulrike Protzer^{6,7}, Yun Peng Liu³. ¹Peking Union Medical College Hospital, Liver Surgery, Beijing, China; ²Zhongshan Hospital, Fudan University, Medical Oncology, Shanghai, China; ³The First Hospital of China Medical University, Medical Oncology, Shenyang, China; ⁴The Sixth People's Hospital of Shenyang, Hepatobiliary Surgery, Shenyang, China; ⁵SCG Cell Therapy, Shanghai, China; ⁶Technical University of Munich, Institute of Virology, Munich, Germany; ⁷Helmholtz Munich, Institute of Virology, Munich, Germany
Email: cmu_trial@163.com

Background and aims: Adoptive cell therapy with TCR-T cells targeting HBV antigens represents an innovative approach for treatment of HBV-related HCC. SCG101 is a first-in-class genetically modified autologous TCR-T with a natural high-avidity TCR directed towards the HLA-A*02-restricted HBsAg peptide S₂₀₋₂₈. We here report first results from an ongoing pilot, investigator-initiated trial (IIT) conducted to evaluate the safety as well as the antiviral and antitumor activity of SCG101.

Method: Patients with HBV-related HCC (HBsAg positive, HBeAg negative and HBV DNA $\leq 2 \times 10^3$ IU/ml), who are HLA-A*02 positive and have received at least two lines of systemic therapy including small-molecule tyrosine kinase inhibitors and PD-1 checkpoint inhibitors were eligible. Following leukapheresis, SCG101 TCR-T cells were manufactured using an automated closed system. Prior to intravenous infusion of SCG101, patients receive lymphodepleting

chemotherapy (fludarabine 25 mg/m²/day and cyclophosphamide 500 mg/m²/day for 3 consecutive days. Ascending dose levels of SCG101 at 1×10^7 /kg to 2×10^8 /kg TCR-transduced T cells were permitted according to protocol and safety assessment including dose-limiting toxicity (DLT) was adjudicated by a Safety Review Committee.

Results: As of Feb 28th, 2022, three HLA-A*02:01⁺ patients have been enrolled: subjects ST1301 and ST1401 received 5×10^7 /kg TCR-T cells, subject ST1204 received 1×10^8 /kg. Transduced T cells were detectable in peripheral blood of all three patients up to last visit. Two patients, ST1301 and ST1204 showed a rapid HBsAg reduction of >1.7 log within 28 days after infusion and sustained with continuous decline thereafter. The HBsAg drop was correlated with a transient ALT/AST flare without significant change of other liver function markers including albumin, bilirubin, etc. Tumor response assessment by mRECIST showed that these two patients had stable disease (SD) with target lesion reduction of 14.5% and 6.2%, respectively, and maintained SD up to last visit (96+ and 55+ days). Patient ST1401 had a transient HBsAg drop of ~ 0.2 log from day 1–4 post treatment and was diagnosed with progressive disease (PD) at day 28. For all patients, no DLT or drug-related serious adverse events (SAEs) have been observed to date. Drug-related adverse events were typical for a T-cell therapy associated cytokine-release syndrome and transient or reversible after treatment.

Conclusion: Systemic SCG101 TCR-T cell therapy was well tolerated and showed promising early signs of clinical efficacy in advanced HBV-related HCC patients who have exhausted available targeted and immunotherapy options. Early and sustained HBsAg reduction demonstrates encouraging antiviral activity with target engagement of SCG101 and might serve as a potential predictive marker of antitumor efficacy. Preliminary data support further systematic clinical evaluation.

THU592

Current trends and in-hospital mortality of transarterial chemoembolization (TACE) in Germany: a systematic analysis of hospital discharge data between 2010 and 2019.

Sven H Loosen¹, Sarah Krieg¹, Tobias Eßing¹, Andreas Krieg², Christoph Roderburg¹, Tom Lüdde². ¹University Hospital Düsseldorf, Clinic for Gastroenterology, Hepatology and Infectious Diseases, Düsseldorf, Germany; ²University Hospital Düsseldorf, Department of Surgery (A), Düsseldorf, Germany
Email: Sven.Loosen@med.uni-duesseldorf.de

Background and aims: Transarterial chemoembolization (TACE) represents a standard of care for intermediate-stage hepatocellular carcinoma (HCC) and is also increasingly performed in patients with cholangiocarcinoma (CCA) or liver metastases. Recently, newer particle-based TACE procedures have been introduced but comprehensive data on clinical trends of TACE as well as its in-hospital mortality in Germany are missing. A systematic evaluation of existing data sets and their careful interpretation can support a rational discussion aiming at further optimizing framework conditions of TACE.

Method: Based on standardized hospital discharge data provided by the German Federal Statistical Office, we systematically evaluate current clinical developments, associated post-interventional complications as well as in-hospital mortality of TACE in Germany between 2010 and 2019.

Results: A total of 49,595 individual cases undergoing TACE were identified within the observation period. The overall in-hospital mortality was 1.00% and significantly higher in females compared to males (1.12% vs. 0.93%; $p < 0.001$). We identified several post-interventional complications such as liver failure (51.49%), sepsis (33.87%), renal failure (23.9%) and liver abscess (15.87%), which were associated with a significantly increased in-hospital mortality. Moreover, in-hospital mortality significantly differed between the underlying indication for TACE (HCC: 0.83%, liver metastases: 1.22%,

and CCA: 1.40%) as well as between different embolization agents (liquid embolization: 0.80%, loaded microspheres: 0.92%, spherical particles: 1.54% and non-spherical particles: 2.84%), for which we observed large geographic differences in their frequency of use. Finally, in-hospital mortality was significantly increased in centers with a low annual TACE case volume (<15 TACE/year: 2.08% vs. >275 TACE/year: 0.45%).

Conclusion: We identified a variety of factors such as post-interventional complications, the embolization method used as well as the hospitals' annual case volume, which are associated with an increased in-hospital mortality following TACE. These data might help to further reduce mortality of this routinely performed local-ablative procedure in the future.

THU593

Pre-treatment cross-talk between the tumoural and peripheral immune system predicts response to checkpoint inhibition in advanced HCC: a single-cell study

Sarah Cappuyns^{1,2,3,4}, Gino Philips^{2,3}, Vincent Vandecaveye^{5,6}, Chris Verslype^{1,7}, Eric Van Cutsem^{1,7}, Diether Lambrechts^{2,3}, Jeroen Dekervel^{1,7}. ¹Digestive Oncology, Department of Gastroenterology, University Hospitals Leuven, Leuven, Belgium; ²Laboratory for Translational Genetics, Department of Human Genetics, KU Leuven, Leuven, Belgium; ³VIB Center for Cancer Biology, Leuven, Belgium; ⁴Mount Sinai Liver Cancer Program, Divisions of Liver Diseases, Tisch Cancer Institute, Icahn School of Medicine at Mount Sinai, New York, United States; ⁵Radiology Department, University Hospitals Leuven, Leuven, Belgium; ⁶Laboratory of Translational MRI, Department of Imaging and Pathology, KU Leuven, Leuven, Belgium; ⁷Laboratory of Clinical Digestive Oncology, Department of Oncology, KU Leuven, Leuven, Belgium

Email: sarah.cappuyns@kuleuven.be

Background and aims: Checkpoint inhibitors have radically changed the treatment of advanced hepatocellular carcinoma (aHCC), albeit that only a subset of patients achieve durable disease control. We aimed to characterize both the tumoural and peripheral immune system of aHCC using single-cell sequencing technology and identify features associated with response and/or resistance to immunotherapy targeting the PD (L)1 axis.

Method: Patients with aHCC were prospectively enrolled prior to initiation of systemic therapy. Clinical response was defined as mRECIST objective response or durable stable disease. Pre-treatment tissue biopsies (n = 31) and both pre- and on-treatment peripheral immune cell samples (n = 58) were subjected to simultaneous single-cell transcriptome, T-cell receptor (TCR) and proteome sequencing, resulting in data from 377 975 single cells.

Results: PD1 and PDL1 were expressed in tumour-infiltrating T-cells versus myeloid cells and tumour cells, respectively. Myeloid cells from tumours responding to immunotherapy expressed significantly higher levels of PDL1 at baseline (p = 0.014), driven by pro-inflammatory PDL1-expressing CXCL10+ macrophages involved in T-cell recruitment. In contrast, non-responding tumours were infiltrated by immature 'monocyte-like' CX3CR1+ and CCR2+ macrophages (p = 0.009 and p = 0.01, respectively). Responding tumours were also characterized by a more clonal baseline TCR repertoire (p = 0.007) and a higher degree of TCR sharing (p = 0.008) with peripheral blood that decreased significantly on-treatment (p = 0.026). In peripheral T-cells, TCRs shared between tumour and blood displayed a higher TCR clonality (p = 0.003), while in the tumour they were present in recently activated CD8+ effector T-cells, characterized by high levels of cytotoxic markers.

Conclusion: Response to checkpoint inhibition in aHCC is driven by the pre-treatment presence of clonally expanded, recently activated cytotoxic CD8+ effector T-cells, infiltrating from peripheral blood and supported by a pro-inflammatory tumoural myeloid component.

THU594

The influence of fasting on tumor-targeted drug delivery

Svea Becker¹, Diana Möckel², Ilaria Biancacci², Jan-Niklas May², Qingbi Wang¹, Huan Sun¹, Marek Weiler², Twan Lammers², Maximilian Hatting¹, Christian Trautwein¹. ¹Medical Department III, Universitätsklinikum Aachen, Aachen, Germany; ²Experimentelle Molekulare Bildgebung, RWTH Aachen, Aachen, Germany
Email: svbecker@ukaachen.de

Background and aims: Hepatocellular carcinoma is increasing in industrialized countries. Disease progression is accelerated by a number of risk factors, although it can be reduced to some extent by using intermittent fasting. Tumorous cells are stressed by regular food deprivation because they are constantly proliferating. Fasting has also been established in recent clinical research to be a new therapeutic before tumor therapy leading to maintenance and repair processes such as autophagy. As a result, tumor therapy can be more precise and patients can show a higher survival rate. Here, we aimed to show how fasting induces changes in the tumor microenvironment facilitating tumor-targeted drug delivery.

Method: We used a well-established syngeneic tumor model with the murine liver hepatoma cell line Hep-55.1C. The tumor was implanted subcutaneously and grew over 3.5 weeks. During tumor growth, the mice were either fasted intermittently every 12 h (IF), once overnight after 20 d for 12 h (STF), or fed *ad libitum* (a.l.). After 21 d, DSPE-Cy7 labeled liposomes were injected i.v. and the biodistribution of the nanoparticles was observed longitudinally up to 72 h p.i. via hybrid computed- and fluorescence tomography (CT-FLT).

Results: Our analysis demonstrates that mice in the a.l. group have little to no liposome-signal in the tumor but have substantial levels of uptake in reticuloendothelial system organs (RES). The STF group has tumor signals, but the RES-organs still have significant signals. The IF mice had the most signal in the tumor, while the RES-organs had fewer liposome signals detected by the CT-FLT.

In addition, intermittent fasting alters the microenvironment of tumors. Collagen1A1 levels in the IF group were considerably lower. This was accompanied by a considerable rise in the number of vessels that were positive for Lectin. In these tests, there was no difference between STF and a.l. mice.

Conclusion: Our findings show that intermittent fasting prior to tumor therapy improves the likelihood of a more precise and direct delivery method. Fasting softens the tissue and increases blood flow, making it easier to deliver (nano-)therapeutics into the tumor through the bloodstream.

THU595

CXCR2 inhibition sensitises NASH-HCC to immunotherapy

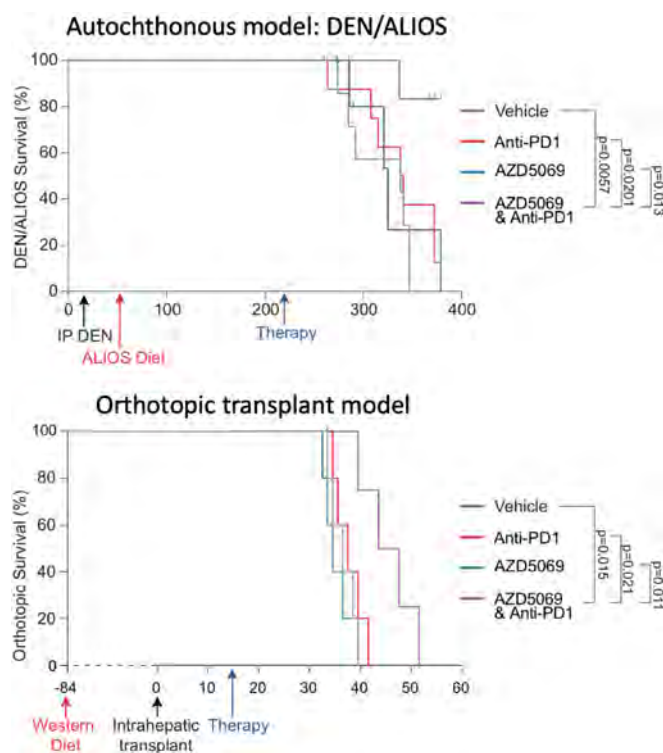
Jack Leslie¹, John B. G. Mackey², Thomas Jamieson², Helen L. Reeves¹, Josep M. Llovet³, Carlin Leo², Thomas G Bird², Owen Sansom², Derek A Mann¹. ¹Newcastle University Medical School, United Kingdom; ²Beatson Institute for Cancer Research, Bearsden, United Kingdom; ³Institut d'Investigacions Biomèdiques August Pi i Sunyer (IDIBAPS), Barcelona, Spain
Email: jack.leslie@ncl.ac.uk

Background and aims: Non-alcoholic steatohepatitis (NASH) is increasingly a major underlying cause of hepatocellular carcinoma (HCC). Immunotherapy offers great promise for HCC therapy; however, recent published data suggests that NASH is the cause of immune changes that negatively impacts on the efficacy of conventional immune checkpoint inhibition (ICI). Here we aimed to sensitise NASH-HCC to anti-PD1 therapy by targeting neutrophils using a CXCR2 small molecule inhibitor (AstraZeneca-AZD5069).

Method: Neutrophil infiltration was characterised in multiple models of murine HCC and in human patient biopsies. Late-stage intervention with anti-PD1 and/or AZD5069 was performed in two NASH-HCC models (orthotopic and autochthonous). The tumour microenvironment was characterised by a combination of immunohistochemistry, flow cytometry and RNA-seq.

POSTER PRESENTATIONS

Results: CXCR2⁺ neutrophils were found to be highly represented in both murine and human NASH-HCC. In models of NASH-HCC lacking response to ICI, the combination of AZD5069 with anti-PD1 effectively suppressed tumour burden and extended survival (Fig 1). The combination therapy increased intratumoral CD103⁺ CXCR1⁺ dendritic cells and CD8⁺ T cells that are associated with anti-tumoural immunity. The therapeutic effect was lost upon genetic impairment of dendritic cells or antibody mediated depletion of CD8⁺ T cells. Combination therapy resulted in an unexpected increase in tumour-associated neutrophils (TANs). These TANs were found to be proliferative and by the use of image mass cytometry to be located within immunological hubs in direct contact antigen presenting cells and CD8⁺ T cells. These immune hubs were enriched for the cytotoxic anti-tumoural protease granzyme B which was found at increased levels in tumours co-treated with CXCR2 antagonist and anti-PD1 compared with monotherapy groups.



TANs in combination-treated tumours displayed a switch from a pro-tumour to anti-tumour progenitor-like neutrophil phenotype, closing resembling a recently characterised acute-inflammatory immature-Ly6G^{int} neutrophil population isolated from lipopolysaccharide- (LPS)-treated mice. Intravenous infusion of these neutrophils into orthotopic tumour bearing mice, sensitised to anti-PD1 therapy, promoting dendritic cell and CD8⁺ T cell recruitment and activation.

Conclusion: CXCR2-inhibition induces multi-cellular reprogramming of the tumour immune microenvironment that promotes ICI treatment of HCC in the context of NASH.

THU596

Combination of systemic immune-inflammation index and albumin-bilirubin score predict prognosis of sequential therapy with sorafenib and regorafenib in unresectable hepatocellular carcinoma

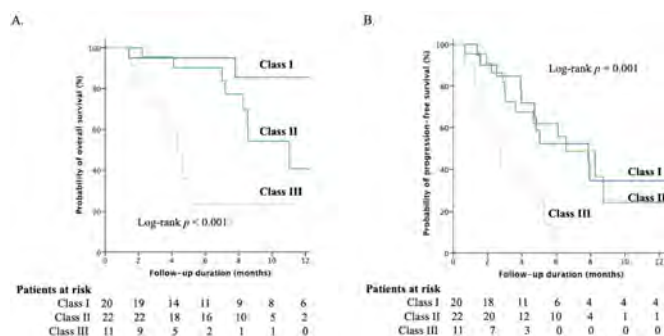
Tai-An Cheng¹, Wei Teng², Po-Ting Lin³, Chen-Chun Lin³, Chun-yen Lin³, Shi-Ming Lin³. ¹Chang Gung Memorial Hospital, Taiwan; ²Chang Gung University, Taiwan; ³Taipei Chang Gung Memorial Hospital, Taiwan

Email: lsmipaicyto@gmail.com

Background and aims: Sequential therapy with sorafenib and regorafenib had shown promising results to improve outcomes for unresectable hepatocellular carcinoma (uHCC) patients. Although there have been several reports regarding the efficacy of sequential therapy in real-world, the role of specific inflammation markers for predicting the prognosis are still unclear. This study aimed to investigate prognostic value of systemic inflammatory markers in patients with HCC who received sorafenib-regorafenib sequential therapy.

Method: A total of 122 uHCC patients who received sorafenib-regorafenib sequential therapy from August 2016 to August 2021 were retrospectively enrolled for analysis. Treatment response was evaluated by modified Response Evaluation Criteria in Solid Tumors (mRECIST) criteria. The pre-treatment host factors, tumor status, biochemistry markers and inflammatory index (NLR, PLR, MLR, SIRI, SIRI, ILIS) were collected. Progression-free survival (PFS) and overall survival (OS) were assessed using the Kaplan-Meier survival curves. The Cox regression model was used to identify independent predictors of PFS and OS.

Results: Among the 122 patients, the median age was 66 years old and 84% were male gender. Regorafenib was used as the second and third lines of therapy in 97 (80%) and 25 (20%) patients respectively. Most patients were Child-Pugh A (96%), ABLI grade II (52%) and BCLC stage C (73%) at baseline. The overall response rate (ORR) and disease control rate (DCR) was 7.4% and 46.7%, respectively. The median OS from the initiation of sorafenib was 39.4 (95%CI: 32.9–45.8) and the median PFS after sorafenib was 3.4 (95%CI: 3.0–3.8) months. Multivariate Cox regression analysis showed that baseline ALBI grade I and systemic inflammatory index (SII) <330 were independent factors associated with good OS (hazard ratio [HR] = 0.655, p = 0.031 and HR = 0.570, p = 0.039) and PFS (HR = 0.725, p = 0.040 and HR = 0.341, p = 0.016). We further stratified our patients into 3 risks group (A: SII ≤330 and ALBI grade I, B: SII >330 or ALBI grade II/III, C: SII >330 and ALBI grade II/III). The combination of SII ≤330 and ALBI grade I showed the best OS (A vs. B vs. C = NR vs. 17.9 vs. 7.5 months, log-rank p = 0.003) and PFS (A vs. B vs. C = NR vs. 3.7 vs. 2.9 months, log-rank p = 0.001) than other two groups.



Conclusion: The combination of baseline ALBI grade and SII index can be used as a promising prognostic tool to predict prognosis of uHCC patients receiving sorafenib-regorafenib sequential therapy.

THU597

Induce the endogenous tumor suppressor miR-34a by small molecules to inhibit liver metastasis

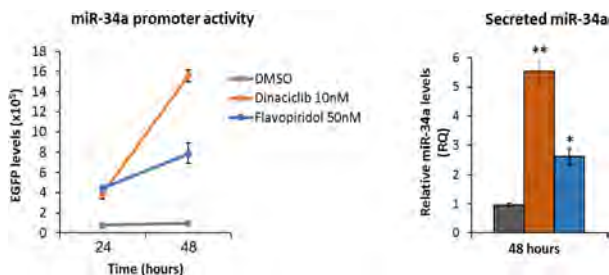
Dayana Yaish¹, Tomer Friehmann¹, Alexander Plotnikov², Shira Levi¹, Hilla Giladi¹, Amnon Peled¹, Haim Barr², Eithan Galun¹. ¹Hadassah University Hospital-Ein Kerem, Goldyne Savad Institute of Gene and Cell Therapy, Jerusalem, Israel; ²Weizmann Institute of Science, The Nancy and Stephen Grand Israel National Center for Personalized Medicine, Rehovot, Israel

Email: dayana.yaish@mail.huji.ac.il

Background and aims: Metastasis originating from different cancers, are commonly spreading to the liver, and as such, are a common cause of death. Recent evidences have indicated the role of microRNAs (miRs) in modulating the metastatic process. There are specific miRs that exhibit tumor-suppressive activity by targeting cancer driver genes. MiR-34a is a well-known tumor suppressor and anti-metastatic miR. We hypothesize that induction of endogenous expression and secretion of miR-34a, could be a new strategy for metastasis therapy.

Method: We performed high throughput screening of synthetic small molecule libraries searching for compounds that induce miR-34a promoter activity and secretion. The compounds were initially tested for their ability to induce EGFP on HepG2 cells carrying a miR-34a-promoter-EGFP reporter. Compounds that induced EGFP levels were tested further for their effect on miR-34a secretion using qRT-PCR analysis performed on RNA extracted from the cell's media.

Results: We identified 6 compounds which induced miR-34a promoter activity. However, only 2 out of these 6 compounds induced miR-34a secretion. Searching databases for predicted activities of these 2 compounds, revealed that both may repress Cyclin Dependent Kinase 5 (CDK5). We therefore, examined the activity of known CDK5 repressors, Dinaciclib and Flavopiridol. Both molecules induced miR-34a promoter activity and secretion.



Conclusion: small molecule induction of miR-34a is a therapeutic approach against liver metastasis.

THU598

Prediction of treatment response using contrast-enhanced ultrasonography in patients treated with Atezolizumab and Bevacizumab for unresectable hepatocellular carcinoma

Hitomi Takada¹, Shinya Maekawa¹, Nobuyuki Enomoto¹. ¹University of Yamanashi, Gastroenterology and Hepatology, Chuo, Japan
Email: takadahi0107@gmail.com

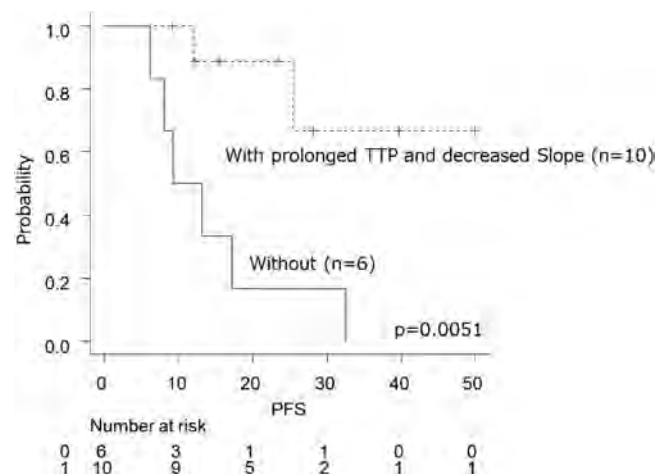
Background and aims: Atezolizumab plus Bevacizumab therapy (AB) was approved for unresectable hepatocellular carcinoma in 2020. However, the prediction of treatment response that can be easily used in clinical practice is still unknown. In this study, we performed Time-intensity curve (TIC) analyses using the arterial phase of contrast-enhanced ultrasonography (CEUS), and examined

its usefulness as a predictive marker of early therapeutic effect after the administration of AB.

Method: Twenty-five patients who received AB for unresectable HCC were included. The initial treatment response after the administration of AB was reported using Response Evaluation Criteria in Solid Tumors (RECIST) after 8–12 weeks. The treatment response was evaluated every 8–12 weeks thereafter. CEUS was performed before administration and early after administration (3–7 days), and TIC analysis was performed using the arterial phase for 2 minutes after injection of the contrast medium. The time to peak (TTP) and the slope of wash-in (Slope) indicators were used for TIC analysis.

Results: The baseline characteristics of 25 patients were 69 (44–81) years old, 20 males, the maximum intrahepatic tumor diameter 64 (21–112) mm, and BCLC stage C 45%. The treatment response was Complete Response 1 case, Partial Response 7 cases, Stable Disease 11 cases, and PD 6 cases.

Patients with prolonged TTP and decreased Slope were 36% using CEUS at 3–7 days, and all cases achieved disease control based on the initial CT after 8–12 weeks. There was a significant difference in the median progression-free survivals (PFSs) between patients with and without prolonged TTP and decreased Slope ($p = 0.0051$). There was a significant difference in the median PFSs between patients with and without decreased α -fetoprotein (AFP) levels ($p = 0.019$). There was also a significant difference in the median PFSs between patients with and without decreased neutrophil-to-lymphocyte ratio (NLR) ($p = 0.038$). PFS stratification was possible by the number of positive numbers among the 3 early markers (TTP prolongation and Slope decrease/AFP decrease/NLR decrease) (0/1 vs. 2/3 8.6 vs. 33 weeks, $p < 0.001$).



Conclusion: Early evaluation using CEUS may be useful in predicting the therapeutic effect in patients treated with Atezolizumab and Bevacizumab for unresectable HCC.

THU599

Efficacy and safety of Atezolizumab plus Bevacizumab-based sequential treatment for unresectable hepatocellular carcinoma: a simulation model

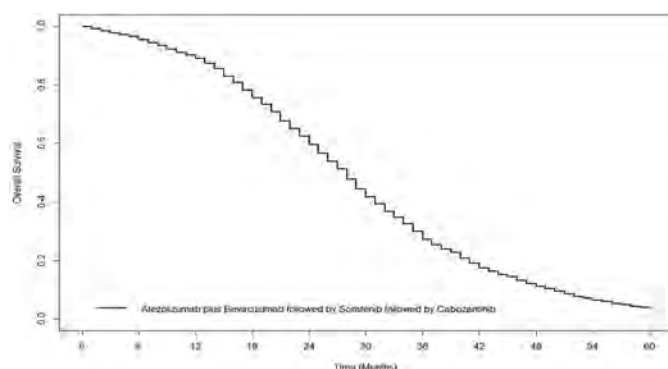
Ciro Celsa¹, Giuseppe Cabibbo¹, Salvatore Battaglia², Paolo Giuffrida¹, Giacomo Emanuele Maria Rizzo¹, Mauro Grova¹, Marco Giacchetto¹, Gabriele Rancatore¹, Caterina Stornello¹, Maria Vittoria Grassini¹, Giuseppe Badalamenti³, Marco Enea¹, Antonio Craxi¹, Vito Di Marco¹, Calogero Camma¹. ¹Section of Gastroenterology and Hepatology,

POSTER PRESENTATIONS

Department of Health Promotion, Mother and Child Care, Internal Medicine and Medical Specialties, PROMISE, University of Palermo, Italy; ²Department of Economics, Business and Statistics (SEAS), University of Palermo, Department of Economics, Business and Statistics (SEAS), University of Palermo, Italy; ³Department of Surgical, Oncological and Oral Sciences (Di.Chir.On.S.), University of Palermo, Department of Surgical, Oncological and Oral Sciences (Di.Chir.On.S.), University of Palermo, Italy
Email: calogero.camma@unipa.it

Background and aims: Systemic therapies for unresectable hepatocellular carcinoma (HCC) have rapidly increased in numbers over recent years and they should be combined in a rationale sequence to offer the best net health benefit. Atezolizumab plus Bevacizumab now represents the standard of care for first-line treatment, but efficacy and safety of subsequent treatment lines still remain unknown. According to hepatological and oncological guidelines, Sorafenib could be an option for second-line treatment after first-line Atezolizumab plus Bevacizumab and Cabozantinib is the only systemic agent tested as third-line treatment. The aim was to estimate the overall survival (OS) of the sequence of Atezolizumab plus Bevacizumab (first-line) followed by Sorafenib (second-line) followed by Cabozantinib (third-line).

Method: A Markov model (Figure 1) was constructed to estimate the OS of the sequence Atezolizumab plus Bevacizumab (first-line) followed by Sorafenib (second-line) followed by Cabozantinib (third-line). The probability of transition between states (first-line treatment, HCC progressions and death) was derived from published randomized controlled trials (RCTs). The proportion of patients who did not receive subsequent lines of therapy due to death was considered when estimating survival. OS was the main outcome. Rates of severe adverse events (SAEs) (defined as \geq grade 3 adverse events) were calculated.



Results: The estimated median OS of the sequential strategy is 28 months (95% Confidence Interval 27–29 months). Rate of SAEs is 67.5%.

Conclusion: This simulation model provides a forecast of the outcomes of the next available sequential systemic treatment of patients with HCC. The sequence including first-line Atezolizumab plus Bevacizumab followed by second-line Sorafenib followed by third-line Cabozantinib leads to a median OS of more than two years, with about two thirds of patients experiencing SAEs. Prospective real-world studies are needed to substantiate the net health benefit of this sequence.

THU600

Risk factors for hepatic encephalopathy in hepatocellular carcinoma after sorafenib or lenvatinib treatment: a real-world study

Bowen Chen^{1,2}, Linzhi Zhang^{2,3}, Jiamin Cheng², Xu Yang⁴, Jin Lei^{2,5}, Tong Wu², Tao Yan², Yinyin Li², Yinying Lu^{1,2}. ¹Peking University 302 Clinical Medical School, Beijing, China; ²The 5th Medical Centre of the PLA General Hospital, Beijing, China; ³Tianjin Medical University Cancer Institute and Hospital, Tianjin, China; ⁴Peking Union Medical College Hospital, Chinese Academy of Medical Sciences and Peking Union Medical College, Department of Liver Surgery, State Key Laboratory of Complex Severe and Rare Diseases, Beijing, China; ⁵Guizhou Medical University, Guiyang, China
Email: luyinying1973@163.com

Background and aims: This study aimed to investigate the incidence rate and risk factors for hepatic encephalopathy (HE) among unresectable hepatocellular carcinoma (uHCC) patients with liver cirrhosis who received sorafenib (SOR) or lenvatinib (LEN) treatment. **Method:** uHCC patients with cirrhosis who received SOR or LEN treatment from September 2014 to February 2021 were continually recruited in our single-centre retrospective study. Hepatic Encephalopathy Scoring Algorithm was used to evaluate occurrence and grade of HE during treatment and logistic regression models were used to further explore risk factors for HE.

Results: 214 patients were enrolled in SOR group, while the other 240 patients were in LEN group, with no statistical difference in baseline characteristics. At time of data cut-off (2021–12), the incidence of HE in SOR group (4.2%, 95%CI: 2%–7%) was significantly lower than that in LEN group (11.3%, 95%CI: 7%–15%) ($p=0.006$). Alcohol-related cirrhosis [OR: 5.857 (95%CI: 1.519–22.591)], Child-Pugh Score >7 [OR: 3.023 (95%CI: 1.135–8.053)], blood ammonia ≥ 38.65 $\mu\text{mol/L}$ [OR: 4.693 (95%CI: 1.782–12.358)], total bile acid ≥ 29.5 $\mu\text{mol/L}$ [OR: 11.047 (95%CI: 4.414–27.650)], LEN treatment [OR: 6.162 (95%CI: 2.258–16.818)] and duration of treatment ≥ 5.6 months [OR: 4.350 (95%CI: 1.701–11.126)] were confirmed as risk factors for HE occurrence during tyrosine kinase inhibitors treatment.

Table 1: Occurrence of Hepatic Encephalopathy.

Variables	SOR Group (n = 214, %)	LEN Group (n = 240, %)	P value
Cases of HE	9 (4.2%)	27 (11.3%)	0.006
Grade of HE			
1	0 (0%)	1 (0.4%)	—
2	3 (1.4%)	14 (5.8%)	—
3	5 (2.3%)	4 (1.7%)	—
4	1 (0.5%)	7 (2.9%)	—
Unknown	0 (0%)	1 (0.4%)	—
Therapeutic Effect of HE			
Cure	8 (3.7%)	20 (8.3%)	—
Void	1 (0.5%)	7 (2.9%)	—
Discontinuation of SOR/LEN Treatment	5 (2.3%)	18 (7.5%)	—

—: not applicable

HE: hepatic encephalopathy, SOR: sorafenib, LEN: lenvatinib.

Conclusion: uHCC patients with cirrhosis who receive LEN are more likely to develop HE than SOR, with alcohol-related cirrhosis, Child-Pugh Score, serum ammonia, total bile acid, and duration of treatment to be risk factors for HE.

Friday 24 June

Acute liver failure and drug induced liver injury

FRI001

Obeticholic acid exacerbates the liver fibrosis of bile duct ligation model by inducing the liver expression of osteopontin

Jie Wang¹, Yuan Zihang¹, Yingying Miao¹, Haoran Zhang¹, Qipeng Wu¹, Xinliang Huang¹, Luyong Zhang^{1,2}, Q. W. Yu¹, Zhenzhou Jiang^{1,3,4}. ¹China Pharmaceutical University, New Drug Screening Center, Jiangsu Center for Pharmacodynamics Research and Evaluation, Nanjing, China; ²Guangdong Pharmaceutical University, Center for Drug Research and Development, Guangdong, China; ³China Pharmaceutical University, Key Laboratory of Drug Quality Control and Pharmacovigilance, Nanjing, China; ⁴China Pharmaceutical University, State Key Laboratory of Natural Medicines, Nanjing, China
Email: jiangcpu@163.com

Background and aims: Liver fibrosis is a dynamic process characterized by the deposition of the accumulated extracellular matrix (ECM). To date, there are still no therapeutic medications approved for fibrosis or cirrhosis. Osteopontin (OPN) is a phosphoglycoprotein of ECM, and has been reported to drive ductular reaction (DR) and the formation of periportal scarring. Obeticholic acid (OCA) is approved for Primary Biliary Cholangitis (PBC), and OCA has been shown to improve the fibrosis in NASH patients evaluated in REGENERATE study. But the applications of OCA are limited due to its side effects. The main objective of this study is to investigate the impact of OCA on liver diseases.

Method: The bile duct ligation model was used to evaluate the effect on fibrosis of OCA assessed by assessment of blood markers of liver injury, pathological section, western blotting, RT-PCR, immunohistochemistry and immunofluorescence staining. OPN and Thr-OPN were detected by ELISA. The primary mouse cholangiocytes and human intrahepatic bile epithelium cells were chosen to investigate in vitro.

Results: Compared to control, OCA treatment (40 mg/kg) aggravated BDL induced liver injury and liver fibrosis in mice, demonstrated by significantly increase in serum ALT, AST, ALP, TGF- β 1, hepatic hydroxyproline, Masson Trichrome, H&E, and Sirius red staining as well as immunohistochemistry staining of α -SMA. The serum and liver content of OPN and its another active form, thrombin-cleaved OPN (Thr-OPN), were obviously increased in OCA-treated BDL mice. Interestingly, there was also a significant increase in the content of Thr-OPN in the liver of OCA-treated sham mice. Next we examined the downstream effects of OPN in liver disease. Immunoblots analysis

and immunohistochemistry staining of CK19 revealed that OCA treatment enhanced ductular reaction induced by BDL, and the immunofluorescence staining of CK19 and Ki67 also proved this. Immunoblots analysis of PCNA and immunohistochemistry staining of Ki67 revealed that OCA treatment weakened liver regeneration. RT-PCR analysis of liver nonparenchymal cells revealed that OCA increased the expression of integrin $\alpha\beta$ 3 receptors in BDL mice, which is OPN targeted.

Conclusion: OCA aggravated the degree of liver injury and fibrosis in obstructive cholestasis probably associated an apparent increase of OPN in serum and liver. OPN may be a biomarker of liver toxicity caused by OCA.

FRI002

A report on the Australian Drug Induced Liver Injury Network: AusDILIN

Beverly Rodrigues¹, Stephen Bloom^{1,2}, Rohit Sawhney^{1,2}, Geoffrey Haar^{1,3}, Maria Bishara¹, Ayushi Chauhan¹, Paul Gow⁴, Simone Strasser⁵, Alan Wigg⁶, Karl Vaz⁴, Fadak Mohammadi⁶, Amanda Nicoll^{1,2}. ¹Eastern Health, Gastroenterology, Australia; ²Eastern Health Clinical School, Monash University, Australia; ³Eastern Health, Pharmacy, Australia; ⁴Austin Health, Gastroenterology, Australia; ⁵Royal Prince Alfred Hospital, Gastroenterology, Australia; ⁶Flinders Medical Centre, Gastroenterology, Australia
Email: beverly.rodrigues91@gmail.com

Background and aims: Drug induced liver injury (DILI) may vary in different regions due to population and prescribing differences. Data on DILI in Australia is limited but is necessary to inform local management. We present prospectively collected data from seventeen Australian liver centres in a new collaboration named AusDILIN. **Method:** A prospective multicentre clinical audit was conducted on reported DILI patients between June 2018 to November 2021 inclusive (41 months).

Results: Data on 150 patients was obtained, and showed the commonest causes were: amoxicillin/clavulanic acid (n = 26, 17%), statins (n = 15, 10%) and cephalosporins (n = 12, 8%). Remdesivir was the identified causative agent in 5 (3%) of cases. Sixteen (11%) of patients were icteric on presentation. The median duration to onset and recovery was 3 \pm 7.4 weeks, and 8 \pm 12.9 weeks, respectively. One hundred and twelve (75%) were managed as inpatients. Forty-seven (31%) received some form of treatment; 11 (7%) were managed with ursodeoxycholic acid and 23 (15%) with corticosteroid monotherapy respectively, although 2 (1%) and 1 (1%) were already on these treatments long-term for chronic conditions. Of the 11 (7%) of patients with unresolving DILI, 4 (3%) were considered for liver transplant. Two (1%) of these were successfully transplanted and 1 (1%) died, with the overall cohort death rate being 4 patients (3%). Fifty patients (33%) were lost to follow up. The DILI persisted beyond 3 and 6 months in 30 (45%) and 10 (7%) of cases, respectively.



Table 1: Baseline characteristics of AusDILIN cohort

Median age (years)	56.37 ± 0.44 [18–94]	
Gender (M: F, n, %)	80 (53%): 70 (47%)	
Ethnicity (n, %)	Caucasian/European	114 (76%)
	SE Asian/Arabic	31 (21%)
	African	2 (1%)
	Unknown	3 (2%)
Pattern of liver injury (n, %)	Hepatic: Cholestatic	54 (36%): 44 (29%)
	Mixed: Unknown	51 (34%): 1 (1%)
Treatment offered (n, %)	CS monotherapy	23 (15%)
	UDCA monotherapy	11 (7%)
	CS plus UDCA combination therapy	5 (3%)
	CS plus IM combination therapy	4 (3%)
	NAC infusion	2 (1%)
Clinical outcomes (n, %)	Self-resolved or resolving	87 (58%)
	Unknown or lost to follow up	50 (33%)
	Persistent or progressed	11 (7%)
	Death (DILI ALF)	4 (3%)
Considered for LTx (n, %)		4 (3%)
	Transplanted	2 (1%)
	Resolved	1 (1%)
	Death	1 (1%)

HTN = hypertension, Chol = cholesterol, DM = diabetes mellitus, CS = corticosteroids, UDCA = Ursodeoxycholic acid, IM = immunomodulator, NAC = N-acetyl cysteine, LTx = liver transplant, ALF = acute liver failure.

Conclusion: DILI is a significant cause of morbidity and mortality in Australia, with a high proportion suffering persistent liver injury, and with the role of treatment remaining undetermined and requiring further study.

FRI003

Incidence, phenotype and prognostic relevance of COVID-19-related liver injury across different age strata

Lukas Hartl^{1,2}, Katharina Haslinger^{1,2}, Martin Angerer^{1,2}, Mathias Jachs^{1,2}, Benedikt Simbrunner^{1,2,3}, David J. M. Bauer^{1,2}, Bernhard Scheiner^{1,2}, Ernst Eigenbauer⁴, Robert Strassl⁵, Monika Breuer⁵, Oliver Kimberger⁶, Daniel Laxar⁶, Michael Trauner¹, Matthias Mandorfer^{1,2}, Thomas Reiberger^{1,2,3}. ¹Medical University of Vienna, Division of Gastroenterology and Hepatology, Department of Medicine III, Vienna, Austria; ²Medical University of Vienna, Vienna Hepatic Hemodynamic Lab, Division of Gastroenterology and Hepatology, Department of Medicine III, Vienna, Austria; ³Medical University of Vienna, Christian Doppler Lab for Portal Hypertension and Liver Fibrosis, Vienna, Austria; ⁴Medical University of Vienna, IT-Systems and Communications, Vienna, Austria; ⁵Medical University of Vienna, Department of Laboratory Medicine, Division of Clinical Virology, Vienna, Austria; ⁶Medical University of Vienna, Department of Anaesthesia, Intensive Care Medicine and Pain Medicine, Vienna, Austria Email: thomas.reiberger@meduniwien.ac.at

Background and aims: Severe acute respiratory distress syndrome-coronavirus-2 (SARS-CoV-2) caused the pandemic of coronavirus disease of 2019 (COVID-19). Variable abnormalities in liver chemistries have been reported in COVID-19 patients. We assessed the prevalence rates and trajectories of elevated liver enzymes after SARS-CoV-2 infection, as well as their prognostic values across different age strata in a large cohort of COVID-19 patients.

Method: Patients with a positive SARS-CoV-2 PCR result between 03/2020–07/2021 at the Vienna General Hospital were included in this study. Patients were stratified for age (i.e. 18–39 vs. 40–69 vs. ≥70 years). Multivariate Cox regression analyses were adjusted for pre-

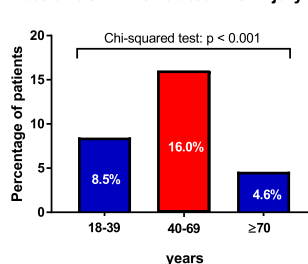
existing liver disease, age, sex, albumin, obesity, diabetes mellitus, cardiovascular disease, lung disease and malignancy.

Results: 900 patients (52.4% male) were included with 32.2% aged 18–39 years, 39.7% 40–69 years, and 28.1% ≥70 years age strata, respectively. Frequency of comorbidities, median D-dimer and C-reactive protein increased with age.

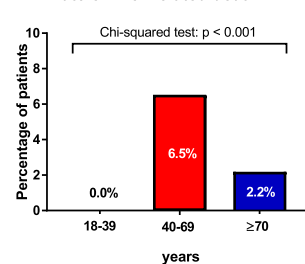
After SARS-CoV-2 infection, parameters of hepatocellular (aspartate aminotransferase [AST]/alanine-aminotransferase [ALT]) and cholestatic liver injury (alkaline phosphatase [ALP]/gamma-glutamyl transferase [GGT]) all significantly increased. AST/ALT and ALP/ALT were elevated in 40.3% (n = 262/650) and 45.0% (n = 287/638) of patients, respectively. The rates of COVID-19-associated liver injury and median levels of liver chemistries were highest in patients aged 40–69 (18–39 years: 8.5% vs. 40–69 years: 16.0% vs. ≥70 years: 4.6%; p < 0.001).

Elevated AST after the first SARS-CoV-2 PCR test was associated with the requirement for hospital admission, ICU admission and intubation throughout all age strata and with a higher frequency of death and liver-related death in patients aged 40–69. Elevated AST and total bilirubin (BIL) at the time of first positive SARS-CoV-2 PCR test independently predicted mortality in the overall cohort (AST: aHR: 1.47; 95%CI: 1.01–2.14; p = 0.043/BIL: aHR: 2.20; 95%CI: 1.22–3.98; p = 0.009) and in patients aged 40–69 years (AST: aHR: 1.78; 95%CI: 1.04–3.06; p = 0.037/BIL: aHR: 2.18; 95%CI: 1.15–4.13; p = 0.017).

Rate of COVID-19-related liver injury



Rate of liver-related death



Conclusion: A considerable proportion of COVID-19 patients show abnormal liver chemistries. The subgroup of patients aged 40–69 years was at particularly high risk for COVID-19-related liver injury; elevated ALT was predictive of liver-related mortality. AST and BIL at the time of first positive SARS-CoV-2 PCR were independent predictors of mortality in the overall group, and particularly in patients aged 40–69 years.

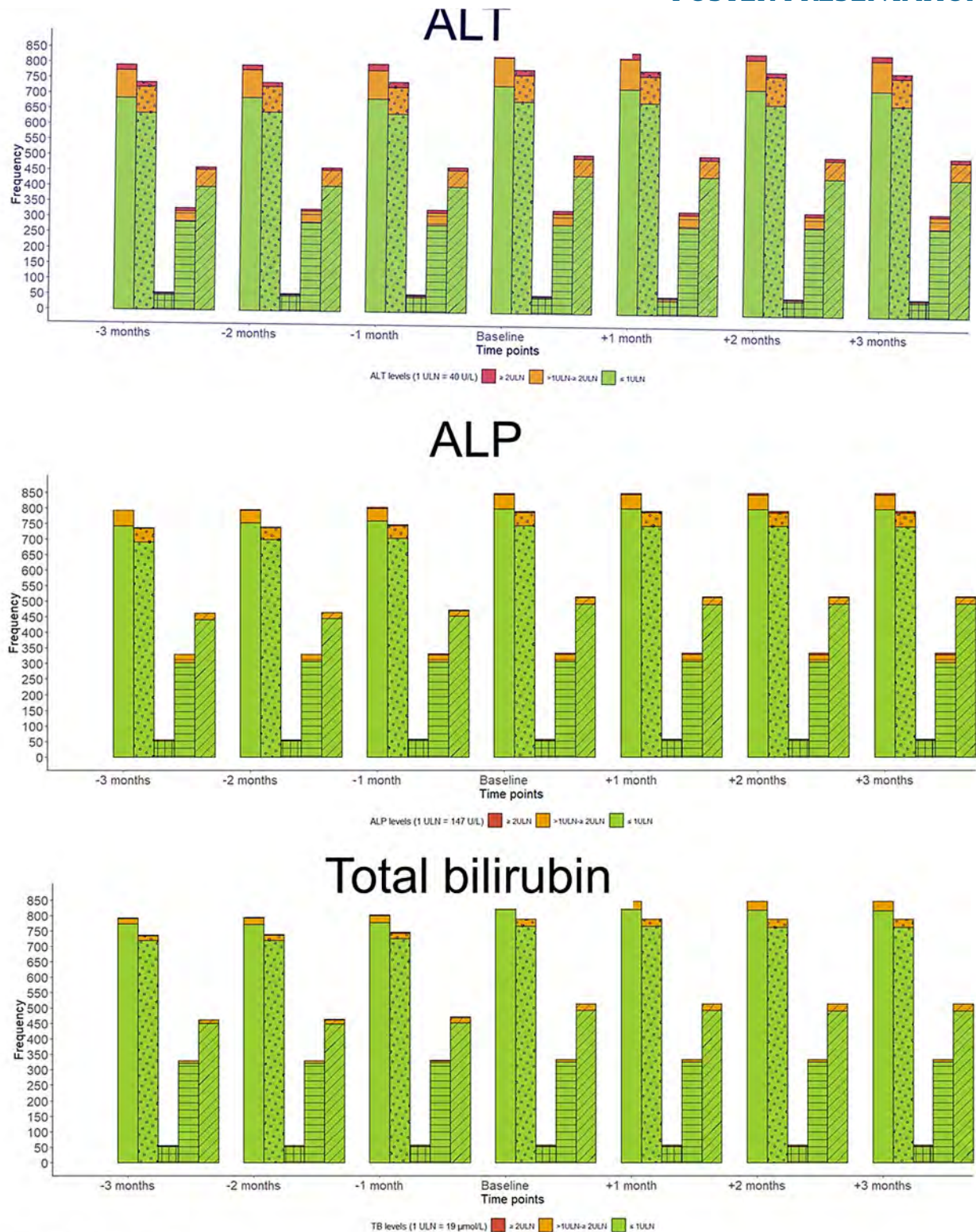
FRI004

Two different types of COVID-19 vaccines and serial liver biochemistries

Grace Lai-Hung Wong¹, Vicki Wing-Ki Hui¹, Terry Cheuk-Fung Yip¹, Yee-Kit Tse¹, Vincent Wai-Sun Wong¹. ¹The Chinese University of Hong Kong, Medical Data Analytic Centre (MDAC), Hong Kong Email: wonglaihung@cuhk.edu.hk

Background and aims: A handful of vaccines against COVID-19 have been approved around the world. These vaccines have excellent safety profiles with few reported side effects. Data concerning the liver safety of COVID-19 vaccines are lacking. We aimed to report the serial liver biochemistries of people before and after receiving COVID-19 vaccines.

Method: This was a territory-wide retrospective observational cohort study in Hong Kong. We identified subjects who had received any of the two COVID-19 vaccines approved in Hong Kong-CoronaVac (the inactivated virus technology platform by Sinovac Biotech (Hong Kong) Limited) and Comirnaty (mRNA technology platform by Fosun Pharma in collaboration with the German drug manufacturer BioNTech, the BNT162b2 mRNA vaccine). Serial liver biochemistries at least 3 months before and after the COVID-19 vaccines were reported, in subjects with or without chronic hepatitis B or C.



Pattern – Group:

Circle – HBV/HCV negative

Crosshatch – HBV/HCV positive

Horizontal stripe – Comirnaty

Diagonal stripe – CoronaVac

Figure: Serial liver biochemistries before and after COVID-19 vaccine.

POSTER PRESENTATIONS

Results: 851 subjects (513 received CoronaVac and 338 received Comirnaty; 56.2% male, median age 52 years old; 6.8% chronic hepatitis B or C) were included. Majority (87%) subjects had normal ALT ($1-2 \times \text{ULN}$: 10.8%; $>2 \times \text{ULN}$: 2.4%), total bilirubin ($1-2 \times \text{ULN}$: 3.3%; $>2 \times \text{ULN}$: 0%) and ALP ($1-2 \times \text{ULN}$: 5.4%; $>2 \times \text{ULN}$: 0.5%) before or at the time of receiving COVID-19 vaccines; these parameters remained stable for up to 3 months after the vaccination-ALT ($1-2 \times \text{ULN}$: 11.6%; $>2 \times \text{ULN}$: 2.1%), total bilirubin ($1-2 \times \text{ULN}$: 3.7%; $>2 \times \text{ULN}$: 0%) and ALP ($1-2 \times \text{ULN}$: 5.4%; $>2 \times \text{ULN}$: 0.8%) at or after the time of receiving COVID-19 vaccines. While patients with chronic viral hepatitis had higher ALT and ALP than those without chronic viral hepatitis at most of the times, these parameters remained normal (ALT: median 24 to 26 U/L vs. 20 to 21 U/L; ALP: median 88 to 90 U/L vs. 80 U/L). Similar serial liver biochemistries were observed in subjects who received CoronaVac and Comirnaty vaccine.

Conclusion: Both types of COVID-19 vaccines have very favourable liver safety profile in people with or without chronic viral hepatitis.

Grant support: This work was supported by the Health and Medical Research Fund (HMRF)-Food and Health Bureau Commissioned Research on COVID-19 (Reference no.: COVID1903002) awarded to Grace Wong.

FRI005

Role of liver biopsy in management of immune checkpoint inhibitors hepatitis: a single-center retrospective study

Kennie Marcin¹, Lucia Parlatti¹, Benoit Terris², Clemence Hollande¹, Anais Vallet Pichard¹, Helene Fontaine¹, Marion Cororuge¹, Loriane Lair Mehiri¹, Vincent Mallet¹, Philippe Sogni¹, Stanislas Pol¹.
¹AP-HP, Centre-Université de Paris, Groupe Hospitalier Cochin Port Royal, DMU Cancérologie et spécialités médico-chirurgicales, Service d'Hépatologie, Paris, France; ²AP-HP, Centre-Université de Paris, Groupe Hospitalier Cochin Port Royal, Service de Pathologie, Paris, France
Email: lucia.parlatti85@gmail.com

Background and aims: Immune check point inhibitors drug induced-liver injury (ICI-DILI) may be associated with chemotherapy dose reduction and cancer progression. It is unclear whether liver biopsy modifies, or not, the management of ICI-DILI. The aim of this study was to explore the impact of liver biopsy on the clinical management and the response to corticosteroids according to histological findings.

Method: We conducted a retrospective, single-center study to evaluate the biochemical, histological and clinical data of 28 patients with ICI-DILI who underwent liver biopsy (June 2015 to January 2021) in a teaching hospital in France. The severity of liver injury was graded according to Common Terminology Criteria for Adverse Events version 5.0 guidelines.

Results: Of the 28 patients (median [interquartile range] age 55 [23–80] years, 36% males), 13 patients (46%) had anti PD1 monotherapy, 6 patients (21%) anti PD1/anti CTLA4 combination therapy and 9 patients (32%) other immunotherapy. ICI-DILI occurred later in the other immunotherapy group than in the anti PD1 monotherapy and anti PD1/anti CTLA4 combination therapy groups (18.6 injections [1–60] vs 4 [1–28] and 3 [1–4] respectively, $p = 0.047$). The type of ICI did not influence the severity of the histological profile of the hepatitis, but patients receiving anti PD1/anti CTLA4 combination therapy had a tendency to more severe hepatitis in comparison to anti PD1 and other immunotherapy (83% of grade 3–4 hepatitis vs 61% and 57% respectively, $p = 0.095$). We did not observe any severe liver injury in our cohort. Corticosteroids were introduced in 6 (100%) patients of the anti PD1/anti CTLA4 combination therapy group, 7 (54%) patients of the anti PD1 monotherapy group and 4 (44%) patients under other therapy. All patients had a favourable clinical evolution after ICI withdrawal with no significative difference in the ALT normalization interval depending on the introduction of corticosteroids. The response to corticosteroids was similar according to the type of ICI and to the histological findings except for the cholangitic profile which seems to have a poorer response. The interval for ALT

normalization was 110 (20–265) days for patients with cholangitic profile without corticosteroids, 120 (18–221) days for patients with cholangitic profile with corticosteroids and 54 (29–79) days for non cholangitic patients (Figure 1).

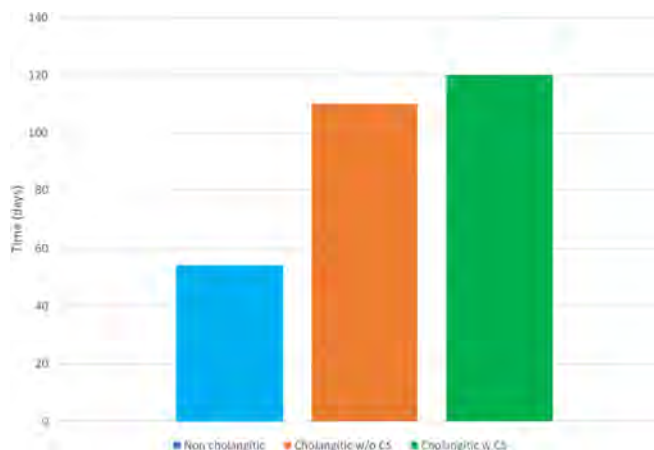


Figure: ALT normalisation interval according to cholangitic histological profile and corticosteroids treatment

Conclusion: In ICI-DILI, liver biopsy must not delay patient care but may be useful in identifying patients with a cholangitic profile who have a poorer response to corticosteroids. Corticosteroids could be reserved to patients who do not improve after ICI withdrawal.

FRI006

Immune checkpoint inhibitors induced liver injury: an observational study

Lina Hountondji¹, Pascale Palassin², Stéphanie Faure¹, Sarah Iltache¹, Marie Dupuy³, Georges-Philippe Pageaux¹, Jean Luc Faillie², Candice Lesage⁴, Elodie Negre⁵, Eric Assenat³, Patricia Rullier⁶, Valérian Rivet³, Xavier Quantin⁷, Alexandre Maria⁶, Lucy Meunier¹.
¹CHU Montpellier, Hepatology, Montpellier, France; ²CHU Montpellier, Pharmacology, Montpellier, France; ³CHU Montpellier, Oncology, Montpellier, France; ⁴CHU Montpellier, Dermatology, Montpellier, France; ⁵CHU Montpellier, Pneumology, Montpellier, France; ⁶CHU Montpellier, Internal Medicine and Multi-Organic Diseases, Montpellier, France; ⁷Montpellier Cancer Institute, Medical Oncology, Montpellier, France
Email: lucy.meunier@chu-montpellier.fr

Background and aims: Immune checkpoint inhibitors (ICI), targeting programmed cell death 1 (PD-1), its ligand (PD-L1) and anti-cytotoxic T lymphocyte-associated protein 4 (CTLA-4) changed the landscape of cancer therapy. Liver toxicity is occurring up to 16% in patients treated with ICI. International guidelines recommend pausing immunotherapy and administering corticotherapy, regardless of the hepatitis phenotype. The aim of our study is to describe the different phenotypes of ICI induced hepatitis and to assess their evolution.

Method: We conduct an observational study in patients with immune-mediated hepatitis due to ICI and submitted to the «ToxImmun» multidisciplinary meeting in Montpellier between December 2018 and October 2021. Data were collected at diagnosis, week 1, 2 and 4, and once a week until hepatitis recovery. Data regarding cancer, hepatitis treatments, and ICI rechallenging were collected. The hepatitis phenotype is defined by the ratio of serum ALT and ALP [$R \text{ value} = (\text{ALT}/\text{ULN})/(\text{ALP}/\text{ULN})$], and categorized as cholestatic ($R \leq 2$), hepatocellular ($R \geq 5$), or mixed ($2 < R < 5$).

Results: Of the 389 patients presented, hepatitis accounted for 14.7% of toxicities due to ICI ($n = 57$), 52 patients were included. 52.8% were men ($n = 28$) and the median age was 66 (range 23–87). PD-1 inhibitor was the most prescribed ICI class ($n = 48$, 92.3%), alone ($n = 31$, 59.6%), or with CTLA-4 inhibitor ($n = 17$, 32.7%). Hepatitis

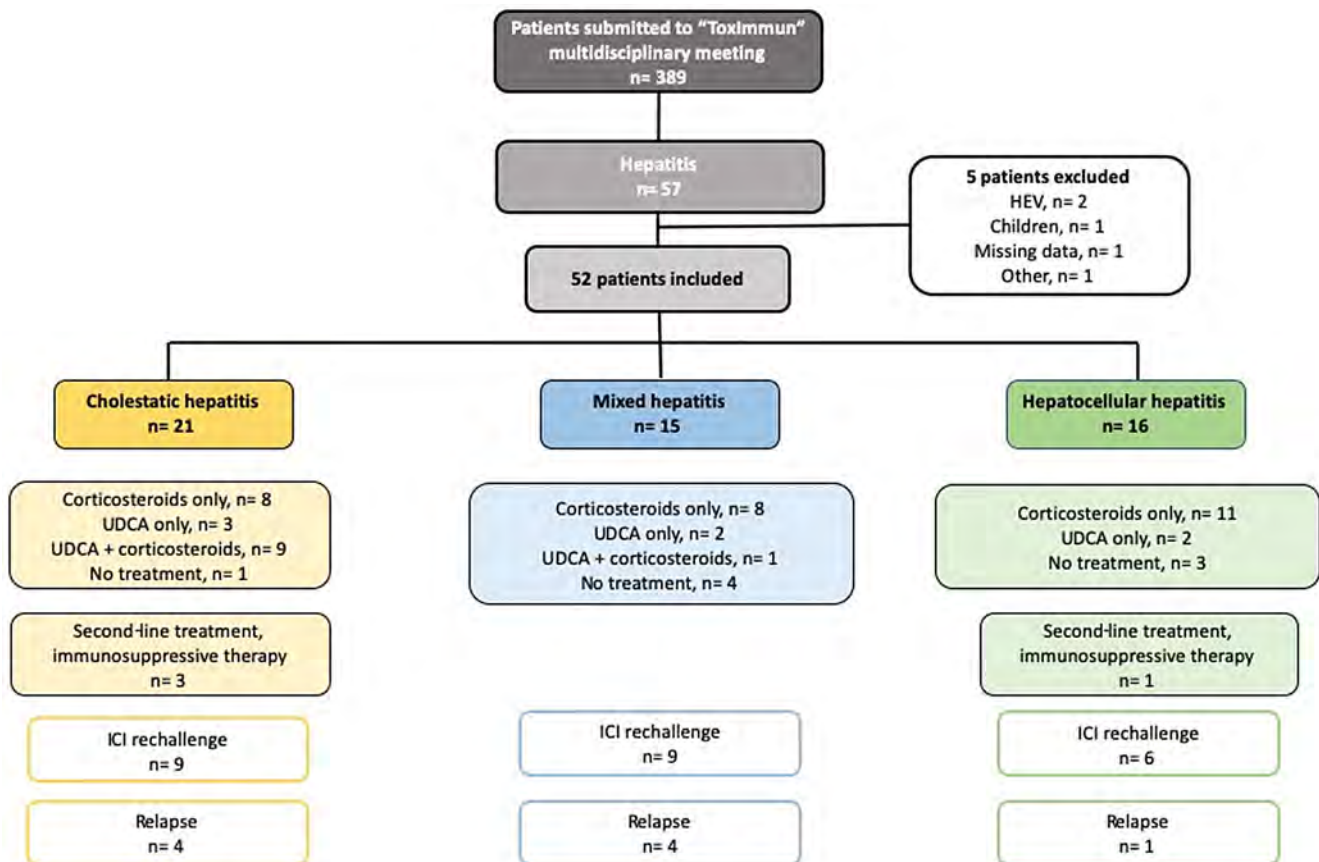


Figure: (abstract: FRI006)

phenotype was cholestatic in 40.4% (n = 21), hepatocellular in 30.8% (n = 16), and mixed in 28.8% (n = 15). Hepatitis were predominantly grade 3, according to the CTCAE system (71.2%, n = 37). No case of severe acute hepatitis has been reported. Liver biopsy was performed in 38.5% (n = 20). Biliary stenosis occurred in 6 patients (28.6%). An extra-hepatic irAE was reported in 46.2% (n = 24). Most patients were treated with corticosteroids (76.9%, n = 40) and ursodeoxycholic acid (UDCA) was in 32.7% (n = 17) patients. ICI was resumed in 46.2% (n = 24), 70.8% received the same ICI (n = 17) and 95.8% received a single ICI (n = 23). The rate of hepatitis recurrence after treatment reintroduction was 37.5% (n = 9). 10 patients died (19.2%), unrelated to ICI.

Conclusion: The frequency of ICI related hepatitis is about 14.7% in our study. This result is consistent with the literature. Future studies should be considered to adapt the treatment to the hepatitis phenotype, particularly in the case of cholestatic pattern, by specifying the place of UDCA.

FRI007

Liver toxicities of immune checkpoints inhibitors for cancer: a multicenter retrospective study

Lucia Parlati¹, Mehdi Sakka², Agnès Bellanger³, Jean François Meritet⁴, Samir Bouam⁵, Aurelia Retbi⁶, Pierre Rufat⁶, Dominique Bonnefont-Rousselot², Rui Batista⁷, Patrick Tilleul⁸, Dominique Thabut⁹, Jean-Philippe Spano¹⁰, Francois Goldwasser¹¹, Philippe Sogni¹², Stanislas Pol¹², Vincent Mallet¹², ¹AP-HP.Centre-Université de Paris, Groupe Hospitalier Cochin Port Royal, DMU Cancérologie et spécialités médico-chirurgicales, Service d'Hépatologie, Paris, France, PARIS 14E ARRONDISSEMENT, France; ²AP-HP.Sorbonne Université, Hôpitaux Universitaires Pitié Salpêtrière-Charles Foix, DMU BioGeM, Service de Biochimie Métabolique, Paris, France; ³AP-HP.

Sorbonne.Université, Hôpitaux Universitaires Pitié Salpêtrière-Charles Foix, DMU PRIME, Pharmacie à Usage Intérieur, France, France; ⁴AP-HP.Centre-Université de Paris, Groupe Hospitalier Cochin Port Royal, DMU BIOPHYGEN, Service de Virologie, Paris, France; ⁵AP-HP.Centre-Université de Paris, Groupe Hospitalier Cochin Port Royal, DMU PRIM, Service d'Information Médicale, Paris, France; ⁶AP-HP.Sorbonne Université, Hôpitaux Universitaires Pitié Salpêtrière-Charles Foix, DMU ESPRIT, Département d'Information Médicale, France; ⁷AP-HP.Centre-Université de Paris, Groupe Hospitalier Cochin Port Royal, DMU PRIME, Pharmacie clinique, Paris, France; ⁸AP-HP.Sorbonne.Université, Hôpitaux Universitaires Pitié Salpêtrière-Charles Foix, DMU PRIME, Pharmacie à Usage Intérieur, France; ⁹AP-HP.Sorbonne.Université, Hôpitaux Universitaires Pitié Salpêtrière-Charles Foix, DMU SAPERE, Service d'Hépatogastroentérologie, Paris France; ¹⁰AP-HP.Sorbonne.Université, Hôpitaux Universitaires Pitié Salpêtrière-Charles Foix, DMU ORPHE, Service d'oncologie médicale, France; ¹¹AP-HP.Centre-Université de Paris, Groupe Hospitalier Cochin Port Royal, DMU Cancérologie et spécialités médico-chirurgicales, Service de Cancérologie, Paris, France; ¹²AP-HP.Centre-Université de Paris, Groupe Hospitalier Cochin Port Royal, DMU Cancérologie et spécialités médico-chirurgicales, Service d'Hépatologie, Paris, France
Email: lucia.parlati85@gmail.com

Background and aims: There are uncertainties on the clinical significance of liver toxicities of immune checkpoint inhibitors (ICI). The aim of our study was to compare liver toxicities under ICI and conventional chemotherapy.

Method: We conducted a retrospective, longitudinal cohort study among cancer patients who received systemic chemotherapy with or without ICI between January 1, 2010, and December 31, 2019, in two teaching hospitals of Assistance Publique-Hôpitaux de Paris (France). We measured the incidence of grade 3–4 liver injury after ICI or

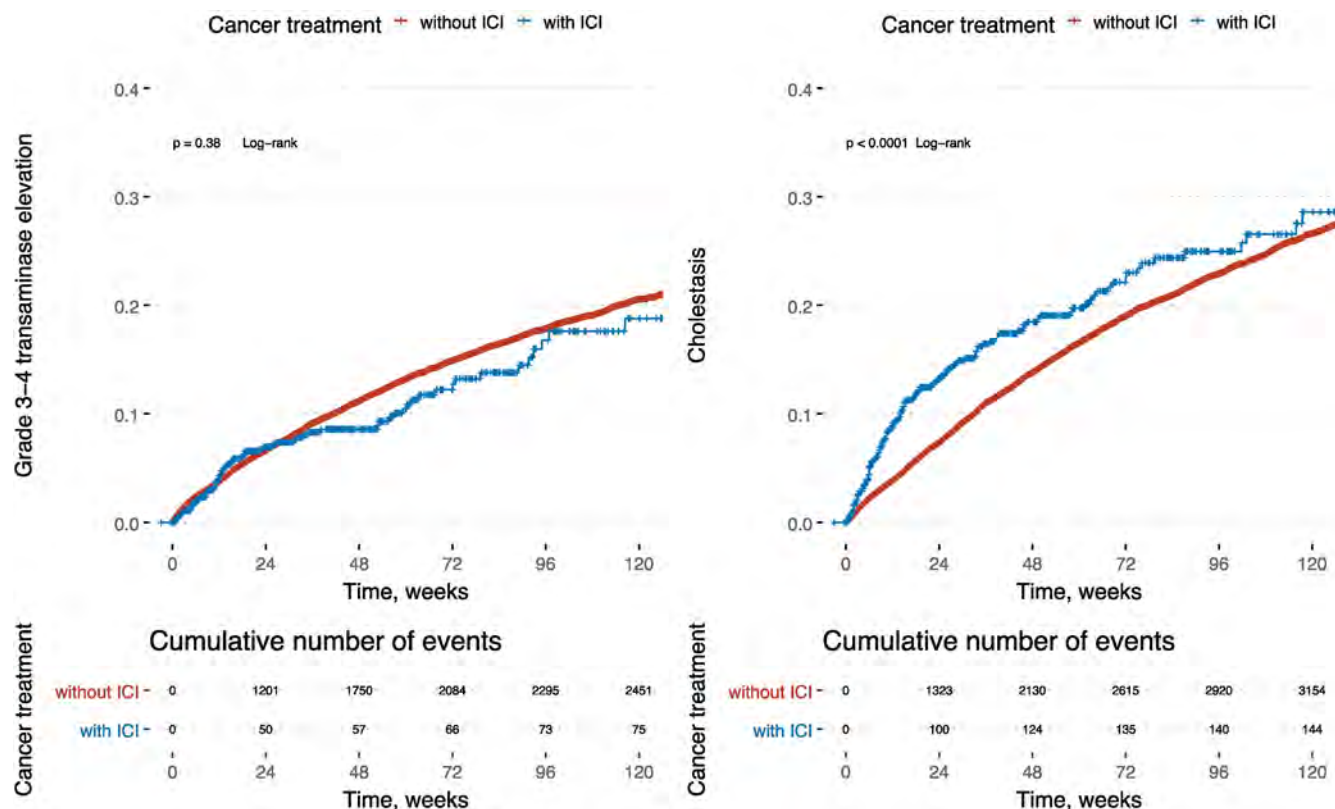


Figure: (abstract: FRI007): Cumulative incidences of liver injury after systemic chemotherapy in a multicenter, retrospective, cohort of cancer patients (N = 22, 206).

conventional chemotherapy, the adjusted hazard ratios [aHR (95% CI)] for hepatocellular injury, cholestasis and jaundice and investigated the management and outcome of patients with ICI drug-induced liver injury (ICI-DILI).

Results: The sample comprised 22, 206 patients (median [interquartile range] age 63 [52–72] years, 54.4% males), including 953 (4.3%) with ICI. The incidence of grade 3–4 liver injury was 209 (21.9%) and 5, 765 (27.1%) for patients treated with and without ICI, respectively (p < 0.001). ICI patients were at risk [aHR 1.46 (1.23–1.75) P < 0.001] for cholestasis without [aHR 0.96 (0.60–1.53) P = 0.860] jaundice. ICI patients were not [aHR 1.12 (0.86–1.45), P = 0.401] at risk for hepatocellular injury. Grade 3–4 liver injury was attributed to ICI-DILI in 26 (2.7%) patients. Grade 4 transaminase and serum bilirubin elevations concerned 6 (0.6%) and 1 (0.1%) ICI-DILI patient, respectively. All patients with ICI DILI had ICI withdrawal, and 11 (42.3%) died thereafter with cancer progression. ICI reintroduction after ICI-DILI was a rare (n = 7; 26.9%) event and was infrequently (n = 1) associated with recurrent liver injury.

Conclusion: Patients treated with ICI were at lower risk of clinically significant liver injury than patients treated with conventional chemotherapy. There may be potential gains from refraining ICI dose reduction in patients with ICI-associated liver injury.

FRI008

Acute severe presentation of autoimmune hepatitis: a 20-year retrospective review of the United States

Thomas Enke¹, Daniel Ganger¹, Jody Rule², Richard Stravitz³, Jorge Rakela⁴, Adrian Reuben⁵, Norman Sussman⁶, Anne Larson⁷, Shannan Tujios², Nathan Bass⁸, Sherry Livingston⁹, Valerie Durkalski-Mauldin⁹, William M. Lee². ¹Northwestern

University Feinberg School of Medicine, Chicago, United States; ²UT Southwestern Medical Center, Dallas, United States; ³Virginia Commonwealth University Medical Center, Richmond, United States; ⁴Mayo Clinic, Phoenix, United States; ⁵Medical University of South Carolina, Columbia, United States; ⁶Baylor College of Medicine, Houston, United States; ⁷University of Washington Medicine, Seattle, United States; ⁸University of California San Francisco, San Francisco, United States; ⁹Medical University of South Carolina, Columbia Email: thomas.enke@northwestern.edu

Background and aims: Autoimmune hepatitis (AIH) is a common cause of acute liver failure (ALF). Treatment includes steroids in those with acute liver injury (ALI) and liver transplantation (LT) in those who fail to respond or develop ALF. The aim of this study is to better characterize the clinical and laboratory data of patients presenting with ALI or ALF secondary to AIH and to identify a combination of clinical variables that predict 21-day transplant-free survival (TFS).

Method: The study included hospitalized adults presenting with ALI or ALF enrolled in the Acute Liver Failure Study Group Registry between 1998 and 2019 from 32 centers within the United States. A review panel adjudicated the etiology of all cases and those identified as AIH were reviewed. ALI was defined as international normalized ratio (INR) ≥ 2.0 without encephalopathy and ALF as any degree of encephalopathy with INR ≥ 1.5. Laboratory and clinical data were reviewed, and variables significantly associated with 21-day TFS were used to develop a multivariable logistic regression model.

Results: A total of 244 of 3364 cases were identified as AIH and reviewed. 161 patients (66%) were diagnosed with ALF and 83 with ALI (34%). At 21 days, 116 patients (48%) had undergone LT, 69 (28%) had TFS and 59 (24%) had died. Patients presenting with ALI had a higher TFS rate (53%) than patients presenting with ALF (16%). Most presenting with ALI received steroids (73%) and were more likely to have TFS (66%) than those who did not receive steroids

(18%). Administration of steroids in those with ALI, admission values of bilirubin, INR, albumin and platelet count were significantly associated with improved TFS and a diagnosis of ALF in those who received steroids was associated with worse TFS in a multivariable logistic regression analysis. The resulting model predicted TFS with a C-statistic of 0.94.

Table 1: Variables associated with 21-day transplant free survival

Multivariate model		
Predictor	Adjusted odds ratio	95% CI ^a
Bilirubin	0.04	(0.01, 0.15)
INR ^b	0.30	(0.16, 0.56)
Platelet count	1.06	(1.01, 1.10)
Albumin	3.10	(1.34, 7.16)
Steroid use with ALI ^c	31.19	(3.35, 290.05)
Steroid use with ALF ^d	1.62	(0.57, 4.58)
ALF without steroid use	0.78	(0.11, 5.51)
ALF with steroid use	0.041	(0.01, 0.171)

^aCI = confidence interval.

^bINR = international normalized ratio.

^cALI = acute liver injury.

^dALF = acute liver failure during hospitalization.

Conclusion: Acute severe presentations of AIH are associated with a high mortality. Steroids remain a cornerstone of treatment and nearly half of patients will require LT. Early identification of those needing LT is critical to prevent delays in listing. We developed a model specifically for AIH that may be helpful in predicting 21-day TFS and early identification of patients in need for expedited LT evaluation. Further assessment of model performance and independent model validation are future work.

FRI009

Single-cell metabolic profiling of primary human hepatocytes shows heterogeneous responses to drug metabolism

Eva Sofía Sánchez Quant¹, Maria Richter¹, Celia Martinez Jimenez^{1,2}, Maria Colome Tatche^{3,4,5}. ¹Helmholtz Zentrum Munich, Helmholtz Pioneer Campus, Munich, Germany; ²Technical University Munich, Faculty of Medicine, Munich, Germany; ³Helmholtz Zentrum Munich, Institute of Computational Biology, Munich, Germany; ⁴Ludwig Maximilian University of Munich, Biomedical Center (BMC), Physiological Chemistry, Munich, Germany; ⁵Technical University Munich, TUM School of Life Sciences Weihenstephan, Munich, Germany
Email: eva.sanchez@helmholtz-muenchen.de

Background and aims: Drugs are primarily metabolized by hepatocytes in the liver, and primary human hepatocytes (PHHs) are the gold standard model for the assessment of drug efficacy, safety and toxicity in the early phases of drug development. Classic approaches assume that all hepatocytes in culture are homogeneous and share a similar metabolic profile. However, advances in single-cell genomics have shown the relevance of cellular heterogeneity in health and disease conditions.^{1,2} Recently, single-cell RNA sequencing has shown that intrahepatic lipid accumulation in Non-alcoholic fatty liver disease (NAFLD) affects the transcriptomic profile of parenchymal and non-parenchymal liver cells.^{3,4} The aim of this study is to investigate the metabolic capacity of individual human hepatocytes *in vitro*, and assess whether the chronic accumulation of lipids enhances cellular heterogeneity.

Method: PHHs isolated from four donors were incubated with a phenotyping 5-probe cocktail (Sanofi-Aventis⁵) using the so-called "cocktail approach." In order to mimic the hepatic steatosis occurring in NAFLD, hepatocytes were loaded with free fatty acids, resulting in intracellular lipid accumulation. Subsequently, cells were incubated with the five-drug cocktail. After 72 h in culture, hepatocytes were collected and single-cell RNA-sequencing was performed using a droplet-based approach.

Results: Four subgroups of hepatocytes were identified consistently, independently of the treatment condition, and across all four donors.

These subgroups displayed differential gene expression upon cocktail treatment, and xenobiotic metabolism-related specialization. Furthermore, lipid accumulation was found to increase transcriptional variability in two subgroups of hepatocytes, and to differentially affect the expression of genes involved in lipid metabolism. In particular, intracellular fat accumulation was shown to diminish the drug-related metabolic capacity of hepatocytes.

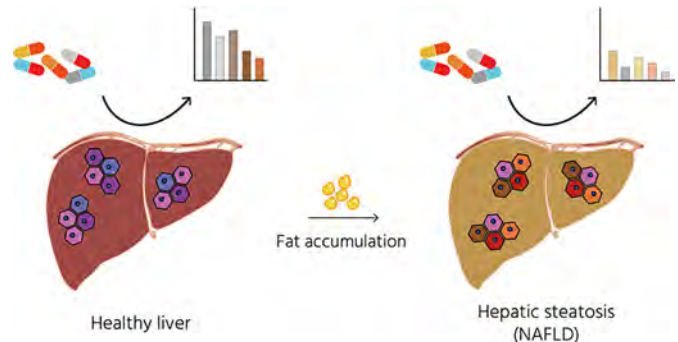


Figure: Graphical abstract summarizing the hypothesis stated.

Conclusion: Our results demonstrate that, upon a metabolic challenge such as exposure to drugs or intracellular fat accumulation, hepatocyte subgroups exhibit heterogeneous transcriptomic responses.

References

1. Richter M. L. *et al.* (2021). *Nat Commun.*
2. Kamies R. and Martinez-Jimenez C. P. (2020). *Mamm Genome.*
3. Xiong X. *et al.* (2019). *Molecular Cell.*
4. Park S. R. *et al.* (2020). *American Journal of Physiology-Endocrinology and Metabolism.*
5. Turpault S. *et al.* (2009). *Br J Clin Pharmacol.*

FRI010

Management of severe, steroid-resistant and steroid-refractory hepatotoxicity in patients treated with checkpoint inhibitor immunotherapy

Nashla Hamdan¹, Marco Iafolla², Yada Kanjanapan², Marcus Butler², Lillian Siu², Philippe Bedard², Kendra Ross², Keyur Patel¹, Anna Spreafico², Jordan Feld¹, Morven Cunningham¹. ¹University Health Network, Toronto Centre for Liver Disease, Toronto, Canada; ²University Health Network, Princess Margaret Cancer Centre, Toronto, Canada
Email: morven_c@hotmail.com

Background and aims: Checkpoint inhibitor immunotherapy (ICI) has revolutionized cancer care and is increasingly used in a range of primary malignancies. Treatment is associated with immune-related toxicities which may require ICI discontinuation and immunosuppressive therapies (IST). Management of severe ICI hepatotoxicity is not well defined, especially for patients who respond poorly to initial corticosteroids. We sought to better understand management of severe ICI hepatotoxicity and responses to IST.

Method: Patients receiving ICI in early phase clinical trials at Princess Margaret Cancer Centre, or treated at the Toronto Centre for Liver Disease for ICI hepatotoxicity, were included. Patients with CTCAE Grade (G)3/4 ICI hepatotoxicity (ALT >5 × ULN) were identified and clinical records reviewed for management and outcomes.

Results: From Aug 2012-Oct 2021, 25 patients with G3/4 ICI hepatotoxicity were identified. Most (17; 68%) had metastatic melanoma. Eleven received anti-CTLA-4/PD-1; 9 anti-PD-1, and 5 anti-CTLA-4 monotherapy. All patients initially received corticosteroids for hepatotoxicity (1–2 mg/kg/day prednisone equivalent). Figure 1 shows response to corticosteroids and sequence of additional IST. 13 patients (52%) were steroid-refractory (no response after 48–72 hours) or steroid-resistant (rebound ALT upon steroid

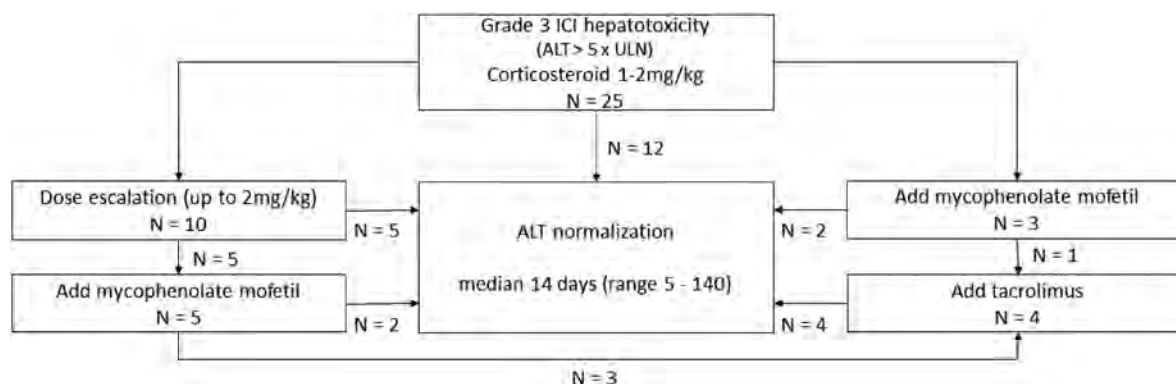


Figure: (abstract: FRI010)

taper). Ten received steroid dose escalation (up to 2 mg/kg/day) with sustained response in five (50%). Eight (32%) received 2nd line IST with mycophenolate (MMF) for steroid resistant/refractory hepatotoxicity, after median 17.5 days of steroid treatment (IQR 9–21). Four (50%; 16% of total cohort) did not respond to MMF and required 3rd line IST (Tacrolimus; dose targeting trough level of 4–6). Age, sex, liver metastases, prior ICI exposure or peak ALT did not predict need for 2nd or 3rd line IST. ALT normalized in all, after median 14 days (IQR 10–27). Patients on corticosteroid alone had shorter total time on IST than those with additional IST (median 86 days, IQR 41–123) vs 113 days (85–235), $p = 0.03$). In those given additional IST, rate of ALT improvement tended to be faster with Tacrolimus than MMF (25.5 IU/day (IQR 22–29.5) vs 10.5 IU/day (IQR –3 to 29.5), $p = ns$ in this small cohort). IST-related adverse events occurred in two patients (vertebral fracture; hyperglycaemia). Over median follow up of 30.6 months (range 2.3–81.5), 12 patients died. No patients died of complications of hepatotoxicity.

Conclusion: Up to a third of patients with severe (G3/4) ICI hepatotoxicity may not respond adequately to corticosteroids and require additional IST. MMF is not consistently effective as 2nd line IST. To expedite resolution and minimize IST exposure, Tacrolimus should be considered 2nd line IST alternative. These results will assist development of treatment algorithms for severe ICI hepatotoxicity, for further prospective evaluation.

FRI011

Activation marker CD69 differentiates non-alcoholic steatohepatitis from drug-induced liver injury

Estefanía Caballano-Infantes¹, Alberto García García¹, Carlos Lopez-Gomez¹, A. Cueto², Mercedes Robles-Díaz³, Aida Ortega-Alonso¹, F. Martin-Reyes¹, Ismael Alvarez-Alvarez², Isabel Arranz-Salas⁴, Francisco Ruiz-Cabello⁵, Maria Isabel Lucena^{2,6}, Eduardo García-Fuentes¹, Raul J. Andrade^{1,3}, Miren Garcia Cortes¹.

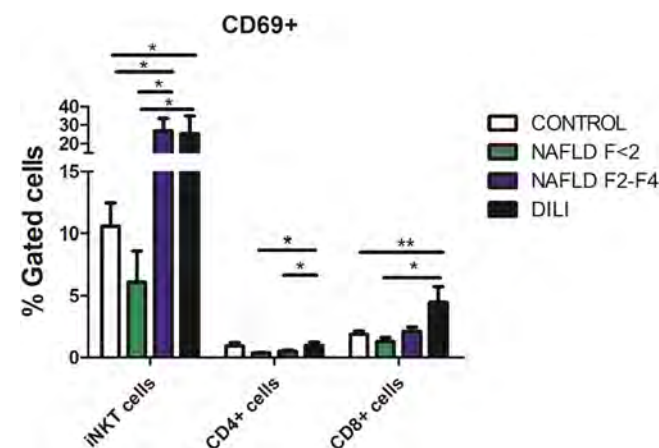
¹IBIMA, Servicio de Aparato Digestivo, Hospital Universitario Virgen de la Victoria, IBIMA, UMA, Malaga, Spain; ²UMA, Departamento de Farmacología, Málaga, Spain; ³UMA, Departamento de Medicina, Málaga, Spain; ⁴IBIMA, Servicio de Anatomía Patológica, Málaga, Spain; ⁵Hospital Universitario Virgen de las Nieves/UGR, Servicio de Análisis Clínicos e Inmunología/Departamento de Bioquímica y Biología Molecular II/Inmunología, Facultad de Medicina, Granada, Spain; ⁶IBIMA, Málaga, Spain
Email: edugf1@gmail.com

Background and aims: Activation of the immune system is involved in both non-alcoholic fatty liver disease (NAFLD) and idiosyncratic drug-induced liver injury (DILI). We aimed to identify activation markers in invariant natural killer T (iNKT) and CD4/CD8+ T cells to better understand the pathophysiology of these disorders.

Method: We analyzed the activation profile (CD69, CD25 and HLA-DR) and NKG2D on iNKT cells, and CD4/CD8 T cells by flow cytometry

in peripheral blood mononuclear cells from NAFLD, with or without significant liver fibrosis, and DILI patients.

Results: There was an increase in iNKT cells in NAFLD patients compared to DILI or control subjects ($p = 0.035$ and $p = 0.031$, respectively). Regarding the cellular activation profile, NAFLD with significant liver fibrosis ($F \geq 2$) displayed higher levels of CD69+ iNKT cells compared to NAFLD with none or mild liver fibrosis ($F \leq 1$) ($p = 0.040$) and control patients ($p = 0.031$). CD69+ iNKT positively correlated with insulin resistance, liver fibrosis indexes FIB4 and APRI, and AST levels. DILI patients showed an increase in CD69+ and HLA-DR+ in both CD4+ and CD8+ T cells, detecting the most relevant difference in the case of CD69+ CD8+ T cells.



Conclusion: CD69+ iNKT may be a biomarker to assess liver fibrosis progression in NAFLD. CD69+ CD8+ T cells were identified as a potential distinctive biomarker for distinguishing DILI from NAFLD. These results support the involvement of the immune system on NAFLD with significant liver fibrosis and DILI development.

FRI012

Natural antibodies are required for necrotic cell debris clearance and liver repair during necrotic liver injury

Matheus Mattos¹, Sofie Vandendriessche¹, Sara Schuermans¹, Romy Mittenzwei², Ari Waisman², Pedro Elias Marques¹. ¹Rega Institute Ku Leuven, Leuven, Belgium; ²Institute for Molecular Medicine, University Medical Center of the Johannes Gutenberg-University Mainz, Mainz, Germany
Email: pedro.marques@kuleuven.be

This abstract is under embargo until Thursday 23 June 2022, 13:30 BST. It will be made publicly available on the congress website once the embargo has lifted.

Journalists, industry, investigators and/or study sponsors must abide by the embargo times set by EASL.

Violation of the embargo will be taken seriously. Individuals and/or sponsors who violate EASL's embargo policy may face sanctions relating to current and future abstract submissions, presentations and visibility at EASL Congresses. The EASL Governing Board is at liberty to ban attendance and/or retract data.

Copyright for abstracts (both oral and poster) on the website and as made available during The International Liver Congress™ 2022 resides with the respective authors. No reproduction, re-use or transcription for any commercial purpose or use of the content is permitted without the written permission of the authors. Permission for re-use must be obtained directly from the authors.

Method: We used the Caco-2 human colorectal adenocarcinoma cell line to represent gut and the human hepatic HepaRG line to represent liver. Caco2 cells were incubated with 0, 5, 10 and 20 mM of APAP for 24 hours. Supernatant was transferred onto fresh HepaRG cells for a further 24 hours. Cell cultures were monitored in real time using the ECIS Z0, an impedance based cellular assay, using multiple frequencies to measure tight junctions, adhesion (4 kHz) and cell membrane integrity (64 kHz). Viability was assessed using PrestoBlue, to monitor cell metabolism, and Promega Celltiter glo for a measure of total ATP. Percentage of APAP metabolized by Caco2 cells was measured using LC-MS/MS. IL-8, IL-1b, IL-6, IL-10, TNF, and IL-12p70 were measured using the CBA Human Inflammatory Cytokines kit flow-cytometry bead assay.

Results: ECIS measurements showed an increase in tight junctions/adhesion in a concentration dependent manner on Caco2 cells. In contrast to previously published work,¹ when using Caco2 preconditioned media, toxicity to HepaRG cells was mitigated with no loss of tight junctions. LC-MS/MS showed that Caco2 cells metabolize 64–68% of total APAP without any adverse effect on their viability. IL-6 and IL-8 produced by HepaRG cells was appropriately reduced suggesting an anti-inflammatory effect of APAP.

Conclusion: We have shown that intestinal cells are capable of removing 2/3 APAP within the intestinal barrier with no compromise of viability or tight junctions mitigating toxicity to hepatic cells. Based on these observations, the intestine is an effective barrier protecting the liver from APAP hepatotoxicity therefore parenteral administration of APAP should be avoided and if no other option intravenous dose should be adjusted accordingly.

Reference

1. Gamal Treskes *et al.* 2017. Low-dose acetaminophen induces early disruption of cell-cell tight junctions in human hepatic cells and mouse liver.

FRI014

A new score to predict mortality at baseline in patients not fulfilling KCH criteria for non acetaminophen induced liver failure-The "SAFE" score (Severity of ALF in emergency)

Harshvardhan Tevethia¹, Rakhi Maiwall¹, Shalini Thapar², Roshan Koul³, Prashant Mohan Agarwal⁴, Guresh Kumar⁵, Ashok Choudhury¹, Shiv Kumar Sarin⁶. ¹Institute of Liver and Biliary Sciences, Hepatology, Delhi, India; ²Institute of Liver and Biliary Sciences, Radiology, Delhi, India; ³Institute of Liver and Biliary Sciences, Neurology, Delhi, India; ⁴Institute of Liver and Biliary Sciences, Critical Care, Delhi, India; ⁵Institute of Liver and Biliary Sciences, Biostatistics, Delhi, India; ⁶Institute of Liver and Biliary Sciences, Hepatology, Delhi, India
Email: harshvardhantevethia@gmail.com

Background and aims: Prognostic scores in ALF such as King's College Hospital (KCH) Score have limited sensitivity in stratifying patients for liver transplant especially related to non-acetaminophen etiology, leading to delayed listing and poor outcomes. The MELD score also has limitations with the use of creatinine which is not a true representative of liver injury. We studied ALF patients not fulfilling KCH criteria; for their clinical course, outcomes, liver volume, markers of cerebral edema like Optic Nerve Sheath Diameter (ONSD) to develop a new score to predict mortality at baseline.

Method: Patients diagnosed to have ALF and not fulfilling KCH criteria at admission were enrolled and electronic data was retrieved [from June 2010 to May 2021] from the HIS using a predefined format. All patients underwent CT imaging (Non contrast) of both Brain and abdomen at admission. The Liver volume was calculated (CT) along with changes of cerebral edema were recorded. Baseline parameters were correlated along with predictors of outcome, need for liver transplant, KCH and MELD scores. Cox regression analysis was done at baseline for prediction of mortality.

Results: A total of 75 patients were screened of which 49 (65.5%) patients did not fulfil the KCH criteria [mean age 33.24 ± 15.5 years,

FRI013

Human paracetamol hepatotoxicity is mitigated by the gut-liver axis in vitro

Katie Morgan¹, Martin Vandeputte¹, Kay Samuel², Steven Morley¹, Natalie Homer³, Martin Waterfall⁴, Jonathan Fallowfield^{1,5}, Peter Hayes¹, John Plevris¹. ¹University of Edinburgh, Hepatology Dept, Edinburgh, United Kingdom; ²Scottish National Blood Transfusion Service, The Jack Copland Centre 52 Research Avenue North, Edinburgh, United Kingdom; ³University of Edinburgh, Mass spectrometry core, Edinburgh, United Kingdom; ⁴University of Edinburgh, Flow Cytometry Core Facility, Edinburgh, United Kingdom; ⁵University of Edinburgh, Centre for Inflammation Research, Edinburgh, United Kingdom
Email: katie.morgan@ed.ac.uk

Background and aims: The gut liver axis is a bidirectional system communicating via signals from the microbiome, immune system, dietary and genetic influences. We have previously shown in vitro that APAP disrupts tight junctions in hepatic HepaRG cells in a concentration dependant manner.¹ The aim of this study, was to develop a model of enterohepatic circulation of paracetamol (APAP) *in vitro* and establish whether intestinal barrier has a hepatoprotective effect in the context of APAP toxicity.

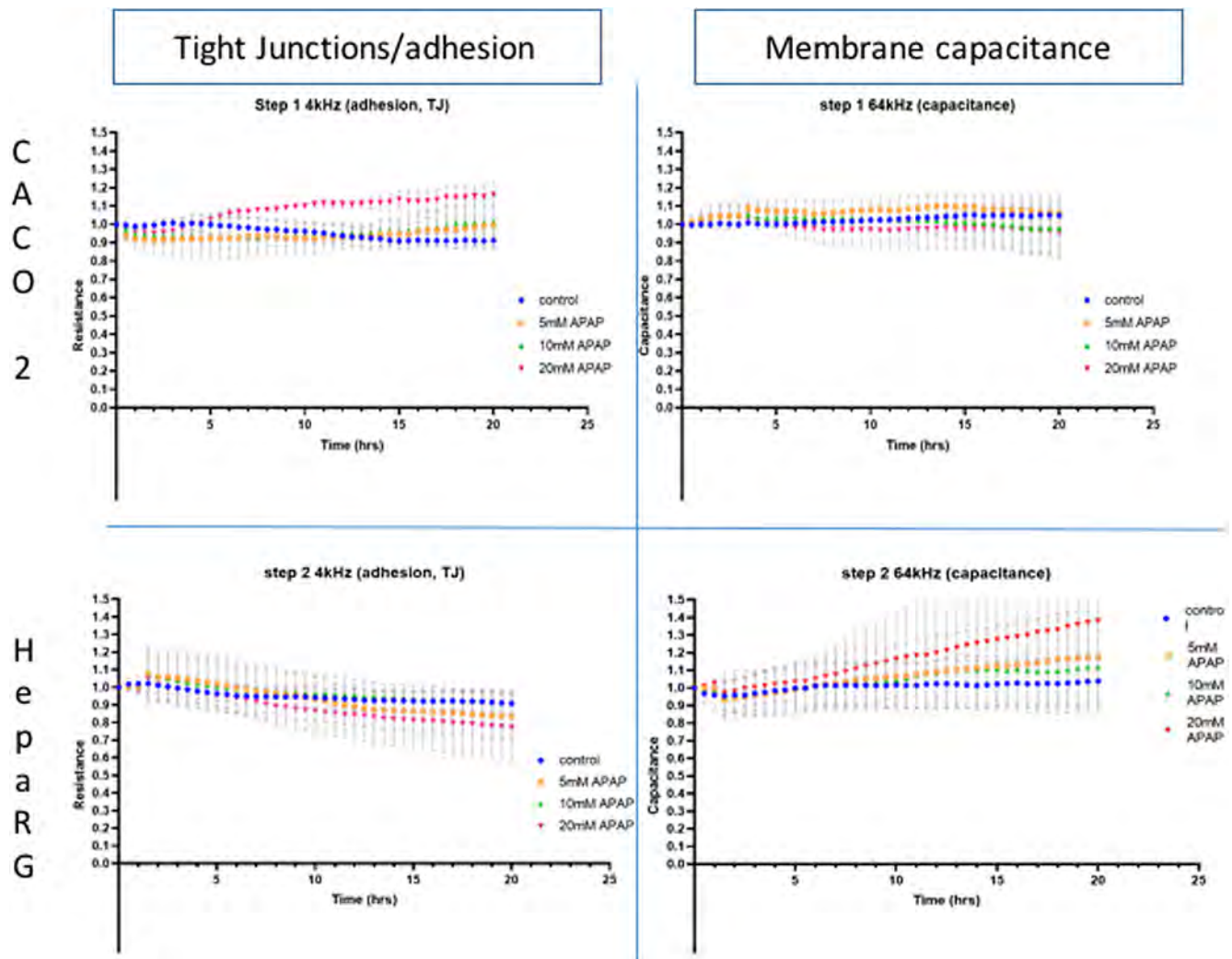
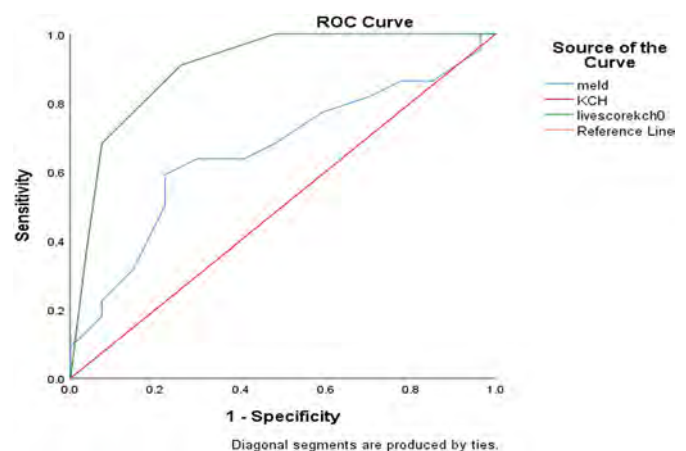


Figure: (abstract: FRI013)

males 59.2%]. The all-cause mortality in patients not meeting the KCH criteria was 44.8%. The most common etiology was hepatitis E (34.7%) followed by indeterminate etiology (28.6%). On the CT imaging of the brain, cerebral edema was seen in 34% patients; with significantly lower liver volume in the ALF non-survivors than survivors ($765 \pm 465 \text{ cm}^3$ vs $1265 \pm 346 \text{ cm}^3$ $p < 0.04$). On univariate analysis Grade >3 Hepatic encephalopathy (HE), ONSD (both right/left eye) $>5 \text{ mm}$, jaundice to HE duration >9 days and liver volume $<980 \text{ cm}^3$ were found to be significant. On multivariate analysis, HE grade 3 (OR- 7.671, 95% C.I- 0.912–64.55), ONSD $>5 \text{ mm}$ (OR- 22.14 95% C.I- 1.943–252.423), jaundice to encephalopathy >9 days (O.R- 24.82 95% C.I- 2.293–268.65) were found to be significant. We developed the “SAFE” score using these variables. A score of 5, gave the AUROC value of 90.9 with $p < 0.01$ (95% CI-82.9–98) with a sensitivity of 90%, specificity of 71%, positive and negative predictive values of 82% and 73% respectively with Youden index at 50%. On comparison with KCH (50, 95% C.I-33.6–64.4) and MELD score (65.9, 95% C.I -50–81.9) the SAFE score was significantly better at predicting mortality in ALF patients at baseline.



Conclusion: In patients not fulfilling the KCH criteria, the newly developed SAFE score was significantly better in predicting worse outcomes. Its variables indicate the presence of cerebral edema and low liver volume as the main causes of mortality in these subset of patients. Application of the SAFE score should be validated and a routine use of CT brain and liver be practiced for better stratification of ALF patients at baseline.

FRI015

Ten-year single center experience in hepatotoxicity due to mushroom poisoning

Ozan Sarıkaya¹, İlker Turan¹, Fulya Günsar¹, Aysenur Arslan², Nilay Daniş³, Ferit Çelik¹, Galip Ersoz¹, Sezgin Ulukaya⁴, Murat Zeytunlu⁵, Omer Ozutemiz¹, Ulus Akarca¹, Zeki Karasu¹. ¹Ege University, Medical Faculty, Gastroenterology, Izmir, Turkey; ²Ege University, Medical Faculty, Internal Medicine, Izmir, Turkey; ³Karabuk University, Gastroenterology, Karabuk, Turkey; ⁴Ege University, Medical Faculty, Anesteziology, Izmir, Turkey; ⁵Ege University, Medical Faculty, General Surgery, Izmir, Turkey
Email: ulusakarca@gmail.com

Background and aims: Mushroom poisoning is quite common in Turkey. It can cause acute liver injury and acute liver failure (ALF) requiring liver transplantation. We investigated the outcomes of patients with acute hepatotoxicity due to mushroom poisoning in our cohort.

Method: We retrospectively evaluated the characteristics of patients with liver toxicity due to mushroom poisoning. We also investigated parameters related to mortality or liver transplantation.

Results: Thirty patients (17/13: F/M, median age 50.4 (22–73)) were included in the study. Twenty-seven patients presented with nausea and vomiting. In addition, fourteen patients had abdominal pain and sixteen had diarrhea. These patients were admitted to our intensive care unit within an average of 2.5 days (6 hours–8 days) after eating mushrooms from the countryside. In 15 patients (fourteen at admission, one during hospitalization), INR increased >1.5, acute liver failure developed in 4 patients (two patients at admission, hepatic encephalopathy developed in two patients during follow-up). The peak levels of ALT, AST and total bilirubin were 2109 ± 1963 U/L, 1828 ± 1675 U/L, 4.92 (0.1–28.56 mg/dl), respectively. In hospital follow-up, the highest INR levels were found to be an average of 2.29 (±1.56). All patients were treated with N-acetylcysteine (NAC). Seven patients were treated with penicillin G, six patients with silymarin, and two patients with both penicillin G and silymarin. Eight patients underwent plasmapheresis (median 6 times). Two of the four patients with ALF underwent emergency liver transplantation, and one patient died 72 days after transplantation. One patient who developed ALF recovered with medical treatment, while the other patient who could not be transplanted died. In multivariate analysis, INR and chlorine levels at hospital admission were found to be statistically significant factors for death and liver transplantation. (respectively; OR: 17.8 and p: 0.04 and OR: 0.54 and p: 0.04)

Conclusion: In our cohort, the mortality rate of mushroom liver toxicity was 10%. High INR levels and detection of hypochloremia have been associated with serious outcomes such as liver transplantation or mortality, and these parameters may be predictive of urgent liver transplantation.

FRI016

CCl4-induced acute liver injury in C57/BL mice model showed elevated expressions of Na⁺ taurocholate cotransporting polypeptide on intestinal stellate cells

Johnny Amer¹, Reem Sbieh¹, Ahmed Salhab¹, Rifaat Safadi¹. ¹Hadassah Hebrew University Hospital, Liver Unit, Jerusalem, Israel
Email: johnnyamer@hotmail.com

Background and aims: The Na⁺ taurocholate cotransporting polypeptide (NTCP/SLC10A1) is believed to be pivotal for hepatic uptake of conjugated bile acids. In the case of acute liver injury (ALI), NTCP is downregulated leading to hepatic and biliary injury, driving inflammatory and fibrotic processes. Several studies linked ALI to cause intestinal mucosa damaged. In this study, we aimed to evaluate whether bile acid (BAs) trafficking interfere with intestinal stellate cells in an ALI of CCl₄ mice model.

Method: C57/BL mice were *i.p* injected (1X) with CCl₄ (xxx) to induce ALI. Livers, intestinal stellate cells (ICS) isolated from intestine and serum were obtained from mice and assessed for inflammatory (H&E

staining, ALT and pro-inflammatory panel of cytokines), fibrosis (Sirius red staining, α-smooth muscle actin, collagen and fibronectin) and metabolic (BAs, cholesterol, triglyceride, glucose tolerance test (GTT) and fasting blood sugar (FBS)) profiles. In addition, ICS were assessed for NTCP and membrane injury of surfactant D (SP-D) and the receptor for advanced glycation end-products (RAGE). BAs trafficking were assessed in ICS and their impact on proliferation and apoptosis were evaluated.

Results: Compared to WT mice, CCl₄-induced ALI and was worsened in the histopathology outcome. In addition, serum showed elevated levels of BAs (3-fold; P = 0.002) associated with increased RAGE, TNF-α, MCP-1, INF-γ, IL-1, IL-6 and IL-8 (p < 0.01). Moreover, CCl₄-induced ALI showed elevated serum levels in liver enzymes, lipids, glucose and metabolic markers (p < 0.01). ICS showed high expressions of αSMA and were correlated with elevated expressions of NTCP. ICS BAs intracellular concentrations were increased (2-fold) with increased SP-D (1.2-fold) as well as elevation in their apoptotic rate (2.1-fold) in the ALI mice model.

Conclusion: NTCP modulatory expressions on ICS could be an important step in the pathogenesis of ALI. Antagonizing BAs uptake may suggest a therapeutic strategy in improving liver-gut axis.

FRI017

The association between chronic Colchicine use and incident decompensated cirrhosis

Michal Carmiel^{1,2}, Fadi Hassan^{2,3}, Vered Rosenberg⁴, Gabriel Chodik^{4,5}, Mohammad Naffaa^{2,3}. ¹Galilee Medical Center, Liver Unit, Nahariya, Israel; ²Bar-Ilan University, The Azrieli Faculty of Medicine, Safed, Israel; ³Galilee Medical Center, Rheumatology Unit, Nahariya, Israel; ⁴Maccabi Healthcare Services, Epidemiology and Database Research, Tel Aviv, Israel; ⁵Tel-Aviv University, Sackler Faculty of Medicine, Tel Aviv, Israel
Email: michalc@gmc.gov.il

Background and aims: Colchicine (COL) is an anti-inflammatory agent, prescribed as a chronic treatment in some medical conditions. Although high doses inhibits microtubule formation resulting in mitotic arrest and hepatotoxicity, in clinical practice COL is considered safe due to relatively low doses. In this study, we examined the association between chronic use of COL and the incidence of decompensated cirrhosis event.

Method: A cohort study using computerized database of 2.3-million member Maccabi Healthcare Services in Israel. All patients ≥18 y/o who initiated COL between Jan. 1 2000 and Dec. 31 2018 were included. Patients were followed until first event of decompensated cirrhosis (DC), leaving MHS, death or Dec. 31 2019. Excluded: patients with a diagnosis of cirrhosis, chronic HBV, HCV, alcoholic or biliary disease at baseline, patients who developed an event within 12 months of follow-up, patients treated <30 days, and patients treated with a mean daily treatment >3 mg/day. COL exposure was evaluated as the Proportion of Months Covered with drug (PMC) and by Mean Daily Dose (MDD). The PMC was categorized as follows: <20%, 20–40%, 40–60%, 60–80%, >80%. Cox regression models were used to calculate the hazard ratios (HR) and confidence intervals (CI) for the development of DC.

Results: A total of 21773 eligible patients initiated COL during study period. During follow-up, 129 incident cases of DC were identified (68.5/100,000 person-years, mean follow-up 8.65 ± 5.53 years). In univariate analysis: COL PMC as well as older age, Familial Mediterranean Fever (FMF), HbA1c ≥ 6.5, BMI > 40 and Fib-4 > 1.45 at baseline were associated with an event of DC. In multivariate analysis: FMF, BMI > 40, FIB-4 > 1.45 and COL PMC were all significantly associated with incident of DC. The highest risk for developing DC (HR 3.68, 95% CI 2.23–6.07) was in '60–80%' PMC group. Restricting analysis to patients treated for >12 and >60 months, the risk for DC in the PMC group '60–80%' was higher, (HR 4.56, 95% CI 2.74–7.58) and (HR 6.69, 95% CI 3.56–12.56), respectively. Patients

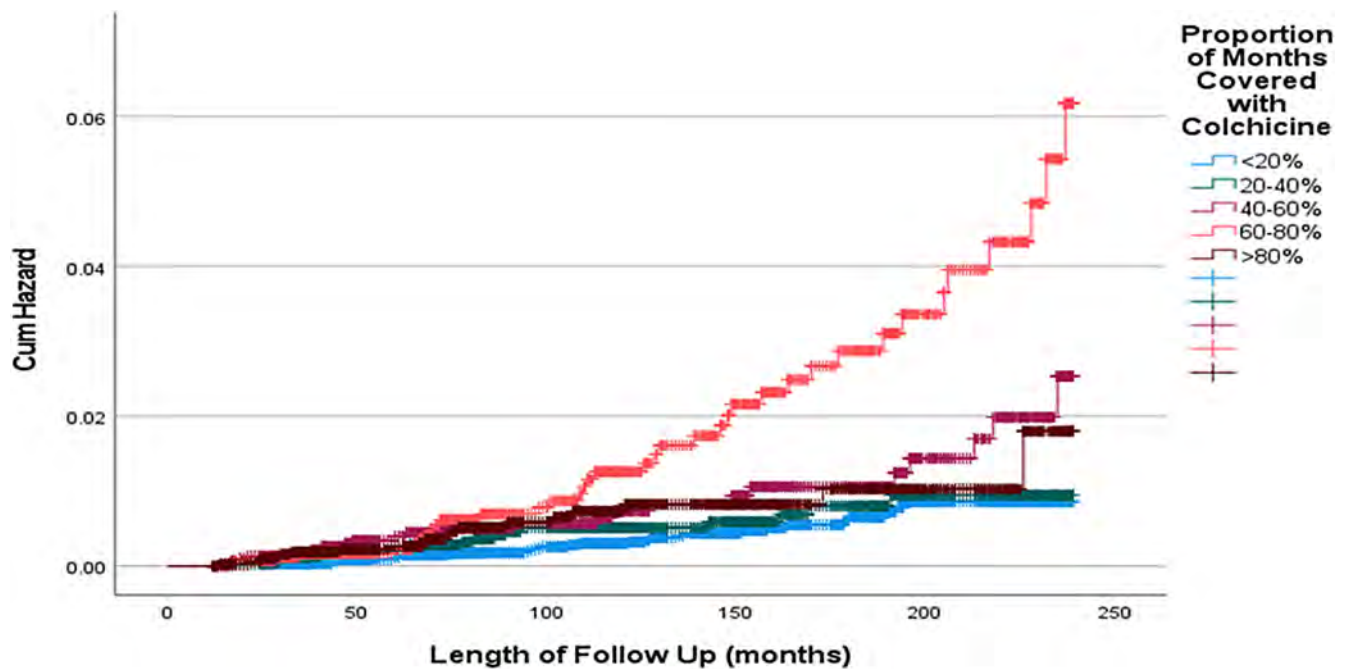


Figure: (abstract: FRI017): Kaplan-Meier analysis for cumulative hazard risk for cirrhosis decompensation related to PMC (%).

with COL PMC '60–80%' had the highest cumulative hazard risk for DC (Kaplan-Meier analysis, LogRank = 47.192, $p < 0.001$).

Conclusion: Chronic colchicine use is associated with incident DC in a cohort of new COL users.

FRI018

Inhibition of C-C motif chemokine receptor 2 (CCR2) using a novel in silico designed peptide attenuates macrophage migration in vitro and intrahepatic monocyte recruitment in vivo

Eline Geervliet^{1,2}, Ralf Weiskirchen², Ruchi Bansal^{1,3}. ¹University of Twente, Medical Cell Biophysics, Enschede, Netherlands; ²RWTH Aachen, Institute of Molecular Pathobiology, Experimental Gene Therapy and Clinical Chemistry, Aachen, Germany; ³University of Twente, Translational Liver Research, Netherlands
Email: ekgeervliet@gmail.com

Background and aims: Acute liver injury is a highly prevalent and a life-threatening disease. Hepatocyte injury induces activation of liver-resident Kupffer cells (KCs) and consequently activation of hepatic stellate cells (HSCs). Hepatocytes, HSCs and KCs secrete C-C motif chemokine ligand 2 (CCL2) and trigger the recruitment of C-C motif chemokine receptor 2 (CCR2) expressing circulating monocytes. This results in chronic liver inflammation that further progresses to liver fibrosis, cirrhosis and/or hepatocellular carcinoma. Blocking the CCR2, using a small molecule CCR2/CCR5 inhibitor cenicriviroc (CVC), has already been proven effective *in vitro*, *in vivo*, and in phase-I and -IIb clinical trials. However, small molecules often have limitations i.e. poor pharmacokinetics and lack of receptor specificity. We designed a CCR2 antagonizing peptide (AP2) with improved pharmacokinetics, and high receptor specificity to reduce monocyte infiltration and disease progression in acute liver injury.

Method: Receptor binding affinity of the AP2 was characterized using surface plasmon resonance imaging (SPRI) *in situ* and *in vitro*. Efficacy

of AP2 on CCL2-driven chemotaxis was examined *in vitro* in mouse RAW 264.7 macrophages and human THP-1 monocytes using transwell assays, and *in vivo* in an acute carbon tetrachloride induced liver injury mouse model. To assess intrahepatic monocyte infiltration *in vivo*, liver tissues were mechanically dissociated using Tissue Grinder, and cell population such as CD45+ leukocytes, resident and monocytes-derived macrophages (MoMFs) (CD11b+/++ and F4/80+/++), and T-cells (CD3+) were analyzed using flow cytometry. Furthermore, effects of AP2 on disease progression (inflammatory and fibrosis markers) were assessed using immunohistochemistry. The effects of AP2 were compared with CVC *in vitro* and *in vivo*.

Results: AP2 ($p < 0.01$) and CVC ($p < 0.05$) showed favorable inhibition of CCL2-driven macrophage/monocyte chemotaxis. *In vivo*, flow cytometric analysis revealed that a decrease in the population of CD45+ cells and CD11b⁺F4/80⁺ MoMFs and (activated) CD11b⁺F4/80⁺ KCs, while CD3+ T cells in CVC and AP2 treated mice were comparable to that of healthy controls. Immunohistochemical analysis evidenced decreased expression of fibrosis markers (collagen-I and alpha-smooth muscle actin) and an increase in Ki-67 positive hepatocytes in the AP2 treated mouse livers. Our data shows effective amelioration of inflammation and fibrosis by inhibition of CCR2 using CCR2-antagonizing peptide. SPRI and *in vitro* peptide binding studies are ongoing alongside with more *in vivo* analysis. The peptide will be evaluated further in a non-alcoholic steatohepatitis (NASH) mouse model.

Conclusion: Our CCR2-antagonizing peptide inhibited migration of macrophages/monocytes *in vitro* and ameliorated inflammation and fibrosis *in vivo* in an acute liver injury mouse model.

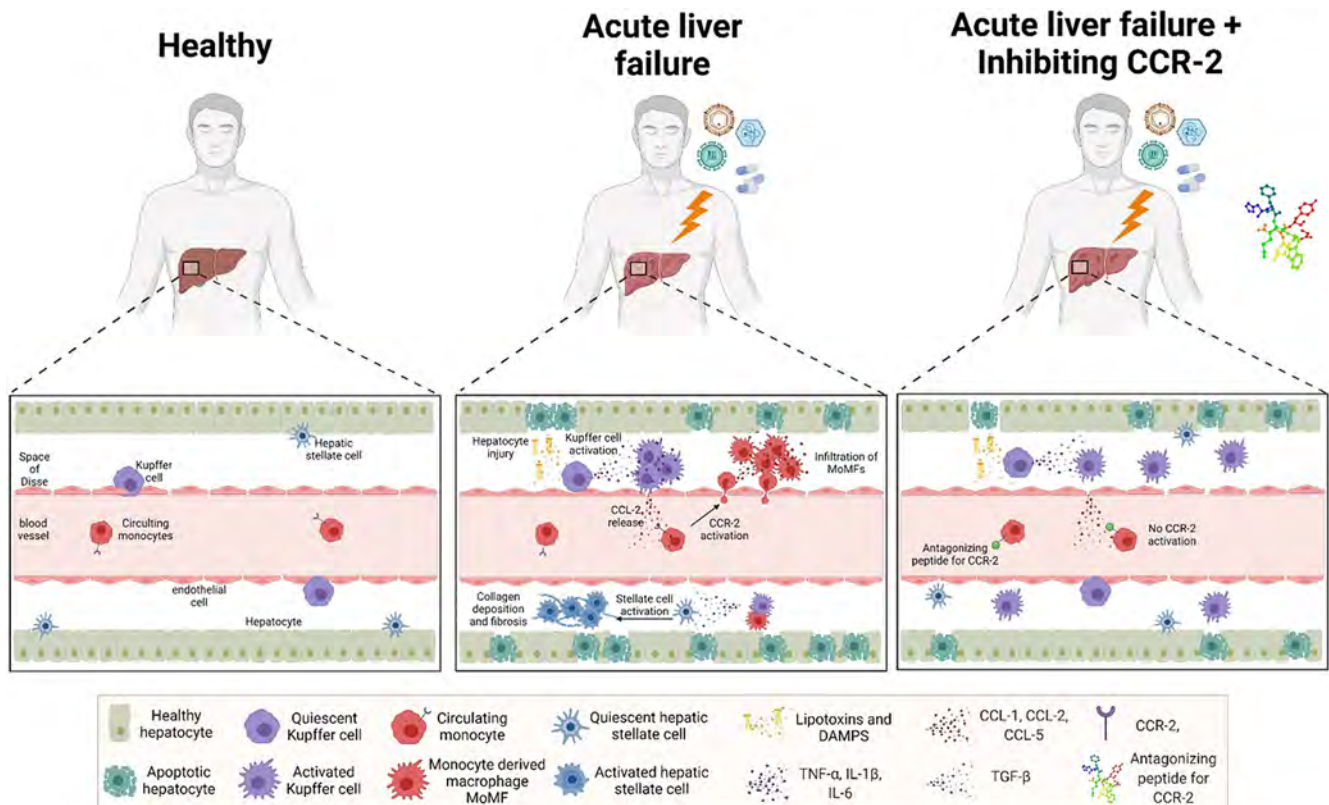


Figure: (abstract: FRI018)

FRI019

Murine intrahepatic regulatory t cells modulate acute liver inflammation by promoting a protective and restorative microenvironment

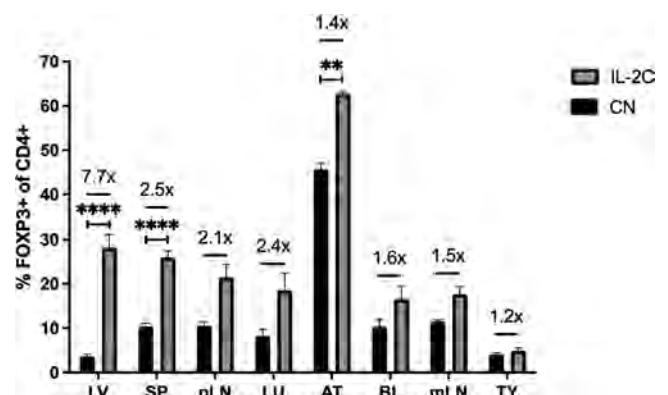
Ada Kurt¹, Karoline Strobl², Tonika Chester¹, Gabriel Osborn¹, Paula Ruiz¹, Elizabeth H. Gray¹, Alberto Sanchez-Fueyo¹, Marc Martinez-Llordella¹. ¹King's College London, Department of Inflammation Biology, London, United Kingdom; ²Medical University of Vienna, Institute for Cancer Research, Vienna, Austria
Email: ada_sera.kurt@kcl.ac.uk

Background and aims: CD4⁺CD25⁺Foxp3⁺ regulatory T cells (Tregs) exert powerful immunomodulatory effects that are essential to maintain immune homeostasis and prevent the development of immune-mediated diseases. In addition to their immunomodulatory role, recent studies have identified that depending on the tissue compartment they migrate to or reside in, Tregs acquire tissue-specific features and develop cytoprotective and regenerative functions. The liver is an organ known to be deprived in IL-2, a cytokine that is essential for the adequate function and survival of Tregs. The extent to which this affects intra-hepatic Treg phenotype and the capacity of these cells to modulate liver damage has not been adequately investigated. In this study, we aimed to explore the phenotypic and functional diversity of liver resident Tregs during homeostasis. Additionally, we investigated their role in ameliorating liver inflammation and tissue damage by depleting Tregs and increasing their pool by exogenous IL-2 complex (IL-2c) administration in murine models.

Method: Flow cytometry phenotyping and microarray analysis was performed on Foxp3-YFP intrahepatic and splenic Tregs in homeostatic conditions and with the administration of IL-2c for 3 consecutive days. Tregs were depleted in Foxp3-DTR mice by intraperitoneal (i.p.) injection of 1 μ g diphtheria toxin and IL-2c were administered i.p. to wild-type C57BL/6 mice. The extent of liver

damage following a single dose of carbon tetrachloride (CCL4) injury was investigated 24 hours later in both models.

Results: Quantification of Foxp3⁺CD4⁺ cells among different tissues showed that the liver exhibited the lowest abundance of Tregs. Analysis in homeostatic conditions revealed that, although intrahepatic Tregs exhibited the core transcriptional Treg signature, they expressed a distinct transcriptional profile. This was characterized by reduced CD25 expression and increased levels of pro-inflammatory Th1 transcripts IL1 β and IFN γ . Depletion of Tregs showed that Tregs effectively reduced the magnitude of systemic and intra-hepatic inflammatory responses following CCL4 injury, but they were not directly involved in ameliorating hepatocyte necrosis. In contrast, the administration of IL-2c markedly increased the number of intra-hepatic Tregs and significantly ameliorated liver damage following CCL4 administration. The cytoprotective effect observed in response to IL-2c was associated with the increased expression by Tregs of markers known to regulate their suppressive function.



POSTER PRESENTATIONS

Conclusion: Our results offer insight into the transcriptome and complex immune network of intrahepatic Tregs and how their number and phenotype may affect their ability to modulate liver inflammation. Strategies capable of selectively increasing the pool of intra-hepatic Tregs could constitute effective therapies in inflammatory liver diseases.

FRI020

Place of steroids and prognosis factors for grade = 3 immune-checkpoint inhibitors induced hepatitis: a 6-year prospective study

Eleonora De Martin¹, Alina Lutu¹, Ariane Laparra-Ramakichenin², Nicolas Golse¹, Astrid Laurent Bellue³, Caroline Robert², Olivier Lambotte⁴, Audrey Coilly¹, Ilias Kounis¹, Edoardo Poli¹, Lea Duhaut¹, Olivier Rosmorduc¹, Catherine Guettier³, Jean-Marie Michot², Didier Samuel¹. ¹Hôpital Paul Brousse, Centre Hépatobiliaire, Villejuif, France; ²Institut Gustave Roussy; ³Hôpital Bicêtre, Anatomopathologie, France; ⁴Hôpital Bicêtre, Médecine interne et Immunologie clinique
Email: eleonora.demartin@aphp.fr

Background and aims: The management of liver toxicity of immune checkpoint inhibitors (ICI) and the role of steroids is controversial. This study aimed to provide a report of a well characterized cohort of patients with ICI-induced hepatitis and their management.

Method: In this prospective cohort study, patients treated with ICI for metastatic cancer and referred to hepatology unit for grade ≥ 3 hepatitis (06/2015–09/2021) were evaluated and the ones with ICI-induced hepatitis, after exhaustive causal investigations, were included. The decision to introduce steroids and/or ursodeoxycholic acid (UDCA) was at physician discretion (oncologist/hepatologist).

Results: Among 64 included patients, 29 (45%) female, median age 61 (33–83) yrs, the most common cancers were metastatic melanoma (n = 30), renal cancer (n = 12) and epidermoid carcinoma (n = 6). The ICI administered were anti-PD1 (n = 29), anti-PDL1 (n = 9), anti-CTLA4 (n = 5), anti-PD1+anti-CTLA4 (n = 21) and ICI+chemotherapy (ex. carboplatin, anti-EGFR) (n = 21). 20% of patients were previously exposed to another ICI. Median time between ICI introduction and first increase of liver tests (LFTs) was 1.80 (0.82–3.42) months and between ICI introduction and peak of LFTs was 2.67 (1.43–5.17) months, median number of doses was 2 (1.75–4). Forty (62%) patients had grade 3 and 24 (38%) grade 4 hepatitis, 33% were symptomatic. At peak median (IQR) LFTs were AST 481 (280–780) IU/l, ALT 320 (164–549) IU/l, total bilirubin 14.5 (10–28) μ mol/l, conjugated 8.85 (5.32–19.2) μ mol/l, GGT 366 (150–800) IU/l, ALP301 (134–513) IU/l, only 2 patients had increased INR. Median IgG were 10.0 (7.8–12.3) g/L, ANA was positive in 49% and ASMA in 3.5% of patients. The diagnosis was histologically confirmed in 91% of patients. Seven patients underwent biliMRI and 3 had cholangitis. No differences were found between patients with grade 3 or 4 hepatitis regarding type of cancer, type of ICI, number of doses, interval between ICI and peak of LFTs. Steroids were introduced in 32 (50%) patients and UDCA was used in 27% of patients. Doses of steroids were 0.5, 1 and 2 mg/kg/day in 8, 21 and 2 patients (not known in 1), respectively. Four patients didn't improve, 1 required increase of steroids, 3 a second immunosuppressive drug, 1 multiple drugs and died of liver failure. Use of steroids was associated with higher AST (p = 0.041), ALT (p = 0.041), total and conjugated bilirubin (p < 0.01 and 0.025) but not with type of ICI, number of doses, interval between ICI introduction and LFTs increase. Among grade 4 patients, 8 (33%) improved without steroids.

Table: Characteristics of patients treated vs not treated with steroids

	Steroids No N=32	Steroids Yes N=32	p
ALT, IU/l	388 [264; 688]	566 [354; 1295]	0.041
AST, IU/l	238 [132; 448]	427 [252; 750]	0.041
Total bilirubin, μ mol/l	11.5 [9.10; 18.8]	20.5 [11.8; 49.2]	<0.01
Conjugated bilirubin, μ mol/l	7.00 [5.05; 10.0]	12.0 [6.00; 38.0]	0.025
GGT, IU/l	390 [155; 659]	315 [184; 981]	0.62
ALP, IU/l	327 [118; 418]	258 [147; 585]	0.59
Interval between first ICI dose and LFTs increase, months	2.07 [0.983; 3.33]	1.38 [0.667; 3.44]	0.67
Interval between first ICI dose and LFTs peak, months	2.53 [1.85; 3.22]	3.42 [1.34; 7.08]	0.51
Number of doses	3.00 [1.50; 4.00]	2.00 [2.00; 4.00]	0.82
Anti-PD1+anti-CTLA4, n(%)	10 (31%)	11 (34%)	0.79
Anti-PD1, n(%)	16 (50%)	13 (41%)	0.45
Anti-PDL1, n(%)	5 (16%)	4 (12%)	1
Anti-CTLA4, n(%)	1 (3.1%)	4 (12%)	0.35

Conclusion: Grade ≥ 3 ICI-induced hepatitis was non-severe in the majority of cases. Steroid therapy was introduced in only half of the patients and was associated with higher ALT and bilirubin level. New cut off to indicate the use of steroid therapy is needed.

FRI021

The role of macrophage ETS Proto-oncogene 2 in acute-on-chronic liver failure

Lulu He¹, Qun Cai¹, Xi Liang², Jiaojiao Xin¹, Jing Jiang¹, Dongyan Shi¹, Keke Ren¹, Yun Li³, Jiaxian Chen¹, Jinjin Luo¹, Jiaqi Li¹, Peng Li¹, Jun Li¹. ¹The First Affiliated Hospital, Zhejiang University School of Medicine, China; ²Taizhou Central Hospital (Taizhou University Hospital), Precision Medicine Center, Taizhou, China; ³Zhejiang University School of Medicine, Institute of Pharmaceutical Biotechnology and the First Affiliated Hospital Department of Radiation Oncology, Hangzhou, China
Email: lijun2009@zju.edu.cn

Background and aims: Acute-on-chronic liver failure (ACLF) is a critical disease caused by acute aggravation of chronic liver disease, with poor prognosis and high mortality. The detailed mechanism of ACLF remains unclear. The purpose of this study was to investigate the value of macrophage ETS Proto-oncogene 2 (ETS2) as a prognostic marker in ACLF, and its role in mouse liver failure model induced by D-GalN/LPS. **Method:** In this study, peripheral blood monocytes from 50 patients with ACLF, 19 patients with chronic liver disease and 14 healthy persons were collected for RNA-SEQ sequencing analysis. ACLF patients were divided into ETS2-high and ETS2-low expression group, and the differentially expressed genes between two groups were analysed. AAV9-ETS2-shRNA were injected to knockdown ETS2 in vivo. And then acute liver failure model of D-GalN/LPS was constructed. Serum biochemical indicators and the expression of inflammatory factors was detected by qPCR and ELISA. HE staining and TUNEL staining were used to observe the inflammatory infiltration and necrosis. Immunohistochemistry was used to detect the expression of high mobility group box 1 (HMGB1). In vitro, CRISPR-Cas9 was used to knockout ETS2 in RAW264.7 cells. The changes of inflammatory factors and related signalling pathways were detected with the intervention of HMGB1.

Results: The mRNA expression of ETS2 in peripheral blood of ACLF group was significantly increased compared with other groups. People who died within 28 days and 90 days showed increased expression of ETS2 compared with people who survived. The activation of innate immune and the suppression of adaptive immune were observed in ETS2- high expression group. In vivo experimental results showed that, ETS2 knockdown increased the liver function impairment and the expression of inflammatory factors

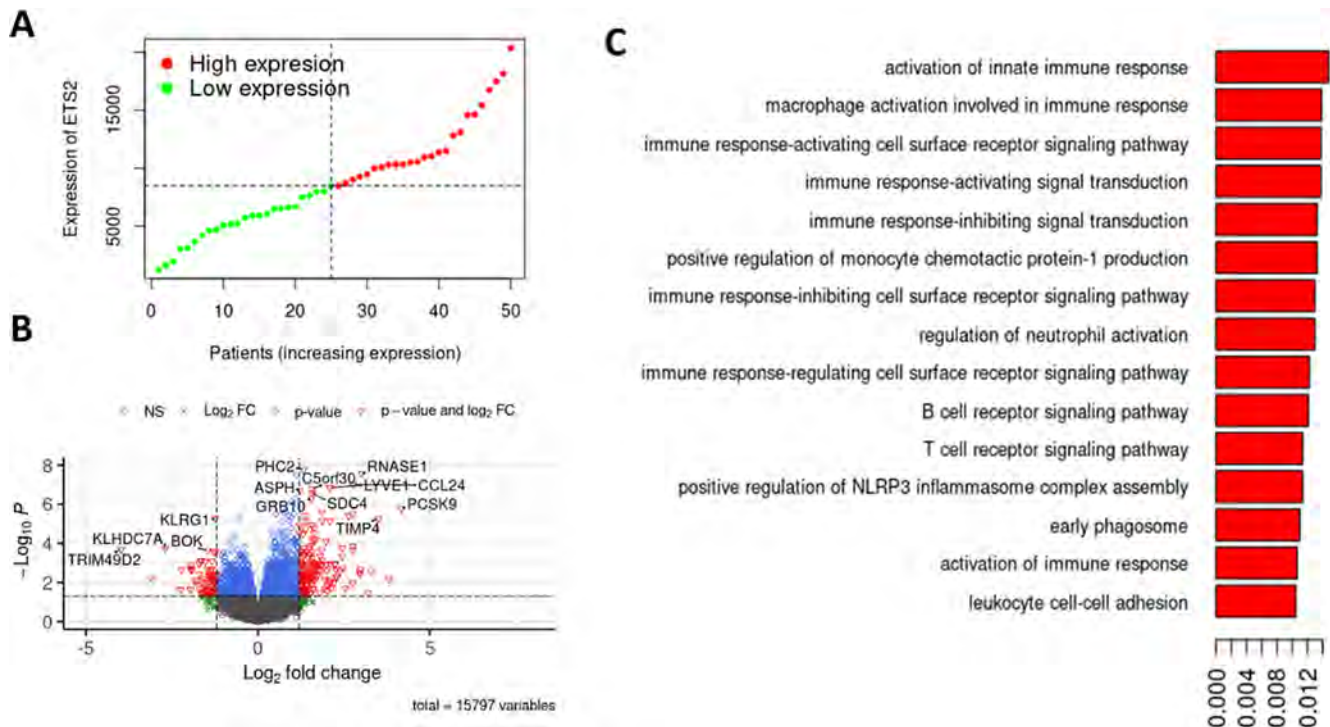


Figure: (abstract: FRI021)

significantly in acute liver failure model. The inflammatory infiltration and necrosis in liver tissue were significantly increased, and the expression of HMGB1 in liver tissue was significantly increased. In vitro results showed that D-GalN could induce HMGB1 release from hepatocytes. Knockout of ETS2 in RAW264.7 significantly increased the expression of HMGB1-induced inflammatory factors, and increased NF-kappa B phosphorylation.

Conclusion: ETS2 was a prognostic marker in ACLF and associated with the activation of innate immune. ETS2 alleviates HMGB1 induced macrophage inflammation by decreasing NF-kappa B activity. Knockdown ETS2 in vivo can increase inflammatory response and further aggravate hepatocyte injury.

FRI022

Novel strategies required to further improve outcomes in acute liver failure

William Bernal¹, Mark J. W. McPhail¹, Anshuman Singh¹, Brian J. Hogan¹, Tasneem Pirani¹, Sameer Patel¹, Robert Loveridge¹, Christopher Willars¹, Michael Heneghan², Varuna Aluvihare², Parthi Srinivasan³, Andreas Prachalias³, Georg Auzinger¹, Nigel Heaton³, Julia Wendon¹. ¹Institute of Liver Studies, King's College Hospital, Liver Intensive Therapy Unit, London, United Kingdom; ²Institute of Liver Studies, King's College Hospital, Hepatology, London, United Kingdom; ³Institute of Liver Studies, King's College Hospital, Liver Transplantation Surgery, London, United Kingdom
Email: william.bernal@kcl.ac.uk

Background and aims: Care for patients with Acute liver injury (ALI) and Failure (ALF) has advanced significantly in recent years through critical care medical therapy and the targeted use of liver transplantation (LT). Case series have shown changes in the character of illness and its outcomes from the 1970 to early 2000s but the current outcomes are poorly characterised. We examined the changing treatment and outcomes of a large cohort of patients with ALF and ALI admitted to a single specialist ICU.

Method: consecutive patients with acute liver disease admitted over the period 1999–2021 were studied, classified in Era 1 (1999–2005),

Era 2 (2006–12) and Era 3 (2013–21) and paracetamol (APAP) and non-APAP aetiologies. ALF was assigned in those with hepatic encephalopathy (HE) and ALI in those without. Severity of illness was assessed by presence of HE and laboratory measures. Data is expressed as n (%) or median (IQR). Data underwent univariate and multivariate analysis including logistic regression for the primary outcome of hospital survival.

Results: The study cohort comprised 1752 patients (median age 36 (27–48) years, 60% female, 56% APAP), of whom 1177 (68%) had/developed ALF. Mortality was 4% in those with ALI and 36% in ALF ($p < 0.001$). Era 1 comprised 628 patients, Era 2: 577 and Era 3: 547. Over the study period the proportion with HE grade 3 on admission rose from 50% to 61% ($p < 0.001$), and in both APAP and non-APAP cases measures of liver injury increased: admission INR: APAP 3.3 (2.4–4.9) in Era 1 to 5.6 (3.6–9.1) in Era 3, non-APAP 2.4 (1.6–4.3) to 3.0 (2.1–4.9) both $p < 0.001$). Survival in ALF rose from 53% in Era 1 to 70% in Era 2 ($p < 0.001$), plateauing at 71% Era 3. In parallel there was a fall in use of LT from 30% of ALF cases in Era 1 to 22% in Era 3 ($p < 0.001$). This was seen in both APAP (22% to 13%, $p < 0.001$) and non-APAP (41% to 31%, $p < 0.001$) cases. 343 patients underwent LT: post-LT survival increased from 72% in Era 1 to 91% in Era 2 and Era 3 ($p < 0.001$). Transplant-free survival (TFS) rose from 54% in Era 1 to 70% in Era 3 for APAP and from 29% to 59% in non-APAP cases (both $p < 0.001$). Non-significant increases in TFS were seen when Eras 2 and 3 were compared (APAP 66% vs. 70% $p = 0.47$, non-APAP 50% vs 59% $p = 0.14$). On multivariate analysis adjusting for age, aetiology and illness severity, Era was associated with improved overall survival: Era 1 to Era 2 (Adjusted Odds Ratio 4.1 (95% CI 2.9–5.9)) and Era 3 (4.7 (3.2–6.9)), but there was no difference in between Era 2 and 3 (1.1 (0.78–1.6)).

Conclusion: Survival for patients with ALF has markedly improved over the last 20 years, despite an increase in illness severity. Patient survival after LT is high, but its use has fallen, particularly in APAP ALF. TFS has progressively improved but outcomes in non-APAP ALF remain inferior. However, overall survival has now plateaued suggesting a need for new medical therapies and/or a re-evaluation of the use of transplantation.

FRI023

Human liver biopsies from people with hemophilia A who received factor VIII gene transfer with valoctocogene roxaparvovec (AAV5-hFVIII-SQ) show unremarkable histopathology and reveal interindividual variability in transgene production

Sylvia Fong¹, Bridget Yates¹, Choong-Ryoul Sihh¹, Aras Mattis^{2,3}, Nina Mitchell¹, Su Liu¹, Chris Russell¹, Benjamin Kim¹, Adebayo Lawal¹, Savita Rangarajan⁴, Will Lester⁵, Stuart Bunting¹, Glenn Pierce⁶, K. John Pasi⁷, Wing Yen Wong¹. ¹BioMarin Pharmaceutical Inc, Novato, United States; ²University of California San Francisco, Department of Pathology, San Francisco, United States; ³University of California San Francisco, Liver Center, San Francisco, United States; ⁴University Hospital Southampton, Southampton, United Kingdom; ⁵University Hospitals Birmingham, Birmingham, United Kingdom; ⁶Voyager Therapeutics, Cambridge, United States; ⁷Barts and the London School of Medicine and Dentistry, London, United Kingdom Email: sfong@bmrn.com

Background and aims: Hemophilia A is an X-linked bleeding disorder caused by deficiency in factor VIII (FVIII), a cofactor in the intrinsic pathway of the coagulation cascade. Factor VIII is made predominantly in liver sinusoidal endothelial cells but gene therapy efforts using adeno-associated viruses (AAV) have targeted heterologous expression in hepatocytes. Factor VIII gene transfer with a single intravenous infusion of valoctocogene roxaparvovec (AAV5-hFVIII-SQ) has been shown to confer clinical benefit through at least 5 years in people with severe hemophilia A. Molecular mechanisms underlying sustained AAV5-hFVIII-SQ-derived FVIII expression in hepatocytes have not been studied in humans.

Method: In a substudy of the phase 1/2 clinical trial (NCT02576795), liver biopsy samples were collected from five participants 2.6–4.1 years after AAV5-hFVIII-SQ gene transfer. The objectives of the substudy were to examine effects on liver histopathology, determine the transduction pattern and percentage of hepatocytes transduced with AAV5-hFVIII-SQ genomes, characterize and quantify episomal forms of vector DNA, and quantify transgene expression (hFVIII-SQ RNA and hFVIII-SQ protein). Separately, we compared patterns and efficiencies of hepatocyte transduction in mice, monkeys, and humans who had all received AAV5-hFVIII-SQ to assess translatability of preclinical findings.

Results: Histopathological examination of human samples revealed no dysplasia, architectural distortion, fibrosis or chronic inflammation. No endoplasmic reticulum stress was detected in hepatocytes expressing hFVIII-SQ protein. Hepatocytes stained positive for vector genomes, and the number of transduced cells increased with AAV5-hFVIII-SQ dose. Molecular analysis demonstrated the presence of stable full-length circular episomal genomes that are associated with long-term expression. Interindividual differences in transgene expression were noted despite the successful administration of identical vector doses. Variability may be related to host-mediated post-transduction mechanisms of vector transcription, hFVIII-SQ protein translation, and secretion. Higher levels of vector genomes were detected in the livers of humans and monkeys than in mice; however, transcription of the vector DNA into RNA occurred more efficiently in mice.

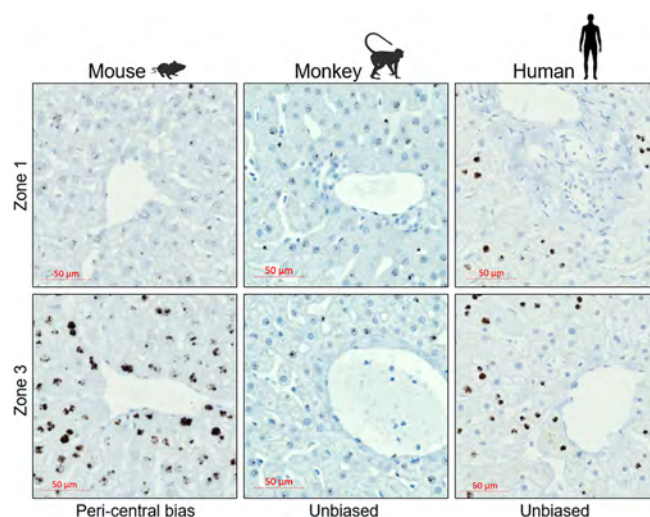


Figure: Cross species comparison of valoctocogene roxaparvovec transduction. In situ hybridization of hFVIII-SQ vector DNA (brown foci) in mouse, monkey, and human liver samples.

Conclusion: Overall, our results showed that liver histopathology was unremarkable following AAV5-hFVIII-SQ administration and that persistent episomal vector structures were formed. This work elucidates several potential mechanisms that may mediate inter-individual variability in FVIII production and advances our understanding of inter-species translatability.

FRI024

Liver toxicity associated to novel cyclin-dependent kinase inhibitor ribociclib in a cohort of advanced breast cancer patients

Miki Scaravaglio¹, Antonio Ciaccio¹, Alice Laffusa¹, Martina Lucà¹, Salvatore Longo², Martina Manna¹, Claudia Maggioni³, Francesca Riva³, Federica Cicchiello³, Marina Elena Cazzaniga⁴, Diego Cortinovis³, Pietro Invernizzi¹. ¹Division of Gastroenterology, Department of Medicine and Surgery, University of Milano-Bicocca, San Gerardo Hospital, Monza, Italy; ²Gastroenterology, Hepatology and Nutrition Division, Department of Life, Health and Environmental Sciences, University of L'Aquila, L'Aquila, Italy, Monza, Italy; ³Division of Medical Oncology, Department of Medicine and Surgery, University of Milano-Bicocca, San Gerardo Hospital, Monza, Italy; ⁴Department of Medical Oncology & Phase 1 Research, University of Milano-Bicocca, San Gerardo Hospital, Monza, Italy, Monza, Italy Email: m.scaravaglio@campus.unimib.it

Background and aims: Three cyclin-dependent kinase 4/6 inhibitors (CKIs) have shown to significantly improve the progression-free survival in patients with hormone receptor (HR)-positive, human epidermal growth factor receptor 2 (HER2)-negative advanced breast cancer (ABC). Among them, ribociclib has recently proved an overall survival benefit, emerging as a first-class option. Nevertheless, clinically significant drug induced liver injury (DILI) has been reported, leading to temporary or definitive withdrawal of anti-neoplastic therapy with related concerns about liver and oncologic outcomes. In a previous analysis of this cohort (manuscript in preparation) we found a significant higher risk of DILI with ribociclib compared to others CKIs. We aimed to assess characteristics and predictors of ribociclib-induced liver toxicity.

Method: All consecutive patients with ABC evaluated between June 2017 and December 2021 at the Oncology Unit of San Gerardo University Hospital, Monza, and received ribociclib for at least a complete cycle of 28 days were included in this retrospective study. Patients with hepatocellular carcinoma and/or chronic advanced liver disease were excluded.

Results: Of 122 ABC patients treated with CKIs, 43 received ribociclib and were included in the analysis, with a median treatment time of 15 months (interquartile range [IQR], 3.5 to 26.5). After a median follow-up time of 21 months (IQR, 15.5 to 30.5) an elevation of liver enzymes of any grade was reported in 13 out of 43 patients (30.2%) and 6 patients (14%) had a DILI, as defined by an ALT $>5 \times$ upper limit of normal (ULN) and/or ALP $>2 \times$ ULN. DILI episodes occurred after a median of 6 months (IQR, 3 to 8) from treatment start and all of them had a hepatocellular pattern. A single case of DILI with autoimmune features was described. Of 6 DILI patients, 1 (17%) underwent temporary and 5 (83%) definitive treatment interruption, achieving liver enzymes normalization within a median of 13 weeks (IQR, 7 to 24). Overall, the occurrence of DILI accounted for over a quarter of the total number of treatment discontinuations. No acute liver failure was reported. Fourteen of 43 patients (33%) died during the study period, none of liver-related cause. Baseline steatosis (RR 13.3, CI 4.5–39.6, $p < 0.01$) and dyslipidemia (RR 3.3, CI 0.8–13.9, $p = 0.05$) were associated with a significant higher risk of DILI. No associations were found when assessing previous exposure to antineoplastic treatments including endocrine agents, concomitant medications, presence of liver metastases, and fibrosis-4 index (FIB-4) at baseline.

Conclusion: Ribociclib is associated with a significant risk of DILI, turning in a relevant rate of antineoplastic treatment discontinuation in ABC patients. Once confirmed in larger prospective studies, baseline assessment of steatosis and dyslipidemia should be warranted to assist pre-treatment risk stratification.

FRI025

Exogenous fibroblast growth factor 7 improved hepatocyte regeneration and ameliorated CCl₄-induced acute liver injury in vivo

Elaine Geervliet^{1,2}, Ruchi Bansal¹. ¹University of Twente, Medical Cell Biophysics, Enschede, Netherlands; ²RWTH Aachen, Institute of Molecular Pathobiochemistry, Experimental Gene Therapy and Clinical Chemistry, Aachen, Germany
Email: ekgeervliet@gmail.com

Background and aims: During acute and chronic liver injury, hepatocyte damage instigates activation of inflammatory responses and ultimately fibrosis. Fibroblast growth factor-7 (FGF7), that binds specifically to FGFR2b (highly expressed on hepatocytes and liver progenitor cells), plays an important role in cholangiocytes/hepatocytes proliferation and liver regeneration as shown in a mouse model of cholangitis and biliary fibrosis, and partial hepatectomy. Unfortunately, during acute and chronic liver disease this ligand is insufficiently expressed resulting in lack of hepatocyte survival, and progression of liver disease. On the other hand, FGFR2b is upregulated during acute and chronic liver disease making it an excellent therapeutic target. In this research, we aim to target FGFR2b with its natural highly specific ligand FGF7 to improve survival and proliferation of hepatocytes, differentiation of liver progenitor cells, and thereby ameliorating liver disease progression in carbon tetrachloride (CCl₄)-induced acute liver injury mouse model.

Method: Acute liver injury was induced by a single injection of CCl₄. Mice were subsequently treated with vehicle or 1 µg/kg FGF7 twice a day for two days. After treatment, the mice were sacrificed, and the organs were harvested for further analysis. Hepatocyte survival and proliferation, inflammation and fibrosis were evaluated by immunohistochemical staining, and gene and protein expression.

Results: Exogenous FGF7 increased liver- and spleen-to-body weight ratio while significantly decreased the liver-to-spleen weight ratio. Immunohistochemical analysis of liver sections showed increased

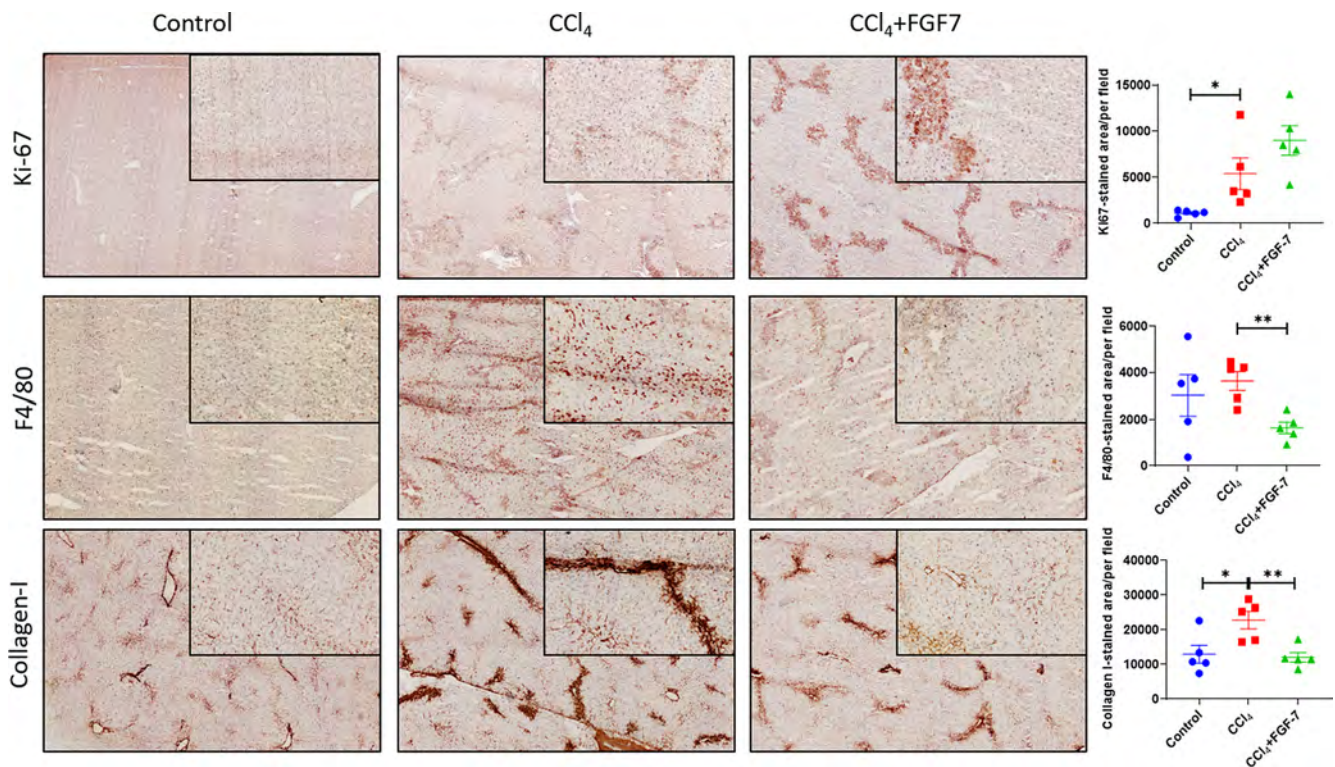


Figure 1: (abstract: FRI025): Representative microscopic images (10x) and quantitative analysis of liver sections of control (healthy, n = 5), CCl₄ (n = 5) and FGF7 (n = 5) treated mice stained with Ki67 (proliferation marker), F4/80 (macrophage marker) and Collagen-I (fibrosis marker). *p < 0.05 and **p < 0.01 denotes significance.

POSTER PRESENTATIONS

proliferation as determined by Ki67 expression. Furthermore, macrophage/inflammation marker, F4/80 and fibrosis marker, collagen-I were significantly decreased upon treatment, see Figure 1. Gene expression analysis of proliferation, inflammation and fibrosis markers followed the similar trend. Extensive protein analysis of hepatocyte survival pathways will be investigated using Western blot. **Conclusion:** Our results show that exogenous administration of FGF7 induces hepatocyte survival and leads to amelioration of inflammatory response and fibrosis in acute liver injury. Our study demonstrates that FGF7, FGF7 derivatives or nano-engineered FGF7 may benefit patients with hepatic dysfunction.

FRI026

Three COVID-19 medications-remdesivir, molnupiravir and ritonavir-boosted nirmatrelvir-and serial liver biochemistries in 22, 456 subjects

Grace Lai-Hung Wong¹, Vicki Wing-Ki Hui¹, Terry Cheuk-Fung Yip¹, Yee-Kit Tse¹, Vincent Wai-Sun Wong¹. ¹The Chinese University of Hong Kong, Medical Data Analytic Centre (MDAC) and Department of Medicine and Therapeutics, Hong Kong
Email: wonglaihung@cuhk.edu.hk

Background and aims: Several medications as treatment for COVID-19 have been approved around the world. These medications have generally good safety profiles, while data concerning the liver safety of these COVID-19 medications and risk of drug-induced liver injury (DILI) are lacking. We aimed to report the serial liver biochemistries of people before and after receiving COVID-19 medications.

Method: This was a territory-wide retrospective observational cohort study in Hong Kong. We identified subjects who had received any of the three COVID-19 medications approved in Hong Kong-remdesivir, molnupiravir and ritonavir-boosted nirmatrelvir. Serial liver biochemistries at least three months before and one month after the COVID-19 medications were reported.

Results: 22, 456 subjects (5, 370 received remdesivir, 13, 127 received molnupiravir and 4, 510 received ritonavir-boosted nirmatrelvir; 551 subjects had received more than one medication) of whom 48.3% male, median age 77 years old, were included. Majority (98.7%) subjects had normal ALT (1–2 × ULN: 0.9%; >2 × ULN: 0.4%) and total bilirubin (normal 91.3%; 1–2 × ULN: 7.2%; >2 × ULN: 1.5%) before or at the time of receiving COVID-19 medications. These parameters remained stable for up to one month after the treatment-ALT (normal 97.7%; 1–2 × ULN: 1.5%; >2 × ULN: 0.8%) and total bilirubin (normal 90.3%; 1–2 × ULN: 7.9%; >2 × ULN: 1.8%). Similar serial liver biochemistries were observed in subjects who received remdesivir, molnupiravir and ritonavir-boosted nirmatrelvir.

Conclusion: Three registered COVID-19 medications (remdesivir, molnupiravir and ritonavir-boosted nirmatrelvir) vaccines have very favourable liver safety profile in people.

Grant support: This work was supported by the Health and Medical Research Fund (HMRF)-Food and Health Bureau Commissioned Research on COVID-19 (Reference no.: COVID1903002) awarded to Grace Wong.

FRI027

Trends in liver transplantation for acute liver failure. A Spanish multicenter study

Isabel Conde^{1,2}, Victoria Aguilera Sancho^{1,2,3}, Sara Martinez⁴, Tommaso Di Maira¹, Maria Senosiain⁵, Rosa María Martín Mateos^{6,6}, Carolina Almohalla⁷, Maria Luisa Gonzalez Dieguez⁸, Sara Lorente Perez⁴, Alejandra Otero⁹, Maria Rodriguez¹⁰, Jose Ignacio Herrero¹¹, Isabel Campos-Varela¹², Ainhoa Fernandez¹³, Marina Berenguer¹. ¹La Fe University and Polytechnic Hospital, València, Spain; ²Instituto de Investigación Sanitaria La Fe de Valencia, Valencia, Spain; ³ISCIII, CIBERehd, Valencia, Spain; ⁴Hospital Clínico Universitario Lozano Blesa, Zaragoza, Spain; ⁵Hospital Universitario Cruces, Barakaldo, Spain; ⁶Hospital Ramón y Cajal, Madrid, Spain; ⁷Rio Hortega University Hospital, Valladolid, Spain; ⁸Central University Hospital of Asturias, Oviedo, Spain; ⁹Hospital Universitario da Coruña (CHUAC), A Coruña, Spain; ¹⁰General University Hospital of Alicante, Alacant, Spain; ¹¹Clínica Universidad de Navarra, Madrid, Spain; ¹²La Vall d'Hebron, Barcelona, Spain; ¹³Gregorio Marañón Hospital, Madrid, Spain
Email: icondemiel@gmail.com

Background and aims: ALF is a critical illness with high morbidity. LT has improved outcome. Aims: to assess if there have been changes in aetiology, profile and outcomes of patients LT due to ALF in a Spanish multicenter cohort and to identify factors associated with mortality.

Method: Retrospective study of LT due to ALF cohort from 11 hospitals between 2001 and 2020. Baseline features, comorbidities, biochemical data, acute complications, early and late outcomes were recorded.

Results: 218 adults LT due to ALF (2001–2020). The cohort was subdivided in 4 time-groups (G1:2001–2005; G2:2006–2010; G3:2011–2015; G4:2016–2020). The number of ALF LT remained stable (G2: 2.5%, G3:2.2%, G4:2.7%). Median age: 41 yrs, 62%women, AHT 11.5%, diabetes 3.7%, dyslipidaemia 8.3%, MELD 34 (29.5–38.1), 83.5% caucasian. Main LT indications were viral (26.2%), cryptogenic (26.1%), autoimmune (22.5%), and DILI (17%). 87% meet King's College criteria. 38% had severe encephalopathy, 22% renal impairment (RI) with haemodialysis, 23% required mechanical ventilation (MV). There was a trend towards an increase of LT for autoimmune (21%, 21%, 31%, 29% in G1–4 respectively, $p=0.88$) and DILI (12.5%, 14%, 18%, 21% in G1–4, $p=0.72$). Women seem more susceptible to ALF TH over time (58%, 53.5%, 65.6% and 67% in G1–4, $p=0.4$). Complications in the early post-LT period were infections (58.7%), RI (25%) and primary dysfunction (24%). Late post-LT complications were AHT (30%), RI (20%) and diabetes (17%). 27% of patients died. Main causes of death were infections (41.5%) and liver-related (20%). Survival was 85%, 81% and 70% at 1, 5 and 10 years. Diabetes, MV, ascites and creatinine were independently associated with poorer survival (HR 4.05, $p=0.054$; HR 2.74, $p=0.037$; HR 2.48, $p=0.048$ and HR 1.47, $p=0.007$, respectively).

Conclusion: LT for ALF remained stable in the last years in Spain. Autoimmune and DILI seem to increase over time, being women more susceptible to ALF TH. Patients with diabetes, ascites, high creatinine levels, and MV were associated with poor outcomes after LT.

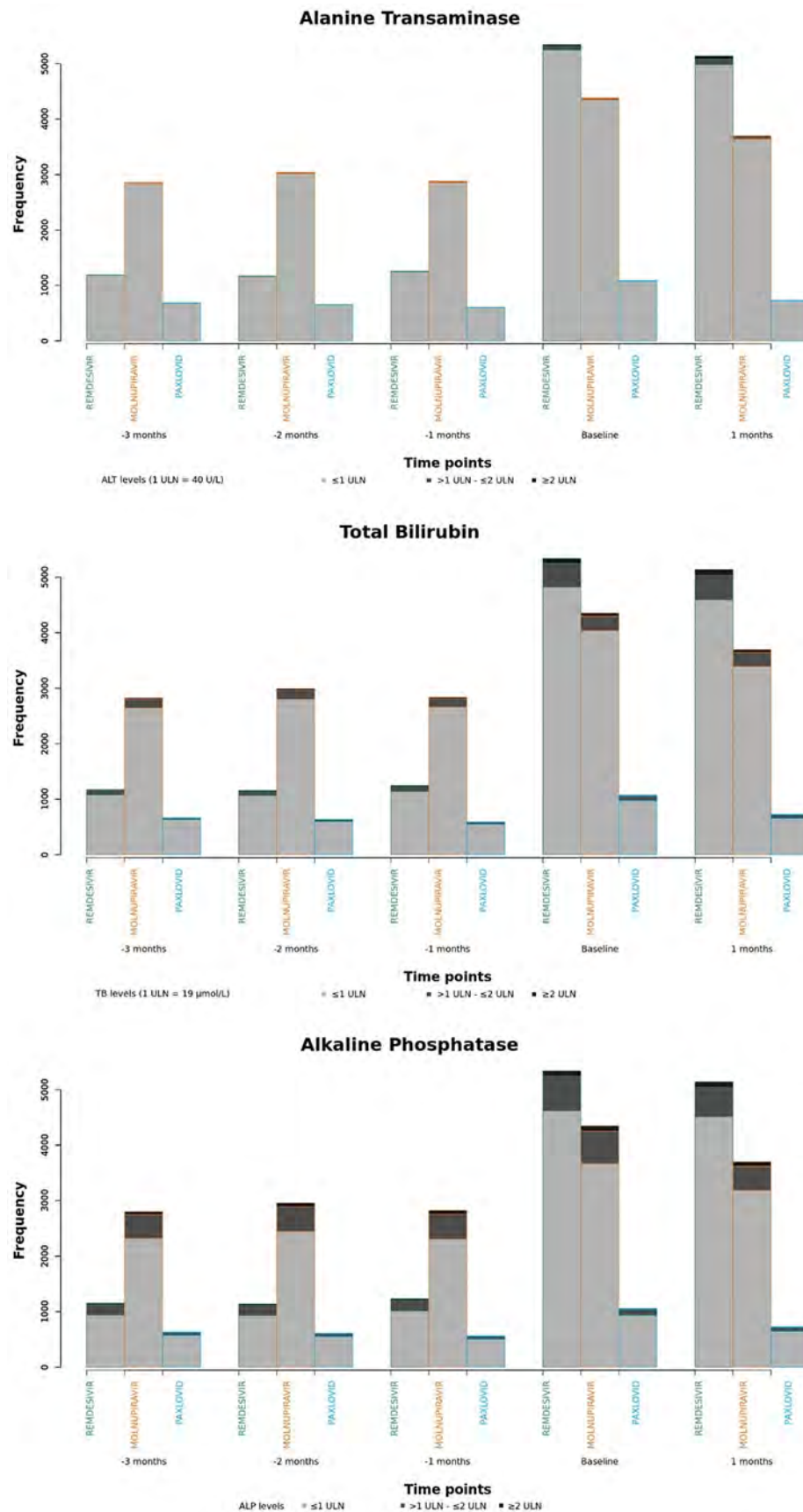


Figure: (abstract: FRI026): Serial liver biochemistries before and after COVID-19 medications.

POSTER PRESENTATIONS

FRI028

Hepatobiliary disease after bone marrow transplant

Maria Dezan^{1,2}, Marco Salvino^{3,4}, Alessandro Almeida^{3,5}, Hugo Silva⁶, Lourianne Cavalcante^{7,8}, Helma Pinchemel Cotrim⁸, Andre Lyra^{7,8}.

¹Hospital São Rafael, Gastroenterology and Hepatology, Salvador, Brazil; ²Federal University of Bahia, Programa de Pós Graduação em Medicina e Saúde, Salvador, Brazil; ³Hospital São Rafael, Hematology, Salvador, Brazil; ⁴Hospital Universitário Professor Edgard Santos-HUPES, Hematology, Salvador, Brazil; ⁵Hospital Universitário Professor Edgard Santos-HUPES, Hematology, Salvador; ⁶Hospital São Rafael, Hematology, Salvador, Brazil; ⁷Hospital São Rafael, Gastroenterology and Hepatology, Salvador, Brazil; ⁸Hospital Universitário Professor Edgard Santos-HUPES, Gastroenterology and Hepatology, Salvador, Brazil
Email: aclyra@live.com

Background and aims: Post-bone marrow transplantation (BMT) hepatobiliary complications (C-HEPBILI) may occur in up to 80% of the cases. We evaluated the frequency and clinical characteristics of C-HEPBILI in patients undergoing BMT at a referral center.

Method: This is a cross-sectional study that analyzed patient data from 2017 to 2021, including demographics, the period between BMT and C-HEPBILI diagnosis, outcome, and length of hospital stay. Drug-induced liver disease (DILI), sepsis-associated liver injury (SALI), sinusoidal obstruction syndrome (SOS), graft versus host disease (GVHD), hypoxic hepatitis (HH), and fulminant hepatitis (FH), among others, were evaluated. We diagnosed DILI according to EASL guidelines. For SALI, we considered the infectious context and a total bilirubin ≥ 2 mg/dL and ALP or ALT $\geq 2 \times$ ULN. We used the EBMT, Seattle, and Baltimore criteria to diagnose SOS and considered hepatic GVHD when patients had skin and/or intestinal GVHD and increased liver enzymes that improved after treatment. For alterations that did not meet the previous criteria, we defined liver enzymes elevation as an increase ≥ 1.5 ULN, named this condition isolated liver enzymes elevation (ILEE), and linked them to a possible etiology whenever clinically pertinent.

Results: Thus far, the study comprised 297 patients, 52% men. The mean age of the total population and the C-HEPBILI patients was 49.6 (± 14.1) and 48.7 (± 13.6) years, respectively; 164 of 297 patients (55%) had C-HEPBILI; 91 of them (55%) were women. Table 1 describes all detected C-HEPBILI. Most patients had ILEE that probably was associated with drugs or infection. We analyzed 201 autologous, 47 allogeneic haploidentical, and 49 allogeneic full-match BMT; C-HEPBILI occurred in 53%, 74%, and 47% of the cases, respectively, and was more frequent among patients with acute lymphoid leukemia. DILI occurred in 15% of patients with C-HEPBILI (44% had cholestatic DILI pattern, 44% hepatocellular, and 12% mixed). The commonest conditioning regimens among patients with DILI used Melphalan. Nine out of 15 SOS patients died. The mean post-BMT hospital stay among C-HEPBILI patients was 25.8 days, while patients without these complications stayed for 17.9 days (mean). Twenty-two of 27 deaths occurred in C-HEPBILI patients, especially among SALI subjects.

Table 1: C-HEPBILI frequency in BMT patients*

	N	Total Population (N = 297)	C-HEPBILI Population (N = 164)
ILEE	120	40, 4%	73, 1%
DILI	25	8, 4%	15, 2%
SOS	15	5, 1%	9, 1%
HH	6	2, 0%	3, 6%
SALI	5	1, 7%	3, 0%
FH	2	0, 7%	1, 2%
GVHD	1	0, 3%	0, 6%

*Some patients progressed with more than one C-HEPBILI.

Conclusion: C-HEPBILI is frequent after BMT, is more common in women, and is associated with considerable morbidity, as well as an

increase in the hospital stay. DILI was a relevant complication. Allogeneic haploidentical BMT was the most associated with C-HEPBILI.

FRI029

FOXA2 prevents hyperbilirubinemia through maintaining apical MRP2 expression in acute liver failure

Sai Wang¹, Rilun Feng², Shanshan Wang³, Hui Liu⁴, Chen Shao⁴, Yujia Li¹, Frederik Link¹, Stefan Munker⁵, Roman Liebe⁶, Christoph Meyer¹, Elke Burgermeister², Matthias Ebert², Steven Dooley², Huiguo Ding⁷, Honglei Weng². ¹Medical Faculty Mannheim, Heidelberg University, Department of Medicine II, Mannheim, Germany; ²Medical Faculty Mannheim, Heidelberg University, Department of Medicine II, Mannheim, Germany; ³Beijing You'an Hospital, Capital Medical University, Beijing Institute of Hepatology, Beijing, China; ⁴Beijing You'an Hospital, Affiliated with Capital Medical University, Department of Pathology, Beijing, China; ⁵University Hospital, LMU Munich, Department of Medicine II, Mannheim, Germany; ⁶Saarland University Medical Center, Saarland University, Department of Medicine II, Germany; ⁷Beijing You'an Hospital, Affiliated with Capital Medical University, Department of Gastroenterology and Hepatology, China
Email: honglei.weng@medma.uni-heidelberg.de

Background and aims: Multidrug resistance protein 2 (MRP2) is a bottleneck in bilirubin excretion. Its loss is sufficient to induce hyperbilirubinemia, a prevailing characteristic of acute liver failure (ALF), that is closely associated with clinical outcome. This study scrutinizes the transcriptional regulation of MRP2 under different pathophysiological conditions.

Method: Thirty-six patients, 14 with quiescent liver cirrhosis and 22 with ALF, were enrolled. Hepatic MRP2, FXR, and FOXA2 expression were examined by immunohistochemistry. Clinicopathologic association was analysed. MRP2 regulatory mechanisms were investigated in primary hepatocytes, *Fxr*^{-/-} mice and LPS-treated mouse model.

Results: In normal hepatocytes, homeostatic MRP2 transcription is mediated by the nuclear receptor FXR/RXR complex. *Fxr*^{-/-} mice lack apical MRP2 expression and rapidly progress into hyperbilirubinemia. In ALF patients, hepatic FXR expression is undetectable, however, the patients without infection maintain apical MRP2 expression and do not suffer from hyperbilirubinemia. These patients express robust FOXA2 in hepatocytes. FOXA2 upregulates MRP2 transcription through binding to its promoter. Physiologically, nuclear FOXA2 translocation is inhibited by insulin. In ALF, high levels of glucagon and TNF- α induce FOXA2 expression and nuclear translocation in hepatocytes. Impressively, ALF patients with sepsis express few FOXA2, lose MRP2 expression, and show severe hyperbilirubinemia. In this case, LPS inhibits FXR expression, induces FOXA2 nuclear exclusion, and thus destroys the compensatory MRP2 upregulation. In both *Fxr*^{-/-} and LPS-treated mice, ectopic FOXA2 expression restored apical MRP2 expression and serum bilirubin levels.

Conclusion: Upregulation of FOXA2 to maintain MRP2 is an efficient strategy to prevent hyperbilirubinemia.

NAFLD: Diagnostics and non-invasive assessment

FRI030

Machine learning encoding of liver biopsy images enables prediction of molecular measurements in a NASH F3/F4 fibrosis clinical cohort

Michael D. Berket¹, Francesco Paolo Casale¹, Rohit Loomba², Arun Sanyal³, Stephen Harrison⁴, Zobair Younossi⁵, Catherine Jia⁶, David Lopez⁶, Li Li⁶, Robert Myers⁶, David Breckinridge⁶, Andrew Billin⁶, Eilon Sharon¹, Matthew Albert¹, Theofanis Karaletsos¹, Daphne Koller¹. ¹Insitro, South San Francisco, United States; ²University of California San Diego, La Jolla, United States; ³Virginia Commonwealth University, Richmond, United States; ⁴University of Oxford, Radcliffe Department of Medicine, United Kingdom; ⁵Inova Fairfax Medical Campus, Falls Church, United States; ⁶Gilead Sciences, Inc., Foster City, United States
Email: research_operations@insitro.com

Background and aims: Machine learning (ML) models of biopsy images have the potential to improve the characterization of liver state by identifying biologically relevant phenotypes that are not captured by standard histological endpoints. To explore this possibility, we develop and compare ML models that predict transcriptomic and genetic endpoints based on standard histology readouts or ML derived histological features. We focus our genetic analysis on the PNPLA3 I148M genotype, which has been robustly linked to NAFLD/NASH risk through GWAS studies (Romeo et al, 2008; Anstee et al, 2020).

Method: Pathologist scores (NASH CRN and Ishak fibrosis scores), quantitative microscopy measurements (alpha-SMA, collagen, and fat content), H&E-stained biopsy images, liver bulk RNA-seq, and PNPLA3 I148M genotypes are curated from the STELLAR3, STELLAR4, and ATLAS clinical trial F3/F4 fibrosis cohorts. We use self-supervised ML methods (trained with no clinician annotations) to generate quantitative embeddings that represent histological phenotypes. We fit generalized linear models to predict the molecular endpoints from the standard and ML-derived biopsy features, training on a random

split of half the data and predicting on held-out samples. All genetic association testing focuses on subjects of European ancestry due to population stratification concerns and considers 10 genotype principal components, age, and sex as covariates.

Results: Predictions of gene expression are improved with the ML biopsy embeddings relative to the standard histological endpoints (A). While the I148M variant is enriched in this cohort relative to the general population (allele frequency $G = 0.46$ vs $G = 0.22$ in gnomAD EUR samples), we do not observe any association between pathologist or quantitative microscopy measurement and I148M genotype ($p > 0.05$). Similarly, genotype predictions from these measurements are not significantly associated with the I148M genotype. However, genotype predictions using the self-supervised ML biopsy embeddings are significantly associated with I148M genotype in the held out samples ($p = 4E-9$, $n = 378$; B). Tiles that influence these genotype predictions are visualized in C.

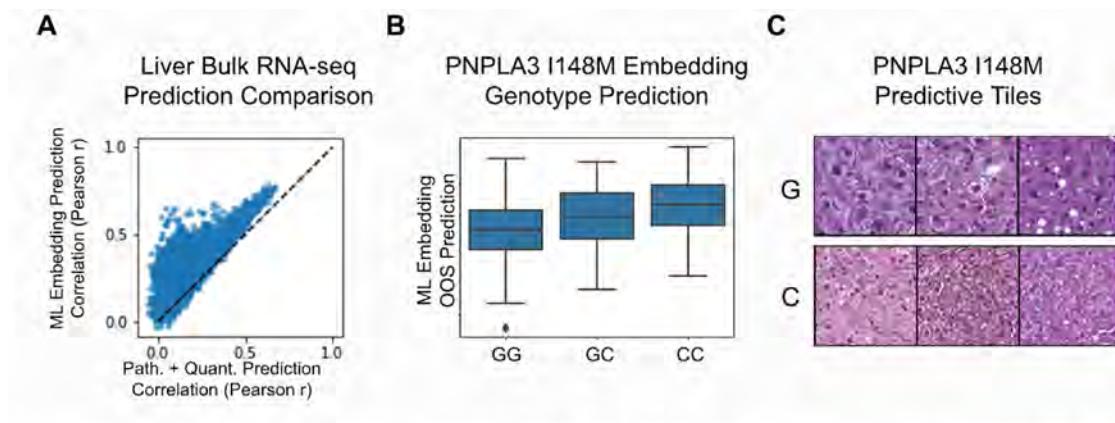
Conclusion: ML models of H&E biopsy images identify histological features that improve predictions of molecular endpoints relative to standard histological readouts. Notably, we identify a histological phenotype associated with PNPLA3 I148M genotype in F3/F4 fibrosis NASH patients that is not captured by standard histological endpoints. This result supports the potential for ML models to provide orthogonal characterizations of histological state, enabling novel insights on the interplay of clinical phenotypes, transcriptomic state, and genetic backgrounds in NASH patients.

FRI031

Validation of AI-assisted method of liver fat measurement in adults with type 2 diabetes

Athena Dworakowski¹, Wenjie Pang¹, Sherif Boulous¹, Sofie De Meyer¹, Jian Yeo², Gaurav Gulsin², Abhishek Dattani², Emer Brady², Joanna Bilak², Sarah Ayton², Alastair Moss², Michael House³, Tim St Pierre³, Gerry McCann². ¹Resonance Health, Burswood, Australia; ²University of Leicester, Department of Cardiovascular Sciences, United Kingdom; ³The University of Western Australia, School of Physics, Crawley, Australia
Email: sofied@resonancehealth.com

Background and aims: Type 2 diabetes (T2D) is strongly associated with the development of non-alcoholic fatty liver disease (NAFLD), which is an emerging independent risk factor for cardiovascular



Prediction of molecular endpoints from histological features. A) Scatter plot of correlations between predicted and observed gene expression using standard histological endpoints (pathologist and quantitative microscopy measurements) or self-supervised ML-derived biopsy embeddings as input features; 3040 / 17648 genes have a difference of at least 0.2 in prediction correlation. B) Box plot of PNPLA3 I148M genotype predicted from self-supervised ML biopsy embeddings. C) Biopsy tiles that most strongly influence the PNPLA3 embedding model predictions.

Figure: (abstract: FRI030)

POSTER PRESENTATIONS

dysfunction. HepaFat-AI® is a software device developed using artificial neural networks (ANN) and provides rapid (less than one minute) automated liver fat quantification from magnetic resonance images without the need for labour-intensive manual image analysis. The aims of this study were to compare HepaFat-AI against the histologically validated HepaFat-Scan® technique as a reference standard in a cohort of asymptomatic adults with T2D.

Method: One hundred and thirty-three adults (97% T2D, mean age 62.6 ± 7.6 years, 60% male) underwent magnetic resonance imaging (MRI) of the liver and heart. Nineteen were excluded due to incorrect imaging parameters or breathing artifacts, leaving a sample of 114 subjects. Volumetric liver fat fraction (VLFF) was analysed twice, first manually with HepaFat-Scan based on the 3-point Dixon principle and then automatically processed using HepaFat-AI. HepaFat-AI was previously trained on 889 individual HepaFat-Scan datasets from both 1.5 T and 3 T scanners and generates a report comprising VLFF measurements, proton density fat fraction (PDFF), and steatosis grade. Bland-Altman analysis was performed to determine the 95% limits of agreement between the two methods of measuring VLFF. The diagnostic performance of HepaFat-AI for predicting HepaFat-Scan steatosis grade 1 or above was also analysed in terms of sensitivity, specificity, and accuracy.

Results: Bland-Altman analysis showed that on average HepaFat-AI yields slightly higher VLFF results with a bias of $+0.42$ (95%CI 0.10–0.74)%VLFF against HepaFat-Scan. The 95% limits of agreement between the two methods were -3.02 and $+3.85$ %VLFF. The sensitivity and specificity of HepaFat-AI for predicting HepaFat-Scan determined steatosis grade of 1 or above were 0.97 (95% CI 0.84–0.99) and 0.88 (95% CI 0.64–0.99) respectively. With HepaFat-Scan as the reference standard, HepaFat-AI had an accuracy of 0.90 (95% CI 84–95) for grading steatosis above or below the grade 0/1 boundary.

Conclusion: HepaFat-AI provides a rapid and automated liver fat quantification analysis of MR images which has important implications for cost and may provide a fast alternative point-of-care testing for patients. The adoption of ANNs in clinical settings has the potential to enhance diagnostic efficiency and medical intervention for T2D adults with liver disease.

FRI032

Identifying advanced liver disease in asymptomatic patients in primary care: an evaluation of patient outcomes 24 months after implementing a primary care liver pathway and community liver service

Tina Reinson¹, Chris Byrne², Mead Mathews³, Janisha Patel⁴.

¹University of Southampton, Primary Care, Population Sciences and Medical Education, Southampton, United Kingdom; ²University of Southampton, Human Development and Health, Southampton;

³St Mary's Surgery, Southampton, United Kingdom; ⁴University Hospital Southampton, Hepatology, Southampton

Email: t.reinson@soton.ac.uk

Background and aims: In 2019, Southampton Clinical Commissioning Group implemented a liver guidance pathway and community liver service to help early detection and reduce the number of deaths from liver disease. The liver guidance pathway supports primary care clinicians identify patients at risk of liver disease to access early intervention before developing to advanced liver disease. The community liver service provides vibration controlled transient elastography (VCTE) assessment to patients who, after following the liver guidance pathway, have been identified as having severe liver fibrosis. This study aims to evaluate the patient outcomes 24 months after implementing the liver pathway and VCTE service.

Method: All patients referred to the Southampton community liver service between January 2019 and December 2020. Demographics recorded included: Age, sex, body mass index (BMI), alcohol consumption (high or low), VCTE reading (kPa), diagnosis (alcohol related liver disease, non-alcoholic fatty liver disease or both) and patient outcomes (stay in primary care or refer to secondary care for clinical management).

Results: 527/632 patients referred to the community liver service received a VCTE assessment. 16.6% ($n = 105$) did not attend their appointment and for 0.9% ($n = 5$), no valid VCTE reading was obtained. The median (IQR) age of patients was 58 (46–65) years, 58.6% were male; median (IQR) BMI was 30.5 (27.1–35.1) kg/m² and alcohol

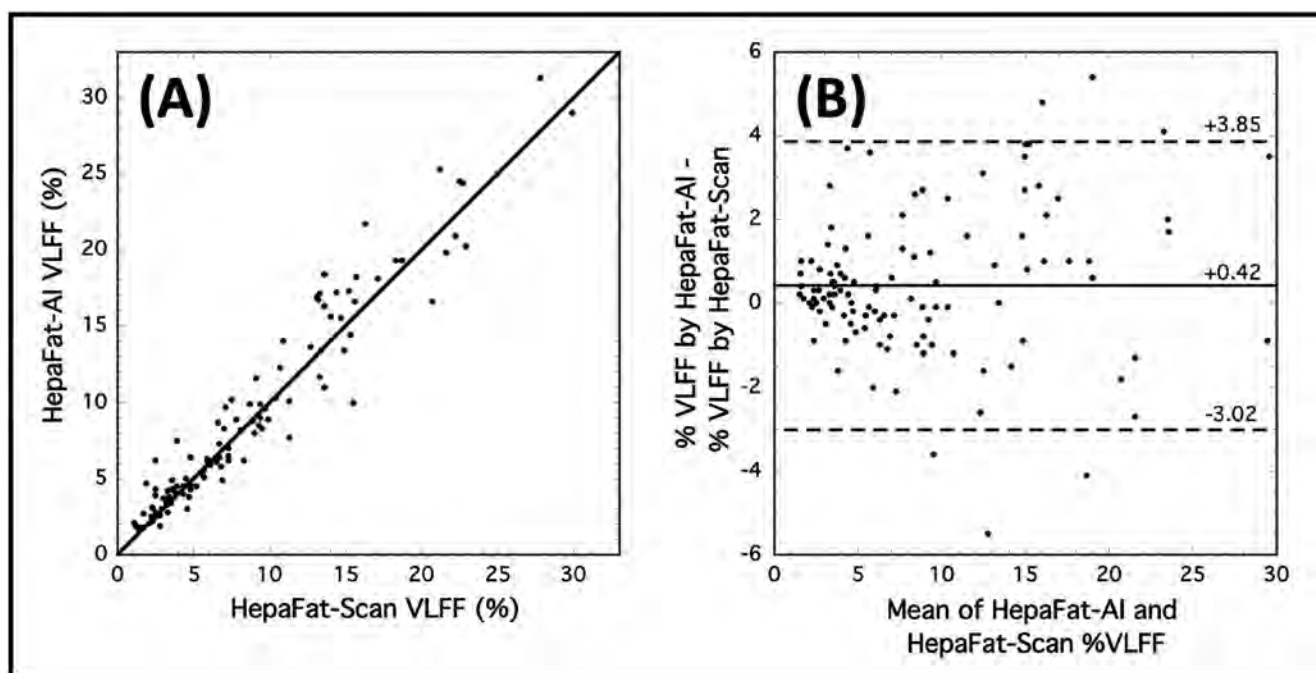


Figure: (abstract: FRI031): (A) VLFF from manual processing (HepaFat-Scan) vs automated processing (HepaFat-AI) with line of equivalence. (B) Bland-Altman plot showing the differences between the HepaFat-AI and HepaFat-Scan VLFF measurements. The solid line shows the mean difference and the dashed lines show the upper and lower 95% limits of agreement between the two methods.

consumption in 23.9% ($n=126$) was graded as high (defined as drinking more than the UK recommended alcohol guidelines). Mean (SD) VCTE was 9.5 (9.2) kPa, of whom 8% ($n=42$) had a reading of >20.0 kPa. 77.4% ($n=408$) were diagnosed with non-alcoholic fatty liver disease (NAFLD); 15.7% ($n=83$) with alcohol related liver disease (ARLD) and 6.8% ($n=36$) with both NAFLD and ARLD. 27.9% ($n=147$) of patients were found to have a liver fibrosis stage of F3/F4 (9.7 kPa–13.5 kPa/ >13.6 kPa) and were referred to secondary care. 71.0% ($n=374$) had a liver fibrosis stage of F0–F2 (between 3.0 kPa and 9.6 kPa) and were referred back to primary care for repeat VCTE assessment in 3 years time.

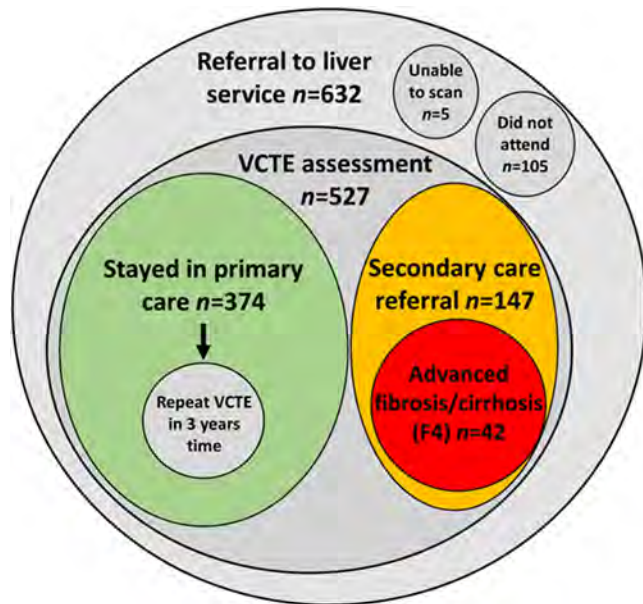


Figure: Summary of patient pathway through the community-based liver scanning service.

Conclusion: 8% asymptomatic patients identified as having advanced liver disease/cirrhosis and ~20% identified as being at risk of developing progressive liver fibrosis, are now being monitored by secondary care. The remaining patients (71%) are being monitored in primary care and will be referred for repeat VCTE assessment in 3 years time. This evaluation demonstrates the usefulness of providing primary care clinicians with a liver guidance pathway with access to VCTE assessment, a service that is still predominantly only accessible in secondary care.

Acknowledgements: Lucie Lleshi, NHS Southampton Clinical Commissioning Group.

FRI033

Predictive survival-time modelling of Non-Alcoholic Steatohepatitis (NASH) fast progressors using real-world evidence

Nils Svängård¹, Christen Gray², Ally Taylor³, Taylor Cohen⁴, Bret Sellman⁴, Claire Donoghue², Faisal Khan⁵, Christopher Rhodes⁶, Philip Ambery⁷, Shameer Khader⁵, John Dillon³. ¹AstraZeneca, Data Science & Artificial Intelligence, Sweden; ²AstraZeneca, Data Science & Artificial Intelligence, Cambridge, United Kingdom; ³University of Dundee, United Kingdom; ⁴AstraZeneca, Microbiome Discovery, Gaithersburg, United States; ⁵AstraZeneca, Data Science & Artificial Intelligence, Gaithersburg, United States; ⁶AstraZeneca, Early CVRM, Gaithersburg, United States; ⁷AstraZeneca, Clinical Metabolism, Gothenburg, Sweden
Email: nils.svangard@astrazeneca.com

Background and aims: Evidence suggests that a subset of patients with Non-Alcoholic Fatty Liver Disease (NAFLD) may progress faster to end stage liver disease via Non-alcoholic Steatohepatitis (NASH). There is a need for methods to identify such sub-populations of fast progressors in order to improve patient care and enable more effective clinical trials. Prior machine learning based approaches to identify progressors, e.g. using binary prediction of progression types, did not consider censored events due to death, transfer out of data source, or end of study period, which can reduce accuracy of the results. The aim of this study is to develop a machine learning survival-time prediction model that can identify NAFLD and NASH patients at risk of fast progression to end stage liver disease based on real-world data, taking censoring of events into account.

Method: We retrospectively evaluated patients in Optum® Clinformatics® Data Mart (de-identified US electronic health records, 2007–2021) aged ≥ 18 with the index-time being the first diagnosis of NAFLD or NASH based on ICD- codes with no prior liver disease. Progression time was defined as the time between index date and the first hard endpoint of NASH or censored at death, transfer out of data source, or end of study period. Progression times were predicted using a machine learning survival-time model robust to missing data, trained on sparse data and 80% of the subjects. Model performance was evaluated using the cumulative dynamic area-under-the-curve on the remaining subjects and compared with five single biomarker baseline models. The most important features were visualized using Shapley Additive exPlanations (SHAP).

Results: A final cohort of 260,180 patients matched the inclusion and exclusion criteria, 3% of the patients had a severe endpoint observed, and the median progression time for these patients was 14 months. The predictive model had an average cumulative dynamic AUC of 0.76 for predicting progression times from index to the end of the study period, compared with 0.64 for the best performing baseline model, the AST/ALT ratio.

Conclusion: The predictive survival-time model outperforms individual biomarkers at characterizing NASH fast progressors both at index time and continuously until the time of event. Future research of the model should include validation in other datasets, including patients in a range of geographic regions, of different ethnicities and with biopsy confirmed NASH.

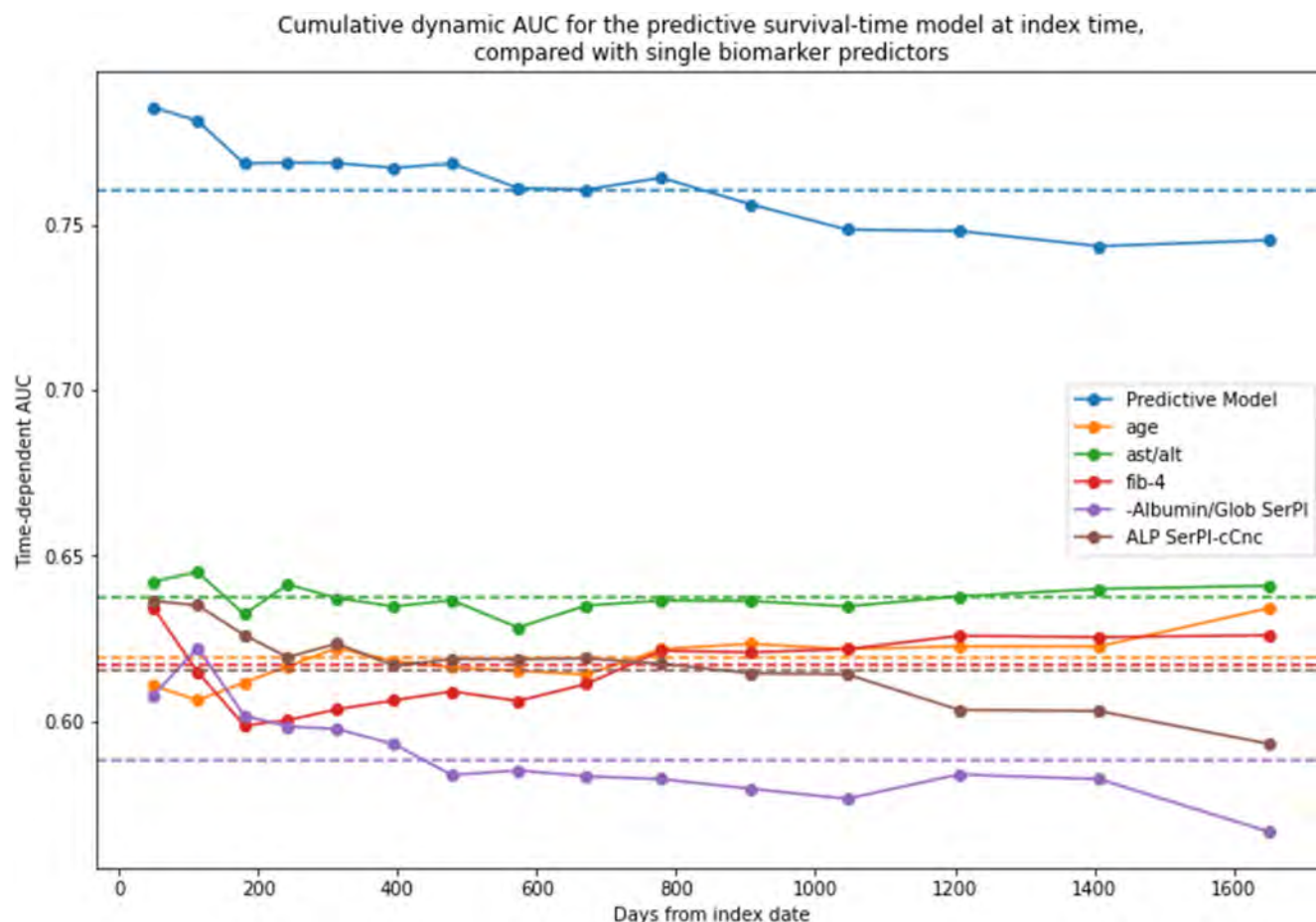


Figure: (abstract: FRI033)

FRI034

Online education significantly improved gastroenterologists' knowledge of the diagnostic and monitoring techniques used in liver fibrosis

James White¹, Elaine Bell¹, Briana Betz², Jörn Schattenberg³.

¹Medscape Global Education, London, United Kingdom; ²Medscape LLC, New York, United States; ³University Medical Center Mainz, I. Department of Medicine, Mainz, Germany

Email: jrwhite@webmd.net

Background and aims: Non-alcoholic steatohepatitis is a leading cause of liver fibrosis. Progression of liver fibrosis to advanced stages is linked to severe outcomes and increased healthcare costs. Non-invasive techniques, including biomarkers and elastography, improve the diagnosis and monitoring of liver fibrosis. Unmet educational needs are one barrier in the use of non-invasive techniques. We assessed whether online continuing medical education (CME) could improve physicians' knowledge and confidence of appropriate diagnostic and monitoring techniques in liver fibrosis.

Method: Gastroenterologists (n = 220) participated in a chapterised video activity entitled "Evolution of Diagnosis and Monitoring for Liver Fibrosis" which covered guideline recommendations, identification of patients at risk of progression, and non-invasive pathways for identifying advanced fibrosis. Educational effect was assessed using a repeated-pair design with pre-/post-assessment. 3 multiple choice questions assessed knowledge and 1 question, rated on a Likert-type scale, assessed confidence. A paired samples t-test was conducted for significance testing on overall average number of correct responses and for confidence rating, and a McNemar's test was conducted at the question level (5% significance level, $p < 0.05$).

Cohen's d with correction for paired samples estimated the effect size of the education on number of correct responses (<0.20 modest, 0.20–0.49 small, 0.59–0.79 moderate, ≥ 0.80 large). Data were collected from 04/01/21 to 09/03/21.

Results: Results showed significant overall improvement in average percentage of correct responses for gastroenterologists (45% pre- to 63% post-education, $p < 0.001$, Cohen's d = 0.56). The percentage of gastroenterologists that answered all questions correctly improved from 9% pre-, to 30% post-education.

Whilst 23% improved and 27% reinforced their knowledge regarding which set of markers is included in the Enhanced Liver Fibrosis (ELF) score, 50% of gastroenterologists still lack this information after education ($p < 0.001$).

Post-activity, 41% of gastroenterologists had a measurable increase in confidence in using non-invasive techniques in clinical practice to identify patients with advanced fibrosis ($p < 0.001$), with an average confidence shift of 58%.

Conclusion: Participation in an online chapterised video activity significantly improved physicians' knowledge and confidence of appropriate diagnostic and monitoring techniques in liver fibrosis. Despite this, further education regarding the markers included in the ELF score is needed for gastroenterologists.

FRI035

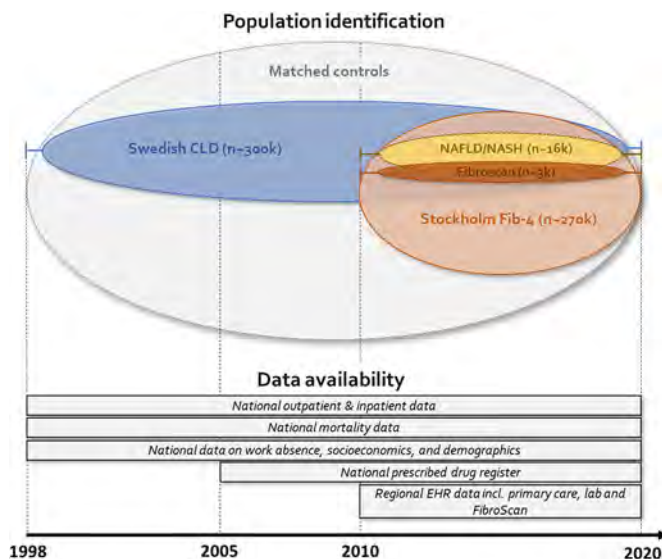
Health outcomes and risk assessment in chronic liver disease (HERALD): a large Swedish research platform

Emilie Toresson Grip^{1,2}, Oskar Ström^{1,2}, Hannes Hagström^{1,3,4},
¹Karolinska Institutet, Department of Medicine Huddinge, Sweden;
²Quantify Research AB, Stockholm, Sweden; ³Karolinska University Hospital, Division of Hepatology, Department of Upper GI Diseases, Stockholm, Sweden; ⁴Karolinska Institutet, Clinical Epidemiology Division, Department of Medicine Solna, Stockholm, Sweden
 Email: emilie.toresson.grip@ki.se

Background and aims: The 'Health outcomes and Risk Assessment in chronic Liver Disease' (HERALD) study is a multi-stakeholder Swedish research-platform linking national and regional registries to investigate the epidemiology and risk factors of liver outcomes, resource-use and costs, in patients with chronic liver diagnoses (CLD) or liver-related laboratory tests. HERALD is also planned to include data from the National Diabetes Register and other countries during 2022, and is open to international collaboration.

Method: A CLD cohort will consist of all patients ≥ 18 years with ≥ 1 CLD diagnosis (ICD-10) in the Swedish Patient Register, or primary care from the Stockholm region. A Fib-4 cohort will consist of patients with laboratory tests (AST, ALT and platelets), required for estimating the non-invasive Fibrosis-4 (Fib-4) score in all care settings in Stockholm. All patients will be linked with longitudinal data on diagnoses, comorbidities, healthcare utilization, prescribed medicines, mortality, work absence, socioeconomic status and demographics. For a subset, other laboratory data and data on transient elastography (FibroScan) are extracted from electronic health records (EHR) and FibroScan-devices, respectively. High-risk subgroups and costs will be compared with matched controls from the general population.

Results: A feasibility study was completed in 2020 and ethical approval for HERALD was granted in August, 2020. During 2001–2019, the number of patients with NAFLD was 16, 285, with at least 46, 122 patient years of follow-up. The number of patients with chronic HCV, AIH or PBC were $n = 53$, 602, $n = 5$, 337 and $n = 5$, 247, respectively. 200, 000 to 300, 000 patients with CLD are expected, partly overlapping with the ~ 270 , 000 patients expected in the Fib-4 cohort.



Conclusion: This study is the result of a research collaboration between academia and analytical and pharmaceutical industry. HERALD will be the largest data collection to date to estimate a contemporary prevalence of liver disease and advanced fibrosis in a

broad, unselected population of healthcare-seeking individuals in Sweden. Furthermore, HERALD will utilize clinical and non-clinical information to characterize patients with different risk profiles and to estimate long-term societal burden associated with severe liver outcomes in clinical practice over a 20-year period.

FRI036

Impact of alcohol use on the diagnostic performance of serum-based indices for fatty liver disease

Oscar Danielsson¹, Markku Nissinen¹, Katja Pahlkala^{2,3,4},
 Terho Lehtimäki^{5,6}, Olli Raitakari^{2,3,7}, Fredrik Åberg⁸. ¹Clinic of Gastroenterology, Helsinki University Central Hospital and University of Helsinki, Helsinki, Finland, Finland; ²Centre for Population Health Research, University of Turku and Turku University Hospital, Turku, Finland, Finland; ³Research Centre of Applied and Preventive Cardiovascular Medicine, University of Turku, Turku, Finland, Finland; ⁴Paavo Nurmi Centre, Unit of Health and Physical Activity, University of Turku, Turku, Finland, Finland; ⁵Department of Clinical Chemistry, Finlab Ltd., Finland, Finland; ⁶Faculty of Medicine and Health Technology, Finnish Cardiovascular Research Center-Tampere, Tampere University, Tampere, Finland, Finland; ⁷Department of Clinical Physiology and Nuclear Medicine, Turku University Hospital, Turku, Finland, Finland; ⁸Transplantation and Liver Surgery, Helsinki University Central Hospital and University of Helsinki, Finland
 Email: oscar.danielsson@hus.fi

Background and aims: Non-alcoholic fatty liver disease (NAFLD) and alcohol-related liver disease (ARLD) frequently co-exist, and recently proposed diagnostic criteria for metabolic-dysfunction associated fatty liver disease (MAFLD) have removed strict cut offs for alcohol use. While several indices exist for detection of NAFLD, there is paucity of study on how alcohol use possibly impact their diagnostic performance. We analysed the effect of various level of alcohol use on the performance of several indices for detecting fatty liver disease (FLD).

Method: From the Cardiovascular Risk in Young Finns study, we included participants who underwent abdominal ultrasound (US) in 2010–2012 for detection of FLD and had serum analyses available from the same time for calculation of the Fatty Liver Index (FLI), Hepatic Steatosis Index (HSI) and Lipid Accumulation Product (LAP). Alcohol use was assessed by questionnaires. Predictive performance for FLD was assessed by AUROC, logistic regression, sensitivity, specificity, and positive and negative predictive values (PPV and NPV) according to alcohol consumption.

Results: Study comprised 1426 individuals (mean age 42.1 years, 42.6% males, mean BMI 26.3 kg/m², mean alcohol use 9.4 g/day), of which 234 (16%) had FLD by US. High risk index-scores were observed in 27.2%, 24.7% and 54.8% (FLI, HSI and LAP, respectively) of the study population. When daily alcohol consumption was < 50 grams, all indices discriminated FLD with AUROCs of 0.82–0.88. Among heavy drinkers (> 50 g/day), AUROCs were 0.61–0.66. Alcohol use correlated weakly with both FLI ($r = 0.09$) and LAP scores ($r = 0.16$, both p -values < 0.001), no significant correlation for HSI.

POSTER PRESENTATIONS

Index	Alcohol/day, g	PPV	NPV
FLI		31.0/45.6%	97.5/94.6%
	<10	28.2/44.6%	97.7/96.0%
	10-20/30*	32.7/45.0%	99.3/93.2%
	20/30-50*	48.5/54.5%	100.0/87.1%
HSI	>50	43.5/53.8%	69.2/69.6%
		23.5/41.5%	97.6/92.4%
	<10	35.1/37.2%	98.5/94.4%
	10-20/30*	21.2/47.7%	97.0/90.1%
LAP	20/30-50*	35.9/62.5%	100.0/88.6%
	>50	44.0/62.5%	70.0/66.7%
		26.6%	96.1%
	<10	23.1%	97.6%
	10-20/30*	32.1%	95.3%
	20/30-50*	43.3%	87.0%
	>50	38.5%	60.0%

Values shown for **lower/higher** cut off values

*Alcohol use categorized using different cut off values for men and women

Conclusion: With alcohol consumption below 50 g/day, FLI, HSI and LAP perform well for detection of FLD, all with comparable performance. With higher alcohol consumption, their diagnostic performance is reduced substantially.

FRI037

Liver stiffness on magnetic resonance elastography and liver-related outcomes in nonalcoholic fatty liver disease: a systematic review and meta-analysis of individual participants

Veeral Ajmera¹, Kun Yang¹, Beom Kyung Kim¹, Abdul Majzoub², Nobuharu Tamaki³, Atsushi Nakajima⁴, Ramazan Idilman⁵, Mesut Gumussoy⁵, Digdem Kuru Öz⁵, Ayse Erden⁵, Natalie Quach⁶, Xin Tu⁶, Xinlian Zhang⁶, Mazen Nouredin⁷, Alina Allen⁸, Rohit Loomba⁶. ¹University of California San Diego; ²Conemaugh Memorial Medical Center; ³Musashino Red Cross Hospital, Japan; ⁴Yokohama City University Medical Center; ⁵Ankara University, Turkey; ⁶University of California San Diego, United States; ⁷Cedars Sinai Medical Center, United States; ⁸Mayo Clinic, United States
Email: v1ajmera@ucsd.edu

Background and aims: Magnetic resonance elastography (MRE) is a reproducible, accurate, continuous biomarker of liver fibrosis,

however, limited data characterize its association with outcomes. We conducted a systematic review and pooled analysis of individual participant data from published studies and additional identified cohorts to evaluate the association between liver stiffness on MRE and liver-related outcomes.

Method: A systematic search identified 6 cohorts of adults at risk for NAFLD who underwent MRE and were assessed for liver-related outcomes. In a pooled analysis, logistic regression and Cox proportional hazards models were used to assess the association between liver stiffness on MRE and liver-related outcomes including a composite primary outcome defined as varices needing treatment, ascites and hepatic encephalopathy. Secondary outcomes included hepatocellular carcinoma (HCC) and death. Cumulative incidence curves evaluated time to first event for the primary outcome.

Results: Our pooled analysis included 2275 patients (54% women) with a mean age 57.5 (±15) years and mean MRE at baseline of 4.01 (±2.17) kPa. A total of 948 events occurred in 458 participants. Each 1 kPa increase in liver stiffness was associated with OR = 1.22 (95% CI: 1.16–1.29, p < 0.001) increased odds of the primary outcomes at baseline. Among 1983 patients with a median (IQR) of 3 (4.14) years of follow up time the 1- and 3-year risk of the primary outcome was 0.6% and 1.5% for MRE <5 kPa, 7.2% and 16.6% for 5–8 kPa and 8.5% and 18.8% for MRE >8 kPa respectively (Figure). The hazard ratio (HR) for the primary outcome, HCC and death for MRE 5–8 kPa were HR = 11.9 (95% CI: 7.58–18.96, p < 0.001), HR = 14.8 (95% CI: 5.53–39.6, p < 0.001) and HR = 2.37 (95% CI: 1.68–3.34, p < 0.001) respectively and for >8 kPa HR = 17.3 (95% CI: 10.1–29.7, p < 0.001), HR = 23.3 (95% CI: 7.94–68.2, p < 0.001) and HR = 4.84 (95% CI: 3.22–7.27, p < 0.001) respectively, compared to <5 kPa. The MEFIB index defined as positive when MRE ≥3.3 kPa and FIB-4 ≥1.6 had a strong association with the primary outcome HR = 21.8 (95% CI: 11.0–43.2, p < 0.001) and excellent negative predictive value for hepatic decompensation (Figure).

Conclusion: Liver stiffness assessed by MRE is associated with liver-related outcomes and death and the combination of MRE and FIB-4 has excellent negative predictive value for hepatic decompensation.

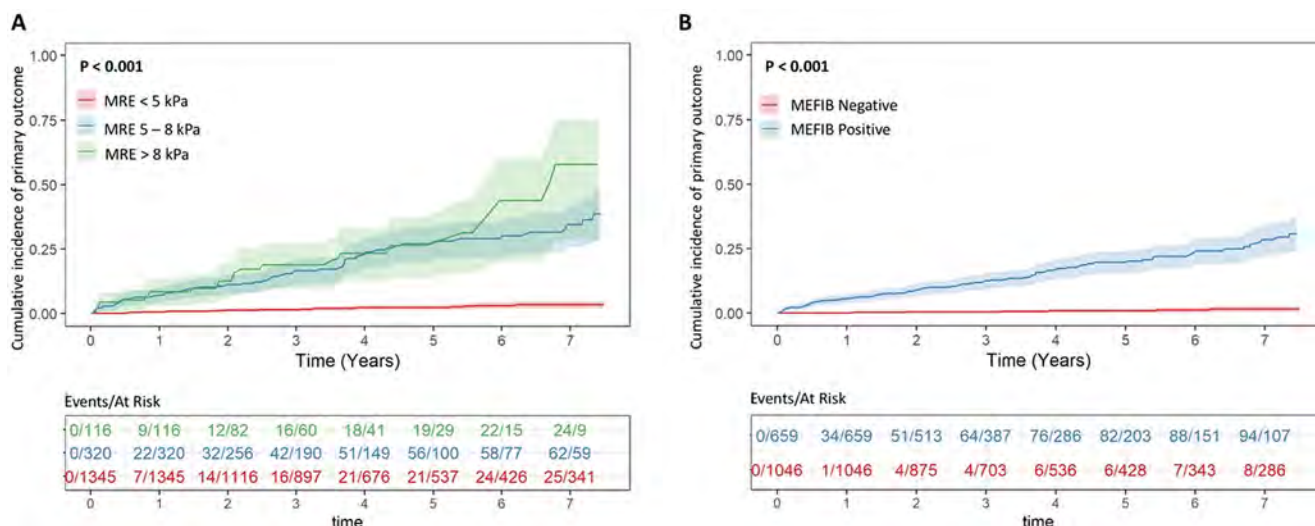


Figure: (abstract: FRI037): Cumulative incidence curves for primary outcome by (a) MRE <5 kPa vs 5–8 kPa and >8 kPa and (b) MEFIB Index.

FRI038

Utilising features of metabolic syndrome to cost-effectively improve metabolic dysfunction-associated fatty liver disease diagnosis rates

Cassandra Baiano¹, Jennifer Nobes¹, Iain Macpherson¹, Callum Livingstone¹, Madeleine Caven¹, Paul Brennan¹, Ellie Dow², John Dillon¹. ¹School of Medicine-University of Dundee, United Kingdom; ²NHS Tayside, United Kingdom
Email: cbaiano@dundee.ac.uk

Background and aims: The international consensus currently defines Metabolic Dysfunction-associated Fatty Liver Disease (MAFLD) as obesity, multiple metabolic risk factors, or type 2 diabetes mellitus plus hepatic steatosis on imaging. To facilitate the diagnosis of liver diseases, like MAFLD, in the community, an algorithm-based diagnostic tool (intelligent liver function testing, iLFT) that uses biochemical tests and clinical information has been developed. 22% of iLFT results are initially descriptive (i.e. isolated raised ALT) with no definitive aetiology but are identified as MAFLD after costly, prolonged investigations. This study aimed to identify whether features of the metabolic syndrome could be used to cost-effectively increase MAFLD diagnosis in the community while decreasing the need for imaging or liver clinic attendance.

Method: A retrospective analysis of iLFT patients from 2018 to 2020 was conducted. Medical records were used to identify BMI, features of metabolic syndrome, and steatosis on ultrasound scan (USS). Logistic regression analyses assessed which features of metabolic syndrome could predict USS steatosis. New MAFLD diagnostic pathways within iLFT were modelled with a cost-benefit analysis.

Results: 2720/6791 patients had no cause for deranged liver function tests identified by iLFT or had suspected MAFLD, of which 646 had sufficient health data for analysis.

While glucose impairment is the only statistically significant feature to predict USS steatosis across BMIs ($p < 0.000$, Sen = 41%, PPV = 88%), prediction can be optimised by stratifying patients into three BMI

categories (≤ 26 , 27–34, ≥ 35). In patients with BMI ≥ 35 ($n = 114$), any one feature of metabolic syndrome is a strong enough predictor of USS steatosis that MAFLD can be diagnosed and managed in the community, and USS and liver clinic can be avoided ($p < 0.003$, Sen = 85%, PPV = 91%). In BMI 27–34 ($n = 275$), glucose impairment is a strong enough predictor of USS steatosis that MAFLD can be diagnosed and managed in the community, and USS and liver clinic can be avoided ($p < 0.007$, Sen = 35%, PPV = 89%). In patients with a high NAFLD fibrosis score or BMI ≤ 26 ($n = 257$), both ultrasound and liver clinic are still required for assessment.

The expert liver team reviewed a sub-cohort of 144/646 patients and found that new MAFLD diagnostic pathways based on this stratification produce the correct MAFLD diagnosis or a fail-safe next step in 96% ($n = 138$) of cases. The new pathways offer a savings of £36.22 for every £1 spent.

Conclusion: New MAFLD diagnostic pathways that stratify patients by BMI and include features of metabolic syndrome to predict fatty infiltration on USS could cost-effectively increase MAFLD diagnosis in the community and reduce referral to USS by 26% while reducing referral to liver clinic by 24% (Sen = 100%, PPV = 98%).

FRI039

Non-invasive assessment of type VII collagen degradation is related to NAFLD activity but not fibrosis stage

Mette Juul Nielsen¹, Peder Frederiksen¹, Morten Karsdal¹, Diana Leeming¹, Jörn Schattenberg². ¹Nordic Bioscience A/S, Herlev, Denmark; ²University Medical Centre of the Johannes Gutenberg-University Mainz, Mainz, Germany
Email: mju@nordicbio.com

Background and aims: Type VII collagen is an anchoring fibril collagen crucial for the function and stability of the extracellular matrix (ECM) by linking basement membrane and interstitial matrix collagens together. Remodeling of the basement membrane is observed in early stage pericellular fibrosis, whereas accumulation

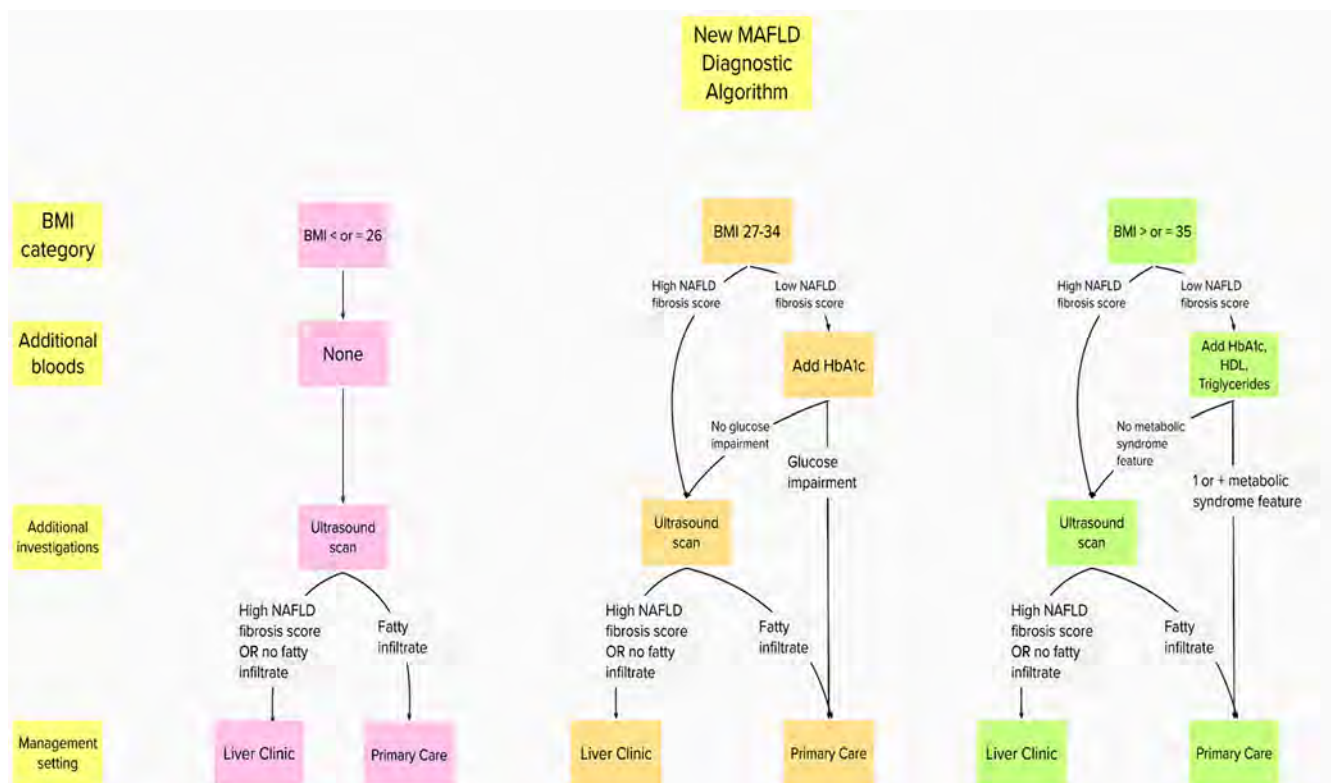


Figure: (abstract: FRI038)

POSTER PRESENTATIONS

of interstitial matrix collagens is observed during advanced fibrosis. The role of type VII collagen in liver fibrosis is unknown. The aim of this study was to investigate the role of type VII collagen using a collagen neoepitope technology in relation to fibrosis development in NAFLD patients.

Method: Degradation of type VII collagen was assessed by the novel neoepitope marker, C7M, developed by Nordic Bioscience A/S, in serum samples from 140 NAFLD patients with biopsy confirmed liver fibrosis F0-F4 and NAS 0-7 in a cross-sectional study design. Histopathological staging of fibrosis, steatosis, hepatocyte ballooning and lobular inflammation was scored according to the Kleiner scoring system.

Results: Patients had median age of 53.5 (IQR 43-60) years and median BMI of 32.2 kg/m² (IQR 29.0-36.1) of which 74 (53%) were male ($p = 0.499$). Serum C7M significantly correlated with the NAS ($r = 0.255$; $p = 0.003$), the grade of hepatocyte ballooning ($r = 0.278$; $p = 0.001$), and steatosis ($r = 0.285$; $p < 0.001$), but not the degree of lobular inflammation ($r = 0.161$; $p = 0.065$) or the histological fibrosis stage ($r = -0.005$; $p = 0.962$). C7M was significantly elevated in patients with NAS ≥ 3 compared to NAS ≤ 2 ($p < 0.001$). A 30% and 18% increase in C7M was observed from hepatocyte ballooning grade 0 to 1-2 ($p = 0.001$) and from steatosis grade 0-1 to 2-3 ($p = 0.004$), respectively. In the same cohort, the levels of the fibrogenic collagen marker, PRO-C3, was increased in the population with advanced vs early fibrosis ($p < 0.0001$), as well as in patients with steatosis ($p = 0.0001$), hepatocyte ballooning ($p = 0.0001$), and lobular inflammation ($p < 0.0001$).

Conclusion: Degradation of type VII collagen may be an early indicator of increased protease activity, related to linkage disruption of the ECM structure between basement membrane and interstitial matrix collagens in liver fibrosis development in patients with NAFLD.

FR1040

Reliability of histologic disease activity measures in non-alcoholic fatty liver disease (NAFLD) and development of an expanded NAFLD activity score

Rish Pai¹, Vipul Jairath^{2,3,4}, Malcolm Hogan⁴, Guangyong Zou^{3,4,5}, Oyedele Adeyi⁶, Quentin Anstee^{7,8}, Bashar Aqel⁹, Cynthia Behling^{10,11}, Elizabeth Carey⁹, Andrew Clouston¹², Kathleen Corey^{13,14}, Brian Feagan^{2,3,4}, David E. Kleiner¹⁵, Christopher Ma^{4,16,17}, Stefanie McFarlane⁴, Mazen Nouredin¹⁸, Vlad Ratziu¹⁹, Mark Valasek²⁰, Zobair Younossi^{21,22}, Stephen Harrison^{23,24}, Rohit Loomba²⁵. ¹Mayo Clinic Arizona, Department of Laboratory Medicine & Pathology, Scottsdale, United States; ²University of Western Ontario, Department of Medicine, Division of Gastroenterology, London, Canada; ³University of Western Ontario, Department of Epidemiology and Biostatistics, London, Canada; ⁴Alimentiv Inc., London, Canada; ⁵Robarts Research Institute, Schulich School of Medicine and Dentistry, University of Western Ontario, London, Canada; ⁶University of Minnesota Medical School, Department of Laboratory Medicine and Pathology, Minneapolis, United States; ⁷Translational & Clinical Research Institute, Newcastle University, Faculty of Medical Sciences, Newcastle upon Tyne, United Kingdom; ⁸Newcastle NIHR Biomedical Research Center, Newcastle upon Tyne Hospitals NHS Foundation Trust, Newcastle upon Tyne, United Kingdom; ⁹Mayo Clinic Arizona, Division of Gastroenterology and Hepatology, Phoenix, United States; ¹⁰Pacific Rim Pathology, San Diego, United States; ¹¹University of California San Diego, Department of Pediatrics, La Jolla, United States; ¹²University of Queensland, Faculty of Medicine and Biomedical Sciences, Saint Lucia, Australia; ¹³Massachusetts General Hospital, Division of Gastroenterology, Boston, United States; ¹⁴Harvard Medical School, Boston, United States; ¹⁵Center for Cancer Research, National Cancer Institute, Laboratory of Pathology, Bethesda, United States; ¹⁶Cumming School of Medicine U C, Division of Gastroenterology & Hepatology, Calgary, Canada; ¹⁷University of Calgary, Department of Community

Health Sciences, Calgary, Canada; ¹⁸Cedars-Sinai Medical Center, Division of Gastroenterology and Hepatology, Department of Medicine, Los Angeles, United States; ¹⁹Pitié Salpêtrière Hospitals, Sorbonne Université, Institute of Cardiometabolism and Nutrition, Paris, France; ²⁰University of California San Diego, Department of Pathology, La Jolla, United States; ²¹Inova Health System, Betty and Guy Beatty Center for Integrated Research, Falls Church, United States; ²²Inova Fairfax Medical Campus, Department of Medicine, Center for Liver Diseases, Falls Church, United States; ²³University of Oxford, Radcliffe Department of Medicine, Oxford, United Kingdom; ²⁴Pinnacle Clinical Research, Medical Director, San Antonio, United States; ²⁵University of California San Diego, NAFLD Research Center, Department of Medicine, La Jolla, United States
Email: roloomba@ucsd.edu

Background and aims: In clinical trials of non-alcoholic steatohepatitis (NASH), the Non-alcoholic Steatohepatitis Clinical Research Network (NASH CRN) histologic scoring system is the current gold standard histology assessment but has demonstrated intra- and inter-observer variability. An expert panel determined in a prior Research and Development/University of California Los Angeles (RAND/UCLA) process that existing histologic scoring systems do not fully capture NASH disease activity and fibrosis. We evaluated the intra- and inter-rater reliability of histologic disease activity measures and correlated these measures with a disease activity visual analogue scale (VAS) to propose an exploratory expanded non-alcoholic fatty liver disease (NAFLD) activity score (NAS) index comprising optimized items.

Method: Four liver pathologists assessed 40 liver biopsies representing the full spectrum of NAFLD. These central readers were blinded to clinical information, completed standardized training, and scored each histologic measure twice, with ≥ 2 weeks between each assessment. Scored measures included existing histologic indices, the component items of these indices, and additional items identified in the prior RAND/UCLA study. Reliability was assessed using intra-class correlation coefficients (ICCs).

Results: The ICCs for existing NAFLD activity indices demonstrated substantial to almost perfect intra-rater reliability (ICC, 0.80-0.85) and moderate to substantial inter-rater reliability (ICC, 0.60-0.72). Ballooning degeneration items (ICC, 0.68-0.79), including those that extended scores from 0 to 2 to 0-4, and steatosis items (ICC, 0.72-0.80) had substantial inter-rater reliability. Fibrosis measures demonstrated substantial to almost perfect inter-rater agreement (ICC, 0.70-0.87). Items for ballooning degeneration and Mallory-Denk bodies (MDBs) had large correlations with the disease activity VAS ($r = 0.66-0.96$) and were used to develop an expanded NAS (intra-rater ICC, 0.90; inter-rater ICC, 0.80). Steatosis items were poorly correlated with the disease activity VAS ($r = -0.02$ to 0.12).

Conclusion: Histologic indices, including the expanded NAS, had almost perfect intra-rater reliability and moderate to substantial inter-rater reliability. Ballooning degeneration and MDBs were used for the expanded NAS based on their strong correlations with disease activity. Future evaluation of the responsiveness of these measures is needed.

FR1041

Evaluating future risk of NAFLD fibrosis in adolescents: prediction and decision curve analysis

Kushala Abeyssekera^{1,2}, Julian Hamilton-Shield¹, James Orr², Fiona Gordon², Laura Howe¹, Jon Heron¹, Matthew Hickman¹. ¹University of Bristol, United Kingdom; ²Bristol Royal Infirmary
Email: k.abeysekera@bristol.ac.uk

Background and aims: Elevated body mass index (BMI) is the major risk factor for nonalcoholic fatty liver disease (NAFLD) development. Using data from the Avon Longitudinal Study of Parents and Children (ALSPAC), we sought to investigate whether other variables from adolescence could improve prediction of future NAFLD fibrosis risk at 24 years, above BMI.

Method: Aged 24 years, 4018 ALSPAC participants had transient elastography (TE) using Echosens 502 Touch. 513 participants with harmful alcohol consumption were excluded. 2.7% had \geq F2 equivalent fibrosis. Logistic regression models examined which factors that were measured at age 17 were predictive of NAFLD fibrosis in young adults. Predictors included sex, BMI, central adiposity, lipid profile, blood pressure, liver function tests, homeostatic model assessment for insulin resistance (HOMA-IR), and steatosis at 17 years (based on ultrasound). A model including all these variables reflected “standard of care” (SoC). Models were compared using area under the receiver operator curve (AUROC) and Bayesian Information Criterion (BIC), analysis, which penalises model complexity. Models were tested in participants with overweight and obese standardised BMIs (BMI SDS) centiles at the 17-year time point. A decision curve analysis (DCA) was performed to evaluate the clinical utility of models at 17-years predicting NAFLD fibrosis at a threshold probability of 0.1. Datasets were imputed up to the number of available TE outcomes.

Results: In adolescents with overweight/obese BMI SDS centiles, the SoC model had the highest AUROC (AUROC 0.84 [SD 0.03]). However following BIC analysis, BMI SDS at 17 years was the best predictor of NAFLD fibrosis at 24 years. A DCA examining overweight/obese adolescent participants demonstrated the model that had greatest net benefit, above a treat all assumption, was the SoC model although the net benefit was marginal (0.0054 [IQR 0.0034–0.0075]). This was equivalent to 5 more NAFLD fibrosis cases being detected per 1000 patients.

Conclusion: SoC measurements are not superior to BMI SDS in adolescence at predicting NAFLD fibrosis development in young adulthood. Additional SoC measurements provide incremental but small benefit in detecting true positive fibrosis cases. Thus, with the agenda of reducing long term morbidity and mortality associated with fibrosis, providing targeted interventions to overweight and obese adolescents is important to prevent progression to fibrosis.

FRI042

Quantification of hepatic steatosis in patients with non-alcoholic fatty liver disease: comparison of sound speed, attenuation coefficient and continuous CAP measurements with MRI-PDFF

Rémi Collin¹, Benjamin Buchard¹, Benoît Magnin², Carine Nicolas¹, Constance Gaillard², Armand Abergel¹. ¹Centre Hospitalier Universitaire Estaing de Clermont-Ferrand, Department of Hepatology and Gastroenterology, Clermont-Ferrand, France; ²Centre Hospitalier Universitaire Estaing de Clermont-Ferrand, Department of Radiology, Clermont-Ferrand, France
Email: rja.collin@gmail.com

Background and aims: Non-alcoholic fatty liver disease (NAFLD) is becoming a major health problem, resulting in hepatic, metabolic and cardio-vascular morbidity. Our study aims at evaluating new ultrasonographic tools to detect and measure hepatic steatosis.

Method: After local approval and patient consent, we included 73 patients addressed to a hepatology consultation for NAFLD suspicion or follow-up. They underwent ultrasonographic measurement of liver sound speed estimation (SSE) and attenuation coefficient (AC) using Aixplorer MACH 30 (Supersonic Imagine, France), and continuous Controlled Attenuation Parameter (cCAP) using Fibroscan (Echosens, France). Hepatic steatosis was then classified according to MRI proton density fat fraction (PDFF). Receiver operating curve (ROC) analysis was performed to evaluate the diagnostic performance in the diagnosis of steatosis.

Results: Our 73 patients (35 males and 38 females) had high mean age, BMI, weight, and waist circumference, respectively 60 years, 29.4 kg/m², 85 kg and 104 cm. 67% had a metabolic syndrome and 15% significant liver fibrosis. According to PDFF, 18 (24.7%) patients had no steatosis (PDFF <6.5%, S0), 30 (41.1%) suffered from mild steatosis (6.5 <PDFF <16.5%, S1), 8 (10.9%) from moderate steatosis (16.5 <PDFF <22%, S2), and 17 (23.3%) from severe steatosis (PDFF >22%, S3). SSE, AC and cCAP correlate with PDFF, with respective Spearman correlation coefficient of -0.50, 0.51 and 0.65 (p < 0.01).

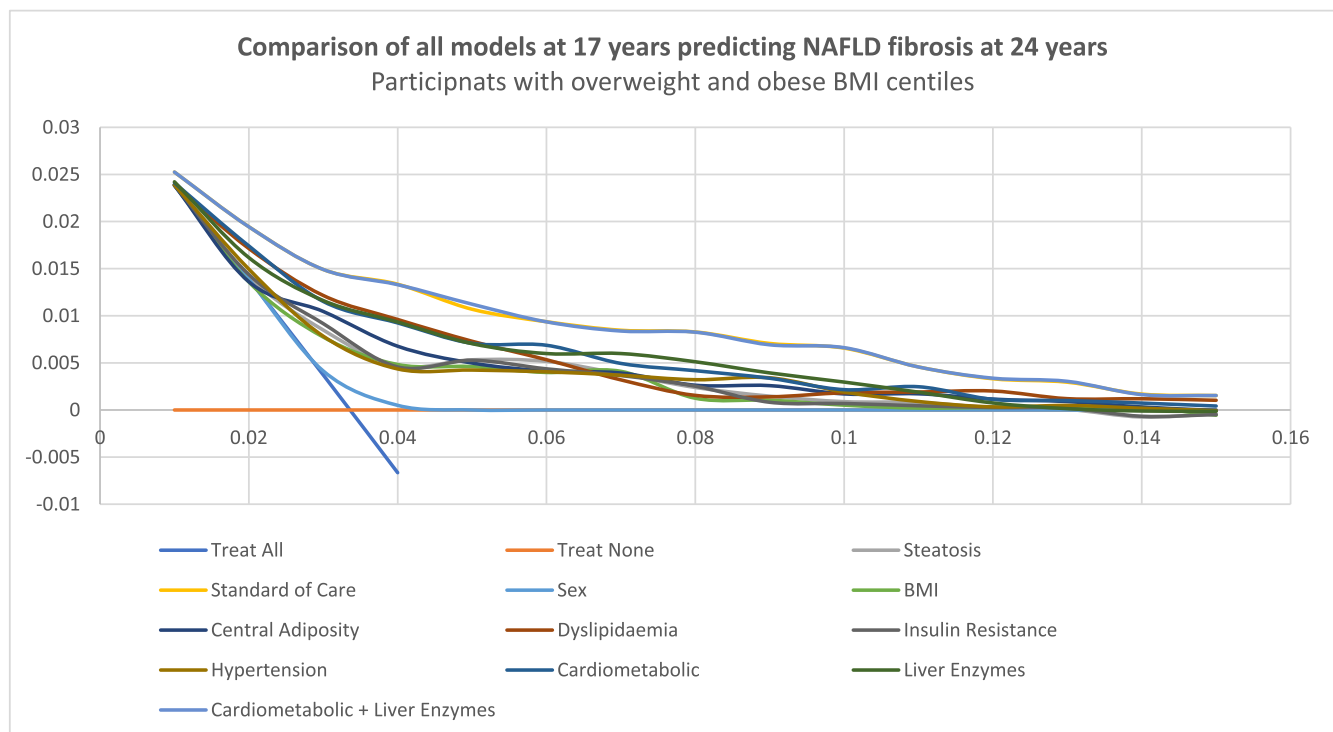
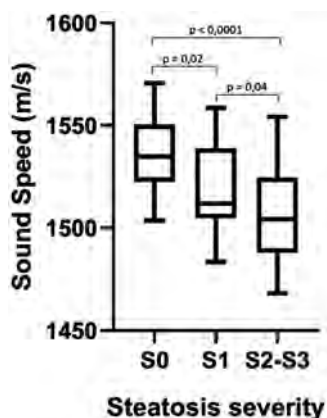


Figure: (abstract: FRI041): Decision curve analysis of different models to predict NAFLD Fibrosis at 24 years in 17 years with overweight or obese BMI centiles.

POSTER PRESENTATIONS

Mean SSE, AC and cCAP values significantly differ between non-steatotic and steatotic patients (S1–S3). SSE values also differs between S1 and S2–S3 steatosis ($p=0.04$). An SSE threshold of 1524 m/s had a sensitivity of 69% and a specificity of 74% for the diagnosis of steatosis (S1–S3). The corresponding area under the ROC curve (AUC) was 0.77 (95% CI 0.66–0.88, $p<0.01$). An AC threshold of 0.41 dB/cm/MHz had a sensitivity of 91% and a specificity of 79% for the diagnosis of steatosis (S1–S3). The corresponding AUC was 0.91 (95% CI 0.84–0.98, $p<0.01$). An cCAP threshold of 263 dB/m had a sensitivity of 82% and a specificity of 78% for the diagnosis of steatosis (S1–S3). The corresponding AUC was 0.92 (95% CI 0.86–0.98, $p<0.01$). The EASL-suggested threshold of 275 dB/m has a sensitivity of 75% and a specificity of 94%.



Conclusion: SSE and AC, simultaneously measured using Aixplorer MACH 30 system, demonstrate their reliability to detect liver steatosis. AC has high sensitivity for all-grade steatosis detection, with AUC >0.90, despite having more than 40% of our patients suffering from mild steatosis (S1).

To be noted that mean SSE values significantly differ between S1 and S2–S3 patients, maybe allowing for future ultrasonographic steatosis grading.

cCAP has good overall performances, but optimal thresholds are yet to be determined, and is not able to distinguish between different grades of steatosis.

FRI043

Community NAFLD screening programme in patients with type 2 diabetes mellitus indicates high burden of undiagnosed liver disease

Emma McCormick¹, Noelle Cullen¹, Suzanne Norris¹, Oonagh O'Hagan², ¹St James's Hospital, Hepatology, Dublin, Ireland; ²Meaghers Pharmacy Group, Dublin, Ireland
Email: emmamccormick@rcsi.ie

Background and aims: NAFLD is the most common liver disease in Western countries, affecting 1 in 4 adults, with prevalence mirroring that of obesity and T2DM. The presence of hepatic fibrosis is an important predictor of premature mortality and liver-related morbidity and mortality. Vibration-controlled transient elastography (VCTE) is a validated non-invasive test with NPV >90% for detection of advanced fibrosis/cirrhosis, but is largely confined to specialist centres. The lack of optimised public health screening strategies to detect liver fibrosis in adults remains a healthcare challenge.

The aim of this study was to assess the feasibility of VCTE as a screening method to detect hepatic fibrosis in patients with identified risk factors for NAFLD in a community healthcare setting.

Method: 206 patients (94 male, 112 female,) with risk factors for NAFLD were identified via dispensing records in community pharmacies and invited to register for VCTE appointment. VCTE assessments were performed in 4 community pharmacies over 14

dates between June and July 2021 and results sent to patients' GPs. Patients with liver stiffness measurements (LSM) >8.2 kPa were referred to a specialist Hepatology clinic for follow up.

Results: The median age was 63 years (range 27–84). 88% of patients had T2DM and 53% had a BMI >30. The median CAP score was 291 dB/m (range 160–400), and 45% of patients had a CAP score ≥300 dB/m. The median LSM was 5.8 kPa. 31% of patients had LSM ≥7.1 kPa, 15% had LSM ≥9.1 kPa and 6.7% had LSM ≥12.5 kPa. Only 19% of patients had both a normal CAP and LSM.

Conclusion: This is the first study to assess VCTE screening for hepatic fibrosis beyond traditional healthcare settings, and demonstrates that community-based risk-stratified screening leads to earlier identification of patients with liver fibrosis. Community pharmacy is a readily accessible healthcare setting in which access to non-invasive assessments of liver fibrosis outside of the hospital setting could be offered with potential significant cost savings to the healthcare system.

FRI044

Non-alcoholic fatty liver disease in patients with type-2 diabetes mellitus in Greenland

Rasmus Hvidbjerg Gantzel^{1,2}, Abdullah Ghassan Farik Muhammad^{1,3}, Frederik Orm Hansen^{1,3}, Karsten Fleischer Rex³, Gerda Elisabeth Villadsen¹, Henning Grønbaek^{1,2}, Michael Lynge Pedersen^{3,4}. ¹Aarhus University Hospital, Department of Hepatology and Gastroenterology, Århus N, Denmark; ²Aarhus University, Department of Clinical Medicine, Århus N, Denmark; ³Steno Diabetes Center Greenland, Nuuk, Greenland; ⁴Institute of Nursing and Health Science, Greenland Center for Health Research, Nuuk, Greenland
Email: ragant@rm.dk

Background and aims: Non-alcoholic fatty liver disease (NAFLD) is the liver manifestation of the metabolic syndrome with a close relation to type-2 diabetes mellitus (T2DM). The prevalence of T2DM is increasing in the Greenlandic population. However, due to genetic variants, diabetic complications may occur less frequently in Greenlanders than non-Greenlanders. We aimed to characterize the prevalence and severity of NAFLD in patients with T2DM in Greenland.

Method: We included 1619 patients with T2DM living in Greenland in a register-based cross-sectional study. 1436 patients were born in Greenland and 183 were born in Denmark. In the absence of histopathology and radiological data, we used alanine aminotransferase (ALT) as surrogate marker of steatosis and estimated the degree of liver fibrosis with the FIB-4 score. Linear regression analyses were performed to assess associations between steatosis and the severity of the metabolic syndrome. A diagnosis of metabolic syndrome required ≥3 of the criteria: T2DM, BMI >30 kg/m², triglycerides >1.7 mmol/l or antilipidemic treatment, HDL <1.0/1.3 mmol/l for men/women or antilipidemic treatment, and systolic/diastolic blood pressure >130/85 mmHg or antihypertensive treatment.

Results: Despite higher BMI and plasma lipid levels, Greenlanders had a better glycemic control with lower HbA1c and a lower proportion on anti-diabetic treatments compared with Danes. The median ALT was similar, though ALT was elevated in a larger proportion of Greenlanders (21%) compared with Danes (11%). The median ALT was statistically significantly higher in Greenlanders with metabolic syndrome compared with Greenlanders without metabolic syndrome (51 vs. 39 U/L, $p<0.001$). Further, ALT increased with 8.0% (95% CI: 5.2–10.9, $p<0.001$) for each metabolic syndrome criteria fulfilled. The Danes had a higher FIB-4 score than Greenlanders (median 0.97 vs. 0.91, $p=0.048$). 84% of Greenlanders and 80% of Danes had a FIB-4 score <1.45 with a very low risk of significant fibrosis, while 13% of Greenlanders and 18% of Danes had a FIB-4 score of 1.45–2.67 with an intermediate risk of fibrosis. Only 2% in both ethnic groups had a FIB-4 score >2.67 suggesting advanced fibrosis.

Conclusion: ALAT elevations are more frequent in Greenlanders than in Danes with T2DM, and ALAT increases with 8.0% for each metabolic syndrome criteria fulfilled. Accordingly, ALAT may be a useful and easily accessible tool to monitor NAFLD in patients with T2DM in Greenland. The median FIB-4 score is lower in Greenlanders compared with Danes, suggesting a lower degree of liver fibrosis. These findings need further evaluations preferably including comparisons with histopathology.

FRI045

A baseline signature of metabolites involving the gut-liver axis predicts MRI-PDFF response to FASN inhibitor TVB-2640: results from the FASCINATE-1 study

Rohit Loomba¹, Marie O'Farrell², Eduardo Martins², Katharine Grimmer², Alithea Zetter², Cristina Alonso³, Ibon Martínez-Arranz³, George Kemble², Stephen Harrison⁴, ¹UC San Diego School of Medicine, Dept of Gastroenterology, La Jolla; ²Sagimet Biosciences, San Mateo, United States; ³OWL Metabolomics, Derio, Spain; ⁴Pinnacle Clinical Research, San Antonio, United States
Email: roloomba@ucsd.edu

Background and aims: TVB-2640 is a potent FASN inhibitor in Ph2b development for NASH. FASN is an attractive target because de novo lipogenesis drives steatosis, causes lipotoxicity, and is necessary for fibrogenesis. A 12 wk Ph2a study FASCINATE-1 was completed and met its primary endpoint. TVB-2640 reduced liver fat by 28.1% ($p = 0.001$) at 50 mg with a 61% MRI-PDFF response rate (decrease $>30\%$, $p = 0.001$), and decreased biomarkers including ALT, PRO-C3, PIIINP, CK-18 and lipotoxins. NASH clinical studies are often confounded by high pbo but relatively low drug response rates. The objective of this work was to identify predictive biomarkers of MRI-PDFF response using metabolomic and SNP profiling of baseline blood samples from patients in FASCINATE-1.

Method: Metabolomic plasma profiling of ~460 species was performed on the OWL platform for pbo, 25 mg, 50 mg. Two machine learning approaches, Random Forest (RF) and Support Vector Machine were applied to baseline data. Using % change in MRI-PDFF as a continuous variable, a signature was developed using 50% of samples and tested using the other 50% with extensive cross-validation for sample size. Genotyping of SNPs relevant to NAFLD was completed for 19 patients to date (6 pbo, 13 on 50 mg, 79% Hispanic). Correlative analysis included metabolomics, genomics and other NASH biomarkers.

Results: A 6-metabolite signature was identified that enriches for MRI-PDFF response to TVB-2640. This showed 79% accuracy, 88% positive predictive value and 63% negative predictive value by the RF method. The components are ursodeoxycholic acid, glyco-ursodeoxycholic acid, DL-2-Aminocaprylic acid, Sarcosine, D (-)-2-Aminobutyric acid and phosphatidyl choline (O-18:0/22:4). The composition of several bile acid derivatives suggests a role for the gut liver axis in TVB-2640 response. Overall, secondary bile acids increased after 12 wk of TVB-2640 across several classes and 9/10 species tested although not statistically significant. Analysis of pbo and independent validation is ongoing to refine this signature. SNP analysis showed allele variants in PNPLA3 rs738409, TM6SF2 rs58542926 and MBOAT7 rs641738 in 68%, 16% and 53% of patients respectively, consistent with literature. MRI-PDFF responders included patients with wild type, hetero- or homozygous PNPLA3 rs738409. The effect of PNPLA3 genotype on baseline metabolomic profile will be assessed. Additional predictive signatures are under development using a combination of metabolomics and genomic profiling.

Conclusion: TVB-2640 decreased liver fat and markers of inflammation, lipotoxicity and fibrosis. Plasma metabolomics identified a baseline predictive signature of MRI-PDFF response to FASN inhibition, which indicates a role for the gut-liver axis. The Ph2b FASCINATE-2 study will incorporate microbiome analysis and the

signature will be retrospectively tested and extended to histology analysis.

FRI046

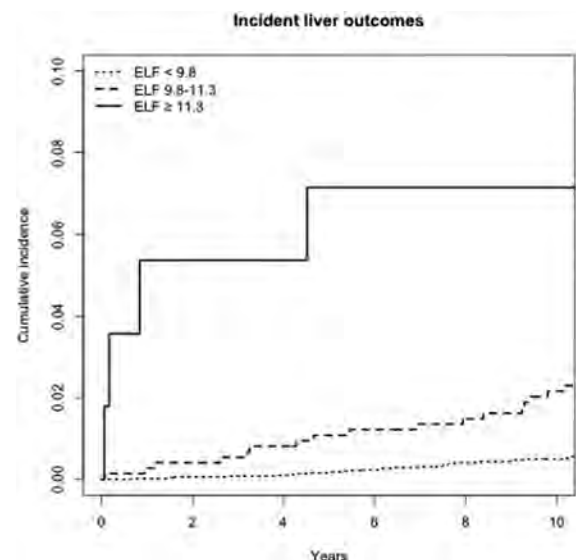
Enhanced Liver Fibrosis test in predicting severe liver-related outcomes in the general population

Kustaa Saarinen^{1,2}, Martti Färkkilä^{1,2}, Antti Jula³, Iris Erlund³, Terhi Vihervaara³, Annamari Lundqvist³, Fredrik Åberg⁴, ¹Helsinki University Hospital, Abdominal Center, Helsinki, Finland; ²University of Helsinki, Helsinki, Finland; ³Finnish Institute for Health and Welfare, Helsinki, Finland; ⁴Helsinki University Hospital, Transplantation and Liver Surgery Clinic, Finland
Email: kustaa.saarinen@gmail.com

Background and aims: Liver fibrosis is the most important prognostic factor for liver-related morbidity and mortality in liver diseases in population including non-alcoholic fatty liver disease and alcohol-related liver disease. Existing methods for liver fibrosis assessment are either not suitable or show suboptimal performance for fibrosis screening in unselected populations. The Enhanced Liver Fibrosis (ELF) test, a composite score based on three serum-based markers of matrix turnover tissue inhibitor metalloproteinase 1 (TIMP-1), human procollagen type III amino terminal propeptide (PIIINP) and hyaluronic acid (HA) can detect advanced fibrosis and predict liver-related outcomes in various types of chronic liver diseases, but studies in large general population cohorts are lacking. We evaluated the performance of the ELF test in predicting liver related outcomes at the population level.

Method: ELF was measured at baseline from frozen serum samples of adult (age >30 years) participants of the Finnish Health 2000 study, a population-based epidemiological survey conducted in year 2000–2001. Subjects with baseline liver disease were excluded. Data were linked with national healthcare registers for hospitalization, cancer and death related to severe liver disease.

Results: The cohort comprised 6040 individuals (46% men, mean age 52.7 ± 15 years, BMI 26.9 kg/m^2 , median alcohol use 74.9 g/week , 10% with diabetes). ELF was <9.8 in 5243 (87%), $9.8–11.3$ in 741 (12%), and ≥ 11.3 in 56 (0.9%). During a median follow-up of 13.1 years, 67 severe liver-related outcomes occurred. By age- and sex-adjusted Cox regression, hazards ratios (HRs) for liver outcomes were 6.44 (95%CI 3.37–12.29) with ELF $9.8–11.3$, and 24.37 (95% CI 8.55–69.50) with ELF ≥ 11.3 , compared to ELF <9.8 . Corresponding cumulative Aalen-Johansen incidences are shown in the figure. The C-statistic of ELF for predicting liver outcomes was 0.82 (95% CI 0.72–0.91) at 5 years and 0.73 (0.65–0.81) at 10 years.



POSTER PRESENTATIONS

Conclusion: The ELF test predicts severe liver-related outcomes in the general population. The ELF test could thus be used for initial stratification of the population regarding risk for future liver disease.

FRI047

Radiowater perfusion PET of the liver, and its value as a biomarker to discriminate between NAFLD and NASH, and activity and fibrosis grade

Olof Eriksson¹, Kerstin Heurling¹, Paul Hockings¹, Edvin Johansson¹, Alkwin Wanders², Håkan Ahlström¹, Lars Johansson¹, Johan Vessby³, Fredrik Rorsman³, Mark Lubberink⁴. ¹Antaros Medical AB, Sweden; ²Aalborg University Hospital, Aalborg, Denmark; ³Uppsala University Hospital, Sweden; ⁴Uppsala University Hospital, Uppsala, Sweden
Email: olof.eriksson@ilk.uu.se

Background and aims: The lack of non-invasive, biopsy free and repeatable assessments for fibrosis and activity stage in NAFL and NASH is a significant hurdle in respect to clinical diagnosis and evaluation of novel interventions. Radiowater PET has been shown to be a sensitive technique to quantify blood flow and identify perfusion defects in e.g. cardiology and neurology. We hypothesized that pathological changes in liver perfusion and arterial and portal blood flow could be detected by radiowater PET. The aim of this clinical study was to assess the value of radiowater PET for distinguishing between NAFL and NASH, as well as predicting activity and fibrosis grade in direct comparison with established biomarkers.

Method: A subset of patients with suspected NAFL/NASH (N = 30) recruited within the NASH AM-02 study was examined by radiowater PET/MRI, as well as transient elastography (FibroScan), in addition to sampling for established biomarkers of liver fibrosis. NAFL/NASH diagnosis as well as activity and fibrosis grade were verified by hepatic biopsy. Dynamic radiowater PET data of the liver was used to assess total hepatic blood flow, portal vein flow, hepatic arterial flow and portal flow fraction. The ROC AUC, the Youden cut-off and sensitivity/specificity were calculated for discrimination between (a) NAFL vs NASH, (b) activity grade 0–1 vs 2–4 and (c) fibrosis grade 0–1 vs 2–4. The correlation between parameters and activity grade 0–4 and fibrosis grade 0–4 was estimated by Spearman's correlation coefficient.

Results: In total 30 patients were examined in this sub-study and diagnosed with NAFL (n = 11) or NASH (n = 19), fibrosis grade 0–1 (n = 17) or 2–4 (n = 13) and activity grade 0–1 (n = 11) or 2–4 (n = 19). The ROC UAS as well as the Spearman's correlation coefficient for each parameter is reported in Table 1.

Conclusion: Radiowater PET has similar value as biomarker for distinguishing between NAFL/NASH and identifying activity grade, but not fibrosis grade, as transient elastography and established plasma markers.

FRI048

The combination of the ELF and FIB-4 scores have high predictive performance for significant fibrosis in patients with NAFLD

Zobair Younossi^{1,2}, Sean Felix², Thomas Jeffers², Elena Younossi², Fatema Nader³, Andrei Racila^{1,2}, Brian Lam², Maria Stepanova³. ¹Inova Health System, Medicine Service Line, Falls Church, United States; ²Betty and Guy Beatty Center for Integrated Research, IHS, Falls Church, United States; ³Center for Outcomes Research in Liver Disease, Washington DC, United States

Email: zobair.younossi@inova.org

Background and aims: Patients with nonalcoholic fatty liver disease (NAFLD) and fibrosis of stage 2 or greater (clinically significant fibrosis) are at risk for adverse outcomes, and are commonly considered to be candidates for clinical trials. Although non-invasive tests (NITs) for fibrosis have good negative predictive value (NPV), they tend to have suboptimal positive predictive value (PPV) for determining significant fibrosis. Our aim was to use a combination of two NITs to rule in and to rule out significant fibrosis among patients with NAFLD.

Method: Data were collected from patients with confirmed NAFLD diagnosis. Serum and liver biopsies were obtained for all patients. The Enhanced Liver Fibrosis (ELF) and FIB-4 NITs were calculated. Liver biopsies were read by a single hepatologist and scored according to the NASH CRN criteria, from stage 0 (no fibrosis) to 4 (cirrhosis). Significant fibrosis stage was defined as stage F2–F4.

Results: There were 463 NAFLD patients included: 48 ± 13 years old, 31% male, 35% type 2 diabetes. Of included patients, 39% had significant fibrosis; mean ELF score was 9.0 ± 1.2, mean FIB-4 score was 1.22 ± 1.05. Patients with significant fibrosis were older, more commonly male, had lower BMI but more components of metabolic syndrome (type 2 diabetes, hypertension, hyperlipidemia), higher ELF and FIB-4 scores (p < 0.0001). The performance of the two NITs in identifying NAFLD patients with significant fibrosis was as follows: AUC (95% CI) = 0.78 (0.74–0.82) for ELF, 0.79 (0.75–0.83) for FIB-4. A combination of ELF score ≥ 9.8 and FIB-4 ≥ 1.96 returned PPV of 95% which can reliably rule in significant fibrosis (sensitivity 22%, specificity >99%), while an ELF score ≥ 7.7 and FIB-4 ≥ 0.30 had NPV of 95% which can be used to rule out significant fibrosis (sensitivity 98%, specificity 22%); based on the latter, a rule to rule out significant fibrosis could be rewritten as follows: ELF < 7.7 or FIB-4 < 0.30.

Conclusion: The combination of ELF and FIB-4 can provide an easy algorithm with both high NPV and high PPV to rule out or rule in significant fibrosis in NAFLD. These data can be used to risk-stratify NAFLD patients in clinical practice as well as identify those who could be candidates for clinical trials.

Table 1: (abstract: FRI047).

	PET Total blood flow [ml/g/min]	PET Portal vein blood flow [ml/g/ min]	PET Portal vein flow fraction [1/1]	Liver stiffness Fibroscan [kPa]	CK18 M30	ALT	AST
NAFL vs NASH, and Activity grade 0–1 vs 2–4 Fibrosis grade 0–1 vs 2–4	ROC AUC (Youden cut-off), p-value ¹ 0.71 (<0.771)*	0.73 (<0.63)*	0.70 (<0.868)*	0.74 (>5.4)*	0.76 (>186)**	0.66 (>0.73)	0.58 (>0.63)
	0.66 (<0.692)	0.68 (<0.612)	0.61 (<0.888)	0.84 (>6.4)**	0.37 (<353)	0.64 (>0.8)	0.66 (>0.74)
Activity grade 0–4 Fibrosis grade 0–4	Spearman's correlation coefficient, p-value –0.40** –0.41**	–0.42** –0.45**	–0.29 –0.27	0.37* 0.68***	0.42** 0.31	0.27 0.37**	0.17 0.41**

¹p-value for testing if variable is able to predict group, i.e. p-value for testing OR differ from 1. *p < 0.1, **p < 0.05, ***p < 0.0001.

FRI049

Association of the biological age and the level of global deoxyribonucleic acid methylation with metabolic parameters in patients with non-alcoholic fatty liver disease

Olena Kolesnikova¹, Anastasiia Radchenko¹, Valentina Galchinskaya².
¹L.T. Mala Therapy National Institute of the National Academy of Medical Sciences of Ukraine, Department of Study of Aging Processes and Prevention of Metabolic-Associated Diseases, Kharkiv, Ukraine; ²L.T. Mala Therapy National Institute of the National Academy of Medical Sciences of Ukraine, Laboratory of Immuno-Biochemical and Molecular-Genetics Researches, Kharkiv, Ukraine
Email: anastasha.radchenko@gmail.com

Background and aims: Changes in the metabolic phenotype occur with age in patients with non-alcoholic fatty liver disease (NAFLD), however, the time of their occurrence and the connection with the processes and markers of aging remain not fully understood. Our aim was to establish the relationship between biological age (BA) and the global methylation level (GML) with metabolic parameters in patients with NAFLD.

Method: Our study included 106 patients with NAFLD with a mean age of 51.4 ± 8.9 years (62.3% women). All patients were divided into groups according to age: group 1-young patients (<45 years), group 2-middle-aged (45–59 years), group 3-the elderly (>60 years). The diagnosis of NAFLD was based on the fatty liver index and fibrosis-4 index. Anthropometric and biochemical parameters were determined in all patients. The GML that is the content of 5-methylcytosine in the DNA of mononuclear blood cells was detected with ELISA as a marker of aging. BA was calculated according to the method of A.G. Gorelkin, B. B. Pinkhasov.

Results: Analysis of anthropometric, lipid profile and liver parameters in patients with NAFLD depending on age revealed significant differences in the level of triglycerides (TG) ($p = 0.043$), BA ($p = 0.002$) between groups 1 and 2, and in BA ($p = 0.002$) between groups 1 and 3. There was a significantly higher proportion of young patients with an increased percentage of body fat (FAT) ($\chi^2 = 4.011$; $p = 0.045$) compared to middle-aged patients. Correlation analysis in group 1 showed a positive association between calendar age (CA) and visceral fat (VIS) ($p = 0.023$) and negative one between CA and alkaline phosphatase (AP) ($p = 0.017$), BA was associated with VIS ($p = 0.016$), and the GML-with ALT ($p = 0.036$). In group 2 there was no relationship between CA and the observed parameters, while BA was positively associated with FAT ($p = 0.012$), VIS ($p = 0.002$), aspartate aminotransferase (AST) ($p = 0.045$), TG ($p = 0.019$), very low-density lipoprotein cholesterol (VLDL-C) ($p = 0.019$) and had a negative relationship with the percentage of skeletal muscle (MUS) ($p = 0.021$) and AP ($p = 0.042$). The GML in this group was associated with body mass index (BMI) ($p = 0.040$), TG ($p = 0.002$), VLDL-C ($p = 0.003$). In group 3, CA had a direct association with VIS ($p = 0.021$) and a reverse one with total cholesterol (TC) ($p = 0.005$), BA was not associated with indicators that were not used for calculation, the GML was directly related to hip circumference (HC) ($p = 0.035$) and AP level ($p = 0.011$).

Conclusion: BA has been associated with anthropometric, lipid and liver parameters in middle-aged patients with NAFLD. The GML has been related to the levels of HC, BMI, TG, VLDL-C, ALT, AP, mainly in middle-aged patients with NAFLD, which may be associated with more pronounced changes in the metabolic profiles of this age group. The data obtained can be useful for the prevention of accelerated aging rates in patients with NAFLD.

FRI050

LEARN algorithm: a novel option for predicting non-alcoholic steatohepatitis

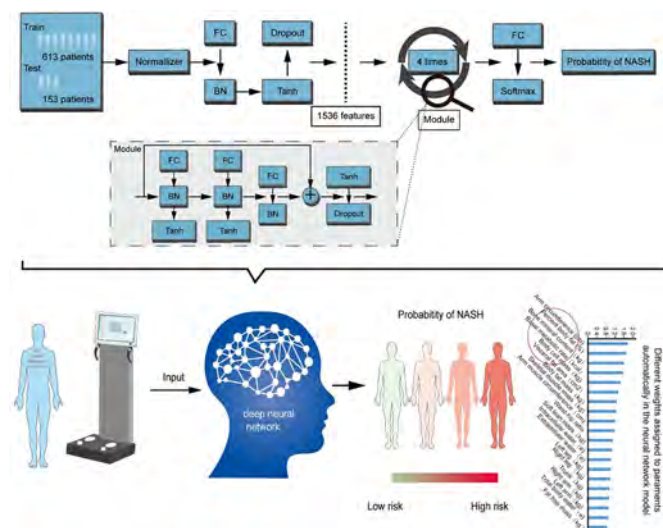
Gang Li¹, Tian-lei Zheng², Xiaoling Chi³, Yong-Fen Zhu⁴, Jinjun Chen⁵, Liang Xu⁶, Jun-Ping Shi⁷, Xiaodong Wang⁸, Wei-Guo Zhao², Chris Byrne⁹, Giovanni Targher¹⁰, Rafael Rios¹, Ou-Yang Huang¹, Liangjie Tang¹, Shi-Jin Zhang², Shi Geng², Huanming Xiao³, Sui-Dan Chen¹¹, Rui Zhang¹², Ming-Hua Zheng¹. ¹the First Affiliated Hospital of Wenzhou Medical University, Wenzhou, China, NAFLD Research Center, Department of Hepatology, Wenzhou, China; ²The Affiliated Hospital of Xuzhou Medical University, Artificial Intelligence Unit, Department of Medical Equipment, Xuzhou, China; ³Guangdong Provincial Hospital of Chinese Medicine, the Second Affiliated Hospital of Guangzhou University of Chinese Medicine, Department of Hepatology, Guangzhou, China; ⁴Sir Run Run Shaw Hospital, Affiliated with School of Medicine, Department of Hepatology and Infection, Hangzhou, China; ⁵Nanfang Hospital, Southern Medical University, Guangzhou, China, Hepatology Unit, Zengcheng Branch, Nanfang Hospital, Southern Medical University, Hepatology Unit, Department of Infectious Diseases, Guangzhou, China; ⁶Tianjin Second People's Hospital, Department of Hepatology, Tianjin, China; ⁷Hangzhou Normal University Affiliated Hospital, Department of Liver Diseases, Hangzhou, China; ⁸the First Affiliated Hospital of Wenzhou Medical University, Key Laboratory of Diagnosis and Treatment for The Development of Chronic Liver Disease in Zhejiang Province, Wenzhou, China; ⁹University Hospital Southampton, Southampton General Hospital, Southampton National Institute for Health Research Biomedical Research Centre, Southampton, United Kingdom; ¹⁰University and Azienda Ospedaliera Universitaria Integrata of Verona, Verona, Italy, Section of Endocrinology, Diabetes and Metabolism, Department of Medicine, Verona, Italy; ¹¹the First Affiliated Hospital of Wenzhou Medical University, Department of Pathology, Wenzhou, China; ¹²the First Affiliated Hospital of Wenzhou Medical University, Department of Nutrition, Wenzhou, China
Email: zhengmh@wmu.edu.cn

Background and aims: There is an unmet need for accurate non-invasive methods to diagnose non-alcoholic steatohepatitis (NASH). Since impedance-based measurements of body composition are simple, repeatable and have a strong association with non-alcoholic fatty liver disease (NAFLD) severity, we aimed to develop a novel and fully automatic machine learning algorithm, consisting of a deep neural network based on impedance-based measurements of body composition to identify NASH (the LEARN algorithm, bioElectrical Impedance Analysis for NASH).

Method: 1, 259 consecutive subjects with suspected NAFLD aged 12–75 years were screened from six medical centers across China from 2016 to 2021. 766 patients with biopsy-proven NAFLD were included in the final analysis. Patients were randomly divided into the training and validation groups, in a ratio of 4:1. The LEARN algorithm (utilizing impedance-based measurements of body composition along with age, sex, history of hypertension and diabetes) was developed in the training group to identify NASH, and subsequently, tested in the validation group.

Results: The LEARN algorithm showed good discriminatory ability for identifying NASH in both the training and validation groups (AUROC: 0.81, 95%CI 0.77–0.84 and 0.80, 0.73–0.87, respectively). This algorithm performed better than serum cytokeratin-18 neopeptide M30 level or other non-invasive NASH scores (including HAIR, ION, NICE) for identifying NASH (p -value <0.001). Additionally, even in a condition of partial missing the data of body composition, LEARN algorithm performed well in identifying NASH (AUROC: 0.82, 95%CI 0.72–0.92). Subgroup analysis showed that the LEARN algorithm performed well in different subgroups.

POSTER PRESENTATIONS



Conclusion: The LEARN algorithm, utilizing simple easily obtained measures, provides a fully automated, simple, non-invasive method for identifying NASH.

Keywords: NAFLD, NASH, LEARN algorithm, body composition.

FRI051

Head to head comparison between MEFIB versus MAST for identification of high-risk patients with NAFLD

Beom Kyung Kim^{1,2}, Nobuharu Tamaki^{1,3}, Jinho Jung¹, Nancy Sutter¹, Claude Sirlin¹, Atsushi Nakajima⁴, Rohit Loomba¹. ¹University of California San Diego; ²Yonsei University College of Medicine; ³Musashino Red Cross Hospital; ⁴Yokohama City University Graduate School of Medicine

Email: roloomba@ucsd.edu

Background and aims: Nonalcoholic fatty liver disease (NAFLD) patients with \geq stage 2 fibrosis are at an increased risk for developing liver-related morbidity and mortality. We performed a head-to-head comparison to evaluate the diagnostic test accuracy and predictive performance of MAST (magnetic resonance imaging-aspartate aminotransferase) versus MEFIB (the combination of magnetic resonance elastography [MRE] and FIB-4).

Method: NAFLD patients with a liver biopsy and MRE were analyzed from two prospective cohorts, the University of California San Diego (n = 414) and Yokohama City University (n = 314). Diagnostic performances for significant fibrosis (stage ≥ 2) were assessed using area under receiver operating characteristic curves (AUROCs).

Results: The mean age was 55.3 years and 48.1% were male. Significant fibrosis was observed in 46.4%. MEFIB was superior than MAST with AUROCs of categorized MEFIB (rule-in, intermediate, and rule-out) and MAST (>0.242 , $0.165\sim 0.242$, and <0.165) being 0.889 (95% confidence interval [CI] $0.864\sim 0.914$) and 0.769 (95% CI $0.733\sim 0.805$), respectively ($p < 0.001$). Positive predictive value for significant fibrosis of MEFIB rule-in criteria was significantly higher, compared to MAST >0.242 (94.2% versus 88.2%, respectively; $p = 0.031$). Negative predictive value for significant fibrosis of MEFIB rule-out criteria was also significantly higher, compared to MAST <0.165 (89.8% versus 73.3%, respectively; $p < 0.001$). When MAST was analyzed as a continuous variable, its AUROC improved to 0.890 (95% CI $0.866\sim 0.914$).

Conclusion: For the identification of high-risk patients with NAFLD, MEFIB is significantly superior to categorized MAST. As continuous MAST score had high AUROC, the optimal cutoffs should be modified. Conversely, MEFIB, as a simple and easy algorithm, has practical advantages with a more reliable diagnostic performance as well as a better rule-in/-out ability.

Key words: NAFLD, significant fibrosis, MEFIB, FAST, MAST, diagnosis, validation

FRI052

MRI assessment (cT1) with LiverMultiScan following VCTE improves the diagnostic yield for high-risk NASH

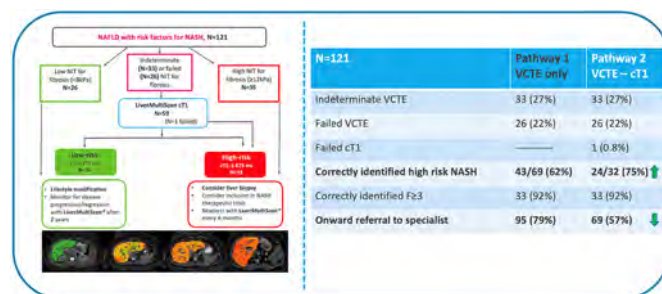
Naim Alkhoury¹, Andrea Dennis², Atsushi Nakajima³, Stephen Harrison⁴, David J. Breen⁵, Daniel Cuthbertson⁶, Mazen Nouredin⁷. ¹Arizona Liver Health, Chandler, United States; ²Perspectum, United Kingdom; ³Department of Gastroenterology and Hepatology, Yokohama City University School of Medicine, Japan; ⁴Division of Cardiovascular Medicine, Department of Medicine, University of Oxford, Oxford, United Kingdom; ⁵University of Southampton, United Kingdom; ⁶Institute of Ageing & Chronic Disease, Faculty of Health & Life Sciences, University of Liverpool, United Kingdom; ⁷Karsh Division of Gastroenterology and Hepatology, Comprehensive Transplant Center, Cedars Sinai Medical Center, Los Angeles, CA, USA, United States

Email: andrea.dennis@perspectum.com

Background and aims: In the diagnostic pathway for NAFLD, EASL recommends the use of non-invasive tests (NITs) for assessing fibrosis. However, NASH, independently of fibrosis stage, is also associated with poor outcomes and thus high costs of care. Accordingly, recent EASL and NICE guidance recommend diagnosis and management of this patient group. As an MRI-derived measure, cT1 is an excellent biomarker to diagnose NASH, shown to predict clinical outcomes, and has become a leading NIT for stratifying patients based on high-disease risk. We compared a clinical pathway using cT1 for stratifying high-risk NASH to the current recommendation using NITs for advanced fibrosis only, to explore diagnostic accuracy and appropriate further referral to specialist care.

Method: We studied NAFLD patients who had undergone NITs; liver stiffness (kPa) from vibration controlled transient elastography (VCTE, FibroScan®), and MRI-derived cT1 (ms) with LiverMultiScan®. All had liver fat $\geq 5\%$ (LiverMultiScan® PDF) and had histologically confirmed NAFLD with liver biopsy. We compared two diagnostic approaches: (1) Utilising VCTE results only, to exclude low risk individuals and identify those with advanced fibrosis suitable for onward referral; (2) VCTE followed by cT1 (for NASH risk stratification). We assessed the number of failed and indeterminate results, % positive predictor value (PPV) for high-risk NASH cases correctly identified, and number referred onto specialist care. Correct identification of fibrosis was based on $F \geq 3$; "high-risk NASH" was $NAS \geq 4$ and $F \geq 2$; established (EASL guidelines) VCTE thresholds were < 8 kPa rule out and ≥ 12 kPa rule in; cT1 threshold was ≥ 875 ms.

Results: Using data from N = 121 patients (60 yrs., 40% female, 59% BMI ≥ 27 kg/m²). The second pathway (VCTE followed by cT1) increased the PPV for high-risk NASH from 62% (43/69 with VCTE ≥ 8 kPa) to 75% (24/32 with cT1 ≥ 875 ms) and reduced subsequent referrals from 95 to 69 individuals. This was driven by better stratification of failed or indeterminate cases, and greater specificity for the identification of those with high-risk NASH by incorporating cT1 (Figure 1).



Conclusion: Investigating suspected advanced fibrosis using positive NIT results, with combined TE and MRI assessment of cT1 increased the diagnostic accuracy of high-risk NASH by 21% and reduced liver biopsy by 28%. Screening tests based on NITs for fibrosis alone are inadequate for risk stratification and diagnosis of NASH. Inclusion of MRI-assessed cT1 in NAFLD/NASH clinical diagnostic pathways improves diagnostic accuracy and reduces the need for biopsy and for specialist referral, which would result in downstream cost savings.

FRI053

The PNPLA3 (rs738409) G/G-genotype is associated with presence of NASH and increased long-term risk of cirrhosis in NAFLD

Magnus Holmer¹, Robin Zenlander¹, Axel Wester¹, Mattias Ekstedt², Patrik Nasr², Stergios Kechagias², Stefano Romeo³, Per Stal¹, Hannes Hagström¹. ¹Karolinska Institutet, Department of Medicine, Huddinge, Stockholm, Sweden; ²Linköping University, Division of Diagnostics and Specialist Medicine, Department of Health, Medicine and Caring Sciences, Linköping, Sweden; ³University of Gothenburg, Department of Clinical and Molecular Medicine, Gothenburg, Sweden
Email: magnus.holmer@ki.se

Background and aims: Mutations in several genes are linked to a worse histopathological profile in patients with nonalcoholic fatty liver disease (NAFLD). It is unclear if these genotypes impact long-term outcomes. Here, we investigated the prognostic importance of PNPLA3, TM6SF2, MBOAT7 and GCKR genotypes on the development of cirrhosis, liver related events (LRE) and all-cause mortality in a well-defined cohort of patients with NAFLD.

Method: DNA samples were collected from 546 patients with NAFLD. Presence of advanced fibrosis was established through liver biopsy (stage 3–4) or elastography (≥ 15 kPa), while presence of nonalcoholic steatohepatitis (NASH) was defined only by histology. A total of 5396 controls matched by age, sex and municipality were identified from the Swedish population. Outcome of cirrhosis, LRE and overall mortality were collected from national registries. Cox regression models were used to estimate adjusted hazard ratios (aHR) for these outcomes.

Results: In patients with NAFLD, the G/G genotype of PNPLA3 (rs738409) was associated with a higher prevalence of NASH at the time of biopsy (OR 3.67 [95% CI = 1.66–8.08]), but not with advanced fibrosis (OR 1.81 [95% CI = 0.79–4.14]). In NAFLD subjects without advanced fibrosis at baseline, the G/G genotype was associated with a higher risk of developing cirrhosis and LRE (aHR 2.41 [95% CI = 1.02–5.71], Figure 1) after adjustments for age, sex, body mass index and type 2 diabetes during a median follow-up of 18.1 years. However, no increased risk was found for patients with advanced fibrosis at baseline (aHR 0.67, [95% CI = 0.13–3.43]). Compared to controls, NAFLD cases had a higher rate of developing cirrhosis and the increased risk correlated to PNPLA3 and GCKR genotypes. Mortality was not affected by any genetic variant.

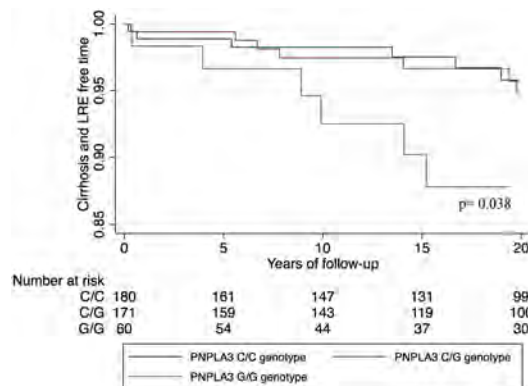


Figure 1: Kaplan-Meier estimate of cirrhosis and LRE-free time in patients with NAFLD without advanced fibrosis at baseline. LRE = Liver related events.

Conclusion: The G/G genotype in PNPLA3 is associated with an increased risk of progression to cirrhosis in NAFLD. This was confined to patients without advanced fibrosis at baseline. Our results suggest that assessment of PNPLA3 genotype can be of clinical relevance in non-cirrhotic patients with NAFLD to individualize monitoring and therapeutic strategies.

FRI054

Hepatic expression of secreted calcium-binding protein 2 by hepatic stellate cells is associated with human non-alcoholic fatty liver disease progression

Frederik Larsen¹, Mike Terkelsen¹, Sofie Bendixen¹, Daniel Hansen¹, Charlotte Wernberg², Mette Lauridsen², Tina Di Caterino³, Fabio Avolio¹, Majken Siersbæk¹, Vineesh Indira Chandran¹, Jonas Graversen¹, Aleksander Krag^{1,3}, Lars Groentved¹, Kim Ravnshjaer¹. ¹University of Southern Denmark, Odense, Denmark; ²Sydvestjysk Sygehus, Esbjerg, Denmark; ³Odense University Hospital, Odense, Denmark
Email: tibert@bmb.sdu.dk

Background and aims: Non-alcoholic fatty liver disease (NAFLD) and its progressive form, non-alcoholic steatohepatitis (NASH), is the hepatic manifestation of obesity-induced metabolic syndrome. Activated Hepatic stellate cells (aHSCs) play a pivotal role in hepatic fibrosis, a defining process of NAFLD pathogenesis. Thus, secreted aHSC-specific proteins may hold promise as non-invasive biomarkers for diagnosis of NASH. Histological assessment of liver biopsies is the golden standard in diagnosis of NASH. Liver biopsy, however, is associated with risk for the patient and does not fully capture the tissue heterogeneity of the fibrotic liver.

Method: RNA sequencing was performed on liver needle biopsies from a histopathological characterized severely obese (BMI >35) discovery cohort (n=30). Bioinformatical analysis was used to identify potential biomarkers and their hepatocellular origin. Detection of mRNA in liver tissue and protein levels in plasma was performed using single molecule fluorescence *in situ* hybridization (smFISH) and ELISA, respectively.

Results: Hepatic expression of secreted modular calcium-binding protein 2 (SMOC2) was upregulated in NASH patients compared to healthy obese patients (padj <0.001). Single-cell RNA sequencing data indicated hepatic SMOC2 expression by quiescent and aHSCs exclusively, which was validated using smFISH. Moreover, plasma [SMOC2] was elevated in NASH patients compared to healthy obese patients (p <0.001) with a predictive accuracy of AUROC 0.88 (steatosis activity score >2).

Conclusion: Plasma [SMOC2] shows promise as a non-invasive biomarker for diagnosis of NASH. Linkage of plasma [SMOC2] to aHSCs, moreover, may directly reflect key cellular changes associated with NASH progression.

FRI055

Clinicians' perspectives on barriers and facilitators for the adoption of non-invasive liver tests: a mixed-method study

Yasaman Vali¹, Roel Eijk², Timothy Hicks³, Will Jones³, Jana Suklan³, Vlad Ratziu⁴, Adriaan G. Holleboom⁵, Miranda Langendam¹, Quentin Anstee⁶, Patrick Bossuyt¹. ¹Amsterdam UMC, University of Amsterdam, Department of Epidemiology and Data Science, Amsterdam, Netherlands; ²Athena Institute, VU University Amsterdam, Faculty of Science, Amsterdam, Netherlands; ³NIHR Newcastle In Vitro Diagnostics Co-Operative, Newcastle University, Newcastle upon Tyne, United Kingdom; ⁴University Paris-Diderot, Assistance Publique-Hôpitaux de Paris, hôpital Beaujon, Paris, France; ⁵Amsterdam University Medical Centres, Department of Internal and Vascular Medicine, Amsterdam, Netherlands; ⁶Newcastle University, The Newcastle Liver Research Group, Translational & Clinical Research Institute, Faculty of Medical Sciences, Newcastle upon Tyne, United Kingdom
Email: y.vali@amc.uva.nl

Background and aims: Multiple non-invasive tests (NITs) have been developed to evaluate NAFLD patients. However, the availability of NITs varies from country to country, and little is known about their implementation and adoption in clinical practice. This study aimed to explore clinicians' perspectives on barriers and facilitators that influence the adoption of NITs.

Method: This cross-sectional study was performed using an exploratory mixed-methods approach. Twenty-seven clinicians from different countries, with a wide age range (from 30 to 63), specialties, and years of experience, were purposefully sampled. All participants filled in a questionnaire; 16 of those participated in a follow-up semi-structured interviews. Qualitative and quantitative data were collected and summarized using the recently published Non-adoption, Abandonment, Scale-up, Spread, and Sustainability (NASSS) framework for new medical technologies in healthcare organizations on seven domains: 1) the condition, 2) the technology, 3) the value proposition, 4) the adopters, 5) the organization, 6) the wider system, and 7) embedding and adaptation over time (see Figure 1).

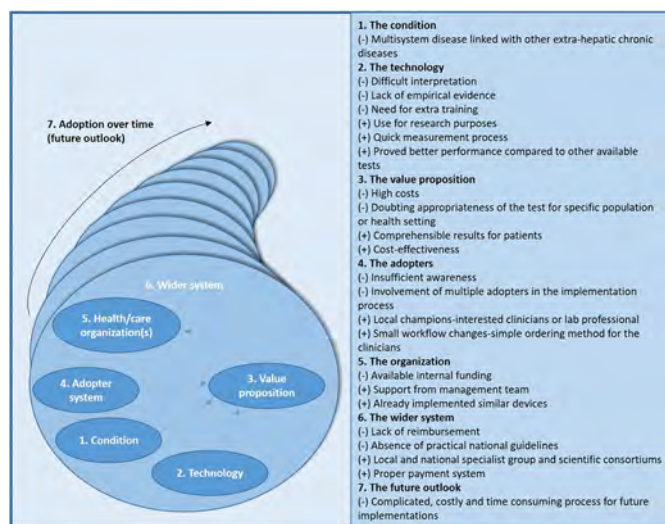


Figure: NASSS (Non-adoption, Abandonments, Scale-Up, Spread, and Sustainability) framework and the main barriers (–) and facilitators (+) of NAFLD tests' adoption in each domain.

Results: Several influencing factors were reported in different domains of the NASSS framework (see Figure 1). Among those, insufficient knowledge and limited awareness, impractical practice guidelines not yet built upon robust evidence for specific patient populations and care settings, need for extra training to perform the tests, difficult interpretation, and absence of sufficient reimbursement systems were perceived as the most important barriers. Other

factors were indicated as important facilitating factors: ease of use and quick measurement process, evidence showing better performance compared to other available tests, local champions (clinicians with special interest in and knowledge about the new test), proper functional payment system and existence of resources in academic hospitals.

Conclusion: Adoption of new diagnostic NAFLD tests is a complex process and can be promoted or restricted by several factors, such as robust evidence, practical guidelines, a proper payment system, and local champions. As this study was restricted to clinicians, future studies could explore other stakeholders' perspectives necessary to improve the adoption of new biomarker-based NITs into clinical practice.

FRI056

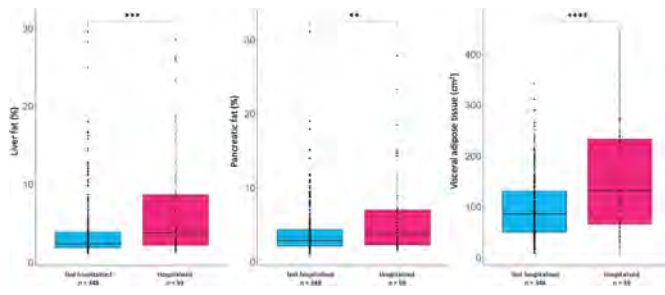
Ectopic fat deposition in the liver and pancreas and the presence of excess visceral adipose tissue significantly increase hospitalisation risk following COVID-19

Tom Waddell^{1,2}, Adriana Roca-Fernandez², John McGonigle², Arun Jandor², Valentina Carapella², Helena Thomaidis-Brears², Andrea Dennis², John Michael Brady², Rajarshi Banerjee². ¹The University of Oxford, Department of Engineering Science, Oxford, United Kingdom; ²Perspectum Ltd, Oxford, United Kingdom
Email: tom.waddell@perspectum.com

Background and aims: In patients with COVID-19, obesity may increase risk of hospitalisation, use of mechanical ventilation and patient mortality. High liver fat, body mass index (BMI) and male sex are significant predictors of hospitalisation risk following COVID-19. However, BMI is a poor indicator of body fat distribution. Here, we studied ectopic fat accumulation within the liver and pancreas and body composition through multiparametric magnetic resonance (mpMR) and compared participants with and without hospitalisation for COVID-19.

Method: Participants with laboratory-confirmed or clinically suspected SARS-CoV-2 infection were recruited to the COVERSCAN study (NCT04369807; median time from initial symptoms = 177 days) and underwent a multi-organ mpMR scan (CoverScan, Perspectum Ltd). Measures of liver and pancreatic fat (PDFF), liver fibroinflammation (cT1) and body composition [visceral adipose tissue (VAT), subcutaneous adipose tissue (SAT), skeletal muscle index (SMI)] were analysed. Differences between participants hospitalised (n = 59) and not hospitalised (n = 348) for COVID-19 were assessed using Wilcoxon signed-rank tests. Univariate and multivariate analyses were performed on all biomarkers to assess the hospitalisation risk. Data presented are median values.

Results: Approximately 6-months after initial symptoms, participants hospitalised following COVID-19 had significantly elevated pancreatic fat (3.8% vs 2.8%, p < 0.01), liver fat (3.8% vs 2.4%, p < 0.01) and liver cT1 (735 ms vs 706 ms, p < 0.01) compared to those who convalesced at home. Though hospitalised participants had a significantly elevated BMI (27 kg/m² vs 25 kg/m², p = 0.014), it was VAT, but not SAT, that was significantly elevated (132 cm² vs 86 cm², p < 0.01). Univariate analysis revealed that male sex, advanced age and elevated BMI, VAT, pancreatic fat, liver fat, and liver cT1 were all significantly predictive of hospitalisation following COVID-19. In multivariate analysis, only age remained significantly predictive of hospitalisation. In hospitalised people with obesity (≥30 kg/m²), VAT, liver cT1 and liver fat, but not BMI nor pancreatic fat, remained significantly elevated [VAT: 220 cm² vs 152 cm², p = 0.01 (Figure 1); liver fat: 9.9% vs 4.2%, p = 0.003; liver cT1: 782 ms vs 742 ms, p = 0.012].



Conclusion: mpMR revealed significantly elevated visceral and ectopic fat deposition within the liver and pancreas in hospitalised participants following COVID-19. In obese participants, BMI was not significantly different in hospitalised, and non-hospitalised patients, whereas visceral fat, liver fibroinflammation and liver fat were significantly elevated. Our work highlights body fat distribution an important consideration for COVID-19 risk profiling, which cannot be sufficiently evaluated based on BMI alone.

FRI057

Genomic and metabolomic profiles and their correlations with preclinical signs of endothelial dysfunction measured by peripheral arterial tonometry in non-alcoholic fatty liver disease

Mario Masarone¹, Jacopo Troisi^{2,3}, Benedetta Maria Motta¹, Martina Lombardi^{2,3}, Pietro Torre¹, Roberta Sciorio¹, Marco Aquino¹, Marcello Persico¹. ¹University of Salerno, Internal Medicine and Hepatology Unit, Department of Medicine, Surgery and Odontostomatology "Scuola Medica Salernitana", Baronissi (Salerno), Italy; ²Theoreo srl, Montecorvino Pugliano (Salerno), Italy; ³University of Salerno, Department of Chemistry and Biology, "A. Zambelli", Fisciano (Salerno), Italy

Email: mario.masarone@gmail.com

Background and aims: NAFLD is associated with insulin resistance, metabolic syndrome (MS) and diabetes and it is an independent CVD risk factor. Endothelial Dysfunction (ED) plays a central role in the pathogenesis of CVD. Preclinical ED can be detected by vascular reactivity studies, such as Peripheral Arterial Tonometry (PAT). Genome Wide Studies (GWAS) identified Single Nucleotide Polymorphisms (SNPs) associated to NAFLD progression. Some of them (ie TM6SF2) have been postulated to influence CVD risk. The use of specific biomarkers related to ED presence in NAFLD may allow an early identification of CVD risk and provide crucial insights into its pathophysiology. This could be addressed through untargeted metabolomics and genomic approaches. Aims: to identify metabolomics signatures able to discriminate the presence of ED by combining data provided by metabolomics analyses with those from PAT, and to correlate them with anthropometric, laboratory and genomic profiles of NAFLD subjects.

Method: Serum was collected from 107 subjects with biopsy-proven NAFLD (55.9% NAFL; 26.6% NASH; 17.5% NASH-Cirrhosis) without clinically evident CVD. Metabolomics analysis was performed by mass spectrometry. The resulting profiles were correlated with PAT scores, revealed by an EndoPAT-2000 device, and with genomic profiles of 4 SNPs of NAFLD (PNAPL3; TM6SF2; GKR; MBOAT).

Results: Class separation in metabolomics profiles between patients with and without ED (EndoPAT cut-off = 0.51) was obtained through a "Partial Least Square Discriminant Analysis" (PLS-DA), which was also used to identify the discriminating metabolites. According to the PLS-

DA score plot, two metabolomics profiles were identified, significantly different, in the two groups ($R^2 = 0.98$, $p < 0.001$). The metabolites profiles are presented in figure 1. By comparing PAT scores of patients with simple steatosis (NAFL) (n:61, 19 with ED), NASH (n:29, 12 with ED), and NASH-cirrhosis (n:17, 9 with ED) no significant difference was observed ($p = 0.34$), suggesting that CVD risk is not associated with the degree of liver disease. Moreover, the clinical and genetic parameters associated to ED were type 2 diabetes, MS and BMI (directly) and TM6SF2 dominant model (CC + CT) (inversely) at the univariate and only MS at a multivariate analysis.

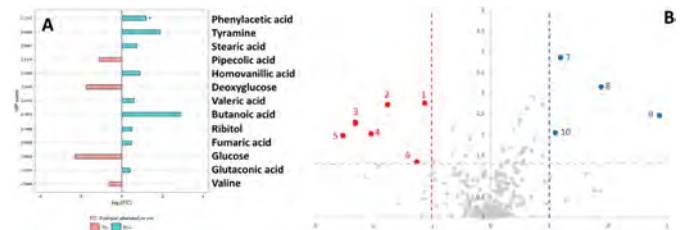


Figure: Metabolomic profiles of NAFLD patients with and without ED. Panel A: Impaired Metabolites. Panel B: Volcano plot of impaired metabolites.

Conclusion: NAFLD patients with and without ED exhibit significant differences in their metabolomics profiles, demonstrating that they could be a useful early diagnostic tool for assessing CVD risk and providing an in-depth understanding of its underlying mechanisms. Among the NAFLD associated SNPs, only TM6SF2 mutation was correlated to a reduced prevalence of ED, but the only independent factor for ED was MS presence.

FRI058

Determinants of liver stiffness measurements in patients with NAFLD-an individual patient data meta-analysis

Ferenc Mozes¹, Emmanuel Selvaraj^{2,3}, Arjun Jayaswal³, Jerome Boursier⁴, Céline Fournier⁵, Elisabetta Bugianesi⁶, Ramy Younes⁷, Salvatore Petta⁸, Sanjiv Mahadeva⁹, Wah-Kheong Chan⁹, Peter Eddowes¹⁰, Philip N. Newsome¹¹, Gideon Hirschfield¹², Vincent Wai-Sun Wong¹³, Victor de Lédinghen¹⁴, Jeremy Cobbold², Won Kim¹⁵, Myoung Seok Lee¹⁶, Christophe Cassinot¹⁷, Geraldine Ooi¹⁸, Atsushi Nakajima¹⁹, Masato Yoneda¹⁹, Ming-Hua Zheng²⁰, Andreas Geier²¹, Theresa Tuthill²², M. Julia Brosnan²², Quentin Anstee²³, Stephen Harrison³, Patrick Bossuyt²⁴, Michael Pavlides^{2,3}. ¹University of Oxford, Oxford Centre for Magnetic Resonance (OCMR), Oxford, United Kingdom; ²University of Oxford, Translational Gastroenterology Unit, Oxford, United Kingdom; ³University of Oxford, Oxford Centre for Magnetic Resonance (OCMR), Oxford, United Kingdom; ⁴Université d'Angers, Laboratoire HIFIH, Angers, France; ⁵Echosens, Paris, France; ⁶University of Turin, Department of Medical Sciences, Turin, Italy; ⁷Boehringer Ingelheim, Ingelheim am Rhein, Germany; ⁸University of Palermo, Section of Gastroenterology and Hepatology, PROMISE, Palermo, Italy; ⁹University of Malaya, Gastroenterology and Hepatology Unit, Department of Medicine, Faculty of Medicine, Malaysia; ¹⁰Nottingham University Hospitals NHS Trust and University of Nottingham, National Institute for Health Research Nottingham Biomedical Research Centre, Nottingham, United Kingdom; ¹¹University Hospitals Birmingham NHS Foundation

POSTER PRESENTATIONS

Trust and the University of Birmingham, National Institute for Health Research Biomedical Research Centre, Birmingham, United Kingdom; ¹²University Health Network, Toronto Centre for Liver Disease, Toronto, Canada; ¹³The Chinese University of Hong Kong, Department of Medicine and Therapeutics, Hong Kong, Hong Kong; ¹⁴Bordeaux University Hospital, Centre d'Investigation de la Fibrose Hépatique, Hôpital Haut-Lévêque, Bordeaux, France; ¹⁵Seoul National University College of Medicine, Division of Gastroenterology and Hepatology, Department of Internal Medicine, Seoul, Korea, Rep. of South; ¹⁶Seoul National University College of Medicine, Department of Radiology, Seoul, Korea, Rep. of South; ¹⁷University Hospital of Montpellier, Department of Diagnostic and Interventional Radiology, Saint-Eloi Hospital, Montpellier, France; ¹⁸Monash University, Centre for Obesity Research and Education, Department of Surgery, Melbourne, Australia; ¹⁹Yokohama City University, Department of Gastroenterology and Hepatology, Yokohama, Japan; ²⁰The First Affiliated Hospital of Wenzhou Medical University, NAFLD Research Center, Department of Hepatology, Wenzhou, China; ²¹University of Wurzburg, Division of Hepatology, Wurzburg, Germany; ²²Pfizer Inc, Internal Medicine Research Unit, Cambridge, United States; ²³Newcastle University, Translational and Clinical Research Institute, Faculty of Medical Sciences, Newcastle upon Tyne, United Kingdom; ²⁴University of Amsterdam, Department of Epidemiology and Data Science, Amsterdam UMC, Amsterdam, Netherlands
Email: ferenc.mozes@cardiov.ox.ac.uk

Background and aims: Liver stiffness measurements (LSM) performed with FibroScan are used in the clinical assessment of patients with non-alcoholic fatty liver disease (NAFLD). Fibrosis is the main determinant of LSM, but the contribution from other determinants and how they vary in patient subgroups is less well studied. Our aim was to describe the dependence of LSM on histological, demographic and laboratory parameters.

Method: Data sets including LSM, demographics, histology- and lab parameters were reported in 2768 patients. Parameters with correlation $r > 0.15$ with LSM were selected as possible determinants of LSM in the entire patient group. Linear regression models were built by adding one predictor at a time to a base model including the log-transformed LSM and fibrosis stages as indicator variables. Partial R^2 values were compared to evaluate the contribution of each variable in explaining the variability of log-transformed LSM. A separate analysis evaluated the interaction between age and fibrosis stage.

Results: NASH CRN fibrosis stage, lobular inflammation and ballooning grades, age, aspartate aminotransferase (AST), platelet count (Plt), gamma-glutamyltransferase (GGT), BMI and presence of T2DM correlated with LSM with $r > 0.15$. Mean age was 51 years, mean BMI was 30 kg/m², 41% of patients had T2DM. Fibrosis stage explained most of the variance ($R^2 = 0.411$) in log-transformed LSM, followed by BMI (partial $R^2 = 0.051$), GGT (partial $R^2 = 0.023$), and AST (partial $R^2 = 0.022$) (see Table). Furthermore, including an interaction term between fibrosis stage and age explained log-transformed LSM better than only considering the main effect of fibrosis stage (F-statistic = 3.171, $p = 0.007$).

Model predictors	Partial R^2
Age	0.0018
BMI	0.0514
Plt	0.0068
AST	0.0221
GGT	0.0232
T2DM	0.0183
Ballooning grade	0.0119
Lobular inflammation grade	0.0132

Conclusion: Our data confirm that fibrosis is the main determinant of LSM in patients with NAFLD, with BMI, GGT and AST explaining most of the remaining variance. However, LSM was less dependent on fibrosis stage in younger patients—a result that deserves further exploration. Our findings should be taken into account when interpreting LSM results from these patients.

FRI059

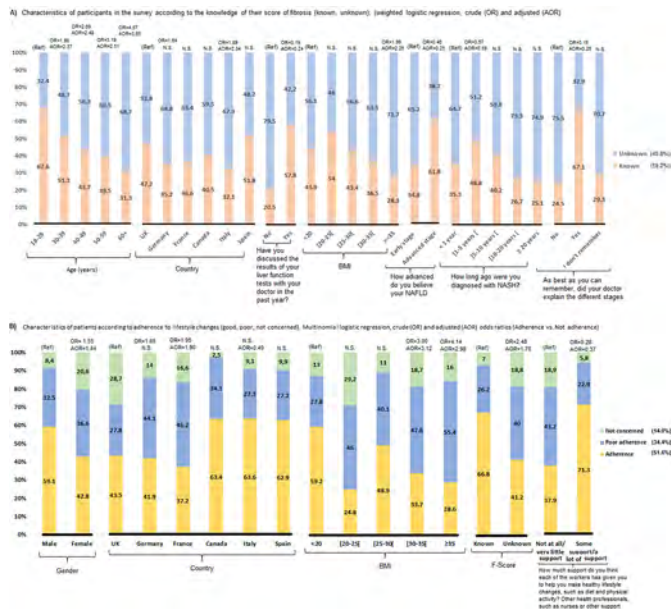
Knowledge of liver fibrosis stage among adults with non-alcoholic fatty liver disease/non-alcoholic steatohepatitis improves adherence to life style changes

Carrieri Patrizia¹, Abbas Mourad¹, Fabienne Marcellin², José Luis Calleja Panero³, Camelia Protopopescu¹, Jeffrey Lazarus^{4,5}.
¹Aix Marseille Univ, Inserm, IRD, SESSTIM, Sciences Economiques & Sociales de la Santé & Traitement de l'Information Médicale, ISSPAM, Marseille, France; ²Aix Marseille Univ, Inserm, IRD, SESSTIM, Sciences Economiques & Sociales de la Santé & Traitement de l'Information Médicale, ISSPAM, Marseille, France; ³Department of Gastroenterology, Hospital Universitario Puerta de Hierro de Majadahonda, Madrid, Spain; ⁴Barcelona Institute for Global Health (ISGlobal), Hospital Clínic, University of Barcelona, Barcelona, Spain; ⁵University of Barcelona, Faculty of Medicine, Barcelona, Spain
Email: abbas.mourad@inserm.fr

Background and aims: Non-alcoholic fatty liver disease (NAFLD) continues to rise in many countries, paralleling the epidemic of obesity worldwide. NAFLD can evolve into non-alcoholic steatohepatitis (NASH) depending on age, lifestyle, and metabolic risk factors. Both diseases are managed with lifestyle interventions, but unawareness of liver disease severity may compromise adherence. An international survey of people living with NAFLD/NASH was conducted for the first time to identify correlates of a lack of knowledge about fibrosis status, and to assess whether this unawareness was associated with poor adherence to lifestyle changes.

Method: We recruited 1411 adults living with NAFLD/NASH in Canada, France, Germany, Italy, Spain, and the United Kingdom who were registered on the online patient community platform Carecity. Weighted binary and multinomial logistic regressions were performed to estimate the effect of explanatory variables on unawareness of fibrosis stage and poor adherence to lifestyle changes, respectively, in univariable and multivariable analyses.

Results: In the study group, men accounted for 54.1%, 15.5% of the participants had obesity, and 75.3% of NAFLD patients reported being in an early fibrosis stage. Of the total, 59.2% were unaware of their fibrosis stage, and 34.4% reported non-adherence to lifestyle changes. After multiple adjustments (Figure 1), older people were found to be at more risk of not knowing their fibrosis stage. Individuals who were aware of their fibrosis stage were more likely to have discussed their liver tests with their physicians throughout the previous year (AOR = 0.24; 95%CI: 0.16–0.36), and to have been diagnosed throughout the 5 years preceding the survey (AOR = 0.59; 95%CI: 0.38–0.91). Individuals with a body mass index (BMI) ≥ 35 were over twice as likely to not know their fibrosis stage (AOR = 2.26; 95%CI: 1.37–3.40). Unawareness about fibrosis stage was significantly associated with poor adherence to lifestyle changes (AOR = 1.70; 95%CI: 1.14–2.41). Individuals with obesity (BMI ≥ 30) had a threefold higher risk of having poor adherence to lifestyle changes (AOR = 3.12; 95%CI: 1.74–5.60). People reporting having received support from nurses and other health staff were more likely to be adherent to lifestyle changes (AOR = 0.37; 95%CI: 0.25–0.54).



Conclusion: As fibrosis stage is becoming the main predictor of NAFLD progression, patients' knowledge of their fibrosis stage should become a priority to improve liver health. Given the seriousness of NASH-related morbidity and mortality, improving patient-provider communication, especially for people with obesity, about liver fibrosis stage, its associated risks, and how to mitigate them, is essential. Training healthcare professionals and promoting patient educational programs to support behavior changes should also be included in the liver health agenda.

FRI060

The MRI and AST (MAST) score is correlated with noninvasive and histologic markers of fibrosis in patients with advanced fibrosis due to NASH

Mazen Nouredin¹, Kris V. Kowdley², Anita Kohli³, Aasim Sheikh⁴, Guy Neff⁵, Bal Raj Bhandari⁶, Nadege Gunn⁷, Stephen Caldwell⁸, Zachary Goodman⁹, Dora Ding¹⁰, Lily Ma¹⁰, Jay Chuang¹⁰, Ryan Huss¹⁰, Chuhan Chung¹⁰, Robert Myers¹⁰, Keyur Patel¹¹, Brian Borg¹², Reem Ghalib¹³, John Poulos¹⁴, Ziad H. Younes¹⁵, Magdy Elkhatab¹⁶, Tarek Hassanein¹⁷, Rajalakshmi Iyer¹⁸, Peter Ruane¹⁹, Mitchell Shiffman²⁰, Simone Strasser²¹, Vincent Wai-Sun Wong²², Rohit Loomba²³, Naim Alkhouri³. ¹Fatty Liver Program, Cedars-Sinai Medical Center, Los Angeles, CA, United States; ²Liver Institute Northwest, Seattle, WA, United States; ³Arizona Liver Health, Chandler, AZ, United States; ⁴GI Specialists of Georgia, Marietta, GA, United States; ⁵Covenant Research, LLC, Sarasota, FL, United States; ⁶Delta Research Partners, LLC, Bastrop, LA, United States; ⁷Pinnacle Clinical Research, Austin, TX, United States; ⁸University of Virginia, Charlottesville, VA, United States; ⁹Inova Fairfax Hospital, Falls Church, VA, United States; ¹⁰Gilead Sciences Inc., Foster City, CA, United States; ¹¹University of Toronto, Toronto, ON, Canada; ¹²Southern Therapy and Advanced Research, Jackson, MS, United States; ¹³Texas Clinical Research Institute, Arlington, TX, United States; ¹⁴Cumberland Research Associates, Fayetteville, NC, United States; ¹⁵Gastro One, Germantown, TN, United States; ¹⁶Toronto Liver Centre, Toronto, ON, Canada; ¹⁷Southern California Research Center, Coronado, CA, United States; ¹⁸Iowa Digestive Disease Center, Clive, IA, United States;

¹⁹Ruane Medical and Liver Health Institute, Los Angeles, CA, United States; ²⁰Bon Secours Mercy Health, Richmond, VA, United States; ²¹Royal Prince Alfred Hospital and The University of Sydney, New South Wales, Australia; ²²Department of Medicine and Therapeutics, The Chinese University of Hong Kong, Hong Kong, Hong Kong; ²³NAFLD Research Center, University of California at San Diego, La Jolla, CA, United States
Email: mazen.nouredin@cshs.org

Background and aims: The MAST Risk score is a noninvasive tool that includes AST and MRI-based assessments of liver stiffness (LS) by elastography (MRE) and steatosis by proton density fat fraction (MRI-PDF), for the identification of patients at risk of progressive NASH. Our aims were to evaluate the effects of cilofexor (CILO) and firsocostat (FIR) on MAST, and associations between treatment-induced changes in MAST with histologic and noninvasive test (NIT) responses in patients with advanced fibrosis due to NASH.

Method: NASH patients with histologically-confirmed, advanced fibrosis (NASH CRN F3-F4) in the phase 2b ATLAS trial were treated with regimens including CILO 30 mg (n = 40), FIR 20 mg (n = 40), CILO + FIR (n = 78), or placebo (n = 39), once daily for 48 weeks (W48). Liver histology was evaluated by a central reader and a machine learning (ML) approach (PathAI; Boston, MA). Endpoints included a ≥ 1 -stage improvement in fibrosis without worsening of NASH (primary endpoint [PE]), ≥ 2 -pt reduction in NAFLD Activity Score (NAS response [NAS-R]), and LS by vibration-controlled transient elastography (VCTE) and ELF responses (ELF-R), defined as $\geq 25\%$ and ≥ 0.5 -unit reductions from baseline (BL) to W48, respectively. Changes in MAST were evaluated using Wilcoxon rank sum and Fisher's exact tests.

Results: At BL, 56% of patients had cirrhosis (F4); median MAST Risk score was higher in those with F4 vs F3 fibrosis (0.36 vs 0.24; p = 0.003). Across study groups, BL MAST was significantly correlated with ELF score (p = 0.53), LS by VCTE (p = 0.48), hepatic collagen content (p = 0.37) and α -SMA expression by morphometry (p = 0.26), serum bile acids (p = 0.44), ML NASH CRN fibrosis score (p = 0.39), and proportionate areas of NASH CRN F4 (p = 0.38), portal inflammation (p = 0.36), and hepatocellular ballooning (p = 0.27; all p < 0.05), but not proportionate areas of steatosis or lobular inflammation. Compared with placebo (median change in MAST from BL to W48: -0.04), greater improvements in MAST at W48 were observed with FIR (-0.23; p = 0.03); differences with CILO (-0.06, p = 0.46) and CILO + FIR (-0.05; p = 0.68) were not statistically significant. Compared to non-responders, greater improvements in MAST from BL to W48 were observed in patients with NAS-R and LS by VCTE-response, but not ELF or PE response (Figure).

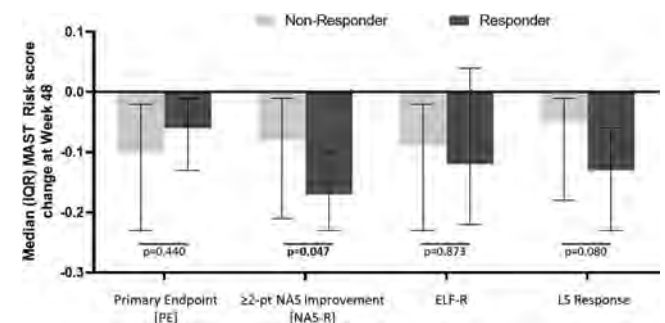


Figure: Change in MAST Risk Score by Histologic and Noninvasive Test Response at Week 48.

Conclusion: In patients with advanced fibrosis due to NASH, the MAST Risk score is correlated with noninvasive and histologic measures of fibrosis and may be a useful marker of treatment response beyond conventional histologic methods.

FRI061

Independent determinants of CAP values in healthy individuals with dysmetabolism

Cristiana Bianco¹, Serena Pelusi¹, Eleonora Giacomuzzi Grigoli², Luigi Santoro¹, Francesco Malvestiti^{1,3}, Melissa Tomasi¹, Ilaria Marini¹, Sara Margarita¹, Rossana Carpani¹, Daniele Prati¹, Luca Valenti^{1,3}.

¹Precision Medicine, Department of Transfusion Medicine and Hematology-Fondazione IRCCS Ca' Granda Ospedale Maggiore Policlinico; ²Università degli Studi di Milano; ³Università degli Studi di Milano, Department of Pathophysiology and Transplantation
Email: biancocristiana.md@gmail.com

Background and aims: Controlled attenuation parameter (CAP) values determined during vibration controlled transient elastography correlate with hepatic fat content and can non-invasively assess the presence of fatty liver with moderate accuracy. Aim of the study was to examine the clinical and metabolic determinants of CAP in a cohort of apparently healthy individuals with dysmetabolism.

Method: We assessed CAP in 953 consecutive blood donors with ≥ 3 dysmetabolism features (hypertension, hyperglycemia, overweight/obesity, low HDL/high tryglicerides), who participated in a primary prevention program (LIVER-BIBLE cohort up to July 2021). CAP determinants were assessed by generalized linear models.

Results: Mean age was 53.9 ± 6.3 yrs, BMI 28.5 ± 3.0 Kg/m², 158 (16.6%) participants were females, 35 (3.7%) diabetics, 704 (73.9%) had hypertension and 383 (40.2%) dyslipidemia, 463 (48.6%) had fatty liver (CAP >275 db/m), and 17 (1.8%) liver stiffness measurement (LSM) ≥ 8 kPa. CAP correlated with LSM ($p < 10^{-16}$). CAP was associated with older age ($p = 0.02$), higher BMI, abdominal circumference, glucose, insulin, ferritin ($p < 0.01$ for all), and lower HDL ($p = 0.03$). No consistent association with CRP, hypertension, diet or lifestyle factors was detected, except for alcohol consumption ($p = 0.003$). At multivariable analysis (Table), abdominal circumference was the main determinant of CAP ($p < 10^{-9}$), with insulin ($p < 10^{-6}$), HbA1c ($p = 0.006$), ferritin ($p = 0.04$) and HDL levels ($p = 0.04$). Independent determinants of CAP ≥ 275 db/m were confirmed to be abdominal circumference ($p < 10^{-5}$), insulin ($p = 0.0003$), HDL, HbA1c, BMI and alcohol consumption ($p < 0.05$ for all). Fatty liver index predicted CAP ≥ 275 db/m with low-moderate accuracy (AUROC = 0.70), whereas ALT with low accuracy (AUROC = 0.60). In the subset of the latest 352 enrolled participants for whom the information was available, we found an independent association between CAP and lower TSH levels (estimate -5.06 ± 2.22 , $p = 0.02$).

	Overall LIVER-BIBLE Cohort			Subgroup with TSH determination (n=352)		
	Estimate	SE	P value	Estimate	SE	P value
Sex, F	1.99	1.84	0.28	3.33	2.76	0.23
Age, years	0.37	0.19	0.06	0.35	0.32	0.27
BMI, kg/m ²	0.79	0.62	0.21	0.42	0.95	0.66
Abdominal circumference, cm	1.41	0.22	1.1×10^{-10}	1.60	0.34	1.9×10^{-6}
HbA1c, mmol/mol	0.61	0.30	6.4×10^{-3}	0.31	0.45	0.49
Insulin, uU/ml	0.70	0.14	2.8×10^{-3}	0.95	0.22	2.0×10^{-5}
HDL, mg/dl	-0.25	0.13	4.9×10^{-2}	-0.15	0.20	0.45
Ferritin, ng/ml	2.91	1.45	4.4×10^{-2}	1.88	2.40	0.43
Alcohol drinks, n/week	0.33	0.22	0.12	0.90	0.34	8.0×10^{-4}
TSH, mIU/l	-	-	-	-5.06	2.22	2.2×10^{-2}

Figure: Independent predictors of CAP values in the LIVER-BIBLE cohort. F: female; BMI: body mass index; HbA1c: glycated hemoglobin; TSH: thyroid stimulating hormone; SE: standard error.

Conclusion: In healthy individuals with dysmetabolism, CAP values were most strongly associated with the severity of hyperinsulinemia and abdominal adiposity. The association between activation of the pituitary-thyroid axis and fatty liver is being evaluated in the whole updated cohort.

FRI062

Performance of liver-related clinical scores in the SAPHIR study

Lorenz Balcar^{1,2}, Georg Semmler^{1,2,3}, Stephan Zandanel¹, David Niederseer⁴, Sophie Gensluckner¹, Alexandra Feldman¹, Christian Datz³, Bernhard Paulweber¹, Elmar Aigner¹. ¹Paracelsus Medical University of Salzburg, First Department of Medicine, Salzburg, Austria; ²Medical University of Vienna, Division of Gastroenterology and Hepatology, Department of Internal Medicine III, Vienna, Austria; ³General Hospital Oberndorf, Department of Internal Medicine, Oberndorf bei Salzburg, Austria; ⁴University Hospital Zurich, Department of Cardiology, Zurich, Switzerland
Email: e.aigner@salk.at

Background and aims: There are several established clinical scores for patients with chronic liver diseases; however, the prognostic value of these scores in the general population is unclear. Therefore, our study aimed to evaluate the value of liver-related risk-scores in a population-based cohort with a 20-year follow-up.

Method: We included participants from the SAPHIR study from the city of Salzburg, Austria. We calculated Cox regression models for (i) overall mortality, (ii) malignancy-related-, (iii) major adverse cardiovascular (CV)-, and (iv) composite CV events (minor/major adverse CV events).

Results: Overall, 1646 patients were included (mean age 52 ± 6 years; 63% male). Mean BMI was 27 ± 4 kg/m² and 15% of patients had metabolic syndrome (MetS) at baseline. Mean Framingham risk score (FRS) was 12 ± 4 points, indicating an intermediate risk for developing CV diseases within 10 years. Median follow-up was 18.7 years (IQR: 15.4–20.5).

In univariable analyses, APRI was associated with overall mortality (hazard ratio [HR]: 5.01 [95% confidence interval (95%CI): 1.27–19.78]; $p = 0.021$), as was FIB-4 (HR: 1.53 [95%CI: 1.18–1.99]; $p = 0.002$), the MetS (HR: 1.28 [95%CI: 1.11–1.49]; $p < 0.001$), the Forns- (HR: 1.24 [95%CI: 1.08–1.42]; $p = 0.002$), and the FLI- (HR: 1.03 [95%CI: 1.01–1.04]; $p = 0.002$), but not the BARD-score (HR: 1.16 [95%CI: 0.97–1.38]; $p = 0.097$). The FLI-score (HR: 1.02 [95%CI: 1.01–1.03]; $p = 0.006$) and the MetS (HR: 1.17 [95%CI: 1.07–1.28]; $p < 0.001$) were univariably associated with malignant events. For major adverse CV events, results were similar (FLI-score: HR: 1.03 [95%CI: 1.02–1.05]; $p < 0.001$; MetS: HR: 1.50 [95%CI: 1.31–1.73]; $p < 0.001$). Furthermore, the Forns- (HR: 1.13 [95%CI: 1.04–1.23]; $p = 0.005$), as well as the FLI-score (HR: 1.03 [95%CI: 1.02–1.04]; $p < 0.001$) and the MetS (HR: 1.32 [1.21–1.43]; $p < 0.001$) were associated with a combined CV endpoint. In multivariable analyses including age, BMI, mean arterial pressure, FRS, and respective scores significantly associated in univariable analyses, none of the scores remained independently associated with overall mortality and malignant outcomes. Interestingly, the MetS remained independently associated with major adverse CV events (aHR: 1.36 [95%CI: 1.11–1.65]; $p = 0.003$) and the FLI-score for combined CV endpoints (aHR: 1.02 [1.01–1.04]; $p = 0.010$).

Conclusion: While specific liver-related scores (i.e., FIB-4, APRI) are strongly associated with outcomes in liver diseased patients, their prognostic value is limited in the general population. Most of the scores of interest were univariably associated with overall mortality; however, these associations vanished when adjusting for other variables. Importantly, the MetS as well as the FLI-score showed independent associations with CV events, suggesting a strong correlation of fatty liver disease and rate of CV outcomes in the general population.

FRI063

Correlations of 2D-Shear wave and transient elastography liver stiffness measurements in patients with non-alcoholic fatty liver disease

Dimitrios Karagiannakis¹, Georgios Markakis¹, Dimitra Lakiotaki¹, Elisavet Michailidou¹, Paraskevi Fytily¹, Evangelos Cholongitis¹, Ioannis Vlachogiannakos¹, George Papatheodoridis¹. ¹Laiko General Hospital, Medical School, National and Kapodistrian University of Athens, Greece

Email: d_karagiannakis@hotmail.com

Background and aim: The performance of transient elastography (TE) has been widely assessed, while 2D-shear wave elastography (2D-SWE) is a newer elastographic technique. The aim of the study was to investigate if liver stiffness measurements (LSM) of 2D-SWE are correlated with LSM of TE for the evaluation of liver fibrosis in patients with non-alcoholic fatty liver disease (NAFLD).

Methods: In total, 552 consecutive patients with NAFLD were included [median age: 55 (range:19–87) years, Males: 288 (52.5%)]. Mean waist circumference was 105 ± 13 cm and median BMI 28.7 (17.3–79.7) kg/m² [Normal BMI (<25): 94 (17%), Overweight (BMI = 25–30): 94 (17%), Obese (BMI > 30): 192 (34.8%)]. Liver fibrosis was assessed by TE (M/XL probe) and 2D-SWE at the same time. CAP was performed for the estimation of the degree of liver steatosis.

Results: Median LSM of TE was 5.5 (2.8–75) kPa and of 2D-SWE 62 (3.7–46.2) kPa. TE (and CAP) and 2D-SWE were not feasible in 18 (3.3%) and 26 (4.7%) patients respectively. Mean CAP value was 290 ± 54 db/m. One hundred and twenty eight patients (23.2%) had mild steatosis (CAP < 250 db/m) and 406 (73.6%) had moderate/severe steatosis (CAP ≥ 250 db/m). LSMs by TE and 2D-SWE were correlated in normal BMI (r: 0.774; p < 0.001), overweight (r: 0.774; p < 0.001) and obese (r: 0.75; p < 0.001) patients, as well as in patients with CAP ≤ 250 db/m (r = 0.63; p < 0.001) and CAP > 250 db/m (r = 0.743; p < 0.001). According to TE measurements, patients were sub-classified to those without moderate fibrosis (F0–F1; LSM by TE < 7 kPa; n = 388 or 70.3%), moderate/severe fibrosis (F2/F3; LSM: 7–13 kPa; n = 117/19.3%) and cirrhosis (F4; LSM > 13 kPa; n = 57/10.3%). A significant correlation between TE and 2D-SWE was found in all these subgroups (r: 0.458; r: 0.624; r: 0.696, respectively; all p < 0.001). The accuracy of 2D-SWE for detecting patients with moderate/severe fibrosis diagnosed by TE was 89.7% (LSM cut-off 6.87 kPa: 87% sensitivity, 81.2% specificity for discrimination between moderate/severe (F2/F3) and no moderate fibrosis (F0–F1). The accuracy of 2D-SWE for diagnosing patients with cirrhosis diagnosed by TE was 99.1% (LSM cut-off 12.16 kPa: 90.4% sensitivity, 95.9% specificity).

Conclusion: LSMs by 2D-SWE correlate with those of TE and therefore 2D-SWE can reliably substitute TE in the evaluation of liver fibrosis in patients with NAFLD. Similar LSM cut-off values of TE and 2D-SWE can be applied in order to classify NAFLD patients into fibrosis stages.

FRI064

Performance of the Enhanced Liver Fibrosis (ELF) test in real world practice versus clinical trials of non-alcoholic steatohepatitis

Maria Stepanova^{1,2,3,4}, Sean Felix^{2,3}, Thomas Jeffers^{2,3}, Elena Younossi^{2,3}, Brian Lam^{2,3}, Linda Henry^{1,2,3,4}, Zobair Younossi^{1,2,3}. ¹Inova Health System, Medicine Service Line; ²Betty and Guy Beatty Center for Integrated Research, IHS; ³Inova Health System, Center for Liver Disease, Department of Medicine; ⁴Center for Outcomes Research in Liver Disease

Email: zobair.younossi@inova.org

Background and aims: The ELF score is calculated using three direct markers of fibrosis [hyaluronic acid (HA), amino-terminal propeptide of type III collagen (PIIINP), tissue inhibitor of matrix metalloproteinase 1 (TIMP-1)]. In NAFLD, advanced stage of fibrosis is the most important predictor of long-term clinical outcomes. Our aim was to assess performance of ELF for identification of advanced fibrosis in

patients with NAFLD enrolled in clinical trials and in patients seen in a real-life hepatology clinic.

Method: Data collected from two non-overlapping samples of NAFLD patients were used in this study (Group 1: real world hepatology practice, Group 2: enrollees from NASH Clinical trials). Both groups were matched according to presence of advanced fibrosis. Clinical data, liver biopsy, and serum were collected for each included patient. ELF scores were calculated using an ADVIA Centaur XP analyzer. Liver biopsies were scored by a single hepatopathologist 0–4 using CRN criteria; advanced fibrosis was defined as stage 3 (bridging fibrosis) or 4 (compensated cirrhosis). Performance of ELF for predicting advanced fibrosis was assessed in both groups.

Results: A total of 1,379 subjects were available [Group 1: N = 467, age 48 ± 13 years old, 31% male, 35% type 2 diabetes, 24.6% advanced fibrosis, mean (SD) ELF score was 9.0 ± 1.2; based on published cutoffs, 78% had ELF < 9.8 (low-risk), 17% 9.8 ≤ ELF < 11.3 (moderate risk), and 5% ELF ≥ 11.3 (high-risk), Group 2: N = 912, age 54 ± 11 years old, 43% male, 55% type 2 diabetes, 26% advanced fibrosis; mean (SD) ELF 9.6 ± 1.0 including 61% with low-risk, 33% moderate risk, 6% high-risk ELF scores]. Area under the ROC curve (AUC) (95%) for predicting advanced fibrosis by ELF was 0.81 (0.77–0.85) in Group 1. The cutoff of ELF ≥ 9.8 returned sensitivity 57% (47%–66%), specificity 89% (86%–92%), positive predictive value (PPV) 63% (54%–70%), negative predictive value (NPV) 86% (83%–89%); in addition, the cut-off of ELF ≥ 11.3 returned specificity 99% (98%–100%), sensitivity 19% (12%–28%), PPV 88% (69%–96%), NPV 79% (77%–80%). In Group 2, ELF had AUC (95% CI) = 0.80 (0.77–0.82) for predicting advanced fibrosis which was identical to that seen in Group 1. The cutoff of ELF ≥ 9.8 returned sensitivity 74% (68%–79%), specificity 74% (70%–77%), positive predictive value (PPV) 50% (45%–55%), negative predictive value (NPV) 89% (86%–91%); in addition, the cut-off of ELF ≥ 11.3 returned specificity 98% (97%–99%), sensitivity 17% (12%–22%), PPV 77% (66%–89%), NPV 77% (74%–80%).

Conclusion: The non-invasive serum-based ELF test performs well in identifying high risk NAFLD patients in both real-life and clinical trial settings.

FRI065

Machine learning using simple non-invasive tests of fibrosis and B-mode ultrasound for the prediction of adverse liver-related outcomes in NAFLD

Heather M. Kosick^{1,2}, Chris McIntosh^{3,4}, Mina Fakhriyehasi³, Chinmay Bera⁵, Oyedele Adeyi⁶, Kartik Jhaveri³, Keyur Patel⁵.

¹University of Toronto, Toronto, Canada; ²University Health Network, Toronto, Canada; ³University Health Network, Joint Department of Medical Imaging, Toronto, Canada; ⁴University Health Network, Peter Munk Cardiac Centre and Joint Department of Medical Imaging, Canada;

⁵University Health Network, Gastroenterology & Hepatology, Toronto, Canada; ⁶University of Minnesota, Department of Laboratory Medicine and Pathology, Minneapolis, United States

Email: heather.evans@medportal.ca

Background and aims: Advanced fibrosis (F3–4) in non-alcoholic fatty liver disease (NAFLD) increases the risk of adverse liver-related outcomes. Serum-based non-invasive tests (NIT) alone are still not yet able to reliably predict NAFLD outcomes. Our aims were to explore the role of machine learning (ML) algorithms based on simple NIT combined with B-mode ultrasound (US), for prediction of adverse liver-related outcomes.

Method: Retrospective observational single center cohort study which included NAFLD patients with biopsy between 2010–2018. Demographics, anthropometric measurements, clinical outcomes, NIT, including FIB-4 and NFS, and US data, including liver/spleen size, steatosis, and features of advanced liver disease, were collected. ML algorithms were generated using the random forest technique to create predictive models for each clinical outcome, including hepatic decompensation, hepatocellular carcinoma (HCC), liver transplant, all-cause and liver-related mortality.

POSTER PRESENTATIONS

Results: 389 NAFLD patients were included with F3–4 prevalence 48.6%, 54.5% male, mean age 48.5±13.2 years, diabetes in 30.1%, and BMI 32.4 ± 7.0 kg/m². Overall, 51 (13.1%) patients had an adverse liver-related outcome over median 3.14 years, and included hepatic decompensation in 9.5%, HCC 4.1%, liver transplant 5.4%, mortality 2.6% and liver-related mortality 2.1%. AUC measures for the ML predictive models were: hepatic decompensation 0.958, HCC 0.770, liver transplant 0.931, all-cause mortality 0.831, and liver-related mortality 0.859. ML feature importance for predictive variables was determined for each outcome. FIB-4, AST:ALT ratio, and age had the greatest feature importance for NIT and clinical variables respectively. US-based parameters did not have significant feature importance for liver-related outcomes compared to clinical or biochemical features.

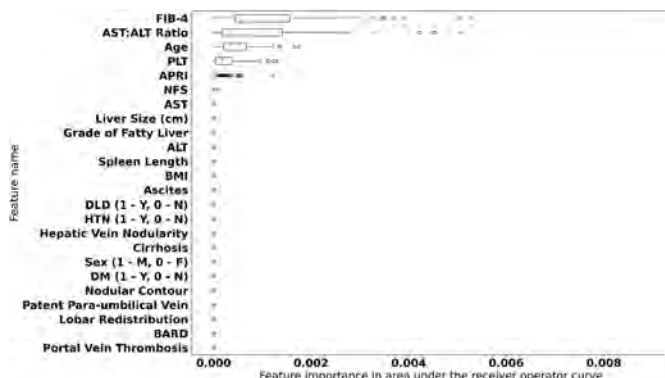


Figure: Feature Importance Box Plot for Machine Learning Algorithm Prediction of Hepatic Decompensation.

Conclusion: ML models based on readily available clinical, biochemical, and US-based variables were able to accurately predict adverse liver-related outcomes in a tertiary cohort of biopsy-proven NAFLD patients. Age, AST:ALT ratio, and FIB-4, but not US-based parameters, contributed significantly to ML predictive models for clinical outcomes.

FRI066

Incorporating a two-tiered liver fibrosis assessment into annual diabetes review in primary care-3 year follow up study

Rajan Bhandari¹, Dina Mansour¹. ¹QE hospital Gateshead, United Kingdom

Email: dmansour299@yahoo.co.uk

Background and aims: We previously presented the outcome of a pathway incorporating 2-tiered fibrosis assessment into annual diabetic reviews in primary care. This 3 year follow up study looks at Outcomes in patients referred into secondary care with moderate-advanced fibrosis

Ongoing service delivery requirements after the first year of case finding

Effectiveness of the pathway in detecting patients with advanced disease, by looking at the number of patients missed in the pathway presenting with advanced disease.

Method: All patients aged >35 years with T2DM attending annual review at two primary care practices in North East England between April 2018 and September 2019 (n=467) had a Fib-4 requested, followed by transient elastography (TE) if the Fib-4 was above the high sensitivity threshold. Those with a liver stiffness >8 kPa were reviewed in secondary care. This pathway was continued in both practices after the end of the initial study period. We reviewed the outcomes of all patients referred to secondary care; the number of patients referred in the subsequent years with ongoing case-finding; and any patients missed from initial screening presenting with decompensated/symptomatic disease.

Results: Of 467 patients in the initial study, 58 were referred for TE, 25 had a LSM>8 kPa and 20 had advanced disease (on imaging/

biopsy/endoscopy). 6/20 (30%) patients with advanced disease have died- 2/20 liver related deaths (hepatocellular carcinoma (HCC) and decompensated cirrhosis); 1 patient diagnosed with HCC was treated with curative transarterial chemoembolisation; 3 patients had varices on OGD (2 started on carvedilol for primary prophylaxis); 12 remain under follow up. In all patients with LSM>8 kPa (n=25): 8/25 (32%) died (3/8 from COVID-19); 24% (6) LSM improved, 8% (2) LSM deteriorated; 32% (8/25) lost weight. No patients missed by the pathway presented with decompensated disease. Serial Fib-4 at annual screening 2019–2021: 4 patients new raised Fib-4 scores-1 DNA, 1 TE is awaited, 1 LSM <8 kPa (discharged), 1 advanced disease (LSM 17.1 kPa).

Conclusion: Incorporation of a two-tiered liver fibrosis assessment into primary care annual diabetic screening significantly improves identification of advanced liver disease and no patients have presented with advanced disease out-with the pathway. It allows for early detection and interventions against the complications associated with advanced liver disease. Mortality in patients with advanced liver disease remains high. Referrals for TE and into secondary care dramatically reduce after the initial year of case finding.

FRI067

New scoring system using MRI with AST for the non-invasive identification of patients with non-alcoholic steatohepatitis with significant activity and fibrosis

Kento Imajo^{1,2}, Yusuke Saigusa³, Takashi Kobayashi¹, Koki Nagai², Shinya Nishida², Nobuyoshi Kawamura², Michihiro Iwaki¹, Yasushi Honda¹, Takaomi Kessoku¹, Yuji Ogawa⁴, Hiroyuki Kirikoshi⁵, Satoshi Yasuda⁶, Hidenori Toyoda⁶, Hideki Hayashi⁷, Hiroyoshi Doi², Shigehiro Kokubu², Daisuke Utsunomiya⁸, Hirokazu Takahashi⁹, Shinichi Aishima¹⁰, Satoru Saito¹, Masato Yoneda¹, Atsushi Nakajima¹.

¹Yokohama City University Graduate School of Medicine, Department of Gastroenterology and Hepatology, Yokohama, Japan; ²Shin-yurigaoka General Hospital, Department of Gastroenterology, Kawasaki, Japan;

³Yokohama City University Graduate School of Medicine, Department of Biostatistics, Yokohama, Japan; ⁴National Hospital Organization Yokohama Medical Center, Department of Gastroenterology, Yokohama;

⁵Yokohama City University Hospital, Department of Clinical Laboratory, Yokohama, Japan; ⁶Ogaki Municipal Hospital, Department of Gastroenterology and Hepatology, Ogaki, Japan; ⁷Gifu City Hospital,

Department of Gastroenterology and Hepatology, Japan; ⁸Yokohama City University Graduate School of Medicine, Department of Radiology,

Yokohama, Japan; ⁹Saga University, Division of Metabolism and Endocrinology, Saga, Japan; ¹⁰Saga University, Department of Pathology & Microbiology, Saga, Japan

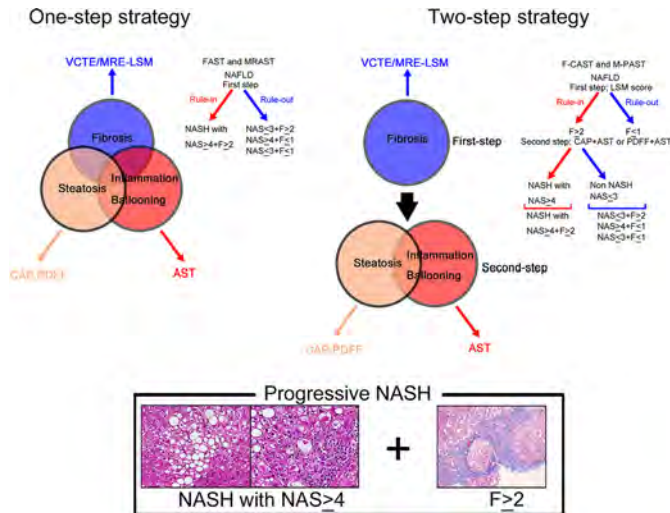
Email: kento318@yokohama-cu.ac.jp

Background and aims: Clinical trials enroll patients with elevated non-alcoholic fatty liver disease (NAFLD) activity score (NAS≥4) and significant fibrosis (F≥2); however, screening failure rates are often high following biopsy. We aimed to develop a new score to identify non-alcoholic steatohepatitis (NASH) with NAS≥4 and F≥2 using magnetic resonance imaging (MRI).

Method: We undertook a prospective primary study of 176 patients and a retrospective validation study of 169 patients with liver biopsy proven NAFLD at three liver centers. Liver stiffness measurement (LSM) by magnetic resonance elastography (MRE), proton density fat fraction (PDFF) measured by MRI, and aspartate aminotransferase (AST) were combined to develop a simple index (MRI with AST; MRAST score) for NASH with NAS≥4 and F≥2, as in FibroScan-AST (FAST) score (One-step strategy).

Results: MRAST score was generally equivalent to FAST (an area under the ROC curve (AUROC)=0.780) for the detection of NASH with NAS≥4 and F≥2 with an AUROC of 0.756, with consistent results in the validation cohort (AUROC=0.812 [MRAST] vs 0.779 [FAST]). We then examined a two-step strategy, VCTE-LSM or MRE-LSM as first-step, following CAP+AST or PDFF+AST as second-step. When used as

the rule-in criteria, the positive predictive value (PPV) was 71.6% for FAST, 74.2% for MRAST, 82.6% for F-CAST, and 78.1% for M-PAST in combined cohort. When used as the rule-out criteria, negative predictive value (NPV) was 85.2% for FAST, 88.8% for MRAST, 85.3% for F-CAST, and 87.3% for M-PAST. Indeterminate patients by the FAST, MRAST, F-CAST and M-PAST were 48.5%, 49.9%, 32.5% and 28.1%, respectively.



Conclusion: MRAST has equal diagnostic accuracy with FAST for NASH with NAS ≥ 4 and F ≥ 2. In addition, our results supported the higher utility of a two-step strategy using F-CAST and M-PAST over one-step method (FAST and MRAST) for detecting NASH with NAS ≥ 4 + F ≥ 2.

FRI068

Impact of artificial intelligence assistive tool on the histopathologic review of fibrosis in non-alcoholic steatohepatitis patients

Aileen Wee¹, Wei Qiang Leow², Gwyneth Soon³, Elaine Chng⁴, Dean Tai⁴, Yayun Ren⁴, Jia Ling Chong⁴, Yee Chen Ng⁴, Feng Liu⁵, Lai Wei⁶, Arun Sanyal⁷. ¹Department of Pathology, Yong Loo Lin School of Medicine, National University of Singapore, Singapore; ²Department of Anatomical Pathology, Singapore General Hospital, Singapore and Duke-NUS Medical School, Singapore; ³Department of Pathology, National University Hospital, Singapore; ⁴HistoIndex Pte. Ltd., Singapore; ⁵Peking University People's Hospital, Peking University Hepatology Institute, Beijing Key Laboratory of Hepatitis C and Immunotherapy for Liver Diseases, Beijing, China; ⁶Hepatopancreatobiliary Center, Beijing Tsinghua Changgung Hospital, Tsinghua University, Beijing, China; ⁷Virginia Commonwealth University, Richmond, Virginia, USA
Email: patweea@nus.edu.sg

Background and aims: Inter-observer variability for categorical scores of liver fibrosis among pathologists ranges from fair to moderate weighted kappa. Artificial intelligence (AI) and advances in digitised whole-slide images (WSI) facilitated the use of an AI-assistive tool in pathology to improve histopathologic interpretation. Second harmonic generation/two-photon excitation fluorescence (SHG/TPEF) microscopy with AI can provide standardised evaluation. This pilot study aims to explore the impact of AI tools on the overall agreement on fibrosis assessment between pathologists.

Method: Unstained sections of liver biopsies from 50 non-treated patients with NASH (F0–F4) were taken from Peking University People's Hospital and fibrosis was quantitated using SHG/TPEF microscopy (qFibrosis). To evaluate performance metrics for assisted and unassisted reads, pathologists interpreted images in both modalities in 2 sessions separated by a wash-out period of at least

3 weeks. H&E and MT-stained images were digitised and uploaded onto a WSI platform, and the assisted reads included an additional SHG image with qFibrosis stage and continuous values. 3 pathologists participated in this study, with experiences ranging from 5 to 40 years.

Results: The qFibrosis AI tool has been validated in studies, showing >95% agreement. When assisted by the qFibrosis AI tool, the concordance rate between pathologists improved to near perfect agreement, with 0.82 linear weighted kappa, as compared to 0.72 for the unassisted review. Mean overall percentage agreement between pathologists improved from 89.38% to 92.93% (p=0.032). Mean linear weighted kappa for intra-observer agreement is also higher, achieving 0.91 kappa compared to 0.79 for unassisted reads. The effect of AI assistance on fibrosis assessment consistency was examined by reviewing the percentage of patients who remained staged between F1–F3 after the initial reads. Using qFibrosis, 95.3% of the patients were retained versus 82% for the unassisted review.

Table: Mean percentage agreement and weighted kappa (linear) for assisted and unassisted reads.

		Unassisted	Assisted
Inter-observer	Mean Percentage Agreement	89.38%	92.92%
	Mean Weighted Kappa (Linear)	0.7157	0.8163
Intra-observer	Mean Percentage Agreement	92.08%	96.46%
	Mean Weighted Kappa (Linear)	0.7861	0.9081

Conclusion: qFibrosis as an AI assistive tool can improve inter-pathologist weighted kappa to near perfect agreement with 93% agreement and 95% retention rate. qFibrosis has been well validated and enable pathologists with varying experience to establish similar performance in fibrosis evaluation. This has important implications in the development of drugs for NASH treatment.

FRI069

PRO-C3 based sequential algorithm can screen high-risk NASH and severe fibrosis in asian NAFLD population

Liang-Jie Tang¹, Gang Li¹, Mohammed Eslam², Pei-Wu Zhu³, Sui-Dan Chen⁴, Howard Ho-Wai Leung⁵, Ou-Yang Huang¹, Grace Lai-Hung Wong^{6,7}, Yu-Jie Zhou⁸, Morten Karsdal⁹, Diana Leeming⁹, Chris Byrne¹⁰, Giovanni Targher¹¹, Jacob George², Vincent Wai-Sun Wong^{6,7}, Ming-Hua Zheng^{1,12,13}. ¹The First Affiliated Hospital of Wenzhou Medical University, NAFLD Research Center, Department of Hepatology, Wenzhou, China; ²Westmead Hospital, Westmead, and University of Sydney, Storr Liver Centre, Westmead Institute for Medical Research, Sydney, Australia; ³The First Affiliated Hospital of Wenzhou Medical University, Department of Laboratory Medicine, Wenzhou, China; ⁴The First Affiliated Hospital of Wenzhou Medical University, Department of Pathology, Wenzhou, China; ⁵The Chinese University of Hong Kong, Department of Anatomical and Cellular Pathology, Hong Kong, China; ⁶The Chinese University of Hong Kong, Department of Medicine and Therapeutics, Hong Kong, China; ⁷The Chinese University of Hong Kong, State Key Laboratory of Digestive Disease, Hong Kong, China; ⁸Shanghai Jiao Tong University, Division of Gastroenterology and Hepatology, Key Laboratory of Gastroenterology and Hepatology, Shanghai, China; ⁹Nordic Bioscience Biomarkers and Research A/S, Herlev, Denmark; ¹⁰University Hospital Southampton, Southampton General Hospital, Southampton National Institute for Health Research Biomedical Research Centre, Southampton, United Kingdom; ¹¹University and Azienda Ospedaliera Universitaria Integrata of Verona, Section of Endocrinology, Diabetes and Metabolism, Department of Medicine, Verona, Italy; ¹²Wenzhou Medical University, Institute of Hepatology, Wenzhou, China; ¹³Key Laboratory of Diagnosis and Treatment for the Development of Chronic Liver Disease in Zhejiang Province, Wenzhou, China
Email: zhengmh@wmu.edu.cn

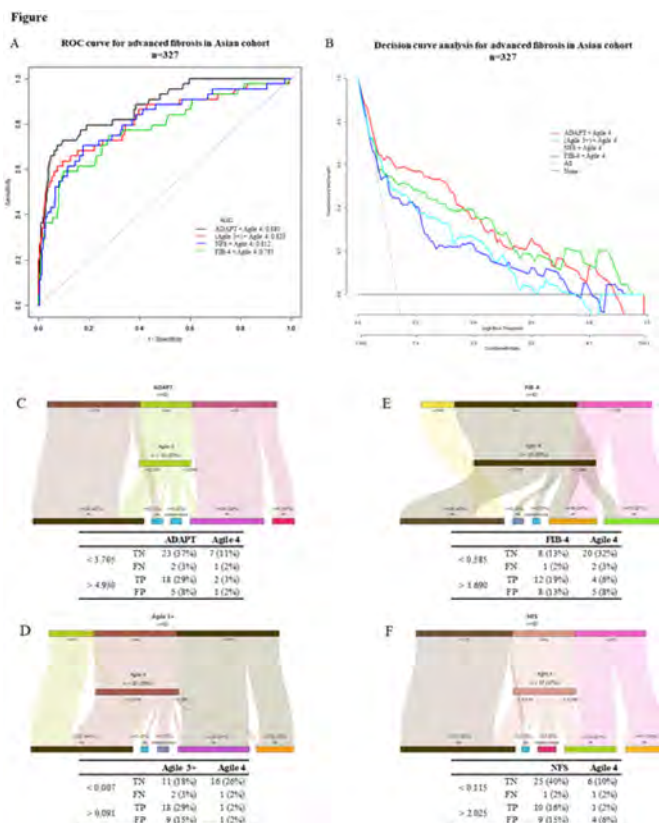
Background and aims: With non-alcoholic fatty liver disease (NAFLD) incidence and prevalence increasing, there is an urgent

POSTER PRESENTATIONS

need for non-invasive diagnostic tests to accurately screen high-risk patients for liver inflammation and fibrosis. We evaluated the diagnostic performance of a new sequential algorithm for assessing liver inflammation and fibrosis in NAFLD.

Method: Data from two prospective Asian cohorts (327 biopsy-confirmed patients with NAFLD [262 from Wenzhou, 65 from Hong Kong]) were studied. The area under the receiver operating characteristic curve (AUROC) was used to test the diagnostic performances of FAST, ADAPT, Agile 3+ and Agile 4, and for comparison with other widely used non-invasive fibrosis scores.

Results: For progressive non-alcoholic steatohepatitis (NASH) patients (NASH + NAFLD activity score (NAS) $\geq 4 + F \geq 2$), the AUROC of FAST score was 0.801 (95% confidence interval (CI): 0.739–0.863), and the negative predictive value (NPV) was 0.951. For advanced fibrosis (F3) and cirrhosis (F4), the AUROC of ADAPT, Agile 3+ and Agile 4 were 0.879 (95% CI: 0.825–0.933), 0.805 (95% CI: 0.725–0.886) and 0.943 (95% CI: 0.892–0.994), and the NPV was 0.972 and 0.992, respectively. A new sequential algorithm of ADAPT + Agile 4 combination was better than other combinations (AUROC = 0.88, 95% CI: 0.824–0.935). This new combination algorithm approach can more accurately screen out high-risk patients (i.e. the number of true positive (TP) groups has increased from 21%, 26%, and 31% to 32%), while reducing the number of patients requiring liver biopsy (including false positive (FP)), false negative (FN) and indeterminate groups from 29% and 26% to 20%) (Figure). At the same time, in all subgroup analyses (stratifying by sex, age, diabetes, NAS, BMI and ALT), ADAPT + Agile 4 had good diagnostic performance.



Conclusion: The new sequential algorithm reliably assesses inflammation and fibrosis in NAFLD patients, making it easier to exclude low-risk patients and recommending high-risk patients for referral treatment, while reducing the need for liver biopsy.

FRI070

Real-world use of the FIB-4 calculator in primary care workflows to screen for advanced non-alcoholic fatty liver disease in a large US health system

George Therapondos¹, Anna Thomas², Douglas T. Dieterich³, Nigel Girgrah¹, Philip Oravetz⁴. ¹Ochsner Health, Multiorgan Transplant, New Orleans, United States; ²NASHNET; ³Icahn School of Medicine, Department of Medicine, New York, United States; ⁴Ochsner Health, Population Health, New Orleans, United States
Email: gtherapondos@ochsner.org

Background and aims: Non-alcoholic fatty liver disease (NAFLD) affects about 25% of the global population. Early identification is needed to appropriately direct patients to expected new therapies. Ochsner Health is a large health system located in Louisiana, USA. The FIB-4 calculation was integrated into the Ochsner Health electronic health record (EHR) to better understand the burden of disease and real-world implications of its use for NAFLD.

Method: The FIB-4 calculation was integrated within the EPIC EHR in Summer 2021 but is not yet available for use by primary care providers. The data presented here are aggregated for exploratory analyses to understand the impact of its use in primary care. The following FIB-4 cut offs were used: if FIB-4 ≥ 2.67 , then high-risk; if FIB-4 from 1.0–2.67 and below 35 years or 1.3–2.67 and 35 to 65 years, or 2.0–2.67 and above 65 years, then medium risk; if FIB-4 < 1.0 and below 35 years or < 1.3 and 35 to 65 years or below 2.0 and over 65 years, then low risk. Data from 2016–2021 were aggregated and a provider-facing dashboard was generated to show patient demographics, comorbidities and FIB-4 scores.

Results: Out of 606, 906 patients, FIB-4 scores were able to be calculated in 283, 880 (46.77%) of these patients. Average age was 52.4 years (60.23% male, 29.71% female). 53.05% identified as White/Caucasian, 37.22% as African American/Black, 0.50% as Asian, and 3.50% as Hispanic or Latino. Prevalence of comorbidities was as follows: obesity (43.45%), diabetes (26.01%), hypertension (24.16%), heart disease (21.83%), hypercholesterolemia/hyperlipidemia (16.21%), and renal disease (9.27%). 60.51% of the total population had two or more comorbidities. Rates of comorbidities amongst the 50 lowest income zip codes in Louisiana were significantly higher than the general population.

20, 013 patients were classified as high-risk for advanced liver fibrosis, and 55, 265 were classified as medium risk. However, only 2.46% of the total population had been referred to hepatology. This trend remained true across multiple subpopulations, including patients with obesity (11.45% were medium/high-risk, 2.35% actually referred), diabetes (9.75% were medium/high-risk, 3.25% referred), heart disease (8.92% were medium/high-risk, 3.24% referred), hypercholesterolemia/hyperlipidemia (6.57% were medium/high-risk, 4.65% referred) and hypertension (9.39% were medium/high-risk, 3.23% referred).

Conclusion: The gap in patients classified as medium and high-risk to the actual rate of referral to hepatology suggests that many patients at-risk for NAFLD are not being identified. This study identified 75, 278 patients who need further hepatology investigation. The implications of this large number of NAFLD patients on the delivery of liver services needs to be further investigated. Additional analysis is needed to understand the impact of health disparities on NAFLD patients.

FRI071

In silico identification and validation of plasma Ficolin-2 (FCN-2) as non-invasive biomarker of fibrosis in Non-alcoholic Fatty Liver Disease (NAFLD)

Pablo J. Giraudi¹, Noel Salvoza^{1,2,3}, Natalia Rosso¹, Claudio Tiribelli¹, Deborah Bonazza⁴, Biagio Casagrande⁵, Nicolo de Manzini^{5,6}, Michela Giurucini⁵, Silvia Palmisano^{6,7}. ¹Fondazione Italiana Fegato Onlus, Basovizza, Italy; ²University of Trieste, Trieste, Italy; ³Philippine Council for Health Research and Development, Taguig, Philippines; ⁴Cattinara Hospital, Surgical Pathology Unit, Trieste, Italy; ⁵Cattinara Hospital, Surgical Clinic Division, Trieste, Italy; ⁶University of Trieste, Department of Medical, Surgical and Health Sciences, Trieste, Italy; ⁷Cattinara Hospital, Trieste, Italy
Email: noel.salvoza@fegato.it

Background and aims: Non-alcoholic fatty liver disease (NAFLD) covers a spectrum of diseases from simple steatosis (SS) to non-alcoholic steatohepatitis (NASH), with a significant risk of progressing to fibrosis. Fibrosis is considered as the most important predictive factor in the prognosis and mortality of NAFLD patients. Liver biopsy is widely accepted as the gold standard for its diagnosis and reliable non-invasive methods are unavailable. We investigated the diagnostic performance of plasma Ficolin-2 (FCN-2), identified by an *in silico* approach for the diagnosis of fibrosis in NAFLD.

Method: For the *in silico* analysis, a biological network was built to identify proteins related to fibrogenesis using molecular databases and bioinformatic tools. Of the several markers identified, FCN-2 met the criteria as one of the most interesting candidates that follows the fibrotic process aside from being secreted in the plasma. For the validation phase, 76 morbidly obese (MO) subjects with biopsy-proven NAFLD were stratified according to fibrosis stage (minimal F0-F1, n = 43; moderate-advanced F2-F3-F4, n = 33). Plasma FCN-2 levels were determined by enzyme-linked immunosorbent assay and the diagnostic performance was assessed.

Results: Although FCN-2 did not differentiate the steatosis stage of NAFLD, plasma FCN-2 levels significantly decreased when liver damage progresses from minimal to moderate/advanced fibrosis ($p < 0.0001$). Interestingly, FCN-2 levels correlated inversely with lobular inflammation ($p = 0.0002$) and portal inflammation ($p = 0.0007$) histological features of NAFLD. When stratified according to sex, the FCN-2 plasma levels are similar between males and females. The diagnostic performance of plasma FCN-2 in detecting $F \geq 2$ fibrosis was higher than those of other current fibrosis' indexes (Forns, FIB-4) (AUROC 0.76, 0.72, and 0.67, respectively). Furthermore, when combined with other tests (GGT and APRI), the score index yield an excellent discrimination power with AUC of 0.80 in identifying advanced fibrosis.

Conclusion: Plasma FCN-2 can be used as potential biomarker for discriminating moderate/advanced from minimal fibrosis in the context of NAFLD. Validation in larger cohorts will be required for its clinical utility. The use of FCN-2 alone or in combination with other tests may provide an alternative to minimize the need for biopsies to detect fibrosis in NAFLD patients.

FRI072

A lower cut-off of liver stiffness measurement (8/13) kPa performs better than Baveno 6 criteria for advanced chronic liver disease in patients with non-alcoholic fatty liver disease

Sagnik Biswas¹, Manas Vaishnav¹, Piyush Pathak¹, Himanshu Narang¹, Shubham Mehta¹, Amit Goel², Shalimar¹. ¹All India Institute of Medical Sciences, New Delhi, Gastroenterology and Human Nutrition, New Delhi, India; ²Sanjay Gandhi Post Graduate Institute of Medical Sciences, Gastroenterology, Lucknow, India
Email: drshalimar@yahoo.com

Background and aims: Patients with $\geq F3$ fibrosis are grouped as compensated advanced chronic liver disease (cACLD). Baveno six consensus recommended the rule in and out liver stiffness measurement (LSM) cut-offs for diagnosing compensated advanced

chronic liver disease (cACLD) as 10 kPa and 15 kPa. Baveno seven suggested lowering the cACLD cut-off for NAFLD, though it is supported by scanty data. We aimed to identify the LS cut-off for cACLD in people with non-alcoholic fatty liver disease (NAFLD).

Method: Included 330 patients with biopsy proved NAFLD (male 173 [52.4%]; age, median [interquartile range] 39 [33–47] years; body mass index 32.6 (25.6–44.4) kg/m²; diabetes 102 (30.9%). All the LS measurements were done by a single operator, after overnight fasting using a standard measurement technique. All the LS measurements were done within four weeks of liver biopsy.

Results: Liver biopsy revealed $\geq F3$ fibrosis, i.e., cACLD, in 70 (21.2%). Measured LS were <10 , 10 to <15 and ≥ 15 kPa in 230 (69.7%), 46 (13.9%) and 54 (16.4%), respectively. Baveno six criteria achieved a sensitivity (rule out) and specificity (rule-in) of 72.9% and 93% for cACLD. The area under receiver operator characteristic (AUROC) curve of LSM for predicting cACLD was 0.862 (0.810–0.914). The LS <8 , 8 to 13, and >13 kPa were present in 182 (55.2%), 82 (24.8%) and 66 (20.0%), respectively. A new cut-off at 8 kPa and 13 kPa showed sensitivity and specificity of 90% each. Univariate analysis identified age, diabetes, and LS as independent predictors of cACLD, but platelet count and albumin were not statistically significant. On multivariate analysis, only LS (OR, 1.201, 95% CI, 1.139–1.267) and diabetes (OR, 2.592, 95% CI, 1.298–5.179) were independent predictors of cACLD. The AUROC for the model with LSM and diabetes was 0.863 compared with 0.862 for LSM alone (DeLong test, $P = 0.934$). The AUROC for predicting cACLD with BMI <25 kg/m² and ≥ 25 kg/m² was 0.945 (0.886–1.000) and 0.844 (0.784–0.904), respectively.

Conclusion: LS cut-offs set at <8 and >13 kPa perform better to diagnose cACLD than the Baveno 6 criteria. The presence of diabetes and body mass index needs to be accounted for while interpreting the cut-offs.

FRI073

High prevalence of multi-organ steatosis and fibroinflammation, identified by multi-parametric magnetic resonance imaging, in people with type 2 diabetes

Nicole Eichert¹, Karyna Gibbons², Azlinda Hamid³, Vashist Deelchand⁴, Jinny Woolgar¹, Rob Suriano¹, Helena Thomaidis-Brears¹, Rajarshi Banerjee¹, Graham Kemp⁵, Sarah Ali⁴, Gaya Thanabalasingham², Daniel Cuthbertson^{3,5}. ¹Perspectum Ltd., Oxford, United Kingdom; ²Oxford University Hospitals NHS Foundation Trust, Oxford Centre for Diabetes, Endocrinology and Metabolism; ³Liverpool University Hospitals NHS Foundation Trust, University Hospital Aintree, United Kingdom; ⁴Royal Free London NHS Foundation Trust, United Kingdom; ⁵University of Liverpool, United Kingdom
Email: nicole.eichert@perspectum.com

Background and aims: Type 2 diabetes (T2D) is a multi-system disease characterized by a high prevalence of micro- and macro-vascular complications, like diabetic nephropathy and cardiovascular disease, and co-morbidities, like metabolic-associated fatty liver disease. These are often only detected at a late stage, particularly when they become clinically manifest. Early detection provides a window to potentially prevent and reverse disease progression, and improve outcomes. The aim of this study was to provide comprehensive assessment of multi-organ health and pre-clinical detection of diabetes-related organ damage with a single, efficient, 30 min non-contrast magnetic resonance imaging (MRI) scan in patients with T2D.

Method: Overall, 138 adults with T2D [62 yr (54–70); 60% male; BMI of 31 kg/m² (28–35); HbA1c 60 mmol/L (51–70); 92% on metformin, T2D duration 11 yr (6–11)] were recruited to the MODIFY study (NCT04114682). MRI data were acquired to derive organ-specific measures of size, fat deposition, fibroinflammation, body composition (visceral adipose tissue, VAT; subcutaneous adipose tissue, SAT; skeletal muscle index, SMI) and aortic distensibility (CoverScan®, Perspectum Ltd.). Normative values of MRI metrics were based on 92

POSTER PRESENTATIONS

healthy volunteers [44 yr (32–53); 66% male; BMI 23 kg/m² (21–25)] and published literature, and the prevalence of abnormalities for each organ was assessed using Fisher's exact tests. Statistical significance of co-prevalence was assessed by simulation assuming that values were independently binomially distributed.

Results: In this cohort of established T2D patients, characterised by abnormal body composition (high SAT and VAT, low SMI), there was a high prevalence of multi-organ abnormality (86% with at least 2 organs affected). There was evidence of fatty infiltration and/or fibroinflammatory changes in the liver (72% of patients), co-occurring with abnormality in pancreas (38%), spleen (44%), kidney (64%), and aorta (71%). High-risk non-alcoholic steatohepatitis (NASH) was significantly more prevalent in the obese ($p < 0.005$). Prevalence of low SMI and elevated pancreatic fat were associated with duration of T2D ($p < 0.05$). Aortic stiffness was significantly associated with organ steatosis ($p < 0.05$, Figure).

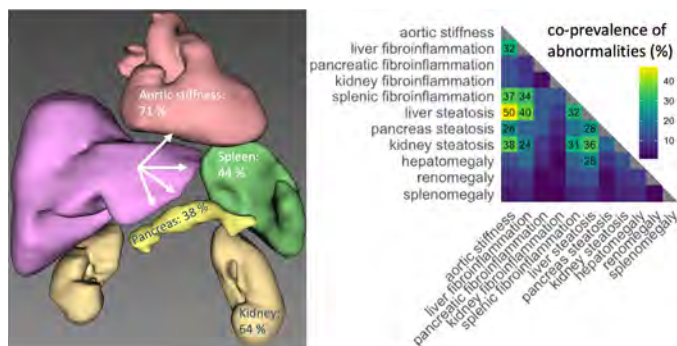


Figure: Left: Co-prevalence of organ abnormality in T2D patients with liver abnormality. Right: Co-prevalence of all abnormalities; pairs with co-prevalence exceeding the significance threshold for association indicated by numeric values.

Conclusion: Elevated levels of fat and fibroinflammation were highly prevalent in the liver, pancreas, spleen, and kidney with evidence of atherosclerosis and sarcopenia in most patients with T2D. The use of glucose-lowering therapies associated with weight loss, such as GLP-1 receptor agonists and SGLT2 inhibitors, are likely to have a beneficial effect on mobilising ectopic fat.

FRI074

Plasma TREM2, a novel non-invasive biomarker for diagnosis of NASH in NAFLD patients with elevated liver stiffness

Charlotte Wernberg^{1,2}, Vineesh Indira Chandran³, Mette Lauridsen², Frederik Larsen⁴, Maria Kløjgaard Skytthe³, Camilla Dalby Hansen¹, Majken Siersbæk⁴, Tina Di Caterino⁵, Sönke Detlefsen⁵, Yaseelan Palarasah³, Kim Ravnskjaer⁴, Lars Groentved⁴, Søren Kragh Møstrup³, Maja Thiele¹, Jonas Graversen³, Aleksander Krag¹. ¹Odense University Hospital, Centre for Liver Research, Department of Gastroenterology and Hepatology, Odense, Denmark; ²University Hospital of South Denmark, Department of Gastroenterology and Hepatology, Esbjerg, Denmark; ³Department of Molecular Medicine, Odense C; ⁴University of Southern Denmark, Department of Biochemistry and Molecular Biology, Odense, Denmark; ⁵Odense University Hospital, Department of Clinical Pathology, Odense, Denmark

Email: charlotte.wilhelmina.wernberg@rsyd.dk

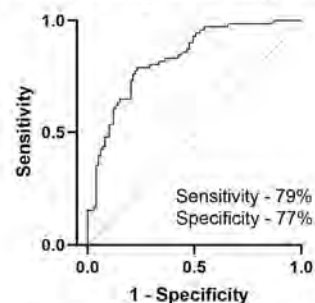
Background and aims: Non-invasive markers of non-alcoholic steatohepatitis (NASH) is still an unmet clinical need, but also represent a key barrier in NASH clinical trials. Here we investigate the diagnostic accuracy of soluble plasma Triggering Receptor Expressed on Myeloid cells 2 (plasma TREM2) as a circulating biomarker for NASH in patients with NAFLD and elevated liver stiffness.

Method: A cross-sectional design with a derivation ($n = 48$) and a validation cohort ($n = 170$) among patient with suspected NAFLD, a valid liver biopsy and liver stiffness measure (LSM) > 7.9 kPa, was

applied. Soluble TREM2 in plasma was measured by quantitative immunoassay. Since patients with low fibrosis score are not eligible for clinical trials, we excluded patients with LSM < 8.0 . At risk NASH was defined as patients with non-alcoholic fatty liver disease (NAFLD) activity score (NAS) ≥ 4 .

Results: Plasma TREM2 levels were significantly elevated in the derivation cohort in at-risk NASH patients with NAS ≥ 4 as compared with NAS < 4 subjects, with an area under the receiver operating characteristics curve (AUROC) 0.92 (95% CI: 0.84–0.99). Plasma TREM2 level was 2.1-fold increased in at-risk NASH patients and a strong diagnostic accuracy was confirmed in the validation cohort with an AUROC 0.83 (95% CI: 0.77–0.89, $p < 0.0001$). TREM2 level was associated with histologic features i.e., steatosis, lobular inflammation, and ballooning ($p < 0.0001$) but not fibrosis. Clinical cut-offs for rule-in and rule-out (90% sensitivity and 90% specificity) were settled and TREM2 values < 38 ng/ml was found to be the optimal rule-out cut-off (sensitivity 90%, specificity 51%) whereas TREM2 level > 65 ng/ml was the optimal rule-in cut off for at-risk NASH (sensitivity 89% and specificity 52%).

TREM2_noNASH vs NASH_validation cohort_NAS4_23092021



Area	0.8306
Std. Error	0.03105
95% confidence interval	0.7698 to 0.8915
P value	< 0.0001

Conclusion: Plasma TREM2 is a promising novel blood-based single biomarker that can rule out or rule in presence of NASH with high accuracy.

FRI075

Unbiased clustering of exhaled breath profiles in metabolic dysfunction-associated fatty liver disease identifies a patient phenotype at higher risk of disease progression

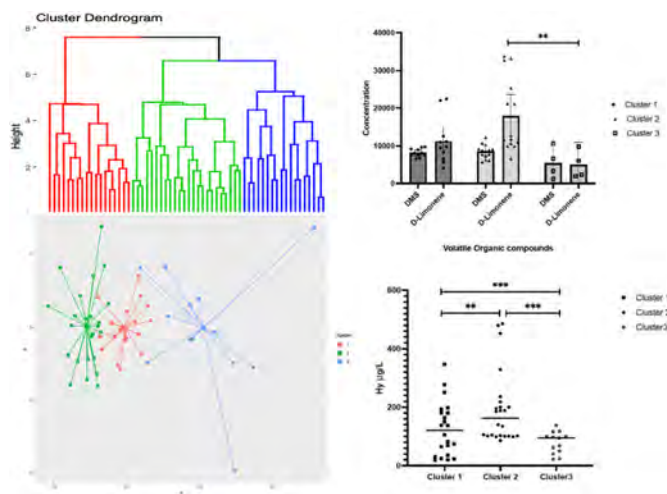
Rohit Sinha¹, Paul Brinkman², Khalida Ann Lockman¹, Alan Jaap³, Peter Hayes¹, John Plevris¹. ¹Hepatology Laboratory and Centre of Liver and Digestive Diseases, The University of Edinburgh, Edinburgh, United Kingdom; ²UMC Amsterdam, The Department of Respiratory Medicine, Amsterdam, Netherlands; ³Edinburgh Centre for Endocrinology & Diabetes, Royal Infirmary of Edinburgh, Edinburgh, United Kingdom
Email: rohit.sinha@nhs.net

Background and aims: Human breath contains numerous volatile compounds which reflect the metabolic activity. Electronic nose (eNose) technology can distinguish metabolic dysfunction-associated fatty liver disease (MAFLD) from healthy with reasonable confidence [1, 2]. We hypothesised breath prints obtained from eNose could identify patient subgroups at higher risk for progression within the MAFLD spectrum.

Method: The study was a prospective single-centre cohort study (ClinicalTrials.gov: NCT02950610). eNose is a custom-made device made up of five-sensor arrays, each containing four sensors, previously validated in respiratory and liver disease [1, 3]. eNose on the exhaled breath was performed on well characterised MAFLD patients ($n = 60$)-Child's A MAFLD cirrhotics ($n = 30$) and non-

cirrhotic MAFLD (n=30), previously described [1]. Data were analysed using R studio (v 2.3.2) and SPSS 21. An unbiased machine learning clustering technique was applied. First hierarchical ward clustering, combined with similarity profile analysis, was used to assess the number of significant cluster groups. Between-cluster comparisons and Games-Howell post hoc analyses of clinical variables at baseline were performed using the Kruskal-Wallis test for continuous data and the chi-square test for categorical data.

Results: Data reduction to 3 principal components (PCs) explained 97.8% of the total variance. Three groups of patients with MAFLD disease were delineated solely based on their exhaled breath profiles. Three clusters were identified; cluster 1 consists of 23 patients, cluster 2 consists of 24 patients, and cluster 3 consists of 13 patients. The clusters were comparable in clinical phenotyping. Cluster 2 was identified as a higher risk group with significant differences in serum hyaluronic acid levels ($p=0.001$), endoscopic evidence for portal hypertension ($p=0.003$) and exhaled breath concentration of dimethyl sulphide ($p=0.041$) and D-limonene ($p=0.015$).



Conclusion: This study shows that unbiased clustering of exhaled breath profiles captured using eNose technology identifies three phenotypes within the MAFLD spectrum. One of the three clusters included most patients with more advanced liver disease. These results warrant prospective studies on the potential of exhaled breath fingerprinting using eNose technology as point-of-care diagnostics in the surveillance of patients with established metabolic dysfunction-associated fatty liver disease.

FR1076

The pericellular basement of the hepatocytes is highly affected by bariatric surgery in obese patients with non-alcoholic fatty liver disease

Ida Lønsmann Lønsmann^{1,2}, Pierre Bel Lassen^{3,4}, Diana Leeming², Morten Karsdal², Mette Juul Nielsen², Karine Clément^{3,4}. ¹University of Southern Denmark, Faculty of Health Research, Odense, Denmark; ²Nordic Bioscience A/S, Biomarkers and Research, Herlev, Denmark; ³Sorbonne Université, INSERM, Paris, France; ⁴Assistance Publique Hôpitaux de Paris, Nutrition Department, Paris, France
Email: llc@nordicbio.com

Background and aims: Bariatric surgery decreases the severity of non-alcoholic fatty liver disease (NAFLD) in patients with severe obesity by improving liver histology and liver function tests. Nevertheless, there is a need for non-invasive biomarkers for monitoring treatment efficacy in NAFLD. The extracellular matrix (ECM) of the liver is subject to major changes during disease progression. The ECM basement membrane (BM) consists of mainly type IV collagen produced by hepatocytes. Changes in BM has been

associated with early liver injury, repair mechanisms and pericellular fibrosis. The aim of this study was to investigate changes in biomarkers targeting two distinct epitopes reflecting BM remodeling of type IV collagen (PRO-C4 and C4M) after bariatric surgery (BS) as well as in relation to baseline liver histology.

Method: 60 weight stable patients with severe obesity (BMI >35 kg/m²) were examined at baseline and 12 months after BS-induced weight loss. Liver biopsies were performed during BS. Serological levels of PRO-C4 and C4M were measured using competitive ELISAs and change from baseline to 12-months follow-up were evaluated using a linear mixed effect model adjusted for type of surgery. Linear regression models adjusted for age, sex, BMI and type 2 diabetes were used to evaluate the association of PRO-C4 and C4M with hepatocyte ballooning, steatosis, lobular inflammation and fibrosis at baseline.

Results: The cohort consisted of 56.7% females with a mean age of 46 and BMI of 49.0 kg/m². 66.7% of the patients were F2. Interestingly, baseline levels of both PRO-C4 and C4M decreased with increasing hepatocyte ballooning ($p<0.0001$) and PRO-C4 decreased with increasing lobular inflammation ($p=0.022$), while this association was borderline significant for C4M ($p=0.055$). No significant associations were observed for collagen type IV remodeling with liver steatosis or fibrosis at baseline. Furthermore, median PRO-C4 and C4M levels decreased significantly from baseline to 12-months post BS by 21% ($p=0.01$) and 14% ($p<0.001$), respectively.

Conclusion: Hepatocytes are embedded in the BM, and changes in hepatocyte health is reflected by remodeling of the adjacent ECM. This study shows that BM remodeling is associated with liver histopathology. Consequently, serological biomarkers of type IV collagen remodeling could be used as markers of treatment efficacy in NAFLD patients.

FR1077

A re-appraisal of the diagnostic performance of ultrasonography for fatty liver disease

Chul-min Lee¹, Eileen Yoon², Jonghyun Lee³, Mi Mi Kim¹, Bo-Kyeong Kang¹, Dae Won Jun², Hyunwoo Oh⁴, Hyo Young Lee⁴, Sang Bong Ahn⁵, Joo Hyun Sohn⁶, Huiyul Park⁷. ¹Hanyang University College of Medicine, Department of Radiology, Seoul, Korea, Rep. of South; ²Hanyang University College of Medicine, Department of Medicine, Seoul, Korea, Rep. of South; ³Hanyang University College of Engineering, Department of Medical and Digital Engineering, Seoul, Korea, Rep. of South; ⁴Uijeongbu Eulji Medical Center, Department of Medicine, Gyeonggi-do, Korea, Rep. of South; ⁵Nowon Eulji Medical Center, Eulji University School of Medicine, Department of Medicine, Seoul, Korea, Rep. of South; ⁶Hanyang University Guri Hospital, Department of Medicine, Gyeonggi-do, Korea, Rep. of South; ⁷Uijeongbu Eulji Medical Center, Department of Family Medicine, Gyeonggi-do, Korea, Rep. of South
Email: bluefish010@naver.com

Background and aims: Previous studies showed that ultrasonography (USG) has high specificity but low sensitivity for diagnosing fatty liver. Especially, the diagnostic performance of USG for mild fatty is low. We tried to re-appraisal the diagnostic performance of USG for fatty liver disease at this point.

Method: We performed a retrospective, multi-nation, multi-center, cross-sectional, and observational study. We included subjects who underwent both the USG and magnetic resonance proton density fat fraction (MR PDFF) within the six-month interval. The diagnostic performance of USG for fatty liver was evaluated as MR PDFF reference standard using sensitivity, specificity, positive and negative predictive value (PPV and NPV), diagnostic accuracy, and area under the receiver operating characteristics curve (AUC).

Results: We included a total of 5056 subjects in this study. The USG showed a sensitivity of 89.1%, specificity of 81.0%, and AUC of 0.850 for diagnosing any fatty liver (MR PDFF $\geq 6.5\%$). Furthermore, the sensitivity, specificity, and AUC of USG for diagnosing mild fatty liver ($6.5\% \leq \text{MR PDFF} \leq 14\%$) were 83.4%, 81.0%, and 0.822,

POSTER PRESENTATIONS

respectively. The mean hepatic fat contents on MR PDFF were significantly different according to the USG fatty liver grading ($p < 0.05$). There was acceptable inter-institution variability of USG for diagnosing fatty liver among six centers.

Conclusion: The USG showed good diagnostic performances for any fatty liver and mild fatty liver, higher than previously known.

FRI078

Cost utility analysis for screening for fibrotic NASH in the type 2 population from European countries

Mazen Nouredin¹, Manuel Romero Gomez^{2,3}, Calum Jones⁴, Kristen Shea⁵, Douglas T. Dieterich⁶, Jörn Schattenberg⁷, Emmanuel Tsochatzis^{8,9}, Elisabetta Bugianesi¹⁰, Vlad Ratziu¹¹.

¹Cedars-Sinai Medical Center, Division of Digestive and Liver Diseases, Department of Medicine, Los Angeles, United States; ²Virgen del Rocío University Hospital, Digestive Diseases Department, Seville, Spain;

³University of Seville, Institute of Biomedicine of Seville, Seville, Spain;

⁴Mtech Access, Bicester, Oxfordshire, United Kingdom; ⁵NASHNET, New York, United States; ⁶Icahn School of Medicine at Mount Sinai, New York, United States; ⁷University Medical Centre Mainz, Department of Medicine, Mainz, Germany; ⁸UCL Institute for Liver and Digestive Health, London, United Kingdom; ⁹Royal Free Hospital, London, United Kingdom; ¹⁰University of Torino, Division of Gastroenterology, Department of Medical Sciences, Torino, Italy; ¹¹Hospital Pitié Salpêtrière, Paris, France

Email: mazen.nouredin@cshs.org

Background and aims: The American Association for the Study of Liver Disease does not recommend screening for non-steatohepatitis (NASH) among patients with type 2 diabetes (T2DM) while the European Association of the liver (EASL) recommends screenings. Both organizations have called for cost effective analysis (CEA) which has been recently published from the US population. Our aim was to assess the value of screening for NASH with significant fibrosis (fibrotic NASH) in five separate European populations.

Method: We performed cost-utility analyses of four separate fibrotic-NASH screening strategies using third-party, public sector payer perspectives for five European countries, each for two separate hypothetical populations initially aged 55 years with either T2DM and fibrotic-NASH, or fibrotic-NASH and no T2DM, and compared it to the strategy of not screening these populations for fibrotic-NASH. Screening methods involved combinations of Fibrosis-4 (FIB-4) followed by Fibroscan® or liver biopsy for detecting fibrotic NASH indicated per recent EASL guidelines. An incremental cost-effectiveness ratio (ICER) of $\leq 50,000$ local currency units per incremental quality-adjusted life year was considered cost-effective.

Results: When screening T2DM+ fibrotic-NASH patients aged 55 years first with FIB-4 followed by Fibroscan®, and then treating detected fibrotic NASH patients with an intensive lifestyle intervention, this is shown to be a cost-effective strategy in all of the country-specific analyses when compared to not screening these patients (Figure 1). These outcomes hold steady both in the base case assessment and in the sensitivity analyses of the model. Screening approaches involving liver biopsy were found non cost-effective in all studied countries. The results have not changed when we assessed the analysis starting screening at age 40.

Treatment	Country	Incremental costs	Incremental utilities	Incremental cost effectiveness ratio (ICER)
ILI	UK*	£274	0.0177	£15,459
	Germany	€90	0.0177	€5,093
	Italy	-€82	0.0177	-€4,643
	France	€148	0.0177	€8,383
	Spain	€109	0.0177	€6,153

UK denotes England and Wales National Health Service (NHS)

Figure: Base case results when screening T2DM+ Fibrotic NASH patients aged 55 years

Conclusion: Screening for fibrotic-NASH in T2D persons over the age of 55 as well as younger patients (over 40 years) is cost effective in European countries. Given the increasing burden of NAFLD/NASH and the expected approved medications, we recommend screening patients with T2D for fibrotic-NASH in Europe.

FRI079

Free Light Chains as a potential biomarker of inflammation and fibrosis in non-alcoholic steatohepatitis

Antonio Liguori^{1,2}, Umberto Basile^{2,3}, Cecilia Napodano^{2,3}, Lidia Tomasello^{1,2}, Fabrizio Mancuso^{1,2}, Luca Di Galleonardo^{1,2}, Giuseppe Marrone^{1,2}, Marco Biolato^{1,2}, Antonio Gasbarrini^{1,2}, Gian Ludovico Rapaccini^{1,2}, Antonio Grieco^{1,2}, Luca Miele^{1,2}.

¹Fondazione Policlinico Universitario A. Gemelli, IRCCS, Dipartimento Scienze Mediche e Chirurgiche, Roma, Italy; ²Università Cattolica del Sacro Cuore, Roma, Italy; ³Fondazione Policlinico Universitario A. Gemelli, IRCCS, Dipartimento Scienze di laboratorio e infettivologiche, Roma, Italy

Email: lig.antonio91@gmail.com

Background and aims: Non-alcoholic fatty liver disease (NAFLD) is the most common chronic liver disease worldwide. Almost 20-30% of NAFLD patient develop steatohepatitis (NASH) characterized by hepatocyte ballooning, lobular inflammation and progressive fibrosis. Inflammation process in NASH is known to be associated with overexpression of pro-inflammatory biomarkers (IL1-beta, IL6, TNF-alfa).

Polyclonal free light chains (FLC) reflect B cell activation and could give insight into the activity of the adaptive immune system in a variety of inflammatory conditions. The aim of this study is to evaluate the potential role of FLC as biomarker of inflammation and fibrosis in NAFLD/NASH.

Method: We enrolled 187 patients with metabolic liver disease at Liver Outpatient clinic at Policlinico A. Gemelli: 48 with NAFLD, 85 with NASH and 54 with cirrhosis. Diagnosis of NASH was histologically assessed. Medical and pharmacological anamnesis, anthropometric measurements and laboratory tests (FLC included, lambda and kappa) were obtained for all patients.

Results: Total FLC (lambda + kappa) were significantly higher in patients with cirrhosis than in patients with NAFLD or NASH (125.2 vs 32.7 mg/L $p < 0.01$). Total FLC, lambda and kappa were higher in NASH patients than in NAFLD although non significantly (respectively 34.5 vs 32.4 mg/L $p = 0.2$, 15.0 vs 13.2 mg/L $p = 0.2$, 19.9 vs 19.1 mg/L $p = 0.8$). In patients with NASH, total FLC are higher in patients with advanced fibrosis ($F > 2$, 39.0 vs 30.3, $p = 0.03$). Total FLC are associated to advanced fibrosis independently from age, sex, BMI and diabetes (OR1.04, CI 1.00-1.08, $p = 0.04$).

Conclusion: In this study we highlight that FLC concentration is significantly higher in patients with cirrhosis than in patients with NAFLD or NASH. In NASH patients, advanced fibrosis is associated with higher serum concentration of total FLC. Serum FLC may represent a useful tool in grading and staging non-alcoholic fatty liver disease.

FRI080

12-week very low calorie diet in NAFLD induces rapid improvements in biomarkers of necro-apoptosis and fibrogenesis of a magnitude comparable to those seen in phase 2 drug trials

Jadine Scragg^{1,2,3,4}, Ida Villesen⁵, Diana Leeming⁵, Olivier Govaere⁶, Guy Taylor¹, Stuart Mcpherson^{2,6,7}, Kate Hallsworth^{2,6,7}, Morten Karsdal⁵, Quentin Anstee^{2,6,7}. ¹Newcastle University, Population Health Sciences, Newcastle upon Tyne, United Kingdom; ²Newcastle Upon Tyne Hospitals NHS Foundation, Newcastle NIHR Biomedical Research Centre, Newcastle upon Tyne, United Kingdom; ³University of Oxford, Nuffield Department of Primary Care Health Sciences, Oxford, United Kingdom; ⁴University of Oxford, NIHR Oxford Biomedical Research Centre, Oxford, United Kingdom; ⁵Nordic Bioscience Biomarkers and Research A/S, Herlev, Denmark; ⁶Newcastle University, Translational and Clinical Research Institute, Newcastle upon Tyne, United Kingdom; ⁷Newcastle Upon Tyne Hospitals NHS Foundation Trust, Liver Unit, Newcastle upon Tyne, United Kingdom
Email: jadine.scragg@phc.ox.ac.uk

Background and aims: Nonalcoholic fatty liver disease (NAFLD) is associated with inflammation and hepatocellular death, leading to activation of fibroblasts and progressive hepatic fibrosis-the single most important factor determining liver-related clinical outcomes and mortality. A range of non-invasive biomarker tests (NITs) are used in drug trials to measure biological response to therapy including routine biochemistry (ALT, AST), markers of necrosis/apoptosis (CK18-M65), and fibrosis (ELF, PRO-C3, and Fibroscan (VCTE)). Although sustained weight loss >10% has been shown to improve histological fibrosis, little is known about its acute effects on NITs.

Method: 26 non-cirrhotic NAFLD patients were prescribed a 12-week very low calorie diet (VLCD) (800kcal/day). Fasted blood samples were taken at weeks 0, 1, 3, 5, 7, 9 and 12 and VCTE measured at weeks 0 and 12. Routine labs as well as hyaluronic acid (HA), TIMP-1, PIINP, PRO-C3, PRO-C4, PRO-C5, CK18-M65 were serially measured and ELF, ADAPT and FIB4 scores calculated. Patients were stratified by weight loss at 12 weeks into <5%, 5–7% and >7% of initial body weight and NIT change from baseline assessed.

Results: After 12-weeks VLCD, 4 patients had lost <5%, 4 had lost 5–7% weight and 18 had lost >7% body weight. No significant difference in NIT values were evident between weight loss groups at baseline. Rapid reductions in multiple collagen biomarkers were apparent after a week of VLCD. At 12-weeks, significant reductions in ELF (ANOVA $p = 0.040$, -5.3 ± 1.8 at >7% weight loss), driven by PIINP (ANOVA $p = 0.004$, -23.7 ± 3.9 at >7% weight loss), and CK18-M65 (ANOVA $p = 0.023$, -43.5 ± 7.6 at >7% weight loss) were seen in patients who lost >7% weight. Similar trends were observed in ALT, AST, PRO-C3, and ADAPT but no difference was seen in FIB4 or VCTE.

Variable	Weight loss group	Baseline NIT value	Significance between baseline NIT values, by weight loss grouping	Percentage change in NIT	Significance of % NIT change from baseline, by weight loss grouping
ELF	<5%	9.4±0.4	0.579	-3.4±2.2	0.040*
	5–7%	9.5±0.2		-2.8±2.5	
	>7%	9.8±0.2		-5.3±1.8*	
PIINP (ng/ml)	<5%	9.7±1.7	0.787	-14.4±17.4	0.004*
	5–7%	9.8±1.3		-3.6±5.6	
	>7%	10.9±1.0		-23.7±3.9*	
TIMP (ng/ml)	<5%	263.1±11.8	0.941	-4.6±6.9	0.463
	5–7%	260.4±45.4		-8.2±3.5	
	>7%	272.1±17.1		-11.4±2.3	
HA (ng/ml)	<5%	67.2±38.6	0.638	-23.5±12.1	0.232
	5–7%	57.6±10.6		-38.5±29.4	
	>7%	105.6±28.3		-39.8±16.9	
ADAPT	<5%	4.9±0.4	0.190	-6.1±8.4	0.458
	5–7%	5.3±0.6		-10.8±6.0	
	>7%	6.1±0.3		-13.9±2.4	
PRO-C3 (ng/ml)	<5%	11.8±2.6	0.666	-10.6±15.4	0.268
	5–7%	11.6±1.6		-24.5±11.7	
	>7%	13.4±1.1		-27.9±3.4	
M65 (IU/l)	<5%	319.4±153.1	0.159	4.6±10.9	0.023*
	5–7%	203.1±35.9		-4.8±6.3	
	>7%	568.0±96.8		-43.5±7.6*	

Conclusion: A 12-week VLCD intervention induced significant weight loss of a level reported to reduce hepatic fibrosis if sustained.

Rapid changes in NITs were observed within a week of commencing VLCD. Significant weight-loss associated improvements in markers of NASH-associated necrosis/apoptosis (CK18-M65), and some but not all markers of fibrogenesis (PIINP, ELF) were present at week-12. These were of a magnitude similar to those reported in Phase 2 drug trials. Changes occurred too rapidly to reflect a drop in hepatic fibrosis stage, suggesting that NITs are sensitive to changes in disease activity and fibrogenesis that precede fibrosis resolution.

FRI081

Signature of circulating hepatic proteins detects fibrosing-steatohepatitis in progressive non-alcoholic fatty liver disease

Olivier Govaere¹, Megan Hasoon², Leigh Alexander³, Simon Cockell², Dina Tiniakos¹, Jerome Boursier⁴, Elisabetta Bugianesi⁵, Vlad Ratziu⁶, Ann K. Daly¹, Quentin Anstee¹. ¹Newcastle University, Translational and Clinical Research Institute, Faculty of Medical Sciences, United Kingdom; ²Newcastle University, Bioinformatics Support Unit, Faculty of Medical Sciences, United Kingdom; ³SomaLogic, Inc., United States; ⁴Angers University Hospital, Hepatology Department, France; ⁵University of Turin, Department of Medical Sciences, Division of Gastro-Hepatology, A. O. Città della Salute e della Scienza di Torino, Italy; ⁶Sorbonne University, Assistance Publique-Hôpitaux de Paris, Hôpital Pitié Salpêtrière, France
Email: olivier.govaere@ncl.ac.uk

Background and aims: Non-alcoholic fatty liver disease (NAFLD) is considered as the hepatic manifestation of the metabolic syndrome and changes in circulating blood proteins have been associated with advanced NAFLD. Yet, it is still unclear which proteins originate from the liver and how these alter during disease progression.

Method: The cohort comprised 256 patients from the European NAFLD Registry with histologically proven NAFLD identified at four specialist centres. The histological semi-quantitative NASH CRN system was used to score the biopsies. 191 plasma and 65 serum samples were processed for proteomics analysis using the SomaScan™ platform. In a subset of 51 cases, snap-frozen liver biopsies underwent high-throughput RNA sequencing (RNAseq). Integrative analysis of these data with publicly available single-cell RNAseq data was used to identify cell of origin. Binary logistic modelling was implemented to predict disease activity.

Results: Comparing patients with advanced fibrosis (F3–4) to mild disease (F0–2) in the discovery cohort of 191 plasma samples identified 156 differentially expressed proteins, while stratifying based on a NAFLD Activity Score (NAS) ≥ 4 identified 79 proteins. Of these, 34 proteins were common to both analyses, including AKR1B10, APOF, THBS2 and TREM2. To determine which proteins originate from the liver, we performed a correlation analysis between plasma proteins identified by the F3–4/NAS ≥ 4 analyses and mRNA within 51 patients, finding 40 proteins/mRNAs reaching the significance threshold. Deconvolution by single-cell RNAseq data indicated the different hepatic cellular changes during disease progression, such as AKR1B10, APOF and GDF15 to originate from epithelial cells, ADAMTSL2 and THBS2 from fibroblasts and TREM2 from macrophages. Finally, to assess potential utility within a non-invasive diagnostic pathway to detect fibrosing-steatohepatitis defined as the presence of NASH, NAS ≥ 4 and F ≥ 2 , we performed logistic regression analysis. Backward elimination of variables identified a composite model that could predict NASH+NAS ≥ 4 +F ≥ 2 with an Area Under the Curve of 0.878 based on markers including circulating ADAMTSL2, AKR1B10, CFHR4 and TREM2. Performance of the model was validated in a cohort of 65 serum samples with an AUC = 0.851 compared to 0.678 for the FIB4 score.

Conclusion: We showed that circulating proteomic changes reflect grade of steatohepatitis and stage of fibrosis that may be used to assess disease severity.

FRI082

Peripheral blood mononuclear cells mitochondrial copy number and adenosine triphosphate inhibition test in non-alcoholic fatty liver disease

Eileen Yoon¹, Dae Won Jun¹, Sang Bong Ahn², Huiyul Park³, Hyo Young Lee⁴, Hyunwoo Oh⁴, Chul-min Lee⁵, Mi Mi Kim⁵, Bo-Kyeong Kang⁵, Joo Hyun Sohn⁶. ¹Hanyang University College of Medicine, Department of Medicine, Seoul, Korea, Rep. of South; ²Nowon Eulji Medical Center, Eulji University School of Medicine, Department of Medicine, Seoul, Korea, Rep. of South; ³UiJeongbu Eulji Medical Center, Department of Family Medicine, Gyeonggi-do, Korea, Rep. of South; ⁴UiJeongbu Eulji Medical Center, Department of Medicine, Gyeonggi-do, Korea, Rep. of South; ⁵Hanyang University College of Medicine, Department of Radiology, Seoul, Korea, Rep. of South; ⁶Hanyang University Guri Hospital, Hanyang University College of Medicine, Department of Medicine, Gyeonggi-do, Korea, Rep. of South
Email: noshin@hanyang.ac.kr

Background and aims: Non-alcoholic fatty liver disease (NAFLD) is known to be associated with mitochondrial dysfunction. The purpose of this study was to develop biomarkers for the assessment of mitochondrial dysfunction in patients with NAFLD.

Method: Mitochondrion-associated transcriptome analysis was performed from the NAFLD and healthy control liver. Peripheral blood mononuclear cells obtained from 88 patients with NAFLD and healthy controls were used to measure mitochondrial DNA (mtDNA) copy number. Mitochondrial inhibition substrate test (ATP assay) was performed in HepG2 cells using patients' serum. Cellular ATP concentration was measured in patient serum was applied at the same quantity as the media.

Results: Hepatic mRNA transcriptome analysis showed that patients with NAFLD exhibited upregulated expression of genes related to mitochondrial tricarboxylic acid (TCA) cycle (E2F1, E2F2, and ORC6) and those related to the mitochondrial envelope (E2F1, MAPK4, and CYP2K6) compared to healthy controls. Gene set enrichment analysis revealed upregulated expression of genes related to the pathways of TCA cycle and DNA replication in patients with NAFLD as compared to that in healthy controls. The mtDNA copy number in the peripheral blood mononuclear cells was 1.28-fold lower in patients with NAFLD than in healthy controls ($p < 0.0001$). Cellular adenosine triphosphate (ATP) concentration decreased 1.2-fold times in NAFLD patients than in healthy controls ($p < 0.0001$). The mtDNA copy number and ATP inhibition test showed negative correlation with degree of hepatic steatosis. And ATP concentration showed positive correlation with mtDNA copy number.

Conclusion: Peripheral blood mononuclear cells mitochondrial copy number and ATP inhibition test can be used biomarkers for the assessment of mitochondrial dysfunction in patients with NAFLD.

FRI083

Comparison of diagnostic performance between FIB-4 and NFS in metabolic-associated fatty liver disease era

Dae Won Jun¹, Eileen Yoon¹, Sang Bong Ahn², Huiyul Park³, Hyo Young Lee⁴, Hyunwoo Oh⁴, Joo Hyun Sohn⁵, Bo-Kyeong Kang⁶, Mi Mi Kim⁶, Chul-min Lee⁶. ¹Hanyang University College of Medicine, Department of Medicine, Seoul, Korea, Rep. of South; ²Nowon Eulji Medical Center, Eulji University School of Medicine, Department of Medicine, Seoul, Korea, Rep. of South; ³UiJeongbu Eulji Medical Center, Department of Family Medicine, Gyeonggi-do, Korea, Rep. of South; ⁴UiJeongbu Eulji Medical Center, Department of Medicine, Gyeonggi-do, Korea, Rep. of South; ⁵Hanyang University Guri Hospital, Hanyang University College of Medicine, Department of Medicine, Gyeonggi-do, Korea, Rep. of South; ⁶Hanyang University College of Medicine, Department of Radiology, Seoul, Korea, Rep. of South
Email: sonjh@hanyang.ac.kr

Background and aims: Fibrosis-4 index (FIB-4) and non-alcoholic fatty liver disease (NAFLD) fibrosis score (NFS) are the two most widely used non-invasive tools for screening of advanced fibrosis in

subjects with NAFLD. Since metabolic dysfunction-associated fatty liver disease (MAFLD) has been proposed as a new category of fatty liver disease, we aimed to compare the diagnostic performance of FIB-4 and NFS in subjects with MAFLD and in various subgroups.

Method: This study was designed as cross-sectional study. Data from 6, 775 subjects who underwent magnetic resonance elastography (MRE) and abdominal ultrasonography at the same time during a health check-up at 13 various health check-up centers were retrospectively reviewed. Advanced fibrosis was defined as an MRE value of ≥ 3.6 kPa.

Results: The area under the receiver operating characteristic curves (AUROCs) of FIB-4 and NFS for diagnosing advanced fibrosis were similar in subjects with MAFLD. However, the AUROC of NFS was lower than that of FIB-4 in the diabetic subgroup of MAFLD (0.809 in FIB-4 vs. 0.717 in NFS, $p = 0.002$). The performances of both FIB-4 and NFS were poor in the subgroup of MAFLD with significant alcohol intake.

Conclusion: The overall diagnostic performance of FIB-4 and NFS for diagnosing advanced fibrosis did not differ among subjects with MAFLD. However, the performance of NFS was lower in the diabetes subgroup of MAFLD. The diagnostic performance of FIB-4 was better for fibrosis in various subgroups of MAFLD.

FRI084

Assessing the applicability of non-invasive diagnostic tests (NITs) in non-alcoholic fatty liver disease: an international qualitative study

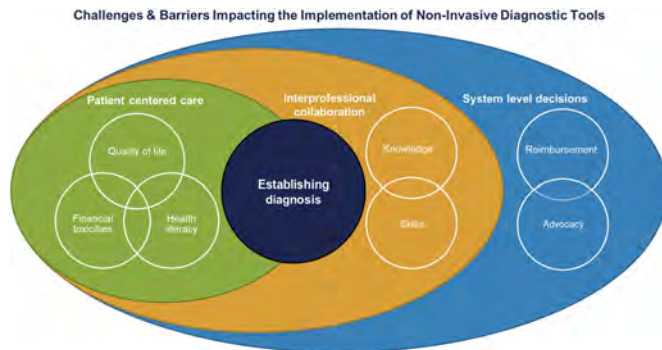
Maja Thiele¹, Sophie Péloquin², Luca Valenti³, Patrice Lazure⁴, Mounia Heddad Masson⁵, Alina Allen⁶, Jeffrey Lazarus⁷, Mazen Nouredin⁸, Mary Rinella⁹, Frank Tacke¹⁰, Suzanne Murray², Emmanuel Tsochatzis¹¹. ¹Center for Liver Research, Odense University Hospital and University of Southern Denmark, Odense, Denmark; ²AXDEV Group Inc., Canada; ³Università degli Studi di Milano, Fondazione IRCCS Ca' Granda Ospedale Maggiore Policlinico, Milan, Italy; ⁴AXDEV Group Inc.; ⁵EASL, Geneva, Switzerland; ⁶Mayo Clinic, Rochester, MN, United States; ⁷Barcelona Institute for Global Health (ISGlobal), Hospital Clinic, University of Barcelona, Barcelona, Spain; ⁸Cedars Sinai Medical Center, Los Angeles, CA, United States; ⁹Northwestern University Feinberg School of Medicine, Chicago, IL, United States; ¹⁰Charité Universitätsmedizin Berlin, Dept. of Hepatology and Gastroenterology, Berlin, Germany; ¹¹UCL Institute for Liver and Digestive Health, Royal Free Hospital and UCL, London, United Kingdom
Email: lazurep@axdevgroup.com

Background and aims: The use of non-invasive tests (NITs) in the field of non-alcoholic fatty liver disease (NAFLD), non-alcoholic steatohepatitis (NASH), and advanced fibrosis has the potential to improve patient care by simplifying the diagnostic process, providing comprehensive data, and reducing the need for biopsies. We assessed the challenges to implementation of NITs in Germany, Italy, the United Kingdom, and the United States.

Method: We conducted a two-phase qualitative assessment consisting of interviews ($n = 29$) followed by an expert workgroup discussion ($n = 8$). Interviews allowed for exploration of challenges with diabetologists, hepatologists, primary care providers (PCPs), patient advocates, clinical/basic researchers, and healthcare administrators/payers. The expert working group discussion included internationally recognized clinicians and researchers in NAFLD and liver fibrosis from the four selected countries. They were asked to review, validate, and expand on the identified challenges and collaboratively discuss potential solutions. Transcripts from both phases were analyzed thematically.

Results: The main challenges related to the implementation of NITs are shown in Figure 1. First, we identified a lack of awareness about NITs and the importance of early detection of NAFLD, NASH, and advanced fibrosis among PCPs and diabetologists. Second, respondents described a need for NITs with more specificity and for their automation to build effective and efficient referral pathways. Some

first phase participants reported that, in the absence of available therapeutic agents, there was no need for novel diagnostic tools. In the opinion of experts, more effort should be made to demonstrate the impact of early diagnosis through NITs. This would help in enhancing patient motivation for improved metabolic health, slowing or halting disease progression and establishing surveillance for the timely detection or prevention of liver related complications. Liver disease was reported to be of low priority among non-hepatologists. This challenge is unlikely to change unless the cost-effectiveness of the more costly NITs and their impact on patient outcomes can be demonstrated.



Conclusion: The results of this qualitative study should inform the development of awareness campaigns and targeted educational interventions focused on diagnosis and risk stratification with NITs. This will facilitate early diagnosis and care and help to raise NAFLD as a public health issue.

FRI085

Evaluation of the performance of a novel digital pathology method for the continuous quantification of steatosis, ballooning and inflammation in liver biopsies and its correlation with NASH-CRN scores in patients with NASH

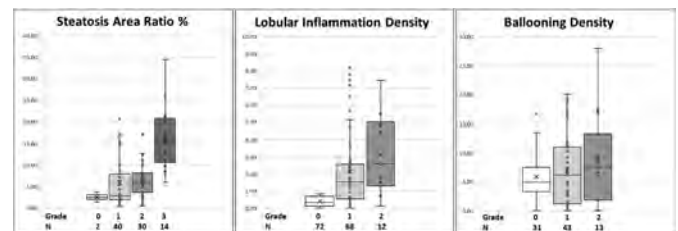
Louis Petitjean¹, Li Chen^{1,2}, Aras Mattis³, Mojgan Hosseini⁴, Michael Goedken⁵, Cynthia Behling⁴, Arun Sanyal⁶, Mathieu Petitjean¹. ¹PharmaNest, Princeton, United States; ²PharmaNest Inc, Princeton, United States; ³University of California San Francisco, San Francisco, United States; ⁴University of California San Diego, La Jolla, United States; ⁵Rutgers University, New Brunswick, United States; ⁶Virginia Commonwealth University, Richmond, United States
Email: mathieu.petitjean@pharmanest.com

Background and aims: We have previously shown that the Phenotypic Fibrosis Composite Score calculated by the FibroNest Quantitative Image analysis and AI methods correlate with the NASH-CRN histological fibrosis stages and steatosis grades established from collagen-stained histology slides. Here, we report the performance of the FibroNest method to quantify Ballooning, Inflammation and Steatosis from digital images of H&E human liver biopsy sections.

Method: This retrospective study comprised a cohort of 87 patients with NASH diagnosed by histologic assessment of liver biopsy according to NASH-CRN criteria with Lobular Inflammation grades of 0 (N = 7), 1 (68), and 2 (12), hepatocyte ballooning grades of 0 (N = 31), 1 (43) and 2 (13), and steatosis grades of 0 (N = 2), 1 (40), 2 (30) and 3 (14). Formalin-fixed, paraffin embedded biopsy sections were H&E stained and imaged with an Operio CS2 scanner at 20X in white light. Quantitative image analysis was performed by FibroNest™ to extract individual features of inflammation (stained nuclei) and tissue texture quantitative layers from the calibrated and normalized images. A subset of 21 representative images was used to develop a machine learning (ML) predictive model using 2.3 K annotations for lobular inflammation, 5.62 K for portal and periportal inflammation,

1.41 for "false" lobular inflammation such as isolated ducts or microscopic necrosis, 1.08 for ballooning and 787 for balloon mimics made by 4 hepatopathologists familiar with the NAS scoring system. The predictive ML model established topographical probability maps for lobular, total inflammation, and hepatocellular ballooning. Confidence thresholds are defined to identify histological features of interest, which are then quantified by several continuous and normalized parameters (biopsy area ration, density count, and 200XFOV normalized count).

Results: The Lobular Inflammation composite score exhibits moderate correlation with the histological grades. Significant disagreement in the assessment of grade 1 lobular inflammation is driven by "confusion" with portal inflammatory features which degrades the specificity between grades 1 and 2 (p = 0.187). The mean values of the Ballooning Density correlate with the histological assessment, but p-values between grades are poor. The mediocre performance of the ML model is driven by the lack of agreement in the annotations provided by pathologists. The steatosis proportion area is in fair agreement with steatosis grades. Disagreement is driven by the fact that the NASH-CRN criteria is based on percent hepatocytes with fat rather than fat area ratio (in full tissue area).



Conclusion: As reported by other teams, liver biopsy Digital Pathology methods based on supervised ML and annotation provided by pathologists (H&E stains, Inflammation, Ballooning) result in continuous quantification methods of moderate performance.

FRI086

Can combination of M2BPGi and APRI help endocrinologists refer patients with advanced hepatic fibrosis to hepatologists?

Mi Mi Kim¹, Bo-Kyeong Kang¹, Chul-min Lee¹, Huiyul Park², Hyo Young Lee³, Hyunwoo Oh³, Sang Bong Ahn⁴, Dae Won Jun⁵, Eileen Yoon⁵, Joo Hyun Sohn⁶. ¹Hanyang University College of Medicine, Department of Radiology, Seoul, Korea, Rep. of South; ²Uijeongbu Eulji Medical Center, Department of Family Medicine, Gyeonggi-do, Korea, Rep. of South; ³Uijeongbu Eulji Medical Center, Department of Medicine, Gyeonggi-do, Korea, Rep. of South; ⁴Nowon Eulji Medical Center, Eulji University School of Medicine, Department of Medicine, Seoul, Korea, Rep. of South; ⁵Hanyang University College of Medicine, Department of Medicine, Seoul, Korea, Rep. of South; ⁶Hanyang University Guri Hospital, Hanyang University College of Medicine, Department of Medicine, Gyeonggi-do, Korea, Rep. of South
Email: mshbogi@naver.com

Background and aims: Although the non-invasive tests (NITs, ex. FIB-4, NAFLD fibrosis score (NFS), AST to platelet ratio index (APRI)) are widely used to diagnose advanced hepatic fibrosis, there is a considerable intermediate zone and diagnostic performance decreased in diabetes subjects. The purpose of this study is to figure out whether combination of M2BPGi with various NITs can help endocrinologist screening for advanced hepatic fibrosis in clinic.

Method: A total of 1,129 subjects visiting endocrinology clinic of tertiary hospital and performed M2BPGi were included (mean age: 53.7 ± 14.8 years). NFS, FIB-4, and APRI were calculated for all subjects. Advanced fibrosis was defined by transient elastography (TE ≥ 8.0 kPa). Sensitivity analysis was also performed.

Results: This study included 426 (37.7%) were diabetes and 703 (62.3%) were non-diabetes who visited the endocrinology

POSTER PRESENTATIONS

department. Mean age was 53.7 ± 14.8 years. Diagnostic performance of predicting advanced hepatic fibrosis was highest in APRI (the area under the receiver operating characteristics curve (AUROC) = 0.811), followed by M2BPGi (0.720) and FIB-4 (0.718). M2BPGi at a cutoff of 0.8 showed similar diagnostic performance to lower cutoff of other NITs (sensitivity: 72.9% in M2BPGi vs. 77.4–82.8% in other NITs; specificity: 57.3% vs. 43.1–65.9%). Diagnostic performance of APRI in diabetes was comparable to non-diabetes group (0.832 vs. 0.811, $P = 0.393$). When the combination of M2BPGi (cutoff of 0.8) and APRI (cutoff of 0.5 and 1.5), the sensitivity and specificity for advanced hepatic fibrosis were 67.4% and 80.4% in endocrinology clinic and 68.9% and 79.2% in diabetic subjects, respectively.

Conclusion: Combination of M2BPGi and APRI can help screening for advanced hepatic fibrosis in endocrinology clinic.

FRI087

The relationship between foetal head circumference growth trajectories and nonalcoholic fatty liver disease in adolescents

Jeffrey Lee¹, Ashish Yadav², Trevor Mori², Rae-Chi Huang³, Leon Adams⁴, Lawrence J. Beilin², Elizabeth McKinnon³, John Olynyk¹, Oyekoya Ayonrinde¹. ¹Fiona Stanley Hospital; ²The University of Western Australia; ³Telethon Kids Institute; ⁴Sir Charles Gairdner Hospital

Email: jeffreylee18@gmail.com

Background and aims: Intrauterine and childhood factors are associated with nonalcoholic fatty liver disease (NAFLD) in adolescents and adults. Previous studies have associated intrauterine growth restriction (IUGR), small for gestational age (SGA) and intrauterine exposures such as smoking in pregnancy, and gestational weight gain, with NAFLD in offspring. Maternal factors and intrauterine influences determine foetal growth patterns and birth weight. Serially measured foetal head circumference (HC) provide a useful measure of foetal growth patterns and IUGR. We aimed to examine associations between foetal HC growth trajectories and subsequent NAFLD during adolescence.

Method: Repeated antenatal ultrasound with foetal morphometry was measured in 1440 pregnant women (Gen1) in the Raine Study, between 16 weeks gestation and delivery. Using standard deviation scores or z-scores for the HC measurements, five foetal HC trajectories were developed (Figure 1). Offspring (Gen2) birth weight was recorded and IUGR, SGA and large for gestational age (LGA) were determined for the live-born neonates. As part of the 17-year follow up of the Gen2 cohort, lifestyle questionnaires, anthropometry, blood tests and liver ultrasound, were performed. A subset of 576 adolescents had both liver ultrasound and foetal ultrasound HC trajectories data.

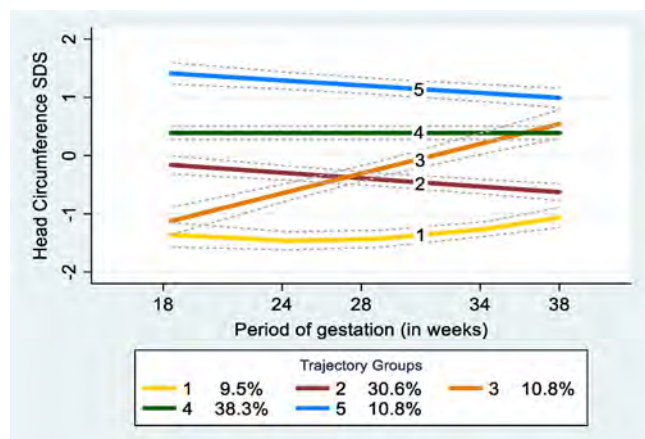


Figure: Head Circumference trajectory groups: 1 Low-stable, 2 Average-falling, 3 Low-rising, 4 Average-stable, 5 High-stable. SDS-standard deviation scores, Dotted lines represent 95% confidence intervals, Percentages represent individual group membership.

Results: NAFLD was diagnosed in 92 of 576 (16%) adolescents (52% male). Adolescents with NAFLD had higher body mass index (BMI), waist circumference, suprailiac skinfold thickness, alanine aminotransferase (ALT), gamma glutamyl transpeptidase, triglycerides, total and low density lipoprotein cholesterol, leptin and Homeostasis Model Assessment for Insulin Resistance (HOMA-IR), but lower high density lipoprotein cholesterol and adiponectin levels compared with those without NAFLD ($p < 0.05$ for all). Birth weight, gestational age, IUGR, SGA and LGA were not associated with NAFLD. Using multivariable logistic regression analysis, low-stable HC trajectory group 1 (OR 3.54; 95% CI, 1.21–10.35, $p = 0.02$), suprailiac skinfold thickness (OR 1.09, 95% CI 1.05–1.13, $p < 0.001$), ALT (OR 1.03, 95% CI 1.01–1.06, $p = 0.02$) and leptin (OR 1.03, 95% CI 1.02–1.05, $p = 0.001$) were associated with NAFLD.

Conclusion: The low-stable HC trajectory associated with a persisting small HC through pregnancy, but not birth characteristics, was associated with increased risk of subsequent NAFLD in adolescents. The association of a low foetal HC trajectory with NAFLD in adolescence supports the Developmental Origins of Health and Disease (DOHaD) hypothesis linking early life events with subsequent disease.

FRI088

Liver stiffness assessed by transient elastography predicts clinical events in patients with T2DM and NAFLD

Jesús Rivera¹, Monica Pons¹, Alejandra Planas², Rafael Simo Canonge², Jordi Bañeras³, Ignacio Ferreira³, Joan Genesca¹, Juan Manuel Pericàs¹. ¹Vall d'Hebron Hospital Universitari, Liver Unit, Barcelona, Spain; ²Vall d'Hebron Hospital Universitari, Diabetes and Metabolism Research Unit, Spain; ³Vall d'Hebron Hospital Universitari, Cardiology Department, Spain

Email: jesusriveraest@gmail.com

Background and aims: Non-alcoholic fatty liver disease (NAFLD) and type 2 diabetes (T2DM) are intimately related entities. T2DM is a major predictor of cardiovascular events (CVE) in NAFLD patients, whereas the role of NAFLD on CVE in T2DM as well as the impact of T2DM on liver-related events (LRE) in NAFLD remain poorly known. The aim of this study was to evaluate the role of NAFLD on the onset of clinical outcomes among T2DM patients.

Method: Prospective cohort with case-control analysis comprising 200 T2DM subjects with no history of CV disease (CVD) and 60 non-diabetic subjects matched by age with available transient elastography (TE) data. Patients were selected from the Outpatient Diabetes Clinic of Vall d'Hebron Hospital and the Primary Healthcare centres within its catchment area (North Barcelona). Overall clinical events (CE) were composed by CVE (coronary, cerebrovascular or peripheral arteriopathy), LRE (liver decompensation or hepatocellular carcinoma) and all-cause mortality. NAFLD was defined as Controlled Attenuation Parameter (CAP) ≥ 275 dB/m and/or Fatty liver index (FLI) ≥ 60 after exclusion of the other liver diseases and alcohol consumption over 30 gr/day in males and 20 gr/day in females. A value of coronary arterial calcium score (CACs) ≥ 400 Agatston units (AU) was considered indicative of high risk of CVD. Cox regression analysis to predict CE was performed.

Results: Overall, 34 (18.2%) T2DM patients presented any CE vs 4 (7.0%) controls ($p = 0.042$) during a median follow-up of 5.6 years. Among patients with T2DM and NAFLD ($n = 134$), 21 (28.4%) CVE were reported, being coronary events the most frequent outcome (11/134; 8.2%). One subject (0.7%) presented LRE and 8 (6%) patients died, 25% of which due to CVD and 37.5% each for malignancy and infectious diseases. T2DM-NAFLD patients with CE showed higher rates of diabetes complications (42.9% vs 22.1%; $p = 0.04$ and 61.9% vs 34.2%; $p = 0.017$ for diabetic retinopathy and nephropathy, respectively), high-risk CVD (CACs ≥ 400 52.6% vs 19.3%, $p = 0.002$) and higher median liver stiffness (6.7 vs 5.4 kPa, $p = 0.007$) than those without CE. No differences were found between groups in terms of T2DM control (fasting glucose; HbA1c) or metabolic syndrome determinants rates

(high blood pressure or obesity). In Cox analysis, development of clinical events among T2DM-NAFLD patients was associated with a higher liver stiffness (HR = 1.05; 95%CI 1.01–1.09, p 0.003) and male gender HR = 4.02; 95%CI 1.29–12.50, p 0.016). No statistical association was found for diabetes complications or CACs ≥ 400 .

Cox regression analysis			
	Hazard Ratio	95% CI	p
Liver stiffness	1.05	1.01-1.09	0.003
Male gender	4.02	1.29-12.50	0.016
Age	1.08	0.99-1.19	0.07
CAC ≥ 400 AU	0.42	0.14-1.19	0.10
Diabetic nephropathy	0.41	0.15-1.11	0.82
Diabetic retinopathy	0.46	0.17-1.24	0.12

Conclusion: Our results suggest that severity of NAFLD is associated with clinical events in patients with T2DM independently of CV disease or T2DM complications. TE might help stratifying T2DM patients with NAFLD at higher risk of developing clinical events and therefore shall be recommended in all T2DM patients.

FRI089

Repeated noninvasive liver biopsy surrogate LIVERFast correlates with BMI and liver enzyme improvements

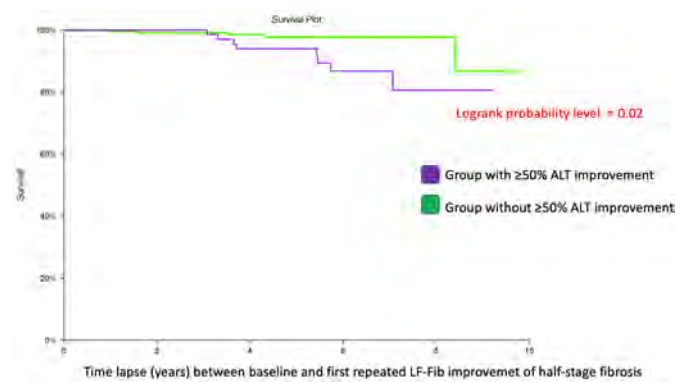
Marie Decraecker¹, Hiriart Jean-Baptiste¹, Marie Irles-Depe¹, Faiza Chermak¹, Juliette Foucher¹, Victor de Lédighen¹. ¹CHU BORDEAUX, Pessac, France
Email: marie.decraecker@gmail.com

Background and aims: MAFLD-related morbi-mortality is increasing worldwide due to epidemics of obesity and type 2 diabetes (T2D). LIVERFast (LF, Fibronostics, US) is a new point-of-care proprietary technology to assess quantitatively (score from 0.00 to 1.00) liver fibrosis (LF-Fib) in MAFLD pts, with prognostic value for liver-related events and overall mortality (Hepatology Suppl.2021). To assess repeated LF-Fib performance for liver fibrosis regression rate (LFR) reflected with significant improvement in clinical endpoints, body mass index BMI $\geq 10\%$ and liver enzymes ALT $\geq 50\%$ from baseline.

Method: Pts with repeated LF-Fib were prospectively included. Significant improvements in clinical endpoints were: BMI decrease of $\geq 10\%$ and ALT decrease $\geq 50\%$ from baseline. Half fibrosis stage improvement was considered with each 0.15 of LF-Fib score. Statistics were descriptive and FPR time dependent using hazard ratios HR (95%CI).

Results: 500 MAFLD patients from a tertiary center were pre-included with LF-Fib at baseline and 401 were included with at least one repeated LF-Fib during follow up; 87 pts had 7 repeated LF-Fib during 9.9 years follow up. 44.3% were female, median (range) age 56 (21–77) yrs, distribution of fibrosis 45%F0, 29%F1, 6%F2, 12%F3 and 8% F4, respectively. 13/401 (3.24%) regressed liver fibrosis as per LF-Fib ≥ 0.15 from baseline score. 109 (27.2%) patients had an ALT regression of $\geq 50\%$ from baseline during FU. 75 (18.7%) experienced an improvement in BMI $\geq 10\%$ during FU. Median LF-FIB was 0.27 and median (range) FU between baseline and last repeated LF-Fib was 3.57 yrs (3–9.9).

Occurrence of half-stage liver fibrosis improvement as per LF-Fib was more probable among those that achieved ALT regression of $\geq 50\%$ from baseline: Cox Mantel Hazard Ratios [HR (95%CI)] 3.47 (1.08–11.19) versus 0.29 (0.09–0.93) in those without $\geq 50\%$ ALT decrease (logrank probability level 0.02) (Figure 1).



HR (95%CI) for LF-Fib half-stage improvement (0.15 score) in the group with BMI improvement of $\geq 10\%$ was 1.78 (0.38–8.39) vs 0.56 (0.12–2.64) in the group that not achieved a BMI improvement of $\geq 10\%$ (logrank probability level = 0.37).

Conclusion: LF-Fib improvement of half-stage was significantly more prevalent in patients that achieved ALT decrease $\geq 50\%$ from baseline and a trend was observed in patients that had $\geq 10\%$ decrease in BMI from baseline. LF-Fib correlates with clinical endpoints and, therefore can be used for long-term monitoring of MAFLD patients.

FRI090

Increased liver stiffness on vibration controlled transient elastography (Fibroscan) as a predictor of all-cause mortality in people with fatty liver disease

Michael Braude^{1,2}, Ammar Majeed^{2,3}, Stuart Roberts^{2,3}, Stephen Bloom^{2,4}, Paul Gow^{5,6}, Anouk Dev^{1,2}, William Sievert^{1,2}, William Kemp^{2,3}. ¹Monash Health-Clayton Hospital Main Entrance, Gastroenterology and Hepatology, Clayton, Australia; ²Monash University Clayton Campus, Clayton, Australia; ³The Alfred, Melbourne, Australia; ⁴Eastern Health, Box Hill, Australia; ⁵Austin Hospital, Heidelberg, Australia; ⁶Melbourne University-Swanston St, Parkville, Australia
Email: mrh.braude@gmail.com

Background and aims: Fatty liver disease, which is often asymptomatic and progressive, is a multi-system, condition which is becoming the leading cause of liver-related morbidity, mortality, and liver transplant. Ascertaining liver disease severity is therefore important to guide management and prognosis. Several studies have shown a correlation between mortality and progressive liver fibrosis on both histopathology and blood-based fibrosis predictive tests. We aimed to assess vibration-controlled transient elastography (VCTE) as a predictor of mortality.

Method: VCTE studies for a primary indication of non-alcoholic fatty liver disease (NAFLD) were collated from consecutive outpatients across 4 Australian tertiary referral centres between July 2008 and April 2019. Patients with VCTE data were linked to Victorian Death Index (VDI) and the Victorian Admitted Electronic Dataset (VAED) via the Centre for Victorian Data Linkage (CVDL). Comorbidity data was derived from International Classification of Diseases 10th Revision (ICD-10) coding within the VAED. Cause of death (COD) was analysed using descriptive statistics. Liver stiffness measurement (LSM, kPa) was analysed as a predictor of all-cause mortality using Cox-proportional regression analysis with multivariable adjustment for age, gender, and comorbidities, including the Charlson Comorbidity Index (CCI).

Results: A total of 7079 individual VCTE records were identified, 6341 of which were matched via data linkage, and 5857 were represented in the VAED. The median follow-up period from VCTE to death/censorship was 3.6 (IQR 2.1–5.5, range 0.2–11.0) years. Mean age at VCTE across the 7079-patient cohort was 55.4 \pm 13.6 years, median LSM was 6.1 kPa (IQR 4.7–9.3) and mean controlled attenuation

POSTER PRESENTATIONS

parameter (CAP) ($n = 3789$) was 287.7 ± 68.7 db/m. In the linked cohort of 6341 patients, 217 deaths occurred during follow-up. Median age of death was 72.3-years (IQR 64.4–79.0). Sepsis ($n = 41$, LSM 12.0 kPa, IQR 5.8–20.2), followed by decompensated liver disease ($n = 33$, LSM 32.2, IQR 18.8–49.1) and non-gastrointestinal malignancy ($n = 25$, LSM 13.9, IQR 6.2–23.9) were the most common primary COD, accounting for 18.9%, 15.2%, and 11.5% of deaths respectively. Hepatocellular carcinoma (HCC) was either a primary or comorbid COD in 8.8% ($n = 19$, LSM 22.8 kPa, IQR 11.7–31.5) of individuals. CAP was not associated with mortality in univariable analysis (HR = 1.00, CI 1.0–1.0, $p = 0.488$). In a multivariable analysis, $n = 5857$ records, increased LSM (HR 1.02, CI 1.01–1.03, $p < 0.001$), increased CCI (HR 1.32, CI 1.27–1.38, $p < 0.001$) and advanced age (HR 1.05, CI 1.03–1.07, $p < 0.001$), but not gender, were associated with increased mortality.

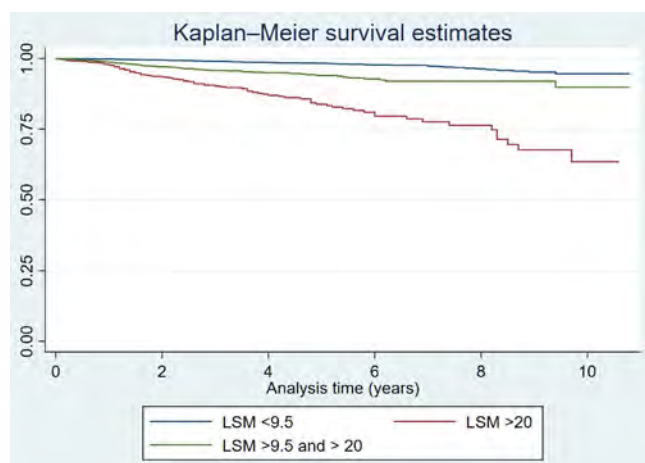


Figure: Kaplan-Meier survival curves based on LSM (kPa).

Conclusion: LSM based on VCTE is independently associated with all-cause mortality in fatty liver disease.

FRI091

Magnetic resonance imaging-based biomarker accurately identifies patients with nonalcoholic steatohepatitis and significant liver fibrosis: a multicentre, international, validation study

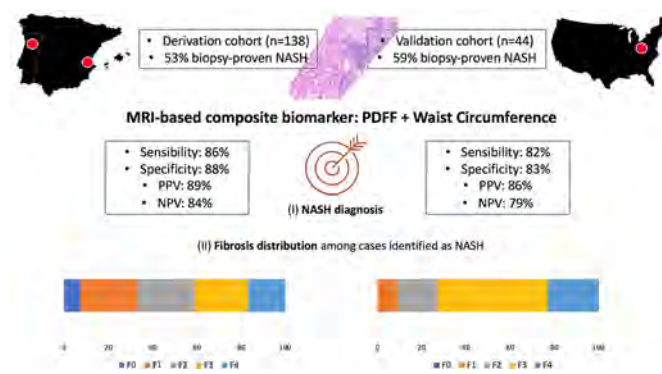
David Marti-Aguado¹, Joud Arnouk², Jaideep Behari², Alessandro Furlan³, Ramon Bataller², Maria Manuela Franca⁴, Ana Gallen⁵, Victor Merino¹, Clara Alfaro-Cervello⁶, Judith Pérez⁷, Salvador Benlloch⁵, Victoria Aguilera Sancho⁸, Desamparados Escudero-García¹, Ana Jimenez-Pastor⁹, Angel Alberich-Bayarri⁹, Miguel Serra¹, Luis Marti-Bonmati⁹. ¹Clinic University Hospital, Valencia, Spain, Department of Gastroenterology and Hepatology, Valencia, Spain; ²University of Pittsburgh Medical Center (UPMC), Hepatology Department, United States; ³University of Pittsburgh Medical Center (UPMC), Radiology Department, Pittsburgh, United States; ⁴Centro Hospitalar Universitário do Porto, Radiology Department, Porto, Portugal; ⁵Hospital Arnau Villanova, Hepatology Department, Valencia, Spain; ⁶Clinic University Hospital, Pathology Department, Valencia, Spain; ⁷Hospital Universitario y Politécnico La Fe, Pathology Department, Valencia, Spain; ⁸Universitario i Politecnico de La Fe, Hepatology Department, Valencia, Spain; ⁹Universitario i Politecnico de La Fe, Radiology Department, Valencia, Spain
Email: davidmmaa@gmail.com

Background and aims: Liver fibrosis is the only histological feature predictive of nonalcoholic steatohepatitis (NASH) progression to cirrhosis and liver-related complications. Currently, the FDA requires the inclusion of patients with biopsy-proven NASH-related fibrosis for therapeutic trials. We aimed to assess the accuracy of simple and

available magnetic resonance imaging (MRI) for the detection of NASH with fibrosis.

Method: We performed a cross-sectional international study that included subjects with NAFLD from three countries evaluated between 2017 and 2021. The training cohort included 138 consecutive patients with contemporaneous MRI and biopsy-proven NAFLD from Spain and Portugal and a validation cohort of 44 patients from USA. Patients with Fibrosis-4 index >4.63 and NAFLD fibrosis score >1.57 were excluded due to high pretest probability of cirrhosis (98% specificity). Disease severity was estimated using the histology NAFLD activity score (NAS), defining NASH as $NAS \geq 4$ and significant fibrosis as $F \geq 2$. Performance parameters of sensitivity, specificity, positive predictive value (PPV) and negative predictive value (NPV) were calculated.

Results: NASH was diagnosed on liver biopsy in 53% of the European and 59% of the US cohorts, while significant fibrosis was found in 50% and 82% patients in the two cohorts, respectively. In the training cohort, MRI-Proton Density Fat Fraction (MRI-PDFF; OR: 1.57; 95%CI 1.31–1.86) and MRI-determined waist circumference (WC; OR: 1.004; 95%CI 1.001–1.007) were imaging biomarkers independently associated with NASH (adjusted for sex, age, height and liver fibrosis). A median MRI-PDFF $>11\%$ combined with a WC >96 cm in women and >107 cm in men, showed 86% sensitivity, 88% specificity, 89% PPV and 84% NPV for the diagnosis of NASH. Among patients that were above these cut-offs, 90% had fibrosis and 63% demonstrated significant fibrosis. In the validation cohort, the combined image biomarkers had 82% sensitivity, 83% specificity, 86% PPV, and 79% NPV for the diagnosis of NASH. All selected patients had fibrosis, including 81% with significant fibrosis.



Conclusion: An MRI-based composite biomarker of PDFF+WC identified patients with NASH and liver fibrosis with high specificity and PPV. This finding offers clinical utility in the management of NAFLD and patient selection for NASH clinical trials.

FRI092

Diagnostic accuracy of MRE for staging hepatic fibrosis in patients with NAFLD

Carmen Lara Romero^{1,2}, Jia-xu Liang³, Isabel Fernández-Lizaranzu⁴, Javier Ampuero^{1,2}, Javier Castell³, Manuel Romero Gomez^{1,2}. ¹Hospital Universitario Virgen del Rocío, Department of Digestive and Liver Diseases; ²Institute of Biomedicine of Seville, Seville, Spain; ³Hospital Universitario Virgen del Rocío, Department of Radiology; ⁴Universidad de Sevilla, Interdisciplinar Physics Group, Seville, Spain
Email: mromerogomez@us.es

Background and aims: To evaluate the diagnostic accuracy of magnetic resonance elastography (MRE) instaging hepatic fibrosis in patients with histologically confirmed nonalcoholic fatty liver disease (NAFLD) and analyze possible confounding factors of MRE.

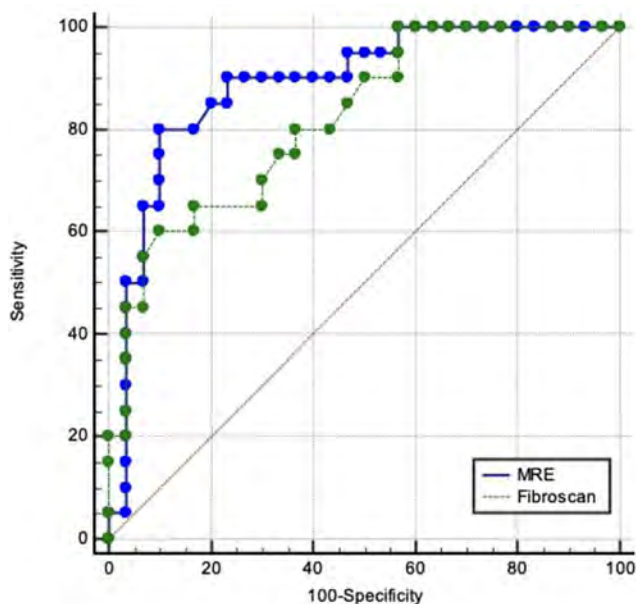
Method: 54 subjects were prospectively enrolled. Liver stiffness measured by MRE and by transient elastography (Fibroscan®) was correlated with the grade of fibrosis determined by liver biopsy.

Patients in our cohort were classified according to the cut-off values obtained from another Meta-analysis of individual patient data (2.61 kpa for F1, 2.97 kpa for F2, 3.62 kpa for F3, 4.69 kpa for F4). We also made an analysis to identify those variables that could underestimate (MRE result lower than biopsy result), overestimate (MRE result higher than biopsy results) or achieve concordance (MRE result consistent with biopsy result).

ANOVA, Kruskal-Wallis test were used for continuous variables and chi-square test or Fisher's exact test for categorical variables. ROC (receiver operator characteristic) curves for diagnostic accuracy were evaluated, and Spearman's correlation was performed to compare histologic liver fibrosis with MRE elastography and Fibroscan.

Results: The area under the ROC curve (AUROC) of MRE for $\geq F2$ was 0.886 vs Fibroscan AUROC 0.842 ($p=0.48$). MRE AUROC for F3 was 0.887 vs Fibroscan AUROC 0.820 ($p=0.27$). Spearman's correlation coefficient of liver fibrosis and Fibroscan was 0.651 ($p<0.0001$) whereas correlation coefficient of liver fibrosis and MRE elastography was 0.704 ($p<0.0001$).

Variables that could overestimate MRE accuracy were AST ($p=0.0005$), ALT ($p=0.0032$) and inflammation activity ($p=0.008$). BMI, weight, or DM did not affect diagnostic accuracy ($p=0.732$, $p=0.816$, $p=0.521$, respectively).



ROC curves for F3 patients

Conclusion: MRE is an effective, non-invasive method for detecting/staging hepatic fibrosis in NAFLD. Although we did not reach statistical significance, MRE showed a higher diagnostic accuracy than transient elastography in discriminating significant and advanced fibrosis. The liver inflammation grade may affect the diagnostic accuracy of MRE in staging hepatic fibrosis in NAFLD patients, but BMI or DM did not.

FRI093

Aldafermin quantitatively improves inflammation in a 24-week clinical trial in patients with nonalcoholic steatohepatitis

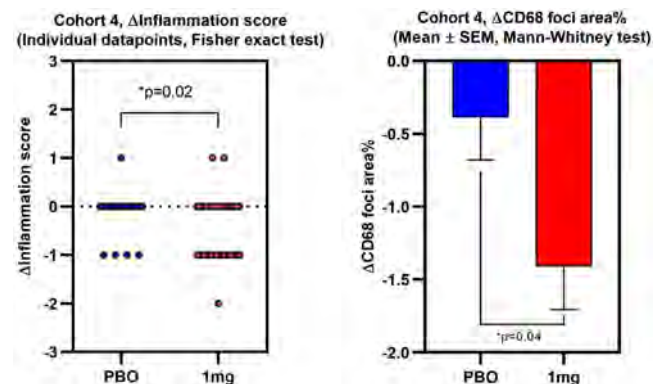
Tian Lan¹, Luong Ruiz¹, Wenhui Liu¹, Amir Ashique¹, Harry Chen¹, Jiping Zha², Alex DePaoli¹, Igor Mikaelian¹, Cynthia Guy³, Eugenia Henry⁴, Corinne Foo-Atkins⁴, William Chang⁴, Hsiao Lieu⁴.

¹NGM Biopharmaceuticals Inc., Translational Science, South San Francisco, United States; ²Adagene Inc., Clinical Development, San Diego, United States; ³Duke University Medical Center, Pathology, Durham, United States; ⁴NGM Biopharmaceuticals Inc., Clinical Research, South San Francisco, United States
Email: tlan@ngmbio.com

Background and aims: Pathologist-based scores are the standard for assessing efficacy in nonalcoholic steatohepatitis (NASH) clinical trials, but are limited by variability in interpretation and insensitivity to small changes, especially for lobular inflammation. Lobular inflammation scores reflect the number of inflammatory foci per microscopic field, which are in part contributed by macrophages. Samples from a Phase 2 clinical trial with aldafermin (NGM282), an engineered fibroblast growth factor 19 analogue, were used to develop and test novel image analysis readouts for liver inflammation based on CD68, a macrophage lysosomal marker.

Method: Liver biopsies were from a 24-week clinical trial with aldafermin: NCT02443116 (Cohort 4, placebo (PBO), $n=18$; 1-mg NGM282, $n=47$). Biopsies and blood for non-invasive biomarkers were collected at baseline and at the end of treatment. A 6-plex immunohistochemistry (IHC) panel that included CD68 was developed to enable two image analysis endpoints: (1) "Type 1 macrophages" (M1 s) based on CD68 expression and cell shape; and (2) "Macrophage foci" to account for focal accumulations of M1 s.

Results: NGM282 decreased lobular inflammation measured by the NASH Clinical Research Network (CRN) criteria ($p=0.02$) and the inflammation measured by the IHC macrophage foci (PBO vs. 1-mg, -0.39% vs. -1.41% , $p=0.04$). The decrease of M1 s did not reach statistical significance in this relatively small study ($p=0.18$). Inflammation reads by CRN criteria and by image analysis did not correlate robustly with the circulating biomarkers, including AST and ALT (r -squared ≈ 0.2).



Conclusion: Quantified IHC readouts can identify histological changes in an automated manner. These histological endpoints do not correlate well with current circulating biomarkers.

FRI094

Clinical and economic evaluation of community-based preventative screening strategies for non-alcoholic fatty liver disease in people with Type-2 diabetes mellitus

Roberta Forlano¹, Tijana Stanic², Sahan Jayawardana², Benjamin H. Mullish¹, Michael Yee¹, Mark Thursz¹, Elias Mossialos^{2,3}, Pinelopi Manousou¹. ¹Department of Metabolism, Digestion and Reproduction, Imperial college London, London, UK, United Kingdom; ²Department of Health Policy, London School of Economics and Political Science, London, UK, United Kingdom; ³Centre for Health Policy, The Institute of Global Health Innovation, Imperial College London, London, UK

Email: r.forlano@imperial.ac.uk

Background and aims: The exact prevalence of Non Alcoholic Fatty Liver Disease (NAFLD) in type 2 diabetes (T2DM) is unknown. We aimed to determine the prevalence and develop a risk stratification and cost analysis for a screening policy in T2DM in primary care. We compared the cost-effectiveness of 5 screening strategies vs standard of care (SoC).

Method: Consecutive T2DM patients underwent blood tests, ultrasound (US) and liver stiffness measurement (LSM). Significant fibrosis and advanced fibrosis were defined by LSM \geq 8.1 kPa and \geq 12.1 kPa. Diagnosis of cirrhosis was clinical, histological or radiological. Markov model included 3 health states: NMD-: no NAFLD; NMD+: NAFLD with LSM \leq 8 kPa; significant liver disease (SLD: LSM \geq 8.1 kPa); compensated cirrhosis (CC) (Fig 1).

The probability of progressing was assumed reduced for those at risk of NAFLD (NMD+) or diagnosed with SLD (SLD+) compared to those at lower risk (NMD-), or with undiagnosed disease (SLD-). The effect of earlier identification, diagnosis and treatment was based on the reduction of transition probabilities for NMD+/SLD+ vs NMD-/SLD-. The base-case analysis was conducted over a lifetime horizon and generated the cost per quality-adjusted life year (QALY) gained. We calculated average cost-effectiveness and the incremental cost-effectiveness ratio (ICER) vs SoC. Life expectancy, lifetime costs, and number of correct diagnoses were estimated. A cost-effectiveness threshold was set at £20,000/QALY gained, as per NICE.

Results: Of 300 patients enrolled, 287 were included; 13 withdrew; 184 (73%) had NAFLD, 28 (10%) other causes of liver disease (alcohol, HBV) and 75 (26%) no liver disease. Significant fibrosis and advanced fibrosis due to NAFLD were 17% (50/287) and 11% (31/287) respectively. The prevalence of cirrhosis was 3% (8/287). Based on predictors of significant fibrosis, the BImAST score (BMI and AST) performed better for diagnosing significant (AUROC 0.81, $p < 0.0001$) and advanced fibrosis (AUROC 0.84, $p < 0.0001$) (Fig 2). Five screening strategies were compared: 1) US + liver function tests (LFTs), 2) FIB-4, 3) NAFLD fibrosis score, 4) BImAST score, 5) fibroscan. In a Markov model, NAFLD screening improved the rate of correct diagnoses by 8–15%, with an exception of the NAFLD fibrosis score strategy, which led to a 2% decrease in correct diagnoses. All screening strategies were associated with QALY gains, ranging from 121–148 years, with fibroscan resulting in the most substantial gains. In all screening strategies, ICER compared to SoC was between £1,970 (BImAST score) and £2,480 (fibroscan) per QALY gained (Tab 1).

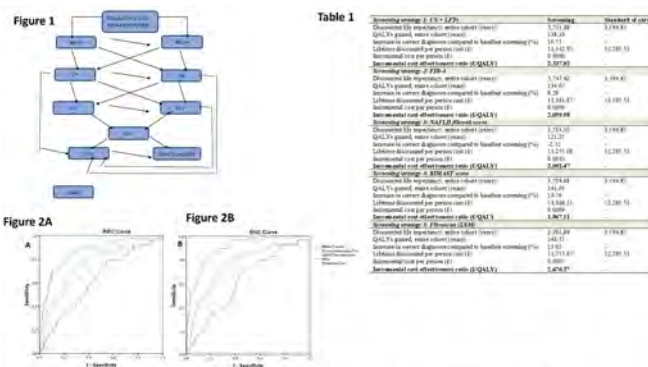


Figure 1. Markov model for the economic evaluation of screening interventions for non-alcoholic fatty liver disease. Abbreviations: –: undiagnosed; +: diagnosed; NAFLD: non-fatty liver disease; T2DM: type-2 diabetes mellitus; NMD: non-mild liver disease (no NAFLD or NAFLD with LSM \leq 8 kPa); SLD: significant liver disease (NAFLD \geq 8.1 kPa); CC: compensated cirrhosis (clinical diagnosis of cirrhosis); DC: decompensated cirrhosis; HCC: hepatocellular carcinoma.

Figure 2. BImAST score vs conventional screening methods for predicting significant (LSM \geq 8.1 kPa, Figure 2A) and advanced (LSM \geq 12.1 kPa, Figure 2B) fibrosis in the diabetic primary care population.

Table 1. Base-case cost-effectiveness analysis of NAFLD screening strategies versus standard of care (baseline screening).

Conclusion: Screening for NAFLD in T2DM improved diagnostic outcomes and was cost-effective in all evaluated scenarios within NICE's cost-effectiveness threshold. Fibroscan followed by BImAST was the screening strategy associated with the greatest clinical gains.

FRI095

Confounding factors in diagnostic performance of magnetic resonance elastography for staging liver fibrosis in patients with non-alcoholic fatty liver disease: an individual patient data meta-analysis

JiaXu Liang^{1,2,3}, Javier Ampuero^{1,2}, Kento Imajo⁴, Mazen Nouredin⁵, Jaideep Behari⁶, Dae Ho Lee⁷, Richard L. Ehman⁸, Juan R. Lacalle⁹, Javier Castell¹⁰, Ferenc Mozes¹¹, Michael Pavlides^{11,12}, Quentin Anstee¹³, Stephen Harrison¹¹, Manuel Romero Gomez^{1,2}.

¹Virgen del Rocío University Hospital, Digestive Diseases Unit, Seville, Spain; ²Institute of Biomedicine of Seville (HUVR/CSIC/US), Seville, Spain, University of Seville, Seville, Spain; ³People's Hospital of Zhengzhou, Radiology, Zhengzhou, China; ⁴Yokohama City University Graduate School of Medicine, Department of Gastroenterology, Yokohama, Japan; ⁵Cedars-Sinai Medical Center, Fatty Liver Program, Karsh Division of Digestive and Liver Diseases, Comprehensive Transplant Program, Los Angeles, CA, United States; ⁶University of Pittsburgh Medical Center, Department of Medicine, Division of Gastroenterology, Hepatology and Nutrition, Center for Liver Diseases, Pittsburgh, United States; ⁷Gachon University Gil Medical Center, Gachon University College of Medicine, Departments of Internal Medicine, Incheon, Korea, Rep. of South; ⁸Mayo Clinic College of Medicine, Department of Diagnostic Radiology, Rochester, United States; ⁹University of Seville, Biostatistics Unit, Department of Preventive Medicine and Public Health, Seville, Spain; ¹⁰Virgen del Rocío University Hospital, Radiology, Seville, Spain; ¹¹Radcliffe Department of Medicine, University of Oxford, Oxford Centre for Clinical Magnetic Resonance Research, Division of Cardiovascular Medicine, United Kingdom; ¹²University of Oxford, Translational Gastroenterology Unit, United Kingdom; ¹³Faculty of Medical Sciences, Newcastle University, Translational and Clinical Research Institute, Newcastle upon Tyne, United Kingdom

Email: mromerogomez@us.es

Background and aims: We conducted an individual patient data meta-analysis to assess potential confounding factors influencing diagnostic accuracy of magnetic resonance elastography in staging liver fibrosis and to determine specific diagnostic cutoff values in patients with non-alcoholic fatty liver disease.

Method: A review of the literature identified studies containing MRE data for grading liver fibrosis in NAFLD patients with liver biopsy as reference standards. The original database was obtained in Excel form the corresponding authors. Pooled diagnostic cutoff value for the

various fibrosis stages were determined in a two-stage meta-analysis as the primary outcome. Multilevel modelling methods were used to analyses potential confounding factors influencing diagnostic accuracy of MRE in staging liver fibrosis.

Results: 6 independent cohorts comprising 483 patients were included in the meta-analysis, yielding liver stiffness cutoffs of 2.77 kPa (area under the receiver operating characteristic curve 0.86 [0.83–0.89]) for any fibrosis ($\geq F1$), 3.09 kPa (0.90 [0.87–0.92]) for significant fibrosis ($\geq F2$), 3.41 kPa (0.93 [0.91–0.96]) for advanced fibrosis ($\geq F3$) and 4.10 kPa (0.91 [0.88–0.93]) for cirrhosis (F4). Notably, cases with mild fibrosis stage (F0–1) with moderate to severe inflammatory activity (A3–4) had exhibited greater stiffness than matched cases of the same fibrosis stage with none to mild inflammation activity. Similarly, higher liver inflammatory activity was an independent variable predicting reduced diagnostic accuracy of MRE [OR (95% CI)=0.404 (0.220–0.740), $p < 0.01$], whereas steatosis degree, BMI, ALT, and AST did not affect the diagnostic accuracy of MRE (Table).

Table: GLMM (generalized linear mixed model) explore variables associated with prediction failure

Variables	OR	95% CI	Estimated (SE)	Z-value	p-value
BMI	1.001	(0.950-1.054)	0.001 (0.026)	0.03	0.97
Age	0.997	(0.972-1.022)	-0.003 (0.013)	-0.24	0.81
Sex (M vs F)	0.898	(0.500-1.612)	-0.108 (0.299)	-0.36	0.72
Population (Asian vs non-Asian)	1.178	(0.636-2.185)	0.164 (0.315)	0.52	0.60
T2DM (yes vs no)	0.788	(0.437-1.422)	-0.238 (0.301)	-0.79	0.43
ALT	0.998	(0.990-1.007)	-0.002 (0.004)	-0.41	0.68
AST	1.002	(0.992-1.012)	0.002 (0.005)	0.36	0.72
platelet	1.002	(0.998-1.006)	0.002 (0.002)	0.84	0.40
Steatosis					
S1	0.703	(0.083-5.924)	-0.353 (1.088)	-0.32	0.75
S2	0.638	(0.069-5.861)	-0.450 (1.132)	-0.40	0.69
S3	0.544	(0.054-5.513)	-0.609 (1.182)	-0.52	0.61
Inflammation activity (Lower vs higher)	0.404	(0.220-0.740)	-0.907 (0.309)	-2.93	<0.01
MRI-PDFF	0.980	(0.940-1.022)	-0.020 (0.021)	-0.94	0.35

Conclusion: MRE has excellent diagnostic performance for determining significant, advanced fibrosis and cirrhosis in patients with NAFLD. Accuracy was not influenced by anthropometric, biochemical, or steatosis degree, but could be influenced by high inflammatory activity.

FRI096

Is it possible to identify nonalcoholic steatohepatitis and the associated degree of fibrosis by noninvasive methods in patients with MAFLD?

José López González¹, Marta Casado¹, Teresa Maria Jordan Madrid¹, Almudena Porcel Martín¹, José Luis Vega Sáenz¹. ¹Torrecedenas University Hospital, Almería, Spain
Email: pepe_1993_17@hotmail.com

Background and aims: Non-alcoholic steatohepatitis (NASH) is a chronic and progressive form of metabolic associated fatty liver disease (MAFLD). NASH diagnosis requires histological evaluation after liver biopsy. Therefore, it is necessary to develop non-invasive diagnostic alternatives to identify NASH and the associated degree of fibrosis. The aim of this study is to analyze the presence of NASH and NASH with advanced fibrosis (AF) in patients with MAFLD and increased liver stiffness (LS), and to identify those associated factors with AF.

Method: We included a prospective cohort of all patients with clinical and ultrasound diagnosis of MAFLD, treated in our department since January 2019, with LS >8 kPa, measured by transient elastography. Presence of NASH and the degree of fibrosis, were evaluated after histological analysis of a liver biopsy. Epidemiological, clinical, analytical, elastographic and histological variables were collected. Patients were classified according to the presence of AF in the liver specimen (grade 3–4) or mild fibrosis (MF) (grade 1–2 or absence).

Results: Our study included 40 patients, whose characteristics are shown in Table 1. Histological analysis demonstrated NASH in 36 patients (90%), 14 patients with AF (35%), and two of them with F4 grade fibrosis. GGT and LS were significantly higher in patients with

NASH and AF vs patients with MF (161.86 ± 115 vs 90.6 ± 56 , $p = 0.04$, 15.9 ± 8.6 vs 10 ± 1.48 , $p = 0.02$). 42% of patients with MF had APRI <0.5 and 57% had APRI between 0.5–1. No patient with MF had APRI >0.5 . Likewise, 50% of patients with AF had APRI >0.5 , and 50% of them, had APRI >1.5 ($p = 0.026$). All patients with APRI >1 and LS >12.1 kPa had AF, and only 29% of patients with AF did not meet both criteria ($p = 0.037$). In addition, all patients with APRI >1.5 and GGT >115.6 IU/ml had AF, compared to 29% of patients with AF who did not meet both analytical criteria ($p = 0.037$).

VARIABLE	RESULTS (n = 40)
AGE	59.78 \pm 8.5
SEX (%)	MALE 20 (50%) FEMALE 20 (50%)
AHT (%)	30 (75%)
DYSLIPIDEMIA (%)	25 (62.5%)
DIABETES (%)	27 (67.5%)
OBESITY (%)	40 (100%)
AST	47.4 \pm 28.2 U/L
ALT	56.1 \pm 33.5 U/L
GGT	115.6 \pm 88 U/L
HEMOGLOBIN A1c	6.5 \pm 1.27%
CHOLESTEROL	202 \pm 33.4 mg/dL
TRIGLYCERIDES	190.4 \pm 95 mg/dL
ADVANCED FIBROSIS (%)	14 (35%)
LIVER STIFFNESS (kPa)	12.1 \pm 5.8 kPa
CAP (n = 23)	334.4 \pm 32.4
FIB-4 (%)	<1.33 13 (32.5%) 1.33–2.66 22 (55%) >2.66 5 (12.5%)
FIB-4	1.8 \pm 1.04
APRI (%)	<0.5 18 (45%) 0.5–1.5 19 (47.5%) >1.5 3 (7.5%)
APRI	0.66 \pm 0.49

Conclusion: Most patients with MAFLD and RH >8 kPa have NASH, one-third of them have AF. Increased GGT, APRI index, and LS were associated with a higher probability of having NASH with AF. LS and APRI combination or APRI and GGT combination, can identify patients with NASH and FA. Therefore, it seems possible to identify patients with MAFLD and high risk of NASH and NASH with AF with non-invasive methods. Nevertheless, further prospective studies are needed to confirm these preliminary results.

FRI097

The potential role of fatigue in identifying patients with NASH and advanced fibrosis who experience disease progression

Zobair Younossi^{1,2,3}, Maria Stepanova^{1,2,4}, Robert Myers⁵, Reem Al Shabeeb³, Issah Younossi⁴, Linda Henry^{1,2,4}. ¹Inova Health System, Medicine Service Line, Falls Church, United States; ²Betty and Guy Beatty Center for Integrated Research, IHS, Falls Church, United States; ³Center for Liver Diseases, Department of Medicine, Falls Church, United States; ⁴Center for Outcomes Research in Liver Disease, Washington DC, United States; ⁵Gilead Sciences, Inc., Foster City, United States
Email: zobair.younossi@inova.org

Background and aims: Fatigue is common in patients with advanced liver disease. We aimed to investigate the association of fatigue with the risk of progression among patients with NASH and advanced fibrosis.

Method: In this post hoc cohort study, enrolled subjects were required to have a liver biopsy consistent with NASH and bridging fibrosis (F3) or compensated cirrhosis (F4), and were followed up for up to two years. Fatigue was quantified using the fatigue domain of the CLDQ-NASH instrument completed by subjects at baseline (score range 1–7, lower score indicates worse fatigue). Cox proportional hazard model was used to determine the relationship between the

POSTER PRESENTATIONS

baseline fatigue score and the time to liver-related clinical events (progression to histologic cirrhosis for F3, developing hepatic decompensation for F4).

Results: There were 1679 advanced NASH patients (N = 802 F3 and 877 patients F4, age 58 ± 9 years, 40% male, 74% type 2 diabetes). During median follow-up of 16 months (IQR 14–18 month, max 26 months), 123 (15%) of F3 patients and 31 (3.5%) F4 patients experienced liver-related clinical events. The mean baseline CLDQ-NASH fatigue score was 4.77 ± 1.36 in F3 and 4.56 ± 1.44 in F4. In both F3 and F4 cohorts, patients with liver-related events in follow-up had higher baseline AST, lower platelet count, and elevated non-invasive test scores for fibrosis (APRI, FIB-4, ELF, Fibrotest, NAFLD Fibrosis Score) in comparison to patients who remained stable in follow-up (all $p < 0.01$). Their baseline fatigue scores were also significantly lower: 4.47 ± 1.36 in progressed F3 vs. 4.83 ± 1.35 in stable F3 ($p = 0.0091$); 3.74 ± 1.31 in progressed F4 vs. 4.59 ± 1.43 in stable F4 ($p = 0.0011$). In multivariate analysis, the association of lower fatigue scores (more fatigue) with the risk of liver-related events was significant: hazard ratio (HR) per 1 fatigue point = 0.84 (0.75–0.93), $p = 0.0012$, in all patients; HR = 0.85 (0.75–0.96), $p = 0.0088$, in F3; HR = 0.67 (0.53–0.85), $p = 0.0014$, in F4. These associations remained significant after adjustment for clinico-demographic confounders: adjusted HR = 0.79 (0.70–0.89), 0.85 (0.74–0.97), and 0.62 (0.48–0.81), respectively (all $p < 0.02$).

Conclusion: Lower baseline fatigue scores were associated with adverse clinical events in patients with advanced NASH. A combination of baseline clinical and fatigue parameters can inform clinicians of which patients with advanced fibrosis due to NASH are at risk of adverse clinical outcomes.

FRI029

Novel digital pathology quantitative image analysis and AI method detects the treatment effects of NASH drug candidates with a performance that benchmarks imaging-based measurements

Li Chen¹, Elizabeth Brown², Anne Minnich², Vipul Baxi², Dimple Pandya², Shuyan Du², Edgar Charles², Zachary Goodman³, Mathieu Petitjean¹, Arun Sanyal⁴. ¹PharmaNest, Inc, Princeton, United States; ²Bristol Myers Squibb, Princeton; ³Inova Health Systems, Falls Church, United States; ⁴Virginia Commonwealth University, Richmond, United States

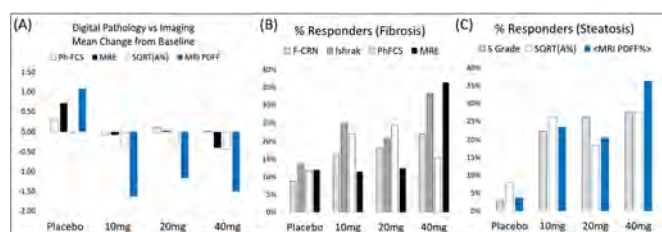
Email: mathieu.petitjean@pharmanest.com

Background and aims: Manual histological evaluation of liver biopsy is the gold standard method for fibrosis and steatosis staging in Non-Alcoholic Steatohepatitis (NASH), but it is limited by its inter and intra-reader variability. Quantitative Digital Pathology image analysis and AI (FibroNest™) as well as quantitative MRI signal analysis methods have the potential to overcome the current limitation of standards. This exploratory post-hoc analysis compared FibroNest digital pathology scoring methods with NASH-CRN categorical stages and imaging-based scores in patients with NASH from the phase 2b FALCON1 study (NCT348699).

Method: Eligible adults were 18–75 years of age (N = 197) with NASH diagnosed by histologic assessment of liver biopsy according to NASH CRN criteria and stage 3 fibrosis. During the 48-week double-blind treatment period, patient received 10 mg, 20 mg, or 40 mg PGBF subcutaneous or placebo once weekly. Liver biopsies were obtained six months before or during screening and at week 24. Most patients underwent imaging resulting in Mean Liver Stiffness (MRE) and Mean Proton Density Fat Fraction (MRI-PDFF) measurements. Formalin-fixed, paraffin embedded sections of the liver biopsies where stained with Masson Trichrome and imaged at 40X. Quantitative image analysis was performed to extract single-fiber quantitative traits (qFTs, N=315) from the fibrosis histological phenotype. A previously validated selection of principal qFTs were normalized and combined into a fibrosis severity score (Ph-FCS, 1 to 10). The non-fibrotic/scar parenchymal tissue area fat ratio (A%) is

measured, and its square root is used as an exploratory marker SQRT (A%). Each digital image was evaluated for quality along 20 dimensions (tissue processing, staining, and scanning) to generate a Digital Biopsy Adequacy Score (DBA).

Results: Patients with biopsies with a DBA lower than 5 (non-adequate, ~10% of the cohort) were not included in the results. Groups sizes ranged from 27 to 45 patient per group. The quantification of the antifibrotic effect of the treatments was similar using the mean change from baseline of the Ph-FCS and MRE. SQRT (A%) was highly correlated to PDFF ($R^2 = 0.660$, N = 334) and demonstrated same anti-steatotic effects as PDFF for each group (Fig. A). Responders were identified with a relative reduction from baseline of MRE, Ph-FCS, PDFF and SQRT (A%) of $\geq 15\%$, $\geq 25\%$, $\geq 30\%$ and $\geq 30\%$ respectively, and with a 1-unit reduction for the histological stage. The agreement between quantitative digital pathology and imaging methods is illustrated in Fig. B, C.



Conclusion: Combined to AI algorithms, quantitative digital pathology image analysis generates continuous scores that enhance conventional histological staging methods. They detect the antifibrotic and anti-steatosis effect of treatment such as PGBF with a performance that benchmarks imaging-based measurements.

FRI099

Translational fibrosis phenotypes between the 3D human NASH spheroidal model and clinical NASH samples

Louis Petitjean¹, Simon Ströbel², Li Chen^{1,3}, Francisco Verdeguer^{2,4}, Radina Kostadinova², Arun Sanyal⁵. ¹PharmaNest, Inc, Princeton, United States; ²InSphero AG, Shlieren, Switzerland; ³PharmaNest Inc, Princeton, United States; ⁴University of Zurich, Zürich, Switzerland; ⁵Virginia Commonwealth University, Richmond, United States

Email: louis.petitjean@pharmanest.com

Background and aims: The use of 3D human spheroidal model for efficacy testing of anti-fibrotic compounds for Non-Alcoholic Steatohepatitis (NASH) has led to the need to understand the relevance of the fibrosis histological phenotypes and their clinical translational relevance. Here, a novel digital pathology quantitative image analysis and AI platform, FibroNest™, was used to measure quantifiable Fibrosis Traits (qFTs) in 3D human NASH models and natural cohort of patients diagnosed with NASH.

Method: 3D liver tissues were either treated for 10 days with free fatty acids and LPS or not to generate NASH (n = 14 tissues) and lean (n = 17 tissues) conditions respectively. The clinical cohort was retrospective and consisted of 104 patients with NASH diagnosed by histologic assessment of liver biopsy according to NASH CRN criteria by pathologists F0 (26), F1 (24), F2 (28), F3 (20), F4 (6). 4 µm FFPE spheroid and liver biopsies sections were stained with Picro Sirius Red, and scanned (40X and 20X) with bright-light whole slide imaging scanners. FibroNest™, was used to quantify the fibrosis histological phenotype including 32 traits for collagen content, fiber morphometry, and architecture, generating 315 qFT. Principal qFTs were automatically detected to best describe the progression of the fibrosis in both models. A Venn diagram approach was used to identify those traits that describe histological fibrosis severity in both models.

Results: The Venn Diagram identifies 97 shared traits between the two fibrosis progression models. qFTs are normalized to their initial

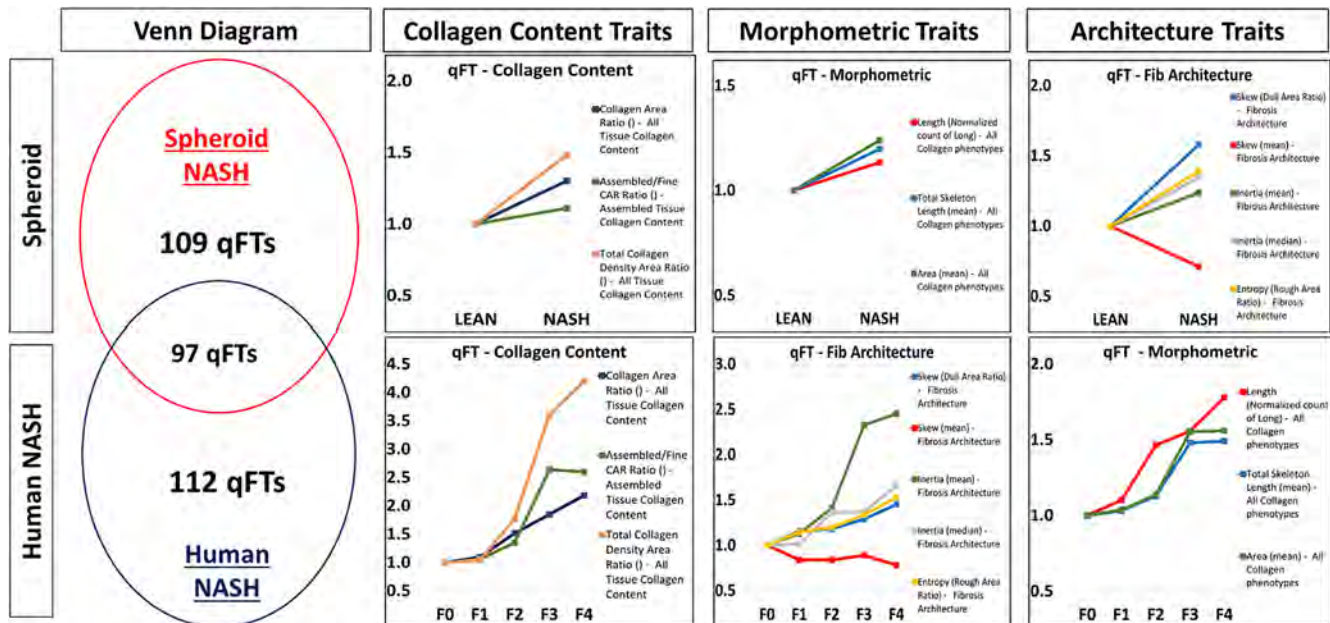


Figure: (abstract: FRI099)

value and their folds describe relative levels of progression benchmarked from a model to another. 10 traits described collagen features such as collagen area ratio, assembled/fine collagen fibers area ratio, and density area ratio (Figure). 61 traits described common morphometric features, such as the proportion of long collagen fibers, the mean fiber skeleton length, and the mean fiber area. 26 traits described common architectural features. The 3D human NASH spheroidal model cannot be directly associated to a specific NASH CRN score, but specific qFTs can be associated with either F2 or F3 stages using their fold values.

Conclusion: We identified 97 histological traits of fibrosis severity phenotype that can be translated from the 3D NASH spheroid model to clinical F2 or F3 NASH CRN stages. These traits will be used to evaluate the anti-fibrotic compounds effect in 3D NASH model to predict their effect in human.

FRI100

Shear wave elastography, transient elastography and enhanced liver fibrosis test use in the assessment of non-alcoholic fatty liver disease (NAFLD) in real- world practices

Sean Felix¹, Elena Younossi^{1,2}, Thomas Jeffers², Evis Hudson³, Nagashree Gundu Rao³, Z. Chris³, Amish Gandhi³, Maria Castillo-Catoni³, Maria Ramirez³, Mehreen Husain³, Evangeline Delgado³, Ambika Baru³, Merica Shrestha³, Romona Satchi³, Yemsrach Gami³, Pegah Golabi³, Andrei Racila⁴, Fatema Nader⁵, Maria Stepanova^{3,5}, Zobia Younossi³. ¹Inova Fairfax Medical Campus, Department of Medicine, Falls Church, United States; ²Inova Fairfax Hospital, Falls Church, United States; ³Inova Health System, Medicine Service Line, Falls Church, United States; ⁴Inova Fairfax Medical Campus, Falls Church, United States; ⁵Center for Outcomes Research in Liver Diseases, Washington, United States
Email: zobair.younossi@inova.org

Background and aims: Risk stratification of NAFLD patients using non-invasive tests can be challenging. In this context, correlation of different radiologic and blood-based NITs to each other can be clinically informative. We aimed to assess the correlation of different NITs to identify high-risk NAFLD/NASH patients seen at real-world primary care provider (PCP) and endocrinology (ENDO) practices and link them to a GI or hepatology practice for specialized care.

Method: Using the electronic health records (EHRs), patients seen at PCP and ENDO clinics were screened for the presence of NASH risk factors. Patients with a diagnosis of type 2 diabetes or those with >2 other components of metabolic syndrome (hypertension, hyperlipidemia, or obesity) were eligible for the second round of assessment using FIB-4. Patients with FIB-4 score ≥ 1.45 were referred to a hepatology practice for transient elastography (TE) by FibroScan™ (Echosens, Paris, France: liver stiffness [LSM] and fat assessment by controlled attenuation parameter [CAP]), shear-wave elastography (SWE) by ACUSON Sequoia Ultrasound System (Siemens Healthineers, Erlangen, Germany: LSM by Point Shear Wave Elastography [pSWE] and ultrasound-derived fat fraction [UDFF]), and the Enhanced Liver Fibrosis (ELF) Test (Siemens Healthineers, Tarrytown, NY, USA).

Results: 13, 953 patients were screened (53% from ENDO practices, 47% from PCP). Of those, 4, 269 (30%) met the criteria for the second round of screening with FIB-4: 1, 286 (30%) agreed to enroll. Based on the FIB-4 risk cut-off, 328 (25%) patients were considered eligible for linkage to hepatology care, of whom 177 (53%) agreed to undergo linkage assessment. Patients who underwent linkage assessment were 67 \pm 10 years of age, 52% male, 61% white, 23% black, 4% Hispanic, and 8% Asian, mean BMI was 31.6 \pm 6.4 kg/m², 90% had clinical history of hyperlipidemia, 79% hypertension, 62% type 2 diabetes, and 23% reported having coronary artery or cardiovascular disease. Mean (SD) FIB-4 score: 1.95 \pm 0.74; ELF score: 9.55 \pm 0.83, LSM by TE: 7.0 \pm 4.0 kPa, CAP 287 \pm 64 dB/m, LSM by SWE: 3.98 \pm 1.55 kPa, UDFF: 13.4 \pm 8.6%, and FAST score: 0.25 \pm 0.24. Of these patients, based on published or recommended by manufacturers cut-offs, 3% were considered high-risk by ELF, 17% by TE, and 8% by SWE; and additional 64% by ELF, 68% by TE, and 84% by SWE were considered low-risk. The correlations among the two stiffness measures (TE and SWE) and ELF were significant: Spearman's rho = +0.51 ($p < 0.0001$) between stiffness by TE and SWE; +0.40 ($p < 0.0001$) between stiffness by SWE and ELF; +0.25 ($p = 0.0028$) between stiffness by TE and ELF.

Conclusion: High-risk NASH patients can be identified by applying a simple clinical algorithm using electronic health records and point-of-care NITs.

POSTER PRESENTATIONS

FRI101

Diagnostic performance of AGILE 3+ score for identification of advanced fibrosis and prediction of liver-related events in patients with non-alcoholic fatty liver disease

Grazia Pennisi¹, Ciro Celsa¹, Marco Enea¹, Alessandra Pandolfo², Michela Antonucci³, Carlo Ciccio¹, Giuseppe Infantino¹, Claudia La Mantia¹, Stefanie Parisi¹, Adele Tulone¹, Vito Di Marco¹, Antonio Craxi¹, Calogero Camma¹, Salvatore Petta¹. ¹Section of Gastroenterology and Hepatology, Department of Health Promotion, Mother and Child Care, Internal Medicine and Medical Specialties (PROMISE), University of Palermo, Italy; ²University of Palermo; ³University of Palermo, Dipartimento di Biomedicina, Neuroscienze e Diagnostica avanzata (BIND)
Email: salvatore.petta@unipa.it

Background and aims: We aimed to assess the diagnostic accuracy of AGILE 3+, a recently developed score based on the combination of AST/ALT ratio, platelet count, diabetes status, sex, age and LSM, respect to FIB-4 and LSM, for the diagnosis of advanced fibrosis and for the prediction of liver-related events (LRE) occurrence in patients with non-alcoholic fatty liver disease (NAFLD).

Method: 614 consecutive patients with biopsy-proven NAFLD or clinical diagnosis of NAFLD-related compensated cirrhosis were enrolled. LRE were recorded during follow-up. FIB-4, LSM by TE and AGILE 3+ were measured. The diagnostic performance of noninvasive criteria for advanced fibrosis and for the prediction of LRE was assessed by AUROC curve and by decision curve analysis (DCA).

Results: In patients with biopsy-proven NAFLD (n = 520), LSM and AGILE 3+ had higher AUROC than FIB-4 (0.88 for LSM and AGILE 3+ vs 0.78 for FIB-4; p < 0.001) for advanced fibrosis, and AGILE 3+ exhibited the lower rate of indeterminate area of the test (25.2% for FIB-4, vs 13.1% for LSM, vs 8.3% for AGILE 3+). In the entire cohort AGILE 3+ had significantly higher AUC for predicting LRE respect to LSM (36-month AUROC 0.95 vs 0.93, p = 0.008; 60-month 0.95 vs 0.92, p = 0.006; 96-month 0.97 vs 0.95, p = 0.001). DCA showed that all scores had modest net benefit for ruling-out advanced fibrosis at the risk threshold of 5%–10% of missing advanced fibrosis. At the risk threshold of 5% of false negative or false positive LRE at 36-, 60-, 96- and 120-month, AGILE 3+ outperformed both FIB-4 and LSM for ruling-out LRE.

Conclusion: AGILE 3+, according to resource availability, clinical setting and the risk scenarios is an accurate and valid alternative to FIB-4 and LSM for the noninvasive assessment of disease severity and prognosis in NAFLD patients.

FRI102

Diagnostic accuracy of non-invasive tests for cirrhotic NASH-an individual participant data meta-analysis

Ferenc Mozes¹, Jenny Lee², Yasaman Vali², Emmanuel Selvaraj¹, Arjun Jayaswal¹, Jerome Boursier³, Elisabetta Bugianesi⁴, Ramy Younes⁵, Monica Lupsor-Platon⁶, Salvatore Petta⁷, Toshihide Shima⁸, Takeshi Okanoue⁸, Sanjiv Mahadeva⁹, Wah-Kheong Chan⁹, Gideon Hirschfield¹⁰, Peter Eddowes¹¹, Philip N. Newsome¹², Vincent Wai-Sun Wong¹³, Victor de Lédinghen¹⁴, Jeremy Cobbald¹⁵, Yoshio Sumida¹⁶, Akira Okajima¹⁷, Jörn Schattenberg¹⁸, Christian Labenz¹⁹, Won Kim²⁰, Myoung Seok Lee²¹, Guruprasad Aithal²², Naaventhana Palaniyappan²², Cristophe Cassinotto²³, Sandeep Aggarwal²⁴, Harshit Garg²⁴, Geraldine Ooi²⁵, Atsushi Nakajima²⁶, Masato Yoneda²⁶, Ming-Hua Zheng²⁷, Céline Fournier²⁸, Andreas Geier²⁹, Theresa Tuthill³⁰, Carla Yunis³⁰, Quentin Anstee³¹, Stephen Harrison¹, Patrick Bossuyt², Michael Pavlides¹. ¹University of Oxford, RDM Cardiovascular Medicine, Oxford, United Kingdom; ²University of Amsterdam, Department of Epidemiology and Data Science, Amsterdam UMC, Amsterdam, Netherlands; ³CHU Angers, Angers, France; ⁴University of Turin, Department of Medical Sciences, Division of Gastroenterology, Turin, Italy; ⁵Boehringer Ingelheim, Binger Strasse 173, Germany; ⁶Iuliu

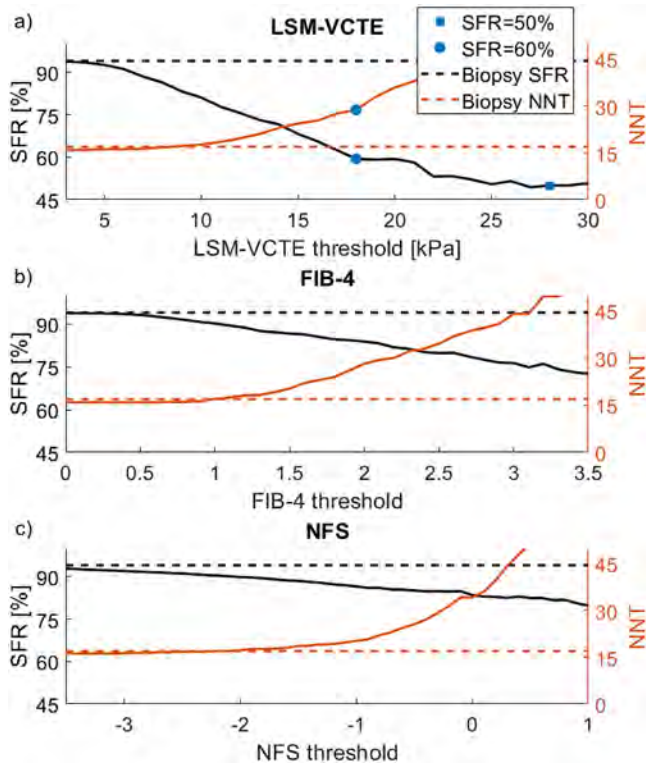
Hațieganu University of Medicine and Pharmacy, Department of Medical Imaging, Romania; ⁷University of Palermo, Department of Gastroenterology and Hepatology Promise, Palermo, Italy; ⁸Saiseikai Suita Hospital, Department of Gastroenterology and Hepatology, Suita, Japan; ⁹University of Malaya, Gastroenterology and Hepatology Unit, Department of Medicine, Faculty of Medicine, Kuala Lumpur, Malaysia; ¹⁰University Health Network, Toronto Centre for Liver Disease, Toronto, Canada; ¹¹Nottingham University Hospitals NHS Trust and University of Nottingham, National Institute for Health Research Nottingham Biomedical Research Centre, Nottingham, United Kingdom; ¹²University Hospitals Birmingham NHS Foundation Trust and the University of Birmingham, National Institute for Health Research Biomedical Research Centre, Birmingham, United Kingdom; ¹³The Chinese University of Hong Kong, Department of Medicine and Therapeutics, Hong Kong, Hong Kong; ¹⁴Bordeaux University Hospital, Centre d'Investigation de la Fibrose Hépatique, Hôpital Haut-Lévêque, Bordeaux, France; ¹⁵University of Oxford, Translational Gastroenterology Unit, Oxford, United Kingdom; ¹⁶Aichi Medical University, Aichi, Japan; ¹⁷Koseikai Takeda Hospital, Kyoto, Japan; ¹⁸University Medical Centre Mainz, Mainz, Germany; ¹⁹University Medical Center of the Johannes Gutenberg-University, Mainz, Germany; ²⁰Seoul Metropolitan Government Boramae Medical Center, Division of Gastroenterology and Hepatology, Department of Internal Medicine, Seoul National University College of Medicine, Seoul, Korea, Rep. of South; ²¹Seoul Metropolitan Government Boramae Medical Center, Department of Radiology, Seoul National University College of Medicine, Seoul, Korea, Rep. of South; ²²University of Nottingham, Nottingham Digestive Diseases Centre, Translational Medical Sciences, School of Medicine, Nottingham, United Kingdom; ²³University Hospital of Montpellier, Department of Diagnostic and Interventional Radiology, Saint-Eloi Hospital, Montpellier, France; ²⁴AIIMS, Department of Surgical Disciplines, New Delhi, India; ²⁵Monash University, Centre for Obesity Research and Education, Department of Surgery, Melbourne, Australia; ²⁶Yokohama City University, Department of Gastroenterology and Hepatology, Yokohama, Japan; ²⁷The First Affiliated Hospital of Wenzhou Medical University, NAFLD Research Center, Department of Hepatology, Wenzhou, China; ²⁸Echosens, Paris, France; ²⁹University Hospital Würzburg, Division of Hepatology, Würzburg, Germany; ³⁰Pfizer, Inc., Cambridge, MA, United States; ³¹Newcastle University, Newcastle upon Tyne Hospitals NHS Foundation Trust, NUTCRI, Framlington, United Kingdom
Email: ferenc.mozes@cardiov.ox.ac.uk

Background and aims: Screening for non-alcoholic steatohepatitis with cirrhosis (NASH+F4), identified by regulators as an unmet medical need, is done by liver biopsy. Given the low prevalence of the condition in typical clinical populations, risk stratification using non-invasive tests (NITs) is desirable to reduce the number of unnecessary liver biopsies. The aim of this study was to evaluate the diagnostic performance of vibration-controlled transient elastography (LSM-VCTE), fibrosis-4 index (FIB-4) and NAFLD fibrosis score (NFS) as screening tests for NASH+F4.

Method: This was an individual participant data meta-analysis of studies evaluating NITs against liver histology. NASH was defined as NAS > 4 with at least grade 1 in each of the components. Diagnostic accuracy was assessed by the area under the receiver operating curve (AUROC). The relationship between NIT cut-off and screen failure rate (SFR) and the number of patients that needed to be tested (NNT) to identify 1 positive case was explored visually. We report on cut-offs that achieved 90% sensitivity, 90% specificity and maximised the Youden-index as well as cut-offs that achieved screen failure rate of 50% and 60%. Sequential combinations of serum NITs followed by LSM-VCTE were also evaluated.

Results: We included 2738 individual patient data from 25 primary studies (43% female, median age 52 years, median BMI 29 kg/m²; 41% had type 2 diabetes; 57% had NASH, 6% had NASH + F4). LSM-VCTE had AUROC = 0.90, higher than 0.80 for FIB-4 and 0.78 for NFS (both p < 0.001). Cut-offs for 90% sensitivity, 90% specificity and maximum

Youden-index were 10.2 kPa (Sp 76%, SFR 80%, NNT = 18), 14.6 (Se 68%, SFR 69%, NNT = 24), and 10.4 kPa (Se 89%, Sp 77%, SFR 79%, NNT = 18) for LSM-VCTE; 1.16 (Sp 52%, SFR 89%, NNT = 18), 2.73 (Se 41%, SFR 79%, NNT = 39) and 1.35 (Se 88%, Sp 61%, SFR 87%, NNT = 18) for FIB-4; -1.637 (Se 53%, SFR 89%, NNT = 18), 0.473 (Se 32%, SFR 82%, NNT = 50) and -0.878 (Se 77%, Sp 69%, SFR 86%, NNT = 21) for NFS (Figure 1). A cut-off combination of FIB4 1.16 or NFS -1.637 followed by LSM VCTE of 16 kPa yielded Se 59%, Sp 93%, SFR 62%, and NNT = 27 and only 10% of the entire patient group would have to undergo liver biopsy while also reducing the number of LSM-VCTE exams to 51%.



Conclusion: Only LSM-VCTE achieved SFR of 50 and 60% which was at the cost of high NNT. Sequential combinations can achieve similar diagnostic accuracy while potentially reducing the number of LSM-VCTE exams and biopsies being performed, which could have favorable cost implications.

FRI103

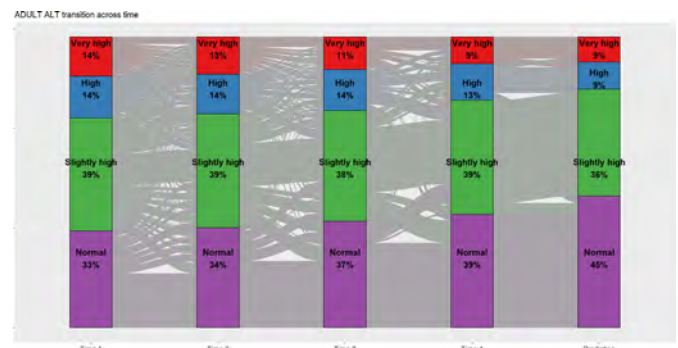
Longitudinal ALT trajectories are generally stable among patients with non-alcoholic fatty liver disease (NAFLD): an investigation using artificial recurrent neural networks

Michael Fried¹, Breda Munoz¹, Jamie Wu¹, Kenneth Cusi², Vincent Wai-Sun Wong³, Peter Mesenbrink⁴, Marcos Pedrosa⁴, Andrea Mospan¹, Miriam Vos⁵, Rohit Loomba⁶, Arun Sanyal⁷. ¹Target RWE, Durham, United States; ²University of Florida, Gainesville, United States; ³The Chinese University of Hong Kong, Hong Kong, China; ⁴Novartis, East Hanover, United States; ⁵Emory University, Atlanta, United States; ⁶University of California at San Diego, San Diego, United States; ⁷Virginia Commonwealth University Medical Center, Richmond, United States
Email: mfried@targetrwe.com

Background and aims: Serum alanine aminotransferase (ALT) is a biomarker used to monitor liver injury. Little is known about ALT fluctuations over short intervals or the influence of patient characteristics on ALT trajectory in patients with NAFLD. This study modelled longitudinal variability in ALT and estimated the probability of a patient transitioning from their baseline level.

Method: TARGET-NASH is a longitudinal study of patients managed for NAFLD in usual clinical practice. Data from patients enrolled in the US with ≥ 3 ALT measures were included. Liver transplant, cholecystitis, liver cancer, sepsis were excluded. ALT categories: normal (≤ 30 U/L), slightly high (1–2X normal), high (2–3X normal), very high ($> 3X$ normal). Using available data, the transition between ALT categories was modelled using a recurrent neural network. 80%–20% data split into training-testing approach was utilized to fit the model and assess accuracy. Age, sex, body mass index (BMI), race/ethnicity, ALT date, hypertension, diabetes, cardiovascular disease and statin use were identified a priori.

Results: 3,664 adult patients were followed over a median of 38.2 months (range: 1.7–87) with 3.9 months (range: 0.5–54.2) between ALT measures. Median age: 59; non-Hispanic (85%), White (76%), BMI 32 kg/m², history of hypertension (74%), type 2 diabetes (54%), cardiovascular disease (22%), statin use (46%); diagnosed with NASH (44.3%), cirrhosis (40.4%), NAFLD (15.3%). Patients in higher ALT categories at baseline were younger with a greater percentage of Hispanic or Latino participants vs. lower ALT categories. At baseline, 33%, 38%, 15%, 14% of patients had normal ALT, slightly high, high, very high ALT levels, respectively. In the unadjusted model, 39% with normal ALT at baseline remained in that category during follow up. Among those with slightly high ALT at baseline, 18% remained within that stratum; 5% and 18% of those with high and very high ALT, respectively, at baseline remained in the same strata. Probability of transitioning from normal or slightly high to very high ALT level was 2% and 6%, respectively, suggesting that transition from low to high ALT levels is uncommon. Risk of transition was higher in NH Whites (24%) and Hispanics (24%), followed by NH Black (21%), Asians (19%). Statin use did not influence transition. Accuracy of the neural network on training and testing data sets was 99% and 82%, respectively. Accuracy of the testing data set improved when limiting to phenotype at baseline: 89% (NAFLD), 84% (NASH), 84% (cirrhosis).



Conclusion: Longitudinal ALT trajectories remained relatively stable among patients with NAFLD. Understanding the course of ALT fluctuations is important for helping to differentiate natural variation from potential hepatotoxic or beneficial effects of therapeutics. Next steps include exploration of ALT trends associated with probability of clinical outcomes.

FRI104

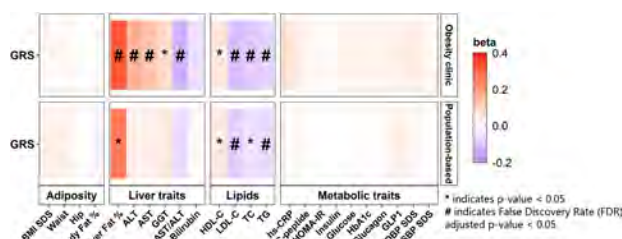
An adult-based genetic risk score for hepatic fat associates with liver and lipid traits in Danish children and adolescents

Yun Huang¹, Sara Stinson¹, Helene Bæk Juel¹, Morten Lund^{2,3}, Louise Aas Holm^{1,3}, Cilius Esmann Fonvig^{1,3,4}, Niels Grarup¹, Oluf Pedersen¹, Michael Michael Christensen^{2,5}, Aleksander Krag^{6,7}, Stefan Stender⁸, Jens-Christian Holm^{1,3,9}, Torben Hansen¹. ¹University of Copenhagen, The Novo Nordisk Foundation Center for Basic Metabolic Research, København, Denmark; ²University of Copenhagen, Department of Biomedical Sciences, Denmark; ³Copenhagen University Holbæk Hospital, Department of Pediatrics; ⁴Kolding Hospital a part of Lillebælt Hospital, Department of Pediatrics; ⁵Statens Serum Institute, Department for Congenital Disorders; ⁶Odense University Hospital, Department of Gastroenterology and Hepatology; ⁷University of Southern Denmark, Institute of Clinical Research; ⁸Rigshospitalet, Department of Clinical Biochemistry; ⁹University of Copenhagen, Faculty of Health and Medical Sciences
Email: torben.hansen@sund.ku.dk

Background and aims: Several genetic variants that associate with hepatic fat content in adults have been identified in genome-wide association studies. Their effects in children and adolescents remain unclear. The aims of this study were to test the effect of genetic variants known to associate with hepatic fat in adults, individually and combined as a genetic risk score (GRS), with cardiometabolic traits, and to investigate the predictive ability of the GRS for hepatic steatosis in children and adolescents.

Method: Children and adolescents with overweight/obesity from an obesity clinic cohort (n = 1, 843, median age 11.7 years, body mass index standard deviation score [BMI SDS] 2.85, 45.2% male) and a population-based cohort of children and adolescents (n = 2, 271, median age 11.6 years, BMI SDS 0.26, 40.1% male) were included. Anthropometrics and biochemical parameters were measured in both cohorts. Liver fat content was measured by magnetic resonance spectroscopy in 539 individuals. We calculated a weighted GRS based on eight genetic variants known to associate with hepatic fat content in adults. Associations of individual genetic variants and the GRS with cardiometabolic traits were tested using multiple linear and logistic regression models. Receiver operating characteristic (ROC) curve analysis was performed on models based on risk factors for hepatic steatosis, defined as hepatic fat $\geq 5\%$, and area under the curve (AUC) was calculated to evaluate model performance.

Results: Variants in *PNPLA3*, *TM6SF2*, *GPAM*, and *GCKR* were significantly associated with higher liver fat content ($p < 0.01$) and with distinct patterns of circulating lipids. The GRS was associated with higher liver fat content and alanine transaminase (ALT), as well as lower LDL-cholesterol and triglycerides in the obesity clinic and population-based cohorts. The GRS was not associated with adiposity or other metabolic traits. The GRS was associated with higher prevalence of hepatic steatosis (odds ratio [OR] per 1-unit GRS-increase: 2.18, $p = 1E-8$), and with lower prevalence of dyslipidemia (OR 0.90, $p = 0.02$). A prediction model for hepatic steatosis including GRS alone yielded cross-validated AUC of 0.76 (95% CI 0.69–0.83). The addition of the GRS to a model containing clinical risk factors for hepatic steatosis (BMI SDS, ALT, homeostatic model assessment of insulin resistance [HOMA-IR]) increased AUC slightly from 0.87 (95% CI 0.82–0.92) to 0.89 (95% CI 0.84–0.94).



Conclusion: The adult-based GRS for hepatic fat was associated with liver fat content, liver enzymes and lipid profiles, but was not associated with adiposity and other metabolic traits in children and adolescents. The GRS could serve as a predictor of the risk for hepatic steatosis in addition to clinical risk factors and could be used for early preventative initiatives.

FRI105

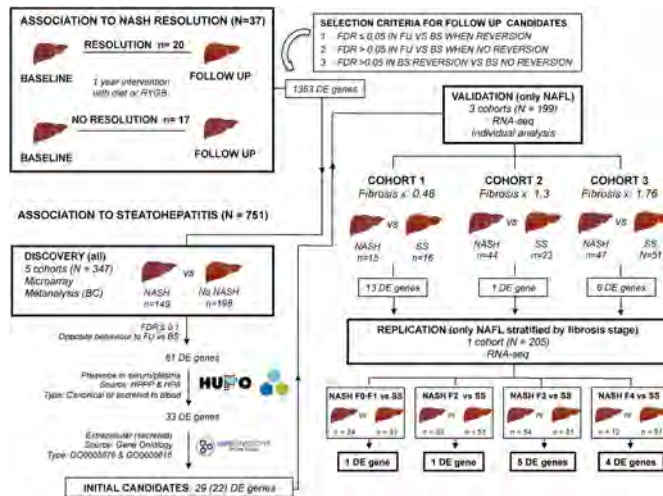
Identification of new potential biomarkers to follow steatohepatitis in patients with non-alcoholic/metabolic-associated fatty liver disease

Douglas Maya^{1,2,3}, Rocío Gallego-Durán^{1,2,3}, María del Rosario García-Lozano^{1,2}, Rocío Muñoz Hernández^{1,3,4}, Angela Rojas Alvarez-Ossorio^{1,2,3}, Antonio Gil-Gomez^{1,2,3}, Javier Ampuero^{1,2,3,4}, Manuel Romero Gomez^{1,2,3,4}. ¹Institute of Biomedicine of Seville, Hepatic, Digestive and Inflammatory Diseases, Sevilla, Spain; ²Centro de Investigación Biomédica en Red en el Área temática de Enfermedades Hepáticas, Spain; ³Hospital Universitario Virgen del Rocío, Gastroenterology and Hepatology, Sevilla, Spain; ⁴Facultad de Medicina, Universidad de Sevilla, Sevilla, Spain
Email: mromerogomez@us.es

Background and aims: To integrate different liver gene-expression datasets to identify novel potential serological biomarkers to follow-up steatohepatitis in NAFLD patients.

Method: Initial candidates were obtained by comparing the gene expression of paired liver biopsies coming from NAFLD patients that were able (n = 20) or not (n = 17) to resolve steatohepatitis at the end of a dietary or a surgical intervention of 1 year (section 1). Association of candidates to steatohepatitis was initially explored in 6 microarray gene expression datasets (n = 317) in which patients were classified as NASH or No NASH according to the SAF score and analysed as a single cohort after batch normalization. Selected candidates were filtered through a series of public datasets to retain exclusively secreted proteins able to reach the bloodstream. Candidates were validated independently in three additional RNA-seq additional datasets in which patients with Bland Steatosis (SS) were compared against patients with steatohepatitis (NASH (Cohort 1: N = 31 15 SS/16 NASH) (Cohort 2 N = 67 23 SS/44 NASH) (Cohort 3 N = 99 51 SS/47 NASH)) introducing age (Cohorts 2 and 3) and sex as covariables in the analysis (all 3). These candidates were further explored in a recently published gene expression (Govaere et al. 2020) in which 163 NASH patients were stratified by fibrosis stage (F0–F1 n = 34; F2 n = 53; F3 n = 54; F4 n = 12) and compared against patients with bland steatosis with no or mild fibrosis (SS n = 51).

Results: Paired liver biopsy analysis identified 1363 genes that significantly change their behaviour specifically in patients achieving NASH resolution. 61 of them showed a positive or a negative association to steatohepatitis in the integrative multiarray comparison in the microarray multicohort dataset. 22 of them are secreted and can reach the bloodstream. Only one of them, IL-32, replicated its behaviour in the microarray cohort (Fold Change (FC): 1.43, p-value 1.3×10^{-9} , FDR: 1.3×10^{-6}) and in all three RNA-seq analysis (Cohort 1 FC: 2.47, p-value 6.2×10^{-4} , FDR 1.0×10^{-2} ; Cohort 2: FC: 1.59, p-value 8.3×10^{-5} , FDR: 9.7×10^{-2} ; Cohort 3 FC: 2.11, p-value 1.15×10^{-7} , FDR: 3.2×10^{-6}). This protein also replicated its behaviour in the last dataset independently from fibrosis stage (NASH F0–F1 vs NAFL FC: 1.64, p-value: 3.78×10^{-6} , q-value: 9.99×10^{-4}) (NASH F2 vs NAFL FC: 1.69, p-value: 5.62×10^{-5} , q-value: 2.90×10^{-2}) (NASH F3 vs NAFL FC: 2.03, p-value: 4.81×10^{-8} , q-value: 8.52×10^{-6}) (NASH F4 vs NAFL FC: 2.16, p-value: 4.80×10^{-5} , q-value: 1.83×10^{-3}).



Conclusion: IL-32 expression in the liver shows the most robust and dynamic association to steatohepatitis and might constitute a useful biomarker for its detection and follow-up in patients.

FRI106

NASH patient's itinerary: Comparison of strategies for screening, referring and management

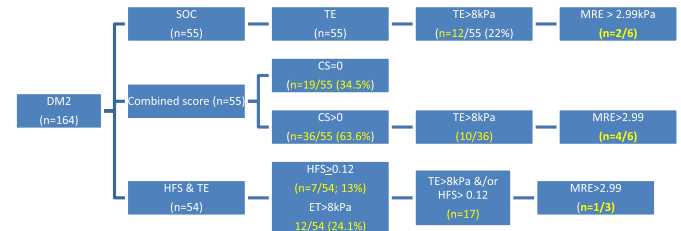
Manuel Romero Gomez^{1,2,3}, Yolanda Sánchez^{2,4}, Silvia García Rey^{2,4}, Francisco Javier Atienza Martín⁵, Pablo Remon⁶, Carmen Lara Romero^{2,6}, María C. Roque-Cuellar^{2,4}, Inmaculada Dominguez⁷, Ioanna-Panagiota Kalafati⁸, Sabine Kahl⁹, Pedro Pablo García-Luna^{7,10}, Jörn Schattenberg¹¹, Michael Roden¹², George Dedoussis⁸, Jeffrey Lazarus¹³. ¹Digestive Diseases Department, Virgen del Rocío University Hospital; ²Institute of Biomedicine of Seville; ³CIBERehd; ⁴Virgen del Rocío University Hospital; ⁵Centro de Salud El Porvenir, Seville, Spain; ⁶Endocrinology and Nutrition Department, Virgen del Rocío University Hospital; ⁷Clinical Biochemistry Department, Virgen del Rocío University Hospital; ⁸Harokopio University Athens; ⁹Deutsches Diabetes-Zentrum; ¹⁰University of Seville; ¹¹University Medical Center Mainz; ¹²German Diabetes Center; ¹³Barcelona Institute for Global Health (ISGlobal), Hospital Clínic, University of Barcelona Email: mromerogomez@us.es

Background and aims: Non-alcoholic fatty liver disease (NAFLD) is a highly prevalent, underdiagnosed, health system burden and impacts on quality of life including comorbidities in the affected population. Cost-effective strategies focusing on clinical pathways to detect and refer patients to care are needed. The aim of this study is to build a stepwise algorithm combining non-invasive freely available methods (FIB-4, NFS, HFS alone or combined) and vibration-controlled transient elastography (VCTE) in diabetic patients from primary care and endocrinology units.

Method: One-hundred sixty-four diabetes patients were recruited from January 2021 to February 2022 and randomized to one of three arms: Arm A (n=55) patients referred following standard of care; Arm B (n=55) patients referred due to altered combined fibrosis score (CFS) (FIB-4>1.3 or NFS>-1.456 or HFS>0.12); and Arm C (n=54) patients referred due to HFS>0.12 or VCTE>8 KPa. Patients at risk of NAFLD-fibrosis (VCTE>8 kPa) underwent magnetic resonance elastography (MRE).

Results: Age average was 55 ± 10 y, 54.3% males, and 66.5% obese (BMI>30 Kg/m²). Transient elastography >8 kPa was found in 35/164 (21.3%); >10 kPa 22/164 (13.4%) and >15 kPa 12/164 (7.3%). No statistical differences were seen among these three arms in biochemical, anthropometric or clinical features. All patients from Arm A were referred and 12/55 showed VCTE>8 kPa and 7 underwent MRE. In Arm B, 36 patients were referred and 10/36 showed VCTE>8 kPa and 9 underwent MRE. In Arm C, 17 were referred and

4 underwent MRE. Two out of six, four out of six and one out of three patients in each arm showed MRE>2.99 kPa (significant fibrosis) in five patients MRE was not valid. Estimated cost for NAFLD patient referral to the liver unit was approximately €570, 78 (Sánchez-Torrijos et al. REED 2019), VCTE €120 and CFS €0.59 per patient with T2DM: cost in Arm A was €31, 392.9; cost in Arm B was €24, 90053 and in Arm C was €16, 215.12



Conclusion: The prevalence of advanced fibrosis in a diabetic cohort reached 7.3% confirmed by transient elastography and MRE. A stepwise algorithm in the management of patients with type 2 diabetes with combined score and VCTE was cost-effective, allowing to save 50% of the budget compared to the standard of care. **Acknowledgement:** Unrestricted grant from Gilead Sciences.

FRI107

Performance of fibrometer-derived biomarker panels for assessment of fibrosis stage in NAFLD: NIMBLE stage 1 and the NASH CRN collaborative Study

Rohit Loomba¹, Sudha Shankar², Katherine Yates³, Clayton Dehn⁴, James Bolognese⁵, Brent Tetri⁶, Kris Kowdley⁷, Raj Vuppalanchi⁸, Cynthia Guy⁹, James Tonascia³, Anthony Samir¹⁰, Claude Sirlin¹¹, Sarah Sherlock¹², Kathryn Fowler¹¹, Helen Heymann¹³, Tania Kamphaus¹³, Roberto Calle¹⁴, Arun Sanyal¹⁵. ¹University of California at San Diego, San Diego, United States; ²Astrazeneca, United States; ³Johns Hopkins University, Bloomberg School of Public Health, United States; ⁴P-value LLC, United States; ⁵Cytel, United States; ⁶Saint Louis University, Department of Gastroenterology and Hepatology, United States; ⁷Liver Institute Northwest, United States; ⁸Indiana University, Division of Gastroenterology and Hepatology, United States; ⁹Duke University, Department of Pathology, United States; ¹⁰Massachusetts General Hospital, Department of Radiology, United States; ¹¹University of California at San Diego, Department of Radiology, United States; ¹²Pfizer, United States; ¹³Foundation for the National Institutes of Health (FNIH), United States; ¹⁴Regeneron Pharmaceuticals, United States; ¹⁵Virginia Commonwealth University, Division of Gastroenterology, Hepatology and Nutrition, Department of Internal Medicine, United States Email: roloomba@ucsd.edu

Background and aims: The intent of the current collaborative study between NIMBLE & the NASH CRN was to further evaluate the performance of Fibrometer-based biomarker panels, including those developed for NAFLD or other liver diseases, with & without VCTE for identification of fibrosis strata in those with NAFLD. This cross-sectional study evaluated the diagnostic-test performance characteristics of four Fibrometer-based biomarker panels for assessing fibrosis in a well-characterized cohort of patients with biopsy-confirmed NAFLD with description of sensitivity & specificity at Youden's cutoff for their intended diagnostic use in a large, multi-center US cohort of patients with NAFLD/NASH.

Method: The performance of Fibrometer Virus (FM-VIRUS), Cirrhometer Virus (CM-VIRUS), Fibrometer NAFLD (FM-NAFLD) & Fibrometer VCTE-Light (FM-VCTE-Light) was evaluated for the assessment of fibrosis. Blood-based parameters were tested from aliquots of the same blood sample from each patient obtained within 90 days of a liver biopsy demonstrating NAFLD of varying activity &

POSTER PRESENTATIONS

stages (Stages 0–4). VCTE measurements were performed in a subgroup of trial participants within this time window. In order to minimize spectrum bias, the cohort was selected a priori to have a similar distribution of fibrosis stages across its entire range. The primary hypothesis was that the AUROC for each panel for its intended use was numerically >0.7 & significantly superior to 0.5. The secondary hypothesis was that the AUROC for each panel for fibrosis was significantly greater than that for FIB-4 (as the common reference).

Results: 1073 patients with biopsy-proven NAFLD including NAFL (n = 220) & NASH (n = 853) were evaluated. The number of patients with fibrosis stages 0, 1, 2, 3 & 4 were 222, 114, 262, 277 & 198, respectively. The dataset for Fibrometer VCTE-Light was smaller as VCTE data were available in only 393 patients. The AUROCs, Youden's cutoff with its sensitivity/specificity are provided below: All 4 panels met criteria for intended use for diagnosis of fibrosis stage ≥ 2 , advanced fibrosis, & cirrhosis. Compared to FIB-4, FM-VIRUS & FM-NAFLD met criteria for diagnosis of advanced fibrosis but not for fibrosis stage ≥ 2 or cirrhosis, while CM-VIRUS was not superior to FIB-4 for any of the intended uses. In contrast, FM-VCTE-Light was significantly superior to FIB-4 for all three intended uses.

	FIB-4	FM-VIRUS	CM-VIRUS	FM-NAFLD	FM-VCTE-Light
Parameters	Age, ALT, AST, PLT	Age, sex, A2M, AST, BUN, GGT, INR, PLT	Age, sex, A2M, AST, BUN, GGT, INR, PLT	Age, weight, AST, ALT, FER, GLU, PLT	Age, sex, A2M, AST, GGT, LSM, PLT
Diagnostic test characteristic	AUROC (Youden cut-off value) [Sensitivity, Specificity]				
F stage ≥ 2	0.796 (1.4) [65.4,80.8]	0.801 (0.4) [69.2,77.4]	0.723 (0.0) [65.2,69.9]	0.809 (0.4) [67.7,80.0]	0.836** (0.4) [71.6,81.1]
F stage ≥ 3	0.793 (1.4) [75.1, 68.6]	0.808* (0.4) [76.4,69.9]	0.764 (0.0) [76.2,63.0]	0.805* (0.4) [77.9,67.0]	0.854** (0.4) [89.9,65.3]
F stage 4	0.81 (1.5) [85, 63.4]	0.826 (0.6) [75.0,73.2]	0.822 (0.1) [65.6,81.5]	0.800 (0.5) [76.7,68.0]	0.899* (0.7) [94.2,74.7]

A2M: alpha2 macroglobulin, AST: aspartate aminotransferase; ALT: alanine aminotransferase, BUN: blood urea nitrogen, FER: ferritin, GGT: Gamma-glutamyl transferase, GLU: fasting glucose, INR: international normalized ratio, LSM: liver stiffness by VCTE, PLT: platelets count.

*p < 0.05 for comparison with FIB-4 for their intended use

**p < 0.001 for comparison with FIB-4 for their intended use

All AUROCs are statistically significant and superior to AUROC=0.5 (p<0.001)

Conclusion: FM-VCTE-Light consistently outperformed FIB-4 for stratification of fibrosis across a spectrum of fibrosis stages. FM-VIRUS & FM-NAFLD appear to be better than FIB-4 for detecting advanced fibrosis but not for other fibrosis stages. These data will be helpful in informing trial design for future studies using these Fibrometer-based non-invasive tools across various intended use populations.

FR1108

Diagnostic accuracy of non-invasive tests for fibrotic NASH-An individual participant data meta-analysis

Ferenc Mozes¹, Jenny Lee², Yasaman Vali², Emmanuel Selvaraj¹, Arjun Jayaswal¹, Jerome Boursier³, Elisabetta Bugianesi⁴, Rami Younes⁵, Monica Lupson-Platon⁶, Salvatore Petta⁷, Toshihide Shima⁸, Takeshi Okanoue⁸, Sanjiv Mahadeva⁹, Wah-Kheong Chan⁹, Gideon Hirschfield¹⁰, Peter Eddowes¹¹, Philip N. Newsome¹², Vincent Wai-Sun Wong¹³, Victor de Lédinghen¹⁴, Jeremy Cobbald¹⁵, Yoshio Sumida¹⁶, Akira Okajima¹⁶, Jörn Schattenberg¹⁷, Christian Labenz¹⁸, Won Kim¹⁹, Myoung Seok Lee²⁰, Guruprasad Aithal²¹, Naaventhana Palaniyappan²¹, Cristophe Cassinotto²², Sandeep Aggarwal²³, Harshit Garg²³, Geraldine Ooi²⁴, Atsushi Nakajima²⁵, Masato Yoneda²⁵, Ming-Hua Zheng²⁶, Céline Fournier²⁷, Michael Trauner²⁸, Andreas Geier²⁹, Theresa Tuthill³⁰, Carla Yunis³⁰, Quentin Anstee³¹, Stephen Harrison¹, Patrick Bossuyt¹, Michael Pavlides¹. ¹University of Oxford, RDM Cardiovascular Medicine, Oxford, United Kingdom; ²University of Amsterdam, Department of Epidemiology and Data Science, Amsterdam

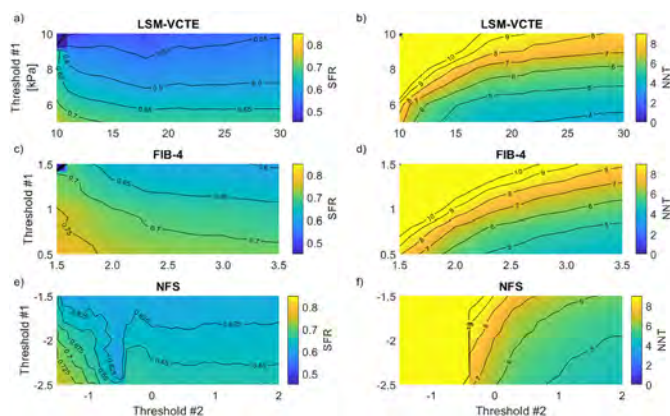
UMC, Amsterdam, Netherlands; ³Centre Hospitalier Universitaire d'Angers, Service d'Hepato-Gastroenterologie et Oncologie Digestive, Angers, France; ⁴University of Turin, Division of Gastroenterology and Hepatology, Department of Medical Sciences, Turin, Italy; ⁵Boehringer Ingelheim, Ingelheim, Germany; ⁶Iuliu Hațieganu University of Medicine and Pharmacy, Department of Medical Imaging, Regional Institute of Gastroenterology and Hepatology "Prof.Dr. Octavian Fodor," Cluj Napoca, Romania; ⁷University of Palermo, Section of Gastroenterology and Hepatology, PROMISE, Palermo, Italy; ⁸Saiseikai Suita Hospital, Department of Gastroenterology and Hepatology, Suita, Japan; ⁹University of Malaya, Gastroenterology and Hepatology Unit, Department of Medicine, Faculty of Medicine, Kuala Lumpur, Malaysia; ¹⁰University Health Network, Toronto Centre for Liver Disease, Toronto, Canada; ¹¹Nottingham University Hospitals NHS Trust and University of Nottingham, National Institute for Health Research Nottingham Biomedical Research Centre, Nottingham, United Kingdom; ¹²National Institute for Health Research Biomedical Research Centre at University Hospitals Birmingham NHS Foundation Trust and the University of Birmingham, Birmingham, United Kingdom; ¹³The Chinese University of Hong Kong, Department of Medicine and Therapeutics, Hong Kong, Hong Kong; ¹⁴Bordeaux University Hospital, Centre d'Investigation de la Fibrose Hépatique, Hôpital Haut-Lévêque, Pessac, France; ¹⁵University of Oxford, Translational Gastroenterology Unit, Oxford, United Kingdom; ¹⁶Aichi Medical University, Division of Hepatology and Pancreatology, Department of Internal Medicine, Aichi, Japan; ¹⁷University Medical Center of the Johannes Gutenberg-University, Metabolic Liver Research Program, I. Department of Medicine, Mainz, Germany; ¹⁸University Medical Center of the Johannes Gutenberg-University, Mainz, I. Department of Medicine, Mainz, Germany; ¹⁹Seoul Metropolitan Government Boramae Medical Center, Division of Gastroenterology and Hepatology, Department of Internal Medicine, Seoul National University College of Medicine, Seoul, Korea, Rep. of South; ²⁰Seoul Metropolitan Government Boramae Medical Center, Department of Radiology, Seoul National University College of Medicine, Seoul, Korea, Rep. of South; ²¹University of Nottingham, Nottingham Digestive Diseases Centre, Translational Medical Sciences, School of Medicine, Nottingham, United Kingdom; ²²University Hospital of Montpellier, Department of Diagnostic and Interventional Radiology, Saint-Elloi Hospital, Montpellier, France; ²³AIIMS, Department of Surgical Disciplines, New Delhi, India; ²⁴Monash University, Centre for Obesity Research and Education, Department of Surgery, Melbourne, Australia; ²⁵Yokohama City University, Department of Gastroenterology and Hepatology, Yokohama, Japan; ²⁶the First Affiliated Hospital of Wenzhou Medical University, NAFLD Research Center, Department of Hepatology, Wenzhou, China; ²⁷Echosens, Paris, France; ²⁸University of Vienna, Vienna, Austria; ²⁹University Hospital Würzburg, Division of Hepatology, Würzburg, Germany; ³⁰Pfizer, Cambridge, United States; ³¹Newcastle University, Translational and Clinical Research Institute, Faculty of Medical Sciences, Newcastle, United Kingdom
Email: ferenc.mozes@cardiov.ox.ac.uk

Background and aims: Histological assessment to confirm non-alcoholic steatohepatitis with significant fibrosis (NASH+F2–3) is needed prior to enrolment in clinical trials. Non-invasive testing (NIT) strategies to identify those with high risk for the target condition are needed to reduce screen failure rates (SFR). Our aim was to evaluate liver stiffness measurements by vibration-controlled transient elastography (LSM-VCTE), alone or in combination with the fibrosis-4 score (FIB-4) and the NAFLD fibrosis score (NFS) in such screening strategies.

Method: This was an individual participant data meta-analysis of studies evaluating LSM-VCTE against liver histology. The target condition was NASH+F2–3. NASH was defined as NAS \geq 4 with at least grade 1 in each of the components. Upper and lower cut-offs were used, with patients with NIT cut-offs between these two thresholds being selected for liver biopsy. Diagnostic performance was tested over a range of lower and upper NIT thresholds for single NITs, and sequential combinations of serum NITs and LSM-VCTE.

Sensitivity (Se), specificity (Sp), SFR, and number of patients that need to be tested to identify one true positive case (NNT) are reported.

Results: We included 2738 individual patient data from 25 primary studies (43% female, median age 52 years, median BMI 29 kg/m²; 41% had type 2 diabetes; 57% had NASH, 28% had NASH+F2–3). Threshold combinations and corresponding SFR and NNT for single NIT strategies are shown in Figure 1. Visual inspection of the SFR and NNT distributions showed that increasing the upper NIT thresholds above 20 kPa, 3.0 and 1.0 for LSM-VCTE, FIB-4 and NFS, respectively, does not improve diagnostic performance, so these were chosen as upper cut-offs. LSM-VCTE thresholds of 6 kPa and 20 kPa (Se 80%, Sp 44%, SFR 64%, NNT 4) had higher sensitivity, higher SFR and lower NNT, than thresholds 10 kPa and 20 kPa (Se 39%, Sp 83%, SFR 53%, NNT 9). FIB-4 thresholds 0.7 and 3.0 (Se 73%, Sp 33%, SFR 67%, NNT 6), only differed in sensitivity and specificity from thresholds 1.0 and 3.0 (Se 58%, Sp 53%, SFR 67%, NNT 6). NFS thresholds –3.0 and 1.0 (Se 79%, Sp 34%, SFR 68%, NNT 5), and –2.6 and 1.0 (Se 73%, Sp 43%, SFR 66%, NNT 5) had similar diagnostic performances.



Sequential combinations of NITs could perform similarly to single NITs, with fewer individuals needing LSM-VCTE and liver biopsy. FIB-4 with cut-offs 0.7 and 4.63 followed by LSM-VCTE with cut-offs 6 and 20 kPa had Se 68%, Sp 59%, SFR 60%, NNT 5. NFS with cut-offs –3.272 and 1.766 followed by LSM-VCTE with cut-offs 6 and 20 kPa had Se 70%, Sp 56%, SFR 62%, NNT 5.

Conclusion: The major benefit of employing a sequential testing strategy was the reduced number of liver biopsies. Additionally, we noticed no further gain in diagnostic accuracy for the upper threshold of NITs above a certain level, suggesting that a judicious choice of thresholds can lead to a reduction in testing costs.

FRI109

Multiparametric MRI biomarker corrected T1 as a prognostic marker in chronic liver disease

Naim Alkhouri¹, Cayden Beyer², Anneli Andersson², Elizabeth Shumbayawonda², Michael Pavlides³, Arjun Jayaswal³, Matt Kelly², Stephen Harrison³. ¹Arizona Liver Health, Fatty Liver Program, Chandler, United States; ²Perspectum, Innovation, United Kingdom; ³Oxford Centre for Magnetic Resonance (OCMR), Headington, United Kingdom
Email: cayden.beyer@perspectum.com

Background and aims: Liver biopsy is an imperfect reference test for non-alcoholic fatty liver disease (NAFLD) and non-alcoholic steatohepatitis (NASH), due to its invasive nature, 2.4% major complication rate, high intra- and inter-reader variability and sampling error. The utility of non-invasive technologies (NITs) as alternative tools for NASH prognosis are assessed by their ability to predict clinical outcomes. Non-invasive multiparametric magnetic resonance imaging (mpMRI) with LiverMultiScan, and specifically corrected T1

(cT1), has previously been shown to predict clinical outcomes. With this study we investigate the association of increasing cT1 thresholds with clinical outcomes.

Method: Imaging and outcomes data were collected at two tertiary centers in the UK between May 2011 and July 2017 from patients referred to clinically indicated biopsy or known liver cirrhosis diagnosis. Clinical outcomes data were collected as a composite endpoint comprising ascites, variceal bleeding, hepatic encephalopathy, hepatocellular carcinoma (HCC), liver transplantation and mortality, more details described by Jayaswal et al. *Liver Intl* (2020) and in NCT01543646. Cox proportional hazard analysis was used to calculate hazard ratios (HRs) for the continuous and grouped variables. Probability of clinical outcome for cT1 as a continuous variable was used as reference and the HRs for each cut-off were used as scaling factors.

Results: 182 patients, including 54% with NAFLD, with 620 years follow up were included in the analysis where 13 patients had liver event occurrences, suggesting the overall risk of complications of 7% within the <72 months follow-up time. The events were ascites (5), variceal bleeding (1), hepatic encephalopathy (2), HCC (3) and mortality (9), with some patients having multiple events. cT1 had a 0.7% increased risk of clinical event for every 1 ms increase in cT1 (HR = 1.007, 95% CI: 1.003–1.011, p = 0.0010), which is equivalent to 91% increase of risk per 100 ms (HR 1.91). Patients with cT1 greater than 875 ms had 3.42 [95% CI: 1.05–11.11, p < 0.05] times higher risk to experience an event before those with cT1 below or equal to 875 ms. The cumulative probability of clinical events over time was higher for patients with cT1 of greater than 875 ms, compared to those with intermediate (800–875 ms) and low (<800 ms) cT1 (Fig. 1).

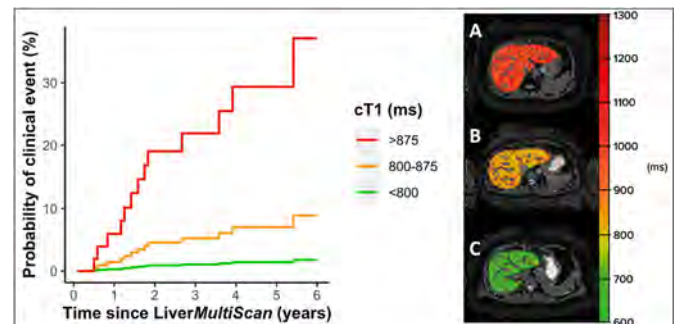


Figure 1: Probability of clinical events in chronic liver disease patients, comparing cT1 cut-offs recommended for clinical pathways and a scale showing the LiverMultiScan cT1 maps of patients with cT1 values of A) 1000ms, B) 833ms and C) 653ms.

Conclusion: This study demonstrates that cT1 above 875 ms is not only able to identify high-risk NASH patients, but also predicts who is at higher risk for clinical events by evaluating patient health records and clinical outcomes. These results show the potential impact non-invasive mpMRI biomarkers can have to inform public health strategies and mitigate the impact of the growing burden of NAFLD.

FRI110

Results of the Non-invasive Biomarkers of Metabolic Liver Disease (NIMBLE) study 1.1 on the reproducibility and repeatability of shear-wave and transient elastography in non-alcoholic fatty liver disease

Theodore Pierce^{1,2}, Arinc Ozturk^{1,2}, Sarah Sherlock³, Guilherme Cunha⁴, Xiaohong Wang⁵, Qian Li^{1,2}, Marian Martin¹, Hannah Edenbaum¹, Kathleen Corey^{2,5}, Yesenia Covarrubias⁴, Sudha Shankar⁶, Helen Heymann⁷, Tania Kamphaus⁷, Roberto Calle⁸, Nancy Obuchowski⁹, Arun Sanyal¹⁰, Rohit Loomba⁴, Claude Sirlin⁴, Kathryn Fowler⁴, Anthony Samir^{1,2}. ¹Massachusetts General Hospital, Radiology, Boston, United States; ²Harvard Medical School, Boston, MA; ³Pfizer; ⁴University of California San Diego, La Jolla; ⁵Massachusetts General Hospital, Fatty Liver Clinic; ⁶AstraZeneca; ⁷Foundation for the National Institutes of Health (FNIH), North Bethesda, United States; ⁸Regeneron, United States; ⁹Cleveland Clinic; ¹⁰Virginia Commonwealth University
Email: asamir@mgh.harvard.edu

Background and aims: The regulatory qualification of non-invasive tests (NITs) for liver fibrosis severity assessment is a major unmet need in non-alcoholic fatty liver disease (NAFLD). Ultrasound-based methods such as shear-wave elastography (SWE) and vibration-controlled transient elastography (VCTE) have the potential, through repeated use, to assess disease response and progression. However, this application has been limited by a paucity of reproducibility data across device manufacturers in the population at risk. The aim of this study from the imaging workstream of the FNIH NIMBLE consortium (NCT04828551), was to address this knowledge gap and contribute to the evidence needed for qualification of ultrasound-based methods.

Method: A prospective two-center study of adults with suspected or established NAFLD stratified by FIB-4 (≤ 1.3 , $>1.3 < 2.67$, ≥ 2.67) to reduce spectrum bias was performed. Each participant underwent 6 examinations on different ultrasound systems and VCTE on two days, each day by a different operator, less than a week apart. Sonographers and clinical investigators were blinded and a pre-specified data chain of custody was maintained. For uniformity, VCTE and SWE measurements were reported and analyzed in units of meters per second by an independent statistician. The primary end point was pooled different-day, different-operator reproducibility coefficient (RDC_{DDDO}). Secondary endpoints included scanner-specific RDC_{DDDO} , same-day/same-operator repeatability coefficient (RC_{SDSO}), and between-vendor RDC_{SDSO} . The study was powered to detect a 95% RDC_{DDDO} upper bound ($UB_{95\%}$) of $\leq 35\%$.

Results: 40 participants (mean age 60 years, 60% female) with low (17), intermediate (15), and high (8) FIB-4 scores were recruited. Mean body mass index was 30.9 kg/m². RDC_{DDDO} was 30.7% ($UB_{95\%}$ 34.4%) for SWE and 35.6% ($UB_{95\%}$ 43.9%) for VCTE. SWE vendor-specific RDC_{DDDO} varied from 24.2%–34.3%. RC_{SDSO} was 21.0% for SWE (13.9%–35.0%, by scanner) and 19.6% for VCTE. Between-vendor RDC_{SDSO} was 52.7% ($UB_{95\%}$ 64.7%).

	Number of Observations	RDC_{DDDO}	Upper 95% Confidence Bound	RC_{SDSO}	Upper 95% Confidence Bound
Vendor 1	24	31.9%	42.0%	19.0%	25.0%
Vendor 2	24	24.2%	32.1%	13.9%	18.3%
Vendor 3	24	29.9%	39.4%	14.2%	18.7%
Vendor 4	24	32.3%	42.5%	14.9%	19.6%
Vendor 5	24	34.3%	45.2%	35.0%	46.1%
Pooled SWE	40	30.7%	34.4%	21.0%	23.5%
VCTE	39	35.6%	43.9%	19.6%	24.1%

Conclusion: SWE demonstrated good RDC_{DDDO} , with slightly higher RDC_{DDDO} observed for VCTE. Considerably higher SWE variability is observed with measurements on different vendor platforms. These estimates are likely to inform ultrasound-based NIT qualification by (1) defining expected variability, (2) establishing that serial examination variability is lower when performed on the same vendor platform, and (3) informing future clinical trial design, including NIMBLE stage 2.

FRI111

Independent association of physical activity with nonalcoholic fatty liver disease and alanine aminotransferase levels

Jun Kyu Lee¹. ¹Dongguk University Ilsan Hospital, Internal Medicine, Goyang, Korea, Rep. of South
Email: jeromee1971@yahoo.co.kr

Background and aims: The aim of the current study was to examine the independent association of physical activity with nonalcoholic fatty liver disease (NAFLD) and aminotransferases while adjusting for obesity and diet.

Method: A data from 32,391 participants aged ≥ 20 years in the Korea National Health and Nutrition Examination Surveys (KNHANES) was analyzed by logistic regression models and general linear models. Physical activity was assessed from the questionnaire by health-enhancing physical activity (HEPA).

Results: The physical activity was negatively associated with NAFLD after adjustment for multiple factors with an odds ratio of 0.66 (95% CI, 0.57–0.76) comparing the most active (HEPA active) and the least active (inactive) participants. Among the participants with NAFLD, physical activity also showed an independent negative association with alanine aminotransferase (ALT) levels but not with aspartate aminotransferase levels. These independent associations were not observed when comparing the minimally active and inactive participants.

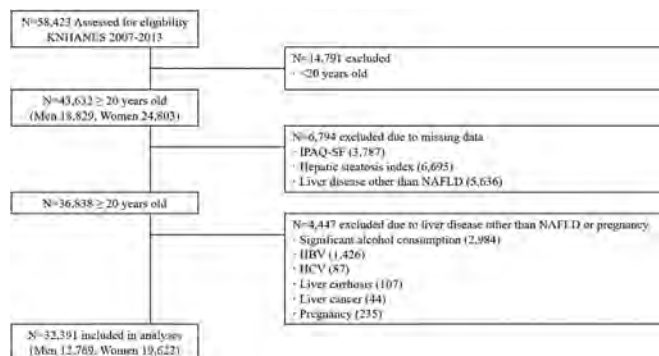


Fig. 1. Flow diagram of participant inclusion and exclusion in the current study using data from Korea National Health and Nutrition Examination Surveys (KNHANES IV, V and VI).

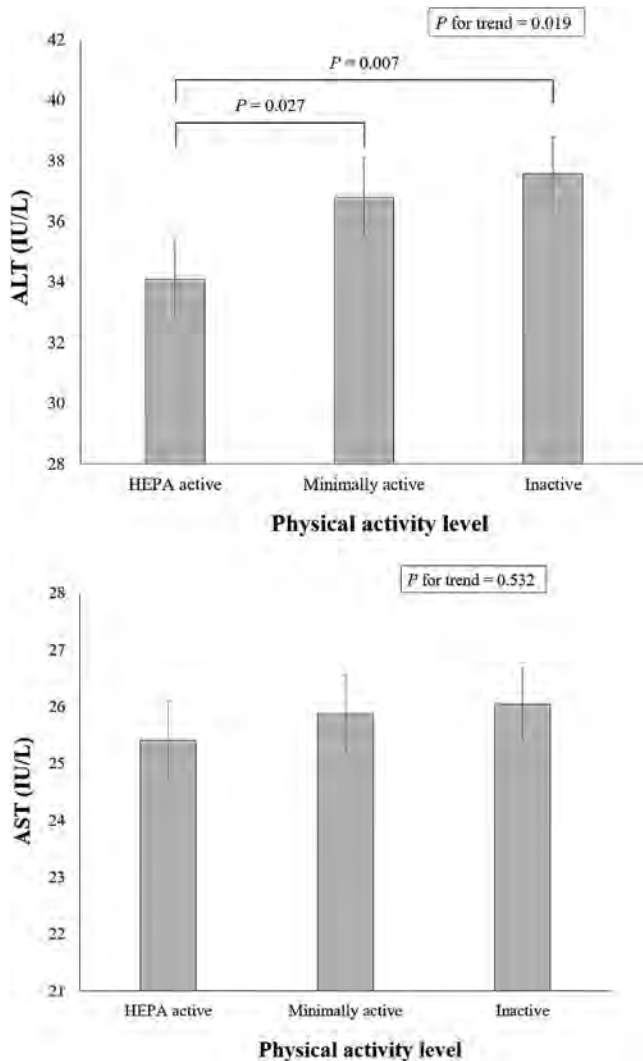


Fig. 2: Adjusted weighted means of ALT (upper) and AST (lower) by the physical activity level among participants with NAFLD (n = 6, 968).

Conclusion: Physical activity is independently associated with the degree of hepatocellular injury in patients with NAFLD as well as the risk of NAFLD in the general population. Sufficiently active physical activity greater than a minimally active level may be needed to lower the risk of NAFLD and ALT levels.

FRI112

In a nonalcoholic steatohepatitis (NASH) clinical trial, baseline and screen failure magnetic resonance elastography (MRE) liver stiffness values calculated as weighted means were not different from values calculated as simple means

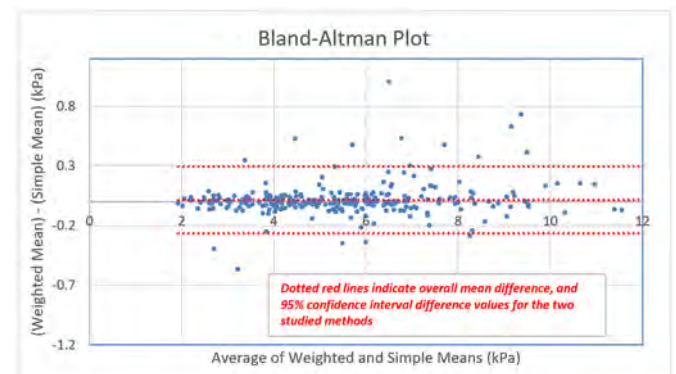
Michael Middleton^{1,2}, Mark Becker³, Walter Henderson¹, Claude Sirlin¹. ¹University of California, San Diego, Radiology, San Diego, United States; ²Quantix Bio, Lewes, United States; ³Intercept Pharmaceuticals, Inc., San Diego, United States
Email: msm@ucsd.edu

Background and aims: Magnetic resonance elastography (MRE) liver stiffness, a quantitative imaging biomarker of hepatic fibrosis, is commonly used in nonalcoholic steatohepatitis (NASH) clinical treatment trials. Typically, four images are acquired through the liver, and means of liver stiffness, weighted based on region-of-interest size are calculated to generate a single representative liver stiffness value for each exam. This is an appropriate method to use in clinical trials, but anecdotally it has been suggested that obtaining simple, rather than weighted means for routine clinical care is easier

and may suffice. The Quantitative Imaging Biomarker Alliance (QIBA) has considered this question as part of their efforts to provide guidelines on how MRE exams should be acquired and analyzed. Data from drug development clinical trials are in many ways ideal to study this kind of question, given that typically such studies are conducted at large numbers of clinical sites using a wide variety of MR scanners of different styles and field strengths, from different MR scanner vendors. Hence, we undertook an analysis of MRE baseline and screen failure imaging data from a clinical trial testing a potential new treatment drug for NASH (NCT03439254; in progress) to determine whether liver stiffness values differed as to whether weighted, or simple means were used to generate final liver stiffness values for each exam.

Method: 308 baseline and screen failure MRE exams were obtained between October 2017 and December 2019 from 49 imaging sites worldwide. 19 MR scanner styles were represented, including 1.5 T and 3 T scanners from GE, Siemens, and Philips, with each exam using either a 2D GRE or a 2D SE-EPI pulse sequence. After exclusion of 13/308 (4.2%) of exams that were not analyzable, and 6/308 (1.9%) of exams for which incorrect images were acquired, 289/308 (93.8%) of exams were included in this analysis. Weighted and simple liver stiffness means were calculated, and compared using regression, Bland Altman, and Student t test analyses.

Results: Weighted liver stiffness means were not different from simple means (5.51 ± 1.97 kPa vs. 5.50 ± 1.94 kPa, respectively; $p = 0.11$). On regression analysis, slope was 0.986, intercept was 0.07 kPa, and the R^2 value was 0.995. On Bland Altman analysis, weighted and simple means differed by 0.01 ± 0.14 kPa. This difference is small compared to typical variability due to inter-scanner reproducibility, and is not clinically meaningful.



Conclusion: In a multi-center NASH clinical trial in which sites were trained and site protocols qualified by a central analysis center before study exams were acquired, no difference was observed between baseline weighted and simple mean MRE liver stiffness values across four acquired slices. This data will help inform ongoing work by QIBA in qualifying MRE liver stiffness as a quantitative imaging biomarker of hepatic fibrosis.

FRI113

Influence of pregnancy on NAFLD-associated lipidomic signatures

Tatyana Kushner¹, Ibon Martínez-Arranz², Marco Arrese³, Mazen Nouredin⁴, Rhoda Sperling¹, Keith Sigel¹, Scott Friedman¹, Pablo Ortiz², Cristina Alonso². ¹Icahn School of Medicine at Mount Sinai; ²OWL Metabolomics, Spain; ³Pontificia Universidad Catolica de Chile; ⁴Cedars Sinai
Email: tatyana.kushner@mssm.edu

Background and aims: Although NAFLD-associated lipidomic signatures have been defined in the general population, there is limited data on the influence of pregnancy on NAFLD-associated

POSTER PRESENTATIONS

lipidomic changes. In this study, we elucidate the deregulated lipidomic serum landscape of pregnant women with NAFLD.

Method: We prospectively screened for NAFLD at 18–22 weeks gestation in pregnant women. Pregnant woman with NAFLD ($n = 6$) and without NAFLD ($n = 7$) were matched 1:1 with retrospectively collected cases from non-pregnant woman with and without NAFLD ($n = 13$) based on age-, BMI- and disease-stage. Lipidomic analysis of serum samples collected under fasting conditions was performed using ultra-high performance liquid chromatography-mass spectrometry, covering lipid species across classes of glycerolipids, glycerophospholipids (phosphatidylinositol, acyl- and ether-linked phosphatidylethanolamine (PE) and phosphatidylcholine (PC)), sphingolipids (ceramides, monohexosylceramides and sphingomyelins), fatty acids and sterols (cholesteryl esters, steroids and bile acids). Lipidomic profiles in pregnant females with vs. without NAFLD and in pregnant females vs. non-pregnant matched female controls were compared.

Results: Pregnant women with NAFLD had higher PE, lysoPE and lower ceramides compared to non-pregnant women with NAFLD (see Figure). Pregnant women with NAFLD had lower triglycerides compared to non-NAFLD pregnant women; non-pregnant females with NAFLD had higher triglycerides compared to non-pregnant females without NAFLD. Pregnant women without NAFLD were significantly more likely to have lower saturated (SFA), monounsaturated (MUFA), and polyunsaturated fatty acids (PUFA) ($p < 0.05$), but have significantly higher triglyceride levels than non-pregnant women with NAFLD ($p < 0.05$). Non-NAFLD pregnant women also had lower ceramides and ether linked-lysoPC compared to non-pregnant women.

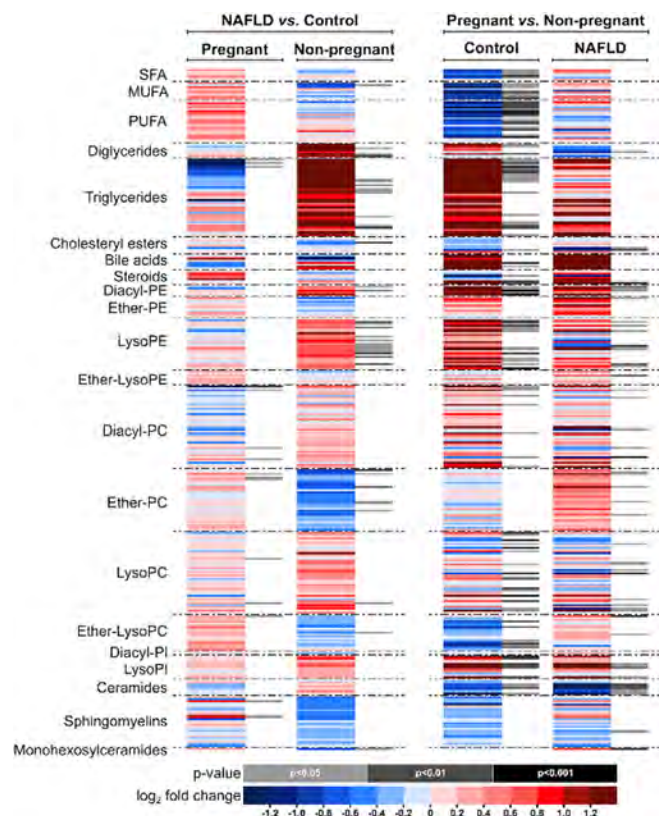


Figure: Heatmaps of lipidomic profiles in pregnant women (with and without NAFLD) compared to non-pregnant controls (with and without NAFLD).

Conclusion: Our findings suggest that NAFLD associated lipidomic signatures may be significantly impacted by pregnancy. NAFLD in pregnancy appears to be associated with a depletion in serum triglycerides and ceramides. Further workup should evaluate pregnancy-trimester specific changes as well as the role these lipid changes may play on NAFLD-associated adverse pregnancy outcomes such as gestational diabetes or effects on the newborn.

FRI114

Plasma sgp130 is an independent predictor of non-alcoholic fatty liver disease severity

Aysim Gunes^{1,2,3}, Laurent Bilodeau⁴, Catherine Huet⁴, Assia Belblidia⁴, Cindy Baldwin¹, Jeanne-Marie Giard⁵, Laurent Biertho^{6,7}, Annie Lafortune^{6,7}, Christian Couture^{6,8}, Bich N. Guyen⁹, Eithan Galun¹⁰, Chantal Bemeur^{11,12}, Marc Bilodeau¹², Mathieu Laplante^{3,6,13}, An Tang⁴, May Faraj^{1,3,11}, Jennifer Estall^{1,2,3}.

¹Institut de recherches cliniques de Montréal (IRCM), Montréal, Canada;

²McGill University, Division of Experimental Medicine, Montréal,

Canada; ³Montreal Diabetes Research Centre, Canada; ⁴Hôtel Dieu de

Montréal-CHUM, Département de radiologie, Montréal, Canada; ⁵Hôtel

Dieu de Montréal-CHUM, Département d'hépatologie, Montréal,

Canada; ⁶University Institute of Cardiology and Respiratory of Quebec,

Québec, Canada; ⁷Laval University, Département de chirurgie, Québec,

Canada; ⁸Department of Molecular Biology, Medical Biochemistry and

Pathology, Québec, Canada; ⁹University of Montreal, Département de

pathologie et biologie cellulaire, Montréal, Canada; ¹⁰Goldyne Savad

Institute of Gene Therapy, Israel; ¹¹University of Montreal, Département

de nutrition, Montréal, Canada; ¹²Research Center Du Chum, Labo

Hépatoneuro, Montréal, Canada; ¹³Laval University, Centre de recherche

sur le cancer de l'Université Laval, Québec, Canada

Email: a.gkizil@gmail.com

Background and aims: Nonalcoholic steatohepatitis (NASH) is a metabolic disease associated with liver failure and cancer. Monitoring of advancing NASH is challenging. Since liver inflammation is a main driver of fibrosis, we investigated relationships between circulating components of the interleukin-6 signaling pathway (IL-6, sIL-6R and sgp130) and liver pathology in subjects with NAFLD and NASH.

Method: Predictive performance of plasma IL-6, sIL-6R and sgp130 were investigated in two independent cohorts: 1) patients with biopsy-confirmed NASH ($n = 49$), where magnetic resonance spectroscopy (MRS), imaging (MRI) and elastography (MRE) assessed liver fat, volume and stiffness; and 2) patients with morbid obesity ($n = 245$) undergoing bariatric surgery where histological staging of steatosis, activity, and fibrosis assessed NASH severity. Correlations were evaluated between IL-6, sIL-6R, sgp130 and anthropomorphic characteristics, plasma markers of metabolic disease or liver pathology.

Results: In patients with NASH, plasma IL-6 and sgp130 strongly correlated with liver stiffness, which for sgp130 was independent of age, sex, BMI, diabetes, hyperlipidemia, hypertension or history of HCC. Plasma sgp130 was the strongest predictor of liver stiffness compared to common biomarkers and risk scores. Plasma sIL-6R correlated with liver volume independent of age, sex, and BMI. In stepwise regression analysis, plasma sgp130 followed by NAFLD fibrosis score and plasma globulin, predicted up to 74% of liver stiffness. In patients with morbid obesity, circulating sgp130 correlated with advanced liver fibrosis.

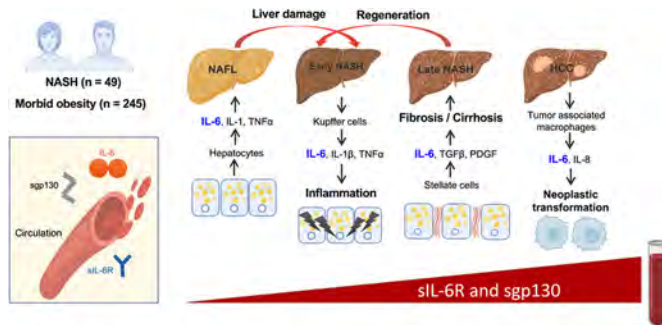


Figure: Advanced NASH is associated with liver failure and cancer; however, its detection in early stages is limited due to lack of non-invasive biomarkers. Interleukin-6 is an important player in NAFLD at all stages, involving multiple signaling mediators that circulate in blood. In biopsy-confirmed NASH, plasma sgp130 was the best predictor of liver stiffness and sIL-6R correlated with liver volume (MRI/MRE). In a second population, high sgp130 was detected in subjects with advanced fibrosis (histology). Circulating sgp130 may be a sensitive biomarker across all stages of NASH linked to metabolic disease independent of sex, age and BMI in progressive NAFLD.

Conclusion: Levels of circulating sgp130 can predict progressing NASH and may be used alone or in combination with other biomarkers as a non-invasive measure of liver disease severity.

FRI115

FIB-4 outperforms other serum non-invasive fibrosis tests in metabolic associated fatty liver disease

Nikoletta Maria Tagkou¹, Giulia Magini^{1,2}, Laurent Spahr¹, Francesco Negro^{1,3}, Jean-Louis Frossard¹, Nicolas Goossens^{1,2}.
¹Hôpitaux Universitaires de Genève (HUG), Division of Gastroenterology and Hepatology, Genève, Switzerland; ²Hôpitaux Universitaires de Genève (HUG), Division of Transplantation, Genève, Switzerland; ³Hôpitaux Universitaires de Genève (HUG), Division of Clinical Pathology, Genève, Switzerland
 Email: tagkounikoletta@gmail.com

Background and aims: Metabolic associated fatty liver disease (MAFLD) is a recently proposed terminology to replace non-alcoholic fatty liver disease (NAFLD) but non-invasive fibrosis scores have not been validated in this population. Additionally, MAFLD definition broadens the disease spectrum by including the overlap with alcohol related liver disease (MAFLD-ALD). We therefore aimed to determine the diagnostic performance of non-invasive fibrosis scores in MAFLD and whether the coexistence of alcohol abuse affects their performance.

Method: We retrospectively collected data of 409 consecutive MAFLD patients undergoing liver biopsy at our institution from 2007 to 2021. We stratified our patients by excessive alcohol consumption defined as >20 g/day in females and >30 g/day in males. The following scores were calculated with previously published cutoffs: NFS, FIB4, APRI and BARD. Advanced fibrosis was considered as F3–4 and cirrhosis as F4 fibrosis on liver biopsy. Diagnostic performance was assessed by analysis of the area under receiver operating characteristic curve (AUROC) and sensitivity/specificity calculations.

Results: Among 409 patients, 277 (66.4%) had pure MAFLD and 132 (31.7%) had MAFLD-ALD. Baseline characteristics in pure MAFLD vs MAFLD-ALD were: age (51.2 vs 58.2, $p < 0.001$), male sex (49.5 vs 87.9%, $p < 0.001$), BMI (36.9 vs 30.4 kg/m², $p < 0.001$), diabetes (51.1 vs 69.2%, $p = 0.001$), advanced fibrosis (27.7 vs 71.2%), cirrhosis (17.5 vs 63.6%), NASH (37.3 vs 32.6%, $p = 0.406$) and median steatosis proportion (50 vs 30%, $p < 0.001$). In pure MAFLD, the AUROCs of FIB4, NFS, APRI, and BARD for advanced fibrosis were 0.88, 0.74, 0.78 and 0.73, respectively (Table). The same AUROCs for predicting cirrhosis were 0.94, 0.82, 0.8 and 0.79, respectively. When comparing the AUROCs, FIB4 performed significantly better than the other non-invasive scores ($p < 0.001$) for the prediction of both advanced

fibrosis and cirrhosis in pure MAFLD. However, FIB4 performed less well for the prediction of cirrhosis in patients with MAFLD-ALD compared to pure MAFLD (AUROC 0.83 vs 0.94, $p = 0.005$), while the other scores performed similarly.

Table: Comparison of the diagnostic performance of non-invasive fibrosis scores in MAFLD

Non-invasive score	AUROC	95% CI	Cut-offs	Sensitivity (%)	Specificity (%)
Advanced fibrosis					
FIB4	0.88	0.83–0.93	1.3	79	75
			2.67	49	98
NFS	0.74*	0.66–0.81	–1.455	90	29
			0.676	43	89
APRI	0.78*	0.72–0.84	0.5	68	72
			1.5	12	97
BARD	0.73*	0.66–0.8	2	84	43
			4	42	90
Cirrhosis					
FIB4	0.94	0.92–0.97	1.3	92	72
			2.67	67	97
NFS	0.82*	0.73–0.91	–1.455	94	28
			0.676	64	89
APRI	0.8*	0.73–0.87	0.5	76	69
			1.5	16	97
BARD	0.79*	0.71–0.86	2	91	41
			4	50	88

* $p < 0.05$ significantly different to FIB4.

Conclusion: FIB4 performs better than other serum non-invasive tests for the prediction of advanced fibrosis and cirrhosis in MAFLD patients, however its performance for the prediction of cirrhosis is reduced in the presence of alcohol abuse.

FRI116

Presence of auto-antibodies has no impact on histological parameters in non-alcoholic fatty liver disease

Ajeet Singh Bhadoria¹, Kavita Jain², Archana Rastogi², Chhagan Bihari².
¹All India Institute of Medical Science Rishikesh, Community and Family Medicine, Rishikesh, India; ²Institute of Liver and Biliary Sciences, New Delhi, India
 Email: ajeetsinghbhadoria@gmail.com

Background and aims: Presence of auto-antibodies have been documented with liver diseases like viral hepatitis, drug induced hepatitis and non-alcoholic fatty liver disease (NAFLD). However, significance and impact of these autoantibodies on histological severity of NAFLD yet needs to be explored. Previous reports on association of autoantibodies with histological severity in other cohorts have revealed inconsistent results. Therefore, this study was undertaken to document the impact of auto-antibodies on histological parameters of NAFLD.

Method: All cases with histological diagnosis of NAFLD during Jan 2016–Jan 2021 were included in the study. Laboratory parameters were recorded and histological assessment was done utilizing Ishak's modified system. Positivity of autoimmune markers was defined as presence of either Anti-nuclear Antibody (ANA; titre of >1:80), anti-smooth muscle antibodies (ASMA), or anti-liver-kidney-microsomal antibodies (LKM-1; titre of >1:40). Demographic, biochemical, serologic and histological characteristics were compared between cases with and without any antibody positivity. Serum levels of CK18-M30 and PIIINP were evaluated by ELISA to assess the subtle changes in necro-inflammatory activity and fibrosis.

Results: Out of 1149 NAFLD cases screened, complete autoantibody status was known for 683 cases. Autoantibodies were present in 281/683 (41.1%, 95% CI 37.4–44.9) patients. ANA, ASMA, ANA plus ASMA was seen in 20.9% (95% CI 17.9–24.2), 14.5% (95% CI 11.9–17.4) and 5.7% (95% CI 4.1–7.7) cases, respectively. LKM-1 was not seen in any case. No significant difference was noted between the two groups in

POSTER PRESENTATIONS

terms of age, gender, body mass index, platelet levels, serum IgG, liver function parameters, ferritin, fasting glucose, fasting insulin, and HbA1c and lipid profile ($p > 0.05$). No significant difference was noted in histological parameters between the groups. However, mean CK18-M30 and PIIINP showed a rising trend with NAFL, NASH, NASH+AIH (χ^2 trend $p < 0.001$). Mean CK18-M30 between cases with negative autoantibody, ANA positivity, ASMA positivity and combined positivity of autoantibody were 178.2 ± 81.8 , 161.6 ± 63.7 , 153.2 ± 70.3 and 169.8 ± 42.9 , respectively ($p = 0.57$).

Conclusion: Auto antibodies were present in more than one third of NAFLD cases, with ANA positivity in one fifth and presence of ASMA in more than one in ten cases. No significant necro-inflammatory activity or fibrosis was seen with presence of auto-antibodies. However, CK-18-M30 and PIIINP showed a significant rising trend from NAFL to NASH to NASH+AIH.

FRI117

Marked underestimation of liver fat content as measured by magnetic resonance versus histology—a systematic review and meta-analysis

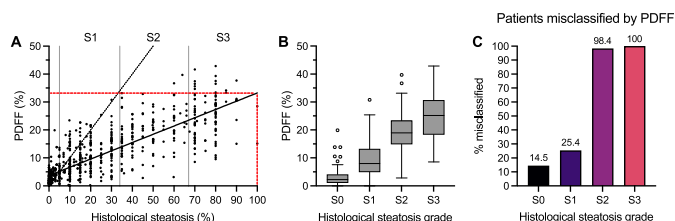
Sami Qadri^{1,2}, Kimmo Porthan^{1,2}, Anne Juuti³, Anne Penttilä³, Juhani Dabek^{1,2}, Tiina E. Lehtimäki⁴, Wenla Seppänen⁴, Johanna Arola⁵, Perttu Arkkila⁶, Hannele Yki-Järvinen^{1,2}. ¹University of Helsinki and Helsinki University Hospital, Department of Medicine, Helsinki, Finland; ²Minerva Foundation Institute for Medical Research, Helsinki, Finland; ³University of Helsinki and Helsinki University Hospital, Department of Gastrointestinal Surgery, Abdominal Centre, Helsinki, Finland; ⁴Helsinki University Hospital, HUS Medical Imaging Centre, Helsinki, Finland; ⁵University of Helsinki and Helsinki University Hospital, Department of Pathology, Helsinki, Finland; ⁶Helsinki University Hospital and University of Helsinki, Department of Gastroenterology, Abdominal Centre, Helsinki, Finland
Email: hannele.yki-jarvinen@helsinki.fi

Background and aims: Magnetic resonance spectroscopy (MRS) and imaging (MRI) measure liver fat via the proton density fat fraction (PDFF), which reflects the tissue volume fraction of hepatic triacylglycerols. Intuitively, PDFF would be predicted to give lower values of steatosis compared to histology, which estimates the percentage of lipid droplet-laden hepatocytes out of all hepatocytes. We conducted a systematic review and meta-analysis of patient-level data to characterise the linearity and agreement between PDFF and histological steatosis across the full spectrum of fatty liver.

Method: Following the PRISMA guideline, we searched PubMed, Scopus, Web of Science, and the Cochrane Library until February 20, 2022, to identify all studies showing data on histological macrovesicular steatosis percentage and MRS/MRI-PDFF in adults with non-alcoholic fatty liver disease (NAFLD) or in living liver donor candidates. We invited authors to submit individual patient data for pooled analysis. Linearity between PDFF and histological steatosis was assessed using Pearson's correlation, linear regression, and mixed-effects models. Agreement was assessed using Bland-Altman analysis and intraclass correlation coefficient (ICC) for continuous data and Cohen's kappa for graded classification. Risk-of-bias was assessed using QUADAS-2.

Results: The eligible studies numbered 11 (3 with MRI-PDFF and 8 with MRS-PDFF; $N = 755$). The relationship between PDFF and histological steatosis was highly linear ($r = 0.82$, $p < 0.0001$), and their values were fairly similar at low levels of liver fat (< 5 – 10%). However, the higher the liver fat, the more PDFF underestimated steatosis as compared to histology (Fig. A). On the average, histological steatosis was 2.7-fold higher than PDFF, and the fractional underestimation by PDFF tended to increase from low to high levels of liver fat. A histological steatosis of 100% corresponded to an average PDFF of 33% (Fig. A). The ICC for absolute agreement between the measures was 0.43, denoting poor reliability, and for consistency between the measures 0.52, denoting moderate reliability. Use of the common NAFLD grading of steatosis (S0: $< 5\%$; S1: 5– 33% ; S2: 34– 66% ;

S3: $> 66\%$) for PDFF resulted in gross misclassification of especially those patients with histological steatosis above grade S1 (kappa = 0.32; Fig. B–C). Median PDFF values corresponding to each steatosis grade were 2.2% for S0, 8.0% for S1, 18.9% for S2, and 25.2% for S3.



Conclusion: Histological and PDFF measurements of liver fat are fundamentally different. While they are in reasonable agreement at levels around the diagnostic threshold for NAFLD ($\sim 5\%$), histological steatosis far surpasses PDFF in patients with moderate-to-severe fatty liver. This difference should be acknowledged in guidelines for NAFLD to prevent misjudgement of the clinical status or treatment effect in patient care.

FRI118

Disease severity assessment of metabolic dysfunction-associated fatty liver disease in Taiwan

Jee-Fu Huang^{1,2,3}, Pei-Chien Tsai¹, Ching-I Huang^{1,3}, Ming-Lun Yeh^{1,3}, Chung-Feng Huang^{1,3}, Chia-Yen Dai^{1,3}, Ming-Lung Yu^{1,3}, Wan-Long Chuang^{1,3}. ¹Kaohsiung Medical University Hospital, Hepatobiliary Division, Department of Internal Medicine, Kaohsiung, Taiwan; ²Kaohsiung Medical University Hospital, Hepatitis Center, Kaohsiung, Taiwan; ³Kaohsiung Medical University, Faculty of Internal Medicine, College of Medicine, Kaohsiung, Taiwan
Email: waloch@kmu.edu.tw

Background and aims: Disease severity in metabolic dysfunction-associated fatty liver disease (MAFLD) has rarely been investigated in Asians. The study aimed to assess the fibrosis stages of MAFLD in a community-based cohort in Taiwan. We also aimed to compare the differences of features between different definitions as well as the interaction between metabolic factors and viral factors.

Method: The retrospective case-control study was performed in adult subjects participating liver disease screening in Southern Taiwan. The items of liver disease screening included HBsAg, anti-HCV, transaminases, and metabolic profiles in a voluntary basis. Abdominal sonography was performed for those who had viral hepatitis or elevated transaminase levels. According to the MAFLD diagnostic criteria we stratified the subjects into: group A for type 2 diabetes, group B for BMI $> 23 \text{ kg/m}^2$, and group C of BMI $\leq 23 \text{ kg/m}^2$ subjects who carried at least 2 metabolic items, respectively. Disease severity was assessed by non-invasive Fibrosis-4 (FIB-4) Index. Advanced fibrosis was defined as FIB-4 value > 3.25 .

Results: From 2009 to 2020, there're 5,180 subjects who had fatty liver index (FLI) > 60 and has fatty liver on sonography. We recruited 1,948 subjects (mean age = 51.5 ± 13.4 years, females 52.1%) who met the diagnostic criteria of MAFLD and had completed results for fibrosis assessment. The study pool included 1,470 (75.5%) NBNC NAFLD subjects and 478 subjects possessing concomitant liver diseases such as viral hepatitis infections and alcoholism. There were 395 (20.3%) of Gr A, 1,818 (93.3%) of Gr B, and 44 (2.3%) subjects of Gr C, respectively. Advanced fibrosis on FIB-4 was observed in 79 (4.1%) subjects. The subjects of Gr C had a significantly higher percentage (20.5%, 9/44) of advanced fibrosis than Gr A (4.1%, 16/395) and Gr B (3.6%, 65/1,818) ($p < 0.001$). Excluding those who had concomitant liver diseases, the subjects of Gr C still had a significantly higher percentage (15%) of advanced fibrosis than Gr A (1.8%) and Gr B (1.4%) ($p = 0.003$). Multivariate regression analysis demonstrated that HBV/HCV co-infection (OR = 16.74, 95% CI = 4.62–60.67, $P <$

0.001), HCV infection (OR = 8.83 95% CI = 4.79–16.30, $P < 0.001$), Gr C (OR = 6.94, 95% CI = 2.65–18.15, $P < 0.001$), and age (OR = 1.08, 95% CI = 1.05–1.11, $P < 0.001$) were significant factors for predicting the subjects with advanced fibrosis.

Conclusion: Lean MAFLD Taiwanese subjects carrying metabolic abnormalities had a higher chance of advanced fibrosis than others in a community-based setting.

FRI119

Optical analysis of liver magnetic resonance images (MRI) 3 T to detect steatohepatitis features: the program DeMILI 3.0.

Isabel Fernández-Lizaranzu^{1,2}, Emilio Gomez-Gonzalez², Sheila Gato Zambrano¹, Rocío Montero-Vallejo¹, Enrique Claudio Fernandez³, Juan Carlos Diaz Martin³, Rebeca Sigüenza⁴, Rocío Aller⁴, Maria Angeles Martin Prats⁵, Manuel Romero Gomez⁶. ¹Institute of Biomedicine of Seville, Seville, Spain; ²Universidad de Sevilla, Higher Technical School of Engineering (ETSI), Group of Interdisciplinary Physics (GFI), Seville, Spain; ³Virgen del Rocio University Hospital, Department of Radiology, Spain; ⁴Hospital Clínico Universitario de Valladolid, Spain; ⁵Universidad de Sevilla, Department of Electronic Engineering, Spain; ⁶Institute of Biomedicine of Seville, Seville, Spain
Email: ifernandez14@us.es

Background and aims: DeMILI in MRI 1.5 T has been proved as useful to detect steatohepatitis in patients with non-alcoholic fatty liver disease (NAFLD) (Gallego-Durán et al. Sci Rep 2016). The aim of this study was to evaluate the potential of optical processing methods applied to non-enhanced contrast liver 3 T MRI to predict steatohepatitis in NAFLD patients.

Method: Seventy-nine biopsy-proven NAFLD patients recruited between October 2019 and December 2021 at 'Virgen del Rocio' University Hospital (HUVR, n = 68) and Valladolid Clinical University Hospital (HCUV, n = 11). Main characteristics: 50.6 % female, 21.5% <45 years old and 32.9% >65 years old, 55.6% showed steatohepatitis in the liver biopsy. 3.0 T MRI was conducted using a whole-body Philips® scanner without contrast medium. 3 different sequences were performed in axial plane: SSFSE-T2 (Single Shot Fast Spin Echo T2-weighted), FAST-STIR (Fast Short inversion Time Inversion Recovery) and DYNAMIC. The entire liver was imaged and 6 consecutive slices, per each sequence, were manually selected covering the whole organ. 84 physical and mathematical feature descriptors (estimators) were computed from every image. Principal Component Analysis was performed to extract the main estimators related to steatohepatitis and two logistic regressions (LR) were built: The first one (DeMILI 3.0-v1) used estimators E63, E12 and E21, n = 43 HUVR patients for training, and n = 36 patients (25 HUVR + 11 HCUV) for validation. The second LR (DeMILI 3.0-v2) was built with estimators E70, E12 and E21 and the same cohort in different subsets: training n = 64 from HUVR, and validation n = 15 (4 HUVR + 11 HCUV). Receiver operating characteristic (ROC) curves were obtained.

Results: ROC curves for DeMILI 3.0-v1 and DeMILI 3.0-v2 are shown in Figure 1. The area under the ROC curves (AUROC) obtained were: i) for DeMILI 3.0-v1, AUROC = 0.7378 for training set and AUROC = 0.7307 for validation set, and ii) for DeMILI 3.0-v2, AUROC = 0.7958 for training set and AUROC = 0.6071 for validation set.

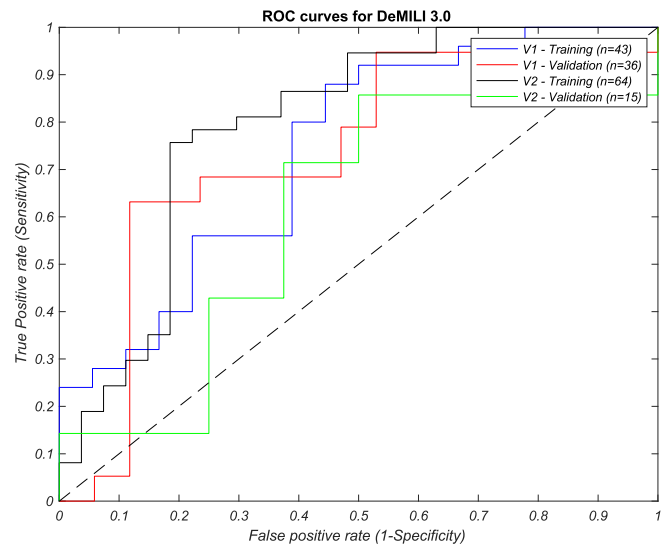


Figure: ROC curves of LRs (v1 and v2) for training and validation subsets.

Conclusion: Initial results with limited cohorts show that DeMILI 3.0 detects steatohepatitis in patients with NAFLD with a diagnosis accuracy of 0.73 (DeMILI 3.0-v1). Validation cohorts include patients from other center than training. DeMILI 3.0-v1 yields results close to DeMILI using 1.5 T MRI.

FRI120

The fibrosis-4 cut-off value for significant fibrosis is dependent on the type of non-alcoholic fatty liver disease patients

Leen Heyens^{1,2,3}, Wouter Robaey^{1,2}, Christophe Van Steenkiste^{4,5}, Sven Francque^{5,6}, Geert Robaey^{1,2,7}. ¹Hasselt University, Faculty of Life Sciences and Medicine, Hasselt, Belgium; ²Ziekenhuis Oost-Limburg, Gastro-enterology and Hepatology, Genk, Belgium; ³Maastricht University, Faculty of Health, Medicine and Life Sciences, Maastricht, Netherlands; ⁴Maria Middelaers, Gastro-enterology and Hepatology, Gent, Belgium; ⁵University of Antwerp, Gastro-enterology and Hepatology, Antwerpen, Belgium; ⁶Antwerp University Hospital, Gastro-enterology and Hepatology, Edegem, Belgium; ⁷UZ Leuven Gasthuisberg Campus, Gastro-enterology, Leuven, Belgium
Email: leen.heyens@uhasselt.be

Background and aims: Non-alcoholic fatty liver disease (NAFLD) has become the most frequent cause of chronic liver disease. The fibrosis stage has been identified as the most important predictor of prognosis. The Fibrosis-4 (FIB-4) is an easy-to-use non-invasive score to predict fibrosis based on routine blood parameters. However, we previously showed that the 1.3 FIB-4 cut-off value had a low performance to detect significant fibrosis ($\geq F2$) in a primary care (PC) population. We aimed to determine whether NAFLD-group-specific optimal FIB-4 cut-off values can be determined to identify patients with a high likelihood of $\geq F2$, considered an at-risk population to be referred for further management.

Method: In a prospective study in the Belgian regions of Limburg, East-Flanders, and Antwerp, patients were screened in seven PC practices. Type 2 diabetes mellitus patients (T2DM) were screened in the hospital of Ziekenhuis Oost-Limburg. As a proxy of the fibrosis stage, liver stiffness was determined using Vibration Controlled Transient Elastography (VCTE) by FibroScan® (Echosens, France) and used as the reference method. The FIB-4 was calculated based on recent laboratory data from the electronic patient file. The Youden Index (J) was used to determine the optimal cut-off value for detecting $\geq F2$ (>7.9 kPa for the M-probe and >7.2 kPa for the XL-probe) in three populations: PC (unselected all-comers), T2DM screened in PC (T2DM-PC, PC subgroup), T2DM screened in a hospital (T2DM-H).

POSTER PRESENTATIONS

Results: Of the 816 (424 (52.0%) PC, 103 (12.6%) T2DM PC, and 289 (35.4%) T2DM-H) screened patients, 534 (65.4%) had FIB-4 values and no other causes of steatosis but NAFLD. Of these, 275 (51.5%) were male, median age was 63 (26–71) years, median BMI 29.8 (26.2–33.46) kg/m², median waist circumference 104.0 (97.0–113.0) cm for men and 98.0 (86.1–110.0) cm for women, and 276 (51.9%) had T2DM. The number of patients with \geq F2 was 30 (11.8%), 20 (30.3%), and 96 (45.7%) for the PC, T2DM-PC, and T2DM-H cohorts. Using logistic regression, both FIB-4 ($p < 0.05$) and the type of NAFLD-group significantly ($p < 0.05$) contributed to \geq F2. The area under the operating curve (AUROC) of the model was 0.76 compared to an AUROC of 0.61 using only FIB-4. The maximum J was 0.40461 and corresponded to a sensitivity of 0.61 and specificity of 0.80. Using the linear predictor, the optimal cut-off value per population was 4.3 for the PC cohort, 2.3 for the T2DM-PC, and 0.66 for the T2DM-H cohort. These cut-off values were not influenced by age or the grade of steatosis as measured by controlled attenuation parameter (CAP).

Conclusion: The optimal cut-off value of the FIB-4 score for detecting NAFLD-associated significant fibrosis depends on the patient groups' characteristics, potentially resulting from the different prevalence of the condition in the respective groups. However, the cut-off values were not influenced by age or the severity of the steatosis.

FRI121

Developing an algorithm to predict NAFLD in clinical trial volunteers-interim report NCT04873258

Jörg Täubel^{1,2,3}, Dominic Pimenta⁴, Aviva Petrie⁵, Lydia Sulaiman⁶, Ulrike Lorch³, Kevin Moore⁵. ¹St George's University of London, United Kingdom; ²Richmond Research Institute, London, United Kingdom; ³Richmond Pharmacology, United Kingdom; ⁴Richmond Research Institute, London, United Kingdom; ⁵University College London, United Kingdom; ⁶King's College London, United Kingdom
Email: d.pimenta@richmondresearchinstitute.org

Background and aims: Non-alcoholic fatty liver disease (NAFLD) affects around 1 in 4 of the global adult population, and ranges in severity from benign fatty liver infiltration, to hepatitis, cirrhosis and hepatocellular carcinoma. NAFLD has important implications for clinical trial volunteers as an occult co-morbidity. NAFLD may modulate drug metabolism, and studies have suggested that Grade III/IV liver reactions are 4x commoner in healthy volunteers with probable NAFLD than without. We therefore aimed to develop a non-invasive tool, utilizing new technology, to predict NAFLD in this population. This is our interim report (NCT04873258)

Method: This is an ongoing observational cross-sectional study design. Volunteers attend the unit for a single day of biomarker assessment, including bioimpedance vector analysis (%visceral fat, total body fat% and skeletal muscle %), anthropometric measurement (BMI, waist circumference), and lab bloods. A FibroScan is performed as a pragmatic gold standard 'outcome' for NAFLD, and E (fibrosis) and CAP (steatosis) scores are recorded. Traditional multivariate linear and logistic regression is performed, correlating biomarkers with linear E and CAP scores, and 'significant' disease (\geq F2, E > 7.5 kPa and \geq S2, CAP > 260 dB) respectively. Alongside this machine learning models are trained (Python {sklearn, TensorFlow}) and performance compared.

Results: Interim results: 290 individuals (of extended target 1500) with demographics as follows; 61% male, 51.5% Caucasian, average age of 39.4 years, 40% of the cohort had diabetes. The overall prevalence of significant fibrosis (E score ≥ 7.5 kPa) was 11.4% and the prevalence of significant steatosis (CAP ≥ 260 dB) was 35.6%. A logistic regression model was trained for E and CAP scores, identifying key features in the dataset as waist circumference and GGT. A prototype clinical score was derived, with an AUC of 0.81 for E and 0.89 for CAP scores. Machine learning models were compared, with the best performing model being Gaussian Naïve Bayes for E (AUC 0.82) and Decision Tree for CAP (0.79). A clinical tool based on a score derived from logistic regression coefficients was created (Figure) for use by

physicians to gauge the risk of NAFLD in volunteers, using two variables (GGT and waist circumference), with high sensitivity and acceptable specificity (E score sensitivity 90%, specificity 45%, CAP score sensitivity 85.5%, specificity 81.9%).

```
Welcome to the RPL NAFLD detection algorithm
Version history: 0.1. ALPHA. 24 Mar 2022. (c) RPL

=====

This is for the detection of NAFLD in trial volunteers - not for use outside of this context.
E Model sensitivity 90%, specificity 45%.
CAP Model sensitivity 85.5%, specificity 81.9% - do not react clinically to results.

=====

Please enter GGT value >> 30
Please enter patients waist circumference in cm >> 86

=====
RPL E Score: -2.845
Clinically significant NAFLD liver fibrosis unlikely. Safe to INCLUDE.

=====
RPL CAP Score: -1.320
Clinically significant fatty liver likely. Advise - discuss with PI/exclude.

=====

Would you like to assess another patient? y/n.
>> y
Resetting model...

Please enter GGT value >> 50
Please enter patients waist circumference in cm >> 105

=====
RPL E Score: -1.185
Clinically significant NAFLD liver fibrosis likely. Advise - EXCLUDE.

=====
RPL CAP Score: 1.028
Clinically significant fatty liver likely. Advise - discuss with PI/exclude.

=====
```

Figure: Prototype NAFLD clinical tool (Alpha).

Conclusion: Our early interim analysis shows promising results, sufficient to prototype a clinical tool with high sensitivity and acceptable specificity for screening out individuals in clinical trials at high probability of occult NAFLD and/or fibrosis. Future work to develop the underlying model, advance machine learning models to further improve performance, and deliver to clinic is underway.

FRI122

Correlation of ultrasound derived fat fraction (UDFF) with MRI (PDFF): possibilities and analysis of confounding factors

Reinhard Kubale^{1,2}, Marcin Krawczyk^{3,4}, Paul Lessenich¹, Arno Bucker¹, Aaron Engel⁵, Andrzej Milkowski⁵, Gunther Schneider². ¹Saarland University Hospital, Homburg, Germany; ²Saarland University, Saarbrücken, Germany; ³Saarland University Hospital, Department of Internal Medicine II-Gastroenterology, Hepatology, Endocrinology, Diabetology, and Nutritional Medicine, Homburg, Germany; ⁴Innere II, Homburg/Saar, Germany; ⁵Siemens Healthineers, Forchheim, Germany
Email: kubale@mac.com

Background and aims: Ultrasound derived Fat fraction (UDFF) is a quantitative sonographic method based on a combination of attenuation and backscatter coefficients. Aim of the study was to evaluate feasibility and correctness in correlation with MRI (PDFF: Proton density fat fraction) and to analyze confounding factors.

Method: Examinations were done with 2 US-machines (Sequoia and S2000: Siemens) with 5C1, DAX and 6C1 transducers with an algorithm based on a phantom corrected combination of attenuation (AC) and backscatter coefficient (BSC). Measurements of a ROI of 9 cm² were correlated with MRI PDFF values of the whole liver and a ROI in the right liver lobe (RLL) in the same position (Vida, Siemens-LiverLab®). To test the reproducibility we examined in a pilot study 20 patients with two UDFF-measurements on different days. The effect of fasting state was tested by performing UDFF before, 1, 3 and 5 hours after a standard meal. The main study consists of 194

Comparison UDFF versus PDFF: 2,1 – 26%

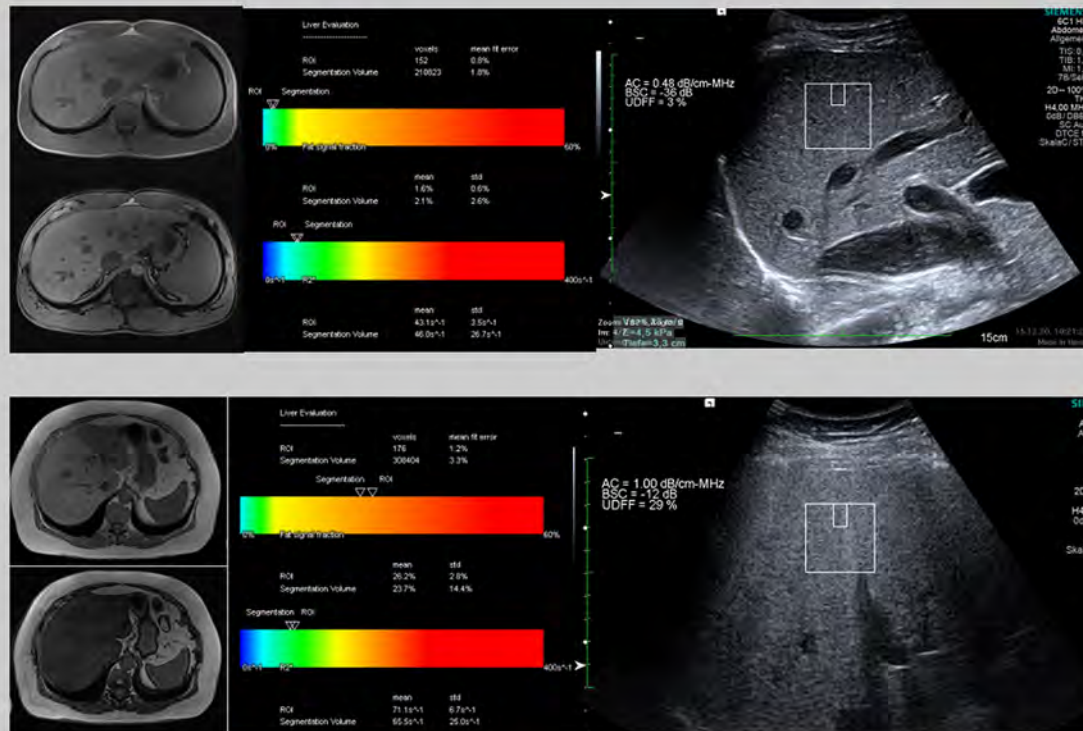


Figure: (abstract: FRI122): Comparison of Multiparametric Assessment of UDFF with PDFF in patients with 2, 1 % and 26%.

consecutive patients (112 male, 82 female), who received a liver MRI for clinical reasons.

Results: In the pilot study (Study I) PDFF of the whole liver ($10.3 \pm 9.4\%$), was significantly higher than in the corresponding ROI ($8.65 \pm 9.6\%$). The correlation of PDFF-measurements with scan heads (5C1, DAX, 6C1) were $r = 0.94/0.91$ and 0.85 . Repeated measurements showed values of $r = 0.99/0.97$ and 0.89 with best reproducibility of the DAX. Measurements before, 1, 3 and 5 hours after meal showed no significant differences between the time points (Friedmann-Test). The main study shows a significant difference in PDFF-measurement of the whole liver ($11.6 \pm 9.1\%$) and the ROI ($8.9 \pm 9.5\%$). Although AC and BSC are not linear related to PDFF the model with both parameters shows a significant correlation between UDFF and PDFF of the whole liver and the corresponding ROI and Voxel for all patients $r = 0.80/0.7$ and 0.6 (6C1). Bland-Altman shows, that main confounding factors are severe liver cirrhosis with a small RLL, chemotherapy/lipiodol application, sarcoidosis and amyloidosis. Problems in MRI arose in severe Hemochromatosis, patients over 150 kg due to artifacts.

Conclusion: UDFF shows a strong positive correlation with PDFF. Confounding factors could be identified hypothetically allowing for improvement in the future. UDFF could be a screening tool for early diagnosis of NAFLD and a biomarker for therapy control.

FRI123

ELF to identify NASH and fibrosis in non-alcohol related fatty liver disease

Richard Parker¹, Peter Eddowes², Natasha McDonald³, Philip N. Newsome², Gideon Hirschfield⁴, Jonathan Fallowfield³, Ian Rowe⁵. ¹Leeds Teaching Hospital Trust, Leeds Liver Unit, Leeds, United Kingdom; ²University of Birmingham, Centre for Liver Research, Birmingham, United Kingdom; ³MRC/University of Edinburgh Centre for Inflammation Research, Queen's Medical Research Institute, Edinburgh, Edinburgh, United Kingdom; ⁴University of Toronto, Division of Gastroenterology, Toronto, Canada; ⁵University of Leeds, Leeds Institute for Medical Research, Leeds, United Kingdom
Email: richardparker@nhs.net

Background and aims: The current paradigm for eligibility for trials in NAFLD requires the presence of NASH and fibrosis of particular severity. We examined whether the ELF score could be repurposed to predict both NASH and fibrosis.

Method: A cohort of 240 patients with biopsy-proven NAFLD was used. Treatment threshold was $NAS \geq 4$ (as per the FLIP algorithm) and fibrosis grade of greater than 2. The cohort was split 60:40 into modelling and validation groups. Internal validation of modelling was done using 2000 bootstrapped samples. Test performance was evaluated with AUROC analysis. Low and high cut-offs at 90% sensitivity or specificity respectively were calculated in the modelling cohort, and negative and positive predictive values (NPV, PPV) and positive and negative diagnostic likelihood ratios (PDLR, NDLR)

POSTER PRESENTATIONS

calculated. The model was calibrated graphically in the validation cohort and test performance confirmed. All statistical tests were done in R using pROC, rms and ggplot2 packages.

Results: The average age of the cohort was 55 years, 117 (66%) were male. All components of the ELF score correlated with NAS and were significantly different between patients with NAS <4 or ≥4. A model ('ELF-t') that included all of the ELF parameters (HA, P3P and TIMP-1) performed best to identify cases suitable for trials or treatment (AUROC 0.74). At a low cut-off ELF-t had a NPV of 91% and the high cut-off gave a PPV of 92%. NDLR was 0.27 (0.12–0.607), PDLR 2.47 (1.15–5.31). Calibration was good in the validation cohort with similar test performance (AUC 0.79, NPV 91%, PPV 93%).

Conclusion: The constituent markers of the ELF test can be repurposed to assess the likelihood of NAFLD with sufficient activity and scarring to meet common eligibility criteria for clinical trials, which are likely to translate into a paradigm for treatment as new drugs come to market. This provides a non-invasive method for assessing patients as an alternative to liver biopsy.

FRI124

Performance of the Steatosis-Associated Fibrosis Estimator (SAFE) to predict F2 fibrosis and higher in a cohort of South Korean patients with non-alcoholic fatty liver disease (NAFLD)

Vivek Charu¹, Allison Kwong¹, Ajitha Mannalithara¹, Eileen Yoon², Dae Won Jun², W. Ray Kim¹. ¹Stanford University School of Medicine, Stanford, United States; ²Hanyang University College of Medicine, Korea, Rep. of South
Email: vcharu@stanford.edu

Background and aims: The Steatosis-Associated Fibrosis Estimator (SAFE) score is a recently developed scoring system to categorize NAFLD patients by their risk of having significant liver fibrosis (F2 or higher). Here we evaluate the performance of the SAFE score in predicting F2 fibrosis based on transient elastography (FibroScan) measurements in a cohort of South Korean patients with NAFLD.

Method: We identified a cohort of adult patients with a clinical diagnosis of NAFLD who underwent FibroScan at Hanyang University from 2020 to 2022. Using the available laboratory information, we calculated SAFE, Fibrosis-4 (FIB-4) and the NAFLD fibrosis score (NFS) for each patient. Our outcome of interest was F2 fibrosis or higher, and a FibroScan threshold of greater than 7 kPa was used. We computed the area under the receiver operating curves (AUROC) to quantify the performance of each non-invasive score to predict F2 fibrosis or greater. We calculated the sensitivity, specificity, positive predictive value and negative predictive values of the SAFE score using an apriori determined threshold of greater than or equal to 100.

Results: We identified 749 patients with a clinical diagnosis of NAFLD who underwent FibroScan testing with clinical/laboratory data to generate SAFE, FIB-4 and NFS scores (Table). SAFE, FIB-4 and NFS were strongly correlated with each other in this cohort (pairwise Spearman's correlations: SAFE-FIB4: 0.83; SAFE-NFS: 0.80; FIB4-NFS: 0.84). We estimated the AUROC for each fibrosis estimator (Table), and found that the AUROC for the SAFE score (0.76) was significantly higher than that for FIB-4 (0.64) and NFS (0.63) (p-values for DeLong's tests: SAFE-FIB4, <2.2e-16; SAFE-NFS, 6.352e-16). FIB-4 and NFS scores had similar AUROC (0.64 and 0.63, p-value for DeLong's test: 0.5822). Using a threshold for the SAFE score of greater than 100 to identify high-risk patients would result in a sensitivity of 0.66 (95%CI: 0.58–0.73), specificity of 0.74 (95%CI: 0.70–0.78), positive predictive value of 0.42 (95%CI: 0.36–0.48) and negative predictive value of 0.88 (95%CI: 0.85–0.91) for predicting F2 fibrosis or higher based on FibroScan measurements.

Sex (N; %)	Male	372 (49.6%)
	Female	377 (50.4%)
Age (median; IQR [years])		55.0 (40.0–63.0)
BMI (median; IQR [kg/m ²])		25.3 (22.9–28.3)
Diabetes (N; %)	Yes	218 (29.1%)
	No	531 (70.9%)
AST (median; IQR [u/L])		36.0 (26.0–53.0)
ALT (median; IQR [u/L])		36.0 (21.0–68.0)
Total Protein (median; IQR [g/dL])		7.7 (7.4–8.0)
Albumin (median; IQR [g/dL])		4.5 (4.3–4.6)
Globulin (median; IQR [g/dL])		3.2 (2.9–3.5)
Platelets (median; IQR [x10 ⁹ /L])		236.0 (196–279)
FibroScan (median; IQR [kPa])		5.4 (4.3–6.8)
FibroScan (N; %)	>7.0 kPa	168 (22.4%)
	≤7.0 kPa	581 (77.6%)
Fibrosis scores		
SAFE (median; IQR)		57.6 (4.2–133.8)
FIB-4 (median; IQR)		1.33 (0.88–2.05)
NFS (median; IQR)		-1.94 (-3.08–-0.82)
AUROC's		
SAFE (estimate; 95%CI)		0.76 (0.72–0.81)
FIB-4 (estimate; 95%CI)		0.64 (0.59–0.69)
NFS (estimate; 95%CI)		0.63 (0.58–0.68)

Conclusion: In a cohort of Korean adults with NAFLD, the SAFE score performs better than FIB-4 or NFS to predict F2 fibrosis or higher based on FibroScan measurement. A SAFE threshold of greater than 100 has reasonable, but not perfect, negative predictive value for identifying F2 fibrosis or greater in this cohort (0.88). Evaluating the performance of the SAFE score in additional diverse cohorts is essential to assess its utility in identifying patients at low risk of having clinically significant fibrosis.

FRI125

FIB-4 combined with positron emission tomography biomarkers detects fibrotic NASH

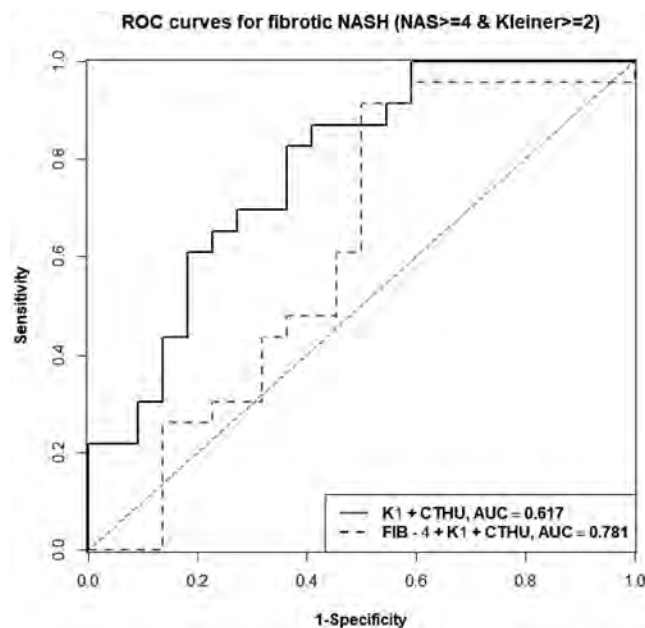
Sean Romeo¹, Connie Chan², Blake Shaw³, Karen Matsukuma⁴, Michael Corwin⁵, Victoria Lyo⁶, Shuai Chen³, Guobao Wang⁵, Souvik Sarkar^{1,7}. ¹University of California, Davis, Internal Medicine/Gastroenterology and Hepatology, United States; ²UC Davis School of Medicine, Sacramento, United States; ³University of California, Davis, Public Health Sciences/Biostatistics, United States; ⁴University of California, Davis, Pathology and Laboratory Medicine, United States; ⁵University of California, Davis, Radiology, United States; ⁶University of California, Davis, Surgery, United States; ⁷Florida Research Institute, Lakewood Ranch, United States
Email: ssarkar@ucdavis.edu

Background and aims: Non-alcoholic steatohepatitis (NASH) is a severe form of non-alcoholic fatty liver disease (NAFLD) that is associated with liver cirrhosis and hepatocellular cancer. Methods for diagnosing NASH without liver biopsy are limited, therefore presenting an urgency to noninvasively detect NASH by characterizing features: steatosis, inflammation, and fibrosis. We combined the well-established non-invasive fibrosis-4 (FIB-4) measurement with a recent ¹⁸F-fluorodeoxyglucose (FDG) positron emission tomography/computed tomography (PET/CT) imaging approach for NASH to elucidate imaging determinant of fibrotic NASH.

Method: The study was approved by the institutional review board. Patients ≥18 years with NAFLD who had undergone liver biopsy were enrolled. FDG transport rate (K₁) by dynamic PET and CT Hounsfield units (CTHU) were determined from liver regions-of-interest (ROI) as previously defined, while FIB-4 was calculated from serum by an established criterion. Liver biopsies were scored per NASH-CRN (Clinical Research Network) criteria. Fibrotic NASH was defined as NAFLD activity score (NAS) ≥4 with Kleiner fibrosis stage ≥2. Severe fibrotic NASH was defined as NAS ≥5, plus fibrosis stage ≥3. Correlations among parameters were calculated using the

Spearman correlation. Receiver operating characteristics (ROC) analyses were performed with cut-off selected based on Youden's Index, where FIB-4, K₁ and CTHU were combined using logistic regression.

Results: Of 45 enrolled patients, 31 were female, 54 ± 13 years, and BMI 34.0 ± 5.7 kg/m²; 16% of patients had inflammation >3, while 58% had NAS >4 and 29% with fibrosis ≥3. FIB-4 correlated with fibrosis significantly ($r = 0.58$, $p < 0.001$), as expected, but not with NAS ($r = 0.2$, $p = 0.178$). K₁ and CTHU showed significant correlations with NAS. As shown prior, the dual-variate model of K₁+CTHU could detect clinical NASH but not fibrotic NASH. When FIB-4 score was combined in the model it was able to detect fibrotic NASH with an AUC of 0.781 (Figure 1) and severe fibrotic NASH with an AUC of 0.845. The triple variate model of $1.46001 \cdot K_1 - 0.04009 \cdot CTHU + 1.27309 \cdot FIB-4 \geq 1.574408$, was able to predict fibrotic NASH with a sensitivity of 83% and a specificity of 64%. While $3.27447 \cdot K_1 + 0.00597 \cdot CTHU + 0.99330 \cdot FIB-4 \geq -1.296305$ predicted severe fibrotic NASH with a sensitivity of 91% and specificity 68%.



Conclusion: Combination of non-invasive serum and imaging tests enabled detection of clinical fibrotic NASH. Studies in larger and diverse cohorts will enable establishing this tool for determination of clinical changes in NAFLD patients.

FRI126

Mitochondria-derived methylmalonic acid is associated with advanced fibrosis risks in metabolic dysfunction-associated fatty liver disease (MAFLD): results from the NHANES 1999–2004

Qi Huang¹, Li Li¹, Linjian Yang¹, Linong Ji¹, Xiantong Zou¹. ¹Peking University People's Hospital, China
Email: evazou@bjmu.edu.cn

Background and aims: Methylmalonic acid (MMA) is related to mitochondrial dysfunction, which is a key process of fatty liver disease. This study aimed to investigate the association between MMA and metabolic dysfunction-associated fatty liver disease (MAFLD) using large epidemiological data.

Method: We included 12, 494 individuals from the National Health and Nutrition Examination Survey (NHANES) 1999–2004. MAFLD was diagnosed with Fatty Liver Index (FLI) ≥60 or USFLI ≥30, and participants with advanced fibrosis risks were identified with elevated non-alcoholic fatty liver disease fibrosis score (NFS), fibrosis-4 (FIB4) or aspartate aminotransferase (AST): platelet ratio

(APRI). Participants were divided into four groups according to MMA levels (<120, 120–175, 175–250 or >250 (nmol/L)).

Results: The prevalence of MAFLD was 38.3, 40.6, 42.1 and 39.8% ($p = 0.068$) and the prevalence of participants with advanced fibrosis risk was 2.0, 3.5, 5.6, 10.6% ($p < 0.001$) in four consecutive MMA groups. Compared with participants with lower MMA levels, higher MMA levels had a higher prevalence of diabetes, hypertension and dyslipidaemia, increased ALT, and decreased vitamin B12, RBC and platelet counts. Higher MMA levels were not independently associated with NAFLD (p for trend: 0.997). MMA >250 nmol/L independently increased the risk of advanced fibrosis by one fold in MAFLD patients (OR 95% confidence interval: 2.05 (1.37, 3.08)), but not in non-MAFLD participants (OR 95%CI: 1.81 (0.93, 3.54)). The association between MMA and fibrosis was consistent among different subgroups stratified by alcohol intake, BMI, blood glucose, pressure or lipids (p for interaction >0.05). The area under the receiver operator characteristics curve (ROC AUC) of MMA in detecting fibrosis in MAFLD was 0.658 (0.658, 0.658), which was higher than that of C-reactive protein 0.540 (0.540, 0.540) ($p < 0.001$). **Conclusion:** MMA was independently associated with advanced fibrosis risks in MAFLD, and this association was unaltered in subgroups stratified by different metabolic profiles or lifestyles. This finding indicated a possibility of using MMA as a novel candidate non-invasive biomarker and therapeutic target for fibrosis in MAFLD.

Fibrosis

FRI146

Hepatic angiocrine HGF attenuates liver fibrogenesis via modulation of PDK1/AKT axis

Jianye Wang¹, Sarah Schulze¹, Victor Olsavsky², Kai Schledzewski², Cyrill Géraud², Helmut Friess¹, Norbert Hueser¹, Daniel Hartmann¹. ¹Klinikum rechts der Isar der Technischen Universität München, München, Germany; ²Medical Faculty Mannheim, Heidelberg University, Mannheim, Germany
Email: jianye.wang@tum.de

Background and aims: Hepatocyte growth factor (HGF) is a complete hepatic mitogen and is believed to play a role in liver fibrogenesis and hepatocarcinogenesis. Liver sinusoidal endothelial cells (LSEC) can recruit inflammatory cells by releasing angiocrine signals to produce HGF in the process of liver fibrosis and cirrhosis, but the precise contributions of HGF from LSEC to liver fibrosis remain elucidated.

Method: To investigate the effects of hepatic angiocrine HGF on liver fibrogenesis, Stab2-Cre^{tg} HGF^{fl/fl} (HGF^{LSEC-KO}) mice, in which HGF is specifically switched off in LSEC, were used. Carbon tetrachloride (CCl₄) injection was performed in these mice and the kinetics of the ratio of liver to body weight, immunohistochemistry for liver fibrosis, Western blot and RT-PCR for fibrotic markers, HGF/c-MET signaling pathways and cell cycle-associated genes were determined after initiation of cirrhosis.

Results: We found that HGF^{LSEC-KO} mice showed no difference in the liver-to-body-weight ratio compared to the control group after early-stage CCl₄ treatment. After fibrogenesis, HGF^{LSEC-KO} mice had a higher expression of collagen 1A1 and alpha-SMA and the proliferation of hepatocytes was significantly impaired in HGF^{LSEC-KO} mice. In addition, the LSEC-specific HGF deficiency reduced the c-met level and thus deactivated the PDK1 (3-phosphoinositide-dependent protein kinase-1)/Akt pathway while hepatic angiocrine HGF did not alter immune cell infiltration.

Conclusion: The hepatic angiocrine HGF signaling pathway plays a crucial role in the early stages of liver fibrogenesis. The hepatic angiocrine HGF signaling pathway is essential not only for liver

POSTER PRESENTATIONS

recovery during fibrogenesis, but also for the growth of the liver and even the entire organism.

Key words: hepatocyte growth factor (HGF), liver sinusoidal endothelial cells (LSEC), hepatocytes, liver, fibrogenesis, liver cirrhosis

FRI147

Bisphosphonate-loaded nanogels attenuate liver fibrosis by repolarization of M2-type macrophages

Leonard Kaps¹, Anne Huppertsberg², Niklas Choteschovsky¹, Adrian Klefenz¹, Feyza Durak³, Barbara Schoers³, Mustafa Diken³, Emma Eichler¹, Sebastian Rosigkeit¹, Sascha Schmitt², Christian Leps⁴, Friedrich Foerster¹, Ernesto Bockamp¹, Bruno Degeest⁵, Federico Marini⁶, Kaloian Koynov⁷, Stefan Tenzer⁴, Detlef Schuppan¹, Lutz Nuhn⁷. ¹University Medical Center Mainz, Institute of Translational Immunology and Research Center for Immune Therapy, Mainz, Germany; ²Max Planck Institute for Polymer Research, Mainz, Germany; ³University Medical Center Mainz, TRON-Translational Oncology, Mainz, Germany; ⁴University Medical Center Mainz, Institute of Immunology, Mainz, Germany; ⁵Ghent University, Department of Pharmaceutics and Cancer Research Institute Ghent (CRIG), Belgium, Belgium; ⁶University Medical Center Mainz, Institute of Medical Biostatistics, Epidemiology and Informatics, Mainz, Germany; ⁷Max Planck Institute for Polymer Research, Mainz
Email: nuhn@uni-mainz.de

Background and aims: In liver fibrosis, M2-type macrophages promote the replacement of functional parenchyma by collagen-rich scar tissue. Bisphosphonates impaired the polarization towards M2-type macrophages and demonstrated an anti-fibrotic/-tumor effect in murine models of mesothelioma and liver cancer [V. JD *et al.*, Br J Cancer. 2010; T. L. Rogers *et al.*, J Transl Med. 2011]. But, pharmacokinetics of bisphosphonates are poor for liver targeting as they are rapidly excreted by the kidneys after intravenous (iv) application. Here, we aimed to treat liver fibrosis by repolarizing liver M2-type macrophages towards an antifibrotic M1-type via a biocompatible, pH-degradable, nanogel carrier system conjugated to the bisphosphonate alendronate (AL).

Method: In primary murine macrophages, AL/NP (~30 µM AL) induced no cytotoxic effect and repolarized M2-type polarized macrophages towards a M1-type, increasing the expression of the M1-type related markers TNF-α, CCL-2 and downregulated the M2-type markers IL-10 and chitinase YM-1 on the transcript and protein level as determined via qPCR and flowcytometry (FACS).

Results: After iv injection in CCl₄ fibrotic Balb/c mice, more than 80% of near-infrared fluorescence labeled (CS800)-AL/NP rapidly accumulated in the liver, whereas CS800-AL were instantly cleared via the kidneys. On the cellular level, CS800-AL/NP were effectively engulfed by non-parenchymal cells (e.g. liver macrophages), while the AL/NP's uptake was significantly lower in parenchymal cells (hepatocytes) as determined by FACS. CS800-AL/NP were well tolerated and showed no overt toxicity. For fibrosis induction, Balb/c mice were gavaged with CCl₄ for 5 weeks. At week 4, mice received two iv injections of AL/NP (~2 mg/kg or 4 mg/kg AL) per week while control groups received equal concentrations of AL or NP, respectively. At the end of week 5, mice were sacrificed and liver collagen and the surrogate marker α-SMA were significantly reduced to physiological levels in AL/NP treated vs. control mice as determined by HYP quantification, Sirius Red readout and immunohistochemistry, while free AL and NP had no significant effect. Transcriptomic and proteomic data from total liver tissue of AL/NP (~4 mg/kg AL) treated vs. control mice (n = 3) revealed an upregulation of proinflammatory pathways and an enrichment of M1-type macrophages related genes in the treated mice, suggesting that AL/NP treatment triggers a switch from M2- to M1-type macrophages. In addition, we showed a downregulation of the M2-type markers YM-1, CD206 and IL-10 in the treated vs. control fibrotic liver both on the transcript and protein expression level.

Conclusion: This nanogel platform and the presented delivered drug conjugate AL/NP may serve as a novel, highly effective tool to treat liver fibrosis and possibly other diseases that are dominated by M2-type macrophages.

FRI148

Preclinical evaluation of the calpain inhibitor BLD-3051 as a therapeutic strategy for liver fibrosis

C. Wong¹, J.-X. Huang¹, W. Yu¹, P. Ibrahim¹, Ravi Rajagopalan¹. ¹Blade Therapeutics, Inc, South San Francisco, United States
Email: rrajagopalan@blademed.com

Background and aims: Calpains are a family of non-lysosomal intracellular calcium-dependent cysteine proteases that perform limited proteolytic cleavage of its substrates that in turn modulate a variety of signaling pathways controlling phenotypic effects like cell proliferation, migration, differentiation, and apoptosis. Elevated dimeric calpain activity levels are implicated in a variety of disease pathologies including fibrotic diseases. Additionally, calpain knock-outs and small molecule dimeric calpain inhibitors are efficacious in animal models of fibrosis. We have generated multiple calpain inhibitors with significantly improved potency, protease selectivity, and ADMET properties that may represent important new anti-fibrotic agents. Here, we describe the properties of BLD-3051, a small molecule dimeric calpain inhibitor and characterize its activity in a therapeutic model of liver fibrosis.

Method: 8-week-old C57BL/6 mice were fed a choline-deficient, L-amino acid, high fat diet (CDAHFD) for the entire 10-week study duration. Oral gavage dosing of BLD-3051 was initiated on week 5 of CDAHFD and continued for 6 weeks. Once daily (QD) doses of 60 and 200 mg/kg and twice daily (BID) doses of 30 and 100 mg/kg were evaluated. Body and liver weight and liver enzyme panel data were collected. Histopathology by modified NAFLD activity score (NAS) and liver hydroxy-proline levels were used to assess anti-fibrotic efficacy.

Results: BLD-3051 reduced NAS scores and liver hydroxy-proline levels in a dose-dependent manner with BID dosing being more efficacious. The lowering of NAS by BLD-3051 is largely driven by an anti-fibrotic effect.



Conclusion: BLD-3051 is a potent, selective, orally bioavailable calpain inhibitor that when dosed therapeutically shows robust anti-fibrotic effects against multiple endpoints in a CDAHFD induced model of liver fibrosis. BLD-3051 is currently in preclinical development.

FRI149

Experimental fibrosis alters matrix-bound vesicles cargo that do not revert after histologic recovery

Toshifumi Sato^{1,2}, Bashar Matour³, Jiang Li², Michael Merchant⁴, Daniel Wilkey⁴, Kenichi Ikejima¹, Stephen Badylak^{3,5}, George Hussey^{5,6}, Melanie Scott^{3,7}, Gavin Arteel^{2,7}. ¹Juntendo University Hospital, Gastroenterology, Bunkyo City, Japan; ²University of Pittsburgh-Department of Medicine, Gastroenterology, Pittsburgh, United States; ³University of Pittsburgh, Surgery, Pittsburgh, United States; ⁴University of Louisville, Medicine, Louisville, United States; ⁵University of Pittsburgh, McGowan Institute for Regenerative Research, Pittsburgh, United States; ⁶University of Pittsburgh, Pathology, Pittsburgh, United States; ⁷Pittsburgh Liver Research Center, University of Pittsburgh, Pittsburgh, United States
Email: tosato@juntendo.ac.jp

Background and aims: Although it is now understood that hepatic fibrosis can resolve, potential therapies to enhance fibrosis resolution are lacking. MBV are nanometer-sized vesicles bound within the ECM collagen network. Changes in MBV cargo may contribute, at least in part, to the phenotypic changes driven by fibrosis and recovery.

Method: Fibrosis was induced by injecting male C57Bl/6J mice with CCl₄ (1 ml/kg 2 × /wk 4wks); animals were sacrificed 1–28 days later. Liver injury and fibrosis was monitored by clinical chemistry, histology and gene expression. MBV were extracted from the livers of mice and the trypsinized MBV proteome cargo was analyzed by LC-MS/MS analysis using a Proxeon EASY-nLC 1000 UHPLC and nano electrospray ionization into an Orbitrap Elite mass spectrometer. Feature data were extracted and analyzed using Proteome Discoverer v2.4. Hierarchical clustering of significantly-changed MBV proteins was performed using StringDB and KEGG classification. To investigate the effect of MBV on the recovery of liver fibrosis, normal MBV from porcine urinary bladder (30 mg/mouse i.p.) were injected for up to 2 weeks after cessation of CCl₄.

Results: Fibrosis caused by CCl₄ rapidly resolved after cessation, reverting to almost normal histology and expression after 28 d recovery. The amount and type of proteins associated with the MBV tended to decrease in fibrosis, which was not reversed even after fibrosis recovery. StringDB and KEGG analysis indicated that the proteins lost in fibrosis/recovery were predominantly RNA-binding proteins associated with the ribosome, which may also impact the RNA cargo of the MBV. Some mice injected with normal MBV accelerated the fibrotic resolution.

Conclusion: Liver MBV alter their protein cargo in response to experimental fibrosis. Importantly, these changes do not revert to baseline levels even after almost complete histological recovery of fibrosis. These data suggest MBV may be a novel prospect for mechanistic insight into hepatic disease progression and recovery.

FRI150

Hepatocyte cell-specific deletion of cathepsin D does not affect liver inflammation and fibrosis during cholestatic-induced liver fibrosis

Maria Fernandez-Fernandez^{1,2}, Paloma Ruiz-Blazquez^{2,3}, Valeria Pistorio^{3,4}, Susana Núñez^{2,5}, M. Carmen Garcia-Ruiz^{2,5,6,7}, José Fernandez-Checa^{2,5,6,7}, Anna Moles^{2,3,6}. ¹Institute of Biomedical Research of Barcelona (IIBB-CSIC), Experimental Pathology, Barcelona, Spain; ²CiberEHD, Spain; ³Institute of Biomedical Research of Barcelona (IIBB-CSIC), Experimental Pathology, Barcelona, Spain; ⁴University of Naples Federico II, Italy; ⁵Institute of Biomedical Research of Barcelona (IIBB-CSIC), Cell Death and Proliferation, Barcelona, Spain; ⁶IDIBAPS, Barcelona, Spain; ⁷USC Research Center for ALPD, United States
Email: anna.moles.fernandez@gmail.com

Background and aims: During liver fibrosis proteolytic activity is regulated in a timely manner in infiltrating and liver-resident cells depending on the cellular demands and controls not only matrix turnover but also, the activation and repression of growth factors and chemokines. Despite our growing understanding of the roles played

by lysosomal proteases, cathepsins, in liver fibrosis, our knowledge of their specific targets and signaling networks remains limited. Thus, the aim of this study was to analyse cathepsin D (CtsD) cell-specific role in hepatocytes during liver fibrosis.

Method: To study the cell-specific role of CtsD we generated a novel knock-out mouse strain by breeding Albumin Cre (hepatocytes) mice with CtsD floxed mice. CtsD cell-specific deletion was confirmed by CtsD WB in primary mouse hepatocytes and dual IF (F4/80-CtsD) in liver sections. Fibrosis was established using bile duct ligation (BDL) for 14 days or chronic administration of CCl₄ (0.5 µl/g) twice a week for 8 weeks in CtsD^{F/F} and CtsD^{ΔHep} mice. Liver damage was determined by serum ALT and H&E staining in liver sections. CtsD was assessed by enzymatic activity assay and RTPCR. Fibrosis was analysed by Sirius Red staining α-SMA IHP and α-SMA, Col1A1 and TGF-beta RTPCR. Liver inflammation was determined by NIMP and F4/80 IHP and TNF-α, CCL2 and CCL3 RTPCR.

Results: First we determined CtsD expression in mouse fibrotic livers, demonstrating CtsD presence in hepatocytes and macrophages. CtsD cell-specific deletion in hepatocytes was validated by CtsD WB in primary mouse hepatocytes and dual IF (F4/80-CtsD) in liver section from CtsD^{F/F} and CtsD^{ΔHep} mice. Of note, CtsD expression remained unaffected in liver non-parenchymal cells. In addition, adult unchallenged CtsD^{ΔHep} mice displayed normal liver damage determined by ALT and H&E staining in liver sections. Next, fibrosis was established for 14d using BDL. CtsD deletion in CtsD^{ΔHep} livers was confirmed by CtsD activity assay and gene expression. CtsD deletion in hepatocytes, did not affect liver damaged (ALT) and liver fibrosis as determined by Sirius red staining, α-SMA IHP and hepatic α-SMA, Col1A1 and TGF-beta gene expression. Furthermore, liver inflammation was also not significantly affected in CtsD^{ΔHep} mice after BDL as assessed by NIMP and F4/80 IHP and TNF-α, CCL2 and CCL3 gene expression. In agreement, no significant changes in liver damage, fibrosis and inflammation were observed after chronic CCl₄ administration between CtsD^{F/F} and CtsD^{ΔHep} mice supporting our results in the BDL model.

Conclusion: CtsD expressed in hepatocytes does not play an essential contribution to liver fibrosis development after cholestatic-induced liver injury.

FRI151

The therapeutic potential of alpha v integrins in liver fibrosis

Syedia Rahman^{1,2,3}, Guruprasad Aithal^{1,3}, Jane Grove^{1,3}, K. Tao Pun⁴, James Roper⁴, Andrew Bennett^{1,2,3}. ¹NIHR Nottingham Biomedical Research Centre, Nottingham University Hospitals NHS Trust and University of Nottingham, Nottingham, United Kingdom; ²FRAME Alternatives Laboratory University of Nottingham Medical School, Life Sciences, Nottingham, United Kingdom; ³Nottingham Digestive Diseases Centre, Medicine, Nottingham, United Kingdom; ⁴GlaxoSmithKline, Novel Human Genetics Research Unit, United Kingdom
Email: syedia.rahman@nottingham.ac.uk

Background and aims: Hepatic stellate cells (HSC) are the primary effector cells in liver fibrosis and they secrete inactive transforming growth factor beta (TGFβ) which, when activated through proteins known as alpha v integrins, contributes to liver fibrosis. These integrins are composed of beta 1, 3, 5, 6 and 8 subunits. Specific inhibitors which target alpha v integrins and their particular beta subunit have shown to reduce fibrosis progression in mouse models but their role has not been explored in human liver disease. We aimed to assess integrin expression on activated human HSCs and the level of integrin expression in human liver samples from patients with varying degrees of fibrosis. Subtype selective integrin inhibitors were tested to determine their capability to inhibit HSC activation and their effect on TGFβ activity. This has previously never been performed before using human samples.

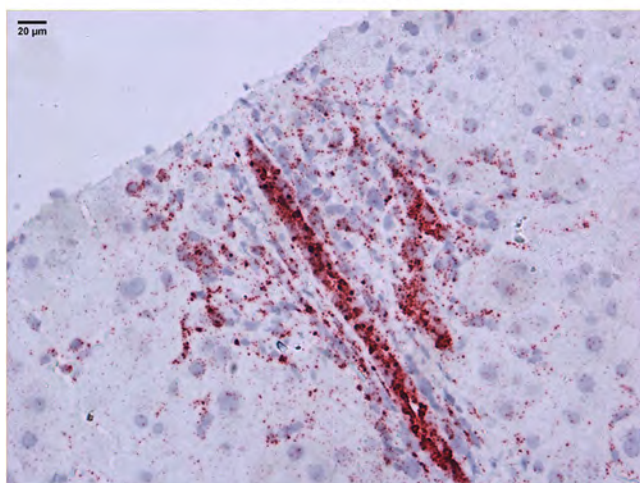
Method: HSCs were isolated from healthy individuals, integrin gene and protein expression was measured using qPCR and western blot. Tissue expression of integrins on fibrotic human liver tissue was

POSTER PRESENTATIONS

examined using a novel technique known as RNAscope®. To assess TGFbeta activity in HSCs, HSCs were co-cultured with mink lung epithelial TGFbeta reporter cells which were used to detect levels of active TGFbeta.

Results: There was gene and protein expression of alpha v, beta 1, 3 and 5 integrins with the exception of beta 6 on activated human HSCs. There was high gene expression of alpha v, beta 1, 3, 5 and 8, normalized to beta-actin. We show, for the first time, an identical pattern of integrin expression observed in fibrotic human liver tissue which showed increased expression compared to healthy controls. In co-culture assays, antibodies to alpha v, beta 1 and beta 3 integrins inhibited the increase in active TGFbeta, while antibodies to beta 5 and beta 6 integrins did not have any effect. From the subtype selective compounds tested, a beta 1 inhibitor, prevented the TGFbeta increase in a dose-dependent manner while a beta 6 inhibitor did not.

Fibrotic human liver tissue stained with haematoxylin and RNAscope® probe detecting B1 integrin



Conclusion: In activated HSCs, there was gene and protein expression of integrins beta 1, 3 and 5 with similar integrins expressed on fibrotic human liver tissue, not reported previously. A beta 1 integrin inhibitor compound successfully inhibited TGFbeta activation in a dose-dependent manner. This shows the exciting potential of beta 1 integrin specifically being a successful treatment target for liver fibrosis.

FRI152

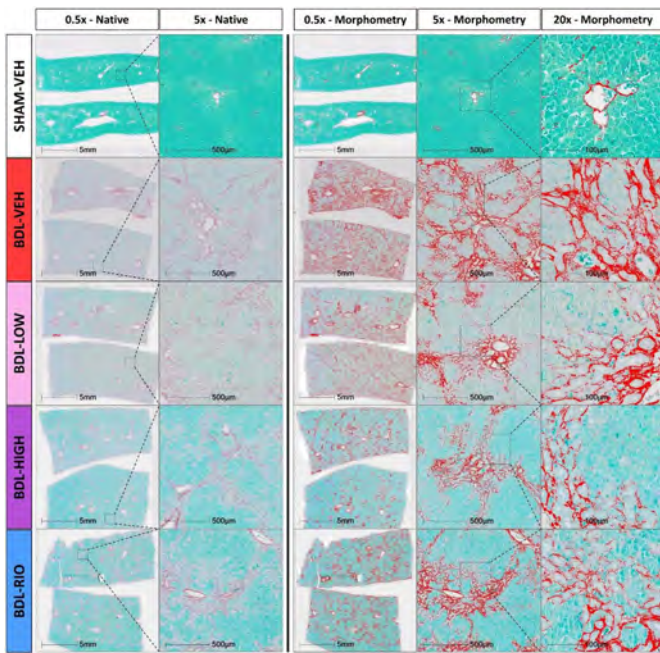
Dual inhibition of integrins alpha-v/beta-6 and alpha-v/beta-1 decreases portal pressure and liver fibrosis in rats with biliary cirrhosis

Philipp Königshofer^{1,2,3,4,5}, Johanna Schaub⁶, Ksenia Brusilovskaya^{1,2,3,4,5}, Benedikt Hofer^{1,2,3}, Benedikt Simbrunner^{1,2,3,4,5}, Oleksandr Petrenko^{1,2,3,4,5}, Hubert Scharnagl⁷, Tatjana Stojakovic⁷, Philipp Schwabl^{1,2,3,4,5}, Eric Lefebvre⁶, Scott Turner⁶, Thomas Reiberger^{1,2,3,4,5}. ¹Medical University of Vienna, Division of Gastroenterology and Hepatology, Vienna, Austria; ²Medical University of Vienna, Vienna Experimental Hepatic Hemodynamic Lab (HEPEX), Vienna, Austria; ³Medical University of Vienna, Christian Doppler Laboratory for Portal Hypertension and Liver Fibrosis, Vienna, Austria; ⁴Ludwig Boltzmann Institute for Rare and Undiagnosed Diseases (LBI-RUD), Vienna, Austria; ⁵CeMM Research Center for Molecular Medicine of the Austrian Academy of Sciences, Vienna, Austria; ⁶Pliant Therapeutics, Inc., South San Francisco, United States; ⁷University Hospital Graz, Clinical Institute of Medical and Chemical Laboratory Diagnostics, Graz, Austria
Email: elefebvre@pliantrx.com

Background and aims: Transforming growth factor-beta (TGF-beta) signalling is a key driver of liver fibrosis. In primary sclerosing cholangitis (PSC), integrins overexpressed on injured cholangiocytes (alpha-v/beta-6) and myofibroblasts (alpha-v/beta-1) regulate TGF-beta activity; they bind and activate latent TGF-beta thereby promoting liver fibrosis. We investigated the effects of PLN-75068, a tool alpha-v/beta-6 and alpha-v/beta-1 inhibitor compound, on liver fibrosis and portal hypertension in rats with cholestatic biliary cirrhosis.

Method: Male Sprague Dawley rats underwent bile duct ligation (BDL) or sham operation (SHAM). Two weeks post-surgery, BDL rats received PLN-75068 100 mg/kg (BDL-LOW), 300 mg/kg (BDL-HIGH), riociguat ([RIO], BDL-RIO; positive control) 0.5 mg/kg or vehicle ([VEH], BDL-VEH), and SHAM rats received VEH (SHAM-VEH) twice daily via oral gavage for 2 weeks. Portal pressure (PP), mean arterial pressure (MAP), heart rate and splanchnic/portal blood flow were measured at end of treatment. Alanine transaminase (ALT), aspartate transaminase (AST), alkaline phosphatase (ALP) and bilirubin (BIL) were assessed. Fibrosis was quantified by automated morphometry of collagen proportionate area (CPA) on Picro-Sirius red-stained full liver lobe sections and assessment of hydroxyproline (HP).

Results: Cirrhotic vehicle control rats (BDL-VEH) showed significantly higher values of PP (12.2 ± 1.9 vs 6.8 ± 0.9 mmHg; $p < 0.001$) and CPA (13.8 ± 4.3 vs $1.1 \pm 0.2\%$; $p < 0.001$) compared with SHAM-VEH. Elevated PP in BDL rats was lowered with treatment: BDL-LOW (-10% ; $p = 0.009$), BDL-HIGH (-9% ; $p = 0.26$) and BDL-RIO (-10% ; $p = 0.02$). MAP was significantly reduced in all treated groups (BDL-LOW: -22% ; BDL-HIGH: -27% ; BDL-RIO: -24% ; all $p < 0.001$) vs BDL-VEH. CPA was decreased with treatment: BDL-LOW (-28% ; $p = 0.04$), BDL-HIGH (-41% ; $p = 0.003$) and BDL-RIO (-29% ; $p = 0.03$) compared with BDL-VEH (Figure). HP levels were comparable across all BDL rats (VEH: 489 ± 163 ug/g; LOW: 508 ± 111 ug/g; HIGH: 473 ± 114 ug/g; RIO: 476 ± 174 ug/g). ALT was significantly lower with treatment: BDL-LOW (63 ± 10 U/L; -26%), BDL-HIGH (58 ± 12 U/L; -32%) and BDL-RIO (59 ± 9 U/L; -31%) all $p < 0.001$, compared with BDL-VEH (85 ± 17 U/L). Treatment with RIO significantly reduced AST ($p = 0.03$), but ALP and BIL remained unchanged in all treated animals compared with BDL-VEH. Weight loss was observed in BDL-HIGH but was not statistically significant.



Quantification of fibrosis by collagen proportionate area on Picro-Sirius red-stained full liver lobe sections. SHAM-VEH, sham operated rats administered vehicle; BDL-VEH, bile duct ligated rats administered vehicle; BDL-LOW, bile duct ligated rats administered PLN-75068 100 mg/kg; BDL-HIGH, bile duct ligated rats administered PLN-75068 300 mg/kg; BDL-RIO, bile duct ligated rats administered riociguat 0.5 mg/kg.

Conclusion: In rats with biliary cirrhosis, dual α -v/ β -6 and α -v/ β -1 inhibition by PLN-75068 ameliorated portal hypertension, exerted dose-dependent anti-fibrotic effects as assessed by CPA and significantly reduced ALT levels. A multinational Phase 2a evaluation of PLN-74809 in participants with PSC is ongoing (INTEGRIS-PSC; EudraCT: 2020-001428-33; NCT04480840).

FRI153

Dual roles of PSMP/MSMP in the progression of hepatic fibrosis and hepatocellular carcinoma

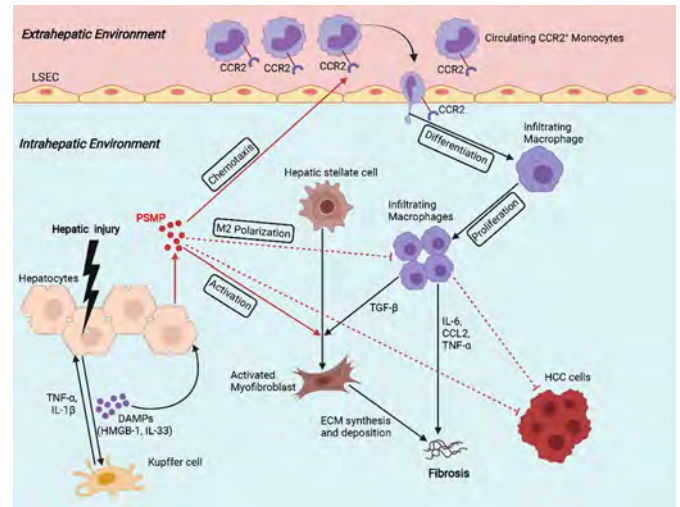
Shaoping She¹, Liying Ren², Pu Chen¹, Dongbo Chen¹, Hongsong Chen¹. ¹Peking University People's Hospital, Peking University Hepatology Institute, Beijing Key Laboratory of Hepatitis C and Immunotherapy for Liver Diseases, Beijing, China; ²Affiliated Hospital of Guilin Medical University, Laboratory of Hepatobiliary and Pancreatic Surgery, Guilin, China
Email: chen hongsong@bjmu.edu.cn

Background and aims: Chemokines are a family of cytokines that orchestrate the migration and positioning of immune cells within tissues and are critical for the function of the immune system. PC3 secreted microprotein (PSMP) or microprotamine (MSMP) is a novel chemotactic cytokine discovered through genome-wide bioinformatics analysis and chemoattractant platform screening, which can act as a CCR2 ligand to recruit peripheral blood monocytes and lymphocytes. CCR2 participates in liver pathology, including acute liver injury, chronic hepatitis, fibrosis/cirrhosis and tumor progression, by mediating the recruitment of immune cells to inflammation and tumor sites. In the present study, we investigated the expression and role of PSMP in liver fibrosis/cirrhosis and hepatocellular carcinoma (HCC).

Method: PSMP expression was studied in patients and murine models of fibrosis/cirrhosis and HCC. The role of PSMP *in vivo* was evaluated in PSMP gene knockout mice. The direct effects of PSMP on macrophages, hepatic stellate cells and tumor cells were studied *in vitro*.

Results: In this study, we found that PSMP is highly expressed in fibrotic/cirrhotic tissues from patients with multiple etiologies. PSMP is also overexpressed in human liver cancer-adjacent tissues, and its

expression level is positively correlated with patients' survival. PSMP deficiency (*Psmf*^{-/-}) resulted in a marked amelioration of hepatic fibrosis, but promoted liver tumor growth in mice. Damage-associated molecular patterns molecules HMGB-1 and IL-33 significantly induced hepatocytes to produce PSMP. In CCl₄-induced hepatic injury, the infiltration of CCR2⁺ monocytes and macrophages into the liver is significantly decreased in *Psmf*^{-/-} mice. In HCC, knockout of PSMP can inhibit the infiltration of tumor-infiltrating CD8⁺ lymphocytes and promote M2-polarization of tumor-associated macrophages (TAMs) in mice. At the cellular level, we found that PSMP can directly promote the M1 polarization of bone marrow-derived macrophages and the activation of LX-2 cells, and also inhibit the proliferation and migration of HCC cells.



Conclusion: In conclusion, PSMP can promote liver fibrosis, while inhibit liver carcinogenesis. These results indicate that PSMP may play different or even opposite functions in different stages of liver disease, suggesting that PSMP is a potential target for the treatment of chronic liver disease and HCC.

FRI154

NKT cells promote both type 1 and type 2 inflammatory responses in the non-obese diabetic inflammation and fibrosis (NIF) mouse model

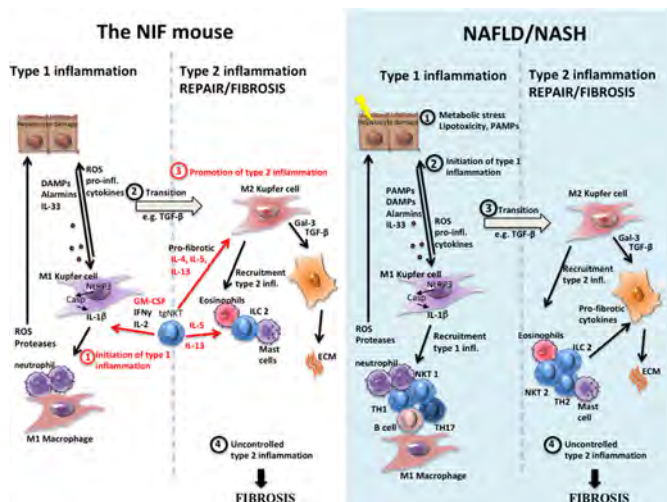
Julia Nilsson^{1,2}, Maria Hörnberg¹, Kajsa Linde¹, Dan Holmberg^{1,2}, Sofia Mayans¹. ¹Inficure Bio AB, Umeå, Sweden; ²Lund University, Experimental Medical Science, Malmö, Sweden
Email: sofia.mayans@inficurebio.com

Background and aims: Sterile liver inflammation and fibrosis are associated with many liver disorders of different etiologies. Both type 1 and type 2 inflammatory responses have been reported to contribute to liver pathology and the mechanisms controlling the balance between these responses are largely unknown. Here we use the non-obese diabetic inflammation and fibrosis (NIF) mouse model for chronic liver inflammation and fibrosis to investigate the role of NKT cells in the different phases of sterile liver inflammation.

Method: Transgenic mice overexpressing a NKT cell population in the presence or absence of an adaptive immune system was analyzed and the role of this population in the generation of chronic liver inflammation and fibrosis was examined.

Results: We demonstrate that transgenic NKT cells, when developing in an immunodeficient *Rag2*^{-/-} genetic background (the NIF mouse), expresses a mixed Th1/Th2 cytokine profile, which induces IL-1 β production through the NLRP3 pathway that initially result in the development of chronic liver inflammation. This phase is followed by the development of a type 2 inflammatory response including the

expression of the IL-33 alarmin, production of anti-inflammatory/profibrotic cytokines, the activation of the TGF β pathway, and recruitment of activated hepatic stellate cells (HSC) which results in the development of liver fibrosis. This process is controlled by the adaptive immune system since littermate controls carrying one functional *Rag2* allele and developing a normal adaptive immune system, fail to develop chronic liver inflammation and fibrosis.



Conclusion: Our data illustrates how plasticity in NKT cells can drive an initial type 1 inflammatory response and promote the transition into a type 2 inflammatory response thus overlapping key cellular and molecular events characterizing human liver diseases such as e.g. NAFLD/NASH. Further, the data suggests that this process is controlled by some component (s) of the adaptive immune system. The observed mechanistic overlap with human liver disease suggest that the NIF mouse model represents a unique tool for drug efficacy tests in liver inflammation and/or fibrosis with large translational potential as illustrated in the figure.

FRI155

Using qFibrosis analysis to predict disease and survival outcome of patients with hepatocellular carcinoma after curative treatment

Chih-Yang Hsiao^{1,2}, Dean Tai³, Yayun Ren³, Kai-Wen Huang^{1,2}.

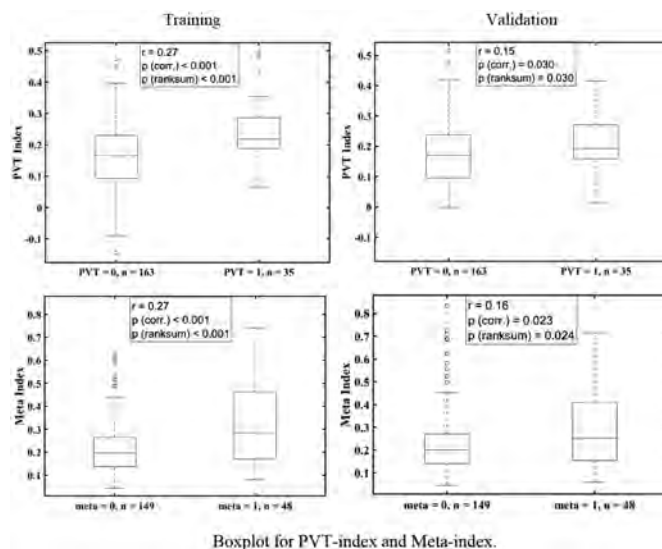
¹National Taiwan University Hospital, Department of Surgery, Taipei, Taiwan; ²National Taiwan University, Graduate Institute of Clinical Medicine, College of Medicine, Taipei, Taiwan; ³HistoIndex Pte Ltd, Research, Singapore, Singapore
Email: skvntuh@gmail.com

Background and aims: Stromal remodelling in tumor microenvironment plays an important role in cancer progression. It is featured by collagen realignment in the stromal compartment, collagen fibers and basal membrane. There remains a lack of studies addressing the stromal background and fibrosis features and its prognostic value in liver cancer. qFibrosis is a system of second harmonic generation and two photon emission (SHG/TPE) microscopy which can identify, quantify and visualize the fibrosis features from biopsy samples. qFibrosis has been validated for its application in diagnosis and prognosis of hepatitis B and non-alcoholic steatohepatitis. In this study, we aim to establish a prognostic estimation model by using qFibrosis analysis in liver cancer.

Method: Total of 198 patients with HCC underwent curative tumor resection were included. Their disease status, survival time, and clinical outcomes of whether portal vein thrombosis (PVT) and metastasis (Meta) developed during follow-up after surgery were analyzed. Liver tissue and liver tumor from the 198 patients were

imaged and assessed using qFibrosis system, and generated a total of 33 and 156 collagen parameters from liver tissue and tumor part, respectively. We used these collagen parameters to build two models, PVT-index and Meta-index, to differentiate the patient's clinical outcome of PVT and Meta, respectively. The models were validated using leave-one-out method.

Results: Both developing PVT and metastasis were significant indicators for poor prognosis. Seven parameters were selected from the parameters of liver tissue and tumor part to build the PVT-index and Meta-index, respectively. The PVT-index well differentiates patients developing PVT ($p < 0.001$ for training, $p = 0.030$ for validation, Figure), and the Meta-index also well differentiate patients developing metastasis during follow-up ($p < 0.001$ for training, $p = 0.024$ for validation, Figure).



Conclusion: Prognostic estimation models consist of collagen parameters in qFibrosis system could be built to predict HCC patient's clinical outcomes of developing PVT and Meta during follow-up after radical treatment. Our results demonstrated the potentials of using qFibrosis system to transform the histopathological features into quantifiable data that could be used to correlate with patient outcome as other clinical biomarkers.

FRI156

Multi-target engagement effect of a novel long-acting Glucagon/GIP/GLP-1 triple agonist, HM15211, in animal model of NASH/fibrosis

Jong Suk Lee¹, Jung Kuk Kim¹, Seonmyeong Lee¹, Yohan Kim¹,
Jaehyuk Choi¹, Hyunjoo Kwon¹, Eun Jin Park¹, Sung Min Bae¹,
Sang Hyun Lee¹, In Young Choi¹. ¹Hanmi Pharm.Co., Ltd., Seoul, Korea,
Rep. of South
Email: jychoi@hanmi.co.kr

Background and aims: Although its benefits were confirmed for NASH resolution, semaglutide failed to improve fibrosis in human. Recently, benefits of glucagon and GIP in addition to GLP-1 have been suggested beyond metabolism such as fibrosis. Thus, optimal use of these incretins simultaneously could be a promising strategy for NASH and fibrosis treatment. For this purpose, a novel long-acting Glucagon/GIP/GLP-1 triple agonist, HM15211, was developed. Here, beneficial effect of HM15211 via multi-target engagement was evaluated in animal models of NASH/fibrosis.

Method: AMLN-diet induced NASH mice and CDA-HFD induced nash.fibrosis mice were administered either with HM15211 or acylated GLP-1, GLP-1/GIP, or GLP-1/Glucagon agonist. Choline-deficient, L-amino acid-defined, and high fat diet (CDA-HFD)

induced NASH and fibrosis mice were also utilized. After treatment for 8 ~ 12 weeks, histologic analysis including NAFLD Activity Score (NAS) and hepatic hydroxyproline (HP) were determined. Liver transcriptome analysis was performed to investigate differentially expressed genes (DEGs) for diverse biological pathways.

Results: In AMLN mice, HM15211 treatment led to greater reduction in each component and composite NAS (6.1, 4.9, 3.6, 4.9, 2.0 for vehicle, acylated GLP-1, GLP-1/GIP, GLP-1/Glucagon, HM15211) than incretin analogs, and more NASH resolution achievement were confirmed for HM15211. In CDA-HFD mice, HM15211 treatment was consistently associated with greater reduction of NAS than incretin analogs. More reduction in hepatic HP and collagen contents (−4.2, −10.0, 7.1, and −26.5% vs. vehicle for acylated GLP-1, acylated GLP-1/GIP, acylated GLP-1/Glucagon, and HM15211) than incretin analogs were confirmed, indicating potential benefits of HM15211 for liver fibrosis. To understand underlying mechanisms for improved therapeutic effects of HM15211 on NASH and fibrosis, DEG analysis was performed and compared to acylated GLP-1, HM15211 treatment was associated with more favourable DEG signature in diverse pathways including bile acid metabolism, inflammation and fibrosis in addition to lipid metabolism, highlighting its multi-targeting MoA for the treatment of NASH and fibrosis.

Conclusion: In NASH/fibrosis animal models, more therapeutic benefits of HM15211 over other incretins were demonstrated. Notably, DEG analysis supports the basis for multi-target engagement effects of HM15211. Thus, HM15211 might be a novel therapeutic option for NASH and fibrosis. Human study is ongoing to assess the clinical relevance of these findings.

FRI157

Direct anti-inflammatory and anti-fibrotic effects of a novel long-acting Glucagon/GIP/GLP-1 triple agonist, HM15211, in thioacetamide-induced mouse model of liver injury and fibrosis

Jung Kuk Kim¹, Jong Suk Lee¹, Yohan Kim¹, Seonmyeong Lee¹, Jaehyuk Choi¹, Hyunjoo Kwon¹, Eun Jin Park¹, Sung Min Bae¹, Dae Jin Kim¹, Sang Hyun Lee¹, In Young Choi¹. ¹Hanmi Pharm.Co., Ltd. Email: iychoi@hanmi.co.kr

Background and aims: HM15211 is a novel long-acting triple agonist consisting of rationally designed Glucagon/GIP/GLP-1 triple agonist conjugated to human IgG FC fragment via short PEG linker. Previously, therapeutic benefits of HM15211 were demonstrated in diet-induced animal models of NASH and/or fibrosis. Here, we evaluate direct anti-inflammatory and -fibrotic effects of HM15211 in TAA (thioacetamide)-induced liver injury and severe fibrosis mouse, and investigate underlying MoA.

Method: To induce liver injury and liver fibrosis, escalating doses of dose of TAA was injected to mouse for 12 weeks. HM15211 was administered during last 10 weeks. Hepatic hydroxyproline (HP) contents were measured and Sirius red staining was conducted. qPCR was performed to evaluate relevant marker gene expression. Multiplex assay was performed to measure blood level of pro-inflammatory cytokines. For mechanistic study, THP-1 cell and LX2 cell were used.

Results: HM15211 treatment significantly reduced HP content (−51% vs. Veh., $p < 0.01$), Sirius red positive area (−65% vs. Veh., $p < 0.001$), and fibrosis score (0.7 for HM15211 vs. 3.0 for Veh., $p < 0.001$) in TAA mice. Considering baseline fibrosis score at week 2 (1.0), HM15211 could confer both potential reversal effect on pre-existing fibrosis and prevention effect on fibrogenesis. Consistently, expression of hepatic marker genes for fibrosis (i.e. collagen) and inflammation (i.e. F4/80 and TNF- α) were significantly reduced in HM15211-treated group. Furthermore, multiplex analysis revealed that HM15211 treatment was associated with robust reduction across pro-inflammatory cytokines such as TNF- α , IL-1 β , IL-6, and etc. Significant reduction in blood level of liver enzymes was also confirmed. Mechanistically, PMA/LPS-induced THP-1 cell adhesion and subsequent cytokine secretion were significantly attenuated by

HM15211. TGF- β -induced collagen production was also reduced in LX2 cell. Based on *in vitro* results, observed benefits in TAA mice might primarily results from direct anti-inflammatory and -fibrotic effects of HM15211.

Conclusion: HM15211 markedly improved liver inflammation and fibrosis in TAA mice, and related MoAs were elaborated by *in vitro* studies. Together with previous results, generalized anti-inflammatory and -fibrotic effects of HM15211 were corroborated. Thus, HM15211 could be a novel therapeutic option for fibrosis due to NASH. Human study is ongoing to assess the clinical relevance of these findings.

FRI158

Loss of bile salt export pump (BSEP/ABCB11) protects mice from development of carbon tetrachloride (CCl₄) induced hepatic fibrosis

Claudia Fuchs¹, Emmanuel Dauda Dixon¹, Philipp Königshofer^{1,2,3,4,5}, Veronika Mlitz¹, Hubert Scharnagl⁶, Tatjana Stojakovic⁷, Thomas Reiberger^{1,2,3,4,5}, Michael Trauner¹. ¹Medical University of Vienna, Division of Gastroenterology and Hepatology, Internal Medicine III, Vienna, Austria; ²Medical University of Vienna, Vienna Experimental Hepatic Hemodynamic lab (HEPEX); ³Medical University of Vienna, Christian Doppler laboratory for Portal Hypertension and Liver Fibrosis; ⁴Ludwig Boltzmann Institute for Rare and Undiagnosed Diseases (LBI-RUD); ⁵CeMM Research Center for Molecular Medicine of the Austrian Academy of Sciences; ⁶Medical University of Graz, Clinical Institute of Medical and Chemical Laboratory Diagnostics; ⁷University Hospital Graz, Clinical Institute of Medical and Chemical Laboratory Diagnostics Email: michael.trauner@meduniwien.ac.at

Background and aims: Loss of BSEP/ABCB11 was shown to protect mice from acquired cholestasis due to preconditioning with a hydrophilic bile acid (BA) pool, with tetrahydroxylated BAs as the most prominent species. In this study we aimed to investigate whether loss of BSEP and subsequent increase in hydroxylation/detoxification of BAs protects mice from development of carbon tetrachloride (CCl₄) induced hepatic fibrosis.

Method: BSEP WT and KO mice were injected every other day with CCl₄ for 8 weeks as model of hepatic fibrosis. *In vitro*, the hepatic stellate cell line LX2 was challenged with TGF- β with and without cotreatment of tetrahydroxylated BAs. RNA profiling was performed by RT-PCR. Liver histology/immunohistochemistry (IHC), immunofluorescence (IF) and immunoblot were assessed.

Results: In contrast to WT mice, serum parameter ALT and AST were not elevated in BSEP KO mice by CCl₄ injection. In line, mRNA expression of inflammatory markers *Cxcl1*, *Cxcl2*, *Ccl2*, *Ccl5* remained unchanged in BSEP KO mice injected with CCl₄, while in WT CCl₄ mice these markers were significantly increased (3fold, 20fold, 20fold, 2fold, respectively). Accordingly, numbers of MAC-2 positive cells were significantly lower in BSEP KO CCl₄ injected mice when compared to CCl₄ WT mice. Fibrotic markers *Col1a1*, *Col1a2* as well as Sirius red were significantly reduced in BSEP KO CCl₄ mice compared to WT CCl₄ mice (by 40%, 60%, 65% respectively). Accordingly, alpha-SMA (marker of activated hepatic stellate cells) (IF) remained at basal levels in BSEP KO CCl₄ mice. Mechanistically, we could demonstrate that hepatic protein expression of pJNK (known to be involved in development of CCl₄ induced hepatic fibrosis) was reduced in BSEP KO CCl₄ mice in comparison to challenged WT mice. *In vitro*, activated phenotype of LX2 cells was ameliorated with treatment of tetrahydroxylated BAs, as reflected by significant reductions of alpha-SMA and Col1a1 gene expression.

Conclusion: Loss of BSEP and subsequent hydroxylation of the bile pool protects mice from CCl₄ induced hepatic fibrosis via suppression of hepatic pJNK signalling and attenuation of HSC activation.

FRI159

Large-scale multicenter study for the clinical utility of the non-invasive biomarkers Gas6 and soluble Axl in hepatocellular carcinoma, liver fibrosis and end-stage liver disease

Katharina Staufer^{1,2}, Heidemarie Huber³, Jasmin Zessner-Spitzenberg³, Rudolf E. Stauber⁴, Armin Finkenstedt⁵, Heike Bantel⁶, Thomas Weiss⁷, Markus Huber⁸, Patrick Starlinger⁹, Thomas Grünberger^{9,10,11}, Thomas Reiberger², Susanne Sebens¹², Gail McIntyre¹³, Ray Tabibiazar¹³, Amato Giaccia¹³, Heinz Zoller⁵, Michael Trauner², Wolfgang Mikulits³. ¹Medical University of Vienna, Department of General Surgery, Division of Transplantation, Wien, Austria; ²Medical University of Vienna, Department of Internal Medicine III, Division of Gastroenterology & Hepatology, Wien, Austria; ³Medical University of Vienna, Department of Medicine I, Division: Institute of Cancer Research, Comprehensive Cancer Center Vienna, Vienna, Austria; ⁴Medical University of Graz, Division of Gastroenterology and Hepatology, Department of Internal Medicine, Graz, Austria; ⁵Medizinische Universität Innsbruck, Department of Medicine I, Gastroenterology, Hepatology and Endocrinology, Innsbruck, Austria; ⁶Hannover Medical School, Department of Gastroenterology, Hepatology and Endocrinology, Hannover, Germany; ⁷University Hospital Regensburg, Center for Liver Cell Research, Children's University Hospital (KUNO), Regensburg, Germany; ⁸University Hospital Bern, Department of Anesthesiology and Pain Therapy, Inselspital, Bern, Switzerland; ⁹Medical University of Vienna, Department of Surgery, Division of General Surgery, Wien, Austria; ¹⁰Clinic Favoriten, HPB Center, Health Network Vienna, Surgery, Vienna, Austria; ¹¹Sigmund Freud Private University, HPB Surgery, Vienna, Austria; ¹²Christian-Albrechts-University Kiel (CAU), Institute for Experimental Cancer Research, Kiel, Germany; ¹³Aravive Biologics, Houston, United States
Email: wolfgang.mikulits@meduniwien.ac.at

Background and aims: The expression of the receptor tyrosine kinase Axl and the release of its cleavage product soluble Axl (sAxl) are highly elevated in hepatocellular carcinoma (HCC), advanced fibrosis, and cirrhosis. Recent studies suggest that the expression of Gas6, the high affinity ligand of Axl, is also enhanced during liver fibrogenesis and HCC. In this study, we evaluated the diagnostic accuracy of sAxl and Gas6 in a large cohort of patients with HCC, liver fibrosis and end-stage liver disease.

Method: Levels of sAxl and Gas6 were analyzed by enzyme-linked immunosorbent assays (ELISAs) in serum samples of patients with HCC, cholangiocarcinoma, colorectal liver metastases, chronic liver disease of all fibrosis stages, end-stage liver disease, and healthy controls from five centers in Europe. ELISAs were optimized to exclusively analyze either free sAxl or bioactive Gas6 levels.

Results: A total of 1111 patients (median age 57.8y, 67.3 % male) was included in the study. sAxl, Gas6 as well as their albumin (alb) ratios showed high diagnostic accuracy for the detection of HCC in comparison to healthy controls (AUC 0.765–0.942). sAxl/alb was confirmed as an accurate biomarker of advanced liver fibrosis and cirrhosis, and was even outperformed by Gas6/alb, which showed good accuracy (AUC 0.818–0.897) comparable to ELF™ test for the detection of liver cirrhosis. sAxl, Gas6 and their albumin ratios detected hepatic decompensation (Gas/alb: AUC 0.878), and were predictors of transplant-free survival.

Conclusion: Gas6/alb shows high accuracy for the detection of significant to advanced fibrosis and liver cirrhosis, as well as decompensated liver cirrhosis superior to sAxl/alb.

FRI160

Multispectral analysis of liver biopsies from patients with chronic hepatitis C reveals unique macrophage phenotypes and spatial interactions associated with fibrosis progression

Omar Saldarriaga¹, Santhoshi Krishnan², Morgan Oneka², Arvind Rao³, Joseph Gosnell¹, Daniel Millian¹, Timothy Wanner¹, Jingjing Jiao⁴, Laura Beretta⁴, Heather Stevenson¹. ¹University of Texas Medical Branch, Department of Pathology, Galveston, United States; ²Rice University, Department of Electrical and Computer Engineering, Houston, United States; ³University of Michigan, Department of Computational Medicine and Bioinformatics, Ann Arbor, United States; ⁴University of Texas MD Anderson Cancer Center, Department of Molecular and Cellular Oncology, Houston, United States
Email: omsaldar@utmb.edu

Background and aims: Despite availability of direct-acting antivirals, viral hepatitis C (HCV) still impacts ~58 million people world-wide and ~70% progress to chronic infection. Chronic hepatitis develops after the virus restricts pro-inflammatory macrophage activation necessary to control infection, contributing to T cell dysfunction and viral persistence. Intrahepatic macrophages represent ~20% of non-parenchymal cells and greatly impact the hepatic microenvironment, host immune response to liver injury and the development of fibrosis. We hypothesized that variations in the heterogeneity of macrophages determine disease progression in HCV + patients.

Method: We used multispectral imaging to phenotype and quantify resident Kupffer cells (CD68 +), monocyte-derived macrophages (Mac387 +), pro-fibrogenic macrophages (CD163 +), and co-expression of pro-inflammatory (CD14) and anti-inflammatory (CD16) in patients with minimal (fibrosis stage: 0/6; n=5) or advanced (fibrosis stage: 6/6; n=6) fibrosis. Next, we compared differences in the spatial distribution of the identified phenotypes (i.e., enrichment or depletion) within the hepatic microenvironment. Multiplex stained liver biopsies were scanned with a spectral imaging microscope (Vectra 3, Akoya Biosciences) and multi-component TIFF images and cell_seq_data files were analyzed to determine the heterogeneity of these various cell phenotypes. Both phenotype matrices and t-distributed stochastic neighbour embedding plots (t-SNE) were used (Visiopharm®; MATLAB 2020a, MathWorks inc.). Phenotypes that were significantly enriched were selected for spatial proximity analysis using G-function calculations.

Results: Phenotype matrix analysis revealed the enrichment of unique pathogenic macrophage phenotypes (CD163 + CD16 +, CD68 +, CD68 + MAC387 +) in the HCV + patients with advanced fibrosis (p < 0.05). Increased CD68 +, CD68 + MAC387 + macrophage populations, in certain individuals, correlated with poor clinical outcome (increased prothrombin time and decreased platelet counts). Spatial analysis showed significant (p < 0.05) enrichment of CD14 +, CD68 + CD14 + CD163 +, CD68 + MAC387 +, and MAC387 + macrophage populations near CD68 + cells and depletion of CD163 + CD16 + population to CD14 + cells. Enriched interactions between MAC387 + and CD163 + MAC387 + positive macrophages were exclusively observed in the HCV + patients with advanced fibrosis.

Conclusion: Multispectral imaging with spatial analysis enabled detailed evaluation of intrahepatic macrophages and their relationship with neighbouring cells phenotypes. Unique phenotypes and interactions were observed among HCV patients with advanced fibrosis and in those that had disease progression. This approach identified novel potential targets for inhibiting fibrosis development and development of future personalized medicine approaches.

FRI161

Neutrophil-specific NLRP3 activation triggers liver inflammation and fibrosis

Benedikt Kaufmann^{1,2}, Yanfang Peipei Zhu¹, Aleksandra Leszczynska¹, Agustina Reca¹, Laela M. Booshehri¹, Alexander Wree³, Helmut Friess², Daniel Hartmann², Hal M. Hoffman¹, Ben Croker¹, Ariel Feldstein¹. ¹Department of Pediatrics, University of California San Diego, La Jolla; ²Department of Surgery, TUM School of Medicine, Klinikum rechts der Isar, Technical, University of Munich; ³Charité, Campus Virchow Klinikum and Charité, Campus Mitte, Department of Hepatology and Gastroenterology, Universitätsmedizin Berlin
Email: benedikt_kaufmann@hotmail.com

Background and aims: Neutrophils have a key role in the acute inflammatory response during liver inflammation and fibrosis and are hypothesized to promote chronic inflammation and liver fibrosis if they are not efficiently cleared by macrophages. The NLRP3 inflammasome is crucial in liver inflammation and fibrogenesis. In this study the role of neutrophil-specific NLRP3 inflammasome over-activation in liver pathobiology was investigated.

Method: Neutrophil-specific mutant NLRP3 knock-in mice were generated by crossing Nlrp3 knock-in mouse strains with the presence of an intronic floxed neomycin resistance cassette with mice expressing Cre recombinase under the control of Calcium-binding protein A8. Liver tissue and bone marrow were analysed by immunohistochemistry, flow cytometry, and real-time quantitative polymerase chain reaction.

Results: Mutant mice with neutrophil-specific NLRP3 activation showed shortened survival, poor growth, and severe liver inflammation. Furthermore, neutrophil-specific NLRP3 activation resulted in systemic changes in hematopoiesis and an accumulation of inflammatory neutrophils, the key cells in the initial phase of inflammation, in the liver. Infiltrative inflammatory neutrophils were identified by elevated CD162 (PSGL-1) and increased expression of CD16/32 (FcγRIII/II) analyzed by flow cytometry as well as increased positive myeloperoxidase staining in the liver of mutant mice. Inflammation of liver tissue in mutant mice resulted in a decrease of resident macrophages evident by reduced CLEC4f and F4/80 expression in both IHC staining and qRT-PCR. In contrast, pro-inflammatory macrophage population was increased in mutant mice demonstrated by Ly6C staining and upregulation of inducible nitric oxide synthase 2 (iNOS2). Sirius Red staining revealed liver fibrosis in mutant mice, whereas WT mice showed a healthy liver. The expression of the pro-fibrotic genes metalloproteinases 1 (TIMP1) and connective tissue growth factor (CTGF) was upregulated in the liver tissue of mutant mice.

Conclusion: Neutrophil-specific NLRP3 overactivation resulted in severe liver inflammation with accumulation of inflammatory neutrophils and pro-inflammatory macrophage polarization. Furthermore, it induced liver fibrosis and a pro-fibrotic gene expression pattern. This data provides novel insights into the complex relationship between liver neutrophil-driven inflammation, macrophage polarization and liver fibrosis.

FRI162

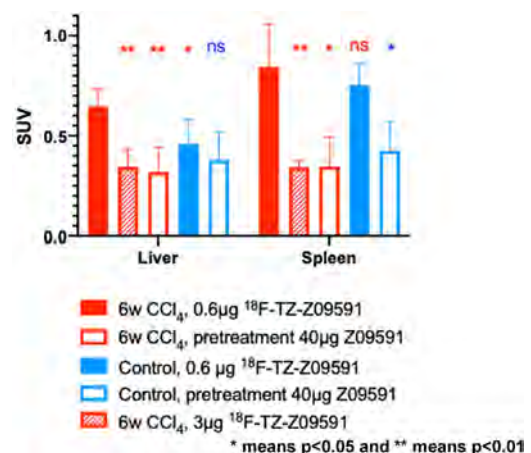
Imaging of fibrosis in metabolic associated liver disease by a radiolabeled affibody targeting PDGFRB

Olivia Wegrzyniak¹, Johanna Rokka², Bo Zhang¹, Maria Rosestedt¹, Bogdan Mitran^{1,3}, Pierre Cheung¹, Emmi Puuvuori¹, Sofie Ingvast⁴, Frederik Ponten⁴, Frederik Frejd⁵, Olle Korsgren⁴, Jonas Eriksson^{1,6}, Olof Eriksson^{1,7}. ¹Uppsala University, Department of Medicinal Chemistry, Uppsala, Sweden; ²Uppsala University, Department of Public Health and Caring Sciences, Uppsala, Sweden; ³Antaros Medical AB, Mölndal, Sweden; ⁴Uppsala University, Department of Immunology, Genetics and Pathology, Uppsala, Sweden; ⁵Affibody AB, Solna, Sweden; ⁶Uppsala University Hospital, PET Center, Uppsala, Sweden; ⁷Antaros Tracer AB, Mölndal, Sweden
Email: olivia.wegrzyniak@ilk.uu.se

Background and aims: The pathological formation of fibrosis, is an important feature in liver in Metabolic Associated Fatty Liver Disease (MAFLD) as well as in many different other diseases. Platelet-derived growth factor receptor beta (PDGFRB) is a known biomarker of activated hepatic stellate cells, and thus play a key role in fibrosis in MAFLD. Today, the treatment and monitoring of hepatic fibrosis is hampered by the lack of suitable methods for detecting and diagnosing the disease. Therefore, it is of crucial importance to develop non-invasive methods in order to detect, diagnose, stage and study fibrosis. Herein, we report the preparation, characterization, and evaluation of fluorine-18-labelled Affibody molecule Z09591, in a mouse model of non-alcoholic steatohepatitis (NASH).

Method: Affibody molecule Z09591 was labelled with fluorine-18 via tetrazine/trans-cyclooctene click chemistry. ¹⁸F-TZ-Z09591 was evaluated in a 6 weeks CCl₄ treatment mouse model of liver fibrosis by a PET study, including *ex vivo* biodistribution and autoradiography. Binding results were correlated to staining and PDGFRB immunohistochemistry (IHC) on *post-mortem* biopsies.

Results: Affibody molecule Z09591 was successfully radiolabelled with fluorine-18 with high purity and reproducible yield. PET studies demonstrated that liver uptake of ¹⁸F-TZ-Z09591 was higher in mice with induced hepatic fibrosis compare to healthy liver (Figure). The liver binding could also be blocked by pre-treatment with Z09591 in excess, indicating receptor specific binding. *Ex vivo* autoradiography demonstrated high signal intensity in positive hepatic sinusoids affected by fibrosis, as confirmed by Sirius red staining and PDGFRB IHC.



Conclusion: We describe the radiolabelling and evaluation of the PDGFRB binding affibody Z09591. ¹⁸F-TZ-Z09591 exhibited specific binding to hepatic fibrotic lesions. ¹⁸F-TZ-Z09591 is a promising tool for PET imaging of fibrosis in MAFLD. The use of such a tracer clinically could represent a non-invasive diagnostic, prognostic as well as predictive tool for MAFLD patients.

POSTER PRESENTATIONS

FRI163

Liver complications in greek patients with sickle cell disease: a multicenter retrospective analysis from eight thalassemia and sickle cell units across Greece

Konstantinos Manganas¹, Sophia Delicou¹, Aikaterini Xydaki¹, Alexandra Kourakli², Loukia Evliati³, Euthimia Vlahaki⁴, Evangelos Klironomos⁵, Michail Diamantidis⁶, Ioannis Lafiatis⁷, Antonis Kattamis⁸, Ioannis-Georgios Koskinas¹. ¹Ippokrateio General Hospital of Athens, Athens, Greece; ²General University Hospital of Patras, Rio, Greece; ³Evangelismos General Hospital, Athens, Greece; ⁴Ippokrateio-General Hospital of Thessaloniki, Thessaloniki, Greece; ⁵Venizeleio General Hospital, Heraklion, Greece; ⁶General University Hospital of Larissa, Larissa, Greece; ⁷General Hospital of Mytilene, Mytilene, Greece; ⁸Agia Sofia Children's Hospital, Athens, Greece
Email: kmagganas92@gmail.com

Background and aims: Sickle cell disease (SCD) is one of the most common monogenic disorders worldwide and liver complications, acute and chronic, are common in this group of patients. Our study aims to highlight the prevalence and predisposing factors of liver fibrosis in SCD patients.

Method: Eight Thalassemia and Sickle Cell Units across Greece and 219 patients enrolled in our study and history of liver related disease complications was recorded, as well as a full laboratory and imaging analysis concerning their liver function. Patients were divided in two groups, those with indications of advanced liver fibrosis (Fibroscan >13.5 kPa or Fib-4 >3.25 or APRI >1.5) and those without indications of advanced liver fibrosis.

Results: The prevalence of significant liver fibrosis in SCD patients in our study was 10.7%. The presence of liver fibrosis was significantly correlated with advanced age, male gender, cholelithiasis and higher LDH, γ -GT, INR, direct and indirect bilirubin levels. Noteworthy, patients with advanced liver fibrosis had suffered significantly more acute liver crises, acute liver sequestration crises and acute intrahepatic cholestasis in the last five years, while these patients were also receiving transfusion therapy more often and for a longer period of time and had higher Liver Iron Concentration (LIC) levels, but without statistical significance. No correlation was observed with ultra-sound findings of right heart failure or previous viral hepatitis.

	Patients with no significant fibrosis	Patients with significant fibrosis	p < 0.05
Hb (g/dl)	9.50 (1.37)	9.03 (1.09)	0.045**
HbS (%)	60.2% (14.5%)	63.9% (10.5%)	0.252*
HbF (%)	11.57% (8.3%)	13.39% (8.1%)	0.334*
PLTs ($\times 10^9/L$)	337.7 (178.81)	183.0 (145.50)	<0.001*
Ferritin (ng/ml)	772.02 (1432.02)	771.86 (1018.94)	0.668**
AST (U/L)	35.78 (15.15)	55.15 (30.42)	0.007**
ALT (U/L)	27.69 (16.18)	35.21 (30.36)	0.994**
γ -GT (U/L)	44.19 (52.89)	72.33 (115.93)	0.042**
LDH (U/L)	386.21 (124.33)	568.76 (224.02)	0.000**
Direct bilirubin (mg/dl)	0.67 (0.35)	1.25 (0.83)	0.002**
Indirect bilirubin (mg/dl)	1.57 (1.40)	2.77 (1.95)	0.003**
CRP (mg/l)	5.43 (8.92)	2.50 (2.76)	0.336**
INR	1.17 (0.41)	1.33 (0.57)	0.003**
Albumin (g/dl)	4.33 (0.52)	4.17 (0.61)	0.228**
MRI T2* (LIC-mg Fe/gr dry weight)	4.96 (7.19)	6.16 (7.04)	0.865**
Age (years)	46.75 (13.48)	52.56 (12.12)	0.05*
Duration of transfusions (years)	7.85 (13.22)	8.71 (13.34)	0.443**
Transfusions (PRBC/year)	6.06 (8.72)	7.95 (8.95)	0.124**
Acute liver crises (per 5 years)	0 (0.00)	0.16 (0.50)	0.000**
Acute intrahepatic cholestasis (per 5 years)	0 (0.00)	0.11 (0.45)	0.010**
Liver sequestration crises (per 5 years)	0.06 (0.278)	0.38 (0.88)	0.046**

Conclusion: Our study shows that advanced liver fibrosis is a significant cause of morbidity in patients with SCD and is primarily associated acute vaso-occlusive phenomena and chronic intravascular hemolysis of the disease itself.

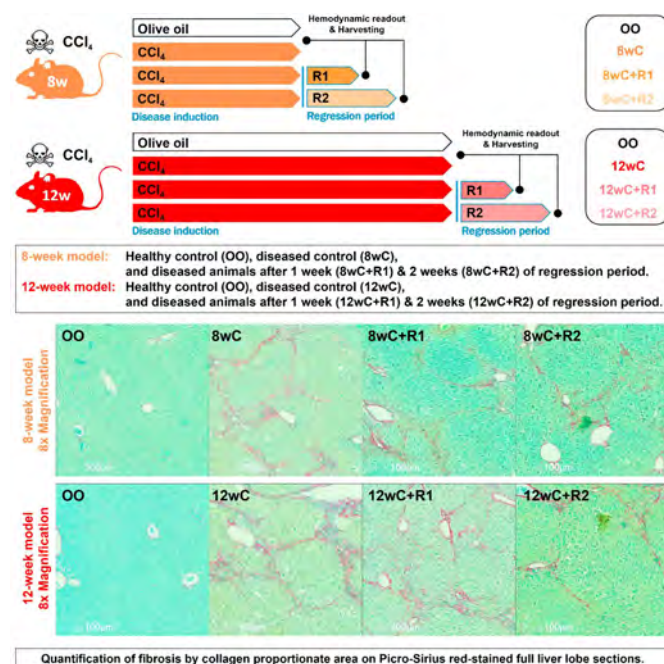
FRI164

Hemodynamic, molecular, and histological characterization of a toxic liver fibrosis regression model

Philipp Königshofer^{1,2,3,4,5}, Ksenia Brusilovskaya^{1,2,3,4,5}, Benedikt Hofer^{1,2,3}, Benedikt Simbrunner^{1,2,3,4,5}, Oleksandr Petrenko^{1,2,3,4,5}, Hubert Scharnagl⁶, Tatjana Stojakovic⁶, Michael Trauner¹, Philipp Schwabl^{1,2,3,4,5}, Stefan Günther Kauschke⁷, Larissa Pfisterer⁷, Thomas Reiberger^{1,2,3,4,5}. ¹Division of Gastroenterology and Hepatology, Department of Internal Medicine III, Medical University of Vienna, Vienna, Austria; ²Vienna Experimental Hepatic Hemodynamic lab (HEPEX), Medical University of Vienna, Vienna, Austria; ³Christian Doppler laboratory for Portal Hypertension and Liver fibrosis, Vienna, Austria; ⁴Ludwig Boltzmann Institute for Rare and Undiagnosed Diseases (LBI-RUD), Vienna, Austria; ⁵CeMM Research Center for Molecular Medicine of the Austrian Academy of Sciences, Vienna, Austria; ⁶Clinical Institute of Medical and Chemical Laboratory Diagnostics, University Hospital Graz, Graz, Austria; ⁷Boehringer Ingelheim Pharma GmbH, Biberach, Germany
Email: thomas.reiberger@meduniwien.ac.at

Background and aims: Portal hypertension (PH) results from 'static' liver fibrosis and 'dynamic' vascular components. Liver disease regression depends on cessation of liver injury to allow liver fibrosis regression and functional regeneration. We aimed to establish a toxic liver disease regression model to investigate the 'regressive' course of PH and fibrosis.

Method: Male C57BL/6J mice were exposed to CCl₄ for eight (8 w) or twelve (12 w) weeks (2 μ L/g in olive oil, 3x/week, per oral), respectively, to induce moderate (8 wC) and severe liver fibrosis (12 wC)-followed by one (+R1) or two (+R2) weeks of regression period, respectively (Figure). Healthy control groups received olive oil only (OO). Portal pressure (PP) was measured at end of each timeline. Blood parameters were assessed. Fibrosis was quantified by collagen proportionate area (CPA) in %. Matrix- and inflammation-related gene-expression was measured in bulk liver tissue.



Results: Diseased animals developed PH with PP (8wC: 8.5 ± 1.3 mmHg vs OO: 4.9 ± 0.8 mmHg; 12 wC: 10.0 ± 1.2 mmHg vs OO: 5.2 ± 0.2 mmHg; all $p < 0.001$) and liver fibrosis with CPA% (8 wC: 8.5 ± 5.0 % vs OO: 1.6 ± 0.9 %; 12 wC: 16.9 ± 3.9 % vs OO: 0.8 ± 0.2 %; all $p < 0.001$). In both models, PP regressed after one (8wC+R1: -31 %, $p < 0.001$; 12wC+R1: -16 %, $p = 0.01$) and after two weeks (8 wC+R2: -29 %, $p < 0.001$; 12wC+R2: -21 %, $p = 0.002$), respectively. Fibrosis regressed in the 8-weeks (8 wC+R1: -1 %, $p < 0.99$; 8 wC+R2: -37 %, $p = 0.24$) and significantly in the 12-weeks (12 wC+R1: -16 %, $p = 0.002$; 12 wC+R2: -21 %, $p < 0.001$) setting. AST and ALT levels significantly decreased after 1 week of regression (8 wC/12 wC+R1: -99 %) and after 2 weeks of regression, transaminases were similar to healthy controls ($p < 0.001$). Expression of fibrogenesis-related genes was significantly reduced: *Col1a1* (8 wC+R1/2: $-85/-91$ %; 12 wC+R1/2: $-83/-74$ %), *Tgf-beta* (8 wC+R1/2: $-71/-80$ %; 12 wC+R1/2: $-62/-27$ %), and *alpha-Sma* (8 wC+R1/2: $-86/-85$ %; 12 wC+R1/2: $-70/-42$ %). Matrix-metalloproteinase activity was promoted by decreased *Timp1* (8 wC+R1/2: $-94/-95$ %; 12 wC+R1/2: $-92/-85$ %) expression. Pro-inflammatory *Tnf-alpha* (8 wC+R1/2: $-69/-74$ %; 12 wC+R1/2: $-70/-69$ %) expression was also decreased.

Conclusion: The characterization of this toxic model of liver disease regression suggests that the two-week regression period following 12-weeks of CCl₄ exposure includes a suitable therapeutic window to investigate treatments to promote regression of PH and liver fibrosis.

FRI165

The upper limit of normal of alanine aminotransferase (ALT) in diagnosing liver disease and fibrosis by the Intelligent Liver Function Test (iLFT) system

Jeremy Lee¹, John Dillon¹, Iain Macpherson¹. ¹University of Dundee, School of Medicine, Dundee, United Kingdom
Email: jjslee@dundee.ac.uk

Background and aims: There is an increasing prevalence of liver disease in the UK, and mortality from liver disease continues to rise. Liver function tests (LFTs) are often used to investigate for liver disease, but there remains a significant number of patients with undiagnosed liver disease who could benefit from early detection and intervention. The intelligent LFT (iLFT) system is designed to cascade further tests in patients with abnormal LFTs, generating a probable liver diagnosis. This increased the rate of diagnosis of liver disease by 43%. One parameter used by iLFT is serum alanine aminotransferase (ALT) level, using an upper limit of normal (ULN) of 30 U/L, given recent evidence suggesting a lower ULN of ALT to diagnose liver diseases. This study aims to determine the frequency of liver disease and fibrosis at ALT level 31–55 U/L, compared to ALT >55 U/L, and provide evidence for using an ULN of ALT of 30 U/L in the iLFT system.

Method: A retrospective analysis was done on patients undergoing iLFT in 2018–19, comparing ALT levels to iLFT and fibrosis outcomes.

Results: 672 iLFT diagnoses were made in the ALT 31–55 U/L group, with 148 (22.0%) alcoholic liver disease (ALD) diagnoses, 74 (11.0%) non-alcoholic fatty liver disease (NAFLD) diagnoses, 30 (4.5%) combined NAFLD and ALD diagnoses, 15 (2.2%) hepatitis B or C diagnoses, 74 (11.0%) metabolic or autoimmune liver diseases. 1041 diagnoses were made in the ALT >55 U/L group, which is significantly higher ($p < 0.05$) compared to the ALT 31–55 U/L group. There were 137 (20.4%) fibrosis diagnoses in the ALT 31–55 U/L group, compared to 311 (29.9%) in the ALT >55 U/L group.

iLFT fibrosis outcomes	ALT 31-55U/L	ALT >55U/L	p-value
ALD with significant fibrosis	33	68	<0.05
Abnormal ALT, ALP, GGT, negative liver screen, abnormal fibrosis biomarkers	11	31	<0.05
Abnormal ALT, negative liver screen, abnormal fibrosis biomarkers	10	32	<0.05
NAFLD-NASH with significant fibrosis	48	110	<0.05
NAFLD and ALD with abnormal fibrosis biomarkers	24	38	0.075
Abnormal ALT, ALP, GGT, negative liver screen, abnormal fibrosis biomarkers	1	1	-
Abnormal ALT, GGT, negative liver screen, abnormal fibrosis biomarkers	10	31	<0.05

Figure: Frequency of fibrosis according to aetiology between both ALT groups.

Conclusion: There is a significant proportion of patients with ALT 31–55 U/L who have underlying liver disease or fibrosis. Lowering the ULN of ALT has increased the detection rate of liver disease and fibrosis in these patients.

FRI166

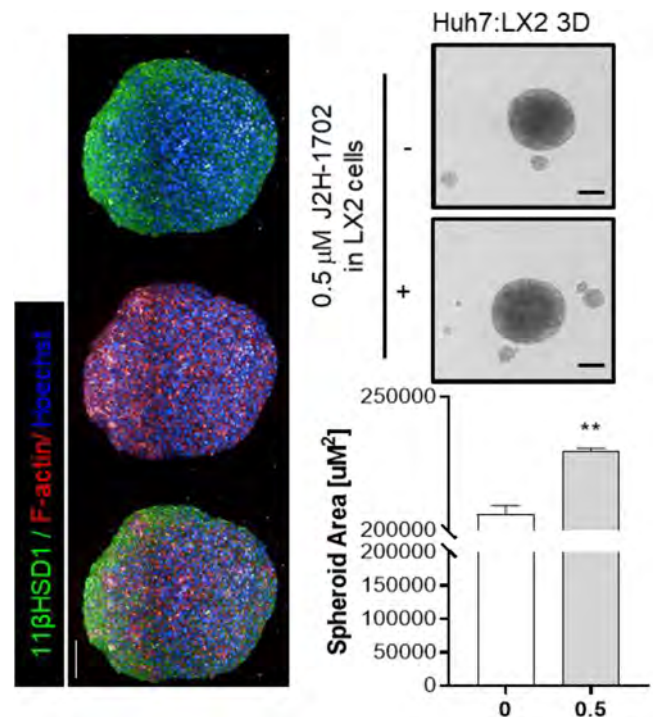
Inhibition of 11beta-hydroxysteroid dehydrogenase 1 relieves fibrosis through depolarizing of hepatic stellate cell in NASH

Su-Yeon Lee¹, Hyung Chul Ryu², Sanghwa Kim¹, Yeonhwa Song¹, Inhee Choi³, Namjeong Kim¹, Jee Woong Lim², Hyo Jin Kang², Jason Kim², Haeng Ran Seo¹. ¹Institut Pasteur Korea, Advanced Biomedical Research Lab, Seongnam-si, Korea, Rep. of South; ²J2H Biotech Inc., R&D Center, Suwon-si, Korea, Rep. of South; ³Institut Pasteur Korea, Medicinal Chemistry, Seongnam-si, Korea, Rep. of South
Email: shr1261@ip-korea.org

Background and aims: 11-beta-hydroxysteroid dehydrogenase type 1 (11betaHSD1) is a key enzyme that catalyses the intracellular conversion of cortisone to physiologically active cortisol. Although 11betaHSD1 has been implicated in numerous metabolic syndromes, such as obesity and diabetes, the functional roles of 11betaHSD1 during progression of nonalcoholic steatohepatitis (NASH) and consequent fibrosis have not been fully elucidated.

Method: the effects of J2H-1702 on steatosis and fibrogenesis were investigated in both multicellular hepatic spheroids (MCHSs) in vitro systems and in vivo mouse models.

Results: We found that pharmacological and genetic inhibition of 11betaHSD1 resulted in reprogramming of hepatic stellate cell (HSC) activation via inhibition of p-SMAD3, alpha-SMA, Snail, and Col1A1 in a fibrotic environment and in multicellular hepatic spheroids (MCHSs). We also determined that 11betaHSD1 contributes to the maintenance of NF-kappaB signalling through modulation of TNF, TLR7, ITGB3, and TWIST, as well as regulating PPAR-alpha signalling and extracellular matrix accumulation in activated HSCs during advanced fibrogenesis in MCHSs. Of great interest, the 11betaHSD1 inhibitor J2H-1702 significantly attenuated hepatic lipid accumulation and ameliorated liver fibrosis in diet- and toxicity-induced NASH mouse models.



POSTER PRESENTATIONS

Conclusion: Together, our data indicate that J2H-1702 is a promising new clinical candidate for the treatment of NASH.

FRI167

Anti-fibrotic effects of microRNA-9-5p and microRNA-122

Dana Eidelstein¹, Eithan Galun¹, Jonathan Axelrod¹. ¹Hadassah University Hospital-Ein Kerem, The Goldyne Savad Institute of Gene and Cell Therapy, Jerusalem, Israel

Email: dana.eidelstein@mail.huji.ac.il

Background and aims: Liver fibrosis is the final consequence of many chronic liver injuries and is an increasingly crucial health problem. MicroRNA's (miR's) are short single-stranded RNAs that regulate post-transcriptional mRNA expression by binding to complementary mRNA sequences, resulting in translational repression and gene silencing. In this *in vitro* study, we sought to identify potential miRNAs that could serve as potential therapeutic targets through which to ameliorate liver fibrosis. We identified and validated fibrosis-reducing miRNAs based on their ability to suppress two key fibrogenic pathways: 1) NADPH Oxidase 4 (NOX4), which maintains stellate cells activation by generation of reactive oxygen species (ROS)-induced oxidative stress and DNA damage; and 2) TGF-beta, a central molecular signaling pathway in fibrosis.

Method: Potential miR candidates were identified by bioinformatics screening for miR seed sequences in the NOX4 3'UTR. Candidate miRNA's were evaluated for anti-fibrotic activity by transfection of synthetic mimic-miRs into LX-2 cells, an established activated human stellate cell (HSC) line, and assessed for reduction of smooth muscle actin (alpha-SMA) protein levels by flow cytometry. Target-sequence specificity of candidate miRs was validated by co-transfection into LX-2 or HEK293 cells of mimic-miRs with a PmiRGLO vector (Promega) containing a cloned NOX4-3'UTR (PmiRGLO-Nox4) or mutant control (PmiRGLO-mutNox4) sequence and analysis of luciferase activity.

Results: Bioinformatics screening identified miR-9-5p and miR-96-5p miRs as having the highest predicted binding potential to NOX4 3' UTR seed sequences and highest potential for NOX4 expression inhibition. miR-9-5p was also predicted to target TGF-beta receptor (TGFbR2) as was miR-122, an important regulator of hepatic metabolism. Co-transfection experiments in HEK293 demonstrated that mimic-miR-9-5p, but neither miR-96-5p nor miR-122, effectively suppressed PmiRGLO-Nox4 directed luciferase expression, but not that of PmiRGLO-mutNox4. miR-96-5p transfection similarly suppressed both NOX4 and TGFbR2 mRNA levels in LX-2 cells. In contrast, both miR9-5p and miR-122, but neither miR-96-5p nor a scrambled control-miR, effectively suppressed alpha-SMA expression in transfected LX-2 cells. Preliminary evidence suggests that LX-2 cells may also inherently express and perhaps secrete both miR-9-5p and miR-122.

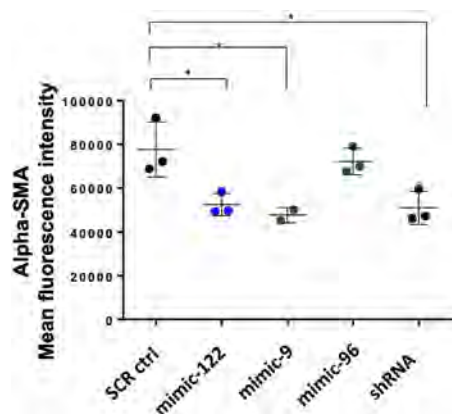


Figure: miR-9-5p and miR-122 suppress alpha-SMA in HSCs *in vitro*. Transfection of LX-2 cells with miRNAs, miR-9-5 and miR-122 decreases alpha-SMA protein expression. * $p < 0.05$ by two-way Student's *t* test.

Conclusion: Our *in vitro* findings demonstrate an anti-fibrotic therapeutic potential of miR-9-5p and miR-122 in activated human stellate cells and liver fibrosis.

FRI168

Higher daily Aramchol dose results in higher effect size in fibrosis improvement in the ARMOR study open label part

Vlad Ratziu¹, Yusuf Yilmaz², Don Lazas³, Scott Friedman⁴, Liat Hayardeny⁵, Shaul Kadosh⁶, Tali Gorfine⁵, Arun Sanyal⁷.

¹Sorbonne Université, Institute for Cardiometabolism and Nutrition (ICAN) and Hôpital Pitié-Salpêtrière, INSERM UMRS 1138 CRC, Paris, France; ²Liver Research Unit, Institute of Gastroenterology, Marmara University, and Department of Gastroenterology, School of Medicine, Marmara University, Istanbul, Turkey; ³ObjectiveGI, Inc., Nashville, United States; ⁴Icahn School of Medicine at Mount Sinai, New York, United States; ⁵Galmed Pharmaceuticals Ltd., Tel Aviv-Yafo, Israel; ⁶Statexcellence Ltd., Israel; ⁷Virginia Commonwealth University, Department of Gastroenterology, Richmond, United States
Email: vlad.ratzu@inserm.fr

Background and aims: Aramchol is a partial inhibitor of hepatic stearyl-CoA desaturase (SCD1) with direct anti-fibrotic activity demonstrated in pre-clinical models. In a 52-week phase 2b study, improvement in fibrosis by ≥ 1 stage without NASH worsening was observed in 17.5%, 21.3% and 29.5%, in the placebo, Aramchol 400 and 600 mg, respectively. A 53% higher exposure is achieved when dividing 600 mg QD Aramchol to 300 mg BID. Since this higher exposure was expected to improve efficacy, Aramchol 300 mg BID was selected for a phase 3 study in patients with NASH and fibrosis. An Open-Label Part is designed to explore the kinetics of histological outcome measures and non-invasive tests as a function of treatment duration

Method: 150 patients with histologically confirmed NASH and fibrosis are being enrolled to receive Aramchol 300 mg BID in the Open-Label Part of the study. Patients are randomized 1:1:1 to perform a post-baseline liver biopsy at weeks 24, 48 or 72. The primary efficacy endpoints are the kinetics of fibrosis improvement without NASH worsening and NASH resolution without fibrosis worsening. Biopsies are read by 3 independent pathologists, followed by a consensus reading

Results: Herein we report the results from the first 20, F1-3 patients that received Aramchol in whom the scheduled post-baseline biopsy was performed. At baseline, mean age \pm SD was 58.5 ± 8.7 years; 70% were females; 75% White; mean BMI 33.5 ± 3.6 kg/m²; 90% had type 2 diabetes; 13 patients had stage 3 fibrosis; 4 stage 2, and 3 stage 1; Mean NAS was 4.8 ± 1.3 . Post-baseline biopsies were performed for 9 patients at 24 weeks, 9 at 48 weeks and 2 at 72 weeks. Altogether 12/20 patients (60%) showed fibrosis improvement by ≥ 1 stage (5/9 after 24 weeks, 6/9 after 48 weeks and 1/2 after 72 weeks). 19/20 patients were either stable or reduced fibrosis measured by liver biopsy. In 5 patients, fibrosis was reduced by 2 points. In 9/20 (45%) patients there was fibrosis improvement without NASH worsening. Statistically significant reductions in ALT, AST and biomarkers associated with liver fibrosis Fib-4 and ProC-3 were also observed corroborating the histological effects. Reductions of a similar magnitude are seen in a cohort of the first 20 patients for which paired biopsy have been analyzed, a cohort of 50 patients for which biomarker data was analyzed (ARCON Cohort) and a cohort of 139 of which ALT, AST and FIB-4 were analyzed. Aramchol showed excellent safety and tolerability. Updated data from the open label study will be presented.

Conclusion: 60% of the 20 patients treated with Aramchol 300 mg BID showed fibrosis improvement. Data is corroborated by congruent changes in fibrosis biomarkers and by a biochemical response in aminotransferases. The data presented here, albeit preliminary, is aligned with the hypothesis that higher Aramchol exposure results in an improved efficacy profile and a direct anti-fibrotic effect may be manifested as early as 24 weeks.

FRI169

Development of a high precision liver biopsy method to improve the accuracy of fibrosis staging and collagen profiling

Morten Christensen¹, Ida Villesen¹, Mette Juul Nielsen¹, Morten Karsdal¹, Diana Leeming¹. ¹Nordic Bioscience, Fibrosis Research, Herlev, Denmark
Email: moc@nordicbio.com

Background and aims: Liver biopsy is the gold standard for diagnosis and staging of hepatic fibrosis, however it is associated with limitations such as the pathologist's inter-variability, small sample size, and patient discomfort. Currently, liver biopsy is required as a primary regulatory outcome in clinical trials on non-alcoholic steatohepatitis (NASH), which has increased the need for regulatory approved biomarkers as clinical endpoints. Additionally, hepatic fibrosis is characterized by the excessive accumulation of extracellular matrix (ECM) proteins such as collagens. Quantifying the ECM might improve the precision of fibrosis staging in the liver biopsy. The aim of this proof-of-concept study was to develop a high precision biopsy method to effectively quantify the fibrosis in the liver of bile duct ligated (BDL) rats using serological collagen degradation biomarkers.

Method: Sprague Dawley rats underwent BDL surgery and were terminated after 2 weeks. Post termination, 160 µg of snap frozen liver tissue was cleaved with matrix metalloproteinase (MMP) -2 and -9 for 3, 24 and 72 hours, and protease activity halted by addition of 1 µM EDTA. MMP-2 and -9 degradation fragments of type III, IV, and VI collagen were measured in the tissue extract by neo-epitope specific competitive ELISAs (C3M and C6M, respectively) based on monoclonal antibodies. The activity of MMP-2 and MMP-9 was confirmed by their ability to cleave carboxymethylated transferrin and visualized by Coomassie blue staining.

Results: Conditioned medium C3M increased significantly with increasing incubation time with MMP-2, thus a 78-fold increase with 3 hour incubation that increased to, 128-fold at 72 hours of incubation. In comparison, MMP-9 showed an increase of 43-fold at 3 hours to, 150-fold at 72 hours. This was significant when compared to tissue extract with no MMP added ($p < 0.0001$). A significant increase was also seen in C6M levels at incubation times of 24 hours (MMP2: 66-fold and MMP9: 103-fold) and 72 hours (MMP2: 14-fold and MMP9: 46-fold) ($p < 0.0001$). MMP-2 and MMP-9 proved successful in cleaving carboxymethylated transferrin.

Conclusion: A proof-of-concept high precision ex vivo model was established in BDL treated rodents showing MMP-2 and MMP-9 degraded collagen type III and VI was released from the liver tissue to the conditioned medium as assessed by C3M and C6M. The high precision biopsy holds potential to improve the current liver biopsy evaluation by providing a quantifiable measurement of liver fibrosis.

FRI170

MAIT cell inhibition promotes liver fibrosis regression by reprogramming macrophage phenotype

Morgane Mabire¹, Hegde Pushpa¹, Hammoutene Adel¹, JingHong Wan¹, Manon Allaire¹, Al Sayegh Rola¹, Tristan Thibault-Sogorb^{1,2}, Emmanuel Weiss^{1,2}, Valérie Paradis^{1,3}, Pierre de la Grange⁴, Hélène Gilgenkrantz¹, Sophie Lotersztajn¹. ¹Université de Paris, Centre de Recherche sur l'Inflammation (CRI), INSERM, U1149, PARIS 18, France; ²Département d'Anesthésie et Réanimation, Hôpital Beaujon, Assistance Publique-Hôpitaux de Paris, 92110, Clichy, France, Clichy, France; ³Département de Pathologie, Hôpital Beaujon, Assistance Publique-Hôpitaux de Paris, 92110, Clichy, France; ⁴GenoSplice Technology, Paris, France
Email: morgane.mabire@inserm.fr

Background and aims: Mucosal-Associated Invariant T (MAIT) cells are non-conventional T cells restricted by the non-classical MHC-1b molecule MR1 that display altered functions during chronic liver diseases. We recently reported that hepatic MAIT cells are activated during fibrosis in human liver samples and in mice models and

display profibrogenic properties (*Nat Commun* 2018). Here, combining studies in human precision-cut liver slices (PCLS) and experimental models, we investigated whether and how targeting MAIT cell activation may impact fibrosis regression.

Method: Liver PCLS were generated from patients with end-stage fibrosis and cultured *ex vivo* with or without the MAIT cell antagonist Acetyl-6-formylpterin (Ac-6-FP) for 48 hrs. Fibrogenic and inflammatory gene expression was evaluated by RT-qPCR and α -SMA by immunostaining. Liver fibrosis was induced in mice by repeated carbon tetrachloride (CCl₄) injections for 4 weeks. For fibrosis regression, CCl₄ injections were discontinued and mice were daily administered with Ac-6-FP for up to 4 days. Comparison of genes differentially regulated by Ac-6-FP in Ly6C^{high} profibrogenic macrophages and Ly6C^{low} restorative macrophages was performed by RNA sequencing.

Results: Human PCLS from patients with end-stage fibrosis exposed to Ac-6-FP showed significant reduction in the expression of fibrogenic genes such as *TGF β* , *ACTA2*, *COL1A1* and *COL1A2*. Concordantly, the number of α -SMA+ cells was reduced in PCLS exposed to Ac-6-FP. Moreover, inhibiting MAIT cells decreased *CCL2* and its receptor *CCR2* expressions. Mice chronically exposed to CCl₄ and daily injected with Ac-6-FP showed accelerated fibrosis regression associated with a decrease in CCR2+ Ly6C^{high} and an increase in Ly6C^{low} macrophages. RNAseq analyzes performed on Ly6C^{high} and Ly6C^{low} macrophages in Ac-6-FP- and vehicle-exposed mice showed reprogramming of macrophage signature by Ac-6-FP. Apoptosis was the most significant pathway deregulated by Ac-6-FP, with upregulation of apoptotic genes in Ly6C^{high} macrophages while induction of survival genes was mainly observed in Ly6C^{low}. Genes of the autophagy pathway, an anti-inflammatory and antifibrogenic mechanism in the liver, were also induced in both populations by Ac-6-FP, together with an increase in the number of LC3II+cells.

Conclusion: Inhibiting MAIT cell activation may offer new perspectives for antifibrogenic therapy, by promoting fibrosis resolution via reprogramming of macrophage profile.

FRI171

The LiverPRO score, a multivariable model for prediction of significant fibrosis in primary care: derivation, validation and comparison with FIB-4 and ELF-test in 5, 000 study participants

Katrine Prier Lindvig^{1,2}, Maria Kjærgaard^{1,2}, Johanne Kragh Hansen^{1,2}, Katrine Thorhauge^{1,2}, Camilla Dalby Hansen^{1,2}, Stine Johansen^{1,2}, Mads Israelsen^{1,2}, Peter Andersen^{1,2}, Nikolaj Torp^{1,2}, Taus Holtug³, Sönke Detlefsen⁴, Morten Beck Trelle⁵, Steen Antonsen⁶, Aleksander Krag^{1,2}, Maja Thiele^{1,2}. ¹Odense University Hospital, Department of Gastroenterology and Hepatology, Odense C, Denmark; ²University of Southern Denmark, Institute of Clinical Research, Odense C, Denmark; ³LT Health, Taastrup, Denmark; ⁴Odense University Hospital, Department of Pathology, Odense C, Denmark; ⁵Odense University Hospital, Svendborg, Department of Clinical Biochemistry, Svendborg; ⁶Odense University Hospital, Svendborg, Department of Clinical Biochemistry, Svendborg, Denmark
Email: katrine.prier.lindvig@rsyd.dk

Background and aims: Significant liver fibrosis is the precursor of progressive liver disease and predicts the risk of liver-related complications. We aimed to generate a decision aid for general practitioners, to evaluate which patients to refer to secondary care, by developing a multivariable model for diagnosis of significant fibrosis in a biopsy-controlled cohort.

Method: We derived the LiverPRO score in a derivation cohort of high-risk patients with an alcohol overuse and biopsy-controlled fibrosis stage (F0–F4). Univariable logistic regression followed by decision tree analysis detected nine routine liver blood markers and age as predictors of significant fibrosis ($\geq F2$). From these, we built the final model as a software combining multiple algorithms derived from fractional polynomial regression that predicts the risk of

POSTER PRESENTATIONS

significant fibrosis in a score range of 0–100%. We validated the LiverPRO score in a screening study of randomly invited Danish citizens at risk of NAFLD or alcohol-related liver disease, using a liver stiffness measurement ≥ 8 kPa as outcome. Finally, we compared the diagnostic accuracy of the LiverPRO score with the serum markers ELF-test and FIB-4.

Results: The derivation cohort included 463 patients, 75% male, with a median age of 57 years (IQR 14). The majority (197/463, 55%) had significant liver fibrosis ($\geq F2$), and 94 (20%) had advanced liver fibrosis ($\geq F3$). The LiverPRO score diagnosed significant fibrosis with good diagnostic accuracy (AUC 0.84; 95% CI 0.81–0.88), similar as the ELF-test (AUC 0.84; 0.80–0.88), and superior to the FIB-4 (AUC 0.77; 95% CI 0.73–0.83). The same was observed for advanced fibrosis (LiverPRO AUC 0.92; 0.88–0.95 versus ELF-test AUC 0.92; 0.89–0.95 versus FIB-4 AUC 0.84; 95% CI 0.79–0.89).

The validation cohort included 4.722 participants, 49% male, median age 57 years (IQR 11), and 299 (6%) had a TE ≥ 8 kPa, of those 50% had risk factors for ALD, 46% for NAFLD and 4% had no risk factors for fatty liver disease. In this low prevalence cohort, the LiverPRO score detected TE ≥ 8 kPa with moderate accuracy (AUC 0.75; 95% CI 0.72–0.77), comparable to the ELF test (AUC 0.74; 95% CI 0.71–0.78) and superior to FIB-4 (AUC 0.64; 95% CI 0.59–0.68).

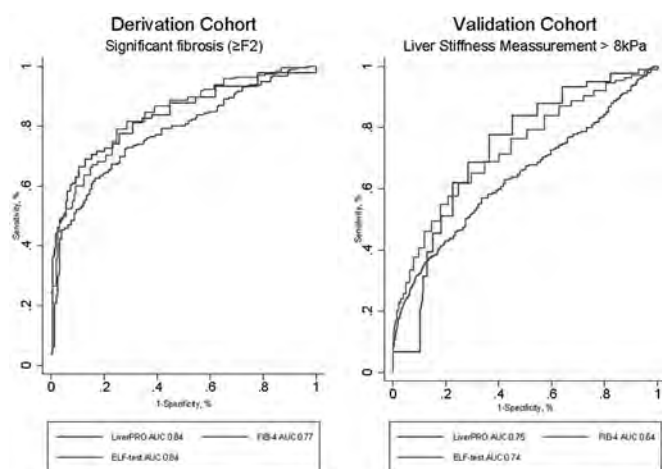


Figure: Overall diagnostic performance for Significant liver fibrosis and Liver Stiffness Measurement > 8 kPa of the LiverPRO score, FIB-4 and ELF-test in the derivation and validation cohort.

Conclusion: The LiverPRO score accurately predicts significant and advanced liver fibrosis in both a high prevalence and a low prevalence cohort. Combined with a very low cost of the routine liver blood markers and an easy interpretable score from 0 to 100%, the score may be a useful screening tool and decision aide for primary care referral pathways.

FRI172

The protective effect of time-caloric restriction in liver fibrosis induced by nitrosamines in rat model

Christian Molina-Aguilar^{1,2}, Fernanda Arriaga-González^{1,2}, Felipe Castañeda^{1,3}, Kevin Villa-Malagon^{4,5}, Irving Simonin-Wilmer¹, Obed Ramírez Sánchez¹, Emilio Calderón Garza⁶, Mayra López Azuara², Osiel Ledesma Juárez⁷, Martín del Castillo Velasco-Herrera⁸, David Adams⁸, Mauricio Díaz-Muñoz⁹, Carla Daniela Robles-Espinoza¹.

¹International Laboratory for Human Genome Research, The Cancer Genetics and Bioinformatics Laboratory, Querétaro, Mexico; ²Centro de Bioingeniería, ITESM, Departamento de Bioingeniería, Querétaro, Mexico; ³Universidad Anáhuac, Facultad de Ciencias de la Salud, Ciudad de México; ⁴Facultad de Biología UMSNH, Morelia, Mexico;

⁵International Laboratory for Human Genome Research, UNAM, The Cancer Genetics and Bioinformatics Laboratory, Querétaro, Mexico; ⁶Facultad de Medicina-UNAM, Ciudad de México, Mexico; ⁷Hospital General de Cadereyta, Cadereyta, Mexico; ⁸Wellcome Sanger Institute, Cambridgeshire, United Kingdom; ⁹Instituto de Neurobiología UNAM, Neurobiología Celular y Molecular, Querétaro, Mexico
Email: cmolina@liigh.unam.mx

Background and aims: Liver fibrosis is the first stage in the progression of cirrhosis and hepatocellular carcinoma (HCC). Around 80% of people with HCC developed cirrhosis as a previous stage, being chronic inflammation a key factor in these maladies' progression. Fibrosis is the only reversible stage of the liver injury progression; however, the cellular and molecular mechanisms of this stage are not fully understood. A better understanding of fibrotic would represents an unprecedented opportunity to avoid complications (cirrhosis and HCC) in patients. It would also help improve patient survival and ease the significant burden on the national health system by reducing drastically the number of HCC patients, which would also lower healthcare costs in many countries. In recent years, our group has explored the beneficial effects that calorie restriction (T-CR) without malnutrition has in rats treated with diethylnitrosamine (DEN), a hepatotoxic that allows us to recapitulate fibrosis-cirrhosis-HCC sequence to characterized better the liver damage and identify potential therapeutic targets. We showed in 2017 that T-CR, in the HCC stage, avoided liver chronic inflammation, the cirrhosis where established in early-stage preserving the hepatic functions, and finally although HCC tumors developed, these had a slower evolution, all compared with rats Ad Libitum (24 h of food access)

Method: Forty male Wistar rats (with an initial weight of 240 ± 20 g) were randomly assigned into one of four experimental groups. AL: Control rats without DEN and 24 h of food access. AL + DEN: Rats with 24 h of food access and DEN treatment weekly during 10 weeks to induce fibrosis. T-CR: Rats with only 2 h of food access per day and without DEN. T-CR+DEN: Rats treated weekly for 10 weeks with DEN and only 2 h of food access.

Results: A) T-CR and T-CR+DEN groups had a reduction of 30 and 37 percent in food intake in comparison with the AL, inducing less corporal weight gain but with normal nutritional state. B) Histopathology, through Ishak stage estimation and blood chemistry assessments, revealed that DEN induces fibrosis and light tissue damage (seen in both groups treated with DEN), but was less aggressive when rats are under caloric restriction. C) Preliminary results suggested a lower "basal chronic inflammatory state" was induced by caloric restriction in both healthy (T-CR) and fibrotic (T-CR +DEN) groups evidenced in total Leucocytes levels. To complement these results, we are analyzing RNAseq data from all these groups and the results will be presented at the congress.

Conclusion: Our results so far suggest that T-CR maintains its beneficial effects at a physiological level despite the damage caused by DEN in fibrosis, and that one of the mechanisms of this effect is through a decrease in the basal inflammatory state of the liver.

FRI173

Macrophage MerTK promotes a profibrogenic cross-talk with hepatic stellate cells via soluble mediators

Mirella Pastore¹, Chiara Raggi¹, Nadia Navari¹, Benedetta Piombanti¹, Giovanni Di Maira¹, Elisabetta Rovida¹, Marie-Pierre Piccinni¹, Letizia Lombardelli¹, Federica Logiodice¹, Krista Rombouts², Salvatore Petta³, Fabio Marra¹. ¹University of Florence, Firenze, Italy; ²University College London, United Kingdom; ³Università degli Studi di Palermo, Palermo, Italy

Email: fabio.marra@unifi.it

Background and aims: Activation of Kupffer cells and recruitment of monocytes are key events in fibrogenesis. These cells release soluble mediators which induce the activation of hepatic stellate cells (HSC), the main fibrogenic cell type within the liver. Mer tyrosine kinase (MerTK) signaling regulates multiple processes in macrophages and has been implicated in the pathogenesis of NASH-related fibrosis. In this study, we explored if MerTK activation in macrophages influences the profibrogenic phenotype of HSCs.

Method: M2c-like (MerTK⁺/CD206⁺/CD163⁺/CD209⁻) macrophages were differentiated from peripheral blood monocytes using M-CSF and IL-10. The role of MerTK was assessed by stimulation with the ligand Gas-6 and by pharmacologic inhibition with UNC569.

Results: MerTK⁺ macrophages exhibited activation of STAT3, ERK1/2, and p38 and increased expression of VEGF-A. Exposure of MerTK⁺ macrophages to Gas-6 increased activation of MerTK and downstream pathways. These events were reverted by pretreatment with UNC569. *MERTK* and *Gas-6* mRNA levels were gradually increased during macrophage polarization towards a M2c-like phenotype and were significantly greater in Kupffer cells than in peripheral blood monocytes. Gas-6 was released both by M2c-like macrophages and Kupffer cells. Activation of MerTK in macrophages induced a secretome which caused a significant increase in migration, proliferation, viability and expression of profibrogenic factors in HSCs. Conditioned medium of Gas-6-stimulated MerTK⁺ macrophages also induced a significant increase in phosphorylation of STAT3 and p38 in HSCs, and upregulation of IL8 expression. These effects were specifically related to MerTK activity in macrophages, as indicated by pharmacologic inhibition.

Conclusion: MerTK activation in M2c-like macrophages modifies the secretome to promote HSC profibrogenic features, indicating that this receptor may be implicated in the pathogenesis of hepatic fibrosis.

FRI174

Comparative fibrosis-reducing activities of farnesoid X receptor (FXR), peroxisome-proliferator activated receptor delta (PPAR) and thyroid hormone receptor (THR) agonists in the carbon tetrachloride mouse model

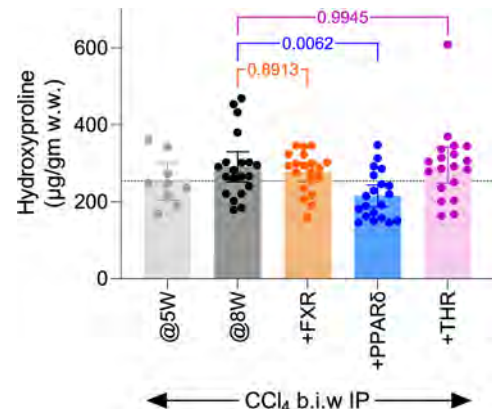
Edward Cable¹, Jeffrey Stebbins¹, Yun-Jung Choi¹, Jiangao Song¹, Prasad Mancham², Sanjay Pandey², Charles McWherter¹. ¹Cymabay Therapeutics Inc., Newark, United States; ²Triangulum Biopharma, Carlsbad, United States

Email: ecable@cymabay.com

Background and aims: Fibrogenesis is a key first step toward cirrhosis in the liver, independent of etiology. A limited number of nuclear receptor agonists that have been tested in diseases with liver fibrosis. The AIM of the current study is to test three of these agonists in established fibrosis in the mouse CCl₄ model. These three selected agonists are: the FXR agonist, obeticholic acid; the PPARδ agonist, seladelpar, and the THRβ agonist, resmetirom. This model's mechanism of liver injury is via the trichloromethyl radical, which is likely harsher than any human disease. The rationale for selecting this model is that fibrosis can be established prior to initiation of treatment and the ability of these receptor agonists can be stringently tested for reduction of established fibrosis.

Method: Male C57B/6 mice were treated with 1 mL of CCl₄ per g BW via IP injection twice per week for 8 weeks. Concurrent with treatment initiation at week 5, a set of animals (n = 10) was sacrificed

to assess the fibrosis levels. Animals (n = 20/group) were dosed daily with OCA (30 mg/kg), seladelpar (10 mg/kg), resmetirom (1 mg/kg) or vehicle in 0.5% CMC, PO for an additional 3 weeks while continuing CCl₄ administration. Liver histology assessments (H&E and PSR) and hydroxyproline content were analyzed as measures of liver fibrosis. **Results:** Average hydroxyproline content at treatment start was 253 mg/g liver. Additional 3 weeks of CCl₄ treatment increased the average hydroxyproline to 290 mg/g. Neither FXR nor THR agonists decreased hydroxyproline content (277 and 291 mg/g, respectively) while PPARδ decreased hydroxyproline to 215 mg/g. In addition to the reduction in total hydroxyproline, the PSR staining demonstrated a reduction in bridging fibrosis with seladelpar compared to both the vehicle at 8 weeks and the starting levels at 5 weeks. No apparent changes in fibrosis staining were observed with the other treatments.



Conclusion: The CCl₄ mouse model may be used to test for molecular targets that will reduce established fibrosis. The combination of total biochemical and histologic measurements are important to assess the topographic changes. Reduction of the PSR positive fibrotic cords between the veins is generally considered beneficial and readily observable in this model. We believe that this 8-week model can be used to dissect some of the molecular mechanisms for fibrogenesis, fibrolysis after cessation of CCl₄, and fibrolysis in the presence of CCl₄. Is treatment-related fibrolysis in the presence of CCl₄ just a reduction in the CCl₄ mediated fibrogenesis or are there separate processes? This model can be used to attempt to answer these questions and build on the findings that PPARδ agonists reduce established fibrosis in the dietary NASH mouse, the *foz/foz* mouse, and the NIF mouse models.

FRI175

A novel role for serine protease Kallikrein 8 in liver fibrosis through cleaving complement C3 and hepatic macrophage polarization

Cichun Wu¹, Yao Liu¹, Ying Li¹, Wei Zhang¹, Lei Fu¹, Xin Ni², Shifang Peng¹. ¹Xiangya Hospital Central South University, Department of Infectious Diseases, Changsha, China; ²Xiangya Hospital Central South University, International Collaborative Research Center for Medical Metabolomics, Xiangya Hospital Central South University, Changsha, China

Email: sfp1988@csu.edu.cn

Background and aims: Kallikrein 8 (KLK8), an emerging serine protease in the family of Kallikrein-related peptidases (KLKs), has been implicated in myocardial and renal fibrosis. To date, it remains unknown whether and how KLK8 is involved in liver fibrosis. In this study, we aimed to determine the role of KLK8 in liver fibrosis and the underlying molecular mechanisms.

Method: KLK8 expression and localization were examined in liver tissues from fibrotic human subjects and rodent models. *In vivo* and *in vitro* silencing or overexpression of KLK8 was used for functional

POSTER PRESENTATIONS

studies. The natural substrates of KLK8 were screened and characterized in the liver. Mechanistic studies were performed to identify the involving KLK8-dependent molecular pathways.

Results: Hepatocyte KLK8 was significantly increased in liver fibrotic patients and rodents, and the greater levels were correlated with the higher degree of liver fibrosis. Notably, liver fibrosis occurred spontaneously in transgenic-mediated overexpression of KLK8 in rats, suggesting a pro-fibrotic effect. With hepatocyte-specific silencing of KLK8 in rodent models, we found that liver fibrosis was significantly attenuated compared with controls. Using immunoprecipitation in combination with mass spectrometry, we identified complement C3 as the natural substrate of KLK8. Furthermore, *in vitro* and *in vivo* mechanistic studies revealed that KLK8 promoted liver fibrosis through cleaving complement C3 to its active fragment C3a, which subsequently induced the macrophage polarization toward M2 phenotype and secretion of transforming growth factor (TGF)- β 1, leading to an indirect activation of hepatic stellate cells.

Fig.S1

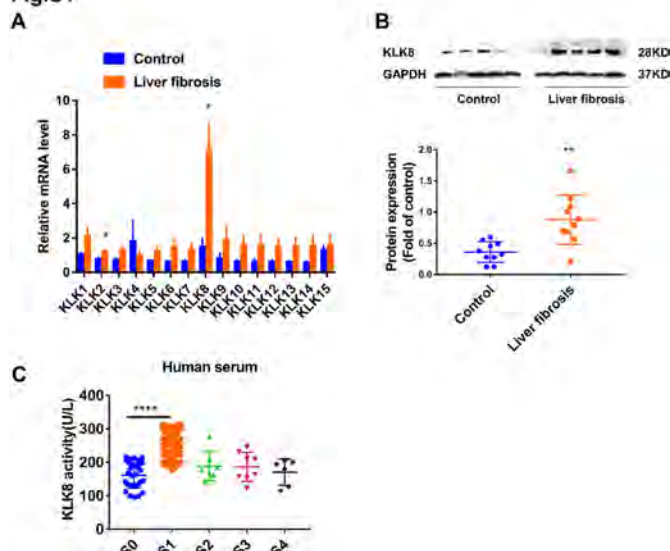
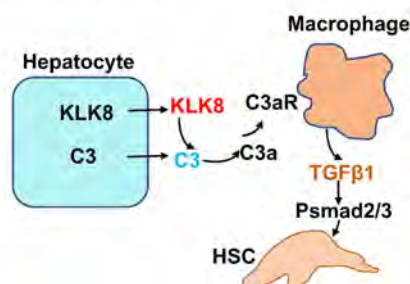


Figure S1. Expression levels of human hepatic KLK8 in liver fibrosis and control. (A) qRT-PCR analysis of the mRNA expression levels of KLK1–KLK15 in the liver fibrosis group (n = 8) and the healthy control group (n = 6); (B) Western blot analysis of KLK8 protein levels in the liver fibrosis group (n = 10) and healthy control group (n = 10); (C) Serum KLK8 in patients with liver fibrosis (n = 108) and healthy control individuals (n = 31); Data are expressed as means \pm SEM; *P < 0.05; **P < 0.01; ***P < 0.001; ****P < 0.0001 vs control.

Proposed mechanisms



Proposed mechanisms. During liver injury, KLK8 secreted by hepatocytes releases the active fragment C3a by shearing complement C3, which in turn activates macrophages to secrete TGF β 1 and promotes the development of liver fibrosis through the TGF β 1/smad2/3 signaling pathway

Conclusion: This study has delineated a novel role for KLK8 in liver fibrosis. As such, the new findings may advance our understanding of

KLK8, and eventually help unleash its therapeutic potential in the development of novel treatments.

FRI176

The modulation of NADPH oxidases by tyrosol-derived phenolic compounds prevents hepatic fibrogenesis

Daniela Gabbia¹, Sara Carpi^{2,3}, Samantha Sarcognato⁴, Ilaria Zanotto¹, Beatrice Polini², Katia Sayaf⁵, Paola Nieri², Francesco Paolo Russo⁵, Maria Guido⁴, Sara De Martin¹. ¹University of Padua, Department of Pharmaceutical and Pharmacological Sciences, Padova, Italy; ²University of Pisa, Department of Pharmacy, Pisa, Italy; ³CNR PISA, NEST, Pisa, Italy; ⁴University of Padua, Department of Medicine, Padova, Italy; ⁵University of Padua, Department of Surgery, Oncology and Gastroenterology, Padova, Italy
Email: sara.demartin@unipd.it

Background and aims: Hepatic NADPH oxidases (NOXs) are devoted to the production of reactive oxygen species (ROS), thus regulating inflammatory and fibrotic processes. Exaggerated NOX expression and activation, particularly of NOX1 and NOX4, have been related to the activation of hepatic stellate cells (HSCs) and the trigger of fibrogenesis. Therefore, compounds modulating the expression and activity of NOXs may represent promising agents for the management of hepatic fibrosis. In this study we investigated the antifibrotic and antioxidant action of the two phenolic compounds tyrosol and hydroxytyrosol, known for their cardioprotective activity, with the aim of unravelling their effect *in vitro* and *in vivo* on NOX-related fibrogenetic pathways.

Method: We evaluated tyrosol and hydroxytyrosol activity by means of LX2 and HepG2 cells, used as *in vitro* models of HSCs and hepatocytes, respectively. A mouse model of liver fibrosis was induced by a 4-week IP CCl₄ administration to 6 Balb/C mice; 6 untreated mice were used as controls. Tyrosol and hydroxytyrosol were administered daily by oral gavage. Levels of hepatic NOX1/4, α SMA, COL1A1, IL-6, IL-10 were assessed by qPCR and Western blot. Hepatic miR-181-5p, miR-221, miR-29b-3p and miR-101 were measured by qPCR.

Results: Tyrosol significantly decreased the production of ROS by HepG2 cells, and the mRNA levels of NOX1/4, α SMA and COL1A1 in TGF β 1-activated LX2 cells, displaying an antifibrotic and antioxidant activity comparable to the prototypical NOX1/4 inhibitor GKT136901. An increase of hepatic ROS (p < 0.0001), α SMA, COL1A1, IL-6 and IL-10 mRNA levels (p < 0.05) were observed in fibrotic mice, as well as a slight increase in NOX1/4 expression. Tyrosol and hydroxytyrosol were able to counteract these effects, by significantly downregulating α SMA, COL1A1, NOX1/4, IL-6 and IL-10 with respect to fibrotic mice. The profibrotic miRNAs miR-181-5p and miR-221 were downregulated by tyrosol, whereas the expression of antifibrotic miRNAs miR-29b-3p and miR-101 was restored to physiological level by both tyrosol and hydroxytyrosol. Liver histology confirmed a reduction of fibrosis in treated mice.

Conclusion: The phenolic compounds tyrosol and hydroxytyrosol ameliorate hepatic fibrosis by reducing hepatic oxidative stress and inflammation and modulating the hepatic expression of miRNAs involved in fibrogenesis. Tyrosol-derived molecules should be evaluated as promising antifibrotic candidates.

FRI177

Exploring gender-related differences in liver fibrosis and regeneration through a new experimental carbon tetrachloride protocol in mice

Katia Sayaf¹, Ilaria Zanotto², Daniela Gabbia², Dafne Alberti³, Giulia Pasqual³, Sara De Martin², Francesco Paolo Russo¹. ¹University of Padova, Department of Surgery, Oncology and Gastroenterology, Padova, Italy; ²University of Padova, Department of Pharmaceutical and Pharmacological Sciences, Padova, Italy; ³University of Padova, Department of Surgery, Oncology and Gastroenterology, Padova, Italy
Email: francescopaolo.russo@unipd.it

Background and aims: The incidence of chronic liver diseases (CLDs) is two-fold higher in men than women and they display clinically relevant differences. Thus, understanding the mechanistic gaps between females and males by pre-clinical studies is fundamental to increase the awareness on gender influence in the pathophysiological and regenerative mechanisms underlying liver fibrosis.

Method: A new experimental protocol based on increasing doses of carbon tetrachloride (CCl₄) has been developed and performed in female and male Balb/C mice, by intraperitoneal injections for 12 weeks, followed by a washout period of 8 weeks. Mice were sacrificed at different timepoints (6, 12 and 20 weeks). Flow cytometry experiments were performed on fresh liver tissues to evaluate the amount of recruited monocytes-derived macrophages (MoMFs). Liver histology was assessed by Masson's trichrome staining, and liver function was evaluated by the hydroxyproline assay. The gene and protein expression of collagen, growth factors, and pro inflammatory elements were evaluated by qPCR and immunohistochemistry, respectively.

Results: Both female and males developed a progressive liver fibrosis during CCl₄ treatment and showed liver regeneration during the washout period. After 6 weeks of treatment, male mice showed more fibrotic areas ($p < 0.05$) and more activated stellate cells (HSCs) than female mice ($p < 0.05$). Furthermore, a higher inflammatory status within male liver was confirmed during the acute damage by the intensive recruitment of pro-inflammatory Ly6C^{high} F4/80^{med to high} CD11b^{high} MoMFS, together with higher levels of gene expression of pro-inflammatory growth factors than females. On the other hand, females developed a worse hepatic condition after 12 weeks of CCl₄ treatment, showing a higher hydroxyproline content, more activated HSCs than males, and elevate amounts of Ly6C^{high} F4/80^{med to high} CD11b^{high} MoMFS. During the washout period, female mice showed less fibrotic areas than males ($p < 0.05$) and the presence of small amounts of MoMFs, while some activated HSCs but no pro-inflammatory MoMFs were detected in males.

Conclusion: This new model of fibrosis obtained with increasing doses of CCl₄ led to the development of liver damage without adaptive responses of the liver to the injury. We observed gender-related differences in liver damage and regeneration, due to the fact that gender influences the recruitment of pro-inflammatory MoMFs and the activation of hepatic stellate cells.

FRI178

Multicenter external validation of FIB-6: a novel, machine-learning, simple bedside score to rule out severe liver fibrosis and cirrhosis in patients with MAFLD

Gamal Shihai¹, Reham Soliman¹, Nabil Mikhail², Khalid Alswat³, Ayman Abdo³, Faisal Sanai⁴, Necati Ormeci⁵, George Dalekos⁶, Amir Anushiravani⁷, Mai Mabrouk⁸, Samir Marzouk⁹. ¹Egyptian Liver Research Institute and Hospital (ELRIAH), Gastroenterology and Hepatology, Egypt; ²Egyptian Liver Research Institute and Hospital (ELRIAH), Biostatistics and Cancer Epidemiology, Egypt; ³College of Medicine, King Saud University, Medicine, Saudi Arabia; ⁴King Abdulaziz Medical City, Gastroenterology, Saudi Arabia; ⁵Ankara University School of Medicine, Gastroenterology, Turkey; ⁶National Expertise Center of Greece in Autoimmune Liver Diseases, Medicine and Research Laboratory of Internal Medicine, Greece; ⁷Tehran University of Medical Sciences, Digestive Disease, Iran; ⁸Misr University for Science and Technology (MUST), Biomedical Engineering, Egypt; ⁹Arab Academy for Science and Technology (AASTMT), Basic and Applied Science Department, Egypt
Email: g_shiha@hotmail.com

Background and aims: Non-invasive tests (NITs) are urgently required to evaluate hepatic fibrosis in MAFLD. We previously developed and validated a non-invasive diagnostic index based on routine laboratory parameters for predicting the stage of hepatic fibrosis in patients with chronic hepatitis C (HCV) called FIB-6 through machine learning with random forests algorithm using retrospective data of 7238 biopsy proven chronic hepatitis C (CHC) patients. Our aim is to validate this novel score in patients with MAFLD.

Method: Performance of the new score was externally validated in cohorts from one site in Egypt ($n = 674$) and in 5 different countries ($n = 1798$) in Iran, KSA, Greece, Turkey and Oman). Biopsy samples were scored by experienced pathologists who used the METAVIR scoring system. Results were also compared with three established tools (FIB-4, APRI, and AAR).

Results: In this study, 2472 patients met the criteria, and their liver biopsy results were included for analysis. Using the optimal cutoffs in the data of FIB-6 indicated a reliable performance in diagnosing cirrhosis, severe fibrosis, and significant fibrosis. Results indicated good sensitivity and NPV. Sensitivity = 70.5%, specificity = 62.9%. PPV = 15.0% and NPV = 95.8% for diagnosis of cirrhosis. For diagnosis of severe fibrosis (F3 and F4), the results were 86.5%, 24.0%, 15.1% and 91.9% respectively, while for diagnosis of significant fibrosis (F2, F3 and F4), the results were 87.0%, 16.4%, 24.8% and 80.0%). Comparing of the results of FIB-6 rule-out cutoffs with those of FIB-4, APRI, and AAR showed that in ruling out severe fibrosis and cirrhosis, FIB-6 gave the highest sensitivity and NPV (97.0% and 94.7%), as compared to FIB-4 (71.6% and 94.7%), APRI (36.4% and 90.7%), and AAR (61.2% and 90.9%).

Table: (abstract: FRI178): Diagnostic performance of FIB-6 optimal cutoffs in all cohorts compared to the liver biopsy results

	Cutoff	Sensitivity	Specificity	PPV	NPV
Cirrhosis (F4 vs. F0123)	2.3159	70.5 (64.0–76.2)	62.9 (60.9–64.9)	15.0 (12.9–17.4)	95.8 (94.7–96.7)
Severe fibrosis (F34 vs. F012)	1.8992	86.5 (82.5–89.8)	24.0 (22.3–25.9)	15.1 (13.6–16.8)	91.9 (89.4–93.9)
Significant fibrosis (F234 vs. F01)	1.7720	87.0 (84.1–89.5)	16.4 (14.8–18.1)	24.8 (23.0–26.7)	80.0 (75.7–83.7)

POSTER PRESENTATIONS

Table: Diagnostic performance of FIB-6 rule-out cutoffs for severe fibrosis (F3) or cirrhosis (F4) in all cohorts compared with that of FIB-4, APRI, and AAR

	Cutoff	Sensitivity	NPV
FIB-6	1.5023	97.0 (94.6–98.4)	94.7 (90.4–97.1)
FIB-4	1.45	71.6 (66.6–76.2)	94.7 (93.6–95.7)
APRI	0.70	36.4 (31.5–41.7)	90.7 (89.5–91.8)
AAR	1.00	61.2 (55.9–66.3)	90.9 (89.3–92.3)

Conclusion: FIB-6 score is an accurate, simple, noninvasive test for ruling out advanced fibrosis and liver cirrhosis in patients with MAFLD better than APRI, FIB-4 and AAR.

FRI179

A bioengineered approach to re-create and study the extracellular matrix-immune cell crosstalk in normal and fibrotic liver

Sara Campinoti¹, Claire McQuitty^{1,2}, Lorenzo Caciolli¹, Bruna Almeida¹, Lai Wei^{1,2}, Luca Zanieri³, Antonio Riva^{1,2}, Alessandro F. Pellegata⁴, Paola Bonfanti^{3,5}, Sara Mantero⁴, Shilpa Chokshi^{1,2}, Luca Urbani^{1,2}. ¹The Roger Williams Institute of Hepatology, London, United Kingdom; ²King's College London, Faculty of Life Sciences & Medicine, United Kingdom; ³The Francis Crick Institute, Epithelial Stem Cell Biology & Regenerative Medicine Lab, United Kingdom; ⁴Politecnico Di Milano, Department of Chemistry, Materials and Chemical Engineering "Giulio Natta", Italy; ⁵University College of London, Division of Infection and Immunity, Royal Free Hospital, United Kingdom

Email: luca.urbani@researchinliver.org.uk

Background and aims: Liver fibrosis is caused by progressive accumulation of extracellular matrix (ECM) coupled with chronic inflammation. Bioengineering allows for the development of disease models to study complex diseases, such as liver fibrosis, where both cellular and extracellular microenvironment components contribute to the pathology. Bioengineered liver models have been developed by combining decellularised liver scaffolds with liver cells. However, the lack of an immune compartment is an important drawback given the role of inflammation in fibrosis. This study aims at establishing a bioengineered liver model to study the immune cell-ECM crosstalk in fibrosis.

Method: We developed two custom-made bioreactors for whole rat livers or human tissue segment culture (WL and HuTS bioreactor respectively). Decellularised normal and fibrotic rat and human livers were obtained following established protocols (detergent-enzymatic treatment). Human peripheral blood mononuclear cells (PBMCs) from healthy donors, were perfused in WL or HuTS bioreactor in absence or presence of decellularised normal or fibrotic liver scaffolds. Viability, phenotype, and cytokine production in the medium were assessed (via FACS and Luminex) in comparison to static culture conditions. Gene expression and cell phenotype of PBMCs present in the scaffolds were examined via qPCR and immunofluorescence.

Results: The bioreactors allowed for perfusion of PBMCs through decellularised rat and human liver scaffolds. Circulated PBMCs maintained cell viability and cell population frequency comparable to static culture conditions. When PBMCs were perfused through decellularised liver scaffolds, a portion of cells infiltrated the matrix, with different cell types and frequency between normal and fibrotic liver scaffolds. In fibrotic scaffolds, the number of circulating T cells decreased, while more liver infiltrating monocytes were found in respect to healthy condition. Cytokine analysis revealed that the ECM triggers the release of innate and adaptive immune system cytokines and those related to pro-regenerative immune response.

Conclusion: Here we show the validation of two bioreactor-based systems which allow to perfuse immune cells through decellularised liver matrix. This perfusion system proved to be suitable for the study

of immune cell interaction with normal or fibrotic ECM, and more in general, with bioengineered constructs, and showed that mechanisms of chronic inflammation observed in fibrosis can be replicated in vitro.

FRI180

Clinical and genetic factors associated with regression of fibrosis in ACLD after etiological therapy

Yuly Mendoza^{1,2}, Mojgan Masoodi³, Sofia Tsouka³, Jaime Bosch², Annalisa Berzigotti^{1,2}. ¹Department of Visceral Surgery and Medicine, Inselspital, Bern University Hospital, University of Bern, Switzerland; ²Department for BioMedical Research, Visceral Surgery and Medicine, University of Bern, Switzerland; ³Institute of Clinical Chemistry, Bern University Hospital, Bern, Switzerland
Email: yuly.mendozajaimes@insel.ch

Background and aims: Liver fibrosis is the main determinant of clinical outcomes in advanced chronic liver disease (ACLD) of any etiology. The introduction of effective etiological therapies has shown that liver fibrosis and even cirrhosis is reversible after eliminating the cause of ACLD. However, not all patients experience fibrosis regression, evidencing that other factors modulate this process. In order to better understand the genetic and molecular mechanisms controlling fibrosis regression we analysed the genetic and transcriptomic pathways in ACLD with or without regression of fibrosis using high-throughput technologies.

Method: We conducted a case-control pilot study of 60 patients with ACLD of different etiology, 30 with histological and/or clinical evidence of regression (Regressors, Re) and 30 without (Non-regressors, NRe), after a minimum of 24 months of etiological therapy. In all patients we performed genotyping (TaqMan assay) of gene variants associated with liver fibrosis (PNPLA3, TM6SF2, SERPINA1, GSKR, TMC4, HSD17B13). Transcriptomic analysis (RNAseq) was done in 30 frozen paired liver biopsies (before and after therapy) of 15 patients. Differentially Expressed Genes (DEGs) analysis were determined using DESeq2 and selected for FDR <0.05. The enrichment of biological pathways was determined with KEGG.

Results: Lack of regression was associated with higher frequency of GSKR-rs1260326 CT-Allele (NRe 63.3% vs Re 36.7%; OR: 0.240, p = 0.020), obesity (63.7% vs. 36.7%, p = 0.041) and higher liver stiffness (33.3 vs. 21.8 kPa, p = 0.032). These three factors remained independently associated with lower likelihood of ACLD regression on multivariate analysis (Figure). RNAseq data comparing Re vs. NRe in the post-therapy samples disclosed 109 significantly DEGs out of 17,243 genes. Downregulated DEGs in Re showed significant enrichment for the Hippo signaling pathway (p < 0.05). Other pathways identified included the PI3K-Akt signaling pathways, ECM-receptor interaction, focal adhesion and relaxin signaling pathways, already known to be involved in liver fibrosis.

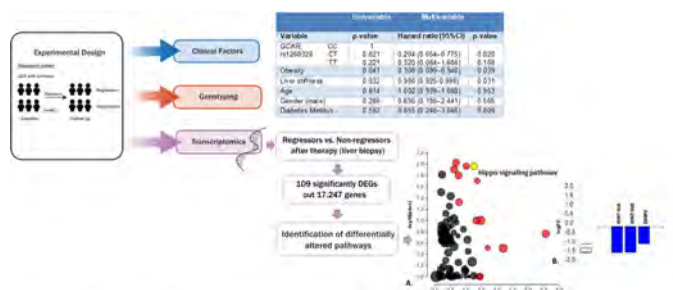


Figure. Study design and schematic illustration. A. Hippo signaling pathway (KEGG: 04390) (yellow) is shown, using negative log of the accumulation and over-representation p-values, along with the other most significant pathways. B. Gene measured expression bar plot with 3 DEGs in Hippo signaling pathway ranked based on their absolute value of log fold change, showing downregulated genes in Regressors.

Conclusion: Presence of obesity, high LSM and GSKR-rs1260326 CT-Allele decrease the likelihood of fibrosis regression of ACLD. The liver transcriptome analysis suggests that the Hippo signaling pathway, a pathway driving hepatic stellate cell activation, is involved in fibrosis

regression and may represent a novel potential therapeutic target to reverse liver fibrosis in ACLD.

FRI181

Addressing the heterogeneity of fibrosis in liver biopsy specimens with qFibrosis – a new paradigm for an old problem

David E. Kleiner¹, Pik Eu Jason Chang², Dean Tai³, Elaine Chng³, Yayun Ren³, Feng Liu⁴, Huiying Rao⁴, Lai Wei⁵, Arun Sanyal⁶.

¹Laboratory of Pathology, Center for Cancer Research, NCI, MD, USA;

²Department of Gastroenterology and Hepatology, Singapore General Hospital, Singapore; ³HistoIndex Pte. Ltd., Singapore; ⁴Peking University People's Hospital, Peking University Hepatology Institute, Beijing Key Laboratory of Hepatitis C and Immunotherapy for Liver Diseases, Beijing, China; ⁵Hepatopancreatobiliary Center, Beijing Tsinghua Changgung Hospital, Tsinghua University, Beijing, 102218, China; ⁶Virginia Commonwealth University, Richmond, Virginia, USA

Email: kleinerd@mail.nih.gov

Background and aims: A 1-stage fibrosis improvement is key for therapeutic benefit assessment in NASH trials. But in trials with a 48-week duration, most patients do not change their fibrosis stage according to the CRN system. This is due to either insufficient change in collagen amount or fibrosis distribution. qFibrosis can analyse these differential changes which has been shown to provide insights on drug effects. The generalisability in this approach beyond NASH has not been established. In this exploratory analysis, a cumulative qFibrosis score was used to identify fibrosis changes in different regions of the liver sections in treated hepatitis C (HCV) subjects who have achieved sustained virological response.

Method: Paired biopsies from 35 patients assessed to have “no-change” in fibrosis. Using qFibrosis, collagen proportionate area (CPA) of 5 pre-defined fibrosis regions [portal, peri-portal (PP), peri-central (PC), peri-sinusoidal (PS) and bridging] were quantified using second harmonic generation/two photon excitation fluorescence technology. CPA values for each region were normalized to a 0–1 range with qFibrosis total weighted score (qF-TWS) calculated as a sum of all 5 CPA values.

Results: The baseline staging of the HCV patients were F0 (n = 1); F1 (n = 2); F2 (n = 2); F3 (n = 7); F4 (n = 9); F5 (n = 2); F6 (n = 12). This cohort was reclassified by qF-TWS as those with progression (n = 9), no change (n = 7) and regression (n = 19). Changes in different regions of the tissue sections and their relationship to overall CPA response of 3 individuals from these representative groups is shown. We observed differential changes in different regions of the liver, with specific changes in the perisinusoidal region even though the conventional fibrosis stage did not change.



Figure: qF-TWS of 3 patients who have no change in fibrosis before and post-treatment. E.g., patient A showed increase in fibrosis (normalized) in 5 regions: 0.11 to 0.22 for portal, 0.17 to 0.30 for PP, 0.18 to 0.21 for PC, 0.21 to 0.33 for bridging, 0.48 to 0.36 for PS.

Conclusion: qF-TWS can differentiate subjects with fibrosis progression and regression post-treatment who were determined as no-change by pathologists' assessment. The ability of qFibrosis to assess fibrosis heterogeneity on a continuous scale provides the potential of detecting subtle fibrosis changes that cannot be captured by current system. A separate study is planned to establish correlation to clinical outcomes.

FRI182

Characterisation of the novel Galectin-3 inhibitor GB1107 on CCl₄-induced liver fibrosis in mice

Alison MacKinnon¹, Ross Mills², Fredrick Zetterberg³, Rob Slack³.

¹Galeto Inc, Edinburgh, United Kingdom; ²University of Edinburgh, Centre for Inflammation Research, Edinburgh, United Kingdom; ³Galeto Inc, Copenhagen, Denmark

Email: AM@galeto.com

Background and aims: Galectin-3 (Gal-3) is a pro-fibrotic β -galactoside binding lectin highly expressed in fibrotic liver (1) and implicated in hepatic fibrosis (2). GB1107 is a novel orally active anti-Gal-3 small molecule inhibitor that has high affinity and selectivity for galectin-3 as well as high oral bioavailability in mice (3).

Method: Liver fibrosis was induced by administration of CCl₄ (1:3 CCl₄:olive oil) at 1 microlitre per g or olive oil control twice weekly by intraperitoneal injection in male C57Bl/6 mice for 8 weeks. GB1107 or vehicle control was administered once daily orally (10 mg/kg) for the last 4 weeks of CCl₄ treatment. Livers were removed and fibrosis assessed by Sirius red staining of liver sections and gene sequencing. Total RNA was extracted and libraries were prepared using the NEBNext Ultra II Directional RNA Library Prep kit and the Poly-A mRNA magnetic isolation module. Paired-end sequencing with a read length of 100 bp was performed using a single P3 flowcell on the NextSeq 2000 platform. The raw reads were aligned to the mouse reference genome assembly GRCh39 using STAR. Pathway enrichment analysis was performed to determine enrichment of differentially expressed genes (DEGs) within Reactome pathways and Gene Ontology (GO) terms.

Results: GB1107 significantly reduced CCl₄-induced liver fibrosis (Sirius red, CCl₄-vehicle 2.70 ± 0.24%; CCl₄-GB1107 1.99 ± 0.10% (p = 0.009)). Using a false discovery rate-adjusted statistical threshold (FDR-adjusted p < 0.05) and a 2-fold change in expression cutoff, 1,659 DEGs were identified with CCl₄ treatment compared to control. Comparing GB1107 treatment with CCl₄ vehicle mice 1147 DEGs were identified. Pathways strongly enriched in up-regulated genes in the CCl₄ group included those related to the extracellular matrix, and collagen biosynthesis and assembly, cell cycle and the immune system whilst pathways related to fatty acid or lipid metabolism were enriched in the down regulated genes. Principal component analysis revealed that GB1107 overlapped significantly with the control group and effectively reversed the CCl₄ induced gene changes.

Conclusion: GB1107 inhibited CCl₄-induced liver fibrosis and reversed CCl₄-induced gene changes. Small molecular weight and orally active inhibitors of galectin-3 show promise as potential new oral anti-fibrotic agents for the treatment of liver fibrosis. A first-in-human study with GB1211, an analogue of GB1107, has shown it to be both safe and well tolerated in man, demonstrating a PK profile that supports twice daily dosing (NCT03809052). GB1211 has now progressed to a phase II study in patients with liver cirrhosis (NCT05009680).

References

- Gudowska M. *et al.* (2015). *Ann. Clin. Lab. Sci.*, 45, 669–673
- Henderson N. C. *et al.* (2006) *Proc Natl Acad Sci U S A* 103, 5060–5065
- Zetterberg *et al.* (2018) *ChemMedChem* 13, 133–137.

FRI183

Quantitative digital pathology of 3D human NASH models establish continuous scores to evaluate the antifibrotic effects of Selonsertib, Firsocostat and Resmetirone

Louis Petitjean², Simon Ströbel³, Li Chen², Eva Thoma³,

Radina Kostadinova³. ¹PharmaNest, Inc, Princeton, United States;

²PharmaNest Inc, Princeton, United States; ³InSphero AG, Schlieren, Switzerland

Email: louis.petitjean@pharmanest.com

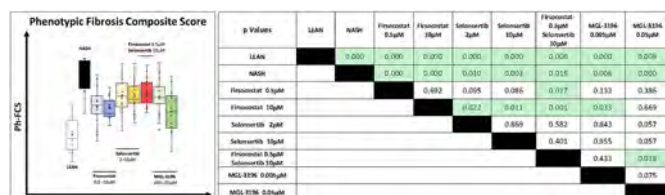
Background and aims: Human in-vitro 3D NASH tissue model have the potential to accelerate the discovery of new anti-fibrotic

POSTER PRESENTATIONS

compounds. We have previously reported the performance of novel Digital Pathology Quantitative AI to generate automatic, continuous and direct fibrosis endpoints to quantify fibrosis severity and compound treatment response. Here, we expand this validation effort to increasing concentrations of Selonsertib, Firsocostat and resmetirone (MGL-3196) and their combinations.

Method: Human in vitro 3D InSight™ liver microtissues containing primary hepatocytes, Kupffer cells, endothelial cells and hepatic stellate cells in 96-well plates were used to model NASH progression using a defined cocktail of free fatty acids, LPS and high levels of sugars. For compound efficacy testing, the 3D NASH tissues were simultaneously treated with selonsertib (2 mM and 10 mM), firsocostat (0.5 mM and 10 mM), MGL-3196 (0.005 mM and 0.05 mM) and combination of selonsertib (10 mM) with firsocostat (0.5 mM) for a total of 9 groups (n = 18 to 21 in each group). Liver microtissues slices were stained with Sirius Red and digitally imaged at 40X. FibroNest™, a cloud-based quantitative image analysis and quantitative AI platform, was used to quantify the fibrosis phenotype along 32 traits for collagen content, morphometry, and architecture. Each trait is described by up to seven quantitative fibrosis traits (qFTs, 315 in total). Principal qFTs are automatically detected and combined into a normalized Phenotypic Composite Fibrosis Score (Ph-FCS). Each qFT is described individually for relative severity (green to red) in Phenotypic Heatcharts.

Results: The Ph-FCS offers a significant detection threshold and dynamic range to evaluate the antifibrotic response the seven treatment arms (box plot chart and p-value table below). Firsocostat (10 mM) and MGL-3196 (0.05 mM) antifibrotic effects are significant and comparable. The combination of selonsertib (10 mM) with the low dose of firsocostat (0.5 mM) does not demonstrate any synergistic effect. The dose response effects are poorly detected except for the MGL-3196 arms (p = 0.075) which demonstrate that the result is driven by the compounds, not the Ph-FCS score and method. Each principal qFT is described individually for relative severity (green to red) in phenotypic heatcharts which can be used to quantified differences in the fibrosis phenotype in each group, and quantify specific effects of each drug (and dose) on the collagen distribution, collagen fibers morphometry and fibrosis architecture.



Conclusion: The combination of FibroNest™ imaging analysis for automated quantification of histological fibrosis severity phenotype within vitro 3D InSight™ human NASH model provide powerful platform for anti-fibrotic drug-candidates response evaluation.

FRI184

Etiology-independent fibrosis severity scoring by quantitative digital pathology image analysis

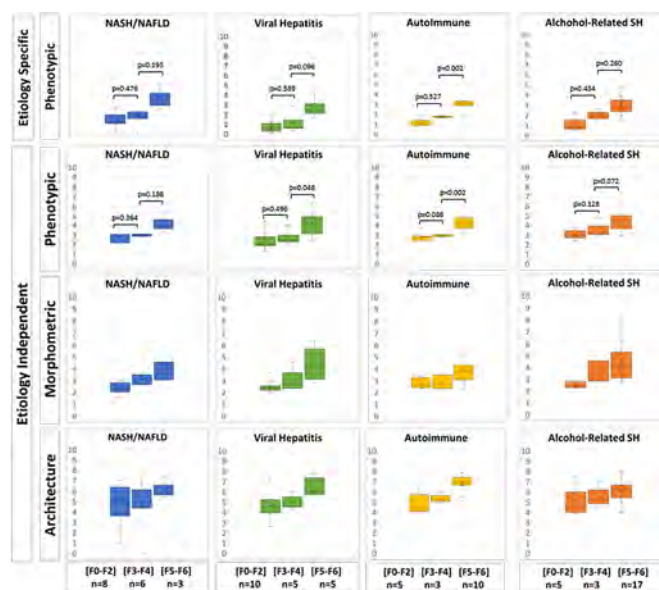
Adam Watson¹, Louis Petitjean², Mathieu Petitjean², Michael Pavlides¹. ¹University of Oxford, Oxford, United Kingdom; ²PharmaNest, Inc, Princeton, United States
Email: mathieu.petitjean@pharmanest.com

Background and aims: While fibrosis is the common end point of many chronic liver disease, little is known about the possible subtle histological differences between etiologies and the related performance of existing fibrosis staging system. Here, we used quantitative Digital Pathology image analysis and quantitative AI to quantify the phenotype of liver fibrosis using histological traits to describe to

collagen content, collagen fiber morphometry and fibrosis architecture. The aim of this study was to identify histological traits common to a variety of liver disease aetiologies and use these to develop a new quantitative etiology-independent fibrosis severity score.

Method: Patients who had undergone liver biopsy for the assessment of diffuse liver disease were included. Liver biopsy histology slides stained with Sirius Red were digitally scanned and categorised as mild (F0–2; n = 28), moderate (F3–4; n = 17) or severe (F5–6; n = 35) fibrosis using the Ishak staging system. Disease etiology was classified as alcohol related liver disease (ARLD; n = 25), non-alcoholic fatty liver disease (NAFLD; n = 17), viral (chronic hepatitis B or C; n = 20), or autoimmune (PBC, PSC or autoimmune hepatitis; AIH; n = 18). FibroNest™ was used to describe the fibrosis phenotype of each etiological group according to quantitative fibrosis traits parameters (qFTs; n = 220) from three phenotypic layers: collagen content, fibers morphometry and fibrosis architecture. For each etiological group, qFTs that showed significant variation (>20%; p < 0.05) between the mild and severe groups of fibrosis were combined to produce an etiology-specific score for fibrosis severity. We also combined qFTs common to all four aetiological groups (n = 77) to produce etiology-independent score for fibrosis severity, morphometry, and architecture.

Results: Our etiology-independent fibrosis phenotypic score (2nd row of Figure 1) correlates with fibrosis stage and distinguishes mild from severe fibrosis with acceptable performance. The etiology-specific phenotypic score (1st row of Figure 1) has a superior performance for mild fibrosis. For each etiology [NAFLD, Viral, Autoimmune, AR-SH], group mean values are comparable for the Mild [2.63;2.67;2.64;3.03], Moderate [3.03;3.04;3.04;2.90] and Severe [4.17;4.26;4.33;4.47] stages. The morphometric and architectural scores (and their related qFTs) can be used to further enrich the understanding of fibrosis phenotypes.



Conclusion: Our data shows that quantitative digital pathology image analysis can phenotype fibrosis and quantify severity in multiple liver disease aetiologies. We used this technology to develop an etiology-independent score to assess the severity of fibrosis from liver biopsies.

FRI185

Liver stiffness and autoimmune profile in a cohort of patients with systemic sclerosis

Davide Di Benedetto^{1,2}, Maria Lorena^{1,2}, Francesca Baorda^{1,2}, Giulia Francesca Manfredi^{1,2}, Antonio Acquaviva^{1,2}, Carla De Benedittis^{1,2}, Cristina Rigamonti^{1,2}, Mattia Bellan^{1,2}, Mario Pirisi^{1,2}. ¹AOU Maggiore della Carità, Division of Internal Medicine, Novara, Italy; ²Università del Piemonte Orientale, Department of Translational Medicine, Novara, Italy
Email: davidedibenedetto304@gmail.com

Background and aims: Systemic sclerosis (SSc) is characterized by skin fibrosis and involvement of esophagus, lungs, heart and kidneys. Liver involvement in SSc is considered rare, but reports addressing this issue are scarce. Here, we evaluated the prevalence of liver fibrosis and hepatic autoimmunity in a cohort of SSc patients.

Method: A retrospective observational study was performed on 97 patients diagnosed with SSc or mixed connective tissue disease with sclerodermic manifestations who underwent transient elastography evaluating liver stiffness (LS) and controlled attenuation parameter (CAP) due to clinical indication; a biochemistry assessment and major antibodies associated to liver autoimmunity were recorded whether performed together to clinical and demographic data.

Results: Among the 97 patients included, 16 (16.5%) had LS ≥ 7.5 kPa, 5 of whom had LS ≥ 12.5 kPa. Predictors of LS ≥ 7.5 were alcohol consumption, waist circumference, elevated alkaline phosphatase (ALP) levels, anti-La and anti-mitochondrial antibody (AMA) positivity. CAP values compatible with steatosis (≥ 280 dB/m) were observed in 6 (6.2%) patients. Waist circumference, body mass index and diabetes mellitus were significant predictors of steatosis. Out of 97 patients, 19 (19.5%) were positive for AMA, 4 (4.2%) for anti-Sp100, 1 (1%) for anti-gp210 and 7 (7.3%) were diagnosed with primary biliary cholangitis.

Conclusion: Among SSc patients, the prevalence of biomarkers of hepatic fibrosis and AMA is relatively high, suggesting the opportunity of performing a transient elastography and a screening for hepatic autoimmunity at diagnosis and/or along the course of the disease.

FRI186

Performance of a p-SWE method implemented on a new ultrasound system for predicting advanced liver fibrosis

Alexandru Popa¹, Roxana Sirli¹, Alina Popescu¹, Andreea Borlea², Felix Bende¹, Victor Baldea¹, Raluca Lupusoru¹, Camelia Foncea¹, Radu Cotrau¹, Pascu Ariana¹, Ioan Sporea¹. ¹Victor Babeş University of Medicine and Pharmacy, Department of Internal Medicine II, Division of Gastroenterology and Hepatology, Center for Advanced Research in Gastroenterology and Hepatology, Timișoara, Romania; ²Victor Babeş University of Medicine and Pharmacy, Department of Internal Medicine II, Division of Endocrinology, Timișoara, Romania
Email: popa.alexandru@umft.ro

Background and aims: Ultrasound based elastography techniques became in the last years reliable tools to predict the severity of liver fibrosis in chronic hepatopathies. Usually, these techniques are integrated in high-end US machines but recently they became available in medium-range ones.

To evaluate the performance of point Shear-Wave Elastography from Siemens, implemented on the new ACUSON Juniper Ultrasound System, for the non-invasive assessment of liver fibrosis, and to identify liver stiffness (LS) cut-off value for predicting advanced fibrosis, using Transient Elastography (TE) as the reference method.

Method: We included 201 consecutive subjects (60% men, mean BMI = 28.7 ± 4.9 kg/m², mean age 59 ± 18.4 years) with or without chronic hepatopathies in whom LS was evaluated in the same session by means of 2 elastography techniques: TE and p-SWE from Siemens. Reliable LS measurements were defined for TE as the median value of 10 measurements with an interquartile range/median (IQR/M) $< 30\%$, and for p-SWE as the median value of 10 measurements acquired in a

homogenous area and an IQR/M $< 30\%$. A cut-off of ≥ 9.5 kPa by TE was used to define advanced fibrosis ($F \geq 3$).

Results: Valid liver stiffness measurements (LSM) were obtained in 97.5% of patients using both elastography methods. Therefore, 196 subjects were included in the final analysis (27.8% with TE ≥ 9.5 kPa). A moderate positive correlation was found between the LS values obtained by the 2 methods: $r = 0.68$, $p < 0.0001$ (Spearman correlation). LS values obtained by p-SWE were significantly lower than those obtained by TE: 8.3 kPa vs. 10.12 kPa ($p < 0.0001$). The best p-SWE cut-off value for advanced fibrosis ($F \geq 3$) was 7.4 kPa (AUC-0.95; Se-81.5%; Sp-98%; PPV-95.7%; NPV-93.3%) (fig 1).

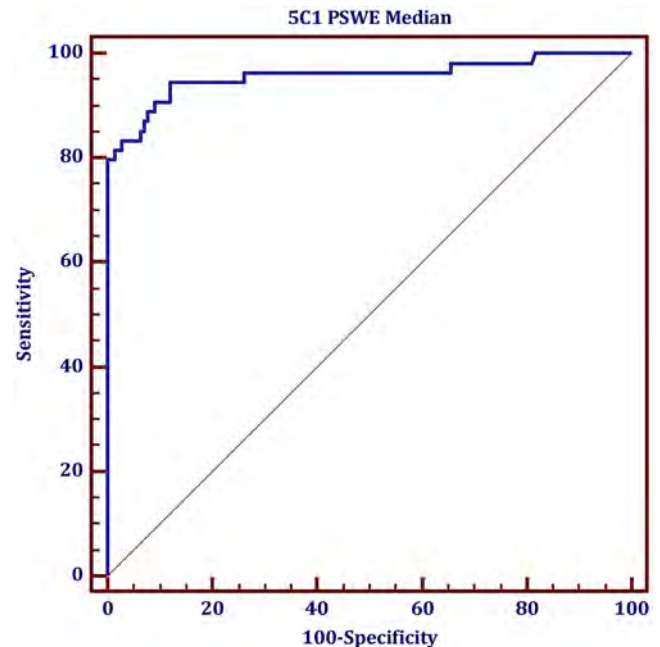


Figure 1: Performance of p-SWE for predicting advanced fibrosis ($F \geq 3$).

Conclusion: Using the new US system, the best p-SWE cut-off value for predicting advanced fibrosis was 7.4 kPa.

FRI187

Inhibition of tumour progression locus 2 (TPL2) halts the progression of liver fibrosis in a stringent long term choline deficient high-fat diet (CdHFD) rat model

Milessa Silva Afonso¹, Rowena Suriben¹, Natalie Sroda¹, Sowjanya Dokku¹, David Hollenback¹, Mehdi Belkhdja¹, Wesley Minto¹, Sangeetha Mahadevan¹, Grant Budas¹, Yeonju Lee¹, Kelli Boyd¹, Eda Canales¹, Bernard Murray¹, Matthew Warr¹, James Taylor¹, James Trevaskis¹, Ruchi Gupta¹. ¹Gilead Sciences, Inc, Foster City, United States
Email: milessa.silvaafonso@gilead.com

Background and aims: Chronic inflammatory stimuli exacerbate liver damage and contribute to the development of fibrosis and NASH. Inhibition of TPL2, a serine-threonine kinase downstream of pattern recognition receptors, could halt or reverse NASH and liver fibrosis. Previously reduced hepatic inflammation and fibrosis was observed with a TPL2 inhibitor (TPL2i) in the rat CDHFD model. Here we explored the effect of TPL2i in an extended disease model.

Method: Male Wistar rats on CDHFD for 8 weeks were treated with TPL2i (100 mg/kg, BID), ACC inhibitor (ACCI, 10 mg/kg, QD), cenicriviroc (CVC, 100 mg/kg BID) or combinations of ACCi (10 mg/kg QD) + TPL2i (100 mg/kg BID) or ACCi (10 mg/kg QD) + FXR agonist cilexifor (CILEX, 30 mg/kg BID) for 10 weeks ($n = 10-15$ /group). Liver fibrosis was assessed by picrosirius red (PSR) and α SMA staining. Hepatic immune cell and cytokine content were assessed by immunohistochemistry and ELISA, respectively. CCR2⁺ and Foxp3⁺/CD3⁺ (TReg)

POSTER PRESENTATIONS

cells were measured by immunofluorescence and quantified using Visiopharm.

Results: TPL2i reduced PSR by 48% and α SMA by 50% vs. vehicle (both $p < 0.001$). The combination TPL2i + ACCi reduced PSR by 63% and α SMA by 72% vs. vehicle. No improvement in these endpoints was observed with either ACCi or CVC. TPL2i reduced the expression of fibrogenic genes and hepatic content of macrophages and T-cells compared to vehicle ($p < 0.001$), but no further reductions were observed with the TPL2i + ACCi combination. A reduced number of CCR2⁺ cells and increased proportion of TRegs were observed in liver from TPL2i-treated rats vs. vehicle. As expected, CVC reduced macrophage number (by 22%, $p < 0.01$) but did not alter T-cells. TPL2i reduced TNF- α by 64%, KC/GRO by 47% and IL-1 β by 46% (vs vehicle, all $p < 0.01$). Further reductions in TNF α and KC/GRO were observed with ACCi + TPL2i combination. CVC reduced TNF- α by 48%, KC/GRO by 32%, and IL-1 β by 34% (vs. vehicle, all $p < 0.05$). As a clinically relevant benchmark, the ACCi + CLO combination reduced PSR and α SMA (by 30% and 52% vs. vehicle, both $p < 0.001$), as well as macrophages and T-cells (by 28% and 32% vs. vehicle, both $p < 0.001$).

Conclusion: TPL2i improved fibrotic and inflammatory endpoints in this extended rat CDHFD model, with greater or equivalent efficacy compared to the clinically validated combination of ACCi + CLO. These results provide rationale for inhibition of TPL2 for the treatment of NASH and suggest potential for its use in novel combination therapies.

FRI188

Evaluation of the antifibrotic effects of naringenin, asiatic acid and icariin by using precision-cut liver slices of mouse and human

Ke Luo¹, Yana Geng¹, Vincent de Meijer², Dorenda Oosterhuis¹, Peter Olinga¹. ¹University of Groningen, Department of Pharmaceutical Technology and Biopharmacy, Groningen, Netherlands; ²University of Groningen, University Medical Center Groningen, Department of Surgery, Groningen, Netherlands
Email: p.olinga@rug.nl

Background and aims: Fibrosis is an exaggerated wound healing response defined by excessive accumulation of extracellular matrix, which may lead to organ dysfunction or even organ failure. Therapies for liver fibrosis are lacking. Naringenin (NRG), asiatic acid (AA) and icariin (ICA) are three compounds that were reported to exert antifibrotic effects in both *in vitro* and *in vivo* animal models of liver fibrosis. However, no human data is available. Our objective was to investigate the potential antifibrotic effects of these three compounds by using the *ex vivo* mouse and human precision-cut liver slices (PCLS) model.

Method: PCLS prepared from mouse liver tissue (mPCLS), healthy human liver tissue (hhPCLS) and cirrhotic human liver tissue (chPCLS) were cultured for 48 h with or without different concentrations of the three compounds. The viability was assessed by evaluating the ATP content of PCLS to study the toxicity of the three

compounds. Gene expression of the fibrotic markers alpha-1 type I collagen (*COL1a1*), heat shock protein 47, alpha-smooth muscle actin, connective tissue growth factor, plasminogen activator inhibitor-1, and inflammatory markers interleukin-1 beta, interleukin-6, tumor necrosis factor alpha were determined by qPCR. Pro-collagen 1a1 (Pcol1a1) excreted by PCLS into the culture medium was determined by an ELISA assay.

Results: NRG concentration-dependently inhibited *COL1a1* gene expression in mouse and human PCLS. The highest non-toxic concentration of NRG (300 μ M in mPCLS, 200 μ M in hhPCLS and chPCLS) suppressed fibrosis and inflammation related genes and reduced the Pcol1a1 in the culture medium by 54 \pm 21 % (mPCLS), 34 \pm 23 % (hhPCLS), and 75 \pm 23 % (chPCLS). The highest non-toxic concentration of AA (30 μ M) decreased only in hhPCLS *COL1a1* and Pcol1a1 by 34 \pm 17 %, and downregulated fibrosis-related gene expression. 25 μ M of ICA, the highest non-toxic concentration, only suppressed in mPCLS *col1a1* gene expression, while decreasing inflammation related genes in all PCLS types.

Conclusion: NRG showed the most promising antifibrotic potency in both mouse and human PCLS, with more profound effects in chPCLS than in the early on-set of fibrogenesis in hhPCLS. Antifibrotic effects of AA were only shown in hhPCLS. ICA only exerted antifibrotic effects on fibrosis related genes in mPCLS.

FRI189

Diagnostic efficacy of Mac-2 binding protein glycosylation isomer for predicting liver fibrosis in patients with metabolic associated fatty liver disease

Se Young Jang¹, Dae Won Jun², Hoon Gil Jo³, Ki Tae Yoon⁴, Young Youn Cho⁵. ¹School of Medicine, Kyungpook National University, Kyungpook National University Hospital, Internal Medicine, Korea, Rep. of South; ²Hanyang University College of Medicine, Internal Medicine, Korea, Rep. of South; ³Wonkwang University Hospital, Wonkwang University School of Medicine, Internal Medicine, Korea, Rep. of South; ⁴Pusan National University Yangsan Hospital, Internal Medicine, Korea, Rep. of South; ⁵Chung-Ang University Hospital, Internal Medicine, Korea, Rep. of South
Email: gongori1004@gmail.com

Background and aims: The definition of metabolic associated fatty liver disease (MAFLD) has newly been proposed. We aimed to investigate the efficacy of Mac-2 binding protein glycosylation isomer (M2BPGi), non-invasive fibrosis marker, for discriminating significant and advanced fibrosis, and cirrhosis, respectively according to MAFLD and NAFLD definitions.

Method: Serum M2BPGi levels were collected and analyzed from 950 fatty liver patients in a tertiary hospital. Liver fibrosis was graded by transient elastography. Diagnostic efficacy of serum M2BPGi and other serum based liver fibrosis markers [fibrosis index based on four factors (FIB-4) and NAFLD fibrosis score (NFS)] was evaluated using correlation analysis and area under the ROC curve (AUC).

Table 1:(abstract: FRI189): Diagnostic efficacy of serum M2BPGi and other serum markers in predicting the liver fibrosis stage in patients with MAFLD.

	AUC (95% CI)	Cut-off value	Sensitivity (%)	Specificity (%)	PPV (%)	NPV (%)	P
M2BPGi							
F >1	0.706 (0.657–0.755)	1.15	48.6	81.2	35.9	88.0	<0.001
F >2	0.719 (0.662–0.776)	1.19	50.5	80.4	24.6	92.8	<0.001
F >3	0.843 (0.774–0.912)	1.31	73.7	85.6	20.1	98.5	<0.001
FIB-4							
F >1	0.703 (0.650–0.756)	1.61	68.8	66.2	30.6	90.7	<0.001
F >2	0.709 (0.643–0.774)	1.63	70.3	65.9	20.7	94.6	<0.001
F >3	0.796 (0.713–0.878)	2.40	65.8	82.8	15.8	98.0	<0.001
NFS							
F >1	0.660 (0.608–0.713)	−0.72	62.5	65.8	28.3	89.0	<0.001
F >2	0.682 (0.616–0.748)	−0.72	68.1	64.4	19.5	94.1	<0.001
F >3	0.787 (0.711–0.863)	−0.70	84.2	63.5	10.2	98.8	<0.001

Results: There were 810 patients and 687 patients by the MAFLD and NAFLD definition, respectively. Serum M2BPGi level and other liver fibrosis markers showed a positive correlation with fibrosis grade. The AUC values of M2BPGi were 0.698, 0.698, and 0.828 for predicting fibrosis (F) >1, F >2, and F >3, respectively in NAFLD group. The AUC values of M2BPGi were 0.706, 0.719, and 0.843 for predicting F >1, F >2, and F >3, respectively in MAFLD group. The AUC values of M2BPGi for predicting severity of fibrosis were greater than those of serum based liver fibrosis markers (Table 1).

Conclusion: M2BPGi showed better diagnostic efficacy for diagnosing the severity of liver fibrosis in MAFLD patients.

FRI190

Multispectral imaging analysis of liver biopsies from patients with non-alcoholic steatohepatitis reveals enrichment of pathogenic macrophage phenotypes associated with disease progression

Joseph Gosnell¹, Omar Saldarriaga¹, Santhoshi Krishnan², Morgan Oneka², Arvind Rao³, Daniel Millian¹, Timothy Wanning¹, Jingjing Jiao⁴, Laura Beretta⁴, Heather Stevenson¹. ¹UTMB Health-University of Texas Medical Branch at Galveston, Pathology, Galveston, United States; ²Rice University, Houston, United States; ³University of Michigan, Ann Arbor, United States; ⁴The University of Texas MD Anderson Cancer Center, Houston, United States
Email: jogosnel@utmb.edu

Background and aims: Non-alcoholic steatohepatitis (NASH) affects 3–6% of the US population and risk factors include obesity, dyslipidemia, metabolic disease, and type 2 diabetes. While many patients diagnosed with NASH will not progress to cirrhosis, identifying which patients will develop advanced fibrosis is a challenge. Intrahepatic macrophages are critical gate keepers in the hepatic microenvironment that assist in maintaining immune tolerance. Upon activation, they can promote a pro-fibrotic hepatic microenvironment. We hypothesized that patient variation in intrahepatic macrophage phenotypes could predict disease progression in patients with NASH.

Method: We used multiplex staining followed by multispectral imaging to phenotype and quantify resident liver macrophages (CD68+), monocyte-derived macrophages (MAC387+), pro-fibrogenic macrophages (CD163+), and their co-expression of pro-inflammatory (CD14) and anti-inflammatory (CD16) markers in the context of hepatic architecture. We compared differences in spatial distribution (i.e., in enrichment and/or depletion) of macrophage populations in patients with NASH and either minimal (n = 6; fibrosis stage: 0–1/4) or advanced (n = 5, fibrosis stage: 4/4) fibrosis. First, multiplexed stained liver biopsies were scanned with a multispectral microscope (Vectra 3, Akoya Biosciences). We then determined the heterogeneity of these various macrophage populations in the study groups using phenotype matrices and t-distributed stochastic neighbor embedding plots (t-SNE) (Visiopharm®; MATLAB 2020a). Phenotypes that were significantly increased in the patients with advanced fibrosis were selected for spatial proximity analysis using G-function equations.

Results: Phenotype matrix analysis revealed the enrichment of unique pathogenic macrophage phenotypes (MAC387+, MAC387 + CD163+, MAC387 + CD163 + CD68+, MAC387 + CD163 + CD16 + CD14 +, MAC387 + CD163 + CD16 + CD14 + CD68+) in NASH patients with advanced fibrosis when compared to those with minimal fibrosis. Pathogenic macrophage populations (MAC387+, CD163 + MAC387+, CD163+, CD68 + CD163+) correlated with poor clinical outcome (increased prothrombin time and decreased platelet counts) in two of the patients with minimal fibrosis. In patients with advanced fibrosis, spatial analysis also showed significant (p < 0.05) infiltration of MAC387+ macrophages near CD68+ Kupffer cells.

Conclusion: Multispectral imaging combined with spatial analysis allows characterization of distinct macrophage subpopulations that

may be able to predict fibrosis progression in patients with NASH. The ability to identify at-risk patients by the presence of pathogenic intrahepatic macrophages may also lead to future precision medicine approaches.

FRI191

Diabetes, but not prediabetes, is associated with significant liver fibrosis

Byung Ik Kim¹, Yong Kyun Cho¹, Won Sohn¹. ¹Kangbuk Samsung Hospital
Email: hand0827@naver.com

Background and aims: This study aimed to assess the risk of liver fibrosis between no glucose intolerance, prediabetes and diabetes in the general population.

Method: A cross-sectional study was conducted based on a cohort from a health examination program which included a magnetic resonance elastography (MRE). The participants were classified into three subgroups according to glucose tolerance: no glucose intolerance, prediabetes and diabetes mellitus. Liver fibrosis was evaluated by liver stiffness measurement (LSM) value using 2-dimensional real-time MRE. The risk of liver fibrosis was compared after adjusting for confounding factors including the presence of liver disease (non-alcoholic fatty liver disease, significant alcohol consumption and viral hepatitis).

Results: A total of 2,090 subjects was included: no glucose intolerance (n = 889); prediabetes (n = 985); and diabetes (n = 216). The mean age was 50.6 years. The mean values of LSM in no glucose intolerance, prediabetes, and diabetes were 2.37 ± 0.43 kPa, 2.41 ± 0.34 kPa, and 2.65 ± 0.70 kPa, respectively (p < 0.001). The proportion of significant fibrosis (LSM ≥ 2.97 kPa) in no glucose intolerance, prediabetes, and diabetes was 3.1%, 4.4%, and 16.7%, respectively (p < 0.001). Compared with no glucose intolerance, the risk of significant fibrosis was higher in diabetes (adjusted odds ratio [aOR] 3.37, 95% confidence interval [CI] = 1.78–6.40, p < 0.001). However, there was no difference between prediabetes and no glucose intolerance (aOR 0.94, 95% CI = 0.54–1.64, p = 0.940). A subgroup analysis also showed that prediabetes is not associated with significant fibrosis unlike diabetes in subjects with or without liver disease.

Conclusion: Diabetes but not prediabetes is a risk factor for significant liver fibrosis regardless of the presence of liver disease.

FRI192

Lysophosphatidylserine may stimulate liver fibrosis

Takako Nishikawa¹, Makoto Kurano², Hitoshi Ikeda², Nobutake Yamamichi¹, Yutaka Yatomi², Kazuhiko Koike³, Mitsuhiro Fujishiro³. ¹The University of Tokyo Hospital, Center for Epidemiology and Preventive Medicine, Tokyo, Japan; ²The University of Tokyo, Clinical Laboratory Medicine, Tokyo, Japan; ³Graduate School of Medicine, the University of Tokyo, Japan, Department of Gastroenterology, Tokyo, Japan
Email: kuranoma-int@h.u-tokyo.ac.jp

Background and aims: Lysophospholipids (LPLs), such as lysophosphatidic acid and sphingosine 1-phosphate are had an interest as second-generation lipid mediators. Lysophosphatidylserine (LysoPS), a phosphatidylserine-derived LPL, has recently been identified as a specific receptor, such as GPR34 and GPR174, P2Y10, and has begun to attract attention as a novel lipid mediator. In this study, we report the effect of LysoPS on liver fibrosis and their physiological roles *in vitro*.

Method: (1) The hepatic myofibroblast-like stellate cell line, CFSC-8B (CFSC), derived from a CCl₄-induced cirrhotic rat liver was utilized. The cells were incubated with the medium added various concentrations of 18: 0 and 18: 1 LysoPS. Expressions of alpha-smooth muscle actin (α-SMA) determined by western blotting. (2) Liver fibrosis was induced by intraperitoneal injection of carbon tetrachloride (CCl₄) two times a week for 8 weeks in mice. (3) The tissue of liver with hepatocellular carcinoma in patient with hepatitis B virus and the plasma in patients with liver dysfunction was utilized. Expressions of

POSTER PRESENTATIONS

GPR34 and GPR174, P2Y10 receptor and LysoPS levels in the plasma were examined.

Results: (1) When the cells were incubated with LysoPS for 24 hours, expressions of α -smooth muscle α -SMA were up-regulated by 10 μ M of 18:0 and 18:1 LysoPS treatment. Expressions of α -SMA were inhibited by inhibitors of Smad3, p38 mitogen-activated Protein kinase and Rho-associated kinase. (2) Expressions of GPR34 and GPR174, P2Y10 receptor were up-regulated along Glisson's capsule in CCl₄ treated mice. 16:1 and 20:4 LysoPS levels in the plasma were increased in CCl₄ treated mice. (3) Expressions of GPR34 and GPR174, P2Y10 receptor, derived from a hepatic myofibroblast-like stellate cell, were up-regulated along fibrous capsule of hepatocellular carcinoma in patient with hepatitis B virus. 16:0 and 18:2 LysoPS levels and phosphatidylserine (PS) levels, as precursor of 16:0 LysoPS, in the plasma were increased in patients with liver fibrosis.

Conclusion: In this study, it was suggested that LysoPS is involved in liver fibrosis in vitro. In vivo study, upregulation of LysoPS receptor was observed in hepatic myofibroblast-like stellate cells, suggesting that LysoPS may also be involved in liver fibrosis. Furthermore, an increase in LysoPS of some fatty acid molecular species was observed in mouse plasma, suggesting the possibility of laboratory medical application of LysoPS as a marker of liver fibrosis.

FRI193

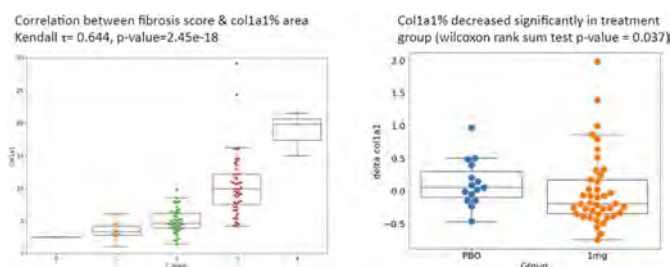
Quantitative assessment of liver fibrosis in NASH patients

Luong Ruiz¹, Tian Lan¹, Wenhui Liu¹, Amir Ashique¹, Harry Chen¹, Jiping Zha², Alex DePaoli¹, Igor Mikaelian¹, Cynthia Guy³, Eugenia Henry¹, William Chang¹, Corinne Foo-Atkins¹, Hsiao Lieu¹.
¹NGM Biopharmaceuticals Inc., Translational Sciences, South San Francisco, United States; ²Adagene Inc, San Diego, United States; ³Duke University Medical Center Greenspace, Department of Pathology, Durham, United States
Email: lruiz@ngmbio.com

Background and aims: The success of clinical trials for the treatment of nonalcoholic steatohepatitis (NASH) is dependent on the efficacy evaluation of the liver fibrosis endpoint. Fibrosis is currently assessed visually using the NASH Clinical Research Network (CRN) staging scheme. However the NASH CRN scheme evaluates patterns of fibrosis that are not related by a linear relationship to the quantified abundance of pathologic collagen deposition. Samples from a Phase 2 clinical trial with aldafermin (NGM282), an engineered fibroblast growth factor 19 analogue, were used to develop a novel image analysis readout for liver fibrosis.

Method: Liver biopsies were from a 24 week clinical trial with aldafermin (NGM282): NCT02443116 (placebo (PBO), n = 22; 1 mg, n = 49). Biopsies and blood for non-invasive biomarkers were collected at baseline and at the end of treatment. A 6-plex immunohistochemistry panel that included Collagen 1A1 (COL1A1) was developed. The image analysis method for COL1A1% area utilized morphological operations to eliminate normal collagen, adaptive thresholding to alleviate uneven signal intensities, and morphological erosion to remove edge effects. Parameters for the methods were tuned on a subset of images and then applied to the whole dataset.

Results: Fibrosis CRN reads correlated robustly with COL1A1% area (Kendall's $\tau = 0.644$, p-value < 0.001). In addition, image analysis identified patients with decreases in COL1A1% area despite no changes in the CRN score. As a consequence, the COL1A1% area identified a statistically significant proportion of responders in the treatment arm (p = 0.037), which represented a 24% decrease in COL1A1% area compared to the PBO group, and which was not reflected by the CRN score (p = 0.12). The COL1A1% area and the CRN score correlated similarly to the non-invasive end points of serum N-terminal type III collagen propeptide and Enhanced Liver Fibrosis (ELF) score (Kendall's $\tau \sim 0.3$ with p < 0.001). Finally, the coefficient of variation for COL1A1 in consecutive liver sections was 7%.



Conclusion: In summary, immunohistochemistry-based quantitative pathology endpoints may identify drug effects that are not captured by categorical CRN endpoints.

FRI194

Second harmonic generation microscopy can quantify and subclassify early stages of NASH fibrosis progression: data from a screen-failure cohort of a NASH phase 2 study

Dominique Brees¹, Dean Tai², Clifford Brass³, Nikolai Naoumov⁴, Elaine Chng², Yayun Ren², Andreas Sailer¹, Douglas Applegate³, Josy George Kochuparampil¹, Juergen Loeffler¹, Li Chen³, Miljen Martic¹, Zachary Goodman⁵, Marcos Pedrosa¹, Quentin Anstee⁶.
¹Novartis Pharma AG, Basel, Switzerland; ²Histoindex Pte. Ltd., Singapore; ³Novartis Pharmaceuticals Corporation, East Hanover, NJ, United States; ⁴London, United Kingdom; ⁵Inova Health System, Director of Hepatic Pathology Consultation and Research, Falls Church, VA, United States; ⁶Newcastle University, Translational & Clinical Research Institute, Faculty of Medical Sciences, Newcastle upon Tyne, United Kingdom
Email: quentin.anstee@newcastle.ac.uk

Background and aims: The semiquantitative liver biopsy grading and staging systems proposed by the non-alcoholic steatohepatitis (NASH) clinical research network (CRN) are widely used in clinical trials due to regulatory authority recommendations. Other, more sensitive methods are available and have potential to provide more detailed and informative analyses of liver histology to inform our understanding of natural history and therapeutic response. Herein we describe the use of second harmonic generation/two-photon excitation fluorescence (SHG/TPEF) microscopy with computer-assisted analyses to provide a standardised and reproducible approach for precise quantitative assessment of NASH fibrosis.

Method: Liver biopsies from 138 patients with non-alcoholic fatty liver disease (NAFLD) who failed screening for a NASH phase 2 clinical trial (TANDEM, NCT03517540) were assessed for liver fibrosis using SHG/TPEF microscopy measured on a continuous scale (qFibrosis). The qFibrosis scores were converted into categorical scores (qF0–qF4) using cut-offs previously reported. qFibrosis was measured in the liver sinusoids from the portal triad to correspond to zones 1, 2, and 3 of the Rappaport acinus, where zones 1 and 3 are defined as 100 μ m away from the end of collagen connected to vessel structures. Independently, all biopsies were assigned a NASH CRN fibrosis stage (F0–F4) by an expert central pathologist.

Results: qFibrosis scores (continuous [$r = 0.59$]; categorical [$r = 0.58$]) correlated moderately with NASH CRN scores (p < 0.001). The main difference in scores between NASH CRN and SHG/TPEF was in F1/qF1 and F2/qF2 patients (F1 [n = 61]; F2 [n = 7] vs qF1 [n = 25]; qF2 [n = 42]). Additionally, SHG/TPEF microscopy classified more patients with stage 3 compared to NASH CRN (F3 [n = 12]; qF3 [n = 29]). The NASH CRN scoring identified differences in the localization of fibrosis in portal, periportal and zone 1 fibrosis, but not in zone 1 alone, between F1 and F2 stages. In contrast, SHG/TPEF microscopy identified significant differences in portal, periportal and zone 1 fibrosis between qF1 and qF2 stages, as well as in zone 1 alone (Table 1). Furthermore, there were no significant differences in mean qFibrosis scores in other acinar zones.

Table 1. Quantitative fibrosis measurements by SHG/TPEF in lobular regions based on staging by SHG/TPEF microscopy and NASH CRN.

SHG/TPEF microscopy staging			
Lobular regions	qF1, mean (n = 25)	qF2, mean (n = 42)	p value
Portal	1.490	2.879	0.004
Periportal	0.659	1.242	<0.001
Perisinusoidal (zone 1)	0.080	0.161	0.005
Perisinusoidal (zone 2)	1.129	1.309	0.342
Perisinusoidal (zone 3)	0.093	0.096	0.881
Pericentral	0.292	0.312	0.688
Central vein	0.339	0.448	0.209
Portal+periportal+perisinusoidal (zone 1)	2.228	4.282	0.001
NASH CRN staging			
Lobular regions	F1, mean (n = 51)	F2, mean (n = 7)	p value
Portal	2.052	5.185	<0.001
Periportal	0.974	1.473	0.030
Perisinusoidal (zone 1)	0.119	0.170	0.211
Perisinusoidal (zone 2)	1.287	1.121	0.658
Perisinusoidal (zone 3)	0.096	0.082	0.678
Pericentral	0.318	0.372	0.549
Central vein	0.401	0.463	0.624
Portal+periportal+perisinusoidal (zone 1)	3.176	6.828	<0.001

CRN, clinical research network; F, fibrosis stage; n, number of patients in group; NASH, non-alcoholic steatohepatitis; SHG/TPEF, second harmonic generation/two-photon excitation fluorescence.

Conclusion: SHG/TPEF microscopy with computer-assisted image analyses is a sensitive and reproducible methodology that may allow categorisation of subtle changes in liver fibrosis that might otherwise not be identified using the NASH CRN staging system. Further research is needed to determine the significance of such changes and parameters to be used when evaluating therapeutic efficacy. SHG/TPEF microscopy may be a useful tool, in combination with the NASH CRN scoring system, in assessing liver fibrosis.

FRI195

Efficacy and safety of prolonged released pirfenidone in patients with compensated cirrhosis. A placebo controlled multicenter study in Mexico

Linda Muñoz¹, Aldo Torre², Laura Esthela Cisneros Garza³, Iaraah Montalvo⁴, René Malé Velazquez⁵, Scherezada Mejia⁶, Juan Ramón Aguilar⁷, Javier Lizardi⁸, Maru Icaza⁴, Frida Gasca⁸, Larissa Hernandez⁸, Paula Cordero-Pérez¹, Luis Chi-Cervera⁴, Lilian Torres Made⁵, Graciela Tapia⁹, Poo Jorge⁸. ¹University Hospital "Dr. Jose E. Gonzalez" UANL, Liver Unit, Monterrey, Mexico; ²INCMN SZ, Gastroenterology, Ciudad de México, Mexico; ³Investigaciones Médicas Cisneros; ⁴Star Médica, Mérida, Mexico; ⁵Instituto de Salud Digestiva y Hepática S.A. de C.V., Guadalajara, Mexico; ⁶Hospital Juárez de México, Ciudad de México, Mexico; ⁷Clinica de Hepatología, Mexico, Mexico; ⁸Clinica REMEDHE, Ciudad de México, Mexico; ⁹Universidad Nacional Autónoma de México, Ciudad de México, Mexico
Email: linda_uanl@hotmail.com

Background and aims: Advanced liver fibrosis (ALF) is a common finding in many chronic liver diseases and considering its predictive value for adverse outcomes new therapies are mandatory. Therefore, we aimed to evaluate efficacy and safety of prolonged release pirfenidone tablets (PR-PFD) in a placebo controlled multicenter study.

Method: 171 patients with ALF were blindly allocated to 3 groups to receive oral PR-PFD 1200 mg (G1) or 1800 mg per day (G2), or placebo (G3) for 24 mos. Response criteria was defined as 30% variation in liver stiffness compared to baseline values estimated by hepatic elastography and considering a reliability criteria as IQR/median less than 30%. Fibrotest was also performed with 10% variation as predictive of response. Patients were classified as regressive fibrotic profile (RFP), stable fibrosis profile (SFP) or progressive fibrotic profile (PFP). Previous decompensation was an exclusion criteria. All participants had ultrasound, and esophageal varices evaluation at baseline, and at 12, and 24 mos.

Results: 150 patients were eligible for efficacy and 171 for safety analysis. At baseline, demographic, etiology, cirrhosis stage, Child-Pugh class or MELD score, Quality of Life or Fatigue scales, as Liver stiffness (kPa) and Fibrotest (units) scores (Mean \pm 1 SE) were similar (ANOVA or Pearson's/Wald's, Chi squared tests) but significantly different at 24 mos (table). According to fibrotic profile in liver stiffness, 58.3 %, 47.4% and 35.1% were RFP; and, 8.3%, 13.3% and 24.3% were PFP, respectively. 19 patients had decompensation due to

variceal bleeding (4), ascites (5), Encephalopathy (5), Hepatocarcinoma (4) without significant difference between groups. ALT levels significantly decreased in groups 1 (44.6 ± 3.9 versus 30.7 ± 4.6 , $p = 0.003$), and 2, (46.8 ± 4.0 versus 37.1 ± 4.6 , $p = 0.007$). Albumin (4.1 ± 0.07 versus 4.4 ± 0.05 , $p = 0.000$), platelets (117 ± 7.9 versus 141 ± 9.2 , $p = 0.000$) and quality of life (80.7 ± 2.2 versus 87.8 ± 2.5 , $p = 0.006$) increased in group 1. Adverse events were mild and affected mainly the GI tract (41, 21 and 45), and skin (14, 9, and 21) and 14 SAEs (5, 6, and 3), in groups 1, 2, and 3, respectively.

Hepatic Elastography	Group 1 (1200 mg)	Group 2 (1800 mg)	Group 3 (Placebo)	Fibrotest Units	Group 1 (1200 mg)	Group 2 (1800 mg)	Group 3 (Placebo)
Baseline	28.7 \pm 2.4	30.6 \pm 2.3	24.7 \pm 1.9	Baseline	0.87 \pm 0.02	0.86 \pm 0.02	0.87 \pm 0.02
24mos	17.3 \pm 1.6	22.3 \pm 1.9	23.1 \pm 2.4	24mos	0.81 \pm 0.02	0.79 \pm 0.02	0.83 \pm 0.02
P value	0.000	0.006	0.481	P Value	0.002	0.015	0.152

Conclusion: PR-PFD at doses of 1200, and 1800mg/day significantly decreased indirect markers of liver fibrosis at 24mos, and improved albumin, platelets and quality of life in patients with compensated cirrhosis. No liver toxicity was detected.

FRI196

Endothelin receptor A antagonist functionalized magnetic nanoparticles as a promising approach for the treatment of liver fibrosis

Marit ten Hove¹, Andreas Smyris¹, Carsten Höltke², Ruchi Bansal¹.

¹University of Twente, Translational Liver Research, Enschede, Netherlands; ²University of Münster, Department of Clinical Radiology, Münster, Germany

Email: r.bansal@utwente.nl

Background and aims: Hepatic injuries, caused by various etiologies such as excessive alcohol intake, fatty liver disease, viral hepatitis, or metabolic disorders, can lead to development of hepatic fibrosis. Hepatic stellate cells (HSCs) activated upon hepatic injury, that proliferate and secrete an excess of extracellular matrix (ECM), remain an attractive target for the treatment of hepatic fibrosis. During liver injury, endothelin-1 (ET-1) levels are upregulated and activate HSCs by interacting with endothelin A (ETA) receptor, which is upregulated on activated HSCs upon hepatic injury. Several studies also indicate that HSCs regulate the sinusoidal blood flow and portal hypertension via ET-1, and hence antagonism of the endothelin pathway using endothelin receptor antagonist (ERA) may offer promising results. However, antagonism of ET pathway using small-molecule ERAs can result in adverse systemic effects since high or frequent dosing will be required to achieve desired therapeutic effects.

In this study, we conjugated ERA to superparamagnetic iron oxide nanoparticles (SPIONs) to improve pharmacokinetics of endothelin receptor antagonist (ERA) and to increase hepatic uptake thereby reducing the high/frequent dosing, reducing the systemic side effects while increasing the therapeutic efficacy. SPIONs are also biocompatible and have magnetic properties, therefore can be detected using magnetic resonance imaging (MRI), making them suitable for theranostic applications.

Method: First, we analyzed the association of ET-1 and ETA with HSCs activation *in vitro*, and with liver fibrosis using human and murine liver tissues. Thereafter, we studied the therapeutic effects of ERA on activated HSCs *in vitro*. We then conjugated ERA on the surface of dextran-PEG coated SPIONs using EDC-NHS conjugation chemistry (see the figure). Next, we examined the therapeutic effects of ERA-SPIONs versus free ERA on activated HSCs *in vitro* and in carbon tetrachloride (CCl₄)-induced liver fibrosis mouse model *in vivo*.



Results: We confirmed the overexpression of ET-1 and ETA in activated HSCs, and human and murine liver fibrosis. ERA dose-dependently inhibited TGF β -induced HSCs activation, collagen-I expression and contractility *in vitro*. ERA-SPIONs were synthesized and attenuated TGF β -induced HSCs activation, ECM production, contractility via antagonizing the endothelin pathway. In CCl $_4$ -induced liver fibrosis mouse model, ERA-SPIONs treatment, compared to ERA treatment, significantly reduced liver weight, ALT levels and inhibited collagen-I deposition indicating attenuation of liver fibrosis.

Conclusion: In this study, we demonstrate that the delivery of ERA using SPIONs is a promising therapeutic approach for the treatment of liver fibrosis that increases the therapeutic efficacy of ERA *in vitro* and *in vivo*.

FRI197

3D human NASH model as a screening-based discovery approach for selecting and prioritizing drug candidates

Radina Kostadinova¹, Simon Ströbel¹, Jana Rupp¹, Katia Fiaschetti¹, Agnieszka Pajak¹, Katarzyna Sanchez¹, Mathieu Petitjean², Li Chen², Manuela Bieri¹, Armin Wolf¹, Sue Grepper¹, Francisco Verdeguer¹.

¹InSphero, Schlieren, Switzerland; ²PharmaNest, Princeton, United States

Email: radina.kostadinova@insphero.com

Background and aims: Non-alcoholic fatty liver disease (NAFLD) is a chronic liver disease, which includes hepatic steatosis that often progresses into steatohepatitis (NASH), characterized additionally by inflammation and fibrosis. We have modeled NASH using 3D human liver microtissues as a high-throughput tool for drug discovery. We present here a novel 3D human NASH model, which incorporates primary hepatocytes, Kupffer cells, liver endothelial cells, and hepatic stellate cells for high-throughput-compatible drug efficacy testing.

Method: We generated liver microtissues by culturing human primary hepatocytes, Kupffer cells, liver endothelial cells, and hepatic stellate cells in InSphero plates. Upon exposure to defined lipotoxic and inflammatory stimuli, including free fatty acids and LPS in media containing high levels of sugar and insulin, this 3D NASH model displayed pathophysiological hallmarks within 10 days of treatment. The accumulation of intracellular triglycerides (bioluminescent assay), secretion of pro-inflammatory cytokines/chemokines (Luminex), and pro-collagens type I and III (HTRF/ELISA) were measured. Quantification of fibrosis based on Sirius Red-stained tissue slices was performed using the PharmaNest imaging platform.

Results: We observed increases in intracellular triglyceride content and the secretion of proinflammatory (e. g. IL-6, IL-1b, TNF-a) and profibrotic (e.g. IL-10, GRO-a, IP-10, MCP-1) cytokines/chemokines in the NASH-treated tissues as compared to the untreated controls. Further, we detected increased fibril collagen deposition, and increased secretion of procollagen type I/III peptides under NASH conditions. Whole transcriptome analysis of NASH-treated tissues versus control revealed activation of pathways and differential regulation of genes associated with lipid metabolism, inflammation, and fibrosis induction. Treatment with the anti-TGF- β antibody and ALK5i (TGF- β RI inhibitor) concentration dependently decreased secretion of pro-collagen type I/III. Decreased deposition of fibril collagens based on quantification of fibrosis of Sirius Red-stained tissues was observed in the presence of anti-TGF- β antibody and ALK5i. The efficacy results of drug clinical candidates Selonsertib and Firsocostat were in line with clinical observations.

Conclusion: In summary, this high-throughput and compatible 3D human NASH model represents a promising approach for NASH drug candidate efficacy selection early within the drug discovery process.

FRI198

Investigating the function of Endothelial-To-Mesenchymal transition during liver fibrogenesis using a Liver-On-A-Chip platform

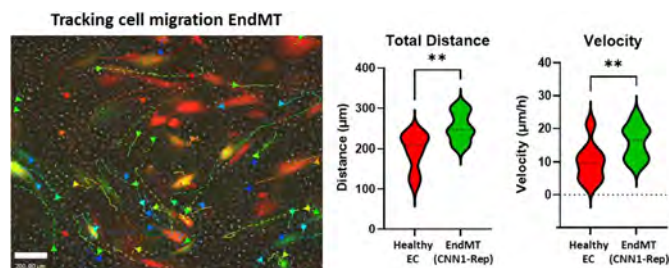
James Whiteford^{1,2}, Samantha Arokiasamy², Clare Thompson¹, William Alazawi¹, Neil Dufton². ¹Queen Mary University of London, United Kingdom; ²Queen Mary University of London, Centre of Microvascular Research, London, United Kingdom

Email: n.dufton@qmul.ac.uk

Background and aims: The plasticity of blood vessels, and particularly the cells that line them, endothelial cells (EC), are fundamental for our body's rapid response to tissue injury. During chronic disease, such as Non-Alcoholic Steatohepatitis (NASH), the specialised liver sinusoidal EC (LSEC) are replaced by the emergence of new disease-associated EC populations. Our research has identified Endothelial-to-mesenchymal transition (EndMT), whereby LSEC loss their liver-specific identity and acquire mesenchymal cell traits, as a key aspect of liver fibrogenesis. The transcriptomic signature of EndMT is now well established but the functional contribution of EndMT to the pathology of liver disease remains largely uninvestigated due to the challenges of performing high-resolution single cell imaging in viable liver tissue. This project aims to understand the cellular characteristics of EndMT by combining novel EndMT reporters with Liver-On-A-Chip (LOAC) platforms to model vascular changes in response to a NASH microenvironment.

Method: Identification, creation, and application of EndMT-specific fluorescent reporter constructs (EndMT-Reps). Transduction of EC using lentiviral packaged CNN1-eGFP construct as an inducible EndMT-Rep (CNN1-Rep) to 2D, 3D and 4D imaging techniques for fixed and live cell imaging. Combined application of live and fixed imaging technologies to measure EndMT using CNN1-Rep on LOAC platform under physiological conditions. Demonstration of the high-resolution single-cell EndMT tracking by live cell time-lapse microscopy and with post-acquisition processing (Volocity software) to perform a comparative study of CNN1-Rep and healthy LSEC within pro-fibrotic (TNF α + TGF β 2) and NASH-like (oleic and palmitic acid) LOAC microenvironment.

Results: We found CNN1-Rep was the most robust EndMT-reporter and was significantly induced in EC treatment with TNF α and TGF β 2 (1 ng/ml and 10 ng/ml respectively) for 48 h. Co-localisation of CNN1-Rep with mesenchymal marker SMA confirmed specificity of the reporter for cell undergoing EndMT. By applying CNN1-Rep within LOAC we were able to track EndMT cells for the first time for up to 24 hours. We show that EndMT cells are significantly more motile in pro-fibrotic and NASH-like than healthy EC within the same LOAC.



Conclusion: The combination of EndMT reporter, CNN1-Rep, with LOAC technology can provide us with unrivalled opportunities to understand the dynamic EndMT behaviour in homeostatic and disease liver microenvironments. Our data support the hypothesis that EndMT cells are migratory and have the potential to be an invasive cell type contributing to fibrotic cellular niche and driving fibrogenesis in the liver.

FRI199

Discovery of AMS-III-1086, a novel LPA1 antagonist for the treatment of liver fibrosis and liver cirrhosis

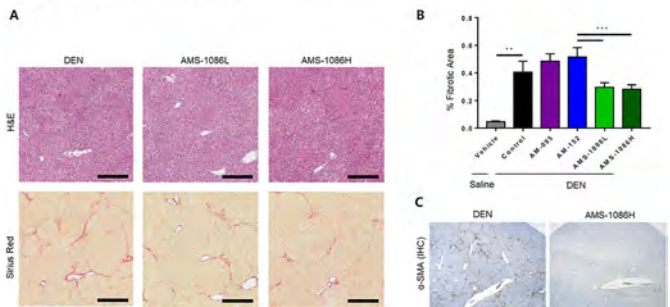
Nakcheol Jeong¹, Peppi Prasit¹, Jung-Hee Kim¹, Misun Lee¹, Bo-Yeong Pak², Sojin Ahn¹, Gil Won Lee¹, Seohyun Min¹, Sanghyeok Lee¹, Yeup Yoon^{3,4,5}, Wonseok Kang^{3,6}, Hyeree Kim^{3,7}. ¹AM Sciences, Seoul, Korea, Rep. of South; ²AM Sciences, Seoul, Korea, Rep. of South; ³Samsung Advanced Institute for Health Sciences and Technology, Sungkyunkwan University, Department of Health Sciences and Technology, Korea, Rep. of South; ⁴Institute for Future Medicine, Samsung Medical Center, Korea, Rep. of South; ⁵Sungkyunkwan University, Department of Biopharmaceutical Convergence, Korea, Rep. of South; ⁶Samsung Medical Center, Sungkyunkwan University School of Medicine, Division of Gastroenterology, Department of Medicine, Korea, Rep. of South; ⁷Institute for Future Medicine, Samsung Medical Center, Korea, Rep. of South
Email: njeong@amsciences.co.kr

Background and aims: Activation of the lysophosphatidic acid 1 (LPA1) receptor has been implicated in a various tissue fibrosis. LPA1 receptor antagonists have shown efficacy in a wide range of animal fibrosis models. Recently a human proof of concept in idiopathic pulmonary fibrosis (IPF) was obtained with the first generation of LPA1 antagonist in a 6-month Phase 2 clinical trial. But the compound was withdrawn from clinical development because of hepatobiliary toxicity, which was unrelated to LPAR1R antagonism but to the inhibition of bile salt export pumps (BSEP). AMS-III-1086 is a novel LPA1 antagonist designed to have a reduced risk of hepatobiliary liability by minimizing bile acids transport inhibition while its efficacy both in vitro and in vivo was improved thus providing a larger therapeutic index.

Method: The potency and selectivity of AMS-III-1086 for LPA1 receptors were determined in vitro by calcium flux and cell chemotaxis assays using B103 cells stably expressing LPA receptors and A2058 cells. LX2 cells were used for evaluating anti-fibrotic activities. Pharmacokinetic (PK) properties were assessed in rodent and non-human primates. N-nitrosodiethylamine (DEN)-induced rat fibrosis model was used for in vivo efficacy studies. BSEP inhibition was determined by BIOIVT. In vivo liver toxicity was evaluated in the cynomolgus monkeys. Human hepatotoxicity was ascertained by in vitro model using Hurel micro liver.

Results: AMS-III-1086 inhibited LPA-stimulated intracellular calcium release (IC₅₀ = 5.3 nM) from B103 cells stably expressing human LPA1 and LPA-induced chemotaxis (A2058 cells; IC₅₀ = 5.7 nM). AMS-III-1086 showed selective antagonism on LPA1 over the other LPA receptors. Treatment with LPA in LX2 cells induced the expressions of the LPA1 gene as well as fibrotic genes, but these were significantly reduced by AMS-III-1086. Functionally, AMS-III-1086 inhibited LPA-induced chemotaxis of LX2 cells. PK results showed good systemic exposure and high oral bioavailability in multiple species. BSEP inhibition was markedly improved, IC₅₀ (20 uM) compared to the first-generation clinical candidates (IC₅₀ = 5 uM). In a DEN-induced rat model of fibrosis and hepatocarcinogenesis, the therapeutic treatment of AMS-III-1086 (oral administration at 10 mg/kg once daily) resulted in the attenuation of fibrogenesis as well as the prevention of cirrhosis after 4 weeks of treatment. There were no significant changes in the levels of AST and ALT in the cynomolgus monkeys. Moreover, a cytotoxicity study using Hurel micro liver predicted that AMS-III-1086 had reduced risk of drug-induced liver injury which was corroborated in vivo in cynomolgus monkey.

DEN-induced liver fibrosis rat model



Conclusion: AMS-III-1086 is a newly identified LPA1 antagonist which shows a good therapeutic index with increased efficacy and improved hepatobiliary toxicity and a favorable preclinical profile.

FRI200

Integrated spatial-temporal mathematical liver lobule model for simulation of fibrotic wall formation

Seddik Hammad¹, Jieliang Zhao^{2,3}, Mathieu de Langlard², Yueni Li¹, Jan G. Hengstler³, Dirk Drasdo^{2,3}, Steven Dooley¹. ¹Heidelberg University, Molecular Hepatology Section, University Medical Center Mannheim, Medical Faculty Mannheim, Mannheim, Germany; ²Institute National de Recherche en Informatique et en Automatique, (INRIA), Salac, France; ³Leibniz Research Centre for Working Environment and Human Factors at the Technical University Dortmund, Dortmund, Germany
Email: steven.dooley@medma.uni-heidelberg.de

Background and aims: Upon different liver injuries, distinct patterns of fibrosis arise i.e. extracellular matrix (ECM) septa (fibrotic walls) connecting pericentral areas due to toxic drugs, or periportal compartments in cholestasis. Organ fibrosis is a highly coordinated and complex multi-cellular process that is difficult to capture with experimental models.

Method: We stepwise developed a computational two liver-lobule model that is continuously refined by iteration between modelers and experimentalists. The model permits to assess the role of biomechanics in the formation of the fibrotic scar. It for the first time integrates the orchestration of hepatocytes and non-parenchymal cells (NPC) during fibrosis development, including their interaction with the ECM network mechanics.

Results: Model predictions are quantitatively confirmed with experimental data. Pattern-characterizing model parameters, e.g. the density of hepatic stellate cells (HSC) and macrophages (Mph) were determined through analysis of experimental 2D and 3D images. A model of the ECM network, NPC and their intercellular communication were integrated as new elements into the existing computational model of the basic liver micro-architecture that already included hepatocytes, sinusoids, central and portal veins. The newly advanced model was applied to test possible mechanisms how the fibrotic scar may form during fibrosis in space and time.

Conclusion: Using this strategy, we propose a scenario that distinguishes regeneration after a single acute toxic injury without scarring versus repeated toxic exposure leading to formation of (etiology dependent) characteristic fibrotic scar patterns, as following: (i) The spatial pattern of CYP2E1 (key metabolizing enzyme) expressing hepatocytes determines the location of ECM deposition (collagen). The tissue response is thereby mediated by the spatial-temporal pattern of certain signaling molecules provided the CYP2E1-positive damaged hepatocytes (DAMPs), leading to activation and attraction of HSC and Mph. (ii) Surviving (CYP2E1-negative) hepatocytes surrounding the CYP2E1 positive (and now damaged) region proliferate and compress the deposited collagen network into the scar like shape. The model may in the future permit us to propose targeted manipulations to reduce scar formation and the transition to cirrhosis.

FRI201

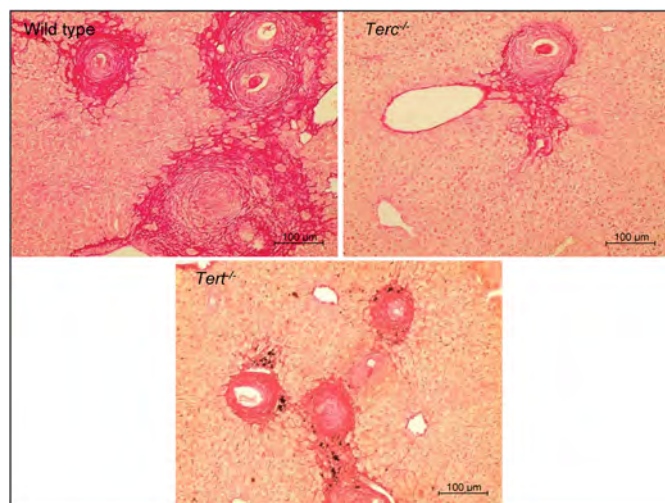
Telomerase-null mice display defective immune activation following the induction of liver fibrosis with *S. mansoni*

William Gomes¹, Vinícius Carvalho¹, Bárbara Santana¹, Leandra Naira Zambelli Ramalho², Rodrigo Calado¹. ¹Ribeirão Preto Medical School, University of São Paulo, Department of Medical Imaging, Hematology, and Clinical Oncology, Ribeirão Preto, Brazil; ²Ribeirão Preto Medical School, University of São Paulo, Department of Pathology and Forensic Medicine, Ribeirão Preto, Brazil
Email: williangomes@usp.br

Background and aims: Telomeres are structures at the end of linear chromosomes constituted by repetitive 5'-TTAGGG-3' sequences associated to protecting proteins. Human patients with germline pathogenic variants in telomere-biology genes present critically short telomeres and usually develop bone marrow failure, but a considerable percentage also manifest pulmonary fibrosis and liver cirrhosis, although the mechanisms for disease development are still unclear. Here, we aim to investigate whether immune-mediated responses are skewed in telomerase- "knockout" (KO) mice challenged with *Schistosoma mansoni*-induced liver fibrosis.

Method: Liver fibrosis was induced by inoculation of approximately 100 cercariae to *Terc*^{-/-} (n = 16), *Tert*^{-/-} (n = 10) and wild-type (WT; n = 8) C57BL/6 mice, which were euthanized after 12 weeks, along with a non-infected group (*Terc*^{-/-} n = 7, *Tert*^{-/-} n = 16 and WT n = 11). Telomere length (TL) in leukocytes and liver fragments was determined by qPCR. Liver tissue samples were stained with haematoxylin-eosin (HE) and Picro-Sirius Red. Immunohistochemical (IHC) staining to F4/80, iNOS and CD206 was performed using diaminobenzidine. Bone-marrow derived macrophages (BMDM) were isolated from a second group of animals (n = 12; 4/each genotype), cultured for 7 days in RPMI and stimulated with lipopolysaccharide (LPS) or interleukin-4 (IL-4) for 24 hours. The polarization to M1 or M2-like phenotypes was determined by nitrite levels and gene expression (*IL-6*, *MMP9*, *TNF-α*, *CD206* and *ARG1*).

Results: TL was significantly shorter in both KO groups (p < 0.01). Infected animals presented hepatosplenomegaly and multiple inflammatory foci in the liver and tissue darkening. Histopathology showed the presence of granulomas surrounding *S. mansoni* eggs trapped within the tissue. *Terc*^{-/-} and *Tert*^{-/-} mice developed less fibrotic areas when compared to the WTs (p < 0.05). IHC staining revealed less macrophage infiltration within the tissue in KO animals. BMDM assay showed that the telomerase KOs impair the classical activation of macrophages, as indicated by nitrite concentrations and the differential expression of *TNF-α*, *IL-6*, and *MMP9*.



Conclusion: Our results suggest that the absence of telomerase causes a limited immune response following *S. mansoni* infection in mice, which mitigates the fibrotic process and cell activation. These findings also reveal that functional telomerase is critical for adequate immune response and, in patients harboring mutations in telomere-biology genes, fibrogenesis must be modulated by other inflammation signaling pathways, which deserves further investigation.

FRI202

Multiplexed digital spatial protein profiling reveals potential non-invasive biomarkers to predict advanced fibrosis

Chang Min Kim¹, Pil Soo Sung², Jung Hoon Cha², Jin Young Park¹, Yun Suk Yu¹, Hee Jung Wang³, Eun Sun Jung², Si Hyun Bae².

¹Cbsbioscience, Research & Business Development, Korea, Rep. of South; ²Catholic University, Korea, Rep. of South; ³Inje University, Korea, Rep. of South

Email: baesh@catholic.ac.kr

Background and aims: Innate and adaptive immune responses are critically associated with the progression of fibrosis in chronic liver diseases. Among the immune cells, intrahepatic mononuclear phagocytes are critical for the initiation and progression of liver fibrosis. In this study, using multiplexed digital spatial profiling, we aimed to develop protein signature which can be used to predict advanced fibrosis in a non-invasive approach.

Method: Snap-frozen liver tissues with various chronic liver diseases at different fibrosis stages were subjected to spatially-defined protein-based multiplexed profiling. CD3, CD68, and α-SMA markers were used to identify specific cell types. Single-cell RNA-Seq analysis was performed using GEO datasets from normal livers and cirrhotic livers. Public miRNA database were used to find miRNA targeting protein signature.

Results: Eighty-eight portal ROIs were selected for the spatial profiling, with 24 ROIs classified into "inflammatory" (high T cell number) and 64 ROIs classified into "non-inflammatory" (low T cell number). In "non-inflammatory" ROIs, which were used for the further analyses, there were liver tissues with various fibrosis grade as F0-2 (n = 31), F3-4 (n = 33). In CD68⁺ areas, protein markers for activation of mononuclear phagocytes were detected significantly stronger in early stage fibrosis (F0, F1, and F2) than advanced fibrosis (F3 and F4). Conversely, CD68 and HLA-DR, which are known to be upregulated in SAMacs rather than KCs, were detected stronger in advanced fibrosis. Using the results from CD68⁺ area, a highly sensitive and specific, unique immune-related protein signature was developed to predict the advanced fibrosis. Combined analysis of single cell RNA-Seq data from GEO datasets (GSE136103) and spatially-defined protein-based multiplexed profiling revealed that most proteins upregulated in F0, F1 and F2 livers in portal CD68⁺ cells were specifically marked in TM (1), TM (3) and SAMacs (1) clusters, whereas proteins upregulated in F3 and F4 livers were marked in SAMacs (1), SAMacs (2), KC (1), and TM (3), highlighting the different phenotypes of portal CD68⁺ cells according to the fibrosis stages. We found the miRNAs targeting the protein signature in a public miRNA database, as the the candidate biomarkers for a non-invasive approach.

Conclusion: By establishing a GeoMx DSP method, we identified an accurate protein signature to predict advanced fibrosis. The spatially-defined protein-based multiplexed profiling demonstrated a critical difference in the phenotypes of mononuclear phagocytes between livers of early stage fibrosis and those of advanced fibrosis. Our results suggest that portal mononuclear phagocytes are critical in inflammation and fibrosis progression, and that miRNAs targeting the protein signature of those cells may be ideal non-invasive biomarker candidates.

FRI203

Sex and diagnosis-specific differences in liver elastography and attenuation

Zhi Tan¹, Marcelle Scagliotta¹, Crystal Connelly¹, Wendy Lam¹, Oyekoya Ayonrinde¹. ¹Fiona Stanley Hospital, Gastroenterology and Hepatology, Murdoch, Australia
Email: oyekoya.ayonrinde@uwa.edu.au

Background and aims: Liver stiffness measurement (LSM) using Transient Elastography (TE), combined with liver attenuation measurement using controlled attenuation parameter (CAP), allows rapid, non-invasive assessment of liver fibrosis and steatosis. We examined the usefulness of TE and CAP for assessment of liver disorders in an adult hepatology outpatient population.

Method: In this cross-sectional study, we investigated the duration and findings of TE and CAP in adult outpatients with known or suspected chronic liver disease, between 2012 and 2021. LSM and CAP were measured using a FibroScan® model 502 Touch. Each procedure was performed by a hepatology nurse with experience of over 500 examinations. Patient age, sex, assessment indication, duration, LSM, CAP, and accuracy of the examination was recorded.

Results: There were 5645 examinations performed on patients with various liver disorders, mean age 55.9 (standard deviation 12.9) years, and 60.7% male. Of these, a medium (M) probe was used for 4212 (74.6%), extra-large (XL) probe for 1422 (25.2%), and small (S) probe without CAP in 11 (0.2%). The most common indications were chronic hepatitis C (CHC, 46%), chronic hepatitis B (CHB, 22%), non-alcoholic fatty liver disease (NAFLD, 15%), and alcohol-related liver disease (ALD, 6%). Median LSM in the cohort was 6.8 (IQR 4.9–11.8) kPa and CAP 252 (IQR 204–307.5) dB/m. Both LSM and CAP were higher in males, compared with females; (LSM 7.1 [5.3–12.2] kPa vs. 6.1 [4.6–10.7] kPa, $p < 0.001$) and (CAP 255 [208–309] dB/m vs. 241 [196–298], $p < 0.001$) respectively. Also, median LSM was highest with ALD (14.5 [7.5–35.3]), compared with CHC (7.6 [5.4–12.5]), NAFLD (7.6 [5.3–13.3]) and CHB (5.4 [4.3–7.1]). Median CAP was highest with NAFLD (315 [261–361] dB/m), compared with ALD (263 [211–329] dB/m), CHC (245 [203–293] dB/m) and CHB (233 [189–283] dB/m). There were sex-differences in CAP, LSM and duration of the examination, across different liver disorders (Table 1).

Diagnosis	Sex		P value
NAFLD	Male n= 302	Female n=379	
LSM (kPa)	7.6 (5.3-14.3)	7.7 (5.4-13.6)	0.75
CAP (dB/m)	323 (264-373)	306 (250-349)	0.01
Duration of exam	231 (94-478)	280 (132-546)	0.01
ALD	Male n= 220	Female n=95	
LSM (kPa)	12.7 (7.2-33.3)	21.8 (8.9-45.7)	0.06
CAP (dB/m)	273 (225-334)	246 (181-298)	0.004
Duration of exam	250 (123-448)	234 (113-490)	0.96
CHC	Male n= 1702	Female n=746	
LSM (kPa)	7.7 (5.7-13.8)	6.8 (4.9-11.5)	<0.001
CAP (dB/m)	250 (208-297)	236 (196-283)	<0.001
Duration of exam	224 (108-463)	250 (124-477)	0.03
CHB	Male n= 701	Female n=524	
LSM (kPa)	5.9 (4.6-7.8)	4.8 (4.0-6.1)	<0.001
CAP (dB/m)	240 (197-294)	219 (182-263)	<0.001
Duration of exam	177 (77-394)	172 (86-403)	0.75

Conclusion: Across various liver disorders, CAP was significantly higher in males overall, suggesting more severe hepatic steatosis. LSM was higher in males with CHC and CHB, compared with females. Severity thresholds for CAP and LSM should consider these differences.

FRI204

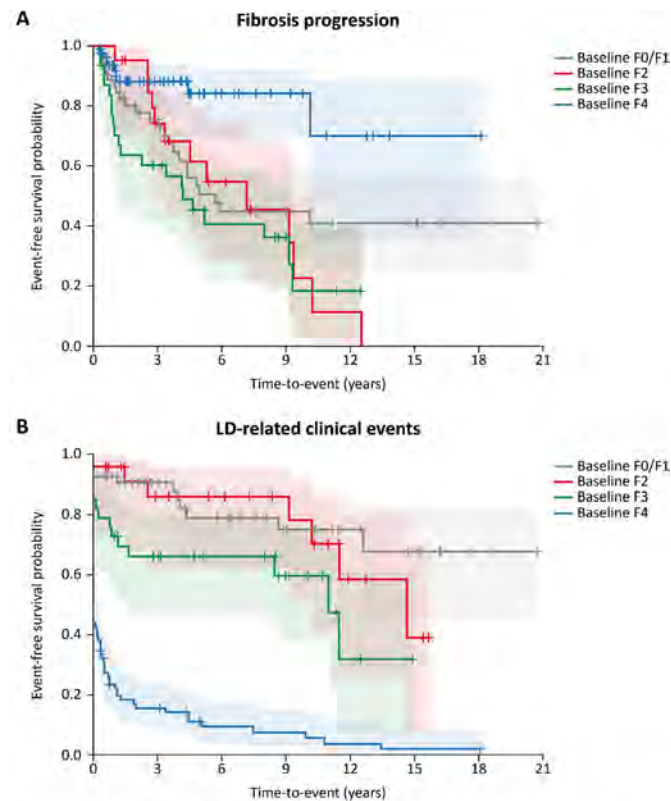
Progression of liver disease among patients with a new diagnosis of protease inhibitor ZZ alpha-1 antitrypsin deficiency

Harmeet Malhi¹, Tiffany Wu¹, May Hagiwara², Gregory Donadio³, Esteban Gnass³, Will Treem², Kaili Ren², Ed G. Marins², Chitra Karki². ¹Mayo Clinic, Rochester, United States; ²Takeda Pharmaceutical Company Limited, Cambridge, United States; ³Inference, Cambridge, United States
Email: malhi.harmeet@mayo.edu

Background and aims: Few studies have characterized disease progression in patients (pts) with alpha-1 antitrypsin deficiency-associated liver disease protease inhibitor ZZ (AATD-LD PiZZ) genotype, who may progress variably with time and may remain asymptomatic despite advanced liver fibrosis. We examined the relationship between progression of disease and LD-related clinical events (LD events) over time in this population.

Method: Data were extracted from the nference database (a proprietary electronic medical record database from the Mayo Clinic Healthcare System) between January 2004 and September 2021. Pts with AATD were defined by the presence of structured diagnosis (dx) codes for AATD, or an alpha-1 antitrypsin serum level of <100 mg/dL. LD was defined based on structured dx codes and surrogate measures. PiZZ genotype was defined by genotype results or unstructured data through natural language processing. Index date was defined as the first date of dx of LD. Fibrosis stage (F0–F4) was assessed at baseline (index date \pm 90 days) and during follow-up using a hierarchical approach: liver biopsy (METAVIR staging), magnetic resonance elastography, Fibroscan, APRI and FIB-4. Pts with <90 days of follow-up were excluded. LD events were defined as development of ascites, spontaneous bacterial peritonitis, variceal bleeding, hepatic encephalopathy, hepatocellular carcinoma and need for liver transplantation. Outcomes were analyzed using descriptive statistics and Kaplan-Meier analysis for time-to-event.

Results: Of 685 000 pts, 6315 had a dx of AATD; of these 501 had the AATD PiZZ genotype, and 316 qualified for the study. Among pts with AATD-LD PiZZ, the mean age was 50.5 years (y), 58.4% were male, 100% were White, and 37.7% were diagnosed with chronic obstructive pulmonary disease, chronic bronchitis, bronchiectasis, or emphysema. At baseline, 197 pts had fibrosis stage: F0/F1, 53; F2, 24; F3, 33; and F4 with compensated cirrhosis (F4cc), 87 (119 pts were not categorized owing to a lack of available data). Of 316 patients with 7.4 y of median follow-up, 17.4% underwent a liver transplant: 2%, 4%, 12% and 44% among pts with baseline stage F0/F1, F2, F3 and F4cc, respectively. Disease progression (\geq 1 fibrosis stage) occurred in 31 pts at \leq 2 y (F0/F1, 22%; F2, 5%; F3, 36%) and in 53 pts at \leq 5 y (F0/F1, 49%; F2, 38%; F3, 55%) (Figure A). At any time during follow-up (median 7.4 years), LD events occurred in 50.1% of pts, with a higher number of events recorded for pts with baseline stage F4cc (98.2%) compared with F3 (68.3%) and F2 (61.0%) (Figure B).



Footnotes: Fibrosis stage (F0–F4) was defined based on liver biopsy (METAVIR staging) and other secondary measures including MELD and CTP scores, MRE, FibroScan, APRI and FIB-4 using this hierarchical order.

F4dc: MELD score increased by 15 or more from the baseline value of < 12 or CTP score increased by > 2 from the baseline; **F4cc:** MRE > 5.0 kPa, APRI > 1.5 or FIB-4 > 3.25; **F3:** 5.0 ≥ MRE > 4.0 kPa, elastography > 12.5 kPa, APRI > 0.63 or FIB-4 > 1.90; **F2:** 4.0 ≥ MRE > 3.5 kPa, elastography > 8.45 kPa, APRI > 0.43 or FIB-4 > 1.43; **F1:** 3.5 ≥ MRE ≥ 3.0 kPa.

AATD-LD PiZZ, alpha-1 antitrypsin deficiency associated liver disease protease inhibitor ZZ; APRI, aspartate aminotransferase to platelet ratio index; cc, compensated cirrhosis; CTP, Child-Turcotte-Pugh; dc, decompensated cirrhosis; FIB-4, Fibrosis-4; KM, Kaplan-Meier; LD, liver disease; MELD, model for end-stage liver disease; METAVIR, meta-analysis of histological data in viral hepatitis; MRE, magnetic resonance elastography; pts, patients.

Figure: KM estimates of fibrosis progression (A) and LD events (B) by baseline fibrosis stage in pts with AATD-LD PiZZ.

Conclusion: Almost 1/3 of F3 pts at baseline progressed to F4 and had LD events in ≤2 y, and >2/3 of F4cc pts had LD events in ≤1 y. These clinically relevant findings need validation in independent cohorts.

FR1205

Perihepatic implantation of matrix-embedded endothelial cells reduce inflammation and collagen deposition in fibrotic mice

Mireia Medrano-Bosch¹, Alazne Moreno-Lanceta^{1,2}, Laura Macias-Muñoz^{2,3}, Elazer Edelman^{4,5}, Wladimiro Jiménez^{1,2,3}, Pedro Melgar-Lesmes^{1,2,4}. ¹Department of Biomedicine, School of Medicine, University of Barcelona, Barcelona, Spain; ²Institut d'Investigacions Biomèdiques August Pi-Sunyer (IDIBAPS), Centro de Investigación Biomédica en Red de Enfermedades Hepáticas y Digestivas (CIBERehd), Barcelona, Spain; ³Biochemistry and Molecular Genetics Service, Hospital Clinic Universitari, Barcelona, Spain; ⁴Institute for Medical Engineering and Science, Massachusetts Institute of Technology, Cambridge, MA, United States; ⁵Cardiovascular Division, Brigham and Women's Hospital, Harvard Medical School, Boston, Massachusetts, United States

Email: pmelgar@ub.edu

Background and aims: Matrix-embedded endothelial cells (MEECs) are endothelial cells grown in a 3D collagen-based scaffold that shields their immunogenicity *in vitro* and *in vivo*. This phenotype conversion minimizes stress and maximizes the secretion of anti-inflammatory and anti-fibrogenic factors. Here, we aimed to test whether the perihepatic implantation of MEECs may interfere with the inflammatory and fibroproliferative processes occurring in fibrotic mice.

Method: Fibrosis was induced in BALB/c mice (n = 12) by i.p. injection of CCl₄ diluted 1:8 v/v in corn oil twice a week for 8 weeks. Acellular matrices or MEECs were surgically implanted between the median and the right lobe in fibrotic mice. After one week, relative fibrosis area was analyzed by Sirius Red staining. Liver function was evaluated in serum samples. The expression of pro-inflammatory genes (nitric oxide synthase 2 (NOS2), ciclooxigenase-2 (COX-2), interleukin 1 beta (IL1-B)), anti-inflammatory genes (arginase 1 (ARG1), mannose receptor C-type 1 (MRC1), resistin (RETN1A)), hepatic stellate cell (HSC) activation factors (oncostatin M (OSM), platelet derived growth factor-BB (PDGFBB), transforming growth factor-beta (TGF-B)) and genes related to the extracellular matrix turnover (collagen-I (COL-I), alpha smooth muscle actin (ALPHA-SMA), tissue inhibitor of metalloproteinases-1 (TIMP1)) was quantified by Real-time PCR.

Results: Implantation of MEECs for seven days promoted a 21% reduction in the hepatic fibrosis area compared with fibrotic livers implanted with acellular matrices. These anti-fibrotic effects translated into a significant improvement of liver function reflected by the reduction of serum transaminases (ALT, 153.3 ± 15.8 vs 100.6 ± 14.5 U/L, p < 0.05; AST, 477 ± 50.4 vs 288 ± 54 U/L, p < 0.05). Perihepatic implantation of MEECs significantly reduced the hepatic expression of pro-inflammatory genes (COX-2, 1.0 ± 0.1 vs 0.6 ± 0.1 fold change (fc), p < 0.05; NOS2, 1.1 ± 0.3 vs 0.5 ± 0.1 fc, p < 0.01; IL1-B, 1.1 ± 0.1 vs 0.5 ± 0.1 fc, p < 0.01) and increased the hepatic expression of anti-inflammatory genes (ARG1, 1.0 ± 0.1 vs 1.6 ± 0.1 fc, p < 0.05; MRC1, 1.0 ± 0.1 vs 1.4 ± 0.1 fc, p < 0.05; RETN1A, 1.1 ± 0.1 vs 14.8 ± 4.8 fc, p < 0.01) on fibrotic mice. Our results also revealed that MEECs promoted a significant decrease in well-known stimulators of HSC (OSM, 1.0 ± 0.2 vs 0.35 ± 0.06 fc, p < 0.05; PDGF-BB, 1.0 ± 0.1 vs 0.57 ± 0.08 fc, p < 0.01, TGF-beta 1.0 ± 0.1 vs 0.69 ± 0.05 fc, p < 0.05). This reduction was associated with a fall in the hepatic expression of genes related to HSC activation (COL-I, 1.0 ± 0.1 vs 0.49 ± 0.06 fc, p < 0.01; ALPHA-SMA, 1.1 ± 0.2 vs 0.63 ± 0.08 fc, p < 0.05, TIMP-1 1.0 ± 0.2 vs 0.56 ± 0.07 fc, p < 0.05).

Conclusion: Perihepatic implants of MEECs display anti-inflammatory and anti-fibrotic activity in liver fibrosis. This study highlights the potential therapeutic utility of MEECs for chronic liver disease.

FR1206

LncRNA XR_592974.2 and circRNA_2599 regulated hypoxic stress response in hepatic stellate cells by targeting the miRNA-145/JMY/P53 pathway

Dan Zhou¹, Jing Gao^{2,3}, Xiao-jun Wang⁴, Yujin Li⁵, Hong Chen⁶, Liting Zhang¹. ¹The First Hospital of Lanzhou University; ²Department of Medicine, Karolinska Institute, Stockholm, Sweden; ³University of Helsinki, Heart and Lung Centre, Helsinki, Finland; ⁴Gansu Provincial Hospital; ⁵Capital Medical University, China; ⁶Xi'an International Medical Center, China

Email: lcheneye@163.com

Background and aims: Non-coding RNAs contribute to the activation of hepatic stellate cells (HSCs) and the progression of liver fibrosis. Hypoxia serves as a pivotal microenvironmental factor that facilitates the activation of HSCs. Our previous study demonstrated differentially expressed mRNAs and miRNAs in hypoxia-induced HSCs. Here, we investigated the interactions among lncRNAs/circRNAs, miRNAs, and mRNAs in HSCs under hypoxic stress.

Method: Hypoxia-induced HSCs model were treated with 400 μmol/L CoCl₂ in HSC-T6 cells. The differentially expressed mRNAs, miRNA, circRNAs, and lncRNAs in hypoxia-induced HSCs were identified using whole-genome sequencing. Next, we constructed the ceRNA network based on the interactions among lncRNAs/circRNAs, miRNAs, and mRNAs in hypoxia-induced HSCs. The functional analyses were performed by the gene ontology analysis and the Kyoto Encyclopedia of Genes and Genomes pathway analysis. Finally, we performed the pathway analysis based on the public database and literature.

Results: A total of 1423 mRNAs, 54 miRNAs, 288 lncRNAs, and 60 circRNAs were differentially expressed in hypoxia-induced HSCs compared to the controls. Combined with our previous identified miRNA-mRNA regulation network in HSCs under hypoxic stress, the results presented that up regulation lncXR_592974.2 and up regulation circRNA_2599 regulated in down regulation miRNAs (miRNA-145-3p and novel 500 mature) -up regulation mRNA (Junction Mediating and Regulatory Protein (JMY, P53 Cofactor)) network, respectively. These ncRNAs/circRNAs-miRNAs- mRNAs were involved in P53 signaling pathway (Figure 1).

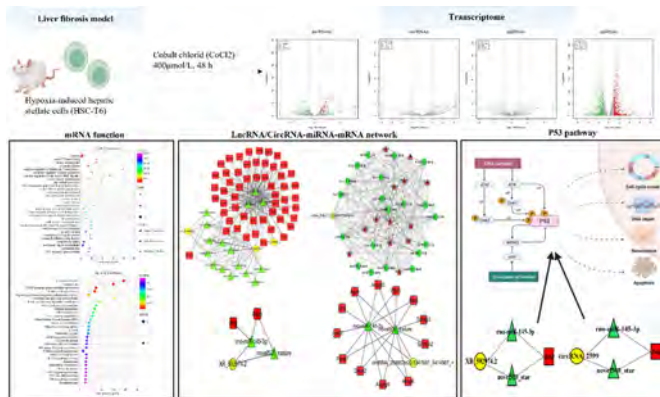


Figure: Illustration of interactions among lncRNAs/circRNAs, miRNAs, and mRNAs in hypoxia-induced hepatic stellate cells in rat.

Conclusion: Our results showed the lncRNAs XR_592974.2/circRNA_2599-miR-145-3p/novel 500 mature -Jmy-p53 regulatory axis that might participate in activated HSCs and might carry potential therapeutic targets for restraining hypoxic stress.

FR1207

Magnetic resonance elastography (MRE) demonstrate the strongest correlation with digital pathology and NASH CRN fibrosis assessments, compared to transient elastography and other assessed non-invasive tests (NITs)

Miljen Martić¹, Dean Tai², Nikolai Naoumov³, Elaine Chng², Clifford Brass⁴, Juergen Loeffler⁵, Jossy George Kochuparampil⁵, Jia Ling Chong², Shenglin Ma⁶, Andreas Sailer⁵, Dominique Brees⁵, Zachary Goodman⁷, Marcos Pedrosa⁵, Quentin Anstee^{8,9}. ¹Novartis Pharma AG, Translational Medicine, Biomarker Development, Basel, Switzerland; ²HistoIndex Pte. Ltd., Singapore, Singapore; ³London, United Kingdom; ⁴Novartis Pharmaceuticals Corporation, East Hanover, NJ, United States; ⁵Novartis Pharma AG, Basel, Switzerland; ⁶Novartis Institutes for BioMedical Research, Translational Medicine, Biomarker Development, Cambridge, MA, United States; ⁷Inova Health System, Director of Hepatic Pathology Consultation and Research, Falls Church, VA, United States; ⁸Translational and Clinical Research Institute, Faculty of Medical Sciences, Newcastle University, Newcastle upon Tyne, United Kingdom; ⁹Newcastle NIHR Biomedical Research Centre, Newcastle Upon Tyne Hospitals NHS Foundation Trust, Newcastle upon Tyne, United Kingdom

Email: miljen.martice@novartis.com

Background and aims: Correlation of a non-invasive test (NIT) with histology-based readouts is one of the key aspects of NIT inclusion in clinical trials and their adoption and impact on patient care. This sub-study aimed to explore correlation of different NITs with liver histology endpoints assessed by standard histology (NASH-CRN) and quantitative digital pathology (HistoIndex, HI-QDP).

Method: As part of the TANDEM NASH Phase 2 trial [NCT 03517540], the cross-sectional pre-treatment data has been collected from 269 patients with NAFLD (138 screen-failed and 131 randomized subjects). Key trial inclusion criteria were based on liver biopsy (NASH with F2 or F3 fibrosis). Only subjects who signed additional

research ICF have been included in this analysis. Liver biopsies were evaluated by a central reader using NASH-CRN scoring system and analyzed by HI-QDP algorithm. ALT, AST, ELF, GGT, FIB-4 and Pro-C3 were analyzed by central laboratory, Fibroscan liver stiffness measurement (LSM) was assessed by a clinical site, while MRE LSM was assessed by a central imaging reader.

Results: Statistical analysis on the entire cohort (n = 269) revealed that MRE had the strongest correlation with both fibrosis assessments (NASH CRN and HI-QDP qFibrosis), followed by a MRI-aspartate aminotransferase (MAST) score (Figure). As MRI and MRE imaging were performed in a random subset of subjects, the MRE based dataset is smaller than for Fibroscan and soluble biomarkers. Interestingly, when correlating with qFibrosis, third and fourth ranked biomarkers were Pro-C3 and ELF, compared to FIB-4 and ELF when correlating with CRN fibrosis assessment. In both cases, Fibroscan LSM and FibroScan-AST (FAST) score ranked fifth and sixth.

Correlation between histology readouts and NITs/R value (p value)		
NITs	qFibrosis continuous	NASH-CRN fibrosis
ALT (qFibrosis n = 266) (NASH-CRN n = 254)	0.07 (p = 0.23)	0.02 (p = 0.75)
AST (qFibrosis n = 266) (NASH-CRN n = 254)	0.26 (p < 0.001)	0.25 (p < 0.001)
ELF (qFibrosis n = 266) (NASH-CRN n = 255)	0.33 (p < 0.001)	0.38 (p < 0.001)
GGT (qFibrosis n = 267) (NASH-CRN n = 255)	0.22 (p < 0.001)	0.18 (p = 0.004)
PRO-C3 (qFibrosis n = 102) (NASH-CRN n = 102)	0.35 (p < 0.001)	0.08 (p = 0.44)
FIB-4 (qFibrosis n = 262) (NASH-CRN n = 251)	0.26 (p < 0.001)	0.40 (p < 0.001)
Fibroscan LSM (kPa) (qFibrosis n = 183) (NASH-CRN n = 181)	0.29 (p < 0.001)	0.21 (p = 0.004)
FAST (qFibrosis n = 151) (NASH-CRN n = 149)	0.26 (p = 0.0011)	0.28 (p < 0.001)
MRE LSM (kPa) (qFibrosis n = 32) (NASH-CRN n = 31)	0.49 (p = 0.005)	0.49 (p = 0.005)
MAST (qFibrosis n = 32) (NASH-CRN n = 31)	0.38 (p = 0.03)	0.43 (p = 0.01)

Conclusion: MRE LSM and MAST score had the strongest correlation with liver fibrosis staging (both NASH CRN and by HI-QDP qFibrosis). Additional evaluation of other individual biomarkers, as well as combination of imaging and soluble biomarkers is still ongoing and will also include separate correlations for randomized and screen failed subjects.

FR1208

Autoantibodies to apolipoprotein A-1 in chronic hepatitis C infection: a role in hepatic fibrosis and cirrhosis?

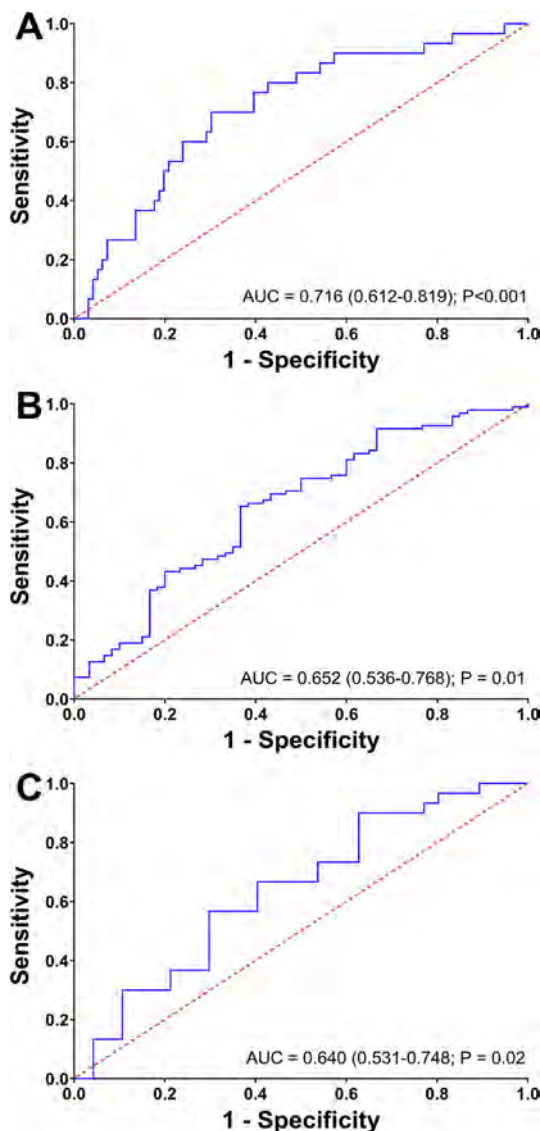
Simon Bridge¹, Sabrina Pagano², David Sheridan³, John Lodge¹, Matthew Cramp⁴, Simon Taylor-Robinson⁵, Dermot Neely⁶, Nicolas Vuilleumier², Margaret Bassendine⁷. ¹Faculty of Health and Life Sciences, Newcastle upon Tyne, United Kingdom; ²Geneva University Hospitals, Geneva, Switzerland; ³Institute of Translational & Stratified Medicine, Hepatology, Plymouth, United Kingdom; ⁴Hepatology, Plymouth, United Kingdom; ⁵Department of Surgery and Cancer, London, United Kingdom; ⁶Clinical Biochemistry, Newcastle upon Tyne, United Kingdom; ⁷Liver Medicine & Hepatology Research Group, United Kingdom

Email: simon.bridge@northumbria.ac.uk

Background and aims: Approximately 40–70% of chronic HCV (CHC) patients develop an autoimmune extrahepatic disorder. IgG autoantibodies against apolipoprotein A-1 (AAA1) are a robust biomarker

POSTER PRESENTATIONS

of cardiovascular disease and predict all-cause mortality [1]. We previously reported the presence of AAA1 in 14/27 CHC patients [2]. Here, we evaluated AAA1 in a larger cohort of CHC patients to explore associations between AAA1, lipoproteins and severity of liver disease. **Method:** Serum samples were obtained from 126 treatment naïve CHC subjects (61 genotype (GT) 1 and 65 GT3) and assayed for AAA1 and lipoprotein profiles. Subjects were classified as cirrhotic by liver imaging and/or histological assessment. Area under receiver operating characteristic curves (AUROC) were calculated for AAA1 and HDL-related parameters and used for predicting patients with cirrhosis. Fibronectin (FN) and messenger RNA (mRNA) were measured in human hepatic stellate cells (LX2) in the presence or absence of AAA1. **Results:** Fifty-nine (47%) CHC patients were AAA1 positive. Twenty-one (70%) of 30 cirrhotic patients were AAA1 positive and the median magnitude of AAA1 was also significantly higher than non-cirrhotic patients (48% vs. 31%; $p < 0.001$). The AUROC for AAA1, ApoA-1 and HDL-C for predicting cirrhosis was 0.72 ($p < 0.001$), 0.65 ($p = 0.01$) and 0.64 ($p = 0.02$) (Figure A, B & C respectively). After 48 hours in the presence of AAA1, LX2 cells showed significantly increased levels of FN compared to LX2 cells alone ($p = 0.02$) and the LX2/IgG control ($p = 0.0016$). This was further confirmed by quantitating FN mRNA, LX2 cells and AAA1 showed an 80% increase in FN mRNA compared to LX2 cells alone ($p = 0.035$) and the LX2/IgG control ($p = 0.028$).



Conclusion: AAA1 are found in a subgroup of CHC patients and are found with higher incidence and magnitude in patients with advanced liver fibrosis. AAA1 are robust biomarkers for predicting cirrhosis. Human hepatic stellate cells in the presence of AAA1 showed a fibrotic phenotype. Further studies are warranted to define the role of AAA1 in the development of fibrosis and cirrhosis.

References

- [1] Antiochos P, Marques-Vidal P, Virzi J, Pagano S, Satta N, Hartley O, et al. Anti-Apolipoprotein A-1 IgG Predict All-Cause Mortality and Are Associated with Fc Receptor-Like 3 Polymorphisms. *Front Immunol* 2017;8:437.
- [2] Bridge SH, Pagano S, Jones M, Foster GR, Neely D, Vuilleumier N, et al. Autoantibody to apolipoprotein A-1 in hepatitis C virus infection: a role in atherosclerosis? *Hepato Int* 2018;12:17–25.

FRI209

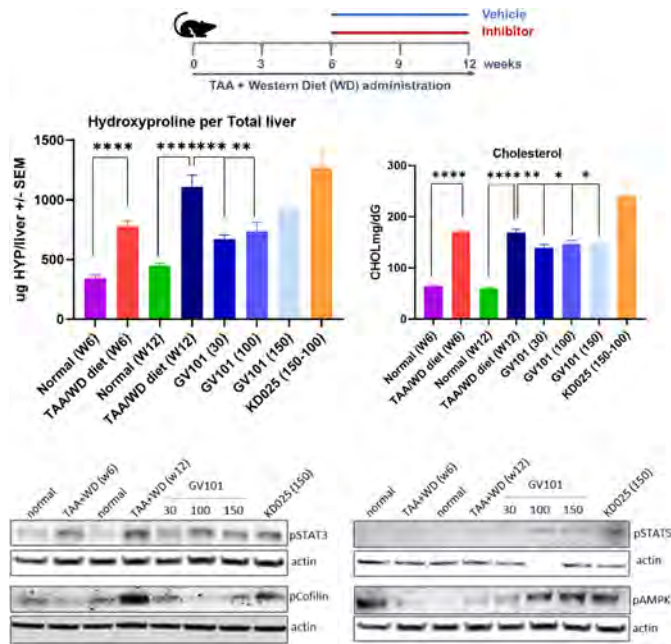
Selectivity matters: novel ROCK2 inhibitor down-regulates established liver fibrosis via concurrent targeting of inflammatory, fibrotic and metabolic pathways

Alexandra Zanin-Zhorov¹, Wei Chen¹, Melanie Nyuydzefe¹, Julien Moretti¹, Iris Zhorov¹, Rashmi Munshi², Malavika Ghosh², Kelli MacDonald³, Bruce Blazar⁴, Sam Waksal¹. ¹Graviton Biosciences, B.V., Translational Medicine, Amsterdam, Netherlands; ²Aragen Biosciences, Morgan Hill, United States; ³QIMR Berghofer Medical Research Institute, Brisbane, Australia; ⁴University of MN, Masonic Cancer Center, Division of Blood & Marrow Transplant & Cellular Therapies, Minneapolis, United States
Email: alexandra.zanin-zhorov@graviton.bio

Background and aims: The pathogenesis of hepatic fibrosis is caused and driven by dysregulated metabolism precipitated by chronic inflammation. Rho-associated coiled-coil-containing protein kinases (ROCKs) have been implicated in these processes, however the ability of selective ROCK2 inhibition to target simultaneously pro-fibrotic, pro-inflammatory and metabolic pathways was not demonstrated yet.

Method: We used the thioacetamide (TAA)-induced liver fibrosis model in combination with or without high fat diet to examine the efficacy of administration of the highly selective ROCK2 inhibitor GV101 to treat liver fibrosis, and its impact on inflammatory, fibrotic, and metabolic pathways in tissues.

Results: We found that therapeutic administration of GV101, a novel ROCK2 inhibitor with more than 1000-fold selectivity over ROCK1, attenuated established liver fibrosis induced by TAA alone or in combination with high fat diet in mice. GV101 treatment significantly reduced hydroxyproline levels in liver and serum AST/ALT ratio, which was associated with downregulation of pCofilin (pro-fibrotic), pSTAT3 (pro-inflammatory), while the levels of pSTAT5 (anti-inflammatory) and pAMPK (anti-metabolic) were increased in tissues of treated mice. In vitro experiments have shown that pharmacological selective ROCK2 inhibition, but not pan-ROCK inhibition down-regulates STAT3-dependent pro-inflammatory cytokine secretion in T cells as well as adipogenesis of both 3T3L1 mouse cells and primary human preadipocytes via AMPK-dependent mechanism.



Conclusion: All together, these data further characterize the ROCK2-specific molecular mechanism of action and highlight the therapeutic potential of highly selective ROCK2 inhibitors in liver fibrosis

FRI210

Aldafermin rebalances collagen turnover in patients with NASH and liver fibrosis in the ALPINE 2/3 study

Manal F. Abdelmalek¹, Lei Ling², Guy Neff³, Naim Alkhouri⁴, Charles Chen², Alex DePaoli², Hsiao Lieu², Diana Leeming⁵, Morten Karsdal⁵, Stephen Harrison⁶. ¹Duke University, Durham, United States; ²NGM Biopharmaceuticals, South San Francisco, United States; ³Covenant Research, Sarasota, United States; ⁴Arizona Liver Health, Tucson, United States; ⁵Nordic Bioscience, Herlev, Denmark; ⁶Pinnacle Clinical Research, San Antonio, United States
Email: lling94080@yahoo.com

Background and aims: The most common method of evaluating liver fibrosis in clinical studies is by microscopic analysis of biopsies stained with Masson's trichrome or sirius red—an approach that may be too simplistic and not able to specifically differentiate among the many different collagen molecules. Recent research has demonstrated that not all collagens are created equal, and that an array of collagen-derived molecules has emerged with novel functions. Whereas the interstitial matrix collagens are increased with more severe disease, the basement membrane collagens are important for regeneration of hepatic tissue (Villesen et al., AASLD 2021). Aldafermin, an engineered analog of the human hormone FGF19, inhibits bile acid synthesis and has improved liver histology in previous phase 2 trials. Here we perform a non-invasive, more granular analysis of both the steady-state and dynamics of collagen turnover in the multicenter, randomized, double-blind, placebo-controlled, phase 2b ALPINE 2/3 study in patients with NASH.

Method: 171 patients were randomized 1:1:1:1 to receive placebo (PBO, n = 43), aldafermin 0.3 mg (n = 43), 1 mg (n = 42), or 3 mg (n = 43) SC QD for 24 weeks at 30 US study sites. Key inclusion criteria included biopsy-proven NASH with NAS_{FL} ≥ 4, stage 2 or 3 fibrosis and absolute liver fat content ≥ 8%. Serum concentrations of Pro-C3, Pro-C4, Pro-C6 and Pro-C8 were measured by ELISA methods.

Results: Demographic and baseline characteristics were similar across the trial groups. At week 24, the LS mean differences in the percent change from baseline in Pro-C3, a marker of interstitial matrix collagen, were -11.7% (SD 7.0%) (p = 0.049 vs PBO) in the

0.3 mg group, -13.8% (SD 7.3%) (p = 0.030 vs PBO) in the 1 mg group, and -30.2% (SD 7.1%) (p < 0.001 vs PBO) in the 3 mg group. The LS mean differences in the percent change from baseline in Pro-C8, a marker of basement membrane collagen, were +21.4% (SD 14.3%) (p = 0.07) in the 0.3 mg group, +49.2% (SD 14.7%) (p < 0.001) in the 1 mg group, and +37.6% (SD 14.4%) (p = 0.005) in the 3 mg group. In contrast, aldafermin did not reach statistical significance on the dose-dependent improvement in fibrosis on liver biopsy (19%, 31%, 15% and 30% of the patients in the placebo, 0.3 mg, 1 mg and 3 mg groups, respectively, achieved fibrosis improvement of ≥ 1-stage without NASH worsening).

Table 1. Percent change from baseline to week 24 in collagen turnover biomarkers

	Placebo (n=43)	Aldafermin 0.3 mg (n=43)	Aldafermin 1 mg (n=42)	Aldafermin 3 mg (n=43)
Pro-C3 (ng/ml)	4.4 (5.0)	-7.3 (5.0)	-9.4 (5.3)	-25.7 (5.2)
Difference vs placebo		-11.7 (7.0)	-13.8 (7.3)	-30.2 (7.1)
P-value vs placebo		0.009	0.007	<0.001
Pro-C4 (ng/ml)	-5.2 (2.5)	-3.2 (2.5)	2.5 (2.7)	-0.5 (2.6)
Difference vs placebo		0 (3.5)	5.6 (3.6)	2.7 (3.6)
P-value vs placebo		0.50	0.06	0.23
Pro-C6 (ng/ml)	10.7 (7.8)	-6.4 (7.9)	5.1 (8.3)	8.4 (8.2)
Difference vs placebo		-17.2 (11.0)	-5.7 (11.3)	-2.3 (11.2)
P-value vs placebo		0.06	0.31	0.62
Pro-C8 (ng/ml)	-10.7 (10.1)	10.7 (10.2)	38.5 (10.8)	26.9 (10.6)
Difference vs placebo		21.4 (14.3)	49.2 (14.7)	37.6 (14.4)
P-value vs placebo		0.07	<0.001	0.005

Values are LS means (SE). Continuous endpoints were analyzed using an analysis of covariance (ANCOVA) model with effects for treatment, baseline fibrosis stage and baseline value as covariates. Analyses were conducted using SAS software, version 9.4.

Conclusion: Our results revealed novel insights into aldafermin biology in reducing the fibrogenesis of type 3 collagen in the interstitial matrix, while strengthening type 8 collagen in the basement membrane. Given the invasive and heterogeneous nature of liver biopsy, these novel, non-invasive fibrosis markers may have the potential to obviate the limitations of liver biopsy by providing important information regarding the state of the liver and extracellular matrix turnover.

Non-invasive assessment of liver disease except NAFLD

FRI214

Use of the enhanced liver fibrosis test to risk stratify patients in the intelligent liver function test pathway: ruling out cirrhosis and advanced fibrosis

Madeline Pearson¹, Iain Macpherson², Jennifer Nobes³, Elizabeth Furrie³, Michael Miller², Ellie Dow³, John Dillon². ¹University of Dundee, School of Medicine, Dundee, United Kingdom; ²University of Dundee, Gut Group, Dundee, United Kingdom; ³Ninewells Hospital, Department of Blood Sciences, Dundee, United Kingdom
Email: mcpearson@dundee.ac.uk

Background and aims: The intelligent liver function testing (iLFT) pathway is an innovative automated system designed to increase detection of liver disease in primary care. Its successful roll-out within NHS Tayside significantly increased liver disease diagnosis, highlighting the need for a second 'rule-out' test to further risk stratify patients and reduce unnecessary burden on secondary care. The enhanced liver fibrosis (ELF) test comprises a panel of three direct serum biomarkers of fibrosis. In July 2020 the ELF score was incorporated into the iLFT pathway in NHS Tayside; it is automatically calculated for all samples with indeterminate or elevated fibrosis scores after an abnormal LFT, and influences recommendations for

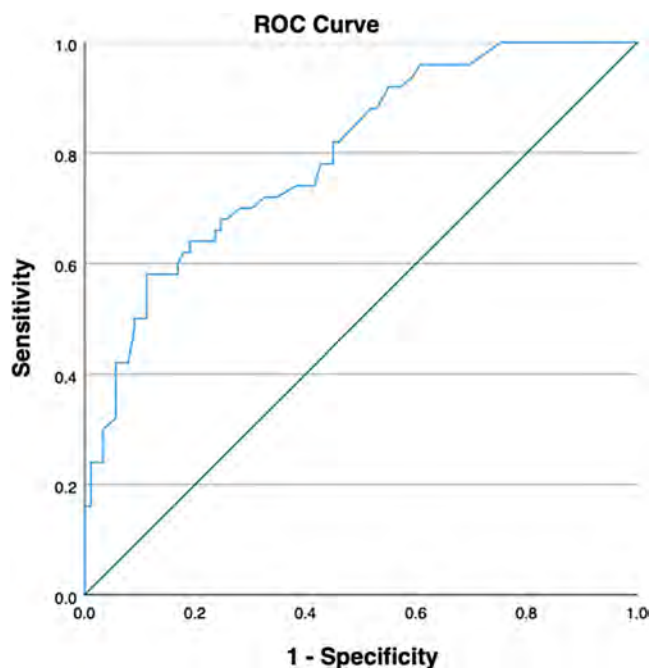
POSTER PRESENTATIONS

patient management. The aim was to investigate if the ELF score could be used safely and effectively as a rule out test for cirrhosis and advanced fibrosis within the iLFT pathway.

Method: Outcomes for all patients who received an ELF test via the iLFT pathway between July 2020 and April 2021 were collected and analysed to compare ELF scores with the incidence of cirrhosis and advanced fibrosis diagnoses. A further analysis of all patients who had undergone ELF testing since its introduction in NHS Tayside, regardless of involvement with iLFT, was undertaken to compare ELF score with Transient Elastography (TE) reading.

Results: 634 patients were included in the study; 62.3% of the patients were male, with a mean age of 62.5 years and mean BMI of 31. 419 (66%) had a 'high' ELF score (≥ 9.8) and 219 had a 'low' ELF score. Median ELF score was 10.2 (IQR 9.5–11.1). 139 patients received TE, with a median ELF score of 10.7 (IQR 9.9–11.4)

57 patients received a clinical diagnosis of cirrhosis; 56 (98%) had a high ELF score ($p < 0.0001$). The negative predictive value (NPV) of ELF as a marker for cirrhosis is 99.5%, with a sensitivity of 98.2%. ELF score was an excellent predictor of advanced fibrosis (F3/4) on TE (AUROC 0.80, $p < 0.001$): the current cut-off value (9.8) had a sensitivity of 100% and specificity of 25%.



Conclusion: The high sensitivity and NPV of the ELF test for cirrhosis and advanced fibrosis confirms the safe implementation of ELF as an additional fibrosis 'rule-out' within the iLFT pathway. It allows for a streamlined, triaged referral system, ensuring that patients requiring secondary care involvement are picked up, whilst reducing unnecessary referrals amongst lower risk patients who can be safely managed in primary care.

FRI215

Comparison of CT, blood test, elastometry and their combination for non-invasive staging of liver fibrosis

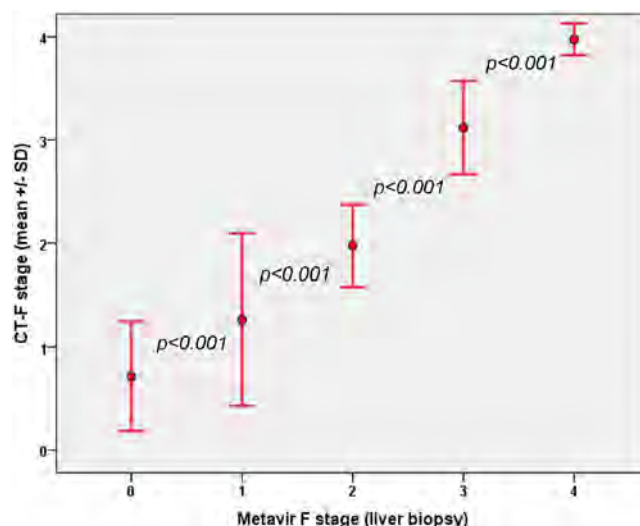
Paul Cales¹, Anita Paisant¹, Clémence M. Canivet¹, Jerome Lebigot¹, Lannes Adrien¹, Carole Vitellius¹, Julien Chaigneau¹, Frédéric Oberti¹, Isabelle Fouchard¹, Sophie Michalak¹, Jerome Boursier¹, Christophe Aubé¹. ¹Angers University, HIFIH Laboratory, Angers, France Email: paul.cales@univ-angers.fr

Background and aims: The EASL 2021 guidelines on non-invasive diagnosis state that imaging does not discriminate initial stages of

liver fibrosis. We sought to evaluate whether liver computed tomography (CT) imaging could discriminate Metavir fibrosis (F) stages.

Method: 111 patients with Metavir F stage by liver biopsy, CT, liver stiffness measurement (LSM), blood test (FM) or their combination (EFM) were retrospectively included. CT was prospectively evaluated by a) an expert radiologist according to the 7 usual signs of cirrhosis + CT-F stage, equivalent to Metavir; b) semi-automated quantitative morphometry (43 signs); c) 70 hepato-gastroenterologists according to CT F-stage in 10 patients (2 per Metavir F stage) for whom 4 independent diagnostic methods agreed for fibrosis stages (method without gold standard). We developed multivariate scores predictive of Metavir F stages using CT signs assessed by the expert radiologist (expert score) or by morphometry (morpho score) and by all non-invasive methods (mixed score including EFM, expert and morpho scores).

Results: 1) Characteristics in all 111 patients were, age: 54.2 ± 12.8 years, male: 60.4%, BMI: 31.2 ± 6.6 kg/m², NAFLD: 75.7%, Metavir: F0: 15.3%, F1: 34.2%, F2: 18.0%, F3: 14.4%, F4: 18.0%. Spearman correlation coefficients (Rs) with Metavir F stages were, expert score: 0.605, FM: 0.648, CT-F stage: 0.661, morpho score: 0.682, LSM: 0.737, EFM: 0.750, mixed score: 0.783. Obuchowski indexes for Metavir F stage discrimination were, expert score: 0.830, FM or CT-F stage: 0.838, morpho score: 0.855, LSM: 0.881, EFM: 0.889, mixed score: 0.909. Concerning discrimination between adjacent Metavir F stages, a significant difference was observed for the following tests, F0 vs F1: FM, LSM, EFM, expert score; F1 vs F2: all tests; F2 vs F3: LSM, EFM; F3 vs F4: CT-F stage, FM, EFM, expert and mixed scores. 2) In the 10 patients evaluated with multiple F references: the Metavir F stages were well-discriminated by CT-F stage with Rs: 0.914, Obuchowski index: 0.950 and significant differences ($p < 0.001$) between all adjacent Metavir F stages (Figure).



Conclusion: A CT expert score discriminates Metavir F0 to F2 stages. The best single test to discriminate all Metavir F stages from each other is a combination of a blood test and elastometry. However, combined methods (blood test, LSM and CT) offer better discrimination. Using multiple concordant F references, a simple CT semiology discriminates between all Metavir F stages very well.

FRI216

Reliability criteria of non-invasive tests for liver fibrosis

Paul Cales¹, Clémence M. Canivet², Lannes Adrien³, Hunault Gilles², Frédéric Oberti³, Valérie Moal³, Isabelle Fouchard³, Sophie Michalak², Jérôme Boursier². ¹Angers University, Hepatology, Angers, France; ²Angers University, HIFIH Laboratory, Angers, France; ³Angers University Hospital, Hepatology, Angers, France

Email: paul.cales@univ-angers.fr

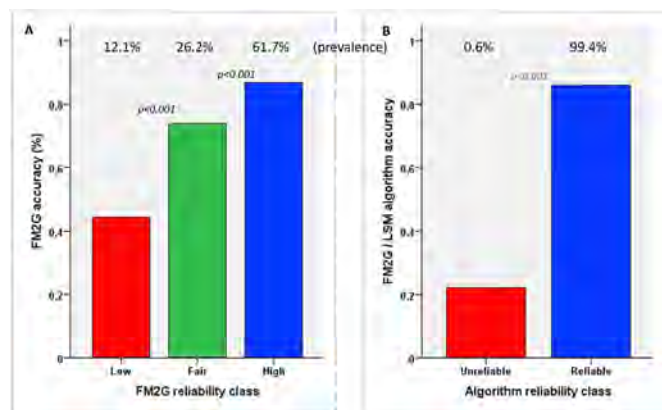
Background and aims: The need for reliability studies on non-invasive tests (NITs) was underlined in the 2021 EASL guidelines. Recently, we developed intrinsic blood test reliability criteria. We sought to validate these criteria and apply them to other NITs.

Method: 6858 patients with chronic liver disease (etiologies: virus, NAFLD, alcohol) were recruited in one (cross-sectional) derivation and two (cross-sectional and longitudinal) validation sets. The main fibrosis measurements were: blood test (FibroMeter FM2G), liver stiffness measurement (LSM), Metavir F (liver biopsy) and survival. We developed a reliability score (RS) for FM2G with Metavir F as reference. It included FM2G markers + etiology and comprised 3 classes: low, fair and high reliability.

Results: 1/In the derivation set, RS estimated FM2G accuracy for fibrosis staging well (agreement coef: 0.96). Thus, cirrhosis AUROCs were, low RS: 0.686, fair RS: 0.824, high RS: 0.924, all: 0.883 ($p < 0.001$ vs each class); accuracy is detailed in the figure.

2/In the cross-sectional validation set, these significant differences were confirmed. Moreover, FM2G RS was well-correlated with the LSM AUROC (Rp: 0.83). Thus, the FM2G RS discriminated the cirrhosis AUROC of LSM better than did reliability criteria based on LSM and the IQR/LSM ratio. Also, the FM2G RS discriminated well the cirrhosis AUROCs of other blood tests (APRI, Fib4, Fibrotest, Hepascore, ELF); e.g. for Fibrotest, low RS: 0.569, fair RS: 0.680, high RS: 0.894 ($p < 0.001$ vs low). The FM2G and LSM reliability classes were complementary. Thus, we developed a sequential algorithm using first FM2G in high RS and otherwise LSM combined with FM2G. The algorithm accuracy was, according to its reliability classes, low (0.6% of patients): 22.2%, high: 86.0%, $p < 0.001$ (Figure). Its overall accuracy was 85.6% vs FM2G: 78.3% or LSM: 81.1% ($p < 0.001$).

3/In the longitudinal validation set, FM2G RS discriminated survival accuracy. Thus, logrank tests for Kaplan-Meier survival estimates of fibrosis stages were, low RS: $p = 2.10^{-7}$, fair RS, $p = 1.10^{-18}$, high RS: 3.10^{-92} . RS was thus validated independently of Metavir F.



Conclusion: A blood test reliability score estimates remarkably its own diagnostic and prognostic accuracies and discriminates diagnostic performances of other NITs. The combination of blood test and elastometry reliability criteria dramatically reduces unreliable NIT prevalence ($\leq 1\%$), improves accuracy and better individualizes patients with under-accuracy.

FRI217

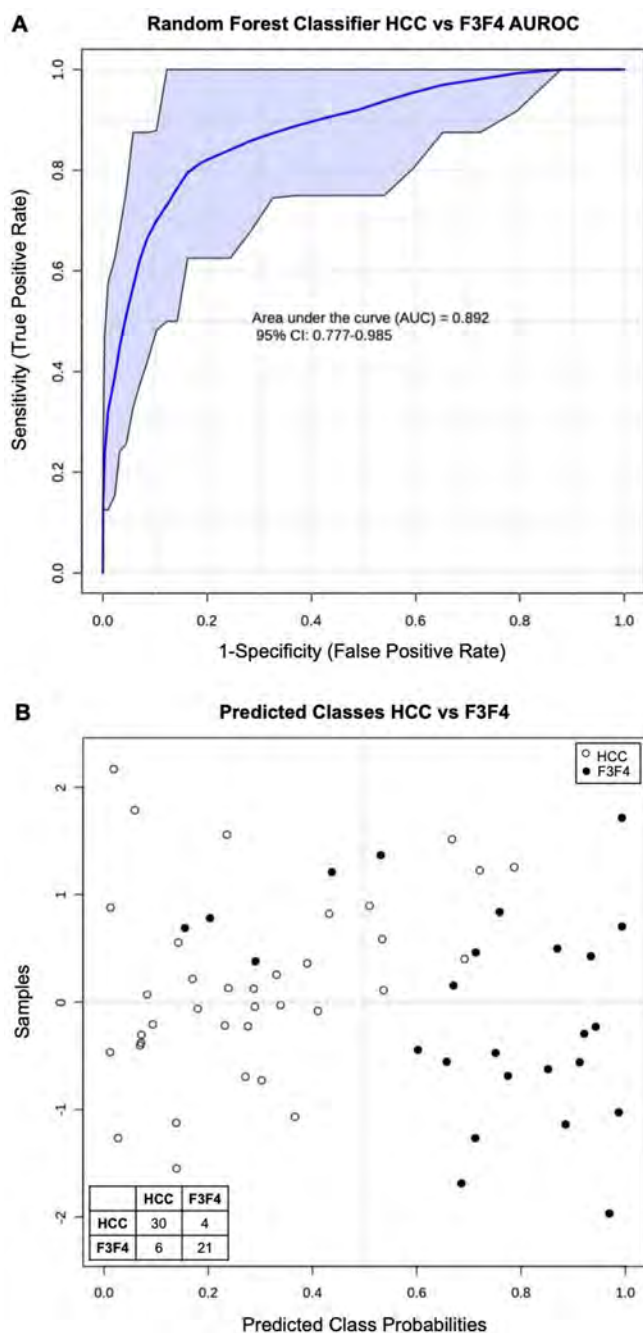
Metabolomic profiling of capillary dry blood samples for the differential diagnoses of hepatocellular carcinoma and liver diseases

Philipp Brunnbauer¹, Jennifer Kirwan^{2,3}, Can Kamali¹, Christian Benzing¹, Katrin Splith¹, Karl Hillebrandt¹, Johann Pratschke¹, Moritz Schmelzle¹, Felix Krenzien¹. ¹Charité-Universitätsmedizin Berlin, Corporate Member of Freie Universität Berlin and Humboldt Universität zu Berlin, Department of Surgery, Experimental Surgery, Berlin, Germany; ²Berlin Institute of Health, Core Unit Metabolomics, Berlin, Germany; ³Max Delbrück Center for Molecular Medicine, Metabolomics, Berlin, Germany
Email: philipp.brunnbauer@charite.de

Background and aims: Hepatocellular carcinoma (HCC) remains the second most common tumour-associated cause of death globally, in part, due to a lack of viable screening options, non-specific clinical presentation and late diagnosis. In fact, alpha-fetoprotein (AFP), the biomarker of choice, is of low diagnostic utility (sensitivity of 41–65%, specificity of 80–94%), which further deteriorates in the presence of cirrhosis or hepatitis. Herein, we present promising preliminary results of an untargeted metabolomics biomarker-discovery study, based on dry blood sampling, demonstrating robust classification accuracy, discriminating HCC (including HCC in cirrhosis) from severe fibrosis or cirrhosis.

Method: Capillary blood samples (10 μ L) were collected from the earlobe of patients using a volumetric absorptive microsampling (VAMS) device. Metabolomic analysis was performed using liquid chromatography (LC) coupled to an electrospray ionisation mass spectrometry (ESI-MS). Raw LC/ESI-MS data were processed using a standard metabolomics workflow and peaks were annotated using an internal database of m/z and retention time with a 30 ppm mass accuracy. Data were further corrected for technical variation and background effects, followed by batch correction and data filtering in MATLAB (R2021a). Random forest classification was conducted in MetaboAnalyst 5.0.

Results: Having analysed dried blood samples from individuals with liver disease and healthy controls, we obtained 297 metabolites from 483 samples (162 patients), deemed suitable for statistical analysis. Although some patients presented with both, for the purpose of classification, we separated preoperative samples into two mutually exclusive groups: HCC (including HCC in cirrhosis, $n = 36$) and severe fibrosis/cirrhosis (F3F4, $n = 25$). From 43 significantly altered metabolites (fold-change ratio = 2.0, evaluated via t-test with $p < 0.05$), we selected a panel of three metabolites (IDs available on request), achieving an AUROC of 0.892 (95% CI: 0.777–0.985, Figure A), and promising predicted class probabilities and confusion matrix (Figure B).



Conclusion: Dry blood sampling can identify promising biomarker candidates that could improve HCC time-to- and stage-at-diagnosis. While our findings will be confirmed in a prospective study, focusing on age and risk factor stratification, we aim to translate our findings into an easy-to-use, low-cost population screening tool for HCC. *MS&FK share senior authorship.*

FRI218

Stable rates of cirrhosis diagnosed by Fibrosan despite changing trends in liver disease epidemiology: a single centre retrospective cohort study

Joan Ericka Flores^{1,2}, Anne Craigie¹, Lucy McDonald¹, Amy Edwards^{1,2}, Tim Papaluca^{1,2}, Michael MacIsaac¹, John Gough¹, Kate New¹, Susanne Glasgow¹, Bradley Whitton¹, Paul Desmond^{1,2}, Marno Ryan^{1,2}, Thai Hong¹, Zina Valaydon², Jacinta Holmes^{1,2}, Barbara Demediuk¹, Catherine Croagh¹, David Iser¹, Kumar Visvanathan^{1,2}, Swee Lin Chen Yi Mei¹, Alexander Thompson^{1,2}, Jessica Howell^{1,2}. ¹St. Vincent's Hospital Melbourne, Fitzroy, Australia; ²University of Melbourne, Parkville, Australia
Email: ericka@flores.com.au

Background and aims: Data for cirrhosis prevalence in Australia are urgently needed to plan health resourcing for hepatocellular carcinoma (HCC) surveillance and liver disease prevention programs. The aim of this study was to describe the prevalence of cirrhosis diagnosed by Fibrosan within an urban tertiary health network and linkage to specialist care.

Method: This retrospective cohort study was conducted at St Vincent's Hospital Melbourne, Australia. Raw Fibrosan data files were extracted from three machines (one static, two portable) used in hospital and community sites, and Fibrosan database. Cirrhosis was defined by aetiology specific cut offs and ≥ 12.5 kPa where aetiology was not available. Individuals with cirrhosis range Fibrosans were cross referenced with hospital record data to describe the proportion of patients referred for follow up. Median time intervals were reported in months (IQR). Proportions of Fibrosans in cirrhotic range and aetiologies compared with Chi square test.

Results: 10,622 Fibrosans were performed in 8727 individuals from 9 April 2010 to 27 April 2021. Fibrosan data from 2012 was not available. Peak number of Fibrosans in 2016, coincided with availability of hepatitis C DAAs. Recorded liver disease aetiologies: 38% chronic hepatitis C (3358/8798), 25% hepatitis B (2231/8798), 15% fatty liver disease (1297/8798) and 10% alcohol (837/8798). 15% (1595/10622) of Fibrosan records were in cirrhosis range. Proportion of Fibrosans with cirrhosis range were similar over time, ranging between 15 and 19% without significant variation ($p=0.68$) (Figure 1a). Proportion of fibrosans with cirrhosis due to most common aetiologies showed significant downtrend with chronic hepatitis C and chronic hepatitis B ($p=0.018$ and $p=0.012$, respectively). An uptrend with MAFLD ($p=0.35$) and alcohol was observed, but only statistically significant for alcohol ($p=0.009$).

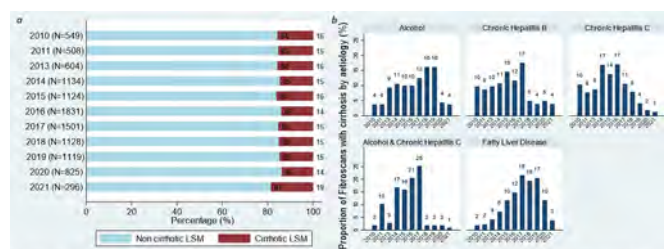


Figure 1 a) Proportion of cirrhotic range Fibrosans by year b) Proportion of cirrhotic range Fibrosans per year by aetiology

1045 patients with cirrhotic Fibrosan range had hospital records: 56% (584/1045) were known to the liver clinic at the time of Fibrosan, 20% (205/1045) were referred following Fibrosan and 24% (252/1045) had no referral. 3% (32/1045) required multiple referrals until patient attendance was recorded and 1% (13/1045) patients never attended liver clinic. Median time from Fibrosan to liver clinic referral was 13 months (IQR 3–34).

Conclusion: The proportion of patients with cirrhosis diagnosed by Fibrosan has remained stable over time, with changing trends of chronic liver disease aetiology from viral hepatitis to fatty liver disease and alcohol related liver disease. Despite this, linkage to care

of people with cirrhosis remains suboptimal. These data are limited by focusing on one hospital's liver clinic and no data of follow-up at other health services, but suggest greater resourcing streamline linkage of people diagnosed with cirrhosis by Fibroscan into specialist care is warranted.

FRI219

Comparative assessment of noninvasive methods (NIMs)-LIVERFAS^t, liver stiffness measurement (LSM) with transient elastography (TE, Fibroscan) ELF and FIB-4 in a prospective cohort with chronic liver diseases (CLD) from a tertiary liver center

Kawin Tangvoraphonkchai¹, Tanita Suttichaimongkol², Prakasit Sangaimwibool³, Wattana Sukeepaisarnjaroen⁴, Churaieat Kularbkaew. ¹*Khon Kaen University, Faculty of Medicine, Division of Gastroenterology, Department of Medicine, Thailand;* ²*Khon Kaen University, Division of Gastroenterology, Department of Medicine, Thailand;* ³*Khon Kaen University, Department of Pathology, Thailand;* ⁴*Khon Kaen University, Department of Pathology, Faculty of Medicine, Thailand*

Email: kawin_tang@hotmail.com

Background and aims: CLD-related mortality in Thailand is increasing due to high prevalence of obesity and not eradicated chronic viral hepatitis B (CHB) and C (CHC). LIVERFAS^t (LF, Fibronostics, US) is a new point-of-care proprietary technology to assess quantitatively liver fibrosis (LF-Fib) and steatosis (LF-Ste). (Hepatology Suppl. 2020) In NAFLD pts, LF-Fib predicted liver-related events and overall mortality (Hepatology Suppl.2021).

To assess: 1/LF-Fib performance for advanced (AF) and bridging fibrosis (BF) vs LSM, FIB-4 and ELF in a prospective tertiary cohort with CLD and LB. 2/LF-Ste performance for mild (\geq S1), moderate (\geq S2) and marked steatosis (S3) vs. imaging methods (CAP) in NAFLD pts, including a CHC/CHB control group without steatosis (S0).

Method: Pts with simultaneous LB, blood biomarkers (LF, FIB4 and ELF) and LSM using TE were prospectively included. LB staging was as per METAVIR for CHB/CHC and NASH-CRN for NAFLD. Statistics were descriptive and using binary area under ROC [BinAUROC (95%CI)].

Results: 192 pts were included with concomitant LF, FIB4 and LSM. N = 157 patients had ELF determined along with LF and other SOC. Main characteristics were: 52.7% males, median (range) age 50 (20–69) yrs, 26.4% NAFLD, 23.9% CHB, 49.8% CHC, BMI 34.9 Kg/m², HbA1c 5.5, LSM 7.5 kPa, LF-Fib 0.29, LF-Act 0.29, LF-Ste 0.35, 49.5% severe NAI, 50.2% AF and 9.5% cirrhosis (F4).

Overall Bin-AUROC (95%CI) for AF were: LSM 0.70 (0.62–0.77), FIB4 0.71 (0.63–0.77) and LF-Fib 0.81 (0.67–0.85) [p = ns vs LSM and p < 0.05 vs FIB4].

In N = 157 patients with concomitant ELF determination, overall Bin-AUROC (95%CI) for AF were: LSM 0.79 (0.71–0.85), FIB4 0.69 (0.61–0.77), ELF 0.63 (0.53–0.71) and LF-Fib 0.77 (0.61–0.77; p = ns vs LSM and p < 0.01 vs FIB4 and ELF, respectively); for BF were: LSM 0.82 (0.71–0.88), FIB4 0.75 (0.63–0.83), ELF 0.64 (0.49–0.77) and LF-Fib 0.77 (0.65–0.85; p = ns vs all).

For \geq S1, \geq S2 and S3 steatosis-when taking into account 17 controls without steatosis (S0)- LF-Ste and CAP performances were: 0.75 (0.59–0.85)/0.75 (0.61–0.85)/0.70 (0.47–0.83) vs 0.81 (0.67–0.89)/0.81 (0.68–0.89)/0.74 (0.55–0.86), respectively, all p = ns.

Conclusion: LIVERFAS^t is a blood biomarker for fibrosis/steatosis staging with similar performances to TE/CAP in a tertiary cohort with CLD. In NAFLD pts, LF can be an alternative to imaging methods (e.g. CAP and LSM) for stratifying the severity of the disease.

FRI220

Diagnostic accuracy of non-invasive imaging modalities for the diagnosis of liver cirrhosis compared to histological assessment in a clinical setting

Liv Hetland¹, Mira Thing¹, Thit Kronborg¹, Beth Hærsted Olsen², Nina Kimer¹, Lise Lotte Gluud^{1,3}. ¹*Hvidovre Hospital, Gastro Unit, Hvidovre, Denmark;* ²*Hvidovre Hospital, Department of Radiology, Hvidovre, Denmark;* ³*Copenhagen University, Department of Clinical Medicine, København, Denmark*

Email: livelinehetland@gmail.com

Background and aims: Diagnostic imaging including abdominal ultrasound (US) and computed tomography (CT) are important tools in the initial evaluation of patients with liver disease. We evaluated the accuracy of US and CT in diagnosing liver cirrhosis using a prospective design with histological assessment as the gold standard.

Method: This study included 369 patients from three prospective cohort studies between January 2017 and November 2021 who underwent diagnostic imaging (US or CT) and a liver biopsy based on clinical indication. Two cohorts (ProDoc, n = 34; StatLiver, n = 78) included patients with suspected cirrhosis and one cohort (FLINC, n = 257) included patients with non-alcoholic fatty liver disease (NAFLD). US and CT scans were performed by experienced radiologists and the results were re-evaluated by a second radiologist in case of inconclusive findings.

Results: The cohorts include 369 patients who underwent a liver biopsy and an US (n = 279) and/or CT scan (n = 129). In addition, 291 patients underwent a Fibroscan. In total 143 patients had histologically confirmed cirrhosis (38.7%). Of patients who underwent US, 78 were correctly diagnosed as having cirrhosis and 159 as correctly being non-cirrhotic; the sensitivity was 0.72, specificity 0.89, positive predictive value (PPV) 0.88 and negative predictive value (NPV) 0.84. Of patients who underwent CT scan, 61 were correctly diagnosed as having cirrhosis and 46 as correctly being non-cirrhotic, giving a sensitivity of 0.75, specificity of 0.96, PPV 0.97 and NPV 0.70. The PPV and NPV for Fibroscan was 0.71 and 0.91.

Conclusion: This study demonstrates that both US and CT provide important diagnostic information for ruling in cirrhosis. However, this study includes a relatively high proportion of patients with cirrhosis and the findings should therefore be re-evaluated in low risk groups.

FRI221

Use of Fibrosis-4 (FIB-4) in liver fibrosis screening: which thresholds to choose?

Denis Ouzan¹, Jeremie Corneille², Guillaume Penaranda³, Jean Marie Dubertrand⁴. ¹*Arnault Institute Tzanck, Saint-Laurent-du-Var, France;* ²*BIOGROUP BIOESTEREL-Laboratoire Mougins-L'espérance, Mougins, France;* ³*BIOGROUP ALPHABIO-Laboratoire Européen, Marseille, France;* ⁴*BIOGROUP BIOESTEREL-Laboratoire Mandelieu-Passero, Mandelieu-la-Napoule, France*

Email: denis.ouzan@wanadoo.fr

Background and aims: Rationale: Screening for liver fibrosis in the general population is a major public health issue. We have shown in a previous study (EASL 2020, Abs FRI225) that FIB-4, a simple score combining age, ALT/AST activity and platelet count, can detect liver fibrosis in general practice and identify a possible cause of chronic liver disease. But the optimal FIB-4 threshold that detects hepatic fibrosis remains to be defined. The FIB-4 thresholds recently proposed by a single study (1) are age-dependent: low risk if <1.30 (<65 years) and <2 (>65 years), intermediate risk between 1.3 and 2.67 (<65 years) and between 2 and 2.67 (>65 years), and high risk if >2.67. The aim of our work is to explore the simpler, age-independent FIB-4 threshold of 2 by performing a second-line ELF (Enhanced Liver Fibrosis) score after automatic calculation of FIB-4.

Method: The FIB-4 score has been automatically generated since October 1, 2020 by all city analysis laboratories in the Alpes-Maritimes French area as soon as ALT/ASAT and platelets are

POSTER PRESENTATIONS

prescribed. The FIB-4 results, calculated by 80 laboratories, were analyzed. The FIB-4 thresholds used are a function of age as defined above. The ELF score was performed in the second line in a group of 183 patients at intermediate or high risk of fibrosis.

Results: During the first 3 months of the implementation of the automatic calculation of the FIB-4, 131, 861 subjects were screened, half of them were older than 65 years, 56% were women and 44% were men. The distribution of fibrosis risk observed by the FIB-4 according to age was as follows: low risk for 107, 148 subjects (81.3%), intermediate risk for 16, 297 subjects (12.4%), and high fibrosis risk for 8, 416 subjects (6.4%). An ELF score >9.8 indicative of advanced fibrosis was observed in 14/54 subjects (26%) of those with a FIB-4 score between 1.3 and 2 and in 102/129 (79%) of those with a FIB-4 >2 ($p < 0.001$).

Conclusion: The automatic calculation of the FIB-4 showed in a large cohort, a risk of hepatic fibrosis in almost 19% of the subjects: intermediate risk 12.4% and high risk of fibrosis 6.4%. The ELF test performed in the second line significantly more often confirmed the existence of advanced fibrosis in subjects with a FIB-4 >2 as compared to those with a FIB-4 between 1.3 and 2 (79 versus 26%). The threshold of 2 could significantly reduce the number of subjects in the intermediate zone of fibrosis, which is debated.

Reference

McPherson S, et al. Age as a Confounding Factor for the Diagnosis of Advanced NAFLD Fibrosis. *Am J Gastroenterol* 2017; 112:740–51.

FRI222

Plasma cell-free DNA methylation as biomarker for hepatocellular carcinoma

María Gárate-Rascón¹, Miriam Recalde¹, Idoia Bilbao², Fabrice Daian³, María Elizalde¹, María Azkona¹, José María Herranz^{1,4}, Carla Rojo¹, Mercedes Iñarrairaegui^{2,4,5}, Itziar Abete⁶, María A. Zulet⁶, Bruno Sangro^{2,4,5}, Maite G. Fernandez-Barrena^{1,4,5}, Loreto Boix⁷, María Reig⁷, Andrea Casadei Gardini⁸, Matías A. Avila^{1,4,5}, Manuel F. Landecheo², Carmen Berasain^{1,4,5}, Maria Arechederra^{1,5}.

¹Center of Applied Medical Research (CIMA), Program of Hepatology, Pamplona, Spain; ²Navarra University Clinic, Hepatology Unit, Pamplona, Spain; ³Developmental Biology Institute of Marseille (IBDM), Marseille, France; ⁴National Institute for the Study of Liver and Gastrointestinal Diseases (CIBERehd, Carlos III Health Institute), Madrid, Spain; ⁵Navarra Institute for Health Research (IdiSNA), Pamplona, Spain; ⁶Food Sciences and Physiology and Center for Nutrition Research, Department of Nutrition, Pamplona, Spain; ⁷Barcelona Clinic Liver Cancer (BCLC), Hospital Clinic de Barcelona, IDIBAPS, Liver Unit, Barcelona, Spain; ⁸IRCCS-San Raffaele Scientific Institute, Unit of Oncology, Milan, Italy

Email: macalderon@unav.es

Background and aims: Hepatocellular carcinoma (HCC) is a global health concern with increasing impact on our societies. Nowadays, there are limited diagnostic methods and most patients are diagnosed at advanced stage when current treatments have little effectiveness. Moreover, although patients in early and intermediate stages might benefit from potentially curative treatments, there is a high rate of recurrence. It is therefore essential to identify new non-invasive reliable biomarkers for the detection of HCC at an early stage and the prediction of recurrence-progression to improve patient survival. In this regard, recent advances have demonstrated that circulating tumor DNA (ctDNA) methylation has a great potential to serve as a blood-based biomarker for early diagnosis and precision treatment. In this project, we aim to identify and validate new ctDNA methylation markers for early HCC detection and HCC recurrence-progression monitoring.

Method: For *in silico* analyses we used available tissue methylation data on control and HCC patients, focusing on CpG islands and lncRNA promoter regions. We set up the protocol to isolate cfDNA from 1 ml of plasma, to treat cfDNA with bisulfite and to perform targeted sequencing. Plasma from control and HCC patients were used for validations.

Results: Using available tissue methylation data on HCC ($n = 670$) and control ($n = 135$) samples from three different studies (GSE56588, GSE54503 and TCGA-LIHC) as well as from blood leukocyte samples of healthy individuals (754 samples, GSE40279) and deep learning approaches we defined a blood-based HCC Methyl Diagnostic panel (HepaMet Panel) consisting on 27 CpG marks located within CpG islands and 2 located within lncRNA promoter regions. HepaMet Panel revealed a robust performance (accuracy of 97.3%) for control and HCC patient classification. *In silico* validation of HepaMet Panel in three independent HCC cohorts (GSE60753, GSE89852 and GSE157341) showed a sensitivity range of 97%–100%. We first set up conditions to analyze 16 of these 29 marks. Validation of this sub-panel using cfDNA from 7 early stage HCCs, 22 advanced HCCs as well as 11 healthy controls succeeded to classify 76% of HCC patients (71% early and 77% advanced).

Conclusion: We have identified a blood-based HCC Methyl Diagnostic panel that effectively classify control and HCC patients. Ongoing analyses will determine HepaMet Panel utility in the early diagnosis of HCC and HCC recurrence-progression monitoring.

FRI223

A derivation and validation study of paired liver and plasma proteomics in 659 individuals reveals circulating biomarkers for alcohol-related liver disease

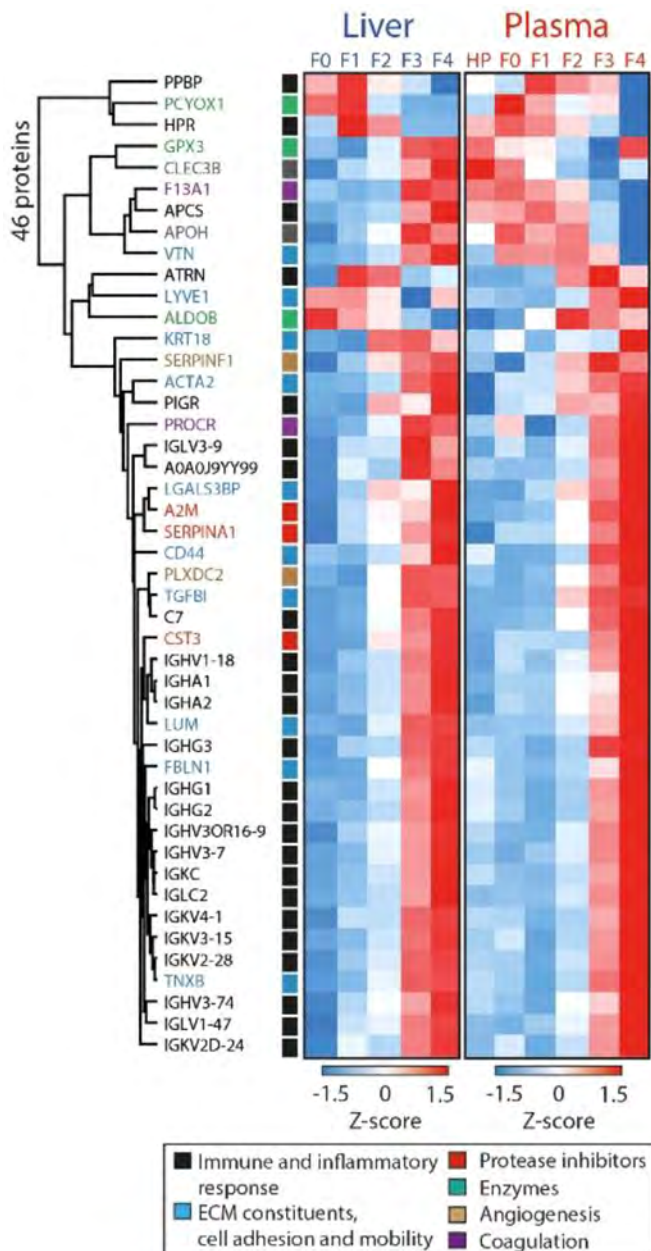
Lili Niu¹, Maja Thiele^{2,3}, Philipp Geyer¹, Ditlev Nytoft Rasmussen², Henry Emanuel Weibel¹, Alberto Delgado¹, Rajat Gupta¹, Florian Meier¹, Maximilian Strauss¹, Maria Kjærgaard^{2,3}, Katrine Prier Lindvig^{2,3}, Mads Israelsen^{2,3}, Simon Rasmussen¹, Torben Hansen⁴, Matthias Mann¹, Aleksander Krag^{2,3}. ¹University of Copenhagen, Center for Protein Research, Copenhagen, Denmark; ²Center for Liver Research, Odense University Hospital, Department of Gastroenterology and Hepatology, Odense, Denmark; ³University of Southern Denmark, Faculty of Health Sciences, Department for Clinical Research, Odense C, Denmark; ⁴University of Copenhagen, Center for Basic Metabolic Research, Denmark
Email: maja.thiele@rsyd.dk

Background and aims: Alcohol-related liver disease (ALD) is the most common cause of liver-related mortality, but diagnosis is often delayed due to lack of accurate, circulating biomarkers. We aimed to develop and validate diagnostic and prognostic protein marker panels of fibrosis, hepatocyte injury with inflammation, and steatosis, using paired liver and plasma proteomics.

Method: We included 459 patients with early ALD in a prospective derivation cohort, used mass spectrometry to measure plasma and liver proteome, and integrated them to determine the tissue origin of circulating proteins. We used machine learning with feature selection to derive three proteomic panels of significant fibrosis ($\geq F2$), mild activity (sum of ballooning and lobular inflammation ≥ 2) and any steatosis ($\geq S1$), and validated their ability to rule out or rule in disease in 137 healthy, age- and gender-matched controls, and 63 liver-biopsied ALD patients from an independent screening cohort. Finally, we evaluated the proteomic biomarkers' ability to predict liver-related events and all-cause mortality, and compared their diagnostic performance with 15 best-in-class existing tests.

Results: The derivation cohort consisted of 76% males, age 57 ± 13 years, 44% significant fibrosis ($\geq F2$), 46% mild activity, 44% steatosis ($\geq S1$). 717 unique proteins were dysregulated during disease progression, accounting for 13% of the measured liver proteome, but only half of liver proteome changes were transmitted to the circulation. Integrative analysis revealed 46 co-dysregulated proteins, representing mostly the downregulation of metabolic functions and upregulation of fibrosis signaling and immune response (figure). Feature selection found that 22 unique plasma proteins could be used in different combinations to derive three proteomic biomarker panels. The panels performed better than all comparators (including elastography, ELF, FIB-4, cytokeratin-18) for detecting significant fibrosis (AUC 0.92) and mild activity (AUC 0.87). The $\geq F2$ proteomic

panel ruled out significant fibrosis in 99% of the healthy controls and had the highest prognostic accuracy for liver-related events and all-cause mortality (Harrell's C 0.90 and 0.79). We successfully reproduced the excellent proteomics performance in the independent validation cohort (AUC 0.87 for significant fibrosis, and AUC 0.81 for mild activity).



Conclusion: Plasma proteomics has a great potential for the diagnosis and prognosis of overall liver health in people with a history of harmful drinking.

FRI224

Development and validation of a hepatic vascular geometrical model for noninvasive diagnosis of clinically significant portal hypertension in cirrhosis (CHESS1802)

Chengyan Wang¹, Yifei Huang², Changchun Liu³, Fuquan Liu⁴, Xumei Hu⁵, Xutong Kuang⁵, Weimin An³, Chuan Liu², Yanna Liu², Xiaolong Qi². ¹Fudan University, Human Phenome Institute, Shanghai, China; ²The First Hospital of Lanzhou University, CHESS Center, Institute of Portal Hypertension, Lanzhou, China; ³Fifth Medical Center of Chinese People's Liberation Army General Hospital, Department of Radiology, Beijing, China; ⁴Beijing Shijitan Hospital, Department of Interventional Therapy, Beijing, China; ⁵Fudan University, Human Phenome Institute, Shanghai, China
Email: qixiaolong@vip.163.com

Background and Aims: Noninvasive and accurate methods are needed to identify patients with clinically significant portal hypertension (CSPH). This study aims to explore the variations of hepatic vascular geometries in patients with CSPH and investigate the capability of using CT/MRI angiographic imaging-based vascular geometrical model (VGM) to identify CSPH in patients with cirrhosis.

Method: The portal vein (PV), hepatic vein (HV), hepatic artery (HA) and inferior vena cava (IVC) were segmented using a pre-trained attention-based convolutional neural network (CNN). A total of 64 vascular geometrical parameters were automatically extracted from those segmented vessels and then fed into the VGM to identify CSPH patients. A total of 853 consecutive liver cirrhosis patients from two centers who underwent contrast enhanced MRI/CT scans within 14 days of transjugular catheterization for hepatic venous pressure gradient (HVPG) measurement were included in this study. The model was trained and validated in a CT cohort (#1) containing 256 patients with cirrhosis and 267 age-matched participants without a history of chronic liver diseases, and tested on another centers including a CT cohort (#2) with 106 patients and an MRI cohort (#3) with 224 patients. CSPH was defined as HVPG ≥ 10 mmHg.

Results: In PV, significant increase of vessel diameter (from 1.50 ± 0.91 to 2.20 ± 0.69 cm) and branch vessel diameter (from 0.41 ± 0.15 vs 0.73 ± 0.56 cm) were observed in CSPH patients. In contrast, significant decrease of PV volume (from 31.01 ± 12.93 to 23.89 ± 9.68 cm³) and tortuosity (from 0.17 ± 0.05 to $0.13 \pm 0.04^\circ$) were observed in CSPH patients. In HV, significant decrease of vessel volume (from 66.52 ± 16.91 to 33.31 ± 28.05 cm³) and length (from 812.42 ± 284.55 to 349.21 ± 185.87 mm) were observed in CSPH patients. In HA, significant increase of vessel length (from 77.26 ± 64.31 to 143.38 ± 57.2 mm) were observed, which indicates significant disruption of hepatic vascular system in CSPH patients. The AUC, accuracy, sensitivity and specificity were 0.90 ± 0.02 (95% CI, 0.88–0.93), 0.84 ± 0.01 (95% CI, 0.84–0.85), 0.87 ± 0.05 (95% CI, 0.80–0.92) and 0.83 ± 0.04 (95% CI, 0.80–0.89) for Cohort #1; 0.84 ± 0.12 (95% CI, 0.67–1), 0.88 ± 0.10 (95% CI, 0.75–1), 0.88 ± 0.10 (95% CI, 0.73–1) and 0.88 ± 0.09 (95% CI, 0.76–1) for Cohort #2; and 0.87 ± 0.11 (95% CI, 0.74–1), 0.91 ± 0.08 (95% CI, 0.8–1), 0.90 ± 0.09 (95% CI, 0.77–1) and 0.92 ± 0.08 (95% CI, 0.82–1) for Cohort #3.

POSTER PRESENTATIONS

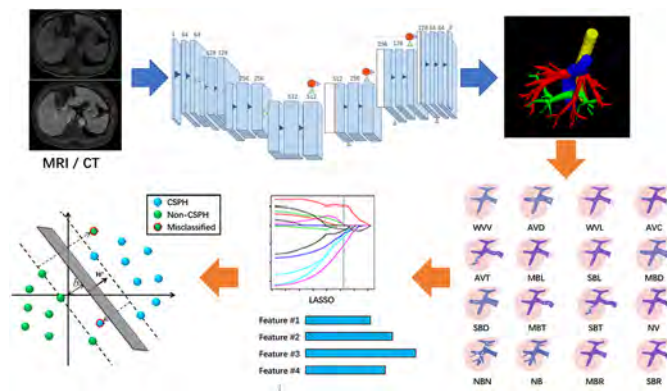


Figure 1: Workflow of the CT/MRI angiographic imaging-based vascular geometrical model.

Conclusion: This study developed and validated a contrast-enhanced CT/MRI-based VGM with good diagnostic consistency to the HVPg measurement. It provided a noninvasive and effective method for diagnosis of CSPH in patients with cirrhosis, which shows good potential for clinical applications.

FRI225

The diagnostic accuracy of ElastQ 2-D shear wave elastography for liver fibrosis risk assessment in a mixed etiology, multinational cohort

David J. M. Bauer^{1,2}, Annalisa De Silvestri³, Laura Maiocchi³, Ruxandra Mare⁴, Ioan Sporea⁴, Theresa Müller-Bucsics^{1,2}, Giovanna Ferraioli³, Thomas Reiberger^{1,2}. ¹Medical University of Vienna, Division of Gastroenterology and Hepatology, Department of Medicine III, Wien, Austria; ²Medical University of Vienna, Vienna Hepatic Hemodynamic Lab, Division of Gastroenterology and Hepatology, Department of Medicine III, Wien, Austria; ³University of Pavia, Fondazione IRCCS Policlinico San Matteo, Pavia, Italy; ⁴Victor Babeş University of Medicine and Pharmacy, Department of Internal Medicine II, Division of Gastroenterology and Hepatology, Center for Advanced Research in Gastroenterology and Hepatology, Timișoara, Romania

Email: thomas.reiberger@meduniwien.ac.at

Background and aims: The 2-D shear wave elastography technique ElastQ (Philips) shows promise for evaluating liver fibrosis risk assessment.

Method: We prospectively recruited 875 patients for simultaneous liver stiffness measurements (LSM) by ElastQ and Vibration Controlled Transient Elastography (VCTE) in 3 European centers. IQR/median $\leq 30\%$ was used as a reliability criterion. The correlation of ElastQ-LSM to VCTE-LSM was assessed by Pearson correlation. The fibrosis stage was classified by VCTE: no significant fibrosis VCTE < 6 kPa, grey area/significant fibrosis VCTE 6–12 kPa, severe fibrosis/cirrhosis VCTE > 12 kPa (EASL CPG 2021). This classification served as a basis for the ROC analysis and definition of 90%-specific rule-in, and 90%-sensitive rule-out cutoffs for ElastQ.

Results: Among 875 participants, ElastQ failed in 26 (2.97%) and VCTE in 7 (0.8%) and was unreliable (IQR/median $> 30\%$) in 24 (2.74%) and 6 (0.69%) participants, respectively. The final population consisted of $n = 813$ patients: 53.9% men ($n = 438$), median age: 57.0 [IQR: 19] years, median BMI: 25.3 [5.8] kg/m². The leading etiologies were HCV (50.1%), NAFLD (16.1%), HBV (12.1%), and ALD (10.1%). Fibrosis stages were no significant fibrosis in $n = 286$ (35.2%), significant fibrosis in $n = 290$ (35.7%), and severe fibrosis/cirrhosis in $n = 237$ (29.2%). The Pearson correlation of VCTE and ElastQ was $R = 0.64$ overall, but higher in VCTE-LSM ≤ 30 kPa ($R = 0.70$, Fig. 1). ElastQ-LSM ruled-out and ruled-in significant fibrosis risk at < 5.3 kPa (Sens.: 91.0%) and at ≥ 6.8 kPa (Spec.: 91.3%), respectively (AUROC: 0.859, $p < 0.001$). Severe fibrosis/cirrhosis risk was ruled-out and

ruled-in at < 6.2 kPa (Sens.: 90.2%) and > 10.2 kPa (Spec.: 90.3%), respectively (AUROC: 0.882, $p < 0.001$).

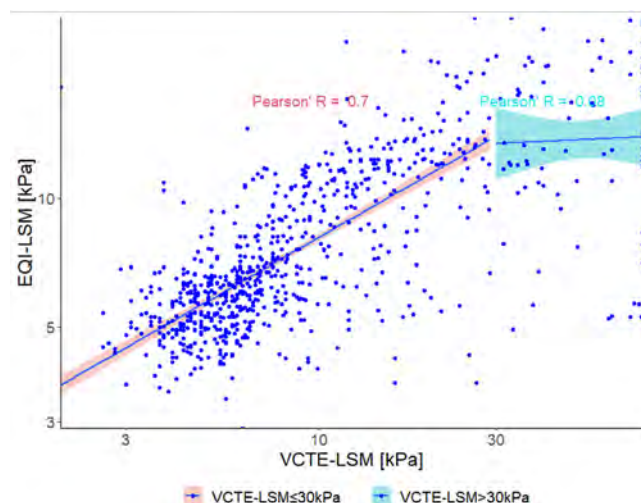


Figure 1: Scatterplot of VCTE-LSM vs. ElastQ-LSM (log10-transformed axis) with Pearson correlation separately shown for VCTE-LSM 0–30 kPa (red) and > 30 kPa (turquoise). Abbreviations: ElastQ-2-D shear wave elastography technique; kPa-kilopascal, LSM-liver stiffness measurement, VCTE-Vibration Controlled Transient Elastography.

Conclusion: This prospective, multicentric study shows a moderate correlation of ElastQ-LSM to VCTE-LSM, with better correlations at VCTE-LSM ≤ 30 kPa. ElastQ-LSM rules out significant fibrosis at < 5.3 kPa and rules in advanced fibrosis/cirrhosis at > 10.2 kPa.

Reference

1. EASL Clinical Practice Guidelines on non-invasive tests for evaluation of liver disease severity and prognosis-2021 update. *J Hepatol.* 2021;75:659–689.

FRI226

Machine learning models for prediction of severe portal hypertension in patients with compensated cirrhosis

Oleksandr Petrenko^{1,2,3,4}, Jiří Reiniš¹, Benedikt Simbrunner^{1,2,3,4}, Benedikt Hofer^{1,2,3,4}, Pierre-Emmanuel Rautou⁵, Lucile Moga⁵, Jonel Trebicka^{6,7}, Wenyi Gu^{6,7}, Philip Georg Ferstl^{6,7}, Lise Lotte Gluud⁸, Flemming Bendtsen⁸, Søren Møller⁹, Agustín Albillos¹⁰, Luis Téllez¹⁰, Sven Francque^{11,12}, Wilhelmus Kwanten^{11,12}, Juan Carlos Garcia Pagan¹³, Valeria Perez¹³, Virginia Hernandez-Gea¹³, Filippo Schepis¹⁴, Marco Scoppettuolo¹⁴, Dario Saltini¹⁴, Cándid Villanueva¹⁵, Anna Brujats¹⁵, Mattias Mandorfer^{3,4}, Thomas Reiberger^{1,2,3,4}. ¹CeMM Research Center for Molecular Medicine of the Austrian Academy of Sciences, Vienna, Austria; ²Ludwig Boltzmann Institute for Rare and Undiagnosed Diseases (LBI-RUD), Vienna, Austria; ³Vienna Hepatic Hemodynamic Lab (HEPEX), Division of Gastroenterology and Hepatology, Department of Internal Medicine III, Medical University of Vienna, Vienna, Austria; ⁴Christian Doppler Laboratory for Portal Hypertension and Liver Fibrosis, Medical University of Vienna, Vienna, Austria; ⁵Service d'Hépatologie, DMU Digest, Hôpital Beaujon, AP-HP, Clichy, France; ⁶Department of Internal Medicine I, Goethe University Clinic, Frankfurt, Germany; ⁷European Foundation for the Study of Chronic Liver Failure, EFCLIF, Barcelona, Spain; ⁸Gastro Unit, Medical Section, Hvidovre Hospital and Department of Clinical Medicine, University of Copenhagen, Copenhagen, Denmark; ⁹Department of Clinical Physiology and Nuclear Medicine, Center for Functional and Diagnostic Imaging and Research, Faculty of Health Sciences Hvidovre Hospital, University of Copenhagen, Hvidovre, Denmark; ¹⁰Department of Gastroenterology, Hospital Universitario Ramón y Cajal, IRYCIS, CIBEREHD, Universidad de Alcalá, Madrid, Spain; ¹¹Department of Gastroenterology and Hepatology, University Hospital Antwerp, Antwerp, Belgium; ¹²Laboratory of

Experimental Medicine and Pediatrics (LEMP), Faculty of Medicine and Health Sciences, University of Antwerp, Antwerp, Belgium; ¹³Barcelona Hepatic Hemodynamic Laboratory, Liver Unit, Hospital Clínic, Institut de Investigacions Biomèdiques August Pi i Sunyer (IDIBAPS), University of Barcelona, Barcelona, CIBEREHD (Centro de Investigación Biomédica en Red Enfermedades Hepáticas y Digestivas), Health Care Provider of the European Reference Network on Rare Liver Disorders; ¹⁴Unit of Gastroenterology, Hepatic Hemodynamic Laboratory, Università degli Studi di Modena e Reggio Emilia (UNIMORE), Modena, Italy; ¹⁵Hospital de la Santa Creu i Sant Pau. Biomedical Research Institute Sant Pau (IIB Sant Pau), Universitat Autònoma de Barcelona, Barcelona, Spain
Email: thomas.reiberger@meduniwien.ac.at

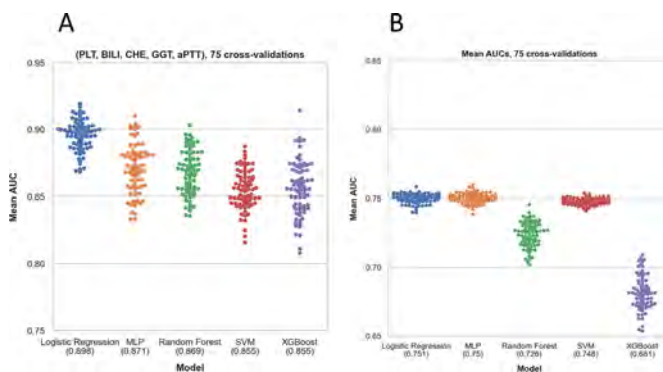
Background and aims: Hepatic venous pressure gradient (HVPG) is the gold standard for evaluation of the severity of portal hypertension (PH). In this multicenter study, we investigated the diagnostic value of different machine learning models trained on standard laboratory parameters to predict severe PH in compensated advanced chronic liver disease (cACLD) patients.

Method: The training cohort included cACLD patients recruited from the prospective VICIS study (NCT03267615). Regression and classification-based prediction models were applied to identify patients with severe PH (i.e., HVPG ≥ 16 mmHg) based on 52 widely available laboratory parameters. After feature selection, the models were applied to an external multicenter validation cohort using a cross-validation approach with the AUC reported as the median value across 75 cross-validations.

Results: The VICIS cohort included 139 cACLD patients (35.2% with HVPG ≥ 16 mmHg), main etiologies were viral hepatitis (32.4%), alcohol-related liver disease (ALD; 21.6%), and non-alcoholic fatty liver disease (NAFLD; 16.5%). The external validation cohort included 834 cACLD patients (36.7% with HVPG ≥ 16 mmHg), with the most prevalent etiologies being viral hepatitis (38.6%), NAFLD (24.2%), and ALD (20.6%).

Recursive feature elimination identified three and five parameters as most suitable for the models.

In the VICIS cohort, internal training-validation with the 5-parameter (platelets, bilirubin, cholinesterase, GGT, aPTT) logistic regression model outperformed the other models with AUC of 0.898 for prediction of HVPG ≥ 16 mmHg (Figure-A).



The best 3-parameter model included platelets, bilirubin, and aPTT. After being applied to the external validation cohort, and following the training-validation split, logistic regression resulted in the highest AUC of 0.751 (Figure-B). The other 3-parameter models yielded median AUC of 0.681 (XGBoost), 0.726 (Random Forest), 0.748 (Support Vector Machine), and 0.750 (Multilayer Perceptron). When trained on the VICIS cohort first and then applied to the external cohorts, the 3-parameter model with logistic regression resulted in AUC spread from 0.472 to 0.872 in the different centers' cohorts.

Conclusion: The VICIS-trained 5-parameter and 3-parameter model performed well to identify HVPG ≥ 16 mmHg in 'local' cACLD patients.

However, the external applicability of the 3-parameter logistic regression model to predict HVPG ≥ 16 mmHg is limited-likely due to differences in laboratory assays and patient characteristics. Training and applying of the models in the subsets of the same cohort resulted in more sustained AUC. Invasive HVPG measurements are hence still needed to reliably identify cACLD with HVPG ≥ 16 mmHg.

FRI227

Reproducibility and applicability of spleen stiffness measurement by vibration controlled transient elastography in patients with and without chronic liver disease

Cristina Rigamonti^{1,2}, Micol Cittone^{1,2}, Giulia Francesca Manfredi^{1,2}, Andrea Sorge³, Riccardo Moia^{1,4}, Maria Francesca Donato⁵, Gianluca Gaidano^{1,4}, Mirella Fraquelli³. ¹Università del Piemonte Orientale, Department of Translational Medicine, Novara, Italy; ²AOU Maggiore della Carità, Division of Internal Medicine, Novara, Italy; ³Fondazione IRCCS Ca' Granda-Ospedale Maggiore Policlinico, Gastroenterology and Endoscopy Unit, Milan, Italy; ⁴AOU Maggiore della Carità, Division of Hematology, Italy; ⁵Fondazione IRCCS Ca' Granda-Ospedale Maggiore Policlinico, Gastroenterology and Hepatology Unit, Italy
Email: cristina.rigamonti@uniupo.it

Background and aims: Spleen stiffness measurement (SSM) by vibration controlled transient elastography (VCTE) has emerged as a promising non-invasive tool with good diagnostic accuracy for predicting the degree of portal hypertension in patients with advanced chronic liver disease (CLD). This study investigated intra-observer and inter-observer agreement and factors influencing SSM reproducibility.

Method: In this prospective multicentre study 297 patients with CLD of different aetiology (187 in Novara and 110 in Milan; 32% cirrhotics) and 123 controls (63 patients with Philadelphia negative (Ph-) myeloproliferative neoplasms in Novara and 60 healthy volunteers in Milan) consecutively underwent VCTE examination for SSM and liver stiffness measurement (LSM). SSM was blindly performed twice by two different operators. Intra-observer and inter-observer agreement was calculated using the intraclass correlation coefficient (ICC) in relationship with different patient-related covariates.

Results: A total of 922 VCTE examinations for SSM were performed in Novara and 680 in Milan, respectively, with an overall failure rate of 3.2% and 3.6%.

In CLD patients from Novara (33% cirrhotic, 26% with splenomegaly) median SSM was 24.9 kPa (IQR 20.6–36.1) and LSM was 6.8 kPa (IQR 4.9–11.3). In CLD patients from Milan (31% cirrhotics, 40% with splenomegaly) median SSM was 29.2 (IQR 16.7–34.5) and median LSM 8.3 kPa (IQR 7.1–10.8).

Median SS value was 26.6 kPa (IQR 24.3 to 36.1) in the overall CLD group, 26.3 kPa (IQR 22.3–33.6) in MPN patients and 16.1 kPa (IQR 14.6–18.7) in healthy volunteers.

In whole CLD group, SSM was significantly correlated with LSM ($r = 0.67$), spleen longitudinal diameter ($r = 0.58$), presence of cirrhosis ($r = 0.54$), and BMI ($r = 0.24$) ($p < 0.0001$ for all comparisons).

In CLD patients the overall inter-observer agreement ICC was 0.90 (0.88–0.92) and factors associated with a reduced agreement were: absence of splenomegaly (ICC 0.87 vs 0.91), BMI > 25 kg/m² (ICC 0.91 vs 0.88) and absence of cirrhosis (ICC 0.84 vs 0.90). Intra-observer agreement ICC for rater 1 and rater 2 respectively were 0.93 (95% CI 0.91–0.95) and 0.96 (95% CI 0.95–0.97) in Novara and 0.91 and 0.94 (95% CI 0.91–0.96) (95% CI 0.87–0.93) in Milan.

Conclusion: SSM is a highly reproducible and feasible technique for assessing SSM in patients with CLD.

FRI228

Validation of the continuous controlled attenuation parameter (CAPc) using the MRI-PDFF as reference

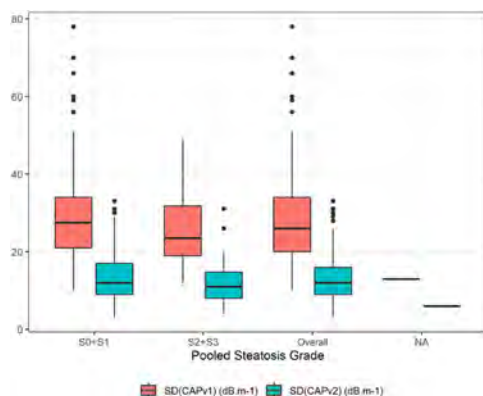
Nathalie Ganne-Carrié¹, Olivier Chazouillères², Jérôme Boursier³, Christophe Aubé⁴, Yves Menu⁵, Olivier Seror⁶, Yves Gandon⁷, Edouard Bardou-Jacquet⁸. ¹Avicenne Hospital (AP-HP), Department of Hepatology, Bobigny, France; ²Hospital Saint-Antoine Ap-Hp, Department of Hepato-gastroenterology, Paris, France; ³Angers University Hospital Center, Department of Hepato-Gastroenterology and Digestive Oncology, Angers, France; ⁴Angers University Hospital Center, Department of Radiology, Angers, France; ⁵Hospital Saint-Antoine Ap-Hp, Department of Radiology, Paris, France; ⁶Jean-Verdier Hospital Ap-Hp, Department of Radiology, Bondy, France; ⁷CHU Rennes-Pontchaillou Hospital, Department of Radiology and Medical Imaging, Rennes, France; ⁸CHU Rennes-Pontchaillou Hospital, Department of Liver Diseases, Rennes, France

Email: edouard.bardou.jacquet@chu-rennes.fr

Background and aims: Controlled Attenuation Parameter (CAP) was first introduced on the FibroScan (FS) device (Echosens, France) in 2010 and has been shown to be well correlated with liver steatosis in patients with various chronic liver diseases [PMID:28039099]. A new acquisition method for CAP (continuous CAP, CAPc) has recently been introduced in order to decrease the intra examination measurement variability (IEMV) [ILC2020;poster FRI073]. The aim of this interim analysis of an ongoing study is to compare the diagnostic performances and the IEMV between CAP and CAPc.

Method: Consecutive patients, all etiologies combined, underwent FS, Magnetic Resonance Imaging (MRI) within 21 days and CAPs obtained by both methods (standard and continuous). A central reading of the MRI images was performed to assess the Proton Density Fat Fraction (PDFF) which was used as the reference to assess the steatosis grades (S >0: PDFF ≥5% and ≤10%; S >1: PDFF ≥10%). The CAPs standard deviations (SD) were compared using the unilateral Wilcoxon signed-rank test. The agreement between CAP and CAPc was assessed with the average bias, the Pearson's coefficient of correlation (CC) and the absolute agreement intraclass coefficient (AA-ICC). The CAPs performances versus the PDFF were estimated with operating characteristics curves (ROC), and their areas under the curves (AUC). AUCs were compared with Delong's bilateral test.

Results: 157 patients were included (41% female, mean BMI = 28.4 ± 5.5 kg/m², mean age = 55.0 ± 13.4 years, Prevalence of S >0 and S >1 were 61% and 22%, respectively). The median CAPc SD (13.1 dB/m²) was significantly lower to median CAP SD (28.4 dB/m²) (p < 0.0001). The median reduction in IEMV was 50% (Fig). The average bias between the CAP and CAPc was 7.9 dB/m. The CC and AA-ICC were 0.90 and 0.89, respectively, highlighting a strong correlation and agreement. AUCs for S >0 were 0.86 (0.79–0.92) and 0.85 (0.78–0.91) for CAP and CAPc, respectively. AUCs for S >1 were 0.85 (0.78–0.92) and 0.86 (0.79–0.93), for CAP and CAPc, respectively. AUCs of CAP and CAPc methods were not significantly different.



Conclusion: By using the continuous method, the intra examination measurement variability of the CAP is decreased with a factor 2, keeping the global performance of the CAP algorithm. Furthermore, the results of CAP and CAPc examinations are strongly correlated and in agreement. Performances of CAP and CAPc are good for S >0 and S >1.

FRI229

A novel non-invasive index for the prediction of liver fibrosis in chronic hepatitis B patients with concurrent nonalcoholic fatty liver disease

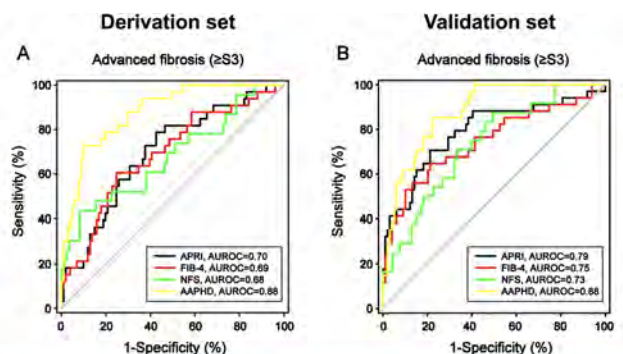
Jian Wang¹, Jiacheng Liu², Yiguang Li³, Li Zhu⁴, Minxin Mao², Weimao Ding⁵, Yuanwang Qiu³, Chuanwu Zhu⁴, Jie Li¹, Rui Huang¹, Chao Wu¹. ¹Nanjing Drum Tower Hospital, The Affiliated Hospital of Nanjing University Medical School, Department of Infectious Diseases, Nanjing, China; ²Nanjing Drum Tower Hospital Clinical College of Traditional Chinese and Western Medicine, Nanjing University of Chinese Medicine, Department of Infectious Diseases, Nanjing, China; ³The Fifth People's Hospital of Wuxi, Department of Infectious Diseases, Wuxi, China; ⁴The Affiliated Infectious Diseases Hospital of Soochow University, Department of Infectious Diseases, Suzhou, China; ⁵Huai'an No. 4 People's Hospital, Department of Hepatology, Huai'an, China

Email: dr.wu@nju.edu.cn

Background and aims: Few accurate non-invasive indexes are available to evaluate liver fibrosis in chronic hepatitis B (CHB) patients with nonalcoholic fatty liver disease (NAFLD). We aimed to establish a predictive index for advanced fibrosis in CHB patients with NAFLD.

Method: A total of 267 treatment-naïve CHB patients with NAFLD underwent liver biopsy were enrolled from four hospitals and randomly divided into a derivation set (n = 134) and a validation set (n = 133). Receiver operating characteristic (ROC) curve was used to compare predicting accuracy of different indexes.

Results: In the derivation set, alanine aminotransferase, aspartate aminotransferase (AST), prothrombin time, presence of hypertension, and type 2 diabetes were significantly associated with advanced fibrosis (≥S3). Based on these parameters, a novel index namely AAPHD for predicting advanced fibrosis was developed. The areas under the ROC curves (AUROCs) of AAPHD index in predicting advanced fibrosis was 0.88 (95%CI:0.82–0.94). The optimal cut-off value of AAPHD was -2.870, with a sensitivity of 72.73% and a specificity of 90.10%. The predicting accuracy of AAPHD for advanced fibrosis was significantly superior to AST-to-platelet ratio index (APRI) (AUROC = 0.70), fibrosis-4 score (FIB-4) (AUROC = 0.69), and NAFLD fibrosis score (NFS) (AUROC = 0.68). In the validation set, the AUROCs of AAPHD (AUROC = 0.88) remains significantly higher than that of FIB-4 and NFS, while it was comparable with APRI for predicting advanced fibrosis.



$$\text{AAPHD} = -17.102 + 1.763 \times \text{hypertension (yes = 1, no = 0)} + 1.975 \times \text{diabetes (yes = 1, no = 0)} + 0.041 \times \text{AST (U/L)} + 0.965 \times \text{PT (s)} - 0.014 \times \text{ALT (U/L)}$$

Figure: Receiver operating characteristic (ROC) curves of non-invasive tests for predicting advanced liver fibrosis in derivation set (A) and validation set (B).

Conclusion: AAPHD is a promising non-invasive index for predicting advanced fibrosis with high accuracy in CHB patients with NAFLD. The application of AAPHD may reduce the necessary for liver biopsy in CHB patients with NAFLD.

FRI230

Comparison between two 2D-SWE techniques using transient elastography as a reference method for liver stiffness assessment

Alina Popescu^{1,2}, Camelia Foncea^{1,2}, Raluca Lupusoru^{1,2,3}, Roxana Sirli^{1,2}, Felix Bende^{1,2}, Alexandru Popa^{1,2}, Victor Baldea^{1,2}, Radu Cotrau^{1,2}, Pascu Ariana^{1,2}, Ioan Sporea^{1,2}. ¹Department of Gastroenterology and Hepatology, Department of Internal Medicine II, Center for Advanced Research in Gastroenterology and Hepatology "Victor Babes" University of Medicine and Pharmacy Timisoara, Romania; ²Center for Advanced Hepatology Research of the Academy of Medical Sciences, Timisoara; ³Center for Modeling Biological Systems and Data Analysis, Department of Functional Sciences, "Victor Babes" University of Medicine and Pharmacy Timisoara, Romania
Email: foncea.camelia@gmail.com

Background and aims: Ultrasound-based liver elastography techniques are non-invasive methods used for the assessment of liver stiffness (LS). In addition to Transient Elastography (TE), new methods were developed. To compare the performance of 2D-SWE technique implemented on two different ultrasound probes from different vendors for the assessment of liver stiffness measurements (LSM) using transient elastography (TE) as reference method.

Method: A prospective study was conducted in which LSM were performed in 201 consecutive patients with or without chronic liver disease, evaluated in the same session by 2D-SWE and TE implemented on the following systems: Siemens ACUSON Sequoia (5C-1 convex transducer and Deep Abdominal Transducer-DAX), Aixplorer Mach 30 (C2-1X convex transducer) and FibroScan Compact M 530 (M and XL probes). Reliable measurements were defined as the median value of 10 measurements and an IQR/M < 0.3. For significant fibrosis a cut-off value for TE of 7 kPa was used, for advanced fibrosis 9.5 kPa and for liver cirrhosis 12 kPa.

Results: From 201 patients, 198 patients had reliable measurements in all techniques and were included in the final analysis, mean age 54.8 ± 13.3 years, mean BMI 28.8 ± 5.0, 58% (116/198) men. 58.5% were without or with mild fibrosis, 14.1% had significant fibrosis, 6.2% had advanced fibrosis and 21.2% had liver cirrhosis. For significant fibrosis the performance was slightly better for 2D-SWE.SSI (AUROC = 0.89, p < 0.0001, >7.3 kPa, Se = 85.1%, Sp = 87.9%) followed by 2D-SWE.5C1 (AUROC = 0.79, p < 0.0001, >6.9 kPa, Se = 33.7%, Sp = 96.7%) and 2D-SWE.DAX (AUROC = 0.78, p < 0.0001, >6.3 kPa, Se = 36.4%, Sp = 96.7%), p = 0.01. For advanced fibrosis the best performance was slightly better by 2D-SWE.SSI (AUROC = 0.92, p < 0.0001, >8.8 kPa, Se = 92.5%, Sp = 91.9%), and by 2D-SWE.DAX (AUROC = 0.86, p < 0.0001, >7.6 kPa, Se = 38.8%, Sp = 99.3%), followed by 2D-SWE.5C1 (AUROC = 0.84, p < 0.0001, >8.6 kPa, Se = 38.8%, Sp = 96.5%), p = 0.02. For liver cirrhosis the performances were similar: 2D-SWE.SSI (AUROC = 0.91, p < 0.0001, >10.3 kPa, Se = 92.8%, Sp = 90.3%), followed by 2D-SWE.DAX (AUROC = 0.90, p < 0.0001, >10 kPa, Se = 23.8%, Sp = 98.7%) and 2D-SWE.5C1 (AUROC = 0.84, p < 0.0001, >9.9 kPa, Se = 33.3%, Sp = 96.7%), p = 0.10. The cut off values for predicting different stages of fibrosis ranged from 6.3–7.3 kPa for F2, 7.6–8.8 kPa for F3 and 9.9–10.3 for F4.

Conclusion: The performance of the evaluated 2D SWE techniques for liver fibrosis assessment was similar.

FRI231

Shear wave elastography is a useful and accurate tool to triage patients with acute liver failure syndromes

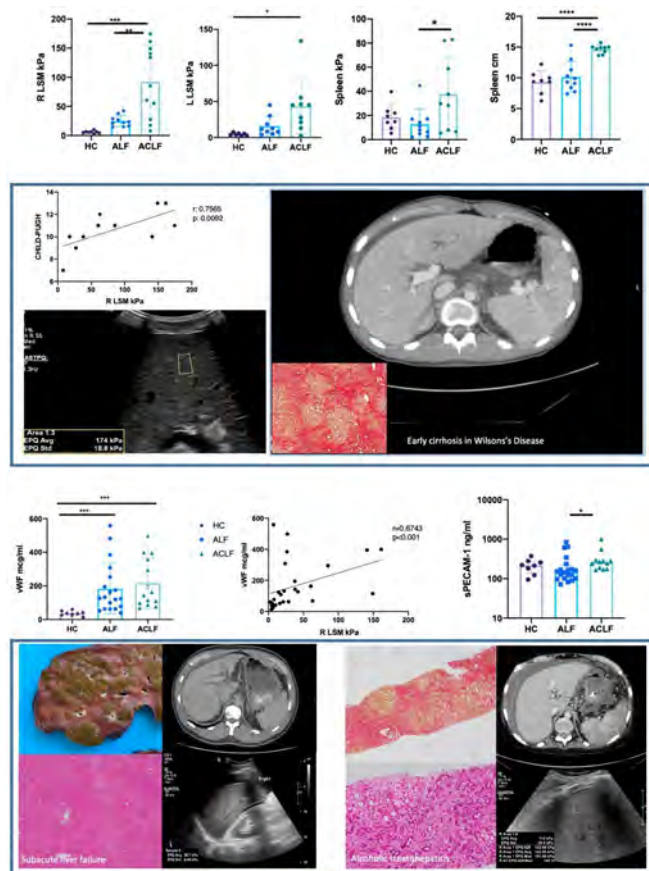
Francesca Maria Trovato¹, Florent Artru¹, Salma Mujib¹, Ellen Jerome¹, Anna Cavazza², William Bernal², Brian J. Hogan², Rosa Miquel², Mark J. W. McPhail¹. ¹Institute of Liver Studies, Department of Inflammation Biology, London, United Kingdom; ²Institute of Liver Studies, London, United Kingdom
Email: trovatofrancesca@gmail.com

Background and aims: Shear wave elastography has been largely used in chronic liver disease to assess liver stiffness non-invasively and estimate the grade of fibrosis. In acute settings, studies were inconclusive since the high stiffness is not related to fibrosis but to a combination of other factors not completely identified, including, inflammation, necrosis and micro-thrombosis. We re-evaluated the usefulness of a non-invasive anatomically directed ultrasound approach to patients with acute liver failure syndromes admitted to intensive care.

Method: 18 patients with index presentation of acute liver failure (ALF) requiring admission to liver intensive care, 3 known cirrhotics in acute on chronic liver failure (ACLF), 8 healthy controls were included in the study. After collateral history, imaging and in some case liver biopsy, acute patients were subsequently re-characterized as 10 ALF and 8 ACLF. Shear wave velocity, hepatic vascular flows, size of liver and spleen were measured using the Philips Affinity 70, and biopsy or explant histological findings were used as comparison. Platelet endothelial cell adhesion molecule-1 (sPECAM-1) and von Willebrand factor were measured in plasma by enzyme-linked immunosorbent assay (ELISA) (n: 8HC, 20 ALF, 12 ACLF).

Results: Liver stiffness measurement of the right lobe (RLSM) accurately identified healthy controls (5.9 ± 2 kPa), acute liver failure (24.87 ± 9.3) and acute on chronic liver failure (92 ± 61.8 kPa) patients. In this population with hyperdynamic circulation, the estimation of the left lobe stiffness was less accurate due to heart beat artifacts. Spleen size, but not spleen stiffness, accurately discriminate between ALF and ACLF. In ACLF, RLSM correlates with both age and severity of liver disease express by Child-Pugh score and the highest values are found in alcoholic hepatitis and Wilson's disease. sPECAM-1 correlates with bilirubin (Spearman r = 0.777, p < 0.001) and MELD (r = 0.05335, p = 0.029) in both acute liver failure syndromes but no correlation was found with liver stiffness. Conversely, vWF is highly directly correlated with RLSM, MELD and SOFA scores (p < 0.001). 3 ALF explants and 4 explants/biopsies confirming the presence of cirrhosis in ACLF patients and higher degree of cholestasis in all compartments (cytoplasmic, canalicular and ductular), had respectively a mean RLSM of 26 ± 17.6 kPa and 109 ± 60 kPa.

POSTER PRESENTATIONS



Conclusion: In patients with acute liver failure syndromes, shear wave elastography can help in the early clinical assessment at admission in intensive care. Plasma vWF is highly correlated RLSM and it can be speculated that the presence of platelets aggregates can be responsible of the increased values. Moreover histological analysis showed high degree of intrahepatic cholestasis in ACLF. Further studies are needed to definitely explain the high level of stiffness reported in these patients.

FRI232

A novel simple and reliable 2D-shear wave elastography (SWE) and ultrasound-guided coefficient attenuation parameter (SCAP) technique for patients with chronic liver disease

Christiane Stern¹, An Ngo², Cristiane Villela-Nogueira³, Dominique Thabut¹, Vlad Ratiu¹. ¹Hôpital Pitié-Salpêtrière, Service d'Hépatogastroentérologie, Paris, France; ²Hôpital Pitié-Salpêtrière, Service d'Hépatogastroentérologie, Paris, France; ³Federal University of Rio de Janeiro, Serviço de Hepatologia, Rio de Janeiro, RJ, Brazil
Email: christiane.stern@gmail.com

Background and aims: Different non-invasive methods are now widely used for first line assessment of liver fibrosis and steatosis in patients with chronic liver disease. The detection of advanced fibrosis using 2D-shear wave elastography (SWE) and significant steatosis using ultraSound-guided CAP (SCAP) measured by Aixplorer MACH 30 (SS) is simple, safe and overcomes several limitations of transient elastography (TE) and CAP measured by FibroScan (FS). Nevertheless, reliability criteria have not been well described for SS. The aims of this study were to define the optimal technical procedure, the performance for the detection of fibrosis and steatosis and the reliability criteria using SS.

Method: 215 consecutive patients with chronic liver disease that underwent non-invasive tests were included. Clinical, biological and

histological data within 6 months were collected. TE and CAP were performed by 2 experienced operators using the classical technique of 10 measurements at the midaxillary line. Measurements of SWE and SCAP were performed in triplicate at the mid (MAL), posterior (PAL) and anterior axillary lines (AAL) (total of 9 values). The technique the simplest to perform and most reliable has been analyzed. Performances of SWE and SCAP for the diagnosis of advanced fibrosis and significant steatosis have been defined using TE (≥ 9.5 kPa) and CAP (≥ 275 dB/m) as reference. Factors associated with discordance have been evaluated.

Results: FS and SS data from 203 patients were analyzed (12 patients excluded due to FS and/or SS failure). Baseline characteristics: mean age 56 ± 14 years; male 58%; MAFLD 59%, viral hepatitis 24%; mean BMI 28.3 ± 5.9 kg/m². Median TE and CAP were 6.5 kPa (2.5–66.9) and 272 dB/m (141–400). Table 1 shows the performances of SCAP according to different technique methods. The median of 3 SWE values and 3 SCAP values (1st measurement at MAL, PAL and AAL) had an AUROC of 0.96 [CI95%: 0.93–0.98] and 0.91 [CI95%: 0.86–0.95] for the diagnosis of advanced fibrosis and significant steatosis, and considered as the best technique. The accuracy of cut-off values for SWE (≥ 8.5 kPa) and SCAP (≥ 0.44) were analyzed in 54 patients with liver biopsy. There was only 1 false-negative for fibrosis (PPV = 50%, NPV = 97%) and 2 false-negatives for steatosis (PPV = 69%, NPV = 87%). The factors associated with discordance were skin-to-liver distance (SLD) ≥ 2.4 cm ($p < 0.001$), depth ≥ 5.5 cm ($p < 0.001$), stability index $< 70\%$ ($p = 0.009$) and viscosity ≥ 2.4 ($p = 0.026$). In logistic regression, the only factor associated with discordance was SLD ($p = 0.012$).

Table 1. Performances of SCAP for the diagnosis of significant steatosis according to different technique methods, taking CAP measured by FibroScan as reference.

SS technique for the diagnosis of steatosis	AUROC	CI95%
SCAP measured 3 times at MAL	0.87	0.82 – 0.92
SCAP measured 3 times at PAL	0.80	0.74 – 0.87
SCAP measured 3 times at AAL	0.85	0.80 – 0.90
SCAP measured 9 times (3 MAL, 3 PAL and 3 AAL)	0.90	0.86 – 0.95
SCAP measured 3 times (1 st MAL, 1 st PAL and 1 st AAL)	0.91	0.86 – 0.95

Conclusion: A quick and reliable non-invasive diagnosis of advanced fibrosis and significant steatosis can be obtained with the median of 3 measurements (1 mid, 1 posterior and 1 anterior axillary line) using SS. The only non-reliable criterion is skin-to-liver distance ≥ 2.4 cm.

Abstract withdrawn

FRI234

Dynamics of liver stiffness predicts hepatocellular carcinoma and ascites occurrence in patients with hepatitis C virus related cirrhosis treated with direct-acting antiviral agents

Alberto Nicoletti¹, Maria Elena Ainora¹, Marco Cintoni², Matteo Garcovich¹, Martina De Siena¹, Barbara Funaro¹, Francesca Ponziani¹, Antonio Grieco³, Laura Riccardi¹, Maurizio Pompili¹, Antonio Gasbarrini¹, Maria Assunta Zocco¹.
¹Fondazione Policlinico Universitario "A. Gemelli" IRCCS, Università Cattolica del Sacro Cuore-Rome, Internal Medicine and Gastroenterology, Rome, Italy; ²Fondazione Policlinico Universitario "A. Gemelli" IRCCS, Università Cattolica del Sacro Cuore-Rome, Clinical Nutrition, Rome, Italy; ³Fondazione Policlinico Universitario "A. Gemelli" IRCCS, Università Cattolica del Sacro Cuore-Rome, Internal Medicine and Liver Transplant, Rome, Italy
 Email: mariaazocco@hotmail.com

Background and aims: The achievement of a sustained virologic response (SVR) with direct acting antivirals (DAAs) has been shown to prevent liver-related events (LREs) in patients with chronic hepatitis C virus (HCV)-related cirrhosis. Bidimensional shear wave elastography (2D-SWE) is an effective and easy to perform technique for the early assessment of liver fibrosis during DAA treatment. The main aim of the study was to evaluate changes in liver stiffness (LS) using 2D-SWE in patients with HCV-related cirrhosis undergoing DAA therapy. Secondary endpoint was to identify any correlation between LS, ultrasound and clinical parameters that predict the occurrence of LREs.

Method: We enrolled 229 consecutive patients who received DAAs based regimens for HCV-related cirrhosis between December 2014 and September 2016. Standard ultrasound, 2D-SWE measured LS, and clinical and laboratory data were assessed before treatment (baseline), 24 weeks after end of treatment (EOT) (T1) and 48 weeks

after EOT (T2). Patients were followed up every 6 months according to international clinical practice guidelines. Any LRE was registered during follow-up. Uni- and multi-variate Cox regression analysis was performed to determine parameters associated with the development of LREs.

Results: At baseline, mean LS was 18.1 ± 6.6 kPa. Levels of LS decreased to a mean of 13.6 ± 6.1 kPa and 12.5 ± 6.1 kPa at T1 ($p < 0.0001$) and T2 ($p < 0.0001$), respectively. The median follow-up was 3.25 years (range 0.2–4.7). HCC was the most frequent LRE (30 patients, 13.1%). 13 patients (5.7%) developed ascites, 11 (4.8%) portal vein thrombosis (PVT), 8 (3.5%) hepatic encephalopathy (HE), 8 (3.5%) infections and 5 (2.2%) variceal bleeding. 9 patients died (3.9%) and 5 were transplanted (2.2%).

Male gender, bilirubin, international normalized ratio (INR), Model for End-stage Liver Disease (MELD) score, prior history of harmful alcohol intake, LS, portal velocity and a change in LS less than 20% at T2 (1-y Delta-LSM) were associated with HCC occurrence by univariate analysis. By Cox regression multivariate analysis, only MELD score (HR 1.16; CI 95% 1.01–1.33; $p = 0.026$) and 1-year Delta LSM $< 20\%$ (HR 2.98; CI 95% 1.01–8.1; $p = 0.03$) were independently associated with HCC risk. Interestingly, 1-year Delta LSM $< 20\%$ was independently associated with the development of ascites with significant hazard ratio (HR 5.08; CI 95% 1.03–25.14; $p = 0.04$). Since the variables maintained their predictive value over time, we combined their HR in a simple model to estimate the probability of HCC occurrence at 24, 36, 48 and 60 months after EOT.

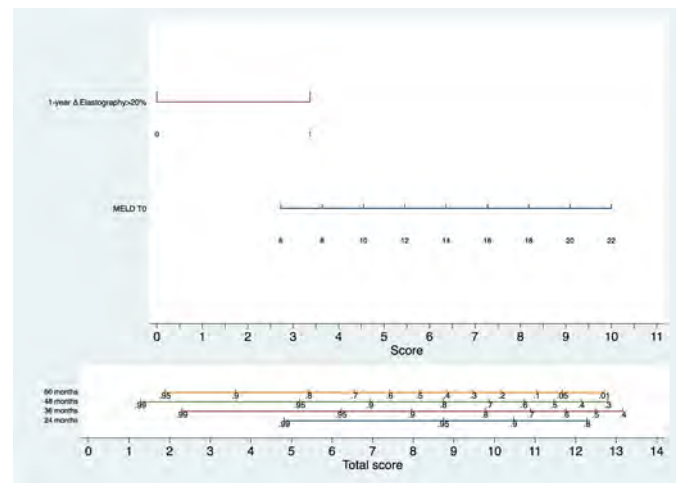


Figure: Predictive model for HCC occurrence.

Conclusion: Alone and in association with clinical and biochemical variables, dynamic changes of 2D-SWE-measured LS after DAA therapy for HCV may be a useful tool to predict HCC and ascites occurrence in cirrhotic patients.

FRI235

The concordance within one blood test improves reliability evaluation of liver fibrosis

Paul Cales¹, Clémence M. Canivet¹, Lannes Adrien¹, Frédéric Oberti¹, Isabelle Fouchard¹, Jerome Boursier¹. ¹Angers University Hospital, Hepatology, Angers, France
 Email: paul.cales@univ-angers.fr

Background and aims: The improved reliability of non-invasive tests of liver fibrosis is defined by agreement between a patented blood test and liver stiffness measurement (LSM) by transient elastography (TE) in 2021 EASL guidelines. The inconvenience is to require two different tests adding cost and reducing availability. Our aim was to apply this agreement rule to a single blood test targeted either for significant fibrosis (FibroMeterV2G: FM2G) or cirrhosis (CirrhoMeterV2G: CM2G) using the same markers.

POSTER PRESENTATIONS

Method: Patients with chronic liver disease of multiple untreated etiologies, with liver biopsy using Metavir F within 6 months of blood test, were included in a derivation (n = 2159) and a validation (n = 1476 with LSM by TE) sets. Agreement grade was calculated as the absolute difference (AD) between fibrosis (F_M) classifications of FM2G and CM2G. The main outcome was severe fibrosis (Metavir $F \geq 3$). Outcome measures were AUROC and accuracy (correct diagnosis).

Results: In the derivation set, FM2G accuracy (and prevalences) were according to agreement grade: high (F_M AD ≤ 0.5): 83.1% (78.6%), fair (F_M AD = 1): 70.2% (16.3%), poor (F_M AD > 1): 50.0% (5.1%), $p < 0.001$. CM2G accuracy was, respectively 83.1%, 67.6%, 50.9% ($p < 0.001$). Then, agreement was classified as concordant or not for Metavir $F \geq 3$. FM2G accuracy (and prevalences) were, concordant: 83.9% (85.9%), discordant: 51.3% (14.1%), $p < 0.001$. FM2G AUROCs were, respectively: 0.866 and 0.519, $p < 0.001$. The overall accuracy of FM2G (79.3%) and CM2G (79.0%) were not different ($p = 0.688$) but they were complementary (kappa: 0.573). So, a CM/FM algorithm was constructed. Its accuracy was significantly increased to 82.2% ($p < 0.001$) vs FM2G or CM2G and different between concordant (85.1%) and discordant (64.1%, $p < 0.001$) blood tests. In the validation set, previous results were confirmed, e.g. CM/FM accuracy was, concordant blood tests: 79.9%, discordant: 60.5% ($p < 0.001$). The concordance prevalence was higher for FM2G vs CM2G (84.9%) than vs LSM (70.9%, $p < 0.001$). Accuracy was globally, LSM: 78.8% vs CM/FM: 77.0%, ($p = 0.173$) or FM2G: 75.5% ($p = 0.011$) but in the 70.9% of concordant FM2G/LSM it was, respectively: 88.0% vs 87.4% ($p = 0.210$) or 88.0% ($p = 1$). The accuracy in concordant tests was however higher in FM2G agreement vs LSM than vs CM2G, e.g. CM/FM: 88.0% vs 79.9% ($p < 0.001$).

Conclusion: The concordance within a blood test significantly increased the concordance prevalence. The limit was a reduced accuracy; the advantages were a reduced cost and liver biopsy recourse by half, and a simpler use (single time and greater ubiquity).

FRI236

Novel and accurate measurement of differential protease activity in diagnosed HCC patients compared to non-HCC cirrhotic patients

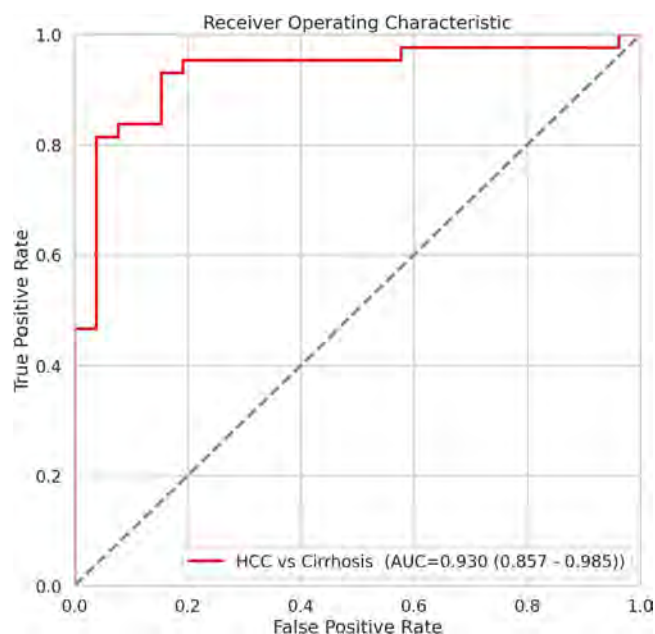
Amit Singal¹, Tram Tran², Ben Holmes², Chris Gulka², Anatoly Myaskovsky², Andrea Shepard², Mackenzie Rowe², Sophie Cazanave², Faycal Touti², Jina Lee², Alejandro Balbin², Wendy Winckler². ¹UT Southwestern Medical Center, Department of Internal Medicine, Dallas, United States; ²Glympse Bio, Cambridge, United States

Email: ttran@glympsebio.com

Background and aims: The incidence of hepatocellular carcinoma (HCC) is rising worldwide and projected to continue increasing through 2030. HCC surveillance using ultrasound with or without AFP has suboptimal sensitivity, missing over one-third of HCC at an early stage. We previously showed a panel of biosensors that interrogate biological pathways implicated in HCC pathogenesis (tumor invasion of extracellular matrix, matrix remodeling, inflammation, and fibrinolysis) was highly effective at differentiating patients with HCC from healthy controls, with AUCs > 0.94 . The aim of this study was to assess accuracy of protease biosensor biomarker panel to distinguish patients with HCC from those with cirrhosis without HCC.

Method: Retrospective plasma samples were obtained from patients diagnosed with HCC (cases) and those with cirrhosis without HCC (controls). Protease biosensor cleavage was assayed from plasma by fluorimetry. The relative signal was used for classification by regularized logistic regression using 100 cross-validation (80% train, 20% validation splits). The maximum point from the Youden's J index in the training set was used to define the optimal cut-off, which was used to calculate sensitivity and specificity for HCC detection in the validation sets.

Results: Plasma protease activity was assessed in 43 HCC cases (65% male, mean age 58 years, 49% HBV/7% HCV/44% unknown etiology) and 26 cirrhosis controls (30% male, mean age 57 years, 100% NASH etiology). Nearly three-fourths (72%) of the cases had early-stage tumors (TNM stage I or II). The most significant biosensors in the classification of HCC vs cirrhosis were substrates of MMPs, DPP4, ANPEP, ARTS-1, KLK14 and Cathepsins (L, S, K, B) and ADAM17. The panel of protease biosensors had high accuracy for differentiating patients with HCC vs those with cirrhosis (AUC = 0.93 [CI 0.86–0.98]) (Figure). Using the Youden's cut-off, sensitivity and specificity of the protease biosensor panel for HCC detection were 0.84 and 0.85, respectively.



Conclusion: Novel non-invasive biosensors measuring protease activity accurately differentiate HCC from cirrhosis and, if validated in larger biomarker studies, may serve as an alternative surveillance tool to improve early HCC detection.

FRI237

FIB-4 predicts severe hematological toxicity and 6-month mortality in older patients with cancer: ELCAPA-LIVER.

Victoire De Salins¹, Antoine Morel², Claudia Martinez-Tapia², Pierre-Emmanuel Rautou³, Florence Canoui-Poitrene², Elena Paillaud⁴, Johanne Poisson⁵. ¹AP-HP, Service de Gériatrie, Hôpital Européen George Pompidou, Paris, France; ²University Paris Est Creteil, INSERM, IMRB, F-94010 Créteil, France, Clinical Epidemiology and Ageing Unit, Institute Mondor de Recherche Biomédicale, Paris-Est University, F-94000 Créteil, France; ³Université Paris-Cité, AP-HP, Hôpital Beaujon, Service d'Hépatologie, DMU DIGEST, Centre de Référence des Maladies Vasculaires du Foie, FILFOIE, ERN RARE-LIVER, Centre de recherche sur l'inflammation, Inserm, UMR 1149, Paris, France; ⁴Université Paris-Cité, AP-HP, Service de Gériatrie, Hôpital Européen George Pompidou, Paris, France, Clinical Epidemiology and Ageing Unit, Institute Mondor de Recherche Biomédicale, Paris-Est University, F-94000 Créteil, France; ⁵Université Paris-Cité, AP-HP, Service de Gériatrie, Hôpital Européen George Pompidou, Centre de recherche sur l'inflammation, Inserm, UMR 1149, Paris, France, France

Email: poisson.johanne@gmail.com

Background and aims: The current increased life expectancy is associated with an increasing incidence of cancer in older patients. Geriatric assessment has improved the management of this heterogeneous population with thorough evaluation of physiologic systems

Nurses and Allied Health Professionals

FRI238

The main thing is to be alive-exploring patients' experiences with weight gain after liver transplantation: a qualitative study

Sonja Beckmann^{1,2}, Patrizia Kuenzler^{1,3}, Kajetan Kabut⁴, Oliver Mauthner^{1,5}. ¹University of Basel, Institute of Nursing Science, Basel, Switzerland; ²University Hospital Zurich, Center Clinica Nursing Science, Zurich; ³Cantonal Hospital St.Gallen, Department of Gastroenterology/Hepatology and Department of Nursing, St.Gallen; ⁴BDH-Klinik Elzach, Zentrum für NeuroRehabilitation, Beatmungs-, und Intensivmedizin, Germany; ⁵University Department of Geriatric Medicine Felix Platter, Basel, Switzerland
Email: sonja.beckmann@usz.ch

Background and aims: Weight gain after liver transplantation (LTx) is common, contributing to the development of new-onset obesity at 2- and 3-years post-LTx in 22% and 38% of patients. These significant weight gains prompt the question of how patients cope with this increase of weight. Unfortunately, few studies examined the patients' perspective. This study aimed to explore how patients' experienced their weight gain after LTx.

Method: Individual interviews followed a guideline with open-ended questions. Transcripts were analyzed according to the six phases of the reflexive thematic analysis approach by Braun and Clarke.

Results: The 12 participants gained 11.5 kg weight (median) over a median of 23 months after LTx. The constitutive theme "The main thing is to be alive" was a recurrent insight, captured in different facets in all three consecutive themes: "The arduous path back to living" was the emotional facet, expressing the ups and downs during the suffering from a life-threatening illness to finally being grateful for the new life. "A pleasurable new phase of life" was the legitimization, reflecting the appreciation of gaining weight and returning to a healthy appearance after having overcome the illness. "I am allowed to look like this now" was the consoling facet after a time of physical and emotional burden due to the increased weight and frustration of being unsuccessful in losing weight. Finally, the awareness of being a LTx survivor outplayed the burden of the excess weight.

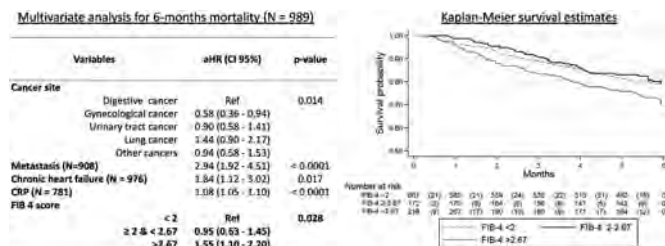
i.e. heart, lung, renal functions for cancer treatment choice, but no study reported a comprehensive analysis of liver parameters and its impact on mortality and toxicity. Yet, aging is thought to be associated with a liver functional decline and is an important risk factor for developing chronic liver disease. FIB-4 has been shown to predict mortality in non-oncological young and older patients without known chronic liver disease. Aims of this study were to evaluate predictive value of FIB-4 for 6-months survival and treatment toxicities in patients age 70 yo or older with cancer.

Method: Patients aged 70 or older with histologically documented solid or hematological cancers and referred for geriatric assessment were included from the multicentric, French prospective open-cohort Elderly Cancer Patients (ELCAPA) from March 2015 to September 2019. In the present study (ELCAPA-LIVER), patients, at any stage, treated by chemotherapy, immunotherapy or targeted therapy in 6 different centers and for whom platelet count and serum AST and ALT measurements were available at baseline, were selected. Patients with known chronic liver diseases were excluded. Geriatric assessment was performed at baseline. FIB-4 cut-off values used to rule out or to rule in advanced fibrosis in elderly patients with liver diseases were used to classify patients into three prognostic groups (cut-offs were decided based on previous papers in older patients). Treatment toxicities (grade 0/I/II vs grade III/IV) and mortality were assessed at 6 months of follow-up.

Results: 989 patients were included: median age: 81 years (IQR: 77–84); female, 58.8%; main cancer sites: digestive 29%, gynecological 28%, urinary tract 14% and lung 12%; metastatic diseases 51%. At 6 months, 763 patients were dead (77%) and 355 patients (59%) experienced grade III/IV anticancer toxicities, including 123 patients (22.4%) with hematological toxicities.

A FIB-4 index >2.67 before treatment was independently associated with hematological toxicities grade III/IV (adjusted OR = 1.92 (95% CI: 1.15–3.22), p = 0.02).

In addition, a FIB-4 index >2.67 was predictive for 6-month mortality independently of cancer site, metastasis, chronic heart failure, and C-Reactive Protein (aHR = 1.55 (1.10–2.20), p = 0.028).



Conclusion: A FIB-4 index >2.67 was an independent predictor for 6-month mortality and severe hematologic toxicity in older patients treated for cancer. This shows the importance of evaluating liver status to improve decision making in older patients with cancer.

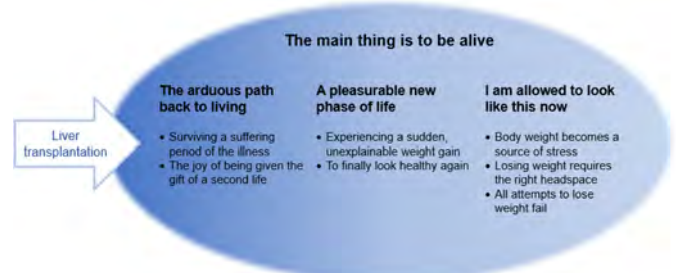


Figure 1. Overview over the four themes and the seven subthemes.

Conclusion: Understanding the patients' dynamic lived experiences, beliefs and motivations on post-LTx weight gain is crucial in providing tailored care. Interventions should be offered early because the comforting insight "I am allowed to look like this now" may hinder the patient's motivation to further engage in weight loss interventions. Our suggestions on time and content of education and self-management support, based on the transtheoretical model, may guide professionals' clinical practice.

POSTER PRESENTATIONS

FRI239

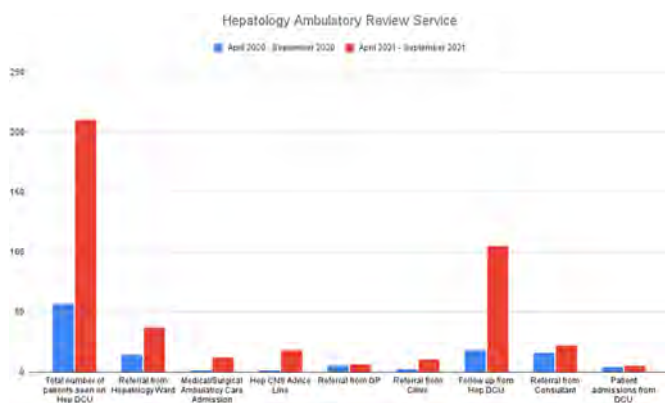
Development of a nurse led hepatology ambulatory review service

Victoria Wharton¹, Bryony Butler¹. ¹John Radcliffe Hospital, Hepatology, Oxford, United Kingdom
Email: victoria.wharton@ouh.nhs.uk

Background and aims: The Liver Unit in Oxford was significantly impacted by COVID-19-highlighting a need for a nurse-led Hepatology ambulatory review service to help minimise inpatient admissions and assess patients with newly diagnosed decompensated liver disease. The Hepatology DCU were providing a nurse led abdominal paracentesis clinic and between appointments the team were able to accommodate clinical reviews. The aims for this service were to reduce Emergency Department (ED) and hospital admissions, facilitate safe and early discharges, expedite care for long term management plans and to allow a single point of access for patients and their families.

Method: Since its creation, the two founding Clinical Nurse Specialists (CNS) have collated key metrics pertaining to the patients treated by the service. These metrics included the route of referral, hospital details, date of referral, the reason for referral and whether they needed a hospital admission. Using this dataset, the effectiveness of the service has been critically assessed.

Results: Between April 2020–September 2021 the Hepatology DCU reviewed a total of 407 patients. 210 patients were seen from April 2021–September 2021; a monthly average increase of 118%, when compared to the previous year. Not included in these figures, were patients reviewed by the hepatology medical team in ED and medical/surgical ambulatory units. Of the 210 patients reviewed in DCU since April 2021, 76 patients were hepatology ward discharges reviewed by either CNS, hepatology specialist registrar or a consultant within 7–10 days of discharge. Furthermore, since starting the service just 3.9% of patients required admission from daycase. 224 (55%) of the patients seen in the ambulatory review service since April 2020 were for ascites/oedema review ± diuretic management. The ambulatory reviews are in addition to the patients' routine follow up appointments-aiding close management of their liver disease and expedition of the relevant investigations required for their long-term management, resulting in early interventions. Following completion of an Independent and Supplementary Prescribing module by the CNS, the ambulatory review service became nurse-led in September 2020.



Conclusion: Although the service is in its infancy, the number of patients reviewed has doubled since starting the hepatology ambulatory review service in April 2020. This has freed up outpatient clinic capacity and prevented delays to assessments. The Hepatology DCU currently provides a five-day service to help reduce ED attendances and reduce inpatient admissions; it is staffed by two full time band 7 CNS.

FRI240

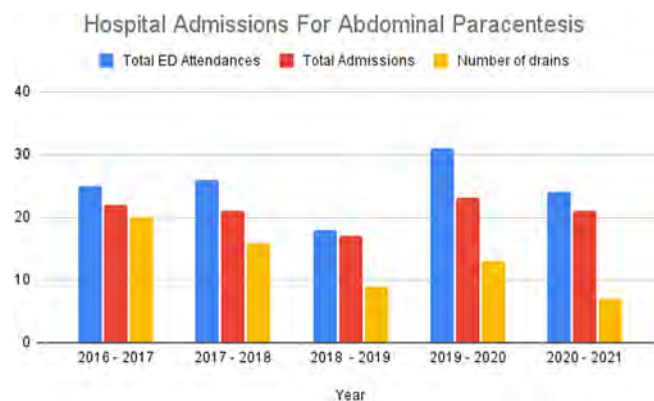
Development of a nurse led daycase abdominal paracentesis service

Victoria Wharton¹, Bryony Butler¹. ¹John Radcliffe Hospital, Hepatology, Oxford, United Kingdom
Email: victoria.wharton@ouh.nhs.uk

Background and aims: Patients living with advanced liver disease often require symptomatic management of ascites with abdominal paracentesis. At Oxford University Hospitals Trust, there was previously no routine care pathway to manage the accumulation of ascites. Instead, patients would frequently present to the emergency department (ED) or to their GP in discomfort and then require emergency admission to the hepatology ward for paracentesis. This resulted in delayed care and often a lengthy hospital admission. A need was identified to provide a nurse-led, daycase paracentesis service for these patients. The aim of this service was to improve patient experience, reduce ED attendances and inpatient admissions, standardise care across the trust and build effective relationships with patients and their families.

Method: The Hepatology Day Case Paracentesis service commenced in October 2018. Initially, clinics occurred once a week, a maximum of four patients were reviewed and paracentesis was performed by a ward-based doctor. However, due to inpatient ward pressures, patients would often experience lengthy delays, when waiting for the doctor to insert their drains. This led to the development of a fully nurse delivered service. To facilitate its creation, a training programme was developed for the Clinical Nurse Specialists, in addition to postgraduate study. A 5-year dataset on patients presenting to ED with ascites (provided by clinical coders) was used to critically assess the effectiveness of the nurse-led daycase paracentesis service.

Results: Since the introduction of a fully nurse-led daycase paracentesis service in January 2020, we have performed 399 ultrasound guided paracentesis in 61 patients up to and including October 2021. Between April 2016–March 2021 a total of 124 patients presented to ED with ascites; 104 of which required an inpatient admission and 65 had a paracentesis. Furthermore, the number of patients needing admission specifically for a paracentesis fell from 20 in 2016–2017 to 7 in 2020–2021. Whilst the number of patients attending ED and requiring admission does not appear to have reduced, the number of patients admitted for paracentesis has reduced significantly.



Conclusion: The number of patients requiring admission to hospital for a paracentesis has reduced by 65% since founding a nurse-led daycase paracentesis service. The nurse-led abdominal paracentesis clinic has reduced the number of patients attending ED for ascites management alone and has provided patients with a single point of contact for managing their ascites requiring paracentesis.

FRI241

Implementing a cirrhosis order set: a qualitative analysis of provider-identified barriers and facilitators

Ashley Hyde¹, Emily Johnson¹, Michelle Carbonneau², Dawn Schroeder², Thea Luig¹, Denise Campbell-Scherer¹, Puneeta Tandon¹. ¹University of Alberta Faculty of Medicine and Dentistry, Edmonton, Canada; ²Alberta Health Services, Edmonton, Canada
Email: ac20@ualberta.ca

Background and aims: Resulting from vascular and hepatocellular injury, cirrhosis is a chronic condition that results in profound impairments in quality of life, and high rates of morbidity and mortality. Hospitalizations and readmissions become more commonplace as cirrhosis advances, with a 90-day readmission rate of 53% noted in a large North American cohort of over 1000 patients. Cirrhosis Care AB (CCAB) is a pragmatic trial which aims to address current gaps in cirrhosis care in Alberta through the implementation of a standardized order set across multiple acute care sites. Prior to implementation of such a large-scale quality improvement initiative, it is essential to understand the implementation contexts, including perceptions of the proposed intervention, and potential barriers and facilitators to implementation.

Method: We used a qualitative descriptive approach to (i) understand participant's past experiences with implementation of standardized order sets, (ii) to identify potential barriers and facilitators to implementation of the cirrhosis order set, and (iii) to develop tailored implementation strategies for each study site. We used the Consolidated Framework for Implementation Research (CFIR) and the Normalisation Process Theory (NPT) to guide development of our interview guide and coding framework. We conducted focus groups using a semi-structured interview guide. Focus groups were recorded and transcribed verbatim. A deductive content analysis approach using the core constructs of CFIR and NPT was used.

Results: We conducted a total of 8 focus groups, that were attended by 54 healthcare providers. Of the attendees, 20% were prescribers (MDs & NPs), with the remainder comprised of nurses, social workers, pharmacists, and physiotherapists. Barriers to implementation of the cirrhosis order set included the significant investment of time and resources required, the "change fatigue" of providers, and poor communication across provider groups. Facilitators included a recognized advantage of the efficiencies offered by the cirrhosis order set, the strength of the evidence on which the order set was based, leadership support of the initiative, and recognition of the need to improve care for patients with cirrhosis.

Conclusion: The findings of this study suggest that healthcare provider's perceptions of the cirrhosis order set were greatly influenced by their past experiences with the implementation of other quality improvement initiatives. Crucial to the success of the cirrhosis order set will be the use of tailored implementation strategies to promote uptake including: (i) the identification of site champions, (ii) use of implementation meetings to share learnings across study sites, and (iii) leveraging the facilitators including highlighting efficiencies in work processes that can be made possible by the cirrhosis order set.

FRI242

Quality of life in patients with advanced cirrhosis. Relationship with the development of complications

Ana Belén Rubio^{1,2,3,4}, Adria Juanola^{1,2}, Martina Perez^{1,2}, Marta Carol^{1,2,3,4}, Carlota Riba^{1,4,5}, Sara Martinez^{1,3,4}, Marta Cervera^{1,2,3,4}, Emma Avitabile^{1,2}, Ann Ma^{1,2}, Laura Napoleone^{1,2}, Octavi Bassegoda^{1,2}, Jordi Gratacós-Gines^{1,2}, Elisa Pose^{1,2,3}, Isabel Graupera^{1,2,3}, Anna Soria^{1,2}, Pere Ginès^{1,2,3,4}, Núria Fabrellas^{1,2,3,4}. ¹Hospital Clinic, Liver Unit, Barcelona, Spain; ²University of Barcelona, Faculty of Medicine and Health Sciences, Barcelona, Spain; ³Instituto de Investigaciones Biomédicas August Pi i Sunyer (IDIBAPS), Barcelona, Spain; ⁴Centro de Investigación Biomédica en Red de Enfermedades Hepáticas y Digestivas (CIBERehd), Madrid, Spain; ⁵Fundació Clínic per la Recerca Biomèdica (FCRB), Barcelona, Spain
Email: a Rubio@clinic.cat

Background and aims: Liver cirrhosis causes an alteration in the Quality of Life (QoL) of patients that is more intense in patients in the decompensated phase. The alteration of QoL affects both the physical and mental dimensions of the patients. It is not known whether the alteration of QoL correlates with a higher risk of developing complications of the disease.

To investigate whether the intensity of QoL alteration is associated with a higher risk of developing complications of cirrhosis.

Method: This study was conducted in the cohort of patients of the MACHT study (*J Hepatol* 2018; PMID: 30138685), a study investigating the effect of midodrine and albumin in patients with decompensated cirrhosis on the liver transplant waiting list. QoL was assessed using the Short Form Health Survey (SF-36) and the Chronic Liver Disease Questionnaire (CLDQ). The relationship between different QoL parameters and the development of complications during follow-up was investigated.

Results: Under baseline conditions the two groups of patients, placebo and treatment, were similar with respect to QoL parameters, and were therefore considered as a single cohort. Of the 159 patients included, 53 (33%) developed complications during follow-up (median 80 days). Patients who developed complications had more marked alterations in CLDQ and most parameters of the physical and mental domains of SF-36 as compared to patients who did not develop complications measured under baseline conditions. The more intense alteration of CLDQ and SF-36 was also associated with a higher risk of developing hepatic encephalopathy during follow-up. In a multivariate analysis, both the mental and physical components of the SF-36 were independent predictive factors of development of hepatic encephalopathy.

Conclusion: In patients with cirrhosis, the QoL parameters are not only useful to assess the degree of the patient's impairment, but also indicate a higher risk of developing complications, especially hepatic encephalopathy. These parameters provide useful clinical information for clinical practice and should be taken into account in clinical studies evaluating the efficacy of new treatments for the disease.

FRI243

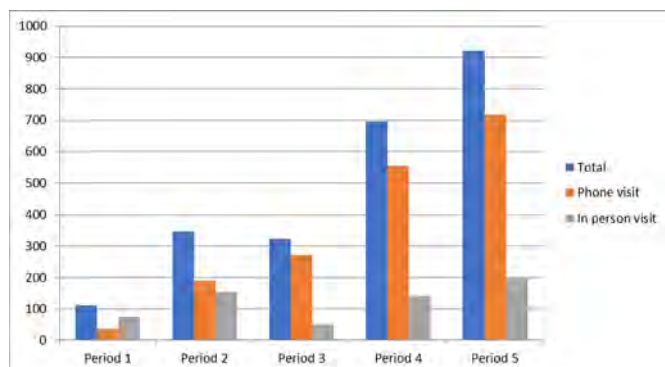
Effects of the COVID-19 pandemic on the activity of an advanced practice nurse clinic on liver cirrhosis

Martina Perez^{1,2,3}, Ann Ma^{1,3,4}, Marta Cervera^{1,2,3,4}, Marta Carol^{1,2,3,4}, Ana Belén Rubio^{1,3,4}, Sara Martínez^{1,3,4}, Carlota Riba^{1,3,4}, Laura Napoleone^{1,3,4}, Jordi Gratacós-Gines^{1,3,4}, Anna Soria^{1,3}, Emma Avitabile^{1,3,4}, Octavi Bassegoda^{1,3,4}, Adria Juanola^{1,3,4}, Elisa Pose^{1,3,4}, Isabel Graupera^{1,3,4}, Pere Ginès^{1,2,3,4}, Núria Fabrellas^{1,2,3,4}. ¹Hospital Clínic de Barcelona, Liver Unit, Barcelona, Spain; ²Facultat de Medicina-Universitat de Barcelona, Barcelona, Spain; ³Centro de Investigación Biomédica en Red de Enfermedades Hepáticas y Digestivas (CIBERehD), Barcelona, Spain; ⁴Institut d'Investigacions Biomèdiques August Pi i Sunyer (IDIBAPS), Barcelona, Spain
Email: maperezgu@clinic.cat

Background and aims: Liver cirrhosis is associated with significant morbidity and mortality and is, in addition, responsible for a high number of hospitalizations, which represent a high burden for health systems. As the disease progresses, serious complications can occur, such as ascites, gastrointestinal bleeding, encephalopathy and jaundice, marking the transition to the decompensated phase. Due to the high progression rate of the disease, these complications tend to recur over time. The role of the nurse is increasingly recognized as instrumental in the management of patients with chronic liver disease, with positive impacts noted on patient education, patient independence and early detection of complications. Nevertheless, patient care was severely impacted in the year 2020 by the COVID-19 pandemic, profoundly changing the internal organisation of hospitals and the type of care we have been able to offer to patients. Therefore, the aim of this study was to evaluate the evolution of the activity of the advanced practice nurse clinic in liver cirrhosis, taking into account its recent implementation and the COVID-19 pandemic.

Method: We performed a retrospective observational descriptive study, analyzing the activity of the liver cirrhosis outpatient nurse clinic of the Hepatology Department of the Hospital Clínic in Barcelona. We included all patients visited by the specialized hepatology nurse over a period of 2.5 years, from 01/03/2019 to 31/08/2021. The data were analyzed considering five periods, each lasting 6 months. The first corresponds to the beginning of the implementation of the advanced practice nurse consultation, the third coincides with the beginning of the pandemic, the fourth and the fifth correspond to the consecutive months until August 2021.

Results: A total of 2398 visits were completed, 1772 (73.8%) by telephone and 626 (26.1%) in person. During the third period (01/03/2020–31/08/2020), face-to-face visits decreased by 30% compared to previous periods, while telephone visits increased by 50%. There was an 8-fold increase in the total number of visits in the last period compared to the first. This increase is due to an increase in telephone visits, a trend that was probably precipitated by the the COVID-19 pandemic, but that has persisted since.



Conclusion: Despite the restrictions on face-to-face visits during the first months of the COVID-19 pandemic, visits in the advanced practice nurse clinic have continued to increase, and it has been possible to respond to patients' care needs. The specialized nurse plays a key role in the management of patients with cirrhosis and has been fundamental in responding to their needs particularly in the context of the COVID-19 pandemic.

FRI244

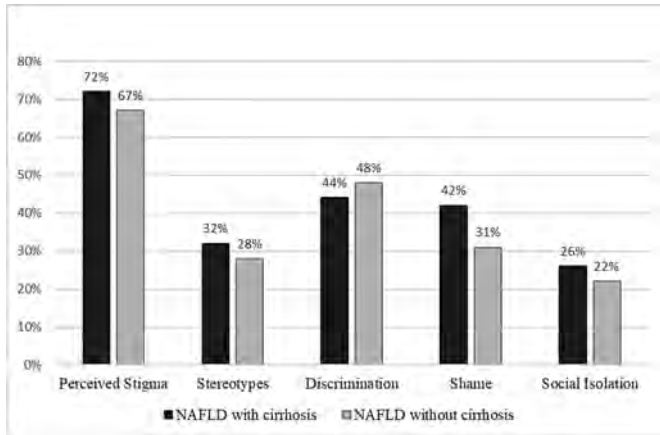
STIGMATIZATION IS COMMON IN PATIENTS WITH METABOLIC ASSOCIATED FATTY LIVER DISEASE AND CORRELATES WITH QUALITY OF LIFE

Marta Carol^{1,2,3,4}, Martina Perez^{1,3,4}, Elsa Solà^{1,2,3,4}, Marta Cervera^{1,2,3,4}, Sara Martínez^{1,2,3}, Adria Juanola^{1,2,3}, Carlota Riba^{1,2,3}, Ann Ma^{1,2,3}, Emma Avitabile^{1,2,3}, Laura Napoleone^{1,2,3}, Elisa Pose^{1,2,3}, Isabel Graupera^{1,2,3}, Maria Honrubia⁴, Marko Korenjak⁵, Ferran Torres^{6,7}, Pere Ginès^{1,2,3,4}, Núria Fabrellas^{1,2,3,4}. ¹Hospital Clínic de Barcelona, Liver Unit, Barcelona, Spain; ²Institut d'Investigacions Biomèdiques August Pi i Sunyer (IDIBAPS), Barcelona, Spain; ³CIBERehD-Centro de Investigación Biomédica en Red de Enfermedades Hepáticas y Digestivas, Madrid, Spain; ⁴Universitat de Barcelona, School of Medicine and Health Sciences, Barcelona, Spain; ⁵ELPA European Liver Patient Organization, Bruxelles, Belgium; ⁶Institut d'Investigacions Biomèdiques August Pi i Sunyer (IDIBAPS), Medical Statistics Core Facility, Barcelona, Spain; ⁷Universitat de Barcelona, Biostatistics Unit, Faculty of Medicine, Barcelona, Spain
Email: mcarol@clinic.cat

Background and aims: Stigmatization is a well-documented problem of some diseases. Perceived stigma is common in alcohol-related liver disease and hepatitis C, but little information exists on stigma in patients with metabolic associated fatty liver disease (MAFLD). Aim of the study was to investigate frequency and characteristics of perceived stigma among patients with MAFLD.

Method: One-hundred and ninety-seven patients seen at the liver clinic were included: a study group of 144 patients with MAFLD, 50 with cirrhosis, and a control group of 53 patients with alcohol-related cirrhosis. Demographic, clinical, and laboratory data were collected. Quality-of-life was assessed by chronic liver disease questionnaire (CLDQ). Perceived stigma was assessed using a specific questionnaire for patients with liver diseases categorized in 4 domains: stereotypes, discrimination, shame, and social isolation.

Results: Perceived stigma was common in patients with MAFLD (99 patients, 69%) and affected all 4 domains assessed. The frequency was slightly higher, yet not significant, in patients with MAFLD cirrhosis vs those without (72% vs 67%, respectively; $p=0.576$). In patients without cirrhosis perceived stigma was unrelated to stage of disease, since frequency was similar in patients with no or mild fibrosis compared to those with moderate/severe fibrosis (66% vs 68%, respectively). Among patients with cirrhosis, stigmatization was more common in alcohol-related vs MAFLD-cirrhosis, yet differences were only significant in two domains. In patients with MAFLD, perceived stigma correlated with poor quality-of-life, but not with demographic or clinical variables.



Conclusion: Perceived stigmatization is common among patients with NAFLD, is associated with impaired quality-of-life, and may be responsible for stereotypes, discrimination, shame, and social isolation, which may affect human and social rights of affected patients.

FRI245

Effect of e-health-based interventions on weight loss in patients with NAFLD: a systematic review and meta-analysis of randomized controlled trials

Ferya Celik¹, Merve Yuksele¹, Hicran Bektaş¹. ¹Akdeniz University, Internal Medicine Nursing, Antalya, Turkey
Email: feryacelik@gmail.com

Background and aims: The only effective treatment is 7%–10% weight loss of non-alcoholic fatty liver disease (NAFLD). Lifestyle changes consisting of diet and physical activity are the cornerstone of weight loss. To synthesize the effect of e-health-based interventions on weight loss in patients with NAFLD.

Design: A systematic review and meta-analysis of randomized controlled trials following Cochrane methods.

Data resources: Systematic searches were conducted in Ovid, Science Direct, Web of Science, CINAHL Complete, PubMed, Cochrane Library, Scopus for studies published in English without year limitations up to January 2022.

Method: The risk of bias in eligible studies was evaluated by two researchers using the Cochrane Collaboration tool. Disagreements were resolved with the third researcher. The meta-analysis data were analyzed using the Comprehensive Meta-Analysis 3 program. PRISMA-2020 was used to report the findings.

Results: Four studies with 253 participants met the inclusion criteria. Lifestyle intervention enabled by e-health-based interventions was dietary and/or physical intervention in all studies. E-health-based interventions were applied by text messages, telephone/video calls, mobile applications. The overall effect of e-health-based interventions on weight loss was statistically significant. E-health-based interventions had a large effect on weight loss in patients with NAFLD ($p = 0.03$, Hedge's $g = -0.91$, 95% confidence interval [CI] -1.75 to -0.07) (Figure 1).

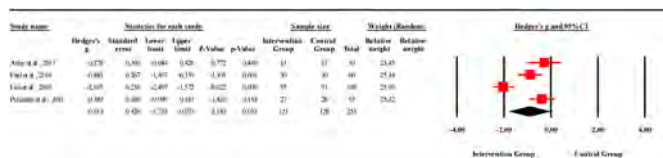


Figure 1: The results of the meta-analysis of the effect of e-health-based interventions on weight loss.

Conclusion: E-health-based interventions had a large effect on weight loss in patients with NAFLD. E-health-based interventions can assist in lifestyle change and weight loss in patients with NAFLD. In this way, liver-related complications can be reduced. Nurses can use affordable, practical and accessible e-health-based interventions to assist with weight loss in patients with NAFLD.

Keywords: e-health-based interventions, liver disease, NAFLD, nursing care, weight loss.

Rare liver diseases (including paediatric and genetic)

FRI246

Role of mutant alpha-1-antitrypsin in determining liver cell fate during embryonic development and in HCC origin

Francesco Annunziata¹. ¹TIGEM, Translational UNIT, Pozzuoli, Italy
Email: f.annunziata@tigem.it

Background and aims: Alpha1-antitrypsin deficiency (AATD) is the most common genetic cause of liver disease in children. The toxic gain-of-function mutation of alpha-1-antitrypsin (ATZ) leads to its accumulation and retention in the endoplasmic reticulum (ER) of the hepatocytes resulting in liver injury and, later in life, in increased risk of hepatocellular carcinoma (HCC). Preliminary data suggest that ATZ starts to be expressed and accumulated as globules early during embryogenesis. However, it is not known whether ATZ may influence liver cell fate commitment and functionality during development. In addition, it has been speculated that globule-devoid (GD) hepatocytes may have a proliferative advantage over globule-containing (GC) hepatocytes and be responsible for HCC development and progression. However, it is not clear yet which cell has to be considered the cell of origin of HCC in AATD patients. Therefore, our aims are: i) study the effects of ATZ expression and accumulation in liver cells during development and differentiation to evaluate alterations in cellular identity that can be harmful during disease progression; ii) lineage trace liver cholangiocytes/progenitors (C/P) cells and mature hepatocytes to identify the cell of origin of HCC in AATD patients.

Method: To characterize the effects of ATZ expression on pathways demonstrated to be crucial for cell fate commitment, we performed RNA sequencing analysis at several stages over embryonic development on liver from the AATD mouse model (PiZ) and wild type (WT) mice. Histological analyses have been performed to confirm alterations in cell fate commitment.

To investigate the cell of origin of the HCC in AATD, we are performing lineage tracing experiments by using C/P- and hepatocyte- specific Cre-recombinase and reporter mouse lines. In addition, to support our *in vivo* experiments, we are investigating the capacity of both C/P cells and hepatocytes to generate liver organoids.

Results: We observed that pathways involved in cell differentiation/proliferation (e.g., Wnt and Hippo pathways) were altered in PiZ compared to WT livers. In addition, immunostainings for C/P- and hepatocyte- specific markers showed hybrid identity of liver cells in PiZ at P0. These results suggest that at very early stages during development ATZ accumulation impairs cell differentiation resulting in immature hepatocytes that are not able to play their crucial role in cell metabolism and homeostasis. Interestingly, we observed that PiZ derived hepatocytes from adult mice are not able to form cysts/organoids as the WT, while C/P form organoids faster than the WT. These results may suggest that C/P cells and not hepatocytes are involved in liver regeneration and are the cell of origin of HCC in PiZ mice.

Conclusion: In summary, our study evaluated the effects of ATZ expression and accumulation in liver cells during embryogenesis and

contribute to identify the cells responsible for HCC development in AATD.

FRI247

A pilot study of biliary atresia newborn screening using dried blood spot matrix metalloproteinase-7

Chee Seng Lee^{1,2}, Yen-Hsuan Ni², Huey-Ling Chen², Jia-Feng Wu², Hong-Yuan Hsu², Yin-Hsiu Chien³, Ni-Chung Lee³, Paul Wuh-Liang Hwu³, Yu-Ju Chen⁴, Yu-Lin Wang⁵, Mei-Hwei Chang².
¹National Taiwan University Hospital Hsin-Chu Branch, Department of Pediatric, Hsinchu County, Taiwan; ²National Taiwan University College of Medicine and Children's Hospital, Department of Pediatric, Taipei, Taiwan; ³National Taiwan University Hospital, Department of Medical Genetics, Taipei, Taiwan; ⁴Institute of Chemistry, Academia Sinica, Taipei, Taiwan; ⁵Institute of NanoEngineering and MicroSystems, National Tsing Hua University, Hsinchu, Taiwan
 Email: mhchangster@gmail.com

Background and aims: Timely diagnosis is a critical challenge and crucial to improved survival of biliary atresia (BA) patients. We aim to evaluate accuracy of Matrix Metalloproteinase-7 (MMP-7) protein as a marker for screening BA at 3 days old.

Method: Using dried blood spot screening for neonatal cholestasis patients (DBS-SCReNC), this study had enrolled pediatric patients with definite diagnosis of BA and compared with non-BA children. Children were recruited from September 12, 2018, to May 14, 2021 and followed-up until at least 6-month-old. The study was conducted in a tertiary hospital, National Taiwan University Children Hospital hepatology clinic, general pediatric clinic and well-child clinic. Stored newborn screen dried blood spot (DBS) at 3 day old of children enrolled in DBS-SCReNC study were retrieved from newborn screening (NBS) centers in Taiwan. There were 25 BA children and 107 non-BA children. MMP-7 on DBS was quantified in 2021 using a sensitive sandwich enzyme-linked immunosorbent assay.

Results: The age of the 25 children with BA (15 male, 10 female) was 3.3 ± 1.3 years, and age of 107 non-BA children (56 male, 51 female) was 2.2 ± 1.2 years old. Of the non-BA children, 3 children were diagnosed with choledochal cyst, 2 with liver hemangioma, 9 with cholestasis diseases and 93 children visited NTUH due to non-hepatobiliary diseases or for well-child visits. The time of BA patients received Kasai operation was at 43 ± 20 days old. The DBS MMP-7 level of BA children was significantly higher than that of non-BA children (19.2 ± 10.4 vs 5.6 ± 2.7 ng/ml, $p < 0.0001$). The DBS MMP-7 level showed good diagnostic accuracy with AUC of 93.7% (95% CI, 87.7%–99.7%). MMP-7 cut-off at 7.8 ng/ml has sensitivity of 92.0% (95% CI, 74.0%–99.0%), specificity of 92.5% (95% CI, 85.8%–96.7%), positive predictive value of 71.9% (95% CI, 56.3%–87.5%), negative predictive value of 98.0% (95% CI, 95.3%–100.0%) ($p < 0.001$).

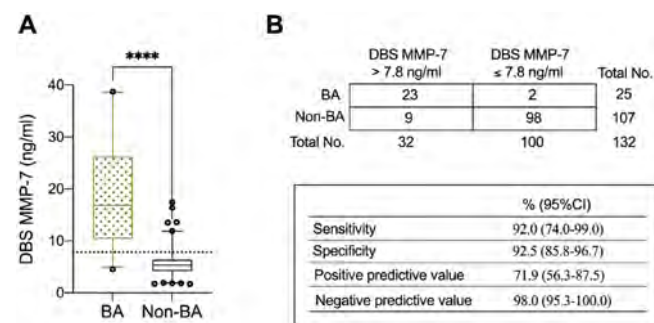


Figure 1. (A) The newborn screening dried blood spot MMP-7 levels within 3-day-old in biliary atresia (BA) and non-biliary atresia (non-BA) children, (B) Diagnosis of BA using DBS MMP-7 at the cut-off of 7.8 ng/ml. (****: $p < 0.0001$).

Conclusion: In this study, DBS MMP-7 is able to distinguish BA from other conditions. This test allows us to screen BA children as early as 3 days old.

FRI248

In vitro rescue of nonsense variations by drug-induced readthrough of premature termination codons in progressive familial intrahepatic cholestasis type 2

Martine Lapalus¹, Elodie Mareux¹, Rachida Amzal¹, Marion Almes^{1,2}, Alice Thebaut^{1,2}, Mounia Lakli¹, Thomas Falguières¹, Sylvie Rebuffat³, Laure Bidou^{4,5}, Olivier Namy⁴, Emmanuel Jacquemin^{1,2}, Emmanuel Gonzalès^{1,2}.
¹Inserm, Physiopathogénèse et traitement des maladies du foie, UMR_S 1193, Université Paris Saclay, HepatinoV, Orsay, France; ²Paediatric Hepatology and Paediatric Liver Transplant Department, National Reference Center for Rare Paediatric Liver Diseases, FILFOIE, ERN RARE LIVER, Assistance Publique-Hôpitaux de Paris, Faculté de Médecine Paris-Saclay, CHU Bicêtre, Le Kremlin-Bicêtre, France; ³Muséum national d'Histoire naturelle, Centre national de la Recherche scientifique, Laboratory Molecules of Communication and Adaptation of Microorganisms (MCAM), UMR 7245 CNRS-MNHN, CP 54, Paris, France; ⁴Institute for Integrative Biology of the Cell (I2BC), CEA, CNRS, Université Paris-Saclay, Gif sur Yvette, France; ⁵Sorbonne Universités, Université Pierre et Marie Curie, UPMC, Paris, France
 Email: martine.lapalus@inserm.fr

Background and aims: Progressive familial intrahepatic cholestasis type 2 (PFIC2) is a severe hepatocellular cholestasis due to biallelic variations in *ABCB11* gene encoding the canalicular bile salt export pump (BSEP/ABCB11). Nonsense variations are responsible for the most severe phenotypes. We previously reported that gentamicin could partially rescue PFIC2-causing *Abcb11* nonsense variations by inducing a pharmacological readthrough (RT). However, due to toxicity issues, there is a medical need to identify alternative therapies. The aim was to assess the ability of H7 (a mushroom extract), 2, 6 diaminopurine (DAP) and CDX5-1 (an aminoglycoside-induced readthrough potentiator) to induce RT of eight *ABCB11* nonsense variations (p.Y354X, p.R415X, p.R470X, p.I528X, p.R1057X, p.R1090X, p.Q1215X and p.E1302X) identified in PFIC2 patients.

Method: The RT levels of the premature termination codon (PTC) in their nucleotide environment were first quantified before and after treatment with aminoglycosides (G418, gentamicin), CDX5-1 combined to gentamicin, H7 and DAP using a dual reporter assay (luciferase/galactosidase) in NIH3T3 cells. Mutagenesis was used to reproduce nonsense variations in a plasmid encoding a rat Bsep-green fluorescent protein. The ability of the drugs to induce RT and to lead to the expression of a full-length protein was studied using immunodetection assays after transfection in human embryonic kidney (HEK293) and Can 10 cells. The function of the drug-induced full-length protein was studied by measuring the ³H taurocholate transport in Madin-Darby canine kidney (MDCK) clones co-expressing *Abcb11* and the rat sodium taurocholate co-transporting polypeptide (Ntcp/Slc10A1).

Results: In NIH3T3 cells, H7 and DAP induced a significant RT of p.R415X, p.R470X, p.R1057X, p.R1090X (UGA nonsense variations) while only H7 increased the RT levels of UAA nonsense variations (p.Y354X et E1302X). CDX5-1 increased the gentamicin-induced RT levels of p.R415X, p.R470X, p.R1057X and p.R1090X (UGA PTCs). H7 and DAP-induced RT levels were significantly higher than gentamicin-induced RT level. Compared to gentamicin alone, CDX5-1 combined to gentamicin, H7 and DAP treatments resulted in an increase of the full-length *Abcb11*^{R1090X} protein expression in HEK293 and Can 10 cells, including at the canalicular membrane of Can 10 cells. Moreover, an additive effect was observed when H7 or DAP were combined to gentamicin. In MDCK cells, these tested drugs increased the bile acid transport of the full-length *Abcb11*^{R1090X} protein.

Conclusion: Our data provide an *in vitro* proof of concept that CDX5-1 (combined to gentamicin), H7 and DAP induce a pharmacological RT leading to a full-length protein expression and increase bile acid transport of *Abcb11*^{R1090X}. These findings provide new insights for the treatment of patients with PFIC2 due to selected nonsense variations.

FRI249

Search for biomarkers and prognostic indicators of liver degeneration in glycogen storage disease type Ia

Roberta Resaz^{1,2}, Davide Cangelosi³, Daniela Segalerba¹, Martina Morini¹, Maria Carla Bosco¹, Sabrina Paci⁴, Annalisa Sechi⁵, Daniela Melis⁶, Maja Di Rocco⁷, David Weinstein⁸, Alessandra Eva¹.
¹IRCCS Istituto Giannina Gaslini, Laboratory of Molecular Biology, Genoa, Italy; ²Università degli Studi di Pavia, Department of Molecular Medicine; ³IRCCS Istituto Giannina Gaslini, Bioinformatic Unit, Genoa, Italy; ⁴Ospedale San Paolo, Clinical Department of Pediatrics, Milan, Italy; ⁵Presidio Ospedaliero Universitario di Udine, Regional Coordinating Center for Rare Diseases; ⁶Università degli Studi di Salerno, Department of Medicine, Surgery and Dentistry "Scuola Medica Salernitana", Section of Pediatrics; ⁷IRCCS Istituto Giannina Gaslini, Department of Pediatrics; ⁸University of Connecticut School of Medicine, Department of Pediatrics, Farmington, United States
 Email: roberta.resaz@hsanmartino.it

Background and aims: Glycogen storage disease type Ia (GSDIa) is an inherited metabolic disorder caused by mutations in the enzyme glucose-6-phosphatase-alpha (G6Pase-alpha). Affected individuals develop renal and liver complications, including the development of hepatocellular adenoma/carcinoma and kidney failure. The purpose of this study was to identify potential biomarkers of the evolution of the disease in GSDIa patients. To this end, we analyzed the expression of exosomal microRNAs (Exo-miRs) in the plasma exosomes of 45 patients aged 6 to 63 years. We found that the altered expression of several Exo-miRs correlates with the pathologic state of the patients and might help to monitor the progression of the disease and the development of late GSDIa-associated complications. In addition, the Exo-miRs expression profile obtained from the patients was correlated with the liver-specific Exo-miRs profile obtained from a mouse model for GSDIa we have generated (LS-G6pc^{-/-}), to derive a common signature that could be specific and prognostic of liver degeneration and connected with biological pathways associated with tumor development and progression.

Method: We analyzed the expression of exosomal microRNAs (Exo-miRs) in the plasma exosomes of 45 patients aged 6 to 63 years. Plasma from age-matched normal individuals were used as controls. microRNAs were purified with exoRNeasy Serum/Plasma Midi kit (Qiagen) from plasma exosomes. TaqMan Array Human microRNA A cards (Thermo Fisher Scientific), enabling the quantification of 381 microRNAs each, were used to analyze exosomes-derived microRNA (ExomiR) expression.

Results: We found several deregulated Exo-miRs that correlate with the pathologic state of the liver patients. We identified microRNAs associated with liver disease and metabolic alterations of glucose and lipid pathways. We also found deregulation of microRNAs relevant in liver tumor development and, finally, several microRNAs whose altered expression has been associated with diabetic and chronic kidney diseases.

Interestingly, we found that deregulated Exo-miR profiles correlate with the altered proteome profile and the altered Exo-miR profile identified in LS-G6pc^{-/-}.

Conclusion: The altered expression of several Exo-miRs correlated with various pathologic liver states associated with the progression of the disease. Thus, our results provide evidence that the Exo-miRs profiles identified may relate to the specific affected organ gene expression and that the long-term consequences of GSDIa can be monitored through Exo-miRs assessment. In conclusion, our results may evolve into protocols to counteract both the progression of liver degeneration leading to HCA and HCC onset as well as kidney disease and failure using circulating microRNAs as biomarkers.

FRI250

Alpha-1 antitrypsin (AAT) augmentation therapy and liver phenotype in individuals with homozygous Pi*Z AAT mutation (Pi*ZZ genotype)

Malin Fromme¹, Karim Hamesch¹, Carolin Victoria Schneider¹, Mattias Mandorfer², Katrine Thorhauge³, Vítor Pereira⁴, Monica Pons⁵, Matthias Reichert⁶, Samira Amzou¹, Robert Bals⁷, Andreas Rembert Koczulla⁸, Marc Miravittles⁹, Sabina Janciauskiene¹⁰, Joan Genesca⁵, Federica Benini¹¹, Joanna Chorostowska-Wynimko¹², Bill Griffiths¹³, Elmar Aigner¹⁴, Alexander Teumer¹⁵, Michael Trauner², Aleksander Krag³, Christian Trautwein¹, Pavel Strnad¹.
¹University Hospital RWTH Aachen, Medical Clinic III, Gastroenterology, Metabolic diseases and Intensive Care, Aachen, Germany; ²Medical University of Vienna, Division of Gastroenterology and Hepatology, Vienna, Austria; ³Odense University Hospital, Department of Gastroenterology and Hepatology, Odense, Denmark; ⁴Centro Hospitalar do Funchal, Department of Gastroenterology, Funchal, Portugal; ⁵Vall d'Hebron University Hospital, Vall d'Hebron Research Institute (VHIR), Liver Unit, Barcelona, Spain; ⁶Saarland University Medical Center, Department of Internal Medicine II, Homburg, Germany; ⁷Saarland University Medical Center, Department of Medicine V, Homburg, Germany; ⁸Marburg University Hospital, Clinic for Pneumology, Marburg, Germany; ⁹Vall d'Hebron Hospital Barcelona, Clinic for Pneumology, Barcelona, Spain; ¹⁰German Center for Lung Research (DZL), Medical University Hannover, Clinic for Pneumology, Hannover, Germany; ¹¹Spedali Civili and University, Gastroenterology Unit, Department of Medicine, Brescia, Italy; ¹²National Institute of Tuberculosis and Lung Diseases, Department of Genetics and Clinical Immunology, Warsaw, Poland; ¹³Cambridge University Hospitals NHS Foundation Trust, Department of Hepatology, Cambridge, United Kingdom; ¹⁴Paracelsus Medical University, First Department of Medicine, Salzburg, Austria; ¹⁵University Medicine Greifswald, Institute for Community Medicine, Greifswald, Germany
 Email: mfromme@ukaachen.de

Background and aims: The homozygous Pi*Z mutation (Pi*ZZ genotype) in the SERPINA1 gene results in severe alpha-1 antitrypsin deficiency (AATD) predisposing to lung and liver disease. While liver transplantation is currently the only treatment option for the liver, intravenous augmentation with purified human AAT is available for the lung. Since AAT administration displays hepatoprotective properties in mouse models of AATD and alcohol-related liver disease, we evaluated its effect on the liver phenotype in Pi*ZZ individuals.

Method: 259 non-augmented Pi*ZZ participants and 315 Pi*ZZ subjects on augmentation therapy were systemically recruited in 11 European countries and subjected to standardized clinical and laboratory evaluation as well as vibration-controlled transient elastography. Participants with hepatic comorbidities and significant alcohol consumption were excluded. Analyses were adjusted for age, sex, body mass index, diabetes mellitus, mean alcohol consumption, and recruitment center. In addition, liver biopsies of 35 non-augmented and 15 augmented Pi*ZZ subjects were evaluated.

Results: As expected, Pi*ZZ individuals on augmentation therapy presented with lower FEV1 values and increased COPD assessment test (CAT) scores. Despite higher age, augmented Pi*ZZ participants displayed lower liver stiffness measurements (LSM), had less frequently significant liver fibrosis (LSM ≥ 7.1 kPa), and significantly lower AST and GGT levels, as compared to Pi*ZZ individuals without augmentation.

Histological evaluation of liver biopsies revealed a lower fibrosis stage (Kleiner 2.0 vs. 4.0, $p = 0.006$) and lower presence of inflammation in augmented vs. non-augmented Pi*ZZ subjects (14.3 vs. 45.7 %, $p = 0.043$).

	Non-augmented n = 259	Augmented n = 315	p value (multivariable) *
Age (years)	50 ± 15	58 ± 10	<0.0001*
Women (%)	48.3	43.8	0.29*
BMI (kg/m ²)	24.4 ± 3.9	24.8 ± 4.5	0.96*
FEV1 (%)	78 ± 26	47 ± 18	<0.0001*
CAT (points)	12 ± 8	19 ± 7	<0.0001*
LSM (kPa)	6.5 ± 5.5	6.1 ± 3.9	0.042
LSM ≥ 7.1 kPa (%)	22.0	19.4	0.020
ALT (% ULN)	76 ± 45	77 ± 42	0.89
AST (% ULN)	74 ± 28	69 ± 26	<0.0001
GGT (% ULN)	92 ± 110	86 ± 74	0.021

Abbreviations: BMI, body mass index; FEV1, forced expiratory volume in 1 second; CAT, COPD assessment test; LSM, liver stiffness measurement; ALT, alanine aminotransferase; AST, aspartate aminotransferase; GGT, gamma-glutamyltransferase; ULN, upper limit of normal. *Univariate.

Conclusion: AAT augmentation therapy seems to have a beneficial association to the liver phenotype of PiZZ individuals. Prospective studies are needed to confirm this observation.

FRI251

Impact of acute hepatic porphyria attack frequency on patient-reported outcomes: results from the porphyria worldwide patient experience research (POWER) study

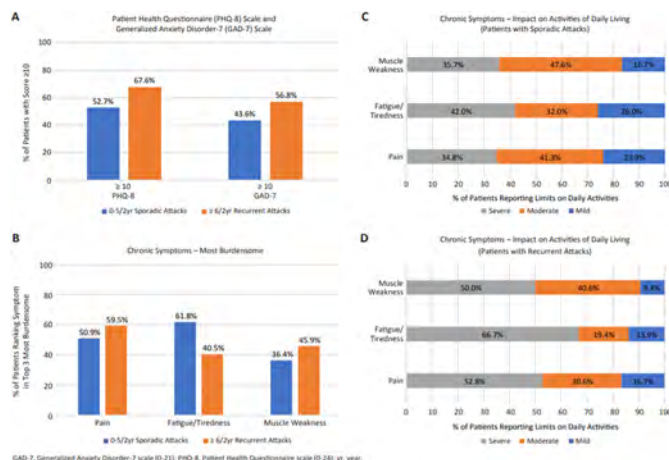
Amy Dickey¹, Kristen Wheeden², Sue Burrell³, Rocco Falchetto⁴, Jasmin Barman-Aksözen^{4,5}, Alison Bulkley⁶, Stephen Meninger⁷, Stephen Lombardelli⁸, Danielle Nance⁹. ¹Massachusetts General Hospital, Boston, United States; ²American Porphyria Foundation, Bethesda, United States; ³Global Porphyria Advocacy Coalition, Durham City, United Kingdom; ⁴Swiss Society for Porphyria, Zurich, Switzerland; ⁵Stadspital Waid and Triemli, Institute of Laboratory Medicine, Zurich, Switzerland; ⁶Kantar Health, New York, United States; ⁷Alnylam Pharmaceuticals, Cambridge, United States; ⁸Alnylam Pharmaceuticals, Maidenhead, United Kingdom; ⁹Banner Health, Gilbert, United States
Email: adickey@mgh.harvard.edu

Background and aims: Acute hepatic porphyria (AHP), a group of rare genetic diseases of haem biosynthesis, is characterised by neurovisceral pain attacks. This study evaluated the impact of AHP on patient-reported outcomes (PROs) and disease burden in AHP patients who experience sporadic or recurrent attacks.

Method: Adult patients having >1 AHP attack within the past 2 years or receiving intravenous hemin and/or glucose for attack prevention were recruited from the United States, Italy, Spain, Australia, Mexico, and Brazil and administered an online survey from January 19 to April 26, 2021. Patients taking givosiran were excluded. Descriptive and bivariate analyses were performed to evaluate differences between patients with sporadic attacks (annualised attack rate [AAR], <6 within past 2 years) and recurrent attacks (AAR, ≥6). Attacks included those leading to a hospitalisation, an emergency room visit, an outpatient doctor visit, or self-management. PROs were assessed with the Generalized Anxiety Disorder-7 (GAD-7) scale (0–21) and the Patient Health Questionnaire (PHQ-8) scale (0–24). Burden of chronic symptoms was also reported.

Results: Of the 92 AHP patients who completed the survey, 55 (60%; mean age, 40.3 years) reported sporadic attacks and 37 (40%; mean age, 42.3 years) reported recurrent attacks. Most patients were female (sporadic, 92.7%; recurrent, 86.5%), and the most frequent diagnosis was acute intermittent porphyria (sporadic, 83.6%; recurrent, 59.4%). A majority of patients in the sporadic (52.7%) and recurrent (67.6%) attack groups reported a PHQ-8 score ≥10, indicating moderate to severe depression; 43.6% and 56.8% of patients in the sporadic and recurrent groups, respectively, reported a GAD-7 score ≥10, indicating moderate to severe anxiety (Figure 1A). Pain was reported as one of the top 3 most burdensome chronic symptoms in the sporadic (50.9%) and recurrent (59.5%) groups (Figure 1B). Of patients reporting their daily activities being limited by severe chronic

symptoms, 83.3% of those in the sporadic (Figure 1C) and 90.6% in the recurrent group (Figure 1D) reported muscle weakness as a top 3 symptom having a moderate to severe impact.



Conclusion: While disease burden appeared greater for AHP patients experiencing recurrent attacks, both sporadic and recurrent group patients experienced a substantial impact on physical, mental, and emotional quality of life.

FRI252

Large-scale, multi-centric prospective validation of the polycystic liver disease complaint-specific assessment (POLCA)

Antoon Billiet¹, Frederik Temmerman¹, Walter Coudyzer², Natalie Van den Ende¹, Isabelle Colle³, Sven Francque⁴, Ho Thien Anh⁵, Stéphane De Maeght⁶, Filip Janssens⁷, Hans Orlent⁸, Dirk Sprengers⁹, Jean Delwaide¹⁰, Sofie Decock¹¹, Jochen Decaestecker¹², Schalk van der Merwe¹, Jef Verbeek¹, Frederik Nevens¹. ¹University Hospitals KU Leuven, Gastroenterology and Hepatology, Leuven, Belgium; ²University Hospitals KU Leuven, Radiology, Leuven, Belgium; ³Algemeen Stedelijk Ziekenhuis Aalst, Gastroenterology and Hepatology, Aalst, Belgium; ⁴Antwerp University Hospital, Gastroenterology and Hepatology, Antwerpen, Belgium; ⁵Université Catholique de Louvain, Nefrology, Brussels, Belgium; ⁶Grand Hôpital de Charleroi, Gastroenterology and Hepatology, Charleroi, Belgium; ⁷Jessa Ziekenhuis, Gastroenterology and Hepatology, Hasselt, Belgium; ⁸AZ Sint Jan Brugge, Gastroenterology and Hepatology, Brugge, Belgium; ⁹GZA Antwerp, Gastroenterology and Hepatology, Antwerpen, Belgium; ¹⁰C.H.U. de Liège, Gastroenterology and Hepatology, Liège, Belgium; ¹¹AZ Sint Lucas Brugge, Gastroenterology and Hepatology, Brugge, Belgium; ¹²AZ Delta, Gastroenterology and Hepatology, Roeselare, Belgium
Email: antoon_billiet@hotmail.com

Background and aims: Polycystic liver disease (PCLD) can lead to extensive hepatomegaly, often associated with severe complaints. Indication for somatostatin-analogues (SA) or liver transplantation (LT) is in part based on subjective, patient-reported symptoms. In 2014 the PCLD-complaint-specific assessment (POLCA) score was developed as a self-report instrument to objectively capture the presence and severity of disease-specific complaints (Temmerman F, J Hepatol 2014).

The aim of this study was to validate the POLCA score and investigate the correlation with liver volume and need for volume-reduction therapy.

Method: A five year prospective multi-centric study in 21 hospitals in Belgium gathered a cohort of 266 PCLD patients. Sequential data including POLCA score, liver volumetry and the need for volume-reduction therapy were recorded. Participants were asked to complete the POLCA questionnaire, as available online

(<https://www.uzleuven.be/polca>). Liver volume was measured using CT-volumetry and adapted as height-adjusted total liver volume (htLV). Combined liver-kidney transplant patients (n=9) were excluded.

Results: For 198 patients, serial POLCA scores were available. The study group consisted of young (54.8y ± 11.3), mostly female (83%) patients with predominant ADPKD (63%). Median time of follow-up was 48 months. Liver volumetry was available for 96 patients, showing a median htLV of 1967 ml.

There was a significant correlation (Spearman's rank) between POLCA severity of perceived illness (SPI) score and htLV ($r = 0.48$; 0.30–0.63). Patients who underwent LT had significantly higher scores on all POLCA subscales and htLV, compared to those not considered to be LT candidates (table 1). SPI score ≥ 16.5 predicted the need of LT with a sensitivity of 81.3% and a specificity of 88.9%.

Table: Comparison of POLCA subscales and htLV

POLCA	No LT (n = 171)	LT (n = 18)	p value
Severity of perceived illness	10.0 (6.0; 15.0)	23.5 (18; 26)	<0, 0001
POLCA	No LT (n = 122)	LT (n = 17)	
GERD complaints	2.0 (0.0; 5.0)	7.0 (4.5; 12.5)	<0, 0001
Impact on food intake	2.0 (0.0; 5.0)	6.0 (4.5; 9.0)	0, 0004
Perception of enlarged LV	6.0 (3.0; 8.0)	10.0 (7.5; 12.0)	<0, 0001
htLV (ml)	No LT (n = 71) 1707 (1173; 2690)	LT (n = 16) 3607 (2901; 4337)	<0, 0001

Longitudinal data showed a significant correlation between the change in SPI score and the change in htLV ($r = 0.45$; 0.26–0.61) and a significant reduction in htLV (–80 ml) by SA resulted in a decrease in SPI score (–6.0 vs +4.5).

Conclusion: This prospective study confirms the use of the POLCA score as a self-report instrument to assess the severity of PCLD-related symptoms. It is a clear reflection of both evolving symptom severity as well as objective changes in liver volume. Our findings highlight the potential of the POLCA score as a tool for longitudinal follow-up of PCLD patients and as a guide for clinicians when evaluating the need for medical or surgical intervention.

FRI253

Improvements in quality of life in odevixibat responders and nonresponders: an analysis of pooled data from the PEDFIC 1 and PEDFIC 2 studies

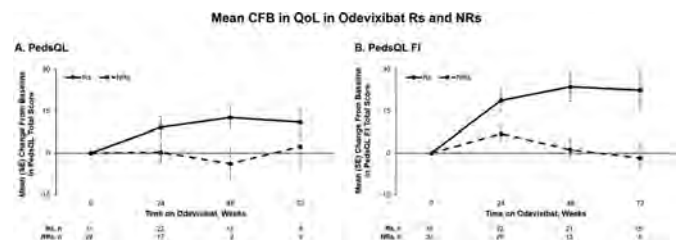
Cara L. Mack¹, Chad Gwaltney², Quanhong Ni³, Qifeng Yu³, Velichka Valcheva³, Lise Kjems³, Patrick Horn³. ¹Children's Hospital Colorado, University of Colorado School of Medicine, Aurora, CO, United States; ²Gwaltney Consulting, Westerly, RI, United States; ³Albireo Pharma, Boston, MA, United States
Email: cara.mack@childrenscolorado.org

Background and aims: Patients with progressive familial intrahepatic cholestasis (PFIC) may have debilitating pruritus that can impact their and their families' quality of life (QoL). The phase 3 PEDFIC 1 and PEDFIC 2 studies evaluated the efficacy and safety of odevixibat, an ileal bile acid transporter inhibitor, in patients with PFIC. In these studies, odevixibat improved serum bile acids (sBAs), pruritus, and sleep; QoL was also evaluated as an exploratory endpoint. Here, using pooled data from these studies, we describe patient- and family-focused QoL changes in odevixibat responders (Rs) and nonresponders (NRs).

Method: In PEDFIC 1, children with PFIC received placebo or odevixibat (40 or 120 µg/kg/day) for 24 weeks. PEDFIC 2 is an ongoing 72-week extension study that enrolled patients from PEDFIC 1 or new patients; all patients in PEDFIC 2 receive odevixibat 120 µg/kg/day. Data from these studies were pooled from patients' first dose of odevixibat to a cut-off date of 4 December 2020. To assess QoL, caregivers of patients ≥ 2 years old completed the Pediatric QoL

Inventory (PedsQL) and family impact (FI) questionnaires, which output total impact scores ranging from 0 to 100; higher scores indicate greater QoL. Treatment R was defined as sBA reductions of $\geq 70\%$ or levels ≤ 70 µmol/L and/or ≥ 1 -point drop from baseline in caregiver-reported pruritus score (on 0–4 scale) at last available assessment.

Results: In the pooled population, 49/84 (58%) met R criteria, and 35/84 (42%) were NRs. In Rs, mean age was 4.8 years and 57% were female; in NRs, mean age was 5.5 years and 37% were female. Among patients with available QoL data (PedsQL: R: n = 31, NR: n = 22; FI: R: n = 46, NR: n = 33), mean (SE) PedsQL and FI total scores at baseline indicated that both Rs (PedsQL: 56.6 [2.3]; FI: 49.9 [2.8]) and NRs (PedsQL: 55.0 [3.5]; FI: 48.9 [3.4]) had impaired QoL at least some of the time, on average. At week 72 in patients with available data, the mean (SE) change from baseline (CFB) in PedsQL total score was 11.0 (4.6) in Rs and 2.3 (8.6) in NRs; the mean (SE) CFB in PedsQL FI total score was 22.5 (7.0) in Rs and –1.7 (4.6) in NRs (Figure).



Conclusion: Odevixibat Rs and, particularly, their families, experienced QoL improvements that were sustained over time; QoL for NRs and their families was largely unchanged with up to 72 weeks of treatment. Further analysis of specific domains within PedsQL and FI that were most highly impacted in Rs is ongoing.

FRI254

Total, primary, and secondary serum bile acid changes and pruritus improvement during odevixibat treatment in patients with progressive familial intrahepatic cholestasis

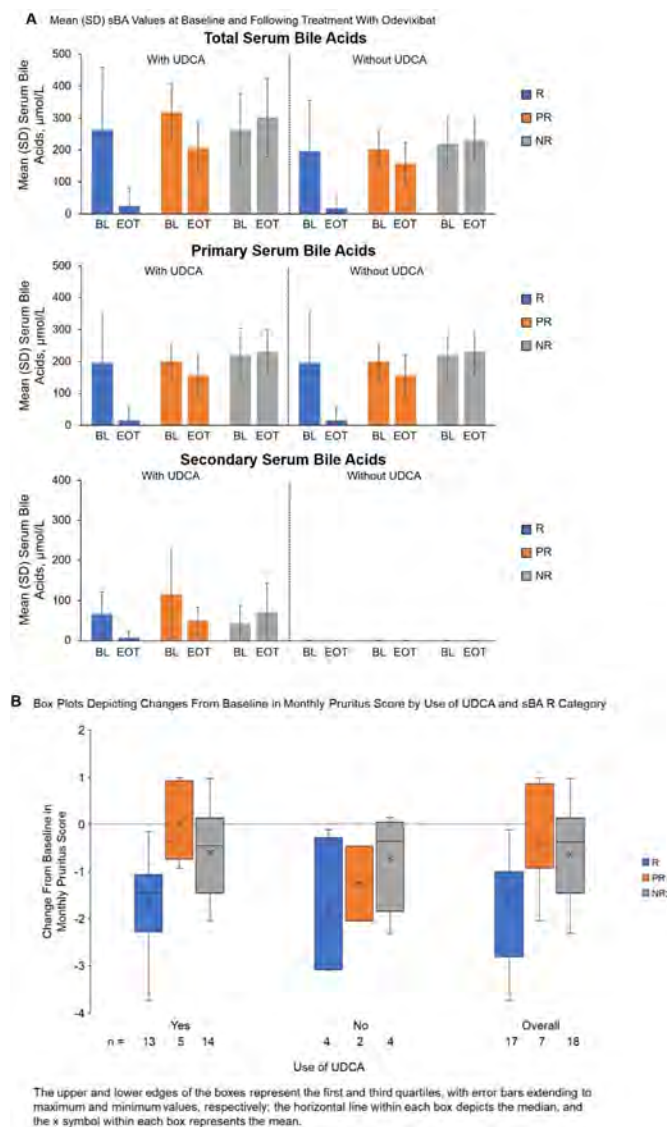
Henkjan J. Verkade¹, Folkert Kuipers¹, Quanhong Ni², Velichka Valcheva². ¹Department of Paediatrics, University of Groningen, Beatrix Children's Hospital/University Medical Centre Groningen, Groningen, Netherlands; ²Albireo Pharma, Inc., Boston, MA, United States
Email: h.j.verkade@umcg.nl

Background and aims: Children with progressive familial intrahepatic cholestasis who received odevixibat in the 24-week PEDFIC 1 study had significant reductions vs placebo-treated patients in total serum bile acids (sBAs) and pruritus. Here, we evaluated changes in sBAs and pruritus in patients from PEDFIC 1 categorised by sBA response (R) level and by factoring in ursodeoxycholic acid (UDCA) use.

Method: Patients eligible for PEDFIC 1 had elevated sBAs and significant pruritus at screening. Concomitant UDCA was allowed provided the patient's dose was stable. Three categories of patients among those randomised to odevixibat (n = 42) were analysed here: sBA Rs (ie, sBAs reduced $\geq 70\%$ from baseline [BL] or levels ≤ 70 µmol/L), sBA partial Rs (PRs [ie, did not meet sBA R criteria but had sBAs reduced $\geq 30\%$], and sBA nonresponders (NRs [ie, did not meet either sBA R or PR criteria). Parameters evaluated included sBA composition (ie, total, primary, and secondary BAs, with UDCA concentration included as secondary BA) as measured by liquid chromatography–tandem mass spectrometry and pruritus as rated by caregivers (range: 0–4; higher scores indicate worse symptoms, with pruritus R defined as a ≥ 1 -point reduction from BL); pruritus outcomes were also compared by whether patients had concomitant UDCA use and/or sBA R.

POSTER PRESENTATIONS

Results: Mean BL total sBAs were higher with vs without UDCA treatment in all 3 sBA R categories (Figure, A), which could be primarily accounted for by UDCA concentrations (66, 116, and 42 $\mu\text{mol/L}$, in sBA Rs, PRs, and NRs, respectively). During odevixibat treatment, sBA Rs ($n=17$) had the largest decreases in total and primary sBAs, whereas sBA PRs ($n=7$) had intermediate decreases, and sBA NRs ($n=18$) had minimal changes. Among all odevixibat-treated patients, sBA Rs experienced greater mean reductions in monthly pruritus scores vs sBA PRs and sBA NRs (Figure, B). sBA PRs who used UDCA had smaller reductions in monthly pruritus score vs those who did not (Figure, B). Among pruritus Rs with UDCA use, the rate of sBA R, PR, and NR was 69%, 0%, and 31%, respectively; among pruritus Rs without UDCA use, these rates were 50%, 25%, and 25%.



Conclusion: UDCA treatment resulted in higher sBAs at BL, but this did not seem to affect sBA R to odevixibat. A sBA PR was not associated with a mean decrease in pruritus with concomitant UDCA use. All sBA R groups included patients for whom pruritus R did not correlate with sBA R.

FRI255

Changes in hepatic parameters, growth, sleep, and biochemical markers with odevixibat treatment across patients with various types of progressive familial intrahepatic cholestasis

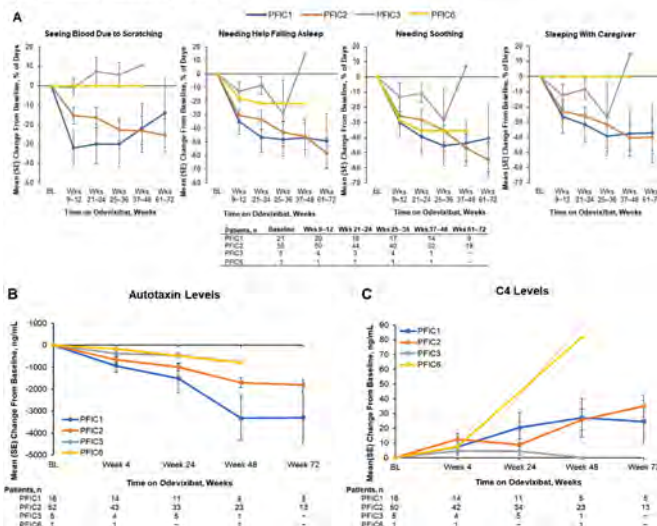
Lorenzo D'Antiga¹, Girish Gupte², Richard J. Thompson³, Ekkehard Sturm⁴, Pier Luigi Calvo⁵, Mohammad Ali Shagrani^{6,7}, Janis M. Stoll⁸, Reha Artan⁹, Buket Dalgıç¹⁰, Hasan Ozen¹¹, Kathleen M. Loomes¹², Jennifer M. Vittorio¹³, Saul J. Karpen¹⁴, Angelo Di Giorgio¹⁵, Quanhong Ni¹⁶, Lise Kjems¹⁶, Patrick Horn¹⁶.
¹Azienda Ospedaliera Papa Giovanni XXIII, Bergamo, Italy; ²Liver Unit and Small Bowel Transplantation, Birmingham Women's and Children's NHS Foundation Trust, Birmingham, United Kingdom; ³Institute of Liver Studies, King's College London, London, United Kingdom; ⁴Paediatric Gastroenterology and Hepatology, University Children's Hospital Tübingen, Tübingen, Germany; ⁵Paediatric Gastroenterology Unit, Regina Margherita Children's Hospital, Azienda Ospedaliera Città della Salute e della Scienza di Torino, Turin, Italy; ⁶King Faisal Specialist Hospital and Research Centre-Organ Transplant Centre, Riyadh, Saudi Arabia; ⁷College Of Medicine-Alfaisal University, Riyadh, Saudi Arabia; ⁸Department of Paediatrics, Washington University School of Medicine, St. Louis, Missouri, United States; ⁹Akdeniz University, Antalya, Turkey; ¹⁰Department of Paediatric Gastroenterology, Gazi University Faculty of Medicine, Ankara, Turkey; ¹¹Hacettepe University Faculty of Medicine, Ankara, Turkey; ¹²Children's Hospital of Philadelphia, Philadelphia, PA, United States; ¹³Department of Surgery, Centre for Liver Disease and Transplantation, Columbia University Medical Centre, New York, NY, United States; ¹⁴Emory University School of Medicine, Children's Healthcare of Atlanta, Atlanta, GA, United States; ¹⁵Paediatric Hepatology Gastroenterology and Transplantation, ASST Papa Giovanni XXIII, Bergamo, Italy; ¹⁶Albireo Pharma, Inc., Boston, MA, United States
 Email: lantiga@asst-pg23.it

Background and aims: PEDFIC 1 and PEDFIC 2 evaluated the safety and efficacy of odevixibat, an ileal bile acid transporter inhibitor, in patients with progressive familial intrahepatic cholestasis (PFIC). Using pooled data from these studies, we analysed secondary and exploratory endpoints in patients with PFIC type 1 (PFIC1), 2 (PFIC2), 3 (PFIC3), and 6 (PFIC6).

Method: PEDFIC 1 was a 24-week, randomised, placebo-controlled study in children with PFIC1 and PFIC2. PEDFIC 2 is an ongoing 72-week extension study in patients with any PFIC type. This pooled analysis spans from patients' first dose of odevixibat to a cut-off of 4 December 2020. Assessments included changes from baseline (BL) in alanine aminotransferase (ALT), total bilirubin, growth, caregiver-reported sleep parameters, autotaxin, and 7 α -hydroxy-4-cholesten-3-one (C4); data are presented to wk72 of odevixibat treatment for patients with PFIC1 and PFIC2 and to wk36 or wk48 for patients with PFIC3 and PFIC6 (who have less time on treatment vs patients with PFIC1 or PFIC2, who could have participated in PEDFIC 1).

Results: Of 84 patients in the pooled population (mean age, 5.0 years), 26% had PFIC1 ($n=22$), 67% PFIC2 ($n=56$), 6% PFIC3 ($n=5$), and 1% PFIC6 ($n=1$). With odevixibat, mean changes in ALT levels to wk72 in patients with PFIC1 ($n=6$) and PFIC2 ($n=15$) who reached this timepoint as of the data cut-off were -14 U/L and -85 U/L, respectively; mean changes in ALT levels to wk36 in patients with PFIC3 ($n=4$) and PFIC6 ($n=1$) were 67 U/L and 89 U/L. Patients with PFIC1 and PFIC2 with available data at wk72 had mean changes in total bilirubin of -6 $\mu\text{mol/L}$ and -5 $\mu\text{mol/L}$, respectively; for patients with PFIC3 and PFIC6, mean changes to wk36 were 18 $\mu\text{mol/L}$ and -83 $\mu\text{mol/L}$. Mean height and weight Z scores increased with odevixibat treatment across the various types of PFIC. Sleep parameters, C4, and autotaxin improved over time in almost all PFIC types (Figure). Across PFIC types, most treatment-emergent adverse events with odevixibat were mild or moderate in severity.

Changes From BL in Sleep Parameters (A), Autotaxin Levels (B), and C4 Levels (C) Over Time With Odevixibat Treatment by PFIC Type



Conclusion: In patients with PFIC treated with odevixibat assessed to date, growth improved, autotaxin levels decreased, and C4 levels increased over time; changes in hepatic and sleep parameters in some PFIC types were more variable (eg, PFIC3, PFIC6), but these conclusions may be limited by the small size of these subgroups, particularly at later timepoints. Odevixibat was generally well tolerated.

FRI256

Analysis of quality of life, hepatic biochemical markers, and sleep in patients with progressive familial intrahepatic cholestasis who had a pruritus response with odevixibat treatment

Girish Gupte¹, Richard J. Thompson², Lorenzo D'Antiga³, Tassos Grammatikopoulos^{2,4}, Emmanuel Gonzales², Florence Lacaille³, Alain Lachaux⁴, Bertrand Roquelaure⁵, Ulrich Baumann⁶, Elke Lainka⁷, Ekkehard Sturm⁸, Eyal Shteyer⁹, Piotr Czubkowski¹⁰, Reha Artan¹¹, Buket Dalgic¹², Hasan Ozen¹³, Kathleen M. Loomes¹⁴, Jennifer M. Vittorio¹⁵, Saul J. Karpen¹⁶, Patrick McKiernan¹⁷, Cara L. Mack¹⁸, Angelo Di Giorgio¹⁹, Qifeng Yu²⁰, Lise Kjems²⁰, Patrick Horn²⁰. ¹Liver Unit and Small Bowel Transplantation, Birmingham Women's and Children's NHS Foundation Trust, Birmingham, United Kingdom; ²Institute of Liver Studies, King's College London, London, United Kingdom; ³Azienda Ospedaliera Papa Giovanni XXIII, Bergamo, Italy; ⁴Paediatric Liver, GI and Nutrition Centre and MowatLabs, King's College Hospital NHS Trust, London, United Kingdom; ⁵Hospital for Sick Children and the University of Toronto, Toronto, ON, Canada; ⁶Paediatric Gastroenterology and Hepatology, Hannover Medical School, Hannover, Germany; ⁷Children's Hospital, Department of Paediatric Gastroenterology, Hepatology, and Transplant Medicine, University Duisburg-Essen, Essen, Germany; ⁸Paediatric Gastroenterology and Hepatology, University Children's Hospital Tübingen, Tübingen, Germany; ⁹Faculty of Medicine, Hebrew University of Jerusalem, Juliet Keidan Department of Paediatric Gastroenterology, Shaare Zedek Medical Centre, Jerusalem, Israel; ¹⁰Department of Gastroenterology, Hepatology, Nutritional Disorders and Paediatrics, The Children's Memorial Health Institute, Warsaw, Poland; ¹¹Akdeniz University, Antalya, Turkey; ¹²Department of Paediatric Gastroenterology, Gazi University Faculty of Medicine, Ankara, Turkey; ¹³Hacettepe University Faculty of Medicine, Ankara, Turkey; ¹⁴Children's Hospital of Philadelphia, Philadelphia, PA, United States; ¹⁵Department of Surgery, Center for Liver Disease and Transplantation, Columbia University Medical Center, New York, NY, United States; ¹⁶Emory University School of Medicine, Children's Healthcare of Atlanta, Atlanta, GA, United States; ¹⁷Division of Gastroenterology/Hepatology/Nutrition,

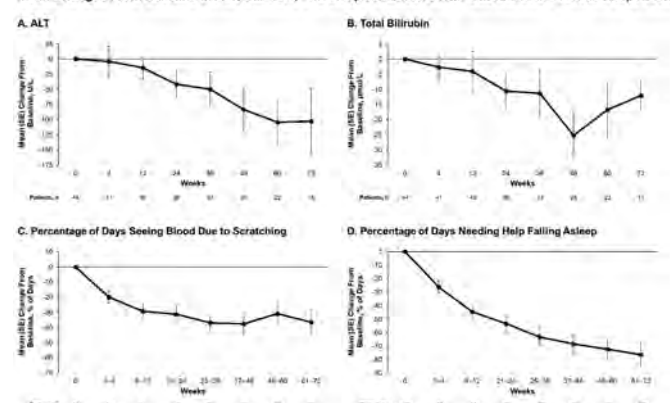
UPMC Children's Hospital of Pittsburgh, Pittsburgh, PA, United States; ¹⁸Children's Hospital of Colorado, University of Colorado School of Medicine, Aurora, CO, United States; ¹⁹Department of Paediatric Gastroenterology Hepatology and Transplantation, ASST Papa Giovanni XXIII, Bergamo, Italy; ²⁰Albireo Pharma, Inc., Boston, MA, United States Email: t.grammatikopoulos@nhs.net

Background and aims: Patients with progressive familial intrahepatic cholestasis (PFIC), a group of rare paediatric cholestatic liver diseases, have debilitating symptoms including severe pruritus that can impact sleep and quality of life (QoL). In the phase 3 PEDFIC 1 and PEDFIC 2 studies, the ileal bile acid transporter inhibitor odevixibat reduced serum bile acids (sBAs) and improved pruritus and sleep in children with PFIC. Using pooled data from these studies, we examined secondary and exploratory efficacy endpoints and safety outcomes in patients who met criteria for a pruritus response with odevixibat treatment.

Method: PEDFIC 1 was a 24-week, randomised, placebo-controlled study in children with PFIC1 or PFIC2. PEDFIC 2 is an ongoing 72-week extension study in patients of with any PFIC type. Pruritus was rated using the Albireo observer-reported outcome instrument (range: 0–4). This pooled analysis spans from patients' first dose of odevixibat to a cut-off of 4 December 2020. We analysed sBAs, QoL (Pediatric QoL Inventory [PedsQL] and PedsQL family impact [FI] questionnaire; higher scores indicate improved QoL), alanine aminotransferase (ALT), total bilirubin, sleep parameters, and treatment-emergent adverse events (TEAEs) in patients with a pruritus response (ie, ≥ 1 -point drop in pruritus score from baseline) following odevixibat treatment.

Results: Of 82 patients in the pooled population (of whom, 49% were female), 44 (54%) were pruritus responders. Of these 44 pruritus responders (mean age, 4.6 years), 24 (55%) were female; 23%, 68%, and 7% had PFIC 1, 2, and 3, respectively. Mean sBA levels were 247 $\mu\text{mol/L}$ at baseline ($n = 44$) and decreased over time by 77% at weeks 70–72 in pruritus responders who reached this timepoint ($n = 18$). Mean PedsQL and FI total scores were 56 ($n = 30$) and 50 ($n = 42$) at baseline and increased by 11 ($n = 8$) and 24 ($n = 14$) at week 72, respectively, in pruritus responders. Mean ALT and total bilirubin levels decreased over time from 109 U/L and 40 $\mu\text{mol/L}$ at baseline to 40 U/L and 18 $\mu\text{mol/L}$ ($n = 15$) (Figure 1A, B), and sleep parameters improved over time in these patients (Figure 1C, D). There were no drug-related serious TEAEs.

Mean Changes From Baseline in ALT, Bilirubin, and Sleep Parameters With Odevixibat in Pruritus Responders



Conclusion: Overall, patients with PFIC with a pruritus response following treatment with odevixibat experienced improvements in sBAs, QoL, hepatic biochemical markers, and sleep parameters that were sustained over time. Odevixibat was generally well tolerated.

POSTER PRESENTATIONS

FRI257

Longitudinal follow-up data on adults with classic, severe alpha-1 antitrypsin deficiency (Pi*ZZ genotype)

Malin Fromme¹, Samira Amzou¹, Barbara Burbaum¹, Philipp Striedl², Matthias Mandorfer³, Elmar Aigner², Christian Trautwein¹, Pavel Strnad¹. ¹University Hospital RWTH Aachen, Medical Clinic III, Gastroenterology, Metabolic Diseases and Intensive Care, Aachen, Germany; ²Paracelsus Medical University, First Department of Medicine, Salzburg, Austria; ³Medical University of Vienna, Division of Gastroenterology and Hepatology, Vienna, Austria
Email: mfromme@ukaachen.de

Background and aims: Homozygous Pi*Z mutation in the *SERPINA1* gene (Pi*ZZ genotype) confers a strong predisposition to lung and liver disease. Since the pace of liver disease progression and suitable prognostic factors remain unknown, we evaluated risk factors (i.e., demographics and lifestyle) and the predictive utility of non-invasive tests in the European Pi*ZZ liver cohort.

Method: 480 Pi*ZZ individuals without concomitant liver diseases or pathological alcohol consumption, decompensated liver disease, or hepatocellular carcinoma were evaluated by a standardized baseline clinical, laboratory, and elastographic assessment. 340 of them had a detailed follow-up interview at least 12 months after their baseline examination.

Results: During a median follow-up of 3.85 years, 23 Pi*ZZ individuals deceased. The main causes of fatality were lung and liver disease, each accounting for 8 deaths. 10/4 individuals received a lung/liver transplant, 3 additional Pi*ZZ individuals developed hepatic decompensation. Compared to the remaining Pi*ZZ participants, 15 individuals who developed a hepatic endpoint (liver transplant/death, or decompensated cirrhosis) presented with significantly higher body mass index (29.3 vs. 24.5 kg/m², $p = 0.003$), liver stiffness measurement (LSM, 14.0 vs. 5.2 kPa, $p = 6.3 \times 10^{-9}$), AST-to-platelet ratio index (APRI, 0.97 vs. 0.31 units, $p = 9.4 \times 10^{-7}$), fibrosis-4 index (FIB-4, 3.6 vs. 1.3, $p = 6.0 \times 10^{-6}$) and liver enzymes in their baseline examination. Multivariate Cox regression analysis revealed LSM ≥ 25 kPa (aHR 30.9, 95% CI 8.0–119.2, $p = 6.1 \times 10^{-7}$) and APRI ≥ 1.0 units (aHR 39.6, 95% CI 10.1–154.7, $p = 1.2 \times 10^{-7}$) as strong predictors of liver-related mortality.

	Pi*ZZ without hepatic endpoint n = 325	Pi*ZZ with hepatic endpoint n = 15	P value (univariable)
Age (years)	57.5 [51.3–65.1]	57.9 [50.8–63.5]	0.828
Women (%)	47.1	20.0	0.040
BMI (kg/m ²)	24.5 [22.0–27.2]	29.3 [24.6–31.6]	0.003
Mean alcohol consumption (g/d)	2.5 [0.0–8.2]	0.0 [0.0–8.2]	0.276
LSM <15 kPa + PLT ≥ 150 (%)	88.9	33.3	8.4×10^{-10}
LSM ≥ 15 kPa (%) ¹	2.8	46.7	4.2×10^{-15}
LSM ≥ 25 kPa (%) ²	1.2	33.3	3.7×10^{-14}
APRI ≥ 1.0 units (%) ³	2.2	46.7	6.4×10^{-17}
FIB-4 ≥ 1.3 (%) ⁴	50.6	93.3	0.001
ALT \geq ULN (%) ⁵	21.5	73.3	4.0×10^{-6}
AST \geq ULN (%) ⁶	13.2	66.7	2.4×10^{-8}
PLT <150/nL (%) ⁷	9.5	60.0	3.1×10^{-9}

Abbreviations: BMI, body mass index; LSM, liver stiffness measurement; APRI, AST-to-platelet ratio index; ALT, alanine aminotransferase; AST, aspartate aminotransferase; PLT, platelet count; ULN, upper limit of normal. Adjusted Hazard ratios with 95%CI: ¹26.2 (7.4–93.2), ²30.9 (8.0–119.2), ³39.6 (10.1–154.7), ⁴14.7 (1.6–135.9), ⁵9.0 (2.4–33.5), ⁶19.3 (5.2–71.8), ⁷17.0 (4.6–62.0).

Conclusion: LSM and APRI accurately stratify Pi*ZZ individuals according to their risk of liver-related events. Thus, these non-invasive tests may facilitate risk stratification in clinical practice as well as patient selection for clinical trials.

FRI258

Gender dependent neurological and hepatic improvement in Wilson disease patients treated with Trientine dihydrochloride: post hoc results from a prospective study

Karl Heinz Weiss¹, Isabelle Mohr², Carlot Kruse³, Aurelia Poujois⁴. ¹Salem Medical Centre, Department of Internal Medicine, Heidelberg, Germany; ²Heidelberg University Hospital, Internal Medicine IV, Department of Gastroenterology, Heidelberg, Germany; ³Univar Solutions B.V., Rotterdam, Netherlands; ⁴Rothschild Foundation Hospital, Rare Disease Reference Centre "Wilson's Disease and Other Copper-Related Rare Diseases," Neurology Department, Paris, France
Email: karlheinz.weiss@stadtmission-hd.de

Background and aims: Wilson disease (WD) is a rare autosomal recessively inherited disorder of the copper metabolism for which liver and neurological manifestations are most common. Trientine dihydrochloride (TETA-2HCl; trientine) is a well-established second line treatment for WD patients intolerant to D-penicillamine. Data on gender differences in WD progression for patients under trientine treatment are limited. The data presented are derived from a post hoc analysis of a single centre prospective study (NCT: 02426905).

Method: This study was a single centre, prospective study in adult WD patients on maintenance treatment with TETA-2HCl 300 mg (equivalent to 200 mg of trientine base) with a follow up of 12 months. All patients were previously treated with D-penicillamine. The neurological disease burden was measured by means of an investigator rated Unified Wilson's Disease Rating Scale (UWDRS) and corresponding changes from baseline to 6 months and 12 months. To investigate corresponding liver disease, the parameters analysed included alanine transferase (ALT) and aspartate transferase (AST) response.

Results: Of the 52 patients enrolled in the study, 51 (98.1%) patients were included in the full analysis set. The mean (SD) duration of trientine treatment was 13.1 (1.62) months (range: 3 to 15 months) with a mean (SD) dose of 1377.6 (368.78) mg per day (range: 150 to 2100 mg per day). The mean (SD) values for UWDRS-assessment were 11.3 (24.31) at baseline, 9.7 (23.85) at month 6 and 8.8 (22.86) at month 12. The decrease of UWDRS values over time was shown to be significant ($p < 0.01$) in a longitudinal regression model with log (UWDRS + 1) as the regressor. Analyses based on gender showed a mean UWDRS of 10.6 ($n = 34$) at baseline, 8.6 ($n = 34$) at 6 months and 8.0 ($n = 34$) for females and 12.6 ($n = 17$) at baseline, 11.9 ($n = 16$) at 6 months and 10.4 ($n = 17$) for males. The gender differences in the UWDRS decrease were significant ($p = 0.02$) in the longitudinal model extended by gender as a covariate. AST and ALT results were stable over time. There appears to be no gender difference in AST and ALT outcomes.

Conclusion: Post hoc analysis indicates that gender might have an influence on neurologic symptom regression and disease course in WD patients on trientine maintenance therapy. The trend of continuous improvement in neurological symptoms is mainly seen in female WD patients-even after long-term therapy. These findings warrant further prospective evaluation and have implications for future study designs.

FRI259

Efficacy and safety of odevixibat over 72 weeks of treatment in patients with progressive familial intrahepatic cholestasis

Richard J. Thompson¹, Emmanuel Gonzalès², Reha Artan³, Winita Hardikar⁴, Florence Lacaille⁵, Alain Lachaux⁶, Bertrand Roquelaure⁷, Ulrich Baumann⁸, Ekkehard Sturm⁹, Eyal Shteyer¹⁰, Pier Luigi Calvo¹¹, Henkjan J. Verkade¹², Mohammad Ali Shagrani^{13,14}, Janis M. Stoll¹⁵, Piotr Czubkowski¹⁶, Buket Dalgıç¹⁷, Girish Gupta¹⁸, Tassos Grammatikopoulos¹⁹, Patrick McKiernan²⁰, Qifeng Yu²¹, Lise Kjems²¹, Patrick Horn²¹.
¹Institute of Liver Studies, King's College London, London, United Kingdom; ²Hépatologie et Transplantation Hépatique Pédiatriques, Centre de Référence de l'Atresie des Voies Biliaires et des Cholestases Génétiques, FSMR FILFOIE, ERN RARE LIVER, Hôpital Bicêtre, AP-HP, Université Paris-Saclay, HépatoInov, Inserm U 1193, Paris, France; ³Akdeniz University, Antalya, Turkey; ⁴Royal Children's Hospital, Melbourne, Australia; ⁵Paediatric Gastroenterology-Hepatology-Nutrition Unit, Hôpital Universitaire Necker-Enfants Malades, Paris, France; ⁶Hospices Civils de Lyon, Hôpital Femme-Mère-Enfant, Service D'hépatogastroentérologie et Nutrition Pédiatrique, Lyon, France; ⁷CHU, Hôpital de la Timone, Marseille, France; ⁸Paediatric Gastroenterology and Hepatology, Hannover Medical School, Hannover, Germany; ⁹Paediatric Gastroenterology and Hepatology, University Children's Hospital Tübingen, Tübingen, Germany; ¹⁰Faculty of Medicine, Hebrew University of Jerusalem, Juliet Keidan Department of Paediatric Gastroenterology, Shaare Zedek Medical Centre, Jerusalem, Israel; ¹¹Paediatric Gastroenterology Unit, Regina Margherita Children's Hospital, Azienda Ospedaliera Città della Salute e della Scienza di Torino, Turin, Italy; ¹²Department of Paediatrics, University of Groningen, Beatrix Children's Hospital/University Medical Centre Groningen, Groningen, Netherlands; ¹³King Faisal Specialist Hospital and Research Centre-Organ Transplant Centre, Riyadh, Saudi Arabia; ¹⁴College Of Medicine-Alfaisal University, Riyadh, Saudi Arabia; ¹⁵Department of Paediatrics, Washington University School of Medicine, St. Louis, Missouri, United States; ¹⁶Department of Gastroenterology, Hepatology, Nutritional Disorders and Paediatrics, The Children's Memorial Health Institute, Warsaw, Poland; ¹⁷Department of Paediatric Gastroenterology, Gazi University Faculty of Medicine, Ankara, Turkey; ¹⁸Istanbul University, Istanbul Faculty of Medicine, Istanbul, Turkey; ¹⁹Liver Unit and Small Bowel Transplantation, Birmingham Women's and Children's NHS Foundation Trust, Birmingham, United Kingdom; ²⁰Division of Gastroenterology/Hepatology/Nutrition, UPMC Children's Hospital of Pittsburgh, Pittsburgh, PA, United States; ²¹Albireo Pharma, Inc., Boston, MA, United States
 Email: richard.j.thompson@kcl.ac.uk

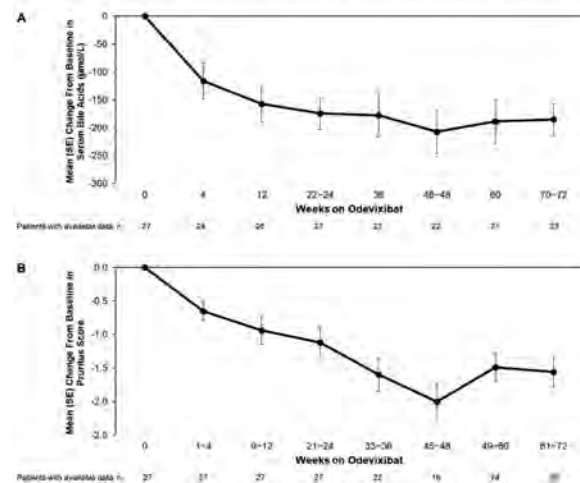
Background and aims: Progressive familial intrahepatic cholestasis (PFIC) is a group of paediatric cholestatic liver diseases characterised by disruption of bile production and transport, pruritus, and progressive liver disease. Here, using pooled data from two phase 3 studies in patients with PFIC (PEDFIC 1 and PEDFIC 2), we describe key long-term outcomes with odevixibat, an ileal bile acid transporter inhibitor, in the subgroup of patients treated with odevixibat for ≥ 72 weeks.

Method: PEDFIC 1 was a 24-week, placebo-controlled, double-blind study of odevixibat in children with PFIC1 or PFIC2. PEDFIC 2 is an ongoing, 72-week extension study in patients of any age with any type of PFIC. This pooled analysis spans from patients' first dose of odevixibat in PEDFIC 1 or PEDFIC 2 to a cut-off of December 4, 2020. The following outcomes are described over time in the subgroup of patients who had ≥ 72 weeks of exposure to odevixibat: serum bile acids (SBAs), caregiver-reported pruritus score (range, 0–4; higher scores indicate worse symptoms), laboratory parameters, growth, and safety.

Results: Of 84 patients in the pooled population, 27 were treated with odevixibat for ≥ 72 weeks (median [range], 92 [76–128] weeks). Of these 27 patients (mean age, 3 years), 52% were male, 70% had PFIC2, and 30% had PFIC1. At baseline, 82% of these 27 patients were using

ursodeoxycholic acid (UDCA), 56% were using rifampicin, and 89% were using UDCA and/or rifampicin. Mean (SE) SBA levels at baseline were 291 (26) $\mu\text{mol/L}$, which decreased by -185 (28) at weeks 70–72 of odevixibat treatment (Figure). Mean (SE) pruritus score at baseline was 2.9 (0.1), which decreased by -1.56 (0.2) at weeks 61–72 (Figure). At week 72 of odevixibat treatment, decreases in alanine aminotransferase (-64.9 U/L), aspartate aminotransferase (-18.8 U/L), and total bilirubin (-5.4 $\mu\text{mol/L}$) were also observed; mean (SE) height and weight Z scores increased by 0.8 (0.1) and 0.5 (0.2), respectively. In this group of patients with ≥ 72 weeks of odevixibat treatment, 26 (96%) patients experienced any treatment-emergent adverse event (TEAE) and 52% experienced drug-related TEAEs. There were no TEAEs leading to discontinuation.

Change From Baseline in sBA Levels (A) and Pruritus (B) in Patients Treated With Odevixibat for ≥ 72 Weeks



Conclusion: Odevixibat was well tolerated and demonstrated durable clinical treatment benefits for up to 72 weeks in improving SBA levels, pruritus scores, hepatic parameters, and growth in patients with PFIC who were treated for at least 72 weeks.

FRI260

In vitro rescue of the bile acid transport function of some ABCB11 variants by CFTR potentiators: a targeted pharmacotherapy in progressive familial intrahepatic cholestasis type 2

Elodie Mareux¹, Martine Lapalus¹, Marion Almes^{1,2}, Pauline Adnot¹, Mounia Lakli¹, Amel Ben Saad¹, Jean-Luc Decout³, Thomas Falguières¹, Isabelle Callebaut⁴, Emmanuel Gonzalès^{1,2}, Emmanuel Jacquemin^{1,2}.
¹Inserm, UMR_S1193 Physiopathogénèse et traitement des maladies du foie, Université Paris-Saclay, HépatoInov, Orsay, France; ²Assistance Publique-Hôpitaux de Paris, Faculté de médecine Paris-Saclay, CHU Bicêtre, Paediatric Hepatology and Paediatric Liver Transplant Department, National Reference Center for Rare Paediatric Liver Diseases, FILFOIE, ERN RARE LIVER, Le Kremlin-Bicêtre, France; ³CNRS, Département de pharmacochimie moléculaire, Université de Grenoble Alpes, Grenoble, France; ⁴CNRS, UMR 7590, Institut de Minéralogie, de Physique des Matériaux et de Cosmochimie, Sorbonne Université, Muséum National d'Histoire Naturelle, Paris, France
 Email: elodie.mareux@universite-paris-saclay.fr

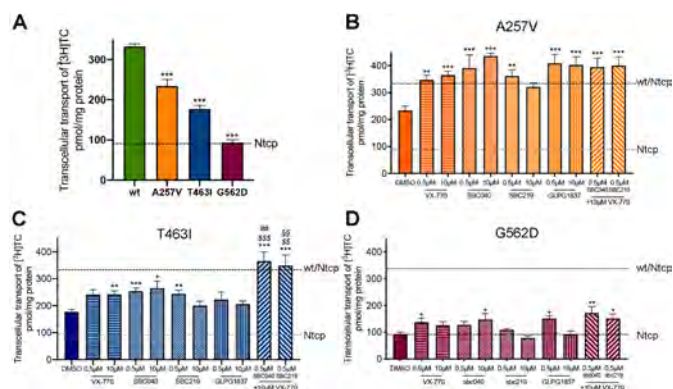
Background and aims: ABCB11 is expressed at the canalicular membrane of hepatocytes and is responsible for biliary bile acid secretion. Variations in the ABCB11 gene cause a spectrum of rare liver diseases. The most severe form is progressive familial intrahepatic cholestasis type 2 (PFIC2). Current medical treatments of these conditions have limited efficacy. Hence, the identification of alternative therapies is a major challenge.

Method: Three ABCB11 disease-causing variations identified in PFIC2 patients (A257 V, T463I and G562D) were studied by 3D structure

POSTER PRESENTATIONS

modelling. The variations were reproduced in a plasmid encoding a rat Bsep—green fluorescent protein. After transfection, the expression and the localisation of the variants were studied in HepG2 and Can 10 cells. Tritiated taurocholate ($[^3\text{H}]\text{TC}$) transport activity and the effect of Ivacaftor (VX-770, Kalydeco®), a clinically approved cystic fibrosis (CF) treatment, GLPG1837 in phase 2 CF clinical trials as well as SBC040 and SBC219, known as potentiators of CFTR were studied in Madin-Darby canine kidney (MDCK) clones co-expressing Abcb11 and the rat sodium taurocholate co-transporting polypeptide (Ntcp/Slc10A1).

Results: As predicted by 3D structure modelling, the three variants were correctly expressed at the canalicular membrane of HepG2 and Can 10 cells but had a defective function when studied in MDCK cells with a $[^3\text{H}]\text{TC}$ transport activity ranging from 28 to 70 % of the one observed in MDCK cells expressing the wild type (wt) Abcb11 (Figure). Ivacaftor, GLPG1837, SBC040 and SBC219 increased the $[^3\text{H}]\text{TC}$ transport activity of A257 V, T463I and G562D by 1.3 to 1.9-fold, allowing the $[^3\text{H}]\text{TC}$ transport activity of the A257 V variant to reach the one of the wt Abcb11. Furthermore, an additive effect was observed for the T463I variant when ivacaftor was combined with SBC040 or SBC219.



Conclusion: Potentiator drugs could increase the pharmacopoeia available for patients with ABCB11 deficiency due to missense variations affecting the transport function and may delay or even suppress the need for liver transplantation in these patients.

FR1261

Plasma-based proteomics profiling of patients with Wilson's disease

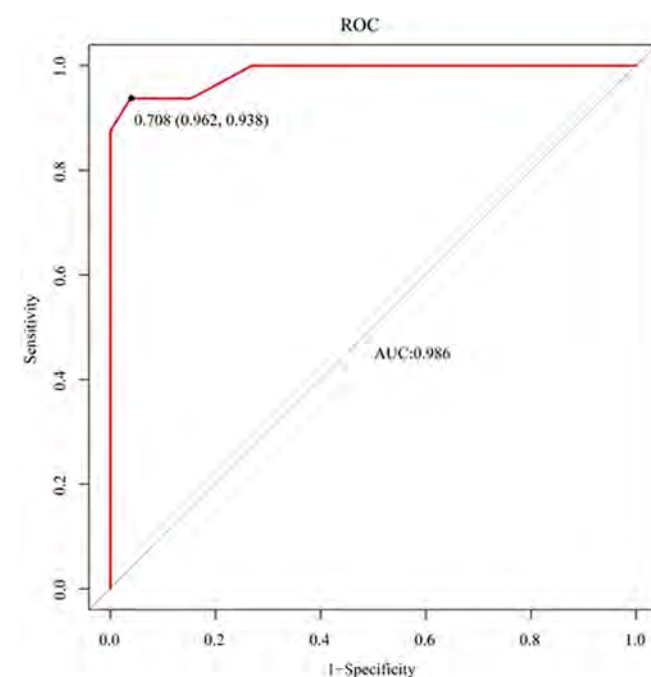
Rui Hua¹, Jie Su¹, HaiTao Qi², Yonggeng Jiao³, Lishuang Qi², Junji Niu¹.
¹The First Affiliated Hospital of Jilin University, Hepatology, Changchun, China; ²Harbin Medical University, College of Bioinformatics Science and Technology, Harbin, China; ³Jilin Province FAW General Hospital, Anesthesiology, Changchun, China
 Email: huar@jlu.edu.cn

Background and aims: Wilson's disease (WD) is an inherited disorder resulting from abnormal copper metabolism. Current diagnostic criteria is inadequacy since biochemical indexes related to copper are unreliable and genetic testing is expensive. The study aimed to reveal WD-related proteomic alterations, from which protein based molecular diagnostic model was developed.

Method: We performed a LTQ-Orbitrap (LC-ESI-MS/MS) comparative quantitative proteomics analysis to reveal the differentially expressed proteins (DEPs) between 20 WD subjects (10 liver type and 10 brain type) and 10 healthy controls. Then, functional enrichment analysis of Gene Ontology (GO) and coexpression protein-protein interaction (PPI) network based on STRING database were performed to reveal the dysregulated biological functions. Next, eXtreme Gradient Boosting (XGboost) was used to construct an optimal classifier to distinguish liver- and brain-type WDs from healthy controls. Finally,

16 independent serum samples were collected, and detected by ELISA method to validate the disease-associated DEPs and the diagnostic classifier.

Results: Of all the identified DEPs of liver-type WD and brain-type WD, there were 62 common DEPs between the two types including 18 were up-regulated and 44 were down regulated. GO enrichment analysis revealed that the common DEPs were mainly involved in inflammation, coagulation cascade, protein transport and activation. And the coexpression PPI network showed that several DEPs interacted with many DEPs implicated in WD, such as Heparin cofactor 2 (SERPIND1), Transthyretin (TTR) and Coagulation factor IX (F9). Hereby, we constructed a classifier consisting of two down-regulated proteins (F9 and C4b-binding protein beta chain (C4BPB)) with 100% accuracy. ELISA test validated the differential down-regulations of F9 and C4BPB in 16 independent WD samples when compared with 26 healthy controls. In the independent samples, the area under the ROC curve (AUC) of the diagnostic classifier was 0.986, and its sensitivity and specificity was 93.8% and 96.2%, respectively.



Conclusion: Our study demonstrates for the first time that mass spectrometry proteomic combined with bioinformatics analysis of serum samples is a potential approach to identify candidate markers associated with WD. Further studies are warranted to evaluate the clinical utility of these biomarkers in patients with WD.

FRI262

Management of hepatic sarcoidosis-multicentric approach

Janina Sollors¹, Andreas Teufel², Christoph Antoni¹, Matthias Ebert², Svetlana Hetjens³, Yuquan Qian¹, Bernhard Schlevogt⁴, Marc-Alexander Woerns⁵, Peter Galle⁵, Cleo-Aron Weis⁶, Raoul Bergner⁷. ¹University Medical Center Mannheim, Department of Internal Medicine II, Mannheim, Germany; ²University Medical Center Mannheim, Medical Faculty Mannheim, Heidelberg University, Department of Internal Medicine II, Mannheim, Germany; ³Medical Faculty University Heidelberg, University Hospital Mannheim, Internal Medicine II, Germany; ⁴University Medical Center Muenster, Department of Medicine B, Muenster, Germany; ⁵University Medical Center Mainz, Department of Internal Medicine I, Mainz, Germany; ⁶University Medical Center Mannheim, Medical Faculty Mannheim, Heidelberg University, Department of Pathology, Mannheim, Germany; ⁷Ludwigshafen Medical Center, Division of Rheumatology, Department of Medicine A, Ludwigshafen, Germany
Email: j.sollors@web.de

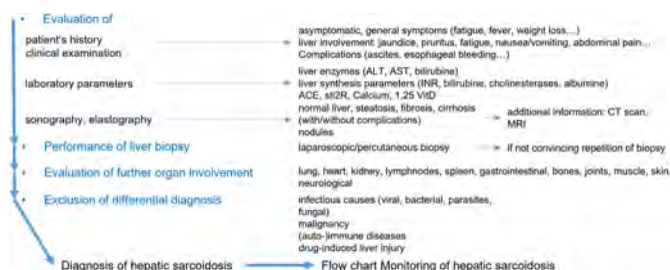
Background and aims: Sarcoidosis is systemic granulomatous disorder of unknown cause, characterized by activation of T-lymphocytes and macrophages involving multiple organs. Main manifestations are bihilar lymphadenopathy, pulmonary densification but also skin, joint and eye involvement. However, liver involvement may occur in up to 60% of all patients. As many patients experience only minor symptoms, a high number of undiagnosed cases must be assumed.

In order to successfully identify patients with hepatic sarcoidosis, a throughout characterization of these patients and their course of disease is necessary. However, the currently available evidence was mostly collected several decades ago.

Method: We collected 40 patients from four German centers to evaluate current treatment standards and course of disease. All of our patients underwent liver biopsy with histologically proven granulomatous hepatitis.

Results: Detailed characterization of these patients showed an overall benign course of disease. Treatment of these patients was very diverse with glucocorticoids for 1 year in 55% (22/40), 5–10 years in 18% (7/40), and permanently in 18% (7/40).

Other treatments included Disease-Modifying Anti-Rheumatic Drugs (DMARDs) of the conventional e.g. non-biological type (metotrexate (MTX), azathioprine (AZA), hydroxychloroquine (HCQ), sulfasalazine (SSZ), leflunomid (LEF)) in 53 %, of these, AZA 81%, MTX 46%, HCQ 10%, furthermore mycophenolatemofetil (MMF) in 10% and cyclophosphamide in 10% and biologicals in 8% of all patients in whom detailed documentation was available.



Conclusion: Despite these very diverse treatments, patients generally showed only slow progression of the disease. Only one patient died due to spontaneous bacterial peritonitis. None of our patients received liver transplantation. Based on our experience, we proposed a diagnostic work up and surveillance strategy as a basis for future, prospective register studies.

FRI263

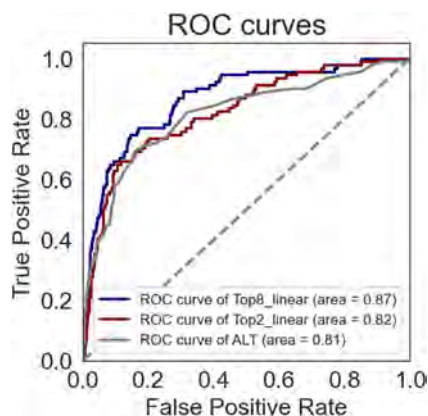
Plasma proteomics identifies hepatic steatosis and sex differences in 2, 147 children and adolescents

Lili Niu^{1,2}, Sara Stinson³, Louise Holm^{3,4}, Morten Lund^{4,5}, Cilius Fonvig^{3,4}, Helene Bæk Juel³, Simon Rasmussen¹, Jens-Christian Holm^{3,4,5}, Torben Hansen³, Matthias Mann^{1,2}. ¹University of Copenhagen, Novo Nordisk Foundation Center for Protein Research, Copenhagen, Denmark; ²Max Planck Institute of Biochemistry, Department of Proteomics and Signal Transduction, Martinsried, Germany; ³University of Copenhagen, Novo Nordisk Foundation Center for Basic Metabolic Research, Copenhagen, Denmark; ⁴Copenhagen University Hospital Holbæk, The Children's Obesity Clinic, Department of Pediatrics, Holbæk, Denmark; ⁵University of Copenhagen, The Faculty of Health and Medical Sciences, Copenhagen, Denmark
Email: mmann@biochem.mpg.de

Background and aims: Childhood obesity constitutes a serious health challenge predisposing children and adolescents to cardio-metabolic- and liver diseases. In particular, the prevalence of pediatric non-alcoholic fatty liver disease (NAFLD) is estimated to be 36% in the context of obesity. Percutaneous liver biopsies are considered the gold standard for diagnosing NAFLD, but due to its invasive nature, its clinical application is limited in children. This study aims to use mass spectrometry-based proteomics to identify non-invasive biomarkers for early detection of hepatic steatosis in children and adolescents, taking into account sex-specific changes in plasma proteins during puberty.

Method: We included 2, 147 children and adolescents, aged 5 through 20, from an obesity clinic cohort and a population-based cohort in Denmark, in a cross-sectional study design. We acquired plasma proteomics data using the Evosep One liquid chromatography system coupled online to an Orbitrap Exploris 480 mass spectrometer. We performed adjusted correlation analysis to identify age-associated proteins. We then used unsupervised hierarchical clustering to identify clusters of protein trajectories changing with age. Liver fat percentage, as quantified by proton magnetic resonance spectroscopy, was available for 764 children (80% of whom were from the obesity clinic). Among these, 13.5% exhibited hepatic steatosis, defined as a liver fat percentage above 5%. We performed student's t-test (two-sided) to identify differentially abundant proteins between children and adolescents with and without hepatic steatosis. Receiver operator characteristics area under the curve (ROC-AUC) was used to identify potential biomarkers. We used the liver damage marker, alanine aminotransferase (ALT) (plasma concentrations) as a benchmark.

Results: On average, 394 proteins were quantified per sample. Among these, 70 proteins significantly correlated with age. Hierarchical clustering identified puberty-related clusters of protein trajectories, which exhibited sex-dependent differences, such as sex hormone-binding globulin. Student's t-test identified 84 significantly differentially abundant proteins, including 44 upregulated and 40 downregulated in the group with hepatic steatosis. The top 20 best-performing proteins which predicted hepatic steatosis, exhibited ROC-AUCs between 0.63 and 0.81. Combining the top two and top eight proteins resulted in an ROC-AUC of 0.82 and 0.87, respectively, which was superior to ALT.



Conclusion: Temporal plasma proteome trajectories reflect sex differences during puberty. A panel of eight proteins shows promising potential as a non-invasive diagnostic marker for hepatic steatosis in children and adolescents. This would need to be externally validated.

FRI264

Pregnancy outcomes in women with Budd Chiari syndrome: a single center experience

Sagnik Biswas¹, Sabreena Sheikh¹, Manas Vaishnav¹, Anshuman Elhence¹, Naba Farooqui², Abhinav Anand¹, Shivanand Gamanagatti³, Shalimar¹. ¹All India Institute of Medical Sciences, New Delhi, Gastroenterology and Human Nutrition, New Delhi, India; ²Mayo Clinic, Rochester, Rochester, United States; ³All India Institute of Medical Sciences, New Delhi, Radiodiagnosis, New Delhi, India

Email: drshalimar@yahoo.com

Background and aims: Budd Chiari Syndrome (BCS) is associated with primary infertility and adverse pregnancy outcomes in affected females. Scant literature is available on the effect of an endovascular intervention on fertility and the outcome of future pregnancies in these patients.

Method: In this retrospective analysis, 121 female patients with BCS attending our liver clinic from 2017 to 2020 were included. Patients were categorized into three groups- no prior conception (group 1), any conception before disease onset but before completion of the family (group 2), and disease onset post completion of the family (group 3). Pregnancy outcomes (live birth, stillbirth, or abortions), mode of delivery, teratogenicity in the fetus, bleeding risk in the mother, decompensation of liver disease, or occlusion of the stent during pregnancy were assessed.

Results: BCS was diagnosed before any conception in 58 women (Group 1; median age: 22 years), during or after pregnancy but before completion of family in 39 (Group 2; median age: 27 years) and after completion of family in 24 women (Group 3; median age: 34 years). Median CTP and MELD scores of the whole cohort were 7, and 12 respectively. The primary infertility rate was 19.8% (24/121). In Group 1: 15 women with primary infertility underwent endovascular intervention with 5/15 (33%) women conceiving subsequently, resulting in 4 live births and 7 abortions. In Group 2: 5 women had developed BCS during pregnancy, and 11 in the postpartum period; 11/39 patients had a history of one or more abortions. Overall, 8/34 (23.5%) patients who underwent endovascular intervention could conceive, resulting in 4/8 (50%) live births. However, no patient developing BCS during pregnancy was able to conceive subsequently despite endovascular intervention. Group 3: No patient had any major complications during past pregnancies. Only one patient developed a TIPSS block in the postpartum period. The mode of delivery was vaginal in 88% of cases. No congenital anomaly/major bleeding episodes/decompensation/maternal mortality occurred.

Conclusion: Infertility is common in patients with BCS. Pregnancy is well tolerated in those with compensated liver disease. Normal vaginal delivery is a safe method of childbirth in these patients. No fetal malformations or major bleeding episodes were noted despite the use of oral anticoagulants.

FRI265

New cases of Budd-Chiari syndrome and splanchnic vein thrombosis after COVID-19 vaccination-a vascular liver disease group (VALDIG) initiative

Raoul Maan¹, Aurélie Plessier², Louise China³, David Patch⁴, Anna Baiges⁵, Juan Carlos Garcia Pagan⁵, Virginia Hernandez-Gea⁵, Marie-Noëlle Hilleret⁶, E.T.T.L. Tjwa⁷, Ilias Kounis⁸, Christophe Bureau⁹, Baptiste Giguët¹⁰, Alexandra Heurgue-Berlot¹¹, Isabelle Ollivier-Hourmand¹², Xavier Causse¹³, Filipe Gaio Castro Nery¹⁴, Mandy Lauw¹⁵, Sarwa Darwish Murad¹. ¹Erasmus University Medical Centre, Department of Gastroenterology and Hepatology, Rotterdam, Netherlands; ²Beaujon Hospital, Department of Hepatology, Paris, France; ³University College London, Institute of Liver and Digestive Health, London, United Kingdom; ⁴Royal Free London NHS Foundation Trust, Hepatology and Liver Transplantation, London, United Kingdom; ⁵Hospital Clinic, Institut de Investigacions Biomèdiques August Pi i Sunyer (IDIBAPS), University of Barcelona, Barcelona, Barcelona Hepatic Hemodynamic Laboratory, Liver Unit, Barcelona, Spain; ⁶CHU Grenoble Alpes, 38043 Grenoble Cedex, Service d'Hépatogastroentérologie, Grenoble, France; ⁷Radboud University Medical Center, Department of Gastroenterology and Hepatology, Nijmegen, Netherlands; ⁸AP-HP Hôpital Paul-Brousse, Inserm, Université Paris-Saclay, UMR-S 1193, Université Paris-Saclay, Inserm, FHU Hépatinov, 94800, Centre Hépatobiliaire; ⁹Physiopathogénèse et traitement des maladies du Foie, Villejuif, France; ¹⁰University Hospital of Toulouse and Toulouse III Paul Sabatier University, Toulouse, France; ¹¹CHU Rennes, Univ Rennes, F-35000, Liver Disease Department, Rennes, France; ¹²CHU Reims, Department of Hepato-Gastroenterology, Reims, France; ¹³University Hospital, Côte de Nacre, Department of Hepatology and Gastroenterology, Caen, France; ¹⁴Department of Hepatology and Gastroenterology, Orleans, France, Orleans, France; ¹⁵Centro Hospitalar Universitário do Porto, EpiUnit, Instituto de Saúde Pública da Universidade do Porto, Porto, Portugal; ¹⁵Erasmus University Medical Centre Rotterdam, Department of Hematology, Rotterdam, Netherlands

Email: r.maana@erasmusmc.nl

Background and aims: Since the world-wide COVID19 vaccination efforts, several studies have reported on a rare side effect of ChAdOx1 nCoV-19 (AstraZeneca) with vaccine-induced immune thrombocytopenia and thrombosis (VITT). We aimed to collect consecutive new cases of splanchnic vein thrombosis (SVT) or Budd-Chiari Syndrome (BCS) following SARSCOV2 vaccination within the Vascular Liver Disease Group (VALDIG) network.

Method: This prospective international cohort study started on 01.05.2021 to include all incident cases of definite VITT (5/5 criteria: onset of symptoms 4–42 days post COVID vaccination, new thrombosis, platelets $<150 \times 10^9$, positive anti-PF4/HIT ELISA and D-dimer >4000 FEU) or otherwise vaccine-related ($<5/5$ criteria) SVT or BCS. Diagnosis was radiologically confirmed, and onset of symptoms was within 6 weeks after 1st or 2nd SARSCOV2 vaccination. Patients with malignancy or cirrhosis were excluded. Statistics were descriptive with frequency (%) and median (range) values. We are presenting our data until 01.11.2021.

Results: In total, 22 patients were included from 13 centers with median age 47 (21–66) and 46 % females. Median time from vaccination (AstraZeneca N=11, Pfizer N=9, Moderna N=1, Johnson N=1) to symptoms was 10 (2–32) and to diagnosis was 16 days (3–56). Patients presented with abdominal pain (86%), ascites (41%), fever (32%), elevated AST (35 U/L; 22–20100), ALT (45 U/L; 17–6928), INR (1.18; 0.88–5.1), D-dimer (6, 570 FEU; 530–63,000), white blood cell count (10, $7 \times 10^9/L$; 4, 2–26) and decreased platelets

($160 \times 10^9/L$; 51–537). Four patients (18%) fulfilled criteria for VIIT. Location of thrombosis was portal vein in 18 (82%), hepatic vein (s) in 8 (36%), superior mesenteric vein in 15 (68%) and splenic vein in 9 (41%). Combined SVT-BCS was present in 18%, and concomitant cerebral/pulmonary/deep vein thrombosis was observed in 23%. An underlying prothrombotic cause was found in only 5 patients (23%; myeloproliferative neoplasm, antiphospholipid syndrome, protein S and antithrombin deficiency, Factor V Leiden). Eight patients (36%) were admitted to the intensive care unit. Eight patients had intestinal ischemia (36%) of whom 5 underwent bowel resection. Patients were treated with LMWH (64%), DOAC (18%) or VKA (59%). Six patients (3/6 with VIIT) received IVIG and six underwent recanalization procedures. One patient died (no VIIT).

Conclusion: Within 6 months, 22 new cases of BCS or SVT following SARS-CoV2 vaccination were identified in 4 countries. Not all were AstraZeneca related. Although definite VIIT was relatively rare, most patients did not have another cause-in contrast to typical SVT or BCS. Also, these patients presented with extensive multiple site thrombosis and high rates of bowel ischemia and ICU admission. Concomitant extra-abdominal thrombosis, rare in typical BCS or SVT, was not uncommon. Further results are awaited from this expanding cohort.

FRI266

Abdominal wall hernia is a frequent complication of polycystic liver disease and associated with hepatomegaly

Thijs Barten¹, Roos-Anne Böklerink¹, Wulphert Venderink², Tom Gevers^{1,3}, Richard ten Broek⁴, J.P.H. Drenth¹. ¹Radboudumc, Department of Gastroenterology and Hepatology, Nijmegen, Netherlands; ²Radboudumc, Department of Radiology, Nijmegen, Netherlands; ³Maastricht UMC, Department of Gastroenterology and Hepatology, Maastricht, Netherlands; ⁴Radboudumc, Department of Surgery, Nijmegen, Netherlands
Email: trmbarten@gmail.com

Background and aims: Polycystic liver disease is related to hepatomegaly which causes an increased mechanical pressure on the abdominal wall. This may lead to abdominal wall herniation. We set out to establish the prevalence of abdominal wall hernia in polycystic liver disease and explore risk factors.

Method: In this cross-sectional cohort study we assessed the presence of abdominal wall hernias from polycystic liver disease patients with at least 1 abdominal computed tomography or magnetic resonance imaging scan. Abdominal wall hernia presence on imaging was independently evaluated by two researchers. Data on potential risk factors were extracted from clinical files.

Results: We included 484 patients of which 40.1% (n = 194) had an abdominal wall hernia. We found a clear predominance of umbilical

hernias (25.8%, n = 125) while multiple hernias were present in 6.2% (n = 30). Using multivariate analysis, male sex (OR 2.727 p < 0.001), abdominal surgery (OR 2.575, p < 0.001) and disease severity according to the Gigot classification (Type 3 OR 2.853, p < 0.001) were identified as risk factors. Total liver volume was an independent PLD specific risk factor in the subgroup of patients with known total liver volume (OR 1.203, p = 0.001). Patients with multiple hernias were older (62.1 vs 55.1, p = 0.001) and more frequently male (22.0 vs 50.0%, p = 0.001).

Abdominal wall hernia	N (%)	Median diameter in mm (IQR) *
Overall	194 (100.0)	12 (7) n = 180
Epigastric	8 (4.1)	18 (6) n = 7
Umbilical	125 (64.4)	11 (6) n = 109
Cicatricial	3 (1.5)	26 (58) n = 3
Inguinal	67 (34.5)	13 (8) n = 53
Other hernia	4 (2.1)	10 (1) n = 2
Multiple hernias	30 (15.5)	13 (7) n = 30
Complex hernia*		
Yes	50 (25.8)	13 (6) (n = 43)
No	131 (67.5)	12 (7) (n = 109)
Unknown	13 (6.7)	Unknown

IQR = interquartile range. * N represents the number of hernias in which the diameter could be measured in two different directions (laterolateral and craniocaudal). ** Complex hernia according to Slater criteria; 13 cases were unknown because hernia repair was performed before the imaging.

Conclusion: Abdominal wall hernias occur frequently in polycystic liver disease with a predominance of umbilical hernias. Hepatomegaly is a clear disease-specific risk factor.

FRI267

MR-derived metrics have utility in identifying paediatric patients with stable autoimmune hepatitis

Piotr Pawliszak¹, Elizabeth Shumbayawonda², Jędrzej Sarnecki¹, Paulina Opyrchal¹, Kamil Janowski³, Piotr Socha³, Małgorzata Woźniak³, Elżbieta Jurkiewicz¹. ¹Children's Memorial Health Institute, Radiology, Warsaw, Poland; ²Oxford, Oxford, United Kingdom; ³Children's Memorial Health Institute, Gastroenterology, Warsaw, Poland
Email: pedro_pawliszak@yahoo.es

Background and aims: Paediatrics with autoimmune hepatitis (AIH) are monitored using liver biochemistry and histology, however, liver biopsy is invasive, expensive and carries the risk of pain and bleeding. Non-invasive imaging techniques (NITs) such as elastography and multiparametric MRI are showing increasing utility in supporting patient management and disease stratification, but have never been compared head-to-head in children. The aim of this study was to investigate the utility of imaging markers to stratify those with stable from those with active disease and thus identify those who may not

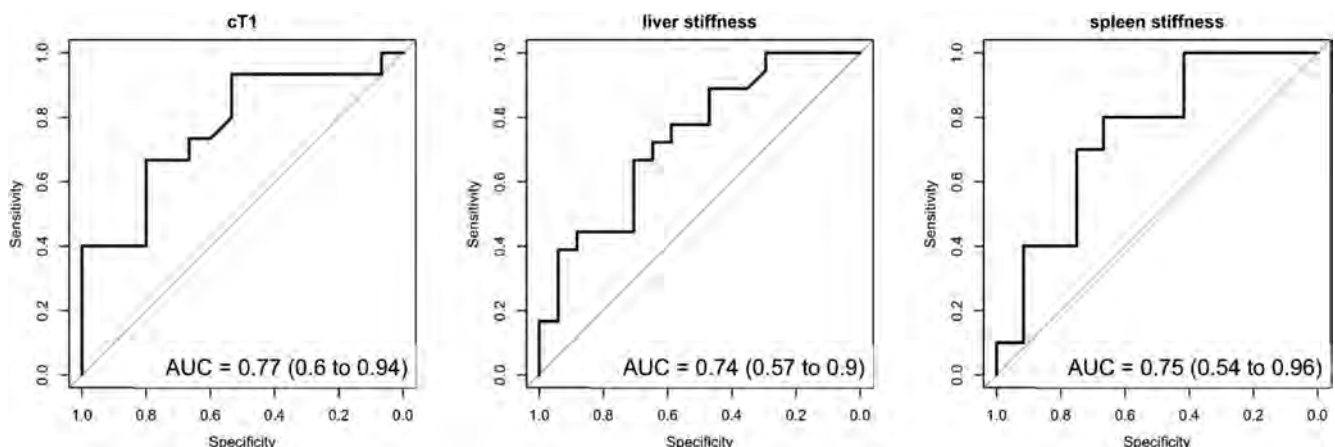


Figure: (abstract: FRI267): Diagnostic accuracy of individual imaging markers to identify AIH patients with stable disease.

POSTER PRESENTATIONS

require a biopsy or in whom it may be delayed leading to improvement in cost-effectiveness of AIH patient management.

Method: N = 36 with biopsy-confirmed AIH (14 ± 3 years) and N = 16 healthy controls [HC; 14 ± 2 years) underwent non-invasive imaging to obtain liver stiffness (LS; magnetic resonance elastography), spleen stiffness (SS) and corrected T1 (cT1). All AIH patients also underwent a liver biopsy. Kruskal-Wallis test was used to compare imaging markers between HC and AIH patients, as well as those with active vs stable disease. Correlations between NITs and histological scores were performed using Spearman's rank tests. Stable disease was defined as having both lobular and portal inflammation ≤1 and Ishak fibrosis ≤2. Discrimination between active and stable disease using NITs was investigated using area under the receiver operator characteristic curve (AUC).

Results: Compared to HC, AIH patients had higher cT1 (827 ms vs 756 ms; $p < 0.001$) and LS (3 kPa vs 2.6 kPa; $p = 0.031$) but not SS (4.9 kPa vs 5.6 kPa, $p = 0.068$). N = 18 had stable disease and lower mean cT1 ($p = 0.011$), LS ($p = 0.017$) and SS ($p = 0.048$) compared to those with active disease. cT1 correlated with fibrosis ($r = 0.37$; $p = 0.049$), lobular ($r = 0.42$, $p = 0.025$) and portal inflammation ($r = 0.5$, $p = 0.005$), LS ($r = 0.42$, $p = 0.007$) and SS ($r = 0.43$, $p = 0.028$). LS correlated with fibrosis ($r = 0.47$, $p = 0.005$), SS ($r = 0.5$, $p = 0.004$) and portal inflammation ($r = 0.37$, $p = 0.029$). For predicting disease activity, cT1 had AUC:0.77 (0.6–0.94), SS had AUC:0.75 (0.54–0.96) and LS had AUC:0.74 (0.57–0.9).

Conclusion: Those with active AIH have higher fibroinflammation, liver and spleen stiffness compared to those with stable AIH. NITs have utility in identifying paediatric patients with stable disease who may not benefit from invasive liver biopsy. Further work exploring the utility of these NITs in the AIH clinical pathway is warranted.

FRI268

Development and validation of a novel ICP-MS method to quantify different copper species in human plasma from patients with Wilson disease

Tao Liang¹, Haiting Zhang², Linwen Zhang¹, Scott Moseley¹, Ping Guo², Meng Chen¹, Tracey Hall¹, Ming Li¹, Eugene Swenson¹, Wei-Jian Pan¹, Brian Meltzer¹, Ryan Peltz¹, Mark Ma¹. ¹Alexion, AstraZeneca Rare Disease, Boston, United States; ²Frontage Laboratories Inc., Exton, United States

Email: mark.ma@alexion.com

Background and aims: Wilson disease (WD) is a rare autosomal recessive genetic disorder. Functional mutation of ATP7B causes inadequate loading of copper (Cu) into ceruloplasmin (CP) and defective Cu excretion into bile, resulting in Cu accumulation in liver and other organs. Currently, WD treatment monitoring lacks reliable and fully validated bioanalytical methods. The calculated non-CP Cu (NCC) method assumes a CP-Cu:CP ratio of 6:1 and can yield negative NCC values, which are biologically implausible. A direct assay is needed to monitor NCC, especially for patients treated with an investigational Cu-binding agent, ALXN1840 (bis-choline tetrathiomolybdate), which mobilizes tissue Cu, contributing to a non-bioavailable pool of circulating Cu.

Method: A novel method utilizing immunocapture of CP, followed by chelation and filtration to isolate different Cu fractions subject to ICP-MS analysis (Figure) was developed to fractionate and directly quantify multiple Cu species from human plasma. It permits measurement of CP-protein via LC-MS method and Cu species including CP bound Cu (CP-Cu), direct NCC, and labile bound Cu (LBC) via one workflow. Methods were validated for precision, accuracy, selectivity and stability following the FDA guidance for Bioanalytical Method Validation. A monoclonal anti-CP antibody was screened and selected for long-term assay use. Samples from healthy volunteers and from patients with WD were assessed for the Cu concentration in the CP fraction and the CP-Cu:CP ratio.

Results: Full validations were successfully performed for each Cu fraction as well as CP-protein and showed a linear range from 5 to

1000 ng/ml (0.08–15.75 μM) for CP-Cu, direct NCC, LBC, and 5.00–800 μg/ml (0.03–5.97 μM) for CP-protein. The mean [95% confidence interval] for the CP-Cu:CP ratio was 4.68 [4.35, 5.00] in healthy volunteers and 4.09 [3.36, 4.82] in patients with WD, both being below the assumed ratio of 6.

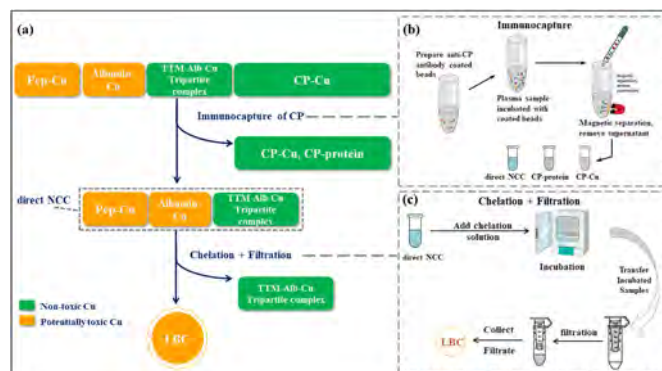


Figure: Method scheme. (a) overview of assay procedure (TTM, the active moiety of ALXN1840 which can bind to Cu and Albumin); (b) Immunocapture steps to obtain direct NCC, CP-protein, and CP-Cu fractions; (c) Chelation and filtration steps to isolate LBC.

Conclusion: Conventional calculated NCC is inaccurate and cannot be used for therapeutic guidance for WD. A novel method was developed that utilizes an immunocapture step and subsequent quantification of various fractions, including CP-Cu, direct NCC, LBC, and CP-protein. Validation data met defined acceptance criteria in terms of precision, accuracy, selectivity and stability. The assay is precise and reproducible and is valuable for accurate quantification of CP-Cu:CP-protein ratio, direct NCC and LBC, which may benefit WD therapy development.

FRI269

Quantitative magnetic resonance cholangiopancreatography identifies features of ductal disease change in primary sclerosing cholangitis: a prospective observational cohort study

Palak Trivedi^{1,2,3,4}, Katherine Arndtz^{1,2,3}, Nadir Abbas^{1,2,3}, Alison Telford⁵, Liam Young⁵, Rajarshi Banerjee⁵, Peter Eddowes^{1,2,6,7}, Kartik Jhaveri⁸, Gideon Hirschfield^{1,2,3,9,10}. ¹National Institute of Health Research (NIHR) Birmingham Biomedical Research Centre (BRC), Centre for Liver and Gastrointestinal Research, University of Birmingham, Birmingham, United Kingdom; ²Institute of Immunology and Immunotherapy, University of Birmingham, Birmingham, United Kingdom; ³Institute of Applied Health Research, University of Birmingham, Birmingham, United Kingdom; ⁴Liver Unit, University Hospitals Birmingham, Birmingham, United Kingdom; ⁵Perspectum Ltd, Oxford, United Kingdom; ⁶NIHR Nottingham BRC, University of Nottingham, Nottingham, United Kingdom; ⁷Nottingham University Hospitals NHS Trust, Nottingham, United Kingdom; ⁸Joint Department of Medical Imaging, University Health Network, University of Toronto, Toronto, Canada; ⁹Toronto Centre for Liver Disease, University Health Network, Toronto, Canada; ¹⁰Department of Medicine, University of Toronto, Toronto, Canada

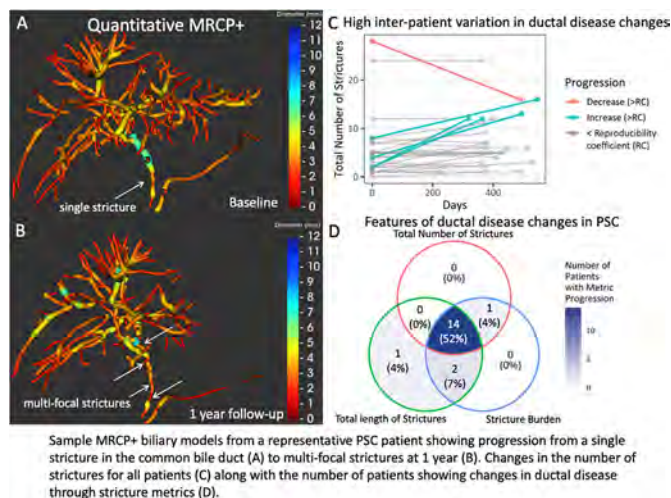
Email: liam.young@perspectum.com

Background and aims: Primary sclerosing cholangitis (PSC) is a chronic, progressive liver disease, characterised by multi-focal stricturing throughout the biliary tree. Biomarkers of parenchymal fibrosis are widely used for risk stratification. However there is a need to better characterise the extent of ductal disease involvement, its evolution over time, and the utility of quantitative biliary metrics for monitoring disease progression longitudinally. This study aimed to evaluate the utility of quantitative MRCP (MRCP+) in characterising

the extent of ductal disease involvement and monitor changes over 1 year in patients with stable biochemical and liver fibrosis readings.

Method: Patients (pts) with PSC were prospectively recruited for standardized heavily T2-weighted MRCP imaging on a Siemens Verio 3 T system at baseline and 1-year thereafter. Scans were processed with MRCP+ to enhance and quantify tubular structures using multi-scale Hessian analysis, gradient vector flow analysis, an intelligent path search algorithm and novel duct modelling algorithms. The 92 metrics generated by MRCP+ were reduced to 24 metrics expected to have clinical significance by an expert hepatopancreatobiliary radiologist. Changes in selected metrics over time were analyzed using linear mixed-effects models assuming patients as random effects.

Results: Non-cirrhotic pts with PSC were enrolled (n = 27; median age 45 yr, 70 % male) with a baseline PSC Mayo Risk Score -0.93 (IQR -1.2-0.3), ALP 142 iU/L (IQR 84-281), ALT 51 iU/L (IQR 26-91), and transient elastography score of 7.7 kPa (IQR 6.2-11.5). Intra- and extra-ductal involvement was seen in 92% and 36% pts with median modified Amsterdam cholangiographic score (MAS) of 2 (IQR 2-2) and 0 (IQR 0-2), respectively. Over a median 371-day follow-up (IQR 365-442), 67% pts manifested features of ductal disease change, evidenced by an increase in the total number of strictures (n = 15, p = 0.036, the total length of strictures (n = 17, p = 0.030), the total stricture burden (n = 17; p = 0.012), or a combination of metrics, which showed a significant dependence on time (Figure 1). Serum ALP (p = 0.51), ALT (p = 0.40), bilirubin (p = 0.39), liver stiffness values (transient elastography, p = 0.07) and biliary strictures assessed using MAS (p = 0.80) did not change significantly over time.



Conclusion: When quantitative imaging is reviewed one year apart, ductal disease change is apparent in the majority of pts with PSC, in the absence of significant variation in liver biochemistry or fibrosis values. Larger scale validation, alongside robust clinical outcome data, is essential to develop quantitative MRCP+ as a radiological toolkit for future PSC clinical trials.

FRI270

Age at diagnosis is associated with mortality in patients with hereditary hemochromatosis

Clare Foley¹, Sophie Diong², Fiona Colclough², John Ryan². ¹Beaumont Hospital, Hepatology, Gastroenterology, Dublin, Ireland; ²Beaumont Hospital, Dublin, Ireland
Email: foleyclare123@gmail.com

Background and aims: Hereditary Haemochromatosis (HH) a disorder of iron metabolism, is the most common autosomal recessive disorder in Caucasians, with Ireland having the highest prevalence in the world. Despite this, no formal screening exists for

the condition. Treatment by therapeutic phlebotomy reduces morbidity and mortality.

Method: This study aimed to identify factors associated with mortality in HH patients attending a Hemochromatosis service.

Results: 1043 patients with HH were identified; 65% were male and 35% were female. Fatigue was the most common presenting complaint (37%), with family history (22%), incidental finding of raised iron studies (16%) and screening programs (13%) being other common causes of referral to the service. Homozygosity for C282Y was the most common HFE genetic mutation in this cohort (68%) with compound HFE heterozygosity accounting for 26%. Median Ferritin at diagnosis was 332 ug/L (range 22-4655 ug/L). Mean Transferrin saturation at diagnosis: 68% (SD ± 17).

At the time of assessment, 0.03% (30/1043) of patients had died, with a median follow up time of 10 years (range 0.06-26). Of those that died, 70% were male, 43% were homozygous for C282Y, and 36% were compound heterozygotes. Median ferritin at diagnosis was 265 ug/L (dead) vs 264 ug/L (alive). Median age at diagnosis was significantly higher in those that died, 63.9 yrs vs 49.1 yrs for those alive at follow up (p < 0.0001). No significant difference was observed between groups based on gender, HFE genotype, or serum ferritin at diagnosis.

Conclusion: In a large sample of patients with patients with Haemochromatosis, age at diagnosis appears to be associated with death. Further investigation is warranted to detail the causes of death, and to determine whether HH screening in an at-risk population would reduce morbidity and mortality.

FRI271

Development of Hepatoblastoma organoids as a patient-derived ex-vivo system

Laura Zanatto¹, Paula Cantallops Vilà¹, Silvia Ariño Mons¹, Beatriz Aguilar-Bravo¹, Juan Carrillo², Laura Royo², Joan Pallares¹, Montserrat Domingo-Sabat², Alvaro del Rio², Juanjo Lozano³, Francisco Hernandez Oliveros⁴, Laura Guerra⁵, Barbara Torres Guerola⁶, Constantino Sábado⁷, Gabriela Guillén⁸, Marta Garrido⁹, José Antonio Salinas¹⁰, Moira Garraus¹¹, María Esther Llinares¹², Silvia Affo¹, Carolina Armengol², Pau Sancho-Bru¹. ¹Institut d'Investigacions Biomèdiques Augustí Pi i Sunyer (IDIBAPS), Liver Cell Plasticity and Tissue Repair, Barcelona, Spain; ²Health Sciences Research Institute Germans Trias i Pujol (IGTP), Childhood Liver Oncology Group (c-LOG), Badalona, Spain; ³Centro de Investigación Biomédica en Red de Enfermedades Hepáticas y Digestivas, Barcelona, Spain; ⁴University Hospital La Paz, Pediatric Surgery Department, Madrid, Spain; ⁵University Hospital La Paz, Pathology Department, Madrid, Spain; ⁶University Hospital La Fe, Medical Oncology Department, Pediatric Oncology Department, Valencia, Spain; ⁷Hospital Vall d'Hebron, Pediatric Oncology Department, Barcelona, Spain; ⁸Hospital Vall d'Hebron, Pediatric Surgery Department, Barcelona, Spain; ⁹Hospital Vall d'Hebron, Pathology Department, Barcelona, Spain; ¹⁰Hospital Universitari Son Espases, Division of Hematology-Oncology, Department of Pediatrics, Palma de Mallorca, Spain; ¹¹Hospital Sant Joan de Déu, Pediatric Cancer Center Barcelona, Barcelona, Spain; ¹²Instituto Murciano de Investigación Biosanitaria (IMIB), Pediatric OncoHematology Service, Clinic University Hospital Virgen de la Arrixaca, Murcia, Spain
Email: LZANATTO@clinic.cat

Background and aims: Hepatoblastoma (HB), the main pediatric liver tumor, is a rare disease with few therapeutic options and increasing incidence. With chemotherapy being the only effective treatment, survivors are doomed to suffer serious side effects and new therapeutic options are urgently needed. The lack of suitable models has strongly compromised the investigation of this pediatric tumor. Here we hypothesize that patient-derived organoids may represent a novel tool to explore the mechanisms involved in HB development and to design new therapeutic options.

Method: Parental tumor (T) and non-tumor (NT) tissues collected from different Spanish hospitals were used to generate a collection of

POSTER PRESENTATIONS

patient-derived organoids. Organoids and primary tissues were characterized through: (i) RT-qPCR to analyze the mutation status; (ii) immunofluorescence analysis to evaluate the expression of HB biomarkers; (iii) transcriptomic studies by performing total- and small- RNA sequencing.

Results: Fourteen stable organoid lines have been successfully generated from T and NT tissues using a specific isolation protocol and have been grown in expansion media enriched in growth factors. T- and NT-organoids present differences in morphology and doubling time, with T organoids growing slower and in darker small structures compared to the NT organoids. Moreover, the T-organoids present the same mutations of the primary tissues. Additionally, T- and NT-organoids show different gene and protein expression of markers associated with hepatocyte- (HNF4) and progenitor-phenotype (KRT19, EpCAM), as well as HB-related genes, such as DLK1; and cytoplasmic localization of both GS and β -catenin. Interestingly, principal component analysis of total RNA and small RNA transcriptome revealed that HB organoids maintain general features of the tumor of origin. Finally, functional analysis has revealed conserved pathways between T- and NT-primary tissues and T- and NT-organoids, among them epigenetic regulation, proliferation, Wnt activation and altered metabolism, indicating the maintenance of tumor features by organoids.

Conclusion: In conclusion, we have developed a new patient-derived *ex vivo* 3D system mimicking HB features, including specific gene and protein expression. Specifically, these data suggest that HB-derived organoids are a reliable model to investigate this poorly understood pediatric tumor towards the development of personalized treatments.

FRI272

High rates of histological findings compatible with porto-sinusoidal vascular disease in patients with constantly elevated gamma-glutamyl transferase levels undergoing a liver biopsy

Nicola Pugliese¹, Luca Di Tommaso¹, Roberto Ceriani¹, Ludovico Alfarone¹, Elisabetta Mastrorocco¹, Maria Terrin¹, Virginia Solitano¹, Francesca Colapietro¹, Chiara Masetti¹, Ana Lleo¹, Luigi Terracciano¹, Alessio Aghemo¹. ¹Humanitas Research Hospital, Cascina Perseghetto, Italy
Email: alessio.aghemo@hunimed.eu

Background and aims: Isolated elevations in gamma-glutamyl transferase (GGT) levels are commonly found in patients referred to liver specialists, however their clinical impact is unknown. Data on the histological findings in these patients are scarce.

Method: All consecutive patients who underwent a liver biopsy between March 1st, 2015 and December 1st, 2020, in our Liver Unit for isolated and persistent (at least 2-fold ULN for three tests within 12 months) elevation of GGT value were retrospectively analyzed for clinical and histological features. Excluded were patients with concomitant ALT or AST elevation, intake of Hepato-toxic drugs or over the counter medications, alcohol intake >20 g/day and metabolic associated fatty liver disease (MAFLD). Data about age, gender, body mass index (BMI), comorbidities (including findings compatible with portal hypertension), smoking habit and disease severity (APRI and FIB-4), were collected. All liver biopsies were blindly reviewed by 2 experts in liver pathology.

Results: During the study period a total of 640 patients performed a liver biopsy. 29 patients (4.5%) met the inclusion criteria and were enrolled. Most of the patients were males (19/29, 65.5%) and their mean age was 49.7 ± 11.4 years (28–73). The mean BMI was 24.5 ± 2.97 (18.8–30) and only two patients presented FIB-4 suggestive of advanced liver disease. The histological findings were compatible with porto-sinusoidal vascular liver disease (PSVD) in 13/29 (45%) patients, hepatic sarcoidosis in 3/29, non-alcoholic steatohepatitis (NASH) in 3 and congenital hepatic fibrosis (CHF) in 3. Histology did not allow a definite diagnosis in 6/29 (21%) patients. Patients with PSVD were male in 10/12 (%), with a mean age of 47 ± 10.9 years (28–

57), without any clinical signs of portal hypertension, in only one patient FIB-4 score was compatible with advanced liver disease. When comparing patients with PSVD to patients with any other liver etiology, we found no difference in gender, age, BMI, smoking habit, FIB-4, GGT, albumin and bilirubin values.

Conclusion: Liver histology in patients with isolated elevated GGT levels is useful as it allows to diagnose chronic liver conditions associated with a significant impact on survival. The high rate of patients with histological findings compatible with PSVD in the absence of signs of portal hypertension, requires careful assessment on how to manage these patients in the long term.

FRI273

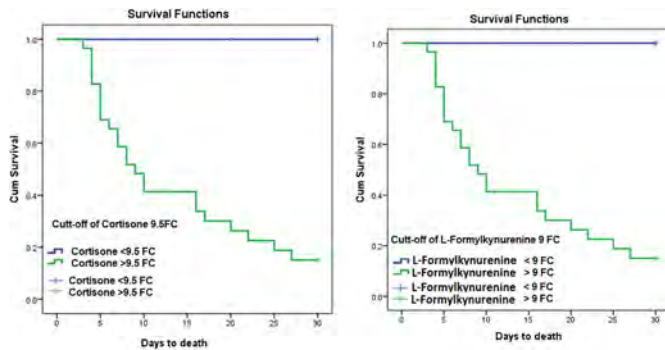
Plasma metabolomics and machine learning characterizes metabolite signature capable of segregating patients with poor outcome in pediatric cirrhosis

Babu Mathew¹, Gaurav Tripathi¹, Vipul Gautam², Akhilesh Saini¹, Manisha Yadav¹, Nupur Sharma¹, Vasundhara Bindal¹, Bikrant Bihari Lal², Vikrant Sood², Rajeev Khanna², Jaswinder Maras¹, Seema Alam². ¹Institute of Liver and Biliary Sciences, Molecular and Cellular Medicine, New Delhi, India; ²Institute of Liver and Biliary Science, Pediatric Hepatology, New Delhi, India
Email: jassi2param@gmail.com

Background and aims: Pediatric cirrhosis is a life-threatening illness with high mortality up to 40%. Primary causes of cirrhosis in children are biliary atresia, genetic-metabolic diseases, autoimmune hepatitis, Wilson's disease and others. Development of cirrhosis in children's predisposes them to early development of sepsis and/or poor outcome. Early diagnosis of cirrhosis, sepsis and/or poor outcome in such patients may increase survival rate; therefore, development of new diagnostic methods is crucial. We investigated whether metabolomics and machine learning (ML) approaches could segregate patients with poor outcome (sepsis/mortality) in pediatric cirrhosis at baseline.

Method: Plasma metabolomics was studied using ultra-high-performance liquid chromatography and high-resolution mass-spectrometry to identify patients with poor outcome (sepsis/mortality) in pediatric cirrhosis at baseline. Altogether, 154 pediatric patients were analysed of them, 54 in derivative [40 Cirrhotics (C) and 14 Non-cirrhotics (NC)] and 100 in validation cohort [75 C, 25 NC]. Differentially expressed metabolites (DEM) with highest AUC and lowest mean decrease in accuracy were identified in cirrhotics, sepsis and were correlated with the severity (PELD score) and outcome (mortality) in pediatric patients.

Results: Of the 762 annotated features (metabolomic/biochemical/spectral databases), at baseline 120 plasma metabolites (Up-109, Downregulated-11) discriminated Cirrhotics from Non-Cirrhotics in pediatric patients (FC > 1.5, $p < 0.05$). Cirrhotics documented significant increase in Tryptophan metabolism, steroid hormone biosynthesis, purine metabolism and others ($p < 0.05$). Most importantly high L-Formylkynurenine (546 Folds), 3-Hydroxy-1H-quinolin-4-one (20 Folds), Cortisone (18 Fold), 12-Hydroxydodecanoic acid (12 Folds), L-Isoleucine (11 Folds), Hypoglycine-A (5 folds), Aminopropylcadaverine (5 Folds), 2, 3, 4, 5-Tetrahydrodipicolinate (3 Folds) and others segregated Cirrhosis from Non-Cirrhosis ($p < 0.05$). Additionally, plasma L-Formylkynurenine, 3-Hydroxy-1H-quinolin-4-one, 12-Hydroxydodecanoic acid, L-Isoleucine and Cortisone segregated sepsis and non-survivors (FC > 2, $p < 0.05$, AUC > 0.8). In validation cohort, baseline plasma L-Formylkynurenine; hazard-ratio (HR) of 3.5 (1.2–5.6), and Cortisone; HR:3 (1.5–5.2) showed high reliability [AUC > 0.95 (0.91–0.97)] for predicting non-survivors and correlated with PELD score ($r^2 > 0.5$, $p < 0.05$). L-Formylkynurenine (9.5 FC), and Cortisone (9 FC) cut-off reliably segregated non-survivors (log-rank $p < 0.01$) and showed <96% accuracy, <95% sensitivity and <95% specificity using Random Forest-based Machine-Learning model.



Conclusion: Plasma metabolite L-Formylkynurenine (>9.5 FC), and Cortisone (>9 FC) can reliably predict cirrhosis, sepsis and poor outcome in pediatric patients.

FRI274

Experience of cholestatic pruritus emphasized by patients with PBC: results from the PBC Foundation app survey

Chris Mitchell¹, James Neuberger², Terri Kim³, Andrew Yeoman⁴, Robert Mitchell-Thain¹. ¹PBC Foundation, Edinburgh, United Kingdom; ²Birmingham Community Healthcare NHS Foundation Trust, United Kingdom; ³Escient Pharmaceuticals, San Diego, United States; ⁴Royal Gwent Hospital: Ophthalmology, United Kingdom
Email: chris@pbcfoundation.org.uk

Background and aims: Pruritus is a common symptom of cholestatic liver disease and treatment has limited efficacy. Patients with pruritus often suffer from intense itch, associated stress, and a negative effect on overall quality of life, including mental health issues.

Using PBC Foundation's App, we collected insights from Primary Biliary Cholangitis patients with pruritus, focussing on what may affect patient's daily experience of itch.

Method: An ongoing itch survey, live for over 6 months, was cross referenced with a previous survey exploring demographics and treatments. Due to cross-referencing, the number of respondents varies between questions. The main survey has 455 respondents. We defined mild, moderate and severe itch as at least 1, 4 and 7 respectively, on a numerical scale of 0 (no itch) to 10 (worse itch).

Results: Overall, similar to other studies 73% respondents suffer from itch. Over half of those itch daily and 3 in 4 patients have moderate to severe itch on their worst day.

In those aged <50 yr itch occurred more likely than in those >50 yr (77% vs 64%) and was more likely to be present daily (53% vs 44%). Itch occurred in the highest frequency in those within the first 5 yr of diagnosis (76%) with the lowest occurring in those >20 yr (45%).

Looking at disease modifying treatments: itch, daily itch, normal day severity and worst day severity for those on obeticholic acid were no worse than other therapies.

Information was only available for those taking cholestyramine, antihistamines or emollients and shows that itch is not present daily while on these therapies suggesting potential benefit. However itch on the worst day was almost exclusively severe and only partially ameliorated by therapy.

Conclusion: This study has a number of limitations, e.g. cross referencing different surveys taken at different times, and the risk of only itch-affected patients engaging. These surveys show that whilst some of the treatments may decrease the incidence of pruritus on a daily basis, severity of pruritus on a normal day is only slightly improved compared to the severity on the worst day. Pruritus can affect anyone within the PBC patient population and does so often and with profound effect.

Table: (abstract: FRI274).

Survey results					
PBC management medication	N	Respondents who itch (%)	Itch daily (%)	Moderate to severe itch on normal day (%)	Modest to severe itch on worst day (%)
Ursodiol	307	69	50	60	85
Obeticholic acid	118	67	52	64	86
Bezafibrate	153	70	49	54	75
Fenofibrate	16	44	30	0	100
Itch remedy					
Cholestyramine	312	87	52	90	99
Antihistamines	390	90	50	76	92
Topical emollients	411	91	49	66	88
Prednisone	42	71	59	62	75
Age in years					
21-30	1	100	100	100	100
31-40	8	75	67	67	100
41-50	21	76	47	61	83
51-60	44	63	55	71	88
61-70	35	63	31	44	74
>70	9	78	43	71	100
Years diagnosed					
<1	22	68	44	63	78
1-2	17	59	36	37	67
3-5	19	100	37	53	83
6-10	21	67	57	67	86
11-15	14	71	70	70	100
16-20	14	57	55	50	78
21-25	10	40	30	40	40
>25	1	100	0	100	100
Sex					
Female	315	72	52	60	80
Male	11	55	45	33	55

FRI275

Cancer risk in acute hepatic porphyria: a nationwide matched cohort study in 1, 245 individuals

Mattias Lissing^{1,2}, Daphne Vassiliou^{3,4,5}, Ylva Floderus^{4,6}, Jacinth Yan⁷, Hannes Hagström^{1,2}, Eliane Sardh^{3,4,5}, Staffan Wahlin^{1,2}.
¹Karolinska University Hospital, Dept of Upper GI Diseases, Sweden; ²Karolinska Institutet, Dept of Medicine, Huddinge, Sweden; ³Karolinska University Hospital, Dept of Endocrinology, Sweden; ⁴Karolinska University Hospital, Centre for Inherited Metabolic Diseases (CMMS), Porphyria Centre Sweden, Sweden; ⁵Karolinska Institutet, Dept of Molecular Medicine and Surgery, Sweden; ⁶Karolinska Institutet, Dept of Medical Biochemistry and Biophysics, Sweden; ⁷Karolinska Institutet, Division of Biostatistics, Institute of Environmental Medicine, Sweden
 Email: mattias.lissing@ki.se

Background and aims: The acute hepatic porphyrias (AHP) are associated with a high risk of hepatocellular carcinoma (HCC). Patients with AHP-associated liver cancer typically do not have a well-defined underlying liver diseases or cirrhosis. Although the carcinogenic mechanisms are unknown, a strong association between HCC and biochemical AHP-activity with elevated porphyrin precursors 5-aminolevulinic acid (ALA) and porphobilinogen (PBG) has been established. The cancerogenic potential of ALA and findings of increased cancer risks in small cohort studies have led to an assumption that AHP is a risk factor for cancer in general. Risk estimates are however uncertain, and little is known about how biochemical activity affects the risk. Our aim was to assess the risks of non-hepatic cancers in correlation to biochemical activity in the largest AHP cohort assembled to date.

Method: All patients in the Swedish porphyria registry with verified AHP were included and matched 1:10 to reference individuals from the general population by age, sex and municipality. Data on incident cancers were collected from the national cancer and cause-of-death registries. Overall cancer incidence and incidence of a predetermined set of specific cancers were compared by incidence rate ratio. Data on biochemical disease activity based on maximal urinary PBG were used to assess the correlation between biochemical AHP activity and cancer risk.

Results: We identified 1, 245 patients with AHP between 1987 and 2015 with a median follow-up of 19 years. Health registries identified 150 AHP-subjects (12.2%) with non-hepatic cancer, similar to 1607 (13.3%) in the matched reference population (n = 12, 367). Preliminary results indicate that AHP patients have a higher risk of kidney cancer 0.8% (n = 10) vs. 0.2% (n = 27) in the matched reference population (p < 0.001), confirming findings in previous smaller cohorts. The risks of other common forms of cancer are however not significantly different in patients with AHP compared to the reference population. More detailed risk estimates regarding each cancer type, combined with subgroup analysis based on biochemical AHP-activity will be presented at the conference.

Conclusion: In addition to the increased risk of hepatocellular carcinoma, patients with AHP have an increased risk of kidney cancer. Preliminary results have not identified increased risks for other non-hepatic cancers.

FRI276

Innovative approach using clinical metagenomics for the diagnosis of non-elucidated liver disease

Anna Sessa^{1,2}, Christophe Rodriguez³, Julien Calderaro¹, Slim Fourati¹, Giuliana Amadeo³, Jean-Michel Pawlotsky¹, Vincent Leroy³. ¹APHP, Hôpital Henri Mondor, Hepatology, Créteil, France; ²Henri Mondor Hospital, Hepatology, Créteil, France; ³APHP, Hôpital Henri Mondor, Hepatology, Créteil, France
 Email: asessa1990@gmail.com

Background and aims: Diagnostic of acute and chronic liver diseases (CLD) may be challenging when main etiologies are absent. Liver histology usually provides hints but often fails to accurately identify the etiologic factor that can be toxic, genetic, auto-immune or

infectious. Clinical metagenomics (CMg) is a new technique based on sequencing of nucleic acids allowing the identification of micro-organisms in an exhaustive manner. Our aim was to evaluate the performance of CMg for the diagnosis of non-elucidated liver diseases.

Method: All patients seen between 2019 and 2021 in a single tertiary centre for a non-elucidated liver disease were included. Inclusion criteria were elevated biochemical liver tests with no definite diagnosis after a comprehensive work-up including a liver biopsy. Patients with known CLD could be included if their features were not consistent with the etiology. The cut-off of 6 months discriminated acute and chronic profiles. Shotgun metagenomics was performed on each liver biopsy specimen with the aim to detect unexpected microorganisms.

Results: 48 patients (median age: 49, male: 58%) were included. Their clinical presentations consisted of acute cytolysis with or without jaundice (n = 9, 19 %, median ALT: 284 IU/L), acute cholestasis or mixed pattern (n = 19, 40 %, median ALP: 225 IU/L), chronic cytolysis (n = 8, 16.7 %, median ALT 166 IU/L) and chronic cholestasis (n = 12, 25%, median ALP: 146 IU/L). 20 patients (42%) had immunosuppression due to solid organ transplantation (n = 9, 19%), HIV infection (n = 6, 13%) and hematopoietic cancer (n = 5, 10%). Results of CMg were negative in 36 (75%), false positive due to contamination in 3 (6%), and positive in 9 (19%) patients. In 7 patients, CMg results allowed an etiologic diagnosis that changed the clinical management. Pathogens identified were adenovirus in one patient presenting with acute hepatitis, HCV in one seronegative liver-transplant recipient with recently acquired infection, HBV in one patient with unexplained cytolysis and low HBV DNA, HDV in 2 seronegative HBsAg (+) patients, Mycobacterium spp in an HIV-infected patient with unexplained granulomatosis, and Shingobium spp in a cirrhotic patient presenting with uncommon ACLF. Additionally, 2 patients had positive results that were considered as putative cofactors. Pathogens were EBV in one HIV-infected patient with tuberculosis, and TTV in one patient on immunotherapy for hematopoietic cancer. Taking the whole population, a definite diagnosis was eventually made after a comprehensive work-up combined to follow-up in 35 patients including 7 infectious diseases diagnosed by CMg (20%), and 13 patients remained with no definite diagnosis.

Conclusion: CMg performed on liver tissue is technically feasible and may bring etiologic diagnostic in patients with non-elucidated acute or chronic liver disease.

FRI277

Accumulation of molybdenum in major organs following chronic oral administration of bis-choline tetrathiomolybdate in Sprague Dawley rats

Kharmen Billimoria¹, Timothy Morley², Maria Estela del Castillo³, Stanislav Stekopytov³, Heidi Goenaga-Infante¹, John Foster⁴. ¹LGC, National Measurement Laboratory, Teddington, United Kingdom; ²Advotox, Harrogate, United Kingdom; ³LGC, National Screening Laboratory, Teddington, United Kingdom; ⁴ToxPath Sciences Ltd, Congleton
 Email: kharmen.billimoria@LGCGroup.com

Background and aims: Molybdenum (Mo) is an essential dietary element, functioning as a cofactor to activate essential enzymes including sulphite, aldehyde and xanthine oxidases. Bis-choline tetrathiomolybdate (BC-TTM) is under development as a therapeutic copper chelating agent for Wilson Disease with doses administered ranging from 15 to 60 mg/day (equivalent to 0.2 to 0.9 mg/kg/day in a 70 kg man). In a rat preclinical model (average bodyweight of 250 g), this would equate to a range of 0.8 to 3.6 mg/kg. The aim of this study was to determine if chronic administration of BC-TTM is associated with accumulation of molybdenum in major organs of a non-WD animal model and if tissue deposits of this metal are associated with haematological and biochemical abnormalities.

Method: Sprague Dawley (SD) rats were randomised to 3 groups of 12 [control, 15 mg/kg (low), 60 mg/kg (high)] and the BC-TTM was dosed by single oral gavage each day at volume of 5 ml/kg for 3 months. This drug exposure was equivalent to 3.75 to 15 mg/day in humans for nine years. Blood samples for clinical monitoring were taken at baseline, monthly and prior to euthanasia. Laser ablation inductively coupled plasma time-of-flight mass spectrometry (LA-ICP-ToF-MS) is an imaging technique used to confirm and spatially resolve the elemental distribution within a tissue. Tissue samples from major organs were prepared for conventional histopathology and LA-ICP-ToF-MS, to produce maps of Mo accumulation, quantified using a novel calibration strategy.

Results: Animals tolerated medication and no adverse clinical observations were made during the study. Dose dependent changes included increasing pigmentation of phagocytic and epithelial cells within each organ using conventional histopathological techniques were observed. However, data from LA-ICP-ToF-MS (Figure shown is from liver and brain) shows scaled spatial distribution of molybdenum deposits by concentration, increasing from blue to red. This accumulation was not associated with either biochemical or haematological abnormalities.

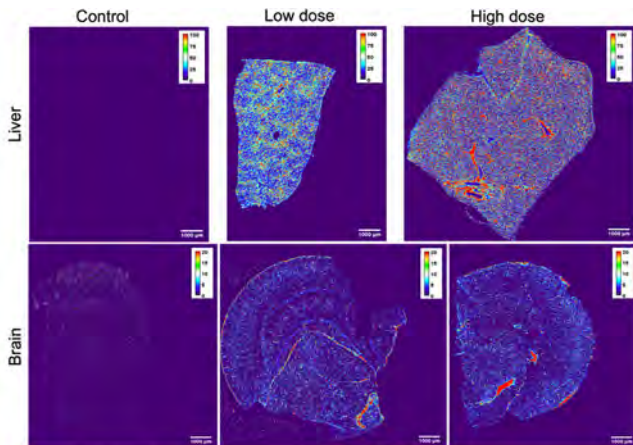


Figure 1: LA-ICP-ToF-MS images showing molybdenum (Mo) in liver and brain tissue sections from the control (vehicle only), low drug dose (15 mg/kg/day) and high drug dose (60 mg/kg/day) groups. The colour scale bar indicates Mo concentration in femtograms molybdenum per pixel. The increase in colour intensity shows a dose dependence on the amount of molybdenum accumulation detected. Spatial resolution = 18 x 20 μ m and the scale bar = 1000 μ m.

Conclusion: LA-ICP-ToF-MS demonstrated dose dependent Mo accumulation in major organs and our findings show the limitations of conventional histopathology to characterise these deposits. SD rats exposed to BC-TTM for 3 months did not exhibit blood or biochemical abnormalities; this may provide false reassurance of molybdenum accumulation following chronic exposure.

FRI279

Liver fibrosis and fat by transient elastography in patients with Alpha-1 antitrypsin deficiency

Hassaan Yousuf^{1,2}, Tobias Maharaj^{1,2}, Daniel Fraughen^{2,3}, Noel G. McElvaney^{2,3}, John Ryan^{1,2}. ¹Beaumont Hospital, Hepatology, Dublin, Ireland; ²Royal College of Surgeons in Ireland, Ireland; ³Beaumont Hospital, Respiratory Medicine, Dublin, Ireland
Email: Hassaanmyousuf@hotmail.com

Background and aims: Alpha-1 Antitrypsin Deficiency (AATD) is a common, inherited disorder which can lead to significant morbidity and mortality. The most severe form is seen in individuals with the homozygous PiZZ variant, with almost no circulating levels of AAT, while heterozygous (PiMZ; PiSZ) variants are associated with milder disease. While AATD effects on the lung have been extensively studied, its effects on the liver are poorly understood. Transient Elastography is widely used to stage liver disease by liver stiffness

measurement (LSM), and provides a measure of hepatic steatosis, the Controlled Attenuation Parameter (CAP).

Our aim is to assess the prevalence of liver fibrosis and steatosis in AATD patients, using transient elastography.

Method: Clinical data along with TE measurement was obtained on adult patients attending a dedicated AATD at our centre over a 4-month period (July–October 2021). LSM cutoffs used were >7.1 kPa for fibrosis, and >10 kPa for advanced fibrosis/cirrhosis

Results: 80 patients were recruited; TE failed on 4 patients; 48 (60%) were female.

39/80 (48%) were homozygous PiZZ, 24/80 PiMZ (30%), 12 PiSZ and 4 were PiSS.

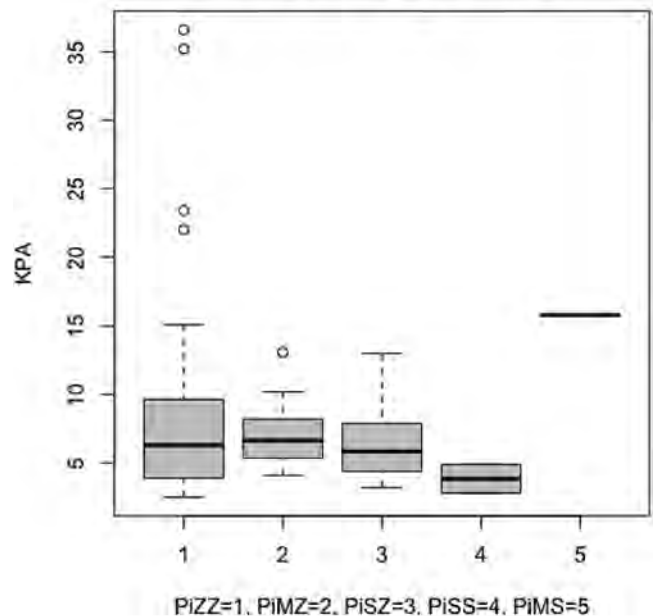
29/76 (38%) had LSM >7.1 kPa; of these 12 (16%) had LSM >10 kPa. Of the patients with advanced fibrosis, 8 were PiZZ, 2 were PiMZ and 1 each of PiSZ and PiMS. 16/39 (41%) PiZZ had evidence of fibrosis; 9 PiMZ (37.5%) had evidence of fibrosis, but only 2 had advanced fibrosis.

For PiZZ homozygotes, the median LSM was 6.3 kPa, and 6.25 kPa for heterozygotes (PiMZ/PiSZ); there was no significant difference in LSM between heterozygotes and homozygotes (Mann-Whitney U test, $p = 0.84$).

The median CAP for homozygotes PiZZ was 252 dB/m, and for heterozygotes (PiMZ/PiSZ) was 282.5 dB/m; there was no statistical significance between the 2 groups (Mann-Whitney U test $p = 0.128$) 6/12 (50%) individuals with advanced fibrosis were obese (BMI >30 kg/m²). In total 17 out of 29 (59%) patients with evidence of fibrosis were either overweight or obese. Of the 29 individuals found to have liver fibrosis by TE, only 6 were known to have chronic liver disease, the rest (79%) were all new diagnoses.

Among the patients with PFTs available, fibrosis was evident on TE in 3/14 (21.4%) patients with GOLD stage IV COPD, 4/14 (28.5%) with GOLD stage II/III COPD, and 10/34 (29.4%) with GOLD stage 0.

Boxplots of KPA~Genotype



Conclusion: In this study, a high rate of undiagnosed advanced liver fibrosis in AATD individuals was evident on routine screening using transient elastography. No association between lung and liver disease severity was noted, nor were there significant differences in liver stiffness or steatosis between AATD genotypes. Of note, a high prevalence of overweight/obesity was seen in those with liver fibrosis.

POSTER PRESENTATIONS

This study highlights the importance of screening AATD patients for liver fibrosis, and the potential clinical utility of transient elastography for these patients.

FRI280

Novel imaging feature in patients with porto-sinusoidal vascular disorder (PSVD)-radiological evaluation guiding diagnosis

Georg Semmler^{1,2}, Katharina Lampichler³, Katharina Wöran⁴, Benedikt Simbrunner^{1,2}, Mathias Jachs^{1,2}, Lukas Hartl^{1,2}, David J. M. Bauer^{1,2}, Lorenz Balcar^{1,2}, Matthias Pinter^{1,2}, Michael Trauner¹, Matthias Mandorfer^{1,2}, Dietmar Tamandl³, Judith Stift⁴, Ahmed Ba-Ssalamah³, Thomas Reiberger^{1,2}, Martina Scharitzer³, Bernhard Scheiner^{1,2}. ¹Medical University of Vienna, Division of Gastroenterology and Hepatology, Department of Internal Medicine III, Vienna, Austria; ²Medical University of Vienna, Vienna Hepatic Hemodynamic Lab, Division of Gastroenterology and Hepatology, Department of Internal Medicine III, Vienna, Austria; ³Medical University of Vienna, Department of Biomedical Imaging and Image-Guided Therapy, Vienna, Austria; ⁴Medical University of Vienna, Clinical Institute of Pathology, Vienna, Austria
Email: georg.semmler@meduniwien.ac.at

Background and aims: Porto-sinusoidal vascular disorder (PSVD) is a recently defined vascular liver disease often complicated by pre-sinusoidal portal hypertension (PH). Diagnosis is challenging and requires liver biopsy, and thus, PSVD is often misdiagnosed as cirrhosis. We investigated radiological features that are distinct between PSVD and cirrhosis.

Method: Demographic, clinical and laboratory parameters of patients with histologically-confirmed PSVD vs. cirrhosis vs. non-cirrhotic liver disease and available CT/MRI scans were retrospectively evaluated. The following imaging features were analyzed: Portosystemic collaterals, ascites, splanchnic vein thrombosis, spleen size, portal tract abnormalities, perfusion disorders, FNH-like lesions, changes in liver morphology and liver surface nodularity.

Results: 54 PSVD, 156 cirrhosis, and 41 non-cirrhotic patients were included. PSVD patients were younger (45.6 ± 16.3 vs. 56.4 ± 12.8 , $p < 0.001$) and had lower HVPG (8 [IQR: $5-12$] mmHg vs. 15 [IQR: $10-21$] mmHg, $p < 0.001$), liver stiffness (8.4 [IQR: $6.8-12.2$] kPa vs. 29.2 [IQR: $16.0-65.1$] kPa, $p < 0.001$), and MELD (9 ± 3 vs. 13 ± 6 points, $p < 0.001$). Specific clinical signs of PH according to PSVD-definition were similarly common in both groups. Intrahepatic portal tract abnormalities (52% vs. 15%; $p < 0.001$), splanchnic vein thrombosis (24% vs. 12%; $p = 0.025$) and FNH-like lesions (33% vs. 1%; $p < 0.001$) were significantly more common in PSVD patients. Hypertrophy of segment I (43% vs. 69%; $p < 0.001$), atrophy of segment IV (24% vs. 46%; $p = 0.004$) and nodular liver surface (19% vs. 87%; $p < 0.001$) were more common in patients with cirrhosis. In patients with adequate gadoteric acid-enhanced MRI (PSVD: $n = 25$, cirrhosis: $n = 95$, non-cirrhotic controls: $n = 41$), we identified the imaging feature of 'periportal hyperintensity' in the hepatobiliary phase (HBP) as very specific for patients with PSVD: 52% in patients with PSVD vs. 1% in cirrhosis vs. 0% in non-cirrhotic controls; $p < 0.001$).

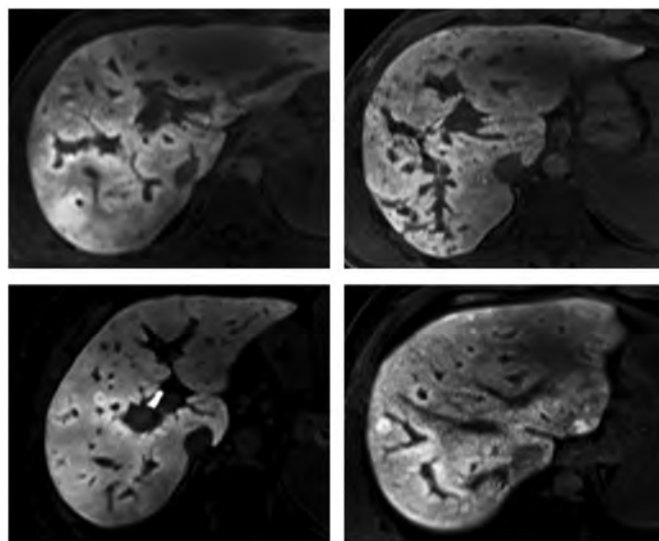


Figure: Periportal hyperintensity on the HBP in patients with PSVD.

Conclusion: Diagnosis of PSVD must be considered in younger patients presenting with clinical features of PH, portal tract abnormalities, splanchnic vein thrombosis, and FNH-like lesions on CT/MRI. 'Periportal hyperintensity' on HBP-MRI was identified as a very specific radiological feature of PSVD patients.

FRI281

Liver involvement in systemic light chain amyloidosis: is the heart guilty?

Margaux Charles¹, Amira Zaroui², Sebastien Mulé², Françoise Roudot Thoraval³, Christophe Duvoux¹, Dany Thibaud², Edouard Reizine³, Vincent Leroy⁴. ¹Hôpital Henri Mondor, Hepatology, Créteil, France; ²Hôpital Henri Mondor, Cardiology, Créteil, France; ³Hôpital Henri Mondor, Radiology, Créteil, France; ⁴Hôpital Henri Mondor, Hepatology, Créteil, France
Email: vleroy.home@wanadoo.fr

Background and aims: Systemic light-chain (AL) amyloidosis is a systemic disease caused by the deposition in organs of unstable monoclonal light chains secreted by clonal plasma cells. Prognosis is mainly related to the degree of cardiac involvement. Elevated liver enzymes and/or hepatomegaly are frequently observed and may be related to deposition of amyloid fibrils in the liver, congestive hepatopathy or confounding factors such as DILI. Diagnostic approach for hepatologists can be extremely challenging, with certain reluctance to perform liver biopsies. The aim of our study was to describe in a large cohort of patients with cardiac AL amyloidosis the characteristics of liver abnormalities, their relationships with cardiac status and their potential prognostic value.

Method: All patients seen from 2008 and 2021 in a single national reference centre for new diagnosis of histologically proven AL amyloidosis with cardiac involvement and available longitudinal liver features were included. Clinical, biological and echocardiographic data were collected. Liver imaging mainly consisted of MRI, or when not available CT-scan. All images were read by a single expert radiologist with specific attention to liver morphometry and signs of congestion.

Results: 200 patients (median age: 66 years, male: 61%) were included. The majority of them had severe heart failure (stage III of Mayo Clinic). Chemotherapy was given in 90% of patients. At baseline, 98 (49%) patients had elevated liver enzymes greater than 1.5 fold the upper limit of normal. Liver abnormalities were associated to higher Pro-BNP and Troponin serum levels. Enzyme patterns were cholestasis, cytolysis and mixed in 81%, 4% and 15%, respectively. Liver abnormalities were significantly associated with higher concentrations of troponin and Pro-BNP. Liver imaging showed hepatomegaly

in 31% of cases, sinusoidal dilation in 43% and hepatic vein dilation in 26%. Compared to patients with normal liver tests, the cholestatic pattern group had more often hepatic vein dilation (40% vs 12%, $p < 0.006$) and sinusoidal dilation (57% vs 30%, $p < 0.04$), these features being significantly associated with lower cardiac flow and echocardiographic features of right ventricular dysfunction. There was no association between liver abnormalities and left ventricular ejection fraction. A liver biopsy was performed in 11 patients and showed amyloid deposits in 9 and features of congestion in 5 patients. During the follow-up, a significant increase of liver tests was observed after 3 months. A cytotoxic pattern was associated with a peak of Pro-BNP and short-term mortality.

Conclusion: Liver involvement is frequent in patients with cardiac AL amyloidosis and seems mainly related to right cardiac dysfunction. The potential role of hepatic amyloid deposits is under investigation by scintigraphy and final results will be presented.

FR1282

The role of the mechanistic target of rapamycin (mTOR) in Alpha-1 Antitrypsin Deficiency

Lisa Bewersdorf¹, Pavel Strnad¹, Annika Gross¹, Yizhao Luo¹, Thorsten Cramer². ¹University Hospital RWTH Aachen, Medical Clinic III, Aachen, Germany; ²University Hospital RWTH Aachen, Clinic for General, Visceral and Transplant Surgery, Aachen, Germany
Email: lbewersdorf@ukaachen.de

Background and aims: Alpha1-antitrypsin (AAT) mutations lead to the retention of the otherwise secreted hepatocellular protein in the endoplasmic reticulum (ER) thereby giving rise to AAT deficiency (AATD). Liver disease arising due to the proteotoxic stress is the second leading cause of mortality in AATD. mTOR signalling acts as the central proteostatic regulator. Our aim was to study the importance of mTOR signalling in AATD.

Method: Animals overexpressing the characteristic AAT mutation (PiZ mice) were cross-bred with rodents harboring a hepatocyte specific-ablation of the interaction partners RAPTOR/RICTOR corresponding to mTOR complexes 1/2 (mTORC1/2) or with mice lacking hepatocellular mTOR.

Results: At two month of age, PiZ-mTOR^{Ahep} and PiZ-RAPTOR^{Ahep} but not PiZ-RICTOR^{Ahep} mice showed elevated liver enzyme levels, signs of increased liver injury and apoptosis despite diminished AAT accumulation. While PiZ-RAPTOR^{Ahep} animals displayed increased levels of the pro-apoptotic protein CHOP, CHOP ablation did not rescue the phenotype. As a potential underlying mechanism, we observed reduced levels of several chaperones, i.e., Hsp90 or Grp94.

Conclusion: mTORC1 but not mTORC2 plays an important role in PiZ induced liver injury.

FR1283

Cerebrotendinous xanthomatosis: long-term course in 5 patients and first description of a successful pregnancy management during therapy with chenodesoxycholic acid (CDCA)

Jan Köhler¹, David Schoeler¹, Petra May¹, Linus Mrozek¹, Renate Kimmerle², Tom Lüdde¹, Stephan vom Dahl¹. ¹University Hospital Duesseldorf, Heinrich-Heine-University, Department of Gastroenterology, Hepatology and Infectious Diseases, Duesseldorf, Germany; ²Endokrinologische Schwerpunktpraxis, Duesseldorf, Germany
Email: JanPhilipp.Koehler@med.uni-duesseldorf.de

Background and aims: Cerebrotendinous xanthomatosis (OMIM #231700) is a rare autosomal-recessive bile acid synthesis defect due to defective mitochondrial sterol 27-hydroxylase CYP27A1, leading to tendon xanthomas, bilateral cataracts, diarrhea and progressive neurologic manifestations. Patients are usually diagnosed during adulthood. Oral therapy with CDCA, a bile acid, reverses the potentially debilitating symptoms and prolongs life span. To our knowledge, this is the first description of a successful pregnancy with CTX.

Method: After biochemical diagnosis, CTX patients were monitored in 6-month intervals with abdominal ultrasound, cMR imaging, ophthalmologic examinations and determination of cholestanol blood levels. Therapy with CDCA (10–15 mg/kg body wt.) was initiated along with lipid-lowering combination therapy and in one female patient, after positive pregnancy testing in 2019, CDCA was continued and monitoring intervals were shortened.

Results: Three siblings, their mother and aunt from a consanguineous family were diagnosed with CTX at ages of 38, 27, 18, 14, and 9 respectively. The aunt was diagnosed in 1997, the mother in 2003 and the siblings in 2005. Mean follow-up in this cohort was 18 ± 2 years. At baseline, tendinous xanthomas were present in 4/5, diarrhea and ataxia in 1/5, hypercholesterolemia and hypertriglyceridemia in all patients. 3/5 patients suffered from cataracts and required surgical therapy. Slight cognitive impairment occurred in 4/5 patients. Ataxia and diarrhea subsided. Total cholesterol (TC), LDL-C and HDL-C at baseline were 217 ± 16 mg/dl, 108 ± 15 mg/dl and 77 ± 5 mg/dl and were reduced to 195 ± 7 mg/dl, 115 ± 12 mg/dl and 53 mg/dl ± 6 mg/dl at last visit. Pretherapeutic cholestanol levels and 7alpha-hydroxycholesterol were 3.1 ± 0.2 mg/dl (ref. range 0.21 to 0.67 mg/dl) and 3857 ± 802 ng/ml (ref. range $< 0, 5$ ng/ml) decreased to 0.3 ± 0.02 mg/dl and 76 ± 10 ng/dl. In a pregnant patient, blood cholestanol and cholesterol levels were stable, and after an uncomplicated pregnancy, she gave birth to a healthy baby boy in term on 08/2020, who was age appropriate and reached normal developmental milestones up to now.

Conclusion: Oral CDCA therapy can help stabilize/reverts the control clinical symptoms of CTX and can successfully be continued during pregnancy. CTX is underdiagnosed and should be suspected in any adult dyslipidemic patients with heterogeneous neurologic manifestations and cataracts.

FR1284

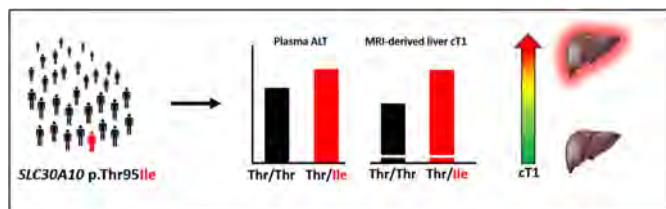
A rare genetic variant in the manganese transporter SLC30A10 and elevated liver enzymes in the general population

Anne-Sofie Seidelin¹, Børge Nordestgaard², Anne Tybjaerg Hansen¹, Hanieh Yaghoobkar³, Stefan Stender¹. ¹Rigshospitalet, Clinical Biochemistry, København, Denmark; ²Herlev Hospital, Clinical Biochemistry, Herlev, Denmark; ³University of Exeter, United Kingdom
Email: stefan.stender@regionh.dk

Background and aim: A rare genetic variant in the manganese transporter SLC30A10 (rs188273166, p.Thr95Ile) was associated with increased plasma alanine transaminase (ALT) in a recent genome-wide association study in the UK Biobank (UKB). The aims of the present study were to validate the association of rs188273166 with ALT in an independent cohort, and to begin to test the clinical, hepatic and biochemical phenotypes associated with the variant.

Method: We included $n = 334, 886$ white participants from UKB, including 14, 462 with hepatic magnetic resonance imaging (MRI), and $n = 113, 612$ individuals from two Danish general population cohorts, the Copenhagen City Heart Study and the Copenhagen General Population Study combined.

Results: Genotyping SLC30A10 p.Thr95Ile identified 816 heterozygotes in the UKB and 111 heterozygotes in the Copenhagen cohort. Compared to non-carriers, heterozygotes had 4 U/L and 5 U/L higher levels of plasma ALT in the UKB and Copenhagen cohort, respectively, and 3 U/L higher plasma aspartate transaminase and gamma glutamyl-transferase in the UKB. Heterozygotes also had higher corrected T1 on liver MRI, a marker of hepatic inflammation ($p = 4 \times 10^{-7}$), but no change in MRI-quantified steatosis ($p = 0.57$). SLC30A10 p.Thr95Ile heterozygotes had an eight-fold increased risk of biliary tract cancer in UKB ($p = 5 \times 10^{-7}$), but this association was not replicated in the Copenhagen cohort.



Conclusion: *SLC30A10* p.Thr95Ile was associated with elevated liver enzymes in two large general population cohorts, and with MRI-quantified hepatic inflammation. We hypothesize that Thr95Ile heterozygosity associates with a mild form of hepatic manganese accumulation leading to liver damage.

FRI285

A small molecule chaperone for alpha-1 antitrypsin deficiency-associated liver disease reduces liver polymer burden in the PiZ mouse model

Britta Handyside¹, Lening Zhang¹, Katina Ngo¹, Ryan Murphy¹, Joseph Chen¹, Nicole Galicia¹, Olivia Gorostiza¹, Glenn Pacheco¹, Lin Xie¹, Donald Mackenzie¹, Heidi Jones¹, Brian Heglar¹, Bing Wang¹, Shripad Bhagwat¹, David Lomas², James Irving², Riccardo Ronzoni², Sherry Bullens¹, Sylvia Fong¹, Stuart Bunting¹. ¹BioMarin Pharmaceutical Inc., Novato, United States; ²University College London, London, United Kingdom
Email: britta.handyside@bmrn.com

Background and aims: Alpha-1 antitrypsin deficiency (AATD) is caused by mutations in the *SERPINA1* gene encoding alpha-1 antitrypsin (AAT). AAT is primarily produced by hepatocytes and is secreted into the blood stream where it functions as a neutrophil elastase inhibitor.

The most clinically severe form of AATD is caused by the Z mutation (Glu342Lys) resulting in expression of the mutant protein Z-AAT. Pathogenic Z-AAT protein can misfold, polymerize and accumulate in the endoplasmic reticulum (ER) of hepatocytes leading to progressive liver fibrosis and low levels of circulating AAT. There is currently no effective treatment for AATD-associated liver disease. Here we tested BMN 349, a molecular chaperone, for its ability to prevent Z-AAT polymerization in hepatocytes while increasing circulating Z-AAT in the PiZ mouse, a model for AATD-associated liver disease.

Method: Young (5 week) and adult (12 week) female heterozygous PiZ mice expressing human Z-AAT were treated twice daily for 30 days with 50 or 100 mg/kg of BMN 349 via oral gavage (10–13 mice per group). Plasma and liver Z-AAT levels were analyzed by ELISA. Z-AAT polymer globules in hepatocytes were evaluated using Periodic Acid-Schiff with Diastase (PAS-D) stains. Liver and plasma pharmacodynamic biomarkers were assessed using mass spectrometry-based proteomics.

Results: Treatment with BMN 349 increased levels of circulating Z-AAT and reduced liver polymer levels in both age groups. In adult mice a dose-response was observed with a liver polymer reduction of 33% with 50 mg/kg ($p = 0.00098$) and 49% with 100 mg/kg ($p < 0.0001$) of BMN 349 compared to vehicle as determined by ELISA. Histological analysis using the PAS-D stain confirmed a significant reduction in liver Z-AAT polymer globules by 25% ($p = 0.0008$) and by 34% ($p = 0.0232$) with 50 or 100 mg/kg of BMN 349, respectively. In young mice, a greater than 80% reduction in liver polymers was detected by ELISA ($p < 0.0001$) and a >85% reduction of Z-AAT polymer globules ($p < 0.0001$) was observed with either dose of BMN 349 compared to vehicle. Together, the data from both age groups showed that a greater effect on liver polymer burden was achieved when treatment was initiated early. Proteomics analysis revealed an increase in ER stress markers including GRP78 in PiZ mouse liver and plasma and reduced levels of circulating liver-derived clotting factor VII in PiZ mouse plasma compared to wildtype mice, suggesting impaired liver function. Treatment with BMN 349 resulted in a

significant decrease of GRP78 and increase of FVII towards wildtype levels, demonstrating BMN 349 helped reduce cellular stress and restore normal biosynthetic function of the liver in PiZ mice in addition to reducing liver polymer burden.

Conclusion: Taken together, these data indicate that BMN 349 is effective in reducing Z-AAT polymer burden, reversing liver damage, and restoring liver function in the PiZ mouse model.

FRI286

A 'melting pot' of genetic variability in Wilson's disease-real world study from London, UK

James Liu Yin¹, Aftab Ala¹. ¹King's College Hospital, Institute of Liver Studies, London, United Kingdom
Email: aftab.ala1@nhs.net

Background and aims: Wilson's disease (WD) has been shown to have more than 600 different variants causing abnormal function of the ATP7B peptide. There is wide global diversity in these variants with different variants appearing to be more prominent in certain geographical areas and populations than others. London, UK is one of the largest, ethnically diverse cities in Western Europe with a growing population of over 9 million. It receives over 100,000 international migrants a year, with the largest proportions from the European Union and Indian Subcontinent. We aimed to review the genetic results at Kings College Hospital, London from patients with abnormal WD genetics and compare this to known global distribution.

Method: We retrospectively collected data on all WD genetic testing done at KCH since becoming one of the national testing centres (2015–present). We further extracted information on specific cDNA, protein change and zygosity status. We subsequently used *WilsonGen*, (Comprehensive genomic variant resource) which has compiled the largest database of variants, (2267 entries currently) to compare whether our variants were unique or previously documented.

Results: We identified 207 WD patients, 30 homozygous, 91 compound heterozygotes and 86 heterozygotes (Mean 28.9 years, range 4–70). Within this, there were 113 different variants identified. The most common was His1069Gln (11%), followed by Cys271Ter (3.6%), Met769Val (3.6%) and Ser1365fs (3.2%). On comparison with the *WilsonGen* database we found that 44 variants were not listed on their records (38.9%). We had ethnicity data accessible for 137 patients, 49% were documented as unspecified and the remaining were; Caucasian (35%), Indian Subcontinent (7%), Middle Eastern (4%), Black/Caribbean (3%), Chinese (1%) and other (<1%).

Conclusion: Our results demonstrate significant genetic variation in London with the most common mutation only accounting for 11% of the overall total. As genetic testing becomes a more utilized tool in furthering diagnostic pathways we need to understand that this variation may have significance. A recently suggested ATP7B-mutation specific diagnostic test would be less effective in a population like London and other Metropolitan cities. This needs to be taken into account in further studies to ensure that genetic variation will not delay or prevent diagnosis of new cases.

The importance of ATP7B genetic variation is yet to be fully understood and characterised with respect to the pathogenesis of WD. Within our cohort, the presence of novel variants was 39% which is a significant portion and higher than previously reported UK data (27% Coffey et al). Considering the wide spread of variation including novel variants, specific mutations have not been shown to confer benefit thus far and therefore further understanding of its significance is needed.

FRI287

The alpha-1 antitrypsin Pi*Z allele is an independent risk factor for liver transplantation/death in patients with advanced chronic liver disease

Lorenz Balcar^{1,2}, Bernhard Scheiner^{1,2}, Markus Urheu¹, Patrick Weinberger¹, Rafael Paternostro^{1,2}, Benedikt Simbrunner^{1,2}, Lukas Hartl^{1,2}, Mathias Jachs^{1,2}, David Jm Bauer^{1,2}, Georg Semmler^{1,2}, Claudia Willheim¹, Matthias Pinter¹, Peter Ferenci¹, Michael Trauner¹, Thomas Reiberger^{1,2}, Albert Stättermayer^{1,2}, Mattias Mandorfer^{1,2}.

¹Medical University of Vienna, Division of Gastroenterology and Hepatology, Department of Internal Medicine III, Vienna, Austria;

²Medical University of Vienna, Vienna Hepatic Hemodynamic Lab, Vienna, Austria

Email: mattias.mandorfer@meduniwien.ac.at

Background and aims: Alpha-1 antitrypsin (AAT) deficiency causes/predisposes for advanced chronic liver disease (ACLD). However, the role of the *SERPINA1* Pi*Z allele in patients who have already progressed to ACLD is unclear. Thus, we aimed to evaluate the impact of the Pi*Z allele on the requirement of liver transplantation/liver-related death in ACLD, while adjusting for the severity of liver disease at inclusion.

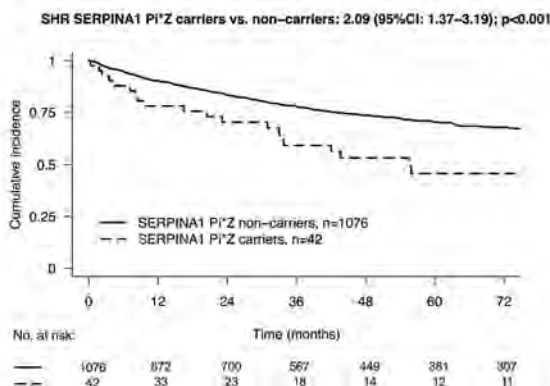
Method: 1118 ACLD patients who underwent HVPG-measurement and genotyping for the Pi*Z/Pi*S allele at the Vienna Hepatic Hemodynamic Lab were included in this retrospective analysis. Requirement of liver transplantation/liver-related death was the outcome of interest, while non-liver-related death and removal of the primary etiological factor were considered as competing risks.

Results: Viral hepatitis was the most common etiology (44%), followed by alcoholic (31%) and non-alcoholic fatty liver disease (11%). Forty-two (4%) and forty-six (4%) patients harboured the Pi*Z and Pi*S variants, respectively.

Pi*Z carriers had more severe portal hypertension (HVPG: 19 ± 6 vs. 15 ± 7 mmHg; $p < 0.001$) and hepatic dysfunction (Child-Turcotte-Pugh: 7.1 ± 1.9 vs. 6.5 ± 1.9 points; $p = 0.050$) at inclusion, as compared to non-carriers. Contrarily, the Pi*S allele was unrelated to liver disease severity.

In competing risk regression analysis, harbouring the Pi*Z allele was significantly associated with an increased probability of liver transplantation/liver-related death (Figure), even after adjusting for liver disease severity at inclusion. The detrimental impact of the common Pi*MM genotype (vs. Pi*MM) was confirmed in a fully adjusted subgroup analysis. In contrast, Pi*S carriers had no increased risk for events.

Figure. Cumulative incidences of liver transplantation/liver-related death in Serpin Family A Member 1 (*SERPINA1*) Pi*Z carriers vs. non-carriers with etiological cure and non-liver-related death as competing risks.



Conclusion: Genotyping for the Pi*Z allele identifies ACLD patients at increased risk for adverse liver-related outcomes, thereby improving prognostication. Therapies targeting accumulated abnormal AAT

should be evaluated as disease-modifying treatments in Pi*Z allele carriers with ACLD.

FRI288

Fontan associated liver disease: a cohort review into the prevalence of portal hypertension

Hannah Donnelly¹, James Orr². ¹Bristol Royal Infirmary, Bristol, United Kingdom; ²Bristol Royal Infirmary, United Kingdom

Email: donnellyhannah@hotmail.com

Background and aims: The Fontan procedure is a palliative operation for patients with functional univentricular congenital heart disease. It directs the systemic venous return directly into the pulmonary circulation without ventricular propulsion preventing mixing of blood. Up to 70 000 Fontan patients are alive worldwide today, and this is expected to double in the next 20 years. Fontan-associated liver disease (FALD) is emerging as a common complication and consensus recommends evaluation for FALD but specific guidelines on screening are not established. The Bristol Liver Unit and Heart Institute are collaborating to review their cohort of patients, particularly looking into the prevalence of portal hypertension.

Method: A database of Fontan patients was gathered, and demographics, bloods, imaging, and endoscopy results were collected from the electronic patient record.

Results: From the 101 Fontan patients on the database 11 had had gastroscopies. 10 patients had gastroscopies to look for signs of portal hypertension, and one due to a hereditary condition. One patient had presented with bleeding, with coffee-ground vomiting, all others were elective. 6/11 had signs of portal hypertension, details in table 1. 5/6 (83%) of those with endoscopic evidence of portal hypertension had either splenomegaly (>13 cm), Fibroscan >20 kPa or thrombocytopenia (platelet count <150). These are all established markers of possible portal hypertension. The patient that did not have any of these had varices shown on a USS and this was confirmed on endoscopy. In the cohort 37% (38/101) met one or more of these criteria.

Table 1: Findings of portal hypertension on endoscopy

Portal hypertensive gastropathy	5/6
(With GOV)	4/6
Oesophageal varices	4/6
Grade 1	
Gastric varix	1/6

Conclusion: Non-invasive markers of portal hypertension seem to predict the presence of portal hypertension detected on endoscopy. Our Fontan patients have a high prevalence of these non-invasive markers and this is with missing data. We plan to explore the prevalence further by establishing a joint clinic with Cardiology to assess the patients and perform gastroscopies if non-invasive markers indicate possible portal hypertension. We will also be looking at the relevance of portal hypertension in this patient group, considering the bleeding risk and impact on transplantation assessment.

FRI289

Senolytic therapies have a place in pediatric biliary cirrhosis

Giulia Jannone¹, Eliano Bonaccorsi², Catherine de Magnée³, Roberto Tambucci³, Jonathan Evraerts¹, Joachim Ravau¹, Mustapha Najimi¹, Etienne Sokal¹. ¹Université catholique de Louvain, IREC Institute, Laboratory of Pediatric Hepatology and Cell Therapy, Brussels, Belgium; ²Université catholique de Louvain, IREC Institute, Laboratory of Experimental Surgery and Transplantation, Brussels, Belgium; ³Cliniques Universitaires Saint-Luc, Pediatric Surgery and Transplantation Unit, Brussels, Belgium

Email: giulia.jannone@student.uclouvain.be

Background and aims: Premature senescence has been extensively characterized in adult chronic hepatobiliary diseases and can worsen liver function and fibrosis evolution. Since new therapeutic options

POSTER PRESENTATIONS

are needed in pediatric biliary cirrhosis to delay liver transplantation, our aim was to investigate the presence of premature senescence in biliary atresia (BA) and to test the senolytic properties of Medicinal Signaling Cells in a preclinical model of biliary cirrhosis.

Method: Senescence was investigated through senescence-associated β -galactosidase activity assay (SA- β -gal) as well as p16 and p21 gene/protein expression in BA livers at the time of hepatoporectomy (n = 5) or liver transplantation (n = 30) as compared to control livers (n = 10). Co-localized expression of senescence (gammaH2AX or p21) with CK19, HNF4alpha, alphaSMA and Ki67 was also assessed. Bile duct ligation (BDL) was performed on 2-months old rats and senescence was characterized in the model through above-mentioned techniques. Human allogeneic liver-derived progenitor cells (HALPC) were injected in BDL rats 48 hours after the surgery at high (12.5×10^6 cells/kg, n = 6) versus low dose (1.25×10^6 cells/kg, n = 6) and compared to the vehicle (n = 6).

Results: Senescence was similarly increased in both BA stages as compared to control livers (SA- β -gal: 5.9 ± 1.4 and 5.4 ± 1 vs 0.6 ± 0.1 %stained area/total, $p < 0.01$) and was also confirmed in BDL livers one and two weeks after the surgery (SA- β -gal: 1.6 ± 0.6 and 6.6 ± 2.4 vs 0.2 ± 0.1 %stained area/total, $p < 0.05$). The pattern of senescence in BA and BDL was similar as senescence first appeared in cholangiocytes of the ductular reaction and subsequently developed in hepatocytes. HALPC transplantation at both doses decreased senescence in BDL rats (p21 gene expression: 0.4 ± 0.04 and 0.5 ± 0.1 vs 1 ± 0.2 fold change; $p < 0.05$).

Conclusion: Premature senescence occurs in BA livers and HALPC display senolytic properties in a preclinical model of biliary cirrhosis.

FR1290

PNPLA3 rs738409 G allele increases the risk of liver cirrhosis in SERPINA1 MZ heterozygotes

Sona Frankova¹, Zuzana Rabekova², Magdalena Neroldova³, Ondrej Fabian⁴, Martin Kveton⁴, Jaroslav A. Hubacek⁵, Julius Spicak¹, Vera Adamkova⁶, Milan Jirsa³, Jan Sperl¹. ¹Institute for Clinical and Experimental Medicine, Department of Hepatogastroenterology, Praha, Czech Republic; ²Institute for Clinical and Experimental Medicine, Department of Hepatogastroenterology, Prague, Czech Republic; ³Institute for Clinical and Experimental Medicine, Laboratory of Experimental Hepatology, Praha, Czech Republic; ⁴Institute for Clinical and Experimental Medicine, Department of Clinical and Transplant Pathology, Praha; ⁵Institute for Clinical and Experimental Medicine, Atherosclerosis Research Laboratory, Praha; ⁶Institute for Clinical and Experimental Medicine, Preventive Cardiology Centre, Praha, Czech Republic
Email: sona.frankova@ikem.cz

Background and aims: Homozygous carriage of mutated Z allele in rs28929474 locus of *SERPINA1* encoding alpha-1-antitrypsin (A1AT) leads to lung emphysema and liver cirrhosis. Recent data show that the *SERPINA1* MZ genotype increases the risk of liver cirrhosis in patients with various liver diseases. The mechanism behind this finding has not been elucidated so far. Our study aimed to demonstrate the synergy between the *SERPINA1* Z allele and unfavourable alleles in other liver disease-modifying genes.

Method: The study group consisted of 1079 liver transplant candidates with liver cirrhosis of various aetiology (642 males, 437 females, average age of 54 years). The aetiology of cirrhosis was as follows: 352 alcoholic, 309 cholestatic, 217 viral, 142 NASH, 59 metabolic. Patients with A1AT deficiency were excluded. The control group consisted of 3329 healthy individuals from the MONICA study (WHO Multinational Monitoring of Trends and Determinants in Cardiovascular Disease Project).

Genomic DNA was isolated from peripheral blood by Qiagen QIAamp kit (Qiagen, Hilden, Germany). *SERPINA1* rs28929474, *PNPLA3* rs738409, *TM6SF2* rs rs58542926 and *GCKR* rs1260326 loci were genotyped by TaqMan RT-PCR SNP assays (Thermo Fisher Scientific, Waltham, MA). Aggregates of A1AT in hepatocytes in liver explants

were stained by PAS-D and immunostained with an anti-A1AT polyclonal rabbit antibody (Cell Marque, Inc., Rocklin, CA, USA).

Results: The frequency of *SERPINA1* MZ heterozygotes was significantly higher in the group with liver cirrhosis in comparison with the control group, 56/1079 (5.2%) vs. 89/3329 (2.7%), $p < 0.0001$, MZ heterozygotes thus have an increased risk of liver cirrhosis (OR 2.0, CI 95% 1.4–2.8).

Re-evaluation of 1009 histopathological reports of the explanted liver specimens revealed that PAS-D positive aggregates were detected in 52/56 (93%) MZ heterozygotes and 18/953 (1.9%) MM homozygotes ($p < 0.0001$). Forty-six out of 56 available specimens of MZ heterozygotes were assessed by immunohistochemistry; A1AT aggregates were confirmed in all cases.

PNPLA3 rs738409 genotype frequencies were 21 CC (37.5%), 24 CG (42.9%), and 11 GG (19.6%) in 56 *SERPINA1* MZ heterozygotes with cirrhosis and 59 CC (66.3%), 26 CG (29.2%) and 4 GG (4.5%) in 59 MZ heterozygotes in the control group. The frequency of the unfavourable *PNPLA3* G allele was significantly higher in *SERPINA1* MZ carriers with cirrhosis than in healthy heterozygotes, and the carriage of the *PNPLA3* G allele increased the risk of liver cirrhosis ($p = 0.001$; OR = 3.278, CI 95% 1.633–6.581). Contrarily, the frequencies of the *TM6SF2* and *GCKR* genotypes in *SERPINA1* MZ heterozygotes did not differ significantly between the patients with cirrhosis and controls.

Conclusion: Our results suggest that the risk genotypes of *PNPLA3* accelerate the progression of fibrosis in *SERPINA1* MZ heterozygotes with chronic liver disease.

FR1291

Patient experience of their Primary Biliary Cholangitis (PBC) management compared to clinical practice guidelines

Chris Mitchell¹, Angela Eddy², James Neuberger³. ¹PBC Foundation, Edinburgh, United Kingdom; ²PBC Foundation, Edinburgh, United Kingdom; ³NHS, Birmingham Queen Elizabeth Medical Centre, Birmingham, United Kingdom
Email: chris@pbcfoundation.org.uk

Background and aims: Primary Biliary Cholangitis (PBC) is a chronic, cholestatic, autoimmune liver disease, which can have a profound impact on patients' quality of life and a significant demand for healthcare services. PBC management guidelines were published in 2017 by European Association for the Study of the Liver (EASL), which include recommendations for daily dosage (13–15 mg/kg) of licensed first-line therapy (ursodeoxycholic acid (UDCA)) and referrals for alternative treatment if UDCA response is inadequate, of which obeticholic acid (OCA) is the only licensed treatment alongside other re-purposed agents.

This study explored the efficacy of patient-clinician collaborations to manage PBC in accordance with EASL guidelines from a patient perspective.

Method: A closed question questionnaire was designed focussing on the application of treatments and the inclusion of patients in the management of their PBC. The questionnaire was piloted with PBC Foundation service users during a focus group testing its reliability and face validity. A convenience sample was used and participants recruited via the PBC Foundation's app during March 2022. Intercept Pharmaceuticals provided financial support and input into the questionnaire, however the PBC Foundation has retained editorial discretion over survey outputs.

Results: 172 patients completed the survey.

154 respondents (90%) take UDCA and 132 respondents (77%) received a timely UDCA prescription (0–3 months after diagnosis). 91% of UDCA patients believe they are taking the recommended dosage however only 54% of UDCA patients report taking dosage within guidelines.

Of those patients who are unresponsive or intolerant to UDCA, 68% were offered alternative treatment and 57% were included in discussions about the most suitable option.

22% of all patients take 2nd line treatment (5% OCA and 17% unlicensed). 8% of all patients take no treatment for PBC management.

54% of patients had no access to face-to-face clinical appointments and 39% had appointments delayed or cancelled during the COVID pandemic. Patient comfort in raising PBC related queries ranges from 86% in face-to-face meetings, 46% on the telephone and 31% on screen-calls.

Latest blood test results were discussed with 73% of patients. 50% of patients believe they understand their test results and 40% say their test results help them manage their PBC.

Conclusion: Unmet PBC patient needs are evident in numerous stages of the life-long clinical journey. Data indicates substantial disparity between published PBC treatment guidelines and actual care delivered to patients, particularly relating to optimal application of PBC management therapies and patient inclusion in important discussions (test results and further treatment referrals). Unmet needs have been exacerbated during the COVID pandemic when timely appointments in patients' preferred formats were adversely affected.

FRI292

Evaluation of the clinical impact of the Ceruloplasmin variant p.Thr551Ile in liver cirrhosis

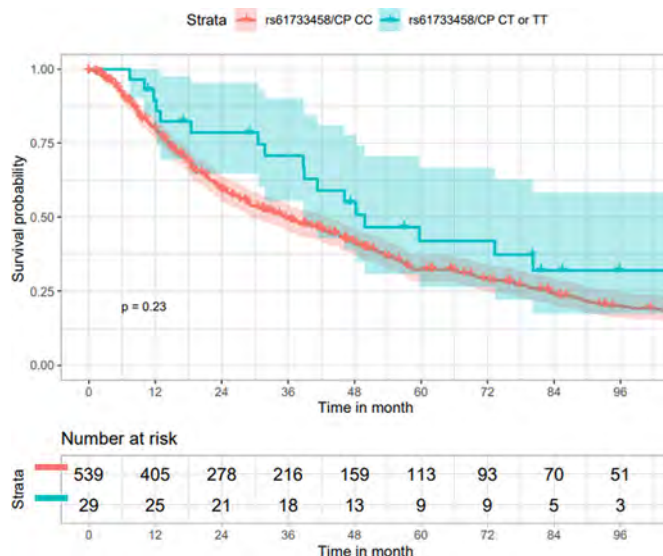
Marlene Panzer^{1,2}, Benedikt Schaefer¹, André Viveiros¹, Herbert Tilg¹, Heinz Zoller^{1,3}. ¹Medical University of Innsbruck, Department of Medicine I, Innsbruck, Austria; ²VASCage Reserch Center of Vasuclar Ageing and Stroke, Innsbruck, Austria; ³Christian Doppler Laboratory on Iron and Phosphate Biology, Innsbruck, Austria
Email: heinz.zoller@i-med.ac.at

Background and aims: Ceruloplasmin is a multicopper oxidase and is involved in cellular iron efflux. Aceruloplasminemia (ACP) is a recessive disease, caused by pathogenic variants in the gene encoding ceruloplasmin (CP). The disease is characterized by iron accumulation in liver, pancreas and brain. Patients typically present in their 5th decade of life with the triad of retinal degeneration, diabetes mellitus and neurodegeneration. Early biochemical signs of ACP include hyperferritinemia and low transferrin saturation. Recent reports suggest that heterozygous variants in CP can also cause hyperferritinemia and hepatic siderosis in patients with non-alcoholic fatty liver. The aim of the present study was to investigate the allele frequency and the clinical impact of the common ceruloplasmin variant p.Thr551Ile in an unselected cohort of patients with liver cirrhosis.

Method: A cohort of patients referred to the Hepatology Laboratory at the Medical University of Innsbruck for PNPLA3 genotyping was retrospectively assessed. Patients diagnosed with liver cirrhosis and available serum CP concentrations were included in this study (n = 568). Demographic, biochemical and clinical parameters were collected by review of patient records. Genotyping for the CP variant p.Thr551Ile (rs61733458) was performed by allelic discrimination PCR.

Results: Genotyping results revealed 2 homozygous and 27 heterozygous patients for p.Thr551Ile. This corresponds to an allele frequency of 2.73% (31 of 1136) in the liver cirrhosis cohort which is not different from the general population as reported in gnomAD (7795 of 282414; 2.76%). Biochemical surrogates of liver disease severity and serum iron parameters did not show significant differences when patients were stratified according to CP genotype. Reduced CP concentrations (≤ 20 mg/dL) were detected in 17.2% of patients carrying the variant p.Thr551Ile and in 11.7% in the normal group, which is not significantly different. Median CP concentrations were also numerically lower in patients heterozygous or homozygous for p.Thr551Ile, but this difference did not reach statistical significance (27.7 mg/dl vs 27.8 mg/dl; p = 0.368). Median time of transplant-free survival was significantly reduced in the group with decreased CP concentration (p = 0.004), but no significant difference

in survival probability was observed when patients were stratified according to CP genotype. Cox regression analysis including age and NaMELD showed that CP serum concentration but not p.Thr551Ile genotype was an independent predictor of transplant-free survival.



Conclusion: Reduced serum ceruloplasmin is common in patients with liver cirrhosis and is independently associated with reduced transplant-free survival in unselected patients with cirrhosis. The CP variant p.Thr551Ile shows no association with serum iron parameters or transplant-free survival.

FRI293

Circulating miR-21 parallels the incidence of IBD in PSC patients

André A. Santos¹, Joana Torres², Susana Saraiva², Catarina Ferreira Gouveia², Catarina Bravo², Marília Cravo², Cecília M. P. Rodrigues¹. ¹Research Institute for Medicines (iMed. ULisboa), Faculty of Pharmacy, Universidade de Lisboa, Lisbon, Portugal; ²Hospital Beatriz Angelo, Loures, Portugal
Email: afasantos@ff.ulisboa.pt

Background and aims: Primary sclerosing cholangitis (PSC) is a chronic and progressive cholestatic liver disease. The major risk factor for developing PSC is having a concomitant diagnosis of inflammatory bowel disease (IBD). Around 71% of PSC patients have IBD. Conversely, PSC is present in only 3–8% of patients with established IBD. Although both diseases run distinct courses, patients with PSC-IBD present a characteristic phenotype, contributing to a high risk of colitis-associated neoplasia. Recently, small non-coding RNAs such as microRNAs (miRNAs) have been correlated with disease onset and progression. miR-21, one of the most studied oncogenic miRNAs, is known to be overexpressed in IBD. Here we aim to further explore miR-21 in patients in a systematic manner and determine its contribution to the typical PSC-IBD phenotype.

Method: In this case-control study we included 12 patients in the PSC-IBD group, 30 patients in the IBD-alone group, and 19 patients in the control group. Serum samples were collected for fasting serum miR-21 expression. Stool samples were used for calprotectin analysis and miR-21 expression. Gut microbiome was investigated using next generation sequencing analysis. During colonoscopy, two biopsies in the right and left colon were performed and expression analysis of miR-21 and inflammation, tight junction and oncogene analysed. In statistical data analysis, outliers were removed (ROUT Q = 1%) and Kruskal-Wallis test or ANOVA Tukey's multiple comparisons test were performed on non-parametric or parametric data, respectively.

POSTER PRESENTATIONS

Results: Serum and fecal miR-21 expression were significantly increased in PSC-IBD patients compared to IBD alone. miR-21 expression in the right colon was similar in both PSC-IBD and IBD alone but increased when compared to controls. The inflammatory marker IL-8 was more elevated in both left and right colon of PSC-IBD patients than in IBD alone. Moreover, macrophage recruitment markers TWIST1, COX2, and CCL2 were also significantly increased in both left and right colon tissue of PSC-IBD patients compared to IBD alone or in control groups. Finally, the genus *Intestinibacter*, often associated with IBD, was elevated in PSC-IBD patients compared to IBD alone.

Conclusion: Our data show that miR-21 in circulation, but not in colon tissue, together with macrophage recruitment and distinct microbiota profiles parallel the incidence of IBD in PSC patients. Given the proinflammatory and oncogenic activities of miR-21, its role in PSC-IBD disease pathogenesis and phenotype merits further evaluation. Supported by FCT CEECIND/04663/2017, GEDII Project Award 2019, and EASL Daniel Alagille Award 2019.

FRI294

Hepatocellular carcinoma in fontan associated liver disease: uncharted territory-are we doing enough?

Michael Christmas¹, Anthony Bergin¹, Wei Lian Tan¹, Myat Khaing¹, Lei Lin¹, Yuming Ding¹, Tony Rahman¹, Ryan Maxwell², Vishva Wijesekera². ¹The Prince Charles Hospital, Gastroenterology, Chermshire, Australia; ²The Prince Charles Hospital, Cardiology, Chermshire, Australia
Email: michael.christmas@health.qld.gov.au

Background and aims: Fontan associated liver disease (FALD) is a well-recognised consequence of the congestion and hypoxia created from the Fontan palliative procedure. Improved clinical management has led to significantly improved life expectancy and thus the paradigm of increased risk of developing FALD and HCC. There are no FALD specific surveillance guidelines for HCC. AASLD and EASL suggest biannual monitoring of serum alpha fetoprotein and ultrasound imaging as the gold standard for HCC screening in the cirrhotic population. This clinical audit seeks identify and audit compliance to the gold standard being offered in our Hepatology clinics.

Method: Retrospective analysis of Fontan patients and clinical, biochemical, radiological and endoscopic databases correlation was undertaken at the Hepatology clinic serving the quaternary regional referral centre for adult congenital heart diseases in Queensland (The Prince Charles Hospital, TPCH). Cirrhosis was identified in patients who had features identified on their liver ultrasound. The current conventional HCC screening requirements were then applied to identified patients.

Results: In the data set of 72 Fontan patients, 49% (35) were female and an average age of 30.3 years. Features of cirrhosis were identified in 44% (32). Of these 32, 90% (29) patients were linked in with an outpatient liver clinic. Only 66% (19) liver clinic patients had standard HCC surveillance. In our data set one patient has had treatment for HCC. Four patients had died due to causes unrelated to HCC.

Conclusion: The majority of cirrhotic patients in this cohort are linked in with a liver clinic. Sub-optimal HCC screening is taking place in this very vulnerable cohort with one third of patients not receiving minimum surveillance potentially leading to missed detection of curable HCC. The young age of this cohort should not disguise or detract from the risk of cirrhosis and HCC. This has identified an opportunity for education to improve the awareness and importance of HCC and screening in this unique population, for staff, patients and carers. International guidelines would be very valuable in this new cohort of cirrhotic patients.

FRI295

Are patients with Fontan-associated liver disease (FALD) appropriately screened for oesophageal varices? Queensland quaternary adult congenital heart disease referral centre experience

Anthony Bergin¹, Yuming Ding¹, Michael Christmas¹, Wei Lian Tan¹, Lei Lin¹, Myat Khaing¹, Alexandra Schlimmer¹, Ann Vandeleur¹, Hayley Thompson¹, Ryan Maxwell¹, Vishva Wijesekera¹, Tony Rahman¹. ¹The Prince Charles Hospital, Gastroenterology, Chermshire, Australia
Email: anthony.bergin@health.qld.gov.au

Background and aims: The Fontan procedure is palliative management of univentricular congenital heart disease. An extracardiac complication of haemodynamic changes from Fontan circulation is Fontan-associated liver disease (FALD). Variceal bleeding is the most severe and life-threatening complication of chronic liver disease and portal hypertension (1). Studies suggest that 15 years post-Fontan procedure greater than 27% of patients had oesophageal varices on oesophago-gastroduodenoscopy (OGD) (2). An ageing Fontan population is a new clinical phenotype due to advances in healthcare. It is thus imperative that cirrhotic Fontan patients are screened for oesophageal varices, however, no formal guidelines currently exist.

Method: Retrospective analysis of Fontan patients and clinical, biochemical, radiological and endoscopic databases correlation was undertaken at the Hepatology clinic serving the quaternary regional referral centre for adult congenital heart diseases in Queensland (The Prince Charles Hospital, TPCH). Cirrhosis was identified in patients who had features identified on their liver ultrasound. The current conventional HCC screening requirements were then applied to identified patients. For each OGD, procedure indication, endoscopic findings and therapeutic interventions were noted.

Results: Seventy-two post-Fontan patients were identified from our database. Of which 49% (n = 35) were female with a mean age of 30.3 years. Only 44% (n = 32) had an OGD, the indications included variceal surveillance, iron deficiency and dyspepsia. Among the cirrhotic FALD patients (n = 32), only 43.7% (n = 14) had an OGD. Of this subgroup 22.8% (n = 7) had grade I oesophageal varices, none of which required treatment. None were taking primary prophylaxis.

Conclusion: FALD patients with cirrhosis should at least have one screening OGD. While 25% of our screened cirrhotic patients had varices, concerning only 43.7% had undergone an OGD. Future multi-centre collaborative research is needed to facilitate the development of guidelines on variceal surveillance for this growing cohort of FALD patients. The majority of cirrhotic patients in this cohort are linked in with a liver clinic. The young age of this cohort should not disguise or detract from the risk of cirrhosis and life threatening variceal bleeding. This study has identified an opportunity for education to improve the awareness and importance of variceal screening and this unique evolving population, for staff, patients and carers.

FRI296

Primary liver malignancies in patients with Wilson's disease

Rodolphe Sobesky^{1,2}, Olivier Guillaud^{2,3}, Aurelia Poujois^{2,4}, Audrey Coilly^{1,2}, Eric Vibert^{1,2}, René Adam^{1,2}, Daniel Cherqui^{1,2}, Cyrille Feray^{1,2}, Didier Samuel^{1,2}, Jean-Charles Duclos-Vallée^{1,2}. ¹CHB-Centre Hépatobiliaire, Villejuif, France; ²Centre référent Maladie de Wilson, France; ³CHU Lyon, Gastro-entérologie, Hépatologie, Lyon, France; ⁴Hôpital Fondation Rothschild, Neurologie, Paris, France
Email: rodolphe.sobesky@aphp.fr

Background and aims: Wilson's disease (WD) can induce chronic liver disease, cirrhosis and its complications. Primary liver cancer in WD patients is currently believed to be rare. Reports of primary hepatobiliary malignancies in these cases are sparse. Our aim was to assess the frequency and characteristics of primary liver cancer in WD patients on long-term follow-up.

Method: We retrospectively analysis a monocentric cohort of WD patients with liver damage from a referral center for rare diseases. Patients of the cohort were regularly assessed with a maximal interval of 6 months. Patients with a history of cirrhosis had a biannual ultrasound examination. Occurrence, treatment and outcome of primary liver tumors were analyzed.

Results: We analyzed 149 WD patients of the cohort, with a mean follow up of 15 years. The mean age at diagnosis of WD was 20.1 years. Sixteen patients were diagnosed with a primary liver tumor during follow up. The mean age at onset of a liver tumor was 52.5 years, with a mean interval between diagnosis of WD and occurrence of tumor of 19.2 years. We diagnosed a hepatocellular carcinoma (HCC) for 10 patients and a cholangiocarcinoma (CCK) for 6 patients. Histological proof could be obtained for 7/10 patients with HCC and for all patients (6/6) with CCK. For the 3 other patient, diagnosis of HCC was based on the morphological aspect (hyper vascular tumor with washout) and elevated AFP markers. All patients who developed a liver tumor had evidence of cirrhosis at the diagnosis of WD. At the diagnostic of tumor, there was no cirrhosis on the pathological examination of the non-tumoral liver for 6 patients (2/10 patients with histological proof of HCC and 4/6 patients with CCK). For all patients with primary liver tumor, a treatment could be proposed. Resection was possible for 8 patients and liver transplantation for 5 patients. During follow up, six patients died from complications of tumor extension (3 from HCC and 3 from CCK).

Conclusion: WD patients with history of cirrhosis are at risk of developing primary liver tumor and require morphological screening, even if there is a regression of fibrosis. The proportion of CCK (37.5%) among these tumors suggests an interest of the biopsy for diagnosis of liver cancer in WD patients.

FRI297

Defining the boundaries for “stability” in Wilson disease patients on maintenance chelation therapy: lessons from the CHELATE trial

C. Omar Kamlin¹, Michael Schilsky², Peter Ott³, Karl Heinz Weiss⁴, Massimo Giovanni Zuin⁵, Aurelia Poujois⁶, Aftab Ala⁷, Koenraad D'Hollander⁸. ¹Orphalan SA France, Medical Affairs, London, United Kingdom; ²Yale University, Division of Internal Medicine and Liver Unit, United States; ³Aarhus University Hospital, Aarhus, Denmark; ⁴Salem Medical Center, Heidelberg, Germany; ⁵University of Milan, Milan, Italy; ⁶Fondation Hopital Rothschild, Department of Neurology, Paris; ⁷Kings College University Hospital, London, United Kingdom; ⁸International Drug Development Institute (IDDI), Belgium
Email: omarkamlin@doctors.org.uk

Background and aims: “Clinical stability” of patients with Wilson disease (WD) is a treatment goal for long-term maintenance therapy and a desired entry point for interventional therapeutic trials in this patient population. Stability evaluation relies on laboratory parameters and clinical assessment. Published guidance and practice guidelines are not aligned, leading to variations in assessments and therapeutic targets. We performed a descriptive secondary analysis of “clinically stable” patients enrolled into the Chelate trial to define the boundaries of biochemical stability (clinicaltrials.gov; NCT03539952).

Method: Clinically stable patients on D-penicillamine (DPA) >1 y were randomised to DPA or trientine tetrahydrochloride if 24-h urinary copper excretion [UCE] was 200–500 mcg/L (amended 100–900), alanine aminotransferase[ALT] <2× ULN IU/L, serum non-caeruloplasmin bound copper[NCC] 50–150 mcg/L, (amended 25–50) determined initially by EDTA method (NCC-Ex). NCC by speciation coupled with ICP-mass spectroscopy (NCC-Sp) was performed retrospectively. Amendments to these ranges and opportunities for biochemical screen failures to re-enter trial were made to improve trial feasibility. We reviewed day 1 data for all screened patients.

Results: Twenty-five of 76 (33%) screened patients had NCC-Sp <50 mcg/L at first sampling, majority (20/25) between 25 and 50 mcg/L. The mean (SD) age was 40.4 (14.3) years; 13 were female. Serum NCC-Sp, UCE, ALT and dose of DPA in mg/kg are shown in the Table. For comparison, graphs of NCC-Sp and NCC-Ex versus UCE at screening are shown in the figure. Though a wide range of UCE was observed, UCE and NCC had a positive correlation. Two subjects with ALT >ULN of 54 (73 and 61) U/L, had corresponding NCC-Sp of 41 and 44.8 mcg/L respectively. UCE ranged widely, however mean UCE was within 200–500. Dose of DPA was 13.2 ± 3.5 mg/kg (7.4–19), within the recommended guidance of 10–15. Sixteen (64%) with NCC -Sp <50, including 3/4 who underwent re-screening, were randomized.

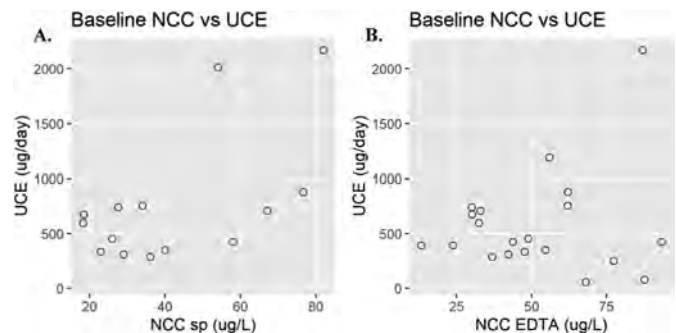


Figure: UCE- NCC scatter plots (A-NCC Sp and B-NCC Ex).

Table: Patients with Serum NCC-Sp <50 mcg/L at trial screening

	Mean	Max	Min	SD
NCC-Sp (mcg/L)	32.4	46.9	17.0	8.9
NCC-Ex	36.5	48.8	13.1	8.5
UCE (mcg/24 hr)	475	798	47	221
ALT (U/L)	26	73	6	16.3
DPA dose (mg/kg)	13.2	19.0	7.4	3.5

Conclusion: Re-screening of patients in clinical trials of rare disease facilitates recruitment. Single and multiple biochemical parameter analyses are helpful in defining the boundaries for “stability” of WD patients and lower values of NCC are common with the optimal lower limit requiring further study. Dosing in patients with very low NCC (<25 mcg/L) should be re-evaluated to avoid overtreatment. NCC may be a useful parameter for response guided dosing of therapy for chelation in WD.

FRI298

Precision-cut liver slices as an ex vivo model to assess impaired hepatic glucose production

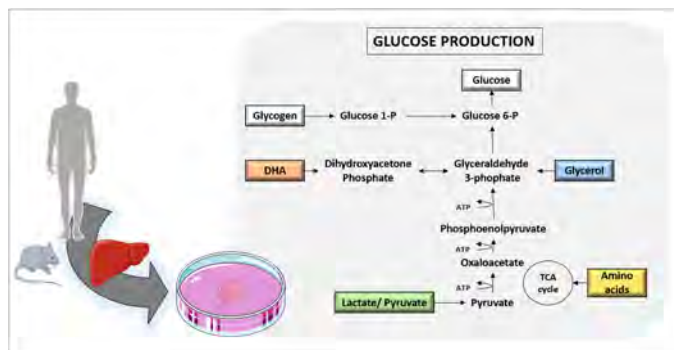
Kishore Alagere Krishnamurthy¹, Ligia Akemi Kiyuna¹, Miriam Langelaar¹, Albert Gerding¹, Trijnie Bos¹, Dorenda Oosterhuis², Peter Olinga², Karen Van Eunen¹, Barbara Bakker¹, Maaik Oosterveer¹. ¹University Medical Center Groningen, Groningen, Netherlands; ²University of Groningen, Groningen, Netherlands
Email: a.k.kishore@umcg.nl

Background and aims: Disturbed glucose metabolism is a common feature of metabolic diseases. For example, fasting hypoglycemia is a severe symptom of various inborn errors of metabolism, among which glycogen storage disease type 1 (GSD I). Due to the liver's central role in endogenous glucose production, the availability of a liver-specific ex vivo model will enable unravelling the mechanisms underlying perturbed glucose homeostasis. Given the limitations of in vitro hepatocyte cultures (e.g. reduced Glucose-6-phosphatase activity, proliferative nature), this study aims to optimize and characterize precision-cut liver slices (PCLS), both from the human and murine liver, as a model to study hepatic glucose production ex vivo.

POSTER PRESENTATIONS

Method: PCLS were prepared from fed and 12h-fasted male C57BL/6 mice and incubated in Williams E glucose-free medium supplemented with gluconeogenic precursors: (1) 10 mM glycerol, (2) 20 mM lactate plus 2 mM pyruvate, or (3) 10 mM dihydroxyacetone (DHA). Net cumulative glucose production was assessed at different time intervals (2 h–24 h). The amino acids in the medium and slice glycogen content were quantified at different time points to assess the source of glucose. Additionally, the efficacy of glucose production in response to fatty acid supplementation (500 μ M palmitate), hormonal (0.1–1 μ M glucagon or insulin), and pharmacological (10–20 μ M forskolin or 50–100 μ M dibutyl-cAMP) stimulation were evaluated. Finally, to study GSD type 1 *ex vivo*, we used either PCLS derived from GSD 1a/1b mouse models (*L-G6PC^{-/-}* and *L-SLC37A4^{-/-}*) or subjected wildtype PCLS to pharmacological inhibition of G6P exchanger SLC37A4 (S4048).

Results: PCLS derived from fed and fasted mice produced glucose, both in the presence and absence of gluconeogenic precursors. The glycogen content in the PCLS was substantially and equally reduced in all conditions after 5 h in culture. No substantial changes were observed in the amino acid concentrations in any condition. Both forskolin and dibutyl-cAMP increased net cumulative glucose production, while palmitate, glucagon or insulin did not alter glucose production. Lastly, PCLS from both pharmacological and genetic models of GSD type 1 showed markedly reduced glucose production and elevated lactate production, in line with the clinical disease phenotype.



Conclusion: PCLS can be used to study glucose production *ex vivo* up to 24 h in culture and DHA seems to result in the higher net glucose production. In ongoing follow-up experiments, ¹³C-labelled DHA and/or glycerol are used to test their role as a gluconeogenic precursor or a gluconeogenic regulator. Finally, PCLS offer the possibility to use patient liver biopsy, murine genetic models and pharmacological intervention. Hence, they are an excellent and promising *ex vivo* platform to study endogenous glucose production in GSD type 1 and other inborn errors of metabolism.

FRI299

Interim 52-week analysis of immunogenicity to the vector capsid and transgene-expressed human FVIII in GENE8-1, a phase 3 clinical study of valoctocogene roxaparvovec, an AAV5-mediated gene therapy for hemophilia A

Brian Long¹, Sylvia Fong¹, Britta Handyside¹, Tara Robinson¹, Jonathan Day¹, Hua Yu¹, Kelly Lau¹, Kathryn Patton¹, Greg de Hart¹, Josh Henshaw¹, Suresh Agarwal¹, Christian Vettermann¹, Soumi Gupta¹. ¹BioMarin Pharmaceutical Inc. San Rafael, CA, USA 94901
Email: brian.long@bmrn.com

Background and aims: Valoctocogene roxaparvovec is an AAV5-mediated gene therapy under investigation for the treatment of hemophilia A and encodes a codon-optimized B-domain deleted human FVIII protein (hFVIII-SQ) under control of a liver-selective promoter. This report describes clinical immunogenicity monitoring data from up to 1 year of follow-up from GENE8-1, an ongoing, fully enrolled, Phase 3, single-arm, open-label study in 134 male participants with severe hemophilia A.

Method: Participants were required to test negative for anti-AAV5 total antibody (AAV5 TAB) utilizing a bridging electrochemiluminescent (ECLA) screening assay being developed as a companion diagnostic by ARUP Laboratories (Salt Lake City, USA). Additionally, all participants were required to be on FVIII prophylaxis and have had at least 150 exposure days to FVIII replacement products without previous clinically detectable FVIII inhibitor development. Following dose administration, plasma was analyzed for AAV5 TAB, and a cell-based AAV5 transduction inhibition (TI) assay was used to further characterize the capsid-neutralizing potential of the anti-AAV5 antibodies. Development of FVIII inhibitors was monitored using the Nijmegen-modified Bethesda assay, and FVIII-specific TAB were assessed by bridging ECLA. Additionally, peripheral blood mononuclear cells were collected for analysis in a validated IFN- γ ELISpot assay for detection of capsid-specific and hFVIII-SQ-specific cellular immune responses.

Results: All participants developed a humoral antibody response to valoctocogene roxaparvovec following dose administration. Transient, low level AAV5 capsid-specific cellular immune responses were detected in the majority of subjects where incidence peaked at Week 2 following dose administration and often declined or reverted to negative over the first 52 weeks. Similarly, sporadic positive FVIII cellular immune responses were detected in a limited number of subjects. No subjects developed FVIII inhibitors following administration of BMN 270.

Conclusion: Immune responses to valoctocogene roxaparvovec were predominantly directed toward the AAV5 capsid, characterized by the production of anti-AAV5 binding and neutralizing antibodies as well as transient AAV5 capsid-specific cellular immune responses. Capsid-specific cellular immune responses showed a moderately positive correlation with plasma levels of the liver enzyme ALT suggesting these responses may be a contributing factor to transient elevations in ALT in some participants. There was no clinical evidence of inhibitor formation in subjects dosed with valoctocogene roxaparvovec.

Friday 24 June

Viral hepatitis C: Clinical aspects except therapy

FRI301

Sex effect on key intrahepatic gene networks in hepatitis C virus infection

Emanuele Marchi¹, Paul Klenerman¹, Narayan Ramamurthy¹, Azim Ansari¹, Eleanor Barnes¹, Caroline Harrer¹. ¹University of Oxford, NDM-Nuffield Department of Medicine, Oxford, United Kingdom
Email: emanuele.marchi@ndm.ox.ac.uk

Background and aims: Spontaneous HCV clearance and successful antiviral therapy rates are largely in favour of women and/or in subjects with a specific IFNL4 genotype. The unfavourable IFNL4 genotype leads to an exaggerated interferon response eventually detrimental for the patient. However, women tend to have a more robust and prompt interferon activity. Beyond this, the causes of sex differences in infections are insufficiently understood. The transcriptional response in the liver during hepatitis C virus (HCV) infection is critical for determining clinical outcomes. This issue remains relatively unexplored as tissue access to address this at scale is usually limited. We aimed to profile the transcriptomics of HCV infected livers to describe the expression networks involved and assess the effect on them of major predictors of clinical outcome such as IFNL4 host genotype and sex.

Method: We took advantage of a large clinical study of hepatitis C therapy accompanied by baseline liver biopsy to examine the drivers of transcription in tissue samples in 195 patients also genotyped genome-wide for host and viral SNPs. We addressed the role of host

factors (disease status, sex, genotype, age) and viral factors (load, mutation) on transcriptional responses.

Results: We observe key modules of transcription which can be impacted differentially by host and viral factors. Underlying cirrhotic state had the most substantial impact, even in a stable, compensated population. Notably, sex had a major impact on antiviral responses in concert with IL28B (interferon lambda) genotype, with stronger interferon and humoral responses in females. Males tended towards a dominant cellular immune response. In both sexes there was a strong influence of the underlying host disease status and of specific viral mutations, and sex-specific eQTLs were also observed.

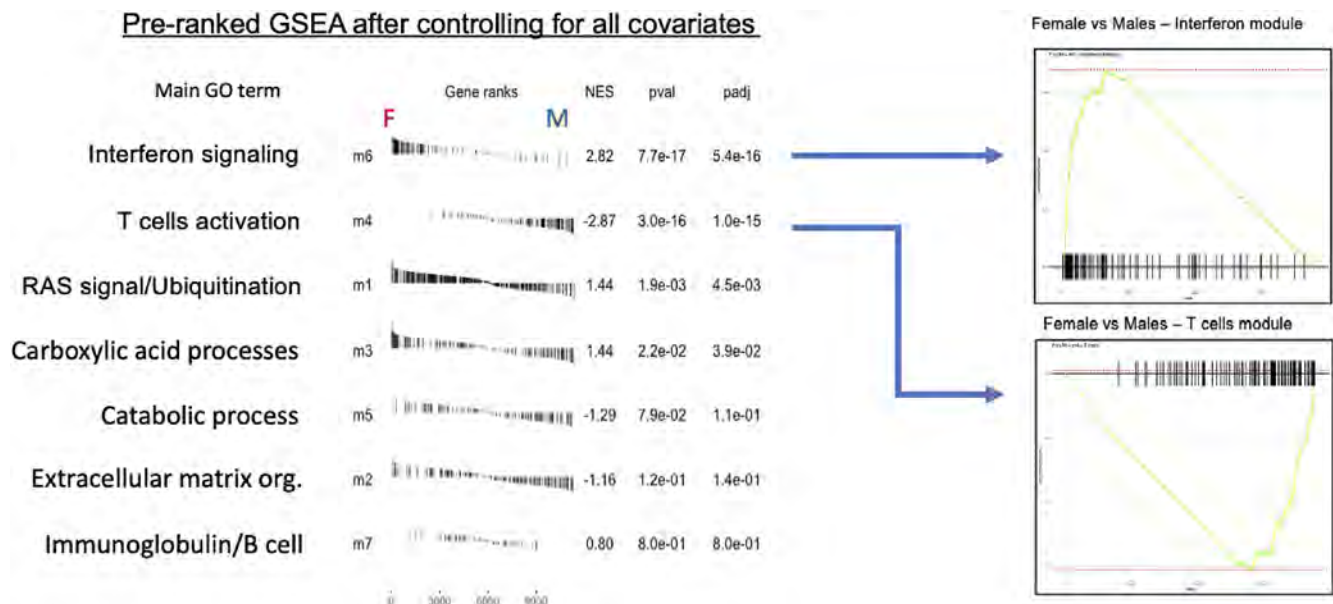
Conclusion: These features help define the major influences on tissue responses in HCV infection, impacting on the response to treatment and with broader implications for responses in other sex-biased infections.

FRI302

Active case management to connect hepatitis C notifications to care and treatment in Australia (CONNECT study), a randomised controlled trial

Tafireyi Marukutira^{1,2}, Karen Moore³, Margaret Hellard¹, Jacqui Richmond¹, Kate Turner³, Alisa Pedrana¹, Shannon M. Melody³, Louise Owen³, Wijnand Van Den Boom¹, Nick Scott¹, Alexander Thompson⁴, David Iser⁴, Tim Spelman¹, Mark Veitch³, Mark Stooze¹, Joseph Doyle¹. ¹Burnet Institute, Melbourne, Australia; ²Monash University, Melbourne, Australia; ³Tasmanian Department of Health, South Launceston, Australia; ⁴St. Vincent's Hospital Melbourne, Fitzroy, Australia
Email: tafireyi.marukutira@burnet.edu.au

Background and aims: Despite the simplicity, tolerability and subsidised access of directly acting antivirals (DAAs), hepatitis C (HCV) treatment uptake in Australia is declining. Initiatives are needed to actively engage people living with HCV to link them to care and treatment. In this study, we measured the impact of using



POSTER PRESENTATIONS

hepatitis C notifications systems to engage diagnosing general practitioners (GPs) and improve patient access to treatment.

Method: The CONNECT study was a randomised controlled trial that compared enhanced case management delivered to clinicians notifying new/repeat HCV diagnoses to standard of care in Tasmania, Australia over 12 months in 2020–2021. GPs were randomised based on their first HCV notification during the study period. The intervention involved a health department nurse specialist contacting notifying GPs directly and providing stepwise support by telephone, and direct patient contact if required. The primary outcome was the proportion of individuals with HCV who initiated DAAs within 12 weeks of HCV antibody notification. Secondary outcomes compared proportion completing pre-treatment HCV RNA testing and blood work-up.

Results: A total of 171 GPs were enrolled and randomised to the intervention (n = 85) or the standard of care (n = 86) arms. Over the observation period, GPs in the intervention notified 111 HCV antibody positive cases compared to 115 in standard of care. A higher proportion of HCV notifications in the intervention compared to standard of care completed HCV RNA testing (96% vs. 86%; p = 0.03) and 33% compared to 30% were HCV RNA+ve (p = 0.19) respectively. Pre-treatment workup among those eligible for treatment (RNA+ve) was similar between intervention and standard of care arms (62% vs. 65%; p = 0.82). The proportion of all HCV notifications that initiated treatment was similar between intervention and standard of care arms (20% vs. 14%; p = 0.24). The proportion of treatment eligible cases initiating treatment within 12 weeks of notification was also similar between study arms (38% vs 32%; p = 0.63) (Figure 1). Most cases who did not initiate were lost to follow up or were referred to a specialist.

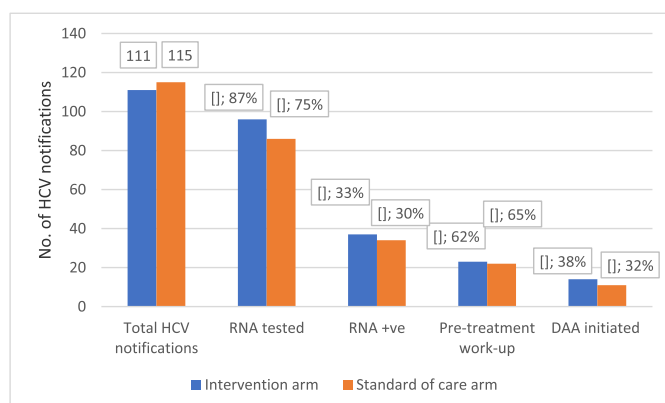


Figure: HCV Testing and Treatment Cascade.

Conclusion: This is the first prospectively randomised study that explored the utilisation of HCV surveillance data to enhance linkage to HCV treatment. While there was no difference in treatment initiation, the intervention encouraged more GPs to complete RNA testing as the initial stage of assessing DAA eligibility. Health Department follow up could potentially augment HCV antibody testing to ensure DAA eligibility is assessed early.

FRI303

Find out HCV patients: systematic study of 2013–2020 HCV files of a MDT viral hepatitis expert unit on the future of patients has made it possible to find out the lost ones and put them into treatment

André-Jean Remy¹, Sonia Djazouli¹, Hakim Bouchkira¹, Jeremy Hervet¹, Berengere Roy¹. ¹Perpignan Hospital, Mobile Hepatitis Team, Perpignan, France

Email: andre.remy@ch-perpignan.fr

Background and aims: Access to direct antiviral agents (DAA) has been progressively needed since 2013. But what happened to the patients, treated or not, seen since that date? Several studies have been conducted to find patients seen in consultation or hospitalization but without assessing the fate of the entire active queue. Our objectives were to evaluate follow-up of patients spent in multidisciplinary team meeting (MDT) within our hospital viral hepatitis expert unit, even when it was no longer mandatory for an DAA, treatment decision in the absence of current healing, to offer them DAA treatment.

Method: All MDT sheets from September 2013 to December 2020 have been reviewed. We contacted GP, patient or private hepatologist by email or telephone for an estimated 5 hours of work per week. Follow-up data were collected via our hospital's computerized file. In the absence of direct contact; national death database was consulted.

Results: As of 31st August 2021, 1158 MDT files were initially studied corresponding to 1032 different patients; there were 683 men and 349 women of average age 37 years and 41% of F3F4 fibrosis; 97 patients were known to have died (69% of non-hepatic cause), 413 cured without liver complications; 153 followed for their cirrhosis and 41 for hepatocellular carcinoma; 328 were lost of sight of 68 previously followed by our team and 146 by liberal hepatologists. As of 31st October 2021, the contact information for 54 patients was missing or incorrect; no information had yet been obtained for 126 patients followed in liberal; 37 additional patients were found within one month of which 8 were already cured and 15 died; 14 were eligible for immediate treatment due to an available positive viral load; 11 patients accepted an appointment for a referral of which 9 had already started the treatment and 2 patients refused the care; there were 90 patients followed by our team to contact or relaunch, which should be achieved within 3 months.

Conclusion: Maintaining MDT transition of all patients with chronic hepatitis C allows for an efficient database and to find untreated and/or untreated patients and offer them treatment. Number of refusals to care remains low, less than 10%. Our study, initially planned as a cohort retrospective analysis, found patients with chronic hepatitis C with RNA positive and untreated and immediately treated. This work shows that there are still patients who know they are infected with HCV but have not yet been treated. The research and treatment of these patients is essential to the elimination of hepatitis C.

FRI304

Effectiveness of a central monitoring system for the continuum of care of hepatitis C in Brazil during COVID-19 pandemic

Paulo Bittencourt¹, Liana Codes¹, Maria Lucia Ferraz¹. ¹Brazilian Liver Institute

Email: plbbr@uol.com.br

Background and aims: Several healthcare facilities dedicated to hepatitis C testing and linkage and retention to care were closed in Brazil due to the COVID-19 pandemic, leading to a 40%–50% reduction in the distribution of HCV rapid tests as well as new treatments for HCV in 2020. To mitigate the adverse impact of the pandemic on the hepatitis C elimination plan, the Brazilian Liver Institute (Ibrafig) sponsored a remote patient support program (PSP) to monitor all aspects of the HCV care continuum (HCV CC) in the public health system. The aims of the present study were to assess the results of this strategy in different steps of the HCV CC in Brazil.

Method: After mapping of the active healthcare facilities offering HCV rapid tests to the general population as well as diagnosis and treatment for HCV, Ibrafig launched a remote PSP to follow-up subjects in all steps of HCV CC from testing of hepatitis C until HCV cure. The remote PSP was comprised by trained healthcare personnel and contacts were made through phone calls, SMS, email or whatsapp according to users preferences. Awareness campaigns concerning hepatitis C elimination were coupled with nationwide advertising of the remote CMS on social media, TV and radio.

Results: From August 2020 to July 2021, 11,049 interactions were recorded between users and CMS, most of them by Whatsapp (91%). Most of them became aware of the PSP by radio and/or TV (41%) and social media (31%). After informed consent, 601 subjects were registered in the PSP including 74 patients already diagnosed with HCV who were lost in the public healthcare system due to the COVID-19 pandemic. Overall, 501 subjects were referred for HCV testing. Fifteen (9%) out of the 115 subjects who reported their test results were positive for HCV. Up to now, 53 (60%) out of 89 HCV positive patients have scheduled their 1st consultation, 12 (13%) are enrolled in care and 14 (16%) are under antiviral treatment. Seven (8%) who achieved end of treatment response are waiting HCV sustained virological response.

Conclusion: Our preliminary data showed that a remote PSP was an effective strategy to monitor the HCV CC. It was capable to refer at risk subjects for HCV testing and to provide linkage and retention to care of those HCV positive subjects in the Brazilian public health system during the COVID-19 pandemic.

FRI305

Retrieval of HCV patients lost to follow-up as a strategy as a strategy for hepatitis C microelimination: results of a brazilian multicentric study

Paulo Bittencourt¹, Maria Lucia Ferraz¹, Gustavo Henrique Santos Pereira², Liana Codes¹, Antonio Andrade², Carlos Brandão-Mello². ¹Brazilian Liver Institute; ²Brazilian Society of Hepatology
Email: plbbr@uol.com.br

Background and aims: Several HCV positive patients in Brazil were lost to follow-up in the last two decades before achievement of sustained virological response (SVR) due to either non-response to interferon-based therapy or lack of treatment due to comorbidity or mild fibrosis. The purpose of the present study was to identify and retrieve those lost patients to offer treatment with the current highly effective direct acting antivirals (DAAs).

Method: All medical charts from three major reference centers for treatment of hepatitis C were retrospectively reviewed by trained healthcare personnel to identify all HCV positive subjects, their treatment status and, in those HCV RNA positive patients, the main reasons for non-achievement of SVR or lack of treatment. After review of a local senior hepatologist, all patients who were not treated or cured were contacted in order to offer therapy with DAAs.

Results: 7,498 medical charts were reviewed, 5,549 (74%) from HCV positive patients (50, 1% males, mean age 51±12 years). Advanced fibrosis or cirrhosis and hepatocellular carcinoma were observed in 1,929 and 95 subjects, respectively. Only 3,272 (59%) were submitted to treatment. SVR, non-response to IFN-based and IFN-free regimens was observed in 2,348 (72%), 658 (20%) and 266 (8%) subjects, respectively. Lack of treatment due to loss of FU (29%) or other reasons (12%) such as comorbidity, mild fibrosis or treatment refusal were reported in the remaining patients. Until October 2021, 2,745 patients were considered eligible to be retrieved by local investigators and 1,593 phone calls were made with a callback success rate of 15%. 43 (2%) patients were retrieved for treatment. Most of the remaining patients have been treated elsewhere (n=61) or have died or underwent liver transplantation (n=69).

Conclusion: Our preliminary data showed that identification and retrieval for treatment of HCV patients lost to FU is an effective microelimination strategy despite the low callback success rate.

FRI306

Reorganizing and simplifying HCV diagnosis and treatment in special populations during COVID pandemic and beyond

Paolo Scivetti¹, Elisa Perfetti¹, Lorenzo Somaini², Sarah Vecchio², Antonio Panero¹, Paola Zaldera³. ¹ASLBI Ospedale degli Infermi, SOC Internal Medicine-Hepatology Centre, Ponderano, Italy; ²ASLbi, Addiction Treatment Centre, Biella, Italy; ³ASLbi, Casa Circondariale-Health Section, Biella, Italy
Email: paolo.scivetti@aslbi.piemonte.it

Background and aims: Hepatitis C infection has a high prevalence among prisoners and in people who use drugs (PWUDs) and his identification and treatment are a pivotal factor to achieve HCV elimination by 2030. However, PWUDs and prisoners often face multiple barriers during the treatment cascade. In our Local Health Unit of Biella we have already developed a shared model of care between Addiction Treatment Centre (SerD), prison and hospital hepatology centre, to gather clinical evaluations within a single visit in order to ameliorate the HCV treatment rate. Subsequently, the treatment journey has been complicated by Covid pandemic. The aim of this study is to describe the new model of care we have developed to overcome old and new barriers to HCV treatment in these special populations.

Method: Since march 2020 a new model of care has been developed and centered on three crucial elements: a collaboration between SerD, prison and hospital hepatology centre; the introduction by AIFA (Italian Agency of Drugs) of the "criterion 12" that allows treatment after ruling out liver fibrosis by APRI and FIB-4 without elastography; the evidence that these scores allow us to exclude severe fibrosis, the risk of a hepatocarcinoma and the need of an ultrasound test. Patients attending SerD performed HCV viral load by mean of on-site fingerstick assay and inmates by mean of salivary test for antiHCV. HCV RNA positive patient's data were recorded into a database shared between the three services. After ruling out severe fibrosis by APRI and FIB-4, hepatologist prescribed the DAAs (direct-acting antiviral agent) with virtual "computer-generated" evaluation of the patients. DAAs were delivered by the SerD's or prison's health professionals. The patients were directly visited by the hepatologist only in the case of severe fibrosis at the scores.

Results: HCV RNA was detected in out of 33/250 SerD patients' and in out of 4/44 inmates, respectively. Linkage to care was possible for a total of 34 patients (30 SerD and 4 Prison). The patients were mostly male, and heroin addicted. Sixteen of them had only a virtual evaluation, conversely 18 patients underwent to direct examination. Overall, 34 patients completed the treatment, and all of them achieved Sustained Virologic Response.

Conclusion: Our new model of care highlights the feasibility of the on-site HCV testing and the efficacy of this simplified virtual "computer-generated" procedure for the treatment of HCV in special populations. This new model of care has allowed us to continue the diagnosis, the linkage to care and the treatment of patients even during COVID-19 pandemic and hopefully beyond.

POSTER PRESENTATIONS

FRI307

The health economic outcomes of trial ACTG5360/MINMON

Benjamin Linas^{1,2}, Michelle Weitz¹, Tannishtha Pramanick³, Mark Sulkowski⁴, Irena Brates⁵, Laura Smeaton⁶, Sandra Cardoso⁷, Sunil Suhas Solomon⁴. ¹Boston Medical Center, Section of Infectious Diseases, Boston, United States; ²Boston University School of Medicine, Medicine, Infectious Diseases, Boston, United States; ³Boston Medical Center, Section of Infectious Diseases, Boston, United States; ⁴Johns Hopkins University School of Medicine, Division of Infectious Diseases, Baltimore, United States; ⁵Harvard T.H. Chan School of Public Health, Center for Biostatistics in AIDS Research (CBAR), Boston, United States; ⁶Harvard T.H. Chan School of Public Health, Center for AIDS Research (CFAR), Boston, United States; ⁷Instituto Nacional de Infectologia Evandro Chagas, Rio de Janeiro, Brazil
Email: tannishtha.pramanick@bmc.org

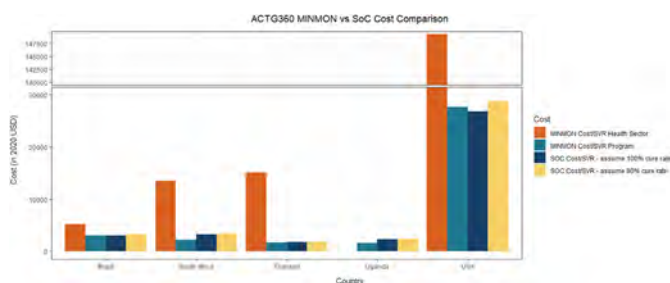
Background and aims: The ACTG MINMON trial demonstrated that HCV treatment with no planned in-person monitoring is safe and efficacious. We report resource utilization and cost in the MINMON trial.

Method: ACTG A5360 (MINMON) was a 5 country, single arm study providing 12 weeks of sofosbuvir/velpatasvir to people with HCV infection with no planned visits prior to SVR evaluation (Week 24). Trial records included planned/unplanned lab tests and visits. Participants completed a 4-week recall questionnaire at weeks 0, 24, and 48 reporting hospital nights, emergency department visits, and ambulatory visits. To cost MINMON, we tabulated consumption and multiplied units of consumption by country-specific cost. We report cost of MINMON per SVR attained (2020 US\$) from the program perspective (includes costs of medications and monitoring from study entry to Week 24), and the health sector perspective (program perspective plus healthcare utilization outside the study prior to cure, plus the additional (or reduced) healthcare utilization observed after HCV treatment).

Sensitivity analyses explored potential cost savings of MINMON compared to the standard of care (SoC). We consulted in-country experts to develop country-specific SoC treatment protocols and employed standard micro costing to estimate cost. We present cost/SVR in MINMON along with that of the simulated SoC, ranging the expected SVR with the SoC.

Results: MINMON cost/SVR (healthcare sector perspective) varied by country from \$5, 256/SVR in Brazil, to \$149, 257/SVR in the U.S. (Graph). The program perspective ranged from \$1, 637/SVR in Uganda to \$27, 641/SVR in the U.S. The cost of pharmaceuticals was the largest component of treatment cost, ranging between 76%–96% of cost from the program perspective.

MINMON had a lower cost/SVR (program perspective) than the SoC across broad assumptions about cure rates. Outside of the U.S., the cost/SVR of MINMON was lower than that of the SoC even when the SoC achieved higher cure than MINMON. In the U.S., the MINMON cost/SVR was lower than the SoC unless the SoC would be expected to achieve at least a 4-percentage point higher cure rate.



Conclusion: MINMON is likely a cost saving strategy compared to the SoC for HCV treatment.

FRI308

Hepatitis C treatment during the COVID-19 pandemic has similar efficacy with less resource utilization: analysis from the British Columbia HCV network

Shirley Jiang¹, Jeanette Feizi¹, Julia MacIsaac¹, Edward Tam², Hin Hln Ko¹, Alnoor Ramji¹. ¹The University of British Columbia, Vancouver, Canada; ²Pacific Gastroenterology Associates, Vancouver, Canada
Email: sjiangx@gmail.com

Background and aims: During the COVID-19 pandemic, a 49% decrease in dispensation of direct-acting anti-virals (DAAs) for hepatitis C (HCV) infection has been observed in Canada. We sought to characterize HCV patients, treatments, and outcomes during the pandemic.

Method: Single-centre retrospective chart review at a site of the British Columbia HCV Network. Patients initiated on DAAs from 17/12/2018–16/3/2020 were included as the pre-pandemic group (pre-PG), and compared to those treated from 17/3/2020–16/6/2021, who were included as the comparison pandemic group (PG).

Results: Over a 15-month period, 139 HCV patients were initiated on treatment as part of the PG compared to 179 patients in the pre-PG, representing a 22% decline. Pandemic patients were significantly younger (mean age 56.1 vs 59.5 years, $p=0.01$) and a greater proportion were on opioid agonist therapy (27% vs 12%, $p<0.01$). Patients had similar HCV genotypes and FIB-4 score. Significantly fewer PG patients had transient elastography (TE) within 6 months of initiating DAAs (52% vs 91%, $p<0.01$). Of patients with TE scores, cirrhosis was found in 12 (8.6%) PG patients compared to 29 (16.2%) pre-PG. Patients treated during the pandemic also had fewer total appointments (median 2 per patient vs 4 per patient pre-PG, $p<0.01$), with fewer office appointments (median 1 per patient vs 2 per patient pre-PG, $p<0.01$) but a similar number of telehealth appointments (median 2 per patient for each group). Treatment patterns were similar with predominant use of glecaprevir/pibrentasvir and sofosbuvir/velpatasvir. Treatment completion rate was higher for the PG vs pre-PG (96% vs 86%, $p<0.01$). Fewer patients obtained lab work for sustained virologic response (SVR) in the PG compared to pre-PG (74% vs 86%, $p<0.01$). SVR rate was similar in both groups at 96% in the PG compared to 99% pre-PG ($p=NS$).

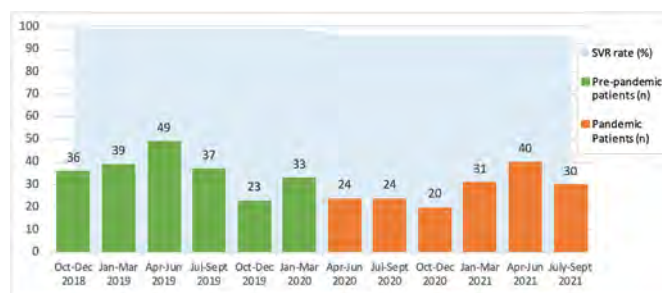


Figure: Patients started on HCV treatment and corresponding SVR rate

Conclusion: Patients with HCV infection treated during the COVID-19 pandemic utilized significantly less resources, had a higher rate of treatment completion, and similar rate of SVR. Treatment simplification through the use of telemedicine, minimizing investigations, and leveraging fewer healthcare resources can maintain high treatment completion and SVR rates.

FRI309

ELIMINATE-interim results of an Austrian HCV macro-elimination project

Caroline Schwarz^{1,2,3}, David Jm Bauer^{1,2}, Livia Dorn⁴, Mathias Jachs^{1,2}, Lukas Hartl^{1,2}, Heidemarie Holzmann⁵, Nikolaus Pfisterer^{1,2,6}, Barbara Hennlich⁶, Florian Mayer⁷, Ralf Schmidt⁷, Astrid Voll-Glaninger⁸, Wolfgang Hübl⁹, Martin Willheim¹⁰, Karin Köhrer¹¹, Sonja Jansen-Skoupy¹², Sabine Tomez¹³, Walter Krugluger^{13,14}, Christian Madl^{6,15}, Michael Schwarz^{1,2,3}, Leonard Brinkmann^{1,2,3}, Lukas Burghart^{1,2,3}, Gerhard Weidinger¹⁶, Florian Riedl⁴, Hermann Laferl¹⁷, Christoph Wenisch¹⁷, Abdelrahman Aburaia¹⁸, Christian Sebesta^{18,19}, Daniela Schmid²⁰, Thomas Reiberger^{1,2}, Andreas Maieron⁴, Michael Gschwantler^{3,15}.

¹Medical University of Vienna, Department for Internal Medicine III, Division of Gastroenterology and Hepatology, Vienna, Austria; ²Medical University of Vienna, Vienna HIV & Liver Study Group, Vienna, Austria; ³Klinik Ottakring, Department for Internal Medicine IV, Vienna, Austria; ⁴University Clinic St. Pölten, Department for Internal Medicine II, St. Pölten, Austria; ⁵Medical University of Vienna, Center for Virology, Vienna, Austria; ⁶Klinik Landstraße, Department for Internal Medicine IV, Vienna, Austria; ⁷Medical University of Vienna, Clinical Institute for Laboratory Medicine, Vienna, Austria; ⁸Klinik Landstraße, Central Laboratory and Blood Bank, Vienna, Austria; ⁹Klinik Ottakring, Central Laboratory, Vienna, Austria; ¹⁰University Clinic St. Pölten, Clinical Institute for Laboratory Medicine, St. Pölten, Austria; ¹¹Landeskrankenhaus Wiener Neustadt, Institute for Medical-Chemical and Molecularbiological Laboratory Diagnostics with Blood Depot, Wiener Neustadt, Austria; ¹²Klinik Favoriten, Institute for Laboratory Diagnostics, Vienna, Austria; ¹³Klinik Donaustadt, Institute for Laboratory Medicine with Blood Depot, Vienna, Austria; ¹⁴Klinik Floridsdorf, Institute for Laboratory Medicine and Blood Depot, Vienna, Austria; ¹⁵Sigmund Freud University, Vienna, Austria; ¹⁶Landeskrankenhaus Wiener Neustadt, Department for Internal Medicine, Gastroenterology and Hepatology, Wiener Neustadt, Austria; ¹⁷Klinik Favoriten, Department for Internal Medicine IV, Vienna, Austria; ¹⁸Klinik Floridsdorf, Department for Internal Medicine and Gastroenterology, Vienna, Austria; ¹⁹Klinik Donaustadt, Department for Internal Medicine II, Vienna, Austria; ²⁰Austrian Agency for Health and Food Safety (AGES), Vienna, Austria

Email: thomas.reiberger@meduniwien.ac.at

Background and aims: The WHO has declared the elimination of HCV until 2030 a global public health goal. We present the preliminary results of an Austrian macro-elimination approach aiming to provide linkage to care and treatment initiation for persons who are recalled based on a “last-positive” HCV-RNA PCR result. Importantly, many of these lost-to-follow-up patients do not belong to known HCV risk groups and are, thus, often not recognized by targeted HCV screening/elimination projects.

Method: First, we identified patients with a “last-positive” HCV-RNA PCR result between 2010 and 2020 in laboratories of Eastern Austria (Burgenland, Lower Austria, Vienna) and (i) described their demographic characteristics. Subsequently, (ii) a systematic recall of these patients to the respective HCV treatment centers was performed, and (iii) HCV-DAA was initiated and SVR was monitored. Here we report the interim results of this ELIMINATE project including data/results from eight centers.

Results: Overall, 22692 patients underwent HCV-RNA PCR testing, 11216 (49.4%) ever showed a positive HCV-RNA result, and in 6223 (27.4%) patients the last available HCV-RNA result was positive (suggesting persisting HCV-viremia).

For this interim report, 1795/6223 HCV-RNA PCR (+) patients were evaluated: 305 (17.0%) were linked to HCV-care. 82 (4.6%) underwent liver disease evaluation and in 64 (3.6%) DAA treatment was initiated. In 10 (0.6%) sustained virologic response was documented.

Main reasons for the suboptimal cascade of care included invalid contact data (663; 36.9%) or patients' unavailability at the time of

recall (172; 9.6%) and death (289; 16.1%). Successful DAA therapy at other centers had already been conducted in 366 patients (20.4%).

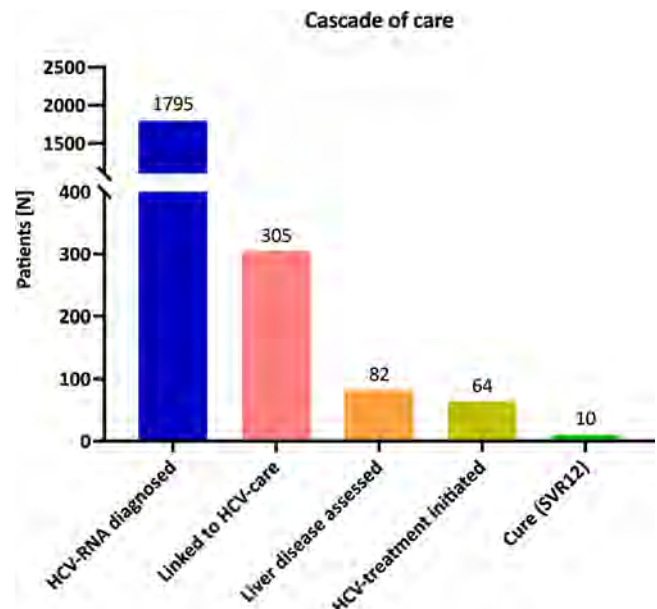


Figure 1: Cascade of care for the ELIMINATE project.

Conclusion: This lab record-based ELIMINATION project identified a considerable number of 6223 HCV patients with potential persisting viremia. Invalid contact data (36.9%) and pre-treatment death (16.1%) represent major problems/barriers. Importantly, at this interim stage 305 (17.0%) patients were successfully linked to care and 64 (3.6%) patients started DAA therapy.

FRI310

The Korean hepatitis C virus care cascade in a tertiary institution: current status and changes in testing, link to care, and treatment

Jonggi Choi¹, Jina Park¹, Danbi Lee¹, Ju Hyun Shim¹, Kang Mo Kim¹, Young-Suk Lim¹, Han Chu Lee¹. ¹Asan Medical Center, University of Ulsan College of Medicine, Department of Gastroenterology, Seoul, Korea, Rep. of South

Email: jkchoi0803@gmail.com

Background and aims: The care cascade for hepatitis C virus (HCV) infection is impeded by multiple barriers, including suboptimal HCV Ab testing, link to care, and diagnosis. We explored the changes in the care cascade of HCV for the past 20 years and its current status in a large cohort from a tertiary referral center.

Method: We analyzed 1, 144, 468 patients who had HCV Ab testing between January 2001 and June 2020. Metrics related to the care cascade of HCV infection and the long-term prognosis of patients were explored.

Results: The seroprevalence of HCV Ab was 1.8%, with a recent decreasing trend. In all, 69.9% of HCV Ab-positive patients performed HCV RNA testing, with a 65.7% positivity. Patients who did not have HCV RNA testing were older and more likely to have a non-hepatocellular carcinoma (HCC) malignancy, normal ALT level, and good liver function. Linkage times for HCV RNA testing from the HCV Ab positivity and for antiviral treatment from HCV diagnosis decreased, notably after 2015, when highly efficacious oral antiviral treatment was introduced to Korea. The average treatment uptake rate was 35.4%, which increased to 38.9% after 2015. Of the 5, 302 patients analyzed regarding long-term prognosis, the annual incidences of HCC were 1.02 and 2.14 per 100 person-years in patients with and without a sustained virological response, respectively.

Cascade steps ^a	Metric ^a	Results ^a
HCV Ab testing ^a	HCV Ab positivity, mean, (range) ^a	1.8% (0.9–2.2) ^a
	Performed HCV RNA testing, mean, (range) ^a	69.6% (65.4–72.4) ^a
	HCV RNA positivity, mean, (range) ^a	65.7% (55.7–83.2) ^a
	Distribution of HCV genotypes ^a	
Link to care for HCV ^a	1b ^a	48.4% ^a
	2 ^a	45.3% ^a
	Linkage time for HCV RNA from the detection of HCV Ab positivity, median ^a	
	Before 2010 ^a	7.3 days ^a
Linkage time for antiviral treatment from confirmed HCV infection, median ^a	2010–2014 ^a	3 days ^a
	After 2015 ^a	1 day ^a
	Before 2010 ^a	226 days ^a
	2010–2014 ^a	192 days ^a
HCV treatment ^a	After 2015 ^a	84 days ^a
	Liver disease status at the time of HCV diagnosis ^a	
	Chronic hepatitis, mean proportion ^a	63.1% ^a
	Liver cirrhosis, mean proportion ^a	14.3% ^a
Rate of antiviral treatment (without HCC) ^a	HCC, mean proportion ^a	22.6% ^a
	Before DAA-era ^a	35.4% ^a
	DAA-era ^a	33.9% ^a
	SVR rate ^a	38.9% ^a
Long-term outcome of HCV ^a	Interferon-based regimen ^a	71.2% ^a
	DAA-based regimen ^a	93.1% ^a
	Annual incidence of HCC ^a	
	With SVR (per 100 person-years) ^a	1.02 ^a
Annual incidence of death or transplantation ^a	Without SVR (per 100 person-years) ^a	2.14 ^a
	With SVR (per 100 person-years) ^a	0.55 ^a
	Without SVR (per 100 person-years) ^a	4.34 ^a

Conclusion: The care cascade of HCV infection has been suboptimal for the past 20 years, despite the recent changes. More effort should be made to increase HCV RNA testing and treatment uptake.

FRI311

Macroeconomic assessment of overall and per-patient healthcare costs of Hepatitis C-infected patients in an integrated health system in the era of direct-acting antiviral therapy

David Kaplan^{1,2}, Claire Durkin¹, Marina Serper¹. ¹University of Pennsylvania, Medicine/Gastroenterology and Hepatology, Philadelphia, United States; ²Corporal Michael J. Crescenz VA Medical Center, Medicine/Gastroenterology and Hepatology, Philadelphia, United States Email: dakaplan@pennmedicine.upenn.edu

Background and aims: Treatment of acute and chronic hepatitis C infection on a national or system-wide scale requires significant investment to acquire, dispense and monitor antiviral therapy with the intent to reduce downstream costs related to reduced liver-related complications. The US Veterans Administration (VA) initiated universal access to HCV direct acting antiviral (DAA) therapy in 2015. The Aim of this study was to quantify the total healthcare costs expended on prior and current hepatitis C-infected individuals before, during after the universal introduction of DAA therapy.

Method: All patients in the VA healthcare system with a positive HCV RNA by a qualitative or quantitative PCR tests at any time between 1999 and 2020 were identified. Exposure to antiviral therapy was identified by prescription fills for interferons and DAA medications. Treatment completion was assigned as 28 days after the final release for a specific regimen and the first date for possible assessment of SVR12 assigned to 84 days after treatment completion. Each course of therapy was characterized based on post-SVR12 date PCR results as cured, relapsed or untested if no PCR test was available. Health Economics Research Center (HERC) average cost estimates and Fee-Basis costs were utilized for outpatient and inpatient care within the VA and external costs, respectively. Cost of outpatient pharmacy were obtained from Managerial Cost Accounting data. For this analysis, total, outpatient, inpatient and pharmacy were aggregated by fiscal year (years 2010–2020) and presented as aggregate or per-patient costs. All costs were inflation-adjusted to year 2021 dollars using the consumer price index and post-treatment costs were discounted by 3% per year.

Results: During fiscal year 2010, 214, 531 unique infected individuals were under care. By 2020, only 68, 086 HCV-infected patients did not have documentation of SVR12 (Figure 1A). Total cost expenditures

prior to DAA availability ranged between \$5.3–5.8B then peaked at \$9.0B in FY2015 due to massive increases in pharmacy-related costs (Figure 1B) then declined to pre-DAA levels by FY2020. Modest increases of outpatient and inpatient costs were observed from FY2010 to FY2018 at which point a significant decline occurred. However, the cost per-patient under care never declined to pre-DAA levels and only a modest decline in outpatient and inpatient expenditures was observed FY2019–2020 (Figure 1C).

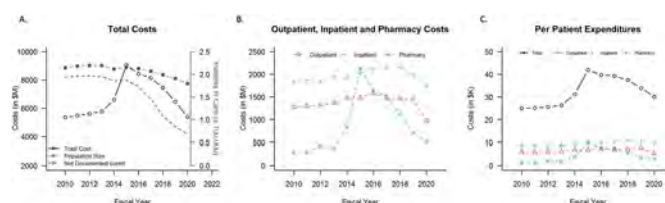


Figure 1. A. Total costs expended on hepatitis C-infected veterans by fiscal year. The number of infected veterans in care (filled circles) and those still viremic (dashed). B. Breakdown of overall costs to outpatient (triangle), inpatient (+) and pharmacy (x). C. Total, outpatient, inpatient and pharmacy costs divided per patient remaining in care.

Conclusion: These data suggest that reductions in overall healthcare costs for a hepatitis C-infected population cannot be observed within the first several years after implementation of universal treatment. Reductions in total cost to pre-DAA levels appear more related to patient attrition than to reduction of average patient treatment costs.

FRI312

Awareness of chronic hepatitis B and C among men who have sex with men (MSM): epidemiological survey and on-site screening

Marie Coessens^{1,2,3}, Tom Holvoet⁴, Jeffery Schouten^{4,5}, Wim Verlinden^{2,5}. ¹VITAZ, Gastroenterology and Hepatology, Sint-Niklaas, Belgium; ²University of Antwerp, Department of Medicine and Health Sciences, Antwerp, Belgium; ³Laboratory of Experimental Medicine and Pediatrics (LEMP), University of Antwerp, Antwerpen, Belgium; ⁴UZ Gent, Gastroenterology and Hepatology, Gent, Belgium; ⁵AZ Nikolaas, Gastroenterology and Hepatology, Sint-Niklaas, Belgium Email: marie.coessens@student.uantwerpen.be

Background and aims: In order to eradicate Hepatitis B (HBV) and Hepatitis C (HCV) by 2030, the WHO focuses on screening in targeted high-risk populations, including men who have sex with men (MSM). The objectives of this study are to assess awareness and knowledge (1) and prevalence (2) of HBV and HCV infections in the MSM population in Flanders and Brussels.

Method: An online questionnaire in Dutch of 5 to 10 minutes was used, as well as face-to-face questionnaire using a tablet at the Belgian and Antwerp Pride (1). In 2018–2020 we joined Sensoa (a Flemish expertise center for sexual health) during outreach projects and tested visitors voluntarily at 14 gay bars, parties and saunas in Flanders by means of an oral quick test for HCV (e.g. OraSure Intercept 2). In addition, HCV test results collected by Ex Aequo (an MSM organization in Brussels that provides sexually transmitted diseases (STD) screening at offices and during on-site actions) in 2019 were analyzed (2).

Results: 300 MSM participated in the online Dutch questionnaire with a median age of 36 years old. HIV status was known to be positive in 7.7%. Knowledge of HBV and HCV infections was poor. Of all participants, 40.5% and 47, 6% thought HBV and HCV patients would always have symptoms; 52.9% thought there was an HCV vaccine; 37.1% thought there was no medication against HCV and of those who knew there was medication, 75% thought that treatment was long and hard. Only 15% and 1%, respectively, knew which sexual practices were with or without risk for HBV and HCV infection. The knowledge of HBV was significantly correlated to the knowledge of HCV ($p < 0.0001$, r_s 0.324) and the degree of education ($p < 0.001$, r_s 0.209). The knowledge of HCV was significantly correlated to the number of sexual partners in the last six months ($p = 0.024$, r_s 0.131), the number of risky sexual practices ($p < 0.0001$, r_s 0.205).

In Sensoa's HCV prevalence study, only 1 of 260 test results was positive (0.38%) and this was an HIV co-infected patient. The Ex Aequo's HCV prevalence study yielded no positive test results. The HIV prevalences were 1, 15% (Sensoa) and 1, 3% (Ex Aequo) and the syphilis prevalence was 2, 5% (Ex Aequo).

Conclusion: There is a big knowledge gap of HBV and HCV infections in the MSM community in Flanders. More awareness campaigns that focus on transmission, disease process, treatment and vaccination need to be created that also target people with a low educational level.

The prevalence of hepatitis C infection and other STD's was low in the MSM population studied of 500 participants. Presumably a young MSM population that voluntarily has themselves tested represents a rather low risk profile for HCV infection. HCV prevalence may be higher in an older population and/or in an illegal environment where more risk factors for HCV infection co-exist and that is more difficult to reach. However, given the high workload and low case finding, an on-site screening approach cannot be recommended.

FRI313

Predictive factors for lost to follow-up pre and post-hepatitis C treatment: Data from the British Columbia hepatitis C virus network

Alnoor Ramji¹, Edward Tam², Julia MacIsaac³, Jean-Philippe Wallach³, Jeanette Feizi², Hin Hin Ko¹. ¹University of British Columbia, Gastroenterology, Vancouver, Canada; ²Pacific Gastroenterology Associates, Vancouver, Canada; ³University of British Columbia, Vancouver, Canada
Email: ramji_a@hotmail.com

Background and aims: In British Columbia (BC) 60% of identified HCV RNA (+) individuals remain untreated. A major challenge is the durable linkage to care of persons who are HCV RNA (+), many are lost to follow-up (LFU) prior to therapy (pre-LFU), or post therapy (post-LFU). Understanding patient profiles will inform resources for HCV elimination. Our aim was to determine predictive factors of HCV patients who are LFU pre- and post-treatment.

Method: Retrospective review of HCV RNA (+) persons in the BC HCV Network to determine the predictive factors of pre-LFU and post-LFU compared to treated persons with SVR12. Chi-square and multi-variable regression analysis were performed.

Results: A total of 4057 patients were included, 2823 (70%) completed HCV therapy, 111 (2.5%) awaiting therapy, and 1123 (27.5%) were pre-LFU. See table. Pre-LFU patients were more likely to be male (70%), have psychiatric disorder (30%), history of injection drug-use (IDU) (37%), and heavy alcohol use (38%) compared to treated patients (64%, 18%, 26%, and 27% respectively, $p < 0.001$). Fewer persons with advanced fibrosis (FIB4 > 3.25 or LSM > 12.5 kPa) were in the pre-LFU group (22%) compared to treated group (30%), $p < 0.001$.

2823 patients completed HCV therapy, 2410 (85.5%) had SVR bloodwork, and 413 (14.5%) did not (post-LFU). Male gender (69%), history of psychiatric disorder (24%), IDU (36%), and heavy alcohol use (35%) were more likely to be post-LFU compared to treated patients (63%, 16%, 26%, 27% respectively, $p < 0.001$). Persons age > 60 years (57%), with a co-morbidity (12%), or advanced fibrosis (20%) were more likely to have SVR12 results documented than the post-LFU group (65%, 17%, and 29% respectively), $p < 0.001$. Multivariable regression for pre and post LFU compared to treated or followed persons, determined that male gender (OR:2.12 and 2.70), psychiatry disease (OR:3.45 and 3.33), IDU (OR:4.25 and 3.05), or heavy alcohol use (OR:3.65 and 2.90) were associated with pre and post-LFU.

	Treated (2823)	Pre-LFU (1123)	p-value
Male	1807 (64%)	786 (70%)	<0.001
Age>60	1843 (65%)	651 (57%)	<0.001
Co-morbidities	484 (17%)	173 (15%)	>0.05
Psychiatry	513 (18%)	336 (30%)	<0.001
IDU	755 (26%)	415 (37%)	<0.001
Alcohol	770 (27%)	426 (38%)	<0.001
Extensive fibrosis	869 (30%)	247 (22%)	<0.001
	Treated and SVR tested (2410)	Post-LFU (413)	p-value
Male	1523 (63%)	284 (69%)	<0.001
Age>60	1608 (66%)	238 (57%)	<0.001
Co-morbidities	420 (17%)	53 (12%)	<0.001
Psychiatry	405 (16%)	102 (24%)	<0.001
IDU	637 (26%)	148 (36%)	<0.001
Alcohol	663 (27%)	144 (35%)	<0.001
Extensive fibrosis	628 (29%)	83 (20%)	<0.001

Figure: Co-morbidity: DM, cardiac, renal, NASH; *p-value based on Chi-square

Conclusion: Male gender, history of psychiatric disorder, IDU, or and heavy alcohol use are predictive of LFU both pre- and post-HCV therapy. Successful HCV elimination strategies will need to incorporate interventions to improve durable engagement of these populations.

FRI314

HCV screening in a tertiary french hospital: just do it !

Si Nafa Si Ahmed¹, Souad Benali¹, Magalie Madau¹, Rania Kibeché¹, Romain Albenois², Michaël Ghez³, Ines Belasri¹, Christine Hernandez¹, Paola Ramirez¹, Julien Negre¹, Laurence Lecomte¹, Floriane Sellier¹, Olivia Pietri¹, Paul Castellani¹, Xavier Adhoute¹, Marc Bourliere¹. ¹Hopital Saint Joseph, Hepatology Unit, Marseille, France; ²Hopital Saint Joseph, Laboratory Unit, Marseille, France; ³Hopital Saint Joseph, DIM, Marseille, France
Email: ssiahmed@hopital-saint-joseph.fr

Background and aims: Universal screening appears to be the most cost-effective strategy to reach the HCV elimination planned by WHO for 2030. All HCV patients have currently access to treatment. In France HCV screening is based on identification of Risk Factor. The aim of the present study was to test universal screening strategy in all hospitalized patients.

Method: From November 2019 to November 2021, we conduct a prospective, longitudinal monocentric study screening all consent patients for HCV regardless identification of Risk Factor. All HCV Ab positive was followed by HCV RNA screening. All replicating patients were proposed to be treated according to the other pathologies for which the patients were hospitalized. The study was authorized by CPP Toulouse.

Because of occurrence COVID 19 pandemics, conducting this study we identify several limitations leading to the prolongation of inclusion time and to develop adaptive measures such as oral consent.

Results: As of September 30, 2021 results are shown in this figure:

Patients	HCV Ab-	HCV Ab+	HCV RNA+
28 806 Hospitalized	4560 included (15.8%)		
N (%)	4436 (97.28)	124 (2.71)	18 (0.4)
Sex Ratio	1.16	2.02	3.5
Prevalence % [IC 95]		2.51 [2.25-3.19]	14.5 [8.32-20.7]
Age mean - (extreme)	66.60 (18-101)	68.21 (21-95)	72.16 (49-95)
Two-sided t test		$p = 0.08$	$p = 0.25$

HCV Ab + patients seemed older; however this difference is not statistically different. Large part of patients (2/3) were unaware of the HCV status.

49 (39.5%) patients come from surgical departments, 38 (30.5%) from the medical department and 37 (30%) are followed in gastroenterology office.

All HCV RNA+ patients have been evaluated for treatment. 8 are eradicated, 2 DAA therapy are still on going, 1 patient refuse treatment (89 years old), 5 patients suffer from HCC and treatment was delayed, 2 patients died during palliative management

POSTER PRESENTATIONS

Conclusion: HCV Ab prevalence recorded is significantly higher than that observed in the general population in France. However only 15.8% of hospitalized patients have been included. Motivation of all health care workers is essential. Final results of the study will be present at the meeting

FRI315

Hepatitis C screening rates by age cohort 1945–1965 in a large community health system before, during and after the COVID pandemic

David Bernstein¹, Nitzan Roth¹, Ben Da¹, Sanjaya Satapathy¹, Henry Bodenheimer¹, Christian Kuntzen¹, Tai Ping Lee¹. ¹Donald and Barbara Zucker School of Medicine at Hofstra/Northwell, Hempstead, United States
Email: dav31475@gmail.com

Background and aims: In the outpatient primary care setting, New York State mandates the offering of hepatitis C (HCV) testing for persons born between 1945 and 1965. Despite this mandate, <50% of HCV screening candidates are offered screening and among those found to be HCV Ab positive, not all patients undergo HCVRNA testing and even fewer are referred for treatment.

Method: We implemented a system where nurse educators personally visited 60 outpatient primary care offices to educate regarding HCV screening. Visits occurred for the first 2 years of the project and then were stopped due to the COVID pandemic. We evaluated our results by birth year, dividing patients into 4 groups, those born between 1945 and 1950, between 1951 and 1955, between 1956 and 1960 and between 1961 and 1965.

Results: From April 1, 2018–August 31, 2021, 50, 047 previously unscreened patients born between 1945 and 1965 were screened with an HCVAB with reflex testing to HCVRNA in all positive HCVABs. 10819 were born between 1945 and 1950, 11573 were born between 1951 and 1955, 13586 were born between 1956 and 1960 and 14069 were born between 1961 and 1965. Screening decreased during the peak pandemic months of March–June 2020 but levels returned to baseline screening numbers by July 2020 and continued at a steady state for the duration of the study.

Subjects born 1945–1950, 234/10819 (2.2%) were HCV AB positive with 67/10819 HCVRNA positive (0.6%). Subjects born 1951–1955, 326/11573 (2.8%) were HCV AB positive with 76/11573 HCVRNA positive (0.7%). Subjects born 1956–1960, 303/13586 (2.2%) were HCV AB positive with 58/13586 (0.4%) HCVRNA positive. Subjects born 1961–1965, 230/14069 (1.6%) were HCV AB positive with 44/14069 (0.3%) HCVRNA positive.

All patients were referred to a hepatitis C treating practitioner. 101 patients completed therapy and 93 remain on treatment. There were no differences by age groups in those accepting DAA treatment, in declining DAA therapy or in the numbers of patients who died during the study.

Conclusion: This large community-based HCV screening program confirmed the NHANES study that approximately 2–2.5% of people born between the years 1945–1965 are HCV AB positive. There were no significant differences by age cohort in this group although there was a trend for patients born between 1956 and 1965 to spontaneously clear the HCV virus without treatment. The COVID pandemic temporarily led to decreased HCV screening but once the pandemic began to ease, screening rates rapidly returned to pre-COVID levels as did DAA treatment rates. The positive effects of in-person nurse educators on primary care providers and their staffs persisted even after these visits were stopped due to COVID.

FRI316

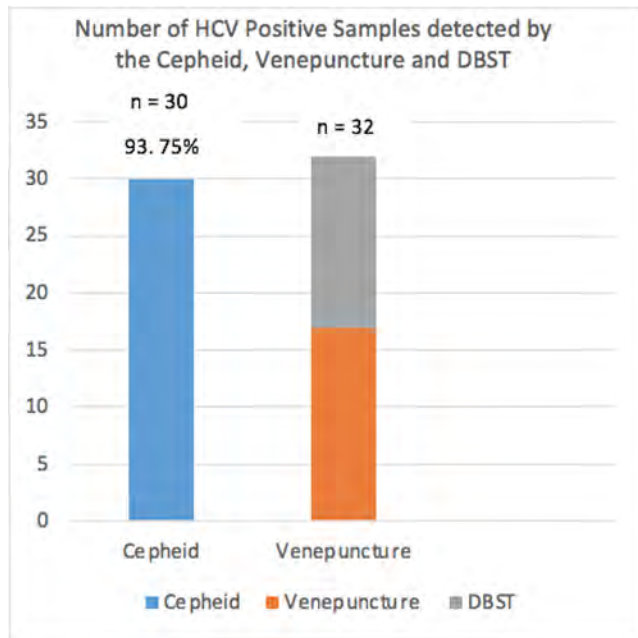
Maximizing the potential of Cepheid, GeneXpert PCR rapid testing for hepatitis C through use of finger prick blood samples collected into EDTA capillary tubes

Anam Choudhry¹, Louise Davies², Nicki Palmer², Jade Davies³, Bazga Ali⁴, Rhys Oakley⁵, James Plant⁶, Louise Evans⁶, Chinlye Chng⁶, Helen Thompson-Jones⁶, Lorraine Wall⁷, Sarah Nicholas⁷, Brendan Healy^{4,8}. ¹Cardiff University School of Medicine, Cardiff, United Kingdom; ²Public Health Wales Cardiff, Cardiff, United Kingdom; ³Public Health Wales Swansea, Swansea, United Kingdom; ⁴University Hospital Wales, Cardiff, United Kingdom; ⁵Cardiff and Vale Pharmacy, United Kingdom; ⁶Swansea Bay UHB BBV Team, Swansea, United Kingdom; ⁷Cardiff and Vale UHB BBV Team, Cardiff, United Kingdom; ⁸Public Health Wales, United Kingdom
Email: choudhrya4@cardiff.ac.uk

Background and aims: The Cepheid, GeneXpert provides hepatitis C virus (HCV) PCR results <90 minutes. A major limitation is the need to load finger prick samples <15 minutes, as patients must be co-located with the machine. Venous blood collected into EDTA tubes can be stored for up to 72 hours at 2–8°C prior to processing. In this project finger-prick blood collected into EDTA capillary tubes and processed >15 minutes after collection was compared with venepuncture (gold standard) and dried-blood spot testing (DBST) to facilitate testing remote from the machine (e.g. prison clinics on different wings remote from a centrally located machine) but still delivering rapid turn-around times with testing in close proximity to the point of need.

Method: Capillary tubes (MiniCollect® Tube 0.25/0.5 ml K3E K3EDTA-450530) were spiked with venepuncture blood from 25 adult patients undergoing HCV testing, processed on the Cepheid and the results compared. HCV positive patients in the community undergoing testing (venepuncture or DBST) were then approached to provide an additional EDTA capillary tube finger-prick sample. Samples were left for >15 minutes <72 hours prior to processing and results compared. As the lower limit of quantification on the Cepheid is 40 IU/ml, results below this level were analysed separately.

Results: Results from the first 36/50 patients are reported here. The time between sample collection and testing ranged from 44 minutes to 94 hours 34 minutes. Samples with longest delays tested positive (no suggestion of the results being affected). Two venepuncture results were detected, viral load <12 IU/ml. Corresponding Cepheid results were negative as expected (results are not included below). One sample registered as “error” (Cepheid) and was not detected by DBST. In one sample the Cepheid result was not detected and the DBST result detected in the “unreliable zone” –10 IU/ml. The LLD of DBST is 1000 IU/ml and this likely is a false positive DBST result. Of the remaining HCV positive samples (n = 32, log viral loads 0.19–2.05 IU/ml). The Cepheid successfully detected HCV in 30 (93.75%) (Figure 1). In the remaining two samples the Cepheid result was “invalid.” This could be due to internal quality standards, probe check failures, system computer failures or PCR process inhibition.



Conclusion: The Cepheid successfully detected 93.75% of the HCV positive samples detected by venepuncture or DBST. The two samples that were not positive returned invalid results which would have prompted retesting. The one discordant result with a very low level DBST result is likely due to a false positive result on DBST. As such, none of the results from finger prick samples collected into EDTA capillary tubes and processed on the Cepheid returned false negative results. This method of sampling is now going to be adopted in Wales with ongoing monitoring of results over the next 12 months.

FR1317

Healthcare resource utilization in treatment-naïve patients with compensated cirrhosis receiving 8-weeks' glecaprevir/pibrentasvir stratified by drug use and socioeconomic status: a retrospective chart review

Juan Isidro Uriz Otano^{1,2}, Armand Abergel³, Alessio Aghemo^{4,5}, Adriana Ahumada⁶, Massimo Andreoni⁷, Tarik Asselah⁸, Abhi Bhagat⁹, Isabel Butrymowicz⁹, Brian Conway¹⁰, Antonio Gasbarrini¹¹, Francisco Jorquera¹², Pietro Lampertico^{13,14}, Maria Luisa Manzano Alonso¹⁵, Lindsay Myles¹⁶, Marcello Persico¹⁷, Alnoor Ramji¹⁸, Dimitri Semizarov⁹, Yanna Song⁹, Erica Villa¹⁹, Qingqing Xu⁹. ¹Navarra Institute for Health Research (IdiSNA), Pamplona, Spain; ²Department of Gastroenterology, Liver Unit, Complejo Hospitalario de Navarra, Pamplona, Spain; ³CHU Estaing, UMR 6602 CNRS Université d'Auvergne, Clermont Ferrand, France; ⁴Department of Biomedical Sciences, Humanitas University, Rozzano, Italy; ⁵Department of Gastroenterology, Humanitas Research Hospital IRCCS, Rozzano, Italy; ⁶Hospital General Universitario Gregorio Marañón, Liver Unit, Madrid, Spain; ⁷University of Tor Vergata, Rome, Italy; ⁸Service d'Hépatologie, Hôpital Beaujon, INSERM UMR 1149, Université de Paris, Clichy, France; ⁹AbbVie Inc., North Chicago, United States; ¹⁰Vancouver Infectious Diseases Center and Simon Fraser University, Vancouver, Canada; ¹¹Internal Medicine and Gastroenterology, Fondazione Policlinico Universitario A. Gemelli IRCCS, Rome, Italy; ¹²Digestive System Service, Complejo Asistencial Universitario de León, IBIOMED and CIBERehd, León, Spain; ¹³Foundation IRCCS Ca' Granda, Ospedale Maggiore Policlinico, Policlinico-Division of Gastroenterology and Hepatology-CRC 'AM and A Migliavacca' Centre for Liver Disease, Milan, Italy; ¹⁴University of Milan, Milan, Italy; ¹⁵Liver Unit, Hospital Universitario 12 De Octubre, Madrid, Spain; ¹⁶Barrie GI Associates, Barrie, Ontario, Canada; ¹⁷Dipartimento di Medicina Clinica Medica, Epatologica e Lungodegenza, AOU OO. RR. San Giovanni di Dio Ruggi e D'Aragona,

Salerno, Italy; ¹⁸University of British Columbia, Vancouver, BC, Canada; ¹⁹UC Gastroenterologia, Dipartimento di SpecialitàMediche, Azienda Ospedaliera Universitaria di Modena, Modena, Italy
Email: ji.uriz.otano@navarra.es

Background and aims: Identifying factors that may influence healthcare resource utilization (HCRU) among patients with hepatitis C virus (HCV) infection is important to support the development of initiatives that reduce healthcare resource burden and allow for more patients to be treated. This study describes HCRU among treatment-naïve, compensated cirrhotic patients treated with 8-weeks' glecaprevir/pibrentasvir (G/P), according to their history of drug use (DU) and socioeconomic status.

Method: Here we present an interim subanalysis of the ongoing, noninterventional, multicenter CREST study which includes chart review data from France, Canada, Italy, and Spain. Demographic and baseline characteristics were reported overall and for patients with history of DU. HCRU was described by history of DU and occupational status. In the group of patients with DU, HCRU was described according to active vs former drug use, and route of drug administration.

Results: This analysis included 206 patients who received ≥ 1 dose of G/P; 139 (67.5%) were male, the median (range) age was 57 (31–88) years (assessed in 203 patients), 185 (89.8%) had stable housing, and 52 (25.2%) were employed full-time. Among 75 (36.4%) patients with history of DU, 52 (69.3%) were intravenous drug users (IVDUs), and 23 (30.7%) were active drug users. Other characteristics included: aged >50 years ($n=51$; 68.0%), stable housing ($n=63$; 84.0%), and employed full-time ($n=16$; 21.3%). Full-time employed patients, compared with those not in full-time employment, had fewer visits to general physicians (0.9 vs 2.0), but more visits to hepatologists (2.0 vs 1.4) and gastroenterologists (0.2 vs 0.1), and a greater number of noninvasive procedures (1.9 vs 0.9). Patients with history of DU, especially IVDUs, had more general physician and nurse visits and fewer hepatologist and gastroenterologist visits than those with no history of DU. Additionally, active drug users had higher on-treatment laboratory test (3.7 vs 2.1) and noninvasive diagnostic procedures (1.7 vs 1.3) compared with former drug users. HCRU in IVDUs was mostly similar to those administering drugs through other routes (Figure).

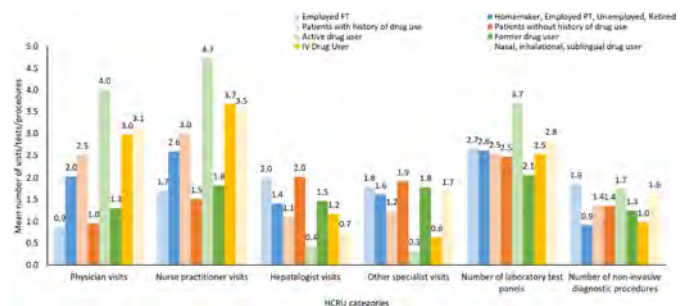


Figure: Healthcare resource utilization stratified by patients' occupational status, history of drug use, and current use of drugs. *Patients with history of illicit drug use included both active and former drug users administering drugs either IV, nasally, through inhalation, or sublingually. FT, full time; IV, intravenous; PT, part time; SD, standard deviation.

Conclusion: In this real-world cohort, HCRU was observed to vary by occupational status and history of DU among patients with HCV receiving G/P, with active drug users having the highest number of physician and nurse practitioner visits. Additional results will be presented at the congress.

FRI318

Progress towards hepatitis C elimination: the feasibility and success of a nurse and harm reduction practitioner led model of care utilising rapid point of care HCV RNA testing at a medically supervised injecting room in Melbourne, Australia

Michael MacIsaac^{1,2}, Bradley Whitton¹, Jenine Anderson³, Matthew Penn³, Anthony Weeks³, Shelley Cogger³, Kasey Elmore³, David Pemberton³, Tim Papaluca^{1,2}, Margaret Hellard^{4,5,6}, Mark Stooze^{4,6}, David Wilson⁴, Alisa Pedrana^{4,6}, Joseph Doyle^{4,5}, Nico Clark^{3,7}, Jacinta Holmes^{1,2}, Alexander Thompson^{1,2}. ¹St Vincent's Hospital Melbourne, Gastroenterology, Fitzroy, Australia; ²University of Melbourne, Faculty of Medicine, Parkville, Australia; ³North Richmond Community Health, Medically Supervised Injecting Room, Richmond, Australia; ⁴Burnet Institute, Disease Elimination Program, Melbourne, Australia; ⁵Alfred Hospital, Infectious Diseases, Melbourne, Australia; ⁶Monash University, School of Public Health and Preventive Medicine, Melbourne, Australia; ⁷The Royal Melbourne Hospital, Addiction Medicine, Parkville, Australia
Email: michael.macisaac@svha.org.au

Background and aims: To achieve HCV elimination targets, efforts must focus on models of care engaging people who inject drugs (PWID). The Xpert® HCV viral load fingerstick point of care (POC) test provides an HCV RNA level within 1 hour, allowing rapid diagnosis and treatment. We previously reported a successful nine-week pilot study incorporating HCV RNA POC testing at a medically supervised injecting room (MSIR) in Melbourne, Australia.¹ We now present the 12-month outcomes of this program.

Method: Prospective cohort study recruiting PWID attending a high-volume MSIR in Melbourne, Australia between 9/11/20 to 9/11/21. Clients were offered HCV screening using the Xpert® HCV RNA POC test. Venepuncture for HBV/HIV screening and fibrosis assessment (APRI/FibroScan) were also offered to clients, regardless of HCV RNA status. HCV RNA results were returned same day if clients were still present, or via phone or at next MSIR visit if they had already departed. POC testing/treatment was led by a full-time hepatology fellow during the initial nine-week pilot program, and a nurse or harm reduction practitioner (HRP) for the remainder of the study period. DAA treatment was prescribed immediately upon return of a positive HCV test if the hepatology fellow was on-site, or by a GP/hepatologist after remote consultation for nurse/HRP assessments. Clients were invited to be followed 4-weekly during treatment and at SVR12. Primary endpoints were number of clients screened for HCV and number commencing DAAs. Testing rates were compared to a historical control period (9/11/18–9/11/19) of standard of care HCV venepuncture testing at the MSIR.

Results: 573 PWID consented to HCV RNA POC testing. By comparison, 180 clients underwent HCV testing during the control period, representing a 218% increase with POC testing. Median age was 42 yrs (IQR 37–49) and 75% male. 161 (28%) were HCV RNA+. An APRI score was calculated for 337 clients and 154 (16/32, 50% with APRI ≥ 1) had a FibroScan performed. Cirrhosis was uncommon (6% HCV RNA+, 5% overall), as was HBV (n = 3, 2%) and HIV co-infection (n = 0). 90% (n = 145/161) of HCV RNA+ clients were prescribed DAA therapy. Median time to treatment start was 8 days (IQR, 2–22); 13 clients (9%) initiated treatment same day as diagnosis. There was no difference in the number of clients linked to treatment with hepatology fellow led on-site prescribing compared to remote prescribing following nurse or HRP assessment (94% vs 88%, p = 0.204). Among those with complete follow up data (n = 43), SVR was 74%. Causes of non-SVR were re-infection (n = 3), relapse (n = 4), and non-response from medication non-adherence (n = 4).

Conclusion: Rapid HCV POC testing in a MSIR rapidly upscales testing and was associated with high rates of treatment initiation. Nurse or HRP led POC testing/treatment with remote prescribing is highly feasible, with similar rates of treatment initiation achieved.

¹ MacIsaac MB, et al. ILC 2021.

FRI319

Screening for hepatitis C in Denmark-the effect of a mobile outreach intervention

Sandra Droese^{1,2,3}, Lone Wulff Madsen^{1,2}, Gustav Bang Harvald¹, Søren Grinderslev¹, Karen Kofoed¹, Lene Kræmer¹, Anne Øvrehus^{1,2}, Peer Christensen^{1,2,3}. ¹Odense University Hospital, Department of Infectious Diseases, Odense, Denmark; ²University of Southern Denmark, Clinical Institute, Odense, Denmark; ³Odense University Hospital, Open Patient Data Explorative Network, Odense, Denmark
Email: peer.christensen@dadlnet.dk

Background and aims: The prevalence of hepatitis C (HCV) in Denmark is low (0.21% of the adult population), 24% of HCV infected are undiagnosed (corresponding to 700 HCV patients in the Region of Southern Denmark (RSD)) and among diagnosed less than half have been cured. As part of the “C-Free-South” program we launched an outreach test and treat center on wheels in the Region of Southern Denmark in June 2020, targeting people with drug or alcohol use and/or psychiatric illnesses as well as festivals and open markets. The aim of this study is to describe the results of the intervention after the first 17 months.

Method: Low threshold non governmental organizations were approached by a mobile unit with medical personnel from the infectious disease department at Odense University Hospital. We used an HCV point of care rapid test for antiHCV, dried blood spot test for HCV RNA and a FibroScan™ Deviser for diagnosis of liver fibrosis. Infected patients were offered treatment either by referral to the nearest clinic or in the mobile unit, as deemed feasible.

Results: 584 persons were tested in 37 different locations of whom 148 were in shelters or other residential institutions. Overall 7% (43) had a positive antiHCV by POC test and 2% (12) had current infection of whom at least 5 (42%) were reinfected after HCV cure. Men constituted 55% of all tested, and 70% of all antiHCV positives (p < 0.05). Median age at test was 50 years (IQR 40–60) with no relation to HCV status. Overall 95% of the 43 antiHCV positives had been tested before, 81% recalled being antiHCV positive at last test, 5% recalled being negative, (suggesting recent infection) and a total of 71% reported to have been cured for HCV (universal treatment for HCV became available Denmark in 2018). The prevalence of antiHCV was 16% (26/162) in facilities open to all (who accepted drug users) and 0% (0/187) in facilities restricted to psychiatric patients or alcohol users. Correspondingly, 91% of the 43 antiHCV positives had injected drugs compared to 8% of antiHCV negatives. We found no infections (0/71) when testing the general population (i.e. at markets).

Conclusion: Our study suggests that most hepatitis C infected in Denmark have been identified and cured, and we found a very low proportion of undiagnosed (5%) compared to the previous national estimate of 24%. However our study is a selected sample of the population at risk for HCV and may not be representative for our region or Denmark. The low absolute number of current infection (2% of tested) suggest that our outreach campaign in its current form is unlikely to diagnose and treat the remaining patients with HCV in our region. An improved case finding strategy is needed to reach the WHO target of 90% diagnosed and 80% cured by 2030. This could be monetary incentives to be tested, and increased use of peer based testing (“snowballing”). A full update of treatment results and new screening methods will be presented at the meeting.

FRI320

Screening for HCV infection combined with SARS-CoV-2 vaccination in the Campania region

Pietro Torre¹, Mario Masarone¹, Roberta Sciorio¹, Monica Annunziata¹, Roberta Coppola¹, Laura Staiano², Carmine Coppola², Marcello Persico¹. ¹University of Salerno, Internal Medicine and Hepatology Unit, Department of Medicine, Surgery and Dentistry, "Scuola Medica Salernitana"; ²OORR Area Stabiese, Plesso Nuovo Gragnano, Naples, Italy, Department of Internal Medicine-Unit of Hepatology and Interventional Ultrasonography
Email: mpersico@unisa.it

Background and aims: The health emergency caused by the SARS-CoV-2 pandemic has negatively impacted the management of HCV infection, potentially jeopardizing the achievement of the goal of eliminate hepatitis C by 2030. To take advantage of the current sanitary situation, associated screening for HCV and SARS-CoV-2 infection have been carried out. We decided to propose HCV screening also to people who undergone SARS-CoV-2 vaccination.

Method: Screening for hepatitis C was carried out by finger-prick test to search for HCV antibodies. It took place in the minutes following the SARS-CoV-2 vaccination, in two different vaccination centers of the Campania region, and in two different time frames. In the period 1 May–20 July 2021, screening for hepatitis C was offered to the general population who got the vaccine at the Fisciano (province of Salerno) vaccination center. In the period 20 September–11 October 2021, screening for hepatitis C was offered to the general population who underwent vaccination at the San Leonardo Hospital (Castellammare di Stabia, metropolitan city of Naples). In both sites, Pfizer-BioNTech, Moderna, or Oxford-AstraZeneca vaccines were used.

Results: Out of 5095 people who underwent vaccination at the Fisciano vaccination center, 1952 (38, 3%, average age 41, 6 years) performed screening for hepatitis C. 5 of these (0, 25%, average age 54, 2 years) resulted HCV-Ab positive; all 5 were aware of their condition; 4 had previous treatment; 1 (0, 05%) was found to have active HCV infection. Out of 2202 people vaccinated at the San Leonardo Hospital, 1207 (54, 8%, average age 43, 1 years) underwent screening for hepatitis C. Among these, 9 (0, 7%, average age 54, 3) resulted positive. 5/9 tested negative on the confirmatory test; 2/9 were aware of their condition and had previous treatment; 1 subject (0, 08%) was found to have active HCV infection; 1 subject is awaiting the results at time of writing.

In both sites a consistent percentage of people refused the HCV-Ab test. Moreover, the prevalence of HCV-Ab positivity and HCV active infection was found to be lower than the national data. Frequent reasons for refusing the test were lack of knowledge of the disease, fear of a positive result, and distrust in the test's effectiveness. Someone refused the test because vaccination was considered a particularly stressful event. The low prevalence of HCV infection found in these projects could be at least partly attributable to the under-participation of the elderly, as at the time the screenings were carried out most of them had probably already received the expected doses of SARS-CoV-2 vaccine.

Conclusion: In conclusion, we believe that SARS-CoV-2 vaccination could be an opportunity to screen for HCV infection, but to maximize the benefits of this screening, the characteristics of the subjects to be tested should be reconsidered, by focusing particularly on the elderly population.

FRI321

Treating children with HCV close to home through a virtual national multidisciplinary network

Deirdre Kelly^{1,2}, Carla Lloyd¹, Maxine Brown¹, Kinza Ahmed¹, Ivana Carey³, Sarah Tizzard³, Joanne Crook³, Penny North-Lewis⁴, Palaniswamy Karthikeyan⁴, Sanjay Bansal³, Graham Foster⁵. ¹Birmingham Children's Hospital, United Kingdom; ²University of Birmingham, United Kingdom; ³King's College Hospital, United Kingdom; ⁴Leeds General Infirmary, United Kingdom; ⁵Barts and The London School of Medicine and Dentistry, United Kingdom
Email: carla.lloyd1@nhs.net

Background and aims: Hepatitis C virus (HCV) infection is a major global health problem in adults & children. The recent efficacy of Direct Acting Anti-viral therapy (DAA) has cure rates of 99% in adults and adolescents. These drugs were licensed for children 3–12 yrs during the recent coronavirus pandemic. To ensure equitable access, safe & convenient supply during lockdown, we established a virtual national treatment pathway for children with HCV in England & evaluated its feasibility, efficacy & treatment outcomes.

Method: A paediatric Multidisciplinary Team Operational Delivery Network (pMDT ODN), supported by NHS England (NHSE), was established with relevant paediatric specialists to provide a single point of contact for referrals & information. Referral & treatment protocols were agreed for HCV therapy approved by MHRA & EMA. On referral the pMDT ODN agreed the most appropriate DAA therapy based on clinical presentation & patient preferences, including ability to swallow tablets. Treatment was prescribed in association with the local paediatrician & pharmacist, without the need for children & families to travel to national centres. All children were eligible for NHS funded therapy; referral centres were approved by the pMDT ODN to dispense medication; funding was reimbursed via a national NHSE agreement. Demographic & clinical data, treatment outcomes & SVR 12 were collected. Feedback on feasibility & satisfaction on the pathway was sought from referrers.

Results: In the first 6 months, 34 children were referred; 30- England; 4- Wales; median (range) age 10 (3.9–14.5) yrs; 15M; 19F: Most were genotype type 1 (17) & 3 (12); 2 (1); 4 (4). Co-morbidities included: obesity (2); cardiac anomaly (1); Cystic Fibrosis (1); Juvenile Arthritis (1). No child had cirrhosis. DAA therapy prescribed: Harvoni (21); Epclusa (11); Maviret (2). 27/34 could swallow tablets; 3/7 received training to swallow tablets; 4/7 are awaiting release of granules. 11/27 have completed treatment and cleared virus; of these 7/11 to date achieved SVR 12. 30 children requiring DAA granule formulation are awaiting referral and treatment.

Referrers found the virtual process easy to access, valuing opportunity to discuss their patient's therapy with the MDT & many found it educational. There were difficulties in providing the medication through the local pharmacy. However there are manufacturing delays in providing granule formulations because suppliers focused on treatments for COVID, leading to delays in referring and treating children unable to swallow tablets.

Conclusion: The National HCV pMDT ODN delivers high quality treatment & equity of access for children & young people, 3–18 yrs with HCV in England, ensuring they receive care close to home with 100% cure rates.

FRI322

Association of sustained virologic response with measures of direct-acting antiviral adherence in patients with Hepatitis C: data from the ASCEND and ANCHOR investigations

Sarah Kattakuzhy¹, Vivian Wang², Catherine Gannon², Sarah Mollenkopf³, Charisse Ahmed², Sanjay Chainani³, Junfeng Sun², Henry Masur², Shyamasundaran Kottilil¹, Elana Rosenthal¹. ¹*Institute of Human Virology, University of Maryland School of Medicine, Baltimore, United States*; ²*National Institutes of Health, Bethesda, United States*; ³*University of Maryland School of Medicine, Baltimore, United States*

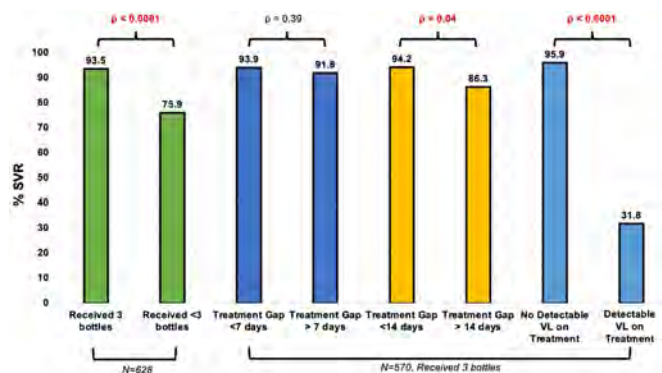
Email: skattakuzhy@ihv.umaryland.edu

Background and aims: While HCV treatment with direct-acting antivirals is highly efficacious in clinical trials, medication receipt and adherence is challenged by both policy and patient-specific barriers in real-world settings. Previous research suggests that sustained virologic response can be achieved with imperfect adherence¹, but current data is unclear on how the amount and timing of nonadherence impacts sustained virologic response (SVR).

Method: Data was pooled from two real-world investigations of HCV treatment using direct-acting antivirals from 2015 to 2020, ASCEND² and ANCHOR³. The analysis was limited to individuals with an anticipated duration of 12 weeks, who were dispensed at least one month of medication, on whom SVR was assessed. Measures of adherence were assessed in three ways: (1) medication receipt (MR), defined as the actual number of 28-pill bottles dispensed; (2) medication gap (MG), defined as the difference in days between expected medication receipt and actual medication receipt; and (3) on treatment detectable viral load (DVL), defined as viral load >1000 IU/ml at week 4 or >100 IU/ml at week 12.

Results: Of 628 individuals, 472 were treated with LDV/SOF (75%), 93 with SOF/VEL (15%), and 63 with ELB/GZV (10%). Overall the cohort was median age 59, majority (69%) male, with 94% Black race, 28% with current heroin use, 16% with current cocaine use, and 27% unstably housed.

Fifteen patients (2.3%) received 1 bottle, 43 (6.8%) received 2 bottles, and 570 (90.8%) received 3 bottles, and MR was significantly associated with SVR ($p < 0.00001$), but was not associated with gender, race, or substance use. Of the 570 who received all 3 bottles, 211 (37%) had a MG of at least 1 day (range 1–197, median 7). MG of 14 days or more was inversely associated with SVR ($p = 0.037$), however MG of 7 days or more was not associated with SVR. Of the 211 with MG, 89 individuals had a gap between months 1 and 2, 79 between months 2 and 3, and 43 between both. There was no association with timing of MG and SVR. Of 567 patients who received 3 bottles and who had on treatment VL assessment, 22 (3.9%) had DVL, which was inversely associated with SVR ($p < 0.0001$). Current cocaine ($p = 0.05$) and opioid use ($p < 0.0001$) were significantly associated with DVL, but race, gender, and housing status were not.



Conclusion: In this analysis of 628 individuals treated with DAA, 10% did not complete treatment, and more than a third had medication gaps, which were inversely associated with SVR. Despite this, patients with imperfect adherence still achieved rates of SVR greater than 75%. These data suggest that while nonadherence to DAA is common, patients should be continued on treatment regardless of imperfect adherence. Finally, these data support removal of policies which can delay medication receipt, such as mandatory on-treatment phone calls, visits, or lab checks.

FRI323

ATA haplotype of the interleukin-10 gene and low phase angle are associated with liver cirrhosis in chronic hepatitis C

Nataly Lopes Viana^{1,2}, Diego Alves Vieira^{2,3}, Thais Pontelo de Vries^{1,2}, Marta Paula Pereira Coelho^{1,2}, Pedro Alves de Castro^{2,3}, Tatiana Bering Bering⁴, Maria Isabel Toulson Davidson Correia⁵, Gifone Aguiar Rocha⁶, Luciana Diniz Silva^{1,2,7}. ¹*UFMG Faculty of Medicine, Sciences Applied to Adult Health Care Post-Graduate Programme, Belo Horizonte, Brazil*; ²*UFMG Faculty of Medicine, Outpatient Clinic of Viral Hepatitis, Instituto Alfa de Gastroenterologia, Faculdade de Medicina, Brazil*; ³*UFMG Faculty of Medicine, Medical Undergraduate Student, Brazil*; ⁴*UFMT-Universidade Federal de Mato Grosso, Department of Food and Nutrition, Brazil*; ⁵*UFMG Faculty of Medicine, Department of Surgery, Brazil*; ⁶*UFMG Faculty of Medicine, Laboratory of Research in Bacteriology, Brazil*; ⁷*UFMG Faculty of Medicine, Department of Internal Medicine, Brazil*

Email: lucianadinizsilva@gmail.com

Background and aims: Chronic infection caused by Hepatitis C virus (HCV) is a major public health problem. It is estimated that, globally, about 71 million people are infected. Approximately 55.0% to 85.0% of the infected individuals will develop chronic hepatitis C. Of those chronically infected by HCV, the risk of liver cirrhosis varies from 15.0% to 30.0% in 20 years. In this context, the progression of hepatic fibrosis may be influenced by host, viral and environmental factors. Among the host factors, the role played by the imbalance between pro- and anti-inflammatory cytokines and the development/progression of liver cirrhosis is highlighted. Interleukin-10 (IL-10) is considered a key cytokine in the control of the secretion of pro-inflammatory mediators. IL-10, single nucleotide polymorphisms (SNPs) in the positions –1082A/G (rs1800896), –819C/T (rs1800871) and –592C/A (rs1800872) in the promoter region of the gene encoding are associated with changing the transcription rates of this gene. Haplotypes GCC, ACC and ATA determine the production of high, intermediate and low levels of IL-10, respectively. Based on these findings, the objective of this present study was to evaluate whether SNPs in the promoter region of the IL-10 coding gene are associated with liver cirrhosis in patients chronically infected with HCV.

Method: We prospectively evaluated 155 patients [mean age, 51.3 ± 11.5 years; 94 (60.6%) men, 60 (38.7%) with cirrhosis]. Diagnosis of cirrhosis was performed based on clinical, laboratory, radiological and histological parameters. SNPs were genotyped by RT-PCR. Phase angle was obtained by electrical bioimpedance analysis. The data were analyzed by SPSS 21.0. The associations were analyzed by logistic regression models. Variables with $p \leq 0.25$ in the univariate analysis were selected for the multivariate model.

Results: Polymorphisms were in balance of Hardy-Weinberg. The ATA haplotype was observed in 43 (72.0%) and in 52 (55.0%) of the patients with and without liver cirrhosis, respectively ($p = 0.04$). In multivariate analysis, ATA haplotype (OR = 2.39; 95.0%CI = 1.10–5.19; $p = 0.03$), phase angle (OR = 0.58; 95.0%CI = 0.38–0.89; $p = 0.01$) and arterial hypertension (OR = 3.55; 95.0%CI = 1.72–7.33, $p = 0.001$) were independently associated with liver cirrhosis.

Conclusion: The ATA haplotype, which is related to lower IL-10 production, associated with liver cirrhosis in patients chronically infected with HCV. Also, phase angle, a nutritional marker that reflects the integrity of cell membranes, was inversely associated with cirrhosis in patients with chronic hepatitis C.

FRI324

Use of Glecaprevir/Pibrentasvir (G/P) for the treatment of HCV infection among fentanyl users: an interim analysis of the GRAND PLAN study

Brian Conway^{1,2}, David Truong¹, Leo Yamamoto¹, Rossitta Yung¹, Shawn Sharma¹. ¹Vancouver Infectious Diseases Centre, Vancouver, Canada; ²Simon Fraser University, Burnaby, Canada
Email: bconway5538@gmail.com

Background and aims: To achieve the World Health Organization mandate of eliminating Hepatitis C Virus (HCV) infection as a public health concern by the end of the decade, we must design and implement plans of intervention for all affected populations, including the most vulnerable and difficult to reach. We describe a community-based program targeting HCV-infected inner-city residents with active fentanyl use.

Method: Through weekly events held at single room occupancy dwellings in the inner city of Vancouver, Canada, we identified subjects with HCV infection and a history of ongoing fentanyl use. We engaged them in a multidisciplinary program of care to meet medical, psychological, social and addiction-related needs and provided HCV treatment with Glecaprevir/Pibrentasvir (G/P) within this context. HCV medications were administered in a way to maximize the likelihood of adherence and follow-up to the sustained virologic response (SVR) 12 time point. This included daily dispensing with opiate agonist therapy or weekly delivery of medications to the place of residence. If a subject was unavailable for weekly check-ins, interventions were immediately implemented to re-integrate into care. This analysis presents the rate of documented cure (achievement of SVR12) in the target population.

Results: We identified 118 eligible HCV-infected fentanyl users who were enrolled in the program. Key demographic characteristics include: 91 (77%) male, median age 47 (26–75) years, 102 (86%) on opiate agonist therapy, F0/1 (86, 73%), ≥F2 (32, 77%), known fentanyl use (74, 63%), other drug use (92, 78%). Of 107 who initiated treatment, 88 completed treatment to date and 82 achieved cure at the SVR12 and/or SVR24 time point. Those lost to follow-up included 2 overdose-related deaths prior to SVR12 time point and 4 disengaged from care. There were no cases of documented virologic failure.

Conclusion: To treat HCV infection among the most vulnerable inner-city populations, specific programs for integration and maintenance in care must be designed and evaluated. We have shown that this can be accomplished even among active fentanyl users who are precariously housed. This may provide the basis for successful interventions among similar populations in different settings.

FRI325

Indigenous methodologies in practice through community engagement and telehealth outreach increase hepatitis C access to care in Alberta, Canada

Kate Dunn¹, Samuel Lee². ¹Indigenous Wellness Core, Calgary, Canada; ²University of Calgary Cumming School of Medicine, Medicine, Calgary, Canada
Email: samlee@ucalgary.ca

Background and aims: Hepatitis C virus (HCV) is a major public health burden in Canada, with prevalence in Indigenous (First Nation, Metis and Inuit) communities 4–6 times higher than non-Indigenous population. Conventional care models have created barriers to curative DAA therapy in remote Indigenous communities. Innovative approaches are required to improve access to HCV services.

Method: The ECHO+ telehealth program in Alberta aims to increase access to HCV treatment through a hub-and-spoke model led by a hepatologist (hub) working with Indigenous communities (spokes) designing a model of care tailored to local needs. We incorporated Indigenous ways of knowing (see figure), including building a predominantly Indigenous team, and embedding the 5 R's of Indigenous Research Methodology (Respect, Relationship, Relevance, Reciprocity, and Responsibility). ECHO+ builds relationships with Indigenous community healthcare teams while using a novel co-design approach to remove barriers while increasing awareness, screening for HCV, and providing telehealth access to specialist care.

Results: Collaborative methods included developing information resources translated into local languages; building infrastructure and supporting community-directed implementation to include other health topics. Due to the COVID-19 pandemic, virtual awareness presentations (HCV awareness topics, community interaction and knowledge sharing, opportunity to follow up with mailed resources packages, and sharing lived experience stories from Indigenous youth and Elders) have been shared with every Indigenous community in Alberta. Practitioners were interviewed to identify barriers to care. Biweekly Zoom meetings with community healthcare teams have expanded during the pandemic to include pandemic topics, and other liver diseases. Collaboration between ECHO+ and Indigenous community leadership and healthcare teams has improved HCV screening, de-stigmatization, increased treatment access, and supported local community healthcare providers to effectively access DAA therapy. Thus, currently 92% of the 53 Indigenous communities in Alberta have engaged with ECHO+, compared to 23% before this approach. This reflects success of the 5R method.



Figure: Five R's as the foundational hub (inner circle) supporting Two-Eyed Seeing framework in community approaches surrounding hepatitis C care as illustrated in wording reflective funding requirement work streams (the outermost arrows) and Western written evidence alongside community directed priorities, oral knowledge and Indigenous perspective of wellness (segments or slices of the circle).

Conclusion: A culturally-sensitive framework combines Indigenous with western approaches to improve access to HCV awareness and care in remote Indigenous communities. This approach has increased community communication and involvement, facilitated engagement with every Indigenous community, and provided practical support throughout the pandemic.

FRI326

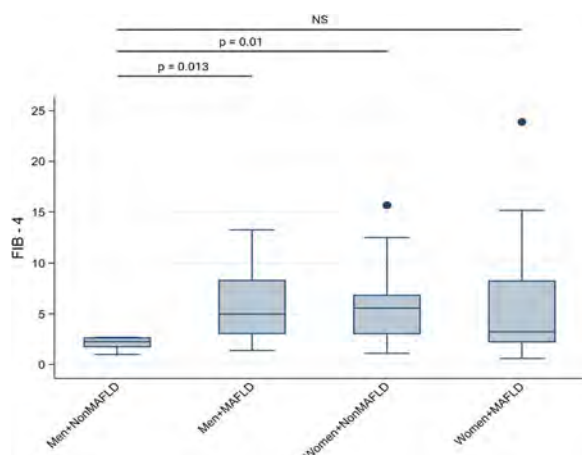
Implication of metabolic associated fatty liver disease and sex differences in the risk of developing liver fibrosis in patients with Hepatitis C

Martín Uriel Vázquez Medina¹, Eira Cerda Reyes², Cruz Vargas-De-León¹, Patty Marlen Ramírez Portillo³, Alejandro Gutierrez Atemis², Juan Armendariz-Borunda². ¹ESM-Escuela Superior de Medicina-IPN, Laboratorio de modelación biomatemática y bioestadística para la salud, Ciudad de México, Mexico; ²Hospital Central Militar Mexico, Ciudad de México, Mexico; ³Benemérita Universidad Autónoma de Puebla, Heroica Puebla de Zaragoza, Mexico
Email: arkiiman@hotmail.com

Background and aims: Hepatitis C (HCV) is a global health problem since it affects about 3% of the world's population. The major complications during the disease are related to the progression of liver fibrosis. Therefore, it is of great importance to study the sociodemographic factors that increase or decrease the risk of developing fibrosis. The aim of this work was to evaluate the involvement of Metabolic associated fatty liver disease (MAFLD) and sex of patients in the risk of developing liver fibrosis during hepatitis C infection.

Method: Cross-section study of Hepatitis C (HCV) newly diagnosed patients, information of age, sex, BMI, comorbidities, and laboratory results were obtained in the first medical consultation with a certified hepatologist, HCV was diagnosed by qualitative RT-PCR test COBAS AMPLICOR and MAFLD was diagnosed according to the international expert consensus statement Eslam (2020). Liver fibrosis was quantified using The Fibrosis-4 (FIB-4) Index. Four groups were formed: 1.- Men+NonMAFLD, 2.- Men+MAFLD, 3.- Women+NonMAFLD and 4. Women+MAFLD. Level of FIB-4 was obtained of each group and global statistical significance (SSi) of the distribution of FIB-4 among groups was evaluated with the Kruskal Wallis test. Post Hoc analysis was performed using the Kruskal Wallis test, alpha was adjusted with the Bonferroni method to obtain the SSi of the FIB-4 distribution within the groups.

Results: A total of 84 patients (26.2% Male) were studied. The median age of the patients were 62 years (IQR 53–71), Distribution in the age and FIB-4 between men and women was not SSi. The prevalence of MAFLD was 73.75%. The difference of MAFLD between sexes was not SSi. The global difference among FIB-4 levels between the four groups was very close to SSi ($p = 0.07$). The Post Hoc analysis (Figure 1) found differences in the levels of FIB-4 between the groups Men+NonMAFLD with Men+MAFLD (2.25 (IQR 1.68–2.67) vs 4.98 (IQR 2.99–8.35), $p = 0.01$) and Men+NonMAFLD with Women+NonMAFLD (2.25 (IQR 1.68–2.67) vs 5.56 (IQR 2.98–6.89), $p = 0.01$). No SSi differences in FIB-4 levels were found between women with and without MAFLD.



Conclusion: In the studied population MAFLD is a risk factor for developing fibrosis in men. Men without MAFLD had lower risk of developing fibrosis than women without MAFLD. Although the literature mentions a lower risk in women of developing fibrosis in hepatitis C, our results could be explained by the age range of our patients in which most of the women were postmenopausal.

FRI327

Micro-eliminating hepatitis C in a network of 47 English Prisons through an industry, prison healthcare and patient organisation partnership

Andrew Jones¹, Nichola Royal², Arran Ludlow-Rhodes², Rob Cheetham², Emily Mongale², Julie Henderson², Katie Abraham², Hayley Cubbage², Samantha Allen², Lee Christensen³, Kate Dorrington¹, Andrew Milner¹, Louise Missen¹, Phil Troke¹. ¹Gilead Sciences Ltd, Medical Affairs, London, United Kingdom; ²Practice Plus Group Health and Rehabilitation, Reading, United Kingdom; ³Hepatitis C Trust, United Kingdom
Email: andy.jones@gilead.com

Background and aims: National Health Service England (NHSE) plans to eliminate Hepatitis C (HCV) in England by 2025, five years earlier than World Health Organisation goals. With a reported HCV prevalence of ~6% in male prisons, and ~12% in female prisons, secure environments are an essential component of this elimination plan. In 2020, NHSE defined HCV micro-elimination as ³95% of prison residents tested within the previous 12 months, ³90% of RNA positive patients treated or initiated on treatment and presence of a robust system to review ongoing testing and treatment performance to ensure these targets are maintained.

Method: To support NHSE in their HCV Elimination Program, a partnership between Gilead Sciences, Practice Plus Group (PPG) and the Hepatitis C Trust (HCT) was formed in 2019. PPG is the provider of healthcare to 47 English prisons with approximately 30, 000 residents. PPG Regional BBV Lead Nurses, and Gilead Medical Scientists worked with prison and HCV stakeholders to optimise test and treat pathways for new prison admissions. Whole prison HCV Intensive Test and Treat events (HITTs) were also run in targeted prisons to ensure testing of residents who were incarcerated before these optimisations were implemented.

Results: Following pathway optimisation across the PPG network of 47 prisons, the HCV screening within 7 days of prison entry increased from 41% in May 2019 to 84% in October 2021. This increase was achieved despite there being significant restrictions to reduce the transmission of COVID-19 being in place across all English prisons. HITTs have been performed in 15 PPG prisons to-date. 1, 909 new RNA+ diagnoses were made during this time with 1, 848 patients started on direct-acting antiviral treatments. By November 2021, 16 out of the 47 prisons have been given micro-elimination status by NHSE with 4 more having submitted data demonstrating achievement of this target and awaiting decision. A further 4 more prisons are on track to achieve micro-elimination by April 2022.

Conclusion: This partnership has demonstrated that, even during a global pandemic, it is possible to achieve the micro-elimination of HCV in a defined setting. Maintenance of micro-elimination status is essential if we are to achieve the WHO HCV targets, requiring robust pathways that are regularly adapted to the changing environment, and systems for tracking performance, both of which have been put in place by this partnership.

FRI328

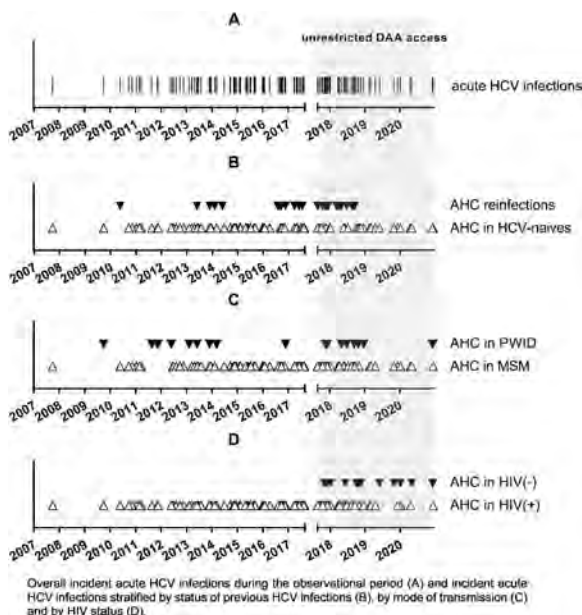
The 'Viennese epidemic' of acute HCV in the era of direct-acting antivirals

David Chromy^{1,2,3}, David Jm Bauer^{1,2}, Benedikt Simbrunner^{1,2}, Mathias Jachs^{1,2}, Lukas Hartl^{1,2}, Philipp Schwabl^{1,2}, Caroline Schwarz^{1,2,4}, Armin Rieger^{2,3}, Katharina Grabmeier-Pfistershammer^{2,5}, Mattias Mandorfer^{1,2}, Michael Trauner¹, Peter Ferenci¹, Michael Gschwantler^{2,4}, Thomas Reiberger^{1,2}. ¹Medical University of Vienna, Division of Gastroenterology and Hepatology, Department of Internal Medicine III, Vienna, Austria; ²Vienna HIV & Liver Study Group; ³Medical University of Vienna, Department of Dermatology, Vienna, Austria; ⁴Wilhelminenspital, Wiener Gesundheitsverbund (WiGeV) der Stadt Wien, Department of Internal Medicine IV, Vienna, Austria; ⁵Medical University of Vienna, Institute of Immunology, Center for Pathophysiology, Infectiology and Immunology, Vienna, Austria
Email: thomas.reiberger@meduniwien.ac.at

Background and aims: An epidemic of acute hepatitis C virus (HCV) infections (AHC)-observed predominantly among men who have sex with men (MSM)-may now decline due to wide availability of direct-acting antivirals (DAAs). This study aimed to investigate changes in the epidemiology of AHC in a Viennese referral center over a 13-year period.

Method: Patients presenting with AHC between 01/2007–12/2020 at the Vienna General Hospital were retrospectively enrolled and followed after virologic clearance/eradication. AHC was defined by the European AIDS treatment network (NEAT) criteria. The introduction of unrestricted DAA-access after 09/17 defined the 'DAA-era', as compared to the 'pre-DAA-era' prior to 09/17.

Results: We identified 134 AHC cases in 119 patients with a mean age of 39 ± 9 years at inclusion. The majority of patients were male (92%), HIV-positive (88%), and MSM (85%). In the DAA-era, a history of prior chronic HCV infection at inclusion was found in 24% (11/46) compared to 7% (5/73) in the pre-DAA-era ($p=0.012$). The annual rate of AHC cases increased in the DAA-era (17.11 per-year) compared to the pre-DAA-era (7.76 per-year). The DAA-era included an AHC-genotype-2 cluster and more HIV-negative AHC cases (0% (0/73) vs. 30% (14/46), $p<0.001$). Patients were followed after spontaneous clearance or sustained virologic treatment response (SVR) for a total of 251.88 patient-years (median 1.39 years per patient). In the DAA-era, we recorded 15 AHC-reinfections-corresponding to an incidence rate of 5.96 (95%CI: 3.57–9.66) re-infections per 100-patient-years.



Conclusion: We observed a high incidence of AHC in Vienna in the DAA-era-primarily among HIV-positive MSM, but increasingly also in HIV-negative MSM. Sufficient screening and prevention strategies combined with fast treatment initiation are needed to confine further spread of HCV.

FRI329

Approaches for a hepatitis C-free city: preliminary results

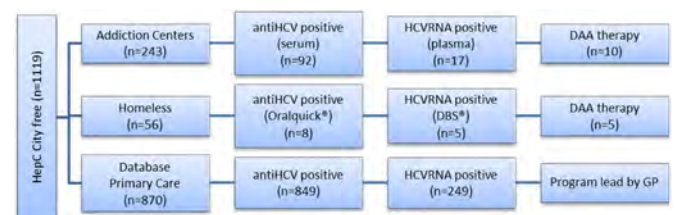
Maria Angelica Luque Gonzalez¹, Yolanda Sánchez^{1,2}, Carmen Lara Romero^{1,2}, Ana Lucena^{1,2}, Javier Ampuero^{1,2,3,4}, Francisco Atienza⁵, Valentin Marquez⁶, Briones Eduardo⁵, Rosa Maria Ufano Lopez⁵, Fernando Martinez⁷, María Carmen Lozano Domínguez⁸, Tinidad Desongles Corrales⁹, Lola Martinez⁷, Rocío Valero¹⁰, Manuel Torralbo¹¹, Diego García¹², Maria Jose Melero¹³, Lutgarda Conde Crespillo⁵, Minerva Blazquez Barba⁵, Miguel Angel Calleja¹⁴, Francisco Javier Garcia-Samaniego Rey^{15,16}, Felipe Fernández-Cuenca¹⁷, Isabel Carmona¹⁸, Susana Padrones⁵, Antonio Sanchez⁷, Manuel Romero Gomez^{1,2,3,4}. ¹University Hospital Virgen del Rocío, Unit of Digestive Diseases, Sevilla, Spain; ²CIBEREHD; ³University of Sevilla; ⁴Ibis-, Biomedicine Institute of Sevilla, Sevilla, Spain; ⁵Primary Health Care Distrito Sevilla; ⁶Médicos del Mundo-Sevilla, Sevilla, Spain; ⁷City Council of Sevilla, Sevilla, Spain; ⁸University Hospital Virgen del Rocío, Microbiology Unit, Sevilla, Spain; ⁹University Hospital Virgen del Rocío, Pharmacy Unit, Sevilla, Spain; ¹⁰Fundación Atenea Grupo Gid, Sevilla, Spain; ¹¹Fundación Triángulo Andalucía, Sevilla, Spain; ¹²Adhara, Sevilla, Spain; ¹³DG Salud Publica; ¹⁴hospital universitario virgen macarena, Pharmacy Unit, Sevilla, Spain; ¹⁵La Paz University Hospital, Madrid, Spain; ¹⁶Coordinador AEHVE; ¹⁷University Hospital Virgen Macarena, Microbiology Unit, Sevilla, Spain; ¹⁸University Hospital Virgen Macarena, Digestive Diseases, Sevilla, Spain
Email: mromerogomez@us.es

Background and aims: We aimed to develop a Hepatitis C elimination program to make Seville a Hepatitis C free city. The main concern was the capability to reach marginal and vulnerable populations. To overcome this drawback, a collaboration between different organizations is needed.

Method: Three groups were addressed: a) patients from primary care health centers database were classified according to anti-HCV status and viral load (HCV RNA); b) patients attended at addiction treatment centers; and c) homeless attended by non-profit organizations like Médicos del Mundo and Fundación Atenea, and social services from City Council in Seville.

Anti-VHC was offered by Oralquick® test in saliva or blood test and, if positive, by dry blood spot (DBS) tests or serum samples to detect HCV RNA. Positive patients got an appointment in clinical hepatology or if not possible, a phone visit can be arranged to allow patient evaluation and remote drug dispensation.

Results: Anti-HCV and HCV RNA tested positive in $n=92/243$ (38%) and 17 (6.9%) [10 treated with AAD] from addiction centers and $n=8/56$ (14%) and 5 (8.9%) [all 5 treated with AAD] in homeless population. In primary care centers $n=849/870$ tested anti-HCV positive and 249 HCV RNA positive. We have identified 271 patients with a positive HCV viral load which may benefit from this Hepatitis C-free city program.



POSTER PRESENTATIONS

Conclusion: Collaborations between health, social and non-profit organizations is key for Hepatitis C elimination. In this sense, enabling HCV detection assays to be performed outside the hospital enhances the chances of identifying positive patients. Moreover, the short-cut for setting up the appointment allows faster access to treatment (presential or remote antiviral dispensation) at hepatology unit. At the same time, the possibility of doing phone visits and remote antiviral dispensation in patients refusing to be attended at the hospital increases treatment success rate. Coordinating these actions together can lead to a Hepatitis C-free city.

Acknowledgement: AEEH and Gilead Science for research grant and SAPD and Abbvie for providing Oralquick® and DBS®.

FRI330

Success of a peer-led community based model of hepatitis C treatment support for marginalised populations

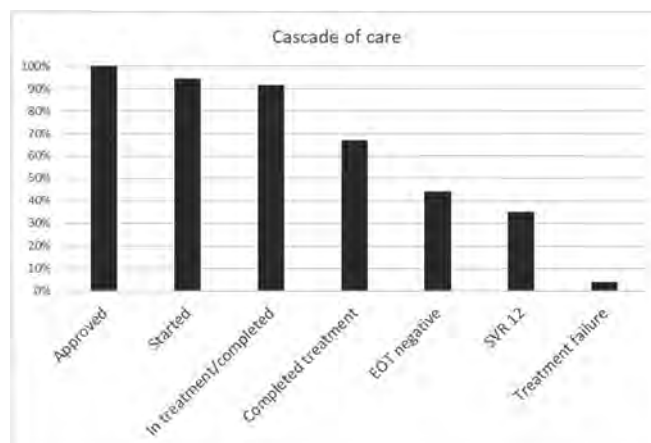
Binta Sultan^{1,2}, John Gibbons¹, Indrajit Ghosh³, Julian Surey^{1,2}, Mark Leonard⁴. ¹University College London Hospital, Find&Treat, United Kingdom; ²University College London; ³Mortimer Market Centre, United Kingdom; ⁴Groundswell, United Kingdom
Email: b.sultan@ucl.ac.uk

Background and aims: Community-based models of HCV care have been developed and shown to be an effective way of supporting marginalised people. Many outreach models of HCV care were scaled down during the pandemic. The Find&Treat team established a peer-led HCV outreach treatment service for vulnerable people in North London during the pandemic, to ensure continued access to care for these patients. We present a description and evaluation of this model of care, which was a multi-component intervention delivered by a highly trained peer.

Method: The model of care was peer-led with clinician support as needed and began in June 2020. Patients with confirmed current HCV infection were referred by drug services, Find&Treat service outreach HCV testing team and local clinics. All patients had a degree of social complexity, which included drug use and or experience of homelessness. The peer and clinician reviewed all patients who were referred. The whole HCV assessment and treatment cascade was managed in the community.

Interventions; Confirmatory bloods and liver fibroscan assessment was undertaken by the peer and a treatment referral was made to the local treatment approval centre. The peer took HCV medication to the patient at their place of residence, provided in monthly or weekly dosset boxes. The peer engaged the patient with appropriate treatment support which included daily text reminders, telephone calls, home visits, video supported care, blood tests for monitoring side effects and treatment response with capillary bloods, and support for hospital appointments. The clinician reviewed patients who had co-morbidities e.g. cirrhosis or other acute health needs and made referrals to secondary care as necessary. The peer supported people with engagement with drug and alcohol services and GP engagement. Routine clinical data was collected in electronic medical records. Data was captured about all interventions and healthcare interactions. This model of care is being evaluated using the integrated HCV candidacy framework developed by Hoj and colleagues (2019).

Results: As of October 2021, 72 patients were referred to the service, all with confirmed HCV infection, 2/72 had HIV co-infection, 2/72 had HBV co-infection, 57 were male, 42/72 had unstable housing, 72/72 had problematic drug or alcohol use. 72/72 had treatment approved, 68/72 have started treatment, 66/72 currently in or completed treatment, 48/72 completed treatment, 25/72 have SVR 12, 1/72 failed treatment.



Conclusion: A peer-led community-based HCV treatment model is effective at supporting people with social complexity to complete treatment. The components of the peer-led intervention addressed multiple domains in the candidacy framework for engagement of vulnerable populations. This model of care is essential to achieving HCV elimination targets and improved health outcomes, especially for vulnerable populations.

FRI331

Impact of hepatitis C virus point-of-care (PoC) viral load assay compared to laboratory-based assays on uptake of testing and treatment, and turnaround times: a systematic review and meta-analysis

Philippa Easterbrook¹, Adam Trickey², Emmanuel Fajardo³, Daniel Alemu³, Adelina Artenie². ¹World Health Organization, Global Hepatitis Programme, Geneva, Switzerland; ²University of Bristol, Bristol, United Kingdom; ³World Health Organization, Geneva, Switzerland
Email: easterbrookp@who.int

Background and aims: The requirement for a confirmatory hepatitis C virus (HCV) viral load (VL) test for diagnosis of chronic HCV infection leads to significant loss to follow-up in the care cascade. Point of care (PoC) HCV VL assays are now being used as an alternate to laboratory-based HCV RNA NAT assays. We undertook a systematic review and meta-analysis to evaluate the impact of using PoC HCV VL compared to laboratory-based standard-of-care approaches on uptake of HCV RNA testing and treatment, and turnaround times (TAT) from HCV antibody (HCVAb) testing to treatment initiation.

Method: We searched PubMed, Embase, and Web of Science on 23/09/2020 for studies in English that used HCV PoC RNA assays and had data on key outcomes. We also searched relevant conference abstracts from 2016 to 2020 not picked up by the main search. We categorised study arms according to whether the PoC HCV VL assay was based on-site at the clinic (Model 1), in a mobile unit (Model 2), or in a laboratory (Model 3) versus a HCV lab-based high-throughput viral load assay (Model 4). For each model, studies were further stratified by whether testing and treatment were delivered at the same or different sites, and on the same day. For TATs we calculated the weighted median of medians. We analysed RNA testing and treatment uptake using random effects meta-analysis. Risk of bias was assessed using a tool adapted from Hoy et al and the ROBINS-I tool.

Results: We included 45 studies with 64 within-study arms: 28 studies among people who inject drugs (PWID)/homeless, 4 among prisoners, 9 among general populations, and 4 among persons with HIV. All were observational studies. The pooled median TAT between HCVAb test and treatment was shorter with PoC RNA assays on site (18.5 days [95% CI: 14–53]) than with use of either lab-based PoC RNA assays (64 [64–64]), or lab-based high-throughput RNA assays (67 [50–67]). Treatment uptake was higher with onsite PoC RNA assays

77% (95% CI: 72%–83%), and PoC assays in a mobile unit 81% (60%–97%) compared to lab-based high-throughput assays 53% (31%–75%), p value = 0.03 (models 1/2 vs 4). The effects were greatest among PWID. 4 studies had direct within-study comparisons between a PoC assay arm and a lab-based assay arm. The pooled relative risk for testing uptake was 1.11 (95% CI: 0.89–1.38) and 1.32 (1.06–1.64) for treatment uptake. Risk of bias was high for 36% of studies and moderate for 40%.

Conclusion: Access to PoC HCV VL was associated with reduced time to treatment initiation and increased treatment uptake, especially among PWID. It is now recommended by WHO guidelines as an additional strategy to promote access to VL testing, especially in marginalised populations with high rates of loss to follow-up.

FRI332

Diagnostic accuracy of point-of-care HCV viral load assays for HCV diagnosis: a systematic review and meta-analysis

Weiming Tang¹, Yusha Tao¹, Emmanuel Fajardo², Elena Ivanova², Roger Chou³, Jo Tucker¹, Philippa Easterbrook². ¹UNC Project-China; ²WHO; ³Oregon Health & Science University
Email: chour@ohsu.edu

Background and aims: Despite the widespread availability of short-course curative HCV treatment, a significant proportion of HCV patients remain undiagnosed and untreated. The requirement for a confirmatory HCV viral load (HCV VL) test can result in substantial care cascade attrition. New point-of-care HCV RNA assays may enhance access to testing by decentralizing HCV RNA testing outside of laboratory settings. We undertook a systematic review and meta-analysis to compare the diagnostic performance of PoC HCV viral load assays to laboratory-based nucleic acid testing.

Method: We searched three databases, used Cochrane methods, and registered the protocol. Studies were eligible if they utilized a laboratory reference standard to evaluate POC HCV RNA assays and if they reported or had raw data that could be extracted to calculate sensitivity, specificity, the limit of detection, and bias. Data were extracted by geographic region, collection year, risk group, and specimen type. Random effects bivariate models were used to summarize estimates and describe the variability in test performance across studies. We used the GRADE approach to assess the certainty of the evidence.

Results: A total of 25 studies including data from 8,791 people were summarized. XX studies in high-income countries and XX in low and middle-income countries. Assays included the Xpert HCV Viral Load assay (Cepheid, USA) Xpert HCV VL Fingerprick (Cepheid, USA) Genedrive HCV ID Kit, Truenat HCV assay, and SAMBA II. Across all assays, the pooled sensitivity and specificity were 99% (95% CI: 98–99%) and 99% (95% CI: 99–100%), respectively, compared to a lab-based reference standard. High sensitivity and specificity were also observed across different study settings (including LMICs and HICs) and populations, using different assays. The evidence was moderate-high certainty. Specificity showed no difference among different specimen types.

Conclusion: POC HCV viral load assays have excellent sensitivity and specificity compared to gold standard laboratory-based nucleic acid testing methods across diverse settings and populations. WHO now recommends the use of POC HCV viral load assays as an additional strategy to promote access to treatment. The adoption of POC viral load assays will be facilitated through increasing availability of integrated molecular multiplex technologies that utilize the same technology for several assays and/or across diseases.

Disclosure: No significant relationships.

FRI333

Hepatitis-C virus viral load reflex testing following an initial positive HCV antibody test: a global systematic review and meta-analysis

Yusha Tao¹, Weiming Tang¹, Mengyuan Cheng¹, Jennifer Bissram², Emmanuel Fajardo³, Lindsey Hiebert⁴, John Ward⁴, Roger Chou⁵, Philippa Easterbrook³, Jo Tucker¹. ¹UNC Project-China; ²UNC Chapel Hill; ³WHO; ⁴Task force/USCDC; ⁵Oregon Health & Science University
Email: weiming_tang@med.unc.edu

Background and aims: A significant proportion of persons who are HCV antibody positive do not in HCV viral load testing following a positive antibody test slow linkage to essential HCV services. HCV programmes have introduced reflex viral load testing (either lab-based reflex testing or clinic based reflex sample collection) as a strategy to reduce the steps in the HCV diagnostic pathway and improve linkage to care. A systematic review evaluated the effectiveness of reflex viral load testing in increasing uptake of HCV viral load testing and treatment, and in reducing turn-around time from HCV Ab screening to viral load testing, linkage to care, and treatment, compared to a standard multi-step viral load testing strategy.

Method: We searched three databases (Medline, EMBASE, and Google Scholar) for studies in English to used either reflex lab-based viral load testing or clinic-based reflex sample collection and had data on the key outcomes. Laboratory-based HCV reflex testing refers to a testing algorithm in which patients have only a single clinical encounter and only one blood draw or specimen taken and sent to the lab. If the sample for anti-HCV testing in the lab is positive, then the same existing or duplicate sample is used for a “reflex” lab-based HCV viral load test. No further visit or sample collection is required. Clinic-based reflex testing refers to a testing algorithm where there is only a single clinical encounter/visit for an initial rapid diagnostic HCV antibody test, but with two blood draws. A fingerstick sample is taken and tested using a rapid diagnostic HCV antibody test, which if positive is then immediately followed by a “reflex” blood draw (either venous blood sample or fingerstick) for HCV viral load confirmation of current infection. Data were extracted by geographic region, collection year, and risk group. Summary estimates (95% confidence intervals [CI]) were calculated using random-effects meta-analyses.

Results: 51 studies met the inclusion criteria reporting laboratory-based reflex testing ($n = 32$) and clinic-based reflex sample collection ($n = 19$). Forty-two were in high-income and nine were in low or middle-income countries. All studies were cross-sectional or cohort studies. Compared to laboratory non-reflex testing, laboratory reflex testing increased the likelihood of viral load testing among patients screened as HCV antibody positive (RR: 1.35 (1.16–1.58)), and may improve linkage to care among patients diagnosed with HCV infection with RNA testing (RR: 1.47 (0.81–2.67)).

Conclusion: HCV viral load reflex testing increased uptake and reduced time to HCV viral load testing and may enhance linkage to care. In addition, laboratory and clinic reflex testing were feasible in a diverse range of LMIC settings. WHO now recommends the adoption of reflex viral load testing as an additional strategy to promote linkage to care.

Disclosure: No significant relationships.

POSTER PRESENTATIONS

FRI334

Finding cases of hepatitis C for treatment using automated screening in the emergency department is effective, but what is the cost?

David Prince^{1,2}, Julia Di Girolamo^{1,3}, Joseph Pipicella^{1,3}, Melissa Fraser¹, Tahrima Kayes¹, Frank Alvaro^{4,5}, Michael Maley^{2,4,5}, Hong Foo^{4,5,6}, Paul Middleton^{2,3,7,8}, Miriam Levy^{1,2,3}. ¹Liverpool Hospital, Gastroenterology and Liver, Liverpool, Australia; ²UNSW Sydney, Medicine, Sydney, Australia; ³Ingham Institute, Liverpool, Australia; ⁴Liverpool Hospital, Pathology, Liverpool, Australia; ⁵NSW Health Pathology, Liverpool, Australia; ⁶Western Sydney University, Medicine, Parramatta, Australia; ⁷Liverpool Hospital, Emergency Department, Liverpool, Australia; ⁸The University of Sydney, Medicine, Camperdown, Australia
Email: david.s.prince@gmail.com

Background and aims: Case detection remains a major challenge for hepatitis C virus (HCV) elimination. We have previously published results from a pilot of an emergency department (ED) semi-automated screening program, SEARCH; Screening Emergency Admissions at Risk of Chronic HCV. In this pilot, 5000 consecutive patients were screened including 4778 overseas born (targeted) from 14, 093 ED presentations. HCVAb was positive in 181 patients (3.6%); 51 (1.0%) were HCV RNA positive. This cost analysis aimed to accurately describe the overall costs of this pilot service. It also aimed to report on costs per patient tested, per HCV Ab positive patient detected and per RNA positive patient treated. We modelled the effect of proposed service refinements (SEARCH 2.0).

Method: All direct costs of HCV testing until direct acting anti-viral (DAA) therapy initiation were calculated. Cost was assessed in 2018 Australian Dollars. A cost analysis of the initial program and refinements are presented. Sensitivity analysis to understand impact of variation in staff time, laboratory test cost, changes in HCV antibody (Ab) prevalence, RNA positivity percentage and rate of linkage to care was conducted. Impact of refinements (SEARCH 2) to cost is presented.

Results: The total SEARCH pilot, testing 5000 patients was estimated to cost \$110, 549.52 (range \$92, 109.79–\$129, 581.24) comprising of \$68, 278.67 for HCV Ab testing, \$21, 568.99 for follow up and linkage to care of positive patients and \$20, 701.86 to prepare HCV RNA positive patients for treatment. Refinements resulted in a 32% cost reduction overall and reduced the cost of HCV antibody screening from \$13.66 to \$8.46 per test and the total cost per positive HCV Ab, positive HCV RNA and treated patient to \$611.77, \$2, 168.64 and \$3, 566.11 respectively. Our sensitivity analysis indicates costs are modest so long as HCV Ab prevalence was 1% or greater.

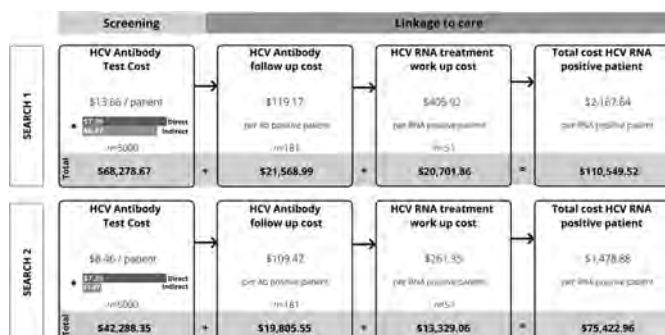


Figure: Costs of HCV screening in SEARCH 1 compared to costs modelled with SEARCH 2 program refinements

Conclusion: ED screening is an affordable strategy for HCV case detection and elimination.

FRI335

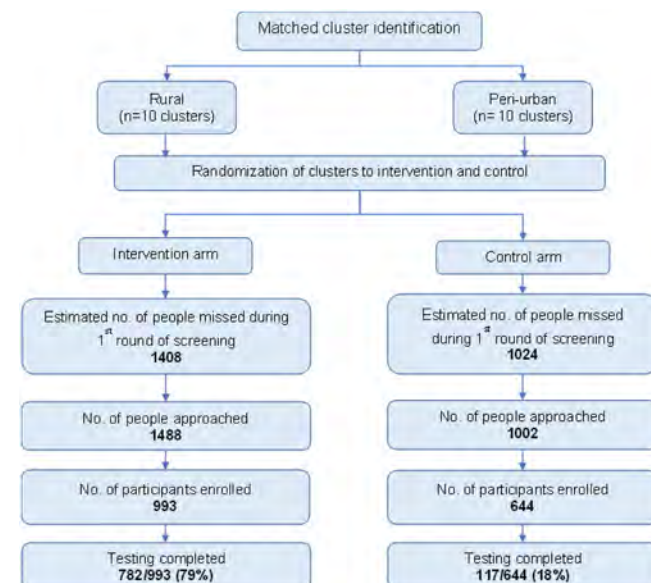
A cluster randomized controlled study of secondary distribution of HCV self-test to support micro-elimination in Karachi, Pakistan.

Aliya Hasnain¹, Sonjelle Shilton², Wasiuddin Shah¹, Jessica Markby², Niklas Luhmann³, Muhammad Jamil³, Elena Ivanova², Saeed Sadiq Hamid⁴. ¹Aga Khan University, Karachi, Pakistan; ²FIND, Geneva, Switzerland; ³WHO, Switzerland; ⁴Aga Khan University, Medicine, Karachi, Pakistan
Email: saeed.hamid@aku.edu

Background and aims: Pakistan has a nationwide HCV prevalence of 6% with majority of cases undiagnosed due to lack of comprehensive screening programmes. Self-testing has shown to acceptable and increases testing uptake for HIV due to its convenience and privacy advantages. This study aims to evaluate the acceptability and effect of a program enabling home delivery of HCV self-testing using the oral-based OraQuick® HCV rapid antibody test. HCV self-testing study is nested within a community-based micro elimination project in an HCV endemic district of Karachi, Pakistan.

Method: This ongoing cluster randomized control study targets persons missed during house-to-house screening done as part of a micro-elimination study in two Union Councils in district Malir of Karachi. During house visits, individuals not found at home are eligible for participation. Target sample size is 1000 participants each in intervention and control group. In the intervention group, an HCV self-test is left with instructions for use explained to a senior household member. In the control group, a pamphlet is left with directions to visit the nearest clinic for HCV screening. Both groups are followed up within 4 weeks to inquire if testing was completed and a brief acceptability survey is conducted with the tester. Results report are incentivized and individuals with positive tests are linked for further management.

Results: 1637 participants were recruited between 29th Nov 2021 and 22nd March 2022, with 993 in the intervention group and 644 in the control group, from rural and peri-urban clusters of the district. Median (IQR) age across both groups is 30 (24–42) years with 82% (1337/1637) male participants. Half (51%) of the participants who completed self-testing had received no formal education. The proportion of participants who reported completing the HCV antibody test was 79% (782/993) in the intervention group compared to 18% (117/644) in the control group ($p < 0.05$). Nearly all (95%) participants who reported completing the test demonstrated willingness to perform HCV self-test in the future.



Conclusion: Preliminary results of this study demonstrate that HCV self-testing increases HCV screening rates in a peri-urban/rural setting consistent of a mostly illiterate population in a low-middle income country like Pakistan.

FRI336

HCV-viral load fingerstick assay to simplify screening and linkage to care of people who use drugs attending Italian addiction treatment centres

Sarah Vecchio¹, Lorenzo Somaini², Luigi Bartoletti³, Daniela Mussi³, Roberta Gaudenzi⁴, Eugenia Vernole⁵, Claudio Leonardi⁶. ¹ASL Biella, Addiction Treatment Center, Biella, Italy; ²ASL Biella, Addiction Treatment Center, Biella, Italy; ³ASL Alessandria, Addiction Treatment Center, Alessandria, Italy; ⁴ASL Umbria 1, Addiction Treatment Center, Perugia, Italy; ⁵ASL Bari, Addiction Treatment Center, Bari, Italy; ⁶ASL Roma 2, Addiction Treatment Center, Roma, Italy
Email: lorenzo.somaini@aslbi.piemonte.it

Background and aims: People who use drugs (PWUDs) are the major drivers of HCV transmission in the world, representing the target population for HCV screening and treatment. In Italy, the estimate prevalence of HCV infection in drug users exceeds the 80%, with 205.000 PWUDs not yet treated. Simplified strategies are required for the screening and diagnosis of hepatitis C infection among PWUDs, and HCV-RNA viral load fingerstick assay can help in overcoming existing challenges and barriers to HCV diagnosis and care. The aims of this prospective study were to evaluate the feasibility and the acceptability of HCV-RNA viral load fingerstick assay use to improve HCV screening and treatment among Italian PWUDs attending different Italian Addiction Treatment Centres (Ser.D) in an outpatient setting.

Method: Between October 2020 and December 2021, the HCV screening was offered to 1258 consecutive PWUDs from 5 Addiction Treatment Centres of 4 Regions of Northern, Central and Southern Italy. HCV analysis was carried out by means of a fingerstick capillary whole blood RNA test. Results were given in 60 minutes.

Results: 1221/1258 (97%) consecutive PWUDs were enrolled. Patients were mostly male (973/1221, 80%), with a mean age of 42.9 years \pm 10.7 and a mean addiction treatment duration of 10.1 years \pm 8.5. The main HCV risk factors identified were heroin addiction (935/1221, 76%), a history of injecting drug use (700/1221, 57%) and tattooing (794/1221, 65%). HCV RNA was identified in 240/1221 patients (20%) participants. The most common HCV genotypes, among available data, were 3 (40/240, 17%) and 1a (38/240, 16%). Among patients with detectable HCV RNA, 89% (214/240) were referred to specialists for HCV treatment and, at the time of writing, 53% (127/240) completed the treatment. All the treated patients achieved SVR (Sustained Virologic Response).

Conclusion: This is one of the largest HCV-RNA screening projects, highlighting the feasibility and the acceptability of onsite testing performed with HCV-RNA viral load fingerstick assay in PWUDs attending Ser.Ds. At present, HCV screening and linkage to care remain worldwide far from comprehensive. The described easy to use approach favours PWUDs engagement and increases HCV treatment and elimination, as evidenced by the high rate of completed treatments.

FRI337

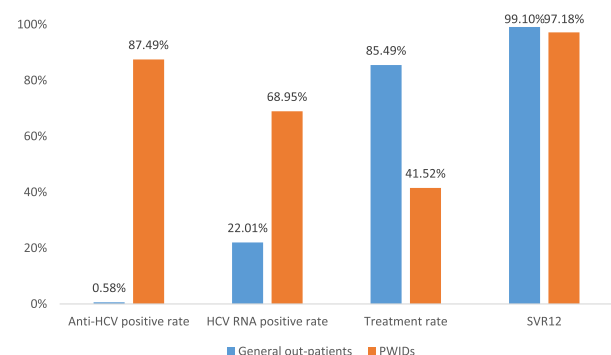
From extensive to intensive screening, co-operations model of hepatitis C elimination in out-patients and people who inject drug population in southwest of China

Qing Lin¹, Youzhi He², Long Chen³, Jingchun He⁴, Xiaojian Yuan⁵, Zhenglin Wang¹, Guohui Wu⁶. ¹The People's Hospital of Jiulongpo District, Chongqing, China; ²Methadone Maintenance Therapy Clinic of Jiulongpo District, Chongqing, China; ³Chongqing Public Health Medical Center, Chongqing, China; ⁴Jiulongpo District Center for Disease Control and Prevention, Chongqing, China; ⁵Xiejiawan Street Community Health Service Center, Jiulongpo District, Chongqing, China; ⁶Chongqing Center for Disease Control and Prevention, Chongqing, China
Email: xiah302@126.com

Background and aims: The Southwest China has a relatively higher HCV prevalence rate among the whole country for large proportion of people who inject drugs (PWID) reside here. We established a co-operation model combined with intensive and extensive HCV screening, and this study aimed to determine its efficacy on the HCV elimination in PWIDs and general out-patients (GOP).

Method: The co-operation network consists of local Centers for Disease Control and Prevention (CDC) and the medical association including 39 community health centers, 15 district hospitals and 1 methadone clinic. The CDC was responsible for educational training, funding and patient-network management. The medical association was responsible for HCV antibody screening and linkage to care with the cascade referral system. Patients with positive HCV antibody were referred to the designated hospital for HCV RNA testing, in which positive patients will receive anti-HCV treatment of sofosbuvir/velpatasvir (SOF/VEL) for 12 weeks with or without RBV. The call-back system in methadone clinic requested the HCV RNA-positive PWID patients to return for further therapy. The patient-education and management were carried out in the district hospitals monthly. Reimbursement and free RNA testing were provided to enhance treatment affordability. The effect and safety of SOF/VEL were evaluated.

Results: From March 2021 to March 2022, 102873 residents and 1,199 PWIDs were screened. The seropositive rate of anti-HCV and HCV RNA were 0.58% (595/101674), 22.01% (131/595) in GOPs and 87.49% (1049/1199, 87.49% (171/248)) in PWIDs, respectively. 85.49% (112/131) GOPs patients and 41.52% (71/171) PWIDs initiated anti-HCV treatment, while only 8% before the model establishment. The genotype distribution is as follows: GT3a 22.13% (29/131), GT3b 20.61% (27/131), GT1b 18.32% (24/131) in GOPs, while GT3a 47.37% (81/171), GT3b 42.69% (73/171) and GT1b 9.94% (17/171) in PWIDs. The percentage of liver fibrosis, cirrhosis and hepatocellular carcinoma was 9.1% (12/131), 9.1% (12/131) and 0.7% (1/131) in GOPs, while 26.31% (45/171), 13.45% (23/171) and 1.75% (3/171) in PWIDs. The co-infection rate of HBV or HIV was 3.8% (5/131) or 1.5% (2/131) in GOPs and 7.6% (13/171) or 14.03% (24/171) in PWIDs. Both groups achieved high SVR12 as 99.10% (111/112) in GOPs and 97.18% (69/71) in PWIDs. None of patients discontinued anti-HCV treatment due to adverse events.



POSTER PRESENTATIONS

Conclusion: The co-operation model was effective in HCV elimination in both groups. The HCV prevalence of PWIDs was significantly higher than GOPs in the district scale. Although PWIDs had lower treatment adherence, the treatment rate in PWIDs were improved significantly by intensive follow-up. Both groups achieved high SVR with good safety profile by SOF/VEL treatment. The co-operations model with intensive and extensive screening was an optimal option for GOP and PWID to eliminate HCV.

FRI338

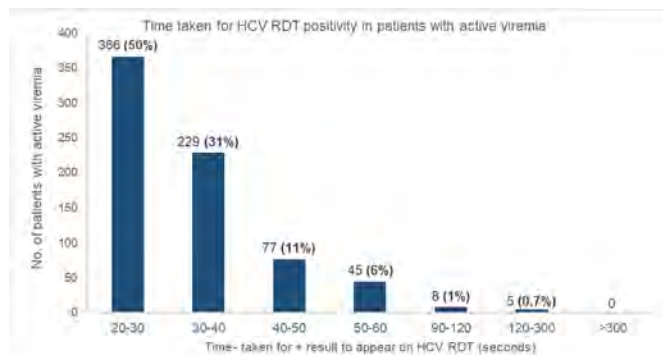
Using time to positivity of hepatitis rapid detection test results to determine active viremia

Saeed Sadiq Hamid¹, Sultan Salahuddin², Wasiuddin Shah², Aliya Hasnain², Muraduddin Gulab², Taj Muhammad², Sabiha Khan².
¹Aga Khan University, Karachi, Pakistan; ²Aga Khan University, Medicine, Karachi, Pakistan
Email: saeed.hamid@aku.edu

Background and aims: The recommended time taken to run the Rapid Diagnostic tests (RDTs) for HCV screening is 20 mins, which is followed by reflex PCR testing for confirmation of chronic HCV infection. Confirmatory viral load testing is a barrier in the HCV cascade of care as it is a cost and time-intensive step. This study hypothesises the correlation between shorter read time and active viremia in HCV infected patients, which can reduce the need for reflex RNA tests and help implement rapid-test-and-treat models for HCV.

Method: The findings from this study were obtained from a community-based micro-elimination study which targets a high burden HCV endemic area in Karachi, Pakistan. Door-to-door visits were performed to conduct rapid screening of individuals with unknown HCV status, using the finger-stick Abbott SD Bioline HCV diagnostic kits. The time taken for the RDT to display a positive result was measured using a stopwatch to record the duration from the point the blood sample was placed in the test kit till the point the test line appeared. Blood samples of individuals with a positive screening test were collected for Hepatitis C core antigen testing, on Abbott Architect i1000SR, to determine viremia.

Results: A total of 1327 participants, median age (IQR) 47 years (39–56), with 70% females, who screened positive on HCV RDT and had HCV core antigen testing done, were included. Overall, 730/1327 (55%) patients were viremic and in all cases, the HCV RDT test was positive within 5 minutes. 50% (366/730) of all viremic cases had a positive screening result within 20–30 seconds. No. of cases with active viremia decreased as the time taken for a positive result to appear on rapid screening increased ($r = -0.63$). Less than 1% of cases with active viremia were found amongst those who had a positive screening result from 120 seconds to 300 seconds.



Conclusion: The time to read SD Bioline HCV RDT can be reduced to 5 mins to identify patients with HCV infection. In patients displaying a positive result between 20 and 30 seconds HCV treatment using DAAs

can be initiated using rapid test-and-treat models reducing loss to follow up and need for HCV RNA testing in resource limited settings.

FRI339

Liver-related mortality among people with hepatitis B and C: a validation study using linked healthcare administrative datasets

Syed Hassan Bin Usman Shah¹, Maryam Alavi², Behzad Hajarizadeh², Gail Matthews², Marianne Martinello², Mark Danta³, Janaki Amin⁴, Matthew Law⁵, Jacob George⁶, Hamish Innes⁷, Gregory Dore².
¹The Kirby Institute, Viral Hepatitis Clinical Research Program, Kensington, Australia; ²The Kirby Institute, Viral Hepatitis Clinical Research Program, UNSW, Kensington, Australia; ³St Vincent's Hospital Sydney, Darlinghurst, Australia; ⁴Macquarie University, Macquarie Park, Australia; ⁵The Kirby Institute, Kensington, Australia; ⁶Westmead Hospital, Westmead, Australia; ⁷Glasgow Caledonian University, United Kingdom
Email: hbinusman@kirby.unsw.edu.au

Background and aims: Routinely collected and linked healthcare administrative datasets could be used to monitor mortality among people with hepatitis B and C virus (HBV and HCV). This study aimed to validate a definition for liver-related mortality among people with an HBV or HCV notification, including any death (i.e. all-cause) following hospitalization for end-stage liver disease (ESLD), which included a first-time hospital admission due to decompensated cirrhosis (DC) or hepatocellular carcinoma (HCC).

Method: In New South Wales, Australia, HBV and HCV notifications (1993–2017) were linked to hospital admissions (2001–2018), all-cause mortality (1993–2018), and cause-specific mortality (1993–2016) databases. Hospitalization-defined ESLD-related mortality was validated in comparison with two death certificate-based definitions of liver deaths coded among primary and secondary cause-specific mortality data, including ESLD-related (deaths due to DC and HCC) and all-liver deaths (ESLD-related and other liver-related causes).

Results: Of 63, 292 and 107, 430 individuals with an HBV and HCV notification, there were 4, 478 (2.6%) post-ESLD hospitalization deaths, 5, 572 (3.3%) death certificate liver disease deaths, and 2, 910 (1.7%) death certificate ESLD deaths. Between 2001 and 2016, 63% (562/891) of HBV post-ESLD hospitalization deaths had death certificate ESLD deaths recorded, including 58% (390/676) of DC and 85% (431/510) of HCC deaths. Further, 83% (741/891) of HBV post-ESLD hospitalization deaths had death certificate liver disease deaths, including 81% (546/676) of DC and 95% (482/510) of HCC deaths. Similarly, 58% (2, 082/3, 587) of HCV post-ESLD hospitalization deaths had death certificate ESLD deaths recorded, including, 56% (1, 817/3, 236) of DC and 82% (1, 007/1, 224) of HCC deaths. Further, 87% (3, 135/3, 587) of HCV post-ESLD hospitalization deaths had death certificate liver disease deaths, including 87% (2, 812/3, 236) of DC and 96% (1, 171/1, 224) of HCC deaths.

Conclusion: Our findings support the use of healthcare administrative datasets as an efficient method and a reliable information source to represent liver-related mortality rates accurately; however, concordance between post-hospitalization and death certificate-based cause of death is clearly higher for HCC than DC.

FRI340

Identifying risk factors associated with hepatitis C virus infection in participants in the national health and nutrition examination survey using Super Learner

Laura Telep^{1,2}, Rachael Phillips³, Anand Chokkalingam^{1,2}.
¹Gilead Sciences, Inc., Foster City, United States; ²University of California, Berkeley, Epidemiology, Berkeley, United States; ³University of California, Berkeley, Biostatistics, Berkeley, United States
Email: laura.telep@gilead.com

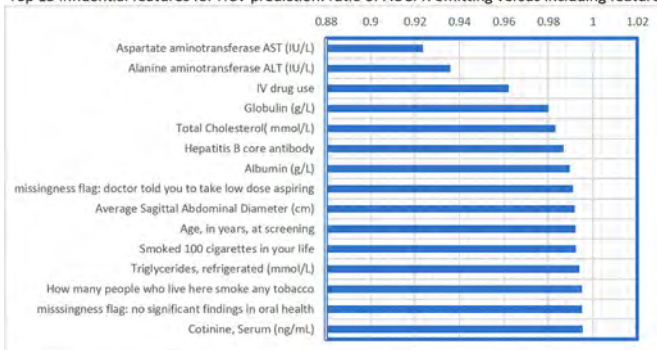
Background and aims: Under-diagnosis is a key impediment to eliminating hepatitis C virus (HCV) infection in the United States (US).

Machine learning methods offer an opportunity to support expanded HCV screening in a resource-optimized way by identifying the characteristics that are most influential in predicting HCV.

Method: The ensemble machine-learning method Super Learner (SL) was used with National Health and Nutrition Examination Survey (NHANES) data collected from 2013 to 2018 to build an HCV infection risk prediction algorithm. Because only 1% of survey participants tested positive for HCV RNA, case-control sampling was used to address class imbalance, with five HCV-uninfected individuals randomly selected for each HCV-infected individual ($n = 1,008$). The SL was fit to the case-control data, its performance was evaluated with the area under the precision-recall curve (AUC-PR), and then it was used to predict HCV infection in the full NHANES dataset ($n = 15,237$). We also identified the features that had the greatest impact on AUC-PR, and thus were most predictive of HCV infection.

Results: The SL's AUC-PR on the full NHANES dataset was 52%, a 47-fold improvement over baseline. At the probability threshold that optimized the F1 score, the SL achieved 55.4% precision and 61.3% recall; that is, if the goal was to identify at least 60% of those infected with HCV, then for every 100 individuals classified as HCV-infected, more than 50% would be true positives. Features that were most predictive of HCV infection included alanine aminotransferase (ALT), aspartate aminotransferase (AST), injection drug use, age, albumin, globulin, and HBV infection status. Additional influential predictors included smoking-related features, risk factors for heart disease or stroke (triglycerides, total cholesterol, recommendations by a doctor to take low dose aspirin), and features related to oral health.

Top 15 influential features for HCV prediction: ratio of AUCPR omitting versus including feature



* Note: a smaller fractional value is associated with greater influence on the AUC-PR

Conclusion: As outreach continues to identify the undiagnosed HCV-infected population in the US, knowledge of the characteristics most predictive of HCV infection should be utilized to guide screening and prevention efforts. Next steps include identifying HCV infection predictors from widely available data such as features collected in a single routine medical care visit and exploring variation in highly predictive features by age category. Algorithms such as the one demonstrated here can be useful tools to support these activities.

Viral Hepatitis C: Post SVR and long term follow up

FRI343

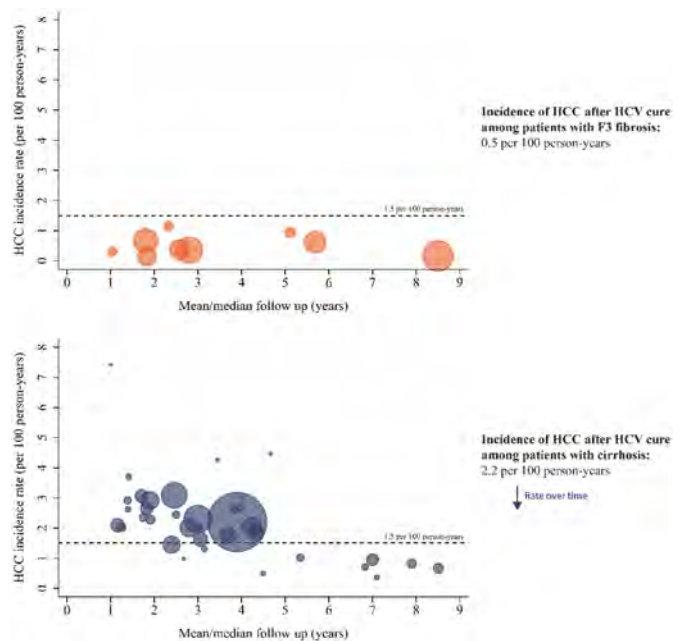
Hepatocellular carcinoma incidence after hepatitis C cure among patients with advanced fibrosis or cirrhosis: a meta-analysis

Ian Lockart^{1,2}, Malcolm Guan Hin Yeo², Behzad Hajarizadeh³, Gregory Dore^{1,3}, Mark Danta^{1,2}. ¹St Vincent's Hospital, Sydney, Australia; ²St Vincent's Clinical School, UNSW Sydney, Australia; ³The Kirby Institute, UNSW Sydney, Australia
Email: m.danta@unsw.edu.au

Background and aims: Hepatitis C virus (HCV) cure reduces but does not eliminate the risk of hepatocellular carcinoma (HCC). HCC surveillance is recommended in populations where the incidence exceeds 1.5% per year. In cirrhosis, HCC surveillance should continue after HCV cure, although it is uncertain if this should be indefinite. For patients with advanced fibrosis (F3), guidelines are inconsistent in their recommendations. This systematic review evaluated the incidence of HCC after HCV cure among patients with F3 fibrosis or cirrhosis.

Method: We searched bibliographic databases and conference abstracts for studies assessing the incidence of HCC after HCV cure among patients with F3 fibrosis or cirrhosis. Meta-analyses were used to cumulate HCC rates and meta-regression was used to explore heterogeneity across studies.

Results: Forty-four studies were included (36,183 patients; 109,385 person-years of follow up). The incidence of HCC was 2.2 per 100 person-years (95% CI 1.9–2.4) among patients with cirrhosis, and 0.5 per 100 person-years (95% CI 0.3–0.7) among patients with F3 fibrosis. In meta-regression analysis among patients with cirrhosis, older age (adjusted rate ratio [aRR] per 10-year increase in mean/median age: 1.34; 95% CI 1.04–1.74) and prior decompensation (aRR per 10% increase in the proportion of patients with prior decompensation: 1.05; 95% CI 1.00–1.11) were associated with an increased incidence of HCC. Longer follow-up after HCV cure was associated with a decreased incidence of HCC (aRR per year increase in mean/median follow-up: 0.87; 95% CI 0.80–0.96).



POSTER PRESENTATIONS

Conclusion: Among patients with cirrhosis, the incidence of HCC decreases over time after HCV cure and is lowest in patients with younger age and compensated cirrhosis. The substantially lower incidence in F3 fibrosis is below the recommended threshold for cost-effective screening.

FRI344

Glycomics-based serum marker as reliable tool for assessment of viral response after treatment with direct-acting antiviral drugs in hepatitis C virus infection

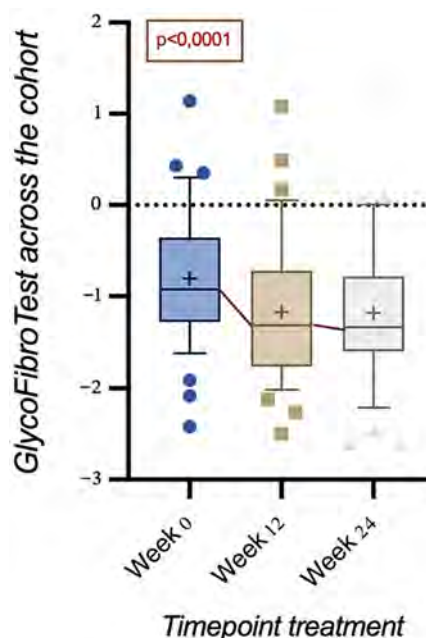
Nicky Somers¹, Elisabeth Vandekerckhove¹, Anja Geerts¹, Helena Degroote¹, Sander Lefere^{1,2}, Lindsey Devisscher², Leander Meuris^{3,4}, Nico Callewaert^{3,4}, Hans Van Vlierberghe¹, Xavier Verhelst¹. ¹Ghent University, Ghent University Hospital, Hepatology Research Unit, Department Internal Medicine and Paediatrics, Liver Research Center Ghent, Ghent University, Ghent University Hospital, Ghent, Belgium, Belgium; ²Ghent University, Gut-Liver Immunopharmacology Unit, Department of Basic and Applied Medical Sciences, Liver Research Center Ghent, Ghent University, Ghent, Belgium, Belgium; ³Vlaams Instituut voor Biotechnologie, Center for Medical Biotechnology, VIB, Ghent, Belgium, Belgium; ⁴Ghent University, Department of Biochemistry and Microbiology, Ghent University, Ghent, Belgium

Email: nicky.somers@ugent.be

Background and aims: Patients with chronic hepatitis C virus (HCV) infection have a genuine risk of developing liver fibrosis and cirrhosis, potentially resulting in hepatocellular carcinoma (HCC), a risk that remains even after sustained viral response (SVR). It is of utmost importance to closely monitor these patients during and after antiviral treatment, which today consists of direct-acting antiviral drugs (DAAs). Glycomics-based biomarkers are an attractive tool to answer this medical need, as alterations in the abundance of N-glycans reflect an altered state of the liver. Progression of liver fibrosis has been linked to changes in serum glycosylation patterns before. Accordingly, our previously developed GlycoFibroTest measures the ratio of NGA2FB to NA3. The aim of this study was to assess the GlycoFibroTest for the evaluation of fibrosis regression during and after treatment of HCV with DAAs.

Method: N-glycosylation patterns were analyzed in sera from 36 HCV-infected patients, collected between January 2015 and June 2016. Patients showed liver biopsy-proven advanced fibrosis (F3, n = 12) or established cirrhosis (F4, n = 24) before therapy initiation, which consisted of a twelve-week oral administration of DAAs. The GlycoFibroTest was measured on serum samples at three timepoints: at the start (week 0), the end (week 12) and during follow up (week 24), by the use of an optimized glycomic technology on a DNA sequencer (DSA-FACE, Applied Biosystems).

Results: All patients achieved SVR after treatment and none of them developed HCC. Figure 1 demonstrates the significant decrease of the GlycoFibroTest ($p < 0.0001$) in all patients (F3 + F4)[12]. More specifically, this decrease was seen from week 0 to weeks 12 and 24, but no significant decline could be retained between weeks 12 and 24. Statistical analysis was performed using IBM SPSS Statistics version 28.0. Since measurements were repeated on the same subject and values were not normally distributed, the non-parametric Friedman's test was used. Statistical significance was set at the alpha level of 0.05.



Conclusion: In this study, we illustrated that changes in serum protein glycosylation that are observed with increasing levels of fibrosis decline after the decrease of viral load during treatment with DAAs of HCV-infected patients (all genotypes). The decrease started early after initiation of treatment and remained stable during post-treatment observation. The rapid decrease of glycomics-based fibrosis biomarkers probably reflects the amelioration of liver inflammation as underlying process rather than the improvement of liver fibrosis itself, which cannot occur in such a short timeframe. In conclusion, this study suggests that GlycoFibroTest shows an excellent correlation with viral response in HCV patients.

FRI345

Post-treatment elevated gamma-glutamyl transferase is the best predictor for future outcomes in HCV patients achieving sustained virological response-data from the german hepatitis C-registry (DHC-R)

Stefan Mauss¹, Hartwig Klinker², Klaus Boeker³, Uta Merle⁴, Ralph Link⁵, Peter Buggisch⁶, Dietrich Hüppe⁷, Markus Cornberg⁸, Christoph Sarrazin^{9,10}, Heiner Wedemeyer^{8,11}, Thomas Berg¹², Frank Tacke¹³, German Hepatitis C-Registry¹¹. ¹Center for HIV and Hepatogastroenterology, Düsseldorf, Germany; ²University Hospital Würzburg, Würzburg, Germany; ³Center of Hepatology, Hannover, Germany; ⁴Heidelberg University Hospital, Heidelberg, Germany; ⁵MVZ-Offenburg GmbH/St. Josefs-Klinik, Offenburg, Germany; ⁶ifi-Institute for Interdisciplinary Medicine, Hamburg, Germany; ⁷Gastroenterologische Gemeinschaftspraxis Herne, Herne, Germany; ⁸Hannover Medical School, Hannover, Germany; ⁹St. Josefs-Hospital, Wiesbaden, Germany; ¹⁰Goethe University Hospital, Frankfurt, Germany; ¹¹Leberstiftungs-GmbH Deutschland, Hannover, Germany; ¹²University Hospital Leipzig, Leipzig, Germany; ¹³Charité-Universitätsmedizin Berlin, Department of Hepatology & Gastroenterology, Campus Virchow-Klinikum and Campus Charité Mitte, Berlin, Germany

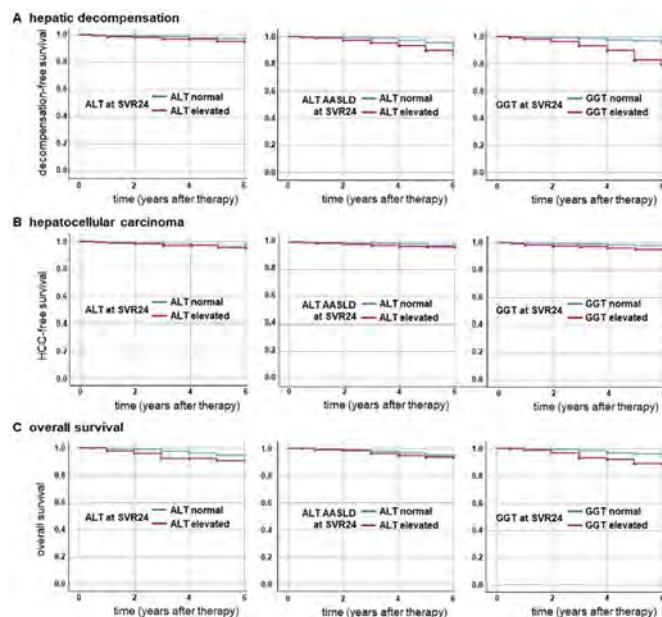
Email: stefan.mauss@center-duesseldorf.de

Background and aims: While direct acting antivirals (DAA) can cure chronic hepatitis C virus (HCV) infection in almost all patients, some patients remain at risk of liver disease despite HCV cure. We aimed at identifying predictors for liver-related morbidity and death after viral cure.

Method: The DHC-R (German Hepatitis C-Registry) is a national multicenter real-world registry. Patients are followed for up to 7 years after DAA therapy. Normal alanine transaminase (ALT; at 37°C) was

defined as (i) ≤ 35 U/l for females and ≤ 50 U/l for males and or (ii) according to AASLD as ≤ 19 U/l for females and ≤ 30 U/l for males. Normal gamma-glutamyl transferase (GGT) (at 37°C) was defined as ≤ 40 U/l (female) and ≤ 60 U/l (male). The present analysis is based on 6982 patients with available data as of January 1st, 2021.

Results: 97.4% of patients achieved sustained virological response (SVR). In patients achieving SVR, elevated ALT at SVR24 was documented in 657/6982 (9.4%), elevated ALT (AASLD) in 2609/6982 (37.4%) and elevated GGT in 1777/6982 (25.5%). At SVR24, elevated ALT was associated with categorized higher body mass index (BMI; $p < 0.05$), liver cirrhosis (OR 2.29, $p < 0.0001$), alcohol consumption ($>30/40$ g/day) (OR 2.93, $p < 0.001$), elevated ALT at baseline (OR 4.46, $p < 0.0001$) and no SVR (OR 43.49, $p < 0.0001$). The same variables were identified using AASLD criteria plus female sex (OR 2.39, $p < 0.001$). Increased GGT at SVR24 was associated with male sex (OR 2.12, $p < 0.001$), higher BMI (OR 1.04, $p < 0.05$), age >50 years (OR 1.60, $p < 0.01$), liver cirrhosis (OR 3.97, $p < 0.0001$), alcohol consumption (OR 2.99, $p < 0.001$), diabetes mellitus (OR 1.63, $p < 0.001$), non-SVR (OR 8.00, $p < 0.0001$) and elevated GGT at baseline (OR 17.12, $p < 0.001$). More importantly, we identified elevated GGT at SVR24 as the best predictor of overall survival, hepatic decompensation or HCC development over elevated ALT or ALT (AASLD; Figure). Combining ALT and GGT did not improve sensitivity substantially.



Conclusion: We here define risk factors for developing clinical complications after cure from HCV infection. In this context, elevated GGT may highlight the relevance of non-alcoholic fatty liver disease (NAFLD), diabetes mellitus, and alcohol consumption.

FR1346

The impact of liver function improvement after direct-acting antiviral therapy on the outcome in hepatitis C virus patients with decompensated cirrhosis

Yuki Tahata¹, Hayato Hikita¹, Satoshi Mochida², Nobuyuki Enomoto³, Norifumi Kawada⁴, Masayuki Kurosaki⁵, Akio Ido⁶, Hitoshi Yoshiji⁷, Daiki Miki⁸, Yasuhiro Takikawa⁹, Ryotaro Sakamori¹, Yoichi Hiasa¹⁰, Hiroshi Yatsushashi¹¹, Kazuhiko Nakao¹², Naoya Kato¹³, Yoshiyuki Ueno¹⁴, Yoshito Itoh¹⁵, Ryosuke Tateishi¹⁶, Goki Suda¹⁷, Taro Takami¹⁸, Kentaro Matsuura¹⁹, Taro Yamashita²⁰, Norio Akuta²¹, Tatsuya Kanto²², Yasunari Nakamoto²³, Yasuhiro Asahina²⁴, Shuji Terai²⁵, Masahito Shimizu²⁶, Ryoko Yamada¹, Takahiro Kodama¹, Tomohide Tatsumi¹, Tomomi Yamada²⁷, Tetsuo Takehara¹. ¹Osaka

University Graduate School of Medicine, Department of Gastroenterology and Hepatology; ²Saitama Medical University, Department of Gastroenterology and Hepatology; ³University of Yamanashi, First Department of Internal Medicine, Faculty of Medicine; ⁴Graduate School of Medicine, Osaka City University, Department of Hepatology; ⁵Musashino Red Cross Hospital, Department of Gastroenterology and Hepatology; ⁶Kagoshima University Graduate School of Medicine and Dental Sciences, Digestive and Lifestyle Diseases, Department of Human and Environmental Sciences; ⁷Nara Medical University, Department of Gastroenterology; ⁸Graduate School of Biomedical and Health Sciences, Hiroshima University, Department of Gastroenterology and Metabolism; ⁹Iwate Medical University, Division of Hepatology, Department of Internal Medicine; ¹⁰Ehime University Graduate School of Medicine, Department of Gastroenterology and Metabolism; ¹¹National Hospital Organization Nagasaki Medical Center, Clinical Research Center; ¹²Nagasaki University of Graduate School of Biomedical Sciences, Department of Gastroenterology and Hepatology; ¹³Graduate School of Medicine, Chiba University, Department of Gastroenterology; ¹⁴Faculty of Medicine, Yamagata University, Department of Gastroenterology; ¹⁵Graduate School of Medical Science, Kyoto Prefectural University of Medicine, Department of Molecular Gastroenterology and Hepatology; ¹⁶Graduate School of Medicine, The University of Tokyo, Department of Gastroenterology; ¹⁷Graduate School of Medicine, Hokkaido University, Department of Gastroenterology and Hepatology; ¹⁸Yamaguchi University Graduate School of Medicine, Department of Gastroenterology and Hepatology; ¹⁹Nagoya City University Graduate School of Medical Sciences, Department of Gastroenterology and Metabolism; ²⁰Kanazawa University Hospital, Department of General Medicine; ²¹Toranomon Hospital, Department of Hepatology; ²²National Center for Global Health and Medicine, The Research Center for Hepatitis and Immunology; ²³Faculty of Medical Sciences, University of Fukui, Second Department of Internal Medicine; ²⁴Tokyo Medical and Dental University, Department of Gastroenterology and Hepatology, Department of Liver Disease Control; ²⁵Graduate School of Medicine and Dental Sciences, Niigata University, Division of Gastroenterology and Hepatology; ²⁶Gifu University Graduate School of Medicine, Department of Gastroenterology/Internal Medicine; ²⁷Osaka University Hospital, Department of Medical Innovation
Email: yuki.tahata@gh.med.osaka-u.ac.jp

Background and aims: Direct-acting antiviral (DAA) therapy can improve liver function in the short term even in patients with hepatitis C virus (HCV)-related decompensated cirrhosis. However, the impact of DAA therapy on long-term outcome among patients with decompensated cirrhosis is unclear.

Method: This study enrolled 396 patients with HCV-related compensated or decompensated cirrhosis who started DAA therapy between February 2019 and December 2020 at 33 Japanese hospitals. Patients were excluded when sustained virologic response (SVR) could not be determined or died before SVR confirmation. SVR was defined as undetectable serum HCV-RNA for at least 12 weeks after the end of treatment (EOT). Our endpoints are the incidence of decompensated cirrhosis events with hospitalization and overall survival. Decompensated cirrhosis events were defined as aggravation of ascites or encephalopathy, rupture of varix, and the onset of spontaneous bacterial peritonitis, sepsis or acute kidney injury. We evaluated the impact of delta MELD score between at baseline and at 12 weeks after the EOT on these endpoints. Delta MELD score was classified into three groups: the MELD score decreased 2 points or more (MELD improved), the MELD score increased 2 points or more (MELD deterioration) and others (MELD stable).

Results: The median age was 70 years. The SVR rates of patients with CP class A, B and C were 100% (224/224), 96% (142/148) and 96% (22/23), respectively. Among 396 patients, delta MELD score were evaluated in 347 patients. The number of patients with MELD improved, MELD stable and MELD deterioration were 41, 275 and 31, respectively. During the median observation period of 20 months, 34 patients experienced decompensated cirrhosis events (the most

frequent event was ascites), 10 patients died, and two patients underwent liver transplantation. In patients with CP class A, five patients experienced decompensated cirrhosis events and two patients died. MELD changes at 12 weeks after the EOT were not associated with the incidence of decompensated cirrhosis events and overall survival. In patients with CP class B or C, the cumulative incidence rate of decompensated cirrhosis event at 2 years with MELD improved, MELD stable, MELD deterioration were 7%, 22% and 58%, respectively. Overall survival rates of patients at 2 years with MELD improved, MELD stable and MELD deterioration were 100%, 97% and 69%, respectively. Patients with MELD deterioration had a higher incidence of decompensated cirrhosis events and poorer overall survival than the other two groups.

Conclusion: In patients with decompensated cirrhosis who were treated with DAA, MELD score deterioration at 12 weeks after the EOT indicated an unfavorable outcome.

FRI347

De-novo occurrence of portal vein thrombosis in patients with HCV-related cirrhosis after sustained virological response: medium to long term observations from the ongoing PITER cohort

Loreta Kondili¹, Maria Giovanna Quaranta¹, Luigina Ferrigno¹, Carmine Coppola², Monica Monti³, Roberto Filomia⁴, Giuseppina Brancaccio⁵, Maurizia Brunetto⁶, Elisa Biliotti⁷, Donatella Ieluzzi⁸, Andrea Iannone⁹, Salvatore Madonia¹⁰, Xhimi Tata¹, Luisa Cavalletto¹¹, Valentina Cossiga¹², Simona Amodeo¹³, Vincenza Calvaruso¹⁴, Elena Rosselli Del Turco¹⁵, Maria Grazia Rumi¹⁶, Maurizio Pompili¹⁷, Alessia Ciano¹⁸, Lucia Brescini¹⁹, Francesco Paolo Russo²⁰. ¹Istituto Superiore di Sanità, Center for Global Health, Roma, Italy; ²Gragnano Hospital, Gragnano (NA), Italy; ³University of Florence, Interdepartmental Centre MASVE, Firenze, Italy; ⁴University Hospital of Messina, Messina, Italy; ⁵University of Padua, Department of Molecular Medicine, Infectious Diseases, Padova, Italy; ⁶University of Pisa, Pisa, Italy; ⁷Umberto I Hospital-“Sapienza” University, Rome; ⁸University Hospital of Verona, Verona, Italy; ⁹University of Bari, Bari, Italy; ¹⁰Azienda Ospedaliera “Ospedali Riuniti Villa Sofia-Cervello”, Palermo, Italy; ¹¹University Hospital of Padua, Padua, Italy; ¹²University of Naples Federico II, Napoli, Italy; ¹³University of Palermo, Gastroenterology and Hepatology Unit (DiBiMiS), Palermo, Italy; ¹⁴University of Palermo, GI & Liver Unit, Department of Health Promotion Sciences Maternal and Infantile Care, Internal Medicine and Medical Specialties (PROMISE), Palermo, Italy; ¹⁵Alma Mater Studiorum-Università di Bologna, Bologna, Italy; ¹⁶San Giuseppe Hospital, Milano, Italy; ¹⁷Fondazione Policlinico Universitario Agostino Gemelli IRCCS, Roma, Italy; ¹⁸Città della Salute e della Scienza of Turin, University Hospital, Turin, Italy; ¹⁹Marche Polytechnic University, Ancona, Italy; ²⁰University of Padua, Gastroenterology Unit, Department of Surgery, Oncology and Gastroenterology, Padova, Italy Email: loreta.kondili@iss.it

Background and aims: Achievement of sustained virological response (SVR) by direct-acting antiviral therapy (DAAs) ameliorates portal hypertension, improves hepatic function, and may reverse hyper-coagulability driven by cirrhosis. However, an unexpected finding of *de-novo* portal vein thrombosis (PVT) immediately after DAAs has been reported. Here, we analyzed the long-term impact of SVR on the development of PVT in patients with cirrhosis.

Method: Consecutive patients with liver cirrhosis, enrolled in the multicenter Italian PITER cohort and treated with DAAs were prospectively evaluated. Patients with history of PVT prior to start of DAAs, and those with no follow-up data after end of treatment (EOT) were excluded. Stepwise Cox regression analysis was used to evaluate factors independently associated with *de-novo* PVT. Kaplan Meier analysis and log rank test evaluated the PVT rates by DAA treatment response.

Results: Of 1632 patients evaluated, 40 (2.5%) developed *de-novo* PVT after DAA treatment. The two year PVT free survival was 99% for

patients who achieved the SVR and 93% for those who didn't ($p = 0.002$). Of 1555 patients who achieved the SVR (median age 65 years, 55% males, 85% Child A and 15% Child B), 34 (2.2%) experienced *de-novo* PVT (median follow-up 36 months after EOT; IQR 24–44.7). Of them, 18 reported HCC development previous or after achieving the SVR; in 6 of whom (17.6%) PVT was of neoplastic nature. The PVT occurrence in patients who achieved the SVR, not related to HCC development, was 1.8% (28 patients); the median time to *de-novo* PVT occurrence was 33.8 months (IQR 17–45 months) after EOT. At pretreatment evaluation, patients who experienced *de-novo* non-neoplastic PVT were more likely Child B (39.3% vs. 14.2%, $p < 0.001$) and by Cox regression analysis, pre-treatment variables independently associated with *de-novo* PVT development were: platelet count $\leq 120,000/\mu\text{L}$ (HR: 3.56, CI 95%: 1.03–12.33), albumin level $< 3.5 \text{ g/dL}$ (HR: 2.66, CI 95%: 1.15–6.15) and bilirubin level $> 1.1 \text{ mg/dL}$ (HR: 2.70, CI 95%: 1.10–6.65). Patients with *de-novo*, non-neoplastic PVT had higher risks of hepatic decompensation (39.3% vs. 4.9%; $p < 0.001$) and liver-related death (13% vs. 2%, $p < 0.001$) regardless the SVR achievement following the DAA treatment.

Conclusion: The risk of *de-novo* non-neoplastic PVT in patients with cirrhosis who achieved the SVR is low and mainly related to the severity of liver disease. Development of *de-novo*, non-neoplastic PVT following the SVR may identify patients with higher risks of hepatic decompensation and mortality despite viral eradication by DAA treatment.

FRI348

Suboptimal follow-up, high re-infection, and drug-related death, among HCV-treated people who inject drugs in Tayside, Scotland

Christopher Byrne^{1,2}, Lewis Beer², Sarah Inglis², Emma Robinson¹, Andrew Radley³, Sharon Hutchinson^{4,5}, David Goldberg^{4,5}, Matthew Hickman⁶, John Dillon^{1,7}. ¹University of Dundee, Molecular and Clinical Medicine, Dundee, United Kingdom; ²University of Dundee, Tayside Clinical Trials Unit, Dundee, United Kingdom; ³NHS Tayside, Public Health, Dundee, United Kingdom; ⁴Glasgow Caledonian University, School of Health and Life Sciences, Glasgow, United Kingdom; ⁵Health Protection Scotland, Glasgow, United Kingdom; ⁶University of Bristol, Population Health Sciences, Bristol, United Kingdom; ⁷NHS Tayside, Gastroenterology, Dundee, United Kingdom Email: c.x.byrne@dundee.ac.uk

Background and aims: In 2017, Tayside, in East Scotland, rapidly scaled-up Hepatitis C Virus (HCV) treatment among People Who Inject Drugs (PWID) using new care pathways. This study aimed to quantify HCV re-infection and routes of re-treatment; mortality; and efficacy of re-infection follow up.

Method: Annual follow-up RNA testing is offered. Re-infection follow-up was measured by calculating the proportion of cases with follow-up tests received in line with local policy. We estimated re-infection incidence, overall and by pathway, per 100 person-years (PY), assuming a Poisson distribution. Mortality was similarly calculated; time-at-risk was from primary HCV treatment to censor date or death.

Results: There were 713 treatments and 577 SVRs. 236 cases among 231 people were followed-up for re-infection. Of cured cases, 39% had ≥ 1 follow-up test. 87 (15%) cases had repeat testing in the first 12 months, in line with policy. Within 2 years, 110 (19%) had a follow-up test. Of those, 20 (18%) were continued follow-up. Within 3 or 4 years, 19 were tested.

Re-infection occurred 39 times over 256.57 PY, yielding a rate of 15.20 per 100 PY (95% CI 10.81–20.78). For recent injectors, there were 26 re-infections over 175.43 PY, yielding a rate of 14.82 per 100 PY (95% CI 9.68–21.72). Re-infection incidence was highest among needle exchanges (table 1), as was subsequent re-treatment.

Table 1: Clinical pathways of re-infected PWID, Tayside 2017–20.

Clinical pathway	n (%)	PY	Incidence per 100 PY*
Pathway prior to re-infection (n = 39)			
Community pharmacy	12 (30.8)	92.25	13.01 (6.72–22.73)
Needle exchange	19 (48.7)	64.08	29.65 (17.85–46.30)
Other [†]	8 (20.5)	77.31	10.35 (4.47–20.39)
Pathway post re-infection (n = 25)			
Drug treatment centre	4 (16.0)		
Needle exchange	15 (60.0)		
Nurse-led community clinic	4 (16.0)		
Prison	2 (8.0)		

Abbreviations: HCV, hepatitis c virus; PWID, people who inject drugs; PY, person-years.

*95% CI in brackets.

Fifty-four patients died over 1, 553.04 PY, all-cause mortality was 3.48 per 100 PY (95% CI 2.61–4.54); 29 were drug related, drug-related mortality was 1.87 per 100 PY (95% CI 1.25–2.68).

Conclusion: Re-infection and drug-related mortality were high in this cohort of HCV-treated PWID, and follow-up was suboptimal. Harm reduction services in Tayside need strengthening alongside comprehensive follow-up RNA testing.

FRI349

Hepatitis C virus reinfection following direct acting antiviral treatment in the prison setting: the SToP-C study

Joanne Carson¹, Gregory Dore¹, Andrew Lloyd¹, Jason Grebely¹, Marianne Byrne¹, Evan B Cunningham¹, Janaki Amin², Peter Vickerman³, Natasha Martin⁴, Carla Treloar⁵, Gail Matthews¹, Behzad Hajarizadeh¹. ¹The Kirby Institute, UNSW Sydney, Sydney, Australia; ²Macquarie University, Sydney, Australia, Faculty of Medicine and Health Sciences, Sydney, Australia; ³University of Bristol, Population Health Sciences, Bristol, United Kingdom; ⁴University of California San Diego, Division of Infectious Diseases & Global Public Health, San Diego, United States; ⁵Centre for Social Research in Health, UNSW Sydney, Sydney, Australia

Email: jcarson@kirby.unsw.edu.au

Background and aims: Ongoing injecting drug use risk behaviours following successful treatment for hepatitis C virus (HCV) may lead to reinfection, reversing benefits of cure, particularly if harm reduction measures are not optimal. This study assessed HCV reinfection risk following direct-acting antiviral therapy in Australian prisons, where opioid agonist therapy is available, but not needle-syringe programs. **Method:** The Surveillance and Treatment of Prisoners with hepatitis C (SToP-C) study enrolled people incarcerated in four prisons in Australia between 2014 and 2019. Participants successfully treated for HCV were followed every 3–6 months to assess for reinfection (identified by HCV sequencing). The incidence of HCV reinfection and associated factors were evaluated.

Results: Among 388 participants receiving treatment, 161 had available post-treatment follow up (92% male; median age 33 years; 67% injecting drug use in prison; median follow-up 9 months). During 145 person-years (py) of follow up, 18 cases of reinfection were identified. Reinfection incidence was 12.5 per 100 py (95%CI: 7.9–19.8) overall and 11.6 per 100 py (95%CI 6.6–20.4) among those continuously incarcerated. Incidence was highest among those injecting in the past month and sharing needles/syringes (28.7 per 100 py; 95%CI 16.3–50.6). In adjusted analysis, injecting drug use with sharing needles/syringes was associated with increased reinfection risk (adjusted hazard ratio 14.62; 95%CI 1.84–116.28; p = 0.011).

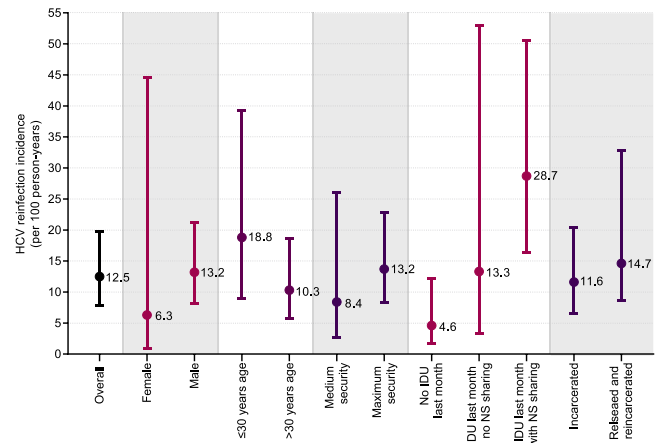


Figure 1. HCV reinfection incidence rates following DAA therapy treatment in the prison setting
Abbreviations: HCV, hepatitis C virus; IDU, injecting drug use; NS, needle or syringe

Conclusion: A high rate of HCV reinfection was observed within a four-prison network. Post-treatment surveillance and retreatment are essential to limit the impact of reinfection. Enhanced access to harm reduction services, including needle and syringe programs, should be considered within prisons.

FRI350

Five-years follow-up of cured HCV patients with or without cirrhosis under real-world interferon-free therapy

Robert Flisiak¹, Dorota Zarębska-Michaluk², Ewa Janczewska³, Magdalena Rogalska¹, Ewa Karpińska⁴, Tomasz Mikula⁵, Beata Bolewska⁶, Jolanta Białkowska⁷, Katarzyna Flejscher-Stępniewska⁸, Krzysztof Tomasiewicz⁹, Kornelia Karwowska¹⁰, Monika Pazgan-Simon¹¹, Piekarska Anna¹², Hanna Berak¹³, Tronina Olga¹⁴, Aleksander Garlicki¹⁵, Jerzy Jaroszewicz¹⁶. ¹Medical University of Białystok, Department of Infectious Diseases and Hepatology, Poland; ²Jan Kochanowski University, Department of Infectious Diseases; ³Medical University of Silesia, Bytom, Department of Basic Medical Sciences, Faculty of Health Sciences in Bytom; ⁴Pomeranian Medical University, Department of Infectious Diseases, Hepatology and Liver Transplantation, Szczecin; ⁵Medical University of Warsaw, Department of Infectious and Tropical Disease and Hepatology, Warsaw; ⁶Poznan University of Medical Sciences, Poznan, Department of Infectious Diseases; ⁷Medical University of Lodz, Department of Infectious and Liver Diseases; ⁸Wroclaw Medical University, Department of Infectious Diseases, Liver Diseases and Immune Deficiencies; ⁹Medical University of Lublin, Department of Infectious Diseases and Hepatology; ¹⁰Collegium Medicum, Nicolaus Copernicus University, Department of Infectious Diseases and Hepatology, Bydgoszcz; ¹¹Wroclaw Medical University, Department of Infectious Diseases and Hepatology; ¹²Medical University of Lodz, Department of Infectious Diseases and Hepatology; ¹³Hospital of Infectious Diseases in Warsaw, Daily Unit; ¹⁴Medical University of Warsaw, Department of Transplantation Medicine, Nephrology and Internal Medicine; ¹⁵Jagiellonian University Medical College, Department of Infectious and Tropical Diseases; ¹⁶Medical University of Silesia, Department of Infectious Diseases and Hepatology, Katowice
Email: robert.flisiak1@gmail.com

Background and aims: Treatment of hepatitis C virus (HCV) infections with direct-acting antivirals (DAA) has demonstrated high efficacy even in patients with liver cirrhosis. The three-year stability of a sustained virological response (SVR) and an improvement in liver function with a persistent risk of hepatocellular carcinoma (HCC) has so far been confirmed in the literature. The purpose of the current study is to evaluate the virologic response, changes in liver function, stiffness and risk of HCC five years following the treatment.

POSTER PRESENTATIONS

Method: A total of 192 patients originally infected with HCV genotype 1 or 4 were analyzed five years after treatment with ombitasvir/paritaprevir/ritonavir with or without dasabuvir and with or without ribavirin. Most of the patients were diagnosed with cirrhosis before treatment (57%) and did not respond to previous treatment attempts (69%).

Results: We confirmed that HCV clearance after DAA treatment is stable regardless of baseline advancement of the disease. We found that SVR is associated with a gradual but significant reduction in liver stiffness over 5 years. Liver function improved during the first 2 years of follow-up and remained stable thereafter. The risk of death due to HCC or any reason persists through 5 years after successful DAA treatment. However, in non-cirrhotic patients, it appears to clear up 3 years after treatment.

Conclusion: Despite the successful treatment of HCV infection 5 years after its completion, patients with cirrhosis are still at risk of developing liver cancer. This justifies screening for HCV, allowing therapy before the development of liver cirrhosis.

FRI351

Clearance of hepatitis C virus infection did not ameliorate the response to hepatitis B vaccine

Ebada Said¹, Tamer Al Eraki², Dalia Abdelhasseb², Shaimaa Ragab², Mona El Awady². ¹Benha University, Egypt; ² Email: ebada.abdelhamid@fmed.bu.edu.eg

Background and aims: In Egypt, citizens older than 30 years did not get the compulsory vaccination against hepatitis B virus (HBV) infection during infancy. Patients with chronic hepatitis C (CHC) are advised to get vaccinated against HBV. The aim was to assess the response to HBV vaccine in CHC patients treated with direct acting antivirals (DDAs) in comparison to treatment-naïve patients and healthy subjects and to identify predictors of weak response.

Method: This prospective study was carried out on 360 adult subjects subdivided into 3 groups. Group I (GI) included 150 consecutive CHC patients who initiated vaccination after getting sustained virologic response (SVR) following treatment with DAAs. Group II comprised 110 consecutive CHC treatment-naïve patients while the control group (GIII) comprised 100 healthy subjects. The mean age of the 3 groups was 50, 45 and 39 year, respectively. Demographic and laboratory variables including HCV-viral load, FIB-4 score, Schistosomal antibody (Ab) titre, and Fibroscan® values were assessed. All the studied groups had received 3 intradermal, 20 µg, doses of HBV-vaccine (Euvax B, LG Life Sciences, Korea) given at 0, 1 & 6 months. Hepatitis B surface antibody (HBsAb) titres were tested 6–8 weeks after the 3rd dose.

Results: Patients of groups I & II showed a mean FIB4 score of 1.4 & 1.8 while a mean fibroscan value of 8.2 & 9.8 KPa, respectively. CHC patients either treated (GI) or treatment-naïve (GII) had highly significant lower mean HBs Ab titre than controls ($p < 0.001$). Twelve patients (8%) in GI had negative response to the HBV-vaccine (HBsAb titres of < 10 mIU/ml) compared to 5 patients (4.5%) in GII and only one subject (1%) in the control group. Those who got HBsAb titres of > 100 mIU/ml were 125/150 (83.3%), 89/110 (85.5%) and 98/100 (98%) in group I, II and III respectively.

Regarding patients with SVR, univariate regression analysis showed that HBsAb titre was negatively associated with higher age ($p < 0.001$), FIB-4 score ($p < 0.001$), fibrosis stage ($p = 0.001$) and ALT levels ($p = 0.03$) while positively associated with platelet count ($p < 0.001$). Higher fibroscan values (KPa) were the most significant predictors of weak response to HBV vaccine. In treatment naïve CHC patients, HBsAb titre was negatively associated with ALT ($p = 0.001$), AST ($p = 0.03$), FIB-4 score ($p = 0.01$) and schistosomal Ab titre ($p < 0.001$) and positively associated with platelet count ($p = 0.001$). Vaccination response showed no association with gender, body mass index, viral load or other variables.

Conclusion: Patients with CHC demonstrate a significantly weak response to HBV-vaccine, particularly those with older age, fibrosis

advancement and schistosomiasis. Treatment and SVR achievement did not ameliorate this response.

FRI352

Reverse Inflammaging: biological age is accelerated in chronic HCV patients and decelerates after HCV cure

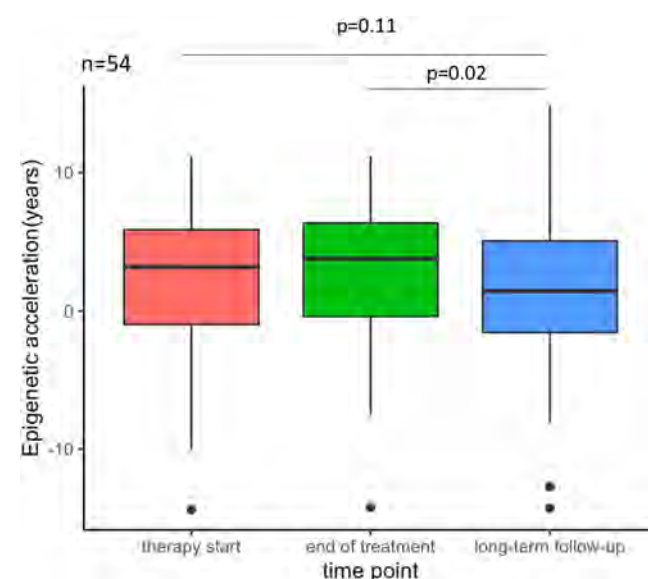
Carlos Oltmanns^{1,2}, Zhaoli Liu¹, Jasmin Mischke^{1,2}, Jan Tauwaldt^{1,2}, Yonatan Mekonnen¹, Heiner Wedemeyer², Anke Kraft^{1,2,3}, Cheng-Jian Xu^{1,2,4}, Markus Cornberg^{1,2,3,4}. ¹TWINCORE a joint venture of Helmholtz Centre for Infection Research and Hannover Medical School Hannover Germany, Hannover, Germany; ²Hannover Medical School, Department of Gastroenterology, Hepatology and Endocrinology, Hannover, Germany; ³German Center for Infection Research, Partner-Site Hannover-Braunschweig, Hannover, Germany; ⁴Centre for Individualised Infection Medicine (CiiM), Hannover, Germany Email: oltmanns.carlos@mh-hannover.de

Background and aims: Recently, HIV and HBV infections have been shown to cause significant biological age acceleration. Accelerated epigenetic or biological age may be a predictor of all-cause and cancer mortality. Thus, we analyzed if HCV is associated with biological age acceleration and if this is reversible after HCV cure.

Method: We included well-characterized 54 patients (mean age 56 years) with chronic hepatitis C at three time points (baseline, end of treatment and follow-up 24–240 (mean 96 weeks) weeks after the end of treatment). Genome-wide DNA methylation data were generated using the illuminaEpic array on PBMC and were used to calculate the epigenetic age acceleration (Horvath clock).

Results: Our results show that chronic HCV infection leads to a significant acceleration of epigenetic age ($p = 3.577e-05$). While chronic HCV patients without evidence of cirrhosis have a lower age acceleration, patients with cirrhosis have a higher biological age. Treatment of HCV patients with DAA results in reversal of age acceleration, but this effect is only detectable at long-term follow-up ($p = 0.02$). Epigenetic age acceleration does not correlate with estimated blood cell counts.

Interestingly, patients who developed HCC after SVR ($n = 8$) have the highest age acceleration and show no evidence of complete reversion after treatment.



Conclusion: Hepatitis C patients with cirrhosis show biological age acceleration that may be reversible after HCV cure. Lack of reversibility appears to be associated with HCC risk. Our findings underline the need for more individualized infectious disease medicine based on biological rather than chronologic age in the future.

FRI353

Overall mortality in patients with chronic hepatitis C: major effects of social vulnerability, tobacco smoking, and history of unhealthy alcohol use (ANRS CO22 HEPATHER cohort)

Lauren Perieres¹, Fabrice Carrat², Marta Lotto¹, Celine Dorival³, Clémence Ramier¹, Fabienne Marcellin¹, Carole Cagnot⁴, Elizabeth Delarocque-Astagneau⁵, Patrizia Carrieri¹, Stanislas Pol⁶, Helene Fontaine⁶, Camelia Protopopescu¹. ¹Aix Marseille Univ, INSERM, IRD, SESSTIM, Sciences Économiques & Sociales de la Santé & Traitement de l'Information Médicale, ISSPAM, Marseille, France; ²Institut National de la Santé et de la Recherche Médicale (INSERM), Institut Pierre Louis d'Epidémiologie et de Santé Publique, Sorbonne Université, Hôpital Saint-Antoine, Unité de Santé Publique, Assistance Publique-Hôpitaux de Paris (AP-HP), Paris, France; ³Institut National de la Santé et de la Recherche Médicale (INSERM), Institut Pierre Louis d'Epidémiologie et de Santé Publique, Sorbonne Université, Paris, France; ⁴ANRS|Emerging Infectious Diseases, Paris, France; ⁵Université Paris-Saclay, UVSQ, Inserm, CESP, Team Anti-infective Evasion and Pharmacoepidemiology, Montigny, France; ⁶Université de Paris, AP-HP, Hôpital Cochin, Département d'Hépatologie/Addictologie, Paris, France
Email: fabienne.marcellin@inserm.fr

Background and aims: The advent of direct acting antivirals has paved the way for a hepatitis C-free world. However, patients with hepatitis C virus (HCV) infection remain at high risk of morbidity and mortality, even after cure. We identify socio-behavioural factors associated with overall (i.e., all-cause) mortality in chronic HCV-infected patients.

Method: We used data collected from August 2012 to June 2018 in the French, multicentre, prospective cohort ANRS CO22 HEPATHER. The study sample comprised chronic HCV-infected patients who attended at least one annual follow-up visit. Analyses focused on the first five years of follow-up. Socio-behavioural data were collected at cohort enrolment (questionnaire administered by a physician). Living in poverty was defined as a standard of living below 1015€ (French poverty threshold in 2015), low educational level as level <high school diploma, unhealthy alcohol use as drinking >2 and >3 alcohol units/day for women and men, respectively, and elevated coffee intake as drinking ≥3 cups of coffee/day. Factors associated with overall mortality were identified using a Cox proportional hazards model. Adjusted population attributable fractions (PAF) were estimated for the modifiable factors of the multivariable analysis.

Results: Of the 10,366 patients in the study sample, 697 died during follow-up. After multivariable adjustment (for sex, age, educational level, HCV genotype, HCV transmission category, and HCV cure), living in poverty (adjusted hazard ratio [aHR]: 1.34 [95% confidence interval, 1.13–1.60]), tobacco smoking (1.70 [1.35–2.14]), and a history of unhealthy alcohol use (1.48 [1.18–1.86]) were independently associated with increased overall mortality. By contrast, elevated coffee intake was associated with lower overall mortality (0.63 [0.52–0.77]). The risk factors accounting for the greatest mortality burden were tobacco smoking, low educational level, living in poverty, and a history of unhealthy alcohol use (PAF: 16.6%, 14.9%, 9.8%, and 7.4%, respectively), whilst HCV cure and elevated coffee intake averted a high proportion of deaths (86.0% and 13.4%, respectively).

Conclusion: In the era of HCV cure, tobacco cessation must be further encouraged in patients with chronic HCV infection, as a modifiable risk factor of mortality. Specific interventions should be developed to target socially vulnerable patients and those with a history of unhealthy alcohol use, who are at higher risk of mortality.

FRI354

Is routine Ribavirin mandatory for genotype 3 hepatitis C compensated cirrhosis patients receiving Sofosbuvir/Velpatasvir? A meta-analysis

Jing Hong Loo¹, Flora Xu¹, Gerald Low¹, Wei Xuan Tay¹, Le Shaun Ang¹, Steve Yew-chong Tam², Prem Harichander Thuraiarajah³, Rahul Kumar⁴, Yu Jun Wong⁵. ¹Yong Loo Lin School of Medicine, National University of Singapore; ²Education Resource Centre, Medical Board, Singapore General Hospital; ³National University Hospital, Division of Gastroenterology & Hepatology, Singapore, Singapore; ⁴Changi General Hospital, Department of Gastroenterology & Hepatology; ⁵Department of Gastroenterology & Hepatology, Changi General Hospital, Singapore
Email: loojinghong@gmail.com

Background and aims: Simplified treatment regimen is crucial for rapid treatment upscale to achieve hepatitis C virus (HCV) elimination. Addition of ribavirin (RBV) to Sofosbuvir/Velpatasvir (SOF/VEL) has been showed improved sustained virological response at 12 weeks (SVR12) in genotype 3 (GT3) decompensated cirrhosis patients. However, the benefits of RBV in GT3 compensated cirrhosis patients receiving SOF/VEL, remains unclear. We aim to systematically review the efficacy and safety of SOF/VEL, with or without RBV in GT3 compensated cirrhosis patients.

Method: With help of medical librarian, we systematically searched four electronic databases (PubMed/MEDLINE, EMBASE, Cochrane Library and Web of Science) from inception up to June 2021 using both free text and MeSH terms. There was no restriction on language, geography, publication dates and publication status. All GT3 compensated cirrhosis patients treated with 12 weeks of SOF/VEL, with or without RBV, were included, regardless of age, gender or prior treatment experience. The primary outcome was the SVR12. The secondary outcome was treatment-related adverse events, as defined by symptomatic anaemia requiring transfusion or a drop in haemoglobin beyond 2 g/dL. The pooled relative risk (RR), 95% confidence interval (CI) and heterogeneity (I^2) were estimated using Review Manager Version 5.3.

Results: From 1,752 citations, a total of 7 studies (2 RCTs, 5 cohort studies) with 1,088 subjects were identified. The SVR12 was similar in GT3 compensated cirrhosis patients, regardless of the use of RBV, for both the intention-to-treat (RR: 1.03, 95%CI: 0.99–1.07; I^2 = 0%) and the per-protocol analysis (RR: 1.03, 95%CI: 0.99–1.07; I^2 = 48%). The overall pooled rate of treatment-related adverse events was 7.2%. Addition of RBV was associated with 4-fold higher risk of treatment-related adverse events in GT3 compensated cirrhosis patients receiving SOF/VEL (RR: 4.20, 95%CI: 1.29–13.68; I^2 = 0%). Subgroup analysis showed that RBV was associated with a numerically higher SVR12 (96% vs 87%, p = 0.12) in GT3 compensated cirrhosis patients with baseline resistance-associated substitutions (RAS). However, addition of RBV did not significantly increase the SVR12 among treatment-experienced GT3 compensated cirrhosis patients.

Conclusion: Ribavirin did not significantly increase the SVR12 in GT3 compensated cirrhosis patients receiving SOF/VEL. Our findings suggest limited role for RBV as routine add-on therapy to SOF/VEL in GT3 compensated cirrhosis patients.

FRI355

High frequency of hepatitis C virus reinfection following antiviral treatment in the North East of England

Sumar Askar¹, Ryan Jelley¹, Kate Mcque¹, Caroline Allsop¹, Francesca McCullough¹, Carolyn Miller¹, Yusri Taha¹, Steven Masson^{1,2}, Stuart Mcpherson^{1,2}. ¹Newcastle Freeman Hospital, Liver Unit, High Heaton, United Kingdom; ²Translational and Clinical Research Institute, Newcastle University, Newcastle Upon Tyne, United Kingdom
Email: sumar.askar@nhs.net

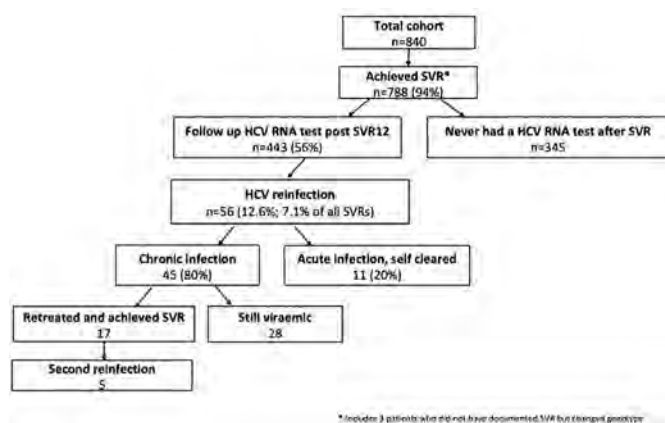
Background and aims: Hepatitis C virus infection (HCV) is common, and injecting drug use (IDU) is the major risk factor for acquisition in

POSTER PRESENTATIONS

Europe. Health services are working towards achieving the WHO target of HCV elimination by 2030. Reinfection following treatment is an important consideration for HCV elimination programmes because this has the potential to hamper elimination efforts. The aim of this work was to assess the rate of HCV reinfection in our region, where IDU is the predominant risk factor (>90%).

Method: All patients who completed treatment with direct acting antiviral (DAA) treatment for HCV in Tyne and Wear, North East England between Jan 2016 and May 2021 were included. Sustained virological response (SVR12) was defined as negative HCV RNA 12 weeks post treatment. Data was collected from our HCV database (HepCare), which automatically gathers laboratory data in real time from our hospital laboratory database. HCV reinfection was defined as a positive HCV RNA after achieving SVR12 or where a genotype has changed after completing DAA treatment when the SVR12 was not documented.

Results: 788 of the 840 patients (76% males; mean age 45.7 ± 11.4 years; 47% G1; 39% G3; 12% Cirrhosis) completing treatment achieved SVR (94%). 459 patients (58%) had a follow-up HCV RNA tested post SVR after a median 0.79 years (range 0.1–5.2 years). 56 reinfections (7.1% of all SVRs and 12.2% of those SVRs who had follow up blood testing) were diagnosed. The median time to reinfection was 1.37 years (range 0.1–5.2 years) and the rate of reinfection was 0.1 per person years. 45 of the 56 (80%) reinfections developed chronic infection, 17 of which were retreated and achieved SVR, while 28 remain viraemic. 5 patients developed a second reinfection. Individuals with reinfection were significantly younger than those maintaining SVR (38.9 ± 7.9 vs 46.2 ± 11.9 years, $p < 0.001$). Reinfection was more common in those with primary G3 infection compared with other genotypes (9.8% vs 5.7% $p = 0.049$). Reinfections were similar between males and females (4.4% females vs 7.4% males $p = 0.15$).



Conclusion: HCV reinfection is common in our cohort and may slow our HCV elimination efforts. In order to address our high reinfection rates we need to improve harm reduction and increase treatment of active IDUs. We aim to implement 'HCV track and trace' for recent infections and reinfections to try to reduce onward HCV transmission.

FRI356

Incidence and risk factors of hepatitis C liver morbidity and mortality in the era of direct-acting antiviral therapies: a population-based linkage study

Maryam Alavi¹, Heather Valerio², Matthew Law¹, Ian Lockart^{3,4}, Mark Danta^{3,4}, Jason Grebely¹, Janaki Amin⁵, Behzad Hajarizadeh¹, Jacob George⁶, Gregory Dore¹. ¹Kirby Institute, UNSW Sydney, Australia; ²Kirby Institute, UNSW Sydney; ³St Vincent's Clinical School, UNSW Sydney, Australia; ⁴St Vincent's Hospital, Sydney, NSW, Australia; ⁵Department of Health Systems and Populations, Macquarie University, Australia; ⁶Storr Liver Centre, Westmead Millennium Institute, University of Sydney, Australia
Email: msalehialavi@kirby.unsw.edu.au

Background and aims: Monitoring trends in hepatitis C virus (HCV) liver morbidity and mortality is increasingly crucial as direct-acting antiviral (DAA) therapy expands and we move towards World Health Organization HCV elimination targets. In New South Wales, Australia, we aimed to evaluate trends in decompensated cirrhosis (DC), hepatocellular carcinoma (HCC), and liver mortality in the pre-DAA (2001–2014) and DAA eras (2015–2020). Further, we assessed factors associated with each liver-related outcome in the DAA era.

Method: HCV notifications (1995–mid 2020) were linked to hospital admissions (2001–2020) and mortality (1995–2020). DC, HCC, and liver death numbers and age-standardised incidence rates [per 100 person-years (PY)] and corresponding 95% CIs were calculated assuming a Poisson distribution. We used Cox Proportional Hazards Regression analyses to evaluate factors associated with each liver-related outcome.

Results: Among 110,022 people with an HCV notification, 5.2% and 2.1% had a DC and HCC diagnosis, respectively, and 4.2% died of liver-related causes. In the pre-DAA era, DC and HCC diagnoses, and liver-related mortality consistently increased, while age-standardised incidence rates were stable or increased: 0.39, 0.15 and 0.13 in 2001 to 0.40, 0.18, and 0.37 per 100 PY in 2014, respectively. Each liver-related outcome declined in the DAA era; in 2020, age-standardised incidence rates of DC, HCC, and liver-related mortality were 0.20 (95% CI 0.17, 0.23), 0.12 (95% CI 0.10, 0.13), and 0.19 (95% CI 0.17, 0.22) per 100 PY, respectively (Figure 1). In the DAA era, a history of alcohol-use disorder was common among people with DC (64%) and HCC (48%). In the DAA era, following older age, a history of alcohol-use disorder was the strongest predictor of DC [adjusted hazard ratio (aHR) 6.70, 95% CI 6.08, 7.39] and HCC diagnoses (aHR 3.53, 95% CI 3.13, 3.99), and liver-related mortality (aHR 5.59, 95% CI 5.08, 6.16).

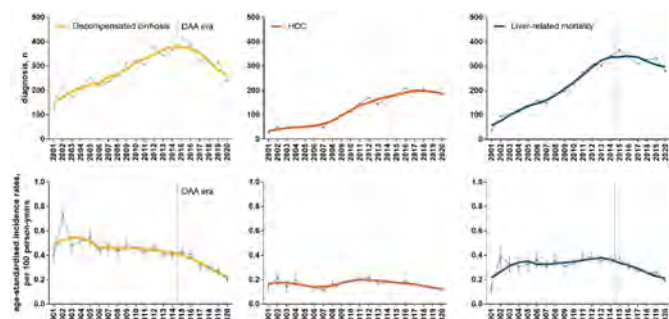


Figure: Trends in diagnoses and age-standardised rates of decompensated cirrhosis, HCC, and liver-related mortality among people with an HCV notification in New South Wales, 1995–mid 2020, n = 110,022.

Conclusion: DAA scale-up in New South Wales, Australia, has reduced the HCV liver disease burden, most remarkably on DC diagnosis and liver-related mortality. However, alcohol-use disorder remains a significant cause of liver disease, both on its own and as a risk factor in the progression of chronic HCV. A broader focus on liver disease prevention is required, encompassing alcohol-use disorder

treatment, to facilitate enhanced declines in advanced liver disease complications in the DAA era.

FRI357

Direct acting antiviral agents improve survival in patients with hepatitis C virus related hepatocellular carcinoma

Hyun Young Woo¹, Won Lim², Jeong Heo¹, Young Joo Park¹. ¹Pusan National University Hospital, Internal Medicine, Busan, Korea, Rep. of South; ²Good Samsun Hospital, Internal Medicine, Busan, Korea, Rep. of South
Email: who54@hanmail.net

Background and aims: Survival data in patients with hepatitis C virus (HCV) associated hepatocellular carcinoma (HCC) treated with direct acting antivirals (DAAs) are limited. Survival rates were compared between patients with HCV-related HCC who were untreated for HCV and who treated with DAA.

Method: From 2010 to 2019, a total of 469 patients who were monoinfected with HCV-related HCC was categorized into patients untreated for HCV and patients treated with DAA. Multivariable Cox regression with HCV treatment status as a time-varying covariate was used to determine mortality risk.

Results: There were 95 untreated group and 94 DAA group. Of DAA group, 42 was active HCC state (patients without viable HCC). Baseline characteristics between untreated group and DAA with active HCC were balanced except genotype. Sustained virologic response rate was 88.2% by per protocol analysis in DAA treated patients. After time-varying adjustment for DAA treatment initiation compared with untreated patients, patients with DAA had significantly higher 5-year overall survival (76.7% vs. 22.4%, $p < 0.001$). Multivariate Cox regression showed that survival was significantly improved in patients with DAA treatment ($p < 0.001$), patients who were treated with curative treatment (0.034) and with history of interferon exposure ($p = 0.045$).

Conclusion: In this study, patients in HCV related HCV who treated DAA achieved 88.2% of SVR and showed significant improvement of survival compared with patients untreated with DAA.

FRI358

Lack of Alpha-fetoprotein reduction after successful Hepatitis C treatment in patients with cirrhosis predicts the development of hepatocellular carcinoma during surveillance-a single unit real-world experience

Aoife Alvain¹, Jack Lee¹, Eileen Shannon¹, Mary Kavanagh¹, Mary Bohan-Keane¹, Margaret Scarry¹, John Lee^{1,2}. ¹University Hospital Galway, Hepatology unit, Galway, Ireland; ²National University of Ireland, Galway, Galway, Ireland
Email: alvaina@tcd.ie

Background and aims: The value and limitation of alpha-fetoprotein (AFP) in hepatocellular carcinoma (HCC) screening is well established. In patients with chronic hepatitis C virus (HCV) infection and cirrhosis, AFP is often elevated in the absence of HCC. The aim of this study was to measure the impact of DAA treatment on AFP levels and correlate this with clinical outcomes. Correlation with changes in transient elastography (Fibroscan) scores were also evaluated.

Method: Patients with established cirrhosis prior to successful direct acting anti-viral (DAA) treatment were included. Patients with HCC were excluded. Laboratory values including AFP, transaminases, platelet count and Fibroscan scores were measured at baseline and post-treatment. Patients were followed-up for the development of HCC. Factors associated with improvement in AFP were investigated. Further analysis was carried out classifying patients based on a clinically relevant threshold.

Results: 77 patients (male $n = 47$, 61.0%) and median follow-up of 5.7 years. 11 (14.3%) have developed HCC during follow-up. Overall, the mean AFP significantly improved with treatment (Mean $17.69 \pm SD 31.44$ vs 7.27 ± 16.80 , $p = 0.0015$). The mean Fibroscan score significantly improved with treatment (22.96 ± 14.07 vs 13.73 ± 9.05 , $p <$

0.001). In linear regression analysis, reduction in AFP was found to positively correlate with reduction in Fibroscan scores (coefficient = 0.04, $p = 0.91$). We defined improvement in AFP levels as a pre-treatment value of >10 which reduced to ≤ 10 after treatment. 47 patients (61.0%) had a normal AFP at baseline, 24 patients (31.2%) improved and 6 (7.8%) remained high. The cumulative HCC risk was 50% for patient whose AFP remained high, 12.5% in those whose AFP improved, and 10.6% those whose AFP remained normal (chi-squared test $p = 0.068$).

Conclusion: The risk of HCC after successful HCV treatment in cirrhotic patients remains high. Overall, AFP levels improve with DAA treatment in patients with cirrhosis. Fibroscan scores improve with DAA treatment. Failure to see an improvement in AFP after treatment predicts the development of HCC. This should be considered in stratifying individual patient HCC risk during real-world follow-up surveillance protocols.

FRI359

Patients with chronic HCV and decompensated cirrhosis are at risk for MELD purgatory

Lisette Krassenburg^{1,2}, Grishma Hirode^{1,3}, Hooman Farhang Zangneh¹, Rael Maan², Alnoor Ramji⁴, Michael P. Manns⁵, Heiner Wedemeyer⁵, Markus Cornberg⁵, Robert De Knecht², Kosh Agarwal⁶, Zillah Cargill⁶, Gonzalo Crespo⁷, Giuseppina Brancaccio⁸, Maria Cristina Morelli⁹, Ilaria Lenci¹⁰, Chiara Mazzarelli¹¹, Paolo Angeli¹², Patrizia Burra¹³, Gabriella Verucchi¹⁴, Maria Francesca Donato¹⁵, Paola Carrai¹⁶, Silvia Martini¹⁷, Paolo Caraceni¹⁸, Francesco Paolo Russo¹⁹, Robert De Man², Harry Janssen¹, Bettina Hansen¹, Adriaan Van der Meer², Jordan Feld¹. ¹Toronto Centre for Liver Disease, Toronto General Hospital, University Health Network, Toronto, Canada; ²Department of Gastroenterology and Hepatology, Erasmus MC University Medical Center Rotterdam, Rotterdam, Netherlands; ³Toronto Viral Hepatitis Care Network (VIRCAN), Toronto, Canada; ⁴Department of Medicine, Division of Gastroenterology, University of British Columbia, Vancouver, Canada; ⁵Department of Gastroenterology, Hepatology and Endocrinology, Hannover Medical School, Hannover, Germany; ⁶Institute of Liver Studies, King's College Hospital, London, United Kingdom; ⁷Liver Transplant Unit, Liver Unit, University of Barcelona, Barcelona, Spain; ⁸Department of Infectious Diseases, Second University of Naples, Naples, Italy; ⁹Department of Organ Failures and Transplantation, Università degli Studi di Bologna Azienda Ospedaliera di Bologna Policlinico Sant'Orsola-Malpighi, Bologna, Italy; ¹⁰Hepatology Unit, Department of Internal Medicine, Tor Vergata University, Rome, Italy; ¹¹Hepatology and Gastroenterology Unit, ASST Ospedale Niguarda, Milan, Italy; ¹²Unit of Internal Medicine and Hepatology (UIMH), University of Padua, Padua, Italy; ¹³Multivisceral Transplant Unit, Department of Surgery, Oncology and Gastroenterology, University Hospital Padua, University of Padua, Padua, Italy; ¹⁴Infectious Diseases Unit, Department of Medical and Surgical Sciences, University of Bologna, Bologna, Italy; ¹⁵Fondazione IRCCS Ca, Granda Ospedale maggiore Policlinico and CRC "A.M. & A. Migliavacca Center for Liver Disease," Division of Gastroenterology and Hepatology, Milan, Italy; ¹⁶Hepatobiliary Surgery and Liver Transplantation, University of Pisa Medical School Hospital, Pisa, Italy; ¹⁷Gastrohepatology Unit, Azienda Ospedaliero Universitaria Città della Salute e della Scienza di Torino, Turin, Italy; ¹⁸Department of Medical and Surgical Sciences, University of Bologna, Bologna, Italy; ¹⁹Department of Surgery, Oncology and Gastroenterology, Gastroenterology/Multivisceral Transplant Section, University/Hospital Padua, Padua, Italy
Email: l.krassenburg@erasmusmc.nl

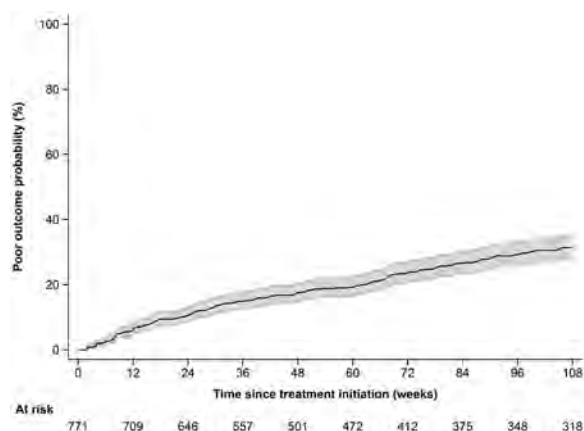
Background and aims: Treatment decisions are challenging in patients with decompensated cirrhosis due to chronic hepatitis C (HCV). Some patients might benefit from delaying HCV treatment until after liver transplantation, as a decrease in MELD-score without clinical benefit may limit transplant eligibility, also known as MELD purgatory. This study aims to predict the probability of a poor

POSTER PRESENTATIONS

outcome among patients who were eligible for a liver transplant at treatment initiation.

Method: Retrospective cohort study including HCV patients with a history of/current decompensated cirrhosis treated with DAAs in Europe and Canada. MELD purgatory was defined as presence of ascites or hepatic encephalopathy with sustained MELD-Na < 15 after treatment initiation. The cumulative probability and factors associated with a poor outcome (sustained MELD purgatory, HCC or death) after treatment initiation were analyzed using Kaplan-Meier plots and multivariable (MV) Cox regression. The risk of death/HCC vs transplantation post-treatment was compared in those who were transplant ineligible at baseline.

Results: Among 877 patients: mean age 55 ± 9 years, 68% male, 86% Caucasian, median BMI 27 [24–30] kg/m², 24% diabetes and 44% history of alcohol abuse. At baseline, median INR was 1.3 (1.2–1.5), ALT was 54 (37–84) U/L, platelets were $77 (55–105) \times 10^9/L$, total bilirubin was 1.9 (1.2–2.8) mg/dL and mean albumin was 32 ± 5.8 g/L. Mean MELD-Na was 15 ± 5.5 . The majority had MELD-Na ≥ 15 (62%), and 51% were decompensated at baseline. A total of 665 (80%) achieved SVR12. During a median follow-up of 35 (8–90) weeks after treatment initiation, 194 (22%) entered sustained MELD purgatory, 114 (13.0%) developed HCC, and 106 died (12.1%). Cumulative probabilities of a poor outcome at 36, 72, and 108 weeks were 15%, 24%, and 32%, respectively (Figure). On MV Cox regression, older age (aHR 1.02, $p = 0.037$), lower sodium (aHR 0.95, $p = 0.014$), and lower albumin (aHR 0.97, $p = 0.032$) at baseline were associated with higher rates of a poor outcome. Of those who met the definition of MELD-purgatory before treatment initiation ($n = 195$), cumulative probabilities of death/HCC were 5.1%, 8.1% and 9.0% at 36, 72, 108 weeks post-treatment start, whereas rates of liver transplant were 4.2%, 9.0% and 12.3% at the same time points.



Conclusion: Patients with chronic HCV and decompensated cirrhosis are at risk for MELD purgatory, HCC or death, even when SVR is achieved. Caution should be taken when treating these patients, especially transplant-eligible patients who may be better off with liver transplantation prior to HCV treatment. Decompensated patients who are not transplant-eligible at treatment start have a similar probability of HCC/death as of receiving a transplant post-treatment, making treatment decisions particularly challenging and highlighting the need for careful post-treatment follow-up.

FRI360

The long-term effect of Hepatitis C eradication by direct-acting antivirals on patient's mood and quality of life as determined by the Beck's Depression Inventory and EQ5D Quality of Life questionnaires-a single unit study

Aoife Alvain¹, Sarah Lanigan¹, Mary Bohan-Keane¹, Margaret Scarry¹, Lynda Jordan¹, Cynthia Garvey¹, Priyanka Jose¹, John Lee^{1,2}. ¹University

Hospital Galway, Hepatology Unit, Galway, Ireland; ²National University of Ireland, Galway, Galway, Ireland
Email: alvaina@tcd.ie

Background and aims: Direct-acting antiviral (DAA) treatments are established to be well tolerated and achieve Hepatitis C virus (HCV) eradication in the quasi-totality of patients. This prevents progression to liver cirrhosis, reduces the risk of hepatocellular carcinoma, and improves overall prognosis. The aim of this study was to investigate the long-term effects of HCV eradication by DAA on patient's mood and quality of life.

Method: HCV patients completed a baseline Beck's Depression Inventory and Quality of Life Questionnaire (EQ5D) prior to DAA treatment and were prospectively evaluated. After anti-viral therapy, the questionnaires were repeated with a minimum of 12 months follow-up. A Beck's score of <10 is considered to be within the normal range of mood variation. An EQ5D of 5 represents optimal quality of life.

Results: A total of 54 patients with a mean age of 49.5 years were included (51.8% male). All patients had a sustained virological response to DAA treatment; the median follow-up was 4.1 years. Prior to treatment, 9 (16.7%) had established cirrhosis, and 14 (25.9%) had at least one psychiatric co-morbidity. The mean Beck's score pre-treatment (Mean $7.88 \pm SD 7.88$) and at long-term follow-up (7.31 ± 6.22) was not significantly different ($p = 0.29$). Median Beck's score pre-treatment (7) and at follow-up (6) were comparable, as were the number of patients with a Beck's score <10 pre-treatment ($n = 37$, 68.5%) and at follow-up ($n = 37$, 68.5%). In the sub-group analysis, no significant difference was found with sub-groups defined by patient's background psychiatric history, pre-treatment cirrhosis status or HCV mode of transmission (pre-treatment and follow-up median scores were comparable and so were the number of patients with a Beck's score <10). There was no significant difference in the EQ5D pre-treatment (6.88 ± 2.30) and at follow-up (6.74 ± 2.45) ($p = 0.39$). Median score pre-treatment (6) and at follow-up were comparable (6), as were the number of patients with EQ5D = 5 pre-treatment ($n = 16$) and at follow-up ($n = 18$).

Conclusion: In this prospective study of patients successfully treated for HCV with DAA treatment, the reported mood and quality of life at long-term follow-up did not significantly change from their pre-treatment baseline. It is expected that quality of life and mood would deteriorate in un-treated patients as they develop complications of chronic HCV and as such this study demonstrate the benefit of DAA treatment on mood and quality of life.

FRI361

Assessing sustained virological response and reinfection from dried blood spots within an on-site hepatitis C diagnosis and treatment model of care in a harm reduction centre

Anna Not¹, Verónica Saludes^{1,2}, Anna Miralpeix^{3,4}, Mont Gálvez^{3,4}, Antoni E. Bordoy¹, Sara González-Gómez¹, Noemí González⁵, Juliana Reyes-Ureña⁶, Xavier Major⁷, Joan Colom⁷, Xavier Fornes^{3,4,8}, Sabela Lens^{3,4,8}, Elisa Martró^{1,2}. ¹Hospital Universitari Germans Trias i Pujol, Institut d'Investigació Germans Trias i Pujol (IGTP), Microbiology Department, Badalona, Spain; ²Consorcio de Investigación Biomédica en Red de Epidemiología y Salud Pública (CIBERESP), Madrid, Spain; ³Hospital Clínic, Liver Unit, Barcelona, Spain; ⁴IDIBAPS, Barcelona, Spain; ⁵REDAN La Mina. Parc de Salut Mar. Sant Adrià del Besòs (Barcelona), Spain; ⁶Center for Epidemiological Studies on HIV/AIDS and STIs of Catalonia (CEEISCAT), ASPCAT, Barcelona, Spain; ⁷Program for the Prevention, Control and Care of HIV, Sexually Transmitted Infections and Viral Hepatitis, ASPCAT, Barcelona, Spain; ⁸Consorcio de Investigación Biomédica en Red de Enfermedades Hepáticas y Digestivas (CIBEREHD), Madrid, Spain

Email: emartro@igtp.cat

Background and aims: Dried blood spot (DBS) samples are a reliable tool to diagnose viremic HCV infection. However, there is scarce data on the usefulness of DBS to assess cure and reinfection after antiviral

therapy. Here, we aimed to evaluate the use of DBS for the assessment of sustained virological response (SVR) and reinfection 12 weeks after on-site treatment with direct-acting antivirals at a harm reduction service (HRS) in Catalonia.

Method: This evaluation was performed within the context of an ongoing micro-elimination study targeting people who inject drugs (PWID) in the largest HRS in Barcelona. At the time of SVR assessment (FU12), HCV-RNA was detected from DBS with an in-house real-time RT-PCR assay (lower limit of detection -LoD-, 541 IU/ml of blood) in comparison with the reference method (viral load in fingerstick capillary blood by GeneXpert®; LoD, 40 IU/ml). Additionally, DBS samples (baseline vs. FU12) were used to assess reinfection vs. treatment failure by an in-house method based on NS5B nested-PCR amplification followed by Sanger sequencing and phylogenetic analysis. When mixed or no signal was obtained, samples were genotyped by a commercial real-time PCR genotyping assay (Abbott).

Results: Among treated patients, 105 DBS samples corresponding to FU12 were tested (55 negative and 50 positive). The DBS-based HCV-RNA assay showed 100% specificity (55/55). Nine cases were not detected, with viral loads between 116 and 4660 IU/ml; sensitivity ranged from 82.0% to 95.0% according to different viral load cut-offs (Table 1). FU12 RNA positive samples ($n = 50$) were genotyped by sequencing ($n = 32$) or by the commercial genotyping assay ($n = 15$) in comparison with baseline DBS samples. Results evidenced the presence of reinfection in 29 cases and of treatment failure in seven cases with high viral loads. The rest of cases could not be classified by any of the two methods: three with low viral loads could not be amplified, one was indeterminate, and in seven cases the same genotype/subtype was detected at FU12 and baseline samples, with phylogenetic classification not assessable from the commercial genotyping assay.

HCV viral load threshold by Xpert HCV	Detected by the DBS assay	
	Proportion	%
Detectable	41/50	82.0
Quantifiable ≥ 100 IU/ml	41/49	83.7
Quantifiable ≥ 1000 IU/ml (EASL Guidelines)	41/46	89.1
Quantifiable ≥ 3000 IU/ml (WHO Testing Guidelines)	38/40	95.0

Conclusion: This study shows the usefulness of DBS samples for assessing cure and differentiating reinfection from relapse after HCV antiviral treatment in the real world, facilitating treatment decentralization in PWID attending HRS. However, some patients presented with low viral loads at FU12, limiting detection and genotyping. While the latter cases might reflect acute infections that may be spontaneously cleared, repeat testing over time would be required to identify all viremic cases.

FRI362

Hepatitis C virus (HCV)-specific T cell confer resistance to HCV re-infection after sustained virologic response in a non-cytolytic fashion among people who inject drugs: results from ANCHOR study

Arshi Khanam¹, Alip Ghosh², Sarah Kattakuzhy¹, Shyamasundaran Kottilil¹, Elana Rosenthal¹. ¹Institute of Human Virology University of Maryland School of Medicine, Division of Clinical Care and Research, Baltimore, United States; ²Institute of Human Virology, University of Maryland School of Medicine, Baltimore, United States

Email: akhanam@ihv.umaryland.edu

Background and aims: People who inject drugs (PWID) remain a major reservoir of chronic hepatitis C virus (HCV) infection. Ongoing injecting drug use is associated with re-infection, however the role of HCV specific immune response in PWID is not understood. In this

study, we evaluated the immune correlates that are associated with re-infection of HCV in PWID after achieving sustained virologic response (SVR).

Method: ANCHOR is a study of 198 people with opioid use disorder, ongoing opioid misuse and chronic HCV. All participants received DAAs, 157 achieved SVR, and 17 were reinfected. We studied 27 patients who achieved SVR without reinfection (Non-RI) and 13 patients who were reinfected (RI). Changes in the phenotypic profile of T cells were determined in the peripheral blood mononuclear cells (PBMCs) by flow cytometry. HCV specific T cell functions were investigated by stimulating the PBMCs with a pool of 21 overlapping peptides from envelop, core and NS3-NS5 regions of HCV. Immune profiles were evaluated at baseline (prior to HCV treatment) and after SVR (prior to reinfection) and compared between the two groups.

Results: At baseline, RI group displayed higher expression of inhibitory receptors including programmed death-1 (PD-1) (CD4 $P = 0.002$, CD8 $P = 0.02$) and 2B4 (CD4 $P = ns$, CD8 $P = 0.01$), and lower expression of activation markers CD38 (CD4 $P = 0.02$, CD8 $P = ns$) and HLA-DR (CD4 & CD8 T cells $P = 0.02$) on T cells than Non-RI group and continuously maintained exhaustive phenotype even after achieving SVR, suggesting persistent exhaustion of T cells in RI. At baseline, RI group constituted lower frequencies of naïve (14% vs. 29%) and terminally differentiated effector memory cells (3% vs. 10%) in CD4 T cell population that did not change upon SVR, while a marked reduction in effector memory cells were observed (48% vs. 31%) at SVR. Moreover, CD8 T cell population exhibited decreased percentage of naïve (17% vs. 35%) and central memory cells (3% vs. 8%) in RI group and similar profile was maintained upon SVR. However, the expression of the transcription factors Tbet and Eomes (CD4: 2% and 5%, CD8: 7% and 20%) was similar between both groups. Further, T cells from RI group persistently produced lower amounts of antiviral cytokines such as IFN- γ and TNF- α at baseline and after achieving SVR compared to the Non-RI (CD4 IFN- γ & TNF- α $P = 0.04$, $P = 0.01$) (CD8 IFN- γ & TNF- α $P = 0.01$, $P = ns$). In fact, polyfunctional T cell response determined by IFN- γ and TNF- α co-producing cells was also impaired in the RI compared to the Non-RI group (CD4 $P = 0.03$ and CD8 $P = 0.04$). However, cytotoxic potential of T cells evaluated by CD107a and perforin expression were maintained between both groups.

Conclusion: Peripheral T cells from PWID who were reinfected with HCV after achieving SVR displayed an exhaustive phenotype and had depressed anti-HCV response after SVR, suggesting a role for protection from re-infection by T cells in a non-cytolytic fashion.

FRI363

Lack of fibrosis remodelling in chronic hepatitis C post SVR, as demonstrated by YKL-40, is predictive of hepatocellular carcinoma occurrence

Maria Guerra Veloz¹, James Lok¹, Chiara Mazzarelli², Mary D Cannon¹, Ivana Carey¹, Kosh Agarwal¹. ¹King's College Hospital, Institute of Liver Studies, United Kingdom; ²ASST Grande Ospedale Metropolitano Niguarda-Milano

Email: maria.guerraveloz@nhs.net

Background and aims: The introduction of new direct-acting antivirals agents (DAA) have revolutionized the natural history of the chronic hepatitis C virus (HCV). However, the course of progressive liver damage, as well as the risk of developing HCC after achieving sustained virological response (SVR), is still uncertain. Our group's preliminary data¹ showed that YKL-40 (acting as a growth factor for fibroblasts and being involved in matrix remodelling) and Hyaluronic acid (HA, acting as promoter of hepatic fibrogenesis) decreased in patients who achieved SVR. The aim of our study was to determine whether YKL-40 and/or HA could be a predictor of HCC occurrence in patients with cirrhosis who achieved SVR.

Method: In this retrospective study, we included patients with hepatitis C related cirrhosis, who achieved SVR after DAA therapy, in whom YKL-40 and HA were measured prior to treatment and at 36

POSTER PRESENTATIONS

weeks post SVR. Cirrhosis was defined based on FibroScan® >14.5 kPa and/or a combination of endoscopy and imaging criteria. Only those treated with DAA therapy between January 2015 and December 2016 were included. Patients were followed-up with until November 2021 or until HCC occurred.

Results: Our study included 71 patients of whom 64.8% were males with a mean age of 61 (±8) years. Of our total cohort, 62% had genotype 1, 55% were Child Pugh A (CPA), 24% were CPA with a previous decompensation, and 21% were CP B/C. During a median follow up of 60 months (IQR 41–70), 25.4% (18) of patients had developed HCC. Patients who developed HCC had more advanced liver disease (CP B/C 53.3% vs 20.5% CPA vs 11.8% CPA previous decompensation; $p = 0.031$), a lower baseline albumin (34.7 vs 38.4; $p = 0.004$) and an elevated YKL-40 at 36 weeks after SVR (4789 vs 3333; $p = 0.036$) compared to those who had not developed HCC (table 1). Between start of treatment and 36 weeks post SVR, the mean decrease in YKL-40 was significantly greater in those who did not develop HCC (from 5098 to 3333, $p < 0.001$; vs 4752 to 4789 $p = 0.987$). There was no difference in the dynamics of HA between the two groups. In the multivariate analysis, YKL-40 at 36 weeks post SVR (HR 1; CI 95% 1–1) was an independent factor associated with HCC. Child Pugh status A (HR 0.36; IC 95% 0.142–0.937) was an independent factor associated with lower HCC.

Characteristics	Total cohort N = 71	No HCC N = 53	HCC N = 18	P
Sex				
Male	46 (64.8)	34 (64.2)	12 (66.7)	0.926
Age	61(±8)	62 (±7.9)	60 (±8.2)	0.512
Alcohol User (yes)	4 (5.6)	3 (5.7)	1 (5.6)	0.565
HT	8 (11.3)	5 (9.4)	3 (16.7)	0.161
DM	17 (23.9)	10 (18.9)	7 (38.9)	0.646
Genotype				
1	44 (62)	35 (66.0)	9 (50)	0.352
3	16 (22.5)	12 (22.6)	4 (22.2)	0.772
CPT				
A previous decompensation	17 (24)	15 (88.2)	2 (11.8)	
A without decompensation	39 (55)	31 (79.5)	8 (20.5)	0.031
B/C	15 (21)	7 (46.7)	8 (53.3)	
MELD	8 (6–11)	8 (6–9)	9 (7–14)	0.137
Baseline AFP IU/L median (IQR)	9(5–23)	9(5–24)	8.5(5.3–15)	0.300
EOT AFP median (IQR)	6(3–9)	6(3–9)	5.5(3.3–8)	0.446
48EOT AFP median (IQR)	4(2–6)	4(2–6)	4(3–6)	0.749
Baseline albumin g/L mean (SD)	37.5 (±4.7)	38.4(±4.27)	34.7(±5.05)	0.004
Baseline Platelet (x10 ⁹ /L)	85(67–120)	89 (69–120)	77(58–114)	0.312
Baseline INR mean (SD)	1.2(±0.19)	1.22 (±0.19)	1.3(±0.17)	0.128
Baseline Bilirubin umol/L mean (SD)	19.5 (±12.3)	17 (±0.95)	24.2(±14.7)	0.057
Baseline YKL-40 pg/ml mean (SD)	5010 (±2933)	5098(±2967)	4752(±2908)	0.687
Baseline HA mean (SD)	919.8 (±556)	926.8 (±585)	896.9 (±467)	0.838
YKL-40 36weeks post SVR mean (SD)	3686(±2425)	3333(±2239)	4789(±2723)	0.036
HA 36weeks post SVR	836 (±507)	893.3 (±522)	638.9 (±404)	0.101

Conclusion: HCC occurrence was higher in patients with CP B/C and those who did not decrease YKL-40 after achieving SVR. YKL-40 could be a predictive factor of HCC occurrence however further studies with a larger sample are necessary to confirm these results.

Mazzarelli C *et al.* Direct fibrosis markers kinetic in patients undergoing antiviral treatment with DAA for chronic hepatitis C. *Journal of Hepatology* 68 (1):S403.

FRI364

HCV reinfection associated with IDU and cocaine use in a cohort of people with OUD: 4 Year follow-up data from the ANCHOR cohort

Elana Rosenthal¹, Junfeng Sun², Britt Gayle¹, Amelia Cover¹, Ashley Davis¹, Shivakumar Narayanan¹, Catherine Gannon², Grace Garrett², Vivian Wang², Meghan Derenoncourt², Henry Masur², Shyamasundaran Kottlil¹, Sarah Kattakuzhy¹. ¹Division of Clinical Care and Research, Institute of Human Virology, University of Maryland School of Medicine, United States; ²National Institutes of Health/Critical Care Medicine Department, Bethesda, United States
Email: erosenthal@ihv.umaryland.edu

Background and aims: People with HCV and opioid use disorder (OUD) who achieve sustained virologic response (SVR) may remain at risk of reinfection. Identification and retreatment of reinfected individuals is critical to HCV elimination. We sought to evaluate the

rate of reinfection and factors associated with reinfection in a cohort of high-risk patients over a 4 year follow-up period.

Method: ANCHOR is a 96 week, prospective cohort study of people with OUD, opioid misuse within a year and chronic HCV. All participants received HCV treatment. Those who achieved SVR were followed for reinfection for 18 months, and subsequently had the option to enroll in LOOP, a 2 year long-term follow-up study. Reinfection was defined as a genotype switch or detectable viral load after SVR. Patients were administered surveys at each visit to assess for ongoing risk behaviors and medication for OUD (MOUD) status. A logistic regression model with GEE was created using covariates with $p < 0.10$ to model the probability of reinfection.

Results: 157 individuals achieved SVR and were followed for 273.2 person-years, median 86.2 weeks (range 12–210 weeks). Subjects were predominantly male (69%), black (84%), middle-aged (median 57 years), and 50.3% unstably housed. Seventeen individuals (10.8%) were reinfected a median of 76.1 weeks (range 21–175 weeks) after HCV treatment, a rate of 6.2/100 person-years. Reinfection was associated with past month IDU ($p = 0.006$), and cocaine positive UDS ($p = 0.03$), however was not associated with age, race, gender, education, or visit specific opioid positive UDS, housing stability, MOUD engagement, or HIV risk score (all $p > 0.05$). Of the 17 reinfected individuals, 12 (71%) initiated HCV re-treatment, with 10 achieving SVR and 2 deaths.

Conclusion: In this cohort of high-risk people with OUD, we found high rates of HCV reinfection which were associated with past-month IDU and cocaine positive UDS at the time of detection. Given the rate and timing of reinfection, these data reinforce the importance of long-term engagement, ongoing HCV testing, and low-barrier treatment of HCV reinfection. Further, in the era of rising stimulant use, these data highlight the importance of assessing for and reducing harms associated with polysubstance use and injection drug use in people with opioid use disorder.

FRI365

Noninvasive prediction of hepatocellular carcinoma development after oral antiviral therapy in patients with chronic hepatitis C: a multicenter study

Yu Rim Lee¹, Jung Gil Park², Min Kyu Kang², Jung Eun Song³, Byoung Kuk Jang⁴, Young Oh Kwon¹, Won Young Tak¹, Se Young Jang¹, Changhyeong Lee³, Byung Seok Kim³, Jae-Seok Hwang⁴, Woo Jin Chung⁴, Soo Young Park¹, Nae-Yun Heo⁵, Jeong Heo⁶, Hyun Young Woo⁶, Yanghyon Baek⁷, Jun Sik Yoon⁸, Joonho Jeong⁹, Jae Young Jang¹. ¹Kyungpook National University, Kyungpook National University Hospital; ²Yeungnam University College of Medicine; ³Daegu Catholic University School of Medicine; ⁴Keimyung University School of Medicine; ⁵Inje University Haeundae Paik Hospital, Inje University College of Medicine; ⁶Pusan National University; ⁷Dong-A University Hospital; ⁸Busan Paik Hospital, Inje University College of Medicine; ⁹University of Ulsan College of Medicine, Ulsan University Hospital
Email: psyong0419@gmail.com

Background and aims: Hepatocellular carcinoma (HCC) can still occur after achieving a sustained virologic response (SVR) to direct-acting antiviral (DAA) therapy in patients with hepatitis C. We aimed to identify non-invasive parameters that predict the HCC development for patient with chronic hepatitis C after SVR.

Method: A total of 3, 489 HCV patients who treated with DAAs and had achieved SVR from nine hospitals in South Korea were included in this study. Predictors of HCC occurrence and HCC risk scores were assessed.

Results: During a median follow-up of 2.3 years, HCC occurred in 158 patients (4.5%). LSM gradually decreased from baseline to SVR and 1 year after treatment ($p < 0.001$). Platelet count, bilirubin, and albumin levels also improved from before treatment to 1 year after treatment (all $P < 0.05$). Multivariate analysis using the Cox regression test identified that age (HR 1.055, 95% CI 1.036–1.074, $P < 0.001$), sex

(HR 1.942, 95% CI 1.326–2.844, $P=0.001$), platelet count (HR 0.987, 95% CI 0.984–0.991, $P<0.001$), and albumin (HR 0.525, 95% CI 0.353–0.780, $P=0.004$) at 1 year follow-up were independently associated with the risk of HCC. HCC risk scores including Modified PAGE-B scores (AUROC = 0.814) and aMAP risk score (AUROC = 0.826) at 1 year after SVR using age, gender, platelet counts, serum albumin levels can discriminate the risk of HCC.

Conclusion: In patients with chronic hepatitis C who have achieved SVR with DAAs, the use of HCC risk scores including Modified PAGE-B scores and aMAP risk score at 1 year after SVR accurately predicted the risk of HCC.

FRI366

Sustained low prevalence of HCV viremia among people who inject drugs following the treatment as prevention for hepatitis C (TraP HepC) nationwide elimination program in Iceland

Magnús Gottfredsson^{1,2}, Valgerdur Runarsdóttir³, Thorvardur J. Löve^{4,5}, Ragnheidur H. Fridriksdóttir⁶, Thorarinn Tyrfinngsson³, Ingunn Hansdóttir³, Ottar M. Bergmann⁶, Einar S. Björnsson^{2,6}, Birgir Johannsson¹, Bryndis Sigurdardóttir¹, Arthur Löve⁷, Guðrún Erna Baldvinsdóttir⁷, Marianna Thordardóttir⁸, Ubaldo Benitez Hernandez⁴, Maria Heimisdóttir⁹, Sigurdur Olafsson^{2,6}. ¹Landspítali University Hospital, Infectious Diseases, Reykjavík, Iceland; ²University of Iceland, Medicine, Reykjavík, Iceland; ³SAA National center for addiction medicine, Reykjavík, Iceland; ⁴Landspítali University Hospital, Science, Reykjavík, Iceland; ⁵University of Iceland, Public Health, Reykjavík, Iceland; ⁶Landspítali University Hospital, Gastroenterology and Hepatology, Reykjavík, Iceland; ⁷Landspítali University Hospital, Virology, Reykjavík, Iceland; ⁸State Epidemiologist, Infectious Diseases, Reykjavík, Iceland; ⁹Icelandic Health Insurance, Reykjavík, Iceland
Email: magnusgo@landspitali.is

Background and aims: Injection drug use (IDU) and sharing of injection equipment and paraphernalia is the main mode of transmission of Hepatitis C Virus (HCV) in most Western societies. People who inject drugs (PWID) therefore need to be diagnosed, treated and cured in order to curb transmission and achieve the WHO goal of eliminating HCV infection as a public health threat by 2030. Starting in 2016, the Treatment as Prevention for Hepatitis C (TraP HepC) program in Iceland has offered direct acting antiviral agents (DAA) to all HCV-infected patients with permanent residence in the country without restrictions. It has from its inception focused on PWID, with special emphasis on active IDU. Vogur addiction hospital screens all patients who report IDU activity upon admission for HCV and therefore is as an ideal sentinel site to monitor the prevalence of HCV viremia in this key population.

Method: We analysed the prevalence of HCV viremia by PCR among PWID who were admitted to Vogur for addiction treatment, 6 years before (2010–2015) and 5 years during the TraP HepC program (2016–2020).

Results: Prior to TraP HepC, 2010–2015 the prevalence of HCV viremia among admitted patients who gave history of ever injecting drugs was stable at 39.5–40.6%. Among those who were currently injecting at the time of admission (injecting within 6 months) the prevalence was stable at 53.2–57.7% during the same period. The prevalence of HCV viremia in the former group dropped to 32.9%, 12.0% and 8.6% during 2016, 2017 and 2018, respectively ($p<0.001$) and subsequently has remained stable at 12.9% and 13.3% in 2019 and 2020.

Conclusion: In the absence of an effective vaccine, treatment with DAA remains the most efficient way to lower the prevalence of HCV. Efficacy among PWID is excellent and treatment has resulted in a sustained drop in HCV viremia in this population but continued monitoring of these patients is needed. Further studies and longer follow-up is needed to evaluate whether this drop eventually translates into a lower nationwide incidence of HCV in Iceland.

FRI367

Direct-acting antiviral treatment in Albanian patients with chronic hepatitis C and advanced liver fibrosis

Liri Cuko¹, Eva Shagla¹, Adriana Babameto¹, Jovan Basho¹, Arlinda Hysenj¹, Stela Taci¹, Irgen Tafaj¹, Eno Pengili¹. ¹Mother Teresa Hospital, Department of Gastrohepatology, Tiranë, Albania
Email: liricuko@yahoo.com

Background and aims: Treatment of chronic hepatitis C with direct-acting antiviral (DAA) is very effective at clearing the infection in more than 90% of people. In Albania treatment with DAA is limited to patients with liver stiffness F3–F4, and with other co-infections. The objective of this study was to evaluate the efficacy of DAA in Albanian patients with genotype 1–5, where most of patients are with advanced liver fibrosis.

Method: This was a retrospective study realized at University Hospital Center of Tirana during 2014–2019, including naïve and experienced patients with genotype 1–5. All patients are evaluated with elastography and most of them were F3–F4. The primary endpoint was SVR-12. In patients without genotype we have used pan genotypic regimen. All patients are treated with genotypic and pangenotypic DAA and are assessed for adverse event during the treatment.

Results: In this study are included 207 patients, main age 48.9 ± 13.1 years, 56% male and 44% female. 152 (73%) were genotype 1, 24 (11.5%) genotype 2, 9 (4.3%) genotype 3, 14 (6.7%) genotype 4, 1 (0.4%) genotype 5, and 7 (3.8%) anassigned genotype. SVR percentage according to genotype is shown in table. SVR to all patients was 93.2%. According to elastography 127 (66%) were F3–F4, 80 (44%) F1–F2. Two patients with decompensated cirrhosis discontinued treatment due to side effect.

Genotype (n, %)	SVR-12 (% n/n)
1 (152, 73%)	95% (145/152)
2 (24, 11.5%)	95.8% (23/24)
3 (9, 4.3%)	88.8% (8/9)
4 (14, 6.7%)	78.5% (11/14)
5 (1, 0.4%)	100% (1/1)
anassigned (4, 6.7%)	71.4% (5/7)

Conclusion: Treatment with DAA proved to be very effective in our patient, most of them with advanced liver fibrosis, compensated or decompensated liver cirrhosis. SVR in total patients was 93.2%. The results about genotype 3, 5, are not significant due to the small number of patients. In our country need to treat all patients with chronic hepatitis C without limitations to reach the objective of WHO.

FRI368

Improved recurrence-free survival rates in patients with HCV-related hepatocellular carcinoma and sustained virological response to direct-acting antivirals

Cristina-Maria Muzica¹, Anca Trifan¹, Laura Huiban¹, Oana Stoica¹, Irina Girleanu¹, Stefan Chiriac¹, Ana-Maria Singeap¹, Camelia Cojocariu¹, Tudor Cuciureanu¹, Sebastian Zenovia¹, Robert Nastasa¹, Carol Stanciu¹. ¹Grigore T. Popa University of Medicine and Pharmacy, Gastroenterology, Iasi, Romania
Email: ancatrifan@yahoo.com

Background and aims: Despite the high efficacy of direct-acting antivirals (DAAs) in chronic HCV infection, a more aggressive pattern of hepatocellular carcinoma (HCC) in patients previously treated with DAAs, has been reported. Tumor aggression in HCV-related HCC after DAAs has been linked to impaired outcome. On this basis, we aimed to assess the pattern of HCC and survival rates in patients previously treated with DAAs therapy.

Method: This is a case-control study investigating the features of HCC and survival rates in patients with chronic HCV infection whom were previously treated with DAAs versus naïve patients. Patients were

POSTER PRESENTATIONS

matched for sex and age in a 1:3 fashion. HCC infiltrative pattern, portal vein thrombosis (PVT), metastases, Milan criteria, Barcelona Clinic Liver Cancer (BCLC) staging, tumor-node-metastasis (TNM) staging, Cancer of the Liver Italian Program (CLIP), as well as the recurrence and overall survival rate at 18 months of follow-up, were compared in the 2 groups. This research was carried out in the Institute of Gastroenterology Iasi, Romania, between January 1st, 2017 and December 31, 2019.

Results: The study included 124 patients that were divided into two groups according to DAAs status: 31 DAAs-treated HCC patients and 93 non-DAAs HCC patients. Overall, 65% were males, and the mean age was 58.9 ± 6.8 years. The mean values of APRI and Fib-4 scores were significantly higher in the DAAs-treated group than in naïve patients ($p < 0.001$). The frequency of the infiltrative HCC pattern, PVT, and metastasis was higher in the non-DAAs group ($p = 0.002$). According to BCLC, CLIP, and TNM, HCC patients in the non-DAAs group had more advanced stages and limited treatment options ($p < 0.001$). Furthermore, HCC recurrence rate was higher in naïve patients than in those DAAs-treated (16, 2% versus 8, 6%, $p = 0.002$). The 18-months overall survival rate was 73.3% in the DAAs-treated group and 43.7% in non-DAAs group ($p = 0.008$).

Conclusion: Our study indicates a better recurrence-free overall survival rate in patients with HCV-related hepatocellular carcinoma with SVR to DAAs compared with naïve patients, demonstrating the beneficial impact on the outcome of these patients.

FRI369

Long-term outcomes associated with task-shifting of HCV treatment by non-specialist providers: five year follow-up from the ASCEND cohort

Sarah Mollenkopf¹, Elana Rosenthal², Gebeyehu Teferi³, Rachel Silk², Nivya George², Henry Masur⁴, Shyamasundaran Kottitil², Sarah Kattakuzhy². ¹University of Maryland School of Medicine, Baltimore, United States; ²Institute of Human Virology, Division of Clinical Care and Research, Baltimore; ³Unity Health Care, Washington, United States; ⁴NIH, Critical Care Medicine Department, Bethesda, United States

Email: skattakuzhy@ihv.umaryland.edu

Background and aims: Since 2015, an increasing body of evidence has supported task-shifting of Hepatitis C (HCV) treatment with direct-acting antivirals (DAA) to non-specialist providers, however, there are limited data on longitudinal outcomes associated with this treatment paradigm. We sought to assess outcomes of patients in the 5 years after initial DAA treatment by specialist and non-specialist providers, to evaluate the longitudinal evidence for task-shifting in the ASCEND cohort.

Method: This analysis included 525 patients treated for HCV with ledipasvir-sofosbuvir in the ASCEND investigation who had long term follow up data available. Chart review and abstraction of variables of interest from date of sustained virologic response (SVR) to June 2020 was completed. Baseline demographic and clinical characteristics were compared using t-tests, while change in outcomes was assessed using McNemar's or chi-squared tests. All analysis was conducted in R, version 4.1.0.

Results: Amongst 525 patients at ASCEND baseline, the mean age was 59.5 years, with majority male (69%), Black race (95%), and genotype 1a (71%), with 20% with HIV, 20% with cirrhosis and 18% IFN-treatment experienced.

In addition to 458 (87.2%) of patients with SVR at the end of the original investigation, 16 patients who were lost to follow up were found to have achieved SVR. Furthermore, of 32 patients with known NSVR, 23 were re-treated, 17 of whom achieved SVR. Therefore, 491 (93.5%) of ASCEND participants ultimately achieved HCV cure during the five-year follow up period.

Of the 458 patients who achieved SVR, 97% returned to clinic, of whom 70% were screened for HCV reinfection. Of 336 patients screened, only two (0.6%) were found to be reinfect.

Twenty-five patients died during the follow up period. There was a significant difference in mortality rates based on SVR status, with 4.1% mortality in those with SVR, compared to 35.7% with NSVR ($p < 0.5$). Of 14 individuals with known cause of death, 5 patients died from HCV-related causes.

When comparing outcomes by original ASCEND treatment provider type, there were no significant differences in rates of loss to follow-up, SVR, HCV re-screening, HCV reinfection or mortality ($p > 0.05$) between nurse practitioners, primary care physicians, and specialist physicians.

		NP	PCP	Specialist	Comparison	
		95% CI	95% CI	95% CI	X ²	p
SVR	#	132	98	261		
	Prop	0.943 (0.891-0.975)	0.916 (0.846-0.961)	0.939 (0.904-0.964)	0.855	0.652
NSVR	#	3	4	7		
	Prop	0.021 (0.004-0.061)	0.037 (0.010-0.093)	0.025 (0.010-0.051)	0.645	0.724
Reinfection [*]	#	0	0	2		
	Prop	0 (0.000-0.028)	0 (0.000-0.037)	0.008 (0.001-0.027)	1.770	0.413
HCV-Related Death [†]	#	2	1	2		
	Prop	0.286 (0.037-0.710)	0.125 (0.003-0.527)	0.200 (0.025-0.556)	0.603	0.740

* Difference between baseline ASCEND and 5-year follow-up values is significant by 3-Sample Test Chi-Squared Test for Equality of Proportions ($p < 0.05$)

† Denominator includes only those people who were tested for reinfection

‡ Denominator includes deaths of all causes

Conclusion: This five-year longitudinal follow-up of the ASCEND cohort identifies an even higher rate of SVR of 93.5% in an urban cohort, with limited reinfection. These data reinforce that task-shifting of HCV therapy to non-specialist providers results in both high rates of HCV cure, as well as favourable long-term outcomes. These data emphasize that restrictions on the basis of treating provider type stand as unnecessary hurdles in the HCV care continuum.

FRI370

Risk stratification of hepatocellular carcinoma in cirrhotic patients after hepatitis C virus eradication: russian single-center experience

Ekaterina Nabatchikova¹, Daria Zazorina¹, Teona Rozina^{1,2}, Elena Nikulkina¹, Elena Tanashchuk¹, Dzhamal Abdurakhmanov¹, Sergey Moiseev^{1,2}. ¹I.M. Sechenov First Moscow State Medical University (Sechenov University), Russian Federation; ²M.V. Lomonosov Moscow State University, Russian Federation

Email: e.nabat4ikova@gmail.com

Background and aims: The risk of hepatocellular carcinoma (HCC) in cirrhotic patients after HCV eradication with direct-acting antivirals (DAAs) is reduced, but not completely eliminated. The aim of our study was to assess incidence, risk factors of HCC and develop a scoring system to predict in patients with HCV-related cirrhosis treated by DAAs.

Method: The prospective single-center cohort study included patients with HCV-related cirrhosis treated by DAAs between July 2015 and May 2020. Exclusion criteria was previous and present HCC. Patients who achieved sustained virological response underwent clinical, laboratory and imaging assessment every 3–6 months after the end of therapy.

Results: A total of 232 cirrhotic patients were enrolled. The median age was 54 (47; 60) years, 49.3% were males, diabetes was present in 19.8%, obesity-in 20.2%, HCV genotype 3-in 25.4% and 29.7% were treatment-experienced. Child-Pugh class B/C were found in 29.3%. Baseline median MELD score was 11 (9; 13), liver stiffness ($n = 133$)–23 (17.4; 30.6) kPa, platelet count $\leq 100 \times 10^3/\text{ml}$ were in 54% of patients, albumin $\leq 35 \text{ g/l}$ –35.3%, bilirubin $\geq 34 \mu\text{mol/l}$ –19.4%, prothrombin time $\leq 60\%$ –19.4%, aspartate aminotransferase-platelet ratio index > 2 –56%, fibrosis-4 score (FIB-4) ≥ 3.25 –67.7%. Esophageal varices 2/3 were in 60.3%, ascites-25.4%. The median follow-up time after EOT was 36 (24; 48) months. De novo HCC occurred in 19 (8.2%) patients. Median alpha-fetoprotein was 6.3 (2.8; 31) IU/ml. Sixteen patients (89%) were within the Milano criteria. The

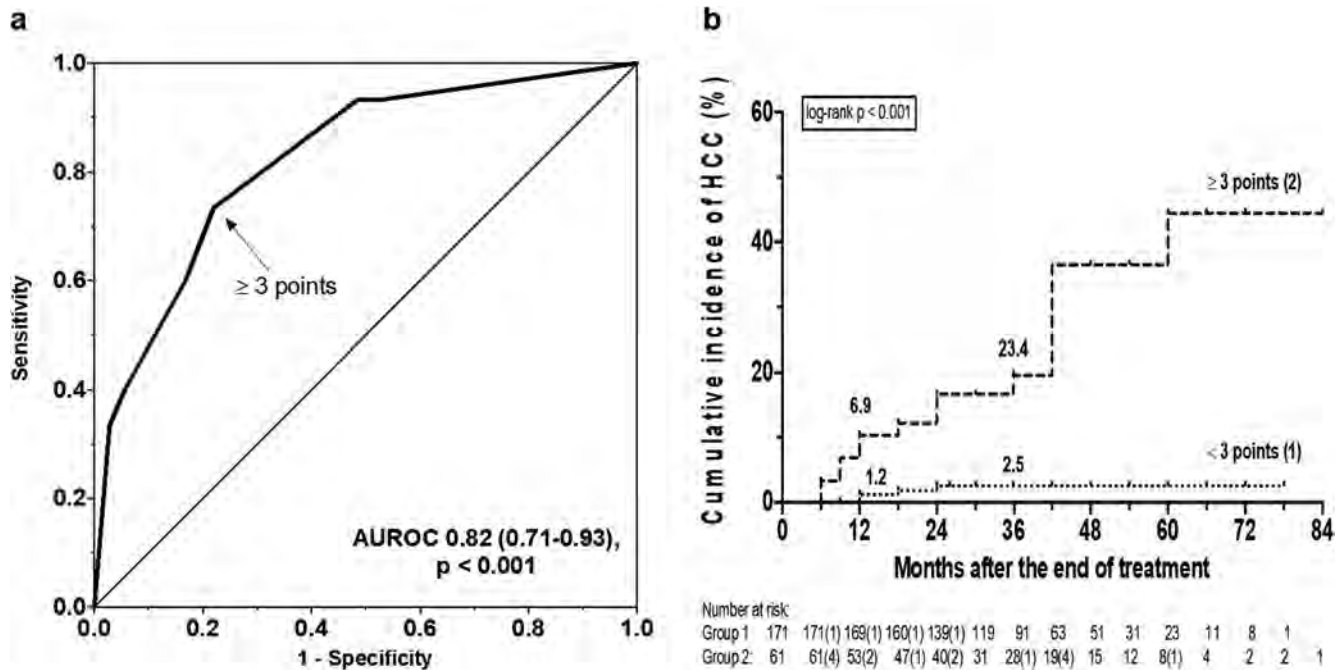


Figure: (abstract: FRI370)

median time from EOT to HCC diagnosis was 18 (12; 42) months. At the multivariate analysis, baseline bilirubin level $\geq 34 \mu\text{mol/l}$ (HR 4.19; $p = 0.002$), baseline ascites (HR 6.6; $p < 0.001$), MELD ≥ 15 (HR 3.82; $p = 0.007$) and FIB-4 > 3.25 (HR 6.4; $p = 0.015$) at the SVR time were independent risk factors for HCC. We determined the weight of each factor equal to HR, and then converted it into an integer: baseline bilirubin level $\geq 34 \mu\text{mol/l}$ -1 point, baseline ascites-2 points, MELD ≥ 15 at the SVR time-1 point, FIB-4 > 3.25 at the SVR time-2 points. The resulting scale allows to set from 0 to 6 points. Patients with HCC had a large sum of points compared to patients without HCC (4 (3; 6) points vs. 1 (0; 2) points, $p < 0.001$). The AUROC of the model was 0.82 (0.71-0.93, $p < 0.001$). The sum of points equal to ≥ 3 has the maximum values of sensitivity (73%) and specificity (78%) and can be used as a threshold value for determining the HCC risk (figure a). The cumulative risk of developing HCC in patients with ≥ 3 points is significantly higher (HR 12.03, log-rank $p < 0.001$) (figure b).

Conclusion: We developed a predictive score using four risk factors, which can help to customize HCC surveillance strategies in cirrhotic patients after HCV eradication.

FRI371

Distinct hepatocellular carcinoma risks in treated chronic hepatitis C patients with different definitions of advanced chronic liver disease

Yen-Chun Liu^{1,2}, Cheng Er Hsu^{1,2}, Ya-Ting Cheng^{1,2}, Chung-Wei Su^{1,2}, Chia-Hung Tai^{1,2}, Yi-Cheng Chen^{1,2}, Yi-Chung Hsieh^{1,2}, Wei Teng^{1,2}, Rachel Wen-Juei Jeng^{1,2}, Chun-yen Lin^{1,2}, Rong-Nan Chien^{1,2}, Tai Dar-In^{1,2}, I-Shyan Sheen^{1,2}. ¹Chang Gung Memorial Hospital, Linkou Branch, Taiwan; ²College of Medicine, Chang Gung University, Taiwan
Email: rachel.jeng@gmail.com

Background and aims: To identify target population for hepatocellular carcinoma (HCC) is an important issue in chronic hepatitis C (CHC) patients after antiviral treatment. Advanced chronic liver disease (ACLD) patients have been suggested by the guideline as the target surveillance group for their remnant HCC risk after sustained virological response (SVR). However, the definition of ACLD composed of different diagnostic tools including liver stiffness measurement (LSM), FIB-4 or both or by ultrasonography image. This study

aims to compare the predictability of HCC among CHC patients with SVR who meet ACLD criteria by different diagnostic measurements.

Method: CHC achieved SVR by interferon-free direct acting anti-viral agents (DAA), whose LSM by transient elastography (TE, Fibroscan) and FIB-4 index were both available before DAA therapy were enrolled. The ACLD was defined as LSM $> 10 \text{ kPa}$ and/or FIB-4 > 3.25 and/or ultrasound signs of cirrhosis. Predictabilities for HCC and 3-year cumulative HCC incidences were compared among four groups of ACLD patients diagnosed by different non-invasive assessments (group A: FIB-4 > 3.25 but LSM ≤ 10 ; group B: FIB-4 ≤ 3.25 but LSM > 10 ; group C: FIB-4 > 3.25 + LSM > 10 ; group D: FIB-4 ≤ 3.25 and LSM ≤ 10 but ultrasonography showed cirrhosis.).

Results: Among 1600 enrolled patients, 922 (58%) patients met criteria of ACLD (group A, N = 128; group B, N = 369; group C, N = 406; group D, N = 19). The mean age was 62 years old, 41% was male and 63% was genotype 1. The annual incidence and 3-year cumulative HCC incidences showed 0.3% and 0.8%, 2.2% and 4.6%, 3.8% and 9.1% and 3.9% and 10.5% in patients with group A, group B, group C and group D (Log-rank $p < 0.01$), respectively (Figure). The negative predictive values (NPVs) for HCC were all the above 95% among these four groups with different ACLD definitions, while the sensitivity was much higher in group C of 62.5% compared to group A (1.4%), B (27.8%) and D (2.8%).

POSTER PRESENTATIONS

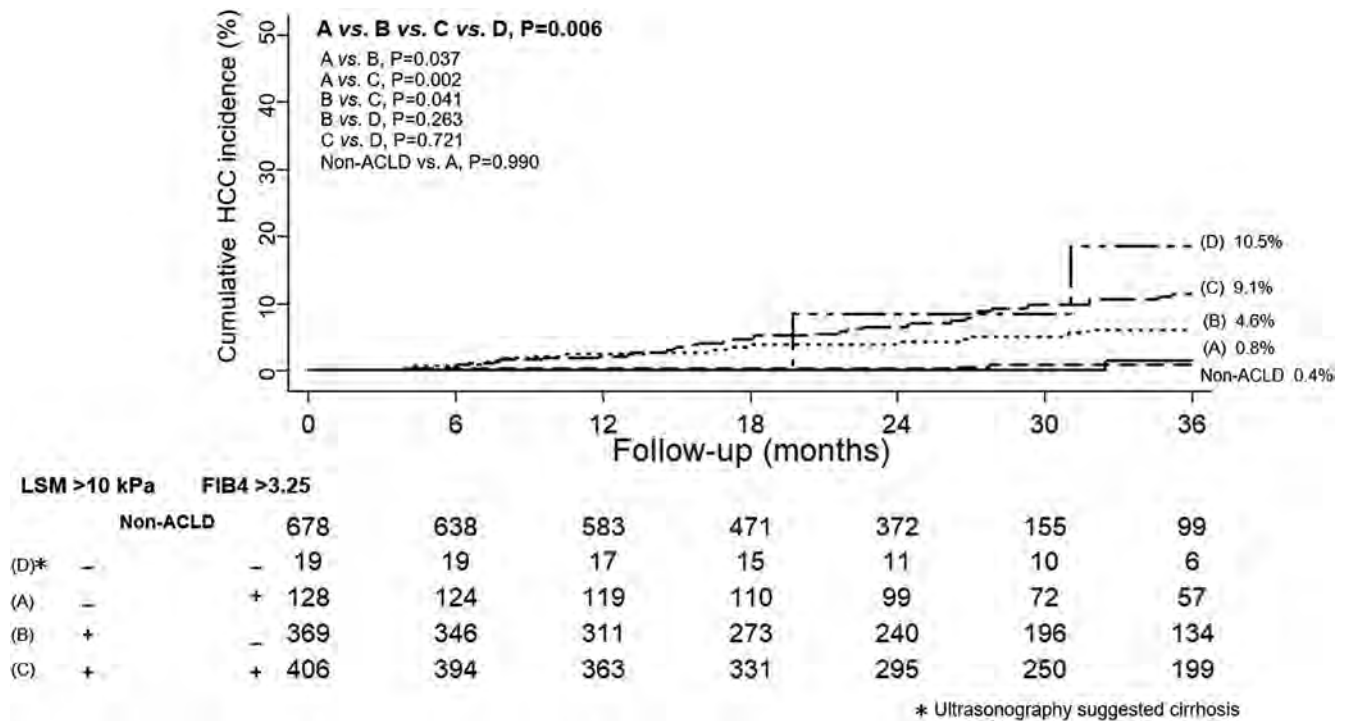


Figure: (abstract: FRI371)

Conclusion: LSM >10 kPa ± FIB-4 >3.25 are more appropriate criteria for ACLD than FIB-4 >3.25 alone which PPV is only 0.8% and its 3-year HCC cumulative incidence be approximate to that of the non-ACLD (0.4%). Those with echo appeared cirrhotic features but not fit the criteria of ACLD due to LSM<10 kPa and FIB-4 < 3.25 were still at high risk of HCC and also shall be under HCC surveillance program.

FRI372

Hepatocellular carcinoma risks of liver fibrosis changes after viral eradication in chronic hepatitis C patients

Yen-Chun Liu^{1,2}, Cheng Er Hsu^{1,2}, Ya-Ting Cheng^{1,2}, Chung-Wei Su^{1,2}, Chia-Hung Tai^{1,2}, Yi-Cheng Chen^{1,2}, Wei Teng^{1,2}, Rachel Wen-Juei Jeng^{1,2}, Chun-yen Lin^{1,2}, Rong-Nan Chien^{1,2}, Tai Dar-In^{1,2}, I-Shyan Sheen^{1,2}. ¹Chang Gung Memorial Hospital, Linkou

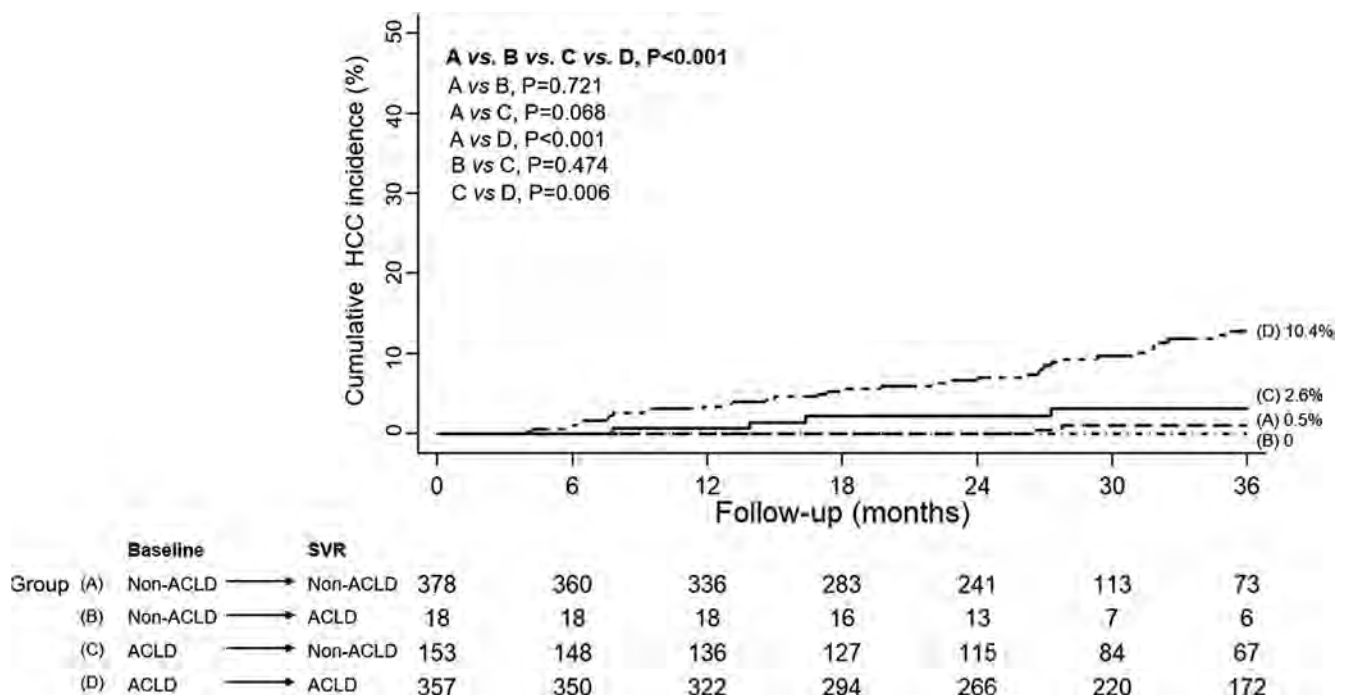


Figure: (abstract: FRI372)

Branch, Taiwan; ²College of Medicine, Chang Gung University, Taiwan
Email: rachel.jeng@gmail.com

Background and aims: Hepatocellular carcinoma surveillance is suggested for chronic hepatitis C (CHC) patients with advanced chronic liver disease (ACLD) by the guideline. It is reported liver fibrosis in patients with advanced fibrosis or cirrhosis can be reversed after viral eradication by direct acting antivirals (DAA). The study aims to investigate the HCC risks among CHC sustained virological response (SVR) patients with fibrosis regression, stationary or progression after SVR, and predictors for ACLD regression.

Method: CHC achieved SVR by interferon-free DAA, whose LSM by transient elastography (TE, Fibroscan) and FIB-4 index were both available before DAA therapy and after SVR were enrolled. The ACLD was defined as LSM >10 kPa and/or FIB-4 >3.25 and/or ultrasound signs of cirrhosis. The 3-year cumulative HCC incidences were compared among four groups of dynamic fibrotic changes (group A: both pre-DAA and post-SVR timepoints: non-ACLD; group B: pre-DAA non-ACLD progressed to post-SVR ACLD; group C: pre-DAA ACLD regressed to post-SVR non-ACLD; group D: both pre-DAA and post-SVR: ACLD). Logistic regression was applied to find predictors for ACLD regression.

Results: There were 906 patients (group A: 378 (42%), group B: 18 (2%), group C: 153 (17%), group D: 357 (39%)) enrolling into the study with mean age of 62 years old, 38% of male and 92% of genotype 1. The 3-year cumulative HCC incidences showed 0.5%, 0%, 2.6% and 10.4% in patients with group A, group B, group C and group D (Log-rank $p < 0.01$), respectively (Figure). Logistic model showed that higher baseline ALT [adjusted OR (aOR): 1.006 (95% CI: 1.002–1.010), $p = 0.007$] was a predictor for ACLD regression, while higher baseline LSM [aOR:0.870 (0.825–0.917), $p < 0.001$] and FIB-4 [aOR:0.655 (0.496–0.864), $p = 0.003$] were unfavorable factors for post-SVR ACLD regression.

Conclusion: Patients with persistent ACLD after SVR posed the highest HCC risks, followed by those with ACLD regression. Those progressed from pre-therapy non-ACLD to post SVR ACLD occurred in 2% of all population with minimal HCC risk as that in the persistent non-ACLD group.

FRI373

Change in fibrosis and clinical progression three years after sustained virological response induced by direct antiviral agents in HIV/HCV subjects

Maria Carnevali Frias¹, Lourdes Dominguez², David Rial Crestelo¹, Otilia Bisbal¹, Rafael Rubio Garcia¹, Federico Pulido Ortega¹. ¹Hospital 12 de Octubre, Medicina Interna, Madrid, Spain; ²King's College Hospital, HIV/Sexual Health, London, United Kingdom
Email: macarfr@gmail.com

Background and aims: Sustained virological response (SVR) achieved after treatment of HCV infection with direct-antiviral agents (DAA) is associated with long-term clinical benefits. We evaluate changes in the estimated fibrosis on SVR confirmation and 3 years after SVR, and if changes on SVR confirmation are related to a decrease in the risk of liver events in people living with HIV (PLWH).

Method: A prospective observational cohort of PLWH with HCV infection and SVR after DAA therapy (January 2015–August 2016) was followed up until December 2020. Liver fibrosis was estimated by non-invasive methods: liver stiffness (LS), APRI and FIB4. Measures were done prior to treatment (baseline), 12 weeks post treatment (SVR12) and 3 years after SVR12 (3 y). Cut-off values for cirrhosis were ≥ 14.6 kPa (LS), ≥ 1 point (APRI), ≥ 3.25 points (FIB4). Cirrhosis regression or non-progression from non-cirrhosis was considered as fibrosis improvement. Clinical outcomes considered were liver-related complications occurred after SVR: death, portal hypertension decompensation (PHD), hepatocarcinoma (HCC) and a composite endpoint of these three.

Results: 393 people were followed-up for a median of 3.8 years (3.5–4.0). There was a significant improvement in LS, APRI and FIB4 from

baseline to 3y [–3.0 kPa (–7.6 to 1.2); –0.4 points (–0.9 to 0.2); –0, 5 points (–1.3 to –0.1)] and major changes were observed from baseline to SVR12. Before the HCV treatment 30.0%, 35.1% and 26.5% subjects were considered as having cirrhosis according to LSM, APRI or FIB4. More than half of them (58.8%, 87.2% and 70.7% respectively) did not remain in that category at the end of the study. Four HCC were detected [3y risk: 0.8% (0.3–2.4)]. At least one episode of PHD was reported in 13 patients [3y risk: 2.6% (1.4–4.8)]. 23 patients died [3 y overall mortality: 3.9% (2.4–6.4)] but only 3 of them due to liver-related causes [3 y related mortality: 0.3% (0.0–1.8)]. 15 patients developed the composite endpoint [3 y risk of any of the covered outcomes: 3.1% (1.8–5.4)]. Estimated liver fibrosis improvement from baseline to SVR12 was associated to lower risk of presenting any of these clinical outcomes, both in the global cohort and in the subgroup of patients with cirrhosis or advanced fibrosis.

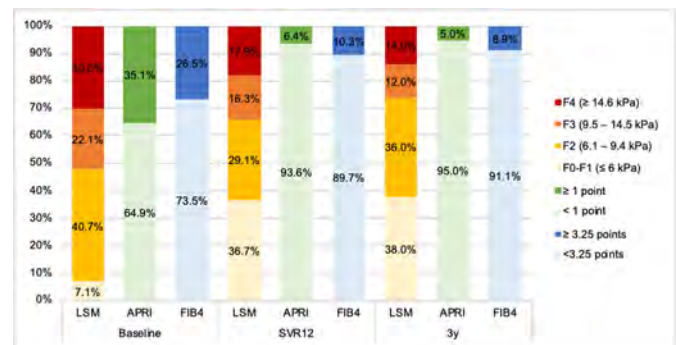


Figure: Patients distribution according to estimated liver fibrosis stage

Conclusion: There is a clinically relevant improvement in non-invasive liver fibrosis markers after 3 years of DAA-induced SVR in PLWH with HCV infection. Estimated fibrosis regression from baseline to SVR12 is associated with a reduction in liver-related complications.

FRI374

FOCUS Project: preliminary results toward hepatitis C Virus screening and elimination in Almería, Spain

Anny Camelo Castillo¹, Marta Casado¹, Teresa Cabezas Fernandez¹, Pedro Amado Villanueva¹, Alba Carrodegua², Diogo Medina², José Luis Vega Sáenz¹, Manuel Rodríguez Maresca¹. ¹TorreCárdenas University Hospital, Almería, Spain; ²GILEAD SCIENCES INC, Madrid, Spain
Email: anjo134@gmail.com

Background and aims: Hepatitis C virus (HCV) elimination is a global challenge, and Spain may be one of the first countries to achieve the World Health Organization's goal of eliminating viral hepatitis by 2030. A 2017–2018 Ministry of Health serosurvey estimated 0.22% active HCV infection among the general Spanish population, 29.4% without prior infection records.

Increasing HCV screening is key, particularly among vulnerable populations with high prevalence. Emergency departments (ED) often act as safety nets due to health equity issues for key populations affected by viral hepatitis, as they often lack optimal links with their primary care providers.

Therefore, we aimed to evaluate HCV screening efficacy in the ED of TorreCárdenas University Hospital, in Almería, Andalusia, Spain.

Method: We implemented opportunistic HCV screening in the ED, using existing infrastructure and staff, aided by electronic health record system modifications to identify eligibility for the test and request serologies automatically. Patients were eligible for testing upon verbal consent if they were between 18 and 69, and had no known diagnosis or test performed in the previous year, and required blood tests in the current visit to the ED.

POSTER PRESENTATIONS

We used the LIAISON®X- Diasorin assay for HCV antibodies (anti-HCV) and the Roche Cobas® 6800 for viral RNA (HCV RNA) in the same specimen (i.e., reflex or single-step testing). Appropriate follow-up or discharge was given, regardless of test results. We contacted positive patients to ensure and monitor linkage to specialist medical care.

Results: We screened 1,131 patients for HCV from August to October 2021, finding 28 (2.47%) anti-HCV positive patients (with an average age of 55, 71% males), and 5 (0.44%) HCV RNA positive patients (80% males), 80% of whom had no prior records or knowledge of their infection.

Conclusion: Undocumented HCV infection among our ED population is higher than estimated in the general population, with twice the active infection rate and nearly two times undiagnosed infection. Thus, opportunistic HCV screening in EDs is feasible, non-disruptive, and effective in increasing diagnosis.

Abstract withdrawn

FRI376

Usefulness of longitudinal assessment of AFP in DAA cured HCV cirrhotic patients to predict the development of HCC

Angelo Sangiovanni¹, Eleonora Alimenti^{1,2}, Riccardo Gattai³, Roberto Filomia⁴, Elisabetta Parente⁵, Luca Valenti^{6,7}, Luca Marzi⁸, Giulia Pieri⁹, Guglielmo Borgia¹⁰, Martina Gambato¹¹, Natalia Terreni¹², Ilaria Serio¹³, Luca Saverio Belli¹⁴, Filippo Oliveri³, Sergio Maimone⁴, Maria Corinna Plaz Torres⁹, Roberta D'Ambrosio¹, Massimo Iavarone¹, Laura Virginia Forzenigo¹⁵, Francesco Paolo Russo¹¹, Maria Grazia Rumi¹⁶, Michele Barone⁵, Anna Ludovica Fracanzani^{7,17}, Giovanni Raimondo⁴, Edoardo Giovanni Giannini¹⁸, Maurizia Brunetto^{3,19}, Erica Villa⁸, Annalisa De Silvestri²⁰, Massimo Colombo²¹, Pietro Lampertico^{1,22}.
¹Foundation IRCCS Ca' Granda Ospedale Maggiore Policlinico, Division of Gastroenterology and Hepatology, Milan, Italy; ²University of Pavia, Department of Medical Sciences, Pavia, Italy; ³University Hospital of Pisa, Hepatology Unit and Laboratory of Molecular Genetics and Pathology of Hepatitis Viruses, Pisa, Italy; ⁴University Hospital of Messina, Division of Clinical and Molecular Hepatology, Messina, Italy; ⁵University of Bari, Gastroenterology Unit, Department of Emergency and Organ Transplantation (D.E.T.O.), Bari, Italy; ⁶Foundation IRCCS Ca' Granda Ospedale Maggiore Policlinico, Division of Transfusion Medicine and Hematology, Milan, Italy; ⁷University of Milan, Department of Pathophysiology and Transplantation, Milan, Italy; ⁸Azienda Ospedaliero-Universitaria Policlinico di Modena, Gastroenterology Unit, Modena, Italy; ⁹University of Genoa, Gastroenterology Unit, Department of Internal Medicine, Genoa, Italy; ¹⁰University of Naples 'Federico II', Department of Clinical Medicine and Surgery, Section of Infectious Diseases, Naples, Italy; ¹¹Padua University Hospital, Multivisceral Transplant Unit, Department of Surgery, Oncology, and Gastroenterology, Padua, Italy; ¹²Valduce Hospital, Division of Gastroenterology, Como, Italy; ¹³University of Bologna, Department of Medical and Surgical Sciences, Bologna, Italy; ¹⁴Ospedale Niguarda, UOC Epatologia e Gastroenterologia, Milan, Italy; ¹⁵Fondazione IRCCS Ca' Granda Ospedale Maggiore Policlinico, Unit of Radiology, Milan, Italy; ¹⁶Ospedale San Giuseppe, Università degli Studi di Milano, Division of Hepatology, Milan, Italy; ¹⁷Foundation IRCCS Ca' Granda Ospedale Maggiore Policlinico, Internal Medicine and Metabolic Diseases, Milan, Italy; ¹⁸University of Genoa, Gastroenterology Unit, Department of Internal Medicine, Genoa, Italy; ¹⁹University of Pisa, Internal Medicine, Department of Clinical and Experimental Medicine, Pisa, Italy; ²⁰Foundation IRCCS Policlinico San Matteo, Clinical Epidemiology and Biometric Unit, Pavia, Italy; ²¹San Raffaele Hospital, Liver Center, Milan, Italy; ²²University of Milan, CRC 'A. M. and A. Migliavacca' Center for Liver Disease, Department of Pathophysiology and Transplantation, Milan, Italy
Email: angelo.sangiovanni@policlinico.mi.it

Background and aims: The usefulness of serum alfafetoprotein (AFP) assessment after sustained virologic response (SVR) in HCV cirrhotic patients treated with direct antiviral agents (DAA) in surveillance programs for the early diagnosis of hepatocellular carcinoma (HCC) is debated. Aim of this study was to evaluate the time course of AFP and its performance in predicting HCC development in this setting. Secondary aim was to define the AFP value predicting HCC development with at least 99% specificity.

Method: In a post-hoc analysis of consecutive cirrhotic patients treated with DAA in a multicenter national study, we enrolled all HCC-free patients with at least one AFP value available at or after SVR and extended the follow-up until 30 September 2020. HCC surveillance program was based on abdominal ultrasound (US) every 6 months. AFP was tested during follow-up on clinical basis depending on the policy of each centre. Joint modelling of

longitudinal data of log AFP and time-to-event endpoint (HCC) were applied for analysis, combining the linear mixed effects model and the Weibull model for survival.

Results: 870 SVR patients, median age 65 (IQR 55–73, 58% males), 92% Child-Pugh A were enrolled. During a median 34 (IQR 14–43) months of post SVR follow-up, 71 patients developed HCC, corresponding to a cumulative incidence at 1, 2 and 3 years of 3.3% (95% CI 2.3–4.8), 5.4% (95% CI 4.0–7.4), 8.3% (95% CI 6.4–10.7), respectively. The joint model considering log AFP values in a time dependent way achieved the best performance to predict the risk of developing HCC, HR 2.44 (95% CI 2.10–2.82, $p < 0.001$). The log-AFP value progressively increased in patients who developed HCC as compared to those who did not ($p < 0.001$). A log AFP increase was associated to increased risk of developing HCC with HR 21.9 (95% CI 4.6–103, $p < 0.001$). By Youden's index an AFP value above 8 ng/ml detected at any time defines the most accurate threshold to predict HCC, corresponding to a 59.6% sensitivity and 96.5% specificity. A 99% specificity was achieved for AFP value >21 ng/ml corresponding to a sensitivity of 23.9%. By Kaplan-Meier curve in a time-dependent association structure, HCC incidence was 10.8 per 100 patient-year (95% CI 7.2–16.1) in patients with AFP >21 ng/ml as compared to 2.2 (95% CI 1.7–3.0) in patients with AFP value ≤ 21 ng/ml ($p < 0.001$).

Conclusion: In cured HCV cirrhotic patients the AFP value over time is associated to HCC development and may help to refine the HCC surveillance strategies. The increase of AFP levels above 21 ng/ml at any time after SVR is associated with a specificity of 99% for the prediction of HCC development, albeit with low sensitivity.

FRI377

A 4 year multi-centre study of persons who inject drugs in Luxembourg, looking at hepatitis C virus seroprevalence, treatment uptake and reinfection rates

Madiha Sharaf¹, Vic Arendt², Thérèse Staub³, Carole Devaux⁴, Emily Montosa Nunes⁴. ¹Centre Hospitalier Luxembourg, Emergency Department, Luxembourg, Luxembourg; ²Centre Hospitalier Luxembourg, National Service of Infectious Diseases, Luxembourg, Luxembourg; ³Centre Hospitalier Luxembourg, National Service of Infectious Diseases, Luxembourg, Luxembourg; ⁴Luxembourg Institute of Health, Department of Infection and Immunity, Esch-sur-Alzette, Luxembourg
Email: madiha.sharaf@gmail.com

Background and aims: The global figure of persons who inject drugs (PWID) stands at 15.6 million persons. 50% of PWID have been estimated to be exposed to the Hepatitis C virus (HCV), and 39% are said to suffer from chronic HCV, in comparison to 1% of the general population. Chronic HCV can result in liver cirrhosis, hepatocellular carcinoma and premature death over 20 to 40 years. The “Hepatitis C among Drug Users”-“HCV-UD” study is the largest multi-centre study in Luxembourg looking at patterns of HCV prevalence amongst PWID, including uptake of treatment and reinfection.

Method: 480 participants were recruited at harm reduction sites throughout the country from November 2015 to December 2019. Participants were offered HCV screening, direct acting anti-viral (DAA) treatment and follow-up with an infectious disease specialist, without cost.

Results: 356 participants (74%) were exposed to HCV versus 124 participants (26%) who had no evidence of exposure. 51% were cured of which 25% were cured through treatment, as evaluated with a sustained viral response at 12 weeks or more. Of these, 27% were reinfected again with HCV. 75% were cured during the course of the study, attributed to previous unrecorded treatment or spontaneous cure. 47% of participants continued to have ongoing infection, of which 7% had undergone treatment, and 93% had not taken any treatment. There was missing data for 6 participants. The results are summarised in the figure below.

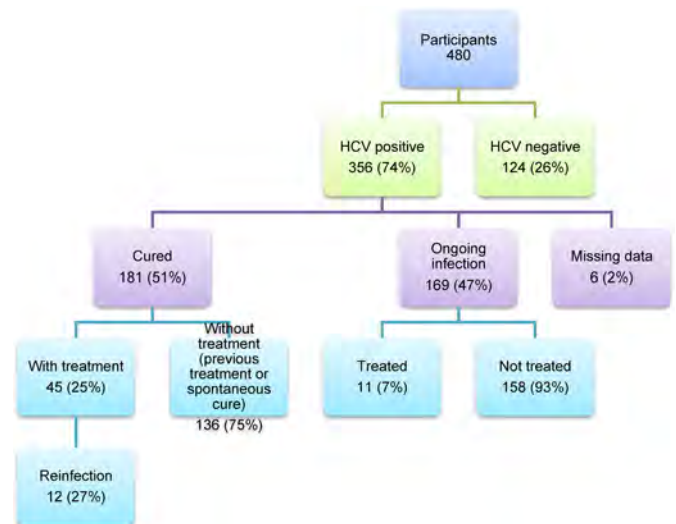


Figure: Patients distribution according to estimated liver fibrosis stage

Conclusion: The outreach set up of the study enabled insights in to the treatment and HCV status of PWID, which the authors feel is a closer representation of reality. HCV prevalence was comparable to other study estimates in the literature. Treatment uptake was low, despite the free DAA treatment offered, however within this subset only 27% went on to be reinfected. What is worrying, however, is that 47% of participants continued to be infected with HCV. This begs the question as to which barriers to care within a psychosocial framework need to be addressed to enable the World Health Organisation's (WHO) target of eradicating HCV as a public health risk by 2030.

Viral hepatitis C: Therapy and resistance

FRI381

Benefits associated with HCV cure in people with mental disorders

Benjamin Rolland¹, Elias Benabadji², Olivier Lada², Pascaline Rabiega³, Fayssol Fouad³, Nabil Hallouche⁴, Stanislas Pol⁵. ¹Université de Lyon-Sud et Service d'Addictologie de Lyon (HCL/CH Vinatier), Lyon, France; ²Gilead Sciences, Boulogne-Billancourt, France; ³IQVIA, France; ⁴GHU Paris Psychiatrie et Neurosciences, Paris; ⁵Université de Paris et Hépatologie de Cochin (AP-HP), Paris, France
Email: stanislas.pol@aphp.fr

Background and aims: Retrospective and prospective studies have reported hepatic and extra-hepatic benefits after direct-acting antivirals (DAAs) treatment of hepatitis C virus (HCV) chronic infection. However, the ability of virologic cure to improve the neuro-cognitive troubles is still questioned: HCV cure could improve neuro-cognitive troubles as the neurotropism of HCV has been suggested (in glial cells and astrocytes). Our main objective was to evaluate, in the subpopulation of patients with psychiatric disorders, the impact of DAAs (assimilated to HCV cure) on hospitalizations, both in general medicine and in psychiatric ward.

Method: All adult patients identified in the French administrative health care databases (SNDS) with DAAs treatment initiation between 2015 and 2018, and with at least one psychiatric disorder, were included. Individuals were assigned into one or several psychiatric disorder sub-groups based on algorithms: “addictive disorders,” “neurotic and mood disorders,” “psychotic disorders” and “other psychiatric disorders.” A longitudinal approach was then used to compare the frequency and the duration of hospitalizations one

POSTER PRESENTATIONS

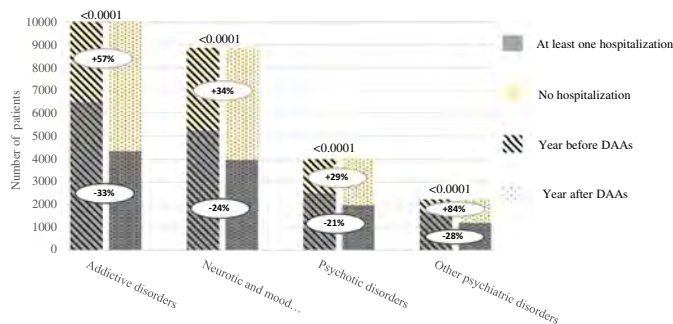
year before and one year after HCV treatment, both in general medicine (all-cause) and in psychiatric ward.

Results: Between 2015 and 2018, a total of 17, 203 HCV patients with at least one psychiatric disorder initiated a treatment in France. 57.4% of the subjects were hospitalized at least once the year before DAAs initiation, while only 41.6% were during the year following treatment ($p < 0.0001$). Put differently, the number of patients with at least one hospitalization decreased by 28% after HCV cure (9, 874 versus 7, 153 patients hospitalized respectively).

The mean number of hospitalizations per patient per year in general medicine department was 1.2 during the pre-DAAs year and decreased to 0.8 the post-treatment year ($p < 0.0001$). Similarly, this number decreased from 1.4 to 1.2 in psychiatric ward.

Among the patients hospitalized at least once in general medicine ($n = 2, 515$), both the year before and the year after treatment, the duration of hospital stays decreased significantly from 20.5 days to 16.7 days after HCV treatment ($p < 0.0001$). In psychiatric wards ($n = 589$) a decreasing trend was also observed from 73, 9 days to 68, 9 days but was not significant ($p = 0.2132$).

Interestingly, similar results were also observed in all four sub-groups and were statistically significant.



Conclusion: DAAs treatment in patients with psychiatric disorders results in a significant reduction in the frequency and the duration of hospitalizations the year following treatment, and even for the patients with severe psychiatric conditions. These results point out both the individual benefit—a better global and psychiatric prognostic—and the collective benefit—fewer resource utilization—of HCV cure in patients with psychiatric disorders.

FRI382

Dismal prognosis for cirrhotic HCV patients after initial DAA treatment failure, rescue therapy may be life-saving

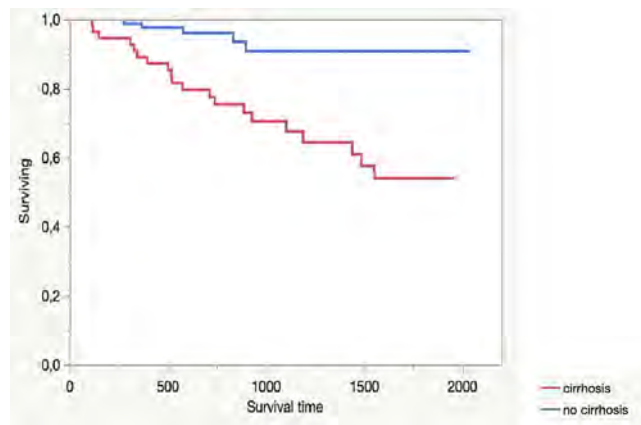
Johan Westin¹, Rune Wejstål¹, Christian Kampmann², Magdalena Ydreborg¹, Ola Weiland³. ¹University of Gothenburg and Sahlgrenska University Hospital, Department of Infectious diseases; ²Skåne University Hospital, Department of Infectious Diseases, Lund, Sweden; ³Karolinska Institute and Karolinska University Hospital, Dept of Medicine, Division of Infectious Diseases, Stockholm, Sweden
Email: johan.westin@gu.se

Background and aims: Effective direct-acting antiviral (DAA) treatment against hepatitis C virus (HCV) infection is universally available. A small portion of HCV patients does not respond, irrespective of treatment regimen. The aim was to study the long-term prognosis after initial DAA treatment failure in HCV infected patients, in a real-life setting.

Method: Data from all adult patients registered in the national Swedish HCV treatment register who did not achieve sustained virological response (SVR) after their initial DAA treatment course, were retrieved from 2014 through 2018.

Results: In total, 288 patients with primary DAA failure were included, of whom 236 underwent a second treatment course as rescue therapy after a median delay of 353 (IQR: 215–650) days. 15

patients received a third treatment course as second rescue treatment after a further median delay of 193 (IQR: 160–378) days. One-hundred-eleven out of 124 (90%) non-cirrhotic and 62/79 (78%) cirrhotic patients achieved SVR following the first rescue treatment. SVR was achieved by 108/112 (96%) patients after a triple DAA regimen. In total 69 (24%) patients were lost to follow-up or died waiting for rescue treatment. Baseline cirrhosis was associated with poor long-term survival. Overall survival 3 years after initial treatment failure was 70% for patients compared with over 90% for patients without baseline cirrhosis (Figure 1).



Conclusion: Our study indicates that rescue therapy in most patients with primary DAA failure have an excellent outcome, in particular when a triple DAA regimen was given. A significant number of patients were lost to follow-up or died waiting for rescue therapy, and the overall long-term prognosis for patients with baseline cirrhosis was poor. This indicates that patients with primary DAA failure should be offered rescue therapy, using a triple DAA regimen, without delay.

FRI383

Requests for drug-drug interaction data on direct-acting antivirals and enzyme inducing anti-epileptic agents: an overview of the HEP Interaction checker database of the University of Liverpool

David Burger¹, David Back², Jasmine Martin², Daryl Hodge², Minou Van Seyen³, Justin Chiong², Alison Boyle², Fiona Marra². ¹Radboud University Medical Center, Pharmacy, Nijmegen, Netherlands; ²University of Liverpool, Liverpool, United Kingdom; ³Jeroen Bosch Ziekenhuis, 's-Hertogenbosch, Netherlands
Email: david.burger@radboudumc.nl

Background and aims: Drug-drug interactions (DDIs) between direct-acting antivirals (DAAs) for hepatitis C virus (HCV) infection and enzyme inducing anti-epileptic agents (eiAEs) are among the most difficult to manage, and form a potential barrier towards elimination of HCV. When patients are not able to switch the eiAE to a non-eiAE, DAA treatment is often deferred. With new data published recently on successful combined treatment of eiAEs and DAAs (Buti et al J Hepatol 2021; Natali et al J Pharm Practice 2021) we wondered how often people are looking for eiAE-DAA interactions at the University of Liverpool's HEP Interaction Checker (www.hep-druginteractions.org) to gauge some information about how widespread this problem may be.

Method: We extracted DDI queries submitted to the HEP Interaction Checker between July 1, 2017 and September 30, 2021. We removed queries on DAAs that are no longer in use (e.g. boceprevir, telaprevir). We only looked at eiAEs (including: carbamazepine, phenytoin, phenobarbital, primidone, oxcarbazepine and eslicarbazepine) as non-eiAEs (e.g. gabapentin, pregabalin) are less of interest from a DDI perspective, and are more often used for other indications such as

neuropathic pain, mood stabilization, etc. Queries to the database are anonymous, the key information that is recorded is the country of origin.

Results: During 51 months of follow-up, a total of 94, 695 queries from 98 countries were recorded by website users to check DDIs between eiAEs and DAAs. The most frequently requested DAAs were glecaprevir/pibrentasvir (GP; 23.3%) and sofosbuvir/velpatasvir (22.3%). Among the eiAEs, carbamazepine was the most frequently requested eiAE (37.9%) followed by phenytoin (19.9%) and oxcarbazepine (18.7%). Until recently, all of these combinations were contra-indicated (red flag). On an individual level, the most frequently requested DDI between an eiAE and a DAA was carbamazepine & GP (n = 7, 773 queries).

Conclusion: During our observation period, we received an average number of 1, 857 requests per month for a potential DDI between an eiAE and a DAA, demonstrating a huge demand globally for advice on concomitant use of these drugs. Our recommendations have recently been updated to reflect recent real-life data. Given the high number of DDI requests involving an eiAE and DAAs, we believe physicians should be informed that treatment options have now been improved, and HCV treatment should no longer be deferred when an eiAE is on board.

FR1384

Changing HCV patient profiles: insights from a large multinational real-world sofosbuvir/velpatasvir (SOF/VEL) dataset

Alessandra Mangia¹, Stefano Fagioli², Vito Di Marco³, Stephen Shafran⁴, Mandana Khalili⁵, Scott Milligan⁶, George Papatheodoridis⁷, Denis Ouzan⁸, Silvia Rosati⁹, Alnoor Ramji¹⁰, Elisabetta Teti¹¹, Montserrat Garcia-Retortillo¹², Francisco Andrés Pérez Hernández¹³, Alexander Wong¹⁴, Chris Fraser¹⁵, Sergio Rodriguez-Tajes¹⁶, Elena Jimenez Mutilloa¹⁷, Luis Enrique Morano Amado¹⁸, Joss O'Loan¹⁹, Francesca Campanale²⁰, Guilherme Macedo²¹, Michele Milella²², Christian Brixko²³, Maria Buti²⁴, María Guerra Veloz²⁵, Roberto Ranieri²⁶, Sergio Borgia²⁷, Annalisa Bascia¹, Conrado Manuel Fernandez Rodriguez²⁸, Brian Conway²⁹, Victor de Ledinghen³⁰, Mary Fenech³¹, Pablo Ryan³², Ivana Maida³³, Alexandra Martins³⁴, Stacey Scherbakovsky³⁵, Ioanna Ntalla³⁶, Candido Hernández³⁷, Kim Vanstraelen³⁷, Juan Turnes³⁸. ¹IRCCS-Ospedale Casa Sollievo Della Sofferenza, San Giovanni Rotondo, Italy; ²Asst Papa Giovanni XXIII-Lombardia HCV Network, Italy; ³Gastroenterology and Hepatology Unit, Department of Health Promotion Sciences Maternal and Infantile Care, Internal Medicine and Medical Specialties, PROMISE, University of Palermo, Italy; ⁴University of Alberta, Edmonton, Canada; ⁵University of California San Francisco, California-TARGET cohort, United States; ⁶Trio Health Analytics, La Jolla, CA, United States; ⁷Department of Gastroenterology, Medical School of National and Kapodistrian University of Athens, Laiko General Hospital of Athens, Greece; ⁸Institut Arnault Tzanck, Saint-Laurent du Var-HELIOS cohort, France; ⁹INMI Lazzaro Spallanzani IRCCS Rome, Italy; ¹⁰University of British Columbia, Vancouver, Canada; ¹¹Infectious Diseases Clinic, Tor Vergata University, Rome, Italy; ¹²Liver Section, Gastroenterology Department, Hospital del Mar Medical Research Institute (IMIM), Parc de Salut Mar, Barcelona, Spain; ¹³Head of Digestive Disease Department, Complejo Hospitalario Nuestra Señora de Candelaria, Santa Cruz, Spain; ¹⁴Department of Medicine, University of Saskatchewan, Regina, Saskatchewan, Canada; ¹⁵Cool Aid Community Health Centre, Victoria, British Columbia, Canada; ¹⁶Liver Unit, Hospital Clinic Barcelona, IDIBAPS, Ciberehd, Spain; ¹⁷Hospital Universitario Insular de Gran Canaria, Spain; ¹⁸Unit of Infectious Diseases, Alvaro Cunqueiro University Hospital, Vigo, Spain; ¹⁹Kombi Clinic and Medeco Inala, Brisbane, Australia; ²⁰Local health department BAT, ASL BAT and Infectious Disease Consultant of Detention Center, Trani, Italy; ²¹Department of Gastroenterology and Hepatology, Centro Hospitalar São João, Porto, Faculty of Medicine, Porto, Portugal; ²²Clinic of Infectious Diseases, University of Bari, Italy; ²³CHR Citadelle, Department of

Gastroenterology and Digestive Oncology, Liege, Belgium; ²⁴Liver Unit, Department of Internal Medicine, Vall d'Hebron University Hospital, Barcelona, Spain; ²⁵Virgen Macarena University Hospital, Seville, Spain; ²⁶Penitentiary Health Service Region Lombardy, San Paolo Hospital University of Milan, Italy; ²⁷Infectious Diseases, William Osler Health System, Brampton, Ontario, Canada; ²⁸Hospital Universitario Fundación Alcorcón, Alcorcón, Spain; ²⁹Vancouver Infectious Diseases Centre, Vancouver, Canada; ³⁰Centre Hospitalier Universitaire Bordeaux, France; ³¹QuilHN Ltd, Better Access Medical Clinic, Brisbane, Australia; ³²Infanta Leonor Hospital, Madrid, Spain; ³³Department of Medical, Surgical and Experimental Sciences, University of Sassari, Italy; ³⁴Hospital Prof Dr Fernando Fonseca, Amadora, Portugal; ³⁵Medical Affairs, Gilead Sciences International, San Francisco, United States; ³⁶Clinical Data Science, Epidemiology, Gilead Sciences Europe Ltd, London, United Kingdom; ³⁷Medical Affairs, Gilead Sciences Europe Ltd, London, United Kingdom; ³⁸Department of Gastroenterology and Hepatology, CHU Pontevedra & IIS Galicia Sur-HEPA-C cohort, Spain
Email: a.mangia@tin.it

Background and aims: The profile of HCV patients (pts) being started on direct-acting antivirals (DAAs) has shifted towards more vulnerable populations. This large real-world analysis describes the diverse profile of these populations according to age and sex.

Method: Adult HCV pts (aged 18+ years [y]) from 37 clinical cohorts across nine countries treated with SOF/VEL for 12 weeks without ribavirin were included. Those with a history of decompensation or prior NS5A-inhibitor exposure were excluded. This descriptive analysis evaluated pt characteristics, time to treatment (TT [time from HCV RNA diagnosis to DAA initiation]), and sustained virological response ≥ 12 weeks after end of treatment (SVR), stratified by age and sex.

Results: Among 6356 pts, 2274 were aged <50 y, 2568 50–65 y, and 1514 >65 y. Within these age strata, 73%, 65%, and 45%, respectively, were male. Vulnerable populations were well represented, and ~20% of all pts had a history of IV drug use. Irrespective of age, male pts were more likely to have compensated cirrhosis and to be infected with HCV genotype (GT) 3 (Table). Within vulnerable populations, higher likelihood of incarceration among male pts was restricted to those aged ≤ 65 y. Significantly fewer mental health disorders were seen in male pts. However, use of antipsychotics appeared similar, irrespective of sex. Median TT was shorter in male pts across the age spectrum.

In 5845 pts with a valid result, SVR was high across age ranges, with no significant differences observed between male and female pts (<50 y: female 98.7%, male 99.2%; 50–65 y: female 98.7%, male 98.1%; >65 y: female 99.3%, male 98.3%). 475 pts did not achieve SVR for a non-virological reason; mostly loss to follow-up, with no differences between males and females across age strata.

Conclusion: SOF/VEL shows high cure rates across different age and sex groups. Antipsychotic drug use appeared similar in males and females, despite significantly fewer mental health disorders in male pts. TT varied from 1 day to >6 months and was shorter in males.

POSTER PRESENTATIONS

Table: (abstract: FRI384): Characteristics of HCV pts in the overall population, stratified by age and sex

	<50 y			50–65 y			>65 y		
	F (n = 608)	M (n = 1666)	p-value	F (n = 905)	M (n = 1663)	p-value	F (n = 833)	M (n = 681)	p-value
F4, %	7.2	13.4	<0.001	18.7	26.1	<0.001	24.2	29.5	<0.05
GT3, %	46.7	48.3	NS	32.5	37.9	<0.01	5.3	10.9	<0.001
Vulnerable*, %	30.4	47.6	<0.001	20.0	24.3	<0.01	17.3	13.1	<0.05
Homeless, %	6.5	12.0	<0.05	2.2	8.4	<0.05	0.0	4.5	<0.05
Imprisoned, %	18.9	45.6	<0.001	5.0	29.0	<0.001	0.7	2.2	NS
Mental health disorder, %	74.6	42.4	<0.001	92.8	62.6	<0.001	99.3	93.3	<0.05
Antipsychotic drug use, %	9.2	11.8	NS	5.1	5.5	NS	2.5	3.1	NS
Median TT, days (IQR)	63 (28–128)	51 (22–113)	–	69 (31–133)	56 (24–115)	–	68 (31–132)	55 (28–112)	–

F, females; M males; NS, not significant; IQR, interquartile range.

*Proportions of patients belonging to vulnerable subpopulations are expressed as % of the total vulnerable population.

FRI385

Sofosbuvir plus velpatisvir for 8 weeks in patients with acute hepatitis C: multicenter, single arm, phase 2 study (The HepNet acute HCV-V study)

Benjamin Maasoumy^{1,2,3}, Patrick Ingiliz⁴, Christoph Spinner⁵, Christiane Cordes⁶, Hans-Jürgen Stellbrink⁷, Julian Schulze zur Wiesch^{8,9}, Stephan M Schneeweiß¹⁰, Katja Deterding¹¹, Tobias Müller¹², Julia Kahlhöfer³, Petra Dörge³, Maria von Karpowitz¹³, Michael P. Manns¹, Heiner Wedemeyer¹, Markus Cornberg^{3,14,15,16}, ¹Hannover Medical School, Department of Gastroenterology, Hepatology and Endocrinology, Hannover, Germany; ²German Center for Infection Research (DZIF), Partner Site Hannover-Braunschweig, Hannover, Germany; ³German Center for Infection Research (DZIF), HepNet Study-House, German Liver Foundation, Hannover, Germany; ⁴Zentrum für Infektiologie Berlin-Prenzlauer Berg, Berlin, Germany; ⁵Technical University of Munich-School of Medicine, Hospital Rechts der Isar, Munich, Germany; ⁶Praxis Dr. Cordes, Berlin, Germany; ⁷Infectiology Center Hamburg (ICH), Hamburg, Germany; ⁸University Medical Center Hamburg-Eppendorf, Medical Department, Hamburg, Germany; ⁹German Center for Infection Research (DZIF), Partner Site Hamburg-Lübeck-Borstel-Riems, Hamburg, Germany; ¹⁰Praxis Hohenstaufenring, Cologne, Germany; ¹¹University Hospital Essen, Department of Gastroenterology and Hepatology, Essen, Germany; ¹²Charité Campus Virchow-Klinikum (CVK), Department of Gastroenterology and Hepatology, Berlin, Germany; ¹³Hannover Medical School, Institute for Biometry, Hannover, Germany; ¹⁴Hannover Medical School, Department of Gastroenterology, Hepatology and Endocrinology, Hannover, Germany; ¹⁵German Center for Infection Research (DZIF), Partner Site Hannover-Braunschweig, Hannover, Germany; ¹⁶Center for Individualized Infection Medicine (CiiM), Hannover, Germany
Email: cornberg.markus@mh-hannover.de

Background and aims: Sofosbuvir plus velpatisvir (SOF/VEL) is highly effective for the treatment of hepatitis C virus (HCV) infection, but it is only approved in chronic hepatitis C. The EASL recommendations suggest 8-weeks of SOF/VEL for the treatment of acute or recently acquired HCV infection. However, to date there are only data published for 6 and 12 weeks for recently acquired HCV infection. The objective of this study was to evaluate the safety and efficacy of 8 weeks of SOF/VEL treatment for acute HCV mono-infection.

Method: In this investigator-initiated, prospective, multicenter, single-arm study, we recruited a total of 20 adults (≥18 years) with acute HCV mono-infection (proven antibody or RNA seroconversion or ALT >10 ULN with known exposure within 4 month) from nine centers in Germany between March 2019 and June 2021. Patients received SOF/VEL (400/100 mg) as a fixed-dose combination tablet once daily for 8 weeks. The primary efficacy endpoint was the proportion of patients with sustained virological response (undetectable HCV RNA 12 weeks after the end of treatment, SVR12). Other endpoints included biochemical response and safety of SOF/VEL.

Results: The median HCV RNA viral load at baseline was 5.0 log₁₀ IU/ml; the distribution of HCV genotypes was as follows: GT1a/1b/2/3/4: n=12/1/1/3/3. Thirteen (65%) of the 20 patients were taking

medication for HIV pre-exposure prophylaxis. Two patients were lost to follow-up. In the per protocol analysis, all patients achieved SVR12 (n = 18/18 [100%]). Median ALT levels were 249 U/L at baseline and 22 U/L 12 weeks after the end of treatment, with all but one patient (94%) achieving ALT normalization. Treatment was well tolerated; by 12 weeks post-treatment, there was one serious adverse event unrelated to study drug and 6 possible or probable drug-related adverse events with only mild symptoms.

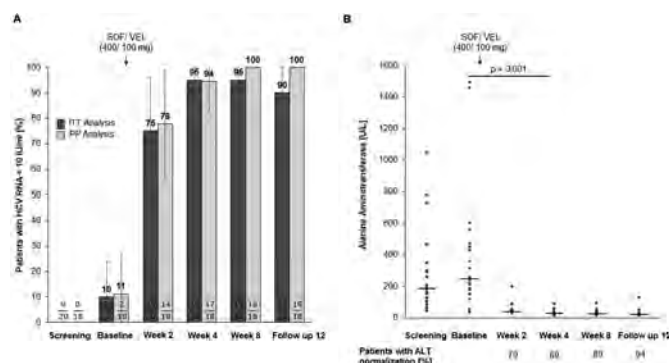


Figure: Response to 8 weeks sofosbuvir (SOF) plus velpatisvir (VEL) (A) Patients with serum HCV RNA levels below <10 IU/ml in the *intention-to-treat* (ITT) and *per protocol* (PP) analysis, percentage ± CI (B) Decline of ALT, median, Friedman test with post hoc analysis

Conclusion: The 8-week treatment with SOF/VEL was well tolerated and highly effective in patients with acute HCV mono-infection. Early treatment of hepatitis C might effectively prevent the spread of HCV in high-risk groups and should therefore be more targeted; ideally, approval for hepatitis C therapy should be pursued independently of chronic hepatitis C.

FRI386

Full-length genome characterization of inherently resistant african HCV genotype 1, subtype 11 in patients failing DAA-based therapy

Slim Fourati^{1,2,3}, Erwan Vo Quang^{2,4}, Christophe Rodriguez^{1,2,3}, Alexandre Soulier^{1,2}, Vanessa Demontant^{1,2}, Stéphane Chevaliez^{1,2,3}, Vincent Leroy^{2,3,4}, Jean-Michel Pawlotsky^{1,2,3}, ¹APHU-Henri Mondor Hospital, Virology, France; ²INSERM U955, "Virus Hepatology, Cancer" Team, Créteil, France; ³Paris-Est Créteil University, Créteil, France; ⁴APHU-Henri Mondor Hospital, Hepatology, Créteil, France
Email: slim.fourati@aphu.fr

Background and aims: Among the so-called "unusual" HCV genotypes, genotype 1, subtype 11 (GT-11) is common in patients of African origin. GT-11 has recently been suggested to be less responsive to NS5A inhibitor-containing regimens than GT-1a or GT-1b. Here, we used shotgun metagenomics based on deep sequencing to generate full-length HCV genome sequences and characterize amino acid substitutions present at baseline and

selected by DAA therapy in regions targeted or not targeted by DAAs in GT-11 infected patients who failed to achieve SVR.

Method: Shotgun metagenomics were used to generate full-length HCV GT-11 genome sequences. Briefly, library preparation was performed using Total RNA and Nextera XT kit (Illumina). Deep sequencing was performed by means of NextSeq500 (Illumina). Full-length HCV sequences were analyzed using our original in-house MetaMIC® software (1% cutoff).

Results: Among 771 patients with HCV infection treated with DAAs who experienced a virological failure and were referred to our center between 2015 and 2019, 316 (41.0%) were infected with genotype 1, and 20 of them (6.3%) with GT-11. All GT-11-infected patients were of African origin. Deep sequencing of full-length HCV GT-11 genomes was performed in 10 patients at baseline and at time of relapse. Treatment regimens were SOF/LDV ± RBV (n = 8), SOF/VEL (n = 1) and SOF/SIM (n = 1).

At baseline, all of the 10 GT-11 patients had ≥3 dominant NS5A resistance-associated substitutions (RASs), including K24G/S (>99%), L31M (>99%) and H58P (>99%). Additionally, baseline NS5A-Q30R was present in 3 patients (>99% in 2 patients; 25% in 1 patient). Sequential analysis of full-length HCV genome sequences showed enrichment of NS5A-Q30R in one patient at failure (>99%) and the selection of NS5A RASs in other patients: baseline K24S (8% and 40%, respectively) replaced by K24G (>99%) in 2 patients; selection of Y93F and Y93H RASs at failure in 2 other patients (20% and 40% respectively).

No NS5B RASs were detected. NS3 R155 K was selected in one patient failing SOF/SIM (30%). No amino acid changes of interest were observed at treatment failure in genome regions other than those targeted by the HCV DAAs administered.

Data on retreatment by triple-combination regimens are ongoing and will be presented.

Conclusion: We report the largest cohort of GT-11-infected African patients failing DAAs thus far. The large number of NS5A RASs present at baseline explains lower SVR rates with NS5A inhibitor-based therapies in these patients. Our results emphasize the need for identifying this subtype and other “unusual” subtypes (e.g. GT-4r) in Africa where they are common, and the urgent need to guarantee equal access to last-generation DAA therapies in Africa.

FRI387

Treating HCV in dual diagnosis acute psychiatric inpatients with substance use disorder

Vera Dreizin¹, Yael Delayahu², David Hovel¹, Gabriela Ilionsky³, Neil Mfaria⁴, Eran Israeli¹. ¹Wolfson Medical center, Institute of Gastroenterology, Holon, Israel; ²Yehuda Abarbanel Mental Health Center, Dual Diagnosis (D) Ward, Bat Yam, Israel; ³Yehuda Abarbanel Mental Health Center, Dual Diagnosis (D) Ward, Bat Yam, Israel; ⁴Yehuda Abarbanel Mental Health Center, Bat Yam, Israel

Email: verpav1@yandex.ru

Background and aims: People with severe mental illness (SMI) and substance use disorder (SUD) are at increased risk for hepatitis C (HCV). However, only 4.7% receive screening for HCV.

Psychiatric patients with dual diagnosis (DD) of SMI and SUD have multiple risk factors for HCV: homelessness, immigration, imprisonment, coinfections such as HIV or hepatitis B.

However, few treatment approaches have been studied in this patient group.

To describe an on-going project of accessing DD patients during their stay at a psychiatric facility for diagnostic work-up, treatment and follow-up.

Method: We initiated a collaboration between Hepatology clinic of a general hospital and Dual Diagnosis acute Ward (DDW) of a psychiatric hospital for treating HCV patients.

All patients admitted to the DDW are screened for HCV AB. Patients positive for HCV are examined at the facility by the project's expert hepatologist and undergo a full diagnostic workup. Treatment is

administered during hospitalization; all patients undergo monthly clinical and laboratory assessment.

Patients discharged from the facility are referred for follow-up to the Hepatology Clinic. We keep close contact with family physicians, rehab centers, medical care providers and families.

Results: From January 2020 to November 2021 we allocated a cohort of 56 HCV patients at different stages of diagnosis and treatment (Table).

We were able to treat 22 patients. 7 have already achieved SVR, 5 have completed treatment and are waiting for SVR, 5 are now being treated and 5 are under investigation. 13 patients had negative HCV PCR due to spontaneous recovery. Two patients died during the follow-up period not due to liver disease. 7 patients were treated for HCV before the psychiatric hospitalization, 12 were not treated. FIB 4 was measured in 30 patients; 43% (13 patients) were with FIB-4 score greater than 1.45. Fibroscan/Fibrotest examination was performed in 26 patients, with evidence of advanced fibrosis in 19% (5 patients). 19 patients were treated by Sofosbuvir/Velpatasvir for 12 weeks and 3 patients were treated with Glecaprevir/Pibrentasvir for 8 weeks. There were no severe adverse events during treatment.

Patients M/F	56 (53/3)
Age	43.6 (24-62)
Multiple psychoactive drugs	56
Substitute treatment	16 (29%)
Active drug users	45 (80%)
Past imprisonment	45 (80%)
Alcohol abuse	43 (77%)
Homeless	36 (64%)
No family	44 (79%)
HIV coinfection	1
HBV coinfection	3
HDV coinfection	1
Liver or kidney transplantation	1
Psychiatric comorbidity	56
Schizophrenia	26 (46%)
Dissocial personality disorder	9 (16%)
Other nonorganic psychosis	21 (38%)
Non psychiatric comorbidity	20 (36%)

Conclusion: We present our ongoing experience of treating HCV in a population of drug dependent patients with SMI during their in-hospital stay. This model has proved efficiency in facilitating their access to care and achieving SVR where no other approach proved successful.

FRI388

Eight-weeks of glecaprevir/pibrentasvir is well tolerated and yields high sustained virological response in HCV-infected treatment-naïve patients with compensated cirrhosis: the CREST study

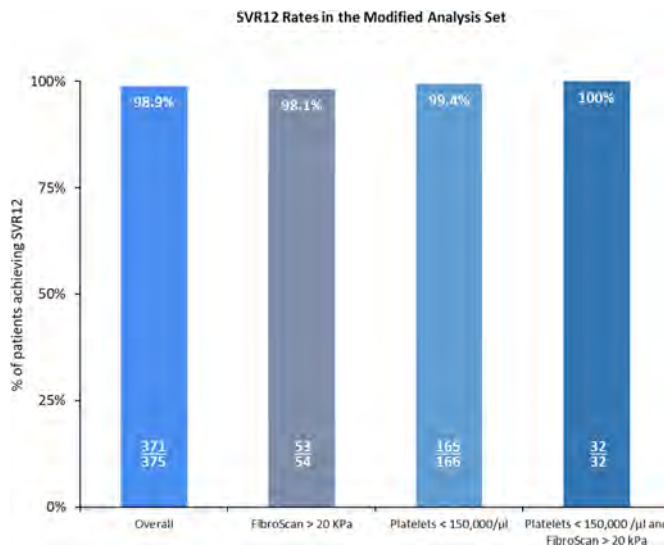
Markus Cornberg¹, Armand Aberger², Alessio Aghemo³, Adriana Ahumada⁴, Massimo Andreoni⁵, Tarik Asselah⁶, Abhi Bhagat⁷, Isabel Butrymowicz⁷, Michal Carmiel^{8,9}, Gabriel Chodik^{10,11}, Brian Conway^{12,13}, Antonio Gasbarrini¹⁴, Dietrich Hüppe¹⁵, Francisco Jorquera¹⁶, Pietro Lampertico^{17,18}, Maria Luisa Manzano Alonso¹⁹, Lindsay Myles²⁰, Marcello Persico²¹, Alnoor Ramji²², Christoph Sarrazin²³, Dimitri Semizarov⁷, Yanna Song⁷, Erica Villa²⁴, Clara Weil¹⁰, Juan Isidro Uriz Otano^{25,26}.
¹Hannover Medical School, Department of Gastroenterology, Hepatology and Endocrinology, Hannover, Germany; ²UMR 6602 CNRS Université d'Auvergne, CHU Estaing; ³Humanitas Research Hospital IRCCS, Department of Biomedical Sciences, Humanitas University, and Department of Gastroenterology, Rozzano, Italy; ⁴Hospital General Universitario Gregorio Marañón, Liver Unit; ⁵University of Tor Vergata, Rome; ⁶Hôpital Beaujon, INSERM UMR 1149, Service d'Hépatologie; ⁷AbbVie Inc., North Chicago, United States; ⁸Galilee Medical Center, Liver Unit; ⁹Bar-Ilan University, The Azrieli Faculty of Medicine; ¹⁰Maccabi Healthcare Services, Maccabitech; ¹¹Tel-Aviv University, Sackler Faculty of Medicine; ¹²Vancouver Infectious Diseases Center; ¹³Simon Fraser University; ¹⁴Fondazione Policlinico Universitario A. Gemelli IRCCS, Internal Medicine and Gastroenterology; ¹⁵Gastroenterologische Gemeinschaftspraxis Herne; ¹⁶Complejo Asistencial Universitario de León, IBIOMED and CIBERehd, Digestive System Service, Spain; ¹⁷Ospedale Maggiore Policlinico, Fondazione IRCCS Ca' Granda; ¹⁸CRC 'AM and A Migliavacca' Centre for Liver Disease, Division of Gastroenterology and Hepatology; ¹⁹Hospital Universitario 12 De Octubre, Liver Unit, Spain; ²⁰Barrie GI Associates; ²¹AOU OO. RR. San Giovanni di Dio Ruggi e D'Aragona, Dipartimento di Medicina Clinica Medica, Epatologica e Lungodegenza; ²²University of British Columbia; ²³Goethe-University Hospital Frankfurt, Department of Internal Medicine and Liver Center, St. Josefs-Hospital Wiesbaden and Viral Hepatitis Research Group; ²⁴Azienda Ospedaliera Universitaria di Modena, UC Gastroenterologia, Dipartimento di SpecialitàMediche; ²⁵Navarra Institute for Health Research (IdiSNA); ²⁶Complejo Hospitalario de Navarra, Department of Gastroenterology, Liver Unit
 Email: cornberg.markus@mh-hannover.de

Background and aims: The direct-acting antiviral glecaprevir/pibrentasvir (G/P) is approved for 8-week treatment of chronic hepatitis C genotypes (GT) 1–6 in patients with or without compensated cirrhosis (CC). To support clinical trials findings, this study assessed real-world effectiveness and safety in treatment-naïve (TN) patients with CC treated with 8-weeks' G/P, with a focus on challenging-to-treat patients with advanced liver disease (platelets <150,000/μl, elasticity >20 kPa [FibroScan®], Echosens, Paris, France), or both), and special populations such as drug users, human immunodeficiency virus coinfection, and psychiatric disorders.

Method: Here we present updated interim results from the CREST study, an ongoing, noninterventional, multicenter study including data from Canada, Germany, Israel, Italy, France, and Spain. The primary endpoint was sustained virologic response at posttreatment Week 12 (SVR12) based on the modified analysis set (MAS) which excluded patients who discontinued G/P for reasons other than nonvirologic failure or with missing SVR12. Safety and laboratory abnormalities were assessed on the full analysis set.

Results: Of 437 patients who received ≥1 dose of G/P, 24.5% (107/437) had GT3, 46.0% (189/411) had platelets <150,000/μl, 16.4% (61/373) had elasticity >20 kPa, and 9.8% (36/366) had platelets <150,000/μl and elasticity >20 kPa. Of 375 patients in the MAS with data available, SVR12 was reached by 371 (98.9%). SVR12 was 97.7% (84/86) in patients with GT3, 99.4% (165/166) in those with platelets <150,000/μl, 98.1% (53/54) in those with elasticity >20 kPa, and 100% (32/32) in those with both elasticity >20 kPa and platelets <150,000/μl (Figure).

Of 117 (26.8%) patients with an adverse event (AE), 5 (1.1%) had a serious AE (SAE), with 1 (0.2%) discontinuing the study drug due to an AE. None of the SAEs were drug related. The most common AEs (>5%) were fatigue (9.6%; 42/437) and headache (6.4%; 28/437). Of 421 patients with laboratory data available, 9 (2.1%) and 10 (2.4%) had alanine or aspartate aminotransferase, respectively, >5x upper limit of normal.



Conclusion: In this real-world cohort, 8-week G/P therapy was well-tolerated, with SVR12 rates similar to those in clinical trials. These results support the use of G/P therapy in TN patients with CC, regardless of liver disease severity or GT, including GT3. Additional efficacy data in special populations will be presented at the congress.

Acknowledgements: The authors would like to express their gratitude to the patients who participated in this study and their families, as well as the study investigators and coordinators of the study. Glecaprevir was identified by AbbVie and Enanta. Medical writing support was provided by Marta Rossi, PhD, of Fishawack Communications Ltd, and funded by AbbVie.

FRI389

HCV-RNA viral load fingerstick assay as a simplified strategy for screening and linkage to care of people who use drugs attending 3 french addiction centers

Denis Ouzan^{1,2}, Joris Herin³, Nicolas Camerlo⁴, Patrick Favot⁵, Bruno Blasi⁴, Maella Lebrun⁶, Henriette Thiercelin⁴, Nathalie Legros⁷, Teresa Namouni⁸, Perrine Roux⁹, Stéphane Chevaliez¹⁰.
¹Arnault Institute Tzanck, Saint-Laurent-du-Var, France; ²RHECCA, NICE, France; ³Bus 31/32, Marseille, France; ⁴CAARUD LOU PASSAGIN, Nice, France; ⁵CSAPA FONDATION DE NICE, France; ⁶Bus 31/32, France; ⁷CSAPA FONDATION DE NICE, France; ⁸CSAPA EMERGENCE, Nice, France; ⁹INSERM, France; ¹⁰CNR HOPITAL MONDOR, France
 Email: denis.ouzan@wanadoo.fr

Background and aims: Rational: The number of people who inject drugs (PWID) that are screened and treated for hepatitis C remains low. Many of them are lost to follow-up after serological testing. It is currently estimated that 20% of patients are treated in Harm reduction centers (CSAPAs) and in Needle exchange structures (CAARUDs). The measurement of the viral load by rapid RT-PCR from capillary blood (Xpert® HCV Viral Load Fingerstick) allows to obtain a result in <1 hour and thus to increase the percentage of HCV-seropositive patients who could benefit from treatment.

Aims: The aims of this prospective study were to evaluate the feasibility and the acceptability of HCV-RNA viral load fingerstick assay use to improve HCV screening and treatment among French PWIDs attending 3 Addiction Centers.

Method: From March 1, 2021, all HCV seropositive PWIDs (previously known positive for serology or determined using a rapid diagnostic test (RDT) simultaneous targeting HCV, HBV, and HIV) followed up in 3 Addiction Centers CAARUD/CSAPA (2 in Nice, 1 in Marseille) were offered a rapid RNA testing using a molecular point of care testing (POCT) (Xpert HCV Viral Load Fingerstick). If the RNA testing was positive, treatment was proposed.

Results: From March 1 to August 31, 2021, 119 PWID were included: 76.5% men with an average age of 45 years, 22 were without social rights, 26 with precarious housing and 22 homeless, 41 declared having injected: heroin, crack, other, 34 inhaled: cocaine, crack, other, 65 having multiple addictions of which cannabis 35 and drugs 11 and 67 excessive alcohol consumption. 46 were receiving substitution treatment. HCV serology was documented in 117 of the 119 DU and was positive in 43 (37%) of them. HBV surface antigen (HBsAg) was positive in 4 and HIV in 3 DU PWID (all previously known). Among 39/43 anti-HCV+ subjects agreed to perform a rapid RNA testing, HCV RNA was positive in 20, i.e. a prevalence of 16%. Antiviral treatment was initiated in 12. The rate of treatment success will be presented.

Conclusion: Despite the high rate of HCV infection among PWIDs, screening and linkage to care remain far from comprehensive. Our HCV-RNA screening project, highlights the feasibility and the acceptability of onsite testing performed with HCV-RNA viral load fingerstick assay in PWIDs. This easy to use approach increases the frequency of HCV RNA testing and the prescription of treatment.

FRI390

Pangenotypic and genotype-specific antivirals in the treatment of genotype 4 infected patients with HIV coinfection

Dorota Zarebska-Michaluk¹, Jerzy Jaroszewicz², Anna Parfieniuk-Kowerda³, Beata Lorenc⁴, Małgorzata Pawłowska⁵, Włodzimierz Mazur⁶, Marek Sitko⁷, Ewa Janczewska⁸, Hanna Berak⁹, Janocha-Litwin Justyna¹⁰, Jakub Klapaczynski¹¹, Krzysztof Tomaszewicz¹², Piekarska Anna¹³, Beata Dobracka¹⁴, Rafał Krygier¹⁵, Jolanta Citko¹⁶, Tronina Olga¹⁷, Krystyna Dobrowolska¹⁸, Robert Flisiak³. ¹Jan Kochanowski University, Department of Infectious Diseases, Kielce, Poland; ²Medical University of Silesia, Department of Infectious Diseases and Hepatology, Katowice, Poland; ³Medical University of Białystok, Department of Infectious Diseases and Hepatology, Białystok, Poland; ⁴Medical University of Gdańsk, Poland; ⁵Ludwik Rydygier Collegium Medicum in Bydgoszcz Faculty of Medicine Nicolaus Copernicus University in Toruń, Bydgoszcz, Poland; ⁶Medical University of Silesia, Katowice, Poland; ⁷Jagiellonian University, Kraków, Poland; ⁸Medical University of Silesia, Bytom, Poland; ⁹Hospital for Infectious Diseases, Warszawa, Poland; ¹⁰Medical University of Wrocław, Wrocław, Poland; ¹¹Central Clinical Hospital of the Ministry of Internal Affairs and Administration, Warszawa, Poland; ¹²Medical University of Lublin, Lublin, Poland; ¹³Medical University of Łódź, Łódź, Poland; ¹⁴MED-FIX, Wrocław, Poland; ¹⁵State University of Applied Sciences, Konin, Poland; ¹⁶Regional Hospital Olsztyn, Olsztyn, Poland; ¹⁷Medical University of Warsaw, Warszawa, Poland; ¹⁸Jan Kochanowski University, Collegium Medicum, Kielce, Poland
Email: dorota1010@tlen.pl

Background and aims: The introduction of the direct-acting antivirals (DAA) has improved substantially the therapy effectiveness in patients with chronic hepatitis C and we aimed to compare the efficacy of pangenotypic and genotype-specific DAA in the cohort of genotype (GT) 4 patients with HCV monoinfection and HIV coinfection.

Method: The analysis included patients selected from the EpiTer-2 database, a large retrospective multicenter national real-world study evaluating DAA treatment in 13, 554 consecutive individuals with hepatitis C virus (HCV) infection.

Results: A total of 662 GT4-infected patients, of whom 168 (25.3%) were coinfecting with HIV, treated in 2015–2020 were enrolled in the analysis. Significantly higher rate of males (67.9% vs. 57.7%), a lower proportion of liver cirrhosis (10.2% vs. 18.1%), and higher of

treatment-naïve patients (87.5% vs. 76.7%) were documented in HIV coinfecting individuals. The overall sustained virologic response after exclusion of non-virologic failures was achieved in 98% with no significant difference between HIV-positive and HIV-negative patients, 96.2% vs. 98.5%, respectively. While the genotype-specific regimens resulted in a similar cure rate regardless of the HIV status, the pangenotypic options were more efficacious in patients with HCV monoinfection as compared to HIV coinfecting (99.3% vs. 94.4%, $p = 0.05$). No significant differences in demographic, clinical, and laboratory parameters were found between 13 virologic nonresponders and responders.

Conclusion: We demonstrated the high effectiveness and good safety profile of DAA regimens in GT4 infected patients with HIV coinfection. However, the current analysis demonstrated lower effectiveness of pangenotypic regimens in HIV/HCV GT4 coinfecting patients compared to genotype-specific regimens.

FRI391

Long-term follow-up of HCV resistance-associated substitutions after DAA treatment failure

Julia Dietz¹, Beat Müllhaupt², Peter Buggisch³, Christiana Graf¹, Kai-Henrik Peiffer¹, Katrin Matschenz³, Jörn Schattenberg⁴, Stefan Mauss⁵, Christoph Antoni⁶, Elena Durmashkina⁷, Claus Niederer⁸, Thomas Discher⁹, Janina Trauth⁹, Georg Dultz¹, Julian Schulze zur Wiesch¹⁰, Felix Piecha¹⁰, Hartwig Klinker¹¹, Tobias Müller¹², Christoph Neumann-Haefelin¹³, Thomas Berg¹⁴, Christoph Berg¹⁵, Stefan Zeuzem¹, Christoph Sarrazin^{1,7}. ¹Goethe University Hospital, Department of Internal Medicine I, Frankfurt, Germany; ²University Hospital Zürich, Zürich, Switzerland; ³Institute for Interdisciplinary Medicine IFI, Hamburg, Germany; ⁴University Medical Center Mainz, Mainz, Germany; ⁵Center for HIV and Hepatogastroenterology, Düsseldorf, Germany; ⁶University Hospital Mannheim, Mannheim, Germany; ⁷St. Josefs-Hospital, Wiesbaden, Germany; ⁸St. Josef-Hospital, Oberhausen, Germany; ⁹Justus Liebig University Gießen, Gießen, Germany; ¹⁰University Medical Center Hamburg-Eppendorf, Hamburg, Germany; ¹¹University Hospital Würzburg, Würzburg, Germany; ¹²Charité Universitätsmedizin Berlin, Berlin, Germany; ¹³University Hospital Freiburg, Freiburg, Germany; ¹⁴University Hospital Leipzig, Leipzig, Germany; ¹⁵University Hospital Tübingen, Tübingen, Germany
Email: julia.dietz@em.uni-frankfurt.de

Background and aims: The approval of direct acting antivirals (DAA) for the treatment of chronic hepatitis C virus (HCV) infection resulted in high sustained virologic response (SVR) rates. Virologic failure is associated with the selection of resistance-associated substitutions (RASs). Long-term persisting RASs may have an impact on retreatment with first generation DAAs in resource-limited settings. This study evaluated the persistence of HCV RASs up to more than 24 months after end of DAA treatment (EOT).

Method: We included samples from $n = 715$ patients with a HCV GT1 and GT3 infection and virologic treatment failure which were collected in the European Resistance Database. HCV NS3, NS5A and NS5B genes were sequenced population-based and RASs conferring a >2-fold increased DAA susceptibility were analyzed and clinical parameters were evaluated retrospectively.

Results: A total of 253 patients with HCV genotype (GT) 1a (35%), 250 with GT1b (35%) and 212 with GT3 (30%) were included and the mean sampling time point after EOT was 7.6 months (0.0–63.0). The majority of patients with GT1 had failed to LDV/SOF (53%) or PrOD (17%) and those with GT3 to DCV/SOF (46%) or VEL/SOF (35%). NS3 RASs reached frequencies of 70–90% after EOT in GT1 and 50% in GT3 after PI failure and disappeared rapidly in GT1b and GT3 after follow-up month 3 (FU3), while in GT1a RASs were stable ($\geq 60\%$), due to Q80 K.

Within NS5B, SOF-resistant RAS S282 T was only found in individual patients with GT3a. Non-nucleoside NS5B RASs were frequent (60%–90%) in GT1 and declined to 27% in GT1a while remaining stable in

POSTER PRESENTATIONS

GT1b. NS5A RASs were very common (90%–95% after EOT) in all GT and even after FU24, RASs were detectable in more than 70% of the patients. RAS patterns in GT1b were dominated by L31M and Y93H and both variants showed a stable course over time (FU24: 95% patients with RASs). Several different RASs were detected in GT1a, most common were M28 T, Q30H/R, L31M and Y93H. However, NS5A RASs slightly decreased in GT1a and GT3a which was mainly caused by the decline of high-level resistant Y93H (FU24: GT1a, 71% and GT3, 73% of patients with RASs).

Conclusion: After DAA failure, NS3 and NS5B RASs disappeared quickly and NS5A RASs persisted beyond two years after EOT. While NS5A RASs remained stable in HCV GT1b, patients with GT1a and GT3 showed a decrease in particular of Y93H two years after EOT.

FRI392

Real-life effectiveness and safety of sofosbuvir/velpatasvir in difficult to treat hepatitis C patients

Hyun Young Woo¹, Jeong Heo¹, Young Joo Park¹. ¹Pusan National University Hospital, Internal Medicine, Busan, Korea, Rep. of South
Email: who54@hanmail.net

Background and aims: In spite of recent advance in the treatment of hepatitis C virus (HCV), there are still difficult to treatment population such as prior direct antiviral agents (DAA) failure, decompensated cirrhosis or presence of hepatocellular carcinoma (HCC). Here we report our experience about these patients treated Sofosbuvir/Velpatasvir (SOF/VEL) in real world setting.

Method: All consecutive patients with HCV receiving SOF/VEL between August 2017–May 2021 in South Korea were enrolled. Sustained virological response (SVR) was defined as undetectable HCV-RNA 12 (SVR12) weeks after the end-of-treatment.

Results: A total of 37 patients were included: median age 65 (45–83) years, 59.5% males, median HCV-RNA 852, 500 (11, 100–10, 800, 000) IU/ml. HCV genotype was 1b in 67.6%, 2 in 29.7%, 1b & 2b in 2.7%. 37.8% have concomitant HCC (BCLC stage A/B/C; 4/8/2). 56.8% have underlying cirrhosis and 7.5% was decompensated cirrhosis. 70.3% have failed prior DAA treatment (Daclatasvir + asunaprevir n = 16, sofosbuvir + ribavirin n = 3, sofosbuvir + ledipasvir n = 2, glecaprevir + pibrentasvir n = 3, boceprevir n = 1) Naïve patients received SOF/VEL for 12 weeks and the patients with prior DAA failure received SOF/VEL for 24 weeks, ribavirin was added in 78.4% of treatment schedules. Undetectable HCV-RNA was achieved by 97.2% of patients at week 4 and end of treatment response was 97.2%. Overall, 36/37 (97.2%) patients by intention to treat analysis and 36/36 (100%) by per protocol analysis achieved SVR12, respectively; One patient was expired due to HCC progression during SOF/VEL treatment. Most patient well tolerated treatment without adverse events.

Conclusion: SOF/VEL is an effective and safe retreatment for difficult to treat HCV population in a real-life setting.

FRI393

Polypharmacy and prevalence of multi drug-drug interactions in hepatitis C patients treated with pangenotypic direct acting antivirals: an analysis from three European countries

Frank Tacke¹, Juan Turnes², Andreas Hintz³, Stefano Fagioli⁴, Antoni Sicras-Mainar⁵, Tim Umland³, Luca Degli Esposti⁶, Ramón Morillo Verdugo⁷, Antonio Garcia Herola⁸, Mehtap Guendogdu⁹, Marinela Mendez¹⁰, Gema Alvarez Nieto¹¹, Kim Vanstraelen¹², Candido Hernández¹², Alessandra Mangia¹³.
¹Charité-Universitätsmedizin Berlin, Berlin, Germany; ²Complejo Hospitalario Universitario de Pontevedra, Gastroenterology and Hepatology, Spain; ³Alexander Apotheke, Hamburg, Germany; ⁴ASST Papa Giovanni XXIII Hospital, Bergamo, Italy; ⁵Atrys health, HEOR, Barcelona, Spain; ⁶Clicon S.r.l., Health Economics and Outcomes Research, Ravenna, Italy; ⁷Hospital Universitario de Valme, Hospital Pharmacy, Sevilla, Spain; ⁸Hospital Marina Baixa, Villajoyosa, Spain; ⁹Gilead Sciences GmbH, Medical Affairs, München, Germany; ¹⁰Gilead Sciences S.L., Medical Affairs, Madrid, Spain; ¹¹Gilead Sciences S.r.l., Medical Affairs, Milan, Italy; ¹²Gilead Sciences, Global Medical Affairs, United Kingdom; ¹³Fondazione "Casa Sollievo della Sofferenza" IRCCS, San Giovanni Rotondo, Italy
Email: a.mangia@tin.it

Background and aims: Current EASL, AASLD and APASL guidelines recommend a thorough drug–drug interaction (DDI) evaluation before starting pangenotypic direct-acting antiviral (pDAA) therapy. Previous studies have analyzed DDIs in HCV patients receiving pDAAs and comedications only by pairwise interactions. However, this does not reflect the polypharmaceutical reality of many HCV patients. The aim of this study was to evaluate the proportion of HCV patients with multiple comedications causing potential DDIs in three European countries.

Method: Comedication prescription data were collected from patients treated with pDAAs in Germany, Italy, and Spain. DDIs were identified using the Liverpool Hep Interaction checker. A multi-DDI profile was defined as the use of ≥ 2 comedications each predicted with a DDI with the administered pDAA. Potential DDI outcomes were summarized as an increase in comedication exposure (impact on safety) or a decrease in DAA exposure (impact on efficacy).

Results: A total of 10,755 HCV patients (mean age: 53.6 years, 64.2% male) treated with either sofosbuvir/velpatasvir (n = 4583) or glecaprevir/pibrentasvir (n = 6172) were included in this multi-national analysis: 4950 from Germany, 4185 from Italy, and 1620 from Spain. Over one-half, 58.9% (6333/10,755) received any comedication during their pDAA therapy, and 20.2% (2177/10,755) were at risk of a DDI with their pDAA. In terms of multi-DDI risk, 566 patients were taking ≥ 2 comedications, each with a potential DDI with their pDAA. This represented 5.3% (566/10,755) of the HCV patient population and 8.9% (566/6333) of patients receiving any comedication. Evaluation of predicted DDI impact revealed that approximately one-quarter (23.9%; 135/566) of patients taking ≥ 2 comedications had a risk of decreasing DAA plasma exposure, mainly caused by gastrointestinal drugs, such as proton-pump inhibitors, and analgesics, such as metamizole. This was observed mainly in Germany and Spain. A further one-quarter of patients (26.5%; 150/566) had a risk of increasing comedication, posing a potential safety risk, mainly in cardiovascular drugs, such as statins, and nervous system drugs, such as antipsychotics.

Conclusion: Across Germany, Italy, and Spain, 8.9% of HCV patients taking medications concomitantly during their pDAA therapy are at risk of multiple DDIs. Accurate prediction of the impact of multiple DDIs on pDAA efficacy and safety is difficult; this should prompt a thorough pDDI assessment before HCV therapy in comorbid patients.

FRI394

Use of comedication in patients with hepatitis C and addiction or drug abuse treated with direct-acting antivirals: implication in drug-drug interactions

Juan Turnes¹, Antonio Garcia Herola², Ramón Morillo Verdugo³, Marinela Mendez Pertuz⁴, Cristina De Alvaro⁵, Candido Hernández⁶, Antoni Sicras-Mainar⁷. ¹CHU, Pontevedra, Gastroenterology and Hepatology Department, Pontevedra, Spain; ²Hospital Marina Baja de Villajoyosa, Digestive Medicine Department, Alicante, Spain; ³Hospital de Valme, AGS Sur de Sevilla, Hospital Pharmacy, Sevilla, Spain; ⁴Gilead Sciences S.L., Madrid, Spain, Medical Affairs, Madrid, Spain; ⁵Gilead Sciences S.L., Madrid, Spain, Medical Affairs, Madrid, Spain; ⁶Gilead Sciences Europe Ltd, Global Medical Affairs, United Kingdom; ⁷Atrys Health, Health Economics and Outcomes Research, Barcelona, Spain
Email: ansicras@atryshealth.com

Background and aims: In previous studies we have analysed drug-drug interactions (DDIs) in the general population. In this sub-analysis we focus on patients with addiction to substance or drug abuse. The objective is to describe the drug use, comedication and the associated risk of drug interactions.

Method: Retrospective observational study, obtained from the BIG-PAC database (Atrys Health), on HCV patients (pts) treated between 2017 and 2020. Possible DDIs with direct-acting antivirals (DAAs) (Sofosbuvir/Velpatasvir [SOF/VEL] and Glecaprevir/Pibrentasvir [GLE/PIB]) were evaluated using the University of Liverpool Interactions for Hepatitis database. The risk of DDIs was analyzed, as well as their potential outcome: increase (↑) in comedication concentration or ↑ DAA (possible impact on safety) and decrease in DAA, ↓DAA (possible impact on efficacy).

Results: 985 pts with history or current consumption of abuse and recreational substances were included, 450 for SOF/VEL (mean age: 53 years; men 65%; F3/4 42%) and 535 with GLE/PIB (mean age: 50 years; men 65% F3/4 30%). The most consumed substances are described in the table, highlighting the higher consumption of opioids in pts treated with SOF/VEL vs GLE/PIB (13% vs 9%, $p < 0.05$, respectively).

The mean number of medications prescribed was 3.9 for SOF/VEL and 2.1 for GLE/PIB ($p < 0.001$). The most prescribed drugs belonged to the nervous system (40%); anti-infectives for systemic use, (13%); cardiovascular (12%) and alimentary system (12%).

GLE/PIB presented a higher percentage of potential DDIs than SOF/VEL, with nervous system medication (8.5% vs 4.9%, $p < 0.01$) and cardiovascular (36.8% vs 13.7%, $p < 0.001$); and similar for alimentary system (45.4% vs 44.7%, ns) and anti-infectives (5.8% vs 6.9%, ns). The most prescribed nervous system drugs with potential DDIs were quetiapine and metamizole.

Table: Addition to substances or drug abuse for HCV patients treated with AADs

Study groups	SOF / VEL	GLE / PIB	Total	p
Number of patients, %	450 (45.7%)	535 (54.3%)	985 (100%)	
Addictions				
Chronic alcoholism	110 (24%)	105 (20%)	215 (22%)	0.068
Opioids	60 (13%)	47 (9 %)	107 (11%)	0.022
Sedatives-anxiolytics	140 (31%)	136 (25%)	276 (28%)	0.048
Cannabis	198 (44%)	235 (44%)	433 (44%)	0.981
Cocaine	116 (26%)	142 (26%)	258 (26%)	0.786
Heroin	80 (18%)	77 (14%)	157 (16%)	0.148

Conclusion: In Spain, 9% of HCV patients with addictions to substance or drug abuse taking ≥ 2 comedications are at risk of multi-DDIs.

FRI395

Five years of progress towards achieving hepatitis C elimination in the country of Georgia, April 2015-October 2021

Tengiz Tsertsvadze^{1,2}, Amiran Gamkrelidze³, Nikoloz Chkhartishvili¹, Akaki Abutidze^{1,2}, Lali Sharvadze^{2,4}, Vakhtang Kerashvili¹, Maia Butsashvili⁵, David Metreveli⁶, Lia Gvinjilia⁷, Tinatin Kuchuloria⁷, Shaun Shadaker⁸, Tamar Gabunia⁹, Ekaterine Adamia¹⁰, Stefan Zeuzem¹¹, Nezam Afdhal¹², Sanjeev Arora¹³, Karla Thornton¹³, Paige A Armstrong⁸. ¹Infectious Diseases, AIDS and Clinical Immunology Research Center, Tbilisi, Georgia; ²Ivane Javakhishvili Tbilisi State University, Tbilisi, Georgia; ³National Center for Disease Control and Public Health, Tbilisi, Georgia; ⁴Clinic Hepa, Tbilisi, Georgia; ⁵Health Research Union, Tbilisi; ⁶Medical Center Mrcheveli; ⁷The Task Force for Global Health; ⁸Centers for Disease Control and Prevention, Division of Viral Hepatitis National Center for HIV, Hepatitis, STD&TB Prevention, Atlanta, USA; ⁹Ministry of IDPs, Labour, Health and Social Affairs of Georgia, Tbilisi, Georgia; ¹⁰Ministry of IDPs from the Occupied Territories, Labour, Health, and Social Affairs of Georgia; ¹¹University of Frankfurt; ¹²Beth Israel Deaconess Medical Center Liver Center; ¹³University of New Mexico
Email: tt@aidcenter.ge

Background and aims: Georgia launched the world's first national hepatitis C elimination program in April 2015. Key strategies include nationwide screening, active case finding, linkage to care, decentralized care, and provision of treatment for all persons with hepatitis C virus (HCV) infection, along with effective prevention interventions. The elimination program aims to achieve the following targets: a) diagnose 90% of HCV-infected persons, b) treat 95% of those diagnosed, and c) cure 95% of those treated. We report progress towards elimination targets 5 years into the elimination program.

Method: The estimated number of persons living with HCV infection was based on a 2015 population-based national seroprevalence survey, which showed that 5.4% of the adult general population had chronic HCV infection (approximately 150,000 persons). We analyzed data in the national HCV screening and treatment databases during April 2015–October 2021.

Results: As of October 31, 2021, 146,533 persons screened positive for HCV antibodies, 145,572 of whom were adults. Of the adults who screened positive, 119,280 (81.9%) underwent HCV viremia testing. A total of 94,891 (79.6%) persons tested had active HCV infection, and 76,149 (80.2%) of them initiated treatment. Of 53,806 patients who were evaluated for sustained virologic response (SVR), 53,230 (98.9%) tested negative for HCV by PCR. Based on the 90-95-95 program goal, Georgia has diagnosed 63.3% of the estimated 150,000 adults living with chronic HCV, treated 59.4% of the target 128,250, and cured 43.7% of the target 121,837.

High cure rates were achieved for all HCV genotypes: 98.9% in genotype 1, 98.9% in genotype 2 and 98.3% in genotype 3, typically the most challenging to treat. Treatment effectiveness was comparable among persons with advanced fibrosis (F3 and F4) with 98.2% achieving SVR, and among patients with mild or no liver fibrosis ($\leq F2$), SVR = 99.1%.

Conclusion: Georgia has made substantial progress towards eliminating hepatitis C. Over 60% of persons with chronic HCV infection have been diagnosed, and most have initiated treatment with high cure rates regardless of fibrosis status. Challenges remain in identifying and linking to care persons living with HCV in Georgia. The Nationwide integrated, decentralized model of HCV treatment, which has already been implemented in many locations, will be critical to improve linkage to care and close gaps in the HCV cascade of care.

POSTER PRESENTATIONS

FRI396

Simplifying mathematical-based response guided therapy for reducing duration of direct acting antivirals in chronic hepatitis C infected patients

Ashish Goyal¹, Alex Churkin², Danny Barash³, Scott Cotler¹, Amir Shlomai^{4,5}, Ohad Etzion⁶, Harel Dahari¹. ¹Program for Experimental & Theoretical Modeling, Division of Hepatology, Department of Medicine, Stritch School of Medicine, Loyola University Chicago, Maywood, United States; ²Department of Software Engineering, Sami Shamoon College of Engineering, Beer-Sheba, Israel; ³Department of Computer Science, Ben-Gurion University, Beer-Sheba, Israel; ⁴Department of Medicine D and The Liver Institute, Rabin Medical Center, Beilinson Hospital, Petah-Tikva; ⁵Sackler Faculty of Medicine, Tel Aviv University, Tel Aviv; ⁶Soroka University Medical Center, Beer-Sheba Email: harel.dahari@gmail.com

Background and aims: We recently reported the first proof-of-concept clinical trial assessing in real-time the utility of response-guided therapy (RGT) with direct-acting antivirals (DAA) in chronic hepatitis C virus (HCV) infected patients, based on a mathematical modeling approach (Etzion et al. *Scientific Reports*. 2020;10:17820). The RGT modeling approach relies on measuring HCV at baseline and days 2, 7, 14 and 28 after initiation of DAA therapy. A simplified on-treatment HCV monitoring procedure is highly warranted.

Method: The mathematical model used in the proof-of-concept study was re-fitted with the measured HCV kinetic data obtained from the 10 patients for whom the model was used to shorten the standard 12-week DAA therapy duration. The fitting procedure consisted of finding the best fits using corrected Akaike Information Criteria. The predicted time to cure (TTC) was defined as the time it takes during DAA therapy to reach less than 1 viral copy in the serum (i.e. 7×10^{-5} copies/ml). The first data point below detection or lower limit of quantification (LLOQ) was assigned a value ($\in [0.2, 15]$ IU/ml) as done in the proof-of-concept study. We next removed either day 2 or day 7 from the 10 patients and repeated the same procedure projecting TTC. Modeling calibration was done using MATLAB R2021a.

Results: We first verified that fitting the model to all the measured data points measured in the proof-of-concept study were in agreement with the current modeling approach (Table 1). Excluding day 2 did not affect maximum TTC projections (Table 1) and TTC were significantly correlated ($r = 0.91$, $p = 0.0007$) with the predicted TTC based on all measured data points. Notably, while excluding day 2 caused potential non-identifiability in estimating HCV viral clearance from circulation, the estimation of TTC remained unaffected. In contrast, excluding day 7 would lead to overestimation of the maximum TTC projections ($r = 0.29$, $p = 0.45$) (Table 1).

Patient	Etzion et al. <i>Scientific Reports</i> .2020;10:17820	Full observed data	Excluding day 2	Excluding day 7
P1	59	59 [59, 59]	59 [59, 59]	60 [52, 67]
P2	46	45 [45, 45]	44 [44, 44]	47 [45, 76]
P3	36	36 [36, 36]	27 [26, 32]	36 [36, 37]
P4	56	58 [58, 58]	58 [58, 58]	93 [93, 93]
P6	43	42 [42, 42]	40 [40, 40]	56 [56, 56]
P7	55	54 [54, 56]	47 [47, 47]	55 [54, 55]
P8	33	31 [30, 34]	34 [33, 34]	35 [35, 35]
P9	56	55 [55, 57]	57 [57, 57]	56 [56, 56]
P10	44	44 [44, 44]	44 [44, 44]	45 [45, 45]
P11	53	53 [53, 53]	53 [53, 53]	44 [42, 46]

Table 1: Modeling predicted time to cure (TTC) in 10 individuals from Etzion et al. The estimates are reported as median [minimum, maximum] in three scenarios, namely, (i) analyzing fully observed data, (ii) analyzing dataset while removing day 2, and (iii) analyzing dataset while removing day 7.

Conclusion: The current analysis indicates that on-treatment day 2 viral load measurement is not necessary to predict TTC. Measuring HCV at baseline and days 7 and 14 after initiation of DAA therapy provides a simplified on-treatment monitoring procedure during modeling-based RGT. Further validation in a large-scale clinical trial, will support the routine implementation of our individualized treatment approach in patients receiving DAA for HCV.

FRI397

Epidemiology of hepatitis B virus infection among hepatitis C (HCV) infected patients treated within HCV elimination program in Georgia

Senad Handanagic¹, Maia Butsashvili², Shaun Shadaker¹, Irina Tskhomelidze^{3,3,3}, Paige A Armstrong¹. ¹Centers for Disease Control and Prevention, Division of Viral Hepatitis, Atlanta, United States; ²Health Research Union, Tbilisi, Georgia; ³The Task Force for Global Health, Tbilisi, Georgia Email: ndv9@cdc.gov

Background and aims: Patients with hepatitis C virus (HCV) and hepatitis B virus (HBV) co-infection are at an increased risk of developing liver disease compared with mono-infected individuals. The Georgia Hepatitis C Elimination Program was established in 2015 and offers free treatment with direct-acting antivirals (DAA) to all persons with HCV infection. The program includes HBV screening for all HCV infected patients. We describe the epidemiology of HBV/HCV co-infection among patients treated within the HCV elimination program.

Method: Data for this analysis comes from the national electronic HCV elimination program treatment database. Persons aged ≥ 18 years with active HCV infection who initiated HCV treatment within the program during May 2015–September 2021 were included. Patients were grouped as HCV mono-infected, HCV/HBV coinfecting (HBV surface antigen [HBsAg] positive), and HBV immune but not infected (HBV surface antibody or HBV core antibody positive, HBsAg negative). We present descriptive analysis and adjusted prevalence ratios (aPR) with 95% confidence intervals (CI) for HCV/HBV coinfection compared to HCV mono-infection for demographic, risk, clinical and treatment outcomes. aPRs were adjusted for age, sex, HCV genotype, and history of injection drug use in a multi-variable model.

Results: As of September 2021, 71,931 adult persons were treated for HCV and screened for HBV within the HCV elimination program in Georgia. The majority were 18–45 years old (48%; median age 46, interquartile range 39–55 years), male (78%), and did not report a history of injection drug use (57%).

Overall, 70% ($n = 50,103$) had HCV mono-infection, 28% ($n = 2,202$) had HCV mono-infection and were immune to HBV, and 2% ($n = 1,626$) had HBV/HCV co-infection. HBV/HCV co-infection was more common among persons who were 18–45 compared to 46–60 years old (aPR: 1.7, 95% CI: 1.5–2.0), male (aPR: 1.3, 95% CI: 1.1–1.6), reported a history of injection drug use (aPR: 1.3, 95% CI: 1.1–1.5), had serum end of treatment (EOT) ALT > 80 U/L compared to < 40 U/L (aPR: 2.3, 95% CI: 1.6–3.4), and did not achieve sustained virologic response (aPR: 1.4, 95% CI: 1.1–1.9).

Conclusion: HBV/HCV co-infection is associated with higher risk of liver disease, elevated EOT ALT, and DAA treatment failure. To improve outcomes for patients with HBV/HCV co-infection, it is essential to evaluate them for HBV treatment. Promoting preventative measures, such as HBV vaccination among patients with HCV infection, is also important to reduce mortality from hepatitis.

FRI398

Direct-acting antivirals and the risk of hepatitis B reactivation in hepatitis B and C coinfecting patients: a systematic review and meta-analysis

Joo Hyun Oh¹, Sang Bong Ahn¹, Jeong-Ju Yoo², Dae Won Jun³, Hyunwoo Oh⁴, Huiyul Park⁵, Joo Hyun Sohn⁶, Hyo Young Lee⁴, Bo-Kyeong Kang⁷, Mi Mi Kim⁷, Eileen Yoon³, Chul-min Lee⁷. ¹Nowon Eulji Medical Center, Eulji University School of Medicine, Department of Medicine, Seoul, Korea, Rep. of South; ²Soonchunhyang University Bucheon Hospital, Department of Medicine, Gyeonggi-do, Korea, Rep. of South; ³Department of Internal Medicine, Hanyang University College of Medicine, Seoul, Korea, Rep. of South; ⁴UiJeongbu Eulji Medical Center, Department of Medicine, Gyeonggi-do, Korea, Rep. of South; ⁵UiJeongbu Eulji Medical Center, Department of Family Medicine, Gyeonggi-do, Korea, Rep. of South; ⁶Hanyang University College of Medicine, Department of Medicine, Gyeonggi-do, Korea, Rep. of South; ⁷Hanyang University College of Medicine, Department of Radiology, Seoul, Korea, Rep. of South
Email: dr486@eulji.ac.kr

Background and aims: Hepatitis B virus (HBV) reactivation may occur in chronic hepatitis C (CHC) coinfecting patients using direct-acting antivirals (DAAs). However, previous studies have reported inconsistent findings on this issue. We investigated the association between DAA and HBV reactivation by conducting a meta-analysis.

Method: Relevant studies were identified by searching Medline, EMBASE, Cochrane Central Register of Controlled Trials, KoreaMed, KMBase, and RISS to September 4th, 2020. The primary outcome was HBV reactivation. Random effect method was used for pooling the data.

Results: We identified 39 articles, comprising 119, 484 patients with chronic (n = 1, 673) or resolved (n = 13, 497) HBV infection who treated with DAA. When all studies were pooled, the rate of HBV reactivation was 12% (95% confidence interval (CI) 0.06–0.19). When stratified by baseline HBV DNA, undetectable HBV DNA (HBV DNA <20 IU/ml) group showed significantly lower risk of reactivation compared to detectable HBV DNA group (odds ratio (OR) 0.30, 95% CI 0.11–0.86). Although patients on prophylactic anti-HBV therapy showed a lower reactivation rate, there was no significant difference (OR 0.27, 95% CI 0.07–1.01). The rate of HBV reactivation was only 0.4% in patients with resolved HBV infection.

Conclusion: The risk of HBV reactivation was not negligible in HCV coinfecting patients using DAAs, indicating watchful attention for HBV reactivation is still needed.

Key Words: Direct-acting antivirals, hepatitis B virus, hepatitis C virus, reactivation

FRI399

Inhibition of high fitness viruses by different antiviral strategies when the infection has started

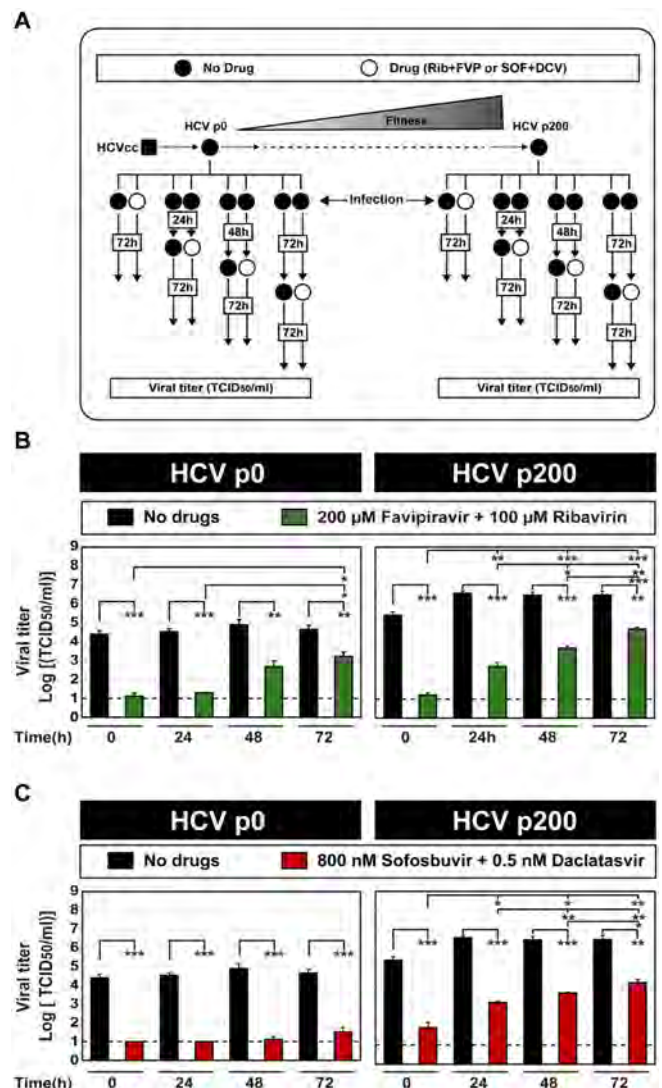
Carlos García-Crespo¹, Lucía Vázquez-Sirvent¹, Maria Eugenia Soria¹, Isabel Gallego¹, Ana Isabel de Ávila¹, Brenda Martínez-González^{1,2}, Esteban Domingo^{1,3}, Celia Perales^{1,2,3}. ¹Centro de Biología Molecular Severo Ochoa, Department of Interactions with the environment, Madrid, Spain; ²Hospital Universitario Fundación Jiménez Díaz, Department of Clinical Microbiology, Madrid, Spain; ³Centro de Investigación Biomédica en Red de Enfermedades Hepáticas y Digestivas, Spain
Email: cperales@cbm.csic.es

Background and aims: Previous results from our laboratory have documented that high fitness hepatitis C virus (HCV) can be a determinant of multidrug resistance, including nucleotide analogues, without the acquisition of specific resistance mutations. However, we recently demonstrated using favipiravir (T-705) and ribavirin that analogue concentrations that individually did not extinguish high fitness HCV in ten serial infections, when used in combination led to extinction in a few passages. With these two nucleotide analogues, we have described for the first time a new synergy mechanism in

lethal mutagenesis against HCV. Here we have investigated the effectiveness of these strategies once the infection has been initiated, as a stringent tests of antiviral efficacy. Combinations of inhibitors and combinations of lethal mutagens were compared. Since new antiviral designs based on sequential inhibitor-mutagenic have proven effective for the extinction of RNA viruses, sequential versus combination therapies have been also examined for suppression of high fitness HCV infectivity once the infection was ongoing.

Method: Low and high fitness HCV populations were used to infect Huh-7.5 hepatoma cells in the absence and presence of mutagenic (favipiravir and favipiravir) and non-mutagenic (sofosbuvir and daclatasvir) antiviral agents. Treatment efficacy was analyzed by measuring virus progeny production when antivirals were administered at different times after infection. In addition, sequential and combination treatments were compared for the extinction these viruses.

Results: The results indicate that low and high fitness viruses were not extinguished by combinations of mutagenic antivirals once the infection is ongoing. Treatment efficacy was lower when time of infection increased. Sequential and combination therapies produced a similar inhibition, without achieving viral extinction.



Conclusion: The time at which antiviral agents were administered once the infection have been initiated influenced viral extinction independently of the mechanism of action of the antivirals (both

POSTER PRESENTATIONS

non-mutagenic and mutagenic agents). Also, the data reinforce that high viral fitness is a determinant of drug resistance independently of the type of therapy used (sequential and combination therapies). No significant differences were observed between both therapies for the extinction of high fitness HCV.

FRI400

Treatment of hepatitis C in primary healthcare in the country of Georgia

Tengiz Tsertsvadze^{1,2}, Amiran Gamkrelidze³, Nikoloz Chkhartishvili¹, Akaki Abutidze¹, Lali Sharvadze^{2,4}, Maia Butsashvili⁵, David Metreveli⁶, Lia Gvinjilia⁷, Tinatin Kuchuloria⁷, Shaun Shadaker⁸, Tamar Gabunia⁹, Ekaterine Adamia⁹, Stefan Zeuzem¹⁰, Nezam Afdhal¹¹, Sanjeev Arora¹², Karla Thornton¹², Paige A Armstrong⁸. ¹Infectious Diseases, AIDS and Clinical Immunology Research Center; ²Ivane Javakhishvili Tbilisi State University; ³National Center for Disease Control and Public Health; ⁴Clinic Hepa; ⁵Health research union; ⁶Medical Center Mrcheveli; ⁷The Task Force for Global Health; ⁸Centers for Disease Control and Prevention, Division of Viral Hepatitis National Center for HIV, Hepatitis, STD&TB Prevention, Atlanta, USA; ⁹Ministry of IDPs, Labour, Health and Social Affairs of Georgia, Tbilisi, Georgia; ¹⁰University of Frankfurt; ¹¹Goethe University Hospital; ¹²University of New Mexico
Email: tt@aidscenter.ge

Background and aims: With technical assistance from the U.S. CDC and support from Gilead Sciences, Georgia launched the world's first national hepatitis C elimination program in April 2015. By October 2021, more than 75 thousand persons initiated treatment, achieving >98% cure rates. Patient enrollment in hepatitis C virus (HCV) treatment sharply increased in 2016, but has since slowed due to challenges in HCV testing and linkage to care. To increase initiation of treatment, Georgia began service decentralization in 2018 by integrating HCV screening and treatment in primary healthcare centers (PHCs).

Method: By July 31 2021, a total of 10 PHCs were providing HCV care services throughout the country. The integrated model is based on "one stop shop" approach, where patients receive all HCV screening and care services in selected PHCs. Treatment naïve patients with no or mild fibrosis (FIB-4 score <1.45) receive care at PHCs and completed examinations according to a simplified diagnostic and treatment monitoring algorithm, and persons with FIB-4 score >1.45 were referred to specialized clinics. Patients received Sofosbuvir/Ledipasvir or Sofosbuvir/Velpatasvir for 12 weeks. Sustained virological response (SVR) was defined as undetectable HCV RNA 12–24 weeks after end of therapy. The Extension for Community Healthcare Outcomes (ECHO) telemedicine model was used to train and support primary healthcare providers. Regular teleECHO videoconferencing was conducted to provide primary care providers with advice and clinical mentoring.

Results: Among persons diagnosed with active HCV infection, 1,454 were evaluated for FIB-4 score. A total of 954 patients initiated treatment, and of them 883 (92.6%) completed treatment. Of 864 patients eligible for SVR testing, 696 (80.6%) had been tested at the time of analysis, and 683 (98.1%) achieved SVR, yielding a >98% cure rate.

Conclusion: Our study reported the effectiveness of a simplified HCV treatment model in PHCs. Expanding this integrated decentralized model of HCV treatment nationwide would provide an opportunity to improve linkage to care and close gaps in the HCV cascade of care.

FRI401

Optimal screening and linkage to care model to achieve hepatitis C elimination targets in Georgia

Tengiz Tsertsvadze^{1,2}, Amiran Gamkrelidze³, Nikoloz Chkhartishvili¹, Akaki Abutidze¹, Lali Sharvadze^{2,4}, Vakhtang Kerashvili¹, Manana Todua², Maia Butsashvili⁵, David Metreveli⁶, Lia Gvinjilia⁷, Tinatin Kuchuloria⁷, Shaun Shadaker⁸, Tamar Gabunia⁹, Ekaterine Adamia⁹, Stefan Zeuzem¹⁰, Nezam Afdhal¹¹, Sanjeev Arora¹², Karla Thornton¹², Paige A Armstrong⁸. ¹Infectious Diseases, AIDS and Clinical Immunology Research Center; ²Ivane Javakhishvili Tbilisi State University; ³National Center for Disease Control and Public Health; ⁴Clinic Hepa; ⁵Health research union; ⁶Medical Center Mrcheveli; ⁷The Task Force for Global Health; ⁸Centers for Disease Control and Prevention, Division of Viral Hepatitis National Center for HIV, Hepatitis, STD&TB Prevention, Atlanta, USA; ⁹Ministry of IDPs, Labour, Health and Social Affairs of Georgia, Tbilisi, Georgia; ¹⁰University of Frankfurt; ¹¹Beth Israel Deaconess Medical Center Liver Center; ¹²University of New Mexico
Email: tt@aidscenter.ge

Background and aims: Access to care and treatment is essential to achieving hepatitis elimination, however, ensuring all patients can navigate the care pathway is challenging and involves multiple steps. Despite marked success of Georgia's National Hepatitis C Elimination Program, with over 75,000 persons initiating treatment April 2015–October 2021, since a peak in October 2016, patient enrollment in treatment has slowed. Developing an optimal model to ensure linkage-to-care at critical steps in the care cascade is paramount for the elimination program.

Method: We evaluated the effectiveness of various linkage-to-care modalities to assess diagnostic yield and engagement in hepatitis C virus (HCV) treatment. HCV care cascades for the period of March 2018–November 2020 were analysed and classified into 6 categories based on where the initial screening was performed: centralized and decentralized hospital sector, primary healthcare, harm reduction, specialized HCV provider sites and integrated HCV/HIV/TB screening locations. We defined linkage to care as: 1) completion of a viremia test after screening HCV antibody (anti-HCV) positive; and 2) establishment of a follow-up appointment for treatment with a hepatitis C specialist.

Results: Analysis included 24,460 anti-HCV positive persons. Persons engaged through the HCV provider site model had the highest rates of both viremia testing and engagement in treatment (91.5% and 87.1%, respectively). These were significantly higher than all other models, including harm reduction (86.2% and 77.8%), decentralized hospital sector (79.5% and 61.6%), integrated HCV/HIV/TB (75.1% and 79.9%), centralized hospital sector (74.5% and 45.6%), and primary healthcare (63.6% and 69.1%) models; all $p < 0.0001$. The primary healthcare model had the lowest rate of viremia testing (63.6%), while the centralized hospital sector had the lowest engagement in treatment (45.6%).

Conclusion: Our data suggest the HCV provider site screening model has been most successful in linking persons to care, for both viremia testing and initiation of treatment. Universal inpatient screening has been effective at testing large numbers of people; among the hospital sector models, the decentralized approach to testing had higher rates of viremia testing and treatment. Decentralization of care is key to providing access to all, but the primary healthcare model showed the lowest rate of viremia testing in our study.

FRI402

Establishing a protocol for management and DAA treatment of HCV during pregnancy: adherence to a co-located care protocol

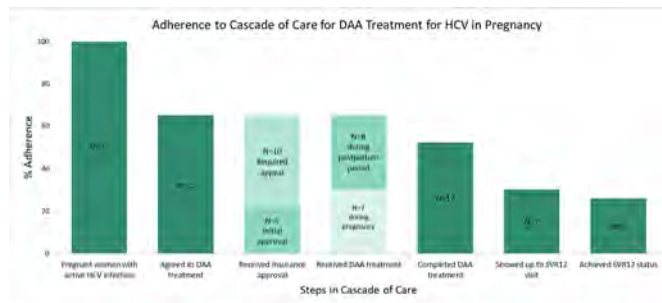
Tatyana Kushner¹, Marcia Lange¹, Rhoda Sperling¹, Douglas T Dieterich¹. ¹Icahn School of Medicine at Mount Sinai
Email: tatyana.kushner@mssm.edu

Background and aims: There are currently no recommendations for directly acting antiviral (DAA) therapy during pregnancy. Emerging

data suggests that DAAs are safe and effective during pregnancy. We evaluated our center experience in implementing DAA treatment during pregnancy.

Method: After establishment of a sub-specialty Women's Liver Clinic (WLC) co-located in the ambulatory obstetrics practice and implementation of universal antepartum HCV screening, we offered DAA treatment during pregnancy to women with active HCV. We evaluated adherence to each step in the HCV treatment cascade of care.

Results: Twenty-three pregnant women with active HCV infection were referred to WLC for consideration for HCV treatment; they were of median age 31 (IQR 24, 36); predominantly white (39%) non-Hispanic (52%), and medicaid-insured (78%); 30% with injection drug use as a risk factor; 9% who acquired HCV through perinatal transmission; 26% with no known risk factors. Fifteen (65%) reported that HCV was initially diagnosed during pregnancy. Adherence to cascade of care is shown in the Figure. Initial DAA ordered was ledipasvir/sofosbuvir for 7 (42%), ledipasvir/velpatasvir for 7 (42%) and glecaprevir/pibrentasvir for 2 (12%). Among those with DAA approval, nine (45%) received their DAA during pregnancy and seven (35%) initiated DAA treatment during pregnancy; eight (40%) initiated postpartum. Twelve (70%) had documented completion of DAA treatment; only 7 (35%) showed up to their SVR12 check; 6/7 (86%) had documented SVR12; one patient required re-treatment. In regards to pregnancy outcomes, 35% had intrahepatic cholestasis of pregnancy; two (9%) had preterm birth; one patient had pregnancy loss prior to DAA treatment initiation. There was one documented mother-to-child transmission in a patient treated with DAA postpartum.



Conclusion: Pregnancy offers an important opportunity to link women with HCV to treatment-the majority were diagnosed initially during routine screening during pregnancy. Cholestasis of pregnancy was a prevalent complication. HCV treatment during pregnancy is feasible and will likely offer benefits to maternal and child health, however significant challenges remain to ensure adherence through the vulnerable postpartum period. Similar to the management of other chronic conditions in the postpartum period, linkage to care and case management programs designed specifically for postpartum women should be evaluated to improve DAA therapy completion and documentation of SVR12.

FRI403

Sofosbuvir/Velpatasvir (S/V) for the treatment of HCV infection among vulnerable inner-city residents: extending the results of clinical trial

Brian Conway^{1,2}, David Truong¹, Leo Yamamoto¹, Rossitta Yung¹, Shawn Sharma¹. ¹Vancouver Infectious Diseases Centre, Vancouver, Canada; ²Simon Fraser University, Burnaby, Canada
Email: bconway5538@gmail.com

Background and aims: The SIMPLIFY study demonstrated that sofosbuvir/velpatasvir (S/V) can be used to treat Hepatitis C Virus (HCV) infection among active drug users, achieving sustained virologic response (SVR) 12 rates comparable to those achieved in

clinical trials enrolling other patient populations. There remains a need to replicate these results in more vulnerable populations, including those using fentanyl and not currently engaged in health care.

Method: Through dedicated outreach events, we identified HCV-infected patients who resided in single room occupancy dwellings who were not currently engaged in health care and who were eligible to receive government-funded antiviral treatment for HCV infection. We offered them the opportunity to enrol in a multidisciplinary program of care to address medical, psychological, social and addiction-related needs and provide S/V therapy in this context, with daily or weekly supervision of adherence, as appropriate. The endpoint of this preliminary analysis is the achievement of SVR12 in those who initiated therapy.

Results: We identified 172 eligible HCV-infected treatment-naïve subjects who were subsequently enrolled in the program. HCV diagnosis was documented 1–41 years before enrolment. Key demographic characteristics include: 126 (73%) male, median age 47 (23–75) years, F0/1 (120, 70%), ≥F2 (52, 30%), opiate/cocaine/amphetamine use (126/66/112, 73%/38%/65%). Once enrolled in care, 38 (22%) initiated addiction care with opiate agonist therapy. Of 142 who initiated treatment, 95 were available at the SVR12 time point to date. Of these, 88 achieved a cure. The main reasons an endpoint was not measured included 3 overdose-related deaths prior to SVR 12 time point and 4 disengaged from care. There were no cases of virologic failure or relapse.

Conclusion: Through dedicated initiatives, it is possible to identify vulnerable inner-city residents who were previously diagnosed with HCV infection and had never been offered treatment for it. These initiatives, combined with dedicated programs to provide HCV treatment in an optimized manner, must be considered to achieve HCV elimination in this unique population.

FRI404

High efficacy and safety of pan-genotypic direct-acting antiviral regimens in adolescents and children: a global systematic review to inform new World Health Organization recommendations

Giuseppe Indolfi¹, Sabrina Giometto², Fariha Malik³, Roger Chou⁴, Philippa Easterbrook⁵, Ersilia Lucenteforte². ¹Università di Firenze, Dipartimento Neurofarba, Firenze, Italy; ²Università di Pisa; ³UCL; ⁴Oregon Health & Science University; ⁵World Health Organization
Email: giuseppe.indolfi@meyer.it

Background and aims: The global hepatitis C virus (HCV) response has to date largely focused on adults who bear the greatest burden of morbidity and mortality. There had been less attention to addressing case-finding and treatment of the estimated 3.26 million HCV infected children and adolescents. The recent regulatory approval of two pan-genotypic regimens down to 3 years provides opportunity to extend treatment opportunities down to all children above 3 years. To inform new World Health Organization (WHO) guidelines, we undertook a systematic review and meta-analysis of treatment outcomes in adolescents and children down to 3 years based on the key pan-genotypic direct-acting antiviral (DAA) regimens.

Method: We searched two databases and key conference abstracts for studies from inception to August 2021 that evaluated three pan-genotypic DAA regimens recommended by WHO for use in adults (sofosbuvir/daclatasvir, SOF/DCV, sofosbuvir/velpatasvir, SOF/VEL, glecaprevir/pibrentasvir, GLC/PIB) in HCV infected adolescents (12–18 years), older children (6–11 years) and young children (3–5 years). Randomised controlled trials (RCT), non-RCT, and prospective observational studies were eligible for inclusion. Key outcomes evaluated were attainment of sustained virological response (SVR12), any adverse events, and discontinuation. Estimates were pooled using random-effects models.

Results: 3 RCTs, 28 non-RCTs and 18 observational studies reported treatment experience in 167 young children (3–5 years), 472 older children (6–11 years), and 2228 adolescents (12–18 years). Across all

POSTER PRESENTATIONS

studies, there were 15 cirrhotic children, 304 treatment-experienced, and 157 with genotype 3 infection. SVR12 was high >95% for all three regimens and across age groups. There was a clear trend towards a higher rate of any adverse event with younger age groups (50% in adolescents, 53% in older children, and 72% in young children) but serious adverse events and treatment discontinuations were uncommon. There were 7 discontinuations of SOD/VEL in young children, because of palatability of the oral formulation.

Conclusion: SOF/DCV, SOF/VEL, and GLC/PIB regimens were highly effective and well tolerated in adolescents and older children, and SOF/VEL and GLC/PIB in young children and are now recommended by WHO. There is currently no direct evidence for SOF/DCV in young children, and studies are planned for 2022. SOF/DCV remains the most affordable and available DAA regimen for adults globally, and alignment of adult and paediatric procurement would simplify supply chain management.

FRI405

Early vs. late treatment for hepatitis C virus discordant solid organ transplantation and direct acting antivirals: a meta-analysis

Madison Gunn¹, George Agyapong², Victor Eligah³, Enoch Chung⁴, Sara Young⁵, Lauren Hulshof⁶, Camilla Mills^{7,8}, Alexandra Gorham⁹, Jordan Feld^{10,11,12}, Raymond Chung^{7,13}. ¹Schulich School of Medicine & Dentistry, London, Canada; ²Yale School of Medicine, Internal Medicine, New Haven, United States; ³Howard University, Pharmaceutical Sciences, Washington DC, United States; ⁴Boston University School of Medicine, Boston, United States; ⁵Boston University School of Medicine, Boston, United States; ⁶Northwestern University, Boston, United States; ⁷Harvard Medical School, Boston, United States; ⁸Boston Children's Hospital, Pediatric Gastroenterology, Hepatology, & Nutrition, Boston, United States; ⁹Johns Hopkins University, Baltimore, United States; ¹⁰Toronto Center for Liver Disease, Toronto, Canada; ¹¹University Health Network, Toronto, Canada; ¹²University of Toronto, Toronto, Canada; ¹³Massachusetts General Hospital, Division of Gastroenterology, Department of Medicine, Boston, United States
Email: madisonccgunn@gmail.com

Background and aims: The advent of curative direct-acting antiviral (DAA) therapy for hepatitis C virus (HCV) has broadened the donor pool for solid organ transplants, allowing the use of organs from HCV + donors that were previously discarded. Although many centers have embraced this practice, the optimal timing of DAA initiation remains unclear. This study aims to summarize the virologic and clinical outcomes of DAA therapy in HCV donor+/recipient- solid organ transplants.

Method: Bibliographic databases were searched for studies published in English between Jan 2013 and Sept 2020. Using random effects models, meta-analysis was performed to pool estimates for sustained virologic response (SVR) and a composite adverse outcome of acute cellular rejection (ACR) and HCV-related complications (fibrosing cholestatic hepatitis and glomerulonephritis). Risk of bias was assessed using a modified Ottawa-Newcastle score.

Results: We included 25 non-randomized trials and observational studies with 635 participants, including 32 observations by organ type: 9 studies reported on heart transplantation (n = 185), 4 on lung (n = 93), 12 on kidney (n = 278) and 7 on liver (n = 79). 16 studies started DAAs <28 days after transplant (early) while 9 initiated DAAs >28 days post-transplant (late). The overall pooled SVR for all organ types was 0.96 (CI 0.95–0.98). SVR for non-liver organs was 0.97 (CI 0.94–0.98) and 0.96 (CI 0.91–1.0) for liver. For studies that had available data, the overall proportion of ACR was 0.10 (CI 0.06–0.15). In subgroup analyses, the SVR for early treatment was 0.97 (CI 0.96–0.99), while the SVR for late treatment was 0.95 (0.91–0.98). The proportion of the composite adverse outcome was 0.06 (CI 0.02–0.09) for early treatment and 0.18 (0.06–0.30) for late treatment. Proportion of ACR was 0.06 (CI 0.02–0.09) for early treatment compared to 0.17 (CI 0.01–0.28) for late treatment. Proportion of HCV-related complications for early treatment was 0.02 (0.01–0.04)

and for late treatment was 0.02 (0.002–0.03). There were no cases of glomerulonephritis reported and only 5 cases of FCH. Of the FCH cases, 4/5 occurred in patients treated >28 after transplant. Early treatment was associated with 30% lower incidence of detectable viremia.

Conclusion: Overall, early DAA initiation (within 28 days) and late initiation (after 28 days) achieved similar SVR rates, although the early strategy reported 30% lower incidence of viremia. Early DAA initiation strategies reported a lower proportion of ACR than the delayed strategy, but this estimate was not statistically significant. On balance these results would support current guidelines recommending early treatment initiation, however randomized clinical trials may be required to more clearly define short-term responses and long-term clinical outcomes for these strategies.

FRI406

Effectiveness of pangenotypic retreatment of HCV infection after prior failure of pangenotypic therapies

Robert Flisiak¹, Justyna Janocha-Litwin², Anna Parfieniuk-Kowierda¹, Dorota Zarębska-Michaluk³, Marek Sitko⁴, Piekarska Anna⁵, Jolanta Białkowska⁵, Dorota Dybowska⁶, Witold Dobracki⁷, Simon Krzysztof², Aleksandra Murawska-Ochab⁸, Małgorzata Pawłowska⁶. ¹Medical University of Białystok, Białystok, Poland; ²Medical University Wrocław; ³Jan Kochanowski University Kielce; ⁴Jagiellonian University, Kraków; ⁵Medical University of Łódź; ⁶Ludwik Rydygier Collegium Medicum in Bydgoszcz Faculty of Medicine Nicolaus Copernicus University in Toruń, Department of Infectious Diseases and Hepatology, Poland; ⁷MED-FIX Wrocław; ⁸Voivodship Hospital, Kielce, Kielce
Email: robert.flisiak1@gmail.com

Background and aims: Pangenotypic therapies for HCV infections, although universal and highly effective, leave the risk of treatment failure. The aim of the analysis was to assess the effectiveness of pangenotypic re-treatment in patients with failure of previous treatment also with pangenotypic drugs; to our knowledge, the results of such real world experience studies have not been published so far.

Method: The analysis included patients selected from the EpiTer-2 database, a large retrospective, multicentre, national real-world study evaluating DAA treatment during 2015–2021 in 14, 450 consecutive subjects with hepatitis C virus (HCV) infection.

Results: A total of 3, 985 patients were treated with pangenotypic regimens, of which 37 (0.9%) received them as retreatment after failure of prior pangenotypic therapy. This group was significantly dominated by males (78%), cirrhotics (49%) and genotype 3 infection (67%) compared to the general population of patients treated with pangenotypic regimens (54%, 21%, 29%, respectively). As shown in figure 1 primary glecaprevir/pibrentasivir (GP) based therapy was changed to velpatasvir/sofosbuvir (VS) based in 18, and VS to GP in 13 patients. In 6 patients, the same regimen was used, extending the duration of therapy or supplementing it with an additional drug (ribavirin (R), sofosbuvir (S), voxilaprevir (V)). The response rate at the end of treatment was 95%, while the overall SVR was 89%. There was no significant difference in SVR between patients retreated with GP (93%) and VS based regimen (87%), which included also two patients on voxilaprevir/VS (VVS) regimen. All four non-responders were cirrhotic males infected with genotype 3 in age of 54–59 years.

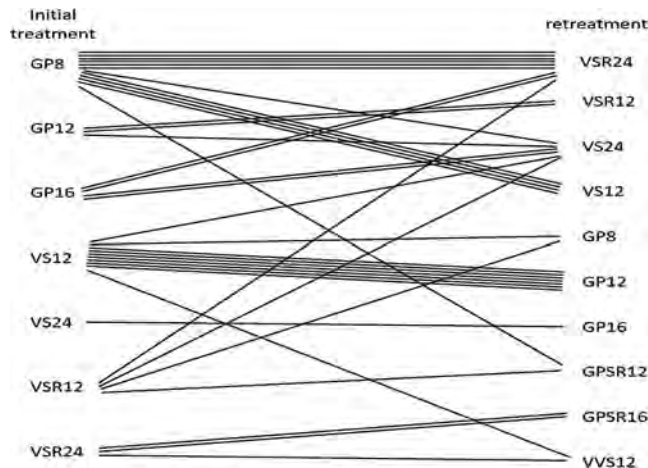


Figure 7: Change from primary to secondary pangenotypic regimens (letter abbreviations in abstract, numbers represent weeks of treatment).

Conclusion: We have demonstrated a high, almost 90% effectiveness of pangenotypic retreatment after failure of the primary pangenotypic therapy. Only men with cirrhosis, infected with genotype 3, did not eliminate HCV infection despite double pangenotypic treatment. We hope to provide data from more patients at the ILC.

FRI407

Infrequent hepatitis C genotypes/subtypes in patients treated with DAA-based regimens: successes and failures

Donald Murphy¹, Isaac Ruiz², Jean-Pierre Villeneuve², Catherine Vincent², Julian Hercun², Daphna Fenyves², Denis Marleau², Helene Castel², Julien Bissonnette², Genevieve Huard², Claire Fournier², Jeanne-Marie Giard², Daniel Corsilli³, Ziad Hassoun², Philippe Willems², Iris Soto², Marc Bilodeau², Bernard Willems². ¹Institut national de santé publique du Québec, Laboratoire de santé publique du Québec (LSPQ), Montréal, Canada; ²Centre hospitalier de l'Université de Montréal (CHUM), Liver Unit, Canada; ³Centre hospitalier de l'Université de Montréal (CHUM), Intensive Care Unit, Canada
Email: isaac.ruiz@me.com

Background and aims: Patients with infrequent Hepatitis C virus (HCV) genotypes/subtypes are characterized by resistance-associated substitution (RAS) profiles that have been associated with lower sustained virological responses (SVR). Real-world data regarding efficacy of direct-acting antiviral (DAA)-based regimens are needed in order to optimize HCV therapy and to further support expert recommendations.

The aim of this study was to evaluate the efficacy of DAA-based regimens in patients infected with infrequent HCV genotypes/subtypes in a real-world cohort at the Centre hospitalier de l'Université de Montréal (CHUM).

Method: A retrospective analysis of every patient referred to the CHUM was performed. Between 2014 and 2021, patients with an infrequent HCV genotype/subtype according to EASL guidelines definition were identified.

Patients treated with at least 1 DAA-based regimen were included. Patients enrolled in clinical trials were excluded. Liver fibrosis was assessed by means of liver elastography or by histological evaluation of liver biopsy. SVR was defined as an undetectable HCV RNA 12 weeks after the end of treatment (SVR12). The choice of the DAA combination was made at the physician's discretion.

Results: Among the 801 patients of the cohort, 106 (13.2%) had an infrequent genotype/subtype. Among them, median age was 64 (17–96), 54 (50.9%) were male, 54 (50.9%) had F3–F4 fibrosis. The overall SVR12 rate following initial treatment with at least one DAA-based regimen was 87.7% (93/106). Twelve patients received a second-line DAA regimen. Before retreatment, 75.0% had F3–F4

fibrosis. SVR12 was 83.3% (10/12). One cirrhotic genotype 1d patient failed 2 one-DAA-based regimens (telaprevir (TPV)/pegylated interferon (pegIFN)/Ribavirin (RBV); sofosbuvir (SOF)/pegIFN/RBV) was successfully retreated with SOF/ledipasvir (LDV). One cirrhotic genotype 1k patient failed 4 DAA-based regimens (SOF/simeprevir (SIM); SOF/LDV 24/48 weeks; SOF/LDV/RBV).

In a subgroup analysis of patients treated with a 2-last generation DAA (SOF/velpatasvir (VEL), SOF/VEL/RBV, glecaprevir (GLE)/pibrentasvir (PIB)), 50 patients were identified. SVR12 was 90.0% (45/50). Among the 106 treated patients, 6 were treated after liver transplantation. One patient presented with fibrosing cholestatic hepatitis. The SVR12 was 83.3% (5/6). A genotype 3b patient failed SOF/VEL for 12 weeks and was successfully retreated with SOF/VEL/voxilaprevir (VOX) for 12 weeks.

Regimen	Genotypes/subtypes									
The successes (SVR12) ¹										
Last generation DAA										
SOF/VEL	2	2c	2i	4	4c	4h	4k	4l	4r	4s
	5a	6	6a	6e	6h	6i	6o	6xc	7	7a
SOF/VEL/RBV	1d	2i								
GLE/PIB	2c	4h	4k	6a	6f					
SOF/VEL/VOX	1	1i	3b	3i	4r					
Past generation DAA										
SOF/PegIFN/RBV	1e	2	4	5a						
SOF/RBV	2	2c	2i	2k	4c	4i	4r	4v	6a	
SOF/SIM	1d									
SOF/LDV	4	5a	6a	6e	6o					
SOF/LDV/RBV	1d	1g	4r	5a	6a	6e				
SOF/DCV/RBV	2									
EBR/GRZ	4c	4k	6o							
EBR/GRZ/RBV	4c	4k								
OBV/PTV/R/RBV	4k									
The failures ²										
Last generation DAA										
SOF/VEL	3i	4b	4r	6p						
SOF/VEL/RBV	3b									
Past generation DAA										
TPV/PegIFN/RBV	1d									
SOF/PegIFN/RBV	1d									
SOF/RBV	2	2i								
SOF/SIM	1k									
SOF/LDV	1	1i	1k	4r	6a					
SOF/LDV/RBV	1k									
OBV/PTV/R/RBV	4k									

¹ n=1, except for 1d (n=3), 2 (n=9), 2c (n=7), 2i (n=6); 4 (n=5); 4c (n=5); 4h (n=2); 4k (n=9); 4l (n=2); 4r (n=8); 5a (n=12); 6 (n=2); 6a (n=11); 6e (n=3), 6h (n=2); 6o (n=3)

² n=1 for all genotypes/subtypes; 1d patient failed both treatments; 1k patient failed all 4 treatments including SOF/LDV 12/48w.

¹ n=1, except for 1d (n=3), 2 (n=9), 2c (n=7), 2i (n=6), 4 (n=5), 4c (n=5), 4h (n=2), 4k (n=9), 4l (n=2), 4r (n=8), 5a (n=12), 6 (n=2), 6a (n=11), 6e (n=3), 6h (n=2), 6o (n=3)

² n=1 for all genotypes/subtypes; 1d patient failed both treatments; 1k patient failed all 4 treatments including SOF/LDV 12/48w.

Conclusion: Our real-world data show that in patients with infrequent HCV genotypes/subtypes treated with 2 last-generation DAA the SVR rate is 90%. Although the data are limited, these results support the possibility of initially treating them with 2 last-generation DAA. More data are needed to determine optimal treatment regimen by genotype/subtype and the benefits of a rational approach based on RAS determination.

FRI408

Preemptive treatment with glecaprevir and pibrentasvir prevents HCV transmission from HCV viraemic donors to solid organ transplant recipients (single centre experience)

Sona Frankova¹, Ondrej Viklicky², Veronika Pitova¹, Janka Slatinska², Jan Sperl¹. ¹Institute for Clinical and Experimental Medicine, Department of hepatogastroenterology, Prague, Czech Republic; ²Institute for Clinical and Experimental Medicine, Department of nephrology, Prague, Czech Republic
Email: sona.frankova@ikem.cz

Background and aims: Organs from hepatitis C viraemic (HCV) donors were not used for transplantation in the past because the transmission of HCV infection to uninfected recipients used to be universal. Treatment of HCV infection in organ transplant recipients was complex and poorly effective before the introduction of direct-

POSTER PRESENTATIONS

acting antivirals (DAA) into clinical practice. Glecaprevir and pibrentasvir (GLE/PIB) represent a pangenotypic anti-HCV DAA combination also approved for patients with severe renal impairment or on maintenance haemodialysis. The study aims to analyze the efficacy and safety of GLE/PIB combination as preemptive therapy of HCV infection when using grafts from HCV viraemic donors.

Method: The solid organ transplant recipients, to whom an organ from HCV viraemic donor was allocated, were given a single dose of GLE/PIB (300 mg/120 mg) 2–6 hours before transplant, followed by a once-daily administration for 12 weeks after transplantation, as recommended for liver and kidney transplant recipients by the manufacturer. HCV RNA levels were assessed weekly in the first four weeks post-transplant, in the treatment weeks 8 and 12, and 12 weeks after the cessation of therapy. The endpoints were negative HCV RNA levels at the end of treatment and 12 weeks post-treatment.

Results: Twelve organs (two liver and ten kidney grafts) from 5 HCV viraemic cadaveric donors were allocated to 12 HCV uninfected recipients. All the recipients presented with an uncomplicated post-transplant course with the rapid development of graft function. None of the recipients presented with an acute rejection episode or severe graft dysfunction during the treatment and follow-up period. All the recipients completed the planned 12 weeks of preemptive antiviral treatment. None of them experienced an adverse event related to antiviral therapy or drug-drug interactions. HCV RNA was undetectable at all checked timepoints in all recipients. HCV infection was transmitted to none of the twelve recipients.

Conclusion: Preemptive treatment with GLE/PIB is safe and effective and allows the use of organs from HCV viraemic donors, so far considered marginal, to uninfected recipients. Organ procurement from HCV viraemic donors became a routine at our centre.

FR1409

Hepatitis C care cascade challenges in the homeless population. A case by case model of delivering care

Maria Guerra Veloz¹, Khin Aye Wint Han¹, Almuthana Mohamed¹, Kathryn Oakes¹, David Robertson¹, Mary D. Cannon¹, Ashley Barnabas¹, Sital Shah¹, Geoffrey Dusheiko¹, Kosh Agarwal¹.

¹Institute of Liver Studies, King's College Hospital, London, United Kingdom, London, United Kingdom

Email: maria.guerraveloz@nhs.net

Background and aims: Given the significant Hepatitis C Virus (HCV) burden, despite curative treatments, efforts focusing on the scaling up of testing and treatment in the homeless population are still needed. The aim of this project was to implement education and flexible onsite HCV incentivised testing, treatment and follow up for the homeless population and evaluate their rates of engagement, therapy initiation and cure in the South London area.

Method: This project was conducted by a multidisciplinary team from Jan 2018 to Sept 2021. A mobile unit "van" for onsite HCV education, flexible screening (InTec HCV Rapid Antibody Test, Cepheid GeneXpert RNA test, DBS or classic venipuncture), treatment and follow up was placed on the street in well-known homeless population areas. Homeless was defined as living in temporary-(hostel/hotel-based) or as being on the street or visiting daily soup kitchens across the area (street-based). Sociodemographic status, risk factors, comorbidities, concomitant medication, clinic data, the rates of treatment initiation and cure were recorded. Treatment adherence was defined as taking $\geq 75\%$ of doses as self-reported by clients.

Results: 940 clients were identified as homeless and 933 (99.3%) participated. Of them 56.2% who were screened were street-based, 243 (26%) tested positive for HCV antibody and of these, 162 (67%) had detectable viremia. Clients with a positive HCV antibody had significantly higher rates of previous injection drug use (71.2 vs 8.6%), previous incarceration (12.3 vs 2.8%), previous HCV tests (28.8 vs 0.1%), as well as being active drug (36.2 vs 3.3%) and alcohol users (43.6 vs 5.2%) than those who were negative. HCV RNA positive clients had significantly more frequent psychiatric disorders, active

drug use, active alcohol consumption, were on opioid substitution therapy, advanced fibrosis (23.5 vs 10%) and had lower rates of previous treatment in comparison with HCV RNA negatives (Figure 1c). The overall treatment initiation was 70.4% (114/162) and SVR 12 was 75.5% (83/110). In the multivariate analysis being screened in temporary housing (OR 2.755, 95%CI 1.356–5.600; $p = 0.005$) and having opioid substitution treatment (OR 2.288, 95%CI 1.041–5.026; $p = 0.039$) were positively associated with treatment initiation. HCV treatment adherence (OR 25.05, $p < 0.001$) was the only factor associated with achieving SVR.

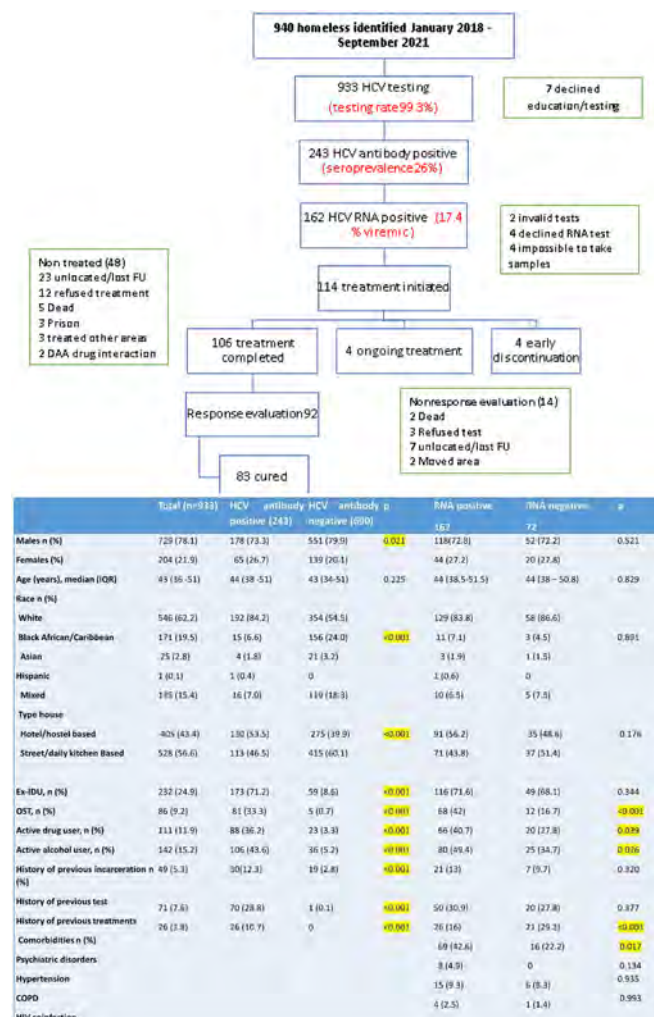


Figure: a) Flow chart project b) Characteristics divided by HCV antibody and RNA status

Conclusion: Promoting education and having flexible onsite-testing and treatment for HCV in the homeless population improves their engagement with the healthcare system, leading to higher rates of treatment initiation and SVR. However, street based homeless people who are not linked with harm reduction services are less likely to initiate HCV treatment, highlighting that there is an urgent need for a broad health inclusion system.

FRI410

Effectiveness and safety of 8-week glecaprevir/pibrentasvir in HCV treatment naïve patients with compensated cirrhosis: real-world experience from Taiwan HCV registry

Chao-Hung Hung¹, Te-Sheng Chang², Chung-Feng Huang³, Hsing-Tao Kuo⁴, Ching-Chu Lo⁵, Chien-Wei Huang⁶, Lee-Won Chong^{7,8}, Pin-Nan Cheng⁹, Ming-Lun Yeh^{10,11}, Cheng-Yuan Peng^{12,13}, Chien-Yu Cheng¹⁴, Jee-Fu Huang^{10,15}, Ming-Jong Bair^{16,17}, Chih-Lang Lin¹⁸, Chi-Chieh Yang¹⁹, Sih-Ren Wang²⁰, Tsai-Yuan Hsieh²¹, Tzong-Hsi Lee²², Pei-Lun Lee⁴, Wen-Chih Wu²³, Chih-Lin Lin²⁴, Wei-Wen Su²⁵, Shengshun Yang²⁶, Chia-Chi Wang^{27,28}, Jui-Ting Hu²⁹, Lien-Juei Mou³⁰, Chun-Ting Chen^{31,32}, Yi-Hsiang Huang^{33,34}, Chun-Chao Chang^{35,36}, Jia-Sheng Huang³⁷, Guei-Ying Chen³⁸, Jian-Neng Gao³⁹, Chi-Ming Tai^{40,41}, Chun-Jen Liu⁴², Mei-Hsuan Lee⁴³, Pei-Chien Tsai¹⁰, Chia-Yen Dai¹⁰, Jia-Horng Kao⁴², Han-Chieh Lin^{33,34}, Wan-Long Chuang¹⁰, Chiyi Chen⁴⁴, Kuo-Chih Tseng^{45,46}, Ming-Lung Yu⁴⁷. ¹ChiaYi Chang Gung Memorial Hospital and College of Medicine, Chang Gung University, Division of Hepatogastroenterology, Department of Internal Medicine; ²ChiaYi Chang Gung Memorial Hospital, Division of Hepatogastroenterology, Department of Internal Medicine, Taiwan; ³Kaohsiung Medical University Hospital, Kaohsiung Medical University, Hepatobiliary Division, Department of Internal Medicine and Hepatitis Center, Taiwan; ⁴Chi Mei Medical Center, Division of Gastroenterology and Hepatology, Department of Internal Medicine, Taiwan; ⁵St. Martin De Porres Hospital, Division of Gastroenterology, Department of Internal Medicine, Taiwan; ⁶Kaohsiung Armed Forces General Hospital, Division of Gastroenterology, Taiwan; ⁷Shin Kong Wu Ho-Su Memorial Hospital, Division of Hepatology and Gastroenterology, Department of Internal Medicine, Taiwan; ⁸Fu-Jen Catholic University, School of Medicine, Taiwan; ⁹National Cheng Kung University Hospital, Division of Gastroenterology and Hepatology, Department of Internal Medicine, Taiwan; ¹⁰Kaohsiung Medical University Hospital, Hepatobiliary Division, Department of Internal Medicine and Hepatitis Center, Taiwan; ¹¹Kaohsiung Municipal Siaogang Hospital, Department of Internal Medicine, Taiwan; ¹²China Medical University Hospital, Center for Digestive Medicine, Department of Internal Medicine, Taiwan; ¹³China Medical University, School of Medicine, Taiwan; ¹⁴Taoyuan General Hospital, Division of Infectious Diseases, Department of Internal Medicine, Taiwan; ¹⁵Kaohsiung Municipal Ta-Tung Hospital, Department of Internal Medicine, Taiwan; ¹⁶Taitung Mackay Memorial Hospital, Division of Gastroenterology, Department of Internal Medicine, Taiwan; ¹⁷Mackay Medical College, Taiwan; ¹⁸Chang Gung Memorial Hospital at Keelung, Liver Research Unit, Department of Hepato-Gastroenterology and Community Medicine Research Center, Taiwan; ¹⁹Show Chwan Memorial Hospital, Department of Gastroenterology, Division of Internal Medicine, Taiwan; ²⁰Yuan's General Hospital, Division of Gastroenterology, Department of Internal Medicine, Taiwan; ²¹Tri-Service General Hospital, Division of Gastroenterology, Department of Internal Medicine, Taiwan; ²²Far Eastern Memorial Hospital, Division of Gastroenterology and Hepatology, Taiwan; ²³Wen-Chih Wu Clinic, Taiwan; ²⁴Renai Branch, Taipei City Hospital, Department of Gastroenterology, Taiwan; ²⁵Changhua Christian Hospital, Department of Gastroenterology and Hepatology, Taiwan; ²⁶Taichung Veterans General Hospital, Division of Gastroenterology and Hepatology, Department of Internal Medicine, Taiwan; ²⁷Taipei Tzu Chi Hospital, Buddhist Tzu Chi Medical Foundation, Taiwan; ²⁸Tzu Chi University, School of Medicine, Taiwan; ²⁹Cathay General Hospital, Liver Center, Taiwan; ³⁰Tainan Municipal Hospital, Division of Gastroenterology, Taiwan; ³¹Tri-Service General Hospital, National Defense Medical Center, Division of Gastroenterology, Department of Internal Medicine, Taiwan; ³²Tri-Service General Hospital Penghu Branch, Division of Gastroenterology, Department of Internal Medicine, Taiwan; ³³Taipei Veterans General Hospital, Division of Gastroenterology and Hepatology, Department of Medicine, Taiwan; ³⁴National Yang-Ming Chiao Tung University, Institute of Clinical Medicine, School of Medicine, Taiwan; ³⁵Taipei Medical University

Hospital, Division of Gastroenterology and Hepatology, Department of Internal Medicine, Taiwan; ³⁶Taipei Medical University, School of Medicine, College of Medicine, Taiwan; ³⁷Yang Ming Hospital, Chiayi, Taiwan; ³⁸Penghu Hospital, Ministry of Health and Welfare, Taiwan; ³⁹National Taiwan University Hospital Hsin-Chu Branch, Taiwan; ⁴⁰E-Da Hospital, Department of Internal Medicine, Taiwan; ⁴¹National Taiwan University Hospital, School of Medicine, Internal Medicine, Taiwan; ⁴²National Taiwan University Hospital, Hepatitis Research Center and Department of Internal Medicine, Taiwan; ⁴³National Yang-Ming Chiao Tung University, Institute of Clinical Medicine, Taiwan; ⁴⁴Ditmanson Medical Foundation Chiayi Christian Hospital, Division of Gastroenterology and Hepatology, Department of Medicine, Taiwan; ⁴⁵Dalin Tzu Chi Hospital, Department of Internal Medicine, Taiwan; ⁴⁶Tzuchi University, School of Medicine, Taiwan; ⁴⁷Kaohsiung Medical University Hospital, Kaohsiung Medical University, Hepatobiliary Division, Department of Internal Medicine and Hepatitis Center Email: fish6069@gmail.com

Background and aims: The once-daily, oral, fixed-dose, direct-acting antiviral combination of glecaprevir/pibrentasvir (G/P) is indicated for chronic hepatitis C (CHC) infection with HCV genotypes 1–6 in patients with or without compensated cirrhosis (CC). Treatment duration of 8 weeks is recommended in most cases. Recent retrospective data from Taiwan revealed that G/P treatment resulted in high SVR12 rates according to label recommendations, comparable to those reported in the pivotal clinical trials. To further validate the data in the real-world setting, this study investigated effectiveness and safety of 8-week G/P therapy in treatment-naïve (TN), CC patients, with an emphasis on those with advanced liver disease in TASL HCV Registry (TACR).

Method: The TACR is an ongoing nationwide registry program organized and supervised by Taiwan Association for the Study of the Liver (TASL), which aims to setup a database and biobank of patients with CHC in Taiwan. Data were analyzed as of 31 October 2021 for patients treated with G/P for TN, CC patients. In this analysis, effectiveness reported as sustained virologic response at post-treatment week 12 (SVR12) was assessed by modified intent-to-treat (mITT) populations that excluded patients who lost to follow-up, underwent treatment and/or traced SVR12 data. Safety profile was assessed in the ITT population.

Results: Of 806 TN, CC patients treated with G/P, 301 patients received 8-week regimen (ITT), and 275 of which had SVR12 data available (mITT). Of the 301 ITT population, mean age was 63.0 years, 53.8% were male, 27.2% were with chronic kidney disease and 2.3% were coinfectd with human immunodeficiency virus. The overall SVR12 rate was 98.2% (270/275) in the mITT population. For selected special patient groups including patients with HCV genotype 3 (GT3), platelets counts <150, 000/μl, FibroScan >20 kPa, or both platelet counts <150, 000/μl and FibroScan >20 kPa, the SVR12 rate was 100% (6/6), 98.0% (144/147), 100.0% (12/12) and 100.0% (7/7), respectively. Overall, 24.9% (75/301) of the patients experienced adverse events (AEs) in the ITT population. Seven patients (2.3%) experienced serious adverse events and two (0.7%) resulted in permanent drug discontinuation. None of them were considered as treatment drug related. The most frequent AEs (>5%) were fatigue (9.0%) and pruritus (7.0%). Laboratory data including international ratio of prothrombin time, total bilirubin, alanine aminotransferase, aspartate aminotransferase and albumin significantly improved after HCV eradication at SVR12.

POSTER PRESENTATIONS

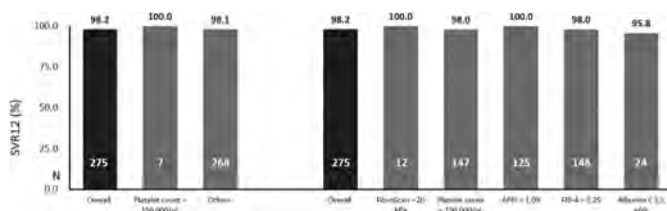


Figure: G/P-treated Patients with SVR12 data available as of Oct 2021 for analysis, n = 275 (mITT).

Conclusion: In this real-world Taiwanese cohort, 8-week G/P therapy was well-tolerated in TN, CC patients. SVR12 rates were similarly high as in the clinical trials, including those with characteristics of advanced liver disease.

FRI411

Reported safety of HCV direct-acting antivirals with opioids: 2017 to 2021

Anthony Martinez¹, Tipu Khan², Doug Dylla³, John Marcinak³, Michelle Collins³, Brad Saget³, Brian Conway⁴. ¹State University of New York, Buffalo, New York, United States; ²Ventura County Medical Center, Ventura, United States; ³AbbVie Inc, United States; ⁴Vancouver Infectious Diseases Centre, Canada
Email: adm35@buffalo.edu

Background and aims: As a result of disengagement in addiction care during the COVID-19 pandemic, there has been a record increase in mortality associated with opioid overdoses (primarily fentanyl), particularly in North America. In the USA there were over 100,000 overdose deaths in 2021, while over 2000 were recorded in the province of British Columbia. As we attempt to develop novel ways to increase HCV treatment following ≥30% declines during the pandemic, we evaluated publicly available adverse events (AEs) reports for opioids and DAAs to assess whether safety concerns from potential drug interactions are warranted, particularly amongst those using fentanyl.

Method: Data were downloaded from the US Food and Drug Administration (FDA) Adverse Event Reporting System (FAERS) Public Dashboard. AEs with the DAAs glecaprevir/pibrentasvir (G/P), sofosbuvir/velpatasvir (SOF/VEL), ledipasvir/sofosbuvir (LDV/SOF), sofosbuvir/velpatasvir/voxilaprevir (SOF/VEL/VOX), and elbasvir/grazoprevir (EBR/GZR) listed as the suspect product were analyzed with an initial received date from July 28, 2017–December 31, 2021, as were opioid-associated AEs for all 2017–2021. Subsequently, AEs were counted based on listed concomitant use of opioids (fentanyl, oxycodone, hydrocodone), or overdose outcomes irrespective of concomitant opioid use. Data are descriptive without any statistical analyses.

Results: In the reporting period, 40 total AEs were recorded with concomitant DAA and fentanyl use, 14 resulting in death (G/P=3, SOF/VEL=11; Table 1); 626 total AEs were recorded with concomitant DAA and oxycodone or hydrocodone use, 28 resulting in death. Separately, overdose events were reported 196 times, 32 resulting in death. The number of overdoses declined each year from 2018 (N=56) to 2021 (N=29). Fentanyl AEs showed no trend year to year.

Table 1: FAERS AEs and deaths with opioids and with concomitant HCV DAAs.

n	Fentanyl AEs (N=58, 001)	Fentanyl deaths (N=29, 850)	Oxycodone/Hydrocodone AEs (N=290, 224)	Oxycodone/Hydrocodone deaths (N=119, 013)	Overdose AEs* (N=98, 037)	Overdose deaths* (N=52, 318)
All DAAs	40	14	626	28	196	32
G/P	13	3	153	6	24	11
SOF/VEL	22	11	269	13	99	14
LDV/SOF	3	0	100	5	50	5
SOF/VEL/VOX	0	0	14	0	8	0
EBR/GZR	2	0	90	4	15	2

*N represents the sum of fentanyl, oxycodone, and hydrocodone overdose AEs and deaths, whereas n's for DAA overdose AEs and deaths are irrespective of concomitant opioids.

Conclusion: With the limitations of FAERS data (under or duplicate reporting, inability to establish causation or incidence), these data show that among ~58,000 fentanyl, ~189,000 oxycodone, and ~100,000 hydrocodone AEs reported to FAERS since 2017, a small proportion (0.19%) have been reported in association with concomitant DAA therapy, with no association between recorded events and a specific DAA regimen. This should reassure HCV treaters on a lack of safety signal for concomitant opioid and DAA use.

FRI414

Impact of the presence of the infectious disease specialist in addiction services (SerDs) as a point-of-care to meet WHO goal of HCV eradication

Chiara Fanelli¹, Eliza Princic¹, Andrea De Vito¹, Claudia Marcia¹, Giordano Madeddu¹, Sergio Babudieri¹, Ivana Rita Maida¹. ¹University of Sassari, Department of Medical, Surgical and Experimental Sciences, Sassari, Italy
Email: chiarfan@hotmail.it

Background and aims: The World Health Organization (WHO) aim for Hepatitis C virus (HCV) elimination by 2030 appears to be threatened by most patients remaining undiagnosed, despite the availability of effective and safe antivirals. The main reservoir of HCV is represented by people who inject drugs (PWIDs). This study aimed to assess the crucial role of the infectologist at the Addiction Services (SerDs) and its potential as a linkage to care of PWID HCV carriers.

Method: This retrospective study compares the number of new diagnosis and treatments among PWIDs before and after the introduction of an infectologist at SerDs Point of Care of Sassari, Italy. Data were collected from February 2015 to August 2020. The watershed day was the 1st of May 2019, when the infectologist was integrated in the personnel of SerD. Logistic regression analysis was performed to assess the relationship between variables before and after the introduction of the infectologist.

Results: From February 2015 to August 2020, 901 users took advantage of at least one dose of under opiate substitution treatment (OST) at the SerDs of Sassari, Italy. In total, 419 users (46.5%) underwent HCV-screening test, of which 333 (79.47%) tested positive and 191 taken in charge by the infectologist. Of 157 patients with detectable HCV-RNA, 138 (87.89%) started HCV treatment. Comparing the group treated with Direct-acting Antiviral Agents (DAA) before and after May 2019, a statistical significance was found in age ($p=0.0018$) and diagnose-to-treatment prescription time ($p<0.001$). When comparing PWIDs taken in charge in the two periods, statistical significance emerged for median age ($p<0.001$), alcohol dependence ($p=0.005$), active PWID ($p=0.01$), cirrhosis ($p=0.006$) and DAA prescription ($p=0.014$) (Table). The number of new diagnoses and treatments from May 2019 until August 2020 was higher than those between February 2015 and May 2019 (respectively, 72 in 15 months versus 66 in 50 months).

Variables	Total (N = 191)	Take-in-charge before May 2019 (N = 81)	Take-in-charge after May 2019 (N = 110)	p-value*
Age, n (IQR)	48, 9 (40, 1–53, 8)	50, 6 (43, 6–55, 4)	45, 7 (38, 6–52, 2)	<0, 001
Male sex, n (%)	177 (92, 7%)	78 (96, 3%)	99 (90%)	0, 099
Alcohol abuse, n (%)	10 (5, 2%)	0 (0%)	10 (9, 1%)	0, 005
Active PWID, n (%)	26 (13, 6%)	5 (6, 2%)	21 (19, 1%)	0, 01
Cirrhosis, n (%)	64 (33, 5%)	36 (44, 4%)	28 (25, 5%)	0, 006
Prescribed DAAs therapy, n (%)	138 (72, 3%)	66 (81, 5%)	72 (65, 5%)	0, 014

*Determined by chi-square test or wilcoxon test. IQR: range interquartile.

Conclusion: The improvement of the Meet-Test-Treat has been related to the introduction of the infectologist at SerDs. This work highlights the increase in patients' compliance to treatment and take-in-charge by a doctor in hard-to-reach population. Furthermore, it provides a higher chance of early diagnosis of patients with a still reversible degree of fibrosis and how to significantly reduce the management time.

FRI415

Eliminating hepatitis C virus infection in prisons: 7 years of experience

Frederico Duarte¹, Luís Manuel Moura¹, Clara Batista¹, Ricardo Correia de Abreu¹, Isabel Neves¹. ¹Unidade Local de Saúde de Matosinhos, Infectious Diseases, Matosinhos, Portugal
Email: frederico.duarte1@gmail.com

Background and aims: Hepatitis C virus (HCV) infection is a major global health problem. The micro-elimination approach implies reaching specific populations, like people living in prisons. The introduction of direct-acting antiviral agents (DAAs) allowed a considerable change in public health.

Since 2015, the use of these drugs in HCV-infected inmates has allowed their cure, resulting from an ongoing optimized care partnership between two prisons and our healthcare unit in Matosinhos, bringing us closer to public health targets in eliminating the infection by 2030.

Method: The authors describe the epidemiological, clinical, analytical and imaging data of inmates with confirmed HCV infection undergoing treatment with DAAs since their availability in our healthcare unit.

Between 2015 and 2022 we identified 118 inmates with positive HCV antibody (65 men, 53 women), 16 have ongoing disease staging, 14 with spontaneous cure and 9 were released before complete staging. Twenty four HIV coinfecting patients, all under treatment, 100% with viral suppression and 75% with CD4⁺ count greater than 500/uL. Four patients were coinfecting with HBV. Almost 55% of the patients were diagnosed with psychiatric illness and were under treatment.

Results: The 79 inmates with confirmed HCV infection (51 men, 28 women) showed an average of 42 years [24–72 years], 11 years of known infection [1–30 years] and 85% had intravenous drug use in the past. HCV genotypes distribution: 1–48%; 3–30%; 4–22%. Liver fibrosis stages ranged from 4 to 64 kPa (F0–F2 85%, F3–F4 15%).

All the 79 patients were initially treated with Sofosbuvir/Ledipasvir and Daclatasvir with or without ribavirin (according to criteria defined in initial protocols) and more recently, Grazoprevir/Elbasvir and pangenotypic drugs, namely Sofosbuvir/Velpatasvir, and

Glecaprevir/Pibrentasvir. All were considered cured by achieving virological response 12 weeks post-treatment.

Conclusion: Our encouraging data is a result from an optimized partnership between the healthcare team in prisons and our hospital, allowing a fast diagnosis, an agile disease staging and adequate treatment, minimizing future risk of transmission and taking us closer to eliminating the infection by 2030.

FRI416

Real-world value and innovation of direct-acting antivirals for the treatment of chronic hepatitis C at Kaiser Permanente Southern California

Lisa Nyberg¹, Ankita Kaushik², Nate Smith³, Fadoua El-Moustaid³, Anders Nyberg¹, Su-Jau Yang⁴, Kevin Chiang⁵, Alon Yehoshua². ¹Kaiser Permanente Hepatology Research, San Diego, United States; ²Gilead Sciences, Inc., Foster City, United States; ³Maple Health Group, New York, United States; ⁴Kaiser Permanente Research and Evaluation, Pasadena, United States; ⁵Kaiser Permanente Pharmacy Analytical Services, Downey, United States
Email: alon.yehoshua@gilead.com

Background and aims: Direct-acting antivirals (DAAs) have been a breakthrough therapeutic innovation in the treatment of chronic hepatitis C virus (HCV) with high efficacy rates and excellent safety and tolerability profiles. The objective of this study was to assess the long-term health and economic benefits associated with direct-acting antivirals (DAAs) vs. no treatment in the Kaiser Permanente Southern California (KPSC) healthcare delivery system.

Method: A hybrid decision-tree and Markov model was used to evaluate the long-term health and cost outcomes associated with treating HCV patients with DAAs (either sofosbuvir/velpatasvir [SOF/VEL] or ledipasvir/sofosbuvir [LDV/SOF]) vs. no treatment in the KPSC setting. A cohort of 7, 255 HCV patients, based on the total number of DAA-treated patients from 2014 to 2019, with an average age of 59 years was simulated over a lifetime (50 year) horizon. Demographic data included baseline distributions of genotype, cirrhosis, prior treatment/naïve, and mix of DAAs. Treatment efficacy by subpopulation was determined from a secondary, real-world, database analysis of HCV patients in the KPSC setting. Utility values, transition probabilities, and health state costs were sourced from published literature, prioritizing data from the KPSC setting where possible. Treatment costs based on wholesale acquisition costs were sourced from publicly available databases. The model considered only direct medical costs, presented in 2021 USD.

Results: Approximately 78% of patients were treated with LDV/SOF and 22% with SOF/VEL in the DAA scenario. DAAs use led to a reduction of 3, 179 cases of compensated cirrhosis (–98%), 3, 318 cases of decompensated cirrhosis (–96%), 646 cases of hepatocellular carcinoma (–80%), 447 cases of liver transplants (–86%), and 3, 078 events of liver-related mortality (–86%) as compared to no treatment. In the DAAs scenario, life-years, and quality-adjusted life-years (QALYs) improved by +25% (+3.21 LYs) and +36% (+3.53 QALYs) vs. the no-treatment scenario. DAAs use also resulted in a reduction of total costs of –72% (–\$144, 592 per person) vs. no treatment. Furthermore, use of DAAs was found to lead to cost savings within 3 years.

Conclusion: Treating patients with DAAs resulted in a reduction in HCV-related morbidity and mortality and significant improvement in QALYs. Furthermore, use of DAAs was dominant (less costly and more effective) as compared to no treatment offering cost-savings within 3 years post-treatment. These findings highlight the substantial value of DAA treatment offered to HCV patients.

Abstract withdrawn

FRI418

Treatment options for hepatitis C in pregnancy: a systematic review of the evidence and future research needs

Neil Gupta¹, Lindsey Hiebert¹, Carolyn Wester², Paige A Armstrong^{1,2}.

¹Task Force for Global Health, Coalition for Global Hepatitis Elimination, United States; ²US Centers for Disease Control and Prevention, Division of Viral Hepatitis, United States

Email: ngupta-consultant@taskforce.org

Background and aims: Treatment for hepatitis C virus (HCV) infection during pregnancy has the potential to substantially increase HCV treatment coverage and prevent mother-to-child transmission. Although direct-acting antiviral (DAA) medications for the treatment of HCV infection have demonstrated excellent safety and efficacy in non-pregnant persons, HCV treatment is not recommended in pregnancy due to a lack of safety data. We assessed the published literature for information on treatment options for HCV infection in pregnancy, including linkage to care and treatment during pregnancy.

Method: We conducted a systematic literature review in PubMed for articles published in English from January 1, 2013–July 1, 2021. We searched using MESH and non-MESH equivalent search terms for “Hepatitis C virus” AND “pregnancy” AND “treatment” OR “direct-acting antivirals.” All articles were reviewed and thematically coded by dual reviewers.

Results: Overall, 486 articles were identified, of which 219 were included as relevant with full-text available. Of these, 118 contained results of primary research and 101 were secondary research. Of the 118 primary research articles, most focused on outcomes of HCV vertical transmission in infants (n = 28, 23.7%), HCV screening results (n = 25, 21.2%), epidemiology of HCV (n = 19, 16.1%), and cost-effectiveness or policies for HCV testing (n = 19, 16.1%). Fourteen (11.9%) assessed linkage to care or follow-up for persons who tested HCV positive. Five (4.2%) studies described results of DAA exposure in pregnancy. This included one prospective trial that reported minor (grade I/II) adverse events in 4 out of 9 participants, one retrospective study that reported no adverse events among 100 participants, one case study with no reported adverse events, and 2 clinical trials that reported DAA discontinuation due to pregnancy in 6 enrolled participants (no clinical outcomes reported). Of the 101 studies without primary research, 13 explicitly included the possibility of HCV treatment during pregnancy.

Conclusion: Despite a substantial body of literature on HCV infection in pregnancy, there are very few reports on maternal linkage to HCV treatment and extremely limited data regarding the safety or effectiveness of DAA treatment in pregnancy. To improve the evidence base on HCV treatment in pregnancy, additional approaches are needed to collect and report relevant data. In response, the Coalition for Global Hepatitis Elimination, with support from the US Centers for Disease Control and Prevention, developed the first clinical case registry to record maternal and infant outcomes for persons exposed to DAAs during pregnancy (“TiP-HepC” Registry). The TiP-HepC registry, in complement to clinical studies and other real-world experiences, will provide urgently needed data to inform optimal treatment options for HCV in pregnancy.

Immune-mediated and cholestatic: Experimental and pathophysiology

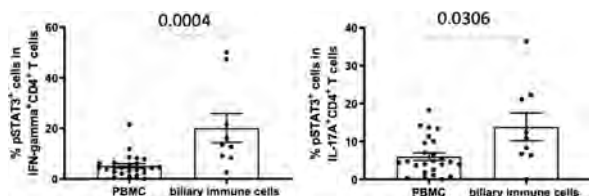
FRI451

Over-responsiveness of the IL-6/STAT3 pathway in inflammatory CD4⁺ T cells of patients with primary sclerosing cholangitis

Leona Dold¹, Leonie Frank¹, Philipp Lutz¹, Tobias Weismüller¹, Dominik Kaczmarek¹, Vittorio Branchi², Marieta Toma², Christian Strassburg¹, Ulrich Spengler¹, Bettina Langhans¹. ¹University Hospital Bonn, Department of Internal Medicine I, Bonn, Germany; ²University Hospital Bonn, Institute of Pathology, Bonn, Germany
Email: Leona.Dold@ukbonn.de

Background and aims: Primary sclerosing cholangitis (PSC) is a chronic inflammatory disorder of the biliary ducts, which leads to fibrosis and predisposes to cholangiocellular carcinoma. Although the exact pathogenesis of PSC remains unclear, proinflammatory CD4⁺ immune cells seem to play a pivotal role. Current treatment options are limited but over-activation of STATs (Signal Transducers and Activators of Transcription protein) was observed in CD4⁺ immune cells and linked to disease activity in various autoimmune diseases. Thus far, activation of STATs has been poorly studied in PSC. **Method:** Using multicolor flow cytometry we analyzed activation of STAT1 and STAT3 at baseline and after in vitro stimulation with recombinant IL-6 and IFN-gamma in immune cells from peripheral blood (PBMC) and from biliary tissue specimens collected by endoscopic retrograde cholangiopancreatography (ERCP) from patients with PSC. In addition, we measured soluble factors in serum and bile via bead-based immunoassay and compared results to healthy controls.

Results: Serum levels of IL-6 (mean ± SEM; 62.1 ± 28.1 pg/ml, p = 0.0279), IFN-gamma (26.7 ± 11.7 pg/ml, p = 0.0082) and IL-17A (9.1 ± 3.0 pg/ml, p = 0.0356), were higher in PSC patients than in healthy controls (IL-6: 10.5 ± 3.6 pg/ml; IFN-gamma: 6.1 ± 2.9 pg/ml; IL-17A: 2.7 ± 1.1 pg/ml). Of note, in PSC patients, inflammatory cytokines were conspicuously higher in bile than in serum. Unlike phospho-STAT1, which was refractory to IFN-gamma and IL-6 stimulation, activation with recombinant IL-6 lead to higher frequencies of phospho-STAT3-positive cells in the IFN-gamma⁺ (80.2 ± 2.3%, p = 0.0055) and IL-17A⁺ CD4⁺ T cell subsets (79.0 ± 2.4%; p = 0.0197) in patients with PSC than in healthy controls (66.1 ± 4.6% in IFN-gamma⁺ and 68.4 ± 4.1% in IL-17A⁺ CD4⁺ T cells). Frequencies of phospho-STAT3-positive cells in the IFN-gamma⁺ and IL-17A⁺ CD4⁺ T-cell subsets were higher in bile duct tissue (from ERCP) when compared to peripheral blood (Fig. 1). Finally, the pan-Jak inhibitor baricitinib dose-dependently reduced IFN-gamma- and IL-17A-secretion of mitogen-stimulated PBMCs from PSC patients in vitro.



Conclusion: Patients with PSC exhibit increased phospho-STAT3 induction in pro-inflammatory CD4⁺ T cells from blood and bile duct tissue, suggesting enhanced responsiveness of the STAT3 pathway in PSC. Although the cause of STAT3 over-responsiveness in PSC remains to be elucidated, targeted STAT3 inhibition may offer a novel approach to modify the course of PSC.

FRI452

Dosing ileal bile acid transporter inhibitors in the fasted state minimizes gastrointestinal adverse effects while maintaining pharmacodynamic effect

Cory Kostrub¹, Rakesh Raman¹, Douglas Mogul¹, Pamela Vig¹. ¹Mirum Pharmaceuticals Inc, Foster City, CA, United States
Email: ckostrub@mirumpharma.com

Background and aims: Ileal bile acid transporter inhibitors (IBATi) interrupt enterohepatic circulation of bile acids (BAs) and increase fecal BA (fBA) excretion, thereby reducing serum BA (sBA). IBATi, including maralixibat (MRX; approved for the treatment of cholestatic pruritus in patients with Alagille syndrome [ALGS] ≥1 year of age) and volixibat (VLX), decrease the toxic accumulation of BAs in the liver and mitigate cholestasis. GI adverse events (AEs; diarrhea, abdominal pain) are side effects of IBATi due to increased excretion of fBA. The aim of this analysis was to assess the impact of timing of IBATi dosing, relative to food, on GI AEs and pharmacodynamic (PD) effects to inform the optimal dosing approach for IBATi.

Method: AE data from 3 phase 1 clinical studies on MRX and VLX in healthy participants were compiled to assess relative tolerability with different timing of IBATi dosing vs mealtime. In Study 1, 75 mg of VLX was dosed fasted (overnight fast and no food for 4 hrs post-dose) vs right after breakfast; in Study 2, 10 mg of MRX was dosed fasted vs immediately before breakfast, and in Study 3, 30 mg of MRX was dosed fasted vs right after breakfast. The PD of IBATi is challenging to directly measure in clinical trials, so the PD impact of IBATi dosing time relative to mealtime was investigated in healthy dogs by measuring fBA excretion over 7 days of dosing, comparing IBATi dosing 4 hr prior, 30 minutes prior, or 4 hours after the daily meal.

Results: Across the 3 phase 1 clinical studies there was a lower rate of GI AEs when dosing IBATi in the fasted state (0%, 0%, and 50% of participants reported a GI AE in Study 1, 2, and 3 respectively) compared to the fed state or at mealtime (75%, 33%, and 100% in Study 1, 2, 3 respectively). In healthy dogs, MRX significantly increased fBA excretion (p < 0.01 vs pretreatment baseline by paired t-test) regardless of dosing time relative to the daily meal, with maximal increases in fBA excretion when dosing 30 minutes prior (231% increase) or 4 hrs after (229% increase) the meal, indicating flexibility in the timing of IBATi dosing vs mealtime to maintain maximal PD effect.

Table: Comparison of the Incidence of GI TEAEs Following IBATi Administration in the Fasted State Versus in the Fed State or At Mealtime in Healthy Participants

	Study 1 ¹		Study 2 ²		Study 3 ³	
	Fasted (n=8)	Fed (n=8)	Fasted (n=6)	At Mealtime (n=6)	Fasted (n=12)	Fed (n=12)
GI TEAE	0 (0%)	6 (75%)	0 (0%)	2 (33%)	6 (50%)	12 (100%)
Diarrhea	-	4 (50%)	-	1 (17%)	6 (50%)	11 (92%)
Loose stools	-	2 (25%)	-	-	-	-
Nausea	-	-	-	1 (17%)	-	3 (25%)
Abdominal pain	-	-	-	-	1 (8%)	5 (42%)
Anorectal discomfort	-	-	-	-	-	1 (8%)

¹ Study FED10634 (Volixibat 75 mg)

² Study NB4-02-06-002 (Maralixibat 10 mg)

³ Study MRX-102 (Maralixibat 30 mg)

Conclusion: These data demonstrate that GI tolerability is improved when dosing an IBATi in the fasted state, versus dosing at mealtime or immediately after food intake. Animal data show that PD effect is maintained regardless of dosing time relative to mealtime, suggesting that efficacy can be maintained while minimizing GI events.

FRI453

Magnesium accumulation by CNNM4 GalNAc-siRNA mediated silencing reduces cholestasis-associated liver fibrosis

Marina Serrano-Macia¹, Naroa Goikotxe², Rubén Rodríguez Agudo², Miren Bravo², Sofia Lachiondo-Ortega², Marcos Fernandez Fondevila³, Petar Petrov^{2,4}, Irene González-Recio², Maria Mercado-Gómez², Claudia Gil-Pitarch², Marta Romero⁵, Teresa Cardoso Delgado², Luis Alfonso Martínez-Cruz², Ruben Nogueiras³, Cesar Martin⁶, Piotr Milkiewicz⁷, Malgorzata Milkiewicz⁸, Ute Schaeper^{9,10}, Daniela Buccella¹¹, Jose Juan G. Marin^{4,5}, Jorge Simón Espinosa^{1,4}, María Luz Martínez-Chantar^{1,4}. ¹CIC bioGUNE-Centro de Investigación Cooperativa en Biociencias, Liver Disease Lab, Derio, Spain; ²CIC bioGUNE-Centro de Investigación Cooperativa en Biociencias, Liver Disease Lab, Derio, Spain; ³CiMUS-Centro Singular de Investigación en Medicina Molecular y Enfermedades Crónicas, Molecular Metabolism Lab, Santiago de Compostela, Spain; ⁴Carlos III National Health Institute, Centro de Investigación Biomédica en Red de Enfermedades Hepáticas y Digestivas (CIBERehd), Madrid, Spain; ⁵Instituto de Investigación Biomédica de Salamanca, Experimental Hepatology and Drug Targeting (HEVEFARM), Salamanca, Spain; ⁶Campus De Bizkaia-Campus of Biscay, Instituto Biofisika, Lejona, Spain; ⁷Medical University of Warsaw, Liver and Internal Medicine Unit, Warszawa, Poland; ⁸Pomeranian Medical University, Department of Medical Biology, Szczecin, Poland; ⁹Silence Therapeutics GmbH, Berlin, Germany; ¹⁰Silence Therapeutics GmbH, Berlin, Germany; ¹¹New York University, Department of Chemistry, New York, United States
Email: jsimon.ciberehd@cicbiogune.es

Background and aims: Primary biliary cholangitis (PBC) and primary sclerosing cholangitis (PSC) are progressive diseases that eventually culminate in cirrhosis and related complications, as liver failure or portal hypertension among others. However, cholestasis is commonly present in these patients. Hepatocytes are adversely affected by the accumulation of bile acids and trigger inflammatory and cell death responses leading to development of fibrosis. Magnesium is known to play an important role in inflammatory and immune responses. Since magnesium distribution can be modulated by silencing Cyclin M4 (CNNM4), CNNM4 expression levels and the effectivity of a CNNM4-targeting therapy were evaluated in preclinical models for cholestasis.

Method: Hepatic CNNM4 expression was evaluated in PBC and PSC biopsies and in samples from rodent models by immunohistochemistry. An *in vitro* cholestasis model was set up by incubating primary hepatocytes with supraphysiological concentrations of glycodeoxycholic acid (GCDCA). Animal models of cholestasis were generated by bile-duct ligation (BDL) for 14 days and by the use of mice lacking *Mdr2* (*Mdr2*^{-/-}) at 3, 5 and 8 months of age. The functional role of CNNM4 in disease progression was characterized in *in vitro* and *in vivo* models of cholestasis via GalNAc-siRNA mediated silencing approach.

Results: CNNM4 upregulation was detected in liver samples of patients with PBC and PSC. Furthermore, we found that CNNM4 expression was enhanced in mice that underwent BDL and in mice lacking *Mdr2*. GalNAc-siRNA mediated silencing of CNNM4 protected primary mouse hepatocytes from GCDCA-induced cell death, mitochondrial dysfunction, oxidative stress and endoplasmic reticulum stress. In rodent models for cholestasis, GalNAc CNNM4 siRNA treatment protected the liver from fibrotic development and inflammation. Silencing *Cnnm4* in hepatocytes induced intracellular magnesium accumulation, which may protect these cells by affecting the bile acid homeostasis.

Conclusion: CNNM4 has been identified as a potential novel therapeutic target for bile acid-induced liver damage. Herein, we show evidence that silencing *CNNM4* by a GalNAc siRNA-approach could also be a novel effective approach for treatment of cholestasis-associated liver fibrosis.

FRI454

Association of bile acids composition and synthetic pathway with therapeutic effect of bezafibrate in chronic cholestatic liver disease

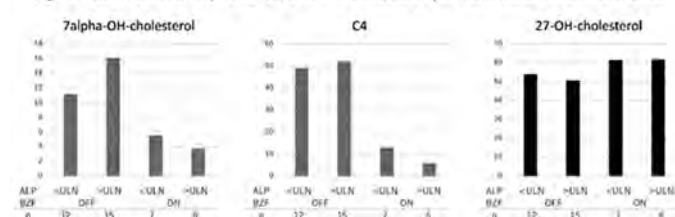
Manami Iida¹, Atsuko Higashide², Shuichi Ohtomo¹, Naoshi Horiba¹, Atsushi Tanaka³. ¹Chugai Pharmaceutical Co., Ltd., Japan; ²Chugai Research Institute for Medical Science, Inc., Japan; ³Teikyo University School of Medicine, Medicine, Japan
Email: iida.manami27@chugai-pharm.co.jp

Background and aims: While ursodeoxycholic acid (UDCA) and bezafibrate (BZF) are therapeutic options in primary biliary cholangitis (PBC) and primary sclerosing cholangitis (PSC), there are treatment resistance cases that do not respond to the combination. Here, we investigated the mechanism of UDCA + BZF treatment resistance in terms of the bile acid composition and synthesis pathway in patients with PBC and PSC.

Method: The subjects were PBC and PSC patients as well as control patients whose liver function test values were all within the normal limits. Fasting plasma was collected and the plasma levels of various bile acids, 7 α -hydroxy cholesterol (7 α -HC), 27-hydroxy cholesterol (27-HC), and C4 were measured by liquid chromatography-tandem mass spectrometry. In addition, various clinical test values tested on the same day and therapeutic agents were collected. The relationship between bile acid composition and synthetic pathway, UDCA and BZF treatment, and liver function tests was examined.

Results: Patients with PBC (n = 30, all females, mean age 67 yrs, UDCA/BZF administration: 26/8), PSC (n = 10, male/female = 7/3, mean age 44 yrs, UDCA/BZF administration: 10/5), and control patients (6 chronic hepatitis B, 23 chronic hepatitis C, 1 dyslipidemia, M/F = 16/14, mean age 66 yrs, UDCA/BZF administration: 3/0) were enrolled in the study. The plasma level of UDCA-related bile acids were high in PBC/PSC, reflecting UDCA administration. Furthermore, GCA, TCA, and TCDCA were higher in PBC/PSC than those in the controls, and the concentrations of these three types of bile acids were significantly correlated with the liver enzymes and bilirubin levels. In terms of the bile acid synthetic pathway, 27-HC was positively correlated with liver enzyme levels, and 27-HC was high in cases with elevated liver enzymes. In relation to BZF administration, BZF-administered PBC/PSC cases (PBC 8, PSC 5) had significantly lower values of 7 α -HC and C4 and higher 27-HC than non-administered cases (PBC 22, PSC 5) (Figure).

Figure. Plasma levels of 7 α -HC, C4, and 27-HC stratified by ALP levels and BZF administration



Conclusion: GCA, TCA, and TCDCA were higher in treatment-resistant PBC/PSC cases with elevated liver enzymes. In addition, 27-HC was elevated, suggesting that the alternative pathway was activated in these treatment resistant cases. In the BZF-administered cases, 7 α -HC and C4 levels were low (Figure), indicating that Cyp7a1 was suppressed and the classical pathway was suppressed as previously reported. On the other hand, 27-HC was not decreased and the alternative pathway was not suppressed, irrespective of liver enzyme levels (Figure). Taken together, BZF treatment failed to inhibit the alternative pathway of bile acids which were activated in cases with elevated liver enzymes, possibly, in part, explaining the mechanism of treatment resistance.

FRI455

Reduced hepatic expression of PPAR alpha in primary biliary cirrhosis is modulated by miR-155

Monika Adamowicz¹, Agnieszka Kempinska-Podhorodecka¹, Joanna Abramczyk¹, Jesus Maria Banales², Piotr Milkiewicz³, Małgorzata Milkiewicz¹. ¹Pomeranian Medical University, Department of Medical Biology, Szczecin, Poland; ²Biodonostia Health Research Institute, Department of Liver and Gastrointestinal Diseases, Donostia University Hospital, Ikerbasque, CIBERehd, San Sebastian, Spain; ³Medical University of Warsaw, Liver and Internal Medicine Unit, Warsaw, Poland
Email: monika.adamowicz@pum.edu.pl

Background and aims: Peroxisome proliferator-activated receptor alpha (PPARα) regulates expression of multiple genes involving lipid metabolism, bile acids (BA) homeostasis, and shows protective effects against inflammation and apoptosis. Progressive diseases such as primary biliary cirrhosis (PBC) and primary sclerosing cholangitis (PSC) result in intrahepatic retention of toxic BA that may lead to liver dysfunction and failure. Small non-coding RNA molecules (miRNAs) regulate gene expression, and miR-155 was associated with silencing of PPARα. Since PPARα activation decreases inflammation and fibrosis we evaluated PPARα and miR-155 expressions in cholestatic livers. We have also analyzed the regulatory effect of miR-155 on PPARα expression *in vitro*.

Method: Liver samples were taken from biopsies at early stages (F1-F2) of PBC (n = 12) or from explanted livers in patients with cirrhotic PBC (n = 11) and PSC (n = 17). The functional role of miR-155 was characterized *in vitro* in hepatocytes (HepG2) and primary cholangiocytes (NHC) where overexpression of miR-155 was induced by mirVana miRNA Mimic. miR-155 expression levels were evaluated after treatment with lipopolysaccharide (LPS), glycodeoxycholic acid (GCDCA), lithocholic acid (LCA) or ursodeoxycholic acid (UDCA).

Results: When compared to controls hepatic PPARα mRNA and protein levels were reduced in cirrhotic PBC (both 50% reduction, P = 0.01), but not in PSC livers. In PBC livers this phenomenon was accompanied with induction of miR-155 (3.7-fold increase, P = 0.004 vs. control). Experimental overexpression of miR-155 in HepG2 led to the inhibition of PPARα (50% reduction, P = 0.02). LPS stimulated miR-155 expression in HepG2 (over 40-fold increase, p = 0.009), whereas the treatment with GCDCA or LCA enhanced the expression of miR-155 in NHC (2-fold p < 0.05, or 2.4 fold p < 0.05, respectively). UDCA suppressed the basal expression of miR-155 in NHC (20% reduction, p = 0.02 vs. control) as well as the LPS-induced miR-155 in HepG2 (p = 0.009 vs LPS).

Conclusion: We showed that PPARα is substantially reduced in PBC livers, and the observed concomitant overexpression of miR-155 induced either by inflammation or bile acids may be accountable for this suppression. Inhibition of miR-155 may be a potential novel therapeutic target in PBC.

FRI456

cholangiocytes-specific deletion of sphingosine-1-phospholipid receptor 1 attenuate cholestasis induced liver injury and fibrosis

Yuan Zihang¹, Jie Wang¹, Yingying Miao¹, Haoran Zhang¹, Xinliang Huang¹, Luyong Zhang^{1,2}, QW Yu¹, Zhenzhou Jiang^{1,3,4}. ¹China Pharmaceutical University, New drug screening center, Jiangsu center for pharmacodynamics research and evaluation, Nanjing, China; ²Guangdong Pharmaceutical University, Center for drug research and development, Guangdong, China; ³China Pharmaceutical University, Key laboratory of drug quality control and pharmacovigilance, Nanjing, China; ⁴China Pharmaceutical University, State key laboratory of natural medicines, Nanjing, China
Email: jiangcpcu@163.com

Background and aims: Cholestasis is a pathophysiological process caused by disorders involving bile secretion and excretion. Chronic cholestasis can cause bile acids (BAs) to accumulate in the liver, induce liver injury, inflammation, and liver fibrosis. Sphingosine-1-

phospholipid receptor 1 (S1PR1) is distributed in various organs, it is the receptor of endogenous substance sphingosine-1-phospholipid (S1P) and participates in a variety of physiological and pathological process. But its role in cholestatic liver disease has not yet been elucidated clearly.

Method: To study the cholangiocyte-specific role of S1PR1, we generated a novel knock-out mouse strains by breeding Krt19Cre mice with S1pr1 floxed mice. S1PR1 cell specific deletion was confirmed in primary isolated intrahepatic cholangiocytes by PCR, WB, and IF, and in liver frozen section by IF. Fibrosis was established by common bile duct ligand (BDL) (14 days) and CA (0.5%) chow diet (4 months). Liver damage was determined by serum ALT, AST, ALP, TBA, and H&E staining. Fibrosis was determined by hepatic hydroxyproline, Masson trichrome staining, Sirius staining, and IHC. Comprehensive serum and liver bile acids profiling were performed using HPLC-MS/MS. RNA-seq was performed in whole liver and primary cholangiocytes after BDL.

Results: First we observed that S1PR1 was more expressed on cholangiocytes after 14 days BDL and 4 months CA chow diet. Interestingly, S1PR1^{Krt19CreERT+/+} mice displayed a trend towards attenuated liver injury and liver fibrosis compared to WT mice after BDL and CA chow diet, demonstrated by significantly decrease in serum ALT, AST, ALP, TBA, hepatic hydroxyproline, Masson Trichrome, H&E, and Sirius red staining as well as immunohistochemistry staining of α-SMA. BA profiling and PCA analysis indicated that S1PR1^{Krt19CreERT+/+} mice alleviates the destruction of bile acid homeostasis induced by BDL and CA chow diet. RNA-seq analysis in BDL liver showed downregulation of ROS, ER stress, and CCR1 chemokine receptor binding signaling in S1PR1^{Krt19CreERT+/+} mice compared to WT mice. WB analysis showed that cholangiocytes-specific deletion of S1PR1 attenuates CHOP induction, phosphorylation of JNK, eif2α, and PERK induced by BDL. Q-PCR analysis showed that cholangiocytes-specific deletion of S1PR1 attenuates the upregulation of Ccl4, Ccl6, and Ccl7 induced by BDL.

Conclusion: Our results illustrate that the cholangiocytes-specific deletion of S1PR1 can alleviate liver fibrosis and injury caused by biliary obstruction or chronic cholestasis, which helps to develop S1PR1 as a target for the treatment of liver fibrosis and cholestasis.

FRI457

Pruriceptor activating compounds in the enterohepatic cycle in cholestatic itch

Frank Wolters¹, Jacqueline Langedijk¹, Dagmar Tolenaars¹, Michel van Weeghel², Rudi de Waart¹, Stan van de Graaf¹, Coen Paulusma^{1,3}, Wendy L. van der Woerd⁴, Henkjan J. Verkade⁵, Arthur Verhoeven¹, Ulrich Beuers¹, Ronald Oude Elferink¹. ¹Amsterdam UMC, Tytgat Institute, Amsterdam, Netherlands; ²Amsterdam UMC, Core Facility Metabolomics, Amsterdam, Netherlands; ³Amsterdam UMC, locatie AMC, Tytgat Institute for Liver and Intestinal Research, Amsterdam, Netherlands; ⁴Utrecht UMC, Department of Pediatric Gastroenterology, Utrecht, Netherlands; ⁵UMC Groningen, Department of Pediatrics, Groningen, Netherlands
Email: r.p.oude-elferink@amc.uva.nl

Background and aims: Pruritus can be a major and debilitating symptom in cholestasis. Treatment is difficult, as the pathophysiology of this symptom remains elusive. This study aims to identify circulating agonists for TRPA1 and other pruriceptors in the enterohepatic circulation, in bile and blood, as a possible cause for itching in cholestatic patients.

Method: Bile of 5 cholestatic patients with and without itch (various cholestatic liver diseases), was fractionated and assessed for *in vitro* pruriceptor activation ([Ca²⁺]_i and luciferase assays) in HEK293T cells. Collected fractions were tested for activation of specific receptors (TRPA1, TRPV1, TRPV3, TRPV4, MRGPRX1, MRGPRX4, FXR) and active fractions were subfractionated and again tested. The content of positive fractions was identified by means of HPLC-MS/MS and, if possible, validated with commercially available standards.

POSTER PRESENTATIONS

Pruritogenic activity of these compounds was assessed by intradermal injection in wild type and TRPA1-deficient mice.

Results: Several fractions from bile activated the TRPA1 receptor (and several other receptors) in vitro. One of these fractions contained a compound with m/z 311.22 which could be identified as a hydrophilic isomer of hydroperoxylinoic acid (HpODE). We could also show that in bile HpODE is rapidly converted into a hydrophilic isomer. Upon biliary diversion of a BRIC type 1 patient we could show that the initial excretion of HpODE and its metabolites is very high with gradual decrease concomitant with the disappearance of itch. In plasma of pruritic cholestatic patients HpODE concentrations were significantly increased compared to cholestatic patients without itch and healthy controls. Wild type mice exhibited scratching behavior upon intradermal injection of HpODE, whereas TRPA1 deficient mice did not.

Conclusion: HpODE, a pruritogen in vitro and in vivo is present in elevated levels in cholestatic patients who experience itch. This compound, and its metabolites is highly secreted into bile upon biliary diversion. Pruriceptor antagonists may be useful in the treatment of cholestatic pruritus.

FRI458

Characterising the early inflammatory landscape of primary sclerosing cholangitis

Calli Dendrou¹, Kate Lynch^{2,3}, Fabiola Curion^{1,4}, Charlotte Rich-Griffin¹, Hing-Yuen Yeung¹, Nicholas Provine², Nicholas Illott², Helen Ferry², Eve Fryer⁵, Holm Uhlig², Roger W.G. Chapman², Satish Keshav², Paul Klenerman². ¹Wellcome Centre for Human Genetics, University of Oxford, Oxford, United Kingdom; ²Translational Gastroenterology Unit, University of Oxford, Oxford, United Kingdom; ³Royal Adelaide Hospital, University of Adelaide, Adelaide, Australia; ⁴Institute of Computational Biology, Helmholtz Munich, Neuherberg, Germany; ⁵John Radcliffe Hospital, Nuffield Division of Clinical and Laboratory Sciences, Oxford, United Kingdom
Email: cdendrou@well.ox.ac.uk

Background and aims: Primary sclerosing cholangitis (PSC) is a chronic inflammatory biliary disease characterised by progressive fibrosis that can lead to cirrhosis and liver failure. Over 70% of PSC patients also have gut co-morbidities, typically ulcerative colitis (UC), suggesting a link between liver pathology and gut microbial dysbiosis. Therapeutic options for PSC are limited, with liver transplantation being most effective, although disease may recur. Thus, there is a dire need to better understand and target the pathological mechanisms of PSC, particularly those acting early on.

A key challenge to characterising early pathology in PSC has been related to acquiring liver biopsies. However, fine needle aspiration (FNA) has emerged as a safe technique for obtaining liver infiltrating immune cells. We sought to assess the experimental efficacy of FNA to adequately sample liver immune cells, and to map the early inflammatory landscape in the liver relative to matched peripheral blood using single-cell profiling technologies. We also sought to assess how inflammation in the liver compares to pathology in the gut of PSC patients presenting with UC.

Method: We obtained liver-infiltrating mononuclear immune cells via FNA and peripheral blood mononuclear cells (PBMCs) from patients with PSC and with non-alcoholic fatty liver disease/steatohepatitis. Cells were analysed by polychromatic flow cytometry and by 10× Genomics single-cell RNA sequencing (scRNAseq). In addition, gut biopsies from PSC-UC patients were obtained and also analysed by scRNAseq.

Results: We obtained liver FNAs from 38 patients (21 PSC, 17 control patients). The median pain score was 0 and no serious adverse effects were reported. Flow cytometry analysis demonstrated a significant enrichment of natural killer (NK) cells, CD8+ T cells, and CD69+ T cells in the liver (all $p < 0.05$). High-resolution profiling of 38, 012 liver immune cells and 78, 751 PBMCs by scRNAseq in a patient subset specifically showed an enrichment of CXCR6+ NK cells, CD8+ central memory T cells, and mucosal-associated invariant T cells in the liver, and a relatively lower abundance of CD4+ regulatory T cells (all $p < 0.05$). Among other immune cell types captured, dendritic cells were enriched in the liver whilst FOShi classical monocytes were reduced ($p < 0.05$). Gene expression analyses also revealed PSC-specific inflammatory pathways, such as an increase in cytokine responsiveness, and analogous analyses were applied to the PSC gut samples.

Conclusion: FNA sampling is a safe approach for obtaining insights into the early inflammatory landscape of the liver in PSC and other diseases, with the application of single-cell methods across tissues revealing tissue-specific and shared inflammatory pathways that may provide a basis for further experimental medicine analyses.

FRI460

Copper accumulation in chronic cholestatic disease augments liver damage by impairment of mitochondrial function

Dennis Koob¹, Judith Nagel^{2,3}, Sebastian Zimny¹, Jingguo Li^{1,4}, Renate Artmann¹, Ralf Wimmer¹, Gerald Denk¹, Martin Roderfeld⁵, Elke Roeb⁵, Hans Zischka^{2,3}, Simon Hohenester¹. ¹University Hospital LMU, Department of Medicine II, Munich, Germany; ²Technical University of Munich, Department of Toxicology and Environmental Hygiene, Munich, Germany; ³Helmholtz Center Munich, Institute of Molecular Toxicology and Pharmacology, Munich, Germany; ⁴Affiliated

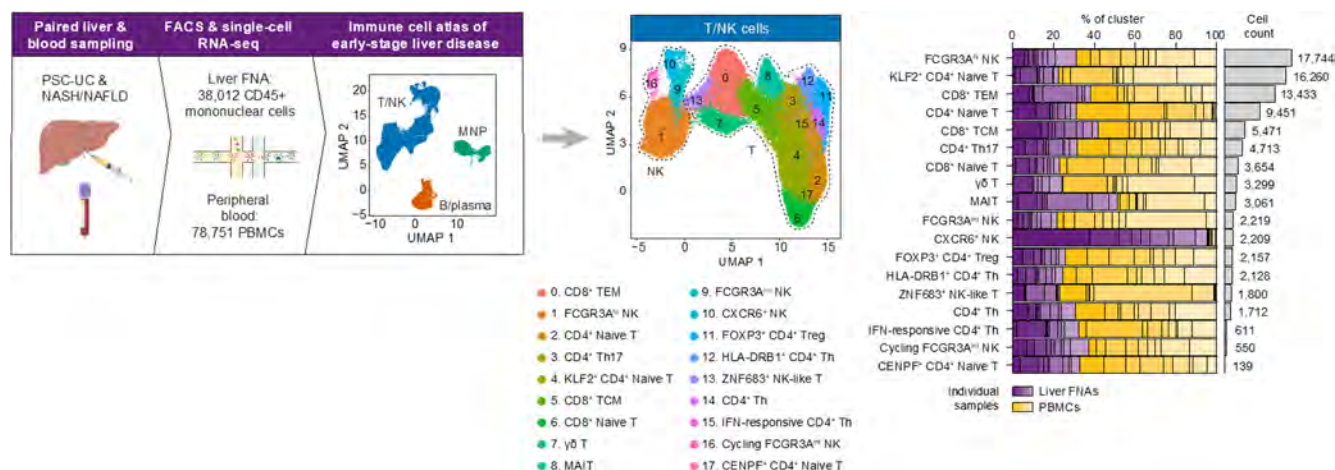


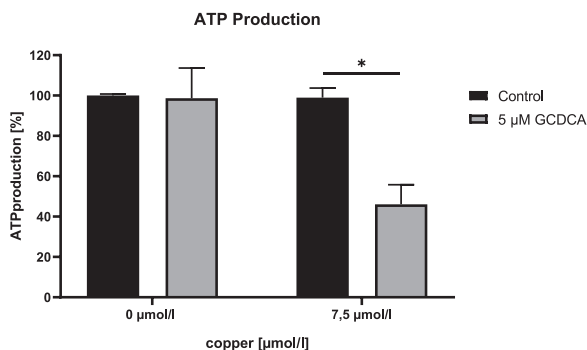
Figure: (abstract: FRI458)

Hospital of Zunyi Medical University, Department of Gastroenterology, Zunyi, China; ²Justus Liebig University, Gastroenterology, Center for Internal Medicine, Gießen, Germany
Email: dennis.koob@med.uni-muenchen.de

Background and aims: Derangement of copper homeostasis, as seen in Wilson's disease, causes liver damage. Copper accumulation also occurs in chronic cholestatic liver disease. In primary sclerosing cholangitis, copper accumulation, i.e. Orcein staining as a component of the Nakanuma score, even predicts reduced transplant-free survival. We hypothesize that copper accumulation might not only be a consequence of cholestasis, but modulate the course of disease. We aimed to investigate the role of copper accumulation in animal models of cholestasis and identify potential molecular targets of copper and bile salt co-toxicity.

Method: Hepatic copper content was determined in wild type and Mdr2^{-/-} animals on both FVB and BALBc backgrounds. Liver damage and liver fibrosis were quantified. Mdr2/FVB animals were fed a copper-enriched diet (2 g/kg). The hepatocyte cell line HepG2 was stably transfected with Ntcp to allow for bile salt uptake and was stimulated with glycochenodeoxycholate (GCDC) and copper (5–10 µM, each). Cell survival, apoptosis, proliferation, and metabolic activity were assessed. In mitochondria from stimulated cells, oxygen consumption and ATP production were quantified.

Results: While hepatic copper content was not different from wildtype in Mdr2/FVB animals, it was increased 1.5 ± 0.2 -fold in Mdr2/BALBc (wt/BALBc vs. Mdr2/BALBc, $n = 5$, $p < 0.05$). Overall, hepatic copper content correlated with liver fibrosis as determined by liver hydroxyproline ($r^2 = 0.8$, $p < 0.05$, $n = 9$). Copper feeding was well tolerated in wt animals and was associated with a slight but insignificant increase in serum ALT only in Mdr2/FVB animals. However, it led to an increase in hepatic copper content (13.5 ± 1.2 vs. 1898.3 ± 445.7 mg/kg, $n = 6$, $p < 0.01$) and liver fibrosis (Desmet score, 0.4 ± 0.5 vs. 1.3 ± 0.5 , $p < 0.05$) in Mdr2/FVB. In HepG2, doses applied of both GCDC and copper were non-toxic in WST assays. Combination of both stimuli, however, led to a marked impairment of metabolic activity to $65.9 \pm 4.3\%$ ($n = 6$, $p < 0.05$). While caspase-3/7 assays excluded apoptosis, reduced proliferative activity was found upon dual treatment. In isolated mitochondria from stimulated HepG2 cells, ATP production was unaffected by each stimulus alone. Combined treatment, however, led to a drop in ATP production from $100 \pm 4.1\%$ to $46.1 \pm 9.7\%$ ($n = 3$, $p < 0.05$) (Figure 1), accompanied by an increase in mitochondrial oxygen consumption.



Conclusion: Hepatic copper deposition in experimental cholestasis is associated with progression of liver fibrosis, mimicking the human phenotype. On a cellular level, bile salt and copper synergistically impair ATP production. Since the respiratory chain was unaffected (increase rather than drop in oxygen consumption), the adenine nucleotide translocator (ANT) is a likely molecular target. These results encourage testing of copper chelating strategies in cholestatic liver disease.

FRI461

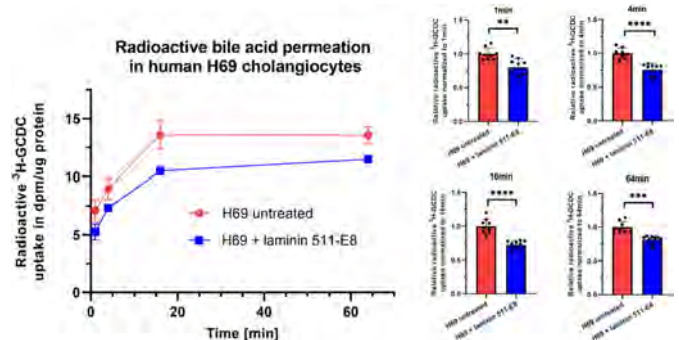
The IgG4-related cholangitis autoantigen laminin 511-E8 stabilizes the biliary bicarbonate umbrella in human cholangiocytes

David Trampert¹, Remco Kersten¹, Dagmar Tolenaars¹, Ronald Oude-Elferink¹, Stan van de Graaf¹, Ulrich Beuers¹. ¹Tytgat Institute for Liver and Intestinal Research, Amsterdam Gastroenterology Endocrinology Metabolism (AGEM), Amsterdam University Medical Centers, Department of Gastroenterology and Hepatology, Amsterdam, Netherlands
Email: u.h.beuers@amsterdamumc.nl

Background and aims: IgG4-related cholangitis (IRC) is the hepatobiliary manifestation of IgG4-related disease (IgG4-RD), a systemic, B-cell driven, fibroinflammatory disorder. To date four autoantigens with pathogenetic relevance have been described by our group and others in IgG4-RD, namely annexin A11, laminin 511-E8, galectin 3 and prohibitin 1 (PMID 28765476, 30089633). We recently demonstrated that patient anti-annexin A11 autoantibodies destabilize the 'biliary bicarbonate umbrella' (PMID 34718050), a protective mechanism against toxic hydrophobic bile acids (PMID 20721884). Another autoantigen, laminin 511-E8, is an extracellular matrix protein that functions as a ligand of the integrin A6B1 (ITGA6B1) receptor (PMID 28879238). Laminin 511-E8 has been shown to upregulate critical components of the 'biliary bicarbonate umbrella' (PMID 27103433) and ITGB1 signaling is important for bile duct development (PMID 22761447). Therefore, we aimed to investigate the role of laminin 511-E8 in human cholangiocytes.

Method: Laminin 511-E8 expression was confirmed in RNA sequencing datasets of human cholangiocyte organoids. Human H69 cells were subjected to shRNA knockdown using lentiviral transduction. Individual knockdown cell lines were generated targeting the mRNA transcripts encoding laminin 511-E8 (LAMA5, LAMB1, LAMC1). Knockdown of LAMB1 and LAMC1 was verified on mRNA and protein level using qPCR and western blot. A parallel approach was taken subjecting H69 cells to recombinant laminin 511-E8 (0.25 µg/cm²). The function of laminin 511-E8 in human cholangiocytes was assessed by three approaches: (i) intracellular pH (pHi) measurements microspectrofluorimetrically using BCECF-AM; (ii) rate of bile acid influx radiochemically by measuring 22, 23-³H-glycochenodeoxycholic acid (³H-GCDC) permeation over time; (iii) GCDC-induced apoptosis determined dynamically by real-time imaging of Caspase-3/7 Green signal and statically by conventional bulk Caspase-3/7 assays.

Results: Screening of the laminin 511-E8 constituent knockdown cell lines revealed that at least LAMB1 and LAMC1 could be of functional importance in cholangiocytes. ³H-GCDC permeation was larger in LAMB1 and LAMC1 knockdown H69 cells compared to Sham controls. Treatment of human cholangiocytes with the recombinant 511-E8 fragment resulted in a decreased pHi and significantly reduced the rate of ³H-GCDC permeation (Figure).



Conclusion: Collectively, our study indicates that the IgG4-RD autoantigen laminin 511-E8 has a protective role in human

POSTER PRESENTATIONS

cholangiocytes against toxic bile acids, similar as recently described for annexin A11. We speculate that autoantibodies against laminin 511-E8 may destabilize the biliary bicarbonate umbrella, thereby contributing to the pathogenesis of IRC.

FRI462

The risk-variant rs56258221 at the BACH2-locus associates with skewed polarization of naive CD4⁺ T cells towards pro-inflammatory phenotypes in primary sclerosing cholangitis

Jonas Bahn¹, Lilly K. Kunzmann¹, Jenny Krause¹, Christian Casar^{1,2}, Silja Steinmann¹, Marcial Sebode¹, Samuel Huber^{1,3}, Ansgar W. Lohse^{1,3}, Andre Franke⁴, Nicola Gagliani^{1,3,5,6}, Dorothee Schwinge¹, Christoph Schramm^{1,3,7}, Tobias Poch¹.

¹University Medical Center Hamburg-Eppendorf, I. Department of Medicine, Hamburg, Germany; ²University Medical Center Hamburg-Eppendorf, Bioinformatics Core, Hamburg, Germany; ³University Medical Center Hamburg-Eppendorf, Hamburg Center for Translational Immunology, Hamburg, Germany; ⁴Christian-Albrechts-University of Kiel, Institute of Clinical Molecular Biology, Kiel, Germany; ⁵University Medical Center Hamburg-Eppendorf, Department for General, Visceral and Thoracic Surgery, Hamburg, Germany; ⁶Karolinska Institute, Immunology and Allergy Unit, Department of Medicine Solna, Stockholm, Sweden; ⁷University Medical Center Hamburg-Eppendorf, Martin Zeitz Center for Rare Diseases, Hamburg, Germany
Email: t.poch@uke.de

Background and aims: Primary sclerosing cholangitis (PSC) is an enigmatic disease of presumably multifactorial pathogenesis, including genetic predisposition and dysregulated immune responses as likely key contributors to the disease development. We have previously described an intrahepatic naive-like population of CD4⁺ T cells in patients with PSC, prone to polarize towards a pro-inflammatory T_H17 phenotype. Genome-wide association studies (GWAS) have linked PSC to several polymorphisms in immune-related genes. We here hypothesized that genetic predisposition contributes to the observed T cell phenotype in patients with PSC.

Method: Patients with PSC (n = 270) were genotyped for the disease-associated risk variants rs56258221 (BACH2), rs80060485 (FOXP1), rs4147359 (IL2RA) and rs7426056 (CD28). To determine T cell function and phenotype, comprehensive immunophenotyping, *in vitro* experiments on polarization and proliferation, microRNA-assays, western blots and single-cell RNA sequencing from peripheral blood naive CD4⁺ T cells was performed. The data generated was correlated to the underlying genotype of the patients.

Results: Functional *in vitro* experiments with naive CD4⁺ T cells from patients with PSC and healthy donors (HD) showed an increased capacity of PSC-derived cells to convert into pro-inflammatory T Helper 1 (T_H1, 50.7% vs. 42.9%, p = 0.027) and T Helper 17 (T_H17, 5, 5% vs. 2, 2%, p = 0.042) subsets, which was accompanied by a lower conversion rate into induced regulatory T cells (iT_{REG}, 9.6% vs. 17.3%, p = 0.022). The observed effects were significantly increased in carriers of the PSC-associated risk variant rs56258221 (BACH2), which was not seen for the other variants in immune-related genes assessed. Interestingly, single-cell RNA sequencing of the T cell compartment in homozygous SNP carriers vs. non-carriers identified a composition skewed towards activated phenotypes in rs56258221-carriers. Reduced expression of BACH2 itself was detected on protein but not mRNA level in naive CD4⁺ T cells, which could be linked to a strongly increased expression of a microRNA located in close genomic proximity to the SNP and imputed to inhibit translation of BACH2.

Conclusion: We here present comprehensive data linking the risk variant rs56258221 at the BACH2-locus to the recently described

dysregulated T cell phenotype in patients with PSC. Decoding how genetic risk contributes to disease pathogenesis is the first step in understanding how the environment interacts with the immune system to fuel disease pathogenesis.

FRI463

Single-cell profiling of liver B cells identifies distinct gene expression and reactivities of expanded B cell clonotypes in primary sclerosing cholangitis

Markus Jördens^{1,2,3}, Tom Hemming Karlsen^{1,2,4,5}, Espen Melum^{1,2,4,5,6}, Johannes R. Hov^{1,2,4,5}, Brian K. Chung^{1,2}.

¹University of Oslo, Norwegian PSC Research Center, Oslo University Hospital and Institute of Clinical Medicine, Oslo, Norway; ²Oslo University Hospital, Research Institute of Internal Medicine, Oslo, Norway; ³University Hospital Düsseldorf, Clinic for Gastroenterology, Hepatology and Infectious Diseases, Medical Faculty, Heinrich Heine University Düsseldorf, Düsseldorf, Germany; ⁴University of Oslo, Institute of Clinical Medicine, Oslo, Norway; ⁵Oslo University Hospital, Section for Gastroenterology, Department of Transplantation Medicine, Division of Surgery, Inflammatory Diseases and Transplantation, Oslo, Norway; ⁶University of Oslo, Hybrid Technology Hub-Centre of Excellence, Institute of Basic Medical Sciences, Faculty of Medicine, Oslo, Norway

Email: b.k.chung@medisin.uio.no

Background and aims: Primary biliary cholangitis (PBC) and primary sclerosing cholangitis (PSC) are autoimmune hepatobiliary diseases with a high prevalence of autoantibodies. In PBC, anti-mitochondrial antibodies (AMA) serve as robust biomarkers whereas autoantibodies against relevant antigens in PSC remain undefined. Using anti-mitochondrial reactivity as a proxy of disease-relevance, we assessed if expanded B cell clonotypes in PBC livers recognize AMA targets and whether analogous B cells in PSC harbour unique gene expression and antigen specificities.

Method: Liver B cells from PBC (n = 3) and PSC explants (n = 3) were enriched by negative bead selection (Stemcell Technologies, Canada) and assessed for B cell receptor (BCR) and total gene expression by single-cell RNA sequencing (scRNAseq). B cell clonality and differential gene expression (DEG) was analyzed by Cell Ranger and Loupe Browser (10X Genomics, USA). Monoclonal antibodies (mAb) generated from BCR sequences of expanded B clonotypes (GenScript, USA) were pooled and screened against >20, 000 human proteins using HuProt v4 microarrays (Cambridge Protein Arrays, UK). A subselection of mAb microarray targets were verified by immunoblotting or enzyme-linked immunosorbent assays (ELISA).

Results: Cumulative frequencies of the five most-expanded B clonotypes as a percentage of total liver clonotypes were similar amongst PBC and PSC explants (mean: 16.8% vs 15.4%, range: 9.1–30.42% to 0.68–41.17%). In contrast, transcriptomes of expanded PBC clonotypes significantly differed from PSC clonotypes; plasma cell markers such as CD38, JSRP1 and MZB1 were significantly higher in PBC clonotypes while the naïve and memory B cell markers MS4A1, CD79A, CD79B and HLA-DP, -DQ, -DR were significantly enriched in PSC clonotypes (log2 fold-change >2.5, p < 0.05, Benjamini-Hochberg corrected). mAbs generated from the BCR sequences of expanded PBC clonotypes strongly recognized the AMA targets PDC-E2, PDHA1, PDHA2, PDHX whereas PSC mAbs did not recognize AMA targets but strongly bound ACTN4, SFMBT2 and RBP (p < 0.001). PBC mAbs (5 of 15) stained a pooled mixture of AMA antigens (PDC-E2, OGDC-E2, BCOADC-E2) by immunoblotting and ACTN4 binding was assigned to a single PSC mAb (1 of 14) by ELISA.

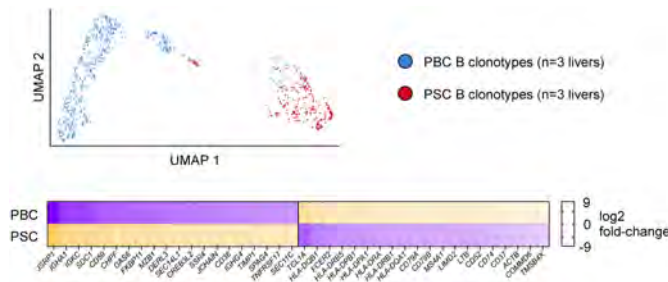


Figure: scRNAseq of expanded B clonotypes in PBC and PSC liver explants. UMAP shows cluster analysis of expanded clonotypes and heatmap indicates comparison of top 20 DEGs amongst expanded PBC and PSC clonotypes.

Conclusion: Our results show that expanded B clonotypes in PBC livers resemble antibody-secreting plasma cells while expanded PSC clonotypes mirror naïve and memory B cell states. These findings may explain the lack of specific antibodies in PSC and underscore the utility of scRNAseq in generating mAbs for future antigen studies in PSC.

FRI464

The rs429358 apolipoprotein E (APOE) polymorphism is associated with increased liver injury in patients with autoimmune hepatitis

Maciej K. Janik¹, Wiktor Smyk², Beata Kruk³, Benedykt Szczepankiewicz⁴, Barbara Górnicka⁴, Susanne N Weber⁵, Piotr Milkiewicz^{1,6}, Marcin Krawczyk^{3,5}. ¹Medical University of Warsaw, Liver and Internal Medicine Unit, Warsaw, Poland; ²Medical University of Gdansk, Department of Gastroenterology and Hepatology, Gdansk, Poland; ³Medical University of Warsaw, Laboratory of Metabolic Liver Diseases, Department of General, Transplant and Liver Surgery, Laboratory of Metabolic Liver Diseases, Centre for Preclinical Research, Warsaw, Poland; ⁴Medical University of Warsaw, Department of Pathology, Warsaw, Poland; ⁵Saarland University Medical Center, Saarland University, Department of Medicine II, Homburg, Germany; ⁶Pomeranian Medical University, Translational Medicine Group
Email: mjanik24@gmail.com

Background and aims: The natural course of autoimmune hepatitis (AIH) varies between patients; therefore, the potential role of genetic modifiers might be suspected. Recent analyses linked the variant rs429358 in apolipoprotein E (APOE) with steatosis and liver injury in fatty liver disease (Jamialahmadi *et al.*, *Gastroenterology* 2021). Here, we analyse this APOE variant in patients with AIH.

Method: The study cohort consisted of 312 non-transplanted (70% women, age 18–83 years) adults with AIH. Pure AIH and its cholestatic variants, namely AIH-primary sclerosing cholangitis (PSC) and AIH-primary biliary cholangitis (PBC), were diagnosed according to the EASL 2015 guidelines. The APOE rs429358 polymorphisms were genotyped using TaqMan assays. The liver fibrosis was assessed by liver biopsy, liver stiffness and serum indices (APRI, FIB-4), whereas liver steatosis was evaluated by controlled attenuation parameter (CAP). The effects of the APOE polymorphism were analysed in combination with the mitochondrial amidoxime-reducing component 1 (MARC1) p.A165T and adiponutrin (PNPLA3) p. I148M variants, which were previously shown to modulate liver injury in AIH.

Results: Among recruited patients, the median duration of the disease was 4 (range 0–33) years. Liver cirrhosis was present in 130 (42%) patients, and 70% of the entire cohort received steroid-based therapy. Sixty (19%) patients were therapy naïve at inclusion. In total, 26% of patients with AIH carry at least one copy of the APOE rs429358 minor allele. The APOE polymorphism was associated with more pronounced liver fibrosis according to APRI score ($p = 0.035$) and liver injury as reflected by increased AST ($p = 0.049$) and a trend for higher ALT ($p = 0.055$) activities in therapy-naïve patients with AIH. A trend

between the genetic variant in APOE and higher ALT was also noticed in the entire cohort ($p = 0.054$). No link was found between the studied variant and results of liver biopsies, transient elastography or CAP (all $P > 0.05$). The protective effect of the MARC1 polymorphism on serum ALT ($p = 0.045$) and AST ($p = 0.024$) activities were more pronounced in patients with APOE wild-type variant. The effect of the PNPLA3 p.I148M polymorphism on liver phenotypes was not modulated by the APOE genotype.

Conclusions: Patients with AIH who carry the APOE polymorphism might manifest a more pronounced liver injury. Variant APOE (rs429358) together with previously detected MARC1 p.A165T polymorphism might help to stratify patients with AIH concerning their risk of progressive liver injury.

FRI465

Intrabiliary injection of MAIT antigens induces cholangitis in mice

Kathrine Sivertsen Nordhus^{1,2,3}, Freeman Zheng^{1,2,3}, Natalie Lie Berntsen^{1,2,3}, Laura Valestrand^{1,2,3}, Jonas Øgaard^{1,2,3}, Tom Hemming Karlsen^{1,2,3,4}, Xiaojun Jiang^{1,2,3}, Espen Melum^{1,2,3,4,5}. ¹Norwegian PSC Research Center, Division of Surgery, Inflammatory Diseases and Transplantation, Oslo University Hospital, Oslo, Norway; ²Research Institute of Internal Medicine, Division of Surgery, Inflammatory Diseases and Transplantation, Oslo University Hospital, Oslo, Norway; ³Institute of Clinical Medicine, University of Oslo, Oslo, Norway; ⁴Section of Gastroenterology, Division of Surgery, Inflammatory Diseases and Transplantation, Oslo University Hospital, Oslo, Norway; ⁵Hybrid Technology Hub-Centre of Excellence, Institute of Basic Medical Sciences, Faculty of Medicine, University of Oslo, Oslo, Norway
Email: espen.melum@medisin.uio.no

Background and aims: Mucosal-associated invariant T (MAIT) cells are a subset of unconventional T-cells that recognize microbial-derived vitamin B metabolites presented by MR1. Previously we have demonstrated that bile from patients with chronic biliary inflammation contains MAIT antigens. Therefore we now aimed to determine if MAIT cells could drive inflammation in the bile ducts by challenging mice with an increased frequency of MAIT cells ($Mr1^+$ B6-MAIT^{CAST} and $iValpha19$ Tg $Calpha^{-/-}$ mice) with intrabiliary injection of MAIT cell activating antigens in terms of fixed *E.coli* and 5-OP-RU.

Method: *E.coli*, 5-OP-RU and PBS were injected into bile ducts of $Mr1^+$ B6-MAIT^{CAST} and $iValpha19$ Tg $Calpha^{-/-}$ mice. Weight and general well-being were monitored daily. The mice were sacrificed after 2, 7 or 14 days. Isolated lymphocytes from liver and spleen were stained with monoclonal antibodies and an MR1 tetramer, then analyzed by flow cytometry. Serum was analyzed for alanine transaminase (ALT).

Results: Intrabiliary fixed *E.coli* injection in $iValpha19$ Tg $Calpha^{-/-}$ mice caused a biliary immune response with increased histological cholangitis score (*E.coli*: 1.29 vs. PBS: 0.24, $p = 0.013$) after 2 days, but with similar weight loss and ALT levels compared to vehicle control. Importantly, a clear activation of hepatic MAIT cells were seen after injection of fixed *E.coli* (MFI CD69 *E.coli* vs. PBS: $p = 0.0015$) in contrast to a minor increase in CD69 MFI for non-MAIT T-cells. In $Mr1^+$ B6-MAIT^{CAST} mice, which has an increased frequency of MAIT cells independent of genetic manipulation, an increased cholangitis score ($p = 0.0485$) was also observed after injection of fixed *E. coli*. In experiments with intrabiliary 5-OP-RU injection in $iValpha19$ Tg $Calpha^{-/-}$ mice a clear increase in proportion of CD69⁺CD25⁺ MAIT cells was observed in the liver (5-OP-RU: 18% vs. PBS: 7%, $p < 0.0001$) that translated into an increased histological cholangitis score (5-OP-RU: 1.78 vs. PBS: 0.47, $p = 0.021$). This suggests that direct activation of MAIT cells leads to cholangitis. A systemic effect, most likely mediated by the portal circulation, was also observed as the proportion of CD69⁺CD25⁺ MAIT cells in the spleen was also increased (5-OP-RU: 6% vs. PBS: 3%, $p = 0.0386$).

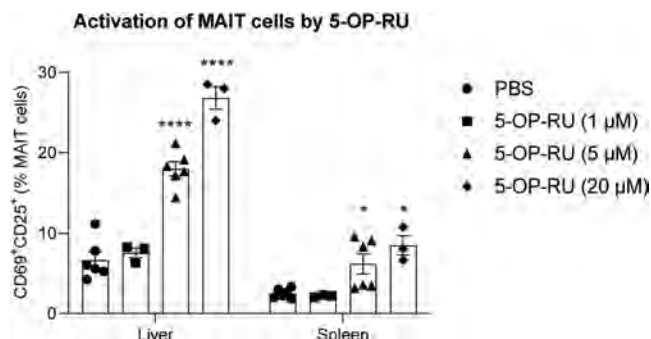


Figure: Intrabiliary 5-OP-RU injection in iValpha19 Tg Calpha^{-/-} mice activates MAIT cells.

Conclusion: We observed a clear activation of hepatic MAIT cells in a mouse model of bile duct inflammation that led to cholangitis. Biliary antigens potentially derived from gut microbiota present in the bile ducts could therefore be speculated to induce an immune response where MAIT cells play a role.

FRI466

TGF beta 2 fuels inflammation and fibrosis in cholestatic liver disease through macrophage and myofibroblast recruitment and activation

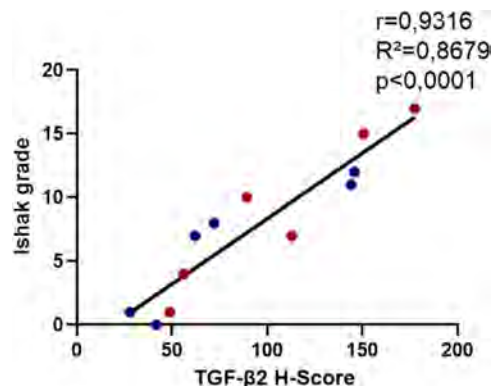
Jan Albin¹, Nadja Meindl-Beinker², Matthias Ebert², Andreas Teufel³, Steven Dooley¹, Anne Dropmann^{1,3}. ¹Medical Faculty Mannheim, Heidelberg University, Department of Medicine II, Molecular Hepatology, Mannheim, Germany; ²Medical Faculty Mannheim, Heidelberg University, Department of Medicine II, Mannheim, Germany; ³Medical Faculty Mannheim, Heidelberg University, Department of Medicine II, Clinical Bioinformatics, Mannheim, Germany
Email: janeinar.albin@medma.uni-heidelberg.de

Background and aims: We have identified TGF-β2 as an important mediator and potential therapeutic target in cholestatic liver disease, in mouse and human. The aim of this study was (1) to correlate TGF-β2 expression with disease activity, fibrotic stage and degree of ductular reaction (DR), and (2) to identify the cell populations in the diseased liver that are source for and target of TGF-β2 and delineate their role in the disease course.

Method: Liver tissues from Abcb4KO, CDE & DDC diet, bile duct ligated and CCl₄ treated mice, as well as patient samples were stained for H&E and Sirius Red. Histologic evaluation of disease activity and stage of fibrosis were determined with the Ishak score and compared to age-matched wild type mice and healthy controls respectively. TGF-β2, pSmad3 and cell type markers were analysed by in-situ hybridisation and immunohistochemistry. TGF-β2 expression levels were evaluated with H-Score.

Results: TGF-β2 is produced by cholangiocytes during disease progression in ABCB4KO mice and primary sclerosing cholangitis patients, especially in regions of DR. This is also seen in BDL and DDC models, both displaying phenotypes of cholestatic liver disease and TGF-β2 expression levels that increase with severity of the injury. In contrast, CDE fed and CCl₄ treated mice show low TGF-β2 expression, even if DRs are present. In patients and mouse models of cholestatic liver disease mRNA expression levels of TGF-β2 highly correlate with disease activity-especially inflammation, stage of fibrosis and extent of DRs. The data suggest that TGF-β2 is a biomarker of cholestatic liver damage, but not of hepatocellular injury without cholestasis. In line with high TGF-β2 levels, Abcb4KO livers show an increased Smad3 phosphorylation in Kupffer cells (KC) and other macrophages, as well as in hepatic stellate cells (HSC) or portal fibroblasts in the portal field area. In contrast Smad3 phosphorylation levels of hepatocytes and cholangiocytes did not change. KC/HSC also show upregulated TGF receptor expression and presence of activation markers (e.g. αSMA in HSC). The numbers of activated non parenchymal cells and the percentage of the pSmad3-positive

fraction in the periportal area correlated with disease progression. Inhibiting TGF-β2 expression with antisense oligonucleotides leads to reduced pSmad3 positive cell numbers, suggesting that TGF-β2 is triggering Smad3 signaling.



Conclusion: TGF-β2 expression is upregulated in cholangiocytes in patients and mouse models with cholestatic liver disease. Neighboring inflammatory and fibrogenic cells display pSmad3 staining and increase in numbers. Next, we search for stress factors and upstream signals that induce TGF-β2 expression during cholestatic liver damage.

FRI467

Liver-specific Tsg101 depletion causes apoptosis, cell death and liver failure

Surui Wang^{1,2}, Revathi Sekar^{1,2}, Jaroslaw Cendrowski³, Ahmed Ghallab⁴, Karsten Motzler^{1,2}, Yun Kwon^{1,2}, Susanne Seitz^{1,2}, Michael Roden^{2,5,6}, Adriano Maida^{1,2}, Jan G. Hengstler⁴, Stephan Herzig^{1,2}, Marta Miaczynska³, Anja Zeigerer^{1,2}. ¹Institute for Diabetes and Cancer, Helmholtz Center Munich, Joint Heidelberg-IDC Translational Diabetes Program, Inner Medicine 1, Heidelberg University Hospital, Neuherberg, Germany; ²German Center for Diabetes Research (DZD), Neuherberg, Germany; ³International Institute of Molecular and Cell Biology, Warszawa, Poland; ⁴Leibniz Research Centre for Working Environment and Human Factors, Dortmund, Germany; ⁵Heinrich Heine University Düsseldorf, Division of Endocrinology and Diabetology, Medical Faculty, Düsseldorf, Germany; ⁶Leibniz Center for Diabetes Research at Heinrich Heine University, Institute for Clinical Diabetology, German Diabetes Center, Dusseldorf, Germany
Email: anja.zeigerer@helmholtz-muenchen.de

Background and aims: The endosomal sorting complexes required for transport (ESCRT) play a key role in lysosomal degradation of membrane signaling receptors. The machinery consists four protein complexes (ESCRT -0 to -III), that are successively recruited to maturing endosomes, sorting ubiquitinated cargos into intraluminal vesicles destined for degradation. Recently, activation of the ESCRT-I has been reported to protect mice against non-alcoholic steatohepatitis (NASH) by targeting TLR4 for degradation, suggesting its potential role for treating non-alcoholic fatty liver disease (NAFLD) and NASH. Thus, the aim of this project is to identify the function of ESCRT-I in liver physiology by interfering with the major regulator of ESCRT-I stability and function, the tumor susceptibility gene 101 (Tsg101).

Method: Tsg101 was downregulated using lipid nanoparticle induced hepatocyte-specific *in vivo* and adenovirus based primary hepatocytes *in vitro* knockdown. The *in vivo* experiments were conducted in time course while serum and livers are collected for functional analysis.

Results: Consistent with previous data, we found Tsg101KD leads to ESCRT-I instability, supporting an essential role of Tsg101 on ESCRT-I function. Remarkably, loss of Tsg101 induces severe liver

inflammation and organ damage leading to animal lethality 8 days after injection. This is associated with a vast elevation of aspartate aminotransferase (AST), alanine aminotransferase (ALT) and bile acid levels in the serum accompanied by a decrease in blood glucose concentrations, indicating severe liver pathologies. Also, the size of the gallbladder is increased in Tsg101KD mice with disrupted bile canaliculi structure, pointing towards impairment of bile acid homeostasis. Initiation of the inflammatory response is dependent on the endosomal accumulation of tumor necrosis factor receptor (TNFR), which leads to the activation of canonical and non-canonical transcription factor nuclear factor κ B (NF- κ B) signaling and the upregulation of downstream cytokines. Moreover, we observe a time-dependent decrease in mitochondrial function, characterized by mitochondrial uncoupling and enhanced proton leak, which manifests into activation of caspase-3 cleavage and induction of apoptosis. The activation of inflammation upon Tsg101 KD is in line with data from NASH patients, where *TSG101* expression is decreased and negatively correlated with interleukin 6 (*IL6*) and 1 beta (*IL1b*) levels, highlighting a potential regulatory function of Tsg101 in liver inflammation.

Conclusion: Altogether, liver-specific Tsg101KD causes a time dependent activation of inflammation and apoptosis, accumulating into hepatocyte death, organ failure and ultimately a lethal phenotype. Our finding suggests a regulatory role of Tsg101 in TNFR signaling and degradation, where Tsg101 protects against liver inflammation.

FRI468

B cell reactivation in autoimmune hepatitis after immunosuppression withdrawal

Elena Perpinan¹, George Koutsoudakis², Laura Patricia Llovet³, Thais Leonel³, Mar Riveiro Barciela⁴, Montserrat García-Retortillo⁵, Mercè Roget⁶, Alberto Sanchez-Fueyo⁷, Maria Carlota Londoño³.
¹King's College Hospital, London, United Kingdom; ²Hospital Clínic Barcelona; ³Hospital Clínic Barcelona, Liver Unit, Barcelona, Spain; ⁴Hospital Vall d'Hebron, Liver Unit, Barcelona, Spain; ⁵Hospital del Mar, Barcelona, Spain; ⁶Consorci Sanitari de Terrassa, Terrassa, Spain; ⁷King's College Hospital, London, United Kingdom
Email: mlondono@clinic.cat

Background and aims: Long-term immunosuppression therapies increase the risk of treatment-related side effects and subsequent reduce quality of life in autoimmune hepatitis (AIH) patients. The optimal strategy for immunosuppression withdrawal (ISW) is still controversial as relapse rates vary between 25 and 100% despite previous sustained complete biochemical response. Moreover, the pathogenesis of AIH is uncertain and no studies have explored the effect of ISW on the immune response. Therefore, we aim to understand the B and T cell repertoire in AIH patients undergoing ISW.

Method: Thirty-seven patients with type 1 AIH, complete biochemical response on first-line treatment for at least 3 years and histological activity index <3 were prospectively included. Detailed characterization of peripheral B and T cell responses was performed through high-dimensional spectral flow cytometry and unsupervised clustering before and after ISW (median time of 9 months).

Results: Fifty-one percent of patients were female ($n=19$) with a median age of 60 years (22–80), and a median time on remission of 4 years (3–11). Most of the patients were on monotherapy with azathioprine at the time of ISW ($n=27$, 74%). After a median follow-up of 31 months (12–34), 21 (57%) patients remained in remission and 16 (43%) patients required reinstitution of therapy (6 of them were still on low-dose immunosuppression when presented the flare). Before ISW, patients who reached remission displayed elevated frequencies of immature transitional 2 marginal zone precursor cells

and early plasmablasts relative to patients who presented a flare ($p=0.02$ and $p=0.03$, respectively). However, both B cell populations together with the transitional T1, T2 and T3 subsets increased in all patients regardless of the outcome of ISW, and positively correlated with serum transaminases and IgG levels after discontinuation of treatment ($p<0.01$). Of note, the expansion of B cell precursors was accompanied by a decrease in the frequency of switched resting memory cells ($p<0.01$). In contrast, no differences were observed in the T cell compartment before or after ISW.

Conclusion: In AIH patients, ISW results in a state of immune activation orchestrated by B cells with no detectable changes in the T cell compartment, regardless of the clinical outcome. This suggests that clinical remission does not entail the restoration of immune tolerance to liver antigens and provides an explanation for late relapses observed after ISW.

FRI469

Serum sterols indicate modified cholesterol homeostasis in cirrhotic patients with PBC and correlate with response to treatment with ursodeoxycholic acid

Wiktor Smyk¹, Beata Kruk², Tadeja Rezen³, Miha Moskon⁴, Ewa Wunsch⁵, Dieter Lütjohann⁶, Frank Lammert⁷, Piotr Milkiewicz^{5,8}, Marcin Krawczyk^{2,9}.
¹Medical University of Gdansk, Department of Gastroenterology and Hepatology, Gdańsk, Poland; ²Medical University of Warsaw, Laboratory of Metabolic Liver Diseases, Department of General, Transplant and Liver Surgery, Centre for Preclinical Research, Warsaw, Poland; ³University of Ljubljana, Centre for Functional Genomics and Bio-Chips, Institute for Biochemistry and Molecular Genetics, Faculty of Medicine, Ljubljana, Slovenia; ⁴University of Ljubljana, Faculty of Computer and Information Science, Ljubljana, Slovenia; ⁵Pomeranian Medical University in Szczecin, Translational Medicine Group, Szczecin, Poland; ⁶University Hospital Bonn, Institute of Clinical Chemistry and Clinical Pharmacology, Bonn, Germany; ⁷Hannover Medical School (MHH), Health Sciences, Hannover, Germany; ⁸Medical University of Warsaw, Liver and Internal Medicine Unit, Department of General, Transplant and Liver Surgery, Warsaw, Poland; ⁹Saarland University, Department of Medicine II, Saarland University Medical Center, Homburg, Germany
Email: marcin.krawczyk@uks.eu

Background and aims: Primary biliary cholangitis (PBC) is a chronic autoimmune cholestatic liver disease of unknown aetiology. Ursodeoxycholic acid (UDCA) is the first-line therapy in PBC however, some patients present insufficient biochemical response to UDCA, indicating worse disease course and survival. Cholesterol is involved in diverse biological activities and derives from de novo synthesis or intestinal absorption. Here, we aim to investigate and correlate serum sterol profiles and PBC phenotypes.

Method: Overall, we included 129 patients with PBC (age 32–93 years, 119 women). A total of 44 individuals presented with cirrhosis at diagnosis, and 13 were transplanted due to PBC before inclusion. Biochemical response to UDCA was assessed according to Barcelona criteria. Follow-up data (range: 1–13 years) were available in 62 (48%) patients. Serum sterol levels were measured by gas chromatography/mass spectrometry (GC/MS) at inclusion. Machine learning (ML) algorithms were used to determine a model that can predict UDCA response.

Results: Cirrhotic patients with PBC demonstrated significantly higher sitosterol ($p=0.0001$), campesterol ($p=0.0042$) and cholesterol ($p<0.0001$) serum concentrations as compared to non-cirrhotic individuals. Patients with cirrhosis showed increased phytosterols:cholesterol but decreased lathosterol:cholesterol ratios (all $p<0.0001$). Desmosterol:cholesterol ratio did not differ between patients with or without cirrhosis. Individuals after transplantation displayed increased serum concentrations of 7 α -hydroxycholesterol

POSTER PRESENTATIONS

compared with non-transplanted patients, which might indicate increased radical oxidation. The ML Support Vector Classifier model including 24-hydroxycholesterol, 27-hydroxycholesterol, campesterol, cholesterol, desmosterol, lanosterol and stigmasterol, revealed high accuracy, precision and sensitivity (all >80%) in predicting non-response to UDCA treatment. In contrast, none of the used sterol models was not able to accurately forecast the deterioration of LFTs during follow-up.

Conclusion: PBC patients with cirrhosis are characterized by decreased cholesterol synthesis and increased sterol absorption as compared to individuals without cirrhosis. Serum levels of algorithmically selected sterols correlate with biochemical non-response to therapy with UDCA in PBC.

FRI470

Preserved MAIT cell proinflammatory function in children with autoimmune liver disease

Suzan Warner¹, Deirdre Kelly², David Wraith¹, Ye Htun Oo³.

¹University of Birmingham, Institute of Immunology and Immunotherapy, Birmingham, United Kingdom; ²Birmingham Children's Hospital, The Liver Unit, Birmingham, United Kingdom; ³University of Birmingham, Centre for Liver and Gastrointestinal Research, Birmingham, United Kingdom

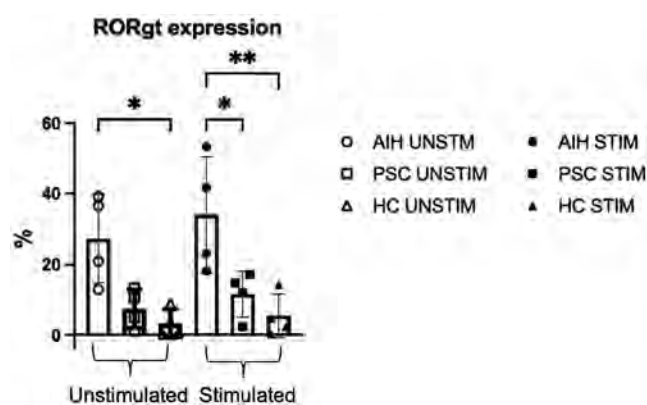
Email: S.Warner@bham.ac.uk

Background and aims: Mucosal-associated invariant T (MAIT) cells are significant players in autoimmune liver disease (AILD), a spectrum of conditions which often starts in childhood. Biological characterisation of MAIT cells and their functional activity in children with AILD has seldom been investigated. We aim to 1) characterise the deep immunophenotype of paediatric MAIT cells in AILD compared to healthy controls and 2) assess their cytokine capabilities.

Method: We performed mass cytometry (CyTOF; Cytometry by time of flight) analysis of peripheral blood mononuclear cells (PBMC) from paediatric patients with AILD (AIH Type 1, N = 4, median age 14 yrs (range 9–14), and PSC, N = 4, median age 14 yrs (range 12–14)) and from healthy children (HC) (N = 4, median age 8.5 years (range 5–14)). These PBMC samples were treated with a cell stimulation cocktail containing phorbol 12-myristate 13-acetate (PMA) and ionomycin and incubated for 4 hours prior to downstream investigation by mass cytometry with a custom MAIT cell CyTOF panel designed by the investigators. Results were compared to controls (unstimulated matched PBMCs from the same patients). Cytobank and GraphPad Prism 9 were used for data analysis.

Results: Compared to the cohort of healthy children, peripheral blood MAIT cells from children with AILD had increased expression of retinoic acid related orphan receptor gamma t (RORγt), a transcription factor of T helper 17 (Th17) cells, and the proinflammatory cytokine interleukin 17A (IL-17A). This was observed at baseline ($p = 0.002$) and post stimulation ($p = 0.001$).

Higher expression of RORγt was observed in AIH Type 1 patients compared to healthy children ($p = 0.005$) Figure 1. There was also a significant difference between AIH Type 1 and PSC IL-17A activity post stimulation ($p = 0.034$). Post-stimulation IL-17A expression was highest in the PSC cohort compared to their unstimulated counterparts ($p = 0.003$). In addition, TNFα, IFNγ and GM-CSF cytokine production were preserved in the children with AILD (AIH Type 1 and PSC), with levels comparable to those in the healthy cohort. This finding was most pronounced in TNFα production ($p = 0.0042$) which differs from peripheral blood MAIT cells in adults with AILD where there is decreased cytokine production.



Conclusion: Peripheral blood MAIT cell cytokine profile in children with AIH Type 1 and PSC are similar to MAIT cells from healthy children. Furthermore, MAIT cells from children with AIH Type 1 and PSC have greater RORγt expression and IL-17A activity at rest and post stimulation, suggesting that MAIT cells with a Th17-like phenotype may play a role in disease pathogenesis.

Cirrhosis and its complications: Portal Hypertension

FRI485

TIPS insertion leads to partial reversal of systemic inflammation in patients with decompensated liver cirrhosis

Lena Stockhoff¹, Anja Tiede¹, Zhaoli Liu², Hannah Schneider³, Valerie Ohlendorf³, Jan Hinrichs⁴, Jennifer Witt³, Denise Menti³, Heiner Wedemeyer³, Bernhard Meyer⁴, Markus Cornberg^{2,3}, Cheng-Jian Xu², Christine Falk⁵, Benjamin Maasoumy^{1,2}. ¹Hannover Medical School, Gastroenterology, Hepatology and Endocrinology, Hannover, Germany; ²Centre for Individualised Infection Medicine (CIIM), Hannover, Germany; ³Hannover Medical School, Gastroenterology, Hepatology and Endocrinology, Hannover, Germany; ⁴Hannover Medical School, Diagnostic and Interventional Radiology, Hannover, Germany; ⁵Hannover Medical School, Institute of Transplant Immunology, Hannover, Germany
Email: maasoumy.benjamin@mh-hannover.de

Background and aims: Patients with decompensated liver cirrhosis are characterized by a state of systemic inflammation (SI), which is closely linked to several complications e.g. sarcopenia. Portal hypertension is widely considered to play a central role in this process. Transjugular intrahepatic portosystemic shunt (TIPS) is an effective treatment option for portal hypertension. The aim of this study was to investigate the impact of TIPS insertion on SI in patients with liver cirrhosis.

Method: In this cross-sectional study a number of 177 consecutive cirrhotic patients receiving a TIPS at Hannover Medical School were included. C-reactive protein (CRP) and white blood cells (WBC) were compared between baseline and 6/12, 24 and 36 months after TIPS insertion. In a subset of 59 patients we were able to perform more detailed analysis on the inflammation status measuring 48 different cytokines. The respective plasma samples were prospectively collected from the cubital vein at baseline as well as 1, 3 and 6 months after TIPS insertion. Blood samples from 5 healthy individuals served as control. Changes of cytokine levels were correlated with the physical status as indicated by body mass index (BMI), hand grip strength (HGS) and mid-arm muscle circumference (MAMC).

Results: Median age of the patients was 56 years and median MELD was 12. Most frequent TIPS indication was refractory ascites (RA)

(76%). Median CRP and WBC were 9.2 mg/L and $5 \times 10^3/\mu\text{L}$, respectively. CRP levels but not WBC significantly decreased after TIPS ($p < 0.001$). Of note, decrease in CRP levels was significantly associated with a better survival ($p = 0.012$). As expected, cytokine levels were significantly higher in the cirrhotic patients as compared to healthy controls affecting 30 of 48 measured cytokines (FDR < 0.05). Pattern of SI did not differ between patients with RA and variceal bleeding except from IL-6, which was significantly higher in patients with RA ($p < 0.001$). One month after TIPS most cytokines were still measured at levels comparable to baseline and some, e.g. IL-2, were even increased. However, during further follow-up we documented a continuous decrease in the majority of cytokines. For 25 cytokines, including IL-6 and IL-2, levels were significantly lower at month 6 compared to the time of TIPS insertion (FDR < 0.05 ; figure). Moreover, 7 of the 30 cytokines (including IL-2), which were elevated prior to TIPS, did not show any statistical difference anymore compared to healthy controls. When correlating cytokine changes with the clinical status, IL-6 appeared to be of particular interest: Decrease in IL-6 was associated with a significant improvement in MAMC and numerical increase in HGS and BMI.

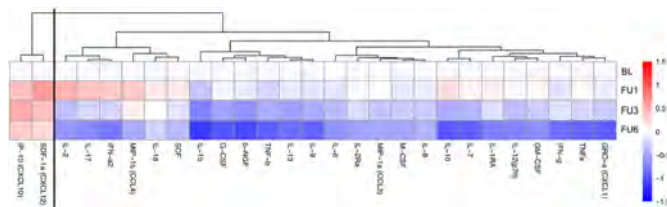


Figure: Decrease in SI after TIPS.

Conclusion: Decreasing portal hypertension via TIPS insertion leads to a significant improvement of SI over time, which is associated with a favorable clinical outcome.

FRI486

RWE evaluating patients with cirrhosis and features of portal hypertension reveals significant comorbidities

Philip Ambery¹, Peter Greasley², Daniel Pettersen², Nerissa Lee³, Steven Kiddle⁴, Phillip Hunt⁵, Victoria Parker⁶. ¹Astrazeneca, Late CVRM clinical research, Gothenburg, Sweden; ²Astrazeneca, Early CVRM, Gothenburg, Sweden; ³University of Bristol, United Kingdom; ⁴Astrazeneca, Health Data Science, Cambridge, United Kingdom; ⁵Astrazeneca, Epidemiology, Washington, United States; ⁶Astrazeneca, Early CVRM, United Kingdom
Email: phil.ambery@astrazeneca.com

Background and aims: Development of portal hypertension is associated with high risk of variceal haemorrhage, ascites, encephalopathy and death. In over 100, 000 individuals identified with portal hypertension we identify significant comorbidities that should be addressed to improve outcomes in this vulnerable population.

Method: Individuals with features of portal hypertension were identified using the TriNetX federated health records. Three groups of patients were identified, Group 1 with confirmed variceal haemorrhage (19, 454 in total, of which 12, 968 were incident), Group 2 with varices but no haemorrhage (43, 583 in total, of which 30, 083 were incident), and Group 3 with portal hypertension but no diagnosed varices (48, 496 in total, of which 31, 611 were incident). Significant comorbidities were identified across all 3 groups.

Results: Higher rates of ischaemic heart disease (IHD), heart failure and chronic kidney disease (CKD) were found in Group 3 versus the other two groups:

	CKD (%)	Heart failure (%)	Ischaemic heart disease (%)
Incident group 1	9.0	8.5	14.5
Incident group 2	11.3	10.2	16.2
Incident group 3	16.3	16.1	19.8

Conclusion: In the absence of variceal haemorrhage portal hypertension is under recognised. Comorbidities affecting patients in group 3 reported at higher levels than in groups 1 and 2 include CKD, IHD and heart failure. In patients with portal hypertension it's important to address comorbidities in addition to the underlying liver disease.

FRI487

Durability of immune response to SARS-CoV-2 vaccination in patients with liver cirrhosis (LC) as compared to healthcare workers (HW)

Alessandra Mangia¹, Valeria Piazzolla¹, Maria Squillante¹, Giovanna Cocomazzi¹, Vito Ciciriello¹, Vincenzo Giambra², Nicola Serra³. ¹Liver Unit, IRCCS "Casa Sollievo della Sofferenza", San Giovanni Rotondo, Italy; ²ISBREM, IRCCS "Casa Sollievo della Sofferenza", San Giovanni Rotondo, Italy; ³University "Federico II", Public Health, Napoli
Email: a.mangia@tin.it

Background and aims: Patients with advanced liver disease have well recognized deficiencies in innate and humoral immunity. Phase 3 trials on both BNT162b2 and mRNA-1273 included an extremely limited number of pts with liver diseases. Real life data on vaccine response in cirrhotics are lacking. To characterize the longitudinal anti-SARS-CoV-2 response in LC as compared to an age and gender matched HW population.

Method: In pts with established diagnosis of LC \pm portal hypertension, levels of binding antibodies at baseline before the first BNT162b2 dose, 7 and 31 days after the first dose and 90 and 180 days after the second dose were evaluated and compared to HW levels at similar time-points. Semiquantitative serological testing for IgG antibodies anti S1 domain was performed by anti-SARS-CoV-2 QuantiVac ELISA (EUROIMMUN); cut-off for positivity = 32.5 BAU/ml. Swab test was performed in suspected cases by RT-PCR kit (ROCHE Diagnostics). Micro neutralization test using wild type virus is ongoing. LC pts were matched 3:1 with HW. Both pts and HW had received BNT162b2 vaccine.

Results: Among 207 LC pts identified so far, 178 have results currently available at the different time-points. After a careful analysis of the swab tests results, 28 pts COVID experienced were identified. Of 150 SARS-CoV-2 naive, 86 (58%) were male, mean age 65.4 ± 4 . Pts with HCV etiology were 67%, pts with portal hypertension 29%. Geometric Mean of anti-SARS-CoV-2 antibody levels overall and by gender among LC pts and HW in the Table. Higher levels of anti-SARS-CoV-2 were observed in HW as compared LC at d7 ($p = 0.007$) and d31 ($p = 0.063$), as well as at d90 ($p = 0.0049$) and d180 ($p = 0.039$). At d180, the number of pts with results lower than the assay's threshold was higher among LC than in HW (5 vs 0, $P = 0.0028$). Irrespective of age, female pts were more likely to have higher anti-SARS-CoV-2 levels as compared to male at late time points.

	HW (n = 50)				LC (n = 150)			
Timepoints	d7	d31	d90*	d180*	d7	d31	d90*	d180*
Total	9.78 (5.94-16.10)	680.66 (532.45-870.13)	305.97 (240.7-388.94)	153.59 (127.15-185.53)	4.04 (2.82-5.79)	442.1 (320.72-609.49)	192.31 (128.43-287.96)	83.1 (38.32-180.19)
Male (54%)	11.92@ (6.24-28.8)	638.78 (477.35-854.81)	246.81 (181.1-336.33)	164.46 (124.09-217.96)	4.33 (2.68-6.99)	470.62 (306.63-722.32)	216.30 (127.23-367.71)	125.94 (32.24-463.2)
Females (46%)	7.89 (3.51-17.71)	732.23 (473.05-1133.42)	389.01* (268.48-563.66)	143.01 (109.15-187.37)	3.68 (2.10-6.43)	409.89 (246.83-682.03)	173.62 (92.07-327.29)	63.61 (21.74-186.13)

*after the second dose; * P = 0.028; @P = 0.024

POSTER PRESENTATIONS

Conclusion: Pts with LC showed an initial response to SARS-CoV-2 vaccination weaker than that of HW. An earlier antibody decline was also observed. The number of pts with absent anti-SARS-CoV-2 after 180 days was higher than in HW. This ongoing study highlights the need of a possibly more intensive vaccination schedule in LC as compared to HW.

FRI488

A simple model for predicting survival in cirrhotic patients undergoing portosystemic shunt embolization

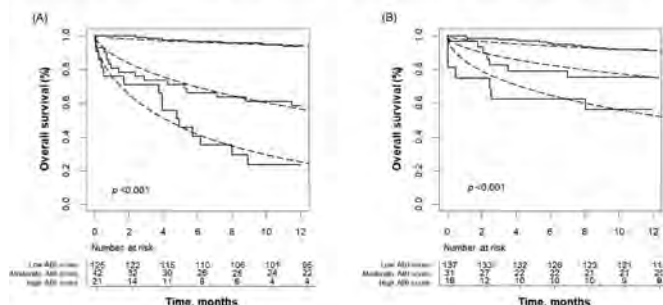
Won-Mook Choi¹, Seungbong Han², Young Seok Kim³, Dong Hyun Sinn⁴, Dong Il Kwon⁵, Young-Suk Lim¹. ¹Asan Medical Center, University of Ulsan College of Medicine, Department of Gastroenterology, Seoul, Korea, Rep. of South; ²Korea University College of Medicine, Department of Biostatistics, Seoul, Korea, Rep. of South; ³Soonchunhyang University Bucheon Hospital, Division of Gastroenterology and Hepatology, Bucheon, Korea, Rep. of South; ⁴Samsung Medical Center, Department of Medicine, Seoul, Korea, Rep. of South; ⁵Asan Medical Center, University of Ulsan College of Medicine, Department of Radiology, Seoul, Korea, Rep. of South
Email: limys@amc.seoul.kr

Background and aims: Portosystemic shunt embolization (PSSE) is an effective treatment for hepatic encephalopathy and gastric varix in patients with portosystemic shunt. However, some of the patients rapidly progress to hepatorenal syndrome and hepatic failure after PSSE. The aim of this study was to develop a prognostic model for predicting survival in patients treated with PSSE.

Method: We included 188 patients with portosystemic shunt who received PSSE for gastric varix or recurrent hepatic encephalopathy to develop a prediction model for 1-year mortality using a Cox proportional-hazard model incorporating significant prognostic factors, which was validated in a separate cohort of 184 patients.

Results: Using multivariable analysis, baseline serum levels of total bilirubin, albumin, and international normalized ratio (INR) were the independent prognostic factors that were significantly associated with the 1-year survival of the patients. An Albumin-Bilirubin-INR (ABI) score was developed assigning 1 point for ≥ 1.5 mg/dL of total bilirubin, <3.0 g/dL of albumin, and ≥ 1.5 for INR, respectively. Time-dependent area under the curve of the ABI score for predicting 6-month and 1-year survival were 0.851 (95% confidence interval [CI], 0.778–0.923) and 0.857 (95% CI, 0.793–0.921) in the development cohort and 0.777 (95% CI, 0.664–0.829) and 0.727 (95% CI, 0.624–0.829) in the validation cohort, which was comparable to the MELD score and the Child-Pugh score, indicating excellent discrimination performance. The ABI score showed a better calibration performance than other scores, especially in patients at high-risk.

Fig. Overall survival in the development cohort (A) and validation cohort (B), according to three risk groups: high (ABI score 3), moderate (ABI score 2), and low (ABI score 0 or 1). Solid lines indicate Kaplan-Meier estimates of overall survival. Dashed lines indicate estimated overall survival according to the Cox proportional hazard model. ABI, Albumin-Bilirubin-INR.



Conclusion: The novel ABI score, which is easier to calculate than MELD or Child-Pugh scores, may help identify a proper indication for PSSE in cirrhotic patients with portosystemic shunt.

FRI489

Blunted cardiovascular effects of beta-blockers in patients with cirrhosis: relation to severity?

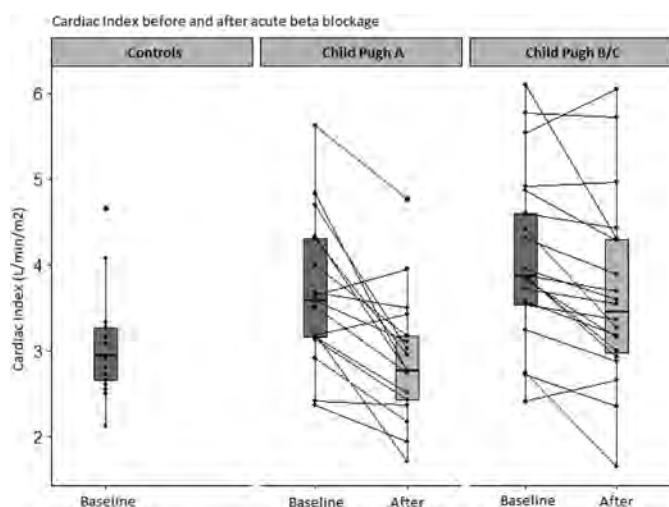
Puria Nabilou¹, Karen Danielsen¹, Nina Kimer², Jens Hove^{3,4}, Flemming Bendtsen^{1,4}, Søren Møller^{4,5}. ¹Hvidovre Hospital, Gastro Unit, Medical Division, Hvidovre, Denmark; ²University of Copenhagen, Bridge Translational Excellence Program, Novo Nordisk Center for Basic Metabolic Research; ³Hvidovre Hospital, Department of Cardiology, Hvidovre, Denmark; ⁴Hvidovre Hospital, Department of Clinical Medicine, Hvidovre, Denmark; ⁵Hvidovre Hospital, Department of Clinical Physiology and Nuclear Medicine, Center for Functional and Diagnostic Imaging and Research, Hvidovre, Denmark
Email: purianabilou@hotmail.com

Background and aims: Patients with cirrhosis and portal hypertension are at high risk of developing complications such as variceal hemorrhage, ascites, and cardiac dysfunction known as cirrhotic cardiomyopathy. Since non-selective betablockers may aggravate hemodynamic complications we investigated the effect of real-time propranolol infusion on cardiac function in patients with varying degrees of cirrhosis.

Method: Thirty-eight patients with Child-Pugh A (n = 17), B (n = 17) and C (n = 4) had liver vein catheterization and cardiac magnetic resonance imaging performed. We assessed the effect of real-time propranolol infusion on the hepatic venous pressure gradient, cardiac index, stroke volume, ejection fraction, heart rate, and contractility. 19 patients were classified responders to beta-blocker therapy.

Results: When pooling Child-Pugh B & C patients, the decrease in cardiac index by beta-blockade was blunted, compared to Child-Pugh A patients (−8.5% vs. −20.5%, p = 0.043).

The effect of NSBB on portal pressure was inversely correlated to the changes on left atrium since the left atrial volume changed by 4 ml ± 18 in the responders compared to 15 ml ± 11 in the non-responders (p = 0.03). Finally, baseline ejection fraction correlated inversely with the decrease in portal pressure r = −0.39, p = 0.02.



Conclusion: We found a blunted effect of beta-blockade on cardiac index in patients with advanced cirrhosis compared to patients with early cirrhosis indicating impaired compensatory cardiac reserve and underlying cirrhotic cardiomyopathy with disease progression. The differential effects of beta-blockade on the left atrium may predict the beta-blocker response on portal pressure but further studies are warranted on this matter.

FRI490

Gender affects the association between serum creatinine levels and clinical response to terlipressin in patients with hepatorenal syndrome type of acute kidney injury

R. Todd Frederick¹, Chris Pappas², Khurram Jamil³. ¹California Pacific Medical Center, Department of Transplant, San Francisco, United States; ²Orphan Therapeutics, LLC, Longboat Key; ³Mallinckrodt Pharmaceuticals, Hampton, United States
Email: fredertz@sutterhealth.org

Background and aims: Hepatorenal syndrome (HRS)-acute kidney injury (AKI) is a rare and serious complication of cirrhosis, with serum creatinine (SCr) used diagnostically. Women generally have less muscle mass and consequently lower SCr levels than men with similar renal function. Terlipressin more effectively reverses HRS when started at lower SCr levels. The largest randomized, prospective database of placebo-controlled studies in patients (pts) with HRS-AKI was examined to assess a gender-based impact on treatment response.

Method: Pooled data from 3 phase III US studies (OT-0401, REVERSE, CONFIRM) were used; pts with HRS-AKI were treated with terlipressin plus albumin (terli) or placebo plus albumin (pbo). Associations between baseline (BL) SCr (SCr upon treatment initiation) and clinical response (complete response [CR]: HRS reversal, SCr [1.5 or less] or partial response [PR]: at least 30% improvement in SCr) stratified by treatment and gender were assessed. Overall response rate (ORR) comprised pts with a CR or PR; p values were calculated using a Fisher's exact test.

Results: Males in the terli group with BL SCr <3 had significant improvements in CR and ORR, relative to pbo, while females did not (Figure). Among pts with a BL SCr of 3–5, both males and females had a significant improvement in ORR (terli vs pbo); however, only males had significant improvements in CR. Across genders, pts with a BL SCr >5 demonstrated limited response to treatment.

Parameter, n (%)	BL SCr <3			BL SCr 3–5			BL SCr >5		
	Terli	Pbo	p value	Terli	Pbo	p value	Terli	Pbo	p value
Male	74	47		112	96		27	22	
HRS	36 (48.6)	13 (27.7)	0.024	35 (31.3)	11 (11.5)	<0.001	2 (7.4)	1 (4.5)	1.000
Reversal									
ORR	42 (56.8)	15 (31.9)	0.009	54 (48.2)	24 (25.0)	<0.001	5 (18.5)	3 (13.6)	0.715
Female	52	37		71	46		16	8	
HRS	26 (50.0)	12 (32.4)	0.129	16 (22.5)	5 (10.9)	0.141	2 (12.5)	0	
Reversal									
ORR	27 (51.9)	13 (35.1)	0.135	24 (33.8)	6 (13.0)	0.016	3 (18.8)	0	0.526

Conclusion: Pts in the terli group had a greater clinical response vs pbo for BL SCr of <5. Males were more likely to have a CR and ORR than females, especially those with BL SCr 3–5. Despite matched SCr, females had a lower response than males, likely reflecting more advanced renal dysfunction upon treatment initiation. New guidance recommending initiation of vasoconstrictor treatment based on SCr change from BL rather than absolute cut-offs may improve outcomes for female pts. Additional biomarkers to evaluate renal dysfunction should also be evaluated.

FRI491

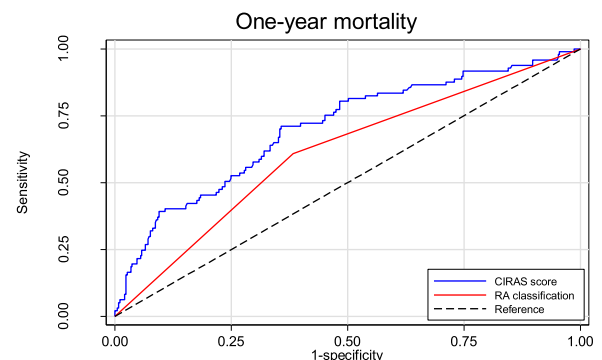
A novel cirrhotic ascites severity score predicts one-year mortality better than the classification into refractory or diuretic-responsive ascites

Rasmus Hvidbjerg Gantzel^{1,2}, Niels Kristian Aagaard¹, Hendrik Vilstrup^{1,2}, Hugh Watson^{1,3}, Peter Jepsen^{1,2}, Henning Grønbaek^{1,2}. ¹Aarhus University Hospital, Department of Hepatology and Gastroenterology, Århus N, Denmark; ²Aarhus University, Department of Clinical Medicine, Århus N, Denmark; ³Virology, Evotec ID, Lyon, France
Email: ragant@rm.dk

Background and aims: Ascites formation is a common manifestation of cirrhosis decompensation and heralds a poor prognosis. Refractory ascites (RA) denotes a worsened state of this condition, where pharmacotherapies are ineffective or induce significant side-effects. The current definition of RA remains largely unaltered through the past 25 years, and rests on a panel of diagnostic criteria including the introduction of intensive diuretic therapy and a modest salt-restrictive diet, and evaluations of renal sodium excretion, weight loss, ascites recurrence rate, and diuretic-induced complications. Further, the traditional binary RA classification may be too simplistic as a predictive measure. We aim to develop a prediction model that relies on easily obtainable ascites-related variables and predicts one-year mortality more accurately than the traditional RA classification. **Method:** We included 478 patients from the placebo-groups of trials for the treatment of cirrhotic ascites. The outcome was mortality hazard during one year of follow-up. Fractional polynomials were included to investigate the functional form of continuous variables. We used Cox regression with stepwise backward variable selection of ascites-related predictors of mortality. Candidate variables were: age, sex, serum sodium, ascites discomfort score, and a categorical variable based on ascites accumulation and diuretic treatment (ascites accumulation with no, moderate, and intensive diuretic treatment, and no ascites accumulation with any diuretic treatment). We compared the final model's discriminative ability (Harrell's C index) with that of the traditional RA classification.

Results: The final prediction model included age, serum sodium, and the categorical accumulation/diuretics variable. The CIRrhotic Ascites Severity (CIRAS) score was computed as $0.041 * (\text{age}-56) - 0.078 * (\text{serum sodium}-137)$ and then add 0.718 if ascites accumulation and no diuretics, or add 0.407 if ascites accumulation and intensive diuretic treatment, or subtract 0.270 if no ascites accumulation and any diuretic treatment.

The CIRAS score had a C index for one-year mortality of 0.70 (95% CI: 0.64–0.75) which was statistically significantly better than the traditional RA classification with a C index of 0.60 (95% CI: 0.55–0.65) ($p < 0.001$, Figure).



Conclusion: The novel CIRAS score combining age, serum sodium, diuretic treatment, and ascites accumulation has better discriminative ability than the traditional RA classification during a one-year follow-up. These findings warrant validation in external cohorts.

FRI492

A network meta-analysis of numbers needed to treat to prevent an episode of overt hepatic encephalopathy in patients with cirrhosis treated for at least 6 months with lactulose alone, or lactulose plus rifaximin-alpha

Juha Halonen¹, Roland Henrar¹, Eric Ngonga Kemadjou². ¹Norgine Ltd, Harefield, United Kingdom; ²JB Medical Ltd, Little Cornard, Sudbury, United Kingdom
Email: jhalonen@norgine.com

Background and aims: Overt hepatic encephalopathy (OHE) occurs in 30–40% of patients with cirrhosis during their clinical course.

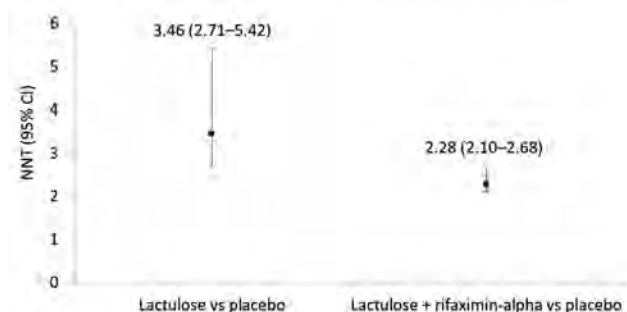
POSTER PRESENTATIONS

Frequent hospitalisations and high mortality make prevention of OHE essential. Current treatment options for OHE include nonabsorbable disaccharides (e.g. lactulose) and antibiotics (e.g. rifaximin-alpha 550 mg). We conducted a network meta-analysis (NMA) of data from a previously published literature review (Hudson M, Schuchmann M. *Eur J Gastroenterol Hepatol* 2019;31:434–50) to determine the comparative long-term efficacy, in terms of number needed to treat (NNT) to prevent an additional OHE episode, of lactulose versus placebo and lactulose + rifaximin-alpha versus placebo.

Method: Literature searches were previously conducted in PubMed of titles and abstracts only, with language restricted to English and the data range unrestricted up to the cut-off date (05 March 2018), using the following search terms: 'hepatic encephalopathy + rifaximin' and 'hepatic encephalopathy + lactulose'. Randomized controlled trials (RCTs) with long-term (≥ 6 months) effectiveness endpoints for lactulose and/or rifaximin-alpha were selected for NNT analysis if statistically significant between-group differences were reported in the rate of OHE recurrence. In this analysis, we conducted an indirect treatment comparison analysis using the odds ratio (OR) for OHE recurrence for NNT mapping. The NMA was conducted using the Mantel-Haenszel approach, with placebo used as the reference treatment and only the fixed effect analysis considered.

Results: A total of 570 articles, including 201 with primary clinical data, were identified. Long-term treatment was reported in 8 articles for lactulose alone and in 19 articles for rifaximin-alpha, alone or in combination with lactulose. NNTs were calculated from 4 studies. When the ORs for the relative efficacy of each treatment versus each of the remaining treatments were calculated, the ORs (95% confidence intervals) for lactulose versus placebo and lactulose + rifaximin-alpha versus placebo were 0.276 (0.164–0.466) and 0.081 (0.042–0.158), respectively. The resulting NNTs were lower for lactulose + rifaximin-alpha versus placebo (2.28) than for lactulose versus placebo (3.46; Figure).

NNT (95% CI) for prevention of one additional OHE episode following long-term (≥ 6 months) treatment with lactulose versus placebo and lactulose + rifaximin-alpha versus placebo. CI, confidence interval; NNT, number needed to treat; OHE, overt hepatic encephalopathy



Conclusion: This NMA based on NNTs demonstrated that, in comparison with placebo, lactulose + rifaximin-alpha may be more effective than lactulose alone in preventing OHE recurrence.

FRI493

Transjugular intrahepatic portosystemic shunt versus balloon-occluded transvenous obliteration for the management of ectopic varices

Ranya Selim¹, Jenna Yousif², Daniel Hillman³, Scott Schwartz³, Kylie Springer⁴, Dilip Moonka¹. ¹Henry Ford Hospital, Gastroenterology and Hepatology, United States; ²Wayne State University School of Medicine, United States; ³Henry Ford Hospital, Radiology, United States; ⁴Henry Ford Hospital, Biostatistics, United States
Email: ranyaselim@gmail.com

Background and aims: Bleeding ectopic or non-gastroesophageal varices occur uncommonly in the setting of portal hypertension. Both

transjugular intrahepatic portosystemic shunt (TIPS) and balloon-occluded antegrade or retrograde transvenous obliteration (BA-RTO) are potential treatment options. Our study is the first to assess and compare TIPS vs. BA-RTO for the management of ectopic varices.

Method: This is a retrospective cohort study at a tertiary liver center. All interventional radiology procedures performed for bleeding varices between 2006 and 2020 were identified. Only patients undergoing TIPS and BA-RTO for bleeding ectopic varices were included. Demographics, pre-procedural data and outcome data was collected and compared between BA-RTO and TIPS groups.

Results: Eleven patients undergoing BA-RTO were compared to seven patients undergoing TIPS. In 6 of the BA-RTO patients, TIPS was deemed unfeasible. Mean age at procedure was 55.6 ± 10.0 . 55.6% were men and 83.3% were white. There were 8 rectal varices, 7 peristomal, one duodenal, one cecal and one superior mesenteric. The mean MELD-Na prior to procedures was 20.8 ± 10.4 in the BA-RTO group vs. 19.0 ± 6.4 in the TIPS groups ($p = 0.69$). In the BA-RTO vs. TIPS groups, respectively, the mean MELD-Na at 30 days after procedure was 18.8 ± 9.9 vs 21.7 ± 5.5 ($p = 0.67$) and at 90 days after procedure was 18.0 ± 4.2 vs 24.0 ± 7.5 ($p = 0.39$). Rebleeding rates during admission were 9.1% for BA-RTO vs. 14.3% for TIPS ($p = 1.00$). The mean length of stay for BA-RTO vs. TIPS was 10.6 ± 8.9 vs. 7.9 ± 8.1 days ($p = 0.41$), mean paracenteses 90 days prior and after procedure were 1.9 ± 3.6 vs. 0.0 ± 0.0 ($p = 0.12$) and 2.0 ± 3.9 vs. 0.0 ± 0.0 ($p = 0.082$), in the BA-RTO vs TIPS groups, respectively. The rates of hepatic encephalopathy in the BA-RTO vs TIPS groups at 90 days before and after the procedure were 45.4% vs. 57.1% ($p = 1.00$) and 28.6% vs 33.3% ($p = 1.00$), respectively. The mortality rates were 27.3% vs 28.6% ($p = 1.00$) in the BA-RTO vs TIPS groups.

Conclusion: Our results demonstrate that both TIPS and BA-RTO are effective treatment modalities for bleeding ectopic varices, with comparable post-procedure outcomes. Patients undergoing BA-RTO had a higher MELD at procedure but lower MELD at 30 and 90 day post-procedure and less HE though no differences were significant. BA-RTO is an excellent option for bleeding ectopic varices, primarily rectal and peristomal, and especially in patients not candidates for TIPS.

FRI494

Identification of potential new serum biomarkers for clinically significant portal hypertension by proteomic profiling of circulating extracellular vesicles

Frane Pastrovic¹, Grgur Salai^{2,3}, Stela Hrkač², Ruder Novak², Lovorka Grgurević^{2,4}, Marko Žarak¹, Kristian Podrug⁵, Tajana Filipec Kanizaj⁶, Tomislav Bokun^{1,7}, Ivica Grgurević^{1,7,8}. ¹University Hospital Dubrava, Zagreb, Croatia; ²Center for Translational and Clinical Research, Department of Proteomics, School of Medicine, University of Zagreb; ³Teaching Institute of Emergency Medicine of the City of Zagreb; ⁴Department of Anatomy, "Drago Perovic", School of Medicine, University of Zagreb; ⁵University Hospital Centre Split, University of Split School of Medicine, Croatia; ⁶KB Merkur; ⁷University of Zagreb Faculty of Pharmacy and Biochemistry; ⁸School of Medicine, University of Zagreb, Zagreb
Email: ivicag72@gmail.com

Background and aims: Portal hypertension (PH) is a driving force for the progression of chronic liver disease. Complications from PH develop when hepatic venous pressure gradient (HVPG) exceeds 10 mmHg, defining the presence of clinically significant portal hypertension (CSPH). However, measuring HVPG is invasive method, with limited availability. Thus, reliable non-invasive tools would be welcome alternative. Circulating extracellular vesicles (ECV) originating from the cells are valuable source of information pertaining the ongoing pathophysiological process including the molecules which might serve as the biomarkers. In this study we aimed to identify potential new serum biomarkers for CSPH in patients with compensated advanced chronic liver disease (cACLD) by proteomic profiling of serum ECV.

Method: Severity of PH was assessed by HVPG measurement that served as the reference standard. Serum samples were pooled based on HVPG measurement in two groups: with and without CSPH. ECV were isolated from the serum pools using ultracentrifugation and vesicle membranes were lysed by sonication. ECV protein cargo was analyzed by Liquid Chromatography-Mass spectrometry (LC-MS). Samples were analyzed in triplicates and proteins identified with at least one peptide were considered relevant for analysis. Functional enrichment analysis of the isolated proteins was conducted using FunRich 3.1.3 analysis tool.

Results: A total of 48 patients were included (30 in the CSPH group and 18 in the non-CSPH group, 75% males; median age: 59, 9 ± 9, 8 years; majority with alcoholic (48%) and non-alcoholic fatty liver disease (23%). LC-MS analysis of ECV content resulted in identification of 733 proteins (38 distinctive for CSPH, and 75 for non-CSPH group), that were further classified based on their cellular origin and function. Proteins involved in platelet degranulation, integrin-mediated signaling pathway, receptor mediated endocytosis and regulation of cholesterol efflux were more represented, whereas those involved in opsonization, phagocytosis, complement activation, immune and inflammatory response were less represented in the CSPH group. Among the individual proteins that showed the most significant difference between the studied groups phospholipid transfer protein and beta-2-glycoprotein 1 were more represented, whereas complement C1q, C1r and C1s subcomponents and annexin A2 were less represented in the CSPH group.

Conclusion: Results of this study provide additional insights into pathophysiological processes taking place along the development of PH in patients with cACLD. Distinctive protein profiles are identified between the patients with respect to the presence of CSPH. Several individual proteins are identified that should be further studied as the potential non-invasive biomarkers of CSPH.

FRI495

Factors influencing survival in cirrhotic patients with hepatic hydrothorax

Sarah Romero¹, Andy Lim², Gurpreet Singh³, Chamani Kodikara¹, Rachel Shingaki-Wells¹, Lynna Chen³, Samuel Hui¹, Marcus Robertson^{1,2}. ¹Monash Health-Clayton Hospital Main Entrance, Gastroenterology, Clayton, Australia; ²Monash University Clayton Campus; ³Department of Medicine, School of Clinical Sciences, Clayton, Australia; ⁴Austin Hospital, Gastroenterology & Liver Transplantation, Heidelberg, Australia
Email: s.romero.md@gmail.com

Background and aims: Hepatic hydrothorax (HH) remains a challenging complication of cirrhosis with limited treatment options. We sought to identify factors associated with mortality in hospitalised patients with confirmed HH treated with current standards-of-care.

Method: We performed a retrospective multi-center cohort study of cirrhotic patients with HH admitted to 3 tertiary hospitals (2010–2018). HH was defined as pleural effusion in the absence of cardiopulmonary disease. The primary outcomes were overall and transplant-free survival at 12-months after the index admission. Cox proportional hazards analysis was used to determine factors associated with the primary outcomes.

Results: 84 patients were included. Mean age 58.3 ± 11.5 years and 54.8% were male. The median Model for End-stage Liver Disease (MELD) score was 29 (IQR 25–33). Management of patients aligned with AASLD guidelines. Diuretics alone achieved resolution of HH in only 12% patients. At least 1 thoracentesis was performed in 73.8% patients, of which 15% were complicated by pneumothorax. Within 12-months of the index admission, 33% patients received liver transplantation (LT) and 11.9% had transjugular intrahepatic portosystemic shunt (TIPS) insertion, none of whom subsequently required LT. At least 1 hospital readmission was required in 63 (75%) patients, most commonly due to recurrent hydrothorax (38%)

and decompensated cirrhosis (41%). Overall and transplant-free survival at 12-months were 68% and 41% respectively. The majority of deaths occurred early after the index admission, with a 45-day overall survival of 80%. The most common cause of deaths was complications of end-stage liver disease and multiorgan failure (75%). No deaths were recorded in patients receiving LT. In the multivariable analysis, increasing age (per 5-year increase, HR 1.3 (CI 1.1–1.7), p = 0.04), increasing MELD score (per 5 points, HR 1.5 (CI 1.1–1.7), p = 0.02), current smoking (HR 8.7 (CI 3.4–21.9), p < 0.01) and acute kidney injury (AKI) (HR 2.9 (CI 1.2–7.0), p = 0.01) were associated with a significantly increased risk of death. After bootstrapping and correcting for MELD score and age, a current smoker had 8.7 times the hazard of death of a non- or ex-smoker and AKI was associated with a 2.9-fold increase in the hazard of death (Figure).

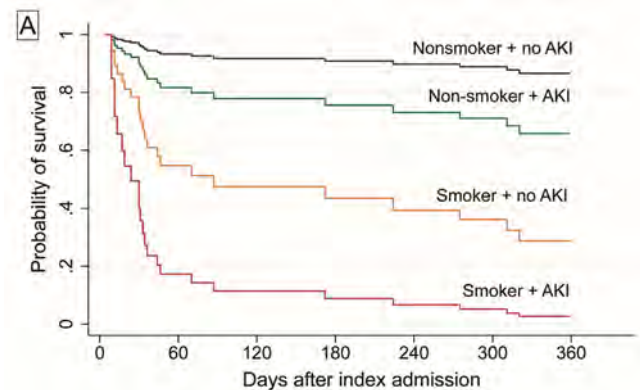


Figure: Multivariable Cox regression of overall patient survival showing survival estimates by smoking and AKI status (age and MELD scores held at mean values).

Conclusion: Cirrhotic patients with HH continue to have a poor 12-month survival despite current treatments and a high-risk of treatment-related complications. LT assessment should be considered in all cases. Current smoking and episodes of AKI are potential modifiable factors affecting survival.

FRI496

Hepatic venous pressure gradient (HVPG) measured at events is lower in non-alcoholic fatty liver disease (NAFLD) associated cirrhosis as compared to alcoholic cirrhosis

Lubomir Skladany¹, Daniela Jancekova¹, Michal Žilínčan², Stanislav Okapec², Janka Vnencakova¹, Svetlana Adamcova Selcanova¹, Michal Kukla³, Tomáš Koller⁴. ¹FD.Roosevelt Teaching Hospital, HEGITO (Div Hepatology, Gastroenterology and Liver Transplant) of the Dept Internal Medicine 2, Banská Bystrica, Slovakia; ²FD.Roosevelt Teaching Hospital, Radiology, Banská Bystrica, Slovakia; ³Faculty of Medicine, Jagiellonian University Medical College, Gastroenterology, Krakow, Poland; ⁴University Hospital of Bratislava, Faculty of Medicine Comenius University, Div Gastroenterology Hepatology of Dept Internal Medicine 5, Bratislava, Slovakia
Email: lubomir.skladany@gmail.com

Background and aims: In our region, alcohol-associated liver disease (ALD) and NAFLD are the most prevalent and the fastest-growing cirrhosis etiologies, respectively. We have recently demonstrated, that a natural history of cirrhosis differs in NAFLD as compared to ALD. HVPG is a strong surrogate of cirrhosis severity but its value in NAFLD is yet to be clarified.

We aimed to compare HVPG in NAFLD with ALD according to the indication (compensated and decompensated disease) with a particular focus on variceal bleeding (VB) and refractory ascites (RA). **Method:** In our hospital system, we have retrospectively identified patients who underwent HVPG measurement and scrutinized them

POSTER PRESENTATIONS

against our RH7 cirrhosis registry (NCT04767945). Then we retrieved patients' etiologies-ALD, NAFLD and other (viral [VIR], autoimmune [AI])-as well as indications for HVPG measurement-VB, RA (or hydrothorax), liver resection, differential diagnosis with transjugular liver biopsy, or implantation of TIPSS. We excluded patients with other etiologies, malignancies, and those with less than 6 months of follow-up.

Results: We enrolled 220 patients. Cirrhosis was due to NAFLD and ALD in 52 and 128 pts (VIR and AI in 26 and 14), respectively. Patients with NAFLD vs. ALD had similar age (60.4 vs. 56.9), a higher proportion of females 67.3 vs. 31.2, lower MELD scores (13.0 vs. 16.0), and a lower white blood cell count (4.9 vs. 6.15). Overall, the median HVPG in NAFLD and ALD (VIR and AI) was 14.0 and 18.0 (12.5 and 10.0) mmHg (P-value for trend <0.001), respectively. In 30 and 19 (17 and 8) compensated pts, HVPG was 11.5 and 10.0 (12.0 and 6.5) mmHg (p = 0.4). Among decompensated pts with VB, in 16 and 51 (7 and 5) the HVPG was 15.5 and 19.0 (13.0 and 18.0) mmHg, respectively (p = 0.02). In 6 and 31 (2 and 1) of pts with RA, the median HVPG was 16.5 and 19.0 (16.0 and 16.0) (p = 0.75). Transplant-free survival at 3 and 6 months did not differ between NAFLD and ALD (84.6 vs. 85.2, and 82.7 vs. 75.8%).

Conclusion: Overall, and in decompensated cirrhosis, the NAFLD etiology was associated with lower values of HVPG compared with ALD, likely reflecting a lower HVPG threshold for VB in NAFLD.

FRI497

Low subcutaneous adipose tissue is associated with mortality independently from portal hypertension in patients with cirrhosis

Xun Zhao¹, Balqis Alabdulkarim¹, Dana Kablawi¹, Marc Deschenes¹, Philip Wong¹, Tianyan Chen¹, Benjamin Rehany¹, Mohamed Abu-Nada¹, David Valenti¹, Ali Bessissow¹, Giada Sebastiani¹, Amine Benmassaoud¹. ¹McGill University Health Centre Glen Site (MUHC), Montréal, Canada
Email: amine.benmassaoud@mcgill.ca

Background and aims: Sarcopenia and adipopenia are associated with worse outcomes in patients with cirrhosis. To this date, it is unclear if muscle and adipose tissue mass predict mortality independently of portal hypertension. The aim of our study was to investigate whether body composition could predict mortality while adjusting for the severity of portal hypertension by using the gold standard, the Hepatic Venous Pressure Gradient (HVPG).

Method: This was a single center retrospective cohort study of adult patients with cirrhosis who underwent HVPG measurement between November 2012 and June 2020 and had available cross-sectional imaging at the 3rd lumbar vertebrae (L3). Participants were excluded if HVPG was not reliable or if imaging was performed more than 12 months before or 1 month after HVPG. Body composition was determined using CoreSlicer, a dedicated radiology software. Total psoas muscle index (PMI), total skeletal muscle index (SMI), subcutaneous and visceral adipose tissue indices (SATI, VATI) were calculated at L3 by measuring their respective areas and dividing by the height squared ((in cm²/m²). Factors associated with death were assessed using univariate and multivariate logistic regression.

Results: We included a total of 81 patients (mean age 60.2 years, 62% males, 31% with non-alcoholic fatty liver disease, 20% with alcohol-related liver disease and 17.3% with viral hepatitis, 52% with HVPG above 10 mmHg, 54% with decompensated cirrhosis at baseline, and median MELD 13). During follow-up, 27 (33.3%) patients died. Patients who died were older (64.6 yrs vs 58 yrs, p = 0.018), had higher HVPG (13.7 mmHg vs 9.2 mmHg, p = 0.004), lower muscle mass (PMI: 4.5 vs 5.6, p = 0.002; SMI: 41.3 vs 48.5, p = 0.002), lower SATI (45.6 vs 74.2, p = 0.002), and tended to have a higher MELD (15.3 vs 12.9, p = 0.067). Sex, BMI and VATI were not associated with mortality. On separate models for each compartment, after adjusting for age and HVPG, SATI (aOR = 0.98, 95%CI 0.96–0.99) was the only body compartment associated with mortality whereas PMI, SMI and

VATI did not. Similarly, when adjusting for age and MELD, SATI (aOR = 0.98, 95%CI 0.97–0.99) and SMI (aOR = 0.94, 95%CI 0.88–0.99) were associated with mortality, but not PMI or VATI.

Conclusion: We have shown that SATI is associated with mortality independently of HVPG. Future larger studies should review the strength of this association separately for males and females and propose cut-offs.

FRI498

Association of low mechano-energetic efficiency and prognosis in liver cirrhosis

Sannia Sjøstedt¹, Signe Wiese², Flemming Bendtsen^{3,4}, Søren Møller^{1,4}. ¹Hvidovre Hospital, Department of Clinical Physiology and Nuclear Medicine, Hvidovre, Denmark; ²Gastro Unit, Medical Division, Hvidovre; ³Hvidovre Hospital, Gastro Unit, Medical Division, Hvidovre; ⁴Copenhagen University, Department of Clinical Medicine, Faculty of Health Sciences, Copenhagen, Denmark
Email: sannia@dadlnet.dk

Background and aims: In cirrhosis, cardiac systolic dysfunction as part of cirrhotic cardiomyopathy (CCM) affects development of complications and course of the disease and prognosis. Myocardial mechano-energetic efficiency (MEE) is an estimate of left ventricular performance and reduced MEE is associated with poor prognosis in heart failure patients. In this study we aimed to investigate the relation of MEE to patient characteristics and its impact on survival in patients with cirrhosis.

Method: We included 283 patients with cirrhosis of different severity according to the Child-Pugh classifications (A/B/C: 106/87/90). All patients had a liver vein catheterization and a hemodynamic investigation performed including determination of cardiac output (CO), stroke volume, and heart rate (HR). These data were used to assess MEE, which was defined as (stroke volume/HR)*1.666.

Results: Eighty-nine percent of the patients had portal hypertension (Hepatic venous pressure gradient >5 mmHg) and 80% indications of a hyperdynamic circulatory state with increased CO and HR. There was no difference in MEE in Child-Pugh class C patients (2.03) vs Child-Pugh class A (1.98) and B (2.05) patients. In Child-Pugh class C patients, low MEE was associated with a poorer prognosis (median survival 886 days vs 2693 days).

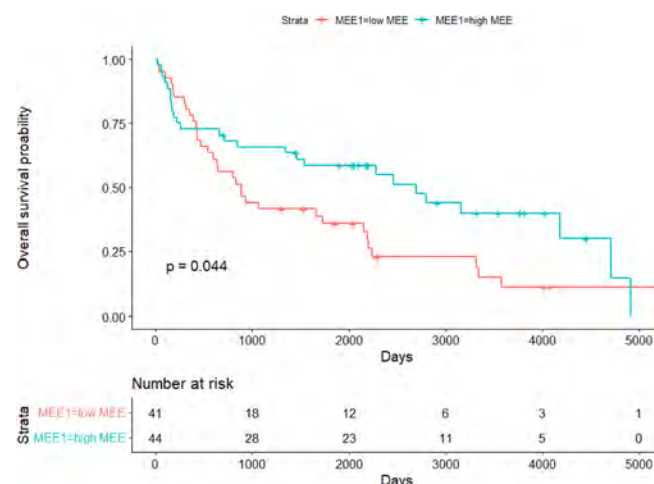


Figure: Kaplan-Meier plot showing differences in survival in liver cirrhosis patients classified as Child C stratified by MEE (low MEE below the median value and high MEE above the median value). A significantly poorer survival is seen in patients with low MEE.

Conclusion: In our study, MEE does not seem to be associated with severity of the liver disease, but in patients with advanced disease low MEE is associated with a poorer prognosis. The prognostic impact of MEE should be further investigated in future prospective studies.

FRI499

Long term albumin administration is associated with reduced healthcare resource use in patients with uncomplicated cirrhotic ascites: results from a simulation model

Kris Bennett^{1,2}, Elisabet Viayna³, Murat Gunal⁴, Duncan Stacey⁵, Anne Davis⁶, David Southern⁷, Matthew Cramp¹. ¹University Hospitals Plymouth NHS Trust, South West Liver Unit, Plymouth, United Kingdom; ²University Hospitals Plymouth NHS Trust, South West Liver Unit, Plymouth, United Kingdom; ³Grifols S.A., Sant Cugat del Vallès, Spain; ⁴Simarter, Istanbul, Turkey; ⁵Grifols UK, Cambridge, United Kingdom; ⁶Employed by Grifols SSNA, NC, United States; ⁷SSB Research Ltd., United Kingdom
Email: kbennett6@nhs.net

Background and aims: Decompensated cirrhosis is associated with high rates of complications and costs. The ANSWER trial showed that long-term human albumin infusions (LTA; 40 g twice/week for 2 weeks, 40 g/week thereafter) added to standard medical treatment (SMT) led to significant reduction of complications and mortality in patients with uncomplicated ascites. We developed a discrete event simulation (DES) model to estimate economic and clinical impacts of LTA in patients with cirrhosis and uncomplicated ascites in the UK. Real-world rates of hospital visits, treatments, and complications in the UK are used as model inputs. The potential benefit of LTA is modelled on data from the ANSWER trial.

Method: We developed a DES model using Simul8 Professional 2021 software to simulate individual patients' disease course by tracking health events (treatments, complications, hospitalizations, death) over time. We compared outputs for 2 patient cohorts: 1) SMT only, 2) SMT + LTA per ANSWER protocol. Model inputs for the SMT cohort were health event probabilities retrieved from Hospital Episode Statistics for 10 UK hospitals between Apr-2016 and Mar-2020. This real-world data gathered from 873 cirrhotic patients with uncomplicated ascites comprised 12-month rates for hospital visits, cirrhosis complications, treatments, and death. These were transformed into costs using NHS tariffs. Reduction in health event probabilities for the SMT + LTA cohort was based on ANSWER trial data.

Results: A hypothetical cohort of 100 patients with cirrhosis and uncomplicated ascites was simulated over 12 months, first with all patients treated with SMT, and then with 30% of patients treated with SMT + LTA; 30% was felt to represent an achievable patient volume for administering LTA in cirrhotic cohorts. In our model, the use of LTA decreased hospital admissions by 12.6% and reduced incidence of cirrhosis-related complications. The development of refractory ascites decreased from 37% to 30% in the LTA group. In the model, SMT + LTA in 30 out of 100 patients with uncomplicated cirrhotic ascites may save up to £264, 589/year in total healthcare costs.



*LTA as per ANSWER protocol: twice weekly for 2 weeks followed by weekly infusions
**Ascites other treatments: Transjugular intrahepatic portosystemic shunt; Liver transplant; Diuretics + other drug management
***Ascites complications: Bacterial peritonitis; Hepatic encephalopathy; Renal dysfunction; Hepatorenal syndrome type I; Gastro-oesophageal varices with bleeding

Figure: Graphical representation of the discrete event simulation model.

Conclusion: Our DES model suggests that, if outcomes reported in the ANSWER trial translate to similar real-world benefits in UK patients, the use of LTA in cirrhotic uncomplicated ascites could lead to cost-savings, even when administered to a proportion of those eligible.

FRI500

Improved survival rates in hepatic encephalopathy after a decade of clinical practice with the addition of rifaximin-alpha to lactulose: a real-world data meta-analysis

Juha Halonen¹, Roland Henrar¹. ¹Norgine Ltd, Harefield, United Kingdom
Email: jhalonen@norgine.com

Background and aims: Hepatic encephalopathy (HE) is a frequent complication of liver cirrhosis with a high risk of both short-term and long-term mortality [1]. Real-world longitudinal data on mortality rates in HE are scarce. This meta-analysis of two available studies compared the survival rates attained over approximately one decade.

Method: In HE, real-world mortality rates over 5 years were initially reported in patients with alcohol-related liver cirrhosis [1] and more recently in patients with HE who received combination treatment with rifaximin-alpha plus lactulose [2, 3]. Our meta-analysis calculated survival rates at 1, 12 and 60 months in the first study, and at 12, 36 and 60 months in the more recent study. Survival rates at 12 and 60 months were compared between studies using two-sided t-tests, assuming equal variance.

Results: The first study (conducted in 1993–2006) included 169 patients with HE and survival rates at 1, 12 and 60 months were 55%, 36% and 15%, respectively. The more recent study (conducted in 2014–2019) included 136 patients with HE and survival rates after 12, 36 and 60 months were 72%, 49% and 35%, respectively. Survival rates were significantly higher in the more recent study in comparison with the previous study at both 12 months (72% vs 36%; $p = 0.029$) and 60 months (35% vs 15%; $p < 0.001$). In the more recent study, all patients received lactulose plus rifaximin-alpha 550 mg; in the previous study, treatments were not reported but were likely to consist of lactulose alone. Notably, the number needed to treat to prevent an HE death, when comparing the more recent study versus the previous study, was 2.8 at 12 months and 4.9 at 60 months.

Conclusion: Direct comparison of the two studies is limited by different countries and by expected clinical improvements over a decade. Nevertheless, these real-world results suggest that treating patients with a combination of rifaximin-alpha 550 mg twice daily plus lactulose, rather than lactulose alone, may improve both 1-year- and 5-year survival rates in HE in current clinical practice.

References

Jepsen P, et al. *Hepatology* 2010;51 (5):1675–82.
Hudson M, et al. *Frontline Gastroenterol* 2017;8 (4):243–51.
Hudson M, et al. *Gut* 2021;70 (S3):A41–2.

FRI501

Risk prediction of hepatic encephalopathy after molecular targeted therapy for hepatocellular carcinoma in patients with cirrhosis

Kisako Fujiwara¹, Takayuki Kondo¹, Sae Yumita¹, Takamasa Ishino¹, Keita Ogawa¹, Miyuki Nakagawa¹, Hidemi Unozawa¹, Terunao Iwanaga¹, Takafumi Sakuma¹, Naoto Fujita¹, Hiroaki Kanzaki¹, Keisuke Koroki¹, Kazufumi Kobayashi¹, Soichiro Kiyono¹, Masato Nakamura¹, Naoya Kanogawa¹, Tomoko Saito¹, Sadahisa Ogasawara¹, Shingo Nakamoto¹, Tetsuhiro Chiba¹, Jun Kato¹, Naoya Kato¹. ¹Graduate School of Medicine, Chiba University, Department of Gastroenterology, Chiba, Japan
Email: kisakoff123@yahoo.co.jp

Background and aims: The management of hepatic encephalopathy (HE) during treatment for advanced hepatocellular carcinoma is crucial because it may cause interruption of molecular targeted therapy. However, the incidence of HE and the risk of its development has not been sufficiently clarified. In this study, we investigated the incidence and risk factors of HE in cirrhotic patients with advanced hepatocellular carcinoma after the first-line chemotherapy.

Method: This retrospective study enrolled 316 cirrhotic patients with advanced hepatocellular carcinoma diagnosed by contrast-enhanced

POSTER PRESENTATIONS

computed tomography (Child-Pugh A 242 cases/B 74 cases) who received molecular targeted agents as first-line chemotherapy between July 2009 and February 2019 and measured ammonia levels before (pre-treatment) and 1 week after treatment (post-treatment). We examined the incidence and predictors of HE within 2 weeks after treatment.

Results: Incidence of HE: Pre-treatment serum ammonia levels elevated significantly compared to post-treatment (56.9 ± 30.6 vs. 79.9 ± 48.3 $\mu\text{mol/L}$, $P < 0.001$), and hepatic encephalopathy was observed in 14 patients (4.4%) within 2 weeks after chemotherapy. Risk factors for the development of HE: Multivariate analysis showed that higher pre-treatment ammonia levels (Odds ratio 1.022 [1.008–1.036], $P = 0.002$) and the greater maximum diameter of portosystemic shunts (Odds ratio 1.094 [1.014–1.179], $P = 0.020$) were significant predictive factors for the development of HE.

Predictive model for the development of HE using a decision-tree-based approach: The final selected tree-discriminated cases were classified according to the following 3 subpopulations; low-risk group (ammonia levels < 73 $\mu\text{mol/L}$; development of HE, 0.9%), intermediate-risk group (ammonia levels ≥ 73 $\mu\text{mol/L}$ and portosystemic shunt diameter < 6.2 mm; development of HE, 4.2%), and high-risk group (ammonia levels ≥ 73 $\mu\text{mol/L}$ and portosystemic shunt diameter ≥ 6.2 mm; development of HE, 20%).

Conclusion: The development of HE after molecular targeted therapy could be clearly risk-segmented according to the ammonia level and the diameter of portosystemic shunts. Therefore, treatment for HE should be considered in cases with higher ammonia levels and large portosystemic shunt before molecular targeted therapy.

FR1502

ABC: a novel algorithm to stratify decompensation risk in patients with cACLD (CHESS2102): an international, multicenter cohort study

Chuan Liu¹, Jia Li², Yu Jun Wong³, Qing Xie⁴, Masashi Hirooka⁵, Hirayuki Enomoto⁶, Tae Hyung Kim⁷, Amr Hanafy⁸, Zhujun Cao⁴, Lili Zhao², Yanna Liu¹, Yifei Huang¹, Xiaoguo Li¹, Ning Kang¹, Yohei Koizumi⁵, Yoichi Hiasa⁵, Takashi Nishimura⁶, Hiroko Iijima⁶, Young Kul Jung⁷, Hyung Joon Yim⁷, Xin Li⁹, Qing-Lei Zeng¹⁰, Xiaolong Qi¹. ¹The First Hospital of Lanzhou University, CHESS Center, Institute of Portal Hypertension, China; ²Department of Gastroenterology and Hepatology, Tianjin Second People's Hospital, Tianjin, China; ³Department of Gastroenterology & Hepatology, Changi General Hospital, Singapore; ⁴Department of infectious disease, Ruijin hospital, Shanghai Jiao Tong university school of medicine, Shanghai, China; ⁵Department of Gastroenterology and Metabolism, Ehime University Graduate School of Medicine; ⁶Department of Internal Medicine, Division of Gastroenterology and Hepatology, Hyogo College of Medicine, Nishinomiya, Japan; ⁷Division of Gastroenterology and Hepatology, Korea University Ansan Hospital, Ansan-si, Gyeonggi-do, Republic of Korea; ⁸Division of Gastroenterology, Hepatology and Endoscopy, Internal Medicine, Zagazig University Faculty of Medicine, Egypt; ⁹Department of radiology, Tianjin second people's hospital, Tianjin, China; ¹⁰Department of Infectious Diseases and Hepatology, The First Affiliated Hospital of Zhengzhou University, Zhengzhou, 450052, China
Email: qixiaolong@vip.163.com

Background and aims: Liver-related death is preceded by clinical decompensation; therefore, the risk stratification of decompensation in compensated advanced chronic liver disease (cACLD) is extraordinary significant. This study intended to investigate a novel algorithm to stratify the decompensation risk in patients with cACLD.

Method: The international, multicenter study included two cohorts from January 2009 to August 2020. In training cohort, the unfavorable Baveno VI criteria patients were used to develop the novel CHESS criteria to stratify decompensation risk. The Algorithm based on Baveno VI criteria plus CHESS criteria (ABC model) was validated in validation cohort.

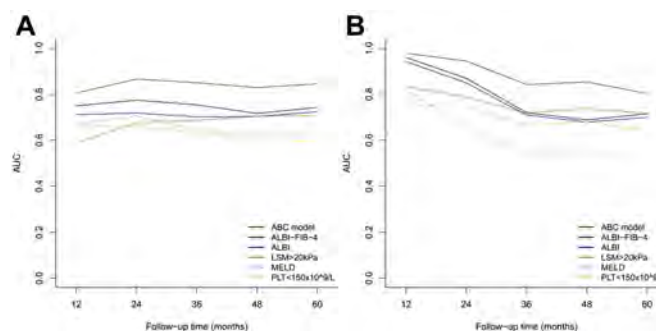


Figure 1. Comparisons of different models for predicting hepatic decompensation in training (A) and validation (B) cohorts.

ABC, Algorithm based on Baveno VI criteria plus CHESS criteria; ALBI-FIB-4, albumin-bilirubin (ALBI) and fibrosis-4 (FIB-4); LSM, liver stiffness measurement; MELD, model of end-stage liver disease; PLT, platelet count.

Results: A total of 1118 cACLD patients were enrolled in training cohort and validation cohort. In training cohort, multivariate analysis revealed that liver stiffness measurement (LSM), platelet count (PLT), albumin, alanine aminotransferase (ALT) and varices were the independent risk factors for hepatic decompensation. The novel CHESS criteria was produced, and < -4.4 , -4.4 to -3.1 and > -3.1 indicated the low risk, medium risk, and high risk of decompensation, with a 3 year-time-dependent area under the curve (tAUC) of 0.851 (0.800–0.901) (Figure 1 A). In validation cohort, the 3 year-tAUC of ABC model was 0.843 (0.742–0.943) (Figure 1 B).

Conclusion: The ABC model can stratify the risk of decompensation in cACLD. HVPG evaluation can be waived in both low risk and high risk cACLD patients as they can be managed by Baveno VI criteria and non-selective β -blockers intervention, respectively, and the remaining medium risk patients need further HVPG evaluation.

FR1503

Quantitative parameters of esophageal varices based on computed tomography may be used for predicting severe varices in patients with liver cirrhosis

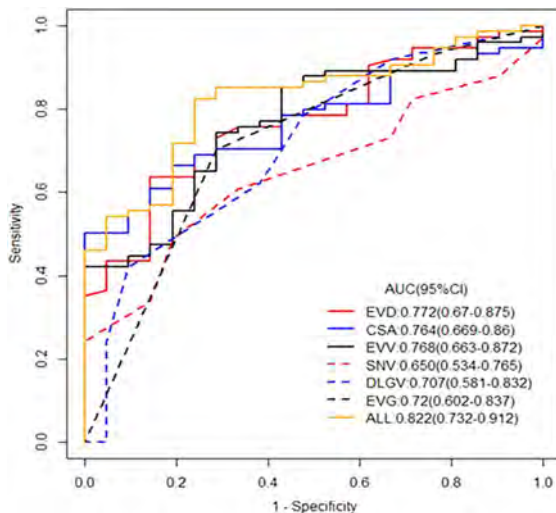
Shang Wan¹, Bin Song¹. ¹West China Hospital, West China School of Medicine, Sichuan University, Radiology, Cheng Du, China
Email: songlab_radiology@163.com

Background and aims: Esophageal varices (EV) are the most common complication in patients with portal hypertension resulted from liver cirrhosis, and the subsequent variceal bleeding is the leading cause of death in those patients. The invasive procedure of endoscopy is now regarded as the reference standard for evaluation of EV, however, the utility of it is limited due to the invasive nature and the high-cost effectiveness. Thus, in this study, we aimed to assess whether the quantitative computed tomography (CT)-derived parameters can noninvasively predict the severity of EV and the risk of esophageal variceal bleeding (EVB).

Method: In this retrospective study, a total of 145 endoscopically confirmed EV patients were included and were divided into a conspicuous (mild-to-moderate EV, $n = 39$) and a non-conspicuous EV group (severe EV, $n = 106$), a bleeding ($n = 89$) and a non-bleeding group ($n = 56$). EV grade (EVG), EV diameter (EVD), cross-sectional surface area (CSA), EV volume (EVV), spleen volume (SV), splenic vein (SNV), portal vein (PV), diameter of left gastric vein (DLGV), and the opening type of LGV were measured independently using 3D-slicer. Univariate and multivariate logistic analysis were used to determine the independent factors and the receiver operating characteristic (ROC) curves were performed to evaluate the diagnostic performance.

Results: The difference of EVG, EVD, CSA, EVV, DLGV, SNV between the conspicuous and non-conspicuous EV group were statistically significant ($p < 0.05$), area under the curves (AUCs) of them for predicting severe EV were 0.72, 0.772, 0.704, 0.768, 0.707, 0.65, with corresponding sensitivities of 70.3%, 63.5%, 50%, 74.3%, 52.7%, 48.6%, specificities

of 71.4%, 85.7%, 100%, 71.4%, 81%, 81% respectively. EVG, CSA (odds ratio (OR):3.258, 95% confidence interval (CI):1.597–6.647; OR:1.029, 95% CI:1.008–1.050) were found to be independent predictive factors. However, there was no significant difference of the included parameters between the bleeding and non-bleeding group ($p > 0.05$).



Conclusion: CT can be used as a noninvasive method to effectively predict the severity of esophageal varices, which may reduce the invasive screening of endoscopy and be used as a supplementary procedure in patients with portal hypertension.

FR1504

A cost-effectiveness evaluation of the GORE® VIATORR® TIPS Endoprosthesis versus large volume paracentesis in the management of portal hypertension complications in the Spanish healthcare system

Mitesh Nakum¹, Thomas Wiersma², Francesca Di Stasi³. ¹W. L. Gore & Associates (UK) Ltd., Health Economics, United Kingdom; ²W.L. Gore & Associates B.V., Tilburg, Netherlands; ³W.L. Gore & Associati Srl, Verona, Italy

Email: mnakum@wlgore.com

Background and aims: The GORE® VIATORR® TIPS Endoprosthesis is widely used in patients for the treatment of portal hypertension and its complications such as refractory ascites in Spain, however little is known about the cost-effectiveness of the GORE® VIATORR® Device in the Spanish healthcare system. The aim of this analysis was to establish the cost-effectiveness of the GORE® VIATORR® Device versus large volume paracentesis (LVP) in refractory ascites with the Spanish healthcare system.

Method: A published markov model¹ was updated to simulate economic outcomes at two years from the Spanish healthcare perspective. Clinical parameters were derived from an updated published literature review². Costing information was gathered from national tariffs, existing literature and expert opinion. Uncertainty was tested using deterministic and probabilistic sensitivity analyses.

Results: The GORE® VIATORR® Device was estimated to be cost-saving by 21,493 Euros versus LVP over the time frame of the analysis. The GORE® VIATORR® Device also resulted in +0.60 QALYs versus LVP and so was cost-effective. Savings with the GORE® VIATORR® Device was from reduced LVP resource utilisation costs and reduced inpatient stay. The GORE® VIATORR® Device also remained over 98% cost-effective in a probabilistic sensitivity analysis versus LVP (see figure below).

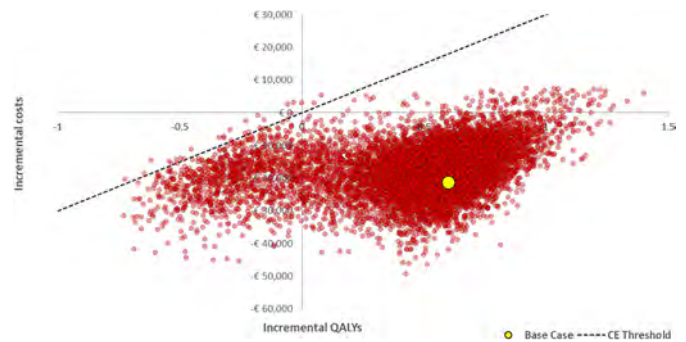


Figure: Probabilistic Sensitivity analysis of incremental Costs versus Incremental QALYs of GORE® VIATORR® TIPS Endoprosthesis versus LVP; CE threshold 30,000 Euros.

Conclusion: From the Spanish healthcare perspective, this economic analysis suggests that the GORE® VIATORR® Device was cost saving and cost-effective at two years compared to LVP. Cost-savings were primarily driven by reduced LVP sessions and decreased inpatient hospital stay. Based on this economic evaluation the consideration of the GORE® VIATORR® Device in refractory ascites is cost-saving to the hospital provider and may improve patient health-related quality of life. Further long term studies are required in providing health economic evidence in this space.

FR1505

Factor VIII/protein C ratio does not reflect coagulation but is linked to pathophysiological mechanisms driving disease progression in patients with advanced chronic liver disease

Lorenz Balcar^{1,2}, Bernhard Scheiner^{1,2}, Rafael Paternostro^{1,2}, Benedikt Simbrunner^{1,2}, Lukas Hartl^{1,2}, Mathias Jachs^{1,2}, David JM Bauer^{1,2}, Albert Stättermayer^{1,2}, Georg Semmler^{1,2}, Matthias Pinter², Peter Quehenberger³, Michael Trauner², Thomas Reiberger^{1,2}, Ton Lisman⁴, Mattias Mandorfer^{1,2}. ¹Medical University of Vienna, Vienna Hepatic Hemodynamic Lab, Division of Gastroenterology and Hepatology, Department of Internal Medicine III, Vienna, Austria; ²Medical University of Vienna, Division of Gastroenterology and Hepatology, Department of Internal Medicine III, Vienna, Austria; ³Medical University of Vienna, Department of Laboratory Medicine, Vienna, Austria; ⁴University Medical Center Groningen, Surgical Research Laboratory and Section of Hepatobiliary Surgery and Liver Transplantation, Department of Surgery, Groningen, Netherlands

Email: j.a.lisman@umcg.nl

Background and aims: We and others have demonstrated that the ratio of procoagulant factor VIII to anticoagulant protein C (FVIII/PC) is a versatile predictor of hepatic decompensation/liver-related death in patients with advanced chronic liver disease (ACLD). Of note, the association between FVIII/PC and thrombomodulin-modified thrombin generation assay (TM-TGA) results is confounded by liver disease severity.

To substantiate the notion that FVIII/PC is unrelated to coagulation potential and provide an alternative explanation for its prognostic value, we investigated its association with (i) bleeding and thrombotic events, and (ii) key pathophysiological mechanisms promoting liver disease progression.

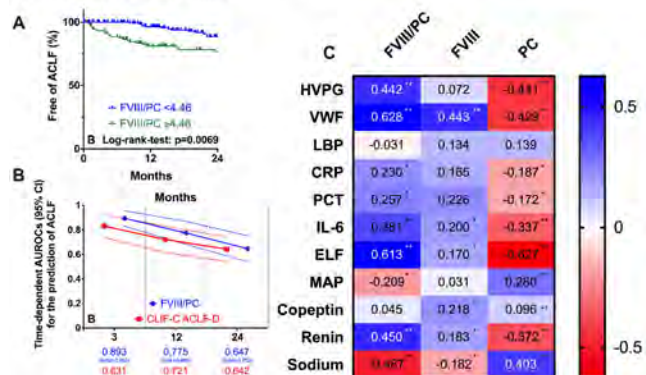
Method: In cohort (i) including ACLD patients undergoing HVPG measurement at the Vienna Hepatic Hemodynamic Lab with information on FVIII/PC ($n = 576$), we evaluated the development of major bleeding as well as arterial/venous thrombotic events (Schulman S, et al, J Thromb Haemost 2010) during follow-up. Moreover, incidence of ACLF was assessed. In cohort (ii), associations between FVIII/PC and pathophysiology-oriented biomarkers were assessed in 142 patients from the prospective Vienna Cirrhosis Study (VICIS).

POSTER PRESENTATIONS

Results: (i) During a follow-up of 31.8 (IQR:12.0–60.3) months, major bleedings were observed in 44 (7.6%) patients and bleedings were attributed to portal hypertension in 35 (6.3%) of the first bleeding events. Non-malignant thrombotic events were diagnosed in 50 (8.7%) patients. FVIII/PC was associated with neither the incidence of major bleedings (hazard ratio [HR]: 1.03[95%CI:0.98–1.09]; $p = 0.272$), nor the occurrence of thrombotic events (HR: 1.03[95%CI:0.98–1.09]; $p = 0.269$). However, it predicted ACLF (adjusted HR: 1.10[95%CI:1.02–1.19]; $p = 0.015$) in decompensated patients, independently of CLIF-C ACLF-D.

(ii) As demonstrated in the attached Figure, FVIII/PC showed moderate to strong correlations with HVPG (Spearman's $\rho = 0.442$; $p < 0.001$), von Willebrand factor ($\rho = 0.628$; $p < 0.001$), serum sodium ($\rho = -0.487$; $p < 0.001$), and renin ($\rho = 0.450$; $p < 0.001$), as well as associations with systemic inflammation: C-reactive protein ($\rho = 0.230$; $p = 0.006$), interleukin-6 ($\rho = 0.381$; $p < 0.001$), and procalcitonin ($\rho = 0.257$; $p = 0.002$). Finally, it also strongly correlated with the enhanced liver fibrosis (ELF) test, as an indicator of fibrogenesis/matrix remodelling ($\rho = 0.613$; $p < 0.001$).

Figure. A Probability of remaining free of ACLF according to the Youden-optimized cut-off for ACLF-development in dACLD patients. **B** Time-dependent AUROC analyses for the prediction of ACLF development in dACLD patients. **C** Correlations of FVIII/PC, FVIII, and PC with portal hypertension severity (HVPG), markers of bacterial translocation (LBP) and systemic inflammation (CRP, PCT, and IL-6) as well as liver fibrogenesis/matrix remodelling (ELF test), and markers of hyperdynamic circulation/systemic hemodynamic impairment (MAP, coepleptin, renin, and serum sodium). *Indicates p -values < 0.05 , whereas **denotes p -values < 0.001 .



Conclusion: Baseline FVIII/PC was associated with neither thrombotic events nor major bleedings during follow-up, i.e., the clinical correlates of coagulation. Hence, results from previous studies on FVIII/PC require reinterpretation. However, FVIII/PC was associated with key pathophysiological mechanisms involved in disease progression, including those promoting further decompensation and ACLF, which may explain its prognostic utility.

FR1506

Prognostic impact of variants in TM6SF2 and MBOAT7 in patients who have progressed to advanced chronic liver disease

Lorenz Balcar^{1,2}, Bernhard Scheiner^{1,2}, Markus Urheu¹, Patrick Weinberger¹, Rafael Paternostro^{1,2}, Benedikt Simbrunner^{1,2}, Georg Semmler^{1,2}, Nicole Auer¹, Claudia Willheim¹, Matthias Pinter¹, Michael Trauner¹, Thomas Reiberger^{1,2}, Mattias Mandorfer^{1,2}, Albert Stättermayer^{1,2}. ¹Medical University of Vienna, Division of Gastroenterology and Hepatology, Department of Internal Medicine III, Vienna, Austria; ²Medical University of Vienna, Vienna Hepatic Hemodynamic Lab, Division of Gastroenterology and Hepatology, Department of Internal Medicine III, Vienna, Austria
Email: mattias.mandorfer@meduniwien.ac.at

Background and aims: Genome-wide association studies revealed genetic variants that modulate the susceptibility for (advanced) chronic liver disease (A)CLD. We have previously shown that a *PNPLA3* variant promotes hepatic decompensation/death in ACLD, while *HSD17B13* did not impact prognosis at this stage. Importantly,

the impact of the *transmembrane 6 superfamily 2 (TM6SF2) rs58542926* and *membrane-bound O-acyltransferase domain-containing 7 (MBOAT7) rs641738* single nucleotide variants (SNV) in patients who have already progressed to ACLD are unknown.

Method: The impact of *TM6SF2*/*MBOAT7* variants on liver-related events was evaluated in 938 ACLD (as defined by HVPG ≥ 6 mmHg; viral hepatitis and alcohol-related or non-alcoholic fatty liver disease) patients undergoing HVPG-measurement at the Vienna Hepatic Hemodynamic Lab.

Results: Mean age was 55 ± 11 years, mean HVPG was 15 ± 7 mmHg and mean MELD was 11 ± 5 points. The main etiologies were viral hepatitis ($n = 495$, 53%) alcohol-related liver disease ($n = 342$, 37%) and non-alcoholic fatty liver disease ($n = 101$, 11%).

While 754 (80%) patients harboured the *TM6SF2* wild-type (C/C), 174 (19%) and 10 (1%) patients had one or two T-alleles, respectively. Patients with at least one *TM6SF2* T-allele had more pronounced portal hypertension (HVPG: 16 ± 7 vs. 15 ± 7 mmHg; $p = 0.031$), higher gamma-glutamyl transferase levels (123 vs. 97 U \times L⁻¹; $p = 0.002$), and more commonly hepatocellular carcinoma (HCC, 17% vs. 12%; $p = 0.049$). Patients with at least one *MBOAT7* T-allele also tended to have a higher HCC prevalence at baseline (14% vs. 10%; $p = 0.051$), while other baseline characteristics were comparable.

In univariable Cox regression analyses, carriers of the *TM6SF2* T-allele showed a trend towards an increased risk for decompensation/liver-related death during follow-up (hazard ratio [HR]: 1.26 [95% confidence interval (95%CI): 0.98–1.62]; $p = 0.072$); in the viral hepatitis subgroup, the association attained statistical significance (HR: 1.53 [95%CI: 1.03–2.29]; $p = 0.036$). After adjusting for age, HVPG, MELD, and albumin levels, neither the *TM6SF2* nor the *MBOAT7* genotype had an effect on decompensation/liver-related death during follow-up.

These results were unaffected by restricting our analysis to patients at increased risk of hepatic decompensation/liver-related death, i.e., those with clinically significant portal hypertension.

Conclusion: While SNVs in *TM6SF2* and *MBOAT7* modulate the risk of progression to ACLD, both genotypes had no independent impact on liver-related outcomes in ACLD patients but were potential risk factors for HCC development. Thus, these variants have limited value for risk stratification in patients with ACLD as HCC screening is warranted anyway.

FR1507

Hepatocellular carcinoma and number of elastic bands per session are strong predictors of bleeding after prophylactic endoscopic variceal bleeding

Renato Medas¹, Rodrigo Liberal¹, Tiago Ribeiro¹, João Afonso¹, Rosa Coelho¹, Hélder Cardoso¹, Guilherme Macedo¹. ¹Centro Hospitalar Universitário São João, Gastroenterology and Hepatology, Porto, Portugal
Email: renatogmedas@gmail.com

Background and aims: Endoscopic variceal band ligation (EVL) is considered a standard care for high-risk varices treatment in cirrhosis. Despite being globally safe, procedure-related bleeding is a potential complication, with an estimated incidence up to 15% in some series, requiring hospitalization and blood transfusion. However, risk factors associated with this serious complication are not well established. The aim of our study was to evaluate factors associated with increased risk for upper gastrointestinal bleeding (UGIB) within 30 days after prophylactic EVL.

Method: We performed a single center retrospective study in a tertiary hospital during a 6-year period (between 09/2015 and 09/2021). All patients with clinically significant portal hypertension due to liver cirrhosis, submitted to prophylactic EVL, were considered eligible for the study. After EVL, all patients received oral proton pump inhibitor and sucralfate, according to an internal protocol. Statistical analysis was performed with SPSS® v.25.0.

Results: A total of 871 prophylactic EVL procedures, performed in 281 patients were analysed. Most procedures were primary prophylaxis (70.3%). 79.9% of patients were male (79.9%) and median age was 60 years (IQR 54–68). Alcohol was the main etiology for cirrhosis (57.9%), followed by hepatitis C virus (14.9%). UGIB 30-days after EVL occurred in 21 cases (2.4% of all EVLs) within a median time of 9 days (IQR 8–17) after index procedure. In 15 patients (68.2%) ligation ulcers were identified as the potential source of bleeding. On univariate analysis the number of elastic bands per session, platelets, albumin, total bilirubin, sodium, hepatocellular carcinoma (HCC) and portal venous thrombosis were associated with increased risk of UGIB 30-days after EVL. After multivariate logistic regression, only the number of elastic bands applied per session [above 7] (odds ratio [OR] 4.76, 95% confidence interval [CI] 1.97–13.02, $p = 0.001$), presence of HCC (OR 3.79, 95% CI 1.16–9.02, $p = 0.006$) and sodium (OR 0.86, 95% CI 0.78–0.95, $p = 0.002$) reached statistical significance. Age, sex, cirrhosis etiology, high-risk varices, concomitant gastric varices, ligation system, creatinine, international normalized ratio, antiplatelet and anticoagulant therapy were not associated with increased risk of bleeding after EVL.

Conclusion: Our study describes a relative low incidence of post-EVL UGIB in accordance with previous reports, reinforcing EVL as a safe procedure for prophylaxis of variceal bleeding. The number of elastic bands applied per session, serum sodium and presence of HCC, rather than platelets or coagulopathy, are predictors of bleeding after prophylactic EVL in patients with liver cirrhosis. These data suggest that prophylactic administration of blood or coagulation products are not necessary. In addition, a minimal EVL strategy should be considered in selected patients.

FRI508

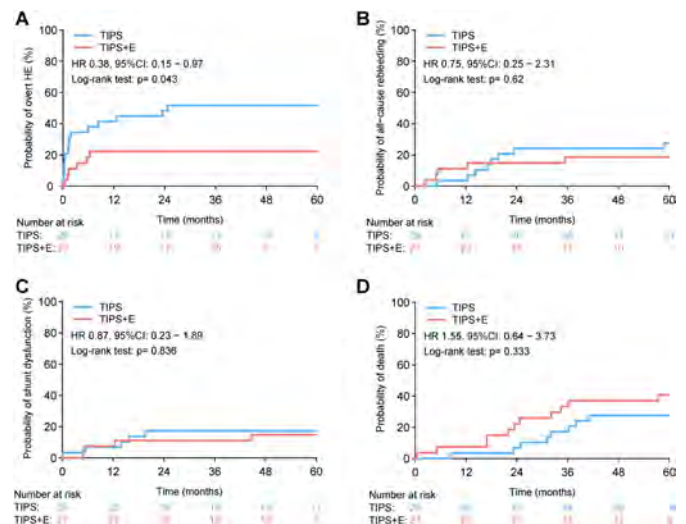
Simultaneous large spontaneous portosystemic shunt embolization for the prevention of overt hepatic encephalopathy after TIPS: a randomized controlled trial

Yong Lv¹, Hui Chen¹, Bohan Luo^{1,2}, Wei Bai^{1,2}, Kai Li¹, Zhengyu Wang^{1,2}, Dongdong Xia^{1,2}, Wengang Guo^{1,2}, Xiaomei Li^{1,2}, Jie Yuan^{1,2}, Zhanxin Yin^{1,2}, Daiming Fan¹, Guohong Han^{1,2}. ¹National Clinical Research Center for Digestive Diseases and Xijing Hospital of Digestive Diseases, Fourth Military Medical University, Department of Liver Diseases and Digestive Interventional Radiology, Xi'an; ²Xi'an International Medical Center Hospital of Digestive Diseases, Department of Liver Diseases and Digestive Interventional Radiology, Xi'an, China
Email: 13991969930@126.com

Background and aims: Large spontaneous portosystemic shunt (SPSS) is associated with increased risk of hepatic encephalopathy (HE) in patients undergoing transjugular intrahepatic portosystemic shunt (TIPS). This study aimed to evaluate whether prophylactic embolization of large SPSS at the time TIPS creation could reduce the incidence of post-TIPS HE in patients with cirrhosis and variceal bleeding.

Method: From June 2014 to August 2017, 56 patients with cirrhosis and large SPSS planning to undergo elective TIPS for the prevention of variceal bleeding were randomly assigned (1:1) to receive TIPS alone (TIPS group, $n = 29$) or TIPS plus simultaneous SPSS embolization (TIPS+E group, $n = 27$). The primary endpoint was overt HE.

Results: TIPS placement and SPSS embolization was successful in all patients. During a median follow-up of 59.0 months in the TIPS group and 45.3 months in the TIPS+E group, the primary endpoint was met in 15 patients (51.7%) in the TIPS group and 6 patients (22.2%) in the TIPS+E group ($p = 0.045$). The 2-year cumulative incidence of overt HE was significantly lower in the TIPS+E group (21.2% vs 48.3%; HR: 0.38, 95%CI, 0.15–0.97; $p = 0.043$) compared with TIPS group. The incidence of recurrent bleeding (18.5% vs 27.6%, $p = 0.627$), shunt dysfunction (14.8% vs 17.2%, $p = 0.995$), death (40.7% vs 31.0%, $p = 0.632$) and other adverse events was not significantly different between the 2 groups.



Conclusion: In patients with cirrhosis treated with TIPS, simultaneous large SPSS embolization reduced the risk for overt HE without increasing other complications. Simultaneous large SPSS embolization should therefore be considered for prophylaxis of post-TIPS HE.

FRI509

Use of second-harmonic generation microscopy for automated detection of septa and nodules in needle liver biopsies of NASH cirrhosis

Mazen Nouredin¹, Dean Tai², Elaine Chng², Yayun Ren², Pol Boudes³, Harold Shlevin³, Stephen Harrison⁴, Guadalupe Garcia-Tsao⁵, Naga Chalasani⁶, Zachary Goodman⁷. ¹Division of Digestive and Liver Diseases, Comprehensive Transplant Center, Cedars-Sinai Medical Center, United States; ²HistoIndex Pte. Ltd., Singapore; ³Galectin Therapeutics, United States; ⁴Pinnacle Clinical Research, San Antonio, TX, USA; ⁵Section of Digestive Diseases, Yale University and CT-VA Healthcare System, Connecticut, USA; ⁶Division of Gastroenterology and Hepatology, Department of Medicine, Indiana University School of Medicine, USA; ⁷Inova Fairfax Hospital, Falls Church, Virginia, USA
Email: mazen.nouredin@cshs.org

Background and aims: Cirrhosis, previously considered irreversible, is now recognized as capable of regression or progression. Most staging systems oversimplify all degrees of cirrhosis into one category. Portal hypertension, defined by hepatic venous pressure gradient (HVPG), correlates with key histological features of cirrhotic liver biopsies, including septa and nodules, which might make a biopsy an acceptable surrogate for clinical outcome. Using second harmonic generation/two-photon excitation fluorescence (SHG/TPEF), this exploratory analysis aims to develop an artificial intelligence (AI) tool based on septa and nodule microscopy for use in natural history monitoring and evaluate treatment response in cirrhotic NASH trials.

Method: 25 liver biopsies from 15 NASH patients with compensated cirrhosis were included from a phase 2a trial. Digitized images stained with Sirius red and immunostain for smooth muscle actin were used by an expert pathologist to identify all septa and cirrhotic nodules. 2 image algorithms were developed to automatically detect septa and nodules based on pathologist's annotations, named qSepta and qNodules, respectively. Agreement between the algorithm detection results and annotations were determined, and the images were rotated to establish repeatability.

Results: Concordance between the pathologist annotations and algorithm identification was determined after excluding technical artifacts. 284 septa were annotated by the pathologist ("true septa") and 294 septa were detected from the SHG/TPEF images using qSepta algorithm. Comparing the qSepta results versus true septa, 91% of the true septa were detected by the algorithm and 85% of the algorithm

POSTER PRESENTATIONS

detection results were true septa. 587 nodules were annotated from 25 H&E images by the pathologist. 525 nodules were detected from the SHG/TPEF images using qNodules. Comparing the qNodules results and true nodules, 82% of the true nodules were detected by the algorithm and 95% of the algorithm detection results were true nodules. The repeatability of qSepta and qNodules were 95% and 99% respectively.

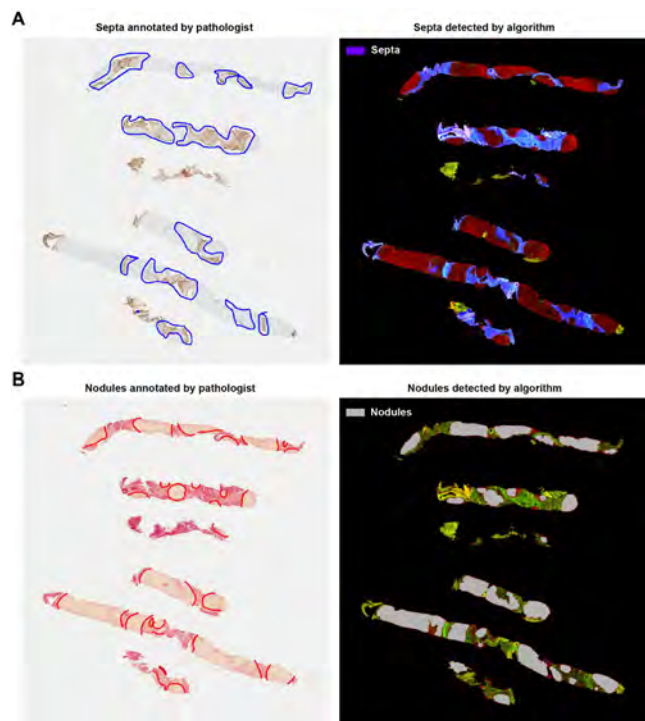


Figure: Examples of septa and nodules detection.

Conclusion: qSepta and qNodules algorithms can accurately detect septa and nodules in NASH cirrhotic patients. This can be used to develop more sophisticated algorithms to correlate with HVP and study the natural history of NASH cirrhosis and treatment response.

FRI510

Hepcidin is higher in patients with more severe liver disease independent of portal hypertension

Robin Greinert¹, Alexander Zipprich², Laura Popp³, Cristina Ripoll².
¹Martin-Luther-University Halle-Wittenberg, Department for Internal Medicine I, Halle (Saale), Germany; ²University of Jena, Department for Internal Medicine IV, Jena, Germany; ³Kreiskrankenhaus Delitzsch GmbH, Innere Medizin, Delitzsch, Germany
 Email: cristina.ripoll@med.uni-jena.de

Background and aims: Hepatocytes are the main source of hepcidin. Hepcidin expression is driven by iron load, although also inflammation, hypoxia and erythropoietic drive. The aim of this study is to evaluate hepcidin in cirrhosis and its association to the main pathophysiological drivers of cirrhosis: portal hypertension, liver insufficiency and systemic inflammation.

Method: Prospective study including consecutive patients between 2014 and 2016 who underwent a hepatic hemodynamic study. Measurement of ferritin, transferrin saturation and hepcidin (in hepatic vein and in peripheral blood) were performed besides standard measurements of liver function. Portal hypertension was estimated by means of HVPG, liver insufficiency was quantified by means of MELD score. SPSS v21 was used. Results are presented as proportions or median with IQR. Categorical variables were evaluated by means of the Chi-square test. Continuous variables were evaluated by the U-Mann Whitney or Spearman correlation as appropriate.

Results: Fifty-one patients (31 male, median age 62 (56–67) years, Child Pugh A 12 (23%), B 28 (55%) C 11 (22%)) were included. Median hepcidin (nmol/L) in the peripheral vein was 2.2 (0.5–7.6) and in the hepatic vein 2.1 (0.5–9.2) with a positive correlation between both (rho Spearman 0.85, $p < 0.001$). 31 and 36% of the patients had levels of hepcidin ≤ 0.5 nmol/L (lower limit of detection) in peripheral and hepatic vein respectively. Those with hepcidin > 0.5 nmol/L had vs those below: greater MELD [16 (11–19) vs 10 (19–12)] and Ferritin (229 (154–473) vs 37 (26–80)). No differences were observed according to CRP & leukocytes. Hepcidin was higher in patients with more severe liver disease [MELD: $r = 0.436$, $p = 0.003$; Child B&C vs A: 2.7 (0.5–11.8) nmol/L vs 0.5 (0.5–3.3) nmol/L $p = 0.05$]. No relevant association to HVP.

Conclusion: No significant differences in peripheral and hepatic vein can be observed, suggesting that the liver remains a main source of hepcidin production even in end-stage liver disease. Increased levels of hepcidin are associated to more severe liver disease and ferritin and have no relevant association to portal hypertension.

FRI511

Effect of thrombocytopenia and platelet transfusion on outcomes of acute variceal bleeding: a real world experience

Sagnik Biswas¹, Manas Vaishnav¹, Piyush Pathak¹, Aditya Vikram Pachisia¹, Rithvik Golla¹, Amit Goel², Dr. Shalimar¹.
¹All India Institute of Medical Sciences, New Delhi, Gastroenterology and Human Nutrition, New Delhi, India; ²Sanjay Gandhi Post Graduate Institute of Medical Sciences, Gastroenterology, Lucknow, India
 Email: drshalimar@yahoo.com

Background and aims: Thrombocytopenia is a feature of portal hypertension. In patients with thrombocytopenia and acute variceal bleeding (AVB), platelet transfusion is recommended by few guidelines and is common in routine clinical practice. However, the effect of thrombocytopenia and platelet transfusion on acute variceal bleeding (AVB) outcomes is unclear. We aimed to assess the outcomes in AVB patients with thrombocytopenia and the effect of platelet transfusion on rebleeding and mortality.

Method: Prospectively maintained database of the patients who presented with AVB were reviewed to study their outcome. Patients were grouped as platelet count $< 20,000/\text{mm}^3$, $20,000\text{--}50,000/\text{mm}^3$ and $> 50,000/\text{mm}^3$. The outcomes were assessed as the risk of rebleeding at days 5 and 42, and risk of death at day 42 from the onset of AVB. Outcomes were compared among patients with and without platelet transfusion during AVB management. Statistical comparisons were done using Kaplan-Meier curves with log-rank tests for rebleeding and logistic regression for 42-day mortality.

Results: A total of 913 patients- males 762 (83.5%); mean age 44.4 ± 12.8 years, MELD 16.6 ± 7.9 ; Child Class A 374 (41.0%), B 361 (39.5%) and C 178 (19.5%); platelet count $< 20,000/\text{mm}^3$, $20,000\text{--}50,000/\text{mm}^3$ and $> 50,000/\text{mm}^3$ in 23 (2.5%), 137 (15.0%) and 753 (82.5%) patients, respectively. Forty-eight (5.2%) patients experienced a rebleed at 5 days with 3 (13%), 7 (5.1%) and 38 (21.3%) patients in each group respectively. Among patients with platelet count $< 20,000/\text{mm}^3$, $20,000\text{--}50,000/\text{mm}^3$ and $> 50,000/\text{mm}^3$, 5 (21.7%), 25 (18.2%) and 108 (14.3%) patients respectively had 42-days rebleeding ($p = 0.296$, log-rank test; figure 1a); similarly, 42-day mortality was 3 (13.0%), 33 (24.1%) and 130 (17.3%), respectively ($p = 0.137$, log-rank test; figure 1b). Ninety-one patients received platelet transfusions-Child A/B/C 8.8%/9.4%/13.5%, respectively; MELD score 16.6 ± 8.0 vs 16.4 ± 7.6 , $p = 0.252$). Among three platelet groups, 10/23 (43.5%), 51/137 (37.2%) and 30/753 (4.0%) ($p < 0.001$) respectively received transfusion. Logistic regression analysis identified MELD score (Odds ratio 1.12 [1.109–1.15], $p < 0.001$) but not the platelet counts or platelet transfusion as predictors of 42-day mortality. Rebleeding rates in patients with platelet count $< 20,000/\text{mm}^3$ were similar in those who underwent endotherapy as compared with those who did not.

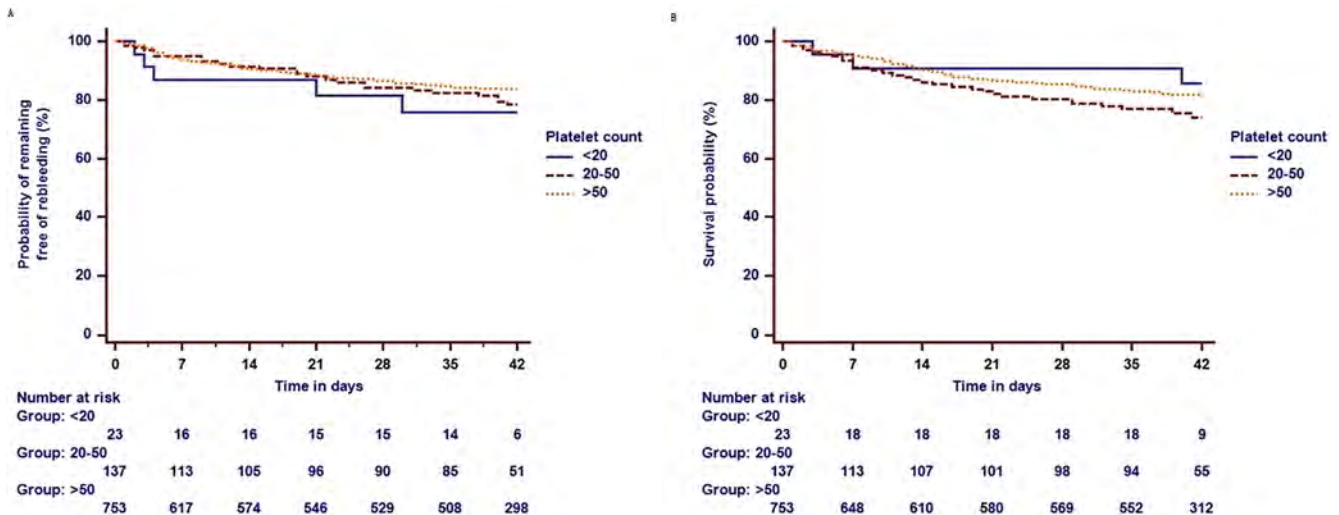


Figure: (abstract FRI511)

Conclusion: Platelet counts and platelet transfusion is not associated with the risk of rebleeding and mortality during follow-up in patients with AVB. Endotherapy is safe in patients with severe thrombocytopenia and not associated with higher rebleed rates.

FRI512

Personalized preemptive TIPS treatment for patients with Child-Pugh B cirrhosis and acute variceal bleeding by applying individualized of prediction of treatment effect

Yong Lv¹, Wei Bai^{1,2}, Kai Li¹, Dongdong Xia^{1,2}, Zhengyu Wang^{1,2}, Bohan Luo^{1,2}, Xiaomei Li^{1,2}, Jie Yuan^{1,2}, Zhanxin Yin^{1,2}, Daiming Fan¹, Guohong Han^{1,2}. ¹National Clinical Research Center for Digestive Diseases and Xijing Hospital of Digestive Diseases, Fourth Military Medical University, Department of Liver Diseases and Digestive Interventional Radiology, Xi'an, China; ²Xi'an International Medical Center Hospital of Digestive Diseases, Department of Liver Diseases and Digestive Interventional Radiology, Xi'an, China
Email: 13991969930@126.com

Background and aims: To evaluate whether individualized treatment effect prediction approach can assist in personalized treatment of acute variceal bleeding (AVB) with pre-emptive transjugular intrahepatic portosystemic shunt (p-TIPS) among patients with Child-Pugh B cirrhosis.

Method: Data of 1021 consecutive patients with Child-Pugh B cirrhosis and AVB from 13 university hospitals in China who were treated with p-TIPS (p-TIPS group, n=297) or standard of care (medical group, n=724) were used to predict treatment effects for individual patients in terms of absolute risk reduction (ARR) of death. Predictions were based on a refitted Chronic Liver Failure Consortium Acute Decompensation score (CLIF-C ADs) and on a newly developed prediction model. The net benefit of different p-TIPS treatment-strategies was compared: (i) treat none, (ii) treat all, (iii) risk-stratification strategy (i.e. selective treatment of patients at high-risk of death), and (iv) prediction-based treatment strategy (i.e. selective treatment of patients whose predicted treatment effect exceeds a decision threshold).

A Nomogram of optimal fit model for predicting mortality on medical treatment and treatment effect from pre-emptive TIPS

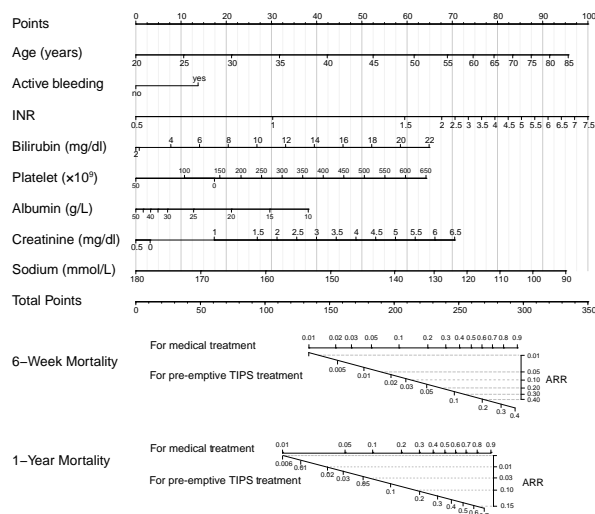
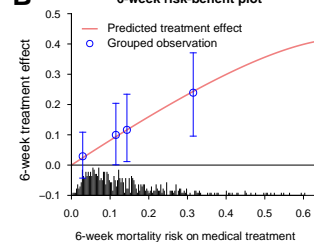
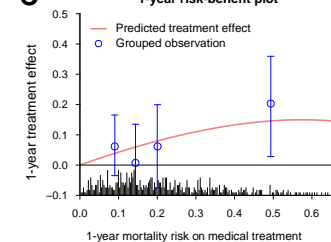


Figure: (abstract FRI512)

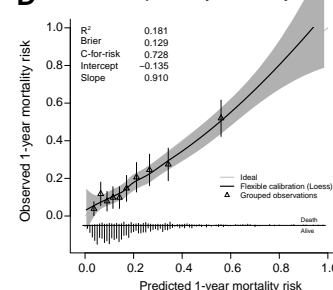
B 6-week risk-benefit plot



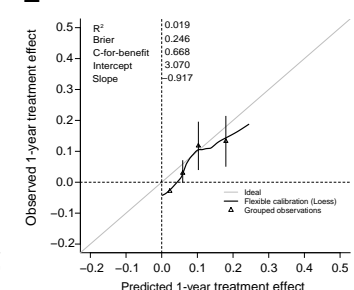
C 1-year risk-benefit plot



D Calibration plot for 1-year mortality risk



E Calibration plot for 1-year treatment effect



POSTER PRESENTATIONS

Results: After propensity score matching, the probability of death was significantly lower in p-TIPS group (15.9% vs 25.6% at 1 year, HR 0.52, 95%CI: 0.35–0.78; $p=0.002$) compared with medical group. A Cox proportional hazards model comprising 9 easy-to-measure clinical predictors (age, active bleeding, albumin, bilirubin, creatinine, INR, sodium, platelet, and treatment status) was built for predicting treatment effects of p-TIPS, which had higher values of concordance-statistic-for-benefit and better calibration compared with the refitted CLIF-CADs model. Net benefit analyses showed that prediction based treatment strategy were associated with more net benefit than other treatment strategies.

Conclusion: The treatment effects of p-TIPS can be predicted for individual patients based on routinely available patient characteristics. Individualized prediction treatment strategy is associated with optimal net benefit.

FRI513

Real-world survival outcomes in patients with decompensated cirrhosis receiving long term human albumin infusions

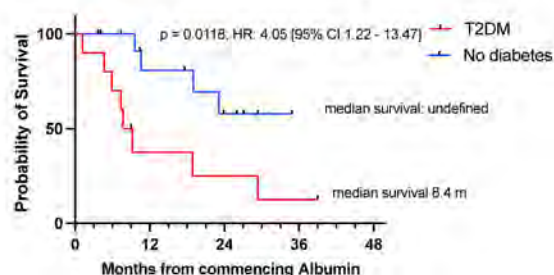
Nicholas Hannah^{1,2}, Douglas Tjandra¹, Ashwin Patwardhan¹, Kelsey Rutland¹, Siddharth Sood^{1,2}. ¹The Royal Melbourne Hospital, Department of Gastroenterology, Parkville, Australia; ²University of Melbourne, Medicine, Dentistry and Health Sciences, Parkville, Australia
Email: nick.m.hannah@gmail.com

Background and aims: The ANSWER study demonstrated the benefit of long term outpatient human albumin (HA) infusions in patients on diuretics for cirrhosis related ascites. HA is commonly used at our institution for cirrhotic patients with refractory ascites requiring repeated paracentesis, including those with ongoing alcohol consumption and renal impairment. We evaluated patient survival outcomes on HA infusions in an unwell but real-world cirrhotic cohort.

Method: We present a single-centre cohort study of patients receiving outpatient HA infusions at The Royal Melbourne Hospital between April 2017–June 2021. Inclusion: age >18 years and cirrhosis with ascites requiring paracentesis. Demographics, clinical data, including outcomes such as time on HA, trans-jugular portosystemic shunt (TIPS), liver transplant and death were recorded. Child-Pugh and Model for End-Stage Liver Disease-Sodium (MELD-Na) score were calculated. Patients received regular outpatient HA infusions up to 40 g/week. Primary outcomes were assessed 12 months after first HA infusion.

Results: 24 patients received at least 1 month of HA infusions (range 1.2–28.2, median 9.3 months). Median age 59.5 years, and 7 were female (29.2%). Aetiology included alcohol (50%), non-alcoholic steatohepatitis (NASH) (16.7%) and viral/alcohol (12.5%). Median MELD-Na 18.5, with Child-Pugh Scores A (4.2%), B (50%) and C (45.8%). Comorbidities included chronic kidney disease 37.5% and Type 2 diabetes mellitus (T2DM) 41.7%. Median follow-up was 16 months and median TIPS/transplant-free survival (TTFS) 10.5 months. Median serum sodium (134 mmol/L to 136.5 mmol/L, $p=0.014$) and albumin (28.5 g/L to 39 g/L, $p=0.003$) increased significantly over 12 months, whilst Child-Pugh score improved from 9 to 7.5 ($p=0.0172$). On multivariate analysis, T2DM (not NASH) had a significant TTFS disadvantage (HR 6.16; 95% CI 1.23–30.84, $p=0.027$), while time on HA infusions showed a TTFS advantage (HR 0.84, 95% CI 0.72–0.99, $p=0.031$). Median TTFS improved in patients with a change in MELD-Na <1 at 1 month: 29.4 months versus 7.7 months ($p=0.011$).

Kaplan-meier analysis of TTFS for those receiving albumin with T2DM



Conclusion: Outpatient HA infusions are associated with increased sodium and albumin levels and improvement in Child-Pugh score in a real-world cohort representing a more unwell population than the original ANSWER trial. T2DM was significantly associated with poorer outcomes, whilst an improvement in MELD-Na score at 1 month may predict those likely to benefit from HA. These results may help targeting of regular HA in decompensated cirrhotic patients.

FRI514

Impact of non-selective beta-blockers on survival and liver-related complications after TIPS-Insertion

Anja Tiede¹, Lena Stockhoff¹, Hannah Schneider¹, Bernhard Meyer², Heiner Wedemeyer¹, Jan Hinrichs², Markus Cornberg^{1,3}, Benjamin Maasoumy^{1,3}. ¹Hannover Medical School, Gastroenterology, Hepatology and Endocrinology, Hannover, Germany; ²Hannover Medical School, Diagnostic and Interventional Radiology, Hannover, Germany; ³Centre for Individualised Infection Medicine (CIIM), Hannover, Germany
Email: maasoumy.benjamin@mh-hannover.de

Background and aims: Non-selective beta-blockers (NSBB) are commonly used to treat portal hypertension in patients with liver cirrhosis. An even more effective reduction and often normalization of portal pressure can be achieved by insertion of a transjugular intrahepatic portosystemic shunt (TIPS). So far, it remains unclear whether NSBB should be stopped immediately after TIPS. Recent data suggest that NSBB exert some additional e.g. anti-inflammatory effects that are independent from pressure reduction and may contribute to a favourable clinical outcome. The aim of this study was to evaluate if NSBB treatment is linked to survival and/or liver-related events after TIPS-insertion.

Method: A number of 235 consecutive cirrhotic patients receiving a TIPS between 2009 and 2019 were included. Patients were followed up for acute kidney injury (AKI), acute-on-chronic liver failure (ACLF), hepatic encephalopathy (HE), infections and mortality for one year after TIPS insertion. Intake of NSBB was assessed prior to TIPS insertion and at the time of hospital discharge. Incidence of periinterventional complications until hospital discharge was analyzed with binary logistic regression adjusting for the recently introduced FIPS-Score. Link between NSBB intake at hospital discharge and further survival and the development of liver-related complications was tested using a multivariable Cox Regression adjusting for TIPS indication (refractory ascites) and FIPS-Score.

Results: Median age of the patients was 59 years, median FIPS –0.15 and median MELD 12.0. TIPS insertion effectively treated portal hypertension in 234 patients (99.6%) as indicated by pressure reduction of >50% or a PSG value <12 mmHg after TIPS. At baseline 136 patients received NSBB therapy (57.9%). Patients in the NSBB group were younger (57 vs 61 years, $p=0.030$) and had lower FIPS (–0.34 vs –0.02, $p=0.002$) and MELD (11.5 vs 12.6, $p=0.014$). Variceal bleeding as TIPS indication was more common in the NSBB group (38.2% vs 8.1%, $p<0.001$). Periinterventional development of AKI, infections and HE as well as in-hospital mortality did not differ between the two groups. In contrast, NSBB therapy prior to TIPS-insertion was associated with a significantly lower incidence of ACLF

during hospitalization ($p=0.012$); however, this did not remain significant after adjusting for FIPs.

Overall, 91 patients (40.3%) were still on NSBB treatment at the time of hospital discharge. NSBB therapy at discharge was neither linked to survival nor to development of AKI, ACLF or incidence of infections during further follow-up in the univariable and multivariable analysis.

Conclusion: Intake of NSBB prior to TIPS is not linked to the risk of periinterventional complications. Use of NSBB after TIPS has no impact on the risk for AKI, ACLF, infections and mortality. Thus, NSBB may be stopped in patients achieving sufficient pressure reduction after TIPS.

FR1515

Real world validation of BAVENO-7 non-invasive diagnosis for clinically significant portal hypertension in compensated advanced chronic liver disease: international cohort study

Yu Jun Wong^{1,2}, Junhui, Garrett Kang³, Elisabetta Degasperis⁴, Giulia Tosetti⁴, Sanchit Sharma⁵, Chuan Liu⁶, Jia Li^{7,8}, Xiaolong Qi⁶, Anoop Saraya⁵, Massimo Primignani⁴. ¹Duke-NUS Medical School, Singapore, Singapore; ²Department of Gastroenterology & Hepatology, Changi General Hospital, Singapore; ³Changi General Hospital, Singapore, Singapore; ⁴Policlinico of Milan, Milano, Italy; ⁵All India Institute Of Medical Sciences, New Delhi, New Delhi, India; ⁶The First Hospital of Lanzhou University, Lanzhou, China; ⁷Tianjin, China; ⁸The Second Hospital of Tianjin, Tianjin, China
Email: eugene.wong.yj@singhealth.com.sg

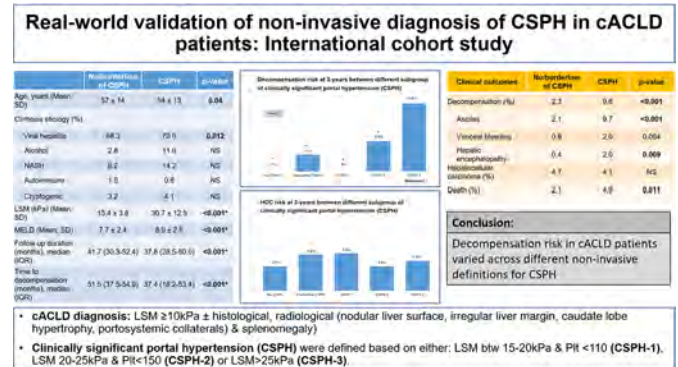
Background and aims: The presence of clinically significant portal hypertension (CSPH) confer a 10-fold higher risk of decompensation in compensated advanced chronic liver disease (cACLD) patients. Recent BAVENO-7 consensus proposed that non-invasive criteria may be used to identify cACLD patients with CSPH using liver stiffness measurement (LSM) and platelet count. Whether non-invasive diagnosis of CSPH could predict clinically meaningful outcomes such as decompensation, hepatocellular carcinoma (HCC) and death, remained unclear. We aim to validate the real-world performance of Baveno-7 CSPH criteria to predict liver decompensation in cACLD patients.

Method: We analysed cACLD patients from 4 countries (Singapore, China, India and Italy). cACLD was diagnosed based on LSM > 10 kPa, with or without histological, radiological or clinical features of liver cirrhosis. CSPH was defined as either LSM between 15 and 20 kPa and platelet < 110 (CSPH-1), LSM 20–25 kPa and platelet < 150 (CSPH-2), or LSM > 25 kPa (CSPH-3). Absence of CSPH was defined as LSM < 15 kPa and platelet > 150. Patients who did not fulfilled either of the above criteria were categorized as borderline CSPH. Exclusion criteria were: prior or current liver decompensation, use of non-selective beta-blocker, untreated viral hepatitis and active alcohol drinking. Primary outcome was liver decompensation; secondary outcome were HCC and death.

Results: The cohort had 1,166 cACLD patients, with a mean age of 55.4 years, 67% male; 69.5% Asian (Chinese 28.6%, Indian 26.6%, Malay 9.7%, Arabic 2.5%, others 2.1%) and Caucasian 30.5%. Primary etiology of cirrhosis was viral hepatitis (77.4%) followed by alcohol (8.8%), NASH (9%), autoimmune (1.1%) and others (3.7%). Total of 54.5% fulfilled diagnosis of CSPH (CSPH-1: 11.6%, CSPH-2: 22.3%, CSPH-3: 66.1%), 12.3% without CSPH and 33.2% were borderline for CSPH. Presence of CSPH predict higher risk of decompensation (HR 4.6, 95%CI: 2.5–8.6) and mortality (HR 2.4, 95%CI: 1.2–4.8) at 3 years.

Decompensation occurred in 7.3% (ascites 6.3%, variceal bleeding 1.5%, encephalopathy 1.3%) over median follow-up of 40 months. The 3-year decompensation risk were 0%, 3.1%, 0%, 5.6%, 12.6% in cACLD patients without CSPH, borderline CSPH, CSPH-1, CSPH-2 and CSPH-3, respectively. The 3-year decompensation risk of CSPH-3 was significantly higher than cACLD patients with CSPH-2, CSPH-1 and borderline CSPH ($p < 0.05$ for all). The 3-year decompensation risk of

CSPH-1 was similar to those without CSPH, and was significantly lower than CSPH-2 (0% vs 5.6%, $p < 0.05$). 3-year HCC risk were similar between CSPH subgroups.



Conclusion: Decompensation risk in cACLD patients varied across different non-invasive definitions of CSPH. LSM > 25 kPa is a reliable, non-invasive diagnosis for CSPH, which correlates with significantly higher risk of decompensation in cACLD patients.

FR1516

Derivation of machine learning histologic scores correlating with portal pressures and the development of varices in NASH patients with cirrhosis

Mazen Nouredin¹, Dean Tai², Elaine Chng², Yayun Ren², Pol Boudes³, Harold Shlevin³, Stephen Harrison⁴, Guadalupe Garcia-Tsao⁵, Zachary Goodman⁶, Naga Chalasani⁷. ¹Division of Digestive and Liver Diseases, Comprehensive Transplant Center, Cedars-Sinai Medical Center; ²HistoIndex Pte. Ltd., Singapore; ³Galectin Therapeutics, United States; ⁴Pinnacle Clinical Research, San Antonio, TX, USA; ⁵Section of Digestive Diseases, Yale University and CT-VA Healthcare System, Connecticut, USA; ⁶Inova Fairfax Hospital, Falls Church, Virginia, USA; ⁷Division of Gastroenterology and Hepatology, Department of Medicine, Indiana University School of Medicine, USA
Email: mazen.nouredin@cshs.org

Background and aims: In clinical trials of non-alcoholic steatohepatitis (NASH) cirrhosis, primary efficacy endpoints have been hepatic venous pressure gradient (HVPG), liver histology and clinical outcomes. Conventional histological assessment of cirrhosis do not include important features such as septa thickness, nodules features, and fibrosis area. We have assessed these with a machine learning (ML) model.

Method: NASH patients with compensated cirrhosis and HVPG ≥ 6 mm Hg (n = 143) were included from the Belapectin phase 2b trial (NCT02462967). Liver biopsies, HVPG measurements, and upper endoscopy were performed at baseline (BL) and at end of treatment (EOT). A second harmonic generation/two-photon excitation fluorescence (SHG/TPEF) imaging-based tool provided an automated quantitative assessment of histologic features: 252 related to septa, 21 related to nodules, and 184 related to fibrosis (SNOF). We also created ML scores and tested their association with HVPG and clinically significant portal hypertension (CSPH: HVPG ≥ 10 mm Hg) and its changes as well as with the presence of varices (SNOF-V).

Results: Samples were divided into training (BL) and validation (EOT). We found that septa [$r = 0.55$ (training) and 0.56 (validation)], nodule [$r = 0.52$ (training), and 0.53 (validation)], and fibrosis [$r = 0.57$ (training) and 0.62 (validation)] parameters correlated individually with HVPG ($P < 0.05$). Combining these parameters in the SNOF score showed better correlations of r of 0.57 (training) and 0.70 (validation) with HVPG ($P < 0.05$). The SNOF score (≥ 11.78) distinguished CSPH at BL and in the validation cohort (BL + EOT) [AUC = 0.85 and 0.74, respectively]. The SNOF-V score (≥ 0.57) distinguished the presence of varices at BL and in the same validation cohort [AUC =

POSTER PRESENTATIONS

0.86 and 0.73, respectively]. The SNOF-C score differentiated those who had >20% change in HVPG against those who did not, with an AUROC of 0.89.

Table: Metrics of SNOF and SNOF-V scores at predicting HVPG and presence of varices

	BL					BL + EOT				
	AUC	Sensitivity	Specificity	PPV	NPV	AUC	Sensitivity	Specificity	PPV	NPV
SNOF score ≥ 11.78 to predict HVPG ≥ 10 (CSPH)	0.85	73%	86%	91%	62%	0.74	65%	76%	83%	54%
SNOF-V score ≥ 0.57 to predict varices	0.86	77%	86%	85%	78%	0.73	64%	78%	74%	70%

Conclusion: The ML algorithm accurately predicted HVPG, CSPH and its changes, development of varices in patients with NASH cirrhosis. Use of ML histology model in NASH cirrhosis trials may improve the assessment of key outcome changes.

FRI517

Ruling out varices needing treatment with a non-invasive score in patients with compensated HBV cirrhosis

Giacomo Emanuele Maria Rizzo¹, Pietro Graceffa¹, Fabrizio Bronte¹, Giuseppe Falco¹, Gabriele Rancatore¹, Ciro Celsa¹, Giada Reina¹, Fabio Simone¹, Sergio Peralta¹, Antonio Craxi¹, Vito Di Marco¹, Vincenza Calvaruso¹. ¹University of Palermo, Gastroenterology and Hepatology Unit, PROMISE, Palermo, Italy
Email: vincenza.calvaruso@unipa.it

Background and aims: Non-invasive criteria to rule-out oesophageal varices needing treatment (VNT) in patients with compensated HBV cirrhosis on long-term treatment with nucleoside analogs (NUCs) are lacking. We have assessed the performance of an algorithm combining platelets and albumin (PLT-ALB) in a cohort of such patients under endoscopic (EGD) surveillance.

Method: All consecutive patients with compensated HBV cirrhosis who achieved HBV DNA suppression on NUCs since at least 1 year were classified at the moment of EGD as: -PLT-ALB IN (low risk for VNT) if platelets were $>120 \times 10^9/L$ plus serum albumin >3.6 g/dL. -PLT-ALB OUT (high risk for VNT) if platelets were $<120 \times 10^9/L$ and/or serum albumin <3.6 g/dL. Primary outcome was the finding of VNT at EGD. Performance of PLT-ALB scoring to predict the outcome was assessed measuring the receiver operating characteristic (AUROC) curve. 87 patients in Child-Pugh A class (mean age 52 years, 75.9% males) were assessed, 46 treated with Entecavir and 41 with Tenofovir. Seven patients (8%) had VNT, all being PLT-ALB OUT.

Results: Among the 41 PLT-ALB IN patients (47.1%) no VNT were found (NPV 100%). The PLT-ALB algorithm showed an AUROC of 0.76, potentially saving 47% of EGDs, with a false negative rate (FNR) of 0% and a false positive rate (FPR) of 48.1%.

Conclusion: APLT-ALB algorithmic approach based on widely available noninvasive parameters can avoid up to 50% EGDs aimed to screen for high-risk varices patients with compensated HBV cirrhosis under NUC suppression. Further validation in larger cohorts are needed before translating this approach into practice.

FRI518

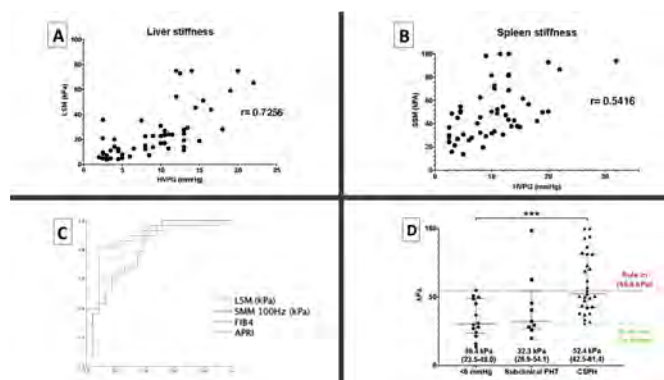
Evaluation of clinically significant portal hypertension with a novel spleen-dedicated probe using transient elastography

Aitor Odriozola Herrán¹, Jose Ignacio Fortea¹, Angela Puente¹, Antonio Cuadrado¹, Emilio Fabrega¹, Maria Teresa Arias Loste¹, Paula Iruzubieta¹, Coral Rivas¹, Juan Carlos Rodriguez Duque¹, Ines García¹, Marina Cobreros¹, María Del Barrio¹, Alex García Tellado², Javier Crespo¹. ¹University Hospital Marqués de Valdecilla, Gastroenterology and Hepatology Service, Santander, Spain; ²University Hospital Marqués de Valdecilla, Internal Medicine, Santander, Spain
Email: aodrihe94@gmail.com

Background and aims: Most studies evaluating the association between spleen stiffness (SS) by transient elastography and the presence of portal hypertension (PH) have used the 50 Hz probe (range: 1.5–75 kPa). Whether the previously reported cut-off values can be extrapolated to those obtained by the spleen-dedicated 100 Hz probe (SSM@100 Hz, range: 6–100 kPa; FibroScan® Expert 630) is uncertain since there is only one study that has assessed its correlation with the hepatic venous pressure gradient (HVPG). In the current study, we aimed to examine its diagnostic accuracy for PH in comparison to other non-invasive tests.

Method: Retrospective single center study. Patients with available liver stiffness (LSM)-SSM and HVPG within 12 months were included. Patients with unstable liver disease (i.e., new decompensated events or any intervention that may impact PH between SSM and HVPG), non-cirrhotic PH, hepatocellular carcinoma (CHC) outside Milan criteria, liver transplants and transjugular intrahepatic portosystemic shunts were excluded. AUROC analysis was conducted to identify dual cut-offs (rule in and out) associated with the presence/absence of clinically significant PH (CSPH).

Results: A total of 56 patients were included with a median interval between HVPG and LSM/SSM of 3.3 months (interquartile range (IQR) 0.4–7.2). LSM and SSM were not feasible in 1 (2%) and 4 (7%) patients. Median age was 60 years (54–70), 71% were males and non-alcoholic fatty liver disease was the most prevalent underlying etiology (50%). Most patients were Child-Pugh A (82%, none C) with a median MELD score of 8 (8–10). A history of decompensation and CHC had occurred in 14 (25%) and 2 (4%) patients. CSPH was present in 29 patients (51.8%), 69% of whom had HVPG ≥ 12 mmHg. Median (IQR) LSM and SSM were 19.2 (10.5–30.8) and 46, 5 (31, 0–62, 5) kPa, and both showed positive correlation with HVPG (Figure 1A/1B). For CSPH, the AUROC of SSM was 0.81 (95% CI 0.68–0.93) and was lower than LSM [0.89 (0.79–0.98), APRI [0.84 (0.74–0.95)], and FIB-4 [0.87 (0.77–0.98)] (Figure 1C). The SSM cutoffs to rule in and out CSPH were 55, 8 (positive predictive value 83, 8%) and 31, 3 kPa (negative predictive value 93.8%) (Figure 1D).



Conclusion: SSM@100 Hz constitutes a good non-invasive test for portal hypertension and can be used to rule in and out clinically significant portal hypertension. However, in our cohort its diagnostic performance was lower than other non-invasive tests, showing LSM the highest accuracy.

FRI519

Are psychometric tests helpful for the prediction of hepatic encephalopathy after TIPS insertion?

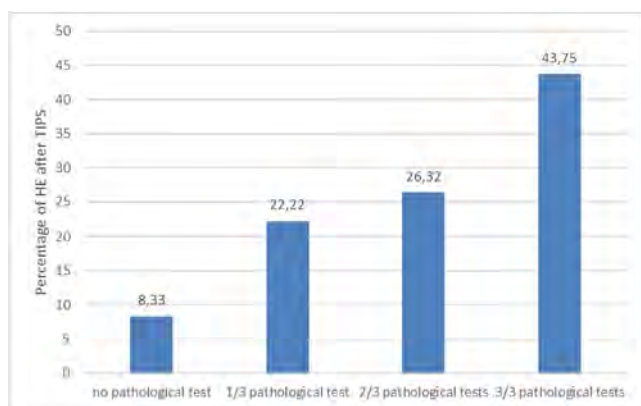
Alena Friederike Ehrenbauer^{1,2}, Hannah Schneider², Lena Stockhoff², Anja Tiede², Meike Dirks¹, Jennifer Witt², Katja Deterding², Henning Pflugrad¹, Maria Magdalena Gabriel¹, Denise Menti², Bernhard Meyer³, Heiner Wedemeyer², Jan Hinrichs³, Karin Weissenborn¹, Benjamin Maasoumy^{2,4}. ¹Hannover Medical

School, Department of Neurology, Hannover, Germany; ²Hannover Medical School, Department of Gastroenterology, Hepatology and Endocrinology, Hannover, Germany; ³Hannover Medical School, Department of Diagnostic and Interventional Radiology, Hannover, Germany; ⁴Center for Individualised Infection Medicine (CIIM), Hannover, Germany
Email: maasoumy.benjamin@mh-hannover.de

Background and aims: Hepatic encephalopathy (HE) is a frequent and severe complication in patients after transjugular intrahepatic portosystemic shunt (TIPS) insertion. Of note, risk factors for post-TIPS HE remain poorly defined. Presence of minimal HE (mHE) is a well-known risk factor for development of overt HE in cirrhotic patients without TIPS. Different psychometric tests, which differ in their diagnostic performance, have been suggested to diagnose mHE. However, their role for the prediction of post-TIPS HE still needs to be determined. We aimed to evaluate the value of three different psychometric tests for the prediction of HE after TIPS.

Method: We prospectively recruited 85 consecutive cirrhotic patients before TIPS insertion and monitored them for 180 days after TIPS insertion for development of HE. 65 patients underwent all psychometric tests: the Portosystemic Encephalopathy Syndrome Test (PSE, Version 2.0; 2020) (cut off <-4), the Animal Naming Test (ANT) (cut-off of <23 animals/minute) and the Critical Flicker Frequency (CFF) (cut-off <39 Hz). Association to HE development was tested using multivariable cox-regression analysis adjusting for all additional parameters with p-value<0.05 in univariable analysis.

Results: Median age was 59 and MELD 12. Indication for TIPS was refractory ascites in 75% of patients. Evaluation for mHE at baseline yielded pathological results in 67%, 24% and 66% of patients according to PSE (gold standard), CFF and ANT, respectively. The highest concordance was observed between PSE and ANT and lowest between PSE and CFF. After TIPS insertion, 24 patients (28%) developed at least one HE episode in the first 180 days. Among all parameters, a larger stent diameter (p=0.049), higher serum-creatinine (p=0.022) and pathological CFF (p=0.001) were significantly associated with HE development in univariable analysis. Of note, pathological CFF values at baseline remained significant in the multivariable model (p=0.001). In contrast, pathological PSE and pathological ANT values were not significantly associated with HE after TIPS neither in univariable (PSE p=0.357 and ANT p=0.098) nor in multivariable analysis (PSE p=0.495 and ANT p=0.050). However, also CFF had a limited value in predicting HE: sensitivity was 61%, specificity 80%, positive predictive value 45% and negative predictive value 85%. Predictive value slightly improved by combining all psychometric tests (figure). Among the 12 patients with normal results in all tests HE incidence was 8% (n=1) compared to 44% (n=7) among those 16 patients with concordant pathological values.



Conclusion: Development of HE after TIPS is a multifactorially influenced event. Psychometric tests, which were designed for diagnosis of mHE, have limited value for predicting HE after TIPS

insertion. The relatively good predictive value of CFF could implicate altered pathomechanism of HE after TIPS.

FR1520

Stratified efficacy of first -line therapy to prevent first variceal bleeding according to previous decompensation of cirrhosis. A competing-risk meta-analyses of individual participant data

Càndid Villanueva^{1,2}, Víctor Sapena³, Gin-Ho Lo⁴, Yeon Seok Seo⁵, Hasnain A. Shah⁶, Virendra Singh⁷, Dhiraj Tripathi⁸, Michael Schepke⁹, Cristian Gheorghe¹⁰, Danielle Q Bonilha¹¹, Rome Jutabha¹², Susana G. Rodrigues¹³, Edilmar Alvarado-Tapias^{1,2}, Anna Brujats², Peter Hayes¹⁴, Tilman Sauerbruch¹⁵, Wen-Chi Chen¹⁶, Speranta Iacob¹⁰, Ermelindo D Libera¹⁷, Dennis M Jensen¹⁸, Pramod Kumar¹⁹, Lee Han Ah²⁰, Huay-Min Wang²¹, Ferran Torres²², Zahid Azam²³, Jaime Bosch^{1,24}. ¹Centro de Investigación Biomédica en Red de Enfermedades Hepáticas y Digestivas (CIBERehd), Madrid; ²Hospital de la Santa Creu i Sant Pau. Biomedical Research Institute Sant Pau (IIB Sant Pau). Universitat Autònoma de Barcelona., Barcelona, Spain; ³Medical Statistics Core Facility, IDIBAPS, Hospital Clinic, Barcelona; ⁴Division of Gastroenterology, Department of Medicine, Kaohsiung Veterans General Hospital, National. Yang-Ming University, Taipei, Taiwan, Republic of China; ⁵Division of Gastroenterology and Hepatology. Department of Internal Medicine. Korea University College of Medicine, Seoul, Korea; ⁶Section of Gastroenterology, Aga Khan University, Karachi, Pakistan; ⁷Department of Hepatology. Post Graduate Institute of Medical Education and Research, Chandigarh, India; ⁸University Hospitals Birmingham NHS Foundation Trust. Birmingham, UK. Institute of Immunology and Immunotherapy, University of Birmingham. UK. Department of Hepatology. Royal Infirmary of Edinburgh, Edinburgh, UK; ⁹Helios Clinic Siegburg, Department Gastroenterology and Hepatology, Ringstr. 49, D-53721 Siegburg, Germany; ¹⁰Center of Gastroenterology & Hepatology, Fundeni Clinical Institute. "Carol Davila" University of Medicine. Bucharest, Romania; ¹¹Department of gastroenterology. Federal University of São Paulo., State University of Campinas. Brasil; ¹²University of Southern California (USC) School of Medicine. Los Angeles, Keck School of Medicine of University of Southern California and Clinical Outreach and Development, Keck Hospital of USC, USA; ¹³University Clinic for Visceral Surgery and Medicine, Inselspital, Bern University Hospital. Hepatology, Department of Biomedical Research, University of Bern, Switzerland; ¹⁴Department of Internal Medicine I, University of Bonn, Bonn, Germany; ¹⁵Department of Internal Medicine I, University of Bonn, Bonn, Germany, Germany; ¹⁶Division of Gastroenterology, Department of Medicine, Kaohsiung Veterans General Hospital, National. Yang-Ming University, Taipei, Taiwan, Republic of China; ¹⁷Division of Gastroenterology, Federal University of São Paulo, Brasil; ¹⁸Department of Medicine, Division of Digestive Diseases, David Geffen School of Medicine at UCLA, Los Angeles, California, USA; ¹⁹Department of Hepatology. Post Graduate Institute of Medical Education and Research, Chandigarh, India, India; ²⁰Division of Gastroenterology and Hepatology. Department of Internal Medicine. Korea University College of Medicine, Seoul, Korea., Korea, Dem. People's Rep. of; ²¹Division of Gastroenterology, Department of Internal Medicine, Kaohsiung Veterans. General Hospital, Kaohsiung, Taiwan. Republic of China; ²²Medical Statistics Core Facility, IDIBAPS, Hospital Clinic, Barcelona. Biostatistics Unit, Faculty of Medicine, Universitat Autònoma de Barcelona, Barcelona; ²³National Institute of Liver & GI Diseases, Dow University of Health Sciences. Karachi, Pakistan., National Institute of Liver & GI Diseases, Dow University of Health Sciences, Karachi, Pakistan., Pakistan; ²⁴Hepatology, Department of Biomedical Research, University of Bern, Switzerland
Email: cvillanueva@santpau.cat

Background and aims: Non-selective β -blockers (NSBB) and endoscopic variceal ligation (EVL) are indicated to prevent first variceal bleeding in cirrhosis. However, compensated and decompensated cirrhosis differ in pathophysiology, prognosis and response to NSBB. Moreover, recent data show that NSBB may prevent ascites in compensated patients. We aimed to assess the efficacy of NSBB vs

POSTER PRESENTATIONS

EVL in patients with high-risk varices treated to prevent first bleeding, stratifying risk according compensation/decompensation of cirrhosis.

Method: A systematic review was performed to identify RCTs comparing NSBBs vs EVL, either in monotherapy or combined, for 1ry prevention of bleeding in cirrhosis. We performed a competing-risk time-to-event meta-analysis using individual patient data (IPD) obtained from principal investigators of RCTs, using an Inverse Probability of the Treatment Weights (IPTW) approach. Analyses were stratified according to present or previous decompensation (bleeding, ascites or encephalopathy). Outcomes included death, prevention of bleeding and prevention of ascites. OLT and death were competing-events.

Results: Among 25 RCTs eligible, 11 providing IPD were included. Overall, 1400 patients were included (656 compensated), 625 treated with NSBB, 546 with EVL and 229 with NSBB+EVL. There were no differences in baseline characteristics between groups. Over 19 months of follow-up, bleeding occurred in 16% compensated vs 16% decompensated (SHR = 1.09, 95% CI = 0.83–1.44, $P = 0.537$), and death in 15% vs 28% respectively (SHR = 2.58, 95% CI = 1.02–3.28, $P < 0.0001$). Overall, risk of death was similar with EVL vs NSBB (SHR = 1.04, 95% CI = 0.71–1.52, $P = 0.848$) and with EVL+NSBB vs either alone, with heterogeneity ($I^2 = 77\%$). In compensated patients, mortality risk was lower with NSBB vs EVL (SHR = 0.57, 95% CI = 0.36–0.90; $P = 0.016$) and was similar with NSBB+EVL vs NSBB ($p = 0.104$), without heterogeneity ($I^2 = 0.0\%$). In decompensated patients, mortality risk was similar with EVL vs NSBB (SHR = 0.81, 95% CI = 0.52–1.26, $P = 0.350$) and with NSBB+EVL vs NSBB ($p = 0.469$) and vs EVL ($p = 0.357$), without heterogeneity ($I^2 = 34\%$). The risk of first bleeding was similar with EVL vs NSBB in compensated ($p = 0.85$) and decompensated patients ($p = 0.64$). The risk of ascites was higher with EVL vs NSBB (SHR = 2.66, 95% CI = 1.36–5.19, $P = 0.004$) in compensated patients and was similar in decompensated ($p = 0.316$).

Conclusion: In patients with compensated cirrhosis and high-risk varices treated to prevent bleeding, NSBB achieved better survival than EVL, without additional benefit by adding EVL to NSBB. The risk of bleeding was similar with both therapies but risk of developing ascites was lower with NSBB. In decompensated patients, survival was similar using NSBB or EVL or combining both. The NSBB may be preferable in compensated patients for prevention of bleeding, while either NSBB or EVL can be used in decompensated.

FRI521

Baseline plasma renin activity (PRA) predicts risk of AKI in patients with cirrhosis: a prospective observational study

Srinivasa Reddy Golamari¹. ¹ILBS/Vasant Kunj Sector A, Hepatology, New Delhi, India

Email: srinivasareddygolamari@gmail.com

Background and aims: Plasma renin activity (PRA), is a measure of the activity of the plasma enzyme renin; which plays a major role in the body's regulation of blood pressure, thirst, and urine output. The degree of impairment in renal function, mainly decrease in renal perfusion and glomerular filtration rate (GFR) correlates with the activity of the endogenous vasoconstrictor system and both correlate with the severity of portal hypertension. Overactive RAAS system leads to renal vasoconstriction, renal injury and failure. We aimed to study the effect of PRA on organ injury/failure in cirrhosis.

Method: A total of 63 patients with cirrhosis, presenting for the first time with grade II/III ascites and no prior ascitic tap, were enrolled in a cross sectional study. At admission and during the hospital stay, presence and development of acute kidney injury (AKI) was studied and correlation with baseline serum PRA was determined.

Results: Altogether, 63 patients with ascites [62% males, with mean age 46.56 ± 12.59 years, CTP, 8.4 ± 1.1 , MELD 18.4 ± 4.1 , and MAP 74 ± 8.2 mmHg] were included. Forty two percent of patients had AKI at baseline. Ninety percent of the patients were on diuretics with a median dose of frusemide 15 mg (10–20) and spironolactone of

37.5 mg (25–50) per day. Mean PRA levels at presentation were 16.07 ± 1.4 (Normal 0.6–4.3 ng/ml/hr.). Baseline serum PRA levels were significantly associated with the presence or development of AKI during the hospital stay ($p = 0.001\%$, OR = 1.22 95% CI: 1.096–1.36]. A PRA value of 16.7 ng/ml/hr increased the risk of AKI with AUC = 0.95%, with a sensitivity of 0.83, and specificity of 0.87. Every 1 ng/ml/hr increase in the PRA level was associated with 0.03 mg/dl increase in serum creatinine from baseline.

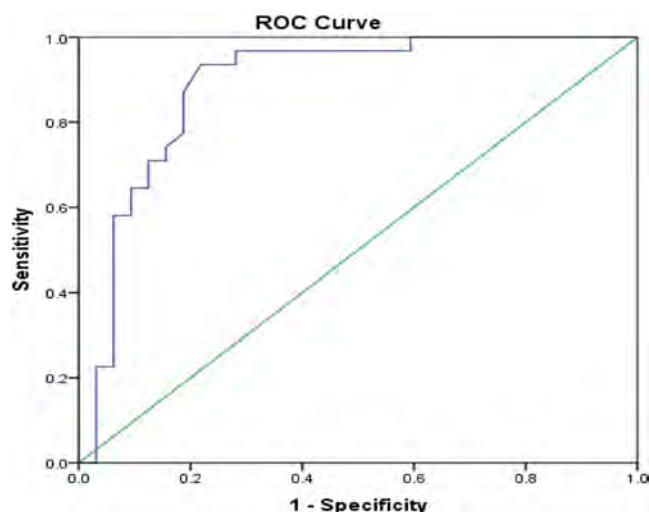


Figure 1: Correlation of serum PRA with AKI-A Kaplan-Meier analysis. [AUC = 0.95%, Sensitivity = 0.83, Specificity = 0.87, 95% CI = 79.8–97.5].

Conclusion: The serum PRA levels closely correlate with the acute kidney injury. Patients with high serum PRAs have a much higher risk of developing AKI. Therefore, baseline serum PRA can serve as a simple and reliable laboratory marker to assist in the prognosis of renal injury in decompensated cirrhosis patients.

FRI522

Performance of spleen stiffness measured by point-shear wave elastography in esophageal varices screening

Mauro Giuffrè^{1,2,3}, Alessia Visintin^{1,2,3}, Cristiana Abazia^{1,2,3}, Flora Masutti^{1,2,3}, Saveria Lory Croce^{1,2,4}. ¹Università Degli Studi Di Trieste, Dipartimento Universitario Clinico Di Scienze Mediche Chirurgiche e Della Salute; ²Fondazione Italiana Fegato Onlus, Basovizza, Italy; ³ASUGI Clinica Patologie del Fegato, Trieste, Italy; ⁴ASUGI Clinica Patologie del Fegato, ospedale cattinara, Trieste, Italy
Email: gff.mauro@gmail.com

Background and aims: According to Baveno VI guidelines, esophago-gastroduodenoscopy (EGD) to stage esophageal varices (EVs) can be avoided in patients with chronic advanced liver disease who have a liver stiffness (LS) <20 kPa and a platelet count $>150 \times 10^3/\mu\text{L}$. Current evidence suggests that spleen stiffness (SS) <46 kPa, measured by transient elastography, can safely predict absence of high-risk varices (HRV). Our aim is to externally validate those data by performing SS measurement with point-shear wave elastography.

Method: We enrolled 500 consecutive patients with compensated liver cirrhosis, of which $n = 208$ (40.4%) had esophageal varices (150 EVs, 58 HRV).

Results: Median SS values were 36 (28.5/45.3) kPa. Patients with EVs had higher median SS values if compared to patients without EVs (45.5 vs. 30 kPa, $p < 0.001$). A similar trend was detected in LS values (23 vs. 15 kPa, $p < 0.001$).

SS showed an AUROC of 0.88 (95% C.I. 0.85–0.9, $p < 0.001$) to discriminate between patients with and without EVs of any kind. Also, SS <30 kPa showed the highest sensitivity to rule-out EVs of any kind (sensitivity 100%, specificity 64%, accuracy 77%); SS >38.5 can rule-in the presence of EVs of any kind with a sensitivity of 87%,

specificity of 89%, accuracy 85%; SS >46 kPa can rule-in the presence of HRV with a sensitivity of 90%, specificity of 89%, accuracy 86%. Furthermore, SS showed a positive linear correlation with splenic bipolar diameter ($R=0.60$, $p<0.001$), splenic area ($R=0.70$, $p<0.001$), and a negative linear correlation with the platelet count ($R=-0.79$, $p<0.001$).

Conclusion: The results of this study show how SS measurements can play an important role in the daily clinical management of cirrhotic patients. The SS (alone or combined with other indicators) may play an important role as a non-invasive screening test to predict the risk of EVs in patients with liver cirrhosis.

FRI523

Portal pressure decreasing effect of beta blockers in cirrhosis with clinically significant portal hypertension, according to the components of metabolic syndrome

Anna Brujats¹, Berta Cuyas¹, Edilmar Alvarado-Tapias^{1,2}, Claudia Pujol¹, Antoni Mombiola¹, Cristina Roig¹, Maria Poca^{1,2}, Xavier Torras¹, Àngels Escorsell^{1,2}, Cándid Villanueva^{1,2}, ¹Hospital de la Santa Creu i Sant Pau, Gastroenterology and Hepatology Department, Biomedical Research Institute Sant Pau (IIB Sant Pau). Universitat Autònoma de Barcelona; ²Centro de Investigación Biomédica en Red de Enfermedades Hepáticas y Digestivas (CIBERehd). Instituto de Salud Carlos III
Email: annabrujats@gmail.com

Background and aims: Patients with cirrhosis due to metabolic associated fatty liver disease (MAFLD) have higher risk of complications related to portal hypertension at any HVPG threshold than patients with HCV cirrhosis. MAFLD is associated with metabolic comorbidities such as obesity, diabetes mellitus (DM), arterial hypertension (AHT) and dyslipidemia (DLP), which may affect vascular response to beta blockers (NSBB). However, whether the unfavorable outcomes in patients with MAFLD can be related to an impact of metabolic comorbidities on the hemodynamic response to NSBB has not been clarified. We aimed to investigate whether the effect of NSBBs on portal pressure may be worse with metabolic comorbidities.

Method: Patients with cirrhosis and high-risk varices, were consecutively included. Hemodynamic measurements were performed at baseline and were repeated 15 to 20 minutes after intravenous administration of propranolol (0.15 mg/Kg). The HVPG response was investigated by grouping patients according to obesity, DM, AHT and DLP. The effect of propranolol was adjusted for baseline differences between groups using propensity score (PS).

Results: 585 patients were included (71% male, mean age 62 ± 11 years), 41% were Child Pugh class A and 59% class B/C, with MELD score of 12 ± 4 . The etiology of cirrhosis was alcohol in 48%, HCV in 36% and MAFLD in 90 (15%). 178 (30%) patients had DM, 116 (20%) obesity, 220 (38%) AHT and 100 (17%) DLP. 191 (33%) had ≥ 1 metabolic comorbidity. After propranolol, mean decrease in HVPG was lower in patients with DM than in those without DM ($9 \pm 10\%$ vs $13.4 \pm 10\%$, $p<0.01$), lower in obesity vs normo-weight ($10.7 \pm 9\%$ vs $13.5 \pm 10\%$, $p=0.04$), lower in AHT vs without ($10.7 \pm 10\%$ vs $13.1 \pm 10\%$, $p=0.02$) and lower in DLP vs without ($9.7 \pm 8\%$ vs $12.7 \pm 10\%$, $p=0.03$). Adjusting by PS only HVPG changes in DM were significant ($p=0.03$). Among metabolic comorbidities, only DM was independently associated with HVPG decrease by multivariate logistic regression (OR = 0.64, 95% CI = 0.41–0.99; $p=0.049$). Patients with DM had lower rates of HVPG decrease $\geq 10\%$ from baseline (46% vs 59%, $p=0.01$) and of HVPG decrease $\geq 20\%$ (8% vs 25%, $p<0.01$). Patients with MAFLD also had lower decrease in HVPG after propranolol than those with

cirrhosis not MAFLD related ($9 \pm 6\%$ vs $14 \pm 10\%$, $p<0.01$). By multivariate logistic regression, only MAFLD and not metabolic comorbidities, was independently associated with HVPG decrease ($p<0.01$). Among patients with MAFLD, HVPG decrease was $<10\%$ in all cases, either with or without each metabolic comorbidity.

Conclusion: Patients with MAFLD cirrhosis had worse hemodynamic response to NSBB than those with cirrhosis not MAFLD related. Among metabolic comorbidities, only the presence of DM has an independent negative influence on acute hemodynamic response to NSBB. However, the influence of MAFLD on hemodynamic response to NSBB was independent of DM or other metabolic comorbidities.

FRI524

Transjugular, intra-hepatic portosystemic shunt (TIPS) in elderly patients: preliminary analysis of a multi center retrospective cohort

Davide Roccarina¹, Laura Turco², Claudia Campani¹, Dario Saltini², Silvia Aspite¹, Vincenza Calvaruso³, Umberto Arena¹, Marco Senzolo⁴, Fabrizio Fanelli⁵, Cristian Caporali², Stefano Gitto¹, Michele Citone⁵, Chiara Di Bonaventura¹, Filippo Schepis², Francesco Vizzutti¹, Oliviero Riggio⁶, Patrizia Burra⁴, Erica Villa², Calogero Camma³, Fabio Marra¹, Marcello Bianchini², ¹University of Florence, Firenze, Italy; ²University of Modena and Reggio Emilia, Modena, Italy; ³Università degli Studi di Palermo, Palermo, Italy; ⁴University of Padua, Padova, Italy; ⁵Careggi University Hospital, Firenze, Italy; ⁶Sapienza University of Rome, Roma, Italy
Email: fabio.marra@unifi.it

Background and aims: TIPS is largely used in patients with cirrhosis affected by portal hypertensive (PH) complications such as bleeding gastro-esophageal varices (GEV) or refractory ascites (RA). However, data regarding its effectiveness and safety in elderly patients are limited. The objective of this study was to evaluate if TIPS might represent an effective and safe option in this group of patients.

Method: We retrospectively analyzed patients with cirrhosis who underwent TIPS implantation for RA and/or bleeding GEV at three Italian referral centers (Florence, Modena, Padua) between 2004 and 2021. A cut-off value of 70 years was considered to define elderly patients. Control of PH consequences, such as ascites and/or bleeding GEV, incidence of complications such as hepatic encephalopathy and deterioration of hepatocellular function, and death were evaluated in the two groups.

Results: A total of 347 consecutive patients, mean age 63.4 ± 8.2 y, 74% males, 35.7% alcohol, 27% HCV and 20% NASH, with a median follow-up of 609 days (IQR 1035) were included and divided into two groups: 252 (72%) were 69 years old or younger (<70 y, mean age 59.4 ± 5.5 y) and 95 (28%) were 70 years or older (≥ 70 y, mean age 74 ± 3.2 y). There were no statistically significant differences between the two groups before TIPS when comparing gender, BMI, TIPS indication, MELD or porta-caval gradient. In the <70 y group there was a higher number of patients with more advanced liver disease (Child-Pugh B and C 68.9% vs 59.3% and 7.5% vs 3.3%, respectively, $p=0.027$), while in the ≥ 70 y group there were significantly more patients with at least one comorbidity (>0.001). During follow-up, no significant differences between the two groups were observed in the overall incidence of all-grade encephalopathy or rebleeding episodes. Moreover, control of ascites or deterioration of hepatocellular function, evaluated at 1, 3, 6, and 12 months, were similar in the two groups. Regarding ascites control, similar results were obtained when the groups were stratified for Child-Pugh classification. Survival was significantly longer in the <70 y group ($p<0.001$). Age and MELD score before TIPS were predictors of mortality.

POSTER PRESENTATIONS

Conclusion: In elderly patients, TIPS implantation is an effective option for the treatment of complications of PH. In this population, the incidence of post-derivative encephalopathy and deterioration of liver function is similar to the one observed in younger patients.

FR1525

Endoscopic glue injection v/s endoscopic human thrombin injection for bleeding gastric varices -a randomized controlled trial

Ashok Jhaharia¹. ¹SMS Medical College, Gastroenterology, Jaipur, India
Email: drashokjhaharia@gmail.com

Background and aims: Acute gastric variceal bleeding (AGVB) is a potentially fatal consequence of portal hypertension, accounting for 10–30% of all variceal bleeding. Although endoscopic cyanoacrylate glue injection is a common treatment for acute hemostasis, it has been linked to significant side effects. In the treatment of AGVB, there is limited evidence of the efficacy and relative safety of endoscopic human thrombin injection over glue injection.

Method: A total of 52 AGVB patients were randomized to receive either thrombin injection (25 patients) or glue injection (27 patients). The primary outcome was the incidence of any glue or thrombin injection-related post-therapy complications. Initial hemostasis, rebleeding, and mortality were all secondary end goals.

Results: Both groups had comparable baseline data. Hemostasis of active bleeding at endoscopy was 100.0% (10/10) in the thrombin group and 87.5% (7/8) in the glue group ($p = 0.44$). Treatment failure after 5 days occurred in two patients (6.1%) in the glue group compared to none in the thrombin group ($p = 0.165$). Between 6 and 42 days after index bleeding, rebleeding occurred in 4 patients in the thrombin group compared to 12 patients in the glue group ($p < 0.03$). In the thrombin group, none of the patients had post treatment ulcers on gastric varices compared to 14.81% (4/27) that occurred in the glue group ($p < 0.045$). Overall, complications occurred in 4 (20%) and 11 (40.7%) patients in the thrombin and glue groups, respectively ($p = 0.105$). Two patients in glue group died.

Conclusion: In order to achieve successful AGVB hemostasis, endoscopic thrombin injection was identical to glue injection. However, glue injection may be linked to a higher rate of rebleeding and post-therapy gastric varices ulcerations.

FR1526

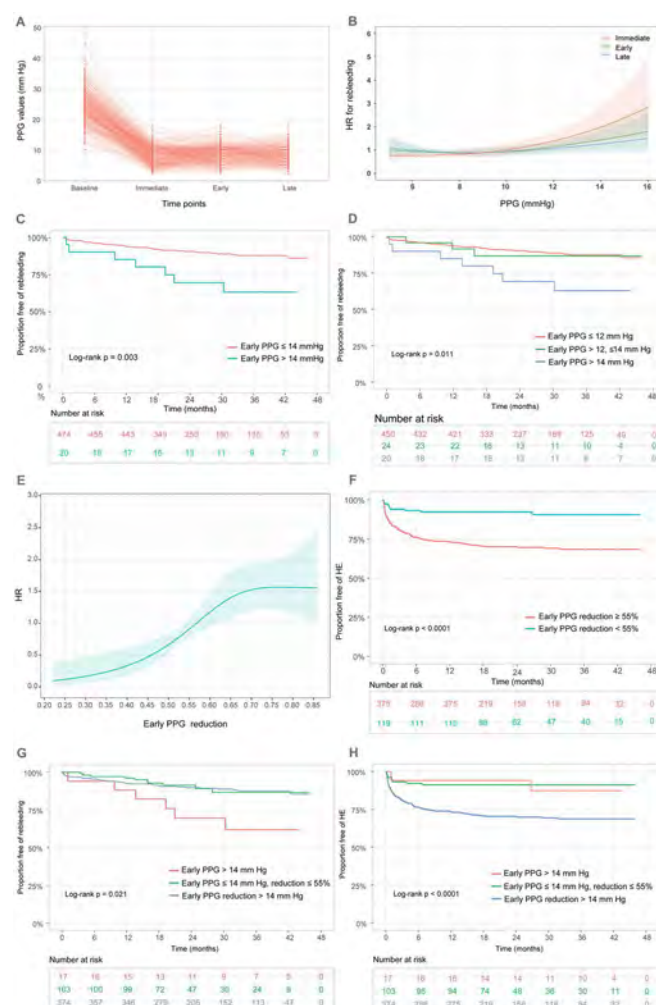
Updating target PPG value to reduce clinical events in patients receiving covered-TIPS for the prevention of variceal rebleeding

Qiuhe Wang¹, Bohan Luo¹, Wei Bai¹, Kai Li¹, Wengang Guo¹, Zhengyu Wang¹, Jie Yuan¹, Xiaomei Li¹, Yong Lv¹, Dongdong Xia¹, Zhanxin Yin¹, Jielai Xia², Guohong Han¹. ¹Department of Liver Diseases and Interventional Radiology, Digestive Diseases Hospital, Xi'an International Medical Center Hospital, Northwestern University, Xi'an, China; ²Department of Medical Statistics, Fourth Military Medical University
Email: 13991969930@126.com

Background and aims: A portosystemic pressure gradient (PPG) value of ≤ 12 mm Hg or $\geq 20\%$ decrease has long been established as the target for TIPS in preventing variceal rebleeding. However, this value was defined in the era of bare stents, when dysfunction rate was high with constantly increased PPG. Moreover, not reaching this target does not necessarily indicate rebleeding. We aimed to confirm the optimal time point to measure PPG as an outcome predictor and update its target value in the scenario of covered TIPS for the prevention of variceal rebleeding.

Method: Consecutive patients receiving TIPS for acute variceal bleeding or secondary prophylaxis of rebleeding during January 1st, 2017 to October 31st, 2019 were included. TIPS procedures with local anesthesia and 8 mm covered stents was performed. PPG was measured preoperatively, immediately after stenting (immediate PPG), within 24–72 h post-operatively (early PPG), and at 1 month (late PPG).

Results: TIPS indications were secondary prophylaxis of rebleeding in 463 (93.7%) patients and pre-emptive TIPS in 31 (6.3%) patients. Median follow-up was 24.4 (17.2–36.7) months. Baseline, immediate, early, and late PPG values were 24.4 ± 5.8 , 8.2 ± 3.0 mm Hg, 8.9 ± 3.1 mm Hg, and 8.7 ± 3.2 mmHg, respectively (Fig. 1A). Absolute early and late PPG were independent predictors of rebleeding in multivariate analyses, with similar HRs (1.11 [1.02–1.21], $p = 0.015$, vs. 1.09 [1.01–1.20], $p = 0.029$) and restrictive cubic spline curves (Fig. 1B). Given the easy access of early PPG before discharge, it was designated as the preferred timepoint. The cut-off value with the best discrimination for early PPG in predicting rebleeding was 14 mm Hg (Fig. 1C). Patients were then stratified into three subgroups: early PPG ≤ 12 mmHg, >12 mm Hg but ≤ 14 mmHg, and >14 mmHg. Patients with early PPG ≤ 14 mm Hg, whether lower than 12 mm Hg or not, had similar rates of variceal rebleeding, yet both strata exhibited lower rebleeding rates compared to that with early PPG >14 mm Hg (log-rank $p = 0.011$, Fig. 1D). As for HE, multivariate analyses indicated that early PPG reduction ($[\text{baseline PPG} - \text{early PPG}] / \text{baseline PPG}$) was an independent predictor (HR 1.05 [1.03–1.07], $p < 0.001$, Fig. 1E), with optimal cut-off being 55% (Fig. 1F). Given these results, the optimal window of PPG should be an absolute early PPG value ≤ 14 mm Hg (to control rebleeding), with early PPG reduction $\leq 55\%$ (to avoid excessive HE). Indeed, this subgroup of patients present the most satisfying results regarding both rebleeding and HE, as compared with other subgroups (Fig 1G, and 1H).



Conclusion: The optimal timepoint to measure PPG as an outcome predictor should be early after the procedure (within 24–72 h). Raising the bar of absolute early PPG value from ≤ 12 mm Hg to

≤14 mm Hg does not affect rebleeding rates, while a relative reduction of 55% might reduce HE in the era of covered TIPS.

FRI527

Impact of alcohol abstinence in patients with alcohol-related cirrhosis and portal hypertension

Benedikt Hofer^{1,2,3}, Benedikt Simbrunner^{1,2,3}, Lukas Hartl^{1,2}, Mathias Jachs^{1,2}, Lorenz Balcar^{1,2}, Rafael Paternostro^{1,2}, Philipp Schwabl^{1,2,3}, Georg Semmler^{1,2}, Bernhard Scheiner^{1,2}, Albert Stättermayer¹, Michael Trauner¹, Mattias Mandorfer^{1,2}, Thomas Reiberger^{1,2,3}. ¹Medical University of Vienna, Division of Gastroenterology and Hepatology, Department of Internal Medicine Iii, Vienna, Austria; ²Medical University of Vienna, Vienna Hepatic Hemodynamic Laboratory, Division of Gastroenterology and Hepatology, Department of Internal Medicine Iii, Vienna, Austria; ³Medical University of Vienna, Christian Doppler Lab for Portal Hypertension and Liver Fibrosis, Vienna, Austria

Email: thomas.reiberger@meduniwien.ac.at

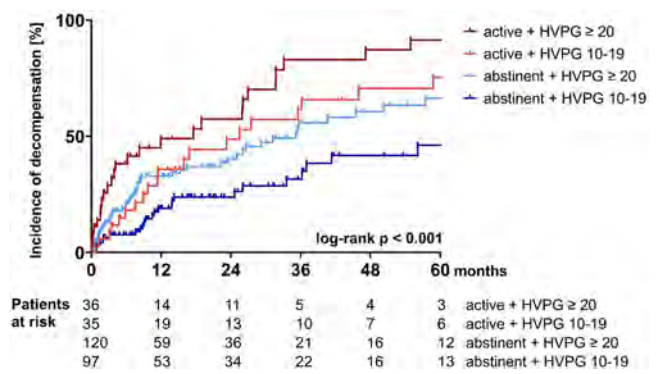
Background and aims: Alcohol-related liver disease (ALD) is a leading cause of liver-related mortality worldwide. Alcohol abstinence is a major determinant of its natural history. However, the impact of abstinence on the disease course in patients who have already progressed to cirrhosis and clinically significant portal hypertension (CSPH) is less well-established. The aim of this study was to examine the impact of alcohol abstinence on decompensation and mortality in ALD patients with CSPH.

Method: Alcohol abstinence, CSPH-related decompensation and mortality were assessed in a cohort comprised of retrospectively and prospectively (Vienna Cirrhosis Study, NCT03267615) recruited ALD patients diagnosed with CSPH (hepatic venous pressure gradient (HVPG) ≥10 mmHg). Patients were classified into four groups according to alcohol abstinence during follow-up and the presence of low (HVPG 10–19 mmHg) or high (HVPG ≥20 mmHg) risk portal hypertension at baseline: abstinent-low (n = 97), abstinent-high (n = 120), active-low (n = 35) and active-high (n = 36).

Results: We included 288 ALD patients (mean age: 56.7 ± 9.9 years; 74.7% male; 88.2% decompensated), who were followed for a median of 21.8 (IQR: 9.1–41.8) months. During the study period, 217 patients (75.3%) remained abstinent, while 71 patients (24.7%) showed continuous alcohol consumption. The mean baseline HVPG of the overall cohort was 20.2 ± 5.0 mmHg (abstinent: 20.2 ± 5.1 vs. active: 20.1 ± 4.8 mmHg; p = 0.858).

First/further hepatic decompensation was less frequent in abstinent patients compared to patients with continued alcohol consumption (26.5% vs. 42.4% at one year; 32.8% vs. 53.0% at two years; log-rank p < 0.001). Importantly, abstinent patients survived significantly longer, with a median transplant-free survival time of 68.2 (95%CI: 37.3–99.1) vs. 41.9 (95%CI: 27.7–56.0) months in patients with ongoing alcohol intake (log-rank p = 0.006).

Following the sub-stratification according to HVPG, the cumulative incidence of hepatic decompensation varied significantly between the subgroups, with 19.0%/23.9% in abstinent-low, 32.8%/40.2% in abstinent-high, 35.7%/48.6% in active-low and 48.9%/57.4% in active-high at one and two years respectively (log-rank p < 0.001). HVPG ≥20 mmHg and continued alcohol intake negatively impacted survival, as demonstrated by a median transplant-free survival time of 94.7 (95%CI: 40.1–149.3) months in abstinent-low, 63.3 (95%CI: 34.1–92.4) months in abstinent-high, 61.3 (95%CI: 32.8–89.8) months in active-low and 36.5 (95%CI: 27.5–45.4) months in active-high (log-rank p = 0.034) ALD patients.



Conclusion: Alcohol abstinence and severity of CSPH are key determinants in the clinical course of ALD patients with cirrhosis and CSPH. ALD patients with low-risk CSPH but a continued alcohol consumption still have a poor prognosis that is similar to abstinent patients with high-risk CSPH.

FRI528

Hepatic recompensation according to Baveno VII criteria significantly reduces liver-related mortality in patients with decompensated alcohol-related cirrhosis

Benedikt Hofer^{1,2,3}, Benedikt Simbrunner^{1,2,3}, Lukas Hartl^{1,2}, Mathias Jachs^{1,2}, Lorenz Balcar^{1,2}, Rafael Paternostro^{1,2}, Philipp Schwabl^{1,2,3}, Georg Semmler^{1,2}, Bernhard Scheiner^{1,2}, Albert Stättermayer¹, Michael Trauner¹, Mattias Mandorfer^{1,2}, Thomas Reiberger^{1,2,3}. ¹Medical University of Vienna, Division of Gastroenterology and Hepatology, Department of Internal Medicine III, Vienna, Austria; ²Medical University of Vienna, Vienna Hepatic Hemodynamic Laboratory, Division of Gastroenterology and Hepatology, Department of Internal Medicine III, Vienna, Austria; ³Medical University of Vienna, Christian Doppler Lab for Portal Hypertension and Liver Fibrosis, Vienna, Austria

Email: thomas.reiberger@meduniwien.ac.at

Background and aims: Abstinence from alcohol constitutes the removal of the primary aetiological factor in alcohol-related cirrhosis and has been linked to an improved outcome. However, the extent and prognostic value of clinical improvements after achieving alcohol abstinence in decompensated alcohol-related cirrhosis have not been sufficiently characterised. Thus, the aim of this study was to examine the impact of hepatic recompensation according to the novel Baveno VII criteria on liver-related mortality and the development of hepatocellular carcinoma (HCC) in patients with decompensated alcohol-related cirrhosis.

Method: Recompensation during follow-up was assessed in patients with decompensated alcohol-related cirrhosis and persistent alcohol abstinence who underwent a baseline hepatic venous pressure gradient (HVPG) assessment. Recompensation was defined according to Baveno VII criteria as resolution of ascites and hepatic encephalopathy (absence of clinical signs and cessation of medical therapy), absence of variceal bleeding and improvement in liver function. Achieving recompensation was regarded as a time-dependent covariate and analysed using Cox proportional-hazards models.

Results: 204 patients with alcohol-related cirrhosis (age: 56.9 ± 9.8 years, 75.0% male) and a median HVPG of 20 (18–24) mmHg were followed-up over a median of 24.4 months. Overall, 37 patients (18.1%) achieved hepatic recompensation. Baseline parameters linked to a higher probability of recompensation in a competing risk analysis included a lower HVPG, a lower Child-Pugh score, higher albumin, higher mean arterial pressure and a lower BMI. Achieving hepatic recompensation nearly abolished the risk of liver-related mortality (HR: 0.071 [95% CI: 0.010–0.527], p = 0.010), even after adjusting for baseline HVPG, MELD, albumin, C-reactive protein and age (adjusted HR: 0.091 [95% CI: 0.012–0.677]; p = 0.019; Table 1). With regard to

POSTER PRESENTATIONS

HCC development, we observed a trend towards a reduced risk in recompensated patients, yet this finding did not reach statistical significance (HR: 0.398 [95% CI: 0.084–1.878], $p = 0.245$).

	Univariate analysis			Multivariate analysis		
	HR	95% CI	p value	aHR	95% CI	p value
Recompensation	0.071	0.010–0.527	0.010	0.091	0.012–0.677	0.019
MELD (per point)	1.072	1.019–1.129	0.007	1.078	1.011–1.149	0.022
Albumin (per g/L)	0.957	0.917–0.999	0.046	1.016	0.961–1.076	0.572
HVPG (per mmHg)	1.101	1.040–1.166	0.001	1.062	1.000–1.129	0.051
CRP (per mg/dL)	1.257	1.079–1.464	0.003	1.068	0.895–1.275	0.465
Age (per year)	1.042	1.012–1.074	0.006	1.039	1.006–1.074	0.020

Conclusion: Hepatic recompensation according to Baveno VII criteria occurred in a considerable proportion of patients with decompensated alcohol-related cirrhosis and was associated with a significantly reduced risk of liver-related mortality. Of note, recompensated patients remain at risk of HCC.

FRI529

Covered TIPS reduces the risk of further decompensation: results from an individual patient data meta-analysis of 3924 patients with cirrhosis

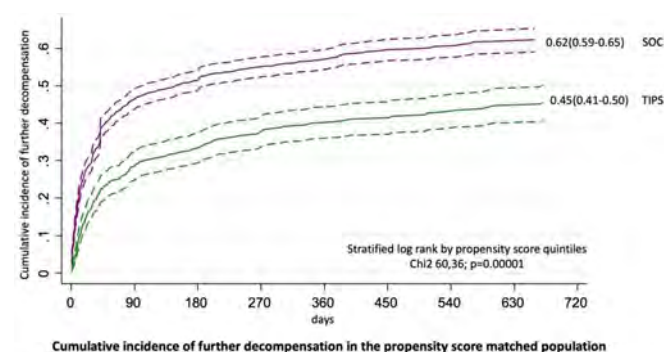
Hélène Larrue^{1,2}, Pol Olivas^{3,4}, Yong Lv⁵, Guohong Han⁶, Theresa Bucsics^{7,8}, Thomas Reiberger^{7,8}, Tilman Sauerbruch⁹, Virginia Hernandez-Gea^{3,4,10,11,12}, Dominique Thabut^{13,14}, Marika Rudler^{13,15}, Jean Marie Peron^{1,2}, Gennaro D'Amico^{16,17}, Juan Carlos Garcia Pagan^{3,4,10,11,12}, Christophe Bureau^{1,2}. ¹Toulouse University Hospital, Department of Hepatology, Toulouse, France; ²Toulouse III-Paul Sabatier University, Toulouse, France; ³Hospital Clínic, Barcelona Hepatic Hemodynamic Lab, Liver Unit, Barcelona, Spain; ⁴Institut d'Investigacions Biomèdiques August Pi i Sunyer (IDIBAPS), Barcelona, Spain; ⁵Fourth Military Medical University, Xijing Hospital of Digestive Diseases, Xi'an, China; ⁶Digestive Diseases Hospital, Xi'an International Medical Center Hospital, Northwestern University, Department of Liver Diseases and Interventional Radiology, Xi'an, China; ⁷Division of Gastroenterology and Hepatology, Medical University of Vienna, Department of Medicine III, Vienna, Austria; ⁸Medical University of Vienna, Vienna Hepatic Hemodynamic Lab, Vienna, Austria; ⁹University of Bonn, Department of Internal Medicine, Bonn, Germany; ¹⁰Universitat de Barcelona, Barcelona, Spain; ¹¹Health Care Provider of the European Reference Network on Rare Liver Disorders (ERN-Liver), Barcelona, Spain; ¹²Centro de Investigación Biomédica Red de Enfermedades Hepáticas y Digestivas (CIBEREHD), Barcelona, Spain; ¹³Groupement hospitalier APHP-Sorbonne Université, Unité de Soins Intensifs d'hépatologie-Gastro-Entérologie, Paris, France; ¹⁴France and Brain Liver Pitié-Salpêtrière Study Group, INSERM UMR_S 938, Centre de recherche Saint-Antoine, Maladies métaboliques, biliaires et fibre-inflammatoires du foie, Institute of Cardiometabolism and Nutrition, Paris, France; ¹⁵Sorbonne Université, INSERM, Centre de Recherche Saint-Antoine, Institute of Cardiometabolism and Nutrition, Paris, France; ¹⁶Azienda Ospedaliera Ospedali Riuniti Villa Sofia-Cervello, Gastroenterology Unit, Palermo, Italy; ¹⁷Clinica La Maddalena, Gastroenterology Unit, Palermo, Italy
Email: bureau.c@chu-toulouse.fr

Background and aims: Baveno VII conference introduced the concept of further decompensation as a prognostic stage of cirrhosis that is associated with an even higher mortality than first decompensation. The effectiveness of transjugular intrahepatic

portosystemic shunt (TIPS) has already been demonstrated for the prevention of rebleeding and recurrent ascites. Nevertheless, the effect of TIPS to decrease the overall incidence of further decompensation events remains unclear-mainly because of the risk of encephalopathy and liver failure. The aim of this study was to assess the incidence of further decompensation after TIPS, defined as new or worsening ascites, new or worsening hepatic encephalopathy or new portal hypertension (PH)-related bleeding or rebleeding, in comparison to standard of care (SOC).

Method: We conducted a review of the medline literature searching for controlled studies (randomized control trials (RCT) and cohorts) assessing TIPS in comparison to SOC in the indication of recurrent ascites, refractory bleeding, and secondary prevention of bleeding since the use of polytetrafluoroethylene-covered stents and until 2020. We collected individual patient data (IPD) to perform an IPD meta-analysis also using a propensity score (PS) matching by multivariate logistic regression. The comparisons were performed by stratified log-rank test by PS quintiles. The primary outcome was the incidence of further decompensation. The secondary outcome was overall survival.

Results: 12 databases among the 14 selected studies (5 RCT, 9 cohorts) were available. The whole population included 3924 patients (SOC: $n = 3077$; TIPS: $n = 847$). After PS matching, 2415 patients (SOC: $n = 1802$; TIPS: $n = 613$) were analyzed: 70% men, mean age 54 ± 12 , alcohol-related cirrhosis 42%, mean Child-Pugh 9 ± 2 , mean MELD score 14 ± 6 without significant differences between groups. The cumulative incidence function of further decompensation at 2 years in the PS-matched population was 0.45 (0.41–0.50) in the TIPS group vs. 0.62 (0.59–0.65) in the SOC group (stratified log-rank $p = 0.00001$), with mortality and liver transplantation as competing risk (figure). The benefit of TIPS was confirmed by IPD meta-analysis adjusted for age, treatment, history of ascites, of encephalopathy, of hepatocellular carcinoma, serum albumin and MELD (hazard ratio 0.47 (0.39–0.57)) without significant heterogeneity ($I^2 = 8.4\%$; $p = 0.365$) and was consistent across study subgroups according to TIPS indication. The overall survival was significantly better in TIPS group: 74% (69%–78%) vs 63% (59%–66%) in SOC group (stratified log rank $p < 0.0001$).



Conclusion: This IPD meta-analysis demonstrates that TIPS decreases the risk of further decompensation in comparison to SOC, in patients with cirrhosis treated for recurrent ascites or in secondary prevention of PH-related bleeding and importantly, also improves survival.

FRI530

Sarcopenia increases the risk of cirrhosis disease progression and death in patients with cirrhosis

Puneeta Tandon¹, Sarah Wang¹, Moon Young Kim², Bart Van Hoek³, Daphne Bot⁴, Jeroen van Vugt⁵, Berend Beumer⁵, Jan Ijzermans⁵, Sunil Taneja⁶, Surender Singh⁶, Maryam Ebadi¹, Aldo J Montano-Loza¹. ¹Division of Gastroenterology (Liver Unit), University of Alberta, Edmonton, Canada; ²Department of Internal Medicine, Yonsei University Wonju College of Medicine, Wonju, Korea, Rep. of South; ³Department of Gastroenterology and Hepatology, Leiden University Medical Center, Leiden, Netherlands; ⁴Department of Dietetics, Leiden University Medical Center, Leiden, Netherlands; ⁵Department of Surgery, Division of HPB & Transplant Surgery, Erasmus MC Transplant Institute, Erasmus MC, University Medical Centre Rotterdam, Rotterdam, Netherlands; ⁶Department of Hepatology, Postgraduate Institute of Medical Education and Research, Chandigarh, India

Email: ptandon@ualberta.ca

Background and aims: Sarcopenia in cirrhosis has been operationalized as low muscle mass. The skeletal muscle index (SMI) is a well-validated tool to identify sarcopenia in cirrhosis and has been associated with increased mortality in patients awaiting liver transplant (LT). To date, the impact of sarcopenia on cirrhosis progression is unknown. In this study, we aimed to explore the relationship between sarcopenia and the risk of: (i) a combined outcome of cirrhosis progression or mortality or (ii) mortality alone. **Method:** The SMI was measured at baseline using abdominal CT imaging at the 3rd lumbar vertebra (L3). Sarcopenia was defined using established cut-offs in patients with cirrhosis awaiting LT as SMI <39 cm²/m² in females and <50 cm²/m² in males. Progression of cirrhosis was defined by an increase in clinical stage from baseline using the D'Amico classification. Factors associated with progression or death or death alone were evaluated using univariate and multivariate Cox regression models.

Results: 1624 adult patients with cirrhosis from five centers across Europe, North America and Asia were included. Mean age was 54 ± 9 years, 26% of patients were female, 31% had compensated disease at baseline, and the mean MELD-Na was 15 ± 7 years. Data on ethnicity was available in 1354 patients (48% Caucasian/European, 46% Asian, and the remainder other ethnicities). The top three etiologies of liver disease were alcohol (40%), hepatitis C (19%) and hepatitis B (13%). Both the SMI as a continuous variable and presence of sarcopenia were associated with the combined outcome of cirrhosis progression or mortality (HR 0.98, 95% CI 0.97–0.99, p < 0.001; and HR 1.37, 95% CI 1.17–1.61, p < 0.001; respectively); and mortality alone (HR 0.98, 95% CI 0.97–0.99, p < 0.001; and HR 1.39, 95% CI 1.16–1.67, p < 0.001; respectively). In multivariate analysis, sarcopenia was associated with increased risk of progression to the next cirrhosis stage or death (HR 1.25, 95% CI 1.06–1.47, p = 0.007) and increased risk of death alone (HR 1.25, 95% CI 1.04–1.50, p = 0.02), after adjusting for age, sex, and MELD score. The 1-year, 5-year and 10-year probabilities of death or progression-free survival were 71%, 37%, and 22% in patients with sarcopenia, compared to 83%, 43%, and 27% in patients without sarcopenia (p < 0.001, log-rank test; Figure 1a). Median survival for patients with sarcopenia was 52 months (95% CI 31–73), compared to 74 months (95% CI 50–97) in patients without sarcopenia (p < 0.001, log-rank test, Figure 1b).

Figure 1a

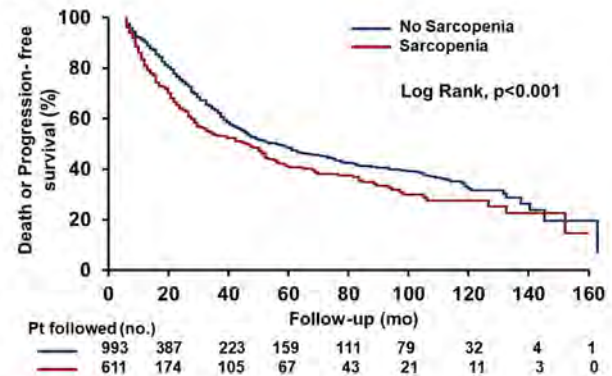


Figure 1b.

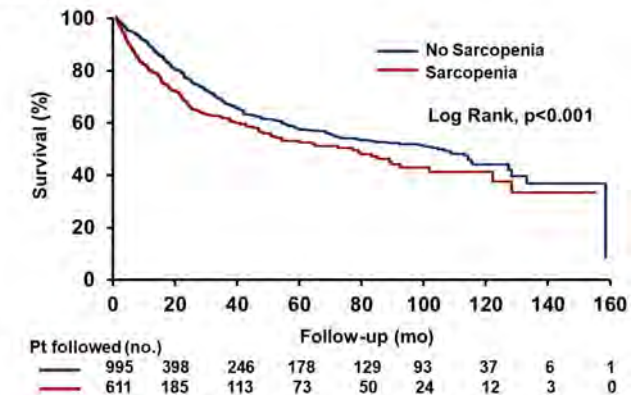


Figure: Survival probabilities for the a) combined outcome of cirrhosis progression or mortality and b) mortality alone in patients with and without sarcopenia.

Conclusion: Sarcopenia was an independent predictor of cirrhosis progression or death or death alone. Future studies are needed to evaluate the possibility of slowing cirrhosis disease progression by reversing or preventing sarcopenia.

FRI531

Substantial reduction of the diagnostic grey zone of the Baveno-VII CSPH criteria by sequential consideration of VITRO

Lukas Hartl^{1,2}, Mathias Jachs^{1,2}, Benedikt Simbrunner^{1,2,3}, David JM Bauer^{1,2}, Rafael Paternostro^{1,2}, Bernhard Scheiner^{1,2}, Lorenz Balcar^{1,2}, Georg Semmler^{1,2}, Albert Stättermayer^{1,2}, Matthias Pinter^{1,2}, Peter Quehenberger⁴, Michael Trauner¹, Thomas Reiberger^{1,2,3}, Mattias Mandorfer^{1,2}. ¹Medical University of Vienna, Division of Gastroenterology and Hepatology, Department of Medicine III, Vienna, Austria; ²Medical University of Vienna, Vienna Hepatic Hemodynamic Lab, Division of Gastroenterology and Hepatology, Department of Medicine III, Vienna, Austria; ³Medical University of Vienna, Christian Doppler Lab for Portal Hypertension and Liver Fibrosis, Vienna, Austria; ⁴Medical University of Vienna, Department of Laboratory Medicine, Vienna, Austria

Email: mattias.mandorfer@meduniwien.ac.at

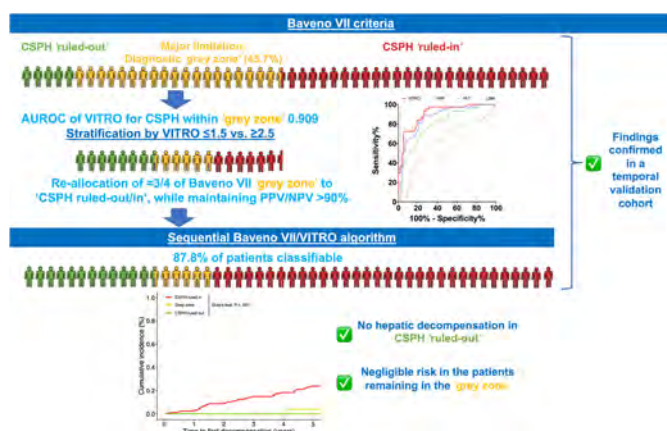
Background and aims: Baveno-VII proposed liver stiffness measurement (LSM) and platelet count (PLT) criteria for non-invasive clinically significant portal hypertension (CSPH) diagnosis in compensated advanced chronic liver disease (cACLD; CSPH 'ruled-out': LSM ≤15 kPa plus PLT ≥150 G/L; CSPH 'ruled-in': LSM ≥25 kPa). However, a substantial share of patients remains in the diagnostic 'grey-zone'. We aimed to refine these criteria by sequential application of von Willebrand factor antigen (VWF)/thrombocytes (VITRO) score.

POSTER PRESENTATIONS

Method: Patients with evidence of cACLD (LSM ≥ 10 kPa) undergoing hepatic venous pressure gradient (HVPG) measurement at the Vienna General hospital between 2004 and 2021 were included. The performance of non-invasive tests (NIT) including VITRO, i.e., the ratio between VWF (%) and PLT (G/L), for the diagnosis of CSPH (HVPG ≥ 10 mmHg) were evaluated in a derivation (2004–2016; n = 221) and a validation (2017–2021; n = 81) cohort. A particular focus was put on patients who were unclassifiable by Baveno-VII criteria.

Results: Overall, viral hepatitis was the predominant etiology (50.7%), followed by alcoholic liver disease (15.2%) and non-alcoholic steatohepatitis (13.2%). CSPH prevalence was 62.3%.

According to Baveno-VII criteria, 45.7% of patients in the derivation cohort remained in the diagnostic 'grey-zone' for CSPH, in which VITRO showed an excellent performance for the detection of CSPH with an area under the receiver operator characteristic curve (AUROC) of 0.909 (95% confidence interval [95%CI]: 0.823–0.965). VITRO ≤ 1.5 'ruled-out' (negative predictive value [NPV]: 97.5%, specificity: 97.7%) and 'ruled-in' (positive predictive value [PPV]: 91.2%, sensitivity: 94.7%) CSPH in patients who were unclassifiable by Baveno-VII criteria. The application of a sequential Baveno-VII-VITRO algorithm re-allocated 73% of initial 'grey-zone' patients to the 'ruled-in'/'ruled-out' group, whilst maintaining a PPV/NPV $>90\%$. Finally, 87.8% of patients were classifiable in regard to CSPH by the Baveno-VII-VITRO sequence. Importantly, all findings were confirmed in a temporal validation cohort.



Of note, not a single patient (0.0%) allocated to the 'CSPH ruled-out' group by the Baveno-VII-VITRO sequence developed decompensation within five years, while 5-year decompensation rates were substantial (23.9%) among 'CSPH ruled-in' patients and negligible (4%) in remaining 'grey-zone' patients.

Conclusion: The sequential application of VITRO ≥ 2.5 to patients who are unclassifiable by Baveno-VII-criteria improves the identification of cACLD patients with a high risk of CSPH and subsequent decompensation. In turn, VITRO ≤ 1.5 'ruled-out' CSPH in Baveno-VII 'grey zone' patients and indicated a favorable prognosis. Less than 15% of cACLD patients remained in the final 'grey zone' when applying the sequential Baveno VII-VITRO algorithm.

FRI532

Causes and predictors of 30-day readmission in patients with gastric varices requiring Balloon-occluded retrograde transvenous obliteration (BRTO)

Mohamed Ahmed¹, Vinay Jahagirdar¹, Wael Mohamed¹, Ifrah Fatima¹, Kevin Kennedy², Alisa Likhitsup³. ¹University of Missouri-Kansas City Volker Campus, Internal medicine, Kansas City, United States; ²Saint Luke's Hospital of Kansas City, Kansas City, United States; ³University of Missouri-Kansas City

Email: mohamedfayez1991@gmail.com

Background and aims: Variceal bleeding is one of the major complications of portal hypertension. Though gastric variceal bleeding is less common, it has a higher mortality than esophageal variceal bleeds. Endoscopic management of gastric varices (GV) is less effective, and Transjugular Intrahepatic Portosystemic Shunts (TIPS) and balloon-occluded retrograde transvenous obliteration (BRTO) are used. In BRTO, the portosystemic gastroduodenal shunt is accessed via the left renal vein, from a trans-jugular or transfemoral approach. The shunt is occluded by a balloon and a sclerosing agent is injected into the variceal system. Studies have shown that BRTO can effectively control active gastric variceal bleeding and is a good alternative to TIPS. Diverting the blood towards the liver improves hepatic function and patient survival, but increased portal pressures may also worsen esophageal varices and ascites.

Method: Patients with GV who underwent BRTO were identified from the 2016–2018 Healthcare Cost and Utilization Project databases (HCUP) using the National readmission database (NRD) by using the International Classification of Diseases Code, 10th Revision Clinical Modification (ICD-10). 30-day readmission rate and diagnosis were identified. Multiple logistic regression model was used to identify the factors associated with readmission. SAS 9.4 was used for data analysis.

Results: Total of 608 patients who underwent BRTO were identified between 2016 and 2018. Mean age was 58.2 ± 12.6 . 39.8% of patients were females. The 30- and 90-days readmission rate was 20.4% and 28.2% respectively. Significant increase length of stay (10.5 ± 10.1 vs 8.4 ± 6.5 ; $p < 0.004$) and total charges (238765 vs 185972 ; $p = 0.001$) was associated with the 30-day readmission patients. Most common diagnosis for 30-day readmissions were hepatic encephalopathy (13%), acute liver failure (8%), gastric varices (6%), Ascites (5%), systemic infection (4%), and acute blood loss anemia (4%). Multiple logistic regression analysis showed that 30-day readmission was associated with renal failure (OR 3.25, 95% CI 1.72–6.16, $P = 0.003$) but not associated with presence of bleeding esophageal varices (OR 1.27, 95%CI, 0.81–1.98), hepatic encephalopathy (OR 1.2, 95% CI 0.75–2.17), liver failure (OR 2.16, 95% CI 0.93–4.99) and DM with chronic complications (OR 1.39, 95% CI 0.91–2.14) at the index admission.

Conclusion: BRTO procedures are associated with high 30-day readmission rate. Patients with renal failure undergoing BRTO are at significantly higher risk of 30-day readmissions with OR of 3.25. Hepatic decompensation, Acute liver failure and systemic infections appears to be the most common causes of 30-days readmission in patient having BRTO.

FRI533

Carvedilol is associated with superior hemodynamic response and rebleeding rates in comparison to propranolol in secondary prophylaxis of variceal bleeding

Mathias Jachs¹, Lukas Hartl¹, Benedikt Simbrunner¹, David JM Bauer¹, Rafael Paternostro¹, Lorenz Balcar¹, Benedikt Hofer¹, Nikolaus Pfisterer¹, Michael Schwarz¹, Bernhard Scheiner¹, Albert Stattermayer¹, Matthias Pinter¹, Michael Trauner¹, Matthias Mandorfer¹, Thomas Reiberger¹. ¹Medical University of Vienna, Division of Gastroenterology and Hepatology, Department of Internal Medicine III, Vienna, Austria

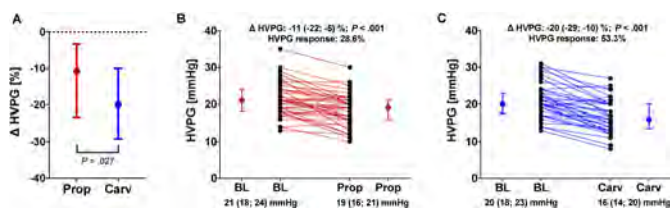
Email: thomas.reiberger@meduniwien.ac.at

Background and aims: In primary prophylaxis of variceal bleeding, carvedilol offers more profound decreases in hepatic venous pressure gradient (HVPG) as compared to propranolol. However, limited data exists on its efficacy and safety after the first variceal bleed, i.e., in secondary prophylaxis.

Method: For this retrospective evaluation, patients who had previously bled and underwent paired HVPG measurements at our centre between 2004 and 2021 to guide non-selective betablocker (NSBB) therapy were included. All patients underwent band ligation in addition to NSBB therapy. The effects of NSBB treatment on HVPG and mean arterial pressure (MAP) was compared between

propranolol and carvedilol users. Long-term follow-up data on rebleeding, acute kidney injury (AKI) and ascites development/progression was recorded and analysed applying competing risk regression.

Results: Eighty-seven (carvedilol/propranolol: n = 45/n = 42) patients were included. Patients underwent their baseline HVPG measurement after a median of 2.2 months following their initial bleed and had a median (NSBB-naïve) baseline HVPG of 21 (IQR: 18; 24) mmHg. Ascites was present in 62% of patients, and 39%, 48% and 13% had Child-Turcotte-Pugh stage A, B and C cirrhosis, respectively. Carvedilol induced more marked reductions in HVPG as compared to propranolol (relative change: -20 [-29;-10] % vs. -11 [-22;-5] %, p=0.027), resulting in a higher proportion of patients achieving chronic HVPG response, i.e., a reduction by ≥20% or to an absolute value ≤12 mmHg (53.3% vs. 28.6%, p=0.034). Carvedilol was thus, associated with a lower cumulative incidence of rebleeding (2.4%/9.9%/10.4% vs. 9.9%/21.6%/34.9% at 1/3/5 years, Gray's test: p=0.015) and liver-related death (5.0%/10.7%/10.7% vs. 7.4%/23.8%/33.9% at 1/3/5 years, p=0.032) during long-term follow-up, as compared to propranolol. Notably, the incidence of AKI did not differ between the two groups (p=0.139) despite more pronounced decreases in MAP induced by carvedilol (relative change: -12 [-17;-6] % vs. -6 [-17; 2] %, p=0.044), and ascites development or worsening was less commonly observed in patients on carvedilol therapy (p=0.034). Stratifying patients by HVPG response status yielded similar results.



Conclusion: Carvedilol was associated with higher rates of HVPG response and lower rebleeding rates in our retrospective study. Of note, the use of carvedilol was also linked to lower rates of non-bleeding further decompensation, i.e., ascites development/progression, whilst having similar impact on the incidence of AKI in our cohort, despite more marked reductions in MAP.

FRI534

Impact of early nasogastric tube feeding after endotherapy for acute variceal bleeding in patients with cirrhosis : a randomized controlled trial

Jatin Yegurla¹, Sanchit Sharma^{1,2}, Namrata Singh¹, Samagra Agarwal¹, Sumaira Qamar¹, Deepak Gunjan¹, Anoop Saraya¹. ¹All India Institute of Medical Sciences, Department of Gastroenterology and Human Nutrition Unit, New-Delhi, India; ²John Radcliffe hospital, Translational Gastroenterology Unit, Oxford, United Kingdom
Email: ansaraya@yahoo.com

Background and aims: Limited data exist on safety of early feeding in patients with cirrhosis after endotherapy for acute variceal bleeding (AVB). We studied the impact of early nasogastric (NG) tube feeding on relevant outcomes in these patients in a randomised controlled trial.

Method: Consecutive patients with cirrhosis undergoing endotherapy for AVB were randomized to receive either liquid diet through an NG tube (n = 40) [early-feeding (EF) group] or sips of water and lemon water orally (n = 40) [standard-of-care (SOC) group] for 48 hours after endotherapy. In early feeding group, 14 Fr NG tube (Ryle's tube) was placed immediately after endotherapy under endoscopic guidance and liquid diet was started one hour later which consisted of commercial polymeric formula feed for first 6 hours followed by home-made milk-based formula feed. Solid diet was resumed 48 hours later in both the groups. Primary end-point was 5-day rebleeding and secondary end-

points included incidence of infections, hepatic encephalopathy during hospitalization and 6-week mortality.

Results: Eighty patients [Mean age: 41 ± 11.5 years; males (82.5%); Alcohol etiology (55%)] were included. Baseline characteristics were comparable in both the groups. The 5-day rebleeding rates in EF and SOC groups were 2.5% and 5%, respectively (p = 0.55). The incidence of infection [2.5% (EF) vs 2.5% (SOC), p = 1.00] and development of HE [5% (EF) vs 2.5% (SOC), p = 0.36] during hospitalisation were comparable. One patient in EF group developed mild epistaxis following NG tube insertion. Average calorie and protein intake by patients in EF group during the 48 hours was 1318 ± 240 Kcal and 43.4 ± 9.2 g of proteins per day. No patient in EF group developed feed intolerance. No significant difference was observed in mortality, rebleeding, infections or decompensations during the 6-week follow-up.

Table: Comparison of baseline characteristics and outcomes between early-feeding (EF) and standard-of-care (SOC) groups. All values are expressed as mean ± SD or frequency (percentage).

	EF group (N = 40)	SOC group (N = 40)	P value
Age (years)	39.4 ± 12.3	42.6 ± 10.5	0.23
Etiology	19 (47.5%)	25 (62.5%)	0.28
Alcohol	8 (20%)	5 (16.25%)	
Cryptogenic	7 (17.5%)	3 (7.5%)	
Hepatitis-B related	6 (15%)	7 (17.5%)	
Others			
MELD Score	13 ± 3.4	14.1 ± 4.5	0.23
Child-Pugh Score	8.7 ± 1.3	8.8 ± 1.6	0.58
Child-Pugh class	33 (82.5%)	28 (70%)	0.23
B	7 (17.5%)	10 (25%)	
C			
Active bleeding at endoscopy	3 (7.5%)	6 (15%)	0.29
Gastric varices	8 (20%)	7 (17.5%)	0.77
Endotherapy	33 (82.5%)	37 (92.5%)	0.46
Endoscopic band ligation	7 (17.5%)	3 (7.5%)	0.17
Glue injection			
Very-early rebleed (48hours-Day 5)	1 (2.5%)	2 (5%)	0.55
Early rebleed (Day 5-Day 42)	4 (10%)	3 (7.5%)	0.69
6-week mortality	1 (2.5%)	4 (10%)	0.16

Conclusion: Early NG tube feeding in patients with cirrhosis after AVB is safe and does not lead to increased risk of rebleeding or encephalopathy. (CTRI/2021/05/043590).

FRI535

A multi-compartmental model of the HepQuant SHUNT test can quantify anatomic shunting and stratify risk for varices: combined results from the HALT-C and SHUNT-V studies

Michael McRae¹, Steve Helmke², Greg Everson². ¹Custom Diagnostic Solutions LLC; ²HepQuant, Denver, United States
Email: michaelpmcrae@gmail.com

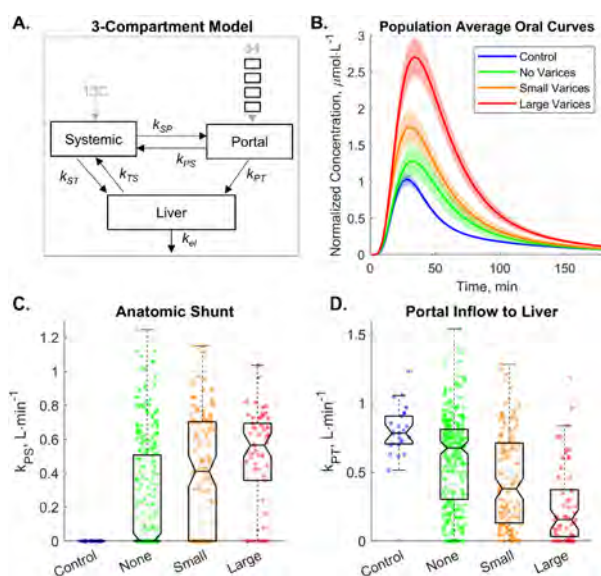
Background and aims: In chronic liver disease (CLD), persistent inflammation and fibrosis impair hepatocyte function and increase portal pressure, resulting in portal venous collaterals and portal-systemic shunting. The HepQuant SHUNT test uses stable non-radioactive isotopes of carbon-13 cholate (13C-CA) intravenously and deuterium cholate (d4-CA) orally to simultaneously measure clearance from both portal and systemic circulations. The aim of this study was to determine whether compartmental analysis of the HepQuant SHUNT test could quantify anatomic shunting in patients with CLD and esophageal varices.

Method: A compartmental model was developed from the HepQuant SHUNT test results from 26 lean controls and 492 CLD patients with esophago-gastro-duodenoscopy findings (291 no varices, 143 small varices, and 58 large varices). Transfer between systemic, portal, and

POSTER PRESENTATIONS

liver compartments was modeled by a system of 18 first-order ordinary differential equations along with assumptions from measured or literature-derived values. The compartmental model and PK parameters were solved for each subject with three parameters estimated by nonlinear least-squares regression including the anatomic shunt flow (kPS). Compartmental analysis was completed using MATLAB Simbiology.

Results: The compartmental model (Fig 1A) fit the data with median adjusted R-squared across all patients of 0.99 for 13C-CA IV curves and 0.95 for d4-CA oral curves. Population-averaged oral curve simulations (Fig 1B) (mean and 95% confidence) from the compartment model show significant differences between controls, no varices, small varices, and large varices. The estimated median anatomic shunt flow, kPS, was 0, 0, 411, and 566 ml/min for controls, none, small, and large varices, respectively with significant difference between all groups (Wilcoxon rank-sum $p < 0.05$) (Fig 1C). In parallel, the model demonstrated reduced portal inflow to the liver (kPT) among varices groups, with median kPT values of 784, 676, 380, and 156 ml/min for controls, none, small, and large varices, respectively with significant difference between all groups ($p < 0.001$) (Fig 1D).



Conclusion: The compartmental model discriminated patients with small and large varices. The model also distinguished the individual contributions of hepatocyte function and anatomic shunting to the hepatic clearance of cholate. The individualized PK parameters estimated from this compartmental model, when combined with artificial intelligence or machine learning algorithms, have significant potential to enhance the diagnostic performance and clinical utility of the HepQuant test of global liver function.

FRI536

Expandable constrained 6 mm transjugular intrahepatic portosystemic shunt: an alternative approach for high-risk patients?

Hannah Schneider¹, Anja Tiede¹, Alena Friederike Ehrenbauer¹, Lena Stockhoff¹, Johanna Luise Charlotte Lorenz¹, Heiner Wedemeyer¹, Richard Taubert¹, Jan Hinrichs², Benjamin Maasoumy¹. ¹Hannover Medical School, Dept. of Gastroenterology, Hepatology and Endocrinology; ²Hannover Medical School, Dept. of Interventional Radiology
Email: schneider.hannah@mh-hannover.de

Background and aims: A transjugular intrahepatic portosystemic shunt (TIPS) can effectively overcome portal hypertension in patients with liver cirrhosis. However, in a considerable proportion of the respective patients relative or absolute contraindications such as

cardiac impairment, recurrent hepatic encephalopathy (HE) or advanced hepatic impairment prevent TIPS insertion. In this study, we investigated whether a response-guided step-up approach using a constrained TIPS with a diameter of 6 mm may pose as an option for otherwise ineligible or high-risk patients.

Method: A number of 38 patients, considered to have a high risk for TIPS related complications due to the presence of relative contraindications, received a constrained 6 mm TIPS at Hannover Medical School between 10/2020 and 03/2022. During the TIPS procedure, a 6 mm stent graft was placed into the parenchymal tract to constrain expansion of the later inserted TIPS endoprosthesis. The 6 mm stent graft can be revised to >8 mm via balloon expansion in case of an insufficient clinical response, increasing shunt volume gradually. A control cohort of patients with conventional (8 mm) TIPS was generated using propensity score matching considering the FIPS (Freiburg index of post TIPS survival), history of HE and diastolic dysfunction. A caliper of 0.25 resulted in 28 patients per group. Patients were followed up for 6 months. Competing risk analysis was performed to evaluate clinical complications.

Results: Median age of patients with constrained TIPS was 61, the majority was male (60.7%), median FIPS was -0.12. Within the high-risk group indication for the constrained TIPS was cardiac impairment, poor liver function or history of HE in 15, 9, and 4 patients, respectively. The constrained TIPS procedure was successful in all patients without any major complication. However, TIPS dysfunction was significantly more frequent in the constrained TIPS cohort ($n = 1$ vs. 6; $p = 0.03$). In 2 patients constrained TIPS did not achieve adequate symptom control. Importantly, in all cases the constrained TIPS was successfully revised and/or dilated to 7/8 mm. While no constrained TIPS had to be reduced or occluded due to clinical complications, TIPS diameter had to be decreased in 2 of the control patients due to recurring HE and cardiac decompensation. Patients treated with the response-guided step-up approach less frequently developed overt HE during follow up ($n = 15$ vs. 5; $p = 0.02$). There was no significant difference concerning the development of cardiac decompensation ($n = 6$ vs. 9; $p = 0.25$) and survival ($n = 4$ vs. 6; $p = 0.38$) between the two groups.

Conclusion: The constrained 6 mm TIPS may offer a more careful step-up approach for selected high-risk TIPS patients. The technical procedure appeared to be safe and well feasible. Larger studies are needed to further explore promising results on TIPS related complications i.e. with regard to HE development.

FRI537

Early treatment with terlipressin in patients with hepatorenal syndrome yields improved clinical outcomes in 3 phase III North American studies

Michael Curry¹, Hugo E. Vargas², Alex Befeler³, Nikolaos T. Pyrsopoulos⁴, Vilas Patwardhan¹, Khurram Jamil⁵. ¹Beth Israel Deaconess Medical Center; ²Mayo Clinic; ³Saint Louis University; ⁴Rutgers-New Jersey Medical School University Hospital; ⁵Mallinckrodt Pharmaceuticals
Email: mcurry@bidmc.harvard.edu

Background and aims: Hepatorenal syndrome (HRS), a serious complication of advanced cirrhosis and a potentially reversible form of acute kidney injury, is associated with a rapid deterioration in kidney function. The vasopressin analogue, terlipressin, successfully reverses HRS. Patients (pts) with higher baseline serum creatinine (SCr) levels have a reduced response to terlipressin. The largest randomized, prospective database of placebo-controlled studies in pts with HRS was examined to assess terlipressin treatment response in pts with varying baseline SCr levels.

Method: Pooled data from 3 Phase III North American-centric, placebo-controlled clinical studies (OT-0401, REVERSE, and CONFIRM) were used. Post hoc analyses examined pooled data from terlipressin-treated pts with HRS (type 1; $n = 352$)—across 3 SCr subgroups (<3 , ≥ 3 to <5 , and ≥ 5 mg/dL)—to

delineate their correlation with HRS reversal (defined as at least 1 SCR level of ≤ 1.5 mg/dL on treatment), renal replacement therapy (RRT)-free survival, transplant-free survival (TFS), and overall survival (OS). Statistical analyses included the Wald test (logistic regression analysis), Chi-square/Fisher's exact test (HRS reversal), and the log rank test (survival estimates).

Results: SCR levels were significantly associated with HRS reversal in univariate and multivariate logistic regression analyses ($p < 0.001$) (Figure). Among pts with HRS, the incidence of HRS reversal inversely correlated with SCR subgroup: < 3 mg/dL, 49.2%; ≥ 3 to < 5 mg/dL, 28.0%; ≥ 5 mg/dL, 9.1% ($p < 0.001$). At Day 30 follow-up, RRT-free survival was significantly higher for pts with HRS in the lower SCR subgroups versus the highest subgroup (< 5 mg/dL vs > 5 mg/dL; $p = 0.01$). Terlipressin-treated pts with HRS who had a lower baseline SCR level had higher OS ($p < 0.001$) and TFS at Day 90 ($p = 0.04$).

Baseline parameters	Terlipressin n	Odds ratio	95% CI	p value
SCR	312	0.518	0.381-0.704	<.001
Model for end-stage liver disease score	312	0.939	0.902-0.977	.002
Prior midodrine and octreotide	312	1.849	1.106-3.091	.019

Figure: Multivariate logistic regression of baseline characteristics on HRS reversal (Terlipressin group, pooled intent-to-treat population)

Conclusion: Terlipressin-treated pts with HRS and a lower baseline SCR level experienced higher HRS reversal and survival outcomes. It is important to identify and treat pts with HRS early when they have lower SCR levels and a greater probability of clinical response to terlipressin.

FRI538

Non-invasive tools are suboptimal to predict the presence of varices needing treatment and risk of clinical decompensation in patients with autoimmune hepatitis related cirrhosis

Randeep Rana¹, Samagra Agarwal¹, Sanchit Sharma^{1,2}, Ujjwal Sonika³, Syed Ahmed¹, Srikanth Gopi¹, Deepak Gunjan¹, Anoop Saraya¹. ¹All India Institute Of Medical Sciences New Delhi, Gastroenterology and Human Nutrition Unit, New Delhi, India; ²Translational Gastroenterology Unit, John Radcliffe Hospital, Oxford, United Kingdom; ³Govind Ballabh Pant Hospital, Gastroenterology, New Delhi, India
Email: ansaraya@yahoo.com

Background and aims: Baveno VII consensus recommend the use of non-invasive tools (NITs) to predict the risk of clinical decompensation (CD) and detecting varices needing treatment (VNTs) in patients with compensated cirrhosis. The present study aimed to validate these recommendations in patients with autoimmune hepatitis (AIH) related cirrhosis.

Method: Diagnostic performance of Baveno-VI (LSM > 20 kPa or platelet $< 150,000/\text{mm}^3$), expanded Baveno-VI (LSM > 25 kPa or platelet $< 110,000/\text{mm}^3$) and platelet-albumin (albumin < 3.6 g/dl or platelet $< 120,000/\text{mm}^3$) criteria for detecting VNTs was assessed against the strategy of endoscopy for all to screen large varices using decision curve analysis (DCA). Patients were stratified using Baveno VII criteria for definite clinically significant portal hypertension (CSPH) (LSM > 25 kPa), possible CSPH (LSM > 15 kPa and platelet $< 150,000/\text{mm}^3$) and no CSPH (LSM < 15 kPa and platelets $> 150,000/\text{mm}^3$). Cumulative incidence of clinical decompensations on follow-up were compared across different strata to assess its clinical relevance.

Results: One hundred ten (110) patients with AIH-related cirrhosis were included, with 37 patients having VNTs. At a threshold probability of 10% missed VNTs, platelet-albumin criteria was the most beneficial among NITs to detect VNTs with a potential to avoid 44 additional endoscopies before 1 additional VNT is missed. Rest of the NITs had similar benefit to performing endoscopy in all patients. At lower thresholds ($< 10\%$ missed VNTs), performing endoscopy in all patients was the most beneficial strategy. Over a median follow-up of 30 months (IQR 13–39 months), 30 of 96 patients with available

follow-up developed clinical decompensation. The 1-year and 3-year rate of clinical decompensation in patients with definite CSPH, possible CSPH and no CSPH was (29.2%, 29.0%, 19.8%) and (35.6%, 39.5%, 29.0%), respectively (log rank test, $p = 0.75$).

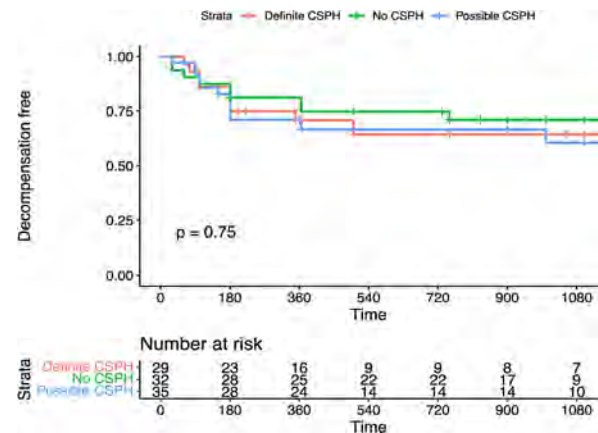


Figure: Figure shows 1-year and 3-year rate of clinical decompensation in patients with definite CSPH, no CSPH and possible CSPH in AIH related cirrhosis.

Conclusion: The strategy of endoscopy for all is superior to all NITs to detect VNTs at lower thresholds for treatment in patients with AIH. The Baveno VII criteria for predicting clinical decompensation is suboptimal to stratify patients of AIH.

FRI539

Improving of hepatic encephalopathy manifestations in cirrhotic patients with clinically significant portal hypertension treated with splenic artery embolization

Sergii Kozlov¹, Pavlo Ivanchov², Elina Manzhaliy³, Iryna Kostishyna⁴, Oleksandr Kozlov², Illia Koshman⁵. ¹Bogomolets National Medical University, Surgery, Kyiv, Ukraine; ²Bogomolets National Medical University, Surgery chair #3, Kyiv, Ukraine; ³Bogomolets National Medical University, Gastroenterology, Kyiv, Ukraine; ⁴Kyiv municipal hospital #12, Surgery, Kyiv, Ukraine; ⁵Kyiv municipal hospital #12, Surgery, Kyiv
Email: sergiinikol@gmail.com

Background and aims: In cirrhotic patients, hepatic encephalopathy (HE) is a severe complication in which hyperammonemia plays a leading role. At the same time, clinically significant portal hypertension with spontaneous venous portosystemic shunts is common clinical finding that aggravated the HE manifestation. Endovascular shunt occlusion considered to be a possible treatment option. We studied the efficacy of splenic artery embolization (SAE) in resolution HE symptoms as a perspective alternative RI treatment option for patients with high risk variceal bleeding.

Method: Selective endovascular embolization of the splenic artery was performed as secondary prophylaxis treatment in 120 patients with one or more episodes of variceal bleedings in history. Partial reduction of excessive splenic artery flow (no more than 70% of baseline levels) was achieved by insertion of several (from 2 to 5) flexible coils into the distal portion of the vessel. Serum levels of albumin and ammonia were evaluated before the procedure, 30 days and 12 months after the procedure. Hepatic encephalopathy grade was evaluated according to West Heaven criteria at the same time points. Standard supportive treatment included non-selective beta-blockers (40–60 mg daily) and UDCA (500–1000 mg daily) with dose adjustment according to BMI.

Results: The plasma ammonia levels improved after SAE from 107 ± 34 to 62 ± 25 $\mu\text{mol/l}$. The mean serum albumin pre and post SAE were 29 ± 0.5 , 27.8 ± 0.4 (1 month), and 32.5 ± 0.7 g/L (12 months) respectively. West Heaven score mean tended to decrease from 2.2 on the baseline to 1.9 (1 month) and 1.4 (12 months). Thus, basic liver

POSTER PRESENTATIONS

functions (protein synthesis and ammonia purification) demonstrated considerable improvement in the long-term observation period due to combined treatment. 65 (54.2%) of 120 patients had no bleeding episodes at the endpoint of 12 months, 39 (32.5%) were hospitalized with 1 (28) or more (11) minor bleedings. Fatal bleedings took place in 11 (9.2%) patients and not related to bleeding deaths-in 4 cases.

Conclusion: From our point of view, the improving of HE manifestations after SAE procedure could be explained by synergetic effects of reduction of the excessive splenic flow, restoring of liver synthetic function due to ameliorating splenic artery steal syndrome, and, as a result, liver tissue rearterialization. SAE showed a long-term reliable prophylactic effect in high-risk patients with CSPH and HE.

FRI540

Sequential algorithm of spleen stiffness measured by a dedicated 100 Hz examination and Baveno VII criteria for clinically significant portal hypertension in compensated cirrhosis

Ruiling He^{1,2}, Chuan Liu¹, Li Jie³, Jianzhong Ma⁴, Ying Guo⁴, Xiaoqing Guo⁴, Shirong Liu⁵, Bo Gao⁶, Ning Liu⁵, Mingkai Chen⁷, Hongwei Zhou⁸, Tianyu Tang⁹, Yu Shi¹⁰, Shenghong Ju⁹, Yan Huadong¹¹, Xiaolong Qi¹. ¹The First Hospital of Lanzhou University, CHESS Center, Institute of Portal Hypertension, China; ²The First Clinical Medical College of Lanzhou University, China; ³Nanjing Drum Tower Hospital, The Affiliated Hospital of Nanjing University Medical School, Department of Infectious Diseases, China; ⁴The third people's Hospital of Taiyuan, Department of Hepatology, China; ⁵Qufu People's Hospital, Department of Infectious Diseases, China; ⁶Qufu People's Hospital, Medical Laboratory, China; ⁷Renmin Hospital of Wuhan University, Department of Gastroenterology, China; ⁸Zhujiang Hospital, Southern Medical University, Department of Laboratory Medicine, China; ⁹Zhongda Hospital Affiliated to Southeast University, Department of Radiology, China; ¹⁰Shengjing Hospital, China Medical University, Department of Radiology, China; ¹¹Shulan (Hangzhou) Hospital Affiliated to Zhejiang Shuren University Shulan International Medical College, Department of Infectious Diseases, China
Email: qixiaolong@vip.163.com

Background and aims: The renewing Baveno VII consensus proposed that liver stiffness measurement (LSM) and spleen stiffness measurement (SSM) can be used to rule in and rule out clinically significant portal hypertension (CSPH) in patients with compensated cirrhosis; however, the thresholds of SSM should be further validated with spleen-dedicated 100 Hz examination. This study aims to assess the performance of sequential algorithm of SSM measured by a dedicated 100 Hz FibroScan® and Baveno VII criteria for CSPH in patients with well-characterized compensated cirrhosis.

Method: This is a prospective multi-center study (NCT05251272). Patients with well-characterized compensated cirrhosis undergoing a 100 Hz specific FibroScan® to evaluate SSM and LSM were consecutively enrolled between August 2021 and March 2022. CSPH was defined as the threshold of hepatic venous pressure gradient measurement above 10 mmHg.

Results: A total of 101 patients (71 male) with a mean age of 52 ± 9 years were recruited from 5 university centers, and 50 (49.5%) patients had CSPH. Applying the Baveno VII criteria for exclusion of CSPH (LSM ≤ 15 kPa and platelet count $\geq 150 \times 10^9/L$), 24/101 (23.8%) patients could rule out CSPH with 8.3% of patients being missed, and the negative predictive value (NPV) and sensitivity were 91.7% and 96.0%. The sequential algorithm for SSM and Baveno VII criteria [SSM < 21 kPa OR (LSM ≤ 15 kPa and platelet count $\geq 150 \times 10^9/L$)] showed that 28/101 (27.7%) patients could rule out CSPH with 7.1% of patients being missed, and the NPV and sensitivity were 92.9% and 96.0%, respectively. Furthermore, the Baveno VII criteria for identification of CSPH (LSM ≥ 25 kPa) had 100% positive predictive value (PPV) and specificity, yet merely 5/101 (5.0%) patients would enable to identify correctly. Comparing with the former, the sequential algorithm of SSM > 50 kPa OR LSM ≥ 25 kPa improved the proportion of ruling in

CSPH (22.8% vs 5.0%, $p < 0.001$) with only 4.3% of patients misclassified, and the PPV and specificity were 95.7% and 98.0%, respectively.

Table: Performance of different methods for ruling out and ruling in clinically significant portal hypertension.

	CSPH Missed	Rule out CSPH	Non-CSPH Missed	Rule in CSPH
LSM ≤ 15 kPa and PLT $\geq 150 \times 10^9/L$	2/23 (8.3%)	24/101 (23.8%)	-	-
SSM < 21 kPa OR (LSM ≤ 15 kPa and PLT $\geq 150 \times 10^9/L$)	2/28 (7.1%)	28/201 (70.5%)	-	-
LSM ≥ 25 kPa	-	-	0	5/101 (5.0%)
SSM > 50 kPa OR LSM ≥ 25 kPa	-	-	1/23 (4.3%)	23/101 (22.8%)***

Data are presented as n (%) or n/N (%), where N is the total number of related cases. CSPH, clinically significant portal hypertension; LSM, liver stiffness measurement; SSM, spleen stiffness measurement; PLT, platelet count. *** $p < 0.001$, LSM ≥ 25 kPa compared to SSM > 50 kPa OR LSM ≥ 25 kPa.

Conclusion: The sequential algorithm of SSM measured by a dedicated 100 Hz examination and Baveno VII criteria is useful to assess CSPH accurately, especially in ruling in CSPH compared to Baveno VII criteria only.

Liver tumours: Experimental and pathophysiology

FRI542

NKG2A hampers tumor surveillance of liver-infiltrating natural killer (NK) cells via TLR4 signaling pathway after liver transplantation

Xinxian Yang^{1,1}, Kwan Man¹. ¹The University of Hong Kong, Surgery, Hong Kong
Email: kwanman@hku.hk

Background and aims: Liver transplantation (LT) provides the best option for selected hepatocellular carcinoma (HCC) patients. However, tumor recurrence occurs at a rate of 10–20% within 5 years. Graft injury during LT significantly affects the outcome of tumor recurrence by changing the regional immune microenvironment. However, the immunological mechanism of hepatic natural killer (NK) cells in graft injury was not completely understood.

Method: 349 HCC patients who underwent LT in Queen Mary Hospital, Hong Kong were recruited in this study. The correlation among the number of intra-graft NK cells, liver function, recurrence free survival (RFS) rate was analyzed. The cytotoxic function of NK cells was evaluated by co-culture with primary HCC cells. Hepatic ischemia-reperfusion injury plus major hepatectomy (IRI + Hx) was performed in C57bl/6 mice to mimic the pathological changes during human LT. Tumor cells (Hepa 1–6) were injected into the liver via portal vein after IRI + Hx in TLR4 knockout and wild-type mice.

Results: The frequency of intra-graft NKG2A+NK cells was significantly increased in patients with tumor recurrence after LT, along with increased expressions of its ligand HLA-E and inflammation signatures (IL-1 β , IL-6, NLRP3, HMGB1, and TLR4). GWR (the ratio of graft volume to estimated standard liver volume) $< 60\%$ was an independent risk factor for tumor recurrence after LT. The frequency of circulating NKG2A + NK cells was significantly increased in the patients with GWR $< 60\%$ compared with GWR $\geq 60\%$ at 3, 6, 9, and 12 months post-LT. The cytotoxic function of NKG2A + NK cells was significantly decreased compared to NKG2A-NK cells when co-cultured with primary HCC cells, characterized by decreased expressions of Granzyme B and CD107a. In IRI+Hx mouse model,

NGK2A+ hepatic (NK1.1+) NK cells were increased at 6, 24, and 48 hours. Interestingly, the expression of NGK2A was increased in liver-infiltrated (CD49a- CD49b+) NK cells but not liver-resident (CD49a+ CD49b-) NK cells. In TLR4 knockout mice subjected to IRI+Hx and tumor cell injection, the tumor growth was significantly hindered and the expression of NGK2A on liver-infiltrated NK cells was significantly decreased compared to wild-type mice at week 4.

Conclusion: Hepatic IRI increased expression of NGK2A on liver-infiltrated NK cells via TLR4 signaling pathway, which provided a favorable immune microenvironment for late-phase tumor recurrence. Understanding the broad spectrum of NK cell functional diversity would help to explore NK cell-based immunotherapy against tumor recurrence.

FRI543

Cancer-associated fibroblasts nurture LGR5 marked liver tumour-initiating cells and promote their metastasis

Jiaye Liu¹, Qiuwei Pan¹. ¹Erasmus University Medical Center Rotterdam, Department of Gastroenterology and Hepatology, Rotterdam, Netherlands

Email: q.pan@erasmusmc.nl

Background and aims: Tumor-initiating cells (TICs) are thought to be the main drivers of cancer development, progression and treatment resistance. We have recently identified the LGR5+ compartment as an important TIC population in liver cancer, representing a viable therapeutic target. Given that cancer-associated fibroblasts (CAFs) constitute a key component of the tumor microenvironment, this study aims to investigate the impact of CAFs on LGR5 marked TICs in liver cancer.

Method: Liver tumor organoids and CAFs were cultured from Diethylnitrosamine-induced liver tumors of LGR5-diphtheria toxin receptor (DTR)-GFP knock-in mice and Rosa 26-mT mice, respectively. 3D co-culture models of LGR5+ TICs with CAFs, based on cell-cell contact or trans-well system, were established *in vitro*. Immunodeficient mouse-based xenograft model was used to investigate the effect on tumor formation and metastasis, as well as diphtheria toxin treatment for specific depletion of LGR5+ cells.

Results: In primary tumors formed in the liver of LGR5-GFP reporter mice, we found high frequency of CAFs marked by alpha-smooth muscle actin surrounding LGR5 expressing cancer cells. In xenograft model, co-engraftment of liver tumor organoids with CAFs resulted in substantially higher number of LGR5+ cells in formed tumors when compared with engrafting tumor organoids alone. Furthermore, *ex vivo* culture of isolated LGR5+ cells from tumors of co-engrafted mice formed significantly larger size of organoids (68.1 ± 36.1 VS. 35.2 ± 18.3 μ m, $n=40$, $p<0.001$), although there is no statistical significance in the number of formed organoids. *In vitro*, co-culture of LGR5+ tumor cells with CAFs, in both cell-cell contact and paracrine signaling based trans-well system, resulted in significantly larger size and number of formed organoids, when compared with culturing LGR5+ cells alone. This promoting effect was eliminated by diphtheria toxin treatment which specifically deplete LGR5 cells due to transgenic expression of DTR. Consistently, subcutaneous co-engraftment of LGR5+ tumor cells with CAFs formed significantly larger tumors compared with engrafting LGR5+ cells alone (0.6 ± 0.2 VS. 0.3 ± 0.2 g, $n=8$, $p<0.05$). Most importantly, co-engraftment dramatically increased the probability of abdominal metastasis (7/8) compared with engraftment of LGR5+ tumor cells alone (1/8). Diphtheria toxin treatment mediated depletion of LGR5+ cells effectively inhibited tumor growth and metastasis in this xenograft model.

Conclusion: We here revealed robust nurturing effects of CAFs in promoting growth and metastasis of LGR5 marked TICs in experimental liver cancer. Understanding their intimate interactions shall help to decipher the mechanistic insight of liver cancer progression and to develop effective treatment for reducing tumor burden and preventing metastasis.

FRI544

Molecular insights into the tumour suppressor role of Protein Phosphatase 2A B56 delta complex in human liver, and its clinically relevant inhibition by cancerous inhibitor of PP2A

Judit Domenech Omella¹, Bob Meeusen², Emanuela Cortesi³, Karen Zwaenepoel⁴, Rita Derua¹, Chris Verslype⁵, Patrick Pauwels⁴, Jukka Westermarck⁶, Tania Roskams⁷, Jos van Pelt⁵, Veerle Janssens¹.

¹KU Leuven, Cellular and Molecular Medicine, Leuven, Belgium;

²University of Copenhagen, Novo Nordisk Foundation Center for Protein Research, Copenhagen, Denmark; ³KU Leuven, Imaging and pathology, Leuven, Belgium; ⁴Universitair Ziekenhuis Antwerpen, Pathology, Antwerpen, Belgium; ⁵KU Leuven, Oncology, Leuven, Belgium;

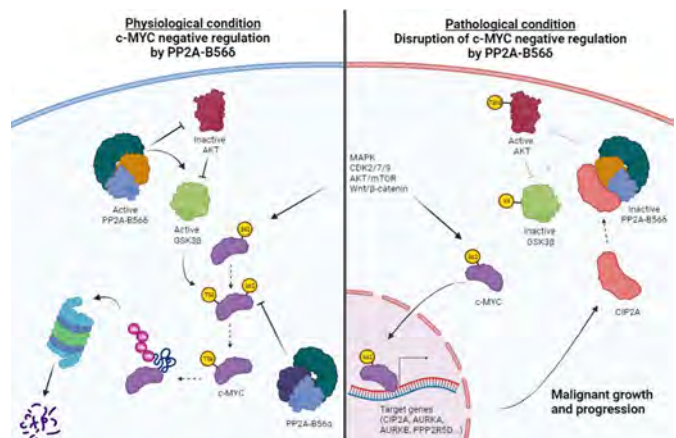
⁶University of Turku, Turku Bioscience, Turku, Finland; ⁷KU Leuven, Imaging and pathology, Leuven, Belgium

Email: judit.domenechomella@kuleuven.be

Background and aims: The clinical prognosis of hepatocellular carcinoma (HCC) remains disappointing due to an incomplete understanding of the molecular mechanisms underlying HCC progression. Recently, we reported increased spontaneous HCC development in *Ppp2r5d* KO mice, devoid of Protein Phosphatase 2A (PP2A) regulatory B56delta subunit expression. All cases presented c-MYC Ser62 hyperphosphorylation, known to increase c-MYC stability and oncogenicity. Hence, our data underscored a tumor suppressive role of PP2A-B56delta in mouse liver. Here, we aimed to investigate the role of PP2A-B56delta as a tumor suppressor in human liver, and define PP2A-B56delta status in human HCC.

Method: B56delta was stably depleted in three human HCC cell lines using shRNA, and effects on colony formation (anchorage-independent growth) and tumor growth (xenograft assays) were assessed. mRNA expression of 28 'PP2A' genes was evaluated in four published HCC datasets and Spearman correlation analysis was performed. Expression of B56delta, c-MYC and Cancerous Inhibitor of PP2A (CIP2A) was analyzed by immunohistochemistry (IHC) in 19 human HCC samples. CIP2A interactors were identified by immunoprecipitation and mass spectrometry. Diethylenetriamine was injected in two-week-old wildtype and CIP2A KO mice to study HCC latency in a chemical-induced HCC mouse model.

Results: B56delta depletion resulted in increased colony formation *in vitro* and tumor growth *in vivo*, and correlated with increased c-MYC protein expression, hyperphosphorylation of AKT and GSK3beta, and upregulation of c-MYC target gene expression. B56delta and CIP2A gene expression correlated positively with patient HCC tumors, and their high mRNA expression was associated with a worse prognosis and decreased overall survival. IHC analysis of human HCC tissue did not show significantly altered B56delta protein expression, but identified increased co-expression of c-MYC and CIP2A. In addition, we identified B56delta as a CIP2A interactor. Underscoring an oncogenic role for CIP2A, its depletion resulted in decreased tumor growth *in vivo* and increased HCC latency.



Conclusion: Our work provides insights into how PP2A-B56delta suppresses human hepatocarcinogenesis and progression, and how its tumor suppressor activity is impaired in human HCC. Specifically, we show that PP2A-B56delta prevents c-MYC protein stabilization via regulation of AKT and GSK3beta, and PP2A-B56delta inactivation is mediated by CIP2A overexpression.

FRI545

Identification of new dominant neoantigens in hepatocellular carcinoma based on a single plasmid system with co-expressing patient's HLA and antigen

Pu Chen¹, Dongbo Chen¹, Shaoping She¹, Yao Yang¹, Liying Ren², Bigeng Zhao², Ruifeng Yang¹, Weijia Liao², Hongsong Chen¹. ¹Peking University Hepatology Institute, Beijing Key Laboratory of Hepatitis C and Immunotherapy for Liver Disease, Peking University People's Hospital, China; ²Laboratory of Hepatobiliary and Pancreatic Surgery, Affiliated Hospital of Guilin Medical University, China
Email: chenhongsong@bjmu.edu.cn

Background and aims: Hepatocellular carcinoma (HCC) is the sixth most common malignancy worldwide. Compared with plentiful neoantigens in melanoma, the paucity and inefficient identification of effective neoantigens in HCC remain enormous challenges in effectively treating this malignancy.

Therefore, we tried to identify new dominant neoantigens in HCC based on an innovative plasmid system.

Method: We established a single plasmid system with co-expressing patient's human leukocyte antigen (HLA) and antigen. To verify whether the system works normally, we connected a reported KRAS G12D neoantigen sequence in HCC and its corresponding wild antigen sequence to the antigen linker regions of the vectors respectively, which carry the corresponding HLA sequence. Subsequently, they were inserted into viral vectors and transduced to the target cells. Moreover, T cell receptor (TCR) T cells that could recognize the neoantigen were constructed and co-cultured with the target cells. Then, the cytotoxicity was detected by enzyme-linked immunospot assay (ELISPOT) and enzyme-linked immunosorbent assay (ELISA). Finally, the proliferation of TCR-T cells was detected by flow cytometry assay.

Besides, next-generation sequencing (NGS) was performed for the samples such as HCC tissue, portal vein tumor thrombosis (PVTT) and tumor infiltrating lymphocyte (TIL) to analyse gene variations, candidate neoantigens and tumor immune microenvironment (TIME). Then, tetramer staining assay was used to detect the specific T cells induced by the predicted candidate neoantigens. Finally, the positive candidate neoantigens were further validated by the single plasmid system.

Results: An innovative plasmid system was established, which includes 39 high-frequency HLA vectors for Asian. Then, we successfully constructed TCR-T cells which could recognize KRAS G12D neoantigen in HCC and used the single plasmid system to verify the immunogenicity of the neoantigen. Interestingly, we found TCR-T cells co-cultured with the target cells which express KRAS G12D could be specifically activated and proliferate. Hence, the single plasmid system works normally, which provides an efficient molecular tool for immunogenicity validation of antigen.

We found some new gene variations in 14 HCC patients and predicted candidate neoantigens. Moreover, we produced some tetramers for the detection of the specific T cells and identified several positive candidate neoantigen-specific T cells. Finally, we successfully identified several new dominant neoantigens produced by ALG1 A55S mutation (ENST00000586840) and other gene variations in HCC, based on our single plasmid system.

Conclusion: Based on our single plasmid system with co-expressed patient's HLA and antigen, we successfully identified several new dominant neoantigens in HCC. These neoantigens could be as potential immunotherapeutic targets for HCC.

FRI546

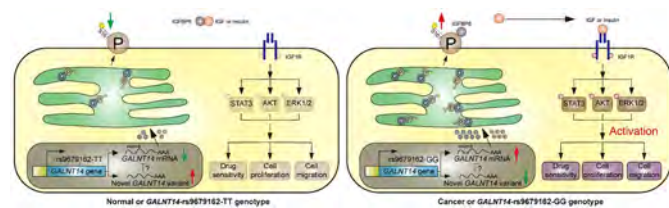
Polypeptide N-acetylgalactosaminyltransferase 14 mediated O-glycosylation on prohibitin-2 serine 161 modulates cell growth, migration and drug susceptibility in hepatocellular carcinoma

Chau-Ting Yeh¹, Yu-De Chu². ¹Chang Gung Memorial Hospital, Liver Research Center, Taoyuan, Taiwan; ²Chang Gung Memorial Hospital, Liver Research Center, Taoyuan
Email: chautingy@gmail.com

Background and aims: Worldwide, hepatocellular carcinoma (HCC) remained a leading cause of cancer-related death. A single nucleotide polymorphism (SNP), rs9679162, located on *Polypeptide N-Acetylgalactosaminyltransferase 14* (GALNT14) gene, differentially predicted the therapeutic outcomes for various gastrointestinal cancers including HCC, while the molecular mechanisms remained largely unknown.

Method: For clinical outcome analysis, 300 HCC patients having received surgical resection were retrospectively enrolled. Their paired liver tissue samples were subjected for SNP genotyping, RNA isolation, western blot, and immunohistochemical analysis. The key GALNT14 substrate was identified by the differential lectin capture method. Functional assessments of the candidate substrate protein were performed following site-directed mutagenesis.

Results: The GALNT14 level was significantly upregulated in the cancerous parts of HCCs. Higher cancerous/noncancerous ratios of GALNT14 were associated with rs9679162-GG genotype and unfavourable postoperative prognosis. A novel exon-6-skipped GALNT14 mRNA variant was identified preferentially in the rs9679162-TT genotype, and was associated with lower GALNT14 expression and favourable clinical outcomes. Cell-based experiments showed that elevated GALNT14 levels promoted HCC growth, migration, and anticancer-drugs susceptibility. Differential lectin capture analysis identified prohibitin-2 (PHB2) as a major GALNT14-mediated O-glycosylation substrate. Site-directed mutagenesis experiments revealed serine-161 (Ser161) as the O-glycosylation site. Complementation assays demonstrated that PHB2-Ser161 O-glycosylation was required for GALNT14-mediated modulation of cell growth, migration, and anticancer drugs susceptibility. PHB2 O-glycosylation was positively correlated with GALNT14 expression in HCC. Finally, PHB2-Ser161 O-glycosylation was crucial for its interaction with Insulin-like Growth Factor-Binding Protein-6 (IGFBP6) and Insulin-like Growth Factor-1 Receptor (IGF1R) mediated signalling activation.



Conclusion: GALNT14 SNP genotypes were associated with GALNT14 levels and differential expression of a novel GALNT14 mRNA variant, linking to postoperative prognosis in HCC. The elevated GALNT14 level promoted HCC growth via O-glycosylation on PHB2-Ser161, leading to activation of the IGF1R-mediated cascade.

FRI547

Gut bacteria modulate anti-tumour immunity in patients with hepatocellular carcinoma

Dhruti Devshi^{1,2}, Sandra Phillips^{1,2}, Helen Edwards^{1,2}, Nicola Harris^{1,2}, Melissa Preziosi³, Abid Suddle³, Antonio Riva^{1,2}, Shilpa Chokshi^{1,2}. ¹The Roger Williams Institute of Hepatology (Foundation for Liver Research), United Kingdom; ²Faculty of Life Sciences and Medicine (King's College London), United Kingdom; ³King's College Hospital, London, United Kingdom
Email: s.chokshi@researchinliver.org.uk

Background and aims: The gut microbiota and their metabolites play a key role in the response to checkpoint receptor (CR) inhibitors. Interestingly, antibiotics can also limit cancer progression by modulating the gut microbiota and their metabolites. The role of bacteria and their metabolites in modulating anti-tumour immunity in hepatocellular carcinoma (HCC) is not understood and is the focus of this study.

Method: Peripheral blood mononuclear cells (PBMCs) from HCC patients were stimulated *in vitro* with a peptide pool spanning seven HCC tumour-associated antigens with/without priming with formaldehyde-fixed *Escherichia coli* DH5a (EC, 50 bacteria-per-cell) or EC supernatants (20% v/v, representing bacterial metabolites). After 3 days, the expression of inhibitory immune checkpoints and functional markers (including PD-1, PD-L1, Granzyme-B, Perforin, IL-10 and IFN γ) were assessed on CD4, CD8 and MAIT T cells by flow cytometry. Thirty-four secreted cytokines (including IL-6, IL-23, IL-2, IL-1a, IL-10, IL-18 and IFN γ) were measured in PBMC culture supernatants by Luminex. For the analysis, peptide-only PBMC cultures were compared with EC-cell-primed or EC-supernatant-primed peptide-stimulated PBMC cultures.

Results: Immunosuppressive PD-1, PD-L1 and IL-10 expression was significantly higher in bacteria-primed HCC-specific CD4⁺ T-cells ($p = 0.024$, 0.0061 and 0.037 respectively) compared to HCC peptide-stimulated only PBMCs. A significant increase in pro- and anti-inflammatory cytokines (including IL-6, IL-23, IL-2, IL-1a, IL-18, IL-10 and IFN gamma) was observed in bacteria-primed HCC peptide-stimulated PBMC cultures compared to HCC peptide-only stimulated PBMCs ($p = 0.037$, 0.037 , 0.0098 , 0.0061 , 0.0061 , 0.0061 , respectively). No significant differences were seen in MAIT cells, or granzyme-B/perforin expression between HCC peptide-stimulated only and bacteria-primed HCC peptide-stimulated PBMC cultures.

Conclusion: These results reveal that bacterial priming induces inhibitory checkpoint receptor expression on anti-tumour T-cells and promotes an immunosuppressive inflammatory landscape in HCC. Further studies investigating bacterial modulation of anti-tumour immunity in HCC are warranted.

FRI548

Lack of the E3-ubiquitin ligase TRIM21 promotes higher emergence of hepatocellular carcinoma nodules in diabetic mice with non-alcoholic steatohepatitis

Ghania Kara-Ali¹, Imerzoukene Ghiles¹, Melanie Simoeseguenio¹, Luis Cano², Annaig Hamon¹, Huma Hameed¹, Claire Piquet-Pellorce¹, Sarah Dion¹, Celine Raguenes-Nicol¹, Stefano Caruso³, Jessica Zucman-Rossi³, Michel Samson¹, Jacques Le-Seyec¹, Marie-Therese Biotrel¹. ¹Univ Rennes, Inserm, EHESP, Irset (Institut de recherche en santé, environnement et travail)-UMR_S 1085, F-35000 Rennes, France; ²INSERM, INRAE, CHU Pontchaillou, UMR 1241 NUMECAN, Univ. Rennes, Rennes, France; ³Centre de Recherche des Cordeliers, INSERM, Sorbonne Université, Université de Paris, Université Paris 13, Functional Genomics of Solid Tumors Laboratory, Paris, France
Email: ghania.kara-ali@univ-rennes1.fr

Background and aims: The deregulation of the E3 ubiquitin ligase tripartite motif protein 21 (TRIM21), a central protein involved in

different physiological processes such as cell cycle, cell death or immune response, can have serious pathophysiological consequences. Thus, a low TRIM21 expression has been linked to poor survival rate in different cancers such as diffuse large B-cell lymphoma, breast cancer and hepatocellular carcinoma (HCC) without knowing the involved mechanisms.

Method: Male mice of *Trim21*-WT or *Trim21*-KO genotypes, in a hypoinsulinemic state resulting from prior injection of streptozotocin at the neonatal stage, were fed with a high-fat high-cholesterol diet (HFHCD) for 4, 8 or 12 weeks. Mice included in this protocol progressively developed a non-alcoholic steatohepatitis (NASH) which systematically resulted in HCC development.

Results: Induced liver damage was more severe in *Trim21*-KO mice after 12 weeks on HFHCD, as attested by serum transaminase levels. In addition, higher number of HCC nodules arose at 12 weeks. At an earlier stage (4 weeks of HFHCD), a more pronounced pro-inflammatory hepatic microenvironment was already detected in *Trim21*-KO mice. However, 8 weeks later, the number of hepatic macrophages and lymphocytes significantly decreased in *Trim21*-KO mice. At the same timing, the spleen of *Trim21*-KO mice contained more CD4⁺ T cells than in *Trim21*-WT mice. Further analysis showed a higher proportion of CD4⁺PD1⁺ and CD8⁺PD1⁺ T cells in *Trim21*-KO mice spleen.

Conclusion: The E3 ubiquitin ligase TRIM21 limits the emergence of HCC nodules in mouse developing NASH. The establishment of an effective anti-tumor immune response may require TRIM21, potentially by restricting the expression of PD-1 in lymphocytes and of PDL-1 in cancerous cells.

FRI549

Role of autophagy-mediated neuropilin-1 degradation on lenvatinib efficacy in human hepatocarcinoma

Paula Fernández-Palanca^{1,2}, Tania Payo-Serafin^{1,2}, Flavia Fondevila^{1,2}, Carolina Méndez-Blanco^{1,2}, Javier González-Gállego^{1,2}, José Luis Mauriz^{1,2}. ¹Institute of biomedicine (IBIOMED), University of León, León, Spain; ²Centro de investigación biomédica en red de enfermedades hepáticas y digestivas (CIBERehd), Instituto de salud Carlos III, Madrid, Spain
Email: pferp@unileon.es

Background and aims: Hepatocarcinoma (HCC) is one of the main causes of cancer-related death. Despite the effectiveness of therapeutic options such as tyrosine kinase inhibitors, loss of efficacy that leads to resistance acquisition is a frequent problem that needs to be addressed. Neuropilin-1 (NRP1) is a transmembrane glycoprotein whose role in cancer has become of special interest. We aimed to identify the *in vitro* role of NRP1 in the underlying mechanisms of lenvatinib efficacy in human HCC.

Method: The human HCC cell lines Huh-7 and Hep3B were employed. Lenvatinib was used for treatments and 100 nM bafilomycin A1 as specific autophagy inhibitor. Protein expression was analyzed by Western blot and immunocytochemistry, cell viability by Ki67 immunofluorescence, MTT and colony formation assay, and gene silencing was performed via transfection of a pool of NRP1 siRNA. Finally, cell migration ability was analyzed by wound-healing assay. Statistical analysis was done with GraphPad Prism 6, considering significance when $p < 0.05$.

Results: Antitumor efficacy of lenvatinib was observed by a reduction of cell viability and Ki67 proliferation index, showing also a decrease in NRP1 protein expression in both HCC cell lines. To identify the mechanism responsible of lenvatinib-derived NRP1 downregulation, a time-course with bafilomycin A1 alone and combined with lenvatinib was done. Autophagy inhibition prevented the reduction of NRP1 expression when combining with lenvatinib, thus blocking lenvatinib effect. Specific NRP1 gene silencing reduced cell viability,

POSTER PRESENTATIONS

showing even greater results when combining with lenvatinib. Interestingly, NRP1 silencing also blocked the loss of lenvatinib sensitivity in combination with bafilomycin A1, increasing lenvatinib antitumor effects even after inhibiting autophagy-derived NRP1 degradation induced by lenvatinib. Therefore, bafilomycin A1 was only able to revert antitumor effects of lenvatinib when NRP1 was not silenced. Likewise, lenvatinib decreased cell migration, and autophagy blockade re-established migration ability of both cell lines reducing lenvatinib efficacy on migration. However, NRP1 silencing was also able to restore migration inhibition of lenvatinib even when combining with bafilomycin A1.

Conclusion: Autophagy-dependent NRP1 degradation seems to play a key role in lenvatinib efficacy in HCC, highlighting the potential interest of NRP1 silencing as a novel strategy to prevent therapeutic failure in advanced HCC.

FRI550

Different acylcarnitines tissue profiles as metabolomics signatures of human hepatocellular carcinoma in non-alcoholic fatty liver disease according to fibrosis level

Benjamin Buchard¹, Natali Abeywickrama Samarakoon², Estelle Pujos-Guillot³, Stéphanie Durand³, Mélanie Petera³, Delphine Centeno³, Juliette Joubert⁴, Aicha Demidem², Armand Abergel¹. ¹Chu Estaing, Service de médecine digestive et hépatobiliaire, Clermont-Ferrand, France; ²Université Clermont-Auvergne, Unité de Nutrition Humaine, UMR 1019, Clermont-Ferrand, France; ³INRA PFEM, PFEM, Saint-Gènes-Champagnelle, France; ⁴Chu Estaing, Service d'anatomopathologie, Clermont-Ferrand, France
Email: benjamin.buchard@gmail.com

Background and aims: The incidence and prevalence of non-alcoholic fatty liver disease (NAFLD) are rising worldwide with the increase of obesity and diabetes. NAFLD is becoming a growing cause of hepatocellular carcinoma (HCC). NAFLD-HCC may rise in the absence of severe liver fibrosis in 20 to 50% of patients. However, current evidence does not support routine screening for HCC in this population. The aim of this study was therefore to identify metabolic pathways and putative biomarkers of NAFLD-HCC according to fibrosis level (F0F1 vs. F3F4).

Method: A non-targeted metabolomics strategy was applied to two groups of NAFLDHCC according to fibrosis level. We investigated 55 pairs of human HCC and adjacent non-tumoral tissues (NTT) which included 30 HCC developed in severe fibrosis or cirrhosis (HCC-F3F4) and 25 HCC developed in no or mild fibrosis (HCC-F0F1). Most of samples were provided by the French Tumor Biobank. Aqueous tissue extracts were analyzed using liquid chromatography coupled to mass spectrometry analysis. HCC was compared to its own NTT in these two groups.

Results: The comparison between HCC and NTT in each group revealed acylcarnitines (AC) as the main discriminant metabolites (figure). AC are known to allow the transportation of fatty acids (FA) across the mitochondrial membrane preceding mitochondrial beta oxidation for energy production. In HCC-F3F4 we found an accumulation of both medium chain acylcarnitines (MCAC, Carbon 12) and long chain acylcarnitines (LCAC, Carbon 14 -16- 18) while short chain acylcarnitines (SCAC-derived from Isoleucine and leucine) were decreased in comparison with NTT-F3F4. In contrast HCC-F0F1 was characterized by a significant increase of LCAC (Carbon 16 -18- 20) in comparison with NTT-F0F1. Notably, unlike HCC-F3F4, MCAC and SCAC were not detected in HCC-F0F1 group when compared to its own NTT.

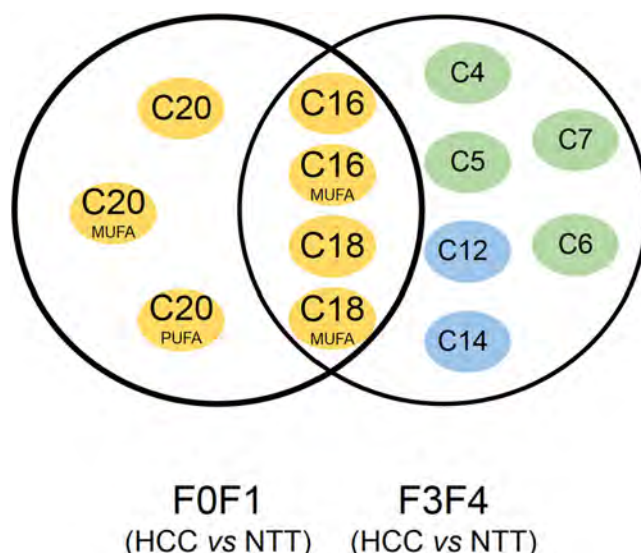


Figure: The Venn diagram displays the acylcarnitine profile that is unique to HCC-F0F1 or HCC-F3F4 and those common to both. MUFA, mono-unsaturated fatty acids; PUFA, poly-unsaturated fatty acids; C, carbon.

In addition, our preliminaries RT-PCR analysis suggest a dysregulation of the main genes coding for enzymes involved in *de novo* lipogenesis and FA oxidation in NAFLD-HCC in comparison with NTT.

Conclusion: Our results are the first one to highlight differences in AC metabolism in NAFLD-HCC and confirm the existence of two distinct metabolomics phenotypes according to underlying non tumoral fibrosis (Buchard et al, Metabolites 2021).

FRI551

Hepatocellular carcinoma alters granulopoiesis to produce neutrophils with an immature phenotype

Daniel Geh¹, Erik Ramon-Gil¹, Maja Laszczewska¹, Saimir Luli¹, Amy Collins¹, Fiona Oakley¹, Jack Leslie¹, Helen L. Reeves^{2,3}, Derek A Mann¹. ¹Newcastle Fibrosis Research Group, Biosciences Institute, Faculty of Medical Sciences, Newcastle University, Newcastle upon Tyne, United Kingdom; ²Translational and Clinical Research Institute, Faculty of Medical Sciences, Newcastle University, Newcastle upon Tyne, United Kingdom; ³Hepatopancreatobiliary Multidisciplinary Team, Newcastle upon Tyne Hospitals NHS Foundation Trust, Freeman Hospital, Newcastle upon Tyne, United Kingdom
Email: daniel.geh@newcastle.ac.uk

Background and aims: Despite immunotherapy being the first line treatment for advanced hepatocellular carcinoma (HCC), the majority of HCCs are resistant, especially in the context of non-alcoholic fatty liver disease (NAFLD). Neutrophils have emerged as important drivers of HCC, exerting pro-tumour functions such as creating an immunosuppressive tumour microenvironment. Despite this little is known about how HCC influences neutrophils. Here we aim to characterize the effect HCC has on neutrophil phenotype.

Method: *In vivo model.* High fat diet induced steatohepatitis plus orthotopic tumour implantations were conducted in C57BL/6J mice. Sham surgeries were conducted for controls. Neutrophils were isolated from the bone marrow, blood, spleen, liver and tumours. *Patient study.* HCC, chronic liver disease and healthy control patient blood samples were collected and neutrophils isolated by density gradient centrifugation. Neutrophils were analyzed by flow cytometry.

Results: In the murine HCC model neutrophil frequency increased across all compartments with disease progression (A). HCC induced altered granulopoiesis with a preferential increase in early neutrophil progenitor populations such as granulocyte-monocyte progenitor cells (GMPs) and pre-neuts (B). Overall neutrophil phenotype mainly corresponded to the tissue of residence and maturation (C), however

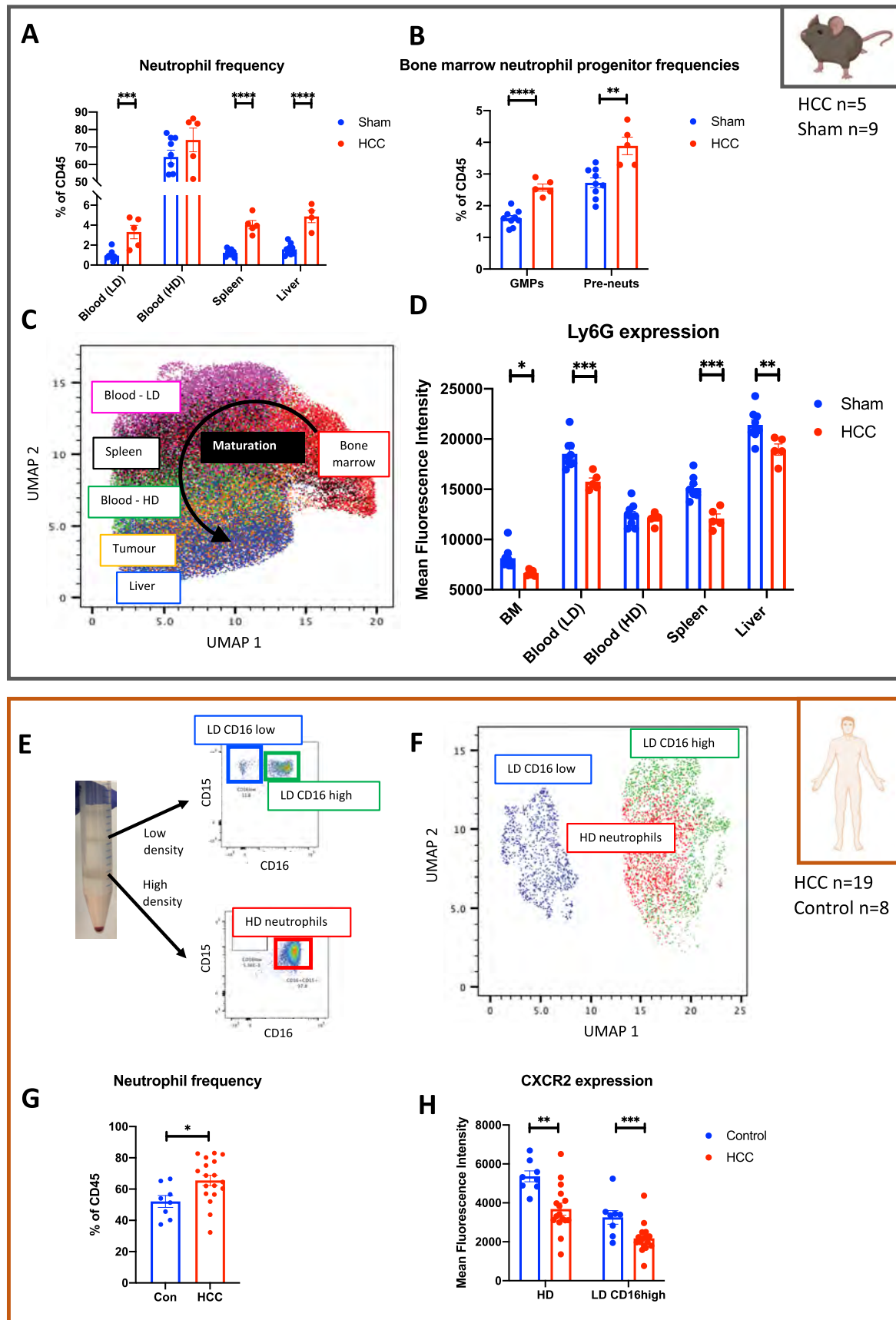


Figure: (abstract: FRI551)

across all compartments HCC gave rise to a more immature neutrophil phenotype as demonstrated by a reduction in Ly6G expression (D). There were also HCC associated changes in neutrophil immune checkpoint and chemokine receptor expression. In patient blood samples 3 neutrophil populations were identified; low density (LD) CD16 low, LD CD16 high and high density (HD) neutrophils (E). These populations could be distinguished based on activation marker and chemokine receptor expression (F). Similar to the murine model there was an increase in neutrophil frequency in HCC patients compared to controls (G) with HCC neutrophils displaying a more immature phenotype as demonstrated by a reduction in CXCR2 expression (H).

Conclusion: HCC induces large shifts in neutrophil dynamics starting during granulopoiesis causing an increase in neutrophil frequency and giving rise to a more immature neutrophil phenotype. We hypothesize that these immature neutrophils have tumour promoting functions, utilized by the HCCs to promote tumour progression. Manipulation of neutrophil maturation may represent an important immune-therapeutic strategy.

FRI552

Hippo inactivation drives BMI1-associated proliferative hepatocarcinogenesis in chronic hepatitis B virus infection

Xufeng Luo^{1,2}, Rui Zhang³, Yaojie Liang², Stefan Schefczyk², Shi Liu⁴, Hideo Baba⁵, Christian Lange⁶, Heiner Wedemeyer⁷, Mengji Lu⁸, Ruth Broering². ¹Affiliated Cancer Hospital of Zhengzhou University, Institute for Lymphoma Research, Zhengzhou, China; ²University Duisburg-Essen, Dept. of Gastroenterology, Hepatology and Transplant Medicine, Essen, Germany; ³Sun Yat-sen University-Sun Yat-sen Memorial Hospital, Department of Hepato-Pancreato-Biliary Surgery, Guangzhou, China; ⁴College of Life Sciences-Wuhan University, State Key Laboratory of Virology, Wuhan, China; ⁵University Duisburg-Essen, Institute for Pathology, Essen, Germany; ⁶Ludwig-Maximilian University of Munich, Department of Internal Medicine, Munich, Germany; ⁷Hannover Medical School, Department of Gastroenterology, Hepatology and Endocrinology, Hannover, Germany; ⁸University Duisburg-Essen, Institute for Virology, Essen, Germany
Email: ruth.broering@uni-due.de

Background and aims: Chronic hepatitis B virus (HBV) infection is one of the foremost sources of hepatocellular carcinoma (HCC). Efficient restraint of HBV viremia and necroinflammation via nucleos (t)ide analogue treatment could reduce the HCC incidence. However, hepatocarcinogenesis still occurs in the absence of active hepatitis, correlating with high hepatitis B surface antigen (HBsAg) serum levels. Nevertheless, the molecular mechanisms leading to neoplastic transformation remain elusive.

Method: Hemizygous HBsAg-transgenic mice (tg[Alb1HBV]44Bri) were investigated as a model of hepatocarcinogenesis. Verteporfin treatment were applied *in vivo* and *in vitro*. Functional analysis included chromatin immunoprecipitation, luciferase-based reporter assays and gain or loss of function assays. HCC tissues with and without HBV infection were analyzed.

Results: Gene set enrichment analysis suggested that signatures in HBsAg-transgenic mice correlated with YAP-downstream, cell cycle, DNA damage and spindle events (GSE84429). Flow cytometry revealed that polyploidy and aneuploidy frequently occurred in hepatocytes of these mice. Quantitative PCR, western blot and immunohistochemical staining revealed the downregulation of MST1/2, loss of YAP phosphorylation and the induction of BMI1 expression. *In vitro*, chromatin immunoprecipitation and the analysis of mutated binding sites in luciferase-based reporter assays indicated that the YAP/TEAD4 transcription factor complex binds and activates the Bmi1 promoter. Furthermore, overexpression or inhibition of YAP or BMI1 directly altered proliferation-associated events, including p16^{INK4a}, p19^{ARF}, p53 and Cyclin D1. Verteporfin treatment of HBsAg-transgenic mice, *in vivo*, and related hepatocytes *in vitro*, attenuated this BMI1-mediated proliferation. Analysis of liver biopsies from

patients chronically infected with HBV revealed positive correlations between HBsAg, YAP and BMI1, which were further associated with proliferation events.

Conclusion: HBsAg-mediated inactivation of Hippo pathway, resulting in increased BMI1 expression, thereby promoting proliferative hepatocarcinogenesis through alterations in the cell cycle and chromosomal stability.

FRI553

RNA-Seq based transcriptome analysis revealed inhibiting methionine aminopeptidase 2 prevented hepatocellular carcinoma with inhibited angiogenesis

Yongtao Wang¹, Mozhdeh Sojoodi¹, Shijia Zhu², Wei Tang³, Guoliang Qiao¹, Shike Wang⁴, Stephen Barrett¹, Michael Lanuti⁵, Motaz Qadan¹, Yujin Hoshida², Kenneth K. Tanabe¹. ¹Massachusetts General Hospital and Harvard Medical School, Division of Gastrointestinal and Oncologic Surgery, Boston, United States; ²University of Texas Southwestern Medical Center, Department of Internal Medicine, Dallas, United States; ³National Cancer Institute, Center for Cancer Research, Bethesda, United States; ⁴The University of Texas MD Anderson Cancer Center, Departments of Thoracic/Head and Neck Medical Oncology, Houston, United States; ⁵Massachusetts General Hospital and Harvard Medical School, Division of Thoracic Surgery, Boston, United States
Email: ktanabe@partners.org

Background and aims: In our previous experiments with molecular and histologic assessments, we demonstrated that in a diethylnitrosamine (DEN)-induced rat hepatocellular carcinoma (HCC) model, inhibition of methionine aminopeptidase 2 (MetAP2) decreased HCC development by inhibiting cirrhosis progression, which was involved with inhibiting angiogenesis and neo-vascularization. In this study we investigated the hypothesis with RNA-Seq analysis, MetAP2 inhibition can reverse the global transcriptomic landscape of DEN-induced HCC with inhibited angiogenesis.

Method: Male Wistar rats received weekly intraperitoneal injections of 50 mg/kg DEN for 18 weeks, and were randomly assigned to 4 groups starting from 9th week: 1) water (control); or 2) MetAP2 inhibitor ZGN1345 (3 mg/kg) by daily gavage; 3) 0.15% DMSO (control); or 4) ZGN-1136 (0.3 mg/kg) by daily subcutaneous injection. Global transcriptomic landscape between DEN-induced rat HCC and normal rat liver, DEN-induced rat HCC before and post-MetAP2 inhibitor treatments were investigated with RNA Sequencing and Gene Set Enrichment Analysis (GSEA) analysis.

Results: Compared with normal rat liver, regulatory signatures of protein maturation, and signatures of collagen containing extracellular matrix, DEN-induced up-regulated genes in liver cancer and cancer keratinization, angiogenesis and vascular invasion in liver cancer were positively enriched in DEN-induced rat HCC. After inhibiting MetAP2 with ZGN1345 treatment, these signatures reflecting enhanced protein maturation, HCC and angiogenesis were significantly reversed in DEN-induced rat HCC. More detailed, regulatory signatures of protein mature were negatively enriched, indicating MetAP2-catalyzed protein maturation and MetAP2 function were inhibited. Signatures of collagen containing extracellular matrix and up-regulated genes in carcinoma associated fibroblast were negatively enriched and suppressed after inhibiting MetAP2. Of notable importance, signatures of cancer keratinization were also negatively enriched and inhibited. Moreover, negative enrichment of signatures of angiogenesis were observed after inhibiting MetAP2, indicating inhibited HCC development was involved with suppressed angiogenesis. Inhibiting MetAP2 with ZGN1136 treatment closely matched and further supported these observations.

Signatures	Protein mature	Collagen	Liver cancer	Angiogenesis
DEN-induced rat HCC vs Normal rat liver	↑	↑	↑	↑
ZGN1345 vs Water control	↓	↓	↓	↓
ZGN1136 vs Vehicle control	↓	↓	↓	↓

Figure 1. Summary of RNA-Seq based transcriptome analysis. ↑ indicates positive enrichment. ↓ indicates negative enrichment.

Conclusion: On the global transcriptomic level, MetAP2 inhibition effectively prevented HCC development, which was involved with inhibited angiogenesis. These data further suggest that inhibition of MetAP2 may represent a new prevention target for HCC.

FRI554

Proteomic analysis of bile in the rat thioacetamide model reveals new mechanisms in human cholangiocarcinogenesis

Leticia Colyn¹, Gloria Álvarez-Sola^{1,2}, Maria U Latasa¹, Iker Uriarte^{1,2}, Jose Maria Herranz^{1,2}, Maria Arechederra^{1,2,3}, Juan Falcon-Perez^{2,4}, Antonio A Pineda⁵, Andrea Casadei Gardini⁶, Coral Barbas⁷, Jesus M Urman^{3,8}, Bruno Sangro^{2,3,9}, Jesus Maria Banales^{2,10}, María Luz Martínez-Chantar^{2,11}, Jose Marin^{2,12}, Fernando Corrales^{2,13}, Maria Iraburu Elizalde¹⁴, Francisco Javier Cubero^{2,15}, Carmen Berasain^{1,2,3}, Maite G Fernandez-Barrena^{1,2,3}, Matías A Avila^{1,2,3}. ¹CIMA, Universidad de Navarra, Hepatology Program, Pamplona, Spain; ²CIBEREHD, Madrid, Spain; ³Instituto de Investigaciones Sanitarias de Navarra IdiSNA, Pamplona, Spain; ⁴CIC-BioGune, Metabolomics Platform, Derio, Spain; ⁵CIMA, Universidad de Navarra, Molecular Therapies Program, Pamplona, Spain; ⁶San Raffaele Hospital, Oncology, Milano, Italy; ⁷Universidad CEU-San Pablo, Centre for Metabolomics and Bioanalysis, Madrid, Spain; ⁸Hospital Universitario de Navarra, Gastroenterology, Pamplona, Spain; ⁹Clínica Universidad de Navarra, Hepatology Unit, Pamplona, Spain; ¹⁰Bio-Donostia Research Institute, San Sebastian, Spain; ¹¹CIC-BioGune, Liver Research Laboratory, Derio, Spain; ¹²Universidad de Salamanca, Physiology and Pharmacology Department, Salamanca, Spain; ¹³CNB-CSIC, Proteomics Unit, Madrid, Spain; ¹⁴Universidad de Navarra, Department of Biochemistry and Genetics, Pamplona, Spain; ¹⁵Universidad Complutense de Madrid, Department of Immunology, Ophthalmology and ENT, School of Medicine, Madrid, Spain
Email: lcolyn@alumni.unav.es

Background and aims: Cholangiocarcinoma (CCA) is a deadly disease usually diagnosed at advanced stages. Animal models enable the understanding of pathological processes and its translation into diagnostic and therapeutic advances. Thioacetamide (TAA)-induced CCA in rats captures key features of the human carcinogenic process, including chronic liver injury, inflammation and stromal reaction. Molecular analysis of bile is an excellent liquid biopsy approach and may also help understanding CCA pathogenesis. Here we performed proteomic analyses of bile from control and TAA-CCA rats. Our findings provide further support to the clinical relevance of this model and allowed us to identify new molecular interactions in CCA.

Method: Male Sprague-Dawley rats were treated with TAA in drinking water for 30 weeks. Serum, bile and liver tissues were collected. We performed LC-MS based proteomic analysis of bile. Most relevant hits were validated by qPCR and immunohistochemistry. In vitro mechanistic studies were performed in human CCA cell lines, including Huh28 cells transduced with KRAS-G12D. Cell

signaling, cell growth, gene regulation and C13-glucose-serine fluxomics analyses were performed.

Results: All TAA-treated rats developed liver fibrosis and CCA. More than 200 proteins were differentially represented in bile from TAA-rats. Ingenuity Pathway Analysis highlighted pathways related to inflammation, cell signaling, oxidative stress and glucose metabolism. The most relevant hits were confirmed by qPCR in rat liver tissues and in human CCA (TCGA). Activation of interleukin-6 (IL6) and epidermal growth factor receptor (EGFR)-ERK1/2 pathways, critical in CCA biology, as well as key genes in cancer-related glucose-serine metabolic reprogramming, were confirmed in TAA-CCA tissues. TAA-CCAs also showed increased expression of G9a histone-methyltransferase and DNA methyltransferase 1 (DNMT1), epigenetic pro-CCA effectors. In CCA cell lines we showed that IL6 expression can be triggered by EGFR-pathway activation and the presence of KRAS-G12D. We also show that the serine-glycine pathway, critically involved in cancer, is enhanced in CCA cells and can be inhibited upon G9a/DNMT1 pharmacological targeting. Mechanistically, KRAS-G12D promoted G9a binding to chromatin in CCA cells, and this was prevented by the inhibition of G9a self-methylation. Finally, we demonstrated that tumorigenic properties conferred by KRAS-G12D to CCA cells such as anchorage-independent growth are highly sensitive to G9a/DNMT1 inhibition.

Conclusion: Our study confirms the rat TAA-CCA model as a key resource for basic and translational CCA research. This model led us to identify the EGFR-ERK1/2 pathway as a critical driver for IL6 production, and to establish the relevance of the glucose-serine pathway in CCA. The G9a/DNMT1 epigenetic complex is further validated as a target for CCA therapy.

FRI555

Expression of hepatitis B surface antigen in vivo and in vitro induces endoplasmic reticulum stress, impairs autophagy and promotes proliferation

Yaojie Liang¹, Xufeng Luo^{1,2}, Stefan Schefczyk¹, Hideo Baba³, Mengji Lu⁴, Ruth Broering¹. ¹University Duisburg-Essen, Medical Faculty, Dept. of Gastroenterology, Hepatology and Transplant Medicine, Essen, Germany; ²The Affiliated Cancer Hospital of Zhengzhou University, Henan Cancer Hospital, Institute for Lymphoma Research, China; ³University Duisburg-Essen, Medical Faculty, Institute for Pathology, Essen, Germany; ⁴University Duisburg-Essen, Medical Faculty, Institute for Virology, Essen, Germany
Email: ruth.broering@uni-due.de

Background and aims: Hepatitis B surface antigen (HBsAg) has been identified to increase the risk and contribute to hepatocellular carcinoma (HCC). However, factors and mechanisms that drive HBsAg-induced hepatocarcinogenesis remain poorly defined, thus hindering the development of new therapeutic strategies. Therefore, we explore how HBsAg mechanistically facilitates the transformation from normal liver cells to HCC.

Method: Data mining of the microarray set GSE84429 (from GEO datasets) indicated the potential candidate signatures of HBsAg-driven intracellular events. Hemizygous tg (Alb1HBV)44Bri/J mice were investigated for this HBsAg-driven carcinogenic events by western blotting, immunohistochemical (IHC) staining. Finally, the findings were verified in HBsAg-overexpressing Hepa1-6 cells, in which functional analysis was performed to study the contribution of these events in hepatocarcinogenesis.

POSTER PRESENTATIONS

Results: Gene set enrichment analysis identified significant signatures in HBsAg-transgenic mice correlating with ER stress, unfolded protein response (UPR), autophagy, cell cycle and proliferation. Clustered heatmap visualized distinct gene expression pattern for endoplasmic reticulum (ER) stress and autophagy in HBsAg-transgenic mice, compared to wild type. These events were further investigated in 2-, 8- and 12-month-old HBsAg-transgenic mice. Elevated BiP expression in HBsAg-transgenic mice indicated induction of UPR. Furthermore, our study indicates that HBsAg impaired the autophagic flux. In HBsAg-transgenic mice autophagy was enhanced at the early stage (increased Beclin1) and blocked at the late stage (increased p62 and LC3B-II). These ER stress and autophagy events could be verified in Hepa1-6 cells overexpressing HBsAg for up to 72 hours. In addition, HBsAg expression changed lysosomal acidification, visualized by acridine orange staining, and promoted proliferation, indicated by Ki67 staining of paraffin-embedded sections and CCK-8 staining and colony formation assay *in vitro*. IHC staining of cleaved caspase3, an apoptosis marker, revealed a slight increase in HBsAg-transgenic mice, indirectly indicating hepatocyte proliferation due to HBsAg accumulation.

Conclusion: Our findings revealed that HBsAg directly induces ER stress, impairs autophagy and promotes proliferation thereby driving hepatocarcinogenesis. Moreover, this study expanded the understanding of HBsAg-mediated intracellular events in carcinogenesis.

FRI556

Cross-talk between cholangiocarcinoma cells and extracellular microenvironment drives desmoplastic matrix deposition

Gilles van Tienderen¹, Oskar Rosmark², Ruby Lieshout¹, Jorke Willemse¹, Floor de Weijer¹, Linda Elowsson Rendin², Gunilla Westergren-Thorsson², Michael Doukas³, Bas Groot Koerkamp¹, Martin van Royen³, Luc J.W. van der Laan¹, Monique M.A. Verstegen¹. ¹ErasmusMC Transplant Institute, Department of Surgery, Rotterdam, Netherlands; ²Lund University, Department of Experimental Medical Science, Lund, Sweden; ³Erasmus MC, Department of Pathology, Rotterdam, Netherlands
Email: g.vantienderen@erasmusmc.nl

Background and aims: Cholangiocarcinoma (CCA) is a highly aggressive tumor which arises from the biliary duct epithelium. Currently available models fail to recapitulate the full complexity of CCA, particularly the desmoplastic environment and the interplay between cancer cells and the extracellular matrix (ECM). We aimed to study the role of tumor cells in ECM deposition and desmoplasia by combining patient-derived CCA organoids (CCAOs) and native liver and tumor scaffolds, obtained by decellularization.

Method: Native human CCA matrix (CCA-M) and tumor-free liver matrix (TFL-M) were decellularized and subsequently recellularized with CCAOs. The decellularized scaffolds were biochemically and mechanically assessed. Tumor cell behavior of CCAOs in CCA-M, TFL-M, and basement membrane extract (BME), was assessed by bulk RNA-sequencing and Stable Isotope Labeling by Amino acids in Cell culture (SILAC)-based mass spectrometry.

Results: Decellularization of CCA tumor and liver tissue resulted in effective removal of cells while preserving ECM structure and retaining important characteristics of the tissue origin, including stiffness and the presence of desmoplasia. When culturing CCAOs in CCA-M, the expression profile of differentially expressed genes much more resembled the transcriptome of primary CCA tumor tissue *in vivo* compared to TFL-M (correlation coefficient (CC) CCA-M 0.83 ±

0.03 vs CC TFL-M 0.70 ± 0.03, $p = 0.004$) and BME (CC CCA-M 0.88 ± 0.04 vs CC BME 0.63 ± 0.06, $p < 0.0001$). Furthermore, CCA-M induced specific extracellular matrix protein production in CCAOs, such as fibronectin 1 (FN1), which is related to desmoplasia and patient survival. In TFL-M, lacking desmoplasia, CCAOs were able to initiate a desmoplastic reaction directly through increased production of multiple collagen types (e.g. COL1A1, COL1A2, COL6A1, COL6A3).

Conclusion: This improved model of cholangiocarcinoma recapitulates key aspects of CCA tumor biology, including transcriptome profiles and ECM protein production. The increased production of extracellular matrix proteins suggests that tumor cells can contribute to their own desmoplastic environment.

FRI557

DNA methylation regulates lncRNAs compromising hepatic identity during hepatocarcinogenesis

Miriam Recalde¹, María Gárate-Rascón¹, José María Herranz^{1,2}, María Elizalde¹, María Azkona¹, Juan Pablo Unfried³, Bruno Sangro^{2,4,5}, Maite G Fernandez-Barrena^{1,2,5}, Puri Fortes^{2,3,5}, Matías A Avila^{1,2,5}, Carmen Berasain^{1,2,5}, Maria Arechederra^{1,5}. ¹Center of Applied Medical Research (CIMA), Program of Hepatology, Pamplona, Spain; ²National Institute for the Study of Liver and Gastrointestinal Diseases (CIBERehd, Carlos III Health Institute), Madrid, Spain; ³Center of Applied Medical Research (CIMA), Department of Gene Therapy and Regulation of Gene Expression, Pamplona, Spain; ⁴Navarra University Clinic, Hepatology Unit, Pamplona, Spain; ⁵Navarra Institute for Health Research (IdiSNA), Pamplona, Spain
Email: macalderon@unav.es

Background and aims: We have previously identified a list of lncRNAs deregulated in hepatocellular carcinoma (HCC). In the present work, we aim to study the mechanism of lncRNA downregulation in HCC and the contribution of this deregulation to the progression of liver tumorigenesis.

Method: We used public RNAseq, methylome and clinical data of HCC and other types of tumor patients from TCGA. Human HCC, peritumoral, cirrhotic and healthy liver samples were obtained from Biobanco Universidad de Navarra (Spain). PLC/PRF/5, HepG2 and well-differentiated HepaRG HCC human cell lines were used to determine the expression of selected lncRNAs and hepatic specific markers by RT-qPCR in control condition and after demethylating treatment with 5-aza-2'-deoxycytidine and lncRNA knockdown with LNA-gapmers. DNA methylation was determined by targeted bisulfite sequencing.

Results: We verified that the in-silico top-ranked downregulated lncRNAs showed decrease expression in HCC compared to paired peritumoral tissues and cirrhotic and healthy livers. As expected, these HCC downregulated lncRNAs were preferentially expressed in liver compared to other organs, yet a set expressed to a lesser extent in other tissues, were also downregulated in the corresponding tumors. Although the promoter regions of these lncRNAs are poorly represented in the published methylome data, we found that the available promoter CpGs were hypermethylated in HCC compared to control tissue, as well as in HCC human cell lines compared to primary hepatocytes. We validated these findings in a cohort of HCC and paired peritumoral tissues. Moreover, demethylating treatment induced the expression of these lncRNAs, thus demonstrating that DNA hypermethylation is responsible for lncRNA downregulation. To determine the relevance of these set of lncRNAs in HCC, we studied the clinical implication of their downregulation. Importantly, TCGA

data showed that their loss of expression was significantly associated with worse survival and poor tumor differentiation, supported by the lower expression of hepatic specific genes such as *Albumin*, *CYP3A4*, *MAT1A* or *HNF4alpha*. Accordingly, in vitro downregulation of a set of these lncRNAs in well-differentiated HepaRG cells resulted in the loss of hepatic specific markers.

Conclusion: All together, our results demonstrate that hepatocarcinogenesis is associated to the downregulation through DNA methylation of a set of lncRNAs essentials to ensure hepatic differentiation.

FRI558

Inhibiting IRE1a-endonuclease activity potentiates the effect of doxorubicin in hepatocellular carcinoma

Maria Kopsida¹, Femke Heindryckx¹, Natasa Pavlovic¹, Hans Lennernas², Jaafar Khaled¹. ¹Uppsala Universitet, Medical Cell Biology, Uppsala, Sweden; ²Uppsala Universitet, Pharmaceutical Biosciences, Uppsala, Sweden
Email: maria.kopsida@mcb.uu.se

Background and aims: Hepatocellular carcinoma (HCC) is the most common form of liver cancer, characterized by a high resistance to chemotherapeutic agents, such as doxorubicin (DOX). One potential contributing factor to this drug resistance, is the activation of the endoplasmic reticulum (ER) stress pathways. This is a cellular stress mechanism that becomes activated when the cell's need for protein synthesis exceeds the ER's capacity to ensure accurate protein folding, and has been implicated in creating drug-resistance in several solid tumors. However, its role in HCC remains unclear and requires further investigation.

Method: Publicly available data from the Human Protein Atlas (HPA) was used to find correlated expression of drug resistance/ER-stress markers in HCC-patients. A chemically induced mouse model for HCC was used and mice were treated twice per week with the ER-stress inhibitor 4u8C and/or DOX for 3 weeks, after the occurrence of tumors. Liver samples were taken for histological and molecular biology analyses.

Results: Data-mining of the HPA revealed that ER-stress markers are highly intertwined with different drug-resistance mechanisms in HCC-patients. Mice with HCC experienced a statistically significant weight loss compared to healthy mice. This was further exacerbated after DOX-treatment, while co-treatment with 4u8C restored weight levels to nearly those of healthy mice. All treatments significantly decreased the number of tumors, with the strongest reduction in the 4u8C + DOX combination treatment. Staining for Ki-67 showed a significant increase in the number of Ki-67 positive cells in mice with HCC, which was significantly reduced in all treatment groups, with the strongest reduction in the 4u8C+DOX combination treatment. In mice with HCC, 4u8C and the combination of 4u8C and DOX significantly increased apoptosis compared to untreated mice. Interestingly, no increase of apoptosis was seen in the DOX-treated group, which could suggest an alternative form of cell death. As DOX is known to induce ferroptosis, Transferrin Receptor-staining in liver tissue was quantified. This showed that DOX increased the area of Transferrin Receptor positive staining, suggesting a possible increase in ferroptosis. Interestingly, treatment with 4u8C reduced this effect, which is in line with previous findings that ferroptosis is-at least in part-dependent on ER-stress pathways.

Conclusion: By using an *in vivo* model known for its similarity to human HCC, we show that using an ER-stress inhibitor can potentiate the cytotoxic effect of DOX. The long-term impact of our study could open the possibility of ER-stress inhibitors as adjuvant treatments for HCC-patients.

FRI559

Genetic ablation of miR-22 fosters hepatic carcinogenesis in mice

Monika Gjorgjieva¹, Cyril Sobolewski¹, Anne-Sophie Ay¹, Daniel Abegg², Marta Sousa¹, Flavien Berthou¹, Margot Fournier¹, Christine Maeder¹, Xavier Montet³, Alexander Adibekian², Michelangelo Foti¹. ¹University of Geneva, PHYME, Geneva, Switzerland; ²The Scripps Research Institute, Chemistry, Jupiter, United States; ³University of Geneva, Radiology, Geneva, Switzerland
Email: monika.gjorgjieva@unige.ch

Background and aims: We previously reported that microRNA-22 (miR-22) deficiency exacerbated diet-induced obesity, hepatomegaly, and liver steatosis in mice by promoting hepatic glycolysis and lipid uptake. In HCC, miR-22 expression/activity is strongly downregulated in both mouse models of HCC and human HCC, suggesting an important role for this microRNA also in pre-cancerous stages and tumorigenesis. Herein, we investigated the role of miR-22 deficiency in HCC development associated or not with diet-induced obesity.

Method: Mir22-knockout (miR22KO) mice were used to investigate hepatic carcinogenesis induced either by DEN, or PTEN-deficiency, in mice fed a normal or obesogenic diet. Proteomic analyses of liver tissues from miR22KO mice were performed and metabolic alterations and cancer processes under the influence of miR-22 were investigated in transformed hepatic cancer cells.

Results: In vivo, the genetic deletion of miR-22 triggers a significant increase in the onset of hepatic tumoural nodules and multiplicity induced by DEN. This miR-22-associated phenotype was further exacerbated in diet-induced obese mice. A similar tumour promoting effect of miR-22 deficiency was observed in a genetic model of HCC spontaneous development induced by the liver specific deletion of the tumour suppressor PTEN (liver-specific miR-22/PTEN double KO mice). Consistent with these phenotypes, proteomic analyses of hepatic tissues from miR-22 KO mice indicate that miR-22 exerts tumour suppressive function in vivo by restraining the expression/activity of several oncogenic factors. Surprisingly, overexpression of miR-22 in Huh7 hepatic cancer cells triggers, in contrast to our in vivo observations, a clear induction of a Warburg effect with an increased glycolysis and an inhibited mitochondrial respiration consistent with an oncogenic role for miR-22 in these cells.

Conclusion: Our study indicates that in vivo miR-22 behaves as a strong tumour suppressive miRNA restraining tumour initiation. Our data further indicate that miR-22 may have a dual role in hepatic carcinogenesis by promoting tumour initiation but inhibiting then tumour progression when cells are already transformed.

FRI560

Focal nodular hyperplasia: a response to portal vein thrombosis followed by a sequence of arterio-portal shunting, hyperperfusion, focal retrograde sinusoidal blood and Wnt flow, and Wnt-induced activation of the bud maturation sequence

IanR Wanless¹, Ashley Stueck¹. ¹Anatomic Pathology, Halifax, Canada
Email: ian2460@gmail.com

Background and aims: Focal nodular hyperplasia (FNH) is a hyperplastic lesion with abnormally high arterial blood flow. Subsequent events in the pathogenesis have not been elucidated. In studies of cirrhosis, we showed that regeneration occurs in the sequence: 1) activation of hepatocyte progenitor cells (HPCs) identified by glutamine synthetase activation (GSA), 2) Hepatocyte (HC) buds with tubular plates, and 3) HC remodeling into single-cell plates. This budding sequence may be initiated by local Wnt secretion. Wnt activates the Wnt/beta-catenin pathway causing regeneration and GSA. GSA in a "map-like pattern" is a defining feature of FNH.

We hypothesize that increased delivery of secreted Wnt to HPCs initiates focal HC hyperplasia. We studied morphology of FNH for an explanation of how Wnt, produced in hepatic veins, could be distributed to the HPC niche in portal tracts.

POSTER PRESENTATIONS

Method: A consecutive series of 50 resected FNH lesions were serially sectioned and stained with GS, CD34, CK19, reticulin.

Results: Most lesions had a large arterio-portal shunt (APS). Proximal sinusoids were mostly lined by CD34-positive sinusoidal endothelial cells (SEC), indicating a high-flow/high-pressure state. HPC activation and tubular HC plate structure confirmed that hyperplasia resulted from budding. Within FNH, GSA was markedly increased near small hepatic veins and absent in high flow areas revealed by CD34-positive SEC. This map-like distribution of GSA suggests that an APS focally pressurizes hepatic veins resulting in focal retrograde sinusoidal flow, delivering increased Wnt concentration to local parenchyma and small bile ducts, inducing HC hyperplasia by activation of budding sequence.

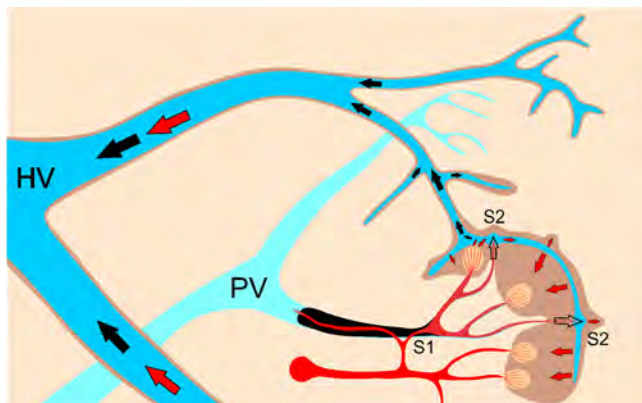


Figure: Early FNH lesion caused by focal portal vein thrombosis. Primary A-PV shunt (S1) and secondary A-HV shunts (S2) pressurize hepatic veins, reversing HV-sinusoid pressure gradients with retrograde Wnt flow, Wnt-driven HC GSA (brown areas), and Wnt-driven budding (yellow ovals). Dotted red lines are CD34+ sinusoids. Arrows red = Wnt flow, black = blood flow.

Conclusion: In FNH, hyperperfusion and focal retrograde sinusoidal flow, can explain the map-like distribution of Wnt effects, such as GSA and bud-derived hyperplasia. Most lesions likely begin with a local portal vein thrombosis with shunt forming during recanalization. Downstream arterialization and A-HV shunting provide the focal and variable HV-to-sinusoidal pressure gradients that determine direction of blood flow. Budd-Chiari lesions likely begin with HV thrombosis giving a distinct lesion (FNH-type 2).

FNH serves as a model for Wnt causing hyperplasia and GSA. Similar blood flow abnormalities occur in chronic liver disease, although in a less predictable and focused pattern. Thus, local Wnt concentration may be an important driver for regeneration in many liver diseases.

FRI561

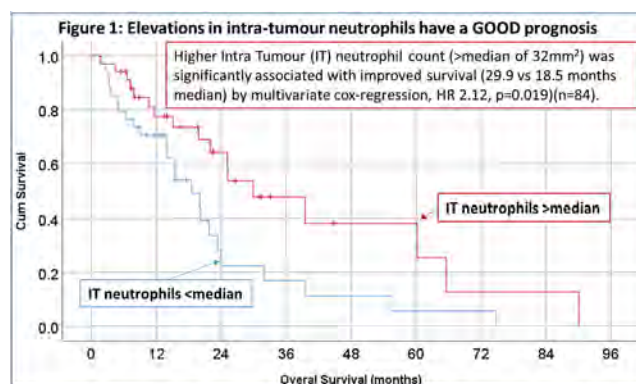
Hepatocellular carcinoma and neutrophils-towards understanding positive and negative impacts on treatments and progression

João Maurício¹, Sandra Murphy², Misti McCain¹, Daniel Geh¹, Marcello Kadhurusman¹, Jack Leslie², Robyn Watson¹, Steven Masson³, Stuart Mcpherson³, Alastair Burt², Ruchi Shukla², Derek A Mann², Caroline Wilson², Helen Louise Reeves^{1,3}. ¹Newcastle University Translational and Clinical Research; ²Newcastle University Biosciences Institute; ³Newcastle upon Tyne Hospitals NHS Foundation Trust, United Kingdom
Email: h.l.reeves@ncl.ac.uk

Background and aims: As deaths from hepatocellular carcinoma (HCC) rise, understanding the tumour-immune axis is key. Elevated circulating neutrophils associate with poor survival in many cancers, including HCC. Understanding the pathophysiological mechanisms and consequences of changes in neutrophil numbers and behaviour may aid novel therapeutic strategies. We explored the human phenotype, function and proteome of circulating neutrophils, associated with tissues distribution and serum cytokines.

Method: 275 subjects (72 healthy; 42 chronic liver disease controls; 161 with HCC-all with Childs Pugh 'A' liver function-of whom 84 had tumor biopsy tissue available). Neutrophil immunohistochemistry (IHC), digital image analysis, serum cyto/chemokine 65-Plex panel (Eve Technologies), FACS, cytospin nuclear maturity, reactive oxygen species (ROS) generation, proteome (Orbitrap Fusion Lumos Tribrid mass spectrometer; MaxQuant and Perseus software) and patient data were analysed.

Results: The IHC density of intra-tumour (IT) CD66B+ neutrophils was higher in earlier TNM stage cancers ($p=0.007$), associated with significantly better responses to therapies and independently with better survival (Figure 1). In contrast, peri-tumour (PT) neutrophils rose as cancers progressed, significantly associated with circulating neutrophil number (0.436; $p=0.002$), size and vascular invasion. Four serum cytokines (IL-8, CXCL10, CXCL13, CCL21) were significantly elevated with HCC, regardless of cirrhotic state. Elevations in IL-8 were early and striking (up to 5X, $p<0.001$), correlating with tumor number (0.531; $p=0.001$), size (0.493; $p=0.020$) and vascular invasion (0.595; $p=0.004$). IT neutrophils correlated with IL-18 (0.587; $p=0.035$) and PT neutrophils with CXCL10 (0.645; $p=0.032$) and MCP-1 (-0.645 ; $p=0.032$).



In the presence of cirrhosis, reductions in nuclear mature (70%>55%) and immature (25%>10%) circulating neutrophils, with increases in hypersegmented (5%<35%) were evident, with a proteome revealing reduced degranulation (MPO, AZU1, CTSG, GM2A, RNASE3). In cancers there was a sharp recovery in immature neutrophils, with a proteome supporting haem metabolism and oxidative phosphorylation (highly significant changes in multiple cytochrome oxidase and haemoglobin subunits and carbonic anhydrase). Functionally, ROS

production was elevated by the NADPH oxidase activator PMA, but less responsiveness to fMLF/receptor signaling.

Conclusion: The development and progression of cancer is associated with changes in chemokines, restoration/elevation in circulating immature neutrophils, metabolic reprogramming and elevated ROS capacity. Elevations in IT neutrophils associated with better responses and outcomes, while accumulation of PT neutrophils associated with circulating neutrophils, and tumor progression.

FRI562

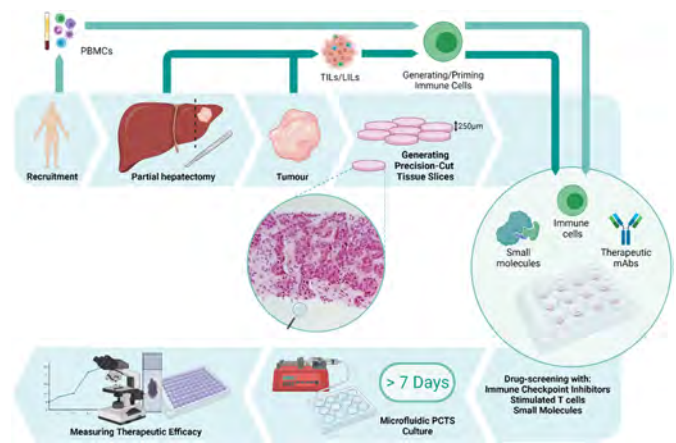
Dynamic organotypic culture of primary liver cancer as a personalised immunocompetent drug screening platform for immuno-oncology

Ravi Jagatia^{1,2,3}, Ewald Doornebal^{1,2,3}, Lorenzo Cacioli^{1,2,4}, Nicola Harris^{1,2}, Una Rastovic^{1,2}, Sara Campinoti^{1,2}, Melissa Preziosi⁵, Marjorie Yumol⁵, Rosa Miquel⁵, Yoh Zen⁵, Andreas Prachalias⁵, Krishna Menon⁵, Sara Mantero⁴, Sandra Phillips^{1,2}, Nigel Heaton⁵, Luca Urbani^{1,2}, Elena Palma^{1,2,6}, Shilpa Chokshi^{1,2,6}. ¹King's College London, Faculty of Life Sciences and Medicine, London, United Kingdom; ²The Roger Williams Institute of Hepatology, London, United Kingdom; ³Contributed Equally; ⁴Politecnico di Milano, Department of Chemistry, Materials and Chemical Engineering "Giulio Natta," Milano, Italy; ⁵Institute of Liver Studies, King's College London, London, United Kingdom; ⁶Corresponding Author
Email: s.chokshi@researchinliver.org.uk

Background and aims: Current primary liver cancer (PLC) models fail to truly encompass the human tumour immune microenvironment, exacerbating a recognised discord between the preclinical and clinical successes of emerging (immuno)therapeutics. The organotypic culture of 3D human Precision Cut Tumour Slice (PCTS) is a cancer explant model which retains tumour specific histoarchitecture, aetiological background, disease phenotype, resident immune landscape, and checkpoint (CP) expression for >5 days ex-vivo. Our study aims to (1) validate PCTS to assess patient specific therapeutic responses and (2) advance culture conditions using a proprietary Multi-well Plate (MuPL) perfusion bioreactor to extend PCTS lifetime and allow perfusion of immune cells through PCTS.

Method: PCTS generated from PLC (HCC & CCA) were treated with approved single agent or combinatory checkpoint inhibitor (CPI), monoclonal antibody (mAb) or kinase inhibitor (KI) therapy for up to 7 days. Therapeutic response was determined by evaluating histology (H&E and Sirius red), apoptosis/cell death (TUNEL, lactate-dehydrogenase release, cytokeratin 18), and proliferative capacity (PC; Ki67). Gene expression was assessed using QuantiGene RNA Assay. Resident immune cells were assessed by immunofluorescence and FACS. In addition, PCTS/immune cells co-cultured in the MuPL bioreactor were longitudinally assessed for viability, histology, and tissue integrity.

Results: Doxorubicin was used as a positive cell death control in all treated patients, decreasing PCTS viability and PC by day5. Overall immunotherapy response was patient specific. Compared to monotherapy, nivolumab + regorafenib therapy decreased the tumour to stroma ratio and PC in all patients by day7. Also, significantly increased apoptosis was detected in one patient, who comparatively showed higher CP expression including PD-1, PD-L1 and CTLA-4. Other combinatorial immunotherapies, including atezolizumab + bevacizumab and nivolumab + ipilimumab, reduced PC without affecting histology or viability. Additionally, PCTS and immune cells cultured in the MuPL bioreactor maintained viability, structural integrity and histoarchitecture for >7 days.



Conclusion: PCTS can be used as a powerful tool to study personalised responses to (immuno)therapeutics. In addition, PCTS can be successfully cultured in a perfusion system, recapitulating tumour-immune cell interactions, allowing assessment of response to cell and vaccine therapy ex-vivo.

FRI563

High plasma level of osteopontin, a potential biomarker in hepatocellular carcinoma, is associated with weakened anti-tumour immunity

Tengfei Si¹, Zhenlin Huang², Shirin Elizabeth Khorsandi^{1,3,4}, Wayel Jassem^{1,3}, Xiaohong Huang¹, Abid Suddle¹, Mark J W McPhail⁵, Francesca Trovato^{1,5}, Salma Mujib¹, Salvatore Napoli¹, Ellen Jerome^{1,3}, Yun Ma¹, Nigel Heaton^{1,3}. ¹King's College Hospital, Institute of Liver Studies, London, United Kingdom; ²Shanghai University of Traditional Chinese Medicine, The MOE Key Laboratory for Standardization of Chinese Medicine, China; ³King's College Hospital, Transplant Service, London, United Kingdom; ⁴the Roger Williams Institute of Hepatology, London, United Kingdom; ⁵King's College Hospital, Liver Intensive Therapy Unit, London, United Kingdom
Email: yunma1@nhs.net

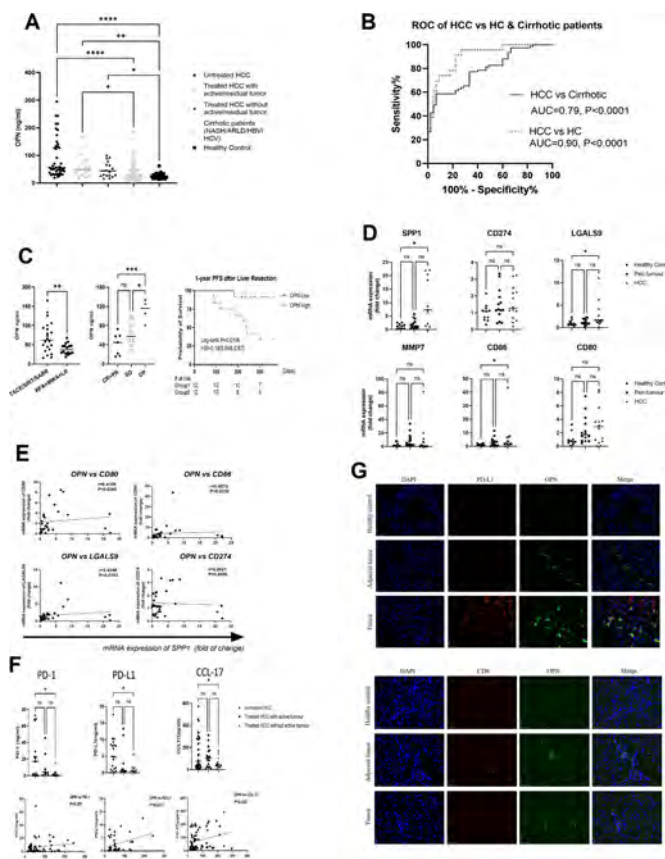
Background and aims: It has been shown that osteopontin (OPN) is closely associated with tumour invasion and metastasis in hepatocellular carcinoma (HCC). The mechanisms for the role of OPN in HCC has been defined in both animal models and carcinoma cell lines, but direct evidence derived from human studies are lacking. We aim to explore OPN's association with clinical outcome and anti-tumour immunity through a comprehensive analysis in a large cohort of HCC patients.

Method: A total of 92 HCC patients, 81 non-HCC patients with underlying liver cirrhosis (NASH/ARLD/HBV/HCV) and 25 healthy controls (HC) were recruited from our centre. Plasma levels of OPN, Th1/Th17 cytokines, soluble PD-1, PD-L1, CTLA-4, CCL17 and CXCL-9 were measured by ELISA. mRNA expression of OPN and ligands for immune checkpoint were assessed by quantitative real-time PCR across HCC and paired adjacent liver tissue (n=16). Immunofluorescence staining was performed to co-stain OPN with CD8 and PD-L1 in HCC, paired adjacent tumour and healthy liver tissues.

Results: The plasma OPN level in untreated HCC (n=48) was significantly higher than other groups (Fig1 A). ELISA results showed good diagnostic performance when compared with both healthy controls (AUC = 0.90, p < 0.0001) and cirrhotic group (AUC = 0.90, p < 0.0001) (Fig1 B). For patients receiving ablation (radio-frequency ablation, RFA; microwave ablation, MWA) or liver resection (LR) (n=16), the OPN levels were much lower than those treated with radiotherapy (selective internal radiation therapy, SIRT; stereotactic ablative radiotherapy, SABR) or chemotherapy (transarterial chemoembolization, TACE) (n=22). In some patients, low OPN level represented better treatment response to TACE and longer

POSTER PRESENTATIONS

progression free survival (PFS) (>1 year) after liver resection (Fig1 C). PCR results showed high expression of OPN in HCC tumour tissue (Fig1 D) and there was a positive correlation between OPN with the ligands of CTLA-4 (CD80/CD86) and TIM-3 (LGALS9) (Fig1 E). Plasma PD-L1 and CCL-17 levels in untreated HCC (n = 48) were both higher when compared to other HCC treated groups (n = 25; n = 19) and positively correlated with OPN. Furthermore, immunofluorescent staining showed that the expression of both OPN and PD-L1 were upregulated in tumour, with high signal of OPN around tumour vasculature. While CD8 was downregulated in tumour and paired adjacent tumour tissue.



Conclusion: OPN has been shown as a potential marker for both diagnosis and prognosis in HCC. The positive correlations between OPN, PD-L1 and chemokine of T-regulatory cells CCL-17 in plasma, suggest that high OPN levels is associated with a weakened anti-tumour immunity. This indication was further confirmed by PCR results and immunofluorescent staining.

FRI564

The uptake of extracellular lipids promotes cholangiocarcinoma progression

Mikel Ruiz de Gauna¹, Francesca Biancaniello^{2,3}, Francisco González-Romero¹, Pedro Miguel Rodrigues^{2,4}, Ainhoa Lapitz², Beatriz Gómez Santos¹, Paula Olaizola², Sabina Di Matteo^{2,3}, Igor Aurrekoetxea^{1,5}, Ibone Labiano², Ane Nieva-Zuluaga¹, Asier Benito-Vicente^{6,7}, María Jesús Perugorria^{2,4}, Maider Apodaka-Biguri¹, Nuno Paiva², Diego Saenz de Urturi¹, Xabier Buque^{1,5}, Igortz Delgado¹, Cesar Augusto Martín^{6,7}, Mikel Azkargorta⁸, Felix Elortza^{4,8}, Diego Calvisi⁹, Jesper Andersen¹⁰, Domenico Alvaro³, Vincenzo Cardinale³, Luis Bujanda^{2,4}, Jesus Maria Banales^{2,4,11,12}, Patricia Aspichueta^{1,4,5}. ¹University of the Basque Country UPV/EHU,

Faculty of Medicine and Nursing, Department of Physiology, Leioa, Spain; ²Department of Liver and Gastrointestinal Diseases, Biodonostia Health Research Institute, Donostia University Hospital, University of the Basque Country UPV/EHU, San Sebastian, Spain; ³Department of Translational and Precision Medicine, "Sapienza" University of Rome, Rome, Italy; ⁴National Institute for the Study of Liver and Gastrointestinal Diseases (CIBERehd, Instituto de Salud Carlos III); ⁵Biocruces Health Research Institute, Cruces University Hospital, Barakaldo, Spain; ⁶Department of Molecular Biophysics, Biofisika Institute (University of Basque Country and Consejo Superior de Investigaciones Científicas (UPV/EHU, CSIC)), Leioa, Spain; ⁷Department of Biochemistry and Molecular Biology, University of the Basque Country (UPV/EHU), Leioa, Spain; ⁸Protemics Platform, Center for Cooperative Research in Bioscience (CIC Biogune), ProteoRed-ISCIII, Bizkaia Science and Technology Park, Derio, Spain; ⁹Institute for Pathology, Regensburg University, Regensburg, Germany; ¹⁰Department of Health and Medical Sciences, Biotech Research & Innovation Centre (BRIC), University of Copenhagen, Copenhagen, Denmark; ¹¹IKERBASQUE, Basque Foundation for Science, Bilbao, Spain; ¹²Department of Biochemistry and Genetics, School of Sciences, University of Navarra
Email: patricia.aspichueta@ehu.eus

Background and aims: One of the hallmarks of cancers is metabolic reprogramming, and its regulation is a possible therapeutic target. There is little information about rearrangements of lipid metabolism in cholangiocarcinoma (CCA), characterised by great heterogeneity and poor prognosis. Previous evidence suggests that *de novo* synthesis of fatty acids (FAs) is decreased in CCA, pointing to exogenous lipids as the main source of FAs. Here, we investigated the alterations in lipid metabolism in CCA and their role in tumour proliferation.

Method: *In vitro* proliferative and migration capacities and *in vivo* tumorigenic capacity of 5 human CCA cell lines were analyzed. Proteome, lipid content and metabolic fluxes were studied in CCA cells, using primary cultures of normal human cholangiocytes (NHC) as a control. Lipid content and metabolic fluxes were analyzed in liver samples of a mouse model of CCA based on the overexpression of *Akt1* and *NOTCH1* intracellular cytoplasmic domain (*Nicd1*).

Results: The proteome of CCA cells showed a dysregulation of pathways involved in lipid and lipoprotein metabolism. The EGI1 CCA cell line showed the highest proliferative and migration capacity. We studied metabolic fluxes with radioisotopes and measured lipid content in high (EGI1) and low (HUCCT1) proliferative cell lines, and in liver tumor tissue from the mouse model of CCA. Both EGI1 and HUCCT1 incorporated more oleic and palmitic acid than NHCs, which resulted in an increased triglyceride storage. Similarly, the CCA mouse model showed a faster clearance and increased liver uptake of intravenous [³H]-oleate. Highly proliferative EGI1 cells showed an increased uptake of very-low density lipoproteins (VLDL) and high density lipoproteins (HDL) than NHC and HUCCT1. This increased uptake of lipids was accompanied by a higher expression of CD36 and fatty acid binding protein FABP5. Unlike glucose or glutamine oxidation, fatty acid oxidation (FAO) rate was increased in EGI1 and downregulated in HUCCT1. Accordingly, FAO-related proteins showed a higher expression in the proteome of EGI1 and, therefore, pharmacological inhibition of FAO induced a more pronounced inhibition on proliferation in EGI1 than in HUCCT1. Expression of the first enzyme involved in FAO, the acyl-CoA dehydrogenase ACADM, whose protein levels are specifically increased in EGI1, was found to correlate with that of the proliferation marker PCNA in tumour tissue from CCA patients.

Conclusion: Highly proliferative human CCA cells are highly dependent on lipid and lipoprotein uptake to sustain an active catabolism of FAs. These results suggest that inhibition of FAO and/or lipid uptake may provide a novel therapeutic strategy for patients of this subclass of CCA.

FRI565

Peroxiredoxin 2 is a target for hepatocellular carcinoma chemoprevention

Emilie Crouchet¹, Eugénie Schaeffer¹, Hussein El Saghire¹, Naoto Fujiwara², Frank Jühling¹, Marine Oudot¹, Clara Ponsolles¹, Nicolas Brignon¹, Sarah Durand¹, Marie Parnot¹, Danijela Heide³, Jenny Hetzer³, Mathias Heikenwälder³, Emanuele Felli^{1,4}, Patrick Pessaix^{1,4}, Nathalie Pochet^{5,6}, Yujin Hoshida², Laurent Mailly¹, Thomas Baumert^{1,4,7}, Catherine Schuster¹. ¹Inserm U1110, Institute of Viral and Liver Disease, University of Strasbourg, Strasbourg, France; ²Liver Tumor Translational Research Program, Simmons Comprehensive Cancer Center, Division of Digestive and Liver Diseases, Department of Internal Medicine, University of Texas Southwestern Medical Center, Dallas, Dallas, United States; ³Division of Chronic Inflammation and Cancer, German Cancer Research Center, Heidelberg, Germany, Heidelberg, Germany; ⁴Institut Hospitalo-Universitaire, Pôle Hépatite-digestif, Nouvel Hôpital Civil, Strasbourg, France, Strasbourg, France; ⁵Department of Neurology, Harvard Medical School, Boston, MA, United States; ⁶Broad Institute of MIT and Harvard, Cambridge, MA, United States; ⁷Institut Universitaire de France, Paris, France
Email: thomas.baumert@unistra.fr

Background and aims: Metabolic liver disease and hepatocellular carcinoma (HCC) are major global health burdens with unsatisfactory treatment options. HCC is the third most common cause of cancer-related death and the leading cause of death among cirrhotic patients. While new treatments for HCC have been recently approved, chemopreventive strategies for advanced fibrosis are lacking. By combining a cell-based system predicting liver disease progression and HCC risk and transcriptome analysis of fibrotic/cirrhotic patient liver tissues, we identified peroxiredoxin 2 (PRDX2) as a driver of disease progression and HCC risk. Here we aimed to uncover the role of PRDX2 in liver disease progression and HCC development.

Method: The role of PRDX2 in liver disease progression and HCC development was investigated by Prdx2 KO in a state-of-art CRISPR/Cas9 mouse model for NASH-induced hepatocarcinogenesis and a cell-line-derived xenograft (CDX) mouse model. The mechanism of action was explored using RNA-Seq analyses of mouse liver tissues and validated by perturbation studies in human liver cell-based models.

Results: In patient liver tissues, PRDX2 expression is increased in tumor, suggesting a role of PRDX2 in hepatocarcinogenesis. In the CRISPR/Cas9 NASH-induced HCC mouse model, KO of Prdx2 improved metabolic liver functions, robustly reduced liver steatosis through improvement of the AMPK/LXRα axis and significantly decreased HCC development. RNA-Seq analyses of mouse liver tissues confirmed that Prdx2 KO restored liver metabolic pathways (i.e. cholesterol, fatty acid and bile acid metabolism), decreased inflammation (IL6/STAT3) and suppressed proliferative and pro-carcinogenic pathways (i.e. EGFR/p38/MAPK, PI3 K/AKT/mTOR). Finally, PRDX2 loss-of-function studies in hepatoma cell-based models and a Huh7-CDX mouse model unraveled that PRDX2 mediates cancer cell proliferation, migration, invasion, and survival.

Conclusion: Our findings demonstrate an important functional role of PRDX2 in metabolic liver disease and hepatocarcinogenesis. Therefore, targeting PRDX2 may be a previously undiscovered therapeutic option for the treatment of metabolic liver diseases and to prevent NASH-induced HCC.

FRI566

Loss of Actin-Binding LIM protein (ABLIM) plays a potential role in migratory cholangiocyte transformation

Lea Duwe¹, Patricia Munoz-Garrido¹, Juan Lafuente-Barquero¹, Colm O'Rourke¹, Jens Marquardt², Jesper Andersen¹. ¹Biotech Research & Innovation Centre, Department of Health and Medical Sciences, University of Copenhagen, Copenhagen N, Denmark; ²University Medical Center Schleswig-Holstein-Campus Lübeck, Department of Medicine I, Lübeck, Germany
Email: jesper.andersen@bric.ku.dk

Background and aims: Actin cytoskeleton aberrations are a major aspect in migration and invasion during cancer development and progression. In bile ducts, rearrangements of the cytoskeleton undertake particularly important roles in polar cholangiocytes and their malignant transformation to invasive cholangiocarcinoma (CCA). Here, we have identified the Actin-Binding LIM protein (ABLIM) as a putative regulator of migratory cholangiocytes by modifying the actin cytoskeleton.

Method: We analyzed ABLIM expression in transcriptome data from 217 CCA patients and 143 surrounding livers (SL), followed by further investigation in TCGA-CHOL (36 CCA, 9 SL) and an additional dataset of microdissected ICCA and matched metastases (GSE40367). ABLIM expression and its localization was visualized in normal bile ducts and CCA tissues by ABLIM immunofluorescence and co-staining of beta-catenin (CTNNB1) for cell-cell adhesion junctions. The expression level was further validated in primary normal human cholangiocytes as well as patient-derived and established CCA cell lines by qRT-PCR, Western blot and immunofluorescence. For functional assays, we generated CRISPR/Cas9 knockouts in the immortalized normal cholangiocyte (H69) line and showed altered migratory phenotype by wound-closure assay.

Results: Transcriptomic analysis revealed a significant downregulation of ABLIM in CCA tissues compared to SL in our cohort ($p < 0.0001$, Mann-Whitney T-test) and TCGA-CHOL ($p = 0.0173$, Mann-Whitney T-test). In metastatic lesions, ABLIM expression levels tend to be lower compared to the primary CCA tumor site ($p = 0.067$, Paired T-test). Genetically mimicking the diminished expression of ABLIM by CRISPR/Cas9 knockout in H69 cholangiocytes revealed a more fibroblast-like morphology with increasing migratory phenotype ($p < 0.0001$, Mixed-effects analysis). In normal human bile ducts, ABLIM co-localizes with beta-catenin in adherens junctions, suggesting a significant role in cell-cell interactions and adhesion complex formation. We have confirmed the decreased expression ($p = 0.004$, Mann-Whitney T-test) and localization of ABLIM in our cell models for future experiments focusing on elucidating the mechanism of ABLIM in cell motility.

Conclusion: ABLIM is aberrantly expressed in CCA patients. Loss of ABLIM leads to an increased migratory phenotype of normal cholangiocytes in culture and may be important for tumor dissemination.

FRI567

Modulation of the cholangiocarcinoma stem-like compartment by monounsaturated fatty acids

Giulia Lori¹, Chiara Raggi¹, Benedetta Piombanti¹, Mirella Pastore¹, Richell Booijink², Elisabetta Rovida¹, Jesper Andersen³, Monika Lewinska³, Paolo Montalto⁴, Fabio Marra¹. ¹University of Florence, Firenze, Italy; ²University of Twente, Enschede, Netherlands; ³Copenhagen University, København, Denmark; ⁴Azienda USL Toscana centro - Firenze - Italy
Email: fabio.marra@unifi.it

Background and aims: Identification of the molecular features of CCA may be helpful in designing new therapeutic approaches. Cancer cells are exposed to a metabolically challenging environment with scarce availability of nutrients, and alterations in lipid metabolism may affect the response of tumor cells to drugs. We hypothesize that fatty acids (FA) modulate the biology of CCA cells and the development of stemness features.

POSTER PRESENTATIONS

Method: CCA cells (HuCCT-1 OR CCLP1) were treated with monounsaturated FA (132mM oleic or 100mM palmitoleic acid). Responsiveness of CCA cells to cytotoxic drugs was tested with crystal violet staining. Epithelial-mesenchymal transition program, stem-like markers, ABC transporters and metabolic markers, were tested with real-time PCR. Self-renewal ability was tested with a colony formation assay. Cancer stem cell- (CSC)-enriched spheres were obtained growing cells in anchorage-independent conditions and selective medium. Five-year overall survival (OS) was analyzed in 104 patients with cholangiocarcinoma sub-grouped based on fatty acid synthase (FASN) expression. NSG mice were injected with spheres obtained from CCLP1 cells and treated for four weeks with the FASN inhibitor orlistat (240 mg/Kg).

Results: Exposure of CCA cell lines to FAs increased cell proliferation and activated growth and survival pathways, including AKT and ERK1/2. Exposure to FA before treatment with chemotherapeutic agents made CCA cells less sensitive to their toxic effects, and modulated the expression of ABC transporters involved in drug resistance. The colony forming ability of CCA cells was increased by FAs, and was associated with upregulation of genes controlling epithelial-mesenchymal transition and stemness. Expression levels of genes involved in lipid metabolism were upregulated in CSC-enriched spheres. In a series of CCA patients, the expression of FASN correlated with OS. FASN inhibition by orlistat decreased cell proliferation and CSC or EMT markers. In a xenograft model of CCA, tumor volume of mice treated with orlistat was significantly lower than in control mice.

Conclusion: Exposure of CCA cells to FA increases growth, invasiveness and resistance to antineoplastic drugs, and modulates stem-like features and self-renewal abilities. In the CCA stem-like subset, several key genes involved in FA synthesis and transport were upregulated, and FASN inhibition decreased cell proliferation and downregulated CSC markers. and FASN expression levels correlate with survival in patients with CCA. These data indicate that lipid metabolism could be a new potential target to affect CCA progression, especially in CSC subset.

FR1568

Cyclophilin D knockout promotes cell death pathways in preventing HCC development in a streptozotocin-induced mouse model of diabetes-linked NASH

Winston Stauffer¹, Joseph Kuo², Daren Ure³, Robert Foster³, Philippe Gallay¹. ¹Scripps Research, Immunology and Microbiology, La Jolla, CA, United States; ²Arena Pharmaceuticals, San Diego, United States; ³Hepion Pharmaceuticals, Edison, NJ, United States
Email: wstauffer@scripps.edu

Background and aims: Cyclophilins are a diverse family of peptidyl prolyl isomerases which promote protein folding and perform a variety of functions in the liver and other tissues. We have previously reported that the pan-cyclophilin inhibitor (CypI) compounds, CRV431, NV556 and Debio-025/Alisporivir, decreased the severity of non-alcoholic steatohepatitis (NASH) and hepatocellular carcinoma (HCC) in a streptozotocin (STZ)-induced HCC murine model. However, it is not known which cyclophilin family member (s) whose inhibition is causing this effect. Here, we report the effects of this HCC model in *Ppif*^{-/-} mice lacking cyclophilin D (CypD), an important component of the mitochondrial permeability transition pore.

Method: 6-week-old male *Ppif*^{-/-} and wild-type (WT) mice were injected with 200 mg/kg STZ to destroy pancreatic beta cells and induce a diabetic phenotype. Mice were nourished with chow with 21.1% fat, 41% sucrose, and 1.25% cholesterol by weight and high sugar solution (23.1 g/L fructose and 18.9 g/L glucose), which continued throughout. After 30 weeks on this diet, mice (n = 10 per group) were sacrificed. Body and liver weight were recorded. Livers were scored for HCC tumor burden. Histological sections of livers stained with H&E were scored for inflammation, steatosis, and ballooning. Liver sections were also stained with Sirius Red for examination of collagen

fibrosis. RNA was extracted from frozen liver tissue for qRT-PCR analysis. PCR apoptosis arrays were purchased from Qiagen. Unpaired Student's t-tests were conducted with GraphPad Prism.

Results: Tumor burden scores were three times higher in WT mice compared to *Ppif*^{-/-} mice, significant by Student's t-test (p = 0.03). Average tumor number was also significantly decreased with *Ppif*^{-/-} mice, of which 8 out of 10 mice had no tumors, compared to just 3 of 10 in WT mice. A trend of reduced collagen deposition was also observed in livers of *Ppif*^{-/-} mice relative to WT, but this was not significant. Inflammation, steatosis, and ballooning were similar between groups. Mechanistically, qPCR arrays for apoptosis genes revealed that the tumor suppressor *Fhit* was significantly elevated in *Ppif*^{-/-} livers, while apoptosis inhibitor and oncogene *Birc5* was decreased.

Conclusion: Cyclophilin inhibition represents a promising avenue for the treatment of HCC development in mouse models. These data show for the first time that mice without CypD are significantly protected from HCC development, suggesting CypD inhibition is at least partly responsible for the previously established anti-tumor effects of CypI antagonist compounds. Molecular analyses suggest CypD inhibition may promote cell death pathways which act as tumor suppressors.

FR1569

Ribosomal protein encoding genes: potential drivers of primary sclerosing cholangitis associated cholangiocarcinoma

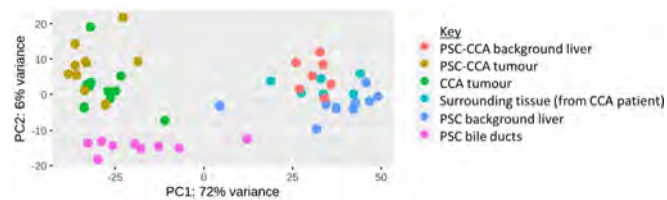
Megan Illingworth^{1,2,3}, Yoh Zen³, Jeremy Nayagam³, Deepak Joshi³, Luca Urbani^{1,2}, Neil Youngson¹, Nigel Heaton³, Shirin Elizabeth Khorsandi^{1,2,3}. ¹The roger williams institute of hepatology, foundation for liver research, London, United Kingdom; ²King's college london, Faculty of life sciences and medicine, London, United Kingdom; ³The institute of liver studies, kings college hospital, London, United Kingdom
Email: megan.illingworth@kcl.ac.uk

Background and aims: Primary sclerosing cholangitis (PSC) patients have a 20% lifetime risk of cholangiocarcinoma (CCA), equating to a 250–1500 fold higher risk than that of the average population. Despite this, stratification of PSC patients at risk of CCA is currently not possible, with PSC patients who progress to CCA facing insufficient and unsuccessful treatment options and thus, a poor prognosis. The degree of similarity between CCA in PSC patients and non-PSC patients is unclear, and therefore the applicability of research into CCA targeted therapeutic for PSC associated CCA (PSC-CCA) patients remains unknown. This work aims to provide novel insight into gene expression in PSC-CCA to aid in the development of biomarkers for risk stratification and targeted therapeutics for this patient cohort. Additionally, this work aims to highlight novel differences in PSC-CCA and CCA not on a PSC background.

Method: Massive analysis of cDNA end (MACE) sequencing of formalin fixed and paraffin embedded tissue from CCA (n = 10), PSC-CCA (n = 10), PSC-CCA surrounding liver (n = 7), PSC bile ducts (n = 9), PSC surrounding liver (n = 9) and CCA adjacent liver (n = 6) was undertaken. Standard bioinformatic analysis was undertaken and differential gene expression determined.

Results: A total of 2567 genes were differentially expressed between PSC-CCA and CCA tumours. Ribosomal processes were significantly downregulated in PSC-CCA tumours when compared to both CCA tumours and PSC bile ducts and ion transport was significantly upregulated. Additionally, 849 of the 2567 genes were long non-coding RNAs, all of which were downregulated in CCA. Analysis of differential expression in the background liver identified 357 genes differentially expressed in PSC-CCA when compared to non-malignant PSC background livers. Apoptotic pathways were upregulated, and ribosomal processes downregulated in PSC-CCA background livers. Comparison of PSC-CCA tumours to PSC bile ducts identified 1717 differentially expressed genes. Ribosomal processes, the complement cascade and extracellular matrix organisation were all

downregulated in PSC-CCA tumours, while mitotic nuclear division and migration were upregulated in PSC-CCA tumours.



Conclusion: This transcriptomic dataset provides novel mechanistic insight into PSC-CCA and highlights a unique role for ribosomal proteins in PSC progression to CCA. The precise mechanism of this is currently unclear, warranting further investigation.

FRI570

Stemness features during cholangiocarcinoma progression in vivo: characterization of primary and metastatic stem-like cells

Margherita Correnti^{1,2,3}, Marco Erreni⁴, Roberta Avigni⁴, Marina Sironi⁵, Matteo Ramazzotti⁶, Caterina Peraldo Neia⁷, Giuliana Cavalloni⁸, Stefania Recalcati², Fabio Marra⁹, Chiara Raggi⁹. ¹Humanitas clinical and research center, Center for autoimmune liver diseases, Rozzano, Italy; ²University of Milan, Dept. of biomedical sciences for health, Milan, Italy; ³University of Milan, Department of Biomedical Sciences for Health, Milan, Italy; ⁴Humanitas clinical and research center, Dept. of immunology, Rozzano, Italy; ⁵Humanitas clinical and research center, Dept. of immunopharmacology, Rozzano, Italy; ⁶University of Florence, Dept. of Experimental and Clinical Biomedical Sciences, Florence, Italy; ⁷Fondazione Edo ed Elvo Tempia Valenta, Cancer genomics lab, Biella, Italy; ⁸IRCCS-Institute Candiolo, Medical oncology division, Candiolo, Italy; ⁹University of Florence, Department of experimental and clinical medicine, Florence, Italy Email: margherita.correnti@gmail.com

Background and aims: Cholangiocarcinoma (CCA) is an extremely heterogeneous adenocarcinoma arising from malignant transformation of biliary tree. Spread of tumor cells in blood or lymphatic circulation as circulating tumor cells (CTCs) plays a major role in recurrence, metastasis and drug unresponsiveness. Assuming that CTCs are heterogeneous, we hypothesized the existence of CCA stem-like relapse-initiating cells. Consistent with cancer stem cells (CSC) hypothesis, stem-like CTCs might represent the potential source for cancer relapse and distant metastasis. The present study aimed to explore the evolution of stemness features during CCA progression.

Method: Enrichment of CCA stem-like subset by sphere culture (SPH) in established CCA cell line (HUCCT1) and primary CCA cell culture (MTCHC-01). Adherent monolayer (MON) cells as control. Set up of CCA orthotopic mouse model by intrahepatic injection of Luciferase-GFP transfected SPH and MON cells. Analysis of GFP+ disseminating tumor cells in target organs and bloodstream by FACS. Isolation of GFP+ tumor cells from primary and metastatic tumors by FACS sorting. Molecular characterization by qRT-PCR arrays focus on CSC, epithelial-to-mesenchymal transition (EMT), angiogenesis and drug resistance. Expression of CSC-like surface markers evaluated by FACS. Molecular data validation in human CCA samples.

Results: CCA SPH-primary tumor derived GFP+ cells showed CSC and EMT-related gene enrichment compared to MON-primary tumors. In accordance, SPH cells were responsible for enhanced tumor spread in secondary organs (lungs, spleen, peritoneum, mesenteric lymph nodes). CD45-/GFP+ tumor cells were detected in bloodstream of very few samples, suggesting that lymphatic circle is the preferential via to CCA dissemination. Notably, lung SPH-disseminated cells showed up-regulation of most of tested CSC, EMT, angiogenesis and drug resistance related genes compared to SPH-primary tumor cells. Despite some differences between cell lines and different mice, a panel of 35 genes commonly up-regulated was found in SPH-

disseminated cells. Some of these genes were significantly up-regulated in 13 recurrent CCA tumor specimens compared to paired primary tumors.

Conclusion: These findings suggest that CCA SPH cells are enriched in stem-like disseminating tumor cells responsible for recurrence and metastasis formation. Moreover, our data indicate that a stemness-core is stably maintained during CCA-evolution starting from primary tumor initiation through disseminating process.

FRI571

miR34a-5p is a target of E2F2 transcription factor in MAFLD-related HCC

Maider Apodaka-Biguri¹, Francisco Gonzalez-Romero¹, Daniela Mestre Congregado¹, Igor Aurrekoetxea¹, Beatriz Gómez Santos¹, Igotz Delgado¹, Xabier Buque^{1,2}, Ane Nieva-Zuluaga¹, Mikel Ruiz de Gauna¹, Idoia Fernández-Puertas¹, Ainhoa Iglesias³, Ana María Aransay^{4,5}, Juanjo Lozano^{5,6}, Cesar Augusto Martín^{7,8}, Irantzu Bernales⁹, Ana Zubiaga³, Patricia Aspichueta^{1,2,5}. ¹Department of Physiology University of the Basque Country UPV/EHU, Faculty of Medicine and Nursing, Leioa, Spain; ²Biocruces Bizkaia Health Research Institute, Cruces University Hospital, Barakaldo, Spain; ³Department of Genetic, Physical Anthropology and Animal Physiology, Faculty of Science and Technology, University of Basque Country UPV/EHU, Leioa, Spain; ⁴Genome analysis platform, Center for Cooperative Research in Biosciences (CIC bioGUNE), Derio, Spain; ⁵National Institute for the Study of Liver and Gastrointestinal Diseases (CIBERehd, Carlos III Health Institute), Madrid, Spain; ⁶Bioinformatic Platform, Clinic Hospital, Barcelona, Spain; ⁷Department of Molecular Biophysics, Biofisika Institute (University of Basque Country and Consejo Superior de Investigaciones Científicas (UPV/EHU, CSIC)), Leioa, Spain; ⁸Department of Biochemistry and Molecular Biology, University of the Basque Country (UPV/EHU), Leioa, Spain; ⁹SGIKER, University of Basque Country UPV/EHU, Leioa, Spain Email: patricia.aspichueta@ehu.eus

Background and aims: Metabolic associated fatty liver disease (MAFLD) is the most common cause of chronic liver disease in Western countries and a risk factor for hepatocellular carcinoma (HCC). E2F2 is a metabolic driver in MAFLD development and progression to HCC. A relationship between E2F2 and microRNAs (miRNAs) expression has been described in different pathologies, but not in liver disease. The aims here were: 1) to identify if liver E2F2 regulates miRNAs involved in MAFLD development and progression to HCC; 2) to investigate the metabolic relationship between E2F2 and the identified miRNAs in liver pathology.

Method: To induce MAFLD-related HCC, diethylnitrosamine (DEN) (25 mg/kg) was administered to 14 day-old *E2f2*^{-/-} and wild-type mice (WT), which were fed a high-fat diet (HFD) until sacrificed at 9 months. Chow diet-fed (CD) 3 month-old *E2f2*^{-/-} and WT mice were also used. E2F2 was specifically upregulated in liver with adeno-associated viruses-serotype 8. miRNA sequencing and transcriptome analysis was performed in 9 month-old DEN-HFD WT and *E2f2*^{-/-} mice livers. Selected differentially expressed liver miRNA candidates and genes were further validated by RT-qPCR analysis. Metabolic fluxes and lipid content were analyzed.

Results: The results obtained from miRNA sequencing and later validation by qPCR showed that in 9 month-old DEN-HFD *E2f2*^{-/-} mice, resistant to MAFLD-related HCC, expression of miR-122-5p was upregulated while that of miR34a-5p, miR155-5p and miR146a-5p were downregulated. Among all, miR34a-5p was the only one decreased in CD-fed *E2f2*^{-/-} while increased when E2F2 was specifically overexpressed in liver, as compared to the corresponding controls. The crosschecked analysis between the upregulated transcriptome genes underlying the resistance to develop MAFLD-related HCC in *E2f2*^{-/-} mice and the miR34a-5p predicted interacting genes showed, among others, the enrichment in "Bile acid transport" and "lipid metabolism" biological pathways. Given the relevance of

POSTER PRESENTATIONS

cholestasis in liver disease, the expression and protein levels of HNF4, a critical regulator of bile metabolism, and of *Etnk2* and *Chpt1*, modulators of the synthesis of phosphatidylethanolamine (PE) and phosphatidylcholine (PC), required for bile secretion, were analyzed. The results showed higher levels of the regulators of bile metabolism in 9 month-old DEN-HFD *E2f2*^{-/-} mice than in DEN-HFD WT mice together with increased PE and PC synthesis which led to higher PE, but not PC liver content, suggesting increased elimination into bile.

Conclusion: miR34a-5p is a target of E2F2 in MAFLD-related HCC. The results suggest that the E2F2-miR34a-5p axis induce inefficient bile secretion during MAFLD development and progression to HCC promoting development of the disease.

FRI572

TIA1 in fatty liver disease and hepatocellular carcinoma

Dobrochna Dolicka¹, Szabolcs Zahoran², Marta Sousa¹, Monika Gjorgjieva¹, Christine Sempoux³, Margot Fournier¹, Christine Maeder¹, Martine Collart², Michelangelo Foti¹, Cyril Sobolewski^{1,4}. ¹University of Geneva, Faculty of Medicine, Department of Cell Physiology and Metabolism, Switzerland; ²University of Geneva, Faculty of Medicine, Department of Microbiology and Molecular Medicine, Switzerland; ³Lausanne University Hospital, University Institute of Pathology, Switzerland; ⁴Institute for Translational Research in Inflammation, Inserm, U1286, Faculty of Medicine, Pole Recherche, France

Email: cyril.sobolewski@univ-lille.fr

Background and aims: Adenylate-Uridylate-rich elements binding proteins (AUBPs) contribute to the development of non-alcoholic fatty liver disease (NAFLD) and hepatocellular carcinoma (HCC) by regulating the expression of genes important for metabolic, inflammatory, and cancerous processes. This effect is mediated by their binding to target mRNAs, which elicits their recruitment into processing bodies (P-bodies) or stress granules (SGs), where mRNAs are degraded or kept translationally silent, respectively. Herein, we aimed at characterizing the role of TIA1, an AUBP with a poorly known function in the liver, in NAFLD and HCC.

Method: TIA1 expression was analyzed in datasets of mouse and human samples of NAFLD and HCC. The role of TIA1 *in vivo* was investigated in mice fed a methionine-choline-deficient (MCD) diet and in a liver-specific PTENKO mouse model of hepatic carcinogenesis, where TIA1 was silenced using AAV8 viruses. Finally, TIA1 functions were characterized *in vitro* in human hepatic cancer cells and a translomic-based approach was used to identify the network of potential TIA1 targets.

Results: *In vitro* analyses indicate that TIA1 promotes cell proliferation and migration. *In vivo*, its silencing worsens NASH induced by the MCD diet and increases tumor number in LPTENKO mice. In agreement, the analysis of polysomal RNAs indicates that TIA1 regulates a whole network of tumor suppressors and oncogenes as well as genes related to lipid metabolism. Finally, TIA1 protein level is strongly downregulated in human HCC and represents an important marker of stress granules upon sorafenib treatment.

Conclusion: Our data emphasize TIA1's dual role in liver carcinogenesis and indicate that its downregulation and association with stress granules may represent potential diagnostic tools and/or therapeutic targets.

FRI573

Mitochondrial damage, revealed as key factor in cabozantinib efficacy against hepatocellular carcinoma, is potentiated by the BH3-mimetic navitoclax

Anna Tutusaus¹, Blanca Cucarull¹, Patricia Rider¹, Carlos Cuño¹, Pablo García de Frutos¹, Loreto Boix^{2,3}, Montserrat Marí¹, Albert Morales^{1,3}. ¹IIBB-CSIC/IDIBAPS, Barcelona; ²Unidad de Hepatología, Hospital Clinic, IDIBAPS, CIBEREHD, Barcelona, Barcelona, Spain; ³Barcelona Clinic Liver Cancer (BCLC), Barcelona, Spain

Email: amorales@clinic.cat

Background and aims: The mitochondrial damage induced by sorafenib and regorafenib plays an important antitumor role in hepatocellular carcinoma (HCC). Both Tyrosine Kinase Inhibitors (TKIs) induce mitochondrial dependent cell death that may be potentiated by specific BH3-mimetics, selective inhibitors of BCL-2 proteins. ABT-263, navitoclax, is a BCL-2 and BCL-xL inhibitor studied in clinical trials, such as with sorafenib in solid tumors (NCT02143401). Mitochondrial effects of cabozantinib have not been previously reported in HCC therapy.

Method: Hepatoma cell lines (HepG2, Hep3B, PLC5) were treated with cabozantinib and BH3-mimetics (ABT-263, navitoclax; BCL-2 and BCL-XL, ABT-199; BCL-2, A-1331852; BCL-xL). Western blots, qPCR and microarrays were performed. Mitochondrial functionality, caspase activation and induction of apoptosis were analyzed. Tumor growth was determined in a mouse syngeneic model after subcutaneous injection of Hepa1-6 cells treated with cabozantinib and/or ABT-263.

Results: Cabozantinib induced mitochondrial Reactive Oxygen Species (ROS) generation and cell death that was potentiated by BH3-mimetics in hepatoma cells. Cabozantinib induced loss of mitochondrial membrane potential, release of apoptogenic proteins and apoptotic cell death, particularly triggered after navitoclax addition. Sorafenib-resistant cells, which exhibited altered levels of BCL-2 proteins, were less sensitive to cabozantinib; effect that was suppressed by navitoclax co-administration. Moreover, the decreased tumor growth in an immunocompetent mice model induced by cabozantinib was potentiated in combination with navitoclax, promoting mitochondrial-dependent death as observed after tumor genetic and proteomic analysis.

Conclusion: Cabozantinib efficacy may be reduced following other TKIs treatments with mitochondrial impact, such as with sorafenib or regorafenib. In contrast, cabozantinib-induced cell death is potentiated in experimental HCC by mitochondrial directed drugs, such as navitoclax, providing a novel strategy for therapy.

FRI574

Mutations in BAP1 drive tumour sensitivity to programmed cell death in patient-derived cholangiocarcinoma organoids

Shaojun Shi¹, Imre F Schene², Indi P. Joore², Henk P. Roest¹, Gilles van Tienderen¹, Ruby Lieshout¹, Bas Groot Koerkamp¹, Petra E. de Ruiter¹, Benedetta Artergiani³, Sabine A Fuchs², Hans Clevers^{3,4}, Luc J.W. van der Laan¹, Monique M.A. Versteegen¹. ¹Erasmus MC Transplant Institute, University Medical Center, Department of Surgery, Rotterdam, Netherlands; ²Wilhelmina Children's Hospital, University Medical Center Utrecht, Department of Metabolic Diseases, Utrecht, Netherlands; ³The Princess Maxima Center for Pediatric Oncology, Utrecht, Netherlands; ⁴OncoCode Institute, Utrecht, the Netherlands; Hubrecht Institute, KNAW (Royal Netherlands Academy of Arts and Sciences), Utrecht, the Netherlands; University Medical Center Utrecht, Cancer Genomics Netherlands, Utrecht, Netherlands

Email: m.versteegen@erasmusmc.nl

Background and aims: Cholangiocarcinoma (CCA) is an aggressive hepatobiliary malignancy associated with high inter-patient heterogeneity. The de-ubiquitinase BRCA-1 associated protein-1 (BAP1) is a tumor suppressor gene found to be mutated in 16–32% of CCA tumors and is strongly associated with CCA progression. However, the biological role of BAP1 in CCA is not well understood. Here, we aimed to determine how mutations in BAP1 impact CCA tumor cell behavior in response to multiple programmed cell death stimuli.

Method: Organoids derived from CCA tumors (CCAOs, n=3) and healthy donor liver (ICOs, n=3). BAP1 mutations in CCAOs were mapped by genomic sequencing. BAP1 loss-of-function in ICOs (ICO^{BAP1-KO}) was introduced by CRISPR/Cas9 gene editing. Programmed cell death was induced in CCAOs and ICO^{BAP1-KO} by exposure to TNF- α (T)/Smac mimic (S) (extrinsic apoptosis) or T/S/Z-VAD-FMK (Z) (necroptosis) or gemcitabine. Sensitivity to cell death induction was presented as a change in cell viability evaluated by an

ATP assay (CellTiterGlo). BAP1 protein and markers for apoptosis (cleaved caspase 3) and necroptosis (phosphorylated MLKL) were determined by immunostaining and immunoblotting.

Results: The three different CCAOs each harbor distinct BAP1 phenotypes: wild type (CCAO^{WT}), loss of heterozygosity (CCAO^{LOH}), and missense mutation combined with LOH (CCAO^{Mut/LOH}). Compared to PDO^{WT}, BAP1 protein expression could not be detected in CCAO^{Mut/LOH} and was greatly declined in CCAO^{LOH}. The cell viability analysis and immunostaining showed that the resistance to either apoptotic or necroptotic induction was significantly increased in CCAO^{Mut/LOH} ($p < 0.001$) compared to CCAO^{WT}. In contrast, CCAO^{LOH} were more sensitive to cell death induction ($p < 0.001$). Similar increased sensitivity was also observed in ICO^{BAP1-KO} compared to wild-type ICOs. Gemcitabine evoked extensive apoptosis in PDO^{WT} (IC50 0.06 μ M), but the sensitivity of both PDO^{LOH} (IC50 0.34 μ M) and PDO^{Mut/LOH} (IC50 0.12 μ M) was significantly lower. Likewise, ICO^{BAP1-KO} displayed drastic resistance to gemcitabine compared to normal ICOs.

Conclusion: Mutations in the BAP1 gene causing loss of function, are associated with a lower sensitivity of CCAOs to extrinsic apoptosis, necroptosis, and gemcitabine cytotoxicity. Correction of the mutation in BAP1 using prime editing is currently effectuated to confirm the role of BAP1 in programmed cell death in CCA. Our findings reveal a promising strategy in CCA precision medicine by targeting BAP1 mutations.

FRI575

Integrative clustering of multiple genomic data using organoid model with application to subtype analysis in intrahepatic cholangiocarcinoma

Hee Seung Lee¹, Dai Hoon Han², Kyung Joo Cho³, Soo Been Park³, Chanyang Kim³, Galam Leem¹, Soon Sung Kwon⁴, Chul Hoon Kim⁴, Jung Hyun Jo¹, Hye Won Lee¹, Si Young Song¹, Jun Yong Park¹. ¹Yonsei University College of Medicine, Division of Gastroenterology, Department of Internal Medicine; ²Yonsei University College of Medicine, Division of Hepatobiliary and Pancreatic Surgery, Department of Surgery; ³Yonsei University College of Medicine; ⁴Yonsei University College of Medicine, Department of Pharmacology
Email: drpjy@yuhs.ac

Background and aims: Intrahepatic cholangiocarcinoma (ICC) has increased rapidly, and the 5-year survival rate is less than 20%. As the genomic analysis technology has been advanced, subgrouping is possible at the histological or molecular level in ICC. But, there was no well-representative model for subtypes of ICC to study developmental differences, carcinogenesis, and personalized drug response. We aimed to develop ICC organoid models that reflect phenotypical, molecular and genetic properties and performed integrative clustering of multiple genomic data using organoid models with subtype analysis.

Method: We enrolled a total of 16 patients who were pathologically diagnosed with cholangiocarcinoma. We made ICC organoid following the previous organoid culture protocol in nature protocol. In accordance with histological characteristics, S100P, N-cadherin, and CD56 expression, the ICC patients were subclassified into small duct type and large duct type. Immunofluorescence (IF), whole exome sequencing, and transcriptomic analysis were performed to characterize and investigate all cancer tissues and matched ICC organoids.

Results: We successfully established ICC organoids within a month. The morphology of ICC organoid was similar to matched primary cancer. Organoid derived xenograft also showed similar phenotype in H&E stain. IF stains showed the expression of cholangiocyte marker (CK19 and Sox9) but negative expression in liver cell marker (AFP and Albumin). The cancer immunotherapy marker, Programmed death-ligand 1 expression between the organoid and tumor tissue was similar. Large and small duct type organoids showed their typical histologic phenotype and stain. ICC organoids shared somatic mutations and showed high concordance of somatic mutation

between primary tumor and organoids. Through the unsupervised PCA clustering showed the separation of each type of ICC. Using the differential gene expression between types, KRAS signaling pathway, TGF β and ERBB2 pathway were significantly enriched in large duct type compared to small duct type ($p < 0.05$). GSEA demonstrated that cholangiocarcinoma class2 signature by Andersen et al. was significantly enriched with LD type (enrichment score = 2.19, $p < 0.001$). Protein-protein interaction network analysis indicated that the significant hub proteins were ZNF217 (Odds ratio 4.96, $P = 0.0105$).

Conclusion: We succeeded in prospective modeling of histological subtype specification in patient-derived ICC organoids. Identification of type specific targetable pathway was possible through gene expression profile of ICC organoids.

FRI576

Role of soluble adenylyl cyclase in the formation and growth of liver tumours

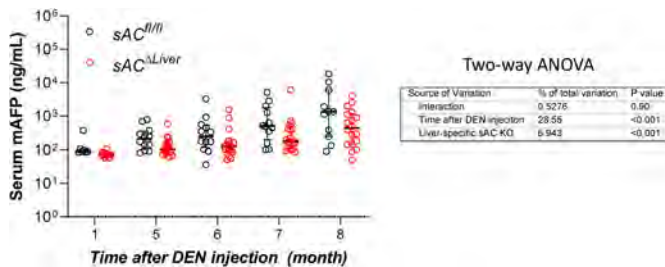
Jung-Chin Chang^{1,2}, Suzanne Duijst¹, Simei Go¹, Dagmar Tolenaars¹, Rachel Thomas², Alain de Bruin², Arthur Verhoeven¹, Ronald Oude-Elferink¹. ¹Amsterdam University Medical Centers, Tytgat Institute for Liver and Intestinal Research, Amsterdam, Netherlands; ²Utrecht University, Department of Biomolecular Health Sciences, Utrecht, Netherlands
Email: j.chang1@uu.nl

Background and aims: Soluble adenylyl cyclase (ADCY10, sAC) mediates the cAMP signaling in the cytoplasm, mitochondria, and the nucleus. sAC is activated by metabolic signals (Ca²⁺, ATP, and bicarbonate) and was recently shown to regulate AMP-activated kinase (AMPK) and transcriptional factor TAZ (WW domain-containing transcription regulator protein 1). The YAP (Yes-associated protein 1)/TAZ signaling pathway regulates the liver size, promotes liver regeneration, and is hyper-activated in liver cancers. Using human liver hepatoma cells HepG2, we recently showed that sAC-cAMP-Epac1 (exchange proteins activated by cyclic AMP 1) signaling regulates mitochondrial Complex I activity and is a metabolic switch between glycolysis and oxidative phosphorylation (PMID: 33412125). We observed that inhibition of sAC activity promotes a Warburg-like metabolic phenotype. Therefore, we hypothesized that reduced sAC activity could promote hepatic tumorigenesis.

Method: Liver carcinogenesis was evaluated in hepatocyte-specific sAC knockout mice (*Adcy10^{fl/fl} × Alb-Cre*) and littermate controls (*Adcy10^{fl/fl}*) following a single dose of 25 mg/kg diethylnitrosamine (DEN) injection at 3–4 weeks of age. Tumor formation was monitored by plasma α -fetoprotein (Afp). Tumor burden was evaluated by liver-to-body weight index. Histologic grading was performed on hematoxylin-eosin stained, formalin-fixed tissues. HepG2 cells were used for the in vitro mechanistic study. Cell proliferation was evaluated by dsDNA quantification; pharmacological agents and intermediate metabolites of lipid and nucleotide synthesis were used to dissect the underlying mechanisms.

Results: Contrary to our expectation, hepatocyte-specific sAC deletion delayed the rise of plasma Afp and reduced the tumor burden in the liver. Preliminary results from histopathology analysis did not suggest a strong correlation between liver-specific sAC deletion and the histological grading of the liver tumors. The in vitro mechanistic study revealed that the suppression of sAC-cAMP-Epac1 signaling activates AMPK and inhibits proliferation of HepG2 cells, which could not be rescued by supplementing intermediates of lipid synthesis or nucleotide. Consistent with AMPK being an established regulator of YAP, we found that sAC inhibition suppressed YAP nuclear translocation.

POSTER PRESENTATIONS



Conclusion: Hepatocyte-specific SAC deletion delays DEN-induced liver carcinogenesis in mice and reduced the overall tumor burden. Pharmacological inhibition of the SAC-cAMP-Epac1 signaling suppresses the growth of human liver cancer cells. The anti-tumor effect of SAC inhibition is likely mediated by the AMPK-dependent suppression of YAP signaling.

FRI577

A targeted screen identifies *Dmbt1* as an oncogene in cholangiocarcinoma

Pooya Shokoohi¹, Saumya Manmadhan¹, Christian Lechler¹, Birgit Kohnke-Ertel¹, Carolin Mogler², Thomas Engleitner^{3,4}, Rupert Öllinger^{3,4}, Roland Rad^{1,3,4}, Roland M Schmid¹, Ursula Ehmer¹. ¹Klinikum rechts der Isar der Technischen Universität München, Internal Medicine II, München, Germany; ²Klinikum rechts der Isar der Technischen Universität München, Institute of Pathology and Unit of Comparative Experimental Pathology, München, Germany; ³Technische Universität München, Institute of Molecular Oncology and Functional Genomics, School of Medicine, München, Germany; ⁴Technische Universität München, Center for Translational Cancer Research (TranslaTUM), School of Medicine, München, Germany
Email: ursula.ehmer@tum.de

Background and aims: Activation of RAS signaling is a common event in human cholangiocarcinoma (CCA). With direct targeting of Ras signaling in its infancy, identification of relevant pathways and genes in RAS-activated cholangiocarcinoma is a prerequisite to the development of novel therapies. To model RAS-activated cholangiocarcinoma, we generated the RPK mouse model that combines liver-specific expression of oncogenic *Kras* with genetic inactivation of the tumor suppressors *Rb* and *p53*. Upon Cre-mediated gene recombination, adult mice developed liver tumors resembling human intrahepatic CCA. To identify potential target genes in the context of activated RAS signaling we employed a targeted screening approach.

Method: Liver tumors from *Rb^{lox/lox}; p53^{lox/lox}; Kras^{LSL-G12D/+}* (RPK) mice and liver tissue of age-matched control mice were micro-dissected and analyzed for RNA and protein expression. A curated subset of top upregulated genes in mRNA microarray analysis of RPK liver tumors were chosen for further investigation. Primary cells lines from RPK mice were transfected with lentiviral shRNA or sgRNA constructs to induce gene knock-down or CRISPR/Cas9-mediated gene mutation, respectively. Cells were analyzed for proliferation and clonogenic assay, followed by RNAseq, GSEA, and cell cycle analysis of cells mutated for the candidate gene *Dmbt1*.

Results: Microarray analysis showed several highly upregulated genes in RPK tumors in comparison to controls. shRNA constructs targeted against top upregulated genes showed a striking decrease in cell proliferation and clonogenic capacity with constructs targeting *Dmbt1*. RPK cells mutant for *Dmbt1* showed an enrichment of gene sets for E2F and G2/M checkpoint activation. Further analysis revealed that reduced proliferation upon inactivation of *DMBT1* is associated with a G2/M cell cycle arrest.

Conclusion: Activation of RAS signaling is a common change in human CCA. In our screen, we identified *Dmbt1* as a potent oncogene in a model of *Ras*-mutant cholangiocarcinoma. While *DMBT1* has been described as a tumor suppressor in other cancers by interacting

with the immune system, we were able to identify a novel cell-autonomous oncogenic role of *DMBT1* in CCA. Our results show that *DMBT1* is essential for cell cycle progression and proliferation in RPK cancer cells. *DMBT1* expression is upregulated in a large subset of human CCA and its potential as a therapeutic target are currently under investigation.

FRI578

ACSL4-dependent ferroptosis promotes HCC progression

Julia Piche¹, Antje Mohs¹, Stephanie Erschfeld¹, Christian Trautwein¹, Tobias Otto¹. ¹Uniklinik RWTH Aachen, Aachen, Germany
Email: jpiche@ukaachen.de

Background and aims: In industrialized countries the prevalence of non-alcoholic fatty liver disease, ranging from steatosis to non-alcoholic steatohepatitis (NASH), is increasing. Mechanisms triggering disease progression towards cirrhosis and hepatocellular carcinoma (HCC) are only incompletely understood. A newly discovered mode of cell death, ferroptosis, is triggered by accumulation of lipid peroxides and is iron-dependent. According to *in vitro* studies, acyl-CoA synthetase long-chain family member 4 (ACSL4) is an essential enzyme for ferroptosis. Interestingly, ACSL4 expression was shown to be upregulated in HCC tissue indicating that ferroptosis might play a role in HCC pathophysiology. Here, we aimed to investigate the relevance of ferroptosis for disease progression using hepatocyte-specific ACSL4 inhibition in experimental HCC models.

Method: We used a well-established fibrosis-driven HCC model. Tumor formation was induced by injecting the carcinogen diethylnitrosamine (DEN), followed by weekly injections of carbon tetrachloride (CCl₄). As a second model we applied the Streptozocin/HFD model. Wild-type (WT) and hepatocyte-specific ACSL4 knockout (ACSL4^{Δhepa}) mice were included to investigate the role of ferroptosis for cancer development.

Results: Our analysis in both models demonstrated that ACSL4-dependent ferroptosis is not involved in HCC initiation, but important for tumor progression. After DEN-CCl₄ treatment, serum transaminase levels were increased, but without significant differences upon ACSL4 deletion. Interestingly, the number of tumors, as well as overall tumor burden were significantly reduced in ACSL4^{Δhepa} mice compared to WT mice. This was accompanied by significantly decreased liver-to-body-weight-ratio in ACSL4^{Δhepa} mice. However, immune cell infiltration was not altered. Furthermore, ACSL4 deletion caused reduced proliferation in the liver and diminished tumor-promoting fibrosis.

Conclusion: Our results demonstrate that ACSL4-dependent ferroptosis promotes tumor progression by enhancing tumor-promoting fibrosis. Therefore, inhibition of ferroptosis or key molecules regulating cell death represents a possible therapeutic treatment for human HCC.

FRI579

Identification of risk factors for HBV-derived HCC using HLA-DPB1 genotype and HBV peptides for genome medicine

Masaya Sugiyama¹, Nao Nishida¹, Katsushi Tokunaga¹, Mizokami Masashi¹. ¹National Center for Global Health and Medicine, Japan
Email: msugiyama@hosp.ncgm.go.jp

Background and aims: Hepatocellular carcinoma (HCC), caused by hepatitis B virus (HBV) infection, is a major problem worldwide. However, no biomarkers for early diagnosis have been discovered so far. In the present study, we focused on the genetic factors associated with HBV-derived HCC. To discover the genetic factors, we analysed the combined genomes of both humans and HBV.

Method: The genome-wide SNPs array and Luminex were applied to 2,996 individuals (408 chronic hepatitis B (CHB) patients, 307 HCC patients with HBV and 2,281 healthy volunteers (HVs)) from 10 hospitals. The obtained SNPs data were filled by imputation: the HBV genome was extracted from sera of CHB or HCC patients and prepared

for next generation sequencing (NGS). All sequence reads were converted into amino acid (AA) sequences to assess the effect of HBV mutations on replication and antigen expression in vitro.

Results: HLA-DPB1*02:01 allele was associated with protection against HCC development ($p < 4.53 \times 10^{-9}$, OR = 0.53). We then analysed the whole HBV genome of patients carrying the HLA-DPB1*02:01 allele. HLA-DPB1*02:01 homozygous patients were divided into HCC and non-HCC groups, matched for age, sex and HBV genotype. HCC with HLA-DPB1*02:01 The proportion of S166 in CHB and HCC was 51.5% and 0%, respectively ($p < 0.05$). In contrast, the proportion of L166 was 34.3% in CHB and 99.4% in HCC ($p < 0.05$). This variation was confirmed using a validation sample set ($p < 0.02$, OR = 18.2). Next, we prepared HLA-DPB1*05:01 homozygous patients and examined the AA variations of HBV protein. We then detected that the K130M and V131I mutations were associated with the HCC group ($p < 0.05$, OR = 8.8); the OR value of the 05:01 population was stronger than that of all patients with HCC (OR = 4.1). Interestingly, mutations in K130M and V131I (nt A1762T and T1764A) were strongly associated with the HLA-DPB1*05:01 homozygous population.

Conclusion: We have identified genetic factors, both host and viral, that are associated with clinical outcome. As only a small proportion of CHB patients develop HCC, these risk factors may be useful in optimising clinical diagnosis and follow-up time. The finding that certain combinations of HLA-DPB1 alleles and viral mutations are associated with a higher risk of developing HCC is novel, and this study is a proof-of-concept study to use genomic data from hepatitis B patients to predict prognosis.

FRI580

Early Kupffer cell depletion does not affect hepatocellular carcinoma progression in mice

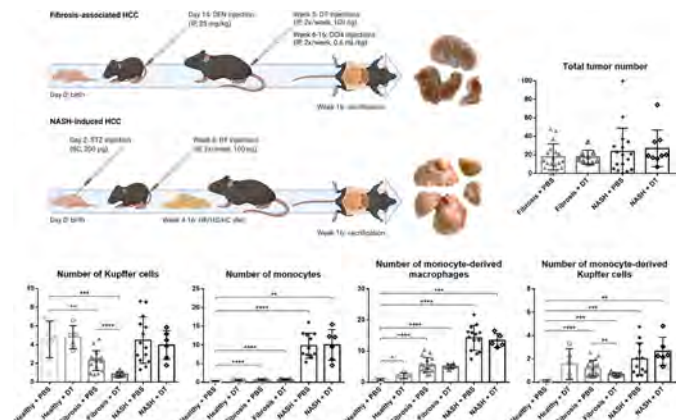
Bart Van Derborgh^{1,2}, Kevin De Muynck^{1,2}, Charlotte Scott^{3,4}, Alain Beschin^{5,6}, Martin Guilliams^{3,7}, Hans Van Vlierberghe^{1,8}, Lindsey Devisscher². ¹Ghent University, Internal Medicine and Pediatrics (Liver Research Center Ghent; Hepatology Research Unit), Ghent, Belgium; ²Ghent University, Basic And Applied Medical Sciences (Liver Research Center Ghent; Gut-Liver Immunopharmacology Unit), Ghent, Belgium; ³Ghent University, Biomedical Molecular Biology, Ghent, Belgium; ⁴VIB-UGent Center for Inflammation Research, Laboratory of Myeloid Cell Biology in Tissue Damage and Inflammation, Ghent, Belgium; ⁵Vrije Universiteit Brussel, Laboratory of Cellular and Molecular Immunology, Brussels, Belgium; ⁶Vrije Universiteit Brussel, Myeloid Cell Immunology Laboratory, Brussels, Belgium; ⁷VIB-UGent Center for Inflammation Research, Laboratory of Myeloid Cell Biology in Tissue Homeostasis and Regeneration, Ghent, Belgium; ⁸Ghent University Hospital, Gastroenterology and Hepatology, Ghent, Belgium Email: lindsey.devisscher@ugent.be

Background and aims: Hepatocellular carcinoma (HCC) represents the majority of primary liver cancer cases. Its aggressive disease behavior and poor prognosis substantiate the critical need to urgently address the lack of effective HCC treatment options. HCC usually occurs in a background of chronic liver disease (CLD), characterized by chronic hepatic inflammation and fibrosis, in which Kupffer cells (KCs), resident liver macrophages, have been proposed to play a role. However, the role of KCs in HCC initiation and progression remains unknown.

Method: In order to investigate the role of KCs in HCC initiation, transgenic Clec4F-diphtheria toxin receptor mice were used. Diphtheria toxin (DT)-mediated KC depletion was performed prior to the introduction of chronic liver damage in both a fibrosis-associated and a non-alcoholic steatohepatitis (NASH)-induced HCC mouse model.

Results: At the time of sacrifice, macroscopic hepatic tumors were present in approximately 100% of the cases in both HCC mouse models without differences between groups. Flow cytometric analysis of the liver tissue showed depletion of KCs and infiltration of monocytes and monocyte-derived macrophages (MoMfs),

confirming previous literature, and the presence of monocyte-derived KCs (MoKCs) in both models. DT-mediated KC ablation at the initiation stage of HCC induction resulted in a decreased number of KCs and MoKCs at end-stage disease in fibrosis-associated HCC but not in the model of NASH-induced HCC. This altered hepatic macrophage pool composition was however not associated with significant changes in tumor burden, HCC markers or inflammatory, angiogenic and fibrotic components of the tumor microenvironment (TME). In NASH-induced HCC, depletion of the KCs resulted in decreased hepatic expression of alpha-smooth muscle actin and vascular endothelial growth factor, however, no differences were detected on histology for tumor burden, steatosis, inflammation and fibrosis, substantiating the limited effect of KC depletion in the initiation phase of HCC pathogenesis.



Conclusion: Despite the tolerogenic function of KCs in homeostasis and the reported role as early activators during inflammation, depletion of KCs during the initiation phase of HCC pathogenesis only has minor effects on the TME and does not affect disease severity or progression in HCC mouse models with different underlying backgrounds.

FRI581

RELB activation drives tumour aggressiveness and predicts prognosis in hepatocellular carcinoma

Luisa Nader¹, Federico Nichetti^{2,3}, Anna-Lena Scherr¹, Christin Ellsner¹, Dirk Ridder⁴, Sarah Fritzsche⁵, Sofia Weiler⁵, Thomas Albrecht⁵, Annika Kessler¹, Nathalie Schmitt¹, Felix Korell⁵, Liangtao Ye⁶, Toni Urbanik¹, Christoph Heilig^{7,8}, Mohammad Rahbari⁹, Lydia Brandl¹⁰, Christoph Springfield^{1,11}, Thomas Longerich⁵, Henning Schulze-Bergkamen¹², Dirk Jäger^{1,9}, Stefan Fröhling⁷, Peter Schirmacher^{5,9}, Beate Straub^{4,13}, Achim Weber¹⁴, Mathias Heikenwälder⁹, Enrico de Toni¹⁵, Benjamin Goeppert^{5,11}, Stephanie Roessler^{5,11}, Kai Breuhahn^{5,11}, Bruno Köhler^{1,11}. ¹National Center for Tumor Diseases (NCT) Heidelberg, University Hospital Heidelberg, Department of Medical Oncology, Heidelberg, Germany; ²Fondazione IRCCS Istituto Nazionale Dei Tumori, Medical Oncology, Milan, Italy; ³National Center for Tumor Diseases (NCT) and German Cancer Research Center (DKFZ), Computational Oncology, Molecular Diagnostics Program, Heidelberg, Germany; ⁴University Hospital, General Pathology, Mainz; ⁵University Hospital Heidelberg, Institute of Pathology, Heidelberg, Germany; ⁶Ludwig-Maximilians-University Munich, Department of Internal Medicine II, Munich, Germany; ⁷German Cancer Consortium (DKTK), Heidelberg, Germany; ⁸NCT Heidelberg and German Cancer Research Center Heidelberg (DKFZ), Department of Translational Medical Oncology, Heidelberg, Germany; ⁹German Cancer Research Center Heidelberg (DKFZ), Division of Chronic Inflammation and Cancer, Heidelberg, Germany; ¹⁰Ludwig-Maximilians-University Munich, Medical Faculty, Institute of Pathology, Munich, Germany; ¹¹University Hospital Heidelberg, Liver Cancer Center Heidelberg, Heidelberg,

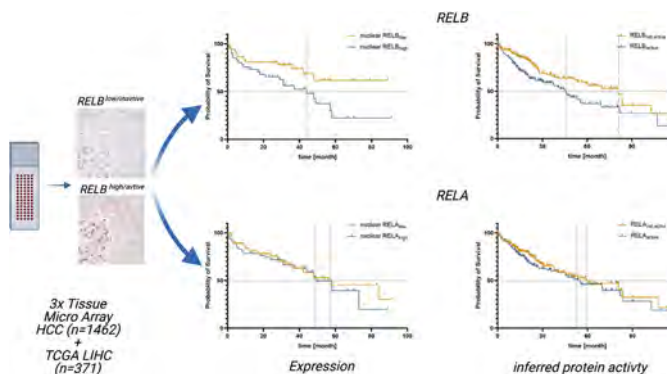
POSTER PRESENTATIONS

Germany; ¹²Marien-Hospital Wesel, Department of Internal Medicine II, Wesel, Germany; ¹³University Hospital Mainz, Department of General Pathology, Mainz, Germany; ¹⁴University and University Hospital Zurich, Department of Pathology and Molecular Pathology, Zurich, Switzerland; ¹⁵Klinikum Grosshadern, Ludwig-Maximilians-University of Munich, Department of Internal Medicine II, Munich, Germany
Email: bruno.koehler@nct-heidelberg.de

Background and aims: Hepatocellular carcinoma (HCC) is the fourth leading cause of cancer death worldwide with increasing incidence rates. Better molecular understanding to identify prognosticators and tailored therapy are urgently needed. The canonical nuclear factor kappa B (NF-kappaB) signaling branch has been shown to play a role in chronic liver disease and hepatocarcinogenesis. However, the role of the non-canonical part with its key transcription factor RELB remains unclear.

Method: Three tissue microarrays (TMA) were immunohistochemically (IHC) stained for NF-kappaB signaling components including RELB and scored for intensity. The TCGA-LIHC cohort served as a third validation set, to comparatively analyze mRNA expression and protein activity as inferred by the VIPER algorithm. Patients were grouped in RELB^{high} and RELB^{low} (expression) and RELB^{active} and RELB^{inactive} (inferred activity). Kaplan-Meier method and Cox proportional hazard models were used for overall survival (OS) analysis. Gene Set Enrichment Analysis (GSEA) was performed on differentially expressed (DE) genes between RELB^{active} and RELB^{inactive} cases.

Results: A total of 1462 (TMA) and 371 (TCGA-LIHC) cases were included. RELB was nuclear enriched in HCC compared to control tissue (IHC score 1.2 vs 6.3, $p \leq 0.0001$). The increase of RELB activity correlated with tumor grading (control vs. G1: $p = \text{n.s.}$; control vs. G2: $p = 0.0193$; control vs. G3/G4: $p = 0.0004$). Patients with a high nuclear RELB expression score had poorer overall survival (OS) compared to those with low RELB expression score ($p = 0.0333$; HR 2.129; 95% CI = 1.087 to 4.17). In the TCGA-LIHC cohort, RELB^{active} cases showed worse OS compared to RELB^{inactive} ones (46 vs 81 months; HR 1.69; 95%CI = 1.20 to 2.39; $p = 0.003$). Through GSEA of DE genes and clustering of functional terms, RELB^{active} tumors showed a significant enrichment of pathways related to cell proliferation, differentiation and metabolic dysregulation.



Conclusion: Non-canonical NF-kappaB signaling drives hepatocarcinogenesis by inducing proliferation and tumor aggressiveness. Activation of its key transcription factor RELB is a prognostic factor for HCC, identifying patients with poor overall survival.

FRI582

An aggressive subgroup of CTNNB1-mutated hepatocellular carcinomas with STEM-cell phenotype and immune tolerance

Lise Desquilles¹, Romain Désert¹, Valérie Monbet², Joyce Madison Giacomini², Luis Cano¹, Clémence Landreau¹, Natalia Nieto³, Anne Corlu¹, Christelle Reynès⁴, Orlando Musso¹.
¹INSERM, INRAE, Univ Rennes 1, Nutrition metabolism and cancer, Rennes, France; ²IRMAR-INRIA, Univ Rennes 1, Rennes, France; ³Department of pathology, Department of medicine (gastroenterology and hepatology), University of Illinois at Chicago, Chicago, United States; ⁴Laboratoire physique industrielle et traitement de l'information, EA2415, Montpellier, France
Email: lise.desquilles@gmail.com

Background and aims: Hepatocellular carcinoma (HCC) is the 3rd cause of cancer-related death worldwide and its heterogeneity impacts patient management. Based on transcriptomic data from over 1300 human HCCs, we described two major dimensions explaining HCC heterogeneity. First, the inverse relationship between proliferation and differentiation. Second, the degree of preservation of periportal and perivenous metabolic zonation. This bidimensional approach revealed four subclasses: PERIportal, PERIVENOUS (PV), EXTRACELLULAR MATRIX and STEM CELL, across a continuum of increasing aggressiveness. The aim of this work was to better understand the mechanisms governing phenotypic diversity within PV-type HCCs, which are characterized by beta-catenin (CTNNB1) gene mutations.

Method: To classify HCCs, we applied Curve Clustering to a transcriptomic training set ($n = 264$) and identified two subgroups of PV-type HCCs with differential aggressiveness: BAD-PV and GOOD-PV. By PLS-DA, we found a 44-gene signature sorting out BAD-PV from GOOD-PV, which was validated in three unrelated datasets (ICGC, $n = 202$; GSE14520¹, $n = 242$; Désert's meta-dataset², $n = 1133$). We integrated these sets with a 15-time point series of HepaRG phenotypic plasticity^{3,4}; and 2 datasets of mouse liver development (GSE87795⁵; GSE90047⁶). To investigate the mechanisms driving aggressiveness in PV-type HCCs, we generated functional gene networks by Weighted Gene Correlation Analysis (WGCNA); assessed HCC mutations in the TCGA and ICGC datasets; gene methylation in TCGA and deconvoluted immune cell populations with the Immunophenoscore and Cibersort algorithms in TCGA and GSE14520 datasets. Finally, we compared BAD-PV and GOOD-PV cytoarchitectural features in the digital TCGA slide collection ($n = 61$).

Results: In BAD-PV HCCs, mRNA transcriptomes matched HepaRG-derived cancer stem/progenitor cells and early stages of mouse liver development; WGCNA identified 3 networks of co-expressed genes related to stemness; DNA methylation analysis revealed 468 key hypo-methylated genes involved in cell proliferation and development. Although CTNNB1-mutated HCCs show no inflammation and don't respond to immune checkpoint inhibitors, BAD-PV had increased Treg lymphocytes, CD4T memory cells and myeloid dendritic cells, high levels of inflammatory molecules, negative immune checkpoints (PDL1; CTLA4) and markers of plasmacytoid dendritic cells. Similarly, histological analysis showed that BAD-PV had higher Edmondson-Steiner's ($p = 1.3e^{-10}$) and inflammation ($p = 3.5e^{-5}$) scores, with higher density of plasma cells ($p = 1.7e^{-7}$).

Conclusion: We identified a subgroup of highly aggressive CTNNB1-mutated HCCs with stem cell phenotype and immune tolerance features.

1. Cancer Res, 70: 10202
2. Hepatology, 66: 1502
3. Hepatology, 45: 957
4. Cancer Res, 79: 1869
5. BMC Genomics, 18: 1
6. Hepatology, 66: 1387

FRI583

Single cell RNAsequencing derived signature of hepatocyte de-differentiation predicts development of hepatocellular carcinoma in patients with liver cirrhosis

Mikhail Gromak¹, Hendrik Luxenburger¹, Tobias Böttler¹, Robert Thimme¹, Maike Hofmann¹, Natascha Röhlen¹. ¹University Medical Center Freiburg, Department of Medicine II, Freiburg, Germany
Email: natascha.roehlen@uniklinik-freiburg.de

Background and aims: Hepatocellular carcinoma (HCC) represents a major complication of liver cirrhosis, occurring at a rate of 1–5% per year. Hepatocytes are believed to represent the origin of malignant transformation in HCC. However, the molecular events determining HCC risk are poorly defined accounting for absence of chemopreventive strategies. Frequent overexpression of immature liver progenitor cell or bile duct markers in HCC suggests de-differentiation of hepatocytes to be involved in its pathogenesis.

Method: Applying single cell RNAsequencing (scRNAseq) derived marker genes of mature hepatocytes, cholangiocytes and progenitor cells we aimed to characterize hepatocyte de-differentiation in liver transcriptome data from different cohorts of patients with chronic liver disease (Geo database: GSE33814, GSE15654, GSE10140). To assess whether hepatocyte-de-differentiation can be investigated non-invasively, serum levels of individual markers were determined by enzyme-linked immunosorbent assay (ELISA) in a cohort of patients with liver cirrhosis with (n = 31) or without (n = 74) HCC development.

Results: Stratification of healthy liver scRNAseq data derived cell cluster marker genes (GSE124395) was used to generate a transcriptomic signature of mature hepatocytes and bile duct-like cells. Gene set enrichment analysis (GSEA) of these scRNAseq derived signatures in liver tissue microarray data of patients with non-alcoholic steatohepatitis (NASH) and Controls suggested enrichment of bile duct-like cells in chronically diseased livers (GSE33814, n = 44, FDR < 0.001). Similar upregulation of progenitor markers on the single cell level in hepatocytes from cirrhotic livers (GSE136103, n = 5 donors) further support this enrichment to occur via de-differentiation of hepatocytes during chronic liver injury. Interestingly, transcriptomic signatures of hepatocyte de-differentiation strongly correlated with risk of HCC development. Indeed, cirrhotic livers of patients with no HCC development within a follow-up period of >10 years showed enrichment of mature hepatocyte marker genes (GSE15654, n = 216, FDR < 0.001), while immature bile duct marker genes were strongly enriched in cirrhotic livers of patients with HCC *de novo* development or recurrence (GSE10140, n = 82, FDR < 0.001). Among the top markers of hepatocyte de-differentiation, we could identify MCAM as a serum biomarker of HCC development (HCC vs. liver cirrhosis = 1064 vs. 413 ng/ml, p = 0.01).

Conclusion: Our results indicate hepatocyte de-differentiation to occur during chronic liver disease progression and to serve as a putative risk factor for HCC development. Detectable serum levels of multiple markers of our scRNAseq derived signature raise the outlook for non-invasive assessment of hepatocyte de-differentiation and its associated clinical HCC risk.

FRI584

Detection of cholangiocarcinoma in mice with protease activity probes

Jesse Kirkpatrick^{1,2}, Pinzhu Huang³, Yuri Popov³, Sangeeta Bhatia^{1,2,4}. ¹Massachusetts Institute of Technology, Harvard-MIT Division of Health Sciences and Technology, Cambridge, United States; ²Koch Institute For Integrative Cancer Research, Cambridge, United States; ³Beth Israel Deaconess Medical Center and Harvard Medical School, Division of Gastroenterology and Hepatology, Boston, United States; ⁴Howard Hughes Medical Institute, Cambridge, United States
Email: jessekirk11@gmail.com

Background and aims: Patients with primary sclerosing cholangitis (PSC) are at a 400-fold increased risk of cholangiocarcinoma (CCA),

and are thus subjected to regular screening with magnetic resonance cholangiopancreatography (MRCP) (Lazaridis *et al.* 2016). Unfortunately, MRCP findings are nonspecific for CCA in the setting of biliary fibrosis, and even invasive endoscopic retrograde cholangiopancreatography with brush cytology and fluorescence *in situ* hybridization often fails to yield a definitive diagnosis (Barr Fritcher *et al.* 2015). We have previously developed a novel class of diagnostic agents, activatable zymography probes (AZPs), analogous to immunofluorescence probes for protease activity, that can be used to visualize tumour-associated protease dysregulation *in situ* and *in vivo* (Soleimany and Kirkpatrick *et al.* 2021). Upon proteolytic cleavage, these probes electrostatically bind to positively charged tissue domains, thereby tagging and labelling proteolytically active cells (Fig. 1A). Because matrix metalloproteases (MMPs), including MMP7 (Leelawat *et al.* 2010) and MMP1 (Metzger *et al.* 2012) have been shown to be dysregulated in CCA, we aimed to develop MMP-sensitive AZPs to enable the differential diagnosis of CCA and benign biliary fibrosis.

Method: We induced CCA tumour formation in *Mdr2*^{-/-} mice via hydrodynamic injection of sleeping beauty transposon-transposase plasmids encoding for *Akt* and *Yap1* (Fig. 1B), and harvested livers of tumour-bearing and untreated *Mdr2*^{-/-} mice 5 weeks later. We then synthesized a panel of nine AZPs with peptide sequences designed to be cleaved by MMPs and applied them to fresh frozen liver tissue sections from CCA and *Mdr2*^{-/-} mice.

Results: We found that four AZPs, most notably AZP6, specifically bound to CCA tumours, and that this binding was significantly abrogated by pre-treatment with broad-spectrum protease inhibitors (p = 0.00015 for AZP6) (Fig. 1C, D). Furthermore, these four AZPs bound significantly less efficiently to fibrotic portal tracts of *Mdr2*^{-/-} mice (p = 4.9 × 10⁻⁸ for AZP6) (Fig. 1C, D). Finally, we incubated a panel of recombinant MMPs, including the CCA-associated MMP1, with a quenched fluorescent version of the AZP6 peptide substrate and found it be efficiently cleaved (Fig. 1E).

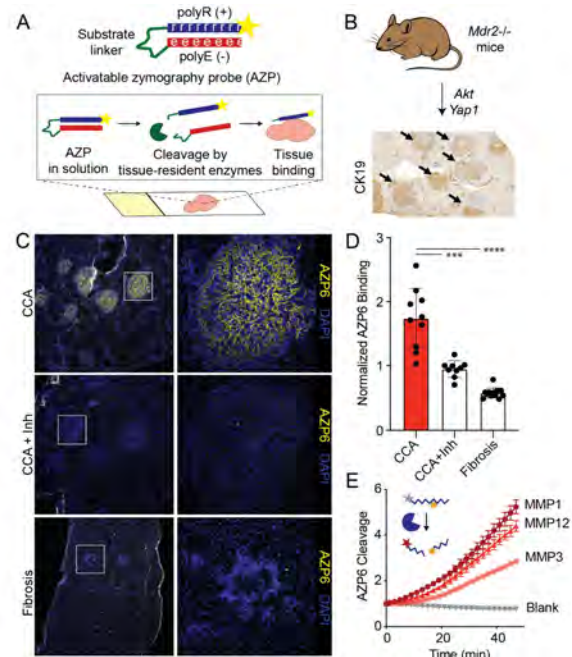


Figure 1: Activatable zymography probes specifically label CCA tumours. A) Principle of AZP staining method. B) Schematic of tumour induction protocol. Mice were sacrificed 5 weeks after hydrodynamic administration of *Akt* and *Yap1* plasmids. Immunohistochemical staining of tumour-bearing livers for CK19 is shown below. C) Fluorescence microscopy images of AZP6-treated liver tissue sections from tumour-bearing ("CCA") mice, without (top) or with (middle) broad-spectrum protease inhibitors ("Inh"), or *Mdr2*^{-/-} ("Fibrosis") mice (bottom). D) Quantification of AZP6 staining. Each point represents one tumour ("CCA") and "CCA + Inh") or one portal tract ("Fibrosis"). ***, p < 0.001; ****, p < 0.0001 by two-tailed t-test. E) A quenched fluorescent version of the AZP6 peptide substrate was incubated with MMP1, 3, or 12 and fluorescence fold change was measured by fluorimetry.

POSTER PRESENTATIONS

Conclusion: MMP dysregulation in a mouse model of CCA is detected by AZPs, enabling differentiation of benign and malignant biliary disease *in situ*. Our next steps will be to adapt these probes for *in vivo* administration and assess their ability to noninvasively distinguish biliary malignancy from fibrosis in mouse models of CCA.

FRI585

Critical investigation on the usability of hepatoma cell lines HepG2 and Huh7 as models for the metabolic representation of resectable hepatocellular carcinoma

Andrea Scheffschick^{1,2}, Gerda Schicht^{1,2}, Lena Seidemann^{1,2}, Sebastian Sperling³, Julia Nerusch^{1,2}, Natalie Herzog⁴, Jonas Babel², Jan Küpper⁴, Daniel Seehofer^{1,2,3}, Georg Damm^{1,2,3}. ¹Saxonian Incubator of Clinical Translation (SIKT), Leipzig, Germany; ²University Hospital, Department of Hepatobiliary Surgery and Visceral Transplantation, Leipzig, Germany; ³Charité University Medicine Berlin, Department of General, Visceral and Transplantation Surgery, Berlin, Germany; ⁴Brandenburg University of Technology Cottbus-Senftenberg, Faculty of Science, Senftenberg, Germany
Email: georg.damm@medizin.uni-leipzig.de

Background and aims: Changes in energy metabolism are a known feature of hepatocellular carcinoma (HCC). Therefore, addressing the energy metabolism in hepatoma cells as a potential treatment is work in progress. Here, we compared the hepatoma cell lines HepG2 and Huh7 with appropriate controls based on primary cells to evaluate their usability in HCC research.

Method: We isolated control primary human hepatocytes (PHHs) from resected livers from non-HCC patients and primary human hepatoma cells (PHCs) and corresponding PHHs (HCC-PHHs) from HCC patients. As a model of proliferating PHHs we used Upcyte® hepatocytes (HepaFH3 clone) generated by lentiviral transduction of PHHs with proliferation-inducing genes. Cell types were characterized for specific HCC markers, enzymes and signaling proteins of the energy metabolism on RNA, protein and functional level.

Results: The characterization for established HCC markers revealed that advanced PHCs are closely related to hepatoma cell lines. In contrast, the identified metabolic key players showed lower expression in PHCs in comparison to hepatoma cell lines and PHHs. Hepatoma cell lines did not reflect anaerobic and fasting characteristics of PHCs. In line with that, clinical data of our donors indicated that their HCC were slowly growing tumors. In contrast, hepatoma cell lines showed similar metabolic characteristics to proliferating PHHs suggesting that the Warburg effect is a general feature of energy shortage in rapidly proliferating cells.

Conclusion: We show that HepG2 and Huh7 cells do not reflect the energy metabolism of PHCs. In particular anaerobic and fasting states of HCCs were not covered by cell lines under standard cell culture conditions.

FRI586

Different immunological microenvironment in patients with different cirrhosis etiology and hepatocellular carcinoma

Andrea Dalbeni¹, Leonardo Natola¹, Filippo Cattazzo¹, Antonio Vella², Marta Garbin¹, Michele Bevilacqua¹, Anna Mantovani¹, Giovanna Zanoni², Alfredo Guglielmi³, Michele Milella⁴, David Sacerdoti¹. ¹AOU Verona, Medicine, Verona, Italy; ²University of Verona, Immunology department, Italy; ³University of Verona, Surgery, Verona, Italy; ⁴Università of Verona, Oncology, Italy
Email: andrea.dalbeni@aovr.veneto.it

Background and aims: Hepatocellular carcinoma (HCC) is the second leading cause of cancer-related death. Most cases (90%) of HCC arise in the setting of a chronic liver disease. The advanced stages of HCC are amendable only to systemic treatment. Systemic therapy has been revolutionized by immune-based therapies. However, a recent meta-analysis of three randomized phase III clinical trials that tested inhibitors of PD-L1 or PD1 in more than 1, 600 patients with

advanced HCC, revealed that immune therapy did not improve survival in patients with non-viral HCC.

The aim of the study was to identify differences in immune cell population of patients with HCC, according to etiopathogenesis of cirrhosis, in order to identify different patterns that may be targeted for immunotherapy.

Method: We analyzed 50 leukocyte sub-populations, using flow cytometric technique, in a cohort of 111 consecutive HCC cirrhotic patients with different etiopathogenesis. Differences between groups were analyzed with the Mann-Whitney U test.

Results: We divided HCC patients with cirrhosis into five groups according to etiology of liver disease: alcoholic, viral (HCV/HBV), metabolic (NAFLD/NASH), overlap between etiological factors and other etiology. Leukocyte sub-populations were significantly different in two groups. Specifically in the group of alcoholic etiology there were increased levels of PMN ($p < 0.01$), monocytes ($p < 0.01$) and NKT cells CD57+RA- (4-8-) ($p = 0.011$), while in viral etiology group there were increased levels of T cells CD57-RA+ (4-8-) ($p = 0.007$) and T cell CD3+ (4-8-) ($p = 0.009$). No specific leukocyte subpopulation was significantly increased in the other groups, in particular in the metabolic one.

Conclusion: These data suggest that in liver disease with different etiopathogenesis there are different immunological microenvironments. Innate and innate-like cells are the principal regulators of immune response in alcoholic HCC, while adaptive immune system is predominant in viral etiology. This suggests that differences in cancer-mediated immune escape could explain the different response to immunotherapy and may be helpful in identification of responder patients to new HCC therapy.

FRI587

Cytokine levels and circulating DNA in plasma could be used as serological biomarkers of response to immunotherapy in hepatocellular carcinoma

Elena Vargas Accarino^{1,2}, Monica Higuera¹, Maria Bermúdez^{1,2,3,4}, Monica Pons^{1,2,3,4}, Maria Torrens¹, Gloria Torres¹, Marta Vila⁵, Francisco Rodríguez-Frías^{4,5}, Xavier Merino⁶, Beatriz Minguez^{1,2,3,4}. ¹Liver Diseases Research Group, Vall d'Hebron Research Institute, Barcelona, Spain; ²Department of Medicine, Universitat Autònoma de Barcelona, Barcelona, Spain; ³Liver Unit, Vall d'Hebron University Hospital, Barcelona, Spain; ⁴CIBERehd, Instituto Carlos III, Barcelona, Spain; ⁵Biochemistry and Microbiology Department, Clinical Laboratories Hospital Universitari Vall d'Hebron, Barcelona, Spain; ⁶Radiology Department, Vall d'Hebron University Hospital, Barcelona, Spain
Email: bminguez@vhebron.net

Background and aims: Immunotherapy and, in particular, immune checkpoint inhibitors (ICIs) have revolutionized the therapeutic landscape for advanced hepatocellular carcinoma (HCC). As monotherapy, they have shown antitumor activity in a subgroup of patients and the combination of anti-PDL1 antibody (atezolizumab) and VEGF-neutralizing antibody (bevacizumab) have become treatment of choice in first-line. One of the unsolved challenges is to identify and validate predictive biomarkers of response to these treatments in patients with HCC. The objective of this study was to identify potential serological markers of response to ICIs.

Method: Prospective cohort of 21 patients treated with ICIs (Nivolumab monotherapy ($n = 15$), Atezolizumab/Bevacizumab combination ($n = 5$) and Durvalumab/Tremelimumab combination ($n = 1$)). Plasma samples were collected at the beginning of ICI treatment and after three months of treatment. Twenty-four inflammatory cytokine levels were analyzed by ELISA as well as the levels of circulating cell free DNA (cfDNA) and its percentage of TERT mutation by ddPCR, at baseline and at 3 months of treatment.

Results: 86% of the study patients were male, with a mean age of 72 years and 76% were BCLC-C at starting ICIs treatment. 48% presented progression (PD), 9% complete response (CR), 14% partial response

(PR) and 29% stable disease (SD) as best radiological response. The underlying liver disease in most cases was hepatitis C virus (HCV) infection (62%). Lymphocyte Activation Gene type 3 (LAG-3) levels measured 3 months after starting ICIs treatment were significantly higher in PD [median (IQR)] 231.4 pg/ml (2668.3) than in CR, PR SD (median (IQR) 126.7pg/ml (245.5) ($p=0.031$). Interleukin-21 (IL-21) levels after three months of treatment were significantly different between patients who presented the best radiological response at follow-up CR/PR (195.5 (155.9) pg/ml), SD (62.7 (29)) or PD (290.6 (689.6) pg/ml) ($p=0.05$). The analysis of MCP-1 (monocyte chemo-attractant protein 1) also showed significantly different levels depending on the response to treatment (CR/PR 88.9 pg/ml (62.4), SD 23 pg/ml (11.9) and PD 12.7 pg/ml (9.8)) ($p=0.002$). The only baseline determination that showed significant differences was total cfDNA, which was significantly higher in patients who presented PD as the best radiological response (8 pg/ml (6.1)) compared to patients who had radiological response (CR/PR) or SD (3 pg/ml (2.9)) ($p=0.024$). Changes in TERT mutation percentage after 3 months of treatment showed a trend to significance between patients experiencing PD and CR/PR/SD patients ($p=0.083$).

Conclusion: Our findings suggest that LAG-3, IL-21 and MCP-1 levels determined after 3 months of ICI treatment and baseline cfDNA levels, could be serological biomarkers of response in patients with advanced HCC. Validation studies are currently ongoing.

FRI588

RuvBL1 haploinsufficiency improves mTOR-driven NASH-HCC development in mice

Alice Guida^{1,2}, Irene Simeone^{1,2}, Simone Polvani¹, Elisabetta Ceni¹, Lucia Picariello¹, Gabriele Dragoni^{1,2}, Andrea Galli¹, Tommaso Mello¹.
¹University of Florence, Clinical and Experimental Biomedical Sciences "Mario Serio", Florence, Italy; ²University of Siena, Genetics, Oncology and Clinical Medicine "GenOMeC" PhD programme, Siena, Italy
Email: tommaso.mello@unifi.it

Background and aims: The AAA+ ATPase RuvBL1 participates in several cellular processes relevant to oncogenic transformation, including DNA repair, gene expression, telomerase complex assembly and mTOR pathway activity. RuvBL1 expression correlates with a worse prognosis in HCC patients, however its role in HCC is largely unexplored. We have previously demonstrated that RuvBL1 haploinsufficiency impairs insulin signalling affecting the PI3K/Akt/mTOR pathway in vivo. Considering the relevance of mTOR pathway hyperactivation in human HCC, we aimed to reduce mTOR-driven hepatocarcinogenesis by targeting RuvBL1 in *Pten*^{hep-/-} mice, a genetic model of NASH progression to HCC.

Method: *Pten*^{hep-/-} and *Ruvbl1*^{hep±} mice were crossed to generate *Pten*^{hep-/-} *Ruvbl1*^{hep±} mice. The impact of RuvBL1 haploinsufficiency on NASH development was assessed by histology at 12 weeks of age. Metabolic and inflammatory markers were evaluated by qPCR and IHC. mTOR pathway cascade was analysed by western blot of liver lysates.

HCC development was assessed in mice aged to 15 months by multiplicity evaluation of macroscopic tumors and by histological classification by Edmondson-Steiner grading system.

Results: Oil red, Sirius red histological stain and F4/80 IHC revealed a significant reduction of steatosis, fibrosis, and inflammation in *Pten*^{hep-/-} *Ruvbl1*^{hep±} compared to *Pten*^{hep-/-} at 12 weeks of age. Quantification of triglycerides extracts confirmed the reduced lipid content in *Ruvbl1* haploinsufficient mice livers. Surprisingly, similar mRNA expression of mTOR-driven lipogenic targets was found in the two mice models. However, expression of *Ppara* and its target CPT1 was increased in *Pten*^{hep-/-} *Ruvbl1*^{hep±}, indicating a lipid-lowering action mediated by PPARalpha in this mouse model. Western blot revealed an increase of p-AMPK and p-RAPTOR protein levels in *Pten*^{hep-/-} *Ruvbl1*^{hep±}, suggesting a role of RuvBL1 at the interplay between mTOR and AMPK in hepatic lipid metabolism. *Pten*^{hep-/-} *Ruvbl1*^{hep±} mice aged to 15 months developed significantly less

macroscopic tumours, which resulted better differentiated and of lower grade than *Pten*^{hep-/-} ones. qPCR analysis showed a significant upregulation of key lipolytic genes, such as *Cpt1a*, *Acadl*, *Acadvl* and *Ppara* in *Pten*^{hep-/-} *Ruvbl1*^{hep±} at 15 months of age.

Conclusion: Targeting RuvBL1 mitigates the NASH metabolic and tumorigenic phenotype driven by mTOR hyperactivation in *Pten*^{hep-/-} mice, likely promoting the switch from mTOR-driven lipogenesis to AMPK-induced fatty acid catabolism.

FRI589

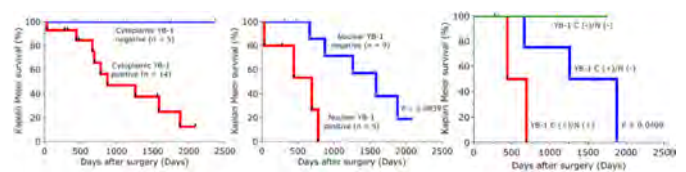
Cold shock protein YB-1 upregulates MDR1 transcription and thus contributes to chemoresistance against cisplatin treatment in cholangiocarcinoma

Tao Lin¹, Jonathan A. Lindquist², Peter Rene Mertens², Matthias Ebert¹, Steven Dooley¹, Jun Li³, Stefan Munker⁴, Honglei Weng¹. ¹UMM; ²uni-magdeburg; ³University Medical Center Hamburg-Eppendorf; ⁴LMU
Email: steven.dooley@medma.uni-heidelberg.de

Background and aims: Cholangiocarcinoma is a liver cancer with high mortality. Chemotherapy with cisplatin or gemcitabine is currently the main approach to treat cholangiocarcinoma patients with advanced stage. However, efficiency of these drugs is poor due to chemoresistance. To date, detailed mechanisms underlying chemoresistance in cholangiocarcinoma are largely unknown. In this study, we demonstrate a crucial role for the cold shock protein Y-box binding protein-1 (YB-1) in cholangiocarcinoma chemoresistance to cisplatin.

Method: Expression of YB-1 was examined by immunohistochemistry in 28 cholangiocarcinoma patients receiving surgery. Among them, 10 patients underwent chemotherapy following operation. Functional studies on the YB-1 effects were performed in cholangiocarcinoma cell lines to delineate the underlying mechanisms.

Results: YB-1 expression in cancer cells, in particular in nuclei, was closely associated with survival of patients. From 10 patients receiving chemotherapy, 2 patients without YB-1 expression, but only 3 out of 8 patients with YB-1 expression survived a 5-year follow-up. In vitro, immunofluorescence staining showed that cisplatin administration induced YB-1 nuclear translocation. ChIP assays demonstrated YB-1 binding to the multidrug resistance gene MDR1 promoter prior to induction of gene expression. Impressively, administration of cisplatin significantly increased MDR1 promoter binding activity of YB-1. Functionally, knockdown of YB-1 by RNAi inhibited cancer cell proliferation and increased cisplatin-dependent apoptosis.



Conclusion: YB-1 nuclear expression plays a crucial role in cholangiocarcinoma chemoresistance to cisplatin treatment through upregulating MDR1 expression. YB-1 expression in cancer cells might be a useful biomarker to predict chemotherapy efficacy in cholangiocarcinoma. Further, disrupting YB-1 function in cholangiocarcinoma is a promising treatment approach in clinical practice.

FRI590

Synergistic anti-tumor activity with a combination of anti-PD1 antibody and the cyclophilin inhibitor, rencofilstat, in the Hep53.4 fatty liver model of hepatocellular carcinoma

Daren Ure¹, Jack Leslie², Bhavesh Variya¹, Robert Foster¹, Jelena Mann³, Derek A Mann^{2,3}. ¹Hepion Pharmaceuticals, Canada; ²Newcastle University, United Kingdom; ³Fibrofind Ltd, United Kingdom
Email: dure@hepionpharma.com

Background and aims: Cyclophilins are a class of protein folding and regulatory enzymes that have been shown in preclinical studies to contribute to progression of several types of cancer, including hepatocellular carcinoma (HCC). Immunomodulation is one of the many therapeutic activities ascribed to cyclophilin inhibition and was the rationale for investigating the clinical phase cyclophilin inhibitor, rencofilstat (CRV431), in combination with anti-PD1 in a murine orthotopic model of HCC.

Method: Murine Hep53.4 HCC cells were implanted into either normal livers or fatty livers of C57BL/6 mice. Fatty livers were generated by feeding mice a western diet with sugar water for 3 months prior to surgical Hep53.4 implantation. Treatments included rencofilstat by once-daily oral gavage and anti-PD1 IgG twice weekly, alone or in combination, starting 2 weeks post-implantation. Anti-cancer effects were assessed by measuring tumor volumes at Week 4 post-implantation, immunohistochemical tumor analysis, and mouse survival in additional cohorts of mice.

Results: Rencofilstat and anti-PD1 IgG treatments, alone or in combination, similarly decreased tumor growth in non-fatty livers by 76–83% over 2 weeks of treatment compared to vehicle treatment. Immunohistochemical analysis showed that rencofilstat and anti-PD1 independently doubled CD4 and CD8 lymphocyte infiltration into tumors. Additionally, rencofilstat decreased the number of tumor neutrophils by 55%, whereas anti-PD1 had no effect on neutrophil infiltration. In the fatty liver model, neither rencofilstat nor anti-PD1 alone produced statistically significant reductions in tumor growth, but the combination decreased tumor growth by 84% compared to 2 weeks of vehicle treatment. Survival analyses in separate cohorts in the fatty liver-HCC model mirrored the tumor measurements in that monotherapies had no effect on survival whereas rencofilstat plus anti-PD1 extended median survival time by 26%.

Conclusion: The different outcomes in non-fatty versus fatty liver HCC models align with previous reports stating that HCC in fatty livers is more resistant to immune checkpoint inhibitor therapy. Combination treatment with rencofilstat and anti-PD1 synergistically decreased tumor growth and extended survival time, which supports clinical investigation in HCC.

FRI591

Rencofilstat, a pan-cyclophilin inhibitor, exerts diverse metabolic and transcriptional anti-tumor activities in a murine NASH-HCC model

Daren Ure¹, Joseph Kuo², Winston Stauffer², Lacey Haddon¹, Patrick Mayo¹, Robert Foster¹, Philippe Gallay². ¹Hepion Pharmaceuticals, Canada; ²Scripps Research Institute, United States
Email: dure@hepionpharma.com

Background and aims: Cyclophilins are protein folding and regulatory enzymes that have been shown in preclinical studies to contribute to progression of several types of cancer, including hepatocellular carcinoma (HCC). They are elevated in most types of cancer, and overexpression is prognostic of shorter survival. Current pharmacologic cyclophilin inhibitors exert anti-cancer activities but target multiple cyclophilin isoforms. The aim of the current study was to elucidate the predominant anti-cancer mechanisms of the pan-cyclophilin inhibitor, rencofilstat (CRV431), in an experimental murine HCC model.

Method: Rencofilstat was studied in a murine NASH-HCC model (streptozotocin + Western diet) characterized by a high mutational burden and spontaneous liver tumor development. Rencofilstat was

administered by once-daily oral gavage from Weeks 20–30 following initiation of Western diet. Liver tumor and non-tumor tissue from vehicle-treated and rencofilstat-treated mice were analyzed by genomic, transcriptomic, and metabolomic methods.

Results: Once-daily, oral rencofilstat treatment decreased tumor burden at Week 30 by 50%. Whole exome sequencing of tumors and nontumor liver tissue revealed a diverse repertoire of somatic mutations that far exceeded the mutation burden of human HCC tumors. This was accompanied by extensive dysregulation of metabolic and transcriptional processes, i.e. changes in approximately 25% of all metabolites and gene expression. Rencofilstat treatment produced many alterations of the metabolic and transcriptional signatures in tumor and nontumor, NASH tissue consistent with anti-cancer effects. At a systems level, 47% of the differential metabolites and 59% of the differential gene expression in tumors were normalized by rencofilstat treatment to levels observed in nontumor tissue. Specific metabolism-related effects of rencofilstat in tumors included normalizations of the oncometabolite, fumarate, and the principal byproduct of methylation reactions, s-adenosylhomocysteine. At the transcriptional level, rencofilstat altered the expression of genes across a spectrum of cellular processes, including oncogenic signaling, cell cycle, cell death, unfolded protein responses, ubiquitination, and several metabolic processes. Noteworthy rencofilstat effects included attenuation of Wnt-β-catenin, Myc, C/EBPβ, Nupr1, Eif2ak3 (PERK), and Rac1.

Conclusion: The clinical phase drug candidate, rencofilstat, decreased tumor burden in an aggressive, hypermutated model of HCC, which was associated with a wide range of metabolic and transcriptional effects. These results suggest that pan-cyclophilin inhibition may be therapeutic across multiple tumor types in HCC or other cancers.

FRI592

Establishing quantitative image analysis methods for tumor microenvironment evaluation

Caner Ercan^{1,2}, Mairene Coto-Llerena^{1,2}, Salvatore Piscuoglio^{1,2}, Luigi Maria Terracciano^{1,3}. ¹University Hospital Basel, University of Basel, Institute of Medical Genetics and Pathology, Basel, Switzerland; ²Department of Biomedicine, University of Basel, Visceral surgery and Precision Medicine Research Laboratory, Basel, Switzerland; ³Humanitas University, Department of Biomedical Sciences, Milan, Italy
Email: caner.ercan@usb.ch

Background and aims: There is growing evidence that supports the role of the tumor microenvironment (TME) in the development and progression of hepatocellular carcinoma (HCC). However, the correlation between its composition and prognosis remain unclear. TME evaluation requires a combination of cell type and spatial information. These information can be obtained with the use of immunohistochemistry on patient derived slides. However, the IHC quantification remains a challenge. Computational methods such as artificial intelligence-based tool, may expedite the detection and classification thousands of different cells, expanding our understanding of the TME. Here, we aim to develop an AI based image analysis pipeline to define morphological and immunological characteristics of HCC-TME, as well as their relationship with clinicopathological features.

Method: We collected 98 HCC samples from liver resections available in the TME composition of the tumors was evaluated and classified as inflamed, immune excluded and immune desert. Tumor slides were stained with a panel of TME markers (CD3, CD8, FOXP3, TIGIT, RORgt, ICOS, GranzymeB CD163, iNOS, PD-1, PD-L1) by IHC. The slides were digitalised and whole slide images were used for the quantification. The samples were split into training (80%) and test (20%) datasets and used to train convolutional neural network (CNN) models. For the quantification of immune cells, we trained two separate CNNs: cell detection and tumor-stroma segmentation. Cell nucleus instance segmentation was achieved using StarDist package

(Schmidt et al 2018). We trained a model with our slides and tested the pretrained model (2D_versatile_he) which is for H&E stained images. Immune cells were classified using random forest classifier in QuPath. Finally, we trained a CNN in UNET architecture with ResNet34 backbone for semantic segmentation of tumor tissue into parenchyma, stroma and debris classes, by fastai deep learning library.

Results: The accuracy of pretrained StarDist model was limited to 72% on IHC slide images. Thus, we trained a new cell nucleus instance segmentation StarDist model with our dataset and it reached 84% accuracy, 91.3% F1-Score, 92% true positive, 90.6% true negative rates on IHC slide images. Random forest classifier annotated immune cells at 98% accuracy. The tissue segmentation model classified tumor regions into parenchyma, stroma and debris at 95, 8% accuracy, 92.5% dice, 86.3% IoU.

Conclusion: In this study we developed a pipeline implementing open-source solutions to quantify IHC slides. The use of this semi-automatized computational pathology workflow can provide robust information in regard of the TME composition augmenting the discovering tumour specific TME features and pave way for the discovery of novel prognostic and therapeutic targets.

FRI593

Development of hepatocellular carcinoma in the extended GAN diet-induced obese mouse model of NASH with advanced fibrosis

Andreas Nygaard Madsen¹, Denise Oró¹, Martin Rønn Madsen¹, Mogens Vyberg², Henrik B. Hansen¹, Michael Feigh¹. ¹Gubra, Hørsholm, Denmark; ²Aalborg University, Center for RNA Medicine, Department of Clinical Medicine, Copenhagen, Denmark
Email: mfe@gubra.dk

Background and aims: Non-alcoholic steatohepatitis (NASH) predispose to the development of severe fibrosis and hepatocellular carcinoma (HCC). Preclinical animal models resembling NASH-driven HCC development are important tools for exploring novel pharmacological interventions for HCC. The present longitudinal study aimed to characterize disease progression in the extended GAN (Gubra-Amylin NASH) diet-induced obese (DIO) mouse model of NASH.

Method: Male C57Bl/6J mice were fed the GAN diet (40% fat, 22% fructose, 10% sucrose, 2% cholesterol) for up to 88 weeks (n = 12–15/group). Disease progression in DIO-NASH mice was evaluated using the clinical NAFLD Activity Score (NAS) and fibrosis staging system, quantitative histology, macroscopic tumor evaluation and liver transcriptomics. Tumor histopathological classification was performed by an expert clinical pathologist.

Results: DIO-NASH animals demonstrated progressive NASH (NAS ≥5) and fibrosis (stage ≥F1) from 28 weeks of GAN diet feeding. Notably, advanced fibrosis (stage F3, bridging fibrosis) was observed ≥80% of animals from 48 weeks of GAN diet. Development of liver tumors was progressively observed with 100% tumor burden after 58 weeks of GAN diet-induction. Tumors demonstrated consistent architectural and cytologic features of HCC, notably loss of reticulin-stained fibers. Progressive HCC development was supported by increased quantitative histological markers of proliferation (Ki67), and hepatic biliary/progenitor cells (CK19). Disease progression was further highlighted by increased quantitative histological markers of steatosis (lipids, hepatocytes with lipid droplets), inflammation (number of inflammatory foci, galectin-3), fibrosis (PSR, collagen 1a1), activated stellate cells (alpha-SMA). Finally, liver whole-tissue transcriptome signatures demonstrated enhanced fibrogenesis (collagens, matrix metalloproteins) and tumorigenesis activity (cell cycle control, growth factors).

Conclusion: DIO-NASH mice show advanced fibrosis and high HCC tumor burden following extended GAN dieting. The GAN DIO-NASH-HCC mouse model is suitable for profiling novel drug therapies for advanced fibrosing NASH-driven HCC.

FRI594

Non-canonical TGF-β signalling contributes to pro tumorigenic Smad3 linker phosphorylation in cholangiocarcinoma

Sophie Alex¹, Jan Albin¹, Diego F. Calvisi², Stefan Munker³, Honglei Weng¹, Nuh N. Rahbari⁴, Matthias Ebert⁵, Anne Dropmann¹, Steven Dooley¹. ¹Medical Faculty Mannheim, University Heidelberg, Molecular Hepatology, Department of Medicine II, Mannheim, Germany; ²University Regensburg, Department of Pathology, Regensburg, Germany; ³Hospital of the University of Munich, Department of Medicine II, Munich, Germany; ⁴Medical Faculty Mannheim, University Heidelberg, Department of Surgery, Mannheim, Germany; ⁵Medical Faculty Mannheim, University Heidelberg, Department of Medicine II, Mannheim, Germany
Email: S.Alex@stud.uni-heidelberg.de

Background and aims: TGF-β signal transduction commences with receptor-mediated C-tail phosphorylation of Smad3, complex formation with Smad4 and nuclear translocation for cytosolic target gene regulation in epithelial cells. Regulatory phosphorylation steps at serine/threonine residues in the Smad linker (L) domain generate phosphorylated forms with mitogenic functions by interfering with transcriptional activity and proteasomal degradation. TGF-β signaling is impaired in several human tumors. We now show that in intrahepatic cholangiocarcinoma (iCCA) pSmad3L levels are increased and we aimed at identifying if this may facilitate tumorigenesis.

Method: We examined 180 healthy and tumorigenic liver tissues from iCCA patients for their Smad3 phosphorylation status, discriminating C-tail (S423 and S425)- and linker residues (S204 and S213), using immunoblotting, immunofluorescence and immunohistochemistry with Smad phosphorylation site-specific antibodies and correlated these with clinical data. For functional studies, we treated cultured iCCA cells with inhibitors for Smad and non-Smad TGF-β signaling pathways in combination with TGF-β1 stimulation and the chemotherapeutics Cisplatin, Gemcitabine, Doxorubicin and 5-FU, and tested chemosensitivity and proliferative activity.

Results: C-tail Smad3 phosphorylation was evident similarly in healthy and tumorigenic liver tissue samples. Elevated pSmad3L levels were exclusively present in tumour tissue with 86% of CCA samples showing increased pSmad3L S213 and only 5% being positive for pSmad3L S204. CCA cell lines show decreased pSmad3C and increased pSmad3L (S213 and S204) levels as compared to non-tumorous cholangiocytes which show strong pSmad3C and weak pSmad3L staining. Treatment with inhibitors indicate a counter regulation of C-terminal versus linker phosphorylation. Intrinsic pSmad3L (S204 and S213) is decreased by treatment with a GSK-3β inhibitor. In this setting, TGF-β1 leads to a stronger phosphorylation of Smad3C. When instead inhibiting ALK5, TGF-β1 treatment enhances nuclear pSmad3L levels. High pSmad3L and low pSmad3C levels result in enhanced proliferation and robust chemoresistance. Interfering with linker phosphorylation of Smad3 by targeting GSK-3β reduces proliferative activity and sensitized the cells for chemotherapy. MMP-9, p21 and c-Myc mRNA expression levels correlate with the respective proliferative activity.

Conclusion: pSmad3L (S204 and S213) phosphorylation is predominant in CCA tissue and interferes with cytosolic pSmad3C (S423/425) signaling in cultured iCCA cells, thereby facilitating proliferative activity and chemoresistance of cancer cells. Canonical ALK5/C-terminal Smad3 phosphorylation and non-canonical Smad3 linker phosphorylation are counterregulated in vitro. A similar scenario in patient samples is currently not confirmed and requires further studies.

FRI595

TGF- β -SOX9 axis-inducible SCUBE3 promotes proliferation, invasion and metastasis in hepatocellular carcinoma via epithelial-to-mesenchymal transition

Hong Ren^{1,2,3,4}, Qiang Luo², Pan Xu¹. ¹Institute for Viral Hepatitis, Chongqing, China; ²Institute for Viral Hepatitis, Chongqing, China; ³Institute for Viral Hepatitis, Yuzhong, Chongqing, China; ⁴Email: renhong0531@cqmu.edu.cn

Background and aims: It was found that secretory SCUBE3 protein is highly expressed in lung cancer and osteosarcoma, is associated with proliferation, invasion and metastasis of lung cancer cells and breast cancer cells. Therefore, the aim is to explore the clinical significance of SCUBE3 in HCC and the specific molecular mechanism of SCUBE3 on the biological function.

Method: TCGA database and IHC were used to detect the SCUBE3 of cancer and paracancerous. CCK8, Clone formation and cell cycle experiment were used to detect the regulation of SCUBE3 on the proliferation of hepatoma cells. The apoptosis and cell cycle after knockdown of SCUBE3 were detected by flow cytometry. Cell migration and invasion were detected by cell scratch and Transwell. The invasion and EMT markers were detected by WB and qPCR. EMT markers in nude mouse tumours was detected by IHC. The cell movement was observed by the RTCA system. ROS reactive oxygen species assay was used to evaluate the effect of SCUBE3 on cell adhesion. The xenograft tumour and metastasis model of liver cancer were constructed. The interacting proteins were verified by confocal and IP assay. TGF β was added on the basis of knocking down SCUBE3. SCUBE3 recombinant protein induced EMT formation. The interaction between Sox9 and SCUBE3 was verified by Chip experiment.

Results: SCUBE3 in hepatocellular carcinoma was different from that in adjacent tissues ($p=0.017$), and SCUBE3 was related to age and stage and grade of hepatocellular carcinoma.

SCUBE3 knockdown inhibit the HCC cell proliferation and colony formation, migration and invasion. The apoptosis increased and the transformation of the cell cycle from the G1 phase to S phase inhibited in KD group. The degree of ROS in different cells was different. The lung metastasis model of liver cancer evaluated the regulatory ability of SCUBE3 on the invasion and metastasis of liver cancer cells. The overexpression of metastatic tumors in the upper lung group was more than that in the control group.

Akt and TGF β were the pathways related to the regulation of hepatoma cell proliferation, metastasis and EMT β /Smad2/3 pathway. SCUBE3 and TGF β R II has interaction. Smad2/3 pathway was also inhibited in KD group. VEGF, N-cadherin also increased, E-cadherin decreased and Smad2/3 expression increased when TGF β was given in KD group. Sox9 and Runx1 were inhibited with SCUBE3 knockdown. The function of Sox9 was related to the prognosis of liver cancer. Chip experiment showed that there was SCUBE3 binding site in chromosome 1657–1665 region of Sox9 transcription factor.

Conclusion: TGF- β -Sox9-SCUBE3 axis regulates the Akt pathway and EMT to promote the proliferation, invasion and metastasis of HCC cells. SCUBE3 may become a new target for clinical diagnosis and treatment of HCC.

Keywords: SCUBE3, Signaling pathway, animal model, hepatoma cells, proliferation and metastasis.

FRI596

Inhibition of Wee1 induces antitumoral effects in preclinical models of hepatocellular carcinoma independently of p53 mutational status

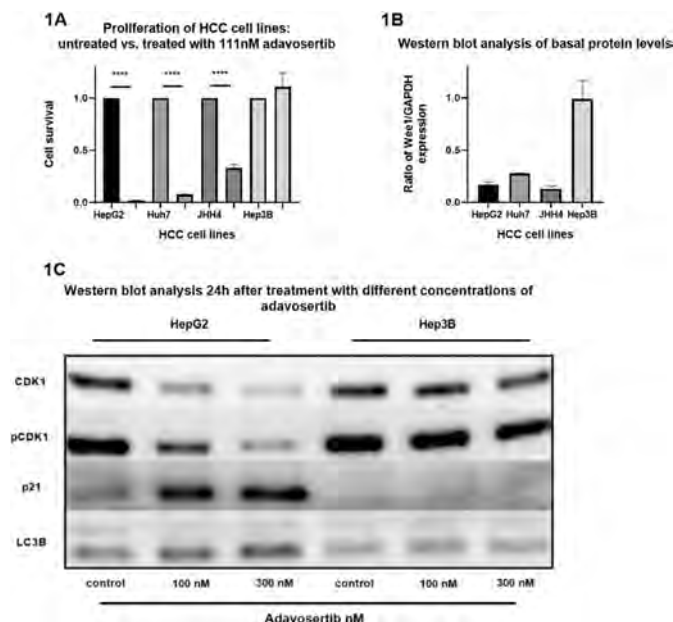
Julia Sophie Schneider¹, Liangtao Ye^{1,2}, Najib Ben Khaled¹, Heike Hermanns³, Claude Haan⁴, Andreas Geier³, Enrico de Toni¹, Florian P Reiter³. ¹University Hospital, LMU Munich, Department of Medicine II, Munich, Germany; ²The Seventh Affiliated Hospital, Sun Yat-sen University, Center for Digestive Diseases, Shenzhen, China; ³University Hospital Würzburg, Division of Hepatology, Department of Medicine II, Würzburg, Germany; ⁴Faculty of Science, Technology and

Medicine (FSTM), University of Luxembourg, Department of Life Sciences and Medicine (DLSM), Belvaux, Luxembourg
Email: schneider-jul@t-online.de

Background and aims: Hepatocellular carcinoma (HCC) is one of the leading causes of cancer-related death worldwide. In the majority of cases HCC is diagnosed in advanced stage when only palliative systemic treatment is feasible. The introduction of immune checkpoint inhibitors has greatly improved survival of HCC patients with advanced-stage HCC. However, the long-term survival characteristically observed in patients responsive to immunotherapy is observed in only a minor proportion of patients. Therefore, understanding tumor biology and establishing new effective and biomarker-guided targeted treatment options remains a priority. Wee1 is a central regulator of cell cycle and a target of several promising inhibitors currently being investigated in clinical trials, including adavosertib. Since Wee1 controls one checkpoint of DNA damage repair, it is postulated that tumors harboring p53 mutations are particularly susceptible to Wee1 inhibition and that mitotic catastrophe occurs in response to the simultaneous impairment of two crucial DNA repair checkpoints. Since p53 is frequently mutated in advanced HCCs, Wee1 inhibition could represent a potentially interesting therapeutic approach for treatment of HCC.

Method: Inhibition of Wee1 was investigated in p53 mutated (Huh7, JHH4, Hep3B) and p53 wildtype HCC cell lines (HepG2) by adavosertib and siRNA. Antitumoral efficacy was assessed by SYBR green assay, FACS analysis and colony formation assays. Western blot was used to assess the underlying mechanisms.

Results: Wee1 inhibition causes a pronounced loss of cell viability in several HCC cell lines (Figure 1A) independently of p53 status, as exemplified by the lack of sensitivity to Wee1 inhibition in Hep3B cells (harboring a loss-of-function p53 mutation). In contrast to resistant Hep3B, Wee1 inhibition mediated a remarkable increase of autophagy and of the G2/M phase cell fraction in sensitive HepG2 cells. Sensitivity to Wee1 inhibition was associated with lower basal Wee1 protein expression and was accompanied by the decrease of CDK1 and a correspondent increase of p21 expression (Figure 1B and 1C).



Conclusion: Wee1 inhibition induces antitumoral effects in HCC by induction of autophagy and impairment of cell cycle control. Further research should address the hypothesis that Wee1 mutational status and/or Wee1 protein expression may serve as biomarkers of response to Wee1 inhibition in systemic HCC treatment.

FRI597

Extracellular concentration of nicotinamid adenine dinucleotide modulates CD203a on TH17 cells and is associated with recurrence of hepatocellular carcinoma

Felix Krenzien¹, Julia Babigan¹, Alexander Arnold², Philipp Brunnbauer¹, Can Kamali¹, Karl Hillebrandt¹, Katrin Splith¹, Moritz Schmelzle¹, Johann Pratschke¹, Christian Benzing¹. ¹Campus Charité Mitte and Campus Virchow-Klinikum, Charité-Universitätsmedizin, corporate member of Freie Universität Berlin, Humboldt-Universität zu Berlin, and Berlin Institute of Health, Department of Surgery, Berlin, Germany; ²Charité-Universitätsmedizin, Corporate Member of Freie Universität Berlin, Humboldt-Universität zu Berlin, Institute of Pathology, Berlin, Germany
Email: felix.krenzien@charite.de

Background and aims: T helper 17 cells (Th17 cells) are a subtype of T helper cells that are involved in a number of pathological processes, one of them being the carcinogenesis of malignant tumors through the secretion of cytokines. Herein, we investigated the influence of extracellular nicotinamide adenine dinucleotide (eNAD⁺) on the ecto-nucleotide pyrophosphatase/phosphodiesterase 1 (CD203a, ENPP1 or PC-1) on Th17 cells with respect to the probability of HCC recurrence following liver resection.

Method: Heparinised blood plasma samples and liver specimen of 59 patients who underwent curative liver resection were compared with 10 control patients free of liver disease. The eNAD⁺ concentration of blood plasma was determined by a heat-based dichotomous pH extraction with a combined enzymatic cycling method, while fibrosis was histologically graded (Desmet score, F0–F4). Flow cytometry was used for cell analysis. Overall, an alpha value of $p < 0.05$ was applied.

Results: Plasma eNAD⁺ concentrations were significantly reduced with increasing liver fibrosis grade ($p < 0.05$). The expression of CD203a on CD4⁺, CCR4⁺, and CCR6⁺ T cells was found to correlate significantly with eNAD⁺ concentrations ($p < 0.05$). Patients with a postoperatively high proportion of CD203a expressing Th17 cells (CD4⁺, CCR6⁺, CCR4⁺) showed a 6-fold increased risk of HCC recurrence and a median recurrence-free survival of 233 days ($p < 0.05$), when compared to low expression CD203a Th17 cells (CCR6⁺, CCR4⁺). Similarly, patients with a postoperatively high proportion of CD203a expressing Th17 cells (CD4⁺, CCR6⁺) showed a 5-fold increased risk for recurrence and a median recurrence-free survival time of 334 days ($p < 0.05$), when compared to low CD203a expressing Th17 cells (CCR6⁺).

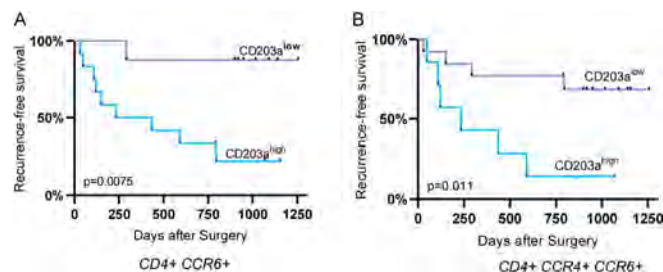


Figure: Frequency of recurrences after liver resection in patients with hepatocellular carcinoma. Patients with a postoperatively high proportion of CD203a expressing Th17 cells (CD4⁺, CCR6⁺, CCR4⁺) showed a 6-fold increased risk of HCC recurrence and a median recurrence-free survival of 233 days ($p < 0.05$), when compared to low expression CD203a Th17 cells (CCR6⁺, CCR4⁺).

Conclusion: Our data show that eNAD⁺ decreases in patients with liver fibrosis/cirrhosis and also correlates with the expression of the ectoenzyme CD203a on Th17 cells. Moreover, the probability of recurrence was significantly increased in patients with high expression of CD203a on Th17 cells, suggesting their potential as valuable prognostic markers and, furthermore, future therapeutic targets.

FRI598

Characterizing and targeting CD44v6+ cells in liver carcinoma

Akshaya Srikanth¹, Klaus Dembowski², Reinhold Schirmbeck¹, André Lechel¹. ¹Ulm University Hospital, Internal Medicine I, Ulm, Germany; ²Amcure GmbH, Stutensee, Germany
Email: akshaya-1.srikanth@uni-ulm.de

Background and aims: Liver carcinoma is one of the leading causes of cancer related deaths worldwide. The hyaluronic acid receptor variant CD44v6 is a marker for tumour stem cells, and has been shown to impact tumour formation and metastasis in several cancers including colorectal cancer and pancreatic cancer. The expression of CD44v6 dramatically increases in liver epithelial cells upon carcinogen exposure. With this study, we aim to target CD44v6 in primary human liver cancer cell lines by using an inhibitor, AMC303, and observe the effects of CD44v6 inhibition on proliferation, migration, invasion and EMT.

Method: CD44v6 expression was investigated in mouse and human liver and tumour tissue by immunohistochemistry. In addition, we used human HCC cell lines (Hep3B and PLC/PRF/5) and human CC cell lines (TFK1 and SZ1) to study the role of CD44v6 inhibition on cell proliferation, migration, invasion and EMT.

Results: Chronic liver damage resulted in the induction of CD44v6 positive epithelial cells in transgenic mouse models with chronic inflammation. The expression patterns of CD44v6+ cells were different in different mouse models of chronic liver damage. We observed clusters of hepatocyte-like cells with CD44v6 expression in a Hepatitis B mouse model and a CCl₄-treated liver fibrosis mouse model, which are characterized by the presence of diffuse inflammation. Interestingly, CD44v6 positive epithelial cells in Hepatitis C Virus- and IKK2/NF- κ B activated- mouse models were located within ectopic lymphoid aggregates and resulted in increased formation of ICC. The number of CD44v6 positive cells was increased upon deletion of Trp53. CD44v6 expression was also upregulated in murine tumours compared to the liver, and coincided with Sox9 expression in the tumours, indicating that CD44v6+ cells were undifferentiated cells. CD44v6 expression was also upregulated in human HCC samples compared to normal adjacent tissue and cirrhotic livers.

Human liver carcinoma cell lines were analysed for CD44 expression and the CC cell lines were found to have a high expression of CD44 with 85–90% of cells positive for CD44 expression. Functional assays (wound healing assay and transwell migration assay) were performed using the CC cell lines. Treatment with the CD44v6 inhibitor AMC303 conferred a reduction in the migration potential of cells in CC cell lines, indicating that CD44v6 is crucial in regulating the migratory capacity of liver tumour cells.

Conclusion: Inhibition of CD44v6 in liver carcinoma cell lines led to a reduction in chemotaxis and migration. In conclusion, CD44v6 appears to be a promising targetable candidate in liver cancer.

FRI599

Coordinating expression of tumorsuppressive microRNAs in hepatocellular carcinoma-a new role for p63 and p73 and their interaction with therapeutic agents

Lisa Kaser¹, Emily Ungermann¹, Claudia Kunst¹, Karsten Guelow¹, Martina Mueller-Schilling¹. ¹University Hospital Regensburg, Internal Medicine I, Regensburg, Germany
Email: claudia.kunst@ukr.de

Background and aims: Hepatocellular carcinoma (HCC) is the most common type of liver cancer. Tumor suppressors such as the p53 family are supposed to prevent carcinogenesis. p53 is the best characterized family member and one of the most frequently mutated genes in tumors. Besides p53, p63 and p73 play an essential role in cellular stress response. Depending on their splice variant-with transactivation domain (TA) or dominant negative (DN), p53 proteins transcriptionally control specific target genes directly via promoter-binding or indirectly, e.g. via regulation of microRNAs (miRs). miRs are small, non-coding RNA molecules with a length of

POSTER PRESENTATIONS

~22 nucleotides. They play an important role in gene regulation and can exert tumor suppressive or oncogenic functions. p53 is known to regulate miRs in a range of cancer entities, but little is known about p63- and p73-dependent control of miRs in HCC. Aim of this study was to evaluate regulation of tumorsuppressive miRs by TAp63 and TA/DNp73 in HCC alone or in combination with HCC-relevant therapeutics.

Method: Hep3B cells were transduced with adenoviral vectors rAd-TAp63, -TAp73, -DNp73 or -GFP to induce expression of the respective p53 family member. (Non-)transduced cells were stimulated with different HCC therapeutics (Doxorubicin, Bleomycin, Regorafenib, Sorafenib, Tivantinib) for up to 72 hours. Expression profiles of tumorsuppressive miRs miR-34a, -145, -149, -192 and -194 were analyzed by RT-qPCR.

Results: Tivantinib induced an increase of all miRs analyzed in non-transduced Hep3B cells, with most effective induction of miR-34a and miR-145 (3.6×/7.4×), while other drugs had no effect. TAp63 transduction moderately increased miR-34a, -149, -192, and -194. TAp73 time-dependently induced miR-34a, -145 and -149, but had no effect on miR-192 and -194. Noteworthy, DNp73 did not induce any of the miRs, underlining the divergent functions of TA and DN isoforms. HCC therapeutics led to a moderate increase of all analyzed miRs in TAp63-transduced cells. In contrast, Tivantinib treatment highly increased (up to 15×) miR-34a, -145 and -149 in TAp73-transduced cells, whereas all other drugs resulted in induction rates of 4–8×. Importantly, in TAp73-transduced cells this reinforcing effect of Tivantinib also displayed a dose-dependency.

Conclusion: TAp63 and TAp73 regulate expression profiles of tumorsuppressive miRs and interact with HCC-relevant therapeutics to control miR expression profiles in HCC. In concordance with our previous data, DNp73 displayed divergent effects regarding miR regulation. Thus, specific combinations of p53 family members and HCC therapeutics—especially TAp73 and Tivantinib—have the capacity to reinforce tumorsuppressive miR expression. These findings provide novel knowledge to the complex network of p53 family-mediated tumor suppression and suggest novel therapeutic scope for the clinical management of HCC.

FR1600

Trusting your gut—a new direction in multikinase inhibitors therapy in hepatocellular carcinoma

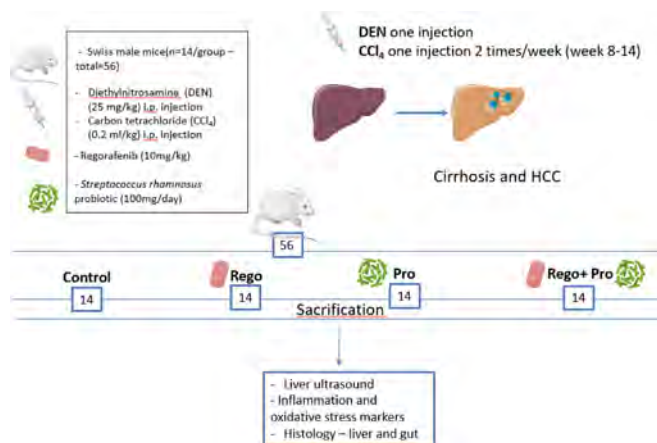
Iuliana Nenu¹, Diana Tudor², Horia Stefanescu¹, Bogdan Procopet¹, Zeno Sparchez¹, Gabriela Adriana Filip². ¹Regional Institute for Gastroenterology and Hepatology “Prof. Dr. O. Fodor”, Hepatology, Cluj-Napoca, Romania; ²Iuliu Hatieganu University of Medicine and Pharmacy, Physiology, Cluj-Napoca, Romania
Email: iuliana.nenu@gmail.com

Background and aims: Hepatocellular carcinoma (HCC) has become a worldwide burden and its incidence is rising. The intestinal microbiota is responsible for inducing resistance to antitumoral drugs. The present study investigated the effects of the combined treatment of Regorafenib (Rego) and probiotic *Streptococcus rhamnosus* (Pro) on HCC bearing mice.

Method: We have induced cirrhosis and hepatocellular carcinoma on two-week Swiss male mice using diethylnitrosamine (DEN- 1 mg/kg) one intraperitoneal injection following carbon tetrachloride (CCl₄-

0.2 ml/kg) intraperitoneal administration two times per week for six weeks (between weeks 8 and 14). Abdominal ultrasound was performed to validate the presence of cirrhosis and liver tumors. Afterward, the mice were divided into four groups: in the first group (control group), the mice were treated with vehicle, the second group received Regorafenib (Rego) (10 mg/kg one time per day for one week), in the third group probiotic (100 mg/day for one week) was administered, and the last group received the combination of Rego and Pro. After the last treatment, liver and intestine fragments were taken for biochemical and histopathological analysis. Liver tumour and intestinal inflammation quantified by ELISA and western blot, oxidative stress and apoptosis markers, histopathological necrosis rate were assessed.

Results: IL-6 and IL-1 levels from both liver and intestine fragments decreased in the groups treated with probiotic compared to control but statistically insignificant ($p > 0.05$). Similarly, malondialdehyde levels dropped when Pro was added to Rego ($p < 0.05$). Tumor necrosis factor-alpha (TNF- α) and TLR-4 have a decreased levels in the combined regimen ($p < 0.05$) and in the Rego group ($p < 0.05$) when compared to the control group and correlate with the histological findings. Likewise, nuclear factor- κ B (NF- κ B) and IKK α expression decreased in the combined regimen. Intestinal inflammation assessed by determination of lipopolysaccharide (LPS) is reduced in the groups where probiotic was administered compared to the control and Rego group ($p < 0.05$). In addition, inducible nitric oxide synthase (iNOS) expression evaluated in intestine homogenate diminished in Rego and Rego associated with the probiotic groups ($p < 0.05$).



Conclusion: The association of *Streptococcus rhamnosus* probiotic with Regorafenib treatment improves the antitumoral activity of the multikinase inhibitor in animals with experimental HCC. Tumoral resistance and systemic adverse effects might be diminished when systemic and intestinal inflammation is lowered. Our results confirmed that the association of Regorafenib with probiotic proves a novel and promising approach. Manipulating and trusting your gut has never been so facile than in the present day for the oncology field.

Saturday 25 June

NAFLD: Experimental and pathophysiology

SAT001

The DNA damage response is involved in the metabolic dysregulation of MAFLD patients via inefficient fatty acid oxidation

Beatriz Gómez Santos¹, Idoia Fernández-Puertas¹, Ane Nieva-Zuluaga¹, Mikel Ruiz de Gauna¹, Maider Apodaka-Biguri¹, Francisco González-Romero¹, Diego Saenz de Urturi¹, Igotz Delgado¹, Igor Aurrekoetxea^{1,2}, Lorena Mosteiro González², Gaizka Errazti Olarteoetxea², Sonia Gaztambide², Luis A Castaño González², Luis Bujanda³, Jesus Maria Banales³, Ana Zubiaga⁴, Xabier Buque¹, Patricia Aspichueta^{1,2}. ¹Faculty of Medicine and Nursing, University of the Basque Country UPV/EHU, Department of Physiology, Leioa, Spain; ²Biocruces Bizkaia Health Research Institute, Barakaldo, Spain; ³Biodonostia Health Research Institute-Donostia University Hospital, University of the Basque Country (UPV/EHU), Department of Liver and Gastrointestinal Diseases, San Sebastián, Spain; ⁴Faculty of Science and Technology, University of Basque Country UPV/EHU, Department of Genetics, Physical Anthropology and Animal Physiology, Leioa, Spain
Email: patricia.aspichueta@ehu.eus

Background and aims: A feature of the metabolic associated fatty liver disease (MAFLD) is the imbalance between processes that regulate lipid input and output. A chronic lipid-rich environment alters the oxidative capacity of the mitochondria generating species involved in the DNA damage response (DDR). The DDR is linked to MAFLD and to E2F transcription factors; however, the effect that the DDR plays in the altered lipid metabolism of MAFLD and the E2F involvement are still unknown. Aims: 1) Evaluate if DDR could be involved in the metabolic dysregulation of MAFLD identifying the involvement of E2F1 and E2F2; 2) Elucidate if the metabolic dysregulation induced by the lipid-rich environment is exacerbated by the DDR.

Method: An obese patient cohort with liver biopsies was used. The activity of mitochondrial complexes, pH2AX (marker of DNA damage) liver levels and liver and serum lipidome were analyzed. A cohort of C57/BL6 mice of different ages was also used. *E2f1* (*E2f1*^{-/-}) and *E2f2* (*E2f2*^{-/-}) knockout mice and their controls, injected with diethylnitrosamine (DEN), were fed a high-fat diet (HFD-DEN) for 10 weeks to induce progressive MAFLD. *In-vitro*, mouse primary hepatocytes were used.

Results: Liver pH2AX levels, increased in obese non-alcoholic steatohepatitis patients (NASH), correlated positively with metabolic features of worse prognosis. Mitochondrial activities were higher in NASH, mainly in those with increased DDR, in which liver triglycerides and diglycerides (DG) were higher; however, serum ketone bodies, an indirect marker of fatty acid oxidation (FAO), remained unchanged when compared with no-NASH patients, suggesting that the increased mitochondrial activity was not linked

to increased FAO. In the mouse cohort, pH2AX levels also correlated with insulin resistance and liver DG content. Interestingly, *E2f1*^{-/-} and *E2f2*^{-/-} mice, protected from steatosis due to an efficient FAO activation, showed decreased pH2AX when treated with HFD-DEN. When hepatocytes were treated with the DDR inducers UV or H₂O₂, they were not able to catabolize the increased intracellular lipid levels when facing a lipid-rich environment. Finally, treatment with fatty acids alone was enough to activate DDR in hepatocytes.

Conclusion: DDR activation triggers metabolic changes related with mitochondrial dysfunction and facilitates lipid accumulation, both linked to disease progression. The results suggest that E2F1 and E2F2 might be intermediates promoting the DDR induced metabolic dysregulation.

SAT002

Hepatic miR-144 drives fumarate activity preventing NRF2 activation during obesity

Valerio Azzimato¹, Ping Chen¹, Emelie Barreby¹, Cecilia Morgantini², Laura Levi¹, Ana Vankova¹, Jennifer Jager³, André Sulen¹, Marina Diotallevi⁴, Joanne X. Shen⁵, Ewa Ellis⁶, Mikael Ryden⁷, Erik Naslund⁸, Anders Thorell⁸, Volker Lauschke⁹, Keith M. Channon⁴, Mark J. Crabtree⁴, Arvand Haschemi¹⁰, Siobhan M. Craige¹¹, Mattia Mori¹², Francesco Spallotta¹³, Myriam Aouadi¹. ¹Center for Infectious Medicine, Medicine, Huddinge, Sweden; ²Karolinska Institutet, Medicine, Huddinge, Sweden; ³Université Côte d'Azur, Inserm, Centre Méditerranéen de Médecine Moléculaire (C3M), Team « Cellular and Molecular Pathophysiology of Obesity and Diabetes », Nice, France; ⁴John Radcliffe Hospital, University of Oxford, Medicine, Oxford, United Kingdom; ⁵Karolinska Institutet, Department of Physiology and Pharmacology, Stockholm, Sweden; ⁶Karolinska Institutet, Department of Clinical Science, Huddinge, Sweden; ⁷Karolinska Institute, Medicine, Huddinge, Sweden; ⁸Karolinska Institutet, Department of Clinical Sciences, Danderyd Hospital, Stockholm, Sweden; ⁹Karolinska Institutet, Department of Physiology and Pharmacology, Stockholm, Sweden; ¹⁰University of Wien, Department of Laboratory Medicine, Austria; ¹¹Virginia Tech, Human Nutrition, Food, and Exercise Department, United States; ¹²University of Siena, Department of Biotechnology, Chemistry, and Pharmacy, Italy; ¹³National Research Council (IASI-CNR), Institute for Systems Analysis and Computer Science "A. Ruberti," Italy
Email: myriam.aouadi@ki.se

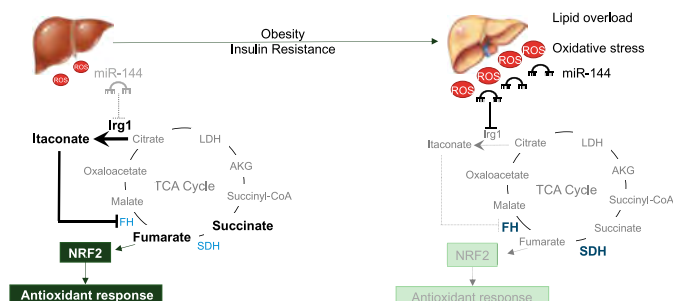
Background and aims: Oxidative stress is central in the development of obesity-associated metabolic complications, including insulin resistance and non-alcoholic fatty liver disease. We recently discovered that microRNA miR-144 regulates the master mediator of the antioxidant response, NRF2. Upon miR-144 silencing, NRF2 target genes were significantly upregulated, suggesting that miR-144 controls NRF2 protein expression and activity. Here we explored a mechanism whereby upon obesity miR-144 inhibited NRF2 activity regulating a tricarboxylic acid (TCA) metabolite, fumarate.

Method: Transcriptomic analysis in liver macrophages (LMs) of obese mice identified the immuno-responsive gene 1 (*Irg1*) as a target of miR-144. IRG1 catalyzes the production of a TCA derivative, itaconate, which inhibits succinate dehydrogenase (SDH). TCA enzyme activities and kinetics were analyzed after miR-144 silencing in obese mice and human liver organoids using single cell activity assays *in situ* and molecular dynamic simulations.



POSTER PRESENTATIONS

Results: miR-144 upregulation in obesity was associated with reduced expression of *Irg1*, which was restored upon miR-144 silencing *in vitro* and *in vivo*. Furthermore, miR-144 overexpression reduces *Irg1* expression and the production of itaconate *in vitro*. In alignment with the reduction in *IRG1* and itaconate levels, SDH activity was upregulated during obesity. Surprisingly, also fumarate hydratase (FH) activity was upregulated in obese livers, leading to fumarate depletion. miR-144 silencing selectively reduced the activities of both SDH and FH resulting in the accumulation of their related substrates succinate and fumarate. Moreover, molecular dynamics analyses revealed the potential role of itaconate as a competitive inhibitor of not only SDH but also FH. Combined, these results demonstrate that miR-144 inhibits the activity of NRF2 through decreased fumarate production in obesity.



Conclusion: miR-144 triggers hyperactivation of FH in the TCA cycle and consumption of its substrate fumarate, eventually inhibiting NRF2 activity. Therefore, herein we unraveled miR-144 immunometabolic role in obesity in the regulation of endogenous antioxidant response.

SAT003

TNFR1 inhibition reduces lipogenesis and improves insulin resistance and fibrosis in NAFLD

Katharina John¹, Stephanie Liebig¹, Silke Marhenke¹, Heiner Wedemeyer¹, Heike Bantel¹. ¹Hannover Medical School, Department of Gastroenterology, Hepatology and Endocrinology, Hannover, Germany
Email: bantel.heike@mh-hannover.de

Background and aims: Non-alcoholic fatty liver disease (NAFLD) shows an increasing prevalence and can result in the development of liver fibrosis/cirrhosis with associated complications. The molecular mechanisms of NAFLD progression remain largely unknown. TNF α has been implicated as an important mediator of NAFLD progression. TNF-mediated liver injury mainly occurs via TNFR1. We therefore investigated the role of TNFR1 signaling for liver steatosis, insulin resistance and fibrosis in NAFLD mice.

Method: HuTNFR1-k/i mice were fed with a high-fat, carbohydrate-rich diet for 32 and treated with anti-TNFR1 or control antibody for 8 weeks. Liver tissues were analysed for lipogenesis, MAP kinase pathway, insulin signaling as well as for NAFLD activity and fibrosis.

Results: Compared to control treatment, TNFR1 inhibition reduced the expression and activation of the transcription-factor SREBP1 and downstream target genes of lipogenesis, which was associated with reduced liver steatosis. NAFLD mice treated with TNFR1 antibody showed also reduced activation of the MAP kinase MKK7 and its target JNK which resulted in decreased insulin receptor substrate (IRS)-1 activation, thus restoring insulin sensitivity. Since SREBP1 transcriptionally repress IRS-2, which contributes to insulin resistance, we additionally analysed IRS-2 expression. We found enhanced IRS-2 mRNA expression in liver tissues from anti-TNFR1 compared to control antibody treated mice. Moreover, TNFR1 inhibition significantly decreased NAFLD activity, liver injury and fibrosis compared to control treatment of NAFLD mice.

Conclusion: The results implicate an important role of TNFR1 signaling for development of steatosis, insulin resistance and fibrotic liver injury in NAFLD. TNFR1 inhibition might therefore represent a promising therapy for fibrotic NASH.

SAT004

Obesity alters the partitioning of glycerol metabolism pathways in NAFLD

Jack Carruthers¹, Patricia Nunes¹, Paul Driscoll², Jim Ellis², James Macrae², Massimo Pinzani³, Dimitrios Anastasiou¹. ¹Francis Crick Institute, Cancer Metabolism Laboratory, London, United Kingdom; ²Francis Crick Institute, Metabolomics Science Technology Platform, London, United Kingdom; ³University College London, Institute of Immunity and Transplantation, United Kingdom
Email: jack.carruthers@crick.ac.uk

Background and aims: Circulating glycerol can originate from the diet and adipose tissue lipolysis, amongst other sources. Glycerol is metabolised by the liver and kidney, both of which express glycerol kinase, an enzyme that phosphorylates glycerol to produce glycerol 3-phosphate. Glycerol is a substrate for gluconeogenesis (GNG) and glycolysis, and can form the backbone of lipids such as triglycerides (TAG). It has been shown that glycerol supports augmented glucose production in type 2 diabetes and provides carbons for circulating TAGs in patients with non-alcoholic fatty liver disease (NAFLD). It is still unclear how glycerol metabolism is partitioned into downstream pathways as these pathological conditions develop. In this study we investigated how risk factors for NAFLD, such as age and obesity, affect the use of glycerol in hepatic glucose and lipid synthetic pathways whilst promoting NAFLD.

Method: C57BL/6J mice were fed either normal chow (NC) or a Western diet (WD) for 12, 25 or 50 weeks. Visceral adiposity and hepatic TAG content were evaluated by magnetic resonance imaging (MRI) and magnetic resonance spectroscopy (MRS). Hepatic insulin signalling was assessed by Western blotting. To measure the capacity of these animals to convert exogenous glycerol into glucose, glycerol tolerance tests were used. To understand whole-body and hepatic glycerol metabolism, mice were infused with ¹³C-glycerol and ¹³C-glucose tracers followed by metabolic analysis using gas chromatography-mass spectrometry (GC-MS) and nuclear magnetic resonance (NMR). Mass-isotopomer distribution analysis was applied to estimate the contribution of glycerol to GNG and TAG esterification.

Results: As expected, WD-fed mice had greater visceral adiposity and higher intrahepatic TAG content at all time points, consistent with the development of NAFLD. Whole-body glycerol turnover increased with age, particularly in WD-fed mice. After 50 weeks, WD-fed mice showed augmented glycaemia in response to a glycerol bolus compared to NC-fed animals. Also at 50 weeks, stable isotope tracing revealed that glycerol to glucose flux was higher in WD- than NC-fed mice. The flux of glycerol carbons into the TAG backbone was higher in WD- than NC-fed mice peaking after 25-weeks of diet. The proportionate contribution of glycerol to TAG was decreased in WD-fed animals. The transition of glycerol flux from TAG esterification to glucose production coincides with the development of changes in hepatic insulin signalling as judged by decreased PI3 K signaling.

Conclusion: Chronic exposure to a WD alters the partitioning of glycerol from TAG to glucose. This transition coincides with the onset of alterations in hepatic insulin signalling. These observations present the possibility that glycerol metabolism could be targeted to alter the pathogenesis of obesity-related NAFLD and insulin resistance.

SAT005

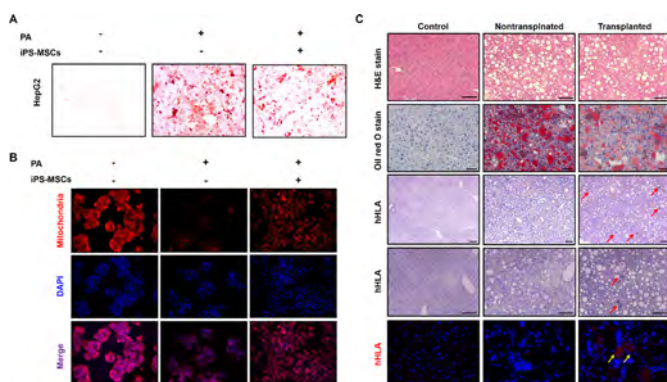
Human induced pluripotent stem cell-derived mesenchymal stem cells ameliorates mitochondrial oxidative dysfunction in non-alcoholic fatty liver disease

Min Kyung Park¹, Yun Bin Lee¹, Se-Mi Jung¹, Yoo-Wook Kwon², Jung-Hwan Yoon¹. ¹Seoul National University College of Medicine, Department of Internal Medicine and Liver Research Institute, Seoul, Korea, Rep. of South; ²Seoul National University Hospital, Biomedical Research Institute, Seoul, Korea, Rep. of South
Email: yblee@snu.ac.kr

Background and aims: Non-alcoholic fatty liver disease (NAFLD) is one of the most common chronic liver diseases worldwide, but its pathophysiology is not fully understood due to the complexity of the mechanisms involved in the disease. Moreover, pharmacological therapy for NAFLD is not yet available. We investigated therapeutic potential of induced pluripotent stem cell-derived mesenchymal stem cells (iPS-MSCs) on hepatic steatosis and mitochondrial oxidative function.

Method: HepG2 cells were treated with palmitic acid (PA) and then co-cultured with iPS-MSCs. Intracellular lipid accumulation was measured by oil red O staining. The mitochondrial oxidative function was assessed by quantifying mitochondrial mass and measuring reactive oxygen species (ROS) and activity of antioxidant enzymes. C57BL/6 mice were chronically fed with choline-deficient, L-amino acid-defined, high-fat diet (CDAHFD). At week 20, mice were injected with either phosphate-buffered saline (nontransplanted) or iPS-MSCs (transplanted; 1×10^6 cells). Four weeks later, liver histology and function were assessed.

Results: PA-induced intracellular lipid accumulation was attenuated when co-cultured with iPS-MSCs (Figure 1A). The functional mitochondrial mass was reduced by PA treatment and then was restored following co-culture with iPS-MSCs (Figure 1B). Increased cellular ROS production by PA treatment was attenuated after co-culture with iPS-MSCs. The activity of superoxide dismutases (SODs) and the ratio of reduced/oxidized glutathione were decreased by PA treatment and were restored by co-culture with iPS-MSCs. After infusion of iPS-MSCs, a successful engraftment of transplanted stem cell was confirmed, leading to amelioration of severe hepatic steatosis in CDAHFD-fed mice (Figure 1C). Decreased mitochondrial DNA content in CDAHFD-fed mice was reinstated to near-control level after transplantation of iPS-MSCs. Augmented hepatic ROS accumulation caused by CDAHFD was attenuated after transplantation of iPS-MSCs with dynamic changes in the activity of SODs and the ratio of glutathione.



Conclusion: Hepatic steatosis and mitochondrial oxidative dysfunction in NAFLD can be ameliorated by transplantation of iPS-MSCs. Our study findings suggest the therapeutic potential of iPS-MSCs in NAFLD and help understanding alterations in hepatic lipid metabolism, which may be restored by iPS-MSCs transplantation.

SAT006

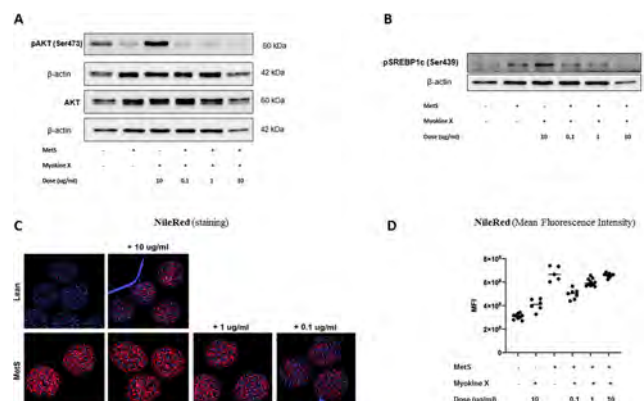
Skeletal muscle-derived myokine affects insulin sensitivity and lipogenesis in a human hepatocyte spheroid model

Jean-Baptiste Potier¹, Achilleas Fardellas², Aurore Dumond¹, Myriam Aouadi², Karim Bouzakri¹. ¹Centre européen d'étude du Diabète, Université de Strasbourg, Strasbourg, France; ²Karolinska Institutet, Centre for Infectious Medicine, Department of Medicine, Huddinge, Sweden
Email: j.potier@ceed-diabete.org

Background and aims: Inter-organ crosstalk has recently emerged as a crucial aspect of body homeostasis, especially in metabolic diseases such as type 2 diabetes (T2D) and NAFLD. Skeletal muscle is highly implied in this crosstalk, through the secretion of specific cytokines called myokines. Among those, our laboratory has focused on the myokine X (MyoX). Due to our previous results on the prevention of diabetes and to the pathophysiological link between this disease and NAFLD, we chose to investigate the effect of the MyoX on the liver. Primary human hepatocytes (PHH) spheroids, the gold standard model for the *in-vitro* study of liver diseases, were used for our experiments.

Method: PHH spheroids were cultured in lean and metabolic syndrome (MetS) conditions treated, or not, with different concentrations of MyoX: 0.1, 1 and 10 $\mu\text{g/ml}$. Spheroids were then stimulated with insulin and protein lysates were collected. Effects of MyoX on the expression of proteins related to glucose (Akt, ERK1/2, GLUT2) and lipid (SREBP1c, FAS, CPT1A) metabolism, two pathways implied in NAFLD development, were assayed by western blot. Furthermore, Nile Red staining was performed for the measurement of triglyceride accumulation.

Results: Concerning glucose metabolism, noticeable effects were observed for the phosphorylation of Akt, which was stronger at a dose of 10 $\mu\text{g/ml}$ in lean condition, suggesting that the MyoX might enhance the intensity of the insulin downstream. Likewise, in the same condition, the slight increase in triglyceride accumulation, observed with the Nile Red staining, could be explained by an insulin-dependent *de novo* lipogenesis mechanism confirmed by the increase of SREBP1c phosphorylation (an insulin-dependent transcription factor responsible for the storage of fatty acid as triglycerides). Concerning MetS conditions, beneficial effects were observed at the lower dose of MyoX, with a decrease in triglyceride amount related to the reduction of SREBP1c phosphorylation, associated with no detrimental effect on p-Akt.



Conclusion: Taken together, our analysis suggest that high doses of MyoX might act as a sensitizer and exacerbates the effects of insulin in PHH in lean condition, enhancing the *de novo* lipogenesis. In MetS condition, potential beneficial effects were noticed for the lower dose of MyoX, suggesting that our protein might be of an interest for the prevention of NAFLD. Further studies should be performed to determine the optimal dose of the myokine.

SAT007

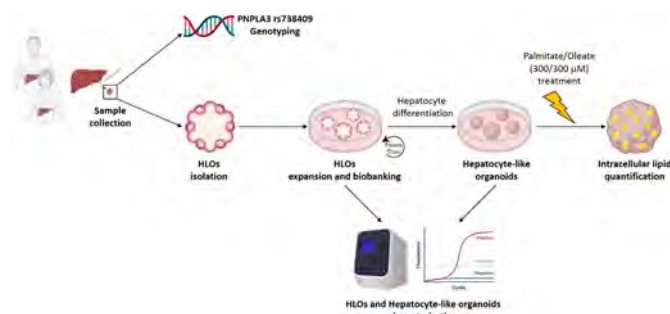
Patient-derived liver organoids to reveal PNPLA3 I148M role in Non-Alcoholic Fatty Liver Disease

Elia Casirati¹, Alessandro Cherubini², Melissa Tomasi², Ilaria Marini², Daniele Prati², Daniele Dondossola³, Luca Valenti^{1,2}. ¹Università degli Studi di Milano, Department of Pathophysiology and Transplantation, Italy; ²Fondazione IRCCS Ca' Granda Ospedale Maggiore Policlinico, Transfusion Medicine and Hematology, Milano, Italy; ³Fondazione IRCCS Ca' Granda Ospedale Maggiore Policlinico, General and Liver Transplant Surgery Unit, Milan, Italy
Email: e.casirati@gmail.com

Background and aims: Non-alcoholic fatty liver disease (NAFLD) heritability is estimated to be within 25–75% and PNPLA3 rs738409 C > G, encoding for the p.I148M protein variant, accounts for a large fraction of disease susceptibility. The p.I148M variant promotes intrahepatic lipid accumulation and progression to advanced fibrosis and hepatocellular carcinoma. A comprehensive human model to study the role and mechanisms of genetic variability in liver disease is still lacking. Aim of this study was therefore to generate patient-derived human liver organoids (HLOs) to clarify the impact and role of PNPLA3 variation in NAFLD onset and progression.

Method: We isolated HLOs from 14 surgical resection specimens. PNPLA3 rs738409 was genotyped by 5' nuclease Taqman assays. Single cells were embedded in Matrigel and a complete organoid medium to instruct signaling cues crucial for the growth of liver epithelial cells. To model fatty liver, HLOs were differentiated toward a hepatocyte-like phenotype (modified from Broutier L, Nat Protoc 2016) and exposed to free fatty acids (FFAs, 300/300 uM palmitic/oleic acid) for 5 days.

Results: We successfully isolated, grew for >150 days and biobanked organoids with different PNPLA3 p.I148M genotypes (7, 1% were GG, 42, 8% were CG, 50, 1% were CC). HLOs showed a monolayer epithelial phenotype with a well-defined apical-basal polarity surrounding a central hollow lumen, and a cholangiocyte-like phenotype expressing KRT19 and SOX9. Differentiated HLOs showed high levels of hepatocyte markers mRNA (albumin, CYP2D6 and ApoA1, Fold Increase 85.8, p=0, 0307; 1.27, p=ns and 324.8, p=0, 0035 respectively; n=5), while the epithelial staminal marker LGR5 was suppressed. The persistent expression of KRT19 suggests the presence of both hepatocellular and cholangiocyte populations, both involved in fibrogenesis. HLOs showed a high expression of PNPLA3 after isolation, which was maintained after hepatocyte differentiation (0.41±0.1 fold compared to liver tissue). When exposed to FFAs, differentiated organoids showed an accumulation of lipid droplets, as examined by Oil Red O (ORO) staining (2.3 fold increase in organoid exposed vs. non-exposed).



Conclusion: We isolated, characterized and biobanked HLOs from 14 patients with different PNPLA3 genotypes, obtaining a 3D in vitro model to investigate NAFLD within a personalized medicine framework with high translational potential.

SAT008

Transcriptomic analysis confirms that PNPLA3 I148M variant is associated with impaired mitochondrial function and antioxidant response in 3D cultured human hepatic stellate cells and liver tissue of patients with NAFLD

Elisabetta Caon¹, Maria Martins¹, Kessarin Thanapirom¹, Ana Levi¹, Walid Al-Akkad¹, Jerjes Abu-Hanna², Pernille Juhl³, Ida Villesen³, Diana Leeming³, Guido Alessandro Baselli⁴, Jan-Willem Taanman⁵, Michele Vacca⁶, Luca Valenti⁴, Stefano Romeo⁷, Giuseppe Mazza¹, Massimo Pinzani¹, Krista Rombouts¹. ¹University College of London, Royal Free Campus, Division of Medicine, Institute for Liver and Digestive Health, London, United Kingdom; ²University College of London, Royal Free Campus, Research Department of Surgical Biotechnology, Division of Surgery and Interventional Science, LONDON, United Kingdom; ³Nordic Bioscience, Biomarkers and Research A/S, Herlev, Denmark; ⁴Università degli Studi di Milano, Fondazione IRCCS Ca' Granda Ospedale Maggiore Policlinico, Dipartimento di Pathophysiology and Transplantation, Milan, Italy; ⁵University College of London, Queen Square Institute of Neurology, Department of Clinical and Movement Neurosciences, London, United Kingdom; ⁶University of Bari "Aldo Moro", Clinica Medica "Frugoni", Interdisciplinary Department of Medicine, Bari, Italy; ⁷University of Gothenburg, Institute of Medicine, Sahlgrenska Academy, Willenberg Laboratory, Department of Molecular and Clinical Medicine, Gothenburg, Sweden
Email: e.caon@ucl.ac.uk

Background and aims: We established that the I148M variant of the patatin-like phospholipase domain-containing 3 (PNPLA3) protein, a key risk locus for fibrogenic progression of chronic liver disease, is associated with mitochondrial dysfunction and defective antioxidant response. The antifibrotic Nuclear Receptor 4A1 (NR4A1) is a key element in mitochondrial metabolism and antioxidant response. By employing transcriptomic analysis we investigated the impact of PNPLA3 I148M mutation on mitochondrial dysfunction, antioxidant response and NR4A1 expression in human hepatic stellate cells (hHSCs) and in an established cohort of patients with NAFLD. 3D culture models were employed to further validate the results.

Method: RNAseq was performed on primary hHSC genotyped for PNPLA3 (I148M) variants CG/GG and cultured on plastic. Biopsies from livers of 125 obese individuals classified as normal liver/simple steatosis/severe NAFLD were genotyped for PNPLA3 (I148M) variants CG/GG and RNAseq was performed. Cell behaviour of hHSCs CC/CG for PNPLA3 variants was evaluated in 3D decellularized scaffolds from human healthy and cirrhotic liver with/without TGFβ1 treatment. QRT-PCR, Western blot, NanoString, PRO-C1/PRO-C3 quantification and cytochrome-c-oxidase activity (COX) assay was performed.

Results: Transcriptomic analysis on liver biopsies genotyped PNPLA3 CC/CG, where the PNPLA3 variant had previously been identified as major driver of NAFLD disease severity and gene expression variability, were compared with transcriptomic data of 2D cultured primary hHSCs PNPLA3 CC/CG genotyped. The comparison highlighted shared dysregulated pathways related to mitochondrial function, antioxidant response and ECM remodelling, the activated upstream regulator TGFβ1 and the target gene NR4A1. Analogous pathways were dysregulated in the analysis of a 700 gene panel in hHSCs CC/CG for PNPLA3 variants cultured in a 3D model of healthy and cirrhotic scaffolds. In particular, the "Oxidative stress" pathway was markedly upregulated by cirrhotic ECM compared to healthy ECM, and PRO-C1/PRO-C3 secretion was increased by TGFβ1. The 3D model was used for further analysis: COX activity and expression, ROS scavenger CYGB gene expression and NRF2-repressor KEAP1 protein were significantly downregulated in CG-PNPLA3 hHSCs compared to CC-PNPLA3 hHSCs and in cirrhotic scaffolds. NR4A1 gene and protein expression were downregulated in CG-PNPLA3 hHSCs vs CC-PNPLA3 hHSCs in healthy scaffolds and by TGFβ1 in cirrhotic scaffolds.

Conclusion: The PNPLA3 I148M variant in hHSCs is linked to disrupted mitochondrial function and antioxidant response. NR4A1, a TGFβ1-regulated antifibrotic gene involved in mitochondrial

metabolism, is downregulated in CG-PNPLA3 hHSCs. Importantly, these defects were maximized in a 3D model recapitulating the ECM microenvironment of cirrhotic human liver.

SAT009

HTD1801 (berberine ursodeoxycholate), a unique single molecule with multiple beneficial effects in metabolic and liver diseases

Meng Yu¹, Ru Bai¹, Xinxiang Fu¹, Zhaobin Chen¹, Weijian Liu¹, Leigh MacConell¹. ¹HighTide Therapeutics USA, LLC, United States
Email: lmacconell@hightidetx.com

Background and aims: A number of chronic liver diseases remain without adequate therapy and may require treatments with multiple mechanisms of action. Ursodeoxycholic acid (UDCA) has been shown to have beneficial effects in some liver diseases primarily through choleric and anti-inflammatory effects. Berberine (BBR) has a long history of use in traditional medicine, emerging as a novel therapeutic with metabolic, antimicrobial, and anti-inflammatory effects. HTD1801 is a new molecular entity consisting of a salt of UDCA and BBR (1:1 stoichiometry), offering the benefits of its parent compounds and novel effects derived from its unique molecular structure. It has been shown to be beneficial in human studies of hyperlipidemia, NASH and PSC.

Method: The physico-chemical properties of HTD1801, BBR and UDCA were compared via x-ray diffraction, Fourier transform infrared spectroscopy, melting point analysis, LogD evaluation, and solubility analysis using fasted and fed state simulated intestinal fluid (FaSSIF and FeSSIF). Efficacy was evaluated in a preclinical NASH model (golden hamsters fed a high fat diet, 8/group) after 6 weeks of daily treatment of HTD1801, UDCA, or BBR-chloride (BBR-Cl).

Results: The crystal form of HTD1801 is a hemi-nonahydrate with a honeycomb-like 3-D structure distinct from BBR-Cl and UDCA. HTD1801 has a lower melting point (~120 °C) compared to BBR-Cl (204–206 °C) and UDCA (200–205 °C). LogD profiles were substantially enhanced for HTD1801 across the pH range for BBR and at pH 6.5 for UDCA vs BBR-Cl or UDCA alone. Dissolution in FaSSIF showed peak concentrations of BBR and UDCA from HTD1801 of ~0.6–0.7 mg/ml in contrast to <0.2 mg/ml for BBR-Cl and UDCA alone. Dissolution in FeSSIF showed peak concentrations of BBR and UDCA from HTD1801 of ~0.3–0.35 mg/ml in contrast to <0.15 mg/ml for BBR-Cl and UDCA alone. Studies in the NASH hamster model showed that HTD1801 at 200 mg/kg for 6 weeks significantly reduced ALT, AST, bilirubin, LDL-c and triglycerides (Table 1). Furthermore, significant histologic improvements were observed in Fibrosis and the NAS with HTD1801. In contrast, UDCA or BBR alone generally resulted in minimal changes in biochemical or histological parameters.

Table 1: Biochemical and Histologic Changes in Hamster Model of NASH After 6 Weeks of Treatment

Group	ALT (U/L)	AST (U/L)	Total Bilirubin (μmol/L)	LDL-c (mmol/L)	Triglycerides (mmol/L)	Fibrosis Score	NAFLD Activity Score (NAS)
Normal Control Group	86.1 ± 15.4	66.0 ± 2.9	0.8 ± 0.1	1.4 ± 0.2	1.4 ± 0.2	0.1 ± 0.1	0.5 ± 0.3
Model Control Group	1334.7 ± 133.0 ^{###}	270.6 ± 25.3 ^{###}	3.2 ± 0.9 ^{###}	7.9 ± 1.0 ^{###}	3.6 ± 0.6 ^{###}	2.0 ± 0.2 ^{###}	7.1 ± 0.4 ^{###}
HTD1801 200 mg/kg	96.6 ± 17.5 ^{**}	66.4 ± 4.6 ^{**}	0.8 ± 0.1 ^{**}	1.3 ± 0.2 ^{**}	2.1 ± 0.4 ^{**}	1.1 ± 0.2 ^{**}	2.5 ± 0.7 ^{**}
UDCA 107.8 mg/kg	934.1 ± 151.3	264.5 ± 73.8	1.7 ± 0.6 [*]	3.8 ± 0.5 ^{**}	2.2 ± 0.2 ^{**}	1.8 ± 0.2	5.3 ± 0.8 [*]
BBR-Cl 102.2 mg/kg	995.5 ± 107.0	232.0 ± 26.0	2.2 ± 0.5	6.5 ± 1.1	3.7 ± 0.4	2.1 ± 0.1	6.3 ± 0.3

Data are Mean (SE).
[#]p<0.05, ^{###}p<0.01 vs the normal control group.
^{*}p<0.05, ^{**}p<0.01 vs the model control group.

Conclusion: These data show that HTD1801 has physico-chemical properties distinct from UDCA or BBR that provide improved dissolution and lipophilicity characteristics which may result in the beneficial effects seen in fibroinflammatory liver diseases.

SAT010

Metabolic, biochemical, histopathological and transcriptomic effects of long-acting FGF21 analogue in the GAN diet-induced obese and biopsy-confirmed mouse model of NASH

Malte H. Nielsen^{1,2}, Denise Oró¹, Henrik B. Hansen¹, Matthew Gillum², Michael Feigh¹. ¹Gubra, Hørsholm, Denmark; ²University of Copenhagen, CBMR, Kbh N, Denmark
Email: mni@gubra.dk

Background and aims: Fibroblast growth factor 21 (FGF21) plays a central role in energy, lipid and glucose metabolism and has been demonstrated to reduce hepatic steatosis, inflammation and fibrosis in rodent models of NASH. The long-acting FGF21 analogue efruxifermin has in a recent phase 2 clinical trial (BALANCED) demonstrated promising efficacy for both NASH resolution and improvement in fibrosis stage as compared to placebo controls (Harrison et al. Nature Medicine, 2021). The present study aimed to evaluate the metabolic, biochemical and histopathological effects of the long-acting FGF21 analogue PF-05231023 in the GAN (Gubra-Amylin NASH) diet-induced obese (DIO) mouse model of NASH with hepatic fibrosis.

Method: Male C57BL/6J mice were fed the GAN diet high in fat, fructose and cholesterol for 34 weeks prior to study start. Only animals with liver biopsy-confirmed NAFLD Activity Score (NAS) ≥5 and fibrosis (stage ≥F1) were included and stratified into treatment groups. DIO-NASH mice received (SC, BIW) vehicle (n = 14) or PF-05231023 (10 mg/kg, n = 14) for 12 weeks. Vehicle-dosed chow-fed C57BL/6J mice (n = 6) served as lean healthy controls. Pre-to-post liver biopsy histopathological scoring was performed for within-subject evaluation of NAS and Fibrosis Stage. Terminal quantitative liver histology, liver whole-transcriptome analysis, blood and liver biochemistry were assessed.

Results: The long-acting FGF21 analogue induced a body weight loss of approx. 8% from baseline and reduced hepatomegaly, plasma transaminases as well as plasma/liver lipids (total cholesterol, triglycerides) as compared to vehicle-treated animals. Notably, PF-05231023 treatment demonstrated ≥2 point significant improvement in NAS and 1-point significant improvement in Fibrosis Stage. Therapeutic effects of PF-05231023 were supported by reduced quantitative histological markers of steatosis (lipids, hepatocytes with lipid droplets) and inflammation (number of inflammatory foci, galectin-3). FGF21 did not improve histomorphometry markers of fibrosis (PSR, collagen 1a1), albeit a marker for activated stellate cells (α-SMA) was significantly reduced, suggesting attenuation of fibrogenesis activity. Finally, PF-05231023 improved NASH-associated transcriptome signatures, including lowered expression of hepatic genes associated with inflammation and fibrogenesis.

Conclusion: Long-acting FGF21 analogue PF-05231023 improved metabolic, biochemical and liver histological markers of steatosis, inflammation and fibrogenesis in biopsy-confirmed DIO-NASH mice. Consistent with clinical findings, PF-05231023 improved NAS and Fibrosis Stage. These findings further validate clinical translatability of the GAN DIO-NASH mouse model.

POSTER PRESENTATIONS

SAT011

NAFLD-induced encephalopathy is associated with low-grade brain tissue hypoxia and inflammation, as well as cerebrovascular, glial, metabolic and behavioural alterations

Anna Hadjihambi^{1,2,3}, Christos Konstantinou^{2,3}, Jan Klohs^{4,5}, Patrick Hosford⁶, Adrien Le Guennec⁷, I. Jane Cox^{2,3}, Rajiv Jalan⁸, Salvatore Lecca⁹, Chris Donnelly^{1,10}, Luc Pellerin^{1,11}. ¹UNIL, Department of Biomedical Sciences, Lausanne, Switzerland; ²Foundation For Liver Research, The Roger Williams Institute of Hepatology, London, United Kingdom; ³KCL, Faculty of Life Sciences and Medicine, United Kingdom; ⁴University of Zurich and ETH Zurich, Institute for Biomedical Engineering, Switzerland; ⁵University of Zurich and ETH Zurich, Neuroscience Centre Zurich, Switzerland; ⁶University College London, Neuroscience, Physiology and Pharmacology, United Kingdom; ⁷KCL, NMR Facility, United Kingdom; ⁸UCL, Institute for Liver and Digestive Health, United Kingdom; ⁹UNIL, The Department of Fundamental Neuroscience, Switzerland; ¹⁰UNIL, Institute of Sports Science, Switzerland; ¹¹Université et CHU de Poitiers, Inserm U1082, France
Email: ucbthad@ucl.ac.uk

Background and aims: Over the last decade, non-alcoholic fatty liver disease (NAFLD) has become increasingly known as a multisystem disease, with its clinical burden not only confined to liver-related morbidity and mortality. Indeed, the most common liver-related complication of NAFLD over a long period of follow-up is encephalopathy. To confirm this, using a mouse model of NAFLD, we investigated alterations in cerebral physiology, metabolism and behaviour.

Method: Behavioural tests were performed in mice (C57BL/6) following 16 weeks of control diet or high fat diet+high fructose/glucose in water (HFDHF/HG). Cerebral blood volume (CBV; indicator of vascular density), brain tissue oxygenation at baseline and in response to systemic hypercapnia (10% CO₂) were monitored under anaesthesia by optoacoustic tomography and optical fluorescence. Cerebral blood flow (CBF) was measured via arterial spin labelling MRI and blood pressure [BP] was monitored via a catheter under anaesthesia. Neuronal activity was assessed by *in vivo* electrophysiology. Cortical mitochondrial respiratory capacities (via oxygen consumption) and brain metabolite and lipid concentrations were measured by high-resolution respirometry and NMR spectroscopy respectively. Meso scale discovery and qPCR were used to evaluate plasma and cortical cytokines. Brain inflammation was further assessed by microglial (Iba-1) and astrocyte (GFAP) immunofluorescence. Liver steatosis was confirmed by histology.

Results: Mice with NAFLD exhibited: an anxiety and depression-related behaviour, but preserved learning and memory lower brain oxygenation attributed to the decreased CBV, brain inflammation, and cortical microglial and astrocytic alterations (increased number, % area covered and volume of cells), which led to elevated oxygen consumption increased lipid concentrations, but a decrease in some metabolites preserved cerebrovascular reactivity, neuronal activity and CBF compensated by the elevated BP.

Conclusion: This study provides evidence indicating a key role of NAFLD in inducing brain dysfunction likely due to the development of low-grade brain tissue hypoxia and inflammation, as well as cerebrovascular, glial, metabolic and behavioural alterations. Such chronic effects are expected to worsen with disease progression, leading to a NAFLD-induced encephalopathy, while increasing patients' risk for neurodegenerative conditions, such as Alzheimer's disease, that share the above pathophysiological mechanisms.

Abstract withdrawn

SAT013

Targeted metabolomics reveals alterations in one-carbon metabolism in NAFLD patients

Mikkel Werge¹, Adrian McCann², Elisabeth Galsgaard³, Dorte Holst³, Anne Bugge², Lise Lotte Gluud¹. ¹Copenhagen University Hospital Hvidovre, Gastro Unit, Denmark; ²Bevital AS, Norway; ³Novo Nordisk A/S-site Måløv, Måløv, Denmark
Email: mikkel.parsberg.werge@regionh.dk

Background and aims: One-Carbon Metabolism (OCM), represents the convergence of numerous metabolic pathways including homocysteine metabolism, glutathione biosynthesis, folate and methionine cycles, transsulphuration pathway, and the choline oxidation pathway. Several mechanisms such as hepatic lipid homeostasis and oxidative stress may link OCM to non-alcoholic fatty liver disease (NAFLD). We aimed to investigate biomarkers and related B-vitamin cofactors coupled to OCM in NAFLD.

Method: This prospective study included 100 patients with histologically verified NAFLD and 50 age and sex matched healthy controls. Targeted metabolomic analyses were performed on fasting plasma samples using tandem mass spectrometry paired with gas or liquid chromatography, or microbiological assay to measure B-vitamin cofactors and metabolites relevant to OCM and glutathione production.

RNA-sequencing was performed on 18 NAFLD liver biopsies with F0 to F4 fibrosis and 6 controls to measure expression levels of cystathionine β -synthase (CBS) and cystathionine γ -lyase (CSE).

Results: The included patients (50% with type 2 diabetes) had NAFLD with fibrosis score of F0 (n = 26), F1 (n = 25), F2 (n = 20), F3 (n = 12), and F4 (n = 17). Patients with NAFLD had higher BMI than controls (mean: 34.7 vs 26.6, $p < 0.0001$). Cystathionine was increased in patients with advanced fibrosis ($p = 0.006$) and the GSG index (glutamate/(serine+glycine)), a proxy measure of glutathione synthesis, was increased in patients with NASH compared to those without NASH ($p = 0.0003$). Plasma concentrations of betaine and pyridoxal 5'-phosphate, the active form of vitamin B6, were lower in NAFLD patients compared to controls. Expression of CSE decreased with increasing fibrosis score ($p = 0.0021$).

	Controls (n = 50)	NAFLD (n = 100)	p	No NASH (n = 36)	NASH (n = 64)	p
Homocysteine	10.3 \pm 3.6	10.8 \pm 3.9	0.40	11.2 \pm 3.5	10.6 \pm 4.1	0.20
Cysteine	296 \pm 42	310 \pm 3	0.03	312 \pm 48	309 \pm 38	0.055
Methionine	27.1 \pm 5.8	26.8 \pm 3.9	0.71	27.4 \pm 7.4	26.5 \pm 5.1	0.89
Serine	118 \pm 22	103 \pm 21	5.1*10 ⁻⁵	108 \pm 20	100 \pm 21	0.94
Glycine	273 \pm 78	215 \pm 53	5.7*10 ⁻⁷	238 \pm 54	208 \pm 48	0.0009
Cystathionine	0.40 \pm 0.36	0.56 \pm 0.59	0.003	0.63 \pm 0.59	0.52 \pm 0.59	0.24
Glutamate	42.9 \pm 17.5	87.1 \pm 37.7	5.1*10 ⁻¹⁵	74.1 \pm 28.7	94.4 \pm 40.3	0.011
GSG index	0.11 \pm 0.05	0.29 \pm 0.13	7.0*10 ⁻¹⁷	0.23 \pm 0.10	0.32 \pm 0.14	0.0003
Choline	8.1 \pm 1.4	8.3 \pm 2.4	0.89	9.1 \pm 2.4	7.8 \pm 2.3	0.0073
Betaine	37.2 \pm 9.5	31.8 \pm 11.6	0.0003	34.7 \pm 14.7	30.2 \pm 9.2	0.22
Dimethylglycine	3.8 \pm 1.1	4.8 \pm 2.3	0.047	5.5 \pm 2.7	4.4 \pm 1.9	0.077
Pyridoxal phosphate	100.2 \pm 91.5	50.8 \pm 32.2	4.6*10 ⁻⁸	52.2 \pm 31.0	50.0 \pm 33.1	0.68

Conclusion: The results suggest demand for metabolites central to OCM may be altered in NAFLD. This could be driven by increased need for glutathione and pyridoxal 5'-phosphate in response to oxidative stress and inflammation, as well as betaine for lipid metabolism in NAFLD patients. Expression of enzymes regulating OCM may be affected by advancing fibrosis.

SAT014

Metabolic NAFLD subtypes align with cardiovascular and genetic risk factors

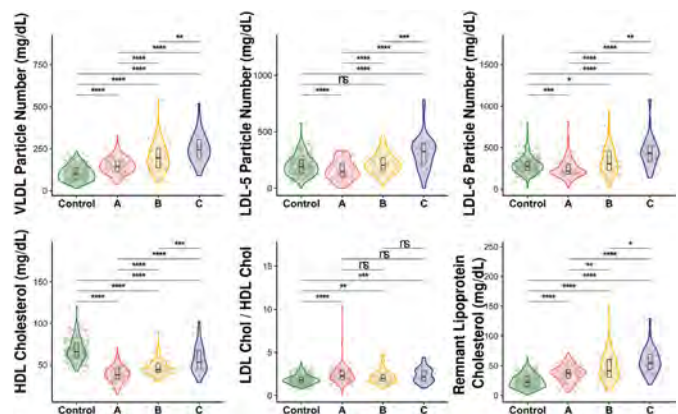
Ibon Martínez-Arranz¹, Chiara Bruzzone², Mazen Nouredin³, Rubén Gil-Redondo², Enara Arretxe¹, Marta Iruarizaga-Lejarreta¹, Maider Bizkarguenaga², Itziar Mincholé¹, David Fernández Ramos^{2,4}, Fernando Lopitz Otsoa², Rebeca Mayo¹, Nieves Embade², Elizabeth Newberry⁵, Bettina Mittendorf⁶, Laura Izquierdo-Sánchez⁷, Ylenia Pérez Castaño⁸, Vaclav Smid⁹, Jorge Arnold¹⁰, Marcin Krawczyk^{11,12}, Paula Iruzubietza¹³, Urko M Marigorta¹⁴, Martine C. Morrison¹⁵, Robert Kleemann¹⁵, Antonio Martín Duce¹⁶, Liat Hayardeny¹⁷, Libor Vitek⁹, Radan Bruha⁹, Rocío Aller¹⁸, Javier Crespo¹³, Manuel Romero Gomez¹⁹, Jesus Maria Banales^{4,7}, Marco Arrese¹⁰, Kenneth Cusi²⁰, Elisabetta Bugianesi²¹, Samuel Klein⁶, Shelly C. Lu³, Quentin Anstee²², Oscar Millet², Nicholas O Davidson⁵, Cristina Alonso¹, José M. Mato^{2,4}. ¹OWL Metabolomics, Derio, Spain; ²CIC bioGUNE-Centro de Investigación Cooperativa en Biotecnología, Precision Medicine and Metabolism, Derio, Spain; ³Cedars-Sinai Medical Center, Karsh Division of Gastroenterology and Hepatology, Los Angeles, United States; ⁴CIBERehd, ISCIII, Madrid, Spain; ⁵Washington University School of Medicine, Department of Medicine and Department of Developmental Biology, St. Louis, United States; ⁶Washington University School of Medicine, Center for Human Nutrition, St. Louis, United States; ⁷Biodonostia Research Institute, Donostia University Hospital, Department of Liver and Gastrointestinal Diseases, San Sebastián, Spain; ⁸Osakidetza Basque Health Service, Donostia University Hospital, Department of Digestive System, San Sebastián; ⁹Faculty General Hospital and the First Faculty of Medicine,

Charles University, Prague, Czech Republic; ¹⁰Pontificia Universidad Católica De Chile, Department of Gastroenterology, School of Medicine, Santiago de Chile, Chile; ¹¹Medical University of Warsaw, Laboratory of Metabolic Liver Diseases, Department of General, Transplant and Liver Surgery, Warsaw, Poland; ¹²Saarland University Medical Center, Department of Medicine II, Homburg, Germany; ¹³Marqués de Valdecilla University Hospital, Cantabria University, Research Institute Marqués de Valdecilla (IDIVAL), Department of Digestive Disease, Santander; ¹⁴Integrative Genomics Lab, CIC bioGUNE, Derio, Spain; ¹⁵The Netherlands Organisation for Applied Scientific Research (TNO), Department of Metabolic Health Research, Leiden, Netherlands; ¹⁶University Hospital Principe De Asturias, Alcalá University, Alcalá, Spain; ¹⁷Galmed Pharmaceuticals Ltd., Tel Aviv-Yafo, Israel; ¹⁸Clinic University Hospital, University of Valladolid, Department of Digestive Disease, Valladolid, Spain; ¹⁹Instituto De Biomedicina De Sevilla (IBiS), Hospital Universitario Virgen Del Rocío/CSIC/Universidad De Sevilla, Seville, Spain; ²⁰University of Florida, Division of Endocrinology, Diabetes and Metabolism, Gainesville, United States; ²¹University of Turin, Gastroenterology Department, Turin, Italy; ²²Translational and Clinical Research Institute, Faculty of Medical Sciences, Newcastle University, Newcastle-upon-Tyne, United Kingdom
Email: director@cicbiogune.es

Background and aims: We previously identified subsets of non-alcoholic fatty liver disease (NAFLD) patients with different metabolic phenotypes. Here we align metabolomic signatures with cardiovascular (CV) and genetic risk factors, and lipid lowering medication.

Method: We analyzed serum from an international cohort of 1143 individuals with biopsy-proven NAFLD using mass spectrometry and NMR based metabolomics. We further analyzed the metabolomes of four mouse models with impaired VLDL-triglyceride (TG) secretion (Mat1a-KO, 0.1MCD, Mttp-LKO, Tm6sf2-LKO), and one (Ldlr-/-Leiden/high fat fed) with normal VLDL-TG secretion.

Results: We identified three metabolic subtypes (A, B, and C; 47%, 27%, and 26% respectively). Subtype A phenocopied the metabolome of mice with impaired VLDL-TG secretion; subtype C phenocopied Ldlr-/-Leiden mice; subtype B showed an intermediate signature. Percentage of patients with NASH and fibrosis were comparably distributed among subtypes, although subtypes B and C exhibited higher ALT, AST, and GGT levels than subtype A. Serum VLDL-TG levels and secretion were lower among subtype A compared to the subtypes B and C. Subtype A VLDL-TG was independent of steatosis, whereas subtypes B and C showed a curvilinear relationship. Serum TG, cholesterol (Chol), VLDL, small dense LDL_{5,6} and remnant lipoprotein Chol, were lower among subtype A compared to subtypes B and C, while LDL-Chol-to-HDL-Chol ratio was similar. Subtype A associated with the TM6SF2 NAFLD risk allele, lower percent of patients with intermediate/high CV disease risk (Framingham risk score $\geq 10\%$ at 10 years), and higher percent of patients with lipid lowering medication.



POSTER PRESENTATIONS

Conclusion: Based on these results, we conclude that NAFLD subtype A stems from multiple nutritional and environmental factors that, acting on a susceptible genetic background, converge in reduced synthesis and export of VLDL-TG and the circulation levels of VLDL-TG exhibiting a reduced CV disease risk. This may account for the variation in hepatic vs. cardiovascular outcomes, offering novel, clinically relevant, risk stratification.

SAT015

Deletion of ATR in hepatocytes improves NAFLD features by increasing mitochondrial function

Maeva Saroul¹, Pierre Cordier¹, Christelle Kabore¹, Romain Donne², Ivan Nemazany³, Fabienne Foufelle⁴, Pascale Bossard⁵, Chantal Desdouets¹. ¹Team Proliferation Stress and Liver Physiopathology, Centre de Recherche des Cordeliers, INSERM, Sorbonne Université, Université de Paris, Paris, France; ²Icahn School of Medicine at Mount Sinai, The Lujambio lab, Oncological sciences, New York, United States; ³Platform for Metabolic Analyses, Structure Fédérative de Recherche Necker, INSERM US24/CNRS UMS 3633, Paris, France; ⁴Team Metabolic Diseases, Diabetes and Co-morbidities, Sorbonne Université, Université de Paris, Paris, France; ⁵Université de Paris, Institut Cochin, INSERM, CNRS, Paris, France
Email: maeva.saroul@inserm.fr

Background and aims: Chronic diseases such as obesity and diabetes are now considered as a social and economic burden. The liver is a central organ affected by these conditions resulting in a high level of fat accumulation, defined as Non-Alcoholic Fatty Liver Disease (NAFLD). Alarming NAFL (steatosis) progresses pejoratively to Non-Alcoholic Steatohepatitis (NASH). NASH has the potential to progress to more severe stages as cirrhosis and hepatocellular carcinoma (HCC). The biological mechanisms underlying NALF/NASH are not entirely understood. In various chronic liver diseases, aberrant DNA Damage Response (DDR) is a hallmark of disease aggravation. In NAFLD, DNA damage are present in human fatty livers and increase with disease progression. We previously showed that fatty hepatocytes division is associated with the activation of the DDR mediated by the kinase ATR. Whether ATR, per se, participates to Non-Alcoholic Fatty Liver Disease remains largely unknown.

Method: We used a hepatic-specific *in vivo* CRISPR/Cas9 approach using AAV vector, to generate ATR^{DHep} mice. C57BL/6J ATR^{DHep} and control (CTR) mice were fed a Choline-Deficient High-Fat Diet (CD-HFD) for 16 and 24 weeks. RNAseq analyses combined with molecular and cellular approaches have been performed on ATR^{DHep} and CTR NAFLD livers. Metabolic parameters have been investigated using Liquid Chromatography associated to Mass-Spectrometry. We also collected data on primary hepatocytes cultures isolated from our NAFLD models.

Results: Unexpectedly, silencing of hepatocyte ATR in murine models of NASH reduced hepatocyte proliferation and cell death. We show, in particular, a decrease in Caspase 8 and cleaved Caspase 3 activities that parallels with a marked increase in *BCL2* expression. We also provide evidence that deletion of hepatic ATR improves fatty acid metabolism by regulating lipogenesis (e.g. *Fas*, *ACC*, *SREBP1C*) and anti-oxidative response (e.g. *NQO1*, *GSTM3*, *HO1*). To go further, we isolated primary hepatocytes from our NAFLD mice models to assess the mitochondrial function. ATR deletion led to activation of mitochondrial respiration in steatotic hepatocytes with a partial restoration of mitochondrial capacities, an improvement of basal/maximal respiration, ATP production and attenuation of proton leak. Flux analyses demonstrated also that ATR^{DHep} hepatocytes increase their glycolysis capacities. Finally, we observe in NAFLD primary hepatocytes that ATR deletion increases the anti-oxidative defense against paraquat-induced oxidative stress.

Conclusion: Inhibition of ATR improves NASH features in CD-HFD fed mice, particularly by acting on mitochondrial function. This suggests that ATR might be a potential marker of mitochondrial dysfunction in NAFLD.

SAT016

The AXL inhibitor bemcentinib reduces inflammation and fibrosis by inducing a dynamic change in macrophages and CD8+T cells subsets during experimental NASH

Sturla M. Groendal¹, Anna Tutusaus², Pablo Garcia de Frutos², Magnus Blø³, Linn Hodneland³, Gro Gausdal³, Akil Jackson⁴, James B Lorens¹, Albert Morales⁵, Montserrat Mari². ¹University of Bergen, Department of Biomedicine, Centre for Cancer Biomarkers, Bergen, Norway; ²IIBB-CSIC/IDIBAPS, Barcelona, Spain; ³BerGenBio ASA, Bergen, Norway; ⁴BerGenBio LTD, Orford, United Kingdom; ⁵IIBB-CSIC/IDIBAPS, Barcelona Clinic Liver Cancer Center (BCLC), Barcelona, Spain
Email: monmari@clinic.cat

Background and aims: Tyro3, AXL and MERTK are receptor tyrosine kinases activated by the ligand GAS6. AXL signalling is increased in non-alcoholic steatohepatitis (NASH) patients and promotes fibrosis through activation of hepatic stellate cells and inflammatory macrophages. Recent data shows that bemcentinib reduces experimental NASH by inhibiting AXL signaling and increasing hepatocyte survival through increased Gas6. In recent years the role of the innate and adaptive immune system in NASH has gained attention. We aim to determine which immune cells express AXL and how AXL inhibition affects the liver immune profile during NASH. This may provide clues for new NASH-directed therapies.

Method: Mice were fed chow or a high-fat methionine-restricted choline-deficient (HFCD) diet for 8 weeks to induce NASH, receiving daily doses of bemcentinib (3–100 mg/kg) or vehicle by oral gavage for the last two weeks. Hepatic inflammatory and fibrotic gene expression were measured by qPCR. Time-of-flight mass cytometry (CyTOF) was utilized to analyze the expression of more than 40 markers on single cells from dissociated livers. Cells were acquired on the Fluidigm Helios and cell populations were studied using machine learning.

Results: Bemcentinib was effective in reducing expression of fibrogenic genes in HFCD-fed mice at all tested dosages (3–100 mg/kg), and inflammatory gene expression at doses >30 mg/kg. CyTOF analysis revealed that Axl was co-expressed with MERTK in infiltrating macrophages and Kupffer cells, but exclusively expressed in conventional type 2 dendritic cells. Compared to chow animals, NASH strongly reduced the amount of Kupffer cells and increased infiltration of monocytes/macrophages and CD8+ T-cells. Bemcentinib partially rescued NASH-induced loss of Kupffer cells and reduced the proportion of both plasmacytoid dendritic cells and subsets of recruited macrophages. Bemcentinib induced a shift in the composition of the resident and recruited macrophages from TGFb^{high} to TGFb^{med} subgroup with an increased influx of CX3CR1^{high} macrophages, associated with tissue remodelling and anti-inflammatory phenotype. Moreover, bemcentinib enhanced the expression of a subtype of CD8+ tissue resident memory T-cells characterized by the expression of CX3CR1 and GranzymeB^{high} known to promote hepatic stellate cell apoptosis.

Conclusion: Bemcentinib reduces inflammation and fibrosis by inducing a dynamic change in liver macrophages and CD8+T cells subsets from pro-inflammatory towards tissue remodeling and anti-fibrotic phenotypes.

SAT017

Human Liver Organoids with myeloid lineages model the multi-cellular crosstalk in Non-Alcoholic Steatohepatitis

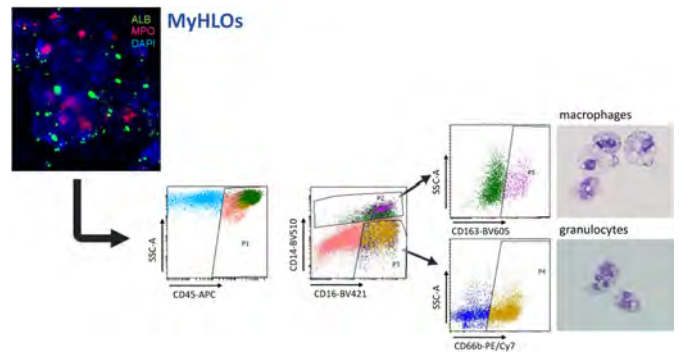
Milad Rezvani^{1,2}, Kyle Lewis², Kentaro Iwasawa², Yuqi Cai², Yuka Milton², Masaki Kimura², RanRan Zhang², Praneet Chaturvedi³, Takanori Takebe^{2,3,4,5,6}. ¹Charité Campus Virchow Clinic, Department of Pediatrics, Division of Gastroenterology, Nephrology and Metabolic Medicine, Berlin, Germany; ²Cincinnati Children's Hospital Medical Center, Department of Pediatrics, Division of Gastroenterology, Hepatology and Nutrition, Cincinnati, United States; ³Cincinnati Children's Hospital Medical Center, Center for Stem Cell and Organoid Medicine (CuSTOM), Cincinnati, United States; ⁴Cincinnati Children's Hospital Medical Center, Division of Developmental Biology, Cincinnati, United States; ⁵Yokohama City University Graduate School of Medicine, Department of Regenerative Medicine, Yokohama, Japan; ⁶Tokyo Medical and Dental University, Institute of Research, Bunkyo City, Japan
Email: milad.rezvani@charite.de

Background and aims: Non-alcoholic Steatohepatitis (NASH) is characterized by hepatocyte injury due to lipotoxicity and inflammatory responses elicited by granulocytes and other myeloid immune cells. Developing therapies against NASH requires platforms modeling both processes. We previously described human liver organoids (HLOs) from induced pluripotent stem cells (iPSCs) recapitulating human hepatogenesis. In turn, studies demonstrated myelopoiesis in human fetal livers. We hypothesized that HLOs may recreate the complex fetal liver microenvironment to co-differentiate hepatocytes and myeloid lineages from iPSCs.

Method: We differentiated human iPSCs into gut spheroids *via* endoderm induction using activin A and Matrigel embedding. We analyzed HLOs *via* qRT-PCR, immunostaining, single-cell RNA sequencing (scRNAseq) and FACS. To generate HLOs with myeloid lineages (MyHLOs), we incorporated combinations of cytokines relevant to the differentiation of neutrophils, monocytes, macrophages, and Kupffer Cells.

Results: scRNAseq data from day 14 cultures revealed mesoderm, ectoderm and an immature hepatocyte population. We also identified a hemogenic endothelial population as putative source of myelopoiesis. We trialed basic myeloid differentiation, added IL-3, followed by GM-CSF and M-CSF, and found abundant macrophages by Giemsa stain. We diversified the myeloid cell subsets using defined cytokine and small molecular cocktails and completed the differentiation protocol with G-CSF. On day 30, we identified *via* Giemsa stain neutrophils, macrophages and their progenitors. We singularized MyHLOs and isolated CD45+CD14-CD16+CD66b+ Neutrophils that phagocytosed at similar levels but migrated faster than primary adult controls. To further assess neutrophil function, we injected MyHLOs into bone marrow-depleted mice modeling sinusoidal obstruction syndrome using Busulfan and Monocrotaline, respectively. Transplanted mice suffered from exacerbated liver injury with neutrophil-infiltrated necrotic foci. Next, we isolated from MyHLOs monocytes that predominantly expressed CD45+CD14+CD16+ with a CD163+ macrophage subset (12%).

Hepatocytes in MyHLOs were immature relative to HLOs by Albumin secretion and CYP3A4 activity. To develop an appropriate NASH model, we defined a hybrid media restoring mature secretory and metabolic function and allowing continued myelopoiesis. We added Palmitic Acid to MyHLOs and detected neutrophil-extracellular traps and reactive oxygen species. This stress response could be alleviated by adding neutrophil or macrophage activation inhibitors, demonstrating cellular crosstalk.



Conclusion: We developed MyHLOs as a novel human liver organoid platform consisting of hepatocytes and syngeneic neutrophils, monocytes and macrophages, which allows to interrogate inter-lineage crosstalk in a human NASH model.

SAT018

Senescence, hand in hand with hepatic iron overload during the progression of NAFLD

Miren Bravo¹, Jorge Simón¹, Naroa Goikotxea¹, Sofia Lachiondo-Ortega¹, Leire Egia-Mendikute², Mate Maus³, Serena Pelusi^{4,5}, Josep Amengual⁶, Ester Gonzalez-Sanchez⁶, Javier Vaquero⁶, Ruben Nogueiras⁷, Asís Palazón², Luca Valenti^{4,5}, Isabel Fabregat⁶, Manuel Serrano^{3,8}, María Luz Martínez-Chantar⁹. ¹CIC bioGUNE-Centro de Investigación Cooperativa en Biociencias, CIBERehd, Liver Disease Lab, Derio, Spain; ²CIC bioGUNE-Centro de Investigación Cooperativa en Biociencias, Cancer Immunology and Immunotherapy Lab, Derio, Spain; ³IRB Barcelona-Institute for Research in Biomedicine, Barcelona, Spain; ⁴Mangiagalli Clinic IRCCS Cà Granda Foundation Ospedale Maggiore Policlinico, Department of Transfusion Medicine and Hematology-Translational Medicine, Milano, Italy; ⁵University of Milan, Department of Pathophysiology and Transplantation, Milano, Italy; ⁶IDIBELL Institut d'Investigació Biomèdica de Bellvitge, CIBERehd, TGF- β and Cancer Group, L'Hospitalet de Llobregat, Spain; ⁷CIMUS, University of Santiago de Compostela-Instituto de Investigación Sanitaria, CIBERobn, Department of Physiology, Santiago de Compostela, Spain; ⁸Catalan Institution for Research and Advanced Studies (ICREA); ⁹CIC bioGUNE-Centro de Investigación Cooperativa en Biociencias, Liver Disease Lab, Derio, Spain
Email: mmlmartinez@cicbiogune.es

Background and aims: Increased hepatic iron stores are observed in non-alcoholic fatty liver disease (NAFLD) patients. Its disturbed homeostasis may potentiate the onset and progression of the disease, increasing oxidative stress and altering lipid metabolism. Moreover, iron dyshomeostasis has been related to senescence, which in turn is involved in the development of chronic metabolic and inflammatory disorders. In this work, we aimed to study the implication of hepatic iron burden and its interrelationship with senescence in the context of NAFLD.

Method: First, a transcriptomic analysis in obese individuals was corroborated in three different diet-induced NAFLD mice models (high fat diet; choline-deficient high fat diet, and 0.1% methionine and choline-deficient diet, 0.1%MCDD), and in primary hepatocytes treated with methionine and choline-deficient medium (MCDM). Second, male C57BL/6 mice fed with 0.1%MCDD were treated with deferiprone (1 mg/ml), an iron chelator, in drinking water.

Results: In 125 obese individuals (transcriptomic cohort), we found a direct correlation between histological NASH and both circulating and liver mRNA levels of ferritin (Ft). Moreover, tissue damage as well as Ft increase, positively correlated with the senescence marker p21 mRNA hepatic levels. All NAFLD models showed a tight correlation between hepatic Ft and p21 overexpression. In accordance, 0.1% MCDD fed mice, showed significantly increased iron levels both in

POSTER PRESENTATIONS

liver and serum. Oral treatment with deferiprone significantly improved liver histopathology (steatosis, inflammation, fibrosis and ROS) and normalized liver-to-body weight ratio. A decrease in hepatic CD45 infiltrating cells was also observed by FACS, where B-cell, granulocyte and macrophage counts were diminished; and serum transaminase (ALT and AST) and iron levels were decreased. Primary hepatocytes isolated from treated mice showed reduced mitochondrial ROS generation (MitoSOX) and increased ATP production. Accordingly, succinate dehydrogenase (SDH) activity and fatty acid oxidation (FAO) were increased. *In vitro*, deferiprone avoided lipid accumulation in MCDM treated primary hepatocytes, also increasing FAO and SDH activity, and prevented mitochondrial membrane potential decrease. Finally, iron chelation decreased the expression of p21 both *in vivo* and *in vitro*. In the latter approach, moreover, senescence-associated beta-galactosidase activity was suppressed.

Conclusion: Our results demonstrate that cellular senescence goes hand in hand with hepatic iron accumulation during the progression of NAFLD. We prove that mitochondrial function recovery by deferiprone plays an essential role in ameliorating lipid metabolism, but also modulating immune response. This points out iron chelation as a potential drug for the treatment of NAFLD, a chronic disease with an increasing prevalence worldwide.

SAT019

Increased liver content of omega-3-derived lipid mediators associates with enhanced mitochondrial oxidative phosphorylation, fatty acid oxidation and metabolic efficiency

Cristina López-Vicario^{1,2,3}, David Sebastián^{4,5}, Mireia Casulleras^{1,3}, Marta Duran-Güell^{1,3}, Roger Flores-Costa^{1,3}, Ferran Aguilar³, Juanjo Lozano², Ingrid Wei Zhang^{1,3}, Esther Titos^{1,2,6}, Jing X Kang⁷, Antonio Zorzano^{4,5}, Makoto Arita⁸, Joan Clària^{1,2,3,6}. ¹Hospital Clínic-IDIBAPS, Barcelona, Spain; ²CIBERehd, Barcelona, Spain; ³European Foundation for the Study of Chronic Liver Failure (EF Clif), Barcelona, Spain; ⁴Institute for Research in Biomedicine (IRB Barcelona), Barcelona, Spain; ⁵CIBERdem, Barcelona, Spain; ⁶Department of Biomedical Sciences, University of Barcelona, Barcelona, Spain; ⁷Laboratory of Lipid Medicine and Technology, Massachusetts General Hospital and Harvard Medical School, Boston, United States; ⁸Laboratory for Metabolomics, RIKEN Center for Integrative Medical Sciences, Yokohama, Japan
Email: jclaria@clinic.cat

Background and aims: Mitochondrial injury is a common finding in metabolic dysfunction associated fatty liver disease (MAFLD). Since the membrane composition in polyunsaturated fatty acids (PUFA) is a major determinant of mitochondrial function, in the current study we investigated the liver mitochondrial phenotype of transgenic *fat-1* mice, which tissues are endogenously enriched with omega-3-PUFAs under resting conditions and following MAFLD induction. The effects of the omega-3-PUFA docosahexaenoic acid (DHA)-derived specialized pro-resolving mediators (SPM) on tumor necrosis factor (TNF) α -induced hepatocyte mitochondrial damage were also investigated.

Method: Liver mitochondria ultrastructure, oxidative phosphorylation, fatty acid β -oxidation (FAO) and bioenergetic metabolic fluxes were examined by transmission electron microscopy (TEM), high-resolution respirometry, radiolabeled [1-¹⁴C] oleate oxidation and NADH/FADH₂ production, respectively. Gene and protein expression were determined by real-time PCR and western blot. Mitochondrial injury was assessed in *fat-1* mice (n=22) and wild-type (WT) counterparts (n=33) induced to MAFLD by an obesogenic high-fat diet (HFD) or a fibrogenic choline-deficient L-amino acid-defined diet in combination with HFD (CDAHFD). Lipidomic analysis was performed using untargeted and targeted LC-MS/MS approaches.

Results: TEM images revealed that mitochondria of hepatocytes from *fat-1* mice had denser inner matrix with intact cristae and higher mitochondrial aspect ratio than WT mice. *Fat-1* mice also had increased TIM44 levels, enhanced oxygen consumption rate, FAO, insulin sensitivity and energy substrate utilization. Notably, *fat-1* mice were protected against HFD-induced MAFLD and CDAHFD-

induced fibrosis. Untargeted lipidomics identified a specific phosphatidylethanolamine DHA-enriched lipid fingerprint in livers from *fat-1* mice. Targeted lipidomics uncovered higher hepatic content of the DHA-derived SPMs resolvin D1 and maresin 1, which in *in vitro* experiments protected hepatocytes from TNF α -induced mitochondrial dysfunction.

Conclusion: These findings indicate that a tissue environment enriched in DHA-derived SPM derivatives optimizes liver mitochondrial efficiency and protects this organ from MAFLD.

SAT020

Factors associated with increased gut permeability and severity of liver disease in diabetic patients with NAFLD

Roberta Forlano¹, Benjamin H. Mullish¹, Laura Martinez-Gili¹, Jesus Miguens Blanco¹, Tong Liu¹, Evangelos Triantafyllou¹, Charlotte Skinner¹, Mark Thursz¹, Julian Marchesi¹, Pinelopi Manousou¹. ¹Imperial College London, Department of Metabolism, Digestion and Reproduction, United Kingdom
Email: r.forlano@imperial.ac.uk

Background and aims: The disruption of the gut-liver axis represents a crucial step towards the development and progression of non-alcoholic fatty liver disease (NAFLD). We investigated gut permeability and factors associated with it in patients with type-2 diabetes mellitus (T2DM) screened for NAFLD in primary care.

Method: Consecutive patients with T2DM were screened for liver disease by bloods, ultrasound and liver stiffness measurement (LSM). Elevated LSM was defined as LSM>8.1 kPa. Faecal metabolites were measured by liquid chromatography-mass spectrometry. Microbiota composition was analysed by 16 s rRNA gene sequencing, faecal cytokines by immunoassay. To assess gut-permeability, we set up an *in-vitro* model with monolayers of Madin-Darby canine kidney cells, whose permeability was estimated by trans-epithelial electric resistance (TEER) on epithelial volt/ohm meter. Faecal water (FW) was added to the model and TEER was measured across the monolayers at different time points. Experiments were replicated pre-treating FW with a cocktail of protease inhibitors. *E. faecalis* spent medium and phosphate-buffered saline (PBS) were used as positive and negative controls respectively.

Results: Three hundred patients were enrolled: 287 were included; 13 withdrew. Overall, 184 (73%) had NAFLD, 28 (10%) other causes of liver disease and 75 (26%) no liver disease.

Proteobacteria were higher in those with normal liver, while *Firmicutes* and *Bacteroidetes* were less abundant in those with NAFLD and elevated LSM (n = 17) compared to those with normal liver (n = 17). An *Anaeroplasma* ASV was less abundant in NAFLD vs normal liver, while *Monoglobus* ASV was less abundant in NAFLD and elevated LSM vs NAFLD and normal LSM. Moreover, those with NAFLD and elevated LSM showed significantly lower levels of faecal IFN- γ (p = 0.02).

Stool samples were used in the model of gut permeability. Overall, FW from patients with NAFLD and elevated LSM caused the greatest change in the TEER vs those with normal liver. When inhibitors of bacterial proteases were added, the effect of FW on TEER was significantly weaker, suggesting a component of bacterial protease activity. In this sub-group of samples, faecal valerate was significantly lower in those with NAFLD and elevated LSM compared to normal liver (0.28 vs 0.47, p = 0.007). Clinically, TEER correlated inversely with BMI (p = 0.029) and waist circumference (p = 0.019) and positively with LSM (p = 0.009) and AST (p = 0.036). No association was found with HbA1c or HOMA-index.

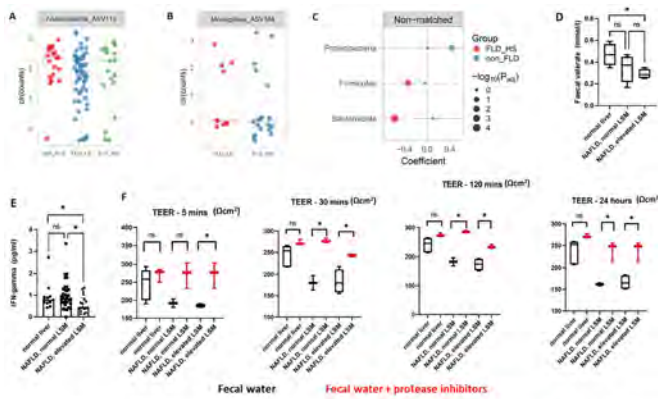


Figure 1. An *Aerospirillum* ASV was less abundant in NAFLD vs normal liver (Figure A), while *Monoglobus* ASV was less abundant in NAFLD and elevated LSM vs NAFLD and normal LSM (Figure B). Proteobacteria were higher in those with normal liver, while Firmicutes and Bacteroidetes were less abundant in those with NAFLD and elevated LSM compared to those with normal liver (Figure C). Faecal valerate (Figure D) and IFN-gamma (Figure E) were significantly lower in those with NAFLD and significant liver disease. In the in-vitro model of gut permeability, the stool samples from those with liver disease caused the greatest drop in TEER (black) compared to normal and this effect was attenuated when inhibitors of bacterial proteases (red) were included in the sample (Figure F).

Conclusion: Diabetics with a diagnosis of NAFLD have lower abundance of pectin-dependent species as well as a pro-inflammatory milieu in the gut. Moreover, patients with NAFLD may have a leakier gut, which correlates with the severity of liver disease and visceral obesity. Measuring intestinal permeability may identify patients who could benefit the most from intestinal barrier interventions.

SAT021

Increased burden of inherited IRF3 rare genetic variants in Europeans with severe Non-alcoholic fatty liver disease

Luigi Santoro¹, Daniele Marchelli², Alessandro Cherubini², Elia Casirati³, Francesco Malvestiti³, Melissa Tomasi², Paola Dongiovanni⁴, Cristiana Bianco², Marica Meroni⁴, Alessandro Federico⁵, Salvatore Petta⁶, Elisabetta Bugianesi⁷, Giorgio Soardo⁸, Umberto Vespasiani Gentilucci⁹, Luca Miele¹⁰, Helen Reeves¹¹, Daniele Prati², Luisa Ronzoni¹, Giodo Baselli¹², Luca Valentini³. ¹Fondazione IRCCS Ca' Granda Ospedale Maggiore Policlinico Milano, Transfusion Medicine and Hematology, Milan, Italy; ²Fondazione IRCCS Ca' Granda Ospedale Maggiore Policlinico Milano, Transfusion Medicine and Hematology, Milan, Italy; ³Università degli Studi di Milano, Milano, Department of Pathophysiology and Transplantation, Milan, Italy; ⁴Fondazione IRCCS Ca' Granda Ospedale Maggiore Policlinico Milano, General Medicine and Metabolic Diseases, Milan, Italy; ⁵Università della Campania "Luigi Vanvitelli", Department of Precision Medicine, Napoli, Italy; ⁶Università di Palermo, PROMISE, Palermo, Italy; ⁷Città della Salute e della Scienza di Torino, Department of Medical Sciences, Torino, Italy; ⁸Università degli Studi di Udine, Liver Unit, Department of Medical Area (DAME), Trieste, Italy; ⁹University Campus Bio-Medico di Roma, Department of Hepatology, Roma, Italy; ¹⁰Università Cattolica di Roma, Department of Translational Medicine and Surgery, Roma, Italy; ¹¹Newcastle University, Translational and Clinical Research Institute, Newcastle, United Kingdom; ¹²Karolinska institutet, Department of Microbiology, Tumor and Cell Biology, Stoccolma, Sweden
Email: nelyl@hotmail.it

Background and aims: Non-alcoholic fatty liver disease (NAFLD) encompasses a wide spectrum of liver damage, and genetic variation accounts for a large fraction of disease variability. Inflammation is involved in the progression of fatty liver to fibrosis and hepatocellular carcinoma (HCC). By performing whole exome sequencing in 72 severe NAFLD patients, defined as advanced fibrosis or HCC, vs 50 local healthy controls plus 33, 123 exome aggregation consortium (ExAC) non-Finnish-Europeans (NFE) individuals, we previously detected increased risk in carriers of interferon regulatory factor (*IRF3*) rs141490768, encoding for the p.A418T variant of the *IRF3*-CL isoform (OR 38.5, 95%CI 15.2–97; exome-wide adjusted $p = 0.015$).

IRF3 is a transcription factor involved in the induction of inflammatory response. The aim was to validate these data and examine the role of *IRF3* across the NAFLD spectrum.

Method: *IRF3* rs141490768 C > T was genotyped in an independent Validation cohort of 241 patients with severe NAFLD, vs. 32, 537 controls from the GnomAD-NFE database without ExAC. In the overall cohort, we tested the enrichment in *IRF3* rare variants (allelic frequency, AF <0.01) by ProxECAT (Proxy External Controls Association Test, accounting for differences in genotyping platforms) between 443 severe NAFLD cases compared to GnomAD-NFE ($n = 64$, 603).

IRF3/p*IRF3* immunohistochemistry (IHC) was performed in 16 NAFLD patients stratified by disease severity.

IRF3 transcriptional activity was assessed in 125 obese individuals severe NAFLD (transcriptomic cohort) by using virtual inference of protein activity by enriched regulon analysis.

Results: We confirmed an enrichment of rs141490768 in the validation (OR 5.84, 95%CI 1.4–24.1; $p = 0.044$) and in the overall cohort (OR 13.6, 95%CI 6.3–29.5; $p = 1.5 \times 10^{-6}$).

Furthermore, we detected an enrichment in *IRF3* rare variants in patients with severe NAFLD vs. controls (ratio of functional mutations to proxies 7.0 in cases vs 0.3 in controls; $p = 1.2 \times 10^{-7}$).

IHC showed a progressive increase in nuclear p*IRF3* staining in both hepatocytes and non-parenchymal cells with NAFLD severity (from normal liver to steatosis to NASH). Consistently, we observed increased expression of transcriptional targets ($\beta = 0.022$ across disease severity; $p = 0.013$).

By using CRISPR/Cas9 genome editing in human HepG2 hepatoma cells, we generated *IRF3*^{-/-}, *IRF3*-CL[±], and rs141490768 knock-in clones to study the functional impact of *IRF3* variation on inflammation and fibrogenesis in 3D multilineage spheroids with hepatocytes and stellate cells.

Conclusion: We found an enrichment of *IRF3* rare variants in patients with severe NAFLD vs. controls. *IRF3* activity was upregulated across the spectrum of NAFLD. Additional studies are required to uncover the mechanism underpinning predisposition to disease progression in carriers of *IRF3* variants.

SAT022

Sex-dependent hepatoprotective role of IL-22 in NAFLD-related fibrosis

Mohamed Noureldin Hassan Ali Abdelnabi¹, Manuel Flores Molina¹, Geneviève Soucy², Vincent Quoc-Huy Trinh², Nathalie Bédard¹, Sabrina Mazouz¹, Jessica Dion¹, Sarah Tran¹, Marc Bilodeau³, Naglaa Shoukry³. ¹Centre de Recherche du Centre hospitalier de l'Université de Montréal (CRCHUM), microbiologie, infectiologie et immunologie, Montreal, Canada; ²Centre de Recherche du Centre hospitalier de l'Université de Montréal (CRCHUM), pathologie et biologie cellulaire, Montreal, Canada; ³Centre de Recherche du Centre hospitalier de l'Université de Montréal (CRCHUM), Département de médecine, Montreal, Canada
Email: mnabdelnabi86@gmail.com

Background and aims: Non-alcoholic fatty liver disease (NAFLD) is a major health problem with complex pathogenesis. The incidence and severity of NAFLD is higher in males than females but the mechanisms underlying this sex difference are not well understood. IL-22 is a pleiotropic cytokine that can be both protective and/or pathogenic during liver injury and inflammation. IL-22 was shown to be hepatoprotective in NAFLD-related liver injury. However, these studies relied primarily on exogenous administration of IL-22 and did not examine the sex-dependent effect of IL-22. Here, we sought to characterize the role of endogenous IL-22 signaling during NAFLD-induced liver injury in males and females.

Method: We used immunofluorescence (IF), flow cytometry, histopathological assessment and gene expression analysis to examine IL-22 production and characterize the intrahepatic immune landscape in human subjects with NAFLD ($n = 20$; 11 males and 9 females) and

POSTER PRESENTATIONS

in an *in vivo* western high fat diet-induced NAFLD model in IL-22RA knock out (IL-22RA KO) mice and their wild type (WT) littermates.

Results: Examination of publicly available datasets from two cohorts with NAFLD demonstrated increased hepatic IL-22 gene expression in females as compared to males ($p=0.0327$ and $p=0.0279$, respectively). Furthermore, our IF analysis of liver sections from NAFLD subjects ($n=20$) demonstrated increased infiltration of IL-22 producing cells in females ($p=0.0002$). We validated the same observation in WT female mice with NAFLD ($p=0.0002$). The lack of endogenous IL-22 signalling (IL-22RA KO) led to exacerbated liver damage, inflammation, apoptosis and liver fibrosis in female but not male mice with NAFLD.

Conclusion: Our data suggest a sex-dependent hepatoprotective antiapoptotic effect of IL-22 during NAFLD-related liver injury in females.

SAT023

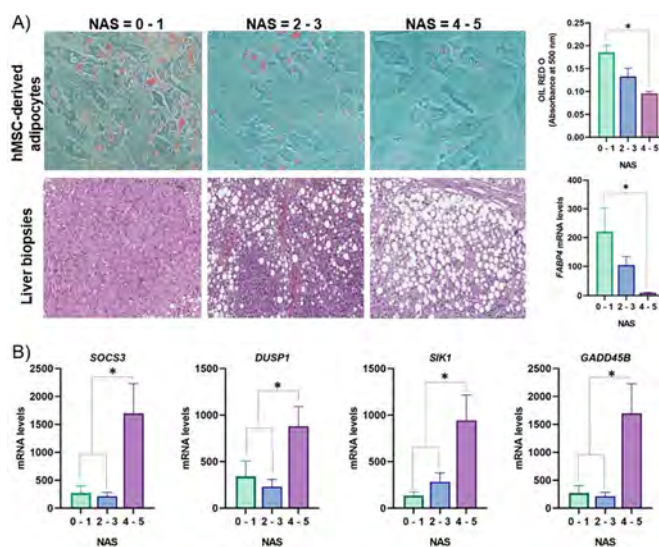
Identification of novel targets in adipose tissue involved in non-alcoholic fatty liver disease progression

Marta Lopez-Yus¹, Silvia Lorente-Cebrian², Carlos Hörndler³, Almudena Sobrino-Prados³, Carmen Casamayor³, Alejandro Sanz Paris³, Vanesa Bernal Monterde³, Jose M Arbones Mainar¹. ¹Instituto Aragonés de Ciencias de la Salud, Zaragoza, Spain; ²University of Zaragoza, Zaragoza, Spain; ³Hospital Universitario Miguel Servet, Zaragoza, Spain
Email: jmarbones.iacs@aragon.es

Background and aims: Obesity is a major risk factor for the development of non-alcoholic fatty liver disease (NAFLD) as dysfunction of subcutaneous adipose tissue (scWAT) may lead to fat accumulation in other organs. It is therefore essential to identify the molecular mechanisms underlying progression of the disease and the role played by the adipose tissue. Our main objectives were: 1) to identify new dysregulated genes in scWAT potentially involved in the development of NAFLD, 2) to establish an *in vitro* model of hMSC-derived adipocytes (hMSC) that could reflect the different stages of NAFLD, and 3) to validate the expression of selected genes in our *in vitro* model.

Method: Biopsies from the abdominal scWAT from 45 patients were obtained and their respective transcriptomes sequenced (RNAseq). Using a computational analysis, we obtained a set of genes upregulated in patients with elevated fatty liver index (FLI). The expression of those genes of interest were validated by qPCR in a different cohort of 50 patients. In this case, the expression in scWAT levels of the genes of interest were correlated with the NAFLD Activity Score (NAS) of liver biopsies. Lastly, hMSC were also isolated from scWAT of patients of this cohort and differentiated into adipocytes to establish an *in vitro* model that could reflect the different stages of NAFLD. Differentiation capacity of these hMSC was compared and expression of selected genes was measured by qPCR in hMSC-derived adipocytes.

Results: We observed reduced expression of the adipocyte differentiation marker FABP4 mRNA, as well as an impaired lipid accumulation, measured by oil red O stain, in hMSC-derived adipocytes of NAFLD patients (Figure 1A). Four genes, first identified in the RNAseq cohort and then confirmed by qPCR in the validation cohort, also showed a differential regulation pattern in hMSC-derived adipocytes, increasing their mRNA expression accordingly to the degree of hepatic steatosis: *SOCS3*, *DUSP1*, *SIK1*, and *GADD45B* (Figure 1B).



Conclusion: Our results constitute a proof-of-concept of the great importance of adipose-liver crosstalk and suggest that impaired adipogenic capacity of hMSC is a critical event in promoting the development of NAFLD. We propose four genes as key players in NAFLD progression.

SAT024

Isoleucine and valine correct hepatic lipid processing, reduce liver steatosis and suppress inflammation in obese mice with manifest NASH

Eveline Gart^{1,2}, Wim van Duyvenvoorde¹, Jaap Keijer², Kanita Salic¹, Martine C. Morrison¹, Robert Kleemann¹. ¹TNO-LOCATIE Leiden-Gaubiusgebouw, Leiden, Netherlands; ²Wageningen University and Research, Wageningen, Netherlands
Email: eveline.gart@tno.nl

Background and aims: Non-alcoholic steatohepatitis (NASH) is associated with disturbed liver lipid handling and excessive accumulation of hepatic fat. Branched-chain amino acids (BCAAs) may beneficially modulate hepatic lipids, however it remains unclear whether individual BCAAs can attenuate already established NASH.

Method: After 26 weeks of obesogenic diet (FFD) run-in, mice were treated with individual BCAA, valine or isoleucine (3% of FFD), for another 12 weeks and were then compared to FFD controls.

Results: Valine and isoleucine did not affect obesity and dyslipidemia compared to FFD, but significantly reduced hyperinsulinemia. Valine and isoleucine significantly reduced ALT, CK-18m30, and total liver steatosis. Microvesicular steatosis was strongly decreased, by 61% (valine) and 71% (isoleucine). Hepatic 4-hydroxynonenal (4-HNE), a marker for oxidative stress induced lipid peroxidation, immunoreactivity was significantly decreased with valine and isoleucine. Functional transcriptome analysis demonstrated an upregulation of BCAA metabolism genes (e.g. BCAT, PP1MK, BCKDHA), deactivation of lipid synthesis regulators (SREBF1, AGT, IGF1) and activation of regulators involved in lipid oxidation (AMPK, ACOX1, EHHADH) and mitochondrial biogenesis (PPARGC1α, CLUH). This correction of critical metabolic pathways by valine and isoleucine was accompanied by significantly decreased lobular inflammation, and suppression of FFD-stimulated inflammatory pathways controlled by IL-1b and TNFα.

Conclusion: The intervention with either valine or isoleucine corrected multiple lipid metabolism processes and reduced NASH-associated steatosis and inflammation which was substantiated by suppression of critical inflammatory pathways.

SAT025

Butyrate protects against diet-induced NASH and liver fibrosis and suppresses specific non-canonical TGF β signaling pathways in human hepatic stellate cells

Eveline Gart^{1,2}, Wim van Duynvenoorde¹, Karin Toet¹, Martien P. M. Caspers¹, Lars Verschuren¹, Aswin L. Menke¹, Roeland Hanemaaijer¹, Jaap Keijer², Kanita Salic¹, Robert Kleemann¹, Martine C. Morrison¹. ¹TNO-Locatie Leiden-Gaubiusgebouw, Leiden, Netherlands; ²Wageningen University and Research, Wageningen, Netherlands
Email: eveline.gart@tno.nl

Background and aims: In obesity-associated non-alcoholic steatohepatitis (NASH), persistent hepatocellular damage and inflammation are key drivers of fibrosis, which is the main determinant of NASH-associated mortality. The short-chain fatty acid butyrate can exert metabolic improvements and anti-inflammatory activities in NASH. However, its effects on NASH-associated liver fibrosis remain unclear.

Method: Putative antifibrotic effects of butyrate were studied in Ldlr^{-/-} mice fed an obesogenic diet (HFD) containing 2.5% (w/w) butyrate for 38 weeks and compared to a HFD-control group. Antifibrotic mechanisms of butyrate were further investigated in TGF- β -stimulated primary human hepatic stellate cells (HSC).

Results: HFD-fed mice developed obesity, insulin resistance, increased plasma leptin levels, adipose tissue inflammation, gut permeability, dysbiosis and NASH-associated fibrosis. Butyrate corrected hyperinsulinemia, lowered plasma leptin levels and attenuated adipose tissue inflammation, without affecting gut permeability or microbiota composition. Butyrate lowered plasma ALT and CK-18M30 levels and attenuated hepatic steatosis and inflammation. Butyrate inhibited fibrosis development as demonstrated by decreased hepatic collagen content, α SMA and Sirius-red-positive area. In TGF- β -stimulated HSC, butyrate dose-dependently reduced collagen deposition and decreased procollagen1 α 1 and PAI1 protein expression. Transcriptomic analysis and subsequent pathway and upstream regulator analysis revealed deactivation of specific non-canonical TGF- β signaling pathways Rho-like GTPases and PI3 K/AKT and other important pro-fibrotic regulators (e.g. YAP/TAZ, MYC) by butyrate, providing a potential rationale for its antifibrotic effects.

Conclusion: Butyrate protects against obesity development, insulin resistance-associated NASH and liver fibrosis. These antifibrotic effects are at least in part attributable to a direct effect of butyrate on collagen production in hepatic stellate cells, involving inhibition of non-canonical TGF- β signaling pathways.

SAT026

Experimental non-alcoholic fatty liver disease causes regional liver functional deficits while total metabolic liver function is preserved

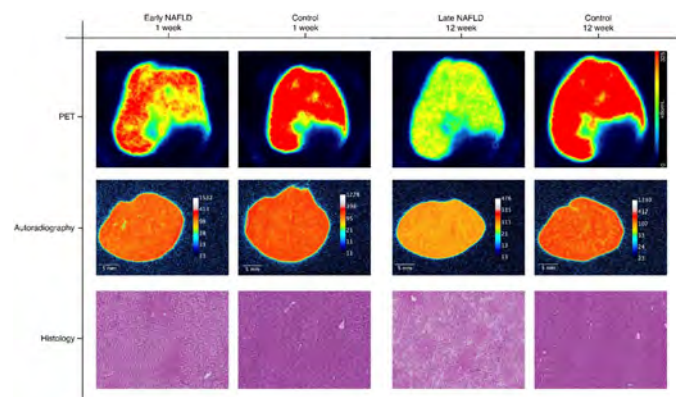
Peter Lykke Eriksen¹, Karen Louise Thomsen¹, Stephen Hamilton-Dutoit², Hendrik Vilstrup¹, Michael Soerensen^{1,3,4}. ¹Aarhus University Hospital, Department of Hepatology and Gastroenterology, Aarhus, Denmark; ²Aarhus University Hospital, Institute of Pathology, Aarhus, Denmark; ³Viborg Regional Hospital, Department of Internal Medicine, Viborg, Denmark; ⁴Aarhus University Hospital, Department of Nuclear Medicine and PET, Aarhus, Denmark
Email: ple@clin.au.dk

Background and aims: The increasing incidence of non-alcoholic fatty liver disease (NAFLD) has imposed a need for understanding how the disease affects metabolic liver function. The aim of this study was to investigate *in vivo* effects of the structural liver changes on hepatic metabolic function assessed by the regional and total capacity for galactose elimination in a rodent model of diet-induced NAFLD of different stages.

Method: Sprague Dawley rats were fed a standard chow (control) or a high-fat, high-cholesterol diet for 1 (n=8) or 12 weeks (n=8), resulting in development of early and late NAFLD, respectively. *In vivo*

liver metabolic function was assessed directly in the liver tissue by 2-[¹⁸F]fluoro-2-deoxy-D-galactose positron emission tomography. *Post mortem* liver tissue was used for autoradiography, histology and fat quantification.

Results: Early NAFLD livers had steatosis with 18 volume % fat. Late NAFLD livers had 32 volume % fat and showed features of non-alcoholic steatohepatitis (NASH) (inflammation, ballooning and fibrosis). Regional galactose metabolism was reduced in both early and late NAFLD with a median hepatic standardised uptake value (SUV) of 9.8 and 7.4 (p=0.02), respectively, compared to ~12.5 in controls. Results were confirmed by the autoradiography measurements. In early NAFLD the decreased SUV was explainable by the degree of fat infiltration. In late NAFLD, SUV was decreased beyond that attributable to fat, likely related to the structural NASH features mentioned. Still, in both groups total capacity for galactose elimination remained intact. In late NAFLD, there was an increase in fat-free liver mass to 21 g vs. 15 g in early NAFLD and control rats (p<0.002).



Conclusion: Metabolic function of the hepatic tissue was compromised by NAFLD. The deficit was related to replacement of liver tissue with fat and in the more advanced disease of late NAFLD probably also to other structural changes. Total liver function was preserved, in the late NAFLD rats by the marked growth of fat-free liver mass. The mechanism behind this functionally compensatory liver growth is not known.

SAT027

Hepatic lipid fingerprint reveals sex-dependent lipid droplet composition in metabolic associated fatty liver disease

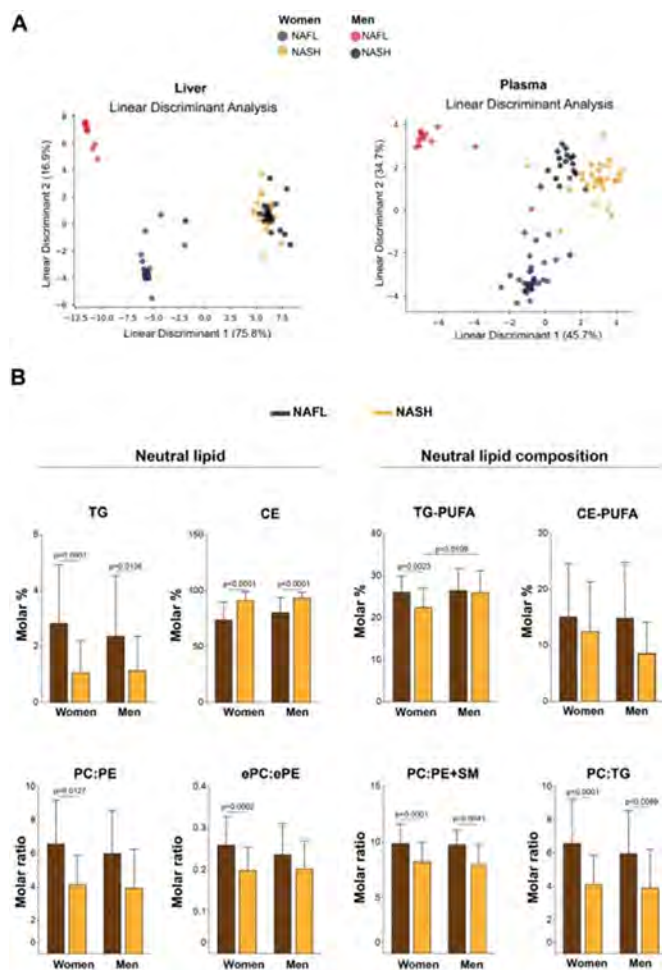
Elisabet Rodríguez-Tomás¹, Gerard Baiges Gaya², Helena Castañé², Andrea Jiménez Franco¹, Jordi Camps Andreu³, Jorge Joven Marié³. ¹Universitat Rovira i Virgili, Medicine and Surgery, Reus, Spain; ²Institut d'Investigació Sanitària Pere i Virgili, Medicine and Surgery, Reus, Spain; ³Hospital Universitari Sant Joan de Reus, Reus, Spain
Email: elisabet.rodriguez@urv.cat

Background and aims: Metabolic Associated Fatty Liver Disease (MAFLD) is a spectrum of heterogenic fatty-liver disorders that affects a quarter of the population. Despite new findings, there is no effective drug treatment and lifestyle interventions to address this disease in a long term. Nevertheless, lipid droplet accumulation is the onset of the natural course of MAFLD being lipid composition a necessary field to approach. In this context, phospholipids are the main constituents of the plasma membrane and changes in its composition are linked with the progression of this disease. How these changes affect women and men is an unsolved question. Thus, the purpose of the study was to identify changes in the lipid signature and phospholipid metabolism during liver disease progression as well as to observe the influence of the liver in the plasma lipidome of morbidly obese women and men.

POSTER PRESENTATIONS

Method: Liquid Chromatography coupled with Mass Spectrometry was used to perform a semi-targeted lipidomic in plasma and liver tissue from morbidly obese patients with non-alcoholic steatohepatitis (NASH) (men = 18; women = 34) and non-alcoholic fatty liver (NAFL) (men = 13; women = 38) who underwent bariatric surgery.

Results: Different lipidome profiles between women and men were observed using linear discriminant analysis in plasma and liver tissue (A). Nevertheless, when the liver disease progress to NASH these sex differences disappear. In addition, we found changes in the lipids associated with hepatic lipid droplet. Concretely, we observed an impairment of triglycerides (TG) and an increase of cholesterol ester levels in both sexes (B). In opposite to liver findings, the plasma TG levels increased in women but not in men. Interestingly, women showed changes in the lipid droplet composition with a loss of polyunsaturated fatty acid (PUFA)-containing TG. In addition, we also observed a decrease in the phospholipid levels in both plasma and liver. Hepatic phosphatidylcholine/phosphatidylethanolamine (PC/PE) and ether-linked PC/PE molar ratio decreased, and fatty acid composition of phospholipids was less polyunsaturated in PC and sphingomyelin (SM) in women between NASH and NAFL. Instead, men did not show any significant difference.



Conclusion: Phospholipid metabolism and hepatic lipid droplet composition seem to be influenced by sex and plasma lipidome seem to mimic the hepatic alterations.

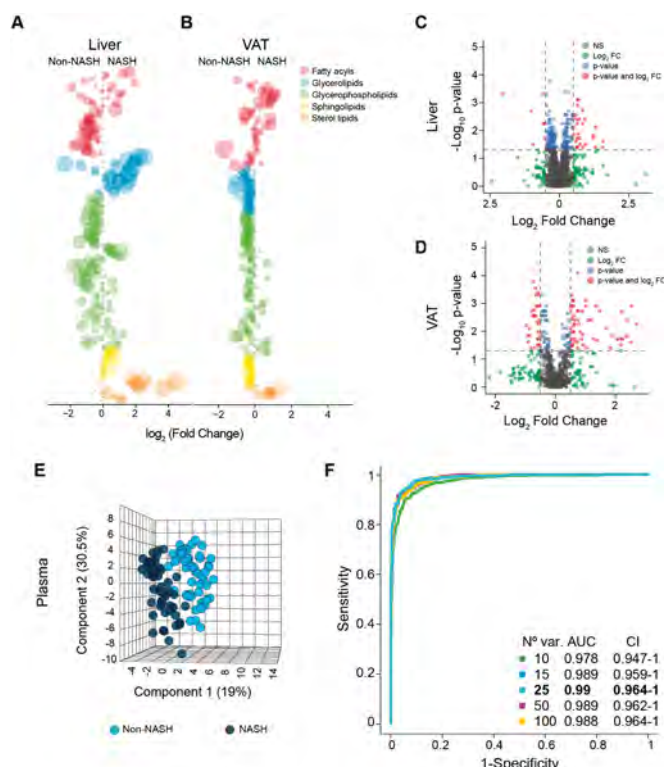
SAT028

Lipidomics and proteomics reveal mitochondrial dysfunction in liver and visceral adipose tissue from patients with non-alcoholic steatohepatitis

Helena Castañé¹, Andrea Jiménez Franco², Elisabet Rodríguez-Tomás², Gerard Baiges Gaya¹, Jordi Camps³, Jorge Joven^{2,3}. ¹Institut d'Investigació Sanitària Pere Virgili, Unitat de Recerca Biomèdica, Reus, Spain; ²Universitat Rovira i Virgili, Medicina i Cirurgia, Reus, Spain; ³Hospital Universitari Sant Joan, Unitat de Recerca Biomèdica, Reus, Spain
Email: helena.castanev@gmail.com

Background and aims: The association of chronic liver disease with obesity and diabetes is clinically important in the context of silent pandemics and there are no pharmacotherapeutic interventions. The initial step of the disease spectrum appears to be a simple accumulation of lipids, steatosis, but can progress to more severe forms initiated by non-alcoholic steatohepatitis (NASH). The pathogenic mechanisms leading to progression are not completely understood but growing evidence likely suggests metabolic dysfunction in multiple and related organs. Lipidomics and proteomics from liver and adipose tissue, with the help of machine learning algorithms, could explain clinical traits and shed light on interorgan crosstalk in patients with NASH. Also, alterations in circulating lipids in patients with NASH have not been previously explored in association with tissue-specific lipid signatures in obesity. We sought to distinguish obese patients with and without NASH identifying the lipidome in plasma, liver, and subcutaneous and visceral adipose tissue.

Method: Patients with extreme obesity (n = 118; n = 58 with NASH diagnostic, and n = 60 were non-NASH) that underwent metabolic surgery donated a liver and a visceral adipose tissue (VAT) biopsy, and blood sample, from which we extracted the lipidome and proteome.



Results: Liver and VAT shared a relatively common lipidome and proteome signature. Regarding lipidomics, mostly all lipid species were altered: glycerophospholipids were diminished in both tissues and tri and diglycerides were increased in liver and decreased in VAT. Volcano plots found more differences between NASH and non-NASH patients in their VAT than in their liver proteome, both tissues had proteins located in mitochondria and with essential roles in energy metabolism altered in NASH. Quantitative enrichment set analysis pointed to impaired mitochondrial beta-oxidation. On the other hand, plasma lipidome and proteome was different enough between NASH and non-NASH patients, thus machine learning algorithms were applied to build a predictive model which had high diagnostic ability.

Conclusion: Lipidomic and proteomic signature not only affects hepatic tissue, but also visceral adipose tissue. The alterations can also be observed in plasma, and the optimal combination of these variables could be a new biomarker of liver severity.

SAT029

Targeting liver glutaminase 1 modulates hepatic ammonia in experimental Non-Alcoholic Steatohepatitis

Maria Mercado-Gómez¹, Naroa Goikoetxea¹, Marina Serrano-Macia¹, Sofia Lachiondo-Ortega¹, Rubén Rodríguez Agudo¹, Petar Petrov², Miren Bravo¹, Claudia Gil-Pitarch¹, Irene González-Recio¹, Jorge Simón Espinosa¹, María Luz Martínez-Chantar¹, Teresa Cardoso Delgado¹. ¹CIC bioGUNE-Centro de Investigación Cooperativa en Biociencias, Derio, Spain; ²La Fe University and Polytechnic Hospital, Valencia, Spain
Email: tcardoso@cicbiogune.es

Background and aims: Hepatic ammonia, a key nitrogen-containing compound, is augmented in NAFLD, specifically in more advanced stages of the disease such as NASH with potential implications in its treatment. Whereas both gut-derived ammonia and decreased hepatic ureagenesis have been shown to contribute to increased hepatic ammonia content under these conditions, the contribution of glutaminase 1 (GLS) expression for hepatic ammonia built-up in NASH has not been previously addressed.

Method: 3-month-old C57BL/6J male mouse were maintained for 6 weeks either on HFD, CD-HFD, CDAA or CDA-HFD. Serum, liver histological analysis (HandE, Oil red, F4/80 immunostaining, Sirius red, Nessler staining of ammonia) and hepatic transcriptional profiling with the nCounter® Metabolic Pathways Panel from nanoString® studies were carried out. Then, animals maintained for 6 weeks on CDA-HFD, a well-established mouse model of diet-induced NASH, presenting increased staining for hepatic ammonia without concomitant blood hyperammonaemia, considered thereby a latency period of abnormal ammonia metabolism, were randomly separated in two experimental groups: hepatic glutaminase 1 (GLS) silencing (n = 6) or non-targeting siRNA control silencing (n = 6) by tail vein injection of the respective siRNA and InvivoFectamine™. After 48 h animals were sacrificed and the expression of key regulators of liver glutamine metabolism assessed, and ammonia content evaluated.

Results: Hepatic transcriptional profiling revealed decreased expression of pathways responsible for amino acid synthesis and arginine metabolism as well as pathways involved in fatty acid metabolism and mitochondrial respiration as the dietary model of NAFLD progressed. On the other hand, pathways associated with hypoxia, DNA damage repair, myc, glutamine metabolism, mTOR and glycolysis, among others, were overexpressed in NASH mouse models. Interestingly, as NAFLD progresses hepatic Nessler staining of ammonia is increased correlating with decreased expression of the enzymes involved in urea cycle, and increased expression of the isoform 1 of glutaminase. In addition, silencing of hepatic glutaminase 1 in CDA-HFD rodents for 48 h results in decreased glutaminase 1 mRNA levels as expected. On the contrary, the expression of urea cycle enzymes, suppressed under NASH conditions, remains

unaltered. Likewise, zonula occludens staining in intestine, a marker for tight junction integrity in the intestinal barrier, is unaffected by hepatic glutaminase 1 silencing. Finally, we have shown that hepatic ammonia content is reduced after glutaminase 1 silencing, and this is associated with a mild reduction in the activation of hepatic stellate cells.

Conclusion: Our results show that targeting liver glutaminase 1 modulates hepatic ammonia in NASH which could be a therapeutic mechanism to halt fibrosis progression.

SAT030

Clinical relevance of an animal model of non-alcoholic steatohepatitis (NASH) and digital pathology with artificial intelligence (DP-AI) analyses of hepatic fibrosis

Yishuang Wei¹, Mengnan Zhang¹, Jiliang Zhang¹, Xiao Teng², Qiang Yang³, Alvin Leong², Gideon Ho², Henry Lu¹, Deming Xu¹. ¹WuXi AppTec, Discovery Biology Unit, WuXi Biology, Shanghai, China; ²HistoIndex Pte Ltd., Singapore, Singapore; ³Hangzhou Choutu Technology Co., Ltd., Hangzhou, China
Email: xu_deming@wuxiapptec.com

Background and aims: Clinical relevance of animal models for NASH is crucial for assessment of in vivo efficacy of compounds in development. The validity of efficacy assessment rests on histopathology of not only steatosis, ballooning and inflammation but also fibrosis. However, hepatic fibrosis varies from model to model. In the current study, we applied an automated quantitative DP-AI system to a mouse model of NASH to evaluate the hepatic fibrosis and the antifibrotic activity of obeticholic acid (OCA), in particular the fibrous septa that are typical in the late-stage of the NASH patients.

Method: In the mouse NASH model, after animals develop steatosis on feeding of high-fat diet (HFD), they are treated with carbon tetrachloride (CCL4) to induce hepatic fibrosis. Test compounds are administered during the CCL4 induction. The liver histopathology is analyzed by the standard means. For DP-AI analyses, second-harmonic generation (SHG)/two-photon excitation fluorescent (TPEF) microscopy is used for imaging of unstained liver sections. Collagen fibers are identified and quantified by an AI-based algorithm that recognizes the portal tract (PT) and the central vein (CV), and examines collagen bundles therebetween, with reference to septa diagnosed in the human NASH livers.

Results: Our previous studies indicated that the combination of HFD and CCL4 induces an extra level of fibrosis that is the target of antifibrotic activity of OCA. DP-AI analyses confirmed this observation. While CCL4 alone induced significant fibrosis, an extra level of fibrosis was induced by the combination, as determined by SHG% (of total area). With the treatment of OCA, the extra fibrosis was suppressed (Fig. 1-B). Although a basal level of fibrosis was observed in both the healthy control and the HFD induction by SHG% (Fig. 1-B), no or minimal septa were present in either (Fig. 1-C). The induction of septa was greatly increased when HFD and CCL4 were combined (septas vs. SHG% in Fig. 1-B and -C). The OCA treatment reduced septa in the HFD+CCL4 model by ~50%, quantitatively much greater than that determined by SHG% (Fig. 1-B and 1-C). We then tested compounds that are in the NASH clinical trials, including agents targeting FXR, ASK1, PPAR-alpha/delta, pan-PPAR, CCR2/CCR5, THR-beta, ACC1/2, SSOA/VAP-1, and GLP1. Their efficacies were largely consistent with the respective clinical outcomes.

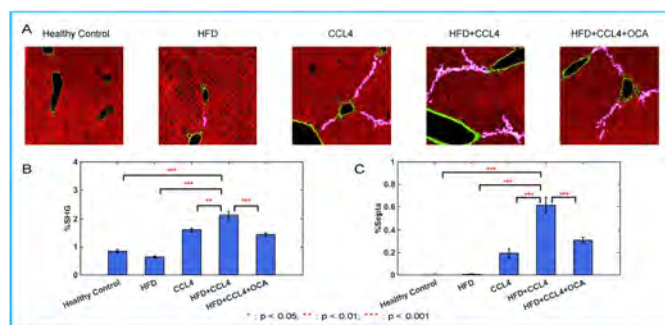


Figure 1. The SHG/TPEF images and the quantification of hepatic fibrosis in the HFD+CCL4 mouse model. A. Images of selected regions of interest from labelled sources for illustration of SHG (in green), TPEF (in red) and septae (in pink). B and C. The total collagen areas (B) and septal collagen areas (C) in whole livers from labelled animal groups, with statistical significance indicated.

Conclusion: Our results demonstrate that the septa identified by the DP-AI system in the HFD+CCL4 model are NASH related, and they are the target of antifibrotic activities of NASH compounds with demonstrated clinical efficacies. Such septa could represent the bridging fibrosis as observed the NASH patients. The HFD+CCL4 model is therefore clinically relevant in terms of histopathological presentation and targets of NASH compounds.

SAT031

Small changes in the metabolism of bile acids by the gut microbiota are associated to NASH pathogenesis

Justine Gillard^{1,2}, Morgane Thibaut², Martin Roumain³, Giulio G. Muccioli³, Anne Tailleur⁴, Bart Staels⁴, Laure Bindels², Isabelle Leclercq¹. ¹UCLouvain, Laboratory of Hepato-Gastroenterology, Institute of Experimental and Clinical Research, Belgium; ²UCLouvain, Metabolism and Nutrition Research Group, Louvain Drug Research Institut, Belgium; ³UCLouvain, Bioanalysis and Pharmacology of Bioactive Lipids, Louvain Drug Research Institut, Belgium; ⁴University of Lille, Inserm, CHU Lille, Institut Pasteur de Lille, U1011-EGID, France
Email: justine.gillard@uclouvain.be

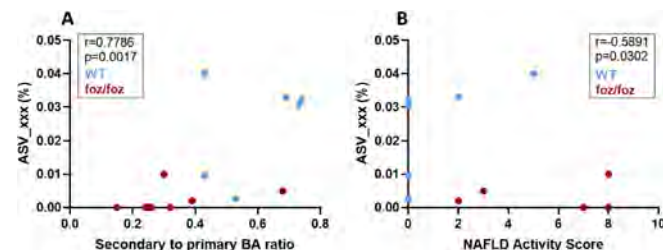
Background and aims: Primary bile acids (BAs) synthesized by the hepatocytes are secreted, modified and reabsorbed in the gut. Specifically, gut bacteria deconjugate BAs through bile salt hydrolase (BSH) activity and transform primary to secondary BAs through 7 α -dehydroxylation. We showed that BAs contribute to NASH pathogenesis and that the enterohepatic BA pool is altered and secondary BAs lowered in experimental NASH, suggesting impaired bacterial biotransformation. Here, our aim is to study the gut microbiota and its BA-metabolizing activities in a NASH experimental model.

Method: We co-housed and fed with HFD for 12 weeks *foz/foz* (NAS \geq 6) and WT (NAS \leq 1) mice and harvested samples after 12 h fasting/4 h refeeding. We analyzed microbial composition of the caecal content using 16S rRNA gene sequencing, BAs by LC-MS/MS and measured BSH activity.

Results: Alpha-diversity (measured by the Shannon and the observed amplicon sequence variant (ASV) indexes); and beta-diversity (reported by the Morisita Horn index) within and among caecal samples were similar in *foz/foz* and WT mice. The proportion of the variance explained by the genotype was low (9.2%, $p=0.32$). The relative abundances of bacterial phyla and families were not significantly different, except for the *Bacteroidaceae* family more abundant in the caecal content of *foz/foz* mice (3.13% vs 1.27% in WT, $p=0.007$).

The BSH activity in caecal content was similar in both groups, matching the similar overall microbial composition. Nevertheless, the low secondary to primary BAs ratio and the low secondary BAs concentration suggested a lower 7 α -dehydroxylase activity in *foz/foz* mice. One specific ASV was detected only in 38% of the *foz/foz* while present in 100% of the WT mice at low abundance. The relative

abundance of this ASV correlated significantly with the secondary to primary BAs ratio (Fig A), with the concentration of the secondary deoxycholic acid ($r=0.8478$, $p=0.0006$) and with the NAFLD activity score (Fig B). We hypothesized that this ASV exhibits a 7 α -dehydroxylase activity, which could explain that its lower prevalence leads to a reduced production of secondary BA, thereby contributing to NASH pathogenesis.



Conclusion: When co-housed and fed the HFD, the overall microbial composition is similar whether mice have NASH or not. Low concentration of secondary BAs in mice with NASH is associated to small changes in bacterial composition that likely impact the microbial 7 α -dehydroxylase activity.

SAT032

Unravelling the landscape of adipose tissue macrophages in human non-alcoholic fatty liver disease

Markus Boesch¹, Hannelie Korff¹, Rita Furtado Feio de Azevedo¹, Ellen Deleus², Matthias Lannoo², Lena Smets¹, Lukas Van Melkebeke^{1,3}, Marie Wallays¹, Tania Roskams⁴, Pierre Bedossa⁵, Andreas Lindhorst^{6,7}, Jef Verbeek^{1,3}, Thierry Voet^{8,9}, Alejandro Sifrim^{9,10}, Martin Gericke^{6,7}, Schalk van der Merwe^{1,3}. ¹KU Leuven, Laboratory of Hepatology, CHROMETA department, Belgium; ²KU Leuven, Department of Abdominal Surgery, Belgium; ³UZ Leuven, Department of Gastroenterology and Hepatology, Belgium; ⁴KU Leuven and University Hospital Leuven, Department of Imaging and Pathology, Belgium; ⁵Beaujon Hospital Paris Diderot University, Department of Pathology, Physiology and Imaging, France; ⁶Martin-Luther-University Halle-Wittenberg, Institute of Anatomy and Cell Biology, Germany; ⁷Leipzig University, Institute of Anatomy, Germany; ⁸Wellcome Trust Sanger Institute, Cancer Genome Project, United Kingdom; ⁹KU Leuven, Department of Human Genetics, Belgium; ¹⁰Wellcome Trust Sanger Institute, Sanger Institute-EBI Single-Cell Genomics Centre, United Kingdom
Email: markus.boesch@kuleuven.be

Background and aims: Non-alcoholic fatty liver disease (NAFLD) is the most common cause of chronic liver disease, thereby affecting 25% of the world population. Patients with non-alcoholic fatty liver (NAFL) can progress further to non-alcoholic steatohepatitis (NASH), characterized by steatosis and hepatic inflammation. It has been postulated that ongoing inflammation in the adipose tissue compartment, potentially driven by macrophages, accounts for this disease transition. Previous studies already showed a significant heterogeneity within the macrophage pool in obese adipose tissue. Here, we aim to unravel the human visceral adipose tissue macrophage population on a single cell level in a well-defined human NAFLD population.

Method: Visceral adipose tissue (VAT) biopsies were collected from obese patients undergoing bariatric surgery (UZ Leuven, Belgium). Liver biopsies were performed and assessed by expert liver pathologists based on the fatty liver inhibition of progression (FLIP) algorithm and steatosis, activity, and fibrosis (SAF) score to distinct patient groups. Adipose tissue macrophages were freshly dissociated and single cell RNA-seq was performed using 10X Genomics 3'v3 on samples of 2 obese controls without NAFLD, 3 NAFL and 4 NASH patients.

Results: The VAT contains multiple macrophage and monocyte subtypes with distinct transcriptional profiles. Among these, we observed an increased influx of pre-inflammatory macrophages and pro-inflammatory monocytes in patients with NASH compared to their obese counterparts. Additionally, anti-inflammatory/angiogenic macrophages were almost completely absent in tissue from NASH patients as compared to obese controls. Velocity and pseudotime analysis also revealed that these macrophages are no longer replenished in NASH patients.

Conclusion: Our study characterized the landscape of human adipose tissue macrophages that points towards a NASH-related loss of anti-inflammatory/angiogenic macrophages. Further studies unraveling their tissue localization and function are ongoing.

SAT033

Atorvastatin attenuates diet-induced non-alcoholic steatohepatitis in ApoE*3-Leiden mice by reducing hepatic inflammation

José A. Inia^{1,2,3}, Anita M. van den Hoek¹, Geurt Stokman¹, Martine C. Morrison¹, Elsbeth Pieterman¹, J. Wouter Jukema^{2,3}, Hans Princen¹. ¹The Netherlands organization for applied scientific research (TNO), Metabolic health research, Leiden, Netherlands; ²Leiden university medical center (LUMC), Einthoven laboratory for experimental vascular medicine, Leiden, Netherlands; ³Leiden university medical center (LUMC), Cardiology, Leiden, Netherlands
Email: jose.inia@tno.nl

Background and aims: Non-alcoholic fatty liver disease (NAFLD) is considered the hepatic manifestation of the metabolic syndrome, and due to the worldwide obesity epidemic, the prevalence of both NAFLD and the more severe form non-alcoholic steatohepatitis (NASH) is rapidly rising. Patients with metabolic syndrome are often prescribed statins to prevent development of cardiovascular disease as a result of a disturbed lipoprotein metabolism. Although the effects of statins on cardiovascular disease are relatively well described, data on their effects on NASH are lacking. Here, we evaluated the effects of atorvastatin on NASH and liver fibrosis development and inflammatory parameters.

Method: ApoE*3-Leiden mice were fed a Westernized diet (WTD) with or without atorvastatin admixture for 32 weeks. Plasma parameters and inflammatory markers were evaluated and hearts and livers were histologically and biochemically examined at study end point.

Results: Atorvastatin significantly reduced the WTD-induced increase in plasma cholesterol levels (-43% , $p < 0.01$) and thereby significantly attenuated the development of atherosclerosis (lesion area -47% , $p < 0.01$ compared to WTD). Atorvastatin significantly reduced hepatic steatosis (-22% , $p < 0.01$) and resulted in a robust decrease of hepatic inflammation (-80% , $p < 0.01$) and fibrosis (-92% , $p < 0.001$) compared to mice that received the WTD only. Interestingly, atorvastatin almost fully blunted the accumulation and formation of hepatic cholesterol crystals (-78% , $p < 0.05$), structures that drive inflammation via inflammasome activation. Analyses on inflammatory markers substantiated this effect and revealed a significant reduction in infiltration of hepatic macrophages, neutrophils and monocytes as well as lower levels of pro-inflammatory cytokines.

Conclusion: Atorvastatin attenuates the development of NASH by reducing intrahepatic cholesterol crystals and cholesterol ester levels, hepatic steatosis, inflammation and fibrosis.

SAT034

Carnitine signature in liver corretales with non-alcoholic fatty liver disease progression

Andrea Jiménez Franco¹, Helena Castañé², Gerard Baiges Gaya², Elisabet Rodríguez-Tomás¹, Jordi Camps Andreu³, Jorge Joven Marié³. ¹Universitat Rovira i Virgili, Medicine and surgery, Reus, Spain; ²Institut

d'investigació Pere Virgili, Medicine and surgery, Reus, Spain; ³Hospital universitari Sant Joan de Reus, Medicine and surgery, Reus, Spain
Email: andreafranco99@gmail.com

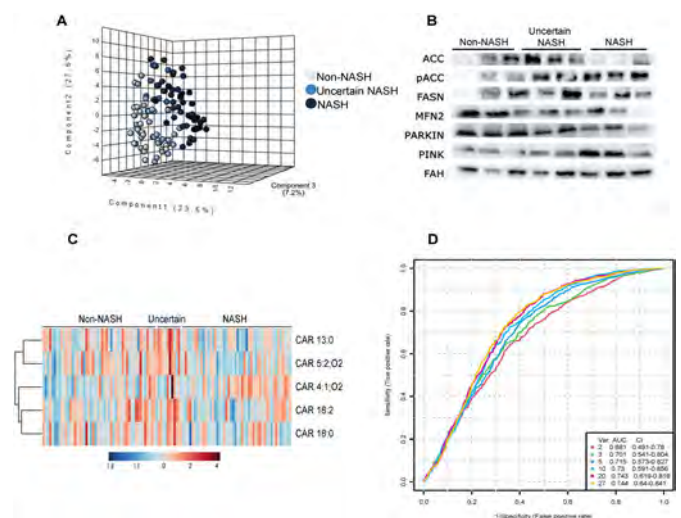
Background and aims: NAFLD is a global silent pandemic that increases in parallel with obesity, that is unknown for most of the population. NAFLD begins with simple inflammation, steatosis, and can become a severer stage known as NASH (Non-alcoholic steatohepatitis), which can only be diagnosed by liver biopsy. In the livers of NASH patients there is mitochondrial dysfunction, which impairs metabolism of the cell, impacting in its global health. Mitochondria is closely related to lipid metabolism: carnitines support the transport of fatty acids into mitochondria for beta-oxidation, thus their concentration may be affected in the development of NAFLD and its progression to NASH.

We sought to distinguish patients with NASH from patients without NASH by measuring carnitine concentrations in both plasma and liver, and to evaluate whether there may be an association between these species and mitochondrial dysfunction.

Method: The study includes 110 morbidly obese participants from the Hospital Sant Joan de Reus who have undergone bariatric surgery. From the liver biopsy we characterized NASH by using NAFLD Activity Score (NAS). 51 patients were classified as Non-NASH, 49 patients as NASH and 10 patients as Uncertain NASH diagnostic.

We performed semi-targeted lipidomics to quantify carnitine species from liver and plasma samples, and we use Western blot to semi-quantify proteins of lipid metabolism and mitophagy in liver samples.

Results: Using multivariate analysis, we have been able to determine that in the liver there was a specific profile of the lipids. By comparing the concentrations in liver of NASH patients with Non-NASH patients revealed that most carnitine concentrations were found to be decreased in NASH. Western blot results determined that both beta-oxidation and autophagy of mitochondria is highly correlated with carnitines and NAFLD. Slight differences were observed between the plasma carnitine concentrations of the different patients. Carnitines could not be used as markers for this disease because were not specific enough.



Conclusion: Beta-oxidation and proteins associated to mitochondrial dynamics and mitophagy were found to be altered as the disease progressed. Mitophagy was activated, and fatty acid beta-oxidation was suppressed. On the other hand, as the liver severity increased, carnitine decreased with a specific signature.

SAT035

Type 2 diabetes and religious fasting: effects on metabolism and liver steatosis

Svenja Sydor¹, Ender Engin¹, Mustafa Özcürümez¹, Anja Figge¹, Josef Pospiech¹, Andreas Jähnert¹, Jan Best¹, Wing-Kin Syn², Ali Canbay¹, Lars Bechmann¹, Paul Manka¹. ¹University Hospital Knappschafts Krankenhaus Bochum, Department of Internal Medicine, Bochum, Germany; ²Medical University of South Carolina, Division of Gastroenterology and Hepatology, Department of Medicine
Email: svenja.sydor@rub.de

Background and aims: Religious fasting during the holy month of Ramadan requires abstaining from food and liquids during the day. After sunset, it is allowed to consume food and drinks in defined periods. Fasting results in a reduced and timed calorie intake and can be regarded as a form of intermittent fasting. Type 2 diabetes (TD2) is a significant risk factor for the development of non-alcoholic steatohepatitis (NASH), the progressive form of non-alcoholic fatty liver disease (NAFLD). Recently several studies suggested some benefits of interval fasting for patients with TD2 and NASH. Here, we aimed to characterize the impact of a one-month interval fasting period on liver health, glucose and lipid metabolism in a cohort of T2D patients.

Method: 20 muslim patients from a German metropolitan region were included. The status of the liver was assessed by Fibroscan®, including the measurement of the controlled attenuation parameter (CAP). Additionally to anthropometric measurements, patients' blood samples were collected at the beginning and end of the four-week fasting period to quantify key parameters of liver injury, lipid and glucose metabolism.

Results: Following the fasting period transient elastography measurements (8.0 ± 1.2 vs. 8.6 ± 1.6 before/after fasting) and CAP values (311.4 ± 9.6 vs. 302.6 ± 10.4 before/after fasting) showed modest changes. In contrast, LFTs, apoptosis marker (M30), and adiponectin significantly decreased after the fasting period. Serum levels of triglycerides were lower following the fasting period. Glucose levels did not change significantly, but serum levels of C-peptide and insulin increased following the fasting period. In addition, the patients experienced a significant weight loss at the end of the fasting month.

Conclusion: In this cohort of T2D patients, we demonstrated that a 4-week intermittent fasting period resulted in an improvement in different serum parameters associated with glucose, liver, and lipid metabolism.

SAT036

The I48M PNPLA3 variant mitigates Niacin beneficial effects: how the genetic screening in non-alcoholic fatty liver disease (NAFLD) patients gains value

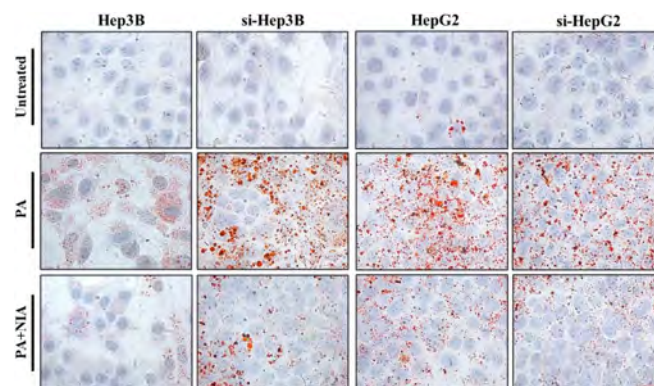
Erika Paolini^{1,2}, Miriam Longo^{1,3}, Marica Meroni¹, Roberto Piciotti^{1,3}, Annalisa Cespiati^{1,4}, Rosa Lombardi^{1,4}, Anna Ludovica Fracanzani^{1,4}, Paola Dongiovanni¹. ¹General medicine and metabolic diseases, Fondazione IRCCS Cà Granda ospedale maggiore policlinico, Milan; ²Università degli Studi di Milano, Milan, Italy, Department of Pharmacological and Biomolecular Sciences, Milan; ³Department of Clinical Sciences and Community Health; ⁴Università degli Studi di Milano, Fondazione IRCCS Cà Granda Ospedale Maggiore Policlinico, Milan, Italy, Department of Pathophysiology and Transplantation
Email: paola.dongiovanni@policlinico.mi.it

Background and aims: The PNPLA3 p.I148M variant is the main genetic predictor of NAFLD and its impact on fat accumulation can be modulated by nutrients. Niacin (NIA) reduces triglycerides (TGs) synthesis and ROS production in NAFLD patients. However, the interplay between NIA and p.I148M polymorphism has not been explored yet. This study aims to: 1) assess the dietary and circulating NIA levels in NAFLD patients stratified according to the presence of the p.I148M variant; 2) examine the efficacy of NIA in Hep3B and HepG2 cells, which are wild-type and homozygous for the p.I148M mutation, respectively.

Method: We enrolled 172 patients (Discovery cohort) with non-invasively assessed NAFLD. Dietary NIA was collected from food diary, while serum NIA was quantified by ELISA. Hepatic expression of genes related to NAD metabolism was evaluated by RNAseq in bariatric NAFLD patients (n=125). HepG2 and Hep3B cells were transfected with a siRNA targeting PNPLA3 and treated with palmitic acid (PA) 0.25 mM alone/plus NIA 0.5 mM for 24 hrs.

Results: At bivariate analysis NAFLD patients showed reduced dietary NIA ($p = 0.01$). The p.I148M variant was correlated with lower levels of alimentary and circulating NIA ($p = 0.01$, $p = 0.03$ vs non-carriers). At multivariate analysis, adjusted for sex, BMI, and alimentary NIA, the p.I148M mutation was associated with reduced serum NIA ($\beta = -18.01$; CI: -35.6–0.57; $p = 0.04$), suggesting that it may independently modulate NIA systemic availability. The expression of enzymes related to NAD biosynthesis was impaired in p.I148M carriers ($p = 0.006$).

NIA supplementation reduced TG synthesis alongside oxidative injury and ER stress in hepatoma cells ($p < 0.001$, $p < 0.05$ vs PA). The efficacy of NIA was hidden by the p.I148M variant in HepG2 cells, suggesting that the loss of lipase activity blunted the NIA protective role. Consistently, PNPLA3 silencing masked the beneficial effect of NIA on TG overload in Hep3B cells, whereas it didn't affect fat accumulation in HepG2 ones ($p < 0.001$, $p < 0.05$ vs PA). The effectiveness of NIA on oxidative/ER stress was maintained in both cell lines silenced for PNPLA3 ($p < 0.001$, $p < 0.05$ vs PA), thus suggesting that it might mitigate the protective role of NIA in lipid handling but not in hepatocellular damage.



Conclusion: NIA levels were reduced in NAFLD patients who carry the p.I148M variant. PNPLA3 silencing compromised the efficacy of NIA in hepatoma cells, thus suggesting its supplementation in NAFLD patients should be preceded by genetic screening.

SAT037

The co-presence of PNPLA3, MBOAT7 and TM6SF2 loss-of-functions impairs mitochondrial morphology and number in severe NAFLD patients

Miriam Longo^{1,2}, Erika Paolini^{1,3}, Marica Meroni¹, Michela Ripolone⁴, Laura Napoli⁴, Roberto Piciotti^{1,2}, Marco Maggioni⁵, Maurizio Moggio⁴, Anna Ludovica Fracanzani^{1,6}, Paola Dongiovanni¹. ¹Fondazione IRCCS Cà Granda Ospedale Maggiore Policlinico, General Medicine and Metabolic Diseases; ²University of Milan, Department of Clinical Sciences and Community Health; ³University of Milan, Department of Pharmacological and Biomolecular Sciences; ⁴Fondazione IRCCS Cà Granda Ospedale Maggiore Policlinico, Neuromuscular and Rare Diseases Unit; ⁵Fondazione IRCCS Cà Granda Ospedale Maggiore Policlinico, Division of Pathology; ⁶University of Milan, Department of Pathophysiology and Transplantation
Email: paola.dongiovanni@policlinico.mi.it

Background and aims: Mitochondrial (mt-) dysfunction is a key event occurring in the progressive forms of non-alcoholic fatty liver

disease (NAFLD) up to hepatocellular carcinoma (HCC). We previously demonstrated that human HepG2 cells, homozygous for the I148M PNPLA3 variant and silenced for *MBOAT7* and *TM6SF2* genes (*MBOAT7*^{-/-}*TM6SF2*^{-/-}) by CRISPR/Cas9, enriched mt-mass and accumulated damaged mitochondria with loss of cristae paralleled by functional defects in the oxidative phosphorylation. In the attempt to translate *in vitro* results in human NAFLD, we aimed to: 1) assess whether mt-morphology, circulating *D*-loop copy number and expression, which reflect mt-mass, correlated with disease severity and number of the 3 at-risk variants (NRV=3) in biopsied NAFLD subjects (n=26, Discovery cohort); 2) evaluate circulating *D*-loop levels in a larger cohort of biopsied NAFLD patients (n=773, Validation cohort), including n=101 NAFLD-HCC. Hepatic *D*-loop levels were evaluated in intra- and extra-tumoral tissues of 3 NAFLD-HCC individuals.

Method: NAFLD patients were stratified according to NRV and to NAFLD activity score (NAS). Mt- morphology was assessed by transmission electron microscopy (TEM).

Results: In the Discovery cohort, NAFLD patients with NRV=3 showed NAS=5–7 along with the highest *D*-loop content compared to patients with 1–2 or no variants ($p<0.01$), reflecting what observed *in vitro*. At TEM, patients carrying NRV=3 showed an enrichment of mt-mass and an elevated pattern of mt-morphological alterations as swollen shapes with loss of internal matrix, rupture of double membranes or giant/elongated mitochondria. In the Validation cohort, the NRV=3 associated with NAS and HCC risk ($p<0.05$) at multivariate analysis adjusted for age, sex, BMI and diabetes. At ordinal regression analysis adjusted as above plus the presence of NRV=3, the *D*-loop levels were independently associated with steatosis, necroinflammation, ballooning, fibrosis, and NAS ($p<0.001$) and were significantly increased in NAFLD patients with NRV=3 ($p=0.03$). Finally, in 3 NAFLD-HCC patients *D*-loop copies were higher in the intra-tumoral tissues compared to extra-tumoral ones, showing the highest number in one patient carrying all 3 at-risk variants.

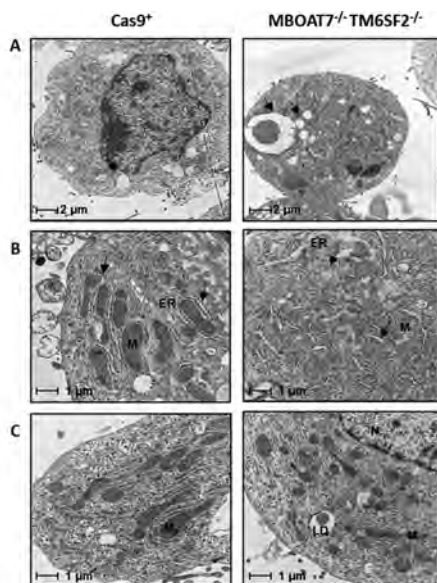


Figure 1: A) Representative TEM images of lipid droplets (LDs) accumulation in the *MBOAT7*^{-/-}*TM6SF2*^{-/-} vs HepG2 Cas9 positive cells exploited as wild-type control (*Cas9*⁺). B-C) Representative TEM images of degenerative mitochondria (M) and mitochondrial biomass. TEM images were obtained by ultrathin 70 nm sections of hepatocytes (bar scale: 1–2 μm). Black arrows indicated LDs (A) or M (B). Capital letters refer to nucleus (N) and endoplasmic reticulum (ER).

Conclusion: PNPLA3, *MBOAT7* and *TM6SF2* loss-of-functions impair mt-functionality and mass *in vitro* and NAFLD patients. The assessment of *D*-loop copies may be a useful biomarker for the evaluation of disease course in genetically predisposed subjects.

SAT038

The association of spleen volume with sex, age, type 2-diabetes, and non-alcoholic fatty liver disease-initial results from more than 35, 000 UK Biobank participants

Samuel Helgesson¹, Sambit Tarai¹, Taro Langner², Håkan Ahlström^{1,2}, Lars Johansson², Joel Kullberg^{1,2}, Elin Lundström^{1,2}. ¹Uppsala University, Department of Surgical Sciences, Radiology, Sweden; ²Antaros Medical AB, BioVenture Hub, Mölndal, Sweden
Email: samuel.helgesson@gmail.com

Background and aims: Non-alcoholic fatty liver disease (NAFLD) is defined as excessive hepatic fat infiltration not related to alcohol/drug abuse. When estimating liver fat with magnetic resonance imaging (MRI), a threshold of 5.56% is typically used for NAFLD (Szczepaniak *et al.* 2004). The contemporary pandemics of obesity and type 2-diabetes (T2D) drive a global increase in NAFLD, with a substantial risk of sequential progression to non-alcoholic steatohepatitis, fibrosis, and cirrhosis. As interconnected to the liver via the hepatic portal vein, the spleen can be enlarged due to increased portal venous pressure as a result of hepatic fibrosis. However, the current knowledge of the spleen volume (SV) distribution in a normal aging cohort, and its association with T2D and early stages of NAFLD, is limited and therefore the subject of investigation in this work.

Method: A deep-learning method for spleen segmentation and SV estimation was developed and validated (training data=85 manual segmentations, Dice score=93%, symmetric mean absolute percentage error=7.88%) on neck-to-knee MRI images from the UK Biobank (UKBB). In total, 37, 019 subjects were included in the study after exclusion of 1, 800 subjects with potential failure segmentations, according to algorithmic quality ratings (Langner *et al.* 2020), and an additional 18 subjects diagnosed with alcoholic liver disease. Liver proton density fat fraction (PDFF) were available for 4, 613 subjects in the UKBB. Using deep regression on the abovementioned MRI images, liver PDFF was inferred for remaining subjects. The cohort was grouped into Controls (unlikely diabetic, n=33, 970) and T2D subjects (n=1, 558), using an algorithm developed on UKBB clinical data (Eastwood *et al.* 2016) and by discarding intermediate/possible diabetic subjects.

Results: Moving average curves of SV vs age, in controls and subjects with T2D, are presented in Fig 1A, with 95% confidence intervals (CI) of the weighted arithmetic average SV displayed. Similar curves of SV vs liver PDFF are presented in Fig 1B. The SV was larger in males than females and in T2D compared to controls, for both sexes, within the approximate age range 55–77 years. There was a similar pattern of age-related decrease in SV in male and female controls. Within certain age intervals, SV appeared to decrease faster with age in T2D subjects compared to in controls. Increasing SV with increasing liver PDFF was observed for both sexes already at low liver PDFF values. For liver PDFF >25%, the measurement uncertainty (CI) was relatively large, as influenced by the low sample size.

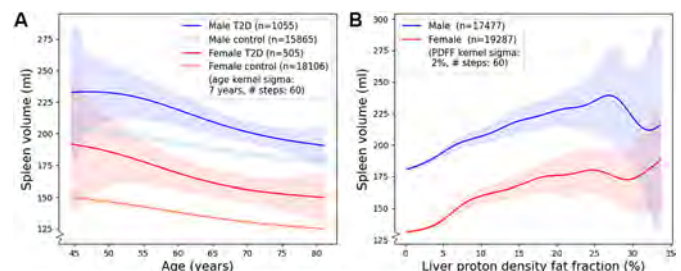


Figure 1. Moving weighted average curves of (A) spleen volume (SV) as a function of age, sex, and type 2-diabetes (T2D), and (B) SV as a function of liver proton density fat fraction (PDFF) and sex. Weighted arithmetic mean values and 95% confidence intervals are based on a gaussian age kernel sigma of 7 years (in A) and a gaussian PDFF kernel sigma of 2% (in B). Wider confidence intervals in the lowest and highest ages (in A) and highest PDFF values (in B) are influenced by the relatively low sample size in these ranges.

Conclusion: Clear patterns demonstrated men, younger subjects, and individuals with T2D and NAFLD to have larger spleens compared to

POSTER PRESENTATIONS

females, older subjects, and disease group controls, respectively. The enlarged spleen observed in disease could reflect an increased portal venous pressure occurring already early in NAFLD.

SAT039

Targeting adipose tissue macrophages ameliorates hepatic injury in a murine model of NAFLD

Celia Martínez Sánchez^{1,2}, Mar Coll¹, Delia Blaya¹, Octavi Bassegoda^{1,3}, Muhammad Fayyaz⁴, Raquel A. Martínez García de la Torre¹, Kelly Swanson⁴, Pau Sancho-Bru¹, Andrew Smith⁵, Pere Ginès^{1,2,3}, Isabel Graupera^{1,3}, Laia Aguilar¹. ¹Institut d'Investigacions Biomèdiques August Pi i Sunyer (IDIBAPS), Liver Unit, Barcelona, Spain; ²Centro de Investigación Biomédica en Red de Enfermedades Hepáticas y Digestivas (CIBERHD), Spain; ³Hospital Clínic de Barcelona, Spain; ⁴University of Illinois at Urbana-Champaign, United States; ⁵University of Illinois at Urbana-Champaign
Email: celiamartinezsa@gmail.com

Background and aims: Adipose tissue dysfunction with infiltration of pro-inflammatory macrophages is a hallmark in obesity leading to an impairment of metabolic homeostasis. Non-alcoholic fatty liver disease (NAFLD) is intimately associated with obesity and it has been shown that pro-inflammatory adipose tissue macrophages (ATMs) induce hepatic inflammation although their role in fibrogenesis is still unknown. The aim of the present study is to assess the role of ATMs in hepatic fibrogenesis by modulating the pro-inflammatory phenotype of ATMs.

Method: Dextran (500 kDa) nanocarriers conjugated with dexamethasone (dexa) were used to modulate ATMs' phenotype in a NAFLD models based on high-fat (HFD) and high fat high cholesterol (HFHC) diets. After feeding animals for 5 months, dextran conjugates were administered i.p. twice per week for 5 additional weeks. In order to study dextran uptake, i.p. administration of dextran-FITC was evaluated by flow cytometry and immunofluorescence. Hepatic and AT macrophages' phenotype switch was assessed by flow cytometry and gene expression analysis. The anti-inflammatory effect of dexa-conjugates in liver and adipose tissue was evaluated by assessing key inflammatory markers expression by qPCR and immunostaining. Changes in hepatic fibrosis and NAS score were explored by histopathological analysis. In-vitro phenotypic modulation of human ATMs incubated with dextran conjugates were evaluated by qPCR. The effect of human ATMs on hepatic stellate cells (HSCs) activation was assessed by culturing HSCs with ATMs conditioned media.

Results: Animals fed with HFHC diet displayed increased liver and adipose tissue macrophage infiltration with an enhanced pro-inflammatory phenotype compared to animals receiving HFD. Compared to HFD, liver tissue from HFHC model showed higher NAS score and fibrosis degree. Dextran-dexa conjugates were predominantly engulfed by macrophages from the AT. Conjugated nanocarriers administration significantly switched the pro-inflammatory phenotype of ATMs without significant differences in liver macrophages. Dextran-dexa treatment caused a significant reduction of hepatic inflammation, NAS score, and hepatic fibrosis in the HFHC model. Human ATMs treated with dextran-dexa attenuated their pro-inflammatory phenotype and reduced HSCs activation.

Conclusion: Dextran-dexamethasone conjugates administrated i.p. are predominantly uptaken by adipose tissue macrophages inducing a switch of their pro-inflammatory phenotype which in turns attenuates liver inflammation and fibrosis. In vitro modulation of human ATMs by dextran nanocarriers reduce activated phenotype of HSCs. These results demonstrate that modulating the pro-inflammatory phenotype of ATMs might be a good strategy to reduce hepatic fibrosis and inflammation in NAFLD.

SAT040

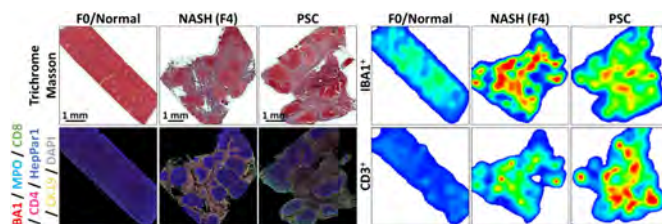
Multiplex immunostaining and transcriptomic profiling identify novel immune cell markers for non-alcoholic steatohepatitis and primary sclerosing cholangitis

Adrien Guillot¹, Marc Winkler¹, Milessa Silva Afonso², Abhishek Aggarwal³, Hilmar Berger¹, David Lopez⁴, Marlene Kohlhepp¹, Hanyang Liu¹, Sangeetha Mahadevan³, Lauri Diehl³, Ruchi Gupta², Frank Tacke¹. ¹Charité Universitätsmedizin Berlin, Department of Hepatology and Gastroenterology, Berlin, Germany; ²Gilead Sciences, Department of Fibrosis Biology, United States; ³Gilead Sciences, Department of Nonclinical safety and Pathobiology, United States; ⁴Gilead Sciences, Department of Research Data Sciences, United States
Email: adrien.guillot@charite.de

Background and aims: The progression of non-alcoholic fatty liver disease (NAFLD) towards non-alcoholic steatohepatitis (NASH) and of primary sclerosing cholangitis (PSC) is accompanied by hepatic infiltration of immune cells. This study aims to combine multiple novel analytic methods for the evaluation of disease stage associated transcriptomic, proteomic and histological changes, and for identifying similarities and differences between NAFLD, NASH, and PSC patients.

Method: Human liver samples (total n = 85) from two independent patient cohorts and mouse samples from a diet induced obesity (DIO) model of NASH and Mdr2-deficient mice (total n = 35) were used. RNA-sequencing and immunostaining by using InSituPlex multiplex immunofluorescence technology were performed on human samples. A specific, adapted sequential immunostaining method for hepatic parenchymal and immune cells was used on all human and mouse samples. Imaging cytometry and clinical or phenotypic data were combined for multidimensional analysis. Key findings on immune cell composition and phenotypes were validated in human clinical samples and functionally tested in mouse models.

Results: NASH and PSC disease stage was associated with significant loss of parenchymal areas, increased fibrosis and defined infiltration of myeloid and lymphoid cell populations. NASH patients predominantly exhibited myeloid cell infiltration, whereas PSC patients had a pronounced lymphoid cell response (Figure). Both diseases displayed intense ionized calcium-binding adapter molecule 1 (IBA1+) macrophage accumulation in the peribiliary areas. Using a machine learning-based algorithm, IBA1 in combination with hepatocyte and ductular cell immunostaining predicted advanced disease stage in NASH and PSC. These findings were validated in mouse models of NASH and PSC and macrophage phenotype was further characterized in rodent samples.



Conclusion: Monocyte/macrophage infiltration and accumulation represents the dominant histological feature associated with the progression of NAFLD, NASH and PSC. Our findings show that IBA1, a pan-macrophage marker, is predictive of disease progression in human and mouse livers.

SAT041

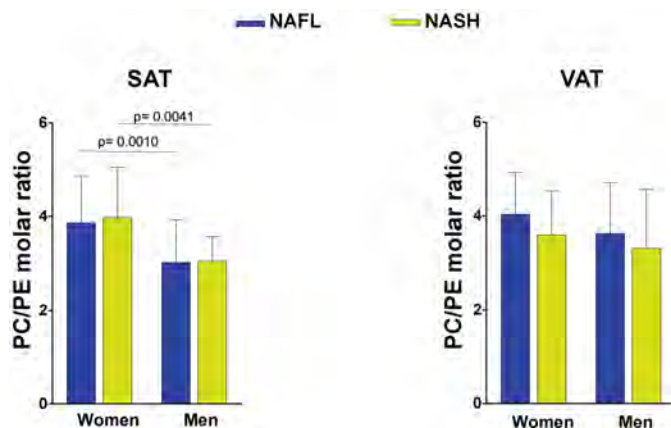
Phospholipid fingerprints reveal sex differences in the adipose tissue phospholipid composition from morbidly obese patients

Gerard Baiges^{1,2}, Elisabet Rodríguez-Tomás², Helena Castañé^{1,2}, Andrea Jiménez Franco², Jordi Camps³, Jorge Joven^{1,2,3}. ¹Fundación Instituto de Investigación Sanitaria Pere Virgili, Tarragona, Spain; ²Rovira i Virgili University, Tarragona, Spain; ³Hospital Universitari Sant Joan de Reus, Reus, Spain
Email: gerardbaiges93@gmail.com

Background and aims: Obesity is a metabolic disease that requires adipose tissue mechanisms of hyperplasia and hypertrophy to ensure energy storage. Nevertheless, men show a higher risk to have insulin resistance, diabetes mellitus and liver disease at a lower weight than women. Phospholipid metabolism plays an important role in the development of adipocytes as well as in determining their size. Concretely an enrichment of phosphatidylcholine (PC) in the plasma membrane of adipocytes increases their fluidity and size too. Thus, the purpose of the study was to explore the phospholipid metabolism in both subcutaneous and visceral adipose tissue to observe if their regulation is influenced by sex and the liver disease severity.

Method: Semi-targeted lipidomic was carried out from abdominal-subcutaneous (SAT) and omental-visceral adipose tissue (VAT) morbidly obese patients candidates to undergoing bariatric surgery. The patients were classified based on pathology severity: non-alcoholic fatty liver (NAFL)- NAFLD activity score (NAS) between 0 and 2 (38 women and 13 men); non-alcoholic steatohepatitis (NASH)-NAS ³ 5 (34 women and 18 men).

Results: We observed the phospholipid levels were not influenced in both tissues by the liver disease progression. Nevertheless, we found that women showed a higher PC/PE molar ratio than men, independently of the disease severity. In addition, we found a less content of polyunsaturated fatty acids in the sn2-position of lysophosphatidylcholines (sn2LPC) between women and men, evidencing different responses in the lipid remodelling. This lipid remodelling in women was associated with an increase of fatty acids (C22) as well as the number of desaturation (n-6). Taken together, C22:6 fatty acid has been associated with anti-inflammatory lipid mediators, indicating women could be more resistant to adipose tissue inflammation than men.



Conclusion: These results demonstrate that women and men have a different phospholipid fingerprint, conferring different biological properties to adipocytes. Thus, the higher PC/PE molar ratio observed in women could explain the intrinsic capability to get more fat in SAT regions than men.

SAT042

Ubiquitination of GSDMD regulated by NEDD4 is involved in hepatocyte pyroptosis of non-alcoholic steatohepatitis

Rui Jin¹, Xiaoxiao Wang², Feng Liu², Huiying Rao². ¹Peking University People's Hospital, Peking University Hepatology Institute, Beijing, China; ²Peking University People's Hospital, Peking University Hepatology Institute, Beijing, China
Email: rao.huiying@163.com

Background and aims: Hepatic injury and death are significant histological features of non-alcoholic steatohepatitis (NASH). Previous studies have shown that gasdermin D (GSDMD)-mediated pyroptosis is involved in the progression of NASH, but its specific mechanism is still unclear. This study intends to clarify further the signaling pathway of GSDMD involved in pyroptosis of liver cells in NASH and further explore the role of ubiquitin enzymes regulating GSDMD in the pathogenesis of NASH.

Method: Methionine-choline deficient (MCD) diet fed male wildtype C57BL/6 mice aged 6–8-week mice to induce NASH mouse model. CRISPR technique (AAVDJ-TBG-GSDMD-SaCas9 system) was used to target and knock down hepatocellular GSDMD in mice. Immunoprecipitation combined with multi-dimensional mass spectrometry was used to identify the ubiquitinase regulating GSDMD. Normal human cell line L02 were also used to investigate the effect of pyroptosis in hepatocytes on liver inflammation and injury.

Results: Compared with control mice, the expression level of GSDMD mRNA in the liver of NASH mice was downregulated, however, the GSDMD protein levels were upregulated, suggesting that GSDMD protein might undergo post-translational modifications. By detecting the expression and cellular localization of GSDMD in the liver by immunohistochemical staining, we found that the GSDMD positive cells in the liver of NASH mice were mainly hepatocytes, suggesting that GSDMD mediated pyroptosis mainly occurred in hepatocytes. We also tried to identify the exact pathway that induced pyroptosis in NASH and found that Caspase1 protein levels and cleavage were increased in NASH mice compared with control ones, whereas Caspase11 protein levels were not significantly changed, suggesting that pyroptosis in the liver is mainly induced by the activation of classical pathway. Further detection found that the ubiquitination level of GSDMD was increased in Caspase1 knockdown mice, suggesting that the decrease of the ubiquitination level of GSDMD during the progression of NASH depends on caspase1. By analyzing immunoprecipitation combined with multi-dimensional mass spectrometry, compared with control mice, the expression level of E3 ubiquitin ligase NEDD4 downregulated in NASH mouse model. We further verified that NEDD4 was an interacting protein of GSDMD.

Conclusion: NEDD4 might be involved in the ubiquitination of with GSDMD to promote hepatocyte pyroptosis which depended on caspase1 in NASH development.

SAT043

Unraveling the transcriptional dynamics of NASH pathogenesis affecting atherosclerosis development

Anita M. van den Hoek¹, Serdar Özsezen², Martien P. M. Caspers², Geurt Stokman¹, Arianne van Koppen¹, Roeland Hanemaaijer¹, Lars Verschuren². ¹The Netherlands Organization for Applied Scientific Research (TNO), Department of Metabolic Health Research, Leiden, Netherlands; ²The Netherlands Organization for Applied Scientific Research (TNO), Department of Microbiology and Systems Biology, Zeist, Netherlands
Email: a.vandenhoeck@tno.nl

Background and aims: The prevalence of non-alcoholic steatohepatitis (NASH) is rapidly increasing and is associated with an increased incidence of cardiovascular disease (CVD). In fact, CVD remains the major overall cause of mortality in patients with NASH. Although NASH and CVD share common risk factors, the mechanisms by which NASH may directly contribute to the development to CVD remain poorly understood. The aim of this study was to gain insight

POSTER PRESENTATIONS

into the dynamics of key molecular processes of NASH that drive atherosclerosis development.

Method: A time-course study was performed in *Ldlr*^{-/-}.Leiden mice, a well-established model for hyperlipidemia that develop NASH with advanced fibrosis and atherosclerosis when fed a high fat diet. NASH and atherosclerosis development in the aortic root were histologically analyzed. Comprehensive transcriptome analysis of liver and aorta was used to identify the temporal dynamics of key processes in both tissues. Dynamical GENIE3 (dynGENIE3) was used for gene regulatory network (GRN) inference using the differentially expressed genes (DEGs) from time series. In this way liver regulators were identified for each aorta target gene by extracting dynamics in the liver that precede dynamics in the aorta and were linked to atherosclerosis development.

Results: The *Ldlr*^{-/-}.Leiden mice developed obesity, hyperlipidemia, insulin resistance in a time-dependent manner with hepatic steatosis and development of hepatic inflammation preceding the atherosclerosis development. Transcriptome analysis of liver and aorta revealed a time-dependent increase of pathways related to NASH and fibrosis followed by an increase in proatherogenic processes the aorta. DynGENIE3 identified specific liver regulators related to lipid metabolism (SC5D and TM7SF2), inflammation (IL1A) and fibrosis (PDGF) linked to a set of aorta target genes related to vascular inflammation (TNFA) and atherosclerosis signaling (VCAM1 and CCL2).

Conclusion: Time-resolved analyses of NASH and atherosclerosis in *Ldlr*^{-/-}.Leiden reveal pathogenic liver processes precede atherosclerosis development in the aorta. Gene regulatory network analysis identified hepatic key regulators and gene modules driving the atherogenic pathways and regulators in the aorta.

SAT044

Repeated weight cycling in obese mice improves hepatic inflammation

Jelle C.B.C. de Jong^{1,2}, Nanda Keijzer¹, Nicole Worms¹, Geurt Stokman¹, Nikki van Trigt¹, Aswin L. Menke¹, Anita M. van den Hoek¹. ¹The Netherlands Organization for Applied Scientific Research (TNO), Metabolic Health Research, Leiden, Netherlands; ²Wageningen University, Human and Animal Physiology, Wageningen, Netherlands
Email: a.vandenhoeck@tno.nl

Background and aims: Lifestyle interventions aimed to reduce body weight remain the current treatment of choice for non-alcoholic steatohepatitis (NASH), but are difficult to maintain and often lead to cycles of weight loss and regain (weight cycling). Although pertaining literature on weight cycling remains controversial, numerous studies indicate that weight cycling leads to an increased risk of developing Type 2 Diabetes or cardiovascular disease. Relative few studies investigated the association between weight cycling and NASH and therefore this was the aim of our study.

Method: *Ldlr*^{-/-}.Leiden mice received a high fat diet (HFD) for 20 weeks to induce obesity and NASH. Mice were then maintained for 16 weeks on the HFD (control group) or were subjected to 4 weight cycling episodes (using diet change). In addition, a group of mice on HFD were added with a similar body weight as the weight cycling group upon sacrifice (weight matched HFD reference group). The effects on body composition, plasma and liver biochemical variable and liver and fat histology were assessed.

Results: Weight cycling tended to slightly decrease body weight and total fat mass as compared to the HFD control group, but adipocyte size and fat inflammation were similar. Weight cycling did not result in a significant change in blood glucose or plasma insulin levels as compared to HFD control group, while plasma alanine transferase (ALT) levels were significantly reduced (with -40%, $p = 0.010$) and tended to be reduced as well as compared to weight matched HFD reference group (with -16%, $p = 0.051$). Hepatic macrovesicular steatosis was similar in the weight cycling and HFD control group (28% and 29%, respectively). Microvesicular steatosis tended to be

increased upon weight cycling (from 17% in HFD control to 24% in weight cycling group, $p = 0.077$), but not as compared to the weight matched HFD reference group (20% microvesicular steatosis). Weight cycling resulted in a robust decrease in hepatic inflammation as compared to both HFD control group (with -67%, $p = 0.004$) and weight matched HFD reference group (with -60%, $p = 0.014$). Hepatic fibrosis was not affected by weight cycling.

Conclusion: The results of our weight cycling experiment argue against the postulate that weight cycling leads to unfavorable metabolic effects and in fact revealed a beneficial effect on hepatic inflammation.

SAT045

The functional roles of BMP10 in the pathogenesis of non-alcoholic fatty liver disease

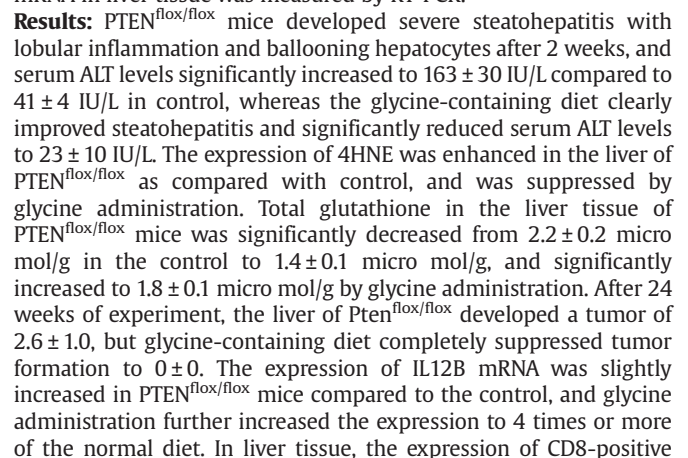
Wenjun Zhang¹, Hanying Chen², Ying Liu³, Zachary Rokop¹, Weinian Shou³, Chandrashekhar Kubal¹. ¹Indiana University School of Medicine, Department of Surgery, Indianapolis, United States; ²Indiana University School of Medicine, Genome Editing Center, Indianapolis, United States; ³Indiana University School of Medicine, Department of Pediatrics, Indianapolis, United States
Email: sakubal@iupui.edu

Background and aims: BMP10 belongs to the Transforming Growth Factor (TGF)-beta superfamily that comprises of more than 45 cytokines based on amino acid sequence homology. Unlike most of other BMP proteins that only function locally at the site of expression (autocrine/paracrine function), BMP10 can act on remote tissue as a circulating cytokine (endocrine function). Recently, BMP10 expression was detected in hepatic stellate cells in human liver. Here we investigated the roles of BMP10 in the regulation of homeostasis of liver metabolism and pathogenesis of non-alcoholic fatty liver disease (NAFLD).

Method: We generated *Bmp10*^{lox/lox} mice and crossed with the *Rosa26-CreERT2* mice to create BMP10 postnatal conditional knockout mice (named as *Bmp10cKO*), which *Bmp10* can be efficiently ablated via activated Cre recombinase activity in all adult tissues/cell types following estrogen agonist-tamoxifen induction in the postnatal mouse. *Bmp10cKO* mice (male, 8-week-old) and controls (*Bmp10*^{lox/lox}) were subjected to high fat high sucrose diet (HFSD) feeding for 20 weeks. A normal chow diet (ND) was used as feeding control. At the end of the diet exposure, we evaluated: (i) liver histology (ii) liver fibrosis by fast green/Sirius red staining; (iii) liver functional tests; (iii) immunoreactivity of selected inflammatory cell markers by IHC (F4/80) and qPCR of inflammatory genes. Total RNA samples for RNA-seq analysis were isolated from *Bmp10pCKO* (BCK) and their littermate control. Finally, we measured circulating BMP10 levels in sera of 9 patients with established cirrhosis undergoing liver transplantation (4 with non-alcoholic steatohepatitis (NASH)) before and after transplantation and compared to 5 healthy controls.

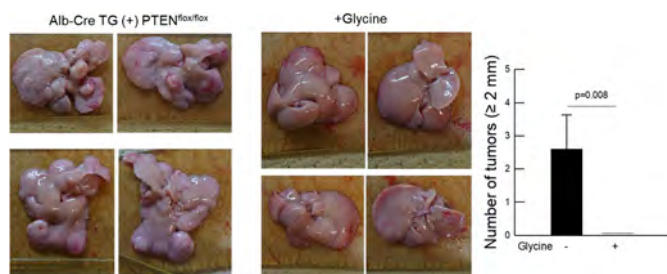
Results: After prolonged HFSD exposure, histological analyses demonstrated a significantly reduced degree of steatosis and fibrosis in the livers from *Bmp10pCKO* mice when compared with controls (Fig. 1A). There were a significantly fewer Kupffer cell (KC) clusters in *Bmp10pCKO* livers when compared to control livers (Fig. 1B). RT-PCR analysis demonstrated that the expression TNF α , IL1B and TGF β were reduced in *Bmp10pCKO* livers. Transcriptomics analysis in combination with Gene Ontology (GO) analysis revealed that leukocyte cell-cell adhesion, fatty acid metabolism, and lipid localization process were among the most altered Biological Process (BP) (Fig. 1C). In cirrhotic patients undergoing liver transplantation, we found that circulating BMP10 levels are significantly elevated prior to transplantation as compared to the post-transplant levels and normal controls, reaching to an average value of 2.89 ± 1.46 ng/ml ($p < 0.001$) (Fig. 1D).

Results: The mean (SD) age and BMI for severe HI pts (n = 8) were 55.5 (3.7) years and 34.3 (12.0) kg/m², respectively, compared with 56.1 (4.1) years and 30.6 (8.3) kg/m², respectively, for normal-matched pts (n = 8). Relative to normal-matched pts, siRNA geometric mean exposure (AUC_(0-T)) was 163% greater in pts with severe HI, and C_{max} was higher by 58% (figure). DPD exposure was 31% higher in pts with severe HI compared with normal-matched pts and C_{max} was 6% higher. The severe HI cohort also had a 452% increase in S104 exposure (88% higher C_{max}), and a 44% increase in HEDC exposure (23% higher C_{max}) compared with normal-matched pts. In total, 3/8 pts had 4 adverse events (AEs) in the severe HI cohort (infusion-related reaction [IRR; n = 2], nausea [n = 1], and dysuria [n = 1]); no normal-matched pts had AEs. Two pts experienced treatment-related AEs that were IRRs of severe back pain/chest tightness that resolved in less than 30 minutes without requiring treatment or study discontinuation.



POSTER PRESENTATIONS

lymphocytes of PTEN^{flox/flox} mice was increased by glycine-containing diet.



Conclusion: Glycine markedly improved steatohepatitis and inhibited hepatic tumorigenesis in hepatocyte-specific PTEN knockout mice. Our findings indicated that glycine acts as anti-oxidative stress to improve steatohepatitis in the early stages, and contributes to the activation of antitumor immunity and suppresses tumor formation in the carcinogenic stage. It was demonstrated that glycine has the potential to prevent NASH-related carcinogenesis.

SAT048

Advanced quantitative phenotypic fibrosis and steatosis scoring is more superior to histology-based conventional staging in NASH animal models

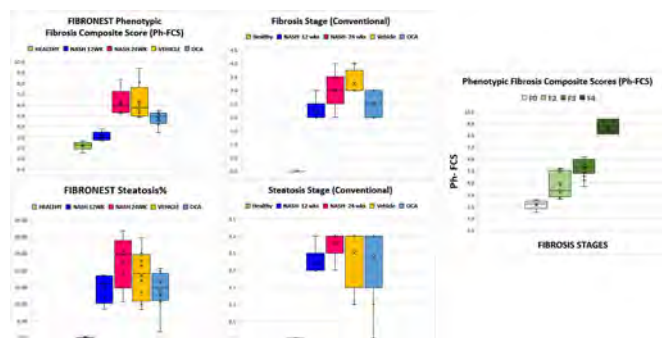
Li Chen^{1,2}, Dipankar Bhattacharya³, Scott Friedman³, Mathieu Petitjean¹. ¹PharmaNest, Princeton, United States; ²PharmaNest Inc, Princeton, United States; ³Icahn School of Medicine at Mount Sinai, New York, United States
Email: li.chen@pharmanest.com

Background and aims: The defining pathologic elements of non-alcoholic steatohepatitis (NASH) are fat accumulation, inflammation, and fibrosis. While conventional histopathology remains the gold standard for diagnosis and staging, this method has limitations, as it uses a narrow range for scoring, qualitative evaluation, and it is also prone to inter-observer variability. The Phenotypic Fibrosis Composite Score (Ph-FCS) calculated by the FibroNest image analysis platform is a novel continuous phenotypic scoring and quantifier of fibrosis and steatosis. Here, we compared Ph-FCS to the conventional scoring in the FAT-NASH model, whose features closely align with human NASH (Tsuchida et al, J. Hepatology 2018; doi: 10.1016/j.jhep.2018.03.011).

Method: Mice (n = 5 per group) were fed a normal diet or the FAT-NASH regimen (high fat, high fructose, high cholesterol, very low dose CCl₄) for 12 or 24 weeks to induce NASH. In other groups, NASH mice (n = 8) were treated with vehicle or with the clinical-stage drug obeticholic acid (OCA, 30 mg/kg, by gavage) for 24 weeks. Liver histological sections were stained with picrosirius red for collagens and imaged at 40X in white light with an Aperio Digital Pathology system. FibroNest®, a cloud-based image analysis platform, was used to quantify the fibrosis phenotype including 32 traits for collagen content and structure, fiber morphometry, and architecture (measures the organization of the fibers). Principal quantitative fibrosis traits (up to 315 qFTs) are automatically detected and combined into a normalized Phenotypic Composite Fibrosis Score (Ph-FCS).

Results: For Healthy vs NASH at 12 wks and 24 wks, FibroNest Ph-FCS FIBROSIS scores (averages) 2.21, 3.08 (p = 0.01), and 6.21 (p = 0.001) respectively, while the conventional method scores 0, 2.2 (p = 0.0003), and 3 (p = 0.0006). For Vehicle vs OCA, FibroNest Ph-FCS FIBROSIS scores were 6.27 and 4.47 (p = 0.03) respectively, while the conventional method scores were 3.3 and 2.5 (p = 0.09). For Healthy vs NASH at 12 wks and 24 wks, FibroNest STEATOSIS scores (averages) were 0.08, 14.71 (p = 0.001), and 22.43 (p = 0.003) respectively, while the conventional scores were 0, 2.2 (p = 0.0003), and 2.8 (p = 0.0001). For Vehicle vs OCA, FibroNest STEATOSIS scores 18.53 and 14.0 (p =

0.2) respectively, while the conventional scores 2.5 and 2.4 (p = 0.8). Thus, both fibrosis and steatosis progress from 0 to 24 wks NASH, however OCA only provided anti-fibrotic but not anti-steatosis effects.



Conclusion: FibroNest shows a markedly wider dynamic range of difference between the groups in the FAT-NASH study. This allows greater detection and sensitivity for subtle changes. FibroNest® provides a more sensitive and reliable evaluation of fibrosis severity and progression in NASH and for the evaluation of therapeutic drug efficacy.

SAT049

Chemical suppression of adipose triglyceride lipase improves non-alcoholic steatohepatitis in a diabetic and hyperlipidemic mouse model

Emmanuel Dauda Dixon¹, Alexander D Nardo¹, Thierry Claudel¹, Claudia Fuchs¹, Veronika Mlitz¹, Tatjana Stojakovic², Hubert Scharnagl³, Gernot Grabner⁴, Robert Zimmermann⁴, Michael Trauner¹. ¹Medical University of Vienna, Hans Popper Laboratory of Molecular Hepatology, Division of Gastroenterology and Hepatology, Department of Internal Medicine III, Wien, Austria; ²University Hospital Graz, Clinical Institute of Medical and Chemical Laboratory Diagnostics, Graz, Austria; ³Medical University of Graz, Clinical Institute of Medical and Chemical Laboratory Diagnostics, Graz, Austria; ⁴University of Graz, Institute of Molecular Biosciences, Graz, Austria
Email: michael.trauner@meduniwien.ac.at

Background and aims: Metabolic comorbidity such as diabetes, obesity and metabolic syndrome plays a key role in the pathogenesis and progression of non-alcoholic fatty liver disease (NAFLD). Increased adipocyte triglyceride lipase (ATGL/PNPLA2) activity, because of insulin resistance, may result in enhanced release of fatty acids from white adipose tissue to the liver, where it precipitates the development and progression of NAFLD. Therefore, ATGL is an attractive target to avert metabolic liver injury. We tested whether the pharmacological ATGL inhibitor Atglstatin hinders metabolic syndrome and improves liver injury in STAM mice as a model of non-alcoholic steatohepatitis (NASH).

Method: Two-days-old C57BL/6j male mice received a single subcutaneous streptozotocin (STZ) injection (100 mg/kg body weight). HFD intervention in the STZ-injected mice representing STAM (diabetic and hyperlipidemia condition) commenced at the age of four weeks and continued for further four weeks. NASH developed within 8 weeks. For the pharmacological inhibition of ATGL, STZ-injected mice were fed an HFD supplemented with 2 mmol/kg Atglstatin for four weeks.

Results: Atglstatin reduced body weight (-2.54 g), despite a comparable consumption of food between the STAM and Atglstatin groups. The bodyweight reduction was due to a decrease in fat (-40%) and liver mass (-23%). Atglstatin treatment significantly improved fasting blood sugar (-12%). Interestingly, the intestinal length was longer (+50%) in the Atglstatin mice in comparison to the STAM mice.

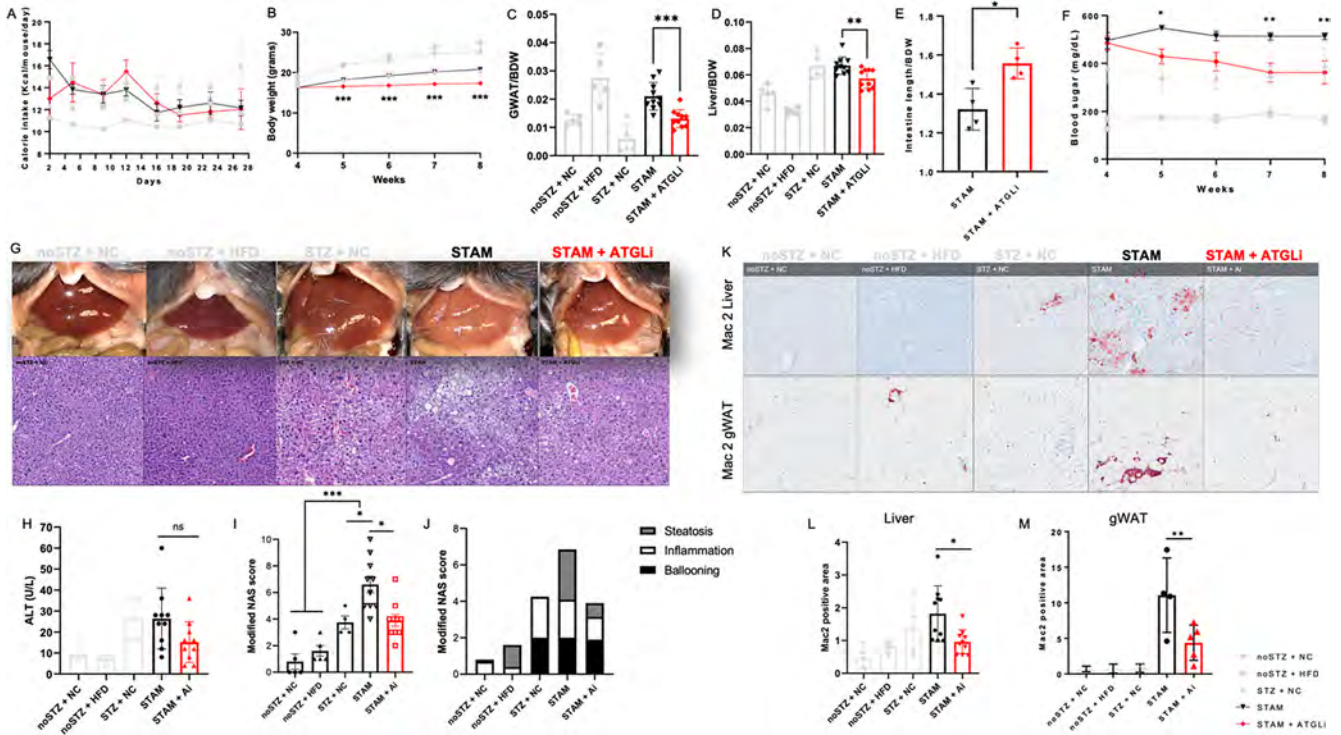


Figure: (abstract: SAT049)

In line with a trend for reduced ALT, there was a significant improvement in histological liver injury assessed by HandE staining and NAFLD score (−45%). The NAFLD score revealed improvement of steatosis (−60%) and inflammation (−35%) but not ballooning in the Atglistatin group. Immunohistochemistry showed that Atglistatin treatment significantly reduces Mac2 positive cells in the liver (−50%) and gonadal white adipose tissues (gWAT) (−60%) compared to the untreated STAM group, indicating a reduced infiltration of immune cells into the liver and gWAT.

Conclusion: Atglitatin improved metabolic features and liver injury in the STAM mice by reducing inflammation and fat accumulation in key metabolic tissues such as the liver, the adipose tissue, and the intestine.

SAT050

Methionine adenosyltransferase 1a antisense oligonucleotides induce the fibroblast growth factor 21-driven recovery from obesity and associated hepatoesteatosis

Xabier Buque¹, Diego Saenz de Urturi¹, Begoña Porteiro^{2,3},
Cintia Folgueira⁴, Alfonso Mora⁴, Teresa Cardoso Delgado^{5,6},
Endika Prieto-Fernández⁷, Paula Olazola^{6,8,9}, Beatriz Gómez Santos¹
Maider Apodaka-Biguri¹, Francisco Gonzalez-Romero¹,
Ane Nieva-Zuluaga¹, Mikel Ruiz de Gauna¹, Naroa Goikoetxea^{5,6},
Juan Luis García Rodríguez⁷, Virginia Gutiérrez de Juan^{5,6},
Igor Aurrekoetxea¹, Valle Montalvo-Romeral⁴, Eva Novoa^{2,6},
Idoia Martín-Guerrero⁷, Marta Varela-Rey^{5,6,10}, Sanjay Bhanot¹¹,
Richard Lee¹¹, Jesus Maria Banales^{6,8,9,12}, Wing-Kin Syn^{1,13,14},
Guadalupe Sabio⁴, María Luz Martínez-Chantar^{5,6},
Ruben Nogueiras^{2,6}, Patricia Aspichueta^{1,6,15}. ¹Basque Country
University, Physiology, Leioa, Spain; ²Department of Physiology, CIMUS,
University of Santiago de Compostela-Instituto de Investigación
Sanitaria, Spain; ³CIBER Fisiopatología de la Obesidad y Nutrición
(CIBERObn), Spain; ⁴Myocardial Pathophysiology, Centro Nacional de
Investigaciones Cardiovasculares (CNIC), Spain; ⁵Liver Disease
Laboratory, CIC bioGUNE-BRTA (Basque Research and Technology
Alliance), Spain; ⁶Centro de Investigación Biomédica en Red de

Enfermedades Hepáticas y Digestivas (CIBERehd), Spain; ⁷Department of Genetics, Physical Anthropology and Animal Physiology, Faculty of Science and Technology and Faculty of Medicine and Nursing, University of the Basque Country UPV/EHU, Spain; ⁸Department of Liver and Gastrointestinal Diseases, Biodonostia Health Research Institute-Donostia University Hospital, University of the Basque Country (UPV/EHU), Spain; ⁹Ikerbasque, Basque Foundation for Science, Spain; ¹⁰Gene regulatory Control in Disease, CIMUS, University of Santiago de Compostela-Instituto de Investigación Sanitaria, Spain; ¹¹IONIS Pharmaceuticals, Inc., United States; ¹²Department of Biochemistry and Genetics, School of Sciences, University of Navarra, Spain; ¹³Section of Gastroenterology, Ralph H Johnson, VAMC, United States; ¹⁴Division of Gastroenterology and Hepatology, Medical University of South Carolina, United States; ¹⁵Biocruces Bizkaia Health Research Institute, Spain
Email: patricia.aspichueta@ehu.eus

Background and aims: High methionine and S-adenosylmethionine (SAME) serum levels are related with obesity and both high and low liver SAME levels promote non-alcoholic fatty liver disease with age. Dietary methionine restriction and deficiency in some enzymes of the methionine cycle confer resistance to obesity development. Here we investigated: i) if the pharmacological knockdown (KD) of methionine adenosyltransferase (*Mat1a*) gene, expressed exclusively in liver and which product synthesizes SAME, provides beneficial outcomes in obesity and comorbidities. ii) The mechanism and molecular agents implicated in these outcomes.

Method: Liver *Mat1a* was silenced in high-fat diet (HFD)-fed and in genetically obese mice using antisense oligonucleotides (ASO). Liver specific fibroblast growth factor (*Fgf*) 21 knockout (KO) mice were used and KD of brown adipose tissue (BAT) β -*klotho* and *Ucp-1* was performed. Changes in body weight, glucose and fat management and energy expenditure were analyzed together with liver and BAT histologies and metabolic fluxes. Primary cultures of hepatocytes from HFD-fed *Mat1a* or control ASO-treated mice were also used

Results: In HFD-fed and in genetically obese mice, *Mat1a* silencing induced thermogenesis leading to a pronounced weight loss and reversal of insulin resistance and hypertriglyceridemia. *Mat1a* ASO

POSTER PRESENTATIONS

treatment induced the recovery from hepatosteatosis reducing liver *de novo* lipogenesis without changing fatty acid oxidation and triglyceride secretion. Serum transaminases and liver fibrotic and inflammatory markers remained unaltered in these mice, while serum FGF21 increased. *In vitro* experiments with hepatocytes from HFD-fed ASO-treated mice and *in vivo* experiments with liver specific *Fgf21*-KO mice showed that liver FGF21 was driving the recovery from obesity. Targeting *Mat1a* in HFD-fed BAT β -*Klotho*- and *Ucp1*-KD mice showed the involvement of thermogenesis in the phenotype. Hepatocyte FGF21 secretion was induced by the nuclear factor erythroid 2-related factor 2 (NRF2), a mediator of antioxidant response, as the binding to the *Fgf21* promoter in *Mat1a* ASO-treated HFD-fed mice hepatocytes and treatments with *Nrf2* siRNA, ML385 -a NRF2 inhibitor-, SAME and the antioxidants glutathione and N-acetylcysteine showed.

Conclusion: Targeting *Mat1a* reverses obesity, dyslipidemia, insulin resistance and hepatosteatosis through the hepatocyte secretion of FGF21 in a mechanism driven by NRF2.

SAT051

NLRP3 inflammasome dependent cell death in myeloid cells drives liver inflammation and fibrosis in murine steatohepatitis

Benedikt Kaufmann^{1,2}, Agustina Reca¹, Aleksandra Leszczynska¹, Andre D. Kim¹, Laela M. Booshehri¹, Helmut Friess², Daniel Hartmann², Lori Broderick¹, Hal M. Hoffman¹, Ariel Feldstein¹.
¹Department of Pediatrics, University of California San Diego, La Jolla;
²Department of Surgery, TUM School of Medicine, Klinikum rechts der Isar, Technical University of Munich
Email: benedikt_kaufmann@hotmail.com

Background and aims: Non-alcoholic fatty liver disease (NAFLD) is the leading cause of chronic liver disease worldwide showing a rapidly rising prevalence among all age groups. Cellular death is crucial in the pathogenesis of NAFLD and driving liver inflammation as well as fibrosis. The NLRP3 inflammasome, a multiprotein complex promoting activation of caspase-1 as well as interleukin 1 β (IL-1 β) release, is recognized to promote programmed cell death in the form of pyroptosis. The cell-specific contribution of the activation of the NLRP3 inflammasome in myeloid cells in NAFLD remains unknown.

Method: A conditional *Nlrp3* knock-out mouse was generated and bred to mice expressing Cre under the control of Lysozyme to investigate the role of NLRP3 inflammasome dependent cell death in myeloid cells, liver inflammation and fibrosis. Both acute (lipopolysaccharide (LPS)/adenosine-triphosphate (ATP)) and chronic (choline-deficient, L-amino acid-defined high-fat diet (CDAA-HFAT)) liver injury models were used to induce *in vivo* NLRP3 activation and fibrotic-non-alcoholic steatohepatitis (NASH). Cell death, liver inflammation and fibrosis were analysed.

Results: Myeloid-specific *Nlrp3* knock-out resulted in a systemic and hepatic decrease of IL-1 β release compared to control mice induced by LPS/ATP injection. NASH-associated cell death and hepatic inflammation was ameliorated in myeloid-specific *Nlrp3* knock-out mice in the CDAA-HFAT model. In addition, fibrosis and hepatic stellate cell activation were decreased in myeloid-specific *Nlrp3* knock-out mice.

Conclusion: This study provides new insights in the role of NLRP3 activation in myeloid cells in the pathogenesis of NAFLD and identifies myeloid specific NLRP3 inflammasome activation as crucial for the progression of NAFLD to fibrotic-NASH.

SAT052

The PNPLA3 I148M variant increases intrahepatic lipolysis and beta oxidation and decreases de novo lipogenesis and hepatic mitochondrial function in humans

Panu Luukkonen^{1,2,3,4}, Kimmo Porthan^{1,3}, Noora Ahlholm^{1,3}, Fredrik Rosqvist^{5,6}, Sylvie Dufour^{2,7}, Xian-Man Zhang^{2,7}, Juhani Dabek^{1,3}, Tiina Lehtimäki⁸, Wenla Seppänen⁸, Marju Orho-Melander⁹, Leanne Hodson⁵, Kitt Falk Petersen^{2,7}, Gerald I. Shulman^{2,7,10}, Hannele Yki-Järvinen^{1,3}.
¹Minerva Foundation Institute for Medical Research, Helsinki, Finland; ²Yale School of Medicine, Department of Medicine, New Haven, United States; ³University of Helsinki, Department of Medicine, Helsinki, Finland; ⁴Helsinki University Hospital, Abdominal Center, Helsinki, Finland; ⁵University of Oxford, Oxford Center for Diabetes, Endocrinology and Metabolism, Oxford, United Kingdom; ⁶Uppsala University, Department of Public Health and Caring Sciences, Clinical Nutrition and Metabolism, Uppsala, Sweden; ⁷Yale School of Medicine, Yale Diabetes Research Center, New Haven, United States; ⁸University of Helsinki and Helsinki University Hospital, Department of Radiology, HUS Medical Imaging Center, Helsinki, Finland; ⁹Lund University, Department of Clinical Sciences, Diabetes and Endocrinology, Malmö, Sweden; ¹⁰Yale School of Medicine, Department of Cellular and Molecular Physiology, New Haven, United States
Email: panu.luukkonen@finnet.fi

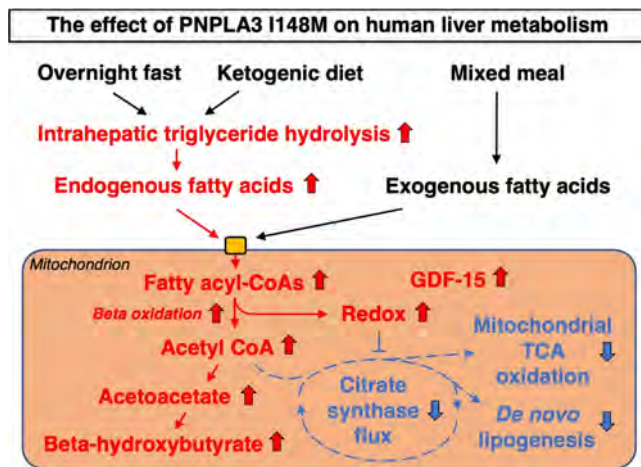
Background and aims: The PNPLA3 I148M variant explains >10% of the risk of cirrhosis but the underlying pathophysiology remains unknown. We studied the effect of this variant on hepatic metabolism *in vivo* under multiple physiological conditions by combining a recruit-by-genotype approach with state-of-the-art stable isotope techniques.

Method: We recruited a total of 93 healthy participants (mean age 53 \pm 1 yrs, BMI 30 \pm 1 kg/m², 19% men; 37 homozygous carriers [148MM] and 56 non-carriers [148II]). Hepatic *de novo* lipogenesis (DNL) was assessed in 48 participants after an overnight fast using D₂O (148MM, n = 19; 148II, n = 36). Hepatic fate of exogenous fatty acids (FA) was determined in 26 participants using a mixed meal enriched in ¹³C-labeled FA (148MM, n = 12; 148II, n = 14). Rates of endogenous glucose production, ketogenesis and hepatic mitochondrial citrate synthase flux were assessed in 12 participants before and after a 6-day ketogenic diet by Positional Isotopomer NMR Tracer Analysis (PINTA) by infusing [3-¹³C]-lactate, [¹³C₄]-beta-hydroxybutyrate (BOHB) and [²H₇]-glucose (148MM, n = 6; 148II, n = 6). Intrahepatic triglycerides (IHTG) were assessed by ¹H magnetic resonance spectroscopy and hepatic mitochondrial redox state was assessed by the ratio of plasma [BOHB] and [acetoacetate].

Results: After an overnight fast, the 148MM group had higher plasma BOHB concentrations (+104%, p < 0.05) and lower DNL (-47%, p < 0.01) than the 148II group, independent of plasma FA and insulin concentrations. After a mixed meal, exogenous ¹³C-labeled FAs in the 148MM group were channeled more towards ketogenesis (+265%, p < 0.001), which was associated with an increased hepatic mitochondrial redox state (+36%, p < 0.05). During a ketogenic diet, the 148MM group manifested higher rates of intrahepatic lipolysis as reflected by a larger reduction in IHTG (77%, p < 0.05) than the 148II group, which was associated with: 1) increased plasma BOHB concentrations (+90%, p < 0.05), 2) increased mitochondrial redox state and 3) decreased rates of hepatic mitochondrial citrate synthase flux (-31%, p < 0.01). Plasma concentrations of GDF-15, a mitochondrial stress marker, were also increased by 40% (p < 0.01) in the 148MM group compared to the 148II group.

Conclusion: Homozygous PNPLA3 I148M carriers have alterations in both intrahepatic anabolic/catabolic processes and mitochondrial function as reflected by increased rates of intrahepatic lipolysis, decreased rates of DNL and increased hepatic mitochondrial beta oxidation/ketogenesis. These changes in turn were associated with an increased mitochondrial redox state and reductions in hepatic mitochondrial citrate synthase flux. Taken together these results

provide new insights in the mechanisms by which the PNPLA3 I148M variant promotes liver disease (Figure).



SAT053

Two diseases, one model-assessing the suitability of FOZ mice to examine CVD in NAFLD

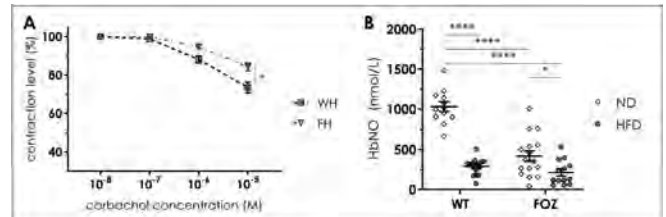
Sebastian Bott¹, Laurent Dumas², Dessy Chantal², Isabelle Leclercq³, Evangelos-Panagiotis Daskalopoulos⁴, Hrag Esfahani⁴. ¹Institute of Experimental and Clinical Research (IREC), Laboratory for Hepato-gastroenterology (GAEN), Brussels, Belgium; ²Institute of Experimental and Clinical Research (IREC), Pole of Pharmacology and Therapeutics (FATH), Université catholique de Louvain (UCL), Belgium; ³Institute of Experimental and Clinical Research (IREC), Laboratory for Hepato-gastroenterology (GAEN), Belgium; ⁴Pole of Cardiovascular Research (CARD), Institut de Recherche Expérimentale et Clinique (IREC), Université catholique de Louvain (UCLouvain), Brussels, Belgium
Email: sebastian.bott@uclouvain.be

Background and aims: Non-alcoholic fatty liver disease (NAFLD) is an umbrella term which describes different states of liver disease, ranging from simple steatosis to non-alcoholic steatohepatitis (NASH), cirrhosis and finally hepatocellular carcinoma. NAFLD case numbers are constantly rising for three decades with around one quarter of the global population being affected today. Patients with NAFLD are at higher risk of developing cardiovascular disease (CVD)-whereby most fatalities in CVD relate to atherosclerosis. Actually, CVD-dependent mortality is more frequent in patients with NAFLD in comparison to liver-related mortality. This association is related to the common metabolic risk factors such as obesity, dyslipidemia, diabetes, and hypertension shared by both NAFLD and CVD. Even more, NAFLD itself is considered as an independent risk factor for CVD (the leading cause of death globally), the link for this latter association is however still unknown. Established pre-clinical animal models only focus on one of the two diseases, yet. Therefore, the aim of this study was to assess the opportunity of using a single mouse model to examine NASH and cardiovascular disease concurrently to facilitate analysis of potential mechanistic links between both diseases.

Method: Male fat aussie mice (FOZ) and their age-matched wildtype (WT) controls were fed regular chow and high fat diet (60% kcal fat) for 24 weeks. Animals were then sacrificed, liver samples were gathered for histological assessment of the hepatic conditions, blood was sampled for determination of nitrosylated hemoglobin (HbNO) levels via electron paramagnetic resonance spectroscopy (EPR), the aorta was searched for atherosclerotic plaques and rings of first order mesenteric arteries were isolated and utilized in a wire myograph to assess carbachol (10^{-8} M to 10^{-5} M)-triggered nitric oxide (NO)-

dependent relaxation to search for endothelial dysfunction, an early hallmark of atherosclerosis.

Results: FOZ mice on high fat diet (FH) featured all hepatic characteristics of progressive NASH (steatosis, ballooning, inflammation, fibrosis; NAFLD activity score = 8). Although no plaques in the aorta were found, a significant reduction in their mesenteric arterial NO-dependent relaxation at a carbachol-concentration of 10^{-5} M compared with wildtype mice on high-fat diet (WH) was detected; [$p < 0.05$]; (A). In addition, EPR showed the lowest HbNO-level in FOZ mice fed a high-fat diet (B).



Conclusion: These results demonstrate suitability of the FOZ mouse model for studies to examine CVD in NAFLD since it develops all key characteristics of progressive liver disease and endothelial dysfunction, an essential hallmark in the development of atherosclerosis which represents the main cause of death in CVD.

SAT054

Oleic acid-induced acute lung injury in Ob/Ob mice fed with high-fat-diet exacerbate bile acid uptake and liver injury that was reversed by antagonizing their entry

Johnny Amer¹, Ahmed Salhab¹, Rifaat Safadi¹. ¹Hadassah Hebrew University Hospital, Liver Unit, Jerusalem, Israel
Email: johnnyamer@hotmail.com

Background and aims: Acute respiratory distress syndrome (ARDS) is a serious complication of COVID-19 and present in a large percentage of COVID-19 deaths. Many studies suggest that people with obesity are at increased risk of severe COVID-19, however, mechanism on liver-lung axis remains unknown. We aimed to evaluate whether bile acid (BAs) trafficking interfere with acute lung injury (ALI) in animal model with obesity.

Method: Leptin deficient (*ob/ob*) mice fed with high-fat-diet (*Ob/Ob^{HFD}*) were *i.p* injected with oleic acid (OA) to induce ALI. To modulate BAs uptake, mice were *i.p* treated with neutralizing antibody for sodium taurocholate co-transporting polypeptide (NTCP; BAs-transporter). Broncho-alveolar lavage fluid (BALF), lungs, livers and serum were obtained from mice and assessed for inflammatory (H&E staining, ALT and pro-inflammatory panel of cytokines), fibrosis (Sirius red staining, α -smooth muscle actin, collagen and fibronectin) and metabolic (BAs, cholesterol, triglyceride, glucose tolerance test (GTT) and fasting blood sugar (FBS)) profiles. In addition, alveolar-capillary membrane injury of surfactant D (SP-D) and the receptor for advanced glycation end-products (RAGE). BAs trafficking were assessed in primary lung cells and their impact on proliferation and apoptosis were evaluated.

Results: Compared to WT-littermates, OA-induced lung injury and was worsened in the *Ob/Ob^{HFD}* in the histopathology outcome. In addition, BALF of the *Ob/Ob^{HFD}* showed elevated levels of BAs (3-fold; $P = 0.002$) associated with increased GM-CSF, INF-g, IL-1, IL-6 and IL-8 ($p < 0.01$). Moreover, *Ob/Ob^{HFD}* with OA showed elevated serum levels in liver enzymes, lipids, glucose and metabolic markers ($p < 0.01$). In addition, *Ob/Ob^{HFD}* livers showed an exacerbated fibrosis profile. NTCP neutralizing antibody in *Ob/Ob^{HFD}* while inhibited BAs uptake/trafficking in both primary alveolar type II (BALF showed 4-fold increase in BAs) and primary hepatocytes (serum showed 3-fold increase in BAs). SP-D, RAGE and serum metabolic

POSTER PRESENTATIONS

markers were suppressed to normal in line with enhance lung and liver histology and maintaining cell viability.

Conclusion: Modulation of BAs trafficking from the liver of obese mice to the lungs could be an important step in the pathogenesis of ALL. Antagonizing BAs uptake may suggest a therapeutic strategy in improving liver-lung axis.

SAT055

The ubiquitin-like modifier FAT10 is upregulated during NASH and impairs PPAR-alpha activity

Ludivine Clavreul¹, Alexia Cotte¹, Lucie Bernard¹, Joel Haas¹, Nathalie Hennuyer¹, An Verrijken^{2,3}, Luc Van Gaal^{2,3}, Sven Francque^{2,4}, Guillaume Lassailly⁵, Bart Staels¹, Réjane Paumelle¹.

¹University of Lille, EGID, Inserm, CHU Lille, Institut Pasteur de Lille, U1011, Lille, France, UMR 1011, LILLE, France; ²Faculty of Medicine and Health Sciences, University of Antwerp, Laboratory of Experimental Medicine and Paediatrics, Antwerp, Belgium; ³Antwerp University Hospital, University of Antwerp, Department of Endocrinology, Diabetology and Metabolism, Antwerp, Belgium; ⁴Antwerp University Hospital, Department of Gastroenterology and Hepatology, Antwerp, Belgium; ⁵CHU of Lille, University of Lille, Department of digestive system diseases, U995, LIRIC, Lille, France

Email: ludivine.clavreul.etu@univ-lille.fr

Background and aims: PPAR-alpha is a nuclear receptor involved in the regulation of lipid metabolism and inflammation in the liver. This transcriptional factor is known to prevent Non-alcoholic Steatohepatitis (NASH), a liver disease characterized by steatosis, inflammation, and ballooning. Indeed, PPAR-alpha is a promising target for the cure of this disease but its gene expression is decreased during NASH development. We show that FAT10, an ubiquitin-like protein known to be involved in proteasomal degradation, is overexpressed in NASH patient's livers and is inversely correlated to PPAR-alpha expression suggesting a role for FAT10 on PPAR-alpha modulation in hepatocytes during NASH progression.

Method: FAT10 and PPAR-alpha hepatic expressions during NASH development were characterized in mice fed two or five weeks with a choline-deficient (CDAA) diet inducing NASH by transcriptomic analysis and immunofluorescence and correlated to histological grade of NASH. The impact of FAT10 modulation on PPAR-alpha expression was then investigated *in vitro* in HepG2 cell line using either a stable overexpression and cytokine treatment inducing FAT10, or siRNA inhibiting FAT10. QPCR and western-blot were performed to assess FAT10 and PPAR-alpha expressions and functional effects on lipid metabolism were quantified by BODIPY staining and Seahorse. Finally, the interaction between FAT10 and PPAR-alpha was observed with co-immunoprecipitation and Proximity Ligation Assay (PLA).

Results: *In vivo*, FAT10 expression is increased in murine NASH livers and associated to a decreased PPAR-alpha expression. *In vitro*, FAT10 overexpression reduces the expression of PPAR-alpha target genes while FAT10 down-regulation increases them. Moreover, FAT10 overexpressing cells accumulate more lipid droplets and have an impaired fatty acid beta-oxidation. Finally, PPAR-alpha and FAT10 co-immunoprecipitate in human hepatocytes, and this interaction was confirmed by PLA *in vitro* and *in vivo*.

Conclusion: These observations show that FAT10 is overexpressed during NASH and correlates negatively with PPAR-alpha expression. Furthermore, FAT10 overexpression is associated with an impaired PPAR-alpha transcriptional activity leading to an inhibition of lipid metabolism in hepatocytes. The interaction observed between FAT10 and PPAR-alpha suggests that FAT10 could be a new modulator of PPAR-alpha activity in hepatocytes during NASH progression.

SAT056

TNF-alpha knockout mice are protected from diet-induced NAFLD in a model of non-obese NAFLD

Katharina Burger¹, Finn Jung¹, Anja Baumann¹, Annette Brandt¹, Raphaela Staltner¹, Victor Sánchez¹, Ina Bergheim¹. ¹University of Vienna, Department of Nutritional Sciences, Wien
Email: ina.bergheim@univie.ac.at

Background and aims: By now, non-alcoholic fatty liver disease (NAFLD) is the most common liver disease worldwide being strongly associated with obesity and insulin resistance but also with dietary pattern. The pro-inflammatory cytokine tumor necrosis factor alpha (TNF-alpha) is thought to be a critical factor in many overweight associated diseases including NAFLD; however, the impact of dietary pattern herein has not yet been fully understood. In the present study we determined the effect of a fat-, sucrose- and cholesterol rich diet in the development of NAFLD in the absence of obesity in TNF-alpha knock out mice (KO) and wild-type animals.

Method: Male TNF-alpha KO and wild-type C57BL/6J mice (6–8 weeks old, n = 8) were pair-fed either a liquid control diet (C) or a liquid fat-, sucrose-, and cholesterol-rich diet (FSC) for 9 weeks. A glucose tolerance test (GTT) was performed in week 8. Markers of liver damage and inflammation as well as insulin signaling were determined in liver tissue. TLR 2 and TLR 4 ligands e.g. lipoteichoic acid and endotoxin were determined using a SEAP reporter activity cell assay in portal plasma.

Results: Despite similar body weight FSC-fed wild-type mice developed liver steatosis with beginning inflammation and insulin resistance when compared to C-fed wildtype mice, whereas FSC-fed TNF-alpha KO mice were significantly protected from inflammatory alterations in liver and impaired glucose tolerance. In line with these findings, mRNA expression of interleukin 1 beta (*IL-1β*) and interleukin 6 (*IL-6*), as well as levels of NO_x were also significantly higher in livers of FSC-fed wild-type mice while being almost at level of control in FSC-fed TNF-alpha KO mice. Expression of insulin receptor substrate 1 (*Irs1*) in liver tissue was also significantly higher in livers of FSC-fed mice compared to all other groups, whereas expression in liver of FSC-fed TNF-alpha KO mice was at the level of controls. Levels of TLR 2 and TLR 4 ligands in portal plasma of both FSC-fed groups were higher than in C-fed groups.

Conclusion: Taken together results of the present study suggest that a lack of TNF-alpha may attenuate the development of diet-induced insulin resistance and NAFLD in mice also in settings of non-obesity induced NAFLD. (This project was funded in part by the Austrian Science Fund)

SAT057

Low dose thyroid hormone improves hepatic mitochondrial fatty acid oxidation and rescues non-alcoholic fatty liver disease in mice

Raghu Ramanathan^{1,2}, Saraha Johnson^{3,4}, Jamal Ibdah^{2,3,5}. ¹University of Missouri-Columbia, Department of Medicine-Gastroenterology and Hepatology, Columbia, United States; ²Harry S. Truman Memorial Veterans' Hospital (VA), Columbia, United States; ³University of Missouri-Columbia, Department of Medicine-Gastroenterology and Hepatology, Columbia, United States; ⁴Harry S. Truman Memorial Veterans' Hospital (VA), Columbia, United States; ⁵University of Missouri-Columbia, Department of Medical Pharmacology and Physiology, Columbia, United States
Email: ibdahj@health.missouri.edu

Background and aims: Non-alcoholic fatty liver disease (NAFLD) is the most common chronic liver disease in the world, with limited therapeutic options. Mitochondrial dysfunction and decreased hepatic mitochondrial fatty acid oxidation (FAO) have been linked to its etiology. Thyroid hormone (TH) is an important regulator of lipid metabolism and may have the potential to treat NAFLD but its use is associated with adverse systemic effects. We hypothesized that

low dose thyroid hormone, which has the advantage of reduced potential for systemic effects, is effective in improving hepatic FAO and rescue of NAFLD. To test this hypothesis, we compared the effects of TH dose on hepatic FAO, mitochondrial quality, and NAFLD histological features in mice.

Method: Six-month-old wild-type male mice with a C57BL/6 background maintained on chow diet were used to compare the effects of TH dose on hepatic FAO. Phosphate buffered saline (PBS) was given intraperitoneally (ip) to control mice (n=8) for 7 days; treatment groups (n=8 per group) received low doses of triiodo-thyronine (T3) at 1 and 5 mcg/100 g weight and a higher dose of 25 mcg/100 g weight ip for 7 days. Complete FAO levels in fresh liver lysate were determined after sacrifice. Mitochondrial trifunctional protein (MTP), the main enzyme complex that catalyzes the last three steps of mitochondrial FAO, and key genes regulating mitochondrial biogenesis and mitophagy were also evaluated. In addition, two-month-old male mice were fed western diet (Research Diets Inc, D12451 Rodent Diet, 45 kcal percent fat, 1 percent cholesterol) for 16 weeks to induce NAFLD, then injected with either PBS (n=6) or 1 and 25 mcg T3/100 g weight ip for 7 days (n=6 per group). Effects on hepatic FAO, mitochondrial quality markers, and liver histology were assessed.

Results: As shown in Figure 1, T3 at various doses resulted in a 4-fold increase in total hepatic CO₂ production in mice fed chow diet (p <0.001) and a 2-fold increase in mice fed a western diet (p <0.05). There was no statistical difference between effects of lower and higher doses of T3 on FAO. Hepatic MTP protein and RNA expression levels remained unchanged in mice injected with T3 compared to control mice suggesting that T3-induced FAO is not due to increased FAO enzyme expression. RNA expression studies suggest that T3 improves mitochondrial mitophagy and biogenesis. Both lower and higher doses of T3 were effective in rescue of NAFLD in western diet-fed mice with significant histological improvement of steatosis and inflammation, and reduction of ALT levels (p <0.05) compared to control mice.

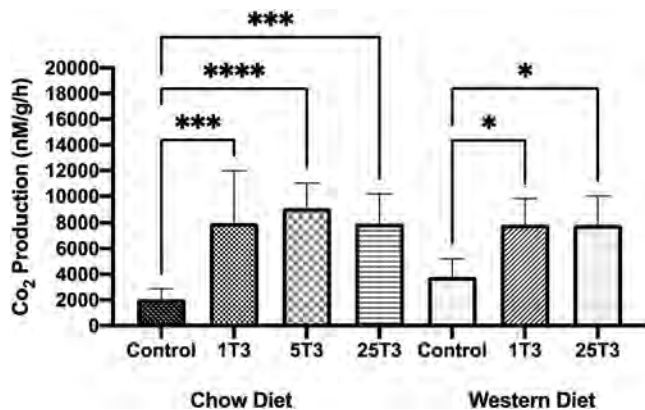


Figure 1. TH dose and hepatic FAO. 1T3, 5T3, and 25T3 denote 1, 5 and 25 mcg T3/100 g weight, respectively. Values expressed as Mean ± S.D. * p < 0.05; *** p < 0.001; **** p < 0.0001

Conclusion: TH at low dose improves hepatic FAO and rescues NAFLD in mice. This study suggests that low dose thyroid hormone is a potential treatment modality for NAFLD.

SAT058

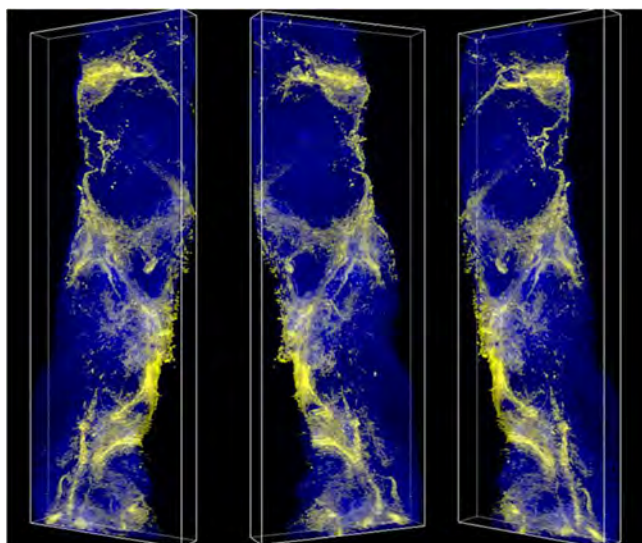
Three-dimensional imaging of cleared human liver tissues reveals extensive fibrosis heterogeneity in non-alcoholic fatty liver disease

Buket Yigit¹, Ekin Ozgonul², Omer Yaman², Burge Ulukan¹, Yagmur Cetin Tas³, Berna Morova², Musa Aydin⁴, Yigit Uysalli², Elif Demirtas⁵, Mert Erkan⁶, Yasemin Gursay Ozdemir³, Sercin Karahuseyinoglu⁷, Cihan Yurdaydin⁸, Murat Akyildiz⁸, Abhishek Sheth⁹, Hale Kirimlioglu¹⁰, Murat Dayangac¹¹, Onur Ferhanoglu¹², Alper Kiraz², Mujdat Zeybel^{9,13}. ¹Koc University, School of Medicine, Gastroenterology and Hepatology, Istanbul, Turkey; ²Koc University, Physics, Istanbul, Turkey; ³Koc University, School of Medicine, Neuroscience, Istanbul, Turkey; ⁴ES.M university, Computer Engineering, Istanbul, Turkey; ⁵Koc University, Graduate School of Health Sciences, Istanbul, Turkey; ⁶Acibadem University, Faculty of Medicine, General Surgery, Istanbul, Turkey; ⁷Koc University, School of Medicine, Histology, Istanbul, Turkey; ⁸Koc University, School of Medicine, Gastroenterology and Hepatology, Istanbul, Turkey; ⁹University of Nottingham NHS Trust, NIHR Biomedical Research Centre, Nottingham, United Kingdom; ¹⁰Acibadem University, Faculty of Medicine, Pathology, Istanbul, Turkey; ¹¹Medipol University, Faculty of Medicine, General Surgery, Istanbul, Turkey; ¹²Istanbul Technical University, Electronics and Communication Engineering, Istanbul, Turkey; ¹³Koc University, School of Medicine, Gastroenterology and Hepatology, Istanbul, Turkey
Email: mzeybel@ku.edu.tr

Background and aims: Liver fibrosis is a dynamic process of fibrogenesis and fibrolysis traditionally evaluated by liver biopsy. Accurate assessment of hepatic fibrosis is vital for optimal biomarker and drug development in the era of NASH clinical trials. The limitations of biopsy-based fibrosis staging include semi-quantitative assessment, sampling, and observer variability. In this study, we aimed to perform 3D imaging of optically transparent whole liver biopsy samples by light sheet fluorescence microscopy (LSFM) to quantify extra-cellular matrix proteins.

Method: Fifty seven NAFLD patients and eleven subjects without hepatic fibrosis were included into the study. Liver tissues were cleared by hydrogel embedding, polymerisation and clearing steps of CLARITY. Histological scoring was performed by an expert pathologist. 2D assessment of Sirius red staining was performed through collagen proportionate area (CPA) analysis. 3D imaging of collagen I and elastin was performed via in-house LSFM by acquiring multiple optical sections. Collagen proportionate volume (CPV) and Elastin proportionate volume (EPV) were calculated using over 100 optical sections per sample.

Results: We demonstrated a method which optically cleared various fibrotic stages of liver tissues and optimized non-destructive slide-free fibrosis pathology of whole liver biopsy samples. Cut-offs for CPV and EPV were established for fibrosis stages of NASH. CPV and EPV analysis showed a considerable optical section heterogeneity resulting in at least a fibrosis stage of variance within the sample. While coefficient variation of CPV sections demonstrating 61.5% of intermediate and 23.1% of high level variation, EPV sections showed 69.2% of intermediate and 15.4% of high level variation.



Conclusion: We report for the first time the 3D imaging of liver fibrosis pathology using an in-house developed light-sheet fluorescence microscopy system. Through the imaging of slide-free whole core liver biopsies, we showed that fibrosis variability occurs even in the different optical sections of the biopsy sample. Comprehensive mapping of hepatic extracellular matrix proteins and imaging of slide-free biopsy samples can improve the accuracy of histological assessment and stratification of NASH patients.

SAT059

In vivo functional genetic screen with a pooled-shRNA library for therapeutic targets of non-alcoholic fatty liver disease

Yong-An Lee¹, Chee Chong Lek¹, Amanpreet Kaur¹, Rong Gao¹, Agnes Bee Leng Ong¹, Yee Siang Lim², Shirleen Soh², Winston Chan³, Yock Young Dan⁴, Huck Hui Ng², Torsten Wuestefeld^{1,5,6}. ¹Genome Institute of Singapore (GIS), Laboratory of in vivo genetics and gene therapy, Singapore, Singapore; ²Genome Institute of Singapore (GIS), Laboratory of Precision Disease Therapeutics, Singapore, Singapore; ³Guangzhou Regenerative Medicine and Health Guangdong Laboratory, China; ⁴National University of Singapore, Department of Medicine, Singapore, Singapore; ⁵National Cancer Centre Singapore, Singapore, Singapore; ⁶Nanyang Technological University, School of Biological Sciences (SBS), Singapore, Singapore
Email: wustefeldt@gis.a-star.edu.sg

Background and aims: With a rapidly increasing prevalence, non-alcoholic fatty liver disease (NAFLD) is recognized as the most common cause of chronic liver disease worldwide. The massive growth of NAFLD is causing a significant burden in health care with social and economic implications. However, unlike other highly prevalent diseases, it remains an underrepresented disease with limited therapeutic possibilities due to the absence of current approved pharmacological treatments. Therefore, there is an urgent need to develop innovative therapies. To address this, we are combining patient samples' transcriptomic profiling with the disease mouse models and in vivo functional genetic screens with the hope of developing therapeutics for this dreaded disease.

Method: We sequenced liver tissues from 130 patients covering different stages of NAFLD to determine dysregulated genes in the patients. Based on the transcriptomic data, a pooled transposon-based shRNA library targeting the dysregulated genes was generated for in vivo genetic screening. The library was directly and stably delivered into hepatocytes of two different mouse models by using hydrodynamic injection. Mice were fed with "Western Diet" supplemented with high fructose and Choline deficient L-amino acid defined high-fat diet (CDHFD) for two different models,

respectively, to recapitulate human pathology of the NAFLD. As a control, normal chow-fed animals were served. Our approach's underlying idea is that shRNAs that confer benefits to the hepatocyte in the detrimental environment of the disease will be enriched over time. At the end of diet treatment, livers were harvested, and the abundance of each shRNA was determined by deep sequencing. Highly enriched shRNAs were validated for their potential therapeutic impact by various studies, including in vitro assays for proliferation and in vivo by repopulating FAH^{-/-} mice so that every hepatocyte expresses the shRNA of interest. Repopulated mice were exposed to NAFLD-inducing diets, and histopathology parameters were evaluated.

Results: Our screens have identified novel shRNAs highly enriched in the disease models. One of the shRNAs has been validated for reducing liver fibrosis in the CDHFD model, the aggressive NAFLD model. From the various in vitro and in vivo assays, the candidate gene silencing showed promoted regeneration of hepatocytes without tumor developments.

Conclusion: We show that combining the study of NAFLD patient liver transcriptome with in vivo functional genetic screening in the disease mice models could discover new candidates as therapeutic targets of the disease. We identified and validated a new target for treating NAFLD through our approach. We are currently investigating the underlying molecular mechanisms. Our study may contribute to new insights into the therapeutic development of the disease.

SAT060

Hepatic insulin resistance is the basis of bile acid dysmetabolism in non-alcoholic fatty liver disease

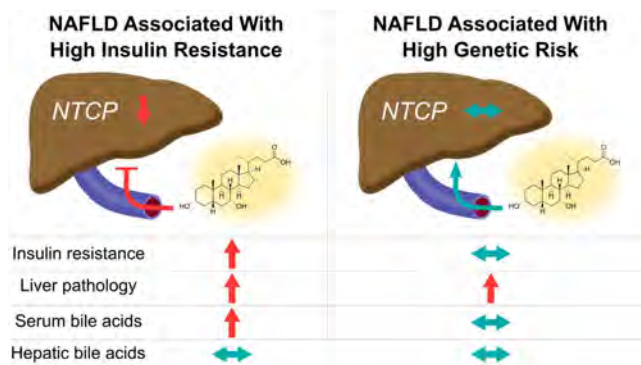
Sami Qadri^{1,2}, Emilia Vartiainen³, Noora Ahlholm^{1,2}, Kimmo Porthan^{1,2}, Anne Juuti⁴, Henna Sammalkorpi⁴, Anne Penttilä⁴, Johanna Arola⁵, Taru Tukiainen³, Matej Orešič^{6,7}, Tuulia Hyötyläinen⁸, Hannele Yki-Järvinen^{1,2}. ¹University of Helsinki and Helsinki University Hospital, Department of Medicine, Helsinki, Finland; ²Minerva Foundation Institute for Medical Research, Helsinki, Finland; ³University of Helsinki, Institute for Molecular Medicine Finland, FIMM, Helsinki, Finland; ⁴University of Helsinki and Helsinki University Hospital, Department of Gastrointestinal Surgery, Abdominal Center, Helsinki, Finland; ⁵University of Helsinki and Helsinki University Hospital, Department of Pathology, Helsinki, Finland; ⁶Örebro University, School of Medical Sciences, Örebro, Sweden; ⁷University of Turku and Åbo Akademi University, Turku Bioscience Centre, Turku, Finland; ⁸Örebro University, School of Science and Technology, Örebro, Sweden
Email: hannele.yki-jarvinen@helsinki.fi

Background and aims: Non-alcoholic fatty liver disease (NAFLD) is associated with increased circulating bile acids (BAs). It is unknown whether this reflects altered intrahepatic BA metabolism due to NAFLD or the associated insulin resistance (IR). To dissociate steatosis from IR, we compared BA metabolism in NAFLD associated with either IR or high genetic risk.

Method: In 106 patients undergoing a liver biopsy, we analysed serum/liver BAs, the hepatic transcriptome (RNA-seq), and concentrations of plasma FGF-19 (marker of intestinal BA metabolism). Using HOMA-IR and a validated weighted Polygenic Risk Score (PRS) for NAFLD, we divided the patients into matched groups to compare the effects of NAFLD associated with IR ('High HOMA-IR' vs. 'Low HOMA-IR') or with high genetic risk ('High PRS' vs. 'Low PRS') on BA metabolism.

Results: An untargeted analysis identified distinct clusters of patients with simultaneously increased BAs, HOMA-IR, and liver fat content. Compared to 'Low HOMA-IR', patients with 'High HOMA-IR' had significantly higher total (+57%, $P = 0.011$) and especially conjugated (+82%, $P = 0.002$) serum BAs, but unchanged hepatic BAs. Expression of the primary hepatic BA uptake transporter NTCP was down-regulated, while plasma FGF-19 was unchanged. Despite having the same degree of steatosis and NASH compared to the 'High HOMA-IR' group, patients with 'High PRS' had similar serum/liver BAs

compared to those with 'Low PRS'. Stage F3-F4 liver fibrosis independently predicted higher serum BAs.



Conclusion: In NAFLD without advanced fibrosis, serum BAs are increased due to IR, which may impair hepatocellular BA uptake. Intrahepatic BAs are unchanged in NAFLD.

SAT061

Non-alcoholic fatty liver disease features a reduced reverse polyunsaturated fatty acid transport (free fatty acids/high-density lipoprotein) from the periphery to the liver

Gabriele Mocciaro¹, Michael Allison², Benjamin Jenkins³, Vian Azzu², Isabel Huang-Doran², Richard Kay³, Antonio Murgia¹, Davies Susan², Mattia Frontini⁴, Antonio Vidal-Puig³, Albert Koulman³, Julian L. Griffin^{1,5}, Michele Vacca^{1,3,6}. ¹University of Cambridge, Department of Biochemistry, Cambridge, United Kingdom; ²Addenbrooke's Hospital, Cambridge Biomedical Research Centre, Department of Medicine, United Kingdom; ³Wellcome Trust-MRC Institute of Metabolic Science Metabolic Research Laboratories, United Kingdom; ⁴National Institute for Health Research BioResource, Cambridge University Hospitals, United Kingdom; ⁵University of Aberdeen, The Rowett Institute, United Kingdom; ⁶Aldo Moro University of Bari, Department of Interdisciplinary Medicine, Clinica Medica "C. Frugoni", Italy
Email: michele.vacca@uniba.it

Background and aims: Non-alcoholic fatty liver disease (NAFLD) is a cluster of liver diseases, ranging from simple steatosis to steatohepatitis (NASH), cirrhosis, and hepatocellular carcinoma. Steatosis arises when hepatic lipid input exceeds output therefore leading to net hepatic fat accumulation; hepatic steatosis does not correlate with disease outcomes that are instead associated with a relative increase in lipotoxic species (e.g. ceramides or diacylglycerols). Over the years, studies have widely reported characteristic changes in the fatty acid pools of tissue, whole serum and VLDL, pointing to NAFLD/NASH-associated increase in *de novo* lipogenesis, suppression of fatty acid oxidation, and depletion of polyunsaturated fatty acids (PUFA). Surprisingly, high-density lipoproteins (HDL) have been disregarded as a source of hepatic lipids despite being one of the possible routes (together with free fatty acids, FFA) delivering lipids from peripheral tissues to the liver.

By integrating whole serum and lipoprotein (HDL) lipidomics, this study points to HDL as a possible actor in the inter-organ cross-talk between peripheral tissues and the liver in NAFLD and advances our understanding of NAFLD pathophysiology.

Method: We studied 89 patients with a biopsy-proven NAFLD and 20 healthy volunteers (CTRL), matched for age and sex, whole serum (20 CTRL, 36 NAFL, 31 NASH F0-2, 22 NASH F3-4) and the HDL lipoprotein (9 CTRL, 11 NAFL, 11 NASH F0-2, 9 NASH F3-4) lipidomics by liquid

chromatography-mass spectrometry. HDL were isolated via fast protein liquid chromatography. Lipid data were presented as absolute values after normalisation for respective internal standards and, for HDL lipids, also Apo-I concentration.

Results: In whole serum, NAFLD patients showed significantly higher absolute concentrations of saturated FFA coupled with a striking depletion of PUFA compared to controls (Fig. 1A); a similar trend was also observed in other lipid species. The lipoprotein lipidomic analysis showed that PUFA were substantially depleted in HDL, with phosphatidylcholine (PC; Fig. 1B) being the most affected lipid class. Additionally, we found that ceramides (Cer) in HDL were significantly increased in NAFLD compared to controls (Fig. 1C). FFA, HDL-PC, and HDL-Cer were also strongly correlated with insulin resistance and/or hepatic liver enzymes (Fig. 1D) suggesting that the concentration of these lipids in HDL might be associated with peripheral organ dysfunction and/or with the necro-inflammatory milieu in NASH.

Conclusion: Taken together, these data show that NAFLD is associated with a reduced absolute content of polyunsaturated FFA and phospholipids within HDL. We, therefore, speculate that an impaired PUFA transport from peripheral tissues to the liver (via FFA and HDL) might be a contributing factor in NAFLD pathophysiology (Fig. 1E).

SAT062

The role of XBP1 in regulating the progression of non-alcoholic steatohepatitis

Haoming Zhou¹, Qi Wang¹, Qingfa Bu¹, Xun Wang¹, Ling Lu¹. ¹The First Affiliated Hospital of Nanjing Medical University, Hepatobiliary Center
Email: hmzhou@njmu.edu.cn

Background and aims: Non-alcoholic steatohepatitis (NASH) is associated with the dysregulation of lipid metabolism and hepatic inflammation. The mechanism underlying NASH is unclear. We aim to investigate the role of X-box binding protein-1 (XBP1) in the progression of NASH.

Method: Human liver tissues obtained from patients with NASH and control group were used to assess XBP1 expression. NASH models were developed in hepatocyte-specific Xbp1 knockout (Xbp1ΔHep), macrophage specific Xbp1 knockout (Xbp1ΔMφ), macrophage-specific Nlrp3 knockout, and wild-type (Xbp1FL/FL or Nlrp3FL/FL) mice fed with high-fat diet for 26 weeks or methionine/choline deficient diet for 6 weeks.

Results: The expression of XBP1 was significantly upregulated in the liver samples from NASH patients. Hepatocyte-specific Xbp1 deficiency inhibited the development of steatohepatitis in the mice fed with the high-fat or methionine/choline deficient diets. Meanwhile, macrophage specific Xbp1 knockout mice developed less severe steatohepatitis and fibrosis than wild-type Xbp1FL/FL mice in response to the high-fat or methionine/choline deficient diets. Macrophage-specific Xbp1 knockout mice showed M2 anti-inflammatory polarization. Xbp1 deleted macrophages reduced steatohepatitis through decreased expression of NLRP3 and secretion of pro-inflammatory cytokines, which mediate M2 macrophage polarization in macrophage-specific Xbp1 knockout mice. Steatohepatitis was less severe in macrophage-specific Nlrp3 knockout mice than in wild-type Nlrp3FL/FL mice. Xbp1 deleted macrophages prevented the hepatic stellate cells activation through decreased expression of TGF-β1. Less fibrotic changes were observed in macrophage-specific Xbp1 knockout mice than in the wild-type Xbp1FL/FL mice. Inhibition of XBP1 suppressed the development of NASH.

Conclusion: XBP1 regulates the development of NASH. XBP1 inhibitors protect against steatohepatitis. XBP1 thus is a potential target for the treatment of NASH.

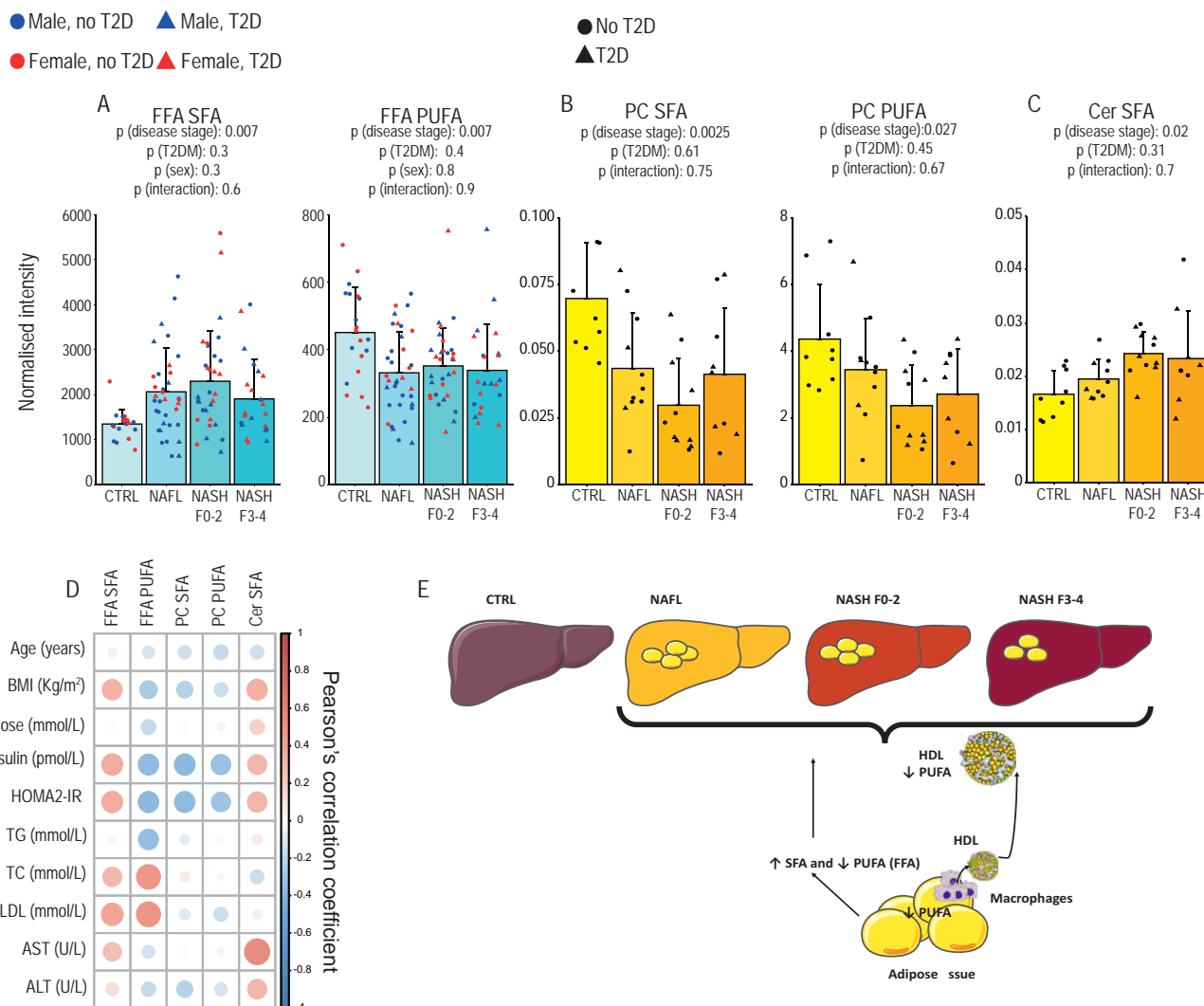


Figure: (abstract: SAT061): Whole serum and HDL lipidomics in NAFLD

SAT063

FXR binding and transcription in the liver is significantly altered in obese patients with NAFLD

Martin Wagner¹, Emilian Jungwirth^{1,2}, Katrin Panzitt¹, David Moore³, Tobias Madl⁴, Gerhard Thallinger², Hanns-Ulrich Marschall⁵.

¹Division of Gastroenterology and Hepatology, Medical University Graz, Graz, Austria; ²Institute of Biomedical Informatics, Graz University of Technology, Graz, Austria; ³Nutritional Sciences and Toxicology, University of California, Berkeley, Berkeley, United States; ⁴Division of Molecular Biology and Biochemistry, Medical University Graz, Graz, Austria; ⁵Department of Molecular and Clinical Medicine/Wallenberg Laboratory, Sahlgrenska Academy, University of Gothenburg, Gothenburg, Sweden

Email: martin.wagner@medunigraz.at

Background and aims: FXR binds to distinct hormone response elements on the chromatin to dictate gene regulation. In mice, these genomic FXR binding profiles are distinct in normal and obese mice, suggesting that FXR activation may produce different outcomes in a different metabolic background. We studied FXR binding profiles and transcriptional outputs in the livers from normal weight and morbidly obese patients with NAFLD, who were treated with either placebo or the FXR ligand obeticholic acid (OCA).

Method: We tested the hepatic FXR cistrome by FXR ChIP-seq and the transcriptome by RNA-seq in liver biopsies of normal and morbidly obese human subjects who had been enrolled in a clinical trial for the treatment with the FXR agonist OCA (NCT0162502). We matched the outcomes of these genomic studies with metabolic profiles of those patients.

Results: In ChIP-seq, a method to determine transcription factor binding on a genome-wide scale, FXR binding sites are inherently different between obese and non-obese patients. In obese patients, FXR bound 26605 sites and only 10270 in non-obese patients. Interestingly, while OCA could recruit additional binding sites in non-obese patients, OCA did not affect FXR binding in obese patients. To explore, which gene sets are selectively targeted by OCA-driven FXR activation in obese patients we integrated the FXR ChIP-seq data with their respective RNA-seq data. In contrast to FXR binding, which remained unaffected by OCA treatment, OCA significantly altered the transcriptome in RNA-seq (1456 genes were up- and 1674 genes downregulated by OCA) in obese patients. Integration of FXR cistromics with transcriptomics revealed activation of "classical" FXR targeted pathways such as bile acid or fatty acid metabolism, however, the top ranked differentially regulated pathways belonged to mitochondrial function. In line with the obese-specific "mitochondrial fingerprint," PGC-1 α , a transcriptional master-regulator of mitochondrial biogenesis, appears to be a direct hepatic FXR target

gene preferentially in obese conditions. Proteomics studies revealed significant changes in proteins of redox metabolism with superoxide dismutase, a first line defence enzyme of oxidative stress, being a specific FXR target. NMR metabolomics studies further showed that in obese conditions glutathione levels significantly dropped in the liver tissue, but could be completely restored by OCA treatment.

Conclusion: The results from FXR cistromics overall suggest that the metabolic background dictates FXR binding and consequently FXR signaling in obese conditions differs from signaling in normal conditions. Activating FXR in obesity may have a major impact on mitochondrial biogenesis and metabolism, which appears to be a selective feature of FXR signaling in the obese condition. A major metabolic effect of OCA in the NAFLD condition may be to balance the redox states.

SAT064

Non-alcoholic fatty liver disease (NAFLD) progression to non-alcoholic steatohepatitis (NASH) and NASH-related hepatocellular carcinoma (HCC) evolves following a differential activation of endoplasmic reticulum stress responses

Alexander Finnemore¹, Jose Maria Herranz^{1,2}, Sergio Barace¹, Stefany Infante^{1,3}, Matías A Avila^{1,2,4}, Guillermo Garcia-Porrero⁵, Sara Arcelus¹, Eva Santamaria^{1,2}, Josepmaria Argemi^{1,2,4,5}. ¹Centro de Investigación Médica Aplicada (CIMA), Hepatology Program, Pamplona, Spain; ²Centro de investigación biomédica en red (CIBER-EHD); ³University of Piura. Lima campus, Miraflores, Peru; ⁴Instituto de Investigación de Navarra (IdisNA); ⁵Clinica Universidad de Navarra, Liver Unit, Pamplona, Spain
Email: jargemi@unav.es

Background and aims: Non-alcoholic fatty liver disease (NAFLD) is notoriously heterogeneous in both its pathophysiology and clinical progression phenotypes. Endoplasmic reticulum stress and the coping response through the Unfolded Protein Response (UPR) have shown to play a significant role in NAFLD-related lipotoxicity. Nevertheless, the dissection of the UPR activation in human and mouse NAFLD progression is poorly understood. The aim of this study was to gain a better understanding of the UPR activation in NAFLD progression.

Method: A total of six main regulators were identified as indicators of activation of different UPR-related pathways. The selected components belonged to the three arms of the UPR, named PERK/ATF4, IRE1A/XBP1 and ATF6. SIRT3 was considered the main regulator of the mitochondrial UPR. An exhaustive compilation of gene expression data was carried out from existing literature and Molecular Signature Database (MSigDB) curated collections and using unpublished RNA-sequencing data of the ATF6-null HCC cell line. Gene signatures were filtered and fine-tuned using controlled in vitro experiment using tunicamycin-treated HCC cell lines. *Mus musculus* gene symbols were replaced by their human orthologs. Gene set variation analysis (GSVA) and single sample Gene Set Enrichment Analysis (ssGSEA) were used to analyze the enrichment of the UPR signatures in human and mouse expression datasets. Statistical analysis was performed using t-student for comparing means of normally distributed continuous variables and Chi-Square was used for comparing categorical variables.

Results: Forty-seven preliminary signatures in both *Homo sapiens* and *Mus Musculus* were defined. After fine-tuning and filtering using controlled ER-stress cell model, a final set of sixteen *bona fide* UPR signatures were derived, which included 358 genes, distributed along 2 ATF4, 2 ATF6, 3 IRE1A, 7 XBP1, 1 PERK and 1 SIRT3 signatures. Using GSVA and ssGSEA these signatures were applied to two NAFLD progression (n = 304 patients, different stage of NAFLD progression F0-4) and two NASH-Hepatocellular Carcinoma (NASH-HCC) (n = 180 samples, including Normal, Cirrhosis, NASH and NASH-HCC and their peritumoral liver counterparts), human data sets. As NAFLD progresses to NASH and NASH-HCC, the expression of UPR branches

is generally decreased. Patients can be split into distinctive groups regarding specific UPR profiles.

Conclusion: NAFLD progresses to NASH and NASH-HCC showing specific patterns of ER stress responses. The application of *bona fide* UPR signatures to human NAFLD gene expression data sets, allows for a UPR-based classification that could have potential prognostic and/or predictive value.

SAT065

MPEP, an mGlu5 receptor allosteric modulator, reduces hepatic steatosis in obese high-fat-diet mice

Laura Giuseppina Di Pasqua¹, Marta Cagna¹, Clarissa Berardo¹, Anna Clea Croce^{2,3}, Ferdinando Nicoletti^{4,5}, Mariapia Vairetti¹, Andrea Ferrigno¹. ¹University of Pavia, Department of Internal Medicine and Therapeutics, Pavia, Italy; ²Institute of Molecular Genetics-Italian National Research Council (CNR), Pavia, Italy; ³University of Pavia, Department of Biology and Biotechnology, Pavia, Italy; ⁴Sapienza University of Rome, Department of Physiology and Pharmacology, Roma, Italy; ⁵IRCCS, Neuromed, Pozzilli, Italy
Email: lauragiuseppin.dipasqua01@universitadipavia.it

Background and aims: The metabotropic glutamate receptor 5 (mGluR5) regulates many central reward pathways as well as those affecting appetite (Bradbury et al., 2005). It is also involved in the alcoholic steatohepatitis regulation (Choi et al., 2019) and recent data proved that mGluR5 modulates body weight, adipose tissue and inflammation in an in vivo model of diet-induced obesity (Oliveira et al., 2021). In an in vitro model of acute hepatic fat accumulation, mGluR5 selective blockade by the negative allosteric modulator MPEP resulted in the reversion of the injury caused by oleic and palmitic acid exposure. On the contrary, the mGluR5 agonist DHPG worsened the fatty acid exposure-induced damage (Ferrigno et al., 2020). Aim of this work was to evaluate the role of MPEP in an in vivo model of hepatic steatosis.

Method: Male 606B6.V mice genetically modified for leptin gene (ob/ob mice), 7-week fed with high fat diet were concomitantly daily administered with MPEP or vehicle (20 mg/kg, IP). At the sacrifice, liver biopsies and hepatic nuclear fractions were collected. Total lipid content was evaluated by Nile Red dye, while lipid droplet areas were calculated by ImageJ software on histological samples fixed in formalin and stained with HandE. Lipid peroxidation and oxidative stress were evaluated by TBARS and ROS assays respectively. Protein analysis for mGluR5, PPAR-alpha, SREBP1, mTOR and NFkB were evaluated by Western blotting on tissue samples or nuclear fractions. The activation of NFkB and mTOR were assessed by calculating the ratio between the phospho-protein and the non-phosphorylated protein expression.

Results: No changes were detected in hepatic mGluR5 protein expression both in MPEP- or vehicle-treated group. MPEP-treated mice displayed a significant reduction in total lipid content compared with vehicle-treated group and lipid droplet areas decreased significantly after MPEP treatment. Levels of hepatic TBARS and ROS diminished significantly after MPEP administration and, in line with these findings, NFkB activation was significantly reduced in MPEP-treated mice with respect to vehicle-treated mice. Nuclear activated PPAR-alpha increased significantly in MPEP group, while nuclear activated SREBP1 was significantly down-regulated by mGluR5 blockade. mTOR activation did not show any significant difference between the two groups in the nuclear fraction.

Conclusion: These results demonstrate that MPEP administration reduces steatosis in obese mice fed by high fat diet. Oxidative stress parameters and inflammation are decreased by mGluR5 blockade, probably via PPAR-alpha that negatively regulates NFkB. Besides, intracellular lipid accumulation is prevented by SREBP1 down-regulation in an mTOR-independent way. Although further investigations are needed, this is the first time that MPEP beneficial effects are reported in an in vivo model of hepatic steatosis.

POSTER PRESENTATIONS

SAT066

Pro-inflammatory liver-homing T cells in peripheral blood, liver and adipose tissue in patients with NASH and changes in post-bariatric surgery samples

James Hallimond Brindley¹, Falguni Tailor¹, Karthik Chandrasekharan¹, Kathryn Waller¹, Wenhao Li¹, Kalpana Devalia², Francesca Rosini³, John Loy², William Alazawi¹.
¹Blizard Institute, Queen Mary University of London, Barts Liver Centre, London, United Kingdom; ²Homerton University Hospital, London, United Kingdom; ³St Mary's Hospital, Histopathology, London, United Kingdom
Email: halbrindley@gmail.com

Background and aims: Non-alcoholic steatohepatitis (NASH), the inflammatory subtype of non-alcoholic fatty liver disease (NAFLD) associated with obesity and type2 diabetes mellitus (T2DM) can lead to advanced liver disease. There are limited data evaluating T cell subsets in multiple tissue compartments or following weight loss in NAFLD. We hypothesised that circulating and tissue T cells changed in advanced versus mild NASH.

Method: Prospective samples were collected under ethically-approved protocols; peripheral blood from 37 NAFLD patients and 7 controls, with primary comparisons between advanced (elastography >9.7kPa or ≥F3) and mild (elastography <8.2kPa or ≤F2) NAFLD. A subset undergoing bariatric surgery (n = 21) underwent additional simultaneous sampling of liver, visceral (VAT) and subcutaneous adipose tissue (SAT) for flow cytometry immuno-profiling, with further blood samples after weight loss.

Results: Peripheral blood MAIT cells were significantly reduced with greater activation in patients with advanced versus mild NAFLD or controls (0.8% vs 3.1%, 3.2% p < 0.05) although IFN gamma and TNF alpha expression was higher in all NAFLD MAIT cells (IL-17 in advanced) compared to control.

In bariatric patients, Th1 (CD4⁺CXCR3⁺) cells were more abundant in NASH vs no-NASH (33% vs 21% p < 0.05), particularly among patients with diabetes in whom pro-inflammatory Th1 and Th17 cells (CD4⁺CD161⁺) expressed higher levels of liver homing CXCR6.

After weight loss, the proportion of Th1, Th17 cells and activated (CD69⁺) CD8⁺ T cells reduced.

The proportion of CXCR6⁺ Th1 and Th17 cells reduced, as did IFN gamma expressing CXCR6⁺Th17 cells.

In patients with T2DM NASH, intrahepatic Th17 cell numbers were higher and MAIT cells lower compared to other groups, with a similar reduction of MAIT cells in SAT. Conversely, SAT total T cell CXCR6 expression was higher in T2DM NASH than in other patient groups. In T2DM NASH, expression of tissue-retaining CD69 expression on Th1 cells was higher in the liver and lower in VAT.

Conclusion: A peripheral and adipose tissue pro-inflammatory, liver-homing T cell phenotype is evident in patients with T2DM and NASH with improvement in this after weight loss.

SAT067

Therapeutic inhibition of complement component 5 does not reduce NASH progression but does attenuate atherosclerosis development in Ldlr^{-/-}.Leiden mice

Florine Seidel^{1,2}, Robert Kleemann¹, Wim van Duyvenvoorde¹, Nikki van Trigt¹, Nanda Keijzer¹, Sandra van der Kooij³, Cees van Kooten³, Lars Verschuren⁴, Aswin L. Menke¹, Johnathan Winter⁵, Timothy Hughes⁵, Paul Morgan⁵, Frank Baas⁶, Kees Fluiter⁶, Martine C. Morrison¹, Amanda Kiliaan². ¹the Netherlands Organisation for Applied Scientific Research (TNO), Metabolic Health Research, Leiden, Netherlands; ²Radboud University Medical Center, Medical Imaging (Anatomy), Nijmegen, Netherlands; ³Leiden University Medical Center (LUMC), Internal Medicine (Nephrology), Leiden, Netherlands; ⁴the Netherlands Organisation for

Applied Scientific Research (TNO), Systems Biology, Zeist, Netherlands; ⁵Cardiff University, Systems Immunity Research Institute and UK Dementia Research Institute Cardiff, School of Medicine, United Kingdom; ⁶Leiden University Medical Center (LUMC), Clinical Genetics, Leiden, Netherlands
Email: florine.seidel@tno.nl

Background and aims: With the increased mortality that is associated with the obesity-related comorbidities non-alcoholic steatohepatitis (NASH) and atherosclerosis, there is a great need for therapeutic interventions to treat advanced stages of these diseases. Chronic inflammation has been shown to be an important driver in progression of both NASH and atherosclerosis. The complement system, one of the first lines of defence in innate immunity, is thought to play an important role in this chronic inflammatory response. However, the therapeutic value of complement system inhibition in already established disease has not been studied to date. In this study we investigated the potential health effects of therapeutic inhibition of the terminal complement system (via inhibition of complement component 5 (C5)) simultaneously on established NASH and atherosclerosis in a translational model of obesity-related disease.

Method: After 20 weeks of high-fat diet (HFD)-feeding, obese Ldlr^{-/-}.Leiden mice were treated bi-weekly with an established anti-C5 antibody (BB5.1) or vehicle control, and a separate group of mice was kept on a chow diet as a healthy reference. To confirm adequate inhibition of C5, the complement system activity in plasma as well as the membrane-attack complex (MAC) deposition in the liver were quantified. After 12 weeks of treatment, NASH was analysed histopathologically and genome-wide hepatic gene expression was analysed by next-generation sequencing followed by pathway analysis. Atherosclerotic lesion area and severity were quantified histopathologically in the aortic roots.

Results: Anti-C5 treatment considerably reduced complement system activity in plasma and MAC deposition in liver. The histological examination of livers revealed that systemic anti-C5 treatment did not affect NASH progression, showing no effect on steatosis, inflammation or fibrosis. However, on the gene expression level, anti-C5 treatment did affect the pathways Oxidative phosphorylation and Mitochondrial dysfunction. Anti-C5 treatment was also revealed to be beneficial against atherosclerosis, limiting the total lesion size independently of an effect on plasma cholesterol. In addition, C5 inhibition reduced lesion severity, increasing the area of mild type I-III lesions and lowering the area of severe type IV and V lesions.

Conclusion: We show for the first time that targeting the complement system via C5 inhibition in advanced stages of NASH is not sufficient to reduce disease development, while therapeutic intervention against moderately-advanced atherosclerosis is beneficial to limit further progression of the lesions.

SAT068

The overexpression of TM6SF2 and/or MBOAT7 wild-type genes re-establishes the mitochondrial dynamics in an in vitro NAFLD model.

Erika Paolini^{1,2}, Miriam Longo^{1,3}, Marica Meroni¹, Giada Tria¹, Chiara Macchi², Roberto Piciotti^{1,4}, Adele Agresta¹, Massimiliano Ruscica², Anna Ludovica Fracanzani^{1,4}, Paola Dongiovanni¹. ¹General medicine and metabolic diseases, Fondazione IRCCS Cà Granda ospedale maggiore policlinico; ²Università degli Studi di Milano, Milan, Italy, Department of Pharmacological and Biomolecular Sciences; ³Università degli Studi di Milano, Milan, Italy, Department of clinical sciences and community health, Università degli studi di Milano; ⁴Università degli Studi di Milano, Milan, Italy, Department of Pathophysiology and Transplantation
Email: paola.dongiovanni@policlinico.mi.it

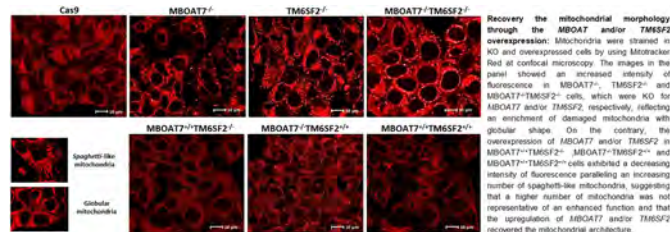
Background and aims: Mitochondria adaptability is hampered in the progression from NASH up to HCC. Recently, we demonstrated that HepG2 cells, homozygous for the PNPLA3 I148M variant, and silenced

for *MBOAT7* and/or *TM6SF2* genes by CRISPR/Cas9 spontaneously developed fat accumulation, exhibited an enrichment of damaged mitochondria, an unbalance in their turnover and finally a higher proliferation rate together with reduced apoptosis.

In the attempt to deepen the impact of *PNPLA3/MBOAT7/TM6SF2* loss-of-function on mitochondrial abnormalities, we aim to assess whether the overexpression of *MBOAT7* and/or *TM6SF2* wild-type forms restores the mitochondrial dynamics which was lost in knock-out (KO) models.

Method: *MBOAT7* and/or *TM6SF2* were overexpressed through lentiviral vectors. Mitochondrial morphology and number were assessed by confocal microscopy and D-loop TaqMan Copy Number Assay whereas the function was evaluated by qRT-PCR, Western Blot, Seahorse assay and immunohistochemistry.

Results: At Oil Red O staining, the overexpressed cells exhibited a reduction of lipids compared to KO models. The upregulation of *MBOAT7* and/or *TM6SF2* lowered D-loop levels and increased spaghetti-like globular shape ratio of mitochondria, enhancing the number of normo-shaped ones. The overexpressed models reduced the mRNA levels of *PGC1 α* , master regulator of mitobiogenesis, which was activated in KO cells in response to fusion-fission unbalance, prompted the expression of *Mfn1* and *Mfn2* (mitochondrial outer membranes proteins involved in fusion) and decreased *FIS1* (fission protein) levels, thus re-establishing the mitochondrial turnover. The increased COX-I/SDHA ratio paralleled the oxygen consumption rate after the overexpression of *MBOAT7* and/or *TM6SF2*, recovering the OXPHOS activity which was impaired in KO cells. Consistently, ROS content, lipid peroxidization and ER/Golgi stress (*ATF4*, *ATF6*, *XPB1* and *GRP78*) decreased, confirming the recovery of mitochondrial derangement. Additionally, the upregulation of *MBOAT7* and/or *TM6SF2* reduced the expression of *DUSP1* (cell proliferation) according to MTS and wound healing assays and fostered the apoptotic pathways, thus attenuating the tumorigenic phenotype.



Conclusion: Genetics may be involved in the mitochondrial maladaptation during NAFLD and the overexpression of *MBOAT7* and/or *TM6SF2* in KO HepG2 cells re-established the mitochondrial dynamics and reduced the proliferation rate.

SAT069

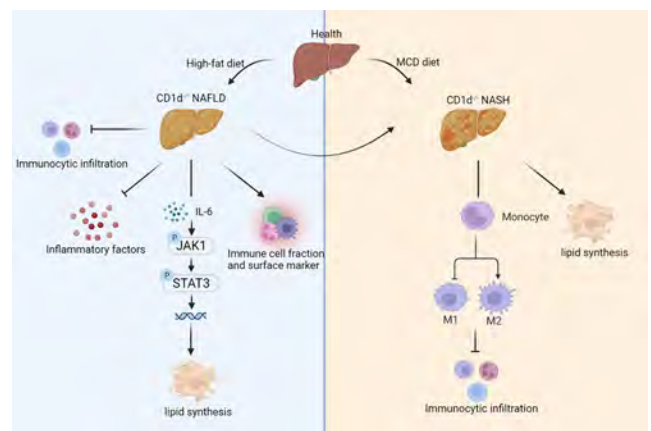
CD1d knockdown promotes NAFL lipid synthesis by activating the IL6-JAK1-STAT3 signal pathway and reduces inflammatory factors in NASH by decreasing macrophage polarisation towards M1 and increasing polarisation towards M2

Dandan Shan^{1,2}, Qiuxian Zheng¹, Zhi Chen¹. ¹Hangzhou, *Diagnosis and Treatment of Infectious Diseases, Hangzhou, China*; ²The First Affiliated Hospital, Zhejiang University School of Medicine, Hangzhou, China
Email: zjuchenzhi@zju.edu.cn

Background and aims: Non-alcoholic fatty liver disease (NAFLD) is a chronic progressive liver disease. NAFLD involves multiple complex biological effects that help activate innate and adaptive immunity and exacerbate NAFLD development. CD1d proteins mediate the delivery of self or microbial lipid and glycolipid antigens to activate immune cells, rapidly produce large amounts of cytokines, and trigger innate and adaptive immune responses. Here, we explored the role for CD1d in NAFLD.

Method: Flow cytometry and Cytometry by Time of Flight (CyTOF) was used to measure and analyze the expression level of markers on the surface of immune cells in liver tissues of NAFL mice, and the distribution map of immune cells was established. M1 and M2 macrophages in liver tissues was also detected.

Results: Compared with the WT HFD group, the CD1d^{-/-} HFD group mice showed a significant increase in liver index, a significant increase in liver steatosis ($p < 0.05$), ALT level ($p < 0.01$), AST level ($p < 0.05$) and a significant increase in serum LDL level ($p < 0.01$). Transcriptome analysis showed that IL6-JAK1-STAT3 signaling pathway was significantly enriched in CD1d^{-/-} HFD group compared with WT HFD group. The gene expression level in CD1d^{-/-} HFD group was significantly increased compared with WT HFD group. In vitro studies showed that CD1d gene knockout aggravated FFA-induced NAFL lipid droplet formation and lipid deposition. AG490 inhibition of IL6-JAK1-STAT3 signaling pathway alleviates liver steatosis and down-regulates the gene expression level of lipid metabolism in THE CD1d knockout NAFL group. The expression level of liver immune cells in CD1d^{-/-} HFD group was lower than that in WT HFD group. Compared with WT NCD group, the expression level of immune cells and inflammatory factors was increased in WT MCD group. The expression levels of liver immune cells and inflammatory factors in CD1d^{-/-} MCD group were lower than those in WT MCD group. The expression level of M2-polarized surface markers in macrophages in CD1d^{-/-} MCD group was higher than that in WT MCD group, while the expression level of M1-polarized surface markers in macrophages was lower. CD1d gene knockout aggravated FFA-induced lipid accumulation in mouse laparoscopic macrophages, inhibited M1 polarization of peritoneal macrophages, and promoted M2 polarization of peritoneal macrophages. CD1d gene knockout aggravated fatty acid induced lipid accumulation in mouse BMDM cells, inhibited M1-type polarization of BMDM cells, and promoted the M2-type polarization.



Conclusion: CD1d plays a protective role in the process of NAFL steatosis, and CD1d deficiency can increase hepatic lipid accumulation and hepatic steatosis by activating il6-JAK1-STAT3 signaling pathway.

In NASH stage, CD1d deficiency can promote M2-type polarization of macrophages by inhibiting M1-type polarization of macrophages, thus reducing the level of liver inflammation.

SAT070

The role of immune semaphorins in NAFLD-a pilot study

Ivana Knezevic Stromar¹, Maja Mijic², Lara Samadan³, Slavko Gasparov², Adriana Vince^{3,4}, Neven Papis^{3,4}. ¹University hospital centre Zagreb, Zagreb, Croatia; ²University hospital Merkur, Zagreb, Croatia; ³School of medicine, University of Zagreb, Zagreb, Croatia; ⁴University hospital for infectious diseases Zagreb, Zagreb, Croatia

Email: npapis@bfm.hr

Background and aims: Non-alcoholic fatty liver disease (NAFLD) is associated with chronic low-grade inflammation, impaired immune response and microvascular endothelial dysfunction. Semaphorins, a large family of biological response modifiers, were recently recognized as one of the key regulators of immune response, possibly also associated with chronic liver diseases. However, their role in NAFLD has not been described. The aim of this study was to identify semaphorins associated with NAFLD and to investigate relationship with steatosis and fibrosis stages.

Method: This was a prospective, multicentric, case-control study. The degree of steatosis was estimated using the controlled attenuation parameter (CAP) and transient elastography (TE) was used to measure fibrosis stage. A routine clinical, demographic, anthropometric and laboratory data were collected and serum semaphorin concentrations (SEMA3A, -3C, -4A, -4D, -5A and -7A) were measured by ELISA. Immunohistochemical staining of liver tissue was performed. The correlation between serum semaphorin concentrations and steatosis and fibrosis grade was analyzed.

Results: Ninety-five patients with NAFLD (51.6% males; median age of 54, IQR 44-56 years) and 35 controls (40% males, 41, IQR 31-52 years) were included. Patients with NAFLD more frequently had diabetes mellitus (30.5% vs 8.6%), arterial hypertension (49.5% vs 8.6%), dyslipidemia (28.4% vs 11.4%) and obesity (BMI 31 kg/m² vs 24 kg/m²). 39 patients with NAFLD had no fibrosis (F0), and in 27, 15, 6 and 8 patients F1 to F4 was detected, respectively. A significantly higher serum concentrations of SEMA3A, -3C and -4D, and lower of SEMA5A and -7A were found in NAFLD group compared to the healthy controls. There was no difference in semaphorin concentrations according to steatosis grade, but there was significant difference according to fibrosis stage, SEMA3A being lower and SEMA3C and -4D higher in advanced fibrosis. Immunohistochemistry confirmed the higher expression of SEMA3C and SEMA4D in advanced fibrosis.

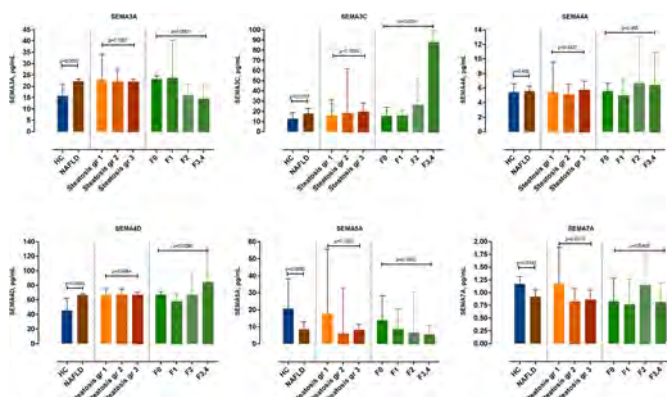


Figure: SEMA3A, -3C, -4A, -4D, -5A and -7A sera concentrations according to the steatosis and fibrosis stage in patients with NAFLD.

Conclusion: We provide the first evidence that immune semaphorins are a promising marker of liver fibrosis in patients with NAFLD. Due to their immunomodulatory role, they could be useful in predicting liver capacity to answer challenges of infection, but also potential diagnostic and therapeutic targets in NAFLD.

SAT071

Machine learning-enabled continuous scoring of histologic features facilitates prediction of clinical disease progression in patients with non-alcoholic steatohepatitis

Janani Iyer¹, Charles Biddle-Snead¹, Quang Le¹, Pratik Mistry¹, Isaac Finberg¹, Victoria Mountain¹, Rob Myers², Chuhan Chung³, Andrew Billin³, Tim Watkins³, Ilan Wapinski¹, Michael Montalto¹, Andrew Beck¹, Murray Resnick¹, Katy Wack¹. ¹PathAI, Boston, United States; ²The Liver Company, Palo Alto, United States; ³Gilead Sciences, Inc., Foster City, United States
Email: kathy.wack@pathai.com

Background and aims: Histologic grading and staging of disease severity are typically performed using ordinal scoring systems, which often lack sufficient sensitivity to characterize changes in histology over short periods of time or in response to treatment during clinical trials. Here we demonstrate the prognostic utility of machine learning-facilitated continuous scoring of histologic features.

Method: Liver biopsies and central pathologist (CP) Ishak and Clinical Research Network (CRN) disease severity scores were collected from subjects enrolled in the Ph3, placebo-controlled STELLAR (ST) trials of selonsertib (NCT03053050, NCT03053063). All subjects had CRN fibrosis stage 3 or 4 at baseline (BL) and were assessed for progression to either cirrhosis or liver-related events (LREs). Treatment arms were combined due to lack of measured drug efficacy. PathAI AI-based measurement of NASH histology (AIM-NASH) models were deployed to generate ML-derived predictions for ordinal and continuous CRN grades/stages for steatosis, hepatocellular ballooning, lobular inflammation, and fibrosis (Figure 1A). Cox proportional-hazards, receiver operating characteristic, and Kaplan-Meier (KM) analyses were employed to assess associations between ML-derived disease severity metrics and patient outcomes.

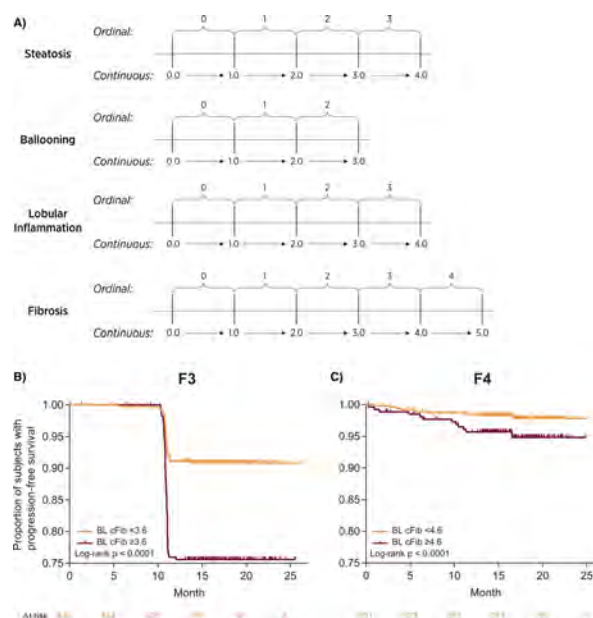


Figure: (A) Mapping of PathAI NASH CRN ordinal to continuous scores; (B) KM analysis showing progression to cirrhosis; (C) KM analysis showing progression to LRE.

Results: During a median follow-up of 16.5 or 15.8 months, 14.9% (N=108/725) of F3 subjects progressed to cirrhosis, and 2.5% (N=20/794) of F4 subjects had liver-related events (LREs) respectively. Progression to cirrhosis in subjects with F3 fibrosis at BL was associated with higher ML continuous and ordinal fibrosis stage and higher manual (Ishak) scoring at BL. Lower ML-derived ordinal but not manual steatosis grade was also associated with progression to cirrhosis. In subjects with F4 fibrosis at BL, lower BL continuous

steatosis grade and ordinal Ishak fibrosis stage were predictive of progression to a LRE. BL continuous fibrosis stage cutoffs of 3.6 and 4.6 stratified subjects into slow vs. rapid progressors to cirrhosis or LREs, respectively (Figures 1B and 1C). ML-derived continuous scoring showed higher discriminatory accuracy to predict progression to cirrhosis and to LREs than ML-derived ordinal scoring (AUROC [90% CI] = 0.66 [0.61, 0.71] vs. 0.59 [0.55, 0.63] and 0.61 [0.52, 0.7] vs. 0.54 [0.47, 0.59] in ST3 and ST4, respectively).

Conclusion: AIM-NASH analysis of biopsies from two completed Ph3 NASH clinical trials demonstrates the prognostic potential of continuous histologic scoring methods. These results support further investigation into the value of ML-based continuous histologic scoring methods for measuring clinically meaningful therapeutic effects in NASH clinical trials.

SAT072

Increasing plasma concentration of aldo-keto reductase family 1 member B10 and its significance in the progression of non-alcoholic fatty liver disease

Hye Eun Lee¹, Dae Ho Lee¹. ¹Gachon University College of Medicine, Gil Medical Center, Incheon, Republic of Korea, Department of Internal Medicine, Incheon, Korea, Rep. of South
Email: esthel0513@gmail.com

Background and aims: Understanding of hepatic gene expression during non-alcoholic fatty liver disease (NAFLD) progression may help to find traceable therapeutic targets. Although efforts to examine the transcriptomic changes that occur as NAFLD progresses have largely used, studies have been limited independent validation. We investigated the feasibility of secretory protein for diagnosis of NAFLD and evaluated the diagnostic accuracy of biomarkers.

Method: We incorporated transcriptomic data on healthy subject and NAFLD patient biopsy-proven samples, representing the full histological range from normal liver tissue to steatohepatitis-cirrhosis-hepatocellular carcinoma in both publicly available data base (n = 853) and a separate replication cohort (n = 102). To validate the finding form the transcriptomic data analysis, we confirmed protein level in serum, blood, and liver tissue form patient. In addition, supporting the biological plausibility of these data, we assessed its expression in primary hepatocytes from mice under various metabolic stresses and other stresses, which caused AKR10B expression.

Results: We discovered tentative secretory proteins that reflect the progression of NAFLD with a consistent and stepwise increasing pattern for the diagnosis of NASH. We found 4 secretory proteins (AKR1B10, annexin A2P2, ZNF468, and CD24) and we showed through our own cohort study that plasma AKR1B10 could be a clinically applicable biomarker for NAFLD (AUROC 0.834) and for advanced fibrosis (AUROC 0.914) at a cutoff level (≥ 1078.2 pg/ml). We applied our protocol to monitor NAFLD in patients undergoing bariatric surgery, showing that plasma AKR1B10 levels decreased markedly after surgery. Translating these findings to the protein level, we optimized in vitro cell model using primary mouse hepatocytes treated with free fatty acid and high glucose.

Conclusion: In the present study, the circulating concentrations of proteins AKR1B10 were strongly associated with disease activity and fibrosis stage. Plasma AKR1B10 could be a useful non-invasive biomarker for the diagnosis of NAFLD as progression of disease. Further validation studies in the future as a biomarker and a probable therapeutic target for NAFLD will be warranted.

SAT073

Validation of the ADAPT score for the diagnosis of clinically significant fibrosis in patients with non-alcoholic fatty liver disease (NAFLD)

Arun Sanyal¹, Sudha Shankar², Katherine Yates³, Clayton Dehn⁴, James Bolognese³, Brent Tetri³, Kris Kowdley³, Raj Vuppalanchi³, Mohammad Siddiqui⁵, Cynthia Behling³, James Tonascia³, Anthony Samir⁶, Claude Sirlin⁷, Sarah Sherlock⁸, Kathryn Fowler³, Helen Heymann⁹, Tania Kamphaus³, Rohit Loomba¹⁰, Roberto Calle¹¹.
¹Virginia Commonwealth University, Department of Internal Medicine, Division of Gastroenterology, Richmond, United States; ²AstraZeneca, Gaithersburg, MD, United States; ³Virginia Commonwealth University, Richmond, VA, United States; ⁴Virginia Commonwealth University, Richmond, VA 23298, United States; ⁵Virginia Commonwealth University, Richmond, United States; ⁶Harvard Medical School/Massachusetts General Hospital, Boston, MA; ⁷University of California San Diego, La Jolla, CA, United States; ⁸Pfizer Inc, 610 Main Street, Cambridge, MA, United States; ⁹Foundation for NIH, North Bethesda, MD, United States; ¹⁰NAFLD research center, San Diego, CA, United States; ¹¹Regeneron Pharmaceuticals Inc., Tarrytown, NY, United States
Email: arun.sanyal@vcuhealth.org

Background and aims: There is an unmet need for validation of diagnostic tools to identify patients with NAFLD who have stage 2 or greater fibrosis that meet regulatory standards for qualification. The ADAPT score is anchored on PROC3, a collagen fragment released during fibrogenesis and being developed for this purpose. PROC3 is measured either with ELISA or on the COBAS platform. The aims of this secondary analysis of the NIMBLE circulating work stream stage 1 dataset were to: (1) evaluate the utility of the ADAPT score (Pro-C3-based fibrosis algorithm that includes Age, Diabetes, Pro-C3 and Platelet count) for the diagnosis of clinically significant fibrosis (\geq stage 2), advanced fibrosis (\geq stage 3) or cirrhosis (stage 4) in patients with NAFLD, and (2) determine if ADAPT performance varies based on whether PROC3 is measured by ELISA or COBAS.

Method: A retrospective analysis of a sample set from the NIDDK NASH CRN DB2 adult cohort curated to avoid spectrum bias by balanced representation of fibrosis stages (0–4) was performed. Histology was independently read by the NASH CRN pathology committee using validated protocols. All samples were obtained within 90 days of a liver biopsy demonstrating NAFLD; a FIB4 score was computed from the same sample as the PROC3. Both ELISA and COBAS based PROC3 results were obtained on each sample. The primary hypothesis was that the ADAPT score would diagnose the fibrosis strata noted above with an AUROC >0.7 with confidence limits that do not intersect 0.5 at the Youden index. The secondary hypothesis was that the AUROC at Youden index would be superior to FIB4 for the same fibrosis strata.

Results: A total of 1070 patients, each providing a single set of the readouts, were studied. The distribution of fibrosis stages was: (0 = 222, 1 = 114, 2 = 262, 3 = 277, 4 = 198). Those with stages 0–1 had more NAFL and had a lower NAFLD activity score compared to those \geq stage 2. Comparison of PROC3 results from ELISA and COBAS methodologies did not show appreciable differences in performance. Data using ELISA are presented below (* primary hypothesis validated, ** secondary hypothesis validated).

	Youden cutpoint	Sensitivity	Specificity	AUROC	FIB4 AUROC
\geq stage 2	≥ 6.2	76.4	76.8	0.849*	0.799**
\geq stage 3	≥ 6.9	74.9	78.7	0.832*	0.790**
Stage 4	≥ 7.1	85.9	68.1	0.824*	0.81

Conclusion: The ADAPT score was validated to diagnose clinically significant and advanced fibrosis in those with NAFLD and was superior to FIB4 for both purposes.

SAT074

Obeticholic acid reduces hepatic matrix metalloproteinase activity in a diet-induced ob/ob mouse model of NASH

Marta Cagna¹, Giuseppina Palladini^{1,2}, Laura Giuseppina Di Pasqua¹, Anna Cleta Croce³, Luciano Adorini⁴, Andrea Ferrigno¹, Mariapia Vairetti¹. ¹University of Pavia, Dept of Internal Medicine and Therapeutics, Pavia, Italy; ²Fondazione IRCCS Policlinico San Matteo, Pavia, Pavia, Italy; ³Institute of Molecular Genetics, Italian National Research Council (CNR), Pavia, Italy; ⁴Intercept Pharmaceuticals, San Diego, California, USA
Email: marta.cagna02@universitadipavia.it

Background and aims: Hepatic matrix metalloproteinases (MMPs) play a role in fibrogenesis of NASH contributing not only to the balance between formation and degradation of connective tissue components, but also to signal transduction for tissue repair. We have previously shown that the FXR agonist obeticholic acid (OCA) reduces hepatic MMP activity by restoring RECK, an MMP regulator tissue reversion-inducing cysteine rich protein with Kazal motifs, after ischemia/reperfusion injury (Ferrigno et al, 2020). Here, the effects of OCA on hepatic MMP activity and RECK content were evaluated in a diet-induced NASH model in ob/ob mice.

Method: Lep^{ob/ob} (ob/ob) NASH mice fed high fat (HF) diet (AMLN-diet; D09100301, with trans-fat, cholesterol and fructose) or control diet were used. After 9 weeks on diet, mice were treated with OCA dosed via dietary admixture 0.05% (30 mg/kg/d) or HF diet for 12 weeks. Liver weight, serum transaminase, alkaline phosphatase, bilirubin, cholesterol, triglycerides, MMP-2 and MMP-9 activity as well as RECK levels were quantified at the end of the study.

Results: HF diet induced a significant increase in liver MMP-9 when compared with mice treated with control diet; OCA administration reduced MMP-9 to levels observed in control diet animals. Although not significant, the same trend occurred for MMP-2. A down-regulation of tissue RECK observed in HF group was recovered by OCA to values comparable to control diet group. A significant increase in liver weight was found in HF diet mice compared to control diet group. OCA treatment reduced liver weight to values comparable with those observed in the control diet group. Serum bilirubin and cholesterol increased in HF diet-treated mice and OCA administration markedly counteracted these increases. OCA did not affect serum transaminase, alkaline phosphatase and triglyceride levels compared to HF diet mice.

Conclusion: Thus, OCA confers protection in a model of NASH, as shown by reduced serum bilirubin and cholesterol levels. This is the first study showing the positive effect of OCA on hepatic MMP-9 via restoration of RECK levels in a NASH model. These are intriguing findings considering a) the crucial role of MMPs in extracellular matrix homeostasis due to stellate cell activation into a profibrogenic phenotype occurring during inflammation and b) the emerging role of RECK in regulating inflammatory and fibrogenic processes. Further studies are necessary to better understand the implications of OCA-induced decrease in hepatic MMPs, and its role in the therapy of NASH.

SAT075

Evaluation of semisynthetic high-fat diets in development of a 4-week mouse NASH model

Ozren Majstorović¹, Maja Antolić¹, Snježana Čužić¹, Lucija Mušak¹, Matea Čedilak², Hrvoje Brzica¹, Martina Bosnar², Ines Glojnarčić¹. ¹Fidelita Ltd, In vivo pharmacology and toxicology, Zagreb, Croatia; ²Fidelita Ltd, In vitro pharmacology, Zagreb, Croatia
Email: ozren.majstorovic@fidelita.eu

Background and aims: Non-alcoholic fatty liver disease (NAFLD) represents the most common chronic liver condition worldwide. Non-alcoholic steatohepatitis (NASH) is characterized by hepatic steatosis, inflammation, hepatocellular damage, and further, fibrosis. At present, no pharmacological NASH therapy was approved by the FDA, creating a necessity for a reliable preclinical model reflecting

disease characteristics seen in humans. Most widely used animal models of NASH are set on nutritional basis, however, their long duration counteracts the need for rapid efficacy testing. In this study, two semisynthetic high-fat diets that act as disease inducers alone, or in combination with 2-hydroxypropyl- β -cyclodextrin (CDX) or fructose, were evaluated with the aim to develop a shorter but reliable mouse NASH model for screening of potential drug candidates.

Method: C57BL/6 male mice were fed with choline-deficient, L-amino acid-defined, high-fat (60 kcal%) diet (CHAHFD) consisting of 0.1% methionine or high-fat (60 kcal%), cholesterol (1.25%), and cholic acid (0.5%) (HFCC) diet. In addition, both dietary regimens were supplemented with either 2% CDX, a cyclic oligosaccharide with high affinity to sterols, or 30% fructose in drinking water. After four weeks of feeding, sera were analysed for biomarkers of liver damage (ALT, AST), cholesterol (CHOL), and fasting glucose levels. Livers were weighed and analysed for triglyceride (TG) content and expression of inflammatory (*Tnf-alpha*, *IL-10*, and *Ccl2*) and fibrosis related genes (*Col1a1*, *Timp1*, *Pai1*, *Ctgf*, *Tgf-beta*, and *Acta2*). Histopathological evaluation was conducted using modified NAS score and immunohistochemistry (IHC) for Collagen 1A1 (COL1A1) and macrophage population (F4/80).

Results: Addition of CDX to HFCC diet resulted in a significant increase in inflammation and fibrosis, as confirmed by NAS, F4/80, and COL1A1 positive area as well as higher expression of both gene panels. In contrast, addition of fructose resulted in a significant increase in steatosis score. CDX addition to CHAHFD resulted in increase of liver damage biomarkers, while inflammation score, COL1A1 surface, and consequently total NAS, where most affected by addition of fructose. When comparing two diets, significantly higher serum CHOL levels were observed in all HFCC groups, while significant increase in liver TG content was achieved in all CHAHFD combinations. Disease progression to perisinusoidal/periportal fibrosis was observed with significantly higher intensity of overall parameters when using CHAHFD, however, accompanied by a transient body weight loss.

Conclusion: This study provides the successful recapitulation of main clinical features of NASH in a 4-week dietary induced mouse model, while favoring use of CHAHFD and emphasizing a need for tailored approach in testing pharmacological candidates based on their targets and mode of action.

SAT076

Tyrosinase mutations, a novel predisposing genetic factor for enhanced non-alcoholic steatohepatitis susceptibility

Kaushalya Kulathunga¹, Arata Wakimoto², Michito Hamada², Satoru Takahashi². ¹Faculty of Medicine-University of Sabaragamuwa Sri Lanka, Department of Physiology, Ratnapura, Sri Lanka; ²University of Tsukuba, department of anatomy and embryology, Tsukuba, Japan
Email: kkulathunga@med.sab.ac.lk

Background and aims: Non-alcoholic fatty liver disease (NAFLD) is an alarmingly rising metabolic disorder. Non-alcoholic steatohepatitis (NASH) is the progressive liver damage with inflammation, leading to fibrosis and carcinogenesis. Interestingly, enhanced susceptibility for NASH was observed in B6 albino mice (albino) with high cholesterol diet (HCD), compared to wild type B6 black mice (black), a phenotype not reported before. This study was led to understand the underline mechanism of elevated NASH susceptibility of albino mice.

Method: B6 albino mice carry G291 T point mutation in tyrosinase (*Try*) gene and this is the only genetic difference compared to B6 black mice. Albino and black mice were fed with HCD for 10 weeks. Normal diet fed mice used as controls. Body weights, blood indices and liver damage related serum parameters were monitored. Liver samples were histologically analyzed. Small intestinal lipid absorption and the expression of intestinal cholesterol transporters were investigated. Mice carrying only the G291 T mutation were developed using

CRISPR/Cas9 technology and employed to confirm that the observed phenotype is resulted from that specific mutation.

Results: Liver injury with elevated ALT, AST levels were observed in albino mice from post day 1 HCD feeding. 2 weeks of HCD induced NASH in albino mice, but no symptom was observed in black mice even after 10 weeks of diet. Histological analysis of albino mice livers revealed significant inflammatory cells and lipid infiltration, and severe fibrosis. Increased serum chylomicron and very low density lipoprotein levels were observed in albino mice partly because of the low serum lipoprotein lipase levels and partly as the expression changes in small intestinal cholesterol transporters. Similar to B6 albino, CRISPR generated mice exhibited the same liver damage phenotype, confirming the contribution of G291 T mutation.

Conclusion: To validate our data in human context, in-silico analysis was carried out investigate the allele frequencies of two main *Try* single nucleotide polymorphisms (SNPs). Interestingly, it was revealed that Hispanic populations with highest prevalence of NAFLD/NASH exhibit relatively high allele frequencies with two main *Try* SNPs, G140A and G316C. This work uncovered a novel possible genetic factor for NASH development. Further studies are carried out to uncover the contribution of human *Try* SNPs in the development of NAFLD/NASH.

SAT077

SIRT5 rs12216101 T > G variant is associated with mitochondrial dysfunction and disease severity in patients with NAFLD

Federico Salomone¹, Rosaria Maria Pipitone², Francesco Malvestiti³, Paola Dongiovanni³, Miriam Longo³, Angela Maria Amorini⁴, Alfio Distefano⁴, Giovanni Li Volti⁴, Giuseppe Lazzarino⁴, Ester Ciociola⁵, Grazia Pennisi², Rossana Porcasi², Daniela Cabibi², Antonio Craxi², Anna Ludovica Fracanzani³, Luca Valenti³, Salvatore Petta², Stefania Grimaudo². ¹Azienda Sanitaria Provinciale di Catania; ²University of Palermo; ³University of Milan; ⁴University of Catania; ⁵University of Gothenburg
Email: federicosalomone@rocketmail.com

Background and aims: Sirtuin 5, encoded by the SIRT5 gene, is a NAD⁺-dependent deacetylase modulating mitochondrial metabolic processes through post-translational modifications. In this study, we aimed to examine the impact of SIRT5 rs12216101 T > G non-coding SNP on disease severity in patients with non-alcoholic fatty liver disease (NAFLD).

Method: The rs12216101 was genotyped in 2606 consecutive European patients with biopsy-proven NAFLD. Transcriptomic analysis was performed in a subset. Effects of SIRT5 pharmacological inhibition was evaluated in HepG2 cells exposed to excess free fatty acids (FFA) and mitochondrial energetics was investigated by HPLC.

Results: In the whole cohort, the frequency distribution of SIRT5 rs12216101 TT, TG and GG genotypes was 47.0%, 42.3% and 10.7%, respectively. At multivariate logistic regression analysis adjusted for gender, age > 50 years, diabetes, and PNPLA3 rs738409 status, SIRT5 rs12216101 T > G variant was associated with presence of NASH (OR 1.20, 95% C.I. 1.03–1.40) and F2–F4 fibrosis (OR 1.18, 95% C.I. 1.00–1.37). Transcriptomic analysis showed that rs12216101 T > G variant was associated with altered SIRT5 mRNA splicing and upregulation of transcripts involved in mitochondrial metabolic pathways, including the oxidative phosphorylation system (OXPHOS), thus suggesting that the G risk allele may confer an overall gain of function of SIRT5. Consistently, western blot analysis demonstrated an up-regulation of OXPHOS complexes III, IV and V. Administration of a pharmacological SIRT5 inhibitor to HepG2 treated with FFA preserved mitochondrial function as evidenced by restored ATP/ADP, NAD⁺/NADH and NADP⁺/NADPHs ratios.

Conclusion: The SIRT5 rs12216101 T > G variant is associated with liver damage, heightened SIRT5 activity and impaired mitochondrial function in patients with NAFLD, thus highlighting SIRT5 as a novel candidate target for NAFLD therapy.

SAT078

Recapitulating insulin resistance in a 3D human liver model for efficacy testing of drug candidates

Radina Kostadinova¹, Lisa Hoelting¹, Simon Hutter¹, Arianna Menghini¹, Anna Zehnder¹, Wolfgang Moritz¹, Francisco Verdeguer¹, Olivier Frey¹. ¹InSphero, Schlieren, Switzerland
Email: radina.kostadinova@insphero.com

Background and aims: There is a close link between metabolic liver diseases, type 2 diabetes, and obesity resulting in a severe dysregulation of glucose and lipid metabolism. Understanding the mechanism of inter-cellular and tissue crosstalk and how it relates to metabolic homeostasis, offers a great potential to identify novel therapeutic opportunities. Conventional cell culture models lack complex multi-cellular interactions found in the human body and are unable for accurate disease modeling and predictive drug efficacy testing *in vitro*. Here, we modeled *de novo* lipogenesis (DNL) and steatosis conditions by the recapitulation of glucose metabolism in 3D human liver co-culture and for efficacy testing of anti-steatotic and anti-diabetic compounds.

Method: We have cultured 3D human liver tissues (hLiMTs) consisting of primary hepatocytes, Kupffer cells and liver endothelial cells in a 96-well format under pathophysiological insulin and glucose conditions in absence (DNL model) or presence of free fatty acids (FFA, OA:PA, steatosis model). After incubation of the tissues with disease stimuli, the insulin and glucagon sensitivity of hLiMTs was assessed by measurement of the tissue triglyceride levels as well as quantifying glycogen content and gluconeogenesis (GNG) upon hormonal stimulation.

Results: Glucagon induced glycogen storage depletion in hLiMTs. Additional, assay conditions were optimized to quantify GNG by measuring glucose release from fasted hLiMTs. The amount of glucose produced through GNG increased in the presence of increasing concentrations of glucagon. In contrast, increasing concentrations of insulin resulted in reduced glucose release from hLiMTs, indicating an inhibition of GNG. Importantly, insulin resistance was observed in hLiMTs incubated in high glucose and high insulin with and without FFA. Triglyceride levels were increased by about 10-fold in the DNL model and 20-fold in the steatosis model as compared to the healthy control. Treatment with 0.5 μ M Firsocostat, an ACC1 inhibitor, decreased significantly the triglyceride levels in the DNL model.

Conclusion: The presented 3D human liver model replicates the features of glucose and lipid handling in a highly scalable format and its application for efficacy testing of anti-steatotic and anti-diabetic compounds. It constitutes one of the three central elements for building a multi-tissue MPS besides pancreatic islets and adipose microtissues to study human glucose and lipid homeostasis.

SAT079

Novel endosomal trafficking adaptor for the regulation of NAFLD to NASH progression

Karsten Motzler¹, Karsten Nalbach², Revathi Sekar¹, Ana Alfaro¹, Martin Hrabe de Angelis³, Matthias Blüher⁴, Michael Roden⁵, Stephan Herzig¹, Natalie Krahmer⁶, Christian Behrends², Anja Zeigerer¹. ¹Institute for Diabetes and Cancer, Helmholtz Center Munich, Neuherberg, Germany; ²Munich Cluster for Systems Neurology (SyNergy), Medical Faculty, Ludwig-Maximilians University Munich; ³Institute of Experimental Genetics, Helmholtz Center Munich; ⁴Helmholtz Institute for Metabolic, Obesity and Vascular Research; ⁵Institute for Clinical Diabetology, German Diabetes Center; ⁶Institute for Diabetes and Obesity, Helmholtz Center Munich
Email: karsten.motzler@helmholtz-muenchen.de

Background and aims: Membrane trafficking through the endosomal transport system has gained increased attention for metabolic regulation in recent years. Cells within organs sensitive to metabolic cues, such as the liver, need to reorganize e.g. transporters and hormone receptors upon alterations in nutrient availability. This

POSTER PRESENTATIONS

reorganization is achieved by the endosomal trafficking machinery and is especially important in highly polarized hepatocytes for the secretion or delivery of certain proteins to apical (biliary) membranes while other proteins must be transported to basolateral (sinusoidal) membranes. Part of the needed specificity is given by different adaptor proteins (APs), aiding cargo recognition and coat protein recruitment during vesicle formation. Here, we are reporting on a novel role of the epsilon subunit of the AP-4 complex (AP4E1) in metabolism and implications for NAFLD to NASH progression. Connecting the two fields of endocytosis and metabolism offers a more thorough understanding of NAFLD and NASH and might help to identify new drug targets.

Method: Using mice with hepatocyte-specific knockout (KO) of Ap4e1 and different models of diet-induced NASH together with proteomic and RNA sequencing approaches, we aim to dissect the crosstalk of hepatocytes with other cell-entities within the liver. By assessing the membranome and secretome of primary hepatocytes, we try to identify novel cargo proteins of Ap-4 and how this transport is affecting the transition of NAFLD to NASH.

Results: Here, we identify a thus far unknown role for an endocytic membrane trafficking adaptor protein, Ap4e1, in NASH development and progression. Interestingly, we find Ap4e1 to be upregulated both in livers of human NASH patients, and in livers of multiple mouse models of NASH. This is associated with a positive correlation of Ap4e1 protein levels with hepatic fibrosis in mice, suggesting a potential connection between Ap4e1 and NASH progression. Indeed, reduction of Ap4e1 exacerbates the development of fibrosis, indicating a regulatory role of Ap4e1 in NASH. Membranome and secretome assessment of primary hepatocytes depleted of Ap4e1 reveal interesting hits on novel cargo proteins of this adaptor that are connected to fibrosis development and are currently investigated further. In addition, ongoing scRNAseq analysis of KO NASH livers is conducted to provide insights into the crosstalk between hepatocytes and other cell types within fibrotic mouse livers to shed light onto the intrahepatic communication pathways that drive disease progression.

Conclusion: Taken together, our data reveal a novel role of Ap4e1 in the regulation of NAFLD to NASH transition. As Ap4e1 depletion exacerbates disease outcome, we aim to identify the responsible cargo proteins that could reveal a new mechanism to understand NASH development and potentially serve as targets for therapeutic applications.

SAT080

Enzymatic activity dysfunction of the mitochondrial respiratory chain, in the full spectrum of the metabolic associated fatty liver disease

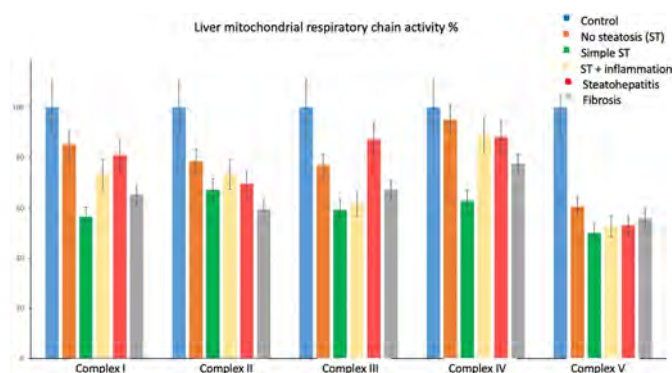
Alberto García Picazo¹, Pilar Gómez Rodríguez¹, Pilar del Hoyo Gordillo², Carolina Ibarrola de Andrés³, Javier Salamanca Santamaría³, Elías Rodríguez Cuéllar¹, Cristina Martín-Arriscado⁴, Jennifer Villa⁵, Ana Martín Algibez⁶, Inmaculada Fernández Vázquez⁶, Miguel Ángel Martín Casanueva⁴, Mercedes Pérez-Carreras⁶. ¹12th October University Hospital, General Surgery, Madrid, Spain; ²12th October University Hospital, Mitochondrial disease, Spain; ³12th October University Hospital, Pathology, Spain; ⁴12th October University Hospital, Imas 12 Research Institute, Spain; ⁵12th October University Hospital, Microbiology, Spain; ⁶12th October University Hospital, Gastroenterology, Spain
Email: alberto.gpicazo@gmail.com

Background and aims: Patients with morbid obesity (MO) develop a huge range of histological injuries related to the metabolic associated fatty liver disease (MAFLD). Those lesions could be a trustful model to study their relation with the mitochondrial dysfunction, which appears in this disease. The main objective is to determine the existence of mitochondrial liver dysfunction in patients with MO and MAFLD.

Method: A prospective case-control study was designed, the case group was composed of MO patients having received bariatric

surgery, whereas the control group was non-hepatopathy patients. In both groups surgical liver biopsy was performed between 2019 and 2021. Demographic, anthropometric, metabolic, blood test and histological (SAF classification) variables were measured. All patients were divided according to their histological injury grade and the dysfunction of the mitochondrial breath chain, and compared to the control group. Liver mitochondrial respiratory chain (MRC) activity was measured by spectrophotometry. The variables were analysed with Stata version 16 software, statistical significance was set at $p < 0.05$.

Results: Case group ($n = 53$): 66% women, 48 ± 11 years, BMI 45 ± 6 ; Control group ($n = 10$): 50% women, 54 ± 13 years, BMI 24 ± 2 . MRC activity in case group vs control group: Complex I, 39.8 vs 53.9 ($p = 0.01$), II- 190.3 vs 275.2 ($p < 0.001$), III-87.6 vs 119 ($p = 0.04$), IV- 92.6 vs 115 ($p = 0.02$) and V- 82.8 vs 155.8 ($p < 0.001$). Figure 1: decreased percentage in the MRC activity related with the histological damage: No steatosis (10/53), simple steatosis (7/53), steatosis + inflammation (7/53), steatohepatitis (17/53), Fibrosis (12/53). A relation between HOMA-IR and high levels of insulin with the activity in the complexes I and II ($p < 0.05$) was identified.



Conclusion: The enzymatic activity of the 5 complexes of the liver MRC are decreased in patients with MO and MAFLD. This alteration affects the synthesis of ATP (complex V). Insulin resistance and insulinemic index are associated with defects in complexes I and II. Mitochondrial dysfunction already appears in subjects with MO without liver injury and is different according to histological severity. There is less enzymatic activity in early and advanced stages of MAFLD, while it increases with MAFLD inflammatory activity. These enzymatic changes could be due to adaptive disorders of the mitochondria in MAFLD.

SAT081

Lipid-induced phenotypic differences in human non-alcoholic fatty liver disease models determined by matrix-assisted laser desorption/ionization mass spectrometry

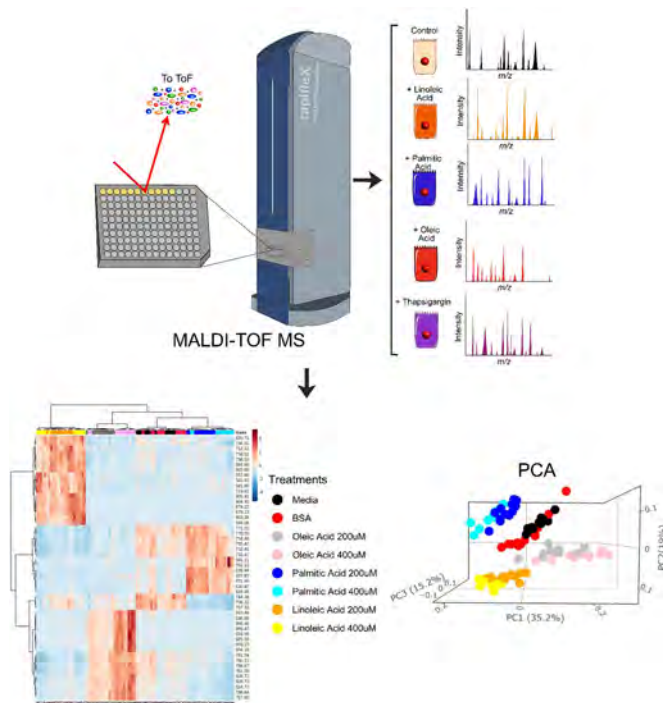
Ruth Walker¹, Michalina Zatorska², Jose Luis Marin-Rubio¹, Matthias Trost¹, Maria Emilia Dueñas¹, Olivier Govaere². ¹Biosciences Institute, Faculty of Medical Sciences, Newcastle upon Tyne, United Kingdom; ²Translational and Clinical Research Institute, Faculty of Medical Sciences, Newcastle upon Tyne, United Kingdom
Email: olivier.govaere@newcastle.ac.uk

Background and aims: Accumulation of lipids is a key part of the pathogenesis of non-alcoholic fatty liver disease (NAFLD) and has recently been associated with endoplasmic reticulum (ER) stress. *In vitro* lipid loading is often used as an experimental model for NAFLD, though a high-throughput screening platform to understand metabolic changes and lipotoxicity is still lacking. Matrix-assisted laser desorption/ionisation-time-of-flight mass spectrometry (MALDI-TOF MS) is a fast, reproducible, and label-free technology, used for assays in pharmaceutical research and development, drug discovery and

chemical biology. This offers the potential to perform comprehensive phenotypic characterisation of biomolecules, including metabolites, and screen for novel therapeutic strategies. The aim of this work was to establish a fast and robust high-throughput screening technique for determining metabolite and peptide/protein changes in a NAFLD cell model.

Method: Human hepatoma HepG2 cells were treated with saturated and unsaturated fatty acids including linoleic, oleic and palmitic acid at concentrations of 200 μ M and 400 μ M, or with the ER stress inducer thapsigargin (1 mM). Cells were mixed one-to-one with 2, 5-dihydroxyacetophenone matrix and analysed by MALDI-TOF MS to determine differences in the phenotypic profiles of metabolites and high molecular weight (HMW) biomolecules. Principal component, hierarchical clustering and multivariate analysis were carried out to identify differences.

Results: Overall, 1372 metabolite and 753 protein unique features were identified by MALDI-TOF MS. Distinctive metabolite profiles were established for each condition, allowing multiplexing and identification of biomarkers. A dose-dependent effect is evident for all lipids and whilst linoleic and oleic acid are often used interchangeably in the field, they induce significant differences in cellular metabolic profiles, having 243 and 76 unique metabolites respectively. Moreover, although thapsigargin and high concentrations of palmitic acid induces ER stress and cellular cytotoxicity respectively, they present substantial differences, indicating that mechanistic differences between these two conditions. Of the lipid treatments, only 400 μ M palmitic acid has a significant effect on the profiles of HMW biomolecules, having 605 unique biomolecules, and 47 common proteins.



Conclusion: Taken together, we have developed a fast MALDI-TOF MS comparative screening technique for determining metabolite and HMW biomolecule changes in a human in vitro NAFLD models. Moreover, our data provides distinctive metabolic and stress fingerprints that are relevant during the progression of NAFLD. Biomarkers from these fingerprints may be used as a screening method for therapeutic interventions.

SAT082

Regulation of NEAT1 in NAFLD by RNA-binding proteins

Lisa Ahne¹, Ahmad Barghash², Shinichi Nakagawa³, Alexandra K. Kierner⁴, Sonja Keßler¹. ¹Institute of Pharmacy, Experimental Pharmacology for Natural Sciences, Halle (Saale), Germany; ²School of Electrical Engineering and Information Technology, Amman, Jordan; ³Faculty of Pharmaceutical Sciences, RNA Biology Laboratory, Sapporo, Japan; ⁴Institute of Pharmacy, Pharmaceutical Biology, Saarbrücken, Germany

Email: lisa.ahne@pharmazie.uni-halle.de

Background and aims: The long non-coding RNA *NEAT1* with its two most abundant transcripts *NEAT1_v1* and *NEAT1_v2* has been shown to play a role in NAFLD. *NEAT1* is strongly regulated via stability and closely associated with paraspeckles and mitochondria. However, the underlying interactions remain unclear so far. RNA-binding proteins (RBPs) are major regulators of post-transcriptional regulation. Aim of this study was to investigate the role of RBPs in the regulation of *NEAT1* in NAFLD.

Method: Experiments were performed either in wildtype, hepatocytic *TTP*^{-/-}, or *Neat1*^{-/-} mice. Mice were fed either a high-fat diet (HFD), a methionine-choline deficient diet (MCD), a Lieber De Carli diet (LDC), or a control diet. Gene expression was analyzed by qPCR, gene arrays, or RNA-Seq. RIP of HuR/ELAVL1 was performed. In vitro experiments were conducted in HepG2, HUH7, or PLC/PRF/5 cells and two human data sets (GEO) were analyzed.

Results: *Neat1* was upregulated in livers of HFD-, Lieber de Carli, and MCD-fed mice. *Neat1*^{-/-} mice gained less weight on an HFD. Hepatic gene expression data of these *Neat1*^{-/-} mice revealed several enriched GO terms related to metabolism. Concordantly, in an *in vitro* steatosis model, treatment of HepG2 cells with oleic acid or palmitic acid induced *NEAT1* expression, particularly of the long *NEAT1* variant. Interestingly, gene expression of paraspeckle RBPs *Sfpq* and *Pspc1* were also significantly increased in the MCD-fed animals. The increase of *Neat1*, *Sfpq*, and *Pspc1* expression seems to particularly take place in hepatocytes, since expression levels were unchanged in Kupffer cell depleted livers. In inflammatory conditions, two oppositely regulated RBPs play a major role in the regulation of inflammatory factors: *TTP/ZFP36* and *HuR/ELAVL1*. Human data sets revealed a contrary deregulation of both RBPs in human steatohepatitis and murine NAFLD models. The target AU-rich motifs of *TTP* and *HuR* could be found above average in the *NEAT1_v2* sequence. Both RBPs exhibit a large overlap of target RNAs containing AU-rich sequences that are stabilized by *HuR* but degraded by *TTP*. In *TTP*^{-/-} livers, a significant induction of *Neat1* expression was observed. Overexpression of *TTP* in liver cells decreased *NEAT1_v1* and *NEAT1_v2* levels. For *HuR*, RIP experiments in total HUH7 cell lysates confirmed binding of *HuR* to human *NEAT1* in liver cells.

Conclusion: Our data suggest that *NEAT1* is regulated by the RBPs *TTP* and *HuR* in steatohepatitis.

SAT083

Anti-inflammatory effect of simvastatin-ezetimibe combination therapy via inhibition of macrophage in NASH related mouse model

Han Seul ki¹, Moon Young Kim¹. ¹Wonju Severance Christian Hospital, Department of Internal Medicine, Division of Gastroenterology and Hepatology, Wonju-si, Korea, Rep. of South

Email: drkimmy@yonsei.ac.kr

Background and aims: There are few clinical options for management of Non-alcoholic steatohepatitis (NASH)-related cirrhosis. In both vivo and vitro studies, we aimed to investigate the effects of statin and ezetimibe combination therapy and putative anti-inflammation capacity in NASH-related liver fibrosis.

Method: A High-fat diet and Thioacetamide (300 mg/kg, intraperitoneal injection twice a week for 8 weeks) was given to establish mice models with non-alcoholic steatohepatitis (NASH) related

POSTER PRESENTATIONS

histological change. Statin (5 mg/kg) and ezetimibe (10 mg/kg) were administered during last 4 weeks.

Results: Ezetimibe, statin monotherapy and combination therapy were improved hepatic steatosis.

We got liver tissue showing histologically NASH-related change from high fat diet for 12 weeks and administration of TAA for 8 weeks. The improvement of steatosis and inflammation was more pronounced in the statin group, ezetimibe group and combination group. In particular, ezetimibe shows lower fat contents and statin shows improvement of inflammation.

Simvastatin mono treatment and combination with ezetimibe treatment suppress hepatic fibrosis

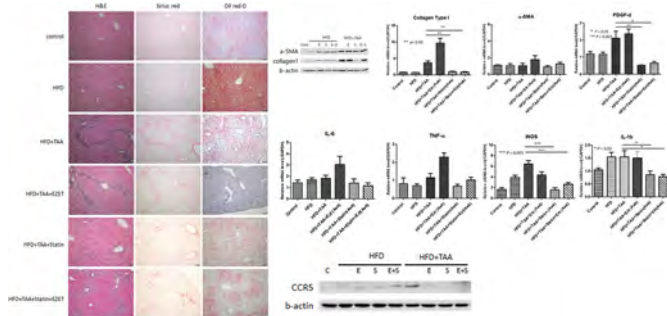
The improvement of fibrosis was more pronounced in the statin and ezetimibe group. These results were confirmed as decreased α -SMA and collagen protein level by Western analysing. In PCR transcription, there was lower transcription level of collagen type I and PDGF-d, suggesting there is lowering fibrosis in statin, ezetimibe treated group. There was elevation of collagen type I and α -SMA, PDGF-d in ezetimibe monotherapy group, but it was not correlated a histological finding.

Simvastatin and ezetimibe combination treatment suppresses hepatic inflammation.

The effects about IL-6, IL-1b, and TNF- α were evaluated by quantitative real-time PCR. And it is suggesting that simvastatin mono-treatment and simvastatin, ezetimibe combination therapy exhibits anti-inflammatory effects. IL-6, TNF- α , IL-1b and iNOS was decreased in statin and combination group. In this study, Ezetimibe mono-treatment group shows elevation of IL-6, TNF- α .

Simvastatin and ezetimibe combination therapy inhibits macrophage migration via downregulating CCR 5 and macrophage activation

In vitro, Statin and ezetimibe downregulate of expression of CCR5. Many macrophages were also observed in HFD-TAA histology and the number of macrophages was decreased in simvastatin, simvastatin + ezetimibe combination treatment group.



Conclusion: In the NASH-cirrhosis mouse model, ezetimibe showed the improvement of steatosis and statin showed anti inflammatory effect. And the combination therapy showed improvement of fibrosis through macrophage migration and suppression, resulting in TNF- α inhibition. Ezetimibe mono-treatment in NASH-cirrhosis need to be evaluated because of potential side effects.

SAT084

The different modulation of KLB expression impacts on liver damage in NAFLD patients and in an in vitro model: a novel druggable target?

Marica Meroni¹, Nadia Panera², Giada Tria³, Roberto Picciotti^{3,4}, Miriam Longo^{3,5}, Erika Paolini^{3,6}, Antonella Mosca⁷, Annalisa Crudele², Anna Ludovica Fracanzani^{3,4}, Anna Alisi², Paola Dongiovanni¹. ¹Fondazione IRCCS Cà Granda Ospedale Maggiore Policlinico, Milan, Italy; ²General Medicine and Metabolic Diseases, Milan, Italy; ³Bambino Gesù Children's Hospital-IRCCS, Research Unit of Molecular Genetics of Complex Phenotypes, Rome; ⁴Fondazione IRCCS Cà Granda Ospedale Maggiore Policlinico, Milan, Italy; ⁵General Medicine

and Metabolic Diseases, Milan; ⁴University of Milan, Department of Pathophysiology and Transplantation, Milan; ⁵University of Milan, Department of Clinical Sciences and Community Health, Milan; ⁶University of Milan, Department of Pharmacological and Biomolecular Sciences, Milan; ⁷Bambino Gesù Children's Hospital-IRCCS, Hepatology Gastroenterology and Nutrition, Rome
Email: paola.dongiovanni@policlinico.mi.it

Background and aims: We previously shown that the rs17618244 variant in β -Klotho (KLB) gene, encoding the hepatic co-receptor of fibroblast growth factor receptor 4 (FGFR4), increases the risk of developing severe NAFLD, NASH and fibrosis both in adults and children, due to lower KLB hepatic/plasma levels. Aim of this study was to investigate the impact of another variant in KLB, the rs12152703, on liver damage in NAFLD patients and to evaluate the effect of KLB *in vitro* genetic ablation on fat accumulation, oxidative/ER stress, inflammation and cell proliferation.

Method: We evaluated the effect of the rs12152703 variant in 1311 biopsied NAFLD patients of whom 261 were children. Hepatic and circulating KLB levels were measured in a subset of patients (n = 125 and n = 290, respectively). Next, we generated a full knock-out model of KLB gene in HepG2 cells (KLB^{-/-}) by CRISPR/Cas9.

Results: At multivariate analysis, the rs12152703 KLB variant was associated with reduced transaminase levels and with protection against NASH and advanced NAFLD activity score (NAS) (p < 0.05). Hepatic and circulating KLB concentrations were increased in NAFLD patients carrying the variant (p < 0.05).

Concerning the *in vitro* model, KLB mRNA and protein levels were strongly dampened in KLB^{-/-} cells (p < 0.01), along with the expression of genes implicated in cholesterol metabolism, suggesting an overall altered KLB signaling (p < 0.05). KLB^{-/-} cells displayed a reduced intra-cellular triglyceride (TG) content (p < 0.05), related to the suppression of genes involved in lipogenesis and TG synthesis (p < 0.05). KLB deletion strongly induced oxidative and ER stress, increasing ROS/RNS production, aldehyde derivate concentrations and ROS-induced DNA damage (p < 0.05). These events triggered the release of pro-inflammatory cytokines into the KLB^{-/-} cultured media (p < 0.05), resembling severe NAFLD. Finally, KLB^{-/-} cells also showed an elevated proliferative rate and invasiveness (p < 0.05).

Conclusion: In sum, the rs12152703 KLB variant protected against severe NASH, whereby enhancing KLB levels differently from the rs17618244 at-risk variation.

Our *in vitro* results outlined that KLB shutdown may be causally involved in the switching towards progressive forms of liver damage, by inducing ER/oxidative stress, inflammation, and enhanced proliferation, even in the absence of excessive fat accumulation. Thus, KLB may constitute a novel druggable target for the prevention of severe NAFLD.

SAT085

Utilization of gluconeogenic glucose-6-phosphate via pentose phosphate pathway is increased in mice fed a high fat/high sugar diet compared to a high sugar diet alone

Getachew Debas Belew^{1,2}, Ana Costa¹, Maria Joao Meneses³, Ludgero Tavares¹, Paula Macedo³, John Jones¹. ¹University of Coimbra, Center for Neuroscience and Cell Biology, Coimbra, Portugal; ²Addis Ababa Science and Technology University, Biotechnology, Addis Ababa, Ethiopia; ³CEDOC-Chronic Diseases Research Center, NOVA Medical School, Nova University of Lisbon, Lisbon, Portugal
Email: gechap4@gmail.com

Background and aims: In hepatocytes, the pentose phosphate pathway (PPP) is an important generator of NADPH for *de novo* lipogenesis (DNL) and for the maintenance of reduced glutathione in antioxidant defense. The development of non-alcoholic fatty liver disease (NAFLD) secondary to high sugar and/or high fat intake is characterized by elevated DNL rates and increased oxidative stress. It is not known whether PPP fluxes are modified in these settings. We developed a double tracer method that provides information on both

DNL and PPP fluxes in feeding mice. We applied this to compare DNL and PPP fluxes in mice fed a normal chow diet supplemented with high-fructose corn syrup (HFCS-55) with a more obesogenic diet composed of high fat chow supplemented with HFCS-55.

Method: Twelve C57BL/6 mice were provided with standard chow (SC) with the drinking water supplemented with 30% (w/v) of HFCS-55 (55/45 mixture of fructose and glucose) for 18 weeks. Eleven mice were placed on high-fat chow (HFC) with the same HFCS-55 supplement over the same period. At the beginning of the final evening, all mice were administered with 99% deuterated water containing and the HFCS-55 fructose component was enriched to 20% with [U-¹³C]₆fructose. On the following morning, mice were deeply anesthetized with ketamine/xylazine and sacrificed by cardiac puncture. Arterial blood was collected and centrifuged to isolate plasma, livers were freeze-clamped, and the samples were stored at -80°C until further processing. Liver triglyceride and glycogen were purified and analyzed for ²H and ¹³C-enrichments by NMR. DNL rates were quantified from lipid ²H-enrichment and adjusted for liver triglyceride levels. Whole body adiposity was estimated from body water ²H enrichment. The fraction of gluconeogenic glucose-6-phosphate (G6P) utilized by the PPP was quantified from glycogen ¹³C-isotopomer analysis.

Results: Mice fed HFC + HFCS-55 had greater body weight (50 ± 1 vs 37 ± 1 g, *p* < 0.0001), higher whole-body adiposity (29 ± 1 vs 16 ± 2%, *p* < 0.0001), and higher liver triglyceride levels (15 ± 2 vs 8 ± 2 g/100 g liver, *p* < 0.025) compared to those fed SC + HFCS-55. DNL rates were not significantly different between the two groups although the high-fat chow mice had a tendency for higher rates (1.02 ± 0.1 vs 0.75 ± 0.1 g/100 g liver, *p* = 0.2109). However, the fraction of gluconeogenic G6P utilized by the PPP was significantly higher for the high-fat chow mice (17.0% versus 13.8%, *p* = 0.034).

Conclusion: A diet high in both fat and sugar is more obesogenic than a diet high in sugar alone. In the presence of high fat, DNL rates were sustained while PPP utilization of G6P derived from gluconeogenesis was significantly increased. This may be explained by additional demand for NADPH above and beyond that consumed by DNL, possibly in response to increased oxidative stress.

SAT086

A novel microwell platform to analyse single-cell secretion dynamics and cell communication in NAFLD progression

Ricell Booiijink^{1,2}, Ruchi Bansal^{1,2}, Leon Terstappen¹. ¹University of Twente, Medical Cell Biophysics, Science and Technology, Netherlands; ²University of Twente, Translational Liver Research, Medical Cell BioPhysics

Email: r.s.booiijink@utwente.nl

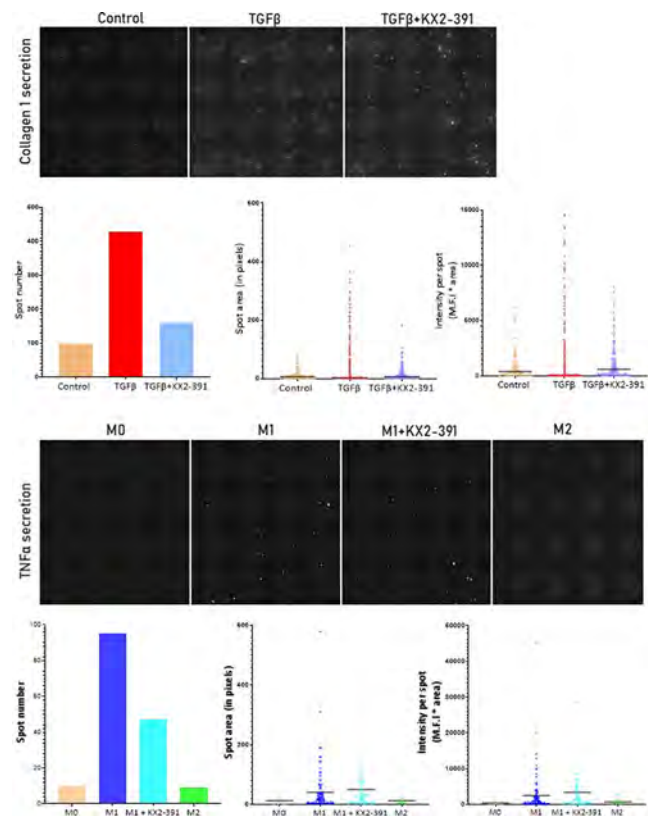
Background and aims: Liver inflammation and fibrosis are the hallmarks of non-alcoholic steatohepatitis (NASH). Here, activated and differentiated hepatic stellate cells (HSCs) together with infiltrating and activated immune cells maintain a continuous cycle of cellular activation, inflammation and fibrogenesis. To do this, these non-parenchymal cell populations in the liver microenvironment secrete factors including cytokines and proteins to communicate with their surroundings. Many studies confirmed heterogeneity within these cells on a genomic level. However, how this heterogeneity translates to cellular secretion and communication, and its influence on NALFD progression remains unclear.

We propose a novel model that enables simultaneous analysis and correlation of single-cell secretion, phenotype, genome and transcriptome, using a self-sorting microwell platform.

Method: The self-sorting microwell chip is developed containing 6400 microwells with a diameter of 70 µm, volume of 1.4 nl and 5 µm single pore at the bottom of each well. While placing a cell suspension

on the chip, single cells are distributed over the wells, and identified by fluorescent microscopy. The chip is brought into contact with a PVDF membrane, which collects secreted molecules from the single cells. Upon removing the membrane, the concentration of secreted molecules can be determined and correlated to the individual cell that produced them. Thereafter, cells of interest can be isolated from the chip and used for further molecular (DNA and RNA) analysis, by punching out the bottom of the microwell into a PCR tube.

Results: To validate the model, human HSCs (LX2) and PMA-differentiated human macrophages (THP1) are used to measure collagen-I and TNF-alpha secretion respectively. Upon TGF-β activation, we observed an increase in the number of HSC-secreted collagen-I spots with increased spot intensity and area, which varied greatly per individual cell, confirming the cellular heterogeneity in collagen-I secretion in non-activated and activated cells. Interestingly, treatment with Src kinase inhibitor, KX2-391, led to an average decrease again with large variety in the amount of collagen-I secretion.



Furthermore, upregulation of TNF-alpha secretion was observed in pro-inflammatory LPS-stimulated M1 macrophages, seen by an increased number of cells that produced detectable TNF-alpha spots. Again, we saw a heterogeneous distribution in TNF-alpha secretion, and treatment with KX2-391 led to a reduction in the amount of TNF-alpha secreted per cell.

Conclusion: We established a method to determine the phenotype and secretome, that can be integrated with genome and transcriptome, of single cells in the NASH microenvironment. Building upon this model by multiplexing cell populations and multiple secreted molecules allows us to map the NASH secretome, exploring novel avenues for NASH treatment.

SAT087

Dysregulation of the urea cycle enzymes determines a more severe NAFLD phenotype in a DIAMOND preclinical model

Rocío Gallego-Durán^{1,2}, María del Rosario García-Lozano^{1,2}, Douglas Maya^{1,2}, Lucía López-Bermudo^{3,4}, Rocío Montero-Vallejo^{1,2}, Sheila Gato Zambrano^{1,2}, Antonio Cárdenas-García^{3,4}, Vanessa García Fernández^{1,2}, Blanca Escudero-López^{3,4}, Rocío Muñoz Hernández^{1,2}, Antonio Gil-Gómez^{1,2}, Angela Rojas Álvarez-Ossorio^{1,2}, Helena Pastor^{1,2}, Franz Martin-Bermudo^{3,4}, Manuel Romero Gómez^{1,2,5}, Javier Ampuero^{1,2,5}. ¹Instituto de Biomedicina de Sevilla/CSIC/ Universidad de Sevilla, SeLiver Group, Spain; ²Hepatic and Digestive Diseases Networking Biomedical Research Centre (CIBERehd); ³Andalusian Center of Molecular Biology and Regenerative Medicine (CABIMER)-CABIMER-, University Pablo Olavide-University of Seville-CSIC, Spain; ⁴Biomedical Research Network on Diabetes and Related Metabolic Diseases (CIBERDEM); ⁵Hospital Universitario Virgen del Rocío, Digestive Diseases Unit
Email: jampuero-ibis@us.es

Background and aims: Non-alcoholic fatty liver disease (NAFLD) is one of the most prevalent liver diseases worldwide, showing a plethora of different pathogenic factors. In this scenario, previous studies have shown an association between the urea cycle dysregulation and different stages of hepatic injury in both patients and preclinical models of NAFLD. The main aim was to evaluate changes in urea cycle enzymes (UCEs) in a DIAMOND preclinical animal model of NAFLD under different dietary interventions.

Method: DIAMOND mice (n = 28) were randomized to three dietary regimens: high-fat diet supplemented with fructose/glucose in drinking water (HF-HFD), choline-deficient high-fat diet model supplemented with 0.1% methionine (CDA-HFD) or standard diet, which was used as a control. HF-HFD and control animals were sacrificed after 21 or 30 weeks of diet intake. CDA-HFD animals were sacrificed after 12 weeks to avoid weight loss along with other adverse outcomes linked to more prolonged exposure to this type of diet intervention. Liver damage characterization includes well-established markers for fibrosis (collagen deposition and COL3A1, COL1A1, and α -SMA expression levels) and inflammation (TNF- α and IL-6 expression), together with body weight and standard biochemical measurements recorded each week or month, respectively. UCEs and glutaminase (GLS) expression levels were evaluated by qRT-PCR.

Results: HF-HFD animals displayed signs of dyslipidemia (hypercholesterolemia), insulin resistance (higher glucose levels), and liver damage (raised AST and ALT levels) together with a 25% and 300% increase in body and liver weight, respectively. CDA-HFD animals displayed similar AST levels, higher ALT levels, and a 200% increase in liver weight but did not show any of the other metabolic disturbances observed in HF-HFD animals. Both diet interventions promoted a general upregulation of fibrotic markers (COL3A1, COL1A1, α -SMA, and collagen deposition) along with a significant upregulation of the pro-inflammatory marker TNF- α . Transcriptomic evaluation of UCEs revealed a significant mRNA downregulation in carbamoyl phosphate synthetase-1 (CPS1) and ornithine transcarbamylase (OTC1) in both CDA-HFD and HF-HFD animals versus controls, together with an increase in GLS1 expression in all groups of animals.

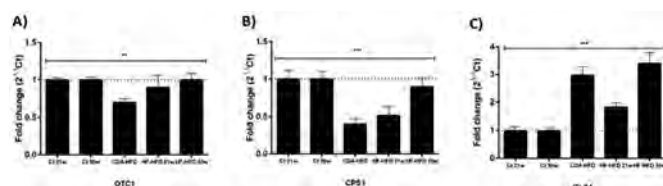


Figure: Hepatic expression of UCEs and GLS1 in DIAMOND mice stratified according to ALT tertiles. A) OTC1 B) CPS1 C) GLS1.

Conclusion: DIAMOND mice, a preclinical model that mimics NAFLD, showed urea cycle dysregulation under different dietary interventions. These enzymes could play a key role in the development and progression of NAFLD.

SAT088

Quantitative multimodal anisotropy imaging enables automated fibrosis assessment of HandE-stained tissue

Yibo Zhang¹, Jun Zhang¹, Michael Drage¹, Janani Iyer¹, Brian Gosink¹, Tan Nguyen¹, Waleed Tahir¹, Victoria Mountain¹, Murray Resnick¹, Michael Montalto¹, Aditya Khosla¹, Andrew Beck¹, Justin Lee¹. ¹PathAI, Boston, United States
Email: justin.lee@pathai.com

Background and aims: Clinical Research Network (CRN) histologic scoring of non-alcoholic steatohepatitis (NASH) requires staining two tissue sections per FFPE block: one with HandE (for grading steatosis, inflammation, and ballooning) and one with Masson's Trichrome (MT; for staging fibrosis). This multi-stain procedure is cumbersome, costly, and inconsistent, introducing interpretability challenges due to variability in staining and intra-biopsy sample heterogeneity. In this study, we develop and evaluate a tool for automated fibrosis assessment based on quantitative multimodal anisotropy imaging (QMAI) of HandE-stained NASH tissue sections. We demonstrate that quantifying HandE-derived fibrosis proportionate area (FPA) using QMAI yields results that correlate strongly with MT-stain color-based fibrosis quantification.

Method: 24 liver core needle biopsies from NASH patients with paired HandE and MT sections (48 slides, CRN fibrosis stages 0–4) were used in this study. HandE sections were imaged using a custom-built multimodal microscope, and MT sections were imaged using a Leica Aperio AT2 scanner. Whole-slide images were reviewed by a board-certified expert NASH pathologist and regions of tissue artifact were excluded from analysis. A pixel-intensity threshold was applied to QMAI images of HandE sections to locate fibrotic regions and compute FPA. For MT sections, color-based segmentation was employed to obtain a binarized fibrosis heatmap from which FPA was quantified. For all sections, a background/foreground algorithm generated the denominator for fibrosis proportion measurements. Concordance between HandE and MT-derived FPA was evaluated via Lin's Concordance.

Results: Slide-level FPA quantification from paired HandE and MT sections showed strong correlation (Lin's CCC = 0.950). Visual examination of detected fibrosis on HandE and MT sections corroborates this result and explains discrepancies between QMAI vs. MT fibrosis quantification (Fig. 1).

Conclusion: Quantitative multimodal anisotropy imaging enables fibrosis quantification from HandE-stained NASH biopsy samples that is consistent with conventional fibrosis quantification from MT-stained tissue. By eliminating the need for MT-stained slides, automated fibrosis quantification and staging from HandE sections may simplify and reduce the cost of NASH studies as well as lessen the impact of MT stain-variability and intra-sample heterogeneity on subject screening and end point assessment. Additionally, detecting fibrosis from HandE sections may enable improved interrogation of spatial relationships between fibrosis and various NASH features commonly assessed on HandE (e.g., steatosis, ballooning, and/or inflammation).

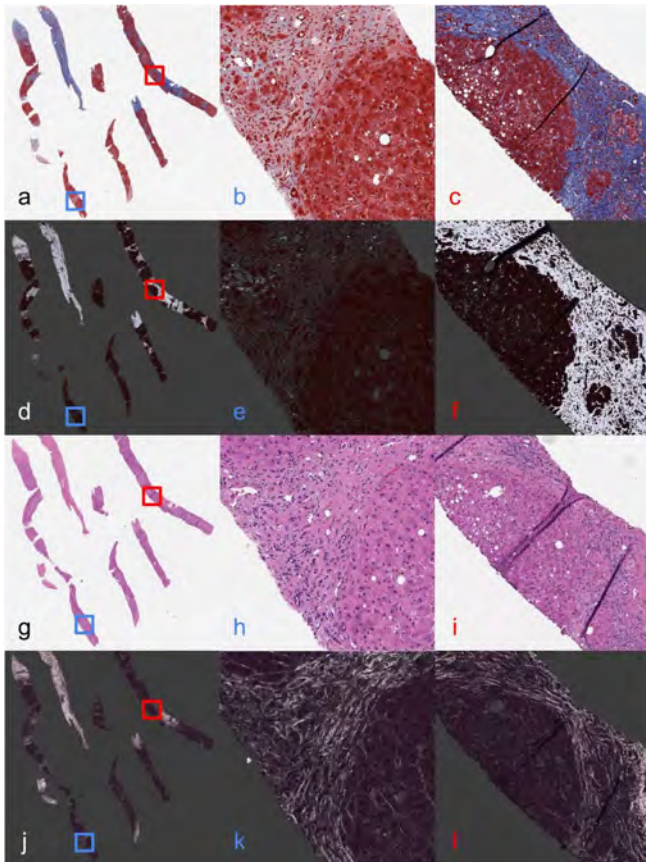


Figure 1: Example paired MT (a-c) and HandE (g-i) tissue areas and their corresponding fibrosis overlays (d-f and j-l, respectively).

SAT089

Zonated quantification of immunohistochemistry in steatotic livers

Cédric Peleman^{1,2}, Winnok De Vos^{3,4,5}, Isabel Pintelon^{3,4,5}, Ann Driessen⁶, Christophe Van Steenkiste^{1,7}, Annelies Van Eyck¹, Luisa Vonghia^{1,8}, Joris De Man¹, Benedicte De Winter^{1,8}, Tom Vanden Berghe⁹, Sven Francque^{1,8}, Wilhelmus Kwanten^{1,2}.
¹University of Antwerp, Laboratory of Experimental Medicine and Pediatrics, Infla-Med Centre of Excellence, Wilrijk, Belgium; ²Antwerp University Hospital, Department of Gastroenterology and Hepatology, Edegem, Belgium; ³University of Antwerp, Laboratory of Cell Biology and Histology, Wilrijk, Belgium; ⁴University of Antwerp, Antwerp Centre for Advanced Microscopy (ACAM); ⁵University of Antwerp, μ Neuro Research Excellence Consortium on multimodal neuromics; ⁶Antwerp University Hospital, Department of Pathology, Edegem, Belgium; ⁷Antwerp University Hospital, Department of Gastroenterology and Hepatology, Edegem, Belgium; ⁸Antwerp University Hospital, Department of Gastroenterology and Hepatology, Edegem, Belgium; ⁹University of Antwerp, Laboratory of Pathophysiology, Infla-Med Centre of Excellence, Wilrijk, Belgium
 Email: cedric.peleman@uantwerpen.be

Background and aims: Immunohistochemical stains (IHC) often reveal differences between different zones of the liver lobule in health and disease, including non-alcoholic fatty liver disease (NAFLD). However, evidence from IHC often depends on

representative images. In NAFLD, lipid vacuoles from macrovesicular steatosis occupy part of the surface and hamper correct interpretation. We developed an image analysis method to quantify IHC staining area of hypoxia marker pimonidazole (Pimo) within different zones of the liver lobule of steatotic livers.

Method: Male C57BL/6J mice were fed the choline-deficient L-amino acid-defined high-fat diet (CDAHFD) or standard diet (SD) for three weeks and received an intraperitoneal injection of Pimo (100 mg/kg) one hour prior to sacrifice (n = 6). Serial sections of formalin-fixed paraffin-embedded liver tissue were stained with haematoxylin-eosin (HandE) and IHC for glutamine synthetase (GS) and Pimo adducts were visualised with 3, 3'-diaminobenzidine (DAB). Whole slide image (WSI) acquisition was performed with the Zeiss Axioscan 1. A script for FIJI open-source image analysis freeware was developed to measure DAB pixel intensities as a function of the relative location (with respect to the central vein and the boundary) within a liver lobule. The autothreshold algorithm 'Percentile' binarised the pixels into positive or negative for Pimo based on the global WSI DAB intensity. Data were processed in R Studio, using the additional package "dplyr" for grouped summary statistics.

Results: CDAHFD induced non-alcoholic steatohepatitis (NASH) with panlobular Pimo positivity, whereas hypoxia was present in the centrolobular area in normal livers in SD group. Liver lobules follow the Voronoi principle wherein each lobule originates from a central vein identified by HandE and centrolobular GS staining. These landmarks were manually annotated for each lobule after which the image analysis script calculated the intensity distribution as a function of the pixel position within the lobule. After exclusion of datapoints belonging to fat vacuoles, the percentage of Pimo positive area was calculated in different parenchymal zones. The Pimo positive area was significantly higher in the periportal zone in NASH livers ($p < 0.05$, Fig. 1). Moreover, the ratio of Pimo positive area in periportal (PP) vs. centrolobular (CV) regions was significantly higher in NASH compared to SD ($p < 0.001$), demonstrating the panlobular nature of Pimo staining in NASH.

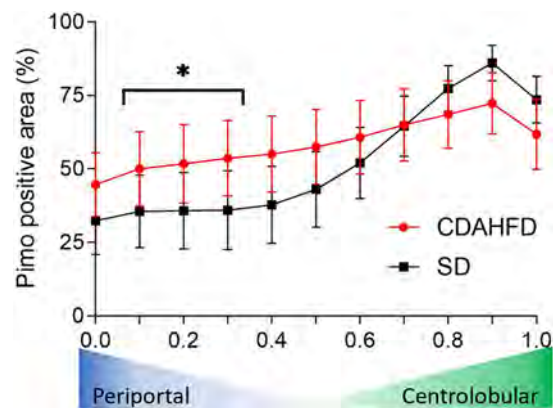


Figure 1. Data presented as mean \pm standard deviation; Mann-Whitney test, * $p < 0.05$.

Conclusion: The method described herein accurately quantifies the difference in zonal distribution of hypoxia marker Pimo in WSI images of NASH and normal livers. This image analysis method should allow for objective zonal quantification of other epitopes assessed by IHC, including livers affected by NAFLD.

SAT090

CD161 expressing CD4⁺ CD25^{hi} T cells accumulate in the liver of obese patients with NASH

Rafael Kaeser¹, Emilia Schlaak¹, Franziska Engels¹, Saskia Killmer¹, Katharina Zoldan¹, Lukas Sturm¹, Lena Mayer¹, Gabriel Seifert², Jodok Matthias Fink², Goran Marjanovic², Thomas Longerich³, Agnieszka Kabat⁴, Edward Pearce⁴, Dominik Bettinger¹, Maike Hofmann¹, Robert Thimme¹, Bertram Bengsch¹, Tobias Böttler¹.

¹University Hospital Freiburg, Department of Internal Medicine II, Freiburg im Breisgau, Germany; ²University Hospital Freiburg, Department of General and Visceral Surgery, Freiburg im Breisgau, Germany; ³University Hospital Heidelberg, Department of Pathology, Germany; ⁴Max Planck Institute of Immunobiology and Epigenetics, Department of Immunometabolism, Freiburg im Breisgau, Germany
Email: rafael.kaeser@uniklinik-freiburg.de

Background and aims: Non-alcoholic fatty liver disease (NAFLD) associated with obesity and metabolic syndrome is emerging as a leading cause of chronic liver disease in western countries. Hepatic steatosis may lead to inflammation resulting in non-alcoholic steatohepatitis (NASH) and progressive liver disease. A role of hepatic T cells in driving inflammation is suspected, however, the immuno-pathogenesis of NASH remains incompletely understood. We therefore set out to characterize the immune landscape in NASH livers and non-inflamed livers in obese patients.

Method: Liver tissue was obtained from heavily obese patients undergoing bariatric surgery. Clinical data and blood samples were collected at baseline and longitudinally after surgery. 52 patients were included in the study and stratified into a group with no indication of inflammation (n=28) and a NASH group with high levels of inflammation (n=24) according to histologic scoring and clinical parameters. Liver and blood samples were characterized by flow cytometry [n=28], validated by mass cytometry [n=20] and subsequently further investigated by single cell RNA sequencing [n=4] for a broad range of immune cell subsets.

Results: CD4T cells were significantly enriched within the inflamed hepatic tissue compared to uninflamed liver samples (Figure A). In contrast, CD8T cells and other immune cells showed no significant differences between the groups. Subsequent cluster analysis confirmed a distinct CD161-expressing CD4⁺ CD25^{hi} T cell subset in the liver, which was enriched in the group of patients with high inflammation (Figure B). Further analysis of this subset by mass cytometry identified CD26, CD127, OX40 and CXCR3 as additional markers defining this inflammation-associated CD4T cell cluster. Interestingly, these differences were only detectable in the liver, but not the peripheral blood, suggesting specific changes of tissue-resident immune populations during NASH.

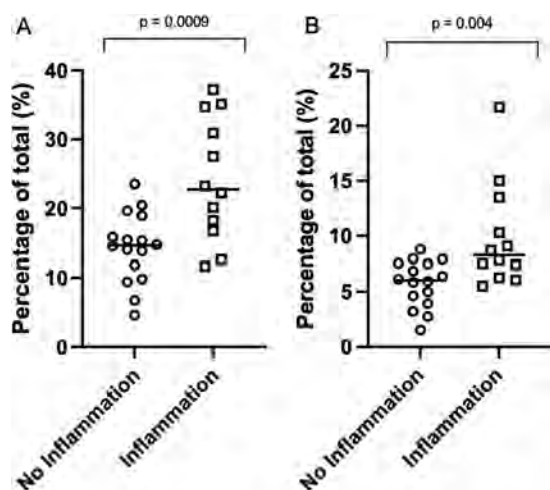


Figure: The proportions of CD4⁺ T cells (A) and CD4⁺ CD25⁺ CD161⁺ T cells (B) in the liver, n = 28, unpaired t-test.

Conclusion: A distinct hepatic CD161-expressing CD4⁺ CD25^{hi} T cell population is significantly enriched in NASH patients from NAFLD patients undergoing bariatric surgery. Further studies are required to dissect their function and mechanistic role in driving inflammation in NASH patients.

SAT091

GL0034, A novel long-acting glucagon-like peptide 1 receptor agonist exhibits significant efficacy in aged db/db mouse model of non-alcoholic fatty liver disease (NAFLD)

Rajamannar Thennati¹, Vinod Burade¹, Adolfo Garcia-Ocana², Richard E Pratley³, Guy Rutter⁴, Tina Vilsbøll⁵, Bernard Thorens⁶. ¹Sun Pharmaceutical Industries Limited, High Impact Innovations-Sustainable Health Solutions (HISHS), Vadodara, India; ²Diabetes Obesity and Metabolism Institute, Icahn School of Medicine at Mount Sinai, New York, United States; ³AdventHealth Translational Research Institute, Orlando, United States; ⁴CR-CHUM, University of Montreal, QC, Montreal, Canada; ⁵Clinical Research, Steno Diabetes Center Copenhagen, Copenhagen, Denmark; ⁶University of Lausanne, Center for Integrative Genomics, Lausanne, Switzerland
Email: rajamannar.thennati@sunpharma.com

Background and aims: Obesity and type 2 diabetes are the major risk factors for non-alcoholic fatty liver disease (NAFLD) and advanced liver fibrosis. GL0034 is a novel long-acting human glucagon-like peptide 1 (GLP-1) receptor agonist, which selectively activates the GLP-1 receptor.

Method: db/db mice (age: 22–24 week) were divided into vehicle control; GL0034 (20 nmol/kg) or semaglutide (20 nmol/kg). Animals were treated with vehicle or test item every third day (q3d) up to day 27. On day 28, HbA1c, plasma triglycerides, serum alanine aminotransferase (ALT), aspartate aminotransferase (AST), liver transforming growth factor β (TGF- β) and malondialdehyde (MDA) were quantified. Liver steatosis was evaluated using Oil- Red O staining and HandE (haematoxylin and eosin) staining.

Results: Subcutaneous treatment with GL0034 led to a significant reduction in HbA1c, body weight, plasma triglycerides, ALT/AST and liver TGF- β (Table). Insulin levels increased (4.5-fold). Reduction in steatosis was confirmed using Oil- Red O/HandE staining and liver MDA (2-fold decrease) level.

	HbA1c (%) Mean±SD		body weight change (%) Mean ± SD	triglycerides (mg/dl) Mean ± SD		serum ALT (U/L) Mean ± SD	serum AST (U/L) Mean ± SD	liver TGF-β (ng/g) Mean ± SD
	d0 (%)	change d28 vs. d0	d28 vs. d0	d0 (mg/dl)	% change d28 vs. d0	d28	d28	d28
Vehicle Control (n = 6)	10.3 ± 1.8	-0.2 ± 1.8	-0.5 ± 1.3	408.7 ± 86.3	46.8 ± 55.8	227.5 ± 36.2	243.8 ± 25.9	24.7 ± 3.2
GL0034 (n = 5) (82.3 μg/kg)	10.3 ± 1.2	-4.9 ± 1.0***	-8.9 ± 1.7***##	443.2 ± 33.1**	-19.8 ± 170.4	69.8 ± 13.4*#	87.4 ± 18.5***##	6.5 ± 2.7***
Semaglutide (n = 5) (synthesized in-house) 20 nmol/kg (82.3 μg/kg)	10.3 ± 1.2	-4.0 ± 1.4***	-3.4 ± 2.9***	431.3 ± 96.1	-6.9 ± 28.8	232.6 ± 141.9	188.6 ± 71.3	12.3 ± 5.2***

Changes in HbA1c (glycated haemoglobin), body weight, triglycerides, ALT (alanine aminotransferase) and AST (aspartate aminotransferase) on day 28. Mean \pm SD using one-way ANOVA followed by Bonferroni's post-test respectively. *p < 0.05, **p < 0.01, ***p < 0.001 vs. vehicle control and #p < 0.05, ##p < 0.01, ###p < 0.001 vs. semaglutide. d0 = day 0 and d28 = day 28.

Conclusion: Hepatic steatosis and increases in triglycerides, ALT/AST in aged db/db mice was suppressed by GL0034, thereby reducing the risk of fibrosis that is accelerated during excessive lipid metabolism in the liver.

SAT092

Development of an ex vivo model for non-alcoholic fatty liver disease using precision-cut liver slices

Mei Li¹, Vincent de Meijer², Peter Olinga¹, Anika Nagelkerke³, Yana Geng¹. ¹University of Groningen, Department of Pharmaceutical Technology and Biopharmacy, Netherlands; ²University Medical Center Groningen, Department of Hepato-, Pancreato-, Biliary Surgery and Liver Transplantation, Netherlands; ³University of Groningen, Department of Pharmaceutical Analysis, Netherlands
Email: yana.geng@rug.nl

Background and aims: Non-alcoholic fatty liver disease (NAFLD) is an emerging healthcare problem, ranging from non-alcoholic fatty liver (NAFL) to non-alcoholic steatohepatitis (NASH), often progresses to fibrosis, cirrhosis along with hepatocellular carcinoma. Progress in this field depends on the availability of reliable preclinical models. In this respect, precision-cut liver slices (PCLS) could provide the preserved multicellular environment allowing for the interplay of various liver cell types. This study aims to investigate NAFLD development in mouse and human PCLS.

Method: Mouse PCLS (mPCLS), from male C57BL/6J mice liver, and human PCLS (hPCLS), obtained from surgical waste material of donor livers, were used. Slices were cultured in GFIPO (William's E Medium supplemented with Glucose (36 mM), Fructose (5 mM), Insulin (1 nM), Palmitic acid (0.12 mM for mPCLS/0.24 mM for hPCLS) and Oleic acid (0.24 mM for mPCLS/0.48 mM for hPCLS)) to mimic the NAFLD-inducing conditions, and WEGG (William's E Medium supplemented with Glucose (25 mM)) as control for up to 96 h. PCLS were collected to assess viability and fat accumulation by measuring ATP levels and triglyceride (TG) content. Inflammation and fibrosis were evaluated by RT-qPCR. Additionally, the conditioned medium of hPCLS were collected for culturing LX2 cells (a human hepatic stellate cell line) at 1:3 (v/v) ratio mixed with LX2 medium. The activation of LX2 cells were evaluated by assessing the protein levels and the mRNA expressions of collagen type 1/*COL1a1* and alpha smooth muscle actin/*ACTA2*.

Results: Slices remained viable for up to 96 hours incubation in both WEGG and GFIPO medium, and TG content was increased 71% (mPCLS) and 92% (hPCLS) in GFIPO compared with WEGG group. In GFIPO, mRNA expression of the inflammatory biomarker interleukin 6 was significantly upregulated compared to WEGG (3-fold in mPCLS, 6-fold in hPCLS), as well as interleukin 1b (3-fold in mPCLS, 42-fold in hPCLS), but no significant differences were observed for tumor necrosis factor α expression. *COL1a1* and *ACTA2* showed an increasing trend in GFIPO in both mPCLS and hPCLS, but only *ACTA2* was significantly increased in hPCLS (2-fold). In LX2 cells, the conditioned medium obtained from hPCLS cultured in GFIPO promoted the activation of LX2 cells comparing to that of hPCLS cultured in WEGG, shown as significantly increased protein level of collagen type 1 (2-fold), albeit not at mRNA expression level.

Conclusion: GFIPO increased the TG content as well as gene expression of inflammatory and fibrosis biomarkers in both mPCLS and hPCLS, without impairing viability. GFIPO introduced a pro-fibrotic environment in hPCLS, and its conditioned medium promoted collagen production in LX2 cells.

SAT093

The neolignan honokiol can improve intestinal barrier dysfunction in fructose-induced liver damage in mice

Anja Baumann¹, Verena Freutsmiedl¹, Julia Jelleschitz¹, Raphaela Staltner¹, Annette Brandt¹, Verena Dirsch², Ina Bergheim¹. ¹University of Vienna, Department of Nutritional Sciences, Vienna, Austria; ²University of Vienna, Department of Pharmacognosy, Vienna, Austria
Email: ina.bergheim@univie.ac.at

Background and aims: Several studies indicate that a fructose-rich diet may be a risk factor in the development of non-alcoholic fatty liver disease (NAFLD). Studies have shown that this is associated with

intestinal barrier dysfunction, and subsequently, with an increased translocation of bacterial toxins. Honokiol, a neolignan found in *Magnolia officinalis* and used in traditional Chinese medicine, has a variety of biological activities including protective effects on the development of intestinal barrier dysfunction. The aim was to determine if an oral supplementation of honokiol improves intestinal barrier dysfunction in fructose-induced NAFLD.

Method: Female C57BL/6J mice (n = 7/group) were fed a 30% fructose solution or plain water \pm 10 mg honokiol per kg body weight per day for 4 weeks. Markers of liver damage and intestinal permeability and toll-like receptor (TLR) 2 as well as TLR4 ligands in portal plasma were measured. In addition, effects of honokiol on fructose-induced intestinal permeability were assessed ex vivo in an everted sac model.

Results: As expected, fructose-fed mice developed liver steatosis which was significantly attenuated in fructose + honokiol-fed mice (NAFLD activity score: fructose vs. fructose + honokiol, $p < 0.05$). These protective effects of honokiol were associated with a significant protection against the increased intestinal permeability found in small intestinal tissue in fructose-fed mice. In line with the latter, TLR2 and 4 ligands were only significantly or by trend higher in portal plasma of fructose-fed mice while being at the level of controls in fructose + honokiol-fed animals. In support of the in vivo findings, honokiol also significantly attenuated fructose-induced permeability in the ex vivo model.

Conclusion: The results of the present study suggest that an oral supplementation of honokiol can improve intestinal barrier dysfunction in settings of fructose-induced liver damage being also associated with a lessened development of NAFLD.

Funded in part by the Interdisciplinary Network of the Faculty of Life Sciences, University of Vienna: Neolignans: new therapeutics in the prevention of diet-induced intestinal barrier dysfunction?

SAT094

Retrospective AI-based measurement of NASH histology (AIM-NASH) analysis of biopsies from Phase 2 study of Resmetirum confirms significant treatment-induced changes in histologic features of non-alcoholic steatohepatitis

Stephen Harrison¹, Janani Iyer², Charles Biddle-Snead², Sara Hoffman², Quang Le², Victoria Mountain², Murray Resnick², Katy Wack², Jim Hennan³, Rebecca Taub³. ¹Pinnacle Clinical Research, San Antonio, United States; ²PathAI, Boston, United States; ³Madrigal Pharmaceuticals, Conshohocken, United States
Email: becky@madrigalpharma.com

Background and aims: Biopsy-based end points are recommended for assessing treatment efficacy in non-alcoholic steatohepatitis (NASH) clinical trials. While manual scoring of NASH histology is subject to intra- and inter-rater variability, AI-powered pathology may enable accurate and reproducible histologic assessment. Here we demonstrate the utility of an AI-based tool (AIM-NASH), for scoring NASH histology in a retrospective analysis of clinical trial liver biopsies.

Method: PathAI AIM-NASH algorithms were deployed on whole slide images of liver biopsies from 104 subjects enrolled in a Phase 2 (Ph2), placebo-controlled, 36-week study of the efficacy of MGL-3196 treatment in patients with NASH and NASH CRN stage 1–3 fibrosis (NCT02912260). Models predicted ordinal and continuous Clinical Research Network (CRN) scores in addition to exploratory features such as portal inflammation. Concordance between clinical pharmacology and AIM-NASH scores and features was evaluated. Differences in end point response rates and in changes in continuous scores and exploratory features between treated and placebo subjects were computed.

Results: All biopsy-based end points that were met via manual histologic scoring were also met by AIM-NASH (Table 1). ML continuous scoring revealed a statistically significant reduction in steatosis and a greater sub-ordinal reduction in fibrosis in treated versus placebo subjects. The measured reduction in continuous

POSTER PRESENTATIONS

fibrosis score was greater than the reduction in collagen proportionate area (CPA) in treated subjects. Change in ML-derived area proportion of portal inflammation was significantly correlated with change in portal inflammation scores from both central readers ($p = 0.009$ and $p = 0.011$, respectively), while concordance between both central readers for portal inflammation scoring was kappa = 0.298.

Table 1: Response rates per end point via manual vs. AI-based scoring

End point	Scorer	Response rate (MGL)	Response rate (Pbo)	p value
2-point or greater improvement in NAS	AIM-NASH	0.41	0.19	0.0327
	Central reader	0.56	0.26	0.0044
	Reader 2	0.42	0.19	0.0321
NASH resolution without worsening fibrosis	AIM-NASH	0.26	0.07	0.0301
	Central reader	0.25	0.06	0.0226
	Reader 2	0.21	0.03	0.0190

Conclusion: This ML approach detected similar proportions of primary end point responders as manual scoring. ML-derived continuous features demonstrated sensitivity to changes in NASH histology and enabled more granular exploration of sub-ordinal treatment effects. Such AI-based tools show promise as assistive devices for NASH pathologists in clinical trial settings.

SAT095

Insights to molecular mechanism of Essentiale: In vitro studies in hepatic cell lines HepaRG and steatotic HepaRG

Dominik Wupperfeld¹, Gert Fricker¹, Beatrice Bois De Fer², Branko Popovic³. ¹Ruprecht-Karls University of Heidelberg, Heidelberg, Germany; ²Sanofi, Gentilly, France; ³Sanofi, Frankfurt, Germany
Email: branko.popovic@sanofi.com

Background and aims: Non-alcoholic fatty liver disease is the most common liver disease worldwide and treatment options are limited. Essential Phospholipids (EPL, Essentiale®), comprising of multiple unsaturated fatty acids, have shown therapeutic effects but the molecular mechanism remains to be investigated. Here, we report the impact of EPL on hepatocyte function through in vitro studies.

Method: Effects of non-cytotoxic concentrations of EPL (0.1 and 0.25 mg/ml) and its constituents polyenylphosphatidylcholine (PPC) and phosphatidylinositol (PI) (both at 0.1 and 1 mg/ml) on the release of pro-inflammatory cytokines caused by treatment with lipopolysaccharide (LPS) and lipid metabolizing enzymes were investigated in human hepatocyte cell lines (HepaRG, steatotic HepaRG) using ELISA and Glucose-6-phosphate dehydrogenase (G6PD) activity assay kits. To induce steatosis in HepaRG cells, differentiated cells were treated with stearic acid and oleic acid for two weeks.

Results: Lipopolysaccharide (1, 5 µg/ml) treatment for 24 h induced release of cytokines. In LPS-treated HepaRG cells EPL (0.25 mg/ml; $p = 0.0063$), PPC (1 mg/ml; $p < 0.0001$), PI (0.1 mg/ml; $p = 0.0396$, 1 mg/ml; $p = 0.0023$) significantly reduced the release of IL-6. Treatment with EPL (0.1 mg/ml; $p < 0.0001$) and PI (1 mg/ml; $p = 0.0029$) increased the release of IL-6 in LPS-treated steatotic HepaRG cells. IL-8 secretion increased significantly ($p < 0.001$) in LPS treated HepaRG and steatotic HepaRG cells in response to all lipid formulations. G6PD activity was unchanged by all treatments in HepaRG and steatotic HepaRG cells. In HepaRG cells human lecithin cholesterol acyltransferase (LCAT) expression was significantly downregulated upon treatment with EPL (0.1 mg/ml; $p < 0.0001$, 0.25 mg/ml; $p = 0.0436$), PPC (1 mg/ml; $p < 0.0001$), PI (1 mg/ml; $p < 0.0001$) and upregulated by PPC (0.1 mg/ml; $p = 0.0009$). However, in steatotic HepaRG cells, a significant increase of expression of LCAT was observed upon treatment with PI

(1 mg/ml; $p = 0.0088$). Endogenous expression of human acyl Coenzyme A oxidase 1 (ACOX1) and fatty acid synthase (FAS) was lower in HepaRG cells compared to steatotic HepaRG cells. While in HepaRG cells ACOX1 expression decreased upon treatment with EPL (0.1 mg/ml; $p = 0.0126$, 0.25 mg/ml; $p = 0.0031$), PPC (0.1 mg/ml; $p = 0.0145$, 1 mg/ml; $p = 0.0434$), PI (1 mg/ml; $p = 0.0404$), none of the treatments affected ACOX1 expression in steatotic HepaRG cells. FAS expression remained unchanged in HepaRG cells upon treatment with lipid formulations. However, in steatotic HepaRG cells, FAS expression was significantly reduced ($p \leq 0.0001$) in response to treatment with all lipid formulations in all concentrations.

Conclusion: In vitro investigations in hepatocyte cell lines provided valuable insights into the impact of EPL on pro-inflammatory cytokine release, lipid-metabolizing enzymes which may improve liver function.

SAT096

Exposure to the SARS-CoV-2 spike protein in an in vitro model of steatosis enhances hepatocyte oxidative stress: implications for COVID-19 and accelerated disease progression

Angus Jacobs¹, Katie Morgan¹, Steven Morley¹, Kay Samuel², Jonathan Fallowfield³, Peter Hayes¹, John Plevris¹. ¹The University of Edinburgh, Hepatology department, Edinburgh, United Kingdom; ²Scottish National Blood Transfusion Service, Tissues, Cells, and Advanced Therapeutics, Edinburgh, United Kingdom; ³The University of Edinburgh, Centre for Inflammation Research, Edinburgh, United Kingdom

Email: anguskerrjacobs@gmail.com

Background and aims: Metabolic dysfunction-associated fatty liver disease (MAFLD) has been identified as a predictor of liver injury in patients hospitalised with coronavirus disease 2019 (COVID-19). The key severe acute respiratory syndrome coronavirus 2 (SARS-CoV-2) receptor, angiotensin converting enzyme 2 (ACE2), is suggested to play a protective role in the pathogenesis of MAFLD. Our unpublished data shows that human hepatic ACE2 expression correlates positively with increasing MAFLD progression, from steatosis through steatohepatitis to cirrhosis. The extent to which COVID-19 may accelerate MAFLD progression remains unclear. Here we use an *in vitro* steatosis model to investigate susceptibility to liver injury following exposure to SARS-CoV-2 spike protein S1 subunit and thus a possible role of COVID-19 in accelerating MAFLD progression.

Method: Following 24 h exposure of fully differentiated (day 14) HepaRG cells were exposed to the SARS-CoV-2 spike protein S1 subunit (0.05 µg/ml, 0.1 µg/ml, and 0.5 µg/ml), changes in cell conformation of the cell layer were measured using electric cell-substrate impedance sensing (ECIS). Cytokine secretion was quantified following exposure to a steatogenic stimulus (oleate) ± S1 subunit using a flow cytometry-based cytokine bead array assay and the metabolic effects assessed by measurement of reactive oxygen species (ROS) and ATP by chemiluminescence assays.

Results: Our data show that 24-h exposure to the SARS-CoV-2 spike protein S1 subunit caused a concentration-dependent alteration in HepaRG cell tight-junction integrity and/or basolateral adhesion. However, the S1 subunit had no significant effect on HepaRG cell viability at any of the tested concentrations. Treatment of HepaRG cells with oleate ± S1 significantly increased secretion of proinflammatory cytokine IL-6 (mean ± SEM; oleate alone: 31.3 ± 0.9 pg/ml; oleate + S1: 33.5 ± 2.9 pg/ml) compared to untreated cells (18.7 ± 2.9 pg/ml, both $p < 0.05$) and cells treated with the S1 subunit alone (16.0 ± 3 pg/ml, both $p < 0.05$). In our *in vitro* steatosis model, the addition of the S1 subunit appeared to have an additive effect, significantly increasing ROS production (mean ± SEM; 63, 700 ± 3500 relative luminescence units (RLU)) compared to untreated cells (40, 500 ± 2100 RLU, $p < 0.05$), but there was no effect on ATP production.

Conclusion: Our data indicate that the SARS-CoV-2 spike protein S1 subunit affects tight junction integrity and promotes oxidative stress in oleate-treated HepaRG cells, and that fat-loading increased

proinflammatory cytokine secretion. This could in turn cause activation of profibrotic signalling pathways and accelerate disease progression in MAFLD.

NAFLD: Therapy

SAT101

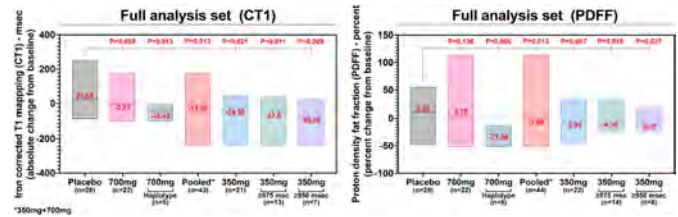
Efficacy and safety of leronlimab in patients with non-alcoholic steatohepatitis: topline results of NASH01 clinical trial

Mazen Nouredin¹, Eric Lawitz², Angela Ritter³, Tarek Hassanein⁴, Kelly Bowman⁵, Scott Kelly⁶, Eisa Mahiyari⁷, Jonah Sacha⁸, Scott Hansen⁸, Christopher Recknor⁶. ¹Cedars Sinai, Liver Disease and Transplant Center, Los Angeles, United States; ²The University of Texas Health Science Center San Antonio, Texas Liver Institute, San Antonio, United States; ³Center for Advanced Research and Education, Gainesville, United States; ⁴Southern California GI and Liver Centers, Coronado, United States; ⁵Sensible Healthcare, Ocoee, United States; ⁶CytoDyn Inc., Vancouver, United States; ⁷Oregon Health and Science University, Genetics, Beaverton, United States; ⁸Oregon Health and Science University, Vaccine and Gene Therapy Institute, Beaverton, United States
Email: crecknor@cytodyn.com

Background and aims: CCR5 modulates key metabolic, inflammatory, and fibrogenic pathways in the pathogenesis of NASH. NASH01 was conducted to determine efficacy, dose and safety of leronlimab, a known CCR5 binding agent, in patients with NASH.

Method: In this multi-center phase 2a, dose ranging, two-part trial, part 1 was designed as a double-blind, randomized, placebo-controlled trial, patients with NASH phenotype who had MRI proton density fat fraction (PDFF) $\geq 8\%$ and corrected T1 (cT1) ≥ 800 were randomly assigned 1:1 weekly SQ leronlimab 700 mg or placebo and part 2 as open label comparing leronlimab 350 mg to part 1 placebo group. Treatment duration was 14 weeks. The primary end point was change from baseline in PDFF and secondary end points were change from baseline in cT1 fibro-inflammatory activity and change in serum cK18 and K18 by M30-M65 ELISA at week 14.

Results: Analyses were conducted on the full analysis set (n = 72) of whom 44% were of Hispanic or Latino ethnicity and 58% with baseline moderate to severe fibro-inflammation (cT1 ≥ 875 ms). Mean percent change from baseline PDFF was significantly reduced in the 350 mg group vs placebo (-5.94% vs +9.85%, p = 0.008) but not in the 700 mg group (+3.75% vs +9.85%, p = 0.135). Mean change cT1 was significantly reduced in the 350 mg group vs placebo (-24.38 ms vs +27.64 ms, p = 0.021) but not in the 700 mg group (-2.73 ms vs +27.64 ms, p = 0.059). Significant reductions were seen in the 350 mg subgroup with baseline cT1 ≥ 875 ms in both PDFF and cT1 vs placebo (-4.37% vs +9.85%, p = 0.020 and -42.00 ms vs +27.64 ms, p = 0.011) respectively. In subjects with cT1 ≥ 950 ms at baseline, PDFF and cT1 were significantly reduced with 350 mg vs placebo (-9.39% vs +9.85%, p = 0.027 and -68.85 ms vs +27.64, p = 0.009) respectively. Mean change in baseline to week 14 for M65 ELISA (cK18 and K18) decreased in the 350 mg group (340.55 to 332.4 U/L; -8.18) while increased in placebo (301.96 to 411.64 U/L; +109.78). In post hoc analyses, mean percent PDFF and mean cT1 were significantly reduced in the pooled 350 + 700 mg group compared to placebo (-1.09% vs +9.85%, p = 0.014 and -13.30 ms vs +27.64 ms, p = 0.013) and in the 700 mg group with genetic haplotypes known to over produce CCR5 compared to placebo (-27.9% vs +9.85%, p = 0.006 and -45.4 ms vs +27.64 ms, p = 0.013). There was no grade 3 or higher drug related treatment emergent adverse event. Injection site reaction and mild diarrhea occurred more frequently with leronlimab than placebo but were not associated with discontinuation.



Conclusion: The primary end point (PDFF) and secondary end points (cT1) were met for the 350 mg group and moderate to severe fibro-inflammation by cT1 350 mg subgroup at baseline. The pooled 350 + 700 mg group also had significant reductions in PDFF, cT1 vs placebo. Treatment with leronlimab was well tolerated. These results are supportive of further trials with leronlimab for NASH.

SAT102

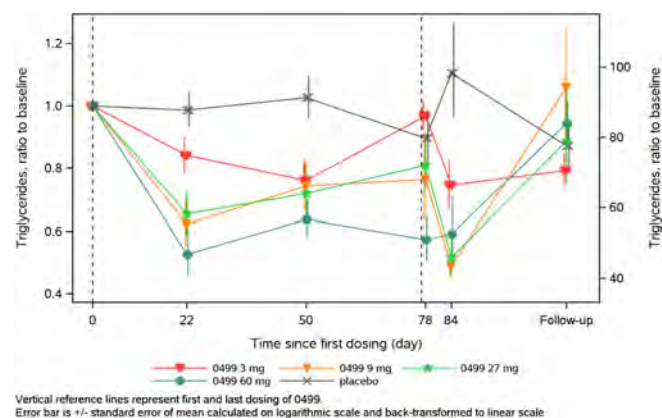
Reduced triglycerides and LDL cholesterol from once-weekly administration of the well-tolerated novel FGF21 analogue 0499

Kirsten Dahl^{1,1}, Jakob Schiøler Hansen², Jesper Clausen¹, Mads Sundby Palle¹, Cassandra Key³, Birgitte Andersen¹. ¹Novo Nordisk A/S, Denmark; ²Novo Nordisk Bio Innovation Hub, United States; ³ICON Early Phase Services, United States
Email: kdhl@novonordisk.com

Background and aims: Activation of the fibroblast growth factor 21 (FGF21) receptor complex has been associated with several attractive effects in preclinical models, including weight loss and decreased hepatic fat content. This has led to the pursuit of FGF21 for pharmacotherapy within obesity and non-alcoholic steatohepatitis (NASH), which has to date been limited by lack of suitable FGF21 analogues. Here we report an investigation of the safety and tolerability of repeated administration of a new FGF21 analogue 0499 in healthy participants.

Method: In a randomized, blinded, placebo-controlled, multiple ascending dose study, healthy males and females with body mass index ~ 30 kg/m² received weekly subcutaneous injections of placebo or 0499 for 12 weeks. FGF21 dose levels were 3, 9, 27, 60 and 120 mg. In each dose cohort, 9 participants were randomized to active treatment and 3 to placebo. Participants were followed for safety monitoring and pharmacokinetic sampling until 36 days after last dose. A total of 57 participants were randomized.

Results: There were no serious adverse events related to treatment. Weekly administration of doses from 3 to 60 mg/week were well tolerated. There were no notable findings from hematology, clinical chemistry or vital signs. Adverse events observed at doses from 3 to 60 mg/week were vomiting, increased appetite, nausea and diarrhea. Nausea and diarrhea were also observed with placebo. Statistically significant weight gain of 4.5%-points (%-pt) (placebo adjusted) was observed in the 3 mg group. In the higher dose groups, weight changes of $\pm 2\%$ -pt were observed (not statistically significant vs placebo). In the 120 mg cohort, all 6 participants who started treatment experienced tolerability issues within the first 3 weeks including moderate gastroesophageal reflux, vomiting, nausea and diarrhea. Further enrolment in the cohort and treatment with 120 mg were stopped. One participant experienced generalized urticaria at 9 mg/week. In total, 25 participants did not complete due to adverse events (n = 5) or other reasons. Withdrawals were distributed (3, 6, 3, 6 and 4 participants in the 3, 9, 27, 60 and 120 mg, and placebo groups, respectively). The plasma half-life of 0499 was ~ 120 hours across dose levels. Low titers of anti-drug antibodies were detected with some neutralizing effect on endogenous FGF21. Sustained reductions in triglycerides (TG) and low-density lipoprotein (LDL) were observed. Placebo-adjusted reductions in the 3, 9, 27 and 60 mg dose cohorts were: for TG, 33%, 52%, 61% and 48%, respectively; for LDL, -7%, 1%, 13% and 20%, respectively (*p < 0.05).



Conclusion: The novel FGF21 analogue was well tolerated at doses up to 60 mg/week for 12 weeks. Treatment was associated with beneficial effects on lipid profile including lowering of TG and LDL levels. These results are encouraging for the further development of 0499 for treatment of NASH.

SAT103

Multimodality assessment of hepatic fibrosis: ranked paired reading and artificial intelligence identifies fibrosis improvement with aramchol missed by conventional staging

Vlad Ratziu¹, Yusuf Yilmaz², Don Lazas³, Scott Friedman⁴, Carolin Lackner⁵, Cynthia Behling⁶, Oscar Cummings⁷, Li Chen⁸, Mathieu Petitjean⁸, Yossi Gilgun-Sherki⁹, Shaul Kadosh¹⁰, Arun Sanyal¹¹. ¹Sorbonne Université, Institute for Cardiometabolism and Nutrition (ICAN) and ²Sorbonne Université, Institute for Cardiometabolism and Nutrition (ICAN) and Hôpital Pitié-Salpêtrière, INSERM UMRs 1138 CRC, Paris, France; ³Liver Research Unit, Institute of Gastroenterology, Marmara University, and Department of Gastroenterology, School of Medicine, Marmara University, Istanbul, Turkey; ⁴ObjectiveHealth, Inc., United States; ⁵Division of Liver Diseases, Icahn School of Medicine at Mount Sinai, United States; ⁶Medical University of Graz, Graz, Austria; ⁷Department of Pathology, Sharp Health System, United States; ⁸Department of Pathology and Laboratory Medicine, Indiana University School of Medicine, Indianapolis, United States; ⁹Pharmanest Ltd., United States; ¹⁰Galmed pharmaceuticals, Israel; ¹¹Statexcellence Ltd., Israel; ¹¹Department of Gastroenterology, Virginia Commonwealth University, United States
Email: vlad.ratzu@inserm.fr

Background and aims: Aramchol is a partial inhibitor of hepatic stearyl-CoA desaturase with direct anti-fibrotic activity in pre-clinical models and histological improvement in a phase 2b trial. This open-label study explored the speed and extent of fibrosis reduction. We compared different methodologies of fibrosis scoring to optimize the design of a registrational placebo-controlled investigation.

Method: 46 Patients (pts) with NASH and fibrosis (28 F3, 11 F2, 7 F1) documented by biopsy were randomized 1:1:1 to receive Aramchol 300 mg BID and underwent a control biopsy at weeks 24, 48 or 72. Biopsies were read by 3 independent pathologists individually, followed by a consensus reading, which determined the final NASH CRN scoring. Three different assessments of the antifibrotic effect were studied on the same slides: 1) a ≥ 1 stage reduction by NASH CRN; 2) a ranked assessment (improvement/worsening/stable) of paired (pre and post baseline) biopsies, blinded to sequence; 3) an automated and continuous score of Fibrosis Composite Severity (FCS), using FibroNest™, a quantitative digital pathology image analysis and artificial intelligence (AI) Method: a 0.3 reduction in FCS (4 fold higher than the analytical variability) identified any reduction in fibrosis; a 25% relative decline in FCS, a strong reduction in fibrosis.

Results: Control biopsies were performed for 26, 15 and 5 pts at 24, 48, and 72 weeks, respectively. Mean (sd) baseline FCS was 5.05

(1.05). Table shows greater fibrosis improvement with longer duration of therapy for both conventional histology and digital pathology readings. Mean FCS reduction was -0.62 ($p=0.017$) at Wk24 and -1.74 ($p<0.0001$) at Wk ≥ 48 . AI evaluation was consistent with paired reading in 21/24 (87.5%) of the pts with fibrosis improvement. When analyzed by AI, 17/23 pts with unchanged NASH CRN stages had any fibrosis response, including 7 with a strong response. Similarly, 13/17 pts with stable ranking had a fibrosis response, including 5 with a strong reduction. No pts with worse CRN stages or worsening ranking had a strong AI fibrosis reduction.

	Wk24, N = 26% (N)	Wk ≥ 48 , N = 20% (N)
Fibrosis reduction		
By NASH CRN ≥ 1 stage	27% (7)	40% (8)
By ranked assessment	42% (11)	65% (13)
By AI reading, any (delta FCS ≥ 0.3)	58% (15)	100% (20)
By AI reading, strong ($\geq 25\%$ FCS)	27% (7)	65% (13)

Conclusion: Aramchol resulted in a high proportion of fibrosis improvement using three separate biopsy reading methodologies, with a larger treatment effect with longer duration of therapy. Both ranked assessments and AI evaluations identified more subjects with fibrosis improvement, indicating greater sensitivity to change vs categorical scoring. Digital pathology quantification by AI reveals a high level of fibrosis improvement that would have been missed by conventional histological measurements. AI technologies are promising for the detection of fibrosis changes in future clinical trials.

SAT104

The effect of glucagon on rates of hepatic mitochondrial oxidation and pyruvate carboxylase flux in man assessed by positional isotopomer tracer analysis (PINTA)

Kitt Falk Petersen¹, Gerald I. Shulman¹. ¹Yale University, Internal Medicine, New Haven, United States
Email: kitt.petersen@yale.edu

Background and aims: Dual GLP-1/glucagon agonists are now in clinical trials for the treatment of T2D and NASH. In addition to promoting further reduction in food intake on top of GLP-1, the glucagon component of these dual agonists may also promote increased rates of hepatic mitochondrial fat oxidation.

Method: In order to investigate this possibility we assessed the glucagon-specific effects of a dual agonist on rates of hepatic mitochondrial oxidation (V_{CS}) and pyruvate carboxylase flux (V_{PC}) in humans by infusing glucagon to achieve a physiological increase in plasma glucagon concentrations in combination with a novel ¹³C PINTA method to assess rates of hepatic V_{CS} and V_{PC} in 15 healthy volunteers using a paired study design. Following an overnight fast a 3-h IV infusion of [3-¹³C]lactate (4.3 μ mol/Kg-min) and [1, 2, 3, 4, 5, 6, 6-²H₇]glucose (0.22 μ mol/Kg-min) was begun and during the last 2 hours glucagon (GLG) was co-infused [6 ng/ (Kg-min)] or no GLG (CON).

Results: The GLG infusion resulted in a ~ 2.4 fold increase in plasma GLG conc. (from 75 ± 11 to 183 ± 20 pg/ml; $P<0.0001$), which was associated with an $\sim 20\%$ increase in both plasma C-peptide (from 1.89 ± 0.17 to 2.30 ± 0.26 ng/ml; $P=0.02$) and plasma insulin conc. (from 9.9 ± 2.0 to 12.0 ± 2.4 μ U/ml; $P=0.06$). Plasma glucose conc. increased from 4.90 ± 0.16 to 5.64 ± 0.19 mmol/L ($p=0.0001$) which was associated with a tendency for increased rates of glucose production (CON: 1042 ± 123 vs. GLG: 1148 ± 122 μ mol/min; $p=0.086$) despite no change in rates of V_{PC} flux (CON: 403 ± 69 vs. GLG: 373 ± 55 μ mol/min; $p=NS$). In contrast, this physiological increase in plasma GLG concentrations caused an 85% increase in rates of hepatic V_{CS} ($p<0.05$).

Conclusion: Taken together these studies demonstrate that a physiological increase in plasma glucagon promotes increased rates of hepatic mitochondrial oxidation in humans, which may provide additional benefits to the anorexic effects of dual GLP-1/glucagon agonists to reduce hepatic steatosis.

SAT105

Identification of biomarkers of histological response in patients with non-cirrhotic NASH treated with Lanifibranor

Jerome Boursier¹, Hugo Herve², Clémence M Canivet², Marine Roux², Pierre Broqua³, Michael Cooreman³, Jean-Louis Junien³, Jean Louis Abitbol³, Philippe Huot-Marchand³, Lucile Dzen³, Sanjaykanumar Patel⁴. ¹Angers University, HIFIH Laboratory UPRES EA3859, Angers; ²Angers University, HIFIH Laboratory UPRES EA3859; ³Inventiva; ⁴Inventiva, France
Email: jeboursier@chu-angers.fr

Background and aims: Lanifibranor, a pan-PPAR agonist, is a promising investigational compound for treating non-alcoholic steatohepatitis (NASH), as shown by histological efficacy in the phase 2b NATIVE trial (Francque SM et al 2021). We aimed to predict lanifibranor treatment response in NATIVE based on serum biomarkers.

Method: Patients receiving lanifibranor 800 or 1200 mg/d were pooled and those with end-of-treatment (EOT) liver biopsies were selected (n = 142). The histological end points 'NASH resolution and fibrosis improvement' (E1) and 'NASH resolution without worsening of fibrosis' (E2) according to NASH-CRN criteria were assessed. A panel of more than 70 biomarkers related to metabolism, inflammation, tissue injury and fibrosis were evaluated by assessing baseline, absolute and relative changes at EOT. Biomarker selection was done using classical univariate analysis, PCA and sPLS-DA, and combined in scores by logistic regression.

Results: 42 (30%) and 63 (44%) patients were respectively E1 and E2 responders; 4 parameters were independently associated with E1 response: baseline adiponectin and ferritin, and relative changes of MMP9 and transferrin. Combining these 4 parameters into an E1-score provided AUROC of 0.81 ± 0.08 for predicting E1 response, with Brier score of 0.17. 632+ bootstrap internal validation confirmed AUROC of 0.80 ± 0.10 and Brier score of 0.17. Negative (NPV) and positive (PPV) predictive value thresholds were 0.299 (rule-out with 80% NPV, corresponding sensitivity: 70%) and 0.592 (rule-in with 80% PPV, corresponding specificity: 95%). Using these thresholds, 72% of patients were biomarker E1 responders of whom 81% were confirmed histologically, leaving only 28% patients in the grey zone between the two thresholds. Baseline CK18 M65, absolute change of hyaluronate, and relative changes of fructosamine and ALT were independently associated with E2 response. The E2-score combining these biomarkers provided AUROC of 0.80 ± 0.08 and Brier score of 0.18 for E2 response (.632+ bootstrap: AUROC 0.78 ± 0.08 , Brier score 0.21). PV thresholds were 0.453 (80% NPV, corresponding 79% sensitivity) and 0.646 (80% PPV, corresponding 89% specificity). Using these thresholds, 80% of patients were biomarker E2 responders (80% confirmed histologically), leaving only 20% patients in the grey zone.

Conclusion: Combined biomarker signatures have good positive and negative predictive value for histological response under lanifibranor treatment in NASH.

SAT106

TERN-101, a farnesoid X receptor agonist, demonstrated similar safety and efficacy in non-alcoholic steatohepatitis patients with coronavirus disease of 2019 (COVID-19) exposure compared to those with no COVID-19 exposure in phase 2a LIFT study

Eric Lawitz¹, Rohit Loomba², Douglas Denham³, Diana Chung⁴, Erin Quirk⁴, Lois Lee⁴, Tonya Marmon⁴, Kris Kowdley⁵. ¹Texas Liver Institute, San Antonio, United States; ²University of California San Diego, La Jolla, United States; ³Clinical Trials of Texas, Inc., San Antonio, United States; ⁴Terns Pharmaceuticals, Foster City, United States; ⁵Liver Institute Northwest, Seattle, United States
Email: llee@ternspharma.com

Background and aims: TERN-101 is a non-steroidal farnesoid X receptor (FXR) agonist with enhanced liver distribution being developed for the treatment of non-alcoholic steatohepatitis (NASH). The phase 2a LIFT study (NCT04328077) was a double-blind, placebo-controlled study in adults with noncirrhotic NASH conducted during the COVID-19 pandemic. TERN-101 (5, 10, and 15 mg) administered for 12 weeks was overall safe and well-tolerated and significantly decreased alanine aminotransferase (ALT) and corrected T1 (cT1) relaxation time. We reviewed COVID-19 exposure in LIFT to explore any potential impact on TERN-101 safety and efficacy.

Method: COVID-19 antibody testing was performed at Screening, and Weeks 0, 6, and 12, and with ad hoc antibody and qualitative virus testing available in the event of COVID-19 symptoms. We evaluated overall safety and key efficacy parameters in patients with COVID-19 exposure, defined as patients with COVID-19 infection as an adverse event (AE) or detectable COVID-19 antibodies during the study.

Results: Of 100 enrolled and treated patients, 96% completed the LIFT study with no discontinuations due to AEs and no deaths; AEs occurred in 38.5% of the placebo and 56.8% of the TERN-101 groups. 97% of the patients had post-baseline COVID-19 antibody results. Of the 24 COVID-19 exposures identified, 4 had documented COVID-19 vaccination during the study (16.7%). COVID-19 infection was reported for 7 patients (7%): 6 who received TERN-101 and had mild to moderate AEs (Grade 1 or 2), and 1 placebo patient who developed a severe AE (Grade 3) that resolved. Among all 24 COVID-19 exposures, non-COVID-19 related treatment-emergent AEs were reported in 7 of 19 (36.8%) patients receiving TERN-101 vs 1 of 5 (20.0%) patients receiving placebo. ALT and cT1 changes at Week 12 among COVID-19 exposures were similar to patients without exposure of COVID-19.

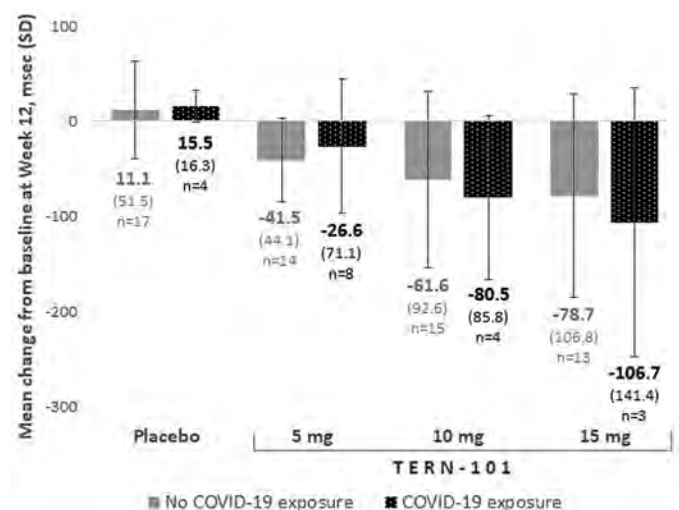


Figure: cT1 changes at Week 12

Conclusion: NASH patient recruitment and retention in the LIFT Study was feasible during the COVID-19 pandemic with successful

POSTER PRESENTATIONS

implementation of COVID-19 testing. The TERN-101 safety profile and cT1 responses were similar between the subset of patients with COVID-19 exposure and those without.

SAT107

Favorable lipid and pruritus profile of liver-distributed farnesoid X receptor agonist TERN-101 at clinically efficacious doses in non-alcoholic steatohepatitis phase 2a LIFT study

Kris Kowdley¹, Eric Lawitz², Rohit Loomba³, Erin Quirk⁴, Daria Crittenden⁴, Diana Chung⁴, Tonya Marmon⁴. ¹Liver Institute Northwest, Seattle, United States; ²Texas Liver Institute, San Antonio, United States; ³University of California San Diego, NAFLD Research Center, La Jolla, United States; ⁴Terns Pharmaceuticals, Foster City, United States

Email: barry.crittenden@gmail.com

Background and aims: TERN-101 is a potent, non-steroidal farnesoid X receptor (FXR) agonist with enhanced liver distribution under investigation for treatment of non-alcoholic steatohepatitis (NASH). Dose-related pruritus and unfavorable lipid effects have raised concerns about FXR agonists as a treatment for NASH. In the phase 2a LIFT study, TERN-101 was overall safe and well-tolerated at all dose levels, with significant reductions in alanine aminotransferase (ALT) and corrected T1 (cT1) relaxation time at 10 and 15 mg. Here we report additional details on lipids and pruritus from LIFT.

Method: LIFT was a double-blind, placebo-controlled study (NCT04328077) evaluating 5, 10 and 15 mg TERN-101 for 12 weeks in 100 adults with non-cirrhotic NASH. Low-density lipoprotein (LDL) and high-density lipoprotein (HDL) cholesterol were assessed at baseline and every 4 weeks. Pruritus was captured as part of routine adverse event (AE) reporting.

Results: No difference in LDL percent change from baseline was observed for 5 and 10 mg TERN-101 vs placebo at any timepoint; 15 mg had significant differences at all timepoints (+15.9% at Week 12). HDL was not different from placebo at Week 12 for 5 and 10 mg TERN-101. Changes in LDL and HDL by thresholds were assessed post-hoc (Table). Pruritus AEs (including pruritic rash) were reported in 11 of 74 (14.8%) patients receiving TERN-101 and none receiving placebo. Onset of pruritus ranged from Day 2 to Day 73. Pruritus resolved with ongoing TERN-101 treatment for 8 of 11 patients. All events were mild or moderate (Grade 1–2), with incidence overall balanced across TERN-101 groups. Grade 2 pruritus occurred in two 10 mg patients (generalized pruritus) and one 15 mg patient (pruritus localized to bilateral forearms). No patient discontinued TERN-101 due to pruritus.

Table: Lipid changes by threshold at Week 12

n (%)	Placebo n = 23	TERN-101		
		5 mg n = 24	10 mg n = 25	15 mg n = 21
LDL increase ≥25 mg/dL	4 (17)	4 (17)	2 (8)	4 (19)
HDL decrease ≥10 mg/dL	1 (4)	1 (4)	2 (8)	5 (24)

Conclusion: LDL and HDL mean changes, and proportion of patients with lipid changes by specified thresholds, were similar for 5 and 10 mg TERN-101 and placebo at Week 12. Pruritus AEs were not dose-dependent and did not lead to treatment discontinuation. These data support an overall differentiated and favorable safety and tolerability profile for TERN-101 at potentially efficacious dose levels.

SAT108

Liver-distributed farnesoid X receptor agonist TERN-101 demonstrates potent target engagement with a favorable exposure-response profile in non-alcoholic steatohepatitis patients

Cara H. Nelson¹, Christopher Jones¹, Kevin Klucher¹, Feng Jin², Tonya Marmon¹, Diana Chung¹, Erin Quirk¹, Daria Crittenden¹. ¹Terns Pharmaceuticals, Foster City, United States; ²Polaris Consulting, Foster City, CA, United States

Email: cnelson@ternspharma.com

Background and aims: TERN-101 is a potent, non-steroidal farnesoid X receptor (FXR) agonist with enhanced liver distribution being developed for treatment of non-alcoholic steatohepatitis (NASH). In the dose-ranging phase 2a LIFT study (NCT04328077), TERN-101 demonstrated significant decreases in alanine aminotransferase (ALT) and corrected T1 (cT1) relaxation time in NASH patients, and was overall safe and well-tolerated with no discontinuations due to adverse events. We present the pharmacokinetic (PK) and pharmacodynamic (PD) results from the LIFT study.

Method: LIFT was a double-blind, placebo-controlled study in adults with noncirrhotic NASH. Patients

(N = 100) were randomized and treated with placebo or TERN-101 (5, 10 or 15 mg) for 12 weeks. All patients had PK and PD samples collected at Week 0 (predose) and at trough timepoints (~24 hours post-dose) on Weeks 2, 4, 6, 8 and 12. Additionally, a subset of patients (N = 26) participated in an intensive PK/PD substudy at Weeks 0 and 12. PD markers of FXR agonism included 7- α -hydroxy-4-cholesten-3-one (C4) and fibroblast growth factor 19 (FGF19). A preliminary population PK model was used to estimate exposures in all patients.

Results: Sustained decreases in C4 were noted with levels significantly lower in the 10 and 15 mg groups vs placebo at most trough timepoints. In the PK/PD substudy, the maximal percent change in C4 and FGF19 occurred at 6 hours postdose. At Week 12, peak C4 decreases were dose-dependent and reached significance in the 10 and 15 mg groups (–56% and –96%, respectively); peak FGF19 change increased with dose and was significant in the 15 mg group (777%). FGF19 returned towards baseline levels at 24 hours postdose in all groups. TERN-101 exposures in the LIFT study were approximately dose proportional with some overlap in exposures between the 10 and 15 mg groups. An exposure-response analysis demonstrated a trend of greater decreases in change of cT1 with increasing exposures of TERN-101.

Conclusion: TERN-101 resulted in significant FXR target engagement in the liver relative to the intestine, as evidenced by sustained decreases in C4 at the 10 and 15 mg doses and transient increases in FGF19. Higher exposures of TERN-101 were associated with greater decreases in cT1, a marker of fibroinflammation improvement in NASH patients. These analyses support further development of TERN-101 for the treatment of NASH, either alone or in combination with other agents.

SAT109

EDP-297: a novel, highly potent, farnesoid X receptor agonist, results of a phase 1 study in healthy subjects

Alaa Ahmad¹, Christine Marotta¹, Ed Luo¹, Jart Oosterhaven², Sjoerd van Marle², Nathalie Adda¹. ¹Enanta Pharmaceuticals Inc, United States; ²PRA, Netherlands

Email: aahmad@enanta.com

Background and aims: EDP-297 is a potent FXR agonist under development for the treatment of non-alcoholic steatohepatitis (NASH). EDP-297 attenuates NASH-relevant pathways of steatosis, liver injury, inflammation, and apoptosis both in vitro and in vivo. Here, we present pharmacokinetic (PK), and pharmacodynamic (PD), food effect (FE), and safety results of a single ascending dose (SAD) and multiple ascending dose (MAD) phase 1 study in healthy subjects (HS).

Method: A randomized, double-blind, placebo-controlled (PBO) study was conducted to evaluate the safety, tolerability, PK/FE, and PD of single and multiple doses of EDP-297 in HS. Subjects received EDP-297 as a single dose (SAD, 5 cohorts, 20–600 µg) or once daily (QD) for 14 days (MAD, 5 cohorts, 5–90 µg), (6 active: 2 PBO/cohort), except in the SAD food effect cohort (8 active: 2 PBO). PD measurements included fibroblast growth factor 19 (FGF-19) and 7- α -hydroxy-4-cholesten-3-one (C4).

Results: A total of 82 subjects (n = 42 in SAD; n = 40 in MAD) received at least one dose of EDP-297 or PBO. EDP-297 was generally well tolerated. No severe adverse events or discontinuations due to adverse events (AEs) in SAD and MAD (up to 60 µg) were observed. Most AEs were mild and not related/unlikely related to study drug. In the SAD part, pruritus was observed in 300 µg (n = 2), 600 µg (n = 2), PBO (n = 1); during the MAD part, pruritus was reported in 30 µg (n = 1), 60 µg (n = 2), and 90 µg (n = 4), PBO (n = 2); the majority were mild or moderate, except for n = 4 severe cases at 90 µg MAD, with n = 1 that led to drug discontinuation. There were no clinically significant abnormal laboratory or abnormal ECG findings, except for n = 1 Grade 2 ALT elevation (MAD 90ug) that was not associated with other liver enzyme abnormalities. There were no clinically meaningful changes in the lipid profile, except for a trend towards decrease in HDL and increase in LDL at MAD 90ug; and mean lipids values were within normal range during the entire study. Plasma exposures increased with increasing single and multiple doses, with mean $t_{1/2}$ following multiple doses of ~9–12.5 hours. No food effect was observed. Strong FXR target engagement was demonstrated, with increase in FGF-19 and decrease in C4 up to 95% and 92%, respectively.

Conclusion: Overall, EDP-297, a potent and selective FXR agonist, was safe and well tolerated with PK suitable for once daily oral dosing, a strong target engagement and no food effect.

SAT110

Weight loss with semaglutide treatment or time-restricted feeding differentially improves non-alcoholic steatohepatitis in diet-induced obese insulin resistant mice

Francois Briand¹, Estelle Grasset¹, Natalia Breyner¹, Thierry Sulpice¹.

¹Physiogenex, Escalquens, France

Email: f.briand@physiogenex.com

Background and aims: Due to its positive correlation with obesity/type 2 diabetes, the prevalence of non-alcoholic steatohepatitis (NASH) is increasing worldwide. Weight loss represents a promising therapeutic strategy for NASH and liver fibrosis. Here we compared the weight loss benefits of the glucagon-like peptide-1 (GLP-1) receptor agonist semaglutide (SEMA) or time-restricted feeding (TRF) on NASH/liver fibrosis in diet-induced obese insulin resistant mice.

Method: Male C57BL/6J mice were fed a 60% high fat/2% cholesterol diet with 10% fructose supplemented drinking water (HFCF diet) for 25 weeks to induce obesity and NASH/liver fibrosis. After the 25-week diet-induction period, mice were kept on HFCF diet and treated with vehicle (control) or SEMA 0.06 mg/kg s.c. QD or placed on TRF from the last 3 hours of the dark cycle till the end of the light cycle, without access to food, but free access to normal drinking water (i.e., without fructose) every day, for 6 weeks. After 6 weeks, blood and liver were collected for biochemistry and histology analysis.

Results: SEMA treatment for 6 weeks induced a 20% lower caloric intake, which led to a 21% lower body weight ($p < 0.001$ vs. control). TRF had a weaker effect on caloric intake (-9%) but also reduced body weight (-11%, $p < 0.05$ vs. control). Both SEMA and TRF reduced the HOMA-IR index of insulin resistance and significantly reduced plasma ALT and AST levels, but these effects were more pronounced with SEMA. TRF, and to a greater extent SEMA, significantly reduced liver weight (SEMA: -37%, TRF: -27%), hepatic fatty acids (SEMA: -61%, TRF: -41%), triglycerides (SEMA: -67%, TRF: -36%, $p < 0.05$) and total cholesterol (SEMA: -48%, TRF: -30%) levels. Accordingly, SEMA showed a stronger reduction in steatosis score than TRF, but both led to significantly lower NAFLD activity score. SEMA and TRF

significantly reduced the hepatic gene expression of MCP-1 (inflammation), alpha-SMA, TGF-beta, Col1alpha1 and TIMP1 (fibrosis). However, SEMA did not alter liver fibrosis (as shown by Sirius Red staining), while TRF showed a clear anti-fibrotic effect in the liver, with significantly lower % Sirius Red labelling ($p < 0.05$ vs. control).

Conclusion: SEMA markedly reduced body weight and liver steatosis but did not improve hepatic fibrosis. Although its weight loss effect was less pronounced, TRF improved both NASH and liver fibrosis. These TRF benefits should be further investigated in the clinical setting.

SAT111

ECC4703, a full thyroid hormone receptor beta (THRβ) agonist, demonstrated excellent selectivity and liver targeting properties and improvement of plasma lipid, NAFLD activity score and fibrosis in NASH animal model

Jianfeng Xu¹, Zhao Yongliang¹, Julie Zhu¹, Jianfeng Xu¹, Jingye Zhou¹.

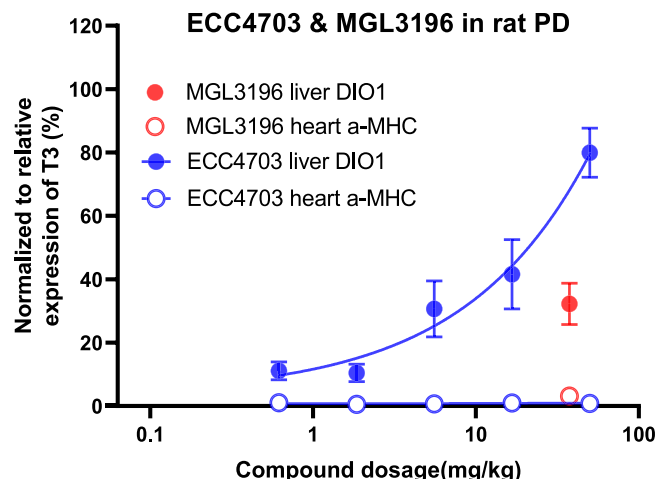
¹Eccogene (Shanghai) Co., Ltd., Shanghai, China

Email: jfxu@eccogene.com

Background and aims: Non-alcoholic steatohepatitis (NASH) is a metabolic liver disease featuring ectopic fat accumulation, hepatocellular damage, chronic inflammation, and progressive fibrosis. Resmetirom (MGL3196) as THRβ agonist has demonstrated THR β selectivity and liver targeting, which translate to plasma lipid lowering, potential of fibrosis improvement and thus NASH resolution in humans. However, MGL3196 is a partial agonist compared to the natural ligand T3 in ligand binding and liver target gene expression. A full agonist may provide superior efficacy for NASH and dyslipidaemia.

Method: Ligand binding to human THRα and THRβ was measured based on recruitment of a coactivating activator peptide to the receptors. Liver targeting was determined in PTU-induced rat hypothyroidism model with induction of THR target gene in liver and heart. Activities in rat and human primary hepatocyte were measured with a reporter gene driven by thyroid response elements. A diet-induced obesity with CCl4 in mice (DIO-CCl4) was applied to evaluate the effect of ECC4703 on plasma lipid and liver pathology.

Results: In a ligand bind assay, ECC4703 is a potent THRβ agonist with relative β vs α selectivity of 49. In PTU rat, ECC4703 elicited robust induction of liver gene DIO1 but no effects on heart gene α-MHC at up to 50 mpk, indicating superior liver targeting. It's noteworthy in both in ligand binding and liver gene expression, ECC4703 showed Emax equivalent to T3 which suggested full agonism. In rat and human hepatocytes, ECC4703 led to potent reporter gene expression, ensuring species translation. In DIO-CCl4 NASH model, ECC4703 treatment resulted in significant decrease in plasma lipid, improvement of liver NAS score and fibrosis, but no effects on heart weight.



POSTER PRESENTATIONS

Conclusion: In summary, ECC4703 is a novel full THR β agonist with excellent *in vitro* and *in vivo* profile, and potentially best-in-class compound for NASH and dyslipidemia treatment.

SAT112

LIVRQNaC increases fatty acid oxidization in a primary human hepatocyte model of non-alcoholic steatohepatitis

Matthew Russell¹, Christopher Newgard^{2,3}, Guofang Zhang², Arianna Nitzel¹, Michael Hamill⁴, Karim Azer¹. ¹Axcella Therapeutics; ²Duke Molecular Physiology Institute; ³Department of Medicine, Duke University Medical Center; ⁴Flagship Pioneering
Email: mrussell@axcellatx.com

Background and aims: Endogenous metabolic modulators (EMM) are naturally occurring compounds with signaling and regulatory properties. When selectively combined, in unique stoichiometric ratios, EMMs can treat complex diseases with system-wide dysregulation of metabolic pathways. LIVRQNaC, an EMM composition of 5 amino acids (AA) and n-acetylcysteine (Nac), decreased liver fat accumulation (*in vivo* and *in vitro*) by reducing triglyceride accumulation. AXA1125, the clinical formulation of these same EMMs, decreased liver fat content in subjects with non-alcoholic fatty liver disease by magnetic resonance imaging measurement of liver proton density fat fraction, MRI-PDFF. The present study investigated the *in vitro* dose-dependent effects of LIVRQNaC on fatty acid oxidation (FAO), the putative mechanism of these effects, in a primary human hepatocyte (PHH) NASH model.

Method: PHHs were plated on collagen coated wells and incubated with 5% CO₂. On day 3, cells were incubated in custom media containing 500 μ M carnitine, 10 μ g/ml insulin, EGF, 1 μ M dexamethasone, and custom AA concentrations (as in healthy human plasma) with and without LIVRQNaC (10X and 30X) and with lipotoxic insult (saturated free fatty acids [2:1 oleate: palmitate] and tumor necrosis factor alpha (1 ng/ml)). After 24 hours, cells were treated for 1 hour with medium containing LIVRQNaC and lipotoxic insult with [U-¹³C] palmitate replacing palmitate and then analyzed for ¹³C-labeled palmitoylcarnitine, acetylcarnitine, acetyl-co-enzyme A, β -hydroxybutyrate, and other metabolites using liquid and gas chromatography-mass spectrometry.

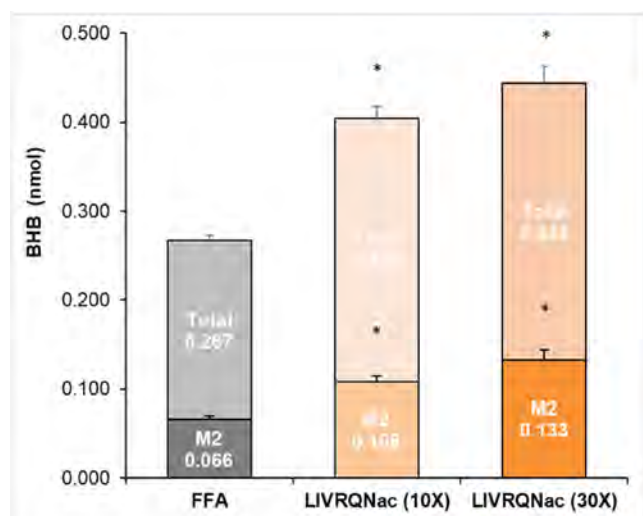


Figure: Increases (%) in labeling of the terminal FAO metabolite BHB, derived from [U-¹³C] palmitate tracer, and total pool size are indicative of the dose-dependent increase in FAO with LIVRQNaC. *p < 0.0001, analysis of variance; BHB, the ketone body, β -hydroxybutyrate; FAO, fatty acid oxidation; M2, mass isotopomers where number represents the number of heavy atoms in the molecule.

Results: ¹³C labeling of fatty acid-derived metabolites (%) was significantly increased by LIVRQNaC treatment vs control. Increases

were observed in labeled palmitoylcarnitine (p < 0.001), acetylcarnitine (p < 0.05), and acetyl-CoA (p < 0.05) in LIVRQNaC- 10X, and 30X treated cells vs control. M2 labeled β -hydroxybutyric acid (terminal FAO product) increased 102% in LIVRQNaC-treated cells (0.108 nmol, 10X; 0.133 nmol, 30X) vs control (0.066 nmol; p < 0.0001; Fig).

Conclusion: Increases in labeled palmitoylcarnitine, acetylcarnitine and acetyl-coA reflected an increase in FAO in PHHs treated with LIVRQNaC. Consistently, there was an increase in total and labelled β -hydroxybutyric acid in LIVRQNaC-treated cells indicating an increase in ketogenesis. These data support a mechanism for AXA1125's clinical effect of decreasing liver fat, by increasing ketogenesis and increasing FAO.

SAT113

Assessment of therapeutic effect of liraglutide in newly established cell culture model of non-alcoholic and drug-induced fatty liver disease

Tea Omanovic Kolaric^{1,2}, Vjera Nincevic², Tomislav Kizivat³, Milorad Zjalic⁴, Lucija Kuna², Ines Bilic-Curcic^{1,5}, Martina Smolic^{1,2}. ¹Faculty of Medicine Osijek, Department of Pharmacology, Osijek, Croatia; ²Faculty of Dental Medicine and Health Osijek, Department of Pharmacology and Biochemistry, Osijek, Croatia; ³University Hospital Centre Osijek, Clinical Department of Nuclear Medicine and Radiation Protection, Osijek, Croatia; ⁴Faculty of Medicine Osijek, Department of Medical Biology and Genetics, Osijek, Croatia; ⁵University Hospital Centre Osijek, Clinical Department of Diabetes, Endocrinology and Metabolism Disorders, Osijek, Croatia
Email: msmolic@mefos.hr

Background and aims: The impact of non-alcoholic fatty liver disease (NAFLD) on global health is becoming more significant with the growing incidence of obesity and drugs consumption. Therefore, more research is necessary in order to enlighten underlying pathophysiologic mechanisms for these conditions and possible therapeutic approaches. Aims of our study were to establish reliable *in vitro* models of non-alcoholic and drug-induced fatty liver disease (DIFLD) and also to investigate possible therapeutic solutions in these *in vitro* models.

Method: HuH7 cell culture models of NAFLD and DIFLD were established by incubation of Huh7 cells with 0, 5 mM oleic acid (OA), 5 μ M to 20 μ M of amiodarone, 1 μ M to 10 μ M of tamoxifen for various time periods (24 h, 48 h), respectively. Cells were cotreated with 1 nM to 100 nM of liraglutide in order to assess its potential beneficial effect in fatty liver models. Cell viability was measured by MTT ((3-(4, 5-dimethylthiazol-2-yl)-2, 5-diphenyltetrazolium bromide) assay. Changes in cell shape and the extent of hepatosteatosis were assessed by fluorescent microscopy as shown in Figure. Cell nuclei were stained with Hoechst, and fat droplets were stained with Oil-Red-O. Triglyceride (TG) accumulation was measured by TGO-PAP method and the results were read on the microplate reader.

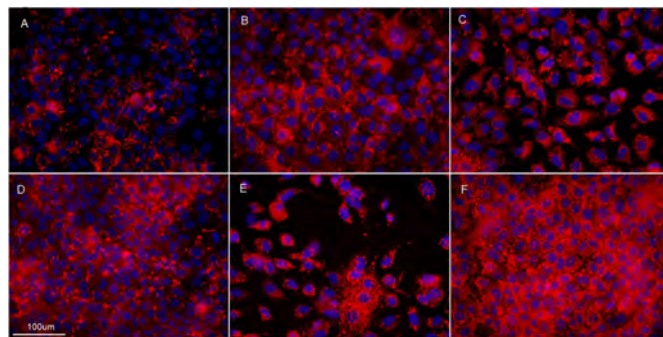


Figure: Effects of tamoxifen, amiodarone and OA on the fat accumulation in Huh7 cell culture after 24 h of treatment with: A- control, B- 10 μ M tamoxifen, C- 20 μ M tamoxifen, D- 20 μ M amiodarone, E- 40 μ M amiodarone, F- 0.5 mM OA.

Results: Tamoxifen significantly reduced cell viability in a dose-dependent manner after just 24 h treatment, compared to amiodarone and OA. Liraglutide co-treatment improved cell viability and the effect was greater after a longer period of treatment, especially in tamoxifen-treated cells for almost 30% ($p < 0.05$). Microscopic observations demonstrated microsteatosis as the predominant form of liver cell injury in this time period, with the greatest accumulation of fat in OA model. Accordingly, TG accumulation was highest in OA model, while liraglutide diminished TG accumulation in all three models.

Conclusion: This newly established cellular Huh7 model of NAFLD and DIFLD could provide a new tool for further studies on these conditions. Nevertheless, further research is needed to better understand the onset of fatty liver changes, drug toxicity, and the possible role of liraglutide in their treatment.

SAT114

Efx treatment improved histopathology and non-invasive markers of liver injury and fibrogenesis to a similar extent in NASH patients with high-risk PNPLA3 genotypes, compared to those with lowest genetic risk: a post-hoc analysis of balanced study

Erik Tillman¹, Reshma Shringarpure², Guy Neff³, Rashmee Patil⁴, Peter Ruane⁵, Bradley Freilich⁶, Cynthia Behling⁷, Erica Fong⁸, Brittany de Temple⁸, Kitty Yale⁹, Stephen Harrison¹⁰, Tim Rolph⁸.
¹Akero Therapeutics, South San Francisco, United States; ²Akero Therapeutics, South San Francisco, United States; ³Covenant Research and Clinics, Fort Meyers, United States; ⁴South Texas Research Institute; ⁵Ruane Clinical Research Group Inc; ⁶Kansas City Research Institute; ⁷Pacific Rim Pathology; ⁸Akero Therapeutics, South San Francisco, United States; ⁹Akero Therapeutics, South San Francisco, United States; ¹⁰Pinnacle Clinical Research
 Email: tim@akerotx.com

Background and aims: The PNPLA3 I148M genetic variant confers increased risk of progressive NAFLD, cirrhosis, and HCC. Concurrent insulin resistance further increases the risk associated with I148M.¹ The aim of this analysis was to evaluate whether I148M presence influenced patients' baseline characteristics and/or response to the long-acting FGF21 analog efruxifermin (EFX) in the BALANCED Main Study.

Method: 80 NASH patients with F1-F3 fibrosis were randomized in a controlled design comparing EFX treatment for 16 weeks with placebo². End-of-treatment liver biopsies were available for patients with $\geq 30\%$ relative reduction in liver fat content (LFC) by MRI-PDFF after 12 weeks of EFX dosing. All EFX-treated patients with MRI-PDFF met this threshold. The PNPLA3 rs738409 SNP was genotyped in all consenting patients. Baseline characteristics and treatment responses were compared across PNPLA3 genotypes: I/I (lowest risk), I/M (intermediate risk), or M/M (highest risk) for all EFX-treated patients with available genotype, biomarker, and histology data.

Results: Of 42 EFX-treated patients genotyped for PNPLA3, 11 were I/I, 22 were I/M, and 9 were M/M.

At Baseline, carriers of the lowest risk (I/I) genotype were older, with more insulin resistance and hypertriglyceridemia, whereas those carrying the highest risk (M/M) genotype were younger, with less insulin resistance and lower triglyceride levels. Histologic response to EFX was observed across all 3 PNPLA3 genotypes, with larger improvements in histopathology seen in patients with M/M genotype. Although the extent of NASH resolution was similar across all genotypes at 40–56%, all 9 M/M carriers achieved ballooning resolution. The extent of fibrosis regression appeared greater in M/M than I/I patients: in EFX-treated patients with paired biopsies that consented to genotyping, 7/9 (78%) M/M carriers had a ≥ 1 -stage improvement in fibrosis compared to 4/10 (40%) of I/I patients, while 4/5 (80%) M/M patients with F2/F3 fibrosis at baseline improved by 2 stages compared to 3/6 (50%) I/I patients. Improvements in metabolic

and liver-related biomarkers were comparable across PNPLA3 genotypes.

Table 1. Baseline Characteristics and Response to Efruxifermin by PNPLA3 Genotype

BALANCED Main Study	PNPLA3 I148 risk variants		
	0 (I/I)	1 (I/M)	2 (M/M)
All EFX-treated patients, N	11	22	9
Age (years)	57.5	51.2	48.2
Hispanic or Latino, n (%)	4 (36%)	14 (65%)	7 (78%)
T2D, n (%)	6 (55%)	9 (41%)	4 (44%)
LFC, MRI-PDFF (%)	17.3	21.3	21.2
Mean Abs CFB to week 12 in LFC, %	-13.1	-15.7	-13.6
Baseline NAFLD Activity Score, mean	5.45	5.45	5.67
Baseline F1, n (%)	4 (36%)	9 (41%)	4 (44%)
Mean ALT at baseline, U/L	65.2	57.2	50.9
ALT mean abs CFB to week 16 (U/L)*	-34.5	-35.5	-26.6
Mean Pro-C3 at baseline, ng/mL	18.0	17.8	17.2
Pro-C3 mean abs CFB to week 16 (ng/mL)*	-7.3	-6.5	-5.8
Mean C-peptide at baseline, ng/mL	7.35	6.57	4.23
Mean HbA1c at baseline (%)	8.6	8.4	8.0
HbA1c mean abs CFB to week 16, %*	-0.85	-0.46	-0.19
Serum TG, mg/dL	226	176	163
Serum TG <150 mg/dL at week 16, n/N (%)*	8/11 (73%)	17/20 (85%)	8/9 (89%)
EFX-treated patients with end-of-study biopsy, N*	10	18	9
NASH resolution, n (%)	4 (40%)	9 (50%)	5 (56%)
≥ 4 -point improvement in NAS	5 (50%)	8 (44%)	5 (56%)
Ballooning resolution, n (%)	4 (40%)	9 (50%)	9 (100%)
≥ 1 -stage improvement in fibrosis, n (%)	4 (40%)	10 (56%)	7 (78%)
2-stage improvement in fibrosis in patients with F2/F3 at baseline, n/N (%)	3/6 (50%)	4/10 (40%)	4/5 (80%)
≥ 1 -stage improvement in fibrosis AND NASH resolution, n (%)	2 (20%)	5 (28%)	4 (44%)

* in EFX-treated patients with measurement at baseline and stated timepoint

Conclusion: EFX significantly improved liver manifestations of metabolic disease including NASH histology across PNPLA3 genotypes, including in patients with highest risk of progression to end-stage liver disease.

1. Barrata *et al.* (2019) *Hepatol Commun* 3:894–907.
2. Harrison *et al.* (2021) *Nat Med* 27:1262–71.

SAT115

Oxygen-nutrient mismatch: a novel concept to explain how Obeticholic acid benefits NASH treatment

Gerond Lake-Bakaar¹, John Robertson², Charles Aardema³.
¹Presbyterian St. Luke's Medical Center, Transplant Center, Denver;
²Blacksburg, Bioengineering, Blacksburg, United States;
³Biomedinnova LLC, Denver, United States
 Email: glakebak@verizon.net

Background and aims: The oxygen-nutrient mismatch concept, first proposed for alcoholic steatohepatitis, ASH, could also apply to non-alcoholic steatohepatitis, NASH. Both are consequences of the unique dual liver blood supply.

The hepatic artery, HA, accounts for 20 percent of liver blood flow. However, it provides over 50 percent of oxygen requirements and has myogenic elements for autoregulation. By contrast, the portal vein, PV, lacks autoregulatory capacity and carries deoxygenated blood, rich in nutrients. Thus, HA oxygen delivery could fail to match excess alcohol (ASH) or nutrient intake (NASH). Furthermore, chronic obstructive sleep apnoea (OSA) and intermittent hypoxia, common in NASH could induce chronic liver damage from tissue hypoxia. Obeticholic acid (OCA), is a highly selective, potent agonist for the Farnesoid-X-receptor (FXR). It effectively treats NASH fibrosis. It can impact vasoactive responsiveness; however, the mechanism of action is unclear.

POSTER PRESENTATIONS

We studied the effects of OCA on HA, PV, and hepatic vein, HV, flow in porcine liver perfused ex vivo with a cardio-emulation pump, the CaVESWave® system to determine whether vascular effects could explain its efficacy in the treatment of NASH

Method: Six fresh porcine livers (two controls) were continuously perfused with phosphate buffered saline (PBS). OCA dosing was delivered in solution with methyl cellulose as carrier, directly into the portal vein catheter. Perfusion was initiated with the HA settings at 120/80 mmHg, PV around 15 mmHg and temperature at 15° C. Flow rates in HA, PV and HV were measured throughout. Carrier only was injected at 30 min intervals in the controls. For the treatment group, 0 mg OCA/kg liver weight, followed by 0.14, 0.28, 0.56 and 1.12 mg/kg, injected at 30 min intervals.

Results: The cardio-emulated waveforms showed little variability, either before or after drug treatment was started (figure 1). HA pressure varied between 117 and 122 mmHg (systolic) and 75–84 mmHg (diastolic); perfusate pH between 7.35 and 7.4; DO between 104 and 105 and temperature 15.8 and 17.5° C.

Control livers (n=2) showed minor changes in flow after treatments with vehicle (figure 2). The maximum percentage increase in HA flow was 3.3 ± 3.5 and HV flow, 4.8 ± 2.8 . By contrast, PV flow was reduced by up to -9.1 ± 5.9 .

In OCA treated livers (n=4), there was a clear dose-relationship between OCA and HA, HV and PV. Hepatic venous outflow and HA flow increased progressively to 11 ± 11.8 and 9.9 ± 8.9 , respectively. Conversely, PV flow was reduced by up to $-19 \pm 16\%$.

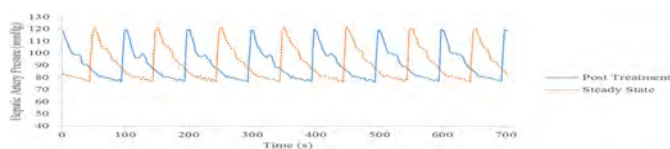


Figure 1:

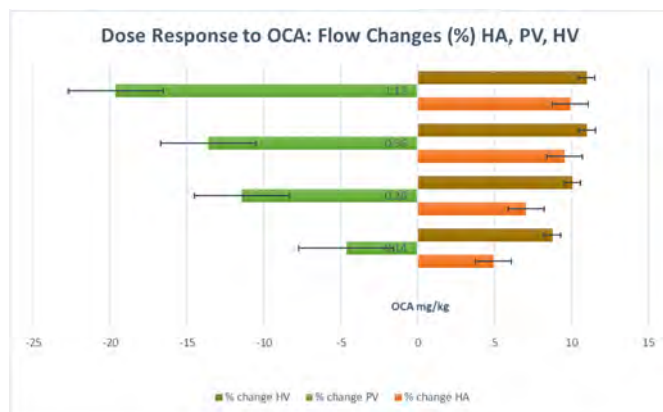


Figure 2:

Conclusion: OCA in dose responsive manner increased HA flow rates and inversely reduced PV flow, consistent with an active hepatic artery buffering response. Thus, increased delivery of oxygen rich HA blood, coupled with reduced nutrient rich PV blood, provides a rational concept for the beneficial effect of chronic OCA in NASH.

SAT116

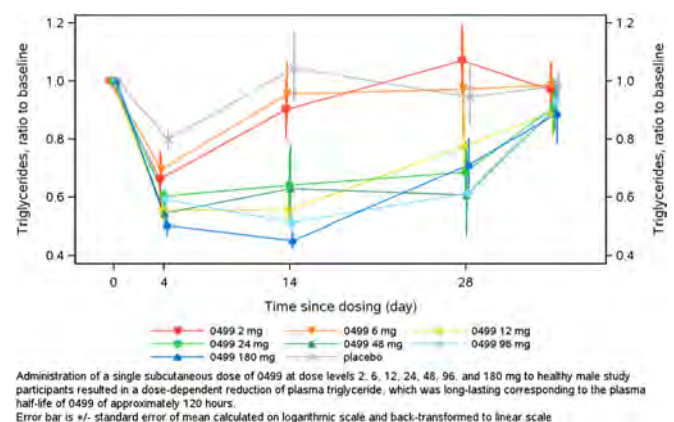
Sustained reduction of triglyceride and LDL cholesterol from single administration of the novel long-acting FGF21 analogue 0499

Kirsten Dahl¹, Martin Friedrichsen¹, Rasmus Ribel-Madsen¹, Jakob Schiøler Hansen², Jesper Clausen¹, Mads Axelsen¹, Mads Sundby-Palle¹, Cassandra Key³, Harumi Murakami⁴, Birgitte Andersen¹. ¹Novo Nordisk A/S, Denmark; ²Novo Nordisk Bio Innovation Hub, United States; ³ICON Early Phase Service, San Antonio, TX, United States; ⁴SOUSEIKAI Sumida Hospital, Tokyo, Japan
Email: kdhl@novonordisk.com

Background and aims: Activation of the fibroblast growth factor 21 (FGF21) receptor complex has been associated with several attractive effects in preclinical models including weight loss and decreased hepatic fat content. This has led to the pursuit of FGF21 for pharmacotherapy within obesity and NASH, which has to date been limited by lack of suitable FGF21 analogues. Here we report the exploration of a new FGF21 analogue 0499 with the purpose of investigating the safety profile, pharmacokinetic (PK) and pharmacodynamic (PD) potential of the new molecule.

Method: In a randomized, blinded, placebo-controlled first human dose (FHD) study, healthy male participants with a BMI around 30 kg/m² received a single subcutaneous administration of either placebo or 0499 at dose level: 2, 6, 12, 24, 48, 96, or 180 mg. In a separate study in Japanese healthy male participants, 3 dose levels: 12, 30, and 96 mg were tested to confirm consistent safety profile and PK characteristics across ethnicity. In both studies, participants were followed for 36 days post-dose while blood samples were obtained for safety evaluation, PK and PD assessments. A total of 78 participants received a single dose of 0499.

Results: The safety profile, as well as PK and PD results were comparable for the two studies. The adverse events observed were mainly related to the gastrointestinal tract including nausea, diarrhea, frequent bowel movements and vomiting. Increased appetite was also observed. Treatment was not associated with changes in heart rate, body temperature, clinical laboratory safety parameters, or body weight. Plasma triglyceride and LDL cholesterol levels were decreased in a dose-dependent manner while HDL cholesterol was increased. The changes in the lipid parameters were sustained for up to 28 days after the single administration. The plasma half-life of 0499 was approximately 120 hours.



Conclusion: From the two studies of 0499 in healthy participants, it was concluded that the novel FGF21 analogue 0499 has an acceptable safety profile at all tested dose levels, and that the PK profile seems compatible with a once-weekly dose regimen. The remarkable improvement on the plasma lipid profile is encouraging for the further development of 0499 for treatment of NASH.

SAT117

Combination of an Acetyl-CoA carboxylase inhibitor and obeticholic acid reduced lipids and bile acids and altered lipid and amino acid metabolism in the liver of humanized mice

Wen-Wei Tsai¹, David Hollenback¹, Andrew Schwab², Megan Showalter², James Trevaskis¹. ¹Gilead Sciences; ²Metabolon
Email: wwtsai76@gmail.com

Background and aims: Inhibition of the acetyl-CoA carboxylase (ACC) isoforms ACC1 and ACC2 reduces lipogenesis, stimulates lipid oxidation, and improves histologic features and fibrosis-related biomarkers in non-alcoholic steatohepatitis (NASH). Obeticholic Acid (OCA), as an FXR agonist, reduces bile acid synthesis and regulates lipid metabolism in the liver. We evaluated the effect of an ACC inhibitor (ACCi) and OCA in combination on lipid and amino acid metabolism in the humanized liver of chimeric PXB mice (PhoenixBio, Japan).

Method: Adult male PXB mice (n = 10, randomized by blood human albumin concentrations) were administered with ACCi (an analog of firsocostat) and/or OCA (10 mg/kg, QD, PO for both compounds) for 18 days and livers were collected 2 h after the last dose. Untargeted metabolomic profiling of liver tissue was performed at Metabolon, Inc (Morrisville, NC, USA) using a combination of LC-MS methods (1).

Results: Humanized liver mice developed spontaneous steatosis due to the lack of FGF19 signalling in the liver as engulfed human hepatocytes did not respond to mouse FGF15. ACCi and OCA combination showed additive effects to reduce neutral lipids (triglycerides, diacylglycerols) and long chain fatty acids, and increase acyl-carnitines and 3-hydroxybutyrate. Although the combination reduced 7-hydroxycholesterol, OCA increased cholesterol and cholesteryl esters alone or in combination with ACCi. Primary and secondary bile acids were mainly decreased by OCA and further reduction was observed in combination. OCA and combination increased N-acetylated amino acids and combination also increased polyamines and nicotinamide adenine dinucleotide hydride.

Conclusion: Metabolomic analysis revealed that lipid metabolism and energetic profile were rapidly changed by ACCi or OCA treatment and combination of both agents reduced lipid synthesis and promoted fatty acid oxidation in the liver of humanized mice. These changes are similar to the clinical findings in NASH patients treated with ACCi and FXR agonist combination, and support the utility of humanized mouse model to elucidate molecular pathways mediated by NASH therapies.

Reference:

1. Evans AM, et al. High resolution mass spectrometry improves data quantity and quality as compared to unit mass resolution mass spectrometry in high-throughput profiling metabolomics. *Metabolomics*. 2014.

SAT118

Identification of a fibrosis endpoint in NAFLD patients more prone to interventions aimed at reducing fibrogenesis

Ida Villesen¹, Jadine Scragg^{2,3,4,5}, Diana Leeming¹, Olivier Govaere^{3,6}, Guy Taylor², Stuart Mcpherson^{3,6,7}, Kate Hallsworth^{3,6,7}, Morten Karsdal¹, Quentin Anstee^{3,6,7}. ¹Nordic Bioscience, Fibrosis, Herlev, Denmark; ²Population Health Sciences Institute, Faculty of Medical Sciences, Newcastle University, Newcastle upon Tyne, United Kingdom; ³Newcastle NIHR Biomedical Research Centre, Newcastle Upon Tyne Hospitals NHS Foundation Trust, Newcastle Upon Tyne, United Kingdom; ⁴Nuffield Department of Primary Care Health Sciences, University of Oxford, Oxford, United Kingdom; ⁵NIHR Oxford Biomedical Research Centre, Oxford, United Kingdom; ⁶Translational and Clinical Research Institute, Faculty of Medical Sciences, Newcastle University, Newcastle upon Tyne, United Kingdom; ⁷Liver Unit, Newcastle Upon Tyne Hospitals NHS Foundation Trust, Newcastle Upon Tyne, United Kingdom
Email: ifv@nordicbio.com

Background and aims: Non-alcoholic fatty liver disease (NAFLD) is associated with inflammation and hepatocellular damage, leading to activation of fibroblasts and fibrosis development. Fibrosis is known to be the single most important factor for predicting liver-related clinical outcomes and is quantifiable by biomarkers of collagens including PRO-C3, PRO-C4 and PRO-C5, measuring formation of type III, IV and V collagen, respectively. However, patient heterogeneity is evident, and it remains largely unknown how to accurately identify patients in most need of treatment. Monitoring fibroblast activity through formation of collagen, may enable identification of fibrosis endotypes; a high or low activity stage of fibrosis formation. This segregation may identify patients more likely to experience anti-fibrotic effect due to therapy or weight loss.

Method: Clinically confirmed NAFLD patients, weight stable ($\pm 3\%$) since diagnoses, were recruited from hepatology clinics at a tertiary centre in the UK. Patients were prescribed an 8–12-week VLCD (~800 kcal/day) intervention. Serum markers were determined at baseline and every second week until end of diet, 4 weeks post-VLCD and at 5 months follow-up. The biomarkers PRO-C3, PRO-C4 and PRO-C5 were quantified by ELISA. For analysis, patients were stratified at baseline into high and low levels of formation of fibrosis, determined by the biomarkers.

Results: 26 patients (mean age 56 and BMI of 42) were included. With a mean weight loss of 9.7% all patients were found to improve liver measures including ALT and AST from baseline to post-VLCD. Yet, patients separated into high and low biomarker levels at baseline, based on the median, were found to differ in response to intervention. Thus, high levels of PRO-C3 (above 11.4 ng/ml) were found to associate with a decrease of 40% from baseline to end of diet while low levels remained unchanged, the same was seen for PRO-C4 (above 263.5 ng/ml) with ~55% decrease and PRO-C5 (above 857.4 ng/ml) with ~ 57% in high-level groups, indicating decreased formation of fibrosis following weight loss, while low biomarker levels remained unchanged throughout the course of the study.

Table 1: Patient baseline characteristics

	High PRO-C3	Low PRO-C3	High PRO-C4	Low PRO-C4	High PRO-C5	Low PRO-C5
BMI, mean (\pm SD)	42 (\pm 9)	39 (\pm 8)	41 (\pm 8)	40 (\pm 8)	41 (\pm 9)	41 (\pm 7)
ALT, mean (\pm SD)	55 (\pm 41)	41 (\pm 17)	56 (\pm 37)	38 (\pm 21)	55 (\pm 39)	40 (\pm 19)
AST, mean (\pm SD)	40 (\pm 21)	29 (\pm 12)	35 (\pm 20)	32 (\pm 16)	33 (\pm 19)	35 (\pm 17)
ELF	10 (\pm 0.9)	10 (\pm 0.7)	10 (\pm 0.8)	10 (\pm 0.8)	10 (\pm 0.8)	10 (\pm 0.8)

p values indicate significant different from high group, calculated using t-test and indicated as *p < 0.05, **p < 0.01

Conclusion: NAFLD patients respond heterogeneously to intervention with regards to their fibrogenesis profile, in which some experience a decrease and other are unchanged, suggesting an endotype of patients more amendable to anti-fibrogenesis intervention.

SAT119

The pan-PPAR agonist lanifibranor improves markers of cardiometabolic health in patients with NASH independent of weight change

Michael Cooreman¹, Sven Francque², Martine Baudin³, Philippe Huot-Marchand³, Lucile Dzen³, Jean-Louis Junien³, Pierre Broqua³, Manal Abdelmalek⁴. ¹Inventiva, United States; ²University Hospital Antwerp, Belgium; ³Inventiva, France; ⁴Duke University School of Medicine, United States
Email: michaelcooreman@msn.com

Background and aims: Lanifibranor therapy resulted in significant efficacy on the histological end point 'NASH resolution and improvement of fibrosis' as well as on markers of cardiometabolic health (CMH) in the phase 2b NATIVE study. Modest weight gain was reported as a PPAR γ effect, which has been ascribed to the maturation of insulin-sensitive, metabolically healthy subcutaneous adipose

POSTER PRESENTATIONS

tissue. We evaluated markers of CMH by changes in weight in the lanifibranor and placebo arms.

Method: NATIVE enrolled 247 patients with SAF activity score 3–4, fibrosis stage F0–F3 in 3 arms: lanifibranor 800, 1200 mg/d and placebo for 24 weeks; 217 (lanifibranor: 144, placebo: 73) patients who completed the trial with weight data at baseline and end of treatment (EOT) were included in the analyses. Mean weight increase at EOT was 2.4 (2.6%) and 2.7 (3.1%) kg for 800 and 1200 mg lanifibranor, respectively; patients were divided in 3 groups according to % weight change: $\leq 2.5\%$ ($n = 73$, 51%); 2.5–5% ($n = 23$, 16%); $> 5\%$ ($n = 48$, 33%). Biomarkers of lipid and glucose metabolism, insulin resistance, inflammation, liver tests, diastolic blood pressure (DBP), hepatic steatosis (NASH-CRN grading) and Controlled Attenuation parameter (CAP) were evaluated at screening and EOT, and compared between the weight change groups.

Results: Improvement of CMH markers at EOT compared to baseline occurred to the same degree in the 3 weight change groups for the pooled lanifibranor arms: increase in HDL-cholesterol, and decrease in total triglycerides, APO-B, APO-B/APO-A1, APO-C3, fasting glucose and insulin levels, HbA1c, HOMA-IR and hs-CRP, along with decreases in hepatic steatosis, ALT, AST, GGT and DBP. Adiponectin, a PPAR γ downstream mediator, increased in all 3 weight change groups, with a higher increase in the $> 2.5\%$ weight increase groups, compared to the $< 2.5\%$ weight increase group. With placebo, 12 (16%) patients with weight change $> 2.5\%$ at EOT had no improvement of CMH markers, no change in adiponectin levels, and had increases in steatosis and worsening of liver tests, HOMA-IR and DBP.

Conclusion: Biomarkers of CMH improve with lanifibranor therapy, independent of weight change. These beneficial effects occur in parallel with a marked increase of adiponectin, which marks adipose tissue health and improves insulin sensitivity; the data provide further evidence that PPAR γ -induced weight gain is metabolically distinct from lifestyle-related weight gain.

SAT120

Lanifibranor therapy reduces the FibroScan-aspartate aminotransferase (FAST) score associated with histological 'NASH resolution and improvement of fibrosis' and biomarker response

Michael Cooreman¹, Manal Abdelmalek², Martine Baudin³, Philippe Huot-Marchand³, Lucile Dzen³, Céline Fournier⁴, Jean-Louis Junien³, Pierre Broqua³, Sven Francque⁵. ¹Inventiva, United States; ²Duke University School of Medicine, United States; ³Inventiva, France; ⁴Echosens, France; ⁵University Hospital Antwerp, Belgium
Email: michaelcooreman@msn.com

Background and aims: Lanifibranor, a pan-PPAR agonist, has shown efficacy on the histological end point 'NASH resolution and improvement of fibrosis' in the phase 2b NATIVE trial. We evaluated the effect of lanifibranor on the FAST score, a promising non-invasive test (NIT) for active NASH with significant fibrosis, and its correlation with histological and biomarker response in NATIVE-enrolled patients with F2–F3 fibrosis.

Method: Patients with non-cirrhotic NASH and SAF-activity score 3–4 enrolled in NATIVE ($n = 247$) received lanifibranor 800, 1200 mg/d or placebo for 24 weeks. A total of 112 patients had baseline F2–F3 fibrosis and FAST scores available at baseline and end of treatment (EOT). FAST combines liver stiffness measurement by vibration controlled transient elastography, controlled attenuation parameter and aspartate aminotransferase levels and provides the probability (between 0 and 1) for active NASH with significant fibrosis ($NAS \geq 4$ and $F \geq 2$): ≥ 0.65 : high-risk, 0.35–0.65: intermediate-risk, ≤ 0.35 low-risk. FAST scores were compared between lanifibranor and placebo arms using a mixed model adjusted for baseline value; the correlation between changes in

FAST scores at EOT and liver histology and biomarkers of metabolism, inflammation and fibrosis was also evaluated.

Results: Mean (SD) FAST score at baseline was 0.55 (0.22), similarly distributed in the 3 treatment arms, with 34% at high-risk NASH, 45% at indeterminate risk and 21% at low-risk. At EOT, FAST significantly decreased from baseline, with mean absolute changes of -0.22 and -0.23 for lanifibranor 800 and 1200 mg respectively (both $p < 0.01$), and -0.09 for placebo. Mean FAST score at EOT was 0.31 for both lanifibranor arms and 0.51 for placebo; 67% in both lanifibranor and 27% in placebo arms had FAST ≤ 0.35 (low-risk) at EOT. Decreases in FAST scores correlated with histological end point 'resolution of NASH and improvement of fibrosis', and with improvement in triglycerides, Apo-C3 and ferritin levels.

Conclusion: Treatment of NASH patients with F2/F3 fibrosis with lanifibranor for 24 weeks leads to a significant reduction of the FAST score compared to placebo and this decrease correlates with improvements in liver histology and biologically relevant biomarkers responses. These results not only support the histological efficacy data but also the potential of the FAST score as a NIT to monitor disease progression and response to therapy.

SAT121

Effect of smartphone-assisted lifestyle intervention in patients with metabolic-associated fatty liver disease (MAFLD): a preliminary analysis of a randomized controlled trial

Suraphon Assawasuwannakit¹, Apichat Kaewdech¹, Chaitong Churuangsuk¹, Naichaya Chamroonkul¹, Pimsiri Sripongpun¹. ¹Prince of Songkla University, Medicine, Hat Yai, Thailand

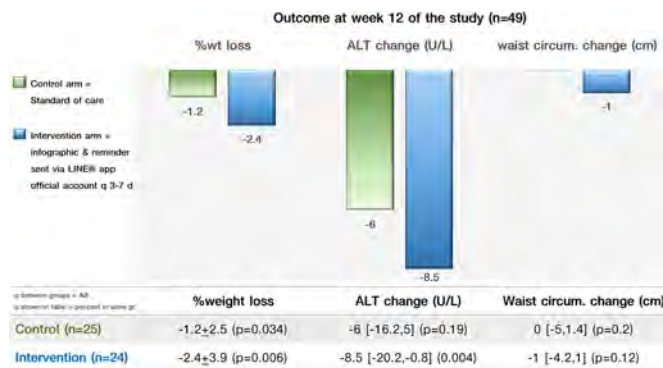
Email: pim072@hotmail.com

Background and aims: Patients with metabolic-associated fatty liver disease (MAFLD) are on the rise globally. While therapeutic medications are being studied, the mainstay of treatment is lifestyle intervention (LSI), but adherence to LSI and weight loss are difficult to achieve. We hypothesized that providing LSI and MAFLD information, as well as encouraging LSI through a social media application, would improve clinical outcomes in MAFLD more than standard of care (SOC).

Method: This is a preliminary result of a randomized controlled study in noncirrhotic MAFLD patients (defined as an international expert consensus statement 2020) aged 18–65 years in Thailand. Patients with active malignancy, current pioglitazone treatment, coexisting other liver diseases, and unstable cardiovascular/neurological conditions were excluded. Eligible patients were randomly assigned to control (SOC) and intervention arm. In the control arm, patients receive standard LSI advice from a single hepatologist; whereas in the intervention arm, in addition to SOC, the investigator sent infographics about MAFLD and LSI information and reminded patients to do LSI every 3–7 days via a social media app popular in Thailand (LINE®) using the study's official account. The outcomes are changes in liver steatosis (measured by controlled attenuated parameter) and fibrosis (measured by liver stiffness) by Fibroscan® at 24 weeks, as well as weight loss, body composition, and serum alanine aminotransferase (ALT) level between the two groups.

Results: So far, 80 patients were enrolled. Of those, 49 patients had week12 follow-ups for weight, waist circumference, and ALT. The mean age of these patients was 51 ± 7 years, 69% were female, mean body mass index (BMI) was 28.3 ± 4.2 kg/m², and 17% had diabetes. There were 25 and 24 patients in the control and intervention arm, respectively. Overall, the patients had a lower BMI at week12 compared to their baseline (median delta BMI -0.4 [IQR: $-0.1, 0.04$] kg/m², $p = 0.003$). Figure 1 depicts the percentage weight loss, ALT,

and waist circumference change in each group. When compared to baseline, patients in the intervention group had a significant reduction in weight (-2.4% , $p=0.006$) and ALT level (-8.5 U/L, $p=0.004$); whereas patients in the control group had a significant decrease in weight (-1.2% , $p=0.034$) but not ALT level (-6 U/L, $p=0.19$). The intervention group had a greater reduction in percent weight loss and ALT than the control group, but the statistically significant levels were not reached.



Conclusion: In this preliminary result, encouraging LSI and delivering MAFLD information via social media application to patients with MAFLD resulted in a significant reduction in weight and ALT level compared to baseline, and the results appeared to be better than SOC. However, the complete data of all eligible patients as well as change in liver steatosis and fibrosis is yet to be confirmed.

SAT122

Efficacy and mechanism of time-restricted fasting in non-alcoholic liver disease

Jiang Deng¹, Dandan Feng¹, Ning Gao¹, Juanjuan Shi¹, Shuangso Dang¹. ¹The Second Affiliated Hospital of Xi'an Jiaotong University, Department of Infectious Disease, Xi'an, China
Email: dang212@126.com

Background and aims: Non-alcoholic fatty liver disease (NAFLD) lacks specific treatment drugs. The aims of this study were to analyze the efficacy and mechanism of time-restricted fasting (TRF) in the treatment of NAFLD.

Method: Thirty-two male rats were randomly divided into three groups: Normal group, which was given a standard diet; NAFLD group, which was given a 60% high-fat diet; and TRF group, which was given a 60% high-fat diet, eating was allowed for 6 hours per day. After 15 weeks, the liver lipidomics and other indicators were determined, detected, and compared.

Results: A total of 1062 metabolites were detected. Compared with the Normal group, weight, body fat ratio, aspartate aminotransferase, total cholesterol, low-density cholesterol, fasting blood glucose, uric acid and the levels of 317 lipids in the NAFLD group were higher, whereas 265 lipids were down-regulated ($p < 0.05$). Compared with the NAFLD group, weight, body fat ratio, daily food intake, and the levels of 253 lipids in the TRF group were lower; 82 lipids were up-regulated ($p < 0.05$), serum triglyceride level was increased, but there was no statistical significance ($p > 0.05$). Kyoto Encyclopedia of Genes and Genomes pathway enrichment was conducted according to the results of differential metabolites, and the results showed that the pathways involved mainly included metabolic pathways, regulation of lipolysis in adipocytes, fat digestion and absorption, etc. Reverse transcription polymerase chain reaction proved that TRF improved the abnormal expression of FAS and PPAR α genes in the NAFLD group ($p < 0.05$).

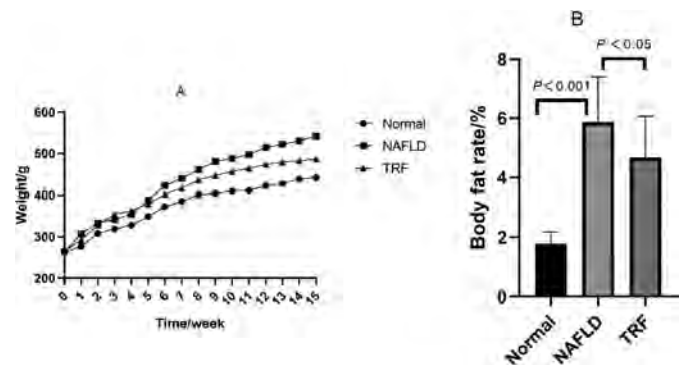


Figure 1: Physical characteristics of rats: (A) Body weight from 1 to 15 weeks (g); (B) body fat rate (%). The data are presented as means \pm SD or the median.

Conclusion: Six hours of time-restricted fasting improves non-alcoholic fatty liver disease by regulating lipid synthesis and metabolism, without an excessive increase in triglyceride levels.

SAT123

Functionalizing novel cancer related genes in liver disease and liver regeneration

Nooshin Nourbakhsh^{1,2}, Torsten Wuestefeld^{1,3,4}, Agnes Bee Leng Ong¹, Rong Gao¹. ¹Genome institute of Singapore, In vivo genetics and gene therapy, Singapore, Singapore; ²Yong Yoo Lin School of Medicine, National university of Singapore, Medicine; ³National Cancer Centre Singapore, Singapore; ⁴Nanyang Technological University, School of Biological Sciences, Singapore
Email: nnourbakhsh@gis.a-star.edu.sg

Background and aims: Caloric abuse and an inactive lifestyle have led to a widespread obesity and metabolic syndrome epidemic. Non-alcoholic fatty liver disease (NAFLD) and non-alcoholic steatohepatitis (NASH) are considered to be the hepatic consequence of it. As NAFLD/NASH condition are highly prevalent and drives a growing incidence rate of HCC, it is considered to be an important and alarming health issue. The critical question how the combination of an inflammatory microenvironment, created by NAFLD/NASH, abnormal metabolism and ongoing liver regeneration contributes to DNA instability and as a consequence promotes cancer is still unanswered. By this project we aim to reveal new relevant biomarkers for early and easier detection, treatment stratification and monitoring as well as approaches to therapies for both prevention and treatment in people who are at high risk for presenting fatty liver associated HCC to improve human health border.

Method: We take advantage of *in vivo* functional genomics screen in a mouse model of progressive fatty liver disease (Choline deficient high fat diet) to address this question. We screened a mir30 based shRNA library targeting 1000 genes, which human orthologs showed dysregulation in cancer. Scoring shRNAs will be validated *in vitro* as well as *in vivo* for influencing cell proliferation, survival and transformation and further will investigate the underlying mechanism with the goal for therapeutic intervention in disease progression.

Results: Computational analysis of shRNA abundance comparing CDHFD vs normal chow group shows selective enrichment for a number for targets. *In vitro* Knockdown of target genes show significant increasing in cell proliferation compared to control group. Short listed targets proceed for *in vivo* validation in NASH mouse model as well as *in vivo* liver repopulation and regeneration assay.

POSTER PRESENTATIONS

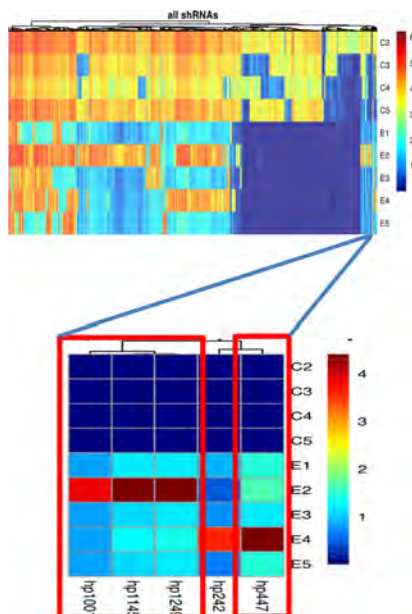


Figure: RNAi screen under CDHF diet, significant enriched shRNAs selected for in detail characterization.

Conclusion: In vivo functional genetic screen identifies new regulators of NASH related liver cancer development.

SAT124

Effect of long-term dietary intervention on liver pathology and markers of hepatocellular senescence in the GAN diet-induced obese mouse model of NASH

Kristoffer Voldum-Clausen¹, Denise Oró¹, Martin Rønn Madsen¹, Mathias Flensted-Jensen², Cecilie Holmegaard Andersen², Steen Larsen², Henrik B. Hansen¹, Michael Feigh¹. ¹Gubra, Hørsholm, Denmark; ²Xlab, University of Copenhagen, Denmark
Email: kristoffervc@gmail.com

Background and aims: Lifestyle change remains the first-line intervention for non-alcoholic steatohepatitis (NASH). This study aimed to evaluate long-term low-caloric dietary intervention on liver disease and markers of hepatocellular senescence in the GAN (Gubra-Amylin NASH) diet-induced obese (DIO) mouse model of NASH with hepatic fibrosis.

Method: Male C57BL/6 mice were fed the GAN diet high in saturated fat, fructose, and cholesterol for 34 weeks prior to study start. A liver biopsy was sampled 4-weeks prior to study start. Only animals with biopsy-confirmed steatosis (score ≥ 2) and fibrosis (stage $\geq F1$) were included and stratified into treatment groups. DIO-NASH mice were kept on the GAN diet or received dietary intervention by switching to chow feeding (chow-reversal) for 8, 16 or 24 weeks (n = 14–16 per group). Chow-fed C57BL/6J mice (n = 10) served as normal controls. Pre-to-post liver biopsy histology was performed for within-subject evaluation of NAFLD Activity Score and Fibrosis Stage. Terminal quantitative liver histology, RNA sequencing, blood and liver biochemistry was assessed. Liver senescence markers included p21 histomorphometry, mitochondrial respiratory capacity and gene expression signatures.

Results: Chow-reversal promoted substantial benefits on metabolic outcomes and liver histology, as demonstrated by robust weight loss, complete resolution of hepatomegaly, hypercholesterolemia,

elevated transaminase levels and hepatic steatosis in addition to attenuation of inflammatory markers. Notably, all DIO-NASH mice demonstrated ≥ 2 point significant improvement in NAFLD Activity Score following dietary intervention. While not improving fibrosis stage, chow-reversal (≥ 16 weeks) reduced quantitative fibrosis markers (PSR, collagen 1a1, α -SMA). Notably, these changes were accompanied by improved liver mitochondrial respiration, complete reversal of p21 overexpression and partial reversal of hepatocellular senescence-associated gene expression signatures.

Conclusion: Chow-reversal substantially improved metabolic, biochemical, and histological hallmarks of fibrosing NASH. Interestingly, molecular signatures of hepatocellular senescence in GAN DIO-NASH mice were also improved following long-term low-caloric dietary intervention, making the model suitable for profiling emerging senotherapeutics targeting senescent hepatocellular cells for the treatment of NASH.

SAT125

Fecal microbiota transplant using endoscopic-placement hydrogel reduces liver fibrosis with no changes in steatosis in a rat model of steatohepatitis with fibrosis

Ramon Bartoli^{1,2}, Ignacio Iborra^{1,3}, Sandra Barbosa⁴, Maria Doladé⁵, Marta Fortuny⁶, Helena Masnou^{2,3}, Rosa M Morillas^{2,3}. ¹Health Research Institute Germans Trias i Pujol (IGTP), Hepatology Unit, Gastroenterology Department, Badalona, Spain; ²Centre for Biomedical Research in Liver and Digestive Diseases Network (CIBERehd), Hepatology Unit, Gastroenterology Department, Badalona, Spain; ³Hospital Germans Trias i Pujol, Hepatology Unit, Gastroenterology Department, Badalona, Spain; ⁴Universitat Autònoma de Barcelona, Department of Cell Biology, Physiology and Immunology, Faculty of Veterinary Medicine, Bellaterra, Spain; ⁵Hospital Germans Trias i Pujol, Clinical Analysis and Biochemistry Department, Badalona, Spain; ⁶Hospital Germans Trias i Pujol, Gastroenterology Department, Badalona, Spain
Email: rbartoli@igtp.cat

Background and aims: Intestinal microbiota (IM) has emerged as a key factor conditioning the development and progression of non-alcoholic fatty liver and although fecal microbiota transplant (FMT) has been proposed as a promising therapeutic strategy, effective colonization of the colon is difficult to achieve. Our group has developed an endoscopic placement hydrogel able to release substances (covergel) that used as a carrier could improve FMT. We aimed to assess the role of IM in the mechanisms leading to steatosis and fibrosis and to compare the efficacy of covergel for FMT delivery with single colonoscopy vs the standard-method, in a rat model of steatohepatitis with fibrosis.

Method: 24 rats were fed with a diet rich in fat/cholesterol/fructose throughout the study (15 weeks) and carbon tetrachloride was injected for 12 weeks (NASH rats). 6 rats (healthy controls) were standard chow fed. At week 12, feces were collected to: 1) assess microbiota phylogenetic profile, and 2) pooled and cryopreserved as "NASH feces" and "healthy feces" for FMT. At week 13, NASH rats were randomized in 3 groups and underwent FMT by single colonoscopy to receive: group 1: 0.5 ml of healthy feces in 3.5 ml of saline (standard method); group 2: 0.5 ml of healthy feces in 3.5 ml covergel (HF-covergel-FMT); group 3: 0.5 ml of NASH feces in 3.5 ml covergel. Rats were euthanized at week 15 and fibrosis (Mason's Trichrome staining) and steatosis (Oil Red staining) degrees were assessed in liver samples. Plasma biochemical parameters were also quantified.

Results: In comparison to control rats, NASH rats didn't develop increased significant body weight gain but an increased in liver to body weight ratio was detected in NASH rats but not in HF-covergel-FMT rats. Levels of albumin, bilirubin, glucose, cholesterol and triglycerides were not altered in any group. ALT and phosphatase alkaline were significantly elevated whereas LDL and HDL-cholesterol significantly reduced in NASH rats. No differences were observed in phosphatase alkaline and LDL-cholesterol between HF-covergel-FMT and control rats.

Standard-FMT was not effective in reversing liver fibrosis, although a non-significant improvement was observed (group 1 vs group 3, $p = 0.084$). In contrast, HF-covergel-FMT was effective in reducing liver fibrosis (group 2 vs group 3; $p = 0.001$). Moreover, HF-covergel-FMT showed a significant improvement on fibrosis compared to standard-FMT (group 1 vs group 2; $p = 0.034$). FMT had no significant effect on steatosis.

Conclusion: HF-covergel-FMT significantly reduces liver to weight ratio, normalizes phosphatase alkaline and LDL-cholesterol and significantly reduces fibrosis without significant attenuation of the ongoing steatosis. The use of covergel would be an advantage, since the prolonged residence time of the hydrogel adhered to the mucosa would facilitate microorganism colonization with a single colonoscopy.

SAT126

Reversing diet-induced steatohepatitis and CCl₄ induced fibrosis with AN1284 treatment

Rinat Abramovitch^{1,2}, Adi Yehezkel², Nathalie Nachmansson^{1,2}, Marta Weinstock³. ¹Hebrew University-Hadassah Medical Center, The Wohl Institute for Translational Medicine, Jerusalem, Israel; ²Hebrew University-Hadassah Medical Center, The Goldyne Savad Institute of Gene Therapy, Jerusalem, Israel; ³Hebrew University, School of Pharmacy, Institute for Drug Research, Jerusalem, Israel
Email: rinat@hadassah.org.il

Background and aims: Non-alcoholic fatty liver disease (NAFLD) is the leading cause of chronic liver disease that can progress to more aggressive non-alcoholic steatohepatitis (NASH). The molecular and metabolic changes occurring in the development and progression of NAFLD to NASH include oxidative stress, chronic hepatic inflammation and fibrosis. So far, there are no effective drug treatments for NASH. AN1284 is an indoline derivative that exhibits potent antioxidant and anti-inflammatory activities in mice with LPS-activated acute liver damage. The aim of the current study was to determine whether AN1284 could reverse steatosis and fibrosis in a mouse model of pre-existing NASH.

Method: The effect of chronic treatment with AN1284 (1 mg/kg/day) by mini-pumps on pre-existing hepatic steatosis and fibrosis, was examined in two mouse models: (I) western dietary (WD) induced NASH for 6 month and (II) CCl₄ induced liver fibrosis. RNA-Seq was used to assess whether changes in cellular processes that occur in human subjects with NASH exists in these mice, and whether they are reversed by AN1284 treatment.

Results: AN1284 treatment (1 mg/kg/day) significantly attenuated liver damage, reduced liver/body ratio, liver fat content and serum ALT levels in dietary induced NASH, and hepatic fibrosis in both models. RNA sequencing showed that the WD significantly elevated the hepatic pathways of steatosis, fibrosis, inflammation, oxidative stress and liver damage seen in human subjects. AN1284 reduced oxidative stress (iNOS) and fibrosis, in association with a decrease in collagen-4 and TGF-beta. RNA-Seq analysis revealed the altered pathways including FXR/RXR, fatty-acid synthase and inflammation (Fig).

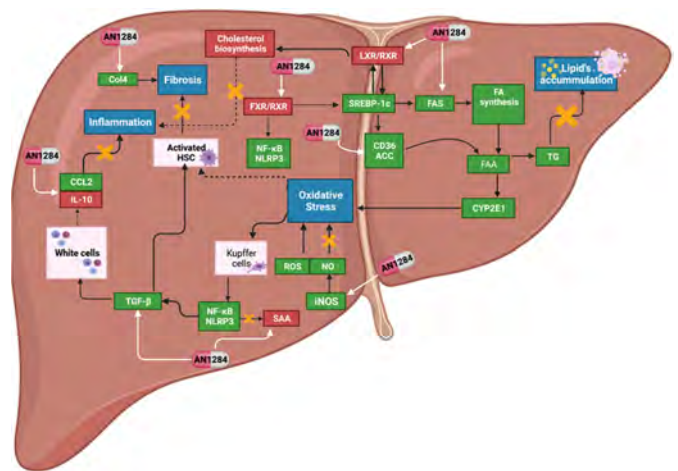


Figure: Summary of changes induced by AN1284 treatment to mice with WD-induced NASH. Up-regulated factors are shown in red and the down-regulated are shown in green.

Conclusion: The diet used in this study reproduced liver pathology in human subjects with NASH. Chronic AN1284 treatment reversed pre-existing steatosis and fibrosis by reducing several factors involved in disease development.

SAT127

Spontaneous and drug-induced histological changes in non-alcoholic steatohepatitis: an assessment by meta-analysis of trials

Grazia Pennisi¹, Ciro Celsa¹, Marco Enea¹, Marco Vaccaro², Vito Di Marco¹, Carlo Ciccioli¹, Giuseppe Infantino¹, Stefanie Parisi¹, Claudia La Mantia¹, Antonio Craxi¹, Calogero Camma¹, Salvatore Petta¹. ¹Section of Gastroenterology and Hepatology, Dipartimento Di Promozione Della Salute, Materno Infantile, Medicina Interna e Specialistica Di Eccellenza (PROMISE), Palermo, Italy; ²Dipartimento di Scienze Economiche, Aziendali e Statistiche, University of Palermo, 90133 Palermo, Italy
Email: graziaipennisi901@gmail.com

Background and aims: Non-alcoholic steatohepatitis (NASH) has a variable rate of progression, making the effect of investigational drugs difficult to assess and compare. In this study, we provide by meta-analysis a reference standard for histological progression of untreated NASH (patients receiving placebo), and perform a network meta-analysis to estimate the relative efficacy of investigational drugs for NASH.

Method: A comprehensive search of several databases was conducted to detect phase 2 and 3 randomized controlled-trials (RCTs) comparing pharmacological interventions in patients with non-cirrhotic NASH. Resolution of NASH without worsening of fibrosis or ≥ 1 stage reduction of fibrosis without worsening of NASH were evaluated as composite outcomes validated by Food and Drug Administration (FDA). Meta-analysis and meta-regressions were performed on placebo arms, and a network meta-analysis on interventions arms.

Results: A total of 15 RCTs met the eligibility criteria. The meta-analysis on untreated patients arms showed a pooled estimate rate of 17% (95% C.I. 12%-23%; $I^2 = 86\%$; $p < 0.01$) and of 21% (95% C.I. 13%-31%; $I^2 = 84\%$; $p < 0.01$) for resolution of NASH without worsening of fibrosis and ≥ 1 stage improvement of fibrosis without worsening of NASH, respectively. Phase 3 RCTs, older age and higher AST levels were associate to a lower rate of spontaneous improvement at univariate meta-regression analysis. By network meta-analysis, semaglutide and pioglitazone, alone or plus Vitamin E, had the highest ranking of effectiveness for NASH resolution without worsening of fibrosis (P-score 0.906, 0.890 and 0.826, respectively). Aldafermin, lanifibranor and obeticholic acid had the highest probability to achieve ≥ 1 stage of fibrosis improvement without

POSTER PRESENTATIONS

worsening of NASH (P-score 0.776, 0.773 and 0.711, respectively). When combining the two outcomes, lanifibranor, semaglutide and aldafermin were the most effective drugs.

Conclusion: Since semaglutide and pioglitazone appear to be more effective on NASH activity while aldafermin, lanifibranor and obeticholic acid perform better on the evolution of fibrosis, combination therapies should be assessed prospectively in subjects who are less likely to improve spontaneously over time, i.e. older patients with biochemically active disease.

SAT128

Synergistic activity of GLP-1 peptide analog XW003 and the long-lasting GIP receptor agonist XW017 in a diet induced obese mouse model

Xinle Wu¹, Haixia Zou¹, Bin Wang¹, Rui Zhu¹, Yan Li¹, Wanjun Guo¹, Catherine Jones², Martijn Fenaux². ¹Sciwind Biosciences, China;

²Sciwind Biosciences, United States

Email: catherine.jones@sciwindbio.com

Background and aims: Glucagon-like peptide-1 (GLP-1) and glucose-dependent insulinotropic peptide (GIP, also known as gastric inhibitory polypeptide) are small peptide hormones termed incretins. Incretins are produced by the gut following food intake and act to stimulate insulin secretion and lower blood sugar. Incretins have additional effects on the digestive tract, liver, pancreas, and central nervous system to maintain metabolic health. GLP-1 receptor agonists have shown promise for treating obesity, type 2 diabetes, and non-alcoholic steatohepatitis (NASH); GIP receptor agonists have the potential to work synergistically with GLP-1 agonists to enhance efficacy.

Method: We investigated GLP-1 peptide analog, XW003 (3 nmol/kg), alone or in combination with a long-lasting GIP peptide analog, XW017 (3, 10, 30, 100 nmol/kg), in the diet induced obese (DIO) mouse model. GLP-1 and GIP peptide analogs were dosed subcutaneously QD for 27 days (n = 6 animals per group). We also evaluated in parallel the activity of a dual GLP-1/GIP receptor agonist, tirzepatide (10 nmol/kg), in this mouse model.

Results: Treatment of mice with the GLP-1 analog XW003 alone resulted in mean body weight loss of 15.6% compared to baseline after 27 days of treatment. Treatment of mice with the GIP analog XW017 alone did not result in significant weight loss (0% compared to baseline at day 27). Combination of XW003 (3 nmol/kg) with XW017 showed an enhanced effect in inducing body weight loss compared to either peptide alone, with mean weight reductions of 24.6% (XW003 + 30 nmol/kg XW017) and 28.3% (XW003 + 100 nmol/kg XW017), respectively, at the end of treatment. In comparison to tirzepatide, combination of XW003 and XW017 showed comparable or higher levels of weight loss. At day 14, tirzepatide (10 nmol/kg) treatment resulted in a 25.8% weight reduction compared to baseline, while the animals treated with a combination of XW003 (10 nmol/kg) and XW017 (100 nmol/kg) produced a mean weight loss of 33.9%.

Conclusion: In conclusion, combinatory treatment of GLP-1 and GIP receptor agonists showed a synergistic effect on promoting weight loss in a mouse model of obesity.

SAT129

Preclinical pharmacology of low molecular weight GLP-1 receptor agonist XW014

Wanjun Guo¹, Xinle Wu¹, Haixia Zou¹, Bin Wang¹, Rui Zhu¹, Catherine Jones², Martijn Fenaux². ¹Sciwind Biosciences, China;

²Sciwind Biosciences, United States

Email: catherine.jones@sciwindbio.com

Background and aims: Glucagon-like peptide-1 (GLP-1) is a peptide hormone produced by the gut in response to food intake and then rapidly degraded. GLP-1 has multiple beneficial effects on metabolism, including delaying gastric emptying and increasing satiety, stimulating insulin secretion and lowering blood sugar, reducing liver fat, and promoting weight loss. GLP-1 peptide analogs have shown

promise for treating obesity, type 2 diabetes, and non-alcoholic steatohepatitis (NASH). XW014 is a small molecule GLP-1 receptor agonist with improved oral bioavailability and cardiovascular safety. Here we evaluated XW014 in vitro and in vivo activity.

Method: GLP-1 receptor agonism was evaluated in vitro by assessing cAMP production in HEK-293 cells. cAMP production in cells treated for 30 minutes with XW014 or comparator was quantified by HTRF-based assay (Cisbio). C57BL/6 mice expressing humanized GLP-1 receptor were dosed with XW014 (50 mg/kg PO BID) or vehicle (n = 4 animals per group) for 4 days. Weight, cumulative food intake, post-prandial glucose, glucose tolerance, and insulin secretion were measured. Cynomolgus monkeys (n = 5) were given a single dose of XW014 (20 mg/kg PO). Intravenous glucose tolerance test (IVGTT) was performed 2 hours after oral dosing.

Results: XW014 showed potent GLP-1 receptor agonist activity in cell culture, with a mean EC₅₀ value of 0.44 ± 0.2 nM. In mice expressing the human GLP-1 receptor, treatment with XW014 (50 mg/kg BID) for 4 days resulted in reduced blood glucose, food intake, and body weight. In cynomolgus monkey, treatment with a single dose of XW014 (20 mg/kg) resulted in improved blood glucose suppression and insulin response during IVGTT compared to baseline.

Conclusion: XW014 is a potent small molecule agonist of the GLP-1 receptor in vitro and induces effective target engagement in two preclinical models, humanized GLP-1 mice and cynomolgus monkeys. The results support the continued development of XW014 for the treatment of metabolic disease.

SAT130

Integrated transcriptomics of CRV431 treatment in a Phase 2a NASH trial confirms anti-fibrotic effect of pan-cyclophilin inhibition and identifies CRV431-specific biomarkers

Patrick Mayo¹, Stephen Harrison², Todd Hobbs¹, Daren Ure¹, Daniel Trepanier¹, Erin Foster¹, Caroline Zhao¹, Robert Foster¹. ¹Hepion Pharmaceuticals, Edison, United States; ²Pinnacle Clinical Research, Austin, United States

Email: pmayo@hepionpharma.com

Background and aims: The progression of liver fibrosis in Non-Alcoholic Steatohepatitis (NASH) has been directly linked to increased mortality and morbidity. To date, numerous drug candidates have failed to show a significant benefit in fibrotic end points for NASH patients enrolled in clinical trials. CRV431, a non-immunosuppressive pan-cyclophilin inhibitor has demonstrated pleiotropic effects well-suited for the treatment of NASH and fibrosis. A new transcriptomic analysis was performed to further elucidate the action of CRV431 in subjects with biomarker defined F2/F3 NASH and explore transcriptomic markers for clinical responsiveness.

Methods: RNA sequencing data was obtained from 27 patients with biomarker confirmed F2/F3 NASH participating in a 28-day, Phase 2a trial of CRV431 (NCT04480710). Subjects were administered CRV431 75 mg, 225 mg, or placebo orally once daily for 28 days. RNA was stabilized and isolated from whole blood on Day 1 and Day 28. RNA sequencing transcripts were evaluated using FastQC, with quantification in Salmon v1.4.0. Differential expression analysis (DEA) was performed using edgeR. Co-expression networks were constructed using weighted gene co-expression network analysis (WGCNA). DEA was combined with WGCNA to enhance the discriminating ability of highly related genes as potential biomarkers. Functional enrichment was performed using clusterProfiler and GeneWalk, followed by key hub gene selection.

Results: Consistent with pre-clinical models, CRV431 down-regulated several collagen genes including COL6A5 (log2Fold = -2.2, p = 0.04), COL7A1 (log2Fold = -4.7, p = 0.0052), COL8A2 (log2Fold = -4.8, p = 0.00076), COL13A1 (log2Fold = -2.4, p = 0.02), COL18A1 (log2Fold = -3.1, p = 0.03). WGCNA analysis identified separate gene modules where CRV431 regulated C6M (r = 0.72, p < 10⁻²⁰⁰), ProC3 (r = 0.78, p < 10⁻²⁰⁰) and ALT (r = 0.59, p = 8.9 × 10⁻¹³⁶) production. The ProC3 module demonstrated involvement in collagen

regulation (COL4A2, COL6A2) while the ALT-module demonstrated a mixture of collagen (COL13A1, COL18A1, COL7A1), anti-inflammatory (IL1RL2, IL17RB) and regulatory effects on cholesterol and ceramide biosynthesis. The C6M module included genes linked to inflammatory and immune responses (IL17RE, IL31RA, IL32, IL7R, LOXL2).

Conclusion: Integrated transcriptomic analysis confirmed anti-fibrotic and anti-inflammatory effects of CRV431 in NASH subjects and suggested regulation of cholesterol and ceramide biosynthesis. Potential biomarker panels were identified to predict ProC3, ALT, and C6M responsivity to CRV431. A paired biopsy Phase 2b study will be conducted to investigate the link of this biomarker panel to NASH histopathology.

SAT131

Pharmacokinetic (PK) and pharmacodynamics (PD) of BIO89-100, a novel glycoPEGylated FGF21, in non-alcoholic steatohepatitis (NASH) patients with compensated cirrhosis

Naim Alkhouri¹, Will Charlton², Hank Mansbach², Maya Margalit³, Kemal Balic², Leo Tseng^{2,4}. ¹Arizona Liver Health; ²89bio, Clinical Development, San Francisco, United States; ³89bio, Clinical Development, Herzliya, Israel; ⁴89bio, Clinical Development, San Francisco

Email: leo.tseng@89bio.com

Background and aims: BIO89-100 is a long-acting glycoPEGylated analogue of fibroblast growth factor 21 (FGF21) in development for the treatment of non-alcoholic steatohepatitis (NASH) and severe hypertriglyceridemia. PK/PD of BIO89-100 was previously characterized in a multiple-ascending dose (MAD) study in noncirrhotic NASH patients (fibrosis stage F1-3). This phase 1 study was designed to characterize the PK/PD properties of BIO89-100 in adult patients with compensated cirrhosis from NASH (F4) and evaluate the effect of cirrhosis on BIO89-100 PK/PD.

Method: This Phase 1, open-label, single-center study in the USA enrolled a total of 8 adult patients with diagnosed compensated cirrhosis (F4) due to NASH based on Liver Forum criteria. Patients received a single 30 mg dose liquid formulation of BIO89-100 via subcutaneous (SC) injection on Day 1. Blood samples for PK and PD assessments were collected before and at predetermined timepoints after BIO89-100 administration. PK parameters were estimated using a non-compartmental approach. As part of exploratory objectives, PD end points from the lipid panel (i.e., triglycerides [TGs], total cholesterol, low-density lipoprotein cholesterol [LDL-C] and high-density lipoprotein cholesterol [HDL-C]) were evaluated as the absolute change and percent change from baseline to Day 8. PK/PD data were consequently compared to historic findings from the MAD study.

Results: A prespecified interim PK/PD analysis was conducted using data from the first 6 patients for PK and all 8 patients for PD. The majority of patients were female (62.5%); mean age was 53.3 years; mean BMI was 37.4 kg/m²; mean VCTE was 28.9 kPa. Following a single 30 mg SC dose in patients with F4 fibrosis, BIO89-100 serum concentration declined in a monophasic fashion with the mean elimination half-life of 62 hours consistent with previous studies. PK exposure differences in F4 patients in this study vs. F1-3 patients in the MAD study were negligible and within a clinical PK variability. Simulated PK profiles using already developed popPK model based on F1-3 data adequately described the F4 PK (Figure). Moreover, BIO89-100 had a robust effect compared to baseline on serum TGs (up to 44% reduction), HDL-C (up to +55% increase), and LDL-C (up to 29% reduction) on Day 8 in patients with F4 NASH. A favorable safety and tolerability profile was observed in this study.

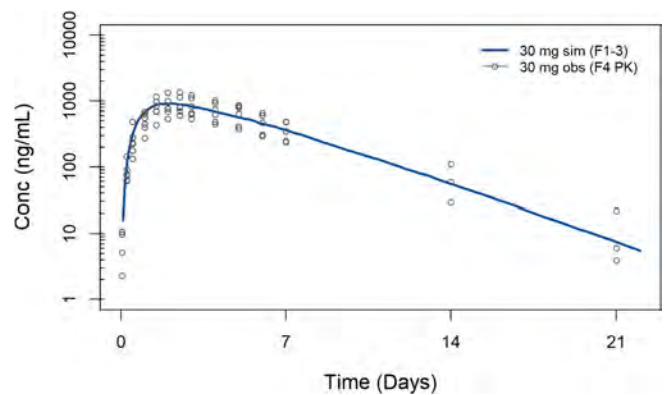


Figure: Simulated (F1-F3) vs. Observed PK Profiles from F4 Patients.

Conclusion: The interim PK/PD data indicate BIO89-100 elicits a robust PK/PD effect independent of NASH fibrosis stage. These findings highlight the feasibility of achieving favorable treatment outcomes in F4 patients with compensated hepatic function without requiring dose adjustment. Overall, these PK/PD properties warrant further investigation to allow assessments of effectiveness of BIO89-100 in a larger F4 population.

SAT132

HEC96719, a novel tricyclic farnesoid X receptor agonist for treatment of non-alcoholic steatohepatitis: results of preclinical study and phase I trial

Shengtian Cao^{1,2}, Xinye Yang¹, Liting Dai¹, Jing Li¹, Ying Jun Zhang¹, Xiaojun Wang¹, Yan Wang². ¹Sunshine Lake Pharma Co Ltd, HEC Pharm Group, HEC Research and Development Center, Dongguan, China; ²Southern Medical University, Biomedical Research Center

Email: yanwang@smu.edu.cn

Background and aims: Current options for therapeutic treatment of NASH are limited. FXR is an effective target modulating important pathways in NASH liver. Here we report the development, preclinical study and phase I trial of HEC96719 a novel tricyclic non-steroidal FXR agonist to identify its potential for NASH treatment.

Method: We designed a series of compounds with structural basis of a prior high-affinity nonsteroidal molecule GW4064. Among these compounds, we identified the ones with no toxicity and higher activity in *in vitro* and *in vivo* models. Then, we tested their distribution and bioavailability in animal models and determined their treatment effect on NASH mice. For the selected compound with the most favorable properties, i.e. HEC96719, we further analyzed its effect on FXR in terms of selectivity and efficacy, and determined its efficacy in various animal models of NASH and liver fibrosis in comparison with obeticholic acid. With supporting data, a phase I trial was then performed in 184 healthy participants at different centers to test the safety, tolerability, pharmacokinetics and surrogate activity of HEC96719 (NCT04546984, NCT04422496, NCT04194242).

Results: We successfully designed several compounds with potent activities and high efficacies on FXR. HEC96719 has a high selectivity for FXR according to the profiling assays with a panel of enzymes, ion channels, nuclear receptors, and G-protein coupled receptors. HEC96719 has a 150-fold higher agonistic potency on FXR than GW4064 and has a good bioavailability and stability. Its distribution in liver and ileum can be respectively 19-fold and 208-fold higher than that in plasma, indicating high effectiveness to sustain FXR activation and FGF15/19 expression. HEC96719 shows better therapeutic efficacy in NASH and liver fibrosis animal models than obeticholic acid. In the healthy participants, HEC96719 was well-tolerated at maximum dose and no severe adverse events were observed. Significant changes of FGF19 and bile acid synthetic intermediate were detected. Their levels were proportional to the increased exposure dosage of HEC96719.

POSTER PRESENTATIONS

Conclusion: These data on pharmacokinetic properties, efficacy and safety profiles overall indicate that HEC96719 is a promising drug candidate for NASH treatment. Planned clinical studies are warranted to further evaluate these effects.

SAT133

Effect of saroglitazar in reducing liver enzymes and liver stiffness in non-alcoholic fatty liver disease: a single arm prospective study

Avisek Chakravorty¹, Swetha Sattanathan², Krishnadas Devadas².

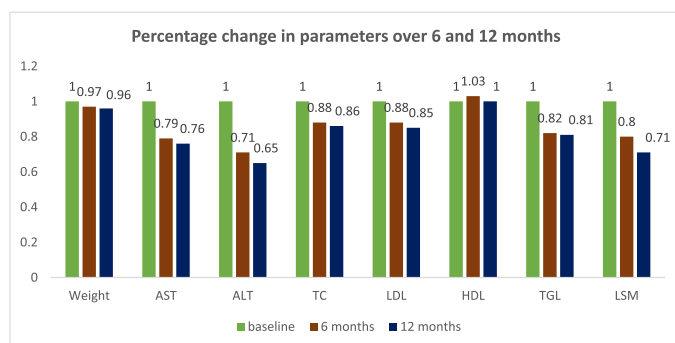
¹Government Medical College Thiruvananthapuram, Medical Gastroenterology, Thiruvananthapuram, India; ²Government Medical College Thiruvananthapuram, Medical Gastroenterology, Thiruvananthapuram, India

Email: avisek.doc@gmail.com

Background and aims: Non-Alcoholic Fatty Liver Disease (NAFLD) is fast becoming the leading cause of cirrhosis worldwide. But the pharmacotherapy of Non-Alcoholic Steatohepatitis (NASH) remains elusive. This trial was conducted to study the effects of the dual peroxisome proliferator-activated receptor (PPAR) agonist Saroglitazar (approved by Drugs Controller General of India for NASH) on liver fibrosis, transaminases and lipid profile in NAFLD patients

Method: Investigator initiated single arm prospective observational study. Consecutive patients of NAFLD (2016 EASL Clinical Practice Guidelines) with raised transaminases and liver stiffness (LSM) ≥ 7 kPa (by Transient Elastography) were started on Tab Saroglitazar 4 mg daily. Patients with pregnancy and lactation were excluded. AST/ALT, Lipid profile and LSM were measured at baseline, 6 months and 1 year

Results: 90 patients were started on Saroglitazar. Data was analysed for all patients at 6 months and for the 57 patients who completed 1 year of therapy. At 6 months and 1 year, there was a significant reduction in transaminases (20.8% and 23.6% reduction for AST, 29.5% and 35.4% reduction for ALT, $p=0.00006$). Mean liver stiffness reduced from 11.6 kPa at baseline to 9.4 at 6 months and 8.3 at 12 months (21.5% and 28.7% reduction, respectively, $p=0.000001$). For those with advanced liver fibrosis at baseline (TE ≥ 9.9 kPa), the reduction in LSM was 28.2% and 36% at 6 and 12 months, respectively. Total cholesterol, Low density lipoproteins (LDL) and triglycerides reduced significantly (14.5%, 15.3% and 18.6% respectively at 1 year, $p<0.05$). No significant difference in High density lipoproteins (HDL) could be found. Significant weight reduction was noted at 6 and 12 months compared to baseline (3.3% and 3.9% reduction respectively, $p=0.00004$). No serious adverse effects were noted in any of the patients while on therapy.



Conclusion: Saroglitazar seems to be a promising option for reduction of liver stiffness and transaminitis in NAFLD. Whether there is similar effect on liver histology has to be proven by biopsy-based studies.

SAT134

Intrahepatic microcirculation disorders and hyperammonemia and their correction at non-alcoholic steatohepatitis patients with initial stages of liver fibrosis

Tatiana Ermolova¹. ¹North-western state medical university named after I.I.Mecnnikov, Internal Medicine and Faculty, St.-Petersburg, Russian Federation

Email: t.v.ermolova@mail.ru

Background and aims: Ammonia is new therapeutic target for chronic liver diseases. Some experimental studies demonstrated, that ammonia increases of activity of hepatic stellate cells, stimulating liver fibrogenesis, impairs liver microcirculation, and these processes are reversible after the using of hypoammonemic medicines. Aims of our study are to estimate blood level of ammonia, intrahepatic microcirculation and efficacy of ornithine (Hepa-Merz) for correction of such disorders at the chronic liver diseases.

Method: We investigated 56 non-alcoholic steatohepatitis (NASH) and 45 HCV patients with initial fibrosis 0–1 stages. Level of ammonia was estimated by biochemical method (PocketChem BA, Arcray, Japan) in capillary blood at the patients and 37 healthy individuals (control), normal ammonia level is less than 60 $\mu\text{mol/L}$. Intrahepatic hemodynamics are determined by polyhepatography (PHG)-modified hepatic impedansometry, non-invasive method for integral estimation of intrahepatic blood flow by checking of tissue resistance to weak electric current. PHG registers a blood flow in projection of zone of hepatic right, left lobes and spleen, integral body impedansography. For correction of blood flow disorders we used hypoammonemic drug ornithine (Hepa-Merz) in dosage 3 grams 3 times daily 4 weeks. Efficacy of LOLA we looked in 2 and 4 weeks via the control PHG and control of ammonia.

Results: Analysis of PHG demonstrated, that at all patients we revealed a liver microcirculation disorders- increased blood resistance, abnormal forms and amplitude of waves in sinusoidal level (out flow zone) at NASH patients and presinusoidal level (inflow zone) at viral patients. Level of ammonia in the NASH patients was 137.2 $\mu\text{mol/L}$, in control group-49.3 $\mu\text{mol/L}$ ($p<0.01$). Hyperammonemia was higher at the NASH patients, compared with viral patients higher (102.3 $\mu\text{mol/L}$) ($p<0.01$). Analysis of efficacy of Hepa-Merz showed, that it was effective for correction of hepatic hemodynamic disorders at all patients, in 2 weeks of the treatment we observed normalization or improvement of the wave form, in 4 weeks-wave amplitude. Level of ammonia was decreased in 2 weeks.

Conclusion: NASH patients with initial stages of liver fibrosis are characterized by hyperammonemia, which is more pronounced in comparison with viral hepatitis. NASH is accompanied by disorders of intrahepatic microcirculation disorders in out flow zone. LOLA improved liver microcirculation and decreases of blood ammonia level at the NASH and HCV patients.

SAT135

Ticagrelor, but not clopidogrel, attenuated hepatic steatosis in a model of non-alcoholic fatty liver disease

Hyunwoo Oh¹, Hyo Young Lee¹, Huiyul Park², Dae Won Jun³, Eileen Yoon³, Sang Bong Ahn⁴, Chul-min Lee⁵, Mi Mi Kim⁵, Bo-Kyeong Kang⁵, Joo Hyun Sohn⁶. ¹UiJeongbu Eulji Medical Center, Department of Medicine, Gyeonggi-do, Korea, Rep. of South; ²UiJeongbu Eulji Medical Center, Department of Family medicine, Gyeonggi-do, Korea, Rep. of South; ³Hanyang University College of Medicine, Department of Medicine, Seoul, Korea, Rep. of South; ⁴Nowon Eulji Medical Center, Eulji University School of Medicine, Department of Medicine, Seoul, Korea, Rep. of South; ⁵Hanyang University College of Medicine, Department of Radiology, Seoul, Korea, Rep. of South; ⁶Hanyang University Guri Hospital, Hanyang University College of Medicine, Department of Medicine, Gyeonggi-do, Korea, Rep. of South

Email: bliss153@hanmail.net

Background and aims: Several studies have suggested that platelets are associated with inflammation and may play an important role in

hepatic inflammation. We tried to evaluate whether antiplatelet drugs could improve non-alcoholic fatty liver disease (NAFLD).

Method: Mice were fed a high-fat diet (HFD) to establish an NAFLD model, which was verified through pre-study liver biopsy at 18 weeks. Animals with an NAFLD activity score (NAS) ≥ 4 were randomized into HFD-only, clopidogrel (CLO; 35 mg/kg/day), and ticagrelor (TIC; 40 mg/kg/day) groups, which were then treated with the respective drug for an additional 15 weeks. Liver and blood samples were collected from all animals at 33 weeks.

Results: The TIC group, but not the CLO group, showed significantly lower degree of steatosis and NAS than the HFD group (HFD: 5.3 ± 0.9 , CLO: 4.6 ± 0.7 , TIC: 3.4 ± 1.2 ; $p = 0.0047$). Hepatic *de novo* lipogenesis markers (SREBP1c, FAS, SCD1, and DGAT2 expression) and mRNA expression of inflammatory markers only decreased significantly in the TIC treatment group. Endoplasmic reticulum (ER) stress markers (CHOP, Xbp1, and GRP78) also decreased significantly in the TIC group, but not in the CLO group. Nile red staining intensity decreased in HepG2 cells following TIC treatment. Hepatic *de novo* lipogenesis markers were decreased significantly in HepG2 cells after TIC treatment.

Conclusion: TIC, but not CLO, attenuated steatosis and NAS via inhibiting fat *de novo* synthesis as well as ER stress in the biopsy proven NAFLD animal model.

SAT136

Lemon balm extract ALS-L1023, an angiogenesis inhibitor, inhibits liver fibrosis in a non-alcoholic fatty liver disease model

Hyo Young Lee¹, Hyunwoo Oh¹, Eileen Yoon², Dae Won Jun², Sang Bong Ahn³, Huiyul Park⁴, Bo-Kyeong Kang⁵, Mi Mi Kim⁵, Chul-min Lee⁵, Joo Hyun Sohn⁶. ¹Uijeongbu Eulji Medical Center, Department of Medicine, Gyeonggi-do, Korea, Rep. of South; ²Hanyang University College of Medicine, Department of Medicine, Seoul, Korea, Rep. of South; ³Nowon Eulji Medical Center, Eulji University School of Medicine, Department of Medicine, Seoul, Korea, Rep. of South; ⁴Uijeongbu Eulji Medical Center, Department of Family medicine, Gyeonggi-do, Korea, Rep. of South; ⁵Hanyang University College of Medicine, Department of Radiology, Seoul, Korea, Rep. of South; ⁶Hanyang University Guri Hospital, Hanyang University College of Medicine, Department of Medicine, Gyeonggi-do, Korea, Rep. of South
Email: novableness@gmail.com

Background and aims: ALS-L1023 is an ingredient extracted from *Melissa officinalis* L. (Labiatae; lemon balm), which grows wild in Europe and the Mediterranean. ALS-L1023 is also known as a natural medicine that suppresses angiogenesis. Herein, we aimed to determine whether ALS-L1023 could alleviate non-alcoholic fatty liver disease (NAFLD).

Method: C57BL/6 wild-type male mice (age, 6-weeks-old) were fed a choline-deficient high-fat diet for 10 weeks to induce NAFLD. Two doses (a low dose, 8 g/kg/day; and a high dose, 12 g/kg/day) of the lemon balm extract, ALS-L1023, were selected and mixed with feed for administration. RNA sequencing was performed for the choline-deficient high-fat diet group, ALS-L1023 responder group, and ALS-L1023 non-responder group.

Results: There was no significant difference between the groups in mean final body weight or food intake. Biochemical analysis revealed that the ALS-L1023 low-dose group had significantly decreased alanine transaminase and aspartate transaminase compared to the choline-deficient high-fat diet group. Based on Sirius red staining, the area of fibrosis significantly decreased due to the administration of ALS-L1023, and the anti-fibrotic effect of ALS-L1023 was greater than that of obeticholic acid. RNA sequencing was performed after mice were divided into responder and non-responder groups. The responder group had lower expression of genes related to the hedgehog-signaling pathway than the non-responder group.

Conclusion: ALS-L1023 may exert anti-fibrotic effects in the NAFLD model.

SAT137

Hepatocyte-specific JNK signaling is protective during progression of NASH

Julia Piche¹, Ines Volkert¹, Marius Maximilian Woitok¹, Tobias Otto¹, Christian Trautwein¹. ¹Uniklinik RWTH Aachen, Aachen, Germany
Email: jpiche@ukaachen.de

Background and aims: The prevalence of non-alcoholic fatty liver disease, ranging from steatosis to non-alcoholic steatohepatitis (NASH), is increasing in developed countries. Mechanism leading to progression towards end-stage cirrhosis and hepatocellular carcinoma (HCC) are incompletely understood.

The c-Jun N-terminal kinases (JNKs) play a crucial role in liver physiology and disease pathogenesis. In the present study, we aimed to investigate the relevance of hepatocyte-specific Jnk1 and Jnk2 inhibition in two experimental NASH models.

Method: NASH was induced by feeding animals a Western-style diet (WSD) or a Choline-deficient high fat diet (CD-HFD) to compare disease development between wild-type (WT) and mice with a hepatocyte-specific deletion of Jnk1 and Jnk2 (JNK1/2^{Δhepa}).

Results: WSD and CD-HFD triggered significantly increased serum transaminases, as well as enhanced steatosis in JNK1/2^{Δhepa} compared to WT animals. Inflammation as evidenced by increased infiltration of immune cells, especially leukocytes and monocyte-derived macrophages, was significantly higher in JNK1/2^{Δhepa} mice. This was further strengthened by strongly increased liver cytokine and chemokine levels as well as an increased oxidative stress response. Furthermore, fibrogenesis was strongly increased in JNK1/2^{Δhepa} animals. Analysis of cell death mechanism revealed strongly increased apoptotic cell death, while necroptosis and pyroptosis was not changed. Thus, we generated JNK1/2^{Δhepa}/caspase 8^{Δhepa} animals and could show that the phenotype was rescued following WSD feeding.

Conclusion: Our results demonstrate that deletion of Jnk 1 and Jnk2 in hepatocytes increases NASH progression. Specifically, an increase in apoptotic cell death is crucial in mediating this effect. Thus, blocking caspase 8 in hepatocytes during an increased stress response may represent a promising therapeutic strategy for NASH.

SAT138

Semaglutide use in adjunct to multidisciplinary lifestyle interventions improves weight and body composition in NAFLD patients

Rochelle Wong¹, Steven Mathews¹, Carolyn Newberry², Sonal Kumar². ¹New York Presbyterian Hospital, Medicine, New York, United States; ²Weill Cornell Medicine, Medicine, New York, United States
Email: sok9028@med.cornell.edu

Background and aims: Non-alcoholic fatty liver disease (NAFLD) is an increasingly prevalent cause of liver disease as obesity rates continue to rise. Recent studies have shown that semaglutide in adjunct to lifestyle intervention is beneficial in treating weight and metabolic syndrome-related comorbidities such as type 2 diabetes (T2DM). Here we describe our single center experience with semaglutide in NAFLD patients.

Method: Patients with NAFLD per transient elastography seen in our multidisciplinary gastroenterology clinic between 2019 and 2021 who were initiated on semaglutide were included. All patients also underwent lifestyle counselling from a team of gastroenterologists, dietitians, and endocrinologists. Primary outcomes were measured by change in weight, body composition analysis via dual bioelectrical impedance analysis, liver chemistries such as alanine aminotransferase (ALT), and metabolic markers such as hemoglobin A1c (HbA1c) and lipid profile in patients on medication for >3 months. Paired t-tests were used for analysis.

Results: Seventy-two patients were prescribed semaglutide. Eleven discontinued due to side effects. Thirty-two were on semaglutide for <3 months at time of analysis. Thirty-three were maintained on semaglutide for at least 3 months and included in the analysis. Of this

cohort, 22 (66.7%) had T2DM, 7 (21.2%) had prediabetes, 5 (15.2%) were overweight, and 24 (72.3%) were obese with BMI >30. All 33 had follow-up labs, 20 with follow-up body composition analysis, and 10 with follow-up transient elastography. Median maximum semaglutide dose was 1.0 mg (IQR 0.5–1.0 mg) with median length of follow-up 281 days (range 92–921 days) after semaglutide initiation. Average weight loss achieved at follow-up was 8.45% ($p=0.001$, Figure 1). Other body composition parameters such as visceral fat area (VFA) (–7.64%, $p=0.01$), percent body fat (–3.46%, $p=0.03$), and truncal segmental fat mass (–7.52%, $p=0.01$) also significantly improved. ALT significantly decreased (–17.5 U/L, $p=0.04$) along with other metabolic parameters HbA1c (–0.7, $p=0.03$). Nausea was the most common adverse event.

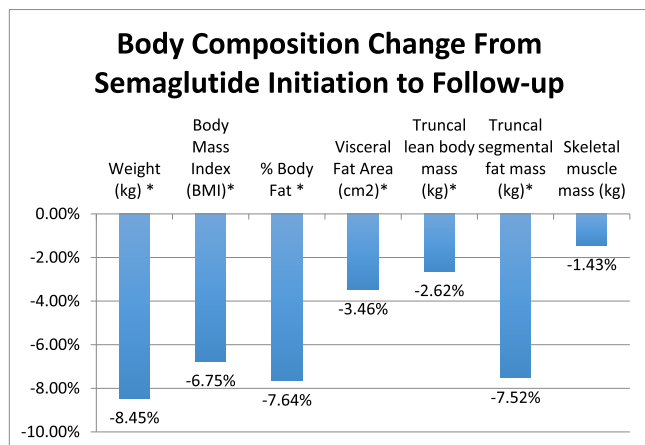


Figure: * indicates $p < 0.05$

Conclusion: Our study is consistent with prior findings of semaglutide achieving clinically significant weight loss when used in combination with lifestyle modifications, and overall being well-tolerated. Semaglutide was also associated with improved body fat distribution parameters, including VFA, which is most associated with cardiometabolic risk factors and metabolic syndrome, given its anatomic location around the internal organs and hyperlipolytic activity. Improving VFA with semaglutide may improve the dysmetabolic profile of NAFLD patients. Further investigation is needed to evaluate the impact of these weight and body composition improvements on cardiovascular outcomes and overall morbidity and mortality.

SAT139

Pegozafermin improved liver histology, liver-related non-invasive tests (NITs) and metabolic profiles in an open-label cohort of a Phase 1b/2a study in subjects with non-alcoholic steatohepatitis (NASH)

Rohit Loomba¹, Naim Alkhouri², Don Lazas³, Pierre Bedossa^{4,5}, Linda Morrow⁶, Shibao Feng⁷, Leo Tseng⁷, Germaine D. Agollah⁷, Will Charlton⁷, Hank Mansbach⁷, Maya Margalit⁸, Stephen Harrison⁹.
¹UCSD NAFLD Research Center, La Jolla, CA, United States; ²Arizona Liver Health, Tucson, AZ, United States; ³Digestive Health Research/ ObjectiveHealth, Nashville, TN, United States; ⁴Liverpat, Paris, France; ⁵Newcastle University, Institute of Translational Research, Newcastle, United Kingdom; ⁶Prosciento Inc., San Diego, CA, United States; ⁷89bio Inc., San Francisco, CA, United States; ⁸89bio Inc., Herzliya, Israel; ⁹Pinnacle Clinical Research, San Antonio, TX, United States
Email: maya.margalit@89bio.com

Background and aims: Pegozafermin (PGZ), a long-acting glycoPEGylated recombinant human FGF21 analog, had significant liver-related and cardiometabolic benefits, with favorable safety and tolerability, in a Phase 1b/2a study in NASH.

Method: In this open label cohort, 20 subjects with biopsy-proven NASH (NAS ≥ 4 , fibrosis stage F2/F3) received SC PGZ 27 mg QW for 20 weeks. Key end points were histology [≥ 2 -point improvement in NAS with ≥ 1 point improvement in ballooning or inflammation; NASH resolution without worsening of fibrosis, and ≥ 1 stage fibrosis improvement without worsening of NASH], and safety and tolerability at week 20 (W20). Change in liver fat and liver and metabolic markers were also assessed. Biopsies were read by one central reader.

Results: BL characteristics included (means): Age 58.4 years, BMI 37.0 kg/m², NAS 5.3 points, MRI-PDFF 21.1%, ALT 47.1 U/L, ProC3 19.3 ng/ml and Fibroscan™ VCTE score 14.3 kPa. 75% of subjects were female, 85% had T2DM, and fibrosis stage was F3 in 65% and F2 in 35% of subjects. 19/20 subjects completed treatment and had W20 biopsies. At W20, 74% of subjects had ≥ 2 pt reduction in NAS (mean absolute change –2.4 pts); 32% and 26% had NASH resolution without fibrosis worsening and improved fibrosis without NASH worsening, respectively. There was a consistent improvement in NITs that assess fibrosis compared to BL [VCTE score –4.6 kPa (–31%; $p < 0.001$), FAST score –0.47 (–76%; $p < 0.001$), FIB4 –0.29 (–19%; $p < 0.01$) and ProC3 –4.3 ng/ml (–20%; $p < 0.001$). 88% of subjects with BL FAST scores in the ‘rule-in’ or ‘indeterminate’ range had ‘rule-out’ FAST scores (≤ 0.35) at W20. At W20, mean relative reduction in MRI-PDFF was 65% ($p < 0.001$), and 100% and 79% of subjects had $\geq 30\%$ and $\geq 50\%$ reductions, respectively. ALT decreased by 46% compared to BL ($p < 0.001$); mean absolute decrease in ALT was –27.8 U/L in subjects with elevated ALT at BL, and ALT decreased ≥ 17 U/L in 71% of these subjects. At W20, significant improvement in HbA1c and lipids, weight loss and increased adiponectin were observed in PGZ-treated subjects. PGZ was safe and well tolerated. There were no deaths, related SAEs or discontinuations due to AEs. Treatment related AEs reported in $\geq 10\%$ of subjects included diarrhea, nausea, vomiting, injection site bruising, injection site erythema and decreased appetite; there were no reports of AEs grade ≥ 3 , hypersensitivity, tremor or adverse effects on vital signs.

Conclusion: PGZ (27 mg QW for 20 weeks) led to meaningful changes in key histology end points and fibrosis-related NITs, reduction in MRI-PDFF and decreased ALT in a cohort of NASH subjects with advanced fibrosis. In addition to these benefits on liver health, PGZ significantly improved metabolic parameters, with good safety and tolerability. These results extend the growing evidence of PGZ’s potential as treatment for NASH. PGZ is currently being evaluated in NASH in the ongoing Phase 2b ENLIVEN study.

SAT140

Identification of new therapeutic targets for hepatic regenerative medicine in Non-Alcoholic Fatty Liver Disease (NAFLD)

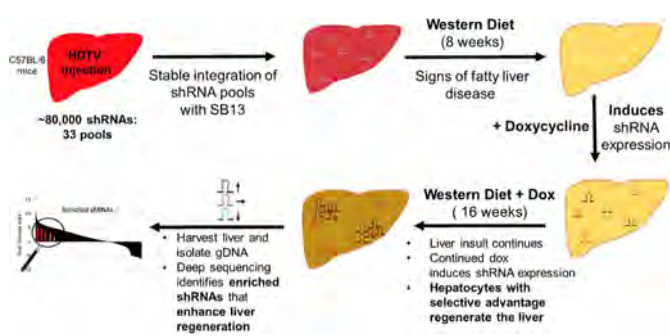
Shainan Hora¹, Rong Gao¹, Viktoriia Iakovleva¹, Agnes Bee, Leng Ong¹, Torsten Wuestefeld¹. ¹Genome Institute of Singapore, Laboratory of In vivo Genetics and Gene Therapy, Singapore, Singapore
Email: Shainan_Hora@gis.a-star.edu.sg

Background and aims: Non-alcoholic fatty liver disease (NAFLD) has emerged as the most common cause of chronic liver disease in the recent years. The massive growth in NAFLD cases is being fueled by an increase in global over-nutrition and obesity. Despite this, NAFLD continues to be an underdiagnosed disease with no current approved treatment and only a handful of drugs in clinical trials. A number of strategies are being employed to reverse this end-stage liver disease, including our unbiased genome wide *in-vivo* functional genetic screen that aims to identify novel regulators of NAFLD and shed light on hepatic regenerative therapy.

Method: Western diet animal model that recapitulates NAFLD in conjunction with RNAi-based functional genetic screen was used to identify gene targets in NAFLD. Specifically, shERWOOD-UltramiR shRNA library targeting the whole mouse genome was shuttled into a transposon-based inducible vector system, followed by hydrodynamic tail vein (HDTV) injections into animal liver. To recapitulate the fatty liver phenotype, mice were fed western diet supplemented

with high fructose. Following diet treatment for 8-weeks, doxycycline was added to induce shRNA expression enabling gene knock-down, along-with western diet for another 16 weeks. Animal livers were harvested, primary NGS analysis was performed and abundance of each shRNA was determined using differential expression analysis method. Top enriched shRNAs were down-selected using a stringent criterion (95% confidence interval with a 4-fold change), validated using a series of experiments *in-vitro* and injected into fumarylacetoacetate hydrolase (FAH)-knockout animals to study liver repopulation following diet treatment.

Results: We have identified several shRNAs that confer a negative or positive effect on the regenerative capacity of hepatocytes when subjected to detrimental environment such as high fat diet. Top enriched shRNAs have been validated using various *in-vitro* assays followed by selection of top scoring shRNAs for their impact on fatty liver disease phenotype using *in-vivo* animal models. Furthermore, we have identified some of the known markers of NAFLD that further validates the authenticity of our screen.



Conclusion: RNAi-based functional genetic screen in combination with high-throughput sequencing will allow the identification of new gene targets and uncover new insights underlying NAFLD development and disease progression.

SAT141

The effects of dietary vitamin E intake on NAFLD and sex differences in serum metabolic profile

Eleonora Scorletti¹, Kate Townsend Creasy², Marijana Vujkovic², Daniel Rader^{1,2}, Kai Markus Schneider³, Carolin Victoria Schneider¹.

¹University of Pennsylvania, Department of Medicine, Philadelphia, United States; ²University of Pennsylvania, Department of Genetics, Philadelphia, United States; ³University of Pennsylvania, Department of Microbiology, Philadelphia, United States

Email: eleonora.scorletti@pennmedicine.upenn.edu

Background and aims: Non-alcoholic fatty liver disease (NAFLD) is characterised by the accumulation of lipid droplets in hepatocytes and affects approximately 20–30% of the general population. Currently, there are no approved pharmacological agents available to treat NAFLD. Growing evidence supports the potential benefits of vitamin E in reducing steatosis and lobular inflammation in nondiabetic patients with NAFLD. Despite previous trials tried to assess the efficacy of vitamin E supplementation in patients with NAFLD, there remains a lack of understanding on the effects of vitamin E. Further, there are reported sex differences in NAFLD etiology and severity, although they have been poorly described.

Method: We analyzed the UK Biobank (UKB) dataset and selected our study population based on the availability of nutritional assessment. We investigated the association between dietary vitamin E intake with various disease phenotypes, serum metabolites and NAFLD prevalence.

Results: Data from >210,000 participants demonstrate that increased dietary vitamin E intake was associated with a lower prevalence of NAFLD and overall mortality. Each standard deviation (SD = 7 mg)

vitamin E increase per kJ energy intake was associated with reduced the risk of NAFLD ICD-10 diagnosis by 12.5% ($p < 0.0001$) and a reduced risk of MRI diagnosis of NAFLD by 24.3% ($p < 0.0001$). Additionally, we found sex differences in the effect of dietary vitamin E on metabolic profiles. Analysis of serum metabolites showed a greater reduction in gamma-glutamyl transferase (GGT) ($p < 1 \times 10^{-92}$) and urate ($p < 1 \times 10^{-68}$) in males, and a greater increase in sex hormone binding globulin (SHBG) in females ($p < 1 \times 10^{-15}$) (Figure 1).

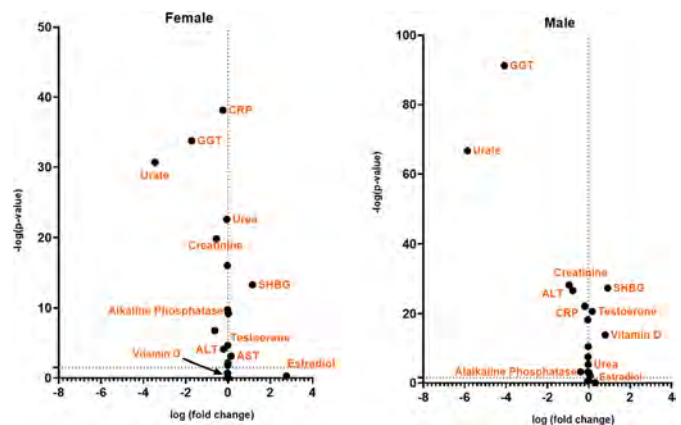


Figure 1: Volcano plot of serum metabolites in males and females.

Conclusion: Our study showed that increased dietary vitamin E intake may be beneficial for preventing NAFLD. Moreover, we found sex differences in the effects of dietary vitamin E on serum metabolic profiles. More randomized clinical trials are needed to identify suitable candidates for vitamin E supplementation in NAFLD patients. [UKB dataset reference number 71300]

SAT142

Favorable safety profile of TERN-201, a highly selective inhibitor of vascular adhesion protein-1, in the non-alcoholic steatohepatitis phase 1b AVIATION study

Mazen Nouredin¹, Eric Lawitz², Naim Alkhouri³, Robert Jenders⁴, Douglas Denham⁵, Bal Raj Bhandari⁶, Christopher Jones⁷, Cara H. Nelson⁷, Tonya Marmon⁷, Swapna Shenvi⁷, Hiba Graham⁷, Daria Crittenden⁷, Erin Quirk⁷, Diana Chung⁷. ¹Cedars-Sinai Medical Center, Cedars-Sinai Fatty Liver Program, Los Angeles, United States; ²Texas Liver Institute, San Antonio, United States; ³Arizona Liver Health, Tucson, United States; ⁴Velocity Clinical Research, La Mesa, United States; ⁵Clinical Trials of Texas, LLC, San Antonio, United States; ⁶Delta Research Partners, Monroe, United States; ⁷Terns Pharmaceuticals, Foster City, United States

Email: equirk@ternspharma.com

Background and aims: TERN-201, an irreversible inhibitor of vascular adhesion protein-1 (VAP-1) with >7000-fold selectivity over monoamine oxidase A or B, has demonstrated sustained target engagement in healthy human subjects. VAP-1 levels are elevated in non-alcoholic steatohepatitis (NASH) patients with fibrosis. Here we report results from Part 1 of the TERN-201, Phase 1b AVIATION trial in patients with NASH.

Method: Part 1 of the two-part AVIATION trial was a double-blind, placebo-controlled study (NCT04897594) in 30 adults with non-cirrhotic NASH phenotype evaluating 10 mg TERN-201 once daily (QD) for 12 weeks followed by off-treatment evaluation at Week 16. The prespecified Part 1 interim analysis primary end point was safety assessed by adverse events (AEs) and laboratory tests; percent change from baseline (BL) in plasma VAP-1 activity was a secondary end point. Exploratory imaging and blood-based biomarkers of liver inflammation and fibrosis were also assessed.

Results: Thirty patients, mean age 49.7 years, 22 (73.3%) women, 4 (13.4%) non-whites, mean (\pm SD) alanine aminotransferase (ALT)

POSTER PRESENTATIONS

67.25 (± 31.25) U/L, liver stiffness (LS) 8.68 (± 2.03) kPa by transient elastography, multiparametric magnetic resonance liver imaging (MRI) corrected T1 (cT1) 899.9 (± 110.2) msec and proton density fat fraction 17.6% ($\pm 7.5\%$) were randomized 2:1 to receive 10 mg TERN-201 or placebo. Nearly all patients (28/30, 95% of TERN-201 and 90% of placebo) completed Part 1. No patient discontinued due to any AE. 10 mg TERN-201 was well-tolerated with a similar incidence of AEs as placebo. All AEs were mild or moderate with no serious AEs or trends in AEs or laboratory abnormalities reported. 10 mg TERN-201 resulted in >98% inhibition of plasma VAP-1 activity in most subjects by Week 2 and sustained suppression through Week 12. There were no statistically significant differences between placebo and 10 mg TERN-201 in change from BL cT1, liver fat fraction, liver enzymes, or cytokeratin-18. At Week 12, tissue inhibitor of metalloproteinase-1 (TIMP1), a marker of hepatic fibrogenesis, decreased by 29.58 (± 9.26) ng/ml in the TERN-201 group and increased by a mean (\pm SE) of 13.56 (± 14.22) ng/ml in the placebo group relative to BL ($p < 0.05$).

Conclusion: TERN-201 was well-tolerated with a safety profile similar to placebo in patients with BL multiparametric MRI and LS values indicating NASH with at least stage 2 fibrosis. While 10 mg TERN-201 led to near complete inhibition of plasma VAP-1 activity and decreased levels of the hepatic fibrogenesis marker TIMP1, no statistically significant differences were observed between TERN-201 and placebo on markers of liver inflammation and injury following 12 weeks of treatment. Overall, these data support further assessment of safety and activity of 20 mg TERN-201 in the ongoing Part 2 of the AVIATION Trial in phenotypic NASH.

SAT143

Pegozafermin led to significant metabolic benefits, in addition to robust beneficial effects on the liver, in an open-label cohort of a Phase 1b/2a study in subjects with non-alcoholic steatohepatitis (NASH)

Naim Alkhouri¹, Rohit Loomba², Juan P Frias³, Linda Morrow⁴, Shibao Feng⁵, Leo Tseng⁵, Germaine D. Agollah⁵, Will Charlton⁵, Hank Mansbach⁵, Maya Margalit⁶, Stephen Harrison⁷. ¹Arizona Liver Health, Tucson, AZ, United States; ²USCD NAFLD Research Center, La Jolla, CA, United States; ³National Research Institute, Los Angeles, CA, United States; ⁴Prosciento Inc., San Diego, CA, United States; ⁵89bio Inc., San Francisco, CA, United States; ⁶89bio Inc., Herzliya, Israel; ⁷Pinnacle Clinical Research, San Antonio, TX, United States
Email: maya.margalit@89bio.com

Background and aims: Metabolic derangements are key drivers of NASH and significant risk factors for cardiovascular (CV) morbidity and mortality in NASH patients, that increases with advancing fibrosis. While treatments for NASH would ideally address both liver injury and metabolic derangements in this population, metabolic liabilities have been a drawback in several NASH drug development programs. Pegozafermin (PGZ), a long-acting glycoPEGylated recombinant human FGF21 analog in development for NASH, significantly improved liver and cardiometabolic parameters, with favorable safety and tolerability, in a Phase 1b/2a study in NASH.

Method: In this open label cohort, 20 subjects with biopsy-proven NASH (NAS ≥ 4 , fibrosis stage F2/F3) received SC PGZ 27 mg QW for 20 weeks. Key end points included histology, safety and tolerability. Change in hemoglobin A1c (HbA1c), body weight (BW), triglycerides (TG), non-HDL cholesterol (non-HDL-C), LDL cholesterol (LDL-C) and adiponectin was assessed at Week 20 (W20).

Results: Baseline (BL) characteristics (means) included age 58.4 years, HbA1c 6.6%, BW 104.6 kg, BMI 37.0 kg/m², TG 170.0 mg/dL, non-HDL-C 125.9 mg/dL, LDL-C 92.0 mg/dL, HDL-C 43.4 mg/dL and adiponectin 3.55 μ g/ml. 75% of subjects were female, and 85% had T2DM. 16/19 (84%) subjects who completed treatment took ≥ 1 anti-diabetic agent (range 1–4 medications, including 15 on metformin and 5 on GLP-1 receptor agonists). 11/19 subjects were treated with statins. At W20, significant improvement in glycemic control, BW and lipid parameters were observed. HbA1c decreased by -0.5% ($p <$

0.001) in the overall population. In subjects with BL HbA1c $\geq 6.5\%$ (N = 10; mean BL HbA1c = 7.3%), who were taking an average of 2 anti-diabetic agents, HbA1c decreased by -0.9% , to a mean of 6.4% ($p < 0.01$). BW decreased by -3.9% ($p < 0.001$). Adiponectin increased by 88.1% ($p < 0.001$). TG decreased by 26% in the overall population, and by 32% in subjects with elevated TG at BL (N = 11, mean BL TG 210 mg/dL; $p < 0.001$ for both comparisons). Non-HDL-C and LDL-C decreased by 18% ($p < 0.001$) and 13% ($p < 0.05$), respectively, and HDL-C increased by 23% ($p < 0.001$). Mean changes in serum lipids in subjects treated with statins were: TG -29.0%; non-HDL-C -22.1%; LDL -16.2% and HDL-C +35.4%.

Conclusion: PGZ (27 mg QW for 20 weeks) led to meaningful reduction in HbA1c and body weight and significant improvement in serum lipids in a cohort of mostly diabetic NASH subjects with advanced fibrosis and significant metabolic derangements, many of whom were already on treatment for diabetes, hyperlipidemia or both. These benefits were additive to robust beneficial effects on liver histology and favorable safety and tolerability, and suggest a potential of PGZ to protect subjects with NASH not only from liver related outcomes, but also from CV risk. PGZ is currently being evaluated in NASH subjects (NAS ≥ 4 , F2-F3) in the ongoing Phase 2b ENLIVEN study.

SAT144

Novel thyroid hormone receptor-beta agonist TG68 safely induces hepatic fat reduction in a non-alcoholic steatohepatitis rat model

Andrea Marco Caddeo¹, Marta Anna Kowalik¹, Marina Serra¹, Simona Rapposelli², Amedeo Columbano¹, Andrea Perra¹. ¹Cagliari, Department of Biomedical Sciences, Monserrato, Cagliari, Italy; ²University of Pisa, Department of Pharmacy, Pisa, Italy
Email: andrea.perra@unica.it

Background and aims: Non-alcoholic fatty liver disease (NAFLD) encompasses a broad spectrum of hepatic pathological conditions ranging from simple steatosis to non-alcoholic steatohepatitis (NASH), in absence of alcohol abuse or hepatic viral infections. Patients affected by NASH can develop fibrosis, cirrhosis and, eventually, hepatocellular carcinoma (HCC). Despite the raising interest in finding a strategy for this condition, no pharmacological approaches have been approved for the treatment of NAFLD. In this respect, thyroid hormones (THs) regulate hepatic lipid metabolism by binding thyroid hormones receptors beta (TR β) in the liver. Alteration of the hepatic TH signaling takes part of the rise and development of liver-associated diseases, such as NAFLD and HCC. To date, the use of THs as therapeutic approach is hindered by the lack of selectivity and adverse extrahepatic side effects, mainly due to their affinity for extrahepatic TR α receptors.

Method: To selectively activate TR β , we designed and synthesized a novel TR β agonist, namely TG68. Rats were fed a high fat diet (HFD) *ad libitum* for 25 weeks, and then animals received orally TG68 (2.8 mg/kg) for three weeks. Blood serum and tissues, including liver, heart and kidney, were collected and analysed after sacrifice.

Results: Blood analysis showed reduced circulating glucose, triglycerides, and cholesterol. Three week-treatment of TG68 significantly reduced liver weight as well as the liver weight/body weight ratio due to an increased fatty acid beta-oxidation and hydrolysis rates highlighted by the overexpression of *Cpt1a* and *Pnpla2*, respectively. Furthermore, TG68 strongly reduced hepatic fat accumulation and ameliorates liver injury in the absence of extrahepatic toxic effects.

Conclusion: Rats fed a HFD and treated orally with TG68 for the last three weeks before sacrifice, ameliorated liver weight/body weight ratio and intrahepatic neutral lipid content. This study strongly suggests that TG68 is an innovative hepatospecific TR β agonist, which might be used as a future therapeutic tool for the treatment of NAFLD.

SAT145

Safety and pharmacokinetics (PK) of single and multiple ascending oral doses of ALG-055009, a thyroid hormone receptor beta agonist for the treatment of non-alcoholic steatohepatitis (NASH), in healthy volunteers and subjects with hyperlipidemia
Hakim Charfi¹, Jean-Louis Pinquier¹, Benedetta Massetto², Kha Le², Christopher Westland², Kusum Gupta², Lawrence Blatt², Sushmita Chanda², John Fry², Matt McClure³. ¹Biotrial, Rennes, France; ²Aligos Therapeutics Inc, South San Francisco, United States; ³Aligos Therapeutics Inc, South San Francisco, United States
Email: bmassetto@aligos.com

Background and aims: Thyroid hormone receptor beta (THR- β) agonists rapidly reduce atherogenic lipids such as low-density lipoprotein cholesterol (LDL-C) and triglycerides in serum and the liver, decrease hepatic fat content and improve liver histology. Therefore, therapeutics targeting THR- β represent a promising mechanism of action to treat patients with NASH. ALG-055009, a novel oral thyroid hormone analogue with high THR- β selectivity and nanomolar potency, is being assessed in a first-in-human study (NCT05090111).

Method: In Part 1 of this multi-part, double blind, randomized, placebo-controlled study, multiple cohorts of 8 healthy volunteers (HV) received single ascending doses of ALG-055009 or placebo (3:1 ratio). In Part 2, multiple cohorts of 10 subjects with mild hyperlipidaemia (LDL-C >110 mg/dL) receive a daily (QD) dose of ALG-055009 or placebo (4:1) for 14 days. Adverse events (AE), vital signs, electrocardiogram (ECG), laboratory parameters, including thyroid stimulating hormones, lipids, sex hormone binding globulin (SHBG), and plasma and urine PK samples are collected. Reported here are the available preliminary blinded safety and PK data in HV from the first five cohorts in Part 1 and the first cohort in Part 2. Pharmacodynamic results and data from additional cohorts will be included at the time of the presentation.

Results: Forty HV and 10 subjects with hyperlipidaemia were enrolled in Part 1 Cohorts 1–5 (0.1 mg, 0.3 mg, 0.9 mg, 2.6 mg, 4 mg) and Part 2 Cohort 1 (0.3 mg), respectively. All HV were male with a mean age of 38 years and a mean body mass index (BMI) of 25 Kg/m². Subjects with hyperlipidaemia were mostly male (90%) with a mean age of 41 years, a mean BMI of 27 Kg/m², and a mean LDL-C of 143.1 mg/dL. All 50 participants completed the study. No serious AE has been reported and no AEs have resulted in premature study drug discontinuation. Seven HV (17.5%) and 3 subjects with hyperlipidaemia (30%) experienced at least one treatment emergent AE (TEAE). All TEAEs were mild or moderate in severity and without dose response. Overall, TEAEs observed in more than 1 subject were: headache (N=2); rhinopharyngitis (N=2); insomnia (N=2). All treatment emergent lab abnormalities were Grade 1, except for two subjects (N=1 in Part 1 Cohort 4; N=1 in Part 2 Cohort 1) who experienced a transient asymptomatic Grade 2 lipase elevation that resolved spontaneously by the following visit. No clinically significant changes in thyroid hormones or SHBG were observed. There were no clinically significant changes in vital signs or ECGs. Plasma ALG-055009 exposures increased dose proportionally between 0.1 and 2.6 mg dose levels (4 mg PK pending), with low variability (CV<36%) and ~1.7-fold accumulation following 14 daily doses.

Conclusion: Single doses of ALG-055009 of up to 4 mg and multiple daily 0.3 mg doses for 14 days were well tolerated with a favourable PK profile.

SAT146

A mediterranean diet intervention has beneficial effects on biomarkers of cardiovascular risk and hepatic fibrosis in non-alcoholic fatty liver disease (NAFLD)

Laura Haigh^{1,2}, Olivier Govaere², Lorna Brownlee³, Sarah Charman², Alasdair Blain², Thomas Wilson⁴, Morten Karsdal⁵, Stuart Mcpherson^{2,3}, John Mathers⁶, Quentin Anstee^{1,2}. ¹NIHR Newcastle Biomedical Research Centre, Newcastle upon Tyne, United Kingdom; ²Institute of Translational and Clinical Research, Faculty of Medical Sciences, Newcastle University, Newcastle upon Tyne, United Kingdom; ³Liver Unit, Newcastle Upon Tyne Hospitals NHS Foundation Trust, Newcastle upon Tyne, United Kingdom; ⁴Institute of Biological, Environmental and Rural Sciences, Aberystwyth University, United Kingdom; ⁵Nordic Bioscience A/S, Herlev, Denmark; ⁶Institute of Population Health Sciences, Faculty of Medical Sciences, Newcastle University, Newcastle upon Tyne, United Kingdom
Email: laura.haigh@nhs.net

Background and aims: Lifestyle interventions are the mainstay of non-alcoholic fatty liver disease (NAFLD) management. We assessed the feasibility and effectiveness of a Mediterranean diet (MD) intervention on patients stratified according to PNPLA3 rs738409 1148M carriage.

Method: 49 participants with NAFLD were recruited from a tertiary hepatology centre in the UK. In a cross-over design, participants completed Diet 1 (MD) and Diet 2 (control) for 4 weeks, in random order (1:1 allocation), separated by a 4-week washout period. Participants completed one-to-one diet and lifestyle consultations at baseline, end of diet phase 1, end of washout and end of diet phase 2. Participants were advised to maintain baseline levels of physical activity and body weight. At each of these time points we assessed; anthropometry; biochemistry, markers of cardiovascular risk (CVR) and biomarkers of hepatic fibrosis.

Changes in physical, biochemical and dietary intake measures after 4-weeks of a MD intervention (n=48)

Participant Characteristics	Baseline	Post-MD Intervention	P-Value
Age (years)	60.0 (52.3–68.8)		
Sex (n, % male)	22 (45.8%)		
PNPLA3 rs738409 (n, %)			
CC	21 (44.7%)		
CG	14 (29.8%)		
GG	12 (25.5%)		
Anthropometrics			
Weight (kg)	93.5 (83.5–109.5)	93.2 (82.0–109.1)	<0.001
BMI (kg/m ²)	35.3 \pm 5.5	34.7 \pm 5.4	<0.001
Waist circumference (cm)	114.6 \pm 13.8	112.7 \pm 13.3	0.002
Body composition (kg): Fat free mass	53.2 (46.8–63.4)	53.9 (45.8–63.1)	0.027
Cardiometabolic measures			
Blood pressure: Systolic (mmHg)	138.9 \pm 16.4	132.8 \pm 14.5	0.013
Diastolic (mmHg)	83.2 \pm 9.8	79.1 \pm 8.5	0.004
Fasting glucose (mmol/L)	6.7 (5.7–9.6)	6.5 (5.5–7.8)	0.017
HOMA-IR	5.2 (3.6–10.3)	4.3 (3.1–6.8)	0.017
Total cholesterol (mmol/L)	4.5 \pm 1.2	4.1 \pm 1.2	<0.001
Triglycerides (mmol/L)	1.5 (1.1–2.1)	1.4 (1.1–2.1)	0.011
HDL (mmol/L)	1.3 (1.1–1.5)	1.2 (1.0–1.4)	0.044
TC:HDL ratio	3.2 (2.7–4.1)	3.1 (2.5–4.0)	0.006
Non-HDL (mmol/L)	3.2 \pm 1.2	2.8 \pm 1.2	<0.001
Liver function			
Albumin (g/L)	45 (43–48)	46 (44–48)	0.024
ALP (IU/L)	89 (77–113)	85 (71–101)	0.014
Hepatic fibrosis			
PRO-C3 (ng/mL)	15.5 (11.4–21.3)	13.5 (10.8–20.1)	0.032
Dietary intake			
MEDAS (0–14)	5.7 \pm 1.9	9.0 \pm 2.1	<0.001

Values are means (SD), medians (IQR), or numbers (percentages)

Results: Retention of participants was high (n = 48, 98%). At 4 weeks MD adoption significantly increased from low to moderate (mean increase, 3.3 points; from 5.7 \pm 1.9 at baseline to 9.0 \pm 2.1) as assessed by MD assessment score. There was no change in physical activity and

POSTER PRESENTATIONS

weight loss was minimal. However, increased MD adoption was associated with significantly improved CVR, minor improvements in liver biochemistry (as measured by albumin and ALP) and significantly improved biomarkers of hepatic fibrosis (as measured by PRO-C3). Effects on CVR were most evident in wildtype *PNPLA3* than carriers of the I148M variant.

Conclusion: We have demonstrated the preliminary feasibility and effectiveness of a MD intervention, which rapidly improved CVR profile with evidence of early benefits on hepatic fibrosis. Carriers of the I148M variant appear to gain less benefit in terms of CVR factors when prescribed a MD intervention. Further validation in larger experimental studies are planned.

Liver development, physiology and regeneration

SAT151

CD44 plays critical role in liver regeneration through enhanced redox balancing

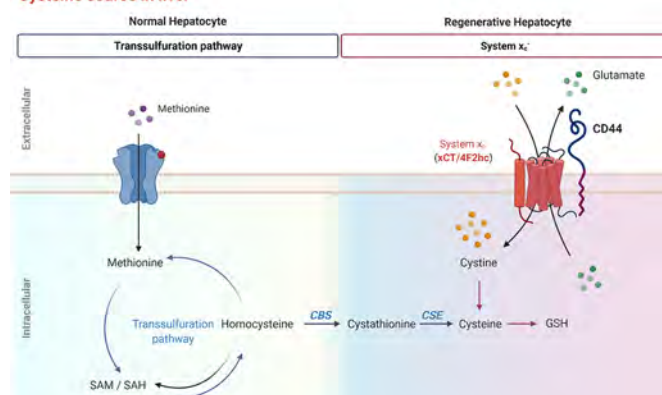
Wan Seob Shim¹, Hyun Young Kim¹, Keon Wook Kang¹, Sang Kyum Kim². ¹Seoul National University, College of Pharmacy and Research Institute of Pharmaceutical Sciences, Seoul, Korea, Rep. of South; ²Chungnam National University, Daedeok Campus, College of Pharmacy, Daejeon, Korea, Rep. of South
Email: kwkang@snu.ac.kr

Background and aims: Liver regeneration triggered by fulminant liver damage accompanies proliferation of hepatic progenitor cells (HPCs). Thus, there has been considerable interest in identifying specific HPC markers. However, the physiological role of HPC markers during liver regeneration is not fully understood. Herein, we identify the mechanistic roles of cluster of differentiation (CD)44, a cell surface marker for hepatic regeneration, in HPC proliferation and redox homeostasis.

Method: Liver regeneration was induced by liver resection or injection of 250 mg/kg acetaminophen. The activity of the system x_c^- antiporter was measured using an extracellular glutamate assay and universal ¹³C₆-cystine isotope tracing. Lentiviral Alb-p-shCD44 (LV-GFP-Alb-p-mCD44-shRNA) delivery system (a construct comprising the gene encoding shCD44 from the albumin promoter) was used to produce hepatocyte-specific CD44 knockdown mice.

Results: After liver resection or exposure to acetaminophen, the CD44 expression level was elevated in mouse primary hepatocytes isolated from regenerative liver tissues. Flow cytometry data identified HPCs, a subpopulation of hepatocytes with a high CD44 expression level and proliferation rate. To elucidate the role of CD44 in HPC proliferation, we knocked it down in AML12 cells. Knockdown of CD44 decreased the expression of xCT as well as the uptake of extracellular cystine through system x_c^- . CD44 ablation resulted in a diminished intracellular cysteine, glutathione (GSH), and a decreased proliferation rate. The proliferation of HPC isolated on a hyaluronic acid-coated dish was highly sensitive to inhibition of system x_c^- . Administration of system x_c^- inhibitor abrogated liver regeneration after acetaminophen (N-acetyl-*p*-aminophenol; APAP)-induced liver injury. Moreover, liver regeneration following APAP injection was significantly inhibited in hepatocyte-specific CD44 knockdown mice.

Cysteine source in liver



Conclusion: The obtained results delineate the central role of CD44 in modulating liver-regenerative capacity. Specifically, CD44 contributes to the intracellular redox balance and cell proliferation by enhancing extracellular cystine uptake through system x_c^- .

SAT152

Development of ECM mimicking 3D-hydrogel scaffolds for liver tissue engineering

Nathan Carpentier¹, Sara Campinoti², Luca Urbani², Peter Dubruel¹, Sandra Van Vlierberghe¹. ¹Ghent University-Campus Sterre-S4, Gent, Belgium; ²Institute of Hepatology, King's College Hospital, United Kingdom
Email: Nathan.carpentier@ugent.be

Background and aims: Annually, millions of people die because of liver failure, while the waiting duration for a donor liver is around 12 months. Herein, we target hybrid 3D-printed scaffolds to serve liver tissue engineering (LTE) applications.

As starting materials gelatin in combination with a polysaccharide was used to develop printable hydrogels. As polysaccharides dextran (Dex) and chondroitin sulphate (CS) were selected as mimics for the liver extracellular matrix (ECM) to explore their effect on the cell response. Methacrylated gelatin (GelMA) served as benchmark. The hydrogel materials were characterized on 2D- as well as on 3D-level. HepG2 cells were used to assess the in vitro biocompatibility of the developed hydrogels.

Method: Thiolated gelatin (GelSH) was crosslinked with the norbornene-functionalized polysaccharides DexNB and CSNB. Gelatin was methacrylated using methacrylic anhydride (GelMA) as reference material.

The different materials were characterized on both 2D- and 3D-level to assess the physico-chemical properties and the biocompatibility. 3D-hydrogel scaffolds of the materials were developed by indirect 3D-printing.

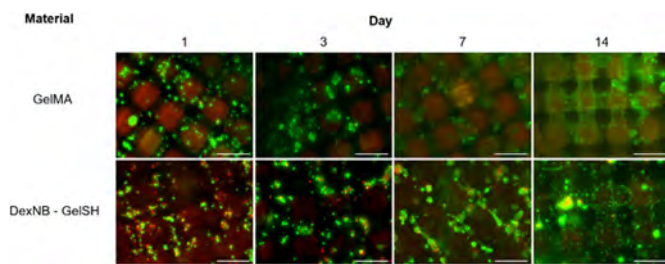
Results: DexNB-GelSH and CSNB-GelSH were superior over GelMA as their crosslinking kinetics were significantly faster and they mimicked natural liver tissue (NLT) to a greater extent with respect to physico-chemical properties. The swelling ratio of GelMA, DexNB-GelSH and CSNB-GelSH were all in line with NLT.

Atomic Force Microscopy (AFM) measurements revealed superior microscale mechanical properties of the DexNB-GelSH compared to the other materials that deviated more from NLT.

On a 3D-level, DexNB-GelSH scaffolds exhibited a compressive modulus of (4.8 ± 1.6) kPa which is in excellent agreement with that of NLT (i.e. 1–5 kPa) as compared to GelMA which resulted in a modulus of (8.5 ± 1.9) kPa and CSNB-GelSH (12.6 ± 1.9) kPa.

So far, the biocompatibility of DexNB-GelSH and GelMA were compared. However, the in vitro biocompatibility of both materials was comparable based on the MTS assay. The live-dead staining showed that the cells grew more into clusters on the DexNB-GelSH

scaffolds compared to the more spread morphology which the cells exhibited on the GelMA material.



Conclusion: DexNB-GelSH and CSNB-GelSH scaffolds are promising hybrid materials to support LTE as they exhibit similar physico-chemical properties compared to NLT (cfr. microscale stiffness, compressive modulus, swelling ratio and chemical composition), while cell viability and proliferation of the hepatocytes were preserved.

In future research, different cell types such as primary hepatocytes and organoids will be included in the biological evaluation. Furthermore decellularized liver ECM will be incorporated into the hydrogel material in order to improve the cell interactivity and proliferation.

SAT153

Three-dimensional conditions in a perfusion bioreactor to support maturation of human amnion epithelial stem cells into functional hepatocyte-like cells

Sara Campinoti¹, Negin Goudarzi^{1,2}, Bruna Almeida¹, I. Jane Cox¹, Roberto Gramignoli³, Luca Urbani^{1,2}. ¹The Roger Williams Institute of Hepatology, London, United Kingdom; ²King's College London, Faculty of Life Sciences and Medicine, United Kingdom; ³Karolinska Institutet, Department of Laboratory Medicine, Sweden
Email: luca.urbani@researchinliver.org.uk

Background and aims: Organ or hepatocyte transplantation are efficient treatments for end stage liver disease, but limited by the shortage of donors. Bioengineered liver transplant is a promising approach, but requires functional liver cells. Perinatal stem cells are promising alternative source of somatic cells. We previously validated epithelial cells isolated from full-term amnion membranes (AEC) as therapeutic strategy to reverse congenital liver disorders or rescue subjects from hepatic failure. AEC cells can mature into hepatocyte-like cells in vivo, supporting their use in regenerative medicine. Decellularized liver extracellular matrix scaffolds (ECM-scaffolds) maintain matrix components and the 3D architecture and can be used to support hepatic maturation and function in vitro. We combined ECM-scaffold technology with primary human AEC and evaluated cell proliferation and functional maturation into hepatocyte-like cells.

Method: primary human AEC were isolated in accordance with current Good Manufacturing Practice (cGMP) and qualified by flow cytometric and biomolecular analysis. Approx. $30\text{--}40 \times 10^6$ AEC from every donor were seeded into rat ECM-scaffolds generated in our lab. The constructs were cultured in custom-made bioreactors both in continuous perfusion and static conditions for 40 days (10 in expansion and 30 in differentiation media). Metabolites and functional products generated by AEC differentiating into hepatocyte-like cells were quantified by NMR, ELISA and luminescent/fluorescent functional assays validated as release criteria for human hepatocyte in clinical use. Additional biomolecular analysis were performed at the end of experimental set.

Results: AEC maintained epithelial characteristics and developed hepatic markers upon maturation. After 2 weeks of hepatic differentiation, AEC expressed hepatoblast markers (AFP). At the end of differentiation, AEC were positive for hepato-specific markers

such as CK18, albumin and CYP3A4, but negative for AFP. Albumin and urea quantifications supported hepatic maturation in bioreactor-cultured scaffolds. Phase 1 and 2 functional assays supported hepatic maturation and comparison with fetal/adult human hepatocytes. NMR analysis highlighted changes in the metabolite in the supernatant of differentiated AEC in ECM-scaffolds.

Conclusion: several groups/companies have proposed stem cells as alternative solution, bounded by genetic and epigenetic instabilities, and limited in hepatic maturation level. Here we show functional differentiation of primary human AEC into hepatocyte-like cells by 3D liver matrix support when maintained in a perfusion bioreactor. We conclude that innovative perfusion ECM-scaffold technology may support maturation for multipotent and eventually pluripotent stem cells, with important repercussion in therapeutic approaches and toxicological studies.

SAT154

Knockdown of Glyoxylate reductase/hydroxypyruvate reductase (GRHPR) accelerates liver regeneration and decreases chronic liver damage

Viktoriia Iakovleva^{1,2}, Anna Potapova¹, Agnes Bee, Leng Ong¹, Rong Gao¹, Yock Young Dan², Torsten Wuestefeld^{1,3,4}. ¹Genome Institute of Singapore (GIS), Laboratory of In vivo Genetics and Gene Therapy, Singapore, Singapore; ²National University of Singapore, Medicine, Singapore, Singapore; ³National Cancer Centre Singapore, Singapore, Singapore; ⁴Nanyang Technological University, Singapore, Singapore

Email: wuestefeldt@gis.a-star.edu.sg

Background and aims: GRHPR dysfunction in humans causes primary hyperoxaluria type 2 (PH2). Excess oxalate leads to kidney stone formation and kidney damage. However, in an in vivo RNAi screen to identify potential modulators of liver regeneration and disease we recently conducted two independent shRNAs targeting GRHPR scored. In addition, GRHPR expression was described to be decreased or lost in a subset of HCC, associated with proliferation rate (Pan et al., Pathobiology 2013;80: 155–162). Intrigued by this, we went on and validated that knockdown of GRHPR in hepatocytes accelerates liver regeneration and protects against liver fibrosis under chronic liver-damaging conditions.

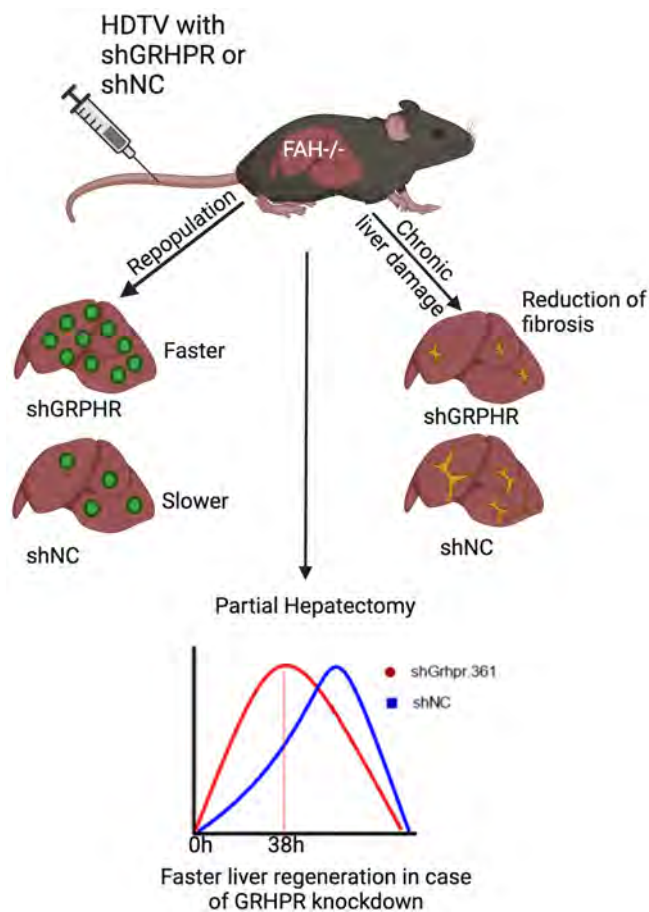
Method: RNAi screen was performed in C57BL/6JInv mice. shRNA pool contained 253 shRNAs and was delivered into the livers of C57BL/6JInv mice by hydrodynamic tail vein injections (HDTV). Thioacetamide (TAA) treatment was applied triweekly for 8 weeks (0.2 mg TAA per g bodyweight) to induce chronic liver damage. The abundance of each RNA was compared to the starting pool. Only enriched candidates were selected for further validation.

GRHPR was then validated in vitro and in vivo. For in vitro studies, a stable liver cell line with GRHPR knockdown was generated and knockdown efficiency was tested by Western Blot. Wound healing assay was performed to validate cell migration in two dimensions. For in vivo studies, we took advantage of the fumarylacetoacetate knockout mouse model (FAH^{-/-}). We delivered an shRNA-expression construct (shGRHPR or shCTRL, non-targeting) into the livers of FAH^{-/-} mice by HDTV, which leads to specific stable integration in hepatocytes. We investigated liver repopulation speed. Furthermore, liver regeneration upon Partial Hepatectomy (PH), and chronic liver damage (TAA model) was investigated on fully repopulated livers, where every hepatocyte expresses the shRNA of interest.

Results: We observed significantly faster cell migration in wound healing assay in case of the GRHPR knockdown. Furthermore, we observed faster clonal expansion in vivo in case of the GRHPR knockdown compared to a non-targeting control. Also, the PH model showed faster liver regeneration at 38 hours and 48 hours' time-points in the experimental group compared to the control group. Chronic liver damage model (TAA model) showed a significant reduction of fibrosis in case of GRHPR knockdown compared to

POSTER PRESENTATIONS

control. In addition, we observed that GRHPR knockdown in hepatocytes *in vivo* does not lead to tumor formation for 1 year.



Conclusion: Hepatocyte-specific knockdown of GRHPR improves liver regeneration and attenuates liver fibrosis. GRHPR knockdown in hepatocytes seems to be safe regarding liver cancer. We did not see any macroscopic impact on the kidney and mice survived for more than one year with hepatocyte-specific GRHPR knockdown. Nevertheless, kidney pathology has to be further evaluated.

SAT155

Expression and function of axon guidance genes in the developing portal tract

Lila Gannoun¹, Catalina De Schrevel¹, Sabine Cordi¹, Frédéric Lemaigre¹. ¹De Duve Institute UCLouvain, LPAD, Woluwe-Saint-Lambert, Belgium
Email: frederic.lemaigre@uclouvain.be

Background and aims: The liver lobules consist of hepatocyte cords and sinusoids that radiate from the portal area to the central vein. The portal area contains a branch of the portal vein, a hepatic artery, a bile duct lined by cholangiocytes, lymphatics, nerves and a heterogeneous mesenchyme. During development, the portal mesenchyme instructs differentiation of cholangiocytes, and normal development of the bile ducts is required for hepatic arteriogenesis (Lemaigre, 2020). Yet, how portal mesenchyme, bile ducts and hepatic artery interact during development remains poorly understood. To address this issue, we hypothesize that the 3D morphogenesis of bile ducts and hepatic artery is guided by signaling interactions with mesenchymal cells in the portal tract.

Method: To investigate this hypothesis, we separately FACS-purified cholangiocytes and adjacent mesenchymal cells at various stages of

liver development in mouse embryos, and subjected the cells to RNAseq analysis. We identified several ligand-receptor pairs where the ligand is differentially expressed in the mesenchyme and the receptor in the cholangiocytes, or vice versa, during duct morphogenesis. These included axon guidance genes, namely genes coding for Slit/Robo proteins, Eph receptors/Ephrins, Semaphorins/Plexins and Netrins/netrin receptors.

Results: We determined the cell-specific and spatial expression of selected genes, and focused our functional analyses on Slit/Robo and Netrin/Netrin receptor pairs due to their preferential location of expression near forming ducts (Fig. 1). Using a Cre-loxP strategy we inactivated selected genes in the developing mesenchyme or cholangiocytes. Functional assays, 2D and 3D imaging identified axon guidance genes required for normal development of bile ducts and hepatic artery.

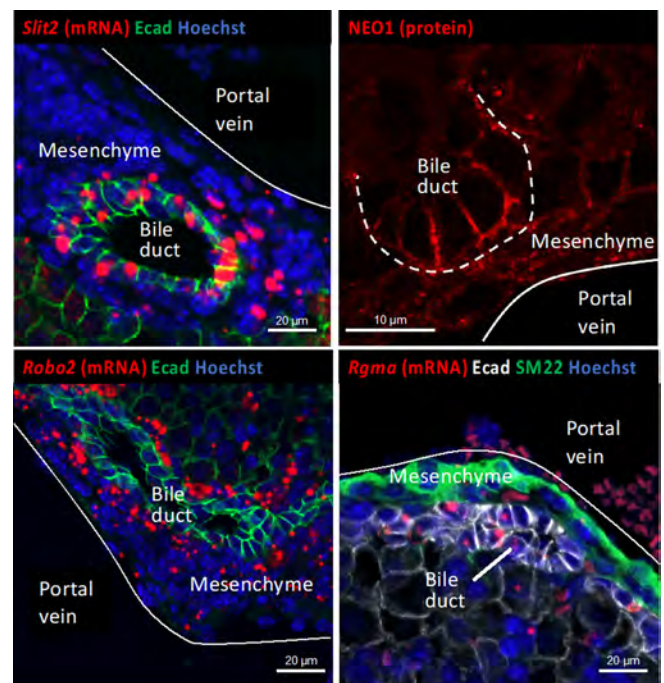


Figure: Expression of axon guidance genes (red) in developing mouse liver at E18.5.

Conclusion: We conclude that axon guidance pathways drive cell-cell interactions that control normal development of bile ducts and hepatic artery in the portal tract.

SAT156

Patients with chronic liver diseases are at risk for diabetes even before development of cirrhosis

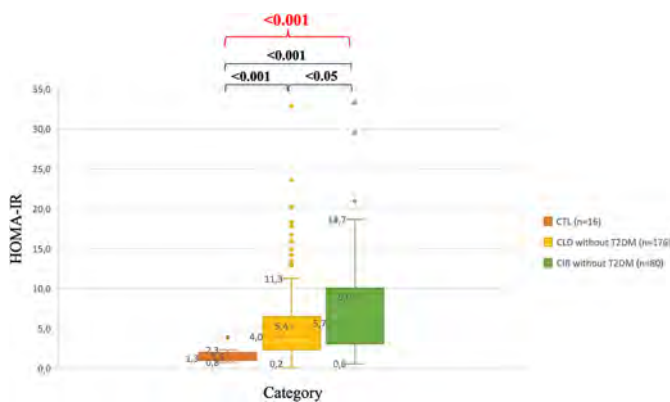
Georgia Bale¹, Frédéric Clarembaut¹, Peter Stärkel^{1,2}, Géraldine Dahlqvist¹, Yves Horsmans^{1,2}, Nicolas Lanthier^{1,1,2}. ¹Cliniques universitaires Saint-Luc, Service d'Hépatogastroentérologie, Brussels, Belgium; ²UCLouvain, Laboratory of Gastroenterology and Hepatology, Brussels, Belgium
Email: nicolas.lanthier@saintluc.uclouvain.be

Background and aims: The prevalence of insulin resistance (IR) and type 2 diabetes mellitus (T2DM) is higher in patients with cirrhosis, compared to control patients without liver disease. The exact mechanism for this is unknown but could include liver inflammation. In this study, we investigate whether cirrhosis is the *primum movens* of IR or if impaired insulin sensitivity is already present in non-cirrhotic patients with chronic liver diseases.

Method: Patients were recruited and divided into three groups: control (CTL), active chronic liver disease without cirrhosis (CLD) and cirrhosis (CIR). In patients not taking pharmacological treatment for

T2DM, IR was quantified using the homeostasis model assessment of insulin resistance (HOMA-IR). The proportion of patients treated for T2DM was recorded in each group. Additionally, HOMA-IR levels among different disease etiologies were compared. The study was approved by the local ethics committee.

Results: 422 patients were included in our study, 16 were controls, 278 had a CLD and 128 were cirrhotic (CIR). The causes of liver disease were as follows: metabolic-dysfunction associated fatty liver disease (MAFLD, n = 206), alcoholic liver disease (ALD, n = 117), active chronic hepatitis C (HCV, n = 59), other cause (n = 24). IR, represented by a HOMA-IR value exceeding 2.5, is already present in patients with non-cirrhotic CLD (median HOMA-IR 4.0). HOMA-IR levels lie between those seen in CTL (median HOMA-IR 1.3) and CIR patients (median HOMA-IR 5.7), with a statistically significant difference between the three groups (p value <0.001) (Figure). Median glycemia in the CLD and CIR groups is the same (98 mg/dL and 99 mg/dL respectively) but insulinemia is different (101.5 pmol/L and 132.3 pmol/L respectively) resulting in distinct HOMA-IR values in CLD and CIR patients (p = 0.018). Compared to CLD patients, patients in the CIR group are also characterised by a higher age, higher AST levels and a lower platelet count consistent with portal hypertension. The number of patients with T2DM is the same in the CLD and CIR groups (36.7 and 37.5% respectively). Finally, HOMA-IR levels differ according to disease etiology (p value <0.001): MAFLD and HCV associated liver disease are associated with higher levels of IR compared to ALD and other causes of CLD.



Conclusion: Chronic liver disease is already a predisposing factor to T2DM, regardless of the presence of cirrhosis. Certain disease etiologies are associated with more severe IR. Cirrhosis is a factor which in itself elicits additional increase in insulin levels. The increased insulin levels in this group may be related to increased IR in this situation or to decreased insulin clearance due to portal hypertension.

SAT157

Characterization of bioengineered liver constructs using hepatoblast organoids (HBOs) and human liver extracellular matrix (ECM) 3D-platforms

Margarita Papatheodoridi¹, Katerina Zacharis², Carola Maria Morell², Elisabetta Caon¹, Luca Frenguelli¹, Andrew Hall³, Ludovic Vallier², Krista Rombouts¹, Giuseppe Mazza¹, Massimo Pinzani¹. ¹University College of London, Royal Free Hospital, Institute for Liver and Digestive Health, London, United Kingdom; ²University of Cambridge, Jeffrey Cheah Biomedical Centre, Wellcome-MRC Cambridge Stem Cell Institute, Cambridge, United Kingdom; ³University College of London, Royal Free Hospital, Academic department of Histopathology, London, United Kingdom

Email: margarita.gpap@gmail.com

Background and aims: Primary fetal hepatoblast organoids (HBOs) derived from human fetal livers have self-renewal ability and can be

consecutively passaged while retaining capacity to differentiate to both the hepatic and biliary lineages. We hypothesized that the environment provided by the decellularised healthy human liver extracellular matrix (ECM) will offer HBOs the natural acellular cues for growth and enhanced metabolic functionality and maturation. Thus, the aim of this study was to demonstrate proof of concept for survival and growth of HBOs in a bio-compatible healthy human liver 3D-platform and assess their functionality.

Method: Healthy human liver unsuitable for transplantation was decellularized. Acellular liver tissue was lyophilized ≥ 24 hours and comminuted to a particulate form. ECM powder was then solubilised, neutralized, sterilised, and mixed with Nanocellulose (Celllink) 70:30 in the resultant ECMgel. HBO cells that had been cultured and expanded on Matrigel were seeded on ECMgel (25 K cells/30 μ L). Standard HBO Matrigel cultures (25 K cells/20 μ L) were used as controls. ECMgel (n = 36) and Matrigel (n = 36) samples for RNA extraction/gene expression, live/dead staining or ELISAs were collected up to day 14.

Results: HBOs repopulated the Matrigel and ECM gel and remained viable for 14 days in maintenance medium. HBO clusters on ECMgel had similar size but displayed a distinctively round shape compared to Matrigel where organoids have a characteristic budding morphology. Albumin gene expression in ECMgel was significantly higher compared to Matrigel samples and showed a significant increase from day 7 to 14. aFP gene expression showed a decreasing trend from day 7 to 14 in both materials. SERPINA and OTC gene expression of HBOs in ECMgel vs Matrigel was also higher on day 14, while CYP3A4 was higher in ECMgel on both timepoints. AURK gene expression in ECMgel was significantly higher than in Matrigel on day 14, suggesting higher proliferation. KRT19 expression was lower on ECMgel on day 7 compared to Matrigel and ranged in very low levels in all samples. Secreted albumin/aFP ratio significantly increased from day 5 to 14 in ECMgel indicating improved maturation but not in Matrigel samples.

Conclusion: Primary HBOs can grow in a healthy human liver ECM 3D-platform *in vitro* for at least 2 weeks and start differentiating towards a hepatocyte phenotype with the signals provided solely by the healthy human liver ECM. Overall, by combining two novel bioengineering technologies we showed the feasibility of constructing *in vitro* small implantable liver tissues that could be used for *in vivo* transplantation in future studies.

SAT158

Novel avenue towards liver regeneration and treatment of acute and chronic liver diseases: safety and PK profile from a first-in human (FIH) clinical trial for HRX-0215 as first in class MKK4 inhibitor

Birgit Jung¹, Markus Weissbach¹, Michael Lutz¹, Roland Selig^{1,2}, Stefan Laufer^{2,3}, Lars Zender^{4,5}, Michael Feigh⁶, Matthias Berse⁷, Jette Penski⁷, Esther Kosmella⁷, Wolfgang Albrecht¹. ¹HepaRegeniX GmbH, Tuebingen, Germany; ²University of Tuebingen, Department of Pharmaceutical Chemistry, Tuebingen, Germany; ³Tuebingen Center for Academic Drug Discovery and Development (TüCAD²), Tuebingen, Germany; ⁴University Hospital Tuebingen, Department of Medical Oncology and Pneumology, Tuebingen, Germany; ⁵University of Tuebingen, iFIT Cluster of Excellence EXC 2180 "Image Guided and Functionally Instructed Tumor Therapies", Tuebingen, Germany; ⁶Gubra, Hørsholm, Denmark; ⁷CRS Clinical Research Services Berlin GmbH, Berlin, Germany

Email: w.albrecht@heparegenix.com

Background and aims: Impaired liver regeneration is a hallmark of acute and chronic liver diseases and to date liver transplantation still represents the only ultimate treatment for acute liver failure and end stage chronic liver diseases. Recent reports validated Mitogen Activated Protein (MAP) Kinase 4 (MKK 4) as a novel target and demonstrated a role as a master regulator of liver regeneration (Wuestefeld et al., Cell 2013). Particularly striking efficacy results

POSTER PRESENTATIONS

accelerated liver regeneration and improved survival were recently obtained in 85% hepatectomy pig model upon treatment with the MKK4 inhibitor HRX-0215 (5 mg/kg i.v.) (Klotz et al., *Hepatology*, 2021). Here, we now report data from a FIH clinical trial for HRX-0215 related to safety, tolerability and pharmacokinetics.

Method: A FIH Clinical trial for HRX-0215 was conducted in 48 healthy volunteers to assess safety, tolerability and pharmacokinetics in a single-center, double-blind, randomized, placebo-controlled manner. In the Single Ascending Dose part volunteers were dosed from 5 to 500 mg, the Multiple Ascending dose part used daily doses between 100 and 500 mg. HRX-0215 was well tolerated at all doses, no relevant changes of any clinical or laboratory parameters were observed. Within a given dosing strength, PK analysis revealed a dose-proportional increase of exposure with very low interindividual variability. Concentration vs. time profiles of HRX-0215 supports a once-daily dose regimen during further clinical development.

Results: In the 4 wk GLP toxicity study in rats and dogs, a NOAEL of 300 mg/kg p.o. and 250 mg/kg p.o. was obtained, respectively. No organ toxicity was observed, which is in line with results from 12 mths ubiquitously, genetically suppressed MKK4 expression in mice. Most importantly, risk mitigation for liver tumor burden was achieved in a diet-induced obese mouse model with biopsy-confirmed NASH (non-alcoholic steatohepatitis) and advanced fibrosis, where HRX-0215 administered at a dose level of 30/kg once daily for 12 weeks attenuated progression in tumor numbers and growth.

Conclusion: Our FIH clinical trial demonstrates a favorable safety profile of HRX-0215 and confirms that pharmacological MKK 4 inhibition is well tolerated. PK characteristics indicate that therapeutic efficacy is achieved with a once-daily dose regimen. This profile enables further clinical development and Phase 2 trials of HRX-0215 in patients with acute and chronic liver diseases.

SAT160

In vivo loss-of-function studies unravel protein tyrosine phosphatase delta as a regulator of liver regeneration during metabolic liver disease

Armando Andres Roca Suarez^{1,2,3,4}, Laurent Mailly^{1,2}, Natascha Roehlen^{1,2}, Alessia Virzi^{1,2}, Nicolas Brignon^{1,2}, Frank Jühling^{1,2}, Christine Thumann^{1,2}, Sarah Durand^{1,2}, Marine Oudot^{1,2}, Eugénie Schaeffer^{1,2}, Romain Martin^{1,2}, Laura Heydmann^{1,2}, Charlotte Bach^{1,2}, Romain Parent^{3,4}, Carole Jamey⁵, Daniel Brumaru^{2,5,6}, Nassim Dali-Youcef^{2,5,7,8,9}, Emanuele Felli^{1,2,10}, Patrick Pessaux^{1,2,10,11}, Atish Mukherji^{1,2}, Catherine Schuster^{1,2}, Thomas Baumert^{1,2,10,11}, Joachim Lupberger^{1,2}.

¹Inserm U1110, Institute for Viral and Liver Disease, Strasbourg, France;

²Université de Strasbourg, Strasbourg, France; ³Inserm U1052, CNRS

UMR-5286, Cancer Research Center of Lyon (CRCL), Lyon, France;

⁴University of Lyon, Université Claude-Bernard (UCBL), Villeurbanne,

France; ⁵Hôpitaux Universitaires de Strasbourg, Laboratoire de

Biochimie et de Biologie Moléculaire, Pôle de Biologie, Strasbourg,

France; ⁶Inserm U1119, Strasbourg, France; ⁷Institut de Génétique et de

Biologie Moléculaire (IGBMC), Illkirch-Graffenstaden, France; ⁸Centre

National de la Recherche Scientifique UMR 7104, Illkirch-Graffenstaden,

France; ⁹Inserm U1258, Illkirch-Graffenstaden, France; ¹⁰Institut

Hospitalo-Universitaire, Pôle Hépatodigestif, Nouvel Hôpital Civil,

Strasbourg, France; ¹¹Institut Universitaire de France, Paris, France

Email: joachim.lupberger@unistra.fr

Background and aims: Signal transduction is tightly regulated by protein phosphatases and dysregulated in many diseases and cancers. Protein tyrosine phosphatase delta (PTPRD) is a STAT3 phosphatase, which was previously described as tumour suppressor. Since STAT3 signalling has a protective but also a pro-oncogenic role in the liver we aimed to study the impact of PTPRD expression on liver disease and development of hepatocellular carcinoma (HCC).

Method: To identify pathways responsive to PTPRD function, we analysed single-cell liver transcriptomics of healthy liver and

transcriptomics and clinical data from patients with liver disease. We established a *Ptpkd*-deficient mouse model, which was subjected to DEN and a choline-deficient diet enabling to study the role of PTPRD in NASH-associated liver cancer in vivo. The impact of PTPRD expression in the liver was validated using primary human hepatocytes and liver progenitor cells (LPCs) including the immortalized cell line HepaRG as well as in transcriptomes of regenerating liver after partial hepatectomy in rodents.

Results: In normal liver, single-cell transcriptomics identified hepatic PTPRD being expressed predominantly in EPCAM⁺ LPCs and in mature hepatocytes. Surprisingly, PTPRD-deficient mice with NASH developed significantly fewer HCC nodules although exhibiting higher fat inclusions compared to wild type mice. This suggests a dual role of PTPRD as a negative regulator of liver regeneration counteracting tumour formation and as a positive regulator hepatic fat metabolism. Indeed, PTPRD expression was strongly impaired after partial hepatectomy in rodent models, correlating with elevated STAT3 signalling in regenerating livers. Differentiated hepatocyte-like human LPCs express higher PTPRD compared to undifferentiated stem-cell like LPCs. Silencing of PTPRD or induction of STAT3 signalling in LPCs promoted de-differentiation and a stem-cell-like phenotype. Hepatocytes of the PTPRD-deficient mice exhibit impaired peroxisomal function, elevated STAT3 signalling and fat accumulation with elevated diabetic markers. Translating these observations to the clinic, obese patients with low hepatic PTPRD expression exhibited increased levels of clinical markers associated with metabolic disease.

Conclusion: Our results suggest a novel role of the STAT3 phosphatase PTPRD as regulator of hepatic regeneration in liver progenitor cells and fat metabolism in hepatocytes during metabolic liver disease.

SAT161

Integrated proteomics and metabolomics analysis reveals canonical and novel regulatory pathways linked to liver regeneration in living donor liver transplant (LDLT) Donors

Gaurav Tripathi¹, Adil Bhat^{1,2}, Manisha Yadav¹, Babu Mathew¹, Nupur Sharma¹, Vasundhara Bindal¹, Viniyendra Pamecha³, Jaswinder Maras¹, Shiv Kumar Sarin⁴. ¹Institute of liver and biliary science, Molecular and cellular medicine, New Delhi, India; ²University of California, Los Angeles, Pathology and Lab Medicine, Los Angeles, United States; ³Institute of liver and biliary science, hepatobiliary surgery, New Delhi, India; ⁴Institute of liver and biliary sciences, hepatology, New Delhi, India

Email: jassi2param@gmail.com

Background and aims: Living donor liver transplant (LDLT) in Donor's provides a unique opportunity to unravel novel biological networks associated to regenerative response. To explore more about liver regeneration, plasma proteomic, metabolomic and the clinical characteristic of LDLT Donors were integrated using network-based modelling with the final aim of uncovering novel biological processes associated to regeneration.

Method: Plasma proteomics and metabolomics were performed on (n = 10) healthy donors at baseline (pre-operative stage) and post-operative stages at Day1, Day3 and Day7. Proteome and metabolome data were analysed using weighted protein/metabolite correlation network analysis W[P/M]CNA to identify clusters of highly correlated proteins and metabolites modules differently expressed in donors at different days. Proteins and metabolites modules were cross correlated to form Multi-Modular Correlation Network (MMCN). Pathway analysis of MMCN identified regeneration linked proteins metabolite network which correlated with post-operative flare in liver enzymes (AST and ALT; p < 0.05).

Results: In comparison to baseline donor sample; post-operative day1 sample showed 232 differentially expressed proteins (DEP; Up-113, Down-119; p < 0.05) and 177 differentially expressed metabolites (DEM; Up-105, Down-72; p < 0.05). At day 1 VEGF, Hedgehog

signaling, Cell cycle, Tryptophan, Sphingolipid metabolism, Primary bile acid metabolism were increased and Calcium ion signaling, Apoptosis, Arachidonic acid metabolism were decreased ($p < 0.05$). At Day3; 264 DEP (Up-157, Down-107; $p < 0.05$) and 267 DEM (Up-136, Down-131; $p < 0.05$) associated to ILGF signaling, IL-12, NFK-B, MAP-K, JAK-STAT signaling, alanine aspartate metabolism and butanoate metabolism were increased whereas Rho-GTPases, interferon-gamma, Cytokine signaling, and fat metabolism were decreased ($p < 0.05$). Day7 showed 232 DEP (Up-97, Down-135; $p < 0.05$) and 299 DEM (Up-133, Down-166; $p < 0.05$) associated to autophagy, RHO-GTPases signalling and primary bile acid biosynthesis increased and Folate metabolism, N-glycan biosynthesis, Arachidonic acid metabolism, JAK-STAT, IL-12 signalling were decreased. Temporal integration performed using W [P/M] CNA identified MMCN clusters ($r^2 > 0.5$). Correlation of these MMCN clusters with the clinical indicator of liver regeneration (liver functions) led to identification of day wise specificity of MMCN cluster e.g. (Day1 specific MMCN-direct correlates with AST and ALT levels ($r^2 > 0.5$, $p < 0.05$)). Pathway enrichment of MMCN cluster identified canonical pathways involving haemostasis and regeneration but also enriched novel pathways linked to regeneration.

Conclusion: Multi-modular network analysis not only validates canonical pathways involving haemostasis and regeneration but also highlight novel pathways linked to liver regeneration.

SAT162

Regulation of extracellular Nicotinamide adenine dinucleotide in patients with liver fibrosis: new insights into conventional hepatobiliary parameters

Can Kamali¹, Alexander Arnold², Philipp Brunnbauer¹, Kaan Kamali¹, Karl Hillebrandt¹, Moritz Schmelze¹, Johann Pratschke¹, Felix Krenzien^{1,3}. ¹Charité-Universitätsmedizin Berlin, Department of Surgery, Berlin, Germany; ²Charité-Universitätsmedizin Berlin, Institute of Pathology, Berlin, Germany; ³Berlin Institute of Health, Berlin, Germany
Email: can.kamali@charite.de

Background and aims: The extension of liver resections represents a challenging surgical decision, depending on many factors, such as the patient's pre-existing conditions, oncological history and expected surgical outcome. A key limiting factor is the hepatic regenerative capacity, which we examined focusing on extracellular nicotinamide adenine dinucleotide (eNAD+) and its implications.

Method: Patients undergoing liver resection were recruited, tissue and blood samples were collected, and postoperative liver insufficiency was graded based on the 50-50 criteria. We utilized an assay that we established in our workgroup to measure concentrations of eNAD+ in the plasma samples. Finally we explored the impact of an eNAD+ treatment on 3D primary murine hepatocyte spheroids.

Results: Patients with low (grade 0 and 1 fibrosis, $n = 56$) and high (grade 2, 3 and 4 fibrosis, $n = 39$) grade fibrosis showed akin transaminase levels (AST, ALT) prior to surgery, while postoperative peak transaminase levels were significantly higher in the low grade fibrosis group (ALT: $p = 0.0008$, AST: $p = 0.0041$). Meanwhile, eNAD+ levels were significantly higher in the low grade fibrosis group (Grade 0 to 4, $p < 0.05$). Conversely, increased expression of catalyzing

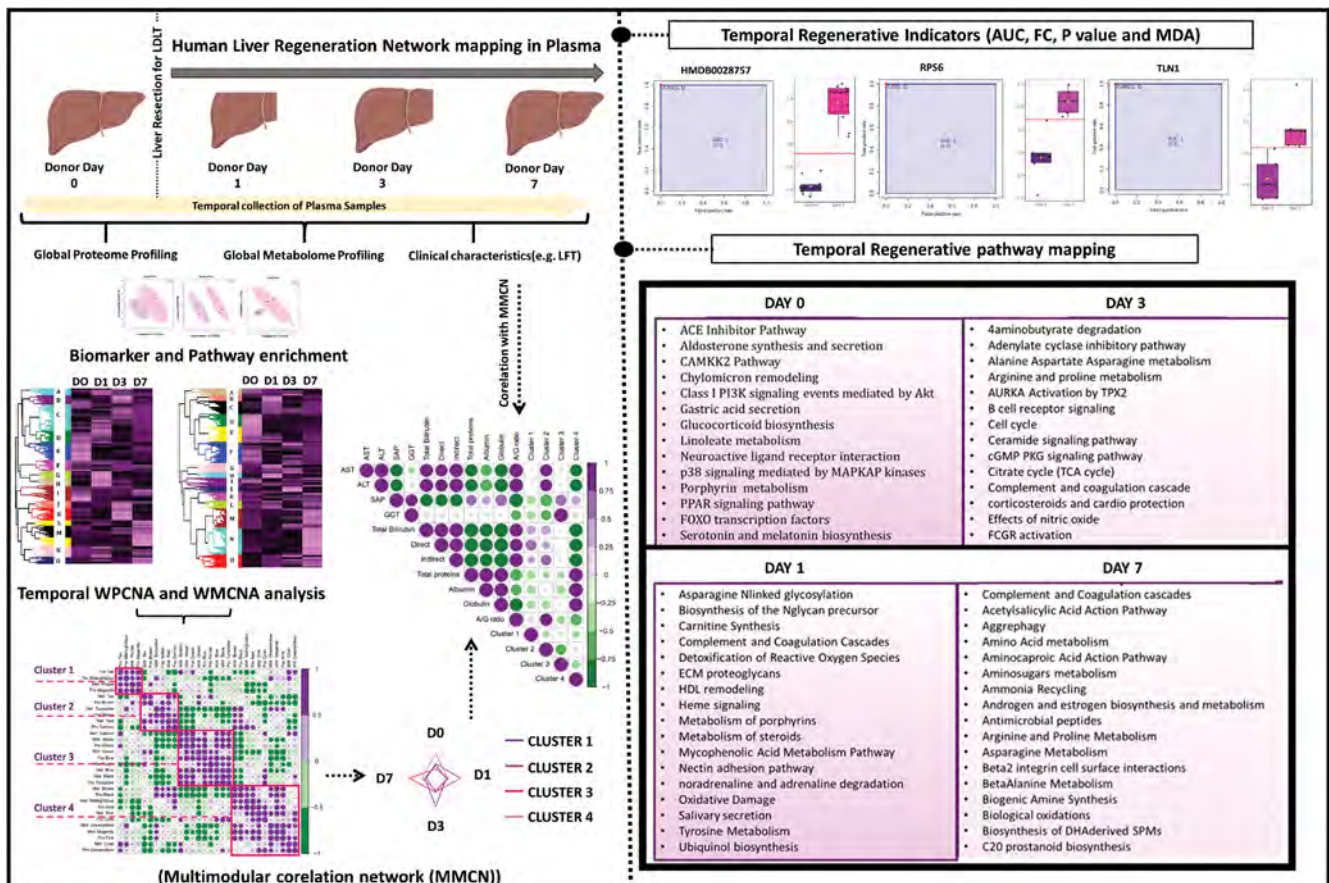
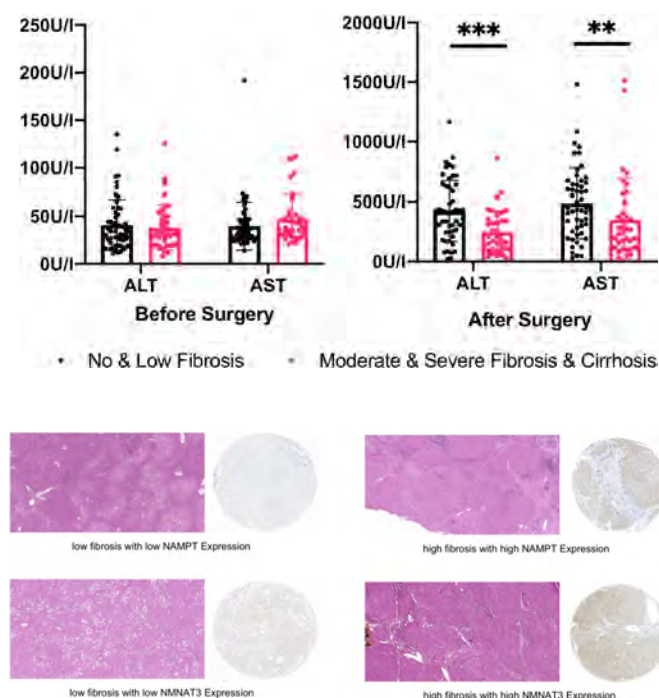


Figure: (abstract: SAT161)

POSTER PRESENTATIONS

enzymes of NAD⁺ synthesis in liver tissue, nicotinamide mononucleotide adenylyltransferase (NMNAT) and nicotinamide phosphoribosyltransferase (NAMPT), were associated with higher fibrosis grade ($p < 0.0001$). Next, we tested whether eNAD⁺ was regulated following liver resection. Indeed, patients revealed a higher postoperative eNAD⁺ decrease than controls ($p < 0.0001$). At the same time, patients who developed postoperative liver insufficiency ($n = 8$), exhibited significantly smaller eNAD⁺ decline than patients who did not develop liver insufficiency ($n = 69$, $p = 0.0325$). Next, 3D primary murine hepatocyte spheroids treated with eNAD⁺ for 12 days demonstrated the highest viability ($p < 0.0001$) when compared to negative controls, TNF alpha treated or combined TNF alpha and eNAD⁺ treated hepatocytes. The eNAD treatment group was followed in superiority of viability in successive order by eNAD⁺ and TNF alpha treated, negative control and finally TNF alpha (lowest viability) treated cell cultures, respectively.



Conclusion: We demonstrated that low grade fibrosis was associated with higher eNAD⁺ levels and compensatory downregulation of catalyzing enzymes of NAD⁺ synthesis in liver tissue. Interestingly, eNAD⁺ was decreased following liver resection and linked to postoperative liver insufficiency. In conclusion, we provide evidence that eNAD⁺ is determined by the degree of fibrosis of the liver and is significantly regulated after liver resection with implications for future therapy targets.

SAT163

Hyaluronan in the prenatal extrahepatic bile duct increases in response to injury

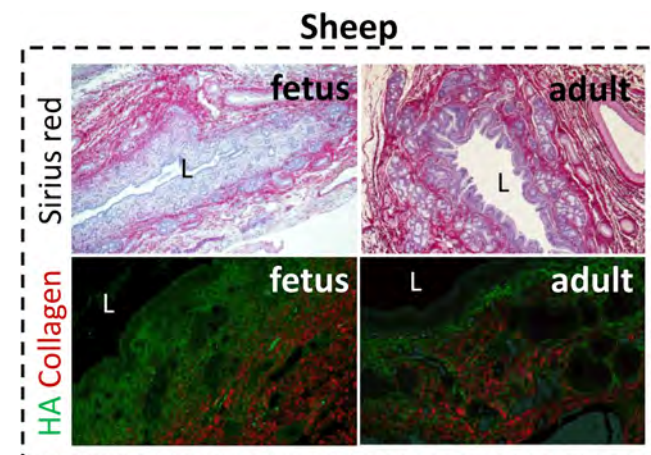
Iris de Jong¹, Mallory Hunt², Kapish Gupta³, Yu Du⁴, Jessica Llewellyn³, Abhishek Dhand⁵, Robert Porte¹, William Gaynor⁶, Rebecca Wells³. ¹University Medical Center Groningen, Department of Surgery, Section Hepato-pancreato-biliary Surgery and Liver Transplantation, Groningen, Netherlands; ²Hospital of the University of Pennsylvania, Department of Surgery, Division of Cardiovascular Surgery, Philadelphia, United States; ³Perelman School of Medicine at the University of Pennsylvania, Division of Gastroenterology, Department of Medicine, Philadelphia, United States; ⁴Perelman School of Medicine at

the University of Pennsylvania, Division of Gastroenterology, Department of Medicine, Philadelphia, United States; ⁵University of Pennsylvania, Department of Bioengineering, Philadelphia, United States; ⁶Children's Hospital of Philadelphia, Division of Cardiothoracic Surgery, Philadelphia, United States
Email: i.e.m.de.jong@umcg.nl

Background and aims: Biliary atresia (BA) is a fibrosing obstructive cholangiopathy and represents the primary cause of obstructive jaundice in infants. The etiology is uncertain, but compelling evidence points toward a prenatal cause. Existing literature on BA focuses mainly on the post-natal period and the early response of the fetal extrahepatic bile duct (EHBD) to injury remains unknown. The objective of this study was to identify unique features of the fetal and neonatal EHBD injury response that had pathophysiological relevance.

Method: Mouse, rat, sheep, and human EHBD samples were studied at different developmental time points. Models included a fetal sheep model of prenatal 14- to 21-day injury, human BA EHBD remnant and liver samples taken at the time of the Kasai procedure, EHBDs isolated from neonatal rats and mice, and spheroids generated from primary neonatal mouse cholangiocytes that were cultured in either collagen, low or high molecular weight hyaluronan. A bile duct-on-a-chip device was used to study swelling of a collagenous matrix with and without hyaluronan.

Results: A thick layer of hyaluronan encircling the lumen was identified as a unique feature of the normal perinatal EHBD. This layer, which was surrounded by collagen, was significantly thicker in ducts subject to prenatal injury, in parallel with extensive PBG hyperplasia and mucus production, and increased serum bilirubin levels. BA remnants and liver samples similarly showed increased hyaluronan centered around ductular structures, compared with age-matched controls. High molecular weight hyaluronan has a positive effect on spheroid growth, supporting the pro-regenerative environment seen *in vivo*. Increased hyaluronan levels in the matrix lead to a decreased lumen diameter.



Conclusion: A dense layer of hyaluronan around the lumen that decreases rapidly after birth is a unique feature of the mammalian fetal and neonatal EHBD. Prenatal injury causes an increased thickness of the hyaluronan layer, with extensive PBG hyperplasia and mucus production, possibly leading to increased bilirubin levels and swelling and obstruction of the EHBD.

SAT164

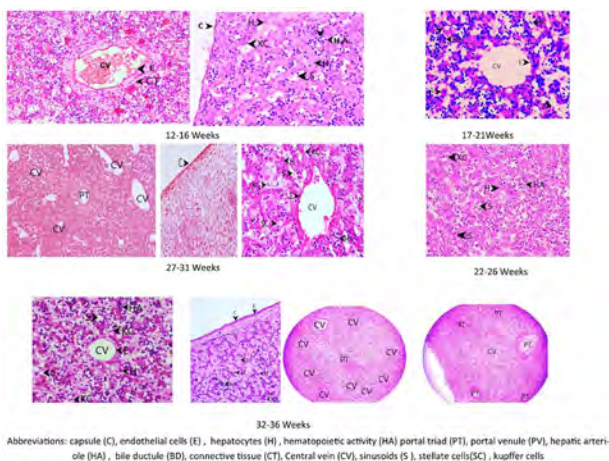
Embryogenesis of human fetal liver at various stages of gestation: a histomorphometric study

Pooja Bhadoria¹, Kavita Modi¹, Brijendra Singh¹. ¹All India Institute of Medical Science Rishikesh, Fetal Autopsy Lab Anatomy, Rishikesh, India
Email: pooja.ana@aiimsrishikesh.edu.in

Background and aims: Correlation of general fetal morphometric parameters with liver dimensions and observation of microscopic features like kupffer cells, hematopoietic activity, stellate cells, glycogen granules, central vein, portal triad carries immense importance in estimation of fetal gestation age, detection of anatomical variations, and identification of congenital anomalies. Hence, we planned to assess prenatal development of human liver between 12 and 36 wks of gestation by evaluating both macroscopic and microscopic parameters using conventional autopsy and histotechniques.

Method: In 33 normal fetuses (gestation age 12–36 wks) were classified in 5 groups as 12–16, 17–21, 22–26, 27–31 and 32–36 wks. Liver parameters like weight, volume, transverse and sagittal diameter, vertical length, length and width of lobes of liver and general morphometric parameters of fetus like weight, crown–rump length, crown–heel length, bi-parietal diameter, head, chest and abdominal circumference, hand and foot length, inner and outer inter-canthal distance were measured. Hematoxylin and Eosin (HandE) sections were studied using Quasmo ISI microscope and image-pro express analyzer.

Results: Out of 33 fetuses (males 27: females 6) and maximum (n = 7) each were in group 17–21 and 27–31 wks. Correlation between gestational age and all general fetal and liver parameters except bi-parietal diameter were statistically significant ($p < 0.05$). Similarly, significant increase amongst all fetal and liver parameters was seen with increasing gestational age ($p < 0.05$). On HandE sections (Fig 1) during 12–16 wks, glisson's capsule, portal triad surrounded by fibrous capsule, central vein, kupffer cells and hematopoietic activity was observed. During 17–21 wks, hepatocytes were present in anastomosing radiating cords with organized hepatic sinusoids and parenchyma. During 22–26 wks, hematopoietic activity became focal, with clear demarcation of hepatic and portal lobule. During 27–31 wks, hepatic and portal lobule was clearly demarcated, hematopoietic activity reduced. Kupffer cells and capsule thickness increased with gestation age. During 32–36 wks, deposition of glycogen granules was observed. Hematopoietic activity became scanty and focal. Hepatic parenchyma became more structured with radiating cords of hepatocytes arising from distinct central vein.



Conclusion: Change in general fetal morphometric parameters and liver parameters except bi-parietal diameter are directly proportional with change in gestation age. Knowledge of morphological and histological features and normal limits of dimensions of liver with

respect to gestation age is a reliable reference. Findings of studies can be used to better understand histology of normal liver and stages of development during fetal life to pick variations and anomalies.

SAT165

Generation of universal low-immunogenic human cholangiocyte organoids for treatment of cholangiopathies

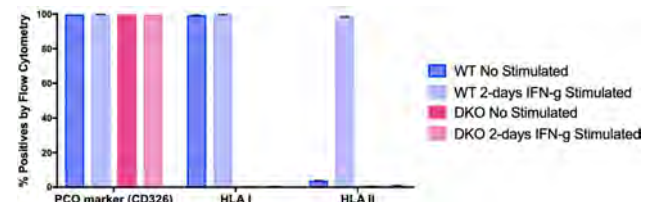
Sandra Petrus-Reurer¹, Adrian Baez-Ortega², Inigo Martincorena², Kourosh Saeb-Parsy¹. ¹University of Cambridge, Surgery, United Kingdom; ²Wellcome Trust Sanger Institute, United Kingdom
Email: sp2016@cam.ac.uk

Background and aims: Other than complex surgery or transplantation, there are no current curative therapies for cholangiopathies affecting the intra- or extrahepatic biliary tree such as Primary Sclerosing Cholangitis (PSC). We have previously shown that human bile duct epithelial cells can be cultured as 3D organoids to generate an unlimited supply of phenotypically- and functionally-mature primary cholangiocyte organoids (PCOs) for the treatment of bile duct disorders. We have used PCOs to generate bioengineered bile ducts to replace the extra-hepatic bile duct, and to treat intrahepatic cholangiopathy in human livers.

Since the generation of autologous PCOs is likely to remain logistically and economically prohibitive for the foreseeable future, immune rejection of allogeneic PCOs remains a key outstanding barrier to their clinical translation. We thus aimed to develop universal low-immunogenic cholangiocyte organoids for regenerative medicine applications.

Method: After systemic testing of numerous conditions, HLA I and II double KO (DKO) 'edited PCOs' (ePCOs) were generated using CRISPR/Cas9 by dissociating PCOs into single cells, electroporation with the guide-Cas9 complex and sorting for the specific double negative cells. Assessment comparing to parental wild-type (WT) cells was carried out by flow cytometry, functional readouts (e.g. Gamma-glutamyl Transferase and Alkaline Phosphatase analyses), and co-culture with CD4⁺ and CD8⁺ lymphocytes *in vitro*, as well as by engraftment under kidney capsule of immunodeficient mice. Mutational load and CRISPR-mediated off-target genetic mutations of parental vs ePCOs were quantified using whole genome sequencing and Nanoseq techniques.

Results: The HLA I and II DKO ePCOs generated maintain a mature PCO phenotype demonstrated by flow cytometry and functional analyses. Immune characterization *in vitro* by co-culture with CD4⁺ and CD8⁺ T cells experiments are ongoing to show that ePCOs have a reduced immunogenicity (Interferon- γ secretion, IFN- γ) compared to WT cells. Moreover, upon engraftment into the kidney capsule of immunodeficient mice, ePCOs survive and engraft expressing cholangiocyte markers (e.g. KRT-7, KRT-19) in a similar manner as WT cells. Finally, pilot data on off-target analysis and mutation burden of parental vs ePCOs do not show CRISPR-mediated off-target sites nor excess mutation in ePCOs. Additional experiments are ongoing to assess the immune response *in vivo* using humanised mouse models.



Conclusion: Human PCOs lacking HLA I and HLA II can be successfully generated using a CRISPR-Cas9 approach. ePCOs retain the phenotypic characteristics of mature PCOs both *in vitro* and *in vivo* upon engraftment in kidney capsule, but show reduced immunogenicity *in vitro* when co-cultured with CD4⁺ and CD8⁺ cells compared to

POSTER PRESENTATIONS

parental cells. Pilot data show no CRISPR-driven off-target mutational burden in ePCOs.

SAT166

Opposite PAR2 roles in liver regeneration from autoimmune or direct damage. Solving the conflict

Gal Reches¹, Netta Rose Blondheim Shraga¹, Florent Carrette², Assaf Malka¹, Natalia Saleev¹, Yehuda Gubbay¹, Offir Ertracht³, Linda M Bradley², Fred Levine⁴, Ron Piran¹. ¹Bar Ilan University, The Azrieli Faculty of Medicine, Safed, Israel; ²Sanford Burnham Prebys Medical Discovery Institute, Infectious and Inflammatory Disease Center, La Jolla, California, United States; ³Galilee Medical Center, Eliachar Research Laboratory, Nahariya, Israel; ⁴Sanford Burnham Prebys Medical Discovery Institute, Sanford Children's Health Research Center, La Jolla, California, United States
Email: galrech@gmail.com

Background and aims: Liver inflammation will cause hepatic damage. In other cases, hepatic injury or poisoning will induce inflammation. Both scenarios will be defined as hepatitis. We chose two distinct hepatitis models that are typical for these two underlying causes. By doing so, we aimed to characterize the role of PAR2 in liver regeneration and inflammation, to reconcile PAR2 confusing role in many damage models, which sometimes aggravates the induced damage and sometimes alleviates it.

Method: WT and PAR2 knock out (PAR2KO) mice were injected with concanavalin A (ConA) for the immune-mediated model, or with carbon tetrachloride (CCl₄) for the direct hepatic damage. In order to separate the immune component from the liver regenerative response we conducted reciprocal bone marrow (BM) replacement of WT and PAR2KO mice and repeated the damage models.

Results: ConA injection caused limited damage in PAR2KO mice livers, while in the WT severe damage followed by leukocytes infiltration was evident. Reciprocal BM replacement of WT and PAR2KO showed that WT BM into PAR2KO displayed marked liver damage, while in PAR2KO BM into WT the tissue was generally protected. In the CCl₄ direct damage model, WT mice hepatocytes regenerated, while PAR2KO failed to recover. Reciprocal BM replacement did not show significant difference in hepatic regeneration comparing to the mice that were not transplanted. In PAR2KO hepatitis was significantly more apparent, while WT recovered regardless of the BM origin.

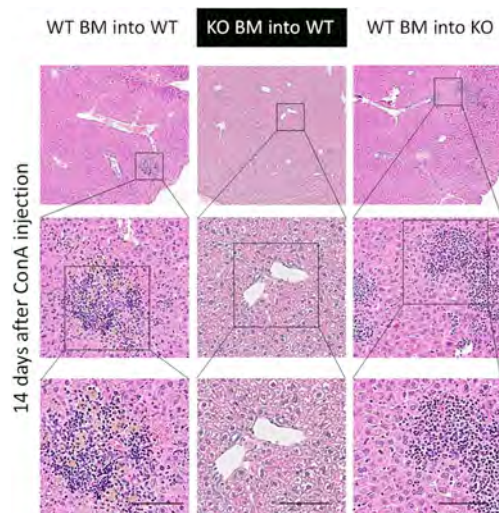


Figure: ConA induced hepatitis is controlled by PAR2 activation in the immune system

Conclusion: We conclude that when PAR2 is predominantly activated in the immune system, it aggravates hepatitis and when it is activated in the damaged tissue it promotes liver regeneration. When we incorporate this finding and revisit the literature reports, we were

able to reconcile the conflicts surrounding PAR2 role in injury, recovery, and inflammation.

SAT167

Chronic injury induces plasticity between cholangiocytes and hepatocytes in the human liver

Vasileios Galanakis^{1,2}, Christopher Gribben¹, Alexander Calderwood¹, Ilias Moutsopoulos¹, Katarzyna Kania³, Emmanouil Athanasiadis⁴, Michael Allison², Irina Mohorianu¹, Ludovic Vallier¹. ¹Wellcome-MRC Cambridge Stem Cell Institute, Cambridge, United Kingdom; ²Addenbrooke's Hospital, Cambridge, United Kingdom; ³Cancer Research UK Cambridge Institute, Cambridge, United Kingdom; ⁴Greek Genom Center, Biomedical Research Foundation, Academy Of Athens, Computational Biology Unit (CBU), Athens, Greece
Email: vasilisgalan@gmail.com

Background and aims: Liver disease is on the rise, resulting in a huge health care burden. The liver's ability to regenerate is unique amongst the human organs. Liver regeneration is believed to mainly be driven by hepatocyte proliferation following acute liver injury or parenchymal volume reduction. However, in the presence of chronic liver injury the regeneration process is more complex and could involve several mechanisms. Indeed, animal studies suggest that 1) liver stem cells activation, 2) dedifferentiation/redifferentiation of cholangiocytes/hepatocytes, 3) transdifferentiation between cholangiocytes and hepatocytes, could be part of this regeneration process. Importantly evidences of regenerative process in human chronic liver diseases, such as in non-alcoholic fatty liver disease (NAFLD), are mainly indicative by histological observations and the underlying mechanisms remain to be fully uncovered.

Method: To define these mechanisms in vivo, we decided to combine state of the art single-nuclei transcriptional analysis (snRNAseq) with functional validations using cholangiocyte organoids. snRNAseq was performed on liver biopsies obtained from over 50 patients across the spectrum of NAFLD. Detailed computational analyses allowed the identification of factors and signalling pathways relevant for regenerative processes. The interest of these factors was further validated using a combination of cholangiocyte organoid system and multiome technology (single nuclei RNAseq and ATAC-Seq) on NAFLD derived cholangiocyte organoids, which were differentiated to hepatocyte like cells in vitro.

Results: Progression of liver disease towards decompensated cirrhosis is accompanied by transcriptomic changes, loss of liver architecture and zonation as well as expansion of ductular cells. Liver plasticity is also observed as evident by the presence of hepatocyte-cholangiocyte bi-phenotyping cells in the late stages of the disease. Similar bi-phenotyping cells can be observed by using the in vitro organoid system thereby suggesting that potential reciprocal plasticity.

Conclusion: Transcriptional analyses of patient biopsies and in vitro modelling suggest that cell plasticity is present in chronically diseased liver. Studying this plasticity may be key to understand the underlying regenerative mechanisms of the chronically injured human liver.

SAT168

In vivo characterization and functional effects of the NAD⁺ transporter, SLC25A51

Sarmistha Mukherjee¹, Beishan Chen¹, Caroline E Perry¹, Melissa Lieu¹, Joseph A Baur¹. ¹Perelman School of Medicine, IDOM, Physiology, Philadelphia, United States
Email: baur@pennmedicine.upenn.edu

Background and aims: SLC25A51 has recently been identified as the NAD⁺ transporter in mammalian mitochondria^{1,2}. SLC25A51 (also known as MCART1) allows mitochondria to take up intact NAD⁺ from the cytoplasm and has previously been identified as a hit of unknown function in screens for essential genes. Although its function is now well established in cell lines, there is little information on SLC25A51

in intact tissues *in vivo*. Here, we are interested in characterizing and understanding the physiological role of hepatic SLC25A51.

Method: We used AAV vectors expressing *Slc25a51* or shRNA targeting under the control of the TBG promoter to overexpress or knock down *Slc25a51*, respectively, in the livers of mice.

Results: Preliminary data show that the *Slc25a51* knockdown mice have significantly higher fasting blood glucose and glucose intolerance, whereas overexpression has no effect. In contrast, overexpression lowers glucose in a pyruvate tolerance test whereas knockdown has no effect. As expected, mitochondrial NAD⁺ and NADH content and redox ratio are significantly higher in the over-expressors without a major change in total tissue NAD. Overexpression of SLC25A51 increased mitochondrial respiration and increased the rate of NAD⁺ uptake into isolated mitochondria. Conversely, loss of SLC25A51 impaired mitochondrial function. In addition, overexpression of SLC25A51 enhanced liver regeneration, significantly improved mitochondrial respiration and increased NAD⁺ uptake in post regenerative isolated mitochondria.

Conclusion: So far, our data suggest a direct enhancement of mitochondrial redox metabolism as the mechanism mediating improved regeneration in the over-expressors. Thus, the role of SLC25A51 appears to be conserved *in vivo* and impacts liver regeneration.

Reference:

- 1 Luongo T. S. Eller J. M. Lu M.-J. Niere M. Raith F. Perry C. Bornstein M. R. Oliphant P. Wang L. McReynolds M. R. Migaud M. E. Rabinowitz D. Johnson F. B. Johnsson K. Ziegler M. Cambronne X. A., and Baur J. A. (2020). SLC25A51 is a mammalian mitochondrial NAD⁺ transporter. *Nature*, 588 (7836), 174–179.
- 2 Kory N. uit de Bos J. van der Rijt S. Jankovic N. Güra M. Arp N. Pena I. A. Prakash G. Chan S. H., Kunchok T. Lewis C. A., and Sabatini D. M. (2020). MCART1/SLC25A51 is required for mitochondrial nad transport. *Science Advances*, 6 (43).

SAT169

The hepatocellular vitamin D receptor regulates liver regeneration after partial hepatectomy

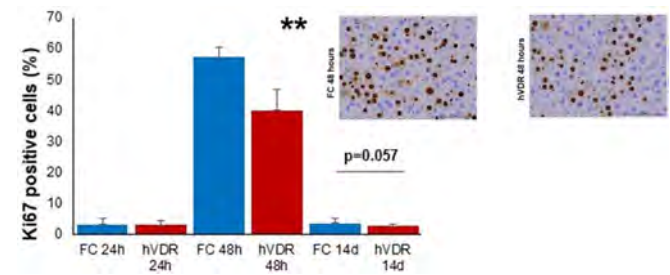
Hari Elangovan^{1,2}, Jeremy Keane¹, Sarinder Chahal^{1,2}, Jennifer Chen¹, Christopher Liddle^{3,4,5}, Jenny Gunton^{1,2,4,5}. ¹Westmead Institute of Medical Research, The Centre for Diabetes, Obesity and Endocrinology Research, Westmead, Australia; ²Garvan Institute of Medical Research, Darlinghurst, Australia; ³The Westmead Institute for Medical Research, The Storr Liver Unit, Westmead, Australia; ⁴Westmead Hospital, Westmead, Australia; ⁵The University of Sydney, Faculty of Medicine and Health, Camperdown, Australia
Email: harendran.elangovan@health.qld.gov.au

Background and aims: There is growing evidence to suggest a role for the vitamin D receptor (VDR) endocrine axis in the modulation of hepatic pathophysiology. However, normal hepatocytes express very low levels of the receptor, and the current dogma suggests that VDR mediates its hepatic functions through paracrine effects from non-parenchymal support tissue. We explored whether hepatocellular VDR (hVDR) might regulate liver regeneration following 2/3 partial hepatectomy (PHx) in a murine model. We hypothesized that hVDR null mice would experience worse regenerative outcomes after PHx.

Method: Hepatocyte-specific VDR null mice (hVDR null) and their floxed control (FC) littermates were bred via albumin promoter driven Cre-LoxP recombination. Utilizing Ki67 immunohistochemistry and polymerase chain reaction of cell cycle and apoptotic regulators, we comparatively analyzed the livers of hVDR null and their controls at 1-, 2- and 14-days post PHx.

Results: hVDR elimination blunted the hepatic regenerative response following PHx ((Ki67 positivity at 48 h hours, $57.1 \pm 3.2\%$ vs $40 \pm 6.5\%$, $p=0.002$) in hVDR null mice (see figure). This reduced cell proliferation appeared to persist into the 14-day mark with a diminution in gross regenerated liver weight (1.03 ± 0.02 g versus 1.11 ± 0.039 g, $p<0.05$) and a reduced liver-to-bodyweight ratio ($3.6 \pm 0.2\%$ vs. $4.0 \pm 0.4\%$, $p<0.005$) in hVDR null mice. Diminished cell

proliferation was associated with reduced mRNA expression of cell cycle drivers Cyclin D ($p<0.05$), Cyclin E1 ($p<0.01$) and Cdk2 ($p<0.05$). We did not identify major differences in the expression of apoptotic regulators at the various time points examined.



Conclusion: hVDR supports liver regeneration following PHx and loss of function appears to stymie this process predominantly through impairment in cell cycle transition, consistent with VDR's function as a transcription factor. These results add further insight into the panoply of mechanisms by which VDR signaling supports hepatic homeostasis following tissue injury. VDR receptor ligands may have therapeutic utility in optimizing regenerative outcomes in the clinical setting.

SAT170

Selective induction of macrophage RNF41 stimulates liver regeneration in hepatectomized healthy and fibrotic mice

Alazne Moreno-Lanceta^{1,2}, Mireia Medrano-Bosch¹, Yilliam Fundora^{2,3}, Meritxell Perramón^{2,4}, Jessica Aspas³, Marina Parra-Robert⁴, Sheila Baena³, Constantino Fondevila^{2,3}, Elazer Edelman^{5,6}, Wladimiro Jiménez^{1,2,4}, Pedro Melgar-Lesmes^{1,2,5}. ¹Department of Biomedicine, School of Medicine, University of Barcelona, Barcelona, Spain; ²Institut d'Investigacions Biomèdiques August Pi-Sunyer (IDIBAPS), Centro de Investigación Biomédica en Red de Enfermedades Hepáticas y Digestivas (CIBERehd), Barcelona, Spain; ³Liver Transplant Unit, Institut Clínic de Malalties Digestives i Metabòliques, Hospital Clínic, University of Barcelona, Barcelona, Spain; ⁴Biochemistry and Molecular Genetics Service, Hospital Clínic Universitari, Barcelona, Barcelona, Spain; ⁵Massachusetts Institute of Technology, Institute for Medical Engineering and Science, Massachusetts Institute of Technology, Cambridge, United States; ⁶Cardiovascular Division, Brigham and Women's Hospital, Harvard Medical School, Boston, Boston, United States
Email: pmelgar@ub.edu

Background and aims: Hepatectomy and liver transplantation are the standard of care in patients with liver tumours and end-stage liver disease, respectively. Macrophage RNF41 is an E3 ubiquitin-protein ligase that has been associated with muscle regeneration but its role in liver repair is unknown. We aimed to evaluate the regenerative effects of macrophage RNF41 induction in mouse models of partial hepatectomy.

Method: Fibrosis was induced with i.p. injections of CCL₄ (1/8 in corn oil) in BALB/c mice (n=12) twice a week for 9 weeks. Partial hepatectomy was carried out in twelve healthy (70% resection, HP70) or fibrotic (40% resection, HP40) mice. Selective macrophage RNF41 induction was achieved with i.v. (50 µg/Kg) injection of a plasmid encoding RNF41 regulated by a CD11b promoter and linked to dendrimer-graphite nanoparticles (pRNF41-DGNP) every 3 days for 9 days. A scrambled pRNF41 composition served as control (pSCR-DGNP). Liver restoration rate, proliferating cell nuclear antigen (PCNA) immunostaining, hepatic function and the expression of growth factors were evaluated. *In vitro* assays were designed to assess hepatocyte proliferation under stimulation with conditioned media from RAW 264.7 macrophages treated with pRNF41-DGNP or pSCR-DGNP.

POSTER PRESENTATIONS

Results: Induction of macrophage RNF41 promoted higher hepatic restoration rate in HP70 mice treated with pRNF41-DGNP than in mice receiving pSCR-DGNP (6.3 ± 0.1 g/body weight, BW vs. 7.1 ± 0.1 g/BW, $p < 0.001$). This effect was highlighted by the higher number of hepatic PCNA positive cells (3.2 ± 0.3 vs. 15.6 ± 0.9 , $p < 0.001$). Induction of RNF41 did not affect hepatic function (AST, 511.8 ± 81.8 vs. 562.6 ± 59.2 U/L, ns; ALT, 117.3 ± 7.3 vs. 122.2 ± 13.3 U/L, ns). Fibrotic mice with HP40 treated with pRNF41-DGNP also showed a higher hepatic restoration rate (6 ± 0.1 g/BW vs. 7 ± 0.1 g/BW, $p < 0.0001$) and increased PCNA positive cells (2.6 ± 0.2 vs. 19.2 ± 2.4 , $p < 0.001$) than fibrotic animals receiving pSCR-DGNP. In contrast to healthy mice with HP70, the selective macrophage RNF41 induction did improve liver function in fibrotic HP40 mice (AST, 742.1 ± 83.7 vs. 325.1 ± 72 U/L, $p < 0.01$; ALT, 175.9 ± 15.15 vs. 65.17 ± 10.2 U/L, $p < 0.001$). The pro-regenerative effect of RNF41 that we observed in both animal models of partial hepatectomy was associated with an increased expression of liver insulin-like growth factor 1 (IGF-1) (HP70, 1 ± 0.1 vs. 4 ± 1 fold change (fc), $p < 0.05$; HP40, 1 ± 0.1 vs. 2.8 ± 0.6 fc, $p < 0.05$). Conditioned media from macrophages treated with pRNF41-DGNP stimulated hepatocyte proliferation (0.2 vs. 0.3 arbitrary units, ai, $p < 0.0001$). This proliferative effect was reduced by IGF-1 blockade with a specific antibody (0.3 vs. 0.2 ai, $p < 0.0001$).

Conclusion: Macrophage RNF41 plays a major role in hepatic regeneration after partial hepatectomy. This work provides a novel therapeutic target for the stimulation of liver regeneration after liver resection.

SAT171

Generation of functional ductal organoid with biliary tree network in decellularized liver scaffold

Jiaxian Chen¹, Xi Liang², Heng Yao¹, Shiwen Ma¹, Hui Yang¹, Deying Chen¹, Jing Jiang¹, Dongyan Shi¹, Jiaojiao Xin¹, Lei Geng³, Yun Li⁴, Jun Li¹. ¹The First Affiliated Hospital, Zhejiang University School of Medicine, State Key Laboratory for Diagnosis and Treatment of Infectious Diseases, Hangzhou, China; ²Taizhou Central Hospital (Taizhou University Hospital), Precision Medicine Center, Taizhou, China; ³The First Affiliated Hospital, Zhejiang University School of Medicine, Hangzhou, China; ⁴Zhejiang University
Email: lijun2009@zju.edu.cn

Background and aims: Developing functional biliary tree organoids is essential for liver regenerative medicine. This study aims to construct a functional ductal organoid (DO) with biliary tree network in decellularized liver scaffold (DLS) with primary cholangiocytes.

Method: Primary cholangiocytes isolated from mouse extrahepatic bile ducts were transplanted into the rat DLS to construct a functional DO. The developed DOs were dynamically characterized by bio-functions and the bio-processes with metabolomics.

Results: Functional DOs were generated in DLS retaining native structure and bioactive factors with mouse primary cholangiocytes expressing enriched biomarkers. The results of morphology assessment showed that the biliary tree-like structures gradually formed from day 3 to day 14. The cholangiocytes in the DOs maintained high viability and highly expressed 9 specific biomarkers (eg. cytokine 7, cytokine 19, EpCAM, aquaporin 1, prominin 1). The basal-apical polarity was observed at day 14 with immunostaining of E-cadherin and alpha-tubulin. The rhodamine 123 transport assay and active collection of cholyl-lysyl-fluorescein revealed that DOs exhibited functions of bile secretion and transportation at day 14, and without observed in monolayer and hydrogel culture systems. The metabolomics analysis with 1075 peak pairs showed that serotonin, as a key molecule of tryptophan metabolism pathway linked to the biliary functions, specifically expressed in functional DO during the period of whole culture process.

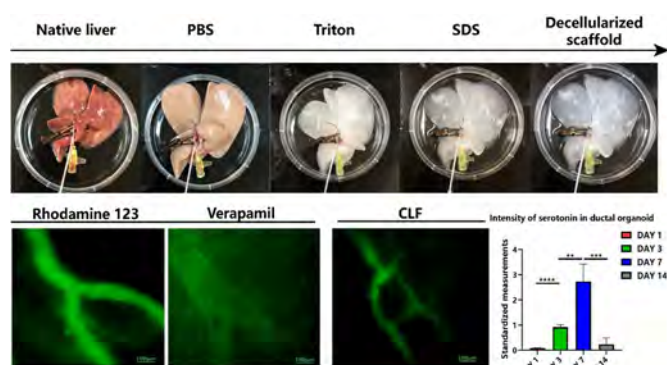


Figure: Primary cholangiocytes generated into functional ductal organoid with biliary tree network in decellularized whole liver scaffold.

Conclusion: A functional DO, with biliary tree network and differential expression of serotonin, was generated with primary cholangiocytes in DLS. It provides the feasibility for disease modeling and drug screening, and paves the way for future clinical therapeutic applications.

SAT172

Molecular basis of hepatic differentiation of human bone marrow mesenchymal stem cell in vivo

Dongyan Shi¹, Xi Liang², Jing Jiang¹, Lunzhi Yuan³, Jiaojiao Xin¹, Suwan Sun¹, Beibei Guo¹, Xingping Zhou¹, Jiaxian Chen¹, Tong Cheng³, Xin Chen⁴, Ningshao Xia³, Jun Li¹. ¹The First Affiliated Hospital, Zhejiang University School of Medicine, State Key Laboratory for Diagnosis and Treatment of Infectious Diseases, National Clinical Research Center for Infectious Diseases, Collaborative Innovation Center for Diagnosis and Treatment of Infectious Diseases, Hangzhou; ²Taizhou Central Hospital (Taizhou University Hospital), Precision Medicine Center, Taizhou, China; ³Xiamen University, State Key Laboratory of Molecular Vaccinology and Molecular Diagnostics, National Institute of Diagnostics and Vaccine Development in Infectious Diseases, School of Life Sciences and School of Public Health, Xiamen, China; ⁴Zhejiang University School of Medicine, Institute of Pharmaceutical Biotechnology and the First Affiliated Hospital Department of Radiation Oncology, Hangzhou, China
Email: lijun2009@zju.edu.cn

Background and aims: The human bone marrow mesenchymal stem cells (hBMSCs) derived hepatocytes are promising in liver regenerative medicine. This study aims to clarify the detailed molecular basis of the hepatocyte differentiation in vivo.

Method: The transcriptomics of hBMSCs-derived hepatocytes isolated from the liver-humanized mice were performed to reveal the differentiation basis.

Results: The cultured hBMSCs-derived hepatocytes isolated from the liver-humanized mice with hBMSCs transplantation exhibited the phenotypical characteristics of mature hepatocytes. Functional analysis of 2385 differentially expressed genes showed the implanted hBMSCs initiated hepatic differentiation at day-2 and gradually matured within 14 days. The bioprocesses of losing of stem cell characteristics, the hepatocyte differentiation and maturation (including glucose biosynthesis, drug metabolism, lipid transport, blood coagulation and complement cascades) were observed at day-1, day-2 and day-14, respectively. Engineering Evaluation by Gene Categorization analysis showed that the proportion of sufficient gene sets of hepatocyte differentiation increased from 4.6% at day-1 to 39.3% at day-14. The hepatocyte specific functional bioprocesses, including organic and carboxylic acid biosynthesis, and sulfur compound and fatty acid metabolism, appeared within 7 days. Transcription factor (TF) predictive analysis revealed that the liver specific TFs (including HNF4A, NR1H4 and FOXA3) initially expressed and regulated the hepatocyte functions from day-2. The increased

expressions of top 10 TFs confirmed their regulation during the hepatic differentiation periods.

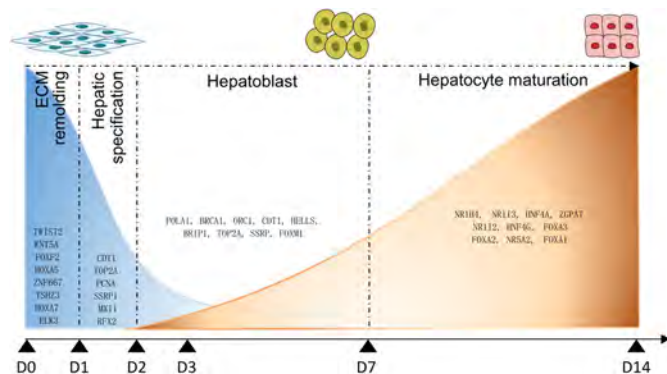


Figure: Process of hepatic differentiation of hBMSCs in vivo.

Conclusion: This study clarified the molecular basis of rapidly hepatocytic differentiation and maturation within 14 days in vivo, which may help for the clinical use of hBMSCs-derived hepatocytes in liver regenerative medicine.

SAT173

Dynamic alterations of metabolites revealed the vascularization progression of bioengineered liver

Qian Zhou¹, Beibei Guo¹, Deying Chen¹, Heng Yao¹, Xi Liang², Jiaojiao Xin¹, Dongyan Shi¹, Keke Ren¹, Hui Yang¹, Jing Jiang¹, Jun Li¹.
¹The First Affiliated Hospital, Zhejiang University School of Medicine, State Key Laboratory for Diagnosis and Treatment of Infectious Diseases, Hangzhou, China; ²Taizhou Central Hospital (Taizhou University Hospital), Precision Medicine Center, Taizhou, China
 Email: lijun2009@zju.edu.cn

Background and aims: Vascularization is a critical but challenging process in developing functional bioengineered liver with the decellularized liver scaffolds (DLSs), in which, the process is accompanied by cell-specific metabolic alterations. The aims of the study were to explore the global change in the metabolic profile of human umbilical vein endothelial cells (HUVECs) during vascularization, and to identify the specific metabolites for evaluating the biological activities and cellular status, thereby providing a foundation for future research on the construction of a functionally vascularized bioengineered liver.

Method: Decellularize the whole rat liver with the most commonly used cocktail of detergents phosphate-buffered saline, 1% (v/v) Triton X-100 and 0.1% (w/v) sodium dodecylsulfate at a flow rate of 20 ml/min. The resulted DLSs were vascularized with HUVECs, and a liquid chromatography mass spectrometry-based metabolomics was performed on culture supernatants collected at 0, 1, 3, 7, 14 and 21 days during the 3 weeks of dynamic perfusion. The 309 positive metabolites were analysed with principal component analysis, partial least squares discriminant analysis and orthogonal partial least-squares discriminant analysis. MetaboAnalyst 5.0 database was then used for metabolic pathway and enrichment analysis.

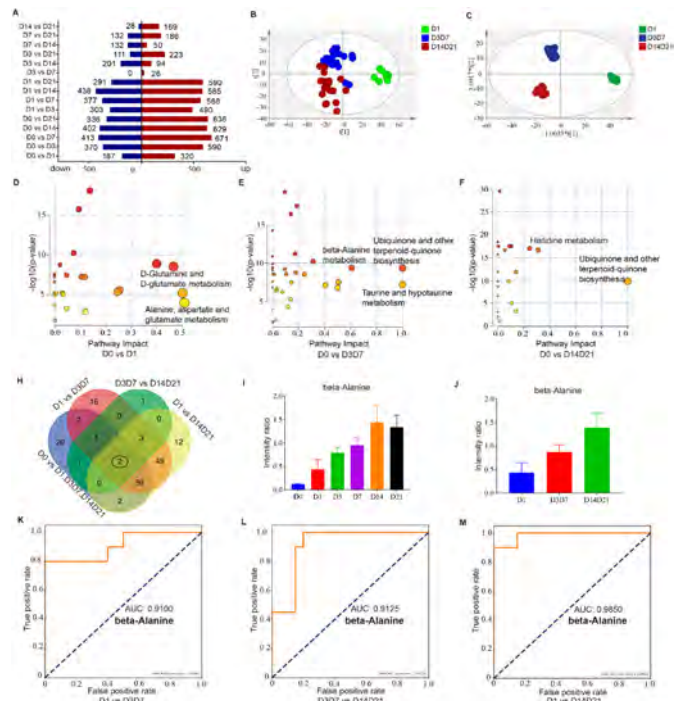
Results: 1. A total of 1698 peak pairs were detected from the culture supernatant, with 309 metabolites being positively identified with high confidence using the dansyl library.

2. Principal component analysis showed a good separation of phase D1 (d0-d1), phase D3D7 (d3-d7), and phase D14D21 (d14-d21).

3. The biological processes of phase D1 were associated with alanine, aspartate and glutamate metabolism, D-Glutamine and D-glutamate metabolism. The metabolites that were activated in phase D3D7 mainly participated in ubiquinone and other terpenoid-quinone biosynthesis, taurine and hypotaurine metabolism, and beta-alanine metabolism. Meanwhile, the metabolites in phase D14D21 were

more relevant to histidine metabolism, and ubiquinone and other terpenoid-quinone biosynthesis.

4. beta-Alanine discriminated any two phases with AUCs of 0.9100, 0.9125 and 0.9850. Its high expression on day 14 predicted the patency of vascularized bioengineered livers.



Conclusion: In this study, we revealed the metabolic alterations that occur during DLS vascularization and divided the vascularization process into 3 phases from metabolic perspective, including phase D1 (cell proliferation and migration), phase D3D7 (vascular lumen formation) and phase D14D21 (functional endothelial barrier formation). A high level of beta-Alanine on day 14 predicted the patency of vascularized bioengineered livers, which confirmed our previous finding that 14 days of in vitro dynamic culture is required for DLS vascularization.

Molecular and cellular biology

SAT177

Pharmacologic inhibition of HSD17B13 is hepatoprotective in mouse models of liver injury

Manuel Roqueta-Rivera¹, Mary Chau¹, Kelsey Garlick¹, Anand Balakrishnan¹, Archie C. Reyes¹, Jonathan Lloyd¹, Sourav Ghorai¹, Jiang Long¹, Joe Panarese¹, Bin Wang¹, Khanh Hoang¹, Tim Greizer¹, Lijuan Jiang¹, Guoqiang Wang¹, Yat Sun Or¹, Bryan Goodwin¹. ¹Enanta Pharmaceuticals, Inc., United States
 Email: mroqueta@enanta.com

Background and aims: Genome wide association studies identified a loss of function variant (rs72613567:TA) in HSD17B13 which confers protection against chronic liver diseases. As a result, HSD17B13 inhibitors may have clinical utility in non-alcoholic steatohepatitis and other liver diseases. Here we describe the identification and characterization of a novel, potent, and selective HSD17B13 inhibitor with hepatoprotective effects in preclinical models of liver injury.

POSTER PRESENTATIONS

Method: Multiple chemical series of HSD17B13 inhibitors were identified and optimized for potency, selectivity, and pharmacokinetic properties. Mass spectrometry was used to monitor HSD17B13 inhibition (HSD17B13i) of dehydrogenase activity in biochemical and cellular assays. *In vivo*, HSD17B13i was evaluated in a mouse model of acute (adenoviral) and chronic liver injury (choline deficient, L-amino acid defined, high fat diet; CDAHFD; A16092201). Markers of inflammation, injury and fibrosis were measured in plasma and liver. Transcriptomics and lipidomics suggested a potential hepatoprotective mechanism for HSD17B13i. Primary human hepatocytes (PHH) carrying the TA allele were used in gain of function studies.

Results: In biochemical assays, a tool compound (EP-036332) inhibited human HSD17B13 with a half-maximal inhibitory concentration (EC_{50}) of 14 nM. In cell based assays, EP-036332 inhibited human and mouse HSD17B13 with EC_{50} s of 47 and 55 nM, respectively. EP-036332 was selective for HSD17B13 over other HSD17B enzymes (>400 fold). In an adenoviral liver injury model, both HSD17B13i and a short hairpin RNA targeting mouse HSD17B13 were hepatoprotective. In addition to reduced plasma ALT and TNF- α , pharmacologic and genetic inhibition of HSD17B13 had overlapping transcriptional effects, including modulation of natural killer cell cytotoxicity (*Ifng*, *Gzmb*), chemokines (*Cxcr6*, *Cxcl9*, *Ccl2*), and necroptosis (*Tnf*, *FasL*). A similar gene expression profile was seen in a CDAHFD liver injury model (3 weeks of diet lead-in and 8 weeks of HSD17B13i). Within one week, HSD17B13i dose-dependently decreased ALT and favored an anti-inflammatory (*Nlrp3*, *S1pr4*), anti-fibrotic (*Tgfb2*, *Ctgf*) gene profile. After 8 weeks of HSD17B13i, liver hydroxyproline, plasma ALT and AST were significantly decreased. Lipidomics revealed HSD17B13i effects on lipid droplet composition (sphingolipids) and lower liver sphingosine-1-phosphate and cholesterol. Consistent with *in vivo* observations, rescue of HSD17B13 in PHH carrying the TA allele resulted in sphingolipid alterations.

Conclusion: Hepatoprotection by HSD17B13i in rodent injury models is characterized by a favorable bioactive lipid profile with a decrease in markers of cytotoxic immune cell activation, cell death, and fibrosis. Overall, these data provide preclinical pharmacologic validation of HSD17B13 inhibitors for the treatment of liver disease.

SAT178

Inhibition of NLRP3 inflammasome by GPR40 agonists

Jeongwoo Park¹, Moo-Yeol Lee², Yoon-Seok Seo², Sung-Chul Lim³, Keon Wook Kang¹. ¹Seoul National University, College of pharmacy, Seoul, Korea, Rep. of South; ²Dongguk University, College of pharmacy, Goyang, Korea, Rep. of South; ³Chosun University, College of medicine, Gwangju, Korea, Rep. of South
Email: kwkang@snu.ac.kr

Background and aims: NOD-like receptor pyrin domain-containing protein 3 (NLRP3) inflammasome is a multi-protein intracellular complex that activates pro-inflammatory cytokines including interleukin (IL)-1 β and IL-18. The activation of inflammasome is known to be related with metabolic inflammation such as the progression of non-alcoholic steatohepatitis. Fasiglifam (TAK875), a selective G-protein coupled receptor 40 (GPR40) agonist with high affinity, significantly improves glucose-dependent insulin secretion and weight gain without hypoglycemia. In this study, we evaluated the functional role of GPR40 agonists in the activation of NLRP3 inflammasome in bone marrow-derived macrophages (BMDMs), kupffer cells and an acute hepatitis mouse model.

Method: Primary BMDMs and kupffer cells were mainly used for cell-based analyses. For NLRP3 inflammasome activation, BMDMs were primed with LPS (100 ng/ml) for 4 h, and then pretreated with GPR40 agonists for 10 min, followed by incubation with ATP (1 mM) for 30 min. To test *in vivo* effects of TAK875, 9 weeks old C57BL/6J male mice were orally administrated with vehicle or 10 mg/kg TAK875 once a day for 4 days. The mice were intraperitoneally injected with 2.5 mg/kg LPS and 750 mg/kg D-galactosamine (D-GalN), and

sacrificed after anaesthetization and blood and liver tissues were collected 4 h after LPS/D-GalN injection.

Results: TAK875 and AMG1638 suppressed activation of NLRP3 inflammasome in BMDMs. TAK875 inhibited the activation of inflammasome by blocking apoptosis-associated speck-like protein containing a CARD (ASC) formation which is a component of inflammasome. TAK875 also suppressed NLRP3 inflammasome-induced pyroptosis of BMDM. Moreover, nuclear factor- κ B (NF- κ B)-dependent priming signal of NLRP3 inflammasome was also partially inhibited by TAK875 and AMG1638. It has been known that intracellular Ca^{2+} increase by ATP, nigericin (pore forming toxin) or endoplasmic reticulum (ER) stress activates NLRP3 inflammasome. Pre-exposure of BMDM to TAK875 suppressed ATP-induced intracellular Ca^{2+} increase, which was reversed by thapsigargin, a sarco/endoplasmic reticulum Ca^{2+} -ATPase (SERCA) inhibitor. Oral administration of mice with TAK875 decreased serum IL-1 β increase in mice treated with lipopolysaccharide/D-galactosamine *in vivo*.

Conclusion: These findings provide an evidence that free fatty acid-sensing GPR40 plays a key role in NLRP3 inflammasome pathway.

SAT179

Role of Monocyte chemoattractant protein-induced protein 1 in liver fibrosis and activation of hepatic stellate cells

Natalia Pydyn¹, Anna Ferenc¹, Justyna Kadłuczka¹, Piotr Major², Edyta Kus³, Tomasz Hutsch^{4,5}, Andrzej Budzyński², Jolanta Jura¹, Jerzy Kotlinowski¹. ¹Faculty of Biochemistry, Biophysics and Biotechnology, Jagiellonian University, Department of General Biochemistry, Kraków, Poland; ²2nd Department of General Surgery, Jagiellonian University Medical College, Poland; ³Jagiellonian Centre for Experimental Therapeutics, Jagiellonian University, Poland; ⁴Laboratory of Centre for Preclinical Research, Medical University of Warsaw, Department of Experimental Physiology and Pathophysiology, Poland; ⁵Veterinary Diagnostic Laboratory ALAB Bioscience, Poland
Email: natalia.pydyn@uj.edu.pl

Background and aims: Monocyte chemoattractant protein-induced protein 1 (MCP1) is a negative regulator of inflammation, acting through cleavage of transcripts coding for proinflammatory cytokines and by inhibition of NF κ B activity. It was shown that Mcp1 is involved in suppression of inflammatory response in liver macrophages. Moreover, overexpression of Mcp1 reduces liver injury in septic mice, by inhibition of inflammatory reaction. On the other hand, Mcp1 deletion in liver epithelial cells in Mcp1^{fl/fl}Alb^{Cre} mice resembles features of primary biliary cholangitis. In this study, we analyzed MCP1 level in human fibrotic livers and hepatic cells isolated from CCl₄-treated mice. We also investigated MCP1 impact on activation status of LX-2 hepatic stellate cell line.

Method: We analyzed liver biopsies isolated from 30 patients with fibrosis stage ranging from 0 to 4. To induce liver fibrosis during *in vivo* experiments, mice were injected with CCl₄ dissolved in corn oil (0, 2 mg/g), 3 times a week for 4 weeks. *In vitro* experiments were performed on LX-2 cells treated with TGF- β (5 or 10 ng/ml) to induce process of their activation.

Results: Analysis of patients' liver biopsies revealed that MCP1 level in liver tissue correlates with the development of fibrosis. To elucidate in which type of liver cells Mcp1 level is induced during fibrotic changes, we analyzed its level in hepatocytes, HSCs and Kupffer cells isolated from fibrotic murine livers. We found that treatment with CCl₄ induces Mcp1 expression in hepatocytes and hepatic stellate cells. On the other hand, Mcp1 level in Kupffer cells from fibrotic livers is decreased. To evaluate role of MCP1 in activation of HSCs, we stimulated LX-2 cell line with TGF- β which resulted in increase of MCP1 level. Moreover, overexpression of MCP1 in LX-2 cells led to decreased mRNA expression of HSCs activation markers e.g. *Acta2*, *Tgfb*, *Col1a1* and α -SMA protein level. Contrary, MCP1 silencing in LX-2 cells resulted in their increased activation status.

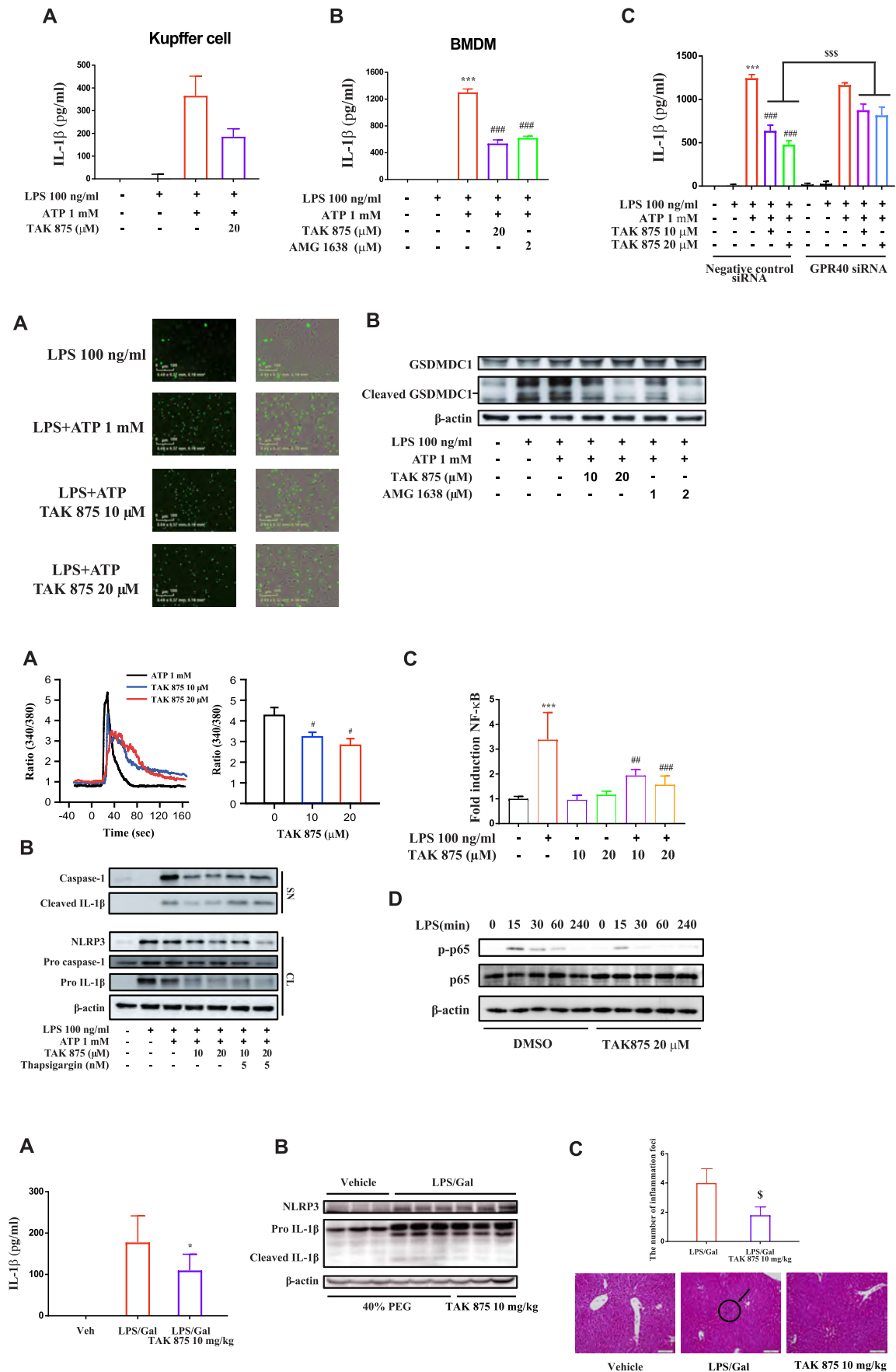


Figure: (abstract: SAT178)

POSTER PRESENTATIONS

Conclusion: In conclusion, we demonstrated a potent MCP1P1 role in liver fibrosis and activation of hepatic stellate cells. MCP1P1 presence in HSCs can be essential to prevent their excessive activation.

Acknowledgments: This study was supported by National Science Centre, grant number K/PBM/000672.

SAT180

The genomic landscape of IDH1 mutant intrahepatic cholangiocarcinoma: a multicentre comprehensive analysis

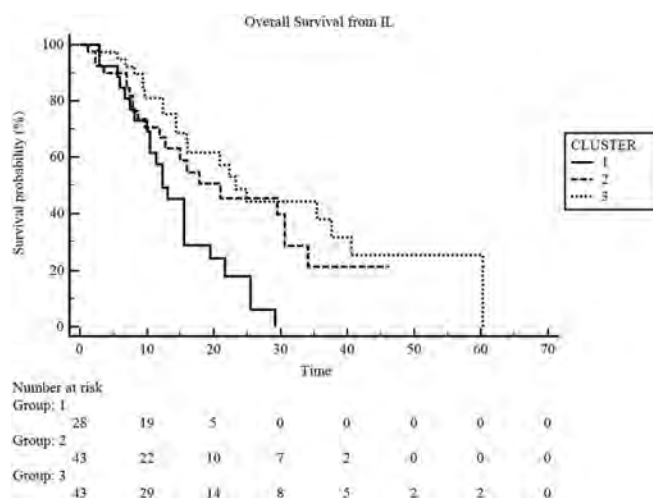
Margherita Rimini¹, Teresa Mercade Macarulla², Valentina Burgio¹, Sara Lonardi³, Monica Niger⁴, Mario Scartozzi⁵, Ilario Raposelli⁶, Giuseppe Aprile⁷, Francesca Ratti¹, Federica Pedica¹, Helena Verdaguer², Floriana Nappo³, Federico Nichetti⁴, Eleonora Lai⁵, Martina Valgiusti⁶, Alessandro Cappetta⁷, Carles Fabregat², Matteo Fassan³, Filippo De Braud⁴, Marco Puzzone⁵, Giovanni Luca Frassinetti⁶, Francesca Simionato⁷, Francesco De Cobelli¹, Luca Aldrighetti¹, Lorenzo Fornaro⁸, Stefano Cascinu¹, Andrea Casadei Gardini¹. ¹Università Vita-Salute, IRCCS-San Raffaele Hospital; ²Vall d'Hebron Institute of Oncology; ³Veneto Institute of Oncology IOV-IRCCS; ⁴Istituto Nazionale Tumori di Milano; ⁵University Hospital of Cagliari; ⁶Istituto Romagnolo per lo Studio dei Tumori "Dino Amadori"-IRST IRCCS; ⁷Azienda ULSS8 Berica, Vicenza; ⁸University Hospital of Pisa
Email: margherita.rimini@gmail.com

Background and aims: The results obtained with new anti-IDH1 drugs in advanced cholangiocarcinoma (CCA) IDH1-mutant (IDH1m) patients, even if positive, didn't show durable responses. A better understanding of the biomolecular pathway, which could be involved in mechanisms of resistance to treatments, is an urgent need.

Method: We performed a retrospective analysis on 247 CCA patients (125 IDH1m and 122 IDH1 wt) tested with the FoundationOne platform. The primary end point was to perform a clustering analysis on IDH1m patients.

Results: From the clustering analysis, three main clusters resulted evident. The cluster 1 presented 84 mutated genes, including PI3K related genes (AKT, EGFR, ERBB2, FGFR2, FLT3, PDGFRA, PIK3CA, PIK3R1, PTEN, RET, SDHB, SDHC, SDHD and TSC1), and RAS related genes (BRAF, CIC, EGFR, ERBB2, FGFR2, FLT3, MAP2K1, MAP3K1, PDGFRA, PTPN11, RER, SSDHB, SDHC and SDHD). The cluster 2 presented 89 mutated genes, including chromatin modification related genes (ARID1A, ASXL1, CREBBP, DAXX, DNMT3A, KDM5C, MLL2, MLL3, NCOR1, PBRM1 and SETD2), DNA damage control related genes (ATM, BAP1, BRCA2, ERCC4, FANCA, MLH1, MSH2, MSH6 and TP53) and cell cycle related genes (ABL1, CASP8, CDK4, CDKN2A, DAXX, PPP2R1A and TP53). The cluster 3 presented 45 mutated genes, including cell cycle related genes (CDKN2A, MED12, NFE2L2, RB1 and TP53). At the univariate analysis for OS from the first line therapy, the inclusion in the cluster 1, 2 or 3 was highlighted to have a prognostic impact. In particular, the IDH1 m patients included in the cluster 1 showed a poorer OS compared with those included in the cluster 2 and 3 ($p=0.0025$).

In the entire sample of patients (IDH1m and IDH1wt) the most frequently mutated or altered genes in our sample were: CDKN2A (27%), ARID1A (20%), CDKN2B (17%), PBRM1 (17%), KRAS/NRAS (16%), BAP1 (16%), TP53 (15%), FGFR2 (10%), BRCA2 (9%), PIK3CA (8.5%), ATM (7%), MTAP (7%) and MAP3K1 (7%). IDH1m patients showed more frequently alterations in CDKN2B ($p=0.04$), and less frequently alterations in TP53, FGFR2, BRCA2, ATM and MAP3K1 ($p=0.0006$, $p=0.0013$, $p=0.0015$, $p=0.047$, $p=0.0053$, respectively). In IDH1m cohort CDKN2A and CDKN2B resulted to negatively impact on DFS, while CDKN2A, CDKN2B and PBRM1 negatively impacted on OS from surgery; no genomic alterations resulted to impact prognosis in IDH1wt cohort. In IDH1m cohort alterations in KRAS/NRAS and TP53 resulted to negatively impact PFS while alterations in TP53 and PIK3CA negatively impacted on OS from I line; in the IDH1wt patients, MTAP negatively impact PFS while TP53 negatively impact OS from I line.



Conclusion: We identified three genomic clusters with prognostic value in IDH1m patients. This new insight in IDH1m CCA could help to identify mechanisms of resistance to treatments, including anti-IDH1.

SAT181

Isolation of hepatocytes from various liver tissues by a novel, semi-automated perfusion technology

Carsten Poggel¹, Timo Adams¹, Ronald Janzen¹, Alexander Hofmann², Olaf Hardt¹, Elke Roeb³, Sarah K. Schröder⁴, Carmen G. Tag⁵, Martin Roderfeld³, Ralf Weiskirchen⁵. ¹Miltenyi Biotec B.V. Co. KG, Bergisch Gladbach, Germany; ²Miltenyi Biotec B.V. Co. KG, Bergisch Gladbach, Germany; ³Justus-Liebig-University Giessen, Department of Gastroenterology, Giessen, Germany; ⁴RWTH University Hospital Aachen, Institute of Molecular Pathobiochemistry, Experimental Gene Therapy and Clinical Chemistry (IFMPEGKC), Germany; ⁵RWTH University Hospital Aachen, Institute of Molecular Pathobiochemistry, Experimental Gene Therapy and Clinical Chemistry (IFMPEGKC), Aachen, Germany
Email: carsten@miltenyibiotec.de

Background and aims: Primary liver cells represent a major tool in biomedical research. Presently, different protocols for the isolation of liver cell subsets have been introduced, which require trained staff to avoid considerable fluctuations in quality and yield. We aimed at establishing an easy workflow for the generation of hepatocytes.

Method: We developed a new semi-automated perfusion technology, which is suitable for the gentle, rapid, and efficient generation of single-cell suspensions from rodent livers. Tissue is clamped into a newly designed disposable (Perfuser) and enzymatically digested using optimized components. Afterwards, single-cells are liberated from the tissue by a short mechanical disruption of the perfused tissue and the sample is applied to a strainer to remove any remaining larger particles from the single cell suspension. Yield, viability and purity of cells were determined. Cells were stimulated with different cytokines and expression of target genes was analyzed by Western blot analysis.

Results: The new perfusion technology is suitable to generate single-cell suspensions from liver tissue. We have constructed a new tube format (Perfuser) which is run in combination with optimized reagents and newly designed sleeves on the gentleMACS instrument for optimal isolation of hepatocytes. The yield isolated from one liver lobe is $\sim 14 \times 10^6$ cells with $\sim 83\%$ viability. In culture, the cells take on the characteristic flattened, hexagonal appearance and can be grown for several days. After stimulation with IL-1 β , the cells express and secrete large quantities of LCN2, previously shown to be a target of IL-1 β . The elaborated protocol takes less preparation time than conventional protocols and also enables the isolation of hepatocytes from other sources such as rat, hamster, and human liver specimens.

Conclusion: The Perfusion Technology allows simple and reliable isolation of primary hepatocytes. Perfuser and appropriate reagents were optimized for parenchymal rodent liver cells but can be adapted to non-parenchymal cells. The semi-automated workflow enabling liver perfusion in a closed system is easy to apply and helps to implement the 3R principle because only one liver lobule is perfused, while others can be used for further experimentation. Nested processing allows simultaneous handling of up to 8 samples. The protocol does not require inconvenient perfusion in living animals avoiding the need of animal ethics approval.

Abstract withdrawn

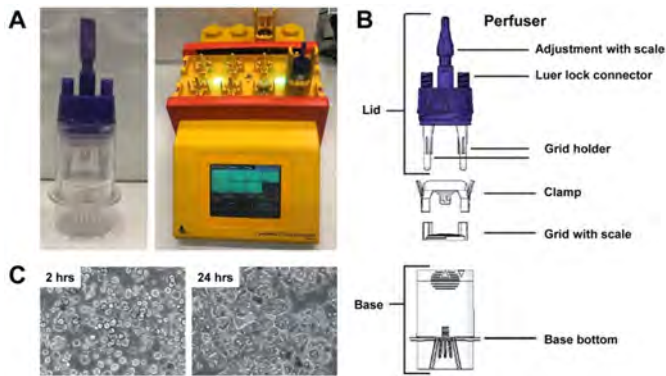


Figure: Semi-automated dissociation of liver tissue. (A) Overview of the Perfusion Technology. (B) Structure of the Perfuser used for generation of single cell cultures from rodent livers. (C) Hepatocytes isolated with optimized reagents after seeding for 2 hours (left) or 24 hours (right).

Conflicts of interest: Carsten Poggel, Timo Adams, Ronald Janzen, Alexander Hofmann and Olaf Hardt are employees of Miltenyi Biotec B.V. and Co. KG.

SAT183

Ptpn1 deletion protects oval cells against lipoapoptosis by favoring lipid droplet formation and dynamics

Pilar Valdecantos^{1,2}, Ines Barahona^{1,2}, Silvia Calero^{1,2}, Ruben Grillo-Risco³, Laura Pereira⁴, Carmen Soler⁵, Lara Lalglesia⁶, M. Jesús Moreno-Aliaga⁶, Laura Herrero⁵, Dolors Serra⁵, Carmelo Garcia-Monzon⁷, Águeda González⁷, Jesus Balsinde⁴, Francisco García-García³, Angela Martinez Valverde^{1,2}. ¹Instituto de Investigaciones Biomédicas Alberto Sols (CSIC-UAM), Metabolism and Cell signalling, MADRID, Spain; ²Centro de Investigación Biomédica en Red de Diabetes y Enfermedades Metabólicas Asociadas (CIBERdem), Spain; ³Príncipe Felipe Research Center, Bioinformatics and Biostatistics Unit, Valencia, Spain; ⁴Instituto de Biología y Genética Molecular (CSIC), Valladolid, Spain; ⁵Institut de Biomedicina de la Universitat de Barcelona (IBUB), Department of Biochemistry and Physiology, School of Pharmacy and Food Sciences. Universitat de Barcelona, Spain; ⁶Center for Nutrition Research, Department of Nutrition, Food Science and Physiology, Spain; ⁷Unidad de Investigación, Hospital Universitario Santa Cristina, Instituto de Investigación Sanitaria del Hospital Universitario de La Princesa, Spain

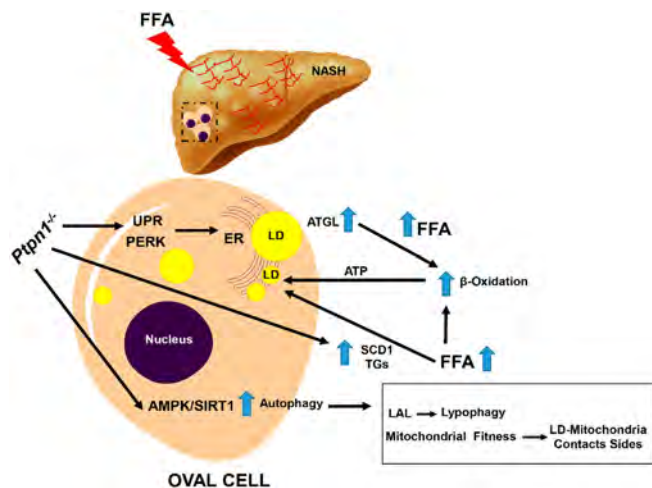
Email: pvaldecantos@iib.uam.es

Background and aims: Activation of oval cells has been related to hepatocyte injury during chronic liver diseases including non-alcoholic fatty liver disease (NAFLD). However, oval cells plasticity can be affected by the pathological environment. We previously found a protection against hepatocyte cell death by inhibiting protein tyrosine phosphatase 1B (PTP1B). Herein, we investigated the molecular and cellular processes involved in the lipotoxic susceptibility in oval cells expressing or not PTP1B.

POSTER PRESENTATIONS

Method: Palmitic acid (PA) induced apoptotic cell death in wild-type (*Ptpn1^{+/+}*) oval cells in parallel to oxidative stress and impaired autophagy. This lipotoxic effect was attenuated in oval cells lacking *Ptpn1* that showed up-regulated antioxidant defences, increased unfolded protein response (UPR) signaling, higher endoplasmic reticulum (ER) content and elevated stearyl CoA desaturase (*Scd1*) expression and activity.

Results: These effects in *Ptpn1^{-/-}* oval cells concurred with an active autophagy, higher mitochondrial efficiency and a molecular signature of starvation, favoring lipid droplet (LD) formation and dynamics. Autophagy blockade in *Ptpn1^{-/-}* oval cells reduced *Scd1* expression, mitochondrial fitness, LD formation and restored lipopoptosis, an effect also recapitulated by *Scd1* silencing. Importantly, oval cells with LDs were found in livers from *Ptpn1^{-/-}* mice with NAFLD.



Conclusion: *Ptpn1* deficiency restrained lipoapoptosis in oval cells through a metabolic rewiring towards a “starvation-like” fate, favoring autophagy, mitochondrial fitness and LD formation. Dynamic LD-lysosomal interactions likely ensured lipid recycling and, overall, these adaptations protect against lipotoxicity. The identification of LDs in oval cells from *Ptpn1^{-/-}* mice with NAFLD opens new therapeutic perspectives to ensure oval cells viability and plasticity under lipotoxic liver damage.

SAT184

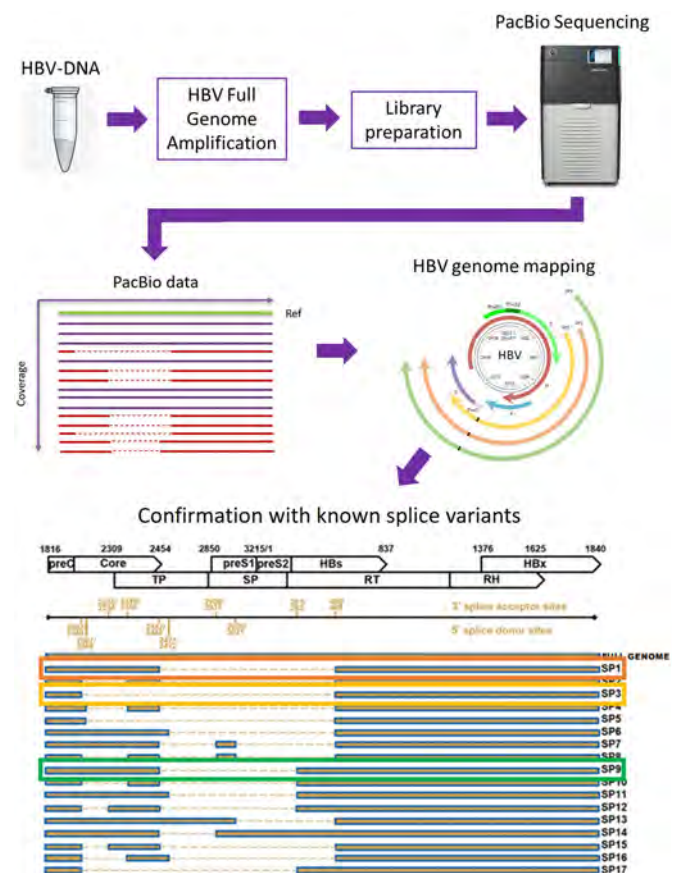
Accurate detection of HBV splice variant DNA by using long-read sequencing

Sanne Hulspas¹, Cornelis Knetsch¹, Michiel Weber¹, Anne Hout¹, Leen-Jan van Doorn¹. ¹Viroclinics-DDL, Rijswijk, Netherlands
Email: sanne.hulspas@ddl.nl

Background and aims: Hepatitis B virus (HBV) RNA splice variants might play an important role in the HBV life cycle and pathogenesis. Although the biological and clinical significance of splice variants remains to be defined, some studies have linked HBV spliced variants to impaired response to interferon- α therapy. In depth HBV genome analysis may help to understand the role of splice variants in disease pathogenesis. With long-read sequencing, a spliced HBV genome can be covered by a single read, in contrast to short reads where the spliced genome is sequenced by multiple fragmented shorter reads. In a mixed population sample with both splice variant and full genomes, these shorter reads may originate either from the spliced template or the original full length genome template. In this study, we report our findings on the accurate detection of HBV splice variant DNAs in plasma (derived from RNA splice variants generated in the liver) with PacBio long-read sequencing.

Method: Starting material for the analysis were plasma sample from HBV-infected patients. Nucleic acid extraction was performed by using the QIAamp MinElute Virus Spin Kit (QIAGEN). The isolated DNA was amplified for HBV full genome by PCR and nested PCR, using the Expand high-fidelity PCR kit (Roche Molecular Systems). Sequencing libraries were prepared using the SMRTbell Express Template Prep Kit 2.0 (Pacific Biosciences). All sequencing reactions were performed on the PacBio Sequel System with the Sequel Sequencing Kit 3.0 chemistry (Pacific Biosciences). Sequencing was performed by using the circular consensus sequencing (CCS) mode, creating HiFi consensus reads. Splice variant analysis was done by using our in-house bioinformatics pipeline Athena.

Results: A first indication of the presence of splice variants is obtained by visualizing the amplification products on gel and looking at the read length distribution after sequencing. In our samples we observed multiple amplicons with varying lengths. After sequencing the read length distribution showed samples with full length HBV genome CCS reads (~3200 bp) and shorter CCS reads of varying size (~1600, ~2000, ~2400 bp). CCS reads were bioinformatically mapped against an HBV reference sequence using minimap2. Consequently, the read mapping was parsed with separate scripting on individual read level, resulting in read counts for each unique start and end splice junction combination. The read counts for potential splice variants were summarized in a table and the most prevalent ones were compared with literature. All identified dominant splice variants were virtually identical to the splice variants described in literature. In the example shown, we specifically identified DNAs, derived from SP1, 3 and 9 (Figure 1).



Conclusion: HBV splice variant DNA can be accurately detected with PacBio long-read sequencing.

SAT185

The identification and characterization of novel bile acid-derived Farnesoid X Receptor agonists

Dannielle Kydd-Sinclair¹, Kimberly A. Watson¹, Alex Weymouth-Wilson², Gemma Packer³. ¹University of Reading, United Kingdom; ²ICE Group, Italy; ³NZP UK Ltd., United Kingdom
Email: dannielle.kydd-sinclair@reading.ac.uk

Background and aims: Since its orphanisation in the early 2000s, the farnesoid X receptor (FXR) has attracted significant attention due to its role in regulating genes involved in bile acid, lipid, glucose metabolism and inflammation. With these metabolic pathways underlying the aetiology of various liver diseases, it is unsurprising that pharmaceutical efforts have targeted FXR also for their treatment. While several FXR agonists, such as obeticholic acid, have been studied in clinical trials, they have been associated with adverse effects arising from the promiscuity of systemic FXR activation and efforts to limit or selectively modulate FXR downstream effects are now being investigated.

Method: *In silico* molecular modelling was performed using Surflex-dock (SYBYL, Tripos) to screen a library of bile acid-derived compounds. Lead compounds were tested further in Lantha screen coactivator recruitment assays (Invitrogen) and in biolayer interferometry assays (Sartorius) using biotinylated, recombinant FXR ligand binding domain. Compounds were added to cultured HepG2 and Huh7 cells for 6 hours, or given to C57BL/6 mice by oral gavage daily for 5 days. After respective treatment, cells or left lobe liver tissue were harvested and total RNA extracted for gene expression analysis by RT-qPCR.

Results: We have identified 2 novel compounds as potent and selective FXR agonists. Docking results, confirmed by the co-crystal structures of FXR LBD complexed with each compound, demonstrates a unique binding mode for each compound, not observed with classic bile acids, including occupancy of a receptor sub-pocket associated with allosteric activation. Both compounds had higher affinities for FXR and were more efficacious than obeticholic acid by up to ten times, and coactivator recruitment assays identified potential differential recruitment dependent on the compound complexed with FXR. *In vitro*, both compounds were more effective than obeticholic acid at regulating FXR target genes, whereas *in vivo*, there appeared to be compound-dependent differential regulation of these genes.

Conclusion: Work here suggests that novel compounds 1 and 2 may be able to achieve gene-specific FXR regulation due to their proposed differential coactivator usage and thus may be promising candidates worthy of further research.

SAT186

SARS-CoV-2 induces pericyte procoagulant response associated with portal vein microthrombosis and intrapulmonary vascular dilations in fatal COVID-19

Alberto Lasagni¹, Massimiliano Cadamuro², Claudia Maria Radu^{3,4}, Arianna Calistri², Matteo Pisan², Clarissa Valle⁵, Pietro Angelo Bonaffini⁵, Adriana Vitiello², Sandro Sironi⁵, Maria Grazia Alessio⁶, Previtali Giulia⁶, Michela Seghezzi⁶, Andrea Gianatti⁷, Mario Strazzabosco⁸, Alastair J Strain⁹, Elena Campello^{1,3}, Luca Spiezia³, Giorgio Palu², Cristina Parolin², Aurelio Sonzogni⁷, Paolo Simioni^{1,3}, Luca Fabris^{1,2,8}. ¹Padua University-Hospital, Division of General Medicine, Padua, Italy; ²University of Padua, Department of Molecular Medicine, Padua, Italy; ³University of Padua, Department of Medicine, Thrombotic and Hemorrhagic Diseases Unit, Padua, Italy; ⁴University of Padua, Department of Women's and Children's Health (SDB), Padua, Italy; ⁵ASST Papa Giovanni XXIII Hospital, Department of Diagnostic Radiology, Bergamo, Italy; ⁶ASST Papa Giovanni XXIII Hospital, Clinical Chemistry Laboratory, Bergamo, Italy; ⁷ASST Papa Giovanni XXIII

Hospital, Department of Pathology, Bergamo, Italy; ⁸Yale University, Digestive Disease Section, Liver Center, New Haven, United States; ⁹University of Birmingham, School of Bioscience, Birmingham, United Kingdom
Email: luca.fabris@unipd.it

Background and aims: Alterations in portal microvasculature have been reported in lethal cases of COVID-19, but underlying mechanisms and clinical significance are unclear. Intrapulmonary vascular dilations (IPVD) arising during chronic or acute liver disease may contribute to hypoxemia. We hypothesize a link between portal vein microthrombosis and persistent hypoxia in patients with severe COVID-19.

Method: Patients who died from COVID-19 (n = 93) and underwent autopsy, were retrospectively analysed for presence of portal vein microthrombosis and IPVD at the capillary level (histology), and hypoxemia (arterial blood gas analysis). Peripheral IPVD was also evaluated by chest-computed tomography (CT), when performed. Hepatic vascular lesions were phenotyped by endothelial (vWF) and pericyte (α SMA or PDGFR- β) markers, tissue factor (TF) and viral nucleoprotein (NP). *In-vitro*, pericytes were infected with SARS-CoV-2 to measure TF expression and effects on endothelial cell (EC) phenotype.

Results: In 15 patients (12 males), portal vein microthrombosis was associated with diffuse IPVD (tissue involvement >75%). They were younger (62 vs 75 years), had a longer illness (27 vs 14 days) with persistent hypoxemia (median PaO₂/FiO₂ = 106) needing more mechanical ventilation (67% vs 24%), than patients with absent or focal lung vascular abnormalities (n = 78, all p < 0, 01). In 13 patients, a significant enlargement of the peripheral intrapulmonary artery diameter unrelated to pulmonary embolism was confirmed by chest-CT (mean = 5, 1 mm, 95% CI 4, 6–5, 5). The small intrahepatic portal veins showed more extensive thrombosis (median = 85 vs 67, 5%, p < 0, 05), with a thicker wall of α SMA⁺ pericytes (median = 10, 63 vs 4, 98%, p < 0, 01), expressing NP around an intact endothelium compared with the other group of deceased COVID-19 patients. The α SMA⁺ area correlated with percentage of thrombosed portal veins (r = 0, 284, p < 0, 05), whereas TF, the initiator of the coagulation cascade, was expressed by pericytes rather than by portal EC. Infection of pericytes *in-vitro* with SARS-CoV-2 induced increased expression of TF in pericytes, whose conditioned medium induced a pro-coagulant phenotype in ECs, characterized by overexpression of vWF.

Conclusion: SARS-CoV-2 infects liver pericytes, eliciting a prothrombotic response and the subsequent hemodynamic changes result in IPVD contributing to the long-lasting respiratory failure. Liver involvement may therefore play a crucial role in a subset of fatal COVID-19.

SAT187

Dual ileal/renal-liver bile acid transporter inhibitors with different transporter selectivity *in vitro* differentially increase faecal and urinary bile acid excretion in organic anion transporting polypeptide 1a/1b knockout mice *in vivo*

Ellen Strångberg¹, Per-Göran Gillberg¹, Ivana Uzelac¹, Ingemar Starke¹, Britta Bonn¹, Jan Mattsson¹, Peter Åkerblad¹, Runa Pal², Ashwani Gaur², Ramesh Kangarajan², Shivendra Singh², Santosh Kulkarni², Paul Dawson³, Erik Lindström¹. ¹Albireo Pharma, Inc., Boston, MA, United States; ²Syngene International Ltd., Bangalore, Karnataka, India; ³Division of Pediatric Gastroenterology, Hepatology and Nutrition, Emory University School of Medicine, Atlanta, GA, United States
Email: ellen.strangberg@albireopharma.com

Background and aims: Bile acids (BAs) play an important role in hepatobiliary injury. The apical sodium-dependent BA transporter (ASBT) and Na⁺-taurocholate cotransporting polypeptide (NTCP) play key roles in maintaining BA homeostasis, and their selective inhibition has shown efficacy in liver diseases. ASBT inhibitors block intestinal and renal BA reuptake and increase faecal BA

POSTER PRESENTATIONS

excretion, whereas NTCP inhibitors block hepatocyte BA uptake, thereby increasing serum BA levels and urinary BA excretion. Dual-acting ASBT/NTCP inhibitors may increase BA excretion via both elimination routes. We aimed to determine the ability of potent dual ASBT/NTCP inhibitors with different transporter selectivity to increase faecal and urinary BA excretion in organic anion transporting polypeptide 1a/1b (OATP) knockout (KO) mice.

Method: Half-maximal inhibitory concentration (IC_{50}) values for inhibition of mouse ASBT and NTCP were determined using transfected cells. Male OATP KO mice ($n=5$ /group) were dosed orally once daily for 7 days at 30 mg/kg. Serum BAs were measured 1 h post-dosing on days 1 and 7. Measurements of plasma 7 α -hydroxy-4-cholesten-3-one (C4), a marker of hepatic BA synthesis, and faecal and urinary BA excretion were performed on day 7.

Results: Systemically bioavailable ASBT/NTCP inhibitors with selective potency toward mouse NTCP (AS0909, AS0918) or ASBT (AS0826, AS0893) were compared (Table). On days 1 and 7, AS0909/AS0918 and AS0826/AS0893 increased serum BAs 20–50-fold and 2–8-fold, respectively, vs vehicle. On day 7, urine BAs increased 2–3-fold in response to AS0909/AS0918 and less than 2-fold with AS0826/AS0893. In contrast, faecal BA excretion was not significantly elevated with AS0909/AS0918 but increased 4–8-fold with AS0826/AS0893. Serum C4 levels were increased 2–3-fold with AS0826/AS0893 and unaffected with AS0909/AS0918.

Table: Mouse potency values (IC_{50} [nM])

Compound	NTCP	ASBT
AS0909	22	183
AS0918	17	438
AS0826	30	16
AS0893	30	2

Conclusion: ASBT-selective dual inhibitors significantly increased hepatic BA synthesis and faecal excretion while modestly increasing serum BA levels and urinary BA excretion. Conversely, NTCP-selective dual inhibitors caused pronounced elevations in serum and urine BAs without significantly affecting BA synthesis or faecal excretion. Dual ASBT/NTCP inhibitors with different selectivity may have a role as part of precision medicine strategy to reduce the BA burden in forms of hepatobiliary disease.

SAT188

Integrated bile lipidome and meta-proteome analysis classifies lipid species and microbial peptides predictive of carcinoma of the gall bladder

Nupur Sharma^{1,2}, Manisha Yadav¹, Gaurav Tripathi¹, Babu Mathew¹, Vasundhara Bindal¹, Hamed Hemati¹, Sadam Hussain Bhat¹, Jaswinder Maras¹. ¹Institute of liver and biliary sciences, Molecular and cellular medicine, New Delhi, India; ²Institute of liver and biliary sciences, Molecular and cellular medicine, New Delhi, India
Email: jassi2param@gmail.com

Background and aims: Histopathological examination is gold standard for detection of gall-stone (GS) or gall bladder carcinoma (CAGB). Bile concentrated in the gall bladder, is expected to recapitulate metagenomics/molecular changes associated to development of CAGB.

Method: Bile samples were screened for lipidomics and metaproteome (microbiome) signatures capable of early detection of cancer. Analysis of training cohort ($n=87$) showed that meta-stability of bile was reduced in CAGB patients ($p<0.05$).

Results: Our results showed that CAGB was associated with the alteration of bile lipidome and microbiome as indicated by multivariate PLS-regression analysis and alpha, beta diversity indexes. Significant reduction of lipid species and increase in bacterial taxa were found associated to development of CAGB with gallstone and without Gallstone ($p<0.05$, Log FC>1.5). Multimodal correlation network (MMCN) created using weighted lipid/Meta-proteomic correlation network analysis (W [L/MP] CNA) showed striking associations between lipid modules and meta-proteomic functionality. A significant and direct correlation of Meta-proteomic modules/functionality and inversely correlation of lipid modules and species with the clinical parameters and bile acid profile was observed in CAGB patients ($p<0.05$). Significant increase in bacterial taxa; Leptospira, Salmonella enterica, Mycoplasma gallisepticum and their functionality showed direct correlation with lipid classes; Lysophosphatidylinositol, Ceramide 1-phosphates, Lysophosphatidylethanolamine, others and development of CAGB ($r^2>0.85$). Lipid/metaproteomic signature based probability for CAGB was >90% whereas probability for gall-stone was >80% ($p<0.05$). Finally, we identified 8 lipid species of diagnostic capability for

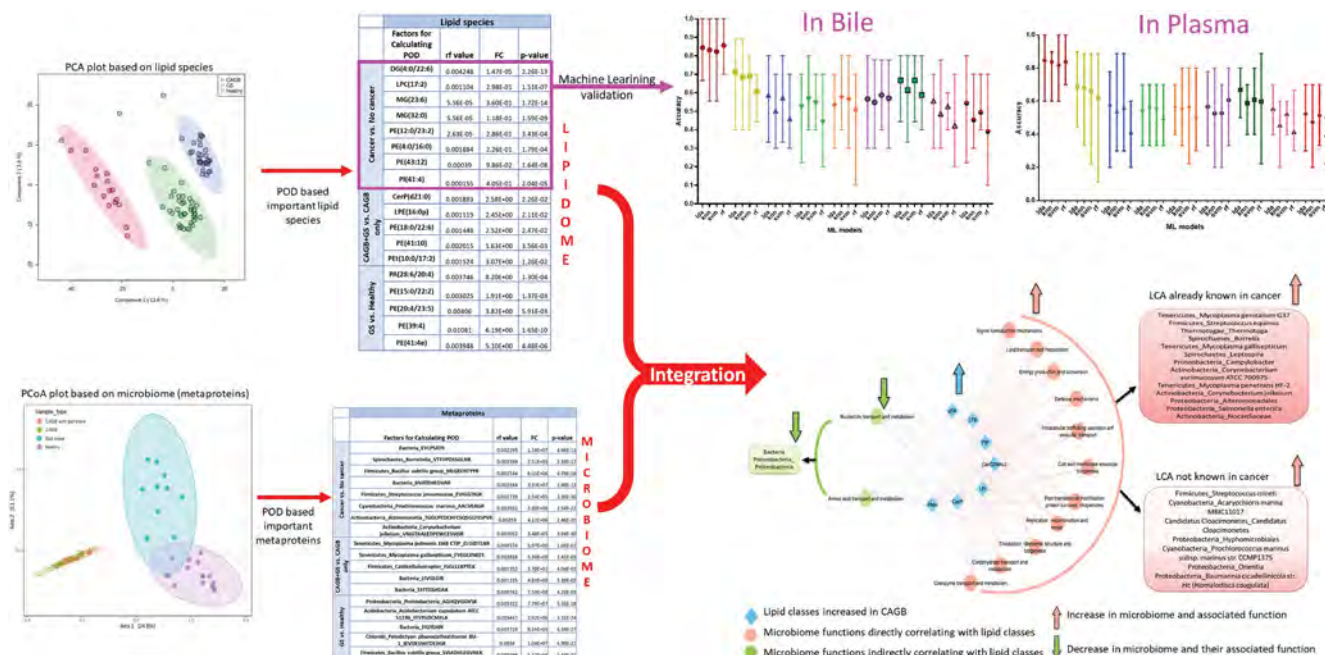


Figure: (abstract: SAT188)

CAGB and cross-validated, using 4 machine learning approaches in two separate test cohorts (n = 38; bile (T1) and paired plasma (T2) cohort, which jointly showed highest accuracy (99%), sensitivity (98%) and specificity (100%) with random forest model for CAGB detection.

Conclusion: Deep and integrated analysis of bile lipidome and metaproteome identify a panel of lipid species/meta-proteome capable of segregating patients predisposed to carcinogenesis of the gall bladder.

SAT189

The effects of apurimic/apirimidinic endonuclease 1 as a sensitizer to sorafenib in hepatocellular carcinoma

Mahzeiar Samadaei¹, Daniel Senfter², Sibylle Madlener², Karolina Uranowska^{3,4}, Christine Hafner^{3,5}, Michael Trauner¹, Nataliya Rohr-Udilova¹, Matthias Pinter¹. ¹Medical University of Vienna, Internal Medicine III, Gastroenterology and Hepatology, Vienna, Austria; ²Medical University of Vienna, Department of Pediatrics and Adolescent Medicine, Vienna, Austria; ³University Hospital St. Poelten, Department of Dermatology, St. Poelten, Austria; ⁴Medical University of Vienna, Institute of Pathophysiology and Allergy Research, Center for Pathophysiology, Infectiology and Immunology, Vienna, Austria; ⁵Karl Landsteiner Gesellschaft, Karl Landsteiner Institute of Dermatological Research, St. Poelten, Austria
Email: nataliya.rohr-udilova@meduniwien.ac.at

Background and aims: Sorafenib, an oral multikinase inhibitor, was the first-generation targeted therapy for patients with hepatocellular carcinoma (HCC). Apurinic/apirimidinic endonuclease 1/redox factor-1 (APE1/Ref-1) is a protein with dual function in redox regulation and DNA repair. APE1/Ref-1 plays a role in development and metastasis but is also linked to inflammation, hypoxia, autophagy and oxidative stress. APE1/Ref-1 also interacts with PI3K/Akt pathway which, in turn, induce sorafenib resistance. Here, we aim to decipher the specific contribution of APE1/Ref-1 repair and redox functions to sorafenib sensitivity of human HCC cells.

Method: Impact of APEX1 expression on overall survival of HCC patients was evaluated by an *in silico* approach using Human Protein Atlas dataset. To check the effects of bifunctional APE1/Ref-1 in five human HCC cell lines (Huh7, SNU398, AKH12, AKH13, 3P), we introduced domain-specific mutations and applied selective inhibitors to block either the repair or the redox function of this protein. These treatments were combined with sorafenib. Neutral red assay was used to evaluate cell viability. To evaluate cytotoxicity, we quantified loss of membrane integrity by LDH release. Clonogenic and invasion ability of HCC cells were measured by colony formation assay and hanging drop method, respectively. Cell cycle distributions as well as characterization of apoptosis were performed by flow cytometry.

Results: *In silico* approach revealed that HCC patients with lower expression of APEX1 reveal longer overall survival: 6.0 ± 0.5 years (low) vs 3.8 ± 0.4 years (high), $p = 0.01$, $n = 365$. APEX1 knock down by siRNA per se as well as in combination with sorafenib-reduced HCC cell viability. All five cell lines which overexpressed either APE1/Ref-1 wild-type or N212A mutants with abrogated DNA repair activity showed consistently delayed response to sorafenib when compared to cells overexpressing mutant redox domain C65S. In line, an inhibitor of APE1/Ref-1 redox function E3330 in combination with sorafenib significantly reduced colony formation (Fig. 1) and invasion of HCC cells.

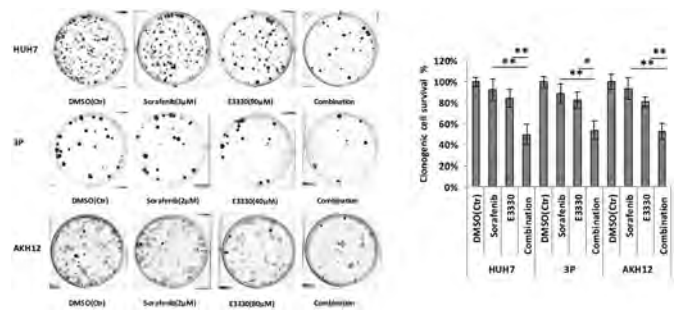


Figure: Impact of E3330, an inhibitor of APE1/Ref-1 redox function, and sorafenib on colony formation in HCC cell lines.

Conclusion: Redox function of APE1/Ref-1 seems to be a promising target in HCC. APE1/Ref-1 redox inhibitor E3330 enhances the anti-tumor effects of sorafenib *in vitro*.

SAT191

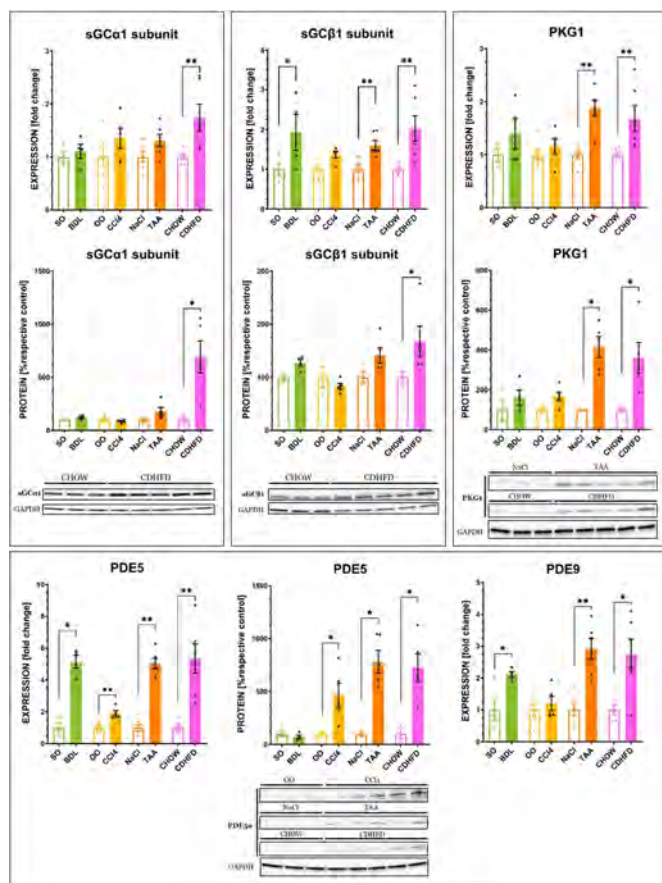
Soluble guanylyl cyclase expression and signaling in different types of liver fibrosis

Ksenia Brusilovskaya^{1,2,3,4}, Philipp Königshofer^{1,2,3,4}, Benedikt Hofer^{1,2,3}, Oleksandr Petrenko^{1,2,3,4,5}, Kerstin Zinöber^{1,2,3}, Martha Seif^{1,2,3}, Stefan Günther Kauschke⁶, Larissa Pfisterer⁶, Philipp Schwabl^{1,2,3,4}, Thomas Reiberger^{1,2,3,4,5}. ¹Medical University of Vienna, Division of Gastroenterology and Hepatology, Department of Medicine III, Vienna, Austria; ²Medical University of Vienna, Vienna Hepatic Hemodynamic Lab (HEPEX), Division of Gastroenterology and Hepatology, Department of Medicine III, Vienna, Austria; ³Medical University of Vienna, Christian-Doppler laboratory for portal hypertension and liver fibrosis, Vienna, Austria; ⁴CeMM Research Center for Molecular Medicine of the Austrian Academy of Sciences, Vienna, Austria; ⁵Ludwig Boltzmann Institute for Rare and Undiagnosed Diseases (LBI-RUD), Vienna, Austria; ⁶Boehringer Ingelheim Pharma GmbH and Co.KG, Biberach, Germany
Email: thomas.reiberger@meduniwien.ac.at

Background and aims: In cirrhosis, impaired NO-soluble guanylyl cyclase (sGC)-cyclic guanosine monophosphate (cGMP)-protein kinase G (PKG-1) signaling contributes to increased intrahepatic vascular resistance and fibrogenesis. We investigated the expression of sGC subunits and the downstream signaling pathway in healthy and diseased liver tissue.

Method: Liver tissue samples of cholestatic (bile duct ligation, BDL-4 weeks), toxic (8 weeks-CCl₄ and 12 weeks-TAA), and metabolic (12 weeks-choline-deficient high fat diet, CDHFD) rat fibrosis models were used. Healthy control tissues were derived from sham-operated (SO), vehicle-injected (OO/NaCl), and normal-diet-fed (CHOW) animals. Gene and protein expression of sGC subunits and key downstream molecules were analyzed by RT-PCR and Western blot.

Results: All models presented severe fibrosis assessed by collagen-proportionate area (CPA: BDL: 13.4%; CCl₄: 4.0%; TAA: 8.0%; CDHFD: 8.5%). The expression of sGC subunits alpha1 and beta1 (sGCα1/β1) increased in all fibrosis models, with the most pronounced upregulation in CDHFD (sGCα1: 1.7 ± 0.3 -fold, $p < 0.01$; sGCβ1: 2.0 ± 0.3 -fold, $p < 0.01$). Accordingly, 6.9-fold sGCα1 ($p = 0.04$) and 1.7-fold sGCβ1 ($p = 0.04$)-higher protein levels were detected in CDHFD group. The expression of PKG-1 was significantly increased in TAA and CDHFD models both on gene (TAA: 1.9 ± 0.2 -fold, $p < 0.01$; CDHFD: 1.7 ± 0.2 -fold, $p < 0.01$) and protein (TAA: 4.1-fold, $p = 0.04$; CDHFD: 3.6-fold, $p = 0.04$) levels. Moreover, upregulation of the cGMP degrading phosphodiesterase enzymes PDE5 (BDL: 5.1 ± 0.4 -fold, $p < 0.01$; CCl₄: 1.9 ± 0.2 -fold, $p < 0.01$; TAA: 5.1 ± 0.3 -fold, $p < 0.01$; CDHFD: 5.3 ± 0.9 -fold, $p < 0.01$), and PDE9 (BDL: 2.1 ± 0.1 -fold, $p = 0.05$; CCl₄: 1.2 ± 0.2 -fold, $p = 0.79$; TAA: 2.9 ± 0.3 -fold, $p < 0.01$; CDHFD: 2.7 ± 0.5 -fold, $p = 0.03$) was observed in cirrhosis. PDE5 protein levels also increased in CCl₄ (4.7-fold, $p = 0.04$), TAA (7.8-fold, $p = 0.04$), and CDHFD (7.2-fold, $p = 0.04$) models-but remained similar in BDL ($p = 0.23$).



Conclusion: Expression of sGC alpha1/beta1 subunits increases in liver cirrhosis in different rat models, paralleled by upregulated cGMP-dependent PKG-1 in toxic and CDHF cirrhosis. In contrast, overexpression of PDE5/9 across all models may indicate insufficient cGMP-related signaling effects in cirrhosis. The functionality of sGC-cGMP signaling in cirrhosis and the impact of pharmacologic activation requires further mechanistic studies.

SAT192

Impact of maternal obesity on liver disease in the offspring: a comprehensive transcriptomic analysis and validation of results

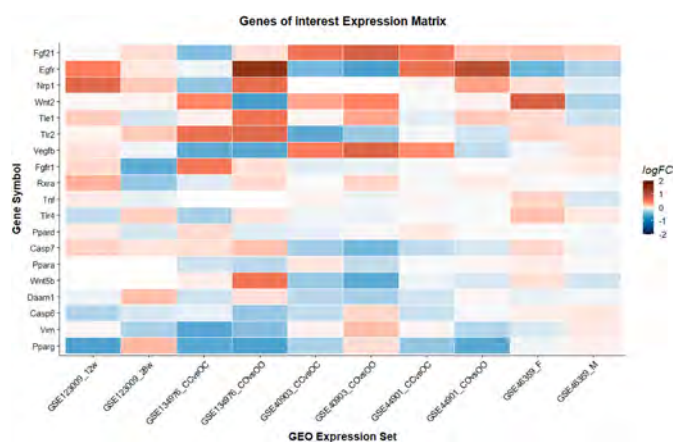
Beat Moeckli^{1,2}, Vaihere Delaune^{1,2}, Julien Prados³, Matthieu Tihy⁴, Andrea Peloso², Graziano Oldani^{1,2}, Thomas Delmi¹, Nicolas Goossens⁵, Laura Rubbia-Brandt⁴, Stéphanie Lacotte¹, Christian Toso^{1,2}. ¹University of Geneva, Faculty of medicine, Geneva, Switzerland; ²Hôpitaux Universitaires de Genève (HUG), Chirurgie, Genève, Switzerland; ³University of Geneva, Bioinformatics Support Platform, Geneva, Switzerland; ⁴Hôpitaux Universitaires de Genève (HUG), Department of clinical pathology, Genève, Switzerland; ⁵Hôpitaux Universitaires de Genève (HUG), Hepatology and gastroenterology, Genève, Switzerland
Email: beat.moeckli@gmail.com

Background and aims: The global obesity epidemic is a major public health concern and particularly affects women of reproductive age. Offspring of obese mothers suffer from an increased risk of liver disease but the molecular mechanisms involved remain unknown. With this study, we uncover new pathways and genes involved in the transmission of liver disease and validate previously identified targets.

Method: We performed an integrative genomic analysis of datasets that investigated the impact of maternal obesity on the hepatic gene expression profile of the offspring in mice. Furthermore, we

developed our own murine model of maternal obesity and validated the top deregulated genes by quantitative real time polymerase chain reaction (qPCR) in our model. Our data is available for interactive exploration on our companion webpage: (<https://genebrowser.unige.ch/maternalobesity>).

Results: We identified five publicly available datasets pertinent to our research question. Pathways involved in metabolism, the innate immune system, the clotting cascade and the cell cycle were consistently deregulated in offspring of obese dams. Concerning genes potentially involved in the development of liver disease, we found *Egfr*, *Vegfb*, *Wnt2* and *Pparg* deregulated in multiple independent datasets (Figure). In our own model, we observed higher tendency towards the development of non-alcoholic liver disease (60 vs 20%) and higher levels of alanine amino transferase (41.0 vs 12.5 IU/l, $p = 0.008$) in female offspring of obese dams. Male offspring presented higher levels of liver fibrosis (2.8 vs. 0.8% relative surface area, $p = 0.045$). Of the top deregulated genes deregulated in the integrative genomic analysis, we validated the deregulation of *Fgf21*, *Pparg* and *Ppard* by qPCR in our own model of maternal obesity.



Conclusion: Maternal obesity represents a looming threat for the liver health of future generations. Our comprehensive transcriptomic analysis discovered new pathways and molecular targets. This will help to better understand the mechanisms of the development of liver disease in the offspring of obese mothers.

SAT193

Liver directed in utero AAV gene therapy for maple syrup urine disease in a neonatal lethal murine model

Kate Mullany^{1,2}, Ian Alexander^{1,3}, Susan Siew². ¹Children's Medical Research Institute, Gene Therapy Research Unit, Westmead, Australia; ²The Children's Hospital at Westmead, Gastroenterology, Westmead, Australia; ³The Children's Hospital at Westmead, Westmead, Australia
Email: kmullany@cmri.org.au

Background and aims: MSUD is a genetic metabolic autosomal recessive condition caused by a deficiency of the mitochondrial enzyme branched chain keto-acid dehydrogenase. Severely affected individuals present in the neonatal period with elevated branched chain amino acid (BCAA) levels leading to encephalopathy and muscle weakness which if untreated progresses to permanent brain injury and/or death. Dietary protein restriction or liver transplantation are current mainstays of therapy, however neither are curative. Liver directed adeno-associated viral (AAV) gene therapy represents a novel potential treatment for MSUD. Our aim is to determine if liver directed AAV gene therapy can rescue the phenotype of a neonatal lethal murine model of MSUD (DBT^{-/-}).

Method: A murine hepatotropic gene addition vector rAAV8.hDBT (5×10^8 vector genome copies per mouse) was administered on DO of life in 9 homozygous knockout pups. Outcome measures included

pup growth, serum BCAA levels through mass spectrometry, DBT protein expression via immunoblotting and vector genome copy via digital droplet PCR. Immunohistochemistry was used to assess presence of DBT protein in liver sections. As neonatal vector administration improved survival but did not rescue all pups, the timing of vector delivery was suspected to be critical, and the same vector was administered *in utero* to pups on E15. Equivalent studies are being initiated to compare outcomes following *in utero* treatment. **Results:** Gene addition with a codon optimised DBT human transgene significantly improved survival, growth and BCAA levels ($p < 0.05$) compared to untreated knockout pups when administered on D0 of life. DBT protein in vector treated homozygous knock out pups was expressed at 2.5 times higher than untreated wild type pups. Immunohistochemistry demonstrated presence of DBT protein in vector treated pups (Figure 1). We will also present the results from the *in utero* vector administration.

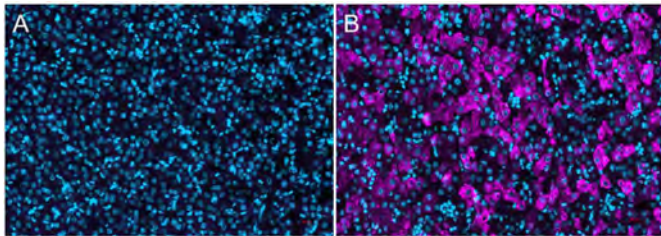


Figure 1. Presence of DBT protein (purple) in murine liver cells in A) untreated DBT^{-/-} and B) D0 vector treated DBT^{-/-} mouse pups. Hepatocyte nuclei were co-stained (blue, DAPI).

Conclusion: Neonatal murine liver transduction with a human DBT transgene significantly improves the disease phenotype in a murine neonatal lethal model of MSUD. Liver directed AAV mediated gene therapy represents a potential novel treatment for MSUD.

SAT194

Patient-derived hepatocellular carcinoma organoids as predictors of Treatment Response

Jun Yong Park^{1,2,3,4}, Kyung Joo Cho^{2,4}, Hye Won Lee^{1,3,4}, Hye Jung Park⁴, Sang Hoon Ahn^{1,3,4}, Hee Seung Lee³, Chul Hoon Kim^{2,5}. ¹Yonsei University College of Medicine, Institute of Gastroenterology, Seoul, Korea, Rep. of South; ²Yonsei University, Brain Korea 21 PLUS Project for Medical Science, Seoul, Korea, Rep. of South; ³Yonsei University College of Medicine, Division of Gastroenterology, Department of Internal Medicine, Seoul, Korea, Rep. of South; ⁴Severance Hospital, Yonsei Liver Center, Seoul, Korea, Rep. of South; ⁵Yonsei University College of Medicine, Department of Pharmacology, Seoul, Korea, Rep. of South
Email: drpjy@yuhs.ac

Background and aims: Organoid models using patient-derived cancer tissues has allowed a better understanding of human cancer as well as development of precision medicine. For advanced HCC treatment, the proper models and the pivotal pathways of cancer stem cells (CSCs) are needed. In this study, we evaluate the sensitivity to anti-cancer drugs using HCC organoids (HCOs) and analyze the relationship between drug resistance group and CSCs-related signal for improving the drug response.

Method: Patient-derived tumor tissue was digested at 37 °C and mixed with Matrigel. After polymerization of Matrigel, medium was added and changed twice a week. To evaluate whether HCO exhibit different sensitivity to drugs, we tested its sensitivity and analyzed the sensitivity in HCO lines with the difference in gene expression.

Results: We successfully established 10 HCOs obtained from 16 HCC patients among. HCOs exhibited heterogeneous morphological features, forming compact structures with or without thick-layered cyst-like structures. HCOs shared somatic mutations and showed high concordance of somatic mutation between primary tumor and

organoids. Through the different gross morphology of HCO showed the differential gene expression. Notably, Wnt pathway was significantly enriched in the compact spherical shape of HCO compared to combined shape ($p < 0.05$). We compared the growth of compact shape of HCOs with and without Wnt pathway-related components, however, they failed to form organoids without Wnt. Also, compact shape of HCOs was resistant to treatment with Lenvatinib *in vitro*.

Conclusion: Our results demonstrated that HCOs with specific structural features provide platform to identify the relationship between drug response and CSC-related signal in HCC.

SAT195

Dissecting A-to-I RNA editome of liver macrophages in non-alcoholic fatty liver disease

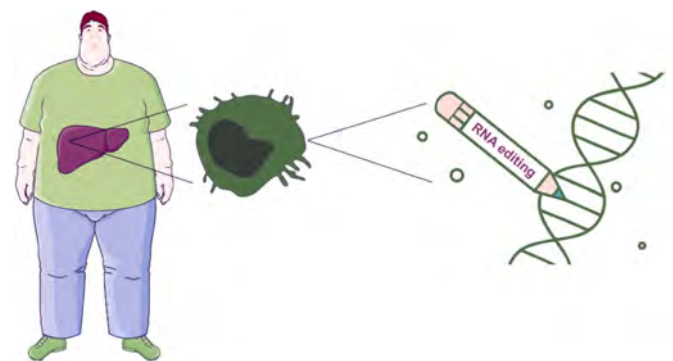
Achilleas Fardellas¹, Myriam Aouadi¹, Sebastian Nock¹, Ping Chen¹, Cecilia Morgantini². ¹Karolinska Institute, Department of Medicine, Center for Infectious Medicine, Huddinge, Sweden; ²Karolinska Institute, Department of Medicine, Cardio Metabolic Unit (CMU), Huddinge, Sweden

Email: myriam.aouadi@ki.se

Background and aims: RNA editing is an epitranscriptomic process referring to modifications in the chemical structure of RNA molecules. Adenosine-to-Inosine (A-to-I) editing is the most common RNA editing event catalysed by a family of enzymes called ADARs (adenosine deaminases acting on RNA). While aberrant RNA editing profiles have been associated with many diseases including neurological disorders and cancers, it has not been previously studied in the setting of non-alcoholic fatty liver disease (NAFLD).

Method: We used RNAseq datasets (GSE135251, GSE126848), which liver biopsies from lean, “healthy” obese and NAFLD patients. Global levels of RNA editing activity were estimated in this cohort using the Alu editing index (AEI), a robust signal with a minimal false-positive rate. Human monocyte-derived macrophages were treated with phRodo-labelled Escherichia coli bioparticles for 2 hours and analyzed via flow cytometry after a 48hour ADAR1-knockdown.

Results: We have recently discovered that IGF1 transcripts in liver macrophage (LMs) of insulin resistant patients underwent A-to-I RNA editing at a high frequency leading to the production of a variant isoform with a higher capacity to regulate insulin signalling. Consistently, preliminary results from RNAseq analysis of 266 liver biopsy samples from two independent studies indicate that the RNA editing rate of NAFLD patients is considerably higher compared to lean and “healthy” obese. However, analyses of the overall RNA editome of LMs revealed that the RNA editing rate is unexpectedly decreased in obesity. To investigate the functional relevance of RNA editing in human macrophages, ADAR1, the key RNA editing enzyme, was silenced and an improved phagocytic capacity of particles was found.



Conclusion: These data suggest that the RNA editome of the liver changes dynamically in the setting of metabolic diseases and interestingly, in a cell-specific manner. Understanding the

POSTER PRESENTATIONS

epitranscriptomic landscape of NAFLD and its role in the disease development may lay the foundation for the development of novel therapeutic strategies and new disease biomarkers.

SAT196

Restoring bone marrow hematopoietic stem cells (BM-HSC) reserve augments regression of fibrosis and regeneration in animal model of cirrhosis

Nidhi Nautiyal^{1,2}, Deepanshu Maheshwari¹, Pranshu E Rao³, Sujata Mohanty³, Anupama Parasar¹, Chhagan Bihari⁴, Subhrajit Biswas², Rakhi Maiwall⁵, Anupam Kumar¹, Shiv Kumar Sarin^{1,5}. ¹Institute of Liver and Biliary Sciences, Molecular and Cellular Medicine, New Delhi, India; ²Amity University Noida, Amity Institute of Molecular Medicine and Stem Cell Research, Noida, India; ³All India Institute of Medical Sciences, Center of Excellence for Stem Cell Research, New Delhi, India; ⁴Institute of Liver and Biliary Sciences, Department of Pathology, New Delhi, India; ⁵Institute of Liver and Biliary Sciences, Department of Hepatology, New Delhi, India
Email: shivsarini@gmail.com

Background and aims: Bone marrow (BM) is a reservoir for hematological and immune cells, plays a central role in resolution of damage and tissue repair. Exhaustion of BM-HSC reserve has been shown to be associated with increased susceptibility to infection, hematological dysfunction and early graft dysfunction post liver transplant in cirrhosis. Whether the loss of BM stem cell (BMSC) reserve in cirrhosis is the cause or a consequence of liver failure is not known. We aim to understand the relation between BM and liver regeneration, and potential therapeutic effect of restoring BM-HSC reserve in the management of chronic liver injury.

Method: C57BL/6 (J) mice were used to develop chronic liver injury through intraperitoneal administration of carbon tetrachloride for 15 weeks (0.1–0.5 ml/kg). Animals were culled at different time points (N = 10 each group; week 3/6/10/15) to study the changes in liver injury, regeneration, BM-HSC and mesenchymal stem cell (MSC) reserve. To restore the BMSC reserve, approximately 4 million healthy whole BM cells (hBM), isolated from GFP-C57BL/6 mice were infused intrafemoral (IF) after 12 weeks of chronic liver injury. Control animals were infused with saline. Animals post BM infusion were sacrificed (N = 10 each group; 24 hours/day 11/day 21) to study the changes in liver injury, regeneration and BMSC reserve.

Results: Histological analysis of liver tissue (figure 1A) showed progressive increase in fibrosis and hepatocyte proliferation till week 10 with development of portal fibrosis at week 3, bridging fibrosis at week 6 and nodular fibrosis (cirrhosis) at week 10. From 10–15 weeks, while the fibrosis was comparable, there was a significant increase ($p < 0.0001$) in TUNEL+ hepatocyte and loss of hepatocyte regeneration with hepatic decompensation [ascites (SAAG 1.4 (1.1–1.7) g/dL), jaundice and rise in ammonia ($p < 0.001$)], suggesting increased hepatocyte injury without compensatory regeneration in development of decompensated cirrhosis. Interestingly, BM studies showed that during the course of chronic liver injury loss of BM MSC occurs between week 3 to 6 followed by loss of LT-HSC between week 6 to 10 followed by regeneration failure (figure 1B). Infusion of hBM in cirrhosis animals (figure 1C) showed that while donor cells disappear by day 21, there was significant increase in total BM LT-HSC reserve by day 11 (figure 1D). hBM recipients showed significant reduction in fibrosis and increased hepatocyte proliferation (figure 1E).

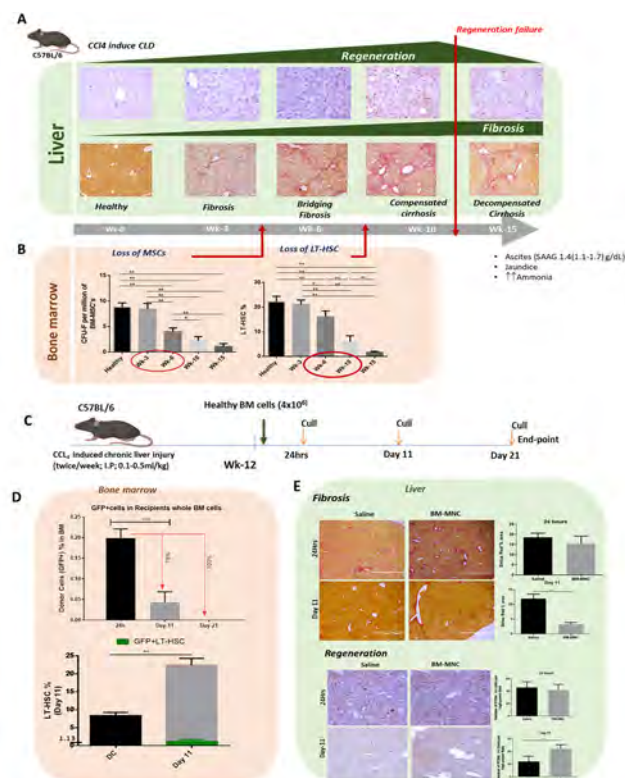


Figure 1: Restoring bone marrow hematopoietic stem cells (BM-HSC) reserve augments regression of fibrosis and regeneration in animal model of cirrhosis. (A) Representative micrograph showing Sirius red staining (bottom) and IHC staining of PCNA+ hepatocyte (top) in liver sections at given time points. (B) Graph showing changes in number of BM-MSC colony forming unit (CFU) (left) and percentage of long term hematopoietic stem cells (LT-HSC) (right) with progression of chronic liver injury (C) Study layout of BM-cell infusion in cirrhosis animals. (D) Graph showing change in percentage of total donor cells (top) and percentage of total LT-HSC (bottom; recipient (gray) and donor (green)) post BM-cell infusion in cirrhosis animals. (E) Representative micrograph (left) and bar graph (right) change in liver fibrosis and hepatocyte regeneration in cirrhotic animals with and without BM infusion

Conclusion: Loss of BM-HSC reserve precedes hepatic regeneration failure indicating seminal role of BM during chronic hepatic injury. IF infusion of hBM induces repopulation of native LT-HSC, accelerates fibrosis resolution and potentiates hepatocyte regeneration in cirrhosis. Hence, restoring BM-HSC reserve can serve as a novel therapeutic approach to augment resolution of fibrosis and native liver regeneration in cirrhosis.

SAT197

Human resident liver macrophages protect against metabolic stress in obesity

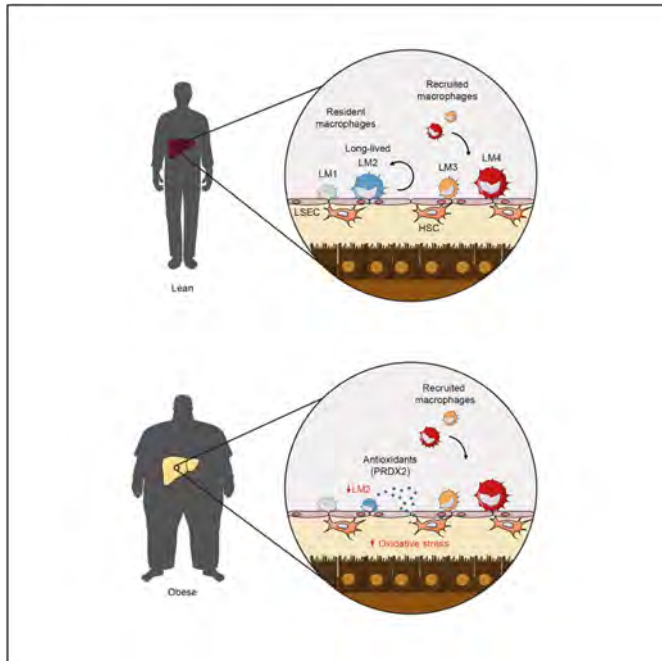
Emilie Barreby¹, Benedikt Strunz¹, Valerio Azzimato¹, Joanne X. Shen², Léa Naudet¹, Isabella Sönnernborg^{1,3}, André Sulen^{1,4}, Sebastian Nock¹, Laura Levi¹, Cecilia Morgantini^{1,5}, Achilleas Fardellas¹, Helene Johansson³, Greg Nowak³, Per Stål⁶, Ewa Ellis³, Erik Naslund⁷, Volker Lauschke^{2,8}, Niklas Björkstöm¹, Ping Chen¹, Myriam Aouadi¹. ¹Karolinska Institutet, Center for Infectious Medicine, Huddinge, Sweden; ²Karolinska Institutet, Section of Pharmacogenetics, Stockholm, Sweden; ³Karolinska Institutet, Division of Transplantation Surgery, Huddinge, Sweden; ⁴University of Bergen, KG Jebsen Center for Autoimmune Diseases, Norway; ⁵Karolinska Institutet, Cardio metabolic unit, Sweden; ⁶Karolinska Institutet, Gastroenterology and Rheumatology Unit, Huddinge, Sweden; ⁷Danderyd Hospital, Karolinska Institutet, Division of Surgery, Department of Clinical Sciences, Stockholm, Sweden; ⁸Dr Margarete Fisher-Bosh Institute of Clinical Pharmacology, Germany
Email: myriam.aouadi@ki.se

Background and aims: Non-alcoholic fatty liver disease has become the most common chronic liver disease, being associated with an increasing prevalence of obesity and type 2 diabetes. Macrophages contribute to the development of these metabolic disorders in

obesity. However, while multiple macrophage populations have been described in the human liver, little is known about their functional role in response to metabolic changes associated with obesity. In this study we characterized liver macrophages (LMs) during the development of metabolic disease in obese individuals.

Method: Liver biopsies from lean and obese individuals undergoing bariatric surgery were characterized by single cell RNA sequencing and flow cytometry. Macrophage ontogeny was examined by studying the replacement of LM subpopulations by monocytes in individuals undergoing liver transplantation, using markers of donor-recipient mismatch. Functional validation was then performed in primary human 3D *in vitro* cultures in which lipid accumulation and oxidative stress was induced as to mimic obese livers.

Results: Here, we identified multiple macrophage populations distinguished by their transcriptomic profiles and origin, rather than their inflammatory status in lean and obese individuals. Interestingly, by studying the dynamics of liver macrophages in individuals undergoing liver transplantation using markers of donor-recipient mismatch, we discovered that liver macrophage turnover differs dramatically in humans and in mice. While the majority of macrophages were monocyte-derived, human livers also contained a distinct population of resident 'long-lived' macrophages. This LM population, denoted LM2, expressed high levels of genes regulating oxidative and metabolic stress in obesity, in particular the antioxidant Peroxiredoxin-2. Moreover, the proportion of these long-lived LM2 decreased during obesity. Finally, removal of LM2 from primary liver 3D cultures reduced PRDX2 levels and increased extracellular ROS.



Conclusion: We discovered a liver resident macrophage population with a protective role that could reduce oxidative stress induced by lipid accumulation. Targeting specific LM populations could thus represent a promising therapeutic strategy for both liver and metabolic disease.

SAT198

Reversal of epithelial-mesenchymal transition in a cholangiocarcinoma cell line by genetic targeting of sulfatide synthesis

Lin Chen^{1,2}, Montserrat Elizalde^{2,3}, Steven Olde Damink^{1,2,4}, Frank Schaap^{1,2,4}, Gloria Álvarez-Sola^{1,2}. ¹Maastricht University Medical Center, Surgery, Maastricht, Netherlands; ²Maastricht University, School of Nutrition and Translational Research in Metabolism, Maastricht, Netherlands; ³Maastricht University Medical Center, Division of Gastroenterology-Hepatology, Department of Internal Medicine, Maastricht, Netherlands; ⁴University Hospital Aachen, Department of General, Visceral and Transplant Surgery, Aachen, Germany
Email: glalvare@gmail.com

Background and aims: Cholangiocarcinoma (CCA) or biliary tract cancer is the second most common liver malignancy with an increasing incidence in Western countries. CCA is a heterogeneous malignant disease with different epidemiological trends among different subtypes of CCA that may reflect genetic and environmental risk factors involved in the incidence of CCA. The lack of effective treatments due to late diagnosis associated with the absence of symptoms highlights the need to search for new therapeutic targets for CCA. A recent study demonstrated the presence of sulfatides, a class of sulfoglycosphingolipids, in the biliary tract in the liver. These lipids are involved in protein trafficking and cell adhesion, showing a protective role in different epithelial cells. Previous work has shown that sulfatides are adhesive molecules related to malignancy, since these lipids induce the binding of platelets to cancer cells promoting immune evasion. Our aim is to study the role of *GAL3ST1*, the gene that encodes the enzyme involved in sulfatide synthesis, in CCA.

Method: We analysed the expression of *GAL3ST1* in 16 non-tumors, 13 tumor tissue specimens of iCCA patients and different CCA cell lines. We used the CRISPRi-Cas9 system in the extrahepatic CCA cell line TFK1 to generate *GAL3ST1* Knockout (KO) cells, and small interfering RNAs to obtain Knockdown (KD) cells. We evaluated the cell proliferation, metabolic activity, epithelial identity and barrier function in these *GAL3ST1* deficient cells.

Results: *GAL3ST1* was up-regulated in CCA cell lines relative to H69 cholangiocyte cells, as well as in iCCA versus non-tumor liver tissue. *GAL3ST1* KO cells showed less proliferative and clonogenic activity *in vitro*. *GAL3ST1* deficient cells displayed a reduction in HIF1 alpha mRNA levels, lower expression of genes involved in glycolysis (e.g., *HK2* and *PGK1*) and less cell viability. Polarized *GAL3ST1* KO cells had increased transepithelial resistance (1.5-fold) and reduced permeability to FITC-dextran (-0.7-fold). Different epithelial markers (Occludin, ZO-1 and E-cadherin) were increased in *GAL3ST1* KO and KD cells. *GAL3ST1*-deficient cells showed reduced basal activation of ERK1/2 MAPK.

Conclusion: *GAL3ST1* was highly expressed in iCCA. The aggregated findings indicate that the modulation of *GAL3ST1* reversed the epithelial-mesenchymal transition in TFK1 cells, thereby reducing their tumorigenic capacity. It will be worth exploring whether targeting *GAL3ST1* has potential in the treatment of CCA.

POSTER PRESENTATIONS

SAT199

Unravelling the circadian transcriptome and epigenome of the human liver

Atish Mukherji¹, Frank Jühling¹, Laurent Mailly¹, Carla Eller¹, Katharina Herzog¹, Cloé Gadenne¹, Clara Ponsolles¹, Alexandre Haller², Philippe Baltzinger^{2,3}, Hiroshi Aikata⁴, Michio Imamura⁴, Catherine Schuster¹, Xiaodong Zhuang⁵, Jacinta Holmes⁶, Jane McKeating⁵, Irwin Davidson², Patrick Pessaix⁷, Joachim Lupberger¹, Thomas Baumert⁸. ¹Université de Strasbourg, Inserm, Institut de Recherche sur les Maladies Virales et Hépatiques Inserm, UMR_S1110, Strasbourg, France; ²Institut de génétique et de biologie moléculaire et cellulaire, Illkirch, France; ³CHU de Strasbourg, Internal Medicine, Endocrinology and Nutrition, Strasbourg, France; ⁴Institute of Biomedical and Health Sciences, Hiroshima University, Department of Gastroenterology and Metabolism, Applied Life Sciences, Hiroshima, Japan; ⁵Nuffield Department of Medicine, University of Oxford, Oxford, United Kingdom; ⁶University of Melbourne, St Vincent's Hospital, Melbourne, Australia; ⁷Université de Strasbourg, Inserm, Institut de Recherche sur les Maladies Virales et Hépatiques Inserm, UMR_S1110, Institut Hospitalo-Universitaire, Pôle Hépatodigestif, Nouvel Hôpital Civil, Strasbourg, Strasbourg, France; ⁸Université de Strasbourg, Inserm, Institut de Recherche sur les Maladies Virales et Hépatiques Inserm, UMR_S1110, Institut Hospitalo-Universitaire, Pôle Hépatodigestif, Nouvel Hôpital Civil, Strasbourg and Institut Universitaire de France, Paris, Strasbourg, France
Email: mukherji@unistra.fr

Background and aims: The role of the circadian clock (CC) as a major regulator of physiology has been well established in the last two decades. Indeed, murine models and epidemiological studies have implicated the disruption of CC-function in several pathologies including liver disease and hepatocellular carcinoma (HCC), which are global health challenges. However, in the human liver, the identity and the epigenetic landscape of CC-regulated gene networks remains largely unknown. Uncovering the identity and transcriptional regulation of circadian genes in human liver is therefore essential to comprehend the molecular understanding of chronic liver disease and HCC.

Method: To identify genes in human liver displaying a circadian expression pattern as well as their associated epigenetic changes under physiological conditions, we performed RNA- and ChIP-sequencing of livers from humanized liver chimeric mice (HM mice) sampled at six timepoints within a 24-hour period. This allowed us to determine temporal transcriptomic and epigenetic changes on a genome-wide level in human hepatocytes. Subsequently, we applied *MetaCycle* and *dryR* to analyze and identify the rhythmic genes and biochemical pathways in human liver cells. Our H3K27ac ChIP-sequencing analyses revealed the kinetics of enhancer activation in human liver in a 24-hour cycle.

Results: Here, we discovered the identity of numerous genes and biochemical pathways which show a rhythmic expression in human liver under physiological conditions. We found that many master transcription factors and associated crucial cellular processes which display circadian rhythmicity uniquely in human liver cells. Importantly, our combined transcriptome and epigenomic analyses uncovered the molecular basis of human liver-specific rhythmic gene networks. Crucially, many of these rhythmically expressed genes and pathways are well-known to get deregulated in chronic liver disease and HCC. These rhythmic genes show a strong correlation between enhancer activation and gene expression.

Conclusion: We have unraveled the identity of circadian genes and gene regulatory networks in human liver cells. This work represents a milestone in understanding the physiology of human liver. Moreover, our findings provide novel opportunities for understanding the molecular relationship between CC in the normal liver but also serve as a reference to understand the perturbation and role of circadian genes in chronic human liver disease and HCC.

SAT200

Single-cell dynamics of interacting mesenchymal and leukocyte populations in advanced NASH

Sofie Bendixen¹, Peter R. Sørensen¹, Mike Terkelsen¹, Daniel Hansen¹, Frederik Adam Bjerre¹, Kamilla Hejn¹, Emma A.H. Scott¹, Ann-Britt Marcher¹, Janusa Vijayathurai¹, Sönke Detlefsen², Kim Ravnskjaer¹, Philip Hallenborg¹, Blagoy Blagoev¹. ¹University of Southern Denmark, Odense, Denmark; ²Odense University Hospital, Odense, Denmark
Email: ravnskjaer@bmb.sdu.dk

Background and aims: Non-alcoholic steatohepatitis (NASH) is an obesity-related disorder caused by extensive fat accumulation in the liver parenchyma. The outcomes are chronic hepatic inflammation and deposition of extracellular matrix (fibrosis) that over time alter the hepatic architecture and function. Disease progression is driven by highly complex interactions between various cell types including hepatic mesenchymal cells and infiltrating immune cells.

Method: To better understand the liver plasticity during NASH development, we performed single-cell RNA sequencing on livers from mice fed a Western diet for 52 weeks and age-matched healthy controls. A single-reference dataset was established through Seurat 3-based integration.

Results: Here, we confidently annotated 11 cell populations including hepatocytes, hepatic stellate cells (HSC), mononuclear phagocytes (MP), and B- and T-cells. The MP-composition showed an expansion of the Kupffer cell-like cell population in NASH and infiltration of monocytes leading to an increase in macrophage heterogeneity. This we confirmed by analysis of RNA velocities predicting profoundly altered MP plasticity in NASH. Also activated HSCs were present to a higher degree in NASH livers exhibiting enhanced extracellular matrix production. Using SCENIC, we identified subpopulation-specific transcriptional networks likely to underlie HSC activation. Combining gene expression levels from individual subpopulations of HSCs and MPs using NicheNet predicted ligand-receptor interactions reflecting possible cross-talk in healthy and diseased livers. Ongoing spatial and loss of function studies will map relative cell locations and function to validate these interactions.

Conclusion: Our results expose dynamical cellular interactions at a hitherto unprecedented resolution, and contribute to the elucidation of hepatic tissue plasticity during NASH development.

SAT201

Dysregulated glutamine metabolism in intrahepatic cholangiocarcinoma: a perspective for targeted therapy

Michela Anna Polidoro¹, Laura Brunelli², Cristiana Soldani¹, Barbara Franceschini¹, Matteo Zampini³, Alessio Aghemo^{4,5}, Matteo Donadon^{4,6}, Guido Torzilli^{4,6}, Roberta Pastorelli², Ana Lleo^{4,5}. ¹Humanitas clinical and research center IRCCS, Hepatobiliary immunopathology lab, Rozzano, Italy; ²Istituto di ricerche farmacologiche Mario Negri IRCCS, Mass spectrometry laboratory, Milano, Italy; ³Humanitas clinical and research center IRCCS, Haematological malignancies genomic lab, Rozzano, Italy; ⁴Humanitas University, Department of biomedical sciences, Pieve Emanuele, Italy; ⁵Humanitas clinical and research center IRCCS, Department of gastroenterology, Rozzano, Italy; ⁶Humanitas clinical and research center IRCCS, Department of surgery, Rozzano, Italy
Email: michela_anna.polidoro@humanitasresearch.it

Background and aims: Intrahepatic cholangiocarcinoma (iCCA) is a deadly cancer arising from biliary epithelial cells (BECs) lining the biliary tree. iCCA is a highly chemoresistant tumor and pharmacological therapies are generally unsuccessful. Furthermore, due to the complexity of the *in-vivo* cellular interactions, metabolic activation pathways are largely unknown. We herein aim to elucidate the metabolic asset of BECs and iCCA cells.

Method: BECs and iCCA cells were isolated from patients resected at the Division of Hepatobiliary and General Surgery, Humanitas Clinical Institute. BECs and iCCA surnatants were analysed by using mass

spectrometry-based untargeted and targeted metabolomic approaches. RNA-seq and Reverse transcriptase-polymerase chain reaction (RT-PCR) analyses were performed to identify altered metabolic pathways in iCCA cells. Moreover, iCCA cell proliferation was assessed at different time points post glutaminase-1 (GLS-1) inhibition (CB-839) and immunofluorescence staining for mitochondria was performed.

Results: iCCA cells were characterized by enhanced mitochondrial activity compared to BECs, resulting in an increased glutamine and glucose uptake. RNA-seq analysis revealed several altered metabolic pathways in iCCA cells attributed to the Warburg effect and glutamine metabolism. To explore the importance of glutamine metabolism, we further evaluated the mRNA expression of ASCT1 and ASCT2, two glutamine transporters, and GLS1, resulted to be significantly upregulated in iCCA cells. CB-839 treatment revealed that GLS1-high iCCA cells were more susceptible to GLS-1 inhibition compared to GLS1-low cells, along with changing in mitochondrial morphology.

Conclusion: Experimental data suggest an impairment of mitochondrial activity of iCCA cells. Resensitizing iCCA cells to metabolic treatments could make them more susceptible to cytotoxic drugs, opening new possibility to improve the outcomes of the iCCA patients.

SAT202

Microfluidic 3-dimensional bioprinting and 2-dimensional micropatterns as tools to bioengineer biliary ducts

Lorena Loarca¹, Cyrille El Khassis¹, Afshan Iqbal², Latifa Bouzahir¹, Alexandra Fuchs³, Erin Bedford⁴, Jean-Charles Duclos-Vallée⁵, Emma Andersson², Pascale Dupuis-Williams^{1,6}. ¹Université Paris-Saclay, Physiopathogénèse et traitement des maladies du foie, Villejuif, France; ²Karolinska Institutet, Cell and Molecular Biology, Solna, Sweden; ³Université de Paris, INSERM, CEA, U 976 HIPI, Paris, France; ⁴Aspect Biosystems, Vancouver, Canada; ⁵FHU Hepatinov, Centre Hépatobiliaire, Villejuif, France; ⁶ESPCI Paris, Université PSL, Paris, France

Email: pascale.dupuis-williams@universite-paris-saclay.fr

Background and aims: There is currently an unmet need of 3D *in vitro* tubular biliary models that replicate the physiopathogenesis of cholestatic disorders to test for novel therapeutic targets.

We are developing several methodologies for the construction of bile tubes:

by microfluidic co-extrusion bioprinting, with the aim of obtaining perfusable tubes of 300 to 500 µm in diameter or by self-organogenesis allowing the development of 3D hollow, polarized, and functional biliary trees grown on 2D micropatterns

Alagille Syndrome (ALGS) is a genetic disorder that affects various organs including the liver. Liver damage in ALGS occurs as a result of defects in the biliary system due to mutations on the JAG1 gene. A mouse model of ALGS (*Jag1^{Ndr/Ndr}*) with a missense mutation in *Jag1* was previously developed showing heart, eyes, and liver abnormalities.

The aim of our study is to show our progress on the construction of 3D bioprinted perfusable human biliary ducts and on the application of our biliary tree model to investigate the organogenesis features observed in ALGS using organoids from the *Jag1^{Ndr/Ndr}* mouse model.

Method: Alginate-collagen I and human primary cholangiocytes were utilized to bioprint tubes of 3 cm in length and 300 µm inner diameter using the RX1 bioprinter and microfluidic printheads (Aspect Biosystems).

Collagen I-coated glass micropatterns and organoids from the *Jag1^{Ndr/Ndr}* mouse model were employed to engineer 3D biliary trees of physiologically relevant geometry and dimensions.

Results: Perfusable human biliary tubes were fabricated via the microfluidic 3D bioprinting technology as assessed by confocal microscopy images of the polarized biliary epithelium.

3D biliary trees from WT and *Jag1^{Ndr/Ndr}* mouse organoids were bioengineered from 2D micropatterns. The *Jag1^{Ndr/Ndr}* biliary trees

exhibited thinner branches with impaired polarity and smaller lumens (Fig 1).

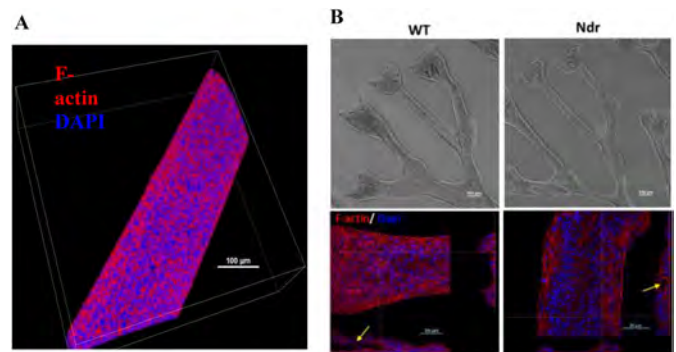


Figure 1. Biliary structures fabricated via microfluidic 3D bioprinting and 3D self-organogenesis on 2D micropatterns (A) 3D reconstruction of confocal Z-stacks of a bioprinted human tube showing F-actin and nuclei labelling (20X). (B) Branches from *Jag1^{Ndr/Ndr}* biliary trees grown on 2D micropatterns are thinner (top panel, phase contrast, 10X) and with smaller lumens (bottom panel, orthogonal views, confocal microscopy (40X)). Yellow arrows pointing at lumens.

Conclusion: Microfluidic 3D bioprinting and 2D micropatterns are two technologies that allow for bioengineering of 3D tubular biliary structures that recapitulate *in vivo* states of health and disease. These models open up opportunities to study organogenesis and physiopathological cues.

The bioprinted tubes could be connected to microfluidic perfusion systems to investigate questions related to bile flow and detoxification. Self-organogenesis of 3D structures on 2D micropatterns is a promising tool to mimic ALGS.

SAT203

Mcpip1 fl/fl LysM Cre mice as an animal model of TNFa-dependent liver endothelial cell dysfunction in humans with chronic inflammation

Dariusz Zurawek¹, Natalia Pydyn¹, Piotr Major², Edyta Kus³, Stefan Chlopicki³, Andrzej Budzyński³, Ewelina Pośpiech⁴, Jolanta Jura¹, Jerzy Kotlinowski¹. ¹Faculty of Biochemistry, Biophysics and Biotechnology, Jagiellonian University, Department of General Biochemistry, Kraków, Poland; ²2nd Department of General Surgery, Jagiellonian University Medical College, Poland; ³Jagiellonian Centre for Experimental Therapeutics, Jagiellonian University, Poland; ⁴Malopolska Centre of Biotechnology, Jagiellonian University, Human Genome Variation Research Group, Poland

Email: j.kotlinowski@uj.edu.pl

Background and aims: Mcpip1 is an RNase involved in a negative regulation of inflammation, which is tightly linked to the function of endothelial cells. Under such pathological state, endothelium is characterized by increased expression of adhesion molecules, enhanced permeability, diminished production of NO, or increased extravasation of leukocytes to the surrounding tissue. The aim of this work was to verify whether Mcpip1 deletion leads to endothelial activation.

Method: We used C57BL/6/J mouse strain with a knock-out of Mcpip1 gene in leukocytes of myeloid lineage (*Mcpip1^{fl/fl}LysM^{Cre}*) as a model of endogenous, sterile inflammation. Multiplex Luminex assay was used to determine serum cytokine profile in these mice. Then, we performed differential expression analysis of genes in CD146⁺ endothelial cells (ECs) isolated from livers of 3 and 6-months-old control (*Mcpip1^{fl/fl}*) and *Mcpip1^{fl/fl}LysM^{Cre}* mice by using next generation sequencing (NGS) and RT-PCR method. NGS was followed by gene ontology enrichment analysis (GO) and signaling pathway impact analysis. Activation of hepatic ECs was analyzed by immunohistochemical (IHC) staining. Finally, results observed in mice were compared to ECs liver histology of a group of 40 patients.

POSTER PRESENTATIONS

Results: Depletion of Mcp1 protein in myeloid leukocytes led to development of sterile and endogenous inflammation in 6-month-old Mcp1^{fl/fl}LysM^{Cre} animals. Mcp1^{fl/fl}LysM^{Cre} mice were characterized by increased serum levels of interleukins (IL-5, IL-6 α , IL-10), chemokines (MCP-2, MCP-5, MIP-3 β , MARC), markers of endothelial damage and TNF α . NGS analysis revealed 1094 differentially expressed genes (fold change >2 or <0.5) in ECs isolated from livers of Mcp1^{fl/fl}LysM^{Cre} mice as compared to control Mcp1^{fl/fl} animals. GO analysis pointed out that 'antigen processing and presentation' and 'cell adhesion molecules' were the mostly affected biological pathways in liver ECs of Mcp1^{fl/fl}LysM^{Cre} mice. Further, RT-PCR and immunohistochemical analysis confirmed significant upregulation of P-selectin, Vcam1 and Icam1 in hepatic ECs of Mcp1^{fl/fl}LysM^{Cre} mice as compared to control littermates. Moreover, we observed significant reduction of the level of liver glycocalyx what was followed by increased serum TNFs levels observed in Mcp1^{fl/fl}LysM^{Cre} mice. Finally, patients with high serum levels of TNF α (>14 pg/ml) showed significant decrease in the levels of glycocalyx in the liver.

Conclusion: Mouse genetic model of endogenous, sterile inflammation (Mcp1^{fl/fl}LysM^{Cre}) has good translational potential in studies of liver ECs activation and damage observed in patients with chronic inflammation.

Acknowledgments: This work was supported by research grant from National Science Centre, Poland grant number 2017/27/B/NZ5/01440 to JK.

SAT204

Peroxisome proliferator activated receptor gamma regulates patatin-like phospholipase domain-containing protein 3 in adipocytes in vitro and in vivo in a mouse model of non-alcoholic steatohepatitis

Emmanuel Dauda Dixon¹, Thierry Claudel¹, Alexander D Nardo¹, Veronika Mlitz¹, Claudia Fuchs¹, Michael Trauner¹. ¹Medical University of Vienna, Hans Popper Laboratory of Molecular Hepatology, Division of Gastroenterology and Hepatology, Department of Internal Medicine III, Wien, Austria

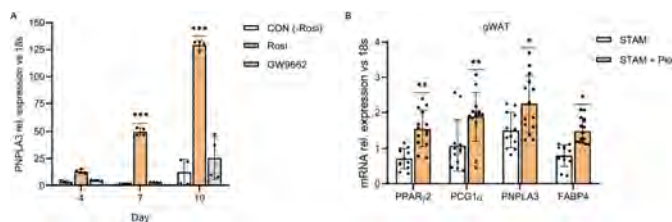
Email: michael.trauner@meduniwien.ac.at

Background and aims: The patatin-like phospholipase domain-containing protein 3 (PNPLA3) is expressed highly in the liver and adipose tissue. Despite its unknown metabolic function, the PNPLA3 mutant I148M is associated with non-alcoholic fatty liver disease development and progression. Hence, there is a growing interest in understanding the role of PNPLA3 in adipose tissue and liver biology, the two main organs/tissues responsible for maintaining metabolic flexibility. Peroxisome proliferator-activated receptor gamma (PPAR gamma) binding activity was shown to be reduced in LX2 cells overexpressing the PNPLA3 I148M variant. Therefore, we explored whether PPAR gamma transcriptionally regulates PNPLA3 in vitro and in vivo in STAM mice as a model of NASH.

Method: A 1 kb DNA fragment of the human PNPLA3 promoter was cloned in front of a luciferase reporter gene and co-transfected into COS-7 cells with a PPAR gamma expression plasmid. Four potential peroxisome proliferator response elements (PPREs) predicted sequences were mapped using NUBIsCan and Genomatix softwares. The predicted PPREs sequences were subjected to gel shift to report the direct interactions between PPAR gamma and PNPLA3. To explore the regulation of PNPLA3 independent of insulin, we investigated the STAM (diabetic and hyperlipidemia condition) model and fed 8 weeks old STAM mice an HFD supplemented with 0.01% pioglitazone for 2 weeks.

Results: Rosiglitazone induced PNPLA3 mRNA expression (+88%) and significantly increased the luciferase activity in co-transfected cells (+50%), demonstrating PPAR gamma-mediated induction of PNPLA3 promoter activity. Interestingly, two PPREs at positions 713–707 (+92%) and 790–780 (+93%) were bound by the PPAR gamma nuclear protein in the differentiated adipocytes. The introduction of two

base-pair mutations into the identified 707mut (~40%) and 780mut2 (~60%) reduced PPAR gamma binding activity, but not 780mut2. Likewise, incubation with an antibody against PPAR gamma also reduced binding (~40%) to the PNPLA3 enhancer regions. In the STAM mouse, pioglitazone treatment increased markedly the expressions of PNPLA3 (+31%) and PPAR gamma (+50%) mRNA and its downstream target genes such as FABP4 and PGC1 alpha in the gonadal white adipose tissue (gWAT). In the liver (with lower PNPLA3 expression compared to white adipose tissue), however, pioglitazone treatment did not significantly increase PNPLA3 (p = 0.56) and PPAR gamma (p = 0.06) gene expression.



Conclusion: This study demonstrates that in the presence of PPAR gamma, PNPLA3 is up-regulated transcriptionally independent of insulin-SREBPs mediated effect. This data suggests that PNPLA3 is a PPAR gamma target gene. However, the pathogenetic and therapeutic relevance of this association with regards to adipose tissue and liver function remains to be determined.

SAT205

Animal variants of sodium-taurocholate co-transporting polypeptide permitting hepatitis B virus infection

Fuwang Chen¹, Jochen Wettengel¹, Florian Gegenfurtner¹, Yi Ni^{2,3}, Stephan Urban^{2,3}, Ulrike Protzer^{1,4}. ¹Institute of Virology, Technical University of Munich/Helmholtz Zentrum München, Munich, Germany; ²Department of Infectious Diseases, Molecular Virology, University Hospital Heidelberg, Heidelberg, Germany; ³German Center for Infection Research (DZIF), partner site Heidelberg, Heidelberg, Germany; ⁴German Center for Infection Research (DZIF), partner site Munich, Munich, Germany

Email: fuwang.chen@tum.de

Background and aims: Evaluation of new therapies to cure chronic hepatitis B virus (HBV) infection is limited by the lack of suitable animal models. Identification of sodium-taurocholate co-transporting polypeptide (NTCP) as a species-specific key factor for HBV entry and infection may allow expanding the HBV host range. Key objective of this study was to analyse species-specific NTCPs for HBV binding and infection in order to advance our knowledge and to discover potential HBV animal models.

Method: NTCPs from various animal species were selected based on their sequence similarity within the human NTCP binding domain (amino acid 157–165). These NTCPs were expressed in HepG2 cells by DNA-plasmid or mRNA transfection. Subsequently, NTCPs expression, bile acid uptake and moreover their capability to support HBV binding and infection were analyzed by luminescence, radiometry, myristoylated HBV-preS1 peptide (MyrB-atto488) staining, flow cytometry and HBeAg-specific ELISA, respectively.

Results: Eighteen animal NTCP variants expressed at comparable levels revealed varying levels of bile acids uptake as physiological function of NTCP. MyrB-atto488 staining and subsequent flow cytometry analysis indicated that all NTCP variants except those from macaque and dolphin were able to bind HBV. Furthermore, HBV infection experiments showed that NTCPs from various species including aardvark, rabbit, whale, big brown bat, cat, rhinoceros and horse support *de novo* HBV infection when expressed on HepG2 cells. In addition, introducing minimal genetic changes into hamster, cow and goat NTCP at amino acid position 82–87 restored the capability to

S761

SAT208

CRISPR perturbation in iPSC-derived hepatic stellate cells reveals role for TNF-driven interferon response in chronic liver disease

Kelly Haston¹, Navpreet Ranu¹, Lorn Kategaya¹, Eric Lubeck¹, Michael D. Berke¹, Francesco Paolo Casale¹, Panagiotis Stanitsas¹, Alicia Lee¹, Owen Chen¹, Bobby Leitmann¹, Srinivasan Sivanandan¹, Ahmed Sandakli¹, Pooja Prasad¹, Rohit Loomba², Arun Sanyal³, Stephen Harrison⁴, Zobair Younossi⁵, Catherine Jia⁶, Grant Budas⁶, James Trevaskis⁶, Robert Myers⁶, David Breckinridge⁶, Ajamete Kaykas¹, Daphne Koller¹, Matthew Albert⁷. ¹insitro, South San Francisco, United States; ²University of California San Diego, La Jolla, United States; ³Virginia Commonwealth University, Richmond, United States; ⁴Oxford University, Radcliffe Department of Medicine, Oxford, United Kingdom; ⁵Inova Fairfax Medical Campus, Fairfax, United States; ⁶Gilead Sciences, Inc., Foster City, United States; ⁷insitro, South San Francisco, United States

Email: research_operations@insitro.com

Background and aims: Activation of hepatic stellate cells (HSC) by inflammatory cytokines plays a central role in the progression of fibrosis. We aimed to: (i) define the interplay between NF-kappa-B and TGF-beta pathways using induced pluripotent stem cell (iPSC)-derived hepatic stellate cells (iHSCs); and (ii) discover insights that align with non-alcoholic steatohepatitis (NASH) progression.

Method: We developed an iHSC model that showed evidence of cellular maturation and extracellular matrix production. We employed Cas9-engineered cells and barcoded guide RNAs to execute pooled optical screening in human cells (POSH); and single-cell RNA-seq to analyze cytokine-treated iHSCs. For characterization of NASH phenotypes, we used 4, 641 whole-slide images of liver biopsies from multiple trials. We trained end-to-end deep convolutional neural networks (CNN) to predict histological features [Casale et al, EASL 2020]. RNA-seq was performed on matched samples. For each clinical end point, we assessed the (multiple-hypothesis corrected) enrichment of TNF-alpha and IL1-beta

response genes at multiple cutoffs using GSEA as implemented in the *gseapy* prerank module.

Results: Using a 400-guide RNA CRISPR library, we characterized the genes critical for TNF-alpha and IL1-beta-mediated activation of NF-kappa-B p65 response in iHSCs (Figure 1A and not shown). Molecular characterization of gene expression changes demonstrated that NF-kappa-B induces type I interferon response genes in iHSCs, constituting a distinct activation state as compared to TGF-beta (Figure 1B). Supporting the disease relevance of these signatures, we observed that TNF-alpha and IL1-beta signatures were enriched for genes associated with the CNN fibrosis stage and progression, as well as the serum fibrosis biomarker ELF score at FDR 5%.

Conclusion: This work constitutes an advancement above the state-of-the-art methodology, with optimized protocols and cell lines for genetic editing of iHSCs. Notably, this constituted the first time that POSH with image-based phenotyping has been achieved in iPSC derived cells. These studies also revealed a model of cytokine-driven fibrosis that aligned with clinical histological and biomarker features of NASH progression. Finally, we highlight the identification of NF-kappa-B p65 induced type I interferon in iHSCs. These results provide insights that will support the development of new therapeutic approaches for NASH.

SAT209

Regulation of cholangiocyte ciliogenesis by soluble adenyllyl cyclase

Hang Lam Li¹, Simei Go¹, Jung-Chin Chang¹, Arthur Verhoeven¹, Ronald Oude Elferink¹. ¹Amsterdam UMC, Tytgat Institute, Amsterdam, Netherlands

Email: r.p.oude-elferink@amc.uva.nl

Background and aims: Sec61 subunit beta (SEC61B) is involved in endoplasmic reticulum (ER) import of nascent plasma membrane, secreted and vacuolar proteins. Mutations in the genes for SEC61B and PC1 are (amongst others) causative for polycystic liver disease

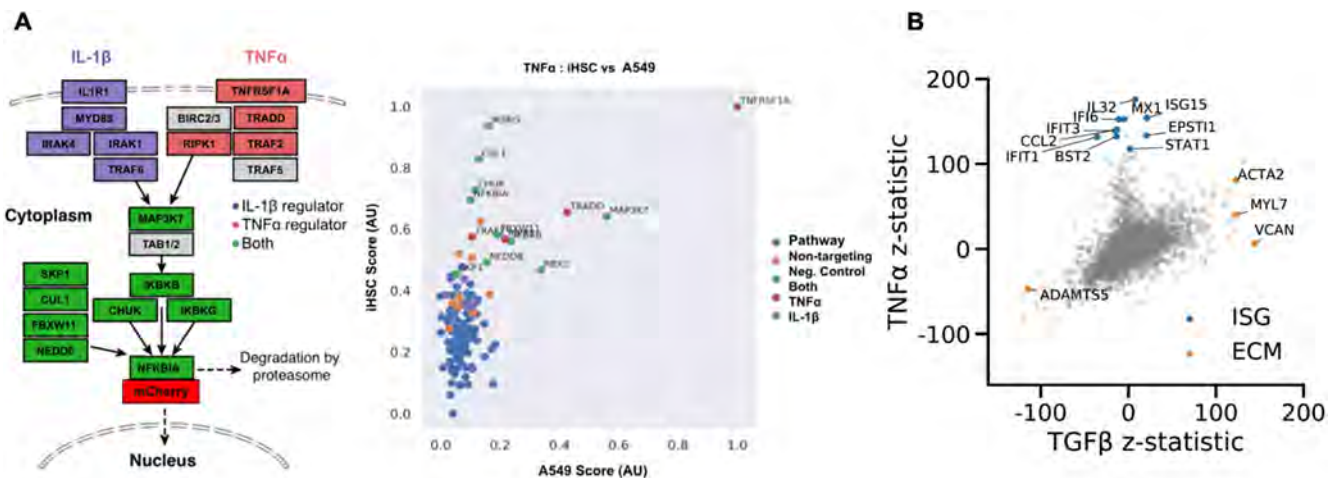


Figure 1 | TNF induced type I interferon stimulated genes mark a unique activation state in iHSCs.

(A) POSH targeting recovered genes responsible for image-based p65-mCherry translocation. iHSC scores were similar in rank to those found in the A549 reference tumor line. IL1-beta specific genes, purple; TNF-alpha specific genes, red; Common NF-kappaB genes, green; and Control genes, orange and blue (pathway modified from Feldman et al., 2019). (B) Scatter plot depicting gene expression levels in iHSCs reveals distinct TNF-alpha-induced type I interferon stimulated gene (ISG) signature, versus common TNF-alpha and TGF-beta cytokine-driven extracellular matrix (ECM) genes.

Figure: (abstract: SAT208)

(PCLD), which is characterized by disturbed ciliogenesis and disturbed cyclic adenosine monophosphate (cAMP) homeostasis. Soluble adenylyl cyclase is highly expressed in H69 cholangiocytes. Therefore, we investigated the role of soluble adenylyl cyclase (sAC, ADCY10) in ciliogenesis of H69 cells.

Method: Phosphoproteomics, western blotting and immunofluorescence staining were performed in H69 cholangiocytes in the presence and absence of the sAC-specific inhibitor LRE1 and by knockdown of sAC with lentiviral shRNA. Deglycosylation of H69 lysates was performed with PNGase F and endo H.

Results: H69 cells incubated with sAC-specific inhibitor LRE1 acutely and drastically reduced phosphorylation of SEC61B at serine 17. The function of this phosphorylation site is currently unknown. We therefore studied the effect of sAC knockdown by lentiviral shRNA on ciliogenesis. Immunofluorescent staining of cilia, with ADP-ribosylation factor-like protein 13B (ARL13B) as a marker, revealed disappearance of cilia upon sAC knockdown. This was accompanied by an intracellular accumulation of ARL13B. Polycystin-1 (PC1), which is largely expressed at the primary cilium of cholangiocytes, was also investigated. sAC knockdown led to impaired glycosylation of PC1, while no difference was observed in its protein levels (as determined by deglycosylation with PNGase F). Conversely, neither protein level, nor glycosylation state of GLUT1, a strongly glycosylated plasma membrane protein that is not associated with the primary cilium, were affected by knockdown of sAC.

Conclusion: These data suggest that sAC-dependent phosphorylation of SEC61B is essential for proper cotranslational glycosylation of a specific set of proteins that travel through the endoplasmic reticulum, including PC1. As a consequence, ablation of sAC expression leads to absence of cilia in cholangiocytes. Our observations suggest that sAC may be a regulator of ciliogenesis.

SAT210

Signal transducer and activator of transcription 3 (STAT3)-driven hepatic transcriptional changes are indicative of a shift from immune tolerance to immune activation in chronic hepatitis B virus (HBV) infection

Jinglin Tang¹, Jiaxuan Zhang¹, Gaoli Zhang¹, Ning Ling¹, Min Chen¹.

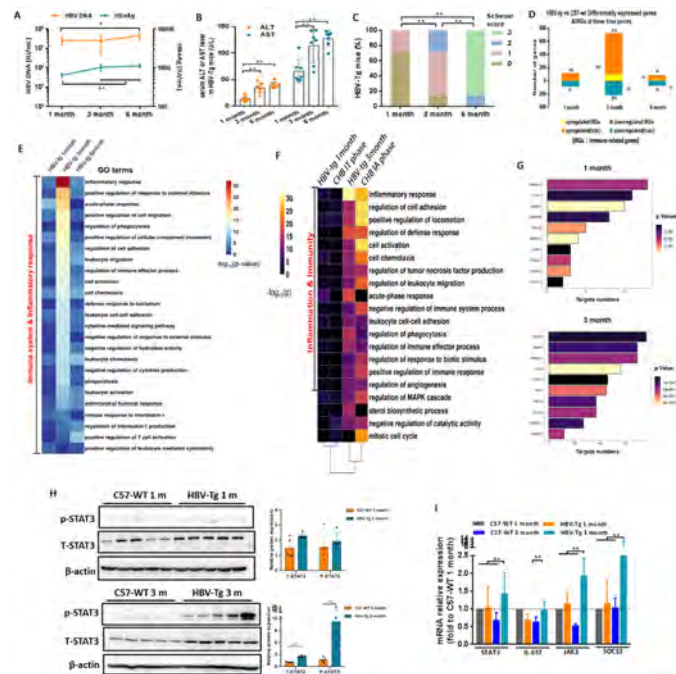
¹Chongqing Medical University, Key Laboratory of Molecular Biology for Infectious Diseases (Ministry of Education), Institute for Viral Hepatitis, The Second Affiliated Hospital, Chongqing, China
Email: mchen@hospital.cqmu.edu.cn

Background and aims: Various immune cells and mediators were reported to be significantly changed in immune activation stage during chronic HBV (CHB) infection. However, it is still unknown what key upstream regulators drive these numerous changes in gene expression, especially during the transition from immune tolerance to immune activation.

Method: A HBV transgenic (HBV-Tg) mice model with spontaneous development of hepatic immune activation was applied to comprehensively investigate the dynamic changes in hepatic gene expression and immune cells by RNA sequencing, flow cytometry and immunohistochemistry. The transcriptomic and immunologic characterizations were analyzed by Gene Set Enrichment Analysis (GSEA) and ImmPort, and upstream transcriptional factors (TFs) were predicted by ENCODE CHIP-seq library in immune tolerance and immune activation phases both in HBV-Tg mice and CHB patients (GSE83148 and GSE65359 from GEO datasets). Expression and activation of predicted transcriptional factors and the signal pathway components were identified and confirmed by western blot and quantitative real time PCR.

Results: Compared to 1-month-old HBV-Tg mice (in immune tolerance phase), a number of inflammatory and immune-related genes and pathways were significantly up-regulated in 3-month-old HBV-Tg mice (in early immune activation phase). Similar hepatic gene expression patterns were found between HBV-Tg mice in 1 month or 3 month and CHB patients in immune tolerance or immune

activation phase respectively. STAT3 was predicted to be the top-ranking transcription factor in early immune activation phase of HBV-Tg mice (3 month). Furthermore, expression of total and phosphorylated STAT3, and several genes involving STAT3 pathway was significantly enhanced in 3-month-old HBV-Tg mice.



A,B,C,D, serum HBV DNA and HBeAg levels (A), serum ALT and AST levels (B), histologic grading of inflammation by Scheuer scoring system (C), and the number of hepatic differentially expressed total or immune-related genes (D) in HBV-Tg mice at 1, 3, or 6 month. E, inflammation and immune-related pathways (GO terms) were significantly up-regulated in 3-month-old HBV-Tg mice by GSEA analysis. F, similar biological processes between HBV-Tg mice in 1 month or 3 month and CHB patients in immune tolerance or immune activation phase separately by cluster analysis. G, STAT3 was the top-ranking transcription factor in 3-month-old HBV-Tg mice predicted by ENCODE tools. H, enhanced protein expression of hepatic total (T) and phosphorylated (P) STAT3 in 3-month-old HBV-Tg mice. I, elevated mRNA expression of several components involving STAT3 signal pathway in 3-month-old HBV-Tg mice.

Conclusion: Activation of STAT3 with enhanced expression of immune- and inflammation-related genes indicated a shift from immune tolerance to immune activation in chronic HBV infection.

SAT211

Polymeric nanomicelles formulation of LY2157299-Galunisertib improves therapeutic outcome by greater reducing fibrosis and ameliorating fatty degeneration in a CCL4-induced hepatic fibrosis rat-model

Elisa Panzarini¹, Stefano Loporatti², Bernardetta Anna Tenuzzo¹, Alessandra Quarta³, Nemany A. N. Hanafy⁴, Gianluigi Giannelli⁵, Camilla Moliterni⁶, Diana Vardanyan¹, Carolina Sbarigia⁶, Stefano Tacconi⁶, Marco Fidaleo^{6,7}, Luciana Dini^{6,7}. ¹University of Salento, Department of Biological and Environmental Sciences and Technologies; ²CNR-NANOTEC-Istituto di Nanotecnologia, Lecce, Italy; ³CNR-NANOTEC-Istituto di Nanotecnologia, Italy; ⁴Kafrelsheikh University, Nanomedicine Department, Institute of Nanoscience and Nanotechnology, Egypt; ⁵National Institute of Gastroenterology, "S. de Bellis" Research Hospital, Italy; ⁶Sapienza University of Rome, Department of Biology and Biotechnology "Charles Darwin", Italy; ⁷Sapienza University of Rome, Research Center for Nanotechnology for Engineering of Sapienza (CNIS), Rome, Italy
Email: luciana.dini@uniroma1.it

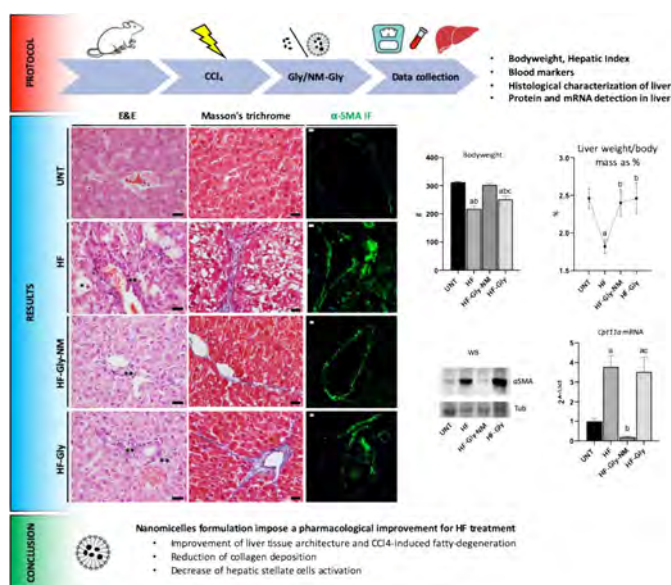
Background and aims: A major cause of liver-related disorders is hepatic fibrosis (HF). TGFβ1, a cytokine, is one of the profibrotic mediators and it affects specific liver cells, including hepatic stellate cells and portal fibroblasts which participate in the overproduction of extracellular matrix. There have been promising results against chronic liver progression in animal models using the TGFβ1 receptor inhibitor LY2157299 (Galunisertib, Gly), despite its low

POSTER PRESENTATIONS

bioavailability. Here, we evaluate in a rat model the possible benefit against HF of encapsulated Gly in polymeric nanomicelles based on polygalacturonic acid and polyacrylic acid (Gly-NMs) previously characterized and known to increase drug bioavailability.

Method: Gly and Gly-NMs role against fibrosis were tested in a CCl₄-induced HF rat model. Morphological, hematic and hepatic data were collected to monitor disease progression.

Results: In terms of body weight, liver weight, and serum parameters of hepatic function, Gly-NM appeared to provide better recovery from hepatic fibrosis than Gly. Molecular markers and histopathological analysis showed that Gly-NMs demonstrated marked antifibrotic properties, reducing collagen deposition in liver tissue and decreasing the activation of hepatic stellate cells. Furthermore, we remarked an improved CCl₄-induced fatty-degeneration following Gly-NMs treatment. The latter was associated with a gene downregulation of carnitine palmitoyl-transferase 1A (*Cpt1a*) which can impose a protective action against CCl₄ insult as reported in the literature for mice lacking the enzyme.



Conclusion: Our results show that encapsulated Gly reduces fibrosis and related disease markers and improve the fatty degeneration better than free drug in a *in vivo* rat model.

SAT212

3D bioprinted hepatocyte and mesenchymal stem cell spheroids as a cell therapy for liver disease

Christopher Dickman¹, Stephanie Campbell¹, Haley Tong¹, Reza Jalili¹, Simon Beyer¹, Tamer Mohamed¹, Sam Wadsworth¹, Spiro Getsios¹.

¹Aspect Biosystems, Vancouver, Canada

Email: chrisd@aspectbiosystems.com

Background and aims: Individuals with severe liver failure or metabolic liver disease, often have limited treatment options aside from transplantation. Liver transplantation is a complex and invasive surgery with limited availability of donor organs. Furthermore, recipients require life-long immune suppression, increasing the risk of infection and cancer. Recently, isolated hepatocytes have been transplanted into pediatric patients with acute liver failure with improvements in survival. Long term function of transplanted hepatocytes remains a challenge for treatment of chronic disease. The goal of this study is to demonstrate the ability of our unique bioprinting technology to generate hepatocyte implants capable of long term viability and function *in vitro* as well as *in vivo* in the intraperitoneal space of transplanted mice.

Method: Primary human hepatocytes (PHHs) were formed into spheroids with the addition of CD166 positive mesenchymal stem cells (MSCs). These spheroids were manufactured into a 3D bioprinted implant using Aspect Biosystems' RX1 bioprinter. Spheroids were embedded in a hydrogel core and surrounded by an immune isolating shell in a core-shell micro-architecture. Live/Dead; albumin, and alpha-1 antitrypsin (A1AT) production as well as ammonia detoxification assays were used to confirm *in vitro* function of printed implants. Hepatocytes were then implanted into the IP space of NOD-*scid* IL2Rgamma^{null} mice. Function was examined over 28 days by monitoring the levels of plasma albumin and A1AT. At day 28 fibers were retrieved to analyze function and viability.

Results: When cultured *in vitro* 1 million cell hepatocyte and MSC implants were able to synthesize >20 ug/million PHH/day. When implanted into mice plasma levels of albumin remained steady for 28 days and reached levels ≥2000ng/ml. The hepatocytes retained function and the ability to detoxify ammonia when retrieved from mice at the study end point.

Conclusion: Our hepatocyte and MSC bioprinted implants demonstrate promise for the treatment of liver disease. We aim to build upon our research with studies demonstration efficacy of these implants in a small and large animal model of acute liver failure.

SAT213

Fibroblast growth factors are therapeutic targets for radiofrequency ablation induced tumorigenesis

Aurelia Markezana¹, Mor Paldor¹, Haixing Liao¹, Muneeb Ahmed², Elina Zorde-Khavlevsky¹, Nir Rozenblum¹, Salome Ganizate¹, Eithan Galun¹, S. Nahum Goldberg¹. ¹Hadassah Hebrew University Hospital, Goldyne Savad Institute of Gene Therapy, Jerusalem, Israel; ²Beth Israel Deaconess Medical Center (BIDMC), Harvard Medical School, Laboratory for Minimally Invasive Tumor Therapies, Boston, United States

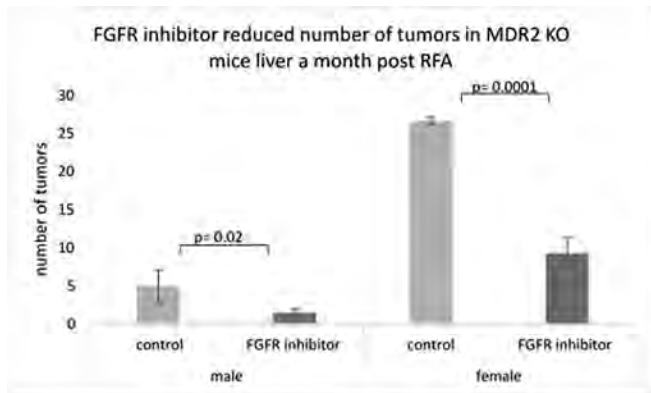
Email: aureliahakoune@gmail.com

Background and aims: Radiofrequency ablation (RFA) is an image-guided method used commonly to treat focal primary and metastatic tumors in the liver and other organs. Despite the advantages of RFA over surgery, the 5-year survival rate of patients treated with RFA remains approximately 50%, with 70%-81% new tumor recurrence in hepatocellular carcinoma (HCC). There is evidence, that local hepatic RFA can promote tumor growth even at a distance from the ablational site. Several potential pro-tumorigenic cytokines and factors, including IL-6, HGF, STAT3, and VEGF, increase following RFA, as we have shown. Additionally, following liver ablation, an increased inflammatory response is observed including recruitment of neutrophils, macrophages, and activated myofibroblasts to the ablated zone. Thus, strategies to identify and suppress local and systemic pro-oncogenic effects of RFA are urgently required to further improve the therapeutic effect.

Method: The proliferative effect of plasma of HCC or Colorectal carcinoma (CRC) patients post liver RFA on several HCC cell lines was tested. Multiplex ELISA protein analysis was performed on these plasmas to identify secreted cytokines and growth factors post RFA and may induce proliferation. Additionally, primary mouse hepatocytes and immortalized human hepatocytes were subjected to moderate hyperthermia *in-vitro*, to mimic the thermal stress induced during ablation in normal parenchymal cells. The medium of these cells was analysed by an unbiased manner protein array and a multiplex ELISA to detect factors secreted to the medium post heating. Next, since we observed increase in the fibroblast growth factors (FGF) post heating *in vitro* and in plasma of human and mice post RFA treatment we used an FGFR inhibitor to inhibit the proliferation observed post RFA *in vivo* and post heating *in vitro*.

Results: Plasma of HCC and CRC patients, 90 min post RFA, induce significant proliferation in HCC cell lines. Multiplex ELISA screening analysis of patient's plasma shows that RFA induced secretion of pro-tumorigenic growth factors and cytokines. Medium of *in-vitro* heated

mouse and human hepatocytes induced significant proliferation of multiple cancer cell lines. Protein analysis shows that hepatocytes subjected to moderate hyperthermia in vitro excrete a wide spectrum of growth factors. A proteomic non-biased array analysis revealed additional growth factors involved in tumorigenesis post RFA, specifically the FGF protein family, which were elevated and secreted from heated hepatocytes and post RFA in human and mouse. In an effort to further substantiate these observations, FGFR inhibitor reduced significantly liver tumor load post RFA in an MDR2 KO inflammation induced HCC mouse model.



Conclusion: Our results indicate that liver RFA, can induce tumorigenesis via the FGF signalling pathway, and its inhibition suppress HCC development.

SAT214

Glycine ameliorates paracetamol-induced liver injury in non-alcoholic fatty liver disease by supporting glutathione biosynthesis

Alia Ghrayeb¹, Shani Drucker¹, Bella Agranovich¹, Daniel Peled¹, Oren Rom^{2,3}, Ifat Abramovich¹, Sara Fernandes¹, Natan Weissman¹, Jonatan Fernandez Garcia¹, James Traylor³, Chen Eugene², Eyal Gottlieb¹, Inbal Mor¹. ¹The Ruth and Bruce Rappaport Faculty of Medicine, Cell Biology and Cancer Science Department, Haifa, Israel; ²University of Michigan, Internal Medicine Department, Ann Arbor, United States; ³Louisiana State University Health Shreveport, Pathology and Translational Pathobiology Department, Shreveport, United States Email: aliaghayeb81@gmail.com

Background and aims: Non-alcoholic fatty liver disease (NAFLD) is the most common chronic liver disease worldwide. NAFLD patients are more susceptible to drug-induced hepatotoxicity compared to healthy individuals, yet a clear understanding of the predisposing factors and dedicated therapeutic interventions are still lacking. Overdose of paracetamol, a common analgesic drug, is one of the leading causes of acute liver injury in general. Paracetamol is oxidized in the liver to N-acetyl-p-benzoquinone imine (NAPQI), a highly reactive metabolite, which is detoxified by the cellular antioxidant, glutathione (GSH). In toxic doses, GSH levels cannot eliminate NAPQI, leading to reactive oxygen species (ROS)-induced damage. Glycine, a substrate of GSH synthesis, is lower in plasma of NAFLD patients and mouse models. It has recently been shown that in mice, administration of glycine can elevate GSH in the liver. We examined the mechanistic link between steatosis and paracetamol toxicity and the role of glycine in glutathione replenishment as therapeutic intervention.

Method: AML12 mouse hepatocyte cell line was incubated with palmitate (PA), which induced an increase in lipid droplets and ROS levels as detected by BOIDPY and DHE staining, respectively. Metabolomics analysis of PA treated cells by liquid chromatography and mass spectrometry demonstrated a decrease in glycine and GSH

levels, which was further exacerbated by exposure to paracetamol. Cell viability analysis showed paracetamol toxicity and PA lipotoxicity were synergistic, indicating lipid accumulation increases oxidative stress and paracetamol toxicity. Glycine supplementation elevated cellular levels of glycine and GSH, even in the presence of paracetamol.

Results: C57BL/6J mice fed western diet (WD) for 8 weeks, demonstrated liver steatosis and decreased circulating glycine compared to mice on standard chow diet (CD). Unbiased metabolomic profiling of liver tissue followed by pathway analysis, exhibited significant changes in GSH and glycine metabolism in WD compared to CD. Following the 8 week diet, mice received a single dose of paracetamol. WD-paracetamol treated mice displayed higher ALT levels and more severe liver histopathology compared to CD-paracetamol treated mice, demonstrating steatosis increased sensitivity to paracetamol hepatotoxicity. Metabolomic analysis of the livers 6hrs following paracetamol administration showed significantly lower GSH and glycine levels in WD compared to CD. Glycine administration to WD-paracetamol treated mice increased hepatic levels of GSH. Indices of liver injury: ALT levels, liver pathology and tissue marker for oxidative stress, were all improved following glycine administration.

Conclusion: These results indicate that decreased glycine in the plasma and the liver in NAFLD lead to lower hepatic GSH synthesis and increase paracetamol sensitivity which can be alleviated by glycine administration.

SAT215

Hepatocyte-specific deletion of the anti-apoptotic Mcl-1 in mice induces polyploidization, mitotic errors and chromosomal instability.

Laure-Alix Clerbaux^{1,2}, Pierre Cordier³, Nina Desboeufs^{1,2}, Kristian Unger⁴, Gabriel Semere², Lap Kwan Chan², Chantal Desdouets³, Massimo Lopes¹, Achim Weber^{1,2}. ¹Institute of Molecular Cancer Research, University of Zürich, Zurich, Switzerland; ²Department of Pathology and Molecular Pathology, Zürich Hospital, Zurich, Switzerland; ³Team Proliferation, Stress and Liver Physiopathology, INSERM, Paris, France; ⁴Research Unit of Radiation Cytogenetics, Helmholtz Zentrum München, Germany Email: laure.alix.clerbaux@gmail.com

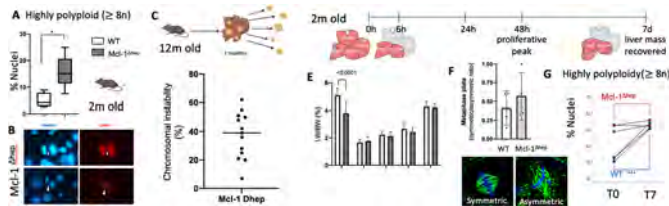
Background and aims: Mcl-1 is a widely recognized pro-survival protein and a promising target for cancer therapy. We previously showed that hepatocyte-specific deletion of Mcl-1 (Mcl-1^{Dhep}) triggers apoptosis and proliferation in livers of young mice, and found that higher apoptotic levels at early age correlate with spontaneous HCC development later on. Aiming to characterize further non-apoptotic roles of Mcl-1, we here investigated its role in ploidy and mitosis *in vivo*.

Method: Mcl-1^{Dhep} livers of 2 months old mice were analyzed for ploidy profile, formation and polarization of mitotic spindles. Whole exome sequencing (WES) of tumors of 12 months old Mcl-1^{Dhep} mice was performed to assess extent of chromosomal instability (CIN) via SNVs and indels frequency. To evaluate the impact of Mcl-1 loss in livers upon induced hyperproliferation, 2 months old Mcl-1^{Dhep} and WT mice were subjected to two-third partial hepatectomy (PHx). Ploidy contingent, mitotic figures and chromosome segregation were analyzed at the peak of proliferation (48 h post-PHx). WES was performed in regenerated livers when hepatocytes stop proliferating (7d post-PHx) to monitor associated genetic alterations.

Results: Mcl-1^{Dhep} livers of young mice displayed a high proportion of polyploid hepatocytes (Fig. A), which were associated neither with higher apoptosis, nor with higher proliferation, age or oxidative stress. Moreover, Mcl-1^{Dhep} hepatocytes entered into mitosis, thus excluding endoreplication. Gene set enrichment analysis showed an association between genes upregulated upon Mcl-1 deletion and genes of the mitotic spindle assembly checkpoint (SAC), which ensures correct chromosomes segregation during mitosis. Around

POSTER PRESENTATIONS

50% of the mitotic events in Mcl-1^{Dhep} livers were aberrant (Fig. B), with abnormal chromosome segregation. WES of Mcl-1^{Dhep} tumors of 12 months old mice showed a mean CIN of 33.8% (Fig. C). Following PHx, liver weight to body weight ratios were similar in Mcl-1^{Dhep} and WT mice during liver regeneration, while Mcl-1^{Dhep} livers were smaller prior to PHx (Fig. E). Mcl-1^{Dhep} hepatocytes progressed faster through G2/M. At the proliferative peak, abnormal mitotic figures were observed with similar frequency in Mcl-1^{Dhep} and WT livers (Fig. F). After regeneration, the ploidy profile was comparable in WT and Mcl-1^{Dhep} livers (Fig. G). Both WT and Mcl-1^{Dhep} livers harbored very low level of SNVs and indels.



Conclusion: In 2 months old mice, hepatocytes lacking Mcl-1 exhibit nuclear polyploidy, mitotic errors and abnormal chromosome segregation leading to CIN. Surprisingly, similar rates of aberrant mitosis were observed in WT and Mcl-1^{Dhep} livers upon hyperproliferation. And after hyperproliferation, WT and Mcl-1^{Dhep} livers exhibited similar levels of abnormal nuclear morphology, of low mutational burden and of high proportion of polyploid nuclei.

SAT216

Hepatic inflammation elicits production of proinflammatory netrin-1 through exclusive activation of translation

Romain Barnault^{1,2,3,4}, Claire Verzeroli^{1,2,3,4}, Carole Fournier⁵, Michelet Maud^{2,3,4,6}, Anna-Rita Redavid^{2,3,4,7}, Ievgeniia Chicherova^{2,3,4,6}, Marie-Laure Plissonnier^{2,3,4,6,8}, Annie Adrait⁹, Olga Khomich^{2,3,4,6}, Fleur Chapus¹⁰, Mathieu Richaud^{2,4,7,8}, Maëva Hervieu^{2,4,7,8}, Veronika Reiterer¹¹, Federica-Grazia Centonze¹¹, Julie Lucifora^{2,4,7,8}, Birke Bartosch^{2,4,7,8}, Michel Rivoire^{2,4}, Hesso Farhan¹¹, Johann Couté⁹, Valbona Mirakaj¹², Thomas Decaens⁵, Patrick Mehlen^{2,3,4,7,8}, Benjamin Gibert^{2,3,4,7}, Fabien Zoulim^{2,3,4,6,13}, Romain Parent^{2,3,4,6}. ¹Centre de Recherche en Cancérologie de Lyon, Inserm U1052-LabEx DEVweCan, France; ²Université de Lyon, France; ³CNRS UMR 5286, France; ⁴Centre Léon Berard, Lyon, France; ⁵Institute for Advanced Biosciences, La Tronche, France; ⁶Pathogenesis of Chronic Hepatitis B and C Laboratory-Centre de Recherche en Cancérologie de Lyon, Inserm U1052-LabEx DEVweCan, France; ⁷Apoptosis, Cancer an development Laboratory-Cancer research Center of Lyon, Inserm U1052-LabEx DEVweCan, France; ⁸Centre de Recherche en Cancérologie de Lyon, Lyon, France; ⁹University of Grenoble-Alpes, Inserm, CEA, UMR biosanté U1292, Grenoble, France; ¹⁰The National Institute of Environmental Health Sciences, Durham, United States; ¹¹Medizinische Universität Innsbruck, Institute of Pathophysiology, Innsbruck, Austria; ¹²Universitätsklinikum Tübingen Anaesthesiology and Intensive care Medicine, Tübingen, Germany; ¹³Service of Hepato-Gastroenterology, Hospice civils de Lyon, Lyon, France

Email: romain.barnault@inserm.fr

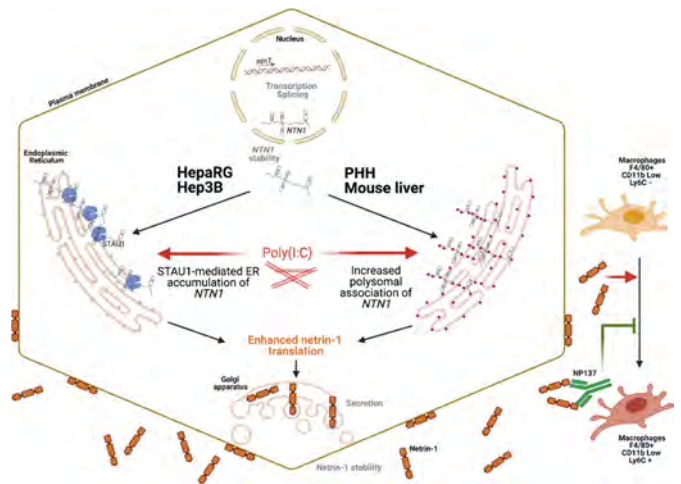
Background and aims: Chronic liver diseases (CLDs) affect more than 1 billion people worldwide. Though CLDs exhibit a high degree of diversity in terms of causal effects, including infectious (HBV and HCV), metabolic, toxic, and genetic, they all converge toward hepatic inflammation and represent a pertinent model for its study. Inflammation in turn drives hepatocyte turnover, extracellular matrix (ECM) accumulation, histological worsening, and the long-term induction of tumorigenic mediators such as IL-6, eventually leading to the development of HCC. Hence, the identification of

factors involved in the harmful consequences of inflammation may lead to its clinical improvement.

Netrin-1 is well known for preventing cellular apoptosis through its binding to “dependence receptors,” and we demonstrated that it is HBV- HCV induced and endowed hepatocytes with resistance to apoptosis during the unfolded protein response (UPR), a hallmark of CLDs and cirrhosis. Owing to the causal link between inflammation, cancer in general, and HCC, we hypothesized that hepatic inflammation and netrin-1 may be reciprocal influencers in the liver. This prompted us to test its inducibility and inflammatory contribution in the liver in the context of previous descriptions in inflammatory bowel disease and colorectal cancer.

Method: A panel of cell biology and biochemistry approaches (RT-qPCR, reporter assays, run-on, polysome fractionation, CLIP, filter binding assay, subcellular fractionation, western blotting, IP, stable isotope labeling by amino acids in cell culture) on in vitro- grown primary hepatocytes and liver cell lines from mouse samples and clinical samples was used

Results: We identify netrin-1 as a hepatic inflammation- inducible factor and decipher its mode of activation through an exhaustive eliminative approach. We show that netrin-1 up- regulation relies on a hitherto unknown mode of induction, namely its exclusive translational activation. This process includes the transfer of NTN1 mRNA to the endoplasmic reticulum and the direct interaction between the Staufen-1 protein and this transcript as well as netrin-1 mobilization from its cell- bound form. Finally, we explore the impact of a phase 2 clinical trial-tested humanized anti-netrin-1 antibody (NP137) in two distinct, toll- like receptor (TLR) 2/TLR3/TLR6-dependent, hepatic inflammatory mouse settings. We observe a clear anti-inflammatory activity indicating the proinflammatory impact of netrin-1 on several chemokines and Ly6C+ macrophages.



Conclusion: These results identify netrin-1 as an inflammation-inducible factor in the liver through an atypical mechanism as well as its contribution to hepatic inflammation.

SAT217

A meta-analysis to identify novel candidate genes in the development of hepatocellular carcinoma

Andrew Walakira¹, Cene Skubic¹, Nejc Nadižar¹, Miha Mraz², Miha Moskon², Tadeja Rezen¹, Damjana Rozman¹. ¹University of Ljubljana, Centre for Functional Genomics and Bio-Chips, Ljubljana, Slovenia; ²University of Ljubljana, Faculty of Computer and Information Science, Ljubljana, Slovenia
Email: andrew.walakira@mf.uni-lj.si

Background and aims: Hepatocellular carcinoma (HCC) is a major health problem worldwide. In 2020, there was about 900,000 new

cases of liver cancer, which is the third-highest number of cancer-related deaths (8.3% of 9.9 million) in the same year. Hepatitis B and C infections are still the major risk factors but with vaccination and effective treatment, these are steadily being overtaken by other factors, such as metabolic associated fatty liver disease and diabetes. Prevention efforts have been useful but the HCC burden is on the rise. To alleviate this problem, there is an urgent need for new tools, such as non-invasive diagnostics and effective treatments. We aim to unravel novel candidate genes that are important in HCC.

Method: We did a meta-analysis using 8 transcriptomics datasets (GSE19665, GSE39791, GSE41804, GSE57957, GSE64041, GSE84402, GSE84598, and HCCDB15/TCGA-LIHC). These datasets were from tumour and surrounding non-tumour tissue biopsies of the liver. First, we did differential gene expression analysis on each of the datasets individually by fitting linear models using the Limma package. This was followed by a meta-analysis by fitting random effects models using log fold change (LogFC) as effect size. Genes were considered significant if their p value was less than 0.05. Significant genes from the meta analysis were further analysed for KEGG pathway enrichment, network analysis in STRING database and searched DisGeNET to discover gene-disease associations. All statistical analyses were done in R software.

Results: After the meta-analysis, 690 genes were significantly differentially expressed. Thirty pathways were enriched with the majority (28) associated with metabolism. The two other enriched pathways were the cell cycle and p53 signalling pathways. Genes in the cell cycle and p53 signalling pathways were generally upregulated, while the genes in metabolism related pathways were generally downregulated. When searched DisGeNET database, 128 genes (of the 690 genes) were found not to be associated with HCC or other forms of liver cancer. Some of these genes like *KIAA0101*, *SERPINA10* and *RDH5* have been associated with HCC in smaller studies. Searching in STRING database revealed several important protein-protein interactions and hubs that are worth further investigation.

Conclusion: Four genes namely; *C8A*, *HAO1*, *PIPOX* and *PROZ* were identified as key hub genes and will be studied further in the laboratory.

SAT218

Characterization of TGR5-mediated Ca²⁺ signaling in cholangiocytes

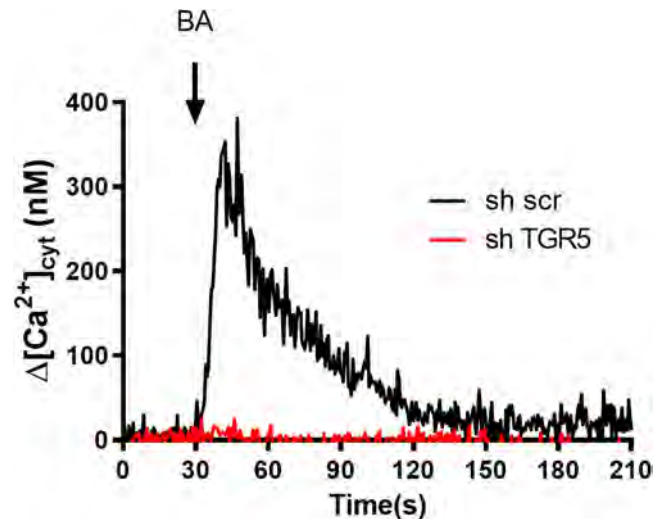
Xuanmeng Chen¹, Amr Al Shebel¹, Thibault Pebrier¹, Thierry Thordjmann¹, Olivier Dellis¹. ¹University of Paris-Saclay, INSERM U1193, Orsay, France
Email: olivier.dellis@universite-paris-saclay.fr

Background and aims: The Bile acid (BA) receptor TGR5 is known to be coupled with cyclic-AMP signaling in cholangiocytes, allowing Cl⁻ and bicarbonate secretion in parallel with water, making a fluid and alkalized bile. Our aim was to decipher TGR5-dependent bile acid-induced Ca²⁺ mobilization in cholangiocytes, a previously overlooked pathway.

Method: using spectrofluorimetry, we measured cytosolic calcium concentration variations in normal human cholangiocytes and cholangiocarcinoma cell lines loaded with the Ca²⁺ dye Indo1, using the BA tauroolithocholate (TLCA) and RO5527239 (RO) as TGR5 agonists. Specific inhibitors for G proteins, P2Y2 receptors and Ca²⁺ transporters like SERCA were used. TGR5 expression was also suppressed using shRNAs.

Results: TLCA and RO5527239 (100 and 300 μM respectively for cell lines and normal cholangiocytes) induced dose dependent Ca²⁺ signals in both normal human cholangiocytes and cholangiocarcinoma cell lines. TGR5-dependent cytosolic Ca²⁺ mobilization occurred through a complex pathway involving: Gαq/11 engagement, Ca²⁺ release from the endoplasmic reticulum and a strong Ca²⁺ influx from the extracellular medium. Furthermore, TGR5-dependent Ca²⁺ increase was dependent on an ATP release and on the activation of P2Y2 receptors (which are also able to induce Ca²⁺ release and Ca²⁺

+ influx), as revealed by using P2Y2-specific inhibitors and apyrase. In the lack of TGR5 expression (TGR5 shRNA treatment), BA-induced Ca²⁺ mobilization was totally impaired (Figure).



Conclusion: Beside the well-known cAMP pathway that stimulates CFTR-dependent Cl⁻ ions secretion, TGR5 stimulation also induces Ca²⁺ signals through a pathway involving ATP release and purinergic P2Y2 stimulation. This new signaling pathway in cholangiocyte may have potential CFTR-independent impact on Cl⁻ ions secretion in bile, and possibly other pathophysiological consequences to be further explored.

Liver transplantation and hepatobiliary surgery: Clinical aspects

SAT229

Outcomes of living liver donors are worse than those of matched healthy controls: nationwide cohort study

Jong Man Kim¹, Jin Yong Choi², Jae Heon Kim³, Hyun Jung Kim⁴, Jae-Won Joh¹. ¹Samsung Medical Center, Sungkyunkwan University School of Medicine, Department of Surgery, Seoul, Korea, Rep. of South; ²Myongji Hospital, Goyang-si, Korea, Rep. of South; ³Soonchunhyang University Seoul Hospital, Korea, Rep. of South; ⁴Korea University, Korea, Rep. of South
Email: jongman94@hanmail.net

Background and aims: Donor death is the most serious complication of living liver donation, but is reported rarely. We investigated the actual mortality of living liver donors (LLDs) compared with matched control groups based on analysis of the Korean National Health Insurance Services (NHIS) database.

Method: This cohort study included 12,372 LLDs who donated a liver graft between 2002 and 2018, and were registered in the Korean Network for Organ Sharing. They were compared to three matched control groups selected from the Korean NHIS and comprising a total of 123,710 subjects: healthy population (Group I); general population without comorbidities (Group II); and general population with comorbidities (Group III).

Results: In this population, 78.5% of living liver donors were 20–39 years old, and 64.7% of all donors were male. Eighty-nine donors (0.7%) in the LLD group died (68 males and 21 females), a mortality rate (1000 person/year) of 0.91 (0.74–1.12). Mortality rate ratio and the adjusted hazard ratio of the LLD group was 2.03 (1.61–2.55) and

POSTER PRESENTATIONS

1.71 (1.31–2.25) compared to Control Group I, 0.75 (0.60–0.93) and 0.63 (0.49–0.82) compared to Control Group II, and 0.58 (0.46–0.71) and 0.49 (0.39–0.60) compared to Control Group III. LLD group, depression, and lower income were risk factors for adjusted mortality. The incidence of liver failure, depression, cancer, diabetes, hypertension, brain infarction, brain hemorrhage, and end-stage renal disease in the LLD group was significantly higher than in Control Group I.

Conclusion: Outcomes of the LLD group were worse than those of the matched healthy control group despite the small number of death and medical morbidities in this group. LLDs should receive careful medical attention for an extended period after donation.

Lay summary: The incidence of mortality, liver failure, depression, cancer, diabetes, hypertension, brain infarction, brain hemorrhage, and end-stage renal disease in the LLD group was significantly higher than in the matched healthy group even though few cases. Careful donor evaluation and selection processes can improve donor safety and enable safe living donor liver transplantation.

SAT230

Pretransplant changes in serum protein glycosylation relate to risk of HCC recurrence after liver transplantation and provide a potential prognostic biomarker: a proof-of-concept study

Xavier Verhelst^{1,2}, Heleen Engels¹, Anja Geerts^{1,2}, Aude Vanlander³, Luis Abreu de Carvalho³, Helena Degroote^{1,2}, Leander Meuris^{4,5}, Frederik Berrevoet³, Nico Callewaert^{4,5}, Hans Van Vlierberghe^{1,2}.
¹Ghent University Hospital, Gastroenterology and Hepatology, Gent, Belgium; ²Ghent University, Liver Research Center Ghent, Gent, Belgium; ³Ghent University Hospital, General, hepatobiliary and transplant surgery, Gent, Belgium; ⁴VIB-Ugent, Center for Medical Biotechnology, Gent, Belgium; ⁵Ghent University, Department of Biochemistry and Microbiology, Gent, Belgium
 Email: xavier.verhelst@uzgent.be

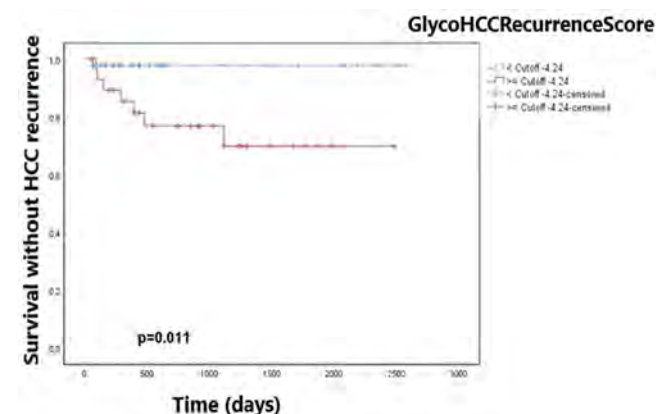
Background and aims: Hepatocellular carcinoma (HCC) recurs after liver transplantation (LT) in 10% of patients. Changes in protein glycosylation have been described during the development of HCC. Study goal was to assess the risk of HCC recurrence after LT, according to changes in serum protein glycosylation before LT.

Method: A prospective study was performed in patients receiving LT between July 2011 and September 2018. A whole serum protein N-glycan profile was assessed using DNA sequencer assisted fluorophore assisted capillary electrophoresis, using a validated high-throughput protocol. For every sample, 13 glycans were quantified. Patients were followed until HCC recurrence or death. Specific changes in serum protein glycosylation profiles were analysed in patients with HCC recurrence compared to patients without.

Results: Amongst 225 consecutive liver transplant patients, 76 patients suffered from HCC before LT. Main indications were related to alcoholic cirrhosis (47.4%), HCV infection (21.1%) and NASH (15.8%). Eight patients (10.5%) developed HCC recurrence after a median follow-up time of 9.5 months after LT. Seventy-four patients (97%) fulfilled Milan criteria.

Significant differences in the relative abundance of 5 serum glycans were present in patients with HCC recurrence compared to patients without (Cox regression analysis). Based on these changes, a composite biomarker was developed (GlycoHCCRecurrenceScore). This score integrates an increased presence of triantennary glycans with and without branch and core fucosylation (NA3, NA3Fc and NA3Fbc) and a decreased presence of undergalactosylated glycans NGA2F and NGA2FB in patients with HCC recurrence. This biomarker panel shows an AUC of 0.855 ($p=0.001$; 95% CI 0.731–0.979) for association with HCC recurrence. Using an optimized cut-off (–4.24), sensitivity was 87.5% and specificity 67.6%. Only 2.1% of patients with a value below this cut-off showed HCC recurrence, compared to 24.1% of patients with values above this cut-off ($p=0.011$). PPV was 72.98% and NPV 84.39%. Figure 1 illustrates the discriminative value of this biomarker. In a univariate cox regression analysis other factors

related to HCC recurrence in this cohort were diameter of the largest lesion before LT and the presence of perineural or lymphovascular invasion in the explant liver. In a multivariate analysis, the biomarker showed an independent relation with HCC recurrence (HR 1.931; $p=0.008$; 1.184–3.149).



Conclusion: A glycomics based serum biomarker panel is strongly associated with tumor recurrence in a cohort of LT patients with HCC, even if adhering to Milan criteria. In a multivariate analysis, this biomarker was the only pretransplant discriminative parameter of HCC recurrence in this cohort. The biomarker could potentially increase the prediction of HCC recurrence and improve allocation strategies in LT candidates with HCC.

SAT231

Liver transplantation for complications of hepatoportal sclerosis

Andrew Keaveny¹, Nadia Khatoon², Murli Krishna², Jason Lewis², Raouf Nakhleh².
¹Mayo Clinic, Transplantation, Jacksonville, United States; ²Mayo Clinic, Pathology, Jacksonville, United States
 Email: keaveny.andrew@mayo.edu

Background and aims: Hepatoportal sclerosis (HPSc) is a rare, often unrecognized condition that leads to non-cirrhotic portal hypertension (PHT). Refractory complications of PHT may necessitate consideration of liver transplantation (LT). There are very limited data on the outcomes post-LT for this condition in the current era of transplantation. In this study, we sought to determine the patient and allograft outcomes of patients transplanted for HPSc at our large volume center.

Method: A 20-year retrospective search for the diagnosis of HPSc was conducted in our surgical pathology files. Twenty-one cases were identified and verified by slide review. The respective patient charts were reviewed for: clinical presentation, background history, biochemical and other laboratory studies, radiographic investigations, histology, treatment, and outcomes.

Results: Of the 21 cases, 12 were male. The age at histological diagnosis ranged from 18 to 83 years, with a median age of 61. Two patients had been referred with and were confirmed to have a diagnosis of HPSc. Six and 4 patients had been documented with ascites and esophageal varices, respectively; 4 patients had a history of hepatic encephalopathy. Relevant history included 5 patients with a prior malignancy treated with chemotherapy, 12 patients with autoimmune disorders, 4 patients with congenital abnormalities related to vascular anomalies, and 2 with HIV. Nine patients underwent LT for decompensated disease not controlled by medical management. One patient required simultaneous liver and kidney transplant. One patient required retransplantation for hepatic artery thrombosis 4 days after the original surgery. Four patients died post-LT. The causes of death at mean of 3.75 years (range: immediate–5 years) post-transplant were intra-operative death at the time of the transplant surgery (1), respiratory failure (1), and multi-organ failure

(2). The remaining 5 patients are alive at a mean of 4 years (range: 2–9 years) post-transplant. One patient was documented to have an occlusive thrombus in an inferior branch of the right portal vein 4 months post-LT and another patient developed a main portal vein thrombosis 3 years post-LT.

Conclusion: Patients presenting with complications of HPSc usually have an underlying risk factor that likely contributed to its development. LT may be required to treat refractory complications, with acceptable long-term outcomes.

SAT232

Discordance in categorization of acute-on-chronic-liver-failure in the national transplant database

Brian Lee¹, Giuseppe Cullaro², Aidan Vosooghi³, Frederick Yao², Sarjukumar Panchal⁴, David Goldberg⁵, Norah Terrault³. ¹University of Southern California, Los Angeles, United States; ²University of California San Francisco; ³University of Southern California; ⁴University of Pennsylvania; ⁵University of Miami
Email: brian.lee@med.usc.edu

Background and aims: Studies regarding acute-on-chronic liver failure (ACLF) among liver transplant (LT) candidates from the United Network for Organ Sharing (UNOS) database are being used to inform LT policy changes worldwide. We assessed the validity of identifying ACLF in UNOS.

Method: We performed random probability sampling among 3 US LT centers between 2013 and 2019 to obtain a representative patient sample across ACLF grades. We compared the concordance of ACLF classification by UNOS vs. blinded manual chart review, according to EASL-CLIF. We compared the association of ACLF by UNOS and chart review with waitlist dropout within 90 days of listing.

Results: Among 481 sampled LT registrants, 250 (52%) had no ACLF, 75 (16%) had ACLF grade 1, 79 (16%) had ACLF Grade 2, and 77 (16%) had ACLF Grade 3 per UNOS categorization. Concordance of ACLF grade by UNOS vs. chart review was: 72%, 64%, 56%, and 64% for no ACLF, Grade 1, Grade 2, and Grade 3, respectively, with overall Cohen's kappa coefficient 0.48 (95%CI 0.42–0.54). Absence of acute decompensation was the most common reason for overestimation, and discordant brain and respiratory failure categorization were the most common reasons for underestimation of ACLF by UNOS. In multivariable analysis, ACLF by chart review was independently associated with waitlist dropout (Grade 1: $p = 0.44$; Grade 2: $p = 0.003$; Grade 3: $p = 0.004$), but this association was not present by UNOS classification (Grade 1: $p = 0.68$; Grade 2: $p = 0.69$; Grade 3: $p = 0.63$).

Concordance Metrics for ACLF Grade and Organ Failure by UNOS vs. Chart Review

		Sensitivity (95% CI)	Specificity (95% CI)	NPV (95% CI)	PPV (95% CI)	AUC (95% CI)
ACLF	None	0.96 (0.91–0.98)	0.72 (0.67–0.77)	0.59 (0.53–0.66)	0.98 (0.95–0.99)	0.84 (0.81–0.87)
	Grade 1	0.64 (0.44–0.81)	0.87 (0.84–0.90)	0.24 (0.15–0.35)	0.98 (0.96–0.99)	0.76 (0.67–0.85)
	Grade 2	0.56 (0.40–0.72)	0.87 (0.84–0.90)	0.28 (0.18–0.39)	0.96 (0.93–0.98)	0.72 (0.64–0.80)
	Grade 3	0.64 (0.53–0.75)	0.93 (0.90–0.95)	0.64 (0.52–0.74)	0.93 (0.90–0.96)	0.79 (0.73–0.84)
Organ Failure	Liver	0.96 (0.92–0.99)	0.98 (0.95–0.99)	0.94 (0.89–0.98)	0.99 (0.97–1.00)	0.97 (0.95–0.99)
	Coagulation	0.93 (0.88–0.97)	0.96 (0.94–0.98)	0.90 (0.83–0.94)	0.98 (0.96–0.99)	0.95 (0.93–0.97)
	Kidney	0.94 (0.89–0.97)	0.98 (0.96–1.00)	0.97 (0.93–0.99)	0.96 (0.94–0.98)	0.96 (0.94–0.98)
	Brain	0.13 (0.09–0.18)	0.92 (0.88–0.95)	0.63 (0.48–0.76)	0.51 (0.46–0.56)	0.53 (0.50–0.55)
	Respiratory	0.36 (0.21–0.53)	0.99 (0.97–1.00)	0.74 (0.49–0.91)	0.95 (0.92–0.96)	0.67 (0.60–0.75)
	Circulatory	0.15 (0.08–0.25)	0.98 (0.96–0.99)	0.52 (0.30–0.74)	0.86 (0.83–0.89)	0.56 (0.52–0.60)

Conclusion: In this retrospective multi-center study, ACLF categorization by UNOS showed weak agreement with manual chart review. We confirmed the independent association of ACLF with waitlist outcomes. These findings are informative for ongoing allocation

policy discussions and highlight the importance of prospective studies regarding ACLF in LT and UNOS reform.

SAT233

Humoral response to 2-dose BNT162b2 mRNA vaccine for COVID-19 in liver transplant recipients

Maria Guarino¹, Ilaria Esposito², Giuseppe Portella³, Valentina Cossiga¹, Ilaria Loperto⁴, Luca Pignata¹, Raffaella Tortora², Maria Rosaria Attanasio¹, Michele Cennamo³, Mario Capasso¹, Daniela Terracciano³, Francesco Maria Cutolo¹, Alfonso Galeota Lanza², Raffaele Lieto¹, Sarah di Somma³, Francesco Paolo Picciotto², Filomena Morisco¹. ¹University of Naples "Federico II," Department of clinical medicine and surgery, Gastroenterology and hepatology Unit, Naples, Italy; ²Hepatology Unit, AORN A. Cardarelli, Naples, Italy; ³Department of translational medical science, University of Naples "Federico II," Naples, Italy; ⁴UOC Epidemiologia e prevenzione e registro tumori, ASL Napoli 1 Centro, Naples, Italy
Email: maria.guarino86@gmail.com

Background and aims: In the context of the Italian SARS-CoV-2 vaccination program, liver transplant (LT) recipients were prioritized for vaccine administration, although the lower response to vaccines is a well known problem in this population. We aimed to evaluate immunogenicity of BNT162b2 mRNA vaccine in LT recipients and healthy controls and to identify factors associated with negative response to vaccine.

Method: We prospectively evaluated a cohort of adult LT patients the humoral response (with anti-Spike protein IgG-LIAISON SARS-CoV-2 S1/S2-IgG chemiluminescent assay) at 1 and 3 months after 2-dose vaccination. A group of 307 vaccinated healthcare workers, matched by age and sex, served as controls.

Results: Overall, 492 LT patients were enrolled (75.41% male, median age 64.85 years). Detectable antibodies were observed in the 75% of patients with a median value of 73.9 AU/ml after 3 months from 2-dose vaccination. At multivariable analysis, older age (>40 years, $p = 0.016$), shorter time from liver transplantation (<5 years, $p = 0.004$), and immunosuppression with antimetabolites ($p = 0.029$) were significantly associated with non-response to vaccination. Moreover, the LT recipients showed antibody titers statistically lower than the control group (103 vs 261 AU/ml, $p < 0.0001$) (figure). Finally, both in controls and LT patients we found a trend of inverse correlation between age and antibody titers (correlation coefficient: -0.2023 and -0.2345 , respectively).

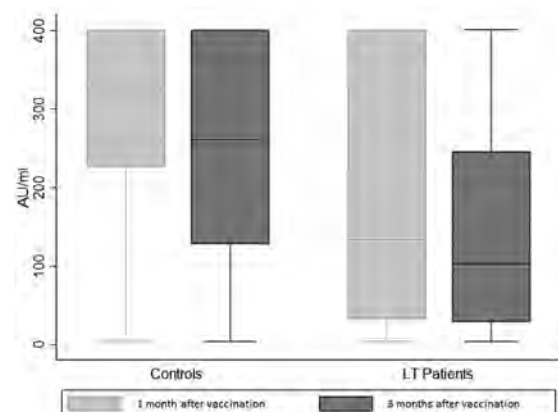


Figure: Humoral response to 2-dose BNT162b2 vaccine after 1 and 3 months in LT patients and healthcare workers (controls).

Conclusion: Three months after vaccination, LT recipients showed humoral response in 75% of cases. Older age, shorter time from transplantation and use of antimetabolites were factors associated with non-response to vaccination and needed to be kept under close monitoring.

SAT234

A predictive model for mortality within one year of liver transplantation at the time of wait-listing for transplant: a novel approach using machine learning algorithms in a large US multi-ethnic cohort

Sripriya Balasubramanian¹, Megha Bhatnagar², Jian Wang², Lisa Edelman³, Malou Valencia³, Aaron Rosenberger², Robert Freed⁴, Amandeep Sahota⁵, Varun Saxena^{5,6}, Nizar Mukhtar⁵, Suk Seo⁵, Brock McDonald⁵, Joanna Ready⁵. ¹Kaiser Permanente, Gastroenterology and Hepatology, Roseville, United States; ²Kaiser Permanente, Information Support for Care Transformation, United States; ³Kaiser Permanente, National Transplant Services; ⁴Kaiser Permanente, Vascular and Interventional Radiology; ⁵Kaiser Permanente, Gastroenterology and Hepatology, United States; ⁶University of California, San Francisco, Hepatology, United States
Email: priya.b.manian@gmail.com

Background and aims: Pre-liver transplant (LT) sarcopenia, malnutrition and frailty are implicated in increased mortality following LT. Tests for these entities are expensive (CT for sarcopenia assessment) or require one-on-one testing not readily available at all centres (frailty testing), limiting widespread use. A predictive tool using readily available clinical data at waitlisting would be valuable to identify patients at risk, allowing for targeted evaluation and intervention.

Method: All Kaiser Permanente adult members nationally who underwent a first LT between 2010 and 19 for indication other than hepatocellular carcinoma were included. Data extracted from the electronic medical record included demographics, laboratory values and diagnoses by ICD 9/10 codes. Frailty was assessed by previously published associated ICD codes; malnutrition by ICD codes and calculated Nutritional Risk Index. One year mortality was calculated from the day of transplant. Vote-based approach was used to identify variables of interest derived from six different machine learning algorithms. Variables with two or more votes were included. Cohort was split 80:20 for model training and validation. Models were developed with repeated iterations and hyperparameter tuning using cross-validation for maximal improvement. Model assessments done with ROC curves, confusion matrix and decile plots with KS statistic.

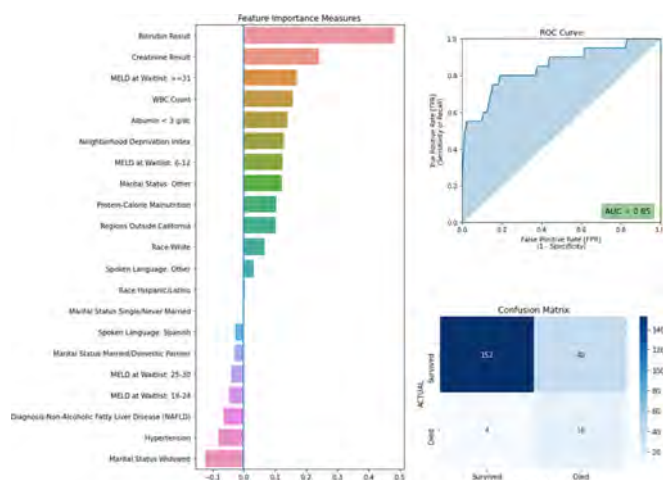


Figure: Combined Feature Importance plot, ROC curve and Confusion matrix for final predictive model: Linear SVC.

Results: A total of 1,056 patient were included, of whom 98 (9.3%) died within one year of surgery. Variables deemed important by the

"vote-based approach" included pre-LT bilirubin, creatinine, WBC count, albumin, MELD at Waitlist ≥ 31 and more (figure). Random forest, decision tree with bagging classifier and linear support vector classifier (SVC) performed best. Linear SVC model was selected as the final model based on sensitivity/recall, specificity, AUC statistic and F1 score. With a threshold of 50%, model had high sensitivity (80%), specificity (79%) and accuracy (79%) in identifying patients with poor outcome. Linear SVC Model performance assessed with KS statistic and decile plots achieved a value of 55 in the 3rd decile with the validation cohort, indicating excellent performance.

Conclusion: We have identified a model that predicts one year mortality after liver transplantation at the time of waitlisting with excellent performance. This enables early detection of patients at risk; studies on targeted interventions to improve post-transplant outcomes are planned.

SAT235

Monitoring patients with anti HBs trough levels can minimise hepatitis B immune globulin therapy after liver transplant

Erica Nicola Lynch¹, Stefania Petrucci², Claudia Campani^{1,3}, Gabriele Dragoni^{1,4}, Tommaso Innocenti¹, Paolo Forte⁵, Stefano Milani¹, Andrea Galli¹. ¹Gastroenterology Research Unit, Department of Experimental and Clinical Biomedical Sciences "Mario Serio," Florence, Italy; ²Hepatobiliary Surgery and Liver Transplantation, University of Pisa Medical School Hospital, Pisa, Italy; ³Department of Experimental and Clinical Medicine, University of Florence, Florence, Italy; ⁴Department of Medical Biotechnologies, University of Siena, Siena, Italy; ⁵Division of Gastroenterology, University Hospital "Careggi," Florence, Italy
Email: ericanicola.lynch@unifi.it

Background and aims: Hepatitis B virus (HBV) is still among the most frequent causes of liver transplantation (LT) in Europe. Combined prophylaxis with anti-HBs immunoglobulins (HBIG) and nucleos(t)ide analogues (NUCs) has virtually eliminated the risk of a disease relapse, although there is growing evidence that HBIG therapy could be safely withheld in most patients. The aim of our study was to evaluate the effectiveness of a combined HBV prophylaxis with a minimised and personalised fixed-dose HBIG therapy and a target anti-HBs trough level of 50–100 UI/L.

Method: All patients transplanted for HBV-related diseases (at least 12 months post LT) who attended our tertiary referral centre between January 2019 and June 2021 were prospectively included in our study. All patients received a combined HBV prophylaxis with NUCs (tenofovir, entecavir, or lamivudine) and intramuscular HBIG therapy administered at individualised multiple-week intervals, aiming at obtaining anti-HBs trough levels of 50–100 UI/L.

Results: Out of a total of 40 patients, there were no cases of HBV-DNA or HBsAg recurrence. The median (IQR) interval between 1000 UI HBIG doses was 5 weeks (4–6 weeks), with a maximum of 9 weeks and a minimum of 4 weeks. No patient characteristic—including LT indication (cirrhosis, hepatocellular carcinoma, or acute hepatitis), HDV coinfection, and type of NUC—was significantly associated with HBIG dosage, nor did the latter correlate with body mass index, estimated glomerular filtration rate, or follow-up duration after LT. The mean anti-HBs trough level reduction per one week increase in inter-HBIG dose interval was 40 UI/L (95% CI 32.96–47.04 UI/L).

Conclusion: Our data support the use of a minimised HBIG for the prevention of HBV recurrence in LT recipients who should prudently continue combined prophylaxis (e. g. HDV coinfection). Anti-HBs trough levels rather than random assessments are rationally a more effective tool to lower the anti HBs level cut-off and therefore minimise HBIG dosage and costs. Individual HBIG consumption

profiles are highly variable and can be as low as <500 UI/month to maintain anti-HBs trough levels of 50–100 UI/L, thus treatment should be personalised.

SAT236

Formal referral networks optimise patient selection for liver transplantation

Oliver Tavabie¹, Victoria Kronsten¹, Talal Valliani², Deepak Joshi¹, Johnny Cash³, Abid Suddle¹, Matthew Cramp⁴, Andreas Prachalias¹, Krishna Menon¹, Kosh Agarwal¹, Michael Heneghan¹, Varuna Aluvihare¹. ¹King's College Hospital, United Kingdom; ²North Bristol NHS Trust, United Kingdom; ³Royal Victoria Hospital, United Kingdom; ⁴Derriford Hospital, United Kingdom
Email: oliver.tavabie@nhs.net

Background and aims: In the United Kingdom, liver transplant (LT) referral pathways for patients (PTs) with chronic liver disease (CLD) are not standardized. This is unlike other conditions with high mortality such as hepatocellular carcinoma (HCC). King's College Hospital (KCH) developed a network of satellite LT centres (SLTCs) with standardized referral pathways to improve access to LT. We aimed to evaluate the impact of SLTCs in LT candidacy evaluation in CLD PTs and those within the established HCC pathway.

Method: All PTs discussed at the KCH LT meeting between 10/2014–10/2019 were included. Second opinions from other LT centres and non-CLD/non-HCC PTs were excluded. Geographic, referral (KCH, SLTC or conventional referrer (CR)), clinical, demographic and laboratory data were retrospectively recorded. HCC PTs had tumor related variables recorded. CLD and HCC PTs were analyzed separately. Univariate (UVA) and multivariate analyses (MVA) were utilized to evaluate the effectiveness of SLTCs in PT selection for LT.

Results: 1102 assessments from CLD PTs (CR = 512 SLTC = 299 KCH = 291) and 240 assessments from HCC PTs (CR = 110 SLTC = 72 KCH = 58) were included. HCC PTs were not more likely to be; referred from any centre, listed or have a contraindication to LT than CLD PTs. 725 CLD PTs were listed and 216 had contraindications to LT. Variables associated with listing were; younger age, autoimmune liver diseases (AILD), biliary atresia (BA), previous LT, higher CLD prognostic scores, shorter referral to decision time and SLTC referral. Variables negatively associated with listing were; non-alcoholic fatty liver disease (NAFLD), alcohol related liver disease (ARLD), hepatitis C and CR referral. MVA including significant and variables of interest was utilized to demonstrate that SLTC referrals were independently associated with listing (adjusted odds ratio (aOR) 2.92 (95% confidence interval (CI) 2.07–4.17)). This was confirmed on sensitivity analyses excluding KCH and ARLD PTs. Variables associated with contraindication to LT were; older age, ARLD, NAFLD, higher CLD prognostic scores and CR referral. Variables negatively associated with contraindication to LT were; AILD, BA, previous LT or SLTC referral. MVA including significant and variables of interest was utilized to demonstrate that SLTC referrals were independently negatively associated with contraindications (aOR 0.33 (95%CI 0.21–0.50)). This was confirmed on sensitivity analyses excluding KCH and ARLD PTs. 168 HCC PTs were listed and 55 had contraindications to LT. No variables were significantly associated with listing including SLTC referral on UVA or MVA. Older HCC PTs were more likely to have a contraindication to LT but SLTC referral did not influence likelihood on UVA or MVA.

Conclusion: Formal referral pathways through SLTCs improve PT selection and access to LT for PTs with CLD but do not impact on the established HCC pathway.

SAT237

Efficacy and safety of SARS-CoV-2 vaccination in liver transplant recipients

Lucy Meunier¹, Mathilde Sanavio¹, Magdalena Meszaros¹, Stéphanie Faure¹, José Ursic Bedoya¹, Maxime Echenne¹, Antoine Debourdeau¹, Georges-Philippe Pageaux¹. ¹CHU Montpellier, St Eloi, Montpellier, France
Email: lucy.meunier@chu-montpellier.fr

Background and aims: Liver transplant recipients have a poorer vaccine responses than the general population (1), so a booster dose is now recommended for these patients. Real-life data on SARS-CoV-2 vaccination in liver transplant recipients are limited. The objective of this study was to evaluate the efficacy and safety of the vaccine and identify factors associated with vaccine response.

Method: This was a retrospective observational study of consecutive liver transplant recipients attending CHU de Montpellier. Inclusion criteria were patients who had received at least one vaccine dose and serological assessment of SARS-CoV-2 spike protein antibody titers. Data on the transplantation indication, immunosuppression, vaccine type, and serology 28 days after the last vaccine dose were collected. Serology below 30 BAU/ml (WHO units) defined non-responders, 30–260 BAU/ml low responders, and >260 BAU/ml responders.

Results: 494 patients were included between 1 January and 15 March 2021. 366 (74%) patients were vaccinated: 280 with 3 doses, 63 with 2 doses, and 23 with 1 dose. 260 patients were excluded from the analysis: 128 (25.9%) unvaccinated, 130 without serology, and 2 with serology prior to the first dose. Complete data were available for 234 patients. 164 (70.1%) patients were male, with a mean age of 59 ± 12 years. Indications for transplantation were alcoholic (n = 92; 39.3%), viral (n = 37; 15.8%), NASH (n = 17; 7.3%), autoimmune (n = 14; 6%), and other cirrhosis (n = 74; 31.6%), with a mean time to transplantation of 4.9 ± 5.9 years. No serious adverse events were reported. Of 201 (85.9%) patients with complete vaccination and post-vaccination serology, 104 (51.7%) were responders, 45 (22.4%) poor responders, and 52 (25.9%) non-responders. In multivariate analysis, factors associated with no or low response were vaccination with Vaxzevria alone (HR 6.8 [1.46–31.67], p = 0.046), mycophenolate mofetil (MMF) therapy (HR 2.1 [1.1–3.9], p = 0.025), no previous SARS-CoV-2 infection prior to vaccination (HR 3.6 [1.025–12.89], p = 0.046), and female gender (HR 2.4 [1.15–4.99], p = 0.02).

Conclusion: Only half of our patients were vaccine responders after three injections. MMF, female gender, and Vaxzevria vaccination were associated with a poorer response, while previous SARS-CoV-2 exposure was associated with a better response. Even after three injections, serological responses were much lower than in the general population. It is now essential to determine the value of a fourth dose, the incidence of COVID-19 in transplant patients with poor serological responses after three doses, and the value of suspending MMF in liver transplant recipients to improve responsiveness.

Reference

1. Rabinowich L, Grupper A, Baruch R, Ben-Yehoyada M, Halperin T, Turner D, et al. Low immunogenicity to SARS-CoV-2 vaccination among liver transplant recipients. *J Hepatol.* 2021 Aug;75 (2):435–8.

SAT238

Immunogenicity and safety of heterologous versus homologous prime-boost regimens with adenoviral vectored and mRNA SARS-CoV-2 vaccine in liver transplant recipients: a prospective study

Supachaya Sriphoosananaphan^{1,2,3}, Sirinporn Suksawatamnuay^{1,2,3}, Nunthiya Srisoonthorn², Nipaporn Siripon², Panarat Thaimai¹, Wanwisar Makhasen², Nawakodchamon Mungnamtrakul², Kessarin Thanapirom^{1,2,3}, Bunthoon Nonthasoot⁴, Pokrath Hansasuta⁵, Piyawat Komolmit^{1,2,3}. ¹Division of Gastroenterology, Department of Medicine, Faculty of Medicine, Chulalongkorn University, Bangkok, Thailand; ²Center of Excellence in Liver Diseases, King Chulalongkorn Memorial Hospital, Thai Red Cross Society, Bangkok, Thailand; ³Liver Fibrosis and Cirrhosis Research Unit, Chulalongkorn University, Bangkok, Thailand; ⁴Department of Surgery, Faculty of Medicine, Chulalongkorn University, Bangkok, Thailand; ⁵Division of Virology, Department of Microbiology, Faculty of Medicine, Chulalongkorn University and King Chulalongkorn Memorial Hospital, Thai Red Cross Society, Bangkok, Thailand
Email: supachaya.sr@gmail.com

Background and aims: Data on immunogenicity of SARS-CoV-2 vaccination in liver transplant (LT) recipients is limited. Homologous vaccination protocol in a number of studies demonstrated variable responses. We aimed to explore SARS-CoV-2 specific humoral response in heterologous prime-boost immunization with ChAdOx1 nCoV-19 AstraZeneca (AZ) and BNT162b2 Pfizer-BioNTech (BNT) among LT patients.

Method: LT recipients receiving SARS-CoV-2 vaccine at King Chulalongkorn Memorial Hospital between April and October 2021 were enrolled. Patients received either heterologous prime-boost protocol (AZ/BNT) or homologous regimen (AZ/AZ) depending on national policies. Blood samples were collected before vaccine administration and 4 weeks after the second dose. SARS-CoV-2 spike receptor-binding-domain (RBD) IgG was measured using electrochemiluminescence immunoassay (Roche Diagnostics) with positive cut-off of ≥ 0.8 U/ml. The neutralizing antibody was detected by enzyme-linked immunosorbent assay-based surrogate virus neutralization test (sVNT) (GenScript) with positive cut-off of $\geq 30\%$ inhibition. Adverse events following vaccination were recorded by questionnaires.

Results: Eighty LT recipients were enrolled; 68.8% male with mean age of 58.0 ± 14.6 years. Median time since transplant was 5.7 years (IQR 2.8–11.8). 58 (72.5%) and 22 (27.5%) patients received AZ/BNT and AZ/AZ, respectively. Comparable seroconversion rate of anti-RBD antibody and sVNT after vaccination were observed in both AZ/BNT and AZ/AZ group (89.7% vs 81.8%, $p = 0.45$ and 77.6% vs 59.1%, $p = 0.10$, respectively). However, median IgG titer was significantly higher in AZ/BNT group compared to AZ/AZ group (843.9 U/ml vs 147.1 U/ml, $p = 0.014$). LT patients receiving AZ/BNT also had significantly higher sVNT than those receiving AZ/AZ (91.2% vs 38.5%, $p < 0.001$) (Figure 1). Use of prednisolone (OR 65.5, 95%CI 4.1–1055.5, $p = 0.003$), low body mass index (OR 1.7, 95%CI 1.1–2.5, $p = 0.008$), and leukopenia (OR 1.01, 95%CI 1.00–1.02, $p = 0.014$) were associated with lack of serological response. Reported adverse events were similar between both regimens.

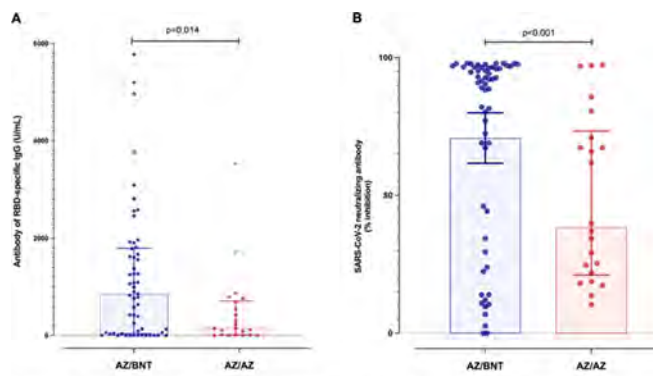


Figure 1. SARS-CoV-2 specific humoral response: A) Antibody of RBD-specific IgG B) Neutralizing antibody

Conclusion: Nearly 90% and 80% of patients had positive anti-RBD antibody and sVNT, respectively, following heterologous prime-boost immunization. AZ/BNT vaccination was well-tolerated and yields greater SARS-CoV-2 specific humoral response than AZ/AZ. Cell-mediated response and immune durability of this mix-and-match strategy among LT recipients are eagerly awaited.

SAT239

Recurrence of primary sclerosing cholangitis after liver transplantation: a french cohort study including 571 patients

Florian Veyre¹, Eleonora De Martin², Domitille Erard³, Claire Francoz⁴, Laure Elkrief⁵, Camille Besch⁶, Olivier Boillot⁷, Karim Boudjema⁸, Filomena Conti⁹, Sebastien Dharancy¹⁰, Christophe Duvoux¹¹, Jean Gugenheim¹², Jean Hardwigsen¹³, Marie-Noëlle Hilleret¹⁴, Isabelle Ollivier-Hourmand¹⁵, Maryline Debette-Gratien¹⁶, Pauline Houssel-Debry¹⁷, Nassim Kamar¹⁸, Jean-Baptiste Hiriart¹⁹, Stéphanie Faure²⁰, Faouzi Saliba²¹, Didier Samuel²², Claire Vanlemmens²³, Christophe Corpechot²⁴, Olivier Chazouillères²⁵, Jérôme Dumortier²⁶. ¹Hospices Civils de Lyon-HCL, Lyon, France; ²Hôpital Paul-Brousse Ap-Hp, Villejuif, France; ³Hôpital Croix-Rousse, Lyon, France; ⁴Beaujon Hospital, Clichy, France; ⁵Chru Hospitals Of Tours, Tours, France; ⁶Chu Strasbourg, Strasbourg, France; ⁷Hospital Édouard Herriot, Lyon, France; ⁸CHU Rennes-Pontchaillou Hospital, Rennes, France; ⁹University Hospitals Pitié Salpêtrière-Charles Foix, Paris, France; ¹⁰Chu De Lille, Lille, France; ¹¹CHU Mondor, Créteil, France; ¹²Hospital Pasteur, Nice, France; ¹³Timone, Marseille, France; ¹⁴Centre Hospitalier Universitaire de Grenoble, La Tronche, France; ¹⁵Chu Caen, Caen, France; ¹⁶CHU Dupuytren 1, Limoges, France; ¹⁷Hospital Center University De Toulouse, Toulouse, France; ¹⁸Chu Bordeaux-Site Pellegrin, Bordeaux, France; ¹⁹University Hospital Center Saint Eloi Hospital, Montpellier, France; ²⁰Hospital Jean-Minjoz, Besançon, France; ²¹Hospital Saint-Antoine Ap-Hp, Paris, France
Email: fl.veyre@gmail.com

Background and aims: Primary sclerosing cholangitis (PSC) is a rare indication of liver transplantation (LT). PSC can recur on the graft with a potential impact on graft survival. The factors associated with recurrence are poorly understood. The goals of our study were to describe the incidence of PSC recurrence (rPSC) and to identify its risk factors from a large cohort with long follow-up.

Method: Were included in a multicenter retrospective cohort study all adult patients transplanted for PSC between 1985 and March 2019, in all French LT centers. Overlap syndrome cases were included.

Results: A total of 571 patients (389 males, 68.1%) with a median age at listing of 42.0 years (IQR 31.5–52.0) were included. The median follow-up time after LT was 104 months (IQR 49.0–180.0). During follow-up, 141 patients (24.7%) developed rPSC, at a median time of 60.0 months (IQR 28.0–107.0) after LT. The cumulative incidence of rPSC was therefore 15.6%, 27.8%, 37.9%, 48.3%, 52.6% at 5, 10, 15, 20, and 25 years after LT, respectively, with a median time to rPSC of 24 years.

In univariate analysis, risk factors associated with rPSC were age <30 years at LT ($p = 0.03$), inflammatory bowel disease (IBD) at inscription on LT waiting list ($p = 0.001$), maintenance steroid therapy ($p < 0.0001$), acute rejection after LT ($p = 0.05$), right liver transplant ($p = 0.02$). Maintenance treatment with mycophenolate mofetil (MMF) was protective ($p = 0.02$). History of CMV infection after LT was not associated with rPSC ($p = 0.09$). MELD score at enrolment, type of biliary anastomosis, year of LT, or “preventive” treatment with Ursodeoxycholic acid were not significantly associated with rPSC. In multivariate analysis, risk factors for rPSC were maintenance steroid therapy (HR = 1.70, CI95% [1.08–2.64]) and the presence of IBD at listing (HR = 1.61, CI95% [1.03–2.54]). During follow-up, after exclusion of patients who died within the first year after LT, 87 patients (16.2%) underwent liver retransplantation (reLT), among whom 59 (68.0%) for rPSC, i.e. 41.8% of patients with rPSC. In the group of patients retransplanted for rPSC, the median time from first LT to rPSC was 59.0 months (IQR 28.0–107.0); this time was significantly shorter compared to patients with rPSC but without the need for reLT (80.5 months, IQR 49.5–144; $p = 0.008$). Fifteen patients underwent a third LT, among whom 12 (80%) due to rPSC, and 7 a fourth LT, among whom 5 for rPSC.

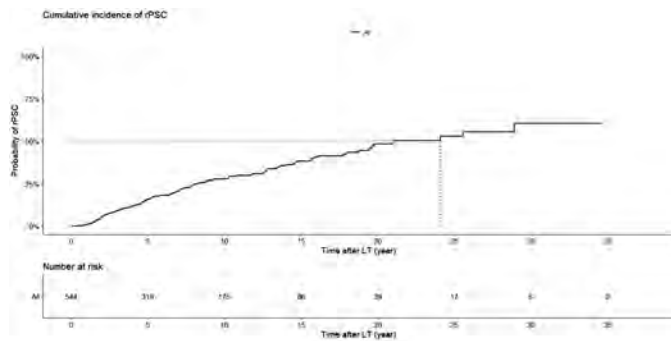


Figure:

Conclusion: Our large study with long follow-up strongly confirms that rPSC after LT for CSP is common, leading in a significant number of cases to one or more reLT. Independent risk factors were the presence of IBD at listing and steroid maintenance therapy. The type of biliary anastomosis had no impact on the risk of rPSC. “Preventive” treatment with AUDC after LT did not reduce the risk of rPSC.

Table: (abstract: SAT240): Joinpoints in trends of monthly LT.

Indication	Northeast		Midwest		South		West	
	Time	Slope (95% CI)	Time	Slope (95% CI)	Time	Slope (95% CI)	Time	Slope (95% CI)
HCV	04/18–05/21	–2.8 (–3.7– –1.9)*	04/18–05/21	–2.1 (–3.2– –1.0)*	04/18–05/21	–2.4 (–3.1– –1.7)*	04/18–05/21	–2.3 (–3.1– –1.4)*
ALD	04/18–05/21	1.9 (1.6–2.3)*	04/18–05/21	1.3 (1.0–1.6)*	04/18–05/21	2.0 (1.7–2.3)*	04/18–11/20 11/20–05/21	1.2 (0.8–1.6)* 6.6 (1.9–11.6)*
NASH	04/18–05/21	–1.0 (–1.8– –0.1)*	04/18–05/21	–0.2 (–0.7–0.3)	04/18–05/21	0.3 (–0.1–0.8)	04/18–05/21	–0.4 (–1.1–0.2)
HCC	04/18–04/20 04/20–05/21	–1.8 (–2.9– –0.7)* –12.4 (–18– –6.0)*	04/18–06/20 06/20–05/21	–0.2 (–1.0–0.7) –15.5 (–21.2– –9.5)*	04/18–10/20 10/20–05/21	–2.0 (–2.6– –1.5)* –24.1 (–33.5– –13.3)*	04/18–06/20 06/20–05/21	–1.3 (–2.2–0.4)* –12.5 (–18.3–6.2)*
ACLF 2–3	04/18–03/20 03/20–05/21	0.6 (–0.1–1.3) 3.4 (2.0–4.8)*	04/18–05/21	0.8 (0.2–1.4)*	04/18–05/21	1.7 (1.3–2.1)*	04/18–05/21	1.1 (0.7–1.5)*
Alcoholic hepatitis	04/18–05/21	3.8 (2.5–5.2)*	04/18–05/21	3.0 (1.7–4.3)*	04/18–05/21	3.3 (1.9–4.8)*	04/18–05/21	4.3 (3.1–5.4)*
All LT**	04/18–05/21	–0.8 (–1.1– –0.4)*	04/18–05/21	–0.6 (–0.9– –0.3)*	04/18–05/21	–0.7 (–1.1– –0.4)*	04/18–010/20 10/20–05/21	–0.2 (–0.7–0.2) –4.7 (–8.8– –0.5)*

* $p < 0.05$.

SAT240

Impact of COVID-19 on the liver transplant activity in the US: variation by the region, etiology, and cirrhosis complications

Ashwani Singal¹, Yong-Fang Kuo², Paul Yien Kwo³, Robert Wong³.

¹University of South Dakota and Avera Transplant Institute, Medicine and Transplant Hepatology; ²university of texas medical branch, Biostatistics; ³stanford university school of medicine, Transplant Hepatology

Email: ashwanisingal.com@gmail.com

Background and aims: To examine Covid-19 impact on liver transplant (LT) activity in the US.

Method: LT listings in UNOS registry stratified to 03/2020–05/2021 (Covid era) and 04/2018–02/2020. Monthly frequency of LT; percentage of etiology (HCV, ALD, NASH, HCC, and ACLF grade 2 or 3); and average MELD score were plotted. Regional analyses performed in northeast (UNOS regions 1, 2, 9), Midwest (regions 7, 8, 10), south (regions 3, 4, 11), and west (regions 5, 6). Joinpoint regression models assessed time trend had significant changes on a log scale.

Results: Of 23, 871 LT recipients (mean age 52 yrs., 62% males, 61% white, 32% ALD, 15% HCC, 30% ACLF grade 2–3, mean MELD score 20.5), 8995 were in Covid era. LT activity decreased since September 2020 by 3.4% every month for any transplant and 22% for HCC. LT activity increased by 4.5% for ALD since 11/2020 and 17% for ACLF 2–3 since 03/2021. LT activity decreased for NASH and HCV by 2.5% and 1% respectively every month and increased for alcoholic hepatitis by 4.5% without any joinpoint in Covid era. Monthly MELD score increased by 0.7 (Std. Error 0.17) and 0.36 (Std. Error 0.13) since 06/2020 for HCV and HCC respectively. Regional analysis showed Covid impact with 12.4–24.1% decrease in LT activity across the four regions. However, this was heterogeneous for overall number of LT, etiology, and for ACLF 2–3 (Table).

Conclusion: Covid-19 pandemic impacted LT activity in the US, with a decrease in LT for HCC, and increase for ALD and severe ACLF. Impact across regions is homogeneous for HCC, but not on other changes. Strategies are needed to reorganize cirrhosis patients in community to overcome after effects of Covid-19.

POSTER PRESENTATIONS

SAT241

Perinatal outcomes in liver transplant patients-possible positive effect of aspirin prophylaxis

Marius Braun¹, Gil Zeevi², Eran Hadar², Arnon Wiznitzer², Alyssa Hochberg², Michal Cohen-Naftaly¹, Assaf Issachar¹, Orly Sneh Arbib¹, Yael Harif¹, Eviatar Neshet³, Evelin Oxtrud¹, Amir Shlomai¹, Ran Tur-Kaspa¹. ¹Liver Institute, Petah Tikva, Israel; ²Ob Gyn, Petah Tikva, Israel; ³Transplant, Petah Tikva, Israel
Email: m_braun_md@yahoo.com

Background and aims: To describe perinatal outcomes in liver transplanted (LT) women and evaluate the effect of low-dose aspirin treatment in these women.

Method: An observational retrospective study examining perinatal outcomes among liver transplant recipients, between 2016 and 2020 at a single university-affiliated tertiary medical center in Israel. Demographic, obstetric and clinical data were obtained from electronic health records. The role of aspirin was explored.

Results: Ten LT patients delivered 13 babies. All the patients received tacrolimus, 9 (69%) low dose prednisone and the liver kidney transplant (LKT) also received azathioprine. The 2 patients that were pregnant during the first year after LT had premature deliveries (week 31, 32). Regarding maternal outcomes, 2 women (16%) developed preeclampsia, 2 (16%) gestational diabetes, three (24%) postpartum infection, and one -postpartum hemorrhage. Median gestational age at delivery was 37 weeks (31–39 weeks), with 6 preterm births (31–36 weeks) and a median birthweight of 3072 g (1450–4100 g). All the babies had high Apgar scores and normal development, but the baby born at week 31 had to be ventilated for a week and is healthy with normal development at 2 year follow-up. Low-dose aspirin (100 mg daily) was administered to LT patients beginning 2018 and was given in 5 (38%) of the pregnancies. Of the women receiving low-dose aspirin, none developed hypertensive disease or suffered excessive bleeding during pregnancy.

Primary disease	Graft type	Week	Fetal weight g	Mode of delivery	Indication for cesarean section	Obstetric complications
ALF HAV	DDLT	38	3836	CS	breech	
ALF HAV	DDLT	35	2556	CS	failed induction	Cholestasis, UTI
ALF	DDLT	37	4100	CS	compound	
ALF in pregnancy	DDLT	31	1450	CS	s/p transplant	liver transplant, ELE, IUGR
ALF -Wilson	DDLT	39	3080	NVD		
Wilson	DDLT	32	1732	CS	NRFHR	sepsis, ele, mild pet
Wilson	LDLT	36	3426	NVD		GDM
Wilson	LDLT	40	3500	NVD		
Hyperoxaluria type 1	SLKT	37	3064	NVD		mild pet
PSC	LDLT	37	2944	VE		GDM1, UTI, cholestasis, cholangitis
			Median 37	Median 3064		
			31–40	1450–410		

DDLT-deceased donor liver transplant; LDLT-living donor liver transplant; SLKT-simultaneous liver kidney transplant; CS-cesarean section; NVD-normal vaginal delivery; VE-vacuum extraction; Pet- preeclampsia.

Conclusion: Successful pregnancy is feasible in stable liver transplant patients. Patients with unstable liver grafts within the first year post transplant have poorer maternal fetal outcomes. Aspirin use is safe in pregnant LT patients and might improve the pregnancy outcome.

SAT242

Antibody response after a third dose of the mRNA-1273 SARS-CoV-2 vaccine in liver transplant recipients

Aitor Odriozola Herrán¹, María Del Barrio¹, Antonio Cuadrado¹, José Ignacio Fortea¹, Lidia Amigo¹, David San Segundo Arribas², María Rodríguez-Cundin³, María Rebollo³, Roberto Fernandez⁴, Federico Castillo⁴, María Achalandabaso⁴, Juan Andrés Echeverri⁴, Juan Carlos Rodríguez-San Juan⁴, Marcos López-Hoyos², Juan Carlos Rodríguez Duque¹, Álex García Tellado⁵, Javier Crespo¹, Emilio Fabrega¹. ¹University Hospital Marqués de Valdecilla, Gastroenterology and Hepatology Service, Santander, Spain; ²University Hospital Marqués de Valdecilla, Immunology, Santander; ³University Hospital Marqués de Valdecilla, Preventive Medicine, Santander, Spain; ⁴University Hospital Marqués de Valdecilla, General Surgery, Santander, Spain; ⁵University Hospital Marqués de Valdecilla, Internal Medicine, Santander, Spain
Email: aodrihe94@gmail.com

Background and aims: Recent studies showed that antibody titers after vaccination against severe acute respiratory syndrome coronavirus 2 (SARS-CoV-2) in liver transplant recipients (LTR) are diminished as compared to the general population, suggesting the possible value of a third booster dose. We aimed to characterize the humoral response after three doses of the Moderna mRNA-1273 vaccine in LTR.

Method: The cohort comprised 129 adult LTR who received a third homologous dose of the mRNA-1273 SARS-CoV-2 vaccine. Humoral response was evaluated using plasma levels of anti-SARS-CoV-2 spike protein S1 immunoglobulin (Abbott® SARS-CoV-2 anti-spike IgG II assay, positive >50 AU/ml) measured a median of 30 days (IQR, 30–33.7 days) after the third vaccine injection.

Results: LTR (median age 63 [IQR, 56–68] years, 76.7% men) had a mean anti-S1 antibody level of 8,388 [SD, ± 10,836.9] AU/ml after the second dose, and 26,134 [SD, 17,136.4] AU/ml after the third dose. All 113 LTR (87, 6%) who had been seropositive before the third dose were still seropositive after the third vaccine injection; and their antibody titers increased significantly from 9426 [SD, 11,057.5] AU/ml to 29,449 [SD, 15,460.5] AU/ml (p = 0.01).

3rd dose of moderna (129)	Seropositive (125)	Seronegative (4)	p
Age (years) (SD)	60.4 (± 10.4)	67.8 (± 1.7)	0.162
Sex (male) (%)	97 (75.2)	2 (1.6)	0.198
Previous medical history (%)			
Hypertension	75 (60)	3 (75)	0.546
Diabetes	44 (35.2)	3 (75)	0.103
Chronic Kidney disease	42 (33.9)	4 (100)	0.007
Cardiovascular disease	33 (26.4)	1 (25)	0.95
Immunosuppressive regimen (%)			<0.001
Without	96 (76.8)	1 (25)	
Mycophenolate			
With mycophenolate	29 (23.2)	3 (75)	
Monotherapy	6 (4.8)	2 (50)	
Association with CN	23 (18.4)	1 (25)	
Immunosuppression (dose-mg) (mean; SD)			
Mycophenolate	1068.9 (± 394.7)	1666.7 (± 577.6)	0.022
Laboratory parameters (SD)			
Haemoglobin (g/dL)	14.9 (± 9.3)	12.7 (± 1.5)	0.635
Platelets (G/L)	169.9 (± 61.3)	150.0 (± 25.2)	0.518
Leukocytes (G/L)	5.9 (± 1.6)	6.5 (± 1.4)	0.474
Lymphocytes (G/L)	3.4 (± 1.8)	1.5 (± 0.8)	0.832
eGFR (ml/min/1.73 m ²)	69.4 (± 18.9)	32.3 (± 17.3)	<0.001

Sixteen patients (12, 4%) were non-responders after the second vaccine dose. After the third dose, twelve of the sixteen (75%) initial non-responders produced anti-spike antibody (3, 633 [SD, 8, 361.1] AU/ml). Non-response after third dose was associated with mofetil mycophenolate treatment (75% vs 23.2%) ($p < 0.001$), a higher dose of this drug (1, 666.7 [SD, \pm 577, 6] vs 1068, 9 [SD, \pm 394, 7]) ($p = 0.02$), and lower estimated glomerular filtration rate (32.3 [SD, \pm 17.3] vs 69.4 [SD, \pm 18.9]) ($p = 0.001$).

Conclusion: our study showed that administration of a third dose of the mRNA-1273 SARS-CoV-2 to LTR improved the immunogenicity of the vaccine. Lower estimated glomerular filtration rate and immunosuppressive regimens with mycophenolate were associated with a poorer response to vaccination.

SAT243

Early post liver transplant rescue treatment with sofosbuvir/velpatasvir/voxilaprevir in patients experienced to NS5A-inhibitors

Margherita Saracco¹, Francesco Tandoi², Alberto Calleri¹, Donatella Cocchis², Giorgia Rizza², Renato Romagnoli², Silvia Martini¹.
¹AOU Città della Salute e della Scienza di Torino, Gastrohepatology Unit; ²AOU Città della Salute e della Scienza di Torino, General Surgery 2U, Liver Transplantation Center
Email: margherita.saracco@gmail.com

Background and aims: Direct acting antivirals (DAA) revolutionized the HCV treatment landscape. In patients (pts) who are HCV viremic at liver transplant (LT), early post-LT DAA therapy (tx) prevents graft damage and extrahepatic HCV involvement. Few data are available regarding pts who are HCV NS5B+NS5A inhibitors experienced at LT. We aimed to describe our first 6 pts treated early after LT with sofosbuvir/velpatasvir/voxilaprevir (SOF/VEL/VOX) for 12 weeks.

Method: From January 1st 2019 to November 1st 2021, 436 pts underwent LT in our Center. Among 46 pts who were viremic at LT, 6 were experienced to NS5A inhibitors. SOF/VEL/VOX was started as soon as graft function was optimal with stable immunosuppression tx (standard combination: steroid, tacrolimus, mycophenolate mofetil).

Results: At LT, the median age of our 6 pts was 54 years and median MELD 13. Median donor age was 70 years. Median cold ischemia time (CIT) 448 minutes. Pt #4 received a graft from a HBCAb-positive donor with 50% macrovesicular steatosis and pt #6 received a graft from a 82-year-old donor; both grafts underwent hypothermic oxygenated machine perfusion. Five pts were HCV genotype (GT) 3 and one 1a; the median post-LT HCV RNA was 618.180 UI/ml, before tx. Pt #6 (GT3) received HCV viremic donor (naïve GT2; Ishak: grading 3/18, fibrosis 1/6) and donor HCV strains replaced the recipient's (shift from GT3 to GT2). The median time from LT to DAA tx was 15 days. Four pts reached sustained virological response after 12 weeks by the end of tx (SVR12) and remained negative after a median follow-up of 587 days, range 42–831 days. Pt #6 is still on tx (week 3 with HCV RNA <15). Pt #3 interrupted the DAA tx at week 8 for cholestatic hepatitis (AST/ALT 62/56 UI/L, GGT/ALP 576/1294 UI/L, bilirubin

12 mg/dL); liver biopsy was consistent with drug-induced hepatitis. Bilirubin dropped to 4 mg/dL at day 7 after tx withdrawal and normalized within 28 days; HCV RNA remained negative from day 14 of tx (follow-up of 400 days). Immunosuppression levels were stable on DAA tx.

Conclusion: Early use of post-LT SOF/VEL/VOX was successful in pts who were HCV viremic at LT and experienced to NS5B+NS5A inhibitors. One pt developed cholestatic hepatitis which reverted after prompt interruption of tx. Early post-LT DAA tx prevented liver damage by HCV and allowed the use of suboptimal grafts (old donor, HCV viremic donor or with moderate macrovesicular steatosis).

SAT244

Inclusion of body composition parameters in MELD score leads to optimization of predictive performance in patients with cirrhosis

Maryam Ebadi¹, Rhonda J. Rosychuk², Elora Rider¹, Abha DunichandHoedl³, Maryam Motamedrad³, Rahima A. Bhanji¹, Aldo J Montano-Loza¹.
¹University of Alberta, Division of Gastroenterology and Liver Unit, Edmonton, Canada; ²University of Alberta, Division of Infectious Diseases, Department of Pediatrics, Edmonton, Canada; ³University of Alberta, Human Nutrition and Metabolism, Edmonton, Canada
Email: montanol@ualberta.ca

Background and aims: Model for end-stage liver disease (MELD) score has been shown to estimate the risk of short-term mortality in patients awaiting liver transplant (LT). Given the decreasing predictive performance of MELD and the improved prognostication using body composition parameters in cirrhosis, inclusion of these parameters may lead to optimization of the organ allocation criteria in LT candidates. The aim of this study was to determine the performance of individual and combined body composition parameters by sex and to compare their performance with MELD in predicting pre-LT mortality.

Method: CT images, from LT evaluation of 860 patients with cirrhosis were used to determine height-normalized indices and radiodensity of muscle, visceral and subcutaneous adipose tissue (SAT) expressed by cm²/m² and Hounsfield Unit (HU), respectively. Performance of body composition features and MELD score for mortality prediction was assessed at 3-, 6-, and 12-months by area under the receiver operating characteristic curve (AUROC) in the presence of competing risks.

Results: Sixty-six percent of the patients were male with the MELD score of 14 \pm 8. Evaluated patients were followed for a mean time of 24 months. Performance of MELD and body composition features for mortality prediction is presented in Table. Among individual body composition features in male patients, SAT radiodensity outperformed other features when considering each time-point. Among various combinations in males, performance of combined skeletal muscle index and SAT radiodensity were superior to that of MELD. Addition of skeletal muscle index and SAT radiodensity to the MELD outperformed MELD at each time point in males. In females, inclusion

Table: (abstract: SAT243)

Patient (recipient of the LT)														
RECIPIENTS								DONORS			AFTER-LT			
Pt #	Age, years	Sex	HCC	MELD at LT	HCV GT	Previous DAA	HCV RNA at LT (UI/ml)	Macrovesicular Steatosis	Age, years	CIT (min)	Days from LT to DAA	HCV RNA pre DAA	HCV RNA <15 UI/ml	SVR12
1	46	M	No	14	3	SOF/VEL	1370000	<5%	55	312	6	26500	Week 1	Y
2	56	M	Yes	8	3	SOF/VEL	7066296	<5%	76	439	9	211200	Week 2	Y
3	48	M	Yes	15	3	SOF/VEL	62400	25%	43	391	21	779000	Week 1	Y
4	57	M	No	20	1a	SOF/LED	3716	50%	63	456	47	457360	Week 2	Y
5	58	M	Yes	9	3	SOF/VEL	1250000	10%	83	511	20	18500000	Week 3	Y
6	51	M	No	11	3	SOF/VEL	1490000	0%	82	578	8	5370000	Week 3	/

POSTER PRESENTATIONS

of SAT and muscle radiodensity within MELD score improved the discriminative performance of MELD, but this was not significant.

	3-month	6-month	12-month
Male			
Skeletal muscle index (SMI)	66.5 (58.2–74.7)	66.5 (59.9–73.1)	62.3 (56.5–68.2)
Subcutaneous adipose (SAT) radiodensity	74.7 (68.0–81.5)	69.1 (62.9–75.3)	62.7 (56.9–68.6)
SAT radiodensity + SMI	76.4 (69.7–83.0)	72.7 (66.9–78.4)	66.1 (60.6–71.7)
MELD	75.3 (68.0–82.5)	68.8 (61.9–75.6)	62.3 (56.3–68.4)
MELD + SAT radiodensity + SMI	81.4 (75.1–87.6)	75.3 (69.3–81.2)	67.4 (61.7–73.0)
P value	0.004	0.001	0.009
Female			
Muscle radiodensity	65.9 (56.6–75.3)	64.8 (56.5–73.1)	63.2 (55.4–70.9)
SAT radiodensity	66.1 (58.3–73.8)	61.5 (53.6–69.5)	62.9 (55.6–70.3)
SAT radiodensity + Muscle radiodensity	72.0 (64.4–79.6)	69.4 (62.3–76.4)	68.7 (62.0–75.5)
MELD	76.9 (69.0–84.7)	71.2 (64.0–78.4)	68.5 (61.7–75.3)
MELD + SAT radiodensity + Muscle radiodensity	80.0 (72.3–87.0)	74.2 (67.3–81.1)	71.3 (64.4–78.1)
P value	0.32	0.23	0.24

Conclusion: Inclusion of skeletal muscle index and SAT radiodensity within MELD was associated with an improvement in the prediction of mortality in male patients with cirrhosis.

SAT245

Long-lasting seropositivity after anti SARS-CoV-2 vaccination in pre liver transplant patients

Alberto Calleri¹, Margherita Saracco¹, Renato Romagnoli², Silvia Martini¹. ¹AOU Città della Salute e della Scienza di Torino, Gastrohepatology Unit, Turin, Italy; ²AOU Città della Salute e della Scienza di Torino, General Surgery 2U, Liver Transplantation Center, Turin, Italy
Email: alberto.calleri.md@gmail.com

Background and aims: Since the beginning of COVID-19 pandemic, global vaccination represents the goal to fight the virus spreading. Anti SARS-CoV-2 vaccines demonstrated a high rate of success in preventing severe COVID-19 and decreasing the infection rate, but few data are available about special population such as pre liver transplant (LT) patients (pts). Serological tests for IgG anti Spike reflect the humoral response to vaccination.

We aimed to evaluate the longevity of the humoral response to mRNA vaccine in pts listed for LT in our Center.

Method: From January 2021 to October 2021 we consecutively enrolled all pts on our LT waiting list who completed anti SARS-CoV-2 mRNA vaccination. Pts with previous COVID-19 received a single vaccine dose within 6 months after infection. All the other pts received 2 doses, administered 21 (Pfizer-BioNTech) or 28 days (Moderna) apart. Pts were tested for SARS-CoV-2 IgG antibodies (LIAISON® SARS-CoV-2 TrimericS IgG assay, positive value ≥ 33.8 BAU/ml) 1 month after mRNA vaccination and then every 2 months until LT. Mask wearing indoors and physical distancing measures were recommended for all pts.

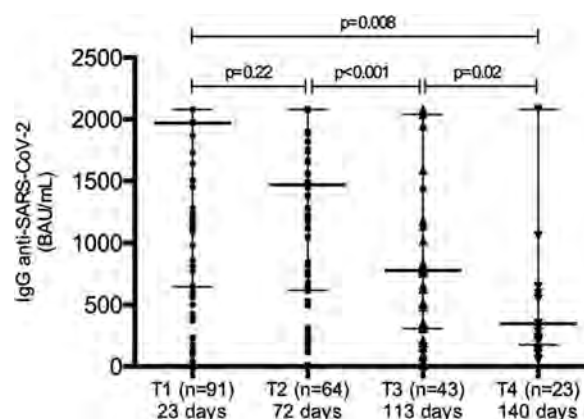
Results: During the study period, 91 pre-LT pts completed the anti-SARS-CoV-2 vaccination: 80 pts received 2 vaccine doses, while 11 pts

received only 1 dose, as per protocol. 94% of the pts received Pfizer-BioNTech and 6% Moderna COVID-19 vaccine. 69% were male, median age 56 years, BMI 25 kg/m², eGFR 95 ml/min, MELD 12 (IQR 8–15). 32% was affected by viral cirrhosis and 43% by hepatocellular carcinoma; 6 pts were treated with steroid and 1 with mycophenolate mofetil due to autoimmune cirrhosis and 1 pt was affected by common variable immunodeficiency.

After a median time of 23 days from the last vaccine dose (T1), 86/91 (95%) seroconverted (median titer 1970 BAU/ml, IQR 645–2080). During follow-up none of retested pts became IgG negative, however their titer progressively decreased:

–after a median time of 72 days from the last vaccine dose (T2), 61/64 (95%) tested again IgG positive (median titer 1480 BAU/ml, IQR 617–2080); –at T3 (113 days from vaccination) 42/43 (98%) pts remained positive and their titer significantly dropped (779 BAU/ml, IQR 307–2040); –23 pts were retested at T4 (140 days after vaccination) and all of them remained IgG positive (median titer 320 BAU/ml, IQR 148–2080). (T1 vs T2, paired $p = 0.22$; T2 vs T3 $p < 0.001$; T3 vs T4, $p = 0.02$; T1 vs T4, $p = 0.008$). (Figure 1).

At the end of a median follow-up period of 190 days (IQR 175–202) from vaccination, none of the patients developed COVID-19. No serious adverse events were registered following vaccination.



Conclusion: In our 91 pre-LT patients, mRNA anti-SARS-CoV-2 vaccination elicited a high rate of seroconversion (95%) within 1 month. We observed a progressive significant decrease in IgG titer during a median follow-up of 190 days after vaccination. Nevertheless, none of our pre-LT pts developed COVID-19.

SAT246

The outcome of living donor versus deceased donor liver transplantation for hepatocellular carcinoma: a systematic review and meta-analysis

Beshoy Effat Elkomos¹, Amr Abdelaal¹, Mostafa Abdo¹, Remon Mamdouh¹. ¹Faculty of Medicine, Ain Shams University, General surgery, cairo, Egypt
Email: beshoy3ft@gmail.com

Background and aims: A potential solution to the deceased donor organ shortage is to expand the organ donor pool to include live donation and to identify patients with lower rates of HCC recurrence to fairly allocate liver grafts. our aims were to detect the long-term outcomes of living donor liver transplant (LDLT) versus deceased donor liver transplant (DDLT) for hepatocellular carcinoma (HCC) and the predictors of recurrence after transplantation.

Method: PubMed, Scopes, Web of science, Cochrane library were searched for eligible studies from inception to 1 July 2021 and a systematic review and meta-analysis were done to detect patient overall survival (OS), Intention to treat overall survival (ITT-OS), disease-free survival (DFS), and recurrence for LDLT vs DDLT recipients.

Outcomes		Studies (n)	Patients (n)	Effect Estimate [RR/HZ (95% CI)]	Favour group	
OS	No. of years					
	1	21	6045	1.04 [1.01, 1.07]	LDLT	
	2	14	4110	1.04 [0.96, 1.14]	None	
	3	19	5859	1.07 [1.01, 1.13]	LDLT	
	4	12	3817	1.09 [1.02, 1.17]		
	5	21	6080	0.99 [0.92, 1.08]		
	6	5	2002	1.14 [0.95, 1.38]	None	
	10	2	1391	1.24 [0.92, 1.67]		
	1	14	3978	1.01 [0.95, 1.06]		
	2	6	1282	0.98 [0.87, 1.09]		
DFS	3	12	3599	1.00 [0.92, 1.09]		
	4	5	1081	0.95 [0.81, 1.11]		
	5	15	4133	1.01 [0.95, 1.08]		
	6	4	1525	0.98 [0.87, 1.11]		
	10	1	896	N/A		
	1	5	2934	1.14 [1.01, 1.28]	LDLT	
	2	3	1419	1.23 [1.00, 1.50]		
3	5	2934	1.26 [1.08, 1.47]			
4	3	1419	1.46 [1.07, 1.99]			
5	5	2934	1.37 [1.09, 1.72]			
6	0		N/A			
10	0		N/A			
Recurrence		16	3617	1.07[0.77, 1.48]	None	
Recipient male sex		3	1491	1.02 [0.70, 1.48]		
Recipient age, y		4	1647	0.99 [0.97, 1.01]		
Beyond MC		4	1647	2.81 [1.69, 4.69]		
AFP >400		3	1019	3.70 [2.11, 6.47]		
Predictors of recurrence	Presence of VI	Microscopic	4	1647	3.73 [2.78, 5.01]	Absence of VI
		Macroscopic	3	1491	3.88 [2.64, 5.70]	
		Poor differentiation	2	840	2.69 [1.29, 5.61]	
						Well/mod. differentiation

Figure: (abstract: SAT246)

Results: 35 studies with total of 7822 patients were included. The 1-, 3-, 4 year-OS showed trivial improvement for LDLT recipients. However, LDLT and DDLT recipients had similar 5-, 6- and 10-year OS. Moreover, our subgroup analysis showed equal long term OS between LDLT and DDLT for those who were within Milan criteria (MC). Nevertheless, beyond MC, there was a better prognosis for the patients who underwent LDLT. In addition to that, a Significant improvement in the ITT-OS was observed for LDLT recipients. Regarding the DFS and recurrence, these studies showed no significant difference between LDLT and DDLT. Moreover, the pooled hazard ratio of the included studies showed that MC, level of alfa feto protein (AFP), presence of vascular invasion (VI), tumor differentiation were predictors of recurrence.

Conclusion: this study is in consonance with the view that the cancer biology (not the graft type) is the most important determinant of recurrence and survival after LT. However, LDLT provided a much better survival benefits to HCC patients especially in regions that suffer from low deceased organ availability.

SAT247

Impact of gender on survival of hepatocellular carcinoma

Chaonan Jin¹, Birgit Schwacha-Eipper¹, Jean-François Dufour², Pompilia Radu². ¹Department for BioMedical Research, Hepatology, University of Bern, Switzerland, Bern, Switzerland; ²Department of Visceral Surgery and Medicine, Hepatology, Inselspital, Bern University Hospital, University of Bern, Switzerland
Email: radupompilia@yahoo.com

Background and aims: Risk of hepatocellular carcinoma (HCC) is considerably higher in men compared to women; however, there is inconclusive evidence on the effect of gender on HCC prognosis. We aimed to evaluate whether gender influences overall survival (OS).

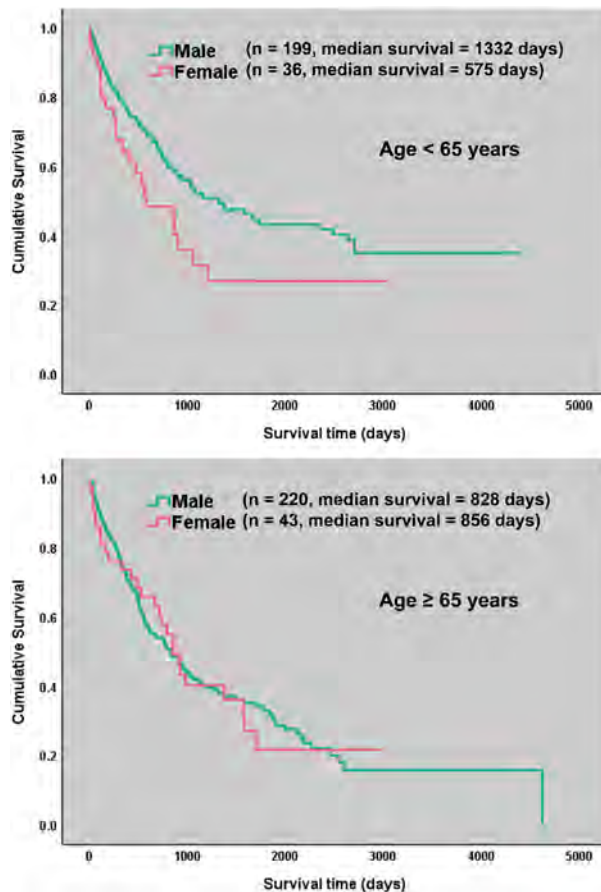
Method: A prospective cohort, consisting of 498 HCC patients included between 2010 and 2020 at University Clinic for Visceral Surgery and Medicine, Inselspital, Bern, was retrospectively analysed.

Patients were grouped by gender and age (>65 and ≤65). The etiology was established based on histology, combined radiological and laboratory features. Treatments were divided into curative (orthotopic liver transplantation, radiofrequency ablation, microwave ablation, surgical resection), non-curative (stereotactic body radiation therapy, transarterial chemoembolization, transarterial embolization, target drugs) and best supportive care (BSC). Cox multivariate regression analysis was performed to identify the risk factors for survival.

Results: The cohort consisted of 419 (84.1%) men, who had a higher median body mass index (26.8 vs 25.4, p=0.037), more frequently both alcoholic and non-alcoholic fatty liver disease (12.9% vs 3.8%, p<0.05), cirrhosis (80.7% vs 70.9%, p=0.050), and diabetes (35.8% vs 22.8%, p=0.025) in comparison to women.

For the patients younger than 65 years of age, the median OS of female vs. male (<65 years) was 575 vs 1332 days (p=0.037) while for the group >65 the median OS was 856 vs 828 days (p=0.920). In <65 group, men had more often both alcoholic and non-alcoholic fatty liver disease (11.6% vs 0.0%, p<0.05), and diabetes (29.2% vs 8.3%, p=0.009). Men younger than 65 years of age were less frequently addressed to best supportive care than women (8.5% vs 22.2%, p<0.05) and frequently to curative therapy, particularly liver transplantation (27.6% vs 8.3%). Both curative and non-curative therapy (95% CI 0.031–0.121, p<0.001 and 95% CI 0.164–0.546, p<0.001, respectively) were independent protective factors.

In ≥65 group, no significant differences with respect to demographic, clinical, and tumor characteristics were observed between men and women. BCLC stage A (95% CI 0.196–0.758, p=0.006), curative therapy (95% CI 0.173–0.525, p<0.001) and non-curative (95% CI 0.393–1.040, p<0.001) were independent protective factors.



Conclusion: Our single-center experience suggests that HCC females <65 years have inferior survival and a lower assignment rate to curative therapies, particularly liver transplantation than HCC males <65 years.

SAT248

Effectiveness of MRI methods in the assessment of hepatic steatosis in living liver donors

Digdem Kuru Öz¹, Zeynep Melekoğlu Ellik², Ayşegül Gürsoy Çoruh¹, Mehmet Adıgüzel^{1,1}, Mesut Gumussoy², Serkan Duman², Ramazan Erdem Er², Onur Kırımker³, Deniz Balci³, Hale Gokcan², Ramazan Idilman², Ayşe Erden¹. ¹Ankara University School of Medicine, Radiology, Ankara, Turkey; ²Ankara University School of Medicine, Gastroenterology; ³Ankara University School of Medicine, General Surgery

Email: digdem_k@hotmail.com

Background and aims: Liver biopsy is still gold standard diagnostic method for accurate quantification of steatosis. However, there is still no consensus in terms of which diagnostic methods to use for donor selection and which threshold value to acceptable. The aims of the present study, to determine utility of proton density fat fraction (PDFF) measurements for quantifying the liver fat content in potential donor candidates, and compare these results with liver biopsy findings.

Method: Between January 2017 and March 2021, a total of 134 living liver donor candidates imaged on a 1.5 tesla Magnetic Resonance Imaging (MRI) device were included. Magnetic resonance spectroscopy (MRS) was performed with a multiecho T2-corrected stimulated echo acquisition mode sequence. MRS fat fraction (FF) was calculated by placing an independent voxel in the right lobe of the liver. PDFF was calculated by 2 radiologists from the parametric FF map obtained with a multi-echo Dixon sequence using at least 4 regions of interest

placed in the right lobe of the liver. The MRI measurement results were compared with pre- and/or intraoperative biopsy results. All liver biopsy specimens were evaluated by the Kleiner's method. Spearman correlation analysis was performed to determine the relationship between MRS and PDFF and histopathology. Receiver Operating Characteristic analysis was used for the diagnostic efficiency of the methods.

Results: Median age was 31 years. The gender was predominantly male (59.7%). On the liver biopsy evaluation, 25 (18.7%) had grade I steatosis, whereas 109 (81.3%) did not have steatosis. Median PDFF calculated with MRI was 3% (0.5–15%).

Signal fat fractions obtained by MRS and PDFF methods were statistically different in the groups with and without steatosis ($p < 0.001$, $p = 0.019$). There was a high degree of positive linear correlation between MRS and PDFF methods ($r = 0.819$, $p < 0.001$). The area under the curve was 0.848 and 0.824 ($p < 0.001$) at the cut-off of 5.05% and 3.25% for MRS and PDFF, respectively.

Conclusion: The present study indicates the MRS and PDFF measurements provided a non-invasive, accurate estimation of the presence and grading of hepatic steatosis in liver donor candidates. Such modalities can be used effectively in donor selection for living donor liver transplantation.

SAT249

Long-term outcomes of donation after cardiac death and living donor liver transplant for primary sclerosing cholangitis

Dilip Moonka¹, Toshihiro Kitajima², Tommy Ivanics², Kelly Collins², Michael Rizzari², Atsushi Yoshida², Marwan Abouljoud², Shunji Nagai². ¹Henry Ford Health System, Gastroenterology and Hepatology, Detroit, United States; ²Henry Ford Health System, Transplant Institute, Detroit
Email: dmoonka1@hfhs.org

Background and aims: The use of donation after circulatory death (DCD) grafts is reported to be a risk factor for worse outcomes after liver transplant (LT) for primary sclerosing cholangitis (PSC) due to a higher risk of biliary complications. However, long-term outcomes comparing DCD, donation after brain death (DBD) donors, and living donor LT (LDLT) have not been fully investigated in a recent cohort. This study aims to assess outcomes of LT for PSC with each graft type.

Method: Using OPTN/UNOS data, we analyzed adult LT patients with PSC or primary biliary cholangitis (PBC) between 2002 and 2020. Patients with exception scores, multi-organ or re-transplant were excluded. One, 5, and 10-year graft survival (GS) were compared between PSC and PBC groups (as control). Next, outcomes were compared between DBD-LT, DCD-LT, and LDLT in each group. In PSC, the three types of donor grafts were compared for cause of graft loss. Finally, transplant outcomes were analyzed in an early era (2002–2010) and late era (2011–2020). Risks were adjusted by recipient variables.

Results: 3,946 PSC and 2,675 PBC patients were eligible. Among PSC patients, 3,099 (78.5%), 151 (3.8%), and 696 (17.7%) received DBD-LT, DCD-LT, and LDLT, respectively. One, 5, and 10-year GS were similar between PSC and PBC groups. In PSC, DCD-LT had significantly higher risks of 1, 5, and 10-year graft loss than DBD-LT (1-year: HR 1.87, $p = 0.007$, 5-year: HR 1.74, $p = 0.001$, 10-year: HR 1.60, $p = 0.003$) whereas LDLT had similar risks of 5 and 10-year graft loss. In contrast, outcomes were comparable between donor types in PBC. As a cause of graft loss, DCD-LT had a significantly higher incidence of both biliary complications and PSC recurrence than other graft types. 16.5% of DCD-LT lost grafts because of PSC recurrence or biliary issues vs 4.5% for DBD-LT and 5.1% for LDLT. Incidence of re-transplant was highest in DCD-LT (DCD-LT 18.5% vs DBD-LT 10.2% vs LDLT 10.6%, $p = 0.005$). This finding was more prominent in the early era, whereas risks of 3- and 5-year graft loss were similar among all graft types in the late era (Figure). When comparing profiles of DCD donors for PSC between eras, CIT was shorter in late era (6.5 vs 5.2 hours, $p = 0.001$)

Adjusted risk of graft loss in PSC in each era

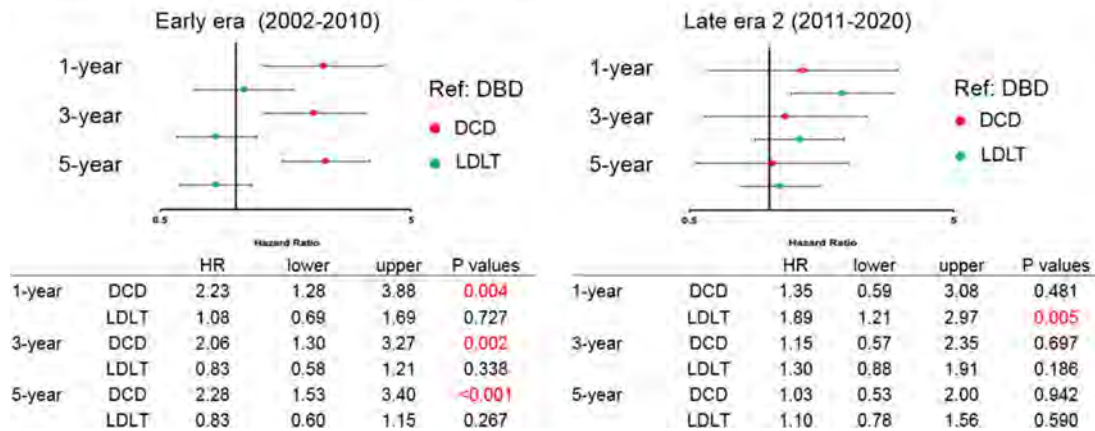


Figure: (abstract: SAT249)

whereas age and proportion of organ sharing were similar between 2 groups.

Conclusion: In PSC patients, the use of DCD grafts was associated with significantly worse post-transplant outcomes because of PSC recurrence and biliary complications. LDLT had similar outcomes to DBD-LT. However, the negative effect of DCD grafts was blunted in the more current era. The use of DCD grafts is an appropriate option for PSC with appropriate donor selection.

SAT250

Patients with acute-on-chronic liver failure have significantly greater healthcare resource utilization after liver transplantation

Vinay Sundaram¹, Christina Lindenmeyer², Kirti Shetty³, Robert Rahimi⁴, Atef Alattar¹, Gianina Flocco², Brett Fortune⁵, Cynthia Gong⁶, Suryanarayana Challa³, Haripriya Maddur⁷, Janice Jou⁸, Michael Kriss⁹, Lance Stein¹⁰, Ross Vyhmeister⁸, Ellen Green⁸, Braidie Campbell⁹, Josh Levitsky¹¹, Constantine Karvellas¹². ¹Cedars-Sinai Medical Center, Los Angeles, United States; ²Cleveland Clinic Main Campus, Cleveland, United States; ³University of Maryland, College Park, United States; ⁴Baylor Scott and White Medical Center-Grapevine, Grapevine, United States; ⁵Weill Cornell Medicine, New York, United States; ⁶University of Southern California, Los Angeles, United States; ⁷Tampa General Hospital, Tampa, United States; ⁸Oregon Health and Science University, Portland, United States; ⁹University of Colorado Denver, Denver, United States; ¹⁰Piedmont Atlanta Hospital, Atlanta, United States; ¹¹Northwestern Medical Center, Chicago, United States; ¹²University of Alberta, Edmonton, Canada
Email: vinaysundaram@yahoo.com

Background and aims: Data is lacking regarding healthcare resource utilization after liver transplantation (LT) for patients with acute-on-chronic liver failure (ACLF).

Method: We retrospectively reviewed data from 10 centers in North America of patients transplanted from years 2018–2019, who required management in the intensive care unit prior to LT. ACLF was identified using the EASL-CLIF criteria.

Results: We studied 318 patients of whom 106 patients (33.3%) had no ACLF, 61 (19.1%) had ACLF-1, 74 (23.2%) had ACLF-2, and 77 (24.2%) had ACLF-3 at LT. Multivariable negative binomial regression analysis demonstrated a significantly longer LOS for patients with ACLF-1 (1.9 days, 95% CI 0.82–7.51), ACLF-2 (6.7 days, 95% CI 2.5–24.3), and ACLF-3 (19.3 days, 95% CI 1.2–39.7), compared to recipients without ACLF. Presence of ACLF-3 at LT was also associated with longer length of dialysis post-LT (9.7 days, 95% CI 4.6–48.8) relative to lower grades. Logistic regression analysis revealed greater likelihood of discharge to a rehabilitation center among recipients with ACLF-1 (OR = 1.79, 95% CI 1.09–4.54), ACLF-2 (OR = 2.23, 95% CI 1.12–5.01) and ACLF-3 (OR =

2.23, 95% CI 1.40–5.73). Development of bacterial infection post-LT also predicted LOS (20.9 days, 95% CI 6.1–38.5) and 30-day readmissions (OR = 1.39, 95% CI 1.17–2.25). (Table) Cost estimates based on post-LT LOS demonstrated that expenditures were significantly greater for patients transplanted with ACLF, and especially for ACLF-3 (No ACLF: \$65,359, ACLF-1: \$102,698, ACLF-2: \$129,893, and ACLF-3: \$244,406, $p < 0.001$).

Table: Multivariable negative binomial regression and logistic regression regarding predictors of post-LT healthcare resource utilization

	Post-LT length of stay (days) (Coefficient, 95% CI)	Post-LT length of dialysis (days) (Coefficient, 95% CI)	30-day readmission (OR, 95% CI)	Discharge to rehabilitation center (OR, 95% CI)
ACLF grade				
No ACLF (reference)	1.9 (0.8, 7.5)	2.1 (-22.4, 16.2)	1.27 (0.62, 2.57)	1.79 (1.09, 4.54)
ACLF-1	6.7 (2.5, 24.3)	5.8 (-1.4, 18.5)	1.37 (0.62, 3.04)	2.23 (1.40, 5.73)
ACLF-2	19.3 (1.2, 38.7)	9.7 (4.6, 48.8)	1.75 (0.87, 3.46)	2.12 (1.11, 5.01)
ACLF-3				1.05 (1.01, 1.09)
Age				5.14 (1.89, 14.0)
Braden score <16	13.2 (5.1, 44.0)			1.36 (1.12, 1.57)
In ICU at LT	7.7 (2.1, 18.1)			
Dialysis at LT	9.2 (2.0, 29.1)	4.9 (1.9, 18.6)		2.00 (1.17, 3.41)
Mechanical ventilation at LT		5.5 (2.96, 16.0)		
Pre-transplant bacterial infection				
Post-transplant bacterial infection	20.9 (6.1, 38.5)		1.39 (1.17, 2.25)	

Conclusion: Patients with ACLF at LT, particularly ACLF-3, have greater post-transplant healthcare resource utilization and costs.

SAT251

Use of statins after liver transplantation is associated with improved survival: results of a nationwide study

Chiara Becchetti¹, Melisa Dirchwolf^{1,2}, Jonas Schropp^{3,4}, Giulia Magini⁵, Beat Müllhaupt⁶, Franz Immer⁷, Jean-François Dufour¹, Banz Vanessa¹, Annalisa Berzigotti¹, Jaime Bosch^{1,8}. ¹Inselspital, University Hospital, University of Bern, Department for Visceral Surgery and Medicine, Berne, Switzerland; ²Hospital Privado de Rosario, Santa Fe, Argentina, Liver Unit, Argentina; ³Open University of Cyprus, Cyprus, Department of Computer Science, Cyprus; ⁴University of Cyprus, Cyprus, Department of Psychology, Cyprus; ⁵Hôpitaux Universitaires de Genève, Geneva, Switzerland, Service de Transplantation, Geneva, Switzerland; ⁶University Hospital Zurich, Switzerland, Swiss HPB (Hepato-Pancreato-Biliary) Center and Department of Gastroenterology and Hepatology, Zürich, Switzerland; ⁷Swisstransplant, the Swiss National Foundation for Organ Donation and Transplantation, Bern, Switzerland, Berne, Switzerland; ⁸University of Bern, Bern, Switzerland, Department of Biomedical Research, Switzerland
Email: becchettichara@tiscali.it

Background and aims: Statins are known to have pleiotropic effects that can act favorably on the liver, including protection from endothelial dysfunction and from ischemia reperfusion injury, as well as to increase cold preservation time in experimental grafts. However, there is limited data on the benefit that statins might confer in the liver transplant (LT) setting, either with regard to statin administration in LT recipients or its use in donors. This study aimed at analyzing the effect of statin exposure on recipient and on graft survival.

Method: We included all consecutive adult LT candidates nationwide who received a liver from a deceased donor. The statistical analysis adopted was a multistate modelling approach examining the effect of statin exposure (recipient under statin treatment or liver from donor exposed to statins) on the transition hazards between LT, biliary and/or vascular (B-V) complications, and death, while allowing for recurring events. The observation time was 3 years.

Results: Overall, 998 (696 male, 70%, mean age 54.5 ± 11.1 years) LT recipients were included. 19% of recipients were exposed to statins during the study period. Over the 3-year follow-up period, 141 patients died; there were 40 re-LT and 363 B-V complications. Recipient statin use protected from mortality after-LT (HR = 0.35; 95%

CI 0.12–0.97; p = 0.039). However, it was not significantly associated with the occurrence of B-V complications (HR = 1.22; 95%CI = 0.83–1.78; p = 0.307) or re-LT (HR, 1.8e-7; 95%CI, 0–Inf; p = 1). In patients developing B-V complications, statin use significantly protected from mortality (HR = 0.10; 95%CI = 0.01–0.75; p = 0.023) and reduced recurrence of B-V complications (HR = 0.42; 95%CI = 0.18–1.00; p = 0.049). Donor statins use prior LT had no significant influence on post-LT outcomes.

Conclusion: Our results show that statin use in recipients appears to confer a survival advantage. Statin administration should therefore be encouraged when indicated.

SAT252

Liver transplantation for hepatocellular carcinoma with extended criteria: performance and applicability of the AFP score after official adoption by the French Organ Sharing Organization ABM: 5-year outcomes

Christophe Duvoux¹, Mathilde Petiet Dumont², Georges-Philippe Pageaux³, Ephrem Salamé⁴, Jérôme Dumortier⁵, Sylvie Radenne⁶, Sébastien Dharancy⁷, Pauline Houssel-Debry⁸, Philippe Bachellier⁹, Laurence Chiche¹⁰, Francois Durand¹¹, Fabrice Muscar¹², Jean Gugenheim¹³, Filomena Conti¹⁴, Jean Hardwigen¹⁵, Christian Jacquelin¹⁶, Corinne Antoine¹⁶, Norbert Ngongang¹⁷, Vincent Leroy¹⁸, Thomas Decaens¹⁹, Daniel Cherqui²⁰, Nadia Oubaya²¹. ¹Henri Mondor Hospital APHP, Paris Est University, Me, Créteil, France; ²Grand Hôpital de l'Est Francilien Site de Meaux, Hepatology and Gastroenterology Department, Meaux, France; ³Saint Eloi Hospital, Liver Department, Montpellier, France; ⁴Trousseau University Hospital, Liver and Digestive Surgery, Liver Transplantation Unit, Tours; ⁵Edouard Herriot University Hospital, Liver Department and Liver Transplantation Unit, Lyon, France; ⁶Hospices Civils de Lyon, Croix Rousse University Hospital, Liver Department and Liver Transplantation Unit, Lyon; ⁷Lille University Hospital, Liver Department and Liver Transplantation Unit, Lille, France; ⁸Rennes University Hospital, Liver Transplantation and Digestive Surgery, Rennes, France; ⁹Strasbourg University Hospital, Liver and Digestive Surgery, Liver Transplantation Unit, Strasbourg, France; ¹⁰Bordeaux University Hospital, Department of Digestive Surgery and Liver Transplantation, Bordeaux, France; ¹¹Beaujon University Hospital-APHP, Liver Department and Liver Transplantation Unit, Clichy, France; ¹²Toulouse

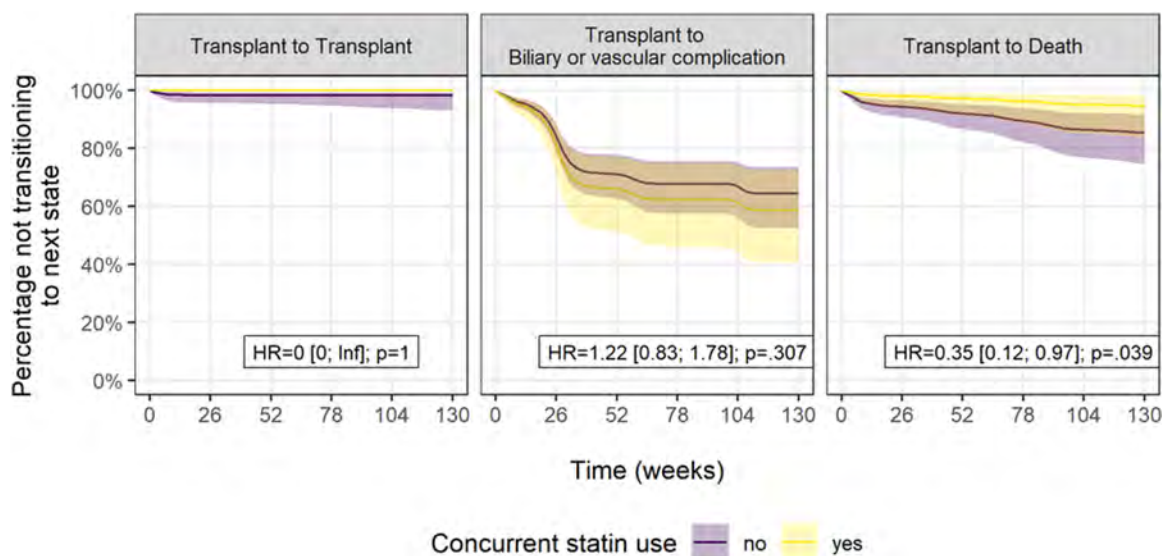


Figure: (abstract: SAT251): Graphical representation of probability of three possible transitions: transplant to transplant; transplant to B-V complication; and transplant to death according to recipients' statin use.

University Hospital, Department of Digestive Surgery and Liver Transplantation, Toulouse, France; ¹³Archet Hospital, University of Nice-Sophia Antipolis, Department of Digestive Surgery; ¹⁴La Pitie Salpêtrière University Hospital APHP, Liver Department and Liver Transplantation Unit, Paris, France; ¹⁵Aix Marseille University, la Timone Hospital, Department of General Surgery and Liver Transplantation, Marseille, France; ¹⁶Agence de la Biomédecine, Biostatistics, Saint Denis, France; ¹⁷Henri Mondor Hospital APHP, Paris Est University, Liver Department and Liver Transplantation Unit, Créteil, France; ¹⁸Henri Mondor Hospital APHP, Paris Est University, Liver Department, Créteil, France; ¹⁹Grenoble University Hospital, Hepatology and Gastroenterology Department, Grenoble, France; ²⁰Paul-Brousse Hospital AP-HP, Centre Hépatobiliaire, Villejuif, France; ²¹Henri Mondor Hospital APHP, Paris Est University, Public Health and Biostatistics, Créteil, France
Email: christophe.duvoux@aphp.fr

Background and aims: Composite scores for selection of patients who are candidates for liver transplantation (LT) for HCC with extended criteria are being considered by scientific societies (EASL), subject to a demonstration of the superiority of these models over the Milan criteria and to their audit. The first composite score developed, the AFP score, has been shown superior to Milan criteria and adopted by the French Organ Sharing Organization, ABM, in January 2013 as a selection tool. The aim of this study was to evaluate the applicability and performance of this new strategy.

Method: Adult patients listed and then transplanted for HCC in 15 French TH centers between March 1, 2013, and March 1, 2014, were studied. The primary end point was the incidence of recurrence at 5 years in patients with AFP score ≤ 2 , or >2 or after down-staging. The secondary end points were 5-year survival rates in the same subgroups and the % of transplanted patients with an AFP score ≤ 2 . Agreement for extraction of the centralized ABM data was obtained from each center and data were quality-controlled for recurrence and death. The statistical analysis was performed with cumulative incidence of recurrence functions and a competitive risk survival analysis taking into account death as a competitive event of recurrence.

Results: Over the enrolment period, 507 patients were consecutively listed, among whom 334 (65.9%) were transplanted and are the basis of this study. Median age at listing was 60 [55–63] and 84.7% were male. The median MELD was 10 [8; 15]; 74 patients (22.2%) were outside the Milan criteria. The AFP score was assessed in 331 patients (99.4%) at listing and in 333 patients (99.7%) within 3 months prior to LT. Overall, 297 (89.7%), 12 (3.6%) and 22 (6.7%) patients were transplanted with a final AFP score ≤ 2 , >2 , and after down-staging ≤ 2 . The 5-year recurrence rates were 12.2% [8.9; 16.5], 50% [26.4; 79.2], and 22.7% [10.2; 46.3] in patients transplanted with an AFP score ≤ 2 , >2 or after down-staging. Overall 5-year survival rates, or after listing and LT with an AFP score ≤ 2 or score >2 , were 73.5% [95% CI: 63.4; 77.9%), 77.0% (71.8; 81.4%) and 33.3% (10.3; 58.8%), respectively.

Conclusion: In this real-life prospective cohort study, including 22% of patients beyond Milan criteria, applicability of the AFP score was high with only 3.6% of patients transplanted with an AFP score >2 . The 12%-observed recurrence rate in patients listed and transplanted with an AFP score ≤ 2 was in strict agreement with the prediction of the model, with a corresponding 77% 5-year survival rate. The AFP score complies with 2018 EASL requirements for an expansion of Milan criteria and can be proposed as a new selection tool for HCC patients.

SAT253

Tacrolimus drug exposure level in the first year after liver transplantation is an independent risk factor for de novo malignancy in patients transplanted for alcohol-related liver disease

Benedict Vanlerberghe^{1,2,3,4}, Hannah Van Malenstein^{1,2}, Mauricio Sainz-Barriga^{5,6}, Diethard Monbaliu^{5,6}, Schalk van der Merwe^{1,2}, Jacques Pirenne^{5,6}, Frederik Nevens^{1,2}, Jef Verbeek^{1,2}. ¹University Hospitals Leuven, Department of Gastroenterology and Hepatology, Leuven, Belgium; ²KU Leuven, Department of Chronic Diseases and Metabolism, Leuven, Belgium; ³Maastricht University Medical Center +, Department of Internal Medicine, Maastricht, Netherlands; ⁴Maastricht University, NUTRIM School of Nutrition and Translational Research in Metabolism, Maastricht, Netherlands; ⁵University Hospitals Leuven, Abdominal Transplantation Surgery, Leuven, Belgium; ⁶KU Leuven, Department of Microbiology, Immunology and Transplantation, Leuven, Belgium
Email: b.vanlerberghe@maastrichtuniversity.nl

Background and aims: De novo malignancy (DNM) is a major cause of mortality in patients undergoing liver transplantation (LTx) for alcohol-related liver disease (ALD). Immunosuppression protocol may influence the risk on DNM, but evidence is conflicting.

Method: We retrospectively analyzed all patients transplanted for ALD between 1990 and October 2016 at our center (n = 317). Patients with a post-LTx follow-up of <12 months (n = 22), a DNM in the 1st year post-LTx (n = 11) or switch of calcineurin-inhibitor type in the 1st year post-LTx (n = 20) were excluded. Total tacrolimus drug exposure level (TDEL) was calculated by area under the curve of trough levels in the 1st year post-LTx. Risk factors for DNM (excluding non-melanoma skin cancers) within 5 years after LTx were analyzed by Cox regression (presented as hazard ratio (HR) with 95% confidence interval).

Results: 264 patients were included. Median age at LTx was 59 years (interquartile range (IQR): 54–64), 206 (78%) patients were male and median follow-up post-LTx was 96 months (IQR: 65–152). 222 patients received tacrolimus and 42 cyclosporine in the 1st year post-LTx. TDEL was known for 212 patients, mean trough level was 7.44 ng/ml (95%CI: 7.22–7.66). 184 (69.7%) patients had a smoking history (ever smoking), of which 80 (30.3%) smoked until LTx and 63 (23.9%) post-LTx. 35 patients developed 36 DNMs within 5 years post-LTx (lung (n = 9), oro-pharyngolaryngeal (n = 9), bladder (n = 3), esophageal (n = 3) and other (n = 12)). In multivariate analysis, type of immunosuppression (tacrolimus vs. cyclosporin and mycophenolic acid vs. azathioprine), any alcohol relapse and sex were not associated with a higher DNM risk, in contrast with age at LTx and smoking history. In patients on tacrolimus, TDEL was higher in those with than those without DNM (8.35 (95%CI: 7.73–8.97) vs. 7.32 (95%CI: 7.09–7.55), p = 0.003) and a higher TDEL was an independent risk factor for DNM (Table 1).

Table: DNM risk in patients on tacrolimus during the 1st year post-LTx (n = 212)

	Univariate	Sig.	Multivariate	Sig.
TDEL	1.417 (1.128–1.779)	.003*	1.540 (1.208–1.962)	.000*
Age at LTx	1.092 (1.028–1.160)	.004*	1.120 (1.054–1.190)	.000*
Smoking history	11.273 (1.525–83.365)	.018*	11.427 (1.541–84.715)	.017*

Legend: * statistically significant

Conclusion: Tacrolimus dose minimization in the 1st year after LTx might be an approach to lower DNM risk in ALD patients and should be investigated in prospective trials.

SAT254

SARS-CoV-2 vaccination in liver transplant recipients: factors affecting immune response and refusal to vaccine

Joanna Raszeja-Wyszomirska¹, Maciej K. Janik¹, Maciej Wójcicki¹, Piotr Milkiewicz^{1,2}. ¹Medical University of Warsaw, Liver and Internal Medicine Unit, Warszawa, Poland; ²Pomeranian Medical University, Translational Medicine Group, Szczecin, Poland
Email: joanna.wyszomirska@wum.edu.pl

Background and aims: The effectiveness of SARS-CoV-2 vaccination in liver transplant (LT) recipients varies between 47.5% to 81% with majority of reports focusing on the immune response assessed in the first month after the vaccination. Data on LT recipients willingness to receive vaccine is limited to only a few reports. Here, we analysed the immune response to the SARS-CoV-2 vaccination, factors affecting response and reasons for refusal to receive this vaccine.

Method: Among 300 consecutive LT recipients, 225 (75%) were vaccinated. Seventy-four (25%) subjects were not vaccinated, including 45 (15%) who refused to be vaccinated and 29 (10%) who did not get the vaccine due to medical reasons. The humoral response was assessed by quantitative determination of anti-trimeric spike-protein-specific-IgG antibodies to SARS-CoV-2 by LIAISON® SARS-CoV-2 TrimericS IgG assay (Diasorin, Italy), which is a chemiluminescence immunoassay (CLIA). Thirty-four vaccinated patients with prior COVID-19 infection were analysed separately.

Results: Among 192 LT recipients vaccinated without prior COVID-19, 69% of them had an immune response (median time of 125 days after the second dose). Older age, worse kidney function and dual immunosuppression negatively affected the humoral response. Mycophenolate mofetil increased the risk of non-response (OR 3.0, 95% CI 1.43–6.25). LT recipients with prior COVID-19 presented with a robust immune response (100%) and with significantly higher IgG antibodies (median 2080 vs 134 BAU/ml; $p < 0.001$). The antibodies concentration was higher in the first 90 days from the second dose ($p = 0.034$) and stable when compared between patients who received the vaccination within 90–150 or more than 150 days (Figure 1). Female gender, living in rural area, lower BMI (all $p < 0.05$) and younger age ($p < 0.001$) were associated with refusal of the vaccine due to non-medical reasons. In contrast, liver recipients with diabetes and impaired kidney function (both $p < 0.01$) were more prone to get a vaccine.

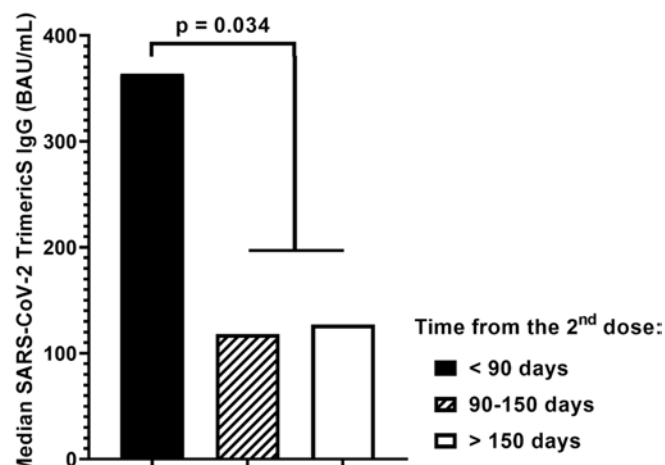


Figure: Median SARS-CoV-2 TrimericS IgG concentration among liver transplant recipients (without prior COVID-19) compared between time from the second dose of the vaccine: <90 days, 90–150 days and >150 days.

Conclusion: Lower immune response after the vaccine among LT recipients may support administration of a third dose. Previous COVID-19 infection dramatically improves response to vaccination in these patients. Sociodemographic factors may play a role in refusal of

being vaccinated but this finding require further investigations in other cohorts of transplanted patients.

SAT255

The effect of clinicopathologic findings of hepatocellular carcinoma on posttransplant survival: a multicenter cohort from TAsL liver transplantation special interest group

Murat Akyildiz¹, Genco Gencdal¹, Volkan Ince², Muhsin Murat Harputluoglu³, Birkan Bozkurt⁴, Murat Zeytinlu⁵, Murat Kılıç⁶, Rasim Farejov⁶, Ilker Turan⁷, Fulya Günsar⁷, Zeki Karasu⁷, Utku Tonguç Yılmaz⁸, Mesut Akarsu⁹, Gökhan Kabaçam¹⁰, Elvan Onur Kırımker¹¹, Ali Atay¹², Meral Akdoğan Kayhan¹², Hale Gökcan¹³, Gupse Adalı¹⁴, Yaman Tokat⁴, Remzi Emiroğlu¹⁵, Kamil Yalçın Polat¹⁶, Sezai Yılmaz², Sedat Karademir¹⁷, Ramazan İdilman¹³. ¹Koç University, School of medicine, Center of Liver Transplantation, Department of Gastroenterology, Turkey; ²Inonu University, School of medicine, Center of Liver Transplantation, Department of General Surgery, Turkey; ³Inonu University, School of medicine, Center of Liver Transplantation, Department of Gastroenterology; ⁴Istanbul Bilim University, School of medicine, Center of Liver Transplantation, Department of General Surgery, Turkey; ⁵Ege University, School of medicine, Center of Liver Transplantation, Department of General Surgery, Turkey; ⁶Izmir kent Hospital, School of medicine, Center of Liver Transplantation, Department of General Surgery, Turkey; ⁷Ege University, School of medicine, Center of Liver Transplantation, Department of Gastroenterology, Turkey; ⁸Acibadem University, School of medicine, Center of Liver Transplantation, Department of General Surgery, Turkey; ⁹Eylül University, School of medicine, Center of Liver Transplantation, Department of Gastroenterology, Turkey; ¹⁰Güven Hospital, Center of Liver Transplantation, Department of Gastroenterology, Turkey; ¹¹Ankara City Research and Training Hospital, Center of Liver Transplantation, Department of General Surgery, Turkey; ¹²Ankara City Research and Training Hospital, Center of Liver Transplantation, Department of Gastroenterology, Turkey; ¹³Ankara University, School of medicine, Center of Liver Transplantation, Department of Gastroenterology, Turkey; ¹⁴Umraniye Research and Training Hospital, Center of Liver Transplantation, Department of Gastroenterology, Turkey; ¹⁵Acibadem University, School of medicine, Center of Liver Transplantation, Department of General Surgery, Turkey; ¹⁶Memorial Atasehir Hospital, Center of Liver Transplantation, Department of General Surgery, Turkey; ¹⁷Güven Hospital, Center of Liver Transplantation, Department of General Surgery
Email: akyildizmr@yahoo.com

Background and aims: The aim of the present study was to determine the effect of clinicopathological findings of hepatocellular carcinoma (HCC) on posttransplant survival.

Method: This was a multicenter retrospective study of patients with HCC undergoing LT from 10 tertiary center in Turkey between 2002 and 2020. Datas were retrieved from standardized electronic case report forms in each center.

Results: A total of 1428 patients with HCC underwent LT were included into the study. Viral hepatitis was the most common etiology accounting for 75.6% of patients. Hepatitis B infection was the most cause (58.6%) followed by hepatitis C (12.6%), and cryptogenic (13.8%). The mean overall survival (OS) was 178.2 months, whereas the mean progression free survival (PFS) was 44 months. The one and five-year estimated overall survival rate was found %89 and 80. Overall and disease-free survival did not significant differ between patients with Living Donor LT and patients with Deceased Donor LT (Log Rank for OS $p = 0.148$ and for PFS $p = 0.137$, respectively). In univariate analysis, serum AFP level, histologic differentiation, tumor size, Milan and UCSF criteria, the number of tumors, the presence of microvascular and macrovascular invasion were significantly associated with patient survival ($p < 0.005$). In multivariate analysis, serum AFP level, poor differentiation

microvascular invasion remained significantly associated with disease free survival ($p < 0.05$).

Table: The correspondance of Recurrence and Non-Recurrence groups

	Recurrence Group	Non-Recurrence Group	P value
Age	54.7 ± 9.8	56.1 ± 8.2	>0.05
Gender (Male)	87.9	84.2	>0.05
Cirrhosis (%)	95.4	93.7	$P = 0.495$
AFP	1825 ± 16311	135.2 ± 739.2	$P < 0.001$
0–9 (%)	35.9	52.3	$P < 0.001$
10–99 (%)	33.1	33.5	$P < 0.001$
100–499 (%)	18.2	10.2	$P < 0.001$
500–999 (%)	5.4	1.9	$P < 0.001$
>1000 (%)	7.4	2.1	$P < 0.001$
Transplantation	80.6/19.4	79.6/20.4	$p > 0.05$
Type: Living donor/			
Cadaveric (%)			
MELD (0–14)%	69.1	67.2	$p > 0.05$
MELD >14%	30.9	32.8	
Total Tumor	79.7 ± 53.8	46.3 ± 37.4	$P < 0.001$
Diameter			
The Largest Tumor	53.8 ± 38.6	33.1 ± 24.4	$P < 0.001$
Diameter			
Total Tumor	4 ± 3.6	2.2 ± 2.2	$P < 0.001$
Number			
Milan (in/out) (%)	38.7/61.3	70.6/29.4	
UCSF (in/out) (%)	49/51	78.3/21.7	
Tumor Biology (%)			
Poor	25	9.4	
differentiated			
Mild	57.3	50	
differentiated			
Well	17.7	40.6	
differentiated			
Lymph node	42.9	24.4	$P < 0.05$
invasion (%)			
Microvascular	59.9	24.5	$P < 0.001$
invasion (%)			
Macrovascular	44.1	17.2	$P < 0.001$
invasion (%)			

Conclusion: Based on the results of the study, viral hepatitis remains the most frequent etiology of HCC in Turkey. High serum AFP levels, poor histologic differentiation and microvascular invasion significantly affect the posttransplant outcome. Donor type does not significantly affect posttransplant survival in patients with HCC.

SAT256

Utility and prognostic value of diagnosing metabolic dysfunction-associated fatty liver disease in patients undergoing liver transplantation for alcohol-related liver disease

Benedict Vanlerberghe^{1,2,3,4}, Hannah Van Malenstein^{1,2}, Mauricio Sainz-Barriga^{5,6}, Diethard Monbaliu^{5,6}, Schalk van der Merwe^{1,2}, Jacques Pirenne^{5,6}, Frederik Nevens^{1,2}, Jef Verbeek^{1,2}. ¹University Hospitals Leuven, Department of Gastroenterology and Hepatology, Leuven, Belgium; ²KU Leuven, Department of Chronic Diseases and Metabolism, Leuven, Belgium; ³Maastricht University Medical Center +, Department of Internal Medicine, Maastricht, Netherlands; ⁴Maastricht University, NUTRIM School of Nutrition and Translational Research in Metabolism, Maastricht, Netherlands; ⁵University Hospitals Leuven, Abdominal Transplantation Surgery, Leuven, Belgium; ⁶KU Leuven, Department of Microbiology, Immunology and Transplantation, Leuven, Belgium
Email: b.vanlerberghe@maastrichtuniversity.nl

Background and aims: Metabolic dysfunction-associated fatty liver disease (MAFLD) is a recently proposed term, which allows diagnosing liver disease associated with metabolic dysfunction in

patients with alcohol-related liver disease (ALD). We assessed the prevalence of MAFLD in ALD patients undergoing liver transplantation (LTx) and its prognostic value on post-LTx outcome.

Method: We retrospectively analyzed all patients transplanted for ALD between 1990 and August 2020 at our center. MAFLD was diagnosed at LTx based on the presence or history of hepatic steatosis and a BMI ≥ 25 kg/m² or type II diabetes (DMII) or ≥ 2 metabolic risk abnormalities (dyslipidemia, hypertension, pre-diabetes). Overall survival and potential risk factors for recurrent liver steatosis (based on imaging or biopsy) and cardiovascular (CV) events were analyzed by Cox regression (presented as hazard ratio (HR) with 95% confidence interval).

Results: Of the 371 included ALD patients, 255 (68.7%) had concomitant MAFLD at LTx. Median follow-up post-LTx was 72 months (Table 1). Patients with ALD-MAFLD were older, more often male, and more frequently had hepatocellular carcinoma (HCC) at LTx (Table 1). Perioperative mortality and overall survival (HR: 0.991 (0.702–1.401); $p = .960$) did not differ between MAFLD and non-MAFLD ALD patients (Table 1). Multivariate analysis identified MAFLD at LTx (HR: 2.092 (1.412–3.098)), weight gain in the 1st year post-LTx (HR: 1.092 (1.043–1.143)) and any alcohol relapse (HR: 4.606 (3.097–6.850)) as independent risk factors for recurrent hepatic steatosis ($p < .001$). MAFLD at LTx was not associated with CV events post-LTx (HR: 1.519 (0.790–2.922); $p = .210$), in contrast with the traditional risk factors age (HR: 1.064 (1.016–1.114); $p = .008$) and DMII (HR: 2.068 (1.134–3.770); $p = .018$).

Table: Patient characteristics (at LTx)

	All (n = 371)	ALD-MAFLD (n = 255)	ALD-non-MAFLD (n = 116)	p value
Age (years)	60.0 (56.0–66.0)	61.0 (56.0–76.0)	58.0 (52.5–64.0)	.001*
Male sex (%)	80.1	86.3	66.4	<.001*
HCC (%)	38.3	44.3	25.0	<.001*
Follow-up (months)	72.0 (34.5–122.0)	68.0 (33.5–116.5)	82.0 (35.5–127.5)	.337
Perioperative mortality (%)	2.43	2.75	1.72	.553

Legend: * statistically significant/IQR: interquartile range

Conclusion: The presence of MAFLD in ALD is associated with a distinct patient profile at LTx and is a risk factor for recurrent hepatic steatosis irrespective of alcohol relapse. These novel findings demonstrate the utility and prognostic value of diagnosing MAFLD at LTx.

SAT257

Severe acute respiratory syndrome coronavirus type 2 (SARS-CoV-2) specific cellular and humoral immunity in Coronavirus Disease-2019 (COVID-19) convalescence after liver transplantation-a prospective six month follow-up

Theresa Kirchner¹, Hagen Sauer¹, Sophia Heinrich¹, Agnes Bonifacius², Ruhl Louisa³, Isabell Pink⁴, Bastian Engel¹, Emily Saunders¹, Joerg Martens², Marius M. Hoepfer⁴, Rainer Blaszczkyk², Heiner Wedemeyer¹, Elmar Jaeckel¹, Christine Falk³, Britta Eiz-Vesper², Richard Taubert¹. ¹Hannover Medical School, Department of Gastroenterology, Hepatology and Endocrinology, Hannover, Germany; ²Institute of Transfusion Medicine and Transplant Engineering, Hannover, Germany; ³Institute of Transplant Immunology, Hannover, Germany; ⁴Department of Pneumology, Hannover Medical School, member of the German Centre for Lung Research (DZL), Hannover, Germany
Email: kirchner.theresa@mh-hannover.de

Background and aims: Data on protective immunity against SARS-CoV-2 in liver transplantation recipients (LTR) after mild/moderate

POSTER PRESENTATIONS

COVID-19 are limited. The aim of the study was to analyse the immune response in LTR convalescents with ongoing immunosuppressive therapy in the first six months and to assess the impact of vaccination in LTR convalescents in comparison to matched convalescents without immunosuppression (non-IS).

Method: Immune response in LTR and non-IS was measured prospectively 1–2 (LTR: n = 15; non-IS: n = 14), 3–5 (LTR: n = 16; non-IS: n = 16) and ≥ 5 (LTR: n = 14; non-IS: n = 36) months after positive PCR test. Immunity after post-COVID-19 booster vaccination in convalescent LTR was measured in n = 11.

Specific T cell reactivity was detected by IFN- γ ELISPOT against 4 antigens (membrane, nucleocapsid, spike protein1/2). Specific antibodies (IgG and A) were detected against 4 different antigens (S1/2, receptor binding domain (RBD), nucleocapsid). Pre-pandemic samples were retrieved from our prospective LTR biorepository.

Results: The majority of LTR (93%) had a mild or moderate COVID-19 (outpatients: 87%). No T cell reactivity or IgG was detectable in pre-pandemic samples.

IgG antibodies in LTR were detectable in 62–85% (1–2 months), 70–90% (3–5 months) and 56–100% (≥ 5 months and vaccination). Although IgG antibodies against nucleocapsid were reduced in LTR in comparison to non-IS, IgG and IgA antibodies against all other antigens including RBD of the spike protein of convalescent LTR were not reduced, neither in frequency nor in concentration.

In initial analysis convalescent LTR had no reduced IFN- γ production normalized to numbers of PBMCs compared to non-IS in the first 6 months. In addition, cellular and humoral immune response did not decline significantly over the first 6 months. However, booster vaccination non-significantly increases cellular (S1 p = .093, S2 p = .058) or humoral (S1 p = .065, S2 p = .096) reactivity against spike protein in convalescent LTR.

The prospective follow-up will be continued for 1 year after COVID-19.

Conclusion: In conclusion, LTR convalescents achieved cellular and humoral immune responses against SARS-CoV-2 comparable to non-IS, even after mild or moderate COVID-19. Cellular and humoral immunity showed no decline but could be boosted with additional vaccination in the first months after COVID-19 in LTR convalescents. The development of a robust immunity without triggered rejection justifies the continuation of immunosuppression during infection.

SAT258

A third dose of the BNT162b2 mRNA vaccine significantly improved immune response among liver transplant recipients

Yana Davidov¹, Victoria Indenbaum², Keren Tsaraf¹, Oranit Cohen-ezra¹, Mariya Likhter¹, Gil Ben Yaacov¹, Rebecca Halperin³, Itzhak Levy^{3,4}, Orna Mor^{2,4}, Nancy Agmon-Levin^{4,5}, Arnon Afek^{4,6}, Galia Rahav^{3,4}, Yaniv Lustig^{2,4}, Ziv Ben Ari^{1,4}. ¹Sheba Medical Center, Liver Diseases Center, Tel Aviv-Yafo, Israel; ²Central Virology Laboratory, Ministry of Health, Tel-Hashomer, Tel Aviv-Yafo, Israel; ³Sheba Medical Center, Infectious diseases unit, Tel Aviv-Yafo, Israel; ⁴Tel Aviv University, Sackler School of Medicine, Tel Aviv-Yafo, Israel; ⁵Sheba Medical Center, Clinical Immunology Angioedema and Allergy Unit, The Zabudowicz Center for Autoimmune Diseases, Tel Aviv-Yafo, Israel; ⁶Sheba Medical Center, Tel Aviv-Yafo, Israel

Email: y.davidov@gmail.com

Background and aims: Immune responses of solid organ transplant recipients to two doses of the BNT162b2 mRNA anti-SARS-CoV-2 vaccine is impaired. The immunogenicity and safety of a third dose among liver transplant (LT) recipients is unknown. This work aimed to evaluate the immune response of LT recipients to a third dose of the BNT162b2 mRNA vaccine.

Method: Consecutive LT recipients (n = 64) in follow-up at Sheba Medical Center were included. Receptor-binding domain (RBD) IgG and neutralizing antibody (NA) titers and T cells levels before (test 2) and 21–28 days a third vaccine dose (test 3) were determined and

compared to their levels measured a median 38 days after the second vaccine dose (test 1). IgG antibody titers ≥ 1.1 IS/CO were defined as positive antibody. Adverse effects after the third dose were monitored.

Results: The LT recipients were of a median age of 64 years; 59.4% were male. The percentage of responders to the second vaccine (69.4%) decreased after a median time of 174 days (54%) and improved significantly after the third vaccine (97%). Geometric mean anti-RBD IgG levels, NA levels and T cell count also increased significantly after the third dose. Anti-RBD IgG and NA titers after the third vaccine negatively correlated with age (p > 0.0001), renal failure (p > 0.0001), mycophenolate mofetil treatment (p = 0.004), and combined immunosuppression vs. calcineurin inhibitors monotherapy (p = 0.001). After the third dose, adverse events were reported by 37% of recipients and were mostly mild (local pain and fatigue).

Conclusion: The immune response after a third BNT162b2 mRNA vaccine improved significantly among LT recipients, without serious adverse effect. Further studies are needed to evaluate immune response durability and to determine the optimal number and schedule of boost vaccines.

SAT259

Everolimus combined with low-dose tacrolimus controls histological graft injury and liver fibrosis as sufficiently as high-dose tacrolimus combined with mycophenolate after liver transplantation

Fabian Dranicki¹, Emily Saunders¹, Theresa Kirchner¹, Bastian Engel¹, Björn Hartleben², Heiner Wedemeyer¹, Elmar Jaecel¹, Richard Taubert¹. ¹Hannover Medical School, Dept. Gastroenterology, Hepatology and Endocrinology, Hannover, Germany; ²Hannover Medical School, Institute for Pathology, Hannover, Germany
Email: dranicki.fabian@mh-hannover.de

Background and aims: After liver transplantation (LTx), there are multiple regimens for immunosuppression (IS). The combination of everolimus (EVR) and low-dose tacrolimus prevents T cell-mediated rejection (TCMR) of liver grafts as sufficiently as the standard of care (SOC) with high-dose tacrolimus (highTAC) and mycophenolate, but is associated with a preserved kidney function within the first years after liver transplantation (LT). However, none of the available studies assessed the histological pattern of graft injury or liver graft fibrosis in surveillance biopsies (svLbx), especially in the first year after LTx.

Method: All surveillance biopsies in our protocol biopsy program taken under at least 1 month of stable immunosuppression with either EVR (aim 3–8 ng/ml) and lowTAC (aim 3–5 ng/ml) or SOC with tacrolimus (aim 3–8 ng/ml) and mycophenolate (500–1500 mg/day) within the first 3–4 years after LTx at our center were included. Patients who were switched to EVR because of insufficient control of alloreactivity through SOC were excluded. Reasons for switches to EVR were malignancies before or after LT, chronic kidney injury, intolerance of SOC or CMV reactivations.

Results: So far, we could include 21 patients for the everolimus/low dose tacrolimus group, and 39 patients for the SOC/high dose tacrolimus group. The switch to EVR took place at a median of 119 days after LTx. EVR/lowTAC group exhibited lower TAC through levels at svLbx than SOC (p < .001). Histological graft injury quantified by the rejection activity index and hepatitis activity index according to Ishak were not significantly different between the EVR/lowTAC group and SOC. Similarly, liver graft fibrosis in all compartments (portal/periportal, sinusoidal, perivenular) was not significantly different between both groups. Likewise, patterns of TCMR, NAFLD/NASH and bile duct abnormalities exhibited similar frequencies in both treatment groups.

Conclusion: The combination of everolimus with low dose tacrolimus seems to control alloreactivity and histological graft injury as sufficiently as SOC with tacrolimus/mycophenolate within the first 3–4 years after LTx. These histological safety data suggest a broader application of this CNI-sparing regimen.

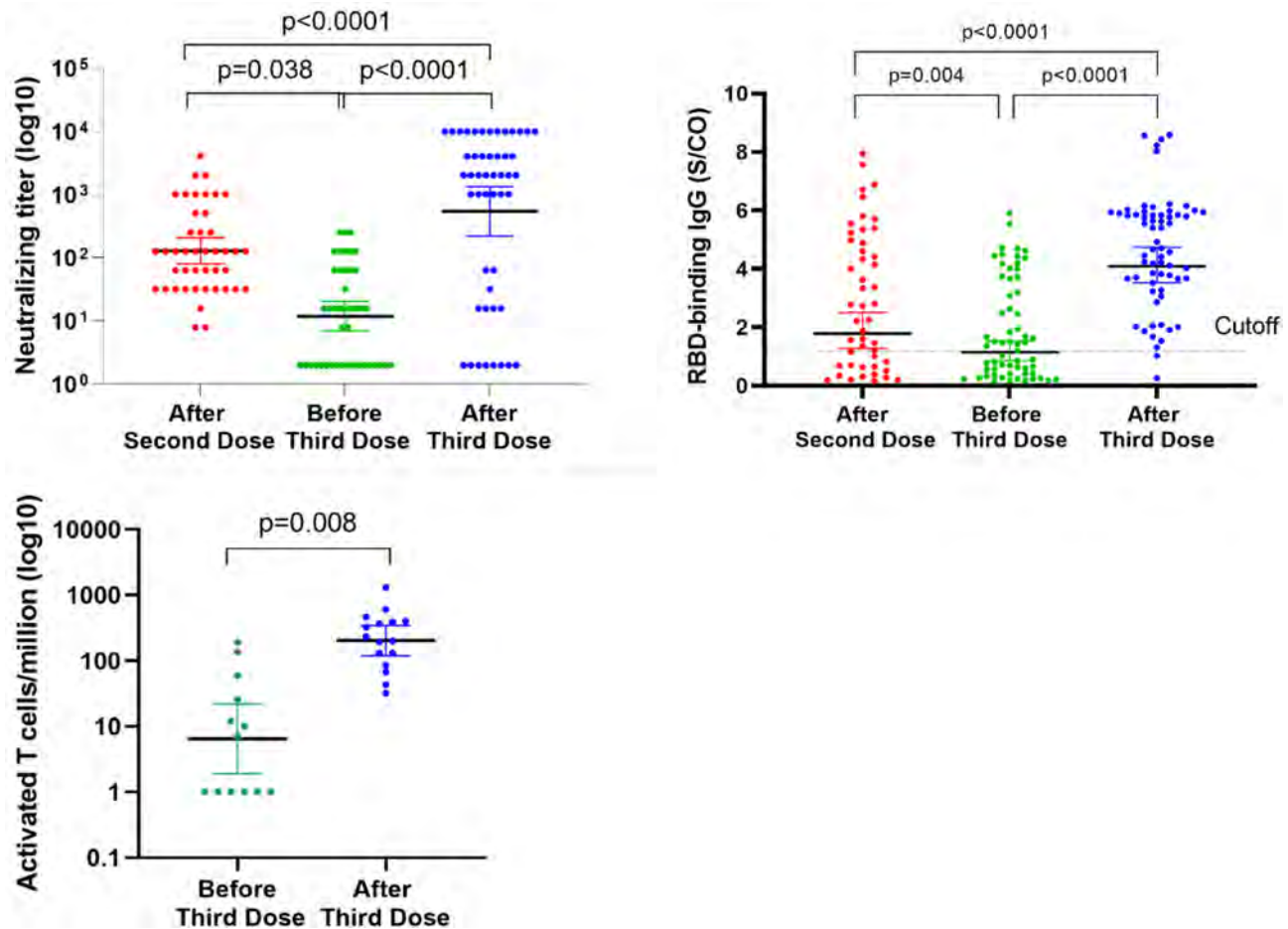


Figure: (abstract: SAT258)

SAT260

The portrait of adult liver transplant recipients in the United States from 2002 to 2020

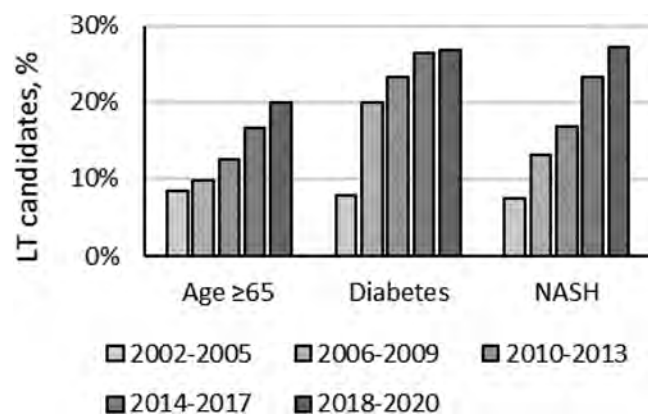
Zobair Younossi^{1,2,3}, Reem Al Shabeeb¹, Michael Harring¹, Janus Ong⁴, Saleh Alqahtani^{5,6}, Linda Henry^{1,7}, Maria Stepanova^{1,7}. ¹Inova Health System, Medicine Service Line; ²Betty and Guy Beatty Center for Integrated Research, IHS; ³Center for Liver Disease, Inova Medicine; ⁴University of the Philippines, College of Medicine; ⁵King Faisal Specialist Hospital and Research Center; ⁶Johns Hopkins University, Division of Gastroenterology and Hepatology; ⁷Center for Outcomes Research in Liver Disease

Email: zobair.younossi@inova.org

Background and aims: Aging population, the epidemics of obesity and metabolic syndrome, and decreasing burden of viral hepatitis are changing the portrait of liver transplant (LT) candidates in the U.S. We aimed to assess changes in demographics and clinical presentation of LT candidates in the U.S. over the last two decades.

Method: The Scientific Registry of Transplant Recipients (SRTR) data 2002–2020 was used to select adult candidates for LT. Patients with acute liver disease, hepatocellular carcinoma, or without known LT etiology were excluded. Trends in the proportions of common LT etiologies of chronic liver disease at the time of LT listing, such as chronic hepatitis B (CHB), chronic hepatitis C (CHC), non-alcoholic steatohepatitis (NASH, including cryptogenic cirrhosis if accompanied by obesity or type 2 diabetes), alcoholic liver disease (ALD) without and with CHC, autoimmune hepatitis (AIH), primary biliary cirrhosis (PBC), and primary sclerosing cholangitis (PSC), were assessed over time along with other clinico-demographic parameters

Results: There were 149,910 LT candidates included in this study: n = 28,581 in 2002–2005, n = 30,158 in 2006–2009, n = 31,824 in 2010–2013, n = 32,925 in 2014–2017, and n = 26,422 in 2018–2020. Over time, the mean ± SD age of LT candidates increased from 52 ± 10 years in 2002–2005 to 55 ± 11 years in 2018–2020, and the proportion of patients ≥65 years increased from 8% to 20% (trend p < 0.0001). The proportion of male candidates decreased from 65% to 60%, respectively, and so did the proportion of white patients: from 75% to 72%, respectively (p < 0.0001). During the same period, the proportion of liver re-transplants decreased from 6.0% to 3.5%, respectively (p < 0.0001). The rates of obesity (BMI >30 kg/m²) and diabetes increased from 33% and 8%, respectively, in 2002–2005 to 40% and 27%, respectively, in 2018–2020 (p < 0.0001) (Figure). In 2002–2005, the most common etiology of chronic liver disease in LT candidates without HCC was CHC without or with ALD (total 45%), while NASH accounted for 7% of listings. In contrast, in 2018–2020, NASH was the second most common LT etiology at 27%, following ALD (38%), while CHC with or without ALD decreased to a total of 10%. Other common etiologies (CHB, AIH, PBC, and PSC) accounted for 2–7% listings each throughout the study period.



Conclusion: The portrait of LT candidates in the U.S. is changing to include more elderly patients, patients with metabolic syndrome, and diagnosis of NASH.

SAT261

Heterologous regimen viral-vector/mRNA produces significantly higher SARS-CoV-2 humoral response than homologous viral-vector and inactivated vaccines in liver transplant recipients

Manuel Mendizabal¹, Nicolas Ducasa², Paula Benencio², Maria Margarita Anders³, Fernando Cairo⁴, Adriana Alter⁵, Patricia Etcheves⁶, Giampaolo Scarton⁶, Mirna Biglione², Ezequiel Mauro⁷. ¹Hospital Universitario Austral, Hepatology and Liver Transplant Unit, Pilar, Argentina; ²Instituto de Investigaciones Biomédicas en Retrovirus y SIDA (INBIRS), CONICET-Universidad de Buenos Aires, Argentina; ³Hospital Aleman, Argentina; ⁴Hospital El Cruce, Argentina; ⁵Fundacion Hemocentro, Argentina; ⁶Bioars, Argentina; ⁷Liver Unit, Hospital Italiano, Buenos Aires, Argentina. Email: mmendizaba@cas.austral.edu.ar

Background and aims: Knowledge of the immunogenicity of vaccines against SARS-CoV-2 in liver transplant recipients (LTR) is mainly limited to mRNA vaccines. We aimed to assess independent predictors of humoral response, in regimens based on homologous non-replicating viral vectors, inactivated vaccines, and heterologous combination.

Method: Multicenter and prospective study, in which consecutive and volunteering LTR and immunocompetent controls were recruited. COVID-19 Spike 1–2 IgG (S-IgG), neutralizing antibodies (NA) and nucleocapsid protein (N) were evaluated 21–90 days after receiving the second doses of vaccine ChAdOx1 (AstraZeneca), rAd26-rAd5 (Sputnik V), inactivated BBIBP-CorV (Sinopharm), and the heterologous combination rAd26/mRNA-1273 (Sputnik V/Moderna), according to the Argentinean immunization program. Vaccine side effects and clinical data was collected.

Results: After excluding 3 LTR for having a positive N protein test, 120 LTR and 27 immunocompetent controls were analyzed. No significant baseline differences were found between LTR and controls. Twenty-four (89%) controls and 74 (61%) LTR were positive for S-IgG ($p = 0.007$). NA titers were significantly higher in controls compared to LTR [64 (8–128) vs 16 (8–64); $p = 0.02$]. The correlation between S-IgG and NA titers was high [Pearson's correlation 0.89 (0.8–0.9); $p < 0.001$]. In a multivariate analysis, Increased BMI [OR 0.8 (0.8–0.9); $p = 0.004$] and the use of MMF [OR 5.1 (2.0–12.8); $p < 0.001$] were independently associated with a negative humoral response, while the use of the rAd26/mRNA-1273 combination [OR 0.11 (0.02–0.6); $p = 0.001$] was independently associated with a higher humoral response rate. No significant differences were detected regarding adverse effects between controls and LTR.

Variable	Detection of S-IgG		P
	Negative N = 46	Positive N = 74	
Age, years (median, IQR)	65 (55–72)	64 (53–70)	0.8
Female sex, n (%)	18 (39)	31 (42.5)	0.7
BMI, (median, IQR)	30 (26–31)	27 (24–31)	0.06
Diabetes, n (%)	20 (44)	23 (31)	0.1
Vaccine, n (%)			
ChAdOx1	19 (41.3)	16 (21.6)	0.02
BBIBP-CorV	13 (28.3)	12 (16.2)	0.1
rAd26-rAd5	12 (26.1)	25 (33.8)	0.3
rAd26/mRNA-1273	2 (4.3)	21 (28.4)	<0.001
Immunosuppression, n (%)			
CNI	44 (95.7)	63 (85.1)	0.1
Prednisone	10 (21.7)	12 (16.2)	0.4
mTOR	5 (10.9)	18 (24.3)	0.09
MMF	25 (54.3)	16 (21.6)	<0.001
Days 2 nd dose-Extraction, (median, IQR)	61 (47–76)	52 (37–68)	0.3
Days between 1st and 2nd dose, (median, IQR)	67 (54–93)	92 (69–114)	0.001
Years since transplantation, (median, IQR)	3.5 (1.4–7.7)	5.6 (3.1–11.4)	0.09

Conclusion: LTR had a significantly lower humoral response than non-immunosuppressed controls. The use of MMF, and a higher BMI, were independently associated with a lower humoral response rate. In contrast, the heterologous combination rAd26/mRNA-1273 was significantly associated with higher S-IgG. New studies are needed in order to characterize the best vaccination scheme in LTR.

SAT262

Evolution of pretransplant cardiac risk factor burden and major adverse cardiovascular events in liver transplant recipients over time

Claire Harrington¹, Paul Levy¹, Elizabeth Cabrera¹, Jing Gao¹, Dyanna Gregory¹, Cynthia Padilla¹, Gonzalo Crespo¹, Lisa VanWagner¹. ¹Northwestern Memorial Hospital, Chicago, United States. Email: claire.harrington@northwestern.edu

Background and aims: Non-alcoholic steatohepatitis (NASH) is associated with high cardiac risk factor burden in liver transplant recipients (LTRs). Major adverse cardiovascular events (MACE) are a major cause of complications in LTRs. The contemporary prevalence and temporal trends in pretransplant cardiac risk factor burden among LTRs are unknown. Therefore, the aim of this study is to evaluate the evolution of MACE and pre-LT cardiac risk factors in LTRs over time.

Method: This is a retrospective cohort of 1739 adult LTRs at a single, large U.S. academic transplant center (2003–2020) using the electronic health record. NASH was defined using primary or secondary listing diagnosis for NASH or cryptogenic cirrhosis plus one metabolic risk factor. MACE was defined as death or hospitalization for myocardial infarction (MI), revascularization, stroke, or heart failure (HF). Logistic regression analysis was used to assess factors *a priori* that are associated with 1-year MACE among LTRs.

Results: Figure 1 shows trends in pre-LT cardiac comorbid conditions. Comparing 2003 and 2020, there was a significant increase in pre-LT obesity, chronic kidney disease (CKD), atherosclerotic (ASCVD) and NASH ($p < 0.05$ for all). There was no significant change in proportion of LTRs with older age (≥ 65 years old), diabetes, or HF. The mean 1-year MACE rate was 18.7%. Higher 1-year MACE was observed in LTRs transplanted for NASH compared to other etiologies (26.4% vs 16.5%, $p < 0.0001$). There was a trend toward a decrease in MACE in 2020 vs 2003 (13.3% vs 25.0%, $p = 0.052$). In multivariable modeling, age, ASCVD, diabetes, HF, and CKD were significantly associated with MACE within 1 year of LT.

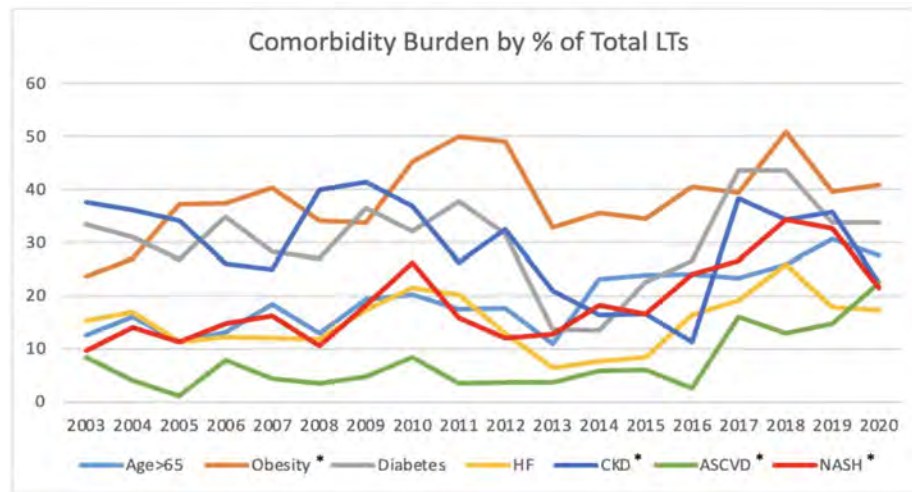


Figure 1: (abstract: SAT262): Comorbidity burden by percent of total LTs over time (2003–2020).

There was an increase in all cardiac risk factors over time. Factors marked with an asterisk had a significant increase between 2003 and 2020 ($p < 0.05$).

Conclusion: There has been an overall increase in cardiac risk factor burden among LTRs between 2003 and 2020 that are also significantly associated with MACE within 1 year of LT. Unexpectedly, overall MACE decreased in our cohort. This may reflect advancement in the identification and management of cardiovascular risk factors in LTRs. With projected continued increase in cardiac risk burden and the proportion of patients transplanted for NASH, it is critical for LT programs to develop and implement quality improvement efforts to improve cardiovascular care in LTRs.

SAT263

Retransplantation (reLT) outcomes of patients who were initially transplanted for ACLF

Gandhi Lanke¹, Feng Li¹, Paul J. Thuluvath^{1,2}. ¹Mercy Medical Center, Baltimore, United States; ²University of Maryland School of Medicine, Baltimore, United States
Email: thuluvath@gmail.com

Background and aims: The outcomes of early retransplantation (within 90-days of initial transplantation) of the liver (reLT) in those who initially underwent LT for acute on chronic liver failure (ACLF) are unknown.

Method: Using the national data from the United Network for Organ Sharing (UNOS) for all adult patients aged ≥ 18 years who were listed for LT in the United States from Jan 11, 2016, to Aug 31, 2020, we identified those who had reLT. We defined organ failure (OF) and graded ACLF as described by EASL-CLIF. The primary outcomes of interest were 3-month mortality and all-time mortality after reLT in those initially transplanted with or without ACLF. Kaplan Meier survival analysis was used to compare survival probabilities.

Results: During the study period, 100 ACLF and 299 non-ACLF patients underwent reLT, and of those 47 ACLF and 159 non-ACLF underwent reLT within 90 days of initial LT. The mean age of ACLF and non-ACLF patients who underwent reLT was 48.6 ± 12.5 and 52.8 ± 11.8 years, respectively ($p < 0.001$). Alcoholic liver disease was the predominant etiology in ACLF patients (58% vs. 24% in non-ACLF, $p < 0.001$). Respiratory (7% vs. 0%, $p < 0.001$) and circulatory (18% vs. 0%, $p < 0.001$) were more common at the time of reLT in the ACLF group compared to non-ACLF group. The overall survival rates in ACLF and non-ACLF groups who underwent reLT within 90 days were similar (72.3% vs. 75.5%, $p = 0.66$). However, patients with 3 or more organ failures ($n = 71$) at the time of reLT (reLT within 90 days of initial LT) had worse outcomes (63.4% vs. 80.7%, $p = 0.006$) compared to those

($n = 135$) with less than 3 organ failures (Figure 1A). Irrespective of the interval between initial LT and reLT (anytime reLT), the survival was lower (68.6% vs. 81.8%, $p = 0.008$) in those with 3 or more organ failures ($n = 86$) at the time of reLT than those ($n = 313$) with less than 3 organ failures (Figure 1B). On multivariable logistic regression analysis, respiratory failure, circulatory failure, and ACLF grade were independent predictors of survival after reLT.

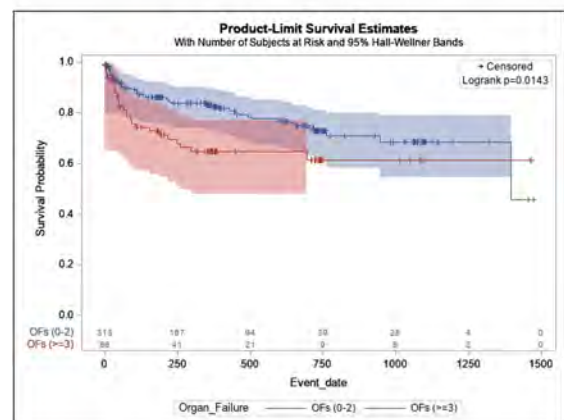
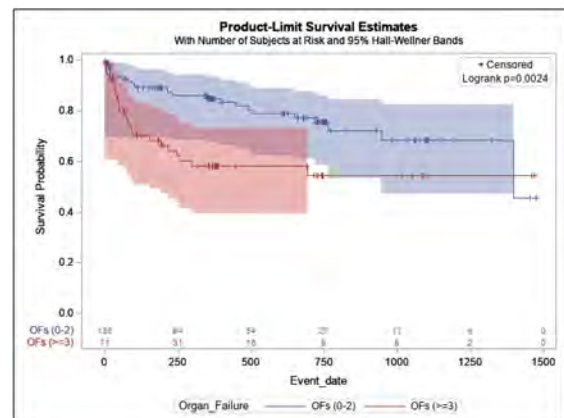


Figure 1: (A) KM survival curves after reLT (within 90 days of initial LT) in those with 0–2 OFs and ≥ 3 OFs at reLT. (B) KM survival curves after reLT (anytime reLT) in those with 0–2 OFs and ≥ 3 OFs at reLT.

POSTER PRESENTATIONS

Conclusion: This large study showed that the post-LT survival outcomes after early or late reLT in patients initially transplanted with ACLF are excellent. Three or more organ failures at the time of reLT were associated with relatively poor outcomes.

SAT264

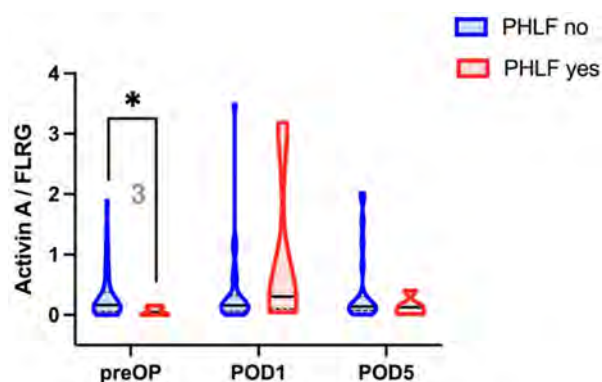
The ratio of Activin A and Follistatin-related gene allows prediction of posthepatectomy liver failure and postoperative morbidity in patients prior to liver surgery

Jonas Santol^{1,2}, David Pereyra², Steffanie Haegele², Daphni Ammon², Anita Pirabe¹, Philipp Jonas³, Stefan Schuster², Sarang Kim², Toni Nguyen², Thomas Grünberger³, Alice Assinger¹, Patrick Starlinger². ¹Medical University of Vienna, Physiology and Pharmacology, Wien, Austria; ²Medical University of Vienna, General Surgery, Wien, Austria; ³Klinik Favoriten, General Surgery, Wien, Austria
Email: jonas.santol@gmail.com

Background and aims: Even though outcome after hepatic resection has improved, patient outcome is significantly worse if posthepatectomy liver failure (PHLF) develops. With no causal treatment available, research focusing on the prediction of PHLF and elucidating its potential causes, is of great importance. Here, we evaluate the predictive potential for PHLF of Activin A and its inhibitory protein Follistatin-related gene (FLRG) and examine their involvement in the development of PHLF.

Method: Activin A and FLRG were measured in plasma of 59 patients undergoing liver resection using commercially available ELISA kits. Plasma was prepared from blood taken prior to the operation (preOP), as well as on the first and fifth postoperative day (POD). Postoperative outcome was prospectively documented.

Results: We saw a significant decrease in plasma for Activin A and FLRG from preOP to POD1 ($p=0.045$ and $p=0.005$, respectively). Subsequently FLRG increased from POD1 to POD5 ($p=0.004$). Interestingly, neither activin A nor FLRG differed between patients with and without PHLF at any timepoint. However, the ratio of Activin A/FLRG was significantly higher in patients without PHLF preOP ($p=0.037$). There was no perioperative dynamic for Activin A/FLRG. PreOP Activin A, FLRG and Activin A/FLRG did not differ between patient in the context of underlying malign or benign liver primary or in the context of low-grade (grade 0–1) or high-grade (grade 2–4) fibrosis. Using Receiver operating curve analysis, we aimed to further investigate the predictive potential of preOP Activin A/FLRG for PHLF. The Activin A/FLRG ratio was able to significantly predict postOP PHLF (Area under the curve = 0.789, $p=0.038$, 95%-CI: 0.609–0.969). Using the median of Activin A/FLRG ratio values, we further divided the cohort in a high and low Activin A/FLRG ratio group. When comparing the 2 groups, we could identify all patients with postOP PHLF in the low Activin A/FLRG ratio group, with none of the patients in the high Activin A/FLRG ratio group developing PHLF (5 of 21 [23.8%] vs 0 of 21 [0.0%], $p=0.017$). Further, patients in the low Activin A/FLRG ratio group were found to suffer from a significantly higher risk for postoperative morbidity (14 of 21 [66.7%] vs 5 of 21 [23.8%], $p=0.005$).



Conclusion: While the circulating dynamics of activin A and FLRG showed no association with PHLF, the preOP ratio of Activin A/FLRG was significantly decreased in patients suffering from PHLF. While further research into the pathophysiology behind these results is needed, Activin A and the ratio of Activin A/FLRG show potential as possible predictors of PHLF and Morbidity.

SAT265

Derivation of a cardiac risk index for use in liver transplantation for non-alcoholic steatohepatitis

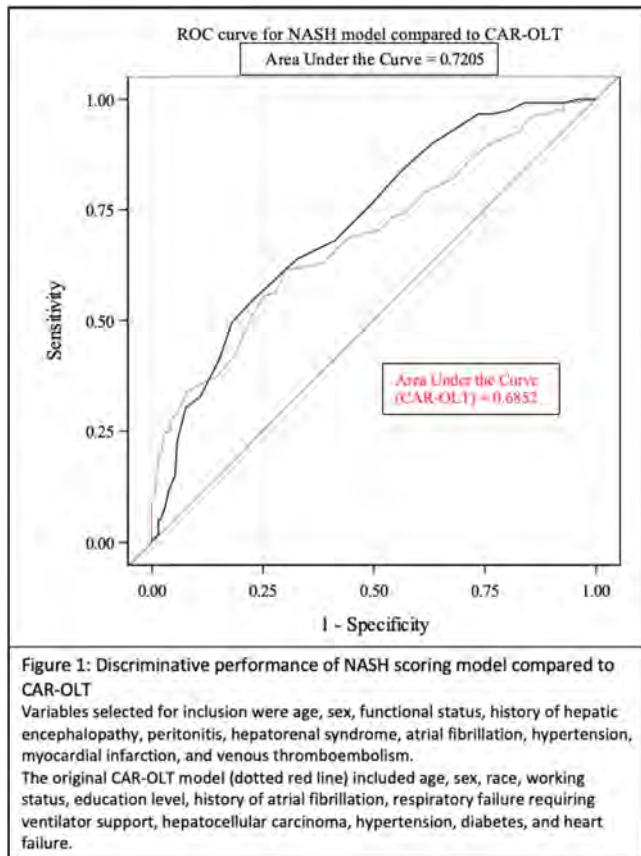
Paul Levy¹, Claire Harrington¹, Elizabeth Cabrera¹, Jing Gao¹, Dyanna Gregory¹, Cynthia Padilla¹, Gonzalo Crespo¹, Lisa VanWagner¹. ¹McGaw Medical Center of Northwestern University, Internal Medicine, Chicago, United States
Email: paul.levy@northwestern.edu

Background and aims: Cardiovascular events (CVEs) are the most common cause of early mortality after liver transplant (LT). LT candidates with non-alcoholic steatohepatitis (NASH) are at highest risk for CVEs. The Cardiovascular Risk in Orthotopic LT (CAR-OLT) score quantifies risk for post-LT CVEs, but its accuracy in LT candidates with NASH is unknown. We propose a new prediction model for risk of CVEs among NASH LT candidates and compare its performance to the CAR-OLT score.

Method: All adults who underwent first LT at a large United States urban transplant center (2/1/2002–12/31/2020) were included. Data were drawn from the Organ Procurement and Transplant Network (OPTN) and linked to data from the electronic health record. Primary outcome was 1-year CVE, defined as death from a CV cause or hospitalization for myocardial infarction (MI), cardiac revascularization, heart failure, atrial fibrillation (AF), cardiac arrest, and/or stroke. NASH was identified based on OPTN primary or secondary listing diagnosis for LT or cryptogenic cirrhosis plus metabolic syndrome comorbidity. All pre-LT variables with $p \leq 0.15$ on bivariate analysis were considered for model inclusion. Akaike Information Criterion was used for model selection using backward selection. Receiver operating curve analysis was used to compare model discrimination.

Results: Among 1788 LT recipients, 330 (18.5%) were listed for NASH. Of these, 115 (34.9%) had 1 year CVE. Variables included in the final model were pre-LT recipient age, sex, functional status, hepatic encephalopathy, peritonitis, hepatorenal syndrome, MI, AF, hypertension, and venous thromboembolism. Only age, sex, history of AF and hypertension were shared risk factors within the CAR-OLT score. The discriminative performance of the new point based score (C statistic = 0.72) was superior to the CAR-OLT score (C statistic = 0.69) for 1-year post-LT CVEs in candidates with NASH (Figure 1).

Conclusion: Patients being considered for LT for NASH cirrhosis have a unique cardiovascular risk profile not captured by existing risk prediction models. This study proposes a novel point based risk prediction tool to guide future cardiac risk stratification in patients with NASH cirrhosis being considered for LT.



SAT266

The prognostic effect of adequate lymphadenectomy in clinically node-negative patients undergoing liver resection for intrahepatic cholangiocarcinoma

Carlo Sposito^{1,2}, Marianna Maspero¹, Francesca Ratti³, Elena Panettieri⁴, Stefano Di Sandro⁵, Fabrizio Di Benedetto⁵, Felice Giuliani⁴, Luca Aldrighetti³, Vincenzo Mazzaferro^{1,2}

¹Fondazione IRCCS Istituto Nazionale Tumori di Milano, HPB surgery and Liver Transplantation, Milano, Italy; ²University of Milan, Oncology and Hemato-Oncology, Milano, Italy; ³Ospedale San Raffaele, Hepatobiliary Surgery Division, Milano, Italy; ⁴Fondazione IRCCS Policlinico Gemelli, General and HPB Surgery, Roma, Italy; ⁵Policlinico di Modena, HPB Surgery and Liver Transplant Unit, Modena, Italy
Email: carlo.sposito@istitutotumori.mi.it

Background and aims: The prognostic effect of lymphadenectomy (LND) in the surgical treatment of intrahepatic cholangiocarcinoma (iCC) with no clinical evidence of lymph-node metastases (clinically node-negative, cN0) is still a matter of debate. The aim of this study is to assess the role of lymphadenectomy in cN0 iCC, and which patients might benefit most.

Method: Consecutive patients who underwent surgery for cN0 iCC at four Italian Centers between 2000 and 2020 were included. A multivariate analysis for factors associated with overall survival (OS) was performed. The cohort was divided into two groups according to LND adequacy, defined as at least 6 excised nodes, and survival analysis was carried out. An analysis of the subgroups of patients that benefited the most from LND was also performed.

Results: Out of 818 surgically resected iCC patients, 632 were cN0. In this cohort, 359 (57%) patients received adequate LND (AD-LND

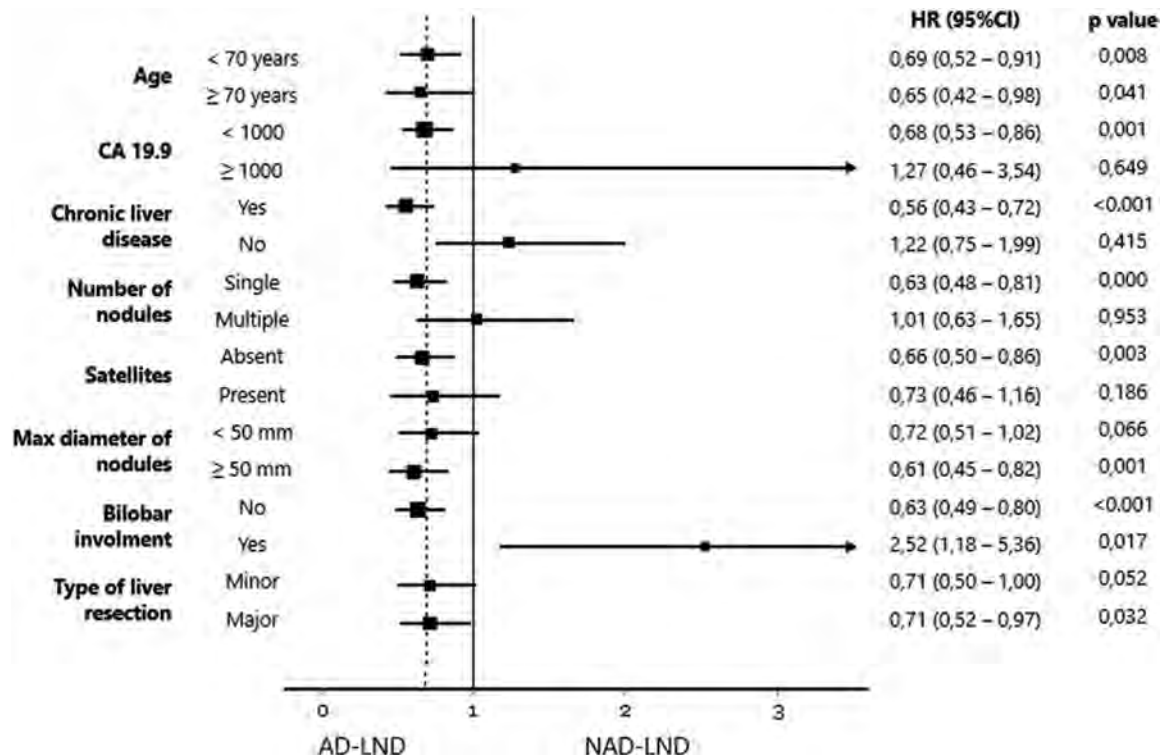


Figure: (abstract: SAT266)

POSTER PRESENTATIONS

group). Patient who did not receive adequate lymphadenectomy (NAD-LND group) were more likely to have an underlying chronic liver disease, a multifocal ICC and have received a major hepatectomy. Length of hospital stay, 90-day morbidity and mortality were comparable between the two groups. The AD-LND group had a higher number of patients with positive LNs at pathology (46% vs 15%, $p < 0.001$).

With a median follow-up of 57 months, OS and recurrence free survival (RFS) were significantly higher in the AD-LND vs. NAD-LND group (5-year OS 53.8% vs. 41.3%, $p < 0.001$; 5-year RFS 51.8% vs. 35.8%, $p < 0.001$). At multivariable analysis, NAD-LND was independently associated with worse OS together with CA19.9 > 120 , major hepatectomy, multifocal disease, grading > 2 , macrovascular invasion, and presence of positive lymph nodes at histology.

As shown in Figure 1, patients with age < 70 , single nodule or size > 50 mm benefit most from AD-LND. Vice versa, in patients with cirrhosis or satellitosis or Ca19.9 > 1000 , AD-LND did not seem to provide a survival advantage.

Conclusion: Adequate LND is associated with improved outcomes after surgical resection for ICC in patients with no preoperative evidence of lymph-nodal metastases. AD-LND does not seem to provide a survival advantage in patients with advanced disease or cirrhosis.

SAT267

Impact of MELD 3.0 Versus MELD-Na in patients with renal dysfunction

Allison Kwong¹, Ajitha Mannalithara¹, W. Ray Kim¹. ¹Stanford University, Gastroenterology and Hepatology, Redwood City, United States

Email: allison.kwong@gmail.com

Background and aims: MELD 3.0 is a proposed model that improves upon MELD-Na, incorporating sex and albumin as additional variables, updating existing coefficients and adding relevant interactions, and resetting the upper bound of serum creatinine to 3.0 from 4.0 mg/dL. This analysis evaluates the impact of replacing MELD-Na with MELD 3.0 on waitlist priority among patients with advanced renal dysfunction.

Method: New adult waitlist registrations for liver transplantation from June 15, 2016 to June 30, 2021 were identified using OPTN data. MELD, MELD-Na, and MELD 3.0 scores from registration were calculated by the following equations:

$MELD = 9.57 \times \log_e(\text{creatinine}) + 3.78 \times \log_e(\text{bilirubin}) + 11.20 \times \log_e(\text{INR}) + 6.43$;

$MELD-Na = MELD + 1.32 \times (137 - Na) - [0.033 \times MELD \times (137 - Na)]$;

$MELD\ 3.0 = 1.33$ (if female) $+ 4.56 \times \log_e(\text{bilirubin}) + 0.82 \times (137 - Na) - 0.24 \times (137 - Na) \times \log_e(\text{bilirubin}) + 9.09 \times \log_e(\text{INR}) + 11.14 \times \log_e(\text{creatinine}) + 1.85 \times (3.5 - \text{albumin}) - 1.83 \times (3.5 - \text{albumin}) \times \log_e(\text{creatinine}) + 6$.

Differences between MELD-Na and MELD 3.0 were evaluated by sex and serum creatinine at listing.

Results: There were 68, 111 new waitlist registrations for liver transplantation during the study period. The median serum creatinine at listing was 1.0 (IQR 0.7–1.5), with 1439 (2.1%) of listings with creatinine between 3 and 4 mg/dL and 6369 (9.4%) receiving maximum points for being on dialysis. On average, MELD 3.0 added 1.47 points for women and 0.14 for men compared to MELD-Na. For patients where the initial creatinine was between 3 and 4 mg/dL, MELD 3.0 added an average of 1.66 points for women and 0.50 for men compared to MELD-Na, whereas for patients on dialysis, MELD 3.0 added 0.16 points for women and subtracted 1.14 for men. Compared to MELD-Na, MELD 3.0 reduced the maximum number of potential creatinine-derived points from 13 to 12.

Conclusion: The MELD 3.0 scoring system increases the weight of the serum creatinine and thus the calculated MELD for patients with renal dysfunction – but not those with $Cr \geq 4$ mg/dL or dialysis. If implemented in liver allocation, MELD 3.0 may increase waitlist priority for patients with acute kidney injury (e.g. hepatorenal syndrome); earlier access to liver transplant for this population could improve post-transplant renal outcomes including the need for kidney transplant.

SAT268

Sustainability of humoral immunity induced by the SARS-CoV-2 vaccine and response to booster dose among Liver Transplant recipients

Liane Rabinowich¹, Ayelet Grupper², Inbal Houry³, Sharon Levy³, Merav Ben-Yehoyada³, Tami Halperin⁴, Oren Shibolet³, Helena Katzman³. ¹Tel-Aviv Sourasky Medical Center, Department of Gastroenterology and Hepatology, Tel Aviv, Israel; ²Tel-Aviv Sourasky Medical Center, Nephrology Department, Tel Aviv, Israel; ³Tel-Aviv Sourasky Medical Center, Department of Gastroenterology and Hepatology, Tel Aviv, Israel; ⁴Tel-Aviv Sourasky Medical Center, Department of infectious diseases, Tel Aviv, Israel

Email: lianer@tlvmc.gov.il

Background and aims: Liver Transplant (LT) recipients were among the first to receive the BioNTech-BNT162b2 SARS-CoV-2 vaccine, with preliminary data indicating reduced humoral response compared to the general population. Our aim was to assess immunogenicity to the SARS-CoV-2 vaccine, durability over time and response to a third booster dose.

Method: LT recipients followed at the Tel-Aviv Sourasky Medical Center and healthy volunteers were tested for SARS-CoV-2 IgG antibodies against the Spike-protein (S) and Nucleocapsid-protein (N) at four time points: 10–20 days after the second Pfizer-BioNTech BNT162b2 SARS-CoV-2 vaccine dose, after 3 months follow-up, prior to (6 months follow-up) and 10–20 days after a third booster dose.

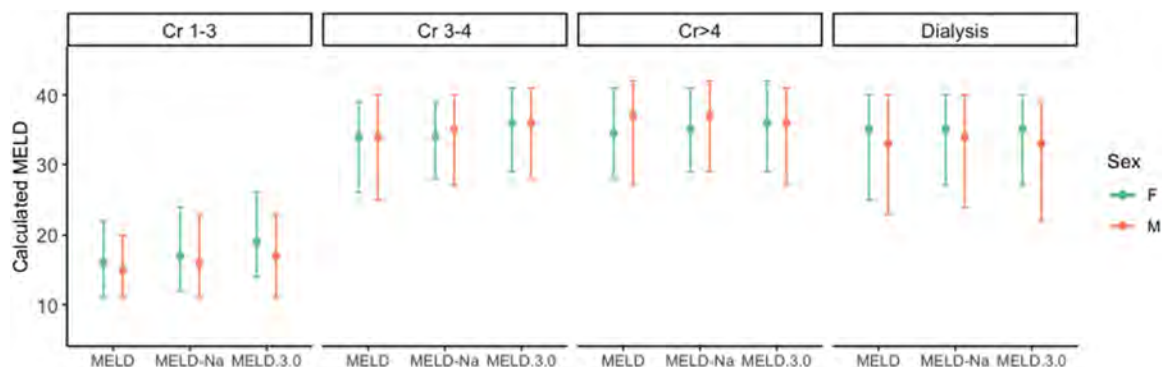


Figure: (abstract: SAT267): Median and interquartile range of calculated MELD using each scoring system (MELD, MELD-Na, and MELD 3.0), stratified by creatinine at listing and sex.

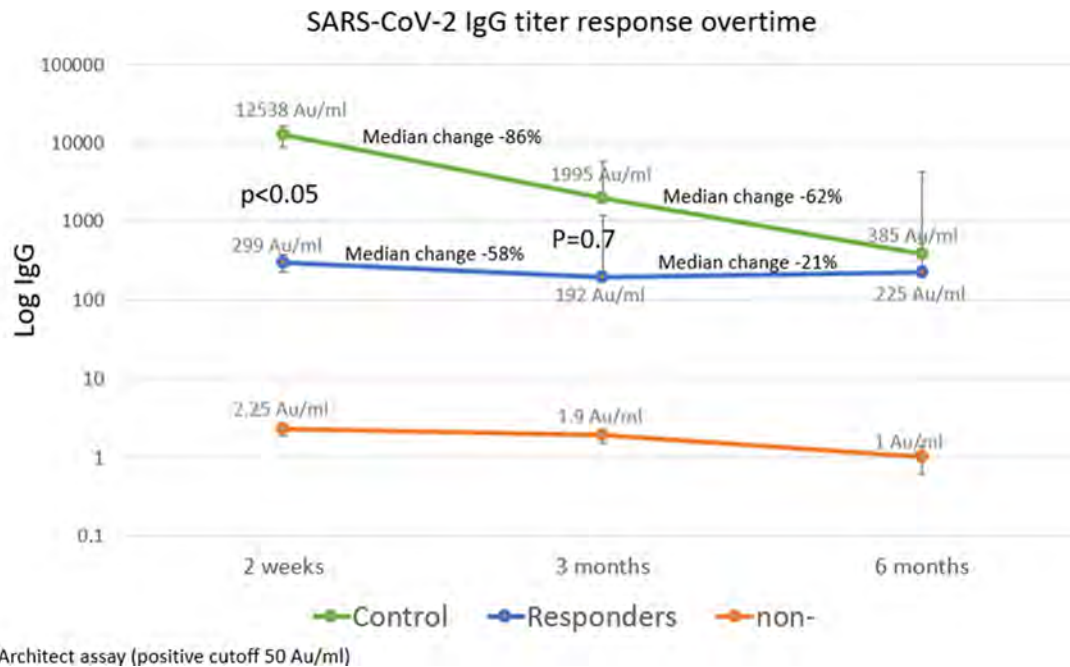


Figure: (abstract: SAT268)

Information regarding vaccine side effects and clinical data was collected from patients and medical records.

Results: Following the second vaccine dose, immunogenicity among 80 LT recipients was significantly lower compared to the control group, with positive serology in 52% compared to 100% among controls ($p < 0.001$). Antibody titer was also significantly lower among LT recipients (median 368.3 AU/ml vs. 12,538 AU/ml in controls, $p < 0.001$). After 3 months follow-up, the antibody titer declined by 58% among LT compared to 86% decline in the controls (median titer 192 AU/ml vs 1,995 AU/ml, $p = 0.7$). By 6 months the titers decreased by 21% and 62% in the LT and controls, respectively (median titer 225 AU/ml vs 385 AU/ml). Following a third dose given to 61 LT recipients received a third booster dose positive response rate increased to 85%. The median antibody titer significantly increased in both groups, but remained lower in LT recipients (3,542 AU/ml vs. 28,358 AU/ml among controls). Predictors for negative response among LT recipients were older age, lower eGFR, and treatment with high dose steroids and MMF.

Conclusion: LT recipients are at risk for lower humoral response to Pfizer-BioNTech SARS-CoV-2 mRNA based vaccine. The decline overtime is lesser in comparison to the general population. A booster dose was able to increase the response rate significantly, although antibody titers remained lower in comparison to control.

SAT269

Acute-on-chronic liver failure due to severe intrahepatic vaso-occlusion and recurrence of the initial disease: 2 major features in liver transplantation for severe sickle-cell-related hepatopathy

Christophe Duvoux¹, Francky Mubenga², Jean Jacques Matimbo¹, Lorraine Blaise³, Eric Levesque⁴, Jean Claude Merle⁵, Norbert Ngongang⁶, Justine Gellen-Dautremer⁷, Maryvonnick Carmagnat⁸, Frederic Galacteros⁹, Daniel Cherqui¹⁰, Vincent Leroy⁶, Alexis Laurent¹¹, Anoosha Habibi⁹, Pablo Bartolucci⁹.
¹Henri Mondor Hospital APHP, Paris Est University, Medical Liver Transplant Unit, liver Unit, Créteil, France; ²Agence Régionale de Santé, Guyenne, Cayenne, France; ³Avicenne University Hospital, Liver Department, Bobigny, France; ⁴Henri Mondor Hospital APHP, Paris Est University, Anesthesiology and Intensive Care, Créteil, France; ⁵Henri Mondor Hospital APHP, Paris Est University, Department of Anesthesiology and Intensive Care, Créteil, France; ⁶Henri Mondor Hospital APHP, Paris Est University, Medical Liver Transplant Unit, liver Unit, Créteil, France; ⁷Poitiers University Hospital, Internal Medicine, Poitiers, France; ⁸Saint Louis University Hospital, Immuno Histocompatibility Laboratory, Paris, France; ⁹Henri Mondor Hospital APHP, Paris Est University, Red Cells Genetic Disorders Unit, Créteil, France; ¹⁰Paul Brousse Hospital, Centre Hépatobiliaire, Villejuif, France; ¹¹Henri Mondor Hospital APHP, Paris Est University, Department of Digestive Surgery, Créteil, France
 Email: christophe.duvoux@aphp.fr

Background and aims: The prognosis of severe sickle cell disease hepatopathy (SCDH) is dismal. Liver transplantation (LT) can be a salvage option but the worldwide experience, less than 70 reported LTs, is very limited and results controversial. The aim of this study was to describe presentation patterns and outcomes of LT for severe SCDH in a reference center for sickle cell disease.

Method: 24 patients, 16 men and 8 women, median age 37.4 years, transplanted between 1992 and 2020 were studied. Data on complications and management of SCD before LT, patterns of SCDH, liver explants, and post-LT outcomes were reviewed.

Results: SCD was SS, SC and S/β thal in 62, 8 and 30% of cases. The indications for LT were.

ACLF in 14 (58%) cases, triggered by severe intrahepatic vaso-occlusive (VOC).

POSTER PRESENTATIONS

in 11/14 (78.5%) cases, severe acute liver failure (ALF) in 5 cases, due to massive VOC in 4 cases and autoimmune hepatitis in 1 case. Five patients were transplanted electively: cirrhosis without ACLF in 3 cases (12.5%) (HCV 2, alcoholic hepatitis on cirrhosis 1), sclerosing cholangitis (SC) (8.5%) in 2 cases, with mild intrahepatic vaso-occlusive injury in 3 cases. Among patients with ACLF, 3 patients were ACLF grade 2, and 9 (64%) grade 3, with a median number of organ failures of 3; the underlying liver disease consisted of chronic SCD-related liver hepatopathy in 11/14 cases (71.5%).

The median MELD score at LT was 37.4, reaching 40 in ACLF patients. Median bilirubin was 700, 553, and 293 $\mu\text{mol/L}$, in ACLF, ALF and elective patients, respectively. 16 patients (67%) received induction immunosuppression. The incidence of acute cellular rejection was 13%. Six patients (25%) developed serious neurological complications (seizures 4 and/or PRES syndrome 3). Postoperative mortality was 0, 20% and 30% in elective patients, ALF and ACLF. The 5-year overall survival was 63%, ranging from 100% in elective patients to 60 and 50% in patients transplanted in ALF and ACLF. With a median post LT Fu of 6.4 years, a liver biopsy was performed in 10/19 patients beyond the 3rd month post LT because of liver lab tests suggestive of rejection. The recurrence of VOC injury was observed in 8/10 cases, significant graft fibrosis, F2/F3, in 4 cases (HCV 1 case). Recurrent SCD vaso-occlusive injury in the graft justified a preventive strategy combining transfusion exchanges and/or hydroxurea, with HbS target <30%.

Conclusion: This largest worldwide series of LT for SCDH shows that severe intrahepatic VOC causes ALF or ACLF in 75% of cases. Associated organ failures account for results inferior to those observed in other indications. In this rare indication, LT was associated with a reasonable 60% 5-year survival yet, transforming the prognosis of severe SCDH. LT should therefore be considered in expert multidisciplinary centers as a treatment option for SCDH. Identification of ACLF patients at high risk of post-operative death should be improved.

SAT270

Post-operative complications and short-term survival in obese cirrhotic patients undergoing liver transplantation

Javier Tejedor-Tejada¹, Carmen Alonso Martín¹, Samuel Juan Fernández Prada¹, Laura Juan¹, Violeta Mauriz², Abdelaleem Helal³, Rifaat Safadi⁴, Esteban Fuentes Valenzuela¹, Carolina Almohalla¹, Félix García Pajares¹. ¹Hospital Universitario Río Hortega, Department of Gastroenterology, Hepatology and Liver Transplantation Unit, Spain; ²Complejo Hospitalario Universitario de Santiago de Compostela, Department of Gastroenterology, Spain; ³National Liver Institute, Menoufia University, Hepatology and Gastroenterology Department, Egypt; ⁴Hadassah Medical Organization, Hadassah Hebrew University Medical Centre, The Liver Unit, Israel Email: jtejedor1991@gmail.com

Background and aims: Obesity is considered a risk factor for perioperative complications, but its effect on patients undergoing liver transplantation (LT) remains unclear. This study was conducted to analyze the impact of the body mass index (BMI) on morbidity and mortality risk following LT.

Method: A multicenter study of outcomes in patients submitted to LT between 2001 and 2019. Recipients were stratified in obese (BMI $\geq 30 \text{ kg/m}^2$) and non-obese patients (BMI <30 kg/m^2). The following exclusion criteria were considered: Patients with no BMI available, refractory ascites, polycystic liver disease or multiorgan transplantation. Post-LT outcomes and 1-year patient and graft survival were compared.

Results: A total of 1410 patients were included in the study, non-obese (989, 70.1%) and obese patients (421, 29.9%). There were not significant differences in Charlson comorbidity score, race, MELD, waiting time, total ischemia time, length of stay, ICU stay (Table 1). The rate of postoperative vascular and biliary complications were significantly higher in the obese recipients (23.3%, p 0.015 and 36.6%,

$p < 0.01$) versus the non-obese recipients (17% and 27.1%). There was a significantly increased risk for long-term graft failure. However, There was no difference in patient survival after LT.

	Non-obese N= 989	Obese N= 421	P value
Sex (male/female)	745/244	337/84	$P= 0.063$
Age (years), mean (SD)	53.9 (10.4)	55.4 (8.8)	$P= 0.012$
BMI (kg/m^2), mean (SD)	25.1 (3.1)	33.6 (3.2)	$P < 0.001$
Waiting list (days), mean (SD)	134 (323)	141 (345)	$P= 0.718$
Charlson comorbidity score, mean (SD)	2.4 (1.3)	2.7 (1.3)	$P= 0.803$
MELD score, mean (SD)	16.02 (6.7)	16.76 (6.6)	$P= 0.884$
Total ischemia time (minutes), mean (SD)	445.7 (136.5)	446.7 (142.8)	$P= 0.909$
Vascular complications (%)	168 (17%)	98 (23.3%)	$P= 0.015$
Biliary complications (%)	268 (27.1%)	154 (36.6%)	$P= 0.002$
Infectious complications (%)	257 (26%)	130 (30.9%)	$P= 0.171$
Postoperative bleeding (%)	121 (12.2%)	59 (14%)	$P= 0.517$
Ischemia-Reperfusion-Injury (%)	156 (15.7%)	47 (11.2%)	$P= 0.08$
Primary graft non-function (%)	91 (9.2%)	31 (7.4%)	$P= 0.041$
Acute rejection (%)	96 (9.7%)	54 (12.8%)	$P= 0.178$
Death			
• < 30 days	76 (7.7%)	33 (7.8%)	$P= 0.251$
• < 1 year	111 (12%)	46 (11.8%)	$P= 0.505$
Graft dysfunction			
• < 30 days	58 (6%)	27 (6.5%)	$P= 0.404$
• < 1 year	84 (9.7%)	53 (14%)	$P= 0.016$

Conclusion: Obese patients have significantly increased morbidity in terms of vascular and biliary complications after LT. They have a higher risk for worse 1-year graft survival in comparison to controls.

SAT271

Impact of comorbidities on liver transplantation: a prospective and multicentric study

Trinidad Serrano¹, Sergio Sabroso², Luis M. Esteban³, Miguel Ángel Gómez Bravo⁴, Pablo Ruiz⁵, Rosa Martín-Mateos⁶, Alejandra Otero Ferreiro⁷, Francisco Javier Bustamante Schneider⁸, Sonia Pascual⁹, Carolina Almohalla¹⁰, Marta Guerrero¹¹, Itxarone Bilbao¹², Valle Cadahía-Rodrigo¹³, Ángel Rubín¹⁴, Luis Cortes García¹, Elena Oton¹⁵, Ana Arias¹⁶, Esther Molina¹⁷, Urszula Ewa Gajownik¹⁸, Jose Ignacio Herrero¹⁹, Magdalena Salcedo²⁰. ¹Hospital Clínico Universitario Lozano Blesa, Zaragoza, Spain; ²National Cancer Research Center, Madrid, Spain; ³Escuela Universitaria Politécnica de la Almunia, Matemáticas aplicadas, Zaragoza, Spain; ⁴Hospital Virgen Del Rocío, Sevilla, Spain; ⁵Clinic, Barcelona, Spain; ⁶Hospital Ramón y Cajal, Madrid, Spain; ⁷Coruña University Hospital, A Coruña, Spain; ⁸Hospital Universitario Cruces, Barakaldo, Spain; ⁹General University Hospital of Alicante, Alacant, Spain; ¹⁰Río Hortega University Hospital, Valladolid, Spain; ¹¹Hospital Universitario Reina Sofía, Córdoba, Spain; ¹²Hospital Universitari Vall d'Hebron, Barcelona, Spain; ¹³Central University Hospital of Asturias, Oviedo, Spain; ¹⁴La Fe University and Polytechnic Hospital, Valencia, Spain; ¹⁵Hospital Universitario de Canarias, San Cristóbal de La Laguna, Spain; ¹⁶Puerta de Hierro Majadahonda University Hospital, Majadahonda, Spain; ¹⁷Santiago Clinic Hospital CHUS, Santiago de Compostela, Spain; ¹⁸Parking Hospital Virgen De La Arrixaca, Murcia, Spain; ¹⁹Clinica Universidad de Navarra, Pamplona, Spain; ²⁰Gregorio Marañón Hospital, Madrid, Spain Email: tserrano.aullo@gmail.com

Background and aims: Comorbidity plays an important role in the mortality of patients both on the waiting list and after liver transplantation (LT). To analyze the impact of comorbidities on LT, a prospective and multicentre study (HEPA_TIC) has been launched and the preliminary results are presented here.

Method: Analysis of 996 consecutive patients included in LT waiting list, in 18 Spanish hospitals, from October 2019 to October 2021. Retransplantation, multivisceral transplantation and patients younger than 16 years were excluded. Comorbidities at the time of

listing, and follow-up variables were collected. The analysis of comorbidities was disaggregated by sex.

Results: Patients were predominantly male (77.2%) with a median age of 61 years IQR (56–66); 60 years in females IQR (54–66) and 61 in males (56–66) ($p = n.s$). Median follow-up was 7.9 months IQR (4.9–12.1). Decompensated cirrhosis was the most frequent indication with no differences in both sexes. Hepatocellular carcinoma was significantly more frequent in males (45.9% vs. 24.6%; $p < 0.001$). The most frequent comorbidities were diabetes and arterial hypertension. Diabetes, chronic obstructive pulmonary disease and cardiovascular disease were significantly higher in men ($p < 0.05$), while chronic kidney disease was higher in women ($p < 0.05$). Only 11.7% of the listed patients had no comorbidities. The number of comorbidities was higher in males than in females ($p < 0.001$). 20.3% of the listed men and 15.1% of the women had more than three comorbidities. During follow-up, 4.8% of females and 2.5% of males died on the waiting list. Comorbidity was the cause of 13.3% of these deaths. In our cohort, 735 patients were transplanted during follow-up. Among all analyzed variables, only hyperuricemia was associated with a decrease in intention-to-treat survival ($p = 0.02$). Also, the presence of more than four comorbidities was related to a lower survival, although it did not reach statistical significance ($p = 0.07$).

Conclusion: Comorbidities are highly prevalent in patients with liver disease on the LT waiting list and are the second leading cause of waiting list mortality. Hyperuricemia is the only comorbidity associated with lower survival, although further follow-up is needed to determine the impact of other comorbidities on survival.

SAT272

Liver transplant patients infection rate with SARS-CoV-2 is lower but depend upon the infection rate in the general population and have a better outcome

Michal Cohen-Naftaly¹, Evelin Oxtrud¹, Orly Sneh Arbib¹, Assaf Issachar¹, Yael Harif¹, Amir Shlomai¹, Marius Braun¹. ¹Rabin Medical Center, Liver Institute, Israel
Email: michal_c_n@yahoo.com

Background and aims: Conflicting results regarding the susceptibility to SARS-Cov2 infection and outcome in liver transplant (LT) patients (pts) were reported. Israel adopted early active policies to control the epidemic. Initially of severe travel restrictions and social distancing were enforced, followed by a lockdown. The relaxation of the restrictions led to 2 more severe waves, which triggered 2 new

lockdowns. Israel was the first in the world to begin immunization with BNT162b2 on 20.12.2020, prioritizing first the elderly and immune compromised and rapidly extending to vaccination of the whole adult population. A fourth wave triggered the administration of booster doses in the same order. Guidelines encouraging social distancing, hygiene, and vaccination were disseminated to our pts and active follow-up was maintained using tele medicine. The immune suppression was not changed.

To assess the pattern of COVID19 pandemic among LT pts followed at Rabin Medical Center, compared to the general population in Israel.

Method: Retrospective study from 2019 to 2021. Demographic data on 420 LT pts were collected from the electronic medical records, immunosuppressive therapy, dates of vaccination with BNT162b2, antibody levels after vaccination, data on SARS-COV-19 infection, severity of the disease, treatments and outcome. The data were compared to data reported on the Ministry of Health website: number of those infected in Israel, the vaccination rate. Comparison according to the waves of eruptions in Israel: 1st wave 2–5.2020, 2nd wave 6–11.2020, 3rd 11.2020–4.2021 and 4th wave 6–10.2021. 20.12.2020.

Results: 41 LT pts were diagnosed with Covid-19 out of 420 LT pts followed up : prevalence of 9.7%, significantly less than the 14.53% reported for the whole population ($p < 0.05$).

There were 4, 6, 19 and 12 COVID-19 cases respectively in waves 1 to 4. In waves 3 and four the number a COVID-19 patients that received 1, 2 and 3 vaccine doses was 2, 10 and 3 respectively, vs 16 unvaccinated. The vaccinated pts were infected at a median of 167 and 27 days after the second and third vaccine, respectively. The risk of infection was proportional to the risk in the population. (Fig 1).

Seven patient were hospitalized and treated with steroids, 3 of them died. All the other patients had mild disease, two pts received monoclonal antibodies.

Three pts died from COVID-19 while 4 pts died of unrelated causes. There was no increase in the mortality of LT pts due to the COVID epidemic.

Conclusion: In our LT cohort the outcome of COVID-19 was better than reported in the literature regarding both morbidity and mortality. Our data indicate that despite the population vaccination and the increase in the antibody titer after the third vaccine, there is still a considerable risk for LT recipients to develop COVID19, which is affected by the infection rate in the general population and not the immunization rate.

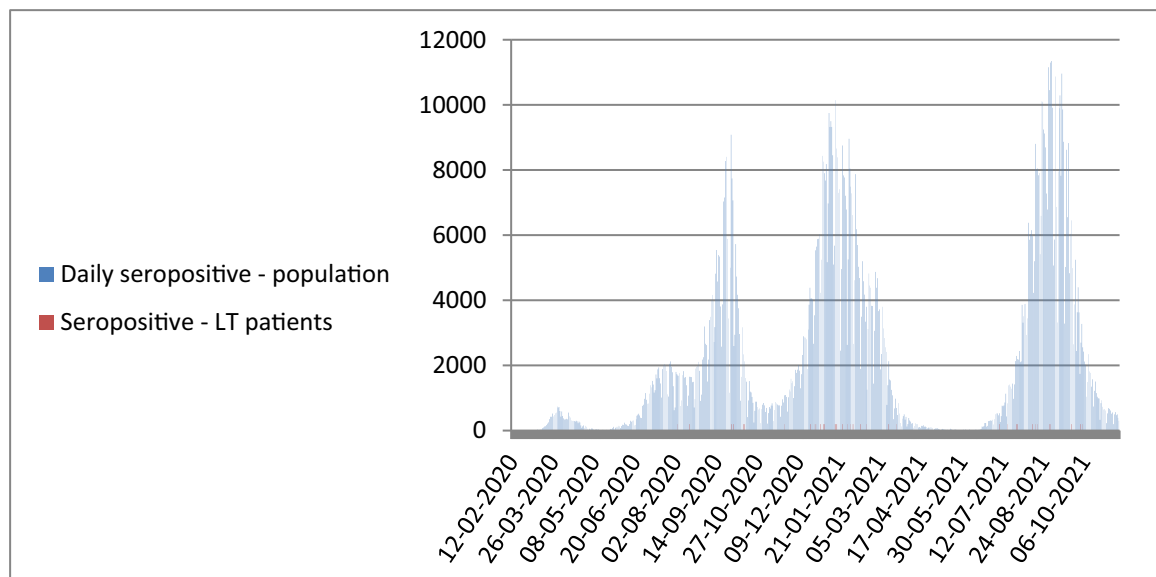


Figure: (abstract: SAT272)

SAT273

Sarcopenia predict complications after hepatic resection for primary hepatocellular carcinoma (HCC) in patients with advanced chronic liver disease (ACLD) and clinically significant portal hypertension (CSPH)

Federico Ravaioli¹, Giovanni Marasco¹, Elton Dajti¹, Vanessa Alemanni¹, Matteo Renzulli¹, Matteo Serenari¹, Matteo Ravaioli¹, Amanda Vestito¹, Giulio Vara¹, Davide Festi¹, Rita Golfieri¹, Matteo Cescon¹, Antonio Colecchia¹. ¹IRCCS Azienda Ospedaliero-Universitaria di Bologna, Department of Medical and Surgical Sciences, Bologna, Italy
Email: f.ravaioli@unibo.it

Background and aims: Patients with advanced chronic liver disease (ACLD) complicated by early-stage hepatocellular carcinoma (BCLC-O/A) are the best candidates for surgical liver resection. Despite the latest improvements in clinical management and surgical techniques, hepatic resection is burdened with an incidence of major complications (MC) and post-hepatectomy hepatic failure (PHLF) with significant perioperative mortality and morbidity. Sarcopenia assessed by measuring skeletal muscle index (SMI) was associated with a higher risk of waiting list mortality and worse outcome after transplantation in patients with ACLD. In the absence of data on the role of sarcopenia in the post-hepatectomy setting, we aimed to investigate the prognostic role of SMI on the incidence of PHLF and surgical complications in patients with ACLD in a third-level European referral centre.

Method: All patients with available preoperative abdominal CT performed 3 months before surgery who underwent hepatic resection for primary HCC enrolled consecutively from 2014 to 2019 were included. Sarcopenia was defined according to the definition endorsed by the EASL as SMI, as measured by CT-images, <50 cm²/m² in males and SMI <39 cm²/m² in females. Surgical complications were assessed according to the Clavien-Dindo classification. The diagnosis of PHLF was performed according to the International Study Group of Liver Surgery (ISGLS) definition.

Results: 159 patients underwent hepatic resection for primary HCC, within inclusion criteria were included in the final analyses. Sarcopenia was present in 82 patients (51.6%). The median SMI was 39.2 (35.7–42.4) cm²/m² and 48.9 (43–55.3) cm²/m² in female and male patients, respectively. SMI values were significantly correlated with age ($r = -0.229$, p value = 0.004) and BMI ($r = 0.369$, p value <0.0001), but not with the of liver disease severity, as assessed by liver stiffness, platelet count, or MELD score. During the 30-days postoperative observation, 13 (8.2%) patients developed MC and 48 PHLF (30.2%; 34 PHLF-A; 14 PHLF-B/C). Overall, the presence of sarcopenia was not independently associated with post-hepatectomy and PHLF complications; however, in the group of patients with clinically significant portal hypertension (CSPH), SMI was independently associated with MC and PHLF B/C (OR 0.889 [0.798–0.990]; p value 0.032). Indeed, the MC rate was significantly higher in patients with (16.3%) than in patients without (0%) sarcopenia ($p = 0.012$).

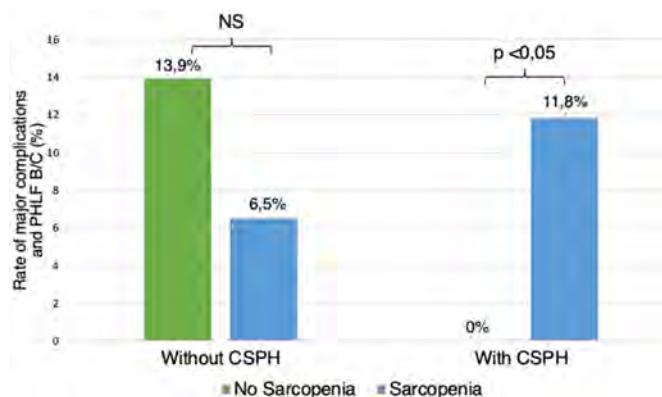


Figure:

Conclusion: The assessment of sarcopenia by SMI may aid physicians and surgeons in preoperative evaluation for hepatectomy for primary hepatocellular carcinoma in patients with advanced chronic liver disease complicated by clinically significant portal hypertension. However, further studies are still needed to evaluate the impact of perioperative nutritional and rehabilitation intervention.

SAT274

A comparison of hispanic living liver donor candidates approved and denied at a high-volume urban transplant center

Dana Toy¹, Brian Horwich¹, Ashwini Mulgaonkar¹, Ana Padilla², Jennifer Dodge^{3,4}, Navpreet Kaur^{2,5}, Hyosun Han^{1,2,4}. ¹University of Southern California, Medicine, Los Angeles, United States; ²University of Southern California, Transplant Institute, Los Angeles, United States; ³University of Southern California, Population and Public Health Sciences, Los Angeles, United States; ⁴University of Southern California, Gastrointestinal and Liver Diseases, Los Angeles, United States; ⁵University of Southern California, Surgery, Los Angeles, United States
Email: dana.toy@med.usc.edu

Background and aims: Hispanics account for 20% of candidates waiting for liver transplantation (LT). Although living donor LT is comparable to deceased donor LT, minorities receive a disproportionately low percentage of living donor LT. From 2018–2019, living donor LT increased by one-third, while percentage of Hispanic living donors decreased. This study aims to compare Hispanic living liver donor candidates who were approved versus declined by a multidisciplinary selection committee at a large urban transplant center.

Method: The Living Liver Donor Referrals Database was reviewed between December 1, 2017 and August 31, 2021 for donor applicants ($n = 195$) who (1) completed a questionnaire and clinic evaluation, (2) were presented at a multidisciplinary selection committee, and (3) were formally approved/declined to serve as living liver donors. Statistical analysis was performed using Student's t-test and chi-squared test.

Results: Of 1,689 living liver donor applicants, 11.5% ($n = 195$) were presented at a multidisciplinary selection committee. Half of those presented were approved (52.3%, $n = 102$), while the other half were declined (47.7%, $n = 93$). Hispanics who were approved ($n = 55$) and declined ($n = 47$) as living liver donor candidates had similar baseline demographics: mean age (34 v. 35 years, $p = 0.71$), mean body mass index (27.9 v. 28.8 kg/m², $p = 0.40$), female (61.8% v. 63.8%, $p = 0.83$). There was no significant difference in social history among Hispanics who were approved and declined: full time employment (62.3% v. 55.6%, $p = 0.50$), some college education (67.9% v. 68.9%, $p = 0.92$), married (47.2% v. 42.2%, $p = 0.62$), without alcohol use (20.6% v. 26.7%, $p = 0.49$). Both approved and declined Hispanic living liver donor candidates had nearly one-fourth who reported no medical insurance (28.3% v. 22.2%, $p = 0.49$) and no primary care doctor (25.5% v. 31.9%, $p = 0.47$). Hispanic living liver donor candidates were referred by intended transplant recipient or their friend/family (74.5% v. 83%, $p = 0.30$). Mean length of time from questionnaire to formal decision by a selection committee did not differ significantly when comparing approved and declined Hispanic candidates (165.4 v. 144.2 days, $p = 0.55$).

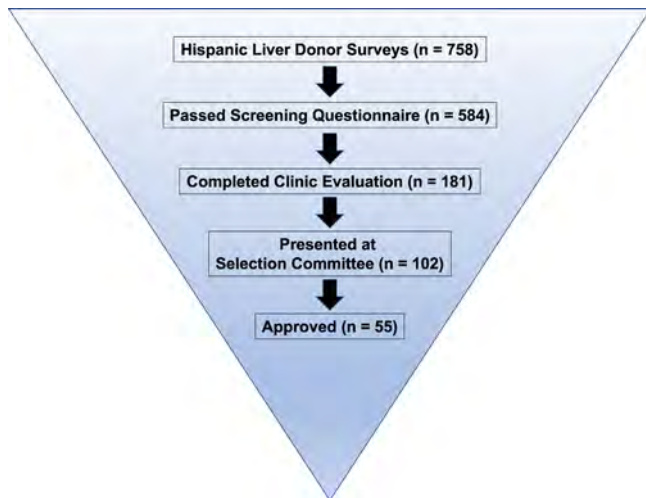


Figure: A schematic of the living liver donor evaluation process, which resulted in 55 approved Hispanic candidates.

Conclusion: The results of our study suggest that there is interest in living donor liver transplantation among Hispanics, given that nearly half (44.9%) of all living liver donor applicants were Hispanic. Our study suggests that the standard demographic and clinical data do not adequately capture factors that influence approval for living liver donor candidacy among Hispanics. There are ongoing efforts to establish comprehensive donor candidate registries that will better elucidate how the donor evaluation process may adapt to reduce racial and ethnic disparities in living donor LT.

SAT275

Liver transplantation in HIV infected subjects: a long-term single center experience

Gian Piero Guerrini¹, Noemi Gualandini², Giovanni Guaraldi³, Paolo Magistri¹, Stefano Di Sandro¹, Nicola De Maria², Fabrizio Di Benedetto¹. ¹Policlinico di Modena, Hepatic-Biliary-Pancreatic Surgery and Liver Transplantation, Modena, Italy; ²Policlinico di Modena, Gastroenterology, Modena, Italy; ³Policlinico di Modena, Infectious Diseases, Modena, Italy
Email: gualandinoemi@gmail.com

Background and aims: Liver diseases, especially cirrhosis and hepatocellular carcinoma (HCC), represent one of the leading causes of death among HIV positive patients. Nowadays, liver transplantation (LT) is a well accepted option for end-stage liver diseases in this category of patients. The aim of the present study was to analyze the results of LT performed in our center comparing the outcome in HIV-positive and negative patients, in particular in HCC LT recipients.

Method: All patients with/without HIV infection who underwent LTs in our center between 2001 and 2020 were considered in the study. Cox regression analysis was used to determine prognostic survival factors, survival was calculated according to Kaplan-Meier method and compared using the log rank test. A subgroup analysis was performed in LT patients with HCC.

Results: 928 LTs were performed between 2001 and 2020, 63 of them in HIV positive recipients. HIV positive patients were younger than HIV negative (49.4 ± 6.6 yrs vs 53.3 ± 10.3 , $p = 0.001$) while no difference was seen regarding MELD score at the time of LT (19 ± 9 vs $19, 1 \pm 9.4$). The mean follow-up was 58 ± 55 months. Five years overall survival in LT recipients HIV positive and negative was 65.3% and 72.7%, respectively ($p = ns$), whereas 5-year graft survival was 65% and 73.2% ($p = ns$). An improvement in survival was recorded in the second period of the study in the HIV-infected group, being 5 yrs survival 46.9% in Era I (2003–2011) and 80.6 in Era 2 (2012–2020, $p < 0.001$). The independent predictive factors of survival in the HIV infected group were: age of the donor (HR 1.07 $p = 0.021$), HCV-RNA

detectable at time of transplant (HR 19.3 $p = 0.011$) and first Era of LT 2001–2010 (HR 12.7 $p = 0.024$). A total of 420 patients underwent LT for HCC, 34 of them were HIV positive and 386 were HIV negative. There were no significant differences between the two groups in terms of HCC macroscopic and histological characteristics. HIV positive subjects showed a better overall survival at 5 years and 10 years although the difference was not significant (71.6% vs 69.6% and 71.6% vs 61%, $p = ns$).

Conclusion: Our study shows that HIV positive LT patients have similar results to HIV negative in terms of survival; survival among HIV-infected LT subjects has improved over time, mainly because of DAAs introduction for HCV and better management of immunosuppression. Excellent results can be achieved for HIV-infected patients with HCC, even better than in HIV-negative patients in our experience, as long as a strategy of good selection of candidates and close surveillance of recurrence is adopted.

SAT276

SARS-CoV-2 infection in liver transplant recipients-a single center case series from Romania

Ioana-Alexandra Husar-Sburlan¹, Raluca Roxana Grigorescu¹, Elena Cristina Radu¹, Daniela Tabacelia¹, Madalina Florescu¹, Florina Nitu², Radu Dumitru^{2,3}, Ana Stanila⁴, Alexandru Martiniuc⁴, Nicolae Boleac⁴, Dragos Chirita⁴, Laura Popa-Dan⁵, Cezar Stroescu⁴, Narcis Copca⁴. ¹Saint Mary Hospital, Gastroenterology, București, Romania; ²Saint Mary Hospital, Radiology, București, Romania; ³Fundeni Clinical Institute, Radiology, București, Romania; ⁴Saint Mary Hospital, Surgery, București, Romania; ⁵Saint Mary Hospital, Anesthesiology and Intensive Care Unit, București, Romania
Email: sburlan.ioana@gmail.com

Background and aims: The COVID-19 pandemic has affected people and medical care and led to changes in solid organ transplant programs. Recipients of liver transplantation (LT) represent a special group of patients with chronic immunosuppression and frequently associated comorbidities that may present with different progression of the disease than the general population.

Method: We report a case series of patients undergoing post-liver transplantation evaluation, from a single centre in Romania, who were diagnosed with SARS-CoV-2 infection by RT-PCR from respiratory swabs. We analysed their clinical traits, prognostic factors, management and outcome.

Results: In this case series, we report 11 cases of SARS-CoV-2 infection in liver transplant recipients at different times after transplant, varying from 7 days to 77 months. 45% of patients included were asymptomatic, while in the symptomatic group dyspnoea was the most common manifestation (83.33%), followed by fever (50%), dry cough and gastrointestinal symptoms. COVID-19 therapies included antibiotics, antivirals, immunomodulators, steroids, low molecular weight heparin, antifungal, high dose vitamin therapy and Quercetine. Dyspnoea as a symptom, and neutrophil-to-lymphocyte-ratio (NLR) as biological marker were significantly associated with a severe clinical course. Other inflammatory markers like leucocytosis, platelet-to-lymphocyte-ratio (PLR), C-reactive protein (CRP), fibrinogen at diagnosis failed to show significant prognostic value. Patients who progressed to severe forms of the disease were often already hypoxic and tachypneic at presentation, highlighting once again that these patients may be presenting at a late stage of their infection, which limited their therapeutic options. In our study in 68% of patients immunosuppression was Tacrolimus, 9% had Tacrolimus with low dose corticoid, 9% had Sirolimus, and two patients were in the induction immunosuppression phase. Tacrolimus immunosuppression remained unchanged during COVID-19 infection in almost all cases. COVID-19-related mortality was 27.27%. No difference was observed in mortality between those infected within one-year vs after one year of liver transplantation.

POSTER PRESENTATIONS

No	Gender	Age	Time post LT-months	Comorbidities	Symptoms	NLR	PLR	CRP	LDH	TGO	TGP	Baseline immunosuppression	Severity	Outcome
1	M	60	23 days	no	dyspnoea	28.82	517.65	279.63	424.22	76	112	Tacrolimus+corticotherapy	severe	dead
2	M	60	7 days	hypertension	fever, productive cough, dyspnoea, diarrhea	58.89	866.67	39.7	222.46	16	105	Syrolimus+corticotherapy	severe	alive
3	M	53	31	no	asymptomatic	1.52	109.84	1	169.57	21	20	Tacrolimus	mild	alive
4	F	44	67	no	asymptomatic	2.09	82.78	2	222	12	7	Tacrolimus	mild	alive
5	M	50	65	type 2 diabetes	asymptomatic	1.88	145.20	1	313.96	42	39	Tacrolimus	mild	alive
6	M	47	59	no	asymptomatic	3.20	121.39	4	185.25	39	40	Tacrolimus	mild	alive
7	M	45	17	chronic obstructive pulmonary disease	asymptomatic	2.26	73.68	1	146.64	29	30	Tacrolimus	mild	alive
8	F	66	59	endometrial carcinoma	fever, chills, myalgia, asthenia, dyspnoea	3.90	240.28	25	354.7	35	25	Syrolimus	moderate	alive
9	F	48	66	no	dysphagia, dry cough	0.99	76.42	12.25	289	86	89	Tacrolimus	moderate	alive
10	M	66	77	type 2 diabetes, obesity, arterial hypertension	fever, dyspnoea	28.00	240.63	15	380	87	133	Tacrolimus+corticotherapy	severe	dead
12	F	66	75	type 2 diabetes, obesity, arterial hypertension	fever, myalgia, dyspnoea, severe asthenia	15.04	387.23	148.85	446.29	45	37	Tacrolimus	severe	dead

Figure: (abstract: SAT276)

Conclusion: In this case series, liver transplant recipients with COVID-19 disease, aged 60 years or older, who presented with dyspnoea and had diabetes mellitus had more severe outcomes. Neutrophil-lymphocyte ratio at diagnosis seems to be a prognostic factor for a more severe course of COVID-19 pneumonia. Other inflammatory markers had failed to show a significant prognostic role. Older liver transplant recipient patients with diabetes, that present dyspnoea related to COVID-19 pneumonia should be admitted and monitored because of the risk of severe course and high risk of mortality.

SAT277

Liver transplantation for hepatocellular carcinoma: outcome and prognostic factors for recurrence

Veronica Paon¹, Ilaria Normelli², Amedeo Carraro³, Paola Violi³, Andrea Dalbeni², Donatella Ieluzzi¹, Andrea Ruzzenente⁴, Alfredo Guglielmi⁴, David Sacerdoti¹. ¹Liver unit AOUI, medicine, Verona, Italy; ²General medicine AOUI, medicine, Verona, Italy; ³Liver transplant unit, surgery, Verona, Italy; ⁴Hepatobiliary surgery, surgery, Verona, Italy

Email: veronica.paon@aovr.veneto.it

Background and aims: Hepatocellular carcinoma (HCC) accounts for approximately 75% of primary liver cancers and is the fourth leading cause of death from malignancy worldwide. The 5-year survival rate is around 10–15%, often due to late diagnosis with detection of advanced neoplastic disease. Liver transplant (LT) is a curative treatment in some patients. The post-transplant recurrence rate of HCC is very wide, between 5 and 30%, due also to different listing policies.

The aim of our study was to evaluate the recurrence rate of HCC after LT and to identify the main risk factors for recurrence.

Method: 230 patients (84% male, mean age 59 yr) with HCC transplanted between February 2007 and December 2020 were followed until recurrence or death. The majority of patients had Mayo End Stage Liver Disease (MELD) scores ≤ 19 , while only 4.8% presented for transplant with MELD scores ≥ 30 . Milan criteria were applied for listing. Etiology, biochemical data, comorbidities, pre-transplant

treatments, and histological evaluation of the native liver were collected.

Results: 57% of patients had viral, 29.6% alcoholic, and 12.6% non-alcoholic fatty liver disease cirrhosis. 37% of patients had type 2 diabetes mellitus (T2DM) and 43.6% hypertension. 69% of patients had undergone pre-transplant treatments (percutaneous ethanol injection, radiofrequency ablation, transarterial chemoembolization, transarterial radioembolization, resection). The mean follow-up was 47 ± 39 months, with 77.4% survival. Average survival of patients without HCC recurrence was 48.6 ± 39.4 months, average survival of patients with recurrence was 23 ± 25.1 months. After LT, 9.1% of patients had HCC recurrence, and 22.6% died. Among those who had HCC recurrence, 57% of patients had recurrence within the first 12 months after transplantation; 19% at 24 months, 19% at 36 months and 5% at 60 months. In 66.6% of patients with relapsed HCC, the tumor started with extrahepatic localizations (lung, lymph nodes, mediastinum).

In the multivariate analysis the only factors that predicted the outcome (death or HCC relapse) were: extranodal microvascular invasion ($p < 0.001$), size of the largest nodule ($p < 0.005$) and number of pre-transplant local-regional treatments ($p < 0.04$). High pre LT MELD and T2DM identified patients with a worse overall outcome and poorer survival.

Conclusion: In our 13 years experience, recurrence of HCC after transplantation was low (9%). Number of pre-transplant treatments, size of nodules and microvascular invasion were the only predictors of recurrence of HCC after transplantation.

SAT278

The liver outcomes and equity (LOEq) index: neighborhood social determinants independently predict outcomes in liver transplantation

Kali Zhou¹, Leane Kuo¹, Jennifer Dodge¹, Laura Thompson¹,
Norah Terrault¹, Myles Cockburn¹. ¹University of Southern California,
Los Angeles, United States
Email: kalizhou@usc.edu

Background and aims: The impact of social determinants of health (SDOH) at the neighborhood-level on patient outcomes in adult liver transplantation (LT) is unknown. We constructed the novel Liver Outcomes and Equity (LOEq) index to characterize area-based SDOH specific to the population with liver disease in the United States (US) and examined association with LT outcomes.

Method: The LOEq index was derived from 16, 713 unique ZIP codes (42% of all US ZIP codes) of adult waitlisted patients in the Scientific Registry of Transplant Recipients database between 6/18/2013–5/18/2018. We selected 38 ZIP code-level variables across five SDOH domains from the 2014–2018 American Community Survey as a comprehensive measure of neighborhood SDOH. Principal component analysis conducted with a structured and iterative process identified the most influential 13 variables to be included in the final index. Primary predictor was the LOEq index categorized into quintiles (Q1 = lowest to Q5 = highest SDOH). Outcomes were 1) waitlist (WL) mortality (= delisting for too sick/death) and 2) post-LT patient survival, examined with competing risk and Cox regression, respectively. Models were adjusted for transplant region and relevant demographic/clinical factors, with insurance tested as an effect modifier.

Results: Adult LT patients disproportionately resided in neighborhoods with higher SDOH, with 14.0% vs 30.3% of waitlisted patients (n = 59, 298) and 13.9% vs 30.2% of transplanted patients (n = 37, 598) in Q1 vs Q5, respectively. Lower LOEq quintiles had higher proportion minorities, public insurance, hepatitis C etiology, diabetes, and obesity. 47% in Q1 vs 17% in Q5 lived in transplant regions with a short wait time to LT; 5.6% in Q5 vs 2.4% in Q1 underwent living donor LT. The 3-year cumulative incidence of WL mortality was higher in Q1 (22.9%) vs Q5 (20.6%), while 3-year post-LT survival was lower in Q1 (85.8%) vs Q5 (87.4%). In the multivariable model of waitlisted

patients, LOEq Q1–4 were associated with increased WL mortality compared to Q5 (all $p < 0.01$), with Q1 patients incurring 23% excess deaths compared to Q5 (HR 1.23, 95% CI 1.16–1.31). Among transplanted, risk of post-LT death was also elevated for LOEq Q1 (HR 1.14, 1.04–1.24) and Q3 (HR 1.12, 1.03–1.21) compared to Q5. There was a non-significant interaction between LOEq and insurance type: higher WL mortality for Q1 vs Q5 (HR 1.28 for private vs 1.15 for public; $p = 0.08$) and lower post-LT deaths for Q1 vs Q5 (HR 1.01 for private vs 1.17 for public; $p = 0.09$).

Conclusion: More LT patients living in higher LOEq quintiles highlights a neighborhood-level disparity in access to LT. Lower neighborhood SDOH predicted worse outcomes in LT independent of patient demographics and clinical characteristics. The liver disease-specific LOEq index might be leveraged to identify the most vulnerable patients for interventions in clinical settings to increase LT equity.

SAT279

Prevalence, prognosis, clinical, biological and histological features of incidentally found hepatocellular carcinoma after liver transplantation

Emilie Kerstens¹, Samuele Iesari^{2,3}, Eliano Bonaccorsi¹,
Laurent Coubeau¹, Géraldine Dahlqvist¹, Olga Ciccarelli¹,
Bénédicte Delire¹. ¹UCLouvain; ²Fondazione IRCCS Ca' Granda Ospedale
Maggiore Policlinico, General surgery and kidney transplantation, Milan,
Italy; ³Institut de Recherche Expérimentale et Clinique, UCLouvain, Pôle
de Chirurgie Expérimentale et Transplantation, Brussels, Belgium
Email: benedicte.delire@saintluc.uclouvain.be

Background and aims: An incidentally found hepatocellular carcinoma (iHCC) is an HCC diagnosed postoperatively after the analysis of the liver explant from patients who underwent liver transplantation (LT) for non-oncological indication. Data about the prevalence and prognosis of iHCC are scarce. The aim of this study is to evaluate the prevalence of iHCC in our LT patients and to compare the mortality, the risk of recurrence and the clinical, biological, and histological features between patients who underwent LT for preoperatively known HCC (pkHCC) and patients with a postoperative diagnosis of iHCC.

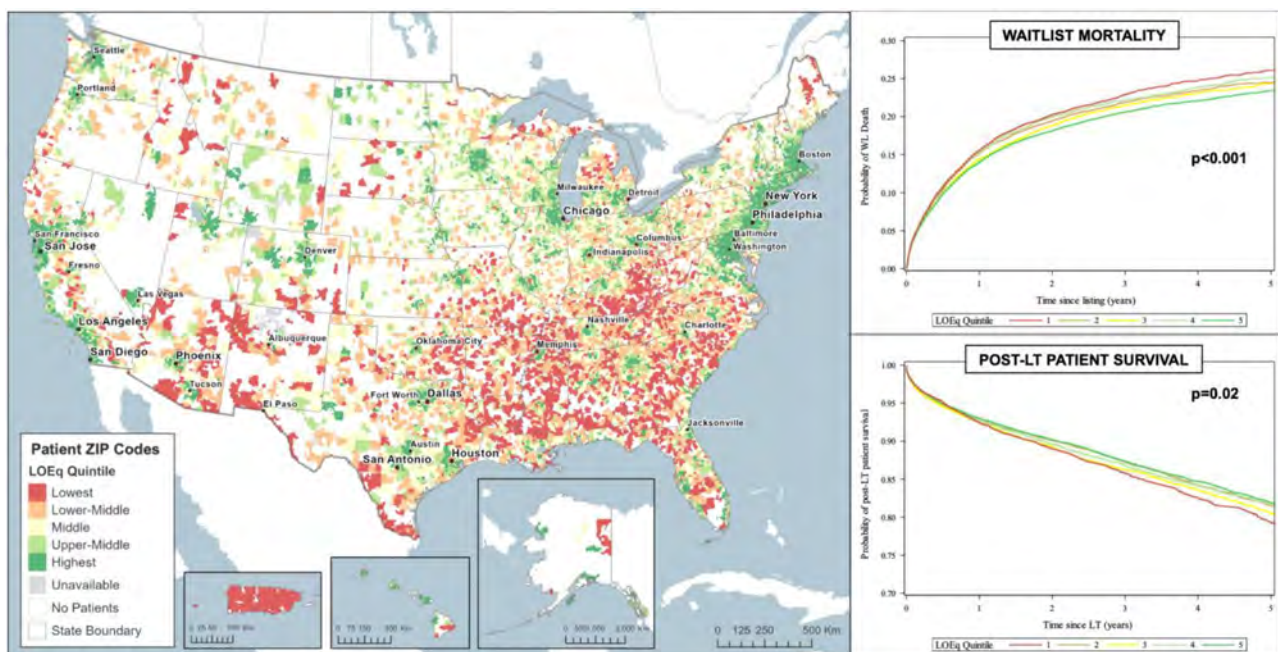


Figure: (abstract: SAT278)

POSTER PRESENTATIONS

Method: We retrospectively reviewed 268 adult patients who underwent LT at the Cliniques Universitaires Saint-Luc, Brussels, Belgium, from January 2010 to January 2020. Results were compared using Fisher's exact test or Mann-Whitney U test as appropriate. The Kaplan-Meier method was used to analyze the rate of death and graft loss. Log-rank tests were run to compare the survival curves. The significance of statistical tests was taken at a P value of <0.05. Analyses were run with SPSS Statistics.

Results: Among the 268 adult patients who underwent LT, 98 cirrhotic patients were transplanted for a pKHC. Prevalence rate of iHCC was 12%. Alcoholic cirrhosis was predominant in the iHCC cohort (88.9% vs 48%, $p = 0.032$). As expected, the patients of the iHCC cohort had a higher MELD score (19.0 (17.0–20.0) vs 10.0 (8.0–13.0); $p < 0.001$) both, at the registration on the waiting list and at LT. Value of Child-Pugh score was also higher for the iHCC cohort compared to pKHC patients (10.0 (9.0–11.0) vs 5.0 (5.0–6.0); $p < 0.001$). None of the iHCC patients got Child-Pugh A score vs 76, 3% of the patients with pKHC ($p < 0.001$). Child-Pugh class C cirrhosis at LT was mainly found in the iHCC cohort (55.6% vs 6.2%; $p < 0.001$). No statistical difference was observed between the 2 cohorts for the level of alpha-fetoprotein, neither at time of registration nor at LT. However, des-carboxy-prothrombin level was significantly higher at time of LT in the iHCC cohort (273.8 (228.9–551.1) vs 42.0 (22.5–96.0); $p = 0.022$). The interval between the last imaging and LT was longer in iHCC cohort than pKHC (2.7 months (1.9–3.7) vs 1.0 (0.5–1.7); $p < 0.004$). Based on histological analysis, Edmondson grade II lesions were more frequently found in the iHCC cohort. However, there was no difference regarding the microvascular invasion rate. None of the 9 iHCC patients got recurrence of HCC post-LT. Cumulated recurrence at 1, 3 and 5 years post-LT for pKHC patients were respectively 3%, 7% and 11%. No significant difference was observed for 1, 3 and 5-year survival rates for iHCC patients compared to pKHC patients (respectively 100%, 88% and 53% vs 90%, 87% and 65%; $p = 0.565$).

Conclusion: While the prevalence of iHCC is not negligible (12% in our patients), it impacts neither the neoplastic recurrence rate nor the survival rate compared to pKHC patients.

SAT280

Survival benefit from liver transplantation for patients with and without hepatocellular carcinoma

Ben Goudsmit¹, Ilaria Prosepe², Maarten Tushuizen¹, Serge Vogelaar³, Ian Alwayn⁴, Bart Van Hoek¹, Andries Braat⁴, Hein Putter². ¹Leiden University Medical Center (LUMC), Gastroenterology and Hepatology, Leiden, Netherlands; ²Leiden University Medical Center (LUMC), Biostatistics, Leiden, Netherlands; ³Foundation Eurotransplant International Foundation, Leiden, Netherlands; ⁴Leiden University Medical Center (LUMC), Surgery, Leiden, Netherlands
Email: b.f.j.goudsmit@lumc.nl

Background and aims: In the US, unequal liver transplantation (LT) access exists between patients with and without hepatocellular carcinoma (HCC). Survival benefit considers survival without and with LT and could equalize LT access. We calculated and compared LT survival benefit scores for patients with (out) HCC, based on longitudinal data in a recent US cohort.

Method: Adult LT candidates with (out) HCC between 2010 and 2019 were included. Waitlist survival over time was contrasted to posttransplant survival, to estimate 5-year survival benefit from the moment of LT. Waitlist survival was modeled with bias-corrected time-dependent Cox regression and posttransplant survival was estimated through Cox proportional hazards regression.

Results: Mean HCC survival without LT was always lower than non-HCC waitlist survival. Below MELD (-Na) 30, HCC patients gained more life-years from LT than non-HCC patients at the same MELD (-Na) score. Only non-HCC patients below MELD (-Na) 9 had negative benefit. Most HCC patients were transplanted below MELD (-Na) 14 and most non-HCC patients above MELD (-Na) 26. Liver function.

(MELD (-Na), albumin) was the main predictor of 5-year benefit. Therefore, during five years, most HCC patients gained 0.12 to 1.96 years from LT, whereas most non-HCC patients gained 2.48 to 3.45 years.

Conclusion: On an individual level, transplanting patients with HCC resulted in survival benefit. However, on a population level, benefit was indirectly wasted, as non-HCC patients were likely to gain more survival due to decreased liver function. Based on these data, we now provide an online calculator to estimate 5-year survival benefit given specific patient characteristics. Survival benefit scores could serve to equalize LT access.

SAT281

Long-term outcomes of liver transplantation (LT) using grafts from donors with active and chronic hepatitis B virus (HBV) infection: multi-center cohort study

Sujin Gang¹, YoungRok Choi¹, Boram Lee¹, Kyung Chul Yoon², Su young Hong¹, Sanggyun Suh¹, Eui Soo Han¹, Suk Kyun Hong¹, Hae Won Lee³, Jai Young Cho³, Nam-Joon Yi¹, Kwang-Woong Lee¹, Kyung-Suk Suh¹. ¹Seoul National University College of Medicine, Department of Surgery; ²Seoul National University Boramae Medical Center, Department of Surgery; ³Seoul National University Bundang Hospital, Department of Surgery
Email: choiyoungrok@gmail.com

Background and aims: We report the long-term outcome of liver transplantation (LT) using grafts from donors with active and chronic hepatitis B virus infection using Hepatitis B immunoglobulin (HBIG) and Nucleos (t)ide analogues (NA).

Method: Among 2260 LTs performed in Seoul National University Hospital, SNU Bundang Hospital, and SNU Boramae Hospital between January 2000 and April 2019, 26 (1.2%) grafts from donors with HBsAg (+), HBeAb (+) or HBV DNA (+) were referred as active and chronic HBV hepatitis grafts and reviewed retrospectively. Demographics and transplantation outcome were analyzed. HBV reactivation redefined as the increase of viral DNA for HBsAg (+) grafts and HBsAg positive seroconversion for chronic hepatitis grafts. Also, we adopted the stage of chronic HBV infection to evaluate and manage of recipients transplanted HBV infected grafts.

Results: Sixteen deceased donor LT were performed with active HBsAg (+) grafts. Ten living donor LT were performed with inactive HBV infected grafts; 8 patients in inactive hepatitis status; HBsAg (–), HBeAb (+) and HBV DNA (+), and 2 patients in chronic HBV hepatitis with seroconversion; HBsAg (–), HBeAb (+) and HBeAg (+). Average follow-up period was 82.6 ± 60.1 months. NA and HBIG were administered during perioperative period depending on donor and recipient's serology. Deaths (n = 8) were occurred 2.0–47.3 months after transplantation. Comparing LT using non-hepatitis virus-infected grafts, there was no difference in patient survival (30.8% vs. 18.6%, $p = 0.247$). Most common causes of death were infection (n = 4) and HCC recurrence (n = 3). HBV reactivation was identified in 1 patient but resolved spontaneously without additional management. All 10 LDLT recipients survived and were in good condition during follow-up. Survivors were in inactive or resolved status for HBV infection under the HBIG and NA. No graft failure was observed. Fourteen patients followed-up more than 5 years were stable and no increase in HCC recurrence rate was observed 5 years after transplantation.

Conclusion: Considering their long-term outcome, liver grafts with active and chronic HBV infection can be safely used in HBV endemic area.

SAT282

Safe use of hepatitis B surface antigen positive (HBsAg (+)) grafts in liver transplantation (LT): a nationwide study based on KOTRY (Korean Organ Transplantation Registry) data

Sujin Gang¹, YoungRok Choi¹, Kwang-Woong Lee¹, Bong Wan Kim², Dong-Sik Kim³, Yang Won Nah⁴, Jong Man Kim⁵, Jae Geun Lee⁶, Je Ho Ryu⁷, Jaehong Jeong⁸, Geun Hong⁹, Shin Hwang⁴. ¹Seoul National University College of Medicine, Department of Surgery; ²Ajou University School of Medicine, Department of Surgery; ³Korea University College of Medicine, Department of Surgery; ⁴University of Ulsan college of medicine, Department of Surgery; ⁵Sungkyunkwan University school of medicine, Department of Surgery; ⁶Yonsei University College of medicine, Department of Surgery; ⁷Pusan National University School of Medicine, Department of Surgery; ⁸School of Medicine, Soonchunhyang University, Department of Surgery; ⁹Ewha Womans University School of Medicine, Department of Surgery
Email: choiyoungrok@gmail.com

Background and aims: In the era of nucleos(t)ide analogues (ANs), we investigate the outcomes of liver transplantation (LT) using HBsAg (+) grafts using Korean national registry database.

Method: Among 4265 LTs which were registered in KOTRY database between April 2014 and January 2020, 20 (0.5%) LTs using HBsAg (+) grafts were identified. We investigated the overall outcomes of LT using HBsAg (+) liver grafts (n = 4100, S (+) group) compared to those of HBsAg (-) liver grafts. S (+) group were compared to those for LT using HBsAg (-) and HBcAb (+) (n = 882, C (+) group) and HBsAg (-) and HBcAb (-) (n = 3132, SC (-) group) after propensity-score matching (1:1).

Results: Twenty HBsAg (+) grafts from deceased donors were transplanted to HBsAg (+) recipients. HBIG was maintained in 16 patients (80%). Most common NA was tenofovir. S (+) group showed comparable patient survival (26.5 ± 21.8 vs 22.8 ± 18.2 months, p = 0.332) and graft survival (26.5 ± 21.8 vs 21.3 ± 18.2 months, p = 0.152) compared to those of HBsAg (-) group.

Age (HR = 1.03, p = 0.016), HCC (HR = 4.61, p < 0.001), MELD score (HR = 2.82, p = 0.001), ascites (HR = 2.14, p = 0.002) and encephalopathy (HR = 2.53, p < 0.001) were the risk factors affecting patient survival. For graft survival, HCC (HR = 4.01, p = 0.001), pre-operative treatment to HCC (HR = 0.54, p = 0.006), MELD score (HR = 2.14, p = 0.012), ascites (HR = 2.52, p < 0.001), and encephalopathy (HR = 1.99, p < 0.001) were significant factors.

After PSM matching between S (+) and C (+), and S (+) and SC (-), there was no significant difference in patient survival (24.3 ± 20.7 vs 38.2 ± 23.0 months, p = 0.863, 24.3 ± 2.7 vs 38.2 ± 23.0 months p = 0.547), and graft survival (26.5 ± 21.8 vs 36.3 ± 17.4 months, p = 0.576, 26.5 ± 21.8 vs 36.3 ± 18.4 months, p = 0.327, respectively).

Conclusion: HBsAg (+) liver grafts can expand the donor pool without compromising the outcomes in the era of NA in the HBV endemic area.

SAT283

A panel of three micro RNAs allows robust prediction of overall survival after liver resection

David Pereyra^{1,2}, Hubert Hackl³, Susanna Skalicky⁴, Jonas Santol^{1,2}, Thomas Grünberger⁵, Matthias Hackl⁴, Alice Assinger², Patrick Starlinger¹. ¹Medical University of Vienna, Department of General Surgery, Division of Visceral Surgery; ²Medical University of Vienna, Center of Physiology and Pharmacology, Institute of Vascular Biology and Thrombosis Research; ³Medical University of Innsbruck, Division of Bioinformatics, Biocenter; ⁴TamiRNA GmbH; ⁵Clinic Favoriten, Department of Surgery, Hepatico-Pancreato-Biliary Center
Email: david.pereyra@meduniwien.ac.at

Background and aims: Overall survival (OS) after liver resection (LR) is influenced by posthepatectomy liver failure (PHLF), disease recurrence, and chronic deterioration of liver function. We previously reported on a panel consisting of the three micro RNAs (miR) miR-122, miR-151a, and miR-192, summed up as the hepatomiR score,

which allows accurate preoperative prediction of PHLF. Here, we aimed for investigation of the hepatomiR score in prediction of long-term OS.

Method: Blood was taken prior to LR in 175 patients followed by optimized plasma preparation. Plasma was used for evaluation of miRs using quantitative polymerase chain reaction, and hepatomiR was calculated. Patients were followed up for disease recurrence and mortality. Statistical analysis was carried out on SPSS version 26 and was based on receiver operating characteristic analysis (ROC), non-parametric tests, log-rank tests, and Cox-regression.

Results: HepatomiR showed a high predictive potential for PHLF with an area under the curve of 0.794 upon ROC. Further, hepatomiR was significantly associated with OS upon univariable Cox-regression (hazard ratio [HR] = 3.104, 95% confidence interval [95%CI] 1.177–8.184, p = 0.022), and remained significant in a multivariable model (HR = 6.326, 95%CI 1.994–20.066, p = 0.022). The previously evaluated cut-offs for hepatomiR (>0.59 and >0.68) were applied in order to divide the cohort into three risk groups. In Kaplan-Meier analysis OS after LR was reduced in the intermediate-risk group (median OS = 44 months, 95%CI 0–96, p = 0.651), and patients in the high-risk group (hepatomiR >0.68) showed a significantly shorter OS (median OS = 11 months, 95%CI 5–18, p = 0.001) when compared to the low-risk group, respectively (median OS = 53 months, 95%CI 31–74). Accordingly, we focused on the high-risk group and observed a significantly higher incidence of 90-day mortality (3.7% vs 27.3%, p = 0.001), and mortality within 1 year (16.3% vs 63.6%, p < 0.001), 3 years (42.9% vs 81.8%, p = 0.012), and 5 years (58.4% vs 90.0%, p = 0.048). An association with disease-free survival could not be observed. In order to evaluate the relevance of hepatomiR for PHLF independent prediction of OS, we further excluded patients with 90-day mortality. We observed that the high-risk cut-off was still able to identify patients with reduced OS (median OS ≤0.68 = 59 months, 95%CI 35–84; median OS >0.68 = 12 months, 95%CI 7–17, p = 0.040), and patients with mortality within 1 year (13.0% vs 50.0%, p = 0.004), 3 years (40.5% vs 75.0%, p = 0.055), and 5 years (56.5% vs 85.7%, p = 0.127).

Conclusion: We here present the hepatomiR score as a marker for risk stratification prior to LR. HepatomiR allows identification of patients at risk for PHLF, and patient with reduced OS after LR independently from PHLF. Accordingly, the evaluation of hepatomiR might improve patient selection and ultimately increase personalized outcome of liver surgery.

SAT284

Liver transplantation for primary sclerosing cholangitis and predictors of disease recurrence

Julie Zhu¹, Dennis Lim², Larry James², Eric Yoshida³, Kevork Peltekian². ¹Dalhousie University, Atlantic Liver Transplant Program, Canada; ²Dalhousie University, Medicine; ³University of British Columbia, Medicine
Email: julie.zhu@ualberta.ca

Background and aims: In liver transplantation (LT) for PSC, pre-transplant colectomy may lower the risk of PSC recurrence (rPSC), and well-controlled or lack of IBD may protect against rPSC, however, these findings are not consistent across all studies. It is unknown whether recipient/donor sex plays a role in rPSC. The aim is to study factors associated with PSC recurrence in the post-transplant population.

Method: This is a retrospective study on adults who received LT for PSC in Halifax NS from 1985 to 2020. Graft and patient outcomes are analyzed by logistic regression models.

Results: A total of 92 patients underwent deceased donor LT for PSC with a mean follow-up time of 9.2 yrs (SD 7.1). Fifty-three remain active in the program, 2 were lost to follow-up and 37 died. The mean age at transplant was 43 (SD13, range 18.9–67.8). Seven patients had a second transplant. The five- and 10-year patient survival rate of the entire cohort was 78.7% and 66% respectively. In the active cohort, the

POSTER PRESENTATIONS

prevalence of rPSC was 23.5% (12/51). Retransplantation for rPSC occurred in 8.3% (1/12). The prevalence of IBD was 82.4% (42/51), consisted of ulcerative pancolitis (64.7%, 33/51), ulcerative proctitis (3.9%), left-sided UC (2%) and Crohn's disease (9.8%). Males are much more likely than females to undergo a colectomy at any time (OR 5.5, 95% CI 1.07–28.22, p 0.041). Refractory IBD was the predominant indication for a colectomy (10/16), followed by dysplasia or colon cancer (6/16). In the post-transplant period, 69% had stable IBD without therapy escalation, 11.9% were escalated to a biologic, 19% underwent a colectomy for active IBD symptoms. Pretransplant colectomy negatively predicted rPSC, in this subgroup 0% (0/6) developed rPSC. Neither recipient sex (OR 1.14, 95% CI 0.26–5.0, p 0.86) or recipient age predicted the likelihood of rPSC. There was no association between donor sex on rPSC (OR 1.25, 95% CI 0.30–5.27, p 0.76). A trend towards increased rPSC was observed in male donors to female recipients versus female-to-female transplants (OR 6, 95% CI 0.33–107.42, p 0.224). Overall, having a post-transplant colectomy, subtotal or total, irrespective of timing, did not significantly impact rPSC (OR 0.389, 95% CI 0.09–1.66, p 0.20). Diagnosis of IBD was not associated with an increased risk of rPSC (OR 1.21, p 0.83).

Conclusion: Several factors were associated with rPSC after liver transplant in patients with PSC and IBD, pre-transplant colectomy was found to be protective, male donor to female recipient was a potential risk factor. It is important to study these factors in multi-centered cohorts to understand the pathogenesis of PSC. Pretransplant total colectomy may be beneficial for several reasons, reducing rPSC, controlling IBD activities, and lowering dysplasia and colon cancer rates in the post-transplant population.

SAT285

Predictive factors of antibody response after anti-SARS-CoV-2 vaccine in liver transplant recipients

Ilias Kounis¹, Bruno Roche¹, Lea Duhaut¹, Rodolphe Sobesky¹, Eleonora De Martin¹, Edoardo Poli¹, Alina Pascale¹, Gabriella Pitta¹, Oriana Ciacio¹, Jean-Charles Duclos-Vallée¹, Didier Samuel¹, Cyrille Feray¹, Audrey Coilly¹. ¹AP-HP Hôpital Paul-Brousse, Centre Hépatobiliaire, Inserm, Université Paris-Saclay, UMR-S 1193, Université Paris-Saclay, Inserm, Physiopathogénèse et traitement des maladies du Foie, FHU Hepatinov, Villejuif, France
Email: ilias.kounis@aphp.fr

Background and aims: A weak immune response to 2 doses of anti SARS-CoV2 vaccine was observed in solid-organ transplant recipients, encouraging the authorities to recommend a third dose in immunosuppressed patients. The aim of our study was to search for predictive factors of an antibody response to the vaccines and describe their efficacy and tolerance in a large population of liver transplant (LT) recipients.

Method: This is retrospective monocenter study conducted at Paul Brousse Hospital in France. All adult LT recipients followed up in our transplant center and vaccinated with at least one dose of vaccine from January 2021 to September 2021 were included. A strong immune response to vaccination was defined as the presence of antibodies titration to SARS-CoV-2 spike protein up to 250 U/ml after 2nd or 3rd dose of vaccine.

Results: 745 patients were included. Of them, 642 (85.5%) had 2 doses and 343 (46%) patients had three. Mean age at vaccination was 59.1 (\pm 14.5) years and mean time from LT to vaccination was 12.1 (\pm 9.7) years. Immunosuppression was due to one immunosuppressive drug in 29.7% of patients, 2 drugs in 57.6% and 3 drugs in 12.5%. The prevalence of anti-SARS-CoV-2 antibodies was 11% (19 patients) before the first dose, 40.8% (53 patients) before the second dose, 66.2% (392 patients) before the third dose, and 72.5% (271 patients) after the third dose. 190 (36.7%) patients had a strong antibody titration after 2nd injection and 139 (47.6%) after 3rd injection. Patients who had strong antibody response had, in time of vaccination, lower Tacrolimus blood concentrations (p = 0.04), lower Mycophenolate (p < 0.001) and corticosteroid doses (p = 0.009), lower creatinine (p =

0.04), higher hemoglobin (p < 0.001) levels and longer time between LT and vaccination (p = 0.004). In multivariate analysis, predictive factors of strong response were time since LT >9.8 years (p = 0.001), while creatinine levels >95 μ mol/l (p = 0.014), use of corticosteroids (p < 0.001) and high mycophenolate dose (p < 0.001) in time of vaccination were correlated with an absence of strong response to the vaccine. Fifteen (2%) patients had COVID after vaccination, 2 of them after 3 doses of vaccine. No serious adverse events were for 99.7% of patients.

Conclusion: A strong immune response was detected to less than a half of LT recipients after 3 doses of anti-SARS-CoV-2 vaccine. These patients remain at risk for Covid-19, especially if they had a recent LT or have high levels of immunosuppression.

SAT286

Immunotherapy before solid organ transplantation: an international transplant community-focused survey

Tommy Ivanics^{1,2,3}, Marco Claasen^{1,4}, David Al-Adra⁵, Gonzalo Sapisochin¹. ¹University Health Network, Multi-Organ Transplant Program, Toronto, Canada; ²Henry Ford Hospital, Department of Surgery, Detroit, United States; ³Uppsala University, Department of Surgical Sciences, Akademiska Sjukhuset, Uppsala, Sweden; ⁴Erasmus MC, Department of Surgery, Rotterdam, Netherlands; ⁵University of Wisconsin-Madison, Division of Transplantation, Madison, United States

Email: tommy.ivanics@uhn.ca

Background and aims: The use of immunotherapy for cancer has increased and is expected to continue to grow. The outcomes after solid organ transplantation (SOT) in patients having received immunotherapy before SOT remain unclear. We sought to evaluate the global transplant surgery community's attitude and experience with patients who have received immunotherapy for malignancy before SOT.

Method: An online-based survey was sent to North American transplant directors in December-2020 and to members of the International Liver Transplant Society (ILTS) in November-2021 to evaluate experiences with, and attitudes towards, SOT in recipients with previous immunotherapy for cancer. Descriptive summary statistics were reported.

Results: 134 respondents provided consent to participate in the survey and 91 completed the survey for a completion rate of 68%. Respondents represented center experience from North America, South America, Europe, Asia, and Australia. Most represented centers from the United States (n = 22, 24%), followed by India (n = 9, 10%), and Spain (n = 4, 4%). Fifty-eight (64%) respondents would consider offering a SOT to a patient with previous history of immunotherapy for cancer. Thirty (33%) respondents were aware of such recipients receiving immunotherapy for cancer before a SOT. The majority (n = 69, 77%) of respondents reported an absence of institutional clinical management policies in this setting.

Conclusion: Though this survey's response rate was relatively low, it provides preliminary insight into the attitudes and experiences with SOT after immunotherapy for cancer in the international transplant community. This represents a clinical scenario for which outcomes should be clarified and consensus guidelines established to inform future clinical management, especially as immunotherapy for cancer is likely to increase in coming years.

Overall (N=139)	
1a. Would you consider offering an organ transplant to a patient with a previous history of immunotherapy treatment for cancer?	
N-Missing	48
Maybe/Don't know	21 (23%)
No	12 (13%)
Yes	58 (64%)
2a. Are you aware of any transplant recipients at your institution that were denied listing for transplantation based on prior immunotherapy exposure?	
N-Missing	48
Don't recall	9 (10%)
No	73 (80%)
Yes	9 (10%)
3a. Are you aware of any transplant recipient in your institution that received immunotherapy for cancer before an organ transplant?	
N-Missing	48
Don't recall	7 (8%)
No	54 (59%)
Yes	30 (33%)
4a. Does your transplant program have any policies in place regarding clinical management of these patients?	
N-Missing	49
Don't know	3 (3%)
No	69 (77%)
Yes	18 (20%)
Time-frame between treatment and transplant - If "yes" to 1a. Would you consider offering an organ transplant to a patient with a previous history of immunotherapy treatment for cancer?	
Overall (N=58)	
1b. What would you consider an acceptable time-frame between the treatment and transplant?	
<4 months	13 (22%)
4-12 months	31 (53%)
12-24 months	6 (10%)
>24 months	8 (14%)
Number of denied listings - If "yes" to 2. Are you aware of any transplant recipients at your institution that were denied listing for transplantation based on prior immunotherapy exposure?	
Overall (N=9)	
2b. How many such patients are you aware of at your institution?	
1-2	4 (44%)
3-5	4 (44%)
>5	1 (11%)
Transplant recipients with prior immunotherapy - If "yes" to 3. Are you aware of any transplant recipient in your institution that received immunotherapy for cancer before an organ transplant?	
Overall (N=30)	
3b. How many patients are you aware of at your institution received immunotherapy for cancer before an organ transplant?	
1-2	20 (67%)
3-5	4 (13%)
>5	6 (20%)
3c. Approximately when did you transplant your first patient who had received prior immunotherapy for cancer?	
Missing	1
Earlier	2 (7%)
2016	1 (3%)
2017	1 (3%)
2018	8 (28%)
2019	9 (31%)
2020	8 (28%)
3d. In the patients that received an organ transplant after immunotherapy receipt for cancer - what was the immunotherapy treatment for?	
Liver cancer	26 (87%)
Other	4 (13%)
3e. What type of immunotherapy was used	
Missing	1
Don't recall	1 (3%)
Immune checkpoint inhibitor	23 (79%)
Immune system modulator	1 (3%)
Monoclonal antibody	3 (10%)
T-cell transfer therapy	1 (3%)
3k. Graft survival: In your opinion and experience, how do the outcomes of these patients compare to the average transplant patient?	
Missing	1
Have not followed them for enough time to make this determination	10 (35%)
Better	1 (3%)
Same	16 (55%)
Worse	2 (7%)
3l. Patient survival: In your opinion and experience, how do the outcomes of these patients compare to the average transplant patient?	
Missing	1
Have not followed them for enough time to make this determination	11 (38%)
Better	1 (3%)
Same	15 (52%)
Worse	2 (7%)
Time-period between immunotherapy and transplant - If "yes" to 4a. Does your transplant program have any policies in place regarding clinical management of these patients	
Overall (N=18)	
4b. Do you require a certain time period between last dose of immunotherapy and transplant?	
No	4 (22%)
Yes, <6 months	10 (56%)
Yes, 6-12 months	2 (11%)
Yes, 12-24 months	1 (6%)
Yes, >24 months	1 (6%)

Figure: (abstract: SAT286)

SAT287

Evaluating the predictive performance and transferability of machine learning-based prediction models using national liver transplant data registries

Tommy Ivanics^{1,2,3}, Delvin So⁴, Marco Claassen^{5,6}, David Wallace^{7,8}, Madhukar Patel⁹, Annabel Gravely⁵, Kate Walker⁷, Thomas Cowling⁷, Lauren Erdman⁴, Gonzalo Sapisochin⁵. ¹University Health Network, Toronto, Canada; ²Henry Ford Hospital, Department of Surgery, Detroit, United States; ³Uppsala University, Department of Surgical Sciences, Uppsala, Sweden; ⁴The Hospital for Sick Children, The Centre of

Computational Medicine, Toronto, Canada; ⁵University Health Network, Multi-Organ Transplant Program, Toronto, Canada; ⁶Erasmus MC Transplant Institute, University Medical Centre Rotterdam, Department of Surgery, division of HPB and Transplant Surgery, Rotterdam, Netherlands; ⁷London School of Hygiene and Tropical Medicine, Department of Health Services Research and Policy, United Kingdom; ⁸Guy's and St Thomas' Hospital, Department of Nephrology and Transplantation, United Kingdom; ⁹University of Texas Southwestern Medical School, Division of Surgical Transplantation, Dallas, United States
Email: tommy.ivanics@uhn.ca

Background and aims: Large, national registries of liver transplant (LT) data are collected in many countries. We compared data from

POSTER PRESENTATIONS

Harmonized - Cross Country Test Set Performance, Mean (range) across 5 imputations

Model (Country model was trained on)	Registry (Country predictions made on)	AUROC	AUPRC
CA	CA	0.58 (0.57 to 0.60)	0.16 (0.16 to 0.19)
	UK	0.68 (0.67 to 0.70)	0.25 (0.24 to 0.26)
	US	0.57 (0.55 to 0.58)	0.21 (0.18 to 0.24)
UK	CA	0.49 (0.49 to 0.50)	0.04 (0.04 to 0.04)
	UK	0.63 (0.62 to 0.64)	0.05 (0.05 to 0.05)
	US	0.65 (0.65 to 0.65)	0.08 (0.08 to 0.08)
US	CA	0.57 (0.56 to 0.58)	0.05 (0.05 to 0.05)
	UK	0.60 (0.60 to 0.60)	0.05 (0.05 to 0.05)
	US	0.63 (0.63 to 0.63)	0.06 (0.06 to 0.07)

Abbreviations: AUPRC: Area under precision-recall curve, AUROC: Area under receiver-operator characteristic, CA: Canada, UK: United Kingdom, US: United States

Figure: (abstract: SAT287)

three national registries and developed machine learning algorithm (MLA)-based models that were used to evaluate performance predictions both within and across these different countries.

Method: We studied adults (≥ 18 -years) who underwent primary LT between Jan-2008 and Dec-2018 from United Network for Organ Sharing (UNOS-US), National Health Service Blood and Transplantation (NHSBT-UK), and the Canadian Organ Replacement Registry (CORR-Canada). MLA models for 90-day post-LT mortality were built firstly on each individual registry's capacity (based on variables inherent to the individual database) and then based on the overlapping variables available in all three registries (based on harmonized variables). The predictive abilities of the harmonized registry models were evaluated externally across countries using area-under-the-receiver-operator-curve (AUROC) and area-under-the-precision-recall-curve (AUPRC).

Results: The total number of patients were as follows: training (2008–2015) (Canada: $n = 827$; UK: $n = 3,388$; US: $n = 40,454$), validation (2016) (Canada: $n = 126$; UK: $n = 621$; US: $n = 6,128$), and testing (2017–2018) (Canada: $n = 261$; UK: $n = 1,278$; US: $n = 12,976$). The best performing MLA-based model was the ElasticNet across both multiply imputed independent and harmonized datasets (best performance in the US: AUROC: 0.70; Range: 0.70–0.71). Model performance diminished from the independent to the harmonized (only using variables that were in common between the three registries) registries, especially in the UK (independent ElasticNet: AUROC: 0.54; Range: 0.52–0.56 to harmonized AUROC: 0.48; Range: 0.48–0.50) and the US (independent ElasticNet: AUROC: 0.70; Range: 0.70–0.71 to harmonized AUROC: 0.65; Range: 0.64–0.65). Model performance after external validation across countries was overall poor (Table 1).

Conclusion: MLA-based models can be constructed using international LT registries, with independent ElasticNet models demonstrating optimal predictive performance. While MLA-based model performance yields fair discriminatory potential, a diminishing number of variables and granularity results in decreased performance. Moreover, the external validity of such MLA-based models is poor when applied to other transplant registries. This is likely due to inherent limitations and variability within each dataset. As such, it is conceivable that these limitations may be overcome in the future by increasing the granularity of datasets (for example, with linkages to other administrative datasets), and placing an increased emphasis on consensus for variable standardization (such as with increased collaboration and communications across transplant data collecting organizations).

SAT288

Liver transplant recipients have a higher incidence of lung cancer than general population

Paula Pujols¹, Fanny Meylin Caballeros², Mercedes Iñarrairaegui³, Javier Zulueta⁴, Gorka Bastarrika Alemañ³, Jose Ignacio Herrero³.

¹University of Navarra, Pamplona, Spain; ²Clínica Universidad de Navarra, Madrid, Spain; ³Clinica Universidad de Navarra, Pamplona, Spain; ⁴Mount Sinai Morningside, New York, United States
Email: iherrero@unav.es

Background and aims: De novo malignancies are frequent complications after liver transplantation. Liver transplant recipients (LTRs) have a higher risk of lung cancer than the general population, but it may be due to a higher frequency of smoking. Our aim was to compare the incidence of lung cancer in LTRs with respect to a matched group of control candidates.

Method: In this retrospective study, 124 LTRs and 496 controls participating in a lung cancer screening program with low-dose computed tomography (LDCT) were compared. Four controls were matched for each LTR according to gender, age (± 10 years), current smoking status, cumulative smoking (± 10 pack-years) and presence of emphysema on initial LDCT examination. The results of our lung cancer screening program in LTRs were also evaluated.

Results: Twelve LTRs (9.7%) and 28 controls (5.6%) were diagnosed with lung cancer. The actuarial risks of lung cancer at 3, 5, 7 and 10 years were 3.3%, 4.5%, 8.3% and 18.2% for LTR and 3%, 3.4%, 4% and 7.1% for controls, respectively ($p = 0.038$). The most important predisposing factors for lung cancer were a higher age and the presence of emphysema.

Ten of the 12 LTRs with lung cancer were diagnosed with stage IA. At the end of the follow-up, six patients had died (two of them from lung cancer progression and one from chemotherapy-related sepsis). Nine patients were free of malignancy at their last follow-up.

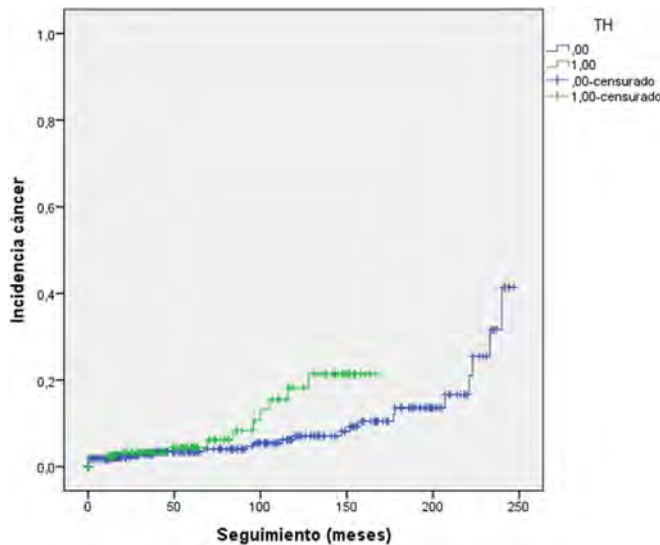


Figure: Comparison of the risk of lung cancer in LTR with respect to controls. (abstract: SAT288)

Conclusion: LTRs have a higher risk of lung cancer than the general population. LDCT allows early diagnosis of lung cancer in tyhis patient population.

SAT289

Survival benefit-based priority of liver transplantation in HBV-related acute-on-chronic liver failure

Peng Li¹, Xi Liang², Jinjin Luo¹, Jiaqi Li¹, Jiaojiao Xin¹, Jing Jiang¹, Dongyan Shi¹, Yingyan Lu³, Hozeifa Mohamed Hassan², Qian Zhou¹, Shaorui Hao¹, Huafeng Zhang¹, Tianzhou Wu², Tan Li¹, Heng Yao¹, Keke Ren¹, Beibei Guo¹, Xingping Zhou¹, Jiaxian Chen¹, Lulu He¹, Hui Yang¹, Wen Hu¹, Shiwen Ma¹, Bingqi Li¹, Shaoli You⁴, Shaojie Xin⁴, Yu Chen⁵, Jun Li¹. ¹The First Affiliated Hospital, Zhejiang University School of Medicine, State Key Laboratory for Diagnosis and Treatment of Infectious Diseases, Hangzhou, China; ²Taizhou Central Hospital (Taizhou University Hospital), Precision Medicine Center, Taizhou, China; ³Tongde Hospital of Zhejiang Province, Key laboratory of cancer prevention and therapy combining traditional Chinese and Western Medicine, Hangzhou, China; ⁴The Fifth Medical Center of PLA General Hospital, Senior Department of Hepatology, Beijing, China; ⁵Beijing Youan Hospital, Capital Medical University, Beijing Municipal Key Laboratory of Liver Failure and Artificial Liver Treatment Research, Fourth Department of Liver Disease, Beijing, China
Email: lijun2009@zju.edu.cn

Background and aims: Acute-on-chronic liver failure (ACLF) is a life-threatening syndrome characterized by multiorgan failure and high short-term mortality rates. Liver transplantation (LT) is an effective therapy but is limited by organ shortages. Survival benefit-based priority for LT is important to decrease the risk of futile transplantation. This study aimed to identify an appropriate prognostic score for determining LT priority for ACLF patients who have a high survival benefit rate.

Method: Hospitalized patients with acute deterioration of hepatitis B virus-related chronic liver disease (n = 4577) from the Chinese Group on the Study of Severe Hepatitis B (COSSH) study cohort were enrolled between January 2015 and December 2020. The performance of five commonly used scores (COSSH-ACLF IIs, COSSH-ACLFs, CLIF-C ACLFs, MELDs and MELD-Nas) for predicting the outcome on the waitlist and post-LT at days 28/90/180/365 were evaluated. The survival benefit based on the extra lifespan derived from LT was calculated by the difference in the area under the survival curve between patients with and without LT.

Results: A total of 368 ACLF patients and 98 non-ACLF patients received LT. The 1-year survival probability of 368 ACLF-LT patients

(77.2%) was significantly higher than that of non-LT patients in both the ACLF entire cohort (52.3%) and the propensity score matching (PSM) cohort (27.6%) (all p < 0.001). However, 98 non-ACLF patients who underwent LT showed a lower survival probability than 2625 without LT (88.8%/92.3%, p = 0.20), and PSM analysis demonstrated no significant improvement in survival probability (88.8%/81.4%, p = 0.16). The receiver operating characteristic curve showed that the COSSH-ACLF II score had the highest performance (0.849) for identifying the 1-year risk of death on the waitlist and was also superior (0.864) for predicting 1-year outcome post-LT to the four other scores (COSSH-ACLFs/CLIF-C ACLFs/MELDs/MELD-Nas, 0.835/0.825/0.796/0.781; all p < 0.05). Survival benefit rate analyses showed that 79.1% of ACLF patients with COSSH-ACLF IIs of 7–10 had a much higher 1-year survival benefit rate (39.2%–64.3%) than those with scores < 7 or > 10 (all p < 0.001).

Conclusion: The COSSH-ACLF IIs not only identified the risk of death on the waitlist but also accurately predicted post-LT mortality and survival benefit rates for ACLF. Patients with COSSH-ACLF IIs of 7–10 should be prioritized for LT. Our findings can help to decrease the risk of futile transplantation and develop new clinical strategies for ACLF patients.

SAT290

Social determinants of health and racial disparities in liver transplant: a nation wide analysis

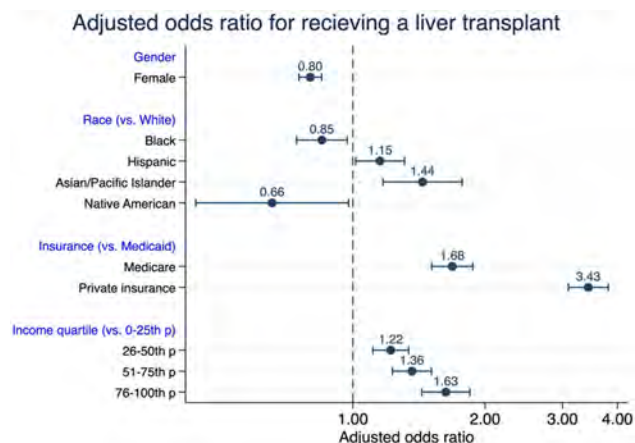
Mahmoud Mansour¹, Adham Obeidat², Mohammad Darweesh³, Ratib Mahfouz⁴, Sanket Basida⁵, Ahmad Ali⁶. ¹University of Missouri Columbia, Internal Medicine, Columbia, Missouri, United States; ²University of Hawaii, Internal Medicine, Honolulu, Hawaii, United States; ³East Tennessee State University, Internal medicine, Johnson City, Tennessee; ⁴Kent Hospital/Brown University, Internal Medicine, Warwick, Rhode Island, United States; ⁵Upadhyay Medical College, Medicine, Gujarat, India; ⁶University of Missouri Columbia, Hepatology, Columbia, Missouri, United States
Email: aliah@health.missouri.edu

Background and aims: Liver transplantation is a life-saving treatment and standard of care for many forms of end-stage liver disease. Unfortunately, 20 percent of patients on liver transplant list die while on the waiting list, with several studies showing racial, gender and socioeconomic disparities among patients receiving a liver transplant. We sought to evaluate disparities amongst patients receiving liver transplant in the United States using the most recently available data from the National Inpatient Sample (NIS).

Method: We performed analysis of discharge data from the NIS between Jan 1st, 2016, to Dec 31st, 2019. We identified adult patients who underwent liver transplant using International Disease Classification of Disease 10th Procedure Coding System (ICD-10-PCS). Multivariate logistic regression was used to evaluate for differences in race, gender and socioeconomic status among those who received a liver transplant.

Results: A total of 29,050 liver transplants were performed during the study period. Compared to White patients, Black and Native America patients had decreased transplant rates (adjusted odds ratio [aOR] 0.85, p = 0.017 and 0.66, p = 0.039; respectively) while Hispanic and Asian/Pacific Islander patients had increased transplant rates (1.15, p = 0.029 and 1.44 p = 0.001; respectively). The increase in income quartile was associated with an incremental increase in transplant rates. Additionally, patients with private insurance had much higher transplant rates compared to those with Medicaid (aOR 3.43, p < 0.001). Female gender was independently associated with decreased transplant rates (aOR 0.80, p < 0.001).

POSTER PRESENTATIONS



Conclusion: Our analysis showed that race and social determinants of health, including gender, income, and insurance status, are associated with the likelihood of receiving a liver transplant in the United States. Our study confirms, on a national level, previously described disparities in receiving liver transplantation. Patient-level studies are needed to understand better why disparities in liver

transplant exist to achieve a more equitable distribution of this scarce resource.

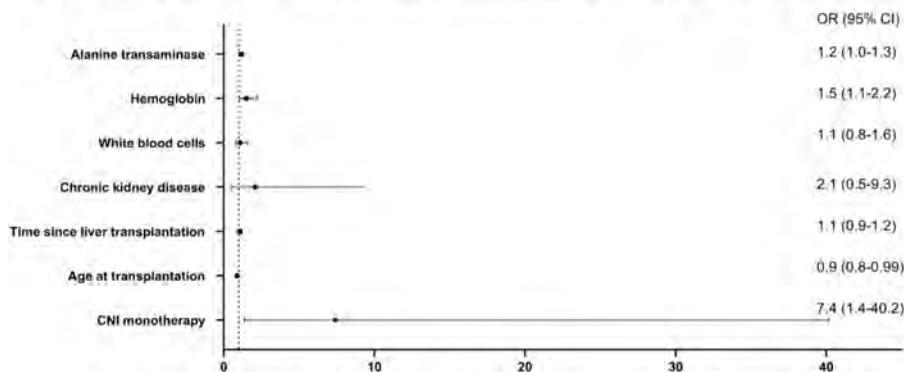
SAT291

Reduced neutralization efficacy against SARS-CoV-2 Omicron variant after third boost of mRNA BNT162 vaccine among liver transplant recipients

Yana Davidov¹, Victoria Indenbaum², Michal Mandelboim^{2,3}, Keren Asraf⁴, Tal Gonen^{2,3}, Keren Tsaraf¹, Oranit Cohen-Ezra¹, Mariya Likhter¹, Gil Ben Yaacov¹, Itai Nemet², Limor Kliker^{2,3}, Orna Mor^{2,3}, Ram Doolman⁴, Carmit Cohen⁵, Arnon Afek^{3,6}, Yitshak Kreiss^{3,6}, Gili Regev^{3,5}, Yaniv Lustig^{2,3}, Ziv Ben Ari^{1,3}. ¹Sheba Medical Center, Liver Diseases Center, Tel Aviv-Yafo, Israel; ²Sheba Medical Center, Central Virology Laboratory, Ministry of Health, Tel-Hashomer, Tel Aviv-Yafo, Israel; ³Tel Aviv University, Sackler School of Medicine, Tel Aviv-Yafo, Israel; ⁴Sheba Medical Center, The Dorman Automated Mega Laboratory, Tel Aviv-Yafo, Israel; ⁵Sheba Medical Center, Infection Prevention and Control Unit, Tel Aviv-Yafo, Israel; ⁶Sheba Medical Center, General Management, Tel Aviv-Yafo, Israel
Email: y.davidov@gmail.com

Background and aims: The immune response of solid organ transplant recipients to the two doses of the BNT162b2mRNA vaccine is impaired (72%). However, improved immune response was noted after the third boost. The durability and effectiveness of the

Predictors of maintained immune response after the third vaccine dose



Neutralization Efficiency against Wild-Type Virus, Delta and Omicron Variants of Concern measured at median time 22 days after the third vaccine

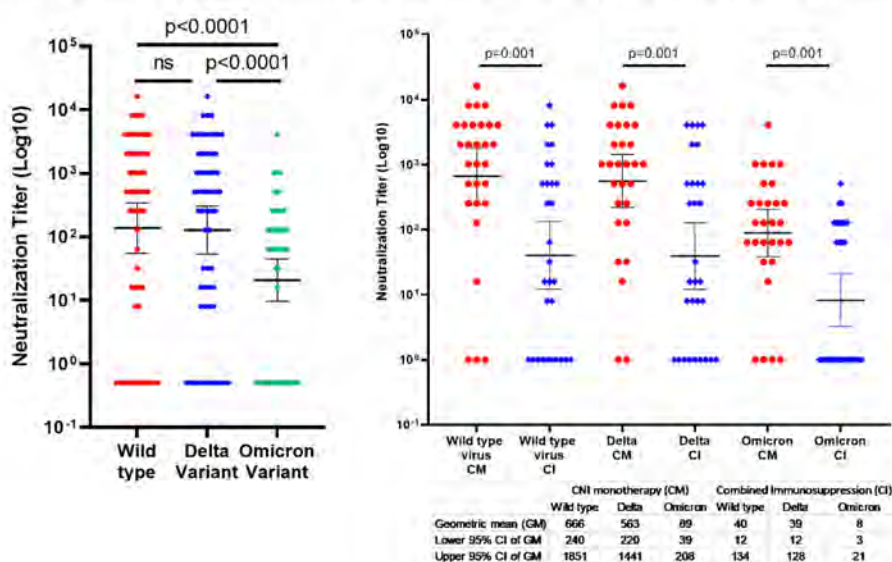


Figure: (abstract: SAT291)

immune response after the third boost are unknown as well as the impact of the emergence of new variants. We aimed to evaluate for the first time, the durability of the response after the third BNT162b2mRNA vaccine among liver transplant recipients, its predictors, and the impact of emerged variants (VOC).

Method: Consecutive 59 liver transplant (LT) recipients, who received three doses of BNT162b2mRNA vaccine and followed-up at the Sheba Medical Center were included. Receptor-binding domain (RBD) IgG, pseudo-virus (pvSARS-2) neutralization antibody (NA) titers, and T cells levels were determined 4 ± 1 weeks and 19 ± 3 weeks after the third vaccine. IgG antibody titer above 21.4 BAU/ml was defined as a positive response. A comparison between the neutralization efficacy of the vaccine among wild type, omicron, and delta variants 4 ± 1 weeks after the third vaccine was conducted.

Results: The 59 LT recipients were of a median age of 61 years (ranges, 25–82); 53.5% were male. Four weeks after the third vaccine, a positive humoral immune response was detected in 81.4%. It decreased significantly 19 ± 3 weeks after the third boost to 76.1%, $p < 0.0001$. The geometric mean titers (GMT) of anti-RBD IgG decreased from 483 BAU/ml to 204 BAU/ml ($p < 0.0001$), pvSARS-2 NA 653 to 450 ($p = 0.2$), and T cell 223 to 30 cells per 10^6 PMC ($p < 0.0001$) four weeks and 19 weeks respectively. Following multivariate analysis, the independent predictors associated with maintaining a positive immune response 19 weeks after the third vaccine were CNI monotherapy ($p = 0.02$) and Hemoglobin > 11.5 g/dl ($p = 0.02$). The GMT of omicron neutralization was significantly lower than wild-type, and delta virus and were 21.72, 140.131, respectively ($p < 0.0001$). We evaluated the impact of CNI monotherapy vs. combined immunosuppression (combination of CNI with MMF or mTOR or prednisone) on neutralization efficacy of VOC. The GMT of the wild type, delta, and omicron variants were significantly higher among LT recipients who received CNI monotherapy than combined immunosuppression and were 666, 563, 89 and 40, 39, 8, respectively, ($p = 0.01$).

Conclusion: The immune response after the third BNT162b2mRNA boost vaccine decreased significantly and rapidly among LT recipients. CNI monotherapy was a predictor of durability. The neutralization efficacy against the omicron variant was reduced significantly. Further studies are needed to evaluate the efficacy of a fourth vaccine dose on the durability of the immune response and protection against symptomatic COVID 19 disease.

SAT292

Long-term outcomes (beyond 5 years) of liver transplant recipients-a transatlantic multicentre study

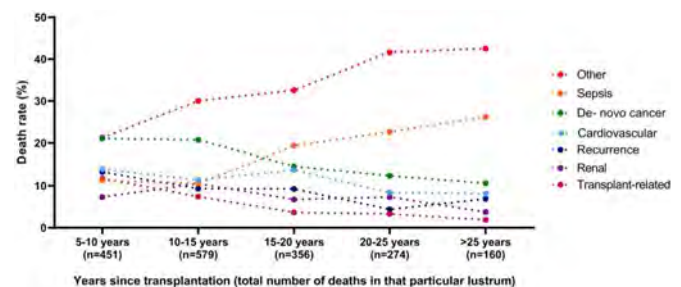
Naaventhana Palaniyappan¹, Emily Peach¹, Fiona Pearce¹, Amritpal Dhaliwal², Isabel Campos-Varela³, Matthew Cant², Cristina Dopazo³, Sapna Divani-Patel², James F. Trotter⁴, Ayiesha Hattar², Laurence Hopkins², Giuliano Testa⁴, Angela Bilbao³, Zain Kasmani², Sarah Faloona², Darius F. Mirza², Goran Klintmalm⁴, Itxarone Bilbao³, Sumeet Asrani⁴, Neil Rajoriya², Aloysious Aravindhan¹. ¹University of Nottingham, Nottingham, United Kingdom; ²Queen Elizabeth Hospital Birmingham, United Kingdom; ³Vall d'Hebron Hospital Universitari, Barcelona, Spain; ⁴Baylor University Medical Center, Dallas, United States
Email: naaventhana.palaniyappan@nottingham.ac.uk

Background and aims: Long-term (>5 year) outcomes following liver transplantation (LT) have not been extensively reported upon, in contrast to established short-term and medium-term outcomes. The aim was to evaluate survival outcomes of recipients who have survived the first 5 years following LT.

Method: A retrospective analysis of prospectively collected data from 3 high volume centres (Dallas, USA; Birmingham, UK; and Barcelona, Spain) was undertaken. Data were extracted of all adult patients, who underwent LT since the inception of the programme in the respective centres to 31 December 2010, and who survived at least 5 years since their first LT. Patient survival was the primary outcome measure. Age-standardised mortality rates stratified by sex were calculated for each

centre and compared with respective jurisdiction mortality rates of the general population.

Results: A total of 3,682 patients who survived at least 5 years following LT were included. Overall, median age at LT was 52 years (IQR 44–58); 53.1% were males; and 84.6% were Caucasians. 49.4% ($n = 1,820$) died during a follow-up period of 36,828 person-years (mean 10 years). 80.2% ($n = 1460$) of all deaths were premature deaths, defined as death before the age of 75 years (USA and UK) and 65 years (Spain). Age-standardised all-cause mortality as compared to general population was 3 times higher for males and 5 times higher for females. On adjusted analysis, besides older recipients (HR 2.09, 95%CI 1.44–3.04) and older donors (1.38, 95%CI 1.11–1.72), predictors of long-term mortality were pre-LT malignancy (HR 1.28, 95%CI 1.02–1.61), pre-LT CVD (HR 1.35, 95%CI 1.11–1.65) and post-LT dialysis (HR 2.40, 95%CI 1.56–3.68).



Conclusion: This study demonstrates an increased mortality rate in LT recipients even after 5 years of transplantation. It is likely that implementation of simple strategies such as non-invasive cancer screening measures, minimisation of immunosuppression and intensive primary/secondary cardiovascular prevention could further improve survival of organ recipients.

SAT293

Hepatic evaluation of patients with telomeropathies

Olivia Portolese¹, Isaac Ruiz¹, Julien Bissonnette¹, Julian Hercun¹, Helene Castel¹, Bernard Willems¹, Marc Bilodeau¹, Jeanne-Marie Giard¹, Catherine Vincent¹, Ziad Hassoun¹, Geneviève Soucy², Bich Ngoc Nguyen², Basil Nasir³, Pasquel Ferraro³, Julie Morisset⁴, Charles Poirier⁴, Genevieve Huard¹. ¹Centre hospitalier de l'Université de Montréal (CHUM), Liver division, Montréal, Canada; ²Centre hospitalier de l'Université de Montréal (CHUM), Department of Pathology, Montréal, Canada; ³Centre hospitalier de l'Université de Montréal (CHUM), Division of Thoracic Surgery; ⁴Centre hospitalier de l'Université de Montréal (CHUM), Division of pulmonary medicine, Canada
Email: isaac.ruiz@me.com

Background and aims: Telomeropathies arise from an inheritable genes mutations resulting in decreased telomere length and impaired telomere maintenance. The most frequent manifestation of telomeropathy in adults is interstitial lung disease (ILD) that can lead to consideration for lung transplantation. Liver and bone marrow involvement have also been described. Liver assessment in this population is not well described in the current literature. The aim of this study was to describe the liver evaluation and findings of patients with telomeropathies and ILD that were evaluated for liver and lung transplantation.

Method: This is a retrospective analysis of a prospectively recruited real-world cohort including all patients between January 2020 and December 2021 who consulted the pulmonary and hepatology units at the Centre hospitalier de l'Université de Montréal (CHUM) for liver and lung transplantation. Diagnosis of telomeropathy was confirmed by sequence analysis and/or telomere length (flow-fish analysis). Demographic, clinical, biological, radiological and pathological data were collected. Liver fibrosis was assessed by elastometry (FibroScan,

POSTER PRESENTATIONS

Echosens, France) and/or histological analysis of a transjugular liver biopsy.

Results: For this analysis, 17 patients were included. Table 1 shows the main characteristics of the cohort. Mean age was 60 years (50–69) and 10 of 17 patients (58.8%) were male. The main reason for the hepatology consultation was pre-operative evaluation for lung or liver transplantation. Sixteen of the 17 (94.1%) patients had at least one comorbidity. The biological evaluation showed a macrocytosis with a mean corpuscular volume of 95.1 fL (83.0–104.0). Mean platelet count was 203.3 x10⁹/L (62.0–485.0).

Transient elastography was available for 15 of 17 (88.2%) patients, mean elasticity was 8.9 kPa (3.7–28.0) and the mean CAP was 247 dB/m (168.0–358.0). Five of 17 (29.4%) patients had a transjugular liver biopsy following abnormal elastography result. Mean gradient was 9.4 (4.0–17.0). Steatosis was present in 4/5 cases (80.0%) and cirrhosis in 4/5 cases (80.0%).

One patient out of 17 (5.9%) had an isolated liver transplantation for decompensated cirrhosis and 10/17 (58.8%) had a lung transplantation. No patient underwent combined lung/liver transplantation.

Conclusion: In patient with telomeropathy undergoing liver/lung transplantation evaluation at least 4/17 (23.5%) had a cirrhosis. Transplantation evaluation should include a hepatology consultation, screening and management of comorbidities, a complete etiological assessment of liver diseases, assessment of the portal hypertension and non-cirrhotic portal hypertension and liver fibrosis via transient elastography and transjugular liver biopsy with hepatic venous pressure gradient measurement.

Characteristics	Cohort
Demographic	n = 17
Age (years), median (IQR)	60 (50-69)
Sex (male), n (%)	10 (58.8)
Femme	7 (41.2)
Ethnicity, n (%)	
White	15 (88.2)
Black	1 (5.9)
Asian	1 (5.9)
Comorbidities, n (%)	
Tobacco use	13 (81.3)
Alcohol consumption	13 (76.4)
Diabetes mellitus	8 (47.0)
Arterial hypertension	6 (35.3)
Dyslipidemia	7 (41.2)
Obesity/overweight	7 (41.2)
BMI, mean (range)	25.6 (19.5-33.5)
Hypothyroidism	6 (35.3)
Rheumatoid arthritis	2 (11.8)
Hepatitis B infection	1 (5.9)
Biology, mean (range)	Normal range
Hemoglobin, (g/L)	136.7 (106.0-169.0) 123.0 - 157.0
Mean corpuscular volume, (fL)	95.1 (83.0-104.0) 80.0 - 100.0
Platelets, (10 ⁹ /L)	203.3 (62.0-485.0) 130.0 - 400.0
Leukocytes, (10 ⁹ /L)	7.1 (2.5-12.3) 4.0 - 5.2
Neutrophils, (10 ⁹ /L)	4.8 (1.6-10.0) 2.0 - 7.0
Lymphocytes, (10 ⁹ /L)	1.3 (0.6-2.0) 1.0 - 4.0
Total bilirubin, (μmol/L)	11.0 (6.0-32.0) 7.0 - 23.0
AST, (IU/L)	25.5 (14.0-57.0) 13.0 - 39.0
ALT, (IU/L)	22.9 (8.0-78.0) 8.0 - 31.0
Alkaline phosphatase, (IU/L)	68.7 (41.0-114.0) 36.0 - 110.0
Gamma-glutamyl Transferase, (IU/L)	37.6 (9.0-107.0) 7.0 - 33.0
Positive Antinuclear Antibodies (>1/160), n (%)	4 (23.5) Negative
Ferritin, (μg/L)	192.8 (42.0-857.0) 10.0 - 307.0
Transferrin saturation, (%)	31.1 (14.0-94.0) 15.0 - 50.0
IgG (n = 10)	12.9 (6.0-20.2) 6.0 - 15.0
Epstein-Barr virus (EBNA IgG +), n (%)	17 (100.0) Negative
Herpes simplex virus -1 (IgG), n (%)	10 (58.8) Negative
Alpha-1-antitrypsin, mean (range)	1.8 (1.2-2.8) 1.0 - 1.9
Radiology	
Transient elastography (Fibroscan), n (%)	15 (88.2)
kPa, mean (range)	8.9 (3.7-28.0)
CAP, dB/m, mean (range)	247.0 (168.0-358.0)
Doppler ultrasound, n (%)	16/17 (94.1)
Portal hypertension signs, n (%)	2/16 (12.5)
Abdominal CT scan, n (%)	7/17 (41.2)
Portal hypertension signs, n (%)	4/7 (57.2)
Thoracic CT scan, n (%)	17/17 (100.0)
Interstitial lung disease, n (%)	17/17 (100.0)
Pulmonary scintigraphy, n (%)	14/17 (82.4)
Pathology	
Transjugular biopsy, n (%)	5 (29.4)
Hepatic venous pressure gradient, (mmHg), mean (range)	9.4 (4.0-17.0)

Figure: Main characteristics of patients.

SAT294

Third dose of SARS-CoV2 mRNA-vaccine in liver transplant recipients: can it bridge the response gap?

Marzia Montalbano¹, Raffaella Lionetti², Ubaldo Visco Comandini¹, Silvia Meschi³, Chiara Agrati³, Federica Conte⁴, Vincenzo Puro³, Paola Piccolo⁵, Giulia Matusali³, Germana Grassi³, Tiziana Mereu¹, Federica Angelone³, Enrico Girardi³, Giuseppe Maria Ettorre⁶, Giampiero D'Offizi¹. ¹National Institute for infectious diseases Lazzaro Spallanzani, POIT; ²National Institute for infectious diseases Lazzaro Spallanzani, POIT; ³National Institute for infectious diseases Lazzaro Spallanzani; ⁴Institute for Systems Analysis and Computer Science "Antonio Ruberti"; ⁵San Giovanni Calibita, Fatebenefratelli Hospital; ⁶San Camillo Hospital, POIT
Email: raffaella.lionetti@inmi.it

Background and aims: Liver transplant recipients (LTRs) show reduced immunological response after 2-dose mRNA vaccine against SARS-CoV2: stronger immunosuppression, time from transplant (TFT) and mycophenolate mofetil (MMF) were related to non-response (NR; D'Offizi, Liver Int 2021). Some studies indicated an additional vaccine dose could improve response. Aim of our study is to assess the effect of a third dose on mRNA vaccine response in LTRs. **Method:** 181 consecutive LTRs (median age 63 years, M/F 149/32) were tested for humoral response before first dose (T0), before second dose (T1), 2 weeks after second dose (T2), before third dose (T3), at 4 (T4) and 12 weeks (T5) after third dose; and for cellular response via Th1 production of interferon-γ (IFN-γ) at T3, T4, T5. Anti-spike IgG (RBD) and neutralizing antibodies (N-Ab) were measured and results expressed as median. NR was defined as titre <7.1 binding antibody units (BAU) for RBD; Micro-Neutralization Assay <5 for N-Ab. NR was defined as <10 pg/ml for IFN-γ. TFT groups were defined by a cut-off of more or less than 6 years.

Results: After 2-dose vaccine, 31 LTRs (17%) were non-responders for RBD and 74 (40.6%) for N-Ab. After third dose, a positive response for RBD and N-Ab was observed in 27 (87%) and 61 (82.4%) LTRs with previous NR, respectively.

Overall, MMF was a significant negative predictive factor for RBD (p <0.001) and N-Ab (p = 0.003) response at T2, but not at T4 and T5. Among responders, RBD titre was lower in LTRs receiving MMF at T2 (180 BAU vs. 278 BAU, p <0.05) and at T4 (2331 BAU vs. 4009 BAU, p <0.05), while N-Ab titre was lower only at T4 (160 vs. 320, p <0.05). Overall, we observed significantly higher response among LTRs with TFT >6 years vs. <6 years at all time points (p = 0.0001 and p = 0.0004; p = 0.026 and p <0.0001; p = 0.025 and p <0.0001 at T2, T4, T5 for RBD and N-Ab, respectively).

Among responders, RBD titre was higher among LTRs with TFT >6 years vs. <6 years at T2 (337 BAU vs. 113 BAU, p <0.05), at T4 (3407 BAU vs. 1402 BAU, p <0.0001), and at T5 (1927 BAU vs. 693 BAU, p <0.0001). N-Ab titre was significantly higher only at T5 (160 vs. 80, p <0.05). IFN-γ production correlated with humoral response at all time points (r = 0.4, p <0.0001 and r = 0.32, p <0.001 at T3; r = 0.29, p = 0.0007 and r = 0.32, p = 0.0004 at T4; r = 0.3, p = 0.0006 and r = 0.35, p <0.0001 at T5 for RBD and N-Ab, respectively). None of the analysed variables influenced IFN-γ response.

Liver disease aetiology and comorbidities (diabetes, cancer, obesity, HIV positivity) did not influence response after third vaccine dose.

Conclusion: A third dose enhances antibody response in LTRs who had a poor response after an initial 2-dose mRNA vaccination to SARS-CoV2. However, MMF and TFT <6 years were associated with lower titres for RBD and N-Ab after the third dose. Further clinical studies should assess whether this enhanced response correlates to a favourable clinical outcome after breakthrough SARS-CoV2 infection.

SAT295

Protein-energy malnutrition is associated with worse outcomes in patients admitted for liver transplant: analysis of national inpatient sample

Mahmoud Mansour¹, Ratib Mahfouz², Mohammad Darweesh³, Adham Obeidat⁴, Nikolaos T. Pyrsopoulos⁵. ¹University of Missouri Columbia, Internal Medicine, Columbia, Missouri, United States; ²Kent Hospital/Brown University, Internal Medicine, Warwick, Rhode Island, United States; ³East Tennessee State University, Internal Medicine, Johnson City, Tennessee, United States; ⁴University of Hawaii, Internal Medicine, Honolulu, Hawaii, United States; ⁵Rutgers-New Jersey Medical School, Gastroenterology and Hepatology, Rutgers, New Jersey, United States
Email: pyrsopni@njms.rutgers.edu

Background and aims: Protein-energy malnutrition (PEM) is a common complication in liver cirrhosis patients, with an estimated prevalence of 25.1 to 65.5%. PEM among cirrhotic patients has been associated with increased morbidity and mortality. The data on the in-hospital outcomes of patients who underwent liver transplantation with co-existing PEM is limited. In this study we sought to evaluate the impact of PEM on patients who underwent liver transplantation.

Method: The United States Nationwide Inpatient Sample was used to search for patients who underwent liver transplantation between Jan 1st, 2016, to Dec 31st, 2019. Using International Classification of Diseases 10th revision codes, we divided patients into two groups based on the presence or absence of PEM. The NIS-provided discharge-level weights were used to reflect prevalence estimates. The primary outcome was in-hospital mortality. Secondary outcomes were intensive care unit (ICU) admission, length of stay (LOS), and hospital charges. Multivariate logistic regression was used to adjust for comorbidities and demographic variables.

Results: Among the 29, 050 patients who underwent liver transplantation, 7, 650 (26.33%) had the diagnosis of PEM. Patients with PEM had higher mortality, ICU admission, mean LOS, and hospital charges compared to those without PEM. After adjusting for potential confounders, PEM was an independent predictor of worse outcomes in patients undergoing liver transplantation. Adjusted odds ratio was 1.64, (p = 0.008) for mortality, and 1.88 (p <0.001) for ICU admission. Adjusted mean for LOS and total hospital charges increased by 14.49 days and \$323, 270, respectively, for liver transplant patients with PEM compared to those without PEM.

Table: In-hospital outcomes of patients undergoing liver transplant with and without a diagnosis of protein-energy malnutrition (PEM).

Outcome	Without PEM	With PEM (p value)	aOR (95% CI)
In-hospital mortality (%)	2.50%	4.05% (<0.001)	1.64 (1.14–2.36)
ICU admission (%)	5.42%	9.76% (<0.001)	1.88 (1.58–2.24)
Mean length of stay (days)	16.40	30.75 (<0.001)	14.49* (12.15–16.82)
Mean hospital charges (US\$)	513, 902	832, 365 (<0.001)	322, 270* (253, 832–392, 708)

*Adjusted mean difference

Abbreviations: PEM: protein energy malnutrition, CI: confidence interval, aOR: adjusted odds ratio

Conclusion: PEM is associated with increased morbidity, mortality, and hospital burden in patients admitted for liver transplantation. Timely nutrition assessment and intervention in liver transplant recipients may improve outcomes.

SAT296

COVID vaccination among liver transplant recipients: A EASL-ESOT/ELITA-ILTS multi society survey

Carmen Vinaixa^{1,2}, Francesco Paolo Russo³, Luca Saverio Belli⁴, Wojciech Polak⁵, Manhal Izzy⁶, Varvara Kirchner^{7,8}, Tommaso Di Maira^{1,2}, Ashwin Rammohan⁹, Thomas Berg¹⁰, Marina Berenguer^{1,2,11}. ¹Hospital Universitario y Politécnico La Fe, Hepatology and Liver Transplantation Section, Digestive Diseases Department, Valencia, Spain; ²Instituto de Salud Carlos III, Madrid, Spain; ³Azienda Ospedale-Università Padova, Gastroenterology and Multivisceral Transplant Unit Department of Surgery, Oncology and Gastroenterology, Padua, Italy; ⁴Dipartimento Medico Polispecialistico, Milan, Italy; ⁵Erasmus MC, Department of Surgery Division of HPB and Transplant Surgery, Rotterdam, Netherlands; ⁶Vanderbilt University, Nashville, United States; ⁷Minnesota, United States; ⁸Stanford University, Division of Abdominal Transplantation, Department of Surgery, Stanford, United States; ⁹Dr Rela Institut and Medical Center, Chennai, India; ¹⁰University Medical Center, Leipzig, Germany; ¹¹University of Valencia, Department of Medicine, Valencia, Spain
Email: vinaixa.carmen@gmail.com

Background and aims: Liver transplant (LT) recipients have been prioritized for vaccination in most parts of the world. The aim of this multi-society survey was to explore and to describe the different policies and outcomes of vaccination in this population in a real-world setting.

Method: A web-based survey was available online from October 2021 to February 2022 to members of the EASL, ESOT/ELITA and ILTS. The survey was divided into 4 domains: (1) Vaccination policies, (2) Safety assessment, (3) Efficacy assessment, and (4) center data. No patient-related data were collected.

Results: 188 eight out of 470 centers responded to the survey. There was a wide geographic distribution: 41% Europe, 24% Asia and 23% North America (Fig 1).

The global response rate to the survey's section on vaccination policies was 90%. Most transplant patients (86%) were vaccinated after 12 months post-LT. Prioritization of transplant patients was very common (85% of centers), this was the case for co-habitants in only 29% of centers. mRNA vaccines were used in most centers (76%); with restrictions to use only these vaccines in transplant recipients in 43% of these centers, followed by viral vector vaccines in 27%. Barriers to vaccination were reported in 23% of cases, related to patient's fear (80%), public health policies (33%) and logistics (20%). Vaccination was ordered by health-care authorities or government in 56% of cases, and by the transplant provider in 30%. Other vaccines as flu were reported to be routinely recommended (92%).

The global response rate to the survey's section on safety assessment was 75.4%. Only 1/3 of centers implemented specific monitoring policies for liver function tests (LFT) and/or immunosuppression (IS) levels post-vaccination, with variable frequencies. Most patients (59%) were monitored in the outpatient clinic, via telemedicine (26%) or patient self-reporting (9%). Only 28% of centers responded to the IS section, and only a minority of them (9%) reported that changes in IS were implemented before vaccination, with variable strategies. Regarding adverse events (AE) post-vaccination, 27% of centers observed LFT elevation, 11% thromboembolic events, 9% acute graft rejection and 17% other AE.

83% of centers answered the vaccine efficacy assessment section: 1/3 of centers tested for SARS-CoV-2 antibodies post-vaccination. COVID-19 positive cases post-vaccination were observed in 65% of the centers, and 33% amongst these were severe.

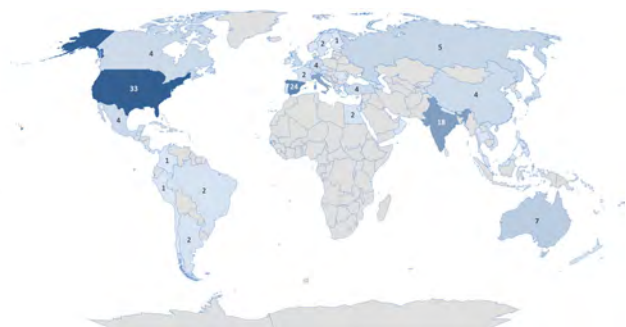


Figure: Geographic distribution of responding centers

Conclusion: COVID-19 vaccination is almost universal amongst LT recipients all over the world, with mRNA vaccines being the main type of vaccine administered. Monitoring for safety and efficacy purposes post-vaccination was only performed in one third of centers, probably reflecting the lack of recommendations. More than half of the centers reported post-vaccination COVID-19 cases.

SAT297

Does m-RNA vaccination protect from Sars-Cov2 (asymptomatic) infection in liver transplant recipients?

Ubaldo Visco Comandini¹, Marzia Montalbano², Raffaella Lionetti², Paola Piccolo³, Daniela Nesticò⁴, Silvia Meschi⁴, Chiara Agrati⁴, Chiara Taibi⁴, Laura Vincenzi², Enrico Girardi⁴, Giuseppe Maria Ettorre⁵, Giampiero D'Offizi². ¹National Institute for infectious diseases Lazzaro Spallanzani, POIT, Rome, Italy; ²National Institute for infectious diseases Lazzaro Spallanzani, POIT; ³San Giovanni Calibita, Fatebenefratelli Hospital; ⁴National Institute for infectious diseases Lazzaro Spallanzani; ⁵San Camillo Hospital
Email: ubaldo.viscocomandini@inmi.it

Background and aims: Vaccination significantly reduces COVID-19 morbidity and mortality, as well as hospitalization, but it is less clear whether vaccination also prevents from asymptomatic infection. Liver Transplant recipients (LTRs) are less prone to develop severe COVID-19 compared to other solid organ transplant recipients (Trapani S, AJT 2021). A high frequency of asymptomatic Sars-CoV2 infections has been described in LTRs (Visco-Comandini, JLT 2021). The study aim is to compare the vaccine-induced humoral response in LTRs who developed Sars-Cov2 infection during or after three dose of mRNA vaccination, with those who did not

Method: The LTRs cohort is composed by 246 subjects, 182 of whom completed a 3-dose vaccination program in 2021. Subjects with Sars-CoV2 infection prior to 1st dose were excluded.

All LTRs were regularly screened through telephone-based questionnaire or clinical visits to detect systemic, respiratory or gastrointestinal symptoms. LTRs reporting symptoms compatible with COVID-19

or close contact to a positive subject underwent nasopharyngeal swab (NPS) to detect active infection.

Sars-CoV2 Receptor Binding Domain antibodies (RBD-Ab, detection limit >7.1 BAU/ml) were prospectively measured at T0 [before 1st dose], T2 [4 weeks (W) after 2nd dose], T3 [before 3rd dose], T4 (4 W after) and T5 (12 W after) in all.

Anti-RBD and neutralizing antibodies (n-Ab, detection limit <1:5 for *alpha* and *delta*, <1:2.5 for *omicron*) were measured at T2, T3, T4 and T5. Neutralizing activity was measured toward *alpha* variant (T2), *alpha* and *delta* variants (T3 and T4), *delta* and *omicron* variants (T5)

Results: Twenty-seven of 164 LTRs were infected by Sars-CoV2 (14.8%) after the 1st dose: 9 between the 2nd and 3rd dose (group A), and 18 after the 3rd dose (group B). Their RBD-Ab and n-Ab titres measured at the last time point before infection, were compared to the remaining vaccinated LTRs who never developed a positive NPS or a positive non RBD-serology (controls, n = 137) (Figure 1).

Moderate to severe COVID19 cases were observed in 2/9 (22.4%) subjects infected after the first/second dose of vaccine (*alpha* or *delta* variant), and in 1/18 (5.5%) infected after the third dose (*delta* or *omicron* variant).

The rate of non-response to vaccination was 22.2% in group A and 22.1% in controls at T2; 0% and 2.9%, in group B and controls respectively at T4.

Absence of neutralizing activity was 77.8% in group A and 46.0% in controls at T2 (p = 0.09); 22.2% and 7.8%, at T4 in group B and controls (p = 0.07).

At T5 infected LTRs showed higher RBD-Ab compared to controls (median 2019, IQR 691–3845 BAU/ml vs 1281, IQR 452–2994 BAU/ml p < 0.05) but similar n-Ab titers

Conclusion: Sars-CoV2 infection between 1st and 3rd vaccination doses was associated with lack of anti-RBD response or lower neutralizing activity, while infection after the 3rd dose seemed to be independent of humoral response to vaccination

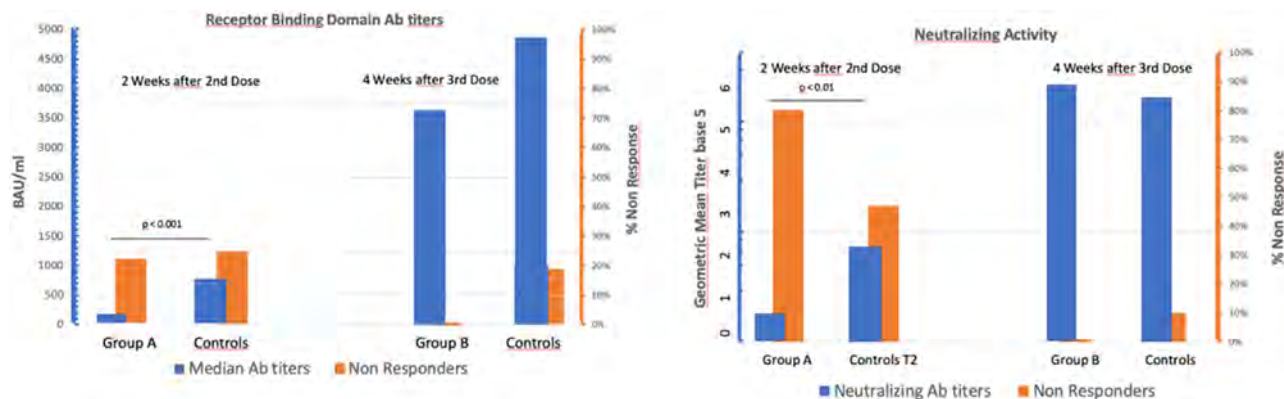


Figure: (abstract: SAT297)

SAT298

Low dose interleukin-2 selectively expands circulating regulatory T cells but fails to promote transplantation tolerance in humans

Tiong Yeng Lim¹, Elena Perpinan¹, Maria Carlota Londoño², Rosa Miquel¹, Paula Ruiz¹, Ada Kurt¹, Elisavet Codela¹, Amy Cross³, Claudia Berlin³, Joanna Hester³, Fadi Issa³, Abdel Douiri⁴, Felix Volmer⁵, Richard Taubert⁵, Evangelia Williams⁶, Jake Demetris⁷, Andrew Lesniak⁷, Gilbert Bensimon⁸, Juanjo Lozano⁹, Marc Martinez-Llordella¹, Timothy Tree⁶, Alberto Sanchez-Fueyo¹.

¹King's College Hospital, Institute of Liver Studies, United Kingdom; ²Hospital Clínic Barcelona, Liver Unit, Barcelona, Spain; ³University of Oxford, Transplantation Research Immunology Group, Oxford, United Kingdom; ⁴King's College London, School of Population Health and Environmental Sciences, London, United Kingdom; ⁵Hannover Medical School, Department of Gastroenterology, Hepatology and Endocrinology, Hannover, Germany; ⁶King's College London, Department of Immunobiology, School of Immunology and Microbial Sciences (SIMS), London, United Kingdom; ⁷University of Pittsburgh, Department of Pathology, Pittsburgh, United States; ⁸Hôpital de la Pitié-Salpêtrière et UPMC Pharmacologie, Département de Pharmacologie Clinique, Paris, France; ⁹Carlos III Health Institute, ioinformatic platform, Biomedical Research Center in Hepatic and Digestive Diseases (CIBEREHD), Barcelona, Spain
Email: lly24@gmail.com

Background and aims: Low dose interleukin-2 (LDIL-2) can expand endogenous circulating CD4+CD25+Foxp3+ regulatory T-cells (Tregs) in vivo, but its role in promoting allograft tolerance in humans has not been investigated. We conducted a clinical trial in stable liver transplant (LT) recipients 2–6 years post-transplant to determine the capacity of LDIL-2 to suppress allospecific immune responses and allow for the complete discontinuation of maintenance immunosuppression.

Method: The LITE trial is a phase IV, open-label, activity, safety and efficacy, prospective single arm clinical trial in which stable LT recipients <50 years old and 2–6 years post-LT receive 6 months of daily 1 million IU injections of LDIL-2. After 4 weeks of LDIL-2 treatment, those recipients in whom circulating Tregs expand >2-fold gradually discontinue their immunosuppressive medication over 3 months. Patients who maintain stable serum liver tests and normal histology 1 year after immunosuppression withdrawal are considered tolerant.

Results: Six patients were recruited with a median age of 34 years (range 22–49) and 38.5 months (range 31–45) post-LT. All patients achieved a marked and sustained increase in circulating Tregs, in keeping with previous studies. Significant increases in circulating eosinophils, basophils, CD56bright NK cells and a reduction in the absolute numbers of circulating B cells were also observed. However, these findings were not associated with the preferential expansion of donor-reactive Tregs and did not promote the accumulation of intra-hepatic Tregs. Furthermore, LDIL-2 induced a marked interferon- γ orchestrated transcriptional response in the liver even before immunosuppression weaning was initiated. The trial was terminated after the first six trial participants failed to reach the primary end point due to rejection requiring immunosuppression reinstitution.

Conclusion: Our trial provides unique insight into the mechanisms of action of immunomodulatory therapies such as LDIL-2 and their limitations in promoting alloantigen-specific effects and immunological tolerance.

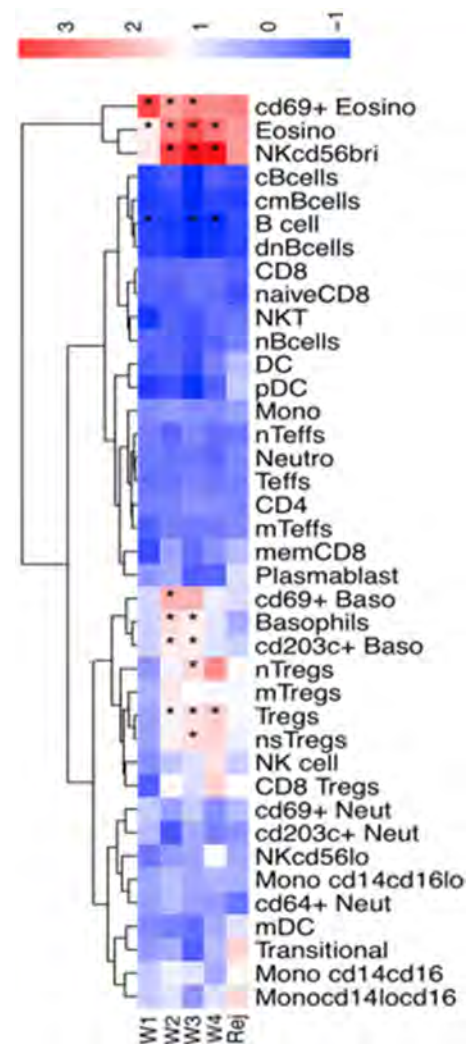


Figure: Sequential changes in mean absolute counts of each circulating immune cell subset following LDIL-2 treatment.

SAT299

Clinical significance of three-dimensional printing of the portal venous system in patients with extrahepatic portal hypertension

Binita Chaudhary¹, Utpal Anand², Rajeev Priyadarshi³. ¹All India Institute of Medical Sciences, Patna, Anatomy, Patna, India; ²All India Institute of Medical Sciences, Patna, Surgical Gastroenterology, Patna, India; ³All India Institute of Medical Sciences, Patna, Radiodiagnosis, Patna, India

Email: binitachaudhary18@gmail.com

Background and aims: Three-dimensional printing (3DP) is a novel technique that can generate 3D virtual image from multidetector computed tomography (MDCT) scan. The aim of the study was to investigate the feasibility of 3DP in visualization of portal venous system of patients with extrahepatic portal vein obstruction (EHPVO) to improve the surgical outcome (surgical time, blood loss).

Method: This retrospective study was performed in the Department of Anatomy in 24 patients of EHPVO who underwent shunt surgery from November 2018 to March 2022. The patients were divided into conventional planning group based on MDCT imaging (n = 12) and

POSTER PRESENTATIONS

planning with 3D printing group based on the 3D reconstruction of portal venous system (n = 12).

The image of MDCT was transferred to D2P software (dicom to print) and saved in a standard format DICOM (digital imaging and communication in medicine). Bone, soft tissue and blood vessels were semi-automatically segmented into separate areas. Segmented regions were combined to create a 3D object. These 3D objects were exported from D2P as STL files. STL files were repaired in 3D design software (Geomagic freeform plus) and a virtual 3D prototype was created. 3D virtual image prepared were used to see the exact location and depth of splenic and renal vein as well as surrounding collaterals.

Results: In conventional planning group, there were 12 patients (8 males and 4 females) with mean age of 24.00 ± 10.91 . The time from day of surgery to the day of discharge from hospital was 7.08 ± 2.53 days. In planning with 3D printing group, there were 12 patients (10 males and 2 females) with mean age of 32.08 ± 16.57 years. The time from day of surgery to the day of discharge in 3D printing group was 7.16 ± 2.20 days.

The mean surgical time in planning with 3D printing group was 252.50 ± 11.579 min, which was significantly lower than that of conventional planning group (298.16 ± 12.87 min); P value < 0.05 . The intraoperative mean blood loss in planning with 3D printing group and conventional planning group were 441.25 ± 44.52 ml and 624.16 ± 123.13 ml respectively; (P value < 0.05).

The rate of complication in the planning with 3D printing group and conventional planning group was 16.66% (2/12) and 8% (1/12) respectively.

Conclusion: Presurgical planning in 3D printing reduces guesswork and thus it remarkably reduces surgical time, blood loss, minimizes complication and improves surgical outcome.

SAT300

Liver transplantation (LT) and ethnicity in the United States: the impact of non-alcoholic steatohepatitis

Zobair Younossi¹, Reem Al Shabeeb², Michael Harring², Dipam Shah², Janus Ong³, Saleh Alqahtani^{4,5}, Linda Henry^{1,6}, Maria Stepanova^{1,2,6}.

¹Inova Health System, Medicine Service Line, Falls Church, United States;

²Inova Fairfax Medical Campus, Department of Medicine, Center for Liver Diseases, FALLS CHURCH, United States; ³College of Medicine, University of the Philippines, Manila, Philippines; ⁴Johns Hopkins Medical Center, Division of Gastroenterology and Hepatology, Baltimore, United States;

⁵King Faisal Specialist Hospital and Research Center, Liver Transplant Center and Biostatistics, Epidemiology and Scientific Computing

Department, Riyadh, Saudi Arabia; ⁶Center for Outcomes Research in Liver Disease, Washington DC, United States

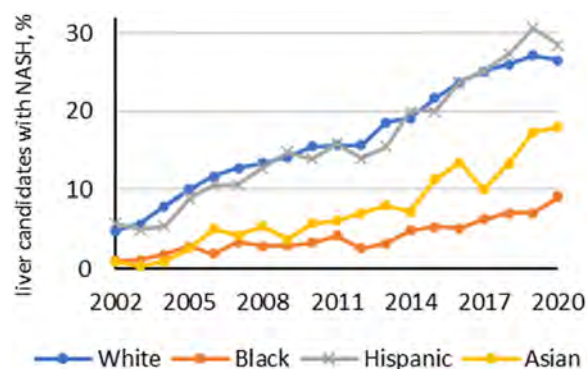
Email: zobair.younossi@inova.org

Background and aims: The burden of chronic liver disease (CLD) may vary by race and/or ethnicity. We aimed to assess distributions and trends of different CLD etiologies among liver transplant (LT) candidates from major racial/ethnic groups in the U.S. over the last two decades.

Method: The Scientific Registry of Transplant Recipients (SRTR) data 2002–2020 was used to select adult (≥ 18) candidates for LT. Patients

without race/ethnicity data (white, black, Hispanic, or Asian) were excluded. Trends in the proportions of common LT etiologies, such as chronic hepatitis B (CHB), chronic hepatitis C (CHC), non-alcoholic steatohepatitis (NASH, including cryptogenic cirrhosis if accompanied by obesity or type 2 diabetes), alcoholic liver disease (ALD) were assessed over time.

Results: 204, 382 LT candidates with known race/ethnicity were included: n = 146, 535 non-Hispanic white (4.1 per 100, 000 per year with reference to the general U.S. population), n = 17, 653 non-Hispanic black or African-American (2.3 per 100, 000), n = 31, 086 Hispanic (2.7 per 100, 000), and n = 9, 108 Asian (2.4 per 100, 000). In whites, the most common etiologies were CHC (27% across all study years) followed by ALD (23%) and NASH (17%). In addition, in whites, there was a decreasing trend in CHC (34% in 2002–2005 to 12% in 2018–2020) but increasing trends in NASH (7% to 27%) (Figure) and ALD (17% to 34%) (all trend $p < 0.0001$). In blacks, CHC (41% in 2002–2005 to 25% in 2018–2020) decreased while ALD increased from 7% to 18% (all $p < 0.0001$). In Hispanics, the trends were similar to whites with CHC decreasing (40% in 2002–2005 to 13% in 2018–2020) while ALD (17% to 34%) and NASH (6% to 29%) increasing (all $p < 0.0001$). Finally, in Asians, the most common etiologies of LT remained CHB and CHC (decreasing from 39% to 28% and from 28% to 11% in 2002–2005 to 2018–2020, respectively) while ALD (3% to 14%) and NASH (1% to 16%) increased (all $p < 0.0001$). The proportions of HCC remained substantially elevated in Asians (28% in 2002–2005, 39% in 2014–2017, and 36% in 2018–2020), and over time was increasing from 2002 to 2005 (7–8%) to 2014–2017 (21–27%) in all other ethnic groups but then decreased in 2018–2020 (17–24%). In multivariate analysis, older age, female gender, obesity and type 2 diabetes were associated with the etiology of NASH in LT candidates of all ethnic groups (all $p < 0.0001$). Higher post-transplant mortality was associated with older age, diabetes, higher MELD score and HCC in all ethnic groups ($p < 0.01$).



Conclusion: CLD etiologies of liver transplant candidates in the U.S. vary across racial/ethnic groups and over time in the U.S. The proportion of NASH among LT candidates increased at least 4-fold between years 2002–2005 and 2018–2020 in all major ethnic groups.

SAT301

Can endothelial biomarkers before liver transplantation together with classical cardiovascular risk factors be useful to predict cardiovascular risk after liver transplantation

Julia Herrerías López¹, Ángela Carvalho-Gomes², Tommaso Di Maira^{1,1}, Marina Berenguer¹, Victoria Aguilera Sancho^{1,2}. ¹La Fe University and Polytechnic Hospital, València, Spain; ²Instituto de Investigación Sanitaria La Fe de Valencia, Valencia, Spain
Email: toyagui@hotmail.com

Background and aims: Cardiovascular (CV) disease is an important cause of morbidity and mortality after liver transplantation (LT). In the general population endothelial biomarkers have been associated to cardiovascular (CV) risk. Little is known about the relationship between endothelial biomarkers in LT candidates. To analyse pre-LT serum biomarkers (day 0) and to evaluate if they have an association with CV risk after LT alone or in combination with classical CV risk factors.

Method: Frozen plasma of 125 LT with a low FRS between 2014–2017 were analyzed. At one year, patients with a high Framingham Risk Score (FRS) or with metabolic syndrome (MS) were considered of high risk, as a surrogate marker for CV events. Endothelial biomarkers measured were: LpPLA2 measured by ELISA and adiponectine, VCAM1, IL6, TNF alpha and proBNP by Luminex. A multivariate analysis with clinical and endothelial biomarkers was done.

Results: Mean age was 56 years, 78% were men, HCV cirrhosis was the most frequent etiology (36%) followed by alcohol (25%). Before LT, 20% had arterial hypertension and 19% diabetes. At one yr post-LT, 33% were considered to have a high CV risk by FRS or MS. Logistic regression showed that age before LT (OR = 1.06; p = 0, 025), DM before LT (OR = 5, 77; p < 0, 001) were associated with high CV risk. Plasma levels of LpPLA2, adiponectine, TNF alpha and ProBNP were associated with Liver function (MELD and Child) (p < 0, 05). LpPLA 2 showed a tendency through a high CV risk (OR = 2.82, p = 0, 089). A model with clinical and endothelial biomarkers was created. DM (OR 9, 63–31 p < 0, 001), obesity (OR 5, 1 IC 1.62–16 p = 0.005), tobacco use (OR 4.44 IC 1.26–15 p = 0, 02) and LpPLA2 (OR 8, 18 IC 1.5–44 p = 0, 015) were statistically significant associated with CV risk post-LT.

Conclusion: Clinical variables such as age, obesity, DM before LT and tobacco use in combination with endothelial biomarkers (LpPLA2) could be useful to predict CV risk after LT.

SAT302

Factors contributing to late evaluation in liver transplant candidates undergoing inpatient liver transplant evaluation

Katherine Cooper¹, Diana Liu¹, Alessandro Colletta^{1,2}, Deepika Devuni^{1,2}. ¹UMass Chan Medical School, Worcester, United States; ²UMass Memorial Medical Center-University Campus, Worcester, United States
Email: katherine.cooper@umassmed.edu

Background and aims: Timely referral for liver transplant evaluation (LTE) is critical in patients with chronic liver disease (CLD) due to the high mortality associated with decompensation. Unfortunately, CLD can be under recognized resulting in the need for urgent transplant evaluation. We aimed to identify the proportion of late referrals in patients undergoing inpatient LTE and potential causes of late LTE.

Method: Patients undergoing inpatient LTE for CLD at our centre between October 2017 and August 2021 were included in the study. Charts were extensively reviewed for liver history focusing on earliest signs of liver dysfunction, imaging evidence of cirrhosis, time of diagnosis, decompensation history and barriers to referral. Patients were considered to have late referrals if they had a Model of End Stage

Liver Disease score (MELD) >15 or decompensation without a substance-related contraindication to transplant.

Results: One hundred fifty-nine patients, mean age 57.7 (SD 9.6) undergoing inpatient transplant evaluation were identified. About half could have been referred earlier for outpatient transplant evaluation. Two-thirds of these patients were diagnosed at least two years prior to their evaluation and had an average of 4.0 (SD 1.3) decompensations (Table 1). Almost all had a primary care physician or saw a health care provider regularly. The most common barriers to referral included failure to obtain MELD labs/calculate MELD and misconceptions about the sobriety period needed for transplant (Table 1).

Diagnosis relative to LTE	
Months since diagnosis	Median: 30 months [IQR: 12.25–60]
0–1 years since diagnosis	33.3%
2–5 years since diagnosis	48.7%
5+ years since diagnosis	17.9%
Decompensation history prior to LTE	
Total Decompensations (#)	4.0 ± 1.3
Jaundice	66.7%
Hepatic Encephalopathy	78.2%
Ascites	96.2%
Hepatorenal syndrome	35.9%
Spontaneous bacterial peritonitis	20.5%
Large volume paracentesis	52.6%
Upper gastrointestinal/Variceal Bleed	35.9%
Hepatic hydrothorax	11.5%
Reason for late LTE	
Failure to obtain/calculate MELD	14.1%
Diagnosis missed or care delayed	12.8%
Misconception about sobriety cut off	12.8%
Understanding of LTE candidacy	5.1%
Insurance or Financial Barriers	10.3%
Care continuity	7.7%
Patient choice	10.3%
No clear reason	19.2%

Conclusion: Many patients are referred for liver transplant late in their clinical course causing unnecessary health care utilization. Efforts to increase timely referral for liver transplant include improving awareness about routine labs and indications for liver transplantation for non-transplant providers. Further, efforts to improve patient insight into their condition may facilitate the referral process.

SAT303

CMV reactivation is associated with lower hepatocellular carcinoma (HCC) recurrence after liver transplantation (LT)

Victoria Aguilera Sancho^{1,2,3}, Sarai Romero Moreno^{1,3}, Isabel Conde^{1,3}, Tommaso Di Maira^{1,3}, Ángela Carvalho-Gomes^{1,4}, Ángel Rubín^{1,3}, Laura Martínez-Arenas¹, F. Xavier Lopez-Labrador⁵, Marina Berenguer^{1,3,6}. ¹Instituto de Investigación Sanitaria La Fe de Valencia, Valencia, Spain; ²CIBERehd Instituto de Salud Carlos III, Valencia, Spain; ³La Fe University and Polytechnic Hospital, Valencia, Spain; ⁴Instituto de Salud Carlos III, CIBERehd; ⁵Fisabio, Valencia, Spain; ⁶Ciberehd, Instituto Carlos II
Email: toyagui@hotmail.com

Background and aims: There are data that link CMV reactivation (rCMV) with post-LT morbidity and mortality. Recent studies though suggest beneficial effects including a potential oncolytic effect

POSTER PRESENTATIONS

resulting in lower HCC recurrence after LT. To assess the effect of rCMV (before tumoral recurrence) in LT-patients with HCC.

Method: We included LT patients with HCC (2018–2020). Exclusion criteria were: late re-LT, early death <1 month and combined Liver Kidney transplant. Variables: (i) Donor (D) and recipient (R) demographics, (ii) related with rCMV (defined if CMV viral load >400c/ml): DR CMV mismatch, preemptive therapy, CMV disease, (iii) related to HCC: bridging, downstage, vascular invasion, baseline AFP. Prophylaxis with valganciclovir was used in high-risk patients while a preemptive approach was used in the remainder. The retreat score was used to establish posttransplant follow-up (AFP and Tomography).

Results: Out of 266 LT, 122 (83% men, median age 59 yrs) fulfilled inclusion criteria; the main etiology was HCV (31%) followed by alcohol (25%) and the functional Meld was 10 (6–27). Most (80%) were intraMilan at LT; 16 (13%) were included after downstaging and 73% received locoregional therapy either for bridging or downstaging. On explant 11.5% had vascular invasion. Median AFP was 43 (1.1–748 ng/ml). A minority were considered high-risk due to CMV Mismatch (11% D/R ±). rCMV occurred in 50 patients (41%); 22 (18%) started early treatment and 5 (4%) developed CMV disease. Overall, 10 patients (8.2%) had HCC recurrence after a median of 288 days (Q1, Q3: 135–445). In multivariate analysis, vascular invasion [HR 11 (IC 3–44), p:0.08] and absence of rCMV were associated with HCC recurrence [HR 0.12 (IC:0.0006–0.25, p:0.004). Survival at 1, 3 and 5 yrs post-LT was 89%, 82% and 77%, respectively.

Conclusion: In our series, vascular invasion, and absence of rCMV were associated with higher risk of HCC recurrence after LT.

SAT304

Managing HBV/HDV co-infection post liver transplant-Exploring a decade of experience

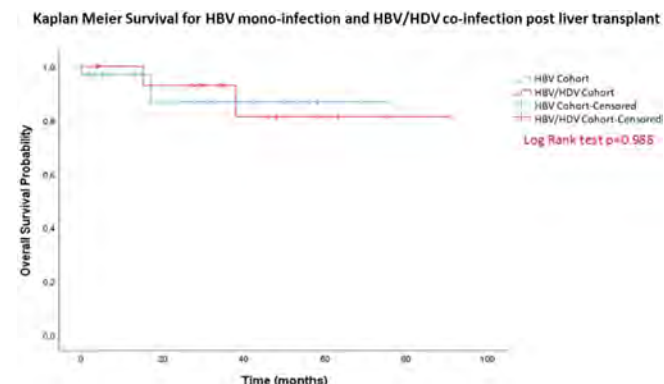
Almuthana Mohamed¹, Lindsay Greenland¹, Maria Guerra Veloz¹, James Lok¹, Khin Aye Wint Han¹, Racquel Beckford¹, Deepak Joshi¹, Michael Heneghan¹, Varuna Aluvihare¹, Abid Suddle¹, Ivana Carey¹, Kosh Agarwal¹. ¹Institute of Liver Studies, King's College Hospital, Hepatology, London, United Kingdom
Email: almuthana700@gmail.com

Background and aims: Liver transplantation is an important treatment modality for hepatitis B patients with delta co-infection (HBV/HDV), including those with hepatocellular carcinoma (HCC) or decompensated cirrhosis. Despite the judicious use of nucleos (t)ide analogues (NA) and hepatitis B immunoglobulins (HBIG), post-transplant management remains challenging, and there is an inherent risk of viral reactivation and graft failure. We describe ten years of experience in managing this patient cohort and explore their long-term clinical outcomes.

Method: In this retrospective study, all patients with HBV/HDV co-infection who underwent liver transplantation at King's College Hospital between 2012 and 2022 were identified. Baseline demographics, date and type of liver transplant, post-surgical management, clinical outcomes, and virological markers (HBV DNA and HDV RNA) pre-, 6- and 12-months post-transplantation were assessed, and Kaplan-Meier's survival curves were generated.

Results: Overall, 16 patients underwent liver transplant, including one individual with concomitant HBV, HDV and HIV infection. The median age was 51 years (Range 29–55, IQR 8), and dominant ethnic groups were Caucasian (n=8, 50%), South Asian and Black African (18.8% each). The most common indication for transplantation was synthetic dysfunction from liver cirrhosis (87.5%). Prior to surgical intervention, 6 patients (37.5%) had detectable HBV DNA levels (Median = 229, Range 71–5.07E3 IU/ml) and 11 individuals (68.8%) had detectable HDV RNA (Median = 2.20E5, Range 1.00E4–3.11E7 IU/ml). In contrast, the vast majority (93.8%) had undetectable HBV DNA and HDV RNA titres at 6- and 12-months post-transplantation. There was also a significant difference in HBsAg levels Pre-transplant, 6- and 12-months post-transplant (p=0.006). All patients were

administered HBIG intra and post-operatively and continued on long-term HBIG and NA. 56% received Tenofovir disoproxil fumarate, 6 individuals (37.5%) were prescribed Entecavir due to underlying renal impairment, and one received tenofovir alafenamide as part of their concurrent HIV treatment. Survival post liver transplant was compared to a control group of HBV mono-infected individuals, the mean survival of HBV/HDV co-infection post liver transplant was 78.6 months, with two fatalities secondary to viral reactivation or transplant-related complications and a mean follow-up of 40.94 months (SD 24.07 months).



Conclusion: This study demonstrates that liver transplantation successfully controls HBV/HDV co-infection expression. Whilst NA and HBIG effectively prevent viral reactivation and are associated with favourable long term outcomes; further work is needed to establish a consensus approach across different transplant centres in this patient group.

SAT305

Durability of SARS-CoV-2 specific immune response following different primary prime-boost vaccine platforms and subsequent humoral response to booster dose among liver transplant recipients

Supachaya Sriphoosanaphan^{1,2}, Sirinporn Suksawatamnuay^{1,2,3}, Nunthiya Srisoonthorn², Nipaporn Siripon², Panarat Thaimai¹, Wanwisar Makhasen², Nawakodchamon Munngnamtrakul², Kessarin Thanapirom^{1,2,3}, Bunthoon Nonthasoot⁴, Pokrath Hansasuta⁵, Piyawat Komolmit^{1,2,3}. ¹Division of Gastroenterology, Department of Medicine, Faculty of Medicine, Chulalongkorn University, Bangkok, Thailand; ²Center of Excellence in Liver Diseases, King Chulalongkorn Memorial Hospital, Thai Red Cross Society, Bangkok, Thailand; ³Liver Fibrosis and Cirrhosis Research Unit, Chulalongkorn University, Bangkok, Thailand; ⁴Department of Surgery, Faculty of Medicine, Chulalongkorn University, Bangkok, Thailand; ⁵Division of Virology, Department of Microbiology, Faculty of Medicine, Chulalongkorn University and King Chulalongkorn Memorial Hospital, Thai Red Cross Society, Bangkok, Thailand
Email: supachaya.sr@gmail.com

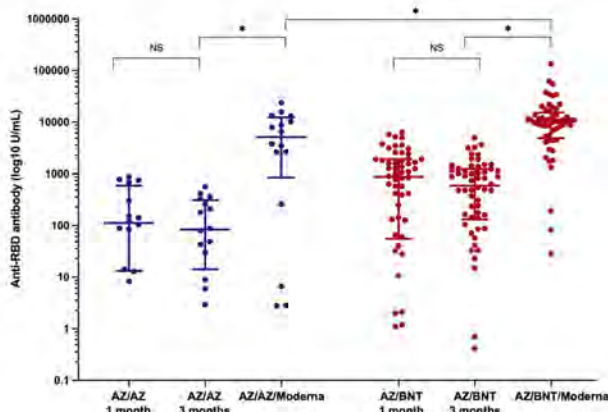
Background and aims: Suboptimal immunogenicity among liver transplant (LT) recipients after primary SARS-CoV-2 vaccination has aroused concerns about the longevity of protection and urgent need of a booster dose. There is a paucity of information on antibody kinetics and response following a third dose vaccine in this population. We aimed to investigate the durability of humoral response after primary immunization induced by different prime-boost vaccine platforms and subsequent response to booster dose in LT recipients.

Method: LT recipients who were vaccinated with ChAdOx1 nCoV-19 (AZ)/AZ or AZ/BNT162b2 (BNT) as primary vaccine series at King Chulalongkorn Memorial Hospital, Bangkok, Thailand, between April and December 2021 were enrolled. The mRNA-1273 (Moderna) was

administered as the booster vaccine at 3 months following the second dose. SARS-CoV-2 spike receptor-binding-protein (RBD) IgG was assessed at 1 month, 3 months after the second dose, and 1 month following the booster vaccine. Anti-RBD antibody was tested using electrochemiluminescence immunoassay (Roche Elecsys). According to the basis of plasma-neutralizing capacity in patients with convalescent SARS-CoV-2 infection, anti-RBD titer of <0.8 U/ml, 0.8–50 U/ml, and >50 U/ml were defined as negative, low-positive, and high-positive, respectively.

Results: Of 74 LT recipients, 51 (68.9%) were male and median age was 61 (IQR 52–68) years. Median time from transplantation was 5.8 (IQR 2.2–10.8) years. Sixty-one (82.4%) patients were taking tacrolimus, 60 (81.1%) anti-metabolite, and 8 (10.8%) steroids. Fifty-eight (78.4%) patients received AZ/BNT as primary vaccine series. Overall, median anti-RBD titers at 1 month after primary immunization were 609.1 (IQR 38.2–1, 632) U/ml and the levels declined to 397.6 (IQR 77.7–1, 098.5) U/ml at 3 months ($p=0.54$). Antibody reduction rate was comparable between two vaccine platforms (32.1% in AZ/AZ versus 43.8% in AZ/BNT, $p=0.25$). After the booster dose, median anti-RBD titers significantly rose to 9, 597.0 (IQR 3, 935–13, 497.5) U/ml ($p<0.001$). The proportion of LT patients with high-positive titers significantly increased from 78.4% at 3 months after primary immunization to 98.6% following the third vaccination ($p<0.001$). Patients who received heterologous prime-boost regimen as primary vaccine series had significantly greater anti-RBD levels after the booster (10, 346.0 U/ml in AZ/BNT/Moderna group versus 5, 134.0 U/ml in AZ/AZ/Moderna group, $p=0.04$). (Figure 1)

Figure 1: Anti-RBD antibody levels at 1 month, 3 months after primary SARS-CoV-2 vaccination, and 1 month after a booster dose in LT recipients (Horizontal lines indicate the median and interquartile range; * p -value <0.05; NS, non-significant)



Conclusion: SARS-CoV-2 specific antibody among LT recipients waned over time after primary immunization regardless of vaccine platforms. The booster strategy substantially provided high protective antibody titers in almost all LT patients. Further studies evaluating duration of protection after the booster as well as clinical effectiveness against the variants of concerns are warranted.

SAT306

Outcome of choledochal cysts with intrahepatic involvement (type IV-A) after extrahepatic cyst excision and roux-en-Y hepaticojejunostomy in adults

Utpal Anand^{1,1}, Rajeev Priyadarshi², Ramesh Kumar³. ¹All India Institute of Medical Sciences, Patna, Surgical Gastroenterology, Patna, India; ²All India Institute of Medical Sciences, Patna, Radiodiagnosis, Patna, India; ³All India Institute of Medical Sciences, Patna, Gastroenterology, Patna, India
Email: utpalanand2@gmail.com

Background and aims: Type I and type IV-A choledochal cysts (CC) according to Todani's classification are the most frequent types.

Unlike type I CC, in which the dilatation is confined to the extrahepatic bile duct, type IV-A affects both extra and intrahepatic ducts. The aim of this study was to evaluate outcomes in adult patients with type IV-A CC at least 2 years after resection of the extrahepatic bile duct cyst.

Method: Data was collected retrospectively from a cohort of 60 adult patients who underwent extrahepatic cyst resection for type IV-A CC from 2010 to 2020 in our institution. A total of 45 patients were included in the final analysis, with a minimum follow-up of two years

Results: Follow-up time ranged from 2 years to 10 years (median, 25 months). Thirty five patients remained asymptomatic; however, 5 patients had abnormal liver function tests (LFTs), requiring regular monitoring. Late complications in varying combinations were seen in 10 patients (16.6%), which included cholangitis and/or intrahepatic-hepatic stones in 9 (15%), intrahepatic bile duct stenosis with stones in 2, anastomotic stricture with or without stone formation in 6, and left lobar atrophy with intrahepatic stones in 3 patients.

Magnetic resonance cholangiopancreatography and/or Computed tomography scans was done to evaluate the causes of stricture which revealed anastomotic stricture in 6 patients and web like stenosis of the left intrahepatic bile duct in 2 patients. Percutaneous transhepatic biliary dilatation was done in 2 patients with anastomotic stricture without cystolithiasis. Re-do hepaticojejunostomy (HJ) required in the remaining 4 patients. The stenotic bile duct was incised and hepaticojejunostomy was performed in both patients with left intrahepatic web. The median time interval from primary surgery to reintervention was 24 months. The median follow-up period after reoperation was 5 years.

Out of 6 patients who required re-do HJ, three patients had left lobe atrophy with patent HJ anastomosis with recurrent attack of cholangitis on follow-up of 3, 8 and 10 years respectively. Two of them underwent left hepatectomy and refashioning of anastomosis and other was kept on conservative management.

Conclusion: Residual intrahepatic dilatation of type IV-A cyst in adults did adversely affect the postoperative outcome after a conventional surgical repair. A long term follow-up is necessary to recognize and address late complications.

SAT307

The impact of COVID-19 on the duration of the liver transplant process in patients presenting for inpatient liver transplant evaluation

Katherine Cooper¹, Arslan Talat^{1,2}, Diana Liu¹, Alessandro Colletta^{1,2}, Deepika Devuni^{1,2}. ¹UMass Chan Medical School, Worcester, United States; ²UMass Memorial Medical Center-University Campus, Worcester, United States

Email: katherine.cooper@umassmed.edu

Background and aims: The SARS-CoV-2 pandemic (COVID-19) adversely affected liver transplantation internationally. At its peak, COVID-19 was associated with decreased transplant rates and increased waitlist mortality. Though many centres have resumed normal transplant activities, there is concern that reduction in health care services may mean patients present later in their disease course resulting in need for more urgent transplant evaluations. We aimed to evaluate differences in the inpatient liver transplant process before and after the COVID-19 pandemic to understand the impacts on the overall transplant care pathway.

Method: Medical records for all patients undergoing liver transplant evaluation (LTE) from 10/2017–8/2021 were reviewed. Patients undergoing LTE for chronic liver disease (CLD) were included; patients with a history of liver transplant or in fulminant liver failure were excluded. Records were categorized as Pre-COVID if evaluation was before 3/15/2020 and post-COVID if after 3/15/2020. Demographic and clinical history were collected for patients undergoing inpatient LTE. Variables were compared using Fishers exact test and students t-tests; significance was evaluated at $p=.05$.

POSTER PRESENTATIONS

Results: One hundred and fifty-nine evaluations occurred (54% Pre-COVID, 46% Post-COVID). Time from referral to the first day of LTE tended to be longer in the Post-COVID period than the Pre-COVID period. Conversely, there was a significant reduction in days from transplant referral to liver transplant in patients who underwent inpatient LTE in the Post-COVID period ($p = 0.0227$). Time having elapsed There were no differences in age ($p = 0.85$), MELD-Na (0.81), months since diagnosis ($p = 1.0$). About 40% of patients who underwent inpatient LTE in the Post-COVID group had received a transplant at the time of data collection compared to 36.0% in the Pre-COVID group. Further, the rate of transplants performed per month has been about 70% higher for patients evaluated in the Post-COVID period compared to the Pre-COVID period (1.8 vs. 1.1 transplants per month, respectively).

	Pre COVID (n = 86)	Post-COVID (n = 73)	p value
Age (years)	57.6 ± 9.6	57.9 ± 9.7	0.845
Time since diagnosis (months)	49.0 ± 62.30	49.0 ± 77.7	1.0
MELD-Na (points)	27.3 ± 7.8	27.0 ± 8.3	0.81
Process Length			
Referral to Evaluation (days)	9.0 ± 17.9	14.4 ± 29.2	0.1552
Referral to Committee (days)	19.3 ± 26.3	22.9 ± 29.2	0.415
Referral to Transplant (days)	105.7 ± 176.6	55.4 ± 65.9	0.0227*

Conclusion: The COVID-19 pandemic appears to have had a negative impact on the ability to undergo evaluation for liver transplant in the outpatient setting. Despite this, patients seem to be receiving transplants at a faster rate despite no differences in time since diagnosis or MELD-Na at the time of work up. The reason for this is multifactorial and may include hospital capacity, varying disease progression, and clinical presentation.

SAT308

Patients with polycystic liver disease have longer waiting times but better clinical outcomes following liver transplantation in the UK

Matthew Gittus¹, Joanna Moore², Albert Ong¹. ¹The University of Sheffield, United Kingdom; ²Saint James Hospital, United Kingdom
Email: m.gittus@sheffield.ac.uk

Background and aims: Polycystic Liver Disease (PLD) can negatively impact a patient's quality of life with potentially debilitating symptoms secondary to hepatomegaly. Liver transplantation remains the only curative option. Liver transplantation rates and outcomes for people with PLD in the UK are not known. People with PLD are now often registered to the Variant Syndrome waiting list which is currently proportionally allocated liver allografts by NHS Blood and Transplant (NHSBT). Prior to this individual transplant centres allocated to their patients.

Method: Retrospective, national, cohort study using NHSBT data from 01/01/2010 and 31/12/2020. All adult recipients who received an elective liver or liver-kidney allograft in UK transplant centres. Data analysis was performed using SPSS 2020.

Results: There are 156 (2%) PLD recipients and 7686 (98%) non-PLD recipients with longer waiting time for PLD recipients compared to non-PLD recipients (mean 513.3, SD 491.8 vs 114.7 days, SD 199.6) but lower mortality (3.8% vs 8.1%) and graft failure (7.3% vs 14.9%) rates. Significant variation in PLD transplantation rates exists between the seven UK transplant centres ($p < 0.001$, Chi² test); ranging from 0 to 54 over the 10-year period. 69.2% of all PLD liver transplantation were performed by two centres.

Recipient characteristics and outcomes	PLD n = 156 (2.0%)	Non-PLD n = 7530 (98.0%)	Total n = 7686	P value
Liver alone (L): Liver-Kidney (LK)	L:98, LK:58 (62.8%:37.2%)	L:7459, LK:71 (99.1%:0.9%)	L:7557, LK:129 (98.3%:1.7%)	0.289 [†]
Male (M): Female (F): Not Reported (NR)	M:39, F:117 (1:3)	M:4908, F:2621, NR:1 (1.87:1)	M:4947, F:2738, NR:1 (1.8:1)	0.154 [†]
Gender ratio-Male (M): Female (F): Not Reported (NR)				
Mean age (range)	52.3 (20–69)	52.7 (18–76)	52.7	<0.001 [‡]
Mean UKELD (range)	47.8 (40–60)	54.9 (39–83)	54.7	0.362 [‡]
Mean MELD (range)	14.9 (6–60)	16.26 (6–40)	16.6	0.222 [‡]
Mean Cr at registration (umol/l)	281.0	141.3	144.1	0.071 [‡]
Total mean waiting time days (range, SD)	513.3 (0–2307, 491.8)	114.7 (0–2425, 199.6)	152.25	<0.001 [‡]
Liver alone mean waiting time (range, SD)	142.2 (0–2425, 194.3)	426.7 (0–2307, 442.0)	145.9 (0–2425, 202.0)	<0.001 [‡]
Liver-Kidney mean waiting time (range, SD)	656.4 (5–1875, 538.8)	400.9 (0–1759, 438.0)	544.8 (0–1875, 516.5)	0.000 [‡]
Intraoperative death n (%)	1 (0.6%)	29 (0.4%)	30 (0.4%)	0.832 [†]
Patient death* n (%)	15 (9.7%)	1128 (16.2%)	1143 (13.6%)	0.088 [†]
Graft failure (excluding death as cause of failure)* n (%)	9 (12.5%)	936 (20.8%)	1037 (19.3%)	0.014 [†]

*At time of data extraction 16/09/2021

[†]Chi² test for categorical variables

[‡]Independent t test for continuous variables 95% CI

Conclusion: People with PLD have a >4-fold longer waiting time to transplantation than other indications despite better graft and patient outcomes. Transplantation rates for people with PLD varied between centres and may be related to registration criteria interpretation. These disparities deserve further study.

SAT309

Missed referrals for liver transplant evaluation are associated with worse outcomes in patients needing inpatient liver transplant evaluation

Katherine Cooper¹, Daniella Gonzalez^{1,2}, Alessandro Colletta^{1,2}, Deepika Devuni^{1,2}. ¹UMass Chan Medical School, Worcester, United States; ²UMass Memorial Medical Center-University Campus, Worcester, United States
Email: katherine.cooper@umassmed.edu

Background and aims: Guidelines state individuals with chronic liver disease (CLD) should be undergo liver transplant evaluation (LTE) once MELD ≥15 or hepatic decompensation. However, CLD is often under-recognized and undertreated which delays referral for liver transplant evaluation (LTE). We aimed to evaluate the effect of late referral for LTE on outcomes in patients undergoing inpatient LTE. **Method:** In this single centre retrospective study, we reviewed charts for all patients undergoing inpatient LTE for CLD between October 2017 and August 2021. Charts were extensively reviewed for history of liver dysfunction, imaging evidence of cirrhosis, liver decompensations, and cirrhosis management. Group 1 included patients with previously missed opportunity for outpatient referral (documented MELD >15 or decompensation without a substance-related contraindication). Group 2 included those referred in a timely manner based on previous history. Categorical variables were compared between groups using Fishers exact test and associations using logistic models.

Results: About one third (37.7%) of patients undergoing inpatient LTE have received a transplant since evaluation. Less than a quarter (15%) received a transplant during their index admission; with patients referred late tending to be transplanted less often (11.5% vs. 18.5%, $p = 0.21$). Overall, patients with missed referrals were more likely to die after approval (30.8% vs. 17.3% $p = 0.05$) and less likely to receive a transplant than those without missed referrals (28.2% vs. 48.1%, $p = 0.016$). Even when adjusting for MELD-Na, disease etiology, and age, patients not receiving timely LTE referral are 2.2 times less likely to receive a liver transplant.

	Missed (Group 1) (n = 78)	Not Missed (Group 2) (n = 81)	
Demographics			
Age	58.7 ± 10.0	56.8 ± 9.2	0.20
White	79.5%	81.3%	0.84
Non-Hispanic	80.8%	90.1	0.12
Male	59.0	55.6	0.75
MELD	27.2 ± 7.4	27.1 ± 8.7	0.938
Primary Diagnosis			
ETOH	43.6%	53.1%	0.93
NASH	26.9%	21.0%	
HCV	11.5%	8.0%	
PBC/PSC	1.3%	2.5%	
Autoimmune	5.1%	4.9%	
Genetic (A1AT, HH)	7.7%	4.9%	
Other/Cryptogenic	3.8%	3.7%	
Overall Outcome			
No Committee	6.4%	2.5%	0.22
Denied or Not Listed	11.5%	15.8%	0.41
Removed from list	9.0%	3.7%	0.17
Died After Approval	30.8%	17.3%	0.05
On Wait list	14.1%	13.6%	0.92
Transplanted	28.2%	48.1%	0.015

Conclusion: Failure to refer for LTE in a timely manner has an adverse effect on patient outcomes. It is crucial to improve education about liver transplant and for providers to remain up to date on liver transplant candidacy and the transplant referral process.

SAT310

Nutritional intake after liver transplant: systematic review with meta-analysis and meta-regression

Lynsey Spillman^{1,2}, Angela Madden³, Holly Richardson³, Fumiaki Imamura⁴, Kirsten Rennie¹, Linda Oude Griep⁴, Michael Allison⁵, Simon Griffin⁴. ¹University of Cambridge, MRC Epidemiology Unit, Cambridge, United Kingdom; ²Cambridge University Hospitals NHS Foundation Trust, Nutrition and Dietetics, Cambridge, United Kingdom; ³University of Hertfordshire, School of Life and Medical Sciences, Hatfield, United Kingdom; ⁴University of Cambridge, MRC Epidemiology Unit, Cambridge, United Kingdom; ⁵Cambridge University Hospitals NHS Foundation Trust, Cambridge Liver Unit, Cambridge, United Kingdom
Email: lynsey.spillman@addenbrookes.nhs.uk

Background and aims: Diabetes, obesity, hypertension, dyslipidaemia and cardiovascular disease are prevalent after liver transplant (LT) and may be prevented by diet. Understanding dietary behaviours of LT recipients (LTRs) can inform the development of evidence-based behavioural interventions to improve outcomes after LT. We aimed to synthesise evidence on nutritional intake of LTRs and investigate causes of heterogeneity in reported intake between studies.

Method: We searched Cochrane Library, MEDLINE, Embase, AMED, CINAHL, PsycINFO, BNI, Web of Science and OpenGrey electronic databases from the earliest date until 04/07/21 for peer-reviewed original studies of any design that recruited LTRs ≥18 years old and assessed their nutritional intake. Two independent reviewers screened papers, extracted data and assessed risk of bias (ROB). Where necessary data were converted to means and standard

deviations for energy (kcal/day) and macronutrients (percent energy/day). Meta-regression analyses were undertaken.

Results: We included 21 studies, and 19 provided dietary findings for meta-regression. Five studies were at low ROB. The pooled daily mean energy intake was 1,998 kcal (Figure); 17% from protein, 48% from carbohydrate, 34% from total fat, 10% from saturated fat and 20 g fibre. Average fruit and vegetable intake ranged from 105 to 418 g/day. Daily energy intake was lower at <1-month post-LT compared to all later time periods: 1-<6 months (-609kcal mean difference (MD), $p = 0.002$), 6-<12 months (-251kcal MD, $p = 0.003$), and ≥12 months (-135kcal MD, $p = 0.021$). As age of LTRs increased, daily energy intake was estimated to be 49.7kcal higher ($p = 0.018$) and energy from carbohydrates was 1.0% lower ($p = 0.022$). Energy from saturated fat increased as proportion of male participants increased (0.2%, $p = 0.001$). Total energy intake was higher (201kcal, $p = 0.042$), energy from protein lower (-2.5%, $p = 0.004$) and energy from total fat higher (3.7%, $p = 0.005$) in European studies compared to other continents.

Conclusion: Diet quality is a potentially important area for post-operative intervention for LTRs. Compared to recommendations from the European Association for the Study of the Liver (35kcal/kg body weight (BW) and 1.5 g protein/kg BW per day), on average LTRs are unlikely to meet energy or protein requirements for recovery in the first month post-LT. For protein and saturated fat LTRs follow recommendations for a healthy diet, however they consume a diet high in total fat and low in fibre, fruits and vegetables. The high energy diet for recovery may continue for longer than required, leading to energy imbalance and excess weight and body fat.

SAT311

Impact of muscle mass on survival of patients with hepatocellular carcinoma after liver transplantation beyond the Milan criteria

Berend Beumer¹, Jeroen van Vugt¹, Gonzalo Sapisochin², Peter Yoon^{2,3}, Marco Bongini⁴, Di Lu⁵, Xiao Xu⁵, Paolo De Simone⁶, Lorenzo Pintore⁶, Nicolas Golse⁷, Małgorzata Nowosad⁸, William Bennet⁹, Emmanuel Tsochatzis¹⁰, Evaggelia Koutli¹⁰, Fariba Abbassi¹¹, Marco Claassen^{1,2}, Manuela Merli¹², Joanne Orourke¹³, Martina Gambato¹⁴, Alberto Benito¹⁵, Avik Majumdar¹⁶, Ek Khoon Tan¹⁷, Maryam Ebadi¹⁸, Aldo J Montano-Loza¹⁸, Marina Berenguer¹⁹, Herold Metselaar²⁰, Wojciech Polak¹, Vincenzo Mazzaferro⁴, Jan Ijzermans¹. ¹Erasmus MC Transplant Institute, Department of Surgery, Division of HPB and Transplant Surgery; ²University Health Network, University of Toronto, Multi Organ Transplant Program, Toronto, Canada; ³Westmead Hospital, Department of Surgery, Sydney, Australia; ⁴National Cancer Institute of Milan, Gastrointestinal Surgery and Liver Transplantation, Milano, Italy; ⁵First Affiliated Hospital, Zhejiang University School of Medicine, Division of Hepatobiliary and Pancreatic Surgery, Department of Surgery, Hangzhou, China; ⁶Azienda Ospedaliero-Universitaria Pisana, Hepatobiliary Surgery and Liver Transplantation, Pisa, Italy; ⁷Hôpital Paul Brousse, Université Paris-Sud, Centre Hépatobiliaire, Villejuif, France; ⁸Medical university of Warsaw, Department of General Transplant and Liver Surgery, Warsaw, Poland; ⁹Sahlgrenska University Hospital, Sahlgrenska Academy, Transplant Institute, Gothenburg, Sweden; ¹⁰Royal Free Hospital and UCL Institute of Liver and Digestive Health, Royal Free Sheila Sherlock Liver Centre, London, United Kingdom; ¹¹University Hospitals of Geneva, Division of Digestive Surgery, Genève, Switzerland; ¹²Sapienza University of Rome, Gastroenterology, Department of Translational and Precision Medicine, Rome, Italy; ¹³Queen Elizabeth Hospital Birmingham, Edgbaston, The Liver Unit, Birmingham, United Kingdom; ¹⁴University of Padova, Section of Gastroenterology, Department of Surgery, Oncology and Gastroenterology, Padova, Italy; ¹⁵Clinica Universidad de Navarra, Radiología, Navarra, Spain; ¹⁶Royal Prince Alfred Hospital, AW Morrow Gastroenterology and Liver Centre, Sydney, Australia; ¹⁷Singapore General Hospital, Department of Hepatopancreatobiliary and Transplant Surgery, Singapore, Singapore; ¹⁸University of Alberta, Division of Gastroenterology and Liver Unit, Zeidler Leducor Centre, Edmonton, Canada; ¹⁹Hospital Universitario y Politécnico La Fe, Hepatology and

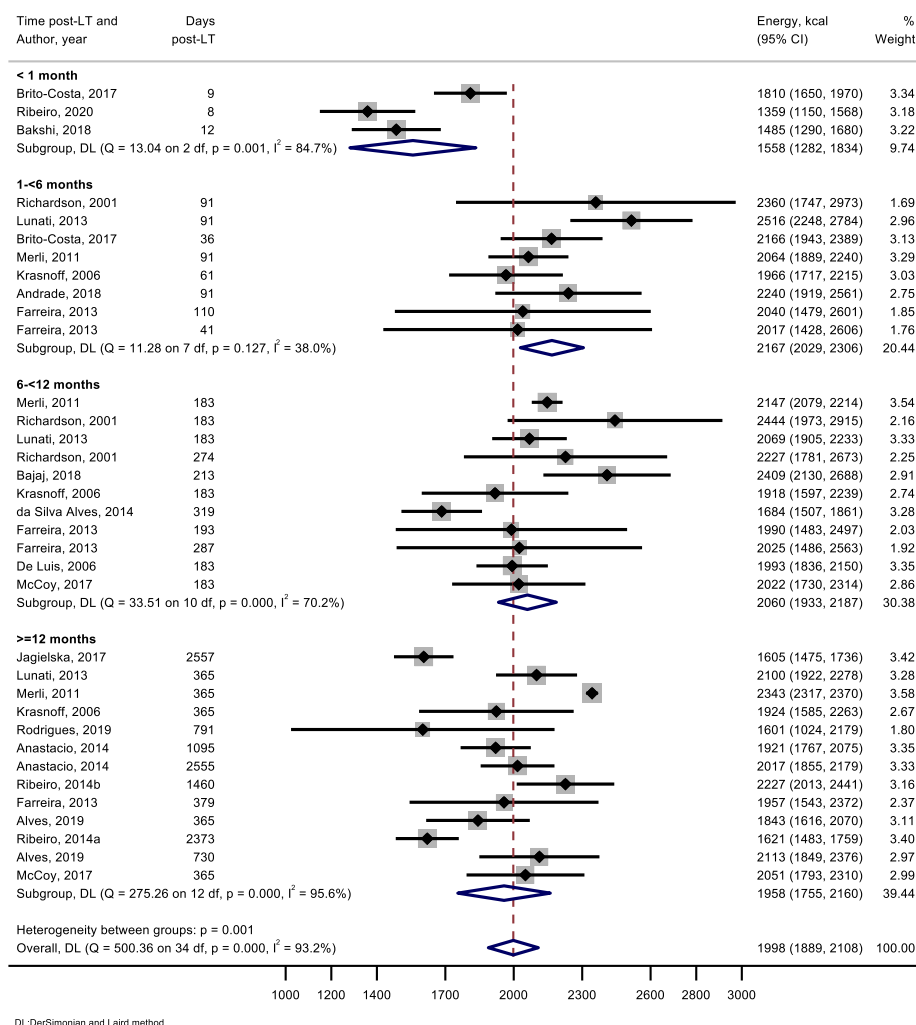


Figure: (abstract: SAT310): Mean daily energy intake categorised by time post-transplant

Liver Transplantation Unit and Ciberehd and ISS La Fe, Valencia, Spain;
²⁰Erasmus MC Transplant Institute, Department of Gastroenterology and Hepatology, Rotterdam, Netherlands
 Email: b.beumer@erasmusmc.nl

Background and aims: When listing for liver transplantation we can transplant as soon as possible or introduce a test of time to better select patients as the tumor's biological behavior is observed. Knowing the degree of harm caused by time itself is essential to advise patients and decide on the maximum duration of the test-of-time. Therefore, we investigated the causal effect of waiting time on post-transplant survival for patients with HCC.

Method: We analyzed the UNOS-OPTN dataset and exploited the natural experiment created by blood groups. Relations between variables were described in a causal graph. Inverse probability weighting was used to address selection bias. Confounding biases were avoided using instrumental variable analysis, with an additive hazards model in the second stage. The causal effect was evaluated as a contrast between a scenario in which all patients waited 2 months and one in which all patients waited 12 months. Upper bounds of the test-of-time were evaluated for probable scenarios by means of simulation.

Results: The F-statistic of the first stage was 86.3. The effect of waiting 12 months versus 2 months corresponded with a significant drop in overall survival of 5.07% 95%CI [0.277; 9.69] and 8.33% 95% CI [0.47; 15.60] at 5- and 10-years post-transplant, respectively. The median survival significantly dropped by 3.41 years from 16.21 years 95%CI

[15.98; 16.60] for those waiting 2 months to 12.80 years 95%CI [10.72; 15.90] for those waiting 12 months. No significant effect modification by tumor size or number was found.

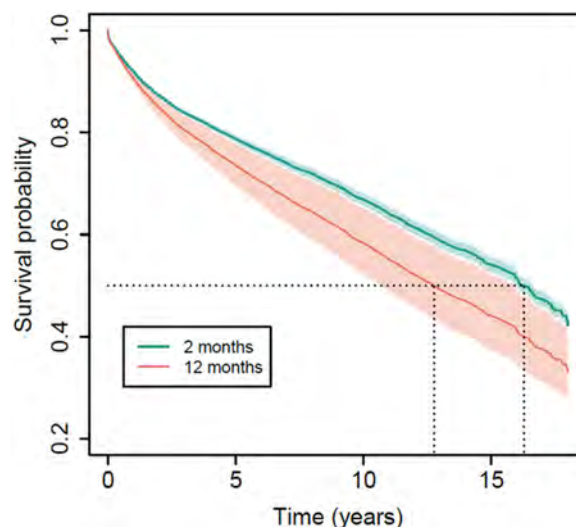


Figure 1: The survival probabilities if all listed HCC patients wait either 2 or 12 months.

Conclusion: From a patient's perspective the choice between ablate-and-wait versus immediate transplantation is in favor of immediate transplantation. From a policy perspective, the extra waiting time can be used to increase the utility of scarce donor livers, although the duration of the test-of-time is bound to be likely less than 8 months.

SAT312

Predictive factors of tumor recurrence after liver transplantation for hepatocellular carcinoma: analysis of a multicenter prospective study including 371 patients

Thomas Decaens¹, René Adam², Sébastien Dharancy³, Laurent Sulpice⁴, Didier Samuel², Emmanuel Boleslawski³, Marianne Latournerie⁵, Georges-Philippe Pageaux⁶, Olivier Scatton², Sylvie Radenne⁷, Eric Savier², Claire Francoz², Claire Vanlemmens⁸, Pierre-Henri Bernard⁹, Jean Hardwigsen¹⁰, Jean Gugenheim¹¹, Christophe Duvoux², Nadia Oubaya². ¹Chu Grenoble Alpes, La Tronche, France; ²Assistance Publique-Hôpitaux de Paris, Paris, France; ³Chu De Lille, Lille, France; ⁴CHU Rennes-Pontchaillou Hospital, Rennes, France; ⁵Chu Dijon, Dijon, France; ⁶Hospital Center University De Montpellier, Montpellier, France; ⁷Hospices Civils de Lyon-HCL, Lyon, France; ⁸Hospital Jean-Minjoz, Besançon, France; ⁹Chu Bordeaux-Site Pellegrin, Bordeaux, France; ¹⁰Hospitals Academics De Marseille, Marseille, France; ¹¹Yespark-La Madeleine/Hôpital l'Archet 2-Nice, Nice, France
Email: tdecaens@chu-grenoble.fr

Background and aims: Hepatocellular carcinoma (HCC) has become the first cause of liver transplantation (LT) in France but also in most countries of the world. Patient selection criteria are based on retrospective studies of cohorts of transplant patients. They are mainly linked to predictive factors of tumor recurrence. The aim of our work was to analyze the predictive factors of tumor recurrence at 24 months after liver transplantation, from a prospective study of patients registered on the LT list for HCC in France.

Method: Prospective multicenter study with 15 French LT centers (NCT01198704). Quantitative variables are presented as mean \pm standard deviation or median with IQR25–75. The qualitative variables are presented in percentage. The overall survival analysis was carried out by the Kaplan Meier method and recurrence-free survival by competitive risk analysis (Fine and Grey) considering death as a competitive event.

Results: 371 patients were included in this study, 18 patients were wrongly included. Among the 353 patients, 72 patients left the list, including 48 (66%) for tumor progression. 281 patients were transplanted, 90% of them men. The median waiting time was 7.56 months (3.78–12.16). During the baseline freeze in October 2021, patients who had not died had a median follow-up of 60.1 months [95% CI: 58.8–61.2]. 45 patients showed tumor recurrence post-transplantation.

The 5-year overall survival was 72% (95%CI 66.2–77.0), the cumulative incidence rate was 16% (95%CI 12.2–21.0) and the median survival of relapsed patients was 16.1 months. (95%CI 13.0–24.0).

The multivariate analysis was divided into two for the construction of tumor recurrence scores based on the data accessible in pre-LT (registration and during the waiting time) and a model based on the data accessible after the transplant (pathology report, surgery data and clinical data within 6 months after LT). The remaining significant pre-LT parameters are the number of HCCs at enrollment >3 (HR = 2.67; $p = 0.002$) and progression of more than 7.5 ng/ml/month of AFP (HR = 2.25; $p = 0.03$). The progression of serum AFP level and the response to the waiting treatment disappear.

The remaining significant transplant and post-LT parameters are the number of viable HCC >3 (HR = 1.91; $p = 0.039$), the presence of satellite nodules (HR = 2.28; $p = 0.01$), and the presence of microscopic vascular invasion (HR = 2.41; $p = 0.0006$). The iron overload, the AFP rate at 6 months disappear.

Conclusion: This prospective multicenter study confirms the importance of the progression of the serum AFP level of more than 7.5 ng/ml/month as a predictive factor of tumor recurrence and underlines the importance of a low number of HCCs upon registration on listing. This study also shows the improvement in the prognosis of patients with tumor recurrence.

SAT313

Evaluation of predictive factors for postoperative nausea and vomiting in hepatobiliary cancer patients

Juliana Fernanda Holanda Bezerra Pereira^{1,2}, Luciano Beltrão Pereira^{3,4}, Zoka Milan¹, Angela Sousa², Claudia Marquez Simões². ¹Kings College Hospital, Anaesthesia and Critical Care, London, United Kingdom; ²State of São Paulo Cancer Institute, Anaesthesia and Pain Care Department, São Paulo, Brazil; ³Kings College Hospital, Institute of Liver Studies, Liver Transplant and Surgery Department, London, United Kingdom; ⁴Liver and Transplant Institute of Pernambuco-IFP, Recife, Brazil
Email: julianafernanda@hotmail.com

Background and aims: Postoperative nausea and vomiting (PONV) is associated with prolonged stay in post anesthesia care unit, patient's dissatisfaction, dehydration, wound dehiscence, bronchoaspiration, acute hypertension, increased intracranial pressure, acid base and electrolyte disorders and delayed hospital discharge. Thus, PONV prophylaxis is mandatory for anesthesia good practice as it poses a significant medical risk. This work aims to validate a simple predictor model for nausea and vomiting in the first 24 postoperative hours in hepatobiliary cancer patients.

Method: This single center retrospective study included adults patients undergoing medium to large hepatobiliary cancer surgeries. It was approved by the Ethics and Research Committee at King's College Hospital. We assessed the PONV incidence after 24 hours. To evaluate possible factors influencing the occurrence of PONV, logistic regression analysis was applied, regression coefficient B, odds ratio (OR), 95% confidence interval of the odds ratio (95% CI OR), and p value were reported. We constructed a receiver operation characteristic (ROC) curve with the area under with possible risk factors for PONV, including the Apfel Score (female sex, non smoking status, postoperative opioid use, history of PONV/sickness).

Results: Over a six months period, a total of 137 patients, predominantly non-smokers (91%), and British race (77%), with the mean age of 61.80 ± 14.41 years and almost equal ratio of males and females (53% vs. 47%), were included in the study. PONV was presented in 29.9% cases; 100% used opioids in the postoperative period; Apfel score ranged from one to four, and most patients had Apfel score two or three (94%). It was obtained that younger age, female gender, and higher Apfel score increased the probability for PONV, while ASA score 3 decreased it. None of the hepatobiliary surgeries was considered potential predictor for PONV. ROC curve for Apfel score as a predictor for PONV was 67.7% ($p = 0.001$) Figure 1.

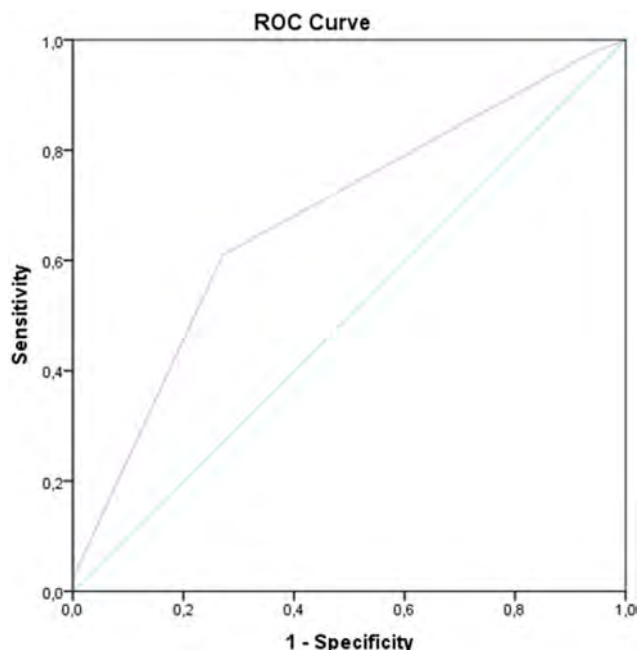


Figure 1. ROC curve for Apfel score as diagnostic marker for postoperative nausea and vomiting in hepatobiliary cancer patients.

Conclusion: We validated the Apfel Score in hepatobiliary cancer patients to guide the prophylaxis for PONV.

Liver transplantation and hepatobiliary surgery: Experimental and pathophysiology

SAT314

Immune responses before and after liver transplantation: a cohort study of the induced immune response

Dina Leth Møller¹, Annemette Hald¹, Andreas Dehlbæk Knudsen^{1,2}, Ranya Houmami¹, Nicoline Stender Arentoft¹, Jens D. Lundgren^{3,4}, Allan Rasmussen⁵, Sisse Rye Ostrowski^{4,6}, Susanne Dam Nielsen^{1,4,5}.

¹Rigshospitalet, University of Copenhagen, Viro-immunology Research Unit, Department of Infectious Diseases 8632, Copenhagen, Denmark;

²Rigshospitalet, University of Copenhagen, Department of Cardiology, Copenhagen, Denmark; ³Rigshospitalet, University of Copenhagen,

Centre of Excellence for Health, Immunity, and Infections, Department of Infectious Diseases, Copenhagen, Denmark; ⁴University of Copenhagen, Department of Clinical Medicine, Copenhagen, Denmark;

⁵Rigshospitalet, University of Copenhagen, Department of Surgical Gastroenterology and Transplantation, Copenhagen, Denmark;

⁶Rigshospitalet, University of Copenhagen, Department of Clinical Immunology, Copenhagen, Denmark

Email: dina.leth.moeller@regionh.dk

Background and aims: Reliable methods to assess the immune function after liver transplantation (LTx) are needed to guide dosing of immunosuppression and thereby prevent infections and rejections. The TruCulture assay is a standardized immunoassay that assesses the induced immune response in whole blood following ligand-stimulation of toll-like receptors (TLR).

We aimed to investigate the induced immune responses using TruCulture in LTx recipients before and three months after LTx and explore associations between methylprednisolone-treated acute rejection and cytokine levels post-LTx.

Method: A prospective observational study including LTx recipients transplanted at Rigshospitalet, Copenhagen University Hospital, Denmark from February 2018 to December 2020.

The TruCulture analysis comprised 4 stimuli and a blank: A) Heat-killed *Candida Albicans* (HKCA, TLR1/2/4/6), B) Lipopolysaccharide (LPS, TLR4), C) Resiquimod R848 (R848, TLR7/8), D) Polyinosinic: polycytidylic acid (poly I:C, TLR3), and E) a blank containing only TruCulture media. After 22 hours of incubation, cytokine concentrations in the supernatants were measured by Luminex (TNF- α , IL-1 β , IL-6, IL-8, IL-10, IL-12p40, IL-17A, IFN- α , and IFN- γ in pg/ml).

Differences in cytokine concentrations before and after LTx were assessed using Wilcoxon signed-rank tests with subsequent Benjamini-Hochberg corrections for multiple comparisons. Associations were assessed using logistic regression.

Results: We included 67 LTx recipients. Median age was 50 years (IQR: 23–70) and 41 were males (61%). Methylprednisolone-treated acute rejection occurred in 10 (15%) recipients a median of 8.5 days (IQR: 7–9) post-LTx.

Most of the stimulated cytokine levels decreased post-LTx (Figure 1). Methylprednisolone-treated acute rejection was significantly associated with an increased relative risk for a large decrease in HKCA-stimulated IL-10 (RR: 2.3 (1.1–5.0), $p = 0.03$), IL-1 β (RR: 2.5 (1.0–5.8), $p = 0.04$) and IL-8 (RR: 2.5 (1.1–5.5), $p = 0.03$), LPS-stimulated IL-10 (RR: 2.1 (1.1–4.1), $p = 0.03$), and Poly I:C-stimulated IL-1 β (RR: 2.1 (1.1–4.0), $p = 0.03$).

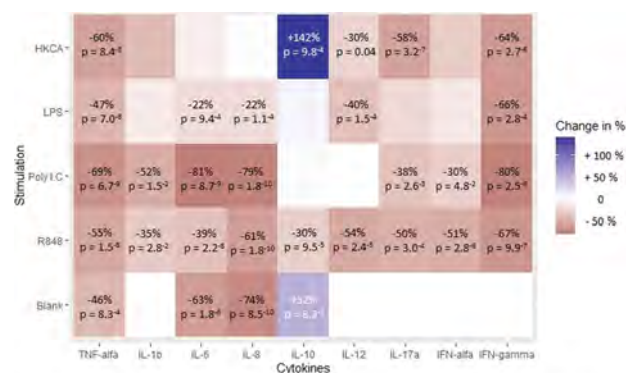


Figure 1: Differences in cytokine concentrations 3 months post-LTx compared to pre-LTx in percentages. Only significant differences are shown in the figure.

Conclusion: Most of the investigated induced immune responses decreased after liver transplantation. Treatment for acute rejection was associated with a larger decrease in a subset of the stimulated cytokines. Thus, TruCulture is feasible and seems promising. Further studies to determine utility for prediction of infections and rejections post-LTx are warranted.

SAT315

Andrographolide can potentially rescue unusable liver grafts by reducing fat content, enhancing mitochondrial function, and inhibiting Th1/Th17 immunity

Zhenlin Huang^{1,2}, Tengfei Si², Xiaohong Huang², Hanish Anand², Celine Filippi², Ragai Mitry², Anil Dhawan², Wayel Jassem², Zhengtao Wang¹, Nigel Heaton², Lili Ji¹, Yun Ma². ¹Shanghai University of Traditional Chinese Medicine, Institute of Chinese Materia Medica, Shanghai, China; ²King's College London, Institute of Liver Studies, London, United Kingdom

Email: yun.ma@kcl.ac.uk

Background and aims: There is a great shortage of good quality donor liver grafts to meet the increasing demand of patients with end-stage liver disease. A large proportion of donated livers are discarded due to suspected sub-optimal quality. One of the major reasons for low quality liver grafts is that the fat content in it being too high (>50%). Normothermic machine perfusion (NMP) is a novel

technique to preserve liver grafts which has been shown to improve marginal liver condition. Andrographolide (Andro), a newly defined active compound from traditional Chinese medicine (Chinese name: 穿心莲), has showed promising early results *in vitro*, so we are exploring using it in the NMP solution to reduce the fat content, improve the mitochondrial function, and inhibit the T cell induced immunity. This work is a deeper investigation of Andro's effects *in vitro* experiments to justify its use during NMP.

Method: Human hepatocytes were isolated from 9 donor fatty liver grafts which were unsuitable for transplantation due to their fat content >50%. Hepatic T cells were isolated from an additional 12

donors' liver perfusates. Hepatocytes and T cells were treated with sequentially increased dosage of Andro (5, 10, 25 μ M) for 48 hours separately. After treatment, free and total cholesterol level in hepatocytes were detected using commercially available kits (Cholesterol Quantification Assay kit, CS0005, Merck); total DNA and RNA was extracted, mitochondrial DNA copy numbers and the expression of anti-oxidative genes was measured by qRT-PCR (SYBRTM Select Master Mix, 4472908, Thermo fisher); lipid droplets were stained using Oil Red (Lipid Staining Kit, MAK194, Merck). Cytokine levels in T cells including TNF- α , IFN- γ and IL-17 were

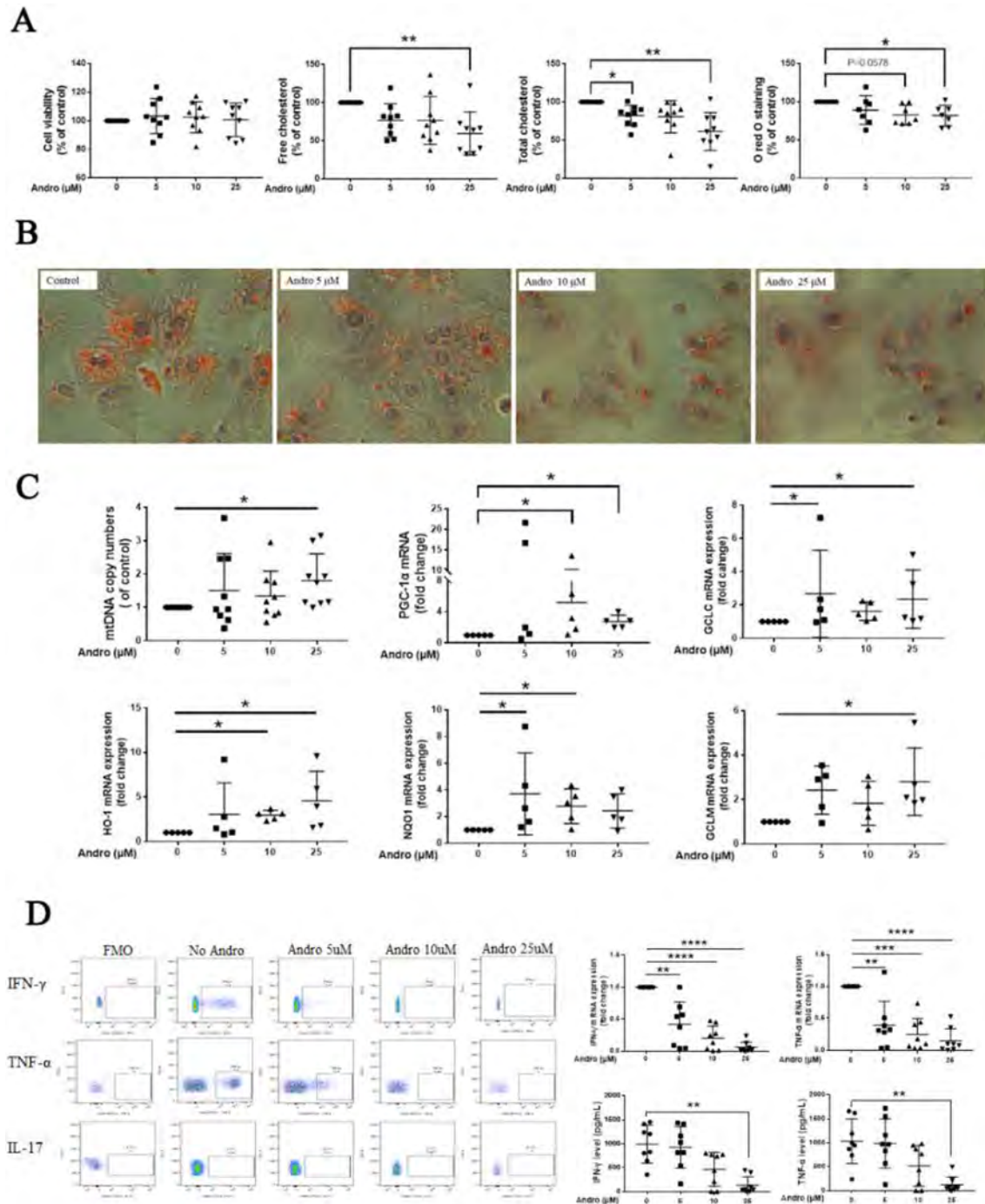


Figure: (abstract: SAT315)

POSTER PRESENTATIONS

measure using flow cytometry; qRT-PCR and ELISA (Human DuoSet ELISA, DY210/DY285B, R&D systems).

Results: In hepatocytes, different dosage of Andro (5, 10, 25 μ M) caused no toxicity. High dosage of Andro (25 μ M) reduced the level of free/total cholesterol ($p < 0.01$) (Figure 1A), decreased amount of lipid droplets (Figure 1B), and increased the mitochondrial DNA copy numbers, mRNA expression of PGC-1 α , GCLC, GCLM, HO-1 and NQO1 ($p < 0.05$) (Figure 1C). Furthermore, Andro (5, 10, 25 μ M) decrease the percentage of TNF- α , IFN- γ or IL-17-producing T cells and reduced mRNA expression of TNF- α and IFN- γ in T cells ($p < 0.05$, $P < 0.01$, $P < 0.0001$). Andro (25 μ M) also decreased the protein level of TNF- α and IFN- γ in T cell culture supernatant ($p < 0.01$) (Figure 1D).

Conclusion: Andro is effective in reducing lipid content, promoting mitochondrial biogenesis and activating anti-oxidative system in hepatocytes. In addition, Andro inhibited Th1 and Th17 immunity. These results show that Andro has a great potential to rescue those marginal liver grafts to ease graft shortage in the setting of human liver transplantation.

SAT316

Trends and causes of etiology in adult liver transplant patients: multicenter study

Mesut Akarsu¹, Murat Harputluoglu², Sezai Yilmaz², Genco Gencdal³, Murat Akyildiz³, Kamil Yalcin Polat⁴, Dinc Dincer⁵, Haydar Adanir⁵, Ilker Turan⁶, Fulya Günsar⁶, Zeki Karasu⁶, Hale Gokcan⁷, Sedat Karademir⁸, Gökhan Kabaçam^{8,9}, Meral Akdogan Kayhan¹⁰, Murat Kiyici¹¹, Murat Taner Gulsen¹², Hatice Yasemin Balaban¹³, Ahmet Bulent Dogrul¹⁴, Suleyman Dolu¹, Ali Senkaya⁶, Zeynep Melekoğlu Ellik⁷, Fatih Eren¹¹, Ramazan Idilman⁷.

¹Department of Gastroenterology, Dokuz Eylül University School of Medicine; ²Liver Transplantation Institute, İnönü University School of Medicine; ³Department of Gastroenterology, Koc University School of Medicine; ⁴Liver Transplant Center, Memorial Ataşehir/Bahçelievler Hospitals; ⁵Department of Gastroenterology, Akdeniz University School of Medicine; ⁶Department of Gastroenterology, Ege University School of Medicine; ⁷Department of Gastroenterology, Ankara University School of Medicine; ⁸Department of Gastroenterology, Güven Hospital; ⁹Yüksek İhtisas University School of Medicine, Internal Medicine, Ankara, Turkey; ¹⁰Department of Gastroenterology, University of Health Sciences, Ankara City Hospital; ¹¹Department of Gastroenterology, Uludağ University School of Medicine; ¹²Department of Gastroenterology, Gaziantep University School of Medicine; ¹³Department of Gastroenterology, Hacettepe University School of Medicine; ¹⁴Department of General Surgery, Hacettepe University, Faculty of Medicine
Email: mesutakarsu71@gmail.com

Background and aims: The indications to liver transplantation (LT) are changing in western population over the years. The aims of the present study were to determine etiological trends in LT in Turkey.

Method: This is multicenter, retrospective study that evaluated the etiological factors of the patients with end-stage chronic liver disease who underwent LT between 2010 and 2020. A total of 5, 080 adult patients with LT was included into the study. The time frame was divided as January 1, 2010 to December 31, 2014 (first period) and January 1, 2015 to December 31, 2020 (second period) (Table 1).

Results: Mean age was 50.3 years; their gender was predominantly female (69.5%). Chronic viral hepatitis (46.4%) was the most common etiological factors leading to transplantation in the overall cohort. Hepatitis B virus (HBV) infection (35.2%) was the main etiology, followed by cryptogenic cirrhosis (CC) (23.5%), hepatitis C virus infection (8.2%), and ALD (6.2%). Hepatocellular carcinoma (HCC) was the LT indication for 939 patients (18.5%). In the second period, the proportion of viral hepatitis was decreased, whereas the proportion of NAFLD-related and ALD-related cirrhosis was increased (Table 1).

Table: Demographic data and etiologic changes in adult liver transplant patients

Demographic and etiologic parameters	Periods		p
	2010–2014 (n:1677)	2015–2020 (n:3403)	
Age (year), mean \pm SD	49.95 \pm 1.92	50.68 \pm 5.75	0.707
Male/Female, n (%)	509 (%30.4)/ 1168 (%69.6)	1037 (%30.5)/ 2366 (%69.5)	0.930
Live LT/Deceased LT, n (%)	1244 (%74.2)/ 433 (%25.8)	2807 (%82.5)/ 596 (%17.5)	<0.001
HCC, n (%)	277 (%16.5)	662 (%19.5)	0.011
Etiology, n (%)			
Viral Hepatitis			
HBV	668 (%39.8)	1125 (%33.1)	<0.001
HCV	196 (%11.7)	223 (%6.6)	<0.001
HDV	148 (%8.8)	110 (%3.2)	<0.001
Autoimmune liver diseases			
AIH	56 (%3.3)	167 (%4.9)	0.010
PBC	24 (%1.4)	64 (%1.9)	0.248
PSC	18 (%1.1)	97 (%2.9)	<0.001
NAFLD	5 (%0.3)	82 (%2.4)	<0.001
ALD	69 (%4.1)	250 (%7.3)	<0.001
Miscellaneous			
CC	347 (%20.7)	849 (%24.9)	0.001
WD	57 (%3.4)	65 (%1.9)	0.001
BCS	28 (%1.7)	103 (%3)	0.004
HC	3 (%0.2)	9 (%0.3)	0.761
AAD	3 (%0.2)	10 (%0.3)	0.564
Others	55 (%3.3)	245 (%7.2)	<0.001

Abbreviations: HBV (Hepatitis B Virus), HCV (hepatitis C Virus), HDV (hepatitis D Virus), AIH (Autoimmune Hepatitis), PBC (Primary Biliary Cholangitis), PSC (Primary Sclerosing Cholangitis), NAFLD (Non-alcoholic fatty liver disease), ALD (Alcoholic Liver Disease), CC (Cryptogenic Cirrhosis), WD (Wilson disease), BCS (Budd- Chiari syndrome), HC (Haemochromatosis), AAD (Alpha-1 Antitrypsin Deficiency)

Conclusion: The present study reports that chronic viral hepatitis as the main cause in indication of LT in Turkey and suggest that the proportion of viral hepatitis is beginning to decline, while the prevalence of fatty liver disease is increasing.

SAT317

A new avatar mouse model to predict the liver immune homeostasis and histologic inflammation of liver transplant patients

Soon Kyu Lee¹, Min-Jung Park², Ho Joong Choi³, Young Kyoung You³, Jeong Won Jang¹, Si Hyun Bae¹, Seung Kew Yoon¹, Pil Soo Sung¹, Mi-La Cho², Jong Young Choi¹. ¹College of Medicine, The Catholic University of Korea, Division of Hepatology, Department of Internal Medicine; ²College of Medicine, The Catholic University of Korea, The Rheumatism Research Center, Catholic Research Institute of Medical Science; ³College of Medicine, The Catholic University of Korea, Department of Surgery, Seoul St. Mary's Hospital
Email: jychoi@catholic.ac.kr

Background and aims: Although liver transplantation (LT) patients have the possibility of rejection or tolerance, there have been no reliable models to predict the liver immune homeostasis of LT patients, which may give clinicians the chance to assess liver immunity and guide future treatment plans. Here, we developed a new patient-derived mouse model to predict the liver immune homeostasis of LT patients.

Method: The patient-derived avatar model was developed by injection of peripheral blood mononuclear cells from healthy controls (HCs) or LT patients with stable, rejection, or tolerance into NSG mice, followed by human hepatic stellate cells and CCl₄ injections. After seven weeks of transferring the cells, the patient's T-cell engraftment

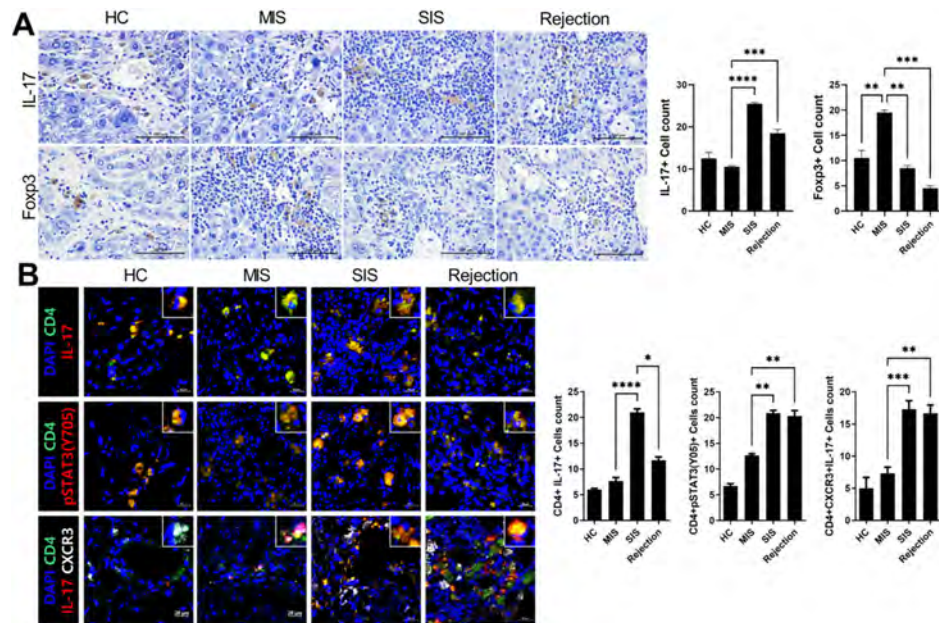


Figure (abstract: SAT317): Comparative analysis of infiltrated T-cell subtypes in the liver of each avatar model group. (A) Representative images of IHC with anti-IL-17, FoxP3 antibodies. (B) Representative confocal microscopy analysis for Th17 cells localization in liver tissues. (×100, original magnification). * $p < 0.05$, ** $p < 0.01$, *** $p < 0.001$, **** $p < 0.0001$. IHC, immunohistochemistry; MIS, mild inflammation with stable; SIS, severe inflammation with stable; NC, negative control; HC, healthy control.

and liver inflammation of the avatar model were evaluated and compared to the liver histology of LT patients.

Results: The CXCR3-dependently engrafted patient's T cells caused different liver inflammation in our model according to the status of the LT patients. The livers of avatar models from rejection patients had severe inflammation with more T helper 17 and fewer regulatory T cells compared to that of the models from tolerance and HCs showing only mild inflammation. Moreover, our model could classify stable post-LT patients into severe and mild inflammation groups, which correlated well with the liver immunity of these patients.

Conclusion: Using our new patient-derived avatar model, we could predict real liver immune homeostasis and histologic inflammation in stable LT patients without liver biopsy.

Conflict of Interest: All authors disclose no conflicts.

Financial Support: This study was supported by a grant of the Korea Health Technology RandD Project through the Korea Health Industry Development Institute (KHIDI), funded by the Ministry of Health and Welfare, Republic of Korea (grant number: HI15C3062). This work was also supported by the National Research Foundation of Korea (NRF) grant funded by the Korea government (MSIT) (No. 2020R1F1A1075816), and was supported by Basic Science Research Program through the National Research Foundation of Korea (NRF) funded by the Ministry of Education (No. 2021R111A1A01050954).

SAT318

Hepatocellular carcinoma and the risk of cancer onset after liver transplantation-role of immune activation and aging profiles

Sarah Shalaby¹, Maria Raffaella Petrara², Elena Ruffoni³, Martina Taborelli⁴, Francesco Carmona³, Paola Del Bianco³, Pierluca Piselli⁵, Francesca D'Arcangelo¹, Debora Bizzaro¹, Marco Senzolo¹, Francesco Paolo Russo¹, Patrizia Boccagni⁶, Umberto Cillo⁶, Paolo Feltracco⁷, Diego Serraino⁴, Anita De Rossi², Patrizia Burra¹. ¹Multivisceral Transplant Unit, Department of Surgery, Oncology and Gastroenterology, Padua University Hospital, Padua, Italy; ²Oncology and Immunology Section, Department of Surgery, Oncology and Gastroenterology, Padua University Hospital, Padua, Italy; ³Immunology and Diagnostic Molecular Oncology Unit, Veneto Institute of Oncology IOV-IRCCS, Padua, Italy; ⁴Cancer Unit, CRO National Cancer Institute, IRCCS, Aviano, Italy; ⁵Department of Epidemiology, National Institute for Infectious Diseases L. Spallanzani, Rome, Italy; ⁶Hepatobiliary Surgery and Liver Transplantation Unit, Department of Surgery, Oncology and Gastroenterology, Padua University Hospital, Padua, Italy; ⁷Section of Anesthesiology and Intensive Care, Department of Medicine-DIMED, Padua, Italy
Email: sarahshalaby18@gmail.com

Background and aims: Patients with hepatocellular carcinoma (HCC) are at higher risk for post-transplant malignancies (PTM). Immune activation and senescence have been frequently implicated in cancer development, however, no data are available concerning their prognostic role in patients undergoing liver transplant (LT). The aim of the study was to analyze these profiles in patients transplanted for HCC (LT-HCC) and for other causes (LT-non-HCC).

Method: Patients who underwent LT between October 2016 and February 2021 at Multivisceral Transplant Unit, Padua University-Hospital were enrolled. Patients characteristics, HCC presence and features and immunosuppression were recorded. Exclusion criteria: ≤18 years old, follow-up shorter than 30 days or previous neoplastic history other than HCC. All PTM were registered. Markers of T (CD3+CD4/8+CD38+) and B (CD19+CD10-CD21-CD27+) cell activation, T (CD3+CD4/8+CD28-CD57+) and B (CD19+IgD-CD27-) cell senescence were evaluated by flow cytometry at transplantation (baseline).

POSTER PRESENTATIONS

Results: A total of 116 patients were included: 45 LT-HCC and 71 LT-non-HCC. LT-HCC patients were older than LT-non-HCC (median 60 vs 53 years, $p=0.011$), but comparable for sex, liver disease etiology, immunosuppressive schedule. At baseline, levels of activated CD8, memory B-cells and senescent CD4, CD8 and B-cells were significantly higher in LT-HCC patients than LT-non-HCC ones. During 27.4 (7.7–41.7) months of follow-up, 6 PTM occurred: 4 in LT-HCC (8.9%) and 2 in LT-non-HCC (2.8%). Patients developing PTM showed significantly higher baseline levels of immune activation than patients without malignancies. Within LT-HCC group, levels of senescent cells were significantly higher in patients with PTM compared to the others [%CD8+CD28-CD57+: 22.45 (17.72–25.86) vs 10.82 (5.21–25.16), $p=0.098$; %CD4+CD28-CD57+: 14.33 (10.23–21.12) vs 2.65 (1.10–13.11), $p<0.001$].

Table: Differences of immunological parameters between LT-HCC and LT-non-HCC at baseline

Median (IQR)	LT-HCC (N = 45)	LT-non-HCC (N = 71)	p value*
%CD8 activation (CD8+CD38+HLA-DR+)	10.89 (5.61–18.52)	6.59 (4.26–9.25)	0.003
%CD4 activation (CD4+CD38+HLA-DR+)	7.23 (4.11–14.12)	6.21 (3.49–9.23)	0.092
%B activated memory (CD19+CD10-CD21-D27+)	10.97 (5.59–20.68)	7.60 (3.00–13.72)	0.040
%CD8 senescence (CD8+CD28-CD57+)	11.06 (6.24–25.16)	5.92 (3.54–10.97)	0.006
%CD4 senescence (CD4+CD28-CD57+)	3.80 (1.36–14.03)	1.80 (0.48–3.41)	0.002
%B senescence (CD19+CD27-IgD-)	12.20 (6.28–17.67)	6.59 (4.24–12.50)	0.019

*Adjusted by age.

Conclusion: Our findings suggest that patients undergoing LT for HCC have a higher immune activation and senescence profile compared to other recipients, possibly representing an additional risk factor for PTM. Moreover, immune activation and senescence may be prognostic factors for PTM occurrence regardless of the cause of transplantation.

SAT319

The crucial role of PARP [poly (ADP-ribose polymerase)] on the post-ischemic liver injury and inflammation

Michitaka Ozaki¹, Sanae Haga¹, Naoki Morita². ¹Hokkaido University, Department of Biological Response and Regulation, Sapporo, Japan; ²National Institute of Advanced Industrial Science and Technology (AIST) Email: ozaki-m@med.hokudai.ac.jp

Background and aims: Ischemia/reperfusion (I/R) of liver is an unavoidable event in liver surgery and transplantation, which sometimes causes serious post-operative liver failure/complications. The mechanism of I/R-induced liver injury, however, is complicated so that we have not elucidated yet. I/R-induced ROS, various types of programmed cell death and the following sterile inflammatory reaction seem to be crucial. In the present study, we investigated the roles of PARP [Poly (ADP-ribose) polymerase] on hypoxia/reoxygenation (H/R)-induced, ROS-mediated programmed cell death and inflammation in mouse liver cells and macrophages.

Method: AML12 cells and Raw264.7 cells were used for the experiments as hepatocytes and macrophages, respectively. Cells were cultured in high-glucose DMEM supplemented with 10% FBS. H₂O₂ were administered directly to the culture medium for oxidative stress. Cellular hypoxic conditions were created and maintained in a chamber by flushing with a 95% N₂/5% CO₂ gas mixture for 10 min and then sealing the chamber. Following 6 h of hypoxia, cells were reoxygenated by opening the chamber and replacing the hypoxic medium with oxygenated medium. Protein and gene expressions were measured by western blot analysis/capillary-based immunoassay and RT-PCR, respectively. Cell survival and death were determined by plating the cells in the xCELLigence System (Roche) and the LDH release.

Results: H/R-induced cell death was inhibited significantly by PJ34, a specific inhibitor of PARP. Because an oxidative stress is one of the

major causes of H/R-induced cell death, we challenged 1 mM H₂O₂ to AML12 liver cells. H₂O₂ induced cell death, PAR [Poly (ADP-ribose)] production and nuclear translocation of AIF (apoptosis inducing factor), which were suppressed significantly by the pre-treatment of PJ34. H₂O₂ also induced Receptor-Interacting Protein (RIP)1/RIP3 binding, which indicates the involvement of necroptosis in H₂O₂-induced cell death. H₂O₂-induced RIP1/RIP3 binding was inhibited by PJ34. These facts indicate that H/R and ROS potentially induce parthanatos and necroptosis in hepatocytes. Furthermore, H/R-induced inflammatory reaction (proinflammatory gene expression) was inhibited by PJ34 both in AML12 cells and Raw264.7 cells.

Conclusion: PARP is potentially involved in H/R- and oxidative stress-induced cell death in mouse liver cells, by inducing programmed cell death (parthanatos and necroptosis) and inflammatory reaction.

SAT320

Mitochondrial transplantation attenuates murine in vivo hepatic ischemia/reperfusion injury

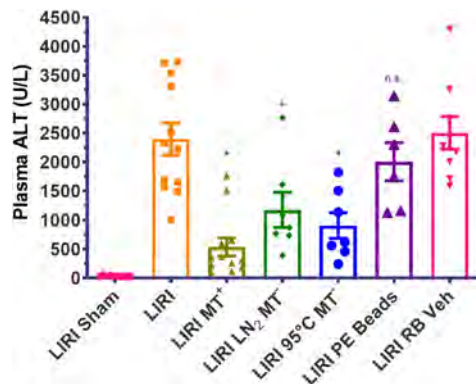
Avinash Mukkala^{1,2}, Raluca Petrut^{2,3}, Zahra Khan^{1,2}, Mirjana Jerkic², Menachem Ailenberg², Shawn Rhind⁴, Marc Jeschke^{5,6,7}, Ana Andreazza⁸, Andras Kapus^{2,7,9}, Ori Rotstein^{1,2,7,10}. ¹University of Toronto, Institute of Medical Science, Toronto, Canada; ²St. Michael's Hospital, Keenan Research Centre for Biomedical Science, Toronto, Canada; ³University of Toronto, Temerty Faculty of Medicine, Toronto, Canada; ⁴Defence Research and Development Canada/Recherche et développement pour la défense Canada, Ottawa, Canada; ⁵University of Toronto, Department of Immunology, Toronto, Canada; ⁶Sunnybrook Health Sciences Centre, Ross Tilley Burn Centre, Toronto, Canada; ⁷University of Toronto, Department of Surgery, Toronto, Canada; ⁸University of Toronto, Department of Pharmacology and Toxicology, Toronto, Canada; ⁹University of Toronto, Department of Biochemistry, Toronto, Canada; ¹⁰St. Michael's Hospital, Department of Surgery, Toronto, Canada Email: avinash.mukkala@mail.utoronto.ca

Background and aims: Liver ischemia/reperfusion injury (LIRI) is a disease process implicated in organ dysfunction following hepatic surgery, traumatic injuries, and liver transplantation. LIRI causes mitochondrial perturbations which lead to organ death. Stringent mitochondrial quality control is vital in reinstating organ integrity in LIRI. Mitochondrial transplantation (MT) has recently surfaced as a biotherapeutic option in IRI. The effect and mechanism of MT in IRI are poorly characterized. We hypothesized that MT, using mitochondria derived from mouse skeletal muscle tissue, is hepatoprotective following murine LIRI.

Method: We utilized an *in vivo* murine model of LIRI by occlusion of the hepatic artery leading to the left lobe for 1 h to achieve lobe-specific ischemia. Mitochondria were isolated from hindlimb mouse skeletal muscle tissue by differential filtration followed by characterization for particle size and number, ATP, membrane potential, ultrastructural morphology, and protein purity. Inactivation of mitochondria was conducted using liquid nitrogen (LN₂) immersion or incubation at 95°C. Active or inactive mitochondria were intrasplenically injected, to access the portal system, at the start of reperfusion. Mouse livers were reperfused for 2 h followed by sacrifice for blood and liver tissue collection for various molecular/histological analyses.

Results: Isolated active mitochondria (1–3 μm) retained membrane potential, cristae architecture and morphology, protein purity, and ATP content. LIRI animals had significantly greater circulating AST and ALT compared to sham animals. In addition, LIRI animals had extensive, left lobe-specific liver necrosis, congestion, and vacuolization, when compared to sham animals. Intrasplenic injection of 80 million active mitochondria into LIRI animals, significantly reduced plasma AST and ALT concentrations and normalized histology. Blinded Suzuki scoring of liver histology showed a significant attenuation of congestion, necrosis, and vacuolization as a result of MT in LIRI animals. Interestingly, inactivated mitochondrial particles (LN₂ or 95°C) also significantly reduced plasma AST and ALT, albeit to

a lesser degree. To rule out a confounding “particle effect” of MT, polyethylene beads (1–4µm) were injected and showed no protective effect against LIRI. Treatment with active mitochondria in LIRI animals significantly increased plasma IL-10 and decreased plasma IL-6 compared to control animals.



Conclusion: MT attenuated LIRI regardless of whether injected mitochondria were active or inactive. Future studies will focus on understanding how MT confers protection from LIRI and how their use in clinical scenarios might be optimized. Future avenues of this research include exploring metabolic reprogramming and liver regeneration as potential explanations for the hepatoprotection afforded by MT.

Viral hepatitis B/D: therapy

SAT341

Bulevirtide treatment of hepatitis D in Germany: multicentre real-world experience

Christopher Dietz¹, Frank Tacke², Caroline Zöllner², Münevver Demir², Hartmut Schmidt³, Christoph Schramm³, Katharina Willuweit³, Christian M. Lange⁴, Gerald Denk⁴, Sabine Weber⁴, Christoph Berg⁵, Julia Grottenthaler⁵, Uta Merle⁶, Alexander Olkus⁶, Stefan Zeuzem⁷, Kathrin Sprinzel⁷, Thomas Berg⁸, Johannes Wiegand⁸, Florian van Bömmel⁸, Toni Herta⁸, Thomas Seufferlein⁹, Eugen Zizer⁹, Nektarios Dikopoulos⁹, Robert Thimme¹⁰, Christoph Neumann-Haefelin¹⁰, Peter Galle¹¹, Martin Sprinzel¹¹, Ansgar W. Lohse¹², Julian Schulze zur Wiesch¹², Jan Kempinski¹², Andreas Geier¹³, Florian P. Reiter¹³, Wolf Peter Hofmann¹⁴, Julia Kahlhöfer¹⁵, Benjamin Maasoumy¹, Kerstin Port¹, Markus Cornberg¹, Heiner Wedemeyer¹, Katja Deterding¹. ¹Medical High School Hannover, Dept. of Gastroenterology, Hepatology and Endocrinology, Hannover, Germany; ²Charité, Dept. of Hepatology and Gastroenterology, Berlin, Germany; ³University Hospital Essen, Dept. of Gastroenterology, Hepatology and Transplantational Medicine, Essen, Germany; ⁴Ludwig Maximilian University Munich, Dept. of Medicine II, München, Germany; ⁵University Tübingen, Medical clinic, Department of Gastroenterology, Hepatology, and Infectiology, Tübingen, Germany; ⁶University Heidelberg, Department of Internal Medicine IV, Heidelberg, Germany; ⁷Goethe University Hospital, Internal Medicine Department, Frankfurt am Main; ⁸University Clinic Leipzig, Division of Hepatology, Clinic and Polyclinic for Gastroenterology, Hepatology, Infectiology, and Pneumology, Leipzig, Germany; ⁹University of Ulm, Department of Internal Medicine I, Ulm, Germany; ¹⁰University Medical Center Freiburg, Faculty of Medicine University Freiburg, Department of Medicine II, Freiburg, Germany; ¹¹University Medical Center of the Johannes-Gutenberg University Mainz, Department of Medicine I, Mainz, Germany; ¹²University Medical

Center Hamburg-Eppendorf, Department of Medicine, Hamburg, Germany; ¹³University Hospital Würzburg, Dept. of Medicine II, Würzburg, Germany; ¹⁴MVZ for Gastroenterology at Bayerischer Platz Berlin, Berlin; ¹⁵German Center for Infection Research (DZIF), HepNet Study-House der Deutschen Leberstiftung, Hannover
Email: dietz.christopher@mh-hannover.de

Background and aims: Infection with hepatitis D virus (HDV) occurs as coinfection with hepatitis B virus. Chronic hepatitis D is the most debilitating form of viral hepatitis with a high risk of liver cirrhosis and hepatocellular carcinoma (HCC). Bulevirtide (BLV) is the first drug with a conditional approval for the treatment of chronic HDV infection in compensated liver disease. The aim of this project is the characterization of treatment response in terms of viral suppression and improvement of hepatic inflammation in a real-world setting.

Method: We collected anonymised longitudinal observational data from fourteen German centres treating patients with 2 mg of BLV. Individual case data from the participating centres were collected in a standardized data sheet. A paired t-test or Wilcoxon signed rank test was used for comparative data analysis. Analyses were carried out with R Studio. Statistical significance was assumed if p values were below 0.05.

Results: Baseline data was collected from 109 patients. In 103 cases BLV was given in combination with a nucleos (t)idanalogue. Currently, 47 and 26 patients reached treatment week 12 and 24 (Table 1). Elevated transaminases improved by 64 IU/ml at average with 24 cases reaching normal ALT levels (<45 U/l) at week 12. A 2log reduction in viral load was achieved by 4 (week 12) and 11 cases (week 24). Liver cirrhosis was present in 43 cases (FIB-4 >3.6) with 4 patients being initially decompensated. Observed improvements regarded the amount of ascites and levels of bilirubin. Hepatic decompensation occurred in two cirrhotic patients. No HCC or other drug-related SAE occurred. Fatigue was the most frequent AE reported (n = 7). A continuous improvement of FIB-4 was noted.

Table: Shown are key characteristics. p values were obtained from paired t-tests or Wilcoxon signed-rank test if medians were compared.

Parameter	Baseline (n = 109)	Week 12 (n = 47)	Week 24 (n = 26)
Log10 HDV-RNA Median	5.7	4.5 (p < 0.001)	3.5 (p < 0.001)
2log reduction	/	4/47	11/26
Viral non-response (<1log reduction)	/	20/47	4/26
ALT (U/l) Mean ± SD	116 ± 105	53 ± 30 (p < 0.001)	47 (p < 0.001)
AST (U/l) Mean ± SD	90 ± 64	49 ± 17 (p < 0.001)	37 (p < 0.001)
Albumin (g/l) Mean ± SD	41 ± 5.4	40 ± 6 (p = 0.36)	42 (p = 0.19)
Bilirubin (µmol/l) Mean ± SD	15 ± 10.4	17 ± 12 (p = 0.75)	14 (p = 0.83)
INR Mean ± SD	1.2 ± 0.1	1.2 ± 0.2 (p = 0.15)	1.1 (p = 0.55)
Platelets (10 ³ /µl) Median	125	115 (p = 0.42)	159 (p = 0.03)
Bile salts (µmol/l) (n = 15)	17 ± 19	60 ± 75 (p < 0.001)	49 ± 49 (p < 0.001)
FIB-4 Median	2.8	2.5 (p < 0.001)	1.9 (p = 0.006)

Conclusion: Decreased platelets and a median FIB-4 of 2.8 indicate advanced liver disease and portal hypertension in patients selected for BLV treatment. After 12 weeks of treatment a decline in viral load is accompanied by a significant improvement in hepatic inflammation and FIB-4. Updated results will be presented at the meeting.

SAT342

Challenges with the cascade of HDV care in Mongolia

Enkhjargal Altangerel¹, Nandintsetseg Tsoggerel¹, Suvd Batbaatar¹, Uyanga Bat-Osor¹. ¹Academy of Medical Professionals, Department of Research, Mongolia
Email: ajargal8@gmail.com

Background and aims: Hepatitis D infection is highly endemic among individuals with chronic HBV infection in Mongolia. The anti-HDV prevalence among HBsAg-positive individuals, indicating likely HBV/HDV coinfection, ranged from 41% to 67% in the two major seroepidemiological studies. The study aimed to define the challenges within the care cascade among HDV patients.

Method: We conducted the cross-sectional survey designed with the inclusion and exclusion criteria for the selection among the patients diagnosed with a coinfection of HBV and HDV. The questionnaire covered topics of care cascade and linkage to the care. In total, 576 participants enrolled in the survey. Both online and paper modes were used to collect the questionnaire. The collected data was analyzed by SPSS 21.0 software.

Results: 65.0% of the participants were from urban areas. Most of the participants were women (59.8%), and the mean age was 43.57 ± 10.9 . The duration of linkage to the specialized doctor varied: the most are within a month (33.3%), within 3–6 months (15.9%), 6–12 months year (17.9%) and more than a year (18.8%). More than half of the participants enrolled to fibrosis assessment within a month (35.0%) and within 3–6 months (26.7%) after linked to the specialized care. However, many (34.5%) didn't attend a specialist's periodic exam and monitoring service after the fibrosis stage was defined. Except for 22.7% of the participants, all were on the antiviral treatment for HBV, including entecavir (11.1%), TAF (36.4%), and the remaining (29.8%) were on a combination of entecavir and TAF. Almost all participants (97.1%) did not get treatment with Peg-interferon, while only (2.9%) underwent the treatment. Peg-interferon treatment patients had the injection at the hospital (70.6%), Family Health Centers (17.6%), and at home (11.8%). The treatment duration was between one months to 1.6 years. The main reasons for the treatment interruption are combination of two or three of the reasons including an inability to bear the side effects, stock out of the injection, and lack of the money to pay for the injection. At the same time, the doctors recommended the Peg-interferon treatment to only 8.7% of the participants.

Conclusion: The most of patients spent a month and more time for the linkage to the care for HDV patients. The patients experience delays in the further steps of the cascade of care, including defining the fibrosis stage and attending periodic monitoring exams. Most doctors do not recommend Peg-interferon treatment, and very few patients are under the treatment. Side effect impact, poor supply, and high cost for injection are the main reasons for treatment interruption. Antivirals treatment for HBV is well practiced.

SAT343

Safety, tolerability and pharmacokinetics of single ascending doses of ALG-020572, a GalNAc-conjugated antisense oligonucleotide, in healthy subjects

Edward J Gane¹, Man-Fung Yuen², Christian Schwabe³, Min Wu⁴, Kha Le⁵, Jen Rito⁶, Kusum Gupta⁴, Christopher Westland⁴, Felix Lai⁴, Meenakshi Venkatraman⁴, Megan Fitzgerald⁴, Tse-I Lin⁴, Lawrence Blatt⁴, Sushmita Chanda⁴, Matt McClure⁴, John Fry⁴, Kosh Agarwal⁵. ¹University of Auckland, Faculty of Medicine, Auckland, New Zealand; ²The University of Hong Kong, Hong Kong; ³Auckland Clinical Studies, Auckland, New Zealand; ⁴Aligos Therapeutics, South San Francisco, United States; ⁵King's College Hospital, Institute of Liver Studies, London, United Kingdom
Email: mwu@aligos.com

Background and aims: To evaluate the safety, tolerability, pharmacokinetics (PK) and antiviral activity of ALG-020572, an antisense oligonucleotide designed to reduce hepatitis B S-antigen (HBsAg) in subjects with chronic hepatitis B (CHB).

Method: This is a two-part, double-blind, randomized, placebo-controlled, single- and multiple ascending dose study. In Part 1, cohorts containing 8 healthy subjects, including at least 4 Asians, were randomized to receive a single ascending subcutaneous (SC) dose of ALG-020572 or placebo in a 3:1 ratio. In Part 2, planned cohorts will consist of 8 CHB subjects that are randomized 3:1 to receive multiple ascending SC doses of ALG-020572 or placebo. Safety assessments, viral markers (Part 2) and plasma/urine PK samples are collected throughout the study. Preliminary blinded results from the first 2 cohorts of Part 1 are reported here. Additional available data will be presented at the conference

Results: In Part 1, the first 2 cohorts of healthy subjects received a single 50 or 150 mg SC dose of ALG-020572 or placebo. Subjects were a mean age of 28 years, 94% male and 50% Asian. ALG-020572 was well tolerated; there were no serious adverse events (AEs) or dose limiting toxicities and all treatment-emergent AEs were mild in severity except one grade 2 injection site tenderness. All treatment-emergent laboratory abnormalities were Grade ≤ 2 . No clinically significant physical examination, vital sign, or ECG abnormalities were reported. Plasma ALG-020572 exposures increased in a slightly greater than dose proportional manner between 50 and 150 mg, with low-to-moderate variability. ALG-020572 showed rapid absorption ($t_{max} \sim 2$ hrs), high volume of distribution, high plasma clearance, and low urinary excretion. No differences in safety or PK were observed between Asian and non-Asian subjects. Based on observed exposures and nonclinical studies, ALG-020572 doses ≥ 150 mg are projected to have antiviral activity in CHB subjects.

Conclusion: ALG-020572 was safe and well tolerated with predictable PK properties when given to healthy subjects as single SC doses of up to 150 mg.

SAT344

Predictors of HBsAg loss after cessation of nucleos(t)ide analogue therapy in asian patients with low HBsAg levels

Milan Sonneveld¹, SM Chiu², Jun Yong Park³, Apichat Kaewdech⁴, Wai-Kay Seto⁵, Yasuhito Tanaka⁶, Ivana Carey⁷, Margarita Papatheodoridis⁸, Florian van Bömmel⁹, Sylvia Brakenhoff¹, Thomas Berg⁹, Fabien Zoulim¹⁰, Sang Hoon Ahn³, George Dalekos¹¹, Nicole Erler¹, Christoph Hoener zu Siederdissen¹², Heiner Wedemeyer¹², Markus Cornberg¹², Man-Fung Yuen⁵, Kosh Agarwal⁷, Andre Boonstra¹, Maria Buti¹³, T Piratvisuth⁴, George Papatheodoridis⁸, Chien-Hung Chen², Benjamin Maasoumy¹². ¹Erasmus MC, Rotterdam, Netherlands; ²Kaohsiung Chang Gung Memorial Hospital, Taiwan; ³Yonsei University College of Medicine, Korea, Rep. of South; ⁴Prince of Songkla University, Tambon Kho Hong, Thailand; ⁵The University of Hong Kong, Hong Kong; ⁶Kumamoto University, Kumamoto, Japan; ⁷King's College Hospital, United Kingdom; ⁸Laiko Hospital, Athens, Greece; ⁹University Hospital Leipzig, Leipzig, Germany; ¹⁰Inserm, Lyon, France; ¹¹General University Hospital of Larissa, Greece; ¹²Medizinische Hochschule, Hannover, Germany; ¹³Hospital Universitari Vall d'Hebron, Barcelona, Spain
Email: m.j.sonneveld@erasmusmc.nl

Background and aims: HBsAg levels ≤ 100 IU/ml can be used to identify HBeAg negative patients most likely to achieve durable remission after cessation of nucleos(t)ide analogue (NUC) therapy. However, the majority of these patients will not achieve HBsAg clearance. We aimed to study predictors of HBsAg loss in patients with low HBsAg levels who discontinued NUC therapy.

Method: We identified Asian patients with low end-of-treatment (EOT) HBsAg levels (≤ 100 IU/ml) from a global database of HBeAg negative patients with undetectable HBV DNA who discontinued long-term NUC therapy. The primary end point for this analysis was HBsAg loss. Patients requiring re-initiation of antiviral therapy were considered non-responders. Determinants of HBsAg loss were explored using backward stepwise elimination in a multivariable Cox regression model considering the following variables: age,

gender, baseline HBeAg status, HBV genotype, and EOT ALT, HBsAg and HBcrAg levels.

Results: We identified 243 patients, of whom the majority were treated with entecavir (62%) or tenofovir disoproxil fumarate (29%). Thirty (12%) patients had been HBeAg positive at start of NUC therapy (all were HBeAg negative at treatment cessation). Median HBsAg levels at EOT were 1.49 log IU/ml (IQR 1.0–1.8) and 172 (71%) had undetectable HBcrAg. HBV genotype B was detected in 107 (44%) patients, and genotype C in 43 (18%); the others had other or unknown genotypes. After therapy cessation, 83 (34%) patients were retreated and 52 (21%) patients cleared HBsAg after a median of 74 (IQR 48–179) weeks of off-treatment follow-up. Multivariable Cox regression identified HBV genotype C (aHR 2.769, $p=0.003$), lower HBsAg (aHR 0.218, $p<0.001$), lower HBcrAg (aHR 0.729, $p=0.010$) and age (aHR 0.958, $p=0.015$) as independent predictors of HBsAg loss.

Conclusion: Among Asian patients with EOT HBsAg levels ≤ 100 IU/ml, HBV genotype C, age and lower HBsAg and HBcrAg levels are associated with a higher probability of HBsAg clearance.

SAT345

Improvement of liver-stiffness after 6 months of therapy: real-life data for HBV/HDV co-infected patients treated with bulevirtide

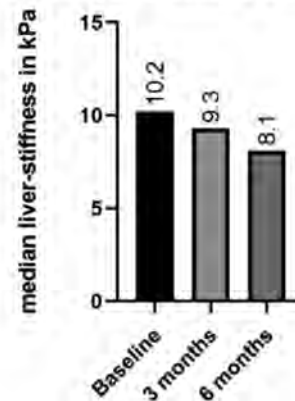
Alexander Killer¹, Mahyar Ghavemi¹, Glisa Smaranda¹, Johannes Bode¹, Björn Jensen¹, Jan Köhler¹, Andreas Walker², Nadine Lübke², Jörg Timm², Tom Lüdde¹, Hans Bock¹. ¹Uniklinik Düsseldorf, Klinik für Gastroenterologie, Hepatologie, Infektiologie, Düsseldorf, Germany; ²Uniklinik Düsseldorf, Institut für Virologie, Düsseldorf, Germany
Email: Alexander.Killer@med.uni-duesseldorf.de

Background and aims: HBV/HDV coinfection is the most aggressive form of chronic viral hepatitis with a high risk for the development of liver cirrhosis and subsequent complications like hepatocellular carcinoma (HCC). In 09/2020 bulevirtide (BLV), a synthetic lipopeptide that blocks HBV/HDV uptake into hepatocytes by binding to the NTCP-receptor, has been approved for the treatment of HDV-related chronic hepatitis in Germany. So far, there is only limited data available on the efficacy of BLV treatment under real-life conditions. We present our single-centre clinical and virological data on 12 patients treated with BLV.

Method: From 11/2020 on, twelve HDV-infected patients with active chronic hepatitis were enrolled. Virological, biochemical and clinical parameters were measured at baseline and at monthly intervals thereafter. Furthermore, we measured liver stiffness by shear wave elastography.

Results: The median age of the 12 patients enrolled (4 female, all HDV-genotype 1) was 42.5. Five patients had compensated liver cirrhosis, ten received NUC-therapy and eight had a history of previous interferon treatment. Mean baseline parameters were: HDV-RNA 597,000 IU/ml, ALT 117 U/l, AST 64 U/l, bile acids 11.5 μ mol/l, platelets 160/nl, HBsAg 23.074 IU/ml, liver stiffness 10.0 kPa. Of note, shear wave elastography results revealed an improvement of liver stiffness to median values of 9.3 kPa after 3 and 8.1 kPa after 6 months. In total, 9 patients (75%) had improved by at least 1 kPa in liver-stiffness. At the time of final analysis (median treatment duration: 8.5 months), no patient had undetectable HDV RNA, 6 patients (50%) had a normalization of ALT and 4 (33%) had reached a combined response of ALT normalization and ≥ 2 Log IU/ml HDV decrease. Mean values of viral loads changed to HDV-RNA 27,600 IU/ml, bile acids 29 μ mol/L, ALT 42 U/l and AST 29 U/l. Treatment was terminated for two patients, one because of non-response at week 48, and one for development of HCC.

Regression of liver-stiffness under BLV treatment



Conclusion: BLV was well-tolerated and led to a biochemical and virological response in the majority of patients. Treatment led to an early and marked decrease of liver-stiffness, suggesting improvement in liver fibrosis in a setting of chronic viral infection. Therefore, an improvement in liver-stiffness could be a way to predict a clinically relevant response and benefit for patients treated with BLV, warranting additional studies in larger patient cohorts.

SAT346

Role of plasmatic and urinary TDF and TAF concentration in a cohort of HBV chronic hepatitis patients

Giacomo Stroffolini¹, Valentina Dodaro¹, Lucio Boglione², Giuseppe Cariti¹, Giovanni Di Perri¹. ¹Amedeo di Savoia Hospital, University of Torino, Medical sciences, Italy; ²University of Piemonte Orientale, Italy
Email: giacomo.stroffolini@unito.it

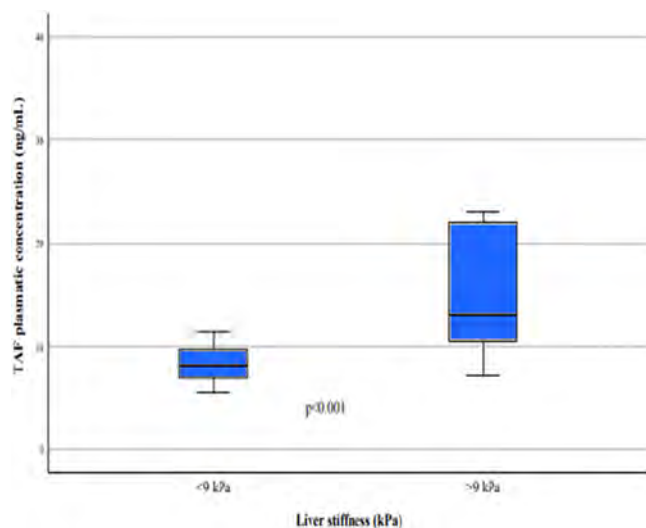
Background and aims: Tenofovir disoproxil fumarate (TDF) is the first-line therapy for chronic HBV infection. Currently, the proximal tubular kidney toxicity of the TDF is debated. Recently, tenofovir alafenamide fumarate (TAF) has been approved; virological and serological effectiveness are equal to TDF, but with lower kidney excretion and tubular toxicity. TAF is currently available for patients over sixty, pretreated with TDF or other NAs, with bone or kidney impairment; however, which categories of patients can benefit the most switching from TDF to TAF is still unclear.

Method: A cross-sectional study was conducted between November 2019 and January 2021. 42 patients were included ($n=42$). At the baseline 17 patients who met the eligibility criteria were switched from TDF to TAF ($n=17$), while the others continued treatment with TDF ($n=25$). Patients were evaluated at baseline and after six months. The plasmatic and urinary dosage was performed for 16 patients treated with TAF ($n=16$) and for 25 patients treated with TDF ($n=25$).

Results: Patients treated with TDF were significantly younger than patients treated with TAF (38 vs 67 years). The plasmatic concentration of TAF was significantly lower for genotype E (27 vs 80 ng/ml) and higher for genotype C (114 vs 36.5 ng/ml) than other genotypes. Higher plasmatic concentration of TAF was found in patients whose liver stiffness was more than 9 kPa (8.20 vs 13.00 ng/ml, see figure). In the TAF group eGFR increased and urinary drug concentration reduced significantly compared to the TDF group (+9 vs 0 ml/min and -4.5 vs +3 ng/ml. eGFR decreased and urinary TDF increased significantly for ADV-pretreated TDF patients compared to not-ADV-pretreated TDF patients (-9 vs +2 ml/min and +9 ng/ml vs +1 ng/ml). The increase of eGFR and the reduction of excreted urinary TDF-TAF in ADV-pretreated TAF group were significant compared to not-ADV-pretreated TAF group (+6.50 vs +1 ml/min and -3.5 vs +2 ng/ml. At linear regression, in univariate analysis the variation of urinary tenofovir concentration was inversely related to age and pretreatment with ADV for TAF patients and directly proportional to eGFR and

POSTER PRESENTATIONS

pretreatment with ADV for TDF patients ($p < 0.005$). In the multivariate analysis only eGFR and pretreatment with ADV for TDF patients resulted significant and directly proportional to the variation of urinary tenofovir concentration (< 0.005).



Conclusion: According to these results, ADV-pretreated patients have a benefit from switching TDF to TAF. The correlation of genotype with plasmatic TAF concentration suggests a possible key role of TDF/TAF transporter polymorphisms. Finally, further studies are needed for a better understanding of TAF pharmacokinetics in relation to liver stiffness

SAT347

Model to predict on-treatment restoration of functional HBV-specific CD8⁺ cell response foresees off-treatment HBV control in eAg-negative chronic hepatitis B

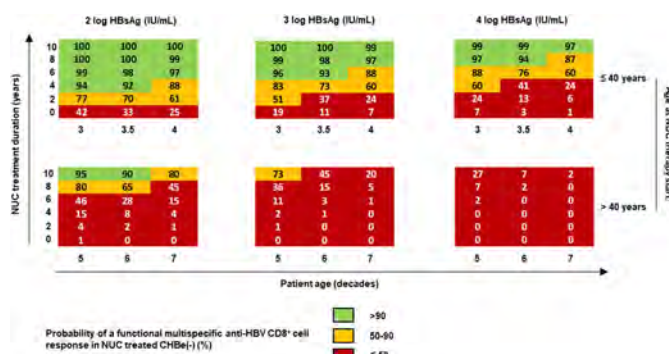
Julia Peña Asensio^{1,2}, Henar Calvo¹, Joaquin Miquel¹, Eduardo Sanz de Villalobos¹, Alejandro González Praetorius¹, Miguel Torralba^{1,3}, Juan Ramón Larrubia^{1,3}. ¹Guadalajara University Hospital, Translational Hepatology Unit, Guadalajara, Spain; ²University of Alcalá, Department of Biology of Systems, Alcalá de Henares, Spain; ³University of Alcalá, Department of Medicine and Clinical Specialties, Alcalá de Henares, Spain
Email: hlnd.julia@gmail.com

Background and aims: Hepatitis B virus (HBV)-specific CD8⁺ cell response restoration during nucleos (t)ide analogue (NUC) treatment could lead to off-treatment HBV control in e-antigen-negative chronic hepatitis B (CHBe (-)). To predict this response with variables involved in T-cell exhaustion for use as treatment stopping tool.

Method: In NUC treated CHBe (-) patients, we considered a functional response in cases with HBV-specific CD8⁺ cells against core and polymerase able to proliferate and secrete type-I cytokines after antigen encounter. We performed a logistic regression model (LRM) to predict the likelihood of developing this response, based on patient age (subrogate of infection length) and, HBsAg level, NUC therapy starting point and duration (antigenic pressure). We discontinued treatment and assessed HBV-DNA dynamics, HBsAg loss and HBsAg decline during off-treatment follow-up, according to LRM likelihood.

Results: We developed a LRM that predicted the presence of a proliferative type-I cytokine-secreting cell response, which correlated positively with treatment duration and negatively with treatment initiation after 40-year age and with age adjusted by HBsAg level. We observed a positive correlation between LRM probability and intensity of proliferation, number of epitopes with functional proliferating response and type-I cytokine secretion level.

Off-treatment, HBsAg loss, HBsAg decline >50% and HBV control were more frequent in the group with >90% LRM probability.



Conclusion: Short-term low-level antigen exposure and early long-term NUC treatment influence the restoration of a functional HBV-specific CD8⁺ cell response. Based on these predictors, high likelihood of detecting this response at treatment withdrawal associates with off-treatment HBV control and HBsAg decline and loss.

SAT348

Antiviral treatment cessation in HBeAg negative chronic hepatitis B: clinical outcome is associated with increase in specific pro-inflammatory cytokines

Marte Holmberg¹, Dag Henrik Reikvam², Olav Dalgard³, Hans Christian Dalsbotten Aass², Ellen Samuelsen³, Niklas Björkström⁴, Asgeir Johannessen¹. ¹Vestfold Hospital Trust, Tønsberg, Norway; ²Oslo University Hospital Ullevål, Oslo, Norway; ³Akershus University Hospital, Lørenskog, Norway; ⁴Karolinska University Hospital, Center for Infectious Medicine, Stockholm, Sweden
Email: marte.holmberg@online.no

Background and aims: Patients with HBeAg negative chronic hepatitis B may experience an immune response after stopping nucleos (t)ide analogue (NA) therapy, which may potentially trigger functional cure (HBsAg loss) or off-therapy sustained viral control. The immunological mechanisms that determine clinical outcome after treatment stop remain poorly understood, and predictors of clinical outcomes are lacking. We hypothesized that markers of systemic inflammation could identify key inflammatory pathways that are associated with and can predict clinical outcome after NA therapy cessation.

Method: Plasma cyto- and chemokines from 57 patients from the ongoing Nuc-Stop study were analyzed by Bio-Plex Pro Human Cytokine 27-plex Assay at baseline and three months after stopping NA therapy. All patients were HBeAg negative, non-cirrhotic, and virally suppressed for at least 24 months prior to stopping NA therapy. Outcome at three months was classified as immune control (HBV DNA <2000 IU/ml and ALT <2x baseline), viral relapse (HBV DNA >2000 IU/ml and ALT <2x baseline), clinical relapse (HBV DNA >2000 IU/ml and ALT >2x baseline), or clinical relapse with restart of treatment. Statistical significance ($p < 0.05$) was determined using Kruskal-Wallis tests or one-way ANOVA followed by Bonferroni post-hoc tests.

Results: After three months, there was a significant increase in interferon gamma-induced protein 10 (IP-10) in patients with clinical relapse who restarted treatment ($p = 0.001$) (Figure). This group also had a stronger ALT flare compared with those who had a clinical relapse without restart (median peak ALT 216 vs. 103 U/L, $p = 0.025$). A significant, but less pronounced, increase in tumor necrosis factor (TNF) was observed in the same group ($p = 0.010$) (Figure). None of the other cyto- or chemokines were associated with clinical outcome at three months.

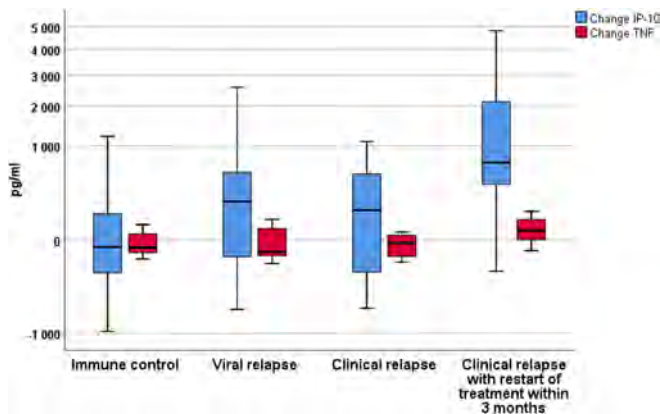


Figure: Changes in IP-10 and TNF 3 months after NA therapy cessation

Conclusion: Clinical relapse requiring restart of antiviral treatment after NA cessation was associated with specific increase in IP-10 and TNF.

SAT349

Tenofovir alafenamide for pregnant chinese women with active chronic hepatitis B: a multicenter, prospective, real-world study

Qing-Lei Zeng¹, Hongxu Zhang², Ji-Yuan Zhang³, Shuo Huang¹, Wei-Zhe Li¹, Guangming Li⁴, Ying-Hua Feng⁵, Guofan Zhang⁶, Jiang-Hai Xu⁷, Wan-Bao Lin⁸, Guang-Hua Xu⁹, Guoqiang Zhang¹⁰, Yan-Li Zeng¹¹, Zu-Jiang Yu¹, Fu-Sheng Wang³. ¹The First Affiliated Hospital of Zhengzhou University, Department of Infectious Diseases and Hepatology, Zhengzhou, China; ²Luohe Central Hospital, Department of Infectious Diseases, China; ³The Fifth Medical Center of Chinese PLA General Hospital, Treatment and Research Center for Infectious Diseases, Beijing, China; ⁴The Sixth People's Hospital of Zhengzhou City, Department of Hepatology, China; ⁵The Sixth People's Hospital of Kaifeng City, Department of Hepatology, China; ⁶The First Affiliated Hospital of Nanyang Medical College, Department of Infectious Diseases, China; ⁷The Fifth People's Hospital of Anyang City, Department of Hepatology, China; ⁸Xinyang Central Hospital, Department of Infectious Diseases, China; ⁹The Affiliated Hospital of Yan'an University, Department of Infectious Diseases, China; ¹⁰Luoyang Central Hospital, Department of Infectious Diseases, China; ¹¹Henan Provincial People's Hospital, Department of Infectious Diseases, China
Email: zengqinglei2009@163.com

Background and aims: Data on long-term tenofovir alafenamide (TAF) therapy for pregnant women with active chronic hepatitis B (CHB, immune clearance and reactivation phases) are lacking. The aim of this study was to investigate the safety and effectiveness of TAF in pregnant women with active CHB and their infants.

Method: Pregnant women with active CHB treated with TAF and tenofovir disoproxil fumarate (TDF) were enrolled in this multicenter (a total of 11 hospitals) prospective study, and infants received standard immunoprophylaxis. The primary outcomes were rates of adverse (safety) events in pregnant women and defects in infants and fetuses. The secondary outcomes were virological responses in pregnant women, infants' safety, hepatitis B surface antigen (HBsAg) status, and growth conditions. Participants were assessed for eligibility from January 1, 2019, to March 31, 2020. The pregnant women and their infants were followed until at least 6 months after delivery and 7 months of age, respectively. The final follow-up date was the November 15, 2021.

Results: One hundred three and 104 pregnant women were enrolled, and 102 and 104 infants were born in the TAF and TDF groups, respectively. In the TAF group, 82 (79.6%) pregnant women were hepatitis B e antigen (HBeAg) positive, and the mean age, gestational age, alanine aminotransferase level, and viral loads at treatment initiation were 29.3 years, 1.3 weeks, 122.2 U/L, and 5.1 log₁₀ IU/ml, respectively. TAF was well tolerated, and the most common adverse

event was nausea (30.1%) during a mean of two years (101.1 ± 24.3 weeks) of treatment. Notably, 1 (1.0%) TAF-treated pregnant woman exposed to agricultural chemicals during early pregnancy who initiated TAF from 12 weeks plus 2 days of gestation underwent induced abortion at 23 weeks plus 4 days of pregnancy due to the diagnosis of cleft lip and palate for the fetus at 22 weeks of gestation, this fetus was regarded as a congenital defect (most likely not related to TAF, because the developmental processes of the lip and palate are completed by 6–10 weeks of embryogenesis). No infants in either group had birth defects. In the TAF group, the HBeAg seroconversion rate of mothers was 20.7% (17/82) at postpartum month 6, infants had normal growth parameters (weight, height, and head circumference) compared with Chinese and WHO standards, and no infants were positive for HBsAg at 7 months of age. As of November 15, 2021, 40 TAF-exposed mother-infant dyads completed the postpartum month 18 follow-up, the cumulative HBeAg seroconversion rate is 28.0% (23/82), and all infants have normal growth parameters compared with Chinese and WHO standards. The TDF group had comparable baseline characteristics, and safety and effectiveness profiles during therapy.



Conclusion: TAF administered throughout or beginning in early pregnancy is generally safe and effective for pregnant women with active CHB and their infants.

SAT350

Suboptimal virological response to antiviral therapy in chronic hepatitis B as an independent predictor for occurrence of HCC and development of severe liver events

Chau-Ting Yeh¹, Chao-Wei Hsu¹. ¹Chang Gung Memorial Hospital, Liver Research Center, Taoyuan, Taiwan
Email: chautingy@gmail.com

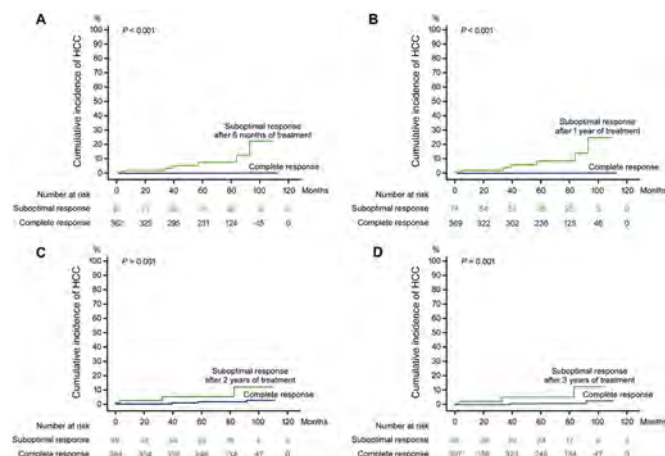
Background and aims: Although several potent antiviral drugs against chronic hepatitis B have been available worldwide with satisfactory virological suppression effect, incomplete virological suppression or suboptimal virological response can occur in a substantial proportion of patients. The definitions of suboptimal virological response varied among different international guidelines in terms of the remaining virological levels and the length of treatment periods. The suggested managements for patients experiencing suboptimal virological responses also varied, from continuation of the present antiviral drugs, switching to a more potent drug, to combination of two or more potent drugs. The long-term outcomes of these patients have never been interrogated.

Method: We retrospectively included 443 patients treated by entecavir in the Liver Clinic, Chang Gung Memorial Hospital, Taiwan, from 2008 to 2013. The HBV-DNA levels were assessed 6 months, 1 year, 2 years and 3 years after initiation of treatment. Suboptimal virological responses were defined as HBV-DNA levels above quantitative limit by Roche TaqMan Assay (>20 IU/ml) after the aforementioned treatment periods. The time-to-development of hepatocellular carcinoma (HCC) as well as the time-to-development of severe liver events (HCC or liver failure related death) were correlated with suboptimal responses and other clinical/virological factors. HBV X genes were sequenced from patients developing HCC.

POSTER PRESENTATIONS

Cell-based experiments were conducted to understand whether the HBV X mutants enhanced cccDNA accumulation.

Results: During the median follow-up period of 69 (range, 4 to 110) months, 6 patients developed HCC and 20 patients developed severe liver events. Kaplan-Meier analysis showed that suboptimal virological response detected at 6 months after treatment was an independent factor to predict HCC occurrence ($p < 0.001$). Univariate and Multivariate Cox proportion hazard ratio analysis showed that suboptimal virological response detected at 6 months after treatment was an independent factor to predict development of severe liver events (unadjusted $p = 0.006$; adjusted $p = 0.001$). Novel HBV X mutations were identified in 5 of the 6 patients developing HCC during the suboptimal response period. These HBV X mutants were capable of enhancing cccDNA accumulation in HCC cells.



Conclusion: Suboptimal response detected at 6 months after antiviral treatment by entecavir was an independent predictor for HCC occurrence and development of severe liver events. Novel HBV X mutations could be selected during the period of suboptimal virological response and these HBV X mutants enhanced cccDNA accumulation in HCC cells.

SAT351

Integrated efficacy analysis of 24-week data from two phase 2 and one phase 3 clinical trials of bulevirtide monotherapy given at 2 mg or 10 mg dose level for treatment of chronic hepatitis delta Pietro Lampertico^{1,2}, Soo Aleman³, Antje Blank⁴, Pavel Bogomolov⁵, Vladimir Chulanov⁶, Nina Mamonova⁶, Morozov Viacheslav⁷, Olga Sagalova⁸, Tatyana Stepanova⁹, Vithika Suri¹⁰, Dmitry Manuilov¹⁰, Lei Ye¹⁰, John F. Flaherty¹⁰, Anu Osinusi¹⁰, Markus Cornberg¹¹, Maurizia Brunetto^{12,13}, Heiner Wedemeyer¹¹.

¹Foundation IRCCS Ca' Granda Ospedale Maggiore Policlinico, Division of Gastroenterology and Hepatology, Milan, Italy; ²CRC "A. M. and A. Migliaiaccà" Center for Liver Disease, University of Milan, Department of Pathophysiology and Transplantation, Milan, Italy; ³Karolinska University Hospital/Karolinska Institutet, Department of Infectious Diseases, Stockholm, Sweden; ⁴Heidelberg University Hospital, Clinical Pharmacology and Pharmacoepidemiology, Heidelberg, Germany; ⁵State budgetary institution of health care of Moscow region "Moscow regional research clinical institute after M.F. Vladimirsky", Moscow, Russian Federation; ⁶FSBI National Research Medical Center for Phthisiopulmonology and Infectious Diseases of the Ministry of Health of the Russian Federation, Moscow, Russian Federation; ⁷LLC Medical Company "Hepatolog," Samara, Russian Federation; ⁸Federal state-funded institution of higher education "Southern Ural State Medical University of Ministry of Health of the Russian Federation", Chelyabinsk, Russian Federation; ⁹Limited liability company "Clinic of Modern Medicine," Moscow, Russian Federation; ¹⁰Gilead Sciences, Foster City,

United States; ¹¹Medizinische Hochschule Hannover, Klinik für Gastroenterologie, Hepatologie und Endokrinologie, Hannover, Germany; ¹²University Hospital of Pisa, Hepatology Unit, Reference Center of the Tuscany Region for Chronic Liver Disease and Cancer, Pisa, Italy; ¹³University of Pisa, Department of Clinical and Experimental Medicine, Pisa, Italy
Email: pietro.lampertico@unimi.it

Background and aims: Bulevirtide (BLV) is a novel first-in-class entry inhibitor for the treatment of chronic HDV infection (CHD) that was conditionally approved in the EU in July 2020. Patients treated with BLV alone have previously shown pronounced viral and biochemical responses (HDV RNA and ALT declines) in 2 phase 2 and 1 phase 3 trials (MYR202, MYR203 and MYR301). Here, we present an integrated efficacy analysis of 24-week data from these studies.

Method: A total of 281 patients with CHD without cirrhosis or with compensated cirrhosis were included in this pooled analysis including 92 and 95 patients treated with BLV at 2 mg or 10 mg given s.c. once daily, respectively, compared with 79 receiving no active anti-HDV treatment (Control) during the analysis period, and 15 patients treated with Peginterferon alfa (Peg-IFN α), the current standard of care (SOC) which is not approved for CHD. The primary efficacy end point assessed at week 24 was the combined response of undetectable HDV RNA or decrease by $\geq 2 \log_{10}$ IU/ml from baseline and ALT normalization; additional end points included viral response (undetectable HDV RNA or decline by $\geq 2 \log_{10}$ IU/ml), ALT normalization and change in HDV RNA levels.

Results: At baseline, demographics of all groups were well balanced. Characteristics of the BLV 2 mg group included: mean (SD) age 42 (9.0) years, 60.9% males, 83.7% White, 44.6% with compensated cirrhosis, 96.7% with HDV genotype 1, 64.1% were on nucleos(t)ide analogues therapy; mean (SD) HDV RNA was 5.2 (1.33) \log_{10} IU/ml and mean (SD) ALT was 107 (70.7) U/L. At Week 24, the combined response was achieved by 31.5% and 32.6% of patients in the BLV 2 mg and 10 mg groups, respectively. While the viral response rate was numerically lower in the BLV 2 mg group than in the BLV 10 mg group (53.3% and 71.6%), rates of ALT normalization were numerically higher for those treated with BLV 2 mg vs 10 mg (51.1% and 42.1%, respectively). For all efficacy end points, response rates were higher in the BLV groups compared to the Control or SOC groups.

Table. Efficacy at week 24.

	BLV 2 mg (N = 92)	BLV 10 mg (N = 95)	Control (N = 79)	Peg-IFN α (SOC) (N = 15)
Combined Response¹: Responder at Week 24	29 (31.5%)	31 (32.6%)	0	0
95% CI	(22.2%, 42.0%)	(23.4%, 43.0%)	(0.0%, 4.6%)	(0.0%, 21.8%)
Viral Response²: Responder at Week 24	49 (53.3%)	68 (71.6%)	3 (3.8%)	4 (26.7%)
95% CI	(42.6%, 63.7%)	(61.4%, 80.4%)	(0.8%, 10.7%)	(7.8%, 55.1%)
Biochemical Response³: Responder at Week 24	47 (51.1%)	40 (42.1%)	5 (6.3%)	0
95% CI	(40.4%, 61.7%)	(32.8%, 52.7%)	(2.1%, 14.2%)	(0.0%, 21.8%)
Change from BL at week 24 in HDV RNA levels (log₁₀ scale): Mean (SD)	-2.07 (1.368)	-2.54 (1.209)	-0.14 (0.773)	-1.16 (2.048)

¹ Undetectable HDV RNA or decrease by $\geq 2 \log_{10}$ IU/ml from baseline and ALT normalization.

² Undetectable HDV RNA or decrease by $\geq 2 \log_{10}$ IU/ml from baseline.

³ ALT normalization.

Undetectable HDV RNA defined as HDV RNA less than limit of detection (LOD), which was 14, 10, and 6 IU/ml in Studies MYR202, MYR203, and MYR301, respectively. Normalization of ALT was defined as an ALT value within the normal range, as defined by central laboratories (all sites in Studies MYR202 and MYR203 and Russian sites in Study MYR301: ≤ 31 U/L for females and ≤ 41 U/L for males; all other sites in Study MYR301: ≤ 34 U/L for females and ≤ 49 U/L for males).

Conclusion: In this integrated efficacy analysis of 24-week data from 281 patients, the combined response rates were comparable in the BLV 2 mg and BLV 10 mg groups; treatment with BLV was better than control or SOC groups. These results provide additional support for the use of BLV 2 mg once daily for treatment of compensated CHD.

SAT352

Integrated safety analysis of 24-week data from three phase 2 and one phase 3 clinical trials of bulevirtide monotherapy given at 2 mg and 10 mg dose level for treatment of chronic hepatitis delta

Pietro Lampertico^{1,2}, Soo Aleman³, Tarik Asselah⁴, Marc Bourliere⁵, Adrian Streinu-Cercel⁶, Pavel Bogomolov⁷, Morozov Viacheslav⁸, Tatyana Stepanova⁹, Stefan Lazar¹⁰, Vithika Suri¹¹, Dmitry Manuilov¹¹, Lei Ye¹¹, John F. Flaherty¹¹, Anu Osinusi¹¹, Maurizia Brunetto^{12,13}, Heiner Wedemeyer¹⁴. ¹Foundation IRCCS Ca' Granda Ospedale Maggiore Policlinico, Division of Gastroenterology and Hepatology, Milan, Italy; ²CRC "A. M. and A. Migliavacca" Center for Liver Disease, University of Milan, Department of Pathophysiology and Transplantation, Milan, Italy; ³Karolinska University Hospital/Karolinska Institutet, Department of Infectious Diseases, Stockholm, Sweden; ⁴Hôpital Beaujon APHP, Université de Paris, INSERM, Clichy, France; ⁵Hôpital Saint Joseph Marseille, Marseille, France; ⁶Matei Bals National Institute of Infectious Diseases, Bucharest, Romania; ⁷State budgetary institution of health care of Moscow region "Moscow regional research clinical institute after M.F. Vladimirovsky", Moscow, Russian Federation; ⁸LLC Medical Company "Hepatolog," Samara, Russian Federation; ⁹Limited liability company "Clinic of Modern Medicine," Moscow, Russian Federation; ¹⁰Dr. Victor Babes Foundation-Infectious and Tropical Diseases Hospital, Bucharest, Romania; ¹¹Gilead Sciences, Foster City, United States; ¹²University Hospital of Pisa, Hepatology Unit, Reference Center of the Tuscany Region for Chronic Liver Disease and Cancer, Pisa, Italy; ¹³University of Pisa, Department of Clinical and Experimental Medicine, Pisa, Italy; ¹⁴Medizinische Hochschule Hannover, Klinik für Gastroenterologie, Hepatologie und Endokrinologie, Hannover, Germany
Email: pietro.lampertico@unimi.it

Background and aims: Bulevirtide (BLV) is a novel first-in-class entry inhibitor of the hepatitis D virus (HDV) that was conditionally approved for treatment of chronic hepatitis delta (CHD) in the EU in July 2020. BLV monotherapy was shown to be generally safe and well tolerated in three phase 2 and one phase 3 trials (MYR202, MYR203, MYR204 and MYR301). Here, we present an integrated safety analysis of 24-week data from these studies.

Method: A total of 355 patients with CHD were included in this pooled analysis: 92 and 145 patients treated with BLV alone at 2 mg or 10 mg given subcutaneous (s.c.) once daily, respectively, compared with 79 receiving no active anti-HDV treatment (Control) during the analysis period, and 39 patients treated with Peginterferon alfa (Peg-IFN α), the current standard of care (SOC) which is not approved for CHD. The assessed safety parameters included graded adverse events (AE) and laboratory abnormalities.

Results: At baseline, demographics of all groups were well balanced. Characteristics of the BLV 2 mg group included: mean (SD) age 42 (9.0) years, 60.9% males, 83.7% White, 44.6% with compensated cirrhosis, 96.7% with HDV genotype 1, 51.1% were interferon experienced; mean (SD) HDV RNA was 5.2 (1.33) log₁₀ IU/ml and mean (SD) ALT was 107 (70.7) U/L. By Week 24, the overall incidence of participants experiencing AEs was similar in BLV 2 mg and BLV 10 mg groups at 67.4% and 73.8%, respectively, compared to rates of 87.2% in the Peg-IFN α group and 49.4% in the control group. There were no serious AEs (SAEs) considered related to BLV and no AEs leading to discontinuation of BLV. The rates of grade 3–4 AEs and grade 3–4 laboratory abnormalities were similar in both BLV and control groups but were higher in the Peg-IFN α group. The AE profile was similar between the BLV groups and the control group, with a few exceptions, including higher rates of headache and total bile acids increased in the BLV treatment arms. Most AEs were mild or moderate in severity. Asymptomatic dose-dependent increase in serum bile acids is expected with BLV treatment based on its mode of action. Injection site reactions, considered as AEs of interest based on daily s. c. BLV administration mode, were more common in the BLV 10 mg group compared to 2 mg.

Number (%) of Participants With Any	BLV 2 mg (N = 92)	BLV 10 mg (N = 145)	Control (N = 79)	Peg-IFN α (N = 39)
AE	62 (67.4%)	107 (73.8%)	39 (49.4%)	34 (87.2%)
AE with Grade 3–4	4 (4.3%)	10 (6.9%)	3 (3.8%)	17 (43.6%)
Grade 3 or 4 Laboratory Abnormalities	6 (6.5%)	11 (7.6%)	6 (7.6%)	16 (41.2%)
AE Related to BLV	45 (48.9%)	87 (60.0%)	0	0
SAE	0	1 (0.7%)	2 (2.5%)	2 (5.1%)
AEs of interest:				
Injection Site Reactions	7 (7.6%)	22 (15.2%)	0	1 (2.6%)

* Related to BLV; † (2.2%) participants in the BLV 2mg group and 5 (3.4%) participants in the BLV 10mg group
Adverse events were coded according to MedDRA Version 24.0.
Severity grades were defined by the CTCAE.
AE = adverse event; BLV = bulevirtide; CTCAE = Common Terminology Criteria for Adverse Events; Peg-IFN α = pegylated interferon alfa; SAE = serious adverse event

Conclusion: Over the 24-week treatment period, monotherapy with BLV at 2 mg and 10 mg dose was generally safe and well tolerated with a low frequency of grade 3–4 AEs, SAEs; and no AEs leading to BLV discontinuation or SAEs considered related to BLV.

SAT353

Virologic response to bulevirtide is delayed in cirrhotic HDV patients with clinically significant portal hypertension

Mathias Jachs^{1,2}, Caroline Schwarz³, Marlene Panzer⁴, Lukas Hartl^{1,2}, Simona Bota⁵, Petra Munda¹, Albert F Stättermayer¹, Ivo Graziadei⁶, Stephan Aberle⁷, Michael Gschwenter³, Heinz Zoller⁴, Michael Trauner¹, Matthias Mandorfer^{1,2}, Peter Ferenci¹, Thomas Reiberger^{1,2}. ¹Medical University of Vienna, Division of Gastroenterology and Hepatology, Department of Internal Medicine III, Vienna, Austria; ²Medical University of Vienna, Vienna Hepatic Hemodynamic Lab, Division of Gastroenterology and Hepatology, Department of Internal Medicine III, Vienna, Austria; ³Klinik Ottakring, Division of Gastroenterology and Hepatology, Department of Internal Medicine IV, Vienna, Austria; ⁴Medical University of Innsbruck, Department of Internal Medicine I, Innsbruck, Austria; ⁵Klinikum Klagenfurt am Wörthersee, Department of Internal Medicine and Gastroenterology, Hepatology, Endocrinology, Rheumatology and Nephrology, Klagenfurt; ⁶Landeskrankenhaus Hall, Department of Internal Medicine, Hall in Tirol; ⁷Medical University of Vienna, Center for Virology, Wien, Austria
Email: thomas.reiberger@meduniwien.ac.at

Background and aims: Bulevirtide (BLV) therapy is licensed for the treatment of hepatitis D virus (HDV)-infection in compensated patients in Europe. Patients with HDV-related advanced chronic liver disease (ACLD) and clinically significant portal hypertension (CSPH) are in urgent need of antiviral treatment due to a substantially increased risk of hepatic decompensation.

Method: The response to BLV therapy was assessed in HDV-related ACLD patients with evidence for CSPH, i.e., liver stiffness measurement (LSM) values ≥ 20 kPa by vibration-controlled transient elastography (VCTE), as compared to patients without evidence for CSPH.

Results: Twenty-one chronic HDV patients (median age: 47.6 years, sex: 10 male/11 female, baseline HDV-RNA: 100 to 21000000 copies/ml, HBV-DNA suppressed in all patients by NA therapy), were treated with BLV for ≥ 24 weeks and underwent pre-treatment VCTE-LSM. Median pre-treatment VCTE-LSM was 17.2 kPa (range: 5.4–48.0 kPa), and seven patients (33.3%) had CSPH by VCTE-LSM ≥ 20 kPa, further evidenced by thrombocytopenia (85.7%), splenomegaly (85.7%), or varices (66.7%).

ALT levels ranged from 22 to 132 U/L in CSPH patients with 5 out of 7 showing ALT ≥ 50 U/L.

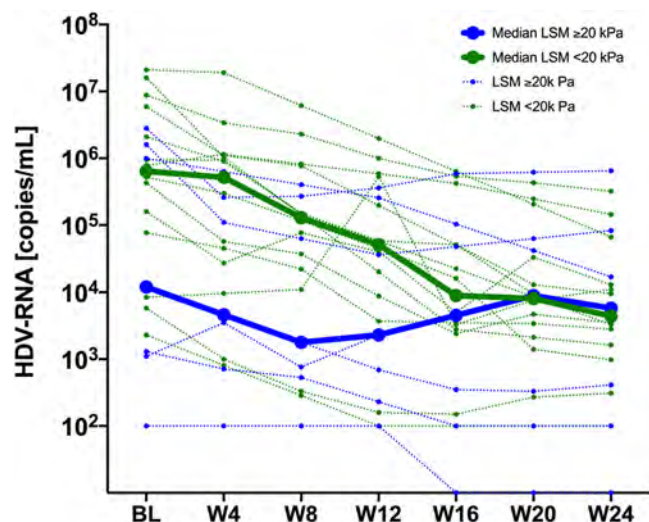
At week 24, virological response (VR, defined by ≥ 2 -log₁₀-decrease or undetectable HDV-RNA) was achieved by only one CSPH patient (14.3%), while five patients (71.4%) showed partial response, i.e. any HDV-RNA decrease (range: -0.63 to -1.77 log₁₀); one patient experienced even an HDV-RNA increase (+0.72 log₁₀). In the 14 HDV patients without evidence for CSPH, seven (50.0%) patients achieved VR at W24, partial response was seen in 6 (42.9%) and one patient showed an increase in HDV-RNA.

POSTER PRESENTATIONS

Interestingly, five (71.4%) CSPH patients achieved normal ALT levels at W24, as compared to 12 out of 14 (85.7%) non-CSPH patients. Four HDV-ACLD patients with CSPH have already reached W48; two (50.0%) achieved HDV-RNA undetectability and all (100%) showed normal ALT levels.

Of note, four out of seven CSPH patients underwent a follow-up VCTE-LSM after one year of BLV therapy (range 40–52 weeks), and three (75.0%) showed VCTE-LSM decreases of $\geq 20\%$, two patients even achieved a reduction to a final VCTE-LSM ≤ 20 kPa (i.e. a clinically relevant decrease as by Baveno VII consensus).

BLV treatment in HDV-CSPH was well tolerated, and no significant adverse events were observed despite substantial increases in serum bile acids levels (median +829% at 4 weeks; maximum levels: 38.0–208.6 $\mu\text{mol/L}$).



Conclusion: Virologic response to BLV in cirrhotic HDV patients with CSPH seems delayed, however, a high rate of decreases in VCTE-LSM suggests a treatment benefit. BLV is safe in patients with CSPH. Data on changes in HVPg as a potential surrogate for treatment efficacy are awaited.

SAT354

Response-guided long-term treatment of chronic hepatitis D patients with bulevirtide-Results of a "real world study"

Mathias Jachs¹, Caroline Schwarz², Marlene Panzer³, Teresa Binter¹, Elmar Aigner⁴, Stephan Aberle⁵, Albert Stättermayer¹, Ivo Graziadei³, Petra Munda¹, Heinz Zoller³, Michael Gschwantler², Michael Trauner¹, Thomas Reiberger¹, Peter Ferenci¹. ¹Medical University of Vienna, Internal Medicine 3, Gastroenterology and Hepatology, Wien, Austria; ²Klinik Ottakring, Internal Medicine 4, Wien, Austria; ³Medical University of Innsbruck, Internal Medicine 1, Innsbruck; ⁴Paracelsus private University/SALK, Salzburg, Austria; ⁵Medical University of Vienna, Center of Clinical Virology, Wien, Austria Email: peter.ferenci@meduniwien.ac.at

Background and aims: Bulevirtide (BLV) blocks hepatic uptake of the hepatitis D Virus (HDV) via the sodium/bile acid cotransporter NTCP. BLV was conditionally approved by EMA, but the optimal treatment duration is unknown. The aim of this real-world study was to define useful efficacy and futility end points.

Method: BLV was provided by MyrPharma (Leipzig/Germany) until 8/2020 and was subsequently prescribed and dosed at the discretion of the investigator. Based on the magnitude of HDV-RNA decline at week 24 patients were classified as responder (≥ 2 log drop), partial responder (>1.0 – <2 log drop), or non-responder (<1 log drop).

Results: 23 patients (m: 10/f:13; mean age: 47.9 years, cirrhosis: n = 15; median ALT:71 IU/ml (range 21–341); HDV-RNA: 9.5×10^5

[range: 1.0 – 2.1×10^7] copies/ml) received BLV (2 mg/d in n=21; 10 mg/day in n=2). 21 patients (84.6%) were on concomitant NUCs (ETV n=3, TDF n=16, TAF n=2), 19 were previous Peginterferon-alfa2a (PEGIFN) non-responders. 22 patients completed at least ≥ 24 weeks of BLV treatment (range: 24–130 weeks), one dropped out at week 8.

Twelve patients (54.5%) were classified as BLV responders: in 2 treatment was terminated as HDV-RNA was undetectable for >6 months after 63 and 130 weeks, respectively. Both became HDV-RNA positive again after 60 and 4 weeks, respectively; in the latter BLV treatment was resumed. One patient underwent liver transplantation at week 25 and one was lost to follow-up after week 26. In 2 patients PEGIFN was added after 39 and 48 weeks, respectively, because of no further decline or re-increase of HDV-RNA. Thus, 7 are still on BLV monotherapy.

Four partial responders (18.2%) are still on BLV monotherapy (24–29 weeks).

Six patients (31.8%) were non-responders. (PEGIFN) was added in 5 except for one who dropped out after 24 weeks. In 4 patients HDV-RNA courses under BLV+PEGIFN are available showing a rapid decline of HDV-RNA within 12 weeks (-0.97 ; -1.19 ; -1.23 ; and -1.54 log-drop, respectively).

ALT levels normalized in 14/22 (63%) at week 24 and 8/10 (80%) at week 48, respectively. Treatment was well tolerated, bile acid levels increased without pruritus. HBsAg levels remained unchanged during BLV therapy.

Conclusion: Long-term BLV is safe and effectively decreases HDV-RNA and ALT. Responders likely require long-term treatment whereas in patients without virologic response, the addition of PEGIFN seems to be of value. Our data indicate the need for an individualized approach for HDV treatment with BLV.

SAT355

HBV RNA levels are associated with virological response to treatment with pegylated interferon alpha in patients with chronic hepatitis D virus infection

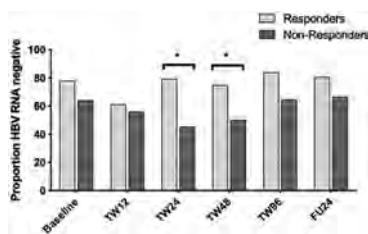
Lisa Sandmann¹, Birgit Bremer¹, Cihan Yurdaydin^{2,3}, Katja Deterding¹, Michael P. Manns^{1,4}, Markus Cornberg^{1,4,5,6}, Heiner Wedemeyer^{1,4,6}, Benjamin Maasoumy^{1,4,5}. ¹Hannover Medical School, Department of Gastroenterology, Hepatology and Endocrinology, Hannover, Germany; ²University of Ankara Medical School, Department of Gastroenterology, Ankara, Turkey; ³Koc University Medical School, Department of Gastroenterology and Hepatology, Istanbul, Turkey; ⁴German Center for Infection Research (DZIF), Partner Site Hannover-Braunschweig, Germany; ⁵Centre for Individualised Infection Medicine (CiM), Helmholtz Centre for Infection Research, Germany; ⁶German Center for Infection Research (DZIF), Partner Site HepNet Study House, Hannover, Germany Email: sandmann.lisa@mh-hannover.de

Background and aims: Chronic hepatitis D virus (HDV) infection causes severe liver disease with rapid progression to liver cirrhosis. Treatment with pegylated interferon alpha (pegIFN α) leads to viral response in approximately 25%, including patients with long-term virological control. Since IFN treatment is accompanied by severe side effects, on-treatment markers to identify patients with high chances of virological response are needed. HBV RNA, which reflects HBV cccDNA activity, may serve as a novel marker during antiviral treatment.

Method: The HIDIT-II study included 120 HBV/HDV co-infected patients. Patients were treated for 96 weeks with pegIFN α and either tenofovir or placebo. 99 patients with HDV RNA results 24 weeks after end of treatment (FU24) were included in this analysis, of whom 32 patients (32.3%) had undetectable HDV RNA at FU24. HBV RNA was measured at baseline, week 12, 24, 48, 96 and FU24 using the Roche Cobas 6800 system (LLOQ 10 cp/ml). Additional virological parameters (HBV DNA, quantitative HBsAg, HBcrAg and HDV RNA) were measured by appropriate assays (Lumipulse® G (Fujirebio-Europe)

for HBcrAg, Roche Cobas TaqMan system with an inhouse assay for HDV RNA).

Results: At baseline, mean HBV RNA levels were 1.71 ± 1.18 log cp/ml and HBV RNA levels were undetectable in 68.8% of patients. During treatment, mean HBV RNA levels did not differ between patients receiving either tenofovir or placebo. When separating between treatment responders (HDV RNA negative at FU24) and non-responders, mean levels of HBV RNA were significantly lower in responders at treatment week 24, 48 and end of treatment. Accordingly, the proportion of patients with undetectable HBV RNA was significantly higher in treatment responders at week 24 and 48 (79% vs. 50%, $p = 0.0031$; 75% vs. 50%, $p = 0.0276$) (Figure). However, HBV RNA levels of patients with viral relapse did not differ from those with maintained response at the end of treatment. No correlation between HBV RNA levels and HBV DNA, qHBsAg, HBcrAg or HDV RNA levels was detected at any time-point during the study. Interestingly, only 36% of patients with undetectable HBV RNA showed undetectable HBcrAg levels at baseline, whereas all but two patients with undetectable HBcrAg were HBV RNA negative ($n = 24/26$, 92%).



Conclusion: On-treatment HBV RNA levels differ significantly between responders and non-responders. Along with other virological parameters, HBV RNA could be a supportive marker to identify patients benefiting from treatment with pegIFNa. However, overall HBV RNA levels were low throughout the study population.

SAT356

Management of chronic hepatitis B virus infection within a large integrated health care setting: treatment patterns among kaiser permanente members in southern california, 2008–2019

Deborah Malden^{1,2}, Prabhu Gounder³, Katherine Oh¹, Amandeep Sahota¹, Robert Wong⁴, Amit Chitnis⁵, Theresa Im¹, Vennis Hong¹, Ana Florea⁶, Sara Tartof^{1,7}. ¹Kaiser Permanente Southern California Department of Research and Evaluation, Pasadena, United States; ²Centers for Disease Control and Prevention, Epidemic Intelligence Service, Division of Scientific Education and Professional Development, Atlanta, United States; ³Los Angeles County Department of Public Health, Los Angeles, United States; ⁴Stanford University School of Medicine, Division of Gastroenterology and Hepatology, Stanford, United States; ⁵Alameda County Public Health, Tuberculosis Section, Division of Communicable Disease Control and Prevention, Oakland, United States; ⁶Kaiser Permanente Southern California Department of Research and Evaluation, Research and Evaluation, Pasadena, United States; ⁷Kaiser Permanente Bernard J Tyson School of Medicine, Department of Health Systems Science, Pasadena, United States
Email: debbie.e.malden@kp.org

Background and aims: An estimated 1.89 million adults in the United States have chronic hepatitis B (CHB). Despite wide availability of treatment for CHB, many treatment-eligible patients remain untreated. To improve treatment rates, we investigated factors associated with receiving treatment among patients with CHB in a large, integrated health care setting in Southern California.

Method: Using data from Kaiser Permanente electronic medical records, we performed a retrospective cohort study among persons aged ≥ 18 years with CHB, defined as having two, positive hepatitis B surface antigen or hepatitis B virus (HBV) DNA tests >6 months apart during 2008–2019. Patients with HIV were excluded. CHB treatment

eligibility was determined according to American Association for the Study of Liver Diseases guidelines based on hepatitis e antigen status, annual serum alanine aminotransferase levels, HBV DNA levels, and presence of fibrosis or cirrhosis. We used multivariate cox proportional hazards regression to estimate adjusted hazard ratios (aHRs) and corresponding 95% CI for treatment receipt among those eligible for CHB treatment during the study period, defined as receiving antiviral treatment according to electronic medical records.

Results: Of 5,314 patients with CHB, 16% ($n = 857$) were eligible for treatment. Treatment-eligible patients were older (mean age 53 vs 48 years) and included a greater proportion of men (56% vs 48%) and persons with diabetes (15% vs 8%), compared with all CHB patients. Among patients eligible for treatment, 49% ($n = 417$) received treatment. Patients who received treatment were on average 4 years younger (mean age 51 vs 55 years), but did not differ greatly by comorbidity status or Body Mass Index than those who did not receive treatment. Women were less likely to receive treatment than men (aHR 0.69; 95% CI: 0.55–0.85). Relative to non-Hispanic Asian race/ethnicity, persons of non-Hispanic White race/ethnicity were less likely to receive treatment (aHR: 0.66; 95% CI: 0.43–0.99). Patients who were referred to a health care specialist (infectious disease, hepatology or gastroenterology) were almost twice as likely to receive treatment, compared with those who were not (aHR 1.85; 95% CI: 1.26–2.70).

Conclusion: Among a large cohort of CHB patients, fewer than half of patients who were eligible for treatment received treatment. Increasing referral of CHB patients to a health care specialist may improve treatment rates.

SAT357

Dose-dependent durability of hepatitis B surface antigen reductions following administration of a single dose of VIR-3434, a novel neutralizing vaccinal monoclonal antibody

Kosh Agarwal¹, Man-Fung Yuen², Heiner Wedemeyer³, Daniel Cloutier⁴, Ling Shen⁴, Andre Arizpe⁴, Sneha V. Gupta⁴, Marie C. Fanger⁴, Lillian Seu⁴, Andrea Cathcart⁴, Audrey H. Lau⁴, Carey Hwang⁴, Edward J. Gane⁵. ¹King's College Hospital, Institute of Liver Studies, London, United Kingdom; ²The University of Hong Kong, Queen Mary Hospital, Hong Kong, China; ³Hannover Medical School, Department of Gastroenterology, Hepatology, and Endocrinology, Hannover, Germany; ⁴Vir Biotechnology, Inc., San Francisco, California, United States; ⁵University of Auckland, Faculty of Medicine, Auckland, New Zealand
Email: kosh.agarwal@kcl.ac.uk

Background and aims: Chronic hepatitis B virus (HBV) infection is associated with significant morbidity and mortality and contributes substantially to the overall global health burden. VIR-3434 is an Fc engineered human monoclonal antibody targeting the conserved antigenic loop of hepatitis B surface antigen (HBsAg) currently in development for the treatment of chronic HBV infection. Here, we report preliminary data from an ongoing phase 1 study evaluating the safety, tolerability, and antiviral activity of VIR-3434 in participants with chronic HBV infection.

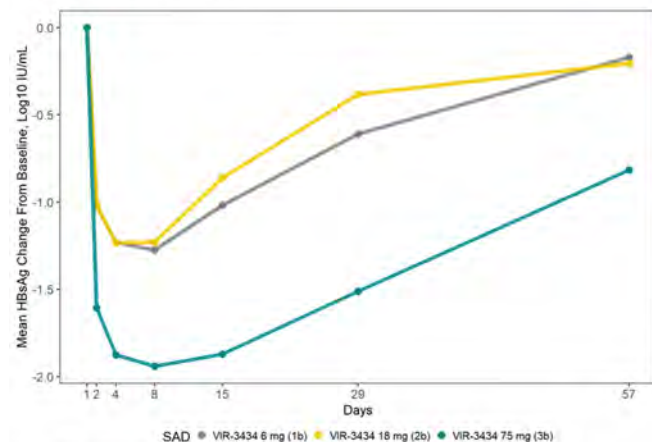
Method: This randomized, double-blind, placebo-controlled, phase 1, single ascending dose study included adults with hepatitis B e antigen (HBeAg)-negative chronic HBV infection without cirrhosis. Participants had HBsAg $<3,000$ IU/ml at screening and had received nucleos (t)ide reverse transcriptase inhibitor (NRTI) therapy for ≥ 2 months. Eight participants in each cohort were randomized 6:2 to receive a single subcutaneous dose of VIR-3434 6 mg, 18 mg, 75 mg, or 300 mg, or placebo. Preliminary data through 8 weeks of follow-up are presented; dose escalation and follow-up are ongoing.

Results: Twenty-four participants were enrolled. Most participants achieved a ≥ 1 log₁₀ IU/ml reduction from baseline in HBsAg within 1–3 days of dosing. The largest and most durable HBsAg reductions were observed in the 75 mg cohort. Among the 6 participants per cohort with >0.2 log₁₀ IU/ml reductions in HBsAg, mean reductions in the

POSTER PRESENTATIONS

6 mg, 18 mg, and 75 mg groups were 1.30, 1.27, and 1.96 log₁₀ IU/mL, respectively, at nadir and 0.17, 0.20, and 0.82 log₁₀ IU/mL, respectively, at week 8 (Figure). Ten adverse events were reported, and all were grade 1 or 2 in severity. No clinically significant laboratory abnormalities or signs of immune complex disease were observed. Pending availability, data from participants receiving a single dose of 300 mg VIR-3434 will also be presented.

Mean HBsAg decline from baseline*



*Excluding 2 participants in each cohort with < 0.2 log₁₀ IU/mL reduction in HBsAg

Conclusion: A single dose of 6 mg, 18 mg, or 75 mg VIR-3434 demonstrated a rapid reduction in HBsAg; the 75 mg dose level was associated with larger and more durable HBsAg reductions through week 8. Preliminary safety data suggest that VIR-3434 was generally safe and well tolerated. These preliminary data support the further evaluation of VIR-3434 for functional cure of patients with chronic HBV infection.

SAT358

Quantification of HBV hepatocyte burden using novel multiplex immunofluorescence staining and image analysis reveals substantial reduction in HBV liver burden with anti-viral treatment

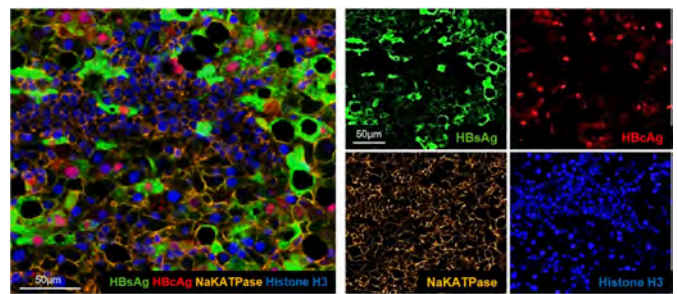
Abhishek Aggarwal¹, Pamela Odorizzi¹, Jens Brodbeck¹, Nicholas Van Buuren¹, Christina Moon¹, Silvia Chang¹, MaryVic Adona¹, Torsten Trowe¹, Scott Turner¹, Patrick Marcellin², Maria Buti³, Anuj Gaggar¹, Lauri Diehl¹, Becket Feierbach¹, Scott Balsitis¹. ¹Gilead Sciences, Inc., Foster City, United States; ²Hospital Beaujon AP-HP, Clichy, France; ³Hospital Universitari Vall d'Hebron, Barcelona, Spain
Email: pamela.odorizzi@gilead.com

Background and aims: Patterns of Hepatitis B virus (HBV) infection and integration before and after nucleotide (NUC) therapy have been previously described, but accurate quantification of HBV-infected hepatocytes in a large liver biopsy collection has not been reported. We developed novel immunofluorescence and image analysis techniques to quantify HBV-positive cells and applied them to over 200 liver biopsies.

Method: A 4-plex immunofluorescence assay was developed with HBsAg, core, membrane (Na⁺/K⁺-ATPase), and nuclear (Histone H3) markers to assign HBV staining to individual cells. An image analysis algorithm was also developed to quantify the percentage of hepatocytes positive for HBV proteins. Biopsies from HBeAg-positive (n = 76) and HBeAg-negative (n = 129) patients before or during NUC (tenofovir disoproxil fumarate or adefovir) treatment for 48 or 240 weeks were analyzed from GS-US-174-0102/0103. When available, matched serum samples were evaluated for HBV DNA, HBsAg, HBcAg, HBV RNA, and ALT. In fifteen cases, two biopsies were

collected from different portions of the liver at the same timepoint and staining was compared to evaluate sampling effects.

Results: Two common and typically mutually exclusive staining patterns were observed: diffuse core staining and foci of HBsAg staining, thought to represent hepatocytes with cccDNA and integrated HBV DNA, respectively. Hepatocytes positive for both core and HBsAg were rare. Biopsies collected from the same patient and timepoint revealed enormous variability in HBV staining within individual patients, indicating that single biopsies are not representative of the entire liver. This intra-patient variability was confirmed in a liver resection sample. On a population level, NUC treatment was associated with >100-fold lower median frequency of core-positive cells (p < 0.001), while reductions in HBsAg-positive cell frequency were modest and not statistically significant. HBeAg-negative Week 240 NUC-treated patients had the lowest HBV burden (median 3.8% hepatocytes positive for core and/or HBsAg). Positive correlations between serum viral biomarkers and liver HBV burden were only observed in HBeAg-positive patients prior to NUC treatment.



Conclusion: Using a novel multiplex imaging method for quantifying HBV burden in a large cohort of liver samples, we demonstrate 1) significant intra-patient variation in liver biopsies and 2) population-level reductions in HBV liver burden associated with HBeAg-negative status and NUC treatment.

SAT359

GST-HG141 inhibits de novo HBV cccDNA formation in cultured primary human hepatocytes

Dong Zhang¹, Wenqiang Wu¹, Shikui Chen¹, Zhou Yu¹, Vadim Bichko¹, John Mao¹, Jiang Zhigan², Haiying He², Li Jian², Shuhui Chen². ¹Fujian Cosunter Pharmaceutical Co., Ltd.; ²Domestic Discovery Service Unit, WuXi AppTec (Shanghai) Co., Ltd.
Email: vbichko@gmail.com

Background and aims: GST-HG141 is a novel, orally-bioavailable HBV capsid assembly modulator (CAM). It inhibits HBV pregenomic RNA packaging, leading to formation of "empty" capsids, devoid of genetic material. However, its mode of action and resistance profile appear to be distinct from other class I CAMs in development. GST-HG141 has an excellent antiviral potency in vitro, as well as efficacy in HBV mouse models. GST-HG141 was safe and well-tolerated in a first-in-man clinical study in healthy volunteers [Li et al, Antimicrob Agents Chemother. 2021; 65 (10)] and is currently under phase Ib evaluation in chronic HBV patients. Here we report antiviral properties of GST-HG141 in cultured primary human hepatocytes (PHH).

Method: Cryopreserved PHHs from a single donor were infected with HepG2.2.15 cell-derived HBV. Treatment with GST-HG141, GLS4, or Entecavir (ETV) started concurrently with infection, or 5 days post-infection. After 7 days of treatment, the effects on the secreted HBV DNA were determined using qPCR. Secreted HBsAg and HBeAg were quantified by ELISA. Southern blot was performed to detect and quantify the HBV covalently closed circular DNA (cccDNA). The identity of the cccDNA band was confirmed by EcoRI digestion.

Results: All three tested compounds reduced secreted HBV DNA levels in a concentration-dependent manner, regardless of when the treatment was started (GST-HG141 EC₅₀ ~ 80 nM). The secreted HBsAg (EC₅₀ ~ 1.5 microM) and HBeAg (EC₅₀ ~ 1.6 microM) levels were also dose-dependently decreased by GST-HG141, but only if treatment started concurrently with infection. Similar observations were made with GLS4. ETV had no effect on HBeAg- and HBsAg levels in cell culture supernatants under neither condition. GST-HG141 potently and dose-dependently inhibited HBV cccDNA formation, but only when treatment started with the infection, and not at day 5 post-infection. No significant cytotoxicity was observed with neither compound in this study (CC₅₀ >10 microM).

Conclusion: These data demonstrate that GST-HG141 prevents *de novo* synthesis of cccDNA, but has no effect on the established cccDNA pools in cultured PHH. It acts on different steps of the HBV life cycle, suggesting dual/multiple mechanisms of antiviral action. Further development of GST-HG141 for chronic HBV infections is warranted. Currently it is undergoing phase Ib-II clinical evaluations. The interim results from the ongoing phase Ib study show robust antiviral efficacy of GST-HG141 monotherapy and good safety/tolerability in chronic HBV patients.

SAT360

Predictive factors of virological response at one year in patients with chronic HBV/HDV co-infected treated with Bulevirtide

Victor de Ledinghen¹, Paul Hermabessière², Sophie Metivier³, Edouard Bardou-Jacquet⁴, Marie-Noelle Hilleret⁵, Veronique Loustaud-Ratti⁶, Nathalie Ganne-Carrié⁷, Laurent Alric^{3,8}, Isabelle Fouchard Hubert⁹, Louis d'Alteroche¹⁰, Bruno Roche⁷, Fabien Zoulim¹¹, Anne Gervais⁷, Helene Fontaine⁷, Anne Minello Franza¹², Christiane Stern⁷, Jérôme Dumortier¹¹, Dominique Roulot⁷, Xavier Causse¹³, Isabelle Ollivier-Hourmand¹⁴, Karine Lacombe⁷, Patrick Miaillhes¹¹, Frederic Heluwaert¹⁵, Leon Muti¹⁶, Isabelle Rosa¹⁷, Valérie Canva¹⁸, Damien Lucidarme¹⁹, Dominique Larrey²⁰, Bernard Prouvost-Keller²¹, Caroline Lascoux-Combe⁷, Juliette Foucher². ¹CHU Bordeaux, France; ²CHU Bordeaux; ³CHU Toulouse; ⁴CHU Rennes; ⁵CHU Grenoble; ⁶CHU Limoges; ⁷APHP; ⁸CHU Rangueil, Digestive Department Toulouse 3 University, Toulouse, France; ⁹CHU Angers; ¹⁰CHU Tours; ¹¹CHU Lyon; ¹²CHU Dijon; ¹³CHR Orleans; ¹⁴CHU Caen; ¹⁵CHG Annecy; ¹⁶CHU Clermont-Ferrand; ¹⁷CHI Créteil; ¹⁸CHU Lille; ¹⁹Hopital Saint Philibert; ²⁰CHU Montpellier; ²¹CHU Nice

Email: victor.deledinghen@chu-bordeaux.fr

Background and aims: BLV monotherapy as well as combination with PEG-interferon α 2a (PEG-IFN α) for 48 weeks induced HDV RNA declines in the French ATU early access program. The aim of this study was to evaluate 12-month predictive factors of virological response in HBV/HDV patients receiving 2 mg BLV with or without PEG-IFN α 2a (real-life study).

Method: 145 patients with chronic HBV/HDV co-infection, with cirrhosis or moderate fibrosis and elevated ALT levels, without liver decompensation, were included. Patients received 2 mg BLV qd sc alone in combination with PEG-IFN α once weekly for 12 months, according to physician's choice. Univariate analysis was performed to evaluate predictive factors of undetectable HDV-RNA after one year of treatment.

Results: Characteristics of the 145 patients were: 99 (68.3%) males, 41 years, cirrhosis N = 91/108 (62.8%), median viral load of 6.2 log₁₀IU/ml. At month 12, in the BLV monotherapy and in the BLV + PEG-IFN group, the median decrease of HDV-RNA was -3.64 et -5.56 log₁₀IU/ml, respectively. Moreover, at month 12, HDV-RNA was undetectable in 39% and 85% of patients treated with BLV monotherapy and BLV + PEG-IFN group, respectively (per-protocol analysis). Factors associated with virological response are indicated in the table.

Table: Factors associated with undetectable HDV-RNA at month 12 (per-protocol analysis)

	Patients treated with BLV 2 mg alone		All patients (BLV with or without PEG-IFN)	
	HR (CI95%)	P	HR (CI95%)	P
Age	1, 00 (0, 95, 1, 05)	0.97	0.99 (0.96, 1.02)	0.62
Gender	2.71 (0.74, 9.95)	0.13	1.04 (0.55, 1.94)	0.91
BMI	0.97 (0.86, 1.09)	0.61	0.96 (0.9, 1.04)	0.31
Liver stiffness	0.96 (0.88, 1.04)	0.33	0.98 (0.95, 1.02)	0.30
FIB-4	0.87 (0.68, 1.12)	0.28	0.94 (0.82, 1.07)	0.31
Cirrhosis	0.39 (0.13, 1.17)	0.09	0.95 (0.52, 1.75)	0.88
HIV	2.49 (0.76, 8.21)	0.13	1.22 (0.48, 3.13)	0.68
HDV-RNA	0.64 (0.42, 0.95)	0.03	0.87 (0.68, 1.11)	0.26
HBe Ag+	2.39 (0.29, 19.73)	0.41	1.6 (0.38, 6.78)	0.53
HBV DNA	0.59 (0.32, 1.08)	0.09	0.96 (0.85, 1.07)	0.64
NUC	1.75 (0.22, 13.86)	0.59	1.11 (0.46, 2.66)	0.81
PEG-IFN	NA		3.06 (1.64, 5.71)	<0.001

Conclusion: In patients treated with BLV 2 mg alone, HDV-RNA is associated with virological response after one year of treatment. In patients treated with or without PEG-IFN, PEG-IFN treatment is associated with virological response. These preliminary results could help physicians for their clinical practice.

SAT361

Impact of baseline viral load on hepatocellular carcinoma risk during antiviral treatment in non-cirrhotic patients with HBeAg-positive chronic hepatitis B

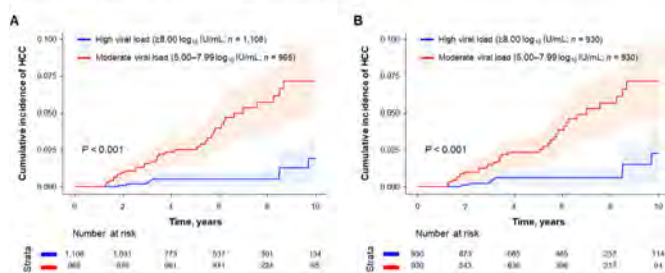
Won-Mook Choi¹, Gi-Ae Kim², Jonggi Choi¹, Seungbong Han³, Young-Suk Lim¹. ¹Asan Medical Center, Department of Gastroenterology, Liver Center, Seoul, Korea, Rep. of South; ²Kyung Hee University School of Medicine, Department of Internal Medicine, Korea, Rep. of South; ³Korea University College of Medicine, Department of Biostatistics, Seoul, Korea, Rep. of South
Email: limys@amc.seoul.kr

Background and aims: Early initiation of anti-viral treatment with high viral load is highly controversial in HBeAg-positive patients with chronic hepatitis B (CHB). Here, we investigated the impact of hepatitis B virus (HBV) DNA levels at the onset of antiviral treatment on the on-treatment risk of hepatocellular carcinoma (HCC) in non-cirrhotic patients with HBeAg-positive CHB.

Method: We conducted a multicenter cohort study including entecavir- or tenofovir-treated non-cirrhotic patients with HBeAg-positive CHB and baseline HBV DNA levels ≥ 5.00 log₁₀ IU/ml at three centers in Korea between January 2007 and December 2016. We compared the on-treatment risk of HCC between high viral load (HBV DNA levels ≥ 8.00 log₁₀ IU/ml) and moderate viral load (5.00–7.99 log₁₀ IU/ml) groups.

Results: Of 2, 073 patients, 1, 108 patients were classified as high viral load group and 965 patients were moderate viral load group. After propensity score (PS)-matching, 930 pairs of patients were generated with well-balanced baseline characteristics. In the entire cohort, HCC was developed in 10 patients (0.15 per 100 person-years) in the high viral load group compared with 37 patients (0.67 per 100 person-years) in the moderate viral load group, during a median 5.7 years of antiviral treatment. Patients with moderate viral load at baseline showed a significantly higher HCC incidence than those with high viral load in both the entire and PS-matched cohorts by Kaplan-Meier analysis (p <0.001 for both; Figure). By multivariable analysis, the moderate viral load group had a significantly higher risk of HCC (hazard ratio, 3.48; 95% confidence interval, 1.72–7.06; P <0.001) than the high viral load group, which was also consistently observed in the PS-weighted, PS-matched, and competing risk analyses.

Fig. Cumulative incidence of HCC during treatment between high vs. moderate viral load groups. (A) Entire cohort and (B) propensity score-matched cohort. High and moderate viral load groups were defined as those who had baseline serum HBV DNA levels $\geq 8.00 \log_{10}$ IU/mL and 5.00–7.99 \log_{10} IU/mL, respectively.



Conclusion: In non-cirrhotic patients with HBeAg-positive CHB, decreased HBV DNA levels at baseline was associated with a significantly high risk of HCC during antiviral treatment. Early initiation of antiviral treatment with a high viral load ($\geq 8.00 \log_{10}$ IU/ml) would retain a low on-treatment risk of HCC in HBeAg-positive CHB patients.

SAT362

Therapeutic vaccination with CLB-3000 in a mouse model of chronic hepatitis B induces anti-HBs responses associated with functional cure

Renae Walsh¹, Hans Netter¹, Chee Leng Lee¹, Rachel Hammond¹, Joan Ho¹, Stephen Locarnini¹, Ronald Farquhar², Bharat Dixit², Aileen Rubio², ¹Victorian Infectious Diseases Services, Parkville, Australia; ²ClearB Therapeutics, Inc., CONCORD, MA, United States
Email: arubio@clearbtherapeutics.com

Background and aims: Our therapeutic vaccine candidates previously achieved functional cure (FC) in a mouse model of chronic hepatitis B (CHB) [EASL 2021 poster 853, AASLD 2021 poster 829]. The vaccines consist of modified HBsAg displaying clearance profile (CP) associated epitopes identified from anti-HBs responses of FC clinical patients. CP-specific antibody responses are distinguished by the occupation of key loop 1 and 2 epitopes within HBsAg “a” determinant [Walsh, R et al 2019. Liver Int 39 (11) pp2066]. The vaccine candidate CLB-3000 consists of 2 modified HBsAg, expressed from *Pichia pastoris* and adjuvanted with Alhydrogel. Therapeutic vaccination with CLB-3000 achieved FC in CHB mice and were assessed for the presence of ‘clearing’ anti-HBs profiles consistent with those observed from clinical FC patients.

Method: CLB-3000 was subcutaneously delivered to CBA/CaJ mice with established CHB infection [Chou H-H et al 2015. PNAS 112 (7) pp2175]. Mice were monitored for FC by serological and liver immunohistochemistry (IHC). The quality of the anti-HBs immune response following FC was assessed for specificity to HBsAg CP epitopes defined clinically, HBsAg immune complexes to confirm serum clearance of HBsAg, and diagnostic anti-HBs titre.

Results: Therapeutic vaccination of CHB mice with CLB-3000 resulted in $>2.5 \log$ IU/ml reduction in serum HBsAg. Liver IHC confirmed clearance of HBV positive cells. Development of a vaccine-elicited CP-associated ‘clearing’ anti-HBs response was concomitantly detected in 80% of CLB-3000 treated CHB mice that achieved FC. Antibody specificity for CP-associated epitopes was detected, targeting both loops 1 and 2 of HBsAg, and mimicked that observed in FC patients. Immune complexes of residual HBsAg and anti-HBs were not typically detected following FC with an established ‘clearing’ anti-HBs response, indicative of complete HBsAg clearance. Placebo treatment resulted in no significant change in virological markers and no anti-HBs seroconversion.

Conclusion: CLB-3000 was highly efficacious in CHB mice as shown by rapid HBsAg decline, clearance from serum and liver, and seroconversion to CP-associated anti-HBs which mirrored clinical FC-associated anti-HBs responses. The data further support CLB-3000 development for the treatment of CHB.

SAT363

Evaluation of the disposition and mass balance recovery of vebicorvir, a first generation hepatitis B core inhibitor, in rats and humans

Katie Zomorodi¹, Luisa M Stamm¹, William Delaney¹, Michael Shen¹, ¹Assembly Biosciences, Inc., South San Francisco, United States
Email: kzomorodi@assemblybio.com

Background and aims: Vebicorvir (VBR) is a first-generation hepatitis B virus (HBV) core inhibitor that targets multiple aspects of the viral replication cycle. VBR is in Phase 2 development for the treatment of chronic HBV infection (cHBV). Here we report the disposition and mass balance recovery of VBR in rats and healthy human subjects.

Method: 27 male rats were dosed with 30 mg/kg [¹⁴C]-VBR radio-labeled with 5.5 MBq/kg. Three animals were placed in metabolism cages for up to 120 h post-dose. Total radioactivity was measured in urine, feces, cage rinse and carcass. Pharmacokinetic (PK) profiles were obtained in blood, plasma and liver samples collected at selected timepoints over 48 h post-dose from three additional terminal animals per timepoint. The human study (NCT04637139) was a single-arm, non-randomized, open-label Phase 1 trial. Following an overnight fast of ≥ 8 hours, 6 healthy subjects received a single oral dose of 300 mg VBR solution containing a microdose of approximately 2 μ Ci of [¹⁴C]-VBR. Samples of blood, urine, and feces were collected for PK, metabolite, and radiolabel assessments for up to 240 h post-dose.

Results: In rats, 86% and 12% of the radio-labeled VBR dose were eliminated in feces and urine, respectively, with excretion of unchanged VBR in the feces accounting for the majority of the administered drug; unchanged VBR was the only radio-component detected in plasma. Total radioactivity showed very high distribution in the liver with partitioning ratios ranging from 18 to 30 over 48 h post-dose (calculated with respect to blood). Similarly, mean cumulative radioactivity recovery in humans was 88%, with 62% excreted in feces and 26% in urine (Figure 1), and unchanged VBR was the major component in both feces (50% of dose) and urine (10% of dose). Unchanged VBR was the predominant component in plasma with low overall circulating metabolite-related radioactivity. Plasma VBR concentrations reached peak by ~ 2.5 h and declined with terminal half-life of 27.7 h. Renal clearance of unchanged VBR (1.62 L/h) was a minor contributor to the total body clearance of VBR (17.9 L/h).

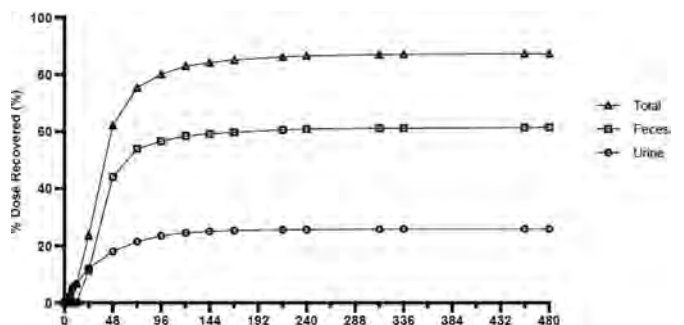


Figure: Mean Cumulative Percent Recovery of Radio-labeled VBR in Feces and Urine in Humans

Conclusion: Fecal excretion of unchanged drug is the primary route of VBR elimination in both rats and humans. VBR is the predominant component in the systemic circulation with low overall circulating metabolite-related radioactivity. VBR showed high liver loading in the rat indicating favourable distribution to the target organ for treatment of chronic HBV infection.

SAT364

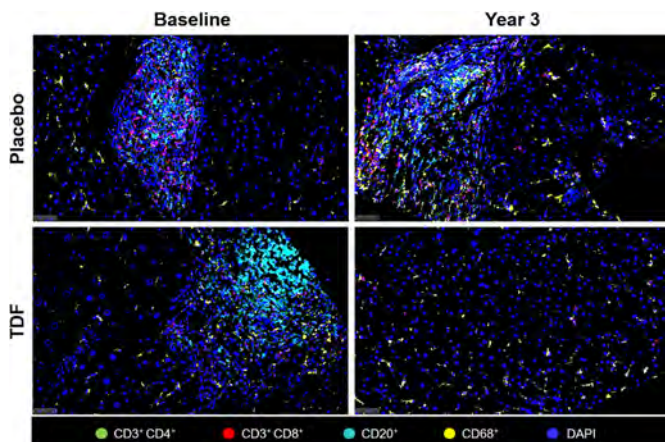
Effect of tenofovir disoproxil fumarate treatment on intrahepatic viral burden and liver immune microenvironment in chronic hepatitis B patients with minimally elevated serum alanine aminotransferase

Abhishek Aggarwal¹, Ricardo Ramirez¹, David Pan¹, Ondrej Podlaha¹, Jeffrey Wallin¹, Jaw-Town Lin², Cheng-Hao Tseng³, Li Li¹, Lauri Diehl¹, Becket Feirbach¹, Simon Fletcher¹, Vithika Suri¹, Yao-Chun Hsu^{3,4}.
¹Gilead Sciences Inc., United States; ²China Medical University Hospital, Taiwan; ³E-Da Cancer Hospital, Taiwan; ⁴I-Shou University, Taiwan
 Email: abhishek.aggarwal5@gilead.com

Background and aims: Integrated analysis of the impact of nucleos (t)ide treatment on intrahepatic HBV antigen expression together with immune cell subset frequency is lacking. In this study, we performed concurrent analysis of the intrahepatic viral burden and the liver immune microenvironment in chronic hepatitis B (CHB) patients with minimally elevated serum alanine aminotransferase (ALT) before and after treatment with tenofovir disoproxil fumarate (TDF).

Method: CHB patients with serum viral load above 2000 IU/ml and mild ALT elevation between 1-2 folds the upper limit of normal were enrolled in a double-blind, placebo-controlled, randomized trial of either oral 300 mg TDF or placebo once daily for 3 years (NCT01522625). Paired core liver biopsies were collected at baseline and year 3 and analyzed by bulk RNA-Seq (n = 56 placebo and n = 64 TDF treated patients) as well as by a custom multiplex immunofluorescence (mIF) assay (Ultivue InsituPlex) in a subset of biopsies (n = 15 placebo and n = 15 TDF treated patients). Cell type proportions from RNA-Seq were calculated using the EPIC algorithm. Quantification of mIF images for immune cell subsets and viral burden was performed using Visiopharm software.

Results: Following 3 years of treatment, patients that received TDF showed significant reduction in serum ALT (p <0.05) and HBV DNA levels (p <0.001) compared to the placebo group. In line with RNA-Seq cell type estimates, mIF analysis revealed a decrease in CD3⁺ T-cell (p <0.001), CD4⁺ T-cell (p <0.001), CD8⁺ T-cell (p <0.001), CD20⁺ B-cell (p <0.01) densities and HBV core⁺ hepatocyte frequency (p <0.001) after 3 years of TDF vs. placebo treatment. PD-1 expression was also significantly reduced on both CD4⁺ and CD8⁺ T-cells (p <0.001) with TDF treatment. Conversely, NK cell and monocyte gene signatures, as well as CD68⁺ macrophage density and HBsAg⁺ hepatocyte frequency did not significantly change with TDF treatment. mIF analysis also showed a reduction in periportal lymphoid aggregates (defined by dense CD20⁺ B-cell clusters, p <0.05) in TDF-treated vs. placebo patients.



Conclusion: Multiparametric analysis of the liver immune microenvironment revealed intrahepatic immune cell infiltration in patients with minimally elevated serum ALT. TDF treatment

significantly reduced the number of HBV core⁺ (but not HBsAg⁺) hepatocytes, which was accompanied by a decrease in both intrahepatic T cells and B cells. These findings suggest that (i) CHB patients with minimally elevated ALT levels may benefit from nucleos (t)ide treatment and (ii) that intrahepatic T and B cell frequency is associated with the HBV core⁺ cell burden.

SAT365

Safety, pharmacokinetics, and antiviral activity of the class II capsid assembly modulator ALG-000184 in subjects with chronic hepatitis B

Man-Fung Yuen¹, Kosh Agarwal², Edward J Gane³, Alina Jucov⁴, Christian Schwabe⁵, Junqi Niu⁶, Jinlin Hou⁷, Kha Le⁸, Benedetta Massetto⁸, Christopher Westland⁸, Qingling Zhang⁸, Felix Lai⁸, Meenakshi Venkatraman⁸, Lawrence Blatt⁸, Tse-I Lin⁸, Sushmita Chanda⁸, Matt McClure⁸, John Fry⁸. ¹Hong Kong, University of Hong Kong, Hong Kong; ²Institute of Liver Studies, Kings College Hospital, United Kingdom; ³University of Auckland, New Zealand, New Zealand; ⁴ARENIA Exploratory Medicine, Republican Clinical Hospital and Nicolae Testemitanu State University of Medicine and Pharmacy, Moldova; ⁵New Zealand Clinical Research, New Zealand; ⁶The First Hospital of Jilin University, Jilin City, China; ⁷Nanjing Hospital of Southern Medical University, China; ⁸Aligos Therapeutics Inc, South San Francisco, United States
 Email: bmassetto@aligos.com

Background and aims: To evaluate the safety, pharmacokinetic, and antiviral activity of ALG-000184, an oral prodrug of ALG-001075, a novel, pan-genotypic class II capsid assembly modulator (CAM) with picomolar potency.

Method: This is an ongoing three-part, multicenter, double-blind, randomized, placebo-controlled study. In Parts 1 and 2, single and multiple doses of ALG-000184 were well tolerated in healthy volunteers (Gane et al, APASL, HBV TAG, 2021). Part 3 is evaluating untreated subjects with chronic hepatitis B (CHB) (N = 10/cohort; 8 active:2 placebo) receiving daily doses of ALG-000184 or placebo × 28 days. Reported here are preliminary blinded safety, PK, and antiviral data.

Results: To date, 36 subjects have completed dosing in Cohorts 1 (100 mg; N = 10 HBeAg neg), 2 (50 mg; N = 10 HBeAg neg), and 4 (100 mg; N = 10 HBeAg pos); enrollment in Cohort 3 (10 mg; N = 6 HBeAg neg) is ongoing. Most subjects were male (56%), Asian (58%), with a mean age of 40 years, a mean BMI of 24.6 Kg/m² and genotype B or D. At baseline, mean HBV DNA by cohort ranged from 4.4 to 8.1 log₁₀ IU/ml and most subjects' (81%) baseline ALT concentrations were within the normal range. Study medication was well tolerated. There was 1 unrelated serious adverse event (hospitalization for back pain management). There were no treatment emergent adverse events (TEAEs) resulting in premature discontinuation. All TEAEs were Grade 1 or 2 in severity, except for three Grade 3 ALT elevations. These were asymptomatic, occurring post dosing and were associated with significant changes in HBV DNA and RNA. There were no changes in synthetic liver function. Plasma ALG-001075 exposures increased dose proportionally between 10, 50 and 100 mg dose levels, with low-to moderate variability and minimal accumulation. A similar magnitude of HBV DNA decline (~3–4 log₁₀ IU/ml) was observed in all cohorts and a similar percentage (≥75%) of HBeAg negative subjects achieved HBV DNA below the lower limit of quantitation (LLOQ; <10 IU/ml). Mean HBV DNA level changes from baseline are shown in Fig 1. HBV RNA declined below LLOQ (10 copies/ml) in 100% of subjects in Cohorts 1 and 2 and by ~3.1 log₁₀ copies/ml at day 28 in Cohort 4.

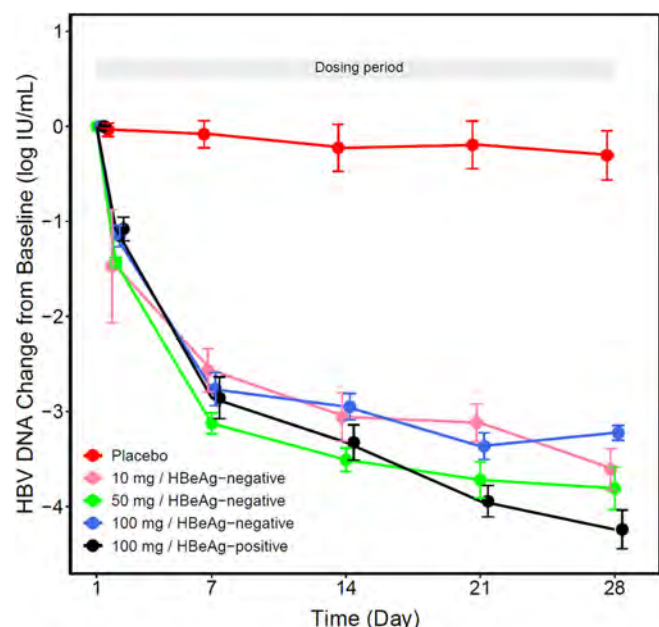


Figure: Mean (SEM) HBV DNA levels change from baseline through the end of the treatment period by Cohort

Conclusion: All dose levels of ALG-000184 were well tolerated, exhibited predictable PK, and resulted in similar, substantial antiviral activity in untreated CHB subjects, regardless of HBeAg status.

SAT366

Deeper virologic suppression with the addition of vebicorvir, a first-generation hepatitis B core inhibitor, to entecavir correlates with reduced inflammation and fibrosis-4 index in treatment naïve patients with HBeAg positive chronic hepatitis B

Mark S Sulkowski¹, Scott K Fung², Xiaoli Ma³, Tuan T Nguyen⁴, Eugene R. Schiff⁵, Hie-Won L Hann⁶, Douglas T Dieterich⁷, Ronald G Nahass⁸, James S Park⁹, Sing Chan¹⁰, Steven-Huy B Han¹¹, Edward J Gane¹², Michael Bennett¹³, Ran Yan¹⁴, Jieming Liu¹⁴, Julie Ma¹⁴, Steven J Knox¹⁴, Luisa M Stamm¹⁴, Maurizio Bonacini¹⁵, Ira M Jacobson⁹, Walid S Ayoub¹⁶, Frank Weilert¹⁷, Natarajan Ravendhran¹⁸, Alnoor Ramji¹⁹, Paul Yien Kwo²⁰, Magdy Elkhatab²¹, Tarek Hassanein²², Ho S Bae²³, Jacob P Lalezari¹⁵, Kosh Agarwal²⁴, Man-Fung Yuen²⁵. ¹Johns Hopkins University School of Medicine, Baltimore, United States; ²University of Toronto, Toronto, Canada; ³Office of Xiaoli Ma, Philadelphia, United States; ⁴T Nguyen Research and Education, Inc., San Diego, United States; ⁵Schiff Center for Liver Diseases, University of Miami School of Medicine, Miami, United States; ⁶Thomas Jefferson University Hospital, Philadelphia, United States; ⁷Icahn School of Medicine, Mount Sinai Hospital, Department of Medicine, Division of Liver Diseases, New York, United States; ⁸Infectious

Disease Care, Hillsborough, United States; ⁹NYU Langone Health, New York, United States; ¹⁰Sing Chan, MD, New York, United States; ¹¹Pfizer Liver Institute, University of California, Los Angeles, United States; ¹²Auckland Clinical Studies Ltd, Auckland, New Zealand; ¹³Medical Associates Research Group, San Diego, United States; ¹⁴Assembly Biosciences, Inc., South San Francisco, United States; ¹⁵Quest Clinical Research, San Francisco, United States; ¹⁶Cedars-Sinai Medical Center, Los Angeles, United States; ¹⁷Waikato Hospital, Hamilton, New Zealand; ¹⁸Gastrohealth of Maryland, Catonsville, United States; ¹⁹Gastrointestinal Research Institute, Vancouver, Canada; ²⁰Stanford University Medical Center, Stanford, United States; ²¹Toronto Liver Centre, Toronto, Canada; ²²Southern California Research Center, Coronado, United States; ²³Asian Pacific Liver Center, Los Angeles, United States; ²⁴Institute of Liver Studies, King's College Hospital, London, United Kingdom; ²⁵Queen Mary Hospital, The University of Hong Kong, Department of Medicine and State Key Laboratory of Liver Research, Hong Kong

Email: msulkowski@jhmi.edu

Background and aims: The goal of NrtI therapy for chronic hepatitis B virus infection (CHBV) is suppression of HBV DNA. While NrtIs reduce HBV DNA in most patients (pts), low-level viremia remains which is associated with disease progression. Therapies providing deeper levels of virologic suppression may improve long-term clinical outcomes. Previous reports from Study 202 (NCT03577171) in treatment-naïve, HBeAg positive pts demonstrated deeper reductions in HBV DNA and pre-genomic RNA (pgRNA) and more rapid normalization of ALT when vebicorvir (VBR) was added to entecavir (ETV). This report explores associations between the reductions in viral parameters with Fibrosis-4 (FIB-4) index, an indicator of liver health.

Method: In Study 202, 13 pts received 300 mg VBR+0.5 mg ETV and 12 pts received PBO+0.5 mg ETV for 24 weeks. Entry criteria included ALT $\leq 10 \times \text{ULN}$, platelets $\geq 100,000/\text{mm}^3$, Metavir F0-F2/Fibroscan $\leq 8 \text{ kPa}$. HBV DNA, pgRNA, and quantitative HBV antigens were measured at each visit. FIB-4 was calculated according to $[(\text{age} \times \text{AST}) / (\text{platelet count} \times \sqrt{\text{ALT}})]$. Correlation analyses were performed, and Pearson correlation coefficients (r) calculated to describe associations between viral parameters and FIB-4.

Results: At Week 24 reductions in ALT and AST were observed with VBR+ETV but not PBO+ETV: ALT -47.2 U/L vs $+1.6 \text{ U/L}$ and AST -25.3 U/L vs $+8.4 \text{ U/L}$ respectively. For platelet counts, the mean change from baseline (CFB) at Week 24 was $+3.5 \times 10^9/\text{L}$ for VBR+ETV and $+23.2 \times 10^9/\text{L}$ for PBO+ETV. Changes in these parameters were reflected in the mean CFB in FIB-4 index, which was significantly greater for VBR+ETV than PBO+ETV: -0.21 vs $+0.05$, $p=0.034$. For VBR+ETV but not PBO+ETV, significant associations were observed between FIB-4 and pgRNA ($r=0.70$; $p=0.008$) and HBcrAg ($r=0.78$; $p=0.003$). There were no significant associations between FIB-4 and HBV DNA for either group.

Conclusion: The addition of VBR to NrtI therapy provides deeper suppression of HBV DNA and pgRNA and more rapid normalization of ALT and AST than NrtI alone over 24 weeks of treatment. The deeper

Figure 1a: FIB-4 Mean Change from Baseline

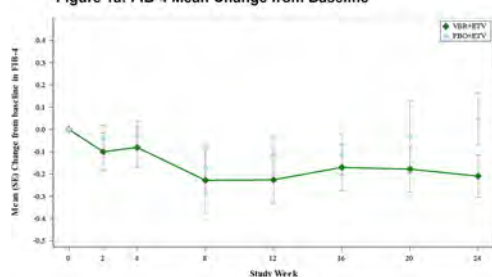


Figure 1b: VBR+ETV: pgRNA and FIB-4

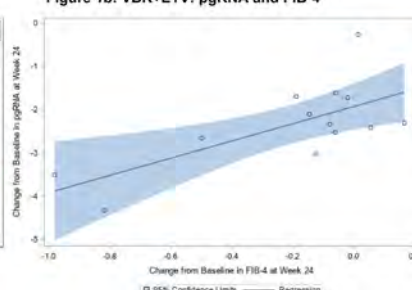


Figure 1c: VBR+ETV: HBcrAg and FIB-4

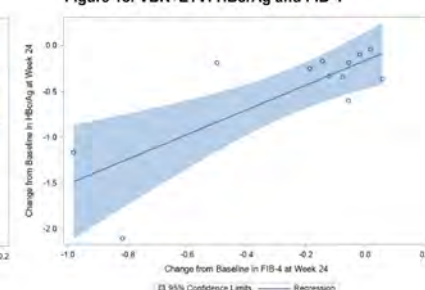


Figure: (abstract: SAT366)

level of viral suppression and reduced inflammation is reflected in greater reductions in FIB-4 for VBR+ETV compared to ETV alone. In post hoc analyses, reductions in pgRNA, a marker for cccDNA replicative activity, and HBcrAg are associated with improvement in FIB-4 over 24 weeks of treatment. Regimens providing deeper levels of viral suppression and reduced inflammation may further improve long-term clinical outcomes including fibrosis, cirrhosis and HCC.

SAT367

Safety, tolerability, pharmacokinetics, and preliminary antiviral activity of the capsid assembly modulator (CAM) ZM-H1505R after multiple escalating oral doses in patients with chronic hepatitis B virus (CHB) Infection

Jiajia Mai¹, Hong Zhang², Min Wu², Hong Chen², Yue Hu², Xiaoxue Zhu², Xiuhong Jiang³, Bo Hua³, Tian Xia³, Gang Liu³, Aiyun Deng³, Bo Liang³, Ruoling Guo³, Hui Lu³, Zhe Wang³, Ming Ren³, Huanming Chen³, Zhijun Zhang³, Junqi Niu², Yanhua Ding². ¹The First Hospital of Jilin University, Jilin, China, Phase I Clinical Research Center, Changchun; ²The First Hospital of Jilin University, Jilin, China, Phase I Clinical Research Center, Changchun, China; ³Shanghai Zhimeng Biopharma, Inc., Shanghai Zhimeng Biopharma, Inc., Shanghai, China
Email: dingyanhua2003@126.com

Background and aims: ZM-H1505R is a newly discovered hepatitis B virus (HBV) capsid inhibitor with a novel pyrazole structure. It interferes with the assembly of HBV particles by inducing the formation of viral capsids devoid of genomic material. The safety, tolerability pharmacokinetics (PK), and preliminary antiviral activity of ZM-H1505R were evaluated in a double-blind, randomized, placebo-controlled, dose escalating study in treatment-naïve chronic hepatitis B (CHB) patients.

Method: Non-cirrhotic and treatment-naïve CHB patients were divided into three cohorts (10 patients each) and randomized within each cohort in a ratio of 4:1 to receive an ascending dose of 50, 100, or 200 mg of ZM-H1505R, or placebo once a day for 28 consecutive days.

Results: All results were analyzed in the blind state, because the blindness was still not uncovered. A total of 30 patients were randomized and completed the study. The cohorts were well matched and balanced with sex, age, baseline HBV DNA level and HBeAg status of the subjects. ZM-H1505R was safe and well tolerated from 50 to 200 mg qd oral administration, with most AEs being grade 1 or 2 and the symptoms being mild to moderate. No SAEs were observed and no withdrawal was caused due to AEs. The rates of AEs were 30%, 60% and 60% in the 50, 100, or 200 mg cohorts, respectively. The most common adverse reactions to ZM-H1505R were the elevation of alanine aminotransferase and aspartate aminotransferase in grade 1 or 2 severity (CTC-AE version 5.0), with the incidence of 10%-50% within a cohort. ZM-H1505R showed a linear pharmacokinetics proportional to the doses. ZM-H1505R reached mean plasma T_{max} at 2.5–3.5 hours postdose with mean terminal half-life of 11.975–12.999 hours after last dosage. A steady-state was achieved following 8 days of daily dosing (no samples were collected during days 2–7). The accumulation rate was similar among the different cohorts (0.941–3.454), which indicates that the accumulation is mild. At day 28, the mean plasma C_{min} were 2.7, 7.0, and 14.6 folds of its protein-binding adjusted HBV DNA EC_{50} for 50, 100, and 200 mg doses, respectively. The mean declines from baseline in HBV DNA were –1.4, –2.3 and –2.5 log₁₀ IU/ml, and in HBcrAg were –0.14, –0.34 and –0.33 log₁₀ IU/ml after 28 days treatment with ZM-H1505R at 50 mg, 100 mg and 200 mg, respectively. The mean decline from baseline in HBV pgRNA were –0.76, and –1.60 log₁₀ IU/ml after 28 days treatment at ZM-H1505R 50 mg and 100 mg, respectively. Most patients experienced viral rebound after last treatment during follow-up period.

Conclusion: Once-a-day oral administration of ZM-H1505R for 28 days was safe and well tolerated. It produced a substantial decrease in

HBV-DNA and HBV pgRNA levels in the serum of CHB patients. On the basis of these results, ZM-H1505R was recommended for further evaluation in phase II trials.

SAT368

Evaluation of renal and bone safety at 4 years in post-liver transplant patients with chronic kidney disease receiving Tenofovir Alafenamide for HBV prophylaxis

Edward J. Gane¹, Rica Dagooc¹, Dominic Ray-Chaudhuri¹, Thomas Mules¹, Frida Abramov², Curtis Holt³, Hongyuan Wang⁴, Vithika Suri², Anu Osinusi², John F. Flaherty². ¹Auckland City Hospital and University of Auckland, New Zealand Liver Transplant Unit, Auckland, New Zealand; ²Gilead Sciences, Inc., Clinical Development, Foster City, United States; ³Gilead Sciences, Inc., Medical Affairs, Foster City, United States; ⁴Gilead Sciences, Inc., Biostatistics, Foster City, United States
Email: frida.abramov@gilead.com

Background and aims: Chronic HBV remains a leading indication for orthotopic liver transplantation (OLT) worldwide. Renal dysfunction and osteopenia are commonly observed long-term complications of maintenance immunosuppression in OLT recipients. In this at-risk population, tenofovir alafenamide (TAF) may have an advantage over tenofovir disoproxil fumarate (TDF) due to its improved renal and bone safety profile. We previously reported similar efficacy and improved safety with TAF vs TDF up to 192 weeks in this population. Presented here is a comprehensive analysis of long-term bone and renal safety.

Method: In this Phase 2 open-label study (NCT02862548), 51 liver transplant recipients on HBV prophylaxis with TDF-containing treatments and ≥Stage 2 chronic kidney disease were randomized 1:1 to TAF 25 mg/day or TDF for 48 weeks, after which all received TAF through Week 192 (i.e. TAF vs. TDF→TAF). Week 192 safety end points included changes in estimated glomerular filtration rate (eGFR) by CG, CKD-EPI, and Chromium-EDTA Renal Scan (Cr-EDTA) methods, serum creatinine (sCr), exploratory markers of renal tubular dysfunction, bone mineral density (BMD) at spine and hip by DXA, and markers of bone turnover.

Results: Baseline characteristics included: mean age 60 years, 75% males, 53% Pacific Islander, median eGFR 50 ml/min/1.73m² with 76% of patients at CKD stage 3 or greater, and median baseline surface area corrected GFR_{Cr-EDTA} was 58 ml/min/1.73². 46/51 (90%) patients completed 192 weeks of treatment. Overall safety results have been previously described. Renal parameters improved from baseline at Week 192 (Table). Increases from baseline in spine and hip BMD were observed with TAF (mean % change at Week 192: 3.4% and 1.1%, respectively) and TDF→TAF after switching to TAF (mean % change at Week 192: 3.8% and 2.1% for spine and hip, respectively); greater decreases in markers of bone turnover were observed in TAF vs TDF→TAF group (Table).

Table: Median (Q1, Q3) Change from Baseline at Week 192

	TAF 25mg (N = 26)	TDF→TAF (N = 24)
eGFR _{CKD-EPI} (ml/min/1.73 m ²)	2.5 (–1.4, 8.2)	1.1 (–6.0, 9.3)
eGFR _{CG} (ml/min)	2.8 (–1.5, 12.3)	0.2 (–9.0, 7.7)
sCr (mg/dL)	–0.08 (–0.19, 0.01)	–0.06 (–0.22, 0.09)
Cr EDTA (ml/min/1.73 m ²)*	0.1 (–7.1, 6.4)	–3.3 (–8.0, 5.6)
RBP:Cr ug/g (%)	–40 (–85, –14)	–38 (–58, 88)
β2M:Cr ug/g (%) [†]	–54 (–87, 278)	–45 (–76, 223)
CTX ng/ml (%)	–39.0 (–60.5, –14.3)	–26.9 (–60.3, 8.9)
P1NP ng/ml (%) [‡]	–36.98 (–55.13, –5.65)	–19.42 (–37.96, 12.75)

*Week 96 results presented

[†]markers of proximal tubular function (retinol-binding protein:Cr [RBP:Cr] and β2-microglobulin:Cr [β2M:Cr])

[‡]markers of bone formation (procollagen type 1 N-terminal propeptide [P1NP]) and resorption (C-type collagen sequence [CTX])

Conclusion: Long-term results after switching from TDF to TAF in an OLT recipient population with a high rate of renal dysfunction show sustained improvements in key bone and renal safety parameters.

SAT369

Functional cure based on pegylated interferon alpha therapy in nucleoside analog-suppressed HBeAg negative chronic hepatitis B: a multicenter real-world study (Everest Project in China)-3.5 years data update

Chan Xie¹, Dongying Xie¹, Lei Fu², Wen-hua Zhang³, Jia Wei⁴,
Guojun Li⁵, Jiahong Yang⁶, Xinyue Chen⁷, Jia-bin Li⁸, Jia Shang⁹,
Yu-juan Guan¹⁰, Yongfang Jiang¹¹, Ying Guo¹², Yi-lan Zeng¹³,
Jiabao Chang¹⁴, Yanzhong Peng¹⁵, Minghua Lin¹⁶, Guangyu Huang¹⁷,
Jia Li¹⁸, Shengwang Gu¹⁹, Jia-wei Geng²⁰, Zhiliang Gao¹. ¹Third
Affiliated Hospital of Sun Yat-sen University, Department of Infectious
Diseases, Guangzhou, China; ²Xiangya Hospital Central South University,
Changsha, China; ³Gansu Wuwei Cancer Hospital, Wuwei, China;
⁴Affiliated Hospital of Yunnan University, Kunming, China; ⁵The Third
People's Hospital of Shenzhen, Shenzhen, China; ⁶People's Hospital of
Deyang City, Deyang, China; ⁷Beijing Youan Hospital, Capital Medical
University, Beijing, China; ⁸The First Affiliated Hospital of Anhui Medical
University, Hefei, China; ⁹Henan Provincial People's Hospital,
Zhengzhou, China; ¹⁰Guangzhou Eighth People's Hospital, Guangzhou,
China; ¹¹The Second Xiangya Hospital of Central South university,
Changsha, China; ¹²The third people's hospital of Taiyuan, Taiyuan,
China; ¹³Chengdu Public Health Medical Center, Chengdu, China; ¹⁴The
Second Hospital of Nanjing, Nanjing, China; ¹⁵Peking University
Shenzhen Hospital, Shenzhen, China; ¹⁶MengChao Hepatobiliary
Hospital of Fujian Medical University, Fuzhou, China; ¹⁷The Fourth
Affiliated Hospital Zhejiang University School Of Medicine, Yiwu, China;
¹⁸Tianjin Second People's Hospital, Tianjin, China; ¹⁹Huaian Medical
District of General Hospital of Eastern Theater Command, Huaian, China;
²⁰The First People's Hospital of Yunnan Province, Kunming, China
Email: gaozhiliang_123@126.com

Background and aims: Add-on or switch to pegylated interferon alpha (PegIFN alpha) in nucleoside analog (NA) treated chronic hepatitis B (CHB) patients is effective strategies to improve functional cure (HBsAg loss) rate. We aimed to investigate the efficacy and safety of “add-on” or “switch-to” therapy in large scale real-world and the predictors for HBsAg loss by pegIFN alpha.

Method: The Everest Project is a multicentre real-world study in China which focused on functional cure of CHB (NCT04035837). Patients who had NA therapy for more than one year, HBV DNA <100 IU/ml, HBeAg negative and HBsAg \leq 1500 IU/ml were recruited since 2018. “Add-on” or “switch to” pegIFN alpha strategy for 48 weeks or up to 96 weeks was decided by doctor and patients. Data on those who have completed 48 weeks of treatment were analysed. mITT population included 5648 patients and PP population included 3988 patients.

Results: In the PP analysis, 81% patients were male, the mean age was 40.9 years and the mean baseline of HBsAg was 380.6 IU/ml. The HBsAg loss rate were 9.5%, 22.0%, 29.0% and 33.2% at 12, 24, 36 and 48 weeks, respectively (figure 1A). HBsAg baseline level, HBsAg decline level at 12, 24 weeks and ALT flare are predictors for HBsAg loss at 48 weeks. 48-week HBsAg loss rate were 56.1% for patients whose baseline HBsAg was 0.05–100 IU/ml. 48-week HBsAg loss rate was decreased with the increase of baseline HBsAg level (figure 1B). Patients achieved HBsAg < 500 IU/ml at 24 weeks had significantly higher 48-week HBsAg loss rate than those with HBsAg ≥ 500 IU/ml (36.7% vs. 1.3%, $p < 0.0001$, figure 1C). For patients with HBsAg decline > 1 log₁₀ IU/ml from baseline to 24 weeks, the 48-week HBsAg loss rate was 58.6%, while 10.0% for those HBsAg decline ≤ 1 log₁₀ IU/ml ($p < 0.0001$) (figure 1C). Patients with higher ALT level at 12 weeks (≥ 5 × ULN) had a higher 48-week HBsAg loss rate (46.3%) (figure 1D). There are 1006 patients (68.4%, 1006/1470) achieved HBsAg ≤ 100 IU/ml at 48 weeks, although they did not achieved HBsAg loss. Those patients might achieve functional cure for further prolonged therapy of PegIFN alpha. There were no severe adverse events during this project.

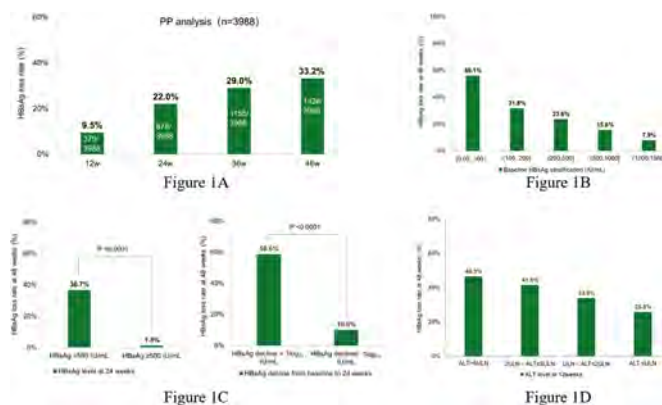


Figure: A. HBsAg loss rate at different time points in PP analysis. B. HBsAg loss rate at 48 weeks by baseline HBsAg stratification. C. HBsAg level or decline range at 24 weeks predicting HBsAg loss at 48 weeks. D. ALT level at 12 weeks predicting HBsAg loss at 48 weeks.

Conclusion: Functional cure could be well achieved in NA-suppressed HBeAg negative CHB patients by pegIFN alpha strategy. Lower HBsAg at baseline, lower HBsAg at 24 weeks, a rapid decline of HBsAg and ALT elevations at 12 weeks are predictors for functional cure at 48 weeks. There are still good chances of functional cure by prolonged treatment for patients who had not achieved HBsAg loss in 48 weeks course. PegIFN alpha therapy was well-tolerated.

SAT370

Understanding the dynamics of HBsAg decline through model-informed drug development (MIDD) of JNJ-3989 and JNJ-6379 for the treatment of chronic hepatitis B virus infection (CHB)

Huybrecht T'jollyn¹, Nele Goeyvaerts¹, Thomas Kakuda¹,
Louis Sandra¹, Tetsuro Ogawa¹, Joris J Vandenbossche¹,
Xavier Woot de Trixhe¹, Oliver Lenz¹, Ronald Kalmeijer¹,
Michael Biermer¹, Juan Jose Perez Ruixo¹, Oliver Ackaert¹. ¹Janssen
Research and Development
Email: htjollyn@its.jnj.com

Background and aims: JNJ-3989 is an N-acetylgalactosamine-conjugated siRNA, consisting of 2 triggers JNJ-3976 and JNJ-3924, designed to target hepatitis B virus (HBV)-derived RNAs, thereby reducing all viral proteins. JNJ-6379 is a capsid assembly modulator inducing formation of 'empty' HBV capsids. The phase 2b study REEF-1 assessed the combination of 40, 100, and 200 mg JNJ-3989 as Q4W subcutaneous injections with or without 250 mg QD oral JNJ-6379 on a background of nucleos (t)ide analogue (NA) (AASLD 2021). The relationship between exposure to JNJ-3989 + NA \pm JNJ-6379 and HBsAg decline was assessed using mechanism-based pharmacokinetic-pharmacodynamic (PK-PD) modeling (see Figure).

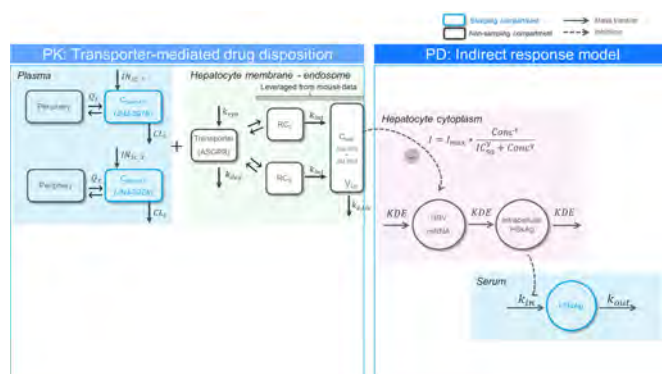


Figure: TMDD-IRM model developed based on Phase 1 and 2 PK and PD data for INI-3989.

Method: This PK-PD model, a Transporter-Mediated Drug Disposition (TMDD) with Indirect Response Model (IRM), was developed based on plasma PK of JNJ-3989 obtained from pooled Phase 1 and 2 studies in healthy, hepatically impaired, and CHB subjects, the latter also providing PD biomarker (HBsAg) data. Asialoglycoprotein (ASGPR)-mediated liver uptake was incorporated by leveraging information from plasma and liver JNJ-3989 concentrations collected in a HBV mouse study. The IRM described the relationship between estimated human liver concentrations and the inhibition of HBsAg production leading to observed HBsAg decline in patients, taking into account the treatment status at baseline [not currently treated (NCT) or virologically suppressed (VS)], and baseline HBeAg status (+ or -). A covariate analysis was performed to investigate treatment- and/or subgroup-specific HBsAg dynamics.

Results: JNJ-3989 liver uptake is saturable through ASGPR resulting in a decreased fraction of the dose that reaches the liver as the dose increases. The dynamics of HBsAg decline were governed by the accumulation of JNJ-3989 in liver, the exposure-dependent inhibition of HBsAg production, and the estimated HBsAg half-life. Covariate analysis indicated that (i) NCT HBeAg+ patients had faster and more pronounced HBsAg decline compared to other subgroups, (ii) combination treatment with JNJ-6379 led to a less pronounced decline in HBsAg, and (iii) JNJ-3989 activity is inversely associated to body weight.

Conclusion: JNJ-3989 showed a non-linear concentration-dependent liver uptake, mediated by ASGPR. HBsAg levels decreased in a dose-dependent manner up to 48 weeks of JNJ-3989 treatment in REEF-1. Covariate analysis identified that HBsAg dynamics display treatment- and subgroup-specific behavior.

SAT371

Serum HBsAg and ddPCR HBV-DNA as predictive parameters of HBsAg loss after nucleos(t)ide analogue (NA) treatment discontinuation in non-cirrhotic patients with chronic hepatitis B

Anna Francesca Guerra¹, Giovanni Tomassoli¹, Lorenzo Piermatteo², Stefano D'Anna², Romina Salpini², Valentina Svicher², Paolo Ventura¹, Gian Luca Abbati¹, Antonello Pietrangeli¹. ¹University of Modena and Reggio Emilia, Internal Medicine, Modena, Italy; ²University of Rome "Tor Vergata", Italy

Email: anna.f.guerra@hotmail.it

Background and aims: According to international guidelines, stopping nucleos(t)ide analogue (NA) treatment in selected non-cirrhotic Chronic Hepatitis B (CHB) patients may promote sustained serological and virological off treatment response. Nevertheless, this approach often leads to virus-induced flares, which may result to life-threatening liver failure. Therefore, in order to assure a safe discontinuation of treatment, reliable predictors of post-NAs remission need to be identified. Here, we aimed to identify predictive parameters of off-NAs response at the end of treatment and, specifically, their association with HBsAg loss or HBsAg <100 IU/ml (known to be predictive of subsequent HBsAg loss).

Method: 38 non-cirrhotic CHB patients, with complete virological suppression (>4 years), were prospectively monitored after suspending NA treatment for a median (IQR) time of 16 (10–19) months. For each patient, a plasma sample at suspension date (baseline, BL) was collected and used to quantify serum HBV-DNA by highly sensitive droplet digital PCR (ddPCR). HBsAg was quantified by the ARCHITECT HBsAg assay at BL, every 2 weeks from suspension in the first month, followed by every month until the sixth month, then every 3 months, in order to assess the achievement of HBsAg <100 IU/ml or HBsAg loss.

Results: At BL, ddPCR revealed that 28 (73.7%) patients had detectable serum HBV-DNA (median [IQR] 5 [2–11] IU/ml), while 10 (26.3%) were completely negative to HBV-DNA. After NA suspension, 7 (18.4%) achieved HBsAg <100 IU/ml (median [IQR]: 43 [35–53] IU/ml) and 8 (21.1%) lost HBsAg at last follow-up.

As expected, patients achieving HBsAg loss had lower HBsAg levels at BL (140 [70–480] IU/ml with vs 1162 [439–3135] without HBsAg loss, $p = 0.014$).

Notably, the negativity to HBV-DNA by ddPCR at BL strongly correlated with the achievement of HBsAg <100 IU/ml or HBsAg loss after NA suspension (outcome observed in 70% [7/10] with vs 28.6% [8/28] without negative BL HBV-DNA; OR [95% CI]: 5.8 [1.3–23.6], $p = 0.03$). Even more, the combination of HBsAg <500 IU/ml + negativity HBV-DNA by ddPCR at BL was the best predictor for achieving HBsAg <100 IU/ml or HBsAg loss (outcome observed in 85.7% with vs 27.6% without this combination; OR [95% CI]: 15.8 (1.6–152.2; $p = 0.008$; PPV = 86%; NPV = 72%).

Conclusion: NA suspension can be an effective strategy to constrain or silence intrahepatic HBV reservoir in accurately selected patients. Residual HBV replicative activity at NA suspension, measured by highly sensitive assays, provides an added value in identifying patients more prone to achieve HBV functional cure.

SAT372

Exploring hepatitis B virus as an immunotherapeutic target for clinical trials of adoptively transferred T cells

Suhasini Lulla¹, Tsung-Yen Chang¹, Spyridoula Vasileiou¹, Manik Kuvalekar¹, Ayumi Watanabe¹, Yovana Velazquez¹, Jenny Stanton², Ann Leen¹. ¹Center for Cell and Gene Therapy, Baylor College of Medicine, Houston Methodist Hospital, Texas Children's Hospital, Houston, United States; ²AlloVir Inc
Email: AMLEEN@texaschildrens.org

Background and aims: Patients chronically infected with hepatitis B virus (HBV) have endogenous T cell deficits including dysfunctional and exhausted HBV-reactive cells, which may be addressed by the adoptive transfer of HBV-reactive T cells from healthy immune individuals. HBsAg-positive, allogeneic, hematopoietic cell transplant (HCT) recipients who received stem cells (and lymphocytes) from donors that were positive for HBc and HBs antibodies have shown high rates of functional cure post-transplant. We explored the feasibility of extending this benefit to all patients with chronic HBV infection by generating a bank of HBV-specific T cells (HBVSTs) from healthy donors that are suitable for off-the-shelf clinical use.

Method: HBVSTs were produced using peptide libraries spanning immunodominant antigens to expand reactive cells. Following a single in vitro stimulation, we achieved a 7.3 ± 0.6 ($n = 9$) fold increase, representing a >6000-fold enrichment of HBV-reactive T cells. The phenotypic profile of these cells was assessed by flow cytometry with antibodies to: CD3, CD4, CD8, CD25, CD69, CD45RO, CD16, CD62L and CD56. The effector profile of reactive cells was assessed using intracellular cytokine staining (ICS), luminex and/or IsoPlexis. In vitro cytolytic capacity was evaluated in a short-term killing assay using antigen-loaded autologous targets and partially HLA-matched HepG2.2.15 cells.

Results: Reactive cells were polyclonal and dominated by CD4+ T cells (mean $72 \pm 4\%$) with a minor CD8+ ($21 \pm 2\%$) component. The cells expressed markers associated with central (CD45RO+/CD62L+: $58 \pm 3\%$) or effector memory (CD45RO+/CD62L-: $30 \pm 3\%$) potential and were activated based on expression of CD25 ($59 \pm 5\%$) and/or CD69 ($21 \pm 3\%$). Post-expansion, these HBVSTs were Th1-polarized and polyfunctional based on their ability to simultaneously produce multiple effector molecules including IFN γ , TNF α , GM-CSF, granzyme B, MIP-1 α and MIP-1 β . Finally, these cells were able to selectively kill virus-expressing autologous targets (40:1 E:T 36% specific lysis) and partially HLA-matched HBV-infected HepG2 cells (71%) with no reactivity against non-infected autologous or allogeneic targets (1% specific lysis each).

Conclusion: This study establishes the feasibility of developing banks of ex vivo expanded HBV-specific T cells that are suitable for clinical use. Further evaluation of these HBVSTs using in vivo models and in chronic HBV patients is warranted.

SAT373

Treatment with Bulevirtide in patients with chronic HBV/HDV co-infection. Safety and efficacy at month 18 in real-world settings

Victor de Ledinghen¹, Sophie Metivier², Edouard Bardou-Jacquet³, Marie-Noëlle Hilleret⁴, Veronique Loustaud-Ratti⁵, Nathalie Ganne-Carrié⁶, Bruno Roche⁶, Isabelle Fouchard Hubert⁷, Anne Gervais⁶, Anne Minello Franza⁸, Tarik Asselah⁶, Christiane Stern⁶, Jérôme Dumortier⁹, Xavier Causse¹⁰, Dominique Roulot⁵, Frederic Heluwaert¹¹, Leon Muti¹², Isabelle Rosa¹³, Valérie Canva¹⁴, Dominique Larrey¹⁵, Caroline Lascoux-Combe⁶, Juliette Foucher¹. ¹CHU Bordeaux; ²CHU Toulouse; ³CHU Rennes; ⁴CHU Grenoble; ⁵CHU Limoges; ⁶APHP; ⁷CHU Angers; ⁸CHU Dijon; ⁹CHU Lyon; ¹⁰CHU Orléans; ¹¹CHG Annecy; ¹²CHU Clermont-Ferrand; ¹³CHI Créteil; ¹⁴CHU Lille; ¹⁵CHU Montpellier
Email: victor.deledinghen@chu-bordeaux.fr

Background and aims: BLV monotherapy as well as combination with PEG-interferon α 2a (PEG-IFN α) for 48 weeks induced HDV RNA declines in HDV patients included in the French ATU early access program started in September 2019. To date, there is no data available evaluating the efficacy and safety of BLV 2 mg at 18 months. The aim of this study was to evaluate 18-month safety and virological response in HBV/HDV patients receiving 2 mg BLV with or without PEG-IFN α 2a included in the French BLV ATU (real-life study).

Method: 145 patients (male gender 99, mean age 41, 3 years, cirrhosis 90) with chronic HBV/HDV co-infection, with cirrhosis or moderate fibrosis and elevated ALT levels, without liver decompensation, were included in the French early access program. Patients received 2 mg BLV qd sc alone (group A) or in combination with PEG-IFN α once weekly (group B), according to physician's choice.

Results: Among these 145 patients, 19 patients switched BLV 2 mg to BLV 10 mg (reason: no response observed after at least 3 months of treatment with 2 mg), 43 patients stopped BLV for many reasons (lost to follow-up, no response, side-effects related to the disease, patient's wish) and 83 always received BLV 2 mg. At M12, HDV-RNA was undetectable in 39% and 85% of patients treated with BLV and BLV + PEG-IFN, respectively. In October 2021, M18 data were already available in 38 patients. Among them, no new severe side-effect was reported. Undetectable HDV-RNA and combined response (HDV-RNA decrease $>2 \log_{10}$ or undetectable and normal ALT <40 IU/L) were observed in 17 (44.7%) and 14 patients (36.8%), respectively. Details are indicated in the table. Among 7 patients treated with BLV 2 mg alone for at least 18 months, HDV-RNA was undetectable in 3 and HDV-RNA decrease $>2 \log_{10}$ or undetectable and normal ALT <40 IU/L was observed in 2.

Characteristics of patients according to response at month 18.

Undetectable HDV-RNA	YES (N = 17)	NO (N = 21)
Cirrhosis	10 (58.8%)	12 (57.1%)
BLV associated with PEG-IFN	12 (70.6%)	8 (38, 1%)
Stop BLV 2 mg before M13	2 (11.8%)	14 (66.7%)
Stop PEG-IFN before M13	8 (47.6%)	6 (28.6%)
Switched to BLV 10 mg during the first 12 months	1 (5.9%)	7 (33.3%)
HDV-RNA decrease $\geq 2 \log_{10}$ or undetectable and normal ALT <40 IU/L	YES (N = 14)	NO (N = 24)
Cirrhosis	8 (57.1%)	14 (58.3%)
BLV associated with PEG-IFN	10 (71.4%)	10 (41.7%)
Stop BLV 2 mg before M13	3 (21.4%)	14 (58.3%)
Stop PEG-IFN before M13	7 (50%)	7 (29.2%)
Switched to BLV 10 mg during the first 12 months	0	7 (29.2%)

Conclusion: In this first real-world cohort and long-term follow-up, daily BLV 2 mg monotherapy is safe and well tolerated during 18 months. Strong antiviral responses against HDV in real-life were observed. Final results (month 18) will be presented during the meeting.

SAT374

Two-year safety and efficacy of tenofovir alafenamide in chronic hepatitis B: a Hellenic multicenter ReAl-life CLInical Study (HERACLIS-TAF)

George Papatheodoridis¹, Konstantinos Mimidis², Spilios Manolakopoulos³, Nikolaos Gatselis⁴, Ioannis Goulis⁵, Andreas Kapatais⁶, Emmanouil Manesis⁷, Themistoklis Vasileiadis⁸, Christos Triantos⁹, Demetrios N. Samonakis¹⁰, Vasilis Sevastianos¹¹, Stylianos Karapathanis¹², Ioannis Elefsiniotis¹³, Melanie Deutsch³, Theodora Mylopoulou², Margarita Papatheodoridi¹, Hariklia Kranidioti³, Polyxeni Agorastou⁵, Theofanie Karaoulani⁶, Anastasia Kyriazidou⁸, Konstantinos Zisimopoulos⁹, George Dalekos⁴. ¹Medical School of National and Kapodistrian University of Athens, Department of Gastroenterology, General Hospital of Athens "Laiko", Athens, Greece; ²Democritus University of Thrace, 1st Department of Internal Medicine, Alexandroupolis, Greece; ³Medical School of National and Kapodistrian University of Athens, 2nd Department of Internal Medicine, Athens, Greece; ⁴General University Hospital of Larissa, Department of Medicine and Research Laboratory of Internal Medicine, Expertise Center of Greece in Autoimmune Liver Diseases, Larissa, Greece; ⁵Aristotle University of Thessaloniki, 4th Department of Internal Medicine, General Hospital of Thessaloniki "Hippokratio", Thessaloniki, Greece; ⁶General Hospital Nikaia-Piraeus Agios Panteleimon, General Hospital of Western Attica Agia Varvara, Piraeus, Greece; ⁷Euroclinic SA, Liver Unit, Athens, Greece; ⁸Aristotle University of Thessaloniki, 3rd Department of Internal Medicine, "Papageorgiou" Hospital, Thessaloniki, Greece; ⁹University Hospital of Patras, Department of Gastroenterology, Patras, Greece; ¹⁰University Hospital of Heraklion, Department of Gastroenterology and Hepatology, Heraklion, Greece; ¹¹Evangelismos General Hospital, 4th Department of Internal Medicine, Athens, Greece; ¹²General Hospital of Rhodes, 1st Department of Internal Medicine, Rhodes, Greece; ¹³General and Oncology Hospital of Kifisia Agioi Anargyroi, University Department of Internal Medicine, Athens, Greece
Email: gepapath@med.uoa.gr

Background and aims: In the phase III trials in chronic hepatitis B (CHB), tenofovir alafenamide (TAF) compared to tenofovir disoproxil fumarate (TDF) had similar efficacy and improved safety in renal function and bone mineral density (BMD) parameters, but patients (pts) with significant renal or BMD disorders were not included. In Greece, TAF has been reimbursed since 02/2018 for CHB pts with estimated glomerular filtration rate (eGFR) <60 ml/min, serum phosphate <2.5 mg/dl or osteoporosis (T-score <-2.5). We assessed the safety and efficacy of 24-month (mo) TAF therapy in CHB pts treated at Greek tertiary liver centers.

Method: Adult CHB pts who started TAF between 02/2018–10/2019 at 13 clinics participating in the HERACLIS-TAF registry were included. Main exclusion criteria were HDV coinfection, active malignancy and bisphosphates use in last 6 months. Clinical and laboratory characteristics were recorded at TAF onset and every 6 mos thereafter until mo-24. MDRD formula was used for eGFR (ml/min) estimation.

Results: TAF was initiated in 176 pts: age 64 ± 12 years, 71% males, 85% undetectable HBV DNA, 86% ALT <40 , 45% eGFR <60 , 94% nucleos (t)ide analogue (NA) experienced (91% directly switched to TAF from another NA–81% from TDF; 3% NA discontinuation >2 mos). There was no TAF-related serious adverse event. At mo-12 and – 24, HBV DNA was undetectable (<15 IU/ml) in 97% and 100% and ALT was ≤ 40 IU/L in 96% and 95% of pts. In pts switching to TAF from other NA, median ALT decreased from onset to mo-12 or – 24 of TAF (23 to 21 or 20 IU/L, $p < 0.001$). Mean eGFR had decreased from previous NA onset (74 ± 28) to TAF onset (66 ± 26 , $p < 0.001$) and then increased at 6 (69 ± 26 , $p = 0.001$) or 12 mos (71 ± 29 , $p < 0.001$) remaining stable at 24 mos (71 ± 31). eGFR difference between 24 mos and TAF onset was >0 in 56% and >10 in 36% of pts; eGFR difference >0 and >10 occurred more frequently in pts with baseline eGFR 30–60 (76% and 48%, $p < 0.030$). In pts starting TAF with phosphate <2.5 , mean phosphate levels increased from onset (2.1) to mo-12 or – 24 (2.7 or 2.9, $p < 0.001$).

Mean BMD (Hip T-score) did not change significantly from TAF onset (-2.1) to mo-12 (-1.8, $P=0.164$) but improved at mo-24 (-1.4, $p=0.016$).

Conclusion: In most NA experienced CHB pts with renal and/or BMD disorders/risks, two-year TAF therapy is safe and effective achieving or maintaining virological suppression and improving ALT, eGFR and serum phosphate levels. eGFR improvement can be achieved in up to 60% of all pts and 75% of those with baseline eGFR 30–60.

SAT375

Treatment of chronic hepatitis B in sub-saharan Africa: 5-year results of a pilot program in Ethiopia

Stian Magnus Staurung Orlie^{1,2}, Hailemichael Desalegn³, Hanna Abera³, Eyerusalem Mamo³, Benon Amare³, Sine Grude⁴, Kristina Hommersand⁴, Nega Berhe^{2,5}, Asgeir Johannessen^{2,4,6}.
¹Vestfold Hospital Trust, Department of Paediatrics, Norway; ²Oslo University Hospital Ullevål, Regional Advisory Unit for Imported and Tropical Diseases, Norway; ³St. Paul's Hospital Millennium Medical College, Ethiopia; ⁴University of Oslo, Faculty of Medicine, Norway; ⁵Addis Ababa University, Akilu Lemma Institute of Pathobiology, Ethiopia; ⁶Vestfold Hospital Trust, Department of Infectious Diseases, Norway
Email: stian@orlien.no

Background and aims: The World Health Organization has set an ambitious goal of eliminating viral hepatitis as a major public health threat by 2030. In sub-Saharan Africa, however, antiviral treatment of chronic hepatitis B (CHB) is virtually unavailable in the public sector. Experiences from real-life CHB cohorts are needed to inform treatment guidelines and policy makers. Here we present 5-year results from one of the first and largest CHB treatment programs on the continent.

Method: Adults with CHB were enrolled in a cohort study at St. Paul's Hospital Millennium Medical College, Addis Ababa, from 2015. Liver function tests, viral markers and transient elastography was assessed at baseline and thereafter at 6-monthly intervals. Tenofovir disoproxil fumarate (TDF) was initiated based on the European Association for the Study of the Liver (EASL) criteria, with some modifications. Changes in laboratory markers were analyzed using Wilcoxon signed-rank tests. Adherence to therapy was measured by pharmacy refill data.

Results: In total, 1303 patients were included in the program; 533 (40.9%) were women and the median age was 31 years (interquartile range 26–40). Co-infections were rare: 29 patients (2.2%) were anti-HCV positive, and 19 (1.5%) were anti-HDV positive.

Overall, 294 individuals (22.6%) started TDF therapy within the first five years of follow-up. Thirty-nine (13.3%) of these patients died, of whom 36 (92.3%) had decompensated cirrhosis at baseline. Eight individuals (2.7%) developed hepatocellular carcinoma.

Liver stiffness declined steadily in patients on TDF therapy; median change from baseline after 1, 3 and 5 years was -2.9 kPa, -5.2 kPa and -5.6 kPa, respectively. Among patients still in care, 141 of 149 (94.6%) had suppressed viraemia (<69 IU/ml). In patients with available pharmacy refill data, 253 of 290 (87.2%) had ≥80% adherence.

Conclusion: This pilot program demonstrated that CHB therapy is feasible in Ethiopia with excellent long-term clinical and virological results. Our findings support rolling out large-scale treatment programs in sub-Saharan Africa.

SAT376

Decrease in the burden of integrated hepatitis B virus DNA in chronic hepatitis B patients with minimally elevated alanine aminotransferase on tenofovir disoproxil fumarate as revealed by long-read DNA-sequencing

David Pan¹, Cameron Soulette¹, Dong Han¹, Ricardo Ramirez¹, Nicholas Van Buuren¹, Jaw-Town Lin², Cheng-Hao Tseng³, Li Li¹, Simon Fletcher¹, Hongmei Mo¹, Becket Feierbach¹, Vithika Suri¹, Yao-Chun Hsu⁴.
¹Gilead Sciences, Inc., Foster City, United States; ²China Medical University, Digestive Medicine Center, Taichung, Taiwan; ³E-Da Cancer Hospital, Division of Gastroenterology and Hepatology, Kaohsiung, Taiwan; ⁴National Yang Ming Chiao Tung University, Institute of Biomedical Bioinformatics, Taipei, Taiwan
Email: david.pan3@gilead.com

Background and aims: Treatment with tenofovir disoproxil fumarate (TDF) was recently shown to reduce the number of distinct, transcriptionally active hepatitis B virus (HBV) integrations in chronic hepatitis B (CHB) patients with mild alanine aminotransferase (ALT) elevation. This short-read RNA-Sequencing (RNA-Seq) analysis was limited to the identification of expressed HBV integrations and hence did not measure the complete burden of integrated HBV DNA. Here, we use targeted long-read DNA Sequencing (DNA-Seq) to enable comprehensive analysis of the effect of TDF treatment on HBV integrations.

Method: A phase 4, randomized, double-blind, placebo-controlled study was conducted to evaluate the efficacy of TDF in CHB patients with mild ALT elevation (>1 fold but <2-fold of the upper limit normal (ULN)) without hepatocellular carcinoma (HCC) (NCT01522625). Targeted long read DNA-Seq was performed on paired liver biopsies (baseline and year 3 post-treatment) from TDF ($n=28$) and placebo ($n=27$) treated patients. The average on-target read length for the long-read DNA-Seq was 5.5 kilobases (kb). The long-read DNA-Seq data was analyzed using the ViraAL Integrations And Translocations (VALIANT) bioinformatics workflow.

Results: All patients had evidence of integrated HBV DNA at baseline with integrations detected near (<5 kb) 2, 165 genes including 13 genes in the Catalogue Of Somatic Mutations In Cancer (COSMIC) database. Of the patients with integrated HBV DNA, 98% ($n=54/55$) had ≥1 integrated HBV sequence (s) flanked by the same human chromosome and 80% (44/55) of patients contained ≥1 integrated HBV sequence (s) flanked by two different human chromosomes, indicating an inter-chromosomal translocation. Consistent with our previous short-read RNA-Seq analysis, there was a significant decrease in integration burden at year 3 post-treatment in TDF-treated ($p=0.0076$) but not placebo-treated ($p>0.05$) patients.

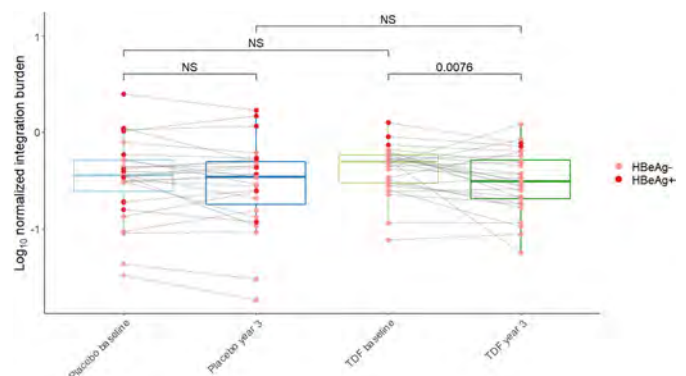


Figure: Normalized integrated HBV DNA burden shows decrease in TDF treated CHB patients but not in patients on placebo.

Conclusion: Targeted long-read DNA-Seq analysis revealed pervasive integrated HBV DNA in CHB patients with minimally elevated ALT, with ≥80% individuals having evidence of HBV-related chromosomal translocation. In line with our previous analysis, TDF treatment

POSTER PRESENTATIONS

significantly decreased the integrated HBV DNA burden in these patients. Together, these results suggest that early treatment of CHB patients with TDF may play a role in reducing the burden of integrated HBV DNA, which is commonly associated with hepatocarcinogenesis.

SAT377

Serum HBV RNA levels are associated with risk of hepatitis flare after stopping NA therapy in HBeAg-negative patients

Kathy Jackson¹, Kumar Visvanathan², Samuel Hall², Gareth Burns³, Sara Bonanzinga¹, Despina Anagnostou², Paul Desmond², Dilip Ratnam⁴, William Sievert⁵, Miriam Levy⁶, Amanda Nicoll⁷, John Lubel⁸, Peter Angus⁹, Marie Sinclair⁹, Simone Strasser¹⁰, Meng Ngu¹¹, Christopher Meredith¹², Gail Matthews¹³, Peter Revill¹, Vijaya Sundararajan¹⁴, Sara Vogrin², Alison Kuchta¹⁵, Jesse Canchola¹⁵, Jason Torres¹⁵, Jasmine Lau¹⁵, Alexander Thompson². ¹Victorian Infectious Diseases Laboratory and the Doherty Institute, Australia; ²St Vincent's Hospital and the University of Melbourne, Gastroenterology, Fitzroy, Australia; ³Western Health, Gastroenterology, Footscray, Australia; ⁴Monash Health, Gastroenterology, Australia; ⁵Monash Health and Monash University, Australia; ⁶Liverpool Hospital and South Western Sydney Clinical School UNSW, Australia; ⁷Eastern Health and Monash University, Australia; ⁸Monash University and the Alfred Hospital, Australia; ⁹Austin Hospital and the University of Melbourne, Australia; ¹⁰Royal Prince Alfred Hospital and UNSW, Australia; ¹¹Concord Hospital and the University of Sydney, Australia; ¹²Bankstown-Lidcombe Hospital, Sydney, Australia; ¹³The Kirby Institute UNSW and St Vincent's Hospital Sydney; ¹⁴Latrobe University and the University of Melbourne, Australia; ¹⁵Roche Molecular Systems, Inc., Pleasanton, CA, United States
Email: alexander.thompson@svha.org.au

Background and aims: Among HBeAg-negative chronic hepatitis B (CHB) patients on long-term nucleos(t)ide analogue (NA) therapy, treatment discontinuation has been associated with HBsAg loss and durable virological suppression, but also hepatitis flares requiring NA therapy to be restarted. The prediction of clinical outcomes after stopping NA therapy remains challenging. Quantification of circulating HBV RNA is a promising biomarker in CHB patients. We have evaluated the role of serum HBVRNA levels to predict clinical outcomes in a large cohort of patients enrolled in a prospective NA-STOP study.

Method: The Melbourne HBV-STOP study was a prospective multicentre study of NA discontinuation in 110 HBeAg-negative non-cirrhotic patients who had achieved long-term virological suppression on treatment. All patients were followed for 96 weeks. In a subset, we performed an exploratory analysis of serum HBVRNA levels for predicting clinical outcomes after stopping NA therapy. HBVRNA levels were measured at baseline and longitudinally using the automated Roche cobas[®] HBVRNA Investigational Assay. Clinical outcomes of interest included rates hepatitis flare (ALT>5xULN), disease remission (HBV DNA<2000 IU/ml and ALT<2xULN) and HBsAg loss, as well as rates of NA re-treatment.

Results: HBVRNA levels were tested at baseline and off-treatment in 65 patients. At baseline, the median age was 56 yrs, 54% were male, and 75% were Asian. Median HBsAg level was 701 (1.6–19912) IU/ml. Following treatment withdrawal, virological reactivation occurred in all participants, 38% experienced a hepatitis flare (ALT>5xULN), 26% restarted NA therapy and 6% (n=4) lost HBsAg by 96 weeks. At baseline, serum HBV RNA was detectable in 16/65 (25%). The detection of HBVRNA in serum at baseline was positively associated with risk of hepatitis flare [ALT>5 xULN, 63% vs 31%, OR = 3.8, 95% CI = (1.2, 12.3), p value = 0.03], as well as lower likelihood of sustained disease remission as well as HBsAg loss. HBVRNA levels were undetectable at baseline in all patients who achieved HBsAg loss. Of patients HBVRNA negative at baseline, HBVRNA levels became detectable in 47/49 patients during follow-up. The time to detection of HBVRNA was shorter for patients stopping TDF than ETV (median

49 vs 90 days, p=0.02). The detection of HBVRNA over time was associated with rising HBVDNA levels>10⁴ IU/ml. HBVRNA levels>10³ cp/ml off-treatment were associated with increased risk of hepatitis flare (ALT>5xULN).

Conclusion: Serum HBVRNA was detectable in a minority of HBeAg-negative patients on long-term NA therapy. The detection of any serum HBVRNA prior to stopping NA therapy, and rising HBVRNA off-treatment, were associated with risk of subsequent hepatitis flare, as well as lower likelihood of HBsAg loss. HBVRNA levels show promise as a biomarker for predicting clinical outcomes after stopping NA therapy in patients with HBeAg-negative CHB.

SAT378

Efficacy and safety of tenofovir alafenamide versus tenofovir disoproxil fumarate in treatment-naïve patients with chronic hepatitis B

Jihye Lim¹, Won-Mook Choi¹, Ju Hyun Shim¹, Danbi Lee¹, Kang Mo Kim¹, Young-Suk Lim¹, Han Chu Lee¹, Jonggi Choi¹. ¹Asan Medical Center, University of Ulsan College of Medicine, Gastroenterology, Korea, Rep. of South
Email: jkchoi0803@gmail.com

Background and aims: We aimed to evaluate the efficacy and safety of tenofovir alafenamide (TAF) compared with tenofovir disoproxil fumarate (TDF) in treatment-naïve patients with chronic hepatitis B (CHB) based on real world data.

Method: We analyzed 2,747 patients with CHB under TAF (n = 502) or TDF (n = 2,245) treatments. Virological response (VR: HBV DNA <15 IU/ml), on-treatment ALT normalization, the incidence of HCC, renal function, and lipid profiles were compared between these groups. Propensity score matching of 495 pairs was also conducted for these comparisons.

Results: The mean age of the total cohort was 48.6 years and 58.2% were male. Cirrhosis had a 33.3% prevalence in this study population. VRs at 12-, 24-, and 36 months were achieved in 70.3%, 81.2%, and 83.3% of the TAF and 67.9%, 84.3% and 86.1% of the TDF cases, respectively (p >0.05 for all). Normalized ALT, as determined by local laboratory criteria (<40 U/L), occurred in 79.7%, 90.6%, and 86.2% of the TAF group and 78.2%, 85.8%, and 85.7% of the TDF group at 12-, 24-, and 36 months, respectively (p >0.05 for all). The HCC risk did not statistically differ across the entire cohort (TAF: 0.80/100 person-years [PYs] vs TDF: 1.45/100 PYs, P=0.30) or in the PS-matched cohort (TAF: 0.82/100 PYs vs TDF: 0.90 PYs, P=0.60). The TAF group showed a lower median increase in serum creatinine from baseline during the early study period. Compared with the TAF group, the TDF group showed significant decreases in total cholesterol, triglyceride, and HDL, but not in LDL.

Conclusion: Real-world data indicate that TAF has comparable efficacies to TDF in terms of VR and ALT normalization, with no higher risk of HCC.

SAT379

Bulevirtide 2 mg/day monotherapy in patients with chronic hepatitis delta with or without cirrhosis: a multicenter european cohort real-life study

Alessandro Loglio¹, Peter Ferenci², Katja Deterding³, Sara Colonia Uceda Renteria⁴, Dana Sambarino¹, Mathias Jachs², Caroline Schwarz⁵, Marta Borghi¹, Kerstin Port³, Riccardo Perbellini¹, Floriana Facchetti¹, Elisabetta Degasper¹, Benjamin Maasoumy³, Thomas Reiberger², Markus Cornberg³, Heiner Wedemeyer³, Pietro Lampertico^{1,6}. ¹Foundation IRCCS Ca' Granda Ospedale Maggiore Policlinico, Division of Gastroenterology and Hepatology, Milan, Italy; ²Medical University of Vienna, Division of Gastroenterology and Hepatology, Vienna, Austria; ³Hannover Medical School, Germany; ⁴Foundation IRCCS Ca' Granda Ospedale Maggiore Policlinico, Clinical Laboratory, Milan, Italy; ⁵Klinik Ottakring, Department of Internal Medicine IV, Vienna, Austria; ⁶University of Milan, CRC "A. M. and A. Migliavacca" Center for Liver Disease, Department of Pathophysiology and Transplantation, Milan, Italy
Email: ale.loglio@gmail.com

Background and aims: Bulevirtide (BLV) has been recently approved for the treatment of HDV-related chronic hepatitis but its 'real-life' effectiveness and safety-especially in patients with cirrhosis-are still poorly known. This study aimed to describe the early virological and biochemical responses in a large European cohort.

Method: All consecutive HDV patients who started BLV 2 mg/day in three EU countries were enrolled in this study. Demographic, clinical and virological features were collected at baseline and during therapy. Primary end point was virological response (≥ 2 Log decline or undetectable HDV-RNA), secondary end points included virological non-response (<1 Log decline), biochemical response (normal ALT), combined response, and safety at week 24. HDV-RNA was quantified by Robogene 2.0 (LOQ 6 IU/ml), in-house RT-PCR (LOQ 100 cp/ml) and Robogene 1.0 (LOQ 80 IU/ml).

Results: 58 patients were enrolled: 47 (25–79) years, 62% males, 97% Caucasian, 78% cirrhotics, 67% varices, spleen diameter 17 (8–25) cm, platelets 88 (28–288) $\times 10^3$ /mmc, transient elastography: 16.3 (1.7–57.8) kPa, CAP 203 (100–320) dB/m; 69% previous interferon therapy, 97% under NA therapy, 2 patients with HCC. At baseline (BLV start): ALT 80 (7–341) U/L (83% $>$ ULN), albumin 4.1 (2.8–4.9) g/dL, HBsAg 3.7 (1.7–4.8) Log IU/ml, 91% HBeAg negative, 86% HBV-DNA undetectable. Baseline HDV-RNA levels were 4.9 (3.3–6.6) Log IU/ml, 4.7 (2.0–7.3) Log cp/ml and 5.8 (1.9–7.5) Log IU/ml, respectively in the three countries. By week 24, ALT levels declined to 34 (18–82) U/L and normalized in 77% of patients. HDV-RNA showed an overall 2.0 (0–3.9) Log decline: virological response was observed in 54% of patients (10% with HDV-RNA $<$ LOQ), while 46% achieved a combined (virological and biochemical) response. A virological non-response (<1 Log decline at week 24) was observed in 27% of patients, even if 60% of them normalized ALT levels. HBsAg levels remained unchanged. BLV was well tolerated, with no significant injection site reactions, including in patients with active HCC or clinically significant portal hypertension.

Conclusion: This real-life multicenter EU cohort study demonstrated the early effectiveness and safety of BLV 2 mg monotherapy even in difficult-to-treat cirrhotic HDV patients. However, the rate of virological non-response at week 24 was higher than previously estimated. The week 48 data will be presented at the meeting.

SAT380

The orally available sodium/taurocholate co-transporting polypeptide inhibitor A2342 blocks hepatitis B and D entry in vitro

Britta Bonn¹, Ellen Strängberg¹, Ivana Uzelac¹, Michael Kirstgen², Nora Goldmann³, Dieter Glebe³, Joachim Geyer², Erik Lindström¹. ¹Albireo Pharma, Inc., Boston, MA, United States; ²Institute of Pharmacology and Toxicology, Justus Liebig University of Giessen, Giessen, Germany; ³Institute of Medical Virology, Justus Liebig University Giessen, Giessen, Germany
Email: britta.bonn@albireopharma.com

Background and aims: A2342 is a novel small molecule, orally available, selective inhibitor of hepatic transporter Na⁺/taurocholate co-transporting polypeptide (NTCP). NTCP mediates uptake of bile acids into hepatocytes and acts as a host receptor for hepatitis B and D viruses (HBV/HDV). The preS1 domain of the large envelope protein of HBV/HDV is essential for binding of these virus particles to NTCP. We previously demonstrated that A2342 lowers HBV DNA viral load in infected human hepatocytes in vitro and also attenuates HBV viral load and HBV antigens in infected humanized mice in vivo. Here, we aim to provide more detail on the NTCP inhibitory mechanism.

Method: Human NTCP-expressing HEK293 cells were used to evaluate inhibition of 1 μ mol/L [³H]taurocholic acid transport and [³H]preS1 peptide binding as surrogate parameter for virus binding. Human NTCP-expressing HepG2 cells were used to evaluate entry inhibition of HDV and HBV via immunostaining against hepatitis D antigen (HDAG) and hepatitis B core antigen (HBcAg), respectively, and measuring hepatitis B e antigen (HBeAg) levels in supernatant of HBV-infected cells. Cryopreserved human hepatocytes infected with a clinical isolate of HBV were used for infection experiments; HBV DNA levels in supernatant were analysed. The peptides preS1 (genotype D) and myrcludex B or tenofovir disoproxil fumarate (TDF) were used as positive controls.

Results: A2342 inhibited [³H]taurocholic acid uptake (half-maximal inhibitory concentration [IC₅₀], 186 nmol/L) and [³H]preS1 peptide binding (IC₅₀, 149 nmol/L) in a concentration-dependent manner. In infection experiments, A2342 (range, 100–400 nmol/L) inhibited numbers of HBcAg-positive cells by 75%–90% and HDAG-positive cells by 40%–60%. HBeAg levels in supernatant were reduced with A2342 by $>90\%$ at all concentrations. In cryopreserved human hepatocytes, A2342 reduced HBV DNA levels in a concentration-dependent manner when given 18 h before infection. A2342 was not effective when given 18 h post-infection. Additive antiviral effects were evident when A2342 was given together with TDF. A2342 was devoid of cellular toxicity in hepatocytes and cell lines.

Conclusion: A2342 inhibits NTCP-mediated bile acid uptake and HBV preS1 peptide binding in similar manners and blocks entry of HBV and HDV. These data further support A2342 as the first orally bioavailable molecule able to inhibit HBV/HDV entry via NTCP in the nanomolar range.

SAT381

Comparative performance analysis between manual and automatic RNA extraction to quantify HDV RNA by RoboGene 2.0 kit in untreated and bulevirtide-treated HDV patients

Sara Colonia Uceda Renteria¹, Alessandro Loglio², Marta Borghi², Dana Sambarino², Riccardo Perbellini², Floriana Facchetti², Sara Monico², Elisabetta Degasper², Ferruccio Ceriotti¹, Pietro Lampertico^{2,3}. ¹Foundation IRCCS Ca' Granda Ospedale Maggiore Policlinico, Clinical Laboratory, Milan, Italy; ²Foundation IRCCS Ca' Granda Ospedale Maggiore Policlinico, Division of Gastroenterology and Hepatology, Milan, Italy; ³University of Milan, CRC "A. M. and A. Migliavacca" Center for Liver Disease, Department of Pathophysiology and Transplantation, Milan, Italy
Email: sara.ucedarenteria@policlinico.mi.it

Background and aims: Diagnosis and management of Chronic Delta Hepatitis (CHD) requires highly sensitive and reliable tests for HDV

RNA quantification coupled with automated lab procedures to optimize time and resources. Aim of the study was to compare two different extraction methods to quantify HDV RNA levels in untreated and Bulevertide (BLV)-treated HDV patients.

Method: This is a single-center retrospective study, evaluating frozen sera from consecutive untreated and BLV treated-HDV patients. HDV RNA levels were quantified by Robogene HDV RNA quantification kit 2.0 (Roboscreen GmbH, Leipzig, Germany; LOQ 6 IU/ml, linear range 5 to 10^9 IU/ml, pangenotypic) by using two different extraction methods: manual method, i.e. INSTANT Virus RNA/DNA kit (Analytik Jena AG, Jena, Germany) versus automatic method, i.e. EZ1 DSP Virus Kit (Qiagen, Hilden, Germany).

Results: 96 frozen sera collected from 18 Caucasians patients with CHD either untreated (baseline) or BLV treated were analyzed. The main baseline features of the patients were the following: 48 (29–77) years, 67% males, 100% HDV-GT1, 100% cirrhotics, all under TDF or ETV treatment, 67% previously interferon-exposed; ALT 106 (32–222) U/L, HBsAg 3.7 (2.5–4.3) Log IU/ml, 94% HBeAg negative, 72% HBV DNA undetectable. Overall, HDV-RNA levels were 3.61 (0.70–6.60) vs 2.66 (0.70–5.52) Log IU/ml, by manual vs automated extraction. Viremia tested undetectable in 0 (0%) vs 1 (1%), while <LOQ in 3 (3%) vs 14 (15%) patients, respectively. Compared to the automated method, manual RNA extraction reported higher HDV-RNA levels in 90 samples [median 0.80 (0.07–2.11) Log IU/ml], similar levels in 3 [two <LOQ samples, and one 197 IU/ml], and lower levels in 3 [0.11 (0.09–0.17) Log IU/ml]. In 15 samples tested “undetectable or <LOQ” by the automated method, HDV-RNA was <LOQ in 3, and positive low-titer [30 (7–92) IU/ml] in 12 samples tested with manual one. During the first 6 months of BLV monotherapy, HDV-RNA progressively declined using both manual [baseline 4.29→3.76→3.52→2.74→2.26 Log IU/ml] and automated extraction [3.59→3.41→2.64→1.61→0.85 Log IU/ml], achieving <LOQ result in 11% vs 47% at month six, respectively.

Conclusion: Quantification of HDV RNA by Robogene 2.0 is significantly influenced by the extraction method, the manual extraction being more sensitive although more time consuming. Therapeutic trials with new anti-HDV therapeutics should consider this important information.

SAT382

Combination therapy in HBeAg-negative chronic hepatitis B patients with low-level viremia to nucleos (tide) analogues

Xin-Yue Chen^{1,2,3}, Shan Ren^{1,2,3}, Junfeng Lu^{2,2}, Lina Ma², Sujun Zheng², Zhongjie Hu². ¹Beijing You'an Hospital, Capital Medical University, Beijing, China; ²Beijing You'an Hospital, Capital Medical University, First Department of Liver Diseases, Beijing, China; ³ Email: chenxydoc@163.com

Background and aims: Considering that the ultimate goals of treatment are to decrease the morbidity and mortality related to chronic hepatitis B (CHB), the recently updated guidelines of liver disease recommend that people with low-level viremia (LLV) to nucleos (tide) analogues (NAs) should switch or add another drug for people with a suboptimal virological response. To compare and evaluate the efficacy and safety of pegylated interferon (peg-IFN) α in combination with NAs and NAs in combination with NAs in HBeAg-negative CHB patients with LLV to NAs, so as to investigate optimal treatment regimen with end point of therapy.

Method: Totally 240 HBeAg-negative CHB patients with LLV to NAs were enrolled in the study, and divided into 2 groups receiving Peg-IFN+NAs (IFN group) or NAs+NAs (NA group) according to administration of NAs. Complete virological response (HBV DNA concentration of less than 20 IU/ml or 10 IU/ml) rate, HBsAg loss/seroconversion rate at 48 weeks of treatment were compared between the 2 groups.

Results: There were 178 patients in IFN group and 89 patients in NA group, and 162 patients in the IFN group and 78 patients in NA group received 48-week treatment duration. At 12 weeks of treatment, the complete virological response rate was 51.1% (40/78) in the NA group,

which was seemed higher than that in the PegIFN group (45.1%, 73/162), but the difference was not statistically significant ($X^2 = 0.52$, $P = 0.47$). At 48 weeks, the complete virological response rates of PegIFN α group and NA group were 97.50% (158/162) and 85.90% (67/78), respectively, with statistically significant differences ($X^2 = 10.56$, $P = 0.001$). There was no significant difference in HBsAg levels at baseline between the PegIFN group and NA group (823.97 vs. 988.50, $t = 0.80$, $P = 0.43$). In the PegIFN α group, HBsAg titer decreased significantly from baseline to week 12 (823.97 vs. 527.7, $t = 2.31$, $P = 0.02$), and then it decreased slowly from week 12 to week 24 (399→324.9 IU/ml). While in the NA group, HBsAg titer did not change significantly from baseline to week 48, there was no statistically significant difference (988.5 vs. 847.1, $t = 0.84$, $P = 0.41$). At week 48, the HBsAg loss/seroconversion rate in PegIFN α group (50/162, 30.9%) was higher than that in NA group (4/78, 5.1%), and the difference was statistically significant ($X^2 = 19.89$, $P < 0.001$).

Conclusion: The treatment regimens of Peg-IFN+NAs and NAs+NAs are effective in suppression of HBV replication in HBeAg-negative CHB patients with LLV to NAs, but Peg-IFN+NAs is superior to NAs+NAs in. Combination therapy with IFN as the basis will achieve reliable end point of therapy in HBeAg-negative CHB patients with LLV to NAs.

[Key words] hepatitis B; chronic; low-level viremia; Peg IFN α ; HBsAg loss/seroconversion; complete virological response;

SAT383

ABI-4334, a novel inhibitor of hepatitis B virus core protein, promotes formation of empty capsids and prevents covalently closed circular DNA formation by disruption of incoming capsids

Nuruddin Unchwaniwala¹, William Delaney¹, Kathryn M Kitrininos¹.

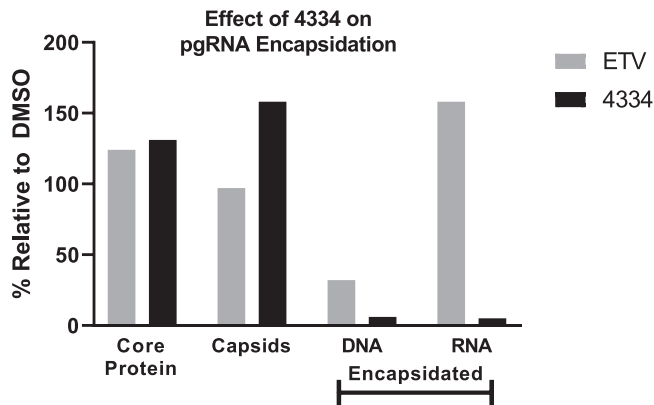
¹Assembly Biosciences, Inc., South San Francisco, United States

Email: kkitrininos@assemblybio.com

Background and aims: Core inhibitors (CIs) are a novel class of antivirals with the potential to improve cure rates in patients with chronic hepatitis B virus infection (CHBV). CIs have demonstrated potent antiviral activity in Phase 1 clinical studies and additive antiviral activity when combined with nucleos (tide) reverse transcriptase inhibitors (NrtIs) compared to NrtIs alone in Phase 2 studies. CIs have multiple mechanisms of action, including inhibition of pre-genomic RNA (pgRNA) encapsidation, preventing assembly and release of infectious viral particles and disruption of incoming capsids, preventing covalently closed circular DNA (cccDNA) formation. ABI-4334 (4334) is a novel CI with single digit nM potency against pgRNA encapsidation and cccDNA formation. Here we further characterize the preclinical profile of 4334.

Method: CI binding pocket variants and NrtI-resistant mutants were assessed for 4334 sensitivity in a HepG2 transient transfection assay. Specificity of 4334 for HBV inhibition was assessed using a panel of 7 different viruses. Effects on pgRNA encapsidation were determined by inducing AD38 cells in the presence of 10x EC₅₀ 4334 for 4 days. Intracellular levels of core protein, HBV DNA, and HBV pgRNA were measured by Western, Southern, and Northern blots, respectively. Intracellular capsid levels were measured by native gels. 4334 effects on cccDNA formation were determined by infecting HepG2-NTCP cells with HBV, treating with 4334 for 3 hours (capsid DNA) or 4 days (cccDNA), and then measuring HBV DNA species by Southern blot.

Results: 4334 demonstrated broad antiviral activity with activity comparable to wild-type for 14/16 CI binding pocket variants and 7/7 NrtI mutants. The antiviral activity of 4334 was specific to HBV, with no activity against any other viruses, including HIV and HCV. 4334 did not impact intracellular core protein levels but inhibited pgRNA encapsidation resulting in empty capsid formation, thus acting as a class II CI. Addition of 4334 also resulted in premature melting of incoming capsids during early infection stages, resulting in significantly lower levels of total HBV DNA deposition and cccDNA formation.



Conclusion: 4334 is a potent CI with broad coverage across CI binding pocket variants and NrtI mutants. The activity of 4334 against pgRNA encapsidation is consistent with a class II CI. 4334 treatment results in melting of cytoplasmic HBV capsids, which prevents cccDNA formation. A Phase 1a first-in-human study with 4334 is planned for 2022.

SAT384

Real-world high adherence to hepatitis B antiviral treatment practice guidelines in Israel

Yana Davidov¹, Fadi Abu Baker², Ariel Israel³, Ziv Ben Ari^{1,4}. ¹Sheba Medical Center, Liver Diseases Center, Tel Aviv-Yafo, Israel; ²Hillel Yaffe Medical Center, Department of Gastroenterology and Hepatology, Hadera, Israel; ³Leumit Health Services, Leumit Research Institute and Department of Family Medicine, Israel; ⁴Tel Aviv University, Sackler School of Medicine, Tel Aviv-Yafo, Israel
Email: y.davidov@gmail.com

Background and aims: Epidemiologic data regarding chronic hepatitis B virus (CHB) infections in Israel are limited as large population-based study have not been performed. This work aimed to evaluate adherence to European Association for the Study of the Liver (EASL) practice guidelines to antiviral treatment in Israel.

Method: Clinical and demographic data of HBsAg-positive patients registered in the Leumit-Health-Service database (one of the four major health maintenance organizations in Israel) between 2000-2019, were retrieved. Patients were compared according to eligibility to antiviral treatment, and type of nucleos (t)ide analogue (NA) treatment.

Results: In total, 1216 patients had documented HBsAg positivity (Israel born: 95.8%, males: 58.6%, mean age: 40.2 ± 14.2 years), 90.6% of whom were HBeAg negative. Cirrhosis was documented for 6% of the patients. Antiviral therapy eligibility was met by 37% of patients, among whom 89% received antiviral therapy. Antiviral therapies include NA with a high barrier to resistance (HBR) (64.5%) (entecavir 36.3% and tenofovir 28.2%) and NA with a low barrier to resistance (LBR) (35.5%) (adefovir 1.7% and lamivudine 33.8%). Compared to patients who received LBR NA, patients receiving HBR NA had shorter treatment (68.7 ± 50 months vs. 161.5 ± 42.6 months, $p < 0.0001$) and follow-up duration (125 ± 68 months vs. 188 ± 48 months, $p < 0.0001$); at the end of follow-up ALT levels and APRI score were higher among patients on LBR NA compared to patients on HBR NA.

Conclusion: Most of the patients infected with HBV were born in Israel and were HBeAg-negative. The majority of the patients received antiviral treatment according to the international practice guidelines. However, one-third of them were treated with a less potent NA probably due to their lower cost. These findings should encourage optimization of HBV care and full compliance with the professional practice guidelines recommendations.

SAT385

No detectable resistance to bulevirtide in participants with chronic hepatitis D (CHD) through 24 weeks of treatment

Julius Hollnberger^{1,2}, Yang Liu³, Ross Martin³, Savrina Manhas³, Thomas Aeschbacher³, Silvia Chang³, Simin Xu³, Bin Han³, Tahmineh Yazdi³, Lindsey May³, Dong Han³, Katrin Schöneweis³, John F. Flaherty³, Vithika Suri³, Dmitry Manuilov³, Roberto Mateo³, Evguenia S Svarovskaia³, Hongmei Mo³, Stephan Urban^{1,4}. ¹University Hospital Heidelberg, Department of Molecular Virology, Heidelberg, Germany; ²German Center for Infection Research (DZIF), Heidelberg; ³Gilead Sciences, Inc., Foster City, United States; ⁴German Center for Infection Research (DZIF), Heidelberg, Germany
Email: stephan.urban@med.uni-heidelberg.de

Background and aims: Bulevirtide (BLV) blocks entry of HDV into hepatocytes via inhibition of the interaction between the HBV preS1 domain and the sodium taurocholate cotransporting polypeptide (NTCP) receptor. Previous studies show that treatment with BLV alone leads to a substantial HDV RNA reduction. Here, we present results from a comprehensive virologic analysis in HDV-infected participants who received BLV at doses of 2 mg, 5 mg, or 10 mg subcutaneously once daily for 24 weeks across two studies (MYR202 [Phase 2] and MYR301 [Phase 3]).

Method: Resistance analysis was performed for participants who experienced a suboptimal response to BLV (virologic non-responder [VNR]; defined as a decline in HDV RNA <1 log₁₀ IU/ml from baseline [BL] at week 24) or virologic breakthrough (VB, defined as two consecutive increases in HDV RNA of ≥2 log₁₀ IU/ml from nadir or two consecutive HDV RNA values ≥LOD if previously <LOD). Virologic partial responder (VPR) and virologic responder (VR) were defined as HDV RNA decline ≥1 but <2 log₁₀ IU/ml and decline ≥2 log₁₀ IU/ml or HDV RNA <LOD at Week 24 respectively. Resistance testing included deep sequencing of the HBV PreS1 BLV region and HDV HDAG region. Additionally, *in vitro* phenotypic testing was performed for clinical isolates at baseline and Week 24 for VNRs and those with VB. For the analysis control, sequencing and/or phenotypic analysis were performed for all available BL samples in the two studies.

Results: Overall, resistance analyses were performed for 26 VNRs and 1 participant with VB representing 13/77 (17%), 9/32 (28%), and 5/80 (6%) participants receiving daily BLV at 2 mg, 5 mg, and 10 mg groups, respectively. No amino acid substitutions at HBV PreS1 BLV region or HDV HDAG associated with resistance to BLV were identified from any participants at BL and Week 24. Clinical isolates carrying the amino acid substitutions remained sensitive to BLV *in vitro*; all the amino acid substitutions were seen in the participants achieving a virologic response. Importantly, by phenotypic analysis, BLV medium EC₅₀ values obtained from 117 baseline samples were similar across VNRs (EC₅₀ = 0.42 nM), VPR (EC₅₀ = 0.38 nM) and VR (EC₅₀ = 0.27 nM) regardless of the presence of HBV and HDV polymorphisms.

Conclusion: This is the largest resistance analysis to date to demonstrate that no genotypic and phenotypic resistance to BLV has been detected through 24 weeks of treatment.

SAT386

The HBV siRNA, ALG-125755, demonstrates a favourable nonclinical profile and significant and durable hepatitis B surface antigen reductions in the AAV-HBV mouse efficacy model

Megan Fitzgerald¹, Kusum Gupta², Kha Le², Sucheta Mukherjee², Jin Hong³, Khiem Nguyen⁴, Alfred Chen⁵, Vivek Rajwanshi⁴, Caroline Williams⁴, Meenakshi Venkatraman⁵, Matthew McClure¹, Sushmita Chanda², John Fry¹, David Smith⁴, Julian Symons⁶, Lawrence Blatt⁷, Leonid Beigelman⁸, Tse-I Lin¹. ¹Aligos Therapeutics, Inc., Clinical Development, South San Francisco, United States; ²Aligos Therapeutics, Inc., TSS, South San Francisco, United States; ³Aligos Therapeutics, Inc., Oligonucleotide Biology, South San Francisco, United States; ⁴Aligos Therapeutics, Inc., Chemistry, South San Francisco, United States; ⁵Aligos Therapeutics, Inc., CMC, South San Francisco, United States; ⁶Aligos Therapeutics, Inc., Chief Scientific Officer, South San Francisco, United States; ⁷Aligos Therapeutics, Inc., Chief Executive Officer, South San Francisco, United States; ⁸Aligos Therapeutics, Inc., President, South San Francisco, United States
Email: mfitzgerald@aligos.com

Background and aims: Currently approved therapies for chronic hepatitis B (CHB) infrequently achieve a functional cure in patients, which requires a sustained loss of hepatitis B surface antigen (HBsAg). In CHB patients, HBV targeted small interfering RNAs (siRNAs) have significantly reduced HBsAg, indicating a potential for their use in a curative therapeutic regimen. Here we evaluate the antiviral activity of ALG-125755, a N-acetylgalactosamine (GalNAc)-conjugated siRNA, in the adeno-associated virus (AAV)-HBV mouse efficacy model and its pharmacokinetic (PK) and safety profile in rats and monkeys.

Method: In the AAV-HBV mouse model, various doses of ALG-125755 or vehicle were administered subcutaneously (SC) once, biweekly for 10 weeks (6 doses), or monthly for 8 weeks (3 doses). For 24 weeks during dosing and follow-up, blood and liver samples were collected for plasma HBsAg and hepatitis B e antigen (HBeAg) assessments and liver ALG-125755 concentrations. The plasma samples were analyzed by LC-hybridization whereas the liver samples were analyzed by LC-MS for ALG-125755 concentration. For PK and toxicity studies, rat and monkey were given single or weekly subcutaneous doses of ALG-125755 and plasma, liver and kidney were collected at various timepoints and analyzed for ALG-125755 concentrations by LC-MS.

Results: A dose dependent inhibition of plasma HBsAg was observed with ALG-125755 in AAV-HBV mice dosed biweekly and monthly at 1.5 and 5 mg/kg/dose. Maximal HBsAg reductions of 1.7, 2.4 and 2.8 log₁₀ IU/ml were observed one-month post-last dose in the 10 mg/kg single dose groups, and 5 mg/kg/dose monthly and biweekly treated groups, respectively. Furthermore, reductions in HBsAg levels were sustained for ≥70 days post-last dose in the single and 5 mg/kg/dose multiple dose groups. Plasma HBeAg was similarly reduced in a dose dependent manner, with reductions up to 1.2 log₁₀ S/CO. Dose and dosing-regimen dependent exposures of ALG-125755 were observed in mouse liver which correlated with the pharmacodynamic effect. High liver exposure of ALG-125755 was observed following single or repeated doses in rats and monkeys. Further, ALG-125755 was well-tolerated in rats and monkeys with no toxicologically relevant findings up to 300 and 100 mg/kg/dose, respectively.

Conclusion: ALG-125755 demonstrated high liver concentrations across species, and significant and durable HBsAg knockdown in the AAV-HBV mouse model. Further development of ALG-125755 as a potential best-in-class HBV siRNA is ongoing.

SAT387

Hepatitis delta management in the United States: an analysis of all-payer claims database

Robert Wong¹, Robert G. Gish^{2,3}, Joseph Lim⁴, Ankita Kaushik⁵, Yan Liu⁵, Emily Acter⁶, Ira M Jacobson⁷. ¹Stanford University School of Medicine, Stanford and VA Palo Alto Healthcare System, Palo Alto, United States; ²University of Nevada, Reno School of Medicine, Kirk Kerkorian School of Medicine at UNLV, Las Vegas, United States; ³UC San Diego Skaggs School of Pharmacy and Pharmaceutical Sciences, Hepatitis B Foundation, La Jolla, United States; ⁴Yale School of Medicine, New Haven, United States; ⁵Gilead Sciences, Inc., Foster City, United States; ⁶STATinMED, Plano, United States; ⁷NYU Grossman School of Medicine, New York, United States
Email: rwong123@stanford.edu

Background and aims: Hepatitis delta (HDV) infection runs a more progressive course than that of hepatitis B (HBV). If left untreated, HDV is associated with an earlier onset of hepatic disease such as cirrhosis, liver failure, and liver cancer compared to HBV. Pegylated-interferon (PEG-IFN) is used off-label as a standard treatment for HDV in the United States (US). Data evaluating HDV treatment patterns is limited. This study describes treatment rates and distribution of provider specialties in management of HDV in the US.

Method: Using the All-Payer Claims Database, adults (≥18 years) with ≥1 inpatient claim or ≥2 outpatient claims ≥30 days apart for HDV infection based on ICD-9/10-CM diagnosis codes were identified from 1/1/2015 to 12/31/2019. First date of HDV diagnosis was defined as the index date. Patients were required to have ≥12 months of continuous enrolment before and after their index date. Treatment patterns for antiviral therapies were assessed over the 12-month postindex period (follow-up). Physician specialty was assessed at diagnosis and during follow-up.

Results: Among the 9, 376 patients identified with HDV during the study period, 6, 719 met inclusion criteria; only 0.1% received treatment with PEG-IFN within the follow-up period. Additionally, only 8.8% were on HBV-specific antiviral therapy including tenofovir disoproxil fumarate (5.3%), entecavir (2.9%), and tenofovir alafenamide (1.0%). The majority (53.0%) of HDV patients were diagnosed by primary care physicians (PCPs), followed by gastroenterology (GI, 9.3%), obstetrics-gynaecology (OBGYN) (4.7%), infectious diseases (ID, 2.4%), and hepatology (0.6%) physicians. During the follow-up period, 62.1% of patients were managed by PCPs, while 12.1%, 4.4%, 2.9%, and 2.7% were seen by GI, OBGYN, ID, and hepatology physicians, respectively.

Conclusion: In a large national US cohort representing ~80% of the insured population, most patients with HDV were diagnosed and cared for by PCPs without specialty referral, and <20% were cared for by specialty providers. Rates of HBV-specific antiviral treatment among HDV patients were <10%, and very few patients were treated with PEG-IFN, the current standard of care for HDV. There is a critical need for greater awareness of the importance of ensuring HDV patients are appropriately treated, and for vigorous efforts to ensure that appropriate healthcare providers are made aware of new HDV therapies in a timely manner.

SAT388

Evaluation of the drug-drug interaction profile of vebicorvir, a first-generation hepatitis B core inhibitor: findings from phase 1 and phase 2a studies

Katie Zomorodi¹, Grace Wang¹, Steven J Knox¹, Julie Ma¹, Luisa M Stamm¹. ¹Assembly Biosciences, Inc., South San Francisco, United States
Email: kzomorodi@assemblybio.com

Background and aims: Vebicorvir (VBR) is a first-generation hepatitis B virus (HBV) core inhibitor that targets multiple aspects of the viral replication cycle. VBR, administered in combination with nucleos (t)ide reverse transcriptase inhibitors (NrtIs) and other agents, is in Phase 2 development for the treatment of chronic HBV

infection (cHBV). In vitro, VBR is not a potent inhibitor of CYP450 s or drug transporters. Here we describe the clinical evaluation of VBR's drug-drug interaction (DDI) potential from Phase 1 and Phase 2a studies.

Method: Studies 201 (NCT03577171; N = 73) and 202 (NCT03576066; N = 25) were Phase 2a, double-blind, placebo-controlled studies evaluating VBR and Nrtls in patients with cHBV in which sparse PK samples were collected. Study 103 was a 3-part Phase 1 DDI study in healthy subjects. Part 1 (N = 20) investigated the potential of VBR to inhibit CYP2C9, 2C19, 2D6, and 2C8 through use of the index substrates tolbutamide, omeprazole, dextromethorphan, and repaglinide, respectively. Parts 2 (N = 18) and 3 (N = 20) evaluated CYP3A4 and 2B6 inhibition/induction, respectively, using midazolam and bupropion. Intensive PK samples were collected, and PK analysis was conducted by non-compartmental methods.

Results: In Studies 201 and 202, there were no clinically significant differences in mean trough VBR or Nrtl concentrations following combination therapy in patients with cHBV (Figure 1a/1b). In Study 103 (Part 1), co-administration of VBR did not change the exposure of omeprazole, dextromethorphan, or repaglinide, suggesting VBR is not an inhibitor of CYPs 2C19, 2D6, or 2C8. Tolbutamide exposure was increased by approximately 30% with VBR co-administration, indicating VBR is a weak inhibitor of CYP2C9. In Part 2, midazolam exposure was reduced by 33% following co-administration with VBR, with no concomitant change in 1-hydroxymidazolam exposure, indicating VBR is not an inhibitor/inducer of CYP3A4. In Part 3, co-administration of VBR did not change the exposure of bupropion, indicating VBR is not an inhibitor/inducer of CYP2B6.

Figure 1A: Plasma VBR Trough Concentrations by Nrtl in Patients with cHBV (Study 201)

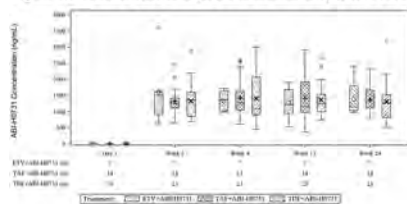
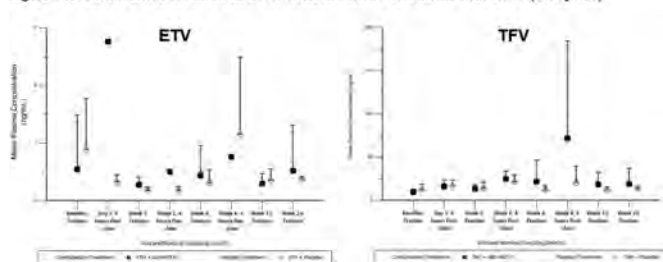


Figure 1b: Plasma Entecavir and Tenofovir Concentrations in Patients with cHBV (Study 201)



Conclusion: The results in Phase 2a studies suggest no clinically significant DDI between VBR and Nrtls. Based on the Phase 1 study, VBR is a weak inhibitor of CYP2C9, but is not an inhibitor of CYP2C19, 2D6, or 2C8, and is not an inhibitor/inducer of CYP3A4 or 2B6. Overall, VBR shows a favorable DDI profile for use in combination treatments including Nrtls and other concomitant medications.

SAT389

Improving the pharmacokinetic profile of the hepatitis B virus core inhibitor ABI-H3733 following oral administration: results from new formulation activities

Michael Shen¹, Zhixin Zong¹, Naqvi Mohammed¹, Katie Zomorodi¹, Luisa M Stamm¹, William Delaney¹, Nicole White¹. ¹Assembly Biosciences, Inc., South San Francisco, United States
Email: mshen@assemblybio.com

Background and aims: ABI-H3733 (3733) is a novel orally administered inhibitor of the hepatitis B virus (HBV) core protein, a viral

structural protein essential for HBV replication. 3733 targets multiple aspects of the viral replication cycle and has the potential to enhance cure rates for patients with chronic HBV infection (cHBV). 3733 is in Phase 1 development and has demonstrated favorable systemic exposure with a half-life of 21 hours using a liquid formulation (LF) in healthy subjects. An initial prototype tablet formulation (T1) only achieved 30% exposure compared to the LF with predicted trough concentrations (C_{min}) approximately 28- and 5.5-fold higher than the protein-adjusted EC_{50} (pa EC_{50}) for pgRNA encapsidation and cccDNA formation, respectively, providing the opportunity to improve formulation for future clinical studies.

Method: The initial LF and T1 formulations of 3733 were tested in dog pharmacokinetic (PK) studies (at a dose of 50 mg) and assessed in healthy subjects at doses ranging from 100 to 500 mg. Due to the low exposure of T1 in both dogs and humans, a new tablet formulation (T2) was designed to improve the absorption and achieve comparable exposure as the LF. The pharmacokinetics of T2 and LF were evaluated in 6 male beagle dogs at 100 mg (3 dogs with T2 and 3 dogs with LF).

Results: In the initial dog PK study, T1 showed 36.7% AUC compared to the LF at 50 mg dose (human equivalent dose of approximately 150 mg). Human PK data were comparable with the dog PK data indicating the dog is a predictive model to evaluate the relative exposure for different formulations. T2 was subsequently tested in the dog PK model at 100 mg dose (predicted human equivalent dose 300 mg) and showed equivalent AUC compared to the LF.

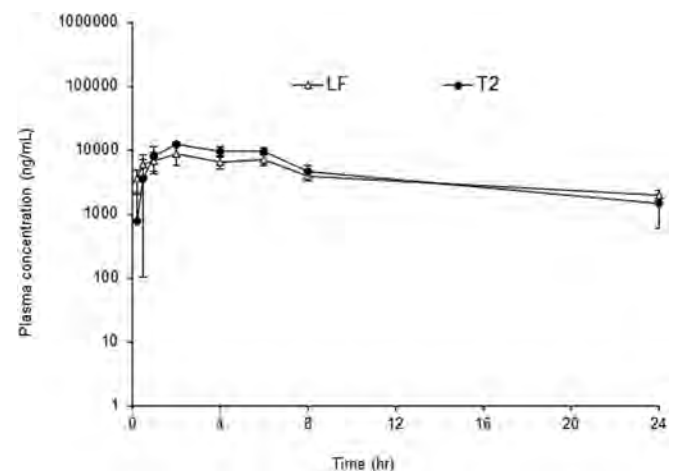


Figure: Mean Plasma Concentration-time Profiles of 3733 After Single Oral Doses of LF and T2 in Male Beagle Dogs

Conclusion: Based on the relative PK data in the dog model, T2 formulation is expected to have similar 3733 exposure as the LF in humans, with predicted C_{min} approximately 150- and 29-fold higher than the pa EC_{50} for pgRNA encapsidation and cccDNA formation, respectively. The improved T2 formulation will be used in an upcoming Phase 1b study conducted with cHBV patients.

SAT390

EDP-514, a novel pangenotypic class II hepatitis B virus core inhibitor: final results of a 28-day phase 1b study in nucleosuppressed chronic hepatitis B patients

Jordan Feld¹, Eric Lawitz², Tuan T Nguyen³, Jacob P Lalezari⁴, Tarek Hassanein⁵, Paul Martin⁶, Steven-Huy B Han⁷, Douglas T Dieterich⁸, Jeanne-Marie Giard⁹, Guy De La Rosa¹⁰, Alaa Ahmad¹⁰, Ed Luo¹⁰, Annie Conery¹⁰, Nathalie Adda¹⁰. ¹Toronto Centre for Liver Disease, University Health Network, Toronto, Canada; ²Texas Liver Institute, San Antonio, Texas, United States; ³Gastroenterology and Hepatology, San Diego, California, United States; ⁴Quest Clinical Research, San Francisco, California, United States; ⁵Southern California Research Center, Coronado, California, United States; ⁶University of Miami, Gastroenterology, Miami, Florida, United States; ⁷University of California, Los Angeles, Los Angeles, California, United States; ⁸Icahn School of Medicine at Mount Sinai, Division of Liver Diseases, New York, New York, United States; ⁹Centre Hospitalier Universitaire de Montréal, Montréal, Québec, Canada; ¹⁰Enanta Pharmaceuticals, Watertown, Massachusetts, United States
Email: gdelarosa@enanta.com

Background and aims: EDP-514, a novel class II HBV core inhibitor, demonstrated nanomolar potency *in vitro*, and a >4-log viral load reduction in an HBV mouse model. Here, we present the safety, pharmacokinetic (PK) and antiviral activity from a phase 1b study of multiple ascending doses (MAD) of EDP-514 in nucleosuppressed chronic hepatitis B (CHB) patients.

Method: This phase 1a/b, randomized, double-blind, placebo-controlled study was conducted in two parts. In Part 1, healthy adult subjects received single or multiple ascending doses of EDP-514 or placebo. In Part 2, noncirrhotic, HBeAg (+) or (-) subjects virologically suppressed on nucleosuppression received EDP-514 or placebo in a 3:1 ratio (24 subjects in 3 cohorts: 200 mg, 400 mg, 800 mg) for 28 days.

Results: The 24 subjects enrolled were mostly male (63%), Asian (67%), HBeAg (-) (88%), treated with tenofovir (92%), with a mean age of 45 years and a mean BMI of 27 kg/m². All TEAEs (n = 20) were mild except for 1 moderate event (200 mg) of abdominal pain that led to drug discontinuation, and 1 severe allergic reaction to aloe cream (800 mg). There were no other grade 3 TEAEs or any SAEs. No clinically significant laboratory abnormalities, liver function tests elevations or clinically relevant ECG or vital signs changes were observed. EDP-514 exhibited PK supportive of once daily (QD) dosing, with trough concentrations of up to ~21-fold above the pEC₅₀. HBV DNA remained undetectable and no virologic failures or breakthroughs were reported through 28 days of treatment. At Day 28, a maximum HBV RNA reduction of 2.3 log in HBeAg (-) and 2.8 log in HBeAg (+) patients was observed in EDP-514 arms compared to 1.2 log in placebo. There were no discernible changes in HBeAg, HBcrAg, and HBsAg.

Conclusion: EDP-514 was safe and well tolerated through 28 days of treatment in CHB nucleosuppressed patients, showed time-linear PK supportive of QD dosing with concentrations of up to ~21-fold above the pEC₅₀, and resulted in a higher log reduction in HBV RNA, up to a maximum of 2.8 log, was observed in HBeAg (+) patients receiving EDP-514.

SAT391

Preclinical activity of small-molecule oral PD-L1 checkpoint inhibitors capable of reinvigorating T cell responses from chronic hepatitis B patients

Emily P. Thi¹, Andrew G. Cole¹, Gavin Heffernan¹, Christina Iott¹, Seyma Ozturk¹, Sharie C Ganchua¹, Dan Nguyen¹, Ingrid Graves¹, Vijay Ahuja¹, Kim Stever¹, Kristi Fan¹, Jorge G. Quintero¹, Steven G. Kultgen¹, Maria Shubina¹, Boya Liu¹, Sunny Tang¹, Troy O. Harasym¹, Angela M Lam¹, Michael J. Sofia¹. ¹Arbutus Biopharma, Warminster, United States
Email: ethi@arbutusbio.com

Background and aims: T cell tolerance is a critical driver in maintaining chronic hepatitis B (CHB) infection. The PD-1/PD-L1

checkpoint axis plays a key role in tolerization and inhibition of this axis by antibody approaches has been associated with loss of hepatitis B surface antigen and seroconversion in CHB patients. Oral small-molecule inhibitors of PD-L1 can enable tuneable on-target engagement with potential for better tissue penetration and improved efficacy. Here we report the preclinical *in vitro* activity of these compounds, as well as *in vivo* efficacy and ability to reinvigorate HBV-specific T cells from CHB patients.

Method: *In vitro* activity was assessed in a Jurkat T cell NFAT reporter assay and PD-L1 reduction was confirmed in CHO-K1 cells expressing human PD-L1 (CHO-K1-hPD-L1) and in peripheral blood mononuclear cells (PBMCs) from healthy donors. T cell activation assays were conducted with PBMCs from healthy donors and CHB patients. Non-specific cytokine release was evaluated in human whole blood. Pharmacokinetic (PK) evaluations were conducted in rodents and non-human primates (NHP). *In vivo* efficacy was evaluated in a MC38 tumor humanized PD-L1 and PD-1 mouse model.

Results: Two optimised PD-L1 inhibitor compounds were evaluated which mediated potent activation of T cells in a NFAT reporter assay (EC₅₀s of 13 and 18 nM). Compound treatment resulted in reduction of PD-L1 expression on the cell surface through a novel internalization mechanism, with EC₅₀s ranging from 1.9–24 nM in CHO-K1-hPD-L1 and primary human myeloid cells. Dose responsive elevations in IL-2 production occurred upon compound treatment of PBMCs stimulated with staphylococcal enterotoxin B. Compound treatment did not elicit non-specific cytokine release in human whole blood, supportive of favourable immune safety. PK profiles showed low systemic clearance in rodents and NHP. In a MC38 tumor model, oral administration of compounds at 10 and 30 mg/kg once daily resulted in profound tumor reduction with T cell activation comparable to anti-PD-L1 antibody. PD-L1 inhibitor treatment of PBMCs from CHB patients *ex vivo* resulted in HBV-specific T cell reinvigoration.

Conclusion: Novel oral small molecule PD-L1 inhibitors able to mediate activation and reinvigoration of HBV-specific T cells from CHB patients were identified. These compounds display *in vivo* anti-tumor efficacy comparable to anti-PD-L1 antibody and possess favourable preclinical profiles for further development.

SAT392

Safety, tolerability, pharmacokinetics (PK), and antiviral activity of the 3rd generation capsid inhibitor AB-836 in healthy subjects (HS) and subjects with chronic hepatitis B (CHB)

Edward J. Gane¹, Alina Jucov², Liudmyla Kolomiichuk³, Timothy Eley⁴, Joanne Brown⁴, Yele King⁴, Elina Medvedeva⁴, Maksym Chernyakhovskyy⁴, Nagraj Mani⁵, Andrew G. Cole⁵, Steven G. Kultgen⁵, Reddy Pamulapati⁵, Emily P. Thi⁵, Troy O. Harasym⁵, Ravi Dugyala⁵, Sachin Chaudhari⁵, Michael J. Sofia⁵, Michael Child⁴, Gaston Picchio⁴, Karen Sims⁴, Man-Fung Yuen⁶. ¹Auckland City Hospital, Auckland, New Zealand; ²Arensia Exploratory Medicine, Chisinau, Moldova; ³Arensia Exploratory Medicine, Kyiv, Ukraine; ⁴Arbutus Biopharma, Clinical Development, Warminster, PA, United States; ⁵Arbutus Biopharma, Research, Warminster, PA, United States; ⁶The University of Hong Kong, Gastroenterology and Hepatology, Hong Kong, Hong Kong
Email: teley@arbutusbio.com

Background and aims: AB-836 is a potent inhibitor of HBV pregenomic RNA encapsidation (a Class II capsid inhibitor). AB-836-001 is an ongoing 3-part study evaluating safety, PK and antiviral activity of AB-836 in HS (Parts 1 and 2) and CHB subjects (Part 3). Preliminary data from Parts 1, 2 and the first 2 cohorts of Part 3 are presented.

Method: In Part 1, HS enrolled into two 8-subject cohorts and were randomized to single doses of AB-836 or placebo (6:2) in 5 alternating dose panels from 10mg-175 mg fasted, and a 6th panel of 125 mg with food. In Part 2, 3 unique cohorts of 10 HS were randomized to 50 mg, 100 mg or 150 mg or placebo (8:2) once daily (QD) for 10 days. In Part 3, 2 ongoing cohorts of 12 HBV DNA+, HBeAg

(+) or (-) CHB subjects will randomize to 50 mg or 100 mg or placebo (10:2) QD for 28 days. Samples are collected for PK in all subjects and antiviral activity in CHB subjects. Safety and tolerability are monitored throughout.

Results: HS (N = 47) were mean age 29 years, mean BMI 24.7 kg/m², all male and 57% white. CHB subjects (N = 10) were mean age 44 years, mean BMI 23.5 kg/m², 60% male, 70% white, 60% HBeAg (-) with mean 5.2 log₁₀ IU/ml HBV DNA at baseline (BL). Preliminary safety data showed AB-836 was well-tolerated in HS. No deaths or serious adverse events (AEs) were observed. One HS (50 mg QD) discontinued on Day 13 due to an AE of agitation. All but 3 AEs were mild (Grade 2 headache, agitation, and bronchitis); only 1 was assessed as related to AB-836 (Grade 1 rash). In ongoing Part 3, there have been no AEs; 1 CHB subject (100 mg) had a transient increase in ALT from BL Grade 1 to Grade 3 at a single visit that resolved with continued dosing. There were no clinically significant abnormalities in clinical laboratory tests in HS and no clinically significant abnormalities in ECGs, vital signs or physical exams in any subject. Single and multiple dose AB-836 PK in HS were dose proportional and support QD dosing with/without food. Mean (SE) HBV DNA log₁₀ change from BL at Day 28 was -2.4 (0.3), -3.1 (0.8) and -0.0 (0.19) at 50 mg, 100 mg, and placebo, respectively. Updated data will be presented.

Conclusion: Single and multiple doses of AB-836 in HS and up to 100 mg QD for 28 days in CHB subjects have been generally safe and well-tolerated. Robust antiviral activity was observed at Day 28 of treatment. These results support further evaluation of AB-836 alone and in combination with other agents, including the GalNAc siRNA AB-729, in CHB subjects.

SAT393

EDP-514, a potent pangenotypic class II hepatitis B virus core inhibitor, demonstrates significant HBV DNA and HBV RNA reductions in a phase 1b study in viremic, chronic hepatitis B patients

Man-Fung Yuen¹, Wan-Long Chuang², Cheng-Yuan Peng³, Rachel Wen-Juei Jeng^{4,5}, Wei-Wen Su⁶, Ting-Tsung Chang^{7,8}, Chi-Yi Chen⁹, Yao-Chun Hsu¹⁰, Guy De Rosa La¹¹, Alaa Ahmad¹¹, Ed Luo¹¹, Annie Conery¹¹, Nathalie Adda¹¹. ¹Queen Mary Hospital, The University of Hong Kong, Department of Medicine, Hong Kong, Hong Kong; ²Kaohsiung Medical University Hospital, Kaohsiung Medical University, Hepatobiliary Division, Department of Internal Medicine, Kaohsiung, Taiwan; ³China Medical University Hospital, China Medical University, Center for Digestive Medicine, Taichung, Taiwan; ⁴Chang Gung Memorial Hospital, Linkou Branch, Department of Gastroenterology and Hepatology, Taiwan; ⁵College of Medicine, Chang Gung University, Taiwan; ⁶Changhua Christian Hospital, Department of Gastroenterology and Hepatology, Taiwan; ⁷National Cheng Kung University Hospital, College of Medicine, National Cheng Kung University, Department of Internal Medicine, Tainan, Taiwan; ⁸National Cheng Kung University, Infectious Disease and Signaling Research Center, Tainan, Taiwan; ⁹Ditmanson Medical Foundation Chia-Yi Christian Hospital, Department of Internal Medicine, Chiayi, Taiwan; ¹⁰E-Da Hospital/I-Shou University, Center for Liver Diseases and School of Medicine, Kaohsiung, Taiwan; ¹¹Enanta Pharmaceuticals, Watertown, Massachusetts, United States
Email: gdelarosa@enanta.com

Background and aims: EDP-514, a novel class II HBV core inhibitor, demonstrated nanomolar anti-HBV potency *in vitro*, and a >4-log viral load reduction in an HBV mouse model. Here, we present the safety, pharmacokinetic (PK) and antiviral activity from a phase 1b study of multiple ascending doses (MAD) of EDP-514 in viremic, chronic hepatitis B (CHB) patients.

Method: A phase 1b, randomized, double-blind, placebo-controlled study was conducted in noncirrhotic, viremic, HBeAg (+) or (-) CHB patients not currently on treatment. Patients received multiple doses

of EDP-514 or matching placebo in a 3:1 ratio (24 planned patients in 3 cohorts: 200 mg, 400 mg, 800 mg QD) for 28 days.

Results: The 25 enrolled subjects were all Asian, mostly male (60%), HBeAg (-) (84%), with a mean age of 46 years, mean HBV DNA of 5.12 log IU/ml, and mean HBV RNA of 3.49 log U/ml at baseline. Overall, 9 subjects reported 22 treatment emergent adverse events (TEAEs), and all of which were mild except for 4 moderate events (n = 2, placebo [GI disorders and urinary tract infection] and n = 2, 200 mg [anaemia and aPTT prolonged], both unlikely related to study drug). No grade 3 TEAEs or SAEs, Grade 3/4 clinical laboratory abnormalities, liver function tests elevations or clinically relevant ECG or vital signs changes were observed in the EDP-514 groups. EDP-514 exhibited trough concentrations of up to ~24-fold above pEC50. At Day 28, mean HBV DNA reductions of 2.9, 3.3, 3.5 and 0.2 log IU/ml, and mean HBV RNA reductions of 2.9, 2.4, 2.0 and 0.02 log U/ml were observed, in the 200 mg, 400 mg, 800 mg and placebo groups, respectively. HBV RNA was undetectable on Day 28 in 11 subjects treated with EDP-514 as compared to none in placebo. HBV DNA was below the LLOQ in 7 subjects treated with EDP-514 as compared to none in placebo. EDP-514 led to a maximum HBV DNA reduction of 4.5 log vs. 0.5 log in placebo, and a maximum HBV RNA reduction of 4.8 log vs. 1.9 log in placebo. There were no discernible changes in HBeAg, HBcAg, and HBsAg levels.

Conclusion: EDP-514 was safe and well tolerated through 28 days of treatment in viremic CHB patients, with a linear PK profile supporting QD dosing and trough concentrations up to ~24-fold above the pEC50. Profound antiviral activity was observed at Day 28 with mean HBV DNA reductions of up to 3.5 log, and mean HBV RNA reductions of up to 2.9 log with EDP-514 treatment. These results support further evaluation of EDP-514 in CHB patients.

SAT394

Increased HBsAg reduction and relapse outcomes in HBeAg negative patients with chronic hepatitis B after nucleos (t)ide analogue withdrawal: 4.5 year follow-up of the Toronto STOP Study

Arif Sarowar¹, Seng Liem^{1,2}, Scott K Fung¹, David Wong¹, Jordan Feld^{1,3}, Colina Yim¹, Seham Noureldin¹, Jenny Chen¹, Bettina Hansen^{1,4}, Harry Janssen¹. ¹Toronto General Hospital, Toronto Centre for Liver Disease, Toronto, Canada; ²Erasmus University Medical Center Rotterdam, Department of Gastroenterology and Hepatology, Canada; ³McLaughlin-Rotman Centre for Global Health, Canada; ⁴University of Toronto, Institute of Health Policy, Management and Evaluation, Canada
Email: arif.sarowar@uhnresearch.ca

Background and aims: Studies have found benefits in nucleos (t)ide analogues (NA) discontinuation in chronic hepatitis B (CHB) patients, but currently heterogeneous outcomes are observed with little understanding of the long-term implications of stopping therapy. This study prospectively evaluates clinical outcome comparisons in HBeAg negative patients who stop or continue NA, and those with eventual retreatment.

Method: 67 HBeAg negative patients in a randomized control study were allocated to stopping (n = 45) or continuing (n = 22) NA therapy and were evaluated over 4.5 years. Patients were retreated based on standardized protocol if they had HBV DNA >20,000 IU/ml, HBeAg seroreversion, or HBV DNA >2000 with ALT >5xULN. Virological relapse (HBV DNA >2000 IU/ml), clinical relapse (HBV DNA >2000 IU/ml and ALT >1.5xULN), HBsAg decline >0.5 IU/ml, and HBsAg loss were compared.

Results: Mean duration of long-term follow-up (LTFU) was 227 weeks. 23/45 (51%) stop patients were retreated, with median time to retreatment of 36 weeks. HBsAg loss was achieved by 2/45 (4%) patients who stopped and 1/21 (5%) continue patients at LTFU. Virological relapse and clinical relapse in the stop group was observed in 41 (91%) patients and 32 (71%) patients, respectively. HBsAg decline >0.5 IU/ml at LTFU was achieved by 12/22 (55%) not

POSTER PRESENTATIONS

retreated stop patients, 10/23 (43%) retreated stop patients, and 3/22 (14%) continue patients. Incidence of HBsAg decline >0.5 IU/ml was higher in the stop group than those in the continue group ($p < 0.05$). Higher mean HBsAg decline was also observed in the stop group (-0.67 IU/ml) compared to continue group (-0.15 IU/ml, $p < 0.05$) by end of follow-up. No patients experienced adverse outcomes, liver decompensation, or death.

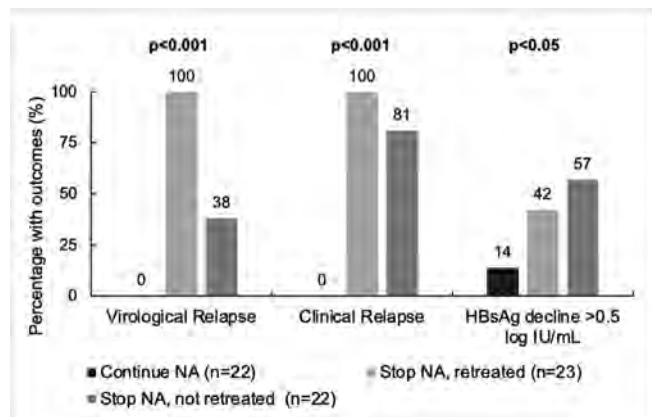


Figure: Clinical Outcomes of STOP Study patients (n = 67)

Conclusion: CHB patients that stop NA have high prevalence of virological relapse and clinical relapse. However, despite a limited HBsAg loss, those that stop therapy exhibited higher HBsAg reduction compared to continued NA treatment.

SAT395

Pharmacodynamics of durable HBsAg suppression by AB-729 short interfering RNA correlates with pharmacokinetics of RNA-induced silencing complex (RISC) loading within liver

Emily P. Thi¹, Maria Shubina¹, Ingrid Graves¹, Angela M Lam¹, Michael J. Sofia¹. ¹Arbutus Biopharma, Warminster, United States
Email: ethi@arbutusbio.com

Background and aims: AB-729 is an N-Acetylgalactosamine (GalNAc)-conjugated short interfering RNA (siRNA), currently in Phase 2a clinical development in combination with other agents for treatment of CHB. AB-729 blocks all HBV RNA transcripts, resulting in durable suppression of viral replication and antigen production, including circulating HBV DNA and the hepatitis B surface antigen (HBsAg). This antiviral effect is mediated through association of AB-729 with the RNA-induced silencing complex (RISC), the RNA:protein complex responsible for mediating cleavage of HBV RNA. Here we investigate the mechanisms underlying the extent and duration of AB-729 activity through assessment of siRNA persistence in liver using an adenovirus-associated HBV (AAV-HBV) mouse model.

Method: Longitudinal serum, plasma and liver samples from AAV-HBV mice receiving a single dose of either a non-HBV targeting control GalNAc siRNA or a surrogate GalNAc siRNA containing the AB-729 siRNA trigger (HBV-siRNA) (1 or 3 mg/kg, n = 8) were assessed for HBsAg and total and RISC-loaded siRNA by chemiluminescent immunoassay, Ago2 immunoprecipitation and stem-loop quantitative reverse-transcription polymerase chain reaction.

Results: A dose responsive decline in serum HBsAg occurred following single doses of 1 and 3 mg/kg of HBV-siRNA, with mean maximum declines of $0.9 \log_{10}$ and $1.9 \log_{10}$ at Day 14, respectively. The kinetics of HBsAg decline did not correlate with that of total intrahepatic concentrations of HBV-siRNA, which peaked at 4-hour post dose and rapidly declined over time. Instead, maximal HBsAg reduction coincided with an increase in the number of RISC-loaded complexes. A decline in the number of RISC-loaded complexes was observed following day 14, mirroring a rebound in HBsAg. HBsAg subsequently returned to baseline 112 days after single doses of HBV-

siRNA, which correlated with the detection of only trace amounts of RISC-loaded complex.

Conclusion: HBsAg suppression mediated by AB-729 in CHB patients is characterized by durable responses which persist up to 48 weeks post-dosing. The mechanisms driving this long duration of activity have not yet been assessed. Our preclinical data reveals that HBsAg reduction coincides with the pharmacokinetics of siRNA RISC-loading. These data suggest that the direct-acting antiviral activity of AB-729, mediated by RNA interference activity, may be a key driver of the prolonged HBsAg suppression observed in CHB patients administered AB-729.

SAT396

Inhibition of hepatitis B surface antigen by RNA interference therapeutic AB-729 is associated with increased cytokine signatures in HBV DNA+ chronic hepatitis B patients

Sharie C Ganchua¹, Bhavna Paratala¹, Christina Iott¹, Man-Fung Yuen², Edward J Gane³, Timothy Eley¹, Karen Sims¹, Kevin Gray¹, Deana Antoniello¹, Angela M Lam¹, Michael J. Sofia¹, Gaston Picchio¹, Emily P. Thi¹. ¹Arbutus Biopharma, Warminster, United States; ²Queen Mary Hospital, Hong Kong; ³Auckland Clinical Studies, New Zealand
Email: ethi@arbutusbio.com

Background and aims: Therapeutic strategies aimed at reducing antigenemia, particularly hepatitis B surface antigen (HBsAg), may result in HBV-specific immune reawakening in chronic hepatitis B (CHB). AB-729 is a single trigger N-Acetylgalactosamine (GalNAc)-conjugated siRNA targeting all HBV transcripts, currently in clinical development in combination with other agents for CHB treatment. Here we report immunological assessment of cytokines and other soluble immune biomarkers in CHB subjects not currently on nucleos(t)ide analog (NA) therapy (HBV DNA+) and compare these profiles to NA-suppressed (HBV DNA-) CHB subjects receiving a single dose of AB-729.

Method: Longitudinal plasma samples from subjects receiving a single dose of AB-729 (90 mg, n = 5 HBV DNA+, n = 6 HBV DNA-) were assessed for cytokines and other soluble immune biomarkers using multiplex Luminex assays.

Results: Following a single dose of AB-729, transient elevations of 2 to 38-fold over pre-dose baseline levels in at least one of IFN γ , CXCL1, IP-10, sBTLA, sLAG3, sTLR2, sGITR, sPD-1, sCTLA4, sPD-L1, sICOS, sCD80, and sCD86 were observed in 5/5 HBV DNA+ subjects. In HBV DNA- subjects, transient elevations of 2 to 7-fold over pre-dose baseline were observed in at least one of IFN γ , IL-17a, CXCL9, CXCL13 and CD163 (3/6 subjects). In HBV DNA+ subjects, transient increases in IFN γ (4/5 subjects) and CXCL1 (3/5 subjects) were associated with transient ALT elevations in the period up to 12 weeks post-dose. In contrast, in HBV DNA- subjects ALT elevation was accompanied by IFN γ increase in only 1/6 subjects. All ALT elevations were mild (Grade 1) and no liver safety markers were considered adverse by the investigators.

Conclusion: We believe this is the first data comparing immunological responses of HBV DNA+ and DNA- CHB subjects undergoing HBsAg reduction following GalNAc-siRNA treatment. Our findings suggest that following AB-729 dosing, a greater breadth of cytokine and soluble immune biomarker responses with IFN γ and T cell activation signatures are observed in HBV DNA+ subjects compared to NA-suppressed CHB patients. Transient elevations in checkpoint-related markers in HBV DNA+ patients were also observed, which were accompanied by mild ALT elevations. These results suggest that HBV DNA+ CHB patients are more immunologically responsive following AB-729 dosing. Assessment of responses following AB-729 repeat dosing in HBV DNA+ subjects with concomitant initiation of NA therapy is ongoing.

SAT397

Reduction of hepatitis B surface antigen mediated by RNA interference therapeutic AB-729 in chronic hepatitis B patients is associated with T cell activation and a decline in exhausted CD8 T cells

Sharie C Ganchua¹, Bhavna Paratala¹, Christina Iott¹, Edward J Gane², Man-Fung Yuen³, Timothy Eley¹, Karen Sims¹, Kevin Gray¹, Deana Antonello¹, Angela M Lam¹, Michael J. Sofia¹, Gaston Picchio¹, Emily P. Thi¹. ¹Arbutus Biopharma, Warminster, United States; ²Auckland Clinical Studies, New Zealand; ³Queen Mary Hospital, Hong Kong
Email: ethi@arbutusbio.com

Background and aims: AB-729 is a GalNAc-conjugated RNA interference (RNAi) therapeutic, currently in Phase 2 clinical development in combination with other agents for the treatment of chronic hepatitis B (CHB). Reduction of antigenemia in CHB, particularly hepatitis B surface antigen (HBsAg), may result in HBV-specific immune reawakening. Here we report immunological assessments in CHB subjects receiving repeat doses of AB-729 after 48 weeks (wks) of treatment and 12 wks of follow-up.

Method: Longitudinal plasma and peripheral blood mononuclear cell (PBMC) samples from virologically suppressed subjects undergoing repeat dosing of AB-729 60 mg every 4 weeks (Q4W, n = 5 for PBMC; n = 6 for plasma assays) or every 8 weeks (Q8W, n = 7 for plasma assays; n = 2 for PBMC) were assessed using Luminex, IFN gamma (IFNγ) T cell fluorospot, immunophenotyping by flow cytometry and thymidine-based T-cell proliferation assays.

Results: By EOT, 5/5 subjects receiving AB-729 Q4W exhibited increases in IFNγ-producing HBV-specific T cells. 3/5 subjects had increases in IFNγ-HBV-specific T cells between wks 16–28 which coincided with a plateau in HBsAg response, mild to moderate transient serum alanine aminotransferase (ALT) elevations (Grade 1–2), and was preceded by T cell proliferation. 2/5 subjects experienced pronounced increases in IFNγ-HBV-specific T cells at EOT or at 12 wks follow-up. HBV-specific T cell IFNγ production was also observed in subjects receiving AB-729 Q8W dosing (2/2). A decline in exhausted CD8 T cells was observed beginning at wk 28 and was present at EOT and at 8–12 wks of follow-up (AB-729 Q4W cohort; 4/6 subjects, Figure). This decline in exhausted CD8 T cells coincided with a plateau in HBsAg response. No significant increases in 41 plasma cytokine/chemokine levels were observed. Mild increases in sBTLA, sCD86, sCTLA-4, SPD-1 were noted in subjects receiving AB-729 Q4W and Q8W (sBTLA, sGITR, sCTLA4). No changes in adverse events related to liver safety markers were noted in either cohort.

Conclusion: Our findings suggest that HBsAg reductions, as a result of treatment with repeat doses of AB-729 every 4 or 8 weeks, is accompanied by HBV-specific T cell activation and proliferation with mild to moderate ALT elevations. A decline in exhausted CD8 T cells at the end of treatment and at 8–12 weeks of follow-up suggest that HBV-specific T cell immune restoration (reawakening) may be durable.

SAT398

Characterizing of hepatitis B virus serum RNA kinetics during TDF plus pegylated interferon alfa-2a with and without nucleic acid polymers

Leeor Hershkovich¹, Louis Shekhtman¹, Michel Bazinet², Mark Anderson³, Mary Kuhns³, Gavin Cloherty³, Scott Cotler¹, Andrew Vaillant², Harel Dahari¹. ¹Program for Experimental and Theoretical Modeling, Division of Hepatology, Department of Medicine, Stritch School of Medicine, Loyola University Chicago, Maywood, United States; ²Replicor Inc., Montreal, Quebec, Canada; ³Abbott Diagnostics, Abbott Park, IL, United States
Email: harel.dahari@gmail.com

Background and aims: Serum HBV RNA (RNA), and HBV core-related antigen (HBcrAg) are markers of cccDNA activity. Little is known about the serum RNA response during tenofovir disoproxil fumarate (TDF), and pegylated interferon alpha-2a (pegIFN) with and without nucleic acid polymer (NAP) treatment. Here we aim to characterize RNA kinetics under TDF and pegIFN with and without NAP combination therapies.

Method: Forty participants with chronic HBV in the REP 401 study (Gastro 2020; 158:2180–94) received 48 weeks of triple combination therapy with NAPs, pegIFN, and TDF. In the experimental group (n = 20), triple combination therapy (TDF + pegIFN + NAPs) followed 24 weeks of TDF. In the control group (n = 20), triple combination therapy followed 24 weeks of TDF monotherapy and 24 weeks of dual therapy (TDF + pegIFN). Abbott RUO assay for RNA (LLOQ 1.65 log₁₀ U/ml) was used every 4 weeks. The threshold for kinetic patterns was defined as a 3-fold change.

Results: Under dual therapy 10 (50%) participants experienced had RNA increase which was followed by a new elevated plateau (n = 6) or by a decline (transient increase, n = 4). All 6 participants establishing a new elevated RNA plateau level experienced a subsequent monophasic decline in RNA following the introduction of NAPs in the control group (Table 1). Under triple therapy in the experimental group 11 (55%) participants had a transient increase. The timing of RNA flares was significantly (p < 0.02) correlated with ALT flares.

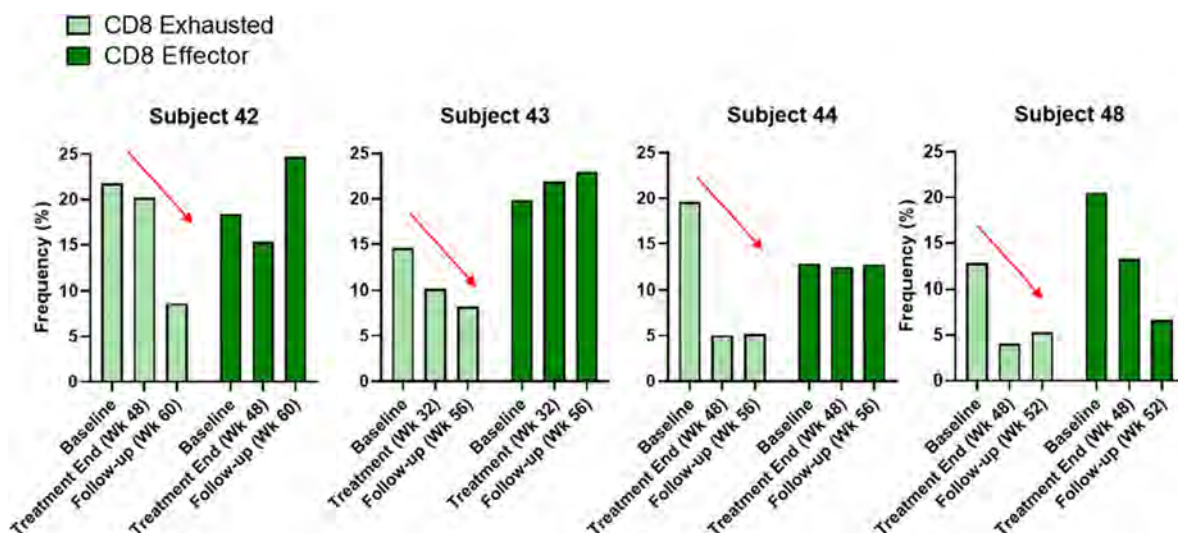


Figure: (abstract: SAT397)

Table 1: RNA kinetics during TDF + pegIFN + NAPs in the REP 401 study

Treatment phase, No. of patients (N)	Mean Pre-treatment RNA (log ₁₀ IU/mL)	Kinetic Patterns				EOT median (IQR) Δ log RNA
		Remain unchanged, N [mean log RNA]	Transient increase, N [mean peak Δ* log RNA] (time of peak [w])	Increase / new elevated plateau, N [mean peak Δ* log RNA] (time of peak [w])	Immediate Decline, N [mean slope (log/wk)]	
pegIFN + TDF (20)*	1.6±0.7	6 [2.3±0.4]	4 [0.0±0.21] (5.0±1.7)	6 [1.9±0.61] (5.3±3.0)	4 [0.17±0.06]	-0.3 (1.7)
pegIFN + TDF + NAP Experimental (20)	1.9±0.4	4 [2.2±0.7]	11 [1.2±0.51] (4.4±3.1)	0	5 [0.26±0.16]	-0.7 (0.6)
pegIFN + TDF + NAP Control † (20)	1.6±0.1	6 [1.5±0.4]	4 [0.55±0.08] (5.0±1.7)	0	10 [0.22±0.14]	-0.6 (0.9)

*Peak Δ log RNA is relative to baseline RNA.

†Control group are five same participants who were treated with pegIFN+TDF.

‡All 6 participants with plateau under pegIFN+TDF went on to have decline under pegIFN+TDF+NAPs.

§All 5 participants with transient increases in pegIFN+TDF remained unchanged with transition to pegIFN+TDF+NAPs.

Conclusion: TDF + pegIFN induces transient increases in serum HBV RNA which either self-resolve or resolve in the presence of NAPs. The correlation of serum HBV RNA elevations with ALT flares suggests release of HBV RNA containing virus subsequent to cytolytic clearance of infected hepatocytes. The mechanism by which pegIFN or NAPs lead to an RNA increase may not indicate an increase in cccDNA activity and requires further research.

SAT399

Early antiviral efficacy of tenofovir alafenamide fumarate in the initial treatment of chronic hepatitis B patients with normal ALT

Huichun Xing¹, Xin Chi¹, Xiu Sun¹, Danying Cheng¹, Shunai Liu².
¹Beijing Ditan Hospital, Capital Medical University, Center of Liver Diseases Division 3, Beijing, China; ²Beijing Ditan Hospital, Capital Medical University, Beijing Key Laboratory of Emerging Infectious Diseases, Institute of infectious disease, Beijing, China
 Email: hchxing@sohu.com

Background and aims: Patients were screened according to antiviral treatment indications recommended by China Guidelines for the prevention and treatment of chronic hepatitis B, some patients (over 30 years old or have a family history of liver cancer) will have ALT in normal range (An upper limit of normal for ALT is 50 U/L for males and 40 U/L for females). This study was designed to investigate the therapeutic effect of tenofovir alafenamide fumarate (TAF) on chronic hepatitis B (CHB) patients with normal alanine transaminase (ALT).

Method: A total of 79 treat-naïve CHB patients treated with TAF antiviral therapy alone in Beijing Ditan Hospital, Capital Medical University from November 2018 to May 2021 were reviewed, including 39 patients in normal ALT group and 40 patients in abnormal ALT group. The clinical data of patients at baseline and 24 weeks after treatment were collected, and the changes of HBV DNA, serum hepatitis B virus e antigen (HBeAg) and hepatitis B virus surface antigen (HBsAg) were compared between the two groups before and after treatment.

Results: After 24 weeks of treatment, in the normal ALT group, HBV DNA decreased significantly from (5.0 ± 2.1) log₁₀ IU/ml to (2.0 ± 1.5) log₁₀ IU/ml (p = 0.000), in abnormal ALT group, HBV DNA decreased from (6.7 ± 1.9) log₁₀ IU/ml to (1.8 ± 1.0) log₁₀ IU/ml (p = 0.000). After 24 weeks of treatment, the rate of complete virological response (CVR) (HBV DNA <20 IU/ml) was 64.1% (25/39) in the normal ALT group, and 50.0% (20/40) in the abnormal ALT group. There was no significant difference between the two groups (p = 0.206). The CVR rates of normal ALT group and abnormal ALT group were 100% at baseline of low viral load (HBV DNA <10³). At 24 weeks, the proportion of HBV DNA target not detected (TND) in the normal ALT group was 43.6% (17/39), significantly higher than that in the abnormal ALT group [12.5% (5/40)] (p = 0.003). Subgroup analysis was performed for the normal ALT group according to the reference upper limit of normal (ULN) recommended by AASLD 2016 (male ≤30 U/L, female ≤19 U/L). In normal ALT group (AASLD 2016), the CVR is 92.3% (12/13), in 30 U/L < ALT < 50 U/L (male) and 19 U/L < ALT < 40 U/L (female) group, the CVR at 24 w is 50% (13/26), respectively, the difference was statistically significant (p = 0.013).

Table: Baseline Demographics and Disease Characteristics

Variables	ALT Normal n = 39	ALT Abnormal n = 40	p values
Mean age, y (SD)	41 (8.4)	38 (8.7)	0.150
Men, n (%)	20 (51)	24 (60)	0.435
Mean ALT, U/L (SD)	30.4 (11.4)	194.3 (196.5)	0.000
Mean AST, U/L (SD)	24.7 (5.9)	101.5 (88.1)	0.000
Mean HBV DNA, log ₁₀ IU/ml (SD)	5.0 (2.1)	6.7 (1.9)	0.001
Mean HBeAg, log ₁₀ IU/ml (SD)	3.6 (1.2)	3.8 (0.6)	0.910
Mean HBeAg, log ₁₀ IU/ml (SD)	1.0 (1.7)	1.5 (1.6)	0.354
HBeAg positive, n (%)	14 (36)	22 (55)	0.088

Conclusion: Tenofovir alafenamide fumarate can obtain better antiviral efficacy in CHB patients with normal ALT, and the efficacy is not lower than that in CHB patients with abnormal ALT.

SAT400

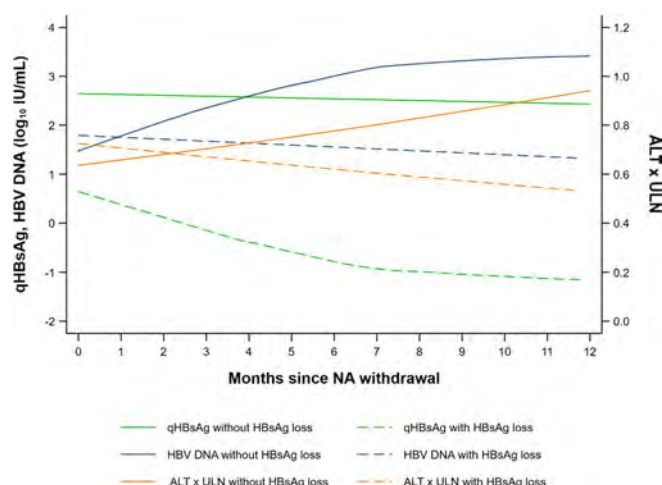
Viral and ALT kinetics after nucleos (t)ide analogue withdrawal among patients who remain off-therapy: results from a global, multi-ethnic cohort of chronic hepatitis B patients (RETRACT-B study)

Grishma Hirode^{1,2,3}, Bettina Hansen^{1,3}, Chien-Hung Chen⁴, Tung-Hung Su⁵, Margarita Papatheodoridi⁶, Sabela Lens⁷, Stijn Van Hees⁸, Sylvia Brakenhoff⁹, Hannah S.J. Choi¹, Rong-Nan Chien¹⁰, Wai-Kay Seto¹¹, Grace Wong¹², Jordan Feld^{1,2,3}, Henry LY Chan¹², Man-Fung Yuen¹¹, Milan Sonneveld⁹, Thomas Vanwolleghem⁸, Xavier Forns⁷, George Papatheodoridis⁶, Jia-Horng Kao⁵, Yao-Chun Hsu¹³, Markus Cornberg¹⁴, Rachel Wen-Juei Jeng¹⁰, Harry Janssen^{1,2,3}. ¹Toronto General Hospital, University Health Network, Toronto Centre for Liver Disease, Toronto, Canada; ²University of Toronto, Institute of Medical Science, Toronto, Canada; ³The Toronto Viral Hepatitis Care Network (VIRCAN), Toronto, Canada; ⁴Kaohsiung Chang Gung Memorial Hospital, Taiwan; ⁵National Taiwan University Hospital, Taiwan; ⁶Medical School of National and Kapodistrian University of Athens, Greece; ⁷Hospital Clinic Barcelona, University of Barcelona, IDIBAPS and CIBERED, Barcelona, Spain; ⁸Antwerp University Hospital, Department of Gastroenterology and Hepatology, Antwerp, Belgium; ⁹Erasmus MC University Medical Center, Department of Gastroenterology and Hepatology, Rotterdam, Netherlands; ¹⁰Chang Gung Memorial Hospital Linkou Medical Center, Chang Gung University, Department of Gastroenterology and Hepatology, Linkou, Taiwan; ¹¹The University of Hong Kong, Hong Kong, Department of Medicine and State Key Laboratory of Liver Research, Hong Kong; ¹²The Chinese University of Hong Kong, Hong Kong; ¹³E-Da Hospital/I-Shou University, Kaohsiung, Taiwan; ¹⁴Centre for Individualized Infection Medicine (CiIM), Hannover Medical School, Department of Gastroenterology, Hepatology and Endocrinology, Hannover, Germany
 Email: grishma.hirode@gmail.com

Background and aims: Recent studies have analyzed the best candidates for nucleos (t)ide analogue (NA) cessation with respect to HBsAg loss. However, whether patients remain off-therapy is often dependent on local reimbursement policies. Patients who remain off-therapy, with/without HBsAg loss, have not been well characterized. We aim to describe this group and analyze early viral and biochemical kinetics after NA cessation.

Method: Virally suppressed, non-cirrhotic CHB patients who were HBeAg negative at NA cessation were included. Patients with coinfection, prior interferon therapy, or prior HCC diagnoses were excluded. We used mixed-effects regression to analyze HBsAg, HBV DNA, and ALT kinetics among patients who remained off-therapy at the end of 1 yr after NA cessation; only patients with follow-up ≥1 yr were included.

Results: Among 804 patients (mean age 52 ± 12 yrs, 71% male, 84% pre-therapy HBeAg negative), 29 (3.6%) achieved HBsAg loss and 775 (96%) remained off-therapy without HBsAg loss at 1 yr. Patients with HBsAg loss (vs without) had a higher proportion of Caucasians (vs Asians) (31% vs 8.3%, $p < .001$), tenofovir-treated patients prior to cessation (vs entecavir-treated) (50% vs 32%, $p = .04$), and lower median HBsAg at end of therapy ($0.4 [-0.6-1.6]$ vs $2.7 [2.2-3.1]$ \log_{10} IU/ml, $p < .001$). Median ALT at end of therapy among the whole group was $0.6 \times (0.4-0.8)$ ULN. Patients with HBsAg loss showed a rapid decline in mean HBsAg in the first 6 mos while those without HBsAg loss showed a modest decrease. There was a decreasing trend in mean HBV DNA among patients with HBsAg loss while HBV DNA increased steadily for the first 6 mos among those without HBsAg loss; however, it stabilized thereafter. Patients with HBsAg loss (vs without) had a lower proportion of virological relapses (HBV DNA >2000 IU/ml: 21% vs 59%; $p < .001$) in the first year. Patients with HBsAg loss experienced a higher proportion of flares (ALT $>5 \times$ ULN: 21% vs 10%, $p = .07$; ALT $>10 \times$ ULN: 10% vs 4.5%, $p = .15$) in the first year but mean ALT decreased over time for that group and increased for those without HBsAg loss. Mean ALT remained normal in both groups. Among those without HBsAg loss, 4 had HBeAg reversions, and 1 decompensated in the first year.



Conclusion: Early kinetics were good indicators of outcomes following NA cessation among patients who remain off-therapy. Patients without HBsAg loss showed increases in HBV DNA and ALT with worse clinical outcomes and only nominal decreases in HBsAg compared to those who achieved HBsAg loss.

SAT401

Discovery of oral PDL1 small molecule inhibitors specifically designed for the treatment of chronic hepatitis B

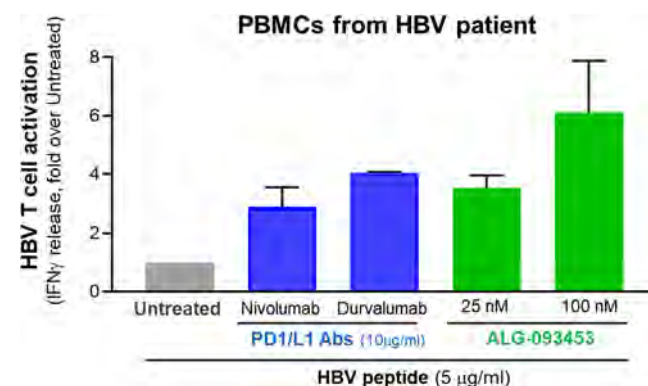
Tongfei Wu¹, Sarah Stevens², Cheng Liu², Kristina Rekstyte-Matiene³, Elke Behaeghel³, Sucheta Mukherjee², Sandra Chang², Ruchika Jaisinghani², Antitsa Stoycheva², Andreas Jekle², Qingling Zhang², Kusum Gupta², Jerome Deval², Julian Symons², Lawrence Blatt², Leonid Beigelman², Pierre Raboisson¹, Francois Gonzalvez¹. ¹Aligos Belgium BVBA, Leuven, Belgium, Belgium; ²Aligos Therapeutics, Inc., South San Francisco, CA, Belgium; ³Novalix, Leuven, Belgium
Email: fgonzalvez@aligos.com

Background and aims: Chronic hepatitis B (CHB) is characterized by high viral replication and exhaustion of virus-specific T cells. In CHB patients, upregulation of PD1 on HBV-specific T cells and PDL1 on liver cells cause T-cell exhaustion and persistent viral infection. Therefore, inhibiting the PD1/PDL1 pathway has recently emerged as an attractive therapeutic strategy to restore a virus-specific T cell response and reverse immune tolerance. Seven PD1/PDL1 antibodies

are currently approved as cancer therapies and nivolumab (anti-PD1) has demonstrated some clinical efficacy in CHB patients. However, the systemic immune-related adverse effects associated with antibodies limit their therapeutic window and therefore, there is a need to develop better tolerated PD1/PDL1 inhibitors for CHB patients. Here, we rationally designed oral PDL1 small molecule inhibitors to localize T cell activation to the liver and thereby mitigate systemic toxicity in CHB patients.

Method: Biochemical PD1/PDL1 interaction was assessed by AlphaLISA®. Cellular activity was measured using a co-culture reporter assay in which NFAT activity of Jurkat T cells is constitutively inhibited by the engagement of PD1 by PDL1-expressing CHO cells. In vivo pharmacokinetic analyses and efficacy were assessed in humanized-PDL1 MC38 subcutaneous xenografts and in the AAV-HBV mouse model. HBV-specific T cell activation assays were performed in PBMCs from an HBV-infected patient and assessed by measuring IFN γ release.

Results: Using structure-based and rationale design, we identified a series of oral PDL1 small molecule inhibitors. In biochemical assays, our lead molecules inhibited PD1/PDL1 interaction with an IC₅₀ value of 16 pM. In PD-1/PDL1 blockade cellular assays, these compounds increased TCR signaling with an EC₅₀ value of 1.5 pM, a similar potency to nivolumab. In mice, our lead molecules displayed good oral bioavailability and high liver/plasma ratios. When dosed orally in MC38 tumor-bearing mice, our lead molecules were well tolerated. Importantly, these compounds showed similar in vivo efficacy to durvalumab in this tumor model that relies on systemic exposure. To test whether our compounds can release exhaustion of HBV-specific T cells, we stimulated PBMCs from an HBV-infected patient with HBV peptide antigens in presence of our lead compounds (Figure). ALG-093453 activated HBV-specific T cells in a dose dependent manner to similar or higher extent as nivolumab and durvalumab.



Conclusion: We designed oral PDL1 small molecule inhibitors specifically for CHB. Our lead molecules show similar in vitro potency and in vivo efficacy in systemic models to FDA-approved PD1/PDL1 antibodies, together with high liver/plasma exposure ratios. Our PDL1 small molecule inhibitors have the potential to activate HBV-specific T cells in the liver, while decreasing bystander T cell activation in the periphery.

SAT402

Incorporation of novel ASO chemistries significantly improves the potency and durability of HBV ASOs in the AAV-HBV mouse model

Jin Hong¹, Laxman Eltepu¹, Saul Martinez Montero¹, Hua Tan¹, Kang Hyunsoon¹, Vivek Rajwanshi¹, John Cortez¹, Dawei Cai¹, Cheng Liu¹, Elen Rosler¹, David Smith¹, Julian Symons¹, Lawrence Blatt¹, Leonid Beigelman¹. ¹Aligos Therapeutics
Email: jhong@aligos.com

Background and aims: We applied proprietary chemistries to develop the best-in-class HBV ASOs, ALG-020572 and ALG-020576, with unique N-Acetylgalactosamine 4 (GalNac4) conjugation. These

POSTER PRESENTATIONS

ASOs target the open reading frames of the small HBsAg and the HBx protein respectively. Both ASOs contain next generation spiropyrrolyl Bridged Nucleic Acid (scp BNA) and nucleobase modified monomers that reduced hepatotoxicity while maintaining efficacy in AAV-HBV mouse model. In this study, we further explored additional BNAs such as guanidine-bridged nucleic acid (GuNA) and other proprietary BNAs in the sequences of ALG-020572 and ALG-020576. We demonstrated that further improvement of *in vitro* and *in vivo* activities could be achieved.

Method: ASOs with LNA and 3rd gen BNA chemistries were synthesized on MerMade 12 and MerMade 48 synthesizers. *In vitro* screening of ASOs was carried out in HepG2.2.15 cells or HBV infected primary human hepatocytes (PHH) using an HBsAg release assay. The AAV-HBV mouse model was used to test efficacy and hepatotoxicity of GalNAc-ASOs by analyzing HBsAg and ALT in mouse plasma.

Results: ALG-021682 and ALG-021639 are GalNAc 4 conjugated ASOs targeting the same site as ALG-020572. ALG-021682 contains GuNA and ALG-021639 contains a novel 3rd gen BNA. Unconjugated ALG-021682 showed a 5-fold lower EC₅₀ than unconjugated ALG-020572 in HepG2.2.15 assay. In HBV infected PHH, the unconjugated ALG-021639 was 5-fold more potent than unconjugated ALG-020572. When tested in the AAV-HBV mouse model, both ALG-021682 and ALG-021639 exhibited a 2-fold lower HBsAg nadir than that of the ALG-020572 analog when dosed at a single dose of 5 mg/kg subcutaneously. None of the ASOs demonstrated ALT elevations. Finally, ALG-021618 is an ALG-020576 derived ASO with a novel structure. It was inactive *in vitro* due to the inability to be metabolically processed by HepG2.2.15 cells. However, in the AAV-HBV mouse model with 3 × 10 mg/kg repeat dosing on days 0, 3 and 7, ALG-021618 achieved a HBsAg nadir of -1.8 log₁₀ IU/ml vs. -1.2 log₁₀ IU/ml for ALG-020576. By day 60, ALG-020576 dosed animals reverted to baseline HBsAg levels but ALG-021618 still suppressed HBsAg by 1 log₁₀ IU/ml.

Conclusion: GuNA and other novel BNAs improved the *in vitro* and *in vivo* activities of our lead ASO ALG-020572. Novel modifications of ALG-020576 significantly improved the *in vivo* depth and durability of HBsAg knockdown. Further investigations combining these chemistries are ongoing.

SAT403

Induction of pre-s antibodies in HBeAg negative chronic hepatitis B patients by therapeutic vaccination with the pre-s based vaccine VVX001-interim analysis

Petra Munda¹, Ina Tulaeva², Rudolf E. Stauber³, Pia Gattringer², Michael Trauner¹, Helmut Brunar^{4,4}, Rudolf Valenta², Peter Ferenci².

¹Medical University of Vienna, Internal Medicine 3, Gastroenterology and Hepatology, Austria; ²Medical University of Vienna, Wien, Austria;

³Medical University of Graz, Internal Medicine 1, Graz, Austria; ⁴Vivaraxx AG, Austria

Email: peter.ferenci@meduniwien.ac.at

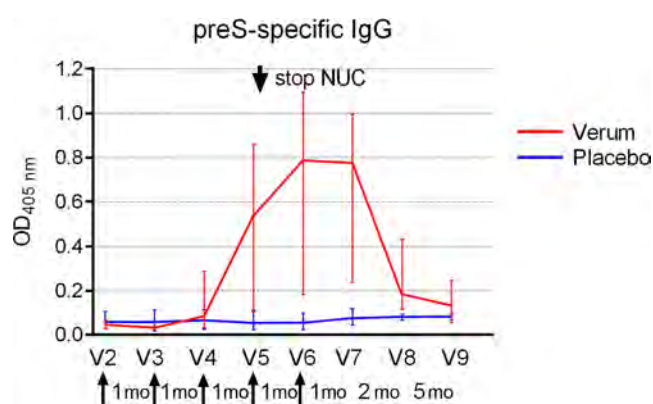
Background and aims: VVX001 is an HBV vaccine candidate based on a HBV-derived preS fused to grass pollen allergen peptides. The aim of this prospective double-blind, placebo-controlled trial (NCT03625934) was to investigate if VVX001 can induce preS-specific antibody and T cell responses in 4 different cohorts including patients with chronic hepatitis B.

Method: This is an interim analysis of non-cirrhotic patients with HBeAg-negative chronic hepatitis B on long-term treatment (>3 years) with nucleos(t)ide analogues (NUCs) (cohort 4a) treated either with 5 s.c. injections (visits 2, 3, 4, 5, 6) of either VVX001 or placebo in 4-week intervals (randomized 3:1), respectively Inclusion criteria: HBV DNA <20 IU/ml (detection limit); HBsAg<1000 IU/ml. After the third vaccination (visit 4) NUCs were stopped. After visit 6, patients were then followed for further 36 weeks (visits 7, 8, 9). preS-specific IgG and CD4+/CD8+ T cell responses were studied by ELISA and FACS analysis CFSE-labeled PBMCs

Results: All 20 patients (m/f:16/4; 19 Caucasians, 1 Asian, age:35–59 years) completed treatment and 17 of them reached visit 9 at this point. Five patients received placebo and 15 received VVX001. All patients in the verum group developed robust preS-specific IgG responses peaking one month after the last injection and declining at month 12. At visit 8 (12 weeks after the last injection) preS-specific IgG levels increased by 139% (median) compared to baseline (p < 0.001). HBsAg decreased from median 365 IU/ml (range: 100 to 1320) to 116 (0–340) (available in 9; p = 0.04) at end of follow-up (FU) in the verum group but did not change in the placebo group (n = 4).

During FU, HBV DNA became quantifiable in 6 verum patients; 2 patients developed ALT flare >10x the upper limit of normal (ULN) and were restarted on NUCs. One had transient ALT increase (7×ULN). In this and in 3 other patients HBV-DNA decreased again below 20 IU/ml. Thirteen verum patients (87%) remained HBV-DNA negative with normal ALT, and none of them required repeated NUC treatment.

Except local injection site-reactions, VVX001 was well tolerated in all participants and no SAEs were reported.



Conclusion: VVX001 is safe and well tolerated and induces a preS-specific immune response in patients with chronic HBeAg-neg hepatitis B. In 87% of vaccinated patients, no repeated treatment with NUCs was necessary after stopping NUCs. A longer follow-up is needed to evaluate the long-term impact of vaccination and stop of NUC therapy.

SAT404

HEC121120, a novel allosteric modulator of HBV core protein demonstrates potent antiviral activities *in vitro* and *in vivo*

Qingying Lai¹, Pu Wang¹, Xinchang Liu², Qingyun Ren², Baohua Gu¹, Jing Li¹, Yunfu Chen¹.

¹State Key Laboratory of Anti-Infective Drug Development (NO. 2015DQ780357), Sunshine Lake Pharma Co., Ltds, Pharmacology and toxicology division, Dongguan, China; ²State Key Laboratory of Anti-Infective Drug Development (NO. 2015DQ780357), Sunshine Lake Pharma Co., Ltds, Dongguan, China

Email: chenyunfu@hec.cn

Background and aims: Capsid assembly modulators (CAMs) represent a clinically validated strategy for the treatment of chronic hepatitis B. Here, we report on HEC121120, a novel class I CAM with improved antiviral activities *in vitro* and *in vivo*.

Method: Antiviral activities on HBV DNA were determined in HepG2.2.15 cells and in HBV-infected primary human hepatocytes (PHH) both *in vitro* and *ex vivo* using quantitative PCR. *In vivo* antiviral efficacy was assessed in the AAV-HBV mouse model with 8 weeks of treatment and 4-week off-treatment follow-up period.

Results: HEC121120 showed potent antiviral activity on HBV DNA production (EC₅₀ = 5.03 nM) in HepG2.2.15 cells with low cytotoxicity (CC₅₀ ≥ 150 μM), similar to that of GLS4 (EC₅₀ = 8.66 nM, CC₅₀ ≥ 150 μM). However, significantly enhanced potency was demonstrated in HBV-infected PHH with EC₅₀ 16.3 nM and 724 nM for HEC121120 and GLS4, respectively. In PHH isolated from chronically infected

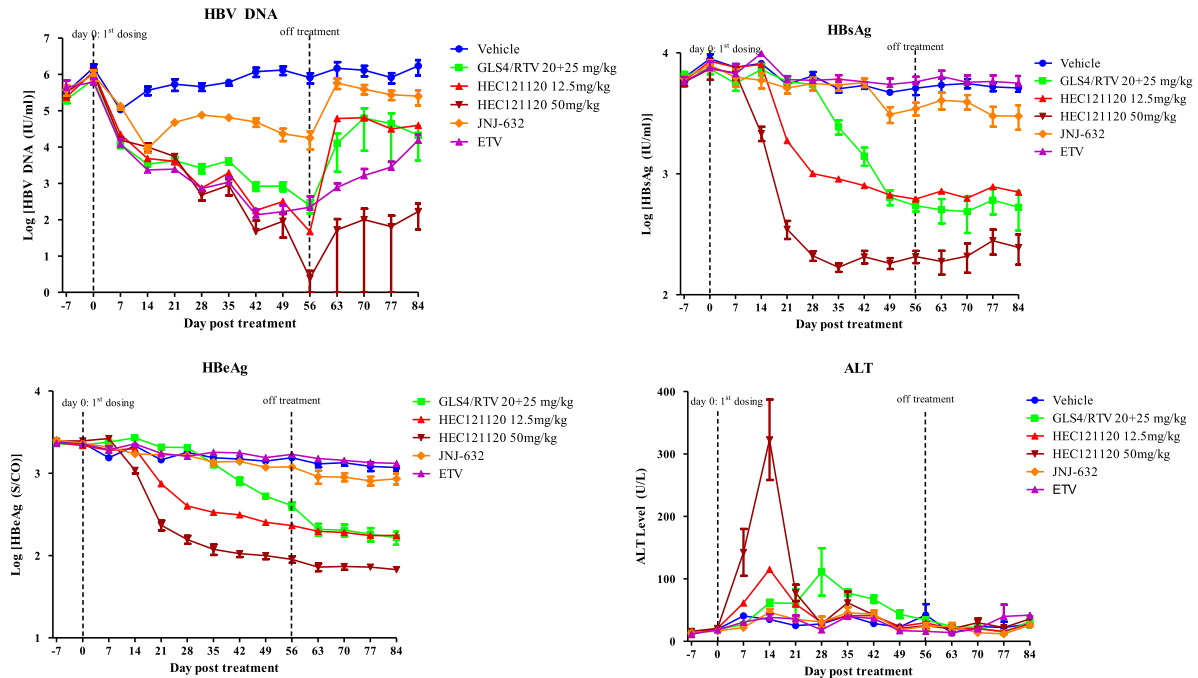


Figure: (abstract: SAT404)

humanized liver mouse, 14 days of GLS4 (5 μ M) and HEC121120 (2 μ M) treatment resulted in suppression of HBV DNA, HBsAg and HBeAg while entecavir (ETV) had no effect on either viral antigen. To compare with similar compounds in AAV-HBV mouse model, treatment with ETV (0.1 mg/kg, QD, p.o.) and JNJ-632 (200 mg/kg, QD, s.c.) resulted in potent reduction of serum HBV DNA but no significant impact on serum HBsAg and HBeAg level. In contrast, both GLS4/RTV (25/20 mg/kg, BID, p.o.) and HEC121120 (12.5 mg/kg or 50 mg/kg, BID, p.o.) potently suppressed HBsAg and HBeAg in addition to HBV DNA. At the end of treatment, HBV DNA declined 3.6, 1.7, 3.5, 4.2, 5.5 log₁₀ for ETV, JNJ-632, GLS4/RTV, HEC121120 (12.5 mg/kg dose) and HEC121120 (50 mg/kg dose), respectively. The mean decline for HBsAg was 1.0, 0.9, 1.4 log₁₀ and the mean decline of HBeAg was 0.6, 0.8, 1.2 log₁₀ for GLS4/RTV, HEC121120 low dose and HEC121120 high dose. There was no significant rebound of viral antigens in GLS4/RTV and HEC121120 treated animals during the 4-week follow-up period. Furthermore, liver IHC showed HBeAg positive hepatocytes were significantly reduced in HEC121120 treated groups compared to control. Similar to GLS4, HEC121120 caused a dose dependent, self-limiting ALT elevations but at an earlier time and with increased magnitude in higher dose group of HEC121120. Concomitantly, the decrease of HBsAg correlated well with the timing and magnitude of ALT, indicative of ALT flare as a therapeutic effect.

Conclusion: HEC121120 is a novel class I CAM, which demonstrated improved antiviral properties both *in vitro* and *in vivo*, further clinical study will be conducted to evaluate the antiviral potency in CHB patients.

SAT405

Evaluation of quantitative HBsAg levels in chronic hepatitis B-a targeted literature review

Anadi Mahajan¹, Saifuddin Kharawala¹, Nitesh Singh¹, Supriya Desai¹, Stuart Kendrick², Emily Lloyd², Vera Gielen². ¹Bridge Medical Consulting, London, United Kingdom; ²GlaxoSmithKline, Research and Development, United Kingdom
Email: anadimahajan@bridgemedical.org

Background and aims: A targeted literature review (TLR) was conducted in patients with chronic hepatitis B (CHB). **Objective 1:**

Hepatitis B surface antigen (HBsAg) titres across disease phases, and their cross-sectional relationship with clinical, biochemical and treatment characteristics. **Objective 2:** Association between HBsAg titres and long-term disease outcomes (cirrhosis, hepatocellular carcinoma [HCC], liver transplant, mortality). **Objective 3:** Change in HBsAg titres and their relationship with the above characteristics. **Method:** Structured searches were performed in MEDLINE® and Embase® (January 2000 to March 2021), with bibliographic searches, hand searches of relevant congress abstracts (2019–2021) and grey literature searches.

Results: Of all studies identified, 59 were selected for reporting, of which 46% were retrospective-cohort and 25% prospective-cohort. HBsAg titres were generally higher in initial Hepatitis B e-antigen (HBeAg)-positive phases than in later HBeAg-negative phases. Cross-sectionally, higher HBsAg titres were consistently associated with higher Hepatitis B Virus (HBV) DNA levels (moderate-to-strong in HBeAg-positive phases; weak-to-moderate in HBeAg-negative phases) and lower age (moderate). Greater decline in HBsAg was consistently associated with subsequent HBsAg seroclearance (hazard ratio [HR]: 1.95 to 43.83) and with lower HBV DNA levels (odds ratio [OR]: 2.82 to 26.52 for virological response). HBsAg titres predicted development of HCC and cirrhosis in treatment-naïve CHB patients by multivariate analysis. Data were limited for prediction of cirrhosis.

Conclusion: HBsAg titres are associated with HBV DNA and age across CHB phases. Decline in HBsAg titres is associated with HBsAg seroclearance and lower HBV DNA levels. HBsAg titres can predict the development of long-term outcomes.

Funding: GlaxoSmithKline (Study 217135).

Conflicts of interest: SKe, VG and EL are employees of GSK and hold stock/shares in the company. SKh, AM, NS and SD are employees of Bridge Medical.

SAT406

Nucleoside/nucleotide analogues monotherapy is safe and efficient for the prevention of HBV flare-ups after liver transplantation in the long term

Orly Sneh Arbib¹, Assaf Issachar^{1,2}, Marius Braun^{1,2}, Michal Cohen-Naftaly^{1,2}, Yael Harif¹, Evelin Oxtrud¹. ¹Beilinson, Petah

POSTER PRESENTATIONS

Tikva, Israel; ²Tel Aviv University, Tel Aviv-Yafo, Israel
 Email: orlysnh@gmail.com

Background and aims: The recurrence rate of HBV after transplantation decreased dramatically due to prophylactic therapy including hepatitis B immunoglobulin (HBIG) and nucleoside/nucleotide (Nuc) analogues. Published data on cessation of HBIG after transplantation and treatment with Nuc analogues as monotherapy are scarce especially in western world
 In 2013 we decided to stop HBIG in liver transplant patients with undetectable HBV DNA in serum during follow-up, more than 2y post LT with good compliance, normal liver function tests that were HBeAg negative and with viral load less than 2000IU/ml at transplantation. Lamivudine was switched to entecavir or tenofovir, before stopping HBIG.. Due to excellent results we decided in 2018 stop HBIG as soon as possible after transplantation in patients who fulfill the other criteria
 We aimed to determine the long-term efficacy of Nuc analogues monotherapy for prevention of HBV seroconversion and flare-up of hepatitis. Overall graft and patient were assessed.
Method: This is a retrospective study on a prospectively maintained data base of transplanted patients in the largest transplant center in Israel. All patients that required LT due to HBV and its complications are followed up by biannual liver function tests, HBV serology, HBV DNA AFP and ultrasound.
Results: 630 liver transplants were performed in our center since 1995, 420 patients are in active follow-up. HBV related disease was the reason for LT in 84 patients, and 25 were eligible for monotherapy (Table 1). The patients were treated with dual therapy for an median time of 7.2 years (IQR 3.4–12.7 years). During a follow-up of median 6.8 years (IQR 4.2–7.4 years) after HBIG discontinuation there were no hepatitis flares, however, two patients treated with entecavir had detectable HBsAg in serum (one of them also temporarily exhibited low titre HBV DNA in serum during follow-up). Two patients had detectable HBsAb, two years after the HBIG was discontinued. There was no recurrence of HCC. There was no graft failure. Five patients received active immunization.

Patients	N
LT d/t HBV	84
Gender male	16
Age (mean)	46
Monotherapy with Nuc analogues	25
Anti HDV Ab prior to transplant	9
HCC prior to transplant	6
Treated with lamivudine before HBIG interruption	12
Treated with tenofovir after HBIG interruption	8
Treated with entecavir after HBIG interruption	17

Conclusion: The Long term follow-up reiterates the safety and efficacy of monotherapy with Nuc analogous in carefully selected Caucasian patients including HCC patients and HBV/HDV co-infected patients.

SAT407
A new method to identify co-variation in hepatitis B virus whole genome sequences identifies networks of polymorphisms associated with drug resistance
 Sheila Lumley¹, Steven Lin², Louise Downs¹, Cori Campbell¹, Anna McNaughton³, Azim Ansari¹, Philippa Matthews⁴. ¹Peter Medawar Building for Pathogen Research; ²Wellcome Trust Centre for Human Genetics; ³University of Bristol; ⁴The Francis Crick Institute
 Email: sheila.lumley@trinity.ox.ac.uk

Background and aims: We developed a model to identify coevolving amino acid (aa) sites within or between hepatitis B virus (HBV) proteins with the aim of identifying structural or functional protein interactions while accounting for the population structure among the isolates (founder effect). Here we present a computationally efficient method to identify co-varying sites across the HBV genome in the context of its phylogeny. We examine the trends in covariation across the genome and apply this to the study of drug resistance associated mutations (RAMs).
Method: We downloaded 9313 genotype A, B C and D whole genome HBV sequences from HBVdb. We aligned, deduplicated and translated them into a sequences. We built a phylogeny for each genotype and

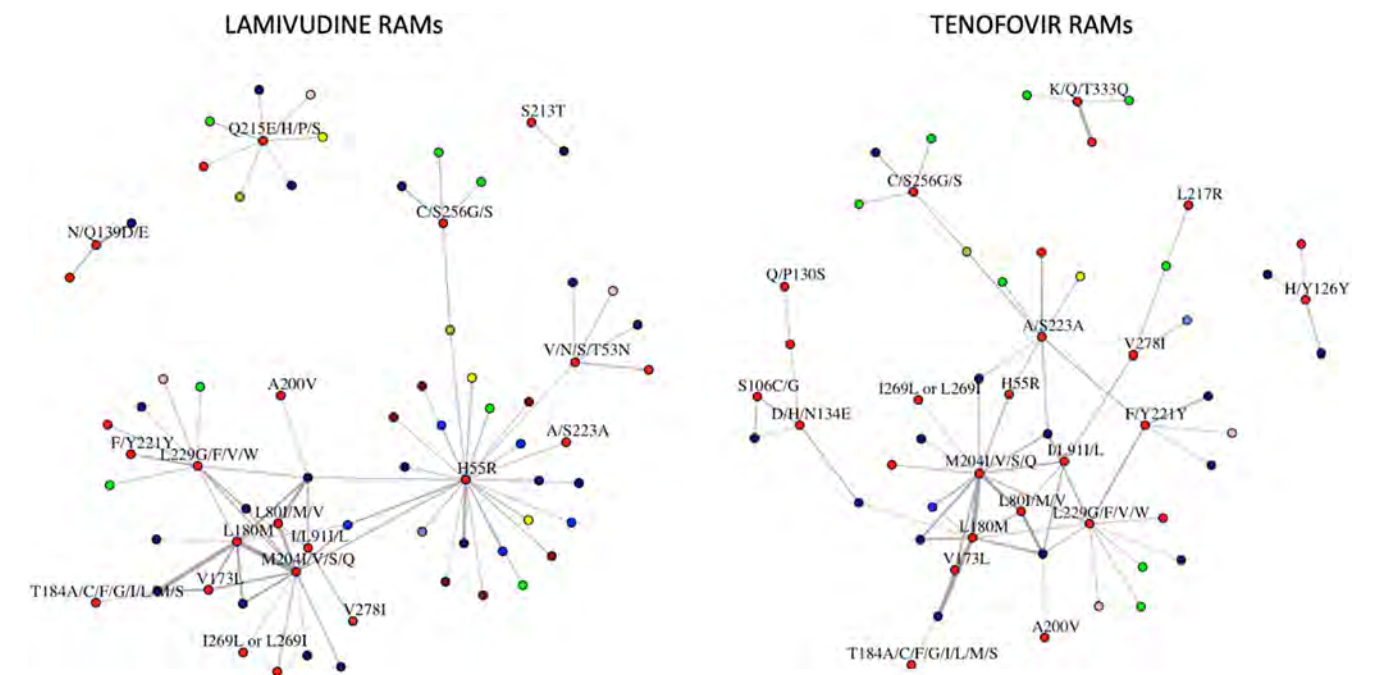


Figure 1: (abstract: SAT407): Network analysis highlighting covarying pairs in which one or more amino acids are Lamivudine or Tenofovir RAMs. Each node represents an amino acid. Node colour indicates the protein; p = reds, C = greens, S = blues, X = yellow. Line width is inversely proportional to the adjusted harmonic mean p value.

reconstructed the ancestral state for each polymorphic site. We used Fisher exact test to investigate covariance between a changes on the tree between two sites. We combined p values using harmonic mean p value and used false discovery rate to account for multiple testing.

Results: We identified 1066 co-varying aa pairs across the genotypes; 547 (51%) pairs involved core protein, 532 (50%) polymerase, 351 (33%) surface, and 87 (8%) X. Core protein was enriched in the proportion of covarying sites relative to other proteins. Within-protein covariations were enriched across all genotypes. Of the 615 within-protein covarying pairs, 53 (9%) were adjacent, and 60 (10%) were ≤ 3 a apart. For genotypes B, C and D, most co-varying sites were linked in a dominant network, the largest of which included 131/186 (70%) covarying amino acids (genotype B). Identification of known primary/secondary RAM pairs in this dataset validated our method; previously reported RAMs were enriched among the covarying sites (OR 2.1, $p < 0.05$). 136 pairs were identified where one or more sites was a known RAM. RAMs co-varied in networks spanning all four proteins (Fig 1), demonstrating the global epistatic connectivity of RAMs.

Conclusion: Covariation analysis reveals a complex, genotype-specific network of a substitutions in HBV. We have shown how this method can describe networks of RAMs, and it could further provide evidence of sites of clinical relevance pertinent to understanding viral evolution and phylogeny, immune escape, and therapeutic vaccine design.

SAT408

Baseline bile acid levels but not bile acid increases during bulevirtide treatment of hepatitis D are associated with HDV RNA decline

Katja Deterding¹, Cheng-Jian Xu^{1,2}, Kerstin Port¹, Benjamin Maasoumy¹, Markus Cornberg^{1,2}, Heiner Wedemeyer¹.

¹Hannover Medical School, Gastroenterology, Hepatology and Endocrinology, Hannover, Germany; ²Center for Individualized Infection Medicine, CiIM, a joint venture between Hannover Medical School and the Helmholtz Center for Infection Research, Hannover, Germany
Email: deterding.katja@mh-hannover.de

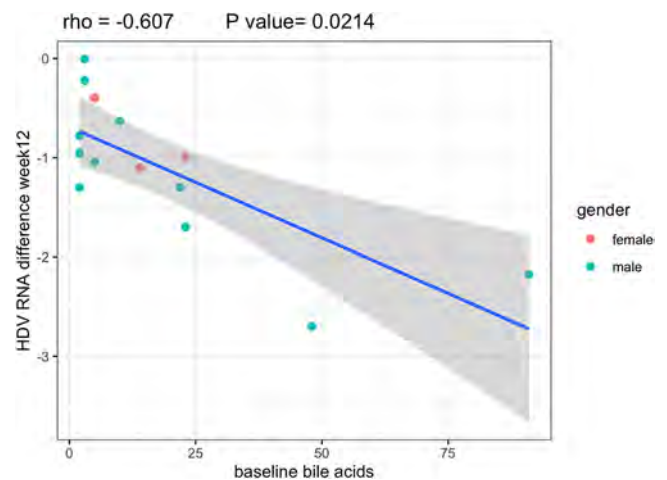
Background and aims: Bulevirtide is an entry inhibitor blocking entry of HBsAg into hepatocytes by interfering with Na⁺-taurocholate cotransporting polypeptide (NTCP), the HBV/HDV receptor. As NTCP is a bile acid transporter, one would expect an increase of bile salts during bulevirtide treatment. Still, there is no data available if the increase in bile acids reflect antiviral efficacy.

Method: We studied 14 patients (11 male, 3 female) with compensated HDV infection receiving bulevirtide 2 mg subcutaneously once daily for at least 12 weeks. The median age of the patients was 48 years (± 12 , 44) and all of the patients had liver cirrhosis or advanced fibrosis and 7 were previously treated with pegylated interferon alfa.

Results: ALT levels improved in all patients over time with 7/14 patients showing normal ALT values at treatment week 12. An HDV RNA drop of at least 50% was evident in 12/14 patients at week 12 including 8 patients with a more than 1log IU/ml and 2 patients achieving a fast response with more a than 2 log HDV RNA decline. Total serum bile acids showed a heterogeneous pattern before and during treatment. Bile salts levels were above the limit of normal already before treatment in 6 patients and increased during bulevirtide administration with different kinetics in most patients. Of note, no patient reported systemic itching. Baseline bile acids were associated with higher transient elastography values ($p = 0.01$) but liver stiffness was not associated with bile acid changes during treatment.

Bile acid levels before the start of treatment were associated with HDV RNA declines at treatments weeks 2, 8 and 12 ($\rho = -0.70$ and $p = 0.005$, $\rho = -0.75$ and $p = 0.002$, $\rho = -0.61$ and $p = 0.02$, respectively; see figure). However, bile acid increases during treatment were not associated with subsequent HDV RNA declines at neither time point ($p = 0.73$; $p = 1$, $p = 0.28$, respectively).

Furthermore, bile acid changes during treatment were also not associated with subsequent ALT declines.



Conclusion: In conclusion, we demonstrate that the bulevirtide-induced increase in bile salts does not correlate with HDV RNA decline in patients with hepatitis D. Thus, blocking HBsAg entry and interfering with the bile acid transporter function of NTCP occur at different concentrations. Thus, in clinical practice, regular measurement of bile salts during bulevirtide treatment does not predict virological response to bulevirtide treatment.

SAT409

Low levels of qHBsAg and tenofovir therapy are associated with successful treatment withdrawal in HBeAg negative chronic hepatitis B: results from spanish multicentric study

Anna Pocurull^{1,2,3,4}, Elena Hoyas⁵, Manuel Rodríguez⁶, Mireia Miquel⁷, Clara Amiama Roig⁸, Sergio Rodríguez-Tajes^{1,2,3,4}, Francisco Javier Garcia-Samaniego Rey⁸, Emilio Suarez⁵, Sabela Lens^{1,2,3,4}. ¹Hospital Clínic de Barcelona, Liver Unit; ²University of Barcelona; ³IDIBAPS; ⁴CIBEREHD; ⁵Hospital Universitario Virgen de Valme, Sevilla; ⁶Hospital Universitario Central de Asturias, Oviedo; ⁷Hospital Parc Taulí, Sabadell; ⁸Hospital La Paz, Madrid
Email: pocurull@clinic.cat

Background and aims: Clinical guidelines suggest that nucleos(t)ide analogues (NA) discontinuation in HBeAg negative chronic hepatitis B (CHB) may increase functional cure rates. However, information about predictive factors in Caucasian patients is still limited also influenced by different re-treatment criteria. We aimed to analyze baseline factors and outcomes after NA withdrawal in 5 Spanish Centers with homogeneous re-treatment criteria.

Method: Prospective inclusion of 96 non-cirrhotic patients with HBeAg-negative CHB in complete viral suppression after >3 years. The re-treatment criteria after NA withdrawal were: ALT >10 upper limit normal (ULN) and bilirubin >2 mg/dl, ALT >5 ULN during 1 month, or ALT >2 ULN and DNA-VHB >2.000UI/ml >6 months.

Results: The median age of the cohort was 55 (IQR: 46–63) years old and 68% were male. Fibrosis values assessed by Fibroscan® were low in all cases (4, 9 (4–6) kPa). At the time of NA withdrawal, 72% received tenofovir and 28% entecavir [median treatment duration of 11 (7–15) years, similar in both groups]. qHBsAg levels ($n = 89$) were 904 (305–2416) UI/ml. After a median follow-up of 28 (24–47) months after NA withdrawal, Twenty-two patients (23%) achieved HBsAg loss. Previous treatment with tenofovir ($p < .05$) and low levels of qHBsAg (<1000 UI/ml) before stopping treatment ($p < .05$) were associated to a higher rate of functional cure. Twenty-six patients (27%) accomplished re-treatment criteria due to ALT >5 ULN ($n = 5$) or >10 ULN ($n = 7$) of which 5 also had bilirubin >2 mg/dl. One patient required liver transplantation due to a fulminant hepatitis.

	HBsAg loss n = 22	HBsAg Persistence n = 74	p
Sex (Male)	17 (77%)	48 (65%)	p = 0, 275
Age (years) (median;IQR)	57, 05; (46–64, 2)	54, 6; (47–63)	p = 0, 365
Genotype (D/A) n = 30	5/2 (16/7%)	18/5 (60/17%)	p = 0, 801
Tenofovir	22 (100%)	47 (64%)	p = 0, 001
LAM Resistance	13 (59%)	21 (28%)	p = 0, 015
ALT ≥5LSN peak without restart treatment	7 (32%)	7 (9%)	p = 0, 068
Baseline qHBsAg (median, IQR)	240 (72–584)	1500 (556–3455)	p = 0, 011
Baseline qHBsAg >1000 IU/L (n = 42)	3 (14%)	39 (53%)	p = 0, 0001
Treatment duration (years) (m; IQR)	12, 97 (9, 1–18, 48)	11, 01 (7, 1–13, 94)	p = 0, 132
Follow-up (months) (m;IQR)	35, 58 (24, 37–57, 6)	33, 36 (24, 39–45, 6)	p = 0, 58

Conclusion: NA withdrawal increases the chance to achieve functional cure also in Caucasian patients, specially those previously treated with tenofovir and very low levels of qHBsAg (<1000 UI/ml). However, a very strict follow-up is strongly recommended so that re-treatment is promptly started.

SAT410

Preliminary results of the effectiveness and safety of Tenofovir Alafenamide Fumarate prophylaxis in HBV-infected individuals, who received chemo/immunosuppressive therapy

Feyza Gunduz¹, Serdar Durak², Yasemin Unsal³, Mehmet Demir⁴, Zeynep Melekoglu Ellik⁵, Abdullah Emre Yildirim⁶, Shahin Mehdiyev¹, Haydar Adanir⁷, Coskun Ozer Demirtas¹, Enver Ucbilek⁸, Yasemin Balaban⁹, Elif Sitre Koç¹⁰, Digdem Ozer Etik¹¹, Pinar Gökçen¹², Derya Ari¹³, Hale Gokcan⁵, Suna Yapali¹⁰, Nergis Ekmen³, Mehmet Arslan², Meral Akdogan Kayhan¹³, Kamil Ozdil¹², Orhan Sezgin⁸, Sedat Boyacioglu¹¹, Halis Simsek⁹, Nurdan Tozun¹⁰, Dinc Dincer⁷, Ramazan Idilman⁵. ¹Marmara University School of Medicine, Turkey; ²Karadeniz Technical University School of Medicine, Turkey; ³Gazi University School of Medicine, Turkey; ⁴Mustafa Kemal University School of Medicine, Gastroenterology, Turkey; ⁵Ankara University School of Medicine, Turkey; ⁶Gaziantep University School of Medicine, Turkey; ⁷Akdeniz University School of Medicine, Turkey; ⁸Mersin University School of Medicine, Turkey; ⁹Hacettepe University School of Medicine, Turkey; ¹⁰Acibadem University School of Medicine, Turkey; ¹¹Başkent University School of Medicine, Turkey; ¹²Health Sciences University, Umraniye Training and Research Hospital, Turkey; ¹³Ankara City Hospital, Turkey
Email: drfgunduz@yahoo.com

Background and aims: There are very limited data regarding the efficacy and safety of tenofovir alafenamide fumarate (TAF) prophylaxis to prevent HBV reactivation in HBV-infected individuals undergoing chemo/immunosuppressive therapy. The aims of the present study were to determine the effectiveness and safety of TAF prophylaxis in HBV-infected individuals, who receive chemo/immunosuppressive therapy.

Method: This is a multicenter, observational study. Data were entered in a standardized electronic case report form (CRF) from each center and collected from the CRF. TAF was administered at a dose of 25 mg/day at the initiation of the chemo/immunosuppressive therapy. The mean follow-up period was 17.1 ± 7.8 months.

Results: A total of 326 HBV-infected individuals with benign and malign diseases received TAF prophylaxis. Among these patients, 158 patients (M/F:83/75) with at least 6 months of follow-up were included into analysis. Mean age was 59.55 ± 12.2 years. Thirty patients had detectable HBV DNA and 5% were HBeAg positive. Solid tumors were the most common primary disease (33.5%), followed by rheumatic

diseases (32.9%) and myeloproliferative diseases (32.2%). Of these patients, 48% received cytotoxic chemotherapy, 17% received B cell depleting therapy, 13% received anti-TNF therapy, 8% were received glucocorticoid therapy, and 12% patients were received other treatments. During the follow-up period, none of the patients had clinical, biochemical, and serological evidence of HBV reactivation under TAF prophylaxis. No HBV-related morbidity and mortality was observed. HBV DNA became negative in 77% of the patients with detectable HBV DNA. All patients maintained their chemo/immunosuppressive therapy without interruption. TAF prophylaxis was well tolerated. The renal function tests and lipid profiles, except triglyceride level did not significantly change from the baseline to the end of the follow-up period (Table 1). No serious adverse events were reported.

Table 1. Laboratory changes during follow-up

w-HB	Baseline		6-months		12-months		18-months		24-months		p-value (pairwise comparisons to baseline)			
	mean±sd	median	mean±sd	median	mean±sd	median	mean±sd	median	mean±sd	median	6-months	12-months	18-months	24-months
ALT, IU/L	34.36±17.33	24.48±21.7	27.81±16.85	27.81±16.85	30.67±16.72	30.67±16.72	30.67±16.72	30.67±16.72	30.67±16.72	30.67±16.72	0.009*	0.204	0.009	0.009
Blood phosphorus, mg/dL	3.52±0.61	3.46±0.71	3.29±0.61	3.29±0.61	3.36±0.59	3.36±0.59	3.36±0.59	3.36±0.59	3.36±0.59	3.36±0.59	0.004*	0.013*	0.009	0.105
GFR, mL/min	83.25±26.48	84.23±23.86	82.88±26.09	84.05±23.77	81.53±27.29	84.23	81.53±27.29	84.23	81.53±27.29	84.23	0.906	0.126	0.906	0.906
Total cholesterol, mg/dL	209.48±55.95	199.48±49.99	222.27±50.05	222.27±50.05	230.73±90.99	232.25±91.09	232.25±91.09	232.25±91.09	232.25±91.09	232.25±91.09	0.322	0.290	0.322	0.187
Triglyceride, mg/dL	147.46±89.11	179.31±11.7	165.17±106.72	169.90±5.51	194.74±7.75	0.050*	0.306	0.003	0.019*	0.019*	0.050*	0.306	0.003	0.019*
HDL, mg/dL	46.15±14.54	43.57±11.49	53.08±16.29	54.97±20.94	60.13±21.66	0.755	0.165	0.154	0.244	0.244	0.755	0.165	0.154	0.244
LDL, mg/dL	125.79±43.82	119.33±35.26	140.63±39.81	149.33±90.73	140.50±1.32	0.789	0.311	0.302	0.877	0.877	0.789	0.311	0.302	0.877
Fasting glucose, mg/dL	110.73±37.06	117.37±37.69	122.87±41.53	122.87±41.53	112.41±39.99	112.95±22.54	0.099	0.033*	0.147	0.099	0.099	0.033*	0.147	0.099

ALT, Alanine transaminase; GFR, Glomerular filtration rate; HDL, High-density lipoprotein; LDL, Low-density lipoprotein

Conclusion: Based on the results of the study, TAF prophylaxis prevents chemo/immunosuppressive therapy-induced HBV reactivation in HBV-infected individuals receiving chemo/immunosuppressive therapy. TAF is safe and tolerable in such individuals.

Keywords: HBV reactivation, HBV prophylaxis, Tenofovir Alafenamide Fumarate

SAT411

Real life efficacy, renal and lipid profile data of tenofovir alafenamide in switched chronic hepatitis B patients

Rahmet Guner¹, Gulsen Yoruk², Oguz Karabay³, Tansu Yamazhan⁴, Nurcan Baykam⁵, Mustafa Yildirim⁶, Nevin Ince⁷, Ilknur Esen Yildiz⁸, İlyas Dökmetaş⁹, Meliye Meriç Koç¹⁰, İftihar Koksall¹¹, Sükran Köse¹², Sabahat Ceken¹³, Dilara Inan¹⁴, I. Bozkurt¹⁵, Kamuran Turker¹⁶, Güven Celebi¹⁷, Ayse Batirel¹⁸, Gulden Unlu¹⁹, Ozgur Parlak²⁰, Levent Gorenk²¹, Fatma Sirmate²², Alper Sener²³, Emine Parlak²⁴, Fehmi Tabak²⁵. ¹Ankara City Hospital, Turkey; ²Istanbul Training and Research Hospital, Turkey; ³Sakarya University School of Medicine, Turkey; ⁴Ege University Faculty of Medicine, Turkey; ⁵Hitit University Faculty of Medicine, Turkey; ⁶Haseki Training and Research Hospital, Turkey; ⁷Duzce University Faculty of Medicine, Turkey; ⁸Recep Tayyip Erdogan University Faculty of Medicine, Turkey; ⁹Sisli Hamideye Etfal Training and Research Hospital, Turkey; ¹⁰Bezmi Alem Vakif University Faculty of Medicine, Turkey; ¹¹Karadeniz Technic University Faculty of Medicine, Turkey; ¹²Izmir Tepecik Training and Research Hospital, Turkey; ¹³Dr. Abdurrahman Yurtaslan Ankara Oncology Training and Research Hospital, Turkey; ¹⁴Akdeniz University Medical Faculty, Department of Infectious Diseases, Turkey; ¹⁵Ondokuz Mayıs University Faculty of Medicine, Turkey; ¹⁶Istanbul Bagcilar Training and Research Hospital, Turkey; ¹⁷Bulent Ecevit University Faculty of Medicine, Turkey; ¹⁸Dr. Lütfi Kırdar Kartal Training and Research Hospital, Turkey; ¹⁹Kocaeli Derince Training and Research Hospital, Turkey; ²⁰Samsun Training and Research Hospital, Turkey; ²¹Istanbul Sultan Abdulhamid Han Training and Research Hospital, Turkey; ²²Bolu Abant İzzet Baysal University Faculty of Medicine, Turkey; ²³18 Mart University Faculty of Medicine, Turkey; ²⁴Atatürk University Faculty of Medicine, Turkey; ²⁵Cerrahapasa University School of Medicine, Turkey
Email: fehmitabak@yahoo.com

Background and aims: Tenofovir alafenamide (TAF) is a new prodrug of tenofovir used for the treatment of HIV-1 and HBV infections. It provides more efficient intracellular tenofovir concentrations at a relatively lower dose than provided by tenofovir disoproxil fumarate (TDF). TAF is expected to have efficacy similar to that of TDF with improved safety profile. TAF is commonly used in HBV treatment in

Turkey. We studied TAF use in chronic hepatitis B patients in a real life setting across the country.

Method: Treatment-experienced chronic HBV patients were included. Twenty-five sites from 15 cities were enrolled. Patients' demographics, laboratory studies before TAF and during TAF treatment were recorded. Data at baseline, in 6th month and in 12th month were compared.

Results: The study included 509 treatment-experienced patients. Among patients, median age was 53 years, male 302 (59.3%), HBeAg-negative 348 (86.1%), median ALT 23 U/L, median fibrosis score 2, and HAI 7. They were previously using TDF (83.9%), entecavir (6.8%), lamivudine (5.5%), telbivudine (3.0%), and adefovir (0.8%). Before TAF, treatment duration <6 months 13 (2.9), 6–12 months 29 (6.5), >12 months 403 (90.6). Indications to switch were osteoporosis 206 (40.5%), blood phosphate level 108 (21.2%), physicians decision 65 (12.8%), glomerular filtration rate (GFR) 62 (12.2%), drug affecting bone mineral density 59 (11.6%), proteinuria/albuminuria 49 (9.6%), transplantation 11 (2.2%), steroids 6 (1.2%), fracture history 2 (0.4), and hemodialysis 2 (0.4%).

Among all patients with HBV-DNA <20 IU/ml was 76.0% at baseline (during switch), 88.0% in 6th month and 84.1% in 12th month ($p < 0.05$). ALT normalization was 72.3% at baseline, 76.9% in 6th month and 81.0% in 12th month ($p < 0.05$). Creatinine levels and estimated (eGFR) remained stable from baseline to 6th and 12th months (0.82 mg/dl, 0.86 mg/dl, and 0.88 mg/dl ($p > 0.05$); 95 ml/min, 84.45 ml/min, and 94.0 ml/min ($p > 0.05$), respectively). Change in HDL, LDL and total cholesterol at baseline, 6th month and 12th month are not significant.

Among all patients, TAF was tolerated well. Side effects were headache 7.7%, nausea 3.1%, fatigue 3.1%, and rash 1.0%.

Conclusion: Although the majority of the patients were using potent nucleos (t)ide analogs, switching to TAF was associated with improved virologic and biochemical responses. Renal functions and lipid parameters remained stable and the drug was well tolerated. Real life data confirmed the efficacy and safety of TAF in treatment-experienced chronic hepatitis B patients.

SAT412

Mathematical modeling of HDV RNA kinetics suggests high peginterferon Lambda efficacy in blocking viral production: insights from the LIMT-1 study

E Fabian Cardozo-Ojeda^{1,2}, Sarah Duehren¹, Saeed Sadiq Hamid³, Yoav Lurie⁴, Edward J Gane⁵, Anat Nevo-Shor⁶, David Yardeni⁶, Scott Cotler¹, Ingrid Choong⁷, Jeffrey Glenn⁸, Harel Dahari¹, Ohad Etzion⁶. ¹Program for Experimental and Theoretical Modeling, Division of Hepatology, Department of Medicine, Stritch School of Medicine, Loyola University Chicago, Maywood, United States; ²Vaccine and Infectious Disease Division, Fred Hutchinson Cancer Research Center, Seattle, United States; ³Aga Khan University, Karachi, Pakistan; ⁴Shaare Zedek, Jerusalem, Israel; ⁵Auckland City Hospital, Auckland, New Zealand; ⁶Soroka University Medical Center, Beer-Sheba, Israel; ⁷Eiger BioPharmaceuticals, Inc., Palo Alto, United States; ⁸Stanford University, Stanford, United States
Email: harel.dahari@gmail.com

Background and aims: We previously reported 5 HDV RNA kinetic patterns under peginterferon-lambda (Lambda) monotherapy therapy (The Liver Meeting, AASLD 2019 #LP12). Here we sought to provide insights into HDV-host dynamics and Lambda efficacy using a mathematical modeling approach.

Method: Thirty-three chronic HDV infected patients participated in a randomized, open-label, Phase 2 clinical study (LIMT-1) of Lambda 120 µg (n = 19) or 180 µg (n = 14), administered once weekly by subcutaneous injections for 48 weeks, with 24 weeks of follow-up. All subjects were on tenofovir or entecavir. Kinetic data was obtained at Week 1 and every four weeks during and post Lambda therapy. HDV RNA was measured by Robogene[®]2.0 (limit of quantification of 14 IU/ml, horizontal dotted line in Fig. 1). Six patients were excluded

from HDV kinetic analysis. The remaining 27 patients were previously categorized into 4 HDV kinetic patterns: monophasic, MP (Fig. 1a), biphasic, BP (Fig. 1b), flat-partial response, FPR (Fig. 1c) and triphasic/staircase, TP (Fig. 1d). We used a mathematical model of virus dynamics with or without proliferation of HDV-susceptible and HDV-infected hepatocytes to recapitulate the 4 HDV kinetic patterns and assess the impact of Lambda in blocking viral production. We fit the models to the HDV data using a population, nonlinear mixed-effects approach. HDV clearance rate was fixed to 0.43 day⁻¹ as previously estimated under Isonafarnib (Lancet Infect Dis 2015;15: 1167–74).

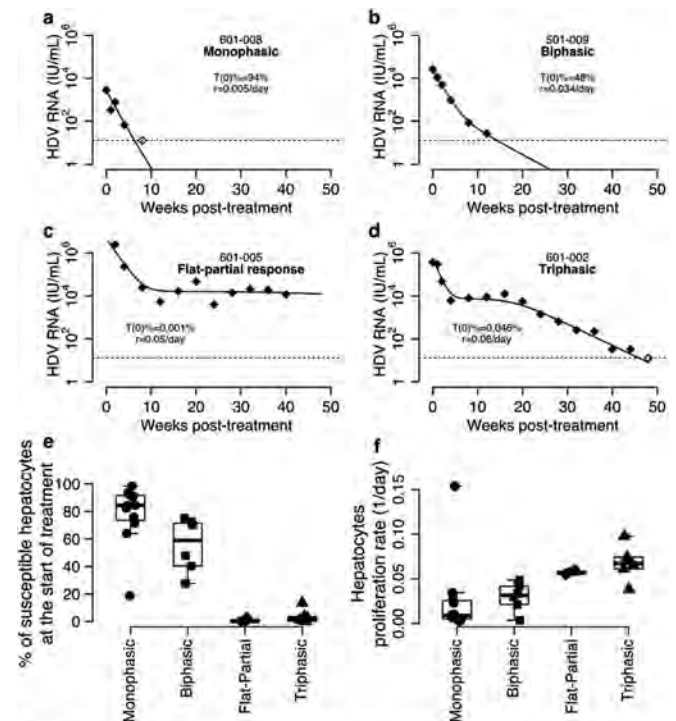


Figure 1. (a-d) Representative modeling calibration (curves) with patient's HDV RNA (symbols) during 48-week Lambda monotherapy. Horizontal lines represent HDV RNA limit of limit of quantification. 'T(0)%' is the estimated percentage of non-infected susceptible hepatocytes at the start of Lambda monotherapy and 'r' is the hepatocytes proliferation rate. Distributions of the estimated (e) T(0)% and (f) r using the best model fits.

Results: We found that only a model with hepatocyte proliferation of HDV-susceptible and HDV-infected cells is able to recapitulate all the 4 HDV kinetic patterns (Fig. 1a-d). The model predicts that population median half-life of HDV-infected hepatocytes is 9 days (equivalent to death/loss rate of 0.08 day⁻¹ [%RSE = 38%]), and that Lambda blocks virus production with population median efficacy of 99% (%RSE = 0.5%). The model predicts that participants with monophasic (Fig. 1a) and biphasic (Fig. 1b) HDV kinetic patterns have a high fraction of noninfected hepatocytes at the start of treatment compared to those with TP and FPR (Fig. 1e). Those with BP kinetics had a ~3.5-fold faster hepatocyte proliferation compared to MP (Fig. 1f). However, hepatocyte proliferation in those with BP was ~2-fold slower than those in the TP and FPR (Fig. 1f).

Conclusion: This study provides, for the first time, a dynamic description of HDV response under Lambda monotherapy. Modeling results predict that Lambda blocks viral production (as estimated under pegylated IFN-α therapy) with high efficacy. The model predicts that the HDV kinetic patterns depend on Lambda efficacy, the fraction of noninfected hepatocytes at the beginning of treatment and their proliferation rates. Further theoretical and experimental efforts are needed to verify and/or refine our understanding of Lambda mode of action against HDV.

SAT413

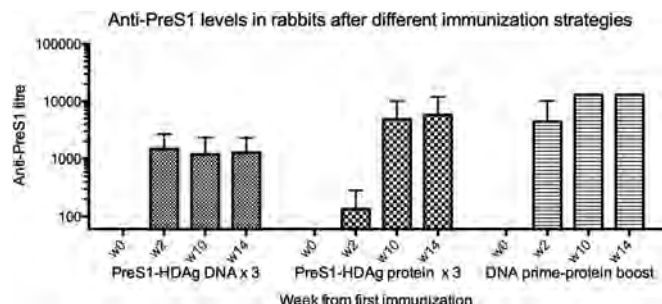
Heterologous prime-boost immunotherapy circumvents tolerance and induces broadly neutralizing antibodies that protects against hepatitis B and D co-infection and hepatitis D super-infection

Lars Frelin¹, Panagiota Maravelia¹, Rani Burm², Yi Ni³, Gustaf Ahlén¹, Lieven Verhoye², Freya Van Houtte², Anna Pasetto¹, Stephan Urban³, Philip Meuleman², Matti Sällberg¹. ¹Karolinska Institutet, Department of Laboratory Medicine, Huddinge, Sweden; ²University of Gent, Laboratory of Liver Infectious Diseases, Belgium; ³University of Heidelberg, Department of Molecular Virology, Germany
Email: lars.frelin@ki.se

Background and aims: Chronic hepatitis B and D virus (HBV/HDV) infections are a major cause of severe liver disease and cancer that generally require lifelong therapy. A hallmark of chronic HBV infection is the profound T cell dysfunction/tolerance to viral proteins, and strategies to break this tolerance may therefore contribute to achieving functional cures. The HDV antigen acts as a heterologous antigen and supports HBV-specific immunoinactivation, leading to enhanced anti-HBV antibody and T cell responses. Its incorporation into an immunotherapeutic approach to enhance neutralizing antibody and T-cell responses to HBV preS1 is therefore being investigated.

Method: Plasmid DNA and fusion proteins containing HBV preS1 and HDAG sequences were expressed in *E. coli*. Antibody and T-cell responses directed against preS1 and HDAG after DNA-prime protein boost immunization were assessed in rabbits and in wild type and HBsAg-transgenic mice. Protection against HBV/HDV co-infection, and HDV super-infection was assessed in uPA-Scid mice repopulated with human hepatocytes against *in vivo*.

Results: A DNA prime protein boost immunization resulted in superior anti-preS1 and anti-HDAG antibody and T-cell responses in mice and rabbits compared to repeated immunization with DNA or protein alone (Figure 1). Antibody titres resulting from immunization were similar across HBV genotypes A-H. The induced antibodies also had broadly neutralizing activity against both HBV and HDV *in vitro*. Immunization of wild-type and HBsAg transgenic C57BL/6 mice resulted in equivalent antibody titres, supporting the role of HDAG in circumventing T cell tolerance to HBV. Passive transfer of antiserum from immunized wild-type mice resulted in protection against HBV/HDV co-infection in 3/3 mice with humanized livers compared to 0/4 control animals that received serum from un-immunized mice. Passive transfer of antiserum from immunized wild-type mice resulted in protection against HDV superinfection in 3/3 mice with humanized livers that had been infected with HBV 8 weeks previously, compared to 0/4 control animals that received serum from un-immunized mice.



Conclusion: This novel prime-boost immunotherapy circumvents immune tolerance and induces endogenous production of high levels of broadly neutralizing preS1 antibodies and T cells against preS1 and HDAG. Our results merits further investigation as a curative strategy for HBV mono-infection and HBV/HDV co-infection.

SAT414

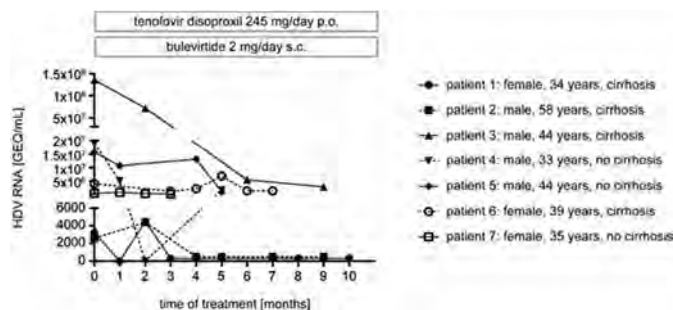
Real-world data on treatment with bulevirtide in patients with chronic hepatitis B and D coinfection

Toni Herta¹, Magdalena Hahn¹, Melanie Maier², Johannes Niemeyer¹, Florian Gerhardt¹, Jonas Schumacher¹, Janett Fischer¹, Johannes Wiegand¹, Thomas Berg¹, Florian van Bömmel¹. ¹Leipzig University Medical Center, Division of Hepatology, Department of Medicine II, Leipzig, Germany; ²Leipzig University Medical Center, Institute of Medical Microbiology and Virology, Leipzig, Germany
Email: florian.vanboemmel@medizin.uni-leipzig.de

Background and aims: The hepatitis B and D virus (HBV/HDV) hepatocyte entry inhibitor bulevirtide (BVL) is available in Europe since July 2020. Real-world data on efficacy and safety of BVL in patients with chronic hepatitis delta (CHD) are sparse. We report efficacy and tolerability of BVL treatment in patients with CHD.

Method: CHD patients were treated with BLV 2 mg/day in combination with tenofovir disoproxil fumarate (TDF) 245 mg/day. HDV RNA and HBV DNA were quantified by real-time PCR based assays (HDV: Roche Diagnostics, lower limit of detection (LLD) 150 genome equivalents (GEQ)/ml; HBV: Abbott Molecular, LLD 10 IU/ml), and HBV surface antigen (HBsAg) by the ARCHITECT assay (Abbott Molecular, sensitivity 0.05 IU/ml).

Results: 7 patients were recruited (4 male, age 41 ± 8.1 years, 5 Caucasians, 2 Asians, 4 with cirrhosis Child-Pugh A). Before BVL treatment initiation, median serum HDV RNA levels were $3.9 \times 10^6 \pm 4.96 \times 10^7$ [range 1.36×10^8] GEQ/ml, median serum HBV DNA 27 ± 203 [range 600] IU/ml, median serum HBsAg 1100 ± 16230 [range 47470] IU/ml and median elevation of alanine aminotransferase (ALT) levels 2.27 ± 1.81 [range 5.13] above upper limit of normal (ULN). After a mean follow-up of 6.7 months, improvement >50% or normalization of ALT was observed in 5/7 patients, suppression of HDV RNA below the detection limit in 2/7, reduction of HDV RNA >2 log GEQ/ml in 2/7, reduction of HDV RNA <2 log GEQ/ml in 2/7 and HDV rebound in 1 patient. Complete virological responders (n = 2, both with cirrhosis) had low HDV RNA levels at baseline (3.22×10^3 and 3.24×10^3 GEQ/ml) and showed a normalization of ALT after 9 or 10 months of treatment. Partial virological responders >2 log GEQ/ml (n = 2, 1 with cirrhosis) presented with higher baseline HDV RNA (1.36×10^8 and 1.57×10^7 GEQ/ml) and showed a reduction of ALT >50% after 5 or 9 months of treatment. Virological non-responders <2 log GEQ/ml (n = 2, 1 with cirrhosis) presented with initial HDV RNA levels of 3.9×10^6 and 3.5×10^5 GEQ/ml, and showed no or <50% reduction of ALT after 3 or 7 months of treatment. 1 patient (no cirrhosis, baseline HDV-RNA 1.9×10^7 GEQ/ml) showed a rebound of serum HDV RNA to 1.48×10^6 GEQ/ml after initial complete response (5 months of treatment), while ALT normalized. HBV DNA was undetectable in 6/7 patients at the end of observation. No BLV related adverse effects were recorded in all individuals.



Conclusion: BVL is well tolerated and leads to a biochemical response in the majority of patients, but the virological response is variable, depending on the viral load at baseline. Further studies should evaluate BLV dose adjustments or peginterferon alfa-2a combination treatments in patients showing insufficient virologic responses.

SAT415

Higher rates of virological relapse after nucleos (t)ide analogue withdrawal in HBeAg-negative versus positive chronic hepatitis B patients: results from a global, multi-ethnic cohort of patients with chronic hepatitis B (RETRACT-B Study)

Hannah S.J. Choi¹, Grishma Hirode^{2,3,4}, Chien-Hung Chen⁵, Tung-Hung Su⁶, Margarita Papatheodoridi⁷, Sabela Lens⁸, Stijn Van Hees⁹, Sylvia Brakenhoff¹⁰, Rong-Nan Chien¹¹, Wai-Kay Seto¹², Grace Wong¹³, Jordan Feld², Henry Ly Chan¹³, Man-Fung Yuen¹², Milan Sonneveld¹⁰, Thomas Vanwolleghem⁹, Xavier Forn⁸, George Papatheodoridis⁷, Jia-Hong Kao⁶, Yao-Chun Hsu¹⁴, Markus Cornberg¹⁵, Bettina Hansen^{2,4}, Rachel Wen-Juei Jeng¹¹, Harry Janssen². ¹University Health Network, Toronto Centre for Liver Disease, Cambodia; ²University Health Network, Toronto Centre for Liver Disease, Canada; ³University of Toronto, Institute of Medical Science, Canada; ⁴The Toronto Viral Hepatitis Care Network (VIRCAN), Canada; ⁵Kaohsiung Chang Gung Memorial Hospital, Taiwan; ⁶National Taiwan University Hospital, Taiwan; ⁷Medical School of National and Kapodistrian University of Athens, Greece; ⁸Hospital Clinic Barcelona, Spain; ⁹Antwerp University Hospital, Belgium; ¹⁰Erasmus University Medical Center, Netherlands; ¹¹Chang Gung Memorial Hospital Linkou Medical Center, Taiwan; ¹²The University of Hong Kong, Hong Kong; ¹³The Chinese University of Hong Kong, Hong Kong; ¹⁴E-Da Hospital/I-Shou University, Taiwan; ¹⁵Hannover Medical School, Germany
Email: sjchoi0731@gmail.com

Background and aims: Whether hepatitis B e antigen (HBeAg) status at the start of nucleos (t)ide analogue (NA) therapy is associated with differential outcomes following NA withdrawal remains unclear. We aimed to compare rates of virological and clinical relapse, ALT flares, and hepatitis B surface antigen (HBsAg) loss in chronic hepatitis B (CHB) patients who were HBeAg-positive versus negative at the start of the most recent NA therapy (SOT).

Method: We investigated outcomes in CHB patients who stopped NA therapy from centres across North America, Europe, and Asia. All included patients were HBeAg-negative and non-cirrhotic at NA discontinuation. Rates of virological (HBV DNA $\geq 2,000$ IU/ml) or clinical (HBV DNA $\geq 2,000$ IU/ml and ALT $\geq 2 \times$ ULN) relapse, ALT flares (≥ 5 or $10 \times$ ULN), and HBsAg loss were compared between SOT HBeAg-positive and -negative patients, using race-stratified Cox regression adjusting for age, sex, NA therapy duration, treatment history, and ALT and HBsAg levels at the end of therapy (EOT).

Results: Of 1,360 CHB patients included, 1,142 were HBeAg-negative and 218 HBeAg-positive at SOT. The HBeAg-negative group was older (54 vs 43 years) and had a higher proportion of males (73% vs 65%), fewer patients previously treated with interferon (8% vs 14%), and lower HBsAg levels at EOT (2.6 vs 3.1 log₁₀ IU/ml), all $p < 0.05$. The duration of NA therapy and racial composition were comparable between the two groups. HBeAg-negativity versus positivity at SOT was significantly associated with a higher rate of virological relapse (adjusted hazard ratio [aHR] 1.9, $p < 0.01$) but not clinical relapse (aHR 1.2, $p = 0.14$). Other significant predictors of virological relapse included higher HBsAg levels at EOT (log₁₀ IU/ml, aHR 1.7), TDF versus ETV treatment (aHR 1.6), and prior use of other NA (aHR 1.2), all $p < 0.05$. For clinical relapse, higher HBsAg (log₁₀ IU/ml, aHR 1.9) and ALT (\times ULN, aHR 1.4) levels at SOT, TDF versus ETV treatment (aHR 1.6), prior use of other NAs (aHR 1.5), and male sex (aHR 1.6) were identified as predictors, all $p < 0.01$. No differences in rates of ALT flares (≥ 5 or $10 \times$ ULN) or HBsAg loss were observed.

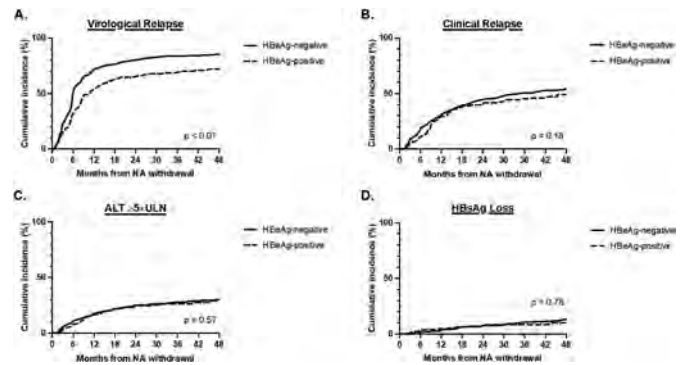


Figure: Unadjusted cumulative incidence of: A) virological relapse; B) clinical relapse; C) ALT flare $\geq 5 \times$ ULN; D) HBsAg loss by HBeAg status at the start of nucleos (t)ide analogue therapy.

Conclusion: CHB patients who were HBeAg-negative versus positive at SOT experienced higher rates of virological relapse, despite having longer time spent in the HBeAg-negative phase of infection. Off-therapy ALT elevations and HBsAg loss were not associated with HBeAg status at SOT.

SAT416

Real life efficacy and tolerability of Tenofovir alafenamide fumarate in liver transplant recipients: a multicenter study

Hale Gokcan¹, Suna Yapali², Murat Harputluoglu³, Zeynep Melekoğlu Ellik¹, Pinar Gökçen⁴, Haydar Adanir⁵, Arif Mansur Cosar⁶, Serdar Durak⁶, Derya Ari⁷, Shahin Mehdiyev⁸, Elif Sitre Koç², Fatih Guzelbulut⁹, Huseyin Alkim¹⁰, Nergis Ekmen¹¹, Abdullah Emre Yıldırım¹², Yasemin Unsul¹¹, Tufan Teker¹³, Digdem Ozer Etik¹⁴, Sezgin Vatansever¹⁵, Hatice Yasemin Balaban¹⁶, Kamil Ozdil⁴, Mehmet Arslan⁶, Meral Akdoğan Kayhan⁷, Feyza Gunduz⁸, Murat Kıyıcı¹³, Sedat Boyacıoğlu¹⁴, Halis Simsek¹⁶, Nurdan Tozun², Dinc Dincer⁵, Ramazan Idilman¹. ¹Ankara University, Gastroenterology, Turkey; ²Acibadem University, Turkey; ³İnönü Üniversitesi Turgut Özal Tıp Merkezi, Turkey; ⁴Sağlık Bilimleri Üniversitesi Ümraniye Eğitim ve Araştırma Hastanesi, Turkey; ⁵Akdeniz Üniversitesi Tıp Fakültesi, E Blok, Antalya, Turkey; ⁶Karadeniz Technical University, Turkey; ⁷Ankara Şehir Hastanesi, Turkey; ⁸Marmara University Research And Education Hospital, Turkey; ⁹SBÜ Haydarpaşa Numune Eğitim ve Araştırma Hastanesi, Turkey; ¹⁰SBÜ Şişli Hamidiye Etfal Eğitim ve Araştırma Hastanesi, Turkey; ¹¹Gazi University Medical Faculty, Turkey; ¹²Gaziantep Üniversitesi Tıp Fakültesi, Turkey; ¹³Uludağ Üniversitesi Tıp Fakültesi Hastanesi, Turkey; ¹⁴Başkent University Ankara Hospital, Turkey; ¹⁵İzmir Atatürk Eğitim Araştırma Hastanesi, Turkey; ¹⁶Hacettepe Üniversitesi, Turkey
Email: sunayapali@gmail.com

Background and aims: We aimed to determine the real-life efficacy and tolerability of tenofovir alafenamide fumarate (TAF) in liver transplant recipients.

Method: This a multicenter retrospective study. A total of 196 recipients were enrolled into the study. The primary end points were virological and biochemical response at week 24 and 48 of the treatment, the secondary end point was tolerability of TAF. Median duration of the TAF treatment was 11.6 months (range: 6–60 months).

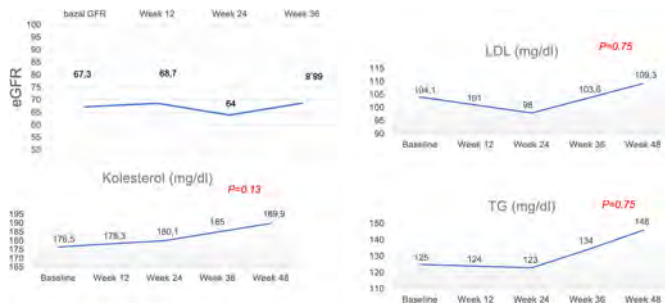
Results: A total of 108 recipients who had at least 6 months follow-up were included in the analysis. Mean age was 58 ± 10 years, 74% were male. Of these, 80% were on tacrolimus-based and 38% on everolimus-based treatments. Median duration from LT to TAF initiation was 24.5 months (range: 0–252 months). Seventeen patients received TAF treatment as first-line therapy, whereas 91 patients switched to TAF treatment. Renal dysfunction and osteoporosis were the most common indications for TAF treatment.

Baseline median serum ALT level was 25 IU/L (range: 10–96 U/L) and baseline median HBV DNA level was 890 IU/ml, respectively. Virological and biochemical response were 90% and 71% at week

POSTER PRESENTATIONS

24, and 100% and 92% at week 48, respectively. From baseline to the last follow-up, improvement in ALT at every 24 weeks compared by linear mixed model was significant; -3.226 IU/ml [95% CI: (-5.62) – (-0.84) ; $p = 0.009$]. After the switch to TAF treatment, none of the patients experienced HBV reactivation.

TAF treatment was well tolerated. Renal functions and lipid profile remained stable during TAF treatment (Figure 1). No serious adverse events were reported. No graft rejection was observed.



Conclusion: The present study indicates that TAF is effective and tolerable in liver transplant recipients.

SAT417

Impact of patient-related factors on the pharmacokinetics of Bulevirtide

Renu Singh¹, Parag Kumar¹, Rory Leisegang¹, Francesco Bellanti², Craig Comisar², Kishore Polireddy², Vithika Suri¹, Dmitry Manuilov¹, John F. Flaherty¹, Sandhya Girish¹. ¹Gilead Sciences, Foster City, United States; ²Certara Inc, Princeton, United States

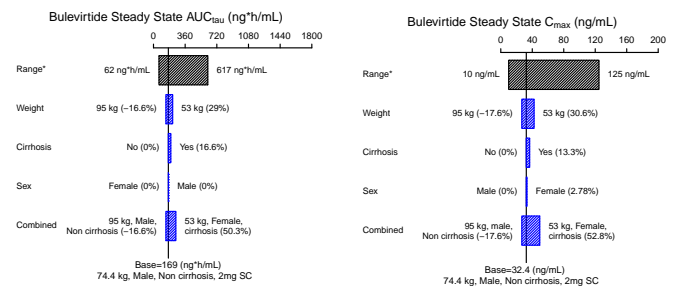
Email: renu.singh16@gilead.com

Background and aims: Bulevirtide (BLV) is a novel, first-in-class, potent, highly selective hepatocyte entry inhibitor of the hepatitis delta virus (HDV) that binds to and inactivates sodium taurocholate cotransporting polypeptide (NTCP), an essential HDV entry receptor. BLV is a 47-amino acid lipopeptide, recommended at a 2 mg dose by daily subcutaneous (SC) injection. Our objective was to characterize the population PK of BLV in participants with or without HDV and evaluate the effect of covariates on its PK to characterize intrinsic/extrinsic factors that might affect BLV exposures.

Method: Comprehensive PK data from participants in 2 Phase 1 studies (N = 48), 3 Phase 2 studies (N = 314), and 1 Phase 3 study (N = 99) were analysed using nonlinear mixed-effects modeling (NONMEM®) software. Individual BLV PK parameter estimates were generated and the impact of patient-specific covariates (eg. baseline (BL) body weight (WT), age, sex, race, BLV dose, health status, BL HDV viral load, creatinine clearance, presence of anti-drug antibodies, liver function tests, comedication (oral antivirals and pegylated interferon alpha) were evaluated.

Results: Nonlinear PK was observed with greater than dose proportional increase in BLV exposure. The final BLV model was described by a 2-compartment model with sequential zero- first-order absorption and first-order elimination from the central compartment. An absolute SC bioavailability of 53.4% was estimated with a dose effect on clearance adequately characterizing the non-linear PK.

WT was the most influential covariate, with a change in BLV exposures ranging from -17.6% to $+30.6\%$ (relative to exposures at the median WT) for participants with extreme covariate values (ie, 5th and 95th WT percentiles), respectively (Figure 1). Additionally, participants with compensated cirrhosis were found to have 17% higher exposure, as compared to participants without cirrhosis.



Conclusion: Across a wide range of participants, BLV exposures were inversely correlated with WT along with slightly higher exposures in participants with cirrhosis. These changes in BLV exposures were not considered clinically meaningful. These data support the use of the recommended 2 mg once daily dose across the spectrum of participants with varied patient-related factors.

SAT418

Reduction of liver stiffness in chronic hepatitis B patients treated with tenofovir disoproxil fumarate: a prospective observational study

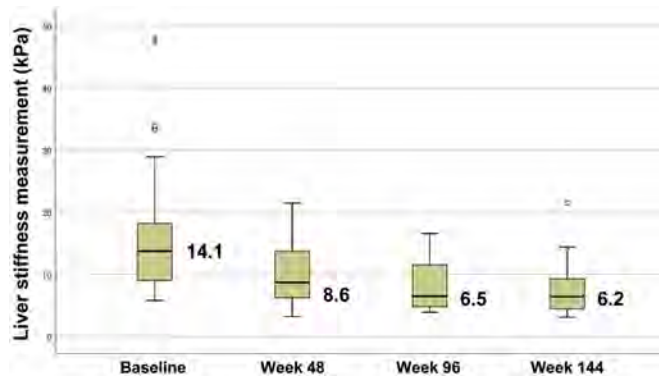
Heejin Cho¹, Yun Bin Lee^{1,2}, Yeonjung Ha², Young Eun Chon², Mi Na Kim², Joo Ho Lee², Seong Gyu Hwang². ¹Department of Internal Medicine and Liver Research Institute, Seoul National University College of Medicine, Seoul, Korea, Rep. of South; ²Department of Internal Medicine, CHA Bundang Medical Center, Seongnam, Korea, Rep. of South

Email: yblee@snu.ac.kr

Background and aims: Regression of hepatic fibrosis during antiviral therapy in patients with chronic hepatitis B has been demonstrated, but data about influence of long-term treatment with tenofovir disoproxil fumarate (TDF) on liver stiffness (LS) measured by transient elastography are scarce. We aimed to investigate changes in LS values during 144-week antiviral therapy with TDF in patients with chronic hepatitis B.

Method: A total of 48 treatment-naïve patients with chronic hepatitis B who initiated TDF therapy were enrolled and followed up for 144 weeks. Laboratory tests and LS measurements were performed at baseline and repeated at weeks 12, 24, 48, 96 and 144. A significant decline of LS was defined as $\geq 30\%$ drop of LS value from the baseline to week 96.

Results: Among the 48 enrolled patients, 11 patients were lost to follow-up before 96 weeks and 37 patients were included in the analysis (median age, 45 years [interquartile range, 35–55.5 years]; 20 men [54.1%]). During antiviral therapy with TDF, the median LS value decreased from 14.1 kPa to 8.6 kPa, 6.5 kPa, and 6.2 kPa at weeks 48, 96 and 144, respectively (all $P < 0.001$; Figure 1). At week 96, virologic and biochemical response were achieved in 34 patients (91.9%) and 33 patients (89.2%), respectively. Moreover, 21 of 36 patients (58.3%) in whom the 96-week LS values were measured showed a significant decline of LS and higher baseline LS value was a single independent predictor of a significant decline of LS (odds ratio, 1.212; 95% confidence interval, 1.027–1.431; $P = 0.023$).



Conclusion: During the long-term antiviral therapy with TDF, LS values declined significantly in treatment-naïve patients with chronic hepatitis B.

SAT419

Toll-like receptor 8 agonism activates monocytes and induces antiviral cytokine production by T-cells in HIV and chronic hepatitis B coinfection

Lydia Tang^{1,2}, Natarajan Ayithan^{1,2}, Shyamasundaran Kottilil^{1,2}.

¹University of Maryland, Baltimore, Baltimore, United States; ²Institute of Human Virology, Baltimore, United States

Email: lydiatang@ihv.umd.edu

Background and aims: In people with HIV/CHB co-infection, progression and mortality from liver disease is worse than among people without HIV. There is no effective cure for CHB. Immune-targeting therapy aimed at recovering HBV-specific immunity is a strategy for CHB cure. Toll-like receptors (TLRs) are a group of pattern recognition receptors identified as immunomodulatory targets for CHB treatment. TLRs activate antigen presenting cells, priming the adaptive immune system. In clinical trial, TLR8 agonism was shown to induce antiviral cytokine production and enhanced HBV-specific B-cell responses in CHB. The aim of this study is to evaluate the effect of HIV co-infection with CHB on HBV-specific immune responses to TLR8 agonism.

Method: CD14⁺ monocytes and CD3⁺ T cells were isolated from autologous peripheral blood mononuclear cell samples by pan T cell negative selection (Miltenyi Biotec) or FACSARIA sorting from people with CHB and HIV/CHB co-infection enrolled in an observational natural history study at the Institute of Human Virology, University of Maryland Baltimore. Monocytes were stimulated with ssRNA40, a TLR8 agonist, then pulsed with HBV peptide and co-cultured with autologous T cells. Activation of monocytes by TLR8 stimulation was evaluated by flow cytometry immunophenotyping and compared with unstimulated monocytes. Activation of HBV-specific CD8 T cells by TLR8 stimulated monocytes was then evaluated by measuring (by intracellular staining and flow cytometry) production of pro-inflammatory cytokines. For statistical analysis student's t-test was used with $p < 0.05$ considered significant.

Results: Samples from 7 patients with CHB and 7 with HIV/CHB were analyzed. At baseline, monocyte population was larger in CHB compared to HIV/CHB ($p = 0.03$) with higher HLA-DR, CD11c and IL6 expression and induced stronger HBV-specific CD8 T cell responses than HIV/CHB with higher induction of TNF alpha ($p = 0.01$), IFN gamma ($p = 0.002$), IL-2 ($p = 0.003$), and IL-21 ($p = 0.03$). *In vitro* treatment of monocytes with ssRNA40 was associated with increased CD40 ($p = 0.03$), CD86 ($p = 0.005$), CD69 and HLA-DR ($p = 0.008$) expression in CHB but not in HIV/CHB. Treatment of autologous T cells with TLR8-stimulated monocytes resulted in increased TNF alpha ($p = 0.02$), IFN gamma ($p = 0.04$), and IL-21 ($p = 0.03$) by CD8 T cells in the HIV/CHB patients. No significant changes were seen in the CHB T cells.

Conclusion: TLR8 agonism activated monocytes. These, in turn, were able to activate HBV-specific antiviral CD8 T cell functions. In HIV/CHB samples, this effect on T cells was seen despite the absence of significant changes in the monocytes with TLR8 treatment, supporting further study of toll-like receptor agonism for CHB treatment in people with HIV/CHB.

SAT420

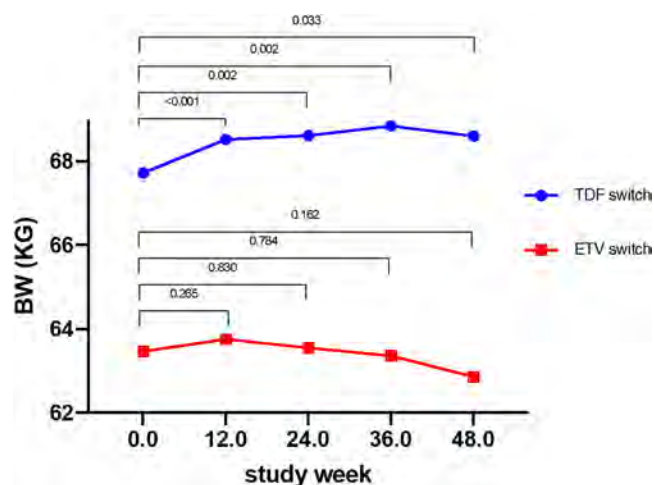
Comparison of body weight and lipid profiles following tenofovir disoproxil fumarate or entecavir switching to tenofovir alafenamide-an interim analysis

Pin-Nan Cheng¹, Chun-Jen Liu², Jyh-Jou Chen³, I-Cher Feng⁴, Hsing-Tao Kuo⁵, Pei-Lun Lee³, Ming-Lung Yu⁵, Yencheng Chiu¹, Chiu Hung-Chih¹, Shih-Chieh Chien¹, Pei-Jer Chen². ¹National Cheng Kung University Hospital, Department of Internal Medicine, Tainan, Taiwan; ²National Taiwan University Hospital, Department of Internal Medicine, Taipei, Taiwan; ³Chi-Mei Medical Center, Liouying, Tainan, Taiwan, Department of Internal medicine, Tainan, Taiwan; ⁴Chi-Mei Medical Center, Tainan, Taiwan, Department of Internal Medicine, Tainan, Taiwan; ⁵Kaohsiung Medical University Hospital, Kaohsiung, Taiwan, Department of Internal Medicine, Kaohsiung, Taiwan
Email: pncheng@mail.ncku.edu.tw

Background and aims: Body weight (BW) and lipid profiles changes have been reported in HIV infected patients treated with tenofovir alafenamide (TAF) containing regimens. Tenofovir disoproxil fumarate (TDF) treated chronic hepatitis B (CHB) patients exhibited lower lipid profiles in phase III study. The impact of TAF, as a new drug for CHB treatment, on BW and lipid profiles remains unclear and needs to investigate.

Method: This was a prospective, multi-center, observational study. CHB patients from five hospitals in Taiwan treated with TDF or entecavir for at least 1 years and then switched to TAF were enrolled. Measurement of biochemical, virological, and atherosclerotic cardiovascular disease (ASCVD) risk score at baseline and then at an interval of 12 weeks or 48 weeks by items. Primary end point was the body weight changes following switching to TAF or entecavir. Secondary end points included ASCVD score changes, and changes of lipid and sugar profiles following switching to TAF.

Results: At the end of October 2021, 99 patients, including 63 males with a mean age of 54.3 years, completed a 48 weeks follow-up were enrolled for analysis. Of them, 65 and 34 patients treated with TDF or entecavir before switching to TAF, respectively. At baseline, significantly lower TG, Chol, and LDL (all $p < 0.05$) in TDF switch group than entecavir switch group. Figure 1 shows the BW changes during 48 weeks of TAF treatment. Following switching to TAF, significant BW gain was present from 12 weeks and maintained thereafter until 48 weeks in TDF switch group comparing with baseline BW. In contrast, BW remained unchanged in entecavir switch group during 48 weeks of observation. In TDF switch group but not entecavir switch group, all of the lipid profiles including TG (88.6 ± 48.3 vs. 104.4 ± 66.6 mg/dL, $p = 0.014$), Chol (160.3 ± 33.1 vs. 188.1 ± 38.9 mg/dL, $p < 0.001$), LDL (104.9 ± 28.9 vs. 121.9 ± 34.2 mg/dL, $p < 0.001$), and HDL (48.2 ± 11.7 vs. 58.2 ± 13.2 mg/dL, $p < 0.001$) were significantly increased following 48-week TAF treatment. ASCVD risk score had a trend toward a significant increase in TDF switch group (6.3 ± 9.5 vs. 7.0 ± 9.4 , $p = 0.051$), but not in entecavir switch group (12.5 ± 16.7 vs. 13.2 ± 18.5 , $p = 0.343$).



Conclusion: Following TDF switch to TAF, BW increased shortly and the lipid-lowering effects of TDF diminished. Combining BW gain and increase of lipid profiles, CVD risk may need to monitor closely.

SAT421

Real life efficacy and tolerability of Tenofovir Alafenamide Fumarate in patients with hepatitis-B virus-related cirrhosis

Suna Yapali¹, Hale Gokcan², Serdar Durak³, Zeynep Melekoğlu Ellik², Fatih Guzelbulut⁴, Sezgin Vatansever⁵, Derya Ari⁶, Shahin Mehdiyev⁷, Haydar Adanir⁸, Elif Sitre Koç¹, Feyza Gunduz⁷, Mehmet Arslan³, Kamil Ozdil⁹, Dinc Dincer⁸, Ramazan Idilman². ¹Acibadem University, Turkey; ²Ankara University Medical School, Turkey; ³KTU Faculty of Medicine, Turkey; ⁴SBÜ Haydarpaşa Numune Eğitim ve Araştırma Hastanesi, Turkey; ⁵Kâtip Çelebi Üniversitesi, İzmir, Turkey; ⁶Ankara Şehir Hastanesi, Turkey; ⁷Marmara University Research And Education Hospital, Turkey; ⁸Akdeniz University, Turkey; ⁹Sağlık Bilimleri Üniversitesi Ümraniye Eğitim ve Araştırma Hastanesi, Turkey
Email: sunayapali@gmail.com

Background and aims: We aimed to determine the real-life efficacy and tolerability of tenofovir alafenamide fumarate (TAF) in patients with hepatitis B virus (HBV)-related cirrhosis

Method: This multicenter study included a total of 91 patients with HBV-related cirrhosis who received TAF treatment as first line treatment or switched to TAF. The primary end points were virological and biochemical response at week 24 and 48 of the treatment, the secondary end point was the assessment of safety and tolerability of TAF. Median follow-up on TAF treatment was 13.7 (range 6–26) months.

Results: Of the 91 patients with cirrhosis, 43 patients who had at least 6 months of follow-up were included in the analysis. Mean age was 64 ± 11 years and 63% was male. Baseline median MELD score was 10 (range: 9–14), and 4 (9.3%) were decompensated. Six (14%) patients received TAF treatment as first-line therapy. Baseline median serum ALT and HBV DNA levels were 25 IU/L (range: 10–96 U/L) and 51000 IU/ml, respectively. Thirty-seven (86%) patients switched to TAF treatment. Renal dysfunction and hypophosphatemia were the most common indications for TAF treatment.

Virological and biochemical responses were 67% and 67% at week 24 and 100% and 83% at week 48, respectively. Serum HBV DNA was undetectable at week 36 among all patients with detectable HBV DNA at baseline. From baseline to the last follow-up, improvement in ALT at every 24 weeks compared by linear mixed model was significant; –1.13 IU/ml [95% CI: (–1.8)–(–0.45), $p = 0.005$]. None of the patients experienced HBV reactivation. During TAF treatment, renal functions and lipid profile were stable (Figure 1). No serious adverse effect was observed.

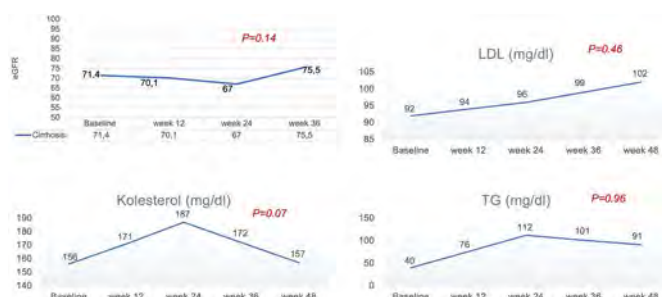


Figure: Changes in estimated glomerular filtration rate (GFR) and lipid profile

Conclusion: Based on the preliminary results of this study, TAF is effective and tolerable in patients with HBV-related compensated and decompensated cirrhosis

SAT422

Effects of the siRNA JNJ-3989 and/or the capsid assembly modulator (CAM-N) JNJ-6379 on viral markers of chronic hepatitis B (CHB): results from the REEF-1 study

Man-Fung Yuen¹, Tarik Asselah², Ira M Jacobson³, Maurizia Brunetto⁴, Harry Janssen⁵, Tetsuo Takehara⁶, Jinlin Hou⁷, Thomas Kakuda⁸, Tom Lambrecht⁹, Ronald Kalmeijer⁸, Carine Guinard-Azadian¹⁰, Cristiana Mayer⁸, John Jerzowski⁸, Thierry Verbinnen⁹, Oliver Lenz⁹, Umesh Shukla⁸, Michael Biermer¹¹. ¹Queen Mary Hospital, Department of Medicine and State Key Laboratory of Liver Research, The University of Hong Kong, Hong Kong, China; ²Université de Paris, INSERM UMR1149 and Hôpital Beaujon, APHP, Clichy, France; ³New York University Grossman School of Medicine, New York, New York, United States; ⁴University of Pisa, Pisa, Italy; ⁵University of Toronto, Toronto, Canada; ⁶Osaka University Graduate School of Medicine, Osaka, Japan; ⁷Nanfeng Hospital, Southern Medical University, Guangzhou, China; ⁸Janssen Research and Development, United States; ⁹Janssen Research and Development, Belgium; ¹⁰Janssen Research and Development, France; ¹¹Janssen Research and Development, Germany
Email: mfyuen@hku.hk

Background and aims: JNJ-3989 is an siRNA targeting all hepatitis B virus (HBV) RNAs thereby reducing viral proteins. JNJ-6379, a CAM-N, prevents the formation of infectious viral genome-containing capsids. The REEF-1 study (NCT03982186) assessed the efficacy and safety of monthly s.c. injections of JNJ-3989 (40, 100, and 200 mg) and/or 250 mg daily oral JNJ-6379 versus placebo in combination with daily oral NA in not currently treated (NCT) or virologically suppressed (VS) HBeAg positive (HBeAg+) or negative (HBeAg-) CHB patients.

Method: In this Phase 2b, multicenter, active-controlled study, CHB patients (N = 470) were randomized and dosed for a 48-week double-blind placebo-controlled treatment period. Changes in viral markers were assessed. Data from week 24 follow-up (FU W24) are presented.

Results: JNJ-3989 reduced HBsAg in a dose dependent manner with the greatest decline at the 200 mg dose (mean [SD] reduction of 2.6 [0.10] log₁₀ IU/ml) at week 48 (W48) versus control (0.22 [0.85] log₁₀ IU/ml; $P < 0.001$). By FU W24, 47.0% of patients in the JNJ-3989 200 mg group had HBsAg <100 IU/ml. HBsAg reduction from baseline (BL) remained ≥1 log for 84.3% and ≥2 log for 37.3% of patients in the JNJ-3989 200 mg group at FU W24. 19.1% and 29.7% of patients met NA stopping criteria (ALT <3x ULN, HBV DNA <LOQ, HBeAg-, HBsAg <10 IU/ml) with JNJ-3989 200 mg at W48 and until FU W24, respectively. Only 3 of 66 (4.5%) patients who met NA stopping criteria met NA re-starting criteria during the follow-up.

Declines in HBeAg and HBcrAg were generally dose dependent and greater in patients with higher baseline (BL) levels, thus reductions were most pronounced in NCT HBeAg+ patients with mean (SD) change from BL at W48 of –2.22 (1.14) log₁₀ IU/ml for HBeAg and –2.56 (0.93) log₁₀ U/ml for HBcrAg in the 200 mg JNJ-3989 group

versus -1.45 (1.67) and -1.69 (1.41) for control; mean (SD) change from BL at FU W24 was -2.52 (1.23) for HBeAg and -2.74 (1.11) for HBcAg with JNJ-3989 200 mg versus -1.50 (1.70) and -1.71 (1.57) for control. Despite lower BL HBeAg and HBcAg levels in VS and/or HBeAg- patients, seroclearance of these markers was infrequent. In NCT HBeAg+ patients, mean (SE) HBV RNA change from BL at W48 was -3.66 (1.11) log₁₀ copies/ml for JNJ-3989 200 mg and -4.68 (1.16) for JNJ-3989 100 mg+JNJ-6379+NA versus -1.34 (1.40) for control. The respective HBV RNA undetectability rates at W48 were 29%, 100% and 0%. Off-treatment HBV RNA levels generally remained stable or declined in the JNJ-3989 arms, but increased in the JNJ-6379 arms consistent with the direct inhibition of HBV RNA release by JNJ-6379. Numerically greater decline in HBV DNA was seen with JNJ-3989 100 and 200 mg and JNJ-6379 containing arms versus control. **Conclusion:** Treatment with JNJ-3989 reduced levels of HBV markers in a dose dependent manner. Reductions in viral markers were most pronounced in NCT HBeAg+ patients.

SAT423

Safety, pharmacokinetics and antiviral activity of GST-HG141, a hepatitis B virus capsid assembly modulator, in subjects with chronic hepatitis B

Jiajia Mai¹, Hong Zhang¹, Min Wu¹, Yanhua Ding¹, Junqi Niu¹, Vadim Bichko², Yanan Tang², Wenhao Yan², John Mao², Dong Zhang², Wenqiang Wu², Hong Ren², George Zhang², Hongming Li², Shikui Chen², Yanhua Zhang², Jiang Zhigan³, Haiying He³, Shuhui Chen³. ¹The First Hospital of Jilin University, Changchun, China; ²Fujian Cosunter Pharmaceutical Co., Ltd., Fuzhou, China; ³Domestic Discovery Service Unit, WuXi AppTec (Shanghai) Co., Ltd., Shanghai, China
Email: vbichko@gmail.com

Background and aims: Hepatitis B virus (HBV) capsid assembly modulators (CAMs) are clinically validated agents for the chronic HBV drug development, with a potential for HBV cure. Safety, tolerability, and pharmacokinetics of GST-HG141, a novel CAM, in healthy subjects (NCT04386915) has been reported previously [Li et al., Antimicrob Agents Chemother. 2021;65 (10)]. The aim of this study was to evaluate safety, PK and antiviral activity of multiple doses of GST-HG141 in patients with chronic hepatitis B (CHB).

Method: A multi-center, randomized, double-blind, placebo-controlled multiple ascending-dose phase Ib study (NCT04868981). Patients with CHB, who were not treated with interferon or nucleosides (>12 or >6 months, respectively), HBeAg-positive or negative (serum HBV DNA $\geq 2 \times 10^5$ or $\geq 2 \times 10^4$ IU/ml, respectively) received oral BID doses of GST-HG141 (25, 50 and 100 mg) for 28 days. Ten patients in each cohort were randomized to receive a drug or placebo (4:1). A validated LC-MS/MS method was used to quantify GST-HG141 in plasma. The PK parameters were calculated with WinNonlin 8.3 software. Serum HBV DNA and HBV pgRNA were determined using Quantitative Real-Time PCR, serum HBV antigens-by ELISA methods. **Results:** Administration of 25, 50 or 100 mg of GST-HG141 BID for 28 days was well tolerated. No SAEs or dose-related increase in number of AEs was reported. There were no TEAEs leading to discontinuation of treatment. A rapid and robust decline in serum HBV DNA was observed (median 2.9, 3.3 and 3.5 log₁₀ IU/ml for 25, 50 and 100 mg dose cohorts, respectively). Serum HBV pgRNA levels decreased by median 2.2 log₁₀ U/ml in all dose cohorts, with a maximum median decrease of 2.40 log₁₀ U/ml in the 100 mg dose cohort at day 29 of treatment. No virus breakthrough was noted. No statistically significant decline in serum HBsAg, HBeAg or HBcAg was observed. However, there was a trend of serum HBeAg and HBcAg decrease in patients, receiving the drug. Plasma GST-HG141 exposure increased relatively proportionally with the dose. Moderate accumulation (mean values 1.67–2.38) was seen with dosing for 28 days.

Conclusion: Oral BID dosing with 25, 50 or 100 mg of GST-HG141 for 28 days was safe and well tolerated. It resulted in rapid, robust and dose-dependent decline in serum HBV DNA. Serum HBV pgRNA

levels also decreased significantly. Plasma GST-HG141 exposure was nearly dose-proportional. Further clinical development of GST-HG141 for CHB is warranted. Phase II drug combination study with GST-HG141 and nucleoside analogs is underway.

SAT424

Predictors of sustained response in hepatitis B surface antigen-negative patients after peginterferon therapy: an observational study

Jun Chen¹, Yan Huang¹. ¹Xiangya Hospital Central South University, Department of Infectious Diseases, Changsha, China
Email: drhyan@126.com

Background and aims: Hepatitis B surface antigen (HBsAg) clearance is considered the functional cure and recommended as the optimal end point of antiviral therapy for chronic hepatitis B (CHB) patients. Although patients could achieve HBsAg clearance after peginterferon treatment, HBsAg reversal occurred in some patients. This study aimed to investigate predictors of sustained response in HBsAg-negative patients after peginterferon therapy.

Method: CHB patients with HBsAg clearance after peginterferon therapy were enrolled from 2018 to 2021. Patients were followed up for 48 weeks after functional cure. Patients with sustained negative HBsAg were non-recurrence group and patients with HBsAg reversal were recurrence group.

Results: A total of 176 patients achieved HBsAg clearance after peginterferon treatment. 113 patients were included at the 48-week follow-up (104 in non-recurrence group, 9 in recurrence group). The cumulative rates of HBsAg reversion at 12 weeks, 24 weeks, 36 weeks, and 48 weeks after achieving functional cure were 2.89%, 3.85%, 6.72%, and 7.92%, respectively. HBsAb at the end of treatment was significantly higher in non-recurrence patients compared with recurrence patients at week 48 ($p < 0.001$).

Table: Analysis of potential predictors for sustained response

Variables	Non-recurrence (N = 104)	Recurrence (N = 9)	p value
HBeAg at baseline (S/CO)	0.36 [0.32, 0.42]	0.35 [0.27, 0.36]	0.171
HBsAb at baseline (mIU/ml)	4.53 [1.65, 18.76]	9.26 [7.24, 30.79]	0.359
HbcAb at baseline (S/CO)	7.64 ± 1.54	7.94 ± 1.27	0.567
HBeAg at the end of treatment (S/CO)	0.46 ± 0.60	7.51 ± 12.40	0.397
HBsAb at the end of treatment (mIU/ml)	416.50 ± 386.61	13.43 ± 8.32	<0.001
HbcAb at the end of treatment (S/CO)	7.89 ± 1.38	8.50 ± 0.65	0.382
Consolidation treatment time, n (%)			0.644
0–12 weeks	15 (14.42)	2 (22.22)	
12–24 weeks	29 (27.89)	1 (11.11)	
24–36 weeks	27 (25.96)	2 (22.22)	
36–48 weeks	33 (31.73)	4 (44.44)	

Conclusion: HBsAb level at the end of treatment is a potential predictor of sustained response. Evaluating HBsAb level when peginterferon discontinued can improve sustained functional cure.

SAT425

Randomized, double-blind, placebo-controlled trial of Tenofovir Alafenamide in children and adolescents with chronic hepatitis B

Kathleen Schwarz¹, Jorge Bezerra², Byung-Ho Choe^{3,4}, Chuan-Hao Lin⁵, Frida Abramov⁶, Anh-Hoa Nguyen⁷, Yang Liu⁸, Rory Leisegang⁹, John F. Flaherty⁶, Daniela Pacurar¹⁰, Kyung Mo Kim¹¹, Iliyar Khaertynova¹², Shalimar¹³, Jia-Feng Wu¹⁴, Manish Tandon¹⁵, Philip Rosenthal¹⁶, Morozov Viacheslav¹⁷, Etienne Sokal¹⁸, Mei-Hwei Chang¹⁹. ¹UC San Diego School of Medicine, Rady Children's Hospital-San Diego, San Diego, United States; ²University of Cincinnati, Cincinnati Children's Hospital, Cincinnati, United States; ³Kyungpook National University School of Medicine, Department of Pediatrics, Daegu, Korea, Rep. of South; ⁴Kyungpook National University School of Medicine, Pediatrics, Daegu, Korea, Rep. of South; ⁵Children's Hospital Los Angeles, Division of Gastroenterology, Hepatology and Nutrition, Los Angeles, United States; ⁶Gilead Sciences, Inc., Clinical Development, Foster City, United States; ⁷Gilead Sciences, Inc., Biostatistics, Foster City, United States; ⁸Gilead Sciences, Inc., Clinical Virology, Foster City, United States; ⁹Gilead Sciences, Inc., Clinical Pharmacology, Foster City, United States; ¹⁰"Carol Davila" University of Medicine and Pharmacy Bucharest, Department of Pediatrics "Grigore Alexandrescu" Emergency Children's Hospital Bucharest, Bucharest, Romania; ¹¹University of Ulsan College of Medicine, Asan Medical Center Children's Hospital, Seoul, Korea, Rep. of South; ¹²Kazan State Medical Academy, Kazan, Russian Federation; ¹³All India Institute of Medical Sciences, Department of Gastroenterology, New Delhi, India; ¹⁴National Taiwan University Hospital, Department of Pediatrics, Taipei, Taiwan; ¹⁵M. V. Hospital and Research Centre, Lucknow, India; ¹⁶University of California, San Francisco, Department of Pediatrics, Division of Gastroenterology, Hepatology and Nutrition, San Francisco, United States; ¹⁷Hepatolog, LLC, Samara, Russian Federation; ¹⁸Université Catholique de Louvain, Cliniques Universitaires Saint-Luc, Pediatric Hepatology and Gastroenterology and Cell Transplant Center, Brussels, Belgium; ¹⁹National Taiwan University and Children Hospital, Department of Pediatrics, Taipei, Taiwan
Email: frida.abramov@gilead.com

Background and aims: Tenofovir Alafenamide (TAF) is a novel prodrug of tenofovir (TFV) with non-inferior efficacy and greater plasma stability resulting in enhanced delivery of TFV and reduced plasma concentrations leading to an improved bone and renal safety profile over tenofovir disoproxil fumarate (TDF). TAF is approved for use in adult patients with Chronic Hepatitis B (CHB). However, safety and efficacy data in pediatric CHB patients are lacking. In a multicenter, randomized, double-blind, placebo-controlled trial we evaluated the safety and efficacy of TAF in children 6 years and older weighing ≥ 25 kg.

Method: Males or females aged 12 to <18 years weighing ≥ 35 kg (Cohort 1), and 6 to <12 years weighing ≥ 25 kg (Cohort 2, Group 1), with HBV DNA $\geq 2 \times 10^4$ IU/ml, ALT $\geq 1.5 \times$ ULN, and creatinine clearance (eGFR; Schwartz method) ≥ 80 ml/min were randomized (2:1) to TAF 25 mg or PBO daily for 24 weeks, after which all patients received open-label TAF for up to Week 240. The co-primary end points were the proportion with HBV DNA <20 IU/ml and safety (treatment-emergent [TE] serious adverse events [SAEs] and all TE adverse events [AEs]) at Week 24; other assessments included serological and biochemical responses, bone mineral density (BMD) (spine and whole body[minus head]), resistance surveillance and pharmacokinetics.

Results: 88 patients were randomized and treated (Cohort 1: TAF 47, PBO 23; Cohort 2 group 1: TAF 12, PBO 6). Baseline (BL) characteristics were similar; overall mean (range) age and mean (SD) weight were 14 (7–17) years and 50.9 (12.9) kg, respectively; 58% were male, 66% Asian, 68% had HBV DNA $\geq 8 \log_{10}$ IU/ml and mean (SD) ALT 107 (118) U/L. 99% were HBeAg-positive, with genotypes D (44%), C (24%), and B (23%) being most common. Overall, at Week 24, 11/59 (19%) TAF and 0/29 PBO patients had HBV DNA <20 IU/ml ($p = 0.0137$); mean (SD) HBV DNA change from BL TAF vs PBO was -4.98 (1.52) \log_{10} IU/ml and -0.10 (0.64) \log_{10} IU/ml ($p < 0.0001$), respectively. High BL viral

load and genotype D were associated with lower rates of viral suppression. A higher proportion of TAF vs PBO patients had ALT normalization (TAF 67%, PBO 4%; $p < 0.0001$), while the rate of HBeAg seroconversion was similar (TAF 7%, PBO 3%). Grade 3 or 4 AEs and SAEs related to study treatment were similar for TAF vs PBO. Slight fluctuations in eGFR were noted for both treatment groups during double blind treatment; however, no patient had eGFR <90 ml/min/ 1.73m^2 at Week 24. Mean % increases from BL to Week 24 in BMD were similar in the TAF vs PBO (spine: +1.6% vs. +1.9%; [$p = 0.77$]; whole body: +1.9% vs. +2.0%; [$p = 0.83$]). Viral resistance was not detected through Week 24. TAF and TFV plasma exposures were within range of adult reference cohorts

Conclusion: In pediatric CHB patients, viral suppression and ALT normalization were superior to placebo, while safety results, including changes in BMD, were similar for TAF and PBO at Week 24

SAT426

The discovery of AMS-I-1274, a high potent and orally active capsid-assembly modulator against hepatitis B virus

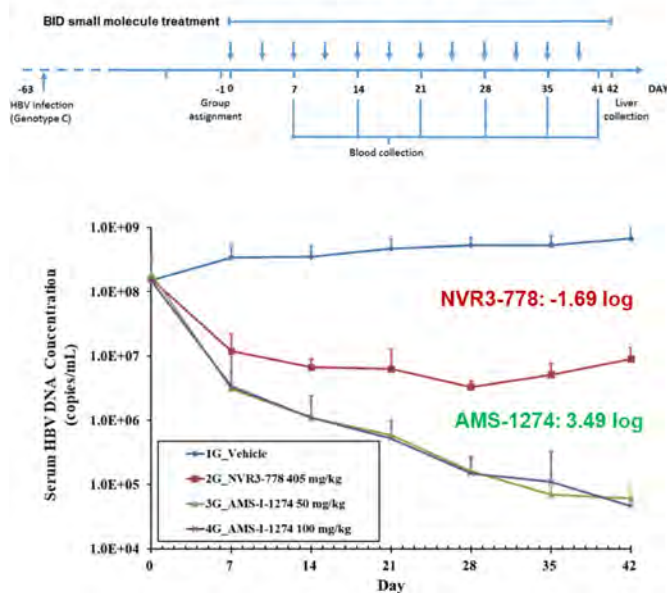
Nakcheol Jeong¹, Peppi Prasit¹, Jung-Hee Kim¹, Misun Lee¹, Heewoo Sim¹, Ryoan Ho Kim¹, Bo-Yeong Pak¹. ¹AM Sciences, Seoul, Korea, Rep. of South
Email: njeong@amsciences.co.kr

Background and aims: Hepatitis B virus (HBV) infection leads to a wide spectrum of liver diseases ranging from acute to chronic hepatitis, cirrhosis, and hepatocellular carcinoma. New drugs that inhibit HBV replication are needed to enhance the treatment of chronic hepatitis B resulting in a higher number of durable responses and functional cures. Capsid-assembly modulators (CAM) are a novel class of HBV antivirals and they have been suggested to be effective anti-HBV agents in both preclinical and clinical studies. Here, we describe the discovery of a novel CAM through high-throughput screening. Lead optimization resulted in the identification of the clinical candidate, AMS-I-1274.

Method: HepAD38 cells were used for the investigation of efficacy including serum-shift assay and mechanism of action studies. HBV genotype (Gt), core-, and NA-resistant variants were evaluated in a HepG2/plasmid DNA transfection system. In vitro anti-viral activity and the effect on the cccDNA level were determined in HBV-infected HepG2-hNTCP cells and primary human hepatocytes (PHH). Pharmacokinetic (PK) properties were assessed in rodents and non-human primates. uPA/SCID mice with humanized liver (PXB-mice) were used for in vivo efficacy studies. Human hepatotoxicity was ascertained by in vitro model using Hurel micro liver.

Results: AMS-I-1274 inhibited HBV replication with an EC₅₀ value of 6.2 nM. The presence of 40% of human serum albumin (HAS) caused a slight reduction in potency (EC₅₀ = 15.6 nM, 2.5-fold increase). It also did not show any significant cytotoxicity (CC₅₀ >100 μM). AMS-I-1274's anti-viral activity was 65-fold more potent compared to Novira 3-778 (EC₅₀ = 5, 700 nM at 40% HSA). Capsid formation assay demonstrated that AMS-I-1274 induced the formation of empty capsid particles devoid of pgRNA and rcDNA (Class II capsid inhibitor). In a de novo HBV infection system, AMS-I-1274 inhibited viral replication with an EC₅₀ value of 1.2 nM against HBV DNA, 8.4 nM against HBsAg, 13.8 nM against HBeAg, and 1.6 nM against intracellular HBV RNA, respectively, and reduced the level of cccDNA (EC₅₀ = 772 nM). AMS-I-1274 showed pan-genotypic activity against isolates from Gt A to H. Most core variants showed no or modest decrease in potency; except for T33N (80-fold). NA-resistant variants remained fully susceptible to AMS-I-1274. PK results showed a good systemic exposure and high oral bioavailability in rodent and non-human primates. In HBV-infected PBX-mice, oral administration of AMS-I-1274 at 50 mg/kg twice daily resulted in robust multi-log reduction ($-3.49 \log_{10}$) of serum HBV DNA after 42 days of treatment.

In HBV-infected PBX-mice model



Conclusion: Taken together, these data support that AMS-I-1274 is a novel class II capsid inhibitor with high anti-HBV potency and a favorable preclinical profile for clinical advancement.

SAT427

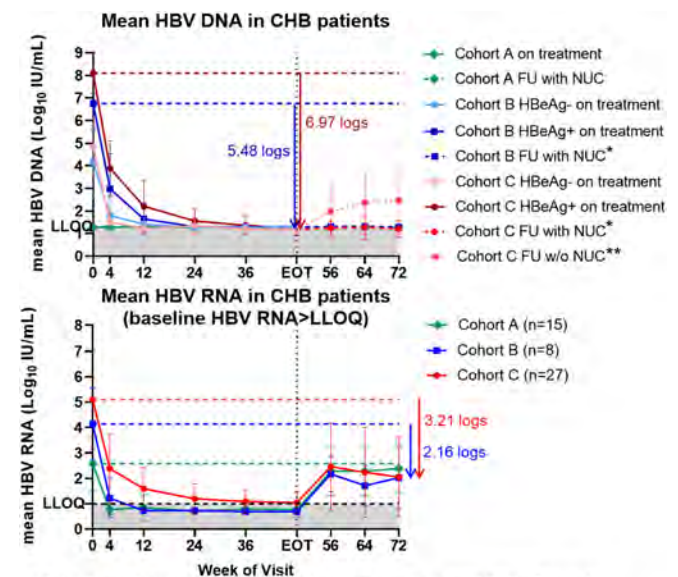
Viral nucleic acids suppression activity of RO7049389 plus NUC with/without Peg-IFN in virologically-suppressed and naïve chronic hepatitis B patients: 48-week treatment and post-treatment follow-up

Man-Fung Yuen¹, Rozalina Balabanska², Jinlin Hou³, Edward J Gane⁴, Tien Huey Lim⁵, WenHong Zhang⁶, Qing Xie⁷, Piyawat Komolmit⁸, Apinya Leerapun⁹, Sheng-Shun Yang¹⁰, Chau-Ting Yeh¹¹, Wen Zhang¹², Xue Zhou¹², Zenghui Xue¹³, Miriam Triyatni¹⁴, Ethan Chen¹³, Rui Li¹², Qingyan Bo¹³. ¹Queen Mary Hospital, The University of Hong Kong, Hong Kong, China, China; ²Acibadem City Clinic Tokuda Hospital EAD, Sofia, Bulgaria; ³Nanfeng Hospital, Southern Medical University, Guangzhou, China; ⁴New Zealand Liver Transplant Unit, The University of Auckland, Auckland, New Zealand; ⁵Middlemore Hospital, Auckland, New Zealand; ⁶Huashan Hospital, Fudan University, Shanghai, China; ⁷Ruijin Hospital, Shanghai Jiaotong University School of Medicine, Shanghai, China; ⁸King Chulalongkorn Memorial Hospital, Bangkok, Thailand; ⁹Maharaj Nakorn Chiang Mai Hospital, Chiang Mai, Thailand; ¹⁰Taichung Veterans General Hospital, Taichung, Taiwan; ¹¹Chang Gung Memorial Hospital, Linkou Branch, Taoyuan, Taiwan; ¹²Roche Pharma Research and Early Development, Roche Innovation Centre Shanghai, Shanghai, China; ¹³Roche (China) Holding, Shanghai, China; ¹⁴F. Hoffmann-La Roche, Basel, Switzerland
Email: qingyan.bo@roche.com

Background and aims: RO7049389 is a Class I HBV core protein allosteric modulator that induces abnormal capsid assembly, leading to depletion of functional core protein thereby inhibiting HBV DNA replication and cccDNA formation. Here we report antiviral and safety results following 48 weeks of RO7049389 plus NUC with/without Peg-IFN-alpha and 24 weeks of follow-up (NCT02952924).

Method: The ongoing open-label study enrolled NUC-suppressed patients to receive RO7049389+NUC (Cohort A, n = 32), and treatment naïve patients to receive RO7049389+NUC without (Cohort B, n = 10) or with (Cohort C, n = 30) Peg-IFN alpha for 48 weeks. At Week 48, all patients except for 5 Cohort C patients who met NUC stopping criteria (HBV DNA <LLOQ and HBsAg <100 IU/ml) entered a 24-week NUC-alone follow-up period.

Results: In Cohort A (11/32 HBeAg+; baseline HBV DNA <LLOQ), 30/32 patients completed the 72-week study with HBV DNA maintained <LLOQ. In all patients with quantifiable HBV RNA at baseline, HBV RNA declined to <LLOQ (10 copies/ml) by Week 4, but rebounded to approximately the baseline level during NUC-alone follow-up. In Cohort B (6/10 HBeAg+; mean baseline HBV DNA 5.7 log₁₀ IU/ml) and Cohort C (19/30 HBeAg+; mean baseline HBV DNA 6.9 log₁₀ IU/ml), a total of 37 patients (10 and 27 respectively) completed the 72-week study. All patients reached HBV DNA <LLOQ except for four Cohort C HBeAg+ patients who had detectable HBV DNA below 150 IU/ml by Week 48. During 24-week follow-up with NUC treatment, except for 2 patients with non-compliance issue, all other patients maintained HBV DNA <LLOQ or at low levels (below 250 IU/ml) and two further patients achieved <LLOQ by Week 72. In 30/33 treatment naïve patients with quantifiable HBV RNA at baseline, HBV RNA decreased <LLOQ at Week 48, and remained an average of >2 log₁₀ copies/ml below baseline at the end of follow-up. RO7049389+NUC ± Peg-IFN was safe and well tolerated up to 72 weeks. No RO7049389-related SAEs occurred; two early terminations in each cohort of A and C were due to non-safety reasons. Most common Grade 2–4 lab abnormalities (ALT elevations) were mainly observed in treatment-naïve patients and were accompanied by a decline in viral markers. ALT elevations resolved spontaneously and were not accompanied by significant changes in liver function.



* Excluded one patient in each cohort of B and C who was non-compliant during NUC-alone FU period
** One patient was retreated with NUC on week 61.

Figure. HBV DNA and HBV RNA levels over 72 weeks.

Conclusion: RO7049389+NUC ± Peg-IFN demonstrated potent effect on viral nucleic acids suppression even in treatment naïve patients. HBV DNA was suppressed and maintained <LLOQ in the majority of treatment-naïve patients. Mean HBV RNA levels remained >2 log₁₀ copies/ml below baseline after the cessation of RO7049389, which may suggest a certain level of suppression in cccDNA level/transcriptional activity in treatment naïve patients. RO7049389 plus current standard of care for 48 weeks was safe and well tolerated, supporting further development in viremic patients.

SAT428

Phase 1b/2a study of heterologous ChAdOx1-HBV/MVA-HBV therapeutic vaccination (VTP-300) combined with low-dose nivolumab (LDN) in virally-suppressed patients with CHB on nucleos (t)ide analogues

Tom Evans¹, Eleanor Barnes². ¹Vaccitech, Oxford, United Kingdom; ²Oxford University, Nuffield Department of Medicine, Oxford, United Kingdom
Email: tom.evans@vaccitech.co.uk

Background and aims: Induction of a CD8+ T cell response to HBV may be required to achieve a functional cure of chronic hepatitis B (CHB). The highest magnitude CD8+ T cell responses achieved to date in man have been induced by replication incompetent adenoviral vectors followed by attenuated poxvirus boosts.

Method: Vaccitech with Oxford University is developing a therapeutic HBV vaccine (VTP-300) using a chimpanzee adenoviral vector (ChAdOx1-HBV) and a Modified vaccine Ankara boost (MVA-HBV), that encode the inactivated polymerase, core, and the entire large S region from a consensus genotype C virus. A Phase 1b/2a trial is enrolling up to 52 patients (10–16 patients in each of 4 groups) with CHB, on antivirals for a minimum of one year with VL undetectable and HBsAg <4,000 IU). Group 1, MVA-HBV (1 × 10⁸ pfu) followed at d28 by homologous MVA-HBV; Group 2, ChAdOx1-HBV (2 × 10⁸ viral particles) followed at d28 by MVA; Group 3, same as group 2 with low dose nivolumab (LDN) (0.3 mg/kg IV) at d28; Group 4 same as Group 2 with LDN at day 0 and day 28. HBV specific T cell responses are assessed using genotype C and D HBV peptides spanning the HBV immunogen in an IFNγ ELISpot assay, before and after (days 7, 28, 35, 84, and 168) vaccination.

Results: As of March 1st 2022, 40 patients had been enrolled with no concerning safety signal or vaccine-associated SAEs reported. Transaminase flares have been observed, associated with SAg decline, in two patients. Groups 2 and 3 have shown reduction in SAg at month 3. In Group 2, only patient with low initial SAg have shown an effect, whereas almost all most patients in Group 3 have shown SAg decline (1 log₁₀ at 6 months in first 6)

HBV genotype C T cell response were assessed in 20 patients to date, targeted HBV core (8/20), sAg (17/20) and pol (8/20) with a mean magnitude of 217, 213 and 118 × SFU/10⁶ PBMC respectively (mean total magnitude 363 SFU) at baseline. After prime vaccination peak mean magnitude (day 7 or day 28) of total HBV specific T cell responses were 437, 244, 688, 332 SFU/10⁶ in groups 1–4 respectively. After boost vaccination peak (day 35) total HBV specific T cell responses were 344, 689, 689, 277 SFU/10⁶ in groups 1–4 respectively. Responses were enhanced from baseline in 13 patients after prime and in 16 patients after boost. Responses were sustained out to 3–6 months in the majority of patients. HBV inter-genotype cross reactive T cell responses were highly cross-reactive with genotype D peptides.

Conclusion: VTP-300 immunotherapy, either alone or combined with nivolumab at the boosting time point, has been immunogenic and shown reduction in SAg in well-controlled CHB patients, while exhibiting an excellent safety profile.

SAT429

Bulevirtide monotherapy for 48 weeks in HDV patients with compensated cirrhosis and clinically significant portal hypertension

Elisabetta Degasper¹, Maria Paola Anolli¹, Colonia Sara², Uceda Renteria², Dana Sambarino¹, Marta Borghi¹, Riccardo Perbellini¹, Caroline Scholtes^{3,4}, Floriana Facchetti¹, Alessandro Loglio¹, Mirella Fraquelli⁵, Andrea Costantino⁵, Ferruccio Ceriotti², Fabien Zoulim^{3,4}, Pietro Lampertico^{1,6}.
¹Foundation IRCCS Ca' Granda Ospedale Maggiore Policlinico, Division of Gastroenterology and Hepatology, Milan, Italy; ²Foundation IRCCS Ca' Granda Ospedale Maggiore Policlinico, Virology Unit, Milan, Italy; ³Hospices Civils de Lyon and Université Claude Bernard Lyon, Lyon, France; ⁴INSERM U1052 Centre de Recherche sur le Cancer de Lyon, Lyon, France; ⁵Foundation IRCCS Ca' Granda Ospedale Maggiore Policlinico, Division of Gastroenterology and Endoscopy, Milan, Italy; ⁶University of Milan, CRC "A. M. and A. Migliavacca" Center for Liver Disease, Department of Pathophysiology and Transplantation, Milan, Italy
Email: elisabetta.degasper@policlinico.mi.it

Background and aims: Bulevirtide (BLV) has been recently approved for the treatment of chronic hepatitis Delta (CHD) in Europe but its long-term effectiveness and safety in patients with compensated cirrhosis and clinically significant portal hypertension (CSPH) are unknown.

Method: Consecutive HDV patients with compensated cirrhosis and CSPH who started BLV 2 mg/day were enrolled in this single-center longitudinal study. Clinical and virological characteristics were collected at baseline, weeks 4, 8 and every 8 weeks thereafter. HDV RNA was quantified by Robogene 2.0 (LOD 6 IU/ml), HBcrAg by LUMIPULSE® G (LOQ 3 Log IU/ml), HBV RNA by cobas® 6800 (LOQ 10 cp/ml).

Results: 18 Caucasian patients with compensated cirrhosis and CSPH under nucleos (t)ide analogue (NUC) treatment were enrolled: 48 (29–77) years, 67% males, 2 active HCC; platelets 70 (37–227) × 10³/mm³, liver stiffness measurement 16.4 (7.8–57.8) kPa, ALT 106 (32–222) U/L, HBsAg 3.7 (2.5–4.3) log IU/ml, HDV RNA 4.9 (3.3–6.6) log IU/ml. During 48 weeks of BLV monotherapy, HDV RNA declined by 3.1 (0.2–4.6) log IU/ml, becoming undetectable in 6 (33%) patients and <100 IU/ml in 9 (50%). A virological response, defined as HDV RNA undetectability or ≥2 log IU/ml decline, was observed in 14 (78%) patients, while 2 (11%) were non-responders. Median ALT declined to 34 (15–76) U/L; a biochemical response (ALT normalization) was observed in 89% of patients while a combined response (virological and biochemical) was observed in 72%. AST, GGT, AFP, albumin, IgG and gammaglobulin levels improved (p < 0.001), while HBsAg, HBV RNA, HBcrAg, platelets and bilirubin did not significantly change. While Child-Pugh Turcotte (CPT) score remained unchanged in all patients with CPT A5 at baseline, 4 out of 5 patients with baseline CPT A6 improved their liver function to CPT A5. No liver-related complications occurred during treatment. BLV was well tolerated: the only adverse event observed was a fully asymptomatic increase of serum bile acids; no site injection reactions were observed. No patient discontinued treatment.

Conclusion: A 48-week course of BLV 2 mg/day monotherapy is safe and effective even for difficult-to-treat HDV patients such as those with compensated cirrhosis and CSPH. Virological response is associated with an improvement of liver function tests and CPT score.

SAT430

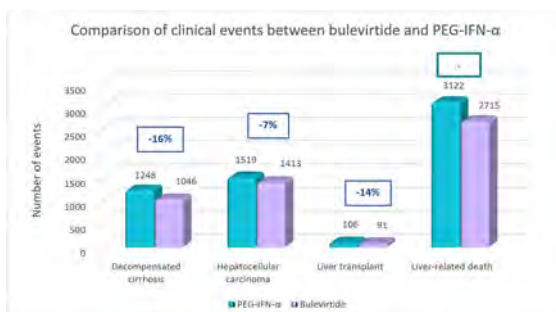
Bulevirtide avoids future clinical events and related costs compared to pegylated-interferon alpha in chronic hepatitis D in Spain

Maria Buti¹, José Luis Calleja Panero², Miguel Ángel Rodríguez Sagrado³, Helena Cantero⁴, Ana de las Heras⁵, Raquel Domínguez-Hernández⁵, Miguel Ángel Casado⁵. ¹Hospital Universitari Vall d'Hebron, Hepatology and Internal Medicine, Barcelona, Spain; ²Puerta de Hierro Majadahonda University Hospital, Gastroenterology and Hepatology, Majadahonda, Spain; ³Hospital Ramón y Cajal, Pharmacy, Madrid, Spain; ⁴Gilead Sciences, Market Access, Madrid, Spain; ⁵Pharmacoeconomics and Outcomes Research Iberia (PORIB), Pozuelo de Alarcón, Spain
Email: rdominguez@porib.com

Background and aims: Chronic Hepatitis D (CHD) is the most severe form of all chronic viral hepatitis. Although it is not approved, pegylated-interferon alpha (PEG-IFN- α) is the most used treatment for patients with CHD. Bulevirtide (Hepcludex[®]) is a novel, first-in-disease and first-in-class entry inhibitor with the European Medicine's Agency conditional approval to treat adults with compensated CHD. The aim of the study was to evaluate the avoided clinical events and their costs of bulevirtide compared to PEG-IFN- α , in patients with CHD in Spain.

Method: The course of the disease was simulated, for a lifetime horizon, through a decision-tree model integrated into a Markov model in order to predict the number of clinical events and derived costs of using bulevirtide in comparison to PEG-IFN- α in CHD patients. A cohort of 3, 882 patients was assumed (national prevalence figures), from which 46.90% were cirrhotic at baseline. "Response to bulevirtide" was defined as achieving the combined response end point (hepatitis D virus-RNA undetectable or ≥ 2 log decline and alanine aminotransferase normalisation) at 24–48 weeks, and "non-response" was considered when the combined response end point was not reached. For bulevirtide, responders remained under treatment beyond 48 weeks, except for patients with HBsAg seroclearance or progression, whereas non-responders stopped treatment at week 48. For PEG-IFN- α , patients were treated until week 48. The parameters of the analysis (patient characteristics, efficacy of bulevirtide and PEG-IFN- α , disease progression and unitary event costs) were extracted from the literature. Only clinical event direct costs were evaluated in the model, from the National Health System perspective (€, 2021). Results were described as avoided events of decompensated cirrhosis (DC), hepatocellular carcinoma (HCC), liver transplant (LT) and liver-related death, and their avoided costs.

Results: In a cohort of 3, 882 patients during a lifetime period, treatment with bulevirtide could avoid 202 DC events, 105 HCC, 15 LT and 407 liver-related deaths in comparison to PEG-IFN- α , resulting in a 16%, 7%, 14% and 13% event reduction, respectively. This would imply a total cost reduction related to events of 12.5 million € with bulevirtide vs PEG-IFN- α (2.3 million € for DC, 1.3 million € for HCC, 7.5 million € for LT and 1.4 million € for liver-related deaths).



Conclusion: Bulevirtide for CHD could avoid a significant number of clinical events compared to PEG-IFN- α , leading to a slower disease progression and cost savings originated by the reduction in the number of negative liver-related events.

SAT431

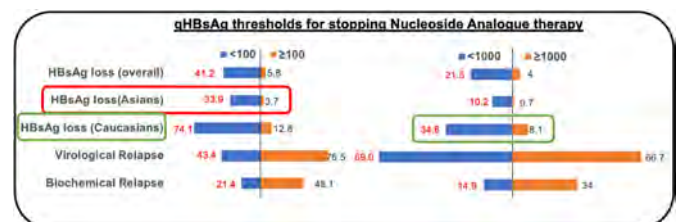
Quantitative HBsAg (qHBsAg) as an end point to stop nucleoside analogues in chronic hepatitis B: a meta-analysis with meta-regression

Seng Gee Lim¹, Ada Ee Der Teo¹, Edwin Shih-Yen Chan², Wah Wah Phyo¹, David Hsing Yu Chen², Carol Anne Hargreaves³. ¹National University Health System, Division of Gastroenterology and Hepatology, Singapore, Singapore; ²Singapore Clinical Research Institute, Singapore; ³National University of Singapore, Data Analytics Consulting Centre, Faculty of Science, Singapore
Email: mdclimsg@nus.edu.sg

Background and aims: Guidelines differ on recommendations for stopping nucleoside analogue (NA) therapy in HBeAg-negative Chronic Hepatitis B (CHB) as the risk-benefit trade-off is unclear. An end-of-treatment quantitative HBsAg (EOTqHBsAg) <100IU/ml or <1000IU/ml has been proposed as criterion to stop NA. We assessed this by meta-analysis and meta-regression.

Method: We searched PubMed, EMBASE and abstracts of major liver conferences for studies of HBeAg-negative CHB NA discontinuation. Risk of bias was assessed by Newcastle-Ottawa tool (modified). Random-effects meta-analysis and meta-regression was performed with covariates of ethnicity (ETHN), EOTqHBsAg (<100 \geq IU/ml [EOT_100], <1000 \geq IU/ml [EOT_1000] and as an ordinal variable [EOT_ORD]), duration of NA therapy (TDUR); dichotomised at 24months[EOT_24] and 36 months[EOT_36]) and duration of follow-up (FUP) after stopping NA. We assessed pooled risk, with 95% confidence intervals (95%CI) of HBsAg loss, virological (VR) and biochemical relapse (BR). Heterogeneity was reported as I². Multivariate meta-regression models examined covariates to explain the heterogeneity.

Results: A total of 42 studies were included (34papers, 8 abstracts). The pooled risks of HBsAg loss, VR and BR for stopping therapy at EOTqHBsAg<100IU/ml were 41.2% (95% CI30.6–52.7%), 43.4% (95% CI30.6–57.2%) and 21.4% (95% CI14.3–30.9%) respectively compared 5.8% (95% CI3.6–9.4%), 75.5% (95% CI64.7–83.8%) and 48.1% (95% CI35.9–60.6%) respectively for those with EOTqHBsAg \geq 100IU/ml. The pooled risks of HBsAg loss, VR and BR for stopping therapy at EOTqHBsAg<1000IU/ml were 21.5% (95% CI 11.8–36.0%), 69.0% (95% CI43.2–86.8%) and 14.9% (95% CI7.6–27.1%) respectively, compared to 4.0% (95% CI1.8–8.9%), 66.7% (95%CI41.8–84.8%) and 34.0% (95% CI20.3–51.1%) respectively for those with EOTqHBsAg \geq 1000IU/ml. ETHN significantly contributed to HBsAg heterogeneity. In Asians, EOTqHBsAg<100IU/ml had HBsAg loss of 33.9% while in Caucasian studies, EOTqHBsAg<1000IU/ml had HBsAg loss of 34.6%, hence a difference in threshold between ethnicities is advocated. Multivariate analysis showed TDUR (continuous) was significant for VR and BR but subgroup analysis of TDUR_24 or TDUR_36 showed no difference.



Conclusion: This meta-analysis provides level 1 evidence to adopt EOTqHBsAg as a criterion to stop NA in HBeAg-negative CHB patients; in Asians EOTqHBsAg<100IU/ml can be advocated, while in Caucasians, EOTqHBsAg<1000IU/ml is appropriate.

POSTER PRESENTATIONS

SAT432

Low level of HBcrAg is beneficial to functional cure obtained with pegylated interferon therapy in inactive HBsAg carriers

Hong Li¹, LiLi Liu¹, Ling Qin², YaLi Liu¹, Zhang Jing¹, Xin-Yue Chen³, Zhenhuan Cao¹. ¹Beijing Youan Hospital, Capital Medical University, The Third Unit, Department of Hepatology, Beijing, China; ²Beijing Youan Hospital, Capital Medical University, Biomedical Information Center, Beijing, China; ³Beijing Youan Hospital, Capital Medical University, The First Unit, Department of Hepatology, Beijing, China
Email: caozhenhuan@ccmu.edu.cn

Background and aims: HBsAg clearance, represented functional cure, is extremely difficult to obtain clinically. Our and other recent studies have shown that IHCs treated with pegylated-interferon (PEG-IFN) results in high HBsAg clearance rates of 44.7% to 65%. Recent study showed that hepatitis B core-related antigen (HBcrAg) could be used as a valuable marker for HBV replication. However, the predictive value of HBcrAg for HBsAg clearance is unclear. This study aims to identify HBcrAg associated with functional cure in IHCs with PEG-IFN therapy.

Method: IHCs received PEG-IFN 135 ug weekly for 96 weeks. Subjects who achieved clearance of HBsAg were considered as responders (R group), and those who did not were considered as non-responders (NR group). To evaluate the factors in predicting HBsAg clearance, univariate and multivariate logistic regression analyses were performed. The receiver operator characteristic curves and the area under the receiver operator characteristic curve (AUROC) were used to evaluate prognostic values.

Results: Our results showed that 39 cases obtained HBsAg clearance (group R), while 21 cases did not (group NR). There was no significant difference in age, ALT, and AST levels between two groups. HBcrAg were all significantly lower in R group than NR group at baseline, 12 and 24 weeks. HBsAg quantification were lower in the R group than in the NR group at 12 and 24 weeks (Table 1). Univariate logistic regression analysis showed that HBcrAg at baseline (OR 10.763, $p = 0.001$), and at 12 weeks (OR 12.511, $p < 0.001$), and 24 weeks (OR 6.955, $p = 0.008$) were all strong predictors of functional cure as well as HBsAg levels at 12 weeks (OR 8.147, $p = 0.004$) and 24 weeks (OR 9.743, $p = 0.002$), HBsAg changes from baseline at 12 weeks (OR 5.468, $p = 0.019$) and 24 weeks (OR 10.719, $p = 0.001$). A multifactor logistic analysis was performed with $Y = 219.227 - 1.269 \times \text{Baseline HBcrAg} - 0.994 \times 12\text{week HBcrAg} - 0.825 \times 24\text{week HBcrAg}$. AUROC was up to 0.916 with 93.5% sensitivity and 85.7% specificity.

Table: Characteristics of R and NR groups at baseline, 12 and 24 weeks of treatment

Parameter	R group n = 39	NR group n = 21	p
Gender (M/F)	27/12	16/5	0.568
Age (years)	38.05 ± 11.25	40.62 ± 11.26	0.368
Baseline			
ALT (U/L)	30.88 ± 14.62	33.17 ± 14.36	0.570
AST (U/L)	27.97 ± 6.89	28.17 ± 8.32	0.946
Ig HBsAg (IU/ml)	1.61 ± 0.97	2.08 ± 0.73	0.067
HBcrAg (mU/ml)	5.45 ± 1.09	6.71 ± 1.16	<0.001
12week			
ALT (U/L)	82.56 ± 89.52	66.05 ± 49.14	0.681
AST (U/L)	64.89 ± 74.50	47.71 ± 28.05	0.545
Ig HBsAg (IU/ml)	0.67 ± 1.21	1.70 ± 0.98	0.001
HBcrAg (mU/ml)	5.79 ± 0.95	7.17 ± 1.31	<0.001
24week			
ALT (U/L)	54.77 ± 50.70	54.45 ± 48.95	0.728
AST (U/L)	46.39 ± 28.24	46.65 ± 45.28	0.636
Ig HBsAg (IU/ml)	-0.29 ± 1.14	1.22 ± 1.27	<0.001
HBcrAg (mU/ml)	5.53 ± 0.93	6.63 ± 1.61	0.003

Conclusion: This study provides evidence supporting serum HBcrAg, as a clinical predictor of HBsAg clearance, which has a higher

predictive value compared to the conventional predictors of HBsAg and ALT.

SAT433

Comparative risk of hepatocellular carcinoma in patients with chronic hepatitis B receiving tenofovir- or entecavir-based regimens: a meta-analysis using individual patient data

Won-Mook Choi¹, Terry Cheuk-Fung Yip², Grace Wong², W. Ray Kim³, Leland Yee⁴, Craig Brooks-Rooney⁵, Tristan Curteis⁶, Harriet Cant⁶, Chien-Hung Chen⁷, Chi-Yi Chen⁸, Yi-Hsiang Huang^{9,10}, Young-Joo Jin¹¹, Dae Won Jun¹², Jin-Wook Kim^{13,14}, Neung Hwa Park^{15,16}, Cheng-Yuan Peng^{17,18}, Hyun Phil Shin¹⁹, Jungwoo Shin¹⁵, Yao-Hsu Yang^{20,21}, Young-Suk Lim¹. ¹University of Ulsan College of Medicine, Department of Gastroenterology, Liver Center, Asan Medical Center, Seoul, Korea, Rep. of South; ²The Chinese University of Hong Kong, CUHK Medical Data Analytics Centre, Department of Medicine and Therapeutics, Hong Kong SAR, Hong Kong; ³Stanford University School of Medicine, Division of Gastroenterology and Hepatology, Stanford, United States; ⁴Gilead Sciences, Foster City, United States; ⁵Costello Medical Consulting Ltd, United States; ⁶Costello Medical Consulting Ltd, Cambridge, United Kingdom; ⁷Kaohsiung Chang Gung Memorial Hospital and Chang Gung University College of Medicine Kaohsiung, Division of Hepatogastroenterology, Department of Internal Medicine, Taiwan; ⁸Ditmanson Medical Foundation Chia-Yi Christian Hospital Chia-Yi, Division of Hepatogastroenterology, Department of Internal Medicine; ⁹Division of Gastroenterology and Hepatology, Department of Medicine, Taipei Veterans General Hospital, Taipei, Taiwan; ¹⁰National Yang Ming Chiao Tung University, Institute of Clinical Medicine, Taipei, Taiwan; ¹¹Digestive Disease Center, Department of Internal Medicine, Inha University Hospital, Inha University School of Medicine, Incheon, Korea, Rep. of South; ¹²Hanyang University College of Medicine, Department of Internal Medicine, Hanyang University Hospital, Seongnam, United States; ¹³Seoul National University Bundang Hospital, Department of Medicine, Seongnam, Korea, Rep. of South; ¹⁴Seoul National University College of Medicine, Department of Internal Medicine, Seoul, Korea, Rep. of South; ¹⁵Ulsan University Hospital, Department of Internal Medicine, University of Ulsan College of Medicine, Ulsan, Korea, Rep. of South; ¹⁶Ulsan University Hospital, Biomedical Research Center, University of Ulsan College of Medicine, Ulsan, Korea, Rep. of South; ¹⁷China Medical University Hospital, Center for Digestive Medicine, Department of Internal Medicine, Taichung, Taiwan; ¹⁸China Medical University, School of Medicine, Taichung, Taiwan; ¹⁹Kyung Hee University School of Medicine, Department of Gastroenterology and Hepatology, Kyung Hee University Hospital at Gangdong, Seoul, Korea, Rep. of South; ²⁰Chiayi Chang Gung Memorial Hospital, Department of Traditional Chinese Medicine, Chiayi, Taiwan; ²¹Chang Gung Memorial Hospital, Health Information and Epidemiology Laboratory, Chiayi, Taiwan
Email: limys@amc.seoul.kr

Background and aims: Chronic hepatitis B (CHB) is associated with a long-term risk of hepatocellular carcinoma (HCC), which can be mitigated by nucleos(t)ide analogue therapies such as tenofovir disoproxil fumarate (TDF) and entecavir (ETV). Aggregate data meta-analyses have been unable to reach a consensus on the relative effectiveness of TDF and ETV to reduce the risk of HCC due to challenges with heterogeneity and different methodologies of included studies. To account for these challenges, this meta-analysis used individual patient data (IPD) to compare the risk of HCC in patients receiving TDF or ETV and identify any subgroup of patients who may benefit more from one treatment than the other.

Method: A literature review identified 20 observational studies from East Asia reporting HCC incidence in patients receiving TDF or ETV, 11 agreed to participate in this study. Eligible patients were adults with CHB who were treatment-naïve before receiving TDF or ETV monotherapy and completed at least 1 year of treatment. After adjustment for potential confounding variables and multiple imputation to account for missing data, a one-stage IPD meta-analysis

evaluated the hazard ratio (HR) of treatment with TDF versus (vs) ETV to reduce HCC risk using a multivariable Cox proportional hazards model. Subgroup analyses for age, sex, HBeAg positivity, cirrhosis status and diabetes status were also conducted.

Results: Data from 42,939 eligible patients (6,979 TDF and 35,960 ETV) were included. The treatments were similar in terms of baseline age (TDF: 48.32 years [yrs] vs ETV: 52.26 yrs), sex (female: 38.64% vs 34.13%), follow-up time (3.71 yrs vs 3.97 yrs) and presence of cirrhosis (38.01% vs 33.69%). Patients receiving TDF were associated with a significantly lower risk of developing HCC: adjusted HR (95% confidence interval [CI]) = 0.77 (0.61–0.98), $p = 0.03$. In all subgroup analyses, TDF showed a lower risk of HCC than ETV (HR <1.0), with the risk difference most pronounced in the HBeAg positive subgroup (Figure).

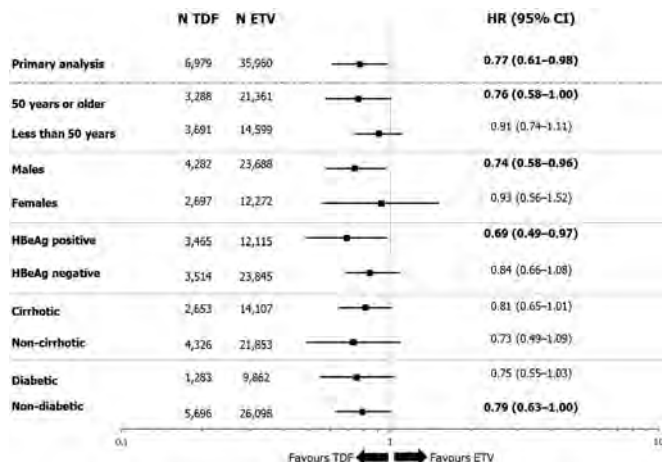


Figure: Analyses for cumulative incidence of HCC in patients with CHB treated with TDF or ETV

*Statistically significant results are in bold. For the '50 years or older' and 'non-diabetic' subgroups, the upper bound of each CI is <1.00, but each has been rounded up to 1.00 when reported to two decimal places.

CHB, chronic hepatitis B; CI, confidence interval; ETV, entecavir; HBeAg, hepatitis B e-antigen; HCC, hepatocellular carcinoma; HR, hazard ratio; TDF, tenofovir disoproxil fumarate

Conclusion: The risk of developing HCC was significantly lower in CHB patients receiving TDF than ETV. TDF was consistently associated with lower HCC risk across all subgroups, but most notably in HBeAg positive patients.

SAT434

VIR-2218 plus VIR-3434 combination therapy reduces hepatitis B virus surface antigen levels in vivo

Julia Noack¹, Jonathan Gall^{1,2}, Hasan Imam¹, Yessenia Anglero-Rodriguez³, Vasant Jadhav³, Michael A. Schmid⁴, Anna Bakardjiev^{1,5}, Lisa A. Purcell¹, Christy Hebner¹, Florian Lempp¹.
¹VIR Biotechnology, San Francisco, United States; ²Genentech, South San Francisco, United States; ³Alnylam Pharmaceuticals, Cambridge, United States; ⁴Humabs Biomed SA, a subsidiary of Vir Biotechnology, Bellinzona, Switzerland; ⁵Denali Therapeutics, South San Francisco, United States

Email: jnoack@vir.bio

Background and aims: Ribonucleic acid (RNA) interference (RNAi) therapeutics targeting hepatitis B virus (HBV) RNAs and monoclonal antibodies (mAbs) targeting HBV surface antigen (HBsAg) represent compelling strategies for potentially enabling a functional cure in chronic HBV patients. VIR-2218 is an investigational siRNA therapeutic that targets a highly conserved region within the HBV X open reading frame and demonstrates potent *in vitro* and *in vivo* antiviral activity. VIR-3434 is an investigational neutralizing monoclonal antibody targeting the antigenic loop of HBsAg with pan-genotypic neutralizing activity *in vitro*, and inhibits viral spread, leading to

elimination of HBsAg *in vivo*. VIR-2218 and VIR-3434 are currently in clinical trials as monotherapy and in combination.

Method: To evaluate the combination activity of VIR-2218 and VIR-3434 versus monotherapy, two *in vivo* studies were conducted using well-established mouse models of HBV infection: C57BL/6 mice transduced with AAV8-HBV (genotype D) or human liver-chimeric PXB-mice infected with HBV (genotype C). The mice were treated with VIR-2218, VIR-3434, entecavir (ETV, AAV8-HBV study only), or a combination of agents at different concentrations. Antiviral activity was determined by evaluation of viral serum/plasma markers including HBV DNA, HBsAg, and HBeAg.

Results: In the AAV-HBV mouse model, VIR-2218 led to a significant reduction of plasma HBsAg, HBeAg and HBV DNA levels (0.89 log, 0.51 log, and 0.65 log maximum mean reduction, respectively), while VIR-3434 monotherapy significantly reduced plasma HBsAg (0.79 log). The combination of VIR-2218 and VIR-3434 further reduced plasma HBsAg and HBV DNA levels when compared to VIR-2218 monotherapy (2.11 log and 2.05 log additional maximum reduction, respectively). The triple combination of VIR-3434, VIR-2218, and ETV significantly enhanced reductions of plasma HBsAg and HBV DNA when compared to ETV monotherapy (2.39 log and 1.26 further maximum reduction, respectively). In HBV-infected PXB mice, VIR-3434 monotherapy resulted in a substantial decrease in serum HBsAg (1.46 log); treatment with the combination of VIR-2218 and VIR-3434 showed an additional ~1 log reduction (2.51 log). VIR-2218 and VIR-3434 combination also showed a clear reduction in serum HBV DNA levels (1.47 log) when compared to the vehicle group, whereas treatment with VIR-3434 alone led to a 0.72 log decrease.

Conclusion: Monotherapy with either the RNAi therapeutic, VIR-2218, or the mAb VIR-3434 is effective in reducing plasma/serum levels of HBsAg in two HBV mouse models. Combined treatment provided improved suppression of HBsAg over monotherapy and represents a promising strategy for HBV functional cure. These data support further clinical development of combination therapy with VIR-2218 and VIR-3434 for the potential treatment of chronic HBV patients.

SAT435

Safety, pharmacokinetics, and antiviral activity of the S-antigen Transport Inhibiting Oligonucleotide Polymers (STOPS) drug candidate ALG-010133 in subjects with chronic hepatitis B

Edward J. Gane¹, Kosh Agarwal², Man-Fung Yuen³, Alina Jucov⁴, Christian Schwabe⁵, Kha Le⁶, Stanley Wang⁶, Christopher Westland⁶, Kim Steel⁷, Qingling Zhang⁶, Vikrant Gohil⁶, Felix Lai⁶, Meenakshi Venkatraman⁶, Lawrence Blatt⁶, Leonid Beigelman⁶, Tse-I Lin⁶, Sushmita Chanda⁶, Matt McClure⁶, John Fry⁶.
¹University of Auckland, Auckland, New Zealand; ²King's College Hospital, Institute of Liver Studies, London, United Kingdom; ³The University of Hong Kong, Queen Mary Hospital, Department of Medicine, School of Clinical Medicine, Hong Kong, Hong Kong; ⁴ARENSIA Exploratory Medicine, Republican Clinical Hospital and Nicolae Testemitanu State University of Medicine and Pharmacy, Chisinau, Moldova; ⁵New Zealand Clinical Research, Auckland, New Zealand; ⁶Aligos Therapeutics, Inc.; ⁷SARPO Consulting, Melbourne, Australia
 Email: swang@aligos.com

Background and aims: To evaluate the safety, pharmacokinetics (PK) and antiviral activity of ALG-010133, a STOPS molecule designed to reduce hepatitis B S-antigen (HBsAg) in chronic hepatitis B (CHB) patients.

Method: This was a 3-part, multicenter, double-blind, randomized, placebo-controlled study. In Parts 1 and 2, single and multiple subcutaneous (SC) doses of ALG-010133 were generally well tolerated in healthy volunteers (Gane et al, EASL 2021). Part 3 evaluated weekly SC doses of ALG-010133 or placebo × 12 weeks in virologically suppressed Hepatitis B e-antigen (HBeAg) negative CHB subjects (N = 10/cohort; 8 active:2 placebo). Reported here are preliminary

POSTER PRESENTATIONS

blinded Part 3 safety, PK, and antiviral data; unblinded data will be presented at the conference.

Results: 31 CHB subjects completed dosing and follow-up in Cohorts 1 (120 mg; N = 10), 2.

(200 mg; N = 10), and 3 (400 mg; N = 11). Most subjects were male (61%) and 48% were white, with mean age 48 years, mean BMI 26.1 kg/m² and baseline HBsAg across cohorts of 3.6 to 3.7 log₁₀ IU/ml. There was 1 unrelated serious treatment emergent adverse event (TEAE) (hospitalization for orchitis) and 1 unrelated TEAE (COVID-19 infection) resulting in premature study drug discontinuation. All TEAEs were Grade 1 or 2 in severity, except for 1 Grade 3 TEAE of injection site erythema (severity based only on surface area criteria of ≥100 cm²; required no treatment and resolved despite continued study drug dosing) and the aforementioned TEAE of orchitis (Grade 3). There was no dose relationship to severity or frequency for any TEAE. The most common (≥3 subjects) TEAEs were injection site erythema (n = 5), increased ALT (n = 4), injection site bruising (n = 4), increased AST (n = 3), and injection site pruritus (n = 3); none were assessed as clinically concerning. Although treatment-emergent ALT and AST elevations (n = 13) were observed, all were Grade 1 (<2.5x upper limit of normal [ULN]) or 2 (≥2.5 to <5x ULN) and none led to premature study drug discontinuation or were associated with symptoms or evidence of liver dysfunction. There were no other clinically significant lab abnormalities. No clinically significant physical examinations, vital signs, or ECG abnormalities were reported. Plasma ALG-010133 exposures increased more than dose proportionally between the 120 to 400 mg dose levels, with moderate variability and minimal accumulation. Compared to baseline, the magnitude of HBsAg decline at Week 12 was <0.1 log₁₀ IU/ml for placebo and across all ALG-010133 dose levels, including the projected efficacious dose level of 400 mg (estimated to maintain total liver exposures >3x EC₉₀ for HBsAg inhibition).

Conclusion: ALG-010133 was safe and well tolerated with predictable PK properties when given to CHB subjects as multiple SC doses of up to 400 mg. No meaningful HBsAg reduction was observed across all cohorts. Further clinical development of ALG-010133 has been discontinued.

SAT436

Costimulation of CD40 and type-I interferon immune pathways by a bifunctional molecule in HBV infection models and healthy non-human primates

Xavier Marniquet¹, Marion Dajon¹, Julie Montegut¹, Maria Elena Giusepponi², Michela Pecoraro², Elena Vicentini², Francesca Morandini², Floriana Zanderigo², Denise Federico², Odile Bonnin¹, Gregory Neveu¹, Charlotte Blanc¹, Christelle Marcou¹, Juliette Lavaux¹, Michel Didier³, Galina Boldina³, Jacques Dumas³, Thomas Bouquin³, Annabelle Milla¹, Hugh Watson¹, Kara Carter¹, Antoine Alam¹. ¹Evotec ID (Lyon), Antiviral Research Unit, Lyon, France; ²Aptuit (Verona) Srl, Verona, Italy; ³Sanofi, Vitry-sur-Seine, France
Email: xavier.marniquet@evotec.com

Background and aims: Type-I interferons (IFN-I) have shown limited ability to cure patients with chronic hepatitis B (CHB), thus more effective treatments are needed to achieve cure in a larger proportion of patients. We aimed to investigate the simultaneous stimulation of CD40 and IFN-I pathways in HBV infection models and non-infected non-human primates (NHP).

Method: HBV-infected primary human hepatocytes (PHH) were used to characterize the effects of IFN-I and CD40 ligand separately and in combination. AAV/HBV-infected mice were subsequently used to confirm these effects in vivo. A single bifunctional molecule with both activities was investigated using reporter cells, HBV-infected PHH and non-infected NHP. Pro-inflammatory cytokine release was assessed in vitro with NHP and human white blood cells (WBC).

Results: The combination of IFN-I and CD40 ligand, on primary human hepatocytes (PHH) and in AAV/HBV-infected mice, showed a significant increase in anti-HBV activity when compared to either

CD40L or IFN-alpha alone. Fusion of IFN-I molecules to an anti-CD40 agonistic mAb yielded a bifunctional molecule active on both CD40 and IFN-I expressed in reporter cells. This fusion molecule reduced pgRNA and HBeAg release from HBV-infected PHH treated at picomolar concentrations starting 4 days after infection, without cytotoxicity. Stimulation of CXCL10 release and anti-HBV activity in infected PHH treated for 1 day was maintained after a washout period of 3 days. Stimulation of WBC in vitro led to low or undetectable release of pro-inflammatory cytokines. Treatment of non-infected NHP with the fusion molecule produced dose-dependent elevation of serum CXCL10, 2'5'OAS and neopterin and stimulated the CD40 pathway without significant systemic release of unwanted pro-inflammatory cytokines.

Conclusion: Target engagement of CD40 and IFN-I receptors with a single bifunctional molecule results in potent activity in HBV-models and stimulates CD40 and type-I IFN immune pathways in vivo.

SAT437

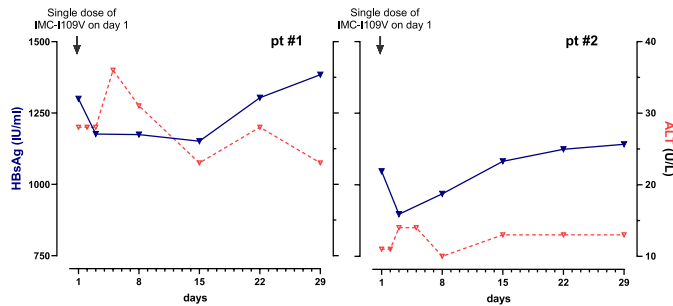
IMC-I109V, a novel T cell receptor (TCR) bispecific (ENVxCD3) designed to eliminate HBV-infected hepatocytes in chronic HBV patients: initial data from a first-in-human study

Stefan Bourgeois¹, Young-Suk Lim², Edward J. Gane³, Hyun Woong Lee⁴, Wendy Cheng⁵, Jeong Heo⁶, Won Kim⁷, Maria Buti⁸, Alexander Thompson⁹, Gail Matthews¹⁰, Ewa Janczewska¹¹, Stephen Ryder¹², Raul J. Andrade¹³, Yuan Yuan¹⁴, Adel Benlahrech¹⁵, Jay Wustner¹⁴, Lucy Dorrell¹⁶, Man-Fung Yuen¹⁷. ¹Ziekenhuis Netwerk Antwerpen, Belgium; ²Asan Medical Centre; ³University of Auckland; ⁴Gangnam Severance Hospital; ⁵Royal Perth Bentley Group; ⁶Pusan National University Hospital; ⁷SMG-SNU Boramae Medical Centre; ⁸Hospital Universitario Valle Hebrón; ⁹St Vincent's Hospital Melbourne; ¹⁰St Vincent's Hospital Sydney; ¹¹ID Clinic Arkadiusz Pisula; ¹²Nottingham University Hospitals NHS Trust; ¹³Hospital Universitario Virgen de la Victoria-IBIMA; ¹⁴Immunocore plc; ¹⁵Immunocore Ltd; ¹⁶Immunocore Ltd, United Kingdom; ¹⁷The University of Hong Kong
Email: lucy.dorrell@immunocore.com

Background and aims: HBsAg clearance is the treatment goal for chronic hepatitis B (CHB). New strategies that enable safe elimination of hepatocytes harbouring HBV genomes are needed. Immune-mobilising monoclonal TCR against viruses (ImmTAV®) are unique bispecific soluble proteins designed to redirect polyclonal T cells, regardless of their specificity, to eliminate virus-infected cells. IMC-I109V is an affinity-enhanced HBV-specific TCR fused to an anti-CD3 scFv T cell activating moiety, that redirects non-exhausted effector T cells to eliminate hepatocytes presenting HLA-bound HBsAg (Env)-derived peptide. Since the mechanism results in hepatocyte lysis, transient liver enzyme increases are expected, necessitating a conservative dosing schedule in our first-in-human study.

Method: IMC-I109V-101 is an open-label Phase 1/2 study evaluating IMC-I109V in HLA-A*02:01 positive patients with CHB who are non-cirrhotic, HBeAg-negative and virally suppressed on nucleos(t)ide analogues. Part 1 is a single ascending dose to identify a safe and pharmacologically active dose. Part 2 is a multiple ascending dose to evaluate safety and anti-HBV activity of repeated doses over 24 weeks. Secondary objectives include PK and effects on serum HBsAg, HBcAg and HBV RNA levels.

Results: Three patients each received a single dose of 0.8 mcg, based on the minimum anticipated biological effect level (MABEL). Doses were well tolerated and not associated with adverse events in any subject. Preliminary PK, HBsAg and liver enzymes were available for the first two participants. PK analysis showed that the maximum serum concentrations were consistent with the dose level. By 12 hours, serum concentrations declined below the lower limit of quantification. Serum HBsAg levels transiently decreased by 11–15% during Days 3–15 post infusion, before returning to baseline within 3 weeks (Figure 1). The decreases coincided with small, transient elevations in ALT, albeit within the normal range.



Conclusion: The concomitant HBsAg declines and ALT elevations indicate that a single, very low dose of IMC-I109V elicited on-target activity consistent with the TCR bispecific (ENVxCD3) mechanism of action, without adverse events. These results are encouraging for the prospect of identifying a tolerable and active treatment regimen with higher and repeat dosing. Enrolment in Part 1 dose escalation continues to evaluate this novel mechanism designed to eliminate HBV-positive hepatocytes. (Eudract no. 2019-004212-64).

SAT438

Long-term outcomes after cessation of antiviral therapy in HBeAg negative patients

Rachel Wen-Juei Jeng^{1,2}, Yen-Chun Liu^{1,2}, Chien-Wei Peng^{1,2,3}, Rong-Nan Chien^{1,2,3}, Yun-Fan Liaw^{2,3}. ¹Linkou Chang Gung Memorial Hospital, Gastroenterology and Hepatology, Taoyuan, Taiwan; ²Chang Gung University, College of Medicine, Taoyuan, Taiwan; ³Linkou Chang Gung Memorial Hospital, Liver Research Unit, Taoyuan, Taiwan
Email: rachel.jeng@gmail.com

Background and aims: We reported a cohort of 691 HBeAg negative chronic hepatitis B patients who had stopping Nuc (Hepatology 2018) with a median follow-up duration about 3 years. We have extended the follow-up to a median of 6.6 (Q1-Q3: 5–8.2) years and to examined the long-term outcome of these patients.

Method: The 691 HBeAg negative CHB patients were followed-up till Dec 2021. Virological relapse (VR) was defined as HBV DNA >2000IU/ml and clinical relapse (CR) as VR plus ALT >2X ULN. Retreatment decision was made according to the Taiwan reimbursement criteria: cirrhosis with detectable HBV DNA or non-cirrhosis with CR prolonged over 3 months or CR with serum bilirubin level >2 mg/dL or INR >1.5 or by joint physician/patient discussion. According to the clinical outcome and management, these patients were categorized into 4 groups: A: no CR and no retreatment (retx); B: no CR but retx; C: CR and no-retx; D: CR and retx.

Results: During a median of 6.6 years follow-up of this observational cohort, 180 (26%) were group A, 27 (4%) were group B, 103 (15%) were group C and 381 (55%) were group D. The cumulative VR, CR, retreatment rate are listed in table. The annual HBsAg decline in group A-D was: – 0.304, – 0.144, – 0.277, – 0.205 log₁₀IU/ml, respectively. Among the 691 patients, 343 (49.6%) achieved HBsAg <100IU/ml (group A-D: 72.8%, 38.5%, 56.3%, 37.8%, respectively) and 112 (16.2%) achieved HBsAg loss by the end of follow-up. The 5 and 10-year cumulative HBsAg loss rate are: group A: 27%, 57%; group B: 0%, 6%; group C: 13%, 38%; group D: 3%, 11%, respectively. Among the retreatment group (N=407), 251 patients (61.7%) had completed additional course of finite therapy with a 10-year cumulative HBsAg loss rate (from the first EOT) of 15%, >2 times higher than 6% in those still under continued treatment. The incidence of HCC and liver related mortality was very low, mostly occurs in cirrhotic patients (Table).

Table: Summary of cumulative events of these 691 HBeAg negative CHB patients

Event	1-year	2-year	3-year	5-year	10-year
Virological relapse	72%	84%	86%	88%	89%
Clinical relapse	42%	60%	65%	70%	72%
Retreatment	21%	39%	48%	57%	63%
HBsAg loss	1%	3%	6%	10%	27%
No CR/no Retx	4%	11%	18%	27%	57%
CR/no Retx	0%	2%	3%	13%	38%
No CR/Retx	0%	0%	0%	0%	6%
CR/ Retx	0%	1%	1%	3%	11%
HCC				4%	6%
Non-cirrhosis				1%	2%
Cirrhosis				8%	11%
Liver-related mortality (due to HCC, hepatic decompensation or cirrhotic complication)				2%	3%
Non-cirrhosis				0%	0%
Cirrhosis				3%	6%

Conclusion: The finite therapy does much increase the functional cure rate, especially in those remain untreated. The HBsAg loss rate accelerated along with follow-up time, especially after year 3.

SAT439

Bepirovirsen, antisense oligonucleotide (ASO) against hepatitis B virus (HBV), harbors intrinsic immunostimulatory activity via Toll-like receptor 8 (TLR8) preclinically, correlating with clinical efficacy from the Phase 2a study

Shihyun You¹, Jared Delahaye¹, Megan Ermler¹, Jennifer Singh¹, William Jordan¹, Avijit Ray¹, Nicholas Galwey², Daren Austin³, Dickens Theodore⁴, Melanie Paffl¹. ¹GlaxoSmithKline, Collegeville, PA, United States; ²GlaxoSmithKline, Stevenage, United Kingdom; ³GlaxoSmithKline, Brentford, United Kingdom; ⁴GlaxoSmithKline, Research Triangle Park, NC, United States
Email: shihyun.k.you@gsk.com

Background and aims: Bepirovirsen (BPV) is a modified ASO targeting HBV RNAs including pregenomic RNA; GSK3389404 (GSK404) is GalNac conjugated BPV. Phase 2a studies (NCT02981602 and NCT03020745) showed more robust dose-related HBsAg reductions and ALT flares with BPV than GSK404, prompting a hypothesis that preferential distribution of BPV to nonparenchymal cells may confer immune activity. To investigate the mechanism of BPV immunostimulatory effect, this post-hoc analysis evaluated changes in soluble proteins measured in study NCT02981602; preclinical models were used to validate the activity.

Method: This study analyzed plasma and serum from 30 patients receiving placebo (PBO) or BPV administered on Days 1, 4, 8, 11, 15 and 22 (treatment naïve: PBO n=6, BPV 150 mg n=6, 300 mg n=12; nucleos[t]ide-treated: PBO n=2, BPV 300 mg n=4). Soluble proteins from plasma (only treatment-naïve groups) collected at 0.5, 4, 6 and 24 hours post dose were evaluated with the Olink 1536 Explore panel for pathway analysis; soluble proteins from serum on Days 1, 2, 8, 15, 22, 23, 29, 36, 57 and 85 were evaluated with the Olink 96 Inflammation panel for correlation analysis. A generalized linear mixed effects model compared changes from baseline at each time point. Mean fold changes and p values were used to select analytes for pathway analyses (Enrichr). A subset of proteins was used in principal component analysis (PCA). BPV was tested in a panel of pattern recognition receptor (PRR)-overexpressing cell lines (InvivoGen) in vitro and TLR8 activity was validated in human TLR8 (hTLR8) transgenic mice in vivo.

Results: Within 6- and 24-hour post BPV dosing, the most significant change was observed in the epithelial mesenchymal transition pathway (p=2.75E-10) and in the inflammatory response pathway (p=4.13E-8), respectively. Notably, induction of IL12B, IFN γ , and IL1Ra, but not type I IFNs were detected, suggestive of TLR8

activation. PCA of TLR8 signature cytokines from longitudinal serum analysis showed that elevation of these cytokines was correlated with reduction of HBsAg in addition to BPV exposure and ALT flare. Transfected BPV showed weak activation of TLR8 among other PRRs in vitro. In hTLR8 mice, BPV elevated cytokines in plasma and livers, in a similar pattern to a TLR8 agonist; lesser effects were observed in wild type. In addition, the IL12B plasma response to BPV was greater than that by scrambled ASO or GSK404, indicating a specificity of BPV activating TLR8 in hTLR8 mice.

Conclusion: TLR8 agonism of BPV was confirmed preclinically. Cytokines/chemokines changed by BPV treatment in the Phase 2a study indicate that an immunostimulatory activity of BPV via TLR8 may be correlated with ASO-mediated HBsAg reduction. These findings support further investigation of a combination of HBsAg reducing agent and TLR8 agonist for treating HBV.

Funding: GSK (NCT02981602)

SAT440

Most patients with advanced cirrhosis treated with bulevirtide monotherapy have a non-monophasic HDV RNA decline patterns: an interim kinetic analysis of real-life setting

Louis Shekhtman^{1,2}, Harel Dahari¹, Scott Cotler¹, Elisabetta Degasperis³, Maria Paola Anolli³, Sara Colonia Uceda Renteria³, Dana Sambarino³, Marta Borghi³, Riccardo Perbellini³, Floriana Facchetti³, Ferruccio Ceriotti⁴, Pietro Lampertico^{3,5}. ¹Program for Experimental and Theoretical Modeling, Division of Hepatology, Department of Medicine, Stritch School of Medicine, Loyola University Chicago, Maywood, United States; ²Network Science Institute, Northeastern University, Boston, United States; ³Foundation IRCCS Ca' Granda Ospedale Maggiore Policlinico, Division of Gastroenterology and Hepatology, Milan, Italy; ⁴Foundation IRCCS Ca' Granda Ospedale Maggiore Policlinico, Virology Unit, Milan, Italy; ⁵CRC "A. M. and A. Migliavacca" Center for Liver Disease, Department of Pathophysiology and Transplantation, University of Milan, Milan, Italy
Email: harel.dahari@gmail.com

Background and aims: Bulevirtide (BLV) was recently approved for treatment of hepatitis D in Europe. Theory predicts that drugs like BLV that block virus infection should lead to a monophasic viral decline that is driven by the rate of loss/death of HDV-infected cells (Shekhtman et al. PMID: 34995688). The current study is the first

to characterize HDV and ALT kinetics under BLV monotherapy in patients with advanced compensated cirrhosis.

Method: Eighteen patients with HDV-related advanced compensated cirrhosis were treated with BLV 2 mg/day monotherapy. All were receiving TDF or ETV for HBV. Blood samples were collected at treatment initiation, weeks 4 and 8, and every 8 weeks thereafter. HDV RNA was measured by Robogene 2.0 (lower limit of quantification, LLoQ = 6 IU/ml). ALT normalization was defined as 41 U/L and 59 U/L for women and men, respectively.

Results: Median baseline HDV and ALT were 4.9 log IU/ml [IQR 4.4–5.8] and 106 U/L [IQR 81–142], respectively. During therapy, patients fit into 6 interim HDV kinetic patterns (Fig. 1): monophasic, MP (n = 3, Fig. 1a), biphasic, BP (n = 7, Fig. 1b), flat-partial response, FPR (n = 4, Fig. 1c), FPR followed by decline (n = 1, Fig. 1d), FPR followed by breakthrough (n = 1, Fig. 1e), and non-responder, NR (n = 2, Fig. 1f). MP patients had significantly (p = 0.039) longer median HDV $t_{1/2}$ of 46 days [range:41–60] compared to BP/FPR patients (26 days [range:11–49]) during the first viral decline phase, suggesting two distinct HDV-infected cell population turnovers. There was no difference (p > 0.18) in HDV $t_{1/2}$, length (median 11 weeks [range 3–22]) and magnitude (median 2.0 log IU/ml [range 1.1–3.3]) of first viral decline phase from baseline between BP and FPR patients. The 2nd slower phase slope of viral decline in BP patients was not significantly different (p = 0.18) than the first phase slope of viral decline in MP patients, suggesting similar HDV-infected cell population turnover. ALT normalization was achieved in 14 (78%) patients at a median of 8 weeks (range: 4 to 16) from initiation of BLV therapy. MP patients had a significantly (p = 0.048) lower median ALT decline slope of 1.4 U/wk [range:0.6–8.9] compared to BP/FPR patients (10.1 U/wk [range:4.5–28.5]), supporting, in part, the theory that HDV decline under BLV reflects the loss/death rate of HDV-infected cells.

Conclusion: While theory predicts a MP viral decline under BLV, this pattern was only identified in 3 patients (17%). In 7 patients (39%) the first rapid phase observed in patients with BP suggests that an additional HDV-infected cell population with a shorter $t_{1/2}$ might exist compared to patients with MP decline. Six patients (33%) experienced a FPR kinetic pattern suggesting suboptimal BLV dosage, which should be further investigated. The current findings will help to develop theoretical models to explain the observed viral dynamics and develop response guided therapy strategies.

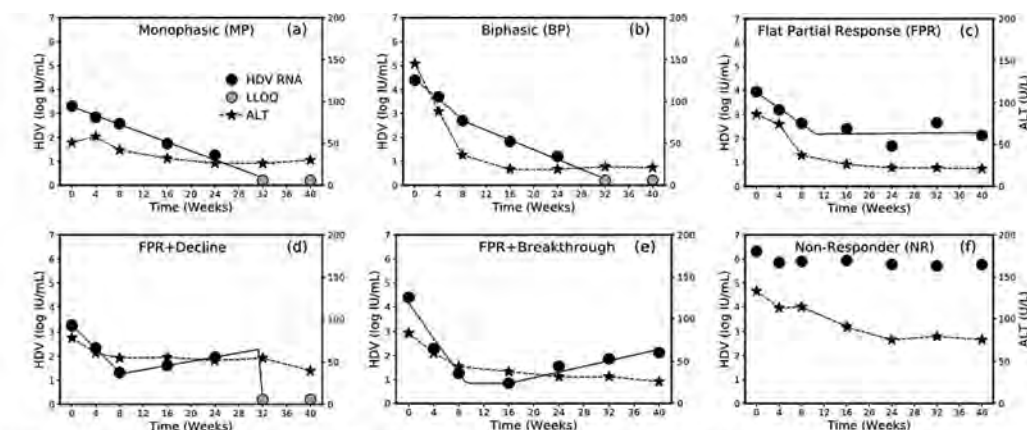


Figure 1. HDV kinetic patterns under BLV monotherapy in patients with advanced liver disease. **(a)** monophasic, MP, i.e., a single phase of viral decline (n=3), **(b)** biphasic, BP, viral decline consisting of a first phase decline that was 2-fold larger than the second phase decline rate (n=7), **(c)** flat-partial response, FPR, defined as a first phase viral decline followed by a plateau that was not significantly (p>0.05) different from slope=0 (n=4), **(d)** FPR followed by decline (n=1), **(e)** FPR followed by breakthrough (n=1), and **(f)** non-responder, NR, defined as having < ~1.0 log IU/mL decline from baseline (n=2). Solid lines for HDV reflect modelling using piecewise linear regression and dashed lines between ALT markers are shown only to highlight the trajectory.

Figure: (abstract: SAT440)

SAT441

Mechanistic pharmacokinetics/pharmacodynamics modelling of the simultaneous effects of bepirovirsen on hepatitis B surface antigen and alanine transaminase changes in chronic hepatitis B patients: phase 2b analysis to inform phase 3 decision-making

Amir Youssef¹, Mohamed Ismail², Mindy Magee¹, Dickens Theodore³, Melanie Paff⁴, Robert Elston⁵, Ahmed Nader¹. ¹GlaxoSmithKline, Clinical Pharmacology Modeling and Simulation, Collegeville, PA, United States; ²Enhanced Pharmacodynamics LLC, Buffalo, NY, United States; ³GlaxoSmithKline, Development, Clinical Sciences Hepatology/GI, Research Triangle, NC, United States; ⁴GlaxoSmithKline, Development, Collegeville, PA, United States; ⁵GlaxoSmithKline, Development, Clinical Sciences Hepatology/GI, Stevenage, Hertfordshire, United Kingdom
Email: amir.s.youssef@gsk.com

This abstract is under embargo until the start of the Late Breaker session on Saturday 25 June 2022, 14:00 BST. It will be made publicly available on the congress website once the embargo has lifted.

Journalists, industry, investigators and/or study sponsors must abide by the embargo times set by EASL.

Violation of the embargo will be taken seriously. Individuals and/or sponsors who violate EASL's embargo policy may face sanctions relating to current and future abstract submissions, presentations and visibility at EASL Congresses. The EASL Governing Board is at liberty to ban attendance and/or retract data.

Copyright for abstracts (both oral and poster) on the website and as made available during The International Liver Congress™ 2022 resides with the respective authors. No reproduction, re-use or transcription for any commercial purpose or use of the content is permitted without the written permission of the authors. Permission for re-use must be obtained directly from the authors.

SAT442

Improved treatment response and bone density in patients with chronic hepatitis B (CHB) switched to tenofovir alafenamide (TAF) from other nucleos (t)ide analogue: 96-week results from a prospective multinational study

Eiichi Ogawa¹, Dae Won Jun², Hidenori Toyoda³, Yao-Chun Hsu⁴, Eileen Yoon^{2,5}, Sang Bong Ahn⁶, Son Do⁷, Huy Trinh⁸, Hirokazu Takahashi^{9,10}, Masaru Enomoto¹¹, Satoshi Yasuda³, Cheng-Hao Tseng⁴, Ming-Lun Yeh^{12,13}, Keigo Kawashima¹⁴, Han Ah Lee⁵, Kaori Inoue⁹, Hiroaki Haga¹⁵, Ai-Thien Do⁷, Mayumi Maeda¹⁶, Joseph Hoang¹⁶, Ramsey C. Cheung^{16,17}, Yoshiyuki Ueno¹⁵, Yuichiro Eguchi^{9,18}, Norihiro Furusyo¹, Ming-Lung Yu^{12,13}, Yasuhito Tanaka^{14,19}, Mindie Nguyen^{16,20}. ¹Kyushu University Hospital, Department of General Internal Medicine, Japan; ²Hanyang University, Department of Gastroenterology, Korea, Rep. of South; ³Ogaki Municipal Hospital, Department of Gastroenterology, Japan; ⁴E-Da Hospital, Division of Gastroenterology and Hepatology, Department of Internal Medicine, Kaohsiung, Taiwan; ⁵Inje University Sanggye Paik Hospital, Department of Internal Medicine, Korea, Rep. of South; ⁶Nowon Eulji Medical Center, Eulji University College of Medicine, Department of Internal Medicine, Korea, Rep. of South; ⁷Digestive Health Associates of Texas, Dallas, United States; ⁸San Jose Gastroenterology, San Jose, United States; ⁹Saga University Hospital, Liver Center, Saga, Japan; ¹⁰Saga University Faculty of Medicine, Division of Metabolism and Endocrinology, Saga, Japan; ¹¹Osaka City University Graduate School of Medicine, Department of Hepatology, Osaka, Japan; ¹²Kaohsiung Medical University Hospital, Hepatobiliary Division, Department of Internal Medicine, Taiwan; ¹³Kaohsiung Medical University, Hepatitis Research Center, College of Medicine and Cohort Research Center, Taiwan; ¹⁴Nagoya City University Graduate School of Medical Sciences, Department of Virology and Liver Unit, Nagoya, Japan; ¹⁵Yamagata University Faculty of Medicine, Department of Gastroenterology, Yamagata, Japan; ¹⁶Stanford University Medical Center, Division of Gastroenterology and Hepatology, Department of Medicine, Palo Alto, United States; ¹⁷Veterans Affairs Palo Alto Health Care System, Division of Gastroenterology and Hepatology, Palo Alto, United States; ¹⁸Locomedical Eguchi Hospital, Locomedical General Institute, Saga, Japan; ¹⁹Kumamoto University Graduate School of Medical Sciences, Department of Gastroenterology and Hepatology, Kumamoto, Japan; ²⁰Stanford University, Department of Epidemiology and Population Health, Palo Alto, United States
Email: mindiehn@stanford.edu

Background and aims: Prior studies comparing TAF with TDF have shown similar efficacy and improved renal/bone safety, but outcome data for patients switched to TAF after other nucleos (t)ide analogues (NA) are limited. We aimed to assess treatment and safety outcomes of CHB patients switched to TAF after at least 1 year of another NA regimen.

Method: We prospectively enrolled adult CHB patients who switched from any NA to TAF at 14 centers in Japan, Korea, Taiwan, and the U.S.

POSTER PRESENTATIONS

All patients gave written informed consent. Primary outcomes were complete viral suppression (CVS, HBV DNA <20 IU/ml), biochemical response (BR, ALT <35/25 U/L men/women), and complete response (CVS+BR). Safety assessments included changes in estimated glomerular filtration rate (eGFR) and bone T-scores.

Results: We enrolled 270 eligible patients. Mean age was 58.1 ± 10.6 , 58.2% were male, 99.6% were Asian, 12.2% had cirrhosis, and 7.8% had chronic kidney disease (CKD). 73.7% switched from entecavir monotherapy, 23% from TDF/adefovir-based therapy (7.8%: combination therapy), 3.3% from another nucleoside analogue, and mean duration of NA treatment prior to TAF was 7.5 ± 4.0 years. Between switch and week 96 follow-up, the proportions of patients with CVS (95.2% to 98.8%), BR (75.2% to 78.7%), and complete response (72.6% to 77.9%) significantly increased (all $p < 0.001$). As shown in Figure, comparing levels at switch vs. week 96 of follow-up, there was no significant difference in mean eGFR (88.4 ± 16.9 vs. 89.5 ± 16.3 , $p = 0.13$) or the distribution of CKD stage ($p = 0.10$). In contrast, between switch and 96-week after switch, mean T-scores significantly improved (from -1.43 ± 1.36 to -1.17 ± 1.38 , $p < 0.001$), more patients had normal bone density (47% vs. 35%) and fewer patients had osteoporosis/osteopenia (53% vs. 65%) or osteoporosis (14% vs. 20%) ($p = 0.019$, Figure). In multivariable analysis, significant factors associated with worsening eGFR were age (adjusted odds ratio [aOR] 1.09, $p = 0.004$) and baseline eGFR, while male sex was associated with lower risk of developing osteopenia/osteoporosis (aOR 0.29, $p = 0.020$). Twelve patients (4.4%, 15/270) did not complete week-96 follow-up. There were 15 SAEs (5.6%, 15/270) and none were related to TAF.

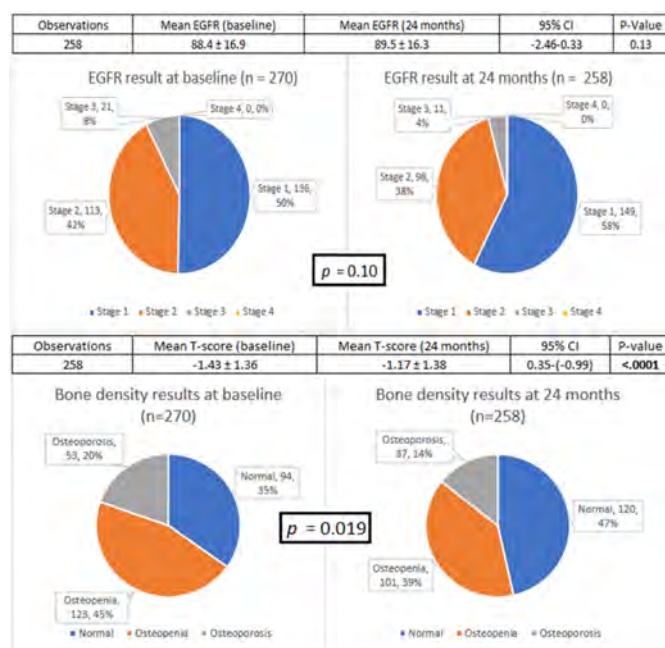


Figure: Week 96 safety results of TAF after other NA treatment

Conclusion: At 96-week following switch to TAF after an average of 7.5 years of treatment with other NA regimen, complete treatment response rate increased while renal function remained stable and bone density significantly improved.

SAT443

Long-term suppression maintained after cessation of AB-729 treatment and comparable on-treatment response observed in HBeAg+ subjects

Man-Fung Yuen¹, Elina Berliba², Wattana Sukeepaisarnjaroen³, Jacinta Holmes⁴, Apinya Leerapun⁵, Pisit Tangkijvanich⁶, Simone Strasser⁷, Alina Jucov², Edward J. Gane⁸, Emily P. Thi⁹,

Heather Sevinsky¹⁰, Elina Medvedeva¹⁰, Varun Sharma¹⁰, Kevin Gray¹⁰, Deana Antonello¹⁰, Gaston Picchio¹⁰, Karen Sims¹⁰, Timothy Eley¹⁰. ¹University of Hong Kong, Gastroenterology and Hepatology, Hong Kong, Hong Kong; ²Arenia Exploratory Medicine, Arenia Exploratory Medicine, Chisinau, Moldova; ³Khon Kaen University, Medicine, Khon Kaen, Thailand; ⁴University of Melbourne, St. Vincent's Hospital, Fitzroy, VIC, Australia; ⁵Chiang Mai University, Internal Medicine, Chiang Mai, Thailand; ⁶Chulalongkorn University, Biochemistry, Bangkok, Thailand; ⁷Royal Prince Alfred Hospital, AW Morrow Gastroenterology and Liver Centre, Camperdown, NSW, Australia; ⁸New Zealand Clinical Research Auckland, Grafton, New Zealand; ⁹Arbutus Biopharma, Research, Warminster, PA, United States; ¹⁰Arbutus Biopharma, Clinical Development, Warminster, PA, United States

Email: teley@arbutusbio.com

Background and aims: AB-729 is an N-Acetylgalactosamine (GalNAc)-conjugated single trigger RNA interference therapeutic that targets all HBV RNA transcripts, including HBx, resulting in suppression of viral replication and all viral antigens. AB-729 is in Phase 2 clinical development for the treatment of chronic hepatitis B (CHB). Here we report additional on treatment and follow-up data from AB-729-001 including a dedicated HBeAg+ cohort.

Method: In AB-729-001 Part 3, 41 non-cirrhotic, CHB subjects received AB-729 60 mg every 4 weeks (Q4W, Cohort E, N = 7), 60 mg every 8 weeks (Q8W, Cohort F, N = 7), 90 mg Q8W (Cohorts I (N = 6), G (N = 7) and K (N = 7)), or 90 mg every 12 weeks (Q12W, Cohort J, N = 7). Cohort G was HBV DNA+ and initiated tenofovir disoproxil fumarate on Day 1; all other Cohorts were virologically suppressed on stable nucleos(t)ide analogue (NA) therapy. Cohort K was all HBeAg+ at baseline. Eligible subjects could continue AB-729 through Week 48. Subjects are followed 48 weeks or more after AB-729 discontinuation.

Results: 40/41 eligible subjects consented to treatment extension. Complete on-treatment data for Cohorts E and F have been reported; at Weeks 32 and 36 post last dose, respectively, mean HBsAg change in Cohorts E and F was $-1.0 \log_{10}$ or more and 4/11 subjects with data remained <100 IU/ml. One subject in Cohort E underwent HBsAg seroconversion after AB-729 discontinuation while still on NA. The mean HBsAg declines for the 90 mg Cohorts I, J, K and G were similar (Table). In Cohorts I, J and G, 12/17 subjects with data were <100 IU/ml and 6 were <10 IU/ml at Week 48. At 20 Weeks post last dose, 11/18 subjects with data were <100 IU/ml and 3 were <10 IU/ml. The mean (SE) \log_{10} change in HBeAg was -0.71 (0.44) at Week 32 in Cohort K. There were no deaths or discontinuations due to AEs. There were 2 unrelated SAEs; all other AEs were Grade 1 or 2.

Baseline and Preliminary Mean (SE) \log_{10} Change in HBsAg

Nominal Visit	HBV DNA-		HBV DNA+		HBeAg+ only Cohort K N=7
	Cohort I N=6	Cohort J N=7 ¹	Cohort G N=7		
Baseline IU/ml	3.36 (0.23)	3.37 (0.28)	3.14 (0.14)	3.23 (0.14)	
Week 12	-1.37 (0.22)	-1.11 (0.35)	-1.56 (0.32)	-1.63 (0.39)	
Week 24	-1.80 (0.23)	-1.56 (0.25)	-1.82 (0.29)	-1.99 (0.35)	
Week 36	-2.06 (0.28)	-1.70 (0.39)	-2.08 (0.32)	-2.28 (0.43)	
Week 48	-1.91 (0.32)	-1.80 (0.41)	-2.16 (0.34)	-	
20 Weeks Post Last Dose ²	-1.42 (0.26)	-1.63 (0.39)	-1.50 (0.13)	-	

¹N = 6 entered treatment extension in J.

²Last dose Cohort J: Week 36, Cohorts I, G, K: Week 40.

Conclusion: AB-729 repeat dosing continues to be generally safe and well tolerated with robust and sustained declines in HBsAg that are comparable across treatment regimens. Neither HBeAg status nor DNA+ at baseline appear to affect response. In 17/31 subjects with data across all cohorts, HBsAg <100 IU/ml was maintained at least 20

weeks post last dose of AB-729. These data support the continued evaluation of AB-729 as the cornerstone of combination CHB treatment.

SAT444

Identification of novel antivirals against hepatitis delta virus infection via high throughput screening

Eirini Tseligka¹, Sophie Clément-Leboube¹, Francesco Negro².

¹University of Geneva Medical School; ²University Geneva Hospital
Email: eirini.tseligka@unige.ch

Background and aims: Chronic hepatitis delta (CHD) is the most severe form of chronic viral hepatitis with major clinical challenges. HDV tight dependence on its helper virus, Hepatitis B Virus (HBV) and the host cell machinery for its life cycle limits the development of drugs directly acting on HDV, while its therapeutic management remains unsatisfactory. We aim to identify compounds that block HDV replication by targeting HDV ribozymes (Rz), specific viral RNA sequences that undergo self-cleavage and ensure an efficient viral replication. We performed a high throughput screening (HTS) of FDA approved drug libraries to identify novel antivirals against HDV infection.

Method: We generated stable Huh7 human hepatoma cells expressing a reporter gene (secreted Gaussia luciferase, Gluc) either downstream (2xRz-Gluc) or upstream (Gluc-2xRz) of two HDV antigenomic Rz sequences. The cis-acting HDV Rz is self-cleaved leading to mRNA degradation and no detection of the secreted luciferase, whereas in the case of its inhibition, the detection of Gluc was monitored. Construct with Gluc alone was used as control. Validation of the assay was performed using a morpholino antisense nucleotide (GeneTools) as a positive control. We performed HTS of FDA approved drug libraries and measured the secreted luciferase as a readout of Rz inhibition after the addition of the molecules. Each plate with Z factor > 0.4 was considered valid. Dose-response effect and toxicity evaluation of the hits with Z-score > 5 was calculated. Analyses and statistic calculations were performed using an excel macro based on Genedata and ActivityBase softwares (IDBS). All data were generated from two independent experiments.

Results: No effect in the luciferase induction was observed in 2xRz-Gluc transfected cells treated with the antisense morpholino, whereas a dose dependent induction of the luciferase expression was detected in Gluc-2xRz transfected cells, implying the efficient inhibition of HDV antigenomic Rz autocatalytic cleavage (EC50 = 27.3 µM). We thus performed HTS on Gluc-2xRz. Gluc cells were included to ensure the specific induction of Gluc due to the inhibition of the HDV antigenomic Rz. The compounds with a Z-score > 5 were selected as positive hits with potentially promising inhibitory effect. We identified six compounds, namely APE000288, APE000286, APE000283, APE000285, APE000916 and APE000445 that showed a specific inhibitory effect on HDV antigenomic Rz in the Gluc-2xRz cells. No sign of toxicity was observed.

Conclusion: Six out of 6644 screened compounds showed a specific inhibitory effect on HDV antigenomic Rz. Further studies investigating the antiviral effect in a relevant cell culture infection model and the mechanism of action are currently ongoing. Drug combinational studies and resistance emergence studies will be additionally performed in the future.

SAT445

Generation and functional analysis of spacer modified HBV-specific chimeric antigen receptors that harbor a Fab fragment as binding domain

Zhe Xie¹, Oliver Quitt¹, Lisa Wolff¹, Elfriede Nöbner¹, Ulrike Protzer^{1,2}.

¹Institute of virology, Technical University of Munich/Helmholtz Zentrum München, München, Germany; ²German Center for Infection Research (DZIF), partner site Munich, Munich, Germany
Email: protzer@tum.de

Background and aims: Chimeric antigen receptor (CAR) T-cell therapy is a promising novel therapeutic approach for cancer, but has recently also been explored in the context of chronic viral infection. CARs are synthetic receptors designed to drive antigen-specific activation of T cells upon binding to cognate antigen, however, some of these artificial receptors have been found to elicit different levels of ligand-independent constitutive signaling. Our study aimed at generating novel CARs using antibody Fab fragments that target the hepatitis B virus envelope protein (HBVenv) on the membrane of HBV-infected cells and to study how their specificity can be guaranteed and which role different spacer lengths play.

Method: We constructed novel CARs that contain the HBVenv-specific human B cell-derived antibody fragment (4D06) as binding domain and CD3- as well as CD28 signaling domains (FabCAR). To determine the impact of spacer length on constitutive signaling, we employed several human immunoglobulin G (IgG) spacers with different lengths (IgG1CH2CH3 (225aa), IgG4CH2CH3 (226aa), IgG4CH3 (116aa) or IgG4Hinge (9aa)) and studied the activation of FabCAR-engrafted T cells in the presence and absence of target antigen. T-cell activation was assessed by quantification of pro-inflammatory cytokines and elimination of HBVenv-transgenic hepatoma cells.

Results: T cells from healthy donors were successfully engrafted with 4D06 FabCARs and efficiently eliminated HBVenv-transgenic Huh7S and HepG2 SML cells. Elimination of target cells was accompanied by secretion of interferon gamma, tumor necrosis factor alpha and granzyme B. However, T cells expressing FabCARs with a long spacer showed high levels of antigen-independent cytokine release and eliminated antigen-negative control cells. This constitutive, ligand-independent T-cell activation correlated with the spacer length and limiting spacer length allowed for antigen-specific T-cell activation. Employing the shortest spacer domains (IgG4 Hinge) completely abolished the constitutive T-cell activation and rendered the FabCAR-engrafted T cells HBV specific.

Conclusion: Our findings demonstrate that the spacer region of a CAR construct can significantly influence ligand-independent signaling and indicate that spacer length modification is an interesting strategy to improve efficacy and safety of CAR T cells. T cells stably transduced with 4D06 FabCARs containing a short spacer efficiently eliminated HBVenv-positive cells in an antigen-dependent manner and represent an interesting novel means to treat chronic hepatitis B and HBV-associated hepatocellular carcinoma.

SAT446

Randomised double-blind study of nitazoxanide for virologically suppressed HBeAg negative chronic Hepatitis B

Yong Chuan Tan^{1,2}, Liang Shen³, Htet Htet Toe Wai Khine¹,

Yuh Ling Amy Tay¹, Celina Adraneda^{1,2}, Jean-Francois Rossignol⁴, Celine Rossignol⁴, Seng Gee Lim^{1,2}. ¹Yong Loo Lin School of Medicine, National University of Singapore, Singapore, Department of Medicine, Singapore, Singapore; ²National University Hospital, Singapore, Singapore; ³Yong Loo Lin School of Gastroenterology and Hepatology, Singapore, Singapore; ⁴Yong Loo Lin School of Medicine, National University of Singapore, Singapore, Biostats Unit, Singapore, Singapore; ⁴Romark L C, United States
Email: mdcv341@nus.edu.sg

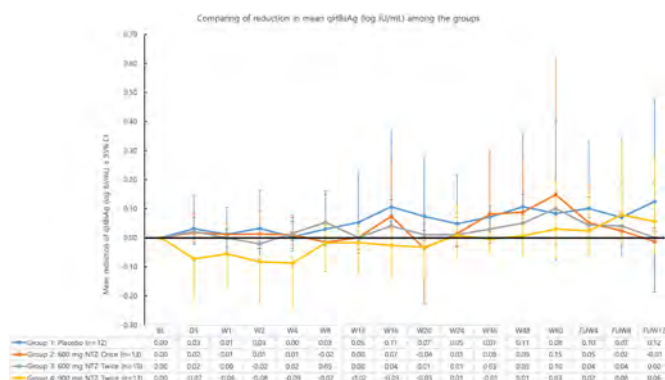
Background and aims: Nitazoxanide (NTZ) is a potential HBV therapeutic agent. NTZ disrupts Hepatitis B x protein (HBx) and host DNA-binding protein 1 (DDB1) interaction and prevents the formation of HBx-DDB1 protein complex responsible for the degradation of host restriction factor-structural maintenance of chromosomes 5/6 (SMC5/6). Restoration of SMC5/6 level after NTZ treatment suppresses Hepatitis B covalently closed circular DNA expression *in vivo*. (Sekiba, Otsuka et al. 2019) A subsequent pilot study demonstrated good anti-viral efficacy with 33% of patients (3 of

POSTER PRESENTATIONS

9 patients) achieving HBsAg loss (Rossignol and Brechot 2019). Consequently, this randomized controlled trial was designed to test NTZ efficacy.

Method: We conducted a phase 2, double-blinded, placebo-controlled, dose-finding, randomized control trial for Hepatitis B e antigen (HBeAg) negative Chronic Hepatitis B patients on long-term (>1 year) nucleos (t)ide analogues (NUCs) (Tenofovir disoproxil fumarate, Tenofovir alafenamide, or Entecavir). Participants were randomized (1:1:1:1) to receive either placebo (Group 1), NTZ 600 mg once daily (Group 2), NTZ 600 mg twice daily (Group 3), or NTZ 900 mg twice daily (Group 4), in addition to their NUC therapy. Primary efficacy end point was defined by the mean change in quantitative Hepatitis B surface antigen (qHBsAg) from baseline to week 48. Secondary end points included sustained off-treatment Hepatitis B surface antigen (HBsAg) loss, qHBsAg reduction, HBsAg seroconversion, Hepatitis B DNA suppression, and change in baseline Fibroscan and/or Fibrosis-4 score

Results: In total, 48 patients were enrolled. 12, 13, 10, and 13 patients were randomized to Group 1, 2, 3, and 4 respectively. There were no statistical differences in the key baseline patient characteristics (age, gender, presence of fatty liver, cirrhosis, Fibroscan score, Fibrosis-4 score, previous PEG-IFN exposure) between treatment groups. Overall, 4 patients who received NTZ and 1 patient who received placebo experienced severe adverse events (SAEs). 4 cases of grade 3 SAEs were deemed to be unrelated to NTZ (hepatocellular carcinoma (n=2); gastroesophageal reflux (n=1); perianal abscess (n=1)). Grade 4 SAE for alanine transaminase and aspartate aminotransferase elevation occurred in 1 patient (group 4) before resolving uneventfully with NTZ dose reduction. The primary and secondary efficacy end points were not met in all groups. No statistical difference in qHBsAg reduction or mean qHBsAg was detected between groups at all study time-points. Analysis of individual patient quantitative HBsAg kinetics did not identify any NTZ responder. The study was terminated early because of the lack of efficacy.



Conclusion: NTZ is safe and tolerable in CHB. Regrettably, the addition of NTZ to NUC therapy did not increase anti-viral efficacy.

SAT447

Low-level viremia in patients with chronic hepatitis B receiving entecavir, tenofovir and tenofovir alafenamide

Xiaohao Wang¹, Dachuan Cai¹, Zhang Juan¹. ¹The Second Affiliated Hospital, Chongqing Medical University, Infectious Diseases, Chongqing, China

Email: cqmuqdc@cqmu.edu.cn

Background and aims: Low-level viremia (LLV) has been reported to be associated with unfavourable outcomes in patients with chronic hepatitis B (CHB). The aims are to evaluate the effect of therapeutic drugs including entecavir (ETV), tenofovir (TDF) and tenofovir alafenamide (TAF) on LLV in CHB patients.

Method: CHB patients who received either ETV, TDF or TAF as a first-line antiviral agent were recruited from July 2020 to March 2021 at the Second Affiliated Hospital of Chongqing Medical University. The demographic characteristics and clinical data were collected. Binary logistic regression analysis was performed to identify the risk factors on the LLV.

Results: In total, 1043 patients (685, 284 and 74 in the ETV, TDF and TAF group) were recruited in this study. At baseline, the mean HBV-DNA level in ETV, TDF and TAF groups was 5.6 (SD:1.3), 5.6 (SD:1.2), and 5.5 (SD:1.1) log₁₀ IU/ml, respectively. About half of the patients were HBeAg positive (46.1%, 56.7% and 54.1%, respectively). After receiving a median of 100.0 (IQR: 66.0–192.0) weeks of antiviral therapy, the incidence of LLV was 30.2% (207/685), 34.9% (99/284) and 28.4% (21/74) in ETV, TDF and TAF groups respectively (p = 0.31). Univariate analysis found that female, age, antiviral time, cirrhosis, and baseline parameters including serum ALT, AST, HBeAg status, HBV-DNA level, albumin, glomerular filtration rate, and high-density lipoprotein-cholesterol were significantly associated with the LLV (p < 0.05). After adjusting for potential confounding factors in the binary logistic regression analysis, it was found that compared with ETV, TDF and TAF could significantly reduce the risk of LLV in patients with CHB (adjust OR: 0.59; 95% CI:0.40–0.88; p = 0.01, adjust OR: 0.50; 95% CI: 0.26–0.96, p = 0.04, respectively).

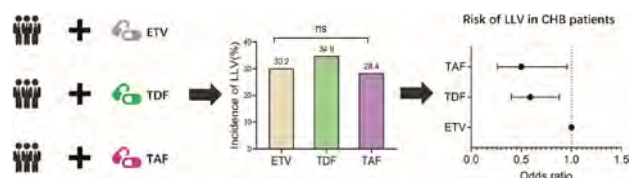


Figure: After receiving a median of 100.0 (IQR: 66.0–192.0) weeks of antiviral therapy, the incidence of LLV was 30.2% (207/685), 34.9% (99/284) and 28.4% (21/74) in ETV, TDF and TAF groups respectively (p = 0.31).

Conclusion: Compared with ETV, TDF and TAF are superior in reducing the risk of LLV in CHB patients.

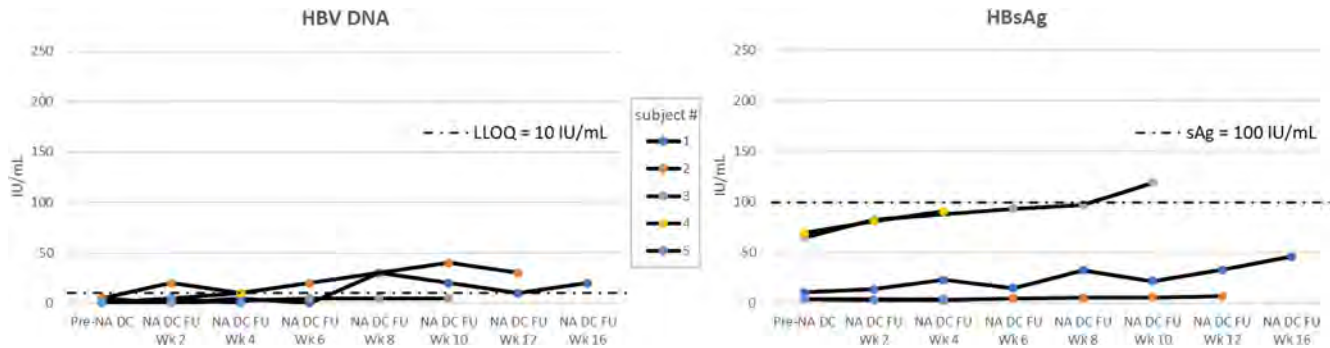
SAT448

Continued suppression of viral markers observed following discontinuation of nucleos (t)ide analogue therapy in chronic hepatitis B subjects with low hepatitis B surface antigen levels after 48 weeks of treatment with AB-729

Man-Fung Yuen¹, Simone Strasser², Wattana Sukeepaisarnjaroen³, Varun Sharma⁴, Deana Antoniello⁴, Elina Medvedeva⁴, Emily P. Thi⁵, Gaston Picchio⁴, Timothy Eley⁴, Karen Sims⁴. ¹The University of Hong Kong, Division of Gastroenterology and Hepatology, Hong Kong; ²Royal Prince Alfred Hospital, AW Morrow Gastroenterology and Liver Centre, Australia; ³Khon Kaen University, Department of Medicine, Thailand; ⁴Arbutus Biopharma, Clinical Development, Warminster, United States; ⁵Arbutus Biopharma, Discovery, Warminster, United States
Email: ksims@arbutusbio.com

Background and aims: AB-729 is an N-Acetylgalactosamine (GalNAc)-conjugated single trigger RNA interference therapeutic that targets all HBV RNA transcripts, including HBx, resulting in suppression of viral replication and all viral antigens. AB-729 is currently in Phase 2 clinical development in combination with other antiviral agents for the treatment of chronic hepatitis B (CHB). Study AB-729-001 assessed up to 48 weeks of AB-729 in combination with nucleos (t)ide analogue (NA) therapy. Here we report early follow-up data for subjects who met protocol eligibility criteria and elected to stop NA therapy at least 24 weeks after their last dose of AB-729.

Method: Subjects participating in study AB-729-001 who received 60 mg or 90 mg of AB-729 every 4 (Q4W), 8 (Q8W), or 12 (Q12W) weeks for 48 weeks were assessed for eligibility to stop NA therapy at least 24 weeks after their last dose of AB-729. Stopping criteria included ALT <2 × ULN, HBeAg negative, HBV DNA undetectable, and HBsAg <100 IU/ml on two separate measurements. Safety and PD



assessments, including HBV DNA, HBsAg, HBV RNA, and HBcrAg were assessed every 2–4 weeks after NA discontinuation.

Results: To date, 27 subjects in the AB-729-001 study have completed at least 24 weeks of follow-up post-last dose of AB-729. Of these, 7 met all eligibility criteria to stop NAs, and 5/7 consented to stop all therapy. NA discontinuation subjects' mean age was 45 years (range 33–59), 3/5 were female, and 4/5 were Asian. One subject was in Cohort E (60 mg Q4W), 3 were in Cohort F (60 mg Q8W) and 1 was in Cohort I (90 mg Q8W). Three were taking entecavir and 2 were taking tenofovir disoproxil fumarate. At study entry, all were HBeAg negative, mean HBsAg was 2886.8 IU/ml (range 1392–6765) and HBcrAg ranged from <3.0 to 4.2 log₁₀ U/ml. At the last visit prior to NA discontinuation (at least 24 weeks-post last AB-729 dose), mean HBsAg was 30.49 IU/ml (range 3.95–69.1) and HBcrAg ranged from <3.0 to 4.5 log₁₀ U/ml. To date, all 5 subjects have completed between 4 and 16 weeks of follow-up off NA therapy, and no subjects have met clinical or viral relapse criteria. No AEs have been reported, no ALT elevations have been observed, and HBV DNA levels have remained either <LLOQ (3 subjects) or have transiently risen to 30 or 40 IU/ml and subsequently decreased in 2 subjects without intervention (Figure). HBsAg levels remain well below pre-study levels for all 5 subjects (Figure).

Conclusion: Discontinuation of NA therapy after AB-729-induced suppression of HBsAg to <100 IU/ml appears to be well-tolerated and leads to continued suppression of HBV DNA and HBsAg without evidence of early clinical or viral relapse. These subjects (and any others from this study who may discontinue NA in the future) will be followed for at least 48 weeks post-NA discontinuation to assess for sustained viral response and evidence of functional cure.

SAT449

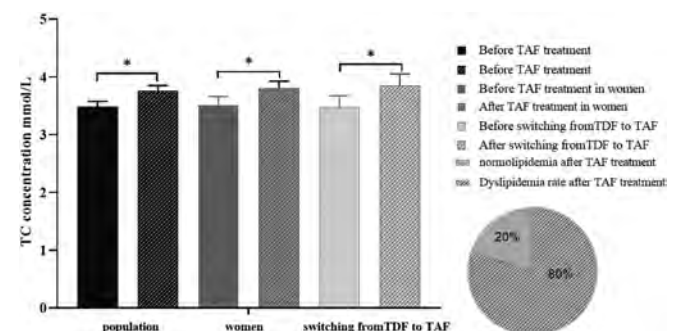
Tenofovir alafenamide fumarate increased lipid levels in hepatitis B virus patients

Wenjuan Zhao¹, Yi Liu², Feng Ye¹, Zixin Cui¹, Shumei Lin¹, Lei Shi¹, Xi Zhang¹, Jianzhou Li¹, Xiaojing Liu¹, Yunru Chen¹. ¹The First Affiliated Hospital of Xi'an Jiaotong University Medical College, Department of infectious disease, Xi'an, China; ²The First Affiliated Hospital of Xi'an Jiaotong University Medical College, traditional Chinese medicine department, Xi'an, China
Email: chenyunru_2002@126.com

Background and aims: Tenofovir alafenamide fumarate (TAF) is among the main drugs for long-term antiviral therapy. Long term administration of TAF can lead to dyslipidemia in HIV patients. Dyslipidemia is associated with arteriosclerosis and hepatocarcinogenesis. Therefore, this study prospectively investigates the effects of TAF on blood lipids after 24 weeks in chronic hepatitis B (CHB) patients.

Method: Forty CHB patients with normal blood lipids were treated with TAF for 24 weeks among them there are 19 female and 21 male patients, 13 patients treated with ETV switching to TAF, 13 patients treated with TDF switching to TAF, 14 patients treated with initial TAF, and 7 patients with fatty liver. The serum level of cholesterol (TC), low density lipoprotein (LDL), high density lipoprotein (HDL-C), and triglyceride (TG) at baseline and 24 weeks treatment were analyzed.

Results: After TAF treatment for 24 weeks, the HDL, LDL and TG levels showed a trend of increasing, and the TC level increased significantly ($p = 0.006$). Typically, the TC level increased significantly in female patients ($p = 0.041$) and in patients with TDF switching ($p = 0.036$). Compared with the non-fatty liver patients, the TG levels increased significantly in the patients with fatty liver ($p = 0.006$). In addition, the dyslipidemia rate increased after TAF treatment, and the LDL abnormal rate (LDL ≥ 2.5 mmol/L) was up to 20% ($p < 0.005$).



TAF: tenofovir alafenamide fumarate; TDF: tenofovir disoproxil; TC total cholesterol; * $P < 0.05$. Before TAF treatment; After TAF treatment; Before TAF treatment in female; After TAF treatment in female; Before TAF treatment in TDF switching to TAF; After TAF treatment in TDF switching to TAF.

Conclusion: TAF treatment for 24 weeks impacted lipid metabolism. Our study indicated that to monitor the blood lipids was necessary in CHB patients with TAF treatment. Especially, the changes in blood lipids should be closely observed in female patients, in switching from TDF to TAF patients, and in patients with fatty liver during TAF treatment. In addition, we only collected 24-week data. The serum lipid profiles after 48 weeks and 96 weeks TAF treatment required further investigation. Lastly, the mechanisms associated with dyslipidemia induced by TAF remained to be clarified in further investigation.

POSTER PRESENTATIONS

SAT450

Off-therapy cure of hepatitis delta after 3 years of bulevirtide monotherapy in a patient with compensated advanced cirrhosis

Maria Paola Anolli¹, Elisabetta Degasperis¹, Colonia Sara Uceda Renteria², Dana Sambarino¹, Marta Borghi¹, Riccardo Perbellini¹, Alessandro Loglio¹, Caroline Scholtes^{3,4}, Floriana Facchetti¹, Mirella Fraquelli⁵, Andrea Costantino⁵, Ferruccio Ceriotti², Fabien Zoulim^{3,4}, Pietro Lampertico^{1,6}.
¹Foundation IRCCS Ca' Granda Ospedale Maggiore Policlinico, Division of Gastroenterology and Hepatology, Milan, Italy; ²Foundation IRCCS Ca' Granda Ospedale Maggiore Policlinico, Virology Unit, Milan, Italy; ³Hospices Civils de Lyon (HCL) and Université Claude Bernard Lyon 1 (UCBL1), Hepatology Department, Lyon, France; ⁴INSERM U1052, Centre de Recherche sur le Cancer de Lyon (CRCL), Lyon, France; ⁵Foundation IRCCS Ca' Granda Ospedale Maggiore Policlinico, Division of Gastroenterology and Endoscopy, Milan, Italy; ⁶University of Milan, CRC "A. M. and A. Migliavacca" Center for Liver Disease, Department of Pathophysiology and Transplantation, Milan, Italy
 Email: maria.anolli@unimi.it

Background and aims: Bulevirtide (BLV) has been recently approved for the treatment of chronic hepatitis Delta (CHD) in Europe, yet the rates of the off-therapy sustained responses following long-term BLV based treatment are currently unknown.

Method: A 54-year Caucasian male with HDV related compensated cirrhosis and clinically significant portal hypertension (CSPH) was treated with BLV monotherapy for 3 years and then followed for 48 week off-therapy. Clinical and virological characteristics were collected every 2 months after BLV withdrawal. HDV RNA was quantified by Robogene 2.0 (LOD 6 IU/ml), HBcrAg by LUMIPULSE® G (LOQ 3 Log U/ml), HBV RNA by cobas® 6800 (LOQ 10 cp/ml).

Results: At the end of the 3 years of BLV monotherapy, ALT were within the normal range, HDV RNA <6 IU/ml and liver function was preserved (CPT score A). During 48 weeks of post-BLV follow-up, HDV RNA levels remained undetectable (HDV RNA <6 IU/ml) and liver function tests within the normal range at all timepoints. While no changes were observed for HBV DNA (always <10 IU/ml) and HBV RNA (always <10 cp/ml) levels, HBsAg and HBcrAg levels declined (4 vs. 3.4 log IU/ml; 4.5 vs. 3.4 log IU/ml, respectively). Compared to baseline, liver stiffness measurement (LSM) by Fibroscan® declined (17.9 vs. 11.5 kPa) and stigmata of portal hypertension improved: PLT normalized (74 vs. 144 × 10³/mm³) and oesophageal varices disappeared. Likewise, autoimmune features secondary to HDV infection, like IgG and γglobulins, normalized. Biliary acids fell into the normal range immediately after BLV withdrawal. A liver biopsy was performed at the end of the post-treatment follow-up: histological response will be presented at the meeting.

Conclusion: A 3-year course of BLV monotherapy may cure HDV infection even in difficult-to-treat cirrhotic patients.

SAT451

Combination treatment of a PAPD5/7 inhibitor with an antisense oligonucleotide bepirovirsin with concurrent dosing shows additive HBsAg decreases in the AAV-HBV mouse model

Jared Delahaye¹, Edward Long¹, Chi Lau¹, Jacob Parsons¹, Bo Wen¹, Zhiyi Cui¹, Melanie Paff¹, Shihyun You¹, Martin Leivers¹.

¹GlaxoSmithKline, Collegeville, PA, United States

Email: martin.leivers@gsk.com

Background and aims: Achieving high levels of functional cure of chronic hepatitis B (CHB) will likely require a treatment regimen containing multiple mechanisms of action. Small molecule inhibitors of the noncanonical poly (A) polymerase 5 and 7 (PAPD5/7) have been shown preclinically to reduce hepatitis B surface antigen (HBsAg) in a mouse model of HBV infection. This current work describes investigation of combinations of a PAPD5/7 inhibitor, GSK3965193, (GSK193) with bepirovirsin (BPV, antisense oligonucleotide against HBV, currently completed a Ph2b study (study NCT04449029)) in a mouse model of HBV infection. Sequential and concomitant

treatment of the two agents were explored and the results used to inform future clinical combination trial design.

Method: The AAV-HBV mouse model of HBV infection was used to establish a dose response for both GSK193 and bepirovirsin as monotherapies. Then, two potential clinical treatment paradigms were tested where both agents were administered concurrently or GSK193 preceding treatment with bepirovirsin in a sequential fashion. GSK193 was dosed at 0.3–30 mg/kg, PO, BID for 28 days and bepirovirsin was dosed at 20 or 40 mg/kg, subcutaneous on days 0, 3, 7, 11, 14 and 21) HBsAg was the key viral end point measured for these studies.

Results: Monotherapy treatment of the PAPD5/7 inhibitor GSK193 resulted in an up to 1 log reduction in HBsAg levels with BID dosing for 28 days. Monotherapy treatment of the antisense oligonucleotide bepirovirsin resulted in an up to 2 log reduction in HBsAg levels with doses on days 0, 3, 7, 11, 14 and 21. When both agents were administered concurrently over 28 days, additional decreases reaching 3 logs in HBsAg were observed over either monotherapy alone. For the sequential treatment of GSK193 followed by bepirovirsin, rapid rebound in HBsAg occurred after discontinuation of GSK193 resulting in no added benefit in this regimen.

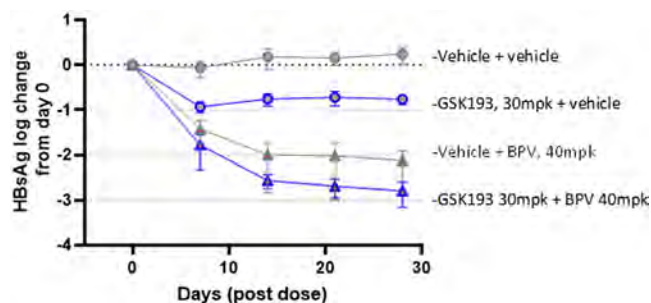


Figure: Reductions in HBsAg with monotherapy or combination dosing of PAPD5/7 inhibitor (GSK193) and ASO (bepirovirsen)

Conclusion: Combinations of a PAPD5/7 inhibitor (GSK193) and antisense oligonucleotide (bepirovirsen) provide additional reductions in HBsAg when dosed concurrently in the AAV-HBV mouse model of HBV. Concurrent dosing of these compounds is also superior in terms of maximal HBsAg suppression to sequential dosing preclinically.

SAT452

Efficacy and safety of bepirovirsin in patients with chronic hepatitis B virus infection not on stable nucleos (t)ide analogue therapy: interim results from the randomised phase 2b B-Clear study

Seng Gee Lim¹, Cristina Pojoga^{2,3}, Harry Janssen⁴, Denis Gusev⁵, Robert Plesniak⁶, Keiji Tsuji⁷, Ewa Janczewska⁸, Corneliu Petru Popescu⁹, Pietro Andreone¹⁰, Jinlin Hou¹¹, Manuela Arbune¹², Adrian Gadano¹³, Diana Petrova¹⁴, Jun Inoue¹⁵, Teerha Piratvisuth¹⁶, Young-Suk Lim¹⁷, Apinya Leerapun¹⁸, Masanori Atsukawa¹⁹, Ji-Dong Jia²⁰, Eternity Labio²¹, Jennifer Cremer²², Robert Elston²³, Tamara Lukic²⁴, Geoff Quinn²³, Stuart Kendrick²³, Punam Bharania²³, Fiona Campbell²³, Melanie Paff²², Dickens Theodore²². ¹National University Health

System, Singapore; ²Regional Institute of Gastroenterology and Hepatology, Romania; ³Babeş-Bolyai University, Department of Clinical Psychology and Psychotherapy, International Institute for Advanced Study of Psychotherapy and Applied Mental Health, Romania; ⁴Toronto General Hospital, Canada; ⁵Center for Prevention and Control of AIDS and Infectious Diseases, Russian Federation; ⁶University of Rzeszow Centrum Medyczne w Lancucie Sp. z o.o., Poland; ⁷Hiroshima Red Cross Hospital, Japan; ⁸Faculty of Health Sciences in Bytom, Medical University of Silesia, ID Clinic, Poland; ⁹Dr Victor Babes Clinical Hospital of Infectious and Tropical Diseases, Carol Davila University of Medicine and Pharmacy, Romania; ¹⁰Azienda Ospedaliero-Universitaria di Modena, Italy; ¹¹Nanfeng Hospital, Southern Medical University, China; ¹²Sf.Cuv. Parascheva Infectious Diseases Clinical Hospital, Romania; ¹³Hospital Italiano de Buenos Aires, Argentina; ¹⁴Diagnostic Consultative Centre Alexandrovsk, Bulgaria; ¹⁵Tohoku University Hospital, Japan; ¹⁶NKC Institute of Gastroenterology and Hepatology, Thailand; ¹⁷Asan Medical Center, University of Ulsan College of Medicine, Korea, Rep. of South; ¹⁸Chiang Mai University, Thailand; ¹⁹Department of Internal Medicine, Division of Gastroenterology and Hepatology, Nippon Medical School, Japan; ²⁰Beijing Friendship Hospital, Capital Medical University, China; ²¹Makati Medical Center, Philippines; ²²GlaxoSmithKline, United States; ²³GlaxoSmithKline, United Kingdom; ²⁴GlaxoSmithKline, United Arab Emirates

Email: jennifer.x.cremer@gsk.com

This abstract is under embargo until the start of the Late Breaker session on Saturday 25 June 2022, 14:00 BST. It will be made publicly available on the congress website once the embargo has lifted.

Journalists, industry, investigators and/or study sponsors must abide by the embargo times set by EASL.

Violation of the embargo will be taken seriously. Individuals and/or sponsors who violate EASL's embargo policy may face sanctions relating to current and future abstract submissions, presentations and visibility at EASL Congresses. The EASL Governing Board is at liberty to ban attendance and/or retract data.

Copyright for abstracts (both oral and poster) on the website and as made available during The International Liver Congress™ 2022 resides with the respective authors. No reproduction, re-use or transcription for any commercial purpose or use of the content is permitted without the written permission of the authors. Permission for re-use must be obtained directly from the authors.

SAT453

Efficacy and safety of bepirovirsen in patients with chronic hepatitis B virus infection on stable nucleos (t)ide analogue therapy: interim results from the randomised phase 2b B-Clear study

Man-Fung Yuen¹, Robert Plesniak², Seng Gee Lim³, Keiji Tsuji⁴, Gheorghe Diaconescu⁵, Adrian Gadano⁶, Ju Hyun Kim⁷, Tarik Asselah⁸, Hyung Joon Yim⁹, Jeong Heo¹⁰, Giuliano Rizzardini¹¹, Harry Janssen¹², Corneliu Petru Popescu¹³, Diana Petrova¹⁴, Alexander Wong¹⁵, Nevin Indriz¹⁶, Cristina Pojoga¹⁷, Yasuhito Tanaka¹⁸, Denis Gusev¹⁹, Ewa Janczewska²⁰, Jennifer Cremer²¹, Robert Elston²², Tamara Lukic²³, Lauren Maynard²², Stuart Kendrick²², Punam Bharania²², Fiona Campbell²², Melanie Paff²², Dickens Theodore²¹. ¹Queen Mary Hospital, China; ²University of Rzeszow, College of Medicine, Centrum Medyczne w Lancucie Sp. z o.o., Poland; ³National University Health System, Singapore; ⁴Hiroshima Red Cross Hospital, Japan; ⁵Spitalul Clinic de Boli Infectioase si Pneumoftiziologie, Romania; ⁶Hospital Italiano de Buenos Aires, Argentina; ⁷Department of Gastroenterology, Gachon University Gil Medical Center, Korea, Rep. of South; ⁸Hôpital Beaujon, France; ⁹Korea University Ansan Hospital, Korea, Rep. of South; ¹⁰College of Medicine, Pusan National University and Biomedical Research Institute, National University Hospital, Korea, Rep. of South; ¹¹Luigi Sacco Hospital, Italy; ¹²Toronto General Hospital, Canada; ¹³Dr Victor Babes Clinical Hospital of Infectious and Tropical Diseases, Carol Davila University of Medicine and Pharmacy, Romania; ¹⁴Alexandrovsk, Bulgaria; ¹⁵Department of Medicine, University of Saskatchewan, Canada; ¹⁶UMHAT Sofamed, Bulgaria; ¹⁷Regional Institute of Gastroenterology and Hepatology, Romania; ¹⁸Kumamoto University, Japan; ¹⁹Center for Prevention and Control of AIDS and Infectious Diseases, Russian Federation; ²⁰ID Clinic, Poland; ²¹GlaxoSmithKline, United States; ²²GlaxoSmithKline, United Kingdom; ²³GlaxoSmithKline, United Arab Emirates

Email: jennifer.x.cremer@gsk.com

This abstract is under embargo until the start of the Late Breaker session on Saturday 25 June 2022, 14:00 BST. It will be made publicly available on the congress website once the embargo has lifted.

Journalists, industry, investigators and/or study sponsors must abide by the embargo times set by EASL.

Violation of the embargo will be taken seriously. Individuals and/or sponsors who violate EASL's embargo policy may face sanctions

relating to current and future abstract submissions, presentations and visibility at EASL Congresses. The EASL Governing Board is at liberty to ban attendance and/or retract data.

Copyright for abstracts (both oral and poster) on the website and as made available during The International Liver Congress™ 2022 resides with the respective authors. No reproduction, re-use or transcription for any commercial purpose or use of the content is permitted without the written permission of the authors. Permission for re-use must be obtained directly from the authors.

Cirrhosis and its complications: Other clinical complications except ACLF and critical illness

SAT486

Evaluation of Interleukin-6 for stepwise diagnosis of minimal hepatic encephalopathy in patients with liver cirrhosis

Simon Johannes Gairing^{1,2}, Julian Anders¹, Leonard Kaps^{1,2}, Michael Nagel^{1,2,3}, Maurice Michel^{1,2}, Wolfgang Maximilian Kremer^{1,2}, Max Hilscher^{1,2,3}, Peter Galle^{1,2}, Jörn Schattenberg^{1,4}, Marcus-Alexander Wörns^{1,2,3}, Christian Labenz^{1,2}. ¹University Medical Center of the Johannes Gutenberg-University, Department of Internal Medicine I, Mainz, Germany; ²University Medical Center of the Johannes Gutenberg-University, Cirrhosis Center Mainz (CCM), Mainz, Germany; ³Dortmund Hospital, Department of Gastroenterology, Hematology, Oncology and Endocrinology, Dortmund, Germany; ⁴University Medical Center of the Johannes Gutenberg-University, Metabolic Liver Research Program, Mainz, Germany
Email: sgairing@uni-mainz.de

Background and aims: Minimal hepatic encephalopathy (MHE) is associated with poor quality of life and dismal prognosis. Psychometric testing is time consuming and therefore often neglected in routine clinical practice. Thus, predictive biomarkers are urgently needed to stratify patients at risk for MHE. This study aimed to evaluate the diagnostic accuracy of interleukin-6 (IL-6) serum levels as part of a stepwise diagnostic algorithm to detect MHE in patients with liver cirrhosis.

Method: The development cohort comprised 197 prospectively recruited patients without evidence of HE grade 1–4. A total of 52 patients served as the independent validation cohort. The Psychometric Hepatic Encephalopathy Score (PHES) was used for MHE diagnosis.

Results: In total, 50 (25.4%) patients of the development cohort were diagnosed with MHE. Serum IL-6 levels were more than twice as high in patients with MHE as in patients without MHE (16 vs 7 pg/ml, $p < 0.001$). In logistic regression analysis, elevated IL-6 levels remained independently associated with MHE (OR 1.036, 95%CI 1.009–1.064, $p = 0.008$) after adjusting for other variables such as MELD, albumin, CRP and history of ascites. Using a cut-off value of IL-6 ≥ 7 pg/ml would have avoided subsequent time-consuming psychometric testing in 38% of all patients (sensitivity 90%, 95%CI 77%–96%; negative predictive value 93%, 95%CI 84%–98%). These results were confirmed in the validation cohort (sensitivity: 94%, NPV: 93%).

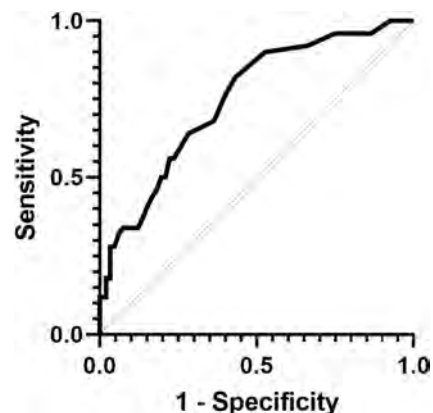


Figure: Discriminative ability of Interleukin-6 to detect minimal hepatic encephalopathy in the development cohort of patients with liver cirrhosis. AUC = 0.751, 95% CI 0.675–0.827, $p < 0.001$.

Conclusion: IL-6 serum levels may serve as biomarker in a stepwise diagnostic algorithm reducing the number of patients requiring elaborate testing with PHES. In particular, IL-6 would be helpful in patients being incapable of performing other tests e.g., due to language barriers.

SAT487

Evaluation of statins as a new therapy to alleviate chronotropic dysfunction in cirrhotic rats

Qamar Niaz^{1,2}, Sania Mehreen³, Mahmoud Ghazi-Khansari¹, Farahnaz Jazaeri¹. ¹Department of Pharmacology, School of Medicine, Tehran University of Medical Sciences, Tehran, Iran; ²Department of Pharmacology and Toxicology, Faculty of Bio-Sciences, University of Veterinary and Animal Sciences, Lahore, Pakistan; ³Department of Zoology, Faculty of Fisheries and Wildlife, University of Veterinary and Animal Sciences, Lahore, Pakistan
Email: fjazaeri@yahoo.com

Background and aims: Liver cirrhosis defines by regenerative nodules and fibrotic septa which causes cirrhotic cardiomyopathy (CCM) with chronotropic hypo-responsiveness. Statins have been reported to decrease inflammation, fibrosis, and portal pressure (PP) in liver cirrhosis through inhibition of Ras homolog family member A (RhoA) and stimulation of endothelial nitric oxide synthase (eNOS). Therefore, we studied the effect of atorvastatin on chronotropic hypo-responsiveness in biliary cirrhotic rats.

Method: Bile duct ligation (BDL) or sham surgery performed on Wistar (*Rattus norvegicus*) male rats and grouped as BDL/Saline, BDL/Ator-7d (days) (Atorvastatin 15 mg/kg/day), and BDL/Ator-14d groups or Sham/Saline, Sham/Ator-7d, and Sham/Ator-14d groups for cirrhosis or control groups respectively. Corrected QT (QTc) interval, chronotropic responses, serum brain natriuretic peptides (BNP), and heart tumour necrosis factor-alpha (TNF-alpha), nuclear factor erythroid 2-related factor 2 (Nrf2), and malondialdehyde (MDA) levels were studied along with liver histopathology, and atrial RhoA and eNOS genes expression.

Results: The chronotropic responses were decreased in BDL/Saline and increased in BDL/Ator-7d group. The QTc interval, BNP, TNF-alpha, and MDA levels were elevated in BDL/Saline and reduced in BDL/Ator-14d group. The Nrf2 level raised non-significantly in BDL/Saline and significantly in BDL/Ator-14d group. The liver inflammation and fibrosis increased in BDL/Saline and were not affected in BDL/Ator-7d and BDL/Ator-14d groups. The RhoA expression down-regulated in BDL/Saline, BDL/Ator-7d, and BDL/Ator-14d groups while the eNOS expression up-regulated non-significantly in BDL/Saline and down-regulated in BDL/Ator-14d group.

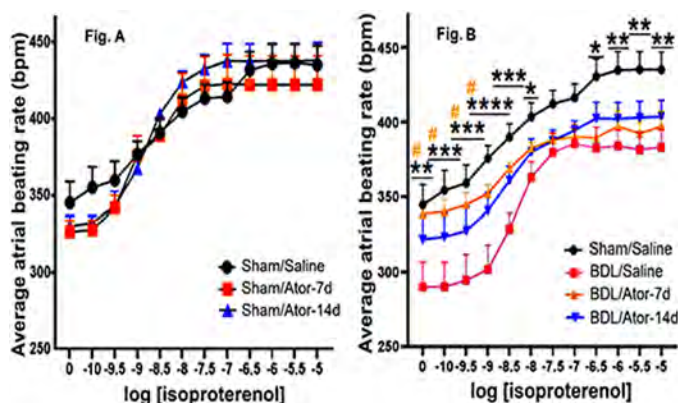


Figure: Average atrial beating rates of sham (control) and BDL (cirrhotic) rats after treatment with saline or atorvastatin (15 mg/kg/day for 7 and 14 days). The atrial beating rates were recorded before, and after stimulation

with 10^{-10} to 10^{-5} M cumulative concentrations of isoproterenol. The data represent the mean \pm SEM. At least, 6–8 rats were included per experimental group. (4B): [*P < 0.05, **P < 0.01, ***P < 0.001 and ****P < 0.0001 BDL/Saline group compared to Sham/Saline group], and [#P < 0.05 BDL/Ator-7d group compared to BDL/Saline group]

Conclusion: Atorvastatin alleviates the chronotropic hypo-responsiveness, and down-regulates the RhoA and eNOS expressions along with anti-inflammatory, anti-oxidant, and anti-stress effects in CCM.

SAT488

The effect of sarcopenia on survival of patients with cirrhosis: a systematic review and meta-analysis

Xinxing Tantai¹, Yi Liu², Yee Hui Yeo³, Michael Praktijn⁴, Ezequiel Mauro⁵, Yuhei Hamaguchi⁶, Cornelius Engelmann⁷, Peng Zhang⁸, Jae Yoon Jeong⁹, Jeroen van Vugt¹⁰, Huijuan Xiao¹¹, Huan Deng¹², Xu Gao¹³, Qing Ye¹⁴, Jiayuan Zhang¹⁵, Longbao Yang¹³, Yaqin Cai¹³, Yixin Liu¹⁶, Na Liu¹⁷, Zongfang Li¹², Tao Han¹⁴, Toshimi Kaido¹⁸, Joo Hyun Sohn¹⁹, Christian Strassburg⁴, Thomas Berg²⁰, Jonel Trebicka²¹, Yao-Chun Hsu²², Jan Ijzermans¹⁰, Jinhai Wang¹³, Grace Su²³, Fanpu Ji²⁴, Mindie Nguyen²⁵. ¹the Second Affiliated Hospital of Xi'an Jiaotong University, Department of Gastroenterology, China; ²the Second Affiliated Hospital of Xi'an Jiaotong University, Department of Infectious Diseases, China; ³Cedars-Sinai Medical Center, Division of General Internal Medicine, United States; ⁴University Hospital Bonn, Department of Internal Medicine I, Germany; ⁵Hospital Italiano de Bs. As., Liver Transplant Unit, Liver Unit, Argentina; ⁶Japanese Red Cross Osaka Hospital, Department of Gastrointestinal Surgery; ⁷Department of Medicine II, Leipzig University Medical Center, Division of Hepatology, Germany; ⁸University of Michigan Medical School, Department of Surgery, United States; ⁹National Medical Center, Department of Gastroenterology and Hepatology, Korea, Rep. of South; ¹⁰Erasmus MC University Medical Centre, Department of Surgery, Division of HPB and Transplant Surgery, Netherlands; ¹¹The Third Central Hospital of Tianjin, Department of Nutrition, China; ¹²The Second Affiliated Hospital of Xi'an Jiaotong University, National and Local Joint Engineering Research Center of Biodiagnosis and Biotherapy, China; ¹³The Second Affiliated Hospital of Xi'an Jiaotong University, Department of Gastroenterology, China; ¹⁴The Third Central Hospital of Tianjin, Department of Gastroenterology and Hepatology, China; ¹⁵Xi'an Jiaotong University, Xi'an Jiaotong University Library, China; ¹⁶The Second Affiliated Hospital of Xi'an Jiaotong University, Department of Gastroenterology, China; ¹⁷the Second Affiliated Hospital of Xi'an Jiaotong University, Department of Gastroenterology, China; ¹⁸St Luke's International Hospital, Department of Gastroenterological and General Surgery, Japan; ¹⁹Hanyang University Guri Hospital, Department of Internal Medicine, Korea, Rep. of South; ²⁰Leipzig University Medical Center, Division of Hepatology, Department of Medicine II, Germany; ²¹Goethe University Clinic Frankfurt, Department of Internal Medicine I, Germany; ²²Fu Jen Catholic University Hospital, Division of Gastroenterology and Hepatology; ²³University of Michigan Medical School, Department of Medicine, United States; ²⁴The Second Affiliated Hospital of Xi'an Jiaotong University, Department of Infectious Diseases, China; ²⁵Stanford University Medical Center, Division of Gastroenterology and Hepatology, United States
Email: jifanpu1979@163.com

Background and aims: The association between sarcopenia and prognosis in patients with cirrhosis remains to be determined. In this study, we aimed to quantify the association between sarcopenia and the risk of mortality in patients with cirrhosis, by sex, underlying liver disease etiology, and severity of hepatic dysfunction.

Method: PubMed, Web of Science, EMBASE, and major scientific conference sessions were searched without language restriction through 13 January 2021 with additional manual search of bibliographies of relevant articles. Cohort studies of ≥ 100 patients

POSTER PRESENTATIONS

with cirrhosis and ≥ 12 months of follow-up that evaluated the association between sarcopenia, muscle mass and the risk of mortality were included.

Results: 22 studies with 6965 patients with cirrhosis were included. The pooled prevalence of sarcopenia in patients with cirrhosis was 37.5% overall (95%CI 32.4%–42.8%), higher in male patients (41.9%), patients with alcohol associated liver disease (ALD) (49.6%), patients with CTP grade C (46.7%), and when sarcopenia was defined in patients by lumbar 3- skeletal muscle index (L3-SMI) (44.4%). Sarcopenia was associated with the increased risk of mortality in patients with cirrhosis (adjusted-hazard ratio [aHR] 2.30, 95% CI 2.01–2.63), with similar findings in sensitivity analysis of cirrhosis patients without HCC (aHR 2.35, 95% CI 1.95–2.83) and in subgroup analysis by sex, liver disease etiology, and severity of hepatic dysfunction (Figure). The 1-, 3-, and 5-year cumulative probabilities of survival in patients with sarcopenia were 76.6%, 64.3%, and 45.3%, compared to 93.4%, 82.0%, and 74.2%, respectively in patients without sarcopenia (all $P < 0.001$). The association between quantitative muscle mass index and mortality further supports the poor prognosis for patients with sarcopenia (aHR 0.95, 95% CI 0.93–0.98).

Group	No. of studies	No. of patients	Adjusted HR(95% CI)	I ² (%)	P-heterogeneity
Overall	16	4645	2.30(2.01–2.63)	0	0.61
With HCC	10	2795	2.35(1.95–2.83)	15	0.31
Without HCC	6	1850	2.25(1.79–2.82)	0	0.85
Sex					
Male	7	898	2.46(1.86–3.25)	0	0.32
Female	6	1467	2.16(1.24–3.79)	49	0.08
Etiology of cirrhosis					
ALD	4	306	2.67(1.60–4.47)	22	0.28
Non-ALD	5	577	2.08(1.34–3.26)	32	0.21
Severity of liver dysfunction					
MELD ≤ 15	6	1057	2.34(1.78–3.09)	0	0.51
MELD ≥ 15	6	1481	1.55(1.15–2.09)	0	0.61
Study location					
Asia	8	2541	2.44(2.01–2.96)	0	0.85
Non-Asia	8	2104	2.25(1.79–2.84)	30	0.19
Study design					
Prospective	3	1025	2.08(1.40–3.09)	50	0.12
Retrospective	13	3620	2.42(2.08–2.83)	0	0.86
Methods for measuring muscle mass					
L3-SMI	10	3144	2.28(1.93–2.70)	0	0.93
Other	6	1501	2.81(2.14–3.69)	0	0.48
Source of cirrhosis cohort					
General patients	11	2536	2.35(1.97–2.82)	13	0.32
Patients evaluated or listed for LT	5	1707	2.25(1.79–2.82)	0	0.85
Study quality score					
NOS score ≥ 9	6	1812	2.16(1.74–2.68)	0	0.89
NOS score < 9	10	2833	2.45(2.01–2.93)	16	0.3

Conclusion: Sarcopenia was highly and independently associated with higher risk of mortality in patients with cirrhosis.

SAT489

Effectiveness of probiotics in the secondary prevention of hepatic encephalopathy among cirrhotic patients

Muhammad Farooq Hanif¹, Abdul Rehman², Raja Omar Fiaz³, Khalid Mahmud Khan⁴. ¹Pakistan Kidney And Liver Institute And Research Centre, Gastroenterology and Hepatology, Lahore, Pakistan; ²Mayo Hospital, Gastroenterology and Hepatology, Lahore, Pakistan; ³Central Park Medical College, Gastroenterology and Hepatology, Lahore, Pakistan; ⁴Jinnah Hospital, Lahore, Gastroenterology and Hepatology, Lahore, Pakistan
Email: farooqdr@hotmail.com

Background and aims: Cirrhosis is one of the leading cause of death around the globe¹. The prevalence of hepatic encephalopathy (HE) which is one of its complication is 10–14% in general, 16–21% with decompensated cirrhosis and 30–40% are of those with cirrhosis at some time during their clinical course². The risk for first bout of overt hepatic encephalopathy is 5–25% within 5 years after cirrhosis³. This study compared the effectiveness of lactulose alone versus combination of lactulose plus probiotics for secondary prevention of hepatic encephalopathy in cirrhotic patients^{4–9}.

Method: Patients with known chronic liver disease admitted with hepatic encephalopathy, were randomized to group A (Lactulose alone) and group B (Lactulose + Probiotics). Probiotic used was Cap. Ecotec 180 mg, 1 trillion CFU (Lacidophilus, Bifidobacterium, S. thermophilus, L.bulgaricus). After discharge each patient was followed for six months for hepatic encephalopathy recurrence. The absence of hepatic encephalopathy at the end of six months treatment for each patient was considered as effective treatment response. Compliance to the treatment and side effects were also noted during this time period.

Results: 166 patients included in the study. Mean age was 55.84 ± 7.82 and 52.37 ± 6.95 in group A and B respectively. Majority of patients were of child class B (75.90%), whereas 6% were child class C and 18% were child class A. Overall encephalopathy occurred in 51.80% and 36.14% of patients in group A and B respectively ($p = 0.02$). Encephalopathy was more common among relatively older females and patients with advanced child class with baseline ammonia more than 80ug/dl. Abdominal bloating, distaste and diarrhea were the common side effects in both groups with no significant difference in the side-effect profile. Patients were compliant to the treatment in both groups.

		Study Groups		p value	Total N = 166
		A N = 83	B N = 83		
Hepatic Encephalopathy	Yes	43 (51.80%)	30 (36.14%)	0.02	73 (43.97%)
	No	31 (37.34%)	48 (57.83%)		79 (47.59%)
	Lost follow-up	09	05		14 (8.43%)
Male		37 (44.57%)	45 (63.85%)		82 (49.39%)
Female		46 (55.42%)	38 (36.14%)		84 (50.60%)
Symptoms free Male		19 (51.35%)	30 (66.66%)		47 (52.22%)
Symptom free Female		12 (26.08%)	18 (47.36%)		32 (42.10%)

Conclusion: In our cohort of cirrhotic patients, combination of lactulose and probiotics showed better response compared to lactulose alone in the long term secondary prevention of hepatic encephalopathy.

SAT490

Sarcopenia as a predictor of mortality and complications in cirrhosis patients-A prospective cohort study

Nidhin Devadas¹, K Sandesh¹, K SunilKumar¹. ¹Government Medical College, Kozhikode, Medical Gastroenterology, Kozhikode, India
Email: niddas@gmail.com

Background and aims: Sarcopenia is a promising tool for prognostication of cirrhosis. EWGSOP2 guidelines define sarcopenia based on muscle strength, muscle quantity or quality and physical performance. Many previous studies didn't use a standardized definition of sarcopenia and was based on skeletal muscle measurement by CT or MRI. Ultrasound guided thigh muscle thickness (TMT) measurement is a validated, cost effective and easy method for assessment of muscle quantity. There is paucity of Indian studies analysing prognostic role of sarcopenia in cirrhosis.

To study the predictive role of sarcopenia on mortality and complications in cirrhosis patients.

Method: This was a prospective cohort study with 120 consecutive patients each in sarcopenia and no sarcopenia groups. Sarcopenia was diagnosed based on EWGSOP2 guidelines using ultrasound guided measurement of TMT. They were followed up for 6 months. Kaplan-Meier analysis with LogRank test was used to compare survival and

Cox proportional hazards model was used for multivariate analysis to determine risk factors of mortality.

Results: Cirrhosis patients with sarcopenia[N1 = 120, M:F = 80:40, Median age-58yrs (51-64)] and without sarcopenia[N2 = 120, M:F = 93:27, Median age-54yrs (46.25-60)] were enrolled. Six month cumulative survival was 56.7% and 76.7% in sarcopenia and no sarcopenia groups respectively ($p = 0.001$). Six month cumulative survival in severe and non-severe sarcopenia was 23.9% and 70% respectively ($p = 0.001$). Age, sex, nutritional status, sarcopenia status, CTP score, MELD score, Bilirubin, Albumin, INR and Sodium were significantly associated with survival. A multivariate analysis showed sarcopenia (HR = 1.283, 95%CI 1.092-2.130, $p = 0.031$), female sex (HR = 1.851, 95%CI 1.106-3.097, $p = 0.019$), CTP class C (HR = 1.447, 95%CI 1.252-1.794, $p = 0.002$) and MELD score >15 (HR = 1.116, 95%CI 1.056-2.203, $p = 0.05$) as independent predictors of mortality. Development of complications like ascites, HE, Covid infection and UGI bleed were significantly higher in sarcopenia group, while SBP, AKI, cellulitis, UTI, HCC and ACLF were not statistically significant between two groups.



Figure 1. Survival curves in both groups (Log rank $p = 0.001$)

Conclusion: Sarcopenia is an independent prognostic marker of mortality in cirrhosis and is associated with increased risk of complications like ascites, HE, Covid infection and UGI bleed. Severe sarcopenia has even poorer outcome. It appears that addition of sarcopenia to existing scoring systems of cirrhosis will improve prognostication of patients.

Key Words: Sarcopenia, Cirrhosis, Thigh muscle thickness, Prognostic tool

SAT491

Diagnosis and pathophysiological analysis of sarcopenia using liver MR in chronic liver disease

Atsushi Nakamura¹, ¹Kawasaki, Japan

Email: naka2722@gmail.com

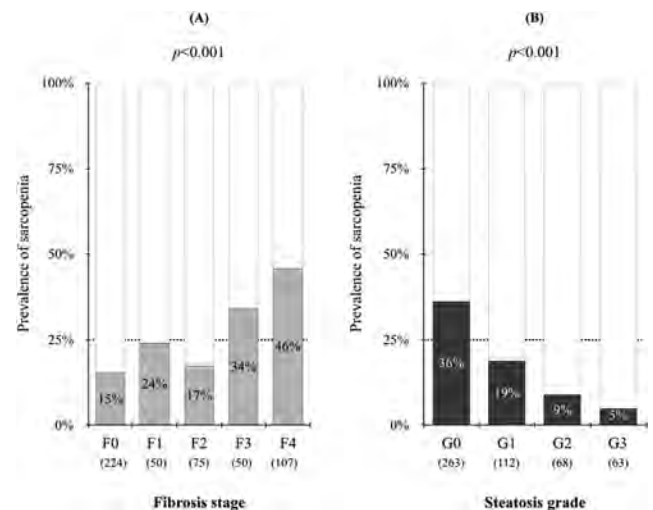
Background and aims: There are a few studies of sarcopenia (SP) diagnosed by magnetic resonance imaging (MRI), and paraspinal muscle area (PSMA) measurement at the level of superior mesenteric artery (SMA) has been reported to be useful (*Hepatology* 2018). However, there are racial differences in body size, and there is no standard for Asians in MRI. On the other hand, in liver cirrhosis (LC), adipopenia (AP) is also associated with worse prognosis, and MRI proton density fat fraction (PDFF) has been shown to reflect body fat mass closely. The aim of this study was to develop SP criteria for MRI based on the GLIM criteria, which are global diagnostic criteria for malnutrition, and to clarify the relationship with patient prognosis. In addition, we analyzed the significance of AP assessment.

Method: This is a retrospective study using imaging data from 506 patients with chronic liver disease (CLD) who underwent MR elastography (mean age 62 years, 60% male, LC 119, HCC 47). The etiologies was HBV/HCV, 241; NAFLD, 153; alcohol, 53; and others, 59. SP was diagnosed by determining the cut off value of PSMI (PSM

index: PSMA/Height²) for each gender based on ROC analysis of body mass index (BMI) against the criteria for malnutrition (in Asian population). AP was also diagnosed by setting the cut off value of MRI-PDFF according to the GLIM criteria by ROC analysis.

Results: 1) SP in CLD: BMI and PSMI were correlated in patients without ascites (M/F: $r = 0.477/0.534$, $p < 0.001$), and the cut off value of SP in males and females was 12.62 and 9.77 cm²/m², respectively (AUC: 0.91/0.77, $p < 0.001$). The prevalence of SP in CLD was 25%, and there was no difference by sex; the prevalence of SP was significantly higher in LC and HCC cases ($p < 0.05$). Furthermore, by MRE fibrosis stage (F0/1/2/3/4), SP increased from F3 and was inversely correlated with steatosis grade ($p < 0.01$). On the other hand, PDFF was significantly correlated with subcutaneous fat area at the SMA level (M/F: $r = 0.558/0.628$, $p < 0.001$) and AP (PDFF < 2.2%) was 17%. In multivariate analysis of factors contributing to SP, age (OR 1.05), Alb (0.23), and PDFF (0.91) were extracted ($p < 0.05$ for each).

2) Prognosis of LC: Child-Pugh classification (A/B/C) was 66/35/18 cases, prevalence of SP was 32/58/82%, AP was 26/33/76%, and SP and AP was 17/42/79%. During the observation period (25 ± 16 m), there were 22 liver-related deaths. The 3-year survival rate by Kaplan-Meier method was 96% in the non-SP group, 55% in the SP group, and 23% in the SP/AP group (log-rank test $p < 0.01$). In the Cox proportional hazard model, Child-Pugh score (HR 1.34) and SP and AP (5.60) were independent prognostic factors ($p < 0.01$).



Conclusion: We demonstrated the validity of new SP diagnostic criteria assessed by SMA levels on MRI in Asians. Our results indicate that the combination of SP and AP is a new phenotype of severe SP, and suggest the need to screen for SP in CLD from the pre-cirrhotic stage.

SAT492

Use of a cirrhosis database can positively impact patient care in United Kingdom practice

Jessica Shearer¹, Dianne Backhouse¹, Lynsey Corless¹. ¹Hull Royal Infirmary, Department of Gastroenterology, Hepatology and Endoscopy, Kingston upon Hull, United Kingdom

Email: lynsey.corless@nhs.net

Background and aims: Screening for oesophageal varices and surveillance for hepatocellular carcinoma (HCC) are advised for patients with cirrhosis but adherence to recommendations is poor. The study aimed to provide descriptive analysis of a new cirrhosis

POSTER PRESENTATIONS

database and evaluate rates of surveillance in a large teaching hospital.

Method: All patients diagnosed with advanced fibrosis/cirrhosis in our centre entered the database sequentially from April 2018. The service covers a population of 600000, with expected prevalence of 600 cirrhotic patients. The database-rather than clinic visits-became the primary means to monitor HCC surveillance/endoscopic screening requests. Subsequent adherence to recommendations was measured in 2021.

Results: 841 patients entered the database over 3 years, with only 200 at inception-less than the predicted cirrhosis prevalence. 36 people died during follow-up and 5 left the area. Of the remaining 800 patients, median age was 60 years; 40% female. 46% of patients had alcohol related disease, 21% non-alcoholic fatty liver disease, 14% viral hepatitis. 63% of the cohort had Childs-Pugh (CP) A or advanced fibrosis, 14% CP-B, 3% CP-C. 21% had no stage recorded. 157 patients (20%) were on primary prophylaxis for variceal bleeding. Of the remaining 643 patients, 237 (37%) were on active endoscopic surveillance and a further 100 (16%) had attended endoscopy in the past 3 years. 43 patients (7%) were overdue, 40 (6%) declined, and 30 (5%) had documented clinical decision not to proceed. 191 patients (24%) had no documentation about screening. 603 (78%) of appropriate patients were up to date with HCC surveillance with a further 105 (14%) awaiting scan, significantly more than our historically reported adherence of 50% ($p < 0.0001$).

Conclusion: The database improved our knowledge of clinical characteristics of our patient population, and provided a way to readily monitor surveillance intervals. Most had appropriate HCC surveillance, surpassing our previous (or nationally reported) adherence rates. A quarter of patients had no documentation of variceal screening, highlighting an area for improvement. Given the rapid rise in cohort size, it is likely the database also reduces numbers lost to follow-up/surveillance in the event of clinic non-attendance, which may be particularly valuable in the post-Covid era of delayed appointments. This study shows the potential of a registry to improve care and outcomes in people with cirrhosis.

SAT493

Psychomotor speed from minimal hepatic encephalopathy testing is associated with physical frailty in patients with end-stage liver disease

Andres Duarte Rojo¹, Rachel K. Grubbs¹, Randi Wong², Pamela M. Bloomer¹, Robert Rahimi³, Alexandra Steinberg⁴, Jennifer Lai². ¹University of Pittsburgh Medical Center; ²University of California San Francisco; ³Baylor University Medical Center; ⁴Axcella Therapeutics
Email: duarterojoa@upmc.edu

Background and aims: The Stroop EncephalApp (StE) is a neuropsychological test assessing psychometric speed and cognitive processing and has been validated to diagnose minimal hepatic encephalopathy (HE). Frailty, as measured by the Liver Frailty Index (LFI), is highly prevalent in end-stage liver disease (ESLD), particularly among patients with HE. While the LFI comprises tests of physical function, it might conceivably also capture the contributions of cognitive impairment to physical frailty in ESLD. This study assessed the relationship between cognitive function (StE) and physical function (LFI) in ESLD.

Method: Patients with ESLD underwent LFI, StE and overt HE testing using modified orientation log (MO-log) and Clinical Hepatic Encephalopathy Staging Scale (CHESS) at 3 centers. Expected StE values were obtained from www.encephalapp.com. Pearson correlation and multivariable linear regression models were used to investigate StE variability. Stroop On, Stroop Off, and their combinations were analyzed separately to characterize StE contribution in

terms of cognitive processing (On-Off) versus psychomotor speed (Off).

Results: Of 172 subjects (58 ± 10 years; 59% male; 93% white; 37% alcohol, 25% NASH), 68% had Child-Pugh B/C cirrhosis, and 69% had prior overt HE. On testing, 97% had normal mentation (MO-log ≥ 23), none had overt HE (CHESS ≥ 3) and 81% had minimal HE. Cognitive function in terms of StE On+Off increased across frailty categories and showed a fair linear relationship with LFI (Fig.), of similar magnitude to that observed for age ($\rho = 0.29$, $p < 0.001$) and education ($\rho = -0.24$, $p < 0.002$). However, StE and LFI correlation weakened from Off ($\rho = 0.37$, $p < 0.001$) to On ($\rho = 0.20$, $p = 0.008$) and On-Off ($\rho = -0.05$, $p = 0.5$) modalities, suggesting that psychomotor speed was the main factor driving the association between cognitive and physical function. On multivariable analysis, adjusted for age, education and sex, only StE On+Off ($\beta = 15.38$, $p < 0.02$) and StE Off ($\beta = 8.95$, $p < 0.001$) remained associated with LFI.

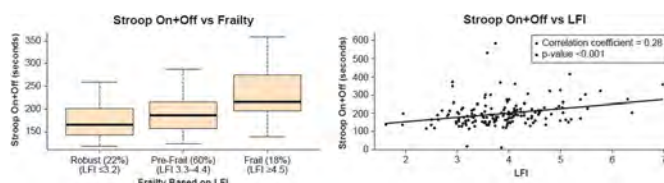


Figure: Box plot of Stroop On+Off value for different categories of frailty; and scatter plot of individual Stroop On+Off and LFI values. Increasing Stroop On+Off time denotes increasing cognitive impairment; increasing LFI denotes increasing frailty.

Conclusion: Using StE and LFI, an association between cognitive and physical function in ESLD was found, likely attributable to psychomotor speed over cognitive processing. Our findings suggest that the comprehensive assessment of minimal HE should include frailty metrics, and vice versa. Also, such brain-muscle relationship further supports investigating interventions targeting both physical and cognitive function in ESLD.

SAT494

A multistrain probiotic increases serum glutamine/glutamate ratio in patients with cirrhosis. A metabolomic analysis

German Soriano^{1,2}, Eva Roman^{2,3,4}, Luca Laghi⁵, Juan Camilo Nieto⁶, Qiuyu Lan⁵, Maria Poca^{1,2}, Edilmar Alvarado-Tapias^{1,2}, Berta Cuyas¹, Silvia Vidal^{4,6}, Candido Juárez⁷, Carlos Guarner^{1,2,4}, Àngels Escorsell¹. ¹Hospital de la Santa Creu i Sant Pau, Department of Gastroenterology, Barcelona, Spain; ²Instituto de Salud Carlos III, CIBERehd, Madrid, Spain; ³School of Nursing EUI-Sant Pau, Barcelona, Spain; ⁴Universitat Autònoma de Barcelona; ⁵University of Bologna, Italy; ⁶Research Institute IIB-Sant Pau, Spain; ⁷Hospital de la Santa Creu i Sant Pau, Department of Immunology, Spain
Email: gsoriano@santpau.cat

Background and aims: Probiotics can improve gut dysbiosis, intestinal barrier, ammonemia and proinflammatory state, as well as cognitive function and risk of falls in patients with cirrhosis. To explore the potential mechanisms underlying these effects, we aimed to analyze the changes in the blood metabolome of patients with cirrhosis after probiotic treatment.

Method: We performed untargeted metabolomics using ¹H-NMR spectroscopy in serum samples from 32 patients with cirrhosis and cognitive dysfunction (Psychometric hepatic encephalopathy score [PHES] < 4) or previous falls. These patients were included in a previous double-blind placebo-controlled trial (Román, Hepatol Commun 2020) and were randomized to receive the multistrain probiotic (brand name Vivomixx in Europe and Visbiome in USA), 450×10^9 cfu bid for 12 weeks, or placebo. Baseline and end of treatment blood samples were analyzed. A false discovery rate (FDR)

5% correction for multiple testing was applied using the Benjamini-Hochberg method.

Results: Patients treated with the probiotic (n = 17) presented a statistically significant improvement in cognitive function and risk of falls (evaluated by the PHES and gait speed, respectively), proinflammatory state (C-reactive protein and TNF- α) and intestinal barrier (fatty acid binding protein [FABP]-6) at the end of treatment. No changes were observed in the placebo group (n = 15). After analyzing 54 metabolites, the main findings were an increase in blood glutamine (FDR p = 0.007), a decrease in glutamate (FDR p = 0.03) and an increase in the glutamine/glutamate ratio in the probiotic group (FDR p = 0.01), while glutamate increased (FDR p = 0.02) and the glutamine/glutamate ratio decreased (FDR p = 0.03) in the placebo group. There was a correlation between the change in the ratio glutamine/glutamate and the change in the PHES (r = 0.34, p = 0.05), change in gait speed (r = 0.47, p = 0.008), and change in FABP-6 (r = -0.37, p = 0.04).

Conclusion: Our results suggest an influence of the multistrain probiotic Vivomixx on the glutamine/glutamate metabolism, and therefore in the capacity of ammonia detoxification, that could contribute to explain the beneficial effects observed in patients with cirrhosis.

SAT495

The composition of the bile acid pool is closely associated with fibrosis in the heart and liver of patients with cirrhosis

Signe Wiese¹, Jens Hove², Henriette Ytting¹, Svend Hoime Hansen³, Søren Møller⁴, Flemming Bendtsen¹. ¹Hvidovre Hospital, Gastro Unit, Medical Division, Denmark; ²Hvidovre Hospital, Dept. Cardiology, Denmark; ³Rigshospitalet, Dept. Clinical Biochemistry; ⁴Hvidovre Hospital, Centre of Functional Imaging and Research, Denmark
Email: signeswiese@gmail.com

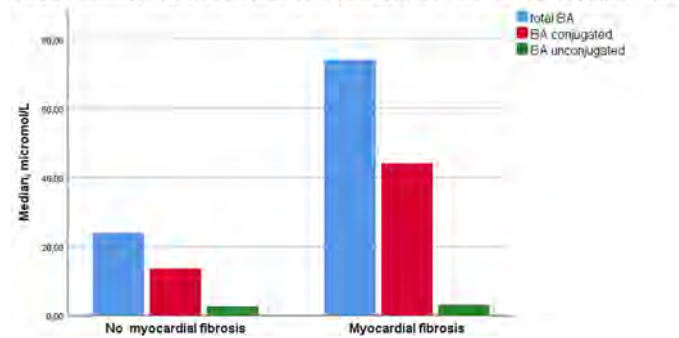
Background and aims: The role of bile acids (BA) in relation to liver fibrosis and signs of heart disease in chronic liver disease are areas of increasing interest. We have previously reported a close association between increased total BA (tBA) concentrations and myocardial fibrosis in patients with cirrhosis, and a strong relationship between the extent of fibrosis in the liver and the heart. These fibrotic changes can accurately be determined by MRI with assessment of myocardial and liver extracellular volume (ECV). Our aim was to identify specific groups or individual BA related to fibrosis in the liver and heart of patients with cirrhosis.

Method: We prospectively included 52 cirrhotic patients. All patients underwent contrast-enhanced MRI with T1-mapping and ECV quantification, and assessments of tBA, a panel of 15 specific BA and C4, a biomarker of de novo BA synthesis.

Results: The BA composition of cirrhotic patients with myocardial fibrosis was altered with increased conjugated BA levels (44 $\mu\text{mol/l}$ (21;87) vs. 14 $\mu\text{mol/l}$ (10;40), p = 0.02), predominantly glycine-conjugated BA (p = 0.01). The following specific BA were markedly increased: glyco-chenodeoxycholic acid (GCDCA) (p = 0.016), glyco-ursodeoxycholic acid (GUDCA) (p = 0.005), glyco-cholic acid (GCA) (p = 0.04) and tauro-ursodeoxycholic acid (TUDCA) (p = 0.026). Similarly, patients with a high liver ECV indicating the most advanced liver fibrosis had increased tBA levels (p < 0.001) and the BA pool consisted predominantly of primary BA (p < 0.001) and conjugated BA (p < 0.001) both glycine- and taurine-conjugated BA (p = 0.001). In these patients the following specific BA were increased: GCDCA (p < 0.001), GCA (p < 0.001), tauro-chenodeoxycholic acid (TCDCA) (p = 0.001), tauro-cholic acid (TCA) (p = 0.001), GUDCA (p = 0.006) and TUDCA (p = 0.001). Moreover, C4 levels were reduced (p = 0.005). When we assessed the relation to disease severity, we found the highest levels of tBA, primary BA and conjugated BA in Child Pugh C patients (p = 0.002, p = 0.003, p = 0.003, respectively).

Conversely, C4 levels decreased with disease severity (p < 0.001). MELD also correlated with BA levels (r = 0.62, p < 0.001) and C4 levels (r = -0.69, p < 0.001).

The bile acid composition in cirrhotic patients with and without myocardial fibrosis, defined as MyoECV > 0.31



Conclusion: The strong associations between myocardial fibrosis and in particular conjugated BA suggest a potential role of BA in the development of structural cardiac abnormalities in cirrhosis. Moreover, the composition of the BA pool is markedly altered in patients with advanced liver fibrosis and is closely related to disease severity.

SAT496

SBP vs. non-SBP bacterial infections at admission have comparable outcomes in a multi-center cohort of inpatients with cirrhosis

Jacqueline O'Leary¹, K. Rajender Reddy², Puneeta Tandon³, Patrick S. Kamath⁴, Guadalupe Garcia-Tsao⁵, Flornce Wong⁶, Jennifer C Lai⁷, Ram Subramanian⁸, Paul J. Thuluvath⁹, Benedict Maliakkal¹⁰, Hugo E. Vargas¹¹, Scott Biggins¹², Leroy Thacker¹³, Jasmohan S Bajaj¹³. ¹Dallas VA Medical Center, Dallas, United States; ²University of Pennsylvania, Philadelphia, United States; ³University of Alberta, Edmonton, Canada; ⁴Mayo Clinic Rochester, MN, Rochester, United States; ⁵Yale University, New Haven, United States; ⁶University of Toronto, Toronto, Canada; ⁷University of California San Francisco, San Francisco, United States; ⁸Emory University, Atlanta, United States; ⁹Mercy Medical Center; ¹⁰University of Tennessee, Knoxville, United States; ¹¹Mayo Clinic, Scottsdale, United States; ¹²University of Washington, Seattle, United States; ¹³VCU, Richmond, United States
Email: dr_jackieo@yahoo.com

Background and aims: Infections in cirrhosis lead to high rates of morbidity and mortality. While there are clear guidelines for diagnosis, treatment and prophylaxis for SBP, non-SBP infections are managed per local standards of care. We hypothesized that admission SBP would have a better prognosis compared to non-SBP bacterial infections in hospitalized patients with cirrhosis. Define outcomes in SBP vs. non-SBP infections in a large inpatient multi-center cohort adjusted for clinically relevant factors.

Method: NACSELD (North American Consortium for study of End-stage Liver Disease) included patients with cirrhosis without HIV or transplant admitted non-electively and followed for 30 days post-discharge. Demographics, cirrhosis details, admission reasons, hospital course and outcomes (ACLF, death, transplant) were recorded. We included patients admitted with bacterial infections (SBP vs others) diagnosed within 48 hours per IDSA guidelines. We excluded those with multiple admission infections, fungal or viral infections. Outcomes of SBP vs non-SBP patients were compared for transplant censored in-hospital mortality, transplant-censored 30-day mortality, transplant and 2nd infections after adjustment for admission factors (MELD, Na, HE, Albumin).

Results: 2,062 total patients were included: 458 had admission infections (103 SBP and 354 non-SBP bacterial infections) and 1605

POSTER PRESENTATIONS

had no admission infection. No differences were seen between the 2 infected groups with respect to ACLF/organ failures, medications and outcomes (Table 1). The adjusted analysis found no difference between the SBP and Non-SBP groups for transplant censored in-patient mortality, transplant, risk for 2nd infection, ACLF and transplant-censored 30-day mortality (Table 2).

Table: Summary of Study Cohort

	SBP Non-SBP No Infection			p value
	(n = 103)	(n = 354)	(n = 1605)	
Age	56.9	56.5	57.5	0.33
Gender (Male)	68%	59%	64%	0.16
MELD	22	19	18	<0.0001
Prior HE	65%	64%	57%	0.01
Hospital course				
ICU Transfer	28%	30%	18%	<0.0001
Brain failure	13%	17%	13%	0.11
Respiratory failure	15%	19%	9%	<0.0001
Circulatory failure	12%	14%	6%	<0.0001
AKI	60%	53%	36%	<0.0001
Renal failure	16%	11%	6%	<0.0001
Clinical Outcomes				
Txp Censored	17%	8%	4%	<0.0001
In-Hospital Mortality				
Txp Censored	19%	13%	8%	<0.0001
30-day Mortality				
Transplant	11%	5%	3%	0.0001
2nd Infection	14%	19%	1%	<0.0001

Table 2: Comparison of Adjusted OR of SBP vs. No-SBP

	OR	p value
Txp Censored In-Hospital Mortality	1.9	0.07
Txp Censored 30-day Mortality	1.3	0.43
Transplant	1.7	0.25
2nd Infection	0.7	0.20
ACLF	0.7	0.35

Conclusion: Patients with bacterial SBP and non-SBP infections were statistically similar with respect to development of 2nd infections, mortality, and transplant requirement after controlling for admission factors. Therefore, all patients with bacterial infections, not just SBP, should be monitored closely to prevent negative outcomes.

SAT497

Natural history of Hepatic Encephalopathy (HE) in a tertiary referral centre for hepatology

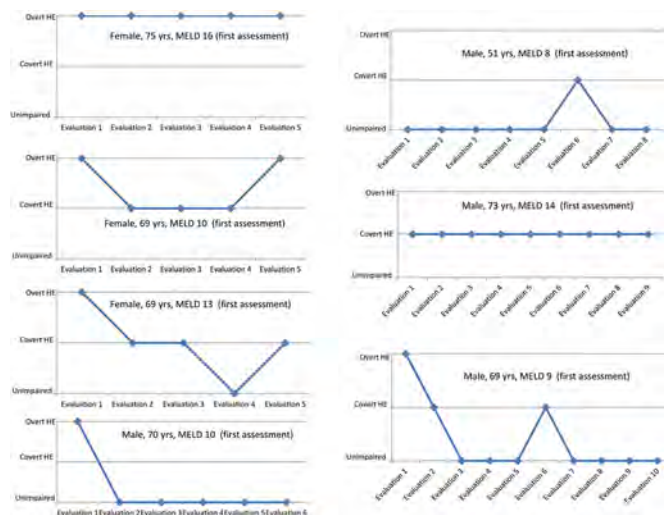
Chiara Mangini¹, Chiara Formentin¹, Alberto Biscontin¹, Gianluca Giusti¹, Paolo Angeli¹, Lisa Zarbonello¹, Sara Montagnese¹.
¹Department of Medicine, Padova, Italy
 Email: sara.montagnese@unipd.it

Background and aims: The occurrence and recurrence of HE mark significant progression in the natural history of cirrhosis. While it is well known that HE is an unfavourable prognostic factor, few data on its evolution over time are available. Our aim was to study the evolution of HE (neuropsychiatric indices, also in relation to HE treatment and severity of liver disease) in patients with varying degree of HE on first assessment.

Method: 87 patients with cirrhosis (age 58 ± 11 years; 72 males) referred to the HE outpatient clinic of the Regional Centre for Liver Diseases at Padova University Hospital between June 2009 and January 2019 were included. They were evaluated from 2 up to 10

times (varying time-intervals), for purposes of liver transplantation selection, differential diagnosis or treatment optimization. The presence/severity of HE was assessed by clinical, neuropsychological (PHES) and neurophysiological (EEG) tools. The severity of liver disease was assessed by the MELD score. Treatment was instituted/modified according to both guidelines and local experience after each evaluation.

Results: On first assessment, 23 patients were classed as unimpaired, 32 as having covert and 32 as having overt HE. Amongst unimpaired patients, on second/third evaluation 56%/6% remained unimpaired, 35%/3% developed covert HE, 9%/0% developed overt HE. Amongst patients with covert HE, on second and third evaluation 25%/10% became unimpaired, 44%/19% remained covert, 31%/13% developed overt HE. Finally, amongst patients with overt HE, 19%/16% became unimpaired, 25%/13% became covert and 56%/25% remained overt. PHES results tended to improve over time in patients with overt HE and the EEG worsened over time (despite remaining within normal limits) in unimpaired patients. These trends were not confirmed after adjustment for HE history, HE treatment and MELD. Finally, in patients with multiple evaluations, HE evolution was manifold and difficult to predict (fig. 1).



Conclusion: While there is obvious HE risk associated with HE on first assessment, our data suggest that evolution over time is extremely variable and largely dependent on HE history/management and MELD. These data also support the concept that HE is an essentially reversible condition.

SAT498

Public knowledge and attitudes toward liver diseases and liver cancer in the Brazilian population

Paulo Bittencourt¹, Liana Codes¹, Maria Lucia Ferraz¹. ¹Brazilian Liver Institute
 Email: plbbr@uol.com.br

Background and aims: Cirrhosis, particularly viral hepatitis (VH) and alcoholic liver disease (ALD), are the 8th leading cause of death in Brazil. Hepatocellular carcinoma (HCC) was also shown to rank 11th among all cancers in terms of mortality. Despite the burden of liver diseases in Brazil, little is known about public awareness of the Brazilian population regarding screening and diagnosis of the most cirrhosis and HCC in the country. To investigate in a representative sample of the Brazilian population public knowledge, level of awareness and attitudes toward cirrhosis and HCC and their most frequent risk factors according to age, gender, average family income,

level of education and place of living. **Method:** Between September 8th to 15th 2021, 1,995 subjects ≥ 18 years (53% women, mean age 44 years and average family income of 654 USD per month) living in five Brazilian regions were prospectively interviewed using a questionnaire consisting of a set of nine questions regarding knowledge about the main causes of cirrhosis and HCC, clinical burden of non-alcoholic fatty liver disease (NAFLD) and information regarding current attitudes toward hepatitis B vaccination, hepatitis B and C testing, alcohol intake as well as previous assessment of liver health by any laboratory or imaging test.

Results: Most of the Brazilian subjects believe that alcohol abuse (63%-87%), NAFLD (29%-53%) and smoking (31%-47%) are the main causes of cirrhosis and HCC. On the contrary, VH were less often linked to either cirrhosis (23%) or HCC (15%). Unexpectedly, more than 2/3 of the Brazilians agreed that NAFLD is a risk factor for cirrhosis, cancer, diabetes and cardiovascular diseases. 55% of the Brazilians were alcohol drinkers and 32% of them claimed to drink more often than once a week. Nearly half of those drinkers use more than three doses of alcohol per day. Previous evaluation of liver disease was referred at least once by 41% of the subjects. Attitudes toward hepatitis B vaccination and hepatitis B and C testing was carried out by 66%, 48% and 40% of the subjects, despite the fact that 80% of them were aware of the availability free of charge of those tests in the public health system. The main reasons for not being tested for VH were perception that there is no need for testing or absence of symptoms. In general, knowledge and attitudes toward prevention of liver diseases were significantly higher in older people and subjects with higher level of education and income ($p < 0.05$).

Conclusion: Despite its major association with liver disease, VH was not considered by the majority of the Brazilian population as the main cause of cirrhosis and HCC, leading a large proportion of those subjects to neglect hepatitis B vaccination and VH testing. Despite the large alcohol consumption and knowledge of its adverse impact in liver health, less than half of the Brazilians have been evaluated at least once for liver disease.

SAT499

The negative impact of the pandemic on hospital admissions, morbidity and 30-day mortality for acute cirrhosis decompensation: a tertiary care perspective

Kohilan Gananandan¹, Alexandra Phillips¹, Anmol Chikhli², Hannah Old², Niharika Thakur³, Konstantin Kazankov⁴, Raj Mookerjee¹, Sharmaine Jia Ying Sim⁵. ¹The Liver Failure Group, Institute for Liver and Digestive Health, United Kingdom; ²Royal Free Hospital, United Kingdom; ³UCL Medical School, United Kingdom; ⁴Aarhus University Hospital, Aarhus, Denmark; ⁵University College London, London, United Kingdom
Email: alexandra.phillips5@nhs.net

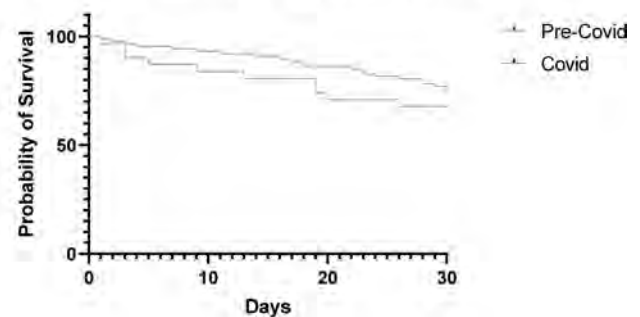
Background and aims: The global pandemic has inevitably diverted resources away from management of chronic diseases, including cirrhosis, where up to 40% of patients are readmitted with new cirrhosis decompensation events. Whilst there is increasing knowledge on COVID-19 infection in liver cirrhosis, little is described on the impact of the pandemic on decompensated cirrhosis admissions and outcomes, which was the aim of this study.

Method: A single-centre, retrospective study, evaluated decompensated cirrhosis admissions to a tertiary London hepatology and transplantation centre, from October 2018 to February 2021. Patients were included if they had an admission with cirrhosis decompensation defined as new onset jaundice or ascites, infection, encephalopathy, portal hypertensive bleeding or renal dysfunction. Admissions

were excluded if they lasted < 24 hours, were elective or occurred post liver-transplant.

Results: There were 351 admissions in the pre-COVID period (October 2018 to February 2020) and 240 admissions during the COVID period (March 2020 to February 2021), with an average of 20.4 admissions per month throughout. Patients transferred in from secondary centres had consistently higher severity scores during the COVID period (UKELD 58 versus 54; $p = 0.007$, MELD Na 22 versus 18; $p = 0.006$, AD score 55.0 versus 51.0; $p = 0.055$). The proportion of ITU admissions pre versus during-COVID stayed constant (22.9% versus 19.2%), but there was a trend towards increased ICU admissions with acute-on-chronic liver failure (ACLF) (73.9% versus 63.8% pre-pandemic). Of those admitted to the intensive care without ACLF, there was a significant increase in EF-CLIF acute decompensation (AD) scores during the COVID period (58 versus 48, $p = 0.009$). In addition, there was a trend towards increased hospital re-admission rates during the COVID period (29.5% versus 21.5%, $p = 0.067$). When censored at 30 days, time to death post discharge was significantly reduced during the COVID period ($p < 0.05$) with a median time to death of 35 days compared to 62 days pre-COVID.

Survival Curve: Comparison of mortality in 30 days after first admission with decompensation



Conclusion: This study provides a unique perspective on the impact that the global pandemic had on the clinical course and characteristics of decompensated cirrhosis admissions. The findings of increased early mortality and re-admissions, and higher AD scores, indicating increased disease morbidity, highlight the need to maintain resourcing on providing high-level hepatology care. Given that COVID-19 will likely be a chronic issue, alternative care pathways such as remote monitoring may need adoption to facilitate continuity of care post-discharge and to reduce readmission rates and morbidity in the future.

POSTER PRESENTATIONS

SAT500

Comparison of recommended daily energy intakes in people with cirrhosis, based on current guidelines, and their directly measured energy requirements: an individual patient data analysis

Clive Jackson¹, Ana Limon-Miro², Tannaz Eslamparast², Hisami Yamanaka-Okumura³, Lindsay Plank⁴, Christiani Jeyakumar Henry⁵, Angela Madden⁶, Livia Garcia Ferreira⁷, César Prieto de Frías⁸, Anne Wilkens Knudsen⁹, Evangelos Kalaitzakis¹⁰, Leah Gramlich¹¹, Maitreyi Raman¹¹, Cathy Alberda¹², Dawn Belland¹³, Vanessa Den Heyer¹³, Puneeta Tandon², Marsha Morgan¹⁴. ¹Department of Clinical Neurophysiology, Royal Free Hospital, Royal Free NHS Foundation Trust, London, United Kingdom; ²Department of Medicine, University of Alberta, Edmonton, Canada; ³Department of Clinical Nutrition and Food Management, Institute of Biomedical Sciences, Tokushima University Graduate School, Tokushima, Japan; ⁴Department of Surgery, University of Auckland, Auckland, New Zealand; ⁵Department of Biochemistry, National University of Singapore, Singapore; ⁶School of Life and Medical Sciences, University of Hertfordshire, Hatfield, United Kingdom; ⁷Postgraduate Program in Nutrition and Health, Nutrition Department, Universidade Federal de Lavras, Brazil; ⁸Department of Gastroenterology, Clínica Universidad de Navarra, Pamplona, Spain; ⁹Medical Division, and Medical Unit, Nutritional Division, Copenhagen University Hospital Hvidovre, Hvidovre, Denmark; ¹⁰Department of Gastroenterology, University Hospital of Heraklion, University of Crete, Heraklion, Greece; ¹¹Department of Medicine, Division of Gastroenterology, University of Calgary, Calgary, Alberta, Canada; ¹²Royal Alexandra Hospital, Alberta Health Services, Edmonton, Canada; ¹³University of Alberta Hospital, Alberta Health Services Nutrition Services, Edmonton, Canada; ¹⁴UCL Institute for Liver and Digestive Health, Division of Medicine, Royal Free Campus, University College London, London, University College London, London, United Kingdom
Email: marsha.morgan@ucl.ac.uk

Background and aims: Weight-based guidelines for the nutritional management of patients with cirrhosis have been formulated by EASL, ESPEN, AASLD and ISHEN. However, the guidance is discordant both in terms of recommended daily energy intakes, which range from 25 to at least 35 kcal/kg, and whether the reference for calculation should be actual, estimate dry or ideal body weight. This study aimed to compare recommended daily energy intakes with daily energy requirements based on direct measurement of resting energy expenditure (REE).

Method: REE was measured, using indirect calorimetry, in 900 patients with cirrhosis (mean [± 1SD] age 55.7 ± 11.6 yr; 70% men); total daily energy requirements were determined, for individual patients, using 1.3 × REE. Daily energy intakes were calculated based on recommended intakes of 25, 30 and 35 kcal/kg referenced to actual body weight; ideal body weight calculated using the Hamwi, Devine, Robinson and Miller formulae, and, in patients with ascites, the estimated dry weight. The limits of agreement for each permutation of the recommended intakes and weight reference standards were compared with the calculated required intakes.

Results: Daily intakes of 25 kcal/kg would provide less energy than required and hence underfeeding in the majority of patients, irrespective of the weight standard used or the presence/absence of ascites. In contrast, daily intakes of 35 kcal/kg would provide more energy than required and hence overfeeding in the majority of patients. Daily intakes of 30 kcal/kg are closest to requirements but would still provide from 452 kcal less to 749 kcal more than required, based on actual body weight in patients without ascites, and from 833 kcal less to 767 kcal more than required based on estimated dry body weight in patients with ascites (Table).

Reference weight (kg)	Cirrhosis: no ascites (n = 770)					
	Recommended daily energy intake					
	25 kcal/kg		30 kcal/kg		35 kcal/kg	
	Mean	LoA	Mean	LoA	Mean	LoA
Actual	-215	-784: 354	148	-452: 749	484	-202: 1170
IBW: Hamwi	-335	-1091: 421	-55	-787: 676	247	-510: 1004
IBW: Devine	-342	-1100: 417	-65	-792: 662	236	-508: 980
IBW: Robinson	-331	-1097: 435	-55	-770: 667	247	-476: 970
IBW: Miller	-284	-1068: 500	-1	-735: 734	311	-416: 1037
Reference weight (kg)	Cirrhosis: ascites (n = 130)					
	Recommended daily energy intake					
	25 kcal/kg		30 kcal/kg		35 kcal/kg	
	Mean	LoA	Mean	LoA	Mean	LoA
Actual	-170	-946: 606	206	-624: 1035	581	-322: 1484
Estimated dry	-369	-1126: 389	-33	-833: 767	303	-560: 1165
IBW: Hamwi	-453	-1301: 396	-134	-1011: 744	185	-733: 1103
IBW: Devine	-470	-1308: 367	-155	-1013: 703	161	-728: 1049
IBW: Robinson	-476	1305: 352	-162	-998: 674	152	-698: 1002
IBW: Miller	-446	-1274: 382	-126	-952: 701	195	-635: 1024

IBW: ideal body weight; LoA: limits of agreement

Conclusion: The current weight-based guideline for determining daily energy intakes in patients with cirrhosis may pose a significant risk of under or overfeeding and need to be urgently reviewed.

SAT501

Rifaximin for the prevention and treatment of hepatic encephalopathy: a systematic review and meta-analysis of randomized clinical trials

Harry D Zacharias¹, Jaclyn Yizhen Tan¹, Fady Kamel¹, Nina Kimer², Lise Lotte Gluud², Marsha Morgan¹. ¹UCL Institute for Liver and Digestive Health, Division of Medicine, Royal Free Campus, University College London, London, London, United Kingdom; ²Gastrounit, Medical Division, Copenhagen University Hospital Hvidovre, Hvidovre, Denmark
Email: marsha.morgan@ucl.ac.uk

Background and aims: Rifaximin has been used for the treatment of hepatic encephalopathy (HE), in patients with cirrhosis, since the 1990s. However, whilst individual studies have shown benefit in acute/recurrent, chronic, and minimal HE, its main licensed indication remains the prevention of recurrent HE in combination with non-absorbable disaccharides (NAD). This systematic review and meta-analyses of randomised clinical trials (RCTs) for the prevention and treatment of HE, in patients with cirrhosis, compared (i) rifaximin vs. placebo/no intervention; (ii) rifaximin vs. NAD; and (iii) rifaximin co-administered with NAD vs. NAD alone.

Method: Electronic/manual searches of the literature were undertaken; further information was obtained from authors/pharmaceutical companies. Meta-analyses were conducted and results presented as relative risks (RR) and 95% confidence intervals (CI). Sources of heterogeneity and the influence of random and systematic errors were evaluated in subgroup/sensitivity analyses.

Results: A total of 38 RCTs involving 4376 people were included; Individual patient data were available for 7 trials and additional information for a further 17; some trials included more than one comparison. Twelve studies compared rifaximin with placebo/no intervention minimal (n=5) or chronic HE (n=3) or for HE prevention (n=4); meta-analysis showed no effects of rifaximin on mortality or serious adverse events (SAEs) but an overall beneficial effect on HE (RR = 0.58, 95% CI 0.56–0.91; NNTB = 5; participants = 969), confirmed in subgroup analyses in minimal HE but not in

chronic HE or for HE prevention. Rifaximin was compared with NADs in 13 studies acute (n = 4), chronic (n = 4) and minimal HE (n = 2) and for HE prevention (n = 3); there were no effects of rifaximin on mortality, SAEs or HE. The effects of rifaximin plus lactulose against lactulose alone were compared in 16 trials in acute HE (n = 8) and for HE prevention (n = 8); rifaximin plus lactulose had a beneficial effect on mortality (RR 0.69, 0.55–0.86; NNTB = 20; participants = 1836), subgroup analyses confirmed mortality benefit in acute HE (RR 0.65, 0.46–0.92; NNTB = 13; participants = 692) but not in HE prevention. Co-administration of the two drugs also had a beneficial effect on HE (RR 0.58, 0.48 to 0.71; n = 2306), with a NNTB of 5. Subgroup analyses confirmed benefit in both the treatment of acute HE (RR 0.62, 0.45 to 0.87) and in HE prevention (RR 0.54, 0.42 to 0.69) (Figure 1); there was no overall effect on SAEs; the evidence was of low to very low quality.

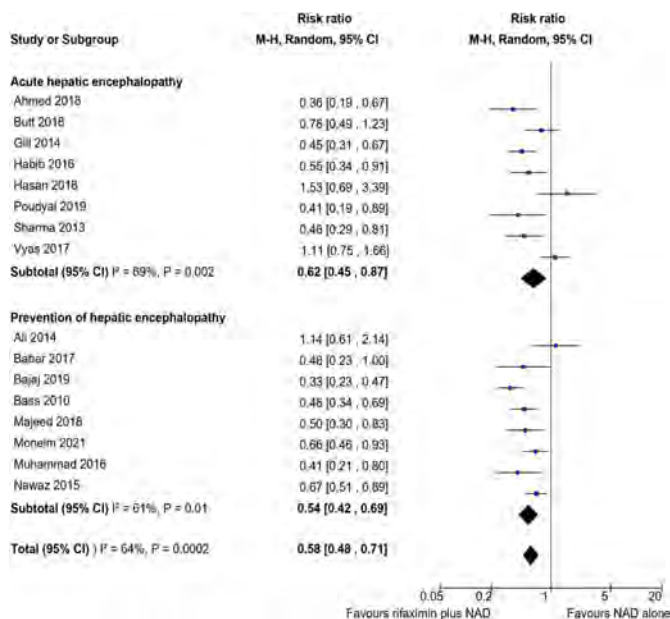


Figure: Random-effects meta-analysis of RCTs comparing the effect of rifaximin plus NAD vs. NAD alone

Conclusion: Rifaximin monotherapy does not convey benefit compared to NADs. However, rifaximin combined with lactulose is a safe and effective intervention for people with cirrhosis and acute HE, and for the prevention of recurrent HE. However, further high-quality studies are needed.

SAT502

Influence of cirrhotic cardiomyopathy defined according to the new multidisciplinary diagnostic criteria on overall mortality among cirrhotic patients

Simona Bota¹, Marcel Razpotnik¹, Philipp Wimmer², Michael Hackl², Gerald Lesnik³, Hannes Alber², Markus Peck-Radosavljevic¹.

¹Klinikum Klagenfurt am Wörthersee, Department of Internal Medicine and Gastroenterology (IMuG) and Emergency Medicine (ZAE), Klagenfurt, Austria; ²Klinikum Klagenfurt am Wörthersee, Department of Internal Medicine and Cardiology (IMuK), Klagenfurt, Austria;

³Klinikum Klagenfurt am Wörthersee, Institut für diagnostische und interventionale Radiologie, Klagenfurt, Austria

Email: bota_simona1982@yahoo.com

Background and aims: New criteria of cirrhotic cardiomyopathy (CCM) were published from a multidisciplinary consortium (Izzy et al. Hepatology 2019 Nov 11. doi: 10.1002/hep.31034) and define systolic dysfunction of the left ventricle as ejection fraction (EF) $\leq 50\%$ and/or global longitudinal strain (GLS) $< -18\%$, while the diastolic dysfunction is diagnosed when three of the following conditions are present:

average E/e' > 14 , peak tricuspid regurgitation velocity > 2.8 m/s, septal e' < 7 cm/s, left atrial volume index > 34 ml/m².

Our aim was to assess the influence of CCM defined according to the new criteria on overall mortality among cirrhotic patients.

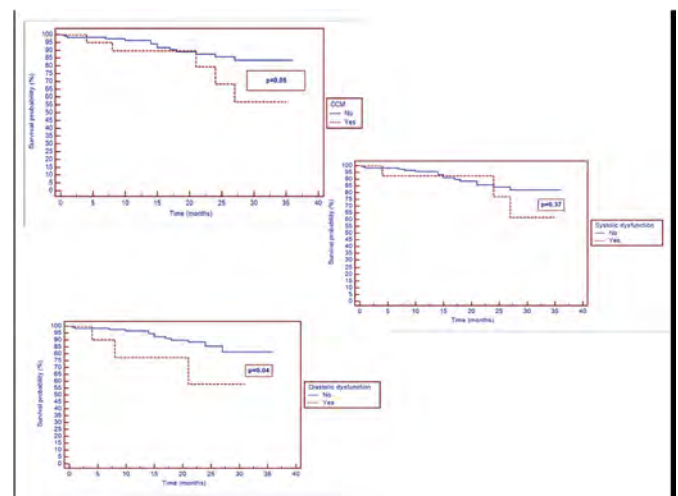
Method: Our prospective study included consecutive patients with liver cirrhosis without structural heart disease, arterial hypertension, HCC outside Milan criteria, portal vein thrombosis, presence of TIPS and with optimal acoustic echocardiography window. The patients were evaluated between 12/2018–11/2021 in our in- and out-patient Department. Conventional and speckle-tracking echocardiography (Vendor GE, EchoPAC PC software) were performed by a single investigator (EACVI TTE certified). The follow-up was performed until the patient was last seen or death.

Results: 412 cirrhotic patients were evaluated during the study period and 133 fulfilled the inclusion criteria and were included in the final analysis. The mean age of patients was 57.1 ± 10.2 years (60.1% males), 70.1% with alcoholic etiology and 48.1% with compensated liver cirrhosis.

CCM (systolic and/or diastolic dysfunction) was present on 15% of patients, only systolic dysfunction on 9.7% and only diastolic dysfunction on 7.5% of the cirrhotic patients.

The median follow-up was 21 (0.5–36) months and 18/133 (13.5%) of cirrhotic patients died during the follow-up.

The presence of diastolic dysfunction was associated with significantly higher mortality ($p = 0.04$) in our cohort of cirrhotic patients (Figure). The presence of CCM (systolic and/or diastolic dysfunction) tends also to increase mortality but did not achieve statistical significance.



Severity of liver disease, assessed by Child-Pugh and MELD score was not correlated with the presence of CCM: $r = -0.0209$, $p = 0.73$ and $r = -0.010$, $p = 0.90$.

Conclusion: Even if the follow-up was relatively short in our study, the presence of CCM (especially diastolic dysfunction) was associated with higher overall mortality among cirrhotic patients. Our data shows the importance of a cardiac (especially echocardiography with strain) evaluation of cirrhotic patients.

SAT503

Risk of herpes zoster infection in patients with cirrhosis: a nationwide population-based study in Korea

Dongsu Jeon¹, Seon-Ok Kim², Ye-Jee Kim², Jonggi Choi¹. ¹Asan Medical Center, Department of Gastroenterology, Liver Center, Seoul, Korea, Rep. of South; ²Asan Medical Center, Biostatistics and Clinical Epidemiology, Seoul, Korea, Rep. of South

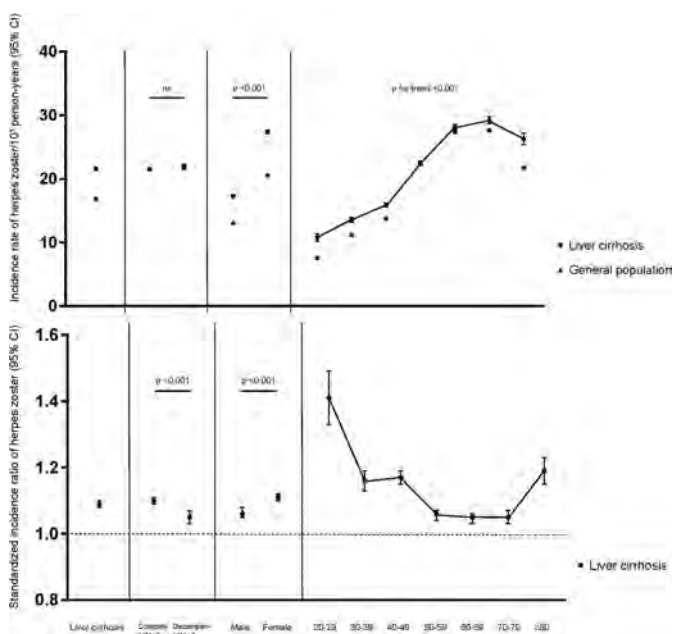
Email: j.choi@amc.seoul.kr

POSTER PRESENTATIONS

Background and aims: Few data are available on the risk of herpes zoster (HZ) infection in patients with liver cirrhosis. We investigated whether patients with liver cirrhosis have an increased risk of HZ infection compared with general population and risk factors associated with HZ infection in patients with cirrhosis.

Method: We performed a nationwide population-based study, using the claim data of the Korean national health insurance database between 2009 and 2019. In total, 505,750 patients with liver cirrhosis were included, yielding 3,266,470 person-years of follow-up. We calculated the incidence rates and standardized incidence ratios (SIRs) of HZ infection in patients with liver cirrhosis to evaluate the risk of HZ infection compared with general population in the same sex and age group. Hazard ratios (HRs) for HZ infection and their 95% confidence intervals (CIs) were estimated using a Cox proportional hazard model for factors associated with increased risk for HZ infection.

Results: In this nationwide population-based study, the overall incidence rate of HZ infection was 21.6/1000 person-years and SIR was 1.09 (95% CI, 1.08–1.10) in patients with liver cirrhosis. Among the patients with liver cirrhosis, the incidence rate and SIR for HZ infection was significantly higher in female patients than male (incidence rate, 27.4 vs. 17.3; SIR, 1.11 vs. 1.06; $p < 0.001$ for both). The incidence rate of HZ increased with age (P trend < 0.001), whereas the SIR of HZ infection showed U-shaped graph in the age curve showing non-linear relationship (Figure 1); The lowest SIR of HZ infection was observed in the patients aged 50–59, 60–69, and 70–79, with peaks in both young and elderly patients. In multivariable analysis adjusting sex, age, and Charlson comorbidity index, viral hepatitis (Hepatitis B for adjusted HRs [95% CI], 1.04 [1.01–1.07], Hepatitis C for 1.05 [1.00–1.10]) as reference to alcoholic cirrhosis showed higher risks of HZ infection. Meanwhile, decompensated cirrhosis was not associated with an increased risk for HZ infection. (adjusted HRs [95% CI], 0.98 [0.96–1.00])



Conclusion: In this population-based study in Korea, we found patients with liver cirrhosis have an increased risk for HZ infection, especially in female, with the peaks of SIR in both young patients under 50 and the elderly over 80. Therefore, zoster vaccination might be considered for patients with liver cirrhosis aged under 50 as well as the elderly.

SAT504

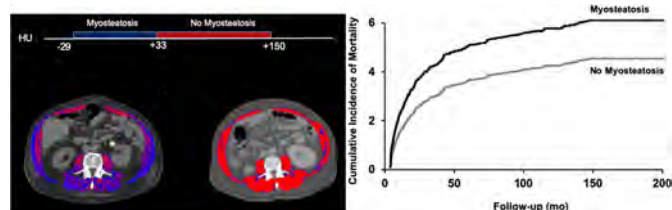
Skeletal muscle pathological fat infiltration (myosteatorosis) associates with higher mortality in patients with cirrhosis

Maryam Ebadi¹, Elora Rider¹, Abha DunichandHoedl², Maryam Motamedrad², Vera C. Mazurak², Vickie Baracos³, Rahima A. Bhanji¹, Aldo J. Montano-Loza¹. ¹University of Alberta, Division of Gastroenterology and Liver Unit, Edmonton, Canada; ²University of Alberta, Human Nutrition and Metabolism, Edmonton, Canada; ³University of Alberta, Department of Oncology, Cross Cancer Institute, Edmonton, Canada
Email: montanol@ualberta.ca

Background and aims: Myosteatorosis (pathological fat accumulation in muscle) is common in patients with cirrhosis and is defined by lower mean skeletal muscle radiodensity on CT. Cut-off points derived from cancer patients have been used to predict myosteatorosis related outcomes in patients with cirrhosis. Given fluid retention in the majority of these patients, the applicability of these cut-offs is questionable. We aimed to determine the optimal cut-offs for myosteatorosis, using a large North American cohort of 855 patients with cirrhosis.

Method: CT images were taken as part of the liver transplant evaluation at the 3rd. lumbar vertebra and were used to determine the skeletal muscle index (SMI) and radiodensity expressed by cm^2/m^2 and Hounsfield Unit (HU), respectively. Sarcopenia was defined using established cut-offs in patients with cirrhosis as $\text{SMI} < 50 \text{ cm}^2/\text{m}^2$ in males and $< 39 \text{ cm}^2/\text{m}^2$ in females. Muscle radiodensity values below the lowest tertile were considered as myosteatorosis. Competing-risk analysis was performed to determine associations between muscle radiodensity and pre-transplant mortality.

Results: Sixty-four percent of the patients were male (64%) with a mean MELD score of 15 ± 8 . Muscle radiodensity less than 33 and 28 HU in males and females, respectively were used as cut-off points (Figure 1a). Using these cut-offs, myosteatorosis was identified in 34% of the patients. Cirrhosis etiology, MELD score, refractory ascites, variceal bleeding, hepatic encephalopathy, sarcopenia and myosteatorosis (sHR 1.56, 95% CI, 1.26–1.92, $p < 0.001$) were predictors of mortality in the univariate competitive risk analysis. Myosteatorosis association with mortality remained significant after adjusting for confounding factors (sHR 1.47, 95% CI, 1.17–1.84, $p = 0.001$). The cumulative incidence of mortality was higher in patients with myosteatorosis (Figure 1b). Sarcopenia was more frequent in patients with myosteatorosis compared to their counterparts (50% vs. 32%, $p < 0.001$). Patients with concurrent presence of myosteatorosis and sarcopenia constituted 17% of the patient population and had the highest risk of mortality (sHR 2.22, 95% CI, 1.64–3.00, $p < 0.001$) when compared to patients without any of these features in an adjusted model.



Conclusion: Myosteatorosis is commonly seen in patients with cirrhosis and is associated with higher mortality. Concomitant presence of myosteatorosis and sarcopenia is associated with an increased risk of worse outcomes.

SAT505

Application of CT-contrast media is not associated with a higher risk for acute kidney injury in patients with decompensated liver cirrhosis

Tammo Lambert Tergast¹, Marie Griemsmann¹, Benjamin Schulte¹, Denise Menti¹, Neslihan Deveci¹, Julia Kahlhöfer², Petra Dörge², Anke Kraft^{1,3}, Heiner Wedemeyer^{1,4}, Markus Cornberg^{1,3,4}, Benjamin Maasoumy^{1,4}. ¹Hannover Medical School, Department of Gastroenterology, Hepatology and Endocrinology, Hannover, Germany; ²Deutsche Leberstiftung, HepNet Study-House, Germany; ³Centre for Individualised Infection Medicine (CiiM), Hannover, Germany; ⁴German Centre for Infection Research (Deutsches Zentrum für Infektionsforschung), partner site Hannover-Braunschweig, Hannover, Germany
Email: tergest.tammo@mh-hannover.de

Background and aims: Acute kidney injury (AKI) is a severe complication in patients with decompensated liver cirrhosis and is associated with a poor prognosis. Identifying and preventing the application of potential trigger substances for AKI is important in the management of these patients. In this context, only insufficient data regarding the nephrotoxic potential of CT-contrast media (CM-CT) is available. Here we investigate the nephrotoxic potential of CM-CT in patients with decompensated liver cirrhosis.

Method: In an exploratory analysis, patients with decompensated liver cirrhosis and ascites that received a paracentesis between 2012 and 2016 at Hannover Medical School (MHH) were included. Patients with AKI or relevant interventional procedures 7 days prior to baseline were excluded from this study. Propensity score matching (PPSM) was conducted, matching for MELD score, leukocyte count, intake of diuretics, presence of diabetes and age. Results were confirmed using data from a prospective registry that collects clinical data and biosamples from patients with liver cirrhosis and ascites that underwent a paracentesis between 2016 and 2020 (validation cohort) at MHH. Analyzed end points were 28-day incidence of AKI, severe AKI and liver transplant (LTx) free survival. Furthermore, measurement of neutrophil gelatinase-associated lipocalin (NGAL), an early marker for AKI, was conducted in plasma-samples from the prospective cohort.

Results: Overall, 140 patients were eligible for analysis in the retrospective cohort, of whom 61 patients received a CM-CT (43%). After PPSM, 51 patients with CM-CT were matched with 51 patients without CM-CT. Baseline parameters like MELD (CM-CT: 15 vs. No CM-CT: 16, $p=0.44$), CRP values (CM-CT: 32 mg/dl vs. No CM-CT: 34 mg/dl, $p=0.80$) and presence of infections at baseline (CM-CT: 35% vs. No CM-CT: 37%, $p=1.00$) were comparable between both groups. The 28-day AKI incidence did not differ between both groups ($p=0.56$). Furthermore, LTx-free survival and incidence of severe AKI was comparable ($p=0.37$ and $p=1.00$). In the validation cohort, CM-CT was noted in 13 patients (11%), while 105 patients had no CM-CT (89%). Incidence of AKI and severe AKI was comparable between the groups ($p=0.85$ and $p=0.54$). Finally, NGAL-levels did not differ significantly between CM-CT and no CM-CT patients (311 ng/ml vs. 266 ng/ml, $p=0.35$).

Conclusion: CM-CT does not increase the risk for AKI in patients with decompensated liver cirrhosis.

SAT506

Proton pump inhibitors are associated with higher mortality risk and higher risk of decompensation in patients with liver cirrhosis-A retrospective cohort study from the Amsterdam metropolitan area

Koos de Wit¹, Thijs Kuipers¹, Koen van der Ploeg¹, Bert Baak², Ulrich Beuers¹, Bart Takkenberg¹. ¹Amsterdam UMC, location AMC, Department of Gastroenterology and Hepatology, Amsterdam, Netherlands; ²OLVG, Department of Gastroenterology and Hepatology, Amsterdam, Netherlands
Email: k.dewit1@amsterdamumc.nl

Background and aims: The clinical course of patients with liver cirrhosis in the Netherlands is insufficiently studied and adherence to

hepatocellular carcinoma (HCC) screening guidelines is unknown. This study was performed to get insight in the clinical course of patients with liver cirrhosis, to determine factors that predict decompensation and transplant-free survival (TFS), and to study adherence to HCC screening guidelines.

Method: A retrospective cohort study of patients with confirmed liver cirrhosis in two large hospitals in Amsterdam, the Netherlands. Patients were identified by ICD-10 code [2014–2020]. Patients were excluded when lost to follow-up within one year after diagnosis (except death) or if there were less than two visits at the outpatient clinic. Clinical parameters, number of decompensation events, development of HCC, hepatic encephalopathy (HE) and medication use were extracted from medical records.

Results: In total 681 patients were included for analyses (67% male, median age 58 years (IQR 50–66)). Main etiologies were alcohol use (40%), chronic hepatitis C (15%) and NAFLD/NASH (10%). Median TFS was 100 months. Decompensated patients at time of diagnosis had a TFS of 86 months compared to 136 months for compensated patients ($p<0.01$). Mortality risk was increased in multivariate analysis by: age at diagnosis (HR 1.05 (1.03–1.07) per year, $p<0.01$), smoking (HR 2.30 (1.50–3.55), $p<0.01$), decompensated initial presentation (HR 1.93 (1.28–2.91), $p=0.03$) and PPI use (HR 1.93 (1.28–2.91), $p<0.01$). In multivariate analysis, risk of future decompensation was increased if patients initially presented decompensated (HR 2.67 (1.72–4.16), $p<0.01$) and used PPIs (HR 1.54 (1.04–2.27), $p=0.03$). PPIs were used by 81% of the patients and in 54% there was no clear indication. In multivariate analysis the risk of development of overt HE was decreased in patients that used statins (HR 0.55 (0.33–0.92), $p=0.02$). A total of 127 patients (19%) developed HCC. Patients who were adequately screened (46%) had a longer TFS (48 months) compared to patients who were not (22 months, $p<0.01$).

Conclusion: In this retrospective cohort study of patients with cirrhosis, PPI use was associated with an increased mortality risk and increased risk of future decompensation, statin use was associated with a reduced risk of HE, and adequate HCC surveillance was associated with markedly better survival.

SAT507

Maintenance of sarcopenia and myosteatosis after liver transplantation

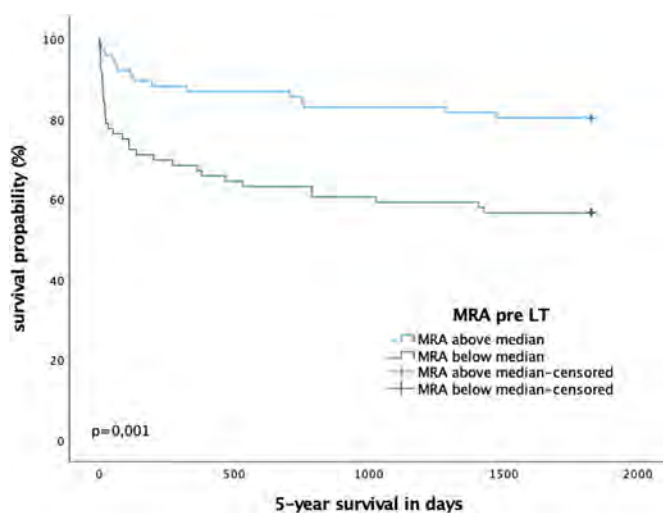
Franziska Recklies¹, Isabel Molwitz², Maria Stark³, Thomas Horvatits¹, Johannes Salamon², Samuel Huber¹, Lutz Fischer⁴, Ansgar Lohse¹, Martina Sterneck¹, Karoline Horvatits¹. ¹University Medical Center Hamburg-Eppendorf, Department of Medicine, Hamburg, Germany; ²University Medical Center Hamburg-Eppendorf, Department of Diagnostic and Interventional Radiology and Nuclear Medicine, Hamburg, Germany; ³University Medical Center Hamburg-Eppendorf, Institute of Medical Biometry and Epidemiology, Hamburg, Germany; ⁴University Medical Center Hamburg-Eppendorf, Department of Hepatobiliary and Transplant Surgery, Hamburg, Germany
Email: k.horvatits@uke.de

Background and aims: Presence of sarcopenia and myosteatosis in liver transplant (LT) candidates is associated with adverse outcomes before and after LT. Aim of this study was to evaluate the course of sarcopenia and myosteatosis before and after LT, and to study its impact on the overall survival.

Method: In this retrospective observational study all patients receiving LT, between 2011–2015 at a tertiary care center, with a CT scan <8 months pre-LT, were studied. Radiological follow-up (FU) was assessed in patients with additional CT scan >6 months post-LT. Clinical characteristics, body mass index (BMI), skeletal muscle index (SMI), sarcopenia (defined as SMI <39 cm²/m² in females and <50 cm²/m² in males), and muscle radiodensity attenuation (MRA) in Hounsfield Units (HU) were assessed. To analyze the development of MRA, SMI, and BMI after LT a linear regression model was applied. For survival analysis, log-rank test, and Cox proportional hazards regression were used.

POSTER PRESENTATIONS

Results: 152 patients (male: 72%; alcoholic liver disease: 35%, viral hepatitis: 22%; HCC 32%) were included in the study. 5-year survival was 68%. Sarcopenia pre-LT was present in 93 (62%) patients. Mean MELD did not differ between patients with and without sarcopenia (21 vs. 22; $p = 0.4$). Mean MRA pre-LT was 37 HU. Reduced MRA pre-LT was associated with higher BMI ($p = 0.033$), age ($p < 0.001$), male sex ($p = 0.019$), and a lower SMI ($p = 0.041$). Patients with hepatorenal syndrome or need of hemodialysis showed a lower MRA than those without ($p = 0.018$; $p = 0.002$). At short-term FU (11 months after LT) mean MRA was 35 HU and 35/50 (70%) fulfilled criteria of sarcopenia, whereas at long-term FU (56 months after LT) mean MRA was 34 HU and 35/52 (67%) were classified as sarcopenic. Neither MRA nor SMI improved after LT. Both, MRA and MELD-score predicted short- and long-term survival (30 days: MRA: HR = 0.913 [95%-CI 0.857; 0.973], $p = 0.005$; MELD-score: HR = 1.061 [95%-CI 1.007; 1.118], $p = 0.027$; 1 year: MRA: HR = 0.952 [95%-CI 0.909; 0.997], $p = 0.037$; MELD-score: HR = 1.046 [95%-CI 1.01; 1.083], $p = 0.011$; 5 years: MRA: HR = 0.956 [95%-CI 0.918; 0.995], $p = 0.029$; MELD-score: HR = 1.03 [95%-CI 1; 1.06], $p = 0.049$).



Conclusion: Neither SMI nor MRA as parameters of sarcopenia improved after transplantation. Besides the MELD score, MRA predicted short- and long-term survival after transplant. MRA and muscle quality should thus be defined prior to transplantation to stratify the patient's risk profile and should be validated in future studies.

SAT508

Clinical and prognostic characterization of the patterns of decompensation of liver cirrhosis

Marta Tonon¹, Simone Incicco¹, Valeria Calvino¹, Alessandra Brocca¹, Antonio Accetta¹, Carmine Gabriele Gambino¹, Marco Cola¹, Daniel Salinas¹, Salvatore Piano¹, Paolo Angeli¹. ¹University of Padova, Unit of Internal Medicine and Hepatology, Department of Medicine, Padova, Italy
Email: salvatorepiano@gmail.com

Background and aims: The clinical course of liver cirrhosis is characterized by two phases, compensated and decompensated cirrhosis, the latter characterized by the onset of complications (ascites, variceal bleeding, hepatic encephalopathy) and a worse prognosis. Recently, Acute Decompensation (AD), i.e. the development of complications that require hospitalization, has been characterized. However, complications of cirrhosis do not necessarily

require hospitalization and can develop progressively. This type of decompensation has recently been defined as Non Acute Decompensation (NAD). At present time, there is no information regarding the incidence and prognostic impact of NAD. The aim of the study was therefore the evaluation of the incidence of NAD and AD in a group of outpatients with liver cirrhosis and the prognostic impact of these two decompensation patterns.

Method: 749 outpatients with cirrhosis were enrolled and consequently followed up until death, liver transplantation or the end of the study (August 2021). Clinical and biochemical data were collected, as well as the development of complications during follow-up, which were considered as AD if they resulted in hospitalization or NAD if they were managed at outpatient clinic.

Results: 379 patients (50.6%) did not develop any decompensation, 163 patients (21.8%) had NAD as first decompensation and 207 (27.6%) had AD. During follow-up, 216 patients (28.8%) died and 145 (19.4%) were transplanted. Survival at 10 years was significantly higher in patients who did not develop decompensations (79.6%) than in patients who developed NAD or AD (33.7% and 21.3%, respectively; $p < 0.001$, Fig. A). Eighty-three patients with NAD (50.9%) subsequently developed AD. There was no significant difference in 10-year survival between patients who developed AD after NAD and those who only had AD, while both of these groups showed shorter survival than patients who had only NAD. In multivariate analysis, age (HR 1.05, $p < 0.001$), MELD (HR 1.10, $p < 0.001$), varices at inclusion (HR 1.48, $p = 0.03$), albumin (HR 0.94, $p < 0.001$), MAP (HR 0.98, $p = 0.006$), effective etiological treatment (HR 0.38, $p < 0.001$) and NAD (HR 2.65, $p < 0.001$) or AD (HR 3.51, $p < 0.001$) were independent predictors of mortality.

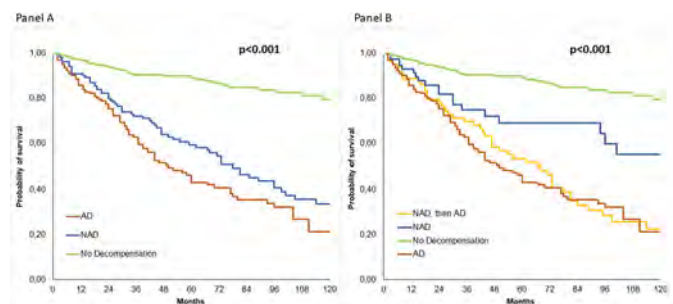


Figure: 120-month survival in patients according to the pattern of decompensation

Conclusion: In more than 20% of patients with cirrhosis the first decompensation is a NAD, which often precedes AD and is associated with a decreased survival. Patients who develop NAD must be monitored closely to prevent any development of AD.

SAT509

Safety, pharmacokinetics and pharmacodynamics of TNP-2092 capsule in chinese liver cirrhosis patients with hyperammonemia: a randomized, double-blind, placebo-controlled, dose-escalation phase Ib/IIa study

Jia Xu¹, Jingrui Liu¹, Jing Chen¹, Zhenkun Ma¹, Yanhua Ding¹, Junqi Niu¹. ¹China
Email: 747740607@qq.com

Background and aims: TNP-2092, a locally acting drug candidate, exhibits broad-spectrum antibacterial activity by inhibiting three essential drug targets RNA polymerase, DNA gyrase and topoisomerase IV. TNP-2092 has a lower propensity for the development of resistance than rifaximin.

Method: Thirty-six liver cirrhosis patients with fasting venous blood ammonia higher than normal were enrolled and received multiple ascending doses of TNP-2092 (100 mg 300 mg and 600 mg, BID for 14 days) or placebo under fed conditions. Patients with Child-Pugh

grade C cirrhosis and grade 2 or above hepatic encephalopathy were excluded.

Results: TNP-2092 was safe and well tolerated in all treatment groups. The most commonly observed treatment emergent adverse events (TEAEs) were neutropenia (29.2%), leucopenia (16.7%) and lipase elevation (12.5%). The most of the TEAEs were mild and lack of dose relationships.

The AUC and C_{max} for TNP-2092 exhibited a dose-proportional increase. The systemic exposure of TNP-2092 increased 2- to 4-fold compared to that in healthy volunteers.

The blood ammonia level decreased in a dose-dependent fashion during and after the treatment (Table 1). TNP-2092 (600 mg BID) reduced the blood ammonia level by 24.03 ug/dL, compared to 15.43 ug/dL produced rifaximin (400 mg, TID) after 14 days of treatment as reported in literature.

Table 1. The change of blood ammonia before and after treatment^a

Dose (mg)		100 mg (N=8)	300 mg (N=8)	600 mg (N=8)	placebo (N=12)
During the treatment (D2-D15), the proportion of blood ammonia measurements returned to normal ^b	Ammonia level returned to normal ^c	13%	22%	32%	7.40%
	P vs. placebo	0.22 ^d	0.01 ^d	0.0004 ^d	...
During the treatment (D2-D15), the proportion of blood ammonia level decreased ^e	Ammonia level decreased ^e	47%	50%	69.40%	52.80%
	P vs. placebo	0.4656 ^d	0.7173 ^d	0.0339 ^d	...
After the treatment (D15), the reduction of blood ammonia level from pretreatment ^f	Change of blood ammonia level (ug/dL) ^g	9.71 ^h	-3.62 ^h	-24.03 ^h	0.85 ^h
	P vs. placebo	0.7128 ^d	0.1393 ^d	0.0353 ^d	...

^a Including blood ammonia measurements conducted on D2,3,4,5,7,9,11,13 and 15.^h

^b The proportion of measurements that decreased from the mean blood ammonia before treatment.^h

^c Fasting blood ammonia on D15 compared to the mean blood ammonia level before treatment.^h

Figure: 120-month survival in patients according to the pattern of decompensation

Conclusion: TNP-2092 was safe and well tolerated with a linear pharmacokinetic and pharmacodynamic profile in liver cirrhosis patients with hyperammonemia. TNP-2092 showed potential to have a stronger effect on the blood ammonia level than rifaximin.

SAT510

Serological assessment of the collagen type III deposition predicts outcome in decompensated liver cirrhosis

Mette Juul Nielsen¹, Robert Schierwagen^{2,3}, Christian Jansen², Frank Uschner^{2,3}, Sabine Klein^{2,3}, Maximilian J Brol^{2,3}, Michael Praktiknjo², Chang Johannes², Morten Karsdal¹, Diana Leeming¹, Jonel Trebicka^{2,3,4,5}. ¹Nordic Bioscience A/S, Denmark; ²University Hospital of Bonn, Department of Internal Medicine I, Bonn, Germany; ³University of Frankfurt, Department of Internal Medicine I, Frankfurt, Germany; ⁴European Foundation for Study of Chronic Liver Failure, Barcelona, Spain; ⁵University Clinic Odense, Department of Hepatology, Odense, Denmark
Email: mju@nordicbio.com

Background and aims: Fibrosis is the result of excessive collagen and extracellular matrix (ECM) accumulation, consequent to an imbalance in collagen formation and degradation. The balance between fibrogenesis and fibrolysis may be of importance for patient management and prognosis. Over time, the collagen fibrils become enzymatically cross-linked resulting in increased stiffness of the tissue. Here we investigated a novel fibrosis resolution biomarker, C-terminal cross-linked type III collagen degradation (CTX-III) in combination with the collagen formation biomarker PRO-C3, and their association with decompensation and predictors of mortality in patients with trans jugular intrahepatic portosystemic shunt (TIPS). **Method:** In 83 patients with decompensated liver cirrhosis, plasma samples were taken from the hepatic vein at the time of TIPS insertion. Fibrogenesis was assessed using PRO-C3 and fibrolysis by the cross-linked collagen fragment CTX-III. The association between individual biomarkers and presence of ascites, Child-Pugh category, and MELD score was investigated. Patients with high fibrogenesis and low fibrolysis and vice versa were identified by CART analysis. The net type III collagen remodeling was defined as the ratio between fibrogenesis and fibrolysis, i.e., the PRO-C3:CTX-III ratio. Kaplan-Meier and Cox regression analyses were used to investigate the association of the balance between fibrogenesis and fibrolysis with 5-year transplant-free survival.

Results: At TIPS insertion, PRO-C3 was significantly elevated in patients with MELD score >11 ($p = 0.014$) and Child-Pugh Class C ($p = 0.017$). Interestingly, the degree of the type III collagen remodeling was not associated with disease severity, including MELD score, presence of ascites, and Child-Pugh class. When stratifying individual biomarkers according to their median, none of the biomarkers was associated with survival. Nevertheless, patients with excessive type III collagen deposition, defined by high fibrogenesis (PRO-C3) and low fibrolysis (CTX-III), at TIPS insertion had significantly shorter survival time compared to those with less type III collagen deposition ($p = 0.020$).

Conclusion: High level of fibrosis resolution is associated with less severe decompensation and better survival in liver cirrhotic patients with TIPS. The balance of collagen formation and collagen degradation provide additional information compared to each biomarker and is essential for the prediction of outcome in cirrhotic patients.

SAT511

Liver frailty index predicts poor outcomes in patients hospitalized for acute decompensation of cirrhosis

Simone Incicco¹, Roberta Gagliardi¹, Marta Tonon¹, Valeria Calvino¹, Nicola Zeni¹, Alessandra Brocca¹, Carmine Gabriele Gambino¹, Paolo Angeli¹, Salvatore Piano¹. ¹Unit of Internal Medicine and Hepatology, Department of Medicine, University of Padova, Padova, Italy
Email: salvatorepiano@gmail.com

Background and aims: Physical frailty is highly prevalent in patients with end stage liver disease and has been associated with poor outcomes. Liver Frailty Index (LFI) is a standardized tool to assess frailty in patients with cirrhosis on liver transplant waiting list. However, there is a paucity of data on the prognostic value of LFI in patients hospitalized for acute decompensation (AD) of cirrhosis. We

POSTER PRESENTATIONS

evaluated LFI in patients hospitalized for AD and the association of LFI with complications occurred during hospitalization and 90-day survival.

Method: We enrolled 117 consecutive patients admitted for AD of cirrhosis from 2019 to 2021. LFI was performed at the time of hospital admission. Occurrence of complications (hepatic encephalopathy [HE], sepsis, organ failures, ACLF) during hospitalization was recorded. Patients were followed up until death, liver transplant or 90 days.

Results: Mean age and MELD-Na were 64 ± 10 and 20 ± 7 , respectively. The majority of patients were male (71%) and had and alcohol-related cirrhosis (56%). Median LFI was 6.1 (IQR 5.0–6.5). LFI showed a weak, but significant, correlation with age ($r = 0.202$; $p = 0.029$), MELD-Na ($r = 0.292$; $p = 0.001$) and parameters of systemic inflammation such as C-Reactive Protein ($r = 0.235$; $p = 0.014$) and white blood cell (WBC) count ($r = 0.207$; $p = 0.025$).

LFI was significantly higher in patients developing hepatic encephalopathy, sepsis, renal failure, circulatory failure, respiratory failure and ACLF than in those who did not (Figure 1). Patients transferred to the ICU had significantly higher LFI than those who did not (Figure 1).

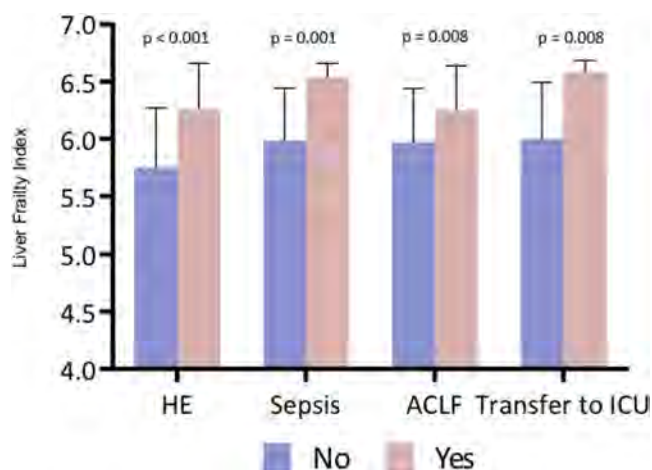


Figure: Liver Frailty Index in patients developing or not complications during hospital stay.

LFI was significantly higher in patients who died than in those who survived during hospitalization (median = 6.5 [IQR = 6.0–6.7] vs 6.0 [IQR 4.8–6.5]; $p = 0.006$) and at 90 days (6.45, IQR 6–6.64 vs 5.87, IQR 4.81–6.37; $p = 0.001$). In multivariate analysis LFI was an independent risk factor of 90-day mortality (HR = 1.88, 95% CI 1.07–3.32; $p = 0.028$), as well as MELD-Na (HR = 1.11, 95% CI 1.04–1.18; $p = 0.01$) and WBC (HR = 1.08, 95% CI 1.00–1.17, $p = 0.046$).

Conclusion: In patients with cirrhosis hospitalized for AD, LFI identifies patients at higher risk of worse outcomes and can be used for the assessment of frailty in these patients.

SAT512

Urinary proteomics identifies oxidative stress and inflammation pathways as key factors differentiating acute-kidney injury-hepatorenal syndrome from acute tubular necrosis in patients with cirrhosis

Pere Ginès^{1,2,3,4}, Laura Napoleone^{1,2,3}, Mikel Azkargorta^{2,5}, Jordi Gratacós-Ginès^{1,2,3}, Cristina Solé^{1,2,3}, Adria Juanola^{1,2,3}, Ann Ma^{1,2,3}, Marta Carol^{1,2,3,4}, Martina Perez^{1,2,3,4}, Ana Belén Rubio^{1,2,3}, Marta Cervera^{1,2,3,4}, Anna Soria^{1,2,3}, Octavi Bassegoda^{1,2,3}, Manuel Morales-Ruiz^{2,3,4,6}, Núria Fabrellas^{1,2,3,4}, Isabel Graupera^{1,2,3,4}, Juanjo Lozano², Elisa Pose^{1,2,3}, Felix Elortza^{2,5}, Elsa Solà^{1,2,3}. ¹Hospital Clinic, Liver Unit, Barcelona, Spain; ²Centro de Investigación Biomédica en Red de Enfermedades Hepáticas y Digestivas (CIBERehd), Madrid, Spain; ³Institut d'Investigacions Biomèdiques August Pi i Sunyer (IDIBAPS), Barcelona, Spain; ⁴School of Medicine and Health Sciences. University of Barcelona, Barcelona, Spain; ⁵CIC bioGUNE, ProteoRed-ISCIII, Bizkaia Science and Technology Park, Derio, Spain; ⁶Hospital Clínic, Biochemistry and Molecular Genetics Department, Barcelona, Spain
Email: pginès@clinic.cat

Background and aims: Acute kidney injury-hepatorenal syndrome (AKI-HRS) and acute tubular necrosis (AKI-ATN) are two common causes of AKI in cirrhosis with differential treatment. Frequently, the distinction between AKI-HRS and AKI-ATN is difficult, in part because there are no objective biomarkers for differential diagnosis. This difficulty is also related to the limited knowledge that exists about the pathogenic mechanisms of these two conditions. The aim of this study was to evaluate the differences between AKI-HRS and AKI-ATN by using proteomics in urine, a technique that allows the identification of large amounts of protein in biological fluids.

Method: Prospective study including 61 patients with a diagnosis of cirrhosis (38 patients with AKI-HRS, 23 patients with AKI-ATN) admitted to the hospital for complications of the disease.

Proteins in urine were analyzed by a nano-flow liquid chromatography technique coupled to tandem mass spectrometry (nLC MS/MS: in Orbitrap XL-ETD system, Thermo).

Differential proteomics (Label Free Quantification) was performed using Progenesis IQ software. Bioinformatics analysis was performed using GenOntology and metabolic pathway analysis was performed using MetaboAnalyst 5.0.

Results: A total of 491 proteins were analyzed. Proteins that were significantly increased in AKI-HRS compared to AKI-ATN corresponded to metabolic pathways related to oxidative stress and inflammation. In particular, some of the most altered pathways corresponded to glycogen metabolism, sucrose metabolism, nitrogen metabolism, glutathione metabolism, riboflavin metabolism, taurine metabolism, arachidonic acid metabolism, tryptophan metabolism and pentose phosphate pathway.

A number of proteins were specifically and differentially up-regulated in both conditions.

Conclusion: These results suggest that oxidative stress and inflammatory pathways play important roles in the pathogenesis of AKI-HRS. This study opens new avenues in the differential diagnosis between AKI-HRS and AKI-ATN in cirrhosis, as well as for new therapies targeting specific proteins or metabolic pathways.

SAT513

Kidney transplant alone recipients with advanced liver disease have similar outcomes to those without advanced liver disease—a single center study of 150 patients

Rohit Nathani¹, Stephanie Rutledge², Carolina Villarroel³, Ron Shapiro⁴, Gene Im⁵. ¹Icahn School of Medicine at Mount Sinai Morningside-West, Department of Medicine, New York, United States; ²Icahn School of Medicine at Mount Sinai, Division of Gastroenterology, Department of Medicine, New York, United States; ³Icahn School of Medicine at Mount Sinai Beth Israel, Department of Medicine, New York, United States; ⁴Icahn School of Medicine at Mount Sinai, Recanati/Miller Transplantation Institute, Department of Surgery, New York, United States; ⁵Icahn School of Medicine at Mount Sinai, Recanati/Miller Transplantation Institute, Division of Liver Diseases, Department of Medicine, New York, United States
Email: rohit.nathani@mountsinai.org

Background and aims: The prevalence of concomitant liver disease (LD) in patients with end-stage renal disease is reported to be 7–40%. The safety of kidney transplant alone (KTA) in those with advanced LD (F3–4) is controversial, with KDIGO guidelines recommending KTA consideration in compensated cirrhosis based on few small studies. The aim of this study was to compare outcomes in KTA patients with advanced LD to KTA patients with non-advanced LD.

Method: Retrospective analysis of all KTA patients at our center from 1/2012–12/2020 was performed. KTA patients with concomitant LD were identified by chart review. Advanced LD and cirrhosis status were determined by clinical criteria and if available, liver biopsy. Matched cohort analysis was performed using matching based on age, time on hemodialysis (HD), sex, and ethnicity. Primary outcome was mortality and secondary outcomes included serious infection (requiring intravenous antibiotics), allograft rejection, allograft failure, and liver decompensation.

Results: Over 8 years 1741 KTAs were performed, with 150 (8.6%) recipients having concomitant LD. KTA with LD cohort was mostly male (81%) and African American (50%) with a median age of 65 years (59–69), median time on HD of 37.5 (8–76.5) months, hepatitis C virus infection as the most common etiology of LD (72%) and a mean follow-up of 1807 (SD ± 960) days. Transjugular liver biopsies were available for 62 (41%) patients with mean hepatic venous pressure gradient of 6.2 (SD ± 3.2) mmHg prior to KTA. We identified 29 (19%) patients with advanced LD at the time of KTA and 27/29 (93%) had compensated cirrhosis, mean MELD 21.8 (SD ± 3.8). The 1-, 3- and 5-year survival rates were 95.5%, 89.8% and 79.5% respectively. KTA patients without advanced LD (n = 46) were selected as a matched cohort. Kaplan-Meier survival analysis showed similar outcomes between KTA with LD subgroups (p = 0.09). On matched cohort analysis, 6 (21%) cases died compared to 9 (20%) controls (p = .9). Mean time to death was 1645 (SD ± 939) days in cases compared to 689 (± 514) days in controls (p = .06). Secondary outcomes were similar between the 2 groups: serious infection 21% vs 28% (p = .51); allograft rejection 14% vs 13%, (p = .55); allograft failure 14% vs 4.3% (p = .2). Liver decompensation occurred in 4 (14%) cases after KTA vs 0 in control group (p = .6), mostly due to ascites (3/4), but also esophageal varices and hepatocellular carcinoma (causing death).

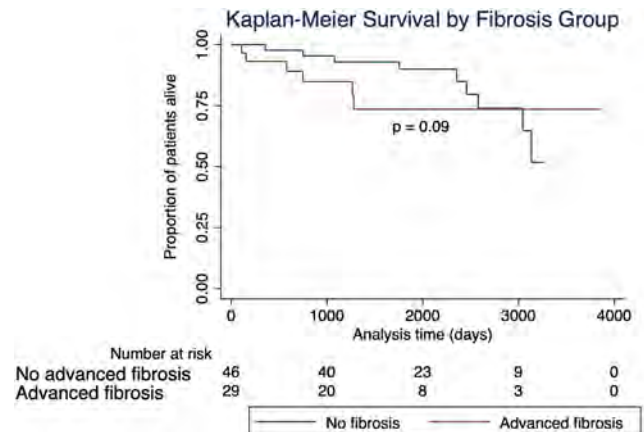


Figure: Similar outcomes in KTA patients with and without advanced LD

Conclusion: This is one of the largest single-center studies comparing outcomes in KTA patients with and without advanced LD. Although limited by small numbers, KTA patients with LD had excellent outcomes, with similar patient, graft, infection and liver decompensation outcomes between advanced LD and those without. This supports the practice of KTA in patients with concomitant LD, even with advanced fibrosis.

SAT514

Clinical features of exacerbation of portal vein thrombosis after discontinuation of anticoagulants

Takayuki Kondo¹, Kisako Fujiwara¹, Sae Yumita¹, Takamasa Ishino¹, Keita Ogawa¹, Miyuki Nakagawa¹, Hidemi Unozawa¹, Terunao Iwanaga¹, Takafumi Sakuma¹, Naoto Fujita¹, Keisuke Koroki¹, Hiroaki Kanzaki¹, Kazufumi Kobayashi¹, Soichiro Kiyono¹, Masato Nakamura¹, Naoya Kanogawa¹, Tomoko Saito¹, Sadahisa Ogasawara¹, Shingo Nakamoto¹, Tetsuhiro Chiba¹, Jun Kato¹, Naoya Kato¹. ¹Graduate School of Medicine, Chiba University, Department of Gastroenterology, Chiba, Japan
Email: takakondonaika@yahoo.co.jp

Background and aims: Portal vein thrombosis (PVT) is not a rare complication in cirrhosis. Currently, optimal management of PVT has been reported in the clinical guidelines. However, recommendations for the discontinuation of anticoagulants are not strictly defined. The present study aimed to clarify the clinical features of exacerbation of PVT after discontinuation of anticoagulants.

Method: This retrospective study included data from our institutional database between 2009 and 2020. This study enrolled 75 consecutive patients diagnosed with PVT by Doppler ultrasound (US) and contrast-enhanced computed tomography (CECT) who received anticoagulants and were followed up with at least one more CECT after diagnosis of PVT. Of the 75 patients, 50 patients discontinued anticoagulants at the physician's discretion. The PVT volume was measured using CECT images that included the whole spleno-portomesenteric axis. The outline of the PVT was traced manually in each slice and obtained at 5-mm intervals, and its volume was calculated by integrating all images. The sum of the diameter of portosystemic shunts diagnosed by Doppler US and CECT were calculated. The therapeutic assessment of the PVT was defined as complete response (0%), partial response (1–50%), slight response (51–75%), no response (76–100%), progression (≥101%).

Results: The PVT volume decreased significantly after anticoagulant therapy (pre-treatment 10.4 ± 10.8 cm³ vs. post-treatment 5.3 ± 7.5 cm³; p < 0.01). Fifty-six patients (74.7%) achieved at least slight response (complete response 38.7%, partial response 26.7%, slight response 9.3%). Fifty patients discontinued anticoagulants, and 31 patients (62.0%) had the exacerbation of PVT after discontinuation of anticoagulants. The cumulative exacerbation rate of PVT was 24.0% at 3 months, 44.6% at 6 months, and 56.4% at 12 months. Multivariate

POSTER PRESENTATIONS

analysis showed that the sum of the diameter of portosystemic shunts ($p=0.02$) and unknown cause of PVT ($p=0.02$) were the significant predictive factors for the exacerbation of PVT after discontinuation of anticoagulants. A predictive model for the exacerbation of PVT after discontinuation of anticoagulants obtained by classification and regression tree analysis indicated the following subpopulations with distinct exacerbation rate: high risk (with unknown cause of PVT, exacerbation rate: 85%); intermediate risk (the sum of portosystemic shunts ≥ 12 mm and without unknown cause of PVT, exacerbation rate: 75%); and low risk (the sum of portosystemic shunts < 12 mm and without unknown cause of PVT, exacerbation rate: 19%).

Conclusion: Patients with unknown cause of PVT or the development of portosystemic shunts should be monitored carefully after discontinuation of anticoagulants because of the high rate of exacerbation of PVT.

SAT515

Systemic inflammatory response syndrome and renal resistive index as early predictors of treatment response to terlipressin in hepatorenal syndrome-acute kidney injury

Vijay Narayanan¹, Avisek Chakravorty², Shivabrata Dhal Mohapatra², Rushil Solanki², Devika Madhu², Ravindra Pal², Krishnadas Devadas³.

¹Government Medical College, Trivandrum, Medical Gastroenterology, Trivandrum, India; ²Government Medical College, Trivandrum, Medical Gastroenterology; ³Government Medical College, Trivandrum, Medical Gastroenterology, Trivandrum, India

Email: vijaynh@gmail.com

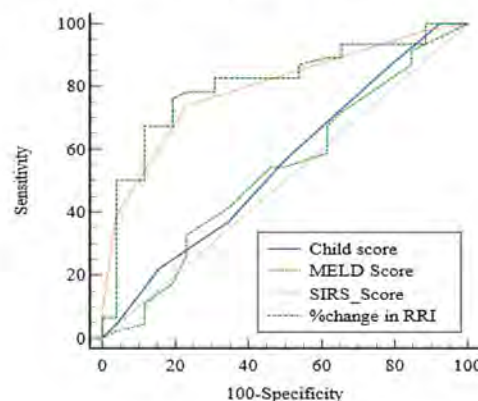
Background and aims: A combination of terlipressin and albumin is the first-line pharmacologic treatment for Hepatorenal Syndrome-Acute Kidney Injury (HRS-AKI). The early identification of patients with a low likelihood of response to treatment is crucial, as they can be fast-tracked for liver transplantation. We assessed the response rates to terlipressin-albumin therapy in patients with decompensated cirrhosis and determined early predictors of treatment response. The mortality between treatment responders and non-responders was compared and predictors of six-month mortality were also assessed.

Method: This was a prospective observational study conducted in the Department of Medical Gastroenterology, Government Medical College, Trivandrum. Patients diagnosed to have HRS-AKI (based on the International Club of Ascites criteria) and treated with terlipressin-albumin were included. Univariate and multivariate logistic regression analysis was used to determine parameters that were predictive of HRS reversal. Best cut-offs of prediction were obtained from ROC curves.

Results: 84 patients with HRS-AKI were included. There was complete response to therapy in 54.8%, partial response in 14.3%, and no response in 31%. The factors associated with complete response to treatment were the presence of systemic inflammatory response syndrome (SIRS) at baseline ($p < 0.001$), a rise in mean arterial pressure (MAP) ≥ 5 mmHg by day 3 of treatment ($p < 0.001$), baseline serum creatinine ≤ 2.5 mg/dL ($p < 0.001$), and a reduction in the renal resistive index (Delta-RRI) $\geq 5\%$ by day 3 of treatment ($p < 0.001$). On multivariate analysis, the independent predictors of complete response to treatment were the presence of SIRS at baseline ($p = 0.016$, OR = 6.19 (CI: 1.40–27)) and Delta-RRI $\geq 5\%$ by day 3 ($p = 0.001$, OR = 24.2 (CI: 3.4–168.6)). The AUROC for predicting complete response to treatment was higher for SIRS Score (0.797) and Delta-RRI (0.803) than CHILD score (0.554) and MELD score (0.503) respectively. Non-responders had significantly higher mortality at 1 month (27% vs 9.5%, $p = 0.04$) and 6 months (74% vs 45%, $p = 0.025$). The factors significantly associated with six-month mortality were the presence of hepatic encephalopathy ($p = 0.05$), stage of AKI ($p = 0.036$), MELD score ($p = 0.014$) and non-resolution of SIRS by day 3 of terlipressin treatment ($p = 0.029$). On multivariate analysis, MELD

>23 was found to be an independent predictor of six mortality ($p = 0.019$, OR = 4.4 (CI: 1.3–15.4)).

Figure: Comparison of AUROC curves to predict treatment response in HRS-AKI



Variable	AUC	SE ^a	95% CI ^b
CHILD score	0.554	0.0713	0.432 to 0.671
MELD Score	0.536	0.0731	0.415 to 0.655
SIRS Score	0.797	0.0617	0.686 to 0.883
% Change in RRI	0.803	0.0550	0.692 to 0.887

Conclusion: SIRS and Delta-RRI are simple parameters to predict treatment response in HRS-AKI. Non-responders have higher mortality and should be identified early to expedite liver transplantation.

In HRS-AKI, the renal resistive index is a measure of the intrarenal vasoconstriction, and SIRS reflects the exaggerated systemic inflammation, both of which are reversed by terlipressin, leading to an enhanced treatment response.

SAT516

A prospective study of global myocardial function in decompensated cirrhosis using advanced echocardiographic techniques and its clinical significance

Jeyamani Ramachandran¹, Purendra Kumar Pati², Teresa Hecker³, Fadak Mohammadi³, Libby John³, Vidyaeha Chandran², Matthew Chapman², Yasmina Tashkent³, Rosemary McCormick³, Kylie Bragg³, Majo Joseph³, James Gunton³, Asif Chinnaratha², Kate Muller³, Alan Wigg³. ¹Flinders Medical Centre, Flinders University, Australia; ²Lyell McEwin Hospital, Elizabeth Vale, Australia; ³Flinders Medical Centre, Bedford Park, Australia

Email: jeyamani.ramachandran@sa.gov.au

Background and aims: Cirrhotic cardiomyopathy (CCM) is cardiac dysfunction due to cirrhosis without a primary cardiac cause. This study investigated CCM using global longitudinal strain (GLS) and global work index (GWI), sensitive measures of myocardial performance and their clinical significance over a 12-month follow-up. Assessed clinical events included acute kidney injury/hepatorenal syndrome (AKI/HRS), refractory ascites, cardiac failure, and death.

Method: Consenting consecutive cirrhotic patients with ascites and those undergoing liver transplant (LT) assessment were studied prospectively after excluding those with prior cardiac diagnosis. Transthoracic echocardiography (TTE) and dobutamine stress echocardiogram (DSE) were performed. GLS by speckle tracking echocardiography (STE) and GWI by combining STE and brachial artery blood pressure were calculated. CCM was defined according to 2019 criteria. **Results:** Since January 2021, 65 cirrhotic patients were studied; Median (interquartile range, IQR) age 56 (13) years; 60% male; 72% related to alcohol misuse; 11 patients on beta-blockers; 28 in Child's

class C, 30 in class B and 7 in class A; Median (IQR) MELD-Na 16 (12). CCM was diagnosed in 16 patients (25%) and was subclinical; systolic dysfunction (SD) in 9 patients, none with left ventricular ejection fraction (LVEF) <50%; Advanced diastolic dysfunction (DD) in 7 patients. If grade 2 DD seen in a further 16 patients were included, the prevalence of CCM reached 49%. A lower MELD-Na was associated with SD (mean MELD-Na 12 Vs 18 in patients with and without SD respectively, $p=0.015$) with no significant association between DD and MELD Na. During the median follow-up of 181 days, 16 patients developed AKI/HRS and 33 patients experienced, refractory ascites, recurrent hydrothorax and or sepsis including peritonitis. No association was seen between SD, DD and CCM and these events. However, age (adjusted odds ratio = 1.018, 95%CI 1.037–1.185, $p=0.002$) and AKI/HRS (adjusted odds ratio = 5.153, 95%CI 1.108–23.959, $p=0.037$) emerged as independent predictors of CCM when grade 2 DD was included. Four patients died and three underwent successful LT. LVEF, GLS and GWI at baseline and on DSE were compared in 53 patients:

	At rest mean (standard deviation)	Peak values on DSE mean (standard deviation)	<i>p</i> value (Mann- Whitney's test)
LVEF	69 (7)	78 (7)	<0.001
GLS (%)	-21 (2)	-20 (3)	0.044
GWI (mmHg)	1917 (370)	1554 (396)	<0.001

GLS and GWI were reduced or unchanged in 30 (57%) and 46 (87%) patients, on DSE. There was no association between this lack of augmentation and clinical events.

Conclusion: A quarter of patients with advanced cirrhosis had CCM as per the new criteria. Low GLS with preserved LVEF and lack of augmentation of GLS and GWI on DSE suggest that advanced cirrhosis is a negative inotropic state. Ongoing follow-up and repeat studies after LT could explore clinical impact and reversibility of CCM.

SAT517

Identification of overt hepatic encephalopathy precipitating factors: a pooled analysis of 3 clinical trials of rifaximin plus lactulose

Arun Jesudian¹, Arun Sanyal², Robert Brown¹, Zeev Heimanson³, Robert Israel³, Jasmohan S Bajaj^{2,4}. ¹Weill Cornell Medicine, New York, United States; ²Virginia Commonwealth University, Richmond, United States; ³Salix Pharmaceuticals, Bridgewater, United States; ⁴McGuire VA Medical Center, Richmond, United States
Email: abj9004@med.cornell.edu

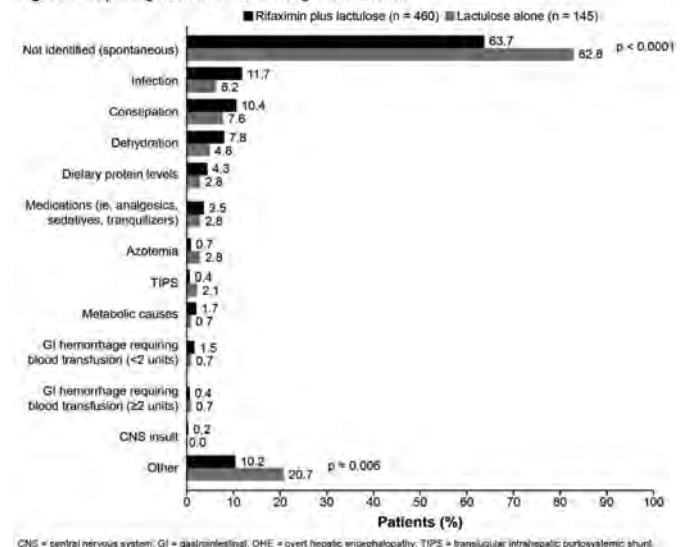
Background and aims: Hepatic encephalopathy (HE) is a cirrhosis-related complication and its occurrence has been linked with several precipitating factors (eg, infection). Guidelines recommend rifaximin as add-on therapy to lactulose for reduction in risk of overt HE (OHE) recurrence. The aim was to summarize precipitating factors associated with breakthrough OHE events, during 3 clinical trials, in patients who received rifaximin plus lactulose or lactulose alone.

Method: Data were pooled from 3 trials: a 6-month, randomized, double-blind, placebo-controlled trial; a 24-month, open-label maintenance trial; and a 6-month, randomized, open-label trial. Adults with cirrhosis who had a history of OHE and were currently in OHE remission (Conn score <2) and received rifaximin 550 mg twice daily plus lactulose or lactulose alone were included. For each OHE episode, investigators were asked to record any contributing factors or precipitating events if they could be identified. *p* values were determined using the Fisher's exact test.

Results: 460 patients treated with rifaximin plus lactulose and 145 patients treated with lactulose alone were included. In the rifaximin plus lactulose group, 60.4% were male, the mean (SD) age was 57.1 (9.3); 38.9% were aged less than 55 y. In the lactulose alone group,

68.3% were male, the mean (SD) age was 56.6 (9.3); 37.2% were aged less than 55 y. The most commonly identified precipitating factors were infection, constipation, and dehydration, each observed in a similar percentage of patients in each group ($p>0.05$; Figure). Precipitating actors were not identified (ie, spontaneous) in a majority of patients in the rifaximin plus lactulose and lactulose alone groups (63.7% vs 82.8%; $p<0.0001$). Results were generally similar when subgrouped by male/female or by age (less than 55 y; at least 55 y).

Figure. Precipitating Factors of Breakthrough OHE Events



Conclusion: Guidelines recommend identification and correction of precipitating factors to improve outcomes. In this analysis, the most commonly identified precipitating factors for OHE events in patients with a history of OHE were infection, constipation, and dehydration. A precipitating factor was not identified in a majority of cases; therefore, empiric therapy should be promptly initiated in the clinic, while factors are being identified. Prevention or early identification of OHE precipitating factors is an important part of cirrhosis disease management strategy to reduce the risk of OHE recurrence and related hospitalizations.

SAT518

Dementia frequently co-exists with hepatic encephalopathy but not other cirrhosis complications in US veterans with cirrhosis

Adeyinka Adejumo¹, Shari Rogal^{1,2}, Patrick Spoutz³, Linda Chia⁴, Jasmohan S Bajaj⁵. ¹University of Pittsburgh, Medicine, Pittsburgh, United States; ²VA Pittsburgh Healthcare System, Center for Health Equity Research and Promotion, Pittsburgh, United States; ³Veterans Integrated Service Network 20, Pharmacy Benefits Management, Vancouver, United States; ⁴Veterans Integrated Service Network 8, Pharmacy Benefits Management, Bay Pines, United States; ⁵Virginia Commonwealth University and Richmond VAMC, Division of Gastroenterology, Hepatology, and Nutrition, Department of Medicine, Richmond, United States
Email: adeyinka_adejumo@yahoo.com

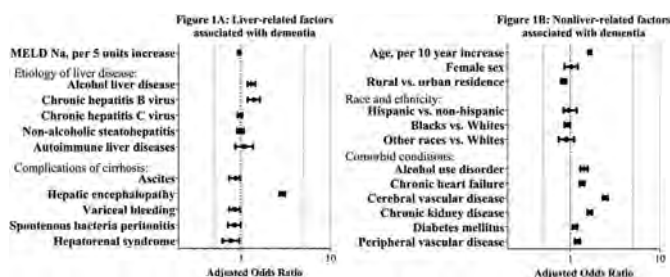
Background and aims: Dementia and hepatic encephalopathy (HE) can manifest similarly in patients with cirrhosis, though the treatments differ. The purpose of this study was to evaluate the prevalence of and risk factors for dementia among Veterans with cirrhosis.

Method: US Veterans with cirrhosis who received VA care between 2019 and 2021 were identified using ICD-10-CM codes. Factors associated with having a diagnosis of dementia were evaluated using multivariate logistic regression models, adjusting for demographic,

POSTER PRESENTATIONS

comorbid illnesses, cirrhosis etiology, and cirrhosis complications (all defined by ICD-10-CM codes).

Results: The cohort included 71,552 veterans with cirrhosis, who were mostly men (96.2%) with a median age of 65.7 years (IQR 61–70). Ten percent ($n = 7,295$) of the overall cohort had a diagnosis code of dementia overall, which increased to 12.4% among patients ≥ 65 years. Dementia was significantly associated with age (adjusted odds ratio and 95% confidence interval, AOR per 10-years: 1.64 [1.58–1.71]), white race (1.09 [1.01, 1.16]), urban residence (1.19 [1.11, 1.27]), alcohol-related cirrhosis (1.30 [1.18–1.44]), hepatitis B (1.39 [1.18–1.62]), alcohol use disorder (1.42 [1.29–1.6]), cerebral vascular disease, peripheral vascular disease, diabetes, chronic kidney disease, and chronic heart failure, and negatively associated with MELD-Na (0.95 [0.92–0.95]/5 points) in multivariate logistic regression (Figures 1A and 1B). Dementia was significantly positively associated with HE (2.87 [2.68–3.08]), but negatively associated with other cirrhosis complications in these models.



Conclusion: Diagnostic codes for dementia were found in 10% of Veterans with cirrhosis and most strongly associated with HE, but not other complications of cirrhosis. Furthermore, alcohol use disorder along with cardiovascular risk factors were associated with dementia, but not NASH itself. Further research is needed to determine strategies to differentiate between HE and dementia and manage this population with specific needs to prevent burden on families, patients and VHA system.

SAT519

Bacterial infections as a predisposing factor for the development of portal vein thrombosis in cirrhotic patients: a prospective study

Leonardo De Marco¹, Filippo Cattazzo¹, Michele Bevilacqua¹, Anna Mantovani¹, Andrea Dalbeni¹, David Sacerdoti¹. ¹Azienda Ospedaliera Universitaria Integrata Verona, Medicina interna C/Liver Unit, Verona, Italy
Email: leonardo.demarco93@gmail.com

Background and aims: Non-malignant portal vein thrombosis (PVT) is one of the complications of liver cirrhosis. The predisposing factors for PVT in cirrhotic patients are not entirely clear. The aim of this study was to identify possible clinical risk factors related to the development of PVT in patients with liver cirrhosis.

Method: We prospectively collected data of 229 consecutive cirrhotic patients followed in our Liver Unit in Verona, enrolled from 2017 to 2020 with a median follow-up of 3.3 years. PVT was determined by ultrasound, computer tomography and/or magnetic resonance imaging. Malignant PVT was considered an exclusion criteria.

Results: Of the 229 patients with liver cirrhosis 26 (11%) developed non-malignant PVT. 17 (65%) were male, with a mean age of 67.3 ± 12.3 y. In patients with non-neoplastic PVT compared to the remaining population, we observed that the prevalence of bacterial infections (sepsis, pneumonia, urinary tract infections, cholangitis, gastroenteritis, bacteraemia, spontaneous bacterial peritonitis) that required hospitalization was significantly higher (50% vs 27.2%; $p = 0.017$). In the multivariate logistic regression analysis, when adjusted for age, sex, type 2 diabetes mellitus and chronic kidney disease, PVT was significantly and independently associated with bacterial

infections (OR 2.72 [95% CI 1, 12 to 6.57; $p = 0.026$]) and hepatocellular carcinoma (HCC) (OR 2.87 [95% CI 1.11 to 7.41; $p = 0.029$]).

Conclusion: Our study showed that bacterial infections requiring hospitalization in patients with liver cirrhosis could be a predisposing factor for the development of PVT. Further studies will be needed to confirm this evidence.

SAT520

Impact of the COVID-19 pandemic on the incidence and type of infections in hospitalized patients with cirrhosis

Berta Cuyas¹, Anna Huerta¹, Maria Poca^{1,2}, Edilmar Alvarado-Tapias^{1,2}, Anna Brujats¹, Eva Roman^{1,2,3}, Carlos Guarner^{1,2}, Àngels Escorsell^{1,2}, German Soriano^{1,2}. ¹Hospital de la Santa Creu i Sant Pau, UAB, Gastroenterology, Barcelona, Spain; ²Centro de Investigación Biomédica en Red de Enfermedades Hepáticas y Digestivas (CIBEREHD), Spain; ³School of Nursing EUI-Sant Pau, Spain
Email: gsoriano@santpau.cat

Background and aims: Infections are a major cause of morbidity and mortality in patients with cirrhosis, especially those caused by multiresistant bacteria. Restrictive measures implemented due to the COVID-19 pandemic have changed hospital protocols: social distancing, hand washing, personal protective equipments. This situation may have changed the incidence and types of infections in patients with cirrhosis during the pandemic. We aimed to compare the infections in patients with cirrhosis hospitalized before the COVID-19 pandemic versus those hospitalized during the pandemic.

Method: We retrospectively analysed the infections in patients with cirrhosis hospitalized in the Gastroenterology department at a high complexity hospital, during the pre-pandemic period (3/2019–2/2020) and during the pandemic (3/2020–2/2021). Baseline characteristics, type of infections, type of bacteria, multiresistance and mortality were evaluated.

Results: A total of 421 episodes of hospitalization were analysed: 252 pre-pandemic and 169 during the pandemic (mean number of hospitalizations/month 21.0 ± 5.2 vs 14.1 ± 3.8 , $p = 0.001$). Patients' baseline MELD was lower in the pre-pandemic group (9 ± 3.7 vs 12 ± 5 , $p < 0.001$). A total of 223 infections were detected in 42% of hospitalizations (40.9% vs 43.8%, $p = 0.55$), and the percentage of nosocomial infections was 43.4% vs 42.6% ($p = 0.89$). Spontaneous bacterial peritonitis and respiratory infections were less frequent during the pandemic (24.8% of total infections in the pre-pandemic period vs 13.8% during the pandemic, and 22.5% vs 17%, respectively) and urinary tract infections were more frequent (22.5% vs 33%) (p NS). Culture positivity rate was similar (55% vs 60.6%, $p = 0.40$), and gram-negative bacteria were the most frequent bacteria isolated in both groups. We found a non-significant trend to a lower rate of multiresistant bacteria in the pandemic group (25.4% vs 19.3%, $p = 0.41$). ACLF incidence was 18.4% vs 12.9% ($p = 0.27$), and 30-day mortality was 14% vs 11.7% ($p = 0.62$).

Conclusion: There were less hospitalizations of patients with cirrhosis in the Gastroenterology department during the COVID-19 pandemic but they had worse baseline liver function. The incidence of infections and the rate of nosocomial infections were similar despite the restrictive measures. A non-significant trend to a lower rate of multiresistant bacteria and spontaneous bacterial peritonitis, and higher percentage of urinary infections were observed during the pandemic.

SAT521

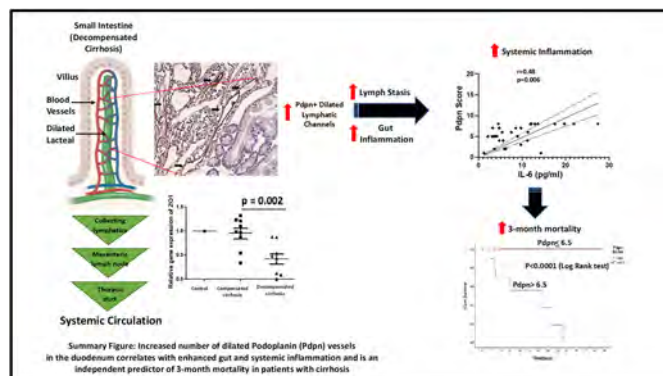
Increased expression of podoplanin, a marker of dilated lymphatic vessels in duodenal biopsies is an independent predictor of three-month mortality in patients with cirrhosis

Savneet Kaur¹, Pinky Juneja¹, S Muralikrishna Shasthy², Guresh Kumar², Dinesh Mani Tripathi¹, Vijayraghavan Rajan², Archana Rastogi², Shiv Kumar Sarin³. ¹Institute of Liver and Biliary Sciences, Molecular and Cellular Medicine, New Delhi, India; ²Institute of Liver and Biliary Sciences, New Delhi, India; ³Institute of Liver and Biliary Sciences, Department of Hepatology, New Delhi, India
Email: shivsarin@gmail.com

Background and aims: The intestinal lymphatic capillaries (lacteals) and the mesenteric collecting vessels regulate gut immunity and fluid homeostasis. In cirrhosis, a dysfunction of the gut lymphatic vessels has been reported. We studied markers of lymphatic vessels in duodenal biopsies and investigated the performance of a highly expressed marker of lymphatic endothelial cells, podoplanin (pdpn), as a predictor of clinical outcomes in cirrhosis.

Method: A prospective, observational, single-centre cohort study was performed in consenting patients with cirrhosis of varying aetiology (n = 31) and matched healthy controls (n = 10). All subjects underwent an upper gastrointestinal tract endoscopy, during which duodenal biopsies were obtained. Gene expression of lymphatic channel markers, such as vascular endothelial growth factor3 (vegfr3), pdpn and lymphatic vessel endothelial hyaluronan receptor 1 (lyve1) were studied in biopsies. Pdpn protein scores were calculated by the number and intensity of pdpn stained lymphatic channels/high power field. Gut inflammation was scored by counting the number of CD3-positive intraepithelial lymphocytes (IELs) in the biopsies and serum levels of TNF-alpha and IL-6 were studied by ELISA.

Results: Gene expression of lymphatic channel markers, vegfr3 and pdpn were enhanced in duodenal biopsies of cirrhosis patients compared to controls. Mean pdpn scores in patients with decompensated cirrhosis (6.91 ± 1.26) were significantly higher than compensated cirrhosis (3.25 ± 1.60 , $P < 0.0001$). Control biopsies showed a weak and minimal pdpn positivity. Pdpn scores were significantly correlated with serum albumin ($r = -0.62$, $p < 0.0001$), bilirubin ($r = 0.69$, $p < 0.0001$) and creatinine ($r = 0.48$, $P = 0.005$). In Cox regression analysis, pdpn score emerged as a significant and independent 3-month mortality predictor (HR: 5.61; 1.08–29.109; $p = 0.04$). Area under the curve for pdpn was 84.2 (70.6–97.8) and the cut-off value of pdpn score for predicting significant mortality was above 6.5 with a sensitivity of 100% and specificity of 75%. Although the number of IELs and TNF-alpha levels were not significantly different in patients with compensated and decompensated cirrhosis; IELs, serum TNF-alpha and IL-6 levels positively correlated with pdpn scores ($p < 0.05$ each). Pdpn score was also inversely associated with expression of gut permeability marker, zona occludin-1 ($r = -0.46$, $p = 0.05$).



Conclusion: An increased number of dilated lymphatic vessels characterized by high pdpn expression, in the duodenal biopsies are a characteristic feature of patients with decompensated cirrhosis and serve as an independent predictor of 3-month mortality. An increased gut permeability and inflammation in cirrhotic patients with dilated duodenal lymphatic channels might be contributing to enhanced systemic inflammatory responses and mortality.

SAT522

Blood metabolomics unveils mitochondrial dysfunction as a potential key feature in the pathogenesis of hepatorenal syndrome

Ann T Ma^{1,2,3}, Adria Juanola^{1,2}, Martina Perez-Guasch^{1,2,3,4}, Marta Carol^{1,2,3,4}, Jordi Gratacós-Gines^{1,2,3}, Laura Napoleone^{1,2,3}, Ana Belén Rubio^{2,3}, Emma Avitabile^{1,2,3}, Anna Soria^{1,2,3}, Marta Cervera^{2,3}, Octavi Bassegoda^{1,2,3}, Carlota Riba^{2,3}, Núria Fabrellas^{2,3,4}, Isabel Graupera^{2,3}, Juanjo Lozano³, Elisa Pose^{1,2,3}, Manuel Morales-Ruiz^{2,3,4,5}, Elsa Solà^{1,2,3}, Pere Ginès^{1,2,3,4}. ¹Liver Unit, Hospital Clínic de Barcelona, Barcelona, Spain; ²Institut d'Investigacions Biomèdiques August Pi i Sunyer (IDIBAPS), Barcelona, Spain; ³Centro de Investigación Biomédica en Red de Enfermedades Hepáticas y Digestivas, Madrid, Spain; ⁴Facultat de Medicina-Universitat de Barcelona, Barcelona, Spain; ⁵Servei de Bioquímica i Genètica Molecular, Hospital Clínic de Barcelona, Barcelona, Spain
Email: pginès@clinic.cat

Background and aims: Important hemodynamic changes occur in hepatorenal syndrome (HRS), including splanchnic vasodilation, decreased cardiac output, and resulting decreased renal perfusion. However, the exact metabolic pathways involved in HRS are unknown. Recently, studies using blood metabolomics have found distinct metabolic alterations in cirrhosis, but no specific studies on HRS have been reported. The aim of this study was to use blood metabolomics to unveil metabolic pathways involved in HRS, as well as identify potential biomarkers for diagnosis of HRS and prediction of treatment response.

Method: Untargeted metabolomics by liquid chromatography coupled to high-resolution mass spectrometry was performed in serum samples of patients with cirrhosis in different disease phases: severe HRS, meeting the definition of type 1 HRS (n = 28), acute tubular necrosis (ATN, n = 16) and acute decompensation of cirrhosis without acute kidney injury (AKI) (AD, n = 16). Of the patients with HRS, blood samples were collected prior to treatment with terlipressin and albumin, and 7–14 days post-treatment (available for 22/28; 17 treatment responders).

Results: Patients were predominantly male (90%), with a median age of 61. Principal component analysis revealed clear differences between AD and the other states (Figure). HRS was characterized by a significant upregulation of pentose and glucuronate interconversions pathways and by an accumulation of fatty acylcarnitines, both of which then decreased towards levels in AD after response to treatment. These findings are consistent with previous data in ACLF, and suggest the presence of mitochondrial dysfunction in HRS. Next, a regression analysis revealed that the combination of 3 metabolites could accurately differentiate HRS from ATN (AUROC of 0.94 (0.88–1.00)). Finally, we found that the combination of 2 metabolites predicted treatment response in HRS (AUROC 0.96 [0.89–1.00]).

POSTER PRESENTATIONS

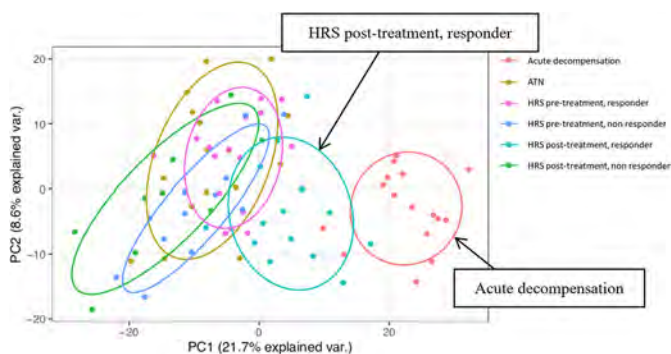


Figure: Principal component analysis of all disease states

Conclusion: The results of this first untargeted blood metabolomics study that specifically investigated the changes in metabolic pathways involved in HRS suggests the presence of mitochondrial dysfunction, which improves following treatment response with terlipressin and albumin. Furthermore, findings may help to uncover novel biomarkers that could be useful in differentiating HRS from ATN, as well as in predicting treatment response.

SAT523

Hyperammonaemia is an independent biomarker of liver-related complications and mortality in clinically stable outpatients with cirrhosis

Tom H Tranah¹, María Pilar Ballester², Juan Antonio Carbonell-Asins³, Annarein Kerbert⁴, Gonçalo Alexandrino⁵, Maria Capilla², Andra Caracostea¹, Desamparados Escudero-García², Karen Louise Thomsen⁶, Miguel Serra², Debbie L. Shawcross¹, Rajiv Jalan⁴. ¹Institute of Liver Studies, Dept of Inflammation Biology, School of Immunology and Microbial Sciences, Faculty of Life Sciences and Medicine, King's College London, London, United Kingdom; ²Hospital Clínico Universitario de Valencia, Digestive Disease Department, Valencia, Spain; ³INCLIVA Biomedical Research Institute, Valencia, Spain; ⁴Institute for Liver and Disease Health, University College London, Royal Free Campus, Liver Failure Group, London, United Kingdom; ⁵Hospital Prof. Doutor Fernando Fonseca, Amadora, Gastroenterology and Hepatology Department, Portugal; ⁶Aarhus University Hospital, Department of Hepatology and Gastroenterology, Denmark
Email: mapibafe@gmail.com

Background and aims: Ammonia is important in the pathogenesis of hepatic encephalopathy (HE). Ammonia has also been implicated in the pathogenesis of liver-related complications such as liver cell death, sarcopenia, immune dysfunction and portal hypertension. We therefore, hypothesized that hyperammonaemia is a risk factor for the development of not only HE but also other liver-related complications and consequent mortality in clinically-stable outpatients with cirrhosis. We aimed to determine the role of ammonia in the risk of liver-related complications and/or mortality and derive a threshold value of ammonia that defines the risk. We also developed a prognostic model defining outcomes.

Method: A prospective observational cohort study of clinically stable cirrhotic outpatients followed-up in three tertiary hospitals was performed. Main outcomes were occurrence of liver-related complications and mortality. As normal ammonia varied across centres, it was normalized according to the upper limit of normality (A_ULN). Multivariable frailty competing risk modelling was performed with either liver-related complications or mortality as events of interest with liver transplantation as a competing risk. AUROC was calculated to compare prediction performance between A-ULN and severity scores at 1-year. Cut-off for A_ULN was calculated using maximally selected rank statistics. Fast unified random forests for survival with 500 trees using log-rank as splitting criteria was used to predict complications and mortality.

Results: 754 patients were included (66% males; mean 56 years) with median follow-up of 223 days (range: 2–2453). A total of 260 (35%) patients developed liver-related complications, infection being the most prevalent (16%). A_ULN was an independent predictor of both complications (HR = 2.27; 95CI = 1.97–2.61; $p < 0.001$) and mortality (HR = 1.59; 95CI = 1.33–1.89; $p < 0.001$). AUROC of A_ULN was 77.9% for 1-year complications; higher than traditional severity scores. Statistical differences in survival were found between high and low levels of A_ULN both for complications and mortality ($p < 0.001$) using 1.4 as cut-off from the training set. A_ULN remained the most important variable for the prediction of complications (Figure 1).

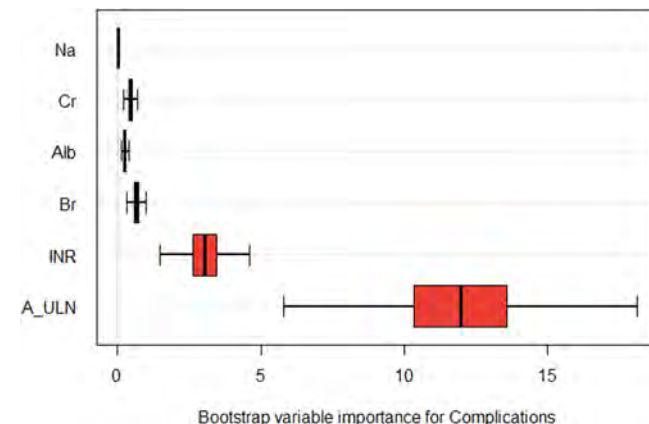


Figure 1: Abbreviations: sodium (Na), creatinine (Cr), albumin (Alb), bilirubin (Br), INR (International Normalized Ratio), ammonia upper limit of normal (A_ULN).

Conclusion: Ammonia is an independent predictor of liver-related complications and mortality in clinically stable outpatients with cirrhosis and performs better than traditional severity scores in predicting complications.

SAT524

Prospective evaluation of the EASL clinical guidelines algorithm of management of acute kidney injury in cirrhosis

Ann T Ma^{1,2,3}, Cristina Solé^{1,2,3}, Laia Escudé¹, Adria Juanola^{1,2,3}, Laura Napoleone^{1,2,3}, Emma Avitabile^{1,2,3}, Martina Perez^{1,2,3,4}, Marta Carol^{1,2,3,4}, Ana Belén Rubio^{1,2,3}, Marta Cervera^{2,3}, Octavi Bassegoda^{1,2,2,3}, Jordi Gratacós-Gines^{1,2,3}, Anna Soria^{1,2,3}, Núria Fabrellas^{2,3,4}, Isabel Graupera^{1,2,3}, Elisa Pose^{1,2,3}, Manuel Morales-Ruiz^{2,3,4,5}, Esteban Poch^{2,4,6}, Elsa Solà^{1,2,3}, Pere Ginès^{1,2,3,4}. ¹Liver Unit, Hospital Clínic de Barcelona, Barcelona, Spain; ²Institut d'Investigacions Biomèdiques August Pi i Sunyer (IDIBAPS), Barcelona, Spain; ³Centro de Investigación Biomédica en Red de Enfermedades Hepáticas y Digestivas (CIBEREHD), Madrid, Spain; ⁴Facultat de Medicina-Universitat de Barcelona, Barcelona, Spain; ⁵Biochemistry and Molecular Genetics Department, Hospital Clínic de Barcelona, Barcelona, Spain; ⁶Nephrology and Kidney Transplantation Department, Hospital Clínic de Barcelona, Barcelona, Spain
Email: pginès@clinic.cat

Background and aims: The EASL guidelines propose an algorithm for managing acute kidney injury (AKI) in cirrhosis. The effectiveness in clinical practice of this algorithm, based on expert opinion, has not been assessed. This study aimed to characterize the clinical outcomes of patients with AKI managed according to this algorithm.

Method: Single center prospective cohort study including consecutive patients admitted for acute decompensation of cirrhosis and AKI from 2019 to 2021. The management of patients followed the recommended EASL AKI algorithm, which includes categorization of patients according to AKI stage (1A or >1A) and albumin administration in the first 48 h for those with a stage >1A. Three crucial groups of patients were identified: 1/AKI 1A responders; 2/AKI >1A responders after albumin therapy; and 3/AKI >1A non-

responders after albumin therapy meeting AKI-HRS criteria. Response rates, defined as resolution of AKI in group 1, resolution or improvement to stage 1A in group 2, and resolution or improvement to a lower AKI stage in group 3, were calculated for each group. Three-month overall survival was also analyzed.

Results: A total of 203 AKI episodes in 138 patients were evaluated (median age 62, 76% male, 67% alcohol-related liver disease, Child-Pugh C 52%). Most patients with AKI-1A had resolution or persistent AKI-1A by day 3 (43% and 26% respectively), while only 31% progressed (Figure). Out of the 173 episodes with AKI>1A, 61 (35%) had resolution or improvement with albumin by day 3. Remarkably, most patients with persistent AKI>1A after albumin administration who met HRS-AKI criteria responded to vasoconstrictors (terlipressin) and albumin (73%). Three-month survival rate of patients in the 3 crucial groups were: 88%, 82%, and 50%, respectively. Non-responders to vasoconstrictor therapy had significantly lower 3-month survival compared to responders (17% vs 65% respectively).

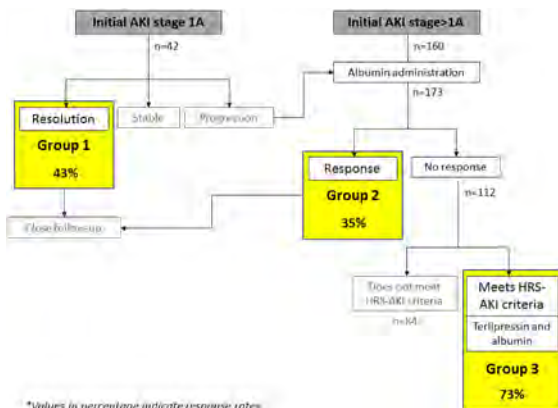


Figure: Flowchart of patients according to the EASL AKI management algorithm*

Conclusion: This study provides real-world data on application of the EASL AKI management algorithm, demonstrating high response rates in the three crucial groups of the algorithm. Specifically, the EASL-AKI algorithm rapidly and accurately identifies patients with AKI-HRS with high response rate to vasoconstrictors and albumin therapy. These findings support the use of this algorithm in clinical practice.

SAT525

MELD 3.0 accurately predicts short term survival of patients with end-stage liver disease

Anna Vidovszky¹, W. Ray Kim¹, Allison Kwong¹, Ajitha Mannalithara¹.
¹Stanford University, Division of Digestive Health, Redwood City, United States

Email: wrkim@stanford.edu

Background and aims: MELD 3.0 is the latest version of the Model for End-stage Liver Disease (MELD) which includes sex and albumin as new variables and updates all of its coefficients. We evaluated calibration of survival prediction of MELD 3.0.

Method: MELD 3.0 was developed based on data from liver transplant waitlist registrants in the US from Jan, 2016 and Dec, 2018. The entire cohort was randomly divided into model training and testing data sets. From the final Cox model for MELD 3.0 derived in the training set, we calculated survival function in mortality prediction. The model was then applied in the testing set to compare the predicted versus observed survival for the score quintiles.

Results: Out of the entire cohort (n = 29, 410), a random 30% (n = 8, 823) was set aside as the testing set. As reported previously, MELD 3.0 is calculated by the following formula: MELD 3.0 = 1.33 (if female) + 4.56 * log_e (bilirubin) + 0.82 * (137-Na) - 0.24 * (137-Na) * log_e (bilirubin) + 9.09 * log_e (INR) + 11.14 * log_e (creatinine) + 1.85 * (3.5-albumin) - 1.83 * (3.5-albumin) * log_e (creatinine) + 6 (online

calculator available at medcalculators.stanford.edu/meld). Survival function for up to 90 days is shown below. The predicted and observed survival up to 30 days of the quintiles based on MELD 3.0 matched closely with no statistically significant difference between the two (GND test, p = 0.11), whereas the comparison based on MELD-Na was significantly different (p = 0.01). Calibration was less robust for 90-day predictions with both scores, with majority of the discrepancy being survival between 30 and 90 days for the highest risk patients (p < 0.01 for both MELD 3.0 and MELD-Na).

t (days)	15	30	45	60	75	90
So (t)	0.991	0.981	0.971	0.963	0.955	0.946

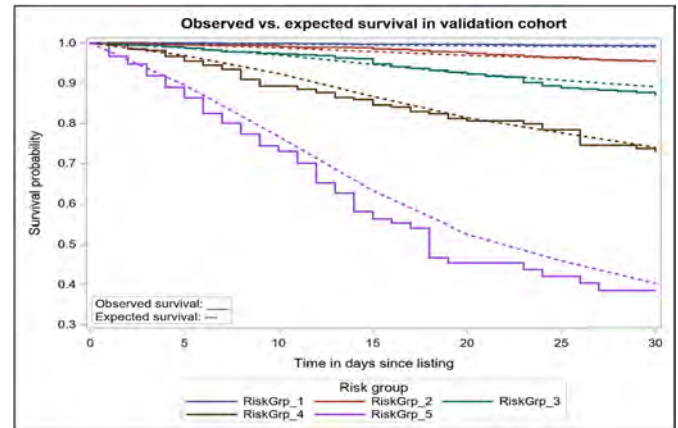


Figure: Survival function for MELD 3.0

Conclusion: While MELD 3.0 is being considered to replace MELD-Na for organ allocation priorities in the US, it provides better calibration of short-term survival than MELD-Na as well, which would be useful for patient management plan and counseling.

SAT526

CyberLiver Animal Recognition Test (CL-ART): a novel remote monitoring tool to assess minimal hepatic encephalopathy

Kohilan Gananandan¹, María Pilar Ballester², Ahmed El Shabrawi^{1,3}, Konstantin Kazankov⁴, Rajiv Jalan¹, Ravan Boddur⁵, Ravi Kumar⁵, Maruthi Raja⁵, Anu Balaji⁵, Karen Louise Thomsen⁴, Raj Mookerjee¹.

¹The Liver Failure Group, UCL Institute for Liver and Digestive Health, United Kingdom; ²Hospital Clínic Universitari, Digestive Disease Department, València, Spain; ³Endemic Hepatology and Gastroenterology, Egypt; ⁴Aarhus University Hospital, Department of Hepatology and Gastroenterology, Aarhus, Denmark; ⁵CyberLiver Limited, United Kingdom

Email: mapibafe@gmail.com

Background and aims: The CyberLiver Animal Recognition Test (CL-ART) is a novel smartphone application (app) that was developed as part of a program for remote monitoring of cirrhosis, and specifically, to diagnose non-overt hepatic encephalopathy and to guide need for intervention. The aim of this study was to compare CL-ART with established tests for minimal hepatic encephalopathy (MHE), as well as to assess its diagnostic performance, and establish an optimal cut-off for MHE.

Method: A prospective study of cirrhosis patients and healthy controls, applying clinical assessment and three different cognitive tests at a tertiary hepatology centre. The CL-ART test involved a timed recognition and appropriate naming of animals using a smartphone app; with time to perform test and failed attempts logged. EncephalApp Stroop Test and Psychometric Hepatic Encephalopathy Score (PHES) (used as the reference to diagnose MHE) were chosen as test comparisons. Pearson rank correlation and

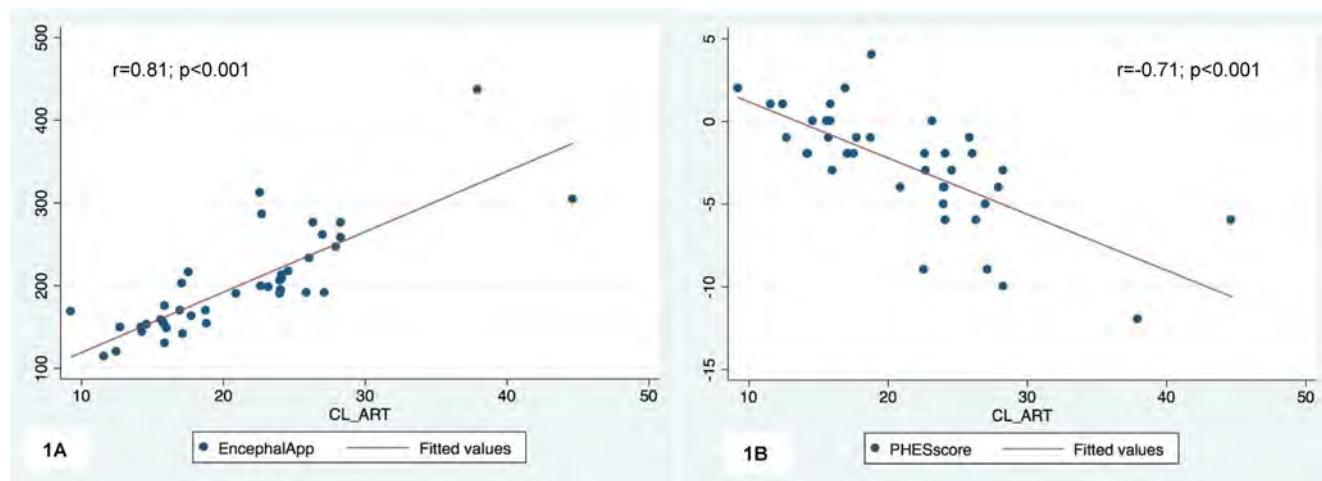


Figure: (abstract: SAT526): Graphs showing correlation between CL-ART with EncephalApp (1A) and PHES (1B)

area under the receiver operator curves (AUROC) were calculated. Youden Index was used to determine a cut-off to diagnose MHE.

Results: 30 cirrhosis patients, deemed at risk of decompensation (67% male; median 56 years, Child-Pugh Score 8[IQR 7–9], MELDNa 15 ± 5.4), and 11 controls with no evidence of liver disease (55% male; median 58 years), were included. Compared to controls, cirrhosis patients performed significantly worse in CL-ART (23 ± 7 vs. 15 ± 4 s; $p < 0.001$), EncephalApp (204 [IQR 173–259] vs 154 [IQR 149–169]; $p < 0.001$) and PHES (-3 [IQR -5 to -2] vs 0 [IQR 0–2]; $p < 0.001$). CL-ART showed a good correlation with both EncephalApp ($r = 0.81$; $p < 0.001$; Figure 1A) and PHES tests ($r = -0.71$; $p < 0.001$; Figure 1B). According to PHES, a total of 9 patients (30%) had MHE. Mean CL-ART was significantly worse in patients with MHE (29 ± 7 vs 21 ± 5 s; $p < 0.001$). AUROC to diagnose MHE was 0.85 (95% CI = 0.70–0.99) and 0.83 (95% CI = 0.65–1.00) for CL-ART and EncephalApp, respectively. A cut-off of >23 seconds in CL-ART showed a sensitivity of 89% and specificity of 62%, to diagnose MHE.

Conclusion: CL-ART is a novel smartphone app, with good patient usability, that is comparable to other established tests and has a good diagnostic performance in MHE. In addition, its rapid testing (usually <30 s) and smartphone application, make for a potential tool for remote monitoring of cirrhosis.

SAT527

Acute kidney injury during hospitalization in patients with liver cirrhosis is associated with increased mortality and chronic kidney disease on follow-up

Anna Cederborg^{1,2}, Björn Lindkvist^{1,2}, Evangelos Kalaitzakis³, Einar S. Björnsson^{4,5}, Hanns-Ulrich Marschall^{1,2}. ¹Institute of Medicine, Sahlgrenska Academy, University of Gothenburg, Gothenburg, Sweden; ²Department of Medicine, Sahlgrenska University Hospital, Gothenburg, Sweden; ³University of Crete, Department of Gastroenterology, University Hospital of Heraklion, Heraklion, Greece; ⁴Department of Internal Medicine, Landspítali University Hospital, Reykjavik, Iceland; ⁵Faculty of Medicine, University of Iceland, Reykjavik, Iceland
Email: anna.cederborg@vgregion.se

Background and aims: Acute kidney failure (AKI) in patients with advanced liver cirrhosis is associated with a poor prognosis. The aim of the study was to evaluate the impact of AKI, AKI progression, infections and acute on chronic liver failure (ACLF) grade 1 and 2 on the development of chronic kidney disease (CKD) and survival.

Method: A total of 313 patients admitted for complications of cirrhosis during a 6-year period were retrospectively evaluated. ACLF grade 1 and 2 was defined according to the European Foundation for

the Study of Chronic Liver Failure Consortium (CLIF-C) ACLF score, AKI according to International Club of Ascites criteria (ICA-AKI), infections as positive cultures or radiological findings, and CKD according to an estimated glomerular filtration rate (eGFR) <60 ml/min/1.73 m².

Results: AKI was present at admission in 27% of patients of whom 72% progressed in AKI stage during hospitalization, with a 3-month survival of 39% versus 78% ($p < 0.001$) in the patients without AKI. ACLF grade 1 or 2 was present in 24% of patients with a 3-month survival of 31% versus 78% among patients without ACLF ($p < 0.001$). Infections developed in 30% of patients during admission. Patients with prior decompensation (45%) had a lower 3-month survival if infected (50%) than compensated patients with infection (73%) and decompensated patients without infection (69%) ($p < 0.001$). Progression of AKI during admission was associated with a hazard ratio for mortality of 2.3 (1.6–3.2), even when adjusting for the presence of ACLF grade 1 or 2 and presence of infection, with a 3-month survival of 32%. Most patients with AKI who survived the first hospitalization presented with CKD at the following admission (82%) with a median follow-up of 2.2 (range 0.3–55.8) months.

Conclusion: Chronic kidney disease was common in patients with liver cirrhosis who survived AKI during the first hospitalization. Even though the presence of infection and ACLF grade 1 or 2 during admission were associated with a worse prognosis, the progression of AKI additionally increased the risk of mortality in patients with liver cirrhosis.

SAT528

Ascites bacterial DNA and IL-6 are promising tools in the diagnosis of spontaneous bacterial peritonitis

Arno Hagenunger¹, Niklas F Aehling¹, Adam Herber¹, Rhea Veelken¹, Sandra Krohn¹, Katharina Zeller¹, Kathrin Jaeger², Daniel Seehofer³, Sebastian Rademacher³, Robert Sucher³, Cornelius Engelmann^{1,4}, Thomas Berg¹. ¹Leipzig University Medical Center, Division of Hepatology Department of Medicine II, Leipzig, Germany; ²Leipzig University Medical Center, IZKF FACS Core Unit, Leipzig, Germany; ³Department of Visceral, Vascular, Thoracic and Transplant Surgery, Leipzig, Germany; ⁴Campus Virchow-Klinikum, Charité-Universitätsmedizin Berlin, Department of Hepatology and Gastroenterology, Berlin, Germany
Email: niklas.aehling@medizin.uni-leipzig.de

Background and aims: Spontaneous bacterial peritonitis (SBP) is a common complication in patients with decompensated cirrhosis or acute on chronic liver failure. Diagnosis is based on an ascitic neutrophil count (PMN) of $\geq 250/\mu\text{l}$. Its sensitivity is limited. We investigated, whether determination of bacterial DNA (bactDNA) or

cytokine levels in ascites could help optimize the diagnostic approach.

Method: Ascites and serum of 98 patients with cirrhosis (42 with SBP and 56 without) as well as serum of 21 control patients without liver disease were collected and analyzed. The majority of patients were male (SBP: n = 29 (69%), Non-SBP: n = 41 (73.2%); controls n = 12 (57.1%)). The main cause of cirrhosis was alcoholic liver disease (SBP: n = 30 (71.4%), Non-SBP: n = 42 (75%)). The mean MELD of patients with SBP was 19.5 (6–40) and 18 (8–38) in patients without SBP. BactDNA was detected using a quantitative 16S rRNA PCR (Molzym, Bremen, Germany). Every detection of bactDNA was seen as positive without any threshold. In addition, the concentrations of IL-1 β , TNF- α , IL-6, IL-8 and IL-10 were determined in serum and ascitic fluid using a LEGENDplex™ (BioLegend, Koblenz, Germany) multi-analyte flow assay. Bacterial DNA and cytokine levels were correlated with clinical outcomes.

Results: BactDNA could be detected in ascites of 24/42 (57.1%) of SBP patients as compared to 5/56 (8.9%) in the non-SBP group ($p < 0.001$). Ascitic fluid culture was positive in 17/42 patients in the SBP group, of which all were positive for bactDNA, and 0/56 patients in the non-SBP group ($p < 0.001$). Serum bactDNA was positive in four patients only, all belonged to the SBP group ($p = 0.031$). The 30-day survival of patients with positive bactDNA in the non-SBP group was 60% as compared to 90.2% in the bactDNA negative ones ($p = 0.042$).

Figure 1 shows different ascites cytokine concentrations between groups. Serum IL-6 levels were significantly higher in the SBP vs non-SBP group and controls (SBP: 733.4 pg/ml (83.4–17550.8) vs 306.1 pg/ml (59.8–3500.8); $p = 0.036$; vs. 35.97 pg/ml (0.98–186.7); $p = 0.005$), respectively. Ascites IL-6 levels showed a similar correlation (SBP: 35293.2 pg/ml (1876.6–507929.7) vs non-SBP 9865.3 pg/ml (1319.0–427434.4); $p < 0.001$). Receiving operator curve analysis revealed an area under the curve of 0.810 (95%CI 0.714–0.905) for the diagnosis of SBP. BactDNA and ascitic IL-6 showed a positive correlation with $r = 0.509$ ($p < 0.001$)

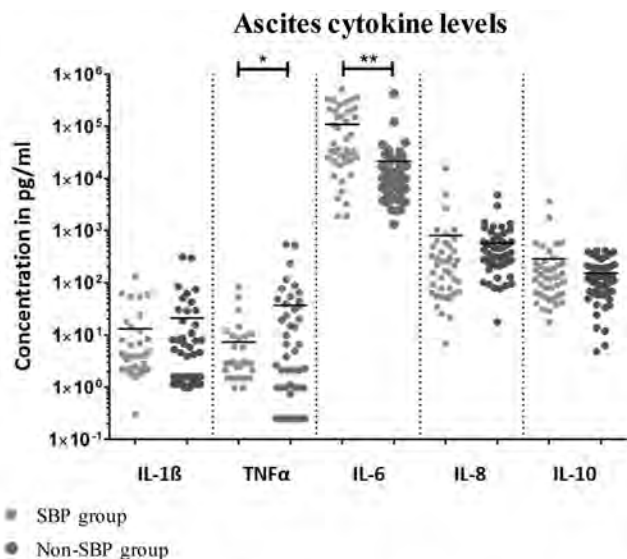


Figure 1: Scatterplots for cytokine concentrations in ascites of patients with cirrhosis with or without SBP. * $p < 0.05$; ** $p < 0.001$

Conclusion: Ascitic BactDNA and IL-6 might be a promising tool in the diagnosis of SBP, perhaps being more sensitive than PMNs. Further analysis in a larger cohort is necessary to prove this.

SAT529

Ascitic fluid mid-regional-pro-adrenomedullin (MR-pro-ADM): a novel rapid-assay sepsis biomarker to diagnose spontaneous bacterial peritonitis in cirrhotic patients

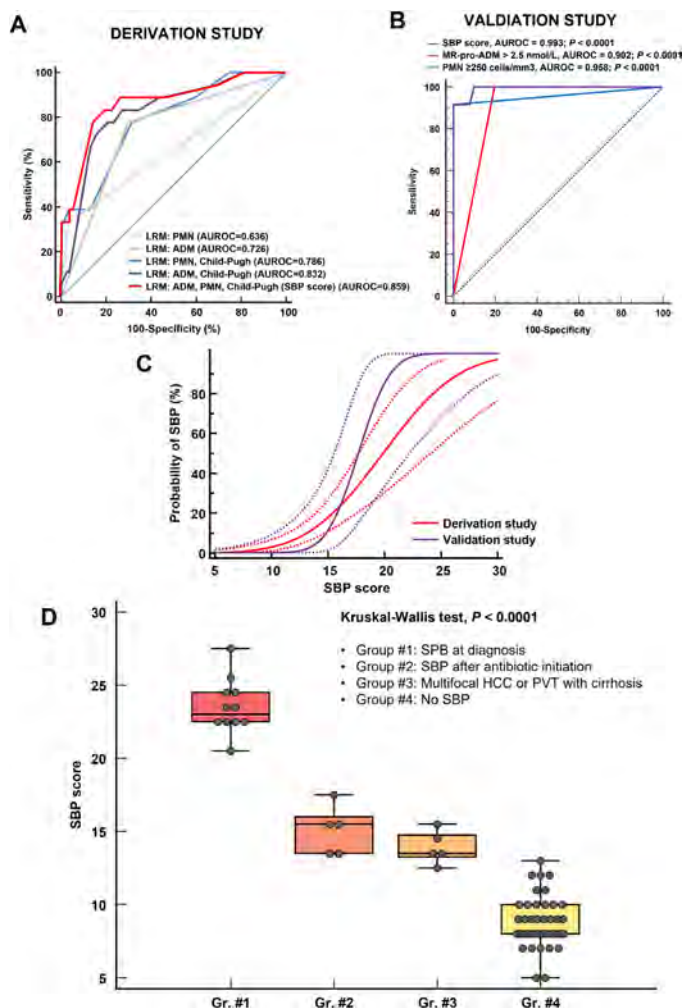
Abderrahim Oussalah¹, Anne-Sophie Lagneaux², Tom Alix¹, Pierre Filhine-Tresarrieu¹, Jonas Callet¹, Janina Ferrand², Jean Jung¹, Julien Broseus³, Sylvain Salignac³, Amandine Luc⁴, Cédric Baumann⁴, Philipp Schuetz⁵, Alain Lozniewski², Katell Peoch⁶, Hervé Puy⁷, Jean-Louis Guéant¹, Jean-Pierre Bronowicki⁸. ¹Department of Molecular Medicine, Division of Biochemistry, Molecular Biology and Nutrition, University Hospital of Nancy, F-54000 Nancy, France; ²Department of Bacteriology, University Hospital of Nancy, F-54000 Nancy, France; ³Laboratory of Hematology, University Hospital of Nancy, F-54000 Nancy, France; ⁴Methodology, Data Management and Statistics Unit, University Hospital of Nancy, F-54000 Nancy, France; ⁵Medical University Clinic, Departments of Internal and Emergency Medicine and Department of Endocrinology, Diabetology and Clinical Nutrition, Kantonsspital Aarau, Switzerland; ⁶Laboratory of Biochemistry, Beaujon Hospital, University of Paris, Clichy, France; ⁷Centre de Recherche sur l'Inflammation, Université de Paris, INSERM, CNRS, 75018 Paris, France, Laboratory of excellence GR-EX, Paris, France; ⁸Department of Gastroenterology and Hepatology University Hospital of Nancy, F-54000 Nancy, France

Email: abderrahim.oussalah@univ-lorraine.fr

Background and aims: Spontaneous bacterial peritonitis (SBP) is a frequent and severe complication of cirrhosis. We determined the diagnostic accuracy of two rapid-assay sepsis-related biomarkers in the ascitic fluid (mid-regional pro-adrenomedullin [MR-pro-ADM] and procalcitonin) to diagnose SBP among patients with cirrhosis.

Method: We performed a two-stage cross-sectional biomarker study. In the derivation study, we assessed the diagnostic accuracy of MR-pro-ADM and procalcitonin in ascitic fluids. The study end point was a diagnosis of SBP with a positive ascitic fluid bacterial culture. We derived the “SBP score” based on the more discriminant criteria from the logistic regression model. In the validation study, we assessed the diagnostic accuracy of the “SBP score” for diagnosing SBP. All SBP and bacteriological diagnoses were adjudicated by a senior gastroenterologist and a senior microbiologist. The “Nancy Biochemical Database” is registered under CNIL #1763197v0.

Results: The derivation study included 236 cases. MR-pro-ADM was significantly higher in ascitic fluids of patients with SBP when compared with those of patients without SBP (3.14 nmol/L [IQR, 2.39–6.74] vs. 1.91 nmol/L [IQR, 1.33–2.80]; $p = 0.0002$). In Bayesian ANOVA, MR-pro-ADM was highly discriminant for SBP diagnosis with a high likelihood ratio (Bayes factor [BF_M], 2505), while procalcitonin showed poor discrimination with a low likelihood ratio (BF_M, 0.45). In ROC analysis, ascitic MR-pro-ADM had an optimal cut-off of ≥ 2.50 nmol/L to diagnose SBP (AUROC, 0.746; 95% CI, 0.685–0.801; $p < 0.0001$) (A). Multivariable logistic regression analysis identified three independent predictors of SBP that were integrated in the “SBP score”: MR-pro-ADM ≥ 2.5 nmol/L (odds ratio [OR], 7.25; 95% CI, 2.04–25.79; $p = 0.002$), absolute polymorphonuclear leukocyte (PMN) count ≥ 250 cells/mm³ (OR, 14.38; 95% CI, 3.17–65.21; $p = 0.0005$), and Child-Pugh score (OR, 1.61; 1.15–2.26; $p = 0.006$). The “SBP score” had improved discrimination when compared to the logistic regression model which only included the absolute PMN count ≥ 250 cells/mm³ and the Child-Pugh score. In the validation study ($n = 63$), the “SBP score” had an AUROC of 0.993 (95% CI, 0.929–1.000; $p < 0.0001$) for diagnosing SBP (B, C). The SBP score was significantly higher among patients with SBP (23; IQR, 22.5–24.5) when compared to those with SBP after antibiotic initiation (15.5; IQR, 13.5–16.0), multifocal hepatocellular carcinoma and/or portal vein thrombosis (13.5; IQR, 13.25–14.75), or those without SBP (8 [IQR, 8–10]) ($p < 0.0001$) (D).



Conclusion: We derived and validated the “SBP score” based on a rapid-assay sepsis-related biomarker (MR-pro-ADM) that significantly improved the diagnostic accuracy of SBP in cirrhotic patients. The usefulness of the “SBP score” deserves formal validation in large prospective studies.

SAT530

Non-invasive prediction of risk of liver-related events in non-alcoholic fatty liver disease patients

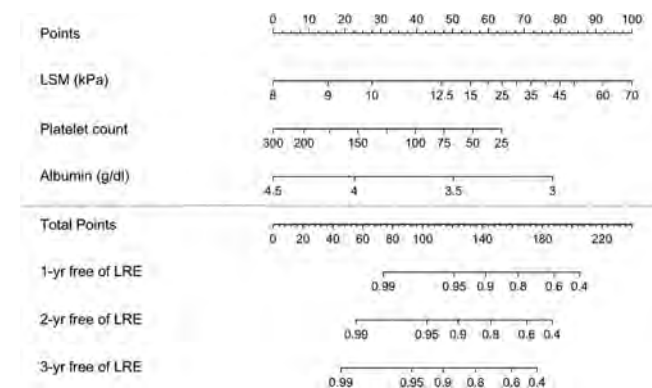
Monica Pons¹, Jesús Rivera¹, Grace Lai-Hung Wong², Terry Cheuk-Fung Yip², Adele Delamarre³, Tracy Davyduke⁴, M Mang⁴, Salvador Augustin¹, Juan Manuel Pericàs^{1,5}, Victor de Lédinghen³, Vincent Wai-Sun Wong², Juan G Abalde⁴, Joan Genesca^{1,5}. ¹Hospital Universitari Vall d'Hebron, Vall d'Hebron Institut de Recerca (VHIR), Vall d'Hebron Barcelona Hospital Campus, Universitat Autònoma de Barcelona, Liver Unit, Department of Internal Medicine, Barcelona, Spain; ²The Chinese University of Hong Kong, Department of Medicine and Therapeutics, Hong Kong; ³Hôpital Haut-Lévêque, Bordeaux University Hospital, Centre d'Investigation de la Fibrose Hépatique, INSERM U1312, Pessac, France; ⁴University of Alberta, Division of Gastroenterology (Liver Unit), Edmonton, Canada; ⁵Centro de Investigación Biomédica en Red de Enfermedades Hepáticas y Digestivas (CIBERehd), Instituto de Salud Carlos III, Madrid, Spain
 Email: monica_xina@hotmail.com

Background and aims: Simple non-invasive tools for predicting liver-related events (LRE) in non-alcoholic fatty liver disease (NAFLD) are needed for prognostic stratification and clinical trial patient selection. We aimed at developing a risk prediction model based on

non-invasive tests (NITs), including liver stiffness measurement (LSM), to determine the risk of developing LRE in NAFLD patients at point-of-care. In addition, we studied LRE incidence in compensated advanced chronic liver disease (cACLD) LSM thresholds.

Method: This is a multicenter retrospective cohort study with NAFLD patients from 4 centers in Canada (n = 72), Hong Kong (n = 1537), France (n = 681) and Spain (n = 348). Patients included had available NITs (LSM by transient elastography and serological tests), had no prior decompensation and a minimum follow-up of 12 months. Patients with concomitant etiologies were excluded. LRE were defined as hepatocellular carcinoma, clinical decompensation, liver transplantation or liver-related death. Risk of LRE was modeled with a Cox regression model using well established predictors and selected by backwards elimination method combined with bootstrapping. The relationship between hazard ratio and NITs was assessed using a cubic spline function. A nomogram was derived from the model.

Results: 2638 patients were included (53% male, mean age 58.4 years (SD 12.4), mean BMI 30.0 kg/m² (SD 5.7), and 60.8% with diabetes mellitus). Among them, 1820 (69%) had LSM <10 kPa, 479 (18%) LSM between 10–15 kPa and 339 (13%) LSM >15 kPa. Forty-five (1.7%) patients developed LRE during a median follow-up of 27 months (IQR 22–35 months). The incidence rate of LRE in patients with LSM <10 kPa was 0.04/100 patient-years, in LSM 10–15 kPa was 0.3/100 patient-years, in LSM 15–25 kPa was 2.1/100 patient-years and in LSM ≥25 kPa was 8.0/100 patient-years. Predictors evaluated in multivariate analysis were diabetes, BMI, platelet count, albumin and LSM. Only platelet count, albumin and LSM were retained in the final model. The performance for predicting LRE based on the area under the receiver operating curve (discrimination) was 0.92, also the calibration of the model was excellent. A nomogram was constructed to assess the individual risk of presenting events at 1, 2 and 3 years of follow-up (figure). The model is currently being validated in 3 external cohorts.



Conclusion: NAFLD patients with LSM <10 kPa (no-cACLD) have a very low incidence of LRE and could be followed in primary care, and the risk increases significantly in patients with LSM >15 kPa. This simple easy-to-use prediction tool for LRE could be very useful for prognostic stratification and selecting NAFLD patients for clinical studies.

SAT531

In-hospital falls and impaired nutritional status are independently associated with in-hospital mortality in patients with liver cirrhosis

Nada Abedin¹, Moritz Hein¹, Christoph Welsch¹, Jörg Bojunga¹, Stefan Zeuzem¹, Georg Dultz¹. ¹Department of Internal Medicine I, University Hospital Frankfurt, Goethe University, Frankfurt am Main, Germany
Email: nada.abedin@kgu.de

Background and aims: Chronic liver disease is associated with severe complications leading to recurrent hospitalization and a high mortality in general. Complications associated with liver cirrhosis are one of the most frequent causes of death in hospitalized patients. This study aimed at detecting risk factors that can be addressed to increase patient safety and outcome.

Method: Hospitalized patients with liver cirrhosis between 2017 and 2019 in the department for gastroenterology at the University Hospital Frankfurt were included in a retrospective analysis. Clinical data, laboratory work and follow-up data from patients' electronic files were gathered and assessed. Statistical analysis was performed using SPSS.

Results: In a total of 1985 hospitalizations our study revealed an in-hospital mortality of 9.6%. Median age was 61 years and 70.5% were male patients. Overall, patients who died during their stay had a significantly longer period of hospitalization (19.1 days vs. 7.7 days, $p < 0.0001$). 1016 cases were from patients with alcoholic liver disease, 15.2% were associated with Hepatitis C, 14.8% were patients with NASH. While there were significant clinical predictors ($p < 0.0001$) for in-hospital mortality in the univariate analysis, such as lower blood pressure, an ongoing infection and different lab values (higher CRP, hyponatremia, leukocytosis, elevation in creatinine), in the uni- and multivariate analysis two factors were independently associated with in-hospital mortality. These include a nutritional risk score >1 ($p = 0.006$, OR 2.029, 95%CI) and a falling incident during hospitalization ($p = 0.002$, OR 3.495, 95%CI). As a general marker for severity of liver disease, the MELD Score was also independently associated with higher in-hospital mortality ($p < 0.001$, OR 4.404, 95%CI).

Conclusion: Patients with liver cirrhosis are at high risk for developing severe complications that can be fatal. Our study reveals two independently associated factors with in-hospital mortality in patients with liver cirrhosis, i.e. nutritional risk and in-hospital falls that can and must be addressed and screened for on admission to alleviate patients' risk and allow for a better outcome.

SAT532

PD-1/PD-L1 pathway is related to infection development and early mortality in patients with cirrhosis

Adria Juanola^{1,2,3}, Elisa Pose^{1,2,3}, Delia Blaya², Cristina Solé¹, Gabriel Mezzano¹, Natalia Jimenez-Esquivel¹, Joaquin Andrés Castillo¹, Jordi Ribera^{2,3,4}, Irene Portoles^{2,3,4}, Martina Perez^{1,2}, Ann Ma^{2,3}, Laura Napoleone^{1,2,3}, Ana Belén Rubio^{2,3}, Marta Cervera^{2,3}, Marta Carol^{2,3}, Octavi Bassegoda^{1,2,3}, Jordi Gratacós-Gines^{1,2,3}, Anna Soria¹, Núria Fabrellas^{2,3,5}, Manuel Morales-Ruiz^{2,3,4}, Mar Coll^{2,3}, Isabel Graupera^{1,2,3}, Gonzalo Crespo^{1,2,3}, Elsa Solà^{1,2,3,6}, Pere Ginès^{1,2,3,5}. ¹Liver Unit, Hospital Clínic de Barcelona, Barcelona, Spain; ²Institut d'Investigacions Biomèdiques August Pi i Sunyer (IDIBAPS), Barcelona, Spain; ³Centro de Investigación Biomédica en Red. Enfermedades Hepáticas y Digestivas (CIBEREHD), Madrid, Spain; ⁴Biochemistry and Molecular Genetics Department, Hospital Clínic de Barcelona, Spain; ⁵Faculty of Medicine and Health Sciences, University of Barcelona, Barcelona, Spain; ⁶Institute for Immunity, Transplantation and Infection, Stanford University, Stanford, CA, USA
Email: juanola@clinic.cat

Background and aims: Infections, often recurrent, are a very characteristic complication of advanced liver cirrhosis and represent a very common cause of hospitalization, acute kidney injury, ACLF and

death. The high risk of infections in cirrhosis is associated, among others, with alterations of the intestinal microbiome as well as defective function in some immune cells. Recent studies in experimental animals suggest the existence of an activation of the PD1-PDL1 pathway (Programmed cell death 1) that would produce an immunoparalysis and predispose to infections. It is unknown whether this pathway participates in the pathogenesis of infections in human cirrhosis. The aim of the present study was to evaluate the activity of the PD-L1 pathway in patients with cirrhosis and its relationship with the development of infections and mortality.

Method: Prospective study of 310 patients with cirrhosis in different disease stages (13% outpatients, 87% hospitalized). PD-1/PD-L1 pathway activity was estimated by measuring serum levels of PD1 and PDL1 (ELISA), which assess the soluble isoform of PD1 (sPD1) and PDL1 (sPDL1) expressed in lymphocytes and monocytes. Main outcomes of the study were infections and ACLF development and death during a 3-month follow-up period.

Results: During follow-up, 99 patients (32%) developed at least one new episode of infection. Baseline serum levels of sPD1 and sPDL1 were higher in patients who developed a new infection compared to those patients who did not develop new infection [sPD1: 2.7 (2.3–3.3) vs 2.5 (2.1–3.0) pg/ml, $p = 0.038$; sPDL1: 160 (115–221) vs 129 (95–172) pg/ml, $p = 0.002$]. On multivariate analysis, sPD1 together with liver function assessed by MELD Sodium, were the only two independent predictive factors of development of new infections during 3-month follow-up. One-hundred forty-eight patients had an active infection at inclusion. Patients with infection at baseline had higher levels of sPDL1 compared to those in patients who did not have infection [164 (115–224) vs 124 (94–161) pg/ml, respectively, $p < 0.001$]. During hospitalization, 30 patients (20%) with infection at baseline died. sPDL1, MELD Sodium and leukocyte count were independently associated with in-hospital mortality among this population. Finally, 16 patients without ACLF at inclusion, developed it during follow-up. sPDL1 was higher among those who developed ACLF [182 (106/242) vs 121 (93–166) pg/ml, $p = 0.001$], irrespective of the presence of infection. Furthermore, sPDL1 was the only independent predictor factor of ACLF at 3 months.

Conclusion: In patients with cirrhosis, serum levels of PDL1 correlate with the development of infections, ACLF and short-term mortality. These results suggest the existence of an activation of the PD1-PDL1 pathway in human cirrhosis that could be an important pathogenic factor for the development of infections and early mortality.

SAT533

Short term intravenous albumin effects in decompensated cirrhosis: about single hospitalization event

Han Seul ki¹, Moon Young Kim¹. ¹Yonsei University Wonju College of Medicine, Department of Internal Medicine, Division of Gastroenterology and Hepatology, Wonju-si, Korea, Rep. of South
Email: drkimmy@yonsei.ac.kr

Background and aims: For intravenous administration of albumin, it is known that long-term administration has a positive effect on the survival rate of cirrhosis. We aimed to investigate the effects of short-term albumin administration on days of hospitalization and change of MELD score, creatinine level, complication during the hospitalization and short-term prognosis.

Method: We investigated patients who were admitted to a single-center hospital, due to acute decompensated events from January 2018 to December 2020. Causes of hospitalization include gastrointestinal bleeding, jaundice, hepatic encephalopathy, newly developed ascites requiring paracentesis and IV antibiotics administration, infection, hepatorenal syndrome, Acute on chronic liver failure. We excluded data about mortality during hospitalization due to aggressive management beyond the standard management.

After investigating the total albumin dose administered to patients during hospitalization, patients who received 40 g or more per week and those who did not were compared and analyzed. The patients

POSTER PRESENTATIONS

receiving 40 g of albumin or more was defined as the high dose albumin group.

Results: In entire cohort, administration of high dose albumin shortened the hospital stay (10.01 vs 12.76 days, $p=0.015$). In subgroup analysis, it showed a better effect in CTP class C (10.18 vs 15.35 days, $p=0.003$), and there is a tendency to reduce complications in all hospitalized patients (9 vs 17 cases, $p=0.21$). After excluding bleeding cases which is expected to have lesser effect of albumin, the shortening of hospitalization period was also remarkably found in high dose albumin administration (9.91 vs 14.25 days, $p=0.008$) and total complications event during hospitalization also tended to decrease (7 vs 10 cases, $p=0.4$).

There was no difference between the two groups in the 3 months survival rate (10 vs 10 case $p=0.88$). And the decrease of creatinine level was not different between two groups (0.53 vs 0.51 $p=0.86$), and that was same in decrease of MELD score (4.35 vs 3.53 $p=0.37$). But in subgroup in CTP class C, the decrease of creatinine level was more prominent in high dose albumin group (0.60 vs 0.48 $p=0.4$).

Conclusion: In the group of patients hospitalized for acute decompensation events, excluding mortality due to disease, albumin administration of 40 g or more per week was reducing the length of hospitalization of patients. In subgroup analysis, in the non-bleeding cases, and the higher CTP patients, the more effective it is. And it is expected that there will also be a creatinine reduction effect, and there seems to be a tendency to reduce the incidence of complications. It is recommended to consider active albumin administration when patients were hospitalized cause of acute decompensation.

SAT534

Myosteatorsis is associated with sarcopenia, frailty and fat body composition abnormalities in liver cirrhosis

Eleni Geladari¹, Theodoros Alexopoulos¹, Meropi Kontogianni², Ilianna Mani¹, Larisa Vasilieva¹, Alexandros-Pantelis Tsigas², Roxani Tenta², Evangelia Stroumpoulis³, Alexandra Alexopoulou¹.

¹Medical School, National and Kapodistrian University of Athens, 2nd Department of Internal Medicine and Research Laboratory, Athens, Greece; ²School of Health Sciences and Education, Harokopio University, Department of Nutrition and Dietetics, Athens, Greece; ³Hippokraton General Hospital, Department of Radiology, Athens, Greece
Email: alexopou@ath.forthnet.gr

Background and aims: Myosteatorsis is defined as increased fat infiltration in skeletal muscle and implies impaired muscle quality. Although it has been included in the recent sarcopenia criteria as suggested by the European Working Group on Sarcopenia in Older People (EWGSOP-2), further research is required exploring myosteatorsis' associations with clinical characteristics of patients with liver cirrhosis (LC). The aim was to investigate the prevalence of myosteatorsis and potential associations with other body composition parameters and clinical characteristics in patients with LC.

Method: Computed tomography (SliceOmaticV4.3 software, Tomovision, Montreal, PQ) was used to assess muscle mass [skeletal muscle index (SMI, cm^2/m^2)] at the third lumbar vertebrae (L3). The same software was utilized to calculate visceral adipose tissue index (VATI, cm^2/m^2), subcutaneous adipose tissue index (SATI, cm^2/m^2) and VATI/SATI (VSR) ratio. Myosteatorsis was defined as muscle radiodensity <33 Hounsfield Units (HU) at L3. Sarcopenia was diagnosed according to EWGSOP-2 criteria, muscle performance was evaluated with the short physical performance battery (SPPB) and frailty using the liver frailty index (LFI).

Results: 167 consecutive patients [67.6% male, MELD 12 (IQR 7–17), 65.3% with decompensated cirrhosis, 43.1%, 23.4% and 33.5% with alcoholic, viral and other causes of liver disease respectively] were included. Myosteatorsis was identified in 59.3%, sarcopenia in 43.1% and frailty in 29.3% of the population.

Patients with myosteatorsis vs those without, were more often female (42.4% vs 17.6%, $p=0.001$), older than 60 years of age (58.6% vs 39.7%,

$p=0.012$), sarcopenic (61.6% vs 16.2%, $p<0.001$), frail (40.4% vs 13.2%, $p<0.001$) and had more often decompensated cirrhosis (71.7% vs 55.9%, $p=0.026$). Moreover, patients with myosteatorsis displayed higher VATI [55.4 (36.6–75.7) vs 32.8 (20.7–56.6), $p<0.001$], SATI [63.3 (37.0–95.1) vs 46.8 (28.7–66.8), $p=0.005$], VSR [0.99 (0.54–1.4) vs 0.69 (0.43–1.18), $p=0.024$] and decreased SPPB [10 (5.5–11) vs 11 (10–12), $p<0.001$]. Liver disease etiology and body mass index did not differ between the groups.

Conclusion: High myosteatorsis prevalence was demonstrated in this sample of patients with cirrhosis. Myosteatorsis was associated with older age, presence of sarcopenia, frailty, decreased performance status, high visceral, and subcutaneous adiposity and more severe liver disease.

SAT535

Correction and prevention of hyponatremia in patients with cirrhosis and ascites-post hoc analysis of the ANSWER study database

Giacomo Zaccherini¹, Maurizio Baldassarre^{1,2}, Manuel Tufoni³, Oliviero Riggio⁴, Paolo Angeli⁵, Carlo Alessandria⁶, Sergio Neri⁷, Francesco Giuseppe Foschi⁸, Fabio Levantesi⁹, Aldo Airolidi¹⁰, Loredana Simone¹¹, Gianluca Svegiati-Baroni¹², Stefano Fagioli¹³, Giacomo Laffi¹⁴, Raffaele Cozzolongo¹⁵, Vito Di Marco¹⁶, Vincenzo Sangiovanni¹⁷, Filomena Morisco¹⁸, Pierluigi Toniutto¹⁹, Annalisa Tortora²⁰, Rosanna De Marco²¹, Silvia Nardelli⁴, Salvatore Piano⁵, Chiara Elia⁶, Mauro Bernardi¹, Paolo Caraceni^{1,2,3}.

¹University of Bologna, Department of Medical and Surgical Sciences, Bologna, Italy; ²University of Bologna, Center for Applied Biomedical Research, Bologna, Italy; ³IRCCS Azienda Ospedaliero-Universitaria di Bologna, Bologna, Italy; ⁴Sapienza University of Rome, Department of Translational and Precision Medicine, Rome, Italy; ⁵University of Padua, Department of Medicine, Padua, Italy; ⁶Città della Salute e della Scienza Hospital, Division of Gastroenterology and Hepatology, Turin, Italy; ⁷Humanitas Medical Care Catania, Internal Medicine, Catania, Italy; ⁸AUSL of Romagna, Internal Medicine, Hospital of Faenza, Faenza, Italy; ⁹AUSL of Bologna, Internal Medicine, Hospital of Bentivoglio, Bentivoglio, Italy; ¹⁰Niguarda Hospital, Department of Hepatology and Gastroenterology, Milan, Italy; ¹¹University Hospital of Ferrara, Gastroenterology Unit, Ferrara, Italy; ¹²Polytechnic University of Marche, Department of Gastroenterology, Ancona, Italy; ¹³Papa Giovanni XXIII Hospital, Gastroenterology and Transplant Hepatology, Bergamo, Italy; ¹⁴University of Florence, Department of Experimental and Clinical Medicine, Florence, Italy; ¹⁵National Institute of Gastroenterology S. De Bellis, Division of Gastroenterology, Castellana Grotte, Italy; ¹⁶University of Palermo, Biomedical Department of Internal and Specialistic Medicine, Palermo, Italy; ¹⁷Azienda Ospedaliera di Rilievo Nazionale dei Colli, Cotugno Hospital of Naples, Naples, Italy; ¹⁸Federico II University of Naples, Department of Clinical Medicine and Surgery, Naples, Italy; ¹⁹University of Udine, Department of Medical Area, Udine, Italy; ²⁰Gemelli Foundation Catholic University, Unit of Gastroenterology, Rome, Italy; ²¹Hospital of Cosenza, Unit of Gastroenterology, Cosenza, Italy
Email: giacomo.zaccherini@unibo.it

Background and aims: Hyponatremia is a frequent and ominous complication in patients with decompensated cirrhosis. Human albumin (HA) administration improves hyponatremia in patients with cirrhosis hospitalized because of acute decompensation, but no data are available on the effects of long-term HA administration. We aimed at determining whether long-term HA administration could help in treating and preventing hyponatremia in outpatients with decompensated cirrhosis and ascites.

Method: We performed a post-hoc analysis on the intention-to-treat population (431 patients) enrolled in the ANSWER trial, grouping patients according to their baseline serum sodium levels. Resolution rates of hyponatremia in hyponatremic patients and incidence rates (IRs) and IR ratios (IRRs) of at least moderate hyponatremia (<130 mmol/l) during a follow-up of 18 months were calculated.

Results: 149 (35%) patients presented hyponatremia (<135 mmol/l) at baseline (74 vs 75 in the standard medical treatment [SMT] and in the SMT+HA arms, respectively). 116 of them (78%) had mild hyponatremia (≥ 130 and <135 mmol/l), while 33 (22%) had at least moderate hyponatremia (<130 mmol/l). Patients with hyponatremia had higher Child-Pugh and MELD scores as compared to normonatremic patients. At baseline, hyponatremic patients randomized to receive long-term HA did not differ from those randomized to SMT. Normalization of hyponatremia (≥ 135 mmol/l) was reached more frequently and faster in SMT+HA than SMT group: 45% vs 28% ($p = 0.042$) after 1 month, and 71% vs 44% ($p = 0.006$) after 3 months. Long-term HA was also effective in preventing episodes of hyponatremia, as the incidence rate of at least moderate hyponatremia was significantly lower in the SMT+HA than in SMT arm, both in hyponatremic and non-hyponatremic patients (incidence rate ratios: 0.245 [CI 0.167–0.359, $p < 0.001$] and 0.539 [CI 0.338–0.859, $p = 0.008$], respectively).

Conclusion: Long-term HA administration appears an effective intervention in managing hyponatremia in outpatients with decompensated cirrhosis and ascites.

SAT536

Low incidence of adverse liver events in a real-world cohort of patients diagnosed with liver disease via a community diagnostic pathway

Alexander Smith^{1,2}, Florina Borca², Julie Parkes¹, Janisha Patel², Hang Phan¹, Callum Robins², Ryan Buchanan¹. ¹University of Southampton, Faculty of Medicine, Southampton, United Kingdom; ²University Hospital Southampton NHS Foundation Trust, Southampton, United Kingdom
Email: asmith49@nhs.net

Background and aims: Community liver diagnostic pathways use non-invasive liver fibrosis tests to identify patients with compensated alcohol-related liver disease (ArLD) and non-alcohol related fatty liver disease (NAFLD). However, the longitudinal association between test scores and adverse liver events is uncertain.

Method: The Southampton Liver Pathway (SLP) involves fibrosis assessment with an enhanced liver fibrosis (ELF) score in primary care and transient elastography (TE). We retrospectively examined the occurrence of adverse liver events in patients with ArLD or NAFLD identified in the SLP. Patients with an ELF test taken between 1st January 2017 and 31st August 2019, TE conducted within 6 months of the ELF test and a negative non-invasive liver screen (e.g. chronic viral hepatitis, autoimmune profile, serum ferritin and transferrin saturation) were included in the analysis. Data were collected at baseline from hospital records including age, sex, BMI, history of alcohol excess, and known type 2 diabetes mellitus (T2DM).

Adverse liver events were defined *a priori* as development of ascites, spontaneous bacterial peritonitis, overt hepatic encephalopathy, variceal bleeding, and hepatocellular carcinoma. We performed a search of hospital electronic records for adverse liver events occurring from the date of ELF test up to 30th April 2021. Kaplan-Meier (KM) curves and hazard ratios (HR) with 95% confidence interval (CI) were produced from univariable cox regression for risk of adverse liver events, stratified by recognised cut-offs for advanced fibrosis for ELF score (>10.5 or ≤ 10.5) and TE (>15 or ≤ 15 kPa).

Results: A total of 324 patients were identified with 57% NAFLD, 37% ArLD, 6% unclassified. Median follow-up was 29 months (IQR 23–40). 213 patients (66%) were male and median age was 61 years (IQR 50–69). Median BMI was 30 kg/m² (IQR 27–35) and 113 patients had T2DM (35%). Median ELF score was 10.5 (IQR 9.8–10.9) and median TE 7.2 kPa (IQR 5.5–11.4). 152 (47%) patients had ELF >10.5 and 54 (17%) had TE >15 kPa.

Only 5 (1.5%) patients experienced an adverse liver event. KM curves are shown in Figure 1. The HR for prediction of adverse liver events according to ELF score was 4.10 (95% CI 0.46–36.68, $p = 0.208$) and for TE result 2.84 (95% CI 0.47–17.01, $p = 0.254$).

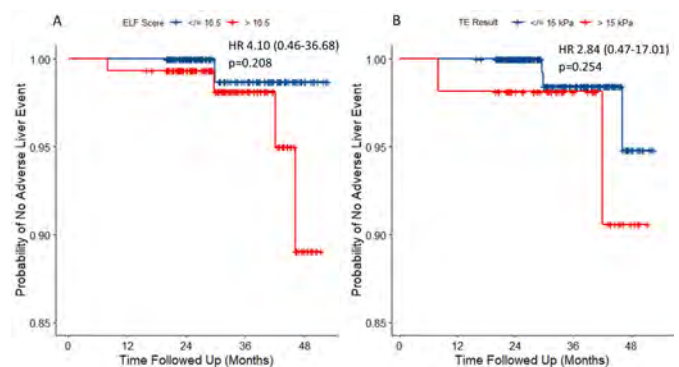


Figure 1: Kaplan-Meier survival curves from univariable Cox regressions for adverse liver events stratified by (A) ELF score and (B) TE result.

Conclusion: Patients from primary care populations with compensated liver disease diagnosed using non-invasive tests have a good medium-term prognosis. High ELF and TE results were not significantly associated with adverse liver events but this was affected by the low incidence of events in the follow-up period.

SAT537

The use of decompensated cirrhosis admission care bundles improves the standard of inpatient care but utilisation is poor across the UK

The Trainee Collaborative for Research and Audit in Hepatology UK¹.
Email: oliver.tavabie@doctors.net.uk

Background and aims: The standard of inpatient care for patients with cirrhosis in the United Kingdom (UK) is variable. Previous reports have demonstrated that less than 50% of inpatients admitted with alcohol-related liver disease (ARLD) receive good care. UK hepatology and gastroenterology societies have developed standards to improve care of patients with decompensated cirrhosis in the first 24 hours of admission. These have been integrated into a number of care bundles. We aimed to audit the uptake of these bundles and assess the impact on patient outcomes across the UK.

Method: Trainees from across UK hospitals were invited to participate in this audit through the ToRCH-UK network. Patients admitted to hospital between 1/11/2019–30/11/2019 with decompensated cirrhosis were identified by coding used for the NHS Cirrhosis Quality Dashboard. Admission clinical, demographic and laboratory data were collected with outcome and trust-specific data. Sites were grouped by NHS region, specialist/non-specialist hepatology centre designation and outcome groups. Univariable and multivariable analyses (MVA) were performed.

Results: 1224 admissions (1168 patients) from 104 hospitals (36 specialist hepatology centres) were included. Median age was 58 (IQR 48–68) and 61.6% were male. 62.3% of admissions were out of hours, 74.8% were for patients with ARLD, 85.1% had an established diagnosis of chronic liver disease with 67.2% having previously decompensated. Median model for end-stage liver disease (MELD) score was 17 (IQR 12–21) and admission inpatient mortality was 15.6%. Admission care bundles were used in 11.4% of admissions and there was significant regional variation in use (see Figure). Care bundle use was higher in patients with; ARLD ($p < 0.0001$), jaundice ($p = 0.005$) and those with higher MELD scores (19 (IQR 14–23) v 16 (IQR 12–21), $p = 0.001$), and reduced in patients with gastrointestinal bleeding ($p = 0.005$). The use of a care bundle was associated with increases in the following; appropriate blood tests requests ($p < 0.0001$), septic screens ($p = 0.0001$), diagnostic paracentesis ($p = 0.005$), appropriate alcohol care ($p = 0.0006$) and acute kidney injury management ($p = 0.0007$). Mortality was higher in patients where a care bundle was used ($p = 0.01$). However, when adjusted for MELD score, age and critical care admission, care bundle use was not associated with mortality (adjusted odds ratio 0.97–2.65, $p = 0.06$).

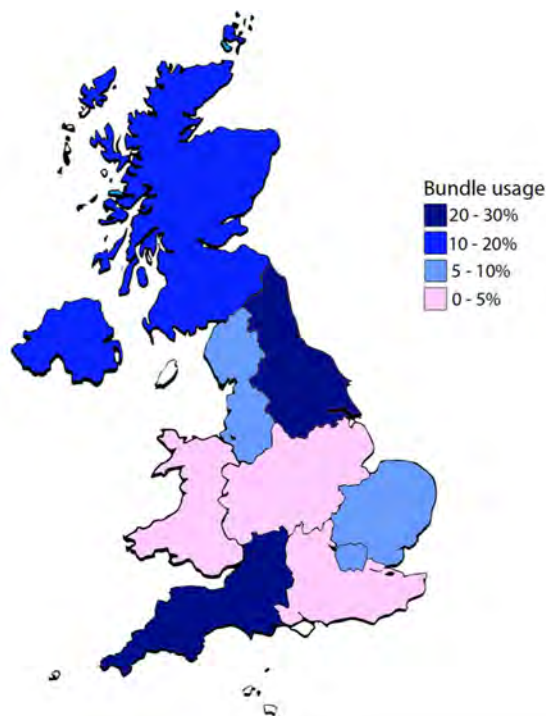


Figure: Heatmap demonstrating regional variation in admission care bundle use across the UK

Conclusion: The use of admission care bundles improves the standard of care of patients with decompensated cirrhosis within the first 24 hours of admission. However, uptake is poor and variable across the UK. Work is required to understand the barriers to use to improve inpatient care for patients with decompensated cirrhosis.

SAT538

Effect of hepatitis B virus treatment on all causes and liver-related death among patients living with HBV with cirrhosis in British Columbia in a population-based cohort study

Makuza Jean Damascene^{1,2,3}, Dahn Jeong^{2,4}, Mawuena Binka², Prince Adu^{2,4}, Georgine Cua², Hector Velasquez^{2,4}, Amanda Yu², Stanley Wong², Maria Alvarez², Sofia Bartlett², Alnoor Ramji⁵, Hin Hin Ko⁵, Eric Yoshida⁵, Mel Krajden², Naveed Janjua^{2,4,6}. ¹The University of British Columbia, School of Population and Public Health, Vancouver, Canada; ²BC Centre for Disease Control, Clinical Prevention Services, Vancouver, Canada; ³Rwanda Biomedical Center (RBC), IHDPC, Kigali, Rwanda; ⁴The University of British Columbia, School of Population and Public Health, Vancouver, Canada; ⁵The University of British Columbia, Division of Gastroenterology, Vancouver, Canada; ⁶St. Paul's Hospital, Centre for Health Evaluation and Outcome Sciences, Vancouver, Canada

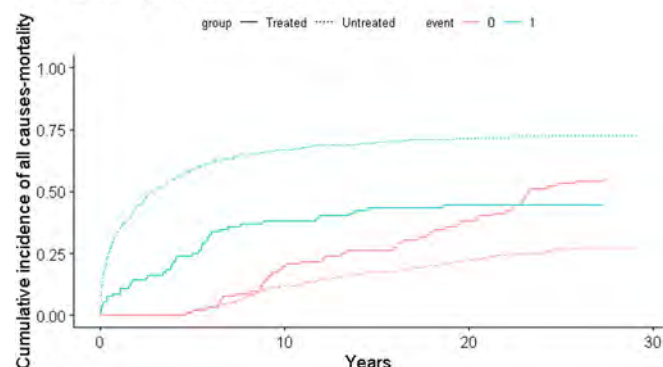
Email: makorofr@gmail.com

Background and aims: The hepatitis B virus (HBV) is a significant burden of liver disease in Canada. We evaluated the effect of HBV treatment on all-cause mortality and liver-related mortality among individuals with HBV and cirrhosis in British Columbia (BC), Canada. **Method:** This analysis used the BC Hepatitis Testers Cohort, which includes all individuals diagnosed with HBV since 1990 in BC, integrated with data on medical visits, hospitalizations, prescription drugs, and mortality. The study population included individuals who tested positive for HBV and were diagnosed with cirrhosis, followed from their HBV first testing date until death or December 31, 2020. We computed all-cause and liver-related mortality rates by HBV treatment status. We used inverse probability of treatment weighting (IPTW) to balance the baseline characteristics with the standardized mean difference (SMD) cut-off of 0.2 for treated and untreated

individuals. We performed multivariable cox proportional hazard modeling to assess the effect of HBV treatment and coinfection with Hepatitis C virus (HCV) on all-cause and liver-related mortality in the overall sample and in the IPTW dataset.

Results: The analysis included 654 HBV-positive individuals with cirrhosis; 100 (15.3%) received HBV treatment. The mean follow-up for treated individuals was 10.29 (SD: 7.61) years and 5.84 (SD: 6.71) years for untreated individuals. A higher proportion of those treated compared to untreated were males [67 (67%) vs 370 (66.8%)], born between 1945 and 1 above [66 (75.9%) vs 330 (65.9%)], those of East and South Asian ethnicity [40 (40.0%) vs 108 (19.5%)], and those with liver cancer [20 (20.0%) vs 68 (12.3%)]. The highest all-cause (124.28; 95%CI: 112.70, 137.04 vs 44.71; 95%CI: 33.49, 59.69 per 1,000 person-years [PYs]); and liver-related mortality (75.74; 95%CI: 66.83, 85.85 vs 29.16; 95%CI: 20.39, 41.70 per 1,000 PYs) rates were higher among individuals who were not treated for HBV compared to those who were treated the liver-related. The multivariable models revealed that HBV-positive cirrhotic individuals who were not treated had a greater risk of dying from all causes (adjusted hazard ratio [aHR] 1.75; 95%CI: 1.25, 2.45) and liver-related mortality (adjusted sub-distribution HR [asHR] 1.78; 95%CI: 1.19, 2.67) compared to treated individuals. Compared to individuals without co-infection HBV/HCV, those co-infected HBV/HCV, not treated for HBV infection had a higher hazard for both all causes and liver-related mortality (aHR 2.60; 95% CI 1.63, 4.14, and 2.93; 95% CI 1.68, 5.14 respectively). Other risk factors for all-cause and liver-related mortality included male sex and HCV infection.

Death by Hepatitis B treatment status



Conclusion: HBV treatment was associated with a significant reduction in all-cause and liver-related mortality among individuals with cirrhosis.

SAT539

Secondary infections in hospitalized patients with cirrhosis: epidemiology, clinical characteristics and prognostic relevance

Gustavo Pereira¹, Caroline Baldin¹, Juliana Piedade¹, Nathalia Galhardi¹, Barbara Rodrigues¹, Raquel Godoy¹, Camila Marques de Alcanatara Barreto¹, Flavia Fernandes¹.

¹Bonsucesso General Hospital, Gastroenterology and Hepatology Unit, Rio de Janeiro, Brazil

Email: ghsperreira@gmail.com

Background and aims: Bacterial infections are frequent in cirrhotic patients and may induce a state of immune paralysis and, consequently, greater susceptibility to secondary infections. There is a paucity of data respect the frequency and clinical characteristics of secondary infections in this population. Our aim was to describe incidence and predictive factors of secondary infections and their correlation with prognosis.

Method: retrospective analysis of patients diagnosed with bacterial infections at admission, originally included in a prospective

observational cohort, followed for 3 months or until death or transplantation.

Results: 225 patients were included (59 ± 12 years, 57% female, HCV ± alcohol etiology in 74%, Child C in 48%, MELD-sodium 21 ± 7, ascites and hepatic encephalopathy in 70 and 38%). Fifty percent of infections were classified as community-based. Skin, SBP and urinary tract i were the most common at admission (25, 23 and 20%). SIRS, qSOFA ≥ 2, and ACLF were observed in 45, 19, and 32 patients. Secondary infection developed in 93 patients (41%) after a median of 11 (7–19) days. The most common secondary infections were respiratory, undetermined site and SBP (27, 23 and 17%). In only 18% of patients the secondary infection developed in same site as the first. The probability of developing secondary infection at the end of the first and second weeks was 12 and 33%. At admission, ACLF (OR 2.84, 95%CI 1.42–5.69, $p=0.003$), non-community infections (OR 7.82, 95%CI 1.69–36.12, $p=0.008$), as well as Child C and age, were predictors of secondary infections. Patients with secondary infections had higher in-hospital mortality (59 vs. 13%, $p<0.001$) as well as at 3 months (64 vs. 26%, $p<0.001$). Development of secondary infection (OR 2.25, 95%CI 1.35–3.73, $p=0.002$) and MELD-sodium (OR 1.1, 95%CI 1.06–1.14, $P<0.001$) were independent predictors of 3-month mortality.

Conclusion: secondary infections are frequent in cirrhotic patients, occurring early and usually in sites other than the index infection. Diagnosis of non-community infections as well as worse liver function at admission were predictors of secondary infections. Development of secondary infections is associated with higher mortality irrespectively of the severity of liver disease.

SAT540

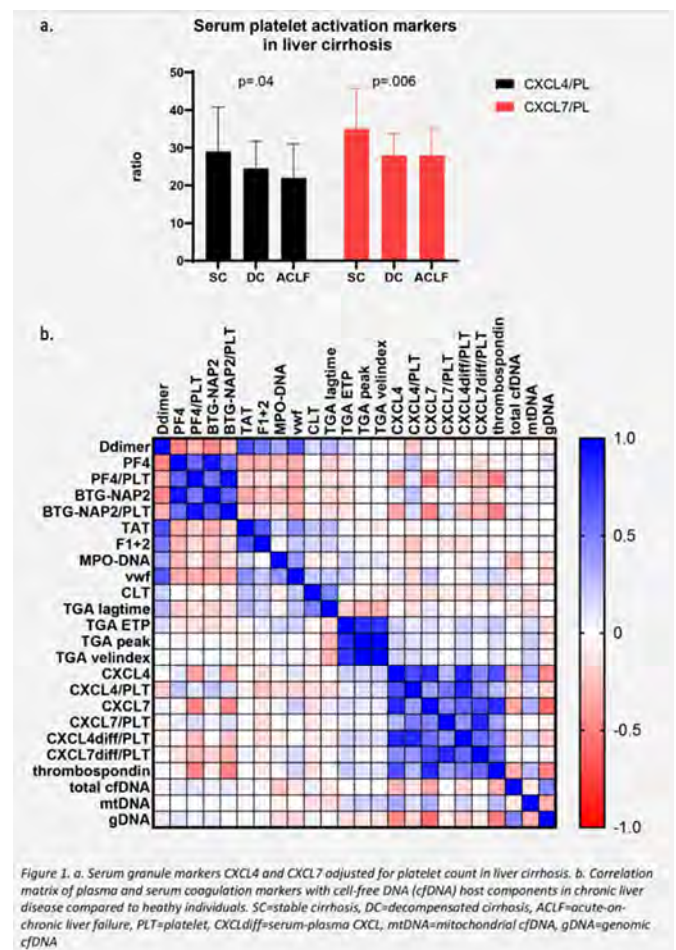
Circulating cell-free DNA levels increment with worsening cirrhosis severity and associate with platelet exhaustion and mortality

Marilena Stamouli¹, Jelle Adelmeijer², Dana Huskens³, Savannah Rivera⁴, Kevin O'Reilly⁵, Elena Palma¹, Neil Youngson¹, William Bernal⁴, Shilpa Chokshi¹, Mark Roest³, Ton Lisman², Vishal Patel^{1,4,6}. ¹The Roger Williams Institute of Hepatology, Foundation for Liver Research, London, United Kingdom; ²Surgical Research Laboratory and Section of Hepatobiliary Surgery and Liver Transplantation, Department of Surgery, University of Groningen, University Medical Center Groningen, Groningen, Netherlands; ³Synapse Research Institute, Cardiovascular Research Institute Maastricht, Maastricht University Medical Center, Maastricht, Netherlands; ⁴Institute of Liver Studies and Transplantation, King's College Hospital, London, United Kingdom; ⁵Department of Critical Care, King's College Hospital NHS Foundation Trust, London, United Kingdom; ⁶School of Immunology and Microbial Sciences, Faculty of Life Sciences and Medicine, King's College London, London, United Kingdom
Email: m.stamouli@researchinliver.org.uk

Background and aims: Chronic liver disease (CLD) is accompanied by changes in pro- and anti-haemostatic pathways, resulting in a fragile restored haemostatic balance. Thrombocytopenia is a common complication in decompensated cirrhosis (DC) and acute-on-chronic liver disease (ACLF), and granule storage pool deficiency has been shown to impair platelet function and favour bleeding. Circulating cell-free DNA (cfDNA) has been proposed to drive organ failure and interact with critical coagulation pathways and platelet function. The aim of this work was to characterise cfDNA in the evolution of CLD, coagulation dysfunction and associated organ failure.

Method: Plasma and serum haemostatic profiles were studied extensively in the full spectrum of CLD of increasing severity: stable cirrhosis (SC, $n=40$), DC ($n=63$), ACLF ($n=50$), and were compared to healthy individuals ($n=40$). Plasma-extracted cfDNA was also characterised by way of its host components (genomic (g) and mitochondrial (mt)). cfDNA content, coagulation and platelet activation markers were compared between groups and correlated with clinical characteristics.

Results: Plasma levels of total cfDNA and its mitochondrial and genomic components were significantly elevated in CLD patients when compared to healthy controls ($p<0.001$). There was no significant difference across the cohorts in plasma coagulation markers, but serum platelet activation markers decreased significantly as liver disease progressed ($p<0.001$) (Figure 1a). Interestingly, both mt- and gDNA correlated with serum platelet activation markers, CXCL4 (mtDNA $r_{(s)}=0.34$, 95% CI 0.19–0.47, gDNA $r_{(s)}=-0.45$, 95% CI 0.57–0.32), CXCL7 (mtDNA $r_{(s)}=0.32$, 95% CI 0.17–0.46, gDNA $r_{(s)}=-0.58$, 95% CI 0.68–0.46) and thrombospondin (mtDNA $r_{(s)}=0.27$, 95% CI 0.11–0.41, gDNA $r_{(s)}=-0.49$, 95% CI 0.60–0.36) (Figure 1b). Host gDNA and platelet granule proteins were significantly associated with patient mortality (30- and 90-day), cirrhosis scores (Child-Pugh, MELD, CLIF-C) and routine haemostasis laboratory tests (platelets, INR, fibrinogen).



Conclusion: cfDNA from mitochondrial and genomic sources share similar pathophysiological properties. cfDNA levels are elevated in patients with advanced CLD, but do not appear to be associated with coagulation activation or inhibition of fibrinolysis. Rather, serum platelet granule content is significantly reduced as cirrhosis progresses and is linked to both mtDNA and gDNA, suggesting that cfDNA may be involved in platelet activation. Our data suggest a mechanism of platelet exhaustion or 'acquired storage pool disease', differentiating patients with and without hepatic decompensation. We conclude that circulating cfDNA is not just a prognostic marker, but may also contribute to changes in platelet content and function.

Liver tumours: Clinical aspects except therapy

SAT554

Sugar sweetened beverage consumption and liver cancer risk

Xuehong Zhang^{1,2,3}, Longgang Zhao⁴, Mace Coday⁵, David O. Garcia⁶, Xinyi Li², JoAnn Manson^{1,2,3}, Katherine McGlynn⁷, Yasmin Mossavar-Rahmani⁸, Michelle Naughton⁹, Melissa Lopez-Pentecost⁶, Nazmus Saquib¹⁰, Howard Sesso^{1,2,3}, Aladdin Shadyab¹¹, Michael Simon¹², Linda Snetselaar¹³, Fred Tabung⁹, Lesley Tinker¹⁴, Deirdre Tobias^{1,2,3}, Trang VoPham¹⁴.
¹Harvard Medical School, Boston, United States; ²Harvard T.H. Chan School of Public Health, Boston, United States; ³Brigham and Women's Hospital, Boston, United States; ⁴University of South Carolina, Columbia, United States; ⁵University of Tennessee, Memphis, United States; ⁶The University of Arizona, Tucson, United States; ⁷National Cancer Institute-Shady Grove, Rockville, United States; ⁸Albert Einstein College of Medicine, United States; ⁹The Ohio State University, Columbus, United States; ¹⁰Sulaiman Al Rajhi University, Al Bukayriyah, Saudi Arabia; ¹¹University of California San Diego, La Jolla, United States; ¹²Wayne State University, Detroit, United States; ¹³The University of Iowa, Iowa City, United States; ¹⁴Fred Hutchinson Cancer Research Center, Seattle, United States

Email: poxue@channing.harvard.edu

Background and aims: Intake of sugar-sweetened beverage (SSB), a postulated risk factor for obesity, diabetes, and cardiovascular disease, may drive insulin resistance and inflammation which are strongly implicated in liver carcinogenesis. However, evidence on the association between SSB intake and liver cancer is scarce. We hypothesized that higher SSB intake would be associated with a greater risk of liver cancer.

Method: We included 97,601 women aged 50–79 years from the Women's Health Initiative Observational Study and Dietary Modification Trial comparison arm. SSB intake was defined as the sum of soft drinks and fruit drinks (1 serving = one 12 fl. oz can or 355 ml), which was assessed by a validated food frequency questionnaire administered at baseline between 1993 and 1998. Incident liver cancers were reported by self-administered questionnaires and further confirmed by medical record review. Cox proportional hazards regression models were used to estimate multivariable hazard ratios (HRs) and 95% confidence intervals (CIs) with adjustment for age, race and ethnicity, education, alcohol intake, smoking status, body mass index, non-steroidal anti-inflammatory drug use, physical activity, total caloric intake, and history of diabetes.

Results: After a median of 19.5 years follow-up, 206 women had confirmed liver cancer. Approximately 6.8% of women consumed ≥ 1 serving/day of SSB at baseline. Higher SSB intake was associated with a 99% greater risk of liver cancer (HR ≥ 1 /day vs never to <3 /month = 1.99, 95%CI = 1.25–3.18, P linear trend = 0.004) as compared to intake of <3 servings/month. Non-statistically significant positive associations with liver cancer were observed for fruit drinks (HR ≥ 1 /day vs never to <3 /month = 1.83, 95%CI = 0.80–4.17) and soft drinks (HR ≥ 1 /day vs never to <3 /month = 1.79, 95%CI = 1.05–3.07). Results were similar after further adjustment for coffee/tea intake, or history of liver diseases, or when liver cancer cases diagnosed within the first 2 years of follow-up or those with history of diabetes were excluded. Substitution analyses indicated replacing SSB with water and/or coffee or tea could significantly lower liver cancer risk.

Conclusion: Our findings suggest SSB as a potential modifiable risk factor for liver cancer in postmenopausal women. Studies in men and diverse populations are needed to examine these associations more comprehensively. If our findings confirmed, reducing SSB consumption might serve as a public health strategy to reduce liver cancer burden.

SAT555

Safety and effectiveness of vaccines against SARS-CoV-2 in patients with liver cancer. VacHep registry: response analysis 4 weeks after the second dose.

Elena Diago Sempere¹, Ana Matilla², Carlos Rodríguez³, Christie Perelló⁴, Beatriz Minguez⁵, Maria Varela⁶, Juan José Urquijo⁷, Javier Ampuero⁸, Janire Prieto⁹, Laura Márquez Pérez², Javier Crespo³, María Bermúdez⁵, Ana María Piedra Cereza⁶, Moises Diago⁷, Belén Ruiz Antoran¹⁰, José Luis Calleja Panero¹¹.
¹Hospital Universitario La Paz, IdiPAZ, Central Unit for Clinical Research and Clinical Trials, Madrid, Spain; ²H.G.U. Gregorio Marañón, Gastroenterology and Hepatology Department, Madrid, Spain; ³Hospital Universitario Marqués de Valdecilla, IDIVAL, Gastroenterology and Hepatology Department, Santander, Spain; ⁴Hospital Universitario Puerta de Hierro, Liver Unit. Gastroenterology and Hepatology Department, Majadahonda, Madrid, Spain; ⁵Hospital Universitario Vall d'Hebron, Liver Unit, Barcelona, Spain; ⁶Hospital Universitario Central de Asturias, Liver Unit. Gastroenterology and Hepatology Department, Oviedo, Spain; ⁷Hospital Universitario General de Valencia, Liver Unit. Gastroenterology and Hepatology Department, Valencia, Spain; ⁸Hospital Universitario Virgen del Rocío, Institute of Biomedicine of Seville (IBIS), Unit for the Clinical Management of Digestive Diseases, Sevilla, Spain; ⁹Hospital Urduliz-Alfredo Espinosa, Gastroenterology and Hepatology Department, Urduliz, Spain; ¹⁰Hospital Universitario Puerta de Hierro Majadahonda, IDIPHIM, Clinical Pharmacology Department, Majadahonda, Madrid, Spain; ¹¹Hospital Universitario Puerta de Hierro, IDIPHIM and CIBEREHD, Department of Gastroenterology and Hepatology, Majadahonda, Madrid, Spain
 Email: eddiagosempere@gmail.com

Background and aims: Vaccines against SARS-Cov2 have been authorized with an efficacy of 95%. However registration studies have not included cancer patients at risk of lower immunogenicity. The aim of this study is to evaluate the immune response and safety after vaccination in patients with liver cancer.

Method: Case-control study, patients with primary liver cancer who received any of the COVID-19 vaccines were included. The immune response was evaluated by detecting tests against Spike protein by electrochemiluminescence. Study titers were defined as undetectable (<0.4 U/ml), suboptimal (0.4–250), and adequate (>250 U/ml). 1 Cancer-free individuals were selected as controls and matched for age and sex. A second control cohort of cirrhotic patients is ongoing. The results of the interim analysis corresponding to 4 weeks after the second dose are presented.

Results: 244 liver cancer patients and 340 controls were prospectively included. Liver cancer patients had a significant lower serologic response (≤ 250 U/ml) 4 weeks after the second dose than the control group (18.9% vs 7, 1%; $p < 0.001$) (Table 1).

	RESPONSE: ADEQUATE IG > 250 U/ ml	RESPONSE: SUBOPTIMAL IG 0, 4– 250 U/ml	IG UNDETECTABLE IG $< 0, 40$ U/ml
HCC PATIENTS	73, 4%	15, 6%	3, 3%
HEALTHY CONTROLS	92, 9%	6, 7%	0, 4%

In patients with liver cancer, age >60 years, recurrence at the time of vaccination, treatment with sorafenib, nivolumab, cabozantinib, Child-Pugh B, and BCLC C/D stage were significantly associated with an inadequate immune response.

The adequate response after vaccination with Pfizer-BioNTech was significantly lower than with Moderna (74% vs 92%, $p < 0.001$). 36% of patients presented adverse effect 28 days after the second dose.

Conclusion: Liver cancer patients develop a significantly lower immune response to SARS-CoV-after two doses in comparison with general population. Factors influencing poorer response include age,

active systemic therapy, tumor stage, and severity of liver disease. The findings confirm the need for a reassessment of vaccination mechanisms in this population.

Reference

Thuluvath PJ, Roberts P, Chauhan M. Analysis of antibody responses after COVID-19 vaccination in liver transplant recipients and those with chronic liver diseases. *J Hepatol.* 2021 Dec;75 (6):1434–1439. doi:10.1016/j.jhep.2021.08.008

SAT556

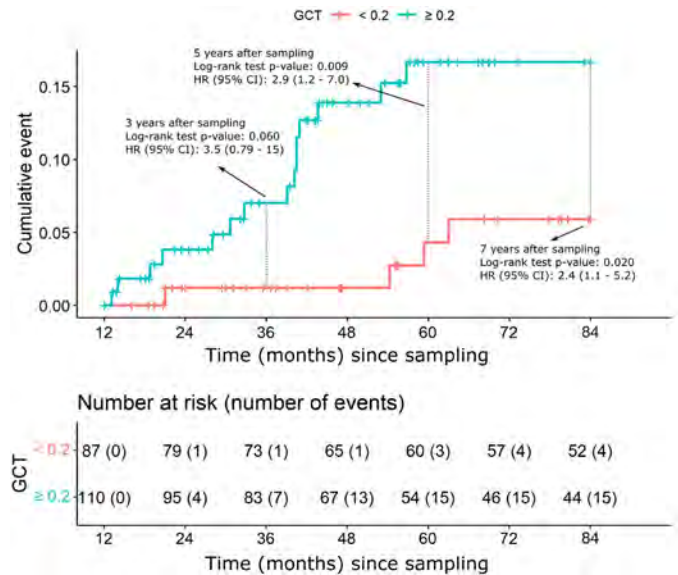
Validation of a glycomics-based test associated with risk of HCC development in cirrhosis

Xavier Verhelst^{1,2}, Leander Meuris³, Roos Colman⁴, Annelies Van Hecke³, Anja Geerts^{1,2}, Nico Callewaert³, Hans Van Vlierberghe^{1,2}. ¹Ghent University Hospital, Gastroenterology and Hepatology, Gent, Belgium; ²Ghent University, Liver Research Center Ghent, Gent, Belgium; ³VIB-Ugent, Center for Medical Biotechnology, Gent, Belgium; ⁴Ghent University, Center for biostatistics, Gent, Belgium
Email: xavier.verhelst@uzgent.be

Background and aims: Cirrhosis is the main risk factor for the development of hepatocellular carcinoma (HCC). Six-monthly screening with ultrasound is advocated for the surveillance of cirrhotic patients. We recently showed that a glycomics-based test (GlycoCirrhoTest [GCT]) can provide additional information regarding the risk of HCC development in cirrhotic patients. The aim of this study is to provide an independent clinical validation of the GCT for the assessment of the risk of HCC development in cirrhosis.

Method: Validation study on serum samples of patients with established compensated cirrhosis (CHILD Pugh A and B) in a tertiary liver center. Serum N-glycan profiling was performed and GCT was calculated at baseline using DNA sequencer assisted fluorophore assisted capillary electrophoresis. During the follow-up period, patients were screened for the presence of HCC every 6 months with ultrasound and alpha foeto protein (AFP) measurements.

Results: A total of 198 cirrhotic patients were followed during a median follow-up time of 7 years. Twenty-nine patients developed HCC and one died during follow-up. At baseline, the mean GCT value was significantly higher in patients who developed HCC within 3 and 5 years compared to patients who did not develop HCC (Welch's t-test, p value 3 years: 0.034, 5 years: 0.022). Hazard ratio for HCC development at 5 years based on GCT was 2.9 (95% CI, 1.2–7.0). Applying the same cut-off as from the proof-of-concept study (0.2), the negative predictive value of GCT for HCC development was 98.9%. Figure 1 illustrates the discriminative power of this biomarker in patients with cirrhosis. GCT is based on changes in serum protein glycosylation related to cirrhosis nodularity and malignant transformation.



Conclusion: This independent validation study confirms that GCT is a glycomics-based test that provides additional information for risk assessment of HCC development in cirrhosis. This information could be used to develop personalised HCC screening programs in cirrhotic patients according to the value of GCT. Moreover, refocusing of the screening resources to the reduced number of cirrhosis patients who truly are at elevated risk for developing HCC may result in earlier detection of more HCC cases, for instance by making contrast-enhanced MRI screening cost-effective.

SAT557

Benefits of tailored HCC surveillance programs on case-fatality rate and cancer-specific mortality using a modelling approach

Massih Ningarhari¹, Abbas Mourad², Claire Delacôte², Line Carolle Ntandja Wandji¹, Guillaume Lassailly¹, Alexandre Louvet¹, Sebastien Dharancy¹, Philippe Mathurin¹, Sylvie Deuffic-Burban³. ¹CHU Lille, Maladies de l'Appareil Digestif, France; ²Université de Lille, INSERM, CHU Lille, U1286-INFINITE, France; ³Université de Paris, INSERM, IAME, France
Email: massih.ningarhari@chu-lille.fr

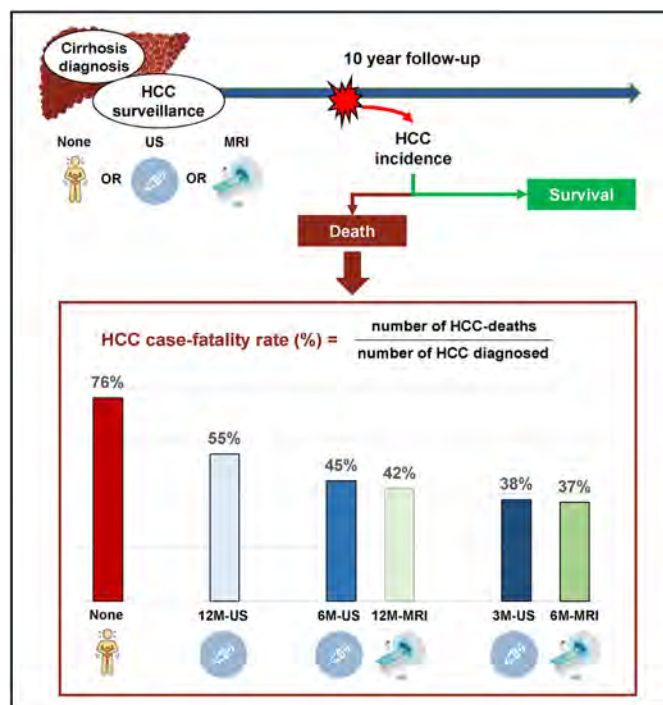
Background and aims: To validate screening programs of solid tumors, expert guidelines now recommend obtaining data supporting reduction of case-fatality rate and cancer-specific mortality. The present study evaluates the benefit of hepatocellular carcinoma (HCC) screening on those outcomes using a modelling approach.

Method: We designed a Markov model to assess 10-year outcomes of HCC surveillance in terms of case-fatality rate (CFR), disease-specific mortality and overall mortality per 100,000 screened patients with compensated cirrhosis. The model simulates the occurrence of HCC, diagnosis through surveillance or symptoms according to tumor growth, treatment, and follow-up. The model evaluates screening in different scenarios varying annual HCC incidence (0.2%, 0.4% or 1.5%), surveillance interval (none, annual (12M), semestrial (6M) or trimestrial (3M)) and imaging modality (US, ultrasound, or MRI, magnetic resonance imaging).

Results: 6M-US screening in comparison to no surveillance reduced 10-year HCC-CFR from 76 to 45%. According to the size of the main tumor, CFRs decreased from 42 to 36% for main nodule size between 1–3 cm, 68 to 61% for main nodule size between 3–5 cm, and 83% to 82% for main nodule size larger than 5 cm. When annual incidences varied from 0.2%, 0.4% to 1.5%, the model predicts reductions of 289, 580 to 2, 110 HCC-related deaths, and of 209, 419 to 1, 521 total deaths, per 100,000 screened patients, respectively. In terms of surveillance modalities, 6M-MRI and 3M-US, in comparison to the

POSTER PRESENTATIONS

recommended 6M-US, yielded reductions of CFRs and cancer-related mortality (−18% and −16%), that were as expected not affected by the variation of incidence. Conversely, effects on overall mortality varied according to annual HCC incidence. In comparison to 6M-US, for incidences varying from 0.2%, 0.4% to 1.5%, 6M-MRI reduced overall mortality from 0.3%, 0.5% to 1.7%, and 3M-US from 0.2%, 0.5% to 1.5%, respectively. Even with extended surveillance interval, 12M-MRI compared to 6M-US leads to a 6% reduction of cancer-related mortality.



Conclusion: Shortening US surveillance or using MRI would reduce HCC case-fatality rate and HCC-related mortality. Conversely, the effect on overall mortality appeared modest. The evaluation of case-fatality rates, absolute numbers of cancer-related and overall deaths, provides additional insights on HCC surveillance.

SAT558

T cell receptor sequencing reveals HCC diversity according to BCLC stages within liver tissue and peripheral blood

Yuwei Zhang¹, Junxiao Wang², Xiubin Li³, Hui Xie², Yijin Wang¹.
¹Southern University of Science and Technology, School of Medicine, Shenzhen, China; ²The Fifth Medical Center of Chinese PLA General Hospital, Department of Invasive Technology, Beijing, China; ³The Third Medical Centre of Chinese PLA General Hospital, Department of Urology, Beijing, China
 Email: yijinwang927015@163.com

Background and aims: T lymphocytes play important roles in human adaptive immune responses and antigen peptides recognition via specific T cell receptors (TCRs). Here we determined the TCR repertoires of tumor, adjacent tissue and PBMC in hepatocellular carcinoma (HCC) patients at different stages, aiming to give a new insight into disease pathogenesis and guiding immune therapy.

Method: We prospectively enrolled 30 patients who were initially diagnosed of HCC at BCLC-A (n = 10), BCLC-B (n = 10), BCLC-C (n = 10), from January 2017 to March 2019 at the 5th Medical Center, Chinese PLA General Hospital. Multi-Immunofluorescence by Tyrosine signal amplification assay was performed in each tumor biopsy to characterize suppressor T lymphocytes with Anti-CD3, Anti-PD1, Anti-CTLA4, and Anti-LAG3 antibodies. Tissue and PBMC samples

were then analyzed by high-throughput deep sequencing of TCR using the ImmuHub TCR profiling system. Ethical approval was obtained from the Institutional Ethics Committee.

Results: The number of CD3+ cells was increased in BCLC_B and BCLC_C stages compared to BCLC_A stages, with the BCLC_B stage being the highest. The ratio of PD1+/CD3+ was significantly higher in BCLC_C than that in BCLC_A and BCLC_B. The number of LAG-3+ cells, as well as the ratio of LAG-3+/CD3+ were gradually increased from BCLC_A to BCLC_C stages (Fig 1).

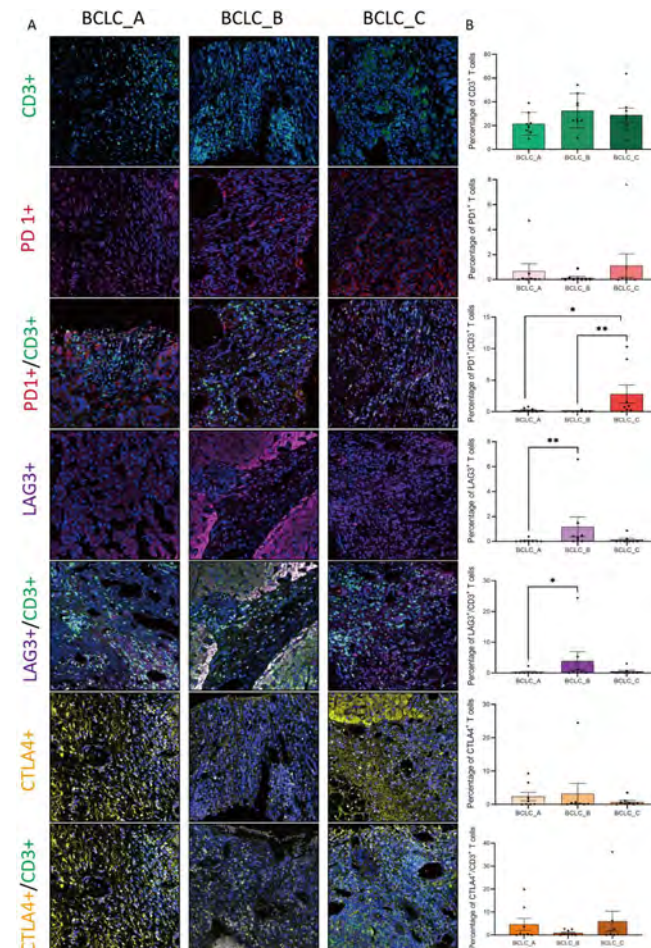


Figure 1:

TCR were successfully sequenced in 78 samples from 28 patients. TRBV5-1, TRBV20-1, TRBJ2-1 and TRBJ2-7 were frequently used in all samples, but seemed no difference between HCC stages. TCR repertoires in tumor tissues are completely different to those in the PBMC, only 4.3% overlaps between tumors and adjacent tissues, and 1.5% overlaps between tumors and PBMCs. Furthermore, a significant expansion of TCR clonality in PBMC, but not in tissues, were observed in BCLC_C patients, compared to BCLC_A and BCLC_B patients (Fig 2A–F). The results were further confirmed by analysis of D75 values (Fig 2G–I) and Shannon index (Fig 2J–L). There was no significant difference in CDR3 length between different stages, neither in PBMC, nor in tissues. Hydrophobic amino acids in both positions 6 and 7 amino acids were less used in BCLC_C than BCLC_A and BCLC_B, either in tumor, adjacent tissues or PBMC (Fig 3).

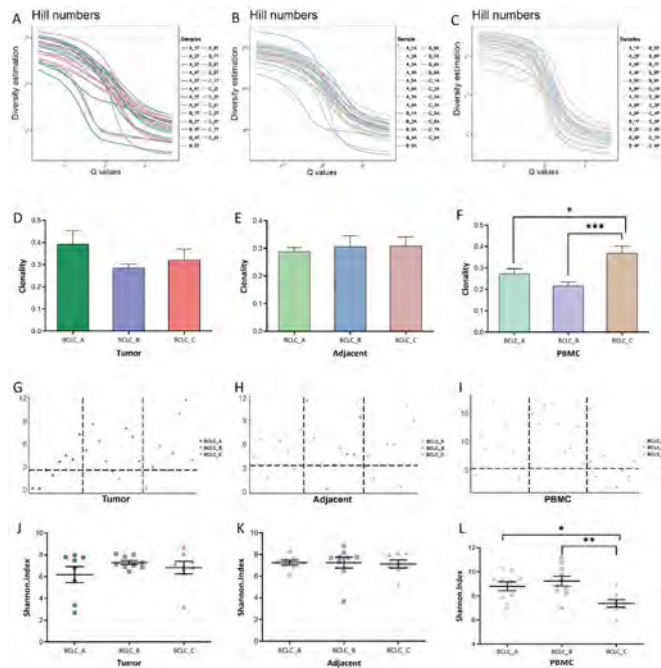


Figure 2:

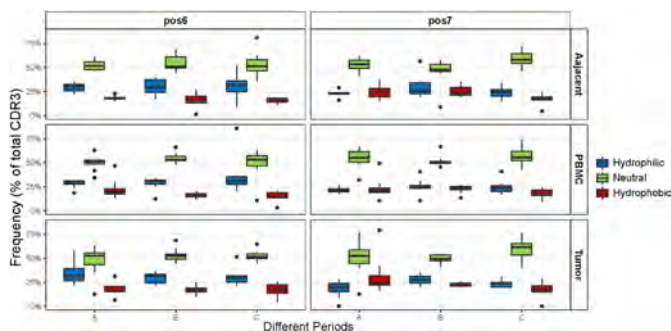


Figure 3:

Conclusion: Despite the number of tumor infiltrating T cells was increased in the BCLC_C stage, most of which were inhibitory T cells, indicating unavailing anti-tumor effect. Through a deep, comprehensive and multidimensional analysis of TCR repertoires, our study found a significant increase in TCR clonality of PBMC in BCLC_C stage, but not in tumors and adjacent. In addition, we found that the use of hydrophobic amino acids at positions 6 and 7 of CDR3 decreased at BCLC_C stage. In conclusion, our findings provide new evidence for future clinical monitoring and immunotherapy of HCC patients.

SAT559

NanoView EV Chip-based profiling in liver cancer differentiation- HCC from intrahepatic CCA-small EVs vs large EVs

Bingduo Wang¹, Tudor Mocan², Sabine K. Urban¹, Adelina Horhat², Dominik Zölzer¹, Zeno Sparchez², Alex Shephard³, Ben Owen³, Arnulf Willms⁴, Ingo G. Schmidt-Wolf⁵, Maria Angeles Gonzalez-Carmona¹, Christian Strassburg¹, Veronika Lukacs-Kornek⁶, Mirosław Kornek¹. ¹University Hospital Bonn, Department of Internal Medicine I, Bonn, Germany; ²Iuliu Hațieganu University of Medicine and Pharmacy, Octavian Fodor Institute for Gastroenterology and Hepatology, Cluj-Napoca, Romania; ³NanoView Biosciences, European Office: Malvern Hills Science Park, Malvern, United Kingdom; ⁴German Armed Forces Central Hospital, Department of General, Visceral and Thoracic Surgery, Koblenz, Germany; ⁵University Hospital Bonn, Center for Integrated Oncology (CIO), Bonn, Germany; ⁶University Hospital Bonn, Institute of Experimental Immunology, Bonn, Germany
Email: wang_bingduo@outlook.com

Background and aims: In spite of recent developments it is still very challenging to differentiate hepatocellular carcinoma (HCC) from intrahepatic cholangiocarcinoma (iCCA). Clinical available methods as CT, MRI and contrast-enhanced ultrasonography demand highest operator skills to achieve a robust differentiation between HCC and iCCA. Here, we utilized NanoView's ExoView® Reader to capture small EVs (sEVs) for further analysis and compared them to large EVs (lEVs) and assessed their clinical performances to differentiate HCC from iCCA. lEVs and sEVs differ in size and biogenesis.

Method: CD44v6⁺, CD133⁺ and double positive cells were confirmed on human CCA and HCC cell lines. sEVs and lEVs from patients' sera were isolated by SEC columns or 10,000 g centrifugation. To quantify lEVs FACS was applied with AnnexinV (AnnV) serving as lEV marker. sEVs were captured with CD9, CD63 and CD81 on ExoView® Tetraspanin Chips according to manufacture's instruction and analyzed for CD44v6 and CD133. Surface analysis of sEVs was performed with ExoView® R100 (NanoView Biosciences, Boston, USA) using their ExoView® Tetraspanin Kit. Data analysis was performed using ExoView® Analyzer 3.0.

Results: 1) CD133 and CD44v6 were differentially expressed in CCA and HCC cell lines, indicating their potential for differential diagnosis. 2) AnnV⁺CD44v6⁺ lEVs were 2.7-fold increased ($p \leq 0.001$) in iCCA patients (AUROC 0.83, 93.3% sensitivity, 71.0% specificity). AnnV⁺CD44v6⁺CD133⁺ lEVs and AnnV⁺CD133⁺ lEVs were not conclusive. 3) Individual sEV subpopulations as characterized by tetraspanins (CD9, CD63 and CD81) plus CD44v6 or CD133 were slightly non-significantly elevated without diagnostic relevancy in iCCA as CD63⁺CD44v6⁺ sEVs (1.36-fold) and CD9⁺CD44v6⁺CD133⁺ (1.43-fold), or reduced as CD9⁺CD44v6⁺ sEVs (0.63-fold). Except and contrary to our lEV data, CD63⁺CD133⁺ sEVs and CD9⁺CD133⁺ sEVs and CD81⁺CD133⁺ sEVs were increased by 6.5-fold ($p = 0.007$) and 3.6-fold ($p = 0.028$) and 9.7-fold ($p = 0.505$). Actually, best clinical performance was observed with CD63⁺CD133⁺ with calculated AUROC of 0.89 ($p = 0.009$) and 87.5% sensitivity and 100% specificity. As expected, no meaningful correlations ($r > 0.5$) were observed with AFP and CA19-9.

Conclusion: Our aim was to differentiate a confirmed liver cancer according to its cancer entity, i.e., if HCC or iCCA and to compare clinical performances of lEVs vs. sEVs. Interestingly, sEVs and lEVs performed contrary. AnnV⁺133⁺ lEVs performed weaker compared to CD63⁺CD133⁺ EVs. Additionally, CD81⁺CD133⁺ sEVs were inferior to CD63⁺CD133⁺ EVs, indicating that sEVs can be further divided into clinical relevant subpopulations by CD9, CD63 and CD81 sEVs plus a biomarker of interest, here CD133, to separate HCC from iCCA via an sEV-based liquid biopsy.

Studies were supported by the German Research Foundation to M.K. (Project# 410853455) and V.L.-K. (Project# 411345524).

POSTER PRESENTATIONS

SAT560

Myosteatorsis and excessive visceral adipose tissue as prognostic factors in patients with hepatocellular carcinoma treated with sorafenib

Min Kyu Kang¹, Yu Rim Lee², Jae Young Jang¹, Jung Eun Song³, Young Oh Kweon², Won Young Tak², SE Young Jang², Changhyeong Lee³, Byung Seok Kim³, Jae-Seok Hwang⁴, Woo Jin Chung⁴, Byoung Kuk Jang⁴, Jeong Ill Suh⁵, Jung Gil Park¹, Soo Young Park². ¹College of Medicine, Yeungnam University, Internal Medicine, Daegu, Korea, Rep. of South; ²School of Medicine, Kyungpook National University, Internal Medicine, Daegu; ³School of Medicine, Daegu Catholic University, Internal Medicine, Korea, Rep. of South; ⁴School of Medicine, Keimyung University, Internal Medicine, Korea, Rep. of South; ⁵College of Medicine, Dongguk University, Korea, Rep. of South
Email: kmggood111@naver.com

Background and aims: Recently, low skeletal muscle mass is significant predictor of mortality in patients with hepatocellular carcinoma (HCC). However, the role of myosteatorsis and visceral adiposity in patients with HCC is not well understood. This study aimed to evaluate the association between body composition and mortality in patients with HCC treated with sorafenib.

Method: From 2008 to 2019, this multicenter, retrospective study included patients with advanced HCC who treated with sorafenib. Body composition parameters were measured using the cross-sectional CT images at the level of L3 vertebra. Visceral adipose tissue index (VATI) and skeletal muscle index (SMI) are defined as the body composition area (cm²) by height squared (m²). Myosteatorsis is defined as mean muscle attenuations values using Hounsfield units (HU).

Results: Of the total 245 patients, 168 (68.6%) died. The non-survival group had higher VATI levels (32.6 vs. 45.7 cm²/m², p = 0.005) and lower HU levels (53.3 vs. 51.0 HU; p = 0.023) than the survival group. By multivariate Cox regression analysis, age (hazard ratio (HR), 0.98, 95% confidence interval (CI), 0.97–1.00; p = 0.018), history of previous treatment (HR, 0.55; 95% CI, 0.40–0.76; p < 0.001), albumin (HR, 0.59; 95% CI, 0.42–0.80; p < 0.001), presence of visceral adiposity (HR, 2.25; 95% CI, 1.49–3.42; p = 0.001), and myosteatorsis (HR, 2.21; 95% CI, 1.53–3.19; p < 0.001) were independently associated with mortality in patients with HCC treated with sorafenib.

Table: Factors associated with mortality by multivariate Cox analysis in HCC patients treated with sorafenib.

Variable	Multivariate analysis		
	Univariate P value*	P value*	Hazard ratio (95% CI)
Age, years	0.148	0.018	0.982 (0.967–0.997)
Male, yes/no	0.955		
BMI, kg/m ²	0.588		
Diabetes, yes/no	0.654		
Hypertension, yes/no	0.905		
Largest tumor diameter, mm	<0.001		
Vessel invasion, yes/no	<0.001		
Extrahepatic metastasis, yes/no	0.698		
Previous treatment history, yes/no	<0.001	<0.001	0.552 (0.400–0.761)
AST, IU/L	<0.001	0.004	1.003 (1.001–1.005)
ALT, IU/L	0.453		
Total bilirubin, mg/dL	0.001		
Albumin, g/dL	0.003	<0.001	0.583 (0.424–0.801)
Total bilirubin, mg/dL	0.831		
Platelet count, 10 ³ /L	0.224		
PT-INR	0.866		
AFP, ng/ml	<0.001	<0.001	1.002 (1.001–1.005)
Creatinine, mg/dL	0.804		
Sarcopenia, yes/no	0.245		
VATI, high/low	0.006	<0.001	2.253 (1.485–3.416)
SATI, high/low	0.146		
Myosteatorsis, yes/no	0.008	<0.001	2.210 (1.533–3.185)

Conclusion: Visceral adiposity and myosteatorsis may be associated with mortality in patients with HCC treated with sorafenib.

SAT561

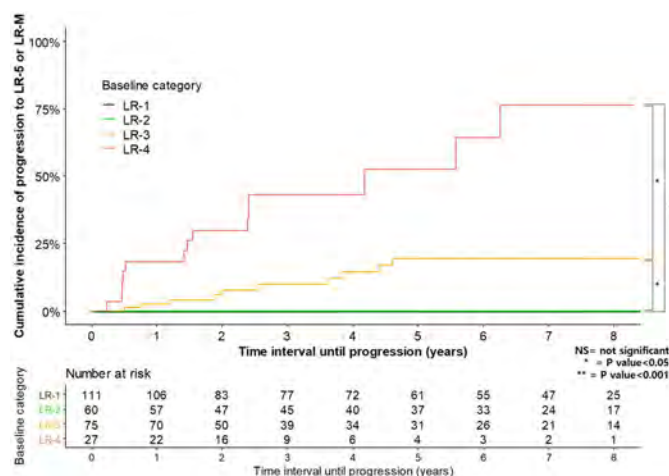
Long term imaging outcomes of liver imaging reporting and data system categories in a prospective hepatocellular carcinoma surveillance cohort

Sang Hyun Choi¹, Byoung Je Kim¹, So Yeon Kim¹, So Jung Lee¹, Jae Ho Byun¹. ¹Asan Medical Center, Radiology, Seoul, Korea, Rep. of South
Email: edwardchoi83@gmail.com

Background and aims: An understanding of the natural history of Liver Imaging Reporting and Data System (LI-RADS) is important. We assessed the imaging outcomes of LI-RADS v2018 categories in prospective hepatocellular carcinoma (HCC) surveillance cohort and determined imaging features significantly predictive of progression to a malignant LI-RADS category.

Method: The imaging outcomes of 183 patients (273 observations) prospectively enrolled between November 2011 and August 2012 were analyzed according to LI-RADS v2018. Cumulative incidences for progression to a malignant category (LR-5 or LR-M) and LR-4 or higher were calculated for each baseline category and compared using log-rank tests. Imaging features significantly predictive of progression to a malignant category were evaluated using Cox proportional hazards modeling.

Results: The 273 observations were initially categorized into 111 LR-1, 60 LR-2, 25 LR-3, and 27 LR-4. For LR-4 observations, the 1-year, 3-year, and 5-year cumulative incidences of progression to a malignant category were 18.5% (95% confidence interval [CI], 6.6–35.2%), 43.0% (95% CI, 23.1–61.5%), and 52.5% (95% CI, 25.9–73.5%), which were significantly higher than those of LR-1, LR-2, and LR-3 (p ≤ 0.009) (Figure). For LR-3, the 1-year, 3-year, and 5-year cumulative incidences of progression to LR-4 or higher were 4.1% (95% CI, 1.1–10.4%), 13.9% (95% CI, 6.7–23.6%), and 23.1% (95% CI, 12.7–35.4%), which were significantly higher than those of LR-1 and LR-2 (p < 0.001). In multivariable analysis, size ≥ 1.0 cm (hazard ratio [HR] = 2.51, 95% CI, 1.08–5.84) and arterial-phase hyperenhancement (HR = 2.91, 95% CI, 1.28–6.62) were significantly independently associated with progression to a malignant category.



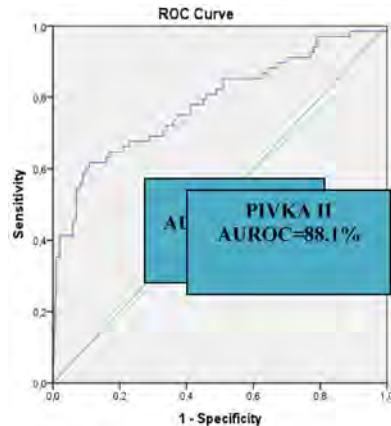
Conclusion: Long-term imaging outcomes differed significantly according to LI-RADS category. Size ≥ 1.0 cm and arterial-phase hyperenhancement were imaging features significantly predictive of progression to a malignant category.

SAT562

Diagnostic accuracy of protein-induced by vitamin K absence (PIVKA-II) for hepatocellular carcinoma (HCC) among caucasian cirrhotic patients with or without diagnostic serum a-fetoprotein (AFP) levels

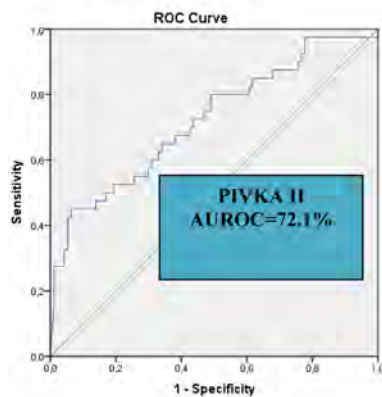
Antonia Syriha^{1,2}, Dionysia Mandilara², Spyridon Pantzios², Ioanna Stathopoulou², Georgia Barla², Petros Galanis^{1,2}, Ioannis Elefsiniotis^{1,2}, ¹General and Oncology Hospital of Kifisia "Agiou Anargyroi," National and Kapodistrian University of Athens, Greece, Academic Department of Internal Medicine-Hepatogastroenterology Unit, Greece
Email: ielefs@nurs.uoa.gr

Background and aims: To evaluate the accuracy of serum biomarkers (AFP, PIVKA-II) for HCC diagnosis among patients with liver cirrhosis. **Method:** 168 consecutive patients with liver cirrhosis (128 males, 91 with CTP score A, 89 with varices, 30 with portal vein thrombosis and 53 with diabetes) with (n = 68, HCC group) or without (n = 100, control group) concomitant histologically confirmed HCC were evaluated for serum levels of the two biomarkers, during a programmed outpatient visit. The mean age of the patients was 65 (\pm 10.8) years and they more often presented with alcoholic or non-alcoholic fatty liver disease (69/168, 41.1%), with the second and third causes of cirrhosis being chronic hepatitis C (44/168, 26.2%) or B (28/168, 16.7%) respectively. Patients with HCC were categorized to stage



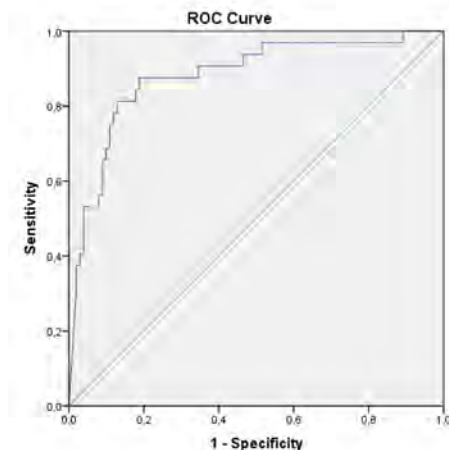
Diagonal segments are produced by ties.

Accuracy of PIVKA-II for the diagnosis of
HCC
in BCLC-C HCC patients
AUROC=0.881 (0.808-0.953)
Proposed Cut-off : 655 mAU/ml



Diagonal segments are produced by ties.

Accuracy of PIVKA-II for the diagnosis of
HCC
excluding HCC patients with AFP >400
ng/ml
AUROC=0.721 (0.622-0.82)
Proposed Cut-off : 1089,53 mAU/ml



Diagonal segments are produced by ties.

Figures: (abstract: SAT562)

POSTER PRESENTATIONS

0/A (n = 11), stage B (n = 16), stage C (n = 32) and stage D (n = 9), according to BCLC staging system.

Results: Mean/median levels of AFP (10835/155 vs 129/4.3, $p < 0.001$) and PIVKA-II (11095/2660 vs 864/46, $p < 0.001$) were significantly higher in HCC group compared to control group. The AUROC curve and the best proposed cut-off value for HCC diagnosis were 82.9% (95%CI 76.3–89.4%)/13.4 ng/ml and 78.4% (95%CI 71.1–85.8%)/654.49 mAU/ml for AFP and PIVKA-II, respectively. The diagnostic accuracy of PIVKA-II among BCLC-C stage HCC patients was the best observed (AUROC = 88.1%, best proposed cut-off value = 655 mAU/ml). Excluding HCC patients with AFP levels above 400 ng/ml, the diagnostic accuracy of PIVKA-II in HCC continued to be significant (best proposed cut-off value 1089.53 mAU/ml) but the AUROC curve (72.1%) for HCC diagnosis was further reduced. It is worth mentioning that extremely high values of PIVKA-II (like those that are noticed in advanced HCC) were observed in 3 cirrhotic patients without HCC following treatment with acenocoumarol (the 2 of them) or having very low levels of vitamin K because of prolonged cholestasis due to sclerosing cholangitis (the third one). In these cases the diagnostic accuracy of the biomarker may be significantly affected.

Conclusion: Both biomarkers showed moderate accuracy for detecting HCC in patients with liver cirrhosis, when they were used separately. The diagnostic accuracy of PIVKA-II in patients with relatively low AFP levels (<400 ng/ml) remained at the same level.

SAT563

An easy to use score to predict survival in patients with hepatocellular carcinoma before the first transarterial chemoembolization session: AFP-DIAM score

Estelle Rebillard², Benjamin Buchard², Nicolas De Abreu³, Mathieu Boulain⁴, Anne Minello Franza⁵, Benoît Magnin³, Maud Reymond², Leon Muti², Bruno Pereira⁶, Armand Aberger².

¹Centre hospitalier Universitaire Estaing de Clermont-Ferrand, Department of Hepatology and Gastroenterology, Clermont-Ferrand, France; ²CHU Estaing, Medecine Digestive et Hepato-Bilaire, Clermont-Ferrand, France; ³CHU Estaing, Radiologie, Clermont-Ferrand, France; ⁴CHU Dijon, Pharmacie, Dijon, France; ⁵CHU Dijon, Hepato-gastroenterologie, Dijon, France; ⁶CHU Gabriel-Montpiéd, Direction de la Recherche Clinique et Innovation, Clermont-Ferrand, France
Email: erebillard@chu-clermontferrand.fr

Background and aims: Transarterial chemoembolization (TACE) is widely used for the treatment of the hepatocellular carcinoma (HCC). TACE is recommended as a palliative treatment for patients with preserved hepatocellular function (either CHILD A or B7 without ascites), with a multinodular HCC without vascular invasion or associated metastasis, with a general preserved state. This profile corresponds to the B stage of the Barcelona Clinic Liver Cancer (BCLC) reference classification. This stage is very heterogeneous with a very different tumor profiles for a single therapeutic option available: TACE. Our aims were to develop a pre-therapeutic easy to use score, to assess the prognosis value of existing scores and to evaluate the prognosis value of the radiological response after two TACE sessions. **Method:** 191 adult cirrhotic patients treated for HCC with TACE in our hospital from 2007 to 2017 were retrospectively included. We investigated the impact of liver function, patient characteristics and tumor burden on overall survival and developed a prognosis score using a regressing model to identify different prognostic groups in patients. Due to the low number of women, the score was only studied in male patients.

Results: Patients had a median age of 66 years and 126 patients were Child A. Two factors were associated with overall survival in the multivariate analysis: AFP > 500 ng/ml and the sum of the diameter of the nodules > 130 mm (AFP-DIAM score). The score distinguishes

two groups with significant difference survival time (median OS 28.3 months for a score = 0 versus 17.7 months for a score > 0). The score developed in this work was validated on an external cohort of 89 patients from Dijon University. Its discrimination capacity (c-index 0.58) is better than the existing scores (c-index STATE 0.55; c-index NIACE 0.54).

After two TACE, the radiological response with a threshold of –65% evaluated by mRECIST, identifies two groups with overall survival significantly different (30.1 versus 25.9 months; Se = 52%, Sp = 70%).

Conclusion: The AFP-DIAM score is a reliable and easy to use score which allows to distinguish two groups with different prognosis before first TACE session. An AFP-DIAM score > 0 identifies patients with dismal prognosis for which the question of a first-line treatment with an immunotherapy-tyrosine kinase inhibitor combination can be raised. Its use could provide further support to BCLC system to guide the therapeutic strategy of patients with HCC.

SAT564

Measurement of protease activity using novel plasma biosensors can accurately detect hepatocellular carcinoma

Tram Tran^{1,2}, Ben Holmes¹, Chris Gulka¹, Anatoly Myaskovsky¹, Andrea Shepard¹, Mackenzie Rowe¹, Sophie Cazanave¹, Fayçal Touti¹, Alejandro Balbin¹, Wendy Winckler¹. ¹Glympse Bio; ²UCLA Division of Digestive Diseases

Email: tttmd@yahoo.com

Background and aims: Hepatocellular carcinoma (HCC) is the 5th leading cancer globally. Suboptimal adherence to routine surveillance and late diagnosis limit treatment options, thus new diagnostic options are needed for at-risk patients. Dysregulated protease activity may occur in HCC in biological pathways including tumor invasion of extracellular matrix, matrix remodeling, inflammation and fibrinolysis. Glympse's novel liquid biopsy (LBx) technology using fluorogenic biosensors and machine learning can sensitively measure protease activity in plasma samples.

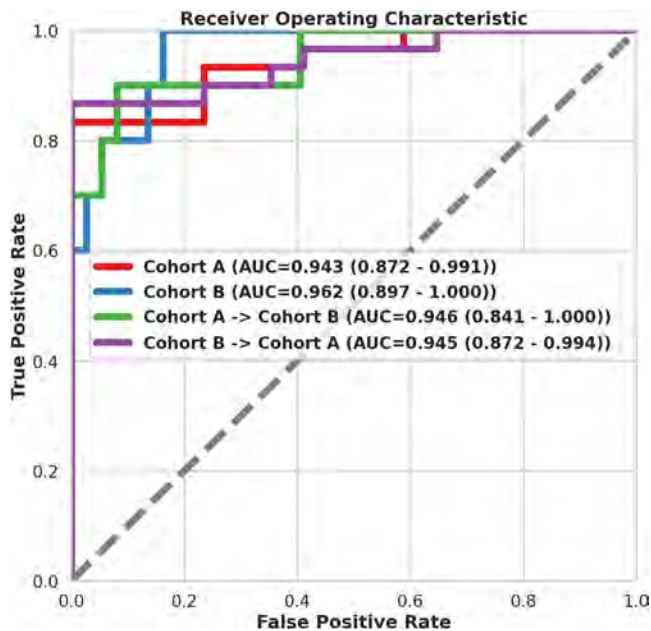
Aims: Assess protease activity changes in plasma of diagnosed HCC patients compared to healthy controls.

Method: We screened >600 peptide substrates to identify a panel of 21 biosensors that interrogate multiple biological pathways implicated in HCC pathogenesis (LBx-HCC). Retrospective plasma samples were obtained from two independent cohorts of patients (pts) diagnosed with HCC (cohorts A and B). Protease biosensor cleavage was assayed from plasma by fluorimetry, and the relative signal was used for classification by regularized logistic regression using 100 cross-validation (80% train, 20% validation splits). Independent classifier models were developed for each cohort and cross-tested without retraining in the second cohort to assess robustness.

Results: In cohort A, 30 pts diagnosed with HCC (M 77%, age 55.8 ± 9.9, BMI 22.3 ± 2.3, Asian 96% and 80% HBV/HCV etiology) were compared to 17 healthy controls (M 59%, age 35.8 ± 12.6, BMI 28.2 ± 4.5, Caucasian 59%/African 24%/Asian 17%).

In cohort B, 10 pts diagnosed with HCC (M 50%, age 59.0 ± 15.4, BMI 23.6 ± 4.7, Caucasian 90% and no underlying viral disease) were compared to 37 healthy controls (M 65%, age 59.2 ± 9.4, BMI 25.8 ± 2.9, Caucasian 100%).

We performed LBx-HCC in all 94 subjects from both cohorts of pts and controls. Protease biosensors were highly effective at differentiating between pts with HCC and healthy controls in both cohorts (cohort A AUC = 0.94 [CI 0.87–1] and cohort B AUC = 0.96 [CI 0.89–1]) (Figure). Importantly, the AUC remains above 0.94 even when naively applying a pre-trained classifier in one cohort to the other despite the differences in the disease etiology of each cohort. The most significant biosensors in HCC were cleaved by DPP4, Cathepsin C, MMP2 and KLK1.



Conclusion: In this study of two independently tested, diverse cohorts of patients with known HCC vs. healthy controls, Glympse's plasma liquid biopsy platform using protease biosensors was highly effective at detecting HCC, with AUCs above 0.94. In the future, this technology could be used in surveillance strategies for earlier, easier, and more accurate diagnosis of HCC.

SAT565

On treatment alpha-fetoprotein reductions predict immunotherapy efficiency in patients with hepatocellular carcinoma

Bernhard Scheiner^{1,2}, Katharina Pomej^{1,2}, Lorenz Balcar^{1,2}, Tobias Meischl^{1,2}, Christian Müller^{1,2}, Michael Trauner¹, Matthias Pinter^{1,2}. ¹Medical University of Vienna, Division of Gastroenterology and Hepatology, Department of Internal Medicine III, Vienna, Austria; ²Medical University of Vienna, Liver Cancer (HCC) Study Group Vienna, Division of Gastroenterology and Hepatology, Department of Internal Medicine III, Vienna, Austria
Email: bernhard.scheiner@meduniwien.ac.at

Background and aims: Immunotherapy with atezolizumab plus bevacizumab represents the new standard of care in systemic front-line treatment of hepatocellular carcinoma (HCC). Biomarkers to predict treatment success are an unmet need. An alpha-fetoprotein (AFP) decrease on treatment might identify patients with a favourable response to immunotherapy.

Method: Patients with HCC treated with PD- (L)1-based immunotherapy between June 2016 and October 2021 at the Medical University of Vienna were included. We investigated the impact of AFP response on radiological response (mRECIST 1.1) as well as time-to-progression (TTP), progression-free survival (PFS) and overall survival (OS). AFP response was defined as AFP decrease by $\geq 25\%$ from baseline at week 6 or AFP within normal range at week 6 after immunotherapy initiation.

Results: Of 83 patients, follow-up AFP values at a median of 6.0 (IQR: 6.0–6.3) weeks after treatment initiation were available in 70 patients and only these patients were included in the final analysis. At baseline, AFP was abnormal in 49 (70%) patients (median: 144 (IQR: 6–1574) ng/ml). In total, 45 (64%) patients achieved an AFP response and this was associated with a significantly better radiological response (which was evaluable in 68 patients): complete/partial response (CR/PR): 38.1% vs. 9.1%, stable disease (SD): 42.9 vs. 27.3%, progressive disease (PD): 19% vs. 63.6% ($p=0.001$), objective

response rate (ORR): 38.1% vs. 9.1% ($p=0.014$). AFP response (OR: 10.5 (IQR: 1.6–67.7), $p=0.014$) remained an independent predictive parameter for ORR even after multivariable adjustment for baseline AFP ≥ 100 ng/ml, C-reactive protein (CRP) ≥ 1 mg/dL, Child-Pugh stage, ECOG PS >1 , presence of macrovascular invasion or extrahepatic metastasis by binary logistic regression analysis. Patients achieving an AFP response also had an improved outcome: time-to-progression (TTP): 11.0 (95%CI: 9.8–12.2) vs. 2.5 (95%CI: 2.0–3.0) months ($p=0.007$); progression-free survival (PFS): 10.4 (95%CI: 5.2–15.5) vs. 2.3 (95%CI: 1.9–2.7) months ($p=0.009$); overall survival (OS): 21.8 (95%CI: 7.4–36.2) vs. 8.5 (95%CI: 0–23.9) months ($p=0.259$).

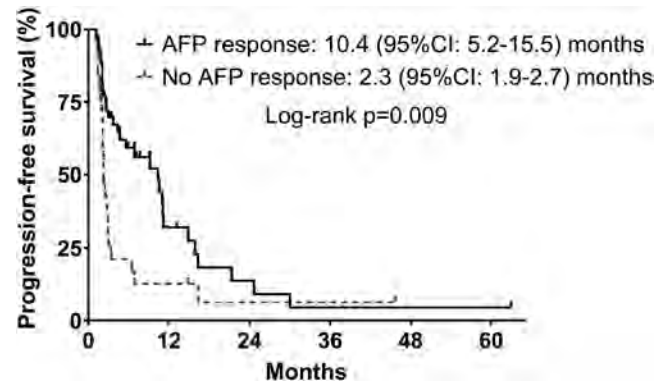


Figure: Comparison of progression-free survival between patients with versus without AFP response (as defined by an AFP decrease $\geq 25\%$ or normal AFP values at week 6)

Conclusion: AFP decrease by $\geq 25\%$ or normal AFP at week 6 after immunotherapy initiation identifies patients with favourable radiological response and survival.

SAT566

Gender differences in hepatocellular carcinoma : is it all due to adherence to surveillance? A study of 1, 716 patients over 3 decades

Wei-Lun Liou¹, Terence Tan¹, Kaina Chen¹, Boon Bee George Goh¹, Pik Eu Jason Chang¹, Chee-Kiat Tan¹. ¹Singapore General Hospital, Department of Gastroenterology and Hepatology, Singapore
Email: liouweilun@gmail.com

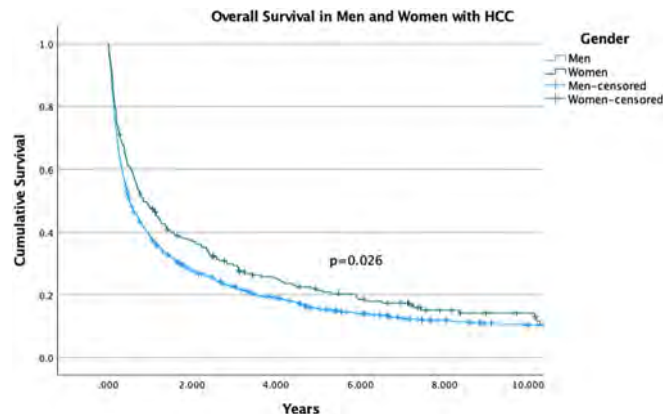
Background and aims: Hepatocellular carcinoma (HCC) is one of the commonest causes of cancer-related death worldwide. There is well-established gender disparity in the incidence of HCC, with men 4 times more common than women. Whether gender is an independent factor for HCC survival is debatable. We study the influence of gender on clinical characteristics of HCC and on survival.

Method: We have an ongoing HCC database since 1988 enrolling patients with HCC seen in our department. Clinical data were prospectively captured. We studied and compared demography, HCC characteristics and survival between men and women. Survival analysis was censored on 31 October 2015 with input from our National Registry of Deaths.

Results: There were 1, 716 HCC patients as of August 2021. 343 (20.0%) were women. Women were significantly older at HCC diagnosis (median 69 vs 62 years, $p<0.001$). Women had a significantly higher incidence of non-viral liver disease (33.8% vs 24%, $p<0.001$). In terms of specific aetiology, autoimmune liver disease was more common (2% vs 0.2%), and alcohol was less common (0.9% vs 5.8%) in women (both $p<0.001$). More women were diagnosed via regular HCC surveillance (37.9% vs 29.6%, $p=0.003$). Hence, women had less-advanced HCC at diagnosis as seen by higher frequency of single lesion (60.8% vs 52.7%, $p<0.001$), smaller median tumour diameter (30 mm vs 39.5 mm, $p=0.038$), lower frequency of portal vein tumour thrombus (19.4% vs 33.4%, $p<0.001$) and less distant metastases (7.7% vs 11%, $p=0.043$). Similarly,

POSTER PRESENTATIONS

significantly more women were in BCLC stages 0/A (39.7% vs 28.4%, $p < 0.001$). The overall median survival was significantly better in women (10.1 vs 6.1 months, $p = 0.003$). When stratified by surveillance status, there was no significant gender difference in survival.



Conclusion: In this large cohort of Asian patients, women diagnosed with HCC were significantly more adherent to HCC surveillance and hence presented with less advanced HCC and had better overall survival than men. The gender difference in survival is likely due to women having better adherence with HCC surveillance.

SAT567

Non-alcoholic fatty liver disease and increased risk of incident primary liver tumours: a meta-analysis of observational cohort studies

Andrea Dalbeni¹, Alessandro Mantovani², Simone Conci², Tommaso Valigi², Alfredo Guglielmi², David Sacerdoti². ¹University of Verona, Medicine, Verona, Italy; ²University of Verona, Verona, Italy
Email: andrea.dalbeni@aovr.veneto.it

Background and aims: We performed a meta-analysis of cohort studies to quantify the magnitude of the association between non-alcoholic fatty liver disease (NAFLD) and risk of incident primary liver tumors, including hepatocellular carcinoma (HCC), cholangiocarcinoma (CC) and hepato-cholangiocarcinoma (HCC-CC).

Method: We systematically searched PubMed, Scopus and Web of Science databases from the inception date to 30 June 2021, using predefined keywords, to identify observational cohort studies conducted in individuals in whom NAFLD was diagnosed by imaging techniques, International Classification of Diseases codes or biopsy. Meta-analysis was performed using random-effects modelling.

Results: We included 9 cohort studies for a total of 9,134,982 middle-aged individuals (10.6% with NAFLD) and 7,026 incident cases of primary liver tumors, over a median follow-up of 10 years. NAFLD was significantly associated with a nearly 2-fold increased risk of developing primary liver tumors (random-effects hazard ratio [HR] 2.07, 95% confidence interval [CI] 1.62–2.65; $I^2 = 97.2\%$). After stratifying the eligible cohort studies by country, we observed that among non-Asian individuals the presence of NAFLD was associated with an approximately 3-fold increased risk of developing primary liver tumors (random-effects HR 2.88, 95% CI 1.78–4.66; $I^2 = 97.2\%$), whereas such association was less strength amongst Asian individuals (random-effects HR 1.55, 95% CI 1.33–1.80; $I^2 = 79.6\%$). Regarding different types of primary liver tumors, NAFLD was associated with a 3.2-fold increased risk of developing HCC (random-effects HR 3.21, 95% CI 1.93–5.33; $I^2 = 96.7\%$), as well as with a 46% increased risk of developing CC or HCC-CC (random-effects HR 1.46, 95% CI 1.27–1.69; $I^2 = 80.7\%$). Sensitivity analyses did not substantially alter these findings. Funnel plot did not reveal any significant publication bias.

Conclusion: This meta-analysis confirms that NAFLD is associated with an increased risk of developing primary liver tumors (especially HCC) over a median follow-up of 10 years. Further research is required to elucidate the complex link between NAFLD and different types of primary liver tumors.

SAT568

Characterization of gut microbiota and exploration of potential predictive model for hepatocellular carcinoma microvascular invasion

Ningning Zhang¹, Zeyu Wang¹, Jiayu Lv², Yang Liu¹, Tian Liu¹, Shuwen Zhang¹, Wang Li¹, Lan Gong^{3,4}, Xiaodong Zhang⁵, Emad El-Omar^{3,4}, Wei Lu¹. ¹Department of Hepatobiliary Oncology, Liver Cancer Center, Tianjin Medical University Cancer Institute and Hospital, National Clinical Research Center for Cancer, Key Laboratory of Cancer Prevention and Therapy, Tianjin Medical University, Tianjin, China; ²Department of Hepatology, Tianjin Third Central Hospital, Tianjin, China; ³Department of Medicine, University of New South Wales, Sydney, Australia; ⁴Microbiome Research Centre, St George and Sutherland Clinical School, University of New South Wales, Sydney, Australia; ⁵Department of Gastrointestinal Cancer Biology, Liver Cancer Center, Tianjin Medical University Cancer Institute and Hospital, National Clinical Research Center for Cancer, Key Laboratory of Cancer Prevention and Therapy, Tianjin Medical University, Tianjin, China
Email: mail4luwei@163.com

Background and aims: The correlation between gut microbiota and microvascular invasion (MVI) in hepatocellular carcinoma (HCC) patients remains unclarified. Prediction of MVI through gut microbiota analysis of HCC patients would be of accurate, non-invasive and very convenient assessment. The aim of the present study was to investigate the characteristics of gut microbiota in HCC-MVI patients and establish a microbial prediction model of HCC-MVI based on microbiome study.

Method: Fecal samples were collected from 59 HCC patients (24 of the total with MVI disease) and 16 healthy controls, and further analyzed by 16S rRNA amplicon sequencing. Bioinformatics methods were used to analyze the obtained sequence data. The diagnostic performance of microbiome characteristics in predicting MVI was assessed by receiver operating characteristic (ROC) curves. The correlation between gut microbiota and tumor microenvironment (TME) in HCC-MVI group were further analyzed with Immunohistochemistry and immunofluorescence assay.

Results: A significant differentiation trend of microbiota composition and structure was observed between the HCC-MVI group and those without vascular invasion (HCC-NVI). Compared with HCC-NVI group and healthy controls, *Klebsiella*, *Proteobacteria*, *Prevotellaceae* and *Enterobacteriaceae* were significantly enriched, whereas *Firmicutes*, *Ruminococcus* and *Monoglobaceae* were significantly decreased in HCC-MVI fecal samples. *Klebsiella* was considered to be the key microbiome signature for HCC-MVI patients. The area under the curve of the established HCC-MVI microbial prediction model was 94.81% (95% confidence interval: 87.63%–100%). The percentage of M2 type tumor-associated macrophage (TAMs) was increased in HCC-MVI group compared with HCC-NVI group ($p < 0.001$). M2-type TAMs in TME was negatively correlated with Shannon and Simpson index of HCC-MVI gut microbiota (all $p < 0.01$). In addition, predicted KEGG pathways showed that the functional differences in metabolic pathways of microbiome varied with groups.

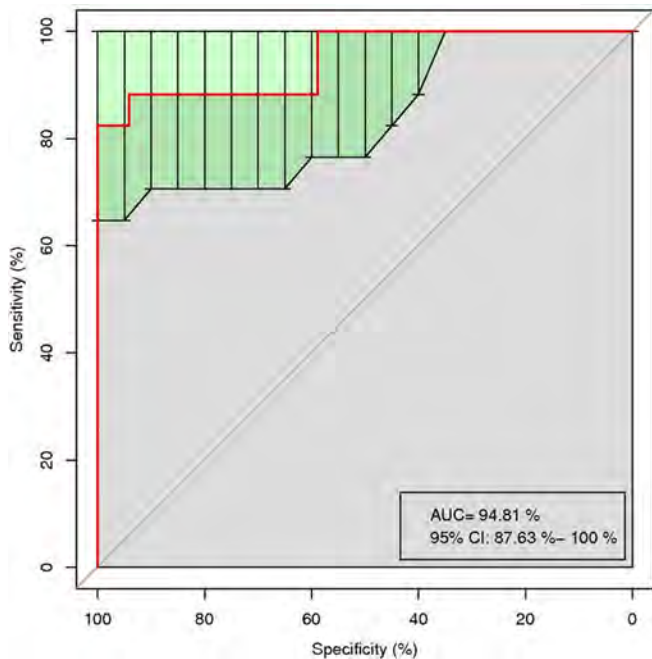


Figure: ROC curves built with twenty significant microbiotas for HCC-MVI predicting.

Conclusion: The results indicated that differences existed in the fecal microbiome of HCC-MVI patients and healthy controls, the prediction model of HCC-MVI established with certain gut bacteria signature may have potential to predict HCC-MVI and the characteristics of fecal microbiome in HCC patients may associate with TME, though future larger-sample studies are required to validate this supposition.

SAT569

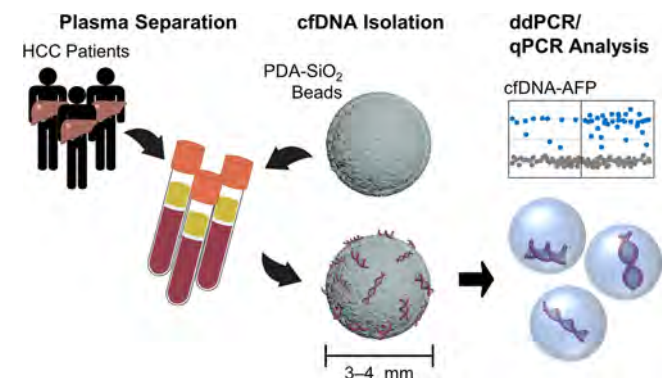
Machine learning algorithm based on dual screening for hepatocellular carcinoma using circulating cell-free DNA and cfDHCC scoring system

Taehee Lee^{1,2}, Piper A. Rawding³, Jiyoung Bu^{3,4}, Sung Hee Hyun⁵, Woo Sun Rou⁶, Kim Seok Hyun^{7,8}, Byung Seok Lee^{7,8}, Luke J. Kubiatowicz³, DaWon Kim^{3,4}, Seungpyo Hong^{3,4,9}, Hyuk Soo Eun^{7,8}. ¹Graduate School, Eulji University, Department of Senior Healthcare, Uijeongbu-si, Korea, Rep. of South; ²Research Institute for Future Medical Science, Chungnam National University Sejong Hospital (CNUSH), Sejong, Korea, Rep. of South; ³University of Wisconsin-Madison, Pharmaceutical Sciences Division, School of Pharmacy, Madison, United States; ⁴University of Wisconsin-Madison, Wisconsin Center for NanoBioSystems (WisCNano), Madison, United States; ⁵Department of Senior Healthcare, Graduate School, Eulji University, Uijeongbu-si, Korea, Rep. of South; ⁶Chungnam National University Sejong Hospital (CNUSH), Department of Internal Medicine, Sejong, Korea, Rep. of South; ⁷Chungnam National University School of Medicine, Department of Internal Medicine, Daejeon, Korea, Rep. of South; ⁸Chungnam National University Hospital, Department of Internal Medicine, Daejeon, Korea, Rep. of South; ⁹Yonsei Frontier Lab and Department of Pharmacy, Yonsei University, Seoul, Korea, Rep. of South Email: hyuksoo@cnu.ac.kr

Background and aims: Hepatocellular carcinoma is diagnosed clinically by computed tomography or magnetic resonance imaging with or without level of serum AFP. However, there is a problem of high cost and radiation hazard to perform the above tests every time for diagnosis. While the current gold standard for diagnosing HCC is tumor biopsies, it only provides a limited snapshot of tumors and vary in sensitivity due to difficulties in identifying lesions. Therefore, we designed a non-invasive, low cost liquid biopsy platform based on the analysis of circulating cell-free DNA (cfDNA) for the early diagnosis and evaluation of prognosis for HCC.

Method: Our platform was consisting of the polydopamine-silica hybrids alginate beads, in order to enhance the cfDNA adsorption. Overall, 249 individuals were enrolled in this study, including 152 patients with HCC, 43 patients with liver cirrhosis (LC), 24 patients with alcoholic liver disease (LA), and 30 healthy individuals (HD). We integrated the expression profiles of plasma cfDNA and cfDNA-AFP to establish a cfDNA score (cfD_{HCC}) specific to HCC patients using a series of machine learning techniques, including the *k*-means cluster analysis, elbow method, and principal component analysis.

Results: Plasma cfDNA levels were the highest among patients with HCC (median: 0.25 ng/μL), followed by LC (0.18 ng/μL), LA (0.11 ng/μL), and HD (0.06 ng/μL), *p* value <0.001. The AUROC of plasma cfDNA levels was 0.713 (*p* = 0.001), 0.592 (*p* = 0.066), and 0.805 (*p* < 0.001) for detecting HCC from LC, LA, and HD groups, respectively. The AUROC of cfDNA-AFP to differentiate HCC from LC, LA, and HD were 0.861 (*p* < 0.001), 0.744 (*p* < 0.001), and 0.971 (*p* < 0.001), respectively. In TACE-treated HCC patients, in the evaluation of overall survival using the cfD_{HCC} score, the group with the high cfD_{HCC} score showed a trend of poorer prognosis than the group with the low cfD_{HCC} score (47.7 ± 5.6 vs. 65.7 ± 4.4 months, *p* = 0.077). Moreover, the group with the high cfD_{HCC} score showed a poorer prognosis than the group with the low cfD_{HCC} score, when the cfD_{HCC} score was used in the evaluation of recurrence-free survival for recurrence with tumor multifocality (23.2 ± 5.5 vs. 54.0 ± 4.6 months, *p* = 0.001) or marginal recurrence (27.4 ± 6.3 vs. 41.1 ± 6.3 months, *p* = 0.061) in TACE-treated HCC patients.



Conclusion: Our novel platform showed high diagnostic and prognostic capabilities. Our results presented herein indicate that cfDNA using polydopamine-silica hybrids alginate beads could be a promising tools for HCC diagnosis and evaluation of prognosis. It could be potentially utilized in the clinic as a reliable system for identifying HCC in early stages, guiding therapeutic decisions, and improving overall survival of HCC patients.

SAT570

Sarcopenia impairs survival and treatment efficacy in patients with hepatocellular carcinoma undergoing immunotherapy

Bernhard Scheiner^{1,2}, Katharina Lampichler³, Katharina Pomej^{1,2}, Lucian Beer³, Lorenz Balcar^{1,2}, Tobias Meischl^{1,2}, Christian Müller^{1,2}, Michael Trauner¹, Martina Scharitzer³, Dietmar Tamandl³, Matthias Pinter^{1,2}. ¹Medical University of Vienna, Division of Gastroenterology and Hepatology, Department of Internal Medicine III, Vienna, Austria; ²Medical University of Vienna, Liver Cancer (HCC) Study Group Vienna, Division of Gastroenterology and Hepatology, Department of Internal Medicine III, Vienna, Austria; ³Medical University of Vienna, Department of Biomedical Imaging and Image-Guided Therapy, Vienna, Austria

Email: bernhard.scheiner@meduniwien.ac.at

Background and aims: Sarcopenia is a common problem in patients with cirrhosis and hepatocellular carcinoma (HCC) and frequently

POSTER PRESENTATIONS

impairs the clinical course of these patients. The impact of baseline sarcopenia on survival and treatment efficacy in HCC patients undergoing immunotherapy has yet to be evaluated.

Method: Patients with HCC treated with PD- (L)1-based immunotherapy between June 2016 and October 2021 at the Medical University of Vienna were included. Sarcopenia was defined by transversal psoas muscle thickness (TPMT) at <12 mm/m in men and <8 mm/m in women at the level of the third lumbar vertebrae using cross-sectional imaging (CT/MRI) at baseline. We investigated the impact of sarcopenia on radiological response (mRECIST 1.1) as well as time-to-progression (TTP), progression-free survival (PFS) and overall survival (OS).

Results: TPMT was evaluated at a median of 20 (IQR 0–38) days prior to first immunotherapy infusion and sarcopenia was present in 37/83 (45%) patients. Sarcopenia at baseline was much more prevalent in men (53%) compared to women (19%, $p = 0.006$) and the presence of sarcopenia was associated with a worse radiological response (which was evaluable in 68 patients): complete/partial response (CR/PR): 11.5% vs. 35.7%, stable disease (SD): 30.8% vs. 40.5, progressive disease (PD): 57.7% vs. 23.8% ($p = 0.011$).

Patients with sarcopenia also had a significantly worse outcome (evaluable in 81 patients due to early loss-of-follow-up in 2 patients): time-to-progression (TTP): 2.5 (95%CI: 1.9–3.1) vs. 10.4 (95%CI: 8.7–12.1) months ($p = 0.010$); progression-free survival (PFS): 2.3 (95%CI: 1.8–2.7) vs. 9.2 (95%CI: 2.5–15.9) months ($p = 0.002$); overall survival (OS): 5.3 (95%CI: 2.5–8.0) vs. 22.6 (95%CI: 8.6–36.6) months ($p = 0.012$). Even after multivariable adjustment for baseline Child-Pugh stage, ECOG PS >1, presence of macrovascular invasion or extrahepatic metastasis and baseline AFP levels (IU/ml), sarcopenia (aHR: 2.24, 95%CI: 1.17–4.31, $p = 0.016$) remained an independent predictor of survival.

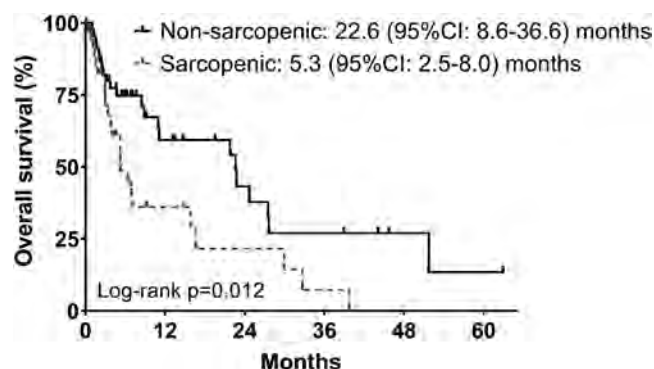


Figure: Comparison of overall survival (OS) between sarcopenic and non-sarcopenic patients prior to initiation of immunotherapy

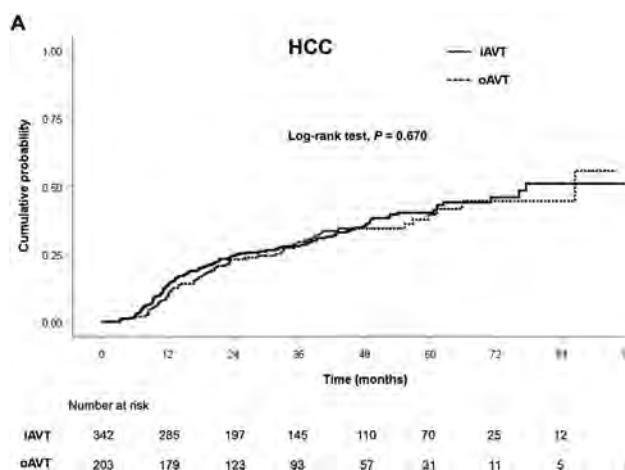


Figure: (abstract: SAT571)

Conclusion: The presence of sarcopenia as determined by TPMT measurement at the level of the third lumbar vertebrae prior to treatment initiation significantly impairs survival and treatment efficacy in HCC patients undergoing immunotherapy.

SAT571

Comparable efficacy between on-going vs. initiation of antiviral therapy at the time of curative treatment for hepatitis B virus-related hepatocellular carcinoma

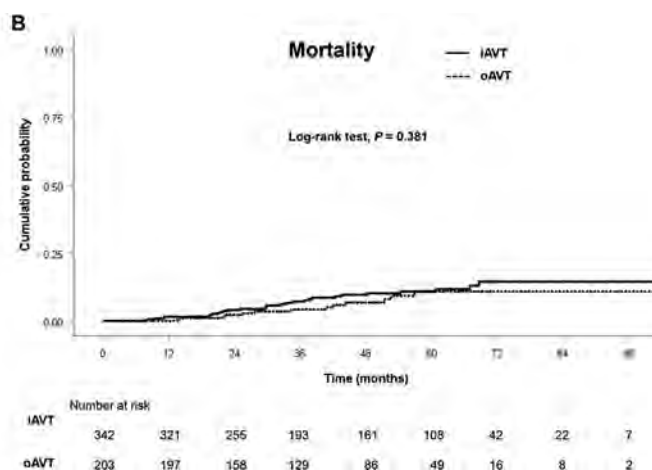
Mi Na Kim¹, Beom Kyung Kim², Su Jong Yu³, Seung Up Kim². ¹CHA Bundang Medical Center, CHA University School of Medicine, Department of Internal Medicine, Seongnam, Korea, Rep. of South; ²Yonsei University College of Medicine, Department of Internal Medicine, Seoul, Korea, Rep. of South; ³Seoul National University College of Medicine, Department of Internal Medicine, Seoul, Korea, Rep. of South
Email: ksukorea@yuhs.ac

Background and aims: Antiviral therapy (AVT) should be applied for patients with newly-diagnosed hepatocellular carcinoma (HCC), if HBV DNA is detectable. We compared the long-term prognosis between patients with on-going AVT and those who initiated AVT at the time of curative treatments for HBV-related HCC.

Method: Between 2013 and 2018, patients with HBV-related HCC who received curative treatments were considered eligible. Primary outcomes were HCC recurrence and overall mortality.

Results: In the study population ($n = 545$), the cumulative probabilities of HCC recurrence at 1, 3, and 5 years was statistically similar between patients in on-going AVT group (oAVT group, 9.9%, 29.4%, and 39.5%, respectively) and those in the initiation AVT group (iAVT group, 13.1%, 27.8%, and 40.2%, respectively) ($p = 0.670$ by log-rank test). The cumulative probabilities of overall mortality was also comparable between the 2 groups (4.2%, 10.8%, and 10.8%, respectively, in oAVT group vs. 1.5%, 7.1%, and 10.8%, respectively, in iAVT group) ($p = 0.381$ by log-rank test). The risk of the early (<2 years) and late (≥ 2 years) recurrence was statistically similar between the 2 groups (all $p > 0.05$ by log-rank tests). Propensity score matching and inverse probability of treatment weighting analysis also yielded a similar risk of HCC recurrence and overall mortality between the 2 groups (all $p > 0.05$ by log-rank tests).

Conclusion: The long-term prognosis of patients who received curative treatments for newly diagnosed HBV-related HCC was comparable regardless of the timing of AVT initiation.



SAT572

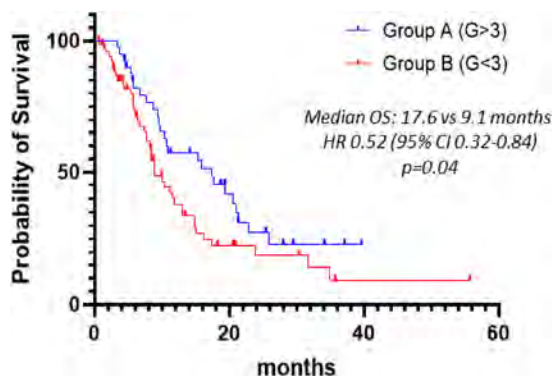
Immune-related adverse events and clinical outcomes in unresectable hepatocellular carcinoma: a single-institute retrospective analysis

Antonella Cammarota^{1,2}, Nicola Personeni^{1,2}, Tiziana Pressiani¹, Antonio D'Alessio^{2,3}, Valentina Zanuso^{1,2}, Silvia Bozzarelli¹, Laura Giordano¹, Lorenza Rimassa^{1,2}, Armando Santoro^{1,2}.
¹Humanitas Research Hospital, Oncology and Hematology Unit, Cascina Perseghetto, Italy; ²Campus Humanitas University, Department of Biomedical Sciences, Pieve Emanuele, Italy; ³Imperial College London, Department of Surgery and Cancer, London, United Kingdom
 Email: antonella.cammarota@humanitas.it

Background and aims: Immune checkpoint inhibitors (ICIs), as monotherapy or in combinations, have broadened the treatment landscape of unresectable hepatocellular carcinoma (HCC), either in first-line or in further lines. The prognostic role of multikinase inhibitors-induced adverse events has been proven in HCC patients (pts) and the development of immune-related adverse events (irAEs) has been associated with improved outcomes in other cancer types, such as melanoma and non-small cell lung cancer. Despite initial evidence of correlation, whether or not irAEs can predict outcomes in unresectable HCC still needs to be confirmed. In this retrospective analysis we aimed to assess the association between grade (G) = 3 irAEs and the efficacy outcomes, namely overall response rate (ORR), overall survival (OS), progression-free survival (PFS) among pts with unresectable HCC treated with ICIs.

Method: ORRs were calculated as the sum of complete and partial responses per RECIST 1.1 and compared using chi-squared test. OS and PFS were estimated using the Kaplan-Meier method and survival curves were compared using log-rank test. Statistical significance was set at $p = 0.05$ and all reported p values are two-sided.

Results: From August 2015 to March 2021, 110 pts with unresectable HCC received ICIs within clinical trials available at our Institution. A total of 58 pts (52.7%) received ICIs as first-line systemic treatment and 36 pts (32.7%) received single-agent ICI. Overall, 38 pts (group A) developed $G \geq 3$ toxicities whereas 72 pts (group B) experienced no or $G < 3$ toxicities. The most common $G \geq 3$ AEs were hepatic (28.9%), dermatological (13.2%) and gastrointestinal (7.9%) toxicities. ORR was 18.4% in group A and 11.1% in group B ($p = 0.96$). Median PFS was 6.9 and 3.9 months (HR 0.66, 95% CI 0.43–0.99, $p = 0.04$) and median OS was 17.6 and 9.1 months (HR 0.52, 95% CI 0.32–0.84, $p = 0.04$) in group A and B, respectively (Figure 1).



Conclusion: Despite the small sample size and the retrospective nature, our analysis suggests that the development of $G \geq 3$ irAEs might correlate with survival outcomes in unresectable HCC. Prospective analyses are needed to confirm these results, hopefully providing further insights on possible predictive biomarkers.

SAT573

Multistage epigenome-wide association study identifies highly accurate epigenomic signatures in association with hepatocellular carcinoma: The HCC epigenome score

Abderrahim Oussalah¹, Ryan Hlady², Sébastien Hergalant¹, Jean-Pierre Bronowicki¹, Jean-Louis Guéant¹, Chen Liu³, Keith Robertson². ¹University of Lorraine, INSERM UMR_S 1256, Nutrition, Genetics, and Environmental Risk Exposure (NGERE), Faculty of Medicine of Nancy, F-54000 Nancy, France; ²Department of Molecular Pharmacology and Experimental Therapeutics, Mayo Clinic, Rochester, MN, 55905, USA; ³Department of Pathology, Yale School of Medicine, New Haven, CT, 06510, USA
 Email: abderrahim.oussalah@univ-lorraine.fr

Background and aims: Hepatocellular carcinoma (HCC) represents the most common primary malignant tumor of the liver. Epigenomic alterations are a common hallmark of human cancer. We recently developed the smoothing method for calculating and visualizing data from epigenome-wide association studies (EWASs) and demonstrated its utility for identifying highly accurate epigenomic signatures in DNA methylation analyses (patent pending, EP21306458). The primary aim was to look for significant epigenomic signatures associated with HCC through a multistage EWAS approach.

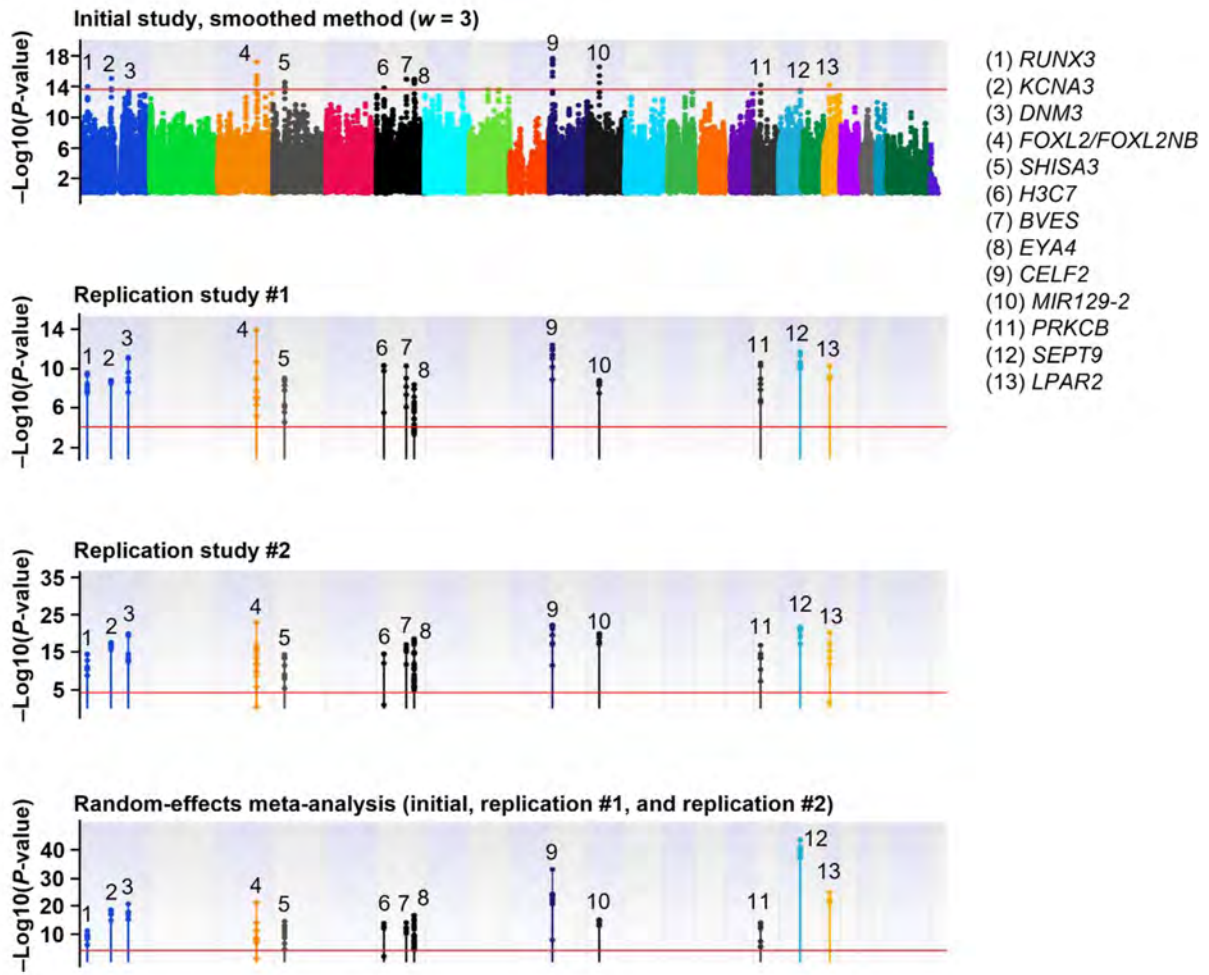
Method: We conducted four-step epigenome association studies of HCC in 357 cases and 239 controls originating from four independent cohorts. In stage #1 (derivation study), we analyzed the epigenome-wide DNA methylome profiles generated from 21 HCC and 100 non-HCC liver tissue samples using the Infinium Human Methylation 450 K BeadChip. We derived an epigenomic score based on the top significant CpG signatures, the “HCC Epigenome Score.” We assessed the diagnostic accuracy of the “HCC Epigenome Score” in two replication cohorts using HCC and non-HCC tissue samples (stage #2: 26 vs. 83; stage #3: 306 vs. 50, respectively). In stage #4, we performed in silico epigenome association study using epigenome-wide DNA methylome profiles generated from 10 plasma samples of patients with ($n = 4$) or without HCC ($n = 6$).

Results: The epigenome-wide association study highlighted 105 CpG probes in 13 top loci (CpG islands) associated with the HCC phenotype (*RUNX3*, *KCNA3*, *DNM3*, *FOXL2/FOXL2NB*, *SHISA3*, *H3C7*, *BVES*, *EYAA*, *CELF2*, *MIR129-2*, *PRKCB*, *SEPT9*, and *LPAR2*) (Figure, **panel A**) (patent pending, EP21306459). In hierarchical clustering analysis, the 105 CpG probes were highly discriminant between HCC and non-HCC samples (Figure, **panel B**). In ROC analysis, the HCC Epigenome Score had an AUROC of 0.960 (95% CI, 0.788–1.00; $p < 0.0001$) for detecting HCC samples. In replication studies on tissue samples (stages #2 and #3), all the 13 loci were significantly associated with the HCC phenotype. Random effect meta-analysis confirmed the significance of the 13 top loci. In ROC analysis that used individual-level data, the HCC Epigenome score had an AUROC of 0.955 (95% CI, 0.935–0.969; $p < 0.0001$) for detecting HCC. According to the underlying chronic liver disease, the HCC Epigenome score had AUROCs of 0.992 (95% CI, 0.968–0.998; $p < 0.0001$); 0.982 (95% CI, 0.935–0.995; $p < 0.0001$); 0.950 (95% CI, 0.671–1.000; $p < 0.0001$); 0.908 (95% CI, 0.845–0.952; $p < 0.0001$), and 0.952 (95% CI, 0.902–1.000; $p < 0.0001$) for HCV, HBV, NASH, alcohol, and other etiologies, respectively. Using plasma circulating cell-free DNA (stage #4), the HCC epigenome score discriminated between HCC and non-HCC patients.

Conclusion: Using four independent cohorts, we derived and validated the HCC epigenome score that showed high diagnostic accuracy for diagnosing HCC.

POSTER PRESENTATIONS

A



B

The HCC Epigenome Score

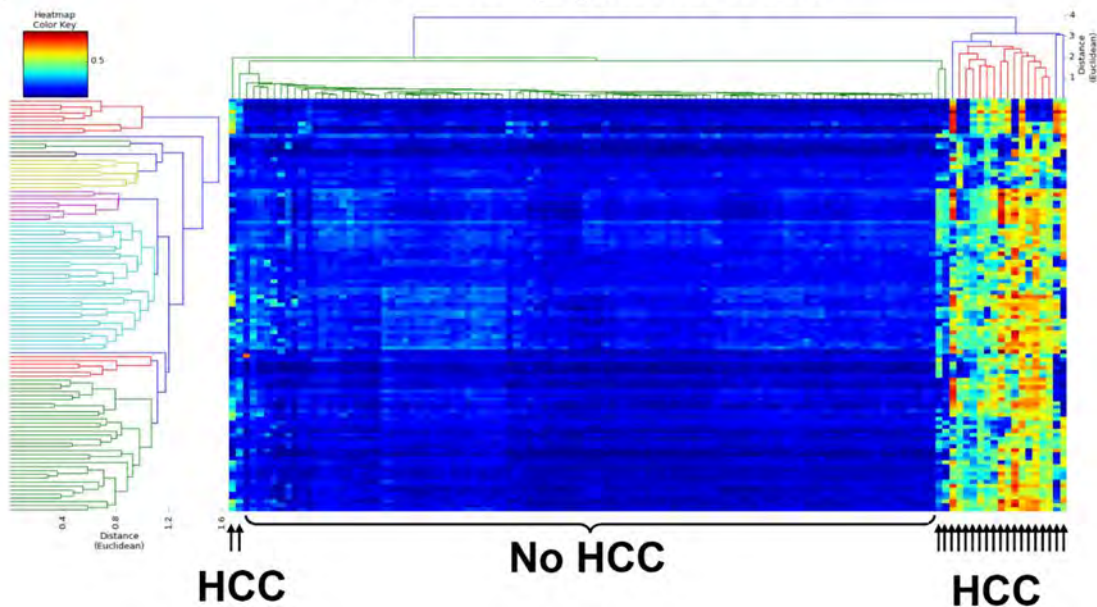


Figure: (abstract: SAT573)

SAT574

Interleukin-6 as a new marker for advanced sarcopenic HCC patients with different cirrhotic aetiology

Andrea Dalbeni¹, Filippo Cattazzo¹, Antonio Vella¹, Giovanna Zanon¹, Michele Bevilacqua¹, Jasmin Kassem¹, Anna Mantovani¹, Simone Conci¹, Tommaso Campagnaro¹, Alfredo Guglielmi¹, Michele Milella¹, David Sacerdoti¹. ¹University of Verona, Medicine, Verona, Italy

Email: andrea.dalbeni@aovr.veneto.it

Background and aims: Hepatocellular carcinoma (HCC) is a major cause of liver cancer-related death worldwide. It usually occurs in cirrhosis with different aetiopathogenesis. Serum IL-6 is a pro-inflammatory cytokine that increases considerably in pathological settings such as trauma, inflammation and neoplasia. Based on pre-clinical data in HCC, IL-6 signalling leads to tumour progression or local recurrence. Aim of our study is to clarify if the levels of IL-6 are associated with HCC progression and its different aetiopathogenesis in cirrhotic patients.

Method: 111 consecutive HCC cirrhotic patients (with different stages and aetiopathogenesis) were enrolled and compared with 36 cirrhotic patients without HCC. Patients were divided according to Child Pugh (CP) class and severity of HCC disease (BCLC). The major anthropometric and biochemical parameters, particularly serum IL-6, were collected. The degree of sarcopenia was also considered using TC dedicated software.

Results: IL-6 levels were different between advanced and not advanced HCC ($p=0.01$), while no difference in IL-6 levels was documented in CP-C with and without HCC; however, IL-6 levels were higher in advanced HCC (OR 4.58 CI: 1.19–17.55; $p<0.001$). IL-6 levels were different also between different etiologies of cirrhosis; in particular, no differences in viral and metabolic cirrhosis, low levels ($p<0.001$) in alcoholic and higher in autoimmune HCC or in combination of different aetiologies. IL-6 correlated also with sarcopenia severity ($p<0.001$) especially in advanced HCC patients ($p<0.001$). In no HCC CP-C patients, IL 6 was not correlated with sarcopenia. In linear regression IL-6 was correlated with AFP ($p<0.001$, $r=0.57$). In multivariate analysis IL-6 was linked with aetiopathogenesis, cancer progression, sarcopenia, CP and lymphocytes count.

Conclusion: These data suggest that IL-6 is higher in inflammatory states (like cirrhosis with CP-C) but it has a closer relation with advanced HCC and could be a marker for the disease itself. IL-6 seems to be also a predictor of sarcopenia especially in advanced HCC patients. Also, cirrhosis aetiopathogenesis has shown different IL-6 levels, documenting a different inflammatory setting. IL-6 could be a new marker to classify advanced HCC and a possible future drug target considering the different cirrhotic aetiopathogenesis.

SAT575

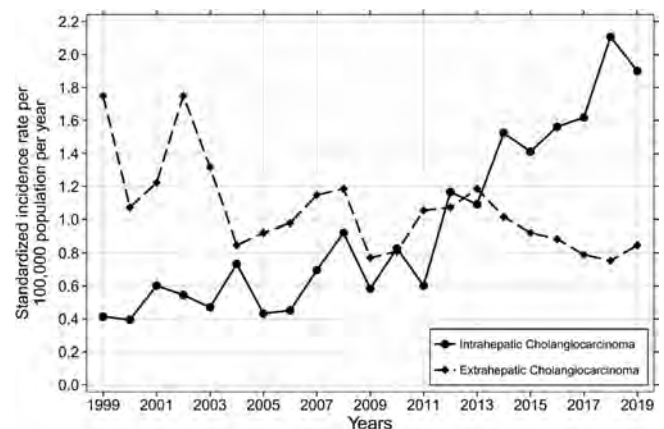
Time-trends in cholangiocarcinoma incidence-a danish nationwide cohort study

Morten Daniel Jensen¹, Joe West^{2,3}, Frank Viborg Mortensen⁴, Peter Jepsen¹. ¹Aarhus University Hospital, Department of Hepatology and Gastroenterology, Aarhus N, Denmark; ²University of Nottingham, Lifespan and Population Health, School of Medicine, NG5 1PB, United Kingdom; ³Nottingham University Hospitals NHS Trust and the University of Nottingham, NIHR Nottingham Biomedical Research Centre (BRC), Nottingham, United Kingdom; ⁴Aarhus University Hospital, Department of Surgical Gastroenterology, Aarhus N, Denmark
Email: moje@clin.au.dk

Background and aims: Cholangiocarcinoma (CCA) is a usually fatal primary liver cancer originating from the biliary epithelium. Extensive surgery is the only curative treatment, and adjuvant chemo- and/or radiotherapy is standard. Up-to-date data on incidence are crucial for our understanding of the disease and for designing trials of interventions. Therefore, we set out to examine incidence of CCA in a nationwide Danish cohort.

Method: We included all Danish patients, $N=2600$, with an ICD-10 diagnosis code of CCA (intrahepatic [iCCA]: C221; extrahepatic [eCCA]: C240) in the Danish Cancer Registry, between 1999-2019. We computed the standardized annual incidence rates of CCA in the Danish population using publicly available data on population demographics and standardized to the Danish population in 1999. We estimated the annual change in CCA incidence using a Poisson regression model.

Results: The standardized incidence rate (SIR) for iCCA increased from 0.41 (95% confidence interval [CI] 0.26–0.63) in 1999 to 1.90 (95% CI 1.55–2.31) in 2019 (Incidence rate ratio [IRR]: 4.59 [95% CI 2.89–7.28]), while the SIR for eCCA decreased from 1.75 (95% CI 1.41–2.14) in 1999 to 0.85 (95% CI 0.62–1.13) in 2019 (IRR: 0.48 [95% CI 0.34–0.69]). The overall SIR of total CCA (iCCA and eCCA) was 1.89 (95% CI 1.78–2.01) for men and 2.13 (95% CI 2.02–2.26) for women, and the trend of increasing IR for iCCA and decreasing IR for eCCA was observed in both sexes. The SIR of total CCA increased from 2.16 (95% CI 1.79–2.60) in 1999 to 2.79 (95% CI 2.35–3.27) in 2019, yielding an IRR of 1.29 (95% CI 1.01–1.64) and an annual increase of 2.51% (95% CI 1.81–3.22).



Conclusion: The incidence of CCA has increased since 1999, driven by a 4-fold increase in incidence of intrahepatic CCA while incidence of extrahepatic CCA has decreased by half. The reasons for this pattern are unclear but are likely due to changing environmental exposures over time.

SAT576

A novel hierarchical fusion strategy of deep learning networks to detect hepatocellular carcinoma from dynamic computed tomography images

I-Cheng Lee¹, Yung-Ping Tsai², Rheun-Chuan Lee¹, Shinn-Ying Ho², Yi-Hsiang Huang¹. ¹Taipei Veterans General Hospital, Taiwan; ²National Yang Ming Chiao Tung University, Institute of Bioinformatics and Systems Biology, Hsinchu, Taiwan
Email: iclee@vghtpe.gov.tw

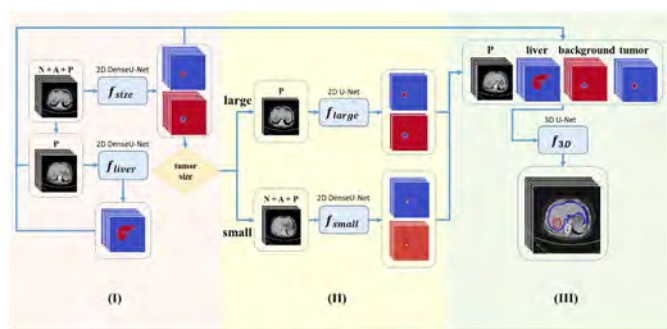
Background and aims: Automatic segmentation of hepatocellular carcinoma (HCC) on computed tomography (CT) scans is in urgent need to assist diagnosis and radiomics analysis. Most existing methods including deep learning for HCC segmentation used single-phase CT images or from small datasets. This study aimed develop a deep learning based network to detect HCC using a large dataset of dynamic CT images.

Method: Dynamic CT images of 595 patients with HCC before resection or radiofrequency ablation from Taipei Veterans General Hospital, Taiwan were used. Tumors in triple phase CT images, including non-contrast, arterial and portal venous phases, were labeled by radiologists. Patients were randomly divided into training, validation and test sets in a ratio of 5:2:3, respectively. The proposed

POSTER PRESENTATIONS

hierarchical fusion strategy of deep learning networks (HFS-Net) consists of three stages based on U-Net and DenseU-Net. The first stage segments tumors in a slice and estimates the tumor size. The second stage uses customized networks for segmenting small and large tumors adaptively. The third stage integrates the outcomes of the first two stages and uses a 3D U-Net to segment 3D liver tumors. Global dice, sensitivity, precision and F1 score were used to measure the performance of HFS-Net model.

Results: The 2D DenseU-Net using triple phase images was more effective for segmenting small tumors, whereas the 2D U-Net using portal venous phase images was more effective for segmenting large tumors. The HFS-Net performed better, compared with the single-strategy deep learning model in segmenting small and large tumors. In the test set, the HFS-Net model achieved good performance in identifying HCC on dynamic CT images, with global dice of 82.8%. The overall sensitivity, precision and F1 score were 84.3%, 75.7% and 0.796 per slice, respectively, and 92.2%, 93.2% and 0.927 per patient, respectively. The sensitivity in tumors <2 cm, 2–5 cm and >5 cm were 57%, 79.2% and 89.5% per slice, respectively, and 72.7%, 93.8% and 100% per patient, respectively.



Conclusion: The HFS-Net model achieved good performance in the detection and segmentation of HCC from dynamic CT images. Automatic 3D tumor segmentation from dynamic CT scans using

HFS-Net can support radiologic diagnosis and facilitate automatic radiomics analysis.

SAT577

Changing global epidemiology of liver cancer from 1990 to 2019: NASH is the fastest growing cause of liver cancer

Daniel Huang^{1,2}, Amit Singal³, Yuko Kono¹, Hashem El-Serag⁴, Rohit Loomba¹. ¹University of California San Diego, La Jolla, United States; ²Yong Loo Lin School of Medicine, Singapore, Singapore; ³UT Southwestern Medical Center, Dallas, United States; ⁴Baylor College of Medicine, Houston, United States
Email: roloomba@ucsd.edu

Background and aims: The major etiologies for liver cancer are hepatitis B virus (HBV), hepatitis C virus (HCV), alcohol, and non-alcoholic steatohepatitis (NASH). Over the last three decades, there have been changes in the etiology and burden of liver cancer due to increasing alcohol consumption, rising obesity rates and advances in prevention and treatment of HBV and HCV. We assessed the temporal trends in the incidence, mortality rates, disability-adjusted life-years (DALYs) secondary to liver cancer, and the contributions of various liver disease etiologies.

Method: We estimated the annual frequencies and age-standardized rates (ASRs) of liver cancer incidence, death and DALYs, from 1990 to 2019 by country, region and etiology using data obtained from the 2019 Global Burden of Disease study.

Results: In 2019 globally, there were 534,000 incident cases, 485,000 deaths, and 12.5 million DALYs due to liver cancer. Between 1990 and 2019, there was a 43% increase in the frequency of incident cases of liver cancer and a 33% increase in liver cancer deaths. However, the incidence ASR fell from 7.0 per 100,000 in 1990 to 6.9 per 100,000 in 2019, and the death ASR fell from 6.8 per 100,000 to 6.3 per 100,000. In 2019, the highest frequency of deaths occurred in the Western Pacific (52%), followed by South-East Asia (15%), Europe (13%), the Americas (10%), the Eastern Mediterranean region (6%) and Africa (4%). The annual percentage change of the death ASRs by country between 1990 and 2019 is shown in Figure 1. The greatest rise in death ASRs occurred in the Americas (annual percentage change [APC]: 1.15%), followed by Europe (APC: 0.71%) and South-East Asia (APC 0.64%). DALYs increased by 175% in the Americas, 131% in the

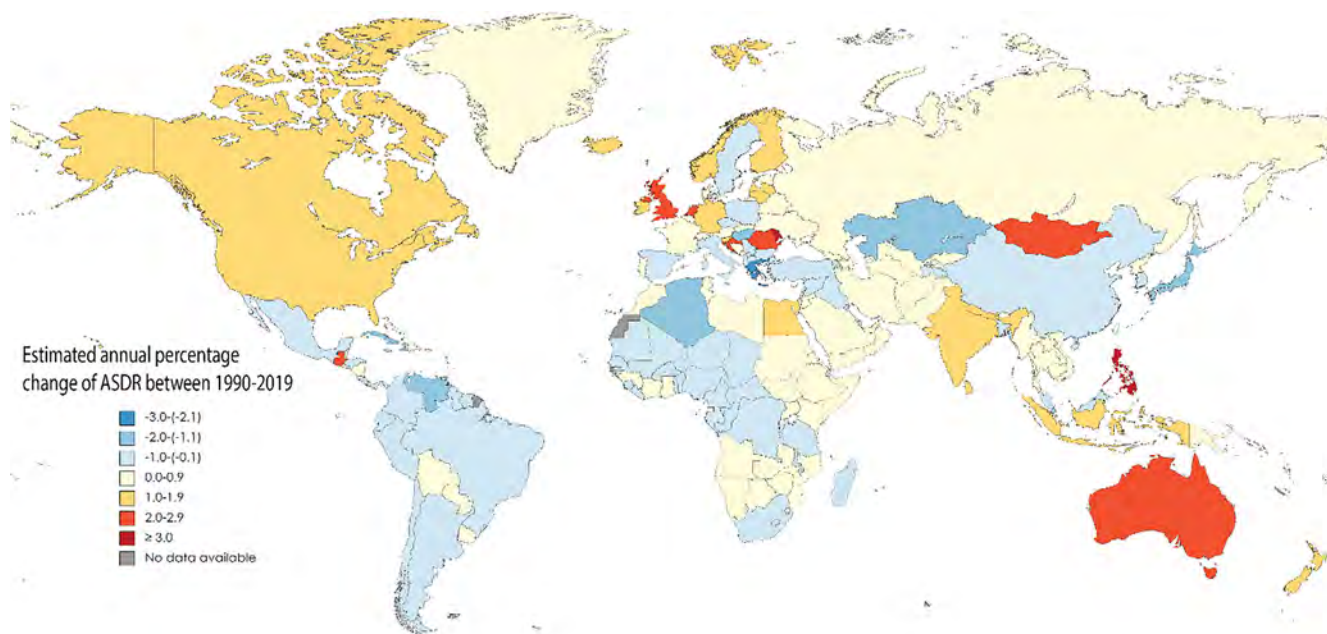


Figure: (abstract: SAT577): Annual percentage change of the age standardized death rate by country, between 1990 and 2019.

Eastern Mediterranean region and 114% in South-East Asia. HBV was the top cause of global liver cancer deaths (40%) in 2019, followed by HCV (29%) and alcohol (19%). NASH (APC: 0.35%) and alcohol (APC: 0.31%) had the fastest growing death ASRs between 1990 and 2019, while HCV grew at a slower rate (APC: 0.16%) and HBV declined (APC – 0.30%).

Conclusion: While the age-adjusted incidence and mortality rates have declined, the frequency of new cases, deaths and DALYs due to liver cancer has increased substantially between 1990 and 2019. The greatest rise in age adjusted liver cancer deaths occurred in the Americas and Europe and were driven by NASH and alcohol. Urgent measures are required to tackle the growing threat of NASH and alcohol-associated liver cancer.

SAT578

Liver resection for single large hepatocellular carcinoma: a prognostic factors study

Giuliana Amadio¹, Vincent Nguyen-Khac¹, Rami Rhaïem², Vincent Leroy¹, Helene Regnault¹, Raffaele Brustia¹, Alexis Laurent¹, Françoise Roudot-Thoraval¹, Daniele Sommacale¹. ¹Henri-Mondor University Hospital, Créteil, France; ²Hospital Robert Debré, Reims, France

Email: giuliana.amadio@aphp.fr

Background and aims: Liver resection is the only curative therapeutic option for large hepatocellular carcinoma (>5 cm), but survival is less good than in smaller tumors mostly because of the high recurrence rate. There is currently no proper tool for relapse risk stratification. We investigated for prognostic factors before and after hepatectomy for a single large HCC.

Method: We retrospectively identified 119 patients who underwent liver resection for a single large HCC in 2 tertiary care French centers, and collected pre and post-operative clinical, biological and radiological features. The primary outcome was overall survival at 5 years. Secondary outcomes were recurrence-free survival at 5 years, and prognostic factors for recurrence.

Results: 84% of the patients were male, and the mean age was 66 years old (58–74). 39 (33%) had Child-Pugh A cirrhosis, and mean Model for End-Stage Liver disease score was 6 (6–6). Etiology of liver disease was predominantly alcohol-related (48%), followed by non-alcoholic steatohepatitis (22%), hepatitis B (18%) and C (10%). Mean tumor size was 70 mm (55–110). Median overall survival was 72.5 months (IC 95% : 56.2–88.7), and five-year overall survival was 55.1 ± 5.5%. The median recurrence-free survival was 26.6 months (IC95% : 16.0–37.1), and five-year recurrence-free survival was 37.8 ± 5%. In multivariate analysis, pre-operative prognostic factors of recurrence were baseline AFP > 7 ng/ml (p < 0.001), portal invasion on imagery (p = 0.003) and cirrhosis (p = 0.020). With these factors, we obtained a simple recurrence-risk scoring system that classified 3 groups with different disease-free survival medians (p < 0.001): no risk factor (65 months), 1 risk factor (36 months), ≥2 risk factors (8.9 months). After liver resection, the presence of satellite nodules was the only significant predictive factor on a multivariate analysis. Adding this value to our pre-operative score, we obtained a pre- and post-operative score that was able to differentiate 4 groups with significantly different disease-free survival medians.

Conclusion: Liver resection is the only curative option for large HCC and we confirmed that survival can be satisfying in experienced centers. Recurrence is the main issue of surgery, and we proposed a simple pre-operative score that could help identifying patients with the most worrying prognosis, possible candidates for combining therapy.

SAT579

Characterization and clinical correlation of the immune contexture in intrahepatic cholangiocarcinoma using multiplex immunohistochemistry

Simon Peter¹, Valery Volk², Charlotte Hoffmann¹, Melanie Bathon¹, Benjamin Goeppert³, Thomas Longerich³, Thomas Albrecht³, Tanja Reineke-Plaas⁴, Friedrich Feuerhake², Arndt Vogel¹, Anna Saborowski¹. ¹Medizinische Hochschule Hannover, Gastroenterologie, Hepatologie und Endokrinologie, Hannover, Germany; ²Medizinische Hochschule Hannover, Institut für Pathologie, Schwerpunkt Neuropathologie, Hannover, Germany; ³Universitätsklinikum Heidelberg, Pathologisches Institut, Heidelberg, Germany; ⁴Medizinische Hochschule Hannover, Institut für Pathologie, Germany

Email: saborowski.anna@mh-hannover.de

Background and aims: Immune checkpoint blockade inhibitors that specifically modify the programmed cell death protein 1/-ligand 1 (PD-1/PD-L1) signaling pathway have been approved for the treatment of various solid cancers, frequently in conjunction with PD-L1 based companion diagnostics. In light of the positive results from the recent TOPAZ-1 trial, a better understanding of the biological behaviour and immune contexture of biliary tumours is prerequisite for a more precise estimation of prognosis and response to immunomodulatory cancer therapies. Using multiplex immunohistochemistry, we set out to spatially resolve and clinically correlate the immune infiltrates, and to delineate the impact of biopsy “site” on established PD-L1 based scoring systems in intrahepatic cholangiocarcinomas (iCCA).

Method: FFPE tissues from 141 resected and clinically annotated iCCAs were stained using a multiplex immunohistochemistry platform (Phenoptics system, Akoya Bioscience) for the following markers: CD4, CD8, CD20, CD68, PD-L1 and pancytokeratin mix AE1/3.

Results: Morphological heterogeneity of resected human iCCA correlated with marked differences in terms of both immune infiltration and PD-L1 expression. Densities of immune infiltrates and PD-L1 positive cells were highest in stroma-rich tumors, but were not influenced by large vs small duct morphology. In addition, we observed a marked intratumoral heterogeneity for immune cell distribution and PD-L1 expression, with highest densities in the tumor margin. Comparative analysis with traditional semiquantitative evaluation methods for determination of PD-L1 signal revealed a profound variability, dependent on which score and tumor area was considered.

Further analyses indicated a favorable prognostic value of tertiary lymphoid structures (TLS). TLS were not only associated with a higher density of diffusely distributed B cells in the tumor but also with a statistically significant enrichment of T cells in spatial proximity to PD-L1 positive macrophages. Of note, PD-L1 expression was not confined to tumor cells and macrophages, but was also evident on a subset of T cells. Similar to PD-L1 positive macrophages, PD-L1 positive T cells were more likely to have not only another but also overall more T cells in a biologically relevant radius around them than their PD-L1 negative counterparts.

Conclusion: Despite a marked inter- as well as intratumoral heterogeneity of immune infiltrates in iCCA, our analysis points towards the existence of recurrent patterns. We delineate the prognostic value of TLS, and suggest a functionally relevant interaction of T cells with PD-L1 positive macrophages and tumor cells. In addition, we posit that annotated PD-L1 based scoring systems will be required in order to serve as an adequate translationally relevant marker, especially in the context of immunotherapy clinical trials.

POSTER PRESENTATIONS

SAT580

Deep view on HCC gene signatures and their comparison with other cancers

Yuquan Qian¹, Timo Itzel^{1,2}, Matthias Ebert^{1,3}, Andreas Teufel^{1,2,3}.
¹Medical Faculty Mannheim, University of Heidelberg, Department of Medicine II, Mannheim, Germany; ²Medical Faculty Mannheim, University of Heidelberg, Division of Hepatology, Division of Bioinformatics, Department of Medicine II, Mannheim, Germany; ³Medical Faculty Mannheim, University of Heidelberg, Clinical Cooperation Unit Healthy Metabolism, Center for Preventive Medicine and Digital Health Baden-Württemberg, Mannheim, Germany
 Email: andreas.teufel@medma.uni-heidelberg.de

Background and aims: Throughout the past two decades, numerous HCC-dependent gene expression signatures have been published, but none of them made it into clinical practice. Setting up a comparative transcriptomics profiling approach, we therefore explored the specificity of these signatures to HCC as this may be a critical with respect to clinical usage.

Method: From the existing publications, we collected HCC gene signatures and evaluate them in independent genome wide gene expression profiles of patients suffering from HCC. Evaluations were performed using four different (commercial and non-commercial) gene expression profiles, particularly a modified version of the ProfileChaser, Oncomine Premium, GENEVA, and SigCom LINC for assigning similar pre-analyzed profiles to our signatures of interests. These results were screened for different cancer entities. We furthermore evaluated common core genes, overlapping pathways, and generation approaches among these HCC gene signatures.

Results: Although the specificity of the investigated HCC signatures varied significantly, none of the signatures exhibited strict specificity to HCC. Many signatures expressed similar profiles in other tumors, especially to renal, breast, and colorectal cancers and particularly those signatures designed to distinguish between good and poor survival of patients. Specificity of HCC gene signatures proved difficult, we furthermore found that no common core genes, few overlapping pathways, and a significant heterogeneity in signature generation approaches among HCC gene signatures may account for this phenomenon.

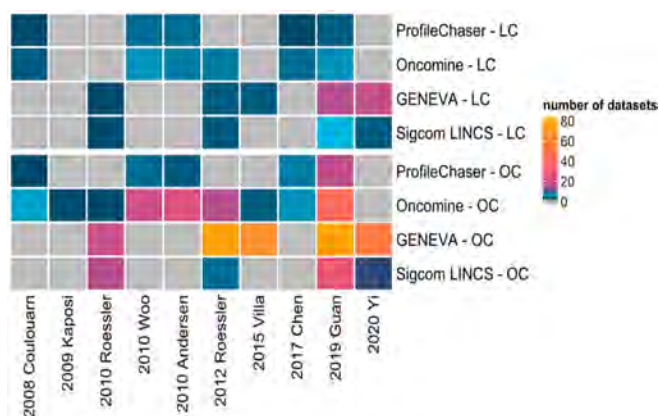


Figure: Gene signature query results of four bio-tools. LC: Liver Cancer, OC: Other Cancers. The color represents the number of datasets matched in each tool; grey means no datasets matched.

Conclusion: Our study shows the poor specificity of current HCC gene signatures, and demonstrates that the clinical use and independent validation of HCC genetic signatures remains challenging. Overall, our data suggest the necessity of standards in tissue preparation and store, as well as signature generation, statistical methods and independent validation.

SAT581

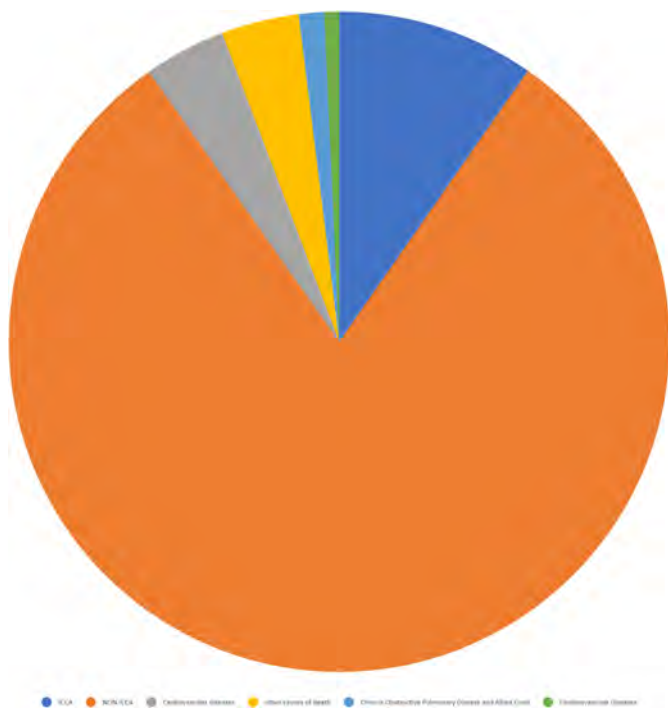
Causes of death after Intrahepatic cholangiocarcinoma diagnosis: a population-based study

Anas Elgenidy¹, Ahmed Abdelwahab², Prasun Jalal². ¹Faculty of medicine, Cairo University, Cairo, Egypt; ²Baylor College of Medicine, Department of Medicine, Gastroenterology and Hepatology Division, Houston, United States
 Email: Ahmed.Abdelwahab@bcm.edu

Background and aims: Intrahepatic cholangiocarcinoma (ICCA) has shown a substantial increase in mortality globally. On the contrary, perihilar cholangiocarcinoma (pCCA) and distal cholangiocarcinoma (dCCA) have been decreasing; however, studies on causes of death in ICCA patients remain limited. We aim to focus on and evaluate the causes of death after ICCA diagnosis.

Method: In this retrospective cohort, we studied 276, 712 ICCA patients diagnosed between 2004 and 2016 in the United States. The standardized mortality ratio (SMRs) with 95% confidence intervals (CIs) for each cause of death using the SEER*Stat software version 8.3.9.2.

Results: Out of the 276, 712 patients diagnosed with ICCA, 203, 914 (73.7%) were between 50 and 79 years (The mean age at diagnosis was 63.51 years); 220, 648 (79.7%) were white, and 144, 942 (52.4%) were females. 35, 814 patients (12.9%) died during the follow-up period with a mean age of 70.83 years. The highest number of deaths (34, 444; 96.2%) occurred within the first year following the diagnosis. During all latency periods, 3, 339 (9.3%) deaths were from ICCA, and 27, 790 (77.6%) were from other cancers. The most common cancer causes were lung and bronchus cancer (9862; 27.5%) followed by pancreatic cancer (3475; 9.7%), and 4, 685 (13.1%) from non-cancer causes. Cardiovascular diseases were the leading non-cancer causes (SMR 1.95; 95% CI (1.85–2.06)), followed by Chronic Obstructive Pulmonary Disease and related Conditions (SMR 2.52; 95% CI (2.29–2.78)).



Conclusion: Following ICCA diagnosis, the most common cause of death was lung and bronchus cancer followed by pancreatic cancer and ICCA, and cardiovascular disease represents a substantial percentage of non-cancer deaths (4.97%). Our findings provide

critical insights into how ICCA survivors should be followed-up and monitored regarding future health risks.

SAT582

Genes modulating liver fat accumulation and lipogenesis predict development of hepatocellular carcinoma among direct antiviral agents treated cirrhotics C with and without viral clearance

Ginevra Mocchetti¹, Antonio Acquaviva^{1,2}, Giulia Francesca Manfredi^{1,2}, Michela Emma Burlone², Francesca Baorda^{1,2}, Davide Di Benedetto^{1,2}, Ramana Mallela Venkata¹, Rosalba Minisini¹, Cristina Rigamonti^{1,2}, Mario Pirisi^{1,2}. ¹Università del Piemonte Orientale, Department of Translational Medicine, Novara, Italy; ²AOU Maggiore della Carità, Division of Internal Medicine, Novara, Italy
Email: michela.burlone@uniupo.it

Background and aims: Genetic risk score (GRS) is a polygenic scoring system that estimates the predisposition to accumulate liver fat combining PNPLA3 (rs738409), TM6SF2 (rs58542926), MBOAT7 (rs641738) and GCKR (rs1260326) polymorphisms. GRS score was related to the probability to de novo hepatocellular carcinoma (HCC) development in HCV cirrhotic patients, treated with direct antiviral agents (DAA). In this setting, it is suggested that HSD17B13: TA variant (rs72613567) exhibits a protective role on fibrosis development and hepatocarcinogenesis. Our aim was to evaluate if HSD17B13 variant together with achievement of viral clearance (SVR) affected the efficacy of GRS in HCC prediction.

Method: 328 HCC-free cirrhotic patients were included. Diagnosis of cirrhosis was based on transient hepatic elastography (liver stiffness ≥ 12.5 kPa) or on clinical diagnosis of liver cirrhosis. Genomic DNA was extracted from whole blood. PNPLA3 and HSD17B13 genotypes were determined using restriction fragment length polymorphism technique. TaqMan® SNP (Life Technologies) genotyping test was used to identify TM6SF2, MBOAT7 and GCKR genotypes. GRS score was calculated as previously described by Degasperis et al, Hepatology 2020.

Results: At the end of the follow-up (median, 7.5 months), n=21 patients were diagnosed with de novo HCC (Group A). Among them, 4 patients were relapsers and 1 was a drop-out, while in HCC-free patients' group (Group B, n=307), 8 relapsers (p=0.001) were observed. The SVR (intention-to-treat) was of 76% in Group A vs. 97% in Group B. In Group A, patients were mainly male, with more advanced liver disease. None of the genes included in the GRS was individually associated with de novo HCC. In a Cox proportional hazards model, a GRS value ≥ 0.457 (75th percentile) predicted the onset of HCC regardless of gender, diabetes, albumin, INR and FIB4 (HR 2.89, C.I. 1.19–7.07, p 0.02). The goodness of the model was improved by adding SVR achievement and presence of HSD17B13 variant; in particular, male gender (HR 6.75, C.I. 1.62–28.2, p 0.009), GRS ≥ 0.457 (HR 4.24, C.I. 1.59–11.33, p 0.004), carriage of the splice variant HSD17B13: TA (HR 0.24, C.I. 0.07–0.75, p 0.015) and failure to achieve SVR (HR 7.7, C.I. 2.38–25, p 0.001), were independent predictors of de novo HCC.

Conclusion: The study results confirmed that genes modulating lipogenesis and liver fat are important risk factors for the development of HCC in HCV cirrhotic patients treated with DAA.

SAT583

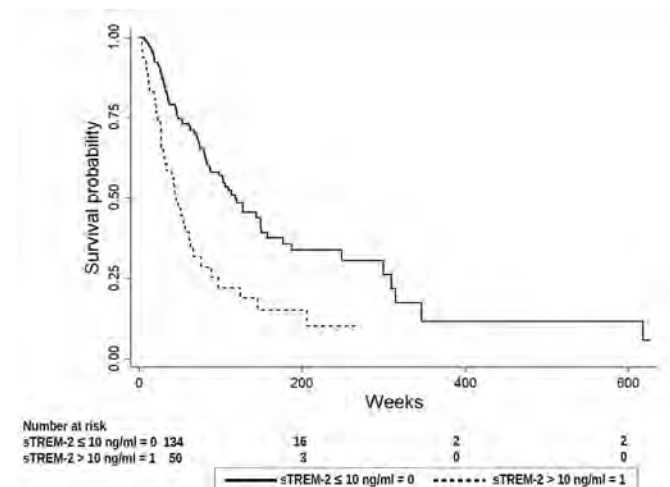
Potential role of soluble triggering receptor expressed on myeloid cells 2 in risk stratification of patients with hepatocellular carcinoma

Francesca Baorda^{1,2}, Federico Ceruti^{1,2}, Antonio Acquaviva^{1,2}, Giulia Francesca Manfredi^{1,2}, Davide Di Benedetto^{1,2}, Michela Emma Burlone², Rosalba Minisini¹, Mattia Bellan^{1,2}, Cristina Rigamonti^{1,2}, Mario Pirisi^{1,2}. ¹Università del Piemonte Orientale, Department of Translational Medicine, Novara, Italy; ²AOU Maggiore della Carità, Division of Internal Medicine, Novara, Italy
Email: michela.burlone@uniupo.it

Background and aims: Triggering receptor expressed on myeloid cells 2 (TREM-2) is a transmembrane receptor of the immunoglobulin superfamily that has been recently studied in many diseases including liver cancer. Nevertheless, its role is still unclear and there are no studies that have evaluated its soluble form (sTREM-2) as a biomarker. Thus, we aimed to explore the prognostic value of serum sTREM-2 in hepatocellular carcinoma (HCC).

Method: An observational cross-sectional study was performed on 184 HCC patients of any etiology, in stage A, B or C of the BCLC classification, enrolled between 2005–2021. Diagnosis of HCC was established according to the AASLD and the EASL guideline criteria. All patients underwent genotyping of TREM-2 polymorphism (rs6918289) through polymerase chain reaction DNA amplification (PCR DNA) and serum sTREM-2 levels were quantified by using an enzyme-linked immunosorbent assay (ELISA).

Results: The median of sTREM-2 was 7.4 ng/ml [5.7–10.4 ng/ml]. sTREM-2 levels had a weak correlation with age (p=0.024) and stronger with AST (p=0.001). From the univariate analysis, an association with the BCLC stage emerged: more advanced stages corresponded to higher values of sTREM-2 (p=0.001). The allele frequency of rs6918289 polymorphism was 92% (339/368) for the ancestral allele (G) and 8% (29/368) for the variant allele (T). The distribution by genotype did not differ from what was expected according to the Hardy-Weinberg equilibrium (p=0.246). At the end of a maximum period of observation (11.9 years), the overall mortality was 58.15% (107/184), with a median survival time of 86 weeks [31–287]. Survival analysis showed that the increase in sTREM-2 levels over the 75th percentile threshold (cutoff=10 ng/ml) was significantly associated with a reduction in overall survival (log rank test with p<0.0001, Figure). The Cox proportional hazards model built having as predictors sTREM-2, sex, age, presence/absence of cirrhosis/HCV infection and BCLC stage, confirmed that serum concentration of sTREM-2 >10 ng/ml is an independent predictor of mortality (HR 1.88, CI 1.22–2.88, p=0.004).



Conclusion: The present study demonstrated the potential negative prognostic role of sTREM-2 on overall HCC survival. However, future prospective studies are necessary to elucidate whether the systematic assessment of sTREM-2 concentrations could be useful to predict the survival in HCC patients.

SAT584

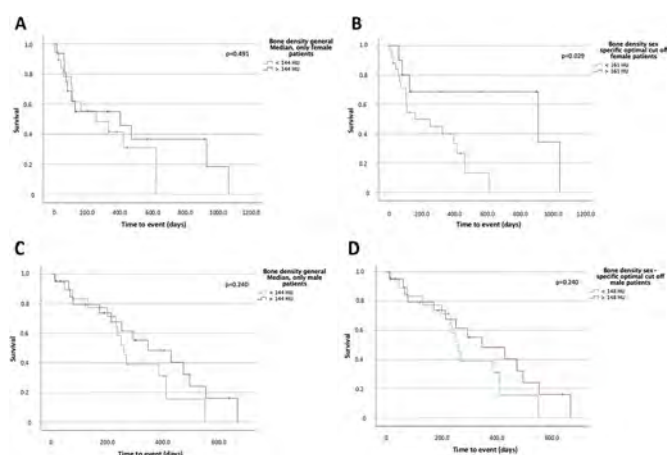
Bone mineral density is a predictor of mortality in female patients with cholangiocarcinoma undergoing palliative treatment

Markus Jördens¹, Linda Wittig¹, Georg Flügel¹, Sven H Loosen¹, Christoph Roderburg¹, Tom Lüdde¹. ¹Düsseldorf
Email: christoph.roderburg@med.uni-duesseldorf.de

Background and aims: Cholangiocellular adenocarcinoma (CCA) is a rare and aggressive malignancy originating from the bile ducts. Its general prognosis is poor as therapeutic options are limited. Often, patients present at advanced stages of disease and palliative chemotherapy remains the only treatment option. So far prognostic markers to assess the outcome of chemotherapeutic treatment in CCA are limited. We evaluated bone mineral density (BMD), a marker for the body composition as prognostic tool in patients with advanced CCA.

Method: 75 patients with advanced CCA that were treated at the department of Gastroenterology, Hepatology and Infectious Diseases or department of General, Visceral and Pediatric Surgery of the University Hospital Düsseldorf were included into this analysis. 64 patients received chemotherapy, 11 best supportive care. Bone mineral density was analyzed at the first lumbar vertebra, using CT scans in venous phase and the local PACS (IntelliSpace PACS, Philips, Amsterdam, The Netherlands).

Results: We identified an optimal cut off of 167 HU for BMD, with patients above that value having a significantly improved overall survival (474 (95%CI: 297–651) days vs. 254 (95%CI: 211–297) days; log rank χ^2 (1) = 6.090; p = 0.014; Figure 3C). The prognostic value for BMD was confirmed using univariate (HR 2.313 (95%CI: 1.170–4.575); p = 0.016) and multivariate (HR 4.143 (95%CI: 1.197–14.343); p = 0.025) Cox regression analysis. Subgroup analysis revealed, that the prognostic value of BMD was only present in women and not in men, suggesting sex specific differences.



Conclusion: Our data suggest, that BMD might represent a valuable and easy accessible independent prognostic marker in patients with advanced CCA for overall survival. Interestingly, subgroup analysis showed sex specificity of this marker only relevant in women.

SAT585

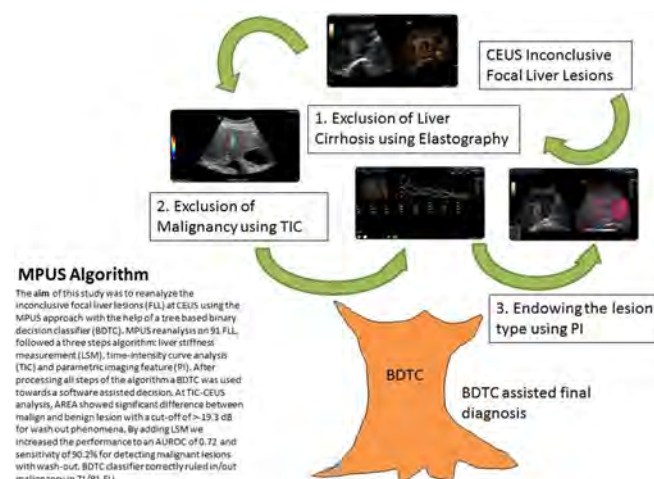
Multiparametric ultrasound approach using a tree based decision classifier for the inconclusive focal liver lesions evaluated by contrast enhanced ultrasound

Tudor-Voicu Moga^{1,2}, Ciprian David³, Alina Popescu¹, Raluca Lupusoru¹, Darius Heredea¹, Ana-Maria Ghiuchici¹, Camelia Foncea¹, Adrian Burdan¹, Roxana Sirli¹, Mirela Danila¹, Ioan Sporea¹. ¹Victor Babes University of Medicine and Pharmacy, Division of Gastroenterology and Hepatology, Department of Internal Medicine II, Center for Advanced Research in Gastroenterology and Hepatology, Timisoara, Romania; ²Victor Babes University of Medicine and Pharmacy, Division of Gastroenterology and Hepatology, Department of Internal Medicine II, Center for Advanced Research in Gastroenterology and Hepatology, Timisoara, Romania; ³Faculty, "Politehnica" University of Timisoara, Electronics and Telecommunications, Timisoara, Romania
Email: moga.tudor@gmail.com

Background and aims: Multi-parametric ultrasound (MPUS) is a concept by which the examiner is encouraged to use the latest features of the ultrasound machine. The aim of this study was to reanalyze the inconclusive focal liver lesions (FLL) at CEUS using the MPUS approach with the help of a tree based decision classifier.

Method: We retrospectively analyzed FLL's that were inconclusive at CEUS examination in our Department over a period of two years (2017–2018). All the reexamined lesions had a second line imaging method performed: (CE-CT), (CE-MRI) or biopsy considered as the reference method. CEUS Inconclusive FLLs had been previously evaluated by ultrasound (US) experts with more than 10 years of experience in CEUS, using a single US machine. MPUS reanalysis followed a three steps algorithm: liver stiffness measurement (LSM), time-intensity curve analysis (TIC) and parametric imaging feature (PI). After processing all steps of the algorithm a binary decision tree classifier (BDTC) was used towards a software assisted decision.

Results: From the 91 inconclusive FLLs evaluated, 34 were HCC, 13 metastasis, 7 haemangioma, 7 regenerative nodules, 5 focal fatty alteration, 3 fatty free areas, 4 cholangiocarcinoma's, 2 abscesses, 5 adenomas and 11 were other benign lesions. AREA was the only TIC-CEUS parameter that showed significant difference between malign and benign lesion with a cut-off of >-19.3 dB for wash out phenomena, (AUROC = 0.58, Se = 74.0%, Sp = 45.7%). By adding the value of elastography we increased the performance to an AUROC of 0.72 and sensitivity of 90.2% for detecting malignant lesions with wash-out. MPUS correctly classified 66/91 lesions with an accuracy of 72.3%. Using the binary decision tree classifier (BDTC) algorithm we correctly classified 71/91 lesions according to their malignant or benign status, with an accuracy of 78.0%, Sensitivity = 62%, Specificity = 45% and Precision = 80%.



Conclusion: By reevaluating the inconclusive FLLs at CEUS using MPUS, we managed to determine that 78% of the lesions were malignant and in 28% of them we establish the lesion type.

SAT586

Adherence to hepatocellular carcinoma screening in patients with hepatitis C cirrhosis treated with direct-acting antivirals against hepatitis C

Elisaul Suarez Zambrano¹, Silvia Acosta-López¹, Dácil Díaz Bethencourt¹, Maria Soledad Garrido¹, Ruth Suarez Darias¹, Francisco Andrés Pérez Hernández¹. ¹Our Lady of Candelaria University Hospital, Santa Cruz de Tenerife, Spain
Email: suarezelisaul@gmail.com

Background and aims: Hepatocellular carcinoma (HCC) screening is indicated for patients with hepatitis C cirrhosis (HCV-C) via biannual ultrasound scan. The risk of HCC and its mortality rate persist after sustained virologic response (SVR), so screening must be maintained. This study aims to analyse HCC screening adherence in patients with HCV-C after SVR and risk factors involved in low adherence. As a secondary aim, we analyse the incidence of HCC and BCLC stage at diagnosis.

Method: A descriptive, trans-sectional, and observational study in which we included patients that have been diagnosed VHC and treated with direct antiviral agents (DAA) between September 2014 and July 2019 with a minimum follow-up period of one year. Demographic and clinical variables were recorded at first specialised consultation. The level of adherence to screening was categorised as 'adequate' if it was conducted within a range of six months. A comparative analysis was carried out, employing nonparametric statistic tests in order to compare the two groups of study (either adequate or inadequate screening processes). Also, a binary logistic regression analysis was carried out in order to determine variables associated to an inadequate screening. For all the analysis, statistical significance was set $p < 0.05$.

Results: 385 patients (114 female) were included. Average age was 57.4 (10.3 SD). The average follow-up was 35.8 months (25 SD). 41.5% had an adequate screening (36.5% for men and 53.5% for women). Screening was adequate only in 20.6% (27/131) for intravenous drug users (IVDU) and 26.4% (24/91) for patients with mental health disorders. The binary multivariate logistic regression analysis showed IVDU history (OR 3.29) and mental health disorders (OR 2.23) as the only independent risk factors for an inadequate HCC screening process. HCC diagnosis was recorded in 45 patients (11.6%), 57.7% with an adequate screening process. The most frequent BCLC stages were stage A (early) in 53.3% of patients, and stage B (intermediate) in 17.8% of them. The average diagnosis of HCC period since the beginning of the screening was 28.6 months. 32.7% of patients abandon the follow-up before the close out, including the 55.6% of those with an inadequate screening. 11.4% of patients (44) deceased during the follow-up period; 40.9% of them (18) were diagnosed with HCC.

Conclusion: There is a low level of adherence to the HCC screening process in patients with hepatitis C cirrhosis after DAA treatment. IVDU medical history and mental health disorders are independent factors for an inadequate screening process. Nevertheless, the screening enables the HCC diagnosis in early stages for most patients in this group. HCC is common and is a mayor cause for mortality in this population.

SAT587

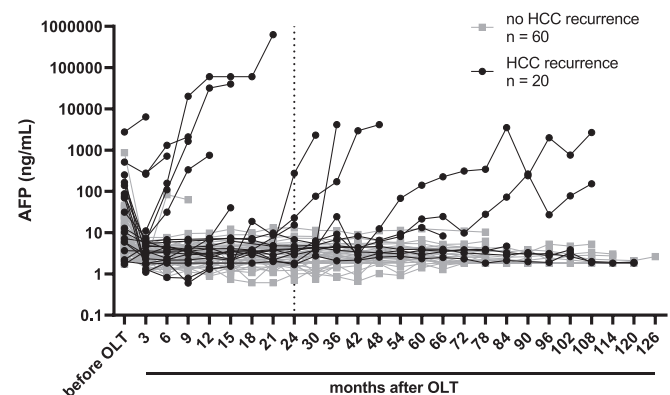
Closely monitored alpha-fetoprotein allows early detection of hepatocellular carcinoma recurrence after orthotopic liver transplantation

Magdalena Hahn¹, Adam Herber¹, Rami Al-Sayegh¹, Janett Fischer¹, Anne Olbrich¹, Sebastian Rademacher², Daniel Seehofer², Sebastian Ebel³, Timm Denecke³, Thomas Berg¹, Florian van Bömmel¹. ¹Leipzig University Medical Center, Division of Hepatology, Department of Medicine II, Leipzig, Germany; ²Leipzig University Medical Center, Department of Visceral, Transplant, Thoracic and Vascular Surgery, Leipzig, Germany; ³Leipzig University Medical Center, Department of Diagnostic and Interventional Radiology, Leipzig, Germany
Email: florian.vanboemmel@medizin.uni-leipzig.de

Background and aims: After orthotopic liver transplantation (OLT) for patients with hepatocellular carcinoma (HCC), HCC recurrence (HCCR) is frequent and has a poor prognosis. An alpha-fetoprotein (AFP) value $>1,000$ ng/ml before OLT is used to identify patients at high risk for HCCR. However, the use of AFP for the detection of HCCR is not established. We have assessed longitudinal AFP levels in patients who underwent OLT for HCC.

Method: In this retrospective monocentric study all patients who underwent OLT due to HCC between 2010 and 2020 in one University Hospital were included. Inclusion criteria were diagnosis of HCC by radiologic or histologic criteria before OLT, availability of serum AFP values measured before OLT, 3 monthly within 24 months after OLT and 6 monthly thereafter, and written informed consent. AFP was measured by COBAS assay (Roche, Switzerland, upper limit of normal (ULN) = 7 ng/ml). AFP levels were correlated to data from patient records.

Results: A total of 80 patients were included and followed for a mean time of 58 ± 40 (range 1–132) months (end of observation = EOBS) after OLT. HCC recurred in 20 patients (25%) after a mean of 33 ± 30 months. In the group without HCCR median serum AFP levels dropped from 5.7 (range 1.7–871) before to 2.7 (1.2–7.7) ng/ml at month 3 after OLT ($p < 0.001$), and remained similar until EOBS (4.1 (1.5–62.8), $p = 0.915$). In contrast, in the HCCR group median AFP level decreased from 76.7 (1.7–2,762) at before OLT to 6.1 (1.1–6,393) ng/ml ($p = 0.010$) at month 3 after OLT, but increased to 751.3 (138–628,400) ng/ml at EOBS ($p = 0.002$) (Figure). In 15 patients (75%) with elevated AFP at HCCR, including two with AFP below ULN until OLT, after OLT AFP increased above ULN by a mean of 3.3 ± 3 (0–9) months before radiologic confirmation of HCCR. Patients with HCCR within the first 12 months after OLT ($n = 7$) had significantly higher median AFP levels at OLT, months 3, 6 and 12 after OLT as compared to patients with HCCR after 12 months or no HCCR (OLT: 165.2 (31.3–2,762) ng/ml vs. 5.9 (1.7–871), $p < 0.001$; 3 months: 11 (4.9–6,393) vs. 2.7 (1.1–7.7), $p < 0.001$; 6 months: 134 (4.6–1,307) vs. 2.31 (0.82–83), $p < 0.001$; 12 months: 16,398.7 (7.3–60,500) vs. 2.8 (0.9–9.7), $p < 0.001$).



Conclusion: Serum AFP levels measured on a longitudinal basis are useful for early detection of AFP positive HCCR after OLT. The optimal frequency of AFP measurement needs to be defined.

SAT588

Predictors of survival of patients with hepatocellular carcinoma in best supportive care

Claudia Campani¹, Laura Bucci², Valentina Adotti¹, Martina Rosi¹, Umberto Arena¹, Stefano Gitto¹, Franco Trevisani², Fabio Marra¹, Ita.Li.Ca. Study Group². ¹University of Florence, Firenze, Italy; ²Alma Mater Studiorum-Università di Bologna, Bologna, Italy
Email: fabio.marra@unifi.it

Background and aims: The prognosis of patients with hepatocellular carcinoma (HCC) is very variable. Patients unfit to receive any type of treatment are managed with best supportive care (BSC), and their median overall survival (OS) is around 3–6 months, although longer values may be observed in clinical practice. Aim of this study was to identify prognostic factors associated with longer survival in patients with HCC treated with BSC.

Method: We retrospectively evaluated the clinical characteristics of 916 patients, recorded in the Ita.Li.Ca. database, who had an indication for BSC. We analyzed both patient and tumor characteristics to identify predictors of better OS.

Results: Median age was 71y and 75% of patients were male. Etiology included chronic viral infection (48.7%), alcohol use disorder (20.7%) and non-alcoholic steatohepatitis (4.1%). Approximately 50% of patients had a performance status 0–1 and were in Child-Pugh B class. Median MELD was 13. 60% of patients had a multifocal HCC with a median number of 2 lesions and a median size of 35 mm. 369 patients had vascular invasion. Median alpha-fetoprotein was 63.2 ng/ml. The median OS was 9 months (CI 7.7; 10.2). No differences in terms of OS were observed considering the etiology of liver disease. Among comorbidities, heart disease was associated with lower OS ($p = 0.015$). Abdominal pain ($p < 0.001$), vomiting ($p = 0.014$), fatigue ($p < 0.001$), edema ($p < 0.001$), jaundice ($p = 0.01$), higher PS ($p = 0.01$), and a worse liver function ($p < 0.001$) were associated with shorter OS. Patients with multifocal HCC had a better OS (12 mo; CI 10–13.9) compared to those with monofocal HCC (8 months; CI 6.5–9.5) ($p < 0.001$). Lack of vascular invasion was also associated with a better OS (14 months, CI 12.2–15.7, $p < 0.001$). No significant differences were observed comparing patients with or without metastasis ($p = 0.310$). Patients who had an active treatment before BSC had significantly longer OS than those for whom BSC was the only treatment (561 patients, $p < 0.001$). Survival in BCLC-A patients was longer than in other stages. No differences in OS were found comparing BCLC-B and -C groups. Patients in BSC with a median OS longer than 6 months had more lesions ($p = 0.005$), higher levels of albumin ($p = 0.003$), lower bilirubin ($p < 0.001$) and alpha-fetoprotein (0, 001), and a lower median MELD ($p < 0.001$). A weak association was found between survival shorter than 6 months and the presence of cirrhosis ($p = 0.012$), alcohol consumption ($p = 0.046$), heart disease ($p = 0.007$), obesity ($p = 0.025$), hypercholesterolemia ($p = 0.002$), hypertriglyceridemia ($p = 0.0036$) symptoms ($p = 0.02$), vascular invasion ($p < 0.001$), and non-multifocal HCC ($p < 0.001$). Similar results were found comparing patients with a mOS longer or shorter than 12 months.

Conclusion: In a large series of patients with HCC in BSC we identified several clinical and tumor characteristics associated with the length of survival.

SAT589

Serum exosomal miRNA-720 as a diagnostic marker for hepatocellular carcinoma

Ji Min Kim¹, Hye Seon Kim¹, Jin Seoub Kim¹, Ji Won Han¹, Soon Kyu Lee¹, Heechul Nam¹, Pil Soo Sung¹, Si Hyun Bae¹, Jong Young Choi¹, Seung Kew Yoon¹, Jeong Won Jang¹. ¹The Catholic University of Korea, Seoul St. Mary's Hospital, Seoul, Korea, Rep. of South
Email: garden@catholic.ac.kr

Background and aims: Hepatocellular carcinoma (HCC) remains with a poor prognosis, largely due to late detection. Highly accurate biomarkers are urgently needed to detect early-stage HCC. Exosomal microRNAs (miRs) recently emerged as a biomarker for various cancers. Our study aims to explore the diagnostic performance of serum exosomal miR-720 for HCC.

Method: Exosomal miRNA was measured by quantitative real-time PCR. A correlation analysis was done between exosomal miR-720 and tumor or clinico-demographic data of patients with HCC. The receiver operating characteristic (ROC) curve was applied to assess the diagnostic capacity of serum exosomal miR-720 for HCC, in comparison with AFP (α -fetoprotein) and prothrombin-induced by vitamin K absence or antagonist-II (PIVKA-II).

Results: miR-720 was chosen as a potential HCC marker through miR microarray, due to significantly differential expression between tumor and non-tumor samples. Serum exosomal miR-720 was significantly upregulated in patients with HCC ($n = 114$) and other liver disease (control, $n = 30$), with the higher area under the ROC curve (AUC = 0.931) than the other markers. Particularly, serum exosomal miR-720 showed superior performance in diagnosing small HCC (< 5 cm; AUC = 0.930) to AFP (AUC = 0.802) or PIVKA-II (AUC = 0.718). Exosomal miR-720 levels marginally correlated with tumor size and number. The proportion of high-level miR-720 increased with intrahepatic tumor stage progression. Unlike AFP or PIVKA-II showing significant correlation with aminotransferase levels, exosomal miR-720 exhibited no correlation with aminotransferase levels.

Conclusion: Serum miR-720 is an excellent biomarker for diagnosis of HCC, with better performance than AFP or PIVKA-II. Its diagnostic utility is maintained even for small HCC and not affected by aminotransferase levels.

Key words: Hepatocellular carcinoma; Exosome; MicroRNA; Biomarkers; Diagnosis.

SAT590

Prospective evaluation of combining three biomarkers and image tools for early detection of hepatocellular carcinoma: an interim analysis

Hyung Joon Yim¹, Tae Hyung Kim¹, Soon Ho Um², Yeon Seok Seo², Young Kul Jung¹, Ji Hoon Kim³, Young-Sun Lee³, Sun Young Yim², Won Hyeok Choe⁴, Jae Young Jang⁵, Byoung Kuk Jang⁶, Dae Won Jun⁷, Eileen Yoon^{8,9}, Yoon Jun Kim¹⁰, Hyung Joon Kim¹¹, Chang Wook Kim¹², Si Hyun Bae¹², Jeong Won Jang¹², Han Ah Lee^{2,9}, Do Young Kim¹³. ¹Korea University Ansan Hospital, Internal Medicine, Ansan, Korea, Rep. of South; ²Korea University Anam Hospital, Internal Medicine, Korea, Rep. of South; ³Korea University Guro Hospital, Internal Medicine, Korea, Rep. of South; ⁴Konkuk University School of Medicine, Internal Medicine, Korea, Rep. of South; ⁵Soonchunhyang University College of Medicine, Internal Medicine, Korea, Rep. of South; ⁶Keimyung University School of Medicine, Internal Medicine, Korea, Rep. of South; ⁷Hanyang University College of Medicine, Internal Medicine, Korea, Rep. of South; ⁸Hanyang University College of Medicine, Internal Medicine; ⁹Inje University College of Medicine, Internal Medicine; ¹⁰Seoul National University College of Medicine, Internal Medicine; ¹¹Chung-Ang University College of Medicine, Internal Medicine; ¹²The Catholic University of Korea, Internal Medicine; ¹³Yonsei University College of Medicine, Internal Medicine
Email: gudwms21@korea.ac.kr

Background and aims: Early detection of hepatocellular carcinoma (HCC) is critically important for the improvement of prognosis.

Although combining AFP and ultrasonography (US) are the standard modalities for surveillance of HCC, combining other tumor biomarkers such as PIVKA-II or AFP L3 with AFP is currently suggested to improve the detection rates of HCC. However, prospective evaluation of combinations of such biomarkers has been rarely performed. The present study aimed to confirm the utility of combination of biomarkers and imaging modalities for early detection of HCC inpatients with liver cirrhosis.

Method: Patients with histologically or clinically confirmed liver cirrhosis were enrolled at 14 tertiary hospitals in Korea. Patients with elevated AFP (>20 ng/ml), hepatic nodule ≥ 1 cm by US or liver CT, or Child-Pugh score ≥ 11 points were excluded. HCC surveillance using AFP, AFP L3, PIVKA-II, and US were performed every 6 months. In addition, liver CT was scanned every 12 months.

Results: A total of 2810 patients/year were followed-up prospectively. Among them, HCC developed in 56 patients. Under this intensive surveillance program, most of HCCs detected were at early stage (50/56 were BCLC stage 0 or A, 48/56 were TNM stage 1, 54/56 were modified UICC stage 1 or 2) and the mean size of HCCs was 1.8 cm (1.3–2.6). The sensitivity of the biomarkers was 42.9% for AFP, 48.2% for AFP L3, 39.3% for PIVKA-II, 59.0% for combination of the three markers when the sensitivity was set to be $\geq 90\%$; Three-combination was the highest and the AFP L3 was the next. We assessed the area under the receiver operating curves (AUROC) for one, two, and three combination of the biomarkers such as AFP (0.598), AFP+AFP L3 (0.646), AFP+PIVKA-II (0.664), and AFP+AFP L3+PIVKA-II (0.688), and found that the three combination was the best. In addition, when incorporated the three biomarkers into GALAD (Gender, Age, L3, AFP, and DCP [= PIVKA-II]) score, the AUROC was 0.778, which is the better. The AUROC improved by adding US (0.820) or liver CT (0.864) on combination of three biomarkers.

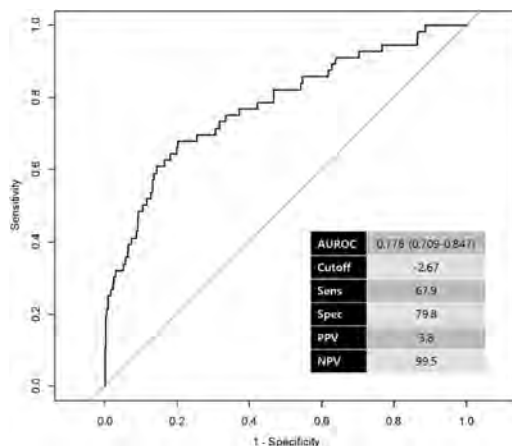


Figure: AUROC of GALAD score in which three biomarkers incorporated.

Conclusion: For early detection of HCCs, a combination of three biomarkers (AFP, AFP L3, PIVKA-II) or GALAD score was shown to be useful in this prospective evaluation. Adding imaging modalities improved the performance further.

SAT591

A natural experiment investigating the impact of waiting time on post-transplant survival for patients with hepatocellular carcinoma: randomization by blood group

Berend Beumer¹, Wojciech Polak¹, Robert De Man², Herold J. Metselaar², Jan Ijzermans¹. ¹Erasmus MC Transplant Institute, Department of Surgery, Division of HPB and Transplant Surgery, Rotterdam, Netherlands; ²Erasmus MC Transplant Institute, Department of Gastroenterology and Hepatology, Rotterdam
Email: b.beumer@erasmusmc.nl

Background and aims: When listing for liver transplantation we can transplant as soon as possible or introduce a test of time to better

select patients as the tumor's biological behavior is observed. Knowing the degree of harm caused by time itself is essential to advise patients and decide on the maximum duration of the test-of-time. Therefore, we investigated the causal effect of waiting time on post-transplant survival for patients with HCC.

Method: We analyzed the UNOS-OPTN dataset and exploited the natural experiment created by blood groups. Relations between variables were described in a causal graph. Inverse probability weighting was used to address selection bias. Confounding biases were avoided using instrumental variable analysis, with an additive hazards model in the second stage. The causal effect was evaluated as a contrast between a scenario in which all patients waited 2 months and one in which all patients waited 12 months. Upper bounds of the test-of-time were evaluated for probable scenarios by means of simulation.

Results: The F-statistic of the first stage was 86.3. The effect of waiting 12 months versus 2 months corresponded with a significant drop in overall survival of 5.07% 95%CI [0.277; 9.69] and 8.33% 95% CI [0.47; 15.60] at 5- and 10-years post-transplant, respectively. The median survival significantly dropped by 3.41 years from 16.21 years 95%CI [15.98; 16.60] for those waiting 2 months to 12.80 years 95%CI [10.72; 15.90] for those waiting 12 months. No significant effect modification by tumor size or number was found.

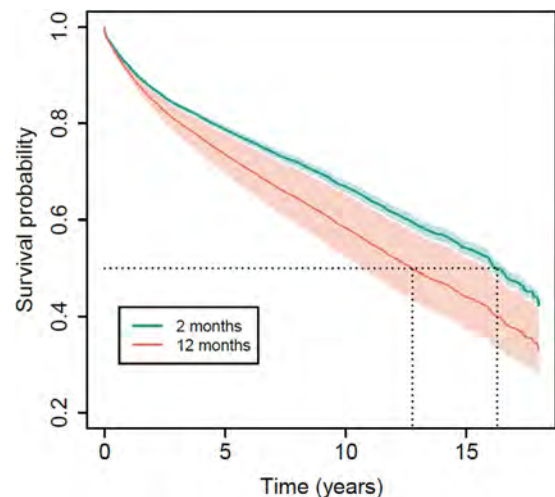


Figure 1: The survival probabilities if all listed HCC patients wait either 2 or 12 months.

Conclusion: From a patient's perspective the choice between ablate-and-wait versus immediate transplantation is in favor of immediate transplantation. From a policy perspective, the extra waiting time can be used to increase the utility of scarce donor livers, although the duration of the test-of-time is bound to be likely less than 8 months.

SAT592

Baveno VII criteria identify varices needing treatment in patients with hepatocellular carcinoma of different BCLC stages undergoing curative hepatectomy

Grace Lai-Hung Wong¹, Terry Cheuk-Fung Yip¹, Angus Wong¹, Brian Chan¹, Matthew Fong¹, Vincent Wai-Sun Wong¹, Stephen L. Chan², Kelvin Ng³. ¹The Chinese University of Hong Kong, Medical Data Analytic Centre (MDAC) and Department of Medicine and Therapeutics, Hong Kong; ²The Chinese University of Hong Kong, State Key Laboratory of Translational Oncology, Department of Clinical Oncology, Hong Kong; ³The Chinese University of Hong Kong, Department of Surgery, Hong Kong
Email: wonglaihung@cuhk.edu.hk

Background and aims: The latest Baveno VII consensus, which was published in late 2021 discussed the use of non-invasive tools for the diagnosis of compensated advanced chronic liver disease (cACLD)

POSTER PRESENTATIONS

and clinically significant portal hypertension (CSPH). We aimed to investigate the predictive value of Baveno VII consensus, as well as other LSM and platelet cutoffs, to predict the presence of varices needing treatment (VNT) in patients with HCC of different stages Barcelona Clinic Liver Cancer staging system (BCLC) undergoing curative hepatectomy.

Method: This was a prospective cohort of patients with confirmed diagnosis of HCC. Patients underwent transient elastography examination before HCC treatment. Patients were prospectively followed for VNT, defined as all grade II to III varices (≥ 5 mm), and small varices found in patients with Child-Pugh C cirrhosis, and any varices presenting red-wale signs, fibrin clot or active bleeding.

Results: 712 patients (83.3% male, median age 62 years old) were recruited from March 2013 to April 2019. Most patients (76%) suffered from chronic hepatitis B infection, 405 (57%) and 595 (84%) patients had platelet count $\leq 150 \times 10^9/L$ and $\geq 110 \times 10^9/L$ respectively. Majority of the patients ($n=389$, 55%) had HCC of BCLC stage A, whereas 69 (10%) patients had stage 0, 131 (18%) patients had stage B and 121 (17%) patients had stage C tumour. The median follow-up duration of patients was 45.8 months. The median liver stiffness measurement (LSM) was 10.5 kPa (Range: 7.0–20.6 kPa); 461 (65%) patients had LSM ≤ 15 kPa, 516 (72.5%) patients had LSM ≤ 20 kPa and 554 (77.8%) patients had LSM ≤ 20 kPa. Patients of BCLC stage 0 and stage A HCC had lower LSM (9.6 kPa and 9.5 kPa respectively), compared to those of BCLC stage B and C HCC (13.2 kPa and 20.6 kPa respectively). VNT occurred in 57 (8.0%) patients, which occurred a bit more commonly in BCLC stage C (12 patients, 10.0%) than earlier stages of HCC (stage 0, 8.7%; stage A, 7.5%; stage B, 7.6%; Table 2). In patients who fulfilled Baveno VII criteria, i.e. LSM ≤ 20 kPa together with a platelet count above $150 \times 10^9/L$, only fourteen (2.0%) patients had VNT. In all BCLC stages of HCC, the proportion of patients with VNT was below 5% (1.5% in stage 0, 1.3% in stage A, 3.1% in stage B, and 3.3% in stage C), which support the validity and applicability of Baveno VII criteria in all BCLC stages of HCC.

	All patients N = 712	BCLC stage 0 N = 69	BCLC stage A N = 389	BCLC stage B N = 131	BCLC stage C N = 121
Any varices	85 (11.9%)	7 (10.1%)	40 (10.3%)	17 (13.0%)	21 (17.4%)
Oesophageal varices ^a	82 (11.5%)	7 (10.1%)	38 (9.8%)	16 (12.2%)	21 (17.4%)
Gastric varices ^a	5 (0.7%)	0 (0%)	4 (1.0%)	1 (0.8%)	0 (0%)
Acute variceal bleeding (AVB)	25 (3.5%)	0 (0%)	14 (3.6%)	4 (3.1%)	7 (5.8%)
Bleeding oesophageal varices ^a	22 (3.1%)	0 (0%)	12 (3.1%)	3 (2.3%)	7 (5.8%)
Bleeding gastric varices ^a	3 (0.4%)	0 (0%)	2 (0.5%)	0 (0%)	0 (0%)
Endoscopic therapy	39 (5.5%)	2 (2.9%)	18 (4.6%)	7 (5.3%)	12 (10.0%)
Varices needing treatment (VNT)	57 (8.0%)	6 (8.7%)	29 (7.5%)	10 (7.6%)	12 (10.0%)
VNT in following subgroups					
LSM ≤ 15 kPa & PLT $\geq 150 \times 10^9/L$	13 (1.8%)	1 (1.5%)	4 (1.0%)	4 (3.1%)	4 (3.3%)
LSM ≤ 15 kPa & PLT $\geq 110 \times 10^9/L$	19 (2.7%)	2 (2.9%)	9 (2.3%)	4 (3.1%)	4 (3.3%)
LSM ≤ 20 kPa & PLT $\geq 150 \times 10^9/L$	14 (2.0%)	1 (1.5%)	5 (1.3%)	4 (3.1%)	4 (3.3%)
LSM ≤ 20 kPa & PLT $\geq 110 \times 10^9/L$	21 (2.9%)	3 (4.3%)	10 (2.6%)	4 (3.1%)	4 (3.3%)
LSM ≤ 25 kPa & PLT $\geq 150 \times 10^9/L$	15 (2.1%)	1 (1.5%)	6 (1.5%)	4 (3.1%)	4 (3.3%)
LSM ≤ 25 kPa & PLT $\geq 110 \times 10^9/L$	23 (3.2%)	3 (4.3%)	11 (2.8%)	4 (3.1%)	5 (4.1%)
Survival (months)	45.8 (21.5–82.5)	66.5 (49–101)	58.9 (32.9–95.4)	26.0 (10.5–54.2)	14.5 (4.9–39.6)

Figure: Varices in different BCLC stages.

Conclusion: This was the first long-term follow-up study of HCC patients undergoing curative hepatectomy supporting the validity and applicability of the new Baveno VII criteria for selecting patients to undergo screening endoscopy for VNT. The validity was consistent across different BCLC stages of HCC.

Grant support: This work was supported by the Health and Medical Research Fund (HMRF)-Food and Health Bureau (Reference no.: 07180216) awarded to Grace Wong.

SAT593

Factors associated with HCC stage at presentation and survival in an ethnically diverse UK population

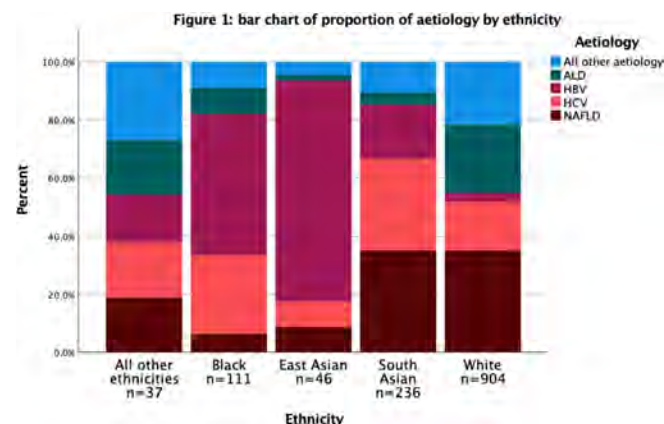
Jessica Spiers¹, Wenhao Li¹, Aloysious Aravinthan², Katharine Caddick³, Yaqza Hussain⁴, Ayman Bannaga⁴, Saad Muhammad⁴, Muhammad Nauman Tahir⁴, Abhishek Sheth², Ankur Srivastava³, Mohsan Subhani², Esther Unitt⁴, Nwe Ni Than⁴, William Alazawi¹. ¹Blizard Institute, Queen Mary University of London, Barts Liver Centre, London, United Kingdom; ²Nottingham University Hospitals NHS Trust, Queen's Medical Centre, United Kingdom; ³North Bristol NHS Trust, Southmead Hospital, Bristol, United Kingdom; ⁴University Hospital Coventry and Warwickshire, Coventry, United Kingdom
Email: jessica.spiers3@nhs.net

Background and aims: Risk factors for hepatocellular carcinoma (HCC) include cirrhosis and diabetes, but patient- and disease-related factors in prognosis have not been widely explored. Evidence highlights ethnic disparity in HCC stage at presentation and survival in the USA; White patients present earlier and survive longer, but there is little evidence evaluating any disparity in the UK.

We sought to evaluate the factors associated with HCC stage at presentation and survival in a UK population.

Method: We retrospectively analysed data from referrals to HCC multidisciplinary teams in 4 regional centres: East London and Essex, Nottingham, Coventry, and Bristol, between 2007 and 2021, where data available. We included all patients with confirmed diagnosis of HCC. Early stage at presentation was defined as Barcelona Clinic Liver Centre (BCLC) Stages 0 and A, late stage was defined as BCLC Stages C and D. Analyses were conducted using Cox regression models for survival and logistic regression models for stage at presentation, all adjusted for age, sex, aetiology of liver disease, HCC surveillance and centre.

Results: We included 1357 patients with a median follow-up of 12 months. 31% of patients had Non-Alcoholic Fatty Liver Disease (NAFLD), 33% had Viral hepatitis, and 18% had Alcoholic Liver Disease (ALD) (Figure 1).



The overall 2-year survival rate was 40%. White ethnicity was independently associated with reduced mortality (Hazard ratio [HR] 0.835, $p=0.043$), but not early-stage presentation (Odds ratio [OR] 1.324, $p=0.089$).

21% of patients had non-cirrhotic HCC. Patients with NAFLD were more likely to develop non-cirrhotic HCC compared with patients with Viral hepatitis and ALD (24% vs. 10%, $p < 0.001$ Chi-square). While HCC surveillance was associated with overall lower risk of mortality (HR 0.699, $p < 0.001$), it was not associated with mortality in the 433 patients with NAFLD (HR 0.806, $p=0.183$). However, it was an independent predictor of early-stage presentation in this cohort (OR 2.313, $p=0.002$).

In patients with diabetes, metformin use was independently associated with early-stage presentation (OR 1.932, $p = 0.008$) and survival (HR 0.674, $p = 0.008$). Diabetes diagnosis was not associated with risk of death (HR 0.912, $p = 0.304$).

Conclusion: In this multi-centre study, White patients were less likely to die following a diagnosis of HCC compared to other ethnicities.

Diabetes status was not an independent predictor of survival but, among patients with diabetes, those on metformin were almost twice as likely to present with early-stage disease, and were less likely to die, consistent with existing evidence for a protective role of metformin in HCC.

HCC surveillance was a predictor of overall survival but not in patients with NAFLD who are at greater risk of developing non-cirrhotic HCC and for whom the current outpatient surveillance programme may require modification.

SAT594

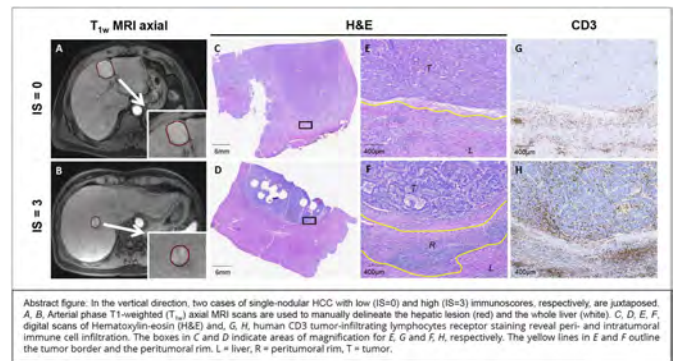
Use of machine learning to predict the histopathological ImmunoScore in hepatocellular carcinoma on multiparametric MRI

Junlin Yang¹, Annabella Shewarega¹, Jessica Santana¹, Vasily Pekurovsky¹, Xuchen Zhang², MingDe Lin¹, David Madoff¹, Lawrence Staib¹, Julius Chapiro¹, James Duncan¹. ¹Yale University, Radiology and Biomedical Engineering, New Haven, United States; ²Yale University, Pathology, New Haven, United States
Email: julius.chapiro@yale.edu

Background and aims: Immunotherapy is the new first-line treatment for advanced-stage hepatocellular carcinoma (HCC) and combinations with locoregional therapies are currently under investigation for intermediate disease stages. However, tumor response to immunotherapy is highly variable and depends on immunological features of the tumor microenvironment at baseline. Histopathologic biomarkers such as the ImmunoScore are potent predictors of response to immunotherapy, however, they are not readily available given the need for tissue sampling. Accordingly, there is an unmet need for non-invasive surrogate markers for the immunological state of HCC prior to allocation of therapy. The purpose of this study is to establish ground proof for the ability of machine learning to extract radiomic features from multi-parametric MRI to predict ImmunoScores in HCC.

Method: This study included 17 individual HCC lesions with whole-tumor gross and histopathology obtained via hepatectomy or orthotopic liver transplantation within 30 days of preoperative abdominal contrast-enhanced MRI. The ImmunoScore, an index indicating the density of CD3⁺, CD4⁺, and CD8⁺ tumor-infiltrating T-lymphocytes both in the tumor center and tumor margin, was assessed by a board-certified pathologist. ImmunoScores of 0–2 signified immunologically “cold” tumors while scores of 3–4 signified immunologically “hot” tumors. Arterial and delayed venous phases of the contrast-enhanced T1-weighted MRI were used to segment both tumors and the whole liver volume. The segmentation masks were used to train an autoencoder with binary cross-entropy and mean squared error (MSE) loss. The latent codes consist of 128 features of each phase and 2 clinical non-imaging features, hepatitis C virus and cirrhosis, resulting in 258 features in total. The latent codes were used for prediction in the following steps. Next, a univariate feature selection was used to select 12 features. Then, linear regression and a random forest model were used to predict ImmunoScores.

Results: Leave-one-out cross-validation was used to evaluate the model performance. The linear regression model showed good performance in predicting the ImmunoScore, with a F1 score 58.42, an AUC of 86.67, and an accuracy of 70.59. The random forest model showed a greater degree of predictiveness with a F1 score 88.24, an AUC of 85.83, and an accuracy of 88.24.



Conclusion: Machine learning-based extraction of radiomic features from multi-phasic MRI may serve as a non-invasive surrogate for ImmunoScore prediction of HCC, potentially facilitating immunophenotyping of tumors prior to allocation to immunotherapy. These results demonstrate a proof of principle and require external validation and prospective evaluation in larger clinical cohorts with tumor response as the next study end point.

SAT595

Value of 18-F fluorodeoxyglucose/choline positron emission tomography imaging for predicting hepatocellular carcinoma recurrence after liver transplantation

Alina Pascale¹, Florent Besson², Nicolas Golse¹, Catherine Guettier³, Maite Lewin⁴, Jean-Charles Duclos-Vallée¹, Rodolphe Sobesky¹, Eleonora De Martin¹, Edoardo Poli¹, Ilias Kounis¹, Lea Duhaut¹, Yasmina Ben Merabet¹, Bruno Roche¹, Tereza Antonini¹, Faouzi Saliba¹, Philippe Ichai¹, Marc Boudon¹, Sophie Sacleux¹, Marie-Amelie Ordan¹, Marc Antoine Allard¹, Gabriella Pittau¹, Oriana Ciacio¹, Antonio Sa Cunha¹, Daniel Azoulay¹, René Adam¹, Eric Vibert¹, Daniel Cherqui¹, Audrey Coilly¹, Olivier Rosmorduc¹, Didier Samuel¹. ¹Paul Brousse Hospital, Hepato-Biliary Center, Villejuif, France; ²Bicetre Hospital, Nuclear Medicine-Molecular Imaging, France; ³Bicetre Hospital, Pathology; ⁴Paul Brousse Hospital, Radiology
Email: alina_pascale@yahoo.com

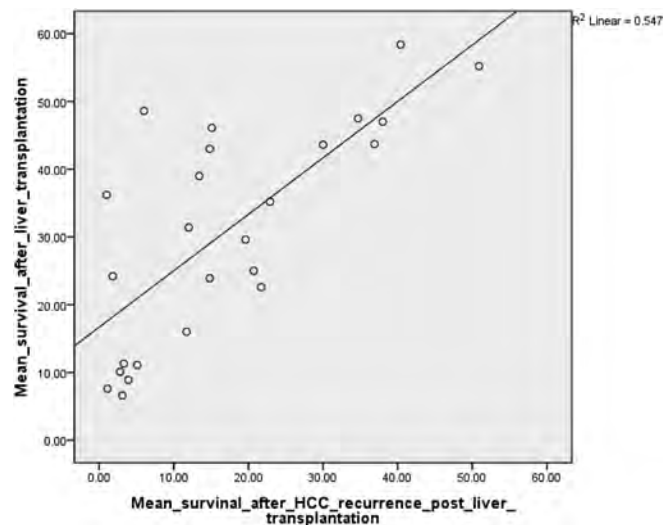
Background and aims: The major issue of liver transplantation (LT) for hepatocellular carcinoma (HCC) is predicting patients at low risk for tumor recurrence. Different criteria, such as Milan criteria, alpha-fetoprotein (AFP) score, are used to select candidates before LT. Despite increasing use of positron emission tomography (PET) imaging in HCC, its value in predicting recurrence after LT is not clear and it is not considered among selection criteria for LT. We studied here the correlation between HCC recurrence after LT and positivity of PET imaging before LT.

Method: We retrospectively analyzed 198 patients consecutively transplanted for HCC in Hepato-Biliary Center, Paul Brousse Hospital, France, between January 2015 and December 2019. We collected demographic data, characteristics of cirrhosis, HCC and PET imaging before LT and post LT data, including histological data. 71 patients had available data before LT on 18F-fluorodeoxyglucose (18F-FDG) and choline PET positivity and SUV analyses. Patients were followed at least two years after LT to detect recurrence. Statistical analyses were performed in SPSS, using Spearman's correlations.

Results: The median age of patients was 61.7 years (range: 34–74) and 166 were males (83.8%). The main etiologies of cirrhosis were: alcohol (40.4%), viral hepatitis (37.8%) and metabolic (13.3%). 76 patients (38.4%) had diabetes. The AFP score at listing was 0 in 62.6% of patients, 1 in 20.7% and 2 in 14.1%. The majority (90.4%) had a bridging treatment before LT. Median waiting time for LT was 5.8 months (range: 0.1–54). 35 (17.7%) patients experienced HCC recurrence after LT. The median time to recurrence was 16.1 months (range: 1–47). HCC recurrence was metastatic at diagnosis in 32 patients (91.4%) and 26 patients had only extrahepatic location. The

POSTER PRESENTATIONS

median follow-up after LT was 30.6 months. The mean survival post HCC recurrence after LT was 17 months (range: 1–50.9). Among the 71 patients with available 18F-FDG PET imaging data, 53 (74.6%) were negative and 18 (25.3%) were positive. Among the 47 patients with available choline-PET imaging data, 25 (53.1%) were negative and 22 (46.8%) were positive. In univariate and multivariate analysis, HCC recurrence after LT is correlated with 18F-FDG PET positivity before LT ($p = 0.03$, $r = 0.262$), but not with choline PET positivity ($p = 0.98$) and histological findings on liver explant: active HCC nodules ($p = 0.002$), microvascular invasion ($p < 0.001$) and macrovascular invasion ($p < 0.001$).



Conclusion: In our cohort, HCC recurrence after LT is a serious adverse event, as it occurs early, is often already metastatic at diagnosis and impacts drastically the survival after LT. HCC recurrence risk after LT could be predicted by the 18F-FDG PET positivity before LT. Further validation is needed but this could be a signal of a potential role of PET imaging for better selecting HCC candidates for LT.

SAT596

Germline genetic risk factors for the development of hepatocellular carcinoma among patients with cirrhosis: a genome-wide association study of U.S. veterans

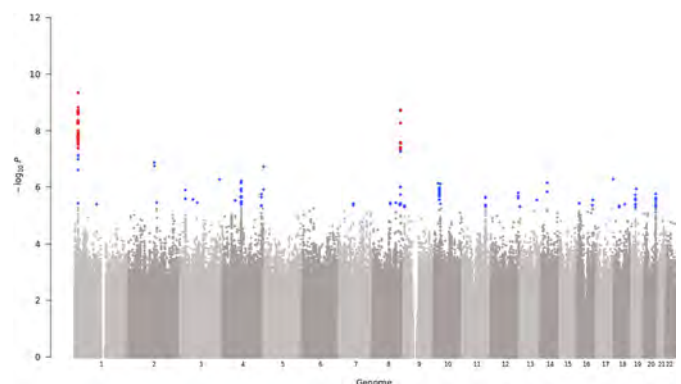
David Kaplan^{1,2}, Marijana Vujkovic^{1,2}, Daniel Dochterman³, Kirk Wengensteen¹, Poornima Devineni⁴, Tae-Hwi Linus Schwantes-An⁵, Anoop Sendamarai⁴, Purushtotham Karnam⁴, Emily Sileo⁴, Tori Anglin³, Trina Norden-Krichmar⁶, Philip Tsao⁷, Timothy Morgan⁸, Saiju Pyarajan⁴, Julie Lynch^{3,9}, Benjamin Voight¹, Kyong-Mi Chang^{1,2}.
¹University of Pennsylvania, Philadelphia, United States; ²Corporal Michael J. Crescenz VA Medical Center, Philadelphia, United States; ³VA Salt Lake City Health Care System, United States; ⁴Center for Data and Computational Sciences, United States; ⁵Indiana University School of Medicine, Indianapolis, United States; ⁶University of California Irvine, Irvine, United States; ⁷VA Palo Alto Healthcare System, Palo Alto, United States; ⁸VA Long Beach Healthcare System, Long Beach, United States; ⁹University of Massachusetts College of Nursing, United States
 Email: dakaplan@pennmedicine.upenn.edu

Background and aims: Hepatocellular carcinoma (HCC) remains a highly mortal cancer with an approximate 20% 5-year survival rate. The primary risk factor for the development of HCC is the presence of cirrhosis, most commonly caused by chronic hepatitis B (HBV) infection, chronic hepatitis C (HCV) infection, alcohol-related liver disease (ALD) and increasingly non-alcoholic fatty liver disease/non-alcoholic steatohepatitis (NAFLD/NASH). Multiple somatic driver gene candidates in HCC including but not limited to TERT, CTNNB1,

TP53, myc, ARID1A, ARID2, AXIN1 have been identified. However, few studies have evaluated germline genetic risk factors for HCC development and none have isolated genes specifically associated with HCC evolving from cirrhosis. The purpose of present study was to identify genetic risk factors for HCC in patients with cirrhosis associated with metabolic and non-metabolic causes of chronic liver disease.

Method: A clinical phenotype consistent with HCC and/or cirrhosis was generated for MVP participants based upon ICD9/10 codes, exclusion of metastatic cancers using VA clinical cancer registry data, FIB-4 scores, and identification of disease etiology using a validated algorithm. Cirrhosis controls were required to have ≥ 3 years follow-up without identification of HCC. Ancestry-specific and multi-ancestry genome-wide association analyses (customized Affymetrix Axiom Array with total 723,305 SNPs) were performed comparing HCC cases and cirrhosis controls, with the covariates of age, age squared, sex, etiology and first 10 principal components of genetically defined ancestry.

Results: From ~650,000 MVP participants, 3,445 HCC cases and 9,626 cirrhosis controls were identified with both metabolic and non-metabolic causes of chronic liver disease. Median time from cirrhosis to HCC diagnosis in cases was 1.9 years [IQR 0.0–5.5], and median cancer-free follow-up of controls was 5.8 years [IQR 4.4–8.1]. Multi-ancestry analysis identified 2 novel trans-ancestry loci associated with carcinogenesis that met genome wide significance (5×10^{-8} , EPHA2/ARHGEF19, LINC00824 marking a cancer risk locus on 8q24.21 with multiple candidate genes including MYC) as well as one additional African-specific locus and one Hispanic-specific locus.



Conclusion: Our effort using population-based MVP biobank has identified novel germline genetic risk loci for HCC evolving out of cirrhosis. Efforts are ongoing to expand our sample size and identify external cohorts for further replication. Future work would include validation of these genetic markers as biomarkers for selection for intensified HCC surveillance.

SAT597

A comparative analysis of Elecsys GALAD and Elecsys GAAD score to detect early-stage hepatocellular carcinoma in an international cohort

Henry LY Chan¹, Arndt Vogel², Thomas Berg³, Enrico de Toni⁴, Masatoshi Kudo⁵, Jörg Trojan⁶, Katharina Malinowsky⁷, Peter Findeisen⁸, Hanns-Georg Klein⁹, Johannes Kolja Hegel¹⁰, Wenzel Schöning¹¹, Konstantin Kroeniger¹², Kairat Madin¹², Ashish Sharma¹³, Teerha Piratvisuth¹⁴. ¹The Chinese University of Hong Kong, Hong Kong; ²Medizinische Hochschule Hannover, Germany; ³Universitätsklinikum Leipzig, Germany; ⁴University Hospital, Ludwig Maximilian University of Munich, Department of Medicine II, Germany; ⁵Kindai University, Japan; ⁶Goethe Universität Frankfurt, Germany; ⁷Microcoat Biotechnologie GmbH, Germany; ⁸MVZ Labor Dr. Limbach Kollegen, Germany; ⁹Zentrum für Humangenetik und Laboratoriumsdiagnostik, Germany; ¹⁰Labor Berlin Charité Vivantes Services GmbH; ¹¹Universitätsmedizin Berlin, Chirurgische Klinik, Campus Charité Mitte und Campus Virchow-Klinikum, Germany; ¹²Roche Diagnostics GmbH, Germany; ¹³Roche Diagnostics International AG, Switzerland; ¹⁴Prince of Songkla University, Thailand
Email: teerha.p@psu.ac.th

Background and aims: The combination of gender (sex) and age plus serum biomarkers alpha-fetoprotein (AFP), Lens culinaris agglutinin-reactive fraction of AFP (AFP-L3) and protein-induced by vitamin K absence-II (PIVKA-II) forms the GALAD algorithm, a promising aid in the detection of early-stage hepatocellular carcinoma (HCC). Here, we present results from the first study comparing the clinical performance of the Elecsys[®] GALAD and Elecsys GAAD (gender [sex], age, AFP and PIVKA-II) algorithms for differentiating early-stage HCC and benign chronic liver disease (CLD).

Method: Adult patients were prospectively enrolled at 9 hospitals in Germany, Thailand, Hong Kong and Japan. Eligible HCC cases had first-time HCC diagnosis confirmed by ultrasound or liver biopsy. Eligible CLD controls had imaging-confirmed absence of HCC (within 12 months), and presence of cirrhosis or non-cirrhotic: chronic hepatitis B/C virus (HBV/HCV), alcoholic liver disease (ALD) or non-alcoholic steatohepatitis (NASH). Serum levels of PIVKA-II, AFP and AFP-L3 were measured using Elecsys assays on the cobas e 601 analyzer. The established cut-offs for HCC detection were 20 ng/ml for AFP, 2.47 for Elecsys GALAD, and 2.57 for Elecsys GAAD scores (range 0–10 for both).

Results: A total of 465 patients (246 with HCC and 219 CLD controls) were included. Among the HCC/CLD cohorts, mean age was 63.5/52.5 years, 81.7%/59.8% were male and 71.1%/28.9% had cirrhosis. Among HCC patients, 43.5% had early-stage HCC (Barcelona Clinic Liver Cancer [BCLC] 0 and A). Of 219 CLD controls, one was excluded from final analysis due to incomplete biomarker data. Elecsys GAAD and GALAD algorithms showed similar performance for discriminating between HCC and CLD (Table): sensitivity for identification of early-stage (72.9% vs 73.8%) and all-stage (85% vs 85.8%) HCC was comparable, and specificity was >90% for both scores. AUCs were similar across cirrhotic (87.6% vs 87.5% for early-stage, 92.9% vs 92.8% for all-stage HCC) and non-cirrhotic (91.2% vs 91.1%; 93.6% both) etiologies. The performance of Elecsys GAAD and GALAD algorithms were superior to AFP alone (Table).

Assay/algorithm (cut-off)	Early-stage HCC			All-stage HCC		
	AUC	Sensitivity	Specificity	AUC	Sensitivity	Specificity
AFP (20 ng/ml)	82.4 (77.4–87.5)	36.4 (27.4–46.3)	98.2 (95.4–99.5)	87.1 (83.9–90.3)	50.4 (44–56.8)	98.2 (95.4–99.5)
GAAD (2.57)	91.3 (88–94.6)	72.9 (63.4–81.0)	92.2 (87.9–95.4)	94.8 (92.9–96.7)	85.0 (79.9–89.2)	92.2 (87.9–95.4)
GALAD (2.47)	91.3 (87.9–94.6)	73.8 (64.4–81.9)	90.8 (86.2–94.3)	94.7 (92.8–96.7)	85.8 (80.8–89.9)	90.8 (86.2–94.3)

All results shown as % (95% CI)

Conclusion: The Elecsys GALAD and GAAD algorithms showed similar performance in differentiating HCC and CLD controls, irrespective of etiology and disease stages. This suggests that the Elecsys AFP-L3 assay had a negligible impact as part of Elecsys GALAD algorithm in the tested cohort.

SAT598

Mixed reality for ultrasound-guided biopsies and ablations of liver tumors: proof of concept using HoloLens as head-mounted display during liver interventions

Fabiola Lugano¹, Irina Bergamin¹, Pamela Meyer-Herbon¹, Lukas Hechelhammer², David Semela¹. ¹Kantonsspital St. Gallen, Division of Gastroenterology and Hepatology, St. Gallen, Switzerland; ²Kantonsspital St. Gallen, Institute of Radiology and Interventional Radiology, St. Gallen, Switzerland
Email: david.semela@kssg.ch

Background and aims: Improving visualization is an important component of facilitating a safe procedure during hepatological interventions. In this context, we have explored whether mixed-reality is feasible and safe in patients undergoing liver biopsy, biopsy of focal liver lesions and interventions such as ultrasound-guided ablation of liver tumors (HCC, liver metastasis) and drainage of liver abscesses. Here we report for the first time the use of SonoEyes[®] (in combination with a HoloLens[®] device as head-mounted display projecting the ultrasound screen).

Method: SonoEyes[®], a CE certified app (class IIa medical device) projects the image from the conventional ultrasound screen onto a mixed-reality headset (HoloLens 2, Microsoft[®]) using a head-mounted display projecting the image from the ultrasound screen in front of the user of the device while the surrounding environment can still be seen and remains unaltered (mixed reality, figure). The system can be connected to any ultrasound device via HDMI. The image can be moved and placed to the comfort of the user (i.e. zooming, position, recording) via voice commands or by using hand gestures even during the procedure while sterile.



Results: This novel imaging technique was used in the clinical setting of biopsies (liver, focal liver lesions) as well as hepatic interventions such as US-guided microwave ablations of liver tumors (figure) and

drainage of liver abscesses (3 hepatologists/1 interventional radiologist, 12/2021 through 03/2022, single center, 400+ biopsies, 50+ ablations annually). To increase visibility of liver lesions (hepatocellular and cholangiocellular carcinoma, metastases) contrast-enhanced ultrasound imaging was used if needed. Use of this mixed reality technology in hepatological interventions was immediate and self-explanatory. Addition of a head-mounted display for the procedures allowed reduced movements of the operating physicians and led to increased focus on the intervention since the examiner stays in situ while having the patient, operating field and the needle in one visual field.

Conclusion: Use of this mixed reality technology in hepatological interventions such as biopsies of focal liver lesions, tumor ablations and liver abscess drainages proved to be useful. This proof of concept showed for the first time that using mixed-reality technology in ultrasound-guided liver interventions is feasible and associated with advantages such less movement during biopsy/ultrasound-guided intervention allowing a better focus on the intervention sight, lower risk of contamination of the sterile field. In addition, live recording by this device was useful for physicians in training in order to review their interventions later.

SAT599

Type 2 diabetes combined with portal vein tumor thrombosis worsens prognosis in patients with hepatocellular carcinoma

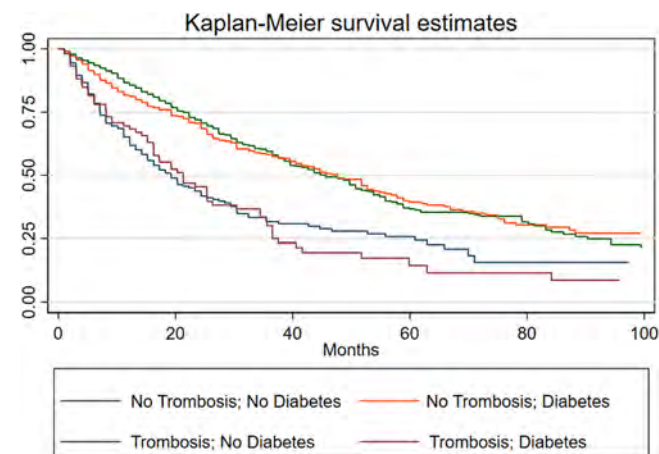
Debora Angrisani¹, Marco Guarracino², Nunzia Farella³, Filomena Morisco⁴, Carmine Coppola⁵, Francesco Izzo⁶, Angelo Salomone Megna⁷, Alessandro Federico⁸, Vincenzo Messina⁹, Gerardo Nardone¹⁰, Guido Piai¹¹, Enrico Ragone¹², Luigi Elio Adinolfi¹³, Giuseppe D'Adamo¹⁴, Maria Stanzione¹⁵, Giampiero Francica¹⁶, Marcello Persico¹⁷, Vincenzo De Girolamo¹⁸, Coppola Nicola¹⁹, Lucia Rocco², Giovan Giuseppe Di Costanzo², Raffaella Tortora². ¹AORN Cardarelli, Hepatology Unit, Naples, Italy; ²AORN Cardarelli, Hepatology Unit, Naples, Italy; ³AORN Ospedale dei colli, Malattie Infettive ad indirizzo ecoinfermentistico, Naples, Italy; ⁴University Federico II, Dipartimento di Medicina Clinica e Chirurgia, Naples, Italy; ⁵OO.RR Area Stabiese; ⁶U.O. di Epatologia ed Ecografia Interventistica, Gragnano, Italy; ⁷Istituto Nazionale per lo studio e la cura dei Tumori, IRCCS Fondazione Pascale; ⁸Chirurgia Oncologica Addominale ad indirizzo Epatobiliare, Naples, Italy; ⁹Azienda Ospedaliera San Pio, OC Malattie Infettive, Benevento, Italy; ¹⁰Università della Campania Vanvitelli, Department of Clinical and Experimental Medicine, Napoli, Italy; ¹¹AORN Sant'Anna e San Sebastiano, UOC Malattie infettive, Caserta, Italy; ¹²Federico II University, Dipartimento di Medicina Clinica e Chirurgia, Naples, Italy; ¹³AORN Sant'Anna e San Sebastiano; ¹⁴UOSD Fisiopatologia Epatica con Servizio di Assistenza ai Trapiantati e Trapiantandi Epatici, Caserta, Italy; ¹⁵AORN Ospedale dei colli, Naples, Italy; ¹⁶Università della Campania Vanvitelli, UO Medicina Interna, Marcanise, Italy; ¹⁷PO Umerto I, UO Medicina Interna, Nocera Inferiore, Italy; ¹⁸Università della Campania Vanvitelli, Dipartimento di Salute Mentale e Fisica e Medicina Preventiva, Naples, Italy; ¹⁹PO Pineta Grande, UO Medicina Interna, Castel Volturno, Italy; ²⁰Ospedale San Giovanni di Dio e Ruggi d'Aragona, Dipartimento di Medicina Clinica Medica, Epatologica e Lungodegenza, AOU OO. RR. San Giovanni di Dio Ruggi e D'Aragona, Salerno, Italy; ²¹ALS Napoli 1-, PSI Napoli EST, Unità complessa di Gastroenterologia, Napoli, Italy; ²²Università della Campania Vanvitelli, Dipartimento di salute mentale e medicina Pubblica, Naples, Italy
Email: deborangrisani@hotmail.it

Background and aims: Type 2 diabetes combined with portal vein tumor thrombosis worsens prognosis in patients with hepatocellular carcinoma.

Method: we analyzed data of 2243 patients from an online region-wide database (Progetto Epatocarcinoma Campania) collected at 18 community and academic centers located in the Campania region, South of Italy. The database covered the period from January 2013 to

April 2021. Kaplan-Meier curves were used to investigate survival in different groups.

Results: There were 398 thrombotic events, 81% of the thrombosis were neoplastic. In 32% of cases the thrombus involved the main trunk, while it involved the right 1st order branch and left 1st order branch in 27% and 11% of cases, respectively. Patients with thrombosis had a risk of death doubled compared to patients without thrombosis. There was no difference in OS in patients with PVTT at the main trunk, or in the left or right portal vein. One hundred and twenty patients with PVTT had type 2 diabetes as comorbidity; in 9% of cases the hepatic disease had a metabolic cause. Patients with diabetes and PVTT had the highest risk of death [HR = 1.02 (0.88–1.18); p = 0.756], although the presence of diabetes was not related to overall survival (Figure).



Conclusion: type 2 diabetes is a risk factor for hepatocellular carcinoma and increases risk of death in patients who develop portal vein tumor thrombosis.

SAT600

British Association for the Study of Liver disease electronic survey on hepatocellular carcinoma UK surveillance practice

Robert Scott¹, Christopher Clarke², Stephen Ryder¹, Shahid Khan³, James Franklin⁴, Aloysious Aravinthan¹. ¹NIHR Nottingham Biomedical Research Centre, Hepatology, Nottingham, United Kingdom; ²Nottingham University Hospitals NHS Trust, Radiology, Nottingham, United Kingdom; ³Imperial College London, St Mary's Hepatology, London, United Kingdom; ⁴Bournemouth University and Royal Bournemouth Hospital, Medical Imaging and Visualisation, Bournemouth, United Kingdom
Email: mszada@nottingham.ac.uk

Background and aims: EASL, AASLD, APSAL recommend eligible patients undergo 6-monthly ultrasound (US) ± alpha fetoprotein (AFP) for HCC surveillance. Provision of this service is variable. There are no guidelines for secondary HCC surveillance. We aimed to survey UK HCC surveillance practice.

Method: An electronic questionnaire was distributed to all NHS hospitals via BASL with responses captured July 2021-January 2022 (single response per centre).

Results: 39 centres responded (15 hepatobiliary (HPB), 6 transplant, and 24 non-HPB centres) from across the UK (Figure 1, summarised in Table 1). NICE eligibility criteria were universally applied, but considerable variability exists otherwise (e.g. surveillance of Child-Pugh C, NASH, autoimmune disease). An estimated 80% undergoing surveillance have cirrhosis. 85% of centres do 6 monthly US and AFP. Compliance was estimated (25% unsure) at 80% but not routinely audited.



Figure: Responding BASL centres

Table 1: **Summary of results.** Median (range). CLD chronic liver disease.

No. of consultants managing CLD	5 (2–19)		
Lead HCC consultant?	90%		
No. of CLD specialist nurses (SN)?	3 (0–13)		
Lead Hepatology nurse?	67%		
iQILS accreditation?	18%		
Database of CLD patients?	33%		
	HPB centres (n = 15)	Non-HPB centres (n = 24)	
Consultants involved in HCC?	8 (3–15)	4 (1–15)	
SNs involved in HCC?	2 (0–10)	1.5 (0–5)	
No. of patients under HCC surveillance	1250 (300–3000)	500 (100–1250)	
Median no. of patients/consultant	156 (27–750)	145 (43–500)	
Median no. of patients/SN	140 (60–1500)	233 (54–1250)	
HCC surveillance programme?	95%		
Administrative support?	10%		
Written protocol for HCC surveillance?	36%		
Is HCC surveillance explained to the patient?	No 8%	Verbal 46%	Written and verbal 46%
Regular audit of HCC detection?	13%		
US reported using a template?	20%		
Agreed pathway for poor views?	Yes 28%	No 72%	
Offer CT or MRI for primary surveillance?	Yes 59%	No 41%	
Secondary HCC surveillance database?	41%		
Written protocol for secondary surveillance?	33%		

General sonographers and/or radiologists perform most surveillance and do not use structured reporting, felt desirable by most respondents. Poor views on US are approached heterogeneously with patients variably offered ongoing US, CT or different MRI protocols. Secondary surveillance is variable, typically using regular CT or MRI with contrast every 3–6 months for 2–5 years before 90% return to US surveillance.

Conclusion: Most responding UK NHS hospitals follow 6-monthly surveillance guidance for primary HCC surveillance. However, data collection regarding compliance, yield and quality. HCC US screening is mostly performed by non-specialists without standardised reporting with inconsistent approaches to poor views. The quality of HCC screening may be improved by consistent resourcing, standardised pathways, data collection and quality assurance.

Author Index

- Aagaard, Niels Kristian, S611 ([FRI491](#))
- Aardema, Charles, S719 ([SAT115](#))
- Aas, Christer F, S221 ([THU257](#))
- Aass, Hans Christian Dalsbotten, S826 ([SAT348](#))
- Abadia, Marta, S90 ([OS127](#))
- Abazia, Cristiana, S626 ([FRI522](#))
- Abbas, Nadir, S96 ([OS137](#)), S526 ([FRI269](#))
- Abbassi, Fariba, S815 ([SAT311](#))
- Abbati, Gian Luca, S839 ([SAT371](#))
- Abbott, Jane, S277 ([THU368](#))
- Abdelaal, Amr, S776 ([SAT246](#))
- Abdelanbi, Mohamed Nouredin Hassan Ali, S675 ([SAT022](#))
- Abdelhasseb, Dalia, S566 ([FRI351](#))
- Abdelmalek, Manal, S721 ([SAT119](#)), S722 ([SAT120](#))
- Abdelmalek, Manal F, S10 ([LB001](#)), S495 ([FRI210](#))
- Abdelrhman, Abo Zed, S137 ([THU035](#))
- Abdelwahab, Ahmed, S928 ([SAT581](#))
- Abdo, Ayman, S479 ([FRI178](#))
- Abdo, Mostafa, S776 ([SAT246](#))
- Abdul-Rahman, Kabbani, S83 ([OS113](#))
- Abdurakhmanov, Dzhamal, S1 ([GS001](#)), S574 ([FRI370](#))
- Abecia, Leticia, S177 ([THU155](#))
- Abedin, Nada, S907 ([SAT531](#))
- Abegg, Daniel, S645 ([FRI559](#))
- Abe, Kanon, S260 ([THU335](#))
- Abergel, Armand, S349 ([THU511](#)), S417 ([FRI042](#)), S549 ([FRI317](#)), S584 ([FRI388](#)), S640 ([FRI550](#)), S918 ([SAT563](#))
- Åberg, Fredrik, S80 ([OS109](#)), S413 ([FRI036](#)), S419 ([FRI046](#))
- Aberle, Stephan, S271 ([THU354](#)), S829 ([SAT353](#)), S830 ([SAT354](#))
- Aberra, Hanna, S841 ([SAT375](#))
- Abete, Itziar, S500 ([FRI222](#))
- Abeysekera, Kushala, S416 ([FRI041](#))
- Abhishek, Abhishek, S22 ([OS013](#))
- Abitbol, Jean Louis, S715 ([SAT105](#))
- Abouda, George, S63 ([OS079](#))
- Abouljoud, Marwan, S778 ([SAT249](#))
- Abraham, Arun, S164 ([THU089](#))
- Abraham, George, S235 ([THU286](#))
- Abraham, Katie, S554 ([FRI327](#))
- Abraham, Michal, S83 ([OS114](#))
- Abrales, Juan, S370 ([THU548](#))
- Abrales, Juan G, S906 ([SAT530](#))
- Abramczyk, Joanna, S601 ([FRI455](#))
- Abramov, Frida, S837 ([SAT368](#)), S866 ([SAT425](#))
- Abramovich, Ifat, S765 ([SAT214](#))
- Abramovitch, Rinat, S83 ([OS114](#)), S725 ([SAT126](#))
- Abreu, Nicolas De, S918 ([SAT563](#))
- Abu-Freha, Naim, S145 ([THU049](#)), S269 ([THU350](#)), S300 ([THU411](#))
- Abugabal, Yehia, S372 ([THU567](#)), S383 ([THU588](#))
- Abu-Hanna, Jerjes, S668 ([SAT008](#))
- Abu Hassan, Muhammad Radzi, S42 ([OS049](#))
- Abu-Nada, Mohamed, S614 ([FRI497](#))
- Aburaia, Abdelrahman, S545 ([FRI309](#))
- Abutaleb, Ameer, S215 ([THU246](#))
- Abutidze, Akaki, S587 ([FRI395](#)), S590 ([FRI400](#)), S590 ([FRI401](#))
- Accarino, Elena Vargas, S212 ([THU240](#)), S658 ([FRI587](#))
- Accetta, Antonio, S18 ([OS007](#)), S92 ([OS131](#)), S894 ([SAT508](#))
- Aceituno, Laia, S114 ([OS169](#)), S316 ([THU450](#))
- Achalandabaso, María, S774 ([SAT242](#))
- Ackaert, Oliver, S838 ([SAT370](#))
- Ackermann, Christin, S197 ([THU197](#))
- Acosta-López, Silvia, S127 ([THU018](#)), S931 ([SAT586](#))
- Acquaviva, Antonio, S483 ([FRI185](#)), S929 ([SAT582](#)), S929 ([SAT583](#))
- Acter, Emily, S280 ([THU372](#)), S846 ([SAT387](#))
- Adali, Gupse, S782 ([SAT255](#))
- Adamia, Ekaterine, S239 ([THU293](#)), S587 ([FRI395](#)), S590 ([FRI400](#)), S590 ([FRI401](#))
- Adamkova, Vera, S536 ([FRI290](#))
- Adamowicz, Monika, S601 ([FRI455](#))
- Adam, René, S538 ([FRI296](#)), S817 ([SAT312](#)), S935 ([SAT595](#))
- Adams, David, S476 ([FRI172](#))
- Adams, Huyen, S134 ([THU030](#))
- Adams, Leon, S440 ([FRI087](#))
- Adams, Timo, S748 ([SAT181](#))
- Adanir, Haydar, S820 ([SAT316](#)), S858 ([SAT410](#)), S861 ([SAT416](#)), S864 ([SAT421](#))
- Adda, Nathalie, S716 ([SAT109](#)), S848 ([SAT390](#)), S849 ([SAT393](#))
- Addeo, Pietro, S20 ([OS010](#))
- Addo, Marylyn, S206 ([THU229](#))
- Adebayo, Danielle, S49 ([OS063](#))
- Adejumo, Adeyinka, S899 ([SAT518](#))
- Adekunle, Femi, S335 ([THU484](#))
- Adel, Hammoutene, S475 ([FRI170](#))
- Adelmeijer, Jelle, S367 ([THU542](#)), S911 ([SAT540](#))
- Adeva, Jorge, S107 ([OS157](#))
- Adeyemo, Mopelola, S155 ([THU070](#))
- Adeyi, Oyedele, S416 ([FRI040](#)), S429 ([FRI065](#))
- Adhoute, Xavier, S547 ([FRI314](#))
- Adibekian, Alexander, S645 ([FRI559](#))
- Adinolfi, Luigi Elio, S938 ([SAT599](#))
- Adisa, Olayinka, S225 ([THU266](#))
- Adigüzel, Mehmet, S778 ([SAT248](#))
- Adler, Andreas, S309 ([THU436](#))
- Adnot, Pauline, S521 ([FRI260](#))
- Adolph, Timon, S126 ([THU017](#))
- Adona, MaryVic, S832 ([SAT358](#))
- Adorini, Luciano, S702 ([SAT074](#))
- Adotti, Valentina, S932 ([SAT588](#))
- Adrait, Annie, S766 ([SAT216](#))
- Adraneda, Celina, S298 ([THU406](#)), S877 ([SAT446](#))
- Adrien, Lannes, S496 ([FRI215](#)), S497 ([FRI216](#)), S507 ([FRI235](#))
- Adu, Prince, S43 ([OS051](#)), S209 ([THU233](#)), S282 ([THU378](#)), S910 ([SAT538](#))
- Aehling, Niklas F, S904 ([SAT528](#))
- Aerssens, Jeroen, S265 ([THU343](#))
- Aerts, Maridi, S107 ([OS156](#))
- Aeschbacher, Thomas, S244 ([THU302](#)), S247 ([THU309](#)), S845 ([SAT385](#))
- Afdhal, Nezam, S587 ([FRI395](#)), S590 ([FRI400](#)), S590 ([FRI401](#))
- Afek, Arnon, S784 ([SAT258](#)), S804 ([SAT291](#))
- Affo, Silvia, S527 ([FRI271](#))
- Afonso, Catarina, S304 ([THU420](#))

*Page numbers for abstracts are followed by the abstract number(s) in parentheses.

- Afonso, João, S28 ([OS024](#)), S618 ([FRI507](#))
- Afonso, Marta B., S7 ([GS009](#))
- Afonso, Milessa Silva, S483 ([FRI187](#)), S684 ([SAT040](#))
- Agarwal, K, S868 ([SAT428](#))
- Agarwal, Kosh, S8 ([GS010](#)), S17 ([OS005](#)), S171 ([THU101](#)), S188 ([THU178](#)), S253 ([THU321](#)), S276 ([THU366](#)), S279 ([THU370](#)), S280 ([THU373](#)), S281 ([THU375](#)), S287 ([THU387](#)), S371 ([THU550](#)), S569 ([FRI359](#)), S571 ([FRI363](#)), S594 ([FRI409](#)), S771 ([SAT236](#)), S812 ([SAT304](#)), S824 ([SAT343](#)), S824 ([SAT344](#)), S831 ([SAT357](#)), S835 ([SAT365](#)), S836 ([SAT366](#)), S871 ([SAT435](#))
- Agarwal, Prashant Mohan, S349 ([THU510](#)), S397 ([FRI014](#))
- Agarwal, Samagra, S369 ([THU547](#)), S633 ([FRI534](#)), S635 ([FRI538](#))
- Agarwal, Suresh, S540 ([FRI299](#))
- Aggarwal, Abhishek, S194 ([THU189](#)), S684 ([SAT040](#)), S832 ([SAT358](#)), S835 ([SAT364](#))
- Aggarwal, Pankaj, S151 ([THU064](#))
- Aggarwal, Sandeep, S448 ([FRI102](#)), S452 ([FRI108](#))
- Aghdaei, Hamid Asadzadeh, S228 ([THU273](#))
- Aghemo, Alessio, S93 ([OS132](#)), S212 ([THU239](#)), S528 ([FRI272](#)), S549 ([FRI317](#)), S584 ([FRI388](#)), S758 ([SAT201](#))
- Agmon-Levin, Nancy, S784 ([SAT258](#))
- Agollah, Germaine D., S730 ([SAT139](#)), S732 ([SAT143](#))
- Agopian, Vatche, S377 ([THU575](#))
- Agorastou, Polyxeni, S840 ([SAT374](#))
- Agranovich, Bella, S765 ([SAT214](#))
- Agrati, Chiara, S806 ([SAT294](#)), S808 ([SAT297](#))
- Agresta, Adele, S698 ([SAT068](#))
- Agudo, Rubén Rodríguez, S48 ([OS060](#)), S84 ([OS116](#)), S132 ([THU027](#)), S600 ([FRI453](#)), S679 ([SAT029](#))
- Aguilar-Bravo, Beatriz, S37 ([OS039](#)), S527 ([FRI271](#))
- Aguilar, Ferran, S674 ([SAT019](#))
- Aguilar, Juan Ramón, S487 ([FRI195](#))
- Aguilar, Laia, S684 ([SAT039](#))
- Aguilera, A., S211 ([THU237](#))
- Aguilera Sancho, Victoria, S442 ([FRI091](#))
- Agwuocha, Chukwuemeka, S225 ([THU266](#))
- Agyapong, George, S592 ([FRI405](#))
- Aharon, Arnon, S27 ([OS022](#))
- Ah, Lee Han, S625 ([FRI520](#))
- Ahlén, Gustaf, S860 ([SAT413](#))
- Ahlholm, Noora, S111 ([OS162](#)), S690 ([SAT052](#)), S694 ([SAT060](#))
- Ahlström, Håkan, S40 ([OS045](#)), S420 ([FRI047](#)), S683 ([SAT038](#))
- Ahmad, Alaa, S716 ([SAT109](#)), S848 ([SAT390](#)), S849 ([SAT393](#))
- Ahmad, Shafqat, S40 ([OS045](#))
- Ahmed, Charisse, S552 ([FRI322](#))
- Ahmed, Kinza, S551 ([FRI321](#))
- Ahmed, Mahmoud, S113 ([OS167](#))
- Ahmed, Mohamed, S632 ([FRI532](#))
- Ahmed, Muneeb, S764 ([SAT213](#))
- Ahmed, Nabil, S215 ([THU246](#))
- Ahmed, Si Nafa Si, S547 ([FRI314](#))
- Ahmed, Syed, S635 ([FRI538](#))
- Ahne, Lisa, S705 ([SAT082](#))
- Ahn, Joseph, S138 ([THU037](#))
- Ahn, Sang Bong, S160 ([THU079](#)), S224 ([THU264](#)), S273 ([THU359](#)), S435 ([FRI077](#)), S589 ([FRI398](#)), S728 ([SAT135](#)), S729 ([SAT136](#)), S875 ([SAT442](#))
- Ahn, Sang Hoon, S100 ([OS144](#)), S755 ([SAT194](#)), S824 ([SAT344](#))
- Ahn, Sojin, S489 ([FRI199](#))
- Ahuja, Vijay, S848 ([SAT391](#))
- Ahumada, Adriana, S549 ([FRI317](#)), S584 ([FRI388](#))
- Aigner, Elmar, S428 ([FRI062](#)), S515 ([FRI250](#)), S520 ([FRI257](#)), S830 ([SAT354](#))
- Aikata, Hiroshi, S758 ([SAT199](#))
- Aikebuse, Melanie, S172 ([THU102](#))
- Ailenberg, Menachem, S822 ([SAT320](#))
- Ainora, Maria Elena, S507 ([FRI234](#))
- Aird, Rhona E., S85 ([OS117](#))
- Airolidi, Aldo, S908 ([SAT535](#))
- Aishima, Shinichi, S430 ([FRI067](#))
- Aithal, Guruprasad, S22 ([OS013](#)), S39 ([OS044](#)), S116 ([OS172](#)), S141 ([THU041](#)), S448 ([FRI102](#)), S452 ([FRI108](#)), S465 ([FRI151](#))
- Ajayi, Lola, S120 ([THU004](#))
- Ajaz, Saima, S171 ([THU101](#))
- Ajmera, Veeral, S414 ([FRI037](#))
- Akanmu, Muhammad-Mujtaba, S225 ([THU266](#))
- Akarca, Ulus, S294 ([THU399](#)), S399 ([FRI015](#))
- Akarsu, Mesut, S782 ([SAT255](#)), S820 ([SAT316](#))
- Akerblad, Peter, S751 ([SAT187](#))
- Akhter, Mohammad Khalil, S240 ([THU295](#))
- Akisik, Fatih, S95 ([OS135](#))
- Akita, Tomoyuki, S229 ([THU274](#))
- Akuta, Norio, S563 ([FRI346](#))
- Akyildiz, Murat, S693 ([SAT058](#)), S782 ([SAT255](#)), S820 ([SAT316](#))
- Ala, Aftab, S1 ([GS001](#)), S22 ([OS013](#)), S61 ([OS077](#)), S534 ([FRI286](#)), S539 ([FRI297](#))
- Alabdulkarim, Balqis, S614 ([FRI497](#))
- Al-Adra, David, S800 ([SAT286](#))
- Al-Akkad, Walid, S668 ([SAT008](#))
- Alam, Antoine, S872 ([SAT436](#))
- Alam, Seema, S528 ([FRI273](#))
- Al-Anbaki, Ali, S104 ([OS152](#))
- Alattar, Atef, S779 ([SAT250](#))
- Alavanja, Marko, S186 ([THU174](#))
- Alavi, Maryam, S302 ([THU415](#)), S560 ([FRI339](#)), S568 ([FRI356](#))
- Alazawi, William, S488 ([FRI198](#)), S698 ([SAT066](#)), S934 ([SAT593](#))
- Albenois, Romain, S547 ([FRI314](#))
- Alberda, Cathy, S890 ([SAT500](#))
- Alber, Hannes, S21 ([OS012](#)), S891 ([SAT502](#))
- Alberich-Bayarri, Angel, S442 ([FRI091](#))
- Albert-Antequera, Cecilia, S222 ([THU261](#))
- Alberti, Dafne, S479 ([FRI177](#))
- Albert, Matthew, S31 ([OS028](#)), S37 ([OS041](#)), S409 ([FRI030](#)), S762 ([SAT208](#))
- Albhaisi, Somaya, S19 ([OS008](#)), S49 ([OS063](#))
- Albillos, Agustin, S115 ([OS169](#)), S334 ([THU482](#)), S370 ([THU548](#)), S502 ([FRI226](#))
- Albin, Jan, S606 ([FRI466](#)), S661 ([FRI594](#))
- Albrechtsen, Nicolai J Wewer, S331 ([THU477](#))
- Albrechtsen, Nicolai J. Wewer, S154 ([THU068](#))
- Albrecht, Thomas, S655 ([FRI581](#)), S927 ([SAT579](#))
- Albrecht, Wolfgang, S132 ([THU026](#)), S737 ([SAT158](#))
- Alcaraz, Estefania, S368 ([THU545](#))
- Alcorn, Joseph, S142 ([THU043](#))
- Aldabe, Rafael, S248 ([THU310](#))
- Aldersley, Mark, S17 ([OS005](#))
- Aldrighetti, Luca, S748 ([SAT180](#)), S789 ([SAT266](#))
- Alejandro, Rafael, S114 ([OS168](#))
- Alemañ, Gorka Bastarrika, S802 ([SAT288](#))
- Alemanni, Vanessa, S91 ([OS129](#)), S794 ([SAT273](#))
- Aleman, Soo, S4 ([GS006](#)), S30 ([OS026](#)), S103 ([OS149](#)), S828 ([SAT351](#)), S829 ([SAT352](#))
- Alemu, Daniel, S556 ([FRI331](#))
- Alenezi, Yusef, S145 ([THU050](#))
- Alessandria, Carlo, S908 ([SAT535](#))
- Alessio, Loredana, S217 ([THU250](#))
- Alessio, Maria Grazia, S751 ([SAT186](#))
- Alexander, Ian, S754 ([SAT193](#))
- Alexander, Leigh, S74 ([OS097](#)), S437 ([FRI081](#))
- Alexandrino, Gonçalo, S51 ([OS065](#)), S902 ([SAT523](#))
- Alexopoulos, Theodoros, S908 ([SAT534](#))
- Alexopoulou, Alexandra, S908 ([SAT534](#))
- Alex, Sophie, S661 ([FRI594](#))
- Alfaro, Ana, S703 ([SAT079](#))
- Alfaro-Cervello, Clara, S442 ([FRI091](#))
- Alfarone, Ludovico, S528 ([FRI272](#))
- Algibez, Ana Martin, S704 ([SAT080](#))
- Al Hinai, Al Shaima, S31 ([OS029](#))
- Ali, Ahmad, S803 ([SAT290](#))
- Ali, Bazga, S548 ([FRI316](#))
- Alibrandi, Angela, S259 ([THU333](#))
- Ali, Fatima, S197 ([THU196](#))
- Alimenti, Eleonora, S578 ([FRI376](#))
- Ali, Sarah, S433 ([FRI073](#))
- Ali Shagrani, Mohammad, S521 ([FRI259](#))
- Alisi, Anna, S706 ([SAT084](#))
- Aliwa, Benard, S68 ([OS088](#)), S179 ([THU159](#))
- Alix, Tom, S905 ([SAT529](#))
- AlKaabi, Saad, S230 ([THU277](#))
- Alkhatib, Mohammad, S284 ([THU381](#))

Author Index

- Alkhazashvili, Maia, S219 (THU253), S221 (THU258), S233 (THU283), S267 (THU347)
- Alkhouri, Naim, S14 (LB005), S75 (OS101), S87 (OS121), S151 (THU064), S159 (THU077), S422 (FRI052), S427 (FRI060), S453 (FRI109), S495 (FRI210), S727 (SAT131), S730 (SAT139), S731 (SAT142), S732 (SAT143)
- Alkim, Huseyin, S861 (SAT416)
- Allah, Belimi Hibat, S19 (OS008), S49 (OS063)
- Allaire, Manon, S65 (OS084), S372 (THU566), S475 (FRI170)
- Allam, Dalia, S19 (OS008), S49 (OS063)
- Allard, Marc Antoine, S935 (SAT595)
- Allen, Alina, S138 (THU037), S414 (FRI037), S438 (FRI084)
- Allen, Kathryn, S138 (THU036)
- Allen, Samantha, S554 (FRI327)
- Allen, Sophie, S364 (THU537)
- Aller, Rocío, S459 (FRI119), S671 (SAT014)
- Alletto, Francesca, S159 (THU078), S167 (THU095)
- Allison, Michael, S7 (GS009), S39 (OS044), S120 (THU005), S122 (THU008), S124 (THU013), S141 (THU041), S695 (SAT061), S742 (SAT167), S815 (SAT310)
- Alloui, Chakib, S271 (THU355)
- Allsop, Caroline, S567 (FRI355)
- Allweiss, Lena, S256 (THU327)
- Almale del Barrio, Laura, S37 (OS040)
- Almasri, Hussam, S230 (THU277)
- Almeida, Alessandro, S408 (FRI028)
- Almeida, Bruna, S120 (THU004), S480 (FRI179), S735 (SAT153)
- Almes, Marion, S514 (FRI248), S521 (FRI260)
- Almohalla, Carolina, S114 (OS168), S406 (FRI027), S792 (SAT270), S792 (SAT271)
- Alonso, Cristina, S419 (FRI045), S455 (FRI113), S671 (SAT014)
- Alonso, Maria Luisa Manzano, S549 (FRI317), S584 (FRI388)
- Alonso-Peña, Marta, S59 (OS074)
- Alqahtani, Saleh, S5 (GS008), S154 (THU069), S785 (SAT260), S810 (SAT300)
- Alric, Laurent, S72 (OS093), S833 (SAT360)
- Al-Rubaiy, Laith, S96 (OS137)
- Al-Sayegh, Rami, S382 (THU586), S931 (SAT587)
- Al-Sayegh, Rola, S65 (OS084)
- Al Shabeeb, Reem, S445 (FRI097)
- AlSoub, Deema, S230 (THU277)
- Alswat, Khalid, S154 (THU069), S479 (FRI178)
- Altangerel, Enkhjargal, S824 (SAT342)
- Altenburg, Arwen, S198 (THU198)
- Altenmüller, Johannes, S321 (THU458)
- Alter, Adriana, S786 (SAT261)
- Altmann, Heidi, S11 (LB002)
- Alukal, Joseph, S48 (OS061)
- Aluvihare, Varuna, S120 (THU005), S371 (THU550), S403 (FRI022), S771 (SAT236), S812 (SAT304)
- Alvain, Aoife, S569 (FRI358), S570 (FRI360)
- Alvarado-Tapias, Edilmar, S64 (OS082), S90 (OS127), S91 (OS128), S137 (THU035), S370 (THU548), S625 (FRI520), S627 (FRI523), S886 (SAT494), S900 (SAT520)
- Álvares-da-Silva, Mario Reis, S19 (OS008), S49 (OS063)
- Alvarez-Alvarez, Ismael, S396 (FRI011)
- Alvarez, Irene Perez, S222 (THU261)
- Alvarez, Laura, S46 (OS056)
- Alvarez, Maria, S17 (OS005), S43 (OS051), S209 (THU233), S282 (THU378), S910 (SAT538)
- Alvarez, Maria Carmen Gallegos, S218 (THU252)
- Álvarez-Navascués, Carmen, S324 (THU464), S328 (THU471)
- Alvarez-Ossorio, Angela Rojas, S450 (FRI105), S708 (SAT087)
- Álvarez-Sola, Gloria, S643 (FRI554), S757 (SAT198)
- Alvaro, Cristina De, S268 (THU348), S587 (FRI394)
- Alvaro, Domenico, S107 (OS157), S648 (FRI564)
- Alvaro, Frank, S558 (FRI334)
- Alves de Castro, Pedro, S552 (FRI323)
- Alves, Rogério, S137 (THU034)
- Alwayn, Ian, S798 (SAT280)
- Amaddeo, Giuliana, S372 (THU566), S375 (THU573), S530 (FRI276), S927 (SAT578)
- Amado, Luis Enrique Morano, S581 (FRI384)
- Amano, Yuichiro, S7 (GS009)
- Amaral, Adam, S58 (OS073)
- Amara, Suneetha, S374 (THU571), S376 (THU574), S383 (THU588)
- Amare, Benon, S841 (SAT375)
- Ambery, Philip, S411 (FRI033), S609 (FRI486)
- Ambros, Raphael, S24 (OS017)
- Amengual, Josep, S673 (SAT018)
- Amer, Johnny, S399 (FRI016), S691 (SAT054)
- Amigo, Lidia, S774 (SAT242)
- Amin, Janaki, S302 (THU415), S560 (FRI339), S565 (FRI349), S568 (FRI356)
- Amin, Naseem, S61 (OS077)
- Amin, Oliver E., S55 (OS070)
- Ammon, Daphni, S788 (SAT264)
- Amodeo, Simona, S564 (FRI347)
- Amorini, Angela Maria, S703 (SAT077)
- Ampuero, Javier, S442 (FRI092), S444 (FRI095), S450 (FRI105), S555 (FRI329), S708 (SAT087), S912 (SAT555)
- Amzal, Rachida, S514 (FRI248)
- Amzou, Samira, S515 (FRI250), S520 (FRI257)
- Anagnostou, Despina, S842 (SAT377)
- Anand, Abhinav, S524 (FRI264)
- Anand, Hanish, S818 (SAT315)
- Anand, Utpal, S170 (THU100), S809 (SAT299), S813 (SAT306)
- Anastasiou, Dimitrios, S666 (SAT004)
- Anastasiy, Igor, S73 (OS095)
- Andersen, Birgitte, S713 (SAT102), S720 (SAT116)
- Andersen, Cecilie Holmegaard, S724 (SAT124)
- Andersen, Jesper, S46 (OS056), S47 (OS058), S77 (OS103), S107 (OS157), S648 (FRI564), S649 (FRI566), S649 (FRI567)
- Andersen, Peter, S2 (GS002), S9 (GS012), S35 (OS036), S131 (THU024), S475 (FRI171)
- Anders, Julian, S882 (SAT486)
- Anders, Malena, S145 (THU051)
- Anders, Maria Margarita, S786 (SAT261)
- Anderson, Jenine, S550 (FRI318)
- Anderson, K, S868 (SAT428)
- Anderson, Mark, S253 (THU321), S279 (THU370), S281 (THU375), S287 (THU387), S851 (SAT398)
- Anderson, Patricia, S342 (THU501)
- Anderson, R. Rox, S364 (THU536)
- Andersson, Anneli, S453 (FRI109)
- Andersson, Emma, S759 (SAT202)
- Andersson, Monique, S23 (OS015)
- Andrade, Antonio, S543 (FRI305)
- Andrade, Raul J., S59 (OS074), S93 (OS132), S308 (THU435), S326 (THU467), S334 (THU482), S396 (FRI011), S872 (SAT437)
- Andreassi, Eleonora, S249 (THU313)
- Andreasson, Anna, S24 (OS016)
- Andréasson, Anne-Christine, S7 (GS009)
- Andreazza, Ana, S822 (SAT320)
- Andreola, Fausto, S366 (THU539)
- Andreone, Pietro, S4 (GS006), S12 (LB004A), S880 (SAT452)
- Andreoni, Massimo, S242 (THU299), S249 (THU313), S549 (FRI317), S584 (FRI388)
- Andresaki, Konstantina, S255 (THU326)
- Andreu, Jordi Camps, S677 (SAT027), S681 (SAT034)
- Andreu-Oller, Carmen, S45 (OS055)
- Andrieu, Thibault, S356 (THU522)
- Ang, Celina, S372 (THU567), S383 (THU588)
- Angelico, Francesco, S161 (THU081), S162 (THU083)
- Angelico, Mario, S249 (THU313)
- Angeli, Paolo, S18 (OS007), S21 (OS011), S49 (OS062), S92 (OS131), S569 (FRI359), S888 (SAT497), S894 (SAT508), S895 (SAT511), S908 (SAT535)
- Angelone, Federica, S806 (SAT294)
- Angel, Peter, S38 (OS042)
- Angerer, Martin, S390 (FRI003)

- Anglero-Rodriguez, Yesseinia, S871 ([SAT434](#))
- Ang, Le Shaun, S567 ([FRI354](#))
- Anglin, Tori, S30 ([OS027](#)), S936 ([SAT596](#))
- Angrisani, Debora, S938 ([SAT599](#))
- Anguita, Juan, S177 ([THU155](#))
- Angus, Peter, S842 ([SAT377](#))
- Anh, Ho Thien, S516 ([FRI252](#))
- Ankarklev, Johan, S199 ([THU200](#))
- Ankavay, Maliki, S97 ([OS138](#))
- Anna, Piekarska, S565 ([FRI350](#)), S585 ([FRI390](#)), S592 ([FRI406](#))
- Annunziata, Francesco, S513 ([FRI246](#))
- Annunziata, Monica, S551 ([FRI320](#))
- Anolli, Maria Paola, S210 ([THU236](#)), S868 ([SAT429](#)), S874 ([SAT440](#)), S880 ([SAT450](#))
- An, Qi, S4 ([GS006](#))
- An, Qian, S233 ([THU283](#))
- Ansari, Azim, S541 ([FRI301](#)), S856 ([SAT407](#))
- Anstee, Quentin, S7 ([GS009](#)), S29 ([OS025](#)), S74 ([OS097](#)), S416 ([FRI040](#)), S424 ([FRI055](#)), S425 ([FRI058](#)), S437 ([FRI080](#)), S437 ([FRI081](#)), S444 ([FRI095](#)), S448 ([FRI102](#)), S452 ([FRI108](#)), S486 ([FRI194](#)), S493 ([FRI207](#)), S671 ([SAT014](#)), S721 ([SAT118](#)), S733 ([SAT146](#))
- Antoine, Benedicte, S37 ([OS039](#))
- Antoine, Corinne, S780 ([SAT252](#))
- Antolić, Maja, S702 ([SAT075](#))
- Antolini, Laura, S96 ([OS136](#))
- Antón Conejero, María Dolores, S325 ([THU465](#))
- Antoni, Christoph, S16 ([OS003](#)), S523 ([FRI262](#)), S585 ([FRI391](#))
- Antonello, Deana, S850 ([SAT396](#)), S851 ([SAT397](#)), S876 ([SAT443](#)), S878 ([SAT448](#))
- Antonini, Teresa, S356 ([THU522](#))
- Antonini, Tereza, S935 ([SAT595](#))
- Antonio Diaz, Luis, S81 ([OS110](#))
- Antonsen, Steen, S475 ([FRI171](#))
- Antonucci, Michela, S448 ([FRI101](#))
- Antoran, Belén Ruiz, S912 ([SAT555](#))
- Anushiravani, Amir, S479 ([FRI178](#))
- Anwar, Masood, S240 ([THU295](#))
- An, Weimin, S501 ([FRI224](#))
- Aoko, Olufemi, S234 ([THU285](#))
- Ao, Ling, S240 ([THU296](#))
- Aouadi, Myriam, S665 ([SAT002](#)), S667 ([SAT006](#)), S755 ([SAT195](#)), S756 ([SAT197](#))
- Aoudjehane, Lynda, S189 ([THU181](#))
- Aoyagi, Katsumi, S295 ([THU401](#))
- Apodaka-Biguri, Maider, S648 ([FRI564](#)), S651 ([FRI571](#)), S665 ([SAT001](#)), S689 ([SAT050](#))
- Applegate, Douglas, S486 ([FRI194](#))
- Aprile, Giuseppe, S748 ([SAT180](#))
- Aqel, Bashar, S15 ([OS002](#)), S416 ([FRI040](#))
- Aquino, Marco, S425 ([FRI057](#))
- Arab, Juan Pablo, S81 ([OS110](#)), S137 ([THU034](#)), S141 ([THU041](#))
- Arabpour, Mohammad, S186 ([THU174](#))
- Aracil, Carlos, S370 ([THU548](#))
- Aracil, Carlos Ferre, S324 ([THU464](#)), S334 ([THU482](#))
- Aragão, Filipa, S305 ([THU421](#))
- Arai, Kumiko, S687 ([SAT047](#))
- Araiza, Adrián Sández, S356 ([THU521](#))
- Arancibia, Juan Pablo, S137 ([THU034](#))
- Aranguren, África Vales, S248 ([THU310](#)), S257 ([THU330](#))
- Aransay, Ana María, S651 ([FRI571](#))
- Araújo, Carlos, S192 ([THU185](#))
- Araujo, Silvia Gómez, S207 ([THU231](#)), S208 ([THU232](#))
- Aravintan, Aloysious, S19 ([OS008](#)), S49 ([OS063](#)), S805 ([SAT292](#)), S934 ([SAT593](#)), S938 ([SAT600](#))
- Arbelaiz, Ander, S77 ([OS103](#))
- Arbib, Orly Sneh, S64 ([OS081](#)), S774 ([SAT241](#)), S793 ([SAT272](#)), S855 ([SAT406](#))
- Arbune, Manuela, S12 ([LB004A](#)), S880 ([SAT452](#))
- Arca, Marcello, S162 ([THU083](#))
- Arcay, Ricardo M, S218 ([THU252](#))
- Arcelus, Sara, S697 ([SAT064](#))
- Archer, Sara, S304 ([THU420](#))
- Ardevol, Alba, S91 ([OS128](#))
- Arechederra, Maria, S112 ([OS165](#)), S500 ([FRI222](#)), S643 ([FRI554](#)), S644 ([FRI557](#))
- Arefaine, Bethlehem, S68 ([OS089](#))
- Arena, Umberto, S627 ([FRI524](#)), S932 ([SAT588](#))
- Arendt, Vic, S579 ([FRI377](#))
- Arendt, Victor, S304 ([THU419](#))
- Arentoft, Nicoline Stender, S818 ([SAT314](#))
- Are, Vijay, S95 ([OS135](#))
- Argemi, Josepmaria, S140 ([THU040](#)), S697 ([SAT064](#))
- Argiriadi, Pamela, S160 ([THU080](#))
- Ariana, Pascu, S483 ([FRI186](#)), S505 ([FRI230](#))
- Arias, Ana, S114 ([OS169](#)), S792 ([SAT271](#))
- Arici, Sena, S297 ([THU405](#))
- Ari, Derya, S858 ([SAT410](#)), S861 ([SAT416](#)), S864 ([SAT421](#))
- Arita, Makoto, S674 ([SAT019](#))
- Ari, Ziv Ben, S292 ([THU395](#)), S784 ([SAT258](#)), S804 ([SAT291](#)), S845 ([SAT384](#))
- Arizpe, Andre, S69 ([OS090](#)), S831 ([SAT357](#))
- Arkkila, Perttu, S458 ([FRI117](#))
- Armendariz-Borunda, Juan, S554 ([FRI326](#))
- Armengol, Carolina, S527 ([FRI271](#))
- Armesto, Susana, S113 ([OS166](#))
- Armijos, Xiimena, S137 ([THU034](#))
- Armstrong, Matthew, S10 ([LB001](#)), S334 ([THU483](#)), S364 ([THU537](#))
- Armstrong, Paige A, S213 ([THU242](#)), S214 ([THU243](#)), S216 ([THU247](#)), S216 ([THU248](#)), S219 ([THU253](#)), S221 ([THU258](#)), S233 ([THU283](#)), S234 ([THU284](#)), S267 ([THU347](#)), S587 ([FRI395](#)), S588 ([FRI397](#)), S590 ([FRI400](#)), S590 ([FRI401](#)), S598 ([FRI418](#))
- Arndtz, Katherine, S526 ([FRI269](#))
- Arnold, Alexander, S663 ([FRI597](#)), S739 ([SAT162](#))
- Arnold, Jorge, S81 ([OS110](#)), S137 ([THU034](#)), S351 ([THU514](#)), S671 ([SAT014](#))
- Arnouk, Joud, S442 ([FRI091](#))
- Arokiasamy, Samantha, S488 ([FRI198](#))
- Arola, Johanna, S111 ([OS162](#)), S312 ([THU441](#)), S327 ([THU469](#)), S458 ([FRI117](#)), S694 ([SAT060](#))
- Arora, Anil, S19 ([OS008](#)), S49 ([OS063](#))
- Arora, Sanjeev, S587 ([FRI395](#)), S590 ([FRI400](#)), S590 ([FRI401](#))
- Arora, Vinod, S53 ([OS066](#))
- Arraez, Dalia Morales, S137 ([THU035](#))
- Arranz, Maria, S44 ([OS052](#))
- Arranz-Salas, Isabel, S396 ([FRI011](#))
- Arrese, Marco, S81 ([OS110](#)), S137 ([THU034](#)), S455 ([FRI113](#)), S671 ([SAT014](#))
- Arretxe, Enara, S671 ([SAT014](#))
- Arriaga-González1, Fernanda, S476 ([FRI172](#))
- Arribas, David San Segundo, S774 ([SAT242](#))
- Arrivè, Lionel, S319 ([THU454](#))
- Arroyo, Vicente, S361 ([THU531](#)), S362 ([THU533](#)), S368 ([THU545](#)), S370 ([THU549](#))
- Arslan, Aysenur, S399 ([FRI015](#))
- Arslan, Mehmet, S858 ([SAT410](#)), S861 ([SAT416](#)), S864 ([SAT421](#))
- Arslanow, Anita, S80 ([OS108](#))
- Arsyad, Nik MA Nik, S19 ([OS008](#)), S49 ([OS063](#))
- Artan, Reha, S518 ([FRI255](#)), S519 ([FRI256](#)), S521 ([FRI259](#))
- Arteaga, Elvis, S155 ([THU070](#))
- Arteel, Gavin, S465 ([FRI149](#))
- Artegiani, Benedetta, S652 ([FRI574](#))
- Artenie, Adelina, S556 ([FRI331](#))
- Arthurs, Callum, S132 ([THU026](#))
- Artmann, Renate, S602 ([FRI460](#))
- Artru, Florent, S116 ([OS171](#)), S135 ([THU031](#)), S352 ([THU516](#)), S355 ([THU520](#)), S505 ([FRI231](#))
- Artzner, Thierry, S20 ([OS010](#))
- Arumugam, Manimozhiyan, S2 ([GS002](#))
- Aryal, Rishi, S244 ([THU302](#)), S247 ([THU309](#))
- Aryan, Mahmoud, S33 ([OS031](#))
- Arzola-Renteria, Erik Jesús, S356 ([THU521](#))
- Asahina, Yasuhiro, S563 ([FRI346](#))
- Ascanio, Mertixell, S285 ([THU383](#)), S286 ([THU384](#)), S300 ([THU410](#))
- Asensio, Julia Peña, S184 ([THU170](#)), S826 ([SAT347](#))
- Asghar, Aliya, S142 ([THU043](#))
- Ashique, Amir, S443 ([FRI093](#)), S486 ([FRI193](#))
- Ashmore-Harris, Candice, S85 ([OS117](#))
- Askari, Fred, S1 ([GS001](#))
- Askar, Sumar, S567 ([FRI355](#))
- Askgaard, Gro, S125 ([THU015](#))
- Aslam, Mujahid, S240 ([THU295](#))

Author Index

- Aslanikashvili, Ana, S214 (THU243), S216 (THU247), S216 (THU248)
- Aslan, Rahmi, S19 (OS008), S49 (OS063)
- Aspas, Jessica, S743 (SAT170)
- Asphaug, Lars, S130 (THU022)
- Aspichueta, Patricia, S46 (OS056), S157 (THU074), S158 (THU076), S648 (FRI564), S651 (FRI571), S665 (SAT001), S689 (SAT050)
- Aspinall, Alexander, S143 (THU045)
- Aspinall, Richard, S22 (OS013), S96 (OS137)
- Aspite, Silvia, S627 (FRI524)
- Asraf, Keren, S804 (SAT291)
- Asrani, Sumeet, S19 (OS008), S49 (OS063), S805 (SAT292)
- Assawasuwannakit, Suraphon, S722 (SAT121)
- Asselah, Tarik, S13 (LB004B), S245 (THU304), S269 (THU350), S288 (THU389), S288 (THU390), S291 (THU393), S300 (THU411), S549 (FRI317), S584 (FRI388), S829 (SAT352), S840 (SAT373), S864 (SAT422), S881 (SAT453)
- Assenat, Eric, S392 (FRI006)
- Assinger, Alice, S788 (SAT264), S799 (SAT283)
- Atallah, Edmond, S22 (OS013), S116 (OS172)
- Atay, Ali, S782 (SAT255)
- Athanasiadis, Emmanouil, S742 (SAT167)
- Athwal, Varinder, S104 (OS152)
- Atienza, Francisco, S555 (FRI329)
- Atif, Mo, S189 (THU181)
- Atik, Cecilia, S374 (THU570), S380 (THU582)
- Atkinson, Stephen, S11 (LB002), S34 (OS034), S122 (THU008), S124 (THU013), S132 (THU026), S135 (THU031), S140 (THU040), S352 (THU516)
- Atsukawa, Masanori, S12 (LB004A), S880 (SAT452)
- Attanasio, Maria Rosaria, S769 (SAT233)
- Attarwala, Nabeel, S133 (THU028)
- Aubé, Christophe, S496 (FRI215), S504 (FRI228)
- Auer, Nicole, S618 (FRI506)
- Augustin, Jeremy, S297 (THU404)
- Augustin, Salvador, S180 (THU161), S370 (THU548), S906 (SAT530)
- Augusto Martín, Cesar, S651 (FRI571)
- Aurrekoetxea, Igor, S648 (FRI564), S651 (FRI571), S665 (SAT001), S689 (SAT050)
- Austin, Andrew, S122 (THU008), S124 (THU013)
- Austin, Daren, S873 (SAT439)
- Auzinger, Georg, S403 (FRI022)
- Avendaño-Reyes, José Manuel, S356 (THU521)
- Averhoff, Francisco, S215 (THU246), S233 (THU283), S267 (THU347)
- Avian, Alexander, S346 (THU506)
- Avigni, Roberta, S651 (FRI570)
- Avila, Gerson, S137 (THU034)
- Avila, Matías A, S132 (THU027), S643 (FRI554), S644 (FRI557), S697 (SAT064)
- Avila, Matías A., S46 (OS056), S48 (OS060), S112 (OS165), S500 (FRI222)
- Avitabile, Emma, S63 (OS080), S136 (THU033), S139 (THU039), S511 (FRI242), S512 (FRI243), S512 (FRI244), S901 (SAT522), S902 (SAT524)
- Avolio, Fabio, S423 (FRI054)
- Awady, Mona El, S566 (FRI351)
- Axelrod, Jonathan, S474 (FRI167)
- Axelsen, Mads, S720 (SAT116)
- Ayada, Ibrahim, S86 (OS120)
- Ay, Anne-Sophie, S645 (FRI559)
- Ayappa, Indu, S169 (THU098)
- Ayares, Gustavo, S81 (OS110), S137 (THU034)
- Aydin, Musa, S693 (SAT058)
- Aydin, Omrum, S9 (GS011)
- Ayers, Andrew, S276 (THU366)
- Ayer, Turgay, S214 (THU244)
- Ayithan, Natarajan, S863 (SAT419)
- Ayonrinde, Oyekoya, S142 (THU044), S164 (THU089), S440 (FRI087), S491 (FRI203)
- Ayoub, Alan, S270 (THU353)
- Ayoub, Walid S, S836 (SAT366)
- Ayton, Sarah, S409 (FRI031)
- Azaceta, María Del Barrio, S157 (THU074), S158 (THU076)
- Azam, Farooq, S240 (THU295)
- Azam, Zahid, S625 (FRI520)
- Azania, Amy, S225 (THU266)
- Azer, Karim, S718 (SAT112)
- Azkargorta, Mikel, S37 (OS039), S46 (OS056), S77 (OS103), S132 (THU027), S365 (THU538), S648 (FRI564), S896 (SAT512)
- Azkona, María, S500 (FRI222), S644 (FRI557)
- Azoulay, Daniel, S935 (SAT595)
- Azuara, Mayra López, S476 (FRI172)
- Azzimato, Valerio, S665 (SAT002), S756 (SAT197)
- Azzu, Vian, S695 (SAT061)
- Baak, Bert, S893 (SAT506)
- Baas, Frank, S698 (SAT067)
- Baatarsuren, Uurtsaikh, S235 (THU287)
- Baba, Hideo, S642 (FRI552), S643 (FRI555)
- Babalís, Daphne, S34 (OS034)
- Baba, Masaya, S295 (THU401)
- Babameto, Adriana, S573 (FRI367)
- Babel, Jonas, S658 (FRI585)
- Babenka, Andrei, S269 (THU351)
- Babigan, Julia, S663 (FRI597)
- Bablon, Pierre, S297 (THU404)
- Babudieri, Sergio, S596 (FRI414)
- Babu, E. Preedia, S197 (THU196)
- Bach, Charlotte, S738 (SAT160)
- Bachelier, Philippe, S20 (OS010), S780 (SAT252)
- Back, David, S580 (FRI383)
- Backhed, Fredrik, S9 (GS011), S94 (OS133)
- Backhouse, Dianne, S63 (OS079), S885 (SAT492)
- Backman, Jens, S30 (OS026)
- Badalamenti, Giuseppe, S387 (THU599)
- Badal, Bryan, S126 (THU016)
- Badia-Aranda, Esther, S127 (THU018)
- Badylak, Stephen, S465 (FRI149)
- Bae, Ho S, S836 (SAT366)
- Baek, Yanghyon, S572 (FRI365)
- Baena, Sheila, S743 (SAT170)
- Bae, Si Hyun, S146 (THU053), S490 (FRI202), S820 (SAT317), S932 (SAT589), S932 (SAT590)
- Bae, Sung Min, S468 (FRI156), S469 (FRI157)
- Baez-Ortega, Adrian, S741 (SAT165)
- Bahn, Jonas, S604 (FRI462)
- Baiano, Cassandra, S415 (FRI038)
- Bai, Chosha, S264 (THU341)
- Baiges, Anna, S90 (OS127), S367 (THU542), S524 (FRI265)
- Baiges, Gerard, S685 (SAT041)
- Bail, Brigitte Le, S372 (THU566)
- Bailey, Adam, S320 (THU456), S320 (THU457), S321 (THU459), S322 (THU460)
- Bailey, Michael, S3 (GS005)
- Bair, Ming-Jong, S595 (FRI410)
- Bai, Ru, S669 (SAT009)
- Bai, Wei, S92 (OS130), S619 (FRI508), S621 (FRI512), S628 (FRI526)
- Bajaj, Jasmohan S, S126 (THU016), S130 (THU023), S176 (THU153), S178 (THU156), S339 (THU494), S887 (SAT496), S899 (SAT517), S899 (SAT518)
- Bajaj, Jasmohan S., S19 (OS008), S49 (OS063), S67 (OS087)
- Bakardjiev, Anna, S871 (SAT434)
- Baker, Fadi Abu, S292 (THU395), S845 (SAT384)
- Bakieva, Shokhista, S235 (THU288)
- Bakker, Barbara, S539 (FRI298)
- Balaban, Hatice Yasemin, S820 (SAT316), S861 (SAT416)
- Balabanska, Rozalina, S299 (THU408), S867 (SAT427)
- Balaban, Yasemin, S858 (SAT410)
- Balaji, Anu, S903 (SAT526)
- Balakrishnan, Anand, S745 (SAT177)
- Balakrishnan, Narmada, S247 (THU308)
- Balasubramanian, Sripriya, S770 (SAT234)
- Balbin, Alejandro, S508 (FRI236), S918 (SAT564)
- Balcar, Lorenz, S18 (OS007), S24 (OS017), S92 (OS131), S354 (THU519), S372 (THU567), S374 (THU571), S376 (THU574), S383 (THU588), S428 (FRI062), S532 (FRI280), S535 (FRI287), S617 (FRI505), S618 (FRI506), S629 (FRI527),

- S629 (FRI528), S631 (FRI531),
S632 (FRI533), S919 (SAT565),
S921 (SAT570)
- Balci, Deniz, S778 (SAT248)
- Baldassarre, Maurizio, S357 (THU523),
S908 (SAT535)
- Baldea, Victor, S483 (FRI186), S505 (FRI230)
- Baldehy, Ignatius, S295 (THU401)
- Balderas, Robert, S189 (THU181)
- Baldin, Caroline, S910 (SAT539)
- Baldvinsdóttir, Guðrún Erna, S573 (FRI366)
- Baldwin, Anne, S37 (OS041)
- Baldwin, Cindy, S456 (FRI114)
- Bale, Georgia, S736 (SAT156)
- Balic, Kemal, S727 (SAT131)
- Ballester, María Pilar, S51 (OS065),
S902 (SAT523), S903 (SAT526)
- Balsinde, Jesus, S749 (SAT183)
- Balsitis, Scott, S832 (SAT358)
- Bals, Robert, S515 (FRI250)
- Baltimore, David, S245 (THU303)
- Baltzinger, Philippe, S758 (SAT199)
- Banales, Jesus Maria, S46 (OS056),
S77 (OS103), S107 (OS157),
S157 (THU074), S158 (THU076),
S192 (THU185), S601 (FRI455),
S643 (FRI554), S665 (SAT001),
S671 (SAT014), S689 (SAT050)
- Bañares, Juan, S316 (THU450)
- Bañares, Rafael, S90 (OS127),
S370 (THU548)
- Bandera, Alessandra, S167 (THU095),
S223 (THU263)
- Bandera, Jose Pinazo, S127 (THU018),
S308 (THU435)
- Bañeras, Jordi, S149 (THU059),
S440 (FRI088)
- Banerjee, Rajarshi, S96 (OS136),
S424 (FRI056), S433 (FRI073),
S526 (FRI269)
- Banerjee, Subham, S105 (OS153)
- Bang, Corinna, S325 (THU466)
- Bannaga, Ayman, S934 (SAT593)
- Bansal, Rajat, S369 (THU547)
- Bansal, Ruchi, S400 (FRI018), S405 (FRI025),
S487 (FRI196), S707 (SAT086)
- Bansal, Sanjay, S551 (FRI321)
- Bansal, V K, S232 (THU280)
- Bantel, Heike, S470 (FRI159), S666 (SAT003)
- Baorda, Francesca, S483 (FRI185),
S929 (SAT582), S929 (SAT583)
- Baptista, Pedro, S65 (OS085)
- Barace, Sergio, S697 (SAT064)
- Baracos, Vickie, S892 (SAT504)
- Barahona, Ines, S749 (SAT183)
- Barash, Danny, S588 (FRI396)
- Barashi, Neta, S47 (OS059)
- Baratta, Francesco, S161 (THU081),
S162 (THU083)
- Barba, Minerva Blazquez, S555 (FRI329)
- Barbancho, Sandra Melitón, S65 (OS085)
- Barbanti, Francesca, S153 (THU067)
- Barbas, Coral, S643 (FRI554)
- Barbato, Anna, S84 (OS115)
- Barbera, Aurora, S180 (THU161),
S365 (THU538)
- Barbera, Thomas, S185 (THU173)
- Barbosa, Sandra, S724 (SAT125)
- Barcena-Varela, Marina, S45 (OS055)
- Barciela, Mar Riveiro, S44 (OS052),
S212 (THU240), S255 (THU325),
S257 (THU330), S269 (THU350),
S277 (THU367), S324 (THU464),
S325 (THU465), S607 (FRI468)
- Barclay, Stephen, S17 (OS005),
S266 (THU345)
- Bardou-Jacquet, Edouard, S504 (FRI228),
S833 (SAT360), S840 (SAT373)
- Barget, Nathalie, S127 (THU019)
- Barghash, Ahmad, S705 (SAT082)
- Barkow, Sophia, S184 (THU169)
- Barla, Georgia, S917 (SAT562)
- Barman-Aksözen, Jasmin, S516 (FRI251)
- Barnabas, Ashley, S594 (FRI409)
- Barnault, Romain, S254 (THU324),
S766 (SAT216)
- Barner-Rasmussen, Nina, S327 (THU469)
- Barnes, E, S868 (SAT428)
- Barnes, Eleanor, S17 (OS005), S54 (OS069),
S57 (OS072A), S58 (OS072B),
S541 (FRI301), S868 (SAT428)
- Barnes, Mathew, S188 (THU178)
- Barnett, Tamara, S240 (THU297)
- Barone, Michele, S578 (FRI376)
- Barreby, Emelie, S665 (SAT002),
S756 (SAT197)
- Barreira, Ana, S44 (OS052), S212 (THU240),
S269 (THU350), S277 (THU367),
S316 (THU450), S324 (THU464),
S325 (THU465), S328 (THU471)
- Barrett, Stephen, S36 (OS037),
S642 (FRI553)
- Barr, Haim, S387 (THU597)
- Barrio, María Del, S624 (FRI518),
S774 (SAT242)
- Barritt, A. Sidney, S223 (THU262)
- Bartels, Alexandra, S381 (THU585)
- Bartels, Emil, S361 (THU532)
- Barten, Thijs, S525 (FRI266)
- Barthemon, Justine, S73 (OS096),
S74 (OS099)
- Bartlett, Sofia, S17 (OS005), S43 (OS051),
S209 (THU233), S282 (THU378),
S910 (SAT538)
- Bartoletti, Luigi, S559 (FRI336)
- Bartolí, Ramon, S724 (SAT125)
- Bartolucci, Pablo, S791 (SAT269)
- Bartosch, Birke, S766 (SAT216)
- Bartres, Concepció, S99 (OS141)
- Baru, Ambika, S447 (FRI100)
- Barutcu, Sezgin, S19 (OS008), S49 (OS063)
- Bascia, Annalisa, S581 (FRI384)
- Baselli, Giodo, S675 (SAT021)
- Baselli, Guido Alessandro, S668 (SAT008)
- Bashir, Mustafa, S14 (LB005), S32 (OS030)
- Basho, Jovan, S573 (FRI367)
- Bashyam, Maria, S345 (THU505)
- Basic, Michael, S262 (THU337)
- Basida, Sanket, S803 (SAT290)
- Basile, Umberto, S436 (FRI079)
- Ba-Salamah, Ahmed, S24 (OS017),
S320 (THU457), S532 (FRI280)
- Bassegoda, Octavi, S63 (OS080),
S139 (THU039), S511 (FRI242),
S512 (FRI243), S684 (SAT039),
S896 (SAT512), S901 (SAT522),
S902 (SAT524), S907 (SAT532)
- Bassendine, Margaret, S493 (FRI208)
- Bassis, Christine, S180 (THU162)
- Bass, Nathan, S394 (FRI008)
- Bastaich, Dustin, S227 (THU270)
- Bastati, Nina, S24 (OS017)
- Bataller, Ramon, S81 (OS110),
S132 (THU027), S137 (THU034),
S137 (THU035), S140 (THU040),
S442 (FRI091)
- Batbaatar, Suvd, S824 (SAT342)
- Batbold, Enkhtuul, S235 (THU287)
- Bathgate, Andrew, S17 (OS005)
- Bathon, Melanie, S927 (SAT579)
- Batirel, Ayse, S858 (SAT411)
- Batista, Clara, S597 (FRI415)
- Batista, Rui, S393 (FRI007)
- Bat-Or, Uyanga, S824 (SAT342)
- Battaglia, Salvatore, S387 (THU599)
- Battezzati, Pier Maria, S335 (THU484)
- Battistella, Sara, S306 (THU423)
- Battisti, Arianna, S284 (THU380)
- Bat-Ulzii, Purevjargal, S235 (THU287)
- Baubeta, Erik Fridh, S333 (THU480)
- Baudin, Martine, S721 (SAT119),
S722 (SAT120)
- Bauer, David J. M., S390 (FRI003),
S502 (FRI225), S532 (FRI280)
- Bauer, David JM, S18 (OS007), S92 (OS131),
S315 (THU449), S359 (THU527),
S617 (FRI505), S631 (FRI531),
S632 (FRI533)
- Bauer, Jens, S198 (THU198)
- Bauer, Ulrike, S189 (THU180)
- Baumann, Anja, S692 (SAT056),
S711 (SAT093)
- Baumann, Cédric, S905 (SAT529)
- Baumann, Ulrich, S519 (FRI256),
S521 (FRI259)
- Baumert, Thomas, S36 (OS038),
S99 (OS142), S246 (THU305),
S649 (FRI565), S738 (SAT160),
S758 (SAT199)
- Baur, Joseph A, S742 (SAT168)
- Bauschen, Alina, S340 (THU495),
S341 (THU498)
- Bauvin, Pierre, S205 (THU227),
S205 (THU228)
- Bawa, Aditi, S137 (THU035)
- Baxi, Vipul, S446 (FRI029)
- Baykam, Nurcan, S858 (SAT411)
- Bayne, David, S19 (OS008), S49 (OS063)
- Bazinet, Michel, S851 (SAT398)
- Beccaria, Maria Garcia, S47 (OS059)
- Becce, Fabio, S355 (THU520)
- Becchetti, Chiara, S780 (SAT251)

Author Index

- Bechmann, Lars, S378 (THU579), S682 (SAT035)
- Beck, Andrew, S700 (SAT071), S708 (SAT088)
- Becker, Britta, S250 (THU315)
- Becker, Hans, S83 (OS113)
- Becker, Mark, S455 (FRI112)
- Becker, Svea, S385 (THU594)
- Beckford, Racquel, S812 (SAT304)
- Beckmann, Sonja, S509 (FRI238)
- Beck-Nielsen, Henning, S9 (GS012)
- Bédard, Nathalie, S675 (SAT022)
- Bedard, Philippe, S395 (FRI010)
- Bed, Cheikh Mohamed, S245 (THU304)
- Bedford, Erin, S759 (SAT202)
- Bedossa, Pierre, S7 (GS009), S680 (SAT032), S730 (SAT139)
- Bedoya, José Ursic, S771 (SAT237)
- Bee, Agnes, S730 (SAT140), S735 (SAT154)
- Beerenwinkel, Niko, S15 (OS001)
- Beer, Lewis, S564 (FRI348)
- Beer, Lucian, S24 (OS017), S921 (SAT570)
- Befeler, Alex, S634 (FRI537)
- Bega, Danny, S1 (GS001)
- Begum, Neelu, S68 (OS089)
- Behaeghel, Elke, S853 (SAT401)
- Behari, Jaideep, S442 (FRI091), S444 (FRI095)
- Behling, Cynthia, S416 (FRI040), S439 (FRI085), S701 (SAT073), S714 (SAT103), S719 (SAT114)
- Behrends, Christian, S703 (SAT079)
- Behrendt, Patrick, S250 (THU315), S263 (THU339)
- Beigelman, Leonid, S846 (SAT386), S853 (SAT401), S853 (SAT402), S871 (SAT435)
- Beilin, Lawrence J., S440 (FRI087)
- Beisel, Claudia, S197 (THU197)
- Bektaş, Hicran, S513 (FRI245)
- Belasri, Ines, S547 (FRI314)
- Belblidia, Assia, S456 (FRI114)
- Belén Rubio, Ana, S512 (FRI243)
- Belew, Getachew Debas, S706 (SAT085)
- Belkhodja, Mehdi, S483 (FRI187)
- Belland, Dawn, S890 (SAT500)
- Bellanger, Agnès, S393 (FRI007)
- Bellan, Mattia, S483 (FRI185), S929 (SAT583)
- Bellantini, Francesco, S862 (SAT417)
- Bell, Elaine, S412 (FRI034)
- Bellet, Jonathan, S17 (OS006)
- Belli, Luca Saverio, S578 (FRI376), S807 (SAT296)
- Bell, John, S277 (THU368)
- Bello, Arnaud Del, S122 (THU009)
- Bell, Sally, S337 (THU488), S342 (THU501)
- Bellue, Astrid Laurent, S402 (FRI020)
- Belmonte, Ernest, S99 (OS141)
- Bemeur, Chantal, S456 (FRI114)
- Benabadj, Elias, S579 (FRI381)
- Benali, Souad, S547 (FRI314)
- Bencheva, Leda, S97 (OS139)
- Bende, Felix, S483 (FRI186), S505 (FRI230)
- Bendixen, Sofie, S423 (FRI054), S758 (SAT200)
- Ben-Dor, Shifra, S83 (OS114)
- Bendtsen, Flemming, S64 (OS083), S331 (THU477), S340 (THU496), S502 (FRI226), S610 (FRI489), S614 (FRI498), S887 (SAT495)
- Benedetti, Livia, S284 (THU380)
- Benedetto, Davide Di, S929 (SAT582)
- Benedetto, Fabrizio Di, S789 (SAT266)
- Benencio, Paula, S786 (SAT261)
- Bengsch, Bertram, S2 (GS003), S100 (OS143), S196 (THU194), S374 (THU571), S376 (THU574), S383 (THU588), S710 (SAT090)
- Bengtsson, Bonnie, S189 (THU179)
- Bengtsson, Johan, S333 (THU480)
- Benini, Federica, S515 (FRI250)
- Benitez, Carlos, S19 (OS008), S49 (OS063), S351 (THU514)
- Benitez, Laura, S114 (OS169)
- Benito, Alberto, S815 (SAT311)
- Benito-Vicente, Asier, S648 (FRI564)
- Benjamin, Jaya, S139 (THU038), S349 (THU510)
- Benlahrech, Adel, S872 (SAT437)
- Benlloch, Salvador, S157 (THU074), S158 (THU076), S222 (THU261), S442 (FRI091)
- Ben, Maria Del, S161 (THU081)
- Benmassaoud, Amine, S31 (OS029), S614 (FRI497)
- Benna, Jamel El, S245 (THU304)
- Bennett, Andrew, S465 (FRI151)
- Bennett, Kris, S615 (FRI499)
- Bennett, Michael, S836 (SAT366)
- Bennet, William, S815 (SAT311)
- Benselin, Jennifer, S17 (OS005)
- Bensimon, Gilbert, S809 (SAT298)
- Benyamini, Hadar, S83 (OS114)
- Ben-Yehoyada, Merav, S790 (SAT268)
- Benzing, Christian, S374 (THU570), S380 (THU582), S497 (FRI217), S663 (FRI597)
- Bera, Chinmay, S429 (FRI065)
- Berak, Hanna, S565 (FRI350), S585 (FRI390)
- Beran, Rudolf, S251 (THU317)
- Berardo, Clarissa, S697 (SAT065)
- Berasain, Carmen, S112 (OS165), S500 (FRI222), S643 (FRI554), S644 (FRI557)
- Berby, Françoise, S246 (THU306), S247 (THU307)
- Bereket, Michael D., S31 (OS028), S409 (FRI030), S762 (SAT208)
- Berenguer, Marina, S114 (OS168), S115 (OS169), S150 (THU061), S192 (THU185), S334 (THU482), S406 (FRI027), S807 (SAT296), S811 (SAT301), S811 (SAT303), S815 (SAT311)
- Berentzen, Tina Landsvig, S29 (OS025)
- Beretta, Laura, S470 (FRI160), S485 (FRI190)
- Beretta-Piccoli, Benedetta Terzioli, S317 (THU452)
- Bergamin, Irina, S937 (SAT598)
- Berg, Christoph, S16 (OS003), S585 (FRI391), S823 (SAT341)
- Berg, Ellen, S31 (OS028)
- Bergentall, Mattias, S94 (OS133)
- Berger, Hilmar, S309 (THU436), S684 (SAT040)
- Berger, Michael, S83 (OS114)
- Bergheim, Ina, S692 (SAT056), S711 (SAT093)
- Berghe, Tom Vanden, S709 (SAT089)
- Bergin, Anthony, S538 (FRI294), S538 (FRI295)
- Bergmann, Andreas, S361 (THU532)
- Bergmann, Ottar M., S573 (FRI366)
- Bergner, Raoul, S523 (FRI262)
- Bergquist, Annika, S27 (OS021), S333 (THU480)
- Berg, Thomas, S11 (LB002), S16 (OS003), S148 (THU057), S184 (THU169), S379 (THU581), S382 (THU586), S383 (THU590), S562 (FRI345), S585 (FRI391), S807 (SAT296), S823 (SAT341), S824 (SAT344), S860 (SAT414), S883 (SAT488), S904 (SAT528), S931 (SAT587), S937 (SAT597)
- Berhe, Nega, S841 (SAT375)
- Bering, Tatiana Bering, S293 (THU396), S552 (FRI323)
- Berliba, Elina, S876 (SAT443)
- Berlin, Claudia, S809 (SAT298)
- Bermúdez, Maria, S658 (FRI587)
- Bermúdez, María, S912 (SAT555)
- Bernal, Carmen, S114 (OS168)
- Bernales, Irantzu, S651 (FRI571)
- Bernal, William, S403 (FRI022), S505 (FRI231), S911 (SAT540)
- Bernardes, Christina, S204 (THU226)
- Bernardi, Mauro, S908 (SAT535)
- Bernard, Lucie, S692 (SAT055)
- Bernardo, Barbara, S7 (GS009)
- Bernard, Pierre-Henri, S817 (SAT312)
- Bernasconi, Davide, S96 (OS136)
- Berney, Thierry, S317 (THU452)
- Bernsmeier, Christine, S192 (THU186), S308 (THU435)
- Bernstein, David, S548 (FRI315)
- Berntsen, Natalie Lie, S605 (FRI465)
- Berres, Marie-Luise, S193 (THU187)
- Berrevoet, Frederik, S107 (OS156), S768 (SAT230)
- Berse, Matthias, S737 (SAT158)
- Bertelli, Cristina, S167 (THU095)
- Berthou, Flavien, S645 (FRI559)
- Bertoletti, Antonio, S223 (THU263)
- Bertoli, Ada, S249 (THU313)
- Bertran, Esther, S48 (OS060)
- Berzigotti, Annalisa, S363 (THU535), S480 (FRI180), S780 (SAT251)
- Besch, Camille, S20 (OS010), S772 (SAT239)
- Beschin, Alain, S655 (FRI580)

- Besombes, Juliette, S258 ([THU331](#))
 Bessissow, Ali, S614 ([FRI497](#))
 Bessone, Fernando, S137 ([THU034](#))
 Besson, Florent, S935 ([SAT595](#))
 Best, Jan, S378 ([THU579](#)), S682 ([SAT035](#))
 Bethencourt, Dácil Díaz, S931 ([SAT586](#))
 Bettinger, Dominik, S19 ([OS008](#)),
 S49 ([OS063](#)), S313 ([THU444](#)),
 S372 ([THU567](#)), S374 ([THU571](#)),
 S376 ([THU574](#)), S383 ([THU588](#)),
 S710 ([SAT090](#))
 Betz, Briana, S412 ([FRI034](#))
 Beudeker, Boris, S194 ([THU190](#))
 Beuers, Ulrich, S93 ([OS132](#)),
 S338 ([THU491](#)), S601 ([FRI457](#)),
 S603 ([FRI461](#)), S893 ([SAT506](#))
 Beumer, Berend, S631 ([FRI530](#)),
 S815 ([SAT311](#)), S933 ([SAT591](#))
 Beumont-Mauviel, Maria, S8 ([GS010](#))
 Bevilacqua, Michele, S658 ([FRI586](#)),
 S900 ([SAT519](#)), S925 ([SAT574](#))
 Bewersdorf, Lisa, S533 ([FRI282](#))
 Beyer, Cayden, S453 ([FRI109](#))
 Beyer, Simon, S764 ([SAT212](#))
 Bezerra, Jorge, S866 ([SAT425](#))
 Bhadoria, Ajeet Singh, S457 ([FRI116](#))
 Bhadoria, Pooja, S741 ([SAT164](#))
 Bhagat, Abhi, S549 ([FRI317](#)), S584 ([FRI388](#))
 Bhagwat, Shripad, S534 ([FRI285](#))
 Bhandal, Khushpreet, S54 ([OS069](#))
 Bhandari, Bal Raj, S427 ([FRI060](#)),
 S731 ([SAT142](#))
 Bhandari, Rajan, S430 ([FRI066](#))
 Bhanji, Rahima A., S775 ([SAT244](#)),
 S892 ([SAT504](#))
 Bhanot, Sanjay, S689 ([SAT050](#))
 Bharania, Punam, S12 ([LB004A](#)),
 S13 ([LB004B](#)), S288 ([THU389](#)),
 S288 ([THU390](#)), S880 ([SAT452](#)),
 S881 ([SAT453](#))
 Bhat, Adil, S128 ([THU020](#)), S738 ([SAT161](#))
 Bhatia, Pujia, S139 ([THU038](#))
 Bhatia, Sangeeta, S657 ([FRI584](#))
 Bhatnagar, Megha, S770 ([SAT234](#))
 Bhat, Sadam Hussain, S752 ([SAT188](#))
 Bhattacharya, Dipankar, S688 ([SAT048](#))
 Bhavani, Ruveena, S19 ([OS008](#)),
 S49 ([OS063](#))
 Bhave, Gautam, S36 ([OS037](#))
 Białkowska, Jolanta, S565 ([FRI350](#)),
 S592 ([FRI406](#))
 Biancacci, Ilaria, S385 ([THU594](#))
 Biancaniello, Francesca, S648 ([FRI564](#))
 Bianchini, Marcello, S627 ([FRI524](#))
 Bianco, Cristiana, S428 ([FRI061](#)),
 S675 ([SAT021](#))
 Bianco, Paola Del, S821 ([SAT318](#))
 Bican, Yesim, S24 ([OS017](#))
 Bichko, Vadim, S832 ([SAT359](#)),
 S865 ([SAT423](#))
 Bickel, Markus, S15 ([OS001](#))
 Biddle-Snead, Charles, S700 ([SAT071](#)),
 S711 ([SAT094](#))
 Bidou, Laure, S514 ([FRI248](#))
 Bieri, Manuela, S488 ([FRI197](#))
 Biermer, Michael, S8 ([GS010](#)),
 S838 ([SAT370](#)), S864 ([SAT422](#))
 Biertho, Laurent, S456 ([FRI114](#))
 Bifani, Pablo, S98 ([OS140](#))
 Biggins, Scott, S19 ([OS008](#)), S49 ([OS063](#)),
 S887 ([SAT496](#))
 Biglione, Mirna, S786 ([SAT261](#))
 Bignamini, Daniela, S159 ([THU078](#))
 Bihari, Chhagan, S20 ([OS009](#)),
 S221 ([THU259](#)), S457 ([FRI116](#)),
 S756 ([SAT196](#))
 Bijvelds, Marcel, S115 ([OS170](#))
 Bilak, Joanna, S409 ([FRI031](#))
 Bilbao, Angela, S805 ([SAT292](#))
 Bilbao, Idoia, S500 ([FRI222](#))
 Bilbao, Itxarone, S792 ([SAT271](#)),
 S805 ([SAT292](#))
 Bilic-Curcic, Ines, S718 ([SAT113](#))
 Biliotti, Elisa, S564 ([FRI347](#))
 Bill, Griffiths, S14 ([LB006](#))
 Billiet, Antoon, S516 ([FRI252](#))
 Billimoria, Kharman, S530 ([FRI277](#))
 Billin, Andrew, S31 ([OS028](#)),
 S318 ([THU453](#)), S409 ([FRI030](#)),
 S700 ([SAT071](#))
 Bilodeau, Laurent, S456 ([FRI114](#))
 Bilodeau, Marc, S456 ([FRI114](#)),
 S593 ([FRI407](#)), S675 ([SAT022](#)),
 S805 ([SAT293](#))
 Bindal, Vasundhra, S34 ([OS033](#)),
 S128 ([THU020](#)), S528 ([FRI273](#)),
 S738 ([SAT161](#)), S752 ([SAT188](#))
 Bindels, Laure, S680 ([SAT031](#))
 Bindels, Patrick, S227 ([THU271](#))
 Binder, Harald, S80 ([OS108](#))
 Bindia, Chabi, S304 ([THU419](#))
 Binka, Mawuena, S17 ([OS005](#)), S43 ([OS051](#)),
 S209 ([THU233](#)), S282 ([THU378](#)),
 S910 ([SAT538](#))
 Binks, Paula, S239 ([THU294](#)),
 S305 ([THU422](#))
 Binter, Teresa, S24 ([OS017](#)), S830 ([SAT354](#))
 Biolato, Marco, S436 ([FRI079](#))
 Biondi, Mia, S294 ([THU400](#))
 Biondi, Roberta, S84 ([OS115](#))
 Biotrel, Marie-Therese, S639 ([FRI548](#))
 Bird, Thomas G, S385 ([THU595](#))
 Birn-Rydder, Rasmine, S314 ([THU446](#))
 Bisbal, Otilia, S577 ([FRI373](#))
 Biscontin, Alberto, S888 ([SAT497](#))
 Bishara, Maria, S389 ([FRI002](#))
 Bi, Sheng, S165 ([THU090](#))
 Bissonnette, Julien, S593 ([FRI407](#)),
 S805 ([SAT293](#))
 Bissram, Jennifer, S557 ([FRI333](#))
 Biswas, Debasis, S252 ([THU320](#))
 Biswas, Sagnik, S433 ([FRI072](#)),
 S524 ([FRI264](#)), S620 ([FRI511](#))
 Biswas, Subhrajit, S756 ([SAT196](#))
 Bittaye, Baboucarr, S258 ([THU332](#))
 Bittencourt, Paulo, S542 ([FRI304](#)),
 S543 ([FRI305](#)), S888 ([SAT498](#))
 Bivegete, Sandra, S256 ([THU328](#))
 Bizkarguenaga, Maider, S671 ([SAT014](#))
 Bizzaro, Debora, S821 ([SAT318](#))
 Bjerre, Frederik Adam, S37 ([OS040](#)),
 S758 ([SAT200](#))
 Björkström, Niklas, S27 ([OS021](#)),
 S189 ([THU179](#)), S756 ([SAT197](#)),
 S826 ([SAT348](#))
 Björnsson, Einar S., S573 ([FRI366](#)),
 S904 ([SAT527](#))
 Blach, Sarah, S43 ([OS050](#)), S230 ([THU278](#)),
 S231 ([THU279](#)), S238 ([THU292](#)),
 S240 ([THU295](#))
 Blagoev, Blagoy, S758 ([SAT200](#))
 Blain, Alasdair, S733 ([SAT146](#))
 Blaise, Lorraine, S791 ([SAT269](#))
 Blanc, Charlotte, S872 ([SAT436](#))
 Blanc, Jean-Frédéric, S372 ([THU566](#)),
 S373 ([THU569](#))
 Blanco, Jesus Miguens, S674 ([SAT020](#))
 Blanes, Marino, S114 ([OS169](#))
 Blank, Antje, S4 ([GS006](#)), S828 ([SAT351](#))
 Blank, Valentin, S148 ([THU057](#))
 Blasczyk, Rainer, S783 ([SAT257](#))
 Blasi, Annabel, S367 ([THU542](#))
 Blasi, Bruno, S584 ([FRI389](#))
 Blatt, Lawrence, S733 ([SAT145](#)),
 S824 ([SAT343](#)), S835 ([SAT365](#)),
 S846 ([SAT386](#)), S853 ([SAT401](#)),
 S853 ([SAT402](#)), S871 ([SAT435](#))
 Blaya, Delia, S139 ([THU039](#)), S684 ([SAT039](#)),
 S907 ([SAT532](#))
 Blazar, Bruce, S494 ([FRI209](#))
 Blázquez-Moreno, Alfonso, S265 ([THU343](#))
 Blissett, Rob, S237 ([THU290](#))
 Bloch, Evan, S219 ([THU253](#))
 Blø, Magnus, S672 ([SAT016](#))
 Blomdahl, Julia, S146 ([THU052](#))
 Blom, Sami, S111 ([OS162](#))
 Bloomer, Pamela M., S886 ([SAT493](#))
 Bloom, Patricia, S180 ([THU162](#))
 Bloom, Stephen, S315 ([THU448](#)),
 S389 ([FRI002](#)), S441 ([FRI090](#))
 Blouin, Karine, S206 ([THU230](#))
 Blue, David Jr, S72 ([OS094](#))
 Blüher, Matthias, S703 ([SAT079](#))
 Boberg, Kirsten Muri, S178 ([THU157](#))
 Boccagni, Patrizia, S821 ([SAT318](#))
 Bocedi, Giulia, S153 ([THU067](#))
 Bockamp, Ernesto, S464 ([FRI147](#))
 Bock, Hans, S257 ([THU329](#)), S825 ([SAT345](#))
 Boddu, Ravan, S903 ([SAT526](#))
 Bode, Johannes, S11 ([LB003](#)), S825 ([SAT345](#))
 Bodenheimer, Henry, S548 ([FRI315](#))
 Bodhani, Jaysal, S310 ([THU438](#))
 Boehlig, Albrecht, S148 ([THU057](#)),
 S379 ([THU581](#))
 Boeke, Caroline, S225 ([THU266](#))
 Boeker, Klaus, S562 ([FRI345](#))
 Boesch, Markus, S346 ([THU507](#)),
 S680 ([SAT032](#))
 Boettcher, Jan, S185 ([THU171](#)),
 S189 ([THU180](#))
 Bogaards, Johannes, S338 ([THU491](#))
 Bogdanov, Alina, S167 ([THU094](#))

Author Index

- Bogdanowicz, Karolina, S34 ([OS034](#))
 Boghici, Dan, S259 ([THU334](#))
 Boglione, Lucio, S825 ([SAT346](#))
 Bogomolov, Pavel, S4 ([GS006](#)),
 S828 ([SAT351](#)), S829 ([SAT352](#))
 Bohan-Keane, Mary, S569 ([FRI358](#)),
 S570 ([FRI360](#))
 Boillet, Gautier, S250 ([THU314](#))
 Boillot, Olivier, S772 ([SAT239](#))
 Boisselle, Carri, S58 ([OS073](#))
 Boix, Loreto, S381 ([THU584](#)), S500 ([FRI222](#)),
 S652 ([FRI573](#))
 Bojunga, Jörg, S353 ([THU517](#)),
 S354 ([THU518](#)), S907 ([SAT531](#))
 Bökkerink, Roos-Anne, S525 ([FRI266](#))
 Bokun, Tomislav, S612 ([FRI494](#))
 Bolca, Selin, S180 ([THU161](#))
 Bolch, Maximilian, S381 ([THU585](#))
 Boldina, Galina, S872 ([SAT436](#))
 Boleac, Nicolae, S795 ([SAT276](#))
 Boleslawski, Emmanuel, S817 ([SAT312](#))
 Bolewska, Beata, S565 ([FRI350](#))
 Bollekens, Jacques, S271 ([THU356](#))
 Bollhagen, Ralf, S251 ([THU316](#))
 Bolognese, James, S451 ([FRI107](#)),
 S701 ([SAT073](#))
 Bolt, Isabelle, S26 ([OS019](#))
 Bolton, Natalie, S280 ([THU373](#)),
 S281 ([THU375](#))
 Bomo, Jeremy, S258 ([THU331](#))
 Bonaccorsi, Eliano, S535 ([FRI289](#)),
 S797 ([SAT279](#))
 Bonacini, Maurizio, S836 ([SAT366](#))
 Bonafede, Machaon, S167 ([THU094](#))
 Bonaffini, Pietro Angelo, S751 ([SAT186](#))
 Bonanni, Paolo, S238 ([THU291](#))
 Bonanzinga, Sara, S842 ([SAT377](#))
 Bonaventura, Chiara Di, S627 ([FRI524](#))
 Bonazza, Deborah, S433 ([FRI071](#))
 Bonder, Alan, S317 ([THU452](#))
 Bonfanti, Paola, S480 ([FRI179](#))
 Bong Ahn, Sang, S438 ([FRI082](#)),
 S438 ([FRI083](#)), S439 ([FRI086](#))
 Bongini, Marco, S815 ([SAT311](#))
 Bonifacius, Agnes, S783 ([SAT257](#))
 Bonilha, Danielle Q, S625 ([FRI520](#))
 Bonino, Ferruccio, S292 ([THU394](#))
 Bonkovsky, Herbert L., S60 ([OS075](#))
 Bonn, Britta, S751 ([SAT187](#)), S843 ([SAT380](#))
 Bonnefont-Rousselot, Dominique,
 S393 ([FRI007](#))
 Bonnin, Odile, S872 ([SAT436](#))
 Booijsink, Richell, S649 ([FRI567](#)),
 S707 ([SAT086](#))
 Boonstra, Andre, S194 ([THU189](#)),
 S194 ([THU190](#)), S251 ([THU317](#)),
 S281 ([THU374](#)), S824 ([SAT344](#))
 Boora, Praveen Kumar, S232 ([THU280](#))
 Booshehri, Laela M., S471 ([FRI161](#)),
 S690 ([SAT051](#))
 Bo, Qingyan, S299 ([THU408](#)), S867 ([SAT427](#))
 Borao, Cristina, S114 ([OS168](#))
 Borca, Florina, S909 ([SAT536](#))
 Bordoy, Antoni E., S570 ([FRI361](#))
 Borg, Brian, S427 ([FRI060](#))
 Borges, Valéria Ferreira de Almeida e,
 S307 ([THU432](#))
 Borghi, Marta, S196 ([THU194](#)),
 S843 ([SAT379](#)), S843 ([SAT381](#)),
 S868 ([SAT429](#)), S874 ([SAT440](#)),
 S880 ([SAT450](#))
 Borgia, Guglielmo, S578 ([FRI376](#))
 Borgia, Sergio, S581 ([FRI384](#))
 Borgmann, Stefan, S339 ([THU493](#))
 Borisovets, Dmitry, S269 ([THU351](#))
 Borlea, Andreea, S483 ([FRI186](#))
 Borman, Meredith, S143 ([THU045](#))
 Bornemann, Lea, S340 ([THU495](#))
 Borrás, Francesc, S361 ([THU531](#))
 Borrós, Salvador, S106 ([OS154](#))
 Borsodi, Christian, S271 ([THU354](#))
 Bosch, Jaime, S90 ([OS127](#)),
 S363 ([THU535](#)), S370 ([THU548](#)),
 S480 ([FRI180](#)), S625 ([FRI520](#)),
 S780 ([SAT251](#))
 Bosch, Miriam, S195 ([THU193](#))
 Bosco, Maria Carla, S515 ([FRI249](#))
 Bosnar, Martina, S702 ([SAT075](#))
 Bossard, Pasacale, S672 ([SAT015](#))
 Bossuyt, Patrick, S74 ([OS097](#)),
 S424 ([FRI055](#)), S425 ([FRI058](#)),
 S448 ([FRI102](#)), S452 ([FRI108](#))
 Bostick, Robert M, S228 ([THU273](#))
 Bos, Trijnie, S539 ([FRI298](#))
 Bota, Simona, S21 ([OS012](#)), S829 ([SAT353](#)),
 S891 ([SAT502](#))
 Botaya, Elena Guillen, S222 ([THU261](#))
 Bot, Daphne, S631 ([FRI530](#))
 Bottai, Matteo, S24 ([OS016](#))
 Böttcher, Katrin, S185 ([THU171](#)),
 S189 ([THU180](#))
 Botteaux, Anne, S124 ([THU012](#))
 Böttler, Tobias, S100 ([OS143](#)),
 S657 ([FRI583](#)), S710 ([SAT090](#))
 Bott, Sebastian, S691 ([SAT053](#))
 Bouam, Samir, S41 ([OS047](#)),
 S393 ([FRI007](#))
 Bouattour, Mohamed, S372 ([THU566](#))
 Boulakira, Hakim, S542 ([FRI303](#))
 Boudes, Pol, S619 ([FRI509](#)),
 S623 ([FRI516](#))
 Boudina, Sihem, S113 ([OS167](#))
 Boudjema, Karim, S772 ([SAT239](#))
 Boudon, Marc, S349 ([THU511](#)),
 S935 ([SAT595](#))
 Bouée, Stéphane, S373 ([THU569](#))
 Boulahouf, Zakaria, S99 ([OS142](#))
 Boulain, Mathieu, S918 ([SAT563](#))
 Boulos, Sherif, S409 ([FRI031](#))
 Boulter, Luke, S85 ([OS117](#))
 Bouma, Gerd, S326 ([THU467](#))
 Bounidane, Ayoub, S313 ([THU444](#))
 Bouquin, Thomas, S872 ([SAT436](#))
 Bourgeois, Stefan, S72 ([OS094](#)),
 S872 ([SAT437](#))
 Bourliere, Marc, S8 ([GS010](#)), S17 ([OS006](#)),
 S101 ([OS146](#)), S250 ([THU314](#)),
 S547 ([FRI314](#)), S829 ([SAT352](#))
 Boursier, Jerome, S73 ([OS096](#)), S74 ([OS097](#)),
 S74 ([OS099](#)), S425 ([FRI058](#)),
 S437 ([FRI081](#)), S448 ([FRI102](#)),
 S452 ([FRI108](#)), S496 ([FRI215](#)),
 S497 ([FRI216](#)), S504 ([FRI228](#)),
 S507 ([FRI235](#)), S715 ([SAT105](#))
 Bousquet, Delphine, S246 ([THU306](#)),
 S247 ([THU307](#))
 Bouzakri, Karim, S667 ([SAT006](#))
 Bouzahir, Latifa, S759 ([SAT202](#))
 Bowlus, Christopher, S318 ([THU453](#)),
 S335 ([THU484](#))
 Bowman, Kelly, S713 ([SAT101](#))
 Boyacioglu, Sedat, S858 ([SAT410](#))
 Boyacioglu, Sedat, S861 ([SAT416](#))
 Boyd, Adam, S58 ([OS073](#))
 Boyd, Kelli, S483 ([FRI187](#))
 Boyd, Sonja, S312 ([THU441](#))
 Boyer, Sylvie, S202 ([THU221](#))
 Boyle, Alison, S580 ([FRI383](#))
 Boyle, Louise H., S198 ([THU198](#))
 Bozkurt, Birkan, S782 ([SAT255](#))
 Bozkurt, I., S858 ([SAT411](#))
 Boztug, Kaan, S315 ([THU449](#)),
 S360 ([THU529](#))
 Bozzarelli, Silvia, S923 ([SAT572](#))
 Bozzi, Giorgio, S167 ([THU095](#))
 Braat, Andries, S798 ([SAT280](#))
 Braconi, Chiara, S107 ([OS157](#))
 Bradley, Linda M, S742 ([SAT166](#))
 Brady, Emer, S409 ([FRI031](#))
 Brady, J Michael, S320 ([THU456](#)),
 S320 ([THU457](#)), S321 ([THU459](#)),
 S322 ([THU460](#))
 Brady, John Michael, S424 ([FRI056](#))
 Bragg, Kylie, S898 ([SAT516](#))
 Brahmania, Mayur, S81 ([OS110](#)),
 S137 ([THU034](#)), S141 ([THU041](#))
 Brakenhoff, Sylvia, S227 ([THU271](#)),
 S281 ([THU374](#)), S824 ([SAT344](#)),
 S852 ([SAT400](#)), S861 ([SAT415](#))
 Brancaccio, Giuseppina, S564 ([FRI347](#)),
 S569 ([FRI359](#))
 Branch, Andrea, S298 ([THU407](#))
 Branchi, Vittorio, S381 ([THU585](#)),
 S599 ([FRI451](#))
 Brandão-Mello, Carlos, S543 ([FRI305](#))
 Brand, Floris van den,
 S326 ([THU467](#))
 Brandl, Lydia, S655 ([FRI581](#))
 Brandt, Annette, S692 ([SAT056](#)),
 S711 ([SAT093](#))
 Brandt, Elisa, S193 ([THU187](#))
 Braniff, Conor, S96 ([OS137](#))
 Brass, Clifford, S486 ([FRI194](#)),
 S493 ([FRI207](#))
 Brates, Irena, S544 ([FRI307](#))
 Braude, Michael, S441 ([FRI090](#))
 Braud, Filippo De, S748 ([SAT180](#))
 Braun, Marius, S774 ([SAT241](#)),
 S793 ([SAT272](#)), S855 ([SAT406](#))
 Bravo, Catarina, S537 ([FRI293](#))
 Bravo, Miguel Ángel Gómez, S114 ([OS168](#)),
 S792 ([SAT271](#))

- Bravo, Miren, S84 (OS116), S87 (OS122), S600 (FRI453), S673 (SAT018), S679 (SAT029)
- Breckinridge, David, S31 (OS028), S409 (FRI030), S762 (SAT208)
- Breen, David J., S422 (FRI052)
- Breen, Leigh, S364 (THU537)
- Brees, Dominique, S486 (FRI194), S493 (FRI207)
- Bremer, Birgit, S248 (THU311), S250 (THU315), S830 (SAT355)
- Brenig, Robert G, S192 (THU186)
- Brennan, Paul, S415 (FRI038)
- Brescini, Lucia, S564 (FRI347)
- Breuer, Monika, S390 (FRI003)
- Brehahn, Kai, S655 (FRI581)
- Breyner, Natalia, S717 (SAT110)
- Briand, Francois, S717 (SAT110)
- Brichler, Segolene, S271 (THU355)
- Bridge, Simon, S493 (FRI208)
- Brigida, Krestina, S235 (THU288)
- Brignon, Nicolas, S36 (OS038), S649 (FRI565), S738 (SAT160)
- Brill, Florian H. H., S250 (THU315)
- Brindley, James Hallimond, S698 (SAT066)
- Brinkmann, Leonard, S545 (FRI309)
- Brinkman, Paul, S434 (FRI075)
- Brito, Matheus Duarte, S293 (THU396)
- Brixko, Christian, S581 (FRI384)
- Briz, Oscar, S59 (OS074)
- Brocca, Alessandra, S18 (OS007), S49 (OS062), S92 (OS131), S894 (SAT508), S895 (SAT511)
- Brodbeck, Jens, S832 (SAT358)
- Broderick, Lori, S690 (SAT051)
- Brodosi, Lucia, S153 (THU067)
- Broekhoven, Annelotte, S120 (THU003), S144 (THU047)
- Broering, Ruth, S264 (THU342), S642 (FRI552), S643 (FRI555)
- Brol, Maximilian J, S895 (SAT510)
- Brønd, Jan Christian, S9 (GS012)
- Bronner, Korbinian, S251 (THU316)
- Bronowicki, Jean-Pierre, S5 (GS007), S373 (THU569), S905 (SAT529), S923 (SAT573)
- Bronsert, Peter, S2 (GS003)
- Bronstein, Jeff, S1 (GS001)
- Bronte, Fabrizio, S624 (FRI517)
- Brooks-Pollock, Ellen, S256 (THU328)
- Brooks-Rooney, Craig, S870 (SAT433)
- Brouqua, Pierre, S715 (SAT105), S721 (SAT119), S722 (SAT120)
- Brosch, Mario, S11 (LB002)
- Broseus, Julien, S905 (SAT529)
- Broschart, Carol, S274 (THU361)
- Brosnan, M. Julia, S7 (GS009), S425 (FRI058)
- Brouwer, Hans, S93 (OS132)
- Brown, A, S868 (SAT428)
- Brown, Elizabeth, S446 (FRI029)
- Browne, Sarah, S88 (OS124)
- Brown, Joanne, S848 (SAT392)
- Brown, Kenneth, S277 (THU368)
- Brownlee, Lorna, S733 (SAT146)
- Brown, Marius, S64 (OS081)
- Brown, Maxine, S551 (FRI321)
- Brown, Robert, S899 (SAT517)
- Brozat, Jonathan Frederik, S193 (THU187), S339 (THU493)
- Bruandet, Amelie, S205 (THU227)
- Brueggemann, Yannick, S250 (THU315)
- Bruggmann, Philip, S238 (THU291)
- Bruha, Radan, S671 (SAT014)
- Bruix, Jordi, S381 (THU584)
- Brujats, Ana, S370 (THU548)
- Brujats, Anna, S91 (OS128), S502 (FRI226), S625 (FRI520), S627 (FRI523), S900 (SAT520)
- Brumaru, Daniel, S738 (SAT160)
- Brunar, Helmut, S854 (SAT403)
- Bruneau, Julie, S206 (THU230)
- Brunelli, Laura, S758 (SAT201)
- Brunetto, Maurizia, S4 (GS006), S292 (THU394), S564 (FRI347), S578 (FRI376), S828 (SAT351), S829 (SAT352), S864 (SAT422)
- Brunnbauer, Philipp, S497 (FRI217), S663 (FRI597), S739 (SAT162)
- Bruns, Tony, S100 (OS143), S335 (THU484), S339 (THU493), S342 (THU500)
- Brusilovskaya, Ksenia, S360 (THU529), S362 (THU534), S466 (FRI152), S472 (FRI164), S753 (SAT191)
- Brustia, Raffaele, S375 (THU573), S927 (SAT578)
- Bruzzzone, Chiara, S671 (SAT014)
- Bryce, Kathleen, S277 (THU368)
- Brzica, Hrvoje, S702 (SAT075)
- Buccella, Daniela, S87 (OS122), S600 (FRI453)
- Bucci, Laura, S382 (THU587), S932 (SAT588)
- Buchanan, Ryan, S42 (OS048), S200 (THU218), S909 (SAT536)
- Buchard, Benjamin, S349 (THU511), S417 (FRI042), S640 (FRI550), S918 (SAT563)
- Buch, Stephan, S11 (LB002)
- Bücker, Arno, S460 (FRI122)
- Buccics, Theresa, S630 (FRI529)
- Budas, Grant, S483 (FRI187), S762 (SAT208)
- Budeebazar, Myagmarjav, S235 (THU287)
- Budzyński, Andrzej, S746 (SAT179), S759 (SAT203)
- Buechter, Matthias, S378 (THU579)
- Buettner, Stefan, S107 (OS157)
- Bugge, Anne, S670 (SAT013)
- Buggisch, Peter, S16 (OS003), S562 (FRI345), S585 (FRI391)
- Bugianesi, Elisabetta, S154 (THU069), S425 (FRI058), S436 (FRI078), S437 (FRI081), S448 (FRI102), S452 (FRI108), S671 (SAT014), S675 (SAT021)
- Bujanda, Luis, S46 (OS056), S59 (OS074), S77 (OS103), S107 (OS157), S648 (FRI564), S665 (SAT001)
- Bu, Jiyoung, S921 (SAT569)
- Bukulatipi, Sarah, S239 (THU294), S305 (THU422)
- Bulato, Cristiana, S358 (THU526)
- Bulbul, Rakibul Hassan, S244 (THU301)
- Bulkley, Alison, S516 (FRI251)
- Bullens, Sherry, S534 (FRI285)
- Buller-Taylor, Terri, S209 (THU233)
- Bungay, Helen, S330 (THU475)
- Bungert, Andreas, S235 (THU287)
- Bunting, Stuart, S404 (FRI023), S534 (FRI285)
- Bu, Qingfa, S695 (SAT062)
- Buque, Xabier, S648 (FRI564), S651 (FRI571), S665 (SAT001), S689 (SAT050)
- Burade, Vinod, S710 (SAT091)
- Burak, Kelly, S143 (THU045)
- Burbaum, Barbara, S520 (FRI257)
- Buridan, Adrian, S930 (SAT585)
- Burden-teh, Esther, S22 (OS013)
- Burdette, Dara, S251 (THU317)
- Bureau, Christophe, S61 (OS076), S524 (FRI265), S630 (FRI529)
- Burger, David, S580 (FRI383)
- Burger, Katharina, S692 (SAT056)
- Burgermeister, Elke, S408 (FRI029)
- Burghart, Lukas, S315 (THU449), S545 (FRI309)
- Burgio, Valentina, S748 (SAT180)
- Burlone, Michela Emma, S929 (SAT582)
- Burman, Julio, S312 (THU442)
- Burm, Rani, S860 (SAT413)
- Burns, Gareth, S842 (SAT377)
- Burns, Keith, S137 (THU035)
- Burra, Patrizia, S49 (OS062), S54 (OS069), S154 (THU069), S306 (THU423), S358 (THU526), S569 (FRI359), S627 (FRI524), S821 (SAT318)
- Burrell, Sue, S516 (FRI251)
- Burt, Alastair, S7 (GS009), S646 (FRI561)
- Burton, Alice, S53 (OS067), S55 (OS070)
- Bush, Brian, S19 (OS008), S49 (OS063)
- Bussey, L, S868 (SAT428)
- Bustamante, Javier, S77 (OS103)
- Buti, Maria, S8 (GS010), S44 (OS052), S103 (OS149), S207 (THU231), S208 (THU232), S212 (THU240), S218 (THU252), S255 (THU325), S257 (THU330), S269 (THU350), S277 (THU367), S285 (THU383), S286 (THU384), S297 (THU405), S300 (THU410), S300 (THU411), S316 (THU450), S581 (FRI384), S824 (SAT344), S832 (SAT358), S869 (SAT430), S872 (SAT437)
- Butler, Bryony, S510 (FRI239), S510 (FRI240)
- Butler, Marcus, S395 (FRI010)
- Butrymowicz, Isabel, S549 (FRI317), S584 (FRI388)
- Butsashvili, Maia, S216 (THU247), S229 (THU275), S587 (FRI395), S588 (FRI397), S590 (FRI400), S590 (FRI401)

Author Index

- Buuren, Nicholas Van, S194 (THU189), S247 (THU308), S832 (SAT358)
- Buxton, Jane, S43 (OS051)
- Byambabaatar, Sumiya, S235 (THU287)
- Byrne, Chris, S410 (FRI032), S421 (FRI050), S431 (FRI069)
- Byrne, Christopher, S564 (FRI348)
- Byrne, Marianne, S565 (FRI349)
- Byrne, Ruth, S253 (THU321)
- Byun, Jae Ho, S916 (SAT561)
- Caballano-Infantes, Estefanía, S396 (FRI011)
- Caballería, Joan, S127 (THU018)
- Caballeria, Llorenç, S25 (OS018)
- Caballero, Francisco J., S46 (OS056)
- Caballeros, Fanny Meylin, S802 (SAT288)
- Cabello, Ricardo, S19 (OS008), S49 (OS063)
- Cabezas, Joaquín, S127 (THU018)
- Cabibbo, Giuseppe, S387 (THU599)
- Cabibi, Daniela, S703 (SAT077)
- Cable, Edward, S86 (OS119), S477 (FRI174)
- Cabrera, Elizabeth, S786 (SAT262), S788 (SAT265)
- Cabrera, Maria, S137 (THU034)
- Cacioli, Lorenzo, S480 (FRI179), S647 (FRI562)
- Cadahía-Rodrigo, Valle, S114 (OS169), S792 (SAT271)
- Cadamuro, Massimiliano, S46 (OS056), S751 (SAT186)
- Caddeo, Andrea Marco, S732 (SAT144)
- Caddick, Katharine, S934 (SAT593)
- Cadoux, Mathilde, S65 (OS084)
- Cadranel, Jean-François David, S270 (THU352)
- Cagigal, María Luisa, S59 (OS074), S113 (OS166)
- Çağlar, Ege Su, S221 (THU257)
- Cagna, Marta, S697 (SAT065), S702 (SAT074)
- Cagnot, Carole, S17 (OS006), S567 (FRI353)
- Cai, Dachuan, S240 (THU296), S878 (SAT447)
- Cai, Dawei, S853 (SAT402)
- Cai, Qun, S402 (FRI021)
- Cairo, Fernando, S137 (THU034), S786 (SAT261)
- Cai, Xianbin, S152 (THU065)
- Cai, Xiujun, S56 (OS071)
- Cai, Yaqin, S883 (SAT488)
- Cai, Yuqi, S673 (SAT017)
- Calado, Rodrigo, S490 (FRI201)
- Calaminus, Moritz, S256 (THU327)
- Calderaro, Julien, S372 (THU566), S375 (THU573), S530 (FRI276)
- Calderón-Mendieta, Francisco, S356 (THU521)
- Calderwood, Alexander, S742 (SAT167)
- Caldwell, Stephen, S318 (THU453), S319 (THU455), S427 (FRI060)
- Calero, Silvia, S749 (SAT183)
- Cales, Paul, S496 (FRI215), S497 (FRI216), S507 (FRI235)
- Calinas, Filipe, S190 (THU182), S211 (THU238)
- Calistri, Arianna, S751 (SAT186)
- Calitz, Carlemi, S368 (THU543)
- Callebaut, Isabelle, S521 (FRI260)
- Calleja, Miguel Angel, S555 (FRI329)
- Callejo-Pérez, Ana, S316 (THU450)
- Calleri, Alberto, S775 (SAT243), S776 (SAT245)
- Calle, Roberto, S451 (FRI107), S454 (FRI110), S701 (SAT073)
- Callet, Jonas, S905 (SAT529)
- Callegaert, Nico, S562 (FRI344), S768 (SAT230), S913 (SAT556)
- Calvaruso, Vincenza, S564 (FRI347), S624 (FRI517), S627 (FRI524)
- Calvino, Valeria, S18 (OS007), S49 (OS062), S92 (OS131), S894 (SAT508), S895 (SAT511)
- Calvisi, Diego, S46 (OS056), S648 (FRI564)
- Calvisi, Diego F., S661 (FRI594)
- Calvo, Henar, S184 (THU170), S826 (SAT347)
- CalvoLassoDeLaVeiga, Esther, S304 (THU419)
- Calvo, Marta, S59 (OS074)
- Calvo, Pier Luigi, S518 (FRI255)
- Camacho-Escobedo, Jesús, S356 (THU521)
- Camara, Salimata, S304 (THU419)
- Cambindo Santana, Verónica, S351 (THU514)
- Cambraia, Rodrigo, S293 (THU396)
- Camerlo, Nicolas, S584 (FRI389)
- Camma, Calogero, S387 (THU599), S448 (FRI101), S627 (FRI524), S725 (SAT127)
- Cammarota, Antonella, S374 (THU571), S923 (SAT572)
- Campagnaro, Tommaso, S925 (SAT574)
- Campanale, Francesca, S581 (FRI384)
- Campani, Claudia, S627 (FRI524), S770 (SAT235), S932 (SAT588)
- Campbell, Braidie, S779 (SAT250)
- Campbell, Cori, S856 (SAT407)
- Campbell, Fiona, S12 (LB004A), S13 (LB004B), S288 (THU389), S291 (THU393), S880 (SAT452), S881 (SAT453)
- Campbell-Scherer, Denise, S511 (FRI241)
- Campbell, Stephanie, S764 (SAT212)
- Campello, Elena, S358 (THU526), S751 (SAT186)
- Campinoti, Sara, S120 (THU004), S480 (FRI179), S647 (FRI562), S734 (SAT152), S735 (SAT153)
- Campins, Magda, S44 (OS052)
- Campion, Loic, S5 (GS007)
- Campos-Varela, Isabel, S114 (OS169), S406 (FRI027), S805 (SAT292)
- Camps, Gracian, S248 (THU310)
- Camps, Gracián, S257 (THU330)
- Camps, Jordi, S678 (SAT028), S685 (SAT041)
- Canales, Eda, S483 (FRI187)
- Canapele, Caterina, S229 (THU276)
- Canbay, Ali, S11 (LB002), S378 (THU579), S682 (SAT035)
- Cancela Penna, Francisco Guilherme, S336 (THU487)
- Canchola, Jesse, S842 (SAT377)
- Cangelosi, Davide, S515 (FRI249)
- Canha, Maria Ines, S190 (THU182)
- Canivet, Clémence M., S715 (SAT105)
- Canivet, Clémence M., S73 (OS096), S74 (OS099), S496 (FRI215), S497 (FRI216), S507 (FRI235)
- Cannella, Luana, S378 (THU578)
- Cannistra, Macarena, S81 (OS110)
- Cannon, Mary D., S571 (FRI363)
- Cannon, Mary D., S594 (FRI409)
- Cano, Luis, S639 (FRI548), S656 (FRI582)
- Canonge, Rafael Simo, S149 (THU059), S440 (FRI088)
- Canoui-Poitaine, Florence, S508 (FRI237)
- Cantalops Vilà, Paula, S37 (OS039)
- Cantero, Helena, S237 (THU289), S869 (SAT430)
- Cant, Harriet, S870 (SAT433)
- Cant, Matthew, S805 (SAT292)
- Canva, Valérie, S833 (SAT360), S840 (SAT373)
- Cao, Di, S89 (OS125)
- Caon, Elisabetta, S668 (SAT008), S737 (SAT157)
- Cao, Shenglian, S727 (SAT132)
- Cao, Wenming, S78 (OS105)
- Cao, Zhenhuan, S870 (SAT432)
- Cao, Zhujun, S19 (OS008), S49 (OS063), S616 (FRI502)
- Capasso, Mario, S769 (SAT233)
- Capela, Tiago, S149 (THU060)
- Capelli, Roberta, S166 (THU093)
- Capilla, Maria, S902 (SAT523)
- Caporali, Cristian, S627 (FRI524)
- Cappellini, Maria Domenica, S60 (OS075)
- Cappetta, Alessandro, S748 (SAT180)
- Cappiello, Giuseppina, S249 (THU313)
- Cappuyens, Sarah, S385 (THU593)
- Caputo, Francesco, S84 (OS115)
- Caraceni, Paolo, S21 (OS011), S357 (THU523), S569 (FRI359), S908 (SAT535)
- Caracostea, Andra, S51 (OS065), S902 (SAT523)
- Carapella, Valentina, S424 (FRI056)
- Caravan, Peter, S36 (OS037)
- Carballo-Folgozo, Lorena, S328 (THU471)
- Carbonell-Asins, Juan Antonio, S51 (OS065), S902 (SAT523)
- Carbone, Marco, S94 (OS134), S96 (OS136), S335 (THU484)
- Carbonetti, Rodolfo, S137 (THU034)
- Carbonneau, Michelle, S511 (FRI241)
- Carceller-Lopez, Elena, S111 (OS163)
- Cárdenas-García, Antonio, S708 (SAT087)
- Cardia Ferraz de Andrade, Antônio Ricardo, S336 (THU487)
- Cardinale, Vincenzo, S107 (OS157), S648 (FRI564)

- Cardona, Concepcion Gimeno, S222 ([THU261](#))
- Cardona, Concepción Gimeno, S229 ([THU276](#))
- Cardon, Anaïs, S185 ([THU172](#))
- Cardoso Delgado, Teresa, S87 ([OS122](#))
- Cardoso, Hélder, S28 ([OS024](#)), S618 ([FRI507](#))
- Cardoso, Sandra, S544 ([FRI307](#))
- Cardozo-Ojeda, E Fabian, S859 ([SAT412](#))
- Card, Timothy, S145 ([THU050](#))
- Carey, Elizabeth, S416 ([FRI040](#))
- Carey, Ivana, S253 ([THU321](#)), S276 ([THU366](#)), S279 ([THU370](#)), S280 ([THU373](#)), S281 ([THU375](#)), S287 ([THU387](#)), S551 ([FRI321](#)), S571 ([FRI363](#)), S812 ([SAT304](#)), S824 ([SAT344](#))
- Cargill, Zillah, S569 ([FRI359](#))
- Carioti, Luca, S249 ([THU313](#)), S284 ([THU380](#))
- Cariou, Bertrand, S73 ([OS096](#))
- Cariti, Giuseppe, S825 ([SAT346](#))
- Carleton, Michael, S112 ([OS164](#))
- Carlos Garcia Pagan, Juan, S57 ([OS072A](#)), S90 ([OS127](#))
- Carlota Londoño, Maria, S57 ([OS072A](#)), S59 ([OS074](#)), S328 ([THU471](#)), S335 ([THU484](#))
- Carmagnat, Maryvonnick, S791 ([SAT269](#))
- Carmiel, Michal, S399 ([FRI017](#)), S584 ([FRI388](#))
- Carmona, Francesco, S821 ([SAT318](#))
- Carmona, Isabel, S555 ([FRI329](#))
- Carnero, Amancio, S48 ([OS060](#))
- Carol, Marta, S63 ([OS080](#)), S139 ([THU039](#)), S511 ([FRI242](#)), S512 ([FRI243](#)), S512 ([FRI244](#)), S896 ([SAT512](#)), S901 ([SAT522](#)), S902 ([SAT524](#)), S907 ([SAT532](#))
- Carotenuto, Pietro, S84 ([OS115](#))
- Carpani, Rossana, S428 ([FRI061](#))
- Carpentier, Nathan, S734 ([SAT152](#))
- Carpino, Guido, S107 ([OS157](#))
- Carpi, Sara, S478 ([FRI176](#))
- Carrai, Paola, S569 ([FRI359](#))
- Carrara, Stefania, S284 ([THU381](#))
- Carraro, Amedeo, S796 ([SAT277](#))
- Carrasco, Natalia Marcos, S114 ([OS169](#))
- Carrasquilla, Germán, S40 ([OS045](#))
- Carrat, Fabrice, S17 ([OS006](#)), S101 ([OS146](#)), S250 ([THU314](#)), S297 ([THU404](#)), S567 ([FRI353](#))
- Carreño, Fernando, S328 ([THU472](#))
- Carrera, Enrique, S137 ([THU034](#))
- Carreras, Maria-Josep, S316 ([THU450](#))
- Carrette, Florent, S742 ([SAT166](#))
- Carrieri, Patrizia, S567 ([FRI353](#))
- Carrillo, Juan, S527 ([FRI271](#))
- Carrillo, Maria Cortes, S188 ([THU178](#))
- Carrión, Laura, S381 ([THU584](#))
- Carrodegua, Alba, S229 ([THU276](#)), S577 ([FRI374](#))
- Carroll, Carin, S160 ([THU080](#))
- Carroll, Miles, S57 ([OS072A](#))
- Carr-Smith, Camilla, S188 ([THU178](#))
- Carruthers, Jack, S666 ([SAT004](#))
- Carson, Joanne, S565 ([FRI349](#))
- Carter, Kara, S872 ([SAT436](#))
- Caruso, Stefano, S639 ([FRI548](#))
- Carvalhana, Sofia, S192 ([THU185](#))
- Carvalho, Armando, S268 ([THU349](#))
- Carvalho-Gomes, Ângela, S114 ([OS169](#)), S150 ([THU061](#)), S192 ([THU185](#)), S811 ([SAT301](#)), S811 ([SAT303](#))
- Carvalho, Vinícius, S490 ([FRI201](#))
- Casado, Marta, S325 ([THU465](#)), S445 ([FRI096](#)), S577 ([FRI374](#))
- Casado, Miguel Ángel, S44 ([OS052](#)), S237 ([THU289](#)), S869 ([SAT430](#))
- Casafont, Fernando, S114 ([OS168](#))
- Casagrande, Biagio, S433 ([FRI071](#))
- Casale, Francesco Paolo, S31 ([OS028](#)), S37 ([OS041](#)), S409 ([FRI030](#)), S762 ([SAT208](#))
- Casamayor, Carmen, S676 ([SAT023](#))
- Casanueva, Miguel Ángel Martín, S704 ([SAT080](#))
- Casar, Christian, S604 ([FRI462](#))
- Cascinu, Stefano, S748 ([SAT180](#))
- Cascio, Antonio, S31 ([OS029](#))
- Cash, Johnny, S771 ([SAT236](#))
- Casillas, Rosario, S255 ([THU325](#))
- Casirati, Elia, S668 ([SAT007](#)), S675 ([SAT021](#))
- Casper, Markus, S11 ([LB002](#)), S369 ([THU546](#))
- Casper, Robert, S88 ([OS124](#))
- Caspers, Martien P. M., S677 ([SAT025](#)), S685 ([SAT043](#))
- Cassiman, David, S61 ([OS077](#)), S346 ([THU507](#))
- Cassinotto, Christophe, S425 ([FRI058](#)), S448 ([FRI102](#)), S452 ([FRI108](#))
- Castañeda, Felipe, S476 ([FRI172](#))
- Castañé, Helena, S677 ([SAT027](#)), S678 ([SAT028](#)), S681 ([SAT034](#)), S685 ([SAT041](#))
- Castano-Garcia, Andrés, S381 ([THU584](#))
- Castañón, Ylenia Pérez, S671 ([SAT014](#))
- Castelain, Vincent, S20 ([OS010](#))
- Castel, Helene, S593 ([FRI407](#)), S805 ([SAT293](#))
- Castellani, Paul, S547 ([FRI314](#))
- Castellanos-Fernandez, Marlen, S154 ([THU069](#))
- Castell, Javier, S442 ([FRI092](#)), S444 ([FRI095](#))
- Castello, Inmaculada, S328 ([THU471](#))
- Castells, Lluís, S115 ([OS169](#))
- Castelnau, Corinne, S245 ([THU304](#))
- Castiella, Agustin, S308 ([THU435](#)), S325 ([THU465](#))
- Castillo, Anny Camelo, S577 ([FRI374](#))
- Castillo-Catoni, Maria, S447 ([FRI100](#))
- Castillo, Federico, S774 ([SAT242](#))
- Castillo, Horacio Romero, S169 ([THU098](#))
- Castillo, Joaquín Andrés, S907 ([SAT532](#))
- Castillo, Mauricio, S19 ([OS008](#)), S49 ([OS063](#))
- Castro, Rui, S192 ([THU185](#))
- Casulleras, Mireia, S361 ([THU530](#)), S361 ([THU531](#)), S362 ([THU533](#)), S370 ([THU549](#)), S674 ([SAT019](#))
- Casu, Stefania, S317 ([THU452](#))
- Cathcart, Andrea, S69 ([OS090](#)), S831 ([SAT357](#))
- Cattazzo, Filippo, S152 ([THU066](#)), S658 ([FRI586](#)), S900 ([SAT519](#)), S925 ([SAT574](#))
- Causse, Xavier, S270 ([THU352](#)), S524 ([FRI265](#)), S833 ([SAT360](#)), S840 ([SAT373](#))
- Caussy, Cyrielle, S181 ([THU163](#))
- Cavalcante, Lourianne, S408 ([FRI028](#))
- Cavalletto, Luisa, S564 ([FRI347](#))
- Cavallone, Daniela, S292 ([THU394](#))
- Cavalloni, Giuliana, S651 ([FRI570](#))
- Cavazza, Anna, S116 ([OS171](#)), S135 ([THU031](#)), S352 ([THU516](#)), S505 ([FRI231](#))
- Caven, Madeleine, S415 ([FRI038](#))
- Cawkwell, Gail, S332 ([THU478](#))
- Cazanave, Sophie, S508 ([FRI236](#)), S918 ([SAT564](#))
- Cazzagon, Nora, S317 ([THU452](#)), S319 ([THU454](#)), S335 ([THU484](#))
- Cazzaniga, Marina Elena, S404 ([FRI024](#))
- Cea, M., S211 ([THU237](#))
- Ceccherini Silberstein, Francesca, S284 ([THU381](#))
- Cecchi, Stefano, S161 ([THU081](#))
- Cederborg, Anna, S904 ([SAT527](#))
- Cedilak, Matea, S702 ([SAT075](#))
- Ceesay, Amie, S258 ([THU332](#)), S295 ([THU401](#))
- Cehelsky, Jeffrey, S58 ([OS073](#))
- Ceken, Sabahat, S858 ([SAT411](#))
- Çekin, Ayhan, S242 ([THU300](#))
- Çekin, Yeşim, S242 ([THU300](#))
- Celebi, Güven, S858 ([SAT411](#))
- Çelik, Ferit, S399 ([FRI015](#))
- Celik, Ferya, S513 ([FRI245](#))
- Celsa, Ciro, S387 ([THU599](#)), S448 ([FRI101](#)), S624 ([FRI517](#)), S725 ([SAT127](#))
- Cendrowski, Jarosław, S606 ([FRI467](#))
- Ceni, Elisabetta, S659 ([FRI588](#))
- Cennamo, Michele, S769 ([SAT233](#))
- Censin, Jenny C., S40 ([OS045](#))
- Centeno, Delphine, S640 ([FRI550](#))
- Centonze, Federica-Grazia, S766 ([SAT216](#))
- Cerceau, Théo, S295 ([THU401](#))
- Cerezal, Ana Maria Piedra, S912 ([SAT555](#))
- Ceriani, Roberto, S528 ([FRI272](#))
- Cerioti, Ferruccio, S223 ([THU263](#)), S843 ([SAT381](#)), S868 ([SAT429](#)), S874 ([SAT440](#)), S880 ([SAT450](#))
- Cerny, Andreas, S308 ([THU435](#))
- Cerocchi, Orlando, S3 ([GS004](#))
- Ceruti, Federico, S929 ([SAT583](#))
- Cervera, Marta, S63 ([OS080](#)), S139 ([THU039](#)), S511 ([FRI242](#)), S512 ([FRI243](#)), S512 ([FRI244](#)),

Author Index

- S896 (SAT512), S901 (SAT522), S902 (SAT524), S907 (SAT532)
- Cescon, Matteo, S794 (SAT273)
- Cespiati, Annalisa, S159 (THU078), S167 (THU095), S682 (SAT036)
- Chaffaut, Cendrine, S127 (THU019)
- Chahal, Sarinder, S743 (SAT169)
- Chaigneau, Julien, S496 (FRI215)
- Chainani, Sanjay, S552 (FRI322)
- Cha, Jung Hoon, S490 (FRI202)
- Chakhunashvili, Giorgi, S233 (THU283), S267 (THU347)
- Chakravorty, Avisek, S728 (SAT133), S898 (SAT515)
- Chalasani, Naga, S619 (FRI509), S623 (FRI516)
- Chalaye, Julia, S375 (THU573)
- Challa, Suryanarayana, S779 (SAT250)
- Challis, Benjamin, S158 (THU075), S179 (THU158)
- Chalouni, Mathieu, S101 (OS146), S250 (THU314)
- Chamley, Marck, S171 (THU101)
- Chamroonkul, Naichaya, S186 (THU175), S187 (THU176), S188 (THU177), S722 (SAT121)
- Chan, Brian, S933 (SAT592)
- Chan, Calvin, S266 (THU346)
- Chan, Connie, S462 (FRI125)
- Chanda, Sushmita, S733 (SAT145), S824 (SAT343), S835 (SAT365), S846 (SAT386), S871 (SAT435)
- Chandramouli, Abhishek Shankar, S148 (THU058), S150 (THU062)
- Chandran, Vidyaleha, S898 (SAT516)
- Chandran, Vineesh Indira, S423 (FRI054), S434 (FRI074)
- Chandrasekharan, Karthik, S698 (SAT066)
- Chang, Chun-Chao, S595 (FRI410)
- Chang, Jiabao, S838 (SAT369)
- Chang, Jung-Chin, S653 (FRI576), S761 (SAT207), S762 (SAT209)
- Chang, Kuo-Kuan, S200 (THU217)
- Chang, Kyong-Mi, S30 (OS027), S936 (SAT596)
- Chang, Mei-Hwei, S514 (FRI247), S866 (SAT425)
- Chang, Pik Eu Jason, S481 (FRI181), S919 (SAT566)
- Chang, Sandra, S853 (SAT401)
- Chang, Silvia, S244 (THU302), S247 (THU309), S832 (SAT358), S845 (SAT385)
- Chang, Te-Sheng, S595 (FRI410)
- Chang, Ting, S14 (LB006)
- Chang, Ting-Tsung, S849 (SAT393)
- Chang, Tsung-Yen, S839 (SAT372)
- Chang, William, S443 (FRI093), S486 (FRI193)
- Chan, Henry LY, S39 (OS043), S101 (OS147), S164 (THU088), S274 (THU362), S302 (THU414), S852 (SAT400), S861 (SAT415), S937 (SAT597)
- Chan, Huan-Keat, S42 (OS049)
- Chan, Lap Kwan, S765 (SAT215)
- Channon, Keith M., S665 (SAT002)
- Chan, Po-Lin, S42 (OS049)
- Chan, Sing, S836 (SAT366)
- Chan, Stephen, S164 (THU088)
- Chan, Stephen L., S933 (SAT592)
- Chantal, Dessy, S691 (SAT053)
- Chantarangkul, Veena, S159 (THU078)
- Chan, Wah-Kheong, S154 (THU069), S209 (THU234), S425 (FRI058), S448 (FRI102), S452 (FRI108)
- Chan, Winston, S694 (SAT059)
- Chao, Daniel, S142 (THU043)
- Chao, Hann-Hsiang, S223 (THU262)
- Chao, Yee, S375 (THU572)
- Chapiro, Julius, S935 (SAT594)
- Chapman, Matthew, S898 (SAT516)
- Chapman, Roger W.G., S602 (FRI458)
- Chapus, Fleur, S766 (SAT216)
- Charfi, Hakim, S733 (SAT145)
- Charles, Edgar, S446 (FRI029), S687 (SAT046)
- Charles, Margaux, S532 (FRI281)
- Charlton, Will, S727 (SAT131), S730 (SAT139), S732 (SAT143)
- Charman, Sarah, S733 (SAT146)
- Charu, Vivek, S462 (FRI124)
- Chaturvedi, Praneet, S673 (SAT017)
- Chaudhari, Rahul, S126 (THU016)
- Chaudhari, Sachin, S848 (SAT392)
- Chaudhary, Binita, S809 (SAT299)
- Chauhan, Ayushi, S389 (FRI002)
- Chau, Hau-Tak, S177 (THU154)
- Chau, Mary, S745 (SAT177)
- Chaves, Roberta, S137 (THU034)
- Chayama, Kazuaki, S252 (THU319)
- Chazouillères, Olivier, S319 (THU454), S504 (FRI228), S772 (SAT239)
- Cheema, Sukhdeep Steven, S134 (THU029)
- Cheetham, Rob, S554 (FRI327)
- Chemin, Isabelle, S258 (THU332), S295 (THU401)
- Chen, Alfred, S846 (SAT386)
- Chen, Beishan, S742 (SAT168)
- Chen, Bowen, S388 (THU600)
- Chen, Charles, S495 (FRI210)
- Chen, Chien-Hung, S102 (OS148), S824 (SAT344), S852 (SAT400), S861 (SAT415), S870 (SAT433)
- Chen, Chien-Jen, S294 (THU398)
- Chen, Chi-Yi, S849 (SAT393), S870 (SAT433)
- Chen, Chiyl, S595 (FRI410)
- Chen, Chun-Ting, S595 (FRI410)
- Chen, Deying, S744 (SAT171), S745 (SAT173)
- Chen, Dongbo, S75 (OS102), S467 (FRI153), S638 (FRI545)
- Chen, Ethan, S299 (THU408), S867 (SAT427)
- Chen, Fuwang, S760 (SAT205)
- Cheng, Benny, S277 (THU368)
- Cheng, Chien-Yu, S595 (FRI410)
- Cheng, Danying, S852 (SAT399)
- Cheng, Ho Ming, S78 (OS105)
- Cheng, Hung-Wei, S192 (THU186)
- Cheng, Jiamin, S388 (THU600)
- Cheng, Mengyuan, S557 (FRI333)
- Cheng, Pin-Nan, S595 (FRI410), S863 (SAT420)
- Cheng, Tai-An, S386 (THU596)
- Cheng, Tong, S744 (SAT172)
- Chen, Guei-Ying, S595 (FRI410)
- Chen, Guofeng, S22 (OS014)
- Cheng, Wendy, S872 (SAT437)
- Cheng, Ya-Ting, S575 (FRI371), S576 (FRI372)
- Chen, Hanying, S686 (SAT045)
- Chen, Harry, S443 (FRI093), S486 (FRI193)
- Chen, Hong, S89 (OS125), S492 (FRI206), S837 (SAT367)
- Chen, Hongsong, S75 (OS102), S467 (FRI153), S638 (FRI545)
- Chen, Hsiu-Hsi, S45 (OS054)
- Chen, Huanming, S837 (SAT367)
- Chen, Huey-Ling, S514 (FRI247)
- Chen, Hui, S92 (OS130), S619 (FRI508)
- Chen, Jacki, S277 (THU368)
- Chen, Jennifer, S743 (SAT169)
- Chen, Jenny, S849 (SAT394)
- Chen, Jiaxian, S66 (OS086), S402 (FRI021), S744 (SAT171), S744 (SAT172), S803 (SAT289)
- Chen, Jilin, S22 (OS014)
- Chen, Jing, S894 (FRI509)
- Chen, Jinjun, S89 (OS125), S344 (THU504), S421 (FRI050)
- Chen, Joseph, S534 (FRI285)
- Chen, Jun, S865 (SAT424)
- Chen, Jyh-Jou, S863 (SAT420)
- Chen, Kaina, S919 (SAT566)
- Chen, Li, S310 (THU438), S439 (FRI085), S446 (FRI029), S446 (FRI099), S481 (FRI183), S486 (FRI194), S488 (FRI197), S688 (SAT048), S714 (SAT103)
- Chen, Lin, S757 (SAT198)
- Chen, Lingzi, S152 (THU065)
- Chen, Long, S559 (FRI337)
- Chen, Lynna, S613 (FRI495)
- Chen, Meng, S526 (FRI268)
- Chen, Min, S240 (THU296), S763 (SAT210)
- Chen, Ming-Huang, S375 (THU572)
- Chen, Mingkai, S636 (FRI540)
- Chen, Owen, S37 (OS041), S762 (SAT208)
- Chen, Pei-Jer, S863 (SAT420)
- Chen, Ping, S665 (SAT002), S755 (SAT195), S756 (SAT197)
- Chen, Pu, S75 (OS102), S467 (FRI153), S638 (FRI545)
- Chen, Qi, S357 (THU524)
- Chen, Qiuying, S133 (THU028)
- Chen, Sam Li-Sheng, S45 (OS054)
- Chen, Shikui, S832 (SAT359), S865 (SAT423)
- Chen, Shuai, S155 (THU070), S462 (FRI125)
- Chen, Shuhui, S832 (SAT359), S865 (SAT423)
- Chen, Sui-Dan, S421 (FRI050), S431 (FRI069)
- Chen, Tianyan, S614 (FRI497)

- Chen, Tsung Po, S162 (THU084)
 Chen, Wanqing, S82 (OS111)
 Chen, Wei, S494 (FRI209)
 Chen, Wen-Chi, S625 (FRI520)
 Chen, Xiaojiao, S182 (THU165)
 Chen, Xin, S744 (SAT172)
 Chen, Xin-Yue, S70 (OS091), S844 (SAT382), S870 (SAT432)
 Chen, Xinyue, S838 (SAT369)
 Chen, Xuanmeng, S767 (SAT218)
 Chen, Yan, S377 (THU577)
 Chen, Yaw-Sen, S119 (THU001)
 Chen, Yi, S1 (GS001)
 Chen, Yi-Cheng, S102 (OS148), S575 (FRI371), S576 (FRI372)
 Chen, Yongping, S70 (OS091)
 Chen, Yu, S74 (OS097), S803 (SAT289)
 Chen, Yu-Ju, S514 (FRI247)
 Chen, Yunfu, S254 (THU323), S854 (SAT404)
 Chen, Yunru, S879 (SAT449)
 Chen, Yutong, S215 (THU245)
 Chen, Zhaobin, S669 (SAT009)
 Chen, Zhenhuai, S22 (OS014), S182 (THU165)
 Chen, Zhi, S699 (SAT069)
 Chen, Zhi-wei, S240 (THU296)
 Cherai, Mustapha, S189 (THU181)
 Chermak, Faiza, S441 (FRI089)
 Chernyakhovskyy, Maksym, S848 (SAT392)
 Cherqui, Daniel, S538 (FRI296), S780 (SAT252), S791 (SAT269), S935 (SAT595)
 Cherubini, Alessandro, S668 (SAT007), S675 (SAT021)
 Chester, Tonika, S401 (FRI019)
 Cheung, Ka-Shing, S272 (THU358), S273 (THU360), S275 (THU364)
 Cheung, Pierre, S471 (FRI162)
 Cheung, Ramsey C., S875 (SAT442)
 Chevaliez, Stéphane, S582 (FRI386), S584 (FRI389)
 Chevret, Sylvie, S127 (THU019)
 Chew, Yun, S120 (THU005)
 Chhatwal, Jagpreet, S214 (THU244)
 Chia, Linda, S126 (THU016), S899 (SAT518)
 Chiang, Chen-Tse, S294 (THU398)
 Chiang, Kevin, S597 (FRI416)
 Chiba, Tetsuhiro, S615 (FRI501), S897 (SAT514)
 Chi-Cervera, Luis, S487 (FRI195)
 Chiche, Jean-Daniel, S355 (THU520)
 Chiche, Laurence, S780 (SAT252)
 Chi, Chen-Ta, S109 (OS160), S375 (THU572)
 Chicherova, Ievgeniia, S766 (SAT216)
 Chien, Elaine, S312 (THU442)
 Chien, Rong-Nan, S102 (OS148), S575 (FRI371), S576 (FRI372), S852 (SAT400), S861 (SAT415), S873 (SAT438)
 Chien, Shih-Chieh, S863 (SAT420)
 Chien, Yin-Hsiu, S514 (FRI247)
 Chi, Huanting, S265 (THU344)
 Chikhliia, Anmol, S889 (SAT499)
 Child, Michael, S848 (SAT392)
 Childs, Kate, S253 (THU321)
 Chimakurthi, Ramu, S332 (THU479)
 China, Louise, S104 (OS151), S342 (THU499), S524 (FRI265)
 Chines, Valeria, S259 (THU333)
 Chinnaratha, Asif, S898 (SAT516)
 Chiong, Justin, S580 (FRI383)
 Chiriac, Stefan, S573 (FRI368)
 Chirita, Dragos, S795 (SAT276)
 Chitadze, Nazibrola, S233 (THU283), S267 (THU347)
 Chitnis, Amit, S831 (SAT356)
 Chiu, Keith Wan Hang, S78 (OS105)
 Chiu, SM, S824 (SAT344)
 Chiu, Yencheng, S863 (SAT420)
 Chi, Xiaoling, S22 (OS014), S421 (FRI050)
 Chi, Xin, S852 (SAT399)
 Chkhartishvili, Nikoloz, S587 (FRI395), S590 (FRI400), S590 (FRI401)
 Chlopicki, Stefan, S759 (SAT203)
 Chng, Chinlye, S548 (FRI316)
 Chng, Elaine, S32 (OS030), S431 (FRI068), S481 (FRI181), S486 (FRI194), S493 (FRI207), S619 (FRI509), S623 (FRI516)
 Chodik, Gabriel, S399 (FRI017), S584 (FRI388)
 Choe, Byung-Ho, S866 (SAT425)
 Choe, Hun Jee, S163 (THU087)
 Cho, Eun Ju, S303 (THU417)
 Choe, Won Hyeok, S932 (SAT590)
 Cho, Heejin, S303 (THU417), S862 (SAT418)
 Choi, Gwang Hyeon, S275 (THU363)
 Choi, Hannah S.J., S852 (SAT400), S861 (SAT415)
 Choi, Ho Joong, S820 (SAT317)
 Choi, Inhee, S473 (FRI166)
 Choi, In Young, S468 (FRI156), S469 (FRI157)
 Choi, Jaehyuk, S468 (FRI156), S469 (FRI157)
 Choi, Jin Yong, S767 (SAT229)
 Choi, Jonggi, S275 (THU363), S545 (FRI310), S833 (SAT361), S842 (SAT378), S891 (SAT503)
 Choi, Jong Young, S820 (SAT317), S932 (SAT589)
 Choi, Moon Seok, S273 (THU359)
 Choi, Sang Hyun, S916 (SAT561)
 Choi, Won-Mook, S610 (FRI488), S833 (SAT361), S842 (SAT378), S870 (SAT433)
 Choi, YoungRok, S798 (SAT281), S799 (SAT282)
 Choi, Yun-Jung, S322 (THU461), S477 (FRI174)
 Cho, Jai Young, S798 (SAT281)
 Cho, Ju-Yeon, S275 (THU363)
 Chokkalingam, Anand, S560 (FRI340)
 Chokshi, Shilpa, S68 (OS089), S120 (THU004), S188 (THU178), S480 (FRI179), S639 (FRI547), S647 (FRI562), S911 (SAT540)
 Cho, Kyung Joo, S653 (FRI575), S755 (SAT194)
 Cholongitas, Evangelos, S429 (FRI063)
 Cho, Mi-La, S820 (SAT317)
 Chong, Jia Ling, S431 (FRI068), S493 (FRI207)
 Chong, Lee-Won, S595 (FRI410)
 Chon, Young Eun, S862 (SAT418)
 Choong, Ingrid, S269 (THU350), S300 (THU411), S859 (SAT412)
 Chopra, Adity, S309 (THU437)
 Chorostowska-Wynimko, Joanna, S515 (FRI250)
 Choteschovsky, Niklas, S464 (FRI147)
 Choudhry, Anam, S548 (FRI316)
 Choudhury, Ashok, S19 (OS008), S53 (OS066), S350 (THU512), S397 (FRI014)
 Choudhury, Gourab, S14 (LB006)
 Chouik, Yasmina, S356 (THU522)
 Chou, Roger, S557 (FRI332), S557 (FRI333), S591 (FRI404)
 Chow, Benjamin, S164 (THU089)
 Choy, Matthew, S134 (THU029)
 Cho, Yong Kyun, S485 (FRI191)
 Cho, Young Youn, S484 (FRI189)
 Christensen, Diana Hedeveg, S172 (THU104)
 Christensen, Hannah, S256 (THU328)
 Christensen, Lee, S554 (FRI327)
 Christensen, Morten, S475 (FRI169)
 Christensen, Peer, S550 (FRI319)
 Christiansen, Michael Michael, S450 (FRI104)
 Christinet, Montserrat Fraga, S253 (THU322)
 Christmas, Michael, S538 (FRI294), S538 (FRI295)
 Chris, Z., S447 (FRI100)
 Chromy, David, S555 (FRI328)
 Chuang, Jay, S427 (FRI060)
 Chuang, Wan-Long, S458 (FRI118), S595 (FRI410), S849 (SAT393)
 Chuang, WL, S868 (SAT428)
 Chulanov, Vladimir, S4 (GS006), S103 (OS149), S828 (SAT351)
 Chu, Lily, S343 (THU502)
 Chung, Brian K., S27 (OS021), S604 (FRI463)
 Chung, Chuhan, S318 (THU453), S319 (THU455), S427 (FRI060), S700 (SAT071)
 Chung, Diana, S88 (OS123), S715 (SAT106), S716 (SAT107), S716 (SAT108), S731 (SAT142)
 Chung, Enoch, S592 (FRI405)
 Chung, Han Yang, S42 (OS049)
 Chung, Raymond, S36 (OS037), S264 (THU341), S592 (FRI405)
 Chung, Woo Jin, S572 (FRI365), S916 (SAT560)
 Churkin, Alex, S588 (FRI396)
 Churuangsuk, Chaitong, S722 (SAT121)
 Chu, Yu-De, S638 (FRI546)
 Chu, Yu-Ju, S294 (THU398)

Author Index

- Ciaccio, Antonio, S404 (FRI024)
Ciacio, Oriana, S800 (SAT285),
S935 (SAT595)
Ciancio, Alessia, S564 (FRI347)
Ciccarelli, Olga, S797 (SAT279)
Cicchello, Federica, S404 (FRI024)
Ciccioli, Carlo, S448 (FRI101), S725 (SAT127)
Ciciriello, Vito, S609 (FRI487)
Cigliano, Riccardo Aiese, S259 (THU333)
Cihlar, Tomas, S244 (THU302)
Cilli, Fiona, S308 (THU434)
Cillo, Umberto, S49 (OS062),
S306 (THU423), S821 (SAT318)
Cingolani, Antonella, S284 (THU381)
Cinque, Felice, S167 (THU095)
Cintoni, Marco, S507 (FRI234)
Ciociola, Ester, S703 (SAT077)
Cisse, Ousseynou, S304 (THU419)
Citko, Jolanta, S585 (FRI390)
Citone, Michele, S627 (FRI524)
Cittone, Micol, S503 (FRI227)
Claar, Ernesto, S212 (THU239)
Claasen, Marco, S109 (OS159),
S800 (SAT286), S801 (SAT287),
S815 (SAT311)
Claeys, Wouter, S106 (OS155)
Clarembau, Frédéric, S736 (SAT156)
Claria, Joan, S346 (THU506)
Clària, Joan, S361 (THU530),
S361 (THU531), S362 (THU533),
S368 (THU545), S370 (THU549),
S674 (SAT019)
Clarke, Christopher, S938 (SAT600)
Clark, Nico, S550 (FRI318)
Claudel, Thierry, S126 (THU017),
S688 (SAT049), S760 (SAT204)
Clausen, Jesper, S713 (SAT102),
S720 (SAT116)
Claveria-Cabello, Alex, S112 (OS165)
Clavreul, Ludivine, S692 (SAT055)
Clemente, Ana, S127 (THU018),
S137 (THU035)
Clement, Guillaume, S205 (THU227)
Clément, Karine, S435 (FRI076)
Clément-Leboube, Sophie,
S877 (SAT444)
Clerbaux, Laure-Alix, S765 (SAT215)
Clere-Jehl, Raphael, S20 (OS010)
Clerici, Mariagrazia, S159 (THU078)
Clevers, Hans, S652 (FRI574)
Cloherty, Gavin, S233 (THU283),
S253 (THU321), S264 (THU341),
S267 (THU347), S279 (THU370),
S281 (THU375), S287 (THU387),
S294 (THU400), S851 (SAT398)
Clouston, Andrew, S416 (FRI040)
Cloutier, Daniel, S69 (OS090),
S831 (SAT357)
Cobbold, Jeremy, S39 (OS044),
S425 (FRI058), S448 (FRI102),
S452 (FRI108)
Cobelli, Francesco De, S748 (SAT180)
Cobrerros, Marina, S328 (THU471),
S624 (FRI518)
Cocchis, Donatella, S775 (SAT243)
Cockburn, Myles, S797 (SAT278)
Cockell, Simon, S7 (GS009), S437 (FRI081)
Cock, Victoria, S228 (THU272)
Coco, Barbara, S292 (THU394)
Cocomazzi, Giovanna, S609 (FRI487)
Cocomello, Nicholas, S161 (THU081),
S162 (THU083)
Coday, Mace, S912 (SAT554)
Codela, Elisavet, S809 (SAT298)
Codes, Liana, S542 (FRI304), S543 (FRI305),
S888 (SAT498)
Codina, Anna Esteve, S113 (OS166)
Codoni, Greta, S308 (THU435)
Coelho, Marta Paula Pereira, S552 (FRI323)
Coelho, Rosa, S618 (FRI507)
Coenraad, Minneke, S120 (THU003),
S144 (THU047)
Coessens, Marie, S546 (FRI312)
Coffin, Carla, S143 (THU045),
S259 (THU334)
Cogger, Shelley, S550 (FRI318)
Cohen, Bracha, S145 (THU049)
Cohen, Carmit, S804 (SAT291)
Cohen, Chari, S277 (THU368)
Cohen-ezra, Oranit, S784 (SAT258),
S804 (SAT291)
Cohen, Jason, S203 (THU224),
S204 (THU225)
Cohen-Naftaly, Michal, S64 (OS081),
S774 (SAT241), S793 (SAT272),
S855 (SAT406)
Cohen, Taylor, S411 (FRI033)
Coilly, Audrey, S349 (THU511),
S402 (FRI020), S538 (FRI296),
S800 (SAT285), S935 (SAT595)
Cojocariu, Camelia, S573 (FRI368)
Cola, Marco, S894 (SAT508)
Colantoni, Alessandra, S161 (THU081),
S162 (THU083)
Colapietro, Francesca, S93 (OS132),
S326 (THU467), S528 (FRI272)
Colavolpe, Lucia, S167 (THU095)
Colclough, Fiona, S527 (THU270)
Cole, Alex, S345 (THU505)
Cole, Andrew G., S848 (SAT391),
S848 (SAT392)
Colecchia, Antonio, S91 (OS129),
S794 (SAT273)
Colecchia, Luigi, S91 (OS129)
Collart, Martine, S652 (FRI572)
Colle, Isabelle, S516 (FRI252)
Colletta, Alessandro, S811 (SAT302),
S813 (SAT307), S814 (SAT309)
Collier, Jane D., S320 (THU456),
S320 (THU457), S321 (THU459),
S322 (THU460)
Collier, Nicholson, S252 (THU319)
Collin, Rémi, S417 (FRI042)
Collins, Amy, S640 (FRI551)
Collins, Jon, S328 (THU472)
Collins, Kelly, S778 (SAT249)
Collins, Kelsey, S169 (THU098)
Collins, Michelle, S596 (FRI411)
Coll, Mar, S684 (SAT039), S907 (SAT532)
Colman, Roos, S913 (SAT556)
Colombatto, Piero, S292 (THU394)
Colombo, Massimo, S210 (THU236),
S578 (FRI376)
Colom, Joan, S570 (FRI361)
Columbano, Amedeo, S732 (SAT144)
Colyn, Leticia, S112 (OS165), S643 (FRI554)
Comandini, Ubaldo Visco, S806 (SAT294),
S808 (SAT297)
Combes, Alain, S349 (THU511)
Comer, Jason, S194 (THU191)
Comisar, Craig, S862 (SAT417)
Conchon, Sophie, S185 (THU172)
Conci, Simone, S920 (SAT567),
S925 (SAT574)
Conde, Isabel, S406 (FRI027), S811 (SAT303)
Conery, Annie, S848 (SAT390),
S849 (SAT393)
Congly, Stephen, S143 (THU045)
Congreave, Susan, S188 (THU178)
Congregado, Daniela Mestre, S651 (FRI571)
Connolly, Crystal, S491 (FRI203)
Connoley, Declan, S337 (THU488),
S366 (THU540)
Conte, Federica, S806 (SAT294)
Conti, Filomena, S189 (THU181),
S772 (SAT239), S780 (SAT252)
Conti, Matteo, S97 (OS139)
Contreras, Bryan J, S362 (THU533)
Contreras, Raul, S137 (THU034)
Conway, Brian, S225 (THU267),
S549 (FRI317), S553 (FRI324),
S581 (FRI384), S584 (FRI388),
S591 (FRI403), S596 (FRI411)
Cook, Charlotte, S200 (THU218)
Cook, Jonathan, S57 (OS072A)
Cook-Wiens, Galen, S159 (THU077)
Cooper, Katherine, S811 (SAT302),
S813 (SAT307), S814 (SAT309)
Cooreman, Michael, S715 (SAT105),
S721 (SAT119), S722 (SAT120)
Copca, Narcis, S795 (SAT276)
Coppola, Carmine, S551 (FRI320),
S564 (FRI347), S938 (SAT599)
Coppola, Nicola, S217 (THU250)
Coppola, Roberta, S551 (FRI320)
Corcoran, Eleanor, S68 (OS089),
S371 (THU550)
Cordero-Pérez, Paula, S487 (FRI195)
Cordes, Christiane, S582 (FRI385)
Cordier, Pierre, S672 (SAT015),
S765 (SAT215)
Cordi, Sabine, S736 (SAT155)
Cordova, Jacqueline, S137 (THU034)
Corey, Kathleen, S416 (FRI040),
S454 (FRI110)
Corless, Lynsey, S63 (OS079), S885 (SAT492)
Corlu, Anne, S656 (FRI582)
Cornberg, Markus, S4 (GS006),
S248 (THU311), S562 (FRI345),
S566 (FRI352), S569 (FRI359),
S582 (FRI385), S584 (FRI388),
S608 (FRI485), S622 (FRI514),

- S823 ([SAT341](#)), S824 ([SAT344](#)), S828 ([SAT351](#)), S830 ([SAT355](#)), S843 ([SAT379](#)), S852 ([SAT400](#)), S857 ([SAT408](#)), S861 ([SAT415](#)), S893 ([SAT505](#))
- Corneille, Jeremie, S499 ([FRI221](#))
- Coronati, Mattia, S161 ([THU081](#))
- Cororuge, Marion, S392 ([FRI005](#))
- Corpechot, Christophe, S317 ([THU452](#)), S319 ([THU454](#)), S335 ([THU484](#)), S772 ([SAT239](#))
- Corradini, Stefano Ginanni, S11 ([LB002](#))
- Corrales, Fernando, S643 ([FRI554](#))
- Corrales, Tinidad Desongles, S555 ([FRI329](#))
- Correa, Elizabeth, S137 ([THU034](#))
- Correia de Abreu, Ricardo, S597 ([FRI415](#))
- Correia, Maria Isabel Toulson Davidson, S293 ([THU396](#)), S552 ([FRI323](#))
- Correnti, Margherita, S651 ([FRI570](#))
- Corsilli, Daniel, S593 ([FRI407](#))
- Corsi, Oscar, S81 ([OS110](#))
- Cortellini, Alessio, S108 ([OS158](#)), S372 ([THU567](#)), S374 ([THU571](#)), S376 ([THU574](#)), S383 ([THU588](#))
- Cortese, Maria Francesca, S255 ([THU325](#)), S257 ([THU330](#))
- Cortesi, Emanuela, S637 ([FRI544](#))
- Cortes, Miren Garcia, S396 ([FRI011](#))
- Cortez, John, S853 ([SAT402](#))
- Cortez, Karina, S113 ([OS167](#))
- Cortez-Pinto, Helena, S192 ([THU185](#))
- Cortinovis, Diego, S404 ([FRI024](#))
- Çoruh, Ayşegül Gürsoy, S778 ([SAT248](#))
- Corwin, Michael, S462 ([FRI125](#))
- Cosar, Arif Mansur, S861 ([SAT416](#))
- Cosgrove, Greg, S308 ([THU434](#))
- Cosma, Chiara, S49 ([OS062](#))
- Cossiga, Valentina, S564 ([FRI347](#)), S769 ([SAT233](#))
- Costa, Ana, S706 ([SAT085](#))
- Costa, Mara, S190 ([THU182](#))
- Costa Mendes, Liliana Sampaio, S336 ([THU487](#))
- Costa, Montserrat, S368 ([THU545](#))
- Costantino, Andrea, S868 ([SAT429](#)), S880 ([SAT450](#))
- Costanzo, Alessia Di, S162 ([THU083](#))
- Costanzo, Giovan Giuseppe Di, S938 ([SAT599](#))
- Costa Silva, Marcelo, S336 ([THU487](#))
- Coste, Marion, S202 ([THU221](#))
- Costentin, Charlotte, S73 ([OS096](#)), S74 ([OS099](#))
- Cotler, Scott, S70 ([OS092](#)), S588 ([FRI396](#)), S851 ([SAT398](#)), S859 ([SAT412](#)), S874 ([SAT440](#))
- Coto-Llerena, Mairene, S660 ([FRI592](#))
- Cotrau, Radu, S483 ([FRI186](#)), S505 ([FRI230](#))
- Cotrim, Helma Pinchemel, S307 ([THU432](#)), S336 ([THU487](#)), S408 ([FRI028](#))
- Cots, Meritxell Ventura, S127 ([THU018](#)), S137 ([THU035](#))
- Cotte, Alexia, S692 ([SAT055](#))
- Cotter, José, S149 ([THU060](#))
- Coubeau, Laurent, S797 ([SAT279](#))
- Coudyzer, Walter, S516 ([FRI252](#))
- Couté, Johann, S766 ([SAT216](#))
- Couto, Cláudia Alves, S137 ([THU034](#))
- Couture, Christian, S456 ([FRI114](#))
- Covarrubias, Yesenia, S454 ([FRI110](#))
- Cover, Amelia, S572 ([FRI364](#))
- Cowling, Thomas, S801 ([SAT287](#))
- Cox, I. Jane, S176 ([THU153](#)), S670 ([SAT011](#)), S735 ([SAT153](#))
- Cox, Sean, S44 ([OS053](#)), S220 ([THU256](#))
- Cozzolongo, Raffaele, S908 ([SAT535](#))
- Crabtree, Mark J., S665 ([SAT002](#))
- Craige, Siobhan M., S665 ([SAT002](#))
- Craigie, Anne, S498 ([FRI218](#))
- Cramer, Thorsten, S533 ([FRI282](#))
- Cramp, Matthew, S493 ([FRI208](#)), S615 ([FRI499](#)), S771 ([SAT236](#))
- Cravo, Marília, S537 ([FRI293](#))
- Craxi, Antonio, S387 ([THU599](#)), S448 ([FRI101](#)), S624 ([FRI517](#)), S703 ([SAT077](#)), S725 ([SAT127](#))
- Creasy, Kate Townsend, S731 ([SAT141](#))
- C-Registry, German Hepatitis, S562 ([FRI345](#))
- Cremer, Jennifer, S12 ([LB004A](#)), S13 ([LB004B](#)), S288 ([THU389](#)), S288 ([THU390](#)), S291 ([THU393](#)), S880 ([SAT452](#)), S881 ([SAT453](#))
- Crespillo, Lutgarda Conde, S555 ([FRI329](#))
- Crespo, Gonzalo, S90 ([OS127](#)), S114 ([OS168](#)), S569 ([FRI359](#)), S786 ([SAT262](#)), S788 ([SAT265](#)), S907 ([SAT532](#))
- Crespo, Javier, S59 ([OS074](#)), S113 ([OS166](#)), S157 ([THU074](#)), S158 ([THU076](#)), S328 ([THU471](#)), S624 ([FRI518](#)), S671 ([SAT014](#)), S774 ([SAT242](#)), S912 ([SAT555](#))
- Crestelo, David Rial, S577 ([FRI373](#))
- Cretet, Clara, S189 ([THU181](#))
- Cristoferi, Laura, S96 ([OS136](#))
- Crittenden, Daria, S88 ([OS123](#)), S716 ([SAT107](#)), S716 ([SAT108](#)), S731 ([SAT142](#))
- Croagh, Catherine, S498 ([FRI218](#))
- Croce, Anna Cleta, S697 ([SAT065](#)), S702 ([SAT074](#))
- Croce, Saveria Lory, S626 ([FRI522](#))
- Croker, Ben, S471 ([FRI161](#))
- Cromhout, Gabriela, S285 ([THU382](#))
- Crook, Joanne, S551 ([FRI321](#))
- Crooks, Colin, S22 ([OS013](#))
- Cross, Amy, S809 ([SAT298](#))
- Cross, Lily, S122 ([THU008](#))
- Cross, Mary, S34 ([OS034](#))
- Crouch, Emilie, S36 ([OS038](#)), S649 ([FRI565](#))
- Crudele, Annalisa, S706 ([SAT084](#))
- Csernalabics, Benedikt, S100 ([OS143](#))
- Cuadrado, Antonio, S114 ([OS169](#)), S624 ([FRI518](#)), S774 ([SAT242](#))
- Cua, Georgine, S282 ([THU378](#)), S910 ([SAT538](#))
- Cubbage, Hayley, S554 ([FRI327](#))
- Cubero, Francisco Javier, S643 ([FRI554](#))
- Cucarull, Blanca, S652 ([FRI573](#))
- Cuciureanu, Tudor, S573 ([FRI368](#))
- Cuellar, Elías Rodríguez, S704 ([SAT080](#))
- Cueto, A., S396 ([FRI011](#))
- Cuevas, Guillermo, S217 ([THU249](#))
- Cui, Yimin, S70 ([OS091](#))
- Cui, Yixiao, S264 ([THU341](#))
- Cui, Zhiyi, S880 ([SAT451](#))
- Cui, Zixin, S879 ([SAT449](#))
- Cuko, Liri, S573 ([FRI367](#))
- Cullaro, Giuseppe, S769 ([SAT232](#))
- Cullen, Noelle, S418 ([FRI043](#))
- Culver, Emma, S320 ([THU456](#)), S320 ([THU457](#)), S321 ([THU459](#)), S322 ([THU460](#)), S330 ([THU475](#))
- Cummings, Oscar, S714 ([SAT103](#))
- Cunha, Antonio Sa, S935 ([SAT595](#))
- Cunha, Guilherme, S454 ([FRI110](#))
- Cunningham, Evan B, S565 ([FRI349](#))
- Cunningham, Morven, S62 ([OS078](#)), S395 ([FRI010](#))
- Cuño, Carlos, S652 ([FRI573](#))
- Curell, Anna, S114 ([OS168](#))
- Curion, Fabiola, S602 ([FRI458](#))
- Curry, Michael, S634 ([FRI537](#))
- Curteis, Tristan, S870 ([SAT433](#))
- Curto, Anna, S370 ([THU549](#))
- Cusi, Kenneth, S449 ([FRI103](#)), S671 ([SAT014](#))
- Cusumano, Caterina, S91 ([OS129](#))
- Cuthbertson, Daniel, S42 ([OS048](#)), S422 ([FRI052](#)), S433 ([FRI073](#))
- Cutolo, Francesco Maria, S769 ([SAT233](#))
- Cutsem, Eric Van, S385 ([THU593](#))
- Cuyas, Berta, S91 ([OS128](#)), S627 ([FRI523](#)), S886 ([SAT494](#)), S900 ([SAT520](#))
- Čužić, Snježana, S702 ([SAT075](#))
- Cyhaniuk, Anissa, S281 ([THU376](#))
- Czlonkowska, Anna, S1 ([GS001](#)), S61 ([OS077](#))
- Czubkowski, Piotr, S519 ([FRI256](#)), S521 ([FRI259](#))
- Czyzewska-Khan, Justyna, S34 ([OS034](#))
- Dabbagh, Karim, S179 ([THU160](#))
- Dabek, Juhani, S458 ([FRI117](#)), S690 ([SAT052](#))
- Da, Ben, S548 ([FRI315](#))
- Dachraoui, Mayssa, S36 ([OS038](#))
- D'Adamo, Giuseppe, S938 ([SAT599](#))
- Daffis, Stephane, S251 ([THU317](#))
- Dagenais, Simon, S151 ([THU063](#))
- Dagooc, Rica, S837 ([SAT368](#))
- Dahari, Harel, S70 ([OS092](#)), S252 ([THU319](#)), S588 ([FRI396](#)), S851 ([SAT398](#)), S859 ([SAT412](#)), S874 ([SAT440](#))
- Dahl, Kirsten, S713 ([SAT102](#)), S720 ([SAT116](#))
- Dahlqvist, Géraldine, S736 ([SAT156](#)), S797 ([SAT279](#))

Author Index

- Dahman, Bassam, S223 (THU262), S227 (THU270)
- Daian, Fabrice, S500 (FRI222)
- Dai, Chia-Yen, S458 (FRI118), S595 (FRI410)
- Daid, Sarav, S203 (THU224), S204 (THU225)
- Dai, Liting, S727 (SAT132)
- Daix, Valérie, S359 (THU528)
- Dajon, Marion, S872 (SAT436)
- Dajti, Elton, S91 (OS129), S794 (SAT273)
- Dalais, Christine, S147 (THU054)
- Dalbeni, Andrea, S152 (THU066), S658 (FRI586), S796 (SAT277), S900 (SAT519), S920 (SAT567), S925 (SAT574)
- Dalbly Hansen, Camilla, S9 (GS012)
- Dalekos, George, S93 (OS132), S326 (THU467), S335 (THU484), S479 (FRI178), S824 (SAT344), S840 (SAT374)
- D'Alessandro, Umberto, S233 (THU282), S258 (THU332), S295 (THU401)
- D'Alessio, Antonio, S108 (OS158), S372 (THU567), S374 (THU571), S376 (THU574), S383 (THU588), S923 (SAT572)
- Dalgard, Olav, S826 (SAT348)
- Dalgic, Buket, S519 (FRI256)
- Dalgic, Buket, S518 (FRI255), S521 (FRI259)
- D'aliberti, Deborah, S259 (THU333)
- Dali-Youcef, Nassim, S738 (SAT160)
- d'Alteroche, Louis, S833 (SAT360)
- Daly, Ann K., S7 (GS009), S437 (FRI081)
- Damascene, Makuza Jean, S43 (OS051), S209 (THU233), S282 (THU378), S910 (SAT538)
- D'Amato, Daphne, S96 (OS136)
- D'Ambrosio, Roberta, S210 (THU236), S223 (THU263), S578 (FRI376)
- D'Amico, Federico, S210 (THU236)
- D'Amico, Gennaro, S630 (FRI529)
- Damink, Steven Olde, S757 (SAT198)
- Damle-Vartak, Amruta, S38 (OS042)
- Damme, Pierre Van, S303 (THU416)
- Damm, Georg, S658 (FRI585)
- Damm, Robert, S378 (THU579)
- Dandri, Maura, S256 (THU327)
- Dang, Shuang suo, S723 (SAT122)
- Dang, Tong, S182 (THU165)
- Daniel, Jules, S122 (THU009)
- Danielle, Adebayo, S19 (OS008)
- Danielsen, Karen, S610 (FRI489)
- Danielsen, Karen Vagner, S340 (THU496)
- Daniels, Samuel, S158 (THU075)
- Danielsson, Oscar, S413 (FRI036)
- Danila, Mirela, S930 (SAT585)
- Daniş, Nilay, S399 (FRI015)
- D'Anna, Stefano, S284 (THU381), S839 (SAT371)
- Danta, Mark, S302 (THU415), S560 (FRI339), S561 (FRI343), S568 (FRI356)
- D'Antiga, Lorenzo, S518 (FRI255), S519 (FRI256)
- Dan, Yock Young, S694 (SAT059), S735 (SAT154)
- Dao, Thong, S61 (OS076)
- Darba, Josep, S285 (THU383), S286 (THU384), S300 (THU410)
- D'Arcangelo, Francesca, S821 (SAT318)
- Darias, Ruth Suarez, S931 (SAT586)
- Dar-In, Tai, S575 (FRI371), S576 (FRI372)
- Darteil, Raphaël, S254 (THU324)
- Darweesh, Mohammad, S803 (SAT290), S807 (SAT295)
- Das, Amit, S138 (THU037)
- Dasarathy, Jaividhya, S33 (OS032), S193 (THU188)
- Dasarathy, Srinivasan, S33 (OS032), S193 (THU188)
- Dasgupta, Ramanuj, S98 (OS140), S247 (THU308)
- Dashdorj, Naranbaatar, S235 (THU287)
- Dashdorj, Naranjargal, S235 (THU287)
- Da Silva, Nathalie, S97 (OS138)
- da Silva, Rita de Cássia Martins Alves, S137 (THU034)
- Daskalopoulos, Evangelos-Panagiotis, S691 (SAT053)
- Das, Panchanan, S299 (THU409)
- Das, Partha Pratim, S299 (THU409)
- Das, Sugato, S327 (THU470)
- Dattani, Abhishek, S409 (FRI031)
- Datz, Christian, S11 (LB002), S428 (FRI062)
- Daud, Juliana, S336 (THU487)
- David, Ciprian, S930 (SAT585)
- David, Joel, S330 (THU475)
- Davidov, Yana, S292 (THU395), S784 (SAT258), S804 (SAT291), S845 (SAT384)
- Davidson, Peter, S7 (GS009)
- Davidson, Mark, S9 (GS011)
- Davidson, Brian R., S55 (OS070)
- Davidson, Irwin, S758 (SAT199)
- Davidson, Nicholas O, S671 (SAT014)
- Davies, Jade, S548 (FRI316)
- Davies, Jane, S239 (THU294), S305 (THU422)
- Davies, Jessica, S53 (OS067), S55 (OS070)
- Davies, Louise, S548 (FRI316)
- Davies, Nathan, S366 (THU539)
- Davis, Anne, S615 (FRI499)
- Davis, Ashley, S572 (FRI364)
- Davis, Brian, S130 (THU023)
- Davis, Joshua Saul, S239 (THU294), S305 (THU422)
- Davis, William, S33 (OS031)
- D'Avola, Delia, S59 (OS074)
- Davydau, Uladzimir, S269 (THU351)
- Davyduke, Tracy, S906 (SAT530)
- Dawe, Joshua, S228 (THU272)
- Dawson, Paul, S751 (SAT187)
- Dayangac, Murat, S693 (SAT058)
- Day, Emily, S34 (OS034)
- Day, Jonathan, S540 (THU299)
- de Almeida e Borges, Valéria Ferreira, S336 (THU487)
- de Andrés, Carolina Ibarrola, S704 (SAT080)
- de Angelis, Martin Hrabe, S703 (SAT079)
- Dear, James, S122 (THU008)
- De, Arka, S232 (THU280)
- de Azevedo, Rita Furtado Feio, S680 (SAT032)
- Debaecker, Simon, S359 (THU528)
- De Benedittis, Carla, S483 (FRI185)
- Debes, Jose, S194 (THU189), S194 (THU190)
- Debette-Gratien, Maryline, S772 (SAT239)
- de Bezenac, Cecile, S233 (THU282)
- De Block, Christophe, S9 (GS011)
- de Boer, Ynto, S93 (OS132), S306 (THU431), S326 (THU467)
- Debourdeau, Antoine, S771 (SAT237)
- De Brauw, Maurits, S9 (GS011)
- de Bruin, Alain, S653 (FRI576)
- Decaens, Thomas, S74 (OS099), S766 (SAT216), S780 (SAT252), S817 (SAT312)
- Decaestecker, Jochen, S516 (FRI252)
- Decaris, Martin, S308 (THU434)
- de Carvalho, Luis Abreu, S768 (SAT230)
- Dechene, Alexander, S378 (THU579)
- Decker, Charlotte, S265 (THU344)
- Decock, Sofie, S516 (FRI252)
- Decout, Jean-Luc, S521 (FRI260)
- Decraecker, Marie, S441 (FRI089)
- De Creus, An, S72 (OS094)
- Dedoussis, George, S451 (FRI106)
- Deeks, Alexandra S., S54 (OS069)
- Deelchand, Vashist, S433 (FRI073)
- De Francesco, Raffaele, S97 (OS139)
- Defreyne, Luc, S107 (OS156)
- de Frías, César Prieto, S890 (SAT500)
- de Frutos, Pablo Garcia, S672 (SAT016)
- Degasperi, Elisabetta, S196 (THU194), S223 (THU263), S623 (FRI515), S843 (SAT379), S843 (SAT381), S868 (SAT429), S874 (SAT440), S880 (SAT450)
- de Gauna, Mikel Ruiz, S651 (FRI571), S665 (SAT001), S689 (SAT050)
- Degeest, Bruno, S464 (FRI147)
- Degerman, Erik, S30 (OS026)
- Degerstedt, Oliver, S368 (THU543)
- de Graaf, Mees N.S., S118 (OS174)
- Degré, Delphine, S124 (THU012)
- de Groof, Joline, S338 (THU491)
- Degroote, Helena, S106 (OS155), S562 (FRI344), S768 (SAT230)
- de Hart, Greg, S540 (FRI299)
- Dehn, Clayton, S451 (FRI107), S701 (SAT073)
- de Jonge, Hugo, S115 (OS170)
- de Jonge, Jeroen, S115 (OS170), S118 (OS174)
- de Jong, Iris, S740 (SAT163)
- de Jong, Jelle C.B.C., S686 (SAT044)
- de Juan, Virginia Gutiérrez, S689 (SAT050)
- Dekervel, Jeroen, S385 (THU593)
- De Knecht, Robert, S41 (OS046), S86 (OS120)
- Delacôte, Claire, S205 (THU227), S205 (THU228), S913 (SAT557)
- De La Fuente, Rocio Aller, S157 (THU074), S158 (THU076)

- de la Grange, Pierre, S65 ([OS084](#)), S475 ([FRI170](#))
- Delagreverie, Heloise, S271 ([THU355](#))
- Delahaye, Jared, S873 ([SAT439](#)), S880 ([SAT451](#))
- Delamarre, Adele, S73 ([OS096](#)), S74 ([OS099](#)), S906 ([SAT530](#))
- Delaney, William, S834 ([SAT363](#)), S844 ([SAT383](#)), S847 ([SAT389](#))
- de Langlard, Mathieu, S489 ([FRI200](#))
- Delarocque-Astagneau, Elizabeth, S567 ([FRI353](#))
- de las Heras, Ana, S869 ([SAT430](#))
- Delataille, Philippe, S359 ([THU528](#))
- de La Tijera, Maria De Fatima Higuera, S137 ([THU034](#))
- de la Torre, Raquel A. Martinez Garcia, S684 ([SAT039](#))
- Delaune, Vaihere, S754 ([SAT192](#))
- Delayahu, Yael, S583 ([FRI387](#))
- Del Barrio, Maria, S328 ([THU471](#))
- Del Ben, Maria, S162 ([THU083](#))
- de Lédinghen, Victor, S72 ([OS093](#)), S73 ([OS096](#)), S74 ([OS099](#)), S101 ([OS146](#)), S250 ([THU314](#)), S425 ([FRI058](#)), S441 ([FRI089](#)), S448 ([FRI102](#)), S452 ([FRI108](#)), S581 ([FRI384](#)), S833 ([SAT360](#)), S840 ([SAT373](#)), S906 ([SAT530](#))
- de Leeuw, Marcel, S180 ([THU161](#))
- Deleus, Ellen, S680 ([SAT032](#))
- Delgado, Alberto, S500 ([FRI223](#))
- Delgado, Evangeline, S447 ([FRI100](#))
- Delgado, Igotz, S648 ([FRI564](#)), S651 ([FRI571](#)), S665 ([SAT001](#))
- Delgado, Teresa Cardoso, S48 ([OS060](#)), S84 ([OS116](#)), S600 ([FRI453](#)), S679 ([SAT029](#)), S689 ([SAT050](#))
- del Hoyo Gordillo, Pilar, S704 ([SAT080](#))
- Delicou, Sophia, S472 ([FRI163](#))
- Delire, Bénédicte, S797 ([SAT279](#))
- Dellis, Olivier, S767 ([SAT218](#))
- Delmi, Thomas, S754 ([SAT192](#))
- Delphine, Degré, S192 ([THU185](#))
- del Rio, Alvaro, S527 ([FRI271](#))
- del Rosario García-Lozano, María, S450 ([FRI105](#))
- Deltenre, Pierre, S11 ([LB002](#)), S131 ([THU025](#))
- Deltoro, Miguel García, S222 ([THU261](#))
- Delwaide, Jean, S516 ([FRI252](#))
- De Maeght, Stéphane, S516 ([FRI252](#))
- de Magnée, Catherine, S535 ([FRI289](#))
- De Man, Robert, S41 ([OS046](#)), S306 ([THU431](#))
- Demant, Jonas, S220 ([THU255](#))
- de Manzini, Nicolo, S433 ([FRI071](#))
- De Martin, Eleonora, S402 ([FRI020](#))
- De Martin, Sara, S478 ([FRI176](#)), S479 ([FRI177](#))
- Dembowsky, Klaus, S663 ([FRI598](#))
- Demediuk, Barbara, S498 ([FRI218](#))
- de Meijer, Vincent, S484 ([FRI188](#)), S711 ([SAT092](#))
- Demetriou, Anna, S202 ([THU220](#))
- Demetris, Jake, S809 ([SAT298](#))
- De Meyer, Sandra, S72 ([OS094](#))
- De Meyer, Sofie, S409 ([FRI031](#))
- Demidem, Aicha, S640 ([FRI550](#))
- Demir, Mehmet, S858 ([SAT410](#))
- Demir, Münevver, S823 ([SAT341](#))
- Demirtas, Coskun Ozer, S858 ([SAT410](#))
- Demirtas, Elif, S693 ([SAT058](#))
- Demontant, Vanessa, S582 ([FRI386](#))
- Dendrou, Calli, S602 ([FRI458](#))
- Denecke, Timm, S379 ([THU581](#)), S383 ([THU590](#)), S931 ([SAT587](#))
- Deng, Aiyun, S837 ([SAT367](#))
- Deng, Guohong, S344 ([THU504](#))
- Deng, Huan, S883 ([SAT488](#))
- Deng, Jiang, S723 ([SAT122](#))
- Deng, Mei, S165 ([THU090](#))
- Deng, Yangyang, S223 ([THU262](#))
- Denham, Douglas, S715 ([SAT106](#)), S731 ([THU142](#))
- Denk, Gerald, S602 ([FRI460](#)), S823 ([SAT341](#))
- Dennis, Andrea, S422 ([FRI052](#)), S424 ([FRI056](#))
- Denys, Alban, S355 ([THU520](#))
- DePaoli, Alex, S443 ([FRI093](#)), S486 ([FRI193](#)), S495 ([FRI210](#))
- de Pascalis, Stefania, S217 ([THU250](#))
- D'Erasmio, Laura, S162 ([THU083](#))
- der Eijk, Annemiek Van, S194 ([THU190](#))
- Derenoncourt, Meghan, S572 ([FRI364](#))
- Deridder, Mathilde, S20 ([OS010](#))
- der Meer, Adriaan Van, S306 ([THU431](#)), S330 ([THU476](#)), S569 ([FRI359](#))
- Derua, Rita, S637 ([FRI544](#))
- de Ruiter, Petra E., S652 ([FRI574](#))
- Desai, Supriya, S855 ([SAT405](#))
- Desalegn, Hailemichael, S19 ([OS008](#)), S23 ([OS015](#)), S49 ([OS063](#)), S841 ([SAT375](#))
- De Salins, Victoire, S508 ([FRI237](#))
- DeSantis, Todd Z., S179 ([THU160](#))
- Desboeufs, Nina, S765 ([FRI215](#))
- Deschenes, Marc, S31 ([OS029](#)), S614 ([FRI497](#))
- de Schepper, Evelien, S227 ([THU271](#))
- Deschler, Sebastian, S185 ([THU171](#)), S189 ([THU180](#))
- Desdouets, Chantal, S672 ([SAT015](#)), S765 ([SAT215](#))
- Désert, Romain, S656 ([FRI582](#))
- De Siena, Martina, S507 ([FRI234](#))
- De Silvestri, Annalisa, S502 ([FRI225](#))
- De Sinno, Andrea, S79 ([OS107](#))
- Desmond, Paul, S498 ([FRI218](#)), S842 ([SAT377](#))
- Desquilles, Lise, S656 ([FRI582](#))
- de Temple, Brittany, S719 ([SAT114](#))
- Deterding, Katja, S248 ([THU311](#)), S582 ([FRI385](#)), S624 ([FRI519](#)), S823 ([SAT341](#)), S830 ([SAT355](#)), S843 ([SAT379](#)), S857 ([SAT408](#))
- Detlefsen, Sönke, S2 ([GS002](#)), S9 ([GS012](#)), S131 ([THU024](#)), S434 ([FRI074](#)), S475 ([FRI171](#)), S758 ([SAT200](#))
- de Toni, Enrico, S655 ([FRI581](#)), S662 ([FRI596](#)), S937 ([SAT597](#))
- de Trixhe, Xavier Woot, S838 ([SAT370](#))
- Deuffic-Burban, Sylvie, S205 ([THU227](#)), S205 ([THU228](#)), S913 ([SAT557](#))
- de Urturi, Diego Saenz, S665 ([SAT001](#)), S689 ([SAT050](#))
- Deutsch, Melanie, S840 ([SAT374](#))
- Devadas, Krishnadas, S728 ([SAT133](#)), S898 ([SAT515](#))
- Devadas, Nidhin, S884 ([SAT490](#))
- Devalia, Kalpana, S698 ([SAT066](#))
- Deval, Jerome, S853 ([SAT401](#))
- Dev, Anouk, S441 ([FRI090](#))
- Devaux, Carole, S579 ([FRI377](#))
- Deveci, Neslihan, S893 ([SAT505](#))
- de Veer, Rozanne, S317 ([THU452](#)), S330 ([THU476](#))
- de Villalobos, Eduardo Sanz, S184 ([THU170](#)), S826 ([SAT347](#))
- Devineni, Poornima, S30 ([OS027](#)), S936 ([SAT596](#))
- Devisscher, Lindsey, S562 ([FRI344](#)), S655 ([FRI580](#))
- De Vito, Andrea, S596 ([FRI414](#))
- de Vries, Elsemieke, S306 ([THU431](#)), S307 ([THU433](#))
- Devshi, Dhruvi, S639 ([FRI547](#))
- Devuni, Deepika, S811 ([SAT302](#)), S813 ([SAT307](#)), S814 ([SAT309](#))
- de Waart, Rudi, S601 ([FRI457](#))
- de Weijer, Floor, S644 ([FRI556](#))
- de Wit, Koos, S893 ([SAT506](#))
- Dezan, Maria, S408 ([FRI028](#))
- Dhabali, Thangjam, S219 ([THU254](#))
- Dhagapan, Amanda, S239 ([THU294](#))
- Dhaliwal, Amritpal, S364 ([THU537](#)), S805 ([SAT292](#))
- Dhanda, Ashwin, S34 ([OS034](#))
- Dhand, Abhishek, S740 ([SAT163](#))
- Dhar, Ameet, S345 ([THU505](#))
- Dharancy, Sebastien, S205 ([THU227](#)), S205 ([THU228](#)), S772 ([SAT239](#)), S913 ([SAT557](#))
- Dharancy, Sébastien, S780 ([SAT252](#)), S817 ([SAT312](#))
- Dharia, Neerav, S126 ([THU016](#))
- Dharmapuri, Sirish, S372 ([THU567](#)), S383 ([THU588](#))
- Dhawan, Anil, S818 ([SAT315](#))
- Dhillon, Tony, S108 ([OS158](#))
- D'Hollander, Koenraad, S539 ([FRI297](#))
- Dhondt, Elisabeth, S107 ([OS156](#))
- Dhurrkay, Roslyn, S305 ([THU422](#))
- Diaconescu, Gheorghe, S13 ([LB004B](#)), S288 ([THU389](#)), S288 ([THU390](#)), S291 ([THU393](#)), S881 ([SAT453](#))
- Diago, Moises, S59 ([OS074](#)), S222 ([THU261](#)), S334 ([THU482](#)), S912 ([SAT555](#))
- Diago, Moisés, S229 ([THU276](#))
- Diallo, Aldiouma, S202 ([THU221](#))

Author Index

- Diallo, Alpha, S17 ([OS006](#))
Diallo, Kalilou, S304 ([THU419](#))
Diamantidis, Michail, S472 ([FRI163](#))
Diatta, Omar, S207 ([THU231](#)), S208 ([THU232](#))
Díaz, Alba, S136 ([THU033](#)), S139 ([THU039](#)), S263 ([THU340](#)), S286 ([THU385](#))
Díaz, Fernando, S114 ([OS168](#))
Díaz-González, Álvaro, S59 ([OS074](#)), S324 ([THU464](#)), S325 ([THU465](#)), S334 ([THU482](#))
Díaz, Luis Antonio, S137 ([THU034](#))
Díaz, María Paz, S218 ([THU252](#))
Díaz-Mejía, Nely, S316 ([THU450](#))
Díaz-Mitoma, Francisco, S100 ([OS145](#))
Díaz-Moreno, Irene, S132 ([THU027](#))
Díaz-Muñoz, Mauricio, S476 ([FRI172](#))
Díaz-Quintana, Antonio, S132 ([THU027](#))
Díaz, Sebastian, S137 ([THU034](#))
Di Benedetto, Davide, S483 ([FRI185](#)), S929 ([SAT583](#))
Di Benedetto, Fabrizio, S795 ([SAT275](#))
Di Caterino, Tina, S423 ([FRI054](#)), S434 ([FRI074](#))
Dickey, Amy, S516 ([FRI251](#))
Dickman, Christopher, S764 ([SAT212](#))
Dickson, Rolland, S15 ([OS002](#))
Didier, Michel, S872 ([SAT436](#))
Dieguez, Maria Luisa Gonzalez, S114 ([OS169](#)), S406 ([FRI289](#))
Diehl, Lauri, S194 ([THU189](#)), S684 ([SAT040](#)), S832 ([SAT358](#)), S835 ([SAT364](#))
Dieterich, Douglas T, S298 ([THU407](#)), S590 ([FRI402](#)), S836 ([SAT366](#)), S848 ([SAT390](#))
Dieterich, Douglas T., S432 ([FRI070](#)), S436 ([FRI078](#))
Dietrich, Peter, S163 ([THU085](#))
Dietz, Christopher, S823 ([SAT341](#))
Dietz, Julia, S15 ([OS001](#)), S16 ([OS003](#)), S585 ([FRI391](#))
Diez, Cristina, S90 ([OS127](#))
Di Fabio, Romano, S97 ([OS139](#))
Di Gialleonardo, Luca, S436 ([FRI079](#))
Di Giorgio, Angelo, S518 ([FRI255](#)), S519 ([FRI256](#))
Di Girolamo, Julia, S558 ([FRI334](#))
Diken, Mustafa, S464 ([FRI147](#))
Dikopoulos, Nektarios, S823 ([SAT341](#))
Dill, Michael, S262 ([THU338](#))
Dillon, John, S17 ([OS005](#)), S411 ([FRI033](#)), S415 ([FRI038](#)), S473 ([FRI165](#)), S495 ([FRI214](#)), S564 ([FRI348](#))
Di Maira, Giovanni, S477 ([FRI173](#))
Di Maira, Tommaso, S114 ([OS168](#)), S406 ([FRI027](#)), S811 ([SAT301](#)), S811 ([SAT303](#))
Di Marco, Vito, S448 ([FRI101](#))
Dimitriadis, Stavros, S57 ([OS072A](#)), S58 ([OS072B](#))
Dimitrova, Dessislava, S72 ([OS094](#))
Dinani, Amreen, S168 ([THU097](#)), S169 ([THU098](#)), S170 ([THU099](#)), S291 ([THU392](#)), S301 ([THU413](#))
Dincer, Dinc, S820 ([SAT316](#)), S858 ([SAT410](#)), S861 ([SAT416](#)), S864 ([SAT421](#))
Ding, Dora, S427 ([FRI060](#))
Ding, Huiguo, S408 ([FRI029](#))
Ding, Wei, S183 ([THU168](#))
Ding, Weimao, S287 ([THU388](#)), S296 ([THU403](#)), S326 ([THU468](#)), S504 ([FRI229](#))
Ding, Yanhua, S89 ([OS125](#)), S837 ([SAT367](#)), S865 ([SAT423](#)), S894 ([SAT509](#))
Ding, Yuming, S538 ([FRI294](#)), S538 ([FRI295](#))
Dini, Luciana, S763 ([SAT211](#))
Diniz, Mariana, S55 ([OS070](#))
Dinkelborg, Katja, S263 ([THU339](#))
Diong, Sophie, S527 ([FRI270](#))
Dion, Jessica, S675 ([SAT022](#))
Dion, Sarah, S639 ([FRI548](#))
Diotallevi, Marina, S665 ([SAT002](#))
Diouf, Assane, S202 ([THU221](#))
Diouf, Boubacar, S304 ([THU419](#))
Diouf, Daouda, S304 ([THU419](#))
Di Pasqua, Laura Giuseppina, S702 ([SAT074](#))
Dirchwolf, Melisa, S137 ([THU034](#)), S780 ([SAT251](#))
Dirks, Meike, S624 ([FRI519](#))
Di Rocco, Maja, S515 ([FRI249](#))
Dirsch, Verena, S711 ([SAT093](#))
Di Sandro, Stefano, S795 ([SAT275](#))
Discher, Thomas, S16 ([OS003](#)), S585 ([FRI391](#))
di Somma, Sarah, S769 ([SAT233](#))
Distefano, Alfio, S703 ([SAT077](#))
di Tocco, Francesca Casuscelli, S259 ([THU333](#))
Di Tommaso, Luca, S528 ([FRI272](#))
Ditt, Vanessa, S197 ([THU197](#))
Divani-Patel, Sapna, S805 ([SAT292](#))
Dixit, Bharat, S834 ([SAT362](#))
Dixon, Dan A., S84 ([OS116](#))
Dixon, Emmanuel Dauda, S469 ([FRI158](#)), S688 ([SAT049](#)), S760 ([SAT204](#))
Djazouli, Sonia, S542 ([FRI303](#))
Do, Ai-Thien, S875 ([SAT442](#))
Dobracka, Beata, S585 ([FRI390](#))
Dobracki, Witold, S592 ([FRI406](#))
Dobrowolska, Krystyna, S585 ([FRI390](#))
Dobson, Susan L., S54 ([OS069](#))
Dochterman, Daniel, S30 ([OS027](#)), S936 ([SAT596](#))
Dodaro, Valentina, S825 ([SAT346](#))
Dodge, Jennifer, S79 ([OS106](#)), S210 ([THU235](#)), S794 ([SAT274](#)), S797 ([SAT278](#))
Dodge, Stephen, S167 ([THU094](#))
D'Offizi, Giampiero, S806 ([SAT294](#)), S808 ([SAT297](#))
Dogrul, Ahmet Bulent, S820 ([SAT316](#))
Doi, Hiroyoshi, S430 ([FRI067](#))
Dokku, Sowjanya, S483 ([FRI187](#))
Dökmetaş, İlyas, S858 ([SAT411](#))
Doladé, Maria, S724 ([SAT125](#))
Dold, Leona, S381 ([THU585](#)), S599 ([FRI451](#))
Dolicka, Dobrochna, S652 ([FRI572](#))
Dolu, Suleyman, S820 ([SAT316](#))
Domenech, Gema, S381 ([THU584](#))
Domenicali, Marco, S357 ([THU523](#))
Domingo, Esteban, S589 ([FRI399](#))
Domingorena, Julieta, S217 ([THU249](#))
Domingo-Sàbat, Montserrat, S527 ([FRI271](#))
Dominguez, Alejandra, S137 ([THU034](#))
Domínguez, Elena Gómez, S334 ([THU482](#))
Domínguez-Hernández, Raquel, S44 ([OS052](#)), S237 ([THU289](#)), S869 ([SAT430](#))
Dominguez, Inmaculada, S451 ([FRI106](#))
Dominguez, Lourdes, S577 ([FRI373](#))
Domínguez, María Carmen Lozano, S555 ([FRI329](#))
Dominici, Massimo, S84 ([OS115](#))
Donadio, Gregory, S491 ([FRI204](#))
Donadon, Matteo, S758 ([SAT201](#))
Donati, Adeline, S131 ([THU025](#))
Donato, Maria Francesca, S317 ([THU452](#)), S503 ([FRI227](#)), S569 ([FRI359](#))
Dondossola, Daniele, S668 ([SAT007](#))
Dongen, Catherine Van, S144 ([THU048](#))
Dongiovanni, Paola, S167 ([THU095](#)), S675 ([SAT021](#)), S682 ([SAT036](#)), S682 ([SAT037](#)), S698 ([SAT068](#)), S703 ([SAT077](#)), S706 ([SAT084](#))
Dong, Ruihua, S89 ([OS125](#))
Dong, Zheng, S377 ([THU577](#))
Donnadieu-Rigole, Hélène, S122 ([THU009](#))
Donnelly, Chris, S670 ([SAT011](#))
Donnelly, Hannah, S535 ([FRI288](#))
Donne, Romain, S672 ([SAT015](#))
Donoghue, Claire, S411 ([FRI033](#))
Donovan, John, S142 ([THU043](#))
Dooley, Steven, S408 ([FRI029](#)), S489 ([FRI200](#)), S606 ([FRI466](#)), S659 ([FRI589](#)), S661 ([FRI594](#))
Doolman, Ram, S804 ([SAT291](#))
Doornebal, Ewald, S647 ([FRI562](#))
Dopazo, Cristina, S114 ([OS168](#)), S805 ([SAT292](#))
Dore, Gregory, S302 ([THU415](#)), S560 ([FRI339](#)), S561 ([FRI343](#)), S565 ([FRI349](#)), S568 ([FRI356](#))
Dörge, Petra, S582 ([FRI385](#)), S893 ([SAT505](#))
Dorival, Celine, S17 ([OS006](#)), S297 ([THU404](#)), S567 ([FRI353](#))
Dorner, Marcus, S55 ([OS070](#))
Dorn, Livia, S545 ([FRI309](#))
Dorrell, Lucy, S872 ([SAT437](#))
Dorrington, Kate, S554 ([FRI327](#))
Doshi, Akash, S223 ([THU262](#)), S227 ([THU270](#))
Do, Son, S875 ([SAT442](#))
Douiri, Abdel, S809 ([SAT298](#))
Doukas, Michael, S194 ([THU189](#)), S644 ([FRI556](#))
Douschan, Philipp, S346 ([THU506](#))
Dow, Ellie, S415 ([FRI038](#)), S495 ([FRI214](#))
Downie, Bryan, S318 ([THU453](#))

- Downs, Louise, S856 (SAT407)
- Doyle, Joseph, S541 (FRI302), S550 (FRI318)
- Drage, Michael, S708 (SAT088)
- Dragoni, Gabriele, S659 (FRI588), S770 (SAT235)
- Dranicki, Fabian, S784 (SAT259)
- Drasdo, Dirk, S489 (FRI200)
- Dreher, Michael, S339 (THU493)
- Dreizin, Vera, S583 (FRI387)
- Drenth, J.P.H., S525 (FRI266)
- Driessen, Ann, S7 (GS009), S709 (SAT089)
- Driever, Ellen, S367 (THU542)
- Driscoll, Paul, S666 (SAT004)
- Drobeniuc, Jan, S219 (THU253), S233 (THU283), S267 (THU347)
- Droese, Sandra, S550 (FRI319)
- Dropmann, Anne, S606 (FRI466), S661 (FRI594)
- Drost, Anne, S240 (THU297)
- Drucker, Shani, S765 (SAT214)
- Duan, Yunfei, S183 (THU168)
- Duarte, Frederico, S597 (FRI415)
- Dubertrand, Jean Marie, S499 (FRI221)
- Dubois, Nicolas, S61 (OS077)
- Dubruel, Peter, S734 (SAT152)
- Duca, Leonardo, S249 (THU313)
- Ducasa, Nicolas, S786 (SAT261)
- Duce, Antonio Martín, S671 (SAT014)
- Duclos-Vallée, Jean-Charles, S538 (FRI296), S759 (SAT202), S800 (SAT285), S935 (SAT595)
- Duehren, Sarah, S70 (OS092), S859 (SAT412)
- Dueñas, Maria Emilia, S704 (SAT081)
- Duengelhof, Paul, S54 (OS069)
- Duffell, Erika, S256 (THU328)
- Dufour, Jean-Francois, S11 (LB002)
- Dufour, Jean-François, S777 (SAT247), S780 (SAT251)
- Dufour, Sylvie, S690 (SAT052)
- Dufton, Neil, S488 (FRI198)
- Duguru, Mary John, S23 (OS015)
- Dugyala, Ravi, S848 (SAT392)
- Duhaut, Lea, S402 (FRI020), S800 (SAT285), S935 (SAT595)
- Duijst, Suzanne, S653 (FRI576)
- Dukewich, Matthew, S33 (OS031)
- Düll, M., S163 (THU085)
- Dultz, Georg, S15 (OS001), S585 (FRI391), S907 (SAT531)
- Duman, Serkan, S778 (SAT248)
- Dumas, Jacques, S872 (SAT436)
- Dumas, Laurent, S691 (SAT053)
- Dumas, Marc-Emmanuel, S179 (THU158)
- Dumitru, Radu, S795 (SAT276)
- Dumond, Aureole, S667 (SAT006)
- Dumont, Mathilde Petiet, S780 (SAT252)
- Dumortier, Jérôme, S72 (OS093), S122 (THU009), S317 (THU452), S772 (SAT239), S780 (SAT252), S833 (SAT360), S840 (SAT373)
- Dunachie, Susanna, S54 (OS069), S57 (OS072A)
- Dunbar, Donald R., S163 (THU086)
- Duncan, James, S935 (SAT594)
- Dung, Nguyen TT, S294 (THU400)
- DunichandHoedl, Abha, S775 (SAT244), S892 (SAT504)
- Dunn, Kate, S553 (FRI325)
- Dunn, Winston, S81 (OS110)
- Duong, Nikki, S126 (THU016)
- Duong, Pham, S294 (THU400)
- Dupin, Julien, S373 (THU569)
- Dupuis-Williams, Pascale, S759 (SAT202)
- Dupuy, Marie, S392 (FRI006)
- Duque, Juan Carlos Rodriguez, S624 (FRI518)
- Duque, Juan Carlos Rodríguez, S774 (SAT242)
- Durak, Feyza, S464 (FRI147)
- Durak, Serdar, S858 (SAT410), S861 (SAT416), S864 (SAT421)
- Durand, Francois, S780 (SAT252)
- Durand, Sarah, S36 (OS038), S99 (OS142), S649 (FRI565), S738 (SAT160)
- Durand, Stéphanie, S640 (FRI550)
- Duran-Güell, Marta, S361 (THU530), S362 (THU533), S370 (THU549), S674 (SAT019)
- Durandel, David, S246 (THU305), S254 (THU324)
- Duran-Vian, Carlos, S113 (OS166)
- Durkalski-Mauldin, Valerie, S394 (FRI008)
- Durkin, Claire, S546 (FRI311)
- Durman, Simon, S334 (THU483)
- Durmashkina, Elena, S16 (OS003), S585 (FRI391)
- Durmuş, Merve Eren, S242 (THU300)
- Duseja, Ajay Kumar, S19 (OS008), S49 (OS063), S154 (THU069), S209 (THU234)
- Dusheiko, Geoffrey, S279 (THU370), S281 (THU375), S305 (THU421), S594 (FRI409)
- Du, Shunda, S384 (THU591)
- Du, Shuyan, S446 (FRI029)
- Dutta, Sangit, S299 (THU409)
- Duvall, Scott, S30 (OS027)
- Duvoux, Christophe, S375 (THU573), S532 (FRI281), S772 (SAT239), S780 (SAT252), S791 (SAT269), S817 (SAT312)
- Duwe, Lea, S649 (FRI566)
- Du, Yu, S740 (SAT163)
- Dwivedi, Girish, S164 (THU089)
- Dworakowski, Athena, S409 (FRI031)
- Dwyer, Benjamin J., S85 (OS117)
- Dybowska, Dorota, S592 (FRI406)
- Dylla, Doug, S596 (FRI411)
- Dyson, Jessica, S311 (THU440), S337 (THU489)
- Dzen, Lucile, S715 (SAT105), S721 (SAT119), S722 (SAT120)
- Dziri, Samira, S271 (THU355)
- Eapen, CE, S19 (OS008), S49 (OS063)
- Easterbrook, Philippa, S203 (THU222), S556 (FRI331), S557 (FRI332), S557 (FRI333), S591 (FRI404)
- Eaton, John, S62 (OS078)
- Ebadi, Maryam, S317 (THU452), S631 (FRI530), S775 (SAT244), S815 (SAT311), S892 (SAT504)
- Ebel, Sebastian, S379 (THU581), S383 (THU590), S931 (SAT587)
- Ebert, Matthias, S408 (FRI029), S523 (FRI262), S606 (FRI466), S659 (FRI589), S661 (FRI594), S928 (SAT580)
- E, Bunthen, S229 (THU274), S260 (THU335), S260 (THU336)
- Echenne, Maxime, S771 (SAT237)
- Echeverri, Juan Andrés, S774 (SAT242)
- Eddowes, Peter, S425 (FRI058), S448 (FRI102), S452 (FRI108), S461 (FRI123), S526 (FRI269)
- Eddy, Angela, S536 (FRI291)
- Edeline, Julien, S372 (THU566)
- Edelman, Elazer, S492 (FRI205), S743 (SAT170)
- Edelman, Lisa, S770 (SAT234)
- Edenbaum, Hannah, S454 (FRI110)
- Edler, Hanan, S47 (OS059)
- Eduardo, Briones, S555 (FRI329)
- Edwards, Amy, S498 (FRI218)
- Edwards, Helen, S639 (FRI547)
- Edwards, Lindsey A, S366 (THU539)
- Ee Der Teo, Ada, S869 (SAT431)
- Egal, Erika, S113 (OS167)
- Egia-Mendikute, Leire, S673 (SAT018)
- Eguchi, Yuichiro, S154 (THU069), S875 (SAT442)
- Ehman, Richard L., S444 (FRI095)
- Ehmer, Ursula, S2 (GS003), S654 (FRI577)
- Ehrenbauer, Alena Friederike, S624 (FRI519), S634 (FRI536)
- Eichelberger, Beate, S362 (THU534)
- Eichert, Nicole, S433 (FRI073)
- Eichler, Emma, S464 (FRI147)
- Eidelshtein, Dana, S474 (FRI167)
- Eigenbauer, Ernst, S390 (FRI003)
- Eijk, Roel, S424 (FRI055)
- Eiliadis, Petros, S255 (THU326)
- Eiz-Vesper, Britta, S783 (SAT257)
- Ekmen, Nergis, S858 (SAT410), S861 (SAT416)
- Ekstedt, Mattias, S146 (THU052), S423 (FRI053)
- Ekvall, Håkan, S30 (OS026)
- Elaborot, Acana Susan, S294 (THU400)
- Elangovan, Hari, S743 (SAT169)
- Elangovan, Lavanya, S188 (THU178)
- Elde, Karen Dombestein, S125 (THU015)
- Elefsiniotis, Ioannis, S840 (SAT374), S917 (SAT562)
- Eley, Timothy, S848 (SAT392), S850 (SAT396), S851 (SAT397), S876 (SAT443), S878 (SAT448)

Author Index

- Elferink, Ronald Oude, S601 ([FRI457](#)), S762 ([SAT209](#))
- Elgavish, Shrona, S47 ([OS059](#)), S83 ([OS114](#))
- Elgenidy, Anas, S928 ([SAT581](#))
- Elhence, Anshuman, S524 ([FRI264](#))
- Elia, Chiara, S908 ([SAT535](#))
- Eligah, Victor, S592 ([FRI405](#))
- Elizalde, María, S500 ([FRI222](#)), S644 ([FRI557](#))
- Elizalde, Maria Iraburu, S643 ([FRI554](#))
- Elizalde, Montserrat, S757 ([SAT198](#))
- El-Karim, Lima Awad, S3 ([CS004](#))
- Elkhashab, Magdy, S427 ([FRI060](#)), S836 ([SAT366](#))
- Elkomos, Beshoy Effat, S776 ([SAT246](#))
- Elkrief, Laure, S127 ([THU019](#)), S372 ([THU566](#)), S772 ([SAT239](#))
- Ellenrieder, Volker, S85 ([OS118](#))
- Eller, Carla, S758 ([SAT199](#))
- Ellik, Zeynep Melekoglu, S858 ([SAT410](#))
- Ellik, Zeynep Melekoğlu, S778 ([SAT248](#)), S820 ([SAT316](#)), S861 ([SAT416](#)), S864 ([SAT421](#))
- Ellis, Ewa, S665 ([SAT002](#)), S756 ([SAT197](#))
- Ellis, Jim, S666 ([SAT004](#))
- Elmore, Kasey, S550 ([FRI318](#))
- El-Moustaid, Fadoua, S597 ([FRI416](#))
- El-Omar, Emad, S920 ([SAT568](#))
- Elortza, Felix, S37 ([OS039](#)), S46 ([OS056](#)), S77 ([OS103](#)), S132 ([THU027](#)), S365 ([THU538](#)), S648 ([FRI564](#)), S896 ([SAT512](#))
- El-Serag, Hashem, S926 ([SAT577](#))
- Elsharkawy, Ahmed, S277 ([THU368](#)), S364 ([THU537](#))
- Elssner, Christin, S655 ([FRI581](#))
- Elston, Robert, S12 ([LB004A](#)), S13 ([LB004B](#)), S288 ([THU389](#)), S291 ([THU393](#)), S875 ([SAT441](#)), S880 ([SAT452](#)), S881 ([SAT453](#))
- Eltepu, Laxman, S853 ([SAT402](#))
- Elwood, Chelsea, S43 ([OS051](#))
- Embade, Nieves, S671 ([SAT014](#))
- Emir, Birol, S151 ([THU063](#))
- Emiroğlu, Remzi, S782 ([SAT255](#))
- Emma Burlone, Michela, S929 ([SAT583](#))
- Emmanouil, Beatrice, S44 ([OS053](#))
- Enea, Marco, S387 ([THU599](#)), S448 ([FRI101](#)), S725 ([SAT127](#))
- Engel, Aaron, S460 ([FRI122](#))
- Engel, Bastian, S783 ([SAT257](#)), S784 ([SAT259](#))
- Engelmann, Cornelius, S883 ([SAT488](#)), S904 ([SAT528](#))
- Engels, Franziska, S710 ([SAT090](#))
- Engels, Heleen, S768 ([SAT230](#))
- Engin, Ender, S682 ([SAT035](#))
- Engleitner, Thomas, S654 ([FRI577](#))
- Enke, Thomas, S394 ([FRI008](#))
- Enomoto, Hirayuki, S616 ([FRI502](#))
- Enomoto, Masaru, S875 ([SAT442](#))
- Enomoto, Nobuyuki, S387 ([THU598](#)), S563 ([FRI346](#))
- Eraki, Tamer Al, S566 ([FRI351](#))
- Erard, Domitille, S356 ([THU522](#)), S772 ([SAT239](#))
- Erasmus, Hans-Peter, S353 ([THU517](#)), S354 ([THU518](#))
- Ercan, Caner, S660 ([FRI592](#))
- Erden, Ayse, S414 ([FRI037](#)), S778 ([SAT248](#))
- Erdman, Lauren, S801 ([SAT287](#))
- Erdmann, Joris, S107 ([OS157](#))
- Eren, Fatih, S820 ([SAT316](#))
- Er Hsu, Cheng, S576 ([FRI372](#))
- Eriksen, Peter Lykke, S677 ([SAT026](#))
- Eriksson, Jan W., S40 ([OS045](#))
- Eriksson, Jonas, S471 ([FRI162](#))
- Eriksson, Olof, S420 ([FRI047](#)), S471 ([FRI162](#))
- Erkan, Mert, S693 ([SAT058](#))
- Erler, Nicole, S824 ([SAT344](#))
- Erlund, Iris, S419 ([FRI046](#))
- Ermler, Megan, S873 ([SAT439](#))
- Ermolova, Tatiana, S728 ([SAT134](#))
- Er, Ramazan Erdem, S778 ([SAT248](#))
- Erreni, Marco, S651 ([FRI570](#))
- Erschfeld, Stephanie, S654 ([FRI578](#))
- Ersoz, Galip, S294 ([THU399](#)), S399 ([FRI015](#))
- Erstad, Derek J., S36 ([OS037](#))
- Ertracht, Offir, S742 ([SAT166](#))
- Eschbach, Erin, S343 ([THU502](#))
- Escorsell, Angels, S64 ([OS082](#)), S91 ([OS128](#)), S627 ([FRI523](#)), S886 ([SAT494](#)), S900 ([SAT520](#))
- Escude, Laia, S90 ([OS127](#)), S902 ([SAT524](#))
- Escudero-García, Desamparados, S157 ([THU074](#)), S158 ([THU076](#)), S442 ([FRI091](#)), S902 ([SAT523](#))
- Escudero-López, Blanca, S708 ([SAT087](#))
- Esfahani, Hrag, S691 ([SAT053](#))
- Eslam, Mohammed, S431 ([FRI069](#))
- Eslamparast, Tannaz, S890 ([SAT500](#))
- Esmat, Gamal, S209 ([THU234](#))
- Espin, Jaime, S237 ([THU290](#))
- Espinosa-Escudero, Ricardo A., S59 ([OS074](#))
- Espinosa, Jorge Simón, S48 ([OS060](#)), S84 ([OS116](#)), S132 ([THU027](#)), S600 ([FRI453](#)), S679 ([SAT029](#))
- Espósito, Ilaria, S769 ([SAT233](#))
- Esposti, Luca Degli, S586 ([FRI393](#))
- Esser, Hannah, S85 ([OS117](#))
- Essex, Whitney, S226 ([THU269](#))
- Eßing, Tobias, S384 ([THU592](#))
- Estall, Jennifer, S456 ([FRI114](#))
- Esteban-Fabró, Roger, S45 ([OS055](#))
- Esteban, Luis M., S792 ([SAT271](#))
- Esteban, Rafael, S44 ([OS052](#)), S212 ([THU240](#)), S237 ([THU289](#)), S257 ([THU330](#)), S277 ([THU367](#)), S297 ([THU405](#))
- Estela del Castillo, Maria, S530 ([FRI277](#))
- Estes, Chris, S43 ([OS050](#)), S230 ([THU278](#)), S231 ([THU279](#)), S235 ([THU288](#))
- Estrella, Federico, S180 ([THU161](#))
- Etcheves, Patricia, S786 ([SAT261](#))
- Etik, Digidem Ozer, S858 ([SAT410](#)), S861 ([SAT416](#))
- Ettorre, Giuseppe Maria, S806 ([SAT294](#)), S808 ([SAT297](#))
- Etzion, Ohad, S70 ([OS092](#)), S145 ([THU049](#)), S269 ([THU350](#)), S300 ([THU411](#)), S588 ([FRI396](#)), S859 ([SAT412](#))
- Eugene, Chen, S765 ([SAT214](#))
- Eunen, Karen Van, S539 ([FRI298](#))
- Eun, Hyuk Soo, S380 ([THU583](#)), S921 ([SAT569](#))
- Eva, Alessandra, S515 ([FRI249](#))
- Evans, Louise, S548 ([FRI316](#))
- Evans, Tom, S868 ([SAT428](#))
- Evason, Kimberley, S113 ([OS167](#))
- Everson, Greg, S633 ([FRI535](#))
- Evert, Katja, S107 ([OS157](#))
- Evliati, Loukia, S472 ([FRI163](#))
- Evole, Helena Hernández, S136 ([THU033](#)), S139 ([THU039](#))
- Evraerts, Jonathan, S535 ([FRI289](#))
- Expósito, Carmen, S25 ([OS018](#))
- Eyck, Annelies Van, S709 ([SAT089](#))
- Eyer, Florian, S11 ([LB002](#))
- Ezeani, Esu, S233 ([THU282](#))
- Fabian, Ondrej, S536 ([FRI290](#))
- Fabrega, Emilio, S114 ([OS168](#)), S115 ([OS169](#)), S334 ([THU482](#)), S624 ([FRI518](#)), S774 ([SAT242](#))
- Fabregat, Carles, S748 ([SAT180](#))
- Fabregat, Isabel, S48 ([OS060](#)), S673 ([SAT018](#))
- Fabrellas, Núria, S25 ([OS018](#)), S63 ([OS080](#)), S139 ([THU039](#)), S511 ([FRI242](#)), S512 ([FRI243](#)), S512 ([FRI244](#)), S896 ([SAT512](#)), S901 ([SAT522](#)), S902 ([SAT524](#)), S907 ([SAT532](#))
- Fabris, Luca, S46 ([OS056](#)), S107 ([OS157](#)), S751 ([SAT186](#))
- Facchetti, Floriana, S54 ([OS069](#)), S223 ([THU263](#)), S843 ([SAT379](#)), S843 ([SAT381](#)), S868 ([SAT429](#)), S874 ([SAT440](#)), S880 ([SAT450](#))
- Fadnes, Lars Thore, S221 ([THU257](#))
- Fagan, Andrew, S67 ([OS087](#)), S130 ([THU023](#)), S176 ([THU153](#)), S339 ([THU494](#))
- Fagioli, Stefano, S96 ([OS136](#)), S210 ([THU236](#)), S581 ([FRI384](#)), S586 ([FRI393](#)), S908 ([SAT535](#))
- Faillie, Jean Luc, S392 ([FRI006](#))
- Faire, Bridget, S16 ([OS004](#))
- Faitot, François, S20 ([OS010](#))
- Fajardo, Emmanuel, S556 ([FRI331](#)), S557 ([FRI332](#)), S557 ([FRI333](#))
- Fakhriyehasl, Mina, S429 ([FRI065](#))
- Falchetto, Rocco, S516 ([FRI251](#))
- Falco, Giuseppe, S624 ([FRI517](#))
- Falcon-Perez, Juan, S77 ([OS103](#)), S643 ([FRI554](#))
- Falguières, Thomas, S514 ([FRI248](#)), S521 ([FRI260](#))
- Falk, Christine, S608 ([FRI485](#)), S783 ([SAT257](#))

- Fallahzadeh, Mohammad Amin, S19 ([OS008](#)), S49 ([OS063](#))
- Fall, Fatou, S23 ([OS015](#))
- Fallowfield, Jonathan, S163 ([THU086](#)), S397 ([FRI013](#)), S461 ([FRI123](#)), S712 ([SAT096](#))
- Fall, Tove, S40 ([OS045](#))
- Faloon, Sarah, S805 ([SAT292](#))
- Fan, Daiming, S92 ([OS130](#)), S619 ([FRI508](#)), S621 ([FRI512](#))
- Fanelli, Chiara, S596 ([FRI414](#))
- Fanelli, Fabrizio, S627 ([FRI524](#))
- Fang, Chengwen, S182 ([THU165](#))
- Fanget, Marie C., S831 ([SAT357](#))
- Fan, Gregory, S203 ([THU224](#)), S204 ([THU225](#))
- Fan, Jian-Gao, S154 ([THU069](#))
- Fan, Kristi, S848 ([SAT391](#))
- Fan, Xiude, S33 ([OS032](#))
- Faraj, May, S456 ([FRI114](#))
- Fardellas, Achilleas, S667 ([SAT006](#)), S755 ([SAT195](#)), S756 ([SAT197](#))
- Farejov, Rasim, S782 ([SAT255](#))
- Farella, Nunzia, S938 ([SAT599](#))
- Fargion, Silvia, S159 ([THU078](#))
- Farhan, Hesso, S766 ([SAT216](#))
- Farinati, Fabio, S358 ([THU526](#))
- Farin-Glattacker, Erik, S80 ([OS108](#))
- Färkkilä, Martti, S80 ([OS109](#)), S312 ([THU441](#)), S327 ([THU469](#)), S419 ([FRI046](#))
- Farooqui, Naba, S524 ([FRI264](#))
- Farquhar, Ronald, S834 ([SAT362](#))
- Farriols, Anna, S316 ([THU450](#))
- Fassan, Matteo, S748 ([SAT180](#))
- Fatima, Ifrah, S632 ([FRI532](#))
- Fatta, Erika, S167 ([THU095](#))
- Fauler, Günter, S68 ([OS088](#))
- Faulkes, Rosemary, S19 ([OS008](#)), S49 ([OS063](#))
- Faure, Stéphanie, S392 ([FRI006](#)), S771 ([SAT237](#)), S772 ([SAT239](#))
- Favot, Patrick, S584 ([FRI389](#))
- Fayyaz, Muhammad, S684 ([SAT039](#))
- Feagan, Brian, S416 ([FRI040](#))
- Federico, Alessandro, S675 ([SAT021](#)), S938 ([SAT599](#))
- Federico, Denise, S872 ([SAT436](#))
- Feder, Molly, S226 ([THU269](#))
- Fehrenbach, Uli, S374 ([THU570](#)), S380 ([THU582](#))
- Feierbach, Becket, S194 ([THU189](#)), S247 ([THU308](#)), S251 ([THU317](#)), S832 ([SAT358](#)), S835 ([SAT364](#)), S841 ([SAT376](#))
- Feigh, Michael, S661 ([FRI593](#)), S669 ([SAT010](#)), S724 ([SAT124](#)), S737 ([SAT158](#))
- Feinman, Leighland, S310 ([THU439](#))
- Feio de Azevedo, Rita Furtado, S346 ([THU507](#))
- Feizi, Jeanette, S544 ([FRI308](#)), S547 ([FRI313](#))
- Feldbacher, Nicole, S68 ([OS088](#))
- Feld, Jordan, S3 ([GS004](#)), S252 ([THU319](#)), S274 ([THU361](#)), S294 ([THU400](#)), S395 ([FRI010](#)), S569 ([FRI359](#)), S592 ([FRI405](#)), S848 ([SAT390](#)), S849 ([SAT394](#)), S852 ([SAT400](#)), S861 ([SAT415](#))
- Feldman, Alexandra, S428 ([FRI062](#))
- Feldstein, Ariel, S471 ([FRI161](#)), S690 ([SAT051](#))
- Felipo, Vicente, S103 ([OS150](#))
- Feliu-Prius, Anna, S212 ([THU240](#))
- Félix, Catarina, S190 ([THU182](#))
- Felix, Sean, S209 ([THU234](#)), S420 ([FRI048](#)), S429 ([FRI064](#)), S447 ([FRI100](#))
- Felli, Emanuele, S36 ([OS038](#)), S99 ([OS142](#)), S649 ([FRI565](#)), S738 ([SAT160](#))
- Feltracco, Paolo, S821 ([SAT318](#))
- Fenaux, Martijn, S726 ([SAT128](#)), S726 ([SAT129](#))
- Fenech, Mary, S581 ([FRI384](#))
- Feng, Bo, S26 ([OS020](#)), S278 ([THU369](#))
- Feng, Dandan, S723 ([SAT122](#))
- Feng, I-Cher, S863 ([SAT420](#))
- Feng, Rilü, S408 ([FRI029](#))
- Feng, Shibao, S730 ([SAT139](#)), S732 ([SAT143](#))
- Feng, Wenke, S35 ([OS035](#))
- Feng, Ying-Hua, S827 ([SAT349](#))
- Fennell, Rebecca, S63 ([OS079](#))
- Fenyyes, Daphna, S593 ([FRI407](#))
- Feray, Cyrille, S5 ([GS007](#)), S538 ([FRI296](#)), S800 ([SAT285](#))
- Fer, Beatrice Bois De, S712 ([SAT095](#))
- Ferenc, Anna, S746 ([SAT179](#))
- Ferenci, Peter, S1 ([GS001](#)), S535 ([FRI287](#)), S555 ([FRI328](#)), S829 ([SAT353](#)), S830 ([SAT354](#)), S843 ([SAT379](#)), S854 ([SAT403](#))
- Ferguson, Catherine, S228 ([THU272](#))
- Ferhanoglu, Onur, S693 ([SAT058](#))
- Fernández-Puertas, Idoia, S651 ([FRI571](#)), S665 ([SAT001](#))
- Fernandes, Christopher C., S332 ([THU478](#))
- Fernandes, Diogo A. E., S192 ([THU185](#))
- Fernandes, Flavia, S910 ([SAT539](#))
- Fernandes, Sara, S765 ([SAT214](#))
- Fernandez, Ainhoa, S406 ([FRI027](#))
- Fernández-Baca, María Victoria, S218 ([THU252](#))
- Fernandez-Barrena, Maite G, S643 ([FRI554](#)), S644 ([FRI557](#))
- Fernandez-Barrena, Maite G., S46 ([OS056](#)), S112 ([OS165](#)), S500 ([FRI222](#))
- Fernandez-Checa, José, S59 ([OS074](#)), S361 ([THU530](#)), S465 ([FRI150](#))
- Fernández-Cuenca, Felipe, S555 ([FRI329](#))
- Fernandez, Emma, S207 ([THU231](#)), S208 ([THU232](#))
- Fernandez, Enrique Claudio, S459 ([FRI119](#))
- Fernandez-Fernandez, Maria, S465 ([FRI150](#))
- Fernandez, Javier, S370 ([THU549](#))
- Fernández, Javier, S362 ([THU533](#))
- Fernández-Lizaranzu, Isabel, S442 ([FRI092](#)), S459 ([FRI119](#))
- Fernández-Palanca, Paula, S639 ([FRI549](#))
- Fernandez, Roberto, S774 ([SAT242](#))
- Fernández-Rodríguez, Conrado, S127 ([THU018](#))
- Fernandez, Teresa Cabezas, S577 ([FRI374](#))
- Fernández, Vanessa García, S708 ([SAT087](#))
- Fernández-Vaquero, Mirian, S47 ([OS059](#))
- Fernández-Yunquera, Ainhoa, S114 ([OS168](#))
- Ferraioli, Giovanna, S502 ([FRI225](#))
- Ferrand, Janina, S905 ([SAT529](#))
- Ferrante, Luigi, S84 ([OS115](#))
- Ferrarese, Alberto, S91 ([OS129](#))
- Ferrari, Erika, S761 ([SAT206](#))
- Ferraro, Pasquel, S805 ([SAT293](#))
- Ferraz, Maria Lucia, S542 ([FRI304](#)), S888 ([SAT498](#))
- Ferreccio, Catterina, S81 ([OS110](#)), S137 ([THU034](#))
- Ferreira, Carlos, S96 ([OS136](#)), S319 ([THU454](#))
- Ferreira-Gonzalez, Sofia, S85 ([OS117](#))
- Ferreira, Ignacio, S149 ([THU059](#)), S440 ([FRI088](#))
- Ferreira, João Pedro Sousa, S28 ([OS024](#))
- Ferreira, Jose Manuel, S304 ([THU420](#))
- Ferreira, Livia Garcia, S890 ([SAT500](#))
- Ferreira, Marcelo Simão, S307 ([THU432](#))
- Ferreira, Raphaella, S227 ([THU270](#))
- Ferreiro, Alejandra Otero, S792 ([SAT271](#))
- Ferrigno, Andrea, S697 ([SAT065](#)), S702 ([SAT074](#))
- Ferrigno, Luigina, S564 ([FRI347](#))
- Ferri, Silvia, S166 ([THU093](#))
- Ferry, Helen, S602 ([FRI458](#))
- Ferstl, Philip, S353 ([THU517](#)), S354 ([THU518](#))
- Ferstl, Philip Georg, S502 ([FRI226](#))
- Fessas, Petros, S374 ([THU571](#))
- Festi, Davide, S91 ([OS129](#)), S794 ([SAT273](#))
- Fettiplace, James, S327 ([THU470](#)), S335 ([THU485](#))
- Feuerhake, Friedrich, S927 ([SAT579](#))
- Feverly, Bart, S72 ([OS094](#))
- Fiaschetti, Katia, S488 ([FRI197](#))
- Fiaz, Raja Omar, S884 ([SAT489](#))
- Fich, Alexander, S145 ([THU049](#))
- Fichtner, Urs, S80 ([OS108](#))
- Fidaleo, Marco, S763 ([SAT211](#))
- Figge, Anja, S682 ([SAT035](#))
- Figredo, Anita, S342 ([THU501](#))
- Figueiredo, Pedro Narra, S190 ([THU182](#))
- Filhine-Tresarrieu, Pierre, S905 ([SAT529](#))
- Filipek, Natalia, S19 ([OS008](#)), S49 ([OS063](#))
- Filip, Gabriela Adriana, S664 ([FRI600](#))
- Filippi, Celine, S818 ([SAT315](#))
- Filippo, Leonardi, S96 ([OS136](#))
- Filmann, Natalie, S15 ([OS001](#))
- Filomia, Roberto, S564 ([FRI347](#)), S578 ([FRI376](#))
- Finberg, Isaac, S700 ([SAT071](#))
- Findeisen, Peter, S937 ([SAT597](#))
- Finkelmeier, Fabian, S15 ([OS001](#)), S313 ([THU444](#)), S353 ([THU517](#)), S354 ([THU518](#))
- Finkenstedt, Armin, S470 ([FRI159](#))

Author Index

- Fink, Jodok Matthias, S710 ([SAT090](#))
 Finnegan, Sarah, S95 ([OS135](#))
 Finnmøre, Alexander, S697 ([SAT064](#))
 Fiorentino, Francesca, S34 ([OS034](#))
 Fischer, Elke, S224 ([THU265](#))
 Fischer, Janett, S11 ([LB002](#)),
 S184 ([THU169](#)), S379 ([THU581](#)),
 S382 ([THU586](#)), S860 ([SAT414](#)),
 S931 ([SAT587](#))
 Fischer, Lutz, S893 ([SAT507](#))
 Fischer, Petra, S193 ([THU187](#))
 Fischer, Susan, S306 ([THU431](#))
 Fishman, Jesse, S167 ([THU094](#))
 Fisseha, Henok, S19 ([OS008](#)), S49 ([OS063](#))
 Fitting, Daniel, S313 ([THU444](#))
 Fitzgerald, Megan, S824 ([SAT343](#)),
 S846 ([SAT386](#))
 Flack, Steve, S96 ([OS137](#))
 Flaherty, John F., S4 ([GS006](#)), S103 ([OS149](#)),
 S244 ([THU302](#)), S828 ([SAT351](#)),
 S829 ([SAT352](#)), S837 ([SAT368](#)),
 S845 ([SAT385](#)), S862 ([SAT417](#)),
 S866 ([SAT425](#))
 Flašhove, Alexander, S193 ([THU187](#))
 Fleischman, M. Wayne, S142 ([THU043](#))
 Flejscher-Stepniewska, Katarzyna,
 S565 ([FRI350](#))
 Flensted-Jensen, Mathias, S724 ([SAT124](#))
 Fletcher, Simon, S53 ([OS067](#)),
 S251 ([THU317](#)), S276 ([THU365](#)),
 S835 ([SAT364](#)), S841 ([SAT376](#))
 Fleury, Hervé, S249 ([THU313](#))
 Flisiak, Robert, S565 ([FRI350](#)),
 S585 ([FRI390](#)), S592 ([FRI406](#))
 Fliss-Isakov, Naomi, S148 ([THU056](#))
 Flocco, Gianina, S779 ([SAT250](#))
 Floderus, Ylva, S530 ([FRI275](#))
 Florea, Ana, S831 ([SAT356](#))
 Floreani, Annarosa, S317 ([THU452](#)),
 S335 ([THU484](#))
 Flores-Costa, Roger, S361 ([THU530](#)),
 S362 ([THU533](#)), S370 ([THU549](#)),
 S674 ([SAT019](#))
 Florescu, Madalina, S795 ([SAT276](#))
 Flores, Joan Ericka, S498 ([FRI218](#))
 Florman, Sander, S343 ([THU502](#))
 Flügen, Georg, S930 ([SAT584](#))
 Fluiter, Kees, S698 ([SAT067](#))
 Foerster, Friedrich, S464 ([FRI147](#))
 Foka, Pelagia, S255 ([THU326](#))
 Foley, Clare, S527 ([FRI270](#))
 Folgueira, Cintia, S689 ([SAT050](#))
 Folsaas, Trine, S77 ([OS103](#)),
 S107 ([OS157](#))
 Foncea, Camelia, S483 ([FRI186](#)),
 S505 ([FRI230](#)), S930 ([SAT585](#))
 Fondevila, Constantino, S743 ([SAT170](#))
 Fondevila, Flavia, S639 ([FRI549](#))
 Fondevila, Marcos Fernandez, S87 ([OS122](#)),
 S600 ([FRI453](#))
 Fong, Erica, S719 ([SAT114](#))
 Fong, Matthew, S933 ([SAT592](#))
 Fong, Sylvia, S404 ([FRI023](#)), S534 ([FRI285](#)),
 S540 ([FRI299](#))
 Fontaine, Helene, S17 ([OS006](#)), S72 ([OS093](#)),
 S101 ([OS146](#)), S250 ([THU314](#)),
 S297 ([THU404](#)), S392 ([FRI005](#)),
 S567 ([FRI353](#)), S833 ([SAT360](#))
 Fontana, Marianna, S58 ([OS073](#))
 Fontela, Fernando Diaz, S150 ([THU061](#)),
 S324 ([THU464](#))
 Fonvig, Cilius, S523 ([FRI263](#))
 Fonvig, Cilius Esmann, S450 ([FRI104](#))
 Foo-Atkins, Corinne, S443 ([FRI093](#)),
 S486 ([FRI193](#))
 Foo, Hong, S558 ([FRI334](#))
 Fooz, Bo De, S303 ([THU416](#))
 Forbes, Stuart, S85 ([OS117](#))
 Forlano, Roberta, S121 ([THU007](#)),
 S179 ([THU158](#)), S444 ([FRI094](#)),
 S674 ([SAT020](#))
 Formentin, Chiara, S888 ([SAT497](#))
 Fornaguera, Cristina, S106 ([OS154](#))
 Fornaro, Lorenzo, S748 ([SAT180](#))
 Forner, Alejandro, S107 ([OS157](#))
 Forns, Xavier, S53 ([OS067](#)), S90 ([OS127](#)),
 S99 ([OS141](#)), S207 ([THU231](#)),
 S208 ([THU232](#)), S263 ([THU340](#)),
 S286 ([THU385](#)), S570 ([FRI361](#)),
 S852 ([SAT400](#)), S861 ([SAT415](#))
 Forrest, Ewan, S19 ([OS008](#)), S34 ([OS034](#)),
 S49 ([OS063](#)), S122 ([THU008](#)),
 S124 ([THU013](#)), S141 ([THU041](#)),
 S266 ([THU345](#)), S352 ([THU516](#))
 Forsman, Cecilia, S333 ([THU480](#))
 Forstén, Aino, S100 ([OS145](#))
 Forstmeyer, Dirk, S383 ([THU590](#))
 Fortea, Jose Ignacio, S90 ([OS127](#)),
 S624 ([FRI518](#)), S774 ([SAT242](#))
 Forte, Paolo, S770 ([SAT235](#))
 Fortes, Puri, S644 ([FRI557](#))
 Fortune, Brett, S779 ([SAT250](#))
 Fortún, Jesús, S114 ([OS169](#))
 Fortuny, Marta, S724 ([SAT125](#))
 Forzenigo, Laura Virginia, S578 ([FRI376](#))
 Foschi, Francesco Giuseppe,
 S908 ([SAT535](#))
 Foster, Erin, S726 ([SAT130](#))
 Foster, Graham, S44 ([OS053](#)),
 S238 ([THU291](#)), S551 ([FRI321](#))
 Foster, John, S530 ([FRI277](#))
 Foster, Neil, S34 ([OS034](#))
 Foster, Robert, S650 ([FRI568](#)),
 S660 ([FRI590](#)), S660 ([FRI591](#)),
 S726 ([SAT130](#))
 Foti, Michelangelo, S645 ([FRI559](#)),
 S652 ([FRI572](#))
 Fouad, Fayssol, S579 ([FRI381](#))
 Fouchard, Isabelle, S73 ([OS096](#)),
 S74 ([OS099](#)), S496 ([FRI215](#)),
 S497 ([FRI216](#)), S507 ([FRI235](#))
 Foucher, Juliette, S441 ([FRI089](#)),
 S833 ([SAT360](#)), S840 ([SAT373](#))
 Foulle, Fabienne, S672 ([SAT015](#))
 Fougerou-Leurent, Claire, S72 ([OS093](#))
 Fouquet, Baptiste, S189 ([THU181](#))
 Fourati, Slim, S530 ([FRI276](#)), S582 ([FRI386](#))
 Fournier, Carole, S766 ([SAT216](#))
 Fournier, Céline, S425 ([FRI058](#)),
 S448 ([FRI102](#)), S452 ([FRI108](#)),
 S722 ([SAT120](#))
 Fournier, Claire, S593 ([FRI407](#))
 Fournier, Margot, S645 ([FRI559](#)),
 S652 ([FRI572](#))
 Fowler, Kathryn, S451 ([FRI107](#)),
 S454 ([FRI110](#)), S701 ([SAT073](#))
 Fracanzani, Anna Ludovica, S159 ([THU078](#)),
 S167 ([THU095](#)), S578 ([FRI376](#)),
 S682 ([SAT036](#)), S682 ([SAT037](#)),
 S698 ([SAT068](#)), S703 ([SAT077](#)),
 S706 ([SAT084](#))
 Franca, Maria Manuela, S442 ([FRI091](#))
 Francesca Manfredi, Giulia, S929 ([SAT583](#))
 Franceschini, Barbara, S758 ([SAT201](#))
 Francica, Giampiero, S938 ([SAT599](#))
 Francione, Paolo, S159 ([THU078](#)),
 S167 ([THU095](#))
 Francioso, Simona, S249 ([THU313](#))
 Franco, Andrea Jimenez, S685 ([SAT041](#))
 Franco, Andrea Jiménez, S677 ([SAT027](#)),
 S678 ([SAT028](#)), S681 ([SAT034](#))
 Franco, Brunella, S84 ([OS115](#))
 Francoz, Claire, S772 ([SAT239](#)),
 S817 ([SAT312](#))
 Francque, Sven, S9 ([GS011](#)), S90 ([OS127](#)),
 S459 ([FRI120](#)), S502 ([FRI226](#)),
 S516 ([FRI252](#)), S692 ([SAT055](#)),
 S709 ([SAT089](#)), S721 ([SAT119](#)),
 S722 ([SAT120](#))
 Franke, Andre, S325 ([THU466](#)),
 S604 ([FRI462](#))
 Frank, Leonie, S599 ([FRI451](#))
 Franklin, James, S938 ([SAT600](#))
 Frankova, Sona, S536 ([FRI290](#)),
 S593 ([FRI408](#))
 Franks, Hester, S116 ([OS172](#))
 Franza, Anne Minello, S72 ([OS093](#)),
 S833 ([SAT360](#)), S840 ([SAT373](#)),
 S918 ([SAT563](#))
 Fraquelli, Mirella, S503 ([FRI227](#)),
 S868 ([SAT429](#)), S880 ([SAT450](#))
 Fraser, Andrew, S17 ([OS005](#))
 Fraser, Chris, S240 ([THU297](#)), S581 ([FRI384](#))
 Fraser, Hannah, S256 ([THU328](#))
 Fraser, Melissa, S558 ([FRI334](#))
 Fraser, Simon, S42 ([OS048](#))
 Frassinetti, Giovanni Luca, S748 ([SAT180](#))
 Fraughen, Daniel, S531 ([FRI279](#))
 Frederick, R. Todd, S611 ([FRI490](#))
 Frederiksen, Peder, S415 ([FRI039](#))
 Freed, Robert, S770 ([SAT234](#))
 Freeman, James, S16 ([OS004](#))
 Freer, Alice, S334 ([THU483](#))
 Freilich, Bradley, S719 ([SAT114](#))
 Freitas, Marta, S149 ([THU060](#))
 Frejd, Frederik, S471 ([FRI162](#))
 Frelin, Lars, S860 ([SAT413](#))
 Frenguelli, Luca, S737 ([SAT157](#))
 Freutsmiedl, Verena, S711 ([SAT093](#))
 Frey, Olivier, S703 ([SAT078](#))
 Frias, Juan P, S732 ([SAT143](#))
 Frias, Maria Carnevali, S577 ([FRI373](#))

- Fricker, Gert, S712 ([SAT095](#))
 Fridriksdottir, Ragnheidur H., S573 ([FRI366](#))
 Friederich, Philip W., S306 ([THU431](#))
 Friedman, Scott, S160 ([THU080](#)),
 S343 ([THU502](#)), S455 ([FRI113](#)),
 S474 ([FRI168](#)), S688 ([SAT048](#)),
 S714 ([SAT103](#))
 Fried, Michael, S449 ([FRI103](#))
 Friedrichsen, Martin, S720 ([SAT116](#))
 Friehmann, Tomer, S387 ([THU597](#))
 Friesland, Martina, S250 ([THU315](#))
 Friess, Helmut, S463 ([FRI146](#)),
 S471 ([FRI161](#)), S690 ([SAT051](#))
 Fritsch, Thea-Charlotte, S380 ([THU582](#))
 Fritzsche, Sarah, S655 ([FRI581](#))
 Fröhling, Stefan, S655 ([FRI581](#))
 Frolkis, Alexandra, S143 ([THU045](#))
 Fromme, Malin, S515 ([FRI250](#)),
 S520 ([FRI257](#))
 Frontini, Mattia, S695 ([SAT061](#))
 Frossard, Jean-Louis, S457 ([FRI115](#))
 Frost, Gary, S179 ([THU158](#))
 Fryer, Eve, S330 ([THU475](#)), S602 ([FRI458](#))
 Fry, John, S733 ([SAT145](#)), S824 ([SAT343](#)),
 S835 ([SAT365](#)), S846 ([SAT386](#)),
 S871 ([SAT435](#))
 Fryknäs, Märten, S368 ([THU543](#))
 Fuchs, Alexandra, S759 ([SAT202](#))
 Fuchs, Bryan C., S36 ([OS037](#))
 Fuchs, Claudia, S469 ([FRI158](#)),
 S688 ([SAT049](#)), S760 ([SAT204](#))
 Fuchs, Michael, S130 ([THU023](#))
 Fuchs, Sabine A, S652 ([FRI574](#))
 Fuentes, A., S211 ([THU237](#))
 Fuentes, Eduardo, S81 ([OS110](#)),
 S137 ([THU034](#))
 Fuhrmann, Lara, S15 ([OS001](#))
 Fujishiro, Mitsuhiro, S485 ([FRI192](#))
 Fujita, Naoto, S615 ([FRI501](#)), S897 ([SAT514](#))
 Fujiwara, Kisako, S615 ([FRI501](#)),
 S897 ([SAT514](#))
 Fujiwara, Naoto, S649 ([FRI565](#))
 Fukada, Hiroo, S687 ([SAT047](#))
 Fukuhara, Kyoko, S687 ([SAT047](#))
 Fu, Lei, S70 ([OS091](#)), S477 ([FRI175](#)),
 S838 ([SAT369](#))
 Fulgenzi, Claudia, S372 ([THU567](#))
 Fulgenzi, Claudia Angela Maria,
 S108 ([OS158](#)), S374 ([THU571](#)),
 S376 ([THU574](#)), S383 ([THU588](#))
 Fuller, Harriett, S104 ([OS151](#))
 Fuller, Karen, S239 ([THU294](#))
 Funaro, Barbara, S507 ([FRI234](#))
 Fundora, Yilliam, S263 ([THU340](#)),
 S286 ([THU385](#)), S743 ([SAT170](#))
 Fung, Scott K, S836 ([SAT366](#)),
 S849 ([SAT394](#))
 Fung, Yan Yue James, S272 ([THU358](#)),
 S273 ([THU360](#)), S275 ([THU364](#))
 Funk, Georg-Christian, S354 ([THU519](#))
 Fu, Rebecca, S265 ([THU344](#))
 Furlan, Alessandro, S442 ([FRI091](#))
 Furrie, Elizabeth, S495 ([FRI214](#))
 Furusyo, Norihiro, S875 ([SAT442](#))
 Fusai, Giuseppe, S55 ([OS070](#))
 Fusaro, Karen, S73 ([OS095](#))
 Fuster, Carla, S365 ([THU538](#))
 Fuster, Daniel, S199 ([THU199](#))
 Fu, Xinxiang, S669 ([SAT009](#))
 Fytli, Paraskevi, S429 ([FRI063](#))
 Gaal, Luc Van, S692 ([SAT055](#))
 Gabbia, Daniela, S378 ([THU578](#)),
 S478 ([FRI176](#)), S479 ([FRI177](#))
 Gabernet, Gisela, S38 ([OS042](#))
 Gabiati, Claudia, S210 ([THU236](#))
 Gabriel, Maria Magdalena, S624 ([FRI519](#))
 Gabunia, Tamar, S587 ([FRI395](#)),
 S590 ([FRI400](#)), S590 ([FRI401](#))
 Gadano, Adrian, S12 ([LB004A](#)),
 S13 ([LB004B](#)), S288 ([THU389](#)),
 S291 ([THU393](#)), S880 ([SAT452](#)),
 S881 ([SAT453](#))
 Gadenne, Cloé, S758 ([SAT199](#))
 Gaggari, Anuj, S251 ([THU318](#)),
 S832 ([SAT358](#))
 Gagliani, Nicola, S83 ([OS114](#)), S604 ([FRI462](#))
 Gagliardi, Roberta, S895 ([SAT511](#))
 Gaidano, Gianluca, S503 ([FRI227](#))
 Gaillard, Constance, S417 ([FRI042](#))
 Gaillard, Vincent, S376 ([THU574](#))
 Gairing, Simon Johannes, S882 ([SAT486](#))
 Gajownik, Urszula Ewa, S792 ([SAT271](#))
 Galacteros, Frederic, S791 ([SAT269](#))
 Galanakis, Vasileios, S742 ([SAT167](#))
 Galanis, Petros, S917 ([SAT562](#))
 Galchinskaya, Valentina, S421 ([FRI049](#))
 Galdavadze, Ketevan, S221 ([THU258](#))
 Gale, Eric, S36 ([OS037](#))
 Gal, Frédéric Le, S271 ([THU355](#))
 Galharia, Nathalia, S910 ([SAT539](#))
 Galicia, Nicole, S534 ([FRI285](#))
 Gallacher, Stuart, S266 ([THU345](#))
 Gallardo, Patricia, S137 ([THU034](#))
 Gallay, Philippe, S650 ([FRI568](#)),
 S660 ([FRI591](#))
 Gallego, Adolfo, S334 ([THU482](#))
 Gallego-Durán, Rocío, S157 ([THU074](#)),
 S158 ([THU076](#)), S450 ([FRI105](#)),
 S708 ([SAT087](#))
 Gallego, Isabel, S589 ([FRI399](#))
 Gallen, Ana, S442 ([FRI091](#))
 Galle, Peter, S80 ([OS108](#)), S145 ([THU051](#)),
 S374 ([THU571](#)), S376 ([THU574](#)),
 S383 ([THU588](#)), S523 ([FRI262](#)),
 S823 ([SAT341](#)), S882 ([SAT486](#))
 Galletto, Athena, S375 ([THU573](#))
 Galli, Andrea, S659 ([FRI588](#)), S770 ([SAT235](#))
 Gall, Jonathan, S871 ([SAT434](#))
 Gall, Maude Le, S65 ([OS084](#))
 Gallo, Camilla, S96 ([OS136](#))
 Galsgaard, Elisabeth, S670 ([SAT013](#))
 Galun, Eithan, S47 ([OS059](#)), S83 ([OS114](#)),
 S387 ([THU597](#)), S456 ([FRI114](#)),
 S474 ([FRI167](#)), S764 ([SAT213](#))
 Gálvez, Mont, S570 ([FRI361](#))
 Galwey, Nicholas, S873 ([SAT439](#))
 Gamanagatti, Shivanand, S524 ([FRI264](#))
 Gambardella, Gennaro, S84 ([OS115](#))
 Gambato, Martina, S306 ([THU423](#)),
 S578 ([FRI376](#)), S815 ([SAT311](#))
 Gambino, Carmine Gabriele, S18 ([OS007](#)),
 S49 ([OS062](#)), S92 ([OS131](#)), S894 ([SAT508](#)),
 S895 ([SAT511](#))
 Gamezardashvili, Ana, S229 ([THU275](#))
 Gami, Yemsrach, S447 ([FRI100](#))
 Gamkrelidze, Amiran, S213 ([THU242](#)),
 S214 ([THU243](#)), S216 ([THU248](#)),
 S219 ([THU253](#)), S221 ([THU258](#)),
 S233 ([THU283](#)), S234 ([THU284](#)),
 S267 ([THU347](#)), S587 ([FRI395](#)),
 S590 ([FRI400](#)), S590 ([FRI401](#))
 Gamkrelidze, Ivane, S43 ([OS050](#)),
 S230 ([THU278](#)), S231 ([THU279](#)),
 S238 ([THU292](#))
 Gamon, Lucie, S122 ([THU009](#))
 Gampa, Anuhya, S372 ([THU567](#)),
 S383 ([THU588](#))
 Gananandan, Kohilan, S889 ([SAT499](#)),
 S903 ([SAT526](#))
 Ganbold, Khatanzul, S235 ([THU287](#))
 Ganchua, Sharie C, S848 ([SAT391](#)),
 S850 ([SAT396](#)), S851 ([SAT397](#))
 Gandhi, Amish, S447 ([FRI100](#))
 Gandicheruvu, Haritha, S137 ([THU035](#))
 Gandon, Yves, S504 ([FRI228](#))
 Gandotra, Akash, S19 ([OS008](#)), S49 ([OS063](#))
 Gane, Edward J., S299 ([THU408](#)),
 S824 ([SAT343](#)), S831 ([SAT357](#)),
 S835 ([SAT365](#)), S836 ([SAT366](#)),
 S837 ([SAT368](#)), S848 ([SAT392](#)),
 S850 ([SAT396](#)), S851 ([SAT397](#)),
 S859 ([SAT412](#)), S867 ([SAT427](#)),
 S871 ([SAT435](#)), S872 ([SAT437](#)),
 S876 ([SAT443](#))
 Gane, Edward J., S16 ([OS004](#)), S58 ([OS073](#)),
 S69 ([OS090](#))
 Ganesh, Nivriti, S98 ([OS140](#))
 Ganger, Daniel, S394 ([FRI008](#))
 Gang, Sujin, S798 ([SAT281](#)), S799 ([SAT282](#))
 Ganiyu, Abdul-Azeez, S110 ([OS161](#))
 Ganizate, Salome, S764 ([SAT213](#))
 Ganne-Carrié, Nathalie, S72 ([OS093](#)),
 S127 ([THU019](#)), S372 ([THU566](#)),
 S504 ([FRI228](#)), S833 ([SAT360](#)),
 S840 ([SAT373](#))
 Gannon, Catherine, S552 ([FRI322](#)),
 S572 ([FRI364](#))
 Gannoun, Lila, S736 ([SAT155](#))
 Ganova-Raeva, Lilia, S221 ([THU258](#))
 Gantzel, Rasmus Hvidbjerg, S418 ([FRI044](#)),
 S611 ([FRI491](#))
 Gao, Bo, S636 ([FRI540](#))
 Gao, Jian-Neng, S595 ([FRI410](#))
 Gao, Jin, S215 ([THU245](#))
 Gao, Jing, S492 ([FRI206](#)), S786 ([SAT262](#)),
 S788 ([SAT265](#))
 Gao, Ning, S723 ([SAT122](#))
 Gao, Rong, S694 ([SAT059](#)), S723 ([SAT123](#)),
 S730 ([SAT140](#)), S735 ([SAT154](#))
 Gao, Xiaoqin, S182 ([THU165](#))
 Gao, Xu, S883 ([SAT488](#))

Author Index

- Gao, Yanhang, S344 ([THU504](#))
Gao, Yinjie, S278 ([THU369](#))
Gao, Zhiliang, S838 ([SAT369](#))
Gárate-Rascón, María, S500 ([FRI222](#)), S644 ([FRI557](#))
Garbin, Marta, S658 ([FRI586](#))
Garcia, Alberto Garcia, S396 ([FRI011](#))
García-Blanco, Agustín, S113 ([OS166](#))
García-Crespo, Carlos, S589 ([FRI399](#))
García-Criado, María Ángeles, S381 ([THU584](#))
Garcia, David O., S912 ([SAT554](#))
Garcia de Frutos, Pablo, S652 ([FRI573](#))
Garcia-Deltoro, Miguel, S229 ([THU276](#))
García, Diego, S555 ([FRI329](#))
Garcia, Federico Garcia, S211 ([THU237](#))
García-Fuentes, Eduardo, S396 ([FRI011](#))
García-García, Francisco, S749 ([SAT183](#))
Garcia-Garcia, Selene, S255 ([THU325](#)), S257 ([THU330](#))
García-Heredia, José Manuel, S48 ([OS060](#))
García, Ines, S624 ([FRI518](#))
Garcia, Jonatan Fernandez, S765 ([SAT214](#))
García-López, Mireia, S53 ([OS067](#)), S99 ([OS141](#)), S263 ([THU340](#)), S286 ([THU385](#))
García-Lozano, María del Rosario, S708 ([SAT087](#))
Garcia, Luis Cortes, S792 ([SAT271](#))
García-Luna, Pedro Pablo, S451 ([FRI106](#))
García-Mediavilla, María-Victoria, S177 ([THU155](#))
Garcia-Monzon, Carmelo, S111 ([OS163](#)), S749 ([SAT183](#))
García-Monzón, Carmelo, S157 ([THU074](#)), S158 ([THU076](#))
García-Nieto, Enrique, S113 ([OS166](#))
Garcia-Ocana, Adolfo, S710 ([SAT091](#))
Garcia-Porrero, Guillermo, S697 ([SAT064](#))
García-Pras, Ester, S99 ([OS141](#)), S263 ([THU340](#)), S286 ([THU385](#))
Garcia, Rafael Rubio, S577 ([FRI373](#))
Garcia-Retortillo, Montserrat, S334 ([THU482](#)), S581 ([FRI384](#))
García-Retortillo, Montserrat, S607 ([FRI468](#))
Garcia-Ruiz, M. Carmen, S59 ([OS074](#)), S361 ([THU530](#)), S465 ([FRI150](#))
Garcia-Tsao, Guadalupe, S339 ([THU494](#)), S619 ([FRI509](#)), S623 ([FRI516](#)), S887 ([SAT496](#))
Garcovich, Matteo, S507 ([FRI234](#))
Gardini, Andrea Casadei, S500 ([FRI222](#)), S643 ([FRI554](#)), S748 ([SAT180](#))
Gargan, Catherine, S239 ([THU294](#))
Garg, Garima, S252 ([THU320](#))
Garg, Harshit, S448 ([FRI102](#)), S452 ([FRI108](#))
Garg, Sumit, S20 ([OS009](#))
Garh, Pratibha, S350 ([THU513](#))
Garlicki, Aleksander, S565 ([FRI350](#))
Garlick, Kelsey, S745 ([SAT177](#))
Garner, Will, S312 ([THU442](#))
Garraus, Moira, S527 ([FRI271](#))
Garrett, Grace, S572 ([FRI364](#))
Garrido, Estefanía Berge, S114 ([OS168](#))
Garrido, Isabel, S282 ([THU377](#))
Garrido, Maria Angeles Lopez, S114 ([OS168](#))
Garrido, Maria Soledad, S931 ([SAT586](#))
Garrido, Marta, S527 ([FRI271](#))
Gart, Eveline, S676 ([SAT024](#)), S677 ([SAT025](#))
Garvey, Cynthia, S570 ([FRI360](#))
Garza, Emilio Calderón, S476 ([FRI172](#))
Garza, Laura Esthela Cisneros, S487 ([FRI195](#))
Gasbarrini, Antonio, S436 ([FRI079](#)), S507 ([FRI234](#)), S549 ([FRI317](#)), S584 ([FRI388](#))
Gasbjerg, Lærke, S121 ([THU006](#))
Gasca, Frida, S487 ([FRI195](#))
Gasparov, Slavko, S700 ([SAT070](#))
Gastaca, Mikel, S114 ([OS168](#))
Gatselis, Nikolaos, S335 ([THU484](#)), S840 ([SAT374](#))
Gattai, Riccardo, S578 ([FRI376](#))
Gattringer, Pia, S854 ([SAT403](#))
Gaudenzi, Roberta, S559 ([FRI336](#))
Gaur, Ashwani, S751 ([SAT187](#))
Gausdal, Gro, S672 ([SAT016](#))
Gautam, Vipul, S528 ([FRI273](#))
Gavalaki, Athena, S218 ([THU251](#))
Gavasso, Sabrina, S358 ([THU526](#))
Gaya, Gerard Baiges, S677 ([SAT027](#)), S678 ([SAT028](#)), S681 ([SAT034](#))
Gayle, Britt, S572 ([FRI364](#))
Gaynor, William, S740 ([SAT163](#))
Gazari, Maria Mercedes Rodriguez, S137 ([THU034](#))
Gaztambide, Sonia, S665 ([SAT001](#))
Geanon, Daniel, S27 ([OS021](#))
Gedara, Chinthaka Mahesh Udamulle, S113 ([OS167](#))
Gee, Heon Yung, S176 ([THU152](#))
Gee Lim, Seng, S13 ([LB004B](#)), S288 ([THU390](#)), S291 ([THU393](#)), S298 ([THU406](#))
Geerts, Anja, S106 ([OS155](#)), S107 ([OS156](#)), S562 ([FRI344](#)), S768 ([SAT230](#)), S913 ([SAT556](#))
Geervliet, Eline, S400 ([FRI018](#)), S405 ([FRI025](#))
Gefen, Maytal, S83 ([OS114](#))
Gegenfurtner, Florian, S760 ([SAT205](#))
Geh, Daniel, S640 ([FRI551](#)), S646 ([FRI561](#))
Geier, Andreas, S166 ([THU092](#)), S425 ([FRI058](#)), S448 ([FRI102](#)), S452 ([FRI108](#)), S662 ([FRI596](#)), S823 ([SAT341](#))
Geisler, Fabian, S11 ([LB003](#)), S38 ([OS042](#)), S189 ([THU180](#)), S339 ([THU493](#))
Geladari, Eleni, S908 ([SAT534](#))
Gellen-Dautremier, Justine, S791 ([SAT269](#))
Gellert-Kristensen, Helene, S161 ([THU082](#))
Gelsomino, Fabio, S84 ([OS115](#))
Gelson, Will, S17 ([OS005](#)), S198 ([THU198](#))
Gemini, Stefano, S91 ([OS129](#))
Gencdal, Genco, S293 ([THU397](#)), S297 ([THU405](#)), S782 ([SAT255](#)), S820 ([SAT316](#))
Genda, Takuya, S172 ([THU103](#))
Genesca, Joan, S149 ([THU059](#)), S180 ([THU161](#)), S365 ([THU538](#)), S370 ([THU548](#)), S440 ([FRI088](#)), S515 ([FRI250](#)), S906 ([SAT530](#))
Geng, Anne, S192 ([THU186](#))
Geng, Jia-wei, S838 ([SAT369](#))
Geng, Lei, S744 ([SAT171](#))
Geng, Shi, S22 ([OS014](#)), S421 ([FRI050](#))
Geng, Yana, S484 ([FRI188](#)), S711 ([SAT092](#))
Genslueckner, Sophie, S428 ([FRI062](#))
Gentilucci, Umberto Vespasiani, S675 ([SAT021](#))
Georgaka, Sokratia, S104 ([OS152](#))
George, Jacob, S19 ([OS008](#)), S49 ([OS063](#)), S154 ([THU069](#)), S302 ([THU415](#)), S431 ([FRI069](#)), S560 ([FRI339](#)), S568 ([FRI356](#))
George, Nivya, S574 ([FRI369](#))
Georgieva, Alexandra, S185 ([THU171](#)), S189 ([THU180](#))
Georgiou, Chrysanthos, S202 ([THU220](#))
Georgopoulou, Urania, S255 ([THU326](#))
Géraud, Cyrill, S463 ([FRI146](#))
Gerber, Athenais, S271 ([THU355](#))
Gerdes, Victor, S9 ([GS011](#))
Gerding, Albert, S539 ([FRI298](#))
Gerhardt, Florian, S148 ([THU057](#)), S379 ([THU581](#)), S860 ([SAT414](#))
Gericke, Martin, S680 ([SAT032](#))
Gerussi, Alessio, S96 ([OS136](#))
Gervais, Anne, S833 ([SAT360](#)), S840 ([SAT373](#))
Getia, Vladimir, S213 ([THU242](#)), S214 ([THU243](#)), S216 ([THU248](#)), S219 ([THU253](#))
Getsios, Spiro, S764 ([SAT212](#))
Gevers, Tom, S306 ([THU431](#)), S308 ([THU435](#)), S315 ([THU447](#)), S525 ([FRI266](#))
Geyer, Joachim, S843 ([SAT380](#))
Geyer, Philipp, S500 ([FRI223](#))
Geyik, Öykü Gönül, S47 ([OS058](#))
Ge, Yueqi, S290 ([THU391](#))
Geyvandova, Natalia, S4 ([GS006](#))
Ghalib, Reem, S427 ([FRI060](#))
Ghallab, Ahmed, S11 ([LB003](#)), S606 ([FRI467](#))
Ghanbari, Mohsen, S86 ([OS120](#))
Ghany, Marc, S264 ([THU341](#))
Ghavemi, Mahyar, S825 ([SAT345](#))
Ghazi-Khansari, Mahmoud, S883 ([SAT487](#))
Gheorghe, Cristian, S625 ([FRI520](#))
Ghesquière, Bart, S346 ([THU507](#))
Ghez, Michaël, S547 ([FRI314](#))
Ghielmetti, Michele, S308 ([THU435](#))
Ghiles, Imerzoukene, S639 ([FRI548](#))
Ghiuchici, Ana-Maria, S930 ([SAT585](#))
Ghorai, Sourav, S745 ([SAT177](#))
Ghorezai, Gul Sabeen Azam, S240 ([THU295](#))
Ghosh, Alip, S571 ([FRI362](#))

- Ghosh, Indrajit, S277 ([THU368](#)), S556 ([FRI330](#))
- Ghosh, Malavika, S494 ([FRI209](#))
- Ghrayeb, Alia, S765 ([SAT214](#))
- Giacchetto, Marco, S387 ([THU599](#))
- Giaccia, Amato, S470 ([FRI159](#))
- Giacofci, Joyce Madison, S656 ([FRI582](#))
- Giambra, Vincenzo, S609 ([FRI487](#))
- Gianatti, Andrea, S751 ([SAT186](#))
- Giannelli, Gianluigi, S763 ([SAT211](#))
- Giannini, Edoardo Giovanni, S578 ([FRI376](#))
- Gian, Yi Lin, S98 ([OS140](#))
- Giard, Jeanne-Marie, S456 ([FRI114](#)), S593 ([FRI407](#)), S805 ([SAT293](#)), S848 ([SAT390](#))
- Gibbons, Carl, S310 ([THU438](#))
- Gibbons, John, S556 ([FRI330](#))
- Gibbons, Karyna, S433 ([FRI073](#))
- Gibert, Benjamin, S766 ([SAT216](#))
- Gielen, Vera, S855 ([SAT405](#))
- Giersch, Katja, S256 ([THU327](#))
- Gigante, Elia, S372 ([THU566](#))
- Giguet, Baptiste, S524 ([FRI265](#))
- Giladi, Hilla, S47 ([OS059](#)), S83 ([OS114](#)), S387 ([THU597](#))
- Gilberg, Mélina, S373 ([THU569](#))
- Gilbert-Marceau, Anika, S373 ([THU569](#))
- Gilgenkrantz, Hélène, S65 ([OS084](#)), S475 ([FRI170](#))
- Gil-Gomez, Antonio, S450 ([FRI105](#)), S708 ([SAT087](#))
- Gilgun-Sherki, Yossi, S714 ([SAT103](#))
- Gillard, Justine, S680 ([SAT031](#))
- Gillberg, Per-Goran, S751 ([SAT187](#))
- Gilles, Hunault, S497 ([FRI216](#))
- Gillevet, Patrick, S67 ([OS087](#)), S130 ([THU023](#))
- Gilligan, Elizabeth, S234 ([THU285](#))
- Gillum, Matthew, S121 ([THU006](#)), S669 ([SAT010](#))
- Gill, Upkar, S55 ([OS070](#)), S284 ([THU380](#))
- Gillyon-Powell, Mark, S44 ([OS053](#))
- Gil, Mar, S365 ([THU538](#))
- Gilmore, Sarah, S251 ([THU317](#))
- Gil-Pitarch, Claudia, S48 ([OS060](#)), S600 ([FRI453](#)), S679 ([SAT029](#))
- Gil-Redondo, Rubén, S671 ([SAT014](#))
- Gilroy, Derek, S55 ([OS070](#))
- Gimeno, Francesc Puchades, S222 ([THU261](#))
- Ginès, Pere, S25 ([OS018](#)), S35 ([OS036](#)), S37 ([OS039](#)), S54 ([OS069](#)), S57 ([OS072A](#)), S63 ([OS080](#)), S136 ([THU033](#)), S139 ([THU039](#)), S157 ([THU074](#)), S158 ([THU076](#)), S511 ([FRI242](#)), S512 ([FRI243](#)), S512 ([FRI244](#)), S684 ([SAT039](#)), S896 ([SAT512](#)), S901 ([SAT522](#)), S902 ([SAT524](#)), S907 ([SAT532](#))
- Gioe, Claudia, S31 ([OS029](#))
- Giometto, Sabrina, S591 ([FRI404](#))
- Giordano, Laura, S923 ([SAT572](#))
- Giosa, Domenico, S259 ([THU333](#))
- Giráldez-Gallego, Alvaro, S127 ([THU018](#))
- Girardi, Enrico, S806 ([SAT294](#)), S808 ([SAT297](#))
- Giraudi, Pablo J., S433 ([FRI071](#))
- Girgrah, Nigel, S432 ([FRI070](#))
- Giri, Dewan, S168 ([THU097](#)), S170 ([THU099](#)), S291 ([THU392](#)), S301 ([THU413](#))
- Girier-Dufournier, Morgane, S297 ([THU404](#))
- Girish, Sandhya, S862 ([SAT417](#))
- Girleanu, Irina, S192 ([THU185](#)), S573 ([FRI368](#))
- Girma, Yabetse, S286 ([THU385](#))
- Girolamo, Vincenzo De, S938 ([SAT599](#))
- Girolstein, Lisann, S145 ([THU051](#))
- Gish, Robert G., S103 ([OS149](#)), S274 ([THU361](#)), S280 ([THU372](#)), S281 ([THU376](#)), S286 ([THU386](#)), S846 ([SAT387](#))
- Gitto, Stefano, S627 ([FRI524](#)), S932 ([SAT588](#))
- Gittus, Matthew, S814 ([SAT308](#))
- Giuffrè, Mauro, S626 ([FRI522](#))
- Giuffrida, Paolo, S387 ([THU599](#))
- Giulante, Felice, S789 ([SAT266](#))
- Giulia, Previtali, S751 ([SAT186](#))
- Giuly, Nathalie, S245 ([THU304](#))
- Giurucin, Michela, S433 ([FRI071](#))
- Giusepponi, Maria Elena, S872 ([SAT436](#))
- Giusti, Gianluca, S888 ([SAT497](#))
- Given, Bruce, S14 ([LB006](#))
- Gjorgjieva, Monika, S645 ([FRI559](#)), S652 ([FRI572](#))
- Glancy, Megan, S266 ([THU345](#))
- Glasgow, Susanne, S498 ([FRI218](#))
- Glebe, Dieter, S843 ([SAT380](#))
- Glenn, Jeffrey, S70 ([OS092](#)), S274 ([THU361](#)), S859 ([SAT412](#))
- Glojnaric, Ines, S702 ([SAT075](#))
- Gluud, Lise Lotte, S154 ([THU068](#)), S331 ([THU477](#)), S499 ([FRI220](#)), S670 ([SAT013](#)), S890 ([SAT501](#))
- Gnass, Esteban, S491 ([FRI204](#))
- Goddard, Chun, S277 ([THU368](#))
- Godoy, Raquel, S910 ([SAT539](#))
- Goedertz, Henri, S304 ([THU419](#))
- Goedken, Michael, S439 ([FRI085](#))
- Goel, Amit, S433 ([FRI072](#)), S620 ([FRI511](#))
- Goel, Ashish, S19 ([OS008](#)), S49 ([OS063](#))
- Goenaga-Infante, Heidi, S530 ([FRI277](#))
- Goeppert, Benjamin, S655 ([FRI581](#)), S927 ([SAT579](#))
- Goetze, Jens Peter, S361 ([THU532](#))
- Goeyvaerts, Nele, S838 ([SAT370](#))
- Goginashvili, Ketevan, S239 ([THU293](#))
- Gogtay, Maya, S235 ([THU286](#))
- Goh, Boon Bee George, S919 ([SAT566](#))
- Gohil, Vikrant, S871 ([SAT435](#))
- Göhlmann, Hinrich, S265 ([THU343](#))
- Goikotxea, Naroa, S48 ([OS060](#)), S84 ([OS116](#)), S87 ([OS122](#)), S132 ([THU027](#)), S177 ([THU155](#)), S600 ([FRI453](#)), S673 ([SAT018](#)), S679 ([SAT029](#)), S689 ([SAT050](#))
- Gokcan, Hale, S778 ([SAT248](#)), S782 ([SAT255](#)), S820 ([SAT316](#)), S858 ([SAT410](#)), S861 ([SAT416](#)), S864 ([SAT421](#))
- Gökçen, Pinar, S858 ([SAT410](#)), S861 ([SAT416](#))
- Golabi, Pegah, S144 ([THU048](#)), S155 ([THU071](#)), S156 ([THU073](#)), S447 ([FRI100](#))
- Golamari, Srinivasa Reddy, S626 ([FRI521](#))
- Goldberg, David, S564 ([FRI348](#)), S769 ([SAT232](#))
- Goldberg, S. Nahum, S764 ([SAT213](#))
- Goldenberg, Daniel, S83 ([OS114](#))
- GoldFarb, David, S43 ([OS051](#))
- Goldin, Robert, S108 ([OS158](#))
- Goldin, Robert D., S34 ([OS034](#)), S132 ([THU026](#))
- Goldmann, Nora, S843 ([SAT380](#))
- Goldring, Amanda, S277 ([THU368](#))
- Goldsmith, Chloe, S246 ([THU306](#))
- Goldsmith, Kerrie, S312 ([THU442](#))
- Goldwasser, Francois, S393 ([FRI007](#))
- Golfieri, Rita, S91 ([OS129](#)), S794 ([SAT273](#))
- Golla, Rithvik, S620 ([FRI511](#))
- Goll, Guro L, S309 ([THU437](#))
- Golovko, George, S194 ([THU191](#))
- Golse, Nicolas, S402 ([FRI020](#)), S815 ([SAT311](#)), S935 ([SAT595](#))
- Gomel, Rachel, S312 ([THU442](#))
- Gomes, Willian, S490 ([FRI201](#))
- Gómez, Alberto, S328 ([THU471](#))
- Gómez- Camarero, Judith, S334 ([THU482](#))
- Gómez-Camarero, Judith, S157 ([THU074](#)), S158 ([THU076](#)), S325 ([THU465](#)), S328 ([THU471](#))
- Gómez, Concepción, S137 ([THU035](#))
- Gomez-Gonzalez, Emilio, S459 ([FRI119](#))
- Gomez, Manuel Romero, S154 ([THU069](#)), S157 ([THU074](#)), S158 ([THU076](#)), S192 ([THU185](#)), S334 ([THU482](#)), S436 ([FRI078](#)), S442 ([FRI092](#)), S444 ([FRI095](#)), S450 ([FRI105](#)), S555 ([FRI329](#)), S671 ([SAT014](#)), S708 ([SAT087](#))
- Gómez, Mercedes Vergara, S334 ([THU482](#))
- Gomez-Muñoz, Neus, S229 ([THU276](#))
- Gómez-Orellana, Antonio M., S3 ([CS005](#)), S114 ([OS168](#))
- Gómez Santos, Beatriz, S651 ([FRI571](#))
- Gompelmann, Daniela, S359 ([THU527](#))
- Gonçalves, João, S192 ([THU185](#))
- Gonen, Tal, S804 ([SAT291](#))
- Gong, Cynthia, S779 ([SAT250](#))
- Gong, Lan, S920 ([SAT568](#))
- Gong, Xiyang, S215 ([THU245](#))
- Goñi, Javier Juampérez, S59 ([OS074](#))
- Gonzaga, Ernesto Robalino, S126 ([THU016](#))
- Gonzalès, Emmanuel, S514 ([FRI248](#)), S519 ([FRI256](#)), S521 ([FRI259](#)), S521 ([FRI260](#))
- González, Águeda, S111 ([OS163](#)), S749 ([SAT183](#))
- Gonzalez, Alvaro Diaz, S328 ([THU471](#))

Author Index

- González-Aseguinolaza, Gloria, S248 (THU310), S257 (THU330)
- González, Belén, S106 (OS154)
- Gonzalez-Carmona, Maria Angeles, S381 (THU585), S915 (SAT559)
- Gonzalez, Daniella, S814 (SAT309)
- González-Gállego, Javier, S177 (THU155), S639 (FRI549)
- González-Gómez, Sara, S570 (FRI361)
- González-Grande, Rocio, S114 (OS168)
- González-Huezo, Maria Sarai, S19 (OS008), S49 (OS063)
- González, José López, S445 (FRI096)
- Gonzalez-Lopez, Marcos Antonio, S113 (OS166)
- González, Lorena Mosteiro, S665 (SAT001)
- González, Luis A Castaño, S665 (SAT001)
- Gonzalez, Maria Angelica Luque, S555 (FRI329)
- González, Noemí, S570 (FRI361)
- González-Recio, Irene, S84 (OS116), S132 (THU027), S600 (FRI453), S679 (SAT029)
- González Rellán, María J., S84 (OS116)
- Gonzalez-Romero, Francisco, S651 (FRI571), S689 (SAT050)
- González-Romero, Francisco, S648 (FRI564), S665 (SAT001)
- Gonzalez-Sanchez, Ester, S673 (SAT018)
- Gonzalo, Ricardo, S368 (THU545)
- Gonzalvez, Francois, S853 (SAT401)
- Goodheart, Richard, S142 (THU044)
- Goodman, Zachary, S318 (THU453), S427 (FRI060), S446 (FRI029), S486 (FRI194), S493 (FRI207), S619 (FRI509), S623 (FRI516)
- Goodwin, Bryan, S745 (THU177)
- Goodyear, Carl, S57 (OS072A)
- Goossens, Nicolas, S457 (FRI115), S754 (SAT192)
- Gopi, Srikanth, S369 (THU547), S635 (FRI538)
- Gora, Baqar, S191 (THU184), S358 (THU525)
- Gordien, Emmanuel, S72 (OS093), S271 (THU355)
- Gordon, Fiona, S416 (FRI041)
- Gordon, Louisa, S204 (THU226)
- Gordon, Michal, S145 (THU049)
- Gordon, Stuart C, S154 (THU069)
- Gorennek, Levent, S858 (SAT411)
- Gores, Gregory, S377 (THU575)
- Gorfine, Tali, S474 (FRI168)
- Gorham, Alexandra, S592 (FRI405)
- Gori, Andrea, S223 (THU263)
- Goria, Odile, S61 (OS076)
- Górnicka, Barbara, S605 (FRI464)
- Gorochov, Guy, S189 (THU181)
- Gorospe, Myriam, S84 (OS116)
- Gorostiza, Olivia, S534 (FRI285)
- Go, Simei, S653 (FRI576), S761 (SAT207), S762 (SAT209)
- Gosink, Brian, S708 (SAT088)
- Gosnell, Joseph, S470 (FRI160), S485 (FRI190)
- Gossez, Morgane, S356 (THU522)
- Gottardi, Davide, S180 (THU161)
- Gottfredsson, Magnús, S573 (FRI366)
- Gottlieb, Eyal, S765 (SAT214)
- Götz, Alexandra, S178 (THU157)
- Goudarzi, Negin, S735 (SAT153)
- Goudsmit, Ben, S798 (SAT280)
- Gough, John, S498 (FRI218)
- Gougol, Amir, S137 (THU035)
- Goulder, Philip, S285 (THU382)
- Goulis, Ioannis, S218 (THU251), S840 (SAT374)
- Gounder, Prabhu, S831 (SAT356)
- Gountas, Ilias, S202 (THU220)
- Gournay, Jérôme, S5 (GS007)
- Gouttenoire, Jérôme, S97 (OS138), S253 (THU322)
- Gouveia, Catarina Ferreira, S537 (FRI293)
- Govaere, Olivier, S7 (GS009), S11 (LB003), S437 (FRI080), S437 (FRI081), S704 (SAT081), S721 (SAT118), S733 (SAT146)
- Govaerts, Liesbeth, S303 (THU416)
- Gow, Paul, S3 (GS005), S389 (FRI002), S441 (FRI090)
- Goyal, Ashish, S588 (FRI396)
- Grabherr, Felix, S126 (THU017)
- Grabmeier-Pfistershammer, Katharina, S555 (FRI328)
- Grabner, Gernot, S688 (SAT049)
- Graceffa, Pietro, S624 (FRI517)
- Grace, Josephine, S134 (THU029)
- Gracen, Lucy, S172 (THU102)
- Graf, Christiana, S15 (OS001), S16 (OS003), S585 (FRI391)
- Graf, Erika, S80 (OS108)
- Graham, Hiba, S731 (SAT142)
- Gramignoli, Roberto, S735 (SAT153)
- Gram-Kampmann, Eva-Marie, S9 (GS012)
- Gramlich, Leah, S890 (SAT500)
- Grammatikopoulos, Tassos, S519 (FRI256), S521 (FRI259)
- Grander, Christoph, S126 (THU017)
- Grandt, Josephine, S154 (THU068), S331 (THU477)
- Grand, Xavier, S246 (THU306)
- Grarup, Niels, S450 (FRI104)
- Grasset, Estelle, S717 (SAT110)
- Grassi, Germana, S806 (SAT294)
- Grassini, Maria Vittoria, S387 (THU599)
- Gratacós-Gines, Jordi, S63 (OS080), S127 (THU018), S136 (THU033), S139 (THU039), S511 (FRI242), S512 (FRI243), S896 (SAT512), S901 (SAT522), S902 (SAT524), S907 (SAT532)
- Graupera, Isabel, S25 (OS018), S35 (OS036), S37 (OS039), S63 (OS080), S91 (OS128), S139 (THU039), S511 (FRI242), S512 (FRI243), S512 (FRI244), S684 (SAT039), S896 (SAT512), S901 (SAT522), S902 (SAT524), S907 (SAT532)
- Graus, Javier, S115 (OS169)
- Gravely, Annabel, S801 (SAT287)
- Graversen, Jonas, S423 (FRI054), S434 (FRI074)
- Graves, Ingrid, S848 (SAT391), S850 (SAT395)
- Gray, Christen, S411 (FRI033)
- Gray, Elizabeth H., S401 (FRI019)
- Gray, Kevin, S850 (SAT396), S851 (SAT397), S876 (SAT443)
- Graziadei, Ivo, S829 (SAT353), S830 (SAT354)
- Grazia Rumi, Maria, S578 (FRI376)
- Grazi, Gianluca, S107 (OS157)
- Greasley, Peter, S609 (FRI486)
- Grebely, Jason, S565 (FRI349), S568 (FRI356)
- Greenaway, Christina, S206 (THU230)
- Green, Ellen, S779 (SAT250)
- Greenland, Lindsay, S812 (SAT304)
- Greenman, Raanan, S27 (OS022)
- Greenwood-Smith, Belinda, S239 (THU294)
- Gregori, Josep, S255 (THU325), S257 (THU330)
- Gregory, Dyanna, S786 (SAT262), S788 (SAT265)
- Greig, Carolyn, S364 (THU537)
- Greinert, Robin, S369 (THU546), S620 (FRI510)
- Greizer, Tim, S745 (SAT177)
- Grelli, Sandro, S249 (THU313)
- Gremmel, Thomas, S362 (THU534)
- Grepper, Sue, S488 (FRI197)
- Grgurević, Ivica, S612 (FRI494)
- Grgurević, Lovorka, S612 (FRI494)
- Gribben, Christopher, S742 (SAT167)
- Grieco, Antonio, S436 (FRI079), S507 (FRI234)
- Griemsmann, Marie, S893 (SAT505)
- Griep, Linda Oude, S815 (SAT310)
- Griffin, Julian L., S695 (SAT061)
- Griffin, Simon, S815 (SAT310)
- Griffiths, Bill, S515 (FRI250)
- Grigoletto, Antonella, S378 (THU578)
- Grigoli, Eleonora Giacomuzzi, S428 (FRI061)
- Grigorescu, Raluca Roxana, S795 (SAT276)
- Grigoriadis, Aristeidis, S333 (THU480)
- Grillo-Risco, Ruben, S749 (SAT183)
- Grimaudo, Stefania, S703 (SAT077)
- Grimm, Dirk, S265 (THU344)
- Grimmer, Katharine, S419 (FRI045)
- Grimsrud, Marit M., S77 (OS103)
- Grinderslev, Søren, S550 (FRI319)
- Gringeri, Enrico, S306 (THU423)
- Grinshpan, Laura Sol, S148 (THU056)
- Grip, Emilie Toresson, S413 (FRI035)
- Gripon, Philippe, S258 (THU331)
- Groba, Sara Reinartz, S313 (THU444)
- Groenbaek, Lisbet, S314 (THU446)
- Groen, Bert, S9 (GS011)
- Groendal, Sturla M., S672 (SAT016)
- Groentved, Lars, S423 (FRI054), S434 (FRI074)
- Gromak, Mikhail, S657 (FRI583)
- Gromski, Mark, S95 (OS135)

- Grønbaek, Henning, S418 (FRI044), S611 (FRI491)
- Grooshuismink, Anthony, S194 (THU190)
- Groot Koerkamp, Bas, S652 (FRI574)
- Gros, Olga, S383 (THU590)
- Gross, Annika, S533 (FRI282)
- Gross, Steve, S133 (THU028)
- Grottenthaler, Julia, S823 (SAT341)
- Grova, Mauro, S387 (THU599)
- Grove, Jane, S22 (OS013), S465 (FRI151)
- Grover, Gagandeep Singh, S232 (THU280)
- Grubbs, Rachel K., S886 (SAT493)
- Grude, Sine, S841 (SAT375)
- Grünberger, Thomas, S470 (FRI159), S788 (SAT264), S799 (SAT283)
- Grupper, Ayelet, S790 (SAT268)
- Grushevskaya, Halina, S269 (THU351)
- Grzyb, Krzysztof, S178 (THU157)
- Gschwantler, Michael, S545 (FRI309), S555 (FRI328), S829 (SAT353), S830 (SAT354)
- Gualandi, Noemi, S795 (SAT275)
- Guan, Yu-juan, S838 (SAT369)
- Guaraldi, Giovanni, S31 (OS029), S795 (SAT275)
- Guarasci, Kellie, S240 (THU297)
- Guarino, Maria, S769 (SAT233)
- Guarner, Carlos, S886 (SAT494), S900 (SAT520)
- Guarracino, Marco, S938 (SAT599)
- Gu, Baohua, S854 (SAT404)
- Gubbay, Yehuda, S742 (SAT166)
- Guckenbiehl, Sabrina, S340 (THU495), S341 (THU498)
- Gudas, Lorraine, S133 (THU028)
- Gudd, Cathrin, S185 (THU173)
- Guéant, Jean-Louis, S905 (SAT529), S923 (SAT573)
- Guedes, Mayra Machado Fleury, S307 (THU432)
- Guedes, Tiago Pereira, S304 (THU420)
- Guelow, Karsten, S241 (THU298), S663 (FRI599)
- Guendogdu, Mehtap, S586 (FRI393)
- Guenneq, Adrien Le, S176 (THU153), S670 (SAT011)
- Guerola, Barbara Torres, S527 (FRI271)
- Guerra, Anna Francesca, S839 (SAT371)
- Guerra, Julia Esteves, S307 (THU432)
- Guerra, Laura, S527 (FRI271)
- Guerra, Manuel Hernández, S237 (THU290), S334 (THU482)
- Guerra, Patricia, S137 (THU034)
- Guerra Veloz, Maria, S594 (FRI409)
- Guerrero, Antonio, S381 (THU584)
- Guerrero, Marta, S150 (THU061), S792 (SAT271)
- Guerrini, Gian Piero, S795 (SAT275)
- Guettier, Catherine, S402 (FRI020), S935 (SAT595)
- Gugenheim, Jean, S772 (SAT239), S780 (SAT252), S817 (SAT312)
- Guglielmi, Alfredo, S658 (FRI586), S796 (SAT277), S920 (SAT567), S925 (SAT574)
- Guha, Neil, S17 (OS005)
- Guida, Alice, S659 (FRI588)
- Guido, Maria, S478 (FRI176)
- Guidotti, Luca, S97 (OS139)
- Guijo-Rubio, David, S3 (GS005)
- Guillaud, Olivier, S538 (FRI296)
- Guillaumet, Montserrat, S64 (OS082)
- Guillén, Gabriela, S527 (FRI271)
- Guillén-Navarro, Encarna, S60 (OS075)
- Guilliams, Martin, S655 (FRI580)
- Guillot, Adrien, S684 (SAT040)
- Guillot, Max, S20 (OS010)
- Guillou, Hervé, S65 (OS084)
- Guinard-Azadian, Carine, S864 (SAT422)
- Guix, Marta García, S91 (OS128)
- Gu, Jiaping, S215 (THU245)
- Gulab, Muraduddin, S560 (FRI338)
- Gulamhusein, Aliya, S62 (OS078), S313 (THU443), S335 (THU484)
- Gulbani, Lasha, S229 (THU275)
- Gulka, Chris, S508 (FRI236), S918 (SAT564)
- Gulsen, Murat Taner, S820 (SAT316)
- Gulsin, Gaurav, S409 (FRI031)
- Gumusoy, Mesut, S293 (THU397), S297 (THU405), S414 (FRI037), S778 (SAT248)
- Gunal, Murat, S615 (FRI499)
- Gunal, Ozgur, S858 (SAT411)
- Gunduz, Feyza, S19 (OS008), S49 (OS063), S858 (SAT410), S861 (SAT416), S864 (SAT421)
- Guner, Rahmet, S858 (SAT411)
- Gunes, Aysim, S456 (FRI114)
- Gunjan, Deepak, S369 (THU547), S633 (FRI534), S635 (FRI538)
- Gunn, Madison, S592 (FRI405)
- Gunn, Nadege, S427 (FRI060)
- Günsar, Fulya, S294 (THU399), S399 (FRI015), S782 (SAT255), S820 (SAT316)
- Gunton, James, S898 (SAT516)
- Gunton, Jenny, S743 (SAT169)
- Gunzer, Matthias, S340 (THU495)
- Guo, Aili, S155 (THU070)
- Guo, Beibei, S66 (OS086), S744 (SAT172), S745 (SAT173), S803 (SAT289)
- Guo, Haitao, S264 (THU341)
- Guo, Ping, S526 (FRI268)
- Guo, Ruoling, S837 (SAT367)
- Guo, Wanjun, S726 (SAT128), S726 (SAT129)
- Guo, Wengang, S92 (OS130), S619 (FRI508), S628 (FRI526)
- Guo, Xiaolin, S70 (OS091)
- Guo, Xiaoqing, S636 (FRI540)
- Guo, Ying, S636 (FRI540), S838 (SAT369)
- Gupta, Ekta, S221 (THU259)
- Gupta, Kapish, S740 (SAT163)
- Gupta, Kusum, S733 (SAT145), S824 (SAT343), S846 (SAT386), S853 (SAT401)
- Gupta, Neil, S598 (FRI418)
- Gupta, Rajat, S500 (FRI223)
- Gupta, Ruchi, S483 (FRI187), S684 (SAT040)
- Gupta, Sneha V., S69 (OS090), S831 (SAT357)
- Gupta, Soumi, S540 (FRI299)
- Gupte, Girish, S518 (FRI255), S519 (FRI256), S521 (FRI259)
- Gur, Merve, S294 (THU399)
- Gusev, Denis, S12 (LB004A), S13 (LB004B), S880 (SAT452), S881 (SAT453)
- Gu, Shengwang, S838 (SAT369)
- Gustein, David, S58 (OS073)
- Gustot, Thierry, S124 (THU012), S192 (THU185)
- Gute, Peter, S15 (OS001)
- Gutierrez Atemis, Alejandro, S554 (FRI326)
- Gut, Marta, S113 (OS166)
- Gu, Wenyi, S353 (THU517), S354 (THU518), S502 (FRI226)
- Guyader, Dominique, S72 (OS093)
- Guy, Cynthia, S443 (FRI093), S451 (FRI107), S486 (FRI193)
- Gu, Ye, S22 (OS014), S70 (OS091), S182 (THU165)
- Guyen, Bich N., S456 (FRI114)
- Guzelbulut, Fatih, S861 (SAT416), S864 (SAT421)
- Guzmán, Elina Muriel, S263 (THU339)
- Gvinjilia, Lia, S214 (THU243), S233 (THU283), S267 (THU347), S587 (FRI395), S590 (FRI400), S590 (FRI401)
- Gwak, Geum-Yon, S273 (THU359)
- Gwaltney, Chad, S517 (FRI253)
- Haan, Claude, S662 (FRI596)
- Haar, Geoffrey, S389 (FRI002)
- Haas, Joel, S692 (SAT055)
- Habboub, Nadeen, S179 (THU158)
- Habibi, Anoosha, S791 (SAT269)
- Habib, Mariam, S188 (THU178)
- Habib, Nagy, S108 (OS158)
- Habtesion, Abeba, S366 (THU539)
- Hackl, Hubert, S799 (SAT283)
- Hackl, Matthias, S799 (SAT283)
- Hackl, Michael, S21 (OS012), S891 (SAT502)
- Hadar, Eran, S774 (SAT241)
- Haddon, Lacey, S660 (FRI591)
- Hadji, Abbas, S294 (THU400)
- Hadjihambi, Anna, S670 (SAT011)
- Hadrup, Sine Reker, S271 (THU356)
- Haegle, Steffanie, S788 (SAT264)
- Haffner-Krausz, Rebecca, S83 (OS114)
- Hafner, Christine, S753 (SAT189)
- Haga, Hiroaki, S875 (SAT442)
- Haga, Hironori, S183 (THU167)
- Haga, Sanae, S822 (SAT319)
- Hagenunger, Arno, S904 (SAT528)
- Hagiwara, May, S491 (FRI204)
- Hagström, Hannes, S24 (OS016), S30 (OS026), S82 (OS112), S119 (THU002), S123 (THU010), S141 (THU041), S189 (THU179),

Author Index

- S413 ([FRI035](#)), S423 ([FRI053](#)),
S530 ([FRI275](#))
- Hahn, Gareth, S188 ([THU178](#))
- Hahn, Magdalena, S860 ([SAT414](#)),
S931 ([SAT587](#))
- Hahn, Sihoun, S1 ([GS001](#))
- Haiden, Lena, S374 ([THU570](#)),
S380 ([THU582](#))
- Haigh, Laura, S733 ([SAT146](#))
- Hajarizadeh, Behzad, S302 ([THU415](#)),
S560 ([FRI339](#)), S561 ([FRI343](#)),
S565 ([FRI349](#)), S568 ([FRI356](#))
- Hald, Annemette, S818 ([SAT314](#))
- Halfon, Philippe, S270 ([THU352](#))
- Halford, Rachel, S44 ([OS053](#)),
S220 ([THU256](#))
- Halilbasic, Emina, S315 ([THU449](#))
- Hall, Andrew, S737 ([SAT157](#))
- Hallenborg, Philip, S758 ([SAT200](#))
- Haller, Alexandre, S758 ([SAT199](#))
- Haller, Rosa, S179 ([THU159](#))
- Hall, Isabelle, S132 ([THU026](#))
- Hallouche, Nabil, S579 ([FRI381](#))
- Hall, Samuel, S842 ([SAT377](#))
- Hallsworth, Kate, S437 ([FRI080](#)),
S721 ([SAT118](#))
- Hall, Tracey, S526 ([FRI268](#))
- Halonon, Juha, S611 ([FRI492](#)),
S615 ([FRI500](#))
- Halperin, Rebecca, S784 ([SAT258](#))
- Halperin, Tami, S790 ([SAT268](#))
- Hamada, Michito, S702 ([SAT076](#))
- Hamaguchi, Yuhei, S883 ([SAT488](#))
- Hamdan, Nashla, S395 ([FRI010](#))
- Hameed, Huma, S639 ([FRI548](#))
- Hamesch, Karim, S313 ([THU444](#)),
S515 ([FRI250](#))
- Hamid, Azlinda, S433 ([FRI073](#))
- Hamid, Saeed Sadiq, S154 ([THU069](#)),
S209 ([THU234](#)), S240 ([THU295](#)),
S274 ([THU361](#)), S558 ([FRI335](#)),
S859 ([SAT412](#))
- Hamill, Michael, S718 ([SAT112](#))
- Hamill, Victoria, S17 ([OS005](#))
- Hamilton, Aaron, S246 ([THU306](#)),
S247 ([THU307](#))
- Hamilton-Dutoit, Stephen, S677 ([SAT026](#))
- Hamilton, James, S14 ([LB006](#))
- Hamilton-Shield, Julian, S416 ([FRI041](#))
- Hammad, Seddik, S489 ([FRI200](#))
- Hammar, Niklas, S24 ([OS016](#)),
S119 ([THU002](#))
- Hammar, Ulf, S40 ([OS045](#))
- Hammond, Nigel, S104 ([OS152](#))
- Hammond, Rachel, S834 ([SAT362](#))
- Hamon, Annaig, S639 ([FRI548](#))
- Hampe, Jochen, S11 ([LB002](#))
- Hanafy, Amr, S616 ([FRI502](#))
- Hanafy, Nemany A. N., S763 ([SAT211](#))
- Han, Bin, S244 ([THU302](#)), S247 ([THU309](#)),
S845 ([SAT385](#))
- Han, Dai Hoon, S653 ([FRI575](#))
- Handanagic, Senad, S214 ([THU243](#)),
S234 ([THU284](#)), S588 ([FRI397](#))
- Hand, James, S188 ([THU178](#))
- Han, Dong, S244 ([THU302](#)), S247 ([THU308](#)),
S247 ([THU309](#)), S841 ([SAT376](#)),
S845 ([SAT385](#))
- Handyside, Britta, S534 ([FRI285](#)),
S540 ([FRI299](#))
- Hanemaaijer, Roeland, S677 ([SAT025](#)),
S685 ([SAT043](#))
- Han, Eui Soo, S798 ([SAT281](#))
- Hanf, Remy, S359 ([THU528](#))
- Han, Guohong, S92 ([OS130](#)), S619 ([FRI508](#)),
S621 ([FRI512](#)), S628 ([FRI526](#)),
S630 ([FRI529](#))
- Han, Hyosun, S794 ([SAT274](#))
- Haniffa, Muzlifah, S55 ([OS070](#))
- Hanif, Muhammad Farooq, S884 ([SAT489](#))
- Han, Ji Won, S932 ([SAT589](#))
- Han, Khin, S134 ([THU030](#))
- Han, Khin Aye Wint, S594 ([FRI409](#)),
S812 ([SAT304](#))
- Han, Kyungdo, S100 ([OS144](#))
- Hanley, Karen Piper, S104 ([OS152](#))
- Hanley, Neil, S104 ([OS152](#))
- Hannah, Nicholas, S622 ([FRI513](#))
- Hann, Hie-Won L, S836 ([SAT366](#))
- Hansasuta, Pokrath, S772 ([SAT238](#)),
S812 ([SAT305](#))
- Hansdottir, Ingunn, S573 ([FRI366](#))
- Hansen, Anne Tybjaerg, S161 ([THU082](#)),
S533 ([FRI284](#))
- Hansen, Bettina, S3 ([GS004](#)), S62 ([OS078](#)),
S281 ([THU374](#)), S313 ([THU443](#)),
S317 ([THU452](#)), S322 ([THU461](#)),
S323 ([THU462](#)), S335 ([THU484](#)),
S569 ([FRI359](#)), S849 ([SAT394](#)),
S852 ([SAT400](#)), S861 ([SAT415](#))
- Hansen, Camilla Dalby, S2 ([GS002](#)),
S129 ([THU021](#)), S131 ([THU024](#)),
S434 ([FRI074](#)), S475 ([FRI171](#))
- Hansen, Daniel, S423 ([FRI054](#)),
S758 ([SAT200](#))
- Hansen, Frederik Orm, S418 ([FRI044](#))
- Hansen, Henrik B., S661 ([FRI593](#)),
S669 ([SAT010](#)), S724 ([SAT124](#))
- Hansen, Jakob Schiøler, S713 ([SAT102](#)),
S720 ([SAT116](#))
- Hansen, Johanne Kragh, S2 ([GS002](#)),
S35 ([OS036](#)), S131 ([THU024](#)),
S475 ([FRI171](#))
- Hansen, Scott, S713 ([SAT101](#))
- Hansen, Svend Hoime, S887 ([SAT495](#))
- Hansen, Torben, S2 ([GS002](#)), S9 ([GS012](#)),
S129 ([THU021](#)), S131 ([THU024](#)),
S450 ([FRI104](#)), S500 ([FRI223](#)),
S523 ([FRI263](#))
- Hanses, Frank, S339 ([THU493](#))
- Han, Seungbong, S275 ([THU363](#)),
S610 ([FRI488](#)), S833 ([SAT361](#))
- Hanslik, Bertrand, S270 ([THU352](#))
- Hanson, Christina, S310 ([THU439](#)),
S332 ([THU478](#))
- Han, Steven-Huy B, S836 ([SAT366](#)),
S848 ([SAT390](#))
- Han, Tao, S883 ([SAT488](#))
- Hao, Shaorui, S803 ([SAT289](#))
- Ha, Phil, S366 ([THU540](#))
- Harasym, Troy O., S848 ([SAT391](#)),
S848 ([SAT392](#))
- Harder, Lea Mørch, S7 ([GS009](#))
- Hardikar, Winita, S521 ([FRI259](#))
- Hardisty, Gareth, S28 ([OS023](#))
- Hardt, Olaf, S748 ([SAT181](#))
- Hardwigsen, Jean, S772 ([SAT239](#)),
S780 ([SAT252](#)), S817 ([SAT312](#))
- Hargreaves, Carol Anne, S869 ([SAT431](#))
- Harif, Yael, S64 ([OS081](#)), S774 ([SAT241](#)),
S793 ([SAT272](#)), S855 ([SAT406](#))
- Harms, Maren, S330 ([THU476](#))
- Harputluoglu, Muhsin Murat,
S782 ([SAT255](#))
- Harputluoglu, Murat, S820 ([SAT316](#)),
S861 ([SAT416](#))
- Harrer, Caroline, S541 ([FRI301](#))
- Harring, Michael, S155 ([THU071](#)),
S785 ([SAT260](#)), S810 ([SAT300](#))
- Harrington, Claire, S786 ([SAT262](#)),
S788 ([SAT265](#))
- Harris, M. Scott, S88 ([OS124](#))
- Harris, Nicola, S120 ([THU004](#)),
S188 ([THU178](#)), S639 ([FRI547](#)),
S647 ([FRI562](#))
- Harrison, Stephen, S14 ([LB005](#)),
S31 ([OS028](#)), S32 ([OS030](#)), S75 ([OS101](#)),
S87 ([OS121](#)), S88 ([OS124](#)),
S409 ([FRI030](#)), S416 ([FRI040](#)),
S419 ([FRI045](#)), S422 ([FRI052](#)),
S425 ([FRI058](#)), S444 ([FRI095](#)),
S448 ([FRI102](#)), S452 ([FRI108](#)),
S453 ([FRI109](#)), S495 ([FRI210](#)),
S619 ([FRI509](#)), S623 ([FRI516](#)),
S711 ([SAT094](#)), S719 ([SAT114](#)),
S726 ([SAT130](#)), S730 ([SAT139](#)),
S732 ([SAT143](#)), S762 ([SAT208](#))
- Harris, Rebecca, S145 ([THU050](#))
- Hartel, Gunter, S204 ([THU226](#))
- Hartleben, Björn, S784 ([SAT259](#))
- Hartl, Johannes, S333 ([THU481](#))
- Hartl, Lukas, S18 ([OS007](#)), S92 ([OS131](#)),
S359 ([THU527](#)), S390 ([FRI003](#)),
S532 ([FRI280](#)), S535 ([FRI287](#)),
S545 ([FRI309](#)), S555 ([FRI328](#)),
S617 ([FRI505](#)), S629 ([FRI527](#)),
S629 ([FRI528](#)), S631 ([FRI531](#)),
S632 ([FRI533](#)), S829 ([SAT353](#))
- Hartmann, Daniel, S185 ([THU171](#)),
S463 ([FRI146](#)), S471 ([FRI161](#)),
S690 ([SAT051](#))
- Harvald, Gustav Bang, S550 ([FRI319](#))
- Harzandi, Azadeh, S68 ([OS089](#))
- Haschemi, Arvand, S665 ([SAT002](#))
- Hasegawa, Akira, S295 ([THU401](#))
- Haselberger, Martina, S339 ([THU493](#))
- Hasenberg, Mike, S264 ([THU342](#))
- Haslinger, Katharina, S390 ([FRI003](#))
- Hasnain, Aliya, S558 ([FRI335](#)),
S560 ([FRI338](#))
- Hasnain, Sumaira, S190 ([THU183](#))
- Hasoon, Megan, S437 ([FRI081](#))

- Hassanein, Tarek, S427 (FRI060), S713 (SAT101), S836 (SAT366), S848 (SAT390)
- Hassan, Fadi, S399 (FRI017)
- Hassan, Hozeifa Mohamed, S357 (THU524), S803 (SAT289)
- Hassoun, Ziad, S593 (FRI407), S805 (SAT293)
- Hastie, David, S203 (THU224), S204 (THU225)
- Haston, Kelly, S31 (OS028), S37 (OS041), S762 (SAT208)
- Hata, Koichiro, S183 (THU167)
- Hatami, Behzad, S228 (THU273)
- Hatano, Etsuro, S183 (THU167)
- Hatchett, Joanne, S312 (THU442)
- Hatta, Ayiesha, S805 (SAT292)
- Hatting, Maximilian, S7 (GS009), S385 (THU594)
- Hatzakis, Angelos, S218 (THU251)
- Hauptmann, Anna, S369 (THU546)
- Haveri, Ajay, S19 (OS008), S49 (OS063)
- Hayakawa, Yuka, S379 (THU580)
- Hayardeny, Liat, S474 (FRI168), S671 (SAT014)
- Hayashi, Hideki, S430 (FRI067)
- Haydel, Brandy, S317 (THU452)
- Hayden, Jennifer, S334 (THU483)
- Ha, Yeonjung, S862 (SAT418)
- Hayes, Peter, S17 (OS005), S19 (OS008), S49 (OS063), S397 (FRI013), S434 (FRI075), S625 (FRI520), S712 (SAT096)
- Haynes, Katelin, S204 (THU226)
- Hay, Ophir, S27 (OS022)
- Hayward, Kelly, S172 (THU102), S204 (THU226)
- Hazarika, Gautam, S299 (THU409)
- Healy, Brendan, S548 (FRI316)
- Heaton, Nigel, S120 (THU004), S403 (FRI022), S647 (FRI562), S647 (FRI563), S650 (FRI569), S818 (SAT315)
- Hebner, Christy, S871 (SAT434)
- Hechelhammer, Lukas, S937 (SAT598)
- Hecke, Annelies Van, S913 (SAT556)
- Hecker, Teresa, S898 (SAT516)
- Heeke, Christina, S271 (THU356)
- Hees, Stijn Van, S852 (SAT400)
- Heffernan, Gavin, S848 (SAT391)
- Hegel, Johannes Kolja, S937 (SAT597)
- Heglar, Brian, S534 (FRI285)
- Hegmar, Hannes, S30 (OS026)
- He, Haiying, S832 (SAT359), S865 (SAT423)
- He, Handan, S70 (OS091)
- Heide, Danijela, S47 (OS059), S649 (FRI565)
- Heider, Dominik, S378 (THU579)
- Heikenwälder, Mathias, S11 (LB003), S38 (OS042), S47 (OS059), S83 (OS114), S649 (FRI565), S655 (FRI581)
- Heil, Franz Josef, S80 (OS108)
- Heilig, Christoph, S655 (FRI581)
- Heil, Marantha, S246 (THU306), S247 (THU307)
- Heimanson, Zeev, S899 (SAT517)
- Heimisdottir, Maria, S573 (FRI366)
- Heim, Kathrin, S54 (OS068), S196 (THU194)
- Heim, Markus, S192 (THU186)
- Heindryckx, Femke, S368 (THU543), S645 (FRI558)
- Heinemann, Melina, S325 (THU466)
- Hein, Moritz, S907 (SAT531)
- Heinrich, Sophia, S783 (SAT257)
- Heinzmann, Alexandra C.A., S193 (THU187)
- Heinz Weiss, Karl, S11 (LB002)
- Hejblum, Gilles, S17 (OS006)
- He, Jingchun, S559 (FRI337)
- Hejn, Kamilla, S758 (SAT200)
- Helal, Abdelaleem, S792 (SAT270)
- Helgesson, Samuel, S683 (SAT038)
- Heling, Dominik, S381 (THU585)
- Hellard, Margaret, S541 (FRI302), S550 (FRI318)
- Heller, Theo, S70 (OS092)
- Hellwig, Kerstin, S339 (THU493)
- Helmke, Steve, S633 (FRI535)
- Helmy, Sherine, S16 (OS004)
- He, Lulu, S402 (FRI021), S803 (SAT289)
- Heluwaert, Frederic, S833 (SAT360), S840 (SAT373)
- Hemati, Hamed, S752 (SAT188)
- Hemming Karlsen, Tom, S605 (FRI465)
- Henderson, Julie, S554 (FRI327)
- Henderson, Louise, S201 (THU219)
- Henderson, Walter, S455 (FRI112)
- Heneghan, Michael, S96 (OS137), S134 (THU030), S371 (THU550), S403 (FRI022), S771 (SAT236), S812 (SAT304)
- Hengstler, Jan G., S11 (LB003), S38 (OS042), S489 (FRI200), S606 (FRI467)
- Henkemeyer, Mark, S113 (OS167)
- Hennan, Jim, S75 (OS101), S711 (SAT094)
- Hennlich, Barbara, S545 (FRI309)
- Hennuyer, Nathalie, S692 (SAT055)
- Henrar, Roland, S611 (FRI492), S615 (FRI500)
- Henrion, Jean, S131 (THU025)
- Henrion, Marc, S23 (OS015)
- Henrique, Mariana Moura, S192 (THU185)
- Henry, Austin, S144 (THU048)
- Henry, Christiani Jeyakumar, S890 (SAT500)
- Henry, Eugenia, S443 (FRI093), S486 (FRI193)
- Henry, Linda, S5 (GS008), S144 (THU048), S154 (THU069), S155 (THU071), S156 (THU073), S429 (FRI064), S445 (FRI097), S785 (SAT260), S810 (SAT300)
- Henshaw, Josh, S540 (FRI299)
- Henze, Lara, S325 (THU466)
- Heo, Jeong, S13 (LB004B), S288 (THU389), S288 (THU390), S291 (THU393), S569 (FRI357), S572 (FRI365), S586 (FRI392), S872 (SAT437), S881 (SAT453)
- Heo, Nae-Yun, S572 (FRI365)
- He, Qibin, S22 (OS014)
- Herber, Adam, S904 (SAT528), S931 (SAT587)
- Herbrecht, Jean-Étienne, S20 (OS010)
- Hercun, Julian, S70 (OS092), S593 (FRI407), S805 (SAT293)
- Heredea, Darius, S930 (SAT585)
- Hergalant, Sébastien, S923 (SAT573)
- Herin, Joris, S584 (FRI389)
- Hermabessiere, Paul, S101 (OS146)
- Hermabessière, Paul, S73 (OS096), S74 (OS099), S833 (SAT360)
- Hermann, Ken, S378 (THU579)
- Hermann, Pernille, S9 (GS012)
- Hermanns, Heike, S662 (FRI596)
- Hermán-Sánchez, Natalia, S48 (OS060)
- Hermans-Borgmeyer, Irm, S83 (OS114)
- Hermie, Laurens, S107 (OS156)
- Hernandez, Anjara, S137 (THU035)
- Hernandez, Anna, S199 (THU199)
- Hernández, Candido, S268 (THU348), S581 (FRI384), S586 (FRI393), S587 (FRI394)
- Hernandez, Christine, S547 (FRI314)
- Hernández, Francisco Andrés Pérez, S581 (FRI384), S931 (SAT586)
- Hernandez-Gea, Virginia, S54 (OS069), S57 (OS072A), S136 (THU033), S367 (THU542), S502 (FRI226), S524 (FRI265), S630 (FRI529)
- Hernandez, Jose Luis Perez, S19 (OS008), S49 (OS063)
- Hernandez, Larissa, S487 (FRI195)
- Hernandez, Nélia, S308 (THU435)
- Hernandez, Rocio Munoz, S450 (FRI105), S708 (SAT087)
- Hernández, Rosario, S63 (OS080)
- Hernandez, Ubaldo Benitez, S573 (FRI366)
- Herola, Antonio Garcia, S268 (THU348), S586 (FRI393), S587 (FRI394)
- Heron, Jon, S416 (FRI041)
- Herraez, Elisa, S59 (OS074)
- Herrán, Aitor Odriozola, S624 (FRI518), S774 (SAT242)
- Herranz, Andrea, S218 (THU252)
- Herranz, Jose Maria, S643 (FRI554), S697 (SAT064)
- Herranz, José María, S112 (OS165), S500 (FRI222), S644 (FRI557)
- Herrema, Hilde, S9 (GS011)
- Herrero, Francisco Sanz, S222 (THU261)
- Herrero, Jose Ignacio, S114 (OS168), S150 (THU061), S406 (FRI027), S792 (SAT271), S802 (SAT288)
- Herrero, Laura, S749 (SAT183)
- Herrmann, Eva, S15 (OS001)
- Hershkovich, Leeor, S851 (SAT398)
- Herta, Toni, S148 (THU057), S823 (SAT341), S860 (SAT414)
- He, Ruiling, S636 (FRI540)
- Hervás, César, S3 (GS005)
- Herve, Hugo, S715 (SAT105)
- Hervet, Jeremy, S542 (FRI303)
- Hervieu, Maëva, S766 (SAT216)

Author Index

- Herzig, Stephan, S606 (FRI467), S703 (SAT079)
- Herzog, Katharina, S758 (SAT199)
- Herzog, Natalie, S658 (FRI585)
- Hessmann, Elisabeth, S85 (OS118)
- Hester, Joanna, S809 (SAT298)
- Hetjens, Svetlana, S523 (FRI262)
- Hetland, Liv, S331 (THU477), S499 (FRI220)
- Hetzer, Jenny, S649 (FRI565)
- Heucke, Niklas, S378 (THU579)
- Heurgue-Berlot, Alexandra, S61 (OS076), S524 (FRI265)
- Heurling, Kerstin, S420 (FRI047)
- Heydmann, Laura, S738 (SAT160)
- Heyens, Leen, S459 (FRI120)
- Heyer, Vanessa Den, S890 (SAT500)
- He, Yining, S215 (THU245)
- Heymann, Helen, S451 (FRI107), S454 (FRI110), S701 (SAT073)
- He, Youzhi, S559 (FRI337)
- He, Zheyun, S301 (THU412), S304 (THU418)
- Hiasa, Yoichi, S563 (FRI346), S616 (FRI502)
- Hickman, Matthew, S256 (THU328), S416 (FRI041), S564 (FRI348)
- Hicks, Amy, S332 (THU479)
- Hicks, Timothy, S424 (FRI055)
- Hidam, Ashini, S51 (OS064), S347 (THU508)
- Hide, Diana, S365 (THU538)
- Hiebert, Lindsey, S229 (THU274), S238 (THU291), S557 (FRI333), S598 (FRI418)
- Higashide, Atsuko, S600 (FRI454)
- Higuchi, Mayu, S379 (THU580)
- Higuera, Monica, S658 (FRI587)
- Hikita, Hayato, S563 (FRI346)
- Hildebrand, Hannah, S372 (THU567), S383 (THU588)
- Hildebrandt, Franziska, S199 (THU200)
- Hildt, Eberhard, S262 (THU337)
- Hillebrandt, Karl, S497 (FRI217), S663 (FRI597), S739 (SAT162)
- Hilleret, Marie-Noëlle, S833 (SAT360)
- Hilleret, Marie-Noëlle, S73 (OS096), S524 (FRI265), S772 (SAT239), S840 (SAT373)
- Hillman, Daniel, S612 (FRI493)
- Hilscher, Max, S882 (SAT486)
- Hindi, Mor, S83 (OS114)
- Hinerman, Amanda S, S264 (THU341)
- Hin Hln Ko, S338 (THU490)
- Hin Ko, Hin, S547 (FRI313)
- Hinrichs, Jan, S608 (FRI485), S622 (FRI514), S624 (FRI519), S634 (FRI536)
- Hintz, Andreas, S586 (FRI393)
- Hipp, Jason, S138 (THU037)
- Hiriart, Jean-Baptiste, S772 (SAT239)
- Hirode, Grishma, S569 (FRI359), S852 (SAT400), S861 (SAT415)
- Hirohara, Junko, S314 (THU445)
- Hirooka, Masashi, S616 (FRI502)
- Hirschberger, Anna, S185 (THU171)
- Hirschfield, Gideon, S62 (OS078), S313 (THU443), S317 (THU452), S322 (THU461), S323 (THU462), S323 (THU463), S335 (THU484), S425 (FRI058), S448 (FRI102), S452 (FRI108), S461 (FRI123), S526 (FRI269)
- Hirsch, Ryan, S337 (THU488), S366 (THU540)
- Hitos, Ana B., S111 (OS163)
- Hjuler, Sara Toftegaard, S7 (GS009)
- Hlady, Ryan, S923 (SAT573)
- Hoang, Joseph, S875 (SAT442)
- Hoang, Khanh, S745 (SAT177)
- Hoare, Matthew, S195 (THU192)
- Hobbs, Todd, S726 (SAT130)
- Hobeika, Christian, S372 (THU566)
- Hobolth, Lise, S64 (OS083), S154 (THU068), S331 (THU477)
- Hochberg, Alyssa, S774 (SAT241)
- Hockings, Paul, S420 (FRI047)
- Hodge, Daryl, S580 (FRI383)
- Hodge, Jacqueline C., S24 (OS017)
- Hodneland, Linn, S672 (SAT016)
- Hodson, Leanne, S690 (SAT052)
- Hoek, Bart Van, S306 (THU431), S631 (FRI530), S798 (SAT280)
- Hoelting, Lisa, S703 (SAT078)
- Hoener zu Siederdisen, Christoph, S824 (SAT344)
- Hoepfer, Marius M., S783 (SAT257)
- Ho, Erwin, S303 (THU416)
- Hofer, Benedikt, S360 (THU529), S362 (THU534), S466 (FRI152), S472 (FRI164), S502 (FRI226), S629 (FRI527), S629 (FRI528), S632 (FRI533), S753 (SAT191)
- Hoffman, Hal M., S471 (FRI161), S690 (SAT051)
- Hoffmann, Charlotte, S927 (SAT579)
- Hoffman, Sara, S711 (SAT094)
- Hofmann, Alexander, S748 (SAT181)
- Hofmann, Maike, S2 (GS003), S54 (OS068), S100 (OS143), S196 (THU194), S657 (FRI583), S710 (SAT090)
- Hofmann, Sarah, S305 (THU421)
- Hofmann, Wolf Peter, S823 (SAT341)
- Hogan, Brian J., S403 (FRI022), S505 (FRI231)
- Hogan, Malcolm, S416 (FRI040)
- Ho, Gideon, S679 (SAT030)
- Hohenester, Simon, S602 (FRI460)
- Højlund, Kurt, S9 (GS012)
- Ho, Joan, S834 (SAT362)
- Holdorf, Meghan, S276 (THU365)
- Hole, Mikal Jacob, S178 (THU157)
- Hollande, Clemence, S372 (THU566), S392 (FRI005)
- Holland-Fischer, Peter, S344 (THU503)
- Holleboom, Adriaan G., S424 (FRI055)
- Hollenbach, Marcus, S313 (THU444)
- Hollenback, David, S483 (FRI187), S721 (SAT117)
- Hollnberger, Julius, S244 (THU302), S845 (SAT385)
- Holmberg, Dan, S467 (FRI154)
- Holmberg, Marte, S826 (SAT348)
- Holmer, Magnus, S423 (FRI053)
- Holmes, Ben, S508 (FRI236), S918 (SAT564)
- Holmes, Elaine, S135 (THU031), S352 (THU516)
- Holmes, Jacinta, S498 (FRI218), S550 (FRI318), S758 (SAT199), S876 (SAT443)
- Holm, Jens-Christian, S450 (FRI104), S523 (FRI263)
- Holm, Kristian, S178 (THU157)
- Holm, Louise, S523 (FRI263)
- Holm, Louise Aas, S450 (FRI104)
- Holm, Sverre, S27 (OS021)
- Hołówko, Wacław, S107 (OS157)
- Holst, Dorte, S670 (SAT013)
- Holt, Andrew, S120 (THU005)
- Holt, Curtis, S837 (SAT368)
- Höltke, Carsten, S487 (FRI196)
- Holtug, Taus, S475 (FRI171)
- Holvoet, Tom, S546 (FRI312)
- Holzhey, Michael, S148 (THU057)
- Holzmann, Heidemarie, S545 (FRI309)
- Homer, Natalie, S397 (FRI013)
- Ho, Ming-Mo, S373 (THU568)
- Hommel, Mirja, S248 (THU310)
- Hommersand, Kristina, S841 (SAT375)
- Honda, Yasushi, S430 (FRI067)
- Hönes, G. Sebastian, S341 (THU498)
- Hong, Geun, S799 (SAT282)
- Hong, Jin, S846 (SAT386), S853 (SAT402)
- Hong, Seungpyo, S921 (SAT569)
- Hong, Suk Kyun, S798 (SAT281)
- Hong, Su young, S798 (SAT281)
- Hong, Thai, S498 (FRI218)
- Hong, Vennis, S831 (SAT356)
- Honnens de Lichtenberg, Kristian, S7 (GS009)
- Honrubia, Maria, S512 (FRI244)
- Hook, Margaret, S342 (THU499)
- Hopkins, Laurence, S805 (SAT292)
- Hora, Shainan, S730 (SAT140)
- Horhat, Adelina, S141 (THU042), S915 (SAT559)
- Horia, Stefanescu, S141 (THU042)
- Horiba, Naoshi, S600 (FRI454)
- Hörnberg, Maria, S467 (FRI154)
- Hörndler, Carlos, S676 (SAT023)
- Horne, Patrick, S310 (THU439)
- Horn, Patrick, S517 (FRI253), S518 (FRI255), S519 (FRI256), S521 (FRI259)
- Horn, Paul, S342 (THU500)
- Horrigan, Stephen, S245 (THU303)
- Horriño, Raquel, S368 (THU545)
- Horscroft, Nigel, S180 (THU161)
- Horsmans, Yves, S135 (THU032), S736 (SAT156)
- Horta, Diana, S127 (THU018), S324 (THU464), S328 (THU471), S334 (THU482)
- Horvath, Angela, S68 (OS088), S179 (THU159)
- Horvatits, Karoline, S893 (SAT507)

- Horvatits, Thomas, S206 (THU229), S224 (THU265), S257 (THU329), S893 (SAT507)
- Horwich, Brian, S794 (SAT274)
- Hosford, Patrick, S670 (SAT011)
- Hoshida, Yujin, S36 (OS037), S642 (FRI553), S649 (FRI565)
- Ho, Shinn-Ying, S925 (SAT576)
- Hosking, Kelly, S239 (THU294), S305 (THU422)
- Hossain, Md. Shafiqul, S260 (THU335)
- Hosseini, Mojgan, S439 (FRI085)
- Houben, Tom, S144 (THU046)
- Houghton, Kathryn, S337 (THU489)
- Hou, Jinlin, S12 (LB004A), S70 (OS091), S299 (THU408), S835 (SAT365), S864 (SAT422), S867 (SAT427), S880 (SAT452)
- Houmami, Ranya, S818 (SAT314)
- Hou, Ming-Chih, S109 (OS160), S375 (THU572)
- Hountondji, Lina, S392 (FRI006)
- Houri, Inbal, S790 (SAT268)
- House, Michael, S409 (FRI031)
- Houssel-Debry, Pauline, S772 (SAT239), S780 (SAT252)
- Housset, Chantal, S297 (THU404)
- Hout, Anne, S750 (SAT184)
- Houtte, Freya Van, S860 (SAT413)
- Hove, Jens, S340 (THU496), S610 (FRI489), S887 (SAT495)
- Hovel, David, S583 (FRI387)
- Hov, Johannes R., S178 (THU157), S309 (THU437), S604 (FRI463)
- Howard, Rob, S269 (THU350), S300 (THU411)
- Howe, Laura, S416 (FRI041)
- Howell, Jessica, S498 (FRI218)
- Hoyas, Elena, S857 (SAT409)
- Hrkač, Stela, S612 (FRI494)
- Hryharovich, Victor, S269 (THU351)
- Hsiao, Chih-Yang, S468 (FRI155)
- Hsieh, Chia-Hsun, S373 (THU568)
- Hsieh, Tsai-Yuan, S595 (FRI410)
- Hsieh, Yi-Chung, S373 (THU568), S575 (FRI371)
- Hsing Yu Chen, David, S869 (SAT431)
- Hsu, Chao-Wei, S827 (SAT350)
- Hsu, Cheng Er, S575 (FRI371)
- Hsu, Christine, S33 (OS031), S201 (THU219)
- Hsu, Heather, S112 (OS164)
- Hsu, Hong-Yuan, S514 (FRI247)
- Hsu, Yao-Chun, S119 (THU001), S835 (SAT364), S841 (SAT376), S849 (SAT393), S852 (SAT400), S861 (SAT415), S875 (SAT442), S883 (SAT488)
- Hua, Bo, S837 (SAT367)
- Huadong, Yan, S344 (THU504), S636 (FRI540)
- Hu, Airon, S301 (THU412), S304 (THU418)
- Huang, Chien-Wei, S595 (FRI410)
- Huang, Ching-I, S458 (FRI118), S595 (FRI410)
- Huang, Daniel, S926 (SAT577)
- Huang-Doran, Isabel, S695 (SAT061)
- Huangfu, Gavin, S164 (THU089)
- Huang, Fung Yu, S177 (THU154)
- Huang, Guangyu, S838 (SAT369)
- Huang, Jee-Fu, S458 (FRI118), S595 (FRI410)
- Huang, Jia-Sheng, S595 (FRI410)
- Huang, Jinhua, S78 (OS105)
- Huang, Jonathan, S319 (THU455)
- Huang, J.-X., S464 (FRI148)
- Huang, Kai-Wen, S468 (FRI155)
- Huang, Ou-Yang, S421 (FRI050), S431 (FRI069)
- Huang, Pinzhu, S657 (FRI584)
- Huang, Qi, S463 (FRI126)
- Huang, Rae-Chi, S440 (FRI087)
- Huang, Rui, S287 (THU388), S296 (THU403), S326 (THU468), S504 (FRI229)
- Huang, Shuo, S827 (SAT349)
- Huang, Xiaohong, S647 (FRI563), S818 (SAT315)
- Huang, Xinliang, S389 (FRI001), S601 (FRI456)
- Huang, Yan, S344 (THU504), S865 (SAT424)
- Huang, Yifei, S22 (OS014), S501 (FRI224), S616 (FRI502)
- Huang, Yi-Hsiang, S109 (OS160), S372 (THU567), S375 (THU572), S383 (THU588), S595 (FRI410), S870 (SAT433), S925 (SAT576)
- Huang, Yun, S450 (FRI104)
- Huang, Zhenlin, S647 (FRI563), S818 (SAT315)
- Huan, Hui, S182 (THU165)
- Huard, Genevieve, S593 (FRI407), S805 (SAT293)
- Hua, Rui, S522 (FRI261)
- Hubacek, Jaroslav A., S536 (FRI290)
- Hübener, Sina, S325 (THU466)
- Huber, Heidemarie, S470 (FRI159)
- Huber, Markus, S470 (FRI159)
- Huber, Samuel, S83 (OS114), S206 (THU229), S224 (THU265), S257 (THU329), S604 (FRI462), S893 (SAT507)
- Hubert, Isabelle Fouchard, S833 (SAT360), S840 (SAT373)
- Huber, Yvonne, S145 (THU051)
- Hübl, Wolfgang, S545 (FRI309)
- Hudson, Evis, S447 (FRI100)
- Huebener, Peter, S325 (THU466)
- Hueffner, Lucas, S250 (THU315), S263 (THU339)
- Huerta, Anna, S900 (SAT520)
- Hueser, Norbert, S463 (FRI146)
- Huet, Catherine, S456 (FRI114)
- Hugger, Mie Balle, S9 (GS012)
- Hughes, Timothy, S698 (SAT067)
- Hu, Guoxin, S70 (OS091)
- Hu, Hui-Han, S294 (THU398)
- Huiban, Laura, S573 (FRI368)
- Huiling, Xiang, S182 (THU165)
- Hui, Rex Wan-Hin, S273 (THU360), S275 (THU364)
- Hui, Samuel, S613 (FRI495)
- Hui, Vicki Wing-Ki, S39 (OS043), S101 (OS147), S164 (THU088), S274 (THU362), S302 (THU414), S390 (FRI004), S406 (FRI026)
- Hu, Jui-Ting, S119 (THU001), S595 (FRI410)
- Hulme, Sam, S195 (THU192)
- Hulshof, Lauren, S592 (FRI405)
- Hulspas, Sanne, S750 (SAT184)
- Hum, Dean, S359 (THU528)
- Hung, Chao-Hung, S595 (FRI410)
- Hung-Chih, Chiu, S863 (SAT420)
- Hung, Ya-Wen, S109 (OS160)
- Hung, Yi-Ping, S375 (THU572)
- Hunsberger, Sally, S235 (THU287)
- Hunt, Mallory, S740 (SAT163)
- Hunt, Phillip, S609 (FRI486)
- Hunyady, Peter, S313 (THU444)
- Huot-Marchand, Philippe, S715 (SAT105), S721 (SAT119), S722 (SAT120)
- Hu, Peng, S181 (THU164), S240 (THU296)
- Hüppe, Dietrich, S562 (FRI345), S584 (FRI388)
- Huppertsberg, Anne, S464 (FRI147)
- Hurtado, Adoración, S218 (THU252)
- Husain, Mehreen, S447 (FRI100)
- Husar-Sburlan, Ioana-Alexandra, S795 (SAT276)
- Hüser, Norbert, S185 (THU171)
- Huskens, Dana, S911 (SAT540)
- Hussain, Md Razeen Ashraf, S229 (THU274)
- Hussain, Tanweer, S240 (THU295)
- Hussain, Yaqza, S934 (SAT593)
- Hussenbux, Arif, S330 (THU475)
- Hussey, George, S465 (FRI149)
- Huss, Ryan, S427 (FRI060)
- Hutchinson, David, S22 (OS013)
- Hutchinson, Sharon, S17 (OS005), S564 (FRI348)
- Hutsch, Tomasz, S746 (SAT179)
- Hu, Tsung-Hui, S45 (OS054)
- Hutter, Simon, S703 (THU078)
- Hu, Wen, S803 (SAT289)
- Hu, Xumei, S501 (FRI224)
- Huyck, Lynn, S107 (OS156)
- Hu, Yue, S89 (OS125), S837 (SAT367)
- Hu, Zhongjie, S272 (THU357), S844 (SAT382)
- Hwang, Carey, S69 (OS090), S831 (SAT357)
- Hwang, Jae-Seok, S572 (FRI365), S916 (SAT560)
- Hwang, Seong Gyu, S100 (OS144), S862 (SAT418)
- Hwang, Shin, S799 (SAT282)
- Hwu, Paul Wuh-Liang, S514 (FRI247)
- Hyde, Ashley, S338 (THU490), S511 (FRI241)
- Hydes, Theresa, S42 (OS048)
- Hylemon, Phillip, S178 (THU156)
- Hyötyläinen, Tuulia, S111 (OS162), S694 (SAT060)

Author Index

- Hyrina, Anastasia, S251 ([THU317](#)), S276 ([THU365](#))
- Hysenji, Arlinda, S573 ([FRI367](#))
- Hyun, Kim Seok, S921 ([SAT569](#))
- Hyun Sohn, Joo, S438 ([FRI082](#)), S438 ([FRI083](#)), S439 ([FRI086](#))
- Hyunsoon, Kang, S853 ([SAT402](#))
- Hyun, Sung Hee, S921 ([SAT569](#))
- Iaccarino, Antonino, S84 ([OS115](#))
- Iacob, Speranta, S625 ([FRI520](#))
- Iafolla, Marco, S395 ([FRI010](#))
- Iakovleva, Viktoriia, S730 ([SAT140](#)), S735 ([SAT154](#))
- Iannacone, Matteo, S97 ([OS139](#)), S259 ([THU334](#))
- Iannone, Andrea, S564 ([FRI347](#))
- Iannone, Giulia, S357 ([THU523](#))
- Iavarone, Massimo, S54 ([OS069](#)), S57 ([OS072A](#)), S223 ([THU263](#)), S578 ([FRI376](#))
- Ibañez, Luis, S90 ([OS127](#)), S157 ([THU074](#)), S158 ([THU076](#))
- Ibarra, Cesar, S77 ([OS103](#))
- Ibdah, Jamal, S692 ([SAT057](#))
- Iborra, Ignacio, S724 ([SAT125](#))
- Ibrahim, P., S464 ([FRI148](#))
- Icaza, Maru, S487 ([FRI195](#))
- Ichai, Philippe, S349 ([THU511](#)), S935 ([SAT595](#))
- Idalsoaga, Francisco, S81 ([OS110](#)), S137 ([THU034](#))
- Idilman, Ramazan, S19 ([OS008](#)), S49 ([OS063](#)), S293 ([THU397](#)), S297 ([THU405](#)), S414 ([FRI037](#)), S778 ([SAT248](#)), S782 ([SAT255](#)), S820 ([SAT316](#)), S858 ([SAT410](#)), S861 ([SAT416](#)), S864 ([SAT421](#))
- Ido, Akio, S563 ([FRI346](#))
- Ieluzzi, Donatella, S564 ([FRI347](#)), S796 ([SAT277](#))
- Iesari, Samuele, S797 ([SAT279](#))
- Igboin, Dolapo, S116 ([OS172](#))
- Iglesias, Ainhoa, S651 ([FRI571](#))
- Iglesias, Teresa, S111 ([OS163](#))
- Igloi-Nagy, Adam, S237 ([THU290](#))
- Ignasi, Olivas, S328 ([THU471](#))
- Ignat, Mina, S141 ([THU042](#))
- Ihdayhid, Abdul, S164 ([THU089](#))
- Iida, Manami, S600 ([FRI454](#))
- Iijima, Hiroko, S616 ([FRI502](#))
- Ijzermans, Jan, S107 ([OS157](#)), S109 ([OS159](#)), S115 ([OS170](#)), S631 ([FRI530](#)), S815 ([SAT311](#)), S883 ([SAT488](#)), S933 ([SAT591](#))
- Ikeda, Hitoshi, S485 ([FRI192](#))
- Ikeda, Yuji, S172 ([THU103](#))
- Ikejima, Kenichi, S465 ([FRI149](#)), S687 ([SAT047](#))
- Ikram, Arfan, S41 ([OS046](#)), S147 ([THU055](#))
- Ikram, Kamran, S147 ([THU055](#))
- Ilionsky, Gabriela, S583 ([FRI387](#))
- Illingworth, Megan, S650 ([FRI569](#))
- Ilott, Nicholas, S602 ([FRI458](#))
- Illiche, Sarah, S392 ([FRI006](#))
- Imajo, Kento, S430 ([FRI067](#)), S444 ([FRI095](#))
- Imam, Hasan, S871 ([SAT434](#))
- Imamura, Fumiaki, S815 ([SAT310](#))
- Imamura, Michio, S252 ([THU319](#)), S291 ([THU393](#)), S758 ([SAT199](#))
- Im, Gene, S33 ([OS031](#)), S343 ([THU502](#)), S897 ([SAT513](#))
- Immer, Franz, S780 ([SAT251](#))
- Imnadze, Paata, S221 ([THU258](#)), S233 ([THU283](#)), S267 ([THU347](#))
- Im, Theresa, S831 ([SAT356](#))
- Im, Yu Ri, S290 ([THU391](#))
- Inan, Dilara, S858 ([SAT411](#))
- Iñarrairaegui, Mercedes, S114 ([OS168](#)), S381 ([THU584](#)), S500 ([FRI222](#)), S802 ([SAT288](#))
- Ince, Nevin, S858 ([SAT411](#))
- Incicco, Simone, S18 ([OS007](#)), S49 ([OS062](#)), S92 ([OS131](#)), S894 ([SAT508](#)), S895 ([SAT511](#))
- Indenbaum, Victoria, S784 ([SAT258](#)), S804 ([SAT291](#))
- Inderson, Akin, S338 ([THU491](#))
- Indolfi, Giuseppe, S203 ([THU222](#)), S591 ([FRI404](#))
- Indriz, Nevin, S13 ([LB004B](#)), S881 ([SAT453](#))
- Infante, Mirtha, S137 ([THU034](#))
- Infante, Stefany, S697 ([SAT064](#))
- Infantino, Giuseppe, S448 ([FRI101](#)), S725 ([SAT127](#))
- Ingiliz, Patrick, S582 ([FRI385](#))
- Inglis, Sarah, S564 ([FRI348](#))
- Ingvast, Sofie, S471 ([FRI162](#))
- Inia, José A., S681 ([SAT033](#))
- Innes, Hamish, S11 ([LB002](#)), S17 ([OS005](#)), S560 ([FRI339](#))
- Innocenti, Tommaso, S770 ([SAT235](#))
- Inoue, Jun, S12 ([LB004A](#)), S880 ([SAT452](#))
- Inoue, Kaori, S875 ([SAT442](#))
- Inoue, Takako, S272 ([THU358](#))
- Invernizzi, Pietro, S94 ([OS134](#)), S96 ([OS136](#)), S335 ([THU484](#)), S404 ([FRI024](#))
- Ioannou, George, S223 ([THU262](#))
- Iott, Christina, S848 ([SAT391](#)), S850 ([SAT396](#)), S851 ([SAT397](#))
- Ippolito, Davide, S96 ([OS136](#))
- Iqbal, Afshan, S759 ([SAT202](#))
- Iqbal, Shahed, S276 ([THU365](#))
- Irles-Depe, Marie, S73 ([OS096](#)), S74 ([OS099](#)), S441 ([FRI089](#))
- Iruarizaga-Lejarreta, Marta, S671 ([SAT014](#))
- Iruetagoiena, Begoña Rodriguez, S84 ([OS116](#))
- Iruzubieta, Paula, S113 ([OS166](#)), S157 ([THU074](#)), S158 ([THU076](#)), S624 ([FRI518](#)), S671 ([SAT014](#))
- Irvine, Katharine, S172 ([THU102](#))
- Irving, James, S534 ([FRI285](#))
- Irving, William, S17 ([OS005](#))
- Irwin, Sophie, S57 ([OS072A](#)), S58 ([OS072B](#))
- Isabel de Ávila, Ana, S589 ([FRI399](#))
- Isabelle, Bordes, S246 ([THU306](#)), S247 ([THU307](#)), S356 ([THU522](#))
- Isabel Lucena, Maria, S308 ([THU435](#))
- Isakov, Vasily, S154 ([THU069](#))
- Isberner, Nora, S339 ([THU493](#))
- Iser, David, S498 ([FRI218](#)), S541 ([FRI302](#))
- Iserte, Gemma, S381 ([THU584](#))
- Ishida, Yuji, S252 ([THU319](#))
- Ishino, Takamasa, S615 ([FRI501](#)), S897 ([SAT514](#))
- Ismail, Marwa, S62 ([OS078](#)), S313 ([THU443](#))
- Ismail, Mohamed, S875 ([SAT441](#))
- Isoniemi, Helena, S312 ([THU441](#))
- Israel, Ariel, S845 ([SAT384](#))
- Israeli, Eran, S583 ([FRI387](#))
- Israel, Robert, S899 ([SAT517](#))
- Israelsen, Mads, S2 ([GS002](#)), S9 ([GS012](#)), S129 ([THU021](#)), S131 ([THU024](#)), S144 ([THU046](#)), S475 ([FRI171](#)), S500 ([FRI223](#))
- Issachar, Assaf, S64 ([OS081](#)), S774 ([SAT241](#)), S793 ([SAT272](#)), S855 ([SAT406](#))
- Issa, Fadi, S809 ([SAT298](#))
- Ita.Li.Ca. Study Group, S932 ([SAT588](#))
- Itoh, Yoshito, S563 ([FRI346](#))
- Itti, Emmanuel, S375 ([THU573](#))
- Itzel, Timo, S928 ([SAT580](#))
- Iuliano, Antonella, S84 ([OS115](#))
- Ivancho, Pavlo, S635 ([FRI539](#))
- Ivanics, Tommy, S109 ([OS159](#)), S778 ([SAT249](#)), S800 ([SAT286](#)), S801 ([SAT287](#))
- Ivanova, Elena, S42 ([OS049](#)), S557 ([FRI332](#)), S558 ([FRI335](#))
- Iwaisako, Keiko, S183 ([THU167](#))
- Iwaki, Michihiro, S430 ([FRI067](#))
- Iwanaga, Terunao, S615 ([FRI501](#)), S897 ([SAT514](#))
- Iwasaki, Hirohiko, S172 ([THU103](#))
- Iwasawa, Kentaro, S673 ([SAT017](#))
- Iyengar, Sowmya, S191 ([THU184](#)), S329 ([THU474](#)), S358 ([THU525](#))
- Iyer, Janani, S700 ([SAT071](#)), S708 ([SAT088](#)), S711 ([SAT094](#))
- Iyer, Rajalakshmi, S427 ([FRI060](#))
- Izquierdo-Altarejos, Paula, S103 ([OS150](#))
- Izquierdo-Sánchez, Laura, S77 ([OS103](#)), S107 ([OS157](#)), S192 ([THU185](#)), S671 ([SAT014](#))
- Izumi, Namiki, S379 ([THU580](#))
- Izzo, Francesco, S938 ([SAT599](#))
- Izzy, Manhal, S807 ([SAT296](#))
- Jaap, Alan, S434 ([FRI075](#))
- Jaber, Samir, S349 ([THU511](#))
- Jachs, Mathias, S18 ([OS007](#)), S92 ([OS131](#)), S359 ([THU527](#)), S390 ([FRI003](#)), S532 ([FRI280](#)), S535 ([FRI287](#)), S545 ([FRI309](#)), S555 ([FRI328](#)), S617 ([FRI505](#)), S629 ([FRI527](#)), S629 ([FRI528](#)), S631 ([FRI531](#)), S632 ([FRI533](#)), S829 ([SAT353](#)), S830 ([SAT354](#)), S843 ([SAT379](#))
- Jack, Kathryn, S277 ([THU368](#))
- Jackson, Akil, S672 ([SAT016](#))

- Jackson, Clive, S125 (THU014), S890 (SAT500)
- Jackson, Kathy, S842 (SAT377)
- Jacobo, Janett, S137 (THU034)
- Jacobs, Angus, S712 (SAT096)
- Jacobson, Ira M, S280 (THU372), S281 (THU376), S836 (SAT366), S846 (SAT387), S864 (SAT422)
- Jacquelinet, Christian, S780 (SAT252)
- Jacquemin, Emmanuel, S514 (FRI248), S521 (FRI260)
- Jadhav, Vasant, S871 (SAT434)
- Jaekel, Elmar, S783 (SAT257), S784 (SAT259)
- Jaeger, Kathrin, S904 (SAT528)
- Jagatia, Ravi, S647 (FRI562)
- Jagdish, Rukmini, S290 (THU391)
- Jagemann, Bettina, S325 (THU466)
- Jäger, Dirk, S655 (FRI581)
- Jager, Jennifer, S665 (SAT002)
- Jäger, Johannes, S80 (OS108)
- Jaggiahgari, Shashidhar, S191 (THU184)
- Jahagirdar, Vinay, S632 (FRI532)
- Jähnert, Andreas, S682 (SAT035)
- Jahnsen, Jørgen, S309 (THU437)
- Jain, Kavita, S457 (FRI116)
- Jairath, Vipul, S416 (FRI040)
- Jaisinghani, Ruchika, S853 (SAT401)
- Jakob, Carolin E. M., S339 (THU493)
- Jakobsson, Gustav, S119 (THU002)
- Jalal, Prasun, S928 (SAT581)
- Jalan, Rajiv, S51 (OS065), S344 (THU503), S366 (THU539), S670 (SAT011), S902 (SAT523), S903 (SAT526)
- Jalili, Reza, S764 (SAT212)
- Jallow, Alpha Omar, S258 (THU332)
- Jaltotage, Biyanka, S164 (THU089)
- James, Joyce, S88 (OS124)
- James, Larry, S799 (SAT284)
- Jamey, Carole, S738 (SAT160)
- Jamieson, Nigel B., S107 (OS157)
- Jamieson, Thomas, S385 (THU595)
- Jamil, Khurram, S611 (FRI490), S634 (FRI537)
- Jamil, Muhammad, S558 (FRI335)
- Jancekova, Daniela, S613 (FRI496)
- Janciauskiene, Sabina, S515 (FRI250)
- Janczewska, Ewa, S8 (GS010), S12 (LB004A), S13 (LB004B), S288 (THU389), S288 (THU390), S291 (THU393), S565 (FRI350), S585 (FRI390), S872 (SAT437), S880 (SAT452), S881 (SAT453)
- Jandor, Arun, S424 (FRI056)
- Janeiro, Mariajoão, S305 (THU421)
- Jang, Byoung Kuk, S572 (FRI365), S916 (SAT560), S932 (SAT590)
- Jang, Jae Young, S572 (FRI365), S916 (SAT560), S932 (SAT590)
- Jang, Jeong Won, S820 (SAT317), S932 (SAT589), S932 (SAT590)
- Jang, Se Young, S377 (THU576), S484 (FRI189), S572 (FRI365), S916 (SAT560)
- Jang, Yeeun, S203 (THU224), S204 (THU225)
- Janik, Maciej K., S315 (THU447), S605 (FRI464), S782 (SAT254)
- Janjua, Naveed, S17 (OS005), S43 (OS051), S209 (THU233), S282 (THU378), S910 (SAT538)
- Jannone, Giulia, S535 (FRI289)
- Janocha-Litwin, Justyna, S592 (FRI406)
- Janowski, Kamil, S525 (FRI267)
- Jansen, Christian, S895 (SAT510)
- Jansen-Skoupy, Sonja, S545 (FRI309)
- Janssen, Harry, S3 (GS004), S12 (LB004A), S13 (LB004B), S281 (THU374), S288 (THU389), S288 (THU390), S291 (THU393), S313 (THU443), S318 (THU453), S569 (FRI359), S849 (SAT394), S852 (SAT400), S861 (SAT415), S864 (SAT422), S880 (SAT452), S881 (SAT453)
- Janssen, Harry LA, S335 (THU484)
- Janssen-Langenstein, Ralf, S20 (OS010)
- Janssens, Filip, S516 (FRI252)
- Janssens, Veerle, S637 (FRI544)
- Janzen, Ronald, S748 (SAT181)
- Jara, Maximilian, S10 (LB001), S29 (OS025)
- Jaramillo-Ramírez, Hiram, S356 (THU521)
- Jargalsaikhan, Ganbolor, S235 (THU287)
- Jaroszewicz, Jerzy, S565 (FRI350), S585 (FRI390)
- Jassem, Wael, S647 (FRI563), S818 (SAT315)
- Jayaswal, Arjun, S425 (FRI058), S448 (FRI102), S452 (FRI108), S453 (FRI109)
- Jayawardana, Sahan, S444 (FRI094)
- Jazaeri, Farahnaz, S883 (SAT487)
- Jean-Baptiste, Hiriart, S441 (FRI089)
- Jeffers, Thomas, S420 (FRI048), S429 (FRI064), S447 (FRI100)
- Jeffery-Smith, Anna, S53 (OS067)
- Jekle, Andreas, S853 (SAT401)
- Jelleschitz, Julia, S711 (SAT093)
- Jelley, Ryan, S567 (FRI355)
- Jen, Chin-Lan, S294 (THU398)
- Jenders, Robert, S731 (SAT142)
- Jeng, Rachel Wen-Juei, S102 (OS148), S294 (THU398), S575 (FRI371), S849 (SAT393), S852 (SAT400), S861 (SAT415), S873 (SAT438)
- Jenkins, Benjamin, S695 (SAT061)
- Jenne, Craig, S259 (THU334)
- Jensen, Anne Sofie, S154 (THU068)
- Jensen, Anne-Sofie Houlberg, S331 (THU477)
- Jensen, Björn, S825 (SAT345)
- Jensen, Dennis M, S625 (FRI520)
- Jensen, Jane, S9 (GS012)
- Jensen, Morten Daniel, S314 (THU446), S925 (SAT575)
- Jeon, Dongsu, S891 (SAT503)
- Jeong, Dahn, S43 (OS051), S209 (THU233), S282 (THU378), S910 (SAT538)
- Jeong, Jaehong, S799 (SAT282)
- Jeong, Jae Yoon, S883 (SAT488)
- Jeong, Joonho, S572 (FRI365)
- Jeong, Nakcheol, S489 (FRI199), S866 (SAT426)
- Jeon, Hong Jae, S380 (THU583)
- Jepsen, Peter, S123 (THU011), S125 (THU015), S172 (THU104), S314 (THU446), S611 (FRI491), S925 (SAT575)
- Jerkic, Mirjana, S822 (SAT320)
- Jermutus, Lutz, S158 (THU075)
- Jerome, Ellen, S116 (OS171), S135 (THU031), S352 (THU516), S505 (FRI231), S647 (FRI563)
- Jerzowski, John, S8 (GS010), S864 (SAT422)
- Jeschke, Marc, S822 (SAT320)
- Jesudian, Arun, S899 (SAT517)
- Jhaisha, Samira Abu, S193 (THU187)
- Jhajharia, Ashok, S628 (FRI525)
- Jhaveri, Kartik, S429 (FRI065), S526 (FRI269)
- Jia, Catherine, S31 (OS028), S409 (FRI030), S762 (SAT208)
- Jia, Haiyan, S89 (OS125)
- Jia, Ji-Dong, S12 (LB004A), S90 (OS127), S880 (SAT452)
- Jiang, Jing, S66 (OS086), S357 (THU524), S402 (FRI021), S744 (SAT171), S744 (SAT172), S745 (SAT173), S803 (SAT289)
- Jiang, Li, S66 (OS086)
- Jiang, Lijuan, S745 (SAT177)
- Jiang, Mengwei, S35 (OS035)
- Jiang, Shirley, S544 (FRI308)
- Jiang, Suwen, S301 (THU412), S304 (THU418)
- Jiang, Wei, S173 (THU151)
- Jiang, Xiaojun, S27 (OS021), S605 (FRI465)
- Jiang, Xiuhong, S837 (SAT367)
- Jiang, Yiwei, S124 (THU012)
- Jiang, Yongfang, S838 (SAT369)
- Jiang, Zhenzhou, S389 (FRI001), S601 (FRI456)
- Jiang, Zicheng, S22 (OS014)
- Jian, Li, S832 (SAT359)
- Jiao, Jingjing, S470 (FRI160), S485 (FRI190)
- Jiao, Yonggeng, S522 (FRI261)
- Ji, Dong, S22 (OS014), S377 (THU577)
- Jie, Li, S636 (FRI540)
- Ji, Fanpu, S883 (SAT488)
- Ji, Lili, S818 (SAT315)
- Ji, Linong, S463 (FRI126)
- Jimenez-Aguero, Raul, S77 (OS103)
- Jimenez, Celia Martinez, S395 (FRI009)
- Jimenez-Esquivel, Natalia, S907 (SAT532)
- Jimenez-Pastor, Ana, S442 (FRI091)
- Jiménez-Pérez, Miguel, S317 (THU452)
- Jiménez, Wladimiro, S106 (OS154), S368 (THU545), S492 (FRI205), S743 (SAT170)
- Jin, Chaonan, S165 (THU090), S777 (SAT247)
- Jindal, Ankur, S22 (OS014)
- Jin, Feng, S716 (SAT108)

Author Index

- Jing, He, S56 ([OS071](#))
Jing, Zhang, S165 ([THU091](#)), S870 ([SAT432](#))
Jin, He, S89 ([OS125](#))
Jin, Rui, S26 ([OS020](#)), S685 ([SAT042](#))
Jin, Young-Joo, S870 ([SAT433](#))
Jirsa, Milan, S536 ([FRI290](#))
Jm Bauer, David, S535 ([FRI287](#)), S545 ([FRI309](#)), S555 ([FRI328](#))
Johannes, Chang, S895 ([SAT510](#))
Johannessen, Asgeir, S23 ([OS015](#)), S826 ([SAT348](#)), S841 ([SAT375](#))
Johannsson, Birgir, S573 ([FRI366](#))
Johansen, Stine, S2 ([GS002](#)), S9 ([GS012](#)), S35 ([OS036](#)), S129 ([THU021](#)), S130 ([THU022](#)), S131 ([THU024](#)), S475 ([FRI171](#))
Johanson, Quinian, S113 ([OS167](#))
Johansson, Edvin, S420 ([FRI047](#))
Johansson, Helene, S756 ([SAT197](#))
Johansson, Kjell Arne, S221 ([THU257](#))
Johansson, Lars, S420 ([FRI047](#)), S683 ([SAT038](#))
Joh, Jae-Won, S767 ([SAT229](#))
John, Aaron, S170 ([THU100](#))
John, Binu, S223 ([THU262](#)), S227 ([THU270](#))
John, Katharina, S666 ([SAT003](#))
John, Libby, S898 ([SAT516](#))
Johnson, Amy, S204 ([THU226](#))
Johnson, Cheryl, S42 ([OS049](#))
Johnson, Emily, S338 ([THU490](#)), S511 ([FRI241](#))
Johnson, Helen, S256 ([THU328](#))
Johnson, Philip, S17 ([OS005](#))
Johnson, Saraha, S692 ([SAT057](#))
Johnstone-hume, Claire, S337 ([THU489](#))
Jo, Hoon Gil, S484 ([FRI189](#))
Jo, Jung Hyun, S653 ([FRI575](#))
Jokelainen, Kalle, S312 ([THU441](#))
Jokl, Elliot, S104 ([OS152](#))
Jonas, Philipp, S107 ([OS157](#)), S788 ([SAT264](#))
Jones, Andrew, S554 ([FRI327](#))
Jones, Calum, S436 ([FRI078](#))
Jones, Catherine, S726 ([SAT128](#)), S726 ([SAT129](#))
Jones, Christopher, S88 ([OS123](#)), S716 ([SAT108](#)), S731 ([SAT142](#))
Jones, Daryl, S134 ([THU029](#))
Jones, David, S94 ([OS134](#)), S96 ([OS137](#)), S311 ([THU440](#)), S327 ([THU470](#)), S337 ([THU489](#))
Jones, Heidi, S534 ([FRI285](#))
Jones, John, S706 ([SAT085](#))
Jones, Rebecca L., S96 ([OS137](#))
Jones, Simon, S364 ([THU537](#))
Jones, Will, S424 ([FRI055](#))
Joore, Indi P., S652 ([FRI574](#))
Jordan, Kelsey, S22 ([OS013](#))
Jordan, Lynda, S570 ([FRI360](#))
Jordan, Veronica Clavijo, S36 ([OS037](#))
Jordan, William, S873 ([SAT439](#))
Jördens, Markus, S604 ([FRI463](#)), S930 ([SAT584](#))
Jorgensen, Kristin, S178 ([THU157](#)), S309 ([THU437](#))
Jorge, Poo, S487 ([FRI195](#))
Jorquera, Francisco, S549 ([FRI317](#)), S584 ([FRI388](#))
Jörs, Simone, S38 ([OS042](#))
Joseph, Majo, S898 ([SAT516](#))
Jose, Priyanka, S570 ([FRI360](#))
José Urquijo, Juan, S912 ([SAT555](#))
Joshi, Deepak, S650 ([FRI569](#)), S771 ([SAT236](#)), S812 ([SAT304](#))
Joshi, Yogendrakumar, S139 ([THU038](#)), S349 ([THU510](#))
Jothamani, Dinesh, S19 ([OS008](#)), S49 ([OS063](#))
Joubert, Juliette, S640 ([FRI550](#))
Jou, Janice, S779 ([SAT250](#))
Joven, Jorge, S678 ([SAT028](#)), S685 ([SAT041](#))
Jovovic, Dusan, S276 ([THU366](#))
Juan, Juan Carlos Rodríguez-San, S774 ([SAT242](#))
Juan, Laura, S792 ([SAT270](#))
Juanola, Adria, S63 ([OS080](#)), S139 ([THU039](#)), S511 ([FRI242](#)), S512 ([FRI243](#)), S512 ([FRI244](#)), S896 ([SAT512](#)), S901 ([SAT522](#)), S902 ([SAT524](#)), S907 ([SAT532](#))
Juan, Zhang, S878 ([SAT447](#))
Juárez, Candido, S886 ([SAT494](#))
Juárez-Fernández, María, S177 ([THU155](#))
Juárez, Osiel Ledesma, S476 ([FRI172](#))
Jucov, Alina, S73 ([OS095](#)), S835 ([SAT365](#)), S848 ([SAT392](#)), S871 ([SAT435](#)), S876 ([SAT443](#))
Judor, Jean-Paul, S185 ([THU172](#))
Juel, Helene Bæk, S129 ([THU021](#)), S131 ([THU024](#)), S450 ([FRI104](#)), S523 ([FRI263](#))
Jühling, Frank, S36 ([OS038](#)), S649 ([FRI565](#)), S738 ([SAT160](#)), S758 ([SAT199](#))
Juhl, Pernille, S668 ([SAT008](#))
Jukema, J. Wouter, S681 ([SAT033](#))
Jula, Antti, S80 ([OS109](#)), S419 ([FRI046](#))
Julian, Gillmore, S58 ([OS073](#))
Jun, Dae Won, S160 ([THU079](#)), S224 ([THU264](#)), S435 ([FRI077](#)), S462 ([FRI124](#)), S589 ([FRI398](#)), S728 ([SAT135](#)), S729 ([SAT136](#)), S870 ([SAT433](#)), S875 ([SAT442](#)), S932 ([SAT590](#))
Juneja, Pinky, S105 ([OS153](#)), S901 ([SAT521](#))
Jung, Birgit, S132 ([THU026](#)), S737 ([SAT158](#))
Jung, Eun Sun, S490 ([FRI202](#))
Jung, Finn, S692 ([SAT056](#))
Jung, Jean, S905 ([SAT529](#))
Jung, Jinho, S74 ([OS098](#)), S422 ([FRI051](#))
Jung, Se-Mi, S667 ([SAT005](#))
Jungwirth, Emilian, S696 ([SAT063](#))
Jung, Young Kul, S616 ([FRI502](#)), S932 ([SAT590](#))
Junhui, S623 ([FRI515](#))
Junien, Jean-Louis, S715 ([SAT105](#)), S721 ([SAT119](#)), S722 ([SAT120](#))
Junker, Anders, S154 ([THU068](#)), S331 ([THU477](#))
Jun, Tomi, S372 ([THU567](#)), S383 ([THU588](#))
Jun Wong, Yu, S623 ([FRI515](#))
Jura, Jolanta, S746 ([SAT179](#)), S759 ([SAT203](#))
Jure, Camila, S137 ([THU034](#))
Jurek, Marzena, S308 ([THU434](#))
Jurkiewicz, Elzbieta, S525 ([FRI267](#))
Ju, Shenghong, S636 ([FRI540](#))
Justyna, Janocha-Litwin, S585 ([FRI390](#))
Jutabha, Rome, S625 ([FRI520](#))
Juul Nielsen, Mette, S435 ([FRI076](#))
Juuti, Anne, S111 ([OS162](#)), S458 ([FRI117](#)), S694 ([SAT060](#))
Jyssum, Ingrid, S309 ([THU437](#))
Kabaçam, Gökhan, S782 ([SAT255](#)), S820 ([SAT316](#))
Kabat, Agnieszka, S710 ([SAT090](#))
Kabbaj, Meriam, S353 ([THU517](#)), S354 ([THU518](#))
Kablawi, Dana, S31 ([OS029](#)), S614 ([FRI497](#))
Kabore, Christelle, S672 ([SAT015](#))
Kabut, Kajetan, S509 ([FRI238](#))
Kachru, Nandita, S285 ([THU383](#)), S286 ([THU384](#)), S300 ([THU410](#))
Kaczmarek, Dominik, S381 ([THU585](#)), S599 ([FRI451](#))
Kadharusman, Marcello, S646 ([FRI561](#))
Kadivar, Mohammad, S271 ([THU356](#))
Kadłuczka, Justyna, S746 ([SAT179](#))
Kadosh, Shaul, S474 ([FRI168](#)), S714 ([SAT103](#))
Kadyan, Sonia, S347 ([THU508](#))
Kaeser, Rafael, S710 ([SAT090](#))
Kaestner, Klaus, S47 ([OS059](#))
Kaewdech, Apichat, S186 ([THU175](#)), S187 ([THU176](#)), S188 ([THU177](#)), S722 ([SAT121](#)), S824 ([SAT344](#))
Kahlhöfer, Julia, S582 ([FRI385](#)), S823 ([SAT341](#)), S893 ([SAT505](#))
Kahl, Sabine, S451 ([FRI106](#))
Kaido, Toshimi, S883 ([SAT488](#))
Kakegawa, Tatsuya, S379 ([THU580](#))
Kakuda, Thomas, S8 ([GS010](#)), S838 ([SAT370](#)), S864 ([SAT422](#))
Kalafati, Ioanna-Panagiota, S451 ([FRI106](#))
Kalaitzakis, Evangelos, S890 ([SAT500](#)), S904 ([SAT527](#))
Kalamitsis, George, S218 ([THU251](#))
Kale, Pratibha Ramchandra, S350 ([THU512](#))
Kalf, Jörg, S381 ([THU585](#))
Kalinowski, Piotr, S156 ([THU072](#))
Kalita, Manash Jyoti, S299 ([THU409](#))
Kalita, Simanta, S299 ([THU409](#))
Kalk, Nicola, S134 ([THU030](#))
Kallin, Nina, S195 ([THU193](#))
Kalmeijer, Ronald, S8 ([GS010](#)), S838 ([SAT370](#)), S864 ([SAT422](#))
Kama, Jibrin, S225 ([THU266](#))
Kamali, Can, S497 ([FRI217](#)), S663 ([FRI597](#)), S739 ([SAT162](#))
Kamali, Kaan, S739 ([SAT162](#))
Kamar, Nassim, S772 ([SAT239](#))

- Kamath, Patrick S., S19 ([OS008](#)),
S49 ([OS063](#)), S81 ([OS110](#)),
S136 ([THU033](#)), S137 ([THU034](#)),
S138 ([THU037](#)), S339 ([THU494](#)),
S887 ([SAT496](#))
- Kamdem, Severin Donald, S113 ([OS167](#))
- Kamel, Fady, S890 ([SAT501](#))
- Kamel, Yasser, S230 ([THU277](#))
- Kamili, Saleem, S221 ([THU258](#))
- Kamkamidze, George, S216 ([THU247](#)),
S229 ([THU275](#))
- Kamkamidze, Tiko, S229 ([THU275](#))
- Kamlin, C. Omar, S61 ([OS077](#)),
S539 ([FRI297](#))
- Kamphaus, Tania, S451 ([FRI107](#)),
S454 ([FRI110](#)), S701 ([SAT073](#))
- Kampmann, Christian, S580 ([FRI382](#))
- Kamzolas, Ioannis, S7 ([GS009](#))
- Kanchelashvili, George, S216 ([THU247](#))
- Kaneko, Atsushi, S295 ([THU401](#))
- Kaneko, Shuichi, S229 ([THU274](#))
- Kaneko, Shun, S379 ([THU580](#))
- Kangarajan, Ramesh, S751 ([SAT187](#))
- Kang, Bo-Kyeong, S160 ([THU079](#)),
S224 ([THU264](#)), S435 ([FRI077](#)),
S438 ([FRI082](#)), S438 ([FRI083](#)),
S439 ([FRI086](#)), S589 ([FRI398](#)),
S728 ([SAT135](#)), S729 ([SAT136](#))
- Kang, Don, S251 ([THU317](#))
- Kang, Garrett, S623 ([FRI515](#))
- Kang, Hyo Jin, S473 ([FRI166](#))
- Kang, Jason, S178 ([THU156](#))
- Kang, Jing X, S674 ([SAT019](#))
- Kang, Keon Wook, S734 ([SAT151](#)),
S746 ([SAT178](#))
- Kang, Min Kyu, S572 ([FRI365](#)),
S916 ([SAT560](#))
- Kang, Ning, S616 ([FRI502](#))
- Kang, Wonseok, S273 ([THU359](#)),
S489 ([FRI199](#))
- Kania, Katarzyna, S742 ([SAT167](#))
- Kanizaj, Tajana Filipec, S612 ([FRI494](#))
- Kanjanapan, Yada, S395 ([FRI010](#))
- Kannt, Aimo, S7 ([GS009](#))
- Kanogawa, Naoya, S615 ([FRI501](#)),
S897 ([SAT514](#))
- Kanto, Tatsuya, S229 ([THU274](#)),
S563 ([FRI346](#))
- Kanzaki, Hiroaki, S615 ([FRI501](#)),
S897 ([SAT514](#))
- Kao, Jia-Horng, S595 ([FRI410](#)),
S852 ([SAT400](#)), S861 ([SAT415](#))
- Kao, Justin, S58 ([OS073](#))
- Kapatais, Andreas, S840 ([SAT374](#))
- Kapil, Umesh, S221 ([THU259](#))
- Kaplan, David, S89 ([OS126](#)),
S223 ([THU262](#)), S227 ([THU270](#)),
S546 ([FRI311](#)), S936 ([SAT596](#))
- Kaplan, David E., S30 ([OS027](#))
- Kaplan, Gilaad, S323 ([THU462](#))
- Kaps, Leonard, S145 ([THU051](#)),
S464 ([FRI147](#)), S882 ([SAT486](#))
- Kaps, Sarah, S166 ([THU092](#))
- Kapus, Andras, S822 ([SAT320](#))
- Kara-Ali, Ghania, S639 ([FRI548](#))
- Karabay, Oguz, S858 ([SAT411](#))
- Karademir, Sedat, S782 ([SAT255](#)),
S820 ([SAT316](#))
- Karagiannakis, Dimitrios, S429 ([FRI063](#))
- Karagozian, Raffi, S203 ([THU224](#)),
S204 ([THU225](#))
- Karahuseyinoglu, Sercin, S693 ([SAT058](#))
- Karaletsos, Theofanis, S31 ([OS028](#)),
S409 ([FRI030](#))
- Karamichali, Eirini, S255 ([THU326](#))
- Karaoulani, Theofanie, S840 ([SAT374](#))
- Karapatanis, Stylianos, S840 ([SAT374](#))
- Karasu, Zeki, S19 ([OS008](#)), S49 ([OS063](#)),
S294 ([THU399](#)), S399 ([FRI015](#)),
S782 ([SAT255](#)), S820 ([SAT316](#))
- Kardashian, Ani, S210 ([THU235](#))
- Karim, Gres, S168 ([THU097](#)),
S170 ([THU099](#)), S301 ([THU413](#))
- Karim, Mohammad Ehsanul,
S282 ([THU378](#))
- Kariv, Revital, S148 ([THU056](#))
- Karki, Chitra, S491 ([FRI204](#))
- Karlas, Thomas, S148 ([THU057](#))
- Karlen, Vanessa, S163 ([THU085](#))
- Karlsen, Tom Hemming, S27 ([OS021](#)),
S77 ([OS103](#)), S178 ([THU157](#)),
S604 ([FRI463](#))
- Karnam, Purushtotham, S936 ([SAT596](#))
- Karnsakul, Wikrom, S308 ([THU435](#))
- Karpen, Saul J., S518 ([FRI255](#)),
S519 ([FRI256](#))
- Karpińska, Ewa, S565 ([FRI350](#))
- Karsdal, Morten, S25 ([OS018](#)),
S415 ([FRI039](#)), S431 ([FRI069](#)),
S435 ([FRI076](#)), S437 ([FRI080](#)),
S475 ([FRI169](#)), S495 ([FRI210](#)),
S721 ([SAT118](#)), S733 ([SAT146](#)),
S895 ([SAT510](#))
- Kartalis, Nikolaos, S333 ([THU480](#))
- Karthikeyan, Palaniswamy, S551 ([FRI321](#))
- Karunanithy, Anu, S42 ([OS049](#))
- Karvellas, Constantine, S779 ([SAT250](#))
- Karwowska, Kornelia, S565 ([FRI350](#))
- Kasavuli, Joyce, S135 ([THU032](#))
- Kaseb, Ahmed, S372 ([THU567](#)),
S383 ([THU588](#))
- Kaser, Lisa, S663 ([FRI599](#))
- Kashyap, Minal, S197 ([THU196](#))
- Kasmani, Zain, S805 ([SAT292](#))
- Kassas, Mohamed El, S154 ([THU069](#)),
S209 ([THU234](#))
- Kassem, Jasmin, S925 ([SAT574](#))
- Katchiuri, Nino, S151 ([THU063](#))
- Katchman, Helena, S49 ([OS063](#))
- Kategaya, Lorn, S31 ([OS028](#)), S37 ([OS041](#)),
S762 ([SAT208](#))
- Kather, Jakob, S11 ([LB003](#))
- Kato, Jun, S615 ([FRI501](#)), S897 ([SAT514](#))
- Kato, Naoya, S563 ([FRI346](#)), S615 ([FRI501](#)),
S897 ([SAT514](#))
- Katsioloudes, Petros, S202 ([THU220](#))
- Katsounas, Antonios,
S378 ([THU579](#))
- Kattakuzhy, Sarah, S552 ([FRI322](#)),
S571 ([FRI362](#)), S572 ([FRI364](#)),
S574 ([FRI369](#))
- Kattamis, Antonis, S472 ([FRI163](#))
- Katzman, Helena, S19 ([OS008](#)),
S790 ([SAT268](#))
- Kaufmann, Benedikt, S471 ([FRI161](#)),
S690 ([SAT051](#))
- Kaufmann, Paul, S361 ([THU532](#))
- Kaur, Amanpreet, S694 ([SAT059](#))
- Kaur, Impreet, S105 ([OS153](#))
- Kaur, Kanudeep, S232 ([THU280](#))
- Kaur, Navpreet, S794 ([SAT274](#))
- Kaur, Savneet, S105 ([OS153](#)),
S901 ([SAT521](#))
- Kauschke, Stefan Günther, S472 ([FRI164](#)),
S753 ([SAT191](#))
- Kaushal, Kanav, S369 ([THU547](#))
- Kaushik, Ankita, S103 ([OS149](#)),
S237 ([THU290](#)), S280 ([THU372](#)),
S281 ([THU376](#)), S285 ([THU383](#)),
S286 ([THU384](#)), S286 ([THU386](#)),
S300 ([THU410](#)), S305 ([THU421](#)),
S597 ([FRI416](#)), S846 ([SAT387](#))
- Kaushik, Vishal, S53 ([OS066](#))
- Kautiainen, Hannu, S312 ([THU441](#)),
S327 ([THU469](#))
- Kavanagh, Mary, S569 ([FRI358](#))
- Kavousi, Maryam, S41 ([OS046](#))
- Kawada, Norifumi, S563 ([FRI346](#))
- Kawai, Hidehiko, S172 ([THU103](#))
- Kawamura, Nobuyoshi, S430 ([FRI067](#))
- Kawashima, Keigo, S875 ([SAT442](#))
- Kayes, Tahrima, S558 ([FRI334](#))
- Kayhan, Meral Akdogan, S782 ([SAT255](#)),
S820 ([SAT316](#)), S858 ([SAT410](#)),
S861 ([SAT416](#))
- Kaykas, Ajamete, S37 ([OS041](#)),
S762 ([SAT208](#))
- Kay, Richard, S695 ([SAT061](#))
- Kazankov, Konstantin, S344 ([THU503](#)),
S889 ([SAT499](#)), S903 ([SAT526](#))
- Keane, Jeremy, S743 ([SAT169](#))
- Keaveny, Andrew, S19 ([OS008](#)),
S49 ([OS063](#)), S768 ([THU231](#))
- Kechagias, Stergios, S146 ([THU052](#)),
S423 ([FRI053](#))
- Keijer, Jaap, S676 ([SAT024](#)), S677 ([SAT025](#))
- Keijzer, Nanda, S686 ([SAT044](#)),
S698 ([SAT067](#))
- Keitel-Anselmino, Verena, S378 ([THU579](#))
- Kelly, Deirdre, S551 ([FRI321](#)), S608 ([FRI470](#))
- Kelly, Matt, S453 ([FRI109](#))
- Kelly, Scott, S713 ([SAT101](#))
- Kemadjou, Eric Ngonga, S611 ([FRI492](#))
- Kemble, George, S419 ([FRI045](#))
- Ke, Mingxia, S240 ([THU296](#))
- Kemp, Graham, S433 ([FRI073](#))
- Kempinska-Podhorodecka, Agnieszka,
S601 ([FRI455](#))
- Kempski, Jan, S823 ([SAT341](#))
- Kemp, William, S441 ([FRI090](#))
- Kendall, Bradley, S147 ([THU054](#))
- Kendall, Tim, S163 ([THU086](#))

Author Index

- Kendrick, Stuart, S12 ([LB004A](#)), S13 ([LB004B](#)), S288 ([THU389](#)), S291 ([THU393](#)), S855 ([SAT405](#)), S880 ([SAT452](#)), S881 ([SAT453](#))
- Kennedy, James, S19 ([OS008](#)), S49 ([OS063](#))
- Kennedy, Kevin, S632 ([FRI532](#))
- Kennedy, Oliver, S42 ([OS048](#))
- Kennedy, Patrick, S55 ([OS070](#)), S72 ([OS094](#)), S188 ([THU178](#)), S284 ([THU380](#)), S286 ([THU386](#))
- Kerashvili, Vakhtang, S587 ([FRI395](#)), S590 ([FRI401](#))
- Kerbert, Annarein, S51 ([OS065](#)), S902 ([SAT523](#))
- Kerbl-Knapp, Jakob, S346 ([THU506](#))
- Kerkar, Nanda, S326 ([THU467](#))
- Kershenobich, David, S238 ([THU292](#))
- Kersten, Remco, S603 ([FRI461](#))
- Kerstens, Emilie, S797 ([SAT279](#))
- Keshav, Satish, S602 ([FRI458](#))
- Keshinro, Rosemary, S34 ([OS034](#))
- Keshvari, Sahar, S190 ([THU183](#))
- Keskin, Onur, S293 ([THU397](#))
- Kessler, Annika, S655 ([FRI581](#))
- Keßler, Sonja, S705 ([SAT082](#))
- Kessoku, Takaomi, S430 ([FRI067](#))
- Kettler, Carla, S95 ([OS135](#))
- Kew, Guan Sen, S298 ([THU406](#))
- Key, Cassandra, S713 ([SAT102](#)), S720 ([SAT116](#))
- Khader, Shameer, S411 ([FRI033](#))
- Khaertynova, Ilsiya, S866 ([SAT425](#))
- Khaing, Myat, S538 ([FRI294](#)), S538 ([FRI295](#))
- Khakoo, Salim, S200 ([THU218](#))
- Khakpoor, Atefeh, S247 ([THU308](#)), S298 ([THU406](#))
- Khaled, Jaafar, S368 ([THU543](#)), S645 ([FRI558](#))
- Khaled, Najib Ben, S662 ([FRI596](#))
- Khalili, Korosh, S3 ([GS004](#))
- Khalili, Mandana, S581 ([FRI384](#))
- Khamri, Wafa, S185 ([THU173](#)), S356 ([THU522](#))
- Khan, Aamir Ghafoor, S240 ([THU295](#))
- Khanam, Arshi, S571 ([FRI362](#))
- Khan, Ambreen, S240 ([THU295](#))
- Khan, Faisal, S411 ([FRI033](#))
- Khanipov, Kamil, S194 ([THU191](#))
- Khan, Juned, S358 ([THU525](#))
- Khan, Khalid Mahmud, S884 ([SAT489](#))
- Khan, Muhammad, S230 ([THU277](#))
- Khanna, Amardeep, S311 ([THU440](#))
- Khanna, Rajeev, S528 ([FRI273](#))
- Khan, Sabiha, S560 ([FRI338](#))
- Khan, Shahid, S938 ([SAT600](#))
- Khan, Tanweer, S94 ([OS133](#))
- Khan, Tipu, S596 ([FRI411](#))
- Khan, Uqba, S372 ([THU567](#)), S383 ([THU588](#))
- Khan, Uzma, S240 ([THU295](#))
- Khan, Zahra, S822 ([SAT320](#))
- Kharawala, Saifuddin, S855 ([SAT405](#))
- Khassis, Cyrille El, S759 ([SAT202](#))
- Khatoon, Nadia, S768 ([SAT231](#))
- Khattab, Nora, S125 ([THU014](#))
- Khazak, Andre, S168 ([THU097](#)), S170 ([THU099](#))
- Khetsuriani, Nino, S233 ([THU283](#)), S267 ([THU347](#))
- Khillan, Vikas, S350 ([THU512](#))
- Khine, Htet Htet Toe Wai, S877 ([SAT446](#))
- Khilghatyan, Davit, S130 ([THU022](#))
- Khomich, Olga, S766 ([SAT216](#))
- Khonelidze, Irma, S213 ([THU242](#))
- Khorsandi, Shirin Elizabeth, S647 ([FRI563](#)), S650 ([FRI569](#))
- Khosdeli, Mina, S318 ([THU453](#))
- Khosla, Aditya, S708 ([SAT088](#))
- Khowaja, Saira, S240 ([THU295](#))
- Khudyakov, Yury, S221 ([THU258](#))
- Khunti, Kamlesh, S29 ([OS025](#))
- Khwairakpam, Giten, S219 ([THU254](#))
- Kibeche, Rania, S547 ([FRI314](#))
- Kiddle, Steven, S609 ([FRI486](#))
- Kiemer, Alexandra K., S705 ([SAT082](#))
- ki, Han Seul, S907 ([SAT533](#))
- Kiliaan, Amanda, S698 ([SAT067](#))
- Killer, Alexander, S825 ([SAT345](#))
- Killmer, Saskia, S2 ([GS003](#)), S710 ([SAT090](#))
- Kilpatrick, Alastair, S85 ([OS117](#))
- Kim, Adam, S33 ([OS032](#)), S193 ([THU188](#))
- Kim, Albert, S37 ([OS041](#))
- Kim, Andre D., S690 ([SAT051](#))
- Kim, Benjamin, S404 ([FRI023](#))
- Kim, Beom Kyung, S74 ([OS098](#)), S414 ([FRI037](#)), S922 ([SAT571](#))
- Kimberger, Oliver, S390 ([FRI003](#))
- Kim, Bong Wan, S799 ([SAT282](#))
- Kim, Byoung Je, S916 ([SAT561](#))
- Kim, Byung Ik, S485 ([FRI191](#))
- Kim, Byung Seok, S572 ([FRI365](#)), S916 ([SAT560](#))
- Kim, Chang Min, S490 ([FRI202](#))
- Kim, Chang Wook, S932 ([SAT590](#))
- Kim, Chanyang, S653 ([FRI575](#))
- Kim, Chul Hoon, S653 ([FRI575](#)), S755 ([SAT194](#))
- Kim, Dae Jin, S469 ([FRI157](#))
- Kim, DaWon, S921 ([SAT569](#))
- Kim, Dong-Sik, S799 ([SAT282](#))
- Kim, DongYun, S176 ([THU152](#))
- Kim, Doohyun, S246 ([THU306](#)), S247 ([THU307](#))
- Kim, Do Young, S932 ([SAT590](#))
- Kim, Elena, S264 ([THU341](#))
- Kimer, Nina, S64 ([OS083](#)), S499 ([FRI220](#)), S610 ([FRI489](#)), S890 ([SAT501](#))
- Kim, Gi-Ae, S275 ([THU363](#)), S833 ([SAT361](#))
- Kim, Hyeree, S489 ([FRI199](#))
- Kim, Hye Seon, S932 ([SAT589](#))
- Kim, Hyung Joon, S932 ([SAT590](#))
- Kim, Hyun Jung, S767 ([SAT229](#))
- Kim, Hyun Young, S734 ([SAT151](#))
- Kim, Irene, S377 ([THU575](#))
- Kim, Jae Heon, S767 ([SAT229](#))
- Kim, Jason, S473 ([FRI166](#))
- Kim, Ji Hoon, S932 ([SAT590](#))
- Kim, Ji Min, S932 ([SAT589](#))
- Kim, Jin Seoub, S932 ([SAT589](#))
- Kim, Jin Un, S290 ([THU391](#))
- Kim, Jin-Wook, S870 ([SAT433](#))
- Kim, Jong Man, S767 ([SAT229](#)), S799 ([SAT282](#))
- Kim, Ju Hyun, S13 ([LB004B](#)), S881 ([SAT453](#))
- Kim, Jung-Hee, S489 ([FRI199](#)), S866 ([SAT426](#))
- Kim, Jung Kuk, S468 ([FRI156](#)), S469 ([FRI157](#))
- Kim, Kang Mo, S545 ([FRI310](#)), S842 ([SAT378](#))
- Kim, Kyung Mo, S866 ([SAT425](#))
- Kim, MeeJ, S312 ([THU442](#))
- Kimmerle, Renate, S533 ([FRI283](#))
- Kim, Mi Mi, S160 ([THU079](#)), S224 ([THU264](#)), S435 ([FRI077](#)), S589 ([FRI398](#)), S728 ([SAT135](#)), S729 ([SAT136](#))
- Kim, Mi Na, S100 ([OS144](#)), S862 ([SAT418](#)), S922 ([SAT571](#))
- Kim, Moon Young, S631 ([FRI530](#)), S705 ([SAT083](#)), S907 ([SAT533](#))
- Kim, Namjeong, S473 ([FRI166](#))
- Kim, Pauline AW Poh, S98 ([OS140](#))
- Kim, Rattana, S260 ([THU335](#))
- Kim, Ryoan Ho, S866 ([SAT426](#))
- Kim, Sanghwa, S473 ([FRI166](#))
- Kim, Sang Kyum, S734 ([SAT151](#))
- Kim, Sarang, S788 ([SAT264](#))
- Kim-Schluger, Leona, S343 ([THU502](#))
- Kim, Seok Hyun, S380 ([THU583](#))
- Kim, Seon-Ok, S891 ([SAT503](#))
- Kim, Seung Up, S283 ([THU379](#)), S922 ([SAT571](#))
- Kim, So Yeon, S916 ([SAT561](#))
- Kim, Sungmin, S377 ([THU576](#))
- Kim, Tae Hyung, S616 ([FRI502](#)), S932 ([SAT590](#))
- Kim, Terri, S529 ([FRI274](#))
- Kimura, Masaki, S673 ([SAT017](#))
- Kimura, Naruhiro, S28 ([OS023](#))
- Kimura, Yusuke, S183 ([THU167](#))
- Kim, Won, S81 ([OS110](#)), S425 ([FRI058](#)), S448 ([FRI102](#)), S452 ([FRI108](#)), S872 ([SAT437](#))
- Kim, W. Ray, S116 ([OS173](#)), S462 ([FRI124](#)), S790 ([SAT267](#)), S870 ([SAT433](#)), S903 ([SAT525](#))
- Kim, Ye-Jee, S891 ([SAT503](#))
- Kim, Yohan, S468 ([FRI156](#)), S469 ([FRI157](#))
- Kim, Yong Ook, S7 ([GS009](#))
- Kim, Yoon Jun, S78 ([OS104](#)), S932 ([SAT590](#))
- Kim, Young Seok, S610 ([FRI488](#))
- Kinast, Volker, S250 ([THU315](#)), S263 ([THU339](#))
- King, Wendy C, S264 ([THU341](#))
- King, Yele, S848 ([SAT392](#))
- Kiraz, Alper, S693 ([SAT058](#))
- Kirchner, Theresa, S317 ([THU452](#)), S783 ([SAT257](#)), S784 ([SAT259](#))
- Kirchner, Varvara, S807 ([SAT296](#))
- Kirikoshi, Hiroyuki, S430 ([FRI067](#))
- Kirimlioglu, Hale, S693 ([SAT058](#))
- Kirkpatrick, Jesse, S657 ([FRI584](#))

- Kirmizigul, Beril, S293 (THU397)
 Kirstein, Martha M, S313 (THU444)
 Kirstgen, Michael, S843 (SAT380)
 Kirwan, Jennifer, S497 (FRI217)
 Kisseleva, Tatiana, S86 (OS119)
 Kitajima, Toshihiro, S778 (SAT249)
 Kita, Yuji, S172 (THU103)
 Kitrinos, Kathryn M, S266 (THU346), S844 (SAT383)
 Kiyici, Murat, S820 (SAT316)
 Kiyono, Soichiro, S615 (FRI501), S897 (SAT514)
 Kiyuna, Ligia Akemi, S539 (FRI298)
 Kizivat, Tomislav, S718 (SAT113)
 Kılıç, Murat, S782 (SAT255)
 Kırımker, Elvan Onur, S782 (SAT255)
 Kırımker, Onur, S778 (SAT248)
 Kıyıcı, Murat, S861 (SAT416)
 Kjærgaard, Maria, S2 (GS002), S9 (GS012), S35 (OS036), S131 (THU024), S144 (THU046), S475 (FRI171), S500 (FRI223)
 Kjaer, Mette, S10 (LB001), S29 (OS025)
 Kjems, Lise, S517 (FRI253), S518 (FRI255), S519 (FRI256), S521 (FRI259)
 Klahr, Emma, S83 (OS114)
 Klapaczynski, Jakub, S585 (FRI390)
 Kleemann, Robert, S671 (SAT014), S676 (SAT024), S677 (SAT025), S698 (SAT067)
 Klefenz, Adrian, S464 (FRI147)
 Kleiner, David E, S264 (THU341)
 Kleiner, David E., S416 (FRI040), S481 (FRI181)
 Klein, Hanns-Georg, S937 (SAT597)
 Klein, Marina B., S206 (THU230)
 Klein, Sabine, S362 (THU533), S895 (SAT510)
 Klein, Samuel, S671 (SAT014)
 Klemm-Kropp, Michael, S306 (THU431)
 Klenerman, Paul, S54 (OS069), S57 (OS072A), S541 (FRI301), S602 (FRI458)
 Klier, Limor, S804 (SAT291)
 Klinker, Hartwig, S562 (FRI345), S585 (FRI391)
 Klinkicht, Markus, S251 (THU316)
 Klintmalm, Goran, S805 (SAT292)
 Klironomos, Evangelos, S472 (FRI163)
 Klohs, Jan, S670 (SAT011)
 Klucher, Kevin, S88 (OS123), S716 (SAT108)
 Klümper, Heinz-Josef, S107 (OS157)
 Kluwe, Johannes, S313 (THU444)
 Knapp, Maximilian, S197 (THU197)
 Knecht, Gaby, S15 (OS001)
 Kneigt, Robert De, S147 (THU055), S227 (THU271), S281 (THU374), S569 (FRI359)
 Knetsch, Cornelis, S750 (SAT184)
 Knolle, Percy A., S185 (THU171), S189 (THU180), S195 (THU193)
 Knop, Filip Krag, S121 (THU006)
 Knox, Steven J, S836 (SAT366), S846 (SAT388)
 Knudsen, Andreas Dehlbæk, S818 (SAT314)
 Knudsen, Anne Wilkens, S890 (SAT500)
 Koay, Tsin Shue, S120 (THU004)
 Kobayashi, Kazufumi, S615 (FRI501), S897 (SAT514)
 Kobayashi, Takashi, S430 (FRI067)
 Kobeiter, Hicham, S375 (THU573)
 Koç, Elif Sitre, S858 (SAT410), S861 (SAT416), S864 (SAT421)
 Koch, Carmo, S282 (THU377)
 Kochuparampil, Jossy George, S486 (FRI194), S493 (FRI207)
 Koç, Meliye Meriç, S858 (SAT411)
 Koczulla, Andreas Rembert, S515 (FRI250)
 Kodama, Takahiro, S563 (FRI346)
 Kodikara, Chamani, S613 (FRI495)
 Koeckerling, David, S345 (THU505)
 Koenen, Rory R., S193 (THU187)
 Koerkamp, Bas Groot, S107 (OS157), S644 (FRI556)
 Kofoed, Karen, S550 (FRI319)
 Koh, Christopher, S70 (OS092)
 Koh, Elaine, S366 (THU540)
 Ko, Hin Hin, S544 (FRI308), S910 (SAT538)
 Koh, Kwang Cheol, S273 (THU359)
 Köhler, Bruno, S655 (FRI581)
 Köhler, Jan, S533 (FRI283), S825 (SAT345)
 Kohlhepp, Marlene, S684 (SAT040)
 Kohli, Anita, S427 (FRI060)
 Kohnke-Ertel, Birgit, S654 (FRI577)
 Köhrer, Karin, S545 (FRI309)
 Koike, Kazuhiko, S485 (FRI192)
 Koizumi, Yohei, S616 (FRI502)
 Ko, Jimin, S33 (OS031)
 Köker, Gökhan, S242 (THU300)
 Ko, Ko, S229 (THU274), S260 (THU335), S260 (THU336)
 Koksai, İftihar, S858 (SAT411)
 Kokubu, Shigehiro, S430 (FRI067)
 Kolaric, Tea Omanovic, S718 (SAT113)
 Kolesnikova, Olena, S421 (FRI049)
 Koller, Daphne, S31 (OS028), S37 (OS041), S409 (FRI030), S762 (SAT208)
 Koller, Tomáš, S613 (FRI496)
 Kolomiichuk, Liudmyla, S848 (SAT392)
 Komolmit, Piyawat, S299 (THU408), S772 (SAT238), S812 (SAT305), S867 (SAT427)
 Kondili, Loreta, S212 (THU239), S232 (THU281), S238 (THU291), S242 (THU299), S564 (FRI347)
 Kondo, Takayuki, S615 (FRI501), S897 (SAT514)
 Kong, Alice Pik-Shan, S39 (OS043)
 Königshofer, Philipp, S360 (THU529), S466 (FRI152), S469 (FRI158), S472 (FRI164), S753 (SAT191)
 Kon, Kazuyoshi, S687 (SAT047)
 Kono, Yuko, S926 (SAT577)
 Konstantinou, Christos, S670 (SAT011)
 Kontogianni, Meropi, S908 (SAT534)
 Koob, Dennis, S602 (FRI460)
 Koo, Bo Kyung, S163 (THU087)
 Kopelman, Yael, S292 (THU395)
 Kopsida, Maria, S368 (THU543), S645 (FRI558)
 Korell, Felix, S655 (FRI581)
 Korenjak, Marko, S512 (FRI244)
 Korf, Hannelie, S120 (THU003), S346 (THU507), S680 (SAT032)
 Kornek, Mirosław, S915 (SAT559)
 Koroki, Keisuke, S615 (FRI501), S897 (SAT514)
 Koro, Konstantin, S259 (THU334)
 Korsavidou-Hult, Nafsika, S333 (THU480)
 Korsgren, Olle, S471 (FRI162)
 Kosari, Kambiz, S377 (THU575)
 Köse, Sükran, S858 (SAT411)
 Koshman, Illia, S635 (FRI539)
 Kosick, Heather M., S429 (FRI065)
 Koskinas, Ioannis-Georgios, S255 (THU326), S472 (FRI163)
 Kosmella, Esther, S737 (SAT158)
 Kostadinova, Radina, S446 (FRI099), S481 (FRI183), S488 (FRI197), S703 (SAT078)
 Kostishyna, Iryna, S635 (FRI539)
 Kostrub, Cory, S599 (FRI452)
 Kotaria, Nato, S221 (THU258)
 Kotlinowski, Jerzy, S746 (SAT179), S759 (SAT203)
 Kotorashvili, Adam, S221 (THU258)
 Kottlilil, Shyamasundaran, S215 (THU246), S552 (FRI322), S571 (FRI362), S572 (FRI364), S574 (FRI369), S863 (SAT419)
 Koulman, Albert, S695 (SAT061)
 Koul, Roshan, S397 (FRI014)
 Kounis, Ilias, S402 (FRI020), S524 (FRI265), S800 (SAT285), S935 (SAT595)
 Kouno, Tetsuya, S86 (OS119)
 Kourakli, Alexandra, S472 (FRI163)
 Kouroufexi, Antri, S202 (THU220)
 Koutli, Evangelia, S815 (SAT311)
 Koutsoudakis, George, S607 (FRI468)
 Kowalik, Marta Anna, S732 (SAT144)
 Kowdley, Kris, S87 (OS121), S312 (THU442), S319 (THU455), S335 (THU484), S451 (FRI107), S701 (SAT073), S715 (SAT106), S716 (SAT107)
 Kowdley, Kris V., S427 (FRI060)
 Koyama, Yukinori, S183 (THU167)
 Koynov, Kaloian, S464 (FRI147)
 Kozlov, Oleksandr, S635 (FRI539)
 Kozlov, Sergii, S635 (FRI539)
 Krackhardt, Angela, S2 (GS003)
 Krämer, Lene, S550 (FRI319)
 Kraft, Anke, S566 (FRI352), S893 (SAT505)
 Krag, Aleksander, S2 (GS002), S9 (GS012), S25 (OS018), S35 (OS036), S129 (THU021), S131 (THU024), S144 (THU046), S423 (FRI054), S434 (FRI074), S450 (FRI104), S475 (FRI171), S500 (FRI223), S515 (FRI250)
 Kragh Hansen, Johanne, S9 (GS012)

Author Index

- Kraglund, Frederik, S123 ([THU011](#)), S172 ([THU104](#))
- Krahmer, Natalie, S703 ([SAT079](#))
- Krajden, Mel, S17 ([OS005](#)), S209 ([THU233](#)), S282 ([THU378](#)), S910 ([SAT538](#))
- Kranidioti, Hariklia, S840 ([SAT374](#))
- Krarup, Niels, S10 ([LB001](#))
- Krassenburg, Lisette, S569 ([FRI359](#))
- Kratzer, Alexander, S241 ([THU298](#))
- Krause, Jenny, S604 ([FRI462](#))
- Krause, Linda, S315 ([THU447](#))
- Kraus, Nico, S362 ([THU533](#))
- Krawczyk, Marcin, S11 ([LB002](#)), S77 ([OS103](#)), S107 ([OS157](#)), S156 ([THU072](#)), S166 ([THU092](#)), S315 ([THU447](#)), S317 ([THU451](#)), S342 ([THU500](#)), S460 ([FRI122](#)), S605 ([FRI464](#)), S607 ([FRI469](#)), S671 ([SAT014](#))
- Krech, Till, S333 ([THU481](#))
- Reiss, Yitshak, S804 ([SAT291](#))
- Kremer, Andreas E, S163 ([THU085](#))
- Kremer, Wolfgang Maximilian, S145 ([THU051](#)), S882 ([SAT486](#))
- Kremsdorf, Dina, S297 ([THU404](#))
- Krenzien, Felix, S374 ([THU570](#)), S380 ([THU582](#)), S497 ([FRI217](#)), S663 ([FRI597](#)), S739 ([SAT162](#))
- Krey, Thomas, S263 ([THU339](#))
- Krieg, Andreas, S384 ([THU592](#))
- Krieg, Sarah, S384 ([THU592](#))
- Krimmel, Laurenz, S2 ([GS003](#))
- Krishna, Murli, S768 ([SAT231](#))
- Krishnamurthy, Kishore Alagere, S539 ([FRI298](#))
- Krishnan, Santhoshi, S470 ([FRI160](#)), S485 ([FRI190](#))
- Krishnan, Vyjayanthi, S88 ([OS124](#))
- Kriss, Michael, S779 ([SAT250](#))
- Kristiansen, Maria, S154 ([THU068](#))
- Kristic, Antonia, S24 ([OS017](#))
- Kroeniger, Konstantin, S937 ([SAT597](#))
- Krohn-Hehli, Louise, S220 ([THU255](#))
- Krohn, Sandra, S904 ([SAT528](#))
- Kronborg, Thit, S340 ([THU496](#)), S499 ([FRI220](#))
- Kronsten, Victoria, S771 ([SAT236](#))
- Krüger, Achim, S83 ([OS114](#))
- Krugluger, Walter, S545 ([FRI309](#))
- Kruk, Beata, S317 ([THU451](#)), S605 ([FRI464](#)), S607 ([FRI469](#))
- Krupa, Łukasz, S107 ([OS157](#))
- Kruse, Carlot, S520 ([FRI258](#))
- Krygier, Rafal, S585 ([FRI390](#))
- Krylova, Nina, S269 ([THU351](#))
- Krzysztof, Simon, S592 ([FRI406](#))
- Ksiazek, Iwona, S7 ([GS009](#))
- Kuang, Xutong, S501 ([FRI224](#))
- Kubal, Chandrashekhar, S686 ([SAT045](#))
- Kubale, Reinhard, S460 ([FRI122](#))
- Kubiatowicz, Luke J., S921 ([SAT569](#))
- Kuchta, Alison, S842 ([SAT377](#))
- Kuchuloria, Tinatin, S214 ([THU243](#)), S216 ([THU247](#)), S219 ([THU253](#)), S221 ([THU258](#)), S587 ([FRI395](#)), S590 ([FRI400](#)), S590 ([FRI401](#))
- Kucykowicz, Stephanie, S55 ([OS070](#))
- Kudo, Hiromi, S121 ([THU007](#)), S132 ([THU026](#))
- Kudo, Masatoshi, S372 ([THU567](#)), S383 ([THU588](#)), S937 ([SAT597](#))
- Kuenzler, Patrizia, S192 ([THU186](#)), S509 ([FRI238](#))
- Kugelmas, Marcelo, S154 ([THU069](#))
- Kuhns, Mary, S851 ([SAT398](#))
- Kuiken, Sjoerd, S93 ([OS132](#))
- Kuiper, Edith, S306 ([THU431](#))
- Kuipers, Folkert, S517 ([FRI254](#))
- Kuipers, Thijs, S893 ([SAT506](#))
- Kujundžić, Petra Dinjar, S270 ([THU353](#))
- Kukla, Michal, S613 ([FRI496](#))
- Kularbkaew, Churaieat, S499 ([FRI219](#))
- Kulathunga, Kaushalya, S702 ([SAT076](#))
- Kulkarni, Anand, S19 ([OS008](#)), S49 ([OS063](#)), S81 ([OS110](#)), S191 ([THU184](#)), S329 ([THU474](#)), S358 ([THU525](#))
- Kulkarni, Santosh, S751 ([SAT187](#))
- Kullberg, Joel, S40 ([OS045](#)), S683 ([SAT038](#))
- Kultgen, Steven G., S848 ([SAT391](#)), S848 ([SAT392](#))
- Kumar, Anupam, S51 ([OS064](#)), S347 ([THU508](#)), S756 ([SAT196](#))
- Kumar, Ashish, S19 ([OS008](#)), S49 ([OS063](#))
- Kumar, Guresh, S51 ([OS064](#)), S139 ([THU038](#)), S349 ([THU510](#)), S397 ([FRI014](#)), S901 ([SAT521](#))
- Kumar, Karan, S358 ([THU525](#))
- Kumar, Manoj, S22 ([OS014](#)), S53 ([OS066](#))
- Kumar, Parag, S862 ([SAT417](#))
- Kumar, Pramod, S625 ([FRI520](#))
- Kumar, Rahul, S567 ([FRI354](#))
- Kumar, Ramesh, S170 ([THU100](#)), S813 ([SAT306](#))
- Kumar, Ravi, S903 ([SAT526](#))
- Kumar Sarin, Shiv, S349 ([THU510](#))
- Kumar, Sonal, S168 ([THU096](#)), S729 ([SAT138](#))
- Kummen, Martin, S178 ([THU157](#))
- Kuna, Lucija, S718 ([SAT113](#))
- Kunderfranco, Paolo, S47 ([OS058](#))
- Kunst, Claudia, S663 ([FRI599](#))
- Kunst, Roni, S26 ([OS019](#))
- Kuntzen, Christian, S548 ([FRI315](#))
- Kunzmann, Lilly K., S604 ([FRI462](#))
- Kuo, Hsing-Tao, S595 ([FRI410](#)), S863 ([SAT420](#))
- Kuo, Joseph, S650 ([FRI568](#)), S660 ([FRI591](#))
- Kuo, Leane, S797 ([SAT278](#))
- Kuo, Yong-Fang, S773 ([SAT240](#))
- Kupcinkas, Juozas, S107 ([OS157](#))
- Kupcinkas, Limas, S308 ([THU435](#))
- Kupfer, Jörg, S163 ([THU085](#))
- Küpper, Jan, S658 ([FRI585](#))
- Kurano, Makoto, S485 ([FRI192](#))
- Kurosaki, Masayuki, S379 ([THU580](#)), S563 ([FRI346](#))
- Kurt, Ada, S401 ([FRI019](#)), S809 ([SAT298](#))
- Kus, Edyta, S746 ([SAT179](#)), S759 ([SAT203](#))
- Kushner, Tatyana, S160 ([THU080](#)), S168 ([THU096](#)), S455 ([FRI113](#)), S590 ([FRI402](#))
- Kuter, David, S60 ([OS075](#))
- Kütting, Fabian, S313 ([THU444](#))
- Kuvalekar, Manik, S839 ([SAT372](#))
- Kuyvenhoven, Johan, S306 ([THU431](#))
- Kveton, Martin, S536 ([FRI290](#))
- Kwak, Soo-Heon, S163 ([THU087](#))
- Kwanten, Wilhelmus, S502 ([FRI226](#)), S709 ([SAT089](#))
- Kweon, Young Oh, S377 ([THU576](#)), S572 ([FRI365](#)), S916 ([SAT560](#))
- Kwon, Dong Il, S610 ([FRI488](#))
- Kwong, Allison, S116 ([OS173](#)), S462 ([FRI124](#)), S790 ([SAT267](#)), S903 ([SAT525](#))
- Kwon, Hyunjoo, S468 ([FRI156](#)), S469 ([FRI157](#))
- Kwon, In Sun, S380 ([THU583](#))
- Kwon, Soon Sung, S653 ([FRI575](#))
- Kwon, Sung, S203 ([THU223](#))
- Kwon, Yoo-Wook, S667 ([SAT005](#))
- Kwon, Yun, S606 ([FRI467](#))
- Kwo, Paul Yien, S773 ([SAT240](#)), S836 ([SAT366](#))
- Kydd-Sinclair, Dannielle, S751 ([SAT185](#))
- Kyprianou, Evi, S202 ([THU220](#))
- Kyriazidou, Anastasia, S840 ([SAT374](#))
- Kyung Kim, Beom, S422 ([FRI051](#))
- Labenz, Christian, S80 ([OS108](#)), S145 ([THU051](#)), S448 ([FRI102](#)), S452 ([FRI108](#)), S882 ([SAT486](#))
- Labiano, Ibone, S648 ([FRI564](#))
- Labio, Eternity, S12 ([LB004A](#)), S880 ([SAT452](#))
- Lacaille, Florence, S519 ([FRI256](#)), S521 ([FRI259](#))
- Lacalle, Juan R., S444 ([FRI095](#))
- La Casta, Adelaida, S77 ([OS103](#)), S107 ([OS157](#))
- Lachaux, Alain, S519 ([FRI256](#)), S521 ([FRI259](#))
- Lachiondo-Ortega, Sofia, S48 ([OS060](#)), S84 ([OS116](#)), S87 ([OS122](#)), S600 ([FRI453](#)), S673 ([SAT018](#)), S679 ([SAT029](#))
- Lackner, Carolin, S11 ([LB002](#)), S714 ([SAT103](#))
- Lacombe, Karine, S72 ([OS093](#)), S833 ([SAT360](#))
- Lacotte, Stéphanie, S754 ([SAT192](#))
- Lada, Olivier, S579 ([FRI381](#))
- Laferl, Hermann, S545 ([FRI309](#))
- Laffi, Giacomo, S908 ([SAT535](#))
- Laffusa, Alice, S404 ([FRI024](#))
- Lafiatis, Ioannis, S472 ([FRI163](#))
- Lafortune, Annie, S456 ([FRI114](#))
- Lafuente-Barquero, Juan, S649 ([FRI566](#))
- Lagging, Martin, S186 ([THU174](#))
- Laghi, Luca, S886 ([SAT494](#))
- Lagneaux, Anne-Sophie, S905 ([SAT529](#))
- Lago, Marilyn Salvat, S2 ([GS003](#))

- Lai, Che To, S39 ([OS043](#)), S164 ([THU088](#)), S302 ([THU414](#))
- Laidlaw, Stephen, S57 ([OS072A](#))
- Lai, Eleonora, S748 ([SAT180](#))
- Lai, Felix, S824 ([SAT343](#)), S835 ([SAT365](#)), S871 ([SAT435](#))
- LaIglesia, Lara, S749 ([SAT183](#))
- Lai, Jennifer, S339 ([THU494](#)), S886 ([SAT493](#))
- Lai, Jennifer C, S887 ([SAT496](#))
- Lai, Kuan-Yu, S162 ([THU084](#))
- Lai, Mandy Sze-Man, S101 ([OS147](#)), S274 ([THU362](#))
- Lainka, Elke, S519 ([FRI256](#))
- Lai, Qingying, S254 ([THU323](#)), S854 ([SAT404](#))
- Lai, Walter, S70 ([OS092](#))
- Lake-Bakaar, Gerond, S719 ([SAT115](#))
- Lakhloufi, Dalila, S124 ([THU012](#))
- Lakiotaki, Dimitra, S429 ([FRI063](#))
- Lakli, Mounia, S514 ([FRI248](#)), S521 ([FRI260](#))
- Lal, Bikrant Bihari, S528 ([FRI273](#))
- Laleman, Wim, S21 ([OS011](#)), S346 ([THU507](#))
- Lalezari, Jacob P, S836 ([SAT366](#)), S848 ([SAT390](#))
- Laloux, Géraldine, S135 ([THU032](#))
- Lam, Angela M, S848 ([SAT391](#)), S850 ([SAT395](#)), S850 ([SAT396](#)), S851 ([SAT397](#))
- Lamarca, Angela, S107 ([OS157](#))
- Lambert, Bieke, S107 ([OS156](#))
- Lambert, Joshua, S124 ([THU013](#))
- Lambotte, Olivier, S402 ([FRI020](#))
- Lambrechts, Diether, S385 ([THU593](#))
- Lambrecht, Tom, S864 ([SAT422](#))
- Lam, Brian, S154 ([THU069](#)), S209 ([THU234](#)), S420 ([FRI048](#)), S429 ([FRI064](#))
- Lam, Laurent, S17 ([OS006](#))
- Lammers, Twan, S385 ([THU594](#))
- Lammers, Willem, S335 ([THU484](#))
- Lammert, Frank, S11 ([LB002](#)), S59 ([OS074](#)), S80 ([OS108](#)), S156 ([THU072](#)), S342 ([THU500](#)), S369 ([THU546](#)), S607 ([FRI469](#))
- Lampertico, Pietro, S4 ([GS006](#)), S8 ([GS010](#)), S57 ([OS072A](#)), S103 ([OS149](#)), S196 ([THU194](#)), S210 ([THU236](#)), S223 ([THU263](#)), S269 ([THU350](#)), S300 ([THU411](#)), S549 ([FRI317](#)), S578 ([FRI376](#)), S584 ([FRI388](#)), S828 ([SAT351](#)), S829 ([SAT352](#)), S843 ([SAT379](#)), S843 ([SAT381](#)), S868 ([SAT429](#)), S874 ([SAT440](#)), S880 ([SAT450](#))
- Lampichler, Katharina, S532 ([FRI280](#)), S921 ([SAT570](#))
- Lam, Shuk Man, S302 ([THU414](#))
- Lam, Wendy, S491 ([FRI203](#))
- Landa-Magdalena, Ana, S107 ([OS157](#))
- Landeche, Manuel F, S500 ([FRI222](#))
- Landis, Charles, S319 ([THU455](#))
- Landreau, Clémence, S656 ([FRI582](#))
- Lange, Christian, S378 ([THU579](#)), S642 ([FRI552](#))
- Lange, Christian M., S340 ([THU495](#)), S341 ([THU498](#)), S823 ([SAT341](#))
- Langedijk, Jacqueline, S601 ([FRI457](#))
- Langelaar, Miriam, S539 ([FRI298](#))
- Lange, Marcia, S160 ([THU080](#)), S168 ([THU096](#)), S590 ([FRI402](#))
- Langendam, Miranda, S424 ([FRI055](#))
- Langer, Mona-May, S340 ([THU495](#)), S341 ([THU498](#))
- Langhans, Bettina, S599 ([FRI451](#))
- Langlois, Lucas, S297 ([THU404](#))
- Langner, Taro, S40 ([OS045](#)), S683 ([SAT038](#))
- Lanigan, Sarah, S570 ([FRI360](#))
- Lani, Lorenzo, S382 ([THU587](#))
- Lanke, Gandhi, S787 ([SAT263](#))
- Lannes, Adrien, S73 ([OS096](#)), S74 ([OS099](#))
- Lanng, Amalie, S121 ([THU006](#))
- Lan, Nick, S164 ([THU089](#))
- Lannoo, Matthias, S680 ([SAT032](#))
- Lan, Qiuyu, S886 ([SAT494](#))
- Lanthier, Nicolas, S736 ([SAT156](#))
- Lan, Tian, S443 ([FRI093](#)), S486 ([FRI193](#))
- Lanuti, Michael, S36 ([OS037](#)), S642 ([FRI553](#))
- Lanza, Alfonso Galeota, S769 ([SAT233](#))
- Lapalus, Martine, S514 ([FRI248](#)), S521 ([FRI260](#))
- Laparra-Ramakichenin, Ariane, S402 ([FRI020](#))
- Laperche, Syria, S251 ([THU316](#))
- Lapidus, Nathanaël, S17 ([OS006](#))
- Lapitz, Ainhua, S77 ([OS103](#)), S648 ([FRI564](#))
- Laplante, Mathieu, S456 ([FRI114](#))
- Lara, Mayra Rojas, S176 ([THU153](#))
- Lark, Christopher, S294 ([THU400](#))
- Larrey, Dominique, S17 ([OS006](#)), S833 ([SAT360](#)), S840 ([SAT373](#))
- Larrubia, Juan Ramón, S184 ([THU170](#)), S826 ([SAT347](#))
- Larrue, Hélène, S630 ([FRI529](#))
- Larsen, Frederik, S423 ([FRI054](#)), S434 ([FRI074](#))
- Larsen, Steen, S724 ([SAT124](#))
- Larson, Anne, S394 ([FRI008](#))
- Lasagni, Alberto, S751 ([SAT186](#))
- Laschinger, Melanie, S185 ([THU171](#))
- Lascaux-Combe, Caroline, S833 ([SAT360](#)), S840 ([SAT373](#))
- Lassailly, Guillaume, S205 ([THU227](#)), S205 ([THU228](#)), S692 ([SAT055](#)), S913 ([SAT557](#))
- Lassen, Pierre Bel, S435 ([FRI076](#))
- Laszczewska, Maja, S640 ([FRI551](#))
- Latasa, Maria U, S643 ([FRI554](#))
- Latasa, Maria U., S112 ([OS165](#))
- Latournerie, Marianne, S817 ([SAT312](#))
- Lau, Audrey H., S831 ([SAT357](#))
- Lauber, David, S24 ([OS017](#))
- Lau, Cathrine, S125 ([THU015](#))
- Lau, Chi, S880 ([SAT451](#))
- Lau, Daryl, S264 ([THU341](#))
- Lauer, Georg, S36 ([OS037](#)), S271 ([THU356](#))
- Laufer, Stefan, S737 ([SAT158](#))
- Lau, Jasmine, S842 ([SAT377](#))
- Lau, Kelly, S540 ([FRI299](#))
- Laurendeau, Caroline, S373 ([THU569](#))
- Laurent, Alexis, S375 ([THU573](#)), S791 ([SAT269](#)), S927 ([SAT578](#))
- Lauridsen, Mette, S423 ([FRI054](#)), S434 ([FRI074](#))
- Lauschke, Volker, S665 ([SAT002](#)), S756 ([SAT197](#))
- Lauw, Mandy, S524 ([FRI265](#))
- Lauzon, Marie, S377 ([THU575](#))
- Lavaux, Juliette, S872 ([SAT436](#))
- Lavery, Gareth, S364 ([THU537](#))
- Lavrijsen, Marla, S86 ([OS120](#))
- Lawal, Adebayo, S404 ([FRI023](#))
- Lawitz, Eric, S10 ([LB001](#)), S687 ([SAT046](#)), S713 ([SAT101](#)), S715 ([SAT106](#)), S716 ([SAT107](#)), S731 ([SAT142](#)), S848 ([SAT390](#))
- Law, Matthew, S302 ([THU415](#)), S560 ([FRI339](#)), S568 ([FRI356](#))
- Laxar, Daniel, S390 ([FRI003](#))
- Layani, Shanny, S83 ([OS114](#))
- Lázaro, Diego Rojo, S114 ([OS169](#))
- Lazar, Stefan, S829 ([SAT352](#))
- Lazarte, Raul, S137 ([THU034](#))
- Lazarus, Jeffrey, S148 ([THU058](#)), S150 ([THU062](#)), S207 ([THU231](#)), S208 ([THU232](#)), S217 ([THU249](#)), S218 ([THU252](#)), S220 ([THU255](#)), S238 ([THU291](#)), S277 ([THU368](#)), S426 ([FRI059](#)), S438 ([FRI084](#)), S451 ([FRI106](#))
- Lazas, Don, S474 ([FRI168](#)), S714 ([SAT103](#)), S730 ([SAT139](#))
- Lazo, Mariana, S81 ([OS110](#)), S137 ([THU034](#))
- Lazure, Patrice, S438 ([FRI084](#))
- Lazzarino, Giuseppe, S703 ([SAT077](#))
- Leaker, Benjamin, S364 ([THU536](#))
- Leal, Carina, S190 ([THU182](#))
- Le Bail, Brigitte, S73 ([OS096](#))
- Lebedel, Louise, S61 ([OS076](#))
- Lebedeva, Elena, S269 ([THU351](#))
- Lebigot, Jerome, S496 ([FRI215](#))
- Lebossé, Fanny, S356 ([THU522](#))
- Lebouche, Bertrand, S31 ([OS029](#))
- Lebrun, Maella, S584 ([FRI389](#))
- Lebwohl, David, S58 ([OS073](#))
- Lecca, Salvatore, S670 ([SAT011](#))
- Lechel, André, S663 ([FRI598](#))
- Lechler, Christian, S654 ([FRI577](#))
- Leclercq, Isabelle, S135 ([THU032](#)), S680 ([SAT031](#)), S691 ([SAT053](#))
- Leclercq, Sophie, S135 ([THU032](#))
- Lecomte, Laurence, S547 ([FRI314](#))
- Lee, Alicia, S31 ([OS028](#)), S37 ([OS041](#)), S762 ([SAT208](#))
- Lee, Boram, S798 ([SAT281](#))
- Lee, Brian, S33 ([OS031](#)), S769 ([SAT232](#))
- Lee, Byung Seok, S380 ([THU583](#))
- Lee, Changhyeong, S572 ([FRI365](#)), S916 ([SAT560](#))
- Lee, Chee Leng, S834 ([SAT362](#))
- Lee, Chee Seng, S514 ([FRI247](#))
- Lee, ChiehJu, S109 ([OS160](#))

Author Index

- Lee, Chul-min, S160 (THU079), S224 (THU264), S435 (FRI077), S438 (FRI082), S438 (FRI083), S439 (FRI086), S589 (FRI398), S728 (SAT135), S729 (SAT136)
- Lee, Dae Ho, S444 (FRI095), S701 (SAT072)
- Lee, Danbi, S545 (FRI310), S842 (SAT378)
- Lee, David Uihwan, S203 (THU224), S204 (THU225)
- Lee, Dong Ho, S78 (OS104), S303 (THU417)
- Lee, DongHo, S163 (THU087)
- Lee, Gil Won, S489 (FRI199)
- Lee, Hae Won, S798 (SAT281)
- Lee, Han Ah, S283 (THU379), S875 (SAT442), S932 (SAT590)
- Lee, Han Chu, S545 (FRI310), S842 (SAT378)
- Lee, Hee Seung, S653 (FRI575), S755 (SAT194)
- Lee, Hye Eun, S701 (SAT072)
- Lee, Hye Won, S653 (FRI575), S755 (SAT194)
- Lee, Hyo Young, S160 (THU079), S224 (THU264), S435 (FRI077), S589 (FRI398), S728 (SAT135), S729 (SAT136)
- Lee, Hyunsuk, S163 (THU087)
- Lee, Hyun Woong, S872 (SAT437)
- Lee, I-Cheng, S109 (OS160), S375 (THU572), S925 (SAT576)
- Lee, Jack, S569 (FRI358)
- Lee, Jae Geun, S799 (SAT282)
- Lee, Jaeeun, S146 (THU053)
- Lee, Jeffrey, S440 (FRI087)
- Lee, Jenny, S74 (OS097), S448 (FRI102), S452 (FRI108)
- Lee, Jeong-Hoon, S78 (OS104), S275 (THU363)
- Lee, Jeremy, S473 (FRI165)
- Lee, Jina, S508 (FRI236)
- Lee, Jiyeon, S35 (OS035)
- Lee, John, S569 (FRI358), S570 (FRI360)
- Lee, Jonghyun, S435 (FRI077)
- Lee, Jong Suk, S468 (FRI156)
- Lee, Joo Ho, S862 (SAT418)
- Lee, Joon Hyeok, S273 (THU359)
- Lee, Jun-Hyuk, S224 (THU264)
- Lee, Jun Kyu, S454 (FRI111)
- Lee, Justin, S708 (SAT088)
- Lee, Kwang-Woong, S798 (SAT281), S799 (SAT282)
- Lee-Law, Pui-Yuen, S46 (OS056)
- Lee, Lois, S88 (OS123), S715 (SAT106)
- Lee, Mei-Hsuan, S595 (FRI410)
- Leem, Galam, S653 (FRI575)
- Leeming, Diana, S25 (OS018), S415 (FRI039), S431 (FRI069), S435 (FRI076), S437 (FRI080), S475 (FRI169), S495 (FRI210), S668 (SAT008), S721 (SAT118), S895 (SAT510)
- Lee, Misun, S489 (FRI199), S866 (SAT426)
- Lee, Moo-Yeol, S746 (SAT178)
- Lee, Myoung Seok, S425 (FRI058), S448 (FRI102)
- Leen, Ann, S839 (SAT372)
- Lee, Nerissa, S609 (FRI486)
- Lee, Ni-Chung, S514 (FRI247)
- Lee, Pei-Chang, S109 (OS160), S375 (THU572), S383 (THU588)
- Lee, Pei-Lun, S595 (FRI410), S863 (SAT420)
- Leerapun, Apinya, S12 (LB004A), S867 (SAT427), S876 (SAT443), S880 (SAT452)
- Lee, Rheun-Chuan, S925 (SAT576)
- Lee, Richard, S689 (SAT050)
- Lee, Samuel, S143 (THU045), S553 (FRI325)
- Lee, Sanghyeok, S489 (FRI199)
- Lee, Sang Hyun, S468 (FRI156), S469 (FRI157)
- Lee, Seonmyeong, S468 (FRI156), S469 (FRI157)
- Lee, So Jung, S916 (SAT561)
- Lee, Soon Kyu, S820 (SAT317), S932 (SAT589)
- Lee, Sunjae, S68 (OS089)
- Lee, Su-Yeon, S473 (FRI166)
- Lee, Taehee, S921 (SAT569)
- Lee, Tai Ping, S548 (FRI315)
- Lee, Tzong-Hsi, S595 (FRI410)
- Lee, William M., S394 (FRI008)
- Lee, Won Kee, S377 (THU576)
- Lee, Yeonju, S483 (FRI187)
- Lee, Yi-Te, S377 (THU575)
- Lee, Yong-An, S694 (SAT059)
- Lee, Young-Sun, S932 (SAT590)
- Lee, Yun Bin, S78 (OS104), S667 (SAT005), S862 (SAT418)
- Lee, Yu Rim, S377 (THU576), S572 (FRI365), S916 (SAT560)
- Lefebvre, Eric, S308 (THU434), S466 (FRI152)
- Lefebvre, Rémy, S181 (THU163)
- Lefere, Sander, S106 (OS155), S562 (FRI344)
- Leff, Phillip, S151 (THU064)
- Legros, Nathalie, S584 (FRI389)
- Legry, Vanessa, S359 (THU528)
- Lehtimäki, Terho, S413 (FRI036)
- Lehtimäki, Tiina, S690 (SAT052)
- Lehtimäki, Tiina E., S458 (FRI117)
- Leibowitz, Randy, S301 (THU413)
- Leicht, Hans Benno, S166 (THU092)
- Lei, Jin, S388 (THU600)
- Leisegang, Rory, S862 (SAT417), S866 (SAT425)
- Leith, Damien, S19 (OS008), S49 (OS063), S290 (THU391)
- Leithead, Joanna, S96 (OS137)
- Leitmann, Bobby, S762 (SAT208)
- Leivers, Martin, S880 (SAT451)
- Lekbaby, Bouchra, S297 (THU404)
- Lek, Chee Chong, S694 (SAT059)
- Le, Kha, S733 (SAT145), S824 (SAT343), S835 (SAT365), S846 (SAT386), S871 (SAT435)
- Le, Khanh, S203 (THU224), S204 (THU225)
- Lemagoarou, Tristan, S270 (THU352)
- Lemaigre, Frédéric, S736 (SAT155)
- Lemaître, Elise, S349 (THU511)
- Lemoine, Maud, S23 (OS015), S233 (THU282), S258 (THU332), S290 (THU391), S295 (THU401), S345 (THU505)
- Lemoine, Sara, S319 (THU454)
- Lemos, Jozelda, S137 (THU034)
- Lempp, Florian, S265 (THU344), S871 (SAT434)
- Lenci, Ilaria, S249 (THU313), S569 (FRI359)
- Lennernas, Hans, S368 (THU543), S645 (FRI558)
- Lenne, Xavier, S205 (THU227)
- Len, Óscar, S114 (OS169)
- Lens, Sabela, S53 (OS067), S55 (OS070), S90 (OS127), S99 (OS141), S207 (THU231), S208 (THU232), S263 (THU340), S286 (THU385), S570 (FRI361), S852 (SAT400), S857 (SAT409), S861 (SAT415)
- Lenzi, Marco, S326 (THU467)
- Lenz, Oliver, S8 (GS010), S838 (SAT370), S864 (SAT422)
- Leo, Carlin, S385 (THU595)
- Leonardi, Claudio, S559 (FRI336)
- Leonard, Mark, S556 (FRI330)
- Leonel, Thais, S99 (OS141), S263 (THU340), S286 (THU385), S607 (FRI468)
- Leong, Alvin, S679 (SAT030)
- Leonhardt, Silke, S309 (THU436)
- Leoni, Gianluca, S249 (THU313)
- Leoni, Laura, S153 (THU067)
- Leoni, Simona, S166 (THU093)
- Leow, Wei Qiang, S431 (FRI068)
- Le Pabic, Estelle, S72 (OS093)
- Le, Phuc, S151 (THU064)
- Leporatti, Stefano, S763 (SAT211)
- Leps, Christian, S464 (FRI147)
- Le, Quang, S700 (SAT071), S711 (SAT094)
- Lequoy, Marie, S372 (THU566)
- Leroy, Vincent, S72 (OS093), S375 (THU573), S530 (FRI276), S532 (FRI281), S582 (FRI386), S780 (SAT252), S791 (SAT269), S927 (SAT578)
- Lesage, Candice, S392 (FRI006)
- Le-Seyec, Jacques, S639 (FRI548)
- Leshno, Moshe, S279 (THU371)
- Leslie, Jack, S385 (THU595), S640 (FRI551), S646 (FRI561), S660 (FRI590)
- Lesniak, Andrew, S809 (SAT298)
- Lesnik, Gerald, S21 (OS012), S891 (SAT502)
- Lessenich, Paul, S460 (FRI122)
- Lester, Will, S404 (FRI023)
- Le, Suong, S342 (THU501)
- Leszczynska, Aleksandra, S471 (FRI161), S690 (SAT051)
- Leung, Howard Ho-Wai, S431 (FRI069)
- Levantesi, Fabio, S908 (SAT535)
- Levesque, Eric, S791 (SAT269)
- Levi, Ana, S668 (SAT008)
- Levi, Laura, S665 (SAT002), S756 (SAT197)
- Levine, Fred, S742 (SAT166)
- Levi, Shira, S387 (THU597)
- Levitsky, Josh, S779 (SAT250)

- Levero, Massimo, S246 (THU306), S247 (THU307), S356 (THU522)
- Levy, Cynthia, S94 (OS134), S318 (THU453), S319 (THU455)
- Levy, Itzhak, S784 (SAT258)
- Levy, Miriam, S558 (FRI334), S842 (SAT377)
- Levy, Paul, S786 (SAT262), S788 (SAT265)
- Levy, Sharon, S790 (SAT268)
- Lewin, Maite, S935 (SAT595)
- Lewinska, Monika, S47 (OS058), S649 (FRI567)
- Lewis, Heather, S345 (THU505)
- Lewis, Jason, S768 (SAT231)
- Lewis, Kyle, S673 (SAT017)
- Leyh, Catherine, S378 (THU579)
- Liang, Bo, S837 (SAT367)
- Liang, Jia-xu, S442 (FRI092)
- Liang, JiaXu, S444 (FRI095)
- Liang, Shan, S165 (THU091)
- Liang, Tao, S526 (FRI268)
- Liang, Xi, S357 (THU524), S402 (FRI021), S744 (SAT171), S744 (SAT172), S745 (SAT173), S803 (SAT289)
- Liang, Xieer, S299 (THU408)
- Liang, Yan, S101 (OS147), S164 (THU088), S274 (THU362), S302 (THU414)
- Liang, Yaojie, S264 (THU342), S642 (FRI552), S643 (FRI555)
- Lian Tan, Wei, S538 (FRI295)
- Liao, Haixing, S764 (SAT213)
- Liao, Jie, S215 (THU245)
- Liao, Weijia, S75 (OS102), S638 (FRI545)
- Liaw, Yun-Fan, S102 (OS148), S873 (SAT438)
- Libera, Ermelindo D, S625 (FRI520)
- Liberal, Rodrigo, S93 (OS132), S282 (THU377), S326 (THU467), S618 (FRI507)
- Li, Bingqi, S803 (SAT289)
- Liddle, Christopher, S743 (SAT169)
- Liebe, Roman, S408 (FRI029)
- Liebig, Stephanie, S666 (SAT003)
- Lieb, Sabine, S382 (THU586)
- Liem, Seng, S849 (SAT394)
- Lieshout, Ruby, S644 (FRI556), S652 (FRI574)
- Lieto, Raffaele, S769 (SAT233)
- Lieu, Hsiao, S443 (FRI093), S486 (FRI193), S495 (FRI210)
- Lieu, Melissa, S742 (SAT168)
- Liew, Danny, S342 (THU501)
- Li, Feng, S48 (OS061), S787 (SAT263)
- Li, Fengyuan, S35 (OS035)
- Li, Gang, S421 (FRI050), S431 (FRI069)
- Ligoria, Regina, S137 (THU034)
- Li, Guangming, S827 (SAT349)
- Li, Guanlin, S164 (THU088)
- Li, Guojun, S838 (SAT369)
- Liguori, Antonio, S436 (FRI079)
- Li, Hai, S344 (THU504), S347 (THU509)
- Li, Hai Jun, S89 (OS125)
- Li, Hang Lam, S761 (SAT207), S762 (SAT209)
- Li, Hong, S870 (SAT432)
- Li, Hongming, S865 (SAT423)
- Li, Hu, S240 (THU296)
- Li, Jia, S22 (OS014), S182 (THU165), S278 (THU369), S616 (FRI502), S623 (FRI515), S838 (SAT369)
- Li, Jia-bin, S838 (SAT369)
- Li, Jiang, S357 (THU524), S465 (FRI149)
- Li, Jianzhou, S879 (SAT449)
- Li, Jiaqi, S402 (FRI021), S803 (SAT289)
- Li, Jie, S215 (THU245), S287 (THU388), S296 (THU403), S326 (THU468), S504 (FRI229)
- Li, Jing, S89 (OS125), S254 (THU323), S310 (THU438), S727 (SAT132), S854 (SAT404)
- Li, Jingguo, S602 (FRI460)
- Li, Jun, S66 (OS086), S357 (THU524), S402 (FRI021), S659 (FRI589), S744 (SAT171), S744 (SAT172), S745 (SAT173), S803 (SAT289)
- Li, Junfeng, S182 (THU165)
- Li, Kai, S92 (OS130), S619 (FRI508), S621 (FRI512), S628 (FRI526)
- Likhitsup, Alisa, S141 (THU041), S632 (FRI532)
- Likhter, Mariya, S784 (SAT258), S804 (SAT291)
- Li, Lewyn, S266 (THU346)
- Li, Li, S22 (OS014), S31 (OS028), S194 (THU189), S247 (THU308), S251 (THU317), S409 (FRI030), S463 (FRI126), S835 (SAT364), S841 (SAT376)
- Lim, Aaron G., S221 (THU257), S256 (THU328)
- Lim, Andy, S613 (FRI495)
- Lim, Dennis, S799 (SAT284)
- Li, Mei, S711 (SAT092)
- Li, Mengying, S144 (THU046)
- Li, Mengyu, S182 (THU165)
- Lim, Hong Kai, S39 (OS044)
- Li, Ming, S296 (THU403), S526 (FRI268)
- Li, Minghui, S278 (THU369)
- Lim, Jee Woong, S473 (FRI166)
- Lim, Jihye, S842 (SAT378)
- Lim, Joseph, S280 (THU372), S281 (THU376), S846 (SAT387)
- Limon-Miro, Ana, S890 (SAT500)
- Lim, Seng Gee, S12 (LB004A), S247 (THU308), S288 (THU389), S869 (SAT431), S877 (SAT446), S880 (SAT452), S881 (SAT453)
- Lim, Sung-Chul, S746 (SAT178)
- Lim, Tien Huey, S299 (THU408), S867 (SAT427)
- Lim, Tiffany, S79 (OS106)
- Lim, Tiong Yeng, S809 (SAT298)
- Li, Musong, S22 (OS014), S182 (THU165)
- Lim, Won, S569 (FRI357)
- Lim, Yee Siang, S694 (SAT059)
- Lim, Young-Suk, S12 (LB004A), S69 (OS090), S275 (THU363), S545 (FRI310), S610 (FRI488), S833 (SAT361), S842 (SAT378), S870 (SAT433), S872 (SAT437), S880 (SAT452)
- Lim, YS, S868 (SAT428)
- Lim, Zixiang, S54 (OS069), S57 (OS072A), S58 (OS072B)
- Lin, Benjamin, S544 (FRI307)
- Lin, Chen-Chun, S373 (THU568), S386 (THU596)
- Lin, Chih-Che, S119 (THU001)
- Lin, Chih-Lang, S595 (FRI410)
- Lin, Chih-Lin, S595 (FRI410)
- Lin, Chih-Wen, S119 (THU001)
- Lin, Chuan-Hao, S866 (SAT425)
- Lin, Chun-yen, S373 (THU568), S386 (THU596), S575 (FRI371), S576 (FRI372)
- Lindblad, Katherine E., S45 (OS055)
- Lindblom, Anna, S7 (GS009)
- Linde, Kajsa, S467 (FRI154)
- Lindell, Gun, S94 (OS133)
- Linden, Daniel, S7 (GS009)
- Lindenmeyer, Christina, S779 (SAT250)
- Linder, Nicolas, S383 (THU590)
- Lindhorst, Andreas, S680 (SAT032)
- Lindkvist, Björn, S904 (SAT527)
- Lindor, Keith D., S335 (THU484)
- Lindquist, Jonathan A., S659 (FRI589)
- Lindström, Erik, S751 (SAT187), S843 (SAT380)
- Lindvig, Katrine Prier, S2 (GS002), S35 (OS036), S129 (THU021), S131 (THU024), S475 (FRI171), S500 (FRI223)
- Ling, Lei, S495 (FRI210)
- Ling, Ning, S240 (THU296), S763 (SAT210)
- Lin, Han-Chieh, S595 (FRI410)
- Lin, Huapeng, S39 (OS043), S164 (THU088)
- Lin, Jaw-Town, S835 (SAT364), S841 (SAT376)
- Lin, Jung-Yi, S372 (THU567)
- Link, Alexander, S11 (LB002)
- Link, Frederik, S408 (FRI029)
- Link, Ralph, S562 (FRI345)
- Lin, Lei, S538 (FRI294), S538 (FRI295)
- Lin, MingDe, S935 (SAT594)
- Lin, Minghua, S838 (SAT369)
- Lin, Po-Ting, S373 (THU568), S386 (THU596)
- Lin, Qing, S559 (FRI337)
- Lin, Ruey-Chang, S200 (THU217)
- Lin, Shi-Ming, S373 (THU568), S386 (THU596)
- Lin, Shumei, S879 (SAT449)
- Lin, Steven, S856 (SAT407)
- Lin, Tao, S659 (FRI589)
- Lin, Tse-I, S824 (SAT343), S835 (SAT365), S846 (SAT386), S871 (SAT435)
- Lin, Wan-Bao, S827 (SAT349)
- Lin, Wen-Yuan, S162 (THU084)
- Lionel, Lerman, S375 (THU573)
- Lionetti, Raffaella, S806 (SAT294), S808 (SAT297)
- Liou, Wei-Lun, S919 (SAT566)

Author Index

- Li, Peng, S357 (THU524), S402 (FRI021), S803 (SAT289)
- Li, Pengfei, S86 (OS120)
- Lipnevich, Igor, S269 (THU351)
- Li, Qian, S454 (FRI110)
- Li, Rui, S867 (SAT427)
- Li, Ruidong, S276 (THU365)
- Li, Shen, S36 (OS037)
- Li, Shuang, S22 (OS014)
- Lisman, Ton, S367 (THU542), S617 (FRI505), S911 (SAT540)
- Lissing, Mattias, S530 (FRI275)
- Li, Tan, S803 (SAT289)
- Li, Tinghong, S182 (THU165)
- Littlejohn, Margaret, S251 (THU318), S305 (THU422)
- Liu, Beibei, S224 (THU265)
- Liu, Boqiang, S56 (OS071)
- Liu, Boya, S848 (SAT391)
- Liu, Changchun, S501 (FRI224)
- Liu, Chao, S182 (THU165)
- Liu, Chen, S923 (SAT573)
- Liu, Cheng, S853 (SAT401), S853 (SAT402)
- Liu, Chuan, S501 (FRI224), S616 (FRI502), S623 (FRI515), S636 (FRI540)
- Liu, Chun-Jen, S595 (FRI410), S863 (SAT420)
- Liu, Dengxiang, S182 (THU165)
- Liu, Diana, S811 (SAT302), S813 (SAT307)
- Liu, Feng, S344 (THU504), S431 (FRI068), S481 (FRI181), S685 (SAT042)
- Liu, Fuquan, S501 (FRI224)
- Liu, Gang, S837 (SAT367)
- Liu, Hanyang, S684 (SAT040)
- Liu, Huan, S22 (OS014)
- Liu, Hui, S408 (FRI029)
- Liu, Jiacheng, S287 (THU388), S296 (THU403), S326 (THU468), S504 (FRI229)
- Liu, Jiaye, S637 (FRI543)
- Liu, Jieming, S836 (SAT366)
- Liu, Jing, S215 (THU245)
- Liu, Jingrui, S89 (OS125), S894 (SAT509)
- Liu, Kara Marie, S37 (OS041)
- Liu, Kuan, S86 (OS120)
- Liu, LiLi, S870 (SAT432)
- Liu, Na, S883 (SAT488)
- Liu, Ning, S636 (FRI540)
- Liu, Peidi, S94 (OS133)
- Liu, Shangbin, S60 (OS075)
- Liu, Shi, S642 (FRI552)
- Liu, Shirong, S636 (FRI540)
- Liu, Shunai, S852 (SAT399)
- Liu, Su, S404 (FRI023)
- Liu, Tian, S920 (SAT568)
- Liu, Tong, S122 (THU008), S132 (THU026), S185 (THU173), S674 (SAT020)
- Liu, Weijian, S669 (SAT009)
- Liu, Wenhui, S443 (FRI093), S486 (FRI193)
- Liu, Xiao, S86 (OS119)
- Liu, Xiaohui, S165 (THU091)
- Liu, Xiaojing, S879 (SAT449)
- Liu, Xinchang, S854 (SAT404)
- Liu, YaLi, S870 (SAT432)
- Liu, Yan, S185 (THU173), S280 (THU372), S281 (THU376), S846 (SAT387)
- Liu, Yang, S244 (THU302), S247 (THU309), S845 (SAT385), S866 (SAT425), S920 (SAT568)
- Liu, Yanna, S501 (FRI224), S616 (FRI502)
- Liu, Yao, S477 (FRI175)
- Liu, Yen-Chun, S102 (OS148), S575 (FRI371), S576 (FRI372), S873 (SAT438)
- Liu, Yi, S879 (SAT449), S883 (SAT488)
- Liu, Yilin, S326 (THU468)
- Liu, Ying, S686 (SAT045)
- Liu, Yixin, S883 (SAT488)
- Liu, Yun Peng, S384 (THU591)
- Liu, Yu-Pei, S182 (THU165)
- Liu, Zhaoli, S566 (FRI352), S608 (FRI485)
- Liu, Zhicheng, S26 (OS020)
- Liu, Zongyi, S181 (THU164)
- Livingstone, Callum, S415 (FRI038)
- Livingston, Sherry, S394 (FRI008)
- Li, Wai Keung, S78 (OS105)
- Li, Wang, S920 (SAT568)
- Li, Wei, S384 (THU591)
- Li, Wei-Zhe, S827 (SAT349)
- Li, Wenhao, S698 (SAT066), S934 (SAT593)
- Liowski, Timur, S325 (THU466)
- Li, Xiaoguo, S616 (FRI502)
- Li, Xiaojiao, S89 (OS125)
- Li, Xiaomei, S92 (OS130), S619 (FRI508), S621 (FRI512), S628 (FRI526)
- Li, Xin, S616 (FRI502)
- Li, Xinyi, S912 (SAT554)
- Li, Xiubin, S914 (SAT558)
- Li, Yan, S726 (SAT128)
- Li, Yiguang, S287 (THU388), S296 (THU403), S326 (THU468), S504 (FRI229)
- Li, Ying, S477 (FRI175)
- Li, Yinyin, S388 (THU600)
- Li, Yizhao, S88 (OS123)
- Li, Yueni, S489 (FRI200)
- Li, Yujia, S408 (FRI029)
- Li, Yujin, S492 (FRI206)
- Li, Yun, S402 (FRI021), S744 (SAT171)
- Lizardi, Javier, S487 (FRI195)
- Li, Zewen, S182 (THU165)
- Li, Zongfang, S883 (SAT488)
- Lkhagva-Ochir, Oyungerel, S235 (THU287)
- Llaneras, Jordi, S44 (OS052), S277 (THU367)
- Llarch, Neus, S381 (THU584)
- Lledó, Jose Luis, S381 (THU584)
- Lleo, Ana, S47 (OS058), S93 (OS132), S107 (OS157), S308 (THU435), S326 (THU467), S335 (THU484), S528 (FRI272), S758 (SAT201), S761 (SAT206)
- Llewellyn, Jessica, S740 (SAT163)
- Llinares, María Esther, S527 (FRI271)
- Llop, Elba, S90 (OS127)
- Llovet, Josep M., S45 (OS055), S385 (THU595)
- Llovet, Laura Patricia, S607 (FRI468)
- Lloyd, Andrew, S103 (OS149), S305 (THU421), S565 (FRI349)
- Lloyd, Carla, S551 (FRI321)
- Lloyd, Emily, S855 (SAT405)
- Lloyd, Jonathan, S745 (SAT177)
- Lloyd, Josephine, S34 (OS034)
- Loarca, Lorena, S759 (SAT202)
- Lobato, Cirley, S137 (THU034)
- Locarnini, Stephen, S251 (THU318), S305 (THU422), S834 (SAT362)
- Lo, Ching-Chu, S595 (FRI410)
- Lockart, Ian, S561 (FRI343), S568 (FRI356)
- Lockman, Khalida Ann, S434 (FRI075)
- Lockwood, Mark, S97 (OS139)
- Lodge, John, S493 (FRI208)
- Loeffler, Juergen, S486 (FRI194), S493 (FRI207)
- Lo, Gin-Ho, S625 (FRI520)
- Logiodice, Federica, S477 (FRI173)
- Loglio, Alessandro, S196 (THU194), S223 (THU263), S843 (SAT379), S843 (SAT381), S868 (SAT429), S880 (SAT450)
- Lohoues, Marie Jeanne, S19 (OS008), S49 (OS063)
- Lohse, Ansgar, S224 (THU265), S257 (THU329), S317 (THU452), S321 (THU458), S333 (THU481), S893 (SAT507)
- Lohse, Ansgar W., S54 (OS069), S206 (THU229), S315 (THU447), S325 (THU466), S604 (FRI462), S823 (SAT341)
- Lok, Anna, S180 (THU162)
- Lok, James, S276 (THU366), S281 (THU375), S571 (FRI363), S812 (SAT304)
- Lomas, David, S534 (FRI285)
- Lombardelli, Letizia, S477 (FRI173)
- Lombardelli, Stephen, S516 (FRI251)
- Lombardi, Andrea, S223 (THU263)
- Lombardi, Martina, S425 (FRI057)
- Lombardi, Rosa, S159 (THU078), S167 (THU095), S682 (SAT036)
- Lombardo, Daniele, S259 (THU333)
- Lonardi, Sara, S748 (SAT180)
- Londoño, Maria Carlota, S54 (OS069), S324 (THU464), S325 (THU465), S334 (THU482), S607 (FRI468), S809 (SAT298)
- Long, Brian, S540 (FRI299)
- Long, Edward, S880 (SAT451)
- Longerich, Thomas, S11 (LB003), S655 (FRI581), S710 (SAT090), S927 (SAT579)
- Longet, Stephanie, S57 (OS072A)
- Long, Jiang, S745 (SAT177)
- Longo, Miriam, S682 (SAT036), S682 (SAT037), S698 (SAT068), S703 (SAT077), S706 (SAT084)
- Longo, Salvatore, S404 (FRI024)
- Longworth, Louise, S39 (OS044)
- Lonjon-Domanec, Isabelle, S8 (GS010), S72 (OS094)
- Lønsmann, Ida Lønsmann, S435 (FRI076)
- Loo, Jing Hong, S567 (FRI354)

- Loomba, Rohit, S10 ([LB001](#)), S14 ([LB006](#)), S31 ([OS028](#)), S74 ([OS098](#)), S409 ([FRI030](#)), S414 ([FRI037](#)), S416 ([FRI040](#)), S419 ([FRI045](#)), S422 ([FRI051](#)), S427 ([FRI060](#)), S449 ([FRI103](#)), S451 ([FRI107](#)), S454 ([FRI110](#)), S701 ([SAT073](#)), S715 ([SAT106](#)), S716 ([SAT107](#)), S730 ([SAT139](#)), S732 ([SAT143](#)), S762 ([SAT208](#)), S926 ([SAT577](#))
- Loomes, Kathleen M., S518 ([FRI255](#)), S519 ([FRI256](#))
- Loosen, Sven H, S384 ([THU592](#)), S930 ([SAT584](#))
- Loperto, Ilaria, S769 ([SAT233](#))
- Lopes, Massimo, S765 ([SAT215](#))
- López-Bermudo, Lucía, S708 ([SAT087](#))
- Lopez, David, S31 ([OS028](#)), S409 ([FRI030](#)), S684 ([SAT040](#))
- López, Flor Noguerras, S114 ([OS168](#))
- Lopez-Gomez, Carlos, S396 ([FRI011](#))
- López-Hoyos, Marcos, S774 ([SAT242](#))
- López, Julia Herreras, S811 ([SAT301](#))
- Lopez-Labrador, F. Xavier, S811 ([SAT303](#))
- López-López, Flora, S107 ([OS157](#))
- López, Néilda, S207 ([THU231](#)), S208 ([THU232](#))
- Lopez-Pentecost, Melissa, S912 ([SAT554](#))
- Lopez, Rosa Maria Ufano, S555 ([FRI329](#))
- López-Rubio, Diana Laura, S356 ([THU521](#))
- López-Vicario, Cristina, S361 ([THU530](#)), S362 ([THU533](#)), S370 ([THU549](#)), S674 ([SAT019](#))
- Lopez-Yus, Marta, S676 ([SAT023](#))
- Lorch, Ulrike, S460 ([FRI121](#))
- Lord, Emma, S34 ([OS034](#)), S121 ([THU007](#)), S122 ([THU008](#)), S124 ([THU013](#)), S132 ([THU026](#))
- Lordick, Florian, S383 ([THU590](#))
- Lord, Janet, S364 ([THU537](#))
- Lorena, Maria, S483 ([FRI185](#))
- Lorenc, Beata, S585 ([FRI390](#))
- Lorens, James B, S672 ([SAT016](#))
- Lorente-Cebrian, Silvia, S676 ([SAT023](#))
- Lorente Perez, Sara, S114 ([OS169](#))
- Lorenz, Johanna Luise Charlotte, S634 ([FRI536](#))
- Lori, Giulia, S649 ([FRI567](#))
- Loste, Maria Teresa Arias, S624 ([FRI518](#))
- Loste, María Teresa Arias, S113 ([OS166](#)), S157 ([THU074](#)), S158 ([THU076](#))
- Lotersztajn, Sophie, S65 ([OS084](#)), S475 ([FRI170](#))
- Lotte Gluud, Lise, S502 ([FRI226](#))
- Lotto, Marta, S567 ([FRI353](#))
- Louisa, Ruhl, S783 ([SAT257](#))
- Lou, Jinfeng, S89 ([OS125](#))
- Loukaki-Gkountara, Domniki, S255 ([THU326](#))
- Lou, Lillian, S215 ([THU246](#))
- Loreiro, Dimitri, S245 ([THU304](#))
- Loustaud-Ratti, Veronique, S72 ([OS093](#)), S270 ([THU352](#)), S833 ([SAT360](#)), S840 ([SAT373](#))
- Louvet, Alexandre, S81 ([OS110](#)), S137 ([THU034](#)), S205 ([THU227](#)), S205 ([THU228](#)), S913 ([SAT557](#))
- Löve, Arthur, S573 ([FRI366](#))
- Loveridge, Robert, S403 ([FRI022](#))
- Löve, Thorvardur J., S573 ([FRI366](#))
- Lövgren-Sandblom, Anita, S94 ([OS133](#)), S329 ([THU473](#))
- Löwe, Bernd, S315 ([THU447](#))
- Low, Gerald, S567 ([FRI354](#))
- Loy, John, S698 ([SAT066](#))
- Lozano, Juanjo, S37 ([OS039](#)), S527 ([FRI271](#)), S651 ([FRI571](#)), S674 ([SAT019](#)), S809 ([SAT298](#)), S896 ([SAT512](#)), S901 ([SAT522](#))
- Lozano, Juan Jose, S139 ([THU039](#))
- Lozniewski, Alain, S905 ([SAT529](#))
- Lubberink, Mark, S420 ([FRI047](#))
- Lubeck, Eric, S762 ([SAT208](#))
- Lubel, John, S842 ([SAT377](#))
- Lübke, Nadine, S825 ([SAT345](#))
- Luc, Amandine, S905 ([SAT529](#))
- Lucà, Martina, S404 ([FRI024](#))
- Lucena, Ana, S555 ([FRI329](#))
- Lucena, Maria Isabel, S326 ([THU467](#)), S396 ([FRI011](#))
- Lucenteforte, Ersilia, S591 ([FRI404](#))
- Lucey, Michael R., S33 ([OS031](#))
- Lucia Ferraz, Maria, S543 ([FRI305](#))
- Luciani, Alain, S375 ([THU573](#))
- Lucidarme, Damien, S833 ([SAT360](#))
- Lucifora, Julie, S246 ([THU305](#)), S766 ([SAT216](#))
- Lüdde, Tom, S11 ([LB003](#)), S384 ([THU592](#)), S533 ([FRI283](#)), S825 ([SAT345](#)), S930 ([SAT584](#))
- Ludewig, Burkhard, S192 ([THU186](#))
- Lu, Di, S815 ([SAT311](#))
- Ludlow-Rhodes, Arran, S554 ([FRI327](#))
- Ludvigsson, Jonas, S82 ([OS112](#))
- Ludwig, Johannes M., S378 ([THU579](#))
- Luetgehetmann, Marc, S54 ([OS069](#)), S256 ([THU327](#)), S257 ([THU329](#))
- Lufadeju, Folu, S225 ([THU266](#))
- Lugano, Fabiola, S937 ([SAT598](#))
- Lu, Henry, S679 ([SAT030](#))
- Luhmann, Niklas, S42 ([OS049](#)), S558 ([FRI335](#))
- Lu, Hui, S837 ([SAT367](#))
- Luigi Calvo, Pier, S521 ([FRI259](#))
- Lui, Gilbert, S78 ([OS105](#))
- Luig, Thea, S511 ([FRI241](#))
- Luisa Ortiz, María, S114 ([OS168](#))
- Lujambio, Amaia, S45 ([OS055](#))
- Lu, Jiajie, S70 ([OS091](#))
- Lu, Junfeng, S844 ([SAT382](#))
- Lukacs-Kornek, Veronika, S915 ([SAT559](#))
- Luketic, Velimir, S318 ([THU453](#)), S319 ([THU455](#))
- Lukic, Tamara, S12 ([LB004A](#)), S13 ([LB004B](#)), S288 ([THU389](#)), S288 ([THU390](#)), S880 ([SAT452](#)), S881 ([SAT453](#))
- Lu, Ling, S695 ([SAT062](#))
- Luli, Saimir, S640 ([FRI551](#))
- Lulla, Suhasini, S839 ([SAT372](#))
- Lu, Mengji, S264 ([THU342](#)), S642 ([FRI552](#)), S643 ([FRI555](#))
- Lu, Ming, S22 ([OS014](#))
- Lumley, Sheila, S856 ([SAT407](#))
- Lundgren, Åsa, S30 ([OS026](#))
- Lundgren, Jens D., S818 ([SAT314](#))
- Lundgren, Karen, S240 ([THU297](#))
- Lund, Jennifer, S201 ([THU219](#))
- Lund-Johansen, Fridtjof, S309 ([THU437](#))
- Lund, Katarina, S30 ([OS026](#))
- Lund, Morten, S450 ([FRI104](#)), S523 ([FRI263](#))
- Lundqvist, Annamari, S80 ([OS109](#)), S419 ([FRI046](#))
- Lundström, Elin, S683 ([SAT038](#))
- Lun, Liou Wei, S19 ([OS008](#)), S49 ([OS063](#))
- Luo, Bohan, S92 ([OS130](#)), S619 ([FRI508](#)), S621 ([FRI512](#)), S628 ([FRI526](#))
- Luo, Ed, S716 ([SAT109](#)), S848 ([SAT390](#)), S849 ([SAT393](#))
- Luo, Jiing-Chyuan, S109 ([OS160](#))
- Luo, Jinjin, S357 ([THU524](#)), S402 ([FRI021](#)), S803 ([SAT289](#))
- Luo, Ke, S484 ([FRI188](#))
- Luo, Qiang, S662 ([FRI595](#))
- Luo, Wun-Sheng, S294 ([THU398](#))
- Luo, Xufeng, S264 ([THU342](#)), S642 ([FRI552](#)), S643 ([FRI555](#))
- Luo, Yizhao, S533 ([FRI282](#))
- Lupberger, Joachim, S36 ([OS038](#)), S99 ([OS142](#)), S738 ([SAT160](#)), S758 ([SAT199](#))
- Luppi, Gabriele, S84 ([OS115](#))
- Lupsor-Platon, Monica, S448 ([FRI102](#)), S452 ([FRI108](#))
- Lupusoru, Raluca, S483 ([FRI186](#)), S505 ([FRI230](#)), S930 ([SAT585](#))
- Lurie, Yoav, S859 ([SAT412](#))
- Lu, Shelly C., S671 ([SAT014](#))
- Lu, Sheng-Nan, S294 ([THU398](#))
- Lusivka-Nzinga, Clovis, S17 ([OS006](#)), S101 ([OS146](#)), S250 ([THU314](#))
- Lustig, Yaniv, S784 ([SAT258](#)), S804 ([SAT291](#))
- Lütge, Mechthild, S192 ([THU186](#))
- Lütjohann, Dieter, S607 ([FRI469](#))
- Lutu, Alina, S402 ([FRI020](#))
- Lutz, Michael, S132 ([THU026](#)), S737 ([SAT158](#))
- Lutz, Philipp, S11 ([LB002](#)), S599 ([FRI451](#))
- Luukkonen, Panu, S690 ([SAT052](#))
- Luukkonen, Panu K., S111 ([OS162](#))
- Luu, Michael, S377 ([THU575](#))
- Lu, Wei, S920 ([SAT568](#))
- Lu, Wei-Yu, S28 ([OS023](#))
- Luxenburger, Hendrik, S657 ([FRI583](#))
- Lu, Xiangyu, S319 ([THU455](#))
- Lu, Xiao-Bo, S344 ([THU504](#))
- Lu, Xiaomin, S319 ([THU455](#))
- Lu, Yingyan, S803 ([SAT289](#))
- Lu, Yinying, S388 ([THU600](#))
- Lu, Yunjie, S183 ([THU168](#))
- Lu, Zhonghua, S296 ([THU403](#))
- Luz Martínez-Chantar, María, S48 ([OS060](#))
- Lv, Jiayu, S920 ([SAT568](#))

Author Index

- Lv, Yong, S92 (OS130), S619 (FRI508), S621 (FRI512), S628 (FRI526), S630 (FRI529)
- Lynch, Erica Nicola, S770 (SAT235)
- Lynch, Julie, S30 (OS027), S936 (SAT596)
- Lynch, Kate, S602 (FRI458)
- Lyo, Victoria, S462 (FRI125)
- Lyra, Andre, S408 (FRI028)
- Lytton, Simon, S244 (THU301)
- Lytvyak, Ellina, S93 (OS132), S313 (THU443), S317 (THU452), S326 (THU467)
- Ma, Anlin, S278 (THU369)
- Ma, Ann, S63 (OS080), S139 (THU039), S511 (FRI242), S512 (FRI243), S512 (FRI244), S896 (SAT512), S907 (SAT532)
- Ma, Ann T, S901 (SAT522), S902 (SAT524)
- Ma, Ann T., S25 (OS018)
- Maan, Raoel, S524 (FRI265), S569 (FRI359)
- Maasoumy, Benjamin, S83 (OS113), S248 (THU311), S250 (THU315), S582 (FRI385), S608 (FRI485), S622 (FRI514), S624 (FRI519), S634 (FRI536), S823 (SAT341), S824 (SAT344), S830 (SAT355), S843 (SAT379), S857 (SAT408), S893 (SAT505)
- Mabile-Archambeaud, Isabelle, S5 (GS007)
- Mabire, Morgane, S65 (OS084), S475 (FRI170)
- Mabrouk, Mai, S479 (FRI178)
- Macarulla, Teresa Mercade, S748 (SAT180)
- Macchi, Chiara, S698 (SAT068)
- Maccioni, Luca, S135 (THU032)
- MacConnell, Leigh, S669 (SAT009)
- Macdonald, Douglas, S17 (OS005)
- Macdonald, Graeme, S147 (THU054), S190 (THU183)
- MacDonald, Kelli, S494 (FRI209)
- MacDonald, Scott, S155 (THU070)
- Macedo, Guilherme, S28 (OS024), S93 (OS132), S282 (THU377), S326 (THU467), S581 (FRI384), S618 (FRI507)
- Macedo, Paula, S706 (SAT085)
- Macera, Margherita, S217 (THU250)
- MacEwan, Joanna, S332 (THU478)
- Machado, Mariana, S190 (THU182)
- MacHale, Siobhan, S234 (THU285)
- Ma, Christopher, S416 (FRI040)
- Macias-Muñoz, Laura, S492 (FRI205)
- Macias, Rocio IR, S46 (OS056), S77 (OS103), S107 (OS157)
- MacIsaac, Julia, S544 (FRI308), S547 (FRI313)
- MacIsaac, Michael, S498 (FRI218), S550 (FRI318)
- Mack, Cara L., S517 (FRI253), S519 (FRI256)
- MacKenzie, Donald, S534 (FRI285)
- Mackey, John B. G., S385 (THU595)
- MacKinnon, Alison, S481 (FRI182)
- Macnaughtan, Jane, S366 (THU539)
- Macpherson, Iain, S415 (FRI038), S473 (FRI165), S495 (FRI214)
- Macrae, James, S666 (SAT004)
- Macrina Lam, Wai Ling, S38 (OS042)
- Madaleno, Joao, S268 (THU349)
- Madau, Magalie, S547 (FRI314)
- Madden, Angela, S815 (SAT310), S890 (SAT500)
- Maddur, Haripriya, S779 (SAT250)
- Madeddu, Giordano, S596 (FRI414)
- Made, Lilian Torres, S19 (OS008), S49 (OS063), S487 (FRI195)
- Ma, Deqiang, S22 (OS014)
- Mader, M, S257 (THU329)
- Madhu, Devika, S898 (SAT515)
- Madin, Kairat, S937 (SAT597)
- Madl, Christian, S545 (FRI309)
- Madlener, Sibylle, S753 (SAT189)
- Madl, Tobias, S68 (OS088), S346 (THU506), S696 (SAT063)
- Madoff, David, S935 (SAT594)
- Madonia, Salvatore, S564 (FRI347)
- Madrid, Teresa Maria Jordan, S445 (FRI096)
- Madsen, Andreas Nygaard, S661 (FRI593)
- Madsen, Anne Broedsgaard, S64 (OS083)
- Madsen, Anne Lundager, S129 (THU021)
- Madsen, Bjørn Stæhr, S2 (GS002), S129 (THU021)
- Madsen, Lone, S125 (THU015)
- Madsen, Lone Wulff, S550 (FRI319)
- Madsen, Martin Rønn, S661 (FRI593), S724 (SAT124)
- Maeda, Mayumi, S875 (SAT442)
- Maeder, Christine, S645 (FRI559), S652 (FRI572)
- Maekawa, Shinya, S387 (THU598)
- Maeso-Gonzalez, Javier, S178 (THU156)
- Maestro, Sheila, S248 (THU310)
- Maeyashiki, Chiaki, S379 (THU580)
- Maffi, Gabriele, S159 (THU078)
- Magalhães, Joana Teixeira, S149 (THU060)
- Magaz, Marta, S367 (THU542)
- Agee, Mindy, S875 (SAT441)
- Mageras, Anna, S298 (THU407)
- Maggioni, Claudia, S404 (FRI024)
- Maggioni, Marco, S682 (SAT037)
- Magini, Giulia, S317 (THU452), S457 (FRI115), S780 (SAT251)
- Magistri, Paolo, S795 (SAT275)
- Magnin, Benoît, S417 (FRI042), S918 (SAT563)
- Mahadevan, Sangeetha, S483 (FRI187), S684 (SAT040)
- Mahadeva, Sanjiv, S425 (FRI058), S448 (FRI102), S452 (FRI108)
- Mahajan, Anadi, S855 (SAT405)
- Maharaj, Tobias, S138 (THU036), S234 (THU285), S531 (FRI279)
- Maheshwari, Deepanshu, S756 (SAT196)
- Maheshwari, Rahul, S319 (THU455)
- Mahfouz, Ratib, S803 (SAT290), S807 (SAT295)
- Mahmood, Hassan, S215 (THU246), S240 (THU295)
- Mahmood, Khalid, S240 (THU295)
- Mahmud, Nadim, S89 (OS126)
- Mahn, Robert, S381 (THU585)
- Mahyari, Eisa, S713 (SAT101)
- Maia, Luís, S304 (THU420)
- Maida, Adriano, S606 (FRI467)
- Maida, Ivana, S581 (FRI384)
- Maier, Melanie, S860 (SAT414)
- Maieron, Andreas, S545 (FRI309)
- Mai, Jiajia, S837 (SAT367), S865 (SAT423)
- Mailly, Laurent, S36 (OS038), S649 (FRI565), S738 (SAT160), S758 (SAT199)
- Maimone, Sergio, S578 (FRI376)
- Mainar, Jose M Arbones, S676 (SAT023)
- Maini, Alex, S104 (OS151)
- Maini, Alexander, S55 (OS070)
- Maini, Mala, S53 (OS067), S55 (OS070), S99 (OS141)
- Maino, Cesare, S96 (OS136)
- Mainz, Dagmar, S80 (OS108)
- Maiocchi, Laura, S502 (FRI225)
- Maira, Tommaso Di, S807 (SAT296)
- Maisonnette, Patrick, S93 (OS132)
- Maitland, Michael, S58 (OS073)
- Maiwald, Bettina, S379 (THU581)
- Maiwall, Rakhi, S51 (OS064), S128 (THU020), S139 (THU038), S347 (THU508), S349 (THU510), S397 (FRI014), S756 (SAT196)
- Majchrzak, Mario, S251 (THU316)
- Majeed, Ammar, S441 (FRI090)
- Ma, Jianzhong, S636 (FRI540)
- Majid, Amir, S290 (THU391)
- Major, Piotr, S746 (SAT179), S759 (SAT203)
- Major, Xavier, S570 (FRI361)
- Majstorović, Ozren, S702 (SAT075)
- Ma, Julie, S266 (THU346), S836 (SAT366), S846 (SAT388)
- Majumdar, Avik, S3 (GS005), S815 (SAT311)
- Majzoub, Abdul, S414 (FRI037)
- Makhasen, Wanwisar, S772 (SAT238), S812 (SAT305)
- Mak, Lung Yi Loey, S78 (OS105), S177 (THU154), S272 (THU358), S273 (THU360), S275 (THU364)
- Mala, Y.M., S197 (THU196)
- Malcus, Peter, S94 (OS133)
- Malcus, Sara, S94 (OS133)
- Malden, Deborah, S831 (SAT356)
- Malecha, Elizabeth, S335 (THU484)
- Malenstein, Hannah Van, S781 (SAT253)
- Maley, Michael, S558 (FRI334)
- Malheiro, Olívio Brito, S293 (THU396)
- Malhi, Harmeet, S136 (THU033), S491 (FRI204)
- Malhotra, Deepa, S151 (THU063)
- Maliakkal, Benedict, S887 (SAT496)
- Malik, Fariha, S203 (THU222), S591 (FRI404)
- Malik, Raza, S203 (THU224), S204 (THU225)
- Ma, Lily, S427 (FRI060)
- Ma, Lina, S844 (SAT382)
- Malinowsky, Katharina, S937 (SAT597)

- Malka, Assaf, S742 ([SAT166](#))
Mallet, Vincent, S41 ([OS047](#)),
S392 ([FRI005](#)), S393 ([FRI007](#))
Malmberg, Filip, S40 ([OS045](#))
Malvestiti, Francesco, S428 ([FRI061](#)),
S675 ([SAT021](#)), S703 ([SAT077](#))
Malysiak, Maryse, S359 ([THU528](#))
Ma, Mark, S526 ([FRI268](#))
Mamdouh, Remon, S776 ([SAT246](#))
Mamo, Eyerusalem, S841 ([SAT375](#))
Mamonova, Nina, S4 ([GS006](#)),
S828 ([SAT351](#))
Manceau, Hana, S127 ([THU019](#))
Manchem, Prasad, S477 ([FRI174](#))
Mancuso, Fabrizio, S436 ([FRI079](#))
Mandal, Sema, S238 ([THU291](#))
Mandelboim, Michal, S804 ([SAT291](#))
Mandilara, Dionysia, S917 ([SAT562](#))
Mandorfer, Mattias, S11 ([LB002](#)),
S14 ([LB006](#)), S18 ([OS007](#)), S24 ([OS017](#)),
S90 ([OS127](#)), S92 ([OS131](#)),
S315 ([THU449](#)), S354 ([THU519](#)),
S359 ([THU527](#)), S362 ([THU534](#)),
S390 ([FRI003](#)), S502 ([FRI226](#)),
S515 ([FRI250](#)), S520 ([FRI257](#)),
S532 ([FRI280](#)), S535 ([FRI287](#)),
S555 ([FRI328](#)), S617 ([FRI505](#)),
S618 ([FRI506](#)), S629 ([FRI527](#)),
S629 ([FRI528](#)), S631 ([FRI531](#)),
S632 ([FRI533](#)), S829 ([SAT353](#))
Manekeller, Steffen, S381 ([THU585](#))
Manero, Estela Florencia, S137 ([THU034](#))
Manesis, Emmanouil, S840 ([SAT374](#))
Manfredi, Giulia Francesca, S483 ([FRI185](#)),
S503 ([FRI227](#)), S929 ([SAT582](#))
Manganas, Konstantinos, S472 ([FRI163](#))
Manganis, Charis, S330 ([THU475](#))
Manga, Noel, S304 ([THU419](#))
Mangia, Alessandra, S581 ([FRI384](#)),
S586 ([FRI393](#)), S609 ([FRI487](#))
Mangini, Chiara, S888 ([SAT497](#))
Mangla, Kamal Kant, S29 ([OS025](#)),
S148 ([THU058](#)), S150 ([THU062](#))
Mang, M, S906 ([SAT530](#))
Manhas, Savrina, S244 ([THU302](#)),
S247 ([THU309](#)), S845 ([SAT385](#))
Mani, Ilianna, S908 ([SAT534](#))
Mani, Nagraj, S848 ([SAT392](#))
Man, Joris De, S709 ([SAT089](#))
Manka, Paul, S378 ([THU579](#)),
S682 ([SAT035](#))
Man, Kwan, S636 ([FRI542](#))
Manmadhan, Saumya, S654 ([FRI577](#))
Mannalithara, Ajitha, S116 ([OS173](#)),
S462 ([FRI124](#)), S790 ([SAT267](#)),
S903 ([SAT525](#))
Manna, Luiza Borges, S329 ([THU473](#))
Manna, Martina, S404 ([FRI024](#))
Mann, Derek A, S385 ([THU595](#)),
S640 ([FRI551](#)), S646 ([FRI561](#)),
S660 ([FRI590](#))
Männistö, Satu, S80 ([OS109](#))
Männistö, Ville Tapio, S80 ([OS109](#))
Mann, Jelena, S660 ([FRI590](#))
Mann, Matthias, S500 ([FRI223](#)),
S523 ([FRI263](#))
Manns, Michael P, S317 ([THU452](#)),
S318 ([THU453](#)), S569 ([FRI359](#)),
S582 ([FRI385](#)), S830 ([SAT355](#))
Manolakopoulos, Spiliot, S840 ([SAT374](#))
Manousou, Pinelopi, S54 ([OS069](#)),
S179 ([THU158](#)), S444 ([FRI094](#)),
S674 ([SAT020](#))
Man, Robert De, S227 ([THU271](#)),
S281 ([THU374](#)), S569 ([FRI359](#)),
S933 ([SAT591](#))
Mansbach, Hank, S727 ([SAT131](#)),
S730 ([SAT139](#)), S732 ([SAT143](#))
Manson, JoAnn, S912 ([SAT554](#))
Mansour, Dina, S430 ([FRI066](#))
Mansouri, Abdel, S245 ([THU304](#))
Mansour, Mahmoud, S803 ([SAT290](#)),
S807 ([SAT295](#))
Mansour, Natalie, S223 ([THU262](#))
Man, Tak Yung, S85 ([OS117](#))
Mantero, Sara, S480 ([FRI179](#)), S647 ([FRI562](#))
Mantia, Claudia La, S448 ([FRI101](#)),
S725 ([SAT127](#))
Mantovani, Alessandro, S152 ([THU066](#)),
S920 ([SAT567](#))
Mantovani, Anna, S658 ([FRI586](#)),
S900 ([SAT519](#)), S925 ([SAT574](#))
Mantry, Parvez, S319 ([THU455](#))
Manuilov, Dmitry, S4 ([GS006](#)),
S103 ([OS149](#)), S244 ([THU302](#)),
S828 ([SAT351](#)), S829 ([SAT352](#)),
S845 ([SAT385](#)), S862 ([SAT417](#))
Manzhali, Elina, S635 ([FRI539](#))
Manzur, Antonio, S158 ([THU075](#))
Mao, John, S832 ([SAT359](#)), S865 ([SAT423](#))
Maomao, Cao, S82 ([OS111](#))
Mao, Minxin, S504 ([FRI229](#))
Mao, Qianguo, S70 ([OS091](#))
Mao, Xiaorong, S182 ([THU165](#))
Mao, Yongwu, S182 ([THU165](#))
Maponga, Tongai Gibson, S23 ([OS015](#))
Maqbool, Nabeel Ahmed, S240 ([THU295](#))
Marasco, Giovanni, S91 ([OS129](#)),
S794 ([SAT273](#))
Maras, Jaswinder, S34 ([OS033](#)),
S128 ([THU020](#)), S528 ([FRI273](#)),
S738 ([SAT161](#)), S752 ([SAT188](#))
Maravelia, Panagiota, S860 ([SAT413](#))
Marcellin, Fabienne, S426 ([FRI059](#)),
S567 ([FRI353](#))
Marcellin, Patrick, S832 ([SAT358](#))
Marcellusi, Andrea, S232 ([THU281](#)),
S242 ([THU299](#))
Marcelo, Julio, S137 ([THU034](#))
Marchand, Lucie, S72 ([OS093](#))
Marchant, Arnaud, S124 ([THU012](#))
Marchelli, Daniele, S675 ([SAT021](#))
Marcher, Ann-Britt, S758 ([SAT200](#))
Marchesi, Julian, S121 ([THU007](#)),
S674 ([SAT020](#))
Marchi, Emanuele, S541 ([FRI301](#))
Marchignoli, Francesca, S153 ([THU067](#))
Marchuk, Svetlana, S269 ([THU351](#))
Marcia, Claudia, S596 ([FRI414](#))
Marciano, Sebastián, S19 ([OS008](#)),
S49 ([OS063](#)), S137 ([THU034](#))
Marcinac, John, S596 ([FRI411](#))
Marcin, Kennie, S392 ([FRI005](#))
Marco, Leonardo De, S900 ([SAT519](#))
Marco, Rosanna De, S908 ([SAT535](#))
Marcou, Christelle, S872 ([SAT436](#))
Marco, Vito Di, S387 ([THU599](#)),
S581 ([FRI384](#)), S624 ([FRI517](#)),
S725 ([SAT127](#)), S908 ([SAT535](#))
Mardinoglu, Adil, S68 ([OS089](#))
Mare, Ruxandra, S502 ([FRI225](#))
Maresca, Manuel Rodriguez, S577 ([FRI374](#))
Mareux, Elodie, S514 ([FRI248](#)),
S521 ([FRI260](#))
Margalit, Maya, S727 ([SAT131](#)),
S730 ([SAT139](#)), S732 ([SAT143](#))
Margarita, Sara, S428 ([FRI061](#))
Marhenke, Silke, S11 ([LB002](#)),
S666 ([SAT003](#))
Maria, Alexandre, S392 ([FRI006](#))
Maria Banales, Jesus, S648 ([FRI564](#))
Maria, Nicola De, S795 ([SAT275](#))
Maried, Jorge Joven, S677 ([SAT027](#)),
S681 ([SAT034](#))
Marigorta, Urko M, S671 ([SAT014](#))
Mari, Jose Maria, S229 ([THU276](#))
Marí, Montserrat, S652 ([FRI573](#)),
S672 ([SAT016](#))
Marinescu, Stefan, S100 ([OS143](#))
Marinho, Carla Maria Moura,
S149 ([THU060](#))
Marinho, Rui, S238 ([THU291](#))
Marini, Federico, S464 ([FRI147](#))
Marini, Ilaria, S428 ([FRI061](#)), S668 ([SAT007](#))
Marin, Jose, S46 ([OS056](#)), S59 ([OS074](#)),
S107 ([OS157](#)), S643 ([FRI554](#))
Marin, Jose Juan G., S600 ([FRI453](#))
Mariño, Zoe, S99 ([OS141](#)), S263 ([THU340](#))
Marin-Rubio, Jose Luis, S704 ([SAT081](#))
Marins, Ed G., S491 ([FRI204](#))
Marins, José Humberto Caetano,
S307 ([THU432](#))
Marionaux, Jonathon, S7 ([GS009](#))
Marjanovic, Goran, S710 ([SAT090](#))
Marjot, Thomas, S54 ([OS069](#)),
S57 ([OS072A](#)), S58 ([OS072B](#))
Markakis, Georgios, S429 ([FRI063](#))
Markby, Jessica, S42 ([OS049](#)),
S558 ([FRI335](#))
Mark, Davwar Pantong, S23 ([OS015](#))
Markezana, Aurelia, S764 ([SAT213](#))
Marleau, Denis, S593 ([FRI407](#))
Marmon, Tonya, S88 ([OS123](#)),
S715 ([SAT106](#)), S716 ([SAT107](#)),
S716 ([SAT108](#)), S731 ([SAT142](#))
Marniquet, Xavier, S872 ([SAT436](#))
Ma, Ronald, S134 ([THU029](#))
Marot, Astrid, S11 ([LB002](#)), S131 ([THU025](#))
Marotta, Christine, S716 ([SAT109](#))
Marquardt, Jens, S313 ([THU444](#)),
S649 ([FRI566](#))
Marquardt, Jens U., S11 ([LB002](#))

Author Index

- Marques de Alcanatara Barreto, Camila, S910 ([SAT539](#))
- Marques, Francisco, S192 ([THU185](#))
- Marques, Pedro Elias, S396 ([FRI012](#))
- Marques, Sara, S268 ([THU349](#))
- Márquez, Andrea, S81 ([OS110](#))
- Marquez, Valentin, S555 ([FRI329](#))
- Marra, Fabio, S47 ([OS058](#)), S477 ([FRI173](#)), S627 ([FRI524](#)), S649 ([FRI567](#)), S651 ([FRI570](#)), S932 ([SAT588](#))
- Marra, Fiona, S580 ([FRI383](#))
- Marrone, Giuseppe, S436 ([FRI079](#))
- Marron, Thomas, S383 ([THU588](#))
- Marron, Thomas U., S372 ([THU567](#))
- Marschall, Hanns-Ulrich, S94 ([OS133](#)), S329 ([THU473](#)), S696 ([SAT063](#)), S904 ([SAT527](#))
- Marsche, Gunther, S346 ([THU506](#))
- Martell, María, S180 ([THU161](#)), S365 ([THU538](#))
- Martens, Joerg, S783 ([SAT257](#))
- Marti-Aguado, David, S127 ([THU018](#)), S137 ([THU035](#)), S442 ([FRI091](#))
- Marti-Bonmati, Luis, S442 ([FRI091](#))
- Martic, Miljen, S486 ([FRI194](#)), S493 ([FRI207](#))
- Martin, Almudena Porcel, S445 ([FRI096](#))
- Martín-Arriscado, Cristina, S704 ([SAT080](#))
- Martin-Bermudo, Franz, S87 ([OS122](#)), S708 ([SAT087](#))
- Martin, Carmen Alonso, S792 ([SAT270](#))
- Martin, Cesar, S600 ([FRI453](#))
- Martín, Cesar Augusto, S48 ([OS060](#)), S87 ([OS122](#)), S648 ([FRI564](#))
- Martincorena, Inigo, S741 ([SAT165](#))
- Martin, Eleonora De, S772 ([SAT239](#)), S800 ([SAT285](#)), S935 ([SAT595](#))
- Martinello, Marianne, S302 ([THU415](#)), S560 ([FRI339](#))
- Martínez, Ana Sánchez, S114 ([OS168](#))
- Martinez, Anthony, S596 ([FRI411](#))
- Martínez-Arenas, Laura, S114 ([OS169](#)), S150 ([THU061](#)), S811 ([SAT303](#))
- Martínez-Arranz, Ibon, S419 ([FRI045](#)), S455 ([FRI113](#)), S671 ([SAT014](#))
- Martínez-Cáceres, Eva, S199 ([THU199](#))
- Martínez-Chantar, María Luz, S46 ([OS056](#)), S84 ([OS116](#)), S87 ([OS122](#)), S132 ([THU027](#)), S177 ([THU155](#)), S600 ([FRI453](#)), S643 ([FRI554](#)), S673 ([SAT018](#)), S679 ([SAT029](#)), S689 ([SAT050](#))
- Martínez-Cruz, Luis Alfonso, S48 ([OS060](#)), S87 ([OS122](#)), S132 ([THU027](#)), S600 ([FRI453](#))
- Martínez-Escudé, Alba, S25 ([OS018](#))
- Martinez, Fernando, S555 ([FRI329](#))
- Martínez-Flórez, Susana, S177 ([THU155](#))
- Martinez Garcia de la Torre, Raquel A., S37 ([OS039](#))
- Martinez-Gili, Laura, S674 ([SAT020](#))
- Martínez-González, Brenda, S589 ([FRI399](#))
- Martinez, Javier, S90 ([OS127](#))
- Martinez-Llordella, Marc, S401 ([FRI019](#)), S809 ([SAT298](#))
- Martinez, Lola, S555 ([FRI329](#))
- Martinez-Roma, Maria, S229 ([THU276](#))
- Martinez, Sara, S63 ([OS080](#)), S406 ([FRI027](#)), S511 ([FRI242](#)), S512 ([FRI243](#)), S512 ([FRI244](#))
- Martinez, Sergio Muñoz, S381 ([THU584](#))
- Martinez-Tapia, Claudia, S508 ([FRI237](#))
- Martín, Francisco Javier Atienza, S451 ([FRI106](#))
- Martin-Guerrero, Idoia, S689 ([SAT050](#))
- Martini, Silvia, S569 ([FRI359](#)), S775 ([SAT243](#)), S776 ([SAT245](#))
- Martiniuc, Alexandru, S795 ([SAT276](#))
- Martin, Jasmine, S580 ([FRI383](#))
- Martin, Javier San, S14 ([LB006](#))
- Martin, Juan Carlos Diaz, S459 ([FRI119](#))
- Martin, Lily, S168 ([THU096](#))
- Martin, Marian, S454 ([FRI110](#))
- Martin-Mateos, Rosa, S114 ([OS169](#)), S127 ([THU018](#)), S157 ([THU074](#)), S158 ([THU076](#)), S792 ([SAT271](#))
- Martin, Natasha, S565 ([FRI349](#))
- Martin, Paul, S223 ([THU262](#)), S848 ([SAT390](#))
- Martin-Reyes, F., S396 ([FRI011](#))
- Martin, Romain, S36 ([OS038](#)), S738 ([SAT160](#))
- Martin, Ross, S244 ([THU302](#)), S247 ([THU309](#)), S845 ([SAT385](#))
- Martins, Alexandra, S581 ([FRI384](#))
- Martin, Sara De, S378 ([THU578](#))
- Martins, Eduardo, S419 ([FRI045](#))
- Martins, Maria, S668 ([SAT008](#))
- Martner, Anna, S186 ([THU174](#))
- Martró, Elisa, S570 ([FRI361](#))
- Marukutira, Tafireyi, S541 ([FRI302](#))
- Marzi, Luca, S578 ([FRI376](#))
- Marzioni, Marco, S107 ([OS157](#))
- Marzorati, Simona, S761 ([SAT206](#))
- Marzouk, Samir, S479 ([FRI178](#))
- Masarone, Mario, S425 ([FRI057](#)), S551 ([FRI320](#))
- Masashi, Mizokami, S654 ([FRI579](#))
- Mascarenhas, Miguel, S28 ([OS024](#))
- Masetti, Chiara, S528 ([FRI272](#))
- Ma, Shenglin, S493 ([FRI207](#))
- Ma, Shiwen, S744 ([SAT171](#)), S803 ([SAT289](#))
- Maslac, Olivia, S251 ([THU318](#))
- Masnou, Helena, S724 ([SAT125](#))
- Mason, Andrew L., S313 ([THU443](#)), S317 ([THU452](#)), S335 ([THU484](#)), S338 ([THU490](#))
- Mason, Hugh, S251 ([THU318](#))
- Masoodi, Mojgan, S363 ([THU535](#)), S480 ([FRI180](#))
- Maspero, Marianna, S789 ([SAT266](#))
- Massaro, Francesco, S84 ([OS115](#))
- Masseli, Johannes, S353 ([THU517](#)), S354 ([THU518](#))
- Más-Serrano, Patricio, S114 ([OS168](#))
- Massetto, Benedetta, S733 ([SAT145](#)), S835 ([SAT365](#))
- Masson, Mounia Heddad, S438 ([FRI084](#))
- Masson, Steven, S34 ([OS034](#)), S120 ([THU005](#)), S122 ([THU008](#)), S124 ([THU013](#)), S141 ([THU041](#)), S567 ([FRI355](#)), S646 ([FRI561](#))
- Mastrocinque, Davide, S212 ([THU239](#))
- Mastrorocco, Elisabetta, S528 ([FRI272](#))
- Masui, Toshihiko, S183 ([THU167](#))
- Masur, Henry, S552 ([FRI322](#)), S572 ([FRI364](#)), S574 ([FRI369](#))
- Masutti, Flora, S626 ([FRI522](#))
- Mateo, Roberto, S244 ([THU302](#)), S247 ([THU309](#)), S845 ([SAT385](#))
- Mateos, Rosa María Martín, S406 ([FRI027](#))
- Mateu, Carlos Alventosa, S222 ([THU261](#))
- Mathers, John, S733 ([SAT146](#))
- Mathew, Babu, S34 ([OS033](#)), S128 ([THU020](#)), S528 ([FRI273](#)), S738 ([SAT161](#)), S752 ([SAT188](#))
- Mathews, Mead, S410 ([FRI032](#))
- Mathews, Steven, S729 ([FRI138](#))
- Mathurin, Philippe, S5 ([GS007](#)), S205 ([THU227](#)), S205 ([THU228](#)), S913 ([SAT557](#))
- Mathur, Rajendra, S347 ([THU508](#))
- Matilla, Ana, S912 ([SAT555](#))
- Matilla, Ana M, S381 ([THU584](#))
- Matimbo, Jean Jacques, S791 ([SAT269](#))
- Mato, José M., S671 ([SAT014](#))
- Matour, Bashar, S465 ([FRI149](#))
- Matschenz, Katrin, S585 ([FRI391](#))
- Matsukuma, Karen, S462 ([FRI125](#))
- Matsumoto, Kosuke, S314 ([THU445](#))
- Matsuura, Kentaro, S563 ([FRI346](#))
- Matteo, Sabina Di, S648 ([FRI564](#))
- Matteucci, Claudia, S249 ([THU313](#))
- Matthaei, Hanno, S381 ([THU585](#))
- Matthews, Gail, S302 ([THU415](#)), S560 ([FRI339](#)), S565 ([FRI349](#)), S842 ([SAT377](#)), S872 ([SAT437](#))
- Matthews, Philippa, S23 ([OS015](#)), S277 ([THU368](#)), S285 ([THU382](#)), S856 ([SAT407](#))
- Mattis, Aras, S404 ([FRI023](#)), S439 ([FRI085](#))
- Mattos, Matheus, S396 ([FRI012](#))
- Mattsson, Jan, S751 ([SAT187](#))
- Matusali, Giulia, S806 ([SAT294](#))
- Matz-Soja, Madlen, S184 ([THU169](#)), S383 ([THU590](#))
- Maucourant, Christopher, S27 ([OS021](#)), S189 ([THU179](#))
- Maud, Michelet, S246 ([THU305](#)), S766 ([SAT216](#))
- Maurer, Lars, S100 ([OS143](#))
- Maurício, João, S646 ([FRI561](#))
- Mauri, Francesco, S372 ([THU567](#))
- Mauriz, José Luís, S639 ([FRI549](#))
- Mauriz, Violeta, S792 ([SAT270](#))
- Mauro, Ezequiel, S90 ([OS127](#)), S786 ([SAT261](#)), S883 ([SAT488](#))
- Maurrer, Lars, S265 ([THU344](#))
- Maus, Mate, S673 ([SAT018](#))
- Mauss, Stefan, S16 ([OS003](#)), S562 ([FRI345](#)), S585 ([FRI391](#))

- Mauthner, Oliver, S509 ([FRI238](#))
 Mavar-Haramija, Marija, S96 ([OS136](#))
 Ma, Xiaoli, S836 ([SAT366](#))
 Maxwell, Ryan, S538 ([FRI294](#)),
 S538 ([FRI295](#))
 Maya, Douglas, S450 ([FRI105](#)),
 S708 ([SAT087](#))
 Mayans, Sofia, S467 ([FRI154](#))
 Mayer, Cristiana, S864 ([SAT422](#))
 Mayer, Cristina, S8 ([GS010](#))
 Mayer, Florian, S545 ([FRI309](#))
 Mayer, Lena, S710 ([SAT090](#))
 Mayers, Douglas, S73 ([OS095](#))
 Ma, Ying, S182 ([THU165](#))
 May, Jan-Niklas, S385 ([THU594](#))
 May, Lindsey, S244 ([THU302](#)),
 S247 ([THU308](#)), S247 ([THU309](#)),
 S845 ([SAT385](#))
 Maynard, Lauren, S13 ([LB004B](#)),
 S881 ([SAT453](#))
 Mayne, Tracy, S310 ([THU439](#)),
 S332 ([THU478](#)), S335 ([THU484](#))
 Mayo, Marilyn J., S317 ([THU452](#)),
 S335 ([THU484](#))
 Mayo, Patrick, S660 ([FRI591](#)), S726 ([SAT130](#))
 Mayo, Rebeca, S671 ([SAT014](#))
 May, Petra, S533 ([FRI283](#))
 Ma, Yun, S647 ([FRI563](#)), S818 ([SAT315](#))
 Mazhar, Samra, S240 ([THU295](#))
 Ma, Zhenkun, S894 ([SAT509](#))
 Mazouz, Sabrina, S675 ([SAT022](#))
 Mazurak, Vera C., S892 ([SAT504](#))
 Mazur, Włodzimierz, S585 ([FRI390](#))
 Mazzaferro, Vincenzo, S789 ([SAT266](#)),
 S815 ([SAT311](#))
 Mazza, Giuseppe, S668 ([SAT008](#)),
 S737 ([SAT157](#))
 Mazzarelli, Chiara, S569 ([FRI359](#)),
 S571 ([FRI363](#))
 Mazzola, Giovanni, S31 ([OS029](#))
 Mazzucco, Veronica, S378 ([THU578](#))
 Mbanya, Dora, S294 ([THU400](#))
 McCain, Misti, S646 ([FRI561](#))
 McCann, Adrian, S670 ([SAT013](#))
 McCann, Gerry, S409 ([FRI031](#))
 McCartney, Erin, S228 ([THU272](#))
 McCaughan, Geoff, S3 ([GS005](#))
 McClain, Craig J., S35 ([OS035](#))
 McClure, Matt, S733 ([SAT145](#)),
 S824 ([SAT343](#)), S835 ([SAT365](#)),
 S871 ([SAT435](#))
 McClure, Matthew, S846 ([SAT386](#))
 McCormick, Emma, S418 ([FRI043](#))
 McCormick, Rosemary, S898 ([SAT516](#))
 McCullough, Francesca, S567 ([FRI355](#))
 McCune, Anne, S141 ([THU041](#))
 McDonald, Brock, S770 ([SAT234](#))
 McDonald, Lucy, S498 ([FRI218](#))
 McDonald, Natasha, S461 ([FRI123](#))
 McElvaney, Noel G., S531 ([FRI279](#))
 McFarlane, Stefanie, S416 ([FRI040](#))
 McGeorge, Sara, S67 ([OS087](#)),
 S130 ([THU023](#)), S176 ([THU153](#)),
 S339 ([THU494](#))
 McGlynn, Katherine, S912 ([SAT554](#))
 McGonigle, John, S424 ([FRI056](#))
 McGuckin, Michael, S190 ([THU183](#))
 Mchunu, Noxolo, S285 ([THU382](#))
 McInnes, Iain B., S57 ([OS072A](#))
 McIntosh, Chris, S429 ([FRI065](#))
 McIntyre, Gail, S470 ([FRI159](#))
 McKeating, Jane, S758 ([SAT199](#))
 McKibben, Andrew, S312 ([THU442](#))
 McKiernan, Patrick, S519 ([FRI256](#)),
 S521 ([FRI259](#))
 McKinnon, Elizabeth, S440 ([FRI087](#))
 McKinnon, Melita, S239 ([THU294](#)),
 S305 ([THU422](#))
 McLaughlin, Megan, S327 ([THU470](#)),
 S335 ([THU485](#))
 McMahan, Lynn, S163 ([THU086](#))
 McMullen, Megan, S33 ([OS032](#))
 McNaughton, Anna, S256 ([THU328](#)),
 S285 ([THU382](#)), S856 ([SAT407](#))
 McNeil, Marian, S163 ([THU086](#))
 McPhail, Mark J W, S135 ([THU031](#)),
 S185 ([THU173](#)), S352 ([THU516](#)),
 S371 ([THU550](#)), S647 ([FRI563](#))
 McPhail, Mark J. W., S116 ([OS171](#)),
 S403 ([FRI022](#)), S505 ([FRI231](#))
 Mcpherson, Stuart, S437 ([FRI080](#)),
 S567 ([FRI355](#)), S646 ([FRI561](#)),
 S721 ([SAT118](#)), S733 ([SAT146](#))
 Mcque, Kate, S567 ([FRI355](#))
 McQuillin, Andrew, S11 ([LB002](#))
 McQuitty, Claire, S480 ([FRI179](#))
 McRae, Michael, S633 ([FRI535](#))
 McWherter, Charles, S322 ([THU461](#)),
 S477 ([FRI174](#))
 Meacham, Georgina, S57 ([OS072A](#)),
 S58 ([OS072B](#))
 Medas, Renato, S618 ([FRI507](#))
 Medel, María Paz, S81 ([OS110](#)),
 S137 ([THU034](#))
 Medhi, Subhash, S299 ([THU409](#))
 Medhus, Asle Wilhelm, S178 ([THU157](#))
 Medina, Diogo, S229 ([THU276](#)),
 S577 ([FRI374](#))
 Medina, Martín Uriel Vázquez,
 S554 ([FRI326](#))
 Medrano-Bosch, Mireia, S492 ([FRI205](#)),
 S743 ([SAT170](#))
 Medrano, Indhira Perez, S324 ([THU464](#))
 Medvedeva, Elina, S848 ([SAT392](#)),
 S876 ([SAT443](#)), S878 ([SAT448](#))
 Meersseman, Philippe, S346 ([THU507](#))
 Meeusen, Bob, S637 ([FRI544](#))
 Megna, Angelo Salomone, S938 ([SAT599](#))
 Mehdiyev, Shahin, S858 ([SAT410](#)),
 S861 ([SAT416](#)), S864 ([SAT421](#))
 Mehiri, Loriane Lair, S392 ([FRI005](#))
 Mehlen, Patrick, S766 ([SAT216](#))
 Mehnert, Ann-Kathrin, S262 ([THU338](#))
 Mehreen, Sania, S883 ([SAT487](#))
 Mehrl, Alexander, S241 ([THU298](#))
 Mehta, R, S868 ([SAT428](#))
 Mehta, Rashmi, S328 ([THU472](#))
 Mehta, Shubham, S433 ([FRI072](#))
 Meier, Florian, S500 ([FRI223](#))
 Meijnikman, Stijn, S9 ([GS011](#))
 Meindl-Beinker, Nadja, S606 ([FRI466](#))
 Meischl, Tobias, S919 ([SAT565](#)),
 S921 ([SAT570](#))
 Meislin, Rachel, S160 ([THU080](#))
 Meiss, Frank, S2 ([GS003](#))
 Meister, Toni Luise, S263 ([THU339](#))
 Mei, Swee Lin Chen Yi, S498 ([FRI218](#))
 Mejia, Scherezada, S137 ([THU034](#)),
 S487 ([FRI195](#))
 Mekonnen, Yonatan, S566 ([FRI352](#))
 Melberg, Hans Olav, S130 ([THU022](#))
 Melero, Maria Jose, S555 ([FRI329](#))
 Melgar-Lesmes, Pedro, S106 ([OS154](#)),
 S492 ([FRI205](#)), S743 ([SAT170](#))
 Melis, Daniela, S515 ([FRI249](#))
 Melis, Marta, S133 ([THU028](#))
 Melkebeke, Lukas Van, S120 ([THU003](#)),
 S680 ([SAT032](#))
 Mello, Tommaso, S659 ([FRI588](#))
 Mells, George, S96 ([OS137](#))
 Melody, Shannon M., S541 ([FRI302](#))
 Meltzer, Brian, S526 ([FRI268](#))
 Melum, Espen, S27 ([OS021](#)), S604 ([FRI463](#)),
 S605 ([FRI465](#))
 Mena, Edward, S319 ([THU455](#))
 Mendes, Liliana Sampaio Costa,
 S137 ([THU034](#))
 Mendes, Milena, S190 ([THU182](#))
 Méndez-Blanco, Carolina, S639 ([FRI549](#))
 Mendez, Marinela, S586 ([FRI393](#))
 Méndez-Sánchez, Nahum, S154 ([THU069](#)),
 S209 ([THU234](#))
 Mendizabal, Manuel, S137 ([THU034](#)),
 S786 ([SAT261](#))
 Mendoza, Yuly, S363 ([THU535](#)),
 S480 ([FRI180](#))
 Mendy, Francis, S258 ([THU332](#))
 Mendy, Maimuna, S295 ([THU401](#))
 Meneses, Maria Joao, S706 ([SAT085](#))
 Menghini, Arianna, S703 ([SAT078](#))
 Meng, Xianmei, S182 ([THU165](#))
 Meng, Zhong-Ji, S344 ([THU504](#))
 Meninger, Stephen, S516 ([FRI251](#))
 Menke, Aswin L., S677 ([SAT025](#)),
 S686 ([SAT044](#)), S698 ([SAT067](#))
 Mennini, Francesco, S242 ([THU299](#))
 Mennini, Francesco Saverio, S232 ([THU281](#))
 Menon, Krishna, S120 ([THU004](#)),
 S371 ([THU550](#)), S647 ([FRI562](#)),
 S771 ([SAT236](#))
 Menti, Denise, S608 ([FRI485](#)),
 S624 ([FRI519](#)), S893 ([SAT505](#))
 Menu, Yves, S504 ([FRI228](#))
 Menzel, Uwe, S40 ([OS045](#))
 Merabet, Yasmina Ben, S935 ([SAT595](#))
 Mera, Jorge, S226 ([THU269](#))
 Mercado-Gómez, Maria, S48 ([OS060](#)),
 S87 ([OS122](#)), S600 ([FRI453](#)),
 S679 ([SAT029](#))
 Mercan, Sercan, S85 ([OS118](#))
 Merchant, Michael, S465 ([FRI149](#))
 Meredith, Christopher, S842 ([SAT377](#))

Author Index

- Mereu, Tiziana, S806 ([SAT294](#))
 Merino, Victor, S442 ([FRI091](#))
 Merino, Xavier, S658 ([FRI587](#))
 Meritet, Jean François, S393 ([FRI007](#))
 Merle, Jean Claude, S791 ([SAT269](#))
 Merle, Philippe, S5 ([GS007](#))
 Merle, Uta, S562 ([FRI345](#)),
 S823 ([SAT341](#))
 Merli, Manuela, S815 ([SAT311](#))
 Meroni, Marica, S167 ([THU095](#)),
 S675 ([SAT021](#)), S682 ([SAT036](#)),
 S682 ([SAT037](#)), S698 ([SAT068](#)),
 S706 ([SAT084](#))
 Meroueh, Chady, S138 ([THU037](#))
 Mertens, Peter Rene, S659 ([FRI589](#))
 Mertins, Philipp, S99 ([OS142](#))
 Meschi, Silvia, S806 ([SAT294](#)),
 S808 ([SAT297](#))
 Mesenbrink, Peter, S449 ([FRI103](#))
 Messina, Vincenzo, S217 ([THU250](#)),
 S938 ([SAT599](#))
 Mestre, Anna, S368 ([THU545](#))
 Meszaros, Magdalena, S122 ([THU009](#)),
 S771 ([SAT237](#))
 Metivier, Sophie, S72 ([OS093](#)),
 S833 ([SAT360](#)), S840 ([SAT373](#))
 Metreveli, David, S587 ([FRI395](#)),
 S590 ([FRI400](#)), S590 ([FRI401](#))
 Metselaar, Herold, S330 ([THU476](#)),
 S815 ([SAT311](#))
 Metselaar, Herold J., S933 ([SAT591](#))
 Meuleman, Philip, S860 ([SAT413](#))
 Meunier, Lucy, S392 ([FRI006](#)),
 S771 ([SAT237](#))
 Meuris, Leander, S562 ([FRI344](#)),
 S768 ([SAT230](#)), S913 ([SAT556](#))
 Meyer, Bernhard, S608 ([FRI485](#)),
 S622 ([FRI514](#)), S624 ([FRI519](#))
 Meyer, Christoph, S408 ([FRI029](#))
 Meyer, Elias Laurin, S90 ([OS127](#))
 Meyer-Herbon, Pamela, S937 ([SAT598](#))
 Meyer, Moritz, S126 ([THU017](#))
 Meyer-Myklestad, Malin Holm,
 S178 ([THU157](#))
 Mezzano, Gabriel, S907 ([SAT532](#))
 Mfaria, Neil, S583 ([FRI387](#))
 Miaczynska, Marta, S606 ([FRI467](#))
 Miaillhes, Patrick, S833 ([SAT360](#))
 Miao, Yingying, S389 ([FRI001](#)),
 S601 ([FRI456](#))
 Michailidou, Elisavet, S429 ([FRI063](#))
 Michalak, Sophie, S73 ([OS096](#)),
 S496 ([FRI215](#)), S497 ([FRI216](#))
 Michałowski, Łukasz, S156 ([THU072](#))
 Michard, Baptiste, S20 ([OS010](#))
 Michel, Maurice, S145 ([THU051](#)),
 S882 ([SAT486](#))
 Micheltorena, Cristina Olague,
 S248 ([THU310](#)), S257 ([THU330](#))
 Michielsen, Peter, S303 ([THU416](#))
 Michot, Jean-Marie, S402 ([THU020](#))
 Middleton, Michael, S455 ([FRI112](#))
 Middleton, Paul, S34 ([OS034](#)),
 S558 ([FRI334](#))
 Mieg, Alexa, S374 ([THU570](#)),
 S380 ([THU582](#))
 Miele, Luca, S436 ([FRI079](#)), S675 ([SAT021](#))
 Mieli-Vergani, Giorgia, S308 ([THU435](#))
 Mijic, Maja, S700 ([SAT070](#))
 Mikaelian, Igor, S443 ([FRI093](#)),
 S486 ([FRI193](#))
 Mikhail, Nabil, S479 ([FRI178](#))
 Miki, Daiki, S563 ([FRI346](#))
 Mi Kim, Mi, S438 ([FRI082](#)), S438 ([FRI083](#)),
 S439 ([FRI086](#))
 Mikula, Tomasz, S565 ([FRI350](#))
 Mikulits, Wolfgang, S470 ([FRI159](#))
 Milani, Stefano, S770 ([SAT235](#))
 Milan, Zoka, S817 ([SAT313](#))
 Milella, Michele, S581 ([FRI384](#)),
 S658 ([FRI586](#)), S925 ([SAT574](#))
 Milic, Jovana, S31 ([OS029](#))
 Milkiewicz, Malgorzata, S77 ([OS103](#)),
 S317 ([THU451](#)), S600 ([FRI453](#))
 Milkiewicz, Malgorzata, S601 ([FRI455](#))
 Milkiewicz, Piotr, S77 ([OS103](#)),
 S315 ([THU447](#)), S317 ([THU451](#)),
 S600 ([FRI453](#)), S601 ([FRI455](#)),
 S605 ([FRI464](#)), S607 ([FRI469](#)),
 S782 ([SAT254](#))
 Milkowski, Andrzej, S460 ([FRI122](#))
 Milla, Annabelle, S872 ([SAT436](#))
 Millar, Jane, S285 ([THU382](#))
 Miller, Carolyn, S567 ([FRI355](#))
 Miller, Keith, S167 ([THU094](#))
 Miller, Mark, S298 ([THU407](#))
 Miller, Michael, S495 ([FRI214](#))
 Millet, Oscar, S671 ([SAT014](#))
 Millian, Daniel, S194 ([THU191](#)),
 S470 ([FRI160](#)), S485 ([FRI190](#))
 Milligan, Scott, S581 ([FRI384](#))
 Mills, Camilla, S592 ([FRI405](#))
 Mills, Ross, S481 ([FRI182](#))
 Milner, Andrew, S554 ([FRI327](#))
 Milton, Yuka, S673 ([SAT017](#))
 Mimche, Patrice, S113 ([OS167](#))
 Mimidis, Konstantinos, S840 ([SAT374](#))
 Mina, Christos, S202 ([THU220](#))
 Mincholé, Itziar, S671 ([SAT014](#))
 Minder, Anna-Elisabeth, S60 ([OS075](#))
 Minguez, Beatriz, S381 ([THU584](#)),
 S658 ([FRI587](#)), S912 ([SAT555](#))
 Minisini, Rosalba, S929 ([SAT582](#)),
 S929 ([SAT583](#))
 Minnich, Anne, S446 ([FRI029](#))
 Min, Seohyun, S489 ([FRI199](#))
 Minto, Wesley, S483 ([FRI187](#))
 Minutolo, Antonella, S249 ([THU313](#))
 Miquel, Joaquin, S184 ([THU170](#)),
 S826 ([SAT347](#))
 Miquel, Mireia, S857 ([SAT409](#))
 Miquel, Rosa, S120 ([THU004](#)),
 S505 ([FRI231](#)), S647 ([FRI562](#)),
 S809 ([SAT298](#))
 Mirabel, Xavier, S5 ([GS007](#))
 Mirakaj, Valbona, S766 ([SAT216](#))
 Miralles, Inmaculada Castelló,
 S222 ([THU261](#))
 Miralpeix, Anna, S570 ([FRI361](#))
 Miranda, Miguel, S110 ([OS161](#))
 Miravittles, Marc, S515 ([FRI250](#))
 Mirza, Darius F., S805 ([SAT292](#))
 Misas, Marta Guerrero, S39 ([OS044](#))
 Mischke, Jasmin, S566 ([FRI352](#))
 Mishra, Gauri, S337 ([THU488](#))
 Mishra, Kajali, S53 ([OS066](#))
 Mishra, Nitu, S252 ([THU320](#))
 Missen, Louise, S554 ([FRI327](#))
 Mistry, Pratik, S700 ([SAT071](#))
 Mistry, Sameer, S188 ([THU178](#))
 Mita, Dorina, S153 ([THU067](#))
 Mitchell, Chris, S96 ([OS137](#)),
 S337 ([THU489](#)), S529 ([FRI274](#)),
 S536 ([FRI291](#))
 Mitchell, Nina, S404 ([FRI023](#))
 Mitchell-Thain, Robert, S96 ([OS137](#)),
 S529 ([FRI274](#))
 Mitnala, Sasikala, S191 ([THU184](#))
 Mitran, Bogdan, S471 ([FRI162](#))
 Mitry, Ragai, S818 ([SAT315](#))
 Mittal, Akaash, S203 ([THU224](#)),
 S204 ([THU225](#))
 Mittendorf, Bettina, S671 ([SAT014](#))
 Mittenzwei, Romy, S396 ([FRI012](#))
 Miyara, Makoto, S189 ([THU181](#))
 Miyata, Tatsunori, S33 ([OS032](#))
 Mlitz, Veronika, S469 ([FRI158](#)),
 S688 ([SAT049](#)), S760 ([SAT204](#))
 Mn, Meenu, S252 ([THU320](#))
 Moal, Valérie, S497 ([FRI216](#))
 Mobsby, Mikaela, S239 ([THU294](#))
 Mocan, Tudor, S915 ([SAT559](#))
 Mocchiatti, Ginevra, S929 ([SAT582](#))
 Mocciano, Gabriele, S695 ([SAT061](#))
 Mochida, Satoshi, S563 ([FRI346](#))
 Mochon, Dolores Ocete, S222 ([THU261](#))
 Möckel, Diana, S385 ([THU594](#))
 Modi, Kavita, S741 ([SAT164](#))
 Moeckli, Beat, S754 ([SAT192](#))
 Moestrup, Søren Kragh, S434 ([FRI074](#))
 Moga, Lucile, S502 ([FRI226](#))
 Moga, Tudor-Voicu, S930 ([SAT585](#))
 Moggio, Maurizio, S682 ([SAT037](#))
 Mogler, Carolin, S2 ([GS003](#)), S654 ([FRI577](#))
 Mogul, Douglas, S599 ([FRI452](#))
 Mohamed, Almuthana, S276 ([THU366](#)),
 S594 ([FRI409](#)), S812 ([SAT304](#))
 Mohamed, Tamer, S764 ([SAT212](#))
 Mohamed, Wael, S632 ([FRI532](#))
 Mohammadi, Fadak, S389 ([FRI002](#)),
 S898 ([SAT516](#))
 Mohammadi, Shahin, S37 ([OS041](#))
 Mohammed, Aaminah, S125 ([THU014](#))
 Mohammed, Naqvi, S847 ([SAT389](#))
 Mohanty, Sujata, S756 ([SAT196](#))
 Mohapatra, Shivabrata Dhal, S898 ([SAT515](#))
 Mo, Hongmei, S244 ([THU302](#)),
 S247 ([THU308](#)), S247 ([THU309](#)),
 S841 ([SAT376](#)), S845 ([SAT385](#))
 Mohorianu, Irina, S742 ([SAT167](#))
 Möhring, Christian, S381 ([THU585](#))
 Mohr, Isabelle, S520 ([FRI258](#))

- Mohr, Raphael, S381 (THU585)
 Mohs, Antje, S654 (FRI578)
 Moia, Riccardo, S503 (FRI227)
 Moigboi, Christiana, S279 (THU370),
 S281 (THU375), S287 (THU387)
 Moiseev, Sergey, S574 (FRI370)
 Mol, Bregje, S338 (THU491)
 Moles, Anna, S465 (FRI150)
 Molina-Aguilar, Christian, S476 (FRI172)
 Molina, Esther, S792 (SAT271)
 Molina, Manuel Flores, S675 (SAT022)
 Molinari, Nicolas, S122 (THU009)
 Moliner, Alba Pueyo, S65 (OS085)
 Moliterni, Camilla, S763 (SAT211)
 Mollenkopf, Sarah, S552 (FRI322),
 S574 (FRI369)
 Møller, Andreas, S331 (THU477)
 Møller, Dina Leth, S818 (SAT314)
 Möller, Lars Christian, S341 (THU498)
 Møller, Søren, S154 (THU068),
 S340 (THU496), S361 (THU532),
 S502 (FRI226), S610 (FRI489),
 S614 (FRI498), S887 (SAT495)
 Molwitz, Isabel, S893 (SAT507)
 Mombiola, Antoni, S627 (FRI523)
 Monbaliu, Diethard, S781 (SAT253),
 S783 (SAT256)
 Monbet, Valérie, S656 (FRI582)
 Monfils, Kathryn, S46 (OS057)
 Monforte, Antonella d'Arminio,
 S284 (THU381)
 Mongale, Emily, S554 (FRI327)
 Monguzzi, Erika, S325 (THU466)
 Monico, Sara, S843 (SAT381)
 Monroy, Susana, S60 (OS075)
 Mons, Silvia Ariño, S37 (OS039),
 S527 (FRI271)
 Mons, Valentín Cuervas, S115 (OS169)
 Montagnese, Sara, S888 (SAT497)
 Montalbano, Marzia, S806 (SAT294),
 S808 (SAT297)
 Montalto, Michael, S700 (SAT071),
 S708 (SAT088)
 Montalto, Paolo, S649 (FRI567)
 Montalvo, Iarah, S487 (FRI195)
 Montalvo-Romeral, Valle, S689 (SAT050)
 Montanari, Noé Axel, S194 (THU189),
 S251 (THU317)
 Montañés, Rosa, S91 (OS128)
 Montano-Loza, Aldo J., S313 (THU443),
 S317 (THU452), S318 (THU453),
 S326 (THU467), S631 (FRI530),
 S775 (SAT244), S815 (SAT311),
 S892 (SAT504)
 Montano-Loza, Aldo J., S93 (OS132)
 Montegut, Julie, S872 (SAT436)
 Monte, Maria, S59 (OS074)
 Monterde, Vanesa Bernal, S127 (THU018),
 S157 (THU074), S158 (THU076),
 S676 (SAT023)
 Montero, Saul Martinez, S853 (SAT402)
 Montero-Vallejo, Rocío, S459 (FRI119),
 S708 (SAT087)
 Montes, Pedro, S137 (THU034)
 Montet, Xavier, S645 (FRI559)
 Monti, Monica, S564 (FRI347)
 Montironi, Carla, S136 (THU033),
 S139 (THU039)
 Montoliu, Carmina, S51 (OS065)
 Mookerjee, Raj, S344 (THU503),
 S889 (SAT499), S903 (SAT526)
 Moon, Andrew, S201 (THU219),
 S223 (THU262)
 Moon, Christina, S194 (THU189),
 S832 (SAT358)
 Mooney, Anne, S169 (THU098)
 Mooneyhan, Ellen, S43 (OS050),
 S230 (THU278), S231 (THU279),
 S238 (THU292), S240 (THU295)
 Moonka, Dilip, S612 (FRI493),
 S778 (SAT249)
 Moore, Celia, S188 (THU178)
 Moore, David, S696 (SAT063)
 Moore-Gillon, Claudia, S345 (THU505)
 Moore, J. Bernadette, S104 (OS151)
 Moore, Joanna, S814 (SAT308)
 Moore, Karen, S541 (FRI302)
 Moore, Kevin, S460 (FRI121)
 Moore, Yvette, S116 (OS172)
 Mora, Alfonso, S689 (SAT050)
 Mora, Andrés Martínez,
 S40 (OS045)
 Mor, Adi, S27 (OS022)
 Moradpour, Darius, S97 (OS138),
 S253 (THU322), S355 (THU520)
 Morales, Albert, S652 (FRI573),
 S672 (SAT016)
 Morales-Ruiz, Manuel, S896 (SAT512),
 S901 (SAT522), S902 (SAT524),
 S907 (SAT532)
 Morandini, Francesca, S872 (SAT436)
 Morão, Bárbara, S190 (THU182)
 Moraras, Kate, S274 (THU361),
 S277 (THU368)
 Moreau, Richard, S245 (THU304)
 Moreea, Sulleman, S22 (OS013)
 Moreira, Teresa, S304 (THU420)
 Morel, Antoine, S508 (FRI237)
 Morell, Carola Maria, S737 (SAT157)
 Morelli, Maria Cristina, S569 (FRI359)
 Morello, Rémi, S61 (OS076)
 Moreno-Aliaga, M. Jesús,
 S749 (SAT183)
 Moreno, Christophe, S124 (THU012),
 S192 (THU185)
 Moreno-Lanceta, Alazne, S106 (OS154),
 S492 (FRI205), S743 (SAT170)
 Moreno-Manzano, Victoria, S103 (OS150)
 Moreno, Sarai Romero, S811 (SAT303)
 Moretti, Julien, S494 (FRI209)
 Morgan, Katie, S397 (FRI013),
 S712 (SAT096)
 Morgan, Marsha, S11 (LB002),
 S125 (THU014), S890 (SAT500),
 S890 (SAT501)
 Morgan, Paul, S698 (SAT067)
 Morgan, Timothy, S30 (OS027),
 S142 (THU043), S936 (SAT596)
 Morgantini, Cecilia, S665 (SAT002),
 S755 (SAT195), S756 (SAT197)
 Morillas, Rosa M, S157 (THU074),
 S158 (THU076), S334 (THU482),
 S370 (THU548), S724 (SAT125)
 Mori, Mattia, S665 (SAT002)
 Morinaga, Maki, S687 (SAT047)
 Mor, Inbal, S765 (SAT214)
 Morini, Martina, S515 (FRI249)
 Morisco, Filomena, S769 (SAT233),
 S908 (SAT535), S938 (SAT599)
 Morriset, Julie, S805 (SAT293)
 Morita, Naoki, S822 (SAT319)
 Mori, Trevor, S440 (FRI087)
 Moritz, Wolfgang, S703 (SAT078)
 Mori, Yasuhiro, S3 (GS004)
 Morley, Steven, S397 (FRI013),
 S712 (SAT096)
 Morley, Timothy, S530 (FRI277)
 Morling, Joanne, S17 (OS005),
 S145 (THU050)
 Mornex, Francoise, S5 (GS007)
 Mor, Orna, S784 (SAT258),
 S804 (SAT291)
 Morova, Berna, S693 (SAT058)
 Morrison, Martine C., S671 (SAT014),
 S676 (SAT024), S677 (SAT025),
 S681 (SAT033), S698 (SAT067)
 Morrow, Linda, S730 (SAT139),
 S732 (SAT143)
 Mortensen, Christian, S154 (THU068),
 S331 (THU477)
 Mortensen, Frank Viborg, S925 (SAT575)
 Mosca, Antonella, S706 (SAT084)
 Moseley, Scott, S526 (FRI268)
 Moskon, Miha, S607 (FRI469),
 S766 (SAT217)
 Moslem, Alireza, S228 (THU273)
 Mospan, Andrea, S449 (FRI103)
 Moss, Adyr, S15 (OS002)
 Moss, Alastair, S409 (FRI031)
 Mossavar-Rahmani, Yasmin,
 S912 (SAT554)
 Mossialos, Elias, S444 (FRI094)
 Mosusaviyarahi, Alireza, S228 (THU273)
 Motamedrad, Maryam, S775 (SAT244),
 S892 (SAT504)
 Motta, Benedetta Maria, S425 (FRI057)
 Motzler, Karsten, S606 (FRI467),
 S703 (SAT079)
 Mouch, Saif Mahmud Abu,
 S292 (THU395)
 Mouchti, Sofia, S95 (OS135)
 Mouhadi, Sanaa El, S319 (THU454)
 Mou, Lien-Juei, S200 (THU217),
 S595 (FRI410)
 Mountain, Victoria, S700 (SAT071),
 S708 (SAT088), S711 (SAT094)
 Mourad, Abbas, S426 (FRI059),
 S913 (SAT557)
 Moura, Luís Manuel, S597 (FRI415)
 Moura, Miguel, S192 (THU185)
 Moussa, Sam, S14 (LB005)
 Moutsopoulos, Ilias, S742 (SAT167)

Author Index

- Mozes, Ferenc, S425 ([FRI058](#)),
S444 ([FRI095](#)), S448 ([FRI102](#)),
S452 ([FRI108](#))
- Mraz, Miha, S766 ([SAT217](#))
- Mrozek, Linus, S533 ([FRI283](#))
- Mrzljak, Anna, S270 ([THU353](#))
- Mubenga, Francky, S791 ([SAT269](#))
- Muccioli, Giulio G., S680 ([SAT031](#))
- Mücke, Marcus, S313 ([THU444](#))
- Mücke, Victoria, S313 ([THU444](#))
- Mueller, Alexandra, S190 ([THU183](#))
- Mueller-Schilling, Martina, S241 ([THU298](#)),
S663 ([FRI599](#))
- Mueller, Sebastian, S11 ([LB002](#))
- Muga, Robert, S199 ([THU199](#))
- Muhammad, Abdullah Ghassan Farik,
S418 ([FRI044](#))
- Muhammad, Saad, S934 ([SAT593](#))
- Muhammad, Taj, S560 ([FRI338](#))
- Muhammed, Ambreen, S372 ([THU567](#)),
S374 ([THU571](#)), S383 ([THU588](#))
- Muir, Andrew, S318 ([THU453](#))
- Mujib, Salma, S116 ([OS171](#)), S135 ([THU031](#)),
S352 ([THU516](#)), S371 ([THU550](#)),
S505 ([FRI231](#)), S647 ([FRI563](#))
- Mukherjee, Sarmistha, S742 ([SAT168](#))
- Mukherjee, Sucheta, S846 ([SAT386](#)),
S853 ([SAT401](#))
- Mukherjee, Sujit, S345 ([THU505](#))
- Mukherji, Atish, S36 ([OS038](#)),
S738 ([SAT160](#)), S758 ([SAT199](#))
- Mukhopadhyay, Sramana, S252 ([THU320](#))
- Mukhtar, Nizar, S770 ([SAT234](#))
- Mukkala, Avinash, S822 ([SAT320](#))
- Mulé, Sebastien, S375 ([THU573](#)),
S532 ([FRI281](#))
- Mules, Thomas, S837 ([SAT368](#))
- Mulgaonkar, Ashwini, S794 ([SAT274](#))
- Mulinacci, Giacomo, S96 ([OS136](#))
- Mullany, Kate, S754 ([SAT193](#))
- Müller, Christian, S919 ([SAT565](#)),
S921 ([SAT570](#))
- Muller, Kate, S898 ([SAT516](#))
- Müller, Sascha, S11 ([LB002](#))
- Müller, Sophie Elisabeth, S342 ([THU500](#))
- Müller, Tobias, S16 ([OS003](#)),
S309 ([THU436](#)), S582 ([FRI385](#)),
S585 ([FRI391](#))
- Müllhaupt, Beat, S16 ([OS003](#)),
S585 ([FRI391](#)), S780 ([SAT251](#))
- Müllhaupt, Daniela, S253 ([THU322](#))
- Mullish, Benjamin H., S54 ([OS069](#)),
S121 ([THU007](#)), S179 ([THU158](#)),
S345 ([THU505](#)), S444 ([FRI094](#)),
S674 ([SAT020](#))
- Müllner-Bucsics, Theresa, S502 ([FRI225](#))
- Munda, Petra, S829 ([SAT353](#)),
S830 ([SAT354](#)), S854 ([SAT403](#))
- Munnamtrakul, Nawakodchamon,
S772 ([SAT238](#)), S812 ([SAT305](#))
- Munker, Stefan, S408 ([FRI029](#)),
S659 ([FRI589](#)), S661 ([FRI594](#))
- Munkhbaatar, Munkhaya, S235 ([THU287](#))
- Munk, Kamilla Kjærgaard, S271 ([THU356](#))
- Muñoz, Beatriz Mateos, S328 ([THU471](#))
- Munoz, Breda, S449 ([FRI103](#))
- Munoz, Chris, S277 ([THU368](#))
- Muñoz-Couselo, Eva, S316 ([THU450](#))
- Munoz-Garrido, Patricia, S649 ([FRI566](#))
- Muñoz, Linda, S487 ([FRI195](#))
- Munshi, Rashmi, S494 ([FRI209](#))
- Munteanu, Daneila, S145 ([THU049](#)),
S300 ([THU411](#))
- Munteanu, Daniela, S269 ([THU350](#))
- Murad, Sarwa Darwish, S524 ([FRI265](#))
- Murakami, Harumi, S720 ([SAT116](#))
- Murata, Ayato, S172 ([THU103](#))
- Muratori, Luca, S166 ([THU093](#))
- Muratori, Paolo, S326 ([THU467](#))
- Murawska-Ochab, Aleksandra,
S592 ([FRI406](#))
- Murgia, Antonio, S695 ([SAT061](#))
- Murphy, Donald, S206 ([THU230](#)),
S593 ([FRI407](#))
- Murphy, Ruth, S22 ([OS013](#))
- Murphy, Ryan, S534 ([FRI285](#))
- Murphy, Sandra, S646 ([FRI561](#))
- Murray, Bernard, S483 ([FRI187](#))
- Murray, Sam, S54 ([OS069](#)), S57 ([OS072A](#)),
S58 ([OS072B](#))
- Murray, Suzanne, S438 ([FRI084](#))
- Murtuza-Baker, Syed, S104 ([OS152](#))
- Murzi-Pulgar, Marianne, S91 ([OS128](#))
- Musabae, Erkin, S235 ([THU288](#))
- Mušak, Lucija, S702 ([SAT075](#))
- Muscari, Fabrice, S780 ([SAT252](#))
- Mushtaq, Kamran, S230 ([THU277](#))
- Musolino, Cristina, S259 ([THU333](#))
- Mussi, Daniela, S559 ([FRI336](#))
- Musso, Orlando, S656 ([FRI582](#))
- Muti, Leon, S833 ([SAT360](#)), S840 ([SAT373](#)),
S918 ([SAT563](#))
- Mutiloa, Elena Jimenez, S581 ([FRI384](#))
- Mutimer, David, S17 ([OS005](#))
- Muyndck, Kevin De, S655 ([FRI580](#))
- Muzaffar, Mahvish, S372 ([THU567](#)),
S374 ([THU571](#)), S376 ([THU574](#)),
S383 ([THU588](#))
- Muzica, Cristina-Maria, S573 ([FRI368](#))
- Myaskovsky, Anatoly, S508 ([FRI236](#)),
S918 ([SAT564](#))
- Myers, Rob, S700 ([SAT071](#))
- Myers, Robert, S31 ([OS028](#)), S318 ([THU453](#)),
S319 ([THU455](#)), S409 ([FRI030](#)),
S427 ([FRI060](#)), S445 ([FRI097](#)),
S762 ([SAT208](#))
- Myles, Lindsay, S549 ([FRI317](#)),
S584 ([FRI388](#))
- Mylopoulou, Theodora,
S840 ([SAT374](#))
- Nabatchikova, Ekaterina, S574 ([FRI370](#))
- Nabeta, Pamela, S42 ([OS049](#))
- Nabilou, Puria, S340 ([THU496](#)),
S610 ([FRI489](#))
- Nachmansson, Nathalie, S83 ([OS114](#)),
S725 ([SAT126](#))
- Nader, Ahmed, S875 ([SAT441](#))
- Nader, Fatema, S156 ([THU073](#)),
S209 ([THU234](#)), S420 ([FRI048](#)),
S447 ([FRI100](#))
- Nader, Luisa, S655 ([FRI581](#))
- Nadižar, Nejc, S766 ([SAT217](#))
- Nadkarni, Devika, S168 ([THU096](#))
- Naffaa, Mohammad, S399 ([FRI017](#))
- Nagai, Koki, S430 ([FRI067](#))
- Nagai, Shunji, S778 ([SAT249](#))
- Nagashima, Shintaro, S260 ([THU335](#)),
S260 ([THU336](#))
- Nagel, Judith, S602 ([FRI460](#))
- Nagelkerke, Anika, S711 ([SAT092](#))
- Nagel, Michael, S80 ([OS108](#)), S882 ([SAT486](#))
- Nagral, Abha, S19 ([OS008](#)), S49 ([OS063](#))
- Nagy, Laura, S33 ([OS032](#)), S193 ([THU188](#))
- Nahass, Ronald G, S836 ([SAT366](#))
- Nahnsen, Sven, S38 ([OS042](#))
- Nahon, Pierre, S17 ([OS006](#)), S101 ([OS146](#)),
S250 ([THU314](#)), S373 ([THU569](#))
- Nah, Yang Won, S799 ([SAT282](#))
- Najimi, Mustapha, S535 ([FRI289](#))
- Nakagawa, Miyuki, S615 ([FRI501](#)),
S897 ([SAT514](#))
- Nakagawa, Shinichi, S705 ([SAT082](#))
- Nakajima, Atsushi, S74 ([OS098](#)),
S414 ([FRI037](#)), S422 ([FRI051](#)),
S422 ([FRI052](#)), S425 ([FRI058](#)),
S430 ([FRI067](#)), S448 ([FRI102](#)),
S452 ([FRI108](#))
- Nakamoto, Shingo, S615 ([FRI501](#)),
S897 ([SAT514](#))
- Nakamoto, Yasunari, S563 ([FRI346](#))
- Nakamura, Atsushi, S885 ([SAT491](#))
- Nakamura, Daichi, S183 ([THU167](#))
- Nakamura, Masato, S615 ([FRI501](#)),
S897 ([SAT514](#))
- Nakanishi, Hiroyuki, S379 ([THU580](#))
- Nakano, Toshiaki, S314 ([THU445](#))
- Nakao, Kazuhiko, S563 ([FRI346](#))
- Nakhleh, Raouf, S768 ([SAT231](#))
- Nakum, Mitesh, S617 ([FRI504](#))
- Nalbach, Karsten, S703 ([SAT079](#))
- Nalinikanta, Rajkumar, S219 ([THU254](#))
- Nam, Heechul, S932 ([SAT589](#))
- Nam, Nguyen Hai, S183 ([THU167](#))
- Namouni, Teresa, S584 ([FRI389](#))
- Namy, Olivier, S514 ([FRI248](#))
- Nance, Danielle, S516 ([FRI251](#))
- Nandez, Ivonne Escalona, S176 ([THU153](#))
- Nankya, Prossie Lindah, S263 ([THU339](#))
- Nan, Yuemin, S278 ([THU369](#))
- Naoumov, Nikolai, S34 ([OS034](#)),
S486 ([FRI194](#)), S493 ([FRI207](#))
- Napodano, Cecilia, S436 ([FRI079](#))
- Napoleone, Laura, S63 ([OS080](#)),
S139 ([THU039](#)), S511 ([FRI242](#)),
S512 ([FRI243](#)), S512 ([FRI244](#)),
S896 ([SAT512](#)), S901 ([SAT522](#)),
S902 ([SAT524](#)), S907 ([SAT532](#))
- Napoli, Laura, S682 ([SAT037](#))
- Napoli, Salvatore, S647 ([FRI563](#))
- Napolitano, Ruben, S212 ([THU239](#))
- Nappo, Floriana, S748 ([SAT180](#))

- Naqash, Abdul Rafeh, S372 (THU567)
 Narang, Himanshu, S433 (FRI072)
 Narayanan, Shivakumar, S572 (FRI364)
 Narayanan, Vijay, S898 (SAT515)
 Narayan, Nicole, S179 (THU160)
 Nardelli, Silvia, S908 (SAT535)
 Nardo, Alexander D, S688 (SAT049), S760 (SAT204)
 Nardone, Gerardo, S938 (SAT599)
 Narguet, Stephanie, S245 (THU304)
 Narmada, Balakrishnan Chakrapani, S98 (OS140)
 Nartey, Yvonne, S226 (THU268)
 Naschberger, Elisabeth, S83 (OS114)
 Nascimento, Leonardo Augusto Dias, S307 (THU432)
 Nasir, Basil, S805 (SAT293)
 Nasir, Nazrila Hairizan Binti, S42 (OS049)
 Naslund, Erik, S665 (SAT002), S756 (SAT197)
 Nasr, Patrik, S30 (OS026), S82 (OS112), S146 (THU052), S423 (FRI053)
 Nassar, Isabelle, S238 (THU291)
 Nastasa, Robert, S573 (FRI368)
 Nathalie, Boyer, S245 (THU304)
 Nathani, Rohit, S291 (THU392), S301 (THU413), S343 (THU502), S897 (SAT513)
 Nathwani, Rooshi, S185 (THU173), S345 (THU505)
 Natola, Leonardo, S658 (FRI586)
 Nattermann, Jacob, S11 (LB002), S339 (THU493), S381 (THU585)
 Naudet, Léa, S756 (SAT197)
 Naughton, Michelle, S912 (SAT554)
 Nault, Jean Charles, S372 (THU566)
 Nautiyal, Nidhi, S756 (SAT196)
 Navaid, Musharraf, S372 (THU567)
 Navalón, María, S106 (OS154)
 Navari, Nadia, S477 (FRI173)
 Navarra, Giuseppe, S259 (THU333)
 Nawaz, Ahmad, S240 (THU295)
 Nayagam, Jeremy, S650 (FRI569)
 İnce, Volkan, S782 (SAT255)
 Ndegwa, Nelson, S82 (OS112), S123 (THU010)
 Ndong, Cilor, S202 (THU221)
 Ndow, Gibril, S233 (THU282), S258 (THU332), S290 (THU391), S295 (THU401)
 Nedumannil, Leya, S134 (THU029)
 Neely, Dermot, S493 (FRI208)
 Neerincx, Andreas, S198 (THU198)
 Neff, Guy, S14 (LB005), S87 (OS121), S427 (FRI060), S495 (FRI210), S719 (SAT114)
 Negre, Elodie, S392 (FRI006)
 Negre, Julien, S547 (FRI314)
 Negro, Francesco, S457 (FRI115), S877 (SAT444)
 Neia, Caterina Peraldo, S651 (FRI570)
 Nelson, Cara H., S88 (OS123), S716 (SAT108), S731 (SAT142)
 Nelson, Mark, S253 (THU321)
 Nema, Shashwati, S252 (THU320)
 Nemazanyy, Ivan, S672 (SAT015)
 Nemet, Ital, S804 (SAT291)
 Nenu, Iuliana, S664 (FRI600)
 Neri, Sergio, S908 (SAT535)
 Nerlander, Lina, S256 (THU328)
 Neroldova, Magdalena, S536 (FRI290)
 Nerusch, Julia, S658 (FRI585)
 Nery, Filipe Gaio Castro, S524 (FRI265)
 Nesher, Eviatar, S774 (SAT241)
 Ness, Erik, S332 (THU478), S335 (THU484)
 Nesticò, Daniela, S808 (SAT297)
 Nestor, John, S88 (OS124)
 Neto, Nadia, S265 (THU343)
 Netter, Hans, S834 (SAT362)
 Neuburger, James, S529 (FRI274), S536 (FRI291)
 Neumann-Haefelin, Christoph, S2 (GS003), S16 (OS003), S100 (OS143), S196 (THU194), S585 (FRI391), S823 (SAT341)
 Neumann, Ulf, S11 (LB003)
 Neurath, Markus F., S163 (THU085)
 Neuveut, Christine, S297 (THU404)
 Nevens, Frederik, S94 (OS134), S120 (THU003), S144 (THU047), S317 (THU452), S335 (THU484), S346 (THU507), S516 (FRI252), S781 (SAT253), S783 (SAT256)
 Nevermann, Nora, S374 (THU570), S380 (THU582)
 Neves, Isabel, S597 (FRI415)
 Neveu, Gregory, S872 (SAT436)
 Nevola, Riccardo, S212 (THU239)
 Nevo-Shor, Anat, S269 (THU350), S300 (THU411), S859 (SAT412)
 Nevo, Yuval, S47 (OS059), S83 (OS114)
 Newberry, Carolyn, S168 (THU096), S729 (SAT138)
 Newberry, Elizabeth, S671 (SAT014)
 Newgard, Christopher, S718 (SAT112)
 New, Kate, S498 (FRI218)
 Newsome, Philip N., S10 (LB001), S425 (FRI058), S448 (FRI102), S452 (FRI108), S461 (FRI123)
 Nga Nguyen, Thi Thu, S61 (OS076)
 Ngele, Jean-René, S270 (THU352)
 Ng, Huck Hui, S694 (SAT059)
 Ng, Kelvin, S933 (SAT592)
 Ngo, An, S506 (FRI232)
 Ngo, Katina, S534 (FRI285)
 Ngongang, Norbert, S780 (SAT252), S791 (SAT269)
 Ngu, Meng, S842 (SAT377)
 Ngu, Natalie, S342 (THU501)
 Ngurruwuthun, Terese, S239 (THU294)
 Nguyen, Anh-Hoa, S866 (SAT425)
 Nguyen, Bich Ngoc, S805 (SAT293)
 Nguyen, Dan, S848 (SAT391)
 Nguyen, Danh, S142 (THU043)
 Nguyen, Diem, S40 (OS045)
 Nguyen, Dung, S57 (OS072A)
 Nguyen, Henry, S143 (THU045)
 Nguyen-Khac, Vincent, S927 (SAT578)
 Nguyen, Khiem, S846 (SAT386)
 Nguyen, Mindie, S214 (THU244), S875 (SAT442), S883 (SAT488)
 Nguyen, Tan, S708 (SAT088)
 Nguyen-Tat, Marc, S80 (OS108)
 Nguyen, Thi Thuy Tu, S264 (THU341)
 Nguyen, Toni, S788 (SAT264)
 Nguyen, Tuan T, S836 (SAT366), S848 (SAT390)
 Ng, Yee Chen, S431 (FRI068)
 Niaz, Qamar, S883 (SAT487)
 Nichetti, Federico, S655 (FRI581), S748 (SAT180)
 Nicholas, Sarah, S548 (FRI316)
 Nicholson, Thomas, S364 (THU537)
 Nicklas, Jule-Marie, S309 (THU436)
 Nicola, Coppola, S938 (SAT599)
 Nicolaidis, Steven, S315 (THU448)
 Nicolas, Carine, S417 (FRI042)
 Nicoletti, Alberto, S507 (FRI234)
 Nicoletti, Ferdinando, S697 (SAT065)
 Nicoll, Amanda, S315 (THU448), S389 (FRI002), S842 (SAT377)
 Nicot, Arnaud, S185 (THU172)
 Niederau, Claus, S16 (OS003), S585 (FRI391)
 Niederseer, David, S428 (FRI062)
 Nielsen, Malte H., S669 (SAT010)
 Nielsen, Mette Juul, S25 (OS018), S415 (FRI039), S475 (FRI169), S895 (SAT510)
 Nielsen, Susanne Dam, S818 (SAT314)
 Niemeyer, Johannes, S382 (THU586), S383 (THU590), S860 (SAT414)
 Nieri, Paola, S478 (FRI176)
 Nieto, Gema Alvarez, S586 (FRI393)
 Nieto, Juan Camilo, S886 (SAT494)
 Nieto, Natalia, S656 (FRI582)
 Nieuwdorp, Max, S9 (GS011)
 Nieva-Zuluaga, Ane, S648 (FRI564), S651 (FRI571), S665 (SAT001), S689 (SAT050)
 Nieves, Andrea Delgado, S168 (THU097), S170 (THU099)
 Niger, Monica, S748 (SAT180)
 Nikolopoulos, Georgios, S202 (THU220)
 Nikulkina, Elena, S574 (FRI370)
 Nilsson, Emma, S333 (THU480)
 Nilsson, Julia, S467 (FRI154)
 Nim, Joseph, S366 (THU540)
 Nincevic, Vjera, S718 (SAT113)
 Ningarhari, Massih, S205 (THU227), S205 (THU228), S372 (THU566), S913 (SAT557)
 Ni, Quanhong, S517 (FRI253), S517 (FRI254), S518 (FRI255)
 Nischalke, Hans Dieter, S11 (LB002)
 Nishida, Nao, S654 (FRI579)
 Nishida, Naoshi, S372 (THU567), S383 (THU588)
 Nishida, Shinya, S430 (FRI067)
 Nishikawa, Takako, S485 (FRI192)
 Nishimura, Takashi, S616 (FRI502)
 Nishio, Takahiro, S183 (THU167)
 Nissen-Meyer, Lise Sofie H., S309 (THU437)

Author Index

- Nissen, Nicholas, S377 ([THU575](#))
 Nissinen, Markku, S413 ([FRI036](#))
 Nistal, Esther, S177 ([THU155](#))
 Nitu, Florina, S795 ([SAT276](#))
 Nitzel, Arianna, S718 ([SAT112](#))
 Nitze, Louise, S29 ([OS025](#))
 Niu, Junqi, S89 ([OS125](#)), S522 ([FRI261](#)), S835 ([SAT365](#)), S837 ([SAT367](#)), S865 ([SAT423](#)), S894 ([SAT509](#))
 Niu, Lili, S500 ([FRI223](#)), S523 ([FRI263](#))
 Ni, Xin, S477 ([FRI175](#))
 Ni, Yen-Hsuan, S514 ([FRI247](#))
 Ni, Yi, S760 ([SAT205](#)), S860 ([SAT413](#))
 Njie, Ramou, S295 ([THU401](#))
 Noack, Julia, S871 ([SAT434](#))
 Nobes, Jennifer, S415 ([FRI038](#)), S495 ([FRI214](#))
 Nock, Sebastian, S755 ([SAT195](#)), S756 ([SAT197](#))
 Nogueira, Paulo, S211 ([THU238](#))
 Nogueiras, Ruben, S84 ([OS116](#)), S87 ([OS122](#)), S600 ([FRI453](#)), S673 ([SAT018](#)), S689 ([SAT050](#))
 Noh, Yung-Kyun, S138 ([THU037](#))
 Nojkov, Borko, S180 ([THU162](#))
 Nomah, Daniel Kwakye, S207 ([THU231](#)), S208 ([THU232](#))
 Nonthasoot, Bunthoon, S772 ([SAT238](#)), S812 ([SAT305](#))
 Norden-Krichmar, Trina, S30 ([OS027](#)), S936 ([SAT596](#))
 Nordestgaard, Børge, S161 ([THU082](#)), S533 ([FRI284](#))
 Nordhus, Kathrine Sivertsen, S605 ([FRI465](#))
 Nörenberg, Pia Maria, S250 ([THU315](#))
 Norero, Blanca, S137 ([THU034](#))
 Normelli, Ilaria, S796 ([SAT277](#))
 Norris, Suzanne, S418 ([FRI043](#))
 North-Lewis, Penny, S551 ([FRI321](#))
 Nölsner, Elfriede, S877 ([SAT445](#))
 Not, Anna, S570 ([FRI361](#))
 Nourbakhsh, Nooshin, S723 ([SAT123](#))
 Nouredin, Mazen, S75 ([OS101](#)), S151 ([THU064](#)), S159 ([THU077](#)), S377 ([THU575](#)), S414 ([FRI037](#)), S416 ([FRI040](#)), S422 ([FRI052](#)), S427 ([FRI060](#)), S436 ([FRI078](#)), S438 ([FRI084](#)), S444 ([FRI095](#)), S455 ([FRI113](#)), S619 ([FRI509](#)), S623 ([FRI516](#)), S671 ([SAT014](#)), S713 ([SAT101](#)), S731 ([SAT142](#))
 Noureldin, Seham, S849 ([SAT394](#))
 Novak, Ruder, S612 ([FRI494](#))
 Novikov, Nikolai, S53 ([OS067](#))
 Novoa, Eva, S689 ([SAT050](#))
 Nowak, Greg, S756 ([SAT197](#))
 Nowosad, Małgorzata, S156 ([THU072](#)), S815 ([SAT311](#))
 Ntalla, Ioanna, S581 ([FRI384](#))
 Ntata, Joyce, S116 ([OS172](#))
 Nuhn, Lutz, S464 ([FRI147](#))
 Nunes, Emily Montosa, S579 ([FRI377](#))
 Nunes, Joao, S122 ([THU008](#))
 Nunes, Patricia, S666 ([SAT004](#))
 Núñez, Susana, S465 ([FRI150](#))
 Nunez, Vanessa, S238 ([THU291](#))
 Nwaogu, Akudo, S276 ([THU366](#))
 Nwobi, Onyeka, S225 ([THU266](#))
 Nyam P, David, S19 ([OS008](#)), S49 ([OS063](#))
 Nyang, Haddy, S258 ([THU332](#))
 Nyberg, Anders, S597 ([FRI416](#))
 Nyberg, Lisa, S597 ([FRI416](#))
 Nytoft Rasmussen, Ditlev, S9 ([GS012](#))
 Nyuydzefe, Melanie, S494 ([FRI209](#))
 Oakes, Kathryn, S594 ([FRI409](#))
 Oakley, Fiona, S7 ([GS009](#)), S640 ([FRI551](#))
 Oakley, Rhys, S548 ([FRI316](#))
 Obeidat, Adham, S803 ([SAT290](#)), S807 ([SAT295](#))
 O'Beirne, James, S172 ([THU102](#))
 Oberhardt, Valerie, S196 ([THU194](#))
 Oberti, Frédéric, S73 ([OS096](#)), S74 ([OS099](#)), S496 ([FRI215](#)), S497 ([FRI216](#)), S507 ([FRI235](#))
 Oberti, Giovanna, S167 ([THU095](#))
 Obon, Pilar, S229 ([THU276](#))
 O'Brien, Alastair, S21 ([OS011](#)), S104 ([OS151](#)), S342 ([THU499](#))
 Obuchowski, Nancy, S454 ([FRI110](#))
 Ocal, Serkan, S242 ([THU300](#))
 Ocete, Maria Dolores, S229 ([THU276](#))
 Ochirsum, Byambasuren, S235 ([THU287](#))
 O'Connell, Malene Barfod, S64 ([OS083](#))
 Odorizzi, Pamela, S832 ([SAT358](#))
 Odriozola, Aitor, S114 ([OS169](#))
 Oechslein, Noémie, S97 ([OS138](#))
 O'Farrell, Marie, S419 ([FRI045](#))
 Ofri, Imri, S279 ([THU371](#))
 Øgaard, Jonas, S605 ([FRI465](#))
 Ogasawara, Sadahisa, S615 ([FRI501](#)), S897 ([SAT514](#))
 Ogawa, Eiichi, S875 ([SAT442](#))
 Ogawa, Eri, S183 ([THU167](#))
 Ogawa, Keita, S615 ([FRI501](#)), S897 ([SAT514](#))
 Ogawa, Tetsuro, S838 ([SAT370](#))
 Ogawa, Yuji, S430 ([FRI067](#))
 Oggioni, Chiara, S223 ([THU263](#))
 Ogilvie, Lauren, S73 ([OS095](#))
 O'Hagan, Oonagh, S418 ([FRI043](#))
 O'Hara, Shaelyn, S160 ([THU080](#))
 Oh, Hyunwoo, S160 ([THU079](#)), S224 ([THU264](#)), S435 ([FRI077](#)), S438 ([FRI082](#)), S438 ([FRI083](#)), S439 ([FRI086](#)), S589 ([FRI398](#)), S728 ([SAT135](#)), S729 ([SAT136](#))
 Oh, Joo Hyun, S224 ([THU264](#)), S273 ([THU359](#)), S589 ([FRI398](#))
 Oh, Katherine, S831 ([SAT356](#))
 Ohlendorf, Valerie, S248 ([THU311](#)), S608 ([FRI485](#))
 Ohtomo, Shuichi, S600 ([FRI454](#))
 Okajima, Akira, S448 ([FRI102](#)), S452 ([FRI108](#))
 Okajima, Hideaki, S183 ([THU167](#))
 Okamoto, Tatsuya, S183 ([THU167](#))
 Okanoue, Takeshi, S448 ([FRI102](#)), S452 ([FRI108](#))
 Okapec, Stanislav, S613 ([FRI496](#))
 Okeke, Edith, S19 ([OS008](#)), S23 ([OS015](#)), S49 ([OS063](#))
 Olafsson, Sigurdur, S573 ([FRI366](#))
 Olaizola, Paula, S46 ([OS056](#)), S648 ([FRI564](#)), S689 ([SAT050](#))
 Olartekoetxea, Gaizka Errazti, S665 ([SAT001](#))
 Olbrich, Anne, S383 ([THU590](#)), S931 ([SAT587](#))
 Oldani, Graziano, S754 ([SAT192](#))
 Oldenburger, Anouk, S7 ([GS009](#))
 Oldham, Stephanie, S7 ([GS009](#))
 Old, Hannah, S889 ([SAT499](#))
 Oldroyd, Christopher, S120 ([THU005](#))
 O'Leary, Jacqueline, S339 ([THU494](#)), S887 ([SAT496](#))
 Olesen, Sara, S9 ([GS012](#))
 Olga, Tronina, S565 ([FRI350](#)), S585 ([FRI390](#))
 Olinga, Peter, S484 ([FRI188](#)), S539 ([FRI298](#)), S711 ([SAT092](#))
 Olivas, Pol, S136 ([THU033](#)), S367 ([THU542](#)), S630 ([FRI529](#))
 Oliveira, Claudia De, S687 ([SAT046](#))
 Oliveri, Filippo, S292 ([THU394](#)), S578 ([FRI376](#))
 Oliveros, Francisco Hernandez, S527 ([FRI271](#))
 Olivo, Ana, S294 ([THU400](#))
 Olkus, Alexander, S823 ([SAT341](#))
 Öllinger, Rupert, S654 ([FRI577](#))
 Ollivier-Hourmand, Isabelle, S61 ([OS076](#)), S524 ([FRI265](#)), S772 ([SAT239](#)), S833 ([SAT360](#))
 O'Loan, Joss, S581 ([FRI384](#))
 Olsavszky, Victor, S463 ([FRI146](#))
 Olsen, Beth Hærsted, S499 ([FRI220](#))
 Oltmanns, Carlos, S566 ([FRI352](#))
 Olynyk, John, S440 ([FRI087](#))
 Omella, Judit Domenech, S637 ([FRI544](#))
 Oneka, Morgan, S470 ([FRI160](#)), S485 ([FRI190](#))
 Ong, Agnes Bee Leng, S694 ([SAT059](#)), S723 ([SAT123](#))
 Ong, Albert, S814 ([SAT308](#))
 Ongarello, Stefano, S42 ([OS049](#))
 Ong, Janus, S5 ([GS008](#)), S154 ([THU069](#)), S209 ([THU234](#)), S785 ([SAT260](#)), S810 ([SAT300](#))
 Ong, Leng, S730 ([SAT140](#)), S735 ([SAT154](#))
 Oniscu, Gabriel, S85 ([OS117](#))
 Önnérhag, Kristina, S30 ([OS026](#))
 Onorato, Lorenzo, S217 ([THU250](#))
 Ooi, Geraldine, S425 ([FRI058](#)), S448 ([FRI102](#)), S452 ([FRI108](#))
 Oosterhaven, Jart, S716 ([SAT109](#))
 Oosterhuis, Dorenda, S484 ([FRI188](#)), S539 ([FRI298](#))
 Oosterveer, Maaike, S539 ([FRI298](#))
 Oo, Ye Htun, S189 ([THU181](#)), S608 ([FRI470](#))
 Opyrchal, Paulina, S525 ([FRI267](#))
 Oravetz, Philip, S432 ([FRI070](#))
 Ordan, Marie-Amelie, S935 ([SAT595](#))
 O'Reilly, Kevin, S911 ([SAT540](#))

- Orešič, Matej, S111 ([OS162](#)), S694 ([SAT060](#))
 Orho-Melander, Marju, S690 ([SAT052](#))
 Ork, Vichit, S260 ([THU335](#))
 Orlent, Hans, S516 ([FRI252](#))
 Orlien, Stian Magnus Staurung, S841 ([SAT375](#))
 Orlova, Valeria, S118 ([OS174](#))
 Ormeci, Necati, S479 ([FRI178](#))
 Oró, Denise, S661 ([FRI593](#)), S669 ([SAT010](#)), S724 ([SAT124](#))
 Orourke, Joanne, S815 ([SAT311](#))
 Orr, James, S416 ([FRI041](#)), S535 ([FRI288](#))
 Ortega-Alonso, Aida, S59 ([OS074](#)), S396 ([FRI011](#))
 Ortega, Federico Pulido, S577 ([FRI373](#))
 Ortega González, Enrique, S229 ([THU276](#))
 Ortiz, Manuel Gahete, S48 ([OS060](#))
 Ortiz, Michael, S113 ([OS167](#))
 Ortiz, Pablo, S455 ([FRI113](#))
 Ortiz-Velez, Carolina, S316 ([THU450](#))
 Ortne, Julia, S80 ([OS108](#))
 Or, Yat Sun, S745 ([SAT177](#))
 Osborn, Gabriel, S401 ([FRI019](#))
 Oshaughnessy, Ana, S116 ([OS172](#))
 Osinusi, Anu, S4 ([GS006](#)), S103 ([OS149](#)), S828 ([SAT351](#)), S829 ([SAT352](#)), S837 ([SAT368](#))
 Osiowy, Carla, S259 ([THU334](#))
 Osti, Valentino, S153 ([THU067](#))
 Ostrowski, Sisse Rye, S818 ([SAT314](#))
 Ostyn, Tessa, S120 ([THU003](#)), S144 ([THU047](#))
 Otano, Juan Isidro Uriz, S549 ([FRI317](#)), S584 ([FRI388](#))
 Otero, Alejandra, S406 ([FRI027](#))
 Oton, Elena, S792 ([SAT271](#))
 Otsoa, Fernando Lopitz, S671 ([SAT014](#))
 Otterdal, Kari, S27 ([OS021](#))
 Otto, Jacobus, S164 ([THU089](#))
 Otto, Tobias, S654 ([FRI578](#)), S729 ([SAT137](#))
 Ott, Peter, S1 ([GS001](#)), S61 ([OS077](#)), S539 ([FRI297](#))
 Oubaya, Nadia, S780 ([SAT252](#)), S817 ([SAT312](#))
 Oude-Elferink, Ronald, S26 ([OS019](#)), S603 ([FRI461](#)), S653 ([FRI576](#)), S761 ([SAT207](#))
 Oudot, Marine, S649 ([FRI565](#)), S738 ([SAT160](#))
 Ouoba, Serge, S229 ([THU274](#)), S260 ([THU335](#)), S260 ([THU336](#))
 Oussalah, Abderrahim, S905 ([SAT529](#)), S923 ([SAT573](#))
 Ou, Xiaojuan, S278 ([THU369](#))
 Ouzan, Denis, S270 ([THU352](#)), S499 ([FRI221](#)), S581 ([FRI384](#)), S584 ([FRI389](#))
 Ovadia, Caroline, S329 ([THU473](#))
 Øvrehus, Anne, S220 ([THU255](#)), S550 ([FRI319](#))
 Owen, Ben, S915 ([SAT559](#))
 Owen, Louise, S541 ([FRI302](#))
 Owino, Collins Oduor, S98 ([OS140](#))
 Owyang, Chung, S180 ([THU162](#))
 Oxtrud, Evelin, S64 ([OS081](#)), S774 ([SAT241](#)), S793 ([SAT272](#)), S855 ([SAT406](#))
 Oyarzabal, Julen, S112 ([OS165](#))
 Ozaki, Michitaka, S822 ([SAT319](#))
 Ozbay, A. Burak, S214 ([THU244](#))
 Ozbek, Umut, S372 ([THU567](#))
 Özcürümez, Mustafa, S378 ([THU579](#)), S682 ([SAT035](#))
 Ozdemir, Yasemin Gursoy, S693 ([SAT058](#))
 Öz, Digidem Kuru, S414 ([FRI037](#)), S778 ([SAT248](#))
 Ozdil, Kamil, S858 ([SAT410](#)), S861 ([SAT416](#)), S864 ([SAT421](#))
 Özdirik, Burcin, S309 ([THU436](#))
 Ozen, Hasan, S518 ([FRI255](#)), S519 ([FRI256](#))
 Ozga, Ann-Kathrin, S206 ([THU229](#))
 Ozgonul, Ekin, S693 ([SAT058](#))
 Ozik, Jonathan, S252 ([THU319](#))
 Özsezen, Serdar, S685 ([SAT043](#))
 Ozturk, Arinc, S454 ([FRI110](#))
 Ozturk, Seyma, S848 ([SAT391](#))
 Ozutemiz, Omer, S399 ([FRI015](#))
 Pacheco, Glenn, S534 ([FRI285](#))
 Pachisia, Aditya Vikram, S620 ([FRI511](#))
 Paci, Sabrina, S515 ([FRI249](#))
 Packer, Gemma, S751 ([SAT185](#))
 Pacurar, Daniela, S866 ([SAT425](#))
 Padaki, Nagaraja Rao, S191 ([THU184](#)), S358 ([THU525](#))
 Padilla, Ana, S794 ([SAT274](#))
 Padilla, Cynthia, S786 ([SAT262](#)), S788 ([SAT265](#))
 Padrones, Susana, S555 ([FRI329](#))
 Paessler, Slobodan, S194 ([THU191](#))
 Paff, Melanie, S12 ([LB004A](#)), S13 ([LB004B](#)), S288 ([THU389](#)), S288 ([THU390](#)), S291 ([THU393](#)), S873 ([SAT439](#)), S875 ([SAT441](#)), S880 ([SAT451](#)), S880 ([SAT452](#)), S881 ([SAT453](#))
 Pagan, Juan Carlos Garcia, S54 ([OS069](#)), S367 ([THU542](#)), S370 ([THU548](#)), S502 ([FRI226](#)), S524 ([FRI265](#)), S630 ([FRI529](#))
 Pagano, Sabrina, S493 ([FRI208](#))
 Pageaux, Georges-Philippe, S72 ([OS093](#)), S122 ([THU009](#)), S392 ([FRI006](#)), S771 ([SAT237](#)), S780 ([SAT252](#)), S817 ([SAT312](#))
 Pagovich, Odelya, S58 ([OS073](#))
 Pahlkala, Katja, S413 ([FRI036](#))
 Pahwa, Prabhjyoti, S197 ([THU196](#))
 Paik, James, S5 ([GS008](#)), S144 ([THU048](#)), S155 ([THU071](#)), S156 ([THU073](#))
 Paik, Seung Woon, S273 ([THU359](#))
 Paik, Yong Han, S275 ([THU363](#))
 Paik, Yong-Han, S273 ([THU359](#))
 Paillaud, Elena, S508 ([FRI237](#))
 Pai, Madhava, S108 ([OS158](#))
 Pai, Rish, S416 ([FRI040](#))
 Paisant, Anita, S496 ([FRI215](#))
 Paiva, Nuno, S648 ([FRI564](#))
 Pajak, Agnieszka, S488 ([FRI197](#))
 Pajares, Félix García, S792 ([SAT270](#))
 Pak, Bo-Yeong, S489 ([FRI199](#)), S866 ([SAT426](#))
 Palaniyappan, Naaventhana, S448 ([FRI102](#)), S452 ([FRI108](#)), S805 ([SAT292](#))
 Palarasah, Yaseelan, S434 ([FRI074](#))
 Palassin, Pascale, S392 ([FRI006](#))
 Palazón, Asís, S673 ([SAT018](#))
 Palazzo, Ana, S137 ([THU034](#))
 Paldor, Mor, S764 ([SAT213](#))
 Palermo, Andrea, S96 ([OS136](#))
 Palladini, Giuseppina, S702 ([SAT074](#))
 Pallares, Joan, S527 ([FRI271](#))
 Palle, Mads Sundby, S713 ([SAT102](#)), S720 ([SAT116](#))
 Pallett, Laura J., S55 ([OS070](#)), S99 ([OS141](#))
 Pallini, Giada, S39 ([OS044](#))
 Palma, Carolina Santos, S192 ([THU185](#))
 Palma, Elena, S120 ([THU004](#)), S647 ([FRI562](#)), S911 ([SAT540](#))
 Palmer, Nicki, S548 ([FRI316](#))
 Palmisano, Elena, S292 ([THU394](#))
 Palmisano, Silvia, S433 ([FRI071](#))
 Palom, Adriana, S212 ([THU240](#)), S255 ([THU325](#)), S269 ([THU350](#)), S277 ([THU367](#)), S297 ([THU405](#))
 Pal, Ravindra, S898 ([SAT515](#))
 Pal, Runa, S751 ([SAT187](#))
 Palu, Giorgio, S751 ([SAT186](#))
 Paluszkiwicz, Rafał, S156 ([THU072](#))
 Pamecha, Viniyendra, S738 ([SAT161](#))
 Pamo, Claudia, S137 ([THU034](#))
 Pamulapati, Reddy, S848 ([SAT392](#))
 Panagiotoglou, Dimitra, S206 ([THU230](#))
 Panarese, Joe, S745 ([SAT177](#))
 Panchal, Sarjukumar, S769 ([SAT232](#))
 Pan, David, S835 ([SAT364](#)), S841 ([SAT376](#))
 Pandolfo, Alessandra, S448 ([FRI101](#))
 Pandya, Dimple, S446 ([FRI029](#))
 Pandey, Sanjay, S477 ([FRI174](#))
 Panera, Nadia, S706 ([SAT084](#))
 Panero, Antonio, S543 ([FRI306](#))
 Panero, José Luis Calleja, S157 ([THU074](#)), S158 ([THU076](#)), S237 ([THU290](#)), S370 ([THU548](#)), S426 ([FRI059](#)), S869 ([SAT430](#)), S912 ([SAT555](#))
 Panettieri, Elena, S789 ([SAT266](#))
 Pang, Jing, S164 ([THU089](#))
 Pang, Wenjie, S409 ([FRI031](#))
 Pan, Liangyu, S182 ([THU165](#))
 Pan, Mei-Hung, S294 ([THU398](#))
 Panning, Marcus, S100 ([OS143](#))
 Pan, Qiwei, S86 ([OS120](#)), S637 ([FRI543](#))
 Pantzios, Spyridon, S917 ([SAT562](#))
 Pan, Wei-Jian, S526 ([FRI268](#))
 Panzarini, Elisa, S763 ([SAT211](#))
 Panzer, Marlene, S537 ([FRI292](#)), S829 ([SAT353](#)), S830 ([SAT354](#))
 Panzer, Simon, S362 ([THU534](#))
 Panzitt, Katrin, S696 ([SAT063](#))
 Paolini, Erika, S682 ([SAT036](#)), S682 ([SAT037](#)), S698 ([SAT068](#)), S706 ([SAT084](#))

Author Index

- Paolo Russo, Francesco, S54 ([OS069](#)), S57 ([OS072A](#)), S479 ([FRI177](#)), S569 ([FRI359](#)), S578 ([FRI376](#))
- Paon, Veronica, S796 ([SAT277](#))
- Papadopoulou, Georgia, S255 ([THU326](#))
- Papagiouvanni, Ioanna, S218 ([THU251](#))
- Papalini, Chiara, S284 ([THU381](#))
- Papaluca, Tim, S498 ([FRI218](#)), S550 ([FRI318](#))
- Papanikolaou, Zafiris, S218 ([THU251](#))
- Papathodoridi, Margarita, S39 ([OS044](#)), S737 ([SAT157](#)), S824 ([SAT344](#)), S840 ([SAT374](#)), S852 ([SAT400](#)), S861 ([SAT415](#))
- Papathodoridis, George, S154 ([THU069](#)), S429 ([FRI063](#)), S581 ([FRI384](#)), S824 ([SAT344](#)), S840 ([SAT374](#)), S852 ([SAT400](#)), S861 ([SAT415](#))
- Papic, Neven, S700 ([SAT070](#))
- Papkiauri, Ana, S221 ([THU258](#))
- Pappas, Chris, S611 ([FRI490](#))
- Paradis, Valérie, S7 ([GS009](#)), S245 ([THU304](#)), S372 ([THU566](#)), S475 ([FRI170](#))
- Parasar, Anupama, S756 ([SAT196](#))
- Paraskevis, Dimitrios, S218 ([THU251](#))
- Paratala, Bhavna, S850 ([SAT396](#)), S851 ([SAT397](#))
- Parente, Elisabetta, S578 ([FRI376](#))
- Parent, Romain, S738 ([SAT160](#)), S766 ([SAT216](#))
- Pares, Albert, S335 ([THU484](#))
- Parés, Albert, S317 ([THU452](#))
- Parfieniuk-Kowerda, Anna, S585 ([FRI390](#)), S592 ([FRI406](#))
- Parikh, Neehar D., S214 ([THU244](#))
- Paris, Alejandro Sanz, S676 ([SAT023](#))
- Parisi, Stefanie, S448 ([FRI101](#)), S725 ([SAT127](#))
- Park, Erica, S308 ([THU434](#))
- Parker, Richard, S34 ([OS034](#)), S120 ([THU005](#)), S141 ([THU041](#)), S213 ([THU241](#)), S461 ([FRI123](#))
- Parker, Victoria, S609 ([FRI486](#))
- Parkes, Julie, S42 ([OS048](#)), S200 ([THU218](#)), S909 ([SAT536](#))
- Park, Eun Jin, S468 ([FRI156](#)), S469 ([FRI157](#))
- Park, Huiyul, S160 ([THU079](#)), S224 ([THU264](#)), S435 ([FRI077](#)), S438 ([FRI082](#)), S438 ([FRI083](#)), S439 ([FRI086](#)), S589 ([FRI398](#)), S728 ([SAT135](#)), S729 ([SAT136](#))
- Park, Hye Jung, S755 ([SAT194](#))
- Park, James S, S836 ([SAT366](#))
- Park, Jeongwoo, S746 ([SAT178](#))
- Park, Jina, S545 ([FRI310](#))
- Park, Jin Young, S490 ([FRI202](#))
- Park, Jung Gil, S572 ([FRI365](#)), S916 ([SAT560](#))
- Park, Jun Yong, S176 ([THU152](#)), S653 ([FRI575](#)), S755 ([SAT194](#)), S824 ([SAT344](#))
- Park, Min-Jung, S820 ([SAT317](#))
- Park, Min Kyung, S78 ([OS104](#)), S667 ([SAT005](#))
- Park, Neung Hwa, S870 ([SAT433](#))
- Park, Soo Been, S653 ([FRI575](#))
- Park, Soo Young, S377 ([THU576](#)), S572 ([FRI365](#)), S916 ([SAT560](#))
- Park, Young Joo, S569 ([FRI357](#)), S586 ([FRI392](#))
- Parlak, Emine, S858 ([SAT411](#))
- Parlar, Yavuz Emre, S293 ([THU397](#))
- Parlati, Lucia, S41 ([OS047](#)), S392 ([FRI005](#)), S393 ([FRI007](#))
- Parnot, Marie, S649 ([FRI565](#))
- Parolin, Cristina, S751 ([SAT186](#))
- Parra-Robert, Marina, S743 ([SAT170](#))
- Parsons, Jacob, S880 ([SAT451](#))
- Parzynski, Craig, S332 ([THU478](#))
- Pascale, Alina, S800 ([SAT285](#)), S935 ([SAT595](#))
- Pascual, Sonia, S114 ([OS168](#)), S792 ([SAT271](#))
- Pasetto, Anna, S860 ([SAT413](#))
- Pasi, K. John, S404 ([FRI023](#))
- Pasqua, Laura Giuseppina Di, S697 ([SAT065](#))
- Pasqual, Giulia, S479 ([FRI177](#))
- Passos-Castilho, Ana Maria, S206 ([THU230](#))
- Pastorelli, Roberta, S758 ([SAT201](#))
- Pastore, Mirella, S47 ([OS058](#)), S477 ([FRI173](#)), S649 ([FRI567](#))
- Pastor, Helena, S708 ([SAT087](#))
- Pastori, Daniele, S161 ([THU081](#)), S162 ([THU083](#))
- Pastor, Tania, S77 ([OS103](#))
- Pastrovic, Frane, S612 ([FRI494](#))
- Pasulapati, Sama Siva Rao, S51 ([OS064](#))
- Pasulo, Luisa, S210 ([THU236](#))
- Pasut, Gianfranco, S378 ([THU578](#))
- Patch, David, S34 ([OS034](#)), S524 ([FRI265](#))
- Patel, Harshil, S323 ([THU462](#))
- Patel, Janisha, S410 ([FRI032](#)), S909 ([SAT536](#))
- Patel, Kajal, S252 ([THU320](#))
- Patel, Keyur, S395 ([FRI010](#)), S427 ([FRI060](#)), S429 ([FRI065](#))
- Patel, Madhukar, S801 ([SAT287](#))
- Patel, Niharika, S350 ([THU512](#))
- Patel, Nishi, S259 ([THU334](#))
- Patel, Poulam, S116 ([OS172](#))
- Patel, Priti, S216 ([THU247](#))
- Patel, Sameer, S403 ([FRI022](#))
- Patel, Sanjaykanumar, S715 ([SAT105](#))
- Patel, Vishal, S911 ([SAT540](#))
- Patel, Vishal C, S135 ([THU031](#)), S352 ([THU516](#)), S371 ([THU550](#))
- Patel, Vishal C., S34 ([OS034](#)), S68 ([OS089](#))
- Paternostro, Rafael, S18 ([OS007](#)), S92 ([OS131](#)), S354 ([THU519](#)), S535 ([FRI287](#)), S617 ([FRI505](#)), S618 ([FRI506](#)), S629 ([FRI527](#)), S629 ([FRI528](#)), S631 ([FRI531](#)), S632 ([FRI533](#))
- Pathak, Piyush, S433 ([FRI072](#)), S620 ([FRI511](#))
- Pathak, Vai, S33 ([OS032](#))
- Pathil-Wartha, Anita, S353 ([THU517](#)), S354 ([THU518](#))
- Patil, Rashmee, S719 ([SAT114](#))
- Pati, Purendra Kumar, S898 ([SAT516](#))
- Patrizia, Carrieri, S426 ([FRI059](#))
- Patten, Daniel, S195 ([THU192](#))
- Patton, Kathryn, S540 ([FRI299](#))
- Paturel, Alexia, S246 ([THU306](#))
- Patwardhan, Ashwin, S622 ([FRI513](#))
- Patwardhan, Vilas, S634 ([FRI537](#))
- Patwa, Yashwi Haresh Kumar, S19 ([OS008](#)), S49 ([OS063](#))
- Paulmann, Dajana, S250 ([THU315](#))
- Paulusma, Coen, S601 ([FRI457](#))
- Paulweber, Bernhard, S428 ([FRI062](#))
- Paumelle, Réjane, S692 ([SAT055](#))
- Pauwels, Patrick, S637 ([FRI544](#))
- Pavel, Oana, S91 ([OS128](#))
- Pavel, Vlad, S241 ([THU298](#))
- Pavlidis, Michael, S320 ([THU456](#)), S320 ([THU457](#)), S321 ([THU459](#)), S322 ([THU460](#)), S425 ([FRI058](#)), S444 ([FRI095](#)), S448 ([FRI102](#)), S452 ([FRI108](#)), S453 ([FRI109](#)), S482 ([FRI184](#))
- Pavlovic, Natasa, S645 ([FRI558](#))
- Pawliszak, Piotr, S525 ([FRI267](#))
- Pawlotsky, Jean-Michel, S530 ([FRI276](#)), S582 ([FRI386](#))
- Pawłowska, Małgorzata, S585 ([FRI390](#)), S592 ([FRI406](#))
- Payance, Audrey, S61 ([OS076](#))
- Payne, Jacques, S88 ([OS124](#))
- Payne, Julia Yang, S151 ([THU064](#))
- Payo-Serafin, Tania, S639 ([FRI549](#))
- Pazgan-Simon, Monika, S565 ([FRI350](#))
- Pazmiño, Galo, S137 ([THU034](#))
- Peach, Emily, S805 ([SAT292](#))
- Pearce, Edward, S710 ([SAT090](#))
- Pearce, Fiona, S805 ([SAT292](#))
- Pearce, Margo, S43 ([OS051](#))
- Pearson, Madeline, S495 ([FRI214](#))
- Pebrier, Thibault, S767 ([SAT218](#))
- Pechlivanis, Alexandros, S135 ([THU031](#)), S352 ([THU516](#))
- Pech, Maciej, S378 ([THU579](#))
- Peck-Radosavljevic, Markus, S21 ([OS012](#)), S891 ([SAT502](#))
- Peck, Ryan, S155 ([THU070](#))
- Pecoraro, Michela, S872 ([SAT436](#))
- Pedde, Anna-Marie, S185 ([THU171](#))
- Pedersen, Mark, S317 ([THU452](#))
- Pedersen, Michael Lynge, S418 ([FRI044](#))
- Pedersen, Oluf, S450 ([FRI104](#))
- Pedica, Federica, S748 ([SAT180](#))
- Pedrona, Alisa, S541 ([FRI302](#)), S550 ([FRI318](#))
- Pedrosa, Marcos, S449 ([FRI103](#)), S486 ([FRI194](#)), S493 ([FRI207](#))
- Pedroto, Isabel, S304 ([THU420](#))
- Peiffer, Kai-Henrick, S313 ([THU444](#))
- Peiffer, Kai-Henrik, S15 ([OS001](#)), S262 ([THU337](#)), S353 ([THU517](#)), S354 ([THU518](#)), S585 ([FRI391](#))
- Peix, Judit, S45 ([OS055](#))
- Pekurovsky, Vasily, S935 ([SAT594](#))
- Peled, Amnon, S27 ([OS022](#)), S47 ([OS059](#)), S83 ([OS114](#)), S387 ([THU597](#))
- Peled, Daniel, S765 ([SAT214](#))
- Peleg, Noam, S279 ([THU371](#))

- Peleman, Cédric, S709 ([SAT089](#))
Pellegata, Alessandro F, S480 ([FRI179](#))
Pellerin, Luc, S670 ([SAT011](#))
Péloquin, Sophie, S438 ([FRI084](#))
Peloso, Andrea, S754 ([SAT192](#))
Peltekian, Kevork, S799 ([SAT284](#))
Pelto, Ryan, S526 ([FRI268](#))
Pelusi, Serena, S428 ([FRI061](#)), S673 ([SAT018](#))
Pemberton, David, S550 ([FRI318](#))
Penaranda, Guillaume, S499 ([FRI221](#))
Peñas, Beatriz, S370 ([THU548](#))
Peng, Cheng-Yuan, S265 ([THU343](#)), S595 ([FRI410](#)), S849 ([SAT393](#)), S870 ([SAT433](#))
Peng, Chien-Wei, S873 ([SAT438](#))
Pengili, Eno, S573 ([FRI367](#))
Peng, Ming-Li, S181 ([THU164](#)), S240 ([THU296](#))
Peng, Shifang, S477 ([FRI175](#))
Peng, Yanzhong, S838 ([SAT369](#))
Peng, Yun, S89 ([OS125](#))
Pennisi, Grazia, S448 ([FRI101](#)), S703 ([SAT077](#)), S725 ([SAT127](#))
Penn, Matthew, S550 ([FRI318](#))
Penski, Jette, S737 ([SAT158](#))
Penttilä, Anne, S111 ([OS162](#)), S458 ([FRI117](#)), S694 ([SAT060](#))
Peoch, Katell, S127 ([THU019](#)), S905 ([SAT529](#))
Peppelenbosch, Maikel, S86 ([OS120](#))
Pera, Guillem, S25 ([OS018](#))
Perales, Celia, S589 ([FRI399](#))
Peralta, Sergio, S624 ([FRI517](#))
Perbellini, Riccardo, S843 ([SAT379](#)), S843 ([SAT381](#)), S868 ([SAT429](#)), S874 ([SAT440](#)), S880 ([SAT450](#))
Pereira, Bruno, S918 ([SAT563](#))
Pereira, Gustavo, S137 ([THU034](#)), S910 ([SAT539](#))
Pereira, Gustavo Henrique Santos, S543 ([FRI305](#))
Pereira, Juliana Fernanda Holanda Bezerra, S817 ([SAT313](#))
Pereira, Laura, S749 ([SAT183](#))
Pereira, Luciano Beltrão, S817 ([SAT313](#))
Pereira, Pedro, S28 ([OS024](#))
Pereira, S., S211 ([THU237](#))
Pereira, Vítor, S515 ([FRI250](#))
Perelló, Christie, S381 ([THU584](#)), S912 ([SAT555](#))
Pereyra, David, S788 ([SAT264](#)), S799 ([SAT283](#))
Perez-Araluce, Maite, S112 ([OS165](#))
Perez, Carla Fiorella Murillo, S335 ([THU484](#))
Pérez-Carreras, Mercedes, S704 ([SAT080](#))
Pérez-del-Pulgar, Sofía, S53 ([OS067](#)), S55 ([OS070](#)), S99 ([OS141](#)), S263 ([THU340](#)), S286 ([THU385](#))
Perez-Guasch, Martina, S901 ([SAT522](#))
Pérez, Judith, S442 ([FRI091](#))
Perez, Laura Marquez, S381 ([THU584](#))
Pérez, Laura Márquez, S912 ([SAT555](#))
Perez, Martina, S25 ([OS018](#)), S63 ([OS080](#)), S136 ([THU033](#)), S139 ([THU039](#)), S511 ([FRI242](#)), S512 ([FRI243](#)), S512 ([FRI244](#)), S896 ([SAT512](#)), S902 ([SAT524](#)), S907 ([SAT532](#))
Perez Medrano, Indhira, S325 ([THU465](#)), S328 ([THU471](#))
Perez, Sara Lorente, S114 ([OS168](#)), S150 ([THU061](#)), S406 ([FRI027](#))
Perez, Valeria, S502 ([FRI226](#))
Perfetti, Elisa, S543 ([FRI306](#))
Perfield, Jim, S7 ([GS009](#))
Pericàs, Juan Manuel, S149 ([THU059](#)), S157 ([THU074](#)), S158 ([THU076](#)), S440 ([FRI088](#)), S906 ([SAT530](#))
Perieres, Lauren, S567 ([FRI353](#))
Perillo, Pasquale, S212 ([THU239](#))
Periyasamy, Giridharan, S98 ([OS140](#))
Perno, Carlo Federico, S284 ([THU381](#))
Perola, Markus, S80 ([OS109](#))
Perone, Ylenia, S372 ([THU567](#))
Peron, Jean Marie, S630 ([FRI529](#))
Perpinan, Elena, S607 ([FRI468](#)), S809 ([SAT298](#))
Perra, Andrea, S732 ([SAT144](#))
Perramón, Meritxell, S106 ([OS154](#)), S743 ([SAT170](#))
Perri, Giovanni Di, S825 ([SAT346](#))
Perrin, Clara, S375 ([THU573](#))
Perry, Caroline E, S742 ([SAT168](#))
Persico, Marcello, S425 ([FRI057](#)), S549 ([FRI317](#)), S551 ([FRI320](#)), S584 ([FRI388](#)), S938 ([SAT599](#))
Personeni, Nicola, S372 ([THU567](#)), S374 ([THU571](#)), S376 ([THU574](#)), S383 ([THU588](#)), S923 ([SAT572](#))
Pertuz, Marinela Mendez, S268 ([THU348](#)), S587 ([FRI394](#))
Perugorria, María Jesús, S46 ([OS056](#)), S77 ([OS103](#)), S648 ([FRI564](#))
Pessaux, Patrick, S36 ([OS038](#)), S99 ([OS142](#)), S649 ([FRI565](#)), S738 ([SAT160](#)), S758 ([SAT199](#))
Peters, Mélanie, S640 ([FRI550](#))
Peter Quehenberger, S359 ([THU527](#))
Petersen, Kitt Falk, S690 ([SAT052](#)), S714 ([SAT104](#))
Petersen, Tim-Ole, S379 ([THU581](#))
Peter, Simon, S927 ([SAT579](#))
Peterson, Troy, S155 ([THU070](#))
Peters, Rory, S330 ([THU475](#))
Petitjean, Louis, S439 ([FRI085](#)), S446 ([FRI099](#)), S481 ([FRI183](#)), S482 ([FRI184](#))
Petitjean, Mathieu, S439 ([FRI085](#)), S446 ([FRI029](#)), S482 ([FRI184](#)), S488 ([FRI197](#)), S688 ([SAT048](#)), S714 ([SAT103](#))
Petra, Fischer, S141 ([THU042](#))
Petrara, Maria Raffaella, S821 ([SAT318](#))
Petrenko, Oleksandr, S315 ([THU449](#)), S360 ([THU529](#)), S466 ([FRI152](#)), S472 ([FRI164](#)), S502 ([FRI226](#)), S753 ([SAT191](#))
Petrie, Aviva, S460 ([FRI121](#))
Petroff, David, S148 ([THU057](#))
Petroni, Maria Letizia, S153 ([THU067](#))
Petrova, Diana, S12 ([LB004A](#)), S13 ([LB004B](#)), S288 ([THU389](#)), S288 ([THU390](#)), S291 ([THU393](#)), S880 ([SAT452](#)), S881 ([SAT453](#))
Petrov, Petar, S84 ([OS116](#)), S600 ([FRI453](#)), S679 ([SAT029](#))
Petrucelli, Stefania, S770 ([SAT235](#))
Petrus-Reurer, Sandra, S741 ([SAT165](#))
Petrut, Raluca, S822 ([SAT320](#))
Petsalaki, Evangelia, S7 ([GS009](#))
Petta, Salvatore, S425 ([FRI058](#)), S448 ([FRI101](#)), S448 ([FRI102](#)), S452 ([FRI108](#)), S477 ([FRI173](#)), S675 ([SAT021](#)), S703 ([SAT077](#)), S725 ([SAT127](#))
Pettersen, Daniel, S609 ([FRI486](#))
Peyvandi, Flora, S159 ([THU078](#))
Pfisterer, Larissa, S472 ([FRI164](#)), S753 ([SAT191](#))
Pfisterer, Nikolaus, S545 ([FRI309](#)), S632 ([FRI533](#))
Pflugrad, Henning, S624 ([FRI519](#))
Pham, Tuan, S113 ([OS167](#))
Phan, Hang, S909 ([SAT536](#))
Phaw, Naw April, S311 ([THU440](#))
Philipp, Stoffers, S353 ([THU517](#))
Phillips, Gino, S385 ([THU593](#))
Phillips, Alexandra, S366 ([THU539](#)), S889 ([SAT499](#))
Phillips, Jonathan, S58 ([OS073](#))
Phillips, Rachael, S560 ([FRI340](#))
Phillips, Sandra, S120 ([THU004](#)), S188 ([THU178](#)), S639 ([FRI547](#)), S647 ([FRI562](#))
Phyo, Wah Wah, S869 ([SAT431](#))
Piai, Guido, S938 ([SAT599](#))
Pianko, Stephen, S342 ([THU501](#))
Piano, Salvatore, S18 ([OS007](#)), S49 ([OS062](#)), S92 ([OS131](#)), S894 ([SAT508](#)), S895 ([SAT511](#)), S908 ([SAT535](#))
Piao, Cindy, S155 ([THU070](#))
Piazzolla, Valeria, S609 ([FRI487](#))
Picariello, Lucia, S659 ([FRI588](#))
Picazo, Alberto García, S704 ([SAT080](#))
Picchio, Camila, S207 ([THU231](#)), S208 ([THU232](#)), S238 ([THU291](#))
Picchio, Gaston, S848 ([SAT392](#)), S850 ([SAT396](#)), S851 ([SAT397](#)), S876 ([SAT443](#)), S878 ([SAT448](#))
Piccinni, Marie-Pierre, S477 ([FRI173](#))
Picciotto, Francesco Paolo, S769 ([SAT233](#))
Piccolo, Paola, S806 ([SAT294](#)), S808 ([SAT297](#))
Pichard, Anais Vallet, S392 ([FRI005](#))
Piche, Julia, S654 ([FRI578](#)), S729 ([SAT137](#))
Piciotti, Roberto, S682 ([SAT036](#)), S682 ([SAT037](#)), S698 ([SAT068](#)), S706 ([SAT084](#))
Pick, Neora, S43 ([OS051](#))
Piecha, Felix, S585 ([FRI391](#))

Author Index

- Piedade, Juliana, S910 ([SAT539](#))
Pierce, Glenn, S404 ([FRI023](#))
Pierce, Theodore, S454 ([FRI110](#))
Pieri, Giulia, S578 ([FRI376](#))
Piermatteo, Lorenzo, S249 ([THU313](#)),
S284 ([THU380](#)), S284 ([THU381](#)),
S839 ([SAT371](#))
Pieterman, Elsbeth, S681 ([SAT033](#))
Pietrangelo, Antonello, S839 ([SAT371](#))
Pietri, Olivia, S547 ([FRI314](#))
Pietschmann, Thomas, S263 ([THU339](#))
Pignata, Luca, S769 ([SAT233](#))
Pilan, Matteo, S751 ([SAT186](#))
Pilebro, Björn, S58 ([OS073](#))
Pillai, Anjana, S372 ([THU567](#)),
S383 ([THU588](#))
Pimenta, Dominic, S460 ([FRI121](#))
Pinato, David J., S108 ([OS158](#)),
S372 ([THU567](#)), S374 ([THU571](#)),
S376 ([THU574](#)), S383 ([THU588](#))
Pineda, Antonio A, S643 ([FRI554](#))
Pineda, Antonio A., S112 ([OS165](#))
Pinheiro, Iris, S180 ([THU161](#))
Pink, Isabell, S783 ([SAT257](#))
Pinpathomrat, Nawamin, S188 ([THU177](#))
Pinquier, Jean-Louis, S733 ([SAT145](#))
Pintelon, Isabel, S709 ([SAT089](#))
Pinter, Matthias, S315 ([THU449](#)),
S354 ([THU519](#)), S372 ([THU567](#)),
S374 ([THU571](#)), S376 ([THU574](#)),
S383 ([THU588](#)), S532 ([FRI280](#)),
S535 ([FRI287](#)), S617 ([FRI505](#)),
S618 ([FRI506](#)), S631 ([FRI531](#)),
S632 ([FRI533](#)), S753 ([SAT189](#)),
S919 ([SAT565](#)), S921 ([SAT570](#))
Pintore, Lorenzo, S815 ([SAT311](#))
Pinyol, Roser, S45 ([OS055](#))
Pinzani, Massimo, S666 ([SAT004](#)),
S668 ([SAT008](#)), S737 ([SAT157](#))
Piombanti, Benedetta, S477 ([FRI173](#)),
S649 ([FRI567](#))
Piombino, Diego, S137 ([THU034](#))
Pipicella, Joseph, S558 ([FRI334](#))
Pipitone, Rosaria Maria, S703 ([SAT077](#))
Piqué-Gili, Marta, S45 ([OS055](#))
Piquet-Pellorce, Claire, S639 ([FRI548](#))
Pirabe, Anita, S788 ([SAT264](#))
Pirani, Tasneem, S403 ([FRI022](#))
Piran, Ron, S742 ([SAT166](#))
Piratvisuth, T, S824 ([SAT344](#))
Piratvisuth, Teerha, S12 ([LB004A](#)),
S186 ([THU175](#)), S187 ([THU176](#)),
S188 ([THU177](#)), S880 ([SAT452](#)),
S937 ([SAT597](#))
Pirenne, Jacques, S781 ([SAT253](#)),
S783 ([SAT256](#))
Pirisi, Mario, S483 ([FRI185](#)), S929 ([SAT582](#)),
S929 ([SAT583](#))
Pirlot, Boris, S135 ([THU032](#))
Pironi, Loris, S153 ([THU067](#))
Piroso, Andrea, S256 ([THU327](#))
Pisano, Giuseppina, S167 ([THU095](#))
Pisapia, Pasquale, S84 ([OS115](#))
Pisaturo, Marianonietta, S217 ([THU250](#))
Piscaglia, Fabio, S79 ([OS107](#)),
S166 ([THU093](#))
Pischke, Sven, S206 ([THU229](#)),
S257 ([THU329](#))
Piscopo, Fabiola, S84 ([OS115](#))
Piscuoglio, Salvatore, S660 ([FRI592](#))
Piselli, Pierluca, S821 ([SAT318](#))
Pistello, Mauro, S292 ([THU394](#))
Pistorio, Valeria, S465 ([FRI150](#))
Pitkänen, Kari, S111 ([OS162](#))
Pitova, Veronika, S593 ([FRI408](#))
Pittau, Gabriella, S800 ([SAT285](#)),
S935 ([SAT595](#))
Plagiannakos, Christina, S62 ([OS078](#)),
S313 ([THU443](#))
Planas, Alejandra, S149 ([THU059](#)),
S440 ([FRI088](#))
Plank, Lindsay, S890 ([SAT500](#))
Plant, James, S548 ([FRI316](#))
Plebani, Mario, S49 ([OS062](#))
Plesniak, Robert, S12 ([LB004A](#)),
S13 ([LB004B](#)), S288 ([THU389](#)),
S288 ([THU390](#)), S291 ([THU393](#)),
S880 ([SAT452](#)), S881 ([SAT453](#))
Plessier, Aurélie, S61 ([OS076](#)),
S524 ([FRI265](#))
Plevris, John, S397 ([FRI013](#)), S434 ([FRI075](#)),
S712 ([SAT096](#))
Plissonnier, Marie-Laure, S246 ([THU306](#)),
S247 ([THU307](#)), S356 ([THU522](#)),
S766 ([SAT216](#))
Plotnikov, Alexander, S387 ([THU597](#))
Poca, Maria, S64 ([OS082](#)), S91 ([OS128](#)),
S370 ([THU548](#)), S627 ([FRI523](#)),
S886 ([SAT494](#)), S900 ([SAT520](#))
Poch, Esteban, S902 ([SAT524](#))
Pochet, Nathalie, S649 ([FRI565](#))
Poch, Tobias, S604 ([FRI462](#))
Pocurull, Anna, S857 ([SAT409](#))
Podlaha, Ondrej, S835 ([SAT364](#))
Podrug, Kristian, S612 ([FRI494](#))
Poen, Alexander, S338 ([THU491](#))
Poetter-Lang, Sarah, S24 ([OS017](#)),
S320 ([THU457](#))
Poggel, Carsten, S748 ([SAT181](#))
Pohl, Junika, S185 ([THU171](#)),
S189 ([THU180](#))
Poirier, Charles, S805 ([SAT293](#))
Poisson, Johanne, S508 ([FRI237](#))
Pojoga, Cristina, S12 ([LB004A](#)),
S13 ([LB004B](#)), S288 ([THU389](#)),
S288 ([THU390](#)), S291 ([THU393](#)),
S880 ([SAT452](#)), S881 ([SAT453](#))
Polak, Wojciech, S109 ([OS159](#)),
S807 ([SAT296](#)), S815 ([SAT311](#)),
S933 ([SAT591](#))
Polanco, Prido, S151 ([THU064](#))
Polat, Kamil Yalcin, S820 ([SAT316](#))
Polat, Kamil Yalçin, S782 ([SAT255](#))
Polidoro, Michela Anna, S758 ([SAT201](#)),
S761 ([SAT206](#))
Poli, Edoardo, S402 ([FRI020](#)),
S800 ([SAT285](#)), S935 ([SAT595](#))
Polini, Beatrice, S478 ([FRI176](#))
Polireddy, Kishore, S862 ([SAT417](#))
Pollicino, Teresa, S259 ([THU333](#))
Pol, Stanislas, S17 ([OS006](#)), S41 ([OS047](#)),
S101 ([OS146](#)), S250 ([THU314](#)),
S297 ([THU404](#)), S392 ([FRI005](#)),
S393 ([FRI007](#)), S567 ([FRI353](#)),
S579 ([FRI381](#))
Polvani, Simone, S659 ([FRI588](#))
Polywka, Susanne, S257 ([THU329](#))
Pomej, Katharina, S24 ([OS017](#)), S92 ([OS131](#)),
S919 ([SAT565](#)), S921 ([SAT570](#))
Pompili, Enrico, S357 ([THU523](#))
Pompili, Maurizio, S507 ([FRI234](#)),
S564 ([FRI347](#))
Ponce, Juan Jose Urquijo, S222 ([THU261](#))
Pons, Caroline, S246 ([THU305](#))
Ponsioen, Cyriel, S338 ([THU491](#))
Ponsioen, Willemijn, S338 ([THU491](#))
Pons-Kerjean, Nathalie, S245 ([THU304](#))
Pons, Monica, S149 ([THU059](#)),
S440 ([FRI088](#)), S515 ([FRI250](#)),
S658 ([FRI587](#)), S906 ([SAT530](#))
Ponsolles, Clara, S649 ([FRI565](#)),
S758 ([SAT199](#))
Pontelo de Vries, Thais, S552 ([FRI323](#))
Ponten, Frederik, S471 ([FRI162](#))
Ponti, Aurora De, S38 ([OS042](#))
Ponziani, Francesca, S507 ([FRI234](#))
Ponz-Sarvisse, Mariano, S107 ([OS157](#))
Popa, Alexandru, S483 ([FRI186](#)),
S505 ([FRI230](#))
Popa-Dan, Laura, S795 ([SAT276](#))
Popescu, Alina, S483 ([FRI186](#)),
S505 ([FRI230](#)), S930 ([SAT585](#))
Popescu, Corneliu Petru, S12 ([LB004A](#)),
S13 ([LB004B](#)), S288 ([THU389](#)),
S288 ([THU390](#)), S291 ([THU393](#)),
S880 ([SAT452](#)), S881 ([SAT453](#))
Popovic, Branko, S712 ([SAT095](#))
Popovic, Vlad, S100 ([OS145](#))
Popov, Yury, S657 ([FRI584](#))
Popp, Laura, S620 ([FRI510](#))
Popp, Oliver, S99 ([OS142](#))
Porcasi, Rossana, S703 ([SAT077](#))
Porrás, David, S177 ([THU155](#))
Porta, Marco, S96 ([OS136](#))
Porteiro, Begoña, S689 ([SAT050](#))
Portella, Giuseppe, S769 ([SAT233](#))
Porte, Robert, S740 ([SAT163](#))
Porthan, Kimmo, S111 ([OS162](#)),
S458 ([FRI117](#)), S690 ([SAT052](#)),
S694 ([SAT060](#))
Portillo, Patty Marlen Ramírez,
S554 ([FRI326](#))
Port, Kerstin, S823 ([SAT341](#)), S843 ([SAT379](#)),
S857 ([SAT408](#))
Portolese, Olivia, S805 ([SAT293](#))
Portoles, Irene, S907 ([SAT532](#))
Posch, Andreas, S192 ([THU185](#))
Pose, Elisa, S54 ([OS069](#)), S57 ([OS072A](#)),
S63 ([OS080](#)), S127 ([THU018](#)),
S136 ([THU033](#)), S139 ([THU039](#)),
S511 ([FRI242](#)), S512 ([FRI243](#)),
S512 ([FRI244](#)), S896 ([SAT512](#)),

- S901 ([SAT522](#)), S902 ([SAT524](#)), S907 ([SAT532](#))
- Pose-Utrilla, Julia, S111 ([OS163](#))
- Pospiech, Ewelina, S759 ([SAT203](#))
- Pospiech, Josef, S682 ([SAT035](#))
- Possamai, Lucia, S345 ([THU505](#))
- Possemiers, Sam, S180 ([THU161](#))
- Postic, Catherine, S65 ([OS084](#))
- Potapova, Anna, S735 ([SAT154](#))
- Poth, Tanja, S38 ([OS042](#))
- Potier, Jean-Baptiste, S667 ([SAT006](#))
- Poujois, Aurelia, S1 ([GS001](#)), S61 ([OS077](#)), S520 ([FRI258](#)), S538 ([FRI296](#)), S539 ([FRI297](#))
- Poulos, John, S427 ([FRI060](#))
- Pourhoseingholi, Mohammadamin, S228 ([THU273](#))
- Powell, Elizabeth, S172 ([THU102](#)), S204 ([THU226](#))
- Powerski, Maciej, S378 ([THU579](#))
- Poyatos-Garcia, Paloma, S51 ([OS065](#))
- Poynard, Thierry, S127 ([THU019](#))
- Pozo-Calzada, Carmen Del, S325 ([THU465](#))
- Prachalias, Andreas, S120 ([THU004](#)), S371 ([THU550](#)), S403 ([FRI022](#)), S647 ([FRI562](#)), S771 ([SAT236](#))
- Prada, Samuel Juan Fernández, S792 ([SAT270](#))
- Pradhan, Pranita, S350 ([THU513](#))
- Praditya, Dimas, S250 ([THU315](#))
- Prados, Julien, S754 ([SAT192](#))
- Praetorius, Alejandro González, S184 ([THU170](#)), S826 ([SAT347](#))
- Prah, Jennifer, S202 ([THU221](#))
- Praktiknjo, Michael, S883 ([SAT488](#)), S895 ([SAT510](#))
- Prallet, Sarah, S262 ([THU338](#))
- Pramanick, Tannishtha, S544 ([FRI307](#))
- Prasad, Babita, S53 ([OS066](#))
- Prasad, Manya, S221 ([THU259](#))
- Prasad, Pooja, S37 ([OS041](#)), S762 ([SAT208](#))
- Prasit, Peppi, S489 ([FRI199](#)), S866 ([SAT426](#))
- Pratelli, Dario, S357 ([THU523](#))
- Prati, Daniele, S428 ([FRI061](#)), S668 ([SAT007](#)), S675 ([SAT021](#))
- Pratley, Richard E, S710 ([SAT091](#))
- Pratschke, Johann, S374 ([THU570](#)), S380 ([THU582](#)), S497 ([FRI217](#)), S663 ([FRI597](#)), S739 ([SAT162](#))
- Prats, Maria Angeles Martin, S459 ([FRI119](#))
- Pratt, Trevor, S155 ([THU070](#))
- Prawira, Angga, S265 ([THU344](#))
- Premkumar, Madhumita, S358 ([THU525](#))
- Pressiani, Tiziana, S372 ([THU567](#)), S374 ([THU571](#)), S376 ([THU574](#)), S383 ([THU588](#)), S923 ([SAT572](#))
- Preziosi, Melissa, S120 ([THU004](#)), S639 ([FRI547](#)), S647 ([FRI562](#))
- Price, Jillian, S209 ([THU234](#))
- Prier Lindvig, Katrine, S9 ([GS012](#))
- Prieto-Fernández, Endika, S689 ([SAT050](#))
- Prieto, Janire, S912 ([SAT555](#))
- Prieto, Jesus, S59 ([OS074](#))
- Primignani, Massimo, S623 ([FRI515](#))
- Prince, David, S558 ([FRI334](#))
- Princen, Hans, S681 ([SAT033](#))
- Princic, Elija, S596 ([FRI414](#))
- Prins, John, S190 ([THU183](#))
- Prinz, Marco, S2 ([GS003](#))
- Prishker, Carlos, S133 ([THU028](#))
- Priyadarshi, Rajeev, S170 ([THU100](#)), S809 ([SAT299](#)), S813 ([SAT306](#))
- Procopet, Bogdan, S141 ([THU042](#)), S664 ([FRI600](#))
- Proctor, Gordon, S68 ([OS089](#))
- Pronier, Charlotte, S258 ([THU331](#))
- Prosepe, Ilaria, S798 ([SAT280](#))
- Protopopescu, Camelia, S426 ([FRI059](#)), S567 ([FRI353](#))
- Protzer, Ulrike, S195 ([THU193](#)), S384 ([THU591](#)), S760 ([SAT205](#)), S877 ([SAT445](#))
- Prouvost-Keller, Bernard, S833 ([SAT360](#))
- Provine, Nicholas, S602 ([FRI458](#))
- Pu, Chunwen, S22 ([OS014](#))
- Puente, Angela, S90 ([OS127](#)), S624 ([FRI518](#))
- Pugliese, Nicola, S528 ([FRI272](#))
- Pujol, Claudia, S91 ([OS128](#)), S137 ([THU035](#)), S627 ([FRI523](#))
- Pujols, Paula, S802 ([SAT288](#))
- Pujos-Guillot, Estelle, S640 ([FRI550](#))
- Puma, Donny, S137 ([THU034](#))
- Pungpapong, Surakit, S15 ([OS002](#))
- Pun, K. Tao, S465 ([FRI151](#))
- Puoti, Massimo, S210 ([THU236](#)), S284 ([THU381](#))
- Purcell, Lisa A., S871 ([SAT434](#))
- Puri, Puneet, S130 ([THU023](#))
- Puro, Vincenzo, S806 ([SAT294](#))
- Purwar, Shashank, S252 ([THU320](#))
- Püschel, Klaus, S224 ([THU265](#))
- Pushpa, Hegde, S475 ([FRI170](#))
- Putignano, Antonella, S124 ([THU012](#)), S192 ([THU185](#))
- Putter, Hein, S798 ([SAT280](#))
- Puustinen, Lauri, S312 ([THU441](#))
- Puuvuori, Emmi, S471 ([FRI162](#))
- Puy, Hervé, S905 ([SAT529](#))
- Puzzoni, Marco, S748 ([SAT180](#))
- Pv, Siva Tez, S347 ([THU508](#))
- Pyarajan, Saiju, S936 ([SAT596](#))
- Pydyn, Natalia, S746 ([SAT179](#)), S759 ([SAT203](#))
- Pyrasopoulos, Nikolaos T., S634 ([FRI537](#)), S807 ([SAT295](#))
- Qadan, Motaz, S642 ([FRI553](#))
- Qadri, Sami, S111 ([OS162](#)), S458 ([FRI117](#)), S694 ([SAT060](#))
- Qamar, Sumaira, S633 ([FRI534](#))
- Qian, Tongqi, S36 ([OS037](#))
- Qian, Yuquan, S523 ([FRI262](#)), S928 ([SAT580](#))
- Qian, Zhiping, S344 ([THU504](#))
- Qiao, Guoliang, S642 ([FRI553](#))
- Qi, HaiTao, S522 ([FRI261](#))
- Qi, Lishuang, S522 ([FRI261](#))
- Qin, Lei, S110 ([OS161](#))
- Qin, Lihui, S133 ([THU028](#))
- Qin, Ling, S870 ([SAT432](#))
- Qiu, Dongdong, S89 ([OS125](#))
- Qiu, Yuanwang, S287 ([THU388](#)), S296 ([THU403](#)), S326 ([THU468](#)), S504 ([FRI229](#))
- Qi, Xiaolong, S22 ([OS014](#)), S182 ([THU165](#)), S501 ([FRI224](#)), S616 ([FRI502](#)), S623 ([FRI515](#)), S636 ([FRI540](#))
- Qosa, Hisham, S687 ([SAT046](#))
- Quach, Natalie, S414 ([FRI037](#))
- Quaglia, Alberto, S34 ([OS034](#))
- Quan, Dongmei, S384 ([THU591](#))
- Quang, Erwan Vo, S582 ([FRI386](#))
- Quant, Eva Sofía Sánchez, S395 ([FRI009](#))
- Quantin, Xavier, S392 ([FRI006](#))
- Quaranta, Maria Giovanna, S564 ([FRI347](#))
- Quarta, Alessandra, S763 ([SAT211](#))
- Qu, Bingqian, S265 ([THU344](#))
- Quehenberger, Peter, S617 ([FRI505](#)), S631 ([FRI531](#))
- Quer, Josep, S257 ([THU330](#))
- Quezada, Julissa Lombardo, S137 ([THU034](#))
- Quinlan, Jonathan, S364 ([THU537](#))
- Quinn, Geoff, S12 ([LB004A](#)), S288 ([THU389](#)), S288 ([THU390](#)), S291 ([THU393](#)), S880 ([SAT452](#))
- Quintero, Jorge G., S848 ([SAT391](#))
- Quirk, Erin, S88 ([OS123](#)), S715 ([SAT106](#)), S716 ([SAT107](#)), S716 ([SAT108](#)), S731 ([SAT142](#))
- Quiros-Roldan, Eugenia, S284 ([THU381](#))
- Quitt, Oliver, S877 ([SAT445](#))
- Qureshi, Huma, S215 ([THU246](#)), S240 ([THU295](#))
- Qu, Xiujuan, S384 ([THU591](#))
- Qu, Zhen, S183 ([THU168](#))
- Rábano, Miriam, S48 ([OS060](#))
- Rabekova, Zuzana, S536 ([FRI290](#))
- Rabiega, Pascaline, S579 ([FRI381](#))
- Rabinowich, Liane, S19 ([OS008](#)), S49 ([OS063](#)), S790 ([SAT268](#))
- Raboisson, Pierre, S853 ([SAT401](#))
- Rachakonda, Vikrant, S137 ([THU035](#))
- Rachmilewitz, Jacob, S83 ([OS114](#))
- Racila, Andrei, S154 ([THU069](#)), S209 ([THU234](#)), S420 ([FRI048](#)), S447 ([FRI100](#))
- Rada, Patricia, S111 ([OS163](#))
- Radchenko, Anastasiia, S421 ([FRI049](#))
- Rademacher, Sebastian, S383 ([THU590](#)), S904 ([SAT528](#)), S931 ([SAT587](#))
- Radenkovic, Silvia, S346 ([THU507](#))
- Radenne, Sylvie, S780 ([SAT252](#)), S817 ([SAT312](#))
- Rader, Daniel, S731 ([SAT141](#))
- Radley, Andrew, S564 ([FRI348](#))
- Rad, Roland, S654 ([FRI577](#))
- Radu, Claudia Maria, S751 ([SAT186](#))
- Radu, Elena Cristina, S795 ([SAT276](#))
- Radu, Pompilia, S777 ([SAT247](#))
- Rafeh Naqash, Abdul, S374 ([THU571](#)), S376 ([THU574](#)), S383 ([THU588](#))

Author Index

- Rafei-Shamsabadi, David, S2 ([GS003](#))
 Raffaele, Brustia, S107 ([OS157](#))
 Raffa, Giuseppina, S259 ([THU333](#))
 Ragab, Shaimaa, S566 ([FRI351](#))
 Raggi, Chiara, S47 ([OS058](#)), S477 ([FRI173](#)), S649 ([FRI567](#)), S651 ([FRI570](#))
 Ragone, Enrico, S938 ([SAT599](#))
 Ragues-Nicol, Celine, S639 ([FRI548](#))
 Rahav, Galia, S784 ([SAT258](#))
 Rahbari, Mohammad, S655 ([FRI581](#))
 Rahbari, Nuh N., S661 ([FRI594](#))
 Rahematpura, Suditi, S19 ([OS008](#)), S49 ([OS063](#))
 Rahimi, Robert, S779 ([SAT250](#)), S886 ([SAT493](#))
 Rahman, Fariyal, S70 ([OS092](#))
 Rahman, Syedia, S465 ([FRI151](#))
 Rahman, Tony, S538 ([FRI294](#)), S538 ([FRI295](#))
 Raimondo, Giovanni, S259 ([THU333](#)), S578 ([FRI376](#))
 Rainer, Florian, S346 ([THU506](#))
 Raitakari, Olli, S413 ([FRI036](#))
 Rajagopalan, Ravi, S464 ([FRI148](#))
 Rajagopal, Poyyamozhi, S108 ([OS158](#))
 Raja, Maruthi, S903 ([SAT526](#))
 Rajan, Vijayraghavan, S901 ([SAT521](#))
 Rajoriya, Neil, S19 ([OS008](#)), S49 ([OS063](#)), S120 ([THU005](#)), S141 ([THU041](#)), S805 ([SAT292](#))
 Rajwanshi, Vivek, S846 ([SAT386](#)), S853 ([SAT402](#))
 Rakela, Jorge, S394 ([FRI008](#))
 Ralton, Lucy, S228 ([THU272](#))
 Ramachandran, Jeyamani, S898 ([SAT516](#))
 Ramachandran, Prakash, S163 ([THU086](#))
 Ramachandran, Sumathi, S221 ([THU258](#))
 Ramalho, Leandra Naira Zambelli, S490 ([FRI201](#))
 Ramamurthy, Narayan, S541 ([FRI301](#))
 Ramanathan, Raghu, S692 ([SAT057](#))
 Raman, Maitreyi, S890 ([SAT500](#))
 Raman, Rakesh, S599 ([FRI452](#))
 Ramazzotti, Matteo, S651 ([FRI570](#))
 Ramberger, Evelyn, S99 ([OS142](#))
 Ramier, Clémence, S567 ([FRI353](#))
 Ramirez, Carolina, S81 ([OS110](#)), S137 ([THU034](#))
 Ramirez, Maria, S447 ([FRI100](#))
 Ramirez, Paola, S547 ([FRI314](#))
 Ramirez, Ricardo, S194 ([THU189](#)), S247 ([THU308](#)), S251 ([THU317](#)), S835 ([SAT364](#)), S841 ([SAT376](#))
 Ramji, Alnoor, S544 ([FRI308](#)), S547 ([FRI313](#)), S549 ([FRI317](#)), S569 ([FRI359](#)), S581 ([FRI384](#)), S584 ([FRI388](#)), S836 ([SAT366](#)), S910 ([SAT538](#))
 Ramkissoon, Resham, S138 ([THU037](#))
 Ramm, Grant, S190 ([THU183](#))
 Rammohan, Ashwin, S807 ([SAT296](#))
 Ramon-Gil, Erik, S640 ([FRI551](#))
 Ramos, David Fernández, S671 ([SAT014](#))
 Ramos, Eva Sanchez, S222 ([THU261](#))
 Ramos, Geraldine, S137 ([THU034](#))
 Ramos, Maria Jimenez, S163 ([THU086](#))
 Rampoldi, Davide, S382 ([THU587](#))
 Ramsauer, Lukas, S189 ([THU180](#))
 Ramsing, Anna Marine Sølling, S123 ([THU011](#))
 Rana, Nisha, S2 ([GS003](#))
 Rana, Randeep, S635 ([FRI538](#))
 Rancatore, Gabriele, S387 ([THU599](#)), S624 ([FRI517](#))
 Randon-Furling, Julien, S233 ([THU282](#))
 Rando-Segura, Ariadna, S44 ([OS052](#)), S99 ([OS141](#)), S207 ([THU231](#)), S208 ([THU232](#)), S212 ([THU240](#)), S255 ([THU325](#)), S257 ([THU330](#)), S277 ([THU367](#))
 Rangarajan, Savita, S404 ([FRI023](#))
 Ranieri, Roberto, S581 ([FRI384](#))
 Rankin, Jamie, S164 ([THU089](#))
 Rank, Kevin, S319 ([THU455](#))
 Ranu, Navpreet, S31 ([OS028](#)), S37 ([OS041](#)), S762 ([SAT208](#))
 Rao, Ankit, S116 ([OS172](#))
 Rao, Arvind, S470 ([FRI160](#)), S485 ([FRI190](#))
 Rao, Huiying, S481 ([FRI181](#)), S685 ([SAT042](#))
 Rao, Krishna, S180 ([THU162](#))
 Rao, Nagashree Gundu, S447 ([FRI100](#))
 Rao Padaki, Nagaraja, S329 ([THU474](#))
 Rao, Pranshu E, S756 ([SAT196](#))
 Rapaccini, Gian Ludovico, S436 ([FRI079](#))
 Raposelli, Ilario, S748 ([SAT180](#))
 Rapposelli, Simona, S732 ([SAT144](#))
 Rashid, Mamunur, S244 ([THU301](#))
 Rashid, Tamir, S140 ([THU040](#))
 Rashu, Elias, S154 ([THU068](#)), S331 ([THU477](#))
 Rasmussen, Allan, S818 ([SAT314](#))
 Rasmussen, Ditlev Nytoft, S2 ([GS002](#)), S131 ([THU024](#)), S500 ([FRI223](#))
 Rasmussen, Simon, S500 ([FRI223](#)), S523 ([FRI263](#))
 Rasponi, Marco, S761 ([SAT206](#))
 Rastogi, Aayushi, S221 ([THU259](#))
 Rastogi, Archana, S51 ([OS064](#)), S457 ([FRI116](#)), S901 ([SAT521](#))
 Rastovic, Una, S120 ([THU004](#)), S647 ([FRI562](#))
 Raszeja-Wyszomirska, Joanna, S782 ([SAT254](#))
 Ratnam, Dilip, S337 ([THU488](#)), S842 ([SAT377](#))
 Ratti, Francesca, S748 ([SAT180](#)), S789 ([SAT266](#))
 Rattray, Magnus, S104 ([OS152](#))
 Ratziu, Vlad, S10 ([LB001](#)), S72 ([OS093](#)), S416 ([FRI040](#)), S424 ([FRI055](#)), S436 ([FRI078](#)), S437 ([FRI081](#)), S474 ([FRI168](#)), S506 ([FRI232](#)), S714 ([SAT103](#))
 Rau, Monika, S166 ([THU092](#))
 Laurell, Imma, S180 ([THU161](#)), S365 ([THU538](#))
 Rautou, Pierre-Emmanuel, S61 ([OS076](#)), S127 ([THU019](#)), S362 ([THU533](#)), S502 ([FRI226](#)), S508 ([FRI237](#))
 Ravaioli, Federico, S91 ([OS129](#)), S153 ([THU067](#)), S794 ([SAT273](#))
 Ravaioli, Matteo, S794 ([SAT273](#))
 Rava, Micol, S259 ([THU334](#))
 Ravau, Joachim, S535 ([FRI289](#))
 Ravendhran, Natarajan, S836 ([SAT366](#))
 Ravnskjær, Kim, S37 ([OS040](#)), S423 ([FRI054](#)), S434 ([FRI074](#)), S758 ([SAT200](#))
 Rawat, Sumit, S252 ([THU320](#))
 Rawding, Piper A., S921 ([SAT569](#))
 Ray, Avijit, S873 ([SAT439](#))
 Ray-Chaudhuri, Dominic, S837 ([SAT368](#))
 Razavi, Homie, S43 ([OS050](#)), S226 ([THU269](#)), S230 ([THU278](#)), S231 ([THU279](#)), S235 ([THU288](#)), S238 ([THU292](#)), S240 ([THU295](#))
 Razavi-Shearer, Devin, S43 ([OS050](#)), S226 ([THU269](#)), S230 ([THU278](#)), S231 ([THU279](#))
 Razavi-Shearer, Kathryn, S43 ([OS050](#)), S230 ([THU278](#)), S231 ([THU279](#)), S235 ([THU288](#))
 Razpotnik, Marcel, S21 ([OS012](#)), S891 ([SAT502](#))
 Ready, Joanna, S770 ([SAT234](#))
 Rebillard, Estelle, S918 ([SAT563](#))
 Rebollo, María, S774 ([SAT242](#))
 Rebuffat, Sylvie, S514 ([FRI248](#))
 Reca, Agustina, S471 ([FRI161](#)), S690 ([SAT051](#))
 Recalcatti, Stefania, S651 ([FRI570](#))
 Recalde, Miriam, S500 ([FRI222](#)), S644 ([FRI557](#))
 Reches, Gal, S742 ([SAT166](#))
 Recklies, Franziska, S893 ([SAT507](#))
 Recknor, Christopher, S713 ([SAT101](#))
 Redavid, Anna-Rita, S766 ([SAT216](#))
 Reddy Katukuri, Goutham, S329 ([THU474](#))
 Reddy, K. Rajender, S887 ([SAT496](#))
 Reddy, Nageshwar, S191 ([THU184](#)), S329 ([THU474](#)), S358 ([THU525](#))
 Reddy, Rajender, S19 ([OS008](#)), S49 ([OS063](#)), S339 ([THU494](#))
 Rees, Tom, S228 ([THU272](#))
 Reeves, Helen, S675 ([SAT021](#))
 Reeves, Helen L., S385 ([THU595](#)), S640 ([FRI551](#))
 Reeves, Helen Louise, S646 ([FRI561](#))
 Regev, Gili, S804 ([SAT291](#))
 Reggiani-Bonetti, Luca, S84 ([OS115](#))
 Reggiani, Giulio Marchesini, S153 ([THU067](#))
 Reggidori, Nicola, S382 ([THU587](#))
 Regnault, Helene, S372 ([THU566](#)), S375 ([THU573](#)), S927 ([SAT578](#))
 Regnier, Maxime, S131 ([THU025](#))
 Rehany, Benjamin, S614 ([FRI497](#))
 Rehman, Abdul, S884 ([SAT489](#))
 Reiberger, Thomas, S11 ([LB002](#)), S18 ([OS007](#)), S24 ([OS017](#)), S90 ([OS127](#)), S92 ([OS131](#)), S315 ([THU449](#)),

- S354 (THU519), S359 (THU527), S360 (THU529), S362 (THU534), S390 (FRI003), S466 (FRI152), S469 (FRI158), S470 (FRI159), S472 (FRI164), S502 (FRI225), S502 (FRI226), S532 (FRI280), S535 (FRI287), S545 (FRI309), S555 (FRI328), S617 (FRI505), S618 (FRI506), S629 (FRI527), S629 (FRI528), S630 (FRI529), S631 (FRI531), S632 (FRI533), S753 (SAT191), S829 (SAT353), S830 (SAT354), S843 (SAT379)
- Reichert, Matthias, S80 (OS108), S342 (THU500), S515 (FRI250)
- Reid, Leila, S220 (THU256)
- Reig, María, S381 (THU584), S500 (FRI222)
- Reikvam, Dag Henrik, S178 (THU157), S826 (SAT348)
- Reilly, Connor, S155 (THU070)
- Reina, Giada, S624 (FRI517)
- Reineke-Plaaf, Tanja, S927 (SAT579)
- Reiniš, Jiří, S502 (FRI226)
- Reinson, Tina, S410 (FRI032)
- Reiterer, Veronika, S766 (SAT216)
- Reiter, Florian P, S166 (THU092), S662 (FRI596), S823 (SAT341)
- Reizine, Edouard, S375 (THU573), S532 (FRI281)
- Rekstyte-Matiene, Kristina, S853 (SAT401)
- Rela, Mohd., S19 (OS008), S49 (OS063)
- Remon, Pablo, S451 (FRI106)
- Remy, André-Jean, S542 (FRI303)
- Renand, Amédée, S185 (THU172)
- Renault, Alain, S72 (OS093)
- Renchindorj, Bishguurmaa, S235 (THU287)
- Rendin, Linda Elowsson, S644 (FRI556)
- Ren, Hong, S181 (THU164), S196 (THU195), S240 (THU296), S662 (FRI595), S865 (SAT423)
- Ren, Kaili, S491 (FRI204)
- Ren, Keke, S66 (OS086), S357 (THU524), S402 (FRI021), S745 (SAT173), S803 (SAT289)
- Ren, Liying, S75 (OS102), S467 (FRI153), S638 (FRI545)
- Ren, Ming, S837 (SAT367)
- Rennie, Kirsten, S815 (SAT310)
- Ren, Qingyun, S854 (SAT404)
- Ren, Shan, S844 (SAT382)
- Renteria, Luis Alejandro Rosales, S356 (THU521)
- Renteria, Sara Colonia Uceda, S843 (SAT379), S874 (SAT440)
- Renteria, Uceda, S868 (SAT429), S880 (SAT450)
- Ren, Yayun, S32 (OS030), S431 (FRI068), S468 (FRI155), S481 (FRI181), S486 (FRI194), S619 (FRI509), S623 (FRI516)
- Renzulli, Matteo, S91 (OS129), S794 (SAT273)
- Resaz, Roberta, S515 (FRI249)
- Resnick, Murray, S700 (SAT071), S708 (SAT088), S711 (SAT094)
- Restrepo, Juan Carlos, S137 (THU034)
- Retbi, Aurelia, S393 (FRI007)
- Reuben, Adrian, S394 (FRI008)
- Reuken, Philipp, S100 (OS143), S339 (THU493)
- Reutlinger, Kristina, S85 (OS118)
- Revill, Peter, S251 (THU318), S266 (THU346), S842 (SAT377)
- Rex, Karsten Fleischer, S418 (FRI044)
- Reyes, Archie C., S745 (SAT177)
- Reyes, Eira Cerda, S554 (FRI326)
- Reyes-Higuera, Gisel Estefania, S356 (THU521)
- Rey, Esther, S111 (OS163)
- Reyes-Ureña, Juliana, S570 (FRI361)
- Rey, Francisco Javier García-Samaniego, S238 (THU291), S555 (FRI329), S857 (SAT409)
- Reymond, Maud, S918 (SAT563)
- Reynès, Christelle, S656 (FRI582)
- Rey, Silvia García, S451 (FRI106)
- Rezen, Tadeja, S607 (FRI469), S766 (SAT217)
- Rezvani, Milad, S673 (SAT017)
- Rhaiem, Rami, S927 (SAT578)
- Rhind, Shawn, S822 (SAT320)
- Rhodes, Christopher, S411 (FRI033)
- Rhu, Hyung Chul, S473 (FRI166)
- Riaño, Ioana, S77 (OS103)
- Riba, Carlota, S63 (OS080), S511 (FRI242), S512 (FRI243), S512 (FRI244), S901 (SAT522)
- Ribeiro, Andrea, S328 (THU472)
- Ribeiro, Tiago, S28 (OS024), S618 (FRI507)
- Ribel-Madsen, Rasmus, S720 (SAT116)
- Ribera, Jordi, S907 (SAT532)
- Riccardi, Laura, S507 (FRI234)
- Ricco, Betrice, S84 (OS115)
- Ricco, Gabriele, S292 (THU394)
- Rice, John, S33 (OS031)
- Richards, Anna, S288 (THU390)
- Richardson, Holly, S815 (SAT310)
- Richardson, Paul, S17 (OS005), S34 (OS034), S122 (THU008), S124 (THU013)
- Richaud, Mathieu, S766 (SAT216)
- Riches, Nicholas, S23 (OS015)
- Rich-Griffin, Charlotte, S602 (FRI458)
- Richmond, Jacqui, S228 (THU272), S541 (FRI302)
- Richter, Maria, S395 (FRI009)
- Riddell, Steven, S277 (THU368)
- Ridder, Dirk, S655 (FRI581)
- Rider, Elora, S775 (SAT244), S892 (SAT504)
- Rider, Patricia, S652 (FRI573)
- Ridzon, Renee, S235 (THU287)
- Riedl, Florian, S545 (FRI309)
- Rieger, Armin, S555 (FRI328)
- Riescher, Alix, S127 (THU019)
- Riester, Elena, S251 (THU316)
- Rieusset, Jennifer, S181 (THU163)
- Rigamonti, Cristina, S483 (FRI185), S503 (FRI227), S929 (SAT582), S929 (SAT583)
- Riggio, Oliviero, S627 (FRI524), S908 (SAT535)
- Rimassa, Lorenza, S372 (THU567), S374 (THU571), S376 (THU574), S383 (THU588), S923 (SAT572)
- Rim, Chai Hong, S283 (THU379)
- Rimini, Margherita, S748 (SAT180)
- Rimola, Jordi, S381 (THU584)
- Rinaldi, Anthony, S7 (GS009)
- Rincón, Mercedes, S177 (THU155)
- Rinella, Mary, S438 (FRI084)
- Ringe, Kristina, S333 (THU480)
- Ringelhan, Marc, S189 (THU180)
- Ringlander, Johan, S186 (THU174)
- Ringström, Gisela, S186 (THU174)
- Rio, Emmanuel, S5 (GS007)
- Rios, Rafael, S421 (FRI050)
- Rio, Thomas Mangana Del, S355 (THU520)
- Ripoll, Cristina, S342 (THU500), S369 (THU546), S620 (FRI510)
- Ripolone, Michela, S682 (SAT037)
- Rita Maida, Ivana, S596 (FRI414)
- Rito, Jen, S824 (SAT343)
- Ritter, Angela, S713 (SAT101)
- Ritter, Timothy, S332 (THU478)
- Riva, Antonio, S480 (FRI179), S639 (FRI547)
- Riva, Francesca, S404 (FRI024)
- Rivas, Coral, S113 (OS166), S624 (FRI518)
- Rivas, Violeta, S137 (THU034)
- Riveiro Barciela, Mar, S316 (THU450), S328 (THU471)
- Rivera, Jesús, S114 (OS168), S149 (THU059), S440 (FRI088), S906 (SAT530)
- Rivera, Jose, S137 (THU034)
- Rivera, Savannah, S371 (THU550), S911 (SAT540)
- Rivero, Montserrat, S113 (OS166)
- Rivet, Valérian, S392 (FRI006)
- Rivoire, Michel, S766 (SAT216)
- Rizza, Giorgia, S775 (SAT243)
- Rizzardini, Giuliano, S13 (LB004B), S210 (THU236), S288 (THU390), S291 (THU393), S881 (SAT453)
- Rizzari, Michael, S778 (SAT249)
- Rizzo, Giacomo Emanuele Maria, S387 (THU599), S624 (FRI517)
- Robaey, Geert, S459 (FRI120)
- Robaey, Wouter, S459 (FRI120)
- Robert, Caroline, S402 (FRI020)
- Roberts, Andrew, S337 (THU488)
- Roberts, Lauren, S121 (THU007)
- Roberts, Lewis, S214 (THU244)
- Robertson, Darren, S158 (THU075)
- Robertson, David, S594 (FRI409)
- Robertson, John, S719 (SAT115)
- Robertson, Keith, S923 (SAT573)
- Robertson, Marcus, S337 (THU488), S366 (THU540), S613 (FRI495)
- Roberts, Scot, S88 (OS124)
- Roberts, Stuart, S154 (THU069), S441 (FRI090)
- Roberts, Surain, S313 (THU443)
- Robins, Callum, S909 (SAT536)
- Robinson, Emma, S564 (FRI348)

Author Index

- Robinson, Tara, S540 ([FRI299](#))
 Roblero, Juan Pablo, S81 ([OS110](#)),
 S137 ([THU034](#))
 Robles-Díaz, Mercedes, S93 ([OS132](#)),
 S317 ([THU452](#)), S326 ([THU467](#)),
 S396 ([FRI011](#))
 Robles-Espinoza, Carla Daniela,
 S476 ([FRI172](#))
 Roca-Fernandez, Adriana, S424 ([FRI056](#))
 Roccarina, Davide, S627 ([FRI524](#))
 Rocco, Lucia, S938 ([SAT599](#))
 Rocha, Cristina Melo, S137 ([THU034](#))
 Rocha, Gifone Aguiar, S293 ([THU396](#)),
 S552 ([FRI323](#))
 Rocha, Haroldo Luis Oliva Gomes,
 S307 ([THU432](#))
 Rocha, Marta, S304 ([THU420](#))
 Roche, Bruno, S800 ([SAT285](#)),
 S833 ([SAT360](#)), S840 ([SAT373](#)),
 S935 ([SAT595](#))
 Rode, Agnès, S5 ([GS007](#))
 Rodenhausen, Aaron Nikolai,
 S193 ([THU187](#))
 Roden, Michael, S451 ([FRI106](#)),
 S606 ([FRI467](#)), S703 ([SAT079](#))
 Roderburg, Christoph, S11 ([LB003](#)),
 S384 ([THU592](#)), S930 ([SAT584](#))
 Roderfeld, Martin, S602 ([FRI460](#)),
 S748 ([SAT181](#))
 Roderick, Paul, S42 ([OS048](#))
 Rodgers, Mary, S294 ([THU400](#))
 Rodney, Kyle, S21 ([OS011](#))
 Rodrigue-Alvarez, Fatima, S176 ([THU153](#))
 Rodrigues, Barbara, S910 ([SAT539](#))
 Rodrigues, Beverly, S315 ([THU448](#)),
 S389 ([FRI002](#))
 Rodrigues, Cecília M. P., S7 ([GS009](#)),
 S537 ([FRI293](#))
 Rodrigues de Freitas, Luiz Antônio,
 S336 ([THU487](#))
 Rodrigues, Pedro Miguel, S46 ([OS056](#)),
 S77 ([OS103](#)), S648 ([FRI564](#))
 Rodrigues, Susana G., S625 ([FRI520](#))
 Rodríguez Agudo, Rubén, S87 ([OS122](#))
 Rodríguez, Antonio González, S114 ([OS168](#))
 Rodríguez, Carlos, S912 ([SAT555](#))
 Rodríguez-Castaneda, Tamara,
 S7 ([GS009](#))
 Rodriguez, Christophe, S530 ([FRI276](#)),
 S582 ([FRI386](#))
 Rodriguez, Conrado Manuel Fernandez,
 S59 ([OS074](#)), S581 ([FRI384](#))
 Rodriguez-Cuenca, Sergio, S7 ([GS009](#))
 Rodríguez-Cundin, María, S774 ([SAT242](#))
 Rodriguez-Duque, Juan Carlos,
 S113 ([OS166](#))
 Rodríguez-Frías, Francisco, S44 ([OS052](#)),
 S99 ([OS141](#)), S207 ([THU231](#)),
 S208 ([THU232](#)), S212 ([THU240](#)),
 S255 ([THU325](#)), S257 ([THU330](#)),
 S277 ([THU367](#)), S658 ([FRI587](#))
 Rodríguez, Héctor, S177 ([THU155](#))
 Rodríguez, Juan Luis García,
 S689 ([SAT050](#))
 Rodríguez, Manuel, S115 ([OS169](#)),
 S127 ([THU018](#)), S857 ([SAT409](#))
 Rodríguez, Marcela Peña, S67 ([OS087](#)),
 S176 ([THU153](#))
 Rodriguez, Maria, S406 ([FRI027](#))
 Rodríguez-Perálvarez, Manuel, S3 ([GS005](#)),
 S114 ([OS168](#)), S115 ([OS169](#)),
 S328 ([THU471](#))
 Rodríguez, Pilar Gómez, S704 ([SAT080](#))
 Rodriguez-Tajes, Sergio, S99 ([OS141](#)),
 S207 ([THU231](#)), S208 ([THU232](#)),
 S263 ([THU340](#)), S286 ([THU385](#)),
 S328 ([THU471](#)), S334 ([THU482](#)),
 S581 ([FRI384](#)), S857 ([SAT409](#))
 Rodríguez-Tomás, Elisabet, S677 ([SAT027](#)),
 S678 ([SAT028](#)), S681 ([SAT034](#)),
 S685 ([SAT041](#))
 Roeb, Elke, S602 ([FRI460](#)), S748 ([SAT181](#))
 Roehlen, Natascha, S36 ([OS038](#)),
 S738 ([SAT160](#))
 Roessler, Stephanie, S655 ([FRI581](#))
 Roest, Henk P., S115 ([OS170](#)), S652 ([FRI574](#))
 Roest, Mark, S911 ([SAT540](#))
 Rogal, Shari, S126 ([THU016](#)), S899 ([SAT518](#))
 Rogalska, Magdalena, S565 ([FRI350](#))
 Rogers, Benjamin, S342 ([THU501](#))
 Roget, Mercé, S607 ([FRI468](#))
 Rohilla, Sumati, S105 ([OS153](#))
 Röhlen, Natascha, S657 ([FRI583](#))
 Rohr-Udilova, Nataliya, S753 ([SAT189](#))
 Roig, Clara Amiama, S857 ([SAT409](#))
 Roig, Cristina, S627 ([FRI523](#))
 Roig, Paula Bufi, S91 ([OS128](#))
 Roinard, Morganer, S245 ([THU304](#))
 Rojo, Andres Duarte, S19 ([OS008](#)),
 S49 ([OS063](#)), S886 ([SAT493](#))
 Rojo, Carla, S500 ([FRI222](#))
 Rokka, Johanna, S471 ([FRI162](#))
 Rokop, Zachary, S686 ([SAT045](#))
 Rola, Al Sayegh, S475 ([FRI170](#))
 Rolland, Benjamin, S579 ([FRI381](#))
 Rolph, Tim, S719 ([SAT114](#))
 Romagnoli, Renato, S775 ([SAT243](#)),
 S776 ([SAT245](#))
 Romagnoli, Veronica, S292 ([THU394](#))
 Roman, Eva, S64 ([OS082](#)), S886 ([SAT494](#)),
 S900 ([SAT520](#))
 Rombouts, Krista, S477 ([FRI173](#)),
 S668 ([SAT008](#)), S737 ([SAT157](#))
 Romeo, Orazio, S259 ([THU333](#))
 Romeo, Sean, S462 ([FRI125](#))
 Romeo, Stefano, S11 ([LB002](#)), S423 ([FRI053](#)),
 S668 ([SAT008](#))
 Römer, Barbara, S80 ([OS108](#))
 Romero, Carmen Lara, S442 ([FRI092](#)),
 S451 ([FRI106](#)), S555 ([FRI329](#))
 Romero Gomez, Manuel, S451 ([FRI106](#)),
 S459 ([FRI119](#))
 Romero, Gustavo, S137 ([THU034](#))
 Romero, Maria Dolores Macia,
 S218 ([THU252](#))
 Romero, Marta, S600 ([FRI453](#))
 Romero, Sarah, S613 ([FRI495](#))
 Rom, Oren, S765 ([SAT214](#))
 Ronot, Maxime, S372 ([THU566](#))
 Ronzoni, Luisa, S675 ([SAT021](#))
 Ronzoni, Riccardo, S534 ([FRI285](#))
 Roos, Floris, S46 ([OS057](#))
 Roper, James, S465 ([FRI151](#))
 Roque-Cuéllar, María C., S451 ([FRI106](#))
 Roquelaure, Bertrand, S519 ([FRI256](#)),
 S521 ([FRI259](#))
 Roqueta-Rivera, Manuel, S745 ([SAT177](#))
 Rorsman, Fredrik, S333 ([THU480](#)),
 S420 ([FRI047](#))
 Rosa, Guy De La, S848 ([SAT390](#))
 Rosa, Isabelle, S833 ([SAT360](#)),
 S840 ([SAT373](#))
 Rosa La, Guy De, S849 ([SAT393](#))
 Rosales, Ricardo Aguilera, S137 ([THU034](#))
 Rosario, Michelle, S188 ([THU178](#))
 Rosas, Alethse De la Torre, S238 ([THU292](#))
 Rosati, Silvia, S581 ([FRI384](#))
 Rosato, Valerio, S212 ([THU239](#))
 Rösch, Thomas, S325 ([THU466](#))
 Rose, Ayub, S240 ([THU295](#))
 Rose-John, Stefan, S47 ([OS059](#)),
 S83 ([OS114](#))
 Rosenberger, Aaron, S770 ([SAT234](#))
 Rosenberg, Nofar, S47 ([OS059](#)), S83 ([OS114](#))
 Rosenberg, Vered, S399 ([FRI017](#))
 Rosenberg, William, S34 ([OS034](#))
 Rosenbluth, Emma, S160 ([THU080](#))
 Rosendahl, Jonas, S11 ([LB002](#))
 Rosenquist, Jenny, S368 ([THU543](#))
 Rosenthal, Elana, S552 ([FRI322](#)),
 S571 ([FRI362](#)), S572 ([FRI364](#)),
 S574 ([FRI369](#))
 Rosenthal, Philip, S866 ([SAT425](#))
 Rosstedt, Maria, S471 ([FRI162](#))
 Rosie, Rajkumari, S219 ([THU254](#))
 Rosigkeit, Sebastian, S464 ([FRI147](#))
 Rosi, Martina, S932 ([SAT588](#))
 Rosina, Arianna, S761 ([SAT206](#))
 Rosini, Francesca, S698 ([SAT066](#))
 Roskams, Tania, S47 ([OS059](#)),
 S120 ([THU003](#)), S144 ([THU047](#)),
 S637 ([FRI544](#)), S680 ([SAT032](#))
 Rosler, Elen, S853 ([SAT402](#))
 Rosmark, Oskar, S644 ([FRI556](#))
 Rosmorduc, Olivier, S402 ([FRI020](#)),
 S935 ([SAT595](#))
 Rosqvist, Fredrik, S690 ([SAT052](#))
 Ross, Christina Cajigas-Du, S193 ([THU188](#))
 Rossen, Noortje, S338 ([THU491](#))
 Ross, Gayle, S60 ([OS075](#))
 Rossi, Anita De, S821 ([SAT318](#))
 Rossignol, Celine, S877 ([SAT446](#))
 Rossignol, Jean-Francois, S877 ([SAT446](#))
 Ross, Kendra, S395 ([FRI010](#))
 Rosso, Natalia, S433 ([FRI071](#))
 Ross, Trenton, S7 ([GS009](#))
 Rosychuk, Rhonda J., S775 ([SAT244](#))
 Röth, Anjali A., S193 ([THU187](#))
 Roth, Nitzan, S548 ([FRI315](#))
 Rotstein, Ori, S822 ([SAT320](#))
 Roudot-Thoraval, Françoise, S375 ([THU573](#)),
 S927 ([SAT578](#))

- Roulot, Dominique, S72 (OS093), S270 (THU352), S271 (THU355), S833 (SAT360), S840 (SAT373)
- Roumain, Martin, S680 (SAT031)
- Rourke, Colm O., S649 (FRI566)
- Rourke, Colm O., S46 (OS056), S77 (OS103)
- Roussos, Sotiris, S218 (THU251)
- Rou, Woo Sun, S380 (THU583), S921 (SAT569)
- Roux, Julien, S192 (THU186)
- Roux, Marine, S73 (OS096), S715 (SAT105)
- Roux, Perrine, S584 (FRI389)
- Rovida, Elisabetta, S477 (FRI173), S649 (FRI567)
- Rowe, Ian, S141 (THU041), S213 (THU241), S461 (FRI123)
- Rowe, Mackenzie, S508 (FRI236), S918 (SAT564)
- Roy, Akash, S350 (THU513)
- Royal, Nichola, S554 (FRI327)
- Roy, Berengere, S542 (FRI303)
- Royo, Laura, S527 (FRI271)
- Rozenblum, Nir, S764 (SAT213)
- Rozina, Teona, S574 (FRI370)
- Rozman, Damjana, S766 (SAT217)
- Ruane, Peter, S427 (FRI060), S719 (SAT114)
- Rubbia-Brandt, Laura, S754 (SAT192)
- Rubín, Ángel, S792 (SAT271), S811 (SAT303)
- Rubio, Aileen, S834 (SAT362)
- Rubio, Ana Belén, S63 (OS080), S139 (THU039), S511 (FRI242), S896 (SAT512), S901 (SAT522), S902 (SAT524), S907 (SAT532)
- Rudler, Marika, S630 (FRI529)
- Rueda-Gotor, Javier, S113 (OS166)
- Ruether, Darius, S313 (THU444), S317 (THU452)
- Rufat, Pierre, S393 (FRI007)
- Ruffoni, Elena, S821 (SAT318)
- Ruge, André, S190 (THU182)
- Rugwani, Hardik, S191 (THU184)
- Ruixo, Juan Jose Perez, S838 (SAT370)
- Ruiz, Beatriz Pacín, S255 (THU325), S257 (THU330)
- Ruiz-Blazquez, Paloma, S465 (FRI150)
- Ruiz-Cabello, Francisco, S396 (FRI011)
- Ruiz de Gauna, Mikel, S648 (FRI564)
- Ruiz, Isaac, S593 (FRI407), S805 (SAT293)
- Ruiz, Lourdes, S316 (THU450)
- Ruiz, Luong, S443 (FRI093), S486 (FRI193)
- Ruiz, Pablo, S317 (THU452), S792 (SAT271)
- Ruiz, Patricia, S114 (OS168)
- Ruiz, Paula, S401 (FRI019), S809 (SAT298)
- Rujeerapaiboon, Natthapat, S186 (THU175), S187 (THU176)
- Rule, Jody, S394 (FRI008)
- Rullier, Patricia, S392 (FRI006)
- Rumi, Maria Grazia, S564 (FRI347)
- Runarsdottir, Valgerdur, S573 (FRI366)
- Rupp, Jana, S488 (FRI197)
- Ruscica, Massimiliano, S698 (SAT068)
- Russell, Anthony, S172 (THU102)
- Russell, Chris, S404 (FRI023)
- Russell, Matthew, S718 (SAT112)
- Russo, Francesco Paolo, S192 (THU185), S306 (THU423), S317 (THU452), S358 (THU526), S478 (FRI176), S564 (FRI347), S807 (SAT296), S821 (SAT318)
- Rustgi, Vinod, S280 (THU372)
- Rutherford, Erica, S179 (THU160)
- Rüthrich, Maria Madeleine, S339 (THU493)
- Rutland, Kelsey, S622 (FRI513)
- Rutledge, Stephanie, S33 (OS031), S343 (THU502), S897 (SAT513)
- Rutter, Guy, S710 (SAT091)
- Ruzzenente, Andrea, S796 (SAT277)
- Ryan, Jennifer, S120 (THU005), S125 (THU014)
- Ryan, John, S39 (OS044), S138 (THU036), S234 (THU285), S527 (FRI270), S531 (FRI279)
- Ryan, Marno, S498 (FRI218)
- Ryan, Pablo, S217 (THU249), S581 (FRI384)
- Ryden, Mikael, S665 (SAT002)
- Ryder, Stephen, S17 (OS005), S122 (THU008), S124 (THU013), S188 (THU178), S872 (SAT437), S938 (SAT600)
- Ryu, Je Ho, S799 (SAT282)
- Saad, Amel Ben, S521 (FRI260)
- Saarinen, Kustaa, S419 (FRI046)
- Sábado, Constantino, S527 (FRI271)
- Sabio, Guadalupe, S111 (OS163), S689 (SAT050)
- Saborowski, Anna, S107 (OS157), S927 (SAT579)
- Sabroso, Sergio, S792 (SAT271)
- Saccomandi, Patrizia, S249 (THU313)
- Sacerdoti, David, S152 (THU066), S658 (FRI586), S796 (SAT277), S900 (SAT519), S920 (SAT567), S925 (SAT574)
- Sacha, Jonah, S713 (SAT101)
- Sacilotto, Federica, S153 (THU067)
- Sacleux, Sophie, S935 (SAT595)
- Sacleux, Sophie-Caroline, S349 (THU511)
- Sadeghlur, Farsaneh, S381 (THU585)
- Sadek, Hesham, S113 (OS167)
- Sadiq Hamid, Saeed, S560 (FRI338)
- Sadirova, Shakhlo, S235 (THU288)
- Sadler, Matthew, S143 (THU045)
- Saeb-Parsy, Kourosh, S741 (SAT165)
- Saed, Hevar Hamah, S186 (THU174)
- Saeed, Anwaar, S372 (THU567), S383 (THU588)
- Saenz de Urturi, Diego, S648 (FRI564)
- Sáenz, José Luis Vega, S445 (FRI096), S577 (FRI374)
- Saez-Palma, Maria, S286 (THU385)
- Safadi, Rifaat, S399 (FRI016), S691 (SAT054), S792 (SAT270)
- Safer, Ricky, S312 (THU442)
- Sagalova, Olga, S4 (GS006), S103 (OS149), S828 (SAT351)
- Sagar, Sagar, S54 (OS068)
- Saget, Brad, S596 (FRI411)
- Saghire, Hussein El, S649 (FRI565)
- Sagrado, Miguel Ángel Rodríguez, S869 (SAT430)
- Sahin, Hacer, S193 (THU187)
- Sahli, Roland, S253 (THU322)
- Sahota, Amandeep, S770 (SAT234), S831 (SAT356)
- Sahuco, Iván, S192 (THU185)
- Saichi, Melissa, S189 (THU181)
- Said, Ebada, S566 (FRI351)
- Saigusa, Yusuke, S430 (FRI067)
- Sailer, Andreas, S486 (FRI194), S493 (FRI207)
- Saini, Akhilesh, S528 (FRI273)
- Sainitin, Donakonda, S195 (THU193)
- Sainz-Barriga, Mauricio, S781 (SAT253), S783 (SAT256)
- Saito, Satoru, S430 (FRI067)
- Saito, Tomoko, S615 (FRI501), S897 (SAT514)
- Saitta, Carlo, S259 (THU333)
- Sajji, Haresh, S190 (THU183)
- Sajous, Jenna, S329 (THU473)
- Sakamori, Ryotaro, S563 (FRI346)
- Sakka, Mehdi, S393 (FRI007)
- Sakuma, Takafumi, S615 (FRI501), S897 (SAT514)
- Salahuddin, Sultan, S560 (FRI338)
- Salai, Grgur, S612 (FRI494)
- Sala, Margarita, S127 (THU018), S334 (THU482)
- Salamé, Ephrem, S780 (SAT252)
- Salamon, Johannes, S893 (SAT507)
- Salatiello, Maria, S84 (OS115)
- Salati, Massimiliano, S84 (OS115)
- Salcedo, Magdalena, S324 (THU464), S325 (THU465), S328 (THU471), S792 (SAT271)
- Salcedo, María Magdalena, S114 (OS169)
- Salcedo, Maria Teresa, S180 (THU161)
- Saldarriaga, Omar, S194 (THU191), S470 (FRI160), S485 (FRI190)
- Saleev, Natalia, S742 (SAT166)
- Salehi, Siamak, S371 (THU550)
- Salhab, Ahmed, S399 (FRI016), S691 (SAT054)
- Saliba, Faouzi, S349 (THU511), S772 (SAT239), S935 (SAT595)
- Salic, Kanita, S676 (SAT024), S677 (SAT025)
- Salie, Henrike, S2 (GS003)
- Salignac, Sylvain, S905 (SAT529)
- Salinas, Daniel, S894 (SAT508)
- Salinas, José Antonio, S527 (FRI271)
- Sällberg, Matti, S860 (SAT413)
- Salloum, Shadi, S36 (OS037)
- Salman, Sidra, S291 (THU392), S301 (THU413)
- Salomaa, Veikko, S80 (OS109)
- Salomão, Frederico Chaves, S336 (THU487)
- Salomone, Federico, S703 (SAT077)
- Salpini, Romina, S249 (THU313), S284 (THU380), S284 (THU381), S839 (SAT371)
- Salta, Sofia, S268 (THU349)

Author Index

- Saltini, Dario, S502 (FRI226), S627 (FRI524)
Saludes, Verónica, S570 (FRI361)
Saluja, Vandana, S349 (THU510)
Salvà, Francisco, S218 (THU252)
Salvatella, Albert, S362 (THU533)
Salvati, Antonio, S292 (THU394)
Salvetti, Anna, S246 (THU305)
Salvino, Marco, S408 (FRI028)
Salvoza, Noel, S433 (FRI071)
Samadaei, Mahzeiar, S753 (SAT189)
Samadan, Lara, S700 (SAT070)
Samadashvili, Tamar, S219 (THU253)
Samanta, Ayan, S368 (THU543)
Samarakoon, Natali Abeywickrama, S640 (FRI550)
Sambarino, Dana, S843 (SAT379), S843 (SAT381), S868 (SAT429), S874 (SAT440), S880 (SAT450)
Sambou, Benjamin, S304 (THU419)
Samer, Al-Dury, S186 (THU174)
Samir, Anthony, S451 (FRI107), S454 (FRI110), S701 (SAT073)
Samji, Hasina, S43 (OS051)
Sammalkorpi, Henna, S111 (OS162), S694 (SAT060)
Samonakis, Demetrious N., S840 (SAT374)
Samson, Michel, S639 (FRI548)
Samuel, Didier, S349 (THU511), S402 (FRI020), S538 (FRI296), S772 (SAT239), S800 (SAT285), S817 (SAT312), S935 (SAT595)
Samuel, Kay, S397 (FRI013), S712 (SAT096)
Samuelsén, Ellen, S826 (SAT348)
Samur, Sumeyye, S214 (THU244)
Sanai, Faisal, S479 (FRI178)
Sanavio, Mathilde, S771 (SAT237)
Sanchez, Abel, S137 (THU034)
Sánchez-Aldehuelo, Rubén, S370 (THU548)
Sanchez, Antonio, S555 (FRI329)
Sánchez-Campos, Sonia, S177 (THU155)
Sanchez, Carlos, S137 (THU034)
Sánchez, Celia Martínez, S684 (SAT039)
Sánchez-Delgado, Jordi, S217 (THU018)
Sanchez-Fueyo, Alberto, S401 (FRI019), S607 (FRI468), S809 (SAT298)
Sanchez-Huertas, Carlos, S103 (OS150)
Sanchez, Jenifer, S55 (OS070)
Sanchez, Jose, S158 (THU075)
Sanchez, Katarzyna, S488 (FRI197)
Sánchez, Marco, S137 (THU034)
Sanchez, Maria Jesus, S238 (THU292)
Sanchez, Mercedes De La Torre, S157 (THU074), S158 (THU076)
Sánchez, Mercedes Latorre, S222 (THU261)
Sánchez, Obed Ramírez, S476 (FRI172)
Sánchez-Rodríguez, M. Belén, S361 (THU531)
Sanchez-Serrano, Jose, S51 (OS065)
Sánchez, Victor, S692 (SAT056)
Sánchez, Yolanda, S451 (FRI106), S555 (FRI329)
Sancho-Bru, Pau, S37 (OS039), S527 (FRI271), S684 (SAT039)
Sancho, Victoria Aguilera, S127 (THU018), S406 (FRI027), S811 (SAT301), S811 (SAT303)
Sandakli, Ahmed, S37 (OS041), S762 (SAT208)
Sandberg, Johan K., S189 (THU179)
Sandesh, K, S884 (SAT490)
Sandmann, Lisa, S830 (SAT355)
Sandra, Louis, S838 (SAT370)
Sandro, Stefano Di, S789 (SAT266)
Sangaimwibool, Prakasit, S499 (FRI219)
Sangiovanni, Angelo, S578 (FRI376)
Sangiovanni, Vincenzo, S908 (SAT535)
Sangro, Bruno, S112 (OS165), S500 (FRI222), S643 (FRI554), S644 (FRI557)
Sanneh, Bakary, S295 (THU401)
Sansom, Owen, S385 (THU595)
Santamaria, Eva, S697 (SAT064)
Santamaría, Javier Salamanca, S704 (SAT080)
Santana, Bárbara, S490 (FRI201)
Santana, Jessica, S935 (SAT594)
Santiago, Jesús González, S59 (OS074)
Santis, Teresa De, S239 (THU294)
Santistevé, Sara Sopena, S255 (THU325)
Santi, Valentina, S382 (THU587)
Santol, Jonas, S788 (SAT264), S799 (SAT283)
Santorio, Armando, S923 (SAT572)
Santorio, Luigi, S428 (FRI061), S675 (SAT021)
Santos, Ana, S28 (OS024)
Santos, André A., S537 (FRI293)
Santos, Beatriz Gómez, S648 (FRI564), S665 (SAT001), S689 (SAT050)
Santos, Cecy Maria de Lima, S293 (THU396)
Santos-Laso, Alvaro, S107 (OS157)
Santos-Laso, Álvaro, S157 (THU074), S158 (THU076)
Santos, Sandra, S21 (OS011)
Sanyal, Arun, S7 (CS009), S10 (LB001), S31 (OS028), S158 (THU075), S179 (THU160), S409 (FRI030), S431 (FRI068), S439 (FRI085), S446 (FRI029), S446 (FRI099), S449 (FRI103), S451 (FRI107), S454 (FRI110), S474 (FRI168), S481 (FRI181), S701 (SAT073), S714 (SAT103), S762 (SAT208), S899 (SAT517)
Sanz-Parra, Arantza, S84 (OS116)
Sapena, Víctor, S625 (FRI520)
Sapisochin, Gonzalo, S109 (OS159), S800 (SAT286), S801 (SAT287), S815 (SAT311)
Saqib, Nazmus, S912 (SAT554)
Saracco, Margherita, S775 (SAT243), S776 (SAT245)
Sara, Colonia, S868 (SAT429), S880 (SAT450)
Saraiva, Rita Catarina, S190 (THU182), S211 (THU238)
Saraiva, Susana, S537 (FRI293)
Saraya, Anoop, S19 (OS008), S49 (OS063), S369 (THU547), S623 (FRI515), S633 (FRI534), S635 (FRI538)
Sarcognato, Samantha, S478 (FRI176)
Sardh, Eliane, S530 (FRI275)
Sarica, Nazim, S297 (THU404)
Sarikaya, Ozan, S399 (FRI015)
Sarin, Sanjay, S219 (THU254), S232 (THU280)
Sarin, Shiv Kumar, S19 (OS008), S20 (OS009), S22 (OS014), S34 (OS033), S49 (OS063), S51 (OS064), S53 (OS066), S105 (OS153), S128 (THU020), S139 (THU038), S221 (THU259), S347 (THU508), S397 (FRI014), S738 (SAT161), S756 (SAT196), S901 (SAT521)
Sarkar, Souvik, S155 (THU070), S462 (FRI125)
Sarmati, Loredana, S249 (THU313), S284 (THU381)
Sarnecki, Jędrzej, S525 (FRI267)
Saroul, Maeva, S672 (SAT015)
Sarowar, Arif, S849 (SAT394)
Sarrazin, Christoph, S15 (OS001), S16 (OS003), S262 (THU337), S562 (FRI345), S584 (FRI388), S585 (FRI391)
Sarrias, Maria-Rosa, S361 (THU531)
Sartor, Ryan Balfour, S178 (THU156)
Sarv, Janeli, S158 (THU075)
Sarwar, Syeda Zahida, S240 (THU295)
Satapathy, Sanjaya, S548 (FRI315)
Satapati, Santhosh, S31 (OS028)
Satchi, Romona, S447 (FRI100)
Sator-Schmitt, Melanie, S38 (OS042)
Sato, Sho, S172 (THU103)
Sato, Shunsuke, S172 (THU103)
Sato, Toshifumi, S465 (FRI149), S687 (SAT047)
Satsangi, Jack, S57 (OS072A), S58 (OS072B)
Sattanathan, Swetha, S728 (SAT133)
Sauerbruch, Tilman, S625 (FRI520), S630 (FRI529)
Sauer, Hagen, S783 (SAT257)
Saunders, Emily, S783 (SAT257), S784 (SAT259)
Sauvé, Laura, S43 (OS051)
Saviano, Antonio, S36 (OS038)
Savner, Eric, S817 (SAT312)
Sawaf, Bisher, S230 (THU277)
Sawhney, Rohit, S315 (THU448), S389 (FRI002)
Saxby, Edward, S342 (THU501)
Saxena, Anoushka, S197 (THU196)
Saxena, Romil, S14 (LB006)
Saxena, Varun, S770 (SAT234)
Sayaf, Katia, S478 (FRI176), S479 (FRI177)
Sayols, Sergi, S40 (OS045)
Sbarigia, Carolina, S763 (SAT211)
Sbieh, Reem, S399 (FRI016)
Scagliotta, Marcelle, S491 (FRI203)
Scalfaro, Pietro, S254 (THU324)
Scanlan, Becky, S256 (THU328)
Scaravaglio, Miki, S96 (OS136), S404 (FRI024)

- Scarry, Margaret, S569 (FRI358), S570 (FRI360)
- Scarton, Giampaolo, S786 (SAT261)
- Scartozzi, Mario, S748 (SAT180)
- Scatton, Olivier, S189 (THU181), S817 (SAT312)
- Schaap, Frank, S757 (SAT198)
- Schachschal, Guido, S325 (THU466)
- Schaefer, Benedikt, S537 (FRI292)
- Schaeffer, Eugénie, S649 (FRI565), S738 (SAT160)
- Schaeper, Ute, S87 (OS122), S132 (THU027), S600 (FRI453)
- Schafmayer, Clemens, S11 (LB002)
- Scharitzer, Martina, S532 (FRI280), S921 (SAT570)
- Scharnagl, Hubert, S466 (FRI152), S469 (FRI158), S472 (FRI164), S688 (SAT049)
- Schattenberg, Jörn, S10 (LB001), S16 (OS003), S75 (OS101), S145 (THU051), S257 (THU329), S412 (FRI034), S415 (FRI039), S436 (FRI078), S448 (FRI102), S451 (FRI106), S452 (FRI108), S585 (FRI391), S882 (SAT486)
- Schaub, Golda, S54 (OS069)
- Schaub, Johanna, S308 (THU434), S466 (FRI152)
- Schefczyk, Stefan, S264 (THU342), S642 (FRI552), S643 (FRI555)
- Scheffschick, Andrea, S658 (FRI585)
- Scheiner, Bernhard, S11 (LB002), S18 (OS007), S92 (OS131), S315 (THU449), S354 (THU519), S359 (THU527), S372 (THU567), S374 (THU571), S376 (THU574), S383 (THU588), S390 (FRI003), S532 (FRI280), S535 (FRI287), S617 (FRI505), S618 (FRI506), S629 (FRI527), S629 (FRI528), S631 (FRI531), S632 (FRI533), S919 (SAT565), S921 (SAT570)
- Scheiter, Alexander, S107 (OS157)
- Schemmerer, Mathias, S257 (THU329)
- Schenck, Maleka, S20 (OS010)
- Schene, Imre F, S652 (FRI574)
- Schepis, Filippo, S502 (FRI226), S627 (FRI524)
- Schepke, Michael, S625 (FRI520)
- Scherbakovsky, Stacey, S581 (FRI384)
- Scherr, Anna-Lena, S655 (FRI581)
- Schiano, Thomas, S317 (THU452), S343 (THU502)
- Schicht, Gerda, S658 (FRI585)
- Schierwagen, Robert, S895 (SAT510)
- Schiff, Eugene R., S836 (SAT366)
- Schilsky, Michael, S1 (GS001), S61 (OS077), S539 (FRI297)
- Schindler, Aaron, S382 (THU586)
- Schirmacher, Peter, S655 (FRI581)
- Schirmbeck, Reinhold, S663 (FRI598)
- Schlaak, Emilia, S710 (SAT090)
- Schledzewski, Kai, S463 (FRI146)
- Schlerman, Franklin, S7 (GS009)
- Schlevogt, Bernhard, S313 (THU444), S523 (FRI262)
- Schlimmer, Alexandra, S538 (FRI295)
- Schluep, Thomas, S14 (LB006)
- Schmelzle, Moritz, S374 (THU570), S380 (THU582), S497 (FRI217), S663 (FRI597), S739 (SAT162)
- Schmid, Daniela, S545 (FRI309)
- Schmid, Michael A., S871 (SAT434)
- Schmid, Roland M., S654 (FRI577)
- Schmid, Roland M., S185 (THU171), S189 (THU180)
- Schmidt, Daniel, S309 (THU436)
- Schmidt, Geske, S85 (OS118)
- Schmidt, Hartmut, S264 (THU342), S823 (SAT341)
- Schmidt, Michael, S251 (THU316)
- Schmidt, Nathalie, S55 (OS070)
- Schmidt, Ralf, S545 (FRI309)
- Schmidt-Wolf, Ingo G., S915 (SAT559)
- Schmist-Arras, Dirk, S47 (OS059), S83 (OS114)
- Schmitt, Nathalie, S655 (FRI581)
- Schmitt, Sascha, S464 (FRI147)
- Schmitz, Sophia M., S193 (THU187)
- Schnabl, Bernd, S86 (OS119), S135 (THU032)
- Schneeberger, Stefan, S85 (OS117)
- Schneeweiß, Stephan M, S582 (FRI385)
- Schneider, Anne, S11 (LB003)
- Schneider, Antoine, S355 (THU520)
- Schneider, Carolin Victoria, S30 (OS027), S515 (FRI250), S731 (SAT141)
- Schneider, Francis, S20 (OS010)
- Schneider, Franciso Javier Bustamante, S792 (SAT271)
- Schneider, Guenther, S460 (FRI122)
- Schneider, Hannah, S83 (OS113), S608 (FRI485), S622 (FRI514), S624 (FRI519), S634 (FRI536)
- Schneider, Julia Sophie, S662 (FRI596)
- Schneider, Kai Markus, S731 (SAT141)
- Schneller, Doris, S38 (OS042)
- Schnuriger, Aurélie, S297 (THU404)
- Schoeler, David, S533 (FRI283)
- Schoers, Barbara, S464 (FRI147)
- Schollmeier, Anja, S262 (THU337)
- Scholtes, Caroline, S72 (OS093), S868 (SAT429), S880 (SAT450)
- Schöneweis, Katrin, S845 (SAT385)
- Schöning, Wenzel, S374 (THU570), S380 (THU582), S937 (SAT597)
- Schotten, Clemens, S378 (THU579)
- Schouten, Jeoffrey, S546 (FRI312)
- Schrader, Jörg, S333 (THU481)
- Schramm, Christoph, S308 (THU435), S315 (THU447), S317 (THU452), S321 (THU458), S325 (THU466), S333 (THU481), S604 (FRI462), S823 (SAT341)
- Schreiber, Richard A., S43 (OS051)
- Schrevel, Catalina De, S736 (SAT155)
- Schröder, Sarah K., S748 (SAT181)
- Schroeder, Dawn, S511 (FRI241)
- Schropp, Jonas, S780 (SAT251)
- Schuermans, Sara, S396 (FRI012)
- Schuetz, Philipp, S905 (SAT529)
- Schulte, Benjamin, S893 (SAT505)
- Schulte, Janun, S361 (THU532)
- Schultheiss, Michael, S2 (GS003), S19 (OS008), S49 (OS063)
- Schulze-Bergkamen, Henning, S655 (FRI581)
- Schulze, Sarah, S463 (FRI146)
- Schulze zur Wiesch, Julian, S4 (GS006), S16 (OS003), S54 (OS069), S57 (OS072A), S582 (FRI385), S585 (FRI391), S823 (SAT341)
- Schulz, Martin, S353 (THU517), S354 (THU518)
- Schumacher, Jonas, S860 (SAT414)
- Schuppan, Detlef, S7 (GS009), S325 (THU466), S464 (FRI147)
- Schurich, Anna, S55 (OS070)
- Schuster, Catherine, S36 (OS038), S99 (OS142), S649 (FRI565), S738 (SAT160), S758 (SAT199)
- Schuster, Stefan, S788 (SAT264)
- Schwab, Andrew, S721 (SAT117)
- Schwabe, Christian, S824 (SAT343), S835 (SAT365), S871 (SAT435)
- Schwabenland, Marius, S2 (GS003)
- Schwabl, Philipp, S90 (OS127), S315 (THU449), S360 (THU529), S466 (FRI152), S472 (FRI164), S555 (FRI328), S629 (FRI527), S629 (FRI528), S753 (SAT191)
- Schwacha-Eipper, Birgit, S777 (SAT247)
- Schwantes-An, Tae-Hwi Linus, S936 (SAT596)
- Schwartz, Scott, S612 (FRI493)
- Schwarz, Caroline, S545 (FRI309), S555 (FRI328), S829 (SAT353), S830 (SAT354), S843 (SAT379)
- Schwarzinger, Michael, S41 (OS047)
- Schwarz, Kathleen, S866 (SAT425)
- Schwärzler, Julian, S126 (THU017)
- Schwarz, Michael, S545 (FRI309), S632 (FRI533)
- Schweiger, Sofia, S21 (OS011)
- Schweiggert, Sabrina, S262 (THU338)
- Schwinge, Dorothee, S604 (FRI462)
- Sciambra, Antonio, S212 (THU239)
- Sciattella, Paolo, S232 (THU281)
- Sciorio, Roberta, S425 (FRI057), S551 (FRI320)
- Scivetti, Paolo, S543 (FRI306)
- Scoppettuolo, Marco, S502 (FRI226)
- Scorletti, Eleonora, S731 (SAT141)
- Scott, Charlotte, S655 (FRI580)
- Scott, Emma A.H., S37 (OS040), S758 (SAT200)
- Scott, Melanie, S465 (FRI149)
- Scott, Nick, S541 (FRI302)
- Scott, Robert, S938 (SAT600)
- Scragg, Jadine, S437 (FRI080), S721 (SAT118)
- Scripcariu, Viorel, S107 (OS157)

Author Index

- Scudeller, Luigia, S223 (THU263)
Sebastián, David, S674 (SAT019)
Sebastiani, Giada, S31 (OS029), S614 (FRI497)
Sebens, Susanne, S470 (FRI159)
Sebesta, Christian, S545 (FRI309)
Sebode, Marcial, S224 (THU265), S308 (THU435), S321 (THU458), S333 (THU481), S604 (FRI462)
Sechi, Annalisa, S515 (FRI249)
Secka, Ousman, S258 (THU332)
Secomandi, Alice, S166 (THU093)
Seehofer, Daniel, S383 (THU590), S658 (FRI585), S904 (SAT528), S931 (SAT587)
Segalerba, Daniela, S515 (FRI249)
Segalés, Paula, S361 (THU530)
Segal-Salto, Michal, S27 (OS022)
Seghezzi, Michela, S751 (SAT186)
Sehrawat, Tejasav, S136 (THU033)
Seidel, Florine, S698 (SAT067)
Seidelin, Anne-Sofie, S533 (FRI284)
Seidemann, Lena, S658 (FRI585)
Seifert, Gabriel, S710 (SAT090)
Seifert, Hendrik, S383 (THU590)
Seif, Martha, S753 (SAT191)
Seitzer, Jessica, S58 (OS073)
Seitz, Susanne, S606 (FRI467)
Sekandarzad, Asieb, S313 (THU444)
Sekar, Revathi, S606 (FRI467), S703 (SAT079)
Selcanova, Svetlana Adamcova, S613 (FRI496)
Selfridge, Marion, S240 (THU297)
Selig, Roland, S737 (SAT158)
Selim, Ranya, S612 (FRI493)
Sellier, Floriane, S547 (FRI314)
Sellman, Bret, S411 (FRI033)
Selvapatt, Nowlan, S345 (THU505)
Selvaraj, Emmanuel, S320 (THU456), S320 (THU457), S321 (THU459), S322 (THU460), S425 (FRI058), S448 (FRI102), S452 (FRI108)
Semela, David, S192 (THU186), S937 (SAT598)
Semere, Gabriel, S765 (SAT215)
Semizarov, Dimitri, S549 (FRI317), S584 (FRI388)
Semmler, Georg, S11 (LB002), S18 (OS007), S24 (OS017), S90 (OS127), S92 (OS131), S354 (THU519), S359 (THU527), S428 (FRI062), S532 (FRI280), S535 (FRI287), S617 (FRI505), S618 (FRI506), S629 (FRI527), S629 (FRI528), S631 (FRI531)
Sempere, Elena Diago, S912 (SAT555)
Sempoux, Christine, S652 (FRI572)
Sem, Xiaohui, S42 (OS049)
Sendamarai, Anoop, S936 (SAT596)
Sener, Alper, S858 (SAT411)
Senfter, Daniel, S753 (SAT189)
Senkaya, Ali, S820 (SAT316)
Sennett, Caileen, S168 (THU097), S170 (THU099)
Senosiáin, Maria, S406 (FRI027)
Sen, Rajashree, S232 (THU280)
Senzolo, Marco, S306 (THU423), S358 (THU526), S627 (FRI524), S821 (SAT318)
Seo, Haeng Ran, S473 (FRI166)
Seok Lee, Byung, S921 (SAT569)
Seok Lee, Myoung, S452 (FRI108)
Seo, Satoru, S183 (THU167)
Seo, Suk, S770 (SAT234)
Seo, Yeon Seok, S283 (THU379), S625 (FRI520), S932 (SAT590)
Seo, Yoon-Seok, S746 (SAT178)
Seppänen, Wenla, S458 (FRI117), S690 (SAT052)
Sepp-Lorenzino, Laura, S58 (OS073)
Sequeira, José Pedro, S268 (THU349)
Serenari, Matteo, S794 (SAT273)
Serenio, Leandro Soares, S238 (THU292)
Sereti, Irini, S235 (THU287)
Serio, Ilaria, S578 (FRI376)
Serizawa, Reza, S154 (THU068), S331 (THU477)
Seron, Daniel, S149 (THU059)
Seror, Olivier, S504 (FRI228)
Serper, Marina, S89 (OS126), S546 (FRI311)
Serra, Dolors, S749 (SAT183)
Serraino, Diego, S821 (SAT318)
Serra, Marina, S732 (SAT144)
Serra, Miguel, S442 (FRI091), S902 (SAT523)
Serra, Nicola, S609 (FRI487)
Serrano, Daniel Bernal, S238 (THU292)
Serrano-Macia, Marina, S46 (OS056), S48 (OS060), S87 (OS122), S132 (THU027), S600 (FRI453), S679 (SAT029)
Serrano, Manuel, S673 (SAT018)
Serrano, Trinidad, S115 (OS169), S792 (SAT271)
Sessa, Anna, S530 (FRI276)
Sesso, Howard, S912 (SAT554)
Setiawan, Veronica, S79 (OS106)
Seto, Wai-Kay, S78 (OS105), S177 (THU154), S272 (THU358), S273 (THU360), S275 (THU364), S824 (SAT344), S852 (SAT400), S861 (SAT415)
Seufferlein, Thomas, S823 (SAT341)
Seu, Lillian, S831 (SAT357)
Seul ki, Han, S705 (SAT083)
Sevastianos, Vasilis, S840 (SAT374)
Sevinsky, Heather, S876 (SAT443)
Sexton, Joseph, S309 (THU437)
Seydi, Moussa, S23 (OS015)
Seyen, Minou Van, S580 (FRI383)
Sezgin, Orhan, S858 (SAT410)
Shabeeb, Reem Al, S785 (SAT260), S810 (SAT300)
Shabrawi, Ahmed El, S903 (SAT526)
Shadaker, Shaun, S213 (THU242), S214 (THU243), S216 (THU247), S216 (THU248), S219 (THU253), S221 (THU258), S233 (THU283), S234 (THU284), S267 (THU347), S587 (FRI395), S588 (FRI397), S590 (FRI400), S590 (FRI401)
Shadyab, Aladdin, S912 (SAT554)
Shafran, Stephen, S581 (FRI384)
Shagla, Eva, S573 (FRI367)
Shagrani, Mohammad Ali, S518 (FRI255)
Shah, Dipam, S810 (SAT300)
Shaheen, Abdel Aziz, S143 (THU045)
Shaheen, Abdel-Aziz, S323 (THU462), S323 (THU463)
Shah, Hasnain A., S625 (FRI520)
Shah, Naina, S134 (THU030)
Shahnavaz, Afshin, S30 (OS026)
Shah, Sabeen, S240 (THU295)
Shah, Sital, S594 (FRI409)
Shah, Syed Hassan Bin Usman, S302 (THU415), S560 (FRI339)
Shah, Vijay, S81 (OS110), S136 (THU033), S137 (THU034), S138 (THU037)
Shah, Wasiuddin, S558 (FRI335), S560 (FRI338)
Shalaby, Sarah, S821 (SAT318)
Shalimar, S433 (FRI072), S524 (FRI264), S620 (FRI511), S866 (SAT425)
Shamsaddini, Amirhossein, S67 (OS087), S130 (THU023)
Shan, Dandan, S699 (SAT069)
Shang, Dazhuang, S280 (THU373)
Shang, Jia, S838 (SAT369)
Shang, Ying, S119 (THU002), S189 (THU179)
Shankar, Sudha, S158 (THU075), S451 (FRI107), S454 (FRI110), S701 (SAT073)
Shannon, Eileen, S569 (FRI358)
Shao, Chen, S408 (FRI029)
Shao, Li, S215 (THU245)
Shapiro, David, S132 (THU026)
Shapiro, Ron, S897 (SAT513)
Sharaf, Madiha, S579 (FRI377)
Sharma, Ashish, S937 (SAT597)
Sharma, Mithun, S19 (OS008), S49 (OS063), S191 (THU184), S329 (THU474), S358 (THU525)
Sharma, Nupur, S34 (OS033), S128 (THU020), S528 (FRI273), S738 (SAT161), S752 (SAT188)
Sharma, Rohini, S11 (LB002), S108 (OS158), S372 (THU567), S374 (THU571), S376 (THU574)
Sharma, Samurailatpam Rajesh, S219 (THU254)
Sharma, Sanchit, S369 (THU547), S623 (FRI515), S633 (FRI534), S635 (FRI538)
Sharma, Shawn, S225 (THU267), S553 (FRI324), S591 (FRI403)
Sharma, Shilpee, S124 (THU012)
Sharma, Shvetank, S128 (THU020)
Sharma, Varun, S876 (SAT443), S878 (SAT448)
Sharon, Eilon, S31 (OS028), S37 (OS041), S409 (FRI030)
Sharvadze, Lali, S587 (FRI395), S590 (FRI400), S590 (FRI401)

- Shasthry, S Muralikrishna, S901 ([SAT521](#))
 Shasthry, Varsha, S349 ([THU510](#))
 Shaw, Blake, S462 ([FRI125](#))
 Shawcross, Debbie L., S51 ([OS065](#)), S902 ([SAT523](#))
 Shaw, David, S228 ([THU272](#))
 Shaw, Jawaid, S19 ([OS008](#)), S49 ([OS063](#))
 Shaw-Saliba, Katy, S235 ([THU287](#))
 Shcherbina, Anna, S31 ([OS028](#))
 Shea, Kristen, S436 ([FRI078](#))
 Shearer, Jessica, S885 ([SAT492](#))
 Shebel, Amr Al, S767 ([SAT218](#))
 Sheen, I-Shyan, S575 ([FRI371](#)), S576 ([FRI372](#))
 Sheikh, Aasim, S427 ([FRI060](#))
 Sheikh, Sabreena, S524 ([FRI264](#))
 Shekhtman, Louis, S851 ([SAT398](#)), S874 ([SAT440](#))
 ShengDi, Wu, S173 ([THU151](#))
 Sheng, Jifang, S165 ([THU090](#))
 Shen, Joanne X., S665 ([SAT002](#)), S756 ([SAT197](#))
 Shen, Liang, S877 ([SAT446](#))
 Shen, Ling, S69 ([OS090](#)), S831 ([SAT357](#))
 Shen, Lu, S215 ([THU245](#))
 Shen, Michael, S834 ([SAT363](#)), S847 ([SAT389](#))
 Shenvi, Swapna, S731 ([SAT142](#))
 Shen, Wei, S181 ([THU164](#))
 Shen, Xinping, S78 ([OS105](#))
 Shen, Yue, S173 ([THU151](#))
 Shepard, Andrea, S508 ([FRI236](#)), S918 ([SAT564](#))
 Shephard, Alex, S915 ([SAT559](#))
 Shephard, Cal, S110 ([OS161](#))
 Shepherd, Liz, S120 ([THU005](#))
 Sheridan, David, S493 ([FRI208](#))
 Sherlock, Sarah, S451 ([FRI107](#)), S454 ([FRI110](#)), S701 ([SAT073](#))
 Sherman, Morris, S3 ([GS004](#))
 Sheshadri, Somya, S19 ([OS008](#)), S49 ([OS063](#))
 She, Shaoping, S467 ([FRI153](#)), S638 ([FRI545](#))
 Sheth, Abhishek, S693 ([SAT058](#)), S934 ([SAT593](#))
 Shetty, Kirti, S779 ([SAT250](#))
 Shetty, Shishir, S195 ([THU192](#))
 Shewarega, Annabella, S935 ([SAT594](#))
 Shibolet, Oren, S148 ([THU056](#)), S790 ([SAT268](#))
 Shi, Dongyan, S66 ([OS086](#)), S357 ([THU524](#)), S402 ([FRI021](#)), S744 ([SAT171](#)), S744 ([SAT172](#)), S745 ([SAT173](#)), S803 ([SAT289](#))
 Shiffman, Mitchell, S318 ([THU453](#)), S427 ([FRI060](#))
 Shiha, Gamal, S479 ([FRI178](#))
 Shih-Yen Chan, Edwin, S869 ([SAT431](#))
 Shi, Juanjuan, S723 ([SAT122](#))
 Shi, Jun-Ping, S421 ([FRI050](#))
 Shi, Junping, S215 ([THU245](#))
 Shi, Lei, S879 ([SAT449](#))
 Shi, Liang, S56 ([OS071](#))
 Shilton, Sonjelle, S42 ([OS049](#)), S219 ([THU254](#)), S232 ([THU280](#)), S558 ([FRI335](#))
 Shimada, Yuji, S172 ([THU103](#))
 Shimakawa, Yusuke, S23 ([OS015](#)), S233 ([THU282](#)), S258 ([THU332](#)), S290 ([THU391](#)), S295 ([THU401](#))
 Shima, Toshihide, S448 ([FRI102](#)), S452 ([FRI108](#))
 Shimizu, Masahito, S563 ([FRI346](#))
 Shimizu, Norikazu, S1 ([GS001](#))
 Shim, Ju Hyun, S545 ([FRI310](#)), S842 ([SAT378](#))
 Shim, Wan Seob, S734 ([SAT151](#))
 Shingaki-Wells, Rachel, S613 ([FRI495](#))
 Shin, Hyun Phil, S870 ([SAT433](#))
 Shin, Jungwoo, S870 ([SAT433](#))
 Shiri-Sverdlov, Ronit, S144 ([THU046](#))
 Shi, Shaojun, S115 ([OS170](#)), S652 ([FRI574](#))
 Shiv Kumar, Sarin, S350 ([THU512](#))
 Shi, Xiaojun, S301 ([THU412](#)), S304 ([THU418](#))
 Shi, Yu, S344 ([THU504](#)), S347 ([THU509](#)), S636 ([FRI540](#))
 Shi, Zhenzhen, S252 ([THU319](#))
 Shlevin, Harold, S619 ([FRI509](#)), S623 ([FRI516](#))
 Shloma, Amir, S64 ([OS081](#)), S279 ([THU371](#)), S588 ([FRI396](#)), S774 ([SAT241](#)), S793 ([SAT272](#))
 Shoaie, Saeed, S68 ([OS089](#))
 Shokoohi, Pooya, S654 ([FRI577](#))
 Shoreibah, Mohamed, S33 ([OS031](#))
 Shoshkes-Carmel, Michal, S47 ([OS059](#))
 Shoukry, Naglaa, S675 ([SAT022](#))
 Shou, Weinian, S686 ([SAT045](#))
 Showalter, Megan, S721 ([SAT117](#))
 Shraga, Netta Rose Blondheim, S742 ([SAT166](#))
 Shrestha, Merica, S447 ([FRI100](#))
 Shrestha, Shreesh, S126 ([THU016](#))
 Shringarpure, Reshma, S719 ([SAT114](#))
 Shteyer, Eyal, S519 ([FRI256](#)), S521 ([FRI259](#))
 Shubina, Maria, S848 ([SAT391](#)), S850 ([SAT395](#))
 Shukla, Ruchi, S646 ([FRI561](#))
 Shukla, Umesh, S864 ([SAT422](#))
 Shulman, Gerald I., S690 ([SAT052](#)), S714 ([SAT104](#))
 Shumbayawonda, Elizabeth, S453 ([FRI109](#)), S525 ([FRI267](#))
 Sia, Daniela, S45 ([OS055](#))
 Sichelschmidt, Stefanie, S340 ([THU495](#))
 Sicras-Mainar, Antoni, S268 ([THU348](#)), S586 ([FRI393](#)), S587 ([FRI394](#))
 Siddiqui, Hamda, S197 ([THU196](#))
 Siddiqui, Mohammad, S701 ([SAT073](#))
 Sieberhagen, Cyril, S34 ([OS034](#))
 Siebert, Matthieu, S65 ([OS084](#))
 Siebner, Hartwig R., S340 ([THU496](#))
 Siegele-Brown, Chloe, S200 ([THU218](#))
 Siegele-Brown, Martin, S200 ([THU218](#))
 Sierralta, Armando, S137 ([THU034](#))
 Siersbæk, Majken, S423 ([FRI054](#)), S434 ([FRI074](#))
 Sievert, William, S342 ([THU501](#)), S441 ([FRI090](#)), S842 ([SAT377](#))
 Siew, Susan, S754 ([SAT193](#))
 Sifrim, Alejandro, S680 ([SAT032](#))
 Sigal, Michael, S309 ([THU436](#))
 Sigel, Keith, S160 ([THU080](#)), S455 ([FRI113](#))
 Sigon, Giordano, S159 ([THU078](#))
 Sigüenza, Rebeca, S459 ([FRI119](#))
 Sigurdardottir, Bryndis, S573 ([FRI366](#))
 Sihni, Choong-Ryoul, S404 ([FRI023](#))
 Sikaroodi, Masoumeh, S67 ([OS087](#)), S130 ([THU023](#))
 Silberstein, Francesca Ceccherini, S249 ([THU313](#)), S284 ([THU380](#))
 Sileo, Emily, S936 ([SAT596](#))
 Siletta, Marianna, S372 ([THU567](#))
 Silk, Rachel, S574 ([FRI369](#))
 Silva, Eliane, S268 ([THU349](#))
 Silva, Geraldine Da, S330 ([THU476](#))
 Silva, Giovanni, S137 ([THU034](#))
 Silva, Hugo, S408 ([FRI028](#))
 Silva, Luciana Diniz, S293 ([THU396](#)), S552 ([FRI323](#))
 Silva, Maria Azevedo, S190 ([THU182](#))
 Silva, Mario Jorge, S190 ([THU182](#)), S211 ([THU238](#))
 Silva, Vítor Macedo, S149 ([THU060](#))
 Silveira, Fabio, S137 ([THU034](#))
 Silvestri, Annalisa De, S578 ([FRI376](#))
 Simao, Adelia, S268 ([THU349](#))
 Simão, André L., S192 ([THU185](#))
 Simbrunner, Benedikt, S24 ([OS017](#)), S315 ([THU449](#)), S354 ([THU519](#)), S359 ([THU527](#)), S360 ([THU529](#)), S362 ([THU534](#)), S390 ([FRI003](#)), S466 ([FRI152](#)), S472 ([FRI164](#)), S502 ([FRI226](#)), S532 ([FRI280](#)), S535 ([FRI287](#)), S555 ([FRI328](#)), S617 ([FRI505](#)), S618 ([FRI506](#)), S629 ([FRI527](#)), S629 ([FRI528](#)), S631 ([FRI531](#)), S632 ([FRI533](#))
 Simeone, Irene, S659 ([FRI588](#))
 Simerzin, Alina, S47 ([OS059](#))
 Sim, Heewoo, S866 ([SAT426](#))
 Simionato, Francesca, S748 ([SAT180](#))
 Simioni, Paolo, S358 ([THU526](#)), S751 ([SAT186](#))
 Simões, Claudia Marquez, S817 ([SAT313](#))
 Simoesegenio, Melanie, S639 ([FRI548](#))
 Simões, Guilherme, S211 ([THU238](#))
 Simone, Fabio, S624 ([FRI517](#))
 Simonelli, Claudia, S232 ([THU281](#))
 Simone, Loredana, S908 ([SAT535](#))
 Simone, Paolo De, S815 ([SAT311](#))
 Simonetto, Douglas, S81 ([OS110](#)), S138 ([THU037](#))
 Simonin-Wilmer, Irving, S476 ([FRI172](#))
 Simón, Jorge, S87 ([OS122](#)), S673 ([SAT018](#))
 Simon, Michael, S912 ([SAT554](#))
 Simpson, Jesse, S155 ([THU070](#))
 Simpson, Kenneth J., S120 ([THU005](#))

Author Index

- Simsek, Halis, S858 ([SAT410](#)), S861 ([SAT416](#))
Sim, Sharmaine Jia Ying, S889 ([SAT499](#))
Sims, Karen, S848 ([SAT392](#)), S850 ([SAT396](#)), S851 ([SAT397](#)), S876 ([SAT443](#)), S878 ([SAT448](#))
Sinclair, Marie, S842 ([SAT377](#))
Singal, Amit, S214 ([THU244](#)), S377 ([THU575](#)), S508 ([FRI236](#)), S926 ([SAT577](#))
Singal, Ashwani, S81 ([OS110](#)), S137 ([THU034](#)), S154 ([THU069](#)), S209 ([THU234](#)), S773 ([SAT240](#))
Singeap, Ana-Maria, S573 ([FRI368](#))
Singh, Anirudh Kumar, S252 ([THU320](#))
Singh, Anshuman, S403 ([FRI022](#))
Singh, Brijendra, S741 ([SAT164](#))
Singh, Gurpreet, S613 ([FRI495](#))
Singh, Hitesh, S347 ([THU508](#))
Singh, Jennifer, S873 ([SAT439](#))
Singh, Khumukcham Lokeshwar, S219 ([THU254](#))
Singh, Mansi, S347 ([THU508](#))
Singh, Meenu, S350 ([THU513](#))
Singh, Namrata, S633 ([FRI534](#))
Singh, Nitesh, S855 ([SAT405](#))
Singh, Renu, S862 ([SAT417](#))
Singh, Shivendra, S751 ([SAT187](#))
Singh, Shiv Kumar, S85 ([OS118](#))
Singh, Shreya, S350 ([THU513](#))
Singh, Surender, S631 ([FRI530](#))
Singh, Veena, S232 ([THU280](#))
Singh, Virendra, S232 ([THU280](#)), S625 ([FRI520](#))
Singh, Yuvaraj, S235 ([THU286](#))
Sinharay, Ricky, S198 ([THU198](#))
Sinha, Rohit, S434 ([FRI075](#))
Sinkala, Edford, S23 ([OS015](#))
Sinn, Dong Hyun, S273 ([THU359](#)), S275 ([THU363](#)), S610 ([FRI488](#))
Siripon, Nipaporn, S772 ([SAT238](#)), S812 ([SAT305](#))
Siriwardena, Ajith, S104 ([OS152](#))
Sirlin, Claude, S74 ([OS098](#)), S422 ([FRI051](#)), S451 ([FRI107](#)), S454 ([FRI110](#)), S455 ([FRI112](#)), S701 ([SAT073](#))
Sirli, Roxana, S483 ([FRI186](#)), S505 ([FRI230](#)), S930 ([SAT585](#))
Sirmatel, Fatma, S858 ([SAT411](#))
Sironi, Marina, S651 ([FRI570](#))
Sironi, Sandro, S751 ([SAT186](#))
Si, Tengfei, S647 ([FRI563](#)), S818 ([SAT315](#))
Sitko, Marek, S585 ([FRI390](#)), S592 ([FRI406](#))
Situ, Jianwen, S249 ([THU312](#))
Siu, Lillian, S395 ([FRI010](#))
Sivanandan, Srinivasan, S762 ([SAT208](#))
Sivell, Chris, S188 ([THU178](#))
Sjöblom, Nelli, S327 ([THU469](#))
Sjöstedt, Sannia, S614 ([FRI498](#))
Skalicky, Susanna, S799 ([SAT283](#))
Skelton, Jessica, S55 ([OS070](#))
Skinner, Charlotte, S121 ([THU007](#)), S674 ([SAT020](#))
Skladany, Lubomir, S613 ([FRI496](#))
Skubic, Cene, S766 ([SAT217](#))
Skyttthe, Maria Kløjgaard, S434 ([FRI074](#))
Slack, Rob, S481 ([FRI182](#))
Slaets, Leen, S72 ([OS094](#))
Slater, Sarah, S108 ([OS158](#))
Slatinska, Janka, S593 ([THU408](#))
Sleiman, Ahmad, S245 ([THU304](#))
Slooter, Charlotte, S326 ([THU467](#))
Smaranda, Glia, S825 ([SAT345](#))
Smeaton, Laura, S544 ([FRI307](#))
Smets, Lena, S346 ([THU507](#)), S680 ([SAT032](#))
Smid, Vaclav, S671 ([SAT014](#))
Smith, Alexander, S909 ([SAT536](#))
Smith, Andrew, S684 ([SAT039](#))
Smith, David, S846 ([SAT386](#)), S853 ([SAT402](#))
Smith, Helen, S327 ([THU470](#))
Smith, Maren, S178 ([THU156](#))
Smith, Nate, S286 ([THU386](#)), S597 ([FRI416](#))
Smith, Rachel, S96 ([OS137](#))
Smith, Stuart, S220 ([THU256](#))
Smolic, Martina, S718 ([SAT113](#))
Smyk, Wiktor, S156 ([THU072](#)), S605 ([FRI464](#)), S607 ([FRI469](#))
Smyris, Andreas, S487 ([FRI196](#))
Snetselaar, Linda, S912 ([SAT554](#))
Soardo, Giorgio, S675 ([SAT021](#))
Sobesky, Rodolphe, S538 ([FRI296](#)), S800 ([SAT285](#)), S935 ([SAT595](#))
Sobolewski, Cyril, S645 ([FRI559](#)), S652 ([FRI572](#))
Sobrinho-Prados, Almudena, S676 ([SAT023](#))
Socaciu, Carmen, S141 ([THU042](#))
Socha, Piotr, S1 ([GS001](#)), S525 ([FRI267](#))
So, Delvin, S801 ([SAT287](#))
Sodergren, Mikael, S108 ([OS158](#))
Soerensen, Michael, S677 ([SAT026](#))
Soffredini, Roberta, S196 ([THU194](#))
Sofia, Michael J., S848 ([SAT391](#)), S848 ([SAT392](#)), S850 ([SAT395](#)), S850 ([SAT396](#)), S851 ([SAT397](#))
Sogni, Philippe, S41 ([OS047](#)), S392 ([FRI005](#)), S393 ([FRI007](#))
Sogukpinar, Özlem, S196 ([THU194](#))
Sohn, Joo Hyun, S160 ([THU079](#)), S224 ([THU264](#)), S435 ([FRI077](#)), S589 ([FRI398](#)), S728 ([SAT135](#)), S729 ([SAT136](#)), S883 ([SAT488](#))
Sohn, Won, S485 ([FRI191](#))
Soh, Shirleen, S694 ([SAT059](#))
Sojoodi, Mozhdah, S36 ([OS037](#)), S364 ([THU536](#)), S642 ([FRI553](#))
Sokal, Etienne, S535 ([FRI289](#)), S866 ([SAT425](#))
Solà, Elsa, S512 ([FRI244](#)), S896 ([SAT512](#)), S901 ([SAT522](#)), S902 ([SAT524](#)), S907 ([SAT532](#))
Solanki, Rushil, S898 ([SAT515](#))
Soldani, Cristiana, S758 ([SAT201](#))
Solé, Cristina, S896 ([SAT512](#)), S902 ([SAT524](#)), S907 ([SAT532](#))
Soler, Carmen, S749 ([SAT183](#))
Soler, María José, S149 ([THU059](#))
Soliman, Reham, S479 ([FRI178](#))
Solis, Francisco, S137 ([THU034](#))
Solitano, Virginia, S528 ([FRI272](#))
Sollors, Janina, S523 ([FRI262](#))
Solomon, Sunil Suhas, S544 ([FRI307](#))
Somaini, Lorenzo, S543 ([FRI306](#)), S559 ([FRI336](#))
Sombie, Roger, S23 ([OS015](#))
Somers, Nicky, S562 ([FRI344](#))
Sommacale, Daniele, S375 ([THU573](#)), S927 ([SAT578](#))
Sonavane, Amey, S19 ([OS008](#)), S49 ([OS063](#))
Sonderup, Mark, S23 ([OS015](#))
Song, Bin, S616 ([FRI503](#))
Song, Jiangao, S477 ([FRI174](#))
Song, Jingjing, S165 ([THU091](#))
Song, Jung Eun, S572 ([FRI365](#)), S916 ([SAT560](#))
Song, Si Young, S653 ([FRI575](#))
Song, Tieying, S182 ([THU165](#))
Song, Yanna, S549 ([FRI317](#)), S584 ([FRI388](#))
Song, Yeonhwa, S473 ([FRI166](#))
Song, Yu, S215 ([THU245](#))
Sonika, Ujjwal, S635 ([FRI538](#))
Sønnerborg, Isabella, S756 ([SAT197](#))
Sonneveld, Milan, S41 ([OS046](#)), S281 ([THU374](#)), S824 ([SAT344](#)), S852 ([SAT400](#)), S861 ([SAT415](#))
Sonzogni, Aurelio, S751 ([SAT186](#))
Sood, Siddharth, S622 ([FRI513](#))
Sood, Vikrant, S528 ([FRI273](#))
Soon, Gwyneth, S431 ([FRI068](#))
Sophie, Schlosser, S241 ([THU298](#))
Sørensen, Peter R., S758 ([SAT200](#))
Sørensen, Simon Langkjær, S35 ([OS036](#)), S131 ([THU024](#))
Sorge, Andrea, S503 ([FRI227](#))
Soria, Anna, S63 ([OS080](#)), S139 ([THU039](#)), S511 ([FRI242](#)), S512 ([FRI243](#)), S896 ([SAT512](#)), S901 ([SAT522](#)), S902 ([SAT524](#)), S907 ([SAT532](#))
Soria, Maria Eugenia, S589 ([FRI399](#))
Soriano, German, S64 ([OS082](#)), S886 ([SAT494](#)), S900 ([SAT520](#))
Soro, Alejandro Fernandez, S222 ([THU261](#))
Sosa, Alejandro Jiménez, S137 ([THU035](#))
Soto-González, Dulce Renée, S356 ([THU521](#))
Soto, Iris, S593 ([FRI407](#))
Sotty, Jules, S297 ([THU404](#))
Soucy, Geneviève, S675 ([SAT022](#)), S805 ([SAT293](#))
Soulette, Cameron, S247 ([THU308](#)), S841 ([SAT376](#))
Soulie, Alexandre, S582 ([FRI386](#))
Soumelis, Vassili, S245 ([THU304](#))
Sousa, Angela, S817 ([SAT313](#))
Sousa, Marta, S645 ([FRI559](#)), S652 ([FRI572](#))
Soussan, Patrick, S245 ([THU304](#)), S297 ([THU404](#))
Southern, David, S615 ([FRI499](#))
Sozzi, Vitina, S251 ([THU318](#))
Spaans, Johanna, S100 ([OS145](#))
Spagnolo, Elia, S192 ([THU185](#))
Spahr, Laurent, S457 ([FRI115](#))
Spalding, Duncan, S108 ([OS158](#))
Spallanzani, Andrea, S84 ([OS115](#))

- Spallotta, Francesco, S665 ([SAT002](#))
Spanier, B.W. Marcel, S338 ([THU491](#))
Spano, Jean-Philippe, S393 ([FRI007](#))
Sparchez, Zeno, S107 ([OS157](#)),
S664 ([FRI600](#)), S915 ([SAT559](#))
Spearman, Wendy, S23 ([OS015](#))
Spector, Seth, S227 ([THU270](#))
Spelman, Tim, S541 ([FRI302](#))
Spence, John, S338 ([THU490](#))
Spengler, Ulrich, S599 ([FRI451](#))
Sperling, Rhoda, S160 ([THU080](#)),
S455 ([FRI113](#)), S590 ([FRI402](#))
Sperling, Sebastian, S658 ([FRI585](#))
Sperl, Jan, S536 ([FRI290](#)), S593 ([FRI408](#))
Spicak, Julius, S536 ([FRI290](#))
Spiers, Harry, S104 ([OS152](#))
Spiers, Jessica, S934 ([SAT593](#))
Spiezia, Luca, S751 ([SAT186](#))
Spillman, Lynsey, S815 ([SAT310](#))
Spinner, Christoph, S582 ([FRI385](#))
Splith, Katrin, S497 ([FRI217](#)),
S663 ([FRI597](#))
Sporea, Ioan, S483 ([FRI186](#)), S502 ([FRI225](#)),
S505 ([FRI230](#)), S930 ([SAT585](#))
Sposito, Carlo, S789 ([SAT266](#))
Spoutz, Patrick, S126 ([THU016](#)),
S899 ([SAT518](#))
Spreafico, Anna, S395 ([FRI010](#))
Sprengers, Dirk, S516 ([FRI252](#))
Springer, David, S271 ([THU354](#))
Springer, Kylie, S612 ([FRI493](#))
Springfield, Christoph, S655 ([FRI581](#))
Sprinzl, Kathrin, S823 ([SAT341](#))
Sprinzl, Martin, S145 ([THU051](#)),
S823 ([SAT341](#))
Sprouse, Francis, S113 ([OS167](#))
Squillante, Maria, S609 ([FRI487](#))
Squires, Katherine, S73 ([OS095](#)),
S97 ([OS139](#))
Sridhar, Siddharth, S249 ([THU312](#))
Srikanth, Akshaya, S663 ([FRI598](#))
Srinivasan, Subash, S310 ([THU438](#))
Srinivasan, Parthi, S403 ([FRI022](#))
Sriphoosanaphan, Supachaya,
S772 ([SAT238](#)), S812 ([SAT305](#))
Sripongpun, Pimsiri, S186 ([THU175](#)),
S187 ([THU176](#)), S188 ([THU177](#)),
S722 ([SAT121](#))
Srisoonthorn, Nunthiya, S772 ([SAT238](#)),
S812 ([SAT305](#))
Srivastava, Ankur, S934 ([SAT593](#))
Sroda, Natalie, S483 ([FRI187](#))
Ssebyatika, George, S263 ([THU339](#))
Stacey, Duncan, S615 ([FRI499](#))
Stadlbauer, Vanessa, S68 ([OS088](#)),
S179 ([THU159](#)), S346 ([THU506](#))
Stæhr Madsen, Bjørn, S9 ([GS012](#))
Staels, Bart, S359 ([THU528](#)), S680 ([SAT031](#)),
S692 ([SAT055](#))
Stahl, Yannick, S250 ([THU315](#))
Stahmeyer, Jona T., S83 ([OS113](#))
Staiano, Laura, S551 ([FRI320](#))
Staib, Lawrence, S935 ([SAT594](#))
Stallmach, Andreas, S339 ([THU493](#))
Stal, Per, S423 ([FRI053](#)), S756 ([SAT197](#))
Staltner, Raphaela, S692 ([SAT056](#)),
S711 ([SAT093](#))
Stamm, Luisa M, S266 ([THU346](#)),
S834 ([SAT363](#)), S836 ([SAT366](#)),
S846 ([SAT388](#)), S847 ([SAT389](#))
Stamouli, Marilena, S68 ([OS089](#)),
S371 ([THU550](#)), S911 ([SAT540](#))
Stanciu, Carol, S573 ([FRI368](#))
Stanic, Tijana, S444 ([FRI094](#))
Stanila, Ana, S795 ([SAT276](#))
Stanitsas, Panagiotis, S37 ([OS041](#)),
S762 ([SAT208](#))
Stankevic, Evelina, S129 ([THU021](#))
Stanton, Jenny, S839 ([SAT372](#))
Stanton, Laura, S143 ([THU045](#))
Stanzione, Maria, S217 ([THU250](#)),
S938 ([SAT599](#))
Stapleton, Joshua, S134 ([THU030](#))
Starke, Ingemar, S751 ([SAT187](#))
Stärkel, Peter, S135 ([THU032](#)),
S736 ([SAT156](#))
Stark, Maria, S893 ([SAT507](#))
Stark, Myriam, S193 ([THU187](#))
Starlinger, Patrick, S470 ([FRI159](#)),
S788 ([SAT264](#)), S799 ([SAT283](#))
Stasi, Francesca Di, S617 ([FRI504](#))
Stathopoulou, Ioanna, S917 ([SAT562](#))
Stättermayer, Albert, S307 ([THU433](#)),
S308 ([THU435](#)), S315 ([THU449](#)),
S535 ([FRI287](#)), S617 ([FRI505](#)),
S618 ([FRI506](#)), S629 ([FRI527](#)),
S629 ([FRI528](#)), S631 ([FRI531](#)),
S632 ([FRI533](#)), S830 ([SAT354](#))
Stättermayer, Albert F, S829 ([SAT353](#))
Stauber, Rudolf E., S11 ([LB002](#)),
S192 ([THU185](#)), S346 ([THU506](#)),
S470 ([FRI159](#)), S854 ([SAT403](#))
Staub, Thérèse, S579 ([FRI377](#))
Staufer, Katharina, S354 ([THU518](#)),
S470 ([FRI159](#))
Staufer, Katharina Katharina,
S353 ([THU517](#))
Stauffer, Winston, S650 ([FRI568](#)),
S660 ([FRI591](#))
Stebbins, Jeffrey, S477 ([FRI174](#))
Stecher, Melanie, S339 ([THU493](#))
Steele, Staci, S88 ([OS124](#))
Steel, Kim, S871 ([SAT435](#))
Steenkiste, Christophe Van, S709 ([SAT089](#))
Stefanescu, Horia, S664 ([FRI600](#))
Stefanini, Benedetta, S79 ([OS107](#)),
S382 ([THU587](#))
Stefanini, Bernardo, S79 ([OS107](#)),
S166 ([THU093](#))
Steinacher, Daniel, S126 ([THU017](#))
Steinberg, Alexandra, S886 ([SAT493](#))
Stein, Lance, S779 ([SAT250](#))
Steinmann, Eike, S250 ([THU315](#)),
S257 ([THU329](#)), S263 ([THU339](#))
Steinmann, Jochen, S250 ([THU315](#))
Steinmann, Joerg, S250 ([THU315](#))
Steinmann, Silja, S604 ([FRI462](#))
Stekopytov, Stanislav, S530 ([FRI277](#))
Stella, Daniele, S249 ([THU313](#))
Stellbrink, Hans-Jürgen, S582 ([FRI385](#))
Stelzer, Dominikus, S80 ([OS108](#))
Stender, Stefan, S161 ([THU082](#)),
S450 ([FRI104](#)), S533 ([FRI284](#))
Stenico, Matteo, S49 ([OS062](#))
Stepanova, Maria, S154 ([THU069](#)),
S209 ([THU234](#)), S420 ([FRI048](#)),
S429 ([FRI064](#)), S445 ([FRI097](#)),
S447 ([FRI100](#)), S785 ([SAT260](#)),
S810 ([SAT300](#))
Stepanova, Tatyana, S4 ([GS006](#)),
S103 ([OS149](#)), S828 ([SAT351](#)),
S829 ([SAT352](#))
Stephan, Christoph, S15 ([OS001](#))
Stéphan, François, S349 ([THU511](#))
Stephan, Schmid, S241 ([THU298](#))
Sterling, Richard, S264 ([THU341](#))
Stern, Christiane, S506 ([FRI232](#)),
S833 ([SAT360](#)), S840 ([SAT373](#))
Sterneck, Martina, S54 ([OS069](#)),
S57 ([OS072A](#)), S893 ([SAT507](#))
Stevenson, Heather, S194 ([THU191](#)),
S470 ([FRI160](#)), S485 ([FRI190](#))
Stevens, Sarah, S853 ([SAT401](#))
Stever, Kim, S848 ([SAT391](#))
Stickel, Felix, S11 ([LB002](#))
Stift, Judith, S532 ([FRI280](#))
Stinson, Sara, S450 ([FRI104](#)), S523 ([FRI263](#))
Stockdale, Alexander, S23 ([OS015](#))
Stockhoff, Lena, S608 ([FRI485](#)),
S622 ([FRI514](#)), S624 ([FRI519](#)),
S634 ([FRI536](#))
Stoelinga, Anna, S307 ([THU433](#))
Stoffers, Philipp, S354 ([THU518](#))
Stoica, Oana, S573 ([FRI368](#))
Stojakovic, Tatjana, S466 ([FRI152](#)),
S469 ([FRI158](#)), S472 ([FRI164](#)),
S688 ([SAT049](#))
Stokman, Geurt, S681 ([SAT033](#)),
S685 ([SAT043](#)), S686 ([SAT044](#))
Stoll, Janis M., S518 ([FRI255](#)), S521 ([FRI259](#))
Stolz, Andrew, S142 ([THU043](#))
Stone, Joanne, S160 ([THU080](#))
Stoove, Mark, S541 ([FRI302](#)), S550 ([FRI318](#))
Stornauiolo, Gianfranco, S217 ([THU250](#))
Stornello, Caterina, S387 ([THU599](#))
Story, Alistair, S277 ([THU368](#))
Stothers, Lisa, S342 ([THU501](#))
Stoycheva, Antitsa, S853 ([SAT401](#))
St Pierre, Tim, S409 ([FRI031](#))
Strain, Alastair J, S751 ([SAT186](#))
Strand, Robin, S40 ([OS045](#))
Strängberg, Ellen, S751 ([SAT187](#)),
S843 ([SAT380](#))
Strassburg, Christian, S11 ([LB002](#)),
S381 ([THU585](#)), S599 ([FRI451](#)),
S883 ([SAT488](#)), S915 ([SAT559](#))
Strasser, Simone, S389 ([FRI002](#)),
S427 ([FRI060](#)), S842 ([SAT377](#)),
S876 ([SAT443](#)), S878 ([SAT448](#))
Strassl, Robert, S390 ([FRI003](#))
Straub, Beate, S655 ([FRI581](#))
Strauss, Maximilian, S500 ([FRI223](#))

Author Index

- Stravitz, Richard, S394 ([FRI008](#))
 Strazzabosco, Mario, S751 ([SAT186](#))
 Stroom, David, S193 ([THU188](#))
 Streinu-Cercel, Adrian, S829 ([SAT352](#))
 Streller, Lea, S313 ([THU444](#))
 Strevens, Helena, S94 ([OS133](#))
 Striedl, Philipp, S520 ([FRI257](#))
 Strnad, Pavel, S14 ([LB006](#)), S515 ([FRI250](#)), S520 ([FRI257](#)), S533 ([FRI282](#))
 Ströbel, Philipp, S85 ([OS118](#))
 Ströbel, Simon, S446 ([FRI099](#)), S481 ([FRI183](#)), S488 ([FRI197](#))
 Strobl, Karoline, S401 ([FRI019](#))
 Strocka, Steffen, S379 ([THU581](#))
 Stroescu, Cezar, S795 ([SAT276](#))
 Stroffolini, Giacomo, S825 ([SAT346](#))
 Ströh, Luisa J, S263 ([THU339](#))
 Stroh, Mark, S58 ([OS073](#))
 Stromar, Ivana Knezevic, S700 ([SAT070](#))
 Ström, Oskar, S413 ([FRI035](#))
 Stroumpouli, Evangelia, S908 ([SAT534](#))
 Strunz, Benedikt, S756 ([SAT197](#))
 Stucchi, Eliana, S96 ([OS136](#))
 Stueck, Ashley, S367 ([THU541](#)), S645 ([FRI560](#))
 Stupia, Roberta, S152 ([THU066](#))
 Sturm, Ekkehard, S518 ([FRI255](#)), S519 ([FRI256](#)), S521 ([FRI259](#))
 Sturm, Lukas, S710 ([SAT090](#))
 Sturm, Nathalie, S73 ([OS096](#)), S74 ([OS099](#))
 Stürzl, Michael, S83 ([OS114](#))
 Stvilia, Ketevan, S213 ([THU242](#))
 Suarez, Armando Andres Roca, S738 ([SAT160](#))
 Suarez, Emilio, S857 ([SAT409](#))
 Subhani, Mohsan, S934 ([SAT593](#))
 Subic-Levrero, Miroslava, S356 ([THU522](#))
 Subramanian, Ram, S339 ([THU494](#)), S887 ([SAT496](#))
 Sucher, Robert, S383 ([THU590](#)), S904 ([SAT528](#))
 Su, Chien-Yu, S294 ([THU398](#))
 Su, Chung-Wei, S575 ([FRI371](#)), S576 ([FRI372](#))
 Sucksdorff, Andrea, S121 ([THU006](#))
 Suda, Goki, S563 ([FRI346](#))
 Suddle, Abid, S134 ([THU030](#)), S639 ([FRI547](#)), S647 ([FRI563](#)), S771 ([SAT236](#)), S812 ([SAT304](#))
 Sugiyama, Aya, S229 ([THU274](#)), S260 ([THU335](#))
 Sugiyama, Masaya, S654 ([FRI579](#))
 Su, Grace, S883 ([SAT488](#))
 Suh, Jeong Ill, S916 ([SAT560](#))
 Suh, Kyung-Suk, S798 ([SAT281](#))
 Suh, Sanggyun, S798 ([SAT281](#))
 Su, Jie, S522 ([FRI261](#))
 Sukeepaisarnjaroen, Wattana, S499 ([FRI219](#)), S876 ([SAT443](#)), S878 ([SAT448](#))
 Suklan, Jana, S424 ([FRI055](#))
 Suk Lee, Jong, S469 ([FRI157](#))
 Sukriti, Sukriti, S105 ([OS153](#))
 Suksawatamnuay, Sirinporn, S772 ([SAT238](#)), S812 ([SAT305](#))
 Sulaiman, Lydia, S460 ([FRI121](#))
 Sulen, André, S665 ([SAT002](#)), S756 ([SAT197](#))
 Sulkowski, Mark, S544 ([FRI307](#))
 Sulkowski, Mark S, S836 ([SAT366](#))
 Sulk, Stefan, S11 ([LB002](#))
 Sullivan, Richard, S305 ([THU422](#))
 Sulpice, Laurent, S817 ([SAT312](#))
 Sulpice, Thierry, S717 ([SAT110](#))
 Sultan, Binta, S556 ([FRI330](#))
 Suman, S, S232 ([THU280](#))
 Sumida, Yoshio, S448 ([FRI102](#)), S452 ([FRI108](#))
 Sundaram, Vinay, S779 ([SAT250](#))
 Sundararajan, Vijaya, S842 ([SAT377](#))
 Sundararaj, Jeya Anice, S276 ([THU366](#))
 Sun, Donglin, S183 ([THU168](#))
 Sung, Pil Soo, S490 ([FRI202](#)), S820 ([SAT317](#)), S932 ([SAT589](#))
 Sun, Haoyu, S121 ([THU007](#))
 Sun, Huan, S385 ([THU594](#))
 SunilKumar, K, S884 ([SAT490](#))
 Sun, Junfeng, S552 ([FRI322](#)), S572 ([FRI364](#))
 Sun, Suwan, S744 ([SAT172](#))
 Sun, Xiu, S852 ([SAT399](#))
 Surace, Lidia, S292 ([THU394](#))
 Surana, Pallavi, S70 ([OS092](#))
 Surey, Julian, S556 ([FRI330](#))
 Surguladze, Sophia, S214 ([THU243](#)), S216 ([THU248](#))
 Suriano, Rob, S433 ([FRI073](#))
 Suriben, Rowena, S483 ([FRI187](#))
 Suri, Vithika, S4 ([GS006](#)), S103 ([OS149](#)), S244 ([THU302](#)), S247 ([THU308](#)), S828 ([SAT351](#)), S829 ([SAT352](#)), S835 ([SAT364](#)), S837 ([SAT368](#)), S841 ([SAT376](#)), S845 ([SAT385](#)), S862 ([SAT417](#))
 Susan, Davies, S7 ([GS009](#)), S695 ([SAT061](#))
 Sussman, Norman, S394 ([FRI008](#))
 Suthram, Silpa, S276 ([THU365](#))
 Sutter, Nancy, S422 ([FRI051](#))
 Suttichaimongkol, Tanita, S499 ([FRI219](#))
 Su, Tung-Hung, S852 ([SAT400](#)), S861 ([SAT415](#))
 Su, Wei-Wen, S45 ([OS054](#)), S595 ([FRI410](#)), S849 ([SAT393](#))
 Su, Ying-Hsiu, S264 ([THU341](#))
 Suyundikov, Anvar, S88 ([OS124](#))
 Svängård, Nils, S411 ([FRI033](#))
 Svarovskaia, Evguenia S, S244 ([THU302](#)), S247 ([THU309](#)), S251 ([THU318](#)), S845 ([SAT385](#))
 Svegiati-Baroni, Gianluca, S908 ([SAT535](#))
 Svenningsen, Jens, S121 ([THU006](#))
 Svicher, Valentina, S249 ([THU313](#)), S284 ([THU380](#)), S284 ([THU381](#)), S839 ([SAT371](#))
 Swadling, Leo, S55 ([OS070](#))
 Swain, Mark G, S143 ([THU045](#)), S323 ([THU462](#)), S323 ([THU463](#))
 Swain, Mark G., S94 ([OS134](#))
 Swanson, Kelly, S684 ([SAT039](#))
 Sweetser, Marianne T., S60 ([OS075](#))
 Swenson, Eugene, S1 ([GS001](#)), S526 ([FRI268](#))
 Swift, Brandon, S328 ([THU472](#)), S335 ([THU485](#))
 Syanda, Adam, S140 ([THU040](#))
 Sydor, Svenja, S378 ([THU579](#)), S682 ([SAT035](#))
 Symons, Julian, S846 ([SAT386](#)), S853 ([SAT401](#)), S853 ([SAT402](#))
 Syn, Wing-Kin, S682 ([SAT035](#)), S689 ([SAT050](#))
 Sypsa, Vana, S218 ([THU251](#))
 Syriha, Antonia, S917 ([SAT562](#))
 Syversen, Silje W, S309 ([THU437](#))
 Szalay, Ferenc, S1 ([GS001](#))
 Szczepankiewicz, Benedykt, S605 ([FRI464](#))
 Szekeres, Thomas, S359 ([THU527](#))
 Taanman, Jan-Willem, S668 ([SAT008](#))
 Tabacelia, Daniela, S795 ([SAT276](#))
 Tabak, Fehmi, S858 ([SAT411](#))
 Tabernero, David, S255 ([THU325](#)), S257 ([THU330](#))
 Tabibiazar, Ray, S470 ([FRI159](#))
 Taborelli, Martina, S821 ([SAT318](#))
 Tabung, Fred, S912 ([SAT554](#))
 Tacconi, Stefano, S763 ([SAT211](#))
 Tacher, Vania, S375 ([THU573](#))
 Taci, Stela, S573 ([FRI367](#))
 Tacke, Frank, S11 ([LB003](#)), S83 ([OS114](#)), S151 ([THU063](#)), S309 ([THU436](#)), S438 ([FRI084](#)), S562 ([FRI345](#)), S586 ([FRI393](#)), S684 ([SAT040](#)), S823 ([SAT341](#))
 Taddei, Tamar, S89 ([OS126](#))
 Taddei, Tamar H, S223 ([THU262](#)), S227 ([THU270](#))
 Tae-Hwi, Linus Schwantes-An, S30 ([OS027](#))
 Tae Yoon, Ki, S484 ([FRI189](#))
 Tafaj, Irgen, S573 ([FRI367](#))
 Tag, Carmen G., S748 ([SAT181](#))
 Tagkou, Nikoletta Maria, S457 ([FRI115](#))
 Tahata, Yuki, S563 ([FRI346](#))
 Taha, Yusri, S567 ([FRI355](#))
 Taheri, Ehsaneh, S228 ([THU273](#))
 Tahir, Muhammad Nauman, S934 ([SAT593](#))
 Tahir, Waleed, S708 ([SAT088](#))
 Taibi, Chiara, S808 ([SAT297](#))
 Tai, Chia-Hung, S575 ([FRI371](#)), S576 ([FRI372](#))
 Tai, Chi-Ming, S595 ([FRI410](#))
 Tai, Dean, S32 ([OS030](#)), S431 ([FRI068](#)), S468 ([FRI155](#)), S481 ([FRI181](#)), S486 ([FRI194](#)), S493 ([FRI207](#)), S619 ([FRI509](#)), S623 ([FRI516](#))
 Tailleux, Anne, S680 ([SAT031](#))
 Tailor, Falguni, S698 ([SAT066](#))
 Tait, Paul, S108 ([OS158](#))
 Takada, Hitomi, S387 ([THU598](#))
 Takahashi, Hirokazu, S430 ([FRI067](#)), S875 ([SAT442](#))
 Takahashi, Kazuki, S260 ([THU335](#)), S260 ([THU336](#))

- Takahashi, Satoru, S702 (SAT076)
 Takami, Taro, S563 (FRI346)
 Takaura, Kenta, S379 (THU580)
 Takebe, Takanori, S673 (SAT017)
 Takehara, Tetsuo, S563 (FRI346), S864 (SAT422)
 Tak, Hyoseon, S246 (THU306), S247 (THU307)
 Takikawa, Yasuhiro, S563 (FRI346)
 Takkenberg, Bart, S893 (SAT506)
 Tak, Won Young, S377 (THU576), S572 (FRI365), S916 (SAT560)
 Talat, Arslan, S813 (SAT307)
 Talbäck, Mats, S24 (OS016), S119 (THU002)
 Talbot, Thomas, S108 (OS158), S383 (THU588)
 Taljaard, Jantjie, S23 (OS015)
 Talukdar, Anjan Jyoti, S299 (THU409)
 Tamaki, Nobuharu, S74 (OS098), S379 (THU580), S414 (FRI037), S422 (FRI051)
 Tamandl, Dietmar, S532 (FRI280), S921 (SAT570)
 Tambucci, Roberto, S535 (FRI289)
 Tam, Edward, S338 (THU490), S544 (FRI308), S547 (FRI313)
 Tam, Joshua, S364 (THU536)
 Tamminga, Matthias, S224 (THU265)
 Tampaki, Athena, S218 (THU251)
 Tam, Steve Yew-chong, S567 (FRI354)
 Tam, Vincent, S110 (OS161)
 Tanabe, Kenneth K., S36 (OS037), S364 (THU536), S642 (FRI553)
 Tanaka, Atsushi, S314 (THU445), S600 (FRI454)
 Tanaka, Junko, S229 (THU274), S260 (THU335), S260 (THU336)
 Tanaka, Shohei, S379 (THU580)
 Tanaka, Yasuhito, S13 (LB004B), S272 (THU358), S295 (THU401), S824 (SAT344), S875 (SAT442), S881 (SAT453)
 Tanang, Alexandre Pissewoewoe, S373 (THU569)
 Tanashchuk, Elena, S574 (FRI370)
 Tan, Chee-Kiat, S919 (SAT566)
 Tandoi, Francesco, S775 (SAT243)
 Tandon, Manish, S866 (SAT425)
 Tandon, Puneeta, S338 (THU490), S339 (THU494), S511 (FRI241), S631 (FRI530), S887 (SAT496), S890 (SAT500)
 Taneja, Sunil, S631 (FRI530)
 Tan, Ek Khoon, S815 (SAT311)
 Tang, An, S456 (FRI114)
 Tang, Jinglin, S763 (SAT210)
 Tangkijvanich, Pisit, S876 (SAT443)
 Tang, Liang-Jie, S431 (FRI069)
 Tang, Liangjie, S421 (FRI050)
 Tang, Lydia, S863 (SAT419)
 Tang, Shanghong, S22 (OS014)
 Tang, Sunny, S848 (SAT391)
 Tang, Tianyu, S636 (FRI540)
 Tanguy, Marion, S127 (THU019)
 Tangvoraphonkchai, Kawin, S499 (FRI219)
 Tang, Wei, S642 (FRI553)
 Tang, Weiming, S557 (FRI332), S557 (FRI333)
 Tang, Xia-Han, S133 (THU028)
 Tang, Yanan, S865 (SAT423)
 Tan, Hiang Keat, S19 (OS008), S49 (OS063)
 Tan, Hua, S853 (SAT402)
 Tanios, Fady, S151 (THU063)
 Tan, Jaclyn Yizhen, S890 (SAT501)
 Tanna, Gian Luca Di, S286 (THU386)
 Tan, Susanna, S251 (THU318)
 Tantai, Xinxing, S883 (SAT488)
 Tan, Terence, S919 (SAT566)
 Tan, Wei Lian, S538 (FRI294)
 Tan, Yong Chuan, S298 (THU406), S877 (SAT446)
 Tan, Zhi, S491 (FRI203)
 Tao, Yusha, S557 (FRI332), S557 (FRI333)
 Tapia, Graciela, S487 (FRI195)
 Tapis, Monica, S137 (THU034)
 Tapper, Elliot, S81 (OS110), S167 (THU094)
 Tarai, Sambit, S683 (SAT038)
 Targher, Giovanni, S421 (FRI050), S431 (FRI069)
 Tariq, Muhammad, S240 (THU295)
 Tarlow, Branden, S116 (OS173)
 Tarp, Jens M., S29 (OS025)
 Tartof, Sara, S831 (SAT356)
 Tashkent, Yasmina, S898 (SAT516)
 Tas, Yagmur Cetin, S693 (SAT058)
 Tata, Kristi, S242 (THU299)
 Tata, Xhimi, S564 (FRI347)
 Tatche, Maria Colome, S395 (FRI009)
 Tateishi, Ryosuke, S563 (FRI346)
 Tateno, Chise, S252 (THU319)
 Tatsumi, Tomohide, S563 (FRI346)
 Täubel, Jörg, S58 (OS073), S460 (FRI121)
 Taubert, Richard, S308 (THU435), S317 (THU452), S634 (FRI536), S783 (SAT257), S784 (SAT259), S809 (SAT298)
 Taub, Rebecca, S14 (LB005), S32 (OS030), S75 (OS101), S87 (OS121), S711 (SAT094)
 Taura, Kojiro, S183 (THU167)
 Tauwaldt, Jan, S566 (FRI352)
 Tavabie, Oliver, S371 (THU550), S771 (SAT236)
 Tavares, Ludgero, S706 (SAT085)
 Tavelli, Alessandro, S284 (THU381)
 Tayek, John, S142 (THU043)
 Taylor, Ally, S411 (FRI033)
 Taylor, Guy, S437 (FRI080), S721 (SAT118)
 Taylor, James, S483 (FRI187)
 Taylor-Robinson, Simon, S493 (FRI208)
 Tay, Wei Xuan, S567 (FRI354)
 Tay, Yuh Ling Amy, S877 (SAT446)
 Tebeka, Nchimunya Nelisa, S140 (THU040)
 Teckman, Jeffrey, S14 (LB006)
 Teerlink, Craig, S30 (OS027)
 Teferi, Gebeyehu, S574 (FRI369)
 Teixeira, Rosangela, S293 (THU396)
 Teixeira, Sofia, S282 (THU377)
 Tejedor-Tejada, Javier, S127 (THU018), S792 (SAT270)
 Teker, Tufan, S861 (SAT416)
 Telep, Laura, S560 (FRI340)
 Telford, Alison, S526 (FRI269)
 Tellado, Álex García, S624 (FRI518), S774 (SAT242)
 Téllez, Érica, S361 (THU531)
 Téllez, Luis, S502 (FRI226)
 Temmerman, Frederik, S516 (FRI252)
 ten Broek, Richard, S525 (FRI266)
 Tenca, Andrea, S312 (THU441)
 Teng, Wei, S373 (THU568), S386 (THU596), S575 (FRI371), S576 (FRI372)
 Teng, Xiao, S679 (SAT030)
 ten Hove, Marit, S487 (FRI196)
 Teniente, Aina, S199 (THU199)
 Tenorio, Laura, S137 (THU034)
 Tenta, Roxani, S908 (SAT534)
 Tenuzzo, Bernardetta Anna, S763 (SAT211)
 Tenzer, Stefan, S464 (FRI147)
 Teo, SL, S868 (SAT428)
 Teoule, François, S17 (OS006), S101 (OS146), S250 (THU314)
 Terai, Shuji, S28 (OS023), S563 (FRI346)
 Tergast, Tammo Lambert, S893 (SAT505)
 Terkelsen, Mike, S37 (OS040), S423 (FRI054), S758 (SAT200)
 Terrabuio, Debora Raquel, S317 (THU452)
 Terracciano, Daniela, S769 (SAT233)
 Terracciano, Luigi, S528 (FRI272)
 Terracciano, Luigi Maria, S660 (FRI592)
 Terrault, Norah, S33 (OS031), S79 (OS106), S160 (THU080), S210 (THU235), S769 (SAT232), S797 (SAT278)
 Terreni, Natalia, S578 (FRI376)
 Terrin, Maria, S528 (FRI272)
 Terris, Benoit, S392 (FRI005)
 Terstappen, Leon, S707 (SAT086)
 Testa, Giuliano, S805 (SAT292)
 Testoni, Barbara, S246 (THU306), S247 (THU307)
 Teti, Elisabetta, S581 (FRI384)
 Tetri, Brent, S451 (FRI107), S701 (SAT073)
 Tetzlaff, Marcus, S325 (THU466)
 Teufel, Andreas, S523 (FRI262), S606 (FRI466), S928 (SAT580)
 Teumer, Alexander, S515 (FRI250)
 Tevethia, Harshvardhan, S53 (OS066), S347 (THU508), S397 (FRI014)
 Thabut, Dominique, S393 (FRI007), S506 (FRI232), S630 (FRI529)
 Thacker, Leroy, S19 (OS008), S49 (OS063), S339 (THU494), S887 (SAT496)
 Thaimai, Panarat, S772 (SAT238), S812 (SAT305)
 Thain, Collette, S96 (OS137)
 Thakur, Niharika, S889 (SAT499)
 Thallinger, Gerhard, S696 (SAT063)
 Thamer, Mae, S341 (THU497)
 Thanabalasingham, Gaya, S433 (FRI073)
 Thanapirom, Kessarinn, S668 (SAT008), S772 (SAT238), S812 (SAT305)
 Thanawala, Vaidehi, S69 (OS090)

Author Index

- Thangapandi, Veera Raghavan, S11 ([LB002](#))
 Thanneeru, Priya, S138 ([THU037](#))
 Than, Nwe Ni, S934 ([SAT593](#))
 Thapar, Manish, S60 ([OS075](#))
 Thapar, Shalini, S397 ([FRI014](#))
 Thebaut, Alice, S514 ([FRI248](#))
 Thennati, Rajamannar, S710 ([SAT091](#))
 Theodore, Dickens, S12 ([LB004A](#)),
 S13 ([LB004B](#)), S288 ([THU389](#)),
 S288 ([THU390](#)), S291 ([THU393](#)),
 S873 ([SAT439](#)), S875 ([SAT441](#)),
 S880 ([SAT452](#)), S881 ([SAT453](#))
 Therapondos, George, S432 ([FRI070](#))
 Thévenot, Thierry, S270 ([THU352](#))
 Theysohn, Jens, S378 ([THU579](#))
 Thibaud, Damy, S532 ([FRI281](#))
 Thibault-Sogorb, Tristan, S475 ([FRI170](#))
 Thibault, Vincent, S258 ([THU331](#))
 Thibaut, Morgane, S680 ([SAT031](#))
 Thiele, Maja, S2 ([GS002](#)), S9 ([GS012](#)),
 S25 ([OS018](#)), S35 ([OS036](#)),
 S129 ([THU021](#)), S130 ([THU022](#)),
 S131 ([THU024](#)), S144 ([THU046](#)),
 S434 ([FRI074](#)), S438 ([FRI084](#)),
 S475 ([FRI171](#)), S500 ([FRI223](#))
 Thi, Emily P., S848 ([SAT391](#)), S848 ([SAT392](#)),
 S850 ([SAT395](#)), S850 ([SAT396](#)),
 S851 ([SAT397](#)), S876 ([SAT443](#)),
 S878 ([SAT448](#))
 Thiercelin, Henriette, S584 ([FRI389](#))
 Thimme, Robert, S2 ([GS003](#)), S54 ([OS068](#)),
 S100 ([OS143](#)), S196 ([THU194](#)),
 S657 ([FRI583](#)), S710 ([SAT090](#)),
 S823 ([SAT341](#))
 Thing, Mira, S331 ([THU477](#)), S499 ([FRI220](#))
 Thioubou, Mame Aisse, S304 ([THU419](#))
 Thirard, Anaïs, S124 ([THU012](#))
 Thirlwell, Kayleigh, S85 ([OS117](#))
 Thi, Viet Loan Dao, S100 ([OS143](#)),
 S262 ([THU338](#)), S265 ([THU344](#))
 Thoma, Eva, S481 ([FRI183](#))
 Thomaides-Brears, Helena, S424 ([FRI056](#)),
 S433 ([FRI073](#))
 Thomas, Anna, S432 ([FRI070](#))
 Thomas, James, S147 ([THU054](#))
 Thomas, Lutz, S15 ([OS001](#))
 Thomas, Rachel, S653 ([FRI576](#))
 Thomas, Robert, S108 ([OS158](#))
 Thomas, Sherin, S51 ([OS064](#))
 Thomas, Sherin Sarah, S221 ([THU259](#))
 Thompson, Alexander, S266 ([THU346](#)),
 S498 ([FRI218](#)), S541 ([FRI302](#)),
 S550 ([FRI318](#)), S842 ([SAT377](#)),
 S872 ([SAT437](#))
 Thompson, Clare, S488 ([FRI198](#))
 Thompson, Hayley, S538 ([FRI295](#))
 Thompson-Jones, Helen, S548 ([FRI316](#))
 Thompson, Laura, S797 ([SAT278](#))
 Thompson, Richard J., S518 ([FRI255](#)),
 S519 ([FRI256](#)), S521 ([FRI259](#))
 Thomsen, Karen L., S51 ([OS065](#))
 Thomsen, Karen Louise, S344 ([THU503](#)),
 S677 ([SAT026](#)), S902 ([SAT523](#)),
 S903 ([SAT526](#))
 Thoraval, Francoise Roudot, S532 ([FRI281](#))
 Thorburn, Douglas, S96 ([OS137](#)),
 S335 ([THU484](#))
 Thordardottir, Marianna, S573 ([FRI366](#))
 Thordjmann, Thierry, S767 ([SAT218](#))
 Thorell, Anders, S665 ([SAT002](#))
 Thorens, Bernard, S710 ([SAT091](#))
 Thorhauge, Katrine, S2 ([GS002](#)), S9 ([GS012](#)),
 S35 ([OS036](#)), S131 ([THU024](#)),
 S475 ([FRI171](#)), S515 ([FRI250](#))
 Thorne, Claire, S203 ([THU222](#))
 Thorne, James, S104 ([OS151](#))
 Thornton, Karla, S587 ([FRI395](#)),
 S590 ([FRI400](#)), S590 ([FRI401](#))
 Thornton, Zak, S256 ([THU328](#))
 Threadgold, Georgia, S44 ([OS053](#))
 Thrift, Aaron, S147 ([THU054](#))
 Thuener, Theresa, S308 ([THU434](#))
 Thuluvath, Paul J., S19 ([OS008](#)),
 S48 ([OS061](#)), S49 ([OS063](#)),
 S339 ([THU494](#)), S787 ([SAT263](#)),
 S887 ([SAT496](#))
 Thumann, Christine, S738 ([SAT160](#))
 Thuraijah, Prem Harichander,
 S567 ([FRI354](#))
 Thursz, Mark, S34 ([OS034](#)), S121 ([THU007](#)),
 S122 ([THU008](#)), S124 ([THU013](#)),
 S132 ([THU026](#)), S135 ([THU031](#)),
 S140 ([THU040](#)), S179 ([THU158](#)),
 S185 ([THU173](#)), S188 ([THU178](#)),
 S258 ([THU332](#)), S295 ([THU401](#)),
 S352 ([THU516](#)), S444 ([FRI094](#)),
 S674 ([SAT020](#))
 Tian, Hua, S266 ([THU346](#))
 Tiede, Anja, S608 ([FRI485](#)), S622 ([FRI514](#)),
 S624 ([FRI519](#)), S634 ([FRI536](#))
 Tihy, Matthieu, S754 ([SAT192](#))
 Tilg, Herbert, S126 ([THU017](#)), S537 ([FRI292](#))
 Tilleul, Patrick, S393 ([FRI007](#))
 Tillman, Erik, S719 ([SAT114](#))
 Timm, Jörg, S825 ([SAT345](#))
 Tiniakos, Dina, S7 ([GS009](#)), S437 ([FRI081](#))
 Tinker, Lesley, S912 ([SAT554](#))
 Tipton, Tom, S57 ([OS072A](#))
 Tiribelli, Claudio, S433 ([FRI071](#))
 Tirona, Kattleya, S313 ([THU443](#))
 Tirucherai, Giridhar, S687 ([SAT046](#))
 Titos, Esther, S674 ([SAT019](#))
 Tizzard, Sarah, S551 ([FRI321](#))
 Tjandra, Douglas, S622 ([FRI513](#))
 T'jollyn, Huybrecht, S838 ([SAT370](#))
 Tjwa, E.T.T.L., S306 ([THU431](#)), S524 ([FRI265](#))
 Tkachuk, Bryce, S323 ([THU463](#))
 Tobias, Deirdre, S912 ([SAT554](#))
 Todo, Tsuyoshi, S377 ([THU575](#))
 Todt, Daniel, S250 ([THU315](#)),
 S257 ([THU329](#))
 Todua, Manana, S590 ([FRI401](#))
 Toet, Karin, S677 ([SAT025](#))
 Tofteng, Flemming, S331 ([THU477](#))
 Tokat, Yaman, S782 ([SAT255](#))
 Tokunaga, Katsushi, S654 ([FRI579](#))
 Tolenaars, Dagmar, S601 ([FRI457](#)),
 S603 ([FRI461](#)), S653 ([FRI576](#))
 Toma, Marieta, S599 ([FRI451](#))
 Tomasello, Lidia, S436 ([FRI079](#))
 Tomasiewicz, Krzysztof, S565 ([FRI350](#)),
 S585 ([FRI390](#))
 Tomasi, Melissa, S428 ([FRI061](#)),
 S668 ([SAT007](#)), S675 ([SAT021](#))
 Tomas, Myreen, S73 ([OS095](#))
 Tomassoli, Giovanni, S839 ([SAT371](#))
 Tomé, Santiago, S127 ([THU018](#))
 Tometten, Lukas, S339 ([THU493](#))
 Tomez, Sabine, S545 ([FRI309](#))
 Tomlinson, Jeremy, S39 ([OS044](#))
 Tommaso, Luca Di, S372 ([THU567](#))
 Tonascia, James, S451 ([FRI107](#)),
 S701 ([SAT073](#))
 Tong, Haley, S764 ([SAT212](#))
 Tong, Steven YC, S305 ([THU422](#))
 Tonini, Maria Manuela, S7 ([GS009](#))
 Toniutto, Pierluigi, S908 ([SAT535](#))
 Tonon, Marta, S18 ([OS007](#)), S49 ([OS062](#)),
 S92 ([OS131](#)), S894 ([SAT508](#)),
 S895 ([SAT511](#))
 Topa, Matilde, S223 ([THU263](#))
 Topazian, Mark, S19 ([OS008](#)), S49 ([OS063](#))
 Törnell, Andreas, S186 ([THU174](#))
 Toro, Luis, S137 ([THU034](#))
 Torp, Nikolaj, S2 ([GS002](#)), S9 ([GS012](#)),
 S129 ([THU021](#)), S131 ([THU024](#)),
 S475 ([FRI171](#))
 Torralba, Miguel, S184 ([THU170](#)),
 S826 ([SAT347](#))
 Torralbo, Manuel, S555 ([FRI329](#))
 Torras, Xavier, S91 ([OS128](#)), S627 ([FRI523](#))
 Torre, Aldo, S19 ([OS008](#)), S49 ([OS063](#)),
 S176 ([THU153](#)), S487 ([FRI195](#))
 Torrens, Maria, S658 ([FRI587](#))
 Torre, Pietro, S425 ([FRI057](#)),
 S551 ([FRI320](#))
 Torres, Daniel Rodrigo, S85 ([OS117](#))
 Torres, Ferran, S370 ([THU548](#)),
 S512 ([FRI244](#)), S625 ([FRI520](#))
 Torres, Gloria, S658 ([FRI587](#))
 Torres, Jason, S842 ([SAT377](#))
 Torres, Joana, S537 ([FRI293](#))
 Torres, Maria Corina Plaz, S39 ([OS044](#))
 Torres, Maria Corinna Plaz, S578 ([FRI376](#))
 Torres-Martín, Miguel, S45 ([OS055](#))
 Tortora, Annalisa, S908 ([SAT535](#))
 Tortora, Raffaella, S769 ([SAT233](#)),
 S938 ([SAT599](#))
 Torzilli, Guido, S758 ([SAT201](#))
 Tosetti, Giulia, S223 ([THU263](#)),
 S623 ([FRI515](#))
 Toso, Christian, S317 ([THU452](#)),
 S754 ([SAT192](#))
 Toucheffeu, Yann, S5 ([GS007](#))
 Tougeron, David, S372 ([THU566](#))
 Touti, Faycal, S508 ([FRI236](#))
 Touti, Fayçal, S918 ([SAT564](#))
 Tout, Issam, S245 ([THU304](#))
 Tovoli, Francesco, S79 ([OS107](#))
 Toy, Dana, S794 ([SAT274](#))
 Toyoda, Hidenori, S17 ([OS005](#)),
 S430 ([FRI067](#)), S875 ([SAT442](#))

- Tozun, Nurdan, S858 (SAT410), S861 (SAT416)
- Tozzi, Giulia, S161 (THU081)
- Trafali, Despina, S218 (THU251)
- Trammell, Samuel, S121 (THU006)
- Trampert, David, S603 (FRI461)
- Tranah, Thomas H., S51 (OS065)
- Tranah, Tom H, S902 (SAT523)
- Tran, Henri, S372 (THU566)
- Tran, Sarah, S675 (SAT022)
- Tran, Tram, S508 (FRI236), S918 (SAT564)
- Trasino, Steven, S133 (THU028)
- Traub, Julia, S68 (OS088)
- Trauner, Michael, S18 (OS007), S24 (OS017), S92 (OS131), S126 (THU017), S315 (THU449), S318 (THU453), S335 (THU484), S354 (THU519), S359 (THU527), S360 (THU529), S390 (FRI003), S452 (FRI108), S469 (FRI158), S470 (FRI159), S472 (FRI164), S515 (FRI250), S532 (FRI280), S535 (FRI287), S555 (FRI328), S617 (FRI505), S618 (FRI506), S629 (FRI527), S629 (FRI528), S631 (FRI531), S632 (FRI533), S688 (SAT049), S753 (SAT189), S760 (SAT204), S829 (SAT353), S830 (SAT354), S854 (SAT403), S919 (SAT565), S921 (SAT570)
- Trauth, Janina, S585 (FRI391)
- Trautwein, Christian, S7 (GS009), S14 (LB006), S193 (THU187), S339 (THU493), S385 (THU594), S515 (FRI250), S520 (FRI257), S654 (FRI578), S729 (SAT137)
- Traylor, James, S765 (SAT214)
- Trebicka, Jonel, S2 (GS002), S11 (LB002), S21 (OS011), S353 (THU517), S354 (THU518), S362 (THU533), S502 (FRI226), S883 (SAT488), S895 (SAT510)
- Treem, Will, S491 (FRI204)
- Treeprasertsuk, Sombat, S19 (OS008), S49 (OS063)
- Tree, Timothy, S809 (SAT298)
- Trehanpati, Nirupma, S197 (THU196)
- Trelle, Morten Beck, S475 (FRI171)
- Treloar, Carla, S565 (FRI349)
- Tremaroli, Valentina, S9 (GS011)
- Trepanier, Daniel, S726 (SAT130)
- Trepo, Eric, S372 (THU566)
- Trépo, Eric, S124 (THU012)
- Trevaskis, James, S276 (THU365), S483 (FRI187), S721 (SAT117), S762 (SAT208)
- Travisani, Franco, S79 (OS107), S382 (THU587), S932 (SAT588)
- Tria, A, S868 (SAT428)
- Tria, Giada, S698 (SAT068), S706 (SAT084)
- Triantafyllou, Evangelos, S116 (OS171), S135 (THU031), S352 (THU516), S674 (SAT020)
- Triantos, Christos, S840 (SAT374)
- Trickey, Adam, S256 (THU328), S556 (FRI331)
- Trifan, Anca, S192 (THU185), S573 (FRI368)
- Trimoulet, Pascale, S249 (THU313)
- Trinh, Huy, S875 (SAT442)
- Trinh, Vincent Quoc-Huy, S675 (SAT022)
- Tripathi, Dhiraj, S625 (FRI520)
- Tripathi, Dinesh Mani, S105 (OS153), S901 (SAT521)
- Tripathi, Gaurav, S34 (OS033), S128 (THU020), S528 (FRI273), S738 (SAT161), S752 (SAT188)
- Tripathi, Harshita, S139 (THU038)
- Tripathi, Kartikeya, S235 (THU286)
- Tripodi, Armando, S159 (THU078)
- Trippler, Martin, S264 (THU342)
- Trivedi, Palak, S54 (OS069), S96 (OS137), S310 (THU438), S334 (THU483), S335 (THU484), S526 (FRI269)
- Trivedi, Parth, S343 (THU502)
- Triyatni, Miriam, S299 (THU408), S867 (SAT427)
- Troisi, Jacopo, S425 (FRI057)
- Troisi, Roberto Ivan, S107 (OS156)
- Trojan, Jörg, S937 (SAT597)
- Troke, Phil, S554 (FRI327)
- Troncone, Giancarlo, S84 (OS115)
- Trost, Matthias, S704 (SAT081)
- Trotter, James F, S805 (SAT292)
- Trovato, Francesca, S135 (THU031), S185 (THU173), S352 (THU516), S371 (THU550), S647 (FRI563)
- Trovato, Francesca Maria, S116 (OS171), S505 (FRI231)
- Trowe, Torsten, S832 (SAT358)
- Truong, David, S225 (THU267), S553 (FRI324), S591 (FRI403)
- Truong, Emily, S159 (THU077)
- Tsai, Ming Chao, S119 (THU001)
- Tsai, Pei-Chien, S458 (FRI118), S595 (FRI410)
- Tsai, Wen-Wei, S721 (SAT117)
- Tsai, Yung-Ping, S925 (SAT576)
- Tsao, Philip, S30 (OS027), S936 (SAT596)
- Tsao, Yo-Yu, S45 (OS054)
- Tsaraf, Keren, S784 (SAT258), S804 (SAT291)
- Tse, Edmund, S228 (THU272)
- Tseligka, Eirini, S877 (SAT444)
- Tseng, Cheng-Hao, S835 (SAT364), S841 (SAT376), S875 (SAT442)
- Tseng, Kuo-Chih, S595 (FRI410)
- Tseng, Leo, S727 (SAT131), S730 (SAT139), S732 (SAT143)
- Tseng, Yuan Tsung, S200 (THU217)
- Tsereteli, Maia, S213 (THU242), S216 (THU247), S221 (THU258), S267 (THU347)
- Tsertsvadze, Tengiz, S587 (FRI395), S590 (FRI400), S590 (FRI401)
- Tse, Yee-Kit, S39 (OS043), S101 (OS147), S164 (THU088), S274 (THU362), S302 (THU414), S390 (FRI004), S406 (FRI026)
- Tsiagka, Dimitra, S218 (THU251)
- Tsigas, Alexandros-Pantelis, S908 (SAT534)
- Tsirogianni, Efrossini, S218 (THU251)
- Tskhomelidze, Irina, S214 (THU243), S216 (THU247), S216 (THU248), S233 (THU283), S234 (THU284), S267 (THU347), S588 (FRI397)
- Tsochatzis, Emmanuel, S3 (GS005), S39 (OS044), S41 (OS047), S90 (OS127), S436 (FRI078), S438 (FRI084), S815 (SAT311)
- Tsoggerel, Nandintsetseg, S824 (SAT342)
- Tsouka, Sofia, S363 (THU535), S480 (FRI180)
- Tsreteli, Maia, S214 (THU243), S216 (THU248), S233 (THU283), S234 (THU284)
- Tsuchiya, Atsunori, S28 (OS023)
- Tsuchiya, Kaoru, S379 (THU580)
- Tsuji, Keiji, S12 (LB004A), S13 (LB004B), S288 (THU389), S288 (THU390), S291 (THU393), S880 (SAT452), S881 (SAT453)
- Tual, Christelle, S72 (OS093)
- Tucker, Jo, S557 (FRI332), S557 (FRI333)
- Tudor, Diana, S664 (FRI600)
- Tuefferd, Marianne, S265 (THU343), S271 (THU356)
- Tufoni, Manuel, S357 (THU523), S908 (SAT535)
- Tujios, Shannan, S394 (FRI008)
- Tukiainen, Taru, S694 (SAT060)
- Tulaeva, Ina, S854 (SAT403)
- Tulone, Adele, S448 (FRI101)
- Tun, Hein, S177 (THU154)
- Tu, Qingli, S182 (THU165)
- Turan, Ilker, S294 (THU399), S399 (FRI015), S782 (SAT255), S820 (SAT316)
- Turco, Elena Rosselli Del, S564 (FRI347)
- Turco, Laura, S627 (FRI524)
- Turdziladze, Alexander, S214 (THU243), S216 (THU248), S219 (THU253)
- Tur-Kaspa, Ran, S64 (OS081), S774 (SAT241)
- Turkenburg, Maud, S338 (THU491)
- Turker, Kamuran, S858 (SAT411)
- Turner, Frances, S163 (THU086)
- Turner, Kate, S541 (FRI302)
- Turner, Scott, S194 (THU189), S308 (THU434), S466 (FRI152), S832 (SAT358)
- Turnes, Juan, S157 (THU074), S158 (THU076), S268 (THU348), S324 (THU464), S581 (FRI384), S586 (FRI393), S587 (FRI394)
- Turon, Fanny, S367 (THU542)
- Turtle, Lance, S54 (OS069)
- Tushuizen, Maarten, S307 (THU433), S798 (SAT280)
- Tuthill, Theresa, S425 (FRI058), S448 (FRI102), S452 (FRI108)
- Tutusaus, Anna, S652 (FRI573), S672 (SAT016)
- Tu, Xin, S414 (FRI037)
- Tveter, Anne T, S309 (THU437)
- Tyagi, Shakun, S197 (THU196)

Author Index

- Tyc, Olaf, S353 ([THU517](#)), S354 ([THU518](#))
 Tyrfinngsson, Thorarinn, S573 ([FRI366](#))
 Tyson, Luke D., S122 ([THU008](#)), S132 ([THU026](#)), S140 ([THU040](#))
- Ucbilek, Enver, S858 ([SAT410](#))
 Uceda Renteria, Sara Colonia, S843 ([SAT381](#))
 Uchiyama, Akira, S687 ([SAT047](#))
 Uemoto, Shinji, S183 ([THU167](#))
 Uemoto, Yusuke, S183 ([THU167](#))
 Ueno, Yoshiyuki, S563 ([FRI346](#)), S875 ([SAT442](#))
 Uhlenbusch, Natalie, S315 ([THU447](#))
 Uhlen, Mathias, S68 ([OS089](#))
 Uhlig, Holm, S602 ([FRI458](#))
 Ulrich, Rainer, S250 ([THU315](#))
 Ulukan, Burge, S693 ([SAT058](#))
 Ulukaya, Sezgin, S399 ([FRI015](#))
 Umair Latif, Muhammad, S85 ([OS118](#))
 Umbro, Ilaria, S162 ([THU083](#))
 Umland, Tim, S586 ([FRI393](#))
 Um, Soon Ho, S932 ([SAT590](#))
 Unchwaniwala, Nuruddin, S844 ([SAT383](#))
 Unfried, Juan Pablo, S644 ([FRI557](#))
 Unger, Kristian, S765 ([SAT215](#))
 Ungermann, Emily, S663 ([FRI599](#))
 Unitt, Esther, S934 ([SAT593](#))
 Unlu, Gulten, S858 ([SAT411](#))
 Unoza, Hidemi, S615 ([FRI501](#)), S897 ([SAT514](#))
 Unsal, Yasemin, S858 ([SAT410](#)), S861 ([SAT416](#))
 Uranowska, Karolina, S753 ([SAT189](#))
 Urbanik, Toni, S655 ([FRI581](#))
 Urbani, Luca, S120 ([THU004](#)), S480 ([FRI179](#)), S647 ([FRI562](#)), S650 ([FRI569](#)), S734 ([SAT152](#)), S735 ([SAT153](#))
 Urban, Sabine K., S915 ([SAT559](#))
 Urban, Stephan, S244 ([THU302](#)), S265 ([THU344](#)), S760 ([SAT205](#)), S845 ([SAT385](#)), S860 ([SAT413](#))
 Ure, Daren, S120 ([THU004](#)), S650 ([FRI568](#)), S660 ([FRI590](#)), S660 ([FRI591](#)), S726 ([SAT130](#))
 Urheu, Markus, S535 ([FRI287](#)), S618 ([FRI506](#))
 Uriarte, Iker, S48 ([OS060](#)), S643 ([FRI554](#))
 Urman, Jesus M, S643 ([FRI554](#))
 Ursic-Bedoya, José, S122 ([THU009](#))
 Usai, Carla, S248 ([THU310](#))
 Uschner, Frank, S353 ([THU517](#)), S354 ([THU518](#)), S895 ([SAT510](#))
 Utomo, Elaine, S330 ([THU476](#))
 Utpatel, Kirsten, S107 ([OS157](#))
 Utsunomiya, Daisuke, S430 ([FRI067](#))
 Uysalli, Yigit, S693 ([SAT058](#))
 Uzelac, Ivana, S751 ([SAT187](#)), S843 ([SAT380](#))
- Vaage, John T, S309 ([THU437](#))
 Vacca, Michele, S7 ([GS009](#)), S668 ([SAT008](#)), S695 ([SAT061](#))
 Vaccaro, Marco, S725 ([SAT127](#))
- Vaillant, Andrew, S851 ([SAT398](#))
 Vairetti, Mariapia, S697 ([SAT065](#)), S702 ([SAT074](#))
 Vaishnav, Manas, S433 ([FRI072](#)), S524 ([FRI264](#)), S620 ([FRI511](#))
 Vajen, Tanja, S193 ([THU187](#))
 Valainathan, Shantha, S127 ([THU019](#))
 Valasek, Mark, S416 ([FRI040](#))
 Valaydon, Zina, S498 ([FRI218](#))
 Valcheva, Velichka, S517 ([FRI253](#)), S517 ([FRI254](#))
 Valdecantos, Pilar, S749 ([SAT183](#))
 Valencia, Jorge, S217 ([THU249](#))
 Valencia, Malou, S770 ([SAT234](#))
 Valenta, Rudolf, S854 ([SAT403](#))
 Valenti, David, S614 ([FRI497](#))
 Valenti, Luca, S11 ([LB002](#)), S428 ([FRI061](#)), S438 ([FRI084](#)), S578 ([FRI376](#)), S668 ([SAT007](#)), S668 ([SAT008](#)), S673 ([SAT018](#)), S675 ([SAT021](#)), S703 ([SAT077](#))
 Valenzuela, Esteban Fuentes, S114 ([OS168](#)), S792 ([SAT270](#))
 Valera, Jose, S137 ([THU034](#))
 Valerio, Heather, S568 ([FRI356](#))
 Valero, Rocio, S555 ([FRI329](#))
 Valery, Patricia, S172 ([THU102](#)), S204 ([THU226](#))
 Valestrand, Laura, S605 ([FRI465](#))
 Valgiusti, Martina, S748 ([SAT180](#))
 Valiakou, Vaia, S255 ([THU326](#))
 Valigi, Tommaso, S920 ([SAT567](#))
 Vali, Yasaman, S74 ([OS097](#)), S424 ([FRI055](#)), S448 ([FRI102](#)), S452 ([FRI108](#))
 Valle, Clarissa, S751 ([SAT186](#))
 Valle, Juan, S107 ([OS157](#))
 Valliani, Talal, S771 ([SAT236](#))
 Vallier, Ludovic, S737 ([SAT157](#)), S742 ([SAT167](#))
 Vallverdú, Julia, S37 ([OS039](#))
 Valsan, Arun, S350 ([THU513](#))
 Valsecchi, Maria Grazie, S96 ([OS136](#))
 Valverde, Angela Martinez, S111 ([OS163](#)), S749 ([SAT183](#))
 Valverde, María Ayala, S137 ([THU034](#))
 van Bömmel, Florian, S8 ([GS010](#)), S148 ([THU057](#)), S379 ([THU581](#)), S382 ([THU586](#)), S383 ([THU590](#)), S823 ([SAT341](#)), S824 ([SAT344](#)), S860 ([SAT414](#)), S931 ([SAT587](#))
 Van Buuren, Nicholas, S251 ([THU317](#)), S841 ([SAT376](#))
 Vandecaveye, Vincent, S385 ([THU593](#))
 van de Graaf, Stan, S26 ([OS019](#)), S601 ([FRI457](#)), S603 ([FRI461](#))
 Vandekerckhove, Elisabeth, S562 ([FRI344](#))
 Vandeleur, Ann, S538 ([FRI295](#))
 van den Berg, Aad, S93 ([OS132](#))
 Van Den Boom, Wijnand, S541 ([FRI302](#))
 Vandenbossche, Joris J, S838 ([SAT370](#))
 van den Brand, Floris F., S93 ([OS132](#))
 Van Den Broeke, Celine, S72 ([OS094](#))
 Vandenbroucke, Roosmarijn, S106 ([OS155](#))
 Vandendriessche, Sofie, S396 ([FRI012](#))
- Van den Ende, Natalie, S317 ([THU452](#)), S516 ([FRI252](#))
 van den Hoek, Anita M., S681 ([SAT033](#)), S685 ([SAT043](#)), S686 ([SAT044](#))
 Van De Parre, Tim, S72 ([OS094](#))
 Vandeputte, Martin, S397 ([FRI013](#))
 Vanderbecq, Quentin, S319 ([THU454](#))
 Van Derborght, Bart, S655 ([FRI580](#))
 van der Kooij, Sandra, S698 ([SAT067](#))
 van der Laan, Luc J.W., S46 ([OS057](#)), S86 ([OS120](#)), S115 ([OS170](#)), S118 ([OS174](#)), S644 ([FRI556](#)), S652 ([FRI574](#))
 Vanderlinden, Axelle, S303 ([THU416](#))
 Van der Meer, Adriaan, S93 ([OS132](#)), S317 ([THU452](#)), S335 ([THU484](#))
 van der Merwe, Schalk, S120 ([THU003](#)), S144 ([THU047](#)), S346 ([THU507](#)), S516 ([FRI252](#)), S680 ([SAT032](#)), S781 ([SAT253](#)), S783 ([SAT256](#))
 van der Ploeg, Koen, S893 ([SAT506](#))
 van der Veen, Jannet, S220 ([THU255](#))
 van der Woerd, Wendy L., S601 ([FRI457](#))
 van der Wouden, Egbert-Jan, S93 ([OS132](#))
 van Doorn, Leen-Jan, S750 ([SAT184](#))
 van Duyvenvoorde, Wim, S676 ([SAT024](#)), S677 ([SAT025](#)), S698 ([SAT067](#))
 van Erpecum, Karel J., S338 ([THU491](#))
 Vanessa, Banz, S780 ([SAT251](#))
 van Ewijk, Reyn, S80 ([OS108](#))
 Van Gulck, Ellen, S72 ([OS094](#))
 Van Haele, Matthias, S47 ([OS059](#))
 Van Hees, Stijn, S861 ([SAT415](#))
 Van Hoecke, Lien, S106 ([OS155](#))
 Van Hoek, Bart, S93 ([OS132](#)), S307 ([THU433](#))
 van Hooff, Maria, S330 ([THU476](#))
 Van Imschoot, Griet, S106 ([OS155](#))
 van Kleef, Laurens, S41 ([OS046](#)), S86 ([OS120](#)), S147 ([THU055](#))
 van Kooten, Cees, S698 ([SAT067](#))
 van Koppen, Arianne, S685 ([SAT043](#))
 Vankova, Ana, S665 ([SAT002](#))
 Vanlander, Aude, S107 ([OS156](#)), S768 ([SAT230](#))
 Vanlangenhove, Peter, S107 ([OS156](#))
 Vanlemmens, Claire, S772 ([SAT239](#)), S817 ([SAT312](#))
 Vanlerberghe, Benedict, S781 ([SAT253](#)), S783 ([SAT256](#))
 Van Malenstein, Hannah, S346 ([THU507](#)), S783 ([SAT256](#))
 van Marle, Sjoerd, S716 ([SAT109](#))
 Van Melkebeke, Lukas, S144 ([THU047](#)), S346 ([THU507](#))
 van Munster, Kim, S338 ([THU491](#))
 van Pelt, Jos, S637 ([FRI544](#))
 Van Remoortere, Pieter, S72 ([OS094](#))
 van Royen, Martin, S644 ([FRI556](#))
 Van Steenkiste, Christophe, S106 ([OS155](#)), S459 ([FRI120](#))
 Vanstraelen, Kim, S581 ([FRI384](#)), S586 ([FRI393](#))

- van Tienderen, Gilles, S46 ([OS057](#)), S118 ([OS174](#)), S644 ([FRI556](#)), S652 ([FRI574](#))
- van Trigt, Nikki, S686 ([SAT044](#)), S698 ([SAT067](#))
- Van Vlierberghe, Hans, S106 ([OS155](#)), S107 ([OS156](#))
- van Vugt, Jeroen, S631 ([FRI530](#)), S815 ([SAT311](#)), S883 ([SAT488](#))
- VanWagner, Lisa, S786 ([SAT262](#)), S788 ([SAT265](#))
- van Weeghel, Michel, S601 ([FRI457](#))
- Vanwolleghe, Thomas, S8 ([GS010](#)), S303 ([THU416](#)), S852 ([SAT400](#)), S861 ([SAT415](#))
- Van Wonterghem, Elien, S106 ([OS155](#))
- Vaqué, Jose Pedro, S113 ([OS166](#))
- Vaquero, Javier, S673 ([SAT018](#))
- Vara, Giulio, S794 ([SAT273](#))
- Varasa, Tomás Artaza, S127 ([THU018](#))
- Vardanyan, Diana, S763 ([SAT211](#))
- Vardeu, A, S868 ([SAT428](#))
- Varela, Jesus, S137 ([THU034](#))
- Varela, Maria, S381 ([THU584](#)), S912 ([SAT555](#))
- Varela-Rey, Marta, S177 ([THU155](#)), S689 ([SAT050](#))
- Vargas-De-León, Cruz, S554 ([FRI326](#))
- Vargas, Hugo E., S19 ([OS008](#)), S49 ([OS063](#)), S339 ([THU494](#)), S634 ([FRI537](#)), S887 ([SAT496](#))
- Variya, Bhavesh, S660 ([FRI590](#))
- Varo, Guillermo Fernández, S106 ([OS154](#)), S368 ([THU545](#))
- Varon, Adrian, S137 ([THU034](#))
- Vartak, Nachiket, S38 ([OS042](#))
- Vartiainen, Emilia, S694 ([SAT060](#))
- Vasileiadis, Themistoklis, S840 ([SAT374](#))
- Vasileiou, Spyridoula, S839 ([SAT372](#))
- Vasilieva, Larisa, S908 ([SAT534](#))
- Vassiliou, Daphne, S530 ([FRI275](#))
- Vatansever, Sezgin, S861 ([SAT416](#)), S864 ([SAT421](#))
- Vatteroni, Maria Linda, S292 ([THU394](#))
- Vaz, Karl, S134 ([THU029](#)), S389 ([FRI002](#))
- Vázquez, Inmaculada Fernández, S127 ([THU018](#)), S704 ([SAT080](#))
- Vázquez-Sirvent, Lucía, S589 ([FRI399](#))
- Vecchio, Mara, S3 ([GS004](#))
- Vecchio, Sarah, S543 ([FRI306](#)), S559 ([FRI336](#))
- Veelken, Rhea, S379 ([THU581](#)), S382 ([THU586](#)), S904 ([SAT528](#))
- Vehreschild, Janne, S339 ([THU493](#))
- Vehreschild, Maria, S339 ([THU493](#))
- Veitch, Mark, S541 ([FRI302](#))
- Velasco-Herrera, Martín del Castillo, S476 ([FRI172](#))
- Velasco, Jose Antonio Velarde-Ruiz, S137 ([THU034](#))
- Velasquez, Hector, S17 ([OS005](#)), S43 ([OS051](#)), S209 ([THU233](#)), S282 ([THU378](#)), S910 ([SAT538](#))
- Vela, Victor, S137 ([THU034](#))
- Velazquez, René Malé, S19 ([OS008](#)), S49 ([OS063](#)), S487 ([FRI195](#))
- Velazquez, Yovana, S839 ([SAT372](#))
- Vella, Antonio, S658 ([FRI586](#)), S925 ([SAT574](#))
- Veloz, Maria Guerra, S171 ([THU101](#)), S276 ([THU366](#)), S571 ([FRI363](#)), S812 ([SAT304](#))
- Veloz, María Guerra, S581 ([FRI384](#))
- Velthuis, Louis, S80 ([OS108](#))
- Veltzke-Schlieker, Wilfried, S309 ([THU436](#))
- Venderink, Wulphert, S525 ([FRI266](#))
- Venet, Fabienne, S356 ([THU522](#))
- Venkatachalapathy, Suresh Vasani, S19 ([OS008](#)), S49 ([OS063](#))
- Venkata, Ramana Mallela, S929 ([SAT582](#))
- Venkatraman, Meenakshi, S824 ([SAT343](#)), S835 ([SAT365](#)), S846 ([SAT386](#)), S871 ([SAT435](#))
- Ventura, Paolo, S839 ([SAT371](#))
- Venuto, Clara De, S357 ([THU523](#))
- Veramendi, Esther, S137 ([THU034](#))
- Verbeek, Jef, S120 ([THU003](#)), S144 ([THU047](#)), S346 ([THU507](#)), S516 ([FRI252](#)), S680 ([SAT032](#)), S781 ([SAT253](#)), S783 ([SAT256](#))
- Verbinnen, Thierry, S8 ([GS010](#)), S864 ([SAT422](#))
- Verdaguer, Helena, S748 ([SAT180](#))
- Verdeguer, Francisco, S446 ([FRI099](#)), S488 ([FRI197](#)), S703 ([SAT078](#))
- Verdonk, Robert, S93 ([OS132](#))
- Verdugo, Ramón Morillo, S268 ([THU348](#)), S586 ([FRI393](#)), S587 ([FRI394](#))
- Vergani, Diego, S308 ([THU435](#))
- Vergis, Nikhil, S34 ([OS034](#)), S121 ([THU007](#)), S122 ([THU008](#)), S124 ([THU013](#)), S132 ([THU026](#)), S135 ([THU031](#)), S352 ([THU516](#))
- Verhagen, Marc A.M.T., S306 ([THU431](#))
- Verheij, Joanne, S9 ([GS011](#))
- Verhelst, Xavier, S106 ([OS155](#)), S107 ([OS156](#)), S307 ([THU433](#)), S317 ([THU452](#)), S335 ([THU484](#)), S562 ([FRI344](#)), S768 ([SAT230](#)), S913 ([SAT556](#))
- Verhoeven, Arthur, S601 ([FRI457](#)), S653 ([FRI576](#)), S761 ([SAT207](#)), S762 ([SAT209](#))
- Verhoye, Lieven, S860 ([SAT413](#))
- Verkade, Henkjan J., S517 ([FRI254](#)), S521 ([FRI259](#)), S601 ([FRI457](#))
- Verlinden, Wim, S546 ([FRI312](#))
- Verma, Manisha, S209 ([THU234](#))
- Verma, Nipun, S350 ([THU513](#))
- Vermeulen, Marion, S251 ([THU316](#))
- Vernole, Eugenia, S559 ([FRI336](#))
- Verrier, Eloi, S99 ([OS142](#)), S246 ([THU305](#))
- Verrijken, An, S692 ([SAT055](#))
- Verschuren, Lars, S677 ([SAT025](#)), S685 ([SAT043](#)), S698 ([SAT067](#))
- Verset, Gontran, S372 ([THU566](#))
- Verslype, Chris, S385 ([THU593](#)), S637 ([FRI544](#))
- Verspagnet, H.W., S144 ([THU047](#))
- Verstegen, Monique M.A., S46 ([OS057](#)), S115 ([OS170](#)), S118 ([OS174](#)), S644 ([FRI556](#)), S652 ([FRI574](#))
- Verucchi, Gabriella, S569 ([FRI359](#))
- Verzeroli, Claire, S766 ([SAT216](#))
- Vesikari, Timo, S100 ([OS145](#))
- Vessby, Johan, S30 ([OS026](#)), S420 ([FRI047](#))
- Vesterhus, Mette, S77 ([OS103](#))
- Vestito, Amanda, S91 ([OS129](#)), S794 ([SAT273](#))
- Vettermann, Christian, S540 ([FRI299](#))
- Vetter, Marcel, S163 ([THU085](#))
- Veyre, Florian, S772 ([SAT239](#))
- Viacheslav, Morozov, S4 ([GS006](#)), S103 ([OS149](#)), S828 ([SAT351](#)), S829 ([SAT352](#)), S866 ([SAT425](#))
- Viana, Nataly Lopes, S552 ([FRI323](#))
- Viayna, Elisabet, S615 ([FRI499](#))
- Vibert, Eric, S538 ([FRI296](#)), S935 ([SAT595](#))
- Vicario, Álvaro, S217 ([THU249](#))
- Vicar, Marta Mac, S137 ([THU034](#))
- Vicentini, Elena, S872 ([SAT436](#))
- Vickerman, Peter, S221 ([THU257](#)), S234 ([THU284](#)), S256 ([THU328](#)), S565 ([FRI349](#))
- Vico-Romero, Judit, S212 ([THU240](#))
- Vidal, Adela, S229 ([THU276](#))
- Vidal, Jordi, S368 ([THU545](#))
- Vidal-Puig, Antonio, S7 ([GS009](#)), S695 ([SAT061](#))
- Vidal, Silvia, S91 ([OS128](#)), S886 ([SAT494](#))
- Vidili, Gianpaolo, S107 ([OS157](#))
- Vidovszky, Anna, S903 ([SAT525](#))
- Vieira, Diego Alves, S552 ([FRI323](#))
- Vigneron, Paul, S372 ([THU566](#))
- Vig, Pamela, S599 ([FRI452](#))
- Vihervaara, Terhi, S419 ([FRI046](#))
- Vijayathurai, Janusa, S758 ([SAT200](#))
- Viklicky, Ondrej, S593 ([FRI408](#))
- Vila, Marta, S255 ([THU325](#)), S658 ([FRI587](#))
- Vilà, Paula Cantallops, S527 ([FRI271](#))
- Vilas-Boas, Filipe, S28 ([OS024](#))
- Vilchez, Tatiana, S21 ([OS011](#))
- Vilella, Àngels, S218 ([THU252](#))
- Vilibic-Cavlek, Tatjana, S270 ([THU353](#))
- Villadsen, Gerda Elisabeth, S418 ([FRI044](#))
- Villa, Erica, S549 ([FRI317](#)), S578 ([FRI376](#)), S584 ([FRI388](#)), S627 ([FRI524](#))
- Villagrasa, Ares, S137 ([THU035](#))
- Villa, Jennifer, S704 ([SAT080](#))
- Villalón, Alejandro, S81 ([OS110](#))
- Villa-Malagon, Kevin, S476 ([FRI172](#))
- Villamil, Maria Alejandra Gracia, S137 ([THU034](#)), S308 ([THU435](#))
- Villanueva, Augusto, S11 ([LB003](#))
- Villanueva, Cándid, S90 ([OS127](#)), S91 ([OS128](#)), S370 ([THU548](#)), S502 ([FRI226](#)), S625 ([FRI520](#)), S627 ([FRI523](#))
- Villanueva, Pedro Amado, S577 ([FRI374](#))
- Villarroel, Carolina, S291 ([THU392](#)), S301 ([THU413](#)), S897 ([SAT513](#))
- Villela-Nogueira, Cristiane, S506 ([FRI232](#))

Author Index

- Villeneuve, Jean-Pierre, S593 ([FRI407](#))
Villeret, Francois, S356 ([THU522](#))
Villesen, Ida, S437 ([FRI080](#)), S475 ([FRI169](#)), S668 ([SAT008](#)), S721 ([SAT118](#))
Villota-Rivas, Marcela, S217 ([THU249](#))
Viltsbøll, Tina, S121 ([THU006](#)), S710 ([SAT091](#))
Vilstrup, Hendrik, S611 ([FRI491](#)), S677 ([SAT026](#))
Vinaixa, Carmen, S807 ([SAT296](#))
Vince, Adriana, S270 ([THU353](#)), S700 ([SAT070](#))
Vincent, Catherine, S593 ([FRI407](#)), S805 ([SAT293](#))
Vincent, Jeanne Perpétue, S295 ([THU401](#))
Vincenzi, Bruno, S372 ([THU567](#))
Vincenzi, Laura, S808 ([SAT297](#))
Vinikoor, Michael, S23 ([OS015](#))
Vintour-Cesar, Emily, S239 ([THU294](#))
Vinuela, L., S211 ([THU237](#))
Vio, Danae, S81 ([OS110](#))
Violi, Paola, S796 ([SAT277](#))
Vionnet, Julien, S355 ([THU520](#))
Virdis, Agostino, S292 ([THU394](#))
Virzi, Alessia, S99 ([OS142](#)), S738 ([SAT160](#))
Visintin, Alessia, S626 ([FRI522](#))
Visvanathan, Kumar, S498 ([FRI218](#)), S842 ([SAT377](#))
Vitale, Alessandro, S306 ([THU423](#))
Vitek, Libor, S671 ([SAT014](#))
Vitellius, Carole, S496 ([FRI215](#))
Vithayathil, Mathew, S345 ([THU505](#)), S374 ([THU571](#))
Vitiello, Adriana, S751 ([SAT186](#))
Vittal, Anusha, S70 ([OS092](#))
Vittorio, Jennifer M., S518 ([FRI255](#)), S519 ([FRI256](#))
Viuff, Marie, S271 ([THU356](#))
Vivanco, Maria, S48 ([OS060](#))
Viveiros, André, S537 ([FRI292](#))
Vizzutti, Francesco, S627 ([FRI524](#))
Vlachogiannakos, Ioannis, S429 ([FRI063](#))
Vlahaki, Euthimia, S472 ([FRI163](#))
Vlierberghe, Hans Van, S562 ([FRI344](#)), S655 ([FRI580](#)), S768 ([SAT230](#)), S913 ([SAT556](#))
Vlierberghe, Sandra Van, S734 ([SAT152](#))
Vnencakova, Janka, S613 ([FRI496](#))
Voet, Thierry, S680 ([SAT032](#))
Vogelaar, Serge, S798 ([SAT280](#))
Vogel, Arndt, S11 ([LB002](#)), S107 ([OS157](#)), S372 ([THU567](#)), S374 ([THU571](#)), S376 ([THU574](#)), S383 ([THU588](#)), S927 ([SAT579](#)), S937 ([SAT597](#))
Vogels, Esther, S26 ([OS019](#))
Vogrin, Sara, S842 ([SAT377](#))
Vogt, Annabelle, S381 ([THU585](#))
Voight, Benjamin, S30 ([OS027](#)), S936 ([SAT596](#))
Voiosu, Andrei, S361 ([THU532](#))
Voitenleitner, Christian, S251 ([THU316](#))
Vold, Jørn-Henrik, S221 ([THU257](#))
Voldum-Clausen, Kristoffer, S724 ([SAT124](#))
Volkert, Ines, S729 ([SAT137](#))
Volk, Valery, S927 ([SAT579](#))
Voll-Glaninger, Astrid, S545 ([FRI309](#))
Volmer, Felix, S809 ([SAT298](#))
Volti, Giovanni Li, S703 ([SAT077](#))
Volz, Tassilo, S256 ([THU327](#))
vom Dahl, Stephan, S533 ([FRI283](#))
Vonderscher, Jacky, S254 ([THU324](#))
von Felden, Johann, S11 ([LB002](#))
Vonghia, Luisa, S709 ([SAT089](#))
von Karpowitz, Maria, S582 ([FRI385](#))
von Maltzahn, Robyn, S327 ([THU470](#)), S335 ([THU485](#))
von Seth, Erik, S82 ([OS112](#))
VoPham, Trang, S912 ([SAT554](#))
Vos, Miriam, S449 ([FRI103](#))
Vosooghi, Aidan, S33 ([OS031](#)), S769 ([SAT232](#))
Vos, Winnok De, S709 ([SAT089](#))
Vucur, Mihael, S11 ([LB003](#))
Vuilleumier, Nicolas, S493 ([FRI208](#))
Vujkovic, Marijana, S30 ([OS027](#)), S731 ([SAT141](#)), S936 ([SAT596](#))
Vuppalachchi, Raj, S95 ([OS135](#)), S451 ([FRI107](#)), S701 ([SAT073](#))
Vyas, Ashish Kumar, S252 ([THU320](#))
Vyberg, Mogens, S154 ([THU068](#)), S331 ([THU477](#)), S661 ([FRI593](#))
Vyhmeister, Ross, S779 ([SAT250](#))
Wack, Katy, S700 ([SAT071](#)), S711 ([SAT094](#))
Waddell, Tom, S424 ([FRI056](#))
Wade, James, S126 ([THU016](#))
Wadsworth, Sam, S764 ([SAT212](#))
Waern, Johan, S186 ([THU174](#))
Wagner, Josef, S251 ([THU318](#))
Wagner, Martin, S696 ([SAT063](#))
Wahl, Alisha, S145 ([THU051](#))
Wahlin, Staffan, S530 ([FRI275](#))
Wah, Phyo Wah, S134 ([THU030](#))
Wai, Clare, S120 ([THU005](#))
Waidmann, Oliver, S313 ([THU444](#))
Waisman, Ari, S396 ([FRI012](#))
Wai-Sun Wong, Vincent, S449 ([FRI103](#)), S452 ([FRI108](#))
Wajcman, Dana Ivancovsky, S148 ([THU056](#))
Wakimoto, Arata, S702 ([SAT076](#))
Waksal, Sam, S494 ([FRI209](#))
Walakira, Andrew, S766 ([SAT217](#))
Waldenström, Jesper, S186 ([THU174](#))
Waleed, Muhammad Furqan, S43 ([OS051](#))
Walkenfort, Bernd, S264 ([THU342](#))
Walker, Andreas, S825 ([SAT345](#))
Walker, Josephine, S234 ([THU284](#)), S256 ([THU328](#))
Walker, Kate, S801 ([SAT287](#))
Walker, Ruth, S704 ([SAT081](#))
Walker, Victoria, S58 ([OS072B](#))
Wallace, David, S801 ([SAT287](#))
Wallach, Jean-Philippe, S547 ([FRI313](#))
Wallays, Marie, S346 ([THU507](#)), S680 ([SAT032](#))
Walldius, Göran, S24 ([OS016](#)), S119 ([THU002](#))
Waller, Kathryn, S698 ([SAT066](#))
Wallin, Jeffrey, S247 ([THU308](#)), S276 ([THU365](#)), S835 ([SAT364](#))
Wall, Lorraine, S548 ([FRI316](#))
Walmsley, Martine, S312 ([THU442](#))
Walsh, Liron, S58 ([OS073](#))
Walsh, Renae, S834 ([SAT362](#))
Walz, Juliane S., S198 ([THU198](#))
Wandeler, Gilles, S23 ([OS015](#))
Wanders, Alkwin, S420 ([FRI047](#))
Wandji, Line Carolle Ntandja, S205 ([THU227](#)), S205 ([THU228](#)), S913 ([SAT557](#))
Wang, Bin, S726 ([SAT128](#)), S726 ([SAT129](#)), S745 ([SAT177](#))
Wang, Bing, S534 ([FRI285](#))
Wang, Bingduo, S915 ([SAT559](#))
Wang, Bo, S281 ([THU375](#))
Wang, Chengyan, S501 ([FRI224](#))
Wang, Chia-Chi, S595 ([FRI410](#))
Wang, Chun Hsiang, S200 ([THU217](#))
Wang, ChunYan, S22 ([OS014](#))
Wang, Chun-Yi, S162 ([THU084](#))
Wangensteen, Kirk, S936 ([SAT596](#))
Wang, Fu-Sheng, S827 ([SAT349](#))
Wang, Grace, S846 ([SAT388](#))
Wang, Guiqiang, S70 ([OS091](#))
Wang, Guobao, S462 ([FRI125](#))
Wang, Guoqiang, S745 ([SAT177](#))
Wang, Hee Jung, S490 ([FRI202](#))
Wang, Hongyuan, S837 ([SAT368](#))
Wang, Hualie, S326 ([THU468](#))
Wang, Huay-Min, S625 ([FRI520](#))
Wang, Jian, S287 ([THU388](#)), S296 ([THU403](#)), S326 ([THU468](#)), S504 ([FRI229](#)), S770 ([SAT234](#))
Wang, Jianye, S463 ([FRI146](#))
Wang, Jie, S389 ([FRI001](#)), S601 ([FRI456](#))
Wang, Jinhai, S883 ([SAT488](#))
Wang, Jinhua, S272 ([THU357](#))
Wang, Jitao, S182 ([THU165](#))
Wang, Junxiao, S914 ([SAT558](#))
Wang, Ling, S86 ([OS120](#))
Wang, Li-Yu, S294 ([THU398](#))
Wang, Ming, S272 ([THU357](#))
Wang, Pu, S254 ([THU323](#)), S854 ([SAT404](#))
Wang, Qi, S695 ([SAT062](#))
Wang, Qingbi, S385 ([THU594](#))
Wang, Qiuhe, S628 ([FRI526](#))
Wang, Ran, S190 ([THU183](#))
Wang, Sai, S408 ([FRI029](#))
Wang, Sarah, S631 ([FRI530](#))
Wang, Shanshan, S408 ([FRI029](#))
Wang, Shike, S642 ([FRI553](#))
Wang, Sih-Ren, S595 ([FRI410](#))
Wang, Stanley, S871 ([SAT435](#))
Wang, Su, S277 ([THU368](#))
Wang, Surui, S606 ([FRI467](#))
Wang, Tongyu, S347 ([THU509](#))
Wang, Vivian, S552 ([FRI322](#)), S572 ([FRI364](#))
Wang, Wenjuan, S182 ([THU165](#))
Wang, Wen-Lung, S119 ([THU001](#))
Wang, Xian-Bo, S344 ([THU504](#))
Wang, Xiaodong, S421 ([FRI050](#))
Wang, Xiaohao, S878 ([SAT447](#))

- Wang, Xiaohong, S454 (FRI110)
Wang, Xiao-jun, S492 (FRI206)
Wang, Xiaojun, S727 (SAT132)
Wang, Xiaoxiao, S685 (SAT042)
Wang, Xun, S695 (SAT062)
Wang, Yan, S22 (OS014), S727 (SAT132)
Wang, Yijin, S914 (SAT558)
Wang, Yinghong, S372 (THU567), S383 (THU588)
Wang, Yongtao, S36 (OS037), S642 (FRI553)
Wang, Yu-Lin, S514 (FRI247)
Wang, Yuting, S240 (THU296)
Wang, Zeyu, S920 (SAT568)
Wang, Zhe, S837 (SAT367)
Wang, Zhenglin, S559 (FRI337)
Wang, Zhengtao, S818 (SAT315)
Wang, Zhengyu, S92 (OS130), S619 (FRI508), S621 (FRI512), S628 (FRI526)
Wang, Zhili, S264 (THU341)
Wang, Zilong, S26 (OS020)
Wan, JingHong, S65 (OS084), S475 (FRI170)
Wanless, IanR, S367 (THU541), S645 (FRI560)
Wanninger, Timothy, S194 (THU191), S470 (FRI160), S485 (FRI190)
Wan, Shang, S616 (FRI503)
Wan, Xueshuai, S384 (THU591)
Wapinski, Ilan, S700 (SAT071)
Ward, Caroline, S108 (OS158)
Ward, John, S229 (THU274), S238 (THU291), S274 (THU361), S557 (FRI333)
Warner, Suzan, S608 (FRI470)
Warrillow, Stephen, S134 (THU029)
Warr, Matthew, S483 (FRI187)
Watanabe, Ayumi, S839 (SAT372)
Watanabe, Takehisa, S295 (THU401)
Waterfall, Martin, S397 (FRI013)
Watkins, Elaine, S322 (THU461)
Watkins, Tim, S700 (SAT071)
Watson, Adam, S482 (FRI184)
Watson, Hugh, S611 (FRI491), S872 (SAT436)
Watson, Kimberly A., S751 (SAT185)
Watson, Robyn, S646 (FRI561)
Watt, Makayla, S338 (THU490)
Watts, Gerald, S164 (THU089)
Webb, Muriel, S148 (THU056)
Webel, Henry Emanuel, S500 (FRI223)
Weber, Achim, S11 (LB003), S655 (FRI581), S765 (SAT215)
Weber, Michiel, S750 (SAT184)
Weber, Sabine, S823 (SAT341)
Weber, Susanne N, S156 (THU072), S605 (FRI464)
Webzell, Ian, S120 (THU005), S134 (THU030)
Wedemeyer, Heiner, S4 (GS006), S83 (OS113), S103 (OS149), S248 (THU311), S250 (THU315), S263 (THU339), S264 (THU342), S274 (THU361), S562 (FRI345), S566 (FRI352), S569 (FRI359), S582 (FRI385), S608 (FRI485), S622 (FRI514), S624 (FRI519), S634 (FRI536), S642 (FRI552), S666 (SAT003), S783 (SAT257), S784 (SAT259), S823 (SAT341), S824 (SAT344), S828 (SAT351), S829 (SAT352), S830 (SAT355), S831 (SAT357), S843 (SAT379), S857 (SAT408), S893 (SAT505)
Wee, Aileen, S431 (FRI068)
Weeks, Anthony, S550 (FRI318)
Weersma, Rinse, S338 (THU491)
Wegrzyniak, Olivia, S471 (FRI162)
Wehmeyer, Malte, S333 (THU481)
Weidinger, Gerhard, S545 (FRI309)
Weidmann, Sören, S333 (THU481)
Weigt, Jochen, S378 (THU579)
Wei, Jia, S838 (SAT369)
Wei, Lai, S278 (THU369), S431 (FRI068), S480 (FRI179), S481 (FRI181)
Weiland, Ola, S580 (FRI382)
Weil, Clara, S584 (FRI388)
Weiler, Marek, S385 (THU594)
Weiler-Normann, Christina, S321 (THU458)
Weiler, Sofia, S655 (FRI581)
Weilert, Frank, S836 (SAT366)
Weinbaum, Sindee, S312 (THU442)
Weinberger, Patrick, S535 (FRI287), S618 (FRI506)
Weinberg, Ethan, S33 (OS031)
Weinmann, Arndt, S374 (THU571), S376 (THU574), S383 (THU588)
Weinstein, David, S515 (FRI249)
Weinstock, Marta, S725 (SAT126)
Wei, Qin, S22 (OS014), S182 (THU165)
Weisberg, Ilan, S170 (THU099), S291 (THU392), S301 (THU413)
Weis, Cleo-Aron, S523 (FRI262)
Weiskirchen, Ralf, S400 (FRI018), S748 (SAT181)
Weismüller, Tobias, S381 (THU585), S599 (FRI451)
Weis, Nina, S220 (THU255)
Weissbach, Markus, S132 (THU026), S737 (SAT158)
Weiss, Emmanuel, S475 (FRI170)
Weissenborn, Karin, S624 (FRI519)
Weissfeld, Lisa, S269 (THU350), S300 (THU411)
Weiss, Felicitas, S313 (THU444)
Weiss, Karl Heinz, S1 (GS001), S61 (OS077), S520 (FRI258), S539 (FRI297)
Weiß, Lena, S38 (OS042)
Weissman, Natan, S765 (SAT214)
Weiss, Thomas, S470 (FRI159)
Weitz, Michelle, S544 (FRI307)
Wei, Yishuang, S679 (SAT030)
Wei Zhang, Ingrid, S362 (THU533)
Wejnaruemarn, Salisa, S19 (OS008), S49 (OS063)
Wejstål, Rune, S580 (FRI382)
Welch, Nicole, S33 (OS032), S193 (THU188)
Wellhöner, Stella, S379 (THU581)
Well, Shauna Vander, S338 (THU490)
Wells, Rebecca, S740 (SAT163)
Welsch, Christoph, S907 (SAT531)
Weltzsch, Jan-Philipp, S308 (THU435)
Wen, Bo, S880 (SAT451)
Wendon, Julia, S403 (FRI022)
Wengenmayer, Tobias, S313 (THU444)
Weng, Honglei, S408 (FRI029), S659 (FRI589), S661 (FRI594)
Wenisch, Christoph, S545 (FRI309)
Wen-Juei Jeng, Rachel, S576 (FRI372)
Wenzel, Jürgen, S257 (THU329)
Werge, Mikkel, S154 (THU068), S331 (THU477), S670 (SAT013)
Wernberg, Charlotte, S423 (FRI054), S434 (FRI074)
Weseslindtner, Lukas, S271 (THU354)
Wester, Axel, S30 (OS026), S123 (THU010), S423 (FRI053)
Wester, Carolyn, S598 (FRI418)
Westergren-Thorsson, Gunilla, S644 (FRI556)
Westermarck, Jukka, S637 (FRI544)
Westerterp, Marit, S144 (THU046)
Westin, Johan, S30 (OS026), S580 (FRI382)
West, Joe, S925 (SAT575)
Westland, Christopher, S733 (SAT145), S824 (SAT343), S835 (SAT365), S871 (SAT435)
Westphal, Max, S74 (OS097)
Wetten, Aaron, S311 (THU440), S337 (THU489)
Wettengel, Jochen, S760 (SAT205)
Wetzel, Alexandre, S355 (THU520)
Wetzstein, Nils, S15 (OS001)
Weymouth-Wilson, Alex, S751 (SAT185)
Wharton, Victoria, S510 (FRI239), S510 (FRI240)
Wheeden, Kristen, S516 (FRI251)
Wheeler, Darren, S332 (THU478)
Whiteford, James, S488 (FRI198)
Whitehouse, Gavin, S34 (OS034)
White, James, S412 (FRI034)
White, Nicole, S847 (SAT389)
Whitton, Bradley, S498 (FRI218), S550 (FRI318)
Wiberg-Itzel, Ewa, S94 (OS133)
Wichert, Marc, S378 (THU579)
Wiegand, Johannes, S148 (THU057), S823 (SAT341), S860 (SAT414)
Wiegard, Christiane, S321 (THU458)
Wiersma, Thomas, S617 (FRI504)
Wiesel, Julian Schulze Zur, S197 (THU197)
Wiesel, Philippe, S94 (OS134)
Wiese, Signe, S340 (THU496), S361 (THU532), S614 (FRI498), S887 (SAT495)
Wigg, Alan, S228 (THU272), S389 (FRI002), S898 (SAT516)
Wiid, Percival, S190 (THU183)
Wijesekera, Vishva, S538 (FRI294), S538 (FRI295)
Wiktorin, Hanna Grauers, S186 (THU174)
Wild, Katharina, S100 (OS143)
Wilkey, Daniel, S465 (FRI149)

Author Index

- Wilkinson, Alex, S195 (THU192)
Willars, Christopher, S403 (FRI022)
Wille, Kai, S339 (THU493)
Willems, Bernard, S593 (FRI407),
S805 (SAT293)
Willemse, Jorke, S118 (OS174),
S644 (FRI556)
Willemse, José, S330 (THU476)
Willems, Philippe, S593 (FRI407)
Willheim, Claudia, S535 (FRI287),
S618 (FRI506)
Willheim, Martin, S545 (FRI309)
Williams, Caroline, S846 (SAT386)
Williams, Evangelia, S809 (SAT298)
Williams, Felicity, S334 (THU483),
S364 (THU537)
Williamson, Catherine, S329 (THU473)
Williams, Roger, S68 (OS089)
Williams, Suzanne, S172 (THU102)
Willis, Todd, S368 (THU545)
Willms, Arnulf, S915 (SAT559)
Wills, Mark R., S198 (THU198)
Willuweit, Katharina, S823 (SAT341)
Wilson, Caroline, S646 (FRI561)
Wilson, David, S550 (FRI318)
Wilson, Phillip, S239 (THU294)
Wilson, Thomas, S733 (SAT146)
Wimmer, Philipp, S21 (OS012),
S891 (SAT502)
Wimmer, Ralf, S602 (FRI460)
Win, Aziza, S203 (THU223)
Winckler, Wendy, S508 (FRI236),
S918 (SAT564)
Winick, Jeffrey, S3 (GS004)
Winkler, Frances, S196 (THU194)
Winkler, Marc, S684 (SAT040)
Winter, Benedicte De, S709 (SAT089)
Winter, Johnathan, S698 (SAT067)
Wintersteller, Hannah, S195 (THU193)
Wint Han, Khin Aye, S276 (THU366)
Winther-Jensen, Matilde, S125 (THU015)
Wirtz, Theresa Hildegard, S193 (THU187)
Wisskirchen, Karin, S384 (THU591)
Wissmann, Jan-Erik, S250 (THU315)
Witherden, Elizabeth, S68 (OS089)
Withers, David, S28 (OS023)
Witschi, Magdalena, S225 (THU266)
Wittig, Linda, S930 (SAT584)
Witt, Jennifer, S608 (FRI485), S624 (FRI519)
Wittkop, Linda, S101 (OS146),
S250 (THU314)
Wittner, Melanie, S54 (OS069),
S197 (THU197)
Wiwa, Owens, S225 (THU266)
Wiznitzer, Arnon, S774 (SAT241)
Woerns, Marcus-Alexander, S523 (FRI262)
Wohlleber, Dirk, S195 (THU193)
Woitok, Marius Maximilian, S729 (SAT137)
Wójcicki, Maciej, S782 (SAT254)
Wolf, Armin, S488 (FRI197)
Wolff, Lisa, S877 (SAT445)
Wolfsberger, Annika, S374 (THU570),
S380 (THU582)
Wolski, Annika, S206 (THU229)
Wolstenholme, Jennifer, S178 (THU156)
Wolters, Frank, S601 (FRI457)
Wong, Alexander, S13 (LB004B),
S288 (THU389), S288 (THU390),
S291 (THU393), S581 (FRI384),
S881 (SAT453)
Wong, Angus, S933 (SAT592)
Wong, C., S464 (FRI148)
Wong, Danny Ka-Ho, S272 (THU358),
S273 (THU360), S275 (THU364)
Wong, Darren, S134 (THU029)
Wong, David, S849 (SAT394)
Wong, Florence, S19 (OS008), S49 (OS063),
S339 (THU494)
Wong, Flornce, S887 (SAT496)
Wong, Grace, S164 (THU088),
S302 (THU414), S852 (SAT400),
S861 (SAT415), S870 (SAT433)
Wong, Grace Lai-Hung, S39 (OS043),
S101 (OS147), S274 (THU362),
S390 (FRI004), S406 (FRI026),
S431 (FRI069), S906 (SAT530),
S933 (SAT592)
Wong, Jason, S209 (THU233)
Wong, Kuan Yau, S190 (THU183)
Wong, Philip, S614 (FRI497)
Wong, Randi, S886 (SAT493)
Wong, Robert, S274 (THU361),
S280 (THU372), S281 (THU376),
S286 (THU386), S341 (THU497),
S773 (SAT240), S831 (SAT356),
S846 (SAT387)
Wong, Rochelle, S729 (SAT138)
Wong, Simon, S308 (THU434)
Wong, Stanley, S17 (OS005), S43 (OS051),
S209 (THU233), S282 (THU378),
S910 (SAT538)
Wong, Steven, S274 (THU361)
Wong, Vincent Wai-Sun, S39 (OS043),
S101 (OS147), S154 (THU069),
S164 (THU088), S274 (THU362),
S302 (THU414), S390 (FRI004),
S406 (FRI026), S425 (FRI058),
S427 (FRI060), S431 (FRI069),
S448 (FRI102), S906 (SAT530),
S933 (SAT592)
Wong, Wing Yen, S404 (FRI023)
Wong, Yu Jun, S22 (OS014), S567 (FRI354),
S616 (FRI502)
Won Jun, Dae, S438 (FRI082),
S438 (FRI083), S439 (FRI086),
S484 (FRI189)
Wood, Kristy, S58 (OS073)
Woo, Hyun Young, S569 (FRI357)
Woolgar, Jinny, S433 (FRI073)
Wöran, Katharina, S532 (FRI280)
Worland, Thomas, S342 (THU501)
Worms, Nicole, S686 (SAT044)
Wörns, Marcus-Alexander, S80 (OS108),
S882 (SAT486)
Wowern, Natasja Von, S125 (THU015)
Woźniak, Małgorzata, S525 (FRI267)
Wraith, David, S608 (FRI470)
Wrba, Thomas, S24 (OS017)
Wree, Alexander, S309 (THU436),
S471 (FRI161)
Wright, Gail, S338 (THU490)
Wright, Mark, S122 (THU008),
S124 (THU013), S200 (THU218)
Wübbolding, Maximilian, S248 (THU311)
Wu, Chao, S287 (THU388), S296 (THU403),
S326 (THU468), S504 (FRI229)
Wu, Chia-Ying, S102 (OS148)
Wu, Chijung, S109 (OS160)
Wu, Cichun, S477 (FRI175)
Wuestefeld, Torsten, S694 (SAT059),
S723 (SAT123), S730 (SAT140),
S735 (SAT154)
Wu, Gang, S185 (THU173)
Wu, Gregory, S203 (THU223)
Wu, Guohui, S559 (FRI337)
Wu, Jamie, S449 (FRI103)
Wu, Jia-Feng, S514 (FRI247), S866 (SAT425)
Wu, Jian, S173 (THU151)
Wu, Jianguo, S33 (OS032)
Wu, Jinzi, S70 (OS091)
Wu, Juan, S78 (OS105)
Wu, Min, S824 (SAT343), S837 (SAT367),
S865 (SAT423)
Wunsch, Ewa, S315 (THU447),
S607 (FRI469)
Wupperfeld, Dominik, S712 (SAT095)
Wu, Qingyan, S262 (THU337)
Wu, Qipeng, S389 (FRI001)
Wu, Shusheng, S249 (THU312)
Wustner, Jay, S872 (SAT437)
Wu, Tianzhou, S803 (SAT289)
Wu, Tiffany, S491 (FRI204)
Wu, Tong, S388 (THU600)
Wu, Tongfei, S853 (SAT401)
Wu, Wei, S384 (THU591)
Wu, Wen-Chih, S595 (FRI410)
Wu, Wenqiang, S832 (SAT359),
S865 (SAT423)
Wu, Xiaoqin, S33 (OS032)
Wu, Xinle, S726 (SAT128), S726 (SAT129)
Wyatt, Brooke, S169 (THU098),
S298 (THU407)
Xavier, Sofia, S149 (THU060)
Xenofontos, Eleni, S202 (THU220)
Xia, Dongdong, S92 (OS130), S619 (FRI508),
S621 (FRI512), S628 (FRI526)
Xia, Jielai, S628 (FRI526)
Xiang, Dejuan, S181 (THU164)
Xiang, Hongyan, S181 (THU164)
Xiang, Huanyu, S181 (THU164)
Xia, Ningshao, S744 (SAT172)
Xiao, Huanming, S421 (FRI050)
Xiao, Huijuan, S883 (SAT488)
Xiao, Jing, S181 (THU164)
Xiao, Nanping, S182 (THU165)
Xiao, Shuang, S181 (THU164)
Xiao, Tian, S147 (THU055)
Xiao, Xiao-he, S377 (THU577)
Xia, Tian, S837 (SAT367)
Xie, Chan, S838 (SAT369)
Xie, Dongying, S838 (SAT369)

- Xie, Hui, S914 ([SAT558](#))
Xie, Lin, S151 ([THU063](#)), S534 ([FRI285](#))
Xie, Qing, S19 ([OS008](#)), S49 ([OS063](#)),
S70 ([OS091](#)), S299 ([THU408](#)),
S616 ([FRI502](#)), S867 ([SAT427](#))
Xie, Yandi, S26 ([OS020](#)), S278 ([THU369](#))
Xie, Yao, S70 ([OS091](#))
Xie, Zhe, S877 ([SAT445](#))
Xing, Huichun, S852 ([SAT399](#))
Xin, Jiaojiao, S66 ([OS086](#)), S357 ([THU524](#)),
S402 ([FRI021](#)), S744 ([SAT171](#)),
S744 ([SAT172](#)), S745 ([SAT173](#)),
S803 ([SAT289](#))
Xin, Shaojie, S803 ([SAT289](#))
Xin, Yongning, S22 ([OS014](#))
Xu, Cheng-Jian, S566 ([FRI352](#)),
S608 ([FRI485](#)), S857 ([SAT408](#))
Xu, Deming, S679 ([SAT030](#))
Xuefeng, Li, S183 ([THU167](#))
Xue, Zenghui, S299 ([THU408](#)),
S867 ([SAT427](#))
Xu, Flora, S567 ([FRI354](#))
Xu, Guang-Hua, S827 ([SAT349](#))
Xu, Jia, S894 ([SAT509](#))
Xu, Jianfeng, S717 ([SAT111](#))
Xu, Jiang-Hai, S827 ([SAT349](#))
Xu, Jun, S318 ([THU453](#)), S319 ([THU455](#))
Xu, Liang, S421 ([FRI050](#))
Xu, Pan, S662 ([FRI595](#))
Xu, Qingqing, S549 ([FRI317](#))
Xu, Simin, S244 ([THU302](#)), S247 ([THU309](#)),
S845 ([SAT385](#))
Xu, Tingfeng, S75 ([OS102](#))
Xu, Xiao, S815 ([SAT311](#))
Xu, Xiaoyuan, S278 ([THU369](#))
Xu, Yuanxin, S58 ([OS073](#))
Xu, Zhongyuan, S89 ([OS125](#))
Xydaki, Aikaterini, S472 ([FRI163](#))

Yaacov, Gil Ben, S784 ([SAT258](#)),
S804 ([SAT291](#))
Yadav, Ashish, S440 ([FRI087](#))
Yadav, Manisha, S34 ([OS033](#)),
S128 ([THU020](#)), S528 ([FRI273](#)),
S738 ([SAT161](#)), S752 ([SAT188](#))
Yaghootkar, Hanieh, S533 ([FRI284](#))
Yaginuma, Reiko, S687 ([SAT047](#))
Yaish, Dayana, S387 ([THU597](#))
Yale, Kitty, S719 ([SAT114](#))
Yamada, Hiroyuki, S3 ([GS004](#))
Yamada, Ryoko, S563 ([FRI346](#))
Yamada, Tomomi, S563 ([FRI346](#))
Yamamichi, Nobutake, S485 ([FRI192](#))
Yamamoto, Gen, S183 ([THU167](#))
Yamamoto, Leo, S225 ([THU267](#)),
S553 ([FRI324](#)), S591 ([FRI403](#))
Yamanaka-Okumura, Hisami,
S890 ([SAT500](#))
Yaman, Omer, S693 ([SAT058](#))
Yamasaki, Kazumi, S260 ([THU336](#))
Yamashina, Shunhei, S687 ([SAT047](#))
Yamashita, Taro, S563 ([FRI346](#))
Yamazhan, Tansu, S858 ([SAT411](#))
Yang, Aruhan, S89 ([OS125](#))

Yang, Bo, S272 ([THU357](#))
Yang, Chi-Chao, S45 ([OS054](#))
Yang, Chi-Chieh, S45 ([OS054](#)),
S595 ([FRI410](#))
Yang, Fengjuan, S323 ([THU462](#)),
S323 ([THU463](#))
Yang, Genren, S66 ([OS086](#))
Yang, Hui, S357 ([THU524](#)), S744 ([SAT171](#)),
S745 ([SAT173](#)), S803 ([SAT289](#))
Yang, Hwai-I, S102 ([OS148](#)), S294 ([THU398](#))
Yang, Hyun, S146 ([THU053](#))
Yang, Jiahong, S838 ([SAT369](#))
Yang, Ju Dong, S214 ([THU244](#)),
S377 ([THU575](#))
Yang, Junlin, S935 ([SAT594](#))
Yang, Ke, S322 ([THU461](#))
Yang, Kun, S414 ([FRI037](#))
Yang, Linjian, S463 ([FRI126](#))
Yang, Longbao, S883 ([SAT488](#))
Yang, Na, S22 ([OS014](#))
Yang, Ping, S272 ([THU357](#))
Yang, Qiang, S679 ([SAT030](#))
Yang, Ruifeng, S638 ([FRI545](#))
Yang, Sheng-Shun, S867 ([SAT427](#))
Yang, Shengshun, S595 ([FRI410](#))
Yang, Shiyong, S182 ([THU165](#))
Yang, Sien-Sing, S119 ([THU001](#))
Yang, Su-Jau, S597 ([FRI416](#))
Yang, Xinxiang, S636 ([FRI542](#))
Yang, Xinye, S254 ([THU323](#)), S727 ([SAT132](#))
Yang, Xu, S388 ([THU600](#))
Yang, Yao, S638 ([FRI545](#))
Yang, Yao-Hsu, S870 ([SAT433](#))
Yang, Ying, S278 ([THU369](#))
Yang, Yongfeng, S70 ([OS091](#)),
S326 ([THU468](#))
Yang, Yongping, S377 ([THU577](#))
Yang, Yuan, S295 ([THU402](#))
Yan, Jacinth, S24 ([OS016](#)), S530 ([FRI275](#))
Yan, Ran, S266 ([THU346](#)), S836 ([SAT366](#))
Yan, Tao, S388 ([THU600](#))
Yan, Wenhao, S865 ([SAT423](#))
Yan, Yuemei, S70 ([OS091](#))
Yao, Frederick, S769 ([SAT232](#))
Yao, Heng, S744 ([SAT171](#)), S745 ([SAT173](#)),
S803 ([SAT289](#))
Yapali, Suna, S858 ([SAT410](#)), S861 ([SAT416](#)),
S864 ([SAT421](#))
Yaquich, Pamela, S137 ([THU034](#))
Yardeni, David, S145 ([THU049](#)),
S269 ([THU350](#)), S300 ([THU411](#)),
S859 ([SAT412](#))
Yashiro, Hiroaki, S7 ([GS009](#))
Yasuda, Satoshi, S430 ([FRI067](#)),
S875 ([SAT442](#))
Yasui, Yutaka, S379 ([THU580](#))
Yates, Bridget, S404 ([FRI023](#))
Yates, Katherine, S451 ([FRI107](#)),
S701 ([SAT073](#))
Yatomi, Yutaka, S485 ([FRI192](#))
Yatsuhashi, Hiroshi, S563 ([FRI346](#))
Yazdi, Tahmineh, S244 ([THU302](#)),
S247 ([THU309](#)), S845 ([SAT385](#))
Ydreborg, Magdalena, S580 ([FRI382](#))

Yee, Leland, S870 ([SAT433](#))
Yee, Michael, S444 ([FRI094](#))
Ye, Feng, S879 ([SAT449](#))
Yegurla, Jatin, S19 ([OS008](#)), S49 ([OS063](#)),
S633 ([FRI534](#))
Yeh, Chau-Ting, S638 ([FRI546](#)),
S827 ([SAT350](#)), S867 ([SAT427](#))
Yehezkel, Adi, S83 ([OS114](#)), S725 ([SAT126](#))
Yeh, Ming-Lun, S458 ([FRI118](#)),
S595 ([FRI410](#)), S875 ([SAT442](#))
Yehoshua, Alon, S237 ([THU290](#)),
S597 ([FRI416](#))
Yeh, Yen-Po, S45 ([OS054](#))
Yekula, Anuroop, S235 ([THU286](#))
Ye, Lei, S828 ([SAT351](#)), S829 ([SAT352](#))
Ye, Liangtao, S655 ([FRI581](#)), S662 ([FRI596](#))
Yeo, Ee Jin, S298 ([THU406](#))
Yeo, Jian, S409 ([FRI031](#))
Yeo, Malcolm Guan Hin, S561 ([FRI343](#))
Yeoman, Andrew, S96 ([OS137](#)),
S529 ([FRI274](#))
Yeon, Yubin, S138 ([THU037](#))
Yeo, Yee Hui, S215 ([THU245](#)), S883 ([SAT488](#))
Ye, Qing, S883 ([SAT488](#))
Yeung, Alan, S266 ([THU345](#))
Yeung, Hing-Yuen, S602 ([FRI458](#))
Yiasemi, Ioanna, S202 ([THU220](#))
Yi, CC, S868 ([SAT428](#))
Yigit, Buket, S693 ([SAT058](#))
Yildirim, Mustafa, S858 ([SAT411](#))
Yildiz, Ilknur Esen, S858 ([SAT411](#))
Yilmaz, Sezai, S782 ([SAT255](#)),
S820 ([SAT316](#))
Yim, Colina, S849 ([SAT394](#))
Yim, Hyung Joon, S13 ([LB004B](#)),
S288 ([THU389](#)), S288 ([THU390](#)),
S291 ([THU393](#)), S616 ([FRI502](#)),
S881 ([SAT453](#)), S932 ([SAT590](#))
Yi, Min, S14 ([LB006](#))
Yim, Sun Young, S932 ([SAT590](#))
Yi, Nam-Joon, S798 ([SAT281](#))
Yin, James Liu, S534 ([FRI286](#))
Yin, Wenwei, S196 ([THU195](#))
Yin, Zhanxin, S92 ([OS130](#)),
S619 ([FRI508](#)), S621 ([FRI512](#)),
S628 ([FRI526](#))
Yip, Terry Cheuk-Fung, S39 ([OS043](#)),
S101 ([OS147](#)), S164 ([THU088](#)),
S274 ([THU362](#)), S302 ([THU414](#)),
S390 ([FRI004](#)), S406 ([FRI026](#)),
S870 ([SAT433](#)), S906 ([SAT530](#)),
S933 ([SAT592](#))
Yip, Vincent, S108 ([OS158](#))
Yıldırım, Abdullah Emre, S19 ([OS008](#)),
S49 ([OS063](#)), S858 ([SAT410](#)),
S861 ([SAT416](#))
Yilmaz, Utku Tonguç, S782 ([SAT255](#))
Yilmaz, Yusuf, S154 ([THU069](#)),
S209 ([THU234](#)), S474 ([FRI168](#)),
S714 ([SAT103](#))
Yki-Järvinen, Hannele, S111 ([OS162](#)),
S458 ([FRI117](#)), S690 ([SAT052](#)),
S694 ([SAT060](#))
Yoh, Tomoaki, S183 ([THU167](#))

Author Index

- Yoneda, Masato, S425 (FRI058), S430 (FRI067), S448 (FRI102), S452 (FRI108)
- Yongliang, Zhao, S717 (SAT111)
- Yoo, Jeongin, S303 (THU417)
- Yoo, Jeong-Ju, S589 (FRI398)
- Yoo, Juhwan, S100 (OS144)
- Yoon, Bo Hyung, S168 (THU097), S170 (THU099), S291 (THU392), S301 (THU413)
- Yoon, Eileen, S160 (THU079), S224 (THU264), S435 (FRI077), S438 (FRI082), S438 (FRI083), S439 (FRI086), S462 (FRI124), S589 (FRI398), S728 (SAT135), S729 (SAT136), S875 (SAT442), S932 (SAT590)
- Yoon, Jung-Hwan, S78 (OS104), S667 (SAT005)
- Yoon, Jun Sik, S572 (FRI365)
- Yoon, Kyung Chul, S798 (SAT281)
- Yoon, Peter, S815 (SAT311)
- Yoon, Seung Kew, S820 (SAT317), S932 (SAT589)
- Yoon, Yeup, S489 (FRI199)
- Yoruk, Gulsen, S858 (SAT411)
- Yoshida, Atsushi, S778 (SAT249)
- Yoshida, Eric, S799 (SAT284), S910 (SAT538)
- Yoshida, Kyoko, S290 (THU391)
- Yoshiji, Hitoshi, S90 (OS127), S563 (FRI346)
- Yoshino, Kenji, S183 (THU167)
- Yoshizawa, Atsushi, S183 (THU167)
- You, Hong, S22 (OS014), S89 (OS125)
- Younes, Ramy, S425 (FRI058), S448 (FRI102), S452 (FRI108)
- Younes, Ziad H., S427 (FRI060)
- Young Lee, Hyo, S438 (FRI082), S438 (FRI083), S439 (FRI086)
- Young, Liam, S526 (FRI269)
- Young, Sara, S592 (FRI405)
- Youngson, Neil, S650 (FRI569), S911 (SAT540)
- Young, TW, S868 (SAT428)
- Young, Vincent B., S180 (THU162)
- Young Woo, Hyun, S572 (FRI365), S586 (FRI392)
- Younossi, Elena, S209 (THU234), S420 (FRI048), S429 (FRI064), S447 (FRI100)
- Younossi, Issah, S154 (THU069), S155 (THU071), S209 (THU234), S445 (FRI097)
- Younossi, Youssef, S5 (GS008), S156 (THU073)
- Younossi, Zobair, S5 (GS008), S31 (OS028), S144 (THU048), S148 (THU058), S150 (THU062), S154 (THU069), S155 (THU071), S156 (THU073), S209 (THU234), S409 (FRI030), S416 (FRI040), S420 (FRI048), S429 (FRI064), S445 (FRI097), S447 (FRI100), S762 (SAT208), S785 (SAT260), S810 (SAT300)
- You, Shaoli, S803 (SAT289)
- You, Shihyun, S873 (SAT439), S880 (SAT451)
- Yousif, Jenna, S612 (FRI493)
- Youssef, Amir, S875 (SAT441)
- Yousuf, Hassaan, S531 (FRI279)
- You, Young Kyoung, S820 (SAT317)
- Ytting, Henriette, S331 (THU477), S887 (SAT495)
- Yu, Amanda, S17 (OS005), S43 (OS051), S209 (THU233), S282 (THU378), S910 (SAT538)
- Yuan, Jie, S92 (OS130), S619 (FRI508), S621 (FRI512), S628 (FRI526)
- Yuan, Lunzhi, S744 (SAT172)
- Yuan, Xiaojian, S559 (FRI337)
- Yuan, Yuan, S872 (SAT437)
- Yuan, Yulin, S182 (THU165)
- Yubao, Zheng, S344 (THU504)
- Yuen, Lilly, S251 (THU318)
- Yuen, Man-Fung, S13 (LB004B), S69 (OS090), S78 (OS105), S177 (THU154), S266 (THU346), S272 (THU358), S273 (THU360), S275 (THU364), S288 (THU389), S288 (THU390), S291 (THU393), S299 (THU408), S824 (SAT343), S824 (SAT344), S831 (SAT357), S835 (SAT365), S836 (SAT366), S848 (SAT392), S849 (SAT393), S850 (SAT396), S851 (SAT397), S852 (SAT400), S861 (SAT415), S864 (SAT422), S867 (SAT427), S871 (SAT435), S872 (SAT437), S876 (SAT443), S878 (SAT448), S881 (SAT453)
- Yu, Hua, S540 (FRI299)
- Yuksel, Merve, S513 (FRI245)
- Yu, Meng, S669 (SAT009)
- Yu, Ming-Lung, S119 (THU001), S154 (THU069), S458 (FRI118), S595 (FRI410), S863 (SAT420), S875 (SAT442)
- Yumita, Sae, S615 (FRI501), S897 (SAT514)
- Yumol, Marjorie, S120 (THU004), S647 (FRI562)
- Yung, Diana, S19 (OS008), S49 (OS063)
- Yung, Rossitta, S225 (THU267), S553 (FRI324), S591 (FRI403)
- Yunis, Carla, S7 (GS009), S448 (FRI102), S452 (FRI108)
- Yu, Philip, S78 (OS105)
- Yu, Qifeng, S517 (FRI253), S519 (FRI256), S521 (FRI259)
- Yu, Q. W., S389 (FRI001)
- Yu, QW, S601 (FRI456)
- Yurdaydin, Cihan, S274 (THU361), S293 (THU397), S297 (THU405), S693 (SAT058), S830 (SAT355)
- Yu, Su Jong, S922 (SAT571)
- Yusupaliev, Bakhodir, S235 (THU288)
- Yu, W., S464 (FRI148)
- Yu, Yun Suk, S490 (FRI202)
- Yu, Zhou, S832 (SAT359)
- Yu, Zu-Jiang, S827 (SAT349)
- Zaanan, Aziz, S372 (THU566)
- Zaccherini, Giacomo, S357 (THU523), S908 (SAT535)
- Zacharias, Harry D, S890 (SAT501)
- Zacharis, Katerina, S737 (SAT157)
- Zachou, Kalliopi, S326 (THU467)
- Zahoran, Szabolcs, S652 (FRI572)
- Zakhashvili, Khatuna, S233 (THU283), S267 (THU347)
- Zaldera, Paola, S543 (FRI306)
- Zali, Mohammadreza, S228 (THU273)
- Zamalloa, Ane, S68 (OS089), S371 (THU550)
- Zambrano, Elisaul Suarez, S931 (SAT586)
- Zambrano, Sheila Gato, S459 (FRI119), S708 (SAT087)
- Zamora, Javier, S114 (OS168), S114 (OS169)
- Zamparelli, Marco Sanduzzi, S381 (THU584)
- Zampini, Matteo, S758 (SAT201)
- Zanaga, Paola, S192 (THU185)
- Zanatto, Laura, S37 (OS039), S527 (FRI271)
- Zandanel, Stephan, S428 (FRI062)
- Zanderigo, Floriana, S872 (SAT436)
- Zanetto, Alberto, S306 (THU423), S358 (THU526)
- Zangneh, Hooman Farhang, S3 (GS004), S569 (FRI359)
- Zanieri, Luca, S480 (FRI179)
- Zaninotto, Martina, S49 (OS062)
- Zanin-Zhorov, Alexandra, S494 (FRI209)
- Zanoni, Giovanna, S658 (FRI586), S925 (SAT574)
- Zanotto, Ilaria, S378 (THU578), S478 (FRI176), S479 (FRI177)
- Zanuso, Valentina, S923 (SAT572)
- Žarak, Marko, S612 (FRI494)
- Zarantonello, Lisa, S888 (SAT497)
- Zarebska-Michaluk, Dorota, S565 (FRI350), S585 (FRI390), S592 (FRI406)
- Zaroui, Amira, S532 (FRI281)
- Zasorina, Daria, S574 (FRI370)
- Zatorska, Michalina, S704 (SAT081)
- Zauner, Christian, S354 (THU519)
- Zazueta, Godolfino Miranda, S19 (OS008), S49 (OS063)
- Zeevi, Gil, S774 (SAT241)
- Zehnder, Anna, S703 (SAT078)
- Zeigerer, Anja, S606 (FRI467), S703 (SAT079)
- Zekrini, Kamal, S61 (OS076)
- Zelber-Sagi, Shira, S148 (THU056)
- Zeller, Katharina, S904 (SAT528)
- Zender, Lars, S132 (THU026), S737 (SAT158)
- Zeng, Ni, S167 (THU094)
- Zeng, Qing-Lei, S616 (FRI502), S827 (SAT349)
- Zeng, Yan-Li, S827 (SAT349)
- Zeng, Yi-lan, S838 (SAT369)
- Zeng, Zheng, S182 (THU165)
- Zeni, Nicola, S895 (SAT511)
- Zenlander, Robin, S423 (FRI053)
- Zenovia, Sebastian, S573 (FRI368)
- Zentar, Marc, S135 (THU031), S352 (THU516)

- Zen, Yoh, S120 (THU004), S308 (THU435), S647 (FRI562), S650 (FRI569)
- Zeo-Sánchez, Daniel E. Di, S326 (THU467)
- Zessner-Spitzenberg, Jasmin, S470 (FRI159)
- Zetter, Alithea, S419 (FRI045)
- Zetterberg, Fredrick, S481 (FRI182)
- Zeuzem, Stefan, S4 (GS006), S15 (OS001), S16 (OS003), S262 (THU337), S313 (THU444), S353 (THU517), S354 (THU518), S585 (FRI391), S587 (FRI395), S590 (FRI400), S590 (FRI401), S823 (SAT341), S907 (SAT531)
- Zeybel, Mujdat, S293 (THU397), S297 (THU405), S693 (SAT058)
- Zeytunlu, Murat, S399 (FRI015), S782 (SAT255)
- Zha, Jiping, S443 (FRI093), S486 (FRI193)
- Zhang, Bai-Hua, S245 (THU303)
- Zhang, Bo, S471 (FRI162)
- Zhang, Dazhi, S240 (THU296)
- Zhang, Dengwei, S177 (THU154)
- Zhang, Dong, S832 (SAT359), S865 (SAT423)
- Zhang, Gaoli, S763 (SAT210)
- Zhang, George, S865 (SAT423)
- Zhang, Guo, S182 (THU165)
- Zhang, Guofan, S827 (SAT349)
- Zhang, Guofang, S718 (SAT112)
- Zhang, Guoqiang, S827 (SAT349)
- Zhang, Haiting, S526 (FRI268)
- Zhang, Haoran, S389 (FRI001), S601 (FRI456)
- Zhang, Hong, S89 (OS125), S837 (SAT367), S865 (SAT423)
- Zhang, Hongxu, S827 (SAT349)
- Zhang, Huafeng, S803 (SAT289)
- Zhang, Huai, S86 (OS120)
- Zhang, Ingrid W., S370 (THU549)
- Zhang, Ingrid Wei, S361 (THU530), S674 (SAT019)
- Zhang, Jiaxuan, S763 (SAT210)
- Zhang, Jiayuan, S883 (SAT488)
- Zhang, Jiliang, S679 (SAT030)
- Zhang, Jiming, S299 (THU408)
- Zhang, Ji-Yuan, S827 (SAT349)
- Zhang, Jun, S708 (SAT088)
- Zhang, Ke, S384 (THU591)
- Zhang, Lei, S89 (OS125)
- Zhang, Lening, S534 (FRI285)
- Zhang, Lihua, S35 (OS035)
- Zhang, Linwen, S526 (FRI268)
- Zhang, Linzhi, S388 (THU600)
- Zhang, Liting, S182 (THU165), S492 (FRI206)
- Zhang, Lukan, S301 (THU412), S304 (THU418)
- Zhang, Luyong, S389 (FRI001), S601 (FRI456)
- Zhang, Mengnan, S679 (SAT030)
- Zhang, Mingxin, S22 (OS014)
- Zhang, Ningning, S920 (SAT568)
- Zhang, Peng, S883 (SAT488)
- Zhang, Qin, S70 (OS091)
- Zhang, Qingge, S182 (THU165)
- Zhang, Qingling, S835 (SAT365), S853 (SAT401), S871 (SAT435)
- Zhang, RanRan, S673 (SAT017)
- Zhang, Rui, S421 (FRI050), S642 (FRI552)
- Zhang, Saisai, S177 (THU154)
- Zhang, Shi-Jin, S421 (FRI050)
- Zhang, Shu, S335 (THU485)
- Zhang, Shuang, S165 (THU091)
- Zhang, Shuangxia, S272 (THU357)
- Zhang, Shujie, S272 (THU357)
- Zhang, Shuwen, S920 (SAT568)
- Zhang, Siyi, S215 (THU245)
- Zhang, Stephanie, S298 (THU407)
- Zhang, Wei, S477 (FRI175)
- Zhang, Wen, S299 (THU408), S867 (SAT427)
- Zhang, Wenhong, S299 (THU408), S867 (SAT427)
- Zhang, Wen-hua, S838 (SAT369)
- Zhang, Wenjun, S686 (SAT045)
- Zhang, Xi, S879 (SAT449)
- Zhang, Xian-Man, S690 (SAT052)
- Zhang, Xiaodong, S920 (SAT568)
- Zhang, Xinlian, S414 (FRI037)
- Zhang, Xinrong, S39 (OS043), S164 (THU088)
- Zhang, Xuchen, S935 (SAT594)
- Zhang, Xuehong, S912 (SAT554)
- Zhang, Yan, S344 (THU504)
- Zhang, Yanhua, S865 (SAT423)
- Zhang, Yi, S341 (THU497)
- Zhang, Yibo, S708 (SAT088)
- Zhang, Ying Jun, S727 (SAT132)
- Zhang, Yingzhi, S196 (THU195)
- Zhang, Yong, S22 (OS014)
- Zhang, Yong-Yuan, S245 (THU303)
- Zhang, Yuchen, S299 (THU408)
- Zhang, Yuwei, S914 (SAT558)
- Zhang, Zhenfeng, S265 (THU344)
- Zhang, Zhijun, S837 (SAT367)
- Zhao, Bigeng, S75 (OS102), S638 (FRI545)
- Zhao, Caroline, S726 (SAT130)
- Zhao, Derrick, S178 (THU156)
- Zhao, Jieling, S489 (FRI200)
- Zhao, Lili, S22 (OS014), S616 (FRI502)
- Zhao, Longgang, S912 (SAT554)
- Zhao, Qianwen, S366 (THU539)
- Zhao, Wei-Guo, S421 (FRI050)
- Zhao, Wenjuan, S879 (SAT449)
- Zhao, Xiaoling, S182 (THU165)
- Zhao, Xin, S332 (THU478)
- Zhao, Xun, S614 (FRI497)
- Zhavoronok, Sergei, S269 (THU351)
- Zheng, Freeman, S605 (FRI465)
- Zheng, Haoyang, S37 (OS041)
- Zheng, Huanwei, S278 (THU369)
- Zheng, Ming-Hua, S86 (OS120), S421 (FRI050), S425 (FRI058), S431 (FRI069), S448 (FRI102), S452 (FRI108)
- Zheng, Qiuxian, S699 (SAT069)
- Zheng, Sujun, S278 (THU369), S844 (SAT382)
- Zheng, Tian-lei, S22 (OS014), S421 (FRI050)
- Zheng, Xin, S344 (THU504)
- Zhigan, Jiang, S832 (SAT359), S865 (SAT423)
- Zhorov, Iris, S494 (FRI209)
- Zhou, Dan, S492 (FRI206)
- Zhou, Haoming, S695 (SAT062)
- Zhou, Hongwei, S182 (THU165), S636 (FRI540)
- Zhou, Huiping, S178 (THU156)
- Zhou, Jian, S78 (OS105)
- Zhou, Jingye, S717 (SAT111)
- Zhou, Kali, S79 (OS106), S797 (SAT278)
- Zhou, Linghua, S72 (OS094)
- Zhou, Qian, S66 (OS086), S745 (SAT173), S803 (SAT289)
- Zhou, Shi-Yi, S180 (THU162)
- Zhou, Taotao, S381 (THU585)
- Zhou, Xin, S272 (THU357)
- Zhou, Xingping, S66 (OS086), S744 (SAT172), S803 (SAT289)
- Zhou, Xiqiao, S182 (THU165)
- Zhou, Xue, S299 (THU408), S867 (SAT427)
- Zhou, Yi, S182 (THU165)
- Zhou, Yuanping, S245 (THU303)
- Zhou, Yuhong, S384 (THU591)
- Zhou, Yu-Jie, S431 (FRI069)
- Zhuang, Xiaodong, S758 (SAT199)
- Zhu, Chenqian, S301 (THU412), S304 (THU418)
- Zhu, Chuanwu, S287 (THU388), S296 (THU403), S326 (THU468), S504 (FRI229)
- Zhu, Dedong, S301 (THU412), S304 (THU418)
- Zhu, Julie, S717 (SAT111), S799 (SAT284)
- Zhu, Li, S287 (THU388), S296 (THU403), S326 (THU468), S504 (FRI229)
- Zhu, Pei-Wu, S431 (FRI069)
- Zhu, Ping, S182 (THU165)
- Zhu, Qianru, S215 (THU245)
- Zhuravleva, Ekaterina, S77 (OS103)
- Zhu, Rui, S726 (SAT128), S726 (SAT129)
- Zhu, Shijia, S36 (OS037), S642 (FRI553)
- Zhu, Xiaoxue, S89 (OS125), S837 (SAT367)
- Zhu, Yanfang Peipei, S471 (FRI161)
- Zhu, Yong-Fen, S421 (FRI050)
- Zhu, Yunxia, S272 (THU357)
- Ziarkiewicz-Wróblewska, Bogna, S156 (THU072)
- Ziayee, Mariam, S154 (THU069)
- Zieniewicz, Krzysztof, S156 (THU072)
- Zihang, Yuan, S389 (FRI001), S601 (FRI456)
- Žilincan, Michal, S613 (FRI496)
- Zimmer, Christine, S27 (OS021)
- Zimmermann, Robert, S688 (SAT049)
- Zimny, Sebastian, S602 (FRI460)
- Zimper, Gudula, S80 (OS108)
- Zinober, Kerstin, S753 (SAT191)
- Ziol, Marianne, S372 (THU566)
- Zipprich, Alexander, S342 (THU500), S369 (THU546), S620 (FRI510)
- Zischka, Hans, S602 (FRI460)
- Zisimopoulos, Konstaninos, S840 (SAT374)
- Zizer, Eugen, S823 (SAT341)
- Zjalic, Milorad, S718 (SAT113)

Author Index

- Zocco, Maria Assunta, S507 ([FRI234](#))
Zoldan, Katharina, S100 ([OS143](#)),
S710 ([SAT090](#))
Zoller, Heinz, S470 ([FRI159](#)), S537 ([FRI292](#)),
S829 ([SAT353](#)), S830 ([SAT354](#))
Zöllner, Caroline, S823 ([SAT341](#))
Zölzer, Dominik, S915 ([SAT559](#))
Zomorodi, Katie, S834 ([SAT363](#)),
S846 ([SAT388](#)), S847 ([SAT389](#))
Zong, Zhixin, S847 ([SAT389](#))
Zorde-Khavlevsky, Elina, S764 ([SAT213](#))
Zorzano, Antonio, S674 ([SAT019](#))
Zougmore, Honore, S270 ([THU352](#))
Zou, Guangyong, S416 ([FRI040](#))
Zou, Guizhou, S70 ([OS091](#))
Zou, Haixia, S726 ([SAT128](#)), S726 ([SAT129](#))
Zoulim, Fabien, S72 ([OS093](#)),
S245 ([THU303](#)), S246 ([THU306](#)),
S247 ([THU307](#)), S356 ([THU522](#)),
S766 ([SAT216](#)), S824 ([SAT344](#)),
S833 ([SAT360](#)), S868 ([SAT429](#)),
S880 ([SAT450](#))
Zou, Xiantong, S463 ([FRI126](#))
Zubiaga, Ana, S651 ([FRI571](#)),
S665 ([SAT001](#))
Zucman-Rossi, Jessica, S639 ([FRI548](#))
Zuin, Massimo Giovanni, S61 ([OS077](#)),
S539 ([FRI297](#))
Zulet, María A., S500 ([FRI222](#))
Zulkhuu, Delgersaikhan, S235 ([THU287](#))
Zuluaga, Paola, S199 ([THU199](#))
Zulueta, Javier, S802 ([SAT288](#))
Zurawek, Dariusz, S759 ([SAT203](#))
Zurera, Coral, S199 ([THU199](#))
zu Siederdisen, Christoph Hoener,
S248 ([THU311](#))
Zwaenepoel, Karen, S637 ([FRI544](#))
Zwanziger, Denise, S341 ([THU498](#))
Zwinderman, Aeilko, S74 ([OS097](#))

Disclosures: no commercial relationships

The following abstract submitters have indicated that they have no relationships with commercial entities that might be perceived as having a connection with their presentation:

Niels Kristian Aagaard	Monika Adamowicz	Charisse Ahmed
Christer F. Aas	David Adams	Mohamed Ahmed
cristiana abazia	Huyen Adams	Syed Ahmed
Nadir Abbas	Leon Adams	Muneeb Ahmed
Fariba Abbassi	Haydar Adanir	Sang Bong Ahn
Gian Luca Abbati	Pietro Addeo	Sang Hoon Ahn
Jane Abbott	Marylyn Addo	Joseph Ahn
Amr Abdelaal	Adeyinka Adejumo	Lisa Ahne
Manal Abdelmalek	Hammoutene Adel	Adriana Ahumada
Abo Zed Abdelrhman	Jelle Adelmeijer	Riccardo Aiese Cigliano
Ahmed Abdelwahab	Jorge Adeva	Hiroshi Aikata
Mostafa Abdo	Mopelola Adeyemo	Maria Elena Ainora
Ayman Abdo	Oyedele Adeyi	Rhona E Aird
Kabbani Abdul-Rahman	Xavier Adhoute	Aldo Airoidi
Kanon Abe	Mehmet Adigüzel	Shinichi Aishima
Leticia Abecia	Luigi Elio Adinolfi	Lola Ajayi
Nada Abedin	Andreas Adler	Saima Ajaz
Stephan Aberle	Pauline Adnot	Veeral Ajmera
Hanna Aberra	Luciano Adorini	Ulus Akarca
Itziar Abete	Valentina Adotti	Mesut Akarsu
Natali Abeywickrama Samarakoon	Annie Adrait	Meral Akdogan Kayhan
George Abouda	Celina Adraneda	Mohammad Khalil Akhter
Marwan Abouljoud	Prince Adu	Tomoyuki Akita
Michal Abraham	Niklas F Aehling	Murat Akyildiz
George Abraham	Maridi Aerts	Al Shaima Al Hinai
Arun Abraham	Nezam Afdhal	Rola Al-Sayegh
Juan Abralles	Arnon Afek	Reem Al Shabeeb
Joanna Abramczyk	Silvia Affo	Amr Al Shebel
Ifat Abramovich	João Afonso	Aftab Ala
Rinat Abramovitch	Marta B. Afonso	Balqis Alabdulkarim
Luis Abreu de Carvalho	Catarina Afonso	Walid Al-Akkad
Fadi Abu Baker	Samagra Agarwal	Seema Alam
Muhammad Radzi Abu Hassan	Pankaj Aggarwal	Ali Al-Anbaki
Samira Abu Jhaisha	Sandeep Aggarwal	Atef Alattar
Saif Mahmud Abu Mouch	Nancy Agmon-Levin	Marko Alavanja
Naim Abu-Freha	Polyxeni Agorastou	Maryam Alavi
Yehia Abugabal	Bella Agranovich	William Alazawi
Jeries Abu-Hanna	Chiara Agrati	Romain Albenois
Mohamed Abu-Nada	Adele Agresta	Hannes Alber
Abdelrahman Aburaia	Ferran Aguilar	Cathy Alberda
Ameer Abutaleb	Laia Aguilar	Angel Alberich-Bayarri
Akaki Abutidze	Juan Ramón Aguilar	Matthew Albert
Antonio Accetta	Beatriz Aguilar-Bravo	Cecilia Albert-Antequera
Laia Aceituno	A. Aguilera	Somaya Albhaisi
María Achalandabaso	Ricardo Aguilera Rosales	Agustin Albillos
Weber Achim	Victoria Aguilera Sancho	Jan Albin
Silvia Acosta-López	George Agyapong	Thomas Albrecht
Antonio Acquaviva	Lee Han Ah	Nicolai J Wewer Albrechtsen
Gupse Adali	Noora Ahlholm	Joseph Alcorn
René Adam	Shafqat Ahmad	Rafael Aldabe
Svetlana Adamcova Selcanova	Nabil Ahmed	Mark Aldersley
Ekaterine Adamia	Kinza Ahmed	Luca Aldrighetti

Disclosures

Rafael Alejandro
Soo Aleman
Vanessa Alemanni
Daniel Alemu
Yusef Alenezi
Carlo Alessandria
Maria Grazia Alessio
Loredana Alessio
Sophie Alex
Leigh Alexander
Adibekian Alexander
Ian Alexander
Fuchs Alexandra
Gonçalo Alexandrino
Theodoros alexopoulos
Alexandra Alexopoulou
Ana Alfaro
Clara Alfaro-Cervello
Lludovico Alfarone
Bazga Ali
Ahmad Ali
Fatima Ali
Angela Alibrandi
Eleonora Alimenti
Anna Alisi
Benard Aliwa
Tom Alix
Saad AlKaabi
Mohammad Alkhatib
Maia Alkhazashvili
Huseyin Alkim
Dalia Allam
Marc Antoine Allard
Sophie Allen
Kathryn Allen
Rocío Aller
Rocio Aller de la Fuente
Francesca Alletto
Michael Allison
Chakib Alloui
Caroline Allsop
Lena Allweiss
Hussam Almasri
Bruna Almeida
Alessandro Almeida
Marion Almes
Carolina Almohalla
Carmen Alonso Martin
Saleh Alqahtani
Laurent Alric
Laith Al-Rubaiy
Rami Al-Sayegh
Deema AlSoub
Khalid Alswat
Enkhjargal Altangere
Arwen Altenburg
Johannes Altenmüller
Adriana Alter
Heidi Altmann
Joseph Alukal
Varuna Aluvihare
Aoife Alvain
Edilmar Alvarado-Tapias
Mario Reis Álvares-da-Silva
Laura Alvarez
Maria Alvarez
Ismael Alvarez-Alvarez
Carmen Álvarez-Navascués

Gloria Álvarez-Sola
del Rio Alvaro
Frank Alvaro
Rogério Alves
Cláudia Alves Couto
Pedro Alves de Castro
Diego Alves Vieira
Ian Alwayn
Giuliana Amaddeo
Pedro Amado Villanueva
Suneetha Amara
Benon Amare
Raphael Ambros
Josep Amengual
Johnny Amer
Clara Amiama Roig
Lidia Amigo
Oliver E Amin
Janaki Amin
Mohammad Amin Fallahzadeh
Daphni Ammon
Simona Amodeo
Angela Maria Amorini
Javier Ampuero
Rachida Amzal
Samira Amzou
Qi An
Weimin An
Qian An
Despina Anagnostou
Abhinav Anand
Hanish Anand
Utpal Anand
Dimitrios Anastasiou
Julian Anders
Maria Margarita Anders
Peter Andersen
Jesper Andersen
Patricia Anderson
R. Rox Anderson
Jenine Anderson
Monique Andersson
Emma Andersson
Raul J. Andrade
Antonio Andrade
Eleonora Andreassi
Anna Andreasson
Ana Andreadza
Pietro Andreone
Thibault Andrieu
Le Shaun Ang
Peter Angel
Francesco Angelico
Federica Angelone
Martin Angerer
Tori Anglin
Debora Angrisani
Juan Anguita
Peter Angus
Geerts Anja
Johan Ankarklev
Maliki Ankavay
Piekariska Anna
Ay Anne-Sophie
Monica Annunziata
Francesco Annunziata
Maria Paola Anolli
Azim Ansari

Corinne Antoine
Benedicte Antoine
Laura Antolini
María Dolores Antón Conejero
Christoph Antoni
Teresa Antonini
Luiz Antônio Rodrigues de Freitas
Steen Antonsen
Michela Antonucci
Amir Anushiravani
Ling Ao
Olufemi Aoko
Myriam Aouadi
Lynda Aoudjehane
Maider Apodaka-Biguri
Giuseppe Aprile
Bashar Aqel
Marco Aquino
Juan Pablo Arab
Mohammad Arabpour
Carlos Aracil
Kumiko Arai
Juan Pablo Arancibia
Ana María Aransay
Carlos Araújo
Aloysious Aravinthan
Ander Arbelaiz
Jose M Arbones Mainar
Marcello Arca
Ricardo M Arcay
Sara Arcelus
Sara Archer
Alba Ardevol
Maria Arechederra
Bethlehem Arefaine
Umberto Arena
Victor Arendt
Nicoline Stender Arentoft
Josep Maria Argemi
Josepmaria Argemi
Pamela Argiriadi
Derya Ari
Pascu Ariana
Ana Arias
María Teresa Arias Loste
Sena Arici
Silvia Ariño Mons
Makoto Arita
Perttu Arkkila
Juan Armendariz-Borunda
Carolina Armengol
Susana Armesto
Xiimena Armijos
Paige A Armstrong
Matthew Armstrong
Katherine Arndtz
Jorge Arnold
Alexander Arnold
Joud Arnouk
Samantha Arokiasamy
Johanna Arola
Anil Arora
Sanjeev Arora
Vinod Arora
Maria Arranz
Isabel Arranz-Salas
Marco Arrese
Fernanda Arriaga-González

Lionel Arrivè
 Vicente Arroyo
 Mehmet Arslan
 Aysenur Arslan
 Anita Arslanow
 Reha Artan
 Tomás Artaza Varasa
 Elvis Arteaga
 Gavin Arteel
 Benedetta Artegiani
 Adelina Artenie
 Callum Arthurs
 Renate Artmann
 Florent Artru
 Thierry Artzner
 Manimozhiyan Arumugam
 Rishi Aryal
 Mahmoud Aryan
 Erikc Jesús Arzola-Renteria
 Hamid Asadzadeh Aghdaei
 Aliya Asghar
 Candice Ashmore-Harris
 Sumar Askar
 Gro Askgaard
 Mujahid Aslam
 Rahmi Aslan
 Ana Aslanikashvili
 Jessica Aspas
 Lars Asphaug
 Richard Aspinall
 Alexander Aspinall
 Silvia Aspite
 Keren Asraf
 Sumeet Asrani
 Suraphon Assawasuwannakit
 Eric Assenat
 Edmond Atallah
 Ali Atay
 Emmanouil Athanasiadis
 Varinder Athwal
 Francisco Atienza
 Francisco Javier Atienza Martín
 Mo Atif
 Cecilia Atik
 Stephen Atkinson
 Masanori Atsukawa
 Maria Rosaria Attanasio
 Nabeel Attarwala
 Payance Audrey
 Nicole Auer
 Jeremy Augustin
 Salvador Augustin
 Igor Aurrekoetxea
 Andrew Austin
 Georg Auzinger
 José Manuel Avendaño-Reyes
 Francisco Averhoff
 Alexander Avian
 Roberta Avigni
 Matías A Avila
 Gerson Avila
 Emma Avitabile
 Fabio Avolio
 Lima Awad El-Karim
 Jonathan Axelrod
 Ibrahim Ayada
 María Ayala Valverde
 Indu Ayappa

Gustavo Ayares
 Omrum Aydin
 Musa Aydin
 Andrew Ayers
 Natarajan Ayithan
 Oyekoya Ayonrinde
 Alan Ayoub
 Zahid Azam
 Maria Azevedo Silva
 Mikel Azkargorta
 María Azkona
 Daniel Azoulay
 Valerio Azzimato
 Vian Azzu
 Henrik B. Hansen
 Frank Baas
 Uurtsaikh Baatarsuren
 Hideo Baba
 Masaya Baba
 Daphne Babalis
 Adriana Babameto
 Jonas Babel
 Andrei Babenka
 Julia Babigan
 Pierre Bablon
 Dr Preedia Babu E
 Sergio Babudieri
 Charlotte Bach
 Philippe Bachellier
 David Back
 Dianne Backhouse
 Jens Backman
 Bryan Badal
 Giuseppe Badalamenti
 Esther Badia-Aranda
 Stephen Badylak
 Si Hyun Bae
 Sung Min Bae
 Si Hyun Bae
 yanghyon baek
 Helene Bæk Juel
 Sheila Baena
 Jonas Bahn
 Wei Bai
 Chosha Bai
 Cassandra Baiano
 Anna Baiges
 Gerard Baiges
 Gerard Baiges Gaya
 Adam Bailey
 Michael Bailey
 Ming-Jong Bair
 Shokhista Bakieva
 Hatice Yasemin Balaban
 Yasemin Balaban
 Hatice Yasemin Balaban
 Rozalina Balabanska
 Narmada Balakrishnan
 Lorenz Balcar
 Deniz Balci
 Maurizio Baldassarre
 Victor Baldea
 Ignatius Baldeh
 Robert Balderas
 Caroline Baldin
 Guðrún Erna Baldvinsdóttir
 Anne Baldwin
 Cindy Baldwin

Georgia Bale
 María Pilar Ballester
 Robert Bals
 Jesus Balsinde
 Philippe Baltzinger
 Jesus Maria Banales
 Juan Bañares
 Rafael Bañares
 Alessandra Bandera
 Jordi Bañeras
 Subham Banerjee
 Corinna Bang
 Ayman Bannaga
 Sanjay Bansal
 Ruchi Bansal
 Rajat Bansal
 V K Bansal
 Heike Bantel
 Francesca Baorda
 Pedro Baptista
 Sergio Barace
 Vickie Baracos
 Ines Barahona
 Danny Barash
 Neta Barashi
 Francesco Baratta
 Francesca Barbanti
 Coral Barbas
 Anna Barbatto
 Thomas Barbera
 Aurora Barbera
 Sandra Barbosa
 Stephen Barclay
 Edouard Bardou-Jacquet
 Nathalie Barget
 Ahmad Barghash
 Sophia Barkow
 Georgia Barla
 Jasmin Barman-Aksözen
 Ashley Barnabas
 Nina Barner-Rasmussen
 Mathew Barnes
 Michele Barone
 Haim Barr
 Emelie Barreby
 Ana Barreira
 Stephen Barrett
 A. Sidney Barritt
 Emil Bartels
 Alexandra Bartels
 Justine Barthemon
 Luigi Bartoletti
 Ramon Bartolí
 Pablo Bartolucci
 Birke Bartosch
 Concepció Bartres
 Ambika Baru
 Sezgin Barutcu
 Annalisa Bascia
 Guido Alessandro Baselli
 Giodo Baselli
 Jovan Basho
 Maria Bashyam
 Michael Basic
 Sanket Basida
 Umberto Basile
 Nathan Bass
 Octavi Bassegoda

Disclosures

Margaret Bassendine
Christine Bassis
Dustin Bastaich
Gorka Bastarrika Alemañ
Nina Bastati
Ramon Bataller
Suvd Batbaatar
Enkhtuul Batbold
Andrew Bathgate
Ayse Batirel
Rui Batista
Clara Batista
Uyanga Bat-Osor
Salvatore Battaglia
Arianna Battisti
Purevjargal Bat-Ulzii
Martine Baudin
Ulrike Bauer
Jens Bauer
Anja Baumann
Cédric Baumann
Anja Baumann
Thomas Baumert
Joseph A Baur
Alina Bauschen
Pierre Bauvin
Aditi Bawa
Nurcan Baykam
David Bayne
Fabio Becce
Chiara Becchetti
Lars Bechmann
Morten Beck Trelle
Britta Becker
Hans Becker
Racquel Beckford
Henning Beck-Nielsen
Cheikh Mohamed Bed
Nathalie Bédard
Erin Bedford
Pierre Bedossa
Lewis Beer
Lucian Beer
Niko Beerenwinkel
Neelu Begum
Jaideep Behari
Cynthia Behling
Christian Behrends
Patrick Behrendt
Lawrence J. Beilin
Hicran Bektaş
Ines Belasri
Assia Belblidia
Elaine Bell
John Bell
Sally Bell
Dawn Belland
Agnès Bellanger
Jonathan Bellet
Luca Saverio Belli
Ernest Belmonte
Luciano Beltrão Pereira
Chantal Bemeur
Ziv Ben Ari
Yasmina Ben Merabet
Amel Ben Saad
Gil Ben Yaacov
Souad Benali

Felix Bende
Sofie Bendixen
Shifra Ben-Dor
Flemming Bendtsen
Livia Benedetti
Paula Benencio
Bertram Bengsch
Johan Bengtsson
Federica Benini
Laura Benitez
Carlos Benitez
Alberto Benito
Asier Benito-Vicente
Jaya Benjamin
Salvador Benlloch
Amine Benmassaoud
William Bennet
Andrew Bennett
Michael Bennett
Kris Bennett
Jennifer Benselin
Gilbert Bensimon
Hadar Benyamini
Christian Benzing
Chinmay Bera
Hanna Berak
Clarissa Berardo
Carmen Berasain
Françoise Berby
Michael D. Bereket
Marina Berenguer
Laura Beretta
Thomas Berg
Christoph Berg
Estefanía Berge Garrido
Hilmar Berger
Michael Berger
Hilmar Berger
Ina Bergheim
Anthony Bergin
Andreas Bergmann
Ottar M. Bergmann
Raoul Bergner
Riika Mari Berg-Pedersen
Annika Bergquist
Nega Berhe
Elina Berliba
Claudia Berlin
Maria Bermúdez
Carmen Bernal
William Bernal
Vanesa Bernal Monterde
Daniel Bernal Serrano
Irantzu Bernales
Lucie Bernard
Pierre-Henri Bernard
Christina Bernardes
Davide Bernasconi
Thierry Berney
Christine Bernsmeier
David Bernstein
Natalie Lie Berntsen
Marie-Luise Berres
Frederik Berrevoet
Matthias Berse
Cristina Bertelli
Ada Bertoli
Esther Bertran

Annalisa Berzigotti
Camille Besch
Alain Beschin
Ali Bessissow
Florent Besson
Fernando Bessone
Jan Best
Dominik Bettinger
Briana Betz
Boris Beudeker
Ulrich Beuers
Berend Beumer
Michele Bevilacqua
Lisa Bewersdorf
Pooja Bhadoria
Ajeet Singh Bhadoria
Khushpreet Bhandal
Bal Raj Bhandari
Rajan Bhandari
Rahima A. Bhanji
Sanjay Bhanot
Adil Bhat
Puja Bhatia
Sangeeta Bhatia
Megha Bhatnagar
Dipankar Bhattacharya
Ruveena Bhavani
Gautam Bhav
Sheng Bi
Jolanta Białkowska
Francesca Biancaniello
Marcello Bianchini
Cristiana Bianco
Yesim Bican
Markus Bickel
Charles Biddle-Snead
Laure Bidou
Laurent Biertho
Pablo Bifani
Scott Biggins
Mirna Biglione
Daniela Bignamini
Chhagan Bihari
Bikrant Bihari Lal
Marcel Bijvelds
Idoia Bilbao
Itxarone Bilbao
Angela Bilbao
Ines Bilic-Curcic
Elisa Biliotti
Griffiths Bill
Antoon Billiet
Kharmen Billimoria
Andrew Billin
Marc Bilodeau
Laurent Bilodeau
Vasundhra Bindal
Laure Bindels
Patrick Bindels
Harald Binder
Chabi Bindia
Mawuena Binka
Paula Binks
Teresa Binter
Nazrila Hairizan Binti Nasir
Marco Biolato
Roberta Biondi
Mia Biondi

Marie-therese Biotrel
 Thomas G Bird
 Kohnke-Ertel Birgit
 Rasmine Birn-Rydder
 Otilia Bisbal
 Alberto Biscontin
 Maria Bishara
 Jennifer Bissram
 Sagnik Biswas
 Debasis Biswas
 Sagnik Biswas
 Subhrajit Biswas
 Baboucarr Bittaye
 Paulo Bittencourt
 Sandra Bivegete
 Maider Bizkarguenaga
 Debora Bizzaro
 Frederik Adam Bjerre
 Niklas Björkström
 Ronny Bjørnstad
 Einar S. Björnsson
 Blagoy Blagoev
 Alasdair Blain
 Lorraine Blaise
 Marino Blanes
 Antje Blank
 Valentin Blank
 Rainer Blaszczyk
 Annabel Blasi
 Delia Blaya
 Minerva Blazquez Barba
 Evan Bloch
 Julia Blomdahl
 Netta Rose Blondheim Shraga
 Stephen Bloom
 Pamela M. Bloomer
 Karine Blouin
 Matthias Blüher
 Kirsten Muri Boberg
 Patrizia Boccagni
 Giulia Bocedi
 Ernesto Bockamp
 Johannes Bode
 Henry Bodenheimer
 Albrecht Boehlig
 Markus Boesch
 Jan Boettcher
 Johannes Bogaards
 Karolina Bogdanowicz
 Dan Boghici
 Lucio Boglione
 Pavel Bogomolov
 Mary Bohan-Keane
 Gautier Boillet
 Olivier Boillot
 Loreto Boix
 Jörg Bojunga
 Roos-Anne Bökkerink
 Tomislav Bokun
 Maximilian Bolch
 Nicolae Boleac
 Emmanuel Boleslawski
 Beata Bolewska
 Isabelle Bolt
 Natalie Bolton
 Eliano Bonaccorsi
 Pietro Angelo Bonaffini
 Paolo Bonanni

Sara Bonanzinga
 Deborah Bonazza
 Alan Bonder
 Paola Bonfanti
 Marco Bongini
 Agnes Bonifacius
 Dominique Bonnefont-Rousselot
 Richell Booijink
 Praveen Kumar Boora
 Laela M. Booshehri
 Cristina Borao
 Florina Borca
 Antoni E. Bordoy
 Valéria Ferreira de Almeida e Borges
 Luiza Borges Manna
 Marta Borghi
 Guglielmo Borgia
 Stefan Borgmann
 Dmitry Borisovets
 Andreea Borlea
 Meredith Borman
 Lea Bornemann
 Francesc Borras
 Christian Borsodi
 Jaime Bosch
 Miriam Bosch
 Maria Carla Bosco
 Pascale Bossard
 Patrick Bossuyt
 Daphne Bot
 Simona Bota
 Sebastian Bott
 Matteo Bottai
 Katrin Böttcher
 Anne Botteaux
 Tobias Böttler
 Samir Bouam
 Pol Boudes
 Karim Boudjema
 Marc Boudon
 Zakaria Boulahtouf
 Mathieu Boulain
 Luke Boulter
 Gerd Bouma
 Ayoub Bounidane
 Delphine Bousquet
 Latifa Bouzahir
 Christopher Bowlus
 Kelly Bowman
 Sedat Boyacioglu
 Sedat Boyacıoğlu
 Sonja Boyd
 Sylvie Boyer
 Alison Boyle
 Louise H. Boyle
 Birkan Bozkurt
 I. Bozkurt
 Silvia Bozzarelli
 Giorgio Bozzi
 Andries Braat
 Linda M Bradley
 Kylie Bragg
 Mayur Brahmania
 Giuseppina Brancaccio
 Andrea Branch
 Vittorio Branchi
 Carlos Brandão-Mello
 Lydia Brandl

Elisa Brandt
 Annette Brandt
 Conor Braniff
 Irena Brates
 Michael Braude
 Miren Bravo
 Catarina Bravo
 David Breckinridge
 David J Breen
 Leigh Breen
 Birgit Bremer
 Robert G Brenig
 Paul Brennan
 Lucia Brescini
 Monika Breuer
 Kai Breuhahn
 Segolene Brichler
 Simon Bridge
 Krestina Brigida
 Nicolas Brignon
 Florian H. H. Brill
 James Hallimond Brindley
 Leonard Brinkmann
 Olívio Brito Malheiro
 Oscar Briz
 Alessandra Brocca
 Lori Broderick
 Lucia Brodosi
 Anne Broedsgaard Madsen
 Annelotte Broekhoven
 Ruth Broering
 Maximilian J Brol
 Korbinian Bronner
 Peter Bronsert
 Jeff Bronstein
 Fabrizio Bronte
 Ellen Brooks-Pollock
 Mario Brosch
 Julien Broseus
 Carol Brosgart
 Hans Brouwer
 Maxine Brown
 Marius Brown
 Lorna Brownlee
 Amelie Bruandet
 Yannick Brueggemann
 Philip Bruggmann
 Radan Bruha
 Anna Brujats
 Ana Brujats
 Daniel Brumar
 Julie Bruneau
 Laura Brunelli
 Philipp Brunnbauer
 Blasi Bruno
 Tony Bruns
 Chiara Bruzzzone
 Kathleen Bryce
 Jiyeon Bu
 Qingfa Bu
 Daniela Buccella
 Laura Bucci
 Stephan Buch
 Ryan Buchanan
 Benjamin Buchard
 Theresa Bucsics
 Myagmarjav Budeebazar
 Andrzej Budzyński

Disclosures

Matthias Buechter
Stefan Buettner
Paula Bufi Roig
Anne Bugge
Peter Buggisch
Elisabetta Bugianesi
Luis Bujanda
Sarah Bukulatjpi
Matteo Bulati
Cristiana Bulato
Rakibul Hassan Bulbul
Alison Bulkley
Terri Buller-Tylor
Helen Bungay
Andreas Bungert
Kelly Burak
Barbara Burbaum
Adrian Burdan
Esther Burden-teh
Christophe Bureau
David Burger
Katharina Burger
Elke Burgermeister
Lukas Burghart
Valentina Burgio
Julio Burman
Gareth Burns
Keith Burns
Patrizia Burra
Alastair Burt
Alice Burton
Rosalía Busà
Brian Bush
Javier Bustamante
Francisco Javier Bustamante Schneider
Maia Butsashvili
Jane Buxton
Sumiya Byambabaatar
Chris Byrne
Christopher Byrne
Marianne Byrne
Ruth Byrne
Jae Ho Byun
Estefanía Caballano-Infantes
Llorenç Caballeria
Joan Caballería
Francisco J. Caballero
Fanny Meylin Caballeros
Ricardo Cabello
Joaquín Cabezas
Teresa Cabezas Fernandez
Daniela Cabibi
Elizabeth Cabrera
maria cabrera
Lorenzo Caciolli
Valle Cadahía-Rodrigo
Massimiliano Cadamuro
Andrea Marco Caddeo
Katharine Caddick
Mathilde Cadoux
María Luisa Cagigal
Ege Su Çağlar
Marta Cagna
Carole Cagnet
Yaqin Cai
Xianbin Cai
Xiujun Cai
Yuqi Cai

Dawei Cai
Dachuan Cai
Qun Cai
Fernando Cairo
Christina Cajigas-Du Ross
Rodrigo Calado
Moritz Calaminus
Julien Calderaro
Emilio Calderón Garza
Francisco Calderón-Mendieta
Alexander Calderwood
Silvia Calero
Filipe Calinas
Arianna Calistri
Isabelle Callebaut
Miguel Angel Calleja
Ana Callejo-Pérez
Alberto Calleri
Jonas Callet
Nico Callewaert
Valeria Calvino
Diego Calvisi
Diego F. Calvisi
Marta Calvo
Henar Calvo
Pier Luigi Calvo
Esther CalvoLassoDelaVeiga
Jesús Camacho-Escobedo
Salimata Camara
Verónica Cambindo Santana
Rodrigo Cambraia
Anny Camelo Castillo
Calogero Camma
Antonella Cammarota
Tommaso Campagnaro
Claudia Campani
Braidie Campbell
Cori Campbell
Denise Campbell-Scherer
Elena Campello
Sara Campinoti
Magda Campins
Loic Campion
Isabel Campos-Varela
Gracian Camps
Jordi Camps
Gracián Camps
Jordi Camps Andreu
Caterina Canapele
Ali Canbay
Jesse Canchola
Davide Cangelosi
Maria Ines Canha
Clémence M Canivet
Luana Cannella
Macarena Cannistra
Mary D Cannon
Luis Cano
Florence Canoui-Poitrine
Matthew Cant
Paula Cantallops Vilà
Valérie Canva
Di Cao
Wenming Cao
ZhuJun Cao
Zhenhuan Cao
Elisabetta Caon
Mario Capasso

Tiago Capela
Roberta Capelli
Maria Capilla
Cristian Caporali
Alessandro Cappetta
Giuseppina Cappiello
Sarah Cappuyns
Francesco Caputo
Paolo Caraceni
Andra Caracostea
Peter Caravan
Lorena Carballo-Folgoso
Juan Antonio Carbonell-Asins
Rodolfo Carbonetti
Michelle Carbonneau
Elena Carceller-Lopez
Claudia Carcione
Timothy Card
Antonio Cárdenas-García
Vincenzo Cardinale
Anaïs Cardon
Sandra Cardoso
Hélder Cardoso
Teresa Cardoso Delgado
E Fabian Cardozo-Ojeda
Ivana Carey
Elizabeth Carey
Ivana Carey
Zillah Cargill
luca carioti
Bertrand Cariou
Giuseppe Cariti
Maryvonnick Carmagnat
Isabel Carmona
Francesco Carmona
Amancio Carnero
Maria Carnevali Frias
Marta Carol
Rossana Carpani
Nathan Carpentier
Guido Carpino
Paola Carrai
Stefania Carrara
Amedeo Carraro
Germán Carrasquilla
Fabrice Carrat
Enrique Carrera
Maria-Josep Carreras
Florent Carrette
Juan Carrillo
Carin Carroll
Miles Carroll
Camilla Carr-Smith
Jack Carruthers
Joanne Carson
Stefano Caruso
Sofia Carvalhana
Vinícius Carvalho
Armando Carvalho
Ângela Carvalho-Gomes
Andrea Casadei Gardini
Marta Casado
Miguel Ángel Casado
Marta Casado
Fernando Casafont
Biagio Casagrande
Francesco Paolo Casale
Carmen Casamayor

Christian Casar
 Stefano Cascinu
 Antonio Cascio
 Johnny Cash
 Rosario Casillas
 Elia Casirati
 Markus Casper
 Martien P. M. Caspers
 Cristophe Cassinotto
 Helena Castañé
 Felipe Castañeda
 Luis A Castaño González
 Andrés Castano-Garcia
 Vincent Castelain
 Javier Castell
 Paul Castellani
 Marlen Castellanos-Fernandez
 Inmaculada Castello
 Inmaculada Castelló Miralles
 Lluís Castells
 Corinne Castelnau
 Agustin Castiella
 Federico Castillo
 Mauricio Castillo
 Joaquin Andrés Castillo
 Maria Castillo-Catoni
 Rui Castro
 Stefania Casu
 Mireia Casulleras
 Francesca Casuscelli di Tocco
 Filippo Cattazzo
 Xavier Causse
 Lourianne Cavalcante
 Luisa Cavalletto
 Daniela Cavallone
 Giuliana Cavalloni
 Anna Cavazza
 Madeleine Caven
 Nora Cazzagon
 Marina Elena Cazzaniga
 M. Cea
 Francesca Ceccherini Silberstein
 Stefano Cecchi
 Amie Ceesay
 Sabahat Ceken
 Yeşim Çekin
 Ayhan Çekil
 Güven Celebi
 Ferya Celik
 Ferit Çelik
 Dorival Celine
 Ciro Celsa
 Jaroslaw Cendrowski
 Elisabetta Ceni
 Michele Cennamo
 Delphine Centeno
 Federica-Grazia Centonze
 Théo Cerceau
 Eira Cerda Reyes
 Roberto Ceriani
 Ferruccio Ceriotti
 Andreas Cerny
 Orlando Cerocchi
 Federico Ceruti
 Marta Cervera
 Matteo Cescon
 Annalisa Cespiati
 Yagmur Cetin Tas

Cendrine Chaffaut
 Sarinder Chahal
 Julien Chaigneau
 Sanjay Chainani
 Giorgi Chakhunashvili
 Avisek Chakravorty
 Julia Chalaye
 Suryanarayana Challa
 Benjamin Challis
 Mathieu Chalouni
 Marck Chamley
 Po-Lin Chan
 Huan-Keat Chan
 Wah-Kheong Chan
 Winston Chan
 Stephen Chan
 Edwin, Shih-Yen Chan
 Brian Chan
 Lap Kwan Chan
 Connie Chan
 Vidyaleha Chandran
 Karthik Chandrasekharan
 Mei-Hwei Chang
 Jiabao Chang
 Tsung-Yen Chang
 Pik Eu Jason Chang
 Ting-Tsung Chang
 Jung-Chin Chang
 Chun-Chao Chang
 Te-Sheng Chang
 Kyong-Mi Chang
 Mei-Hwei Chang
 Kuo-Kuan Chang
 Kyong-Mi Chang
 Keith M. Channon
 Dessy Chantal
 Veena Chantarangkul
 Yee Chao
 Hann-Hsiang Chao
 Daniel Chao
 matthew chapman
 Roger W.G. Chapman
 Fleur CHAPUS
 Hakim Charfi
 Margaux Charles
 Sarah Charman
 Vivek Charu
 Praneet Chaturvedi
 Hau-Tak Chau
 Rahul Chaudhari
 Binita Chaudhary
 Ayushi Chauhan
 Roberta Chaves
 Frederico Chaves Salomão
 Kazuaki Chayama
 Sukhdeep Steven Cheema
 Isabelle Chemin
 Yaw-Sen Chen
 Huey-Ling Chen
 Yu-Ju Chen
 Ping Chen
 Wanqing Chen
 Chien-Hung Chen
 Yu Chen
 Dongbo Chen
 Hongsong Chen
 Pu Chen
 Huanming Chen

Hong Chen
 Yongping Chen
 Xinyue Chen
 Lingzi Chen
 Jinjun Chen
 Sui-Dan Chen
 Kaina Chen
 Lynna Chen
 Tianyan Chen
 Ming-Huang Chen
 Jinjun Chen
 Hong Chen
 guofeng chen
 Zhenhuai Chen
 Jilin Chen
 Jing Chen
 Xin-Yue Chen
 Shuai Chen
 Jenny Chen
 Hui Chen
 Qiuying Chen
 Hui Chen
 Yutong Chen
 Sui-Dan Chen
 Chien-Hung Chen
 Yunfu Chen
 Ping Chen
 Lin Chen
 Yunfu Chen
 Wen-Chi Chen
 Hanying Chen
 Chien-Hung Chen
 Owen Chen
 Yi-Cheng Chen
 Jyh-Jou Chen
 Pei-Jer Chen
 Tsung Po Chen
 Jennifer Chen
 Jiaxian Chen
 Hsiu-Hsi Chao
 Sam Li-Sheng Chen
 Bowen Chen
 Qi Chen
 Chiyi Chen
 Chun-Ting Chen
 Guei-Ying Chen
 Xin-Yue Chen
 Chien-Hung Chen
 Min Chen
 Long Chen
 Yunru Chen
 Jun Chen
 David, Hsing Yu Chen
 Jiaxian Chen
 Hong Chen
 Zhi-Wei Chen
 Min Chen
 Jiaxian Chen
 Zhi Chen
 Xuanmeng Chen
 Beishan Chen
 Shuai Chen
 Zhenhuai Chen
 Xiaojiao Chen
 Mingkai Chen
 Swee Lin Chen Yi Mei
 Benny Cheng
 Ho Ming Cheng

Disclosures

Danying Cheng
Hung-Wei Cheng
Ya-Ting Cheng
Pin-Nan Cheng
Mengyuan Cheng
Tai-An Cheng
Jiamin Cheng
Chien-Yu Cheng
Wendy Cheng
Mustapha Cherai
Faiza Chermak
Daniel Cherqui
Alessandro Cherubini
Tonika Chester
Ka-Shing Cheung
Pierre Cheung
Sylvie Chevreton
Yun Chew
Xiaoling Chi
Chen-Ta Chi
Xin Chi
Huanting Chi
Linda Chia
Kevin Chiang
Tetsuhiro Chiba
Luis Chi-Cervera
Laurence Chiche
Jean-Daniel Chiche
Ievgeniia Chicherova
Yin-Hsiu Chien
Rong-Nan Chien
Shih-Chieh Chien
Anmol Chikhliya
Kate Childs
Ramu Chimakurthi
Louise China
Valeria Chines
Asif Chinnaratha
Justin Chiong
Stefan Chiriac
Dragos Chirita
Nazibrola Chitadze
Amit Chitnis
SM Chiu
Keith Wan Hang Chiu
Yencheng Chiu
Nikoloz Chkhartishvili
Stefan Chlopicki
Chinlye Chng
Elaine Chng
Ju-Yeon Cho
Kyung Joo Cho
Heejin Cho
Young Youn Cho
Jai Young Cho
Yong Kyun Cho
Mi-La Cho
Eun Ju Cho
Gabriel Chodik
Won Hyeok Choe
Byung-Ho Choe
Hun Jee Choe
Moon Seok Choi
Won-Mook Choi
Gwang Hyeon Choi
Jonggi Choi
Won-Mook Choi
In Young Choi

Jaehyuk Choi
Inhee Choi
Won-Mook Choi
Hannah S.J. Choi
YoungRok Choi
Ho Joong Choi
Won-Mook Choi
Shilpa Chokshi
Evangelos Cholongitas
Young Eun Chon
Jia Ling Chong
Lee-Won Chong
Adity Chopra
Joanna Chorostowska-Wynimko
Niklas Choteschovsky
Cheng-Fu Chou
Roger Chou
Anam Choudhry
Ashok Choudhury
Yasmina Chouik
Benjamin Chow
Matthew Choy
Z Chris
Hannah Christensen
Diana Hedevang Christensen
Michael Christmas
Yu-De Chu
Lily Chu
Yu-Ju Chu
Wan-Long Chuang
Vladimir Chulanov
Brian K. Chung
Han Yang Chung
Woo Jin Chung
Enoch Chung
Alex Churkin
Chaitong Churuangsuk
Antonio Ciacio
Oriana Ciacio
olga ciccirelli
Federica Cicchiello
Carlo Ciccioli
Vito Ciciriello
Tomas Cihlar
Umberto Cillo
Antonella Cingolani
Felice Cinque
Marco Cintoni
Ester Ciociola
Laura Esthela Cisneros Garza
Ousseynou Cisse
Jolanta Citko
Michele Citone
Micol Cittone
Marco Claasen
Joan Claria
Joan Clària
Nico Clark
Christopher Clarke
Kunst Claudia
Alex Claveria-Cabello
Veronica Clavijo Jordan
Ludivine Clavreul
Guillaume Clement
Ana Clemente
Sophie Clément-Leboube
Laure-Alix Clerbaux
Raphael Clere-Jehl

Mariagrazia Clerici
Hans Clevers
Andrew Clouston
Marina Cobreros
Donatella Cocchis
Victoria Cock
Myles Cockburn
Simon Cockell
Barbara Coco
Giovanna Cocomazzi
Nicholas Cocomello
Mace Coday
Elisavet Codela
Liana Codes
Greta Codoni
Rosa Coelho
Minneke Coenraad
Shelley Cogger
Jason Cohen
Carmit Cohen
Bracha Cohen
Oranit Cohen-ezra
Michal Cohen-Naftaly
Audrey COILLY
Camelia Cojocariu
Marco Cola
Alessandra Colantoni
Francesca Colapietro
Lucia Colavolpe
Fiona Colclough
Alex Cole
Antonio Colecchia
Luigi Colecchia
Mar Coll
Martine Collart
Isabelle Colle
Alessandro Colletta
Jane D. Collier
Nicholson Collier
Rémi Collin
Amy Collins
Kelly Collins
Kelsey Collins
Roos Colman
Joan Colom
Piero Colombatto
Maria Colome Tatche
Amedeo Columbano
Leticia Colyn
Ubaldo Visco Comandini
Alain Combes
Jason Comer
Pier Giulio Conaldi
Sophie Conchon
Simone Conci
Isabel Conde
Lutgarda Conde Crespillo
Stephen Congly
Susan Congreave
Crystal Connelly
Declan Connoley
UK-PBC Consortium
Federica Conte
Filomena Conti
Bryan J Contreras
Raul Contreras
Charlotte Cook
Jonathan Cook

Katherine Cooper
 Narcis Copca
 Carmine Coppola
 Nicola Coppola
 Carmine Coppola
 Roberta Coppola
 Eleanor Corcoran
 Paula Cordero-Pérez
 Christiane Cordes
 Pierre Cordier
 Jacqueline Cordova
 Lynsey Corless
 Anne Corlu
 Mattia Coronati
 Marion Cororuge
 Christophe Corpechot
 Fernando Corrales
 Elizabeth Correa
 Ricardo Correia de Abreu
 Margherita Correnti
 Oscar Corsi
 Maria Cortes Carrillo
 Luis Cortes Garcia
 Maria Francesca Cortese
 Emanuela Cortesi
 John Cortez
 Diego Cortinovis
 Michael Corwin
 Arif Mansur Cosar
 Chiara Cosma
 Valentina Cossiga
 Mara Costa
 Ana Costa
 Marcelo Costa Silva
 Andrea Costantino
 Marion Coste
 Charlotte Costentin
 Scott Cotler
 Mairene Coto-Llerena
 Radu Cotrau
 Helma Pinchemel Cotrim
 Alexia Cotte
 José Cotter
 Laurent Coubeau
 Walter Coudyzer
 Yohann Couté
 Christian Couture
 Amelia Cover
 I. Jane Cox
 Sean Cox
 Raffaele Cozzolongo
 Mark J. Crabtree
 Siobhan M. Craigie
 Anne Craigie
 Thorsten Cramer
 Matthew Cramp
 Marília Cravo
 Antonio Craxi
 Gonzalo Crespo
 Javier Crespo
 Clara Cretet
 Catherine Croagh
 Anna Cleta Croce
 Saveria Lory Croce
 Ben Croker
 Gabriela Cromhout
 Joanne Crook
 Colin Crooks

Mary Cross
 Lily Cross
 Amy Cross
 Emilie Crouchet
 Annalisa Crudele
 Benedikt Csernalabics
 Georgine Cua
 Antonio Cuadrado
 Francisco Javier Cubero
 Blanca Cucarull
 Tudor Cuciureanu
 Valentín Cuervas Mons
 A Cueto
 Guillermo Cuevas
 Yimin Cui
 Zixin Cui
 Yixiao Cui
 Liri Cuko
 Giuseppe Cullaro
 Noelle Cullen
 Oscar Cummings
 Evan B Cunningham
 Morven Cunningham
 Carlos Cuño
 Anna Curell
 Fabiola Curion
 Anna Curto
 Caterina Cusumano
 Francesco Maria Cutolo
 Berta Cuyas
 Piotr Czubkowski
 Justyna Czyzewska-Khan
 Ben Da
 Nathalie Da Silva
 Geraldine Da Silva
 Juhani Dabek
 Mayssa Dachraoui
 Giuseppe D'Adamo
 Rica Dagooc
 Harel Dahari
 Géraldine Dahlqvist
 Bassam Dahman
 Chia-Yen Dai
 Fabrice Daian
 Sarav Daid
 Elton Dajti
 Andrea Dalbeni
 Umberto D'Alessandro
 Olav Dalgard
 Buket Dalgic
 Buket Dalgic
 Deborah D'aliberti
 Nassim Dali-Youcef
 Hans Christian Dalsbotten Aass
 Louis d'Alteroche
 Ann K Daly
 Daphne D'Amato
 Federico D'Amico
 Gennaro D'Amico
 Amruta Damle-Vartak
 Robert Damm
 Georg Damm
 Yock Young Dan
 Shuangshuo Dang
 Tong Dang
 Abegg Daniel
 Adebayo Danielle
 Karen Vagner Danielsen

Karen Danielsen
 Oscar Danielsson
 Mirela Danila
 Nllay Daniş
 Stefano D'Anna
 Thong Dao
 Viet Loan Dao Thi
 Francesca D'Arcangelo
 Tai Dar-In
 Antonella d'Arminio Monforte
 Mohammad Darweesh
 Amit Das
 Panchanan Das
 Partha Pratim Das
 Srinivasan Dasarathy
 Jaividhya Dasarathy
 Ramanuj Dasgupta
 Naranjargal Dashdorj
 Evangelos-Panagiotis Daskalopoulos
 Christian Datz
 Juliana Daud
 Ciprian David
 Joel David
 Yana Davidov
 Mark Davids
 Brian R Davidson
 Nicholas O Davidson
 Irwin Davidson
 Jessica Davies
 Louise Davies
 Jade Davies
 Nathan Davies
 William Davis
 Brian Davis
 Ashley Davis
 Joshua Saul Davis
 Delia D'Avola
 Uladzimir Davydu
 Tracy Davyduke
 Joshua Dawe
 Murat Dayangac
 Arka De
 Nicolas De Abreu
 Ana Isabel de Ávila
 Carla De Benedittis
 Cecile de Bezenac
 Christophe De Block
 Ynto de Boer
 Filippo De Braud
 Maurits De Brauw
 Alain de Bruin
 Francesco De Cobelli
 Vincenzo De Girolamo
 Joline de Groof
 Jelle C.B.C de Jong
 Iris de Jong
 Jeroen de Jonge
 Hugo de Jonge
 Alethse De la Torre Rosas
 Mercedes De La Torre Sanchez
 Mathieu de Langlard
 Cecy Maria de Lima Santos
 Stéphane De Maeght
 Catherine de Magnée
 Robert De Man
 Joris De Man
 Nicolo de Manzini
 Leonardo De Marco

Disclosures

Rosanna De Marco
Nicola De Maria
Eleonora De Martin
Vincent de Meijer
Kevin De Muynck
Stefania de Pascalis
Aurora De Ponti
Anita De Rossi
Petra E. de Ruiter
Victoire De Salins
Teresa De Santis
Evelien de Schepper
Martina De Siena
Annalisa De Silvestri
Paolo De Simone
Andrea De Sinno
Rozanne de Veer
Clara De Venuto
Andrea De Vito
Winnok De Vos
Elsemieke de Vries
Rudi de Waart
Floor de Weijer
Benedicte De Winter
Koos de Wit
James Dear
Jose Debes
maryline debette-gratien
Antoine Debourdeau
Thomas Decaens
Jochen Decaestecker
Alexander Dechene
Charlotte Decker
Sofie Decock
Jean-Luc Decout
Marie Decraecker
George Dedoussis
Alexandra S Deeks
Vashist Deelchand
Luc Defreyne
Elisabetta Degasperis
Bruno Degeest
Erik Degerman
Helena Degroote
Jeroen Dekervel
María Del Barrio
María Del Barrio Azaceta
Maria Del Ben
Paola Del Bianco
Maria Estela del Castillo
Pilar del Hoyo Gordillo
Carmen Del Pozo-Calzada
Claire Delacôte
Heloise Delagreverie
Adele Delamarre
Elizabeth Delarocque-Astagneau
Vaihere Delaune
Yael Delayahu
Ellen Deleus
Igotz Delgado
Alberto delgado
Igotz Delgado
Evangeline Delgado
Andrea Delgado Nieves
Sophia Delicou
bénédicté delire
Thomas Delmi
Degré Delphine

Pierre Deltene
Jean Delwaide
Klaus Dembowsky
Barbara Demediuk
Anna Demetriou
Jake Demetris
Aicha Demidem
Mehmet Demir
Coskun Ozer Demirtas
Elif Demirtas
Vanessa Den Heyer
Calli Dendrou
Timm Denecke
Huan Deng
Aiyun Deng
Jiang Deng
Yangyang Deng
Mei Deng
Gerald Denk
Alban Denys
Meghan Derenoncourt
Mathilde Deridder
Rita Derua
Hailemichael Desalegn
Nina Desboeufs
Marc Deschenes
Sebastian Deschler
Chantal Desdouets
Romain Désert
Paul Desmond
Tinidad Desongles Corrales
Lise Desquilles
Sönke Detlefsen
Sylvie Deuffic-Burban
Melanie Deutsch
anouk dev
Nidhin Devadas
Kalpana Devalia
Neslihan Deveci
Poornima Devineni
Lindsey Devisscher
Dhruvi Devshi
Deepika Devuni
Maria Dezan
Thangjam Dhabali
Amanda Dhagapan
Amritpal Dhaliwal
Abhishek Dhand
Ashwin Dhanda
Ameet Dhar
Sebastien Dharancy
Sébastien Dharancy
Neerav Dharia
Sirish Dharmapuri
Anil Dhawan
Koenraad D'Hollander
Elisabeth Dhondt
Roslyn Dhurrkay
Fabrizio Di Benedetto
Davide Di Benedetto
Fabrizio Di Benedetto
Chiara Di Bonaventura
Tina Di Caterino
Alessia Di Costanzo
Giovanni Giuseppe Di Costanzo
Luca Di Galleonardo
Angelo Di Giorgio
Julia Di Girolamo

Tommaso Di Maira
Giovanni Di Maira
Tommaso Di Maira
Vito Di Marco
Sabina Di Matteo
Laura Giuseppina Di Pasqua
Giovanni Di Perri
Maja Di Rocco
Stefano Di Sandro
Sarah di Somma
Gian Luca Di Tanna
Luca Di Tommaso
Daniel E. Di Zeo-Sánchez
Gheorghe Diaconescu
Moises Diago
Moisés Diago
Elena Diago Sempere
Aldiouma Diallo
Kalilou Diallo
Alpha Diallo
Michail Diamantidis
Omar Diatta
Fernando Diaz
Luis Antonio Diaz
Sebastian Diaz
Luis Antonio Diaz
Alba Díaz
María Paz Díaz
Alba Díaz
Dácil Díaz Bethencourt
Fernando Diaz Fontela
Alvaro Diaz Gonzalez
Juan Carlos Diaz Martin
Álvaro Díaz-González
Nely Díaz-Mejía
Irene Diaz-Moreno
Mauricio Diaz-Muñoz
Antonio Diaz-Quintana
Rolland Dickson
Lütjohann Dieter
Peter Dietrich
Julia Dietz
Christopher Dietz
Cristina Diez
Mustafa Diken
Nektarios Dikopoulos
Michael Dill
Stavros Dimitriadis
Amreen Dinani
Dinc Dincer
Wei Ding
Yanhua Ding
Weimao Ding
Huiguo Ding
Yuming Ding
Mariana Diniz
Petra Dinjar Kujundžić
Katja Dinkelborg
Sarah Dion
Jessica Dion
Sophie Diong
Marina Diotallevi
Assane Diouf
Daouda Diouf
Boubacar Diouf
Melisa Dirchwolf
Meike Dirks
Verena Dirsch

Thomas Discher
 Alfio Distefano
 Sapna Divani-Patel
 Dan A Dixon
 Sonia Djazouli
 Ai-Thien Do
 Beata Dobracka
 Witold Dobracki
 Krystyna dobrowolska
 Susan L Dobson
 Daniel Dochterman
 Valentina Dodaro
 Jennifer Dodge
 Giampiero D'Offizi
 Ahmet Bulent Dogrul
 Hiroyoshi Doi
 İlyas Dökmetaş
 Maria Doladé
 Leona Dold
 Dobrochna Dolicka
 Suleyman Dolu
 Gema Domenech
 Judit Domenech Omella
 Marco Domenicali
 Esteban Domingo
 Julieta Domingorena
 Montserrat Domingo-Sàbat
 Alejandra Dominguez
 Inmaculada Dominguez
 Raquel Domínguez-Hernández
 Massimo Dominici
 Stelzer Dominikus
 Matteo Donadon
 Adeline Donati
 Maria Francesca Donato
 Daniele Dondossola
 Ruihua Dong
 Zheng Dong
 Paola Dongiovanni
 Romain Donne
 Chris Donnelly
 Hannah Donnelly
 John Donovan
 Steven Dooley
 Ram Doolman
 Ewald Doornebal
 Cristina Dopazo
 Petra Dörge
 Livia Dorn
 Marcus Dörner
 Akash Doshi
 Abdel Douiri
 Michael Doukas
 Philipp Douschan
 Ellie Dow
 Bryan Downie
 Louise Downs
 Joseph Doyle
 Gabriele Dragoni
 Fabian Dranicki
 Dirk Drasdo
 Michael Dreher
 Ann Driessen
 Ellen Driever
 Paul Driscoll
 Jan Drobeniuc
 Anne Dropmann
 Anne Drost

Shani Drucker
 Yu Du
 Yunfei Duan
 Frederico Duarte
 Matheus Duarte Brito
 Nicolas Dubois
 Peter Dubruel
 Leonardo Duca
 Nicolas Ducasa
 Jean-Charles Duclos-Vallée
 Sarah Duehren
 Maria Emilia Dueñas
 Paul Duengelhof
 Erika Duffell
 Jean-François Dufour
 Jean-François Dufour
 Sylvie Dufour
 Neil Dufton
 Mary John Duguru
 Lea Duhaut
 Suzanne Duijst
 Matthew Dukewich
 M. Düll
 Georg Dultz
 Serkan Duman
 Marc-Emmanuel Dumas
 Laurent Dumas
 Radu Dumitru
 Susanna Dunachie
 Donald R. Dunbar
 Nguyen TT Dung
 Abha DunichandHoedl
 Winston Dunn
 Kate Dunn
 Nikki Duong
 Pham Duong
 Pascale Dupuis-Williams
 Marie Dupuy
 Feyza Durak
 Serdar Durak
 Stéphanie Durand
 Francois Durand
 Sarah Durand
 Marta Duran-Güell
 Carlos Duran-Vian
 Valerie Durkalski-Mauldin
 Claire Durkin
 Simon Durman
 Elena Durmashkina
 Ajay Kumar Duseja
 Geoffrey Dushenko
 Sangit Dutta
 Scott Duvall
 Christophe Duvoux
 Girish Dwivedi
 Benjamin J Dwyer
 Dorota Dybowska
 Samira Dziri
 Bunthen E
 CE Eapen
 Philippa Easterbrook
 John Eaton
 Maryam Ebadi
 Sebastian Ebel
 Matthias Ebert
 Maxime Echenne
 Juan Andrés Echeverri
 Peter Eddowes

Angela Eddy
 Lisa Edelman
 Hanan Edler
 Briones Eduardo
 Helen Edwards
 Amy Edwards
 Leire Egia-Mendikute
 Yuichiro Eguchi
 Alena Friederike Ehrenbauer
 Emma Eichler
 Dana Eidshtein
 Ernst Eigenbauer
 Roel Eijk
 Britta Eiz-Vesper
 Nergis Ekmen
 Mattias Ekstedt
 Håkan Ekvall
 Jamel El Benna
 Mohamed El Kassas
 Cyrille El Khassis
 Sanaa El Mouhadi
 Hussein El Saghire
 Ahmed El Shabrawi
 Acana Susan Elaborot
 Lavanya Elangovan
 Hari Elangovan
 Karen Dombestein Elde
 Shrona Elgavish
 Anas ELgenidy
 Anshuman Elhence
 Chiara Elia
 Victor Eligah
 María Elizalde
 Montserrat Elizalde
 Beshoy Effat Elkomos
 Laure Elkrief
 Volker Ellenrieder
 Carla Eller
 Ewa Ellis
 Jim Ellis
 Ewa Ellis
 Kasey Elmore
 Fadoua El-Moustaid
 Felix Elortza
 Linda Elowsson Rending
 Hashem El-Serag
 Christin Ellsner
 Laxman Eltepu
 Chelsea Elwood
 Nieves Embade
 Remzi Emiroğlu
 Beatrice Emmanouil
 Marco Enea
 Bastian Engel
 Cornelius Engelmann
 Heleen Engels
 Franziska Engels
 Ender Engin
 Thomas Engleitner
 Thomas Enke
 Nobuyuki Enomoto
 Hirayuki Enomoto
 Masaru Enomoto
 Ramazan Erdem Er
 Domitille Erard
 Hans-Peter Erasmus
 Caner Ercan
 Ayse Erden

Disclosures

Joris Erdmann
Fatih Eren
Merve Eren Durmuş
Arthur Erhoeven
Graf Erika
Jonas Eriksson
Mert Erkan
Nicole Erler
Iris Erlund
Tatiana Ermolova
Gaizka Errazti Olartekoetxea
Marco Erreni
Stephanie Erschfeld
Galip Ersoz
Derek J Erstad
Offir Ertracht
Ivone Escalona Nandez
Erin Eschbach
Àngels Escorsell
Laia Escude
Desamparados Escudero-García
Blanca Escudero-López
Hrag Esfahani
Mohammed Eslam
Tannaz Eslamparast
Gamal Esmat
Jaime Espin
Ricardo A. Espinosa-Escudero
Ilaria Esposito
Tobias Eßing
Jennifer Estall
Rafael Esteban
Luis M. Esteban
Rafael Esteban
Anna Esteve Codina
Federico Estrella
Patricia Etcheves
Giuseppe Maria Ettorre
Chen Eugene
Hyuk Soo Eun
Alessandra Eva
Louise Evans
Katja Evert
Loukia Evliati
Jonathan Evraerts
Carmen Expósito
Florian Eyer
Esu Ezeani
Emilio Fabrega
Carles Fabregat
Isabel Fabregat
Núria Fabrellas
Luca Fabris
Floriana Facchetti
Lars Thore Fadnes
Andrew Fagan
Jean Luc Faillie
Bridget Faire
François Faitot
Emmanuel Fajardo
Mina Fakhriyehasl
Rocco Falchetto
Giuseppe Falco
Juan Falcon-Perez
Thomas Falguières
Christine Falk
Fatou Fall
Tove Fall

Jonathan Fallowfield
Sarah Faloon
Gregory Fan
Jian-Gao Fan
Xiude Fan
Chiara Fanelli
Chengwen Fang
May Faraj
Achilleas Fardellas
Rasim Farejov
Nunzia Farella
Silvia Fargion
Hesso Farhan
Fabio Farinati
Erik Farin-Glattacker
Naba Farooqui
Anna Farriols
Matteo Fassan
Ifrah Fatima
Erika Fatta
Günter Fauler
Rosemary Faulkes
Stéphanie Faure
Muhammad Fayyaz
Alessandro Federico
Carlo Federico Perno
Uli Fehrenbach
Michael Feigh
Jeanette Feizi
Nicole Feldbacher
Alexandra Feldman
Ariel Feldstein
Anna Feliu-Prius
Sean Felix
Catarina Félix
Emanuele Felli
Paolo Feltracco
Martijn Fenaux
Mary Fenech
Ying-Hua Feng
Wenke Feng
Bo Feng
Dandan Feng
I-Cher Feng
Rilu Feng
Rebecca Fennell
Cyrille Feray
Anna Ferenc
Catherine Ferguson
Onur Ferhanoglu
Idoia Fernández-Puertas
Diogo A. E. Fernandes
Christopher C. Fernandes
Sara Fernandes
Flavia Fernandes
Roberto Fernandez
Emma Fernandez
Javier Fernandez
Ainhua Fernandez
Enrique Claudio Fernandez
Javier Fernández
Marcos Fernandez Fondevila
Jonatan Fernandez Garcia
Samuel Juan Fernández Prada
David Fernández Ramos
Conrado Manuel Fernandez Rodriguez
Conrado Fernández-Rodríguez
Alejandro Fernandez Soro

Guillermo Fernández Varo
Inmaculada Fernández Vázquez
María Victoria Fernández-Baca
Maite G Fernandez-Barrena
José Fernandez-Checa
Felipe Fernández-Cuenca
Maria Fernandez-Fernandez
Isabel Fernández-Lizaranzu
Paula Fernández-Palanca
Miriam Fernández-Vaquero
Ainhoa Fernández-Yunquera
Janina Ferrand
Luigi Ferrante
Alberto Ferrarese
Erika Ferrari
Maria Lucia Ferraz
Carlos Ferre Aracil
Catterina Ferreccio
Marcelo Simão Ferreira
Ignacio Ferreira
Livia Garcia Ferreira
Ignacio Ferreira
Raphaella Ferreira
Jose Manuel Ferreira
Silvia Ferri
Luigina Ferrigno
Andrea Ferrigno
Helen Ferry
Philip Georg Ferstl
Petros Fessas
Davide Festi
Raja Omar Fiaz
Alexander Fich
Anja Figge
Anita Figredo
Pierre Filhine-Tresarrieu
Gabriela Adriana Filip
Tajana Filipec Kanizaj
Natalia Filipek
Celine Filippi
Leonardi Filippo
Natalie Filmann
Roberto Filomia
Ane-Kristine Finbråten
Jodok Matthias Fink
Fabian Finkelmeier
Armin Finkenstedt
Alexander Finnemore
Francesca Fiorentino
Janett Fischer
Susan Fischer
Lutz Fischer
Janett Fischer
Petra Fischer
Elke Fischer
Henok Fisseha
Daniel Fitting
Steve Flack
Alexander Flaßhove
Berthou Flavien
M. Wayne Fleischman
Katarzyna Flejscher-Stepniewska
Mathias Flensted-Jensen
Hervé Fleury
Robert Flisiak
Naomi Fliss-Isakov
Gianina Flocco
Ylva Floderus

Ana Florea
 Annarosa Floreani
 Joan Ericka Flores
 Manuel Flores Molina
 Roger Flores-Costa
 Madalina Florescu
 Sander Florman
 Georg Flügen
 Kees Fluiter
 Clare Foley
 Cintia Folgueira
 Trine Folseraas
 Camelia Foncea
 Flavia Fondevila
 Constantino Fondevila
 Matthew Fong
 Helene Fontaine
 Cilius Fonvig
 Cilius Esmann Fonvig
 Hong Foo
 Roberta Forlano
 Chiara Formentin
 Cristina Fornaguera
 Lorenzo Fornaro
 Ewan Forrest
 Cecilia Forsman
 Dirk Forstmeyer
 Paolo Forte
 Jose Ignacio Fortea
 Puri Fortes
 Jesús Fortún
 Brett Fortune
 Marta Fortuny
 Laura Virginia Forzenigo
 Francesco Giuseppe Foschi
 Neil Foster
 Graham Foster
 Michelangelo Foti
 Isabelle Fouchard
 Isabelle Fouchard Hubert
 Juliette Foucher
 Fabienne Foufelle
 Claire Fougerou-Leurent
 Baptiste Fouquet
 Margot Fournier
 Carole Fournier
 Kathryn Fowler
 Anna Ludovica Fracanzani
 Montserrat Fraga Christinet
 Maria Manuela Franca
 Barbara Franceschini
 Giampiero Francica
 Paolo Francione
 Simona Francioso
 Brunella Franco
 Claire Francoz
 Sven Francque
 Leonie Frank
 Andre Franke
 James Franklin
 Hester Franks
 Mirella Fraquelli
 Simon Fraser
 Hannah Fraser
 Andrew Fraser
 Melissa Fraser
 Giovanni Luca Frassinetti
 Daniel Fraughen

Clarembau Frédéric
 Robert Freed
 James Freeman
 Marta Freitas
 Frederik Frejd
 Verena Freutsmiedl
 Gert Fricker
 Erik Fridh Baubeta
 Philip W. Friederich
 Tomer Friehmann
 Martina Friesland
 Helmut Friess
 Thea-Charlotte Fritsch
 Sarah Fritzsche
 Stefan Fröhling
 Alexandra Frolkis
 Malin Fromme
 Mattia Frontini
 Jean-Louis Frossard
 Gary Frost
 Eve Fryer
 Lei Fu
 Rebecca Fu
 Bryan C. Fuchs
 Michael Fuchs
 Sabine A Fuchs
 A. Fuentes
 Eduardo Fuentes
 Esteban Fuentes Valenzuela
 Lara Fuhrmann
 Mitsuhiro Fujishiro
 Naoto Fujita
 Kisako Fujiwara
 Naoto Fujiwara
 Hiroo Fukada
 Kyoko Fukuhara
 Claudia Fulgenzi
 Claudia Angela Maria Fulgenzi
 Harriett Fuller
 Karen Fuller
 Barbara Funaro
 Yilliam Fundora
 Yan Yue James Fung
 Georg-Christian Funk
 Alessandro Furlan
 Elizabeth Furrie
 Rita Furtado Feio de Azevedo
 Norihiro Furusyo
 Giuseppe Fusai
 Carla Fuster
 Daniel Fuster
 Paraskevi Fytilli
 Jose Juan G. Marin
 Gisela Gabernet
 Claudia Gabiati
 Maria Magdalena Gabriel
 Tamar Gabunia
 Cloé Gadenne
 Nicola Gagliani
 Roberta Gagliardi
 Manuel Gahete Ortiz
 Gianluca Gaidano
 Constance Gaillard
 Filipe Gaio Castro Nery
 Urszula Ewa Gajownik
 Frederic Galacteros
 Vasileios Galanakis
 Petros Galanis

Valentina Galchinskaya
 Ketevan Galdavadze
 Eric Gale
 Alfonso Galeota Lanza
 Nathalia Galhardi
 Stuart Gallacher
 Patricia Gallardo
 Philippe Gallay
 Isabel Gallego
 Adolgo Gallego
 Rocío Gallego-Durán
 Maria Carmen Gallegos Alvarez
 Ana Gallen
 Athena Galletto
 Andrea Galli
 Camilla Gallo
 Alessia Gallo
 Elisabeth Galsgaard
 Eithan Galun
 Mont Gálvez
 Shivanand Gamanagatti
 Gennaro Gambardella
 Martina Gambato
 Carmine Gabriele Gambino
 Ana Gamezardashvili
 Yemsrach Gami
 Amiran Gamkrelidze
 Lucie Gamon
 Anuhya Gampa
 Khatanzul Ganbold
 Amish Gandhi
 Haritha Gandicheruvu,
 Akash Gandotra
 Nivrithi Ganesh
 Sujin Gang
 Daniel Ganger
 Salome Ganizate
 Nathalie Ganne-Carrié
 Catherine Gannon
 Lilia Ganova-Raeva
 Xu Gao
 Rong Gao
 Zhiliang Gao
 yinjie gao
 Ning Gao
 Jing Gao
 Jian-Neng Gao
 Xiaoqin Gao
 Bo Gao
 María Gárate-Rascón
 Marta Garbin
 David O. Garcia
 Ines García
 Diego García
 Maria García Beccaria
 Miren Garcia Cortes
 Miguel García Deltoro
 Vanessa García Fernández
 Alberto García Garcia
 Marta García Guix
 Juan Carlos Garcia Pagan
 Félix García Pajares
 Alberto García Picazo
 Silvia García Rey
 Juan Luis García Rodríguez
 Álex García Tellado
 Agustín García-Blanco
 Carlos García-Crespo

Disclosures

Miguel Garcia-Deltoro
Eduardo García-Fuentes
Selene García-García
Francisco García-García
José Manuel García-Heredia
Mireia García-López
María del Rosario García-Lozano
Pedro Pablo García-Luna
María-Victoria García-Mediavilla
Carmelo García-Monzon
Carmelo García-Monzón
Enrique García-Nieto
Guillermo García-Porrero
Ester García-Pras
Montserrat García-Retortillo
Montserrat García-Retortillo
M. Carmen García-Ruiz
Francisco Javier García-Samaniego Rey
Guadalupe García-Tsao
Matteo Garcovich
Garima Garg
Sumit Garg
Harshit Garg
Catherine Gargan
Pratibha Garh
Aleksander Garlicki
Moirra Garraus
Grace Garrett
Isabel Garrido
Marta Garrido
Maria Soledad Garrido
Eveline Gart
Cynthia Garvey
Lærke Gasbjerg
Frida Gasca
Slavko Gasparov
Mikel Gastaca
Sheila Gato Zambrano
Nikolaos Gatselis
Riccardo Gattai
Pia Gattringer
Roberta Gaudenzi
Vipul Gautam
Athena Gavalaki
Sabrina Gavasso
Britt Gayle
William Gaynor
Sonia Gaztambide
Yueqi Ge
Daniel Geanon
Heon Yung Gee
Anja Geerts
Maytal Gefen
Florian Gegenfurtner
Daniel Geh
Fabian Geisler
Eleni Geladari
Justine Gellen-Dautremer
Helene Gellert-Kristensen
Fabio Gelsomino
Will Gelson
Stefano Gemini
Genco Gencdal
Joan Genesca
Jia-Wei Geng
Shi Geng
Anne Geng
Yana Geng

Sophie Gensluckner
Sokratia Georgakak
Jacob George
Nivya George
Alexandra Georgieva
Chrysanthos Georgiou
Cyrill Géraud
Athenais Gerber
Victor Gerdes
Florian Gerhardt
Martin Gericke
Alessio Gerussi
Anne Gervais
Vladimer Getia
Tom Gevers
Philipp Geyer
Joachim Geyer
Natalia Geyvandova
Aamir Ghafoor Khan
Ahmed Ghallab
Mohsen Ghanbari
Marc Ghany
Mahyar Ghavemi
Cristian Gheorghe
Bart Ghesquière
Michael Ghez
Michele Ghielmetti
Imerzoukene Ghiles
ana-maria ghiuchici
Indrajit Ghosh
Alip Ghosh
Indrajit Ghosh
Alia Ghrayeb
Marco Giacchetto
Amato Giaccia
Joyce Madison Giacofci
Eleonora Giacomuzzi Grigoli
Vincenzo Giambra
Yi Lin Gian
Andrea Gianatti
Edoardo Giovanni Giannini
Jeanne-Marie Giard
Karyna Gibbons
John Gibbons
Benjamin Gibert
Katja Giersch
Baptiste Giguet
Mar Gil
Hilla Giladi
Hélène Gilgenkrantz
Antonio Gil-Gomez
Upkar Gill
Justine Gillard
Patrick Gillevet
Elizabeth Gilligan
Matthew Gillum
Mark Gillyon-Powell
Claudia Gil-Pitarch
Rubén Gil-Redondo
Derek Gilroy
Concepcion Gimeno Cardona
Concepción Gimeno Cardona
Stefano Ginanni Corradini
Claudia Gioe'
Sabrina Giometto
Laura Giordano
Domenico Giosa
Alvaro Giráldez-Gallego

Enrico Girardi
Pablo J Giraudi
Dewan Giri
Morgane Girier-Dufournier
Irina Girleanu
Yabetse Girma
Stefano Gitto
Matthew Gittus
Mauro Giuffrè
Paolo Giuffrida
Previtali Giulia
Felice Giuliente
Nathalie Giuly
Michela Giurucin
Gianluca Giusti
Monika Gjorgjieva
Megan Glancy
Susanne Glasgow
Dieter Glebe
Lise Lotte Gluud
Simei Go
Chun Goddard
Raquel Godoy
Henri Goedertz
Ashish Goel
Amit Goel
Benjamin Goeppert
Jens Peter Goetze
Ketevan Goginashvili
Maya Gogtay
Boon Bee George Goh
Naroa Goikoetxea
Hale Gokcan
Pinar Gökçen
Pegah Golabi
Srinivasa Reddy Golamari
David Goldberg
Daniel Goldenberg
David GoldFarb
Robert D. Goldin
Robert Goldin
Nora Goldmann
Amanda Goldring
Chloe Goldsmith
Kerrie Goldsmith
Francois Goldwasser
Rita Golfieri
Rithvik Golla
George Golovko
Nicolas Golse
Rachel Gommel
Willian Gomes
Alberto Gómez
Concepción Gómez
Silvia Gómez Araujo
Miguel Ángel Gómez Bravo
Judith Gómez-Camarero
Elena Gómez Domínguez
Pilar Gómez Rodríguez
Beatriz Gómez Santos
Neus Gomez-Muñoz
Antonio M. Gómez-Orellana
Daniela Gompelmann
João Gonçalves
Tal Gonen
Cynthia Gong
Xiyang Gong
Öykü Gönül Geyik

Daniella Gonzalez
 Belén González
 Águeda González
 Noemí González
 María Luisa Gonzalez Dieguez
 Alejandro González Praetorius
 María J González Rellán
 Antonio González Rodríguez
 Jesús González Santiago
 Gloria González-Aseguinolaza
 Maria Angeles Gonzalez-Carmona
 Javier González-Gállego
 Sara González-Gómez
 Rocio González-Grande
 Maria Sarai González-Huezo
 Marcos Antonio Gonzalez-Lopez
 Francisco Gonzalez-Romero
 Francisco González-Romero
 Ester Gonzalez-Sanchez
 Carl Goodyear
 Nicolas Goossens
 Srikanth Gopi
 Baqar Gora
 Emmanuel Gordien
 Fiona Gordon
 Louisa Gordon
 Stuart C Gordon
 Michal Gordon
 Levent Gorenek
 Tali Gorfine
 Alexandra Gorham
 Andrea Gori
 Odile Gorla
 Barbara Górnica
 Guy Gorochov
 Myriam Gorospe
 Joseph Gosnell
 Morgane Gossez
 Eyal Gottlieb
 Alexandra Götz
 Negin Goudarzi
 Ben Goudsmit
 John Gough
 Amir Gougol
 Philip Goulder
 Prabhu Gounder
 Ilias Gountas
 Jérôme Gournay
 Jérôme Gouttenoire
 Catarina Ferreira Gouveia
 Olivier Govaere
 Paul Gow
 Ashish Goyal
 Josephine Grace
 Pietro Graceffa
 Christiana Graf
 Roberto Gramignoli
 Leah Gramlich
 xavier grand
 Josephine Grandt
 Niels Grarup
 germana grassi
 Maria Vittoria Grassini
 Jordi Gratacós-Gines
 Hanna Grauers Wiktorin
 Isabel Graupera
 Javier Graus
 Elizabeth H Gray

Gianluca Grazi
 Ivo Graziadei
 Jason Grebely
 Ellen Green
 Christina Greenaway
 Lindsay Greenland
 Belinda Greenwood-Smith
 Josep Gregori
 Dyanna Gregory
 Carolyn Greig
 Sandro Grelli
 Ivica Grgurević
 Lovorka Grgurević
 Christopher Gribben
 Antonio Grieco
 Marie Griemsmann
 Julian L. Griffin
 Raluca Roxana Grigorescu
 Aristeidis Grigoriadis
 Ruben Grillo-Risco
 Stefania Grimaudo
 Dirk Grimm
 Marit M. Grimsrud
 Søren Grinderslev
 Laura Sol Grinshpan
 Philippe Gripon
 Bert Groen
 Lisbet Groenbaek
 Lars Groentved
 Mikhail Gromak
 Henning Grønbaek
 Anthony Grooshuismink
 Olga Gros
 Steve Gross
 Annika Gross
 Mauro Grova
 Jane Grove
 Gagandeep Singh Grover
 Rachel K. Grubbs
 Sine Grude
 Thomas Grünberger
 Halina Grushevskaya
 Krzysztof Grzyb
 Ye Gu
 Shengwang Gu
 Wenyi Gu
 Jiaping Gu
 Baohua Gu
 Wenyi Gu
 Noemi Gualandi
 Yu-juan Guan
 Maria Guarino
 Carlos Guarner
 Marco Guarracino
 Yehuda Gubbay
 Sabrina Guckenbiehl
 Lorraine Gudas
 Cathrin Gudd
 Jean-Louis Guéant
 Mayra Machado Fleury Guedes
 Karsten Guelow
 Julia Esteves Guerra
 Anna Francesca Guerra
 Laura Guerra
 Patricia Guerra
 María Guerra Veloz
 Maria Guerra Veloz
 Marta Guerrero

Marta Guerrero Misas
 Gian Piero Guerrini
 Catherine Guettier
 Jean Eugenheim
 Alfredo Guglielmi
 David Guijo-Rubio
 Francisco Guilherme Cancela Penna
 Olivier Guillaud
 Montserrat Guillaumet
 Gabriela Guillén
 Elena Guillen Botaya
 Martin Guillems
 Max Guillot
 Muraduddin Gulab
 Lasha Gulbiani
 Murat Taner Gulsen
 Mesut Gumussoy
 Ozgur Gunal
 Nagashree Gundu Rao
 Feyza Gunduz
 Rahmet Guner
 Aysim Gunes
 Deepak Gunjan
 Madison Gunn
 Fulya Günsar
 James Gunton
 Jenny Gunton
 Matthias Gunzer
 Ruoling Guo
 Xiaolin Guo
 Ying Guo
 Wanjun Guo
 Aili Guo
 Wengang Guo
 Beibei Guo
 Haitao Guo
 Xiaoqing Guo
 Rajat Gupta
 Ekta Gupta
 Kapish Gupta
 Girish Gupte
 Merve Gur
 Ayşegül Gürsoy Çoruh
 Yasemin Gursoy Ozdemir
 Marta Gut
 Peter Gute
 Alejandro gutierrez atemis
 Virginia Gutiérrez de Juan
 Cynthia Guy
 Dominique Guyader
 Fatih Guzelbulut
 Elina Muriel Guzmán
 Lia Gvinjilia
 Geum-Yon Gwak
 Tom H Tranah
 Thomas H Tranah
 Phil Ha
 Yeonjung Ha
 Claude Haan
 Geoffrey Haar
 Joel Haas
 Nadeen Habboub
 Mariam Habib
 Nagy Habib
 Anoosha Habibi
 Abeba Habtesion
 Michael Hackl
 Hubert Hackl

Disclosures

Eran Hadar
Abbas Hadji
Anna Hadjihambi
Sine Reker Hadrup
Steffanie Haegele
Beth Hærsted Olsen
Rebecca Haffner-Krausz
Christine Hafner
Hironori Haga
Sanae Haga
Hiroaki Haga
Arno Hagenunger
Gareth Hahn
Nguyen Hai Nam
Lena Haiden
Laura Haigh
Behzad Hajarizadeh
Bouchkira Hakim
Philippe Halfon
Rachel Halford
Andrew Hall
Samuel Hall
Isabelle Hall
Philip Hallenborg
Alexandre Haller
Rosa Haller
Nabil Hallouche
Kate Hallsworth
Rebecca Halperin
Michito Hamada
Yuhei Hamaguchi
Hevar Hamah Saed
Nashla Hamdan
Huma Hameed
Karim Hamesch
Saeed Sadiq Hamid
Azlinda Hamid
Saeed Sadiq Hamid
Victoria Hamill
Aaron Hamilton
Stephen Hamilton-Dutoit
Ulf Hammar
Niklas Hammar
Rachel Hammond
Nigel Hammond
Annaig Hamon
Jochen Hampe
Tao Han
Seungbong Han
Khin Aye Wint Han
Kyungdo Han
Khin Han
Hyosun Han
Dai Hoon Han
Eui Soo Han
Ji Won Han
Khin Aye Wint Han
amr hanafy
James Hand
Senad Handanagic
Roeland Hanemaaijer
Muhammad Farooq Hanif
Muzlifah Haniffa
Neil Hanley
Nicholas Hannah
Pokrath Hansasuta
Ingunn Hansdottir
Torben Hansen

Camilla Dalby Hansen
Frederik Orm Hansen
Bettina Hansen
Torben Hansen
Daniel Hansen
Frank Hanses
Bertrand Hanslik
Winita Hardikar
Gareth Hardisty
Jean Hardwigsen
Carol Anne Hargreaves
Yael Harif
Maren Harms
Muhsin Murat Harputluoglu
Murat Harputluoglu
Caroline Harrer
Michael Harring
Claire Harrington
Rebecca Harris
Nicola Harris
Stephen Harrison
Gunter Hartel
Lukas Hartl
Johannes Hartl
Lukas Hartl
Björn Hartleben
Daniel Hartmann
Rune Hartmann
Daniel Hartmann
Gustav Bang Harvald
Azadeh Harzandi
Arvand Haschemi
Akira Hasegawa
Martina Haselberger
Mike Hasenberg
Katharina Haslinger
Sumaira Hasnain
Aliya Hasnain
Megan Hasoon
Fadi Hassan
Tarek Hassanein
David Hastie
Kelly Haston
Koichiro Hata
Behzad Hatami
Etsuro Hatano
Joanne Hatchett
Ayiesha Hatta
Maximilian Hatting
Ajay Haveri
Ophir Hay
Yuka Hayakawa
Liat Hayardeny
Hideki Hayashi
Brandy Haydel
Peter Hayes
Katelin Haynes
Gautam Hazarika
Qibin He
Yining He
Zheyun He
Jingchun He
Youzhi He
Lulu He
Ruiling He
Nigel Heaton
Lukas Hechelhammer
Teresa Hecker

Mounia Heddad Masson
Hannes Hegmar
Danijela Heide
Huber Heidemarie
Dominik Heider
Mathias Heikenwälder
Marintha Heil
Franz Josef Heil
Christoph Heilig
Kathrin Heim
Markus Heim
Kathrin Heim
Maria Heimisdottir
Moritz Hein
Femke Heindryckx
Melina Heinemann
Sophia Heinrich
Alexandra C.A. Heinzmann
Gilles Hejblum
Kamilla Hejn
Abdelaleem Helal
Samuel Helgesson
Dominik Heling
Margaret Hellard
Theo Heller
Kerstin Hellwig
Sherine Helmy
Frederic Heluwaert
Hamed Hemati
Walter Henderson
Michael Heneghan
Jan G. Hengstler
Jim Hennan
Barbara Hennlich
Nathalie Hennuyer
Thiercelin Henriette
Jean Henrion
Marc Henrion
Mariana Moura Henrique
Christiani Jeyakumar Henry
Linda Henry
Austin Henry
Lara Henze
Nae-Yun Heo
Adam Herber
Jean-Étienne Herbrecht
Julian Hercun
Darius Heredeia
Sébastien Hergalant
Paul Hermabessiere
Paul Hermabessière
Ken Hermann
Natalia Hermán-Sánchez
Irm Hermans-Borgmeyer
Laurens Hermie
Nélia Hernandez
Christine Hernandez
Ubaldo Benítez Hernandez
Anjara Hernandez
Larissa Hernandez
Rosario Hernández
Helena Hernández Evole
Manuel Hernández Guerra
Francisco Hernandez Oliveros
Virginia Hernandez-Gea
Anna Hernandez-Rubio
Jon Heron
Elisa Herraiez

Jose Maria Herranz	Alyssa Hochberg	Tom Houben
José María Herranz	Daryl Hodge	Kathryn Houghton
Andrea Herranz	Leanne Hodson	Ranya Houmami
Jose Maria Herranz	Christoph Hoener zu Siederdisen	Lina Hountondji
Hilde Herrema	Marius M. Hoeper	Pauline Housset-Debry
Julia Herreras López	Hal M. Hoffman	Chantal Housset
Jose Ignacio Herrero	Maïke Hofmann	Johannes R. Hov
Laura Herrero	Brian J. Hogan	Jens Hove
Eva Herrmann	Simon Hohenester	David Hovel
Leeor Hershkovich	svend hoime hansen	Jessica Howell
Toni Herta	Juliana Fernanda Holanda Bezerra Pereira	Elena Hoyas
César Hervás	Mikal Jacob Hole	Martin Hrabe de Angelis
Hugo Herve	Clemence Hollande	Stela Hrkáč
Guillou Herve	Peter Holland-Fischer	Victor Hryharovich
Jeremy Hervet	Marcus Hollenbach	Chih-Yang Hsiao
Maëva Hervieu	Julius Hollnberger	Yi-Chung Hsieh
Stephan Herzig	Sverre Holm	Chia-Hsun Hsieh
Katharina Herzog	Jens-Christian Holm	Yi-Chung Hsieh
Natalie Herzog	Louise Holm	Tsai-Yuan Hsieh
Elisabeth Hessmann	Kristian Holm	Yao-Chun Hsu
Joanna Hester	Jens-Christian Holm	Hong-Yuan Hsu
Svetlana Hetjens	Louise Aas Holm	Christine Hsu
Liv Hetland	Marte Holmberg	Chao-Wei Hsu
Jenny Hetzer	Cecilie Holmegaard Andersen	Cheng Er Hsu
Niklas Heucke	Magnus Holmer	Jui-Ting Hu
Alexandra Heurgue-berlot	Jacinta Holmes	Yue Hu
Laura Heydmann	Elaine Holmes	Guoxin Hu
Leen Heyens	Jacinta Holmes	Xumei Hu
Helen Heymann	Wacław Hołowko	Yue Hu
Yoichi Hiasa	Dorte Holst	Zhongjie Hu
Belimi Hibat Allah	Andrew Holt	Hui-Han Hu
Timothy Hicks	Carsten Hölcke	Tsung-Hui Hu
Amy Hicks	Tom Holvoet	Airong Hu
ashini hidam	Michael Holzhey	Peng Hu
Diana Hide	Heidemarie Holzmann	Wen Hu
Lindsey Hiebert	Natalie Homer	Bo Hua
Atsuko Higashide	Mirja Hommel	Rui Hua
Mayu Higuchi	Kristina Hommersand	Yan Huadong
Monica Higuera	Yasushi Honda	Hui Huan
Maria de Fatima Higuera de la Tijera	G. Sebastian Hönes	xinliang huang
Hannah Hildebrand	Thai Hong	Shuo Huang
Franziska Hildebrandt	Vennis Hong	Yi-Hsiang Huang
Eberhard Hildt	Seungpyo Hong	Fung Yu Huang
Karl Hillebrandt	Suk Kyun Hong	Kai-Wen Huang
Marie-Noëlle Hilleret	Su young Hong	Guangyu Huang
Marie-Noëlle Hilleret	Geun Hong	Ou-Yang Huang
Marie-Noëlle Hilleret	Maria Honrubia	Yi-Hsiang Huang
Daniel Hillman	Margaret Hook	Yifei Huang
Max Hilscher	Laurence Hopkins	Yi-Hsiang Huang
Mor Hindi	Shainan Hora	Jinhua Huang
Amanda S Hinerman	Adelina Horhat	Yifei Huang
Jan Hinrichs	Stefanescu Horia	Xinliang Huang
Jason Hipp	Naoshi Horiba	Xiaohong Huang
Grishma Hirode	Paul Horn	Zhenlin Huang
Junko Hirohara	Carlos Hörndler	Yifei Huang
Masashi Hirooka	Yves Horsmans	Jonathan Huang
Ryan Hirsch	Diana Horta	Xiaohong Huang
Anna Hirschberger	Angela Horvath	Zhenlin Huang
Gideon Hirschfield	Thomas Horvatits	Yi-Hsiang Huang
Ana B. Hitos	Karoline Horvatits	Ou-Yang Huang
Ryan Hlady	Thomas Horvatits	Rui Huang
Ming-Mo Ho	Brian Horwich	Rae-Chi Huang
Joan Ho	Patrick Hosford	Yi-Hsiang Huang
Shinn-Ying Ho	Yujin Hoshida	Rui Huang
Joseph Hoang	Kelly Hosking	Qi Huang
Matthew Hoare	Md. Shafiquel HOSSAIN	Yi-Hsiang Huang
Christian Hobeika	Jinlin Hou	Jee-Fu Huang
Lise hobolth	Ming-Chih Hou	Jia-Sheng Huang

Disclosures

Chien-Wei Huang
Ching-I Huang
Yan Huang
Yun Huang
Pinzhu Huang
Isabel Huang-Doran
Gavin Huangfu
Sina Hübener
Samuel Huber
Markus Huber
Samuel Huber
Wolfgang Hübl
Evis Hudson
Peter Huebener
Lucas Hueffner
Anna Huerta
Norbert Hueser
Catherine Huet
Mie Balle Hugger
Timothy Hughes
Rex Wan-Hin Hui
Vicki Wing-Ki Hui
Samuel Hui
Laura Huiban
xiang huiling
Sam Hulme
Lauren Hulshof
Ya-Wen Hung
Yi-Ping Hung
Chao-Hung Hung
Chiu Hung-Chih
Sally Hunsberger
Mallory Hunt
Peter Hunyady
Anne Huppertsberg
Adoración Hurtado
Mehreen Husain
Ioana-Alexandra Husar-Sburlan
Norbert Hüser
Dana Huskens
Md Razeen Ashraf Hussain
Yaqza Hussain
Sadam Hussain Bhat
Arif Hussenbux
George Hussey
David Hutchinson
Tomasz Hutsch
Lynn Huyck
Jae-Seok Hwang
Seong Gyu Hwang
Jae-Seok Hwang
Shin Hwang
Paul Wuh-Liang Hwu
Ashley Hyde
Theresa Hydes
Phillip Hylemon
Tuulia Hyötyläinen
Arlinda Hysenj
Sung Hee Hyun
Kang Hyunsoon
Antonino Iaccarino
Speranta Iacob
Viktoriia Iakovleva
Andrea Iannone
Giulia Iannone
Massimo Iavarone
Luis Ibañez
Cesar Ibarra

Carolina Ibarrola de Andrés
Jamal Ibdah
Ignacio Iborra
Maru Icaza
Philippe ICHAI
Francisco Idalsoaga
Ramazan Idilman
Akio Ido
Donatella Ieluzzi
Samuele Iesari
Dolapo Igboin
Teresa Iglesias
Ainhua Iglesias
Olivas Ignasi
Mina Ignat
Abdul Ihdayhid
Manami Iida
Hiroko Iijima
Jan IJzermans
Hitoshi Ikeda
Yuji Ikeda
Kenichi Ikejima
Gabriela Ilionsky
Megan Illingworth
Nicholas Illott
sarah Iltache
Gene Im
Theresa Im
Gene Im
Yu Ri Im
Kento Imajo
Michio Imamura
Fumiaki Imamura
Franz Immer
Paata Imnadze
Dilara Inan
Mercedes Iñarrairaegui
Nevin Ince
Volkan Ince
Simone Incicco
Victoria Indenbaum
Akin Inderson
Vineesh Indira Chandran
Giuseppe Indolfi
Nevin Indriz
Mirtha Infante
Stefany Infante
Giuseppe Infantino
Sarah Inglis
Sofie Ingvast
José A. Inia
Hamish Innes
Tommaso Innocenti
Kaori Inoue
George Ioannou
Davide Ippolito
Afshan Iqbal
Maria Iraburu Elizalde
Marie Irles-Depe
Paula Iruzubiet
Katharine Irvine
James Irving
Sophie Irwin
Bordes Isabelle
Vasily Isakov
Nora Isberner
David Iser
Takamasa Ishino

Marwa Ismail
Helena Isoniemi
Ariel Israel
Eran Israeli
Mads Israelsen
Fadi Issa
Assaf Issachar
emmanuel itti
Antonella Iuliano
Pavlo Ivanchov
Dana Ivancovsky Wajcman
Tommy Ivanics
Elena Ivanova
Keiko Iwaisako
Michihiro Iwaki
Terunao Iwanaga
Hirohiko Iwasaki
Kentaro Iwasawa
Sowmya Iyengar
Rajalakshmi Iyer
Paula Izquierdo-Altarejos
Laura Izquierdo-Sánchez
Francesco Izzo
Manhal Izzy
Samir Jaber
Kathryn Jack
Clive Jackson
Kathy Jackson
Janett Jacobo
Angus Jacobs
Hodge Jacqueline C.
Christian Jacquelinet
Elmar Jaeckel
Ravi Jagatia
Rukmini Jagdish
Bettina Jagemann
Jennifer Jager
Johannes Jäger
Dirk Jäger
Shashidhar Jaggaiahgari
Vinay Jahagirdar
Andreas Jähnert
Kavita Jain
Carolin E. M. Jakob
Gustav Jakobsson
Prasun Jalal
Alpha Omar Jallow
Biyanka Jaltotage
Larry James
Carole Jamey
Nigel B Jamieson
Thomas Jamieson
Muhammad Jamil
Daniela Jancekova
Sabina Janciauskiene
Byoung Kuk Jang
Jae Young Jang
Yeeun Jang
Jeong Won Jang
Maciej K. Janik
Naveed Janjua
Justyna Janocha-Litwin
Kamil Janowski
Christian Jansen
Sonja Jansen-Skoupy
Ralf Janssen-Langenstein
Veerle Janssens
Filip Janssens

Hiram Jaramillo-Ramírez	Ankur Jindal	Jean Jung
Ganbolor Jargalsaikhan	He Jing	Jinho Jung
Jerzy Jaroszewicz	Zhang Jing	Emilian Jungwirth
Wayel Jassem	Jung Hyun Jo	Anders Junker
Sahan Jayawardana	HOON Gil Jo	Jolanta Jura
Makuza Jean Damascene	Maria Joao Meneses	Camila Jure
dubertrand jean marie	Jae-Won Joh	Elżbieta Jurkiewicz
Hiriart Jean-Baptiste	Chang Johannes	Janocha-Litwin Justyna
Marie Jeanne Lohoues	Asgeir Johannessen	Rome Jutabha
Thomas Jeffers	Birgir Johannsson	Anne Juuti
Anna Jeffery-Smith	Stine Johansen	Ingrid Jyssum
Julia Jelleschitz	Helene Johansson	Sandesh K
Ryan Jelley	Kjell Arne Johansson	Sunilkumar K
Chin-Lan Jen	libby john	Gökhan Kabaçam
Rachel Wen-Juei Jeng	Aaron John	agnieszka kabat
Benjamin Jenkins	Cheryl Johnson	Dana Kablawi
Björn jensen	Amy Johnson	Christelle Kabore
Morten Daniel Jensen	Helen Johnson	Dominik Kaczmarek
Anne Sofie Jensen	Saraha Johnson	Marcello Kadharusman
Jane Jensen	Philip Johnson	Justyna Kadłuczka
Morten Daniel Jensen	Emily Johnson	Shaul Kadosh
Dennis M Jensen	Claire Johnstone-hume	Sonia Kadyan
Anne-Sofie Houlberg Jensen	Kalle Jokelainen	Rafael Kaeser
Dongsub Jeon	Elliot Jokl	Klaus Kaestner
Hong Jae Jeon	Philipp Jonas	Sabine Kahl
Jae Yoon Jeong	Will Jones	Julia Kahlhöfer
Joonho Jeong	Daryl Jones	Toshimi Kaido
Jaehong Jeong	Simon Jones	Tatsuya Kakegawa
Peter Jepsen	Calum Jones	Ioanna-Panagiota Kalafati
corneille jeremie	Rebecca L Jones	Evangelos Kalaitzakis
Bomo Jeremy	John Jones	Pratibha Ramchandra Kale
Ellen Jerome	Indi P. Joore	Jörg Kalff
Marc Jeschke	Lynda Jordan	Piotr Kalinowski
Maria Jesus Sanchez	Teresa Maria Jordan Madrid	Simanta Kalita
Ashok Jhaharia	Markus Jördens	Manash Jyoti Kalita
Kartik Jhaveri	Poo Jorge	Nicola Kalk
Dong Ji	Herin Joris	Can Kamali
Lili Ji	Francisco Jorquera	Kaan Kamali
Haiyan Jia	Simone Jörs	Nassim Kamar
Ji-Dong Jia	Priyanka Jose	Patrick S. Kamath
zhennzhou jiang	majo Joseph	Fady Kamel
Wei Jiang	Deepak Joshi	Yasser Kamel
Xiaojun Jiang	Yogendrakumar Joshi	Saleem Kamili
Mengwei Jiang	Deepak Joshi	George Kamkamidze
Yiwei Jiang	Dinesh Jothimani	Tiko Kamkamidze
Xiuhong Jiang	Janice Jou	Tania Kamphaus
Yongfang Jiang	Juliette Joubert	Christian Kampmann
Shirley Jiang	Jorge Joven	Ioannis Kamzolas
Zicheng Jiang	Jorge Joven Maried	George Kanchelashvili
zhennzhou jiang	Dusan Jovovic	Shun Kaneko
jing jiang	Shenghong Ju	Wonseok Kang
Suwen Jiang	Javier Juampérez Goñi	Min Kyu Kang
Xiaojun Jiang	Laura Juan	Hyo Jin Kang
Suwen Jiang	Adria Juanola	Jing X Kang
Jingjing Jiao	Candido Juárez	Ning Kang
Yonggeng Jiao	María Juárez-Fernández	Bo-Kyeong Kang
Andrea Jimenez Franco	Jean-Paul Judor	Junhui, Garrett Kang
Andrea Jiménez Franco	Frank Jühling	Bo-Kyeong Kang
Alejandro Jiménez Sosa	J. Wouter Jukema	Min Kyu Kang
Raul Jimenez-Aguero	Antti Julia	Jason Kang
Natalia Jimenez-Esquivel	Tomi Jun	Wonseok Kang
Ana Jimenez-Pastor	Dae Won JUN	Keon Wook Kang
Miguel Jiménez-Pérez	Pinky Juneja	Katarzyna Kania
Chaonan Jin	Se-Mi Jung	Yada Kanjanapan
He Jin	Jinho Jung	Naoya Kanogawa
Rui Jin	Young Kul Jung	Hiroaki Kanzaki
Chaonan Jin	Finn Jung	Justin Kao
Young-Joo Jin	Young Kul Jung	Andreas Kapatais

Disclosures

Umesh KAPIL
Gilaad Kaplan
David E Kaplan
Leonard Kaps
Sarah Kaps
Andras Kapus
Ghania Kara-Ali
Oguz Karabay
Sedat Karademir
Dimitrios Karagiannakis
Raffi Karagozian
Sercin Karahuseyinoglu
Theofanie Karaoulani
Stylianios Karapatanis
Zeki Karasu
Ani Kardashian
Mohammad Ehsanul Karim
Gres Karim
Revital Kariv
Thomas Karlas
Vanessa Karlen
Tom Hemming Karlsen
Purushtotham Karnam
Wikrom Karnsakul
Ewa Karpińska
Palaniswamy Karthikeyan
Anu Karunanithy
Constantine Karvellas
Kornelia Karwowska
Joyce Kasavuli
Ahmed Kaseb
Lisa Kaser
Minal Kashyap
Zain Kasmani
Jasmin Kassem
Lorn Kategaya
Katharina Katharina Stauffer
Jakob Kather
Jaeger Kathrin
Jun Kato
Matschenz Katrin
Panzitt Katrin
Petros Katsioloudes
Antonios Katsounas
Sarah Kattakuzhy
Antonis Kattamis
Benedikt Kaufmann
Paul Kaufmann
Benedikt Kaufmann
Savneet Kaur
Impreet Kaur
Navpreet Kaur
Amanpreet Kaur
Kanudeep Kaur
Kanav Kaushal
Vishal Kaushik
Hannu Kautiainen
Mary Kavanagh
Hidehiko Kawai
Nobuyoshi Kawamura
Keigo Kawashima
Richard Kay
Tahrima Kayes
Ajamete Kaykas
Konstantin Kazankov
Mingxia Ke
Jeremy Keane
Andrew Keaveny

Stergios Kechagias
Jaap Keijer
Nanda Keijzer
Verena Keitel-Anselmino
Graham Kemp
William Kemp
Agnieszka Kempinska-Podhorodecka
Jan Kempinski
Patrick Kennedy
Oliver Kennedy
James Kennedy
Kevin Kennedy
Vakhtang Kerashvili
Annarein Kerbert
Jakob Kerbl-Knapp
Nanda Kerkar
David Kershenobich
Remco Kersten
Emilie Kerstens
Satish Keshav
Rosemary Keshinro
Sahar Keshvari
Onur Keskin
Annika Kessler
Sonja Keßler
Takaomi Kessoku
Guan Sen Kew
Ilsiyar Khaertynova
Myat Khaing
Salim Khakoo
Atefeh Khakpoor
Jaafar Khaled
Mandana Khalili
Korosh Khalili
Wafa Khamri
Khalid mahmud Khan
Uqba Khan
Muhammad Khan
Uzma Khan
Sabiha Khan
Shahid Khan
Juned Khan
Zahra Khan
Arshi Khanam
Kamil Khanipov
Amardeep Khanna
Rajeev Khanna
Nadia Khatoon
Nora Khattab
Andre Khazak
Nino Khetsuriani
Vikas Khillan
Htet Htet Toe Wai Khine
Davit Khlghatyan
Olga Khomich
Irma Khonelidze
Shirin Elizabeth Khorsandi
Mina Khoshdeli
Saira Khowaja
Yury Khudyakov
Giten Khwairakpam
Rania Kibeché
Alexandra K. Kierner
Amanda Kiliaan
Murat Kiliç
Saskia Killmer
Jong Man Kim
Beom Kyung Kim

Young Seok Kim
DongYun Kim
Gi-Ae Kim
Byung Seok Kim
So Yeon Kim
Byoung Je Kim
Gi-Ae Kim
Doohyun Kim
Jung Kuk Kim
Yohan Kim
Jung Kuk Kim
Dae Jin Kim
Kang Mo Kim
Seon-Ok Kim
Ye-Jee Kim
Sanghwa Kim
Namjeong Kim
Jason Kim
Kang Mo Kim
DaWon Kim
Tae Hyung Kim
Seung Up Kim
Beom Kyung Kim
Mi Na Kim
Adam Kim
Seung Up Kim
Irene Kim
Chul Hoon Kim
Sungmin Kim
Mi Mi Kim
Sarang Kim
Seok Hyun Kim
Byung Seok Kim
Terri Kim
Jin Un Kim
Andre D. Kim
Chanyang Kim
Chul Hoon Kim
Albert Kim
Jong Man Kim
Bong Wan Kim
Dong-Sik Kim
Byung Ik Kim
Hye Seon Kim
Jin Seoub Kim
Ji Min Kim
Rattana Kim
Ji Hoon Kim
Tae Hyung Kim
Hyung Joon Kim
Chang Wook Kim
Do Young Kim
Yong Ook Kim
Jin-Wook Kim
Moon Young Kim
Beom Kyung Kim
Elena Kim
Hyeree Kim
Moon Young Kim
Ju Hyun Kim
Hyun Young Kim
Sang Kyum Kim
Oliver Kimberger
Nina Kimer
Renate Kimmerle
Leona Kim-Schluger
Yusuke Kimura
Masaki Kimura

Naruhiko Kimura	Iftihar Koksai	Murli Krishna
Volker Kinast	Shigehiro Kokubu	Santhoshi Krishnan
Wendy C King	Olena Kolesnikova	Michael Kriss
Alper Kiraz	Tomáš Koller	Maria Kristiansen
Theresa Kirchner	Daphne Koller	Antonia Kristic
Varvara Kirchner	Liudmyla Kolomiichuk	Sandra Krohn
Hiroyuki Kirikoshi	Piyawat Komolmit	Louise Krohn-Hehli
Onur Kırımker	Kazuyoshi Kon	Thit Kronborg
Elvan Onur Kırımker	Takayuki Kondo	Victoria Kronsten
Hale Kırımlioglu	Yuko Kono	Achim Krüger
Jesse Kirkpatrick	Christos Konstantinou	Walter Krugluger
Beril Kirmizigul	Meropi Kontogianni	Beata Kruk
Martha M Kirstein	Bo Kyung Koo	Łukasz Krupa
Michael Kirstgen	Yael Kopelman	Rafal Krygier
Jennifer Kirwan	Maria Kopsida	Nina Krylova
Tatiana Kisseleva	Felix Korell	Xutong Kuang
Yuji Kita	Marko Korenjak	Chandrashekhar Kubal
Toshihiro Kitajima	Hannelie Korf	Luke J. Kubiawicz
Murat KIYICI	Keisuke Koroki	Alison Kuchta
Murat Kiyıcı	Nafsika Korsavidou-Hult	Tinatin Kuchuloria
Soichiro Kiyono	Olle Korsgren	Stephanie Kucykowicz
Tomislav Kizivat	Kambiz Kosari	Hiromi Kudo
Maria Kjærgaard	Sükran Köse	Masatoshi Kudo
Kamilla Kjærgaard Munk	Illia Koshman	Hiromi Kudo
Emma Klahr	Heather M Kosick	Masatoshi Kudo
Jakub Klapaczynski	Ioannis-Georgios Koskinas	Patrizia Kuenzler
Robert Kleemann	Esther Kosmella	Marcelo Kugelmas
Adrian Klefenz	Iryna Kostishyna	Sjoerd Kuiken
Marina B. Klein	Nato Kotaria	Edith Kuiper
Samuel Klein	Jerzy Kotlinowski	Thijs Kuipers
Sabine Klein	Adam Kotorashvili	Michal Kukla
Hanns-Georg Klein	Shyamasundaran Kottlilil	Churaieat Kularbkaew
David E Kleiner	Roshan Koul	Kaushalya Kulathunga
Michael Klemm-Kropp	Albert Koulman	Anand Kulkarni
Paul Klenerman	Ilias Kounis	Manoj Kumar
Limor Kliker	Tetsuya Kouno	Rahul Kumar
Hartwig Klinker	Alexandra Kourakli	Ashish Kumar
Goran Klintmalm	Antri Kouroufexi	Anupam Kumar
Evangelos Klironomos	Evaggelia Koutli	Manoj Kumar
Jan Klohs	George Koutsoudakis	Guresh Kumar
Ingvild Klundby	Marta Anna Kowalik	Pramod Kumar
Johannes Kluwe	Yukinori Koyama	Ramesh Kumar
Gaby Knecht	Kaloian Koynov	Karan Kumar
Ivana Knezevic Stromar	Sergii Kozlov	Yashwi Haresh Kumar Patwa
Jimin Ko	Oleksandr Kozlov	Martin Kummen
Ko Ko	Angela Krackhardt	Lucija Kuna
Tsin Shue Koay	Lene Kræmer	Paolo Kunderfranco
Kazufumi Kobayashi	Anke Kraft	Roni Kunst
Takashi Kobayashi	Johanne Kragh Hansen	Christian Kuntzen
Kazufumi Kobayashi	Frederik Kraglund	Lilly K. Kunzmann
hicham kobeiter	Natalie Krahmer	Joseph Kuo
Elif Sitre Koç	Mel Krajden	Leane Kuo
Carmo Koch	Hariklia Kranidioti	Hsing-Tao Kuo
Andreas Rembert Koczulla	Lisette Krassenburg	Joseph Kuo
Chamani Kodikara	Alexander Kratzer	Juozas Kupcinskas
David Koeckerling	Nico Kraus	Limas Kupcinskas
Rory R. Koenen	Linda Krause	Jörg Kupfer
Karen Kofoed	Jenny Krause	Jan Küpper
Kwang Cheol Koh	Marcin Krawczyk	Makoto Kurano
Elaine Koh	Till Krech	Ada Kurt
Christopher Koh	Yitshak Kreiss	Digdem Kuru Öz
Jan Köhler	Wolfgang Maximilian Kremer	Edyta Kus
Bruno Köhler	Dina Kremsdorf	Fabian Kütting
Marlene Kohlhepp	Felix Krenzien	johan kuyvenhoven
Karin Köhrer	Thomas Krey	Soo-Heon Kwak
Kazuhiko Koike	Andreas Krieg	Daniel Kwakye Nomah
Yohei Koizumi	Sarah Krieg	Wilhelmus Kwanten
Gökhan Köker	Laurenz Krimmel	Young Oh Kweon

Disclosures

Dong Il Kwon
Yoo-Wook Kwon
Sung Kwon
Hyunjoo Kwon
In Sun Kwon
Soon Sung Kwon
Yun Kwon
Allison Kwong
Dannielle Kydd-Sinclair
Evi Kyprianou
Anastasia Kyriazidou
Karen L Thomsen
Adelaida La Casta
Claudia La Mantia
Christian Labenz
Ibone Labiano
Sofia Lachiondo-Ortega
Carolin Lackner
Karine Lacombe
Stéphanie Lacotte
Giacomo Laffi
Alice Laffusa
Ioannis Lafiatis
Annie Lafortune
Martin Lagging
Luca Laghi
Anne-Sophie Lagneaux
Eleonora Lai
Mandy Sze-Man Lai
Jennifer C Lai
Che To Lai
Qingying Lai
Walter Lai
Kuan-Yu Lai
Che To Lai
Stephen Laidlaw
Lara Laiglesia
Elke Lainka
Loriane Lair Mehiri
Dalila Lakhoulfi
Dimitra Lakiotaki
Mounia Lakli
Wim Laleman
Géraldine Laloux
Brian Lam
Wendy Lam
Shuk Man Lam
Wai Ling Macrina Lam
Laurent Lam
Bieke Lambert
Joshua Lambert
Olivier Lambotte
Diether Lambrechts
Willem Lammers
Frank Lammert
Katharina Lampichler
Qiuyu Lan
Nick Lan
Ana Landa-Magdalena
Manuel F Landecho
Charles Landis
Clémence Landreau
Christian M. Lange
Christian Lange
Marcia Lange
Jacqueline Langedijk
Miranda Langendam
Mona-May Langer

Bettina Langhans
Simon Langkjær Sørensen
Lucas Langlois
Taro Langner
Lorenzo Lani
Sarah Lanigan
Gandhi Lanke
Amalie Lanng
Matthias Lannoo
Nicolas Lanthier
Michael Lanuti
Martine Lapalus
Ariane Laparra-Ramakichenin
Syria Laperche
Nathanaël Lapidus
Ainhua Lapitz
Mathieu Laplante
Carmen Lara Romero
Christopher Lark
Dominique Larrey
Juan Ramón Larrubia
Hélène Larrue
Steen Larsen
Frederik Larsen
Anne Larson
Alberto Lasagni
Melanie Laschinger
Caroline Lascoux-Combe
Guillaume Lassailly
Maja Laszczewska
Maria U Latasa
Muhammad Umair latif
Mercedes Latorre Sánchez
Marianne Latournerie
Cathrine Lau
Jasmine Lau
David Lauber
Georg Lauer
Alexis Laurent
Astrid Laurent Bellue
Mette Lauridsen
Tea Lund Laursen
Mandy Lauw
Marie Lauzon
Gareth Lavery
Marla Lavrijsen
Matthew Law
Daniel Laxar
Shanny Layani
Stefan Lazar
Raul Lazarte
Don Lazas
Mariana Lazo
Giuseppe Lazzarino
Khanh Le
Phuc Le
Suong Le
Brigitte Le Bail
Frédéric Le Gal
Maude Le Gall
Adrien Le Guennec
Estelle Le Pabic
Benjamin Leaker
Carina Leal
Louise Lebedel
Elena Lebedeva
Jerome Lebigot
Fanny Lebossé

Salvatore Lecca
André Lechel
Christian Lechler
Isabelle Leclercq
Sophie Leclercq
Laurence Lecomte
Osiel Ledesma Juárez
Ni-Chung Lee
Joon Hyeok Lee
Nerissa Lee
Brian Lee
Jaejun Lee
Jenny Lee
Brian Lee
Jiyeon Lee
Yu Rim Lee
Changhyeong Lee
So Jung Lee
David Uihwan Lee
Chee Leng Lee
Jong Suk Lee
Sang Hyun Lee
Seonmyeong Lee
Jong Suk Lee
Sang Hyun Lee
Seonmyeong Lee
Han Chu Lee
Danbi Lee
ChiehJu Lee
Pei-Chang Lee
I-Cheng Lee
Dong Ho Lee
Jeremy Lee
William M. Lee
Su-Yeon Lee
Pei-Chang Lee
Han Chu Lee
Danbi Lee
Byung Seok Lee
Taehee Lee
Tai Ping Lee
Rheun-Chuan Lee
Han Ah Lee
Yi-Te Lee
Hye Won Lee
Hee Seung Lee
Yu Rim Lee
Won Kee Lee
Hyo Young Lee
Chul-Min Lee
Jack Lee
John Lee
Jonghyun Lee
Hyo Young Lee
Byung Seok Lee
Yu Rim Lee
Changhyeong Lee
Richard Lee
Jeffrey Lee
Jun-Hyuk Lee
Joo Ho Lee
Hye Won Lee
Hee Seung Lee
Alicia Lee
Kwang-Woong Lee
Boram Lee
Hae Won Lee
Jae Geun Lee

Soon Kyu Lee	Howard Ho-Wai Leung	Hong Li
Pei-Chang Lee	Fabio Levantesi	Yujia Li
Pei-Lun Lee	Eric Levesque	Guanlin Li
Dae Ho Lee	Laura Levi	Mei Li
Young-Sun Lee	Ana Levi	Jianzhou Li
Han Ah Lee	Laura Levi	Yujin Li
Ming-Sui Lee	Shira Levi	Hu Li
Yong-An Lee	Fred Levine	Jiaqi Li
Tzong-Hsi Lee	Josh Levitsky	Peng Li
Mei-Hsuan Lee	Massimo Levvero	Yun Li
Samuel Lee	Miriam Levy	Jingguo Li
Jun Kyu Lee	Paul Levy	Jiaqi Li
Han Ah Lee	Miriam Levy	Peng Li
Hyunsuk Lee	Maite Lewin	Bingqi Li
DongHo Lee	Monika Lewinska	Yun Li
Hyun Woong Lee	Jason Lewis	Mengying Li
Sunjae Lee	Kyle Lewis	Yueni Li
Jenny Lee	Heather Lewis	Wenhao Li
Dae Ho Lee	Catherine Leyh	Musong Li
Hye Eun Lee	Zongfang Li	Mengyu Li
Moo-Yeol Lee	Jiang Li	Tinghong Li
Pui-Yuen Lee-Law	Feng Li	Zewen Li
Galam Leem	Xiubin Li	Junfeng Li
Apinya Leerapun	Guangming Li	Xinyi Li
Rémy Lefebvre	Wei-Zhe Li	Giovanni Li Volti
Sander Lefere	Fengyuan Li	Yan Liang
Phillip Leff	Jia-bin Li	Yaojie Liang
Terho Lehtimäki	Guojun Li	Bo Liang
Tiina Lehtimäki	Jia Li	Yaojie Liang
Tiina E. Lehtimäki	Pengfei Li	Jia-xu Liang
Jin Lei	Gang Li	JiaXu Liang
Randy Leibowitz	Minghui Li	Xieer Liang
Hans Benno Leicht	Wang Li	Xi Liang
Damien Leith	Shen Li	Shan Liang
Joanna Leithead	Xiaojiao Li	Yaojie Liang
Bobby Leitmann	Haijun Li	WeiJia Liao
Chee Chong Lek	Jing Li	Jie Liao
Bouchra Lekbaby	Wai Keung Li	Haixing Liao
Tristan Lemagoarou	Shuang Li	Ermelindo D Libera
Elise Lemaître	Musong Li	Rodrigo Liberal
Sara Lemoine	Li Li	Christopher Liddle
Jozelda Lemos	Xiaoguo Li	Sabine Lieb
Florian Lempp	Xin Li	Roman Liebe
Óscar Len	Yan Li	Seng Liem
Ilaria Lenci	Kai Li	Ruby Lieshout
Xavier Lenne	Xiaomei Li	Raffaele Lieto
Hans Lennernas	Jie Li	Melissa Lieu
Marco Lenzi	Ying Li	Danny Liew
Carlin Leo	Gang Li	Regina Ligorja
Mark Leonard	Jing Li	Antonio Liguori
Claudio Leonardi	Feng Li	Alisa Likhitsup
Thais Leonel	Kai Li	Mariya Likhter
Silke Leonhardt	Xiaomei Li	Andy Lim
Laura Leoni	Jing Li	Jee Woong Lim
Gianluca Leoni	Yiguang Li	Jihye Lim
Simona Leoni	Jie Li	Won Lim
Wei Qiang Leow	Jia Li	Hong Kai Lim
Christian Leps	Hang Lam Li	Aaron G. Lim
Marie Lequoy	Kai Li	Tiffany Lim
Lionel Lerman	Xiaomei Li	Zixiang Lim
Vincent Leroy	Jia-Wei Li	Dennis Lim
Candice Lesage	Ming Li	Yee Siang Lim
Jacques Le-Seyec	Yiguang Li	Tien Huey Lim
Moshe Leshno	Rui Li	Zixiang Lim
Jack Leslie	Yinyin Li	Tiong Yeng Lim
Andrew Lesniak	Jun Li	Zixiang Lim
Gerald Lesnik	Jiang Li	Sung-Chul Lim
Aleksandra Leszczynska	Peng Li	Ana Limon-Miro

Disclosures

Chih-Wen Lin
Chih-Che Lin
Wan-Bao Lin
Jung-Yi Lin
Shi-Ming Lin
Chen-Chun Lin
Chun-yen Lin
Po-Ting Lin
Minghua Lin
Huapeng Lin
Steven Lin
Chun-yen Lin
Wen-Yuan Lin
Shi-Ming Lin
Chen-Chun Lin
Chun-yen Lin
Po-Ting Lin
Han-Chieh Lin
Chih-Lin Lin
Chih-Lang Lin
Huapeng Lin
Tao Lin
Qing Lin
Shumei Lin
Ruey-Chang Lin
Lei Lin
Benjamin Linas
Gun Lindell
Christina Lindenmeyer
Nicolas Linder
Andreas Lindhorst
Keith D. Lindor
Jonathan A. Lindquist
Ning Ling
Ralph Link
Alexander Link
Frederik Link
Raffaella Lionetti
Wei-Lun Liou
Igor Lipnevich
Ton Lisman
Margaret Littlejohn
Yi Liu
Yixin Liu
Na Liu
Zhaoli Liu
Jiaye Liu
Tong Liu
Shi Liu
Gang Liu
Tong Liu
Yan Liu
Kuan Liu
Boqiang Liu
Yanna Liu
Changchun Liu
Chuan Liu
Fuquan Liu
Jingrui Liu
Huan Liu
Zhaoli Liu
Tong Liu
Jingrui Liu
Yanna Liu
Chuan Liu
Chen Liu
Tong Liu
Shunai Liu

Yao Liu
Feng Liu
Cheng Liu
Xinchang Liu
Jiacheng Liu
Yilin Liu
Zhicheng Liu
Hanyang Liu
Jiacheng Liu
Ying Liu
Beibei Liu
Kara Marie Liu
Yen-Chun Liu
Chun-Jen Liu
Jiacheng Liu
Xiao Liu
Chun-Jen Liu
Yali Liu
LiLi Liu
Hui Liu
Diana Liu
Yi Liu
Xiaojing Liu
Zongyi Liu
Xiaohui Liu
Diana Liu
Dengxiang Liu
Yu-Pei Liu
Chao Liu
Chuan Liu
Shirong Liu
Ning Liu
James Liu Yin
Sherry Livingston
Callum Livingstone
Timur Liwinski
Javier Lizardi
Oyungerel Lkhagva-Ochir
Jordi Llaneras
Jessica Llewellyn
María Esther Llinares
Elba Llop
Laura Patricia Llovet
Josephine Lloyd
Carla Lloyd
Andrew Lloyd
Gin-Ho Lo
Ching-Chu Lo
Lorena Loarca
Cirley Lobato
Stephen Locarnini
Ian Lockart
John Lodge
Federica Logiodice
Alessandro Loglio
Ansgar W. Lohse
Ansgar Lohse
James Lok
Anna Lok
Khumukcham Lokeshwar Singh
Letizia Lombardelli
Martina Lombardi
Rosa Lombardi
Andrea Lombardi
Rosa Lombardi
Daniele Lombardo
Julissa Lombardo Quezada
Maria Carlota Londoño

Thomas Longerich
Stephanie Longet
Miriam Longo
Salvatore Longo
Miriam Longo
Jing Hong Loo
Sven H Loosen
Ilaria Loperto
Massimo Lopes
Nataly Lopes Viana
Nélida López
Mayra López Azuara
Maria Angeles Lopez Garrido
José López González
Lucía López-Bermudo
Carlos Lopez-Gomez
Marcos López-Hoyos
F. Xavier Lopez-Labrador
Flora López-López
Melissa Lopez-Pentecost
Diana Laura López-Rubio
Cristina López-Vicario
Marta Lopez-Yus
Fernando Lopitz Otsoa
Ulrike Lorch
Emma Lord
Janet Lord
Florian Lordick
Maria Lorena
Beata Lorenc
Sara Lorente Perez
Silvia Lorente-Cebrian
Johanna Luise Charlotte Lorenz
Giulia Lori
Sophie Lotersztajn
Marta Lotto
Jinfeng Lou
Lillian Lou
Ruhl Louisa
Dimitri Loureiro
Veronique Loustaud-Ratti
Alexandre Louvet
Arthur Löve
Thorvardur J. Löve
Robert Loveridge
Anita Lövgren-Sandblom
Gerald Low
Bernd Löwe
John Loy
Juanjo Lozano
Juan Jose Lozano
Juanjo Lozano
María Carmen Lozano Domínguez
Alain Lozniewski
Yunjie Lu
Mengji Lu
Hui Lu
jiajie lu
Mengji Lu
Shelly C. Lu
Ming Lu
junfeng lu
Xiao-Bo Lu
Zhonghua Lu
Yinying Lu
Di Lu
Mengji Lu
Wei-Yu Lu

Ling Lu
 Eric Lubeck1
 John Lubel
 Nadine Lübke
 Amandine Luc
 Martina Lucà
 Maria Isabel Lucena
 Ana Lucena
 Ersilia Lucenteforte
 Michael R. Lucey
 Alain Luciani
 Damien Lucidarme
 Marchand Lucie
 Julie Lucifora
 Tom Lüdde
 Burkhard Ludewig
 Johannes M. Ludwig
 Marc Luetgehetmann
 Fabiola Lugano
 Niklas Luhmann
 Gilbert Lui
 Thea Luig
 Velimir Luketic
 Saimir Luli
 Suhasini Lulla
 Sheila Lumley
 Morten Lund
 Katarina Lund
 Morten Lund
 Jens D. Lundgren
 Åsa Lundgren
 Annamari Lundqvist
 Xufeng Luo
 Jiing-Chyuan Luo
 Bohan Luo
 Ke Luo
 Wun-Sheng Luo
 Yizhao Luo
 Bohan Luo
 Jinjin Luo
 Qiang Luo
 Xufeng Luo
 Joachim Lupberger
 Gabriele Luppi
 Monica Lupsor-Platon
 Raluca Lupusoru
 Maria Angelica Luque Gonzalez
 Clovis Lusivka-Nzinga
 Yaniv Lustig
 Mechthild Lütge
 Alina Lutu
 Philipp Lutz
 Michael Luu
 Panu K. Luukkonen
 Panu Luukkonen
 Hendrik Luxenburger
 Peter Lykke Eriksen
 Erica Nicola Lynch
 Kate Lynch
 Julie Lynch
 Victoria Lyo
 Andre Lyra
 Simon Lytton
 Ellina Lytvayak
 Roberd M Bostick
 Urko M Marigorta
 Anlin Ma
 Deqiang Ma

Yun Ma
 Zhenkun ma
 Lina Ma
 Ann Ma
 Ronald Ma
 Ann T Ma
 Shiwen Ma
 Ying Ma
 Jianzhong Ma
 Raoel Maan
 Benjamin Maasoumy
 Isabelle Mabile-Archambeaud
 Morgane Mabire
 Mai Mabrouk
 Marta Mac Vicar
 Chiara Macchi
 Luca Maccioni
 Scott MacDonald
 Douglas Macdonald
 Paula Macedo
 Vitor Macedo Silva
 margherita macera
 Joanna MacEwan
 Mariana Machado
 Siobhan MacHale
 Maria Dolores Macia Romero
 Laura Macias-Muñoz
 Michael MacIsaac
 Julia MacIsaac
 Michael MacIsaac
 John B. G. Mackey
 Jane Macnaughtan
 James Macrae
 Joao Madaleno
 Magalie Madau
 Angela Madden
 Haripriya Maddur
 Giordano Madeddu
 M Mader
 Devika Madhu
 Christian Madl
 Tobias Madl
 Sibylle Madlener
 Salvatore Madonia
 Bjørn Stæhr Madsen
 Lone Madsen
 Bjørn Stæhr Madsen
 Anne Lundager Madsen
 Mayumi Maeda
 Christine Maeder
 Shinya Maekawa
 Lebrun Maella
 Javier Maeso-Gonzalez
 Sheila Maestro
 Chiaki Maeyashiki
 Gabriele Maffi
 Marta Magaz
 Marco Maggioni
 Claudia Maggioni
 Giulia Magini
 Paolo Magistri
 Benoît Magnin
 Rahul Maheshwari
 Deepanshu Maheshwari
 Ratib Mahfouz
 Hassan Mahmood
 Khalid Mahmood
 Robert Mahn

Eisa Mahyari
 Jiajia Mai
 Luís Maia
 Ivana Maida
 Adriano Maida
 Ivana Rita Maida
 Melanie Maier
 Andreas Maieron
 Laurent Mailly
 Sergio Maimone
 Alex Maini
 Alexander Maini
 Cesare Maino
 Dagmar Mainz
 Laura Maiocchi
 Patrick Maisonneuve
 Bettina Maiwald
 Rakhi Maiwall
 Mario Majchrzak
 Ammar Majeed
 Amir Majid
 Piotr Major
 Xavier Major
 Avik Majumdar
 Abdul Majzoub
 Lung Yi Loey Mak
 Wanwisar Makhasen
 Y.M. Mala
 Peter Malcus
 Deborah Malden
 René Malé Velazquez
 Michael Maley
 Harmeet Malhi
 Benedict Maliakkal
 Farihah Malik
 Raza Malik
 Farihah Malik
 Assaf Malka
 Vincent Mallet
 Filip Malmberg
 Kristian Malme
 Francesco Malvestiti
 Remon Mamdouh
 Eyerusalem Mamo
 Nina Mamonova
 Tak Yung Man
 Hana Manceau
 Fabrizio Mancuso
 Sema Mandal
 Michal Mandelboim
 Dionysia Mandilara
 Steffen Manekeller
 Estela Florencia Manero
 Emmanouil Manesis
 Giulia Francesca Manfredi
 Noel Manga
 Thomas Mangana Del Rio
 Konstantinos Manganas
 Charis Manganis
 Chiara Mangini
 Ilianna Mani
 Paul Manka
 Saumya Manmadhan
 Derek A Mann
 Matthias Mann
 Martina Manna
 Ajitha Mannalithara
 Ville Tapio Männistö

Disclosures

Satu Männistö
Pinelopi Manousou
JoAnn Manson
Dina Mansour
Natalie Mansour
Mahmoud Mansour
Abdel Mansouri
Sara Mantero
Alessandro Mantovani
Anna Mantovani
Parvez Mantry
Maria Luisa Manzano Alonso
Elina Manzhali
Qianguo Mao
Minxin Mao
Xiaorong Mao
Yongwu Mao
Cao Maomao
Tongai Gibson Maponga
Jaswinder Maras
Giovanni Marasco
Patrick Marcellin
Fabienne Marcellin
Andrea Marcellusi
Julio Marcelo
Arnaud Marchant
Daniele Marchelli
Ann-Britt Marcher
Giulio Marchesini Reggiani
Emanuele Marchi
Francesca Marchignoli
Svetlana Marchuk
Claudia Marcia
Sebastián Marciano
Kennie Marcini
Natalia Marcos Carrasco
Adil Mardinoglu
Ruxandra Mare
Manuel Rodriguez Maresca
Elodie Mareux
Sara Margarita
Jose Maria Mari
Alexandre Maria
Jose Marin
Stefan Marinescu
Federico Marini
Ilaria Marini
Jose Luis Marin-Rubio
José Humberto Caetano Marins
Angelico Mario
Goran Marjanovic
Thomas Marjot
Davwar Pantong Mark
Georgios Markakis
Jessica Markby
Aurelia Markezana
Astrid Marot
Jens Marquardt
Jens U. Marquardt
Pedro Elias Marques
Francisco Marques
Sara Marques
Camila Marques de Alcanatara Barreto
Valentin Marquez
Andrea Márquez
Laura Márquez Pérez
Fiona Marra
Thomas U. Marron

Giuseppe Marrone
Gunther Marsche
María Martell
Joerg Martens
David Marti-Aguado
Luis Marti-Bonmati
Jasmine Martin
Cesar Martin
Paul Martin
Romain Martin
Paul Martin
Cesar Augusto Martín
Ana Martin Algibez
Miguel Ángel Martín Casanueva
Antonio Martín Duce
Rosa Martin-Mateos
Rosa María Martín Mateos
Maria Angeles Martin Prats
Cristina Martín-Arriscado
Franz Martin-Bermudo
Marianne Martinello
Sara Martinez
Javier Martinez
Fernando Martinez
Lola Martinez
sara martinez
Raquel A. Martinez Garcia de la Torre
Celia Martinez Jimenez
Saul Martinez Montero
Andrés Martínez Mora
Celia Martínez Sánchez
Angela Martinez Valverde
Laura Martínez-Arenas
Eva Martínez-Cáceres
Alba Martínez-Escudé
Susana Martínez-Flórez
Laura Martinez-Gili
Brenda Martínez-González
Marc Martinez-Llordella
Maria Martinez-Roma
Claudia Martinez-Tapia
Idoia Martin-Guerrero
Silvia Martini
Alexandru Martiniuc
F Martin-Reyes
Alexandra Martins
Maria Martins
Anna Martner
Tafireyi Marukutira
Luca Marzi
Simona Marzorati
Samir Marzouk
Mario Masarone
Mizokami Masashi
Miguel Mascarenhas
chiara masetti
Olivia Maslac
Helena Masnou
Andrew L. Mason
Hugh Mason
Mojgan Masoodi
Marianna Maspero
Francesco Massaro
Johannes Masseli
Patricio Más-Serrano
Steven Masson
Elisabetta Mastrorocco
Toshihiko Masui

Henry Masur
Flora Masutti
Beatriz matesos Muñoz
John Mathers
Babu Mathew
Mead Mathews
Steven Mathews
Rajendra Mathur
Philippe Mathurin
Jean Jacques Matimbo
Bashar Matour
Karen Matsukuma
Kosuke Matsumoto
Kentaro Matsuura
Claudia Matteucci
Hanno Matthaei
Gail Matthews
Philippa Matthews
Matheus Mattos
Giulia Matusali
Madlen Matz-Soja
Christopher Maucourant
Michelet Maud
Lars Maurer
Francesco Mauri
João Maurício
José Luís Mauriz
Violeta Mauriz
Ezequiel Mauro
Lars Maurrer
Mate Maus
Ryan Maxwell
Douglas Maya
Florian Mayer
Lena Mayer
Marlyn J. Mayo
Sabrina Mazouz
Wlodzimierz Mazur
Vera C. Mazurak
Vincenzo Mazzafferro
chiara mazzarelli
Giovanni Mazzola
Veronica Mazzucco
Dora Mbanya
Misti McCain
Adrian McCann
Erin McCartney
Geoff McCaughan
Craig J. McClain
Emma McCormick
rosemary McCormick
Francesca McCullough
Anne McCune
Brock McDonald
Lucy McDonald
Natasha McDonald
Noel G. McElvaney
Sara McGeorge
Katherine McGlynn
Michael McGuckin
Noxolo Mchunu
Chris McIntosh
Gail McIntyre
Jane McKeating
Elizabeth McKinnon
Melita McKinnon
Lynn McMahon
Megan McMullen

Anna McNaughton	Silvia Meschi	Valbona Mirakaj
Marian McNeil	Vincenzo Messina	Anna Miralpeix
Mark J W McPhail	Daniela Mestre Congregado	Godolfino Miranda Zazueta
Stuart Mcpherson	Magdalena Meszaros	Fraquelli Mirella
Kate Mcque	Sophie Metivier	Darius F. Mirza
Andrew McQuillin	David Metreveli	Jasmin Mischke
Claire McQuitty	Herold Metselaar	Nitu Mishra
Georgina Meacham	Herold J. Metselaar	Kajali Mishra
Renato Medas	Leander Meuris	Gauri Mishra
María Paz Medel	Moritz Meyer	Sameer Mistry
Subhash Medhi	Bernhard Meyer	Dorina Mita
Asle Wilhelm Medhus	Christoph Meyer	Chris Mitchell
Philippe Meersseman	Pamela Meyer-Herbon	Robert Mitchell-Thain
Bob Meeusen	Malin Holm Meyer-Myklestad	Sasikala Mitnala
Shahin Mehdiyev	Gabriel Mezzano	Bogdan Mitran
Ann-Kathrin Mehnert	Neil Mfaria	Ragai Mitry
Alexander Mehrl	Marta Miaczynska	Akaash Mittal
Shubham Mehta	Patrick Mialhes	Bettina Mittendorf
Florian Meier	Yingying Miao	Romy Mittenzwei
Stijn Meijnikman	Vitale Miceli	Makoto Miyara
Nadja Meindl-Beinker	Michael Michael Christiansen	Tatsunori Miyata
Tobias Meischl	Elisavet Michailidou	Meenu MN
Rachel Meislin	Sophie Michalak	Valérie Moal
Toni Luise Meister	Łukasz Michałowski	Mikaela Mobsby
Scherezada Mejia	Baptiste Michard	Ginevra Mocchiatti
Mette Mejlby Hansen	Maurice Michel	Gabriele Mocchiato
Yonatan Mekonnen	Rivoire Michel	Diana Möckel
Hans Olav Melberg	Jean-Marie Michot	Kavita Modi
Zeynep Melekoglu Ellik	Paul Middleton	Beat Moeckli
Zeynep Melekoglu Ellik	Håvard Midgard	Tudor-Voicu Moga
Maria Jose Melero	Alexa Mieg	Maurizio Moggio
Daniela Melis	Luca Miele	Carolin Mogler
Marta Melis	Giorgina Mieli-Vergani	Almuthana Mohamed
Sandra Melitón Barbancho	Jesus Miguens Blanco	Wael Mohamed
Tommaso Mello	Maja Mijic	Almuthana Mohamed
George Mells	Nabiel Mikhail	Hozeifa Mohamed Hassan
Cristina Melo Rocha	Daiki Miki	Fadak Mohammadi
Shannon M Melody	Tomasz Mikula	Shahin Mohammadi
Espen Melum	Wolfgang Mikulits	Aaminah Mohammed
Edward Mena	Stefano Milani	Prashant Mohan Agarwal
Milena Mendes	Michele Milella	Sujata Mohanty
Carolina Méndez-Blanco	Jovana Milic	Michelle Møhlenberg
Nahum Méndez-Sánchez	Malgorzata Milkiewicz	Irina Mohorianu
Manuel Mendizabal	Piotr Milkiewicz	Raphael Mohr
Yuly Mendoza	Malgorzata Milkiewicz	Christian Möhring
Francis Mendy	Piotr Milkiewicz	Antje Mohs
Maimuna Mendy	Małgorzata Milkiewicz	Riccardo Moia
Xianmei Meng	Piotr Milkiewicz	Christiana Moigboi
Aswin L. Menke	Malgorzata Milkiewicz	Sergey Moiseev
Krishna Menon	Piotr Milkiewicz	Bregje Mol
Denise Menti	Jane Millar	Anna Moles
Yves Menu	Michael Miller	Esther Molina
Uwe Menzel	Carolyn Miller	Christian Molina-Aguilar
Maria Mercado-Gómez	Mark Miller	Nicolas Molinari
Sercan Mercan	Oscar Millet	Camilla Moliterni
Michael Merchant	Daniel Millian	Sarah Mollenkopf
Christopher Meredith	Camilla Mills	Lars Christian Möller
tiziana mereu	Yuka Milton	Søren Møller
Melihe Meriç Koç	Christos Mina	Dina Leth Møller
Victor Merino	Anne Minello Franza	Søren Møller
Xavier Merino	Rosalba Minisini	Andreas Møller
Jean François Meritet	Antonella Minutolo	Isabel Molwitz
Jean Claude Merle	Rosa Miquel	Antoni Mombiola
Manuela Merli	Joaquin Miquel	Diethard Monbaliu
Marica Meroni	Rosa Miquel	Valérie Monbet
Chady Meroueh	Mireia Miquel	Kathryn Monfils
Peter Rene Mertens	Rosa Miquel	Erika Monguzzi
Philipp Mertins	Xavier Mirabel	Sara Monico

Disclosures

Sara Montagnese
Marzia Montalbano
Paolo Montalto
Iaarah Montalvo
Valle Montalvo-Romeral
Noé Axel Montanari
rosa montañés
Maria Monte
Rocío Montero-Vallejo
Pedro Montes
Xavier Montet
Monica Monti
Carla Montironi
Carmina Montoliu
Anne Mooney
Dilip Moonka
Karen Moore
Yvette Moore
J. Bernadette Moore
Celia Moore
David Moore
Kevin Moore
Joanna Moore
Claudia Moore-Gillon
Orna Mor
Inbal Mor
Orna Mor
Alfonso Mora
Darius Moradpour
Dalia Morales Arraez
Manuel Morales-Ruiz
Luis Enrique Morano Amado
Bárbara Morão
Richard Moreau
Sulleman Moreea
teresa moreira
Antoine Morel
Carola Maria Morell
Maria Cristina Morelli
Rémi Morello
Christophe Moreno
M. Jesús Moreno-Aliaga
Alazne Moreno-Lanceta
Victoria Moreno-Manzano
Marsha Morgan
Katie Morgan
Marsha Morgan
Timothy Morgan
Paul Morgan
Katie Morgan
Cecilia Morgantini
Mattia Mori
Yasuhiro Mori
Trevor Mori
Rosa M Morillas
Maki Morinaga
Martina Morini
Filomena Morisco
Naoki Morita
Steven Morley
Timothy Morley
Steven Morley
Joanne Morling
Francoise Mornex
Berna Morova
Martine C. Morrison
Linda Morrow
Christian Mortensen

Frank Viborg Mortensen
Christian Mortensen
Antonella Mosca
Miha Moskon
Alireza Moslem
Adyr Moss
Yasmin Mossavar-Rahmani
Elias Mossialos
Lorena Mosteiro González
Alireza MosusaviJarahi
Maryam Motamedrad
Benedetta Maria Motta
Karsten Motzler
Lien-Juei Mou
Miguel Moura
Luís Manuel Moura
Carla Maria Moura Marinho
Abbas Mourad
Ilias Moutsopoulos
Ferenc Mozes
Anna Mrzljak
Francy Mubenga
Giulio G. Muccioli
Marcus Mücke
Victoria Mücke
Alexandra Mueller
Sebastian Mueller
Martina Mueller-Schilling
Robert Muga
Abdullah Ghassan Farik Muhammad
Taj Muhammad
Saad Muhammad
Ambreen Muhammed
Andrew Muir
Salma Mujib
Sujit Mukherjee
Sarmistha Mukherjee
Atish Mukherji
Sramana Mukhopadhyay
Nizar Mukhtar
Avinash Mukkala
Sebastien Mulé
Thomas Mules
Ashwini Mulgaonkar
Giacomo Mulinacci
Kate Mullany
Kate Muller
Tobias Müller
Sophie Elisabeth Müller
Tobias Müller
Christian Müller
Tobias Müller
Christian Müller
Tobias Müller
Sascha Müller
Beat Müllhaupt
Daniela Müllhaupt
Beat Müllhaupt
Nawakodchamon Mungnamtrakul
Stefan Munker
Munkhzaya Munkhbaatar
Chris Munoz
Linda Muñoz
Rocio Munoz Hernandez
Eva Muñoz-Couselo
Daneila Munteanu
Sarwa Darwish Murad
Harumi Murakami

Ayato Murata
Paolo Muratori
Luca Muratori
Aleksandra Murawska-Ochab
Antonio Murgia
Donald Murphy
Sandra Murphy
Ruth Murphy
Sam Murray
Syed Murtuza-Baker
Marianette Murzi P
Erkin Musabae
Fabrice Muscari
Kamran Mushtaq
Cristina Musolino
Daniela Mussi
Orlando Musso
Leon Muti
David Mutimer
Mahvish Muzaffar
Cristina-Maria Muzica
Robert Myers
Theodora Mylopoulou
Bich N Guyen
Mees N.S. de Graaf
Ekaterina Nabatchikova
Pamela Nabeta
Puria Nabilou
Nathalie Nachmansson
Fatema Nader
Luisa Nader
Fatema Nader
Devika Nadkarni
Mohammad Naffaa
Shunji Nagai
Koki Nagai
Shintaro Nagashima
Michael Nagel
Judith Nagel
Anika Nagelkerke
Abha Nagral
Yang Won Nah
Sven Nahnsen
Pierre Nahon
Leandra Naira Zambelli Ramalho
Miyuki Nakagawa
Shinichi Nakagawa
Atsushi Nakajima
Yasunari Nakamoto
Shingo Nakamoto
Daichi Nakamura
Atsushi Nakamura
Masato Nakamura
Hiroyuki Nakanishi
Toshiaki Nakano
Kazuhiko Nakao
Raouf Nakhleh
Karsten Nalbach
Rajkumar Nalinikanta
Heechul Nam
Olivier Namy
Yuemin Nan
Prossie Linda Nankya
Nikolai Naoumov
Cecilia Napodano
Laura Napoleone
Salvatore Napoli
Laura Napoli

Floriana Nappo	An Ngo	Bunthoon Nonthasoot
Abdul Rafah Naqash	Norbert Ngongang	Trina Norden-Krichmar
Himanshu Narang	Meng Ngu	Børge Nordestgaard
Vijay Narayanan	Natalie Ngu	Pia Maria Nörenberg
Shivakumar Narayanan	Terese Ngurruwuthun	Ilaria Normelli
Silvia Nardelli	Mindie Nguyen	Suzanne Norris
Alexander D Nardo	Thi Thu Nga Nguyen	Penny North-Lewis
Gerardo Nardone	Toni Nguyen	Elfriede Nößner
Stephanie Narguet	Diem Nguyen	Anna Not
Balakrishnan Chakrapani Narmada	Dung Nguyen	Nooshin Nourbakhsh
Pedro Narra Figueiredo	Henry Nguyen	Seham Noureldin
Elisabeth Naschberger	Danh Nguyen	Mohamed Noureldin Hassan Ali Abdelanbi
Leonardo Augusto Dias Nascimento	Thi Thuy Tu Nguyen	Ruder Novak
Erik Naslund	Vincent Nguyen-khac	Eva Novoa
Patrik Nasr	Marc Nguyen-Tat	Greg Nowak
Robert Nastasa	Yen-Hsuan Ni	Małgorzata Nowosad
Boyer Nathalie	Xin Ni	Line Carolle Ntandja Wandji
Legros Nathalie	Federico Nichetti	Joyce Ntata
Rohit Nathani	Sarah Nicholas	Lutz Nuhn
Rooshi Nathwani	Thomas Nicholson	Joao Nunes
Leonardo Natola	Jule-Marie Nicklas	Patricia Nunes
Jacob Nattermann	Coppola Nicola	Susana Núñez
Léa Naudet	Steven Nicolaides	Akudo Nwaogu
Michelle Naughton	Carine Nicolas	David Nyam P
Muhammad Nauman Tahir	Camerlo Nicolas	Haddy Nyang
Nidhi Nautiyal	Ferdinando Nicoletti	Anders Nyberg
musharraf navaid	Alberto Nicoletti	Lisa Nyberg
María Navalón	Amanda Nicoll	Colm O'Rourke
Nadia Navari	Arnaud Nicot	Kathryn Oakes
Giuseppe Navarra	Claus Niederau	Fiona Oakley
Ahmad Nawaz	David Niederseer	Rhys Oakley
Jeremy Nayagam	Johannes Niemeyer	Adham Obeidat
Nelson Ndegwa	Juan Camilo Nieto	James O'Beirne
Cilor Ndong	Natalia Nieto	Valerie Oberhardt
Gibril Ndow	Max Nieuwdorp	Giovanna Oberti
Leya Nedumannil	Ane Nieva-Zuluaga	Pilar Obon
Dermot Neely	monica niger	Alastair O'Brien
Andreas Neerincx	Nik Ma Nik Arsyad	Serkan Ocal
Guy Neff	Georgios Nikolopoulos	Maria Dolores Ocete
Elodie Negre	Elena Nikulkina	Dolores Ocete Mochon
Julien Negre	Emma Nilsson	Byambasuren Ochirsum
Francesco Negro	Joseph Nim	Aitor Odriozola
Mark Nelson	Vjera Nincevic	Aitor Odriozola Herrán
Shashwati Nema	Massih Ningarhari	Noémie Oechslin
Ivan Nemazanyy	Hans Dieter Nischalke	Imri Ofri
Ital Nemet	Naoshi Nishida	Jonas Øgaard
Iuliana Nenu	Shinya Nishida	Sadahisa Ogasawara
Sergio Neri	Naoshi Nishida	Eri Ogawa
Lina Nerlander	Nao Nishida	Keita Ogawa
Julia Nerusch	Takako Nishikawa	Yuji Ogawa
Eviatar Neshet	Takashi Nishimura	Chiara Oggioni
Daniela Nesticò	Takahiro Nishio	Chiara Oggioni
James Neuberger	Nicholas Nissen	Joo Hyun Oh
Ulf Neumann	Lise Sofie H. Nissen-Meyer	Katherine Oh
Christoph Neumann-Haefelin	Markku Nissinen	Hyunwoo Oh
Markus F. Neurath	Esther Nistal	Oonagh O'Hagan
Christine Neuveut	Florina Nitu	Shaelyn O'Hara
Nora Nevermann	Lili Niu	Shuichi Ohtomo
Isabel Neves	Junqi Niu	Hideaki Okajima
Yuval Nevo	Lili Niu	Akira Okajima
Anat Nevo-Shor	Ramou Njie	Tatsuya Okamoto
Kate New	Jennifer Nobes	Takeshi Okanoué
Elizabeth Newberry	Sebastian Nock	Stanislav Okapec
Carolyn Newberry	Paulo Nogueira	Edith Okeke
Yee Chen Ng	Ruben Nogueiras	Cristina Olague Micheltorena
Huck Hui Ng	Flor Nogueiras López	Paula Olaizola
Kelvin Ng	Yung-Kyun Noh	Anne Olbrich
Jean-René Ngele	Borko Nojkov	Hannah Old
		Graziano Oldani

Disclosures

Steven Olde Damink
Christopher Oldroyd
Jacqueline O'Leary
Sara Olesen
Tronina Olga
Peter Olinga
Pol Olivas
Filippo Oliveri
Ana Olivo
Alexander Olkus
Rupert Öllinger
Isabelle Ollivier-Hourmand
Victor Olsavszky
Inge Christoffer Olsen
Carlos Oltmanns
John Olynky
Tea Omanovic Kolaric
Morgan Oneka
Agnes Bee Leng Ong
Janus Ong
Albert Ong
Stefano Ongarello
Gabriel Oniscu
Kristina Önerhag
Lorenzo Onorato
Ye Htun Oo
Geraldine Ooi
Dorenda Oosterhui@rug.nl
Paulina Opyrchal
Philip Oravetz
Marie-Amelie Ordan
Kevin O'Reilly
Matej Orešič
Marju Orho-Melander
Vichit Ork
Hans Orlent
Stian Magnus Staurung Orlén
Valeria Orlova
necati ormeci
Denise Oró
Joanne Orourke
James Orr
Enrique Ortega G.
Aida Ortega-Alonso
María Luisa Ortiz
Carolina Ortiz-Velez
Julia Ortne
Gabriel Osborn
Ana Oshaughnessy
Valentino Osti
Sisse Rye Ostrowski
Tessa Ostyn
Alejandra Otero
Alejandra Otero Ferreira
Elena Oton
Kari Otterdal
Tobias Otto
Jacobus Otto
Xiaojuan Ou
Nadia Oubaya
Linda Oude Griep
Ronald Oude-Elferink
Marine Oudot
Serge Ouoba
Abderrahim Oussalah
Denis Ouzan
Louise Owen
Collins Oduor Owino

Chung Owyang
Evelin Oxtrud
Julen Oyarzabal
Michitaka Ozaki
Umut Ozbek
Mustafa Özcürümez
Kamil Ozdil
Burcin Özdirik
Hasan Ozen
Digdem Ozer Etik
Ann-Kathrin Ozga
Ekin Ozgonul
Jonathan Ozik
Serdar Özsezen
Omer Ozutemiz
Aditya Vikram Pachisia
Sabrina Paci
Beatriz Pacín Ruiz
Gemma Packer
Nagaraja Rao Padaki
Cynthia Padilla
Ana Padilla
Susana Padrones
Slobodan Paessler
Duilio Pagano
Sabrina Pagano
Georges-Philippe Pageaux
Katja Pahkala
Prabhjyoti Pahwa
Madhava Pai
Yong-Han Paik
Seung Woon Paik
Yong Han Paik
James Paik
Elena Paillaud
Anita Paisant
Nuno Paiva
Ravindra Pal
Naaventhana Palaniyappan
Yaseelan Palarasah
pascale palassin
Asís Palazón
Ana Palazzo
Mor Paldor
Andrea Palermo
Giuseppina Palladini
Joan Pallares
Giada Pallini
Elena Palma
Carolina Santos Palma
Elena Palma
Nicki Palmer
Silvia Palmisano
Elena Palmisano
Adriana Palom
Giorgio Palu
Rafał Paluszkiwicz
Viniyendra pamecha
Claudia Pamo
Qiuwei Pan
Liangyu Pan
Dimitra Panagiotoglou
Sarjukumar Panchal
Alessandra Pandolfo
Nadia Panera
Antonio Panero
Elena Panettieri
Jing Pang

Marcus Panning
Spyridon Pantzios
Marlene Panzer
Simon Panzer
Marlene Panzer
Erika Paolini
Veronica Paon
Ioanna Papagiouvanni
Chiara Papalini
Tim Papaluca
Zafiris Papanikolaou
Margarita Papatheodoridi
Ana Papkauri
Valérie Paradis
Anupama Parasara
Romain Parent
Elisabetta Parente
Albert Parés
Anna Parfieniuk-Kowerda
Stefanie Parisi
Jun Yong Park
Min Kyung Park
Soo Young Park
Jung Gil Park
Eun Jin Park
Jina Park
Min Kyung Park
Young Joo Park
Jun Yong Park
Hye Jung Park
Soo Young Park
Young Joo Park
Huiyul Park
Jung Gil Park
Huiyul Park
Jun Yong Park
Soo Been Park
Min-Jung Park
Neung Hwa Park
Jeongwoo Park
Julie Parkes
Emine Parlak
Yavuz Emre Parlar
Lucia Parlato
Marie Parnot
Cristina Parolin
Marina Parra-Robert
Craig Parzynski
Alina Pascale
Sonia Pascual
Tania Pastor
Helena Pastor
Mirella Pastore
Roberta Pastorelli
Daniele Pastori
Frane Pastrovic
Sama Siva Rao Pasulapati
David Patch
Janisha Patel
Poulam Patel
Harshil Patel
Kajal Patel
Priti Patel
Niharika Patel
Nishi Patel
Janisha Patel
Sameer Patel
Vishal Patel

Rafael Paternostro	Caterina Peraldo Neia	Camila Picchio
Vai Pathak	Celia Perales	Marie-Pierre Piccinni
Piyush Pathak	Sergio Peralta	Francesco Paolo Picciotto
Anita Pathil-Warth	Riccardo Perbellini	Paola Piccolo
Purendra Kumar Pati	Vitor Pereira	Julia Piche
Favot Patrick	Laura Pereira	Roberto Piciotti
Daniel Patten	Gustavo Henrique Santos Pereira	Neora Pick
alexia paturel	Bruno Pereira	Felix Piecha
Ashwin Patwardhan	S. Pereira	Juliana Piedade
Vilas Patwardhan	Gustavo Pereira	Ana Maria Piedra Cerezal
Dajana Paulmann	Pedro Pereira	Giulia Pieri
Coen Paulusma	Marta Paula Pereira Coelho	Lorenzo Piermatteo
Bernhard Paulweber	Tiago Pereira Guedes	de la grange pierre
Réjane Paumelle	Christie Perelló	Elsbeth Pieterman
Patrick Pauwels	David Pereyra	Antonello Pietrangelo
Oana Pavel	Valeria Perez	Olivia Pietri
Vlad Pavel	Martina Perez	Thomas Pietschmann
Natasa Pavlovic	Judith Pérez	Luca Pignata
Piotr Pawliszak	Irene Perez Alvarez	Charlotte Pihl
Małgorzata Pawłowska	Ylenia Pérez Castaño	Matteo Pilan
Tania Payo-Serafin	Jose Luis Perez Hernandez	Anjana Pillai
Monika Pazgan-Simon	Francisco Andrés Pérez Hernández	Jose Pinazo Bandera
Galo Pazmiño	Indhira Perez Medrano	Antonio A Pineda
Rautou PE	Maite Perez-Araluce	Isabell Pink
Emily Peach	Mercedes Pérez-Carreras	Nawamin Pinpathomrat
Margo Pearce	Sofía Pérez-del-Pulgar	Isabel Pintelon
Fiona Pearce	Martina Perez-Guasch	Lorenzo Pintore
edward pearce	Elisa Perfetti	Benedetta Piombanti
Madeline Pearson	Juan Manuel Pericàs	Diego Piombino
Thibault Pebrier	Lauren Perieres	Karen Piper Hanley
Maciej Pech	Giridharan Periyasamy	Joseph Pipicella
Alexandros Pechlivanis	Markus Perola	Rosaria Maria Pipitone
Ryan Peck	Jean Marie Peron	Claire piquet.pellorce
Anna-Marie Pedde	Ylenia Perone	Anita Pirabe
Mark Pedersen	Elena Perpignan	Ron Piran
Oluf Pedersen	Andrea Perra	Tasneem Pirani
Federica Pedica	Meritxell Perramón	T Piratvisuth
Alisa Pedrana	Clara perrin	Jacques Pirenne
João Pedro Sousa Ferreira	Caroline E Perry	Boris Pirlot
Isabel Pedroto	Marcello Persico	Loris Pironi
Kai-Henrick Peiffer	María Jesús Perugorria	Andrea Piroso
Kai-Henrik Peiffer	Patrick Pessaux	Giuseppina Pisano
Daniel Peled	Mélanie Petera	Pasquale Pisapia
Noam Peleg	Rory Peters	mariantonietta pisaturo
Cédric Peleman	Tim-Ole Petersen	Sven Pischke
Alessandro F Pellegata	Troy Peterson	Fabiola Piscopo
Luc Pellerin	Mathilde Petiet Dumont	Salvatore Piscuoglio
Andrea Peloso	Mathieu Petitjean	Pierluca Piselli
Kevork Peltekian	Fischer Petra	Mauro Pistello
Serena Pelusi	Maria Raffaella Petrara	Valeria Pistorio
David Pemberton	David Petroff	Gabriella Pittau
Julia Peña Asensio	Maria Letizia Petroni	Christina Plagiannakos
Marcela Peña Rodríguez	Petar Petrov	Alejandra Planas
Guillaume Penaranda	Stefania Petruccelli	Lindsay Plank
Beatriz Peñas	Raluca Petrut	James Plant
Yanzhong Peng	Evangelia Petsalaki	Maria Corina Plaz Torres
Yun Peng	Flora Peyvandi	Maria Corinna Plaz Torres
Shifang Peng	Henning Pflugrad	Mario Plebani
Cheng-Yuan Peng	Hang Phan	Aurélie Plessier
Ming-Li Peng	Naw April Phaw	John Plevris
Eno Pengili	Gino Phillips	Marie-Laure Plissonnier
Matthew Penn	Sandra Phillips	Alexander Plotnikov
Grazia Pennisi	Rachael Phillips	Maria Poca
Jette Penski	Wah Wah Phyto	Esteban Poch
Anne Penttilä	Guido Piai	Tobias Poch
Katell Peoch	Stephen Pianko	Nathalie Pochet
Maikel Peppelenbosch	Valeria Piazzolla	Anna Pocurull
Guillem Pera	Lucia Picariello	Kristian Podrug

Disclosures

Alexander Poen
Sarah Poetter-Lang
Pauline AW Poh Kim
Junika Pohl
Johanne Poisson
Cristina Pojoga
Stanislas Pol
Prido Polanco
Kamil Yalçin Polat
Kamil Yalcin Polat
Edoardo Poli
Michela Anna Polidoro
Beatrice Polini
Teresa Pollicino
Simone Polvani
Susanne Polywka
Katharina Pomej
Enrico Pompili
Maurizio Pompili
Caroline Pons
Monica Pons
Willemijn Ponsioen
Cyriel Ponsioen
Nathalie Pons-Kerjean
Clara Ponsolles
Thais Pontelo de Vries
Frederik Ponten
Francesca Ponziani
Alexandru Popa
Laura Popa-Dan
Alina Popescu
Yury Popov
Oliver Popp
Rossana Porcasi
Almudena Porcel Martin
David Porras
Kerstin Port
Marco Porta
Robert Porte
Begoña Porteiro
Giuseppe Portella
Kimmo Porthan
Irene Portoles
Andreas Posch
Elisa Pose
Julia Pose-Utrilla
Josef Pospiech
Ewelina Pośpiech
Lucia Possamai
Catherine Postic
Anna Potapova
Tanja Poth
Jean-Baptiste Potier
John Poulos
Mohammadamin Pourhoseingholi
Elizabeth Powell
Maciej Powerski
Paloma Poyatos-Garcia
Thierry Poynard
Andreas Prachalias
Pranita Pradhan
Dimas Praditya
Julien Prados
Jennifer Prah
Michael Praktiknjo
Sarah Prallet
Tannishtha Pramanick
Babita Prasad

Manya Prasad
Pooja Prasad
Dario Pratelli
Daniele Prati
Johann Pratschke
Trevor Pratt
Angga Prawira
Madhumita Premkumar
Melissa Preziosi
Jillian Price
Katrine Prier Lindvig
Jesus Prieto
Janire Prieto
César Prieto de Frías
Endika Prieto-Fernández
Massimo Primignani
David Prince
Hans Princen
Elija Prinic
John Prins
Marco Prinz
Carlos Prishker
Rajeev Priyadarshi
Bogdan Procopet
Gordon Proctor
Charlotte Pronier
Ilaria Prosepe
Camelia Protopopescu
Bernard Prouvost-Keller
Nicholas Provine
Chunwen Pu
Francesc Puchades Gimeno
Angela Puente
Alba Pueyo Moliner
Nicola Pugliese
Claudia Pujol
Paula Pujols
Estelle Pujos-Guillot
Federico Pulido Ortega
Donny Puma
Surakit Pungpapong
Massimo Puoti
Puneet Puri
Vincenzo Puro
Shashank Purwar
Klaus Püschel
hegde pushpa
Hein Putter
Lauri Puustinen
Emmi Puuvuori
Hervé Puy
Marco Puzzoni
Saiju Pyarajan
Natalia Pydyn
Nikolaos T. Pyrsopoulos
Danielle Q Bonilha
Motaz Qadan
Sami Qadri
Sumaira Qamar
Xiaolong Qi
Lishuang Qi
HaiTao Qi
Xiaolong Qi
Tongqi Qian
Yuquan Qian
Zhiping Qian
Guoliang Qiao
Lihui Qin

Ling Qin
Dongdong Qiu
Yuanwang Qiu
Zhen Qu
Bingqian Qu
Natalie Quach
Alberto Quaglia
Xavier Quantin
Maria Giovanna Quaranta
Alessandra Quarta
Peter Quehenberger
Josep Quer
Jonathan Quinlan
Eugenia Quiros-Roldan
Oliver Quitt
Vincent Quoc-Huy Trinh
Huma Qureshi
Juan R Lacalle
Miriam Rábano
Vikrant Rachakonda
Jacob Rachmilewitz
Andrei Racila
Roland Rad
Patricia Rada
Anastasiia Radchenko
Sebastian Rademacher
Silvia Radenkovic
Sylvie Radenne
Claudia Maria Radu
Elena Cristina Radu
Giuseppina Raffa
Brustia Raffaele
Chiara Raggi
Enrico Ragone
Celine Raguenees-Nicol
Galia Rahav
Mohammad Rahbari
Nuh N. Rahbari
Suditi Rahematpura
Robert Rahimi
Fariar Rahman
Tony Rahman
Giovanni Raimondo
Florian Rainer
Olli Raitakari
Poyyamozi Rajagopal
Vijayraghavan Rajan
Samurailatpam Rajesh Sharma
Neil Rajoriya
Jorge Rakela
Lucy Ralton
Jeyamani Ramachandran
Sumathi Ramachandran
Narayan Ramamurthy
Maitreyi Raman
Raghu Ramanathan
Matteo Ramazzotti
Evelyn Ramberger
Clémence Ramier
Paola Ramirez
Carolina Ramirez
Maria Ramirez
Patty Marlen Ramírez Portillo
Obed Ramírez Sánchez
Resham Ramkissoon
Grant Ramm
Ashwin Rammohan
Erik Ramon-Gil

Geraldine Ramos
 Davide Rampoldi
 Lukas Ramsauer
 Nisha Rana
 Randeep Rana
 Gabriele Rancatore
 Julien Randon-Furling
 Ariadna Rando-Segura
 Roberto Ranieri
 Kevin Rank
 Jamie Rankin
 Navpreet Ranu
 Ankit Rao
 Arvind Rao
 Pranshu E Rao
 Huiying Rao
 Arvind Rao
 Krishna Rao
 Gian Ludovico Rapaccini
 Ilario Raposelli
 Simona Rapposelli
 Mamunur Rashid
 Tamir Rashid
 Elias Rashu
 Ditlev Nytoft Rasmussen
 Allan Rasmussen
 Ditlev Nytoft Rasmussen
 Simon Rasmussen
 Ditlev Nytoft Rasmussen
 Marco Rasponi
 Aayushi Rastogi
 Archana Rastogi
 Una Rastovic
 Dilip Ratnam
 Francesca Ratti
 Magnus Ratray
 Vlad Ratzu
 Imma Raurell
 Pierre-Emmanuel Rautou
 Federico Ravaoli
 Matteo Ravaoli
 Federico Ravaoli
 Joachim Ravau
 Kim Ravnskjaer
 Sumit Rawat
 Piper A. Rawding
 Dominic Ray-Chaudhuri
 Marcel Razpotnik
 Joanna Ready
 Estelle Rebillard
 María Rebollo
 Sylvie Rebuffat
 Agustina Reca
 Stefania Recalcati
 Miriam Recalde
 Gal Reches
 Franziska Recklies
 Anna-Rita Redavid
 Rajender Reddy
 K. Rajender Reddy
 Rajender Reddy
 Nageshwar Reddy
 Tom Rees
 Helen L. Reeves
 Helen Louise Reeves
 Helen Reeves
 Helen L. Reeves
 Luca Reggiani-Bonetti

Nicola Reggidori
 Maxime Regnier
 Benjamin Rehany
 Abdul Rehman
 Matthias Reichert
 Leila Reid
 Connor Reilly
 Giada Reina
 Sara Reinartz Groba
 Jiří Reiniš
 Tina Reinson
 Florian P Reiter
 Veronika Reiterer
 Edouard Reizine
 Mohd. Rela
 Pablo Remon
 Liying Ren
 Yayun Ren
 Ming Ren
 Shan Ren
 Yayun Ren
 Qingyun Ren
 Yayun Ren
 Hong Ren
 Keke Ren
 Amédée Renand
 Alain Renault
 Bishguurmaa Renchindorj
 Kirsten Rennie
 Matteo Renzulli
 Roberta Resaz
 Juan Carlos Restrepo
 Aurelia Retbi
 Adrian Reuben
 Philipp Reuken
 Kristina Reutlinger
 Peter Revill
 Karsten Fleischer Rex
 Esther Rey
 Gisel Estefania Reyes-Higuera
 Juliana Reyes-Ureña
 Maud Reymond
 Christelle Reynès
 Tadeja Rezen
 Milad Rezvani
 Rami Rhaiem
 Shawn Rhind
 Hyung Chul Rhu
 David Rial Crestelo
 Ioana Riaño
 Tiago Ribeiro
 Jordi Ribera
 Antônio Ricardo Cardia Ferraz de Andrade
 Laura Riccardi
 Gabriele Ricco
 Betrice Ricco'
 John Rice
 Paul Richardson
 Mathieu Richaud
 Nicholas Riches
 Charlotte Rich-Griffin
 Jacqui Richmond
 Maria Richter
 Steven Riddell
 Dirk Ridder
 Elora Rider
 Patricia Rider
 Renee Ridzon

Florian Riedl
 Alix Riescher
 Jennifer Rieusset
 Cristina Rigamonti
 Oliviero Riggio
 Chai Hong Rim
 Margherita Rimini
 Kristina Ringe
 Marc Ringelhan
 Johan Ringlander
 Gisela Ringström
 Emmanuel Rio
 Rafael Rios
 Cristina Ripoll
 Michela Ripolone
 Angela Ritter
 Antonio Riva
 Francesca Riva
 Coral Rivas
 Violeta Rivas
 Mar Riveiro Barciela
 Jesús Rivera
 Jose Rivera
 Savannah Rivera
 Montserrat Rivero
 Valérian Rivet
 Giorgia Rizza
 Michael Rizzari
 Giacomo Emanuele Maria Rizzo
 Geert Robaey
 Wouter Robaey
 Ernesto Robalino Gonzaga
 Caroline Robert
 Lauren Roberts
 Surain Roberts
 Stuart Roberts
 Andrew Roberts
 Marcus Robertson
 Keith Robertson
 David Robertson
 Marcus Robertson
 Callum Robins
 Emma Robinson
 Juan Pablo Roblero
 Mercedes Robles-Díaz
 Carla Daniela Robles-Espinoza
 Armando Andres Roca Suarez
 Davide Roccarina
 Lucia Rocco
 Haroldo Luis Oliva Gomes Rocha
 marta rocha
 Bruno Roche
 Agnès Rode
 Michael Roden
 Aaron Nikolai Rodenhausen
 Martin Roderfeld
 Paul Roderick
 Mary Rodgers
 Fatima Rodriguez-Alvarez
 Daniel Rodrigo Torres
 Beverly Rodrigues
 Pedro Miguel Rodrigues
 Susana G. Rodrigues
 Cecília M. P. Rodrigues
 Barbara Rodrigues
 Maria Rodriguez
 Manuel Rodríguez
 Héctor Rodríguez

Disclosures

Carlos Rodríguez
Rubén Rodríguez Agudo
Elías Rodríguez Cuéllar
Juan Carlos Rodríguez Duque
Juan Carlos Rodríguez Duque
Maria Mercedes Rodriguez Gazari
Begoña Rodriguez Iruretagoyena
Sergio Rodriguez-Cuenca
María Rodríguez-Cundin
Juan Carlos Rodríguez-Duque
Francisco Rodríguez-Frías
Juan Carlos Rodríguez-San Juan
Elisabet Rodríguez-Tomás
Elke Roeb
Natascha Roehlen
Stephanie Roessler
Henk P. Roest
Mark Roest
Shari Rogal
Magdalena Rogalska
Benjamin Rogers
Mercé Roget
Sumati Rohilla
Natascha Röhlen
Nataliya Rohr-Udilova
Cristina Roig
Morganer Roinard
Angela Rojas Alvarez-Ossorio
Mayra Rojas Lara
Carla Rojo
Diego Rojo Lázaro
Johanna Rokka
Zachary Rokop
Al Sayegh Rola
Oren Rom
Renato Romagnoli
Veronica Romagnoli
Eva Roman
Stefano Romeo
Orazio Romeo
Sean Romeo
Barbara Römer
Marta Romero
Sarah Romero
Gustavo Romero
Horacio Romero Castillo
Manuel Romero Gomez
Sarai Romero Moreno
Martin Rønn Madsen
Luisa Ronzoni
Riccardo Ronzoni
Floris Roos
María C. Roque-Cuéllar
Bertrand Roquelaure
Fredrik Rorsman
Isabelle Rosa
Luis Alejandro Rosales Renteria
Michelle Rosario
Thomas Rösch
Ayub Rose
Stefan Rose-John
William Rosenberg
Nofar Rosenberg
Vered Rosenberg
Aaron Rosenberger
Emma Rosenbluth
Jonas Rosendahl
Maria Rosestedt

Martina Rosi
Rajkumari Rosie
Sebastian Rosigkeit
Arianna Rosina
Francesca Rosini
Tania Roskams
Elen Rosler
Oskar Rosmark
Olivier Rosmorduc
Fredrik Rosqvist
Gayle Ross
Kendra Ross
Elena Rosselli Del Turco
Noortje Rossen
Natalia Rosso
Rhonda J. Rosychuk
Nitzan Roth
Anjali A. Röth
Ori Rotstein
Woo Sun Rou
Francoise Roudot Thoraval
Françoise Roudot-Thoraval
Dominique Roulot
Martin Roumain
Sotiris Roussos
Marine Roux
Perrine Roux
Julien Roux
Elisabetta Rovida
Ian Rowe
Berengere Roy
Akash Roy
Laura Royo
Nir Rozenblum
Teona Rozina
Laura Rubbia-Brandt
Ángel Rubín
Ana Belén Rubio
Rafael Rubio Garcia
Marika Rudler
Javier Rueda-Gotor
Darius Ruether
Pierre Rufat
Elena Ruffoni
André Ruge
Hardik Rugwani
Patricia Ruiz
Lourdes Ruiz
Pablo Ruiz
Paula Ruiz
Belén Ruiz Antoran
Mikel Ruiz de Gauna
Paloma Ruiz-Blazquez
Francisco Ruiz-Cabello
Natthapat Rujeerapaiboon
Jody Rule
Patricia Rullier
Massimiliano Ruscica
Anthony Russell
Francesco Paolo Russo
Maria Madeleine Rührich
Kelsey Rutland
Stephanie Rutledge
Andrea Ruzzenente
Jennifer Ryan
Pablo Ryan
Marno Ryan
Jennifer Ryan

John Ryan
Mikael Ryden
Stephen Ryder
Je Ho Ryu
Antonio Sa Cunha
Kustaa Saarinen
Constantino Sábado
Gul Sabeen Azam Ghorezai
Guadalupe Sabio
Sergio Sabroso
Patrizia Saccomandi
David Sacerdoti
Federica Sacilotto
Sophie-Caroline Sacleux
Sophie Sacleux
Farsaneh Sadeghlar
Matthew Sadler
Anwaar Saeed
Diego Saenz de Urturi
Maria Saez-Palma
Rifaat Safadi
Ricky Safer
Olga Sagalova
Sagar Sagar
Hacer Sahin
Roland Sahli
Amandeep Sahota
Iván Sahuco
Melissa Saichi
Yusuke Saigusa
Akhilesh Saini
donakonda sainitin
Mauricio Sainz-Barriga
Tomoko Saito
Satoru Saito
Tomoko Saito
Carlo Saitta
Haresh Sajiir
Jenna Sajous
Mehdi Sakka
Takafumi Sakuma
Margarita Sala
Sultan Salahuddin
Grgur Salai
Javier Salamanca Santamaría
ephrem salamé
Johannes Salamon
Massimiliano Salati
Maria Salatiello
María Magdalena Salcedo
Magdalena Salcedo
Maria Teresa Salcedo
Omar Saldarriaga
Natalia Saleev
Siamak Salehi
Ahmed Salhab
Faouzi Saliba
Kanita Salic
Henrike Salie
Sylvain Salignac
Daniel Salinas
José Antonio Salinas
Shadi Salloum
Sidra Salman
Veikko Salomaa
Federico Salomone
Angelo Salomone Megna
Romina Salpini

Sofia Salta
 Dario Saltini
 Verónica Saludes
 Vandana Saluja
 Francisco Salvà
 Marilyn Salvat Lago
 Albert Salvatella
 Antonio Salvati
 Anna Salvetti
 Marco Salvino
 Noel Salvoza
 Mahzeiar Samadaei
 Lara Samadan
 Tamar Samadashvili
 Dana Sambarino
 Benjamin Sambou
 Al-Dury Samer
 Anthony Samir
 Hasina Samji
 Henna Sammalkorpi
 Liliana Sampaio Costa Mendes
 Michel Samson
 Kay Samuel
 Didier Samuel
 Kay Samuel
 Ellen Samuelsen
 David San Segundo Arribas
 Faisal Sanai
 Mathilde Sanavio
 Jenifer Sanchez
 Carlos Sanchez
 Abel Sanchez
 Antonio Sanchez
 Marco Sánchez
 Victor Sánchez
 Yolanda Sánchez
 Ana Sánchez Martínez
 Eva Sofia Sánchez Quant
 Eva Sanchez Ramos
 Sonia Sánchez-Campos
 Jordi Sánchez-Delgado
 Alberto Sanchez-Fueyo
 Carlos Sanchez-Huertas
 M. Belén Sánchez-Rodríguez
 Jose Sanchez-Serrano
 Pau Sancho-Bru
 Ahmed Sandakli
 Johan K. Sandberg
 Adrián Sández Araiza
 Prakasit Sangaimwibool
 Angelo Sangiovanni
 Vincenzo Sangiovanni
 Bakary Sanneh
 Owen Sansom
 Eva Santamaria
 Bárbara Santana
 Valentina Santi
 Céline Santo
 Jonas Santol
 Luigi Santoro
 Ana Santos
 André A. Santos
 Álvaro Santos-Laso
 Eduardo Sanz de Villalobos
 Francisco Sanz Herrero
 Alejandro Sanz Paris
 Arantza Sanz-Parra
 Víctor Sapena

Nazmus Saquib
 Margherita Saracco
 Rita Catarina Saraiva
 Susana Saraiva
 Anoop Saraya
 Eliane Sardh
 Nazim Sarica
 Ozan Sarikaya
 Shiv Kumar Sarin
 Sanjay Sarin
 Shiv Kumar Sarin
 Loredana Sarmati
 Jędrzej Sarnecki
 Maeva Saroul
 Arif Sarowar
 Christoph Sarrazin
 Maria-Rosa Sarrias
 Ryan Balfour Sartor
 Sanjaya Satapathy
 Romona Satchi
 Toshifumi Sato
 Shunsuke Sato
 Sho Sato
 Melanie Sator-Schmitt
 Jack Satsangi
 Swetha Sattanathan
 Hagen Sauer
 Tilman Sauerbruch
 Emily Saunders
 Laura Sauvé
 Antonio Saviano
 Eric Savier
 Bisher Sawaf
 Rohit Sawhney
 Edward Saxby
 Varun Saxena
 Anoushka Saxena
 Katia Sayaf
 Sergi Sayols
 Carolina Sbarigia
 Reem Sbieh
 Marcelle Scagliotta
 Becky Scanlan
 Miki Scaravaglio
 Margaret Scarry
 Giampaolo Scarton
 Mario Scartozzi
 Olivier Scatton
 Frank Schaap
 Guido Schachschal
 Benedikt Schaefer
 Eugénie Schaeffer
 Clemens Schafmayer
 Martina Scharitzer
 Hubert Scharnagl
 Golda Schaub
 Stefan Schefczyk
 Andrea Scheffschick
 Alexander Scheiter
 Mathias Schemmerer
 Maleka Schenck
 Imre F Schene
 Filippo Schepis
 Michael Schepke
 Anna-Lena Scherr
 Thomas Schiano
 Gerda Schicht
 Robert Schierwagen

Aaron Schindler
 Peter Schirmacher
 Reinhold Schirmbeck
 Emilia Schlaak
 Kai Schledzowski
 Bernhard Schlevogt
 Alexandra Schlimmer
 Moritz Schmelzle
 Roland M. Schmid
 Daniela Schmid
 Roland M. Schmid
 Daniel Schmidt
 Nathalie Schmidt
 Geske Schmidt
 Ralf Schmidt
 Michael Schmidt
 Hartmut Schmidt
 Dirk Schmist-Arras
 Sascha Schmitt
 Nathalie Schmitt
 Sophia M. Schmitz
 Stefan Schneeberger
 Hannah Schneider
 Carolin Victoria Schneider
 Hannah Schneider
 Francis Schneider
 Antoine Schneider
 Julia Sophie Schneider
 Hannah Schneider
 Carolin Victoria Schneider
 Anne Schneider
 Doris Schneller
 Aurélie Schnuriger
 Barbara Schoers
 Anja Schollmeier
 Caroline Scholtes
 Wenzel Schöning
 Clemens Schotten
 Jörg Schrader
 Christoph Schramm
 Richard A Schreiber
 Sarah K. Schröder
 Dawn Schroeder
 Jonas Schropp
 Sara Schuermans
 Benjamin Schulte
 Janun Schulte
 Michael Schultheiss
 Martin Schulz
 Sarah Schulze
 Julian Schulze zur Wiesch
 Henning Schulze-Bergkamen
 Jonas Schumacher
 Detlef Schuppan
 Anna Schurich
 Catherine Schuster
 Stefan Schuster
 Catherine Schuster
 Christian Schwabe
 Marius Schwabenland
 Tae-Hwi Linus Schwantes-An
 Scott Schwartz
 Caroline Schwarz
 Michael Schwarz
 Michael Schwarzingen
 Sabrina Schweiggert
 Dorothee Schwingen
 Paolo Sciattella

Disclosures

Roberta Sciorio	Howard Sesso	Dongyan Shi
Paolo Scivetti	Veronica Setiawan	Xiaojun Shi
Marco Scoppettuolo	Han Seul Ki	Lei Shi
Melanie Scott	Vasilis Sevastianos	Xiaojun Shi
Nick Scott	Joseph Sexton	Yu Shi
Emma A.H. Scott	Moussa Seydi	Oren Shibolet
Charlotte Scott	Orhan Sezgin	Gamal Shiha
Robert Scott	Shaun Shadaker	Sonjelle Shilton
Viorel Scripcariu	Aladdin Shadyab	Ju Hyun Shim
Luigia Scudeller	Eva Shagla	Wan Seob Shim
David Sebastián	Mohammad Ali Shagrani	Toshihide Shima
Susanne Sebens	Naina Shah	Yuji Shimada
Christian Sebesta	Vijay Shah	Masahito Shimizu
Marcial Sebode	Hasnain A. Shah	Norikazu Shimizu
Annalisa Sechi	Vijay Shah	Hyun Phil Shin
Ousman Secka	Sital Shah	Jungwoo Shin
Alice Secomandi	Syed Hassan Bin Usman Shah	Rachel Shingaki-Wells
Daniela Segalerba	Sabeen Shah	Harold Shlevin
Paula Segalés	Dipam Shah	Amir Shlomai
Michela Seghezzi	Wasiuddin Shah	Saeed Shoaie
Tejasav Sehrawat	Afshin Shahnavaz	Pooya Shokoohi
Florine Seidel	Sarah Shalaby	Mohamed Shoreibah
Anne-Sofie Seidelin	Shalimar	Michal Shoshkes-Carmel
Lena Seidemann	Amirhossein Shamsaddini	Weinian Shou
Hendrik Seifert	Dandan Shan	Naglaa Shoukry
Gabriel Seifert	Ying Shang	Shreesh Shrestha
Susanne Seitz	Jia Shang	Merica Shrestha
Asieb Sekandarzad	Dazhuang Shang	Eyal Shteyer
Revathi Sekar	Eileen Shannon	Po-Yeh Shu
Ranya Selim	Chen Shao	Ruchi Shukla
Floriane Sellier	Shilpee Sharma	Tengfei Si
Nowlan Selvapatt	Nupur Sharma	Stefanie Sichelschmidt
Emmanuel Selvaraj	Shvetank Sharma	Mohammad Siddiqui
Xiaohui Sem	Mithun Sharma	Hamda Siddiqui
Gabriel Semere	Sanchit Sharma	Cyril Sieberhagen
Christine Sempoux	Eilon Sharon	Matthieu Siebert
Rajashree Sen	Lali Sharvadze	Hartwig R. Siebner
Anoop Sendamarai	Varsha Shasthry	Chloe Siegele-Brown
Alper Sener	S Muralikrishna Shasthry	Martin Siegele-Brown
Daniel Senfter	Jawaid Shaw	Armando Sierralta
Ali Senkaya	David Shaw	Majken Siersbæk
Caileen Sennett	Blake Shaw	William Sievert
Maria Senosiáin	Katy Shaw-Saliba	Susan Siew
Marco Senzolo	Shaoping She	Alejandro Sifrim
Satoru Seo	Jessica Shearer	Michael Sigal
Suk Seo	I-Shyan Sheen	Keith Sigel
Haeng Ran Seo	Sabreena Sheikh	Giordano Sigon
Yeon Seok Seo	Louis Shekhtman	Rebeca Sigüenza
Yoon-Seok Seo	Yue Shen	Bryndis Sigurdardottir
Kim Seok Hyun	Joanne X. Shen	Masoumeh Sikaroodi
Myoung Seok Lee	Xinping Shen	Emily Sileo
Wenla Seppänen	Lu Shen	Marianna Siletta
José Pedro Sequeira	Joanne X. Shen	Rachel Silk
Matteo Serenari	Liang Shen	Mario Jorge Silva
Irin Sereti	Wei Shen	Rita de Cássia Martins Alves da Silva
Ilaria Serio	Jifang Sheng	Giovanni Silva
Reza Serizawa	Wu ShengDi	Hugo Silva
Daniel Seron	Liz Shepherd	Eliane Silva
Olivier Seror	David Sheridan	Fabio Silveira
Marina Serper	Morris Sherman	Sharmaine Jia Ying Sim
Nicola Serra	Somya Sheshadri	Adelia Simao
Dolors Serra	Abhishek Sheth	André L. Simão
Miguel Serra	Kirti Shetty	Alina Simerzin
Marina Serra	Jun-Ping Shi	Francesca Simionato
Diego Serraino	Liang Shi	Paolo Simioni
Trinidad Serrano	Juanjuan Shi	Rafael Simo Canonge
Marina Serrano-Macia	Zhenzhen Shi	Guilherme Simões
Anna Sessa	Shaojun Shi	Claudia Marquez Simões

Melanie Simoeseugenio
 Michael Simon
 Fabio Simone
 Loredana Simone
 Claudia Simonelli
 Douglas Simonetto
 Irving Simonin-Wilmer
 Kenneth J. Simpson
 Jesse Simpson
 Halis Simsek
 Ashwani Singal
 Ana-Maria Singeap
 Shiv Kumar Singh
 Gurpreet Singh
 Anirudh Kumar Singh
 Mansi Singh
 Hitesh Singh
 Virendra Singh
 Meenu Singh
 Shreya Singh
 Brijendra Singh
 Yuvaraj Singh
 Namrata Singh
 Virendra Singh
 Veena Singh
 Surender Singh
 Anshuman Singh
 Ricky Sinharay
 Edford Sinkala
 Dong Hyun Sinn
 Nipaporn Siriporn
 Ajith Siriwardena
 Roxana SIRLI
 Claude Sirlin
 Fatma Sirmatel
 Sandro Sironi
 Marina Sironi
 Marek Sitko
 Jianwen Situ
 Srinivasan Sivanandan
 Chris Sivell
 Kathrine Sivertsen Nordhus
 Nelli Sjöblom
 Jessica Skelton
 Charlotte Skinner
 Maria Kløjgaard Skytthe
 Sarah Slater
 Ahmad Sleiman
 Charlotte Slooter
 Gliga Smaranda
 Laura Smeaton
 Lena Smets
 Vaclav Smid
 Andrew Smith
 Stuart Smith
 Maren Smith
 Rachel Smith
 Nate Smith
 Martina Smolic
 Wiktor Smyk
 Andreas Smyris
 Orly Sneh Arbib
 Linda Snetselaar
 Giorgio Soardo
 Leandro Soares Sereno
 Rodolphe Sobesky
 Cyril Sobolewski
 Almudena Sobrino-Prados

Carmen Socaciu
 Mikael Sodergren
 Michael Soerensen
 Roberta Soffredini
 Philippe Sogni
 Özlem Sogukpinar
 Shirleen Soh
 Joo Hyun Sohn
 Won Sohn
 Mozhdeh Sojoodi
 Etienne Sokal
 Elsa Solà
 Cristiana Soldani
 Cristina Solé
 Carmen Soler
 María José Soler
 Reham Soliman
 Francisco Solis
 Virginia Solitano
 Anna Marine Sølling Ramsing
 Janina Sollors
 Roger Sombie
 Nicky Somers
 Daniele Sommacale
 Amey Sonavane
 Mark Sonderup
 Jung Eun Song
 yeonhwa Song
 Bin Song
 Yu Song
 Jung Eun Song
 Si Young Song
 Jingjing Song
 Tieying Song
 ujwal sonika
 Isabella Sönnernborg
 Aurelio Sonzogno
 Siddharth Sood
 Vikrant Sood
 Gwyneth Soon
 Sara Sopena Santistev
 Schlosser Sophie
 Peter R. Sørensen
 Andrea Sorge
 Anna Soria
 Maria Eugenia Soria
 Anna Soria
 Dulce Renée Soto-González
 Jules Sotty
 Geneviève Soucy
 Alexandre Soulier
 Vassili Soumelis
 Marta Sousa
 Angela Sousa
 Patrick Soussan
 Vitina Sozzi
 Elia Spagnolo
 Laurent Spahr
 Duncan Spalding
 Andrea Spallanzani
 Francesco Spallotta
 B.W. Marcel Spanier
 Jean-Philippe Spano
 Wendy Spearman
 Seth Spector
 Tim Spelman
 John Spence
 Ulrich Spengler

Rhoda Sperling
 Sebastian Sperling
 Harry Spiers
 Jessica Spiers
 Luca Spiezia
 Katrin Splith
 Carlo Sposito
 Patrick Spoutz
 Dirk Sprengers
 Kylie Springer
 David Springer
 Christoph Springfield
 Martin Sprinzl
 Maria Squillante
 Akshaya Srikanth
 Parthi Srinivasan
 Supachaya Sriphoosanaphan
 Nunthiya Srisoonthorn
 Ankur Srivastava
 George Ssebyatika
 Vanessa Stadlbauer
 Yannick Stahl
 Jona T. Stahmeyer
 Laura Staiano
 Per Stal
 Andreas Stallmach
 Raphaela Staltner
 Marilena Stamouli
 Carol Stanciu
 Tijana Stanic
 Ana Stanila
 Panagiotis Stanitsas
 Evelina Stankevici
 Laura Stanton
 maria stanzione
 Joshua Stapleton
 Maria Stark
 Myriam Stark
 Patrick Starlinger
 Ioanna Stathopoulou
 Albert Stättermayer
 Albert F Stättermayer
 Winston Stauffer
 Melanie Stecher
 Horia Stefanescu
 Benedetta Stefanini
 Bernardo Stefanini
 Lance Stein
 Joerg Steinmann
 Jochen Steinmann
 Eike Steinmann
 Silja Steinmann
 Stanislav Stekopytov
 Daniele Stella
 Stefan Stender
 Matteo Stenico
 Tatyana Stepanova
 Maria Stepanova
 Tatyana Stepanova
 Maria Stepanova
 Christoph Stephan
 Schmid Stephan
 François Stéphan
 Christiane Stern
 Martina Sterneck
 Heather Stevenson
 Felix Stickel
 Judith Stift

Disclosures

Sara Stinson
Alexander Stockdale
Lena Stockhoff
Anna Stoelinga
Oana Stoica
Tatjana Stojakovic
Geurt Stokman
Janis M. Stoll
Andrew Stolz
Joanne Stone
Mark Stoove
Gianfranca Stornaiuolo
Caterina Stornello
Alistair Story
Lisa Stothers
Alastair J Strain
Robin Strand
Christian Strassburg
Robert Strassl
Beate Straub
Maximilian Strauss
Richard Stravitz
David Streem
Adrian Streinu-Cercel
Lea Streller
Helena Strevens
Philipp Striedl
Philipp Ströbel
Karoline Strobl
Steffen Strocka
Cezar Stroescu
Giacomo Stroffolini
Luisa J Ströh
Oskar Ström
Evangelia Stroumpouli
Benedikt Strunz
Eliana Stucchi
Ita.Li.Ca. Study Group
Ashley Stueck
Roberta Stupia
Nathalie Sturm
Lukas Sturm
Michael Stürzl
Ketevan Stvilia
Grace Su
Jie Su
Chung-Wei Su
Wei-Wen Su
Ying-Hsiu Su
Emilio Suarez
Ruth Suarez Darias
Elisaul Suarez Zambrano
Mohsan Subhani
Miroslava Subic-Levrero
Ram Subramanian
Robert Sucher
Andrea Sucksdorff
Abid Suddle
Aya Sugiyama
Masaya Sugiyama
Jeong Ill Suh
Kyung-Suk Suh
Sanggyun Suh
Wattana Sukeepaisarnjaroen
Jana Suklan
Sukriti Sukriti
Sirinporn Suksawatamnuay
André Sulen

Stefan Sulk
Richard Sullivan
Laurent Sulpice
S Suman
Yoshio Sumida
Donglin Sun
Haoyu Sun
Xiu Sun
Junfeng Sun
Huan Sun
Vinay Sundaram
Jeya Anice Sundararaj
Vijaya Sundararajan
Lidia Surace
Pallavi Surana
Julian Surey
Sophia Surguladze
Davies Susan
Norman Sussman
Nancy Sutter
Tanita Suttichaimongkol
Gianluca Svegiati-Baroni
Jens Svenningsen
Leo Swadling
Kelly Swanson
Adam Syanda
Svenja Sydor
Wing-Kin Syn
Antonia Syriha
Silje W Syversen
Ferenc Szalay
Benedykt Szczepankiewicz
Thomas Szekeres
Jan-Willem Taanman
Daniela Tabacelia
Fehmi Tabak
David Tabernero
Ray Tabibiazar
Martina Taborelli
Fred Tabung
Stefano Tacconi
Vania Tacher
Stela Taci
Tamar Taddei
Tamar H Taddei
Linus Schwantes-An Tae-Hwi
Irgen Tafaj
Carmen G. Tag
Nikoletta Maria Tagkou
Yusri Taha
Yuki Tahata
Ehsaneh Taheri
Dean Tai
Chia-Hung Tai
Chi-Ming Tai
Chiara Taibi
Anne Tailleur
Falguni Tailor
Won Young Tak
Hyoseon Tak
Hitomi Takada
Hirokazu Takahashi
Kazuki Takahashi
Satoru Takahashi
Kenta Takaura
Yasuhiro Takikawa
Arslan Talat
Mats Talbäck

Thomas Talbot
Jantjie Taljaard
Anjan Jyoti Talukdar
Steve Yew-chong Tam
Joshua Tam
Nobuharu Tamaki
Dietmar Tamandl
Roberto Tambucci
Matthias Tammenga
Athena Tampaki
Jaclyn Yizhen Tan
Chee-Kiat Tan
Terence TAn
Hiang Keat Tan
Hua Tan
Zhi Tan
Yong Chuan Tan
Ek Khoon Tan
Wei Lian Tan
Kenneth K. Tanabe
Atsushi Tanaka
Shohei Tanaka
Yasuhito Tanaka
Junko Tanaka
Elena Tanashchuk
Francesco Tandoi
Puneeta Tandon
Manish Tandon
Puneeta Tandon
Sunil Taneja
Wei Tang
Liangjie Tang
Shanghong Tang
Xia-Han Tang
Liang-Jie Tang
Weiming Tang
An Tang
Jinglin Tang
Tianyu Tang
Pisit Tangkijvanich
Marion Tanguy
Kawin Tangvoraphonkchai
Xinxing Tantai
Lars Tanum
Yusha Tao
Graciela Tapia
Monica Tapias
Sambit Tarai
Giovanni Targher
Branden Tarlow
Sara Tartof
Yasmina Tashkent
Xhimi Tata
Kristi Tata
Ryosuke Tateishi
Tomohide Tatsumi
Jörg Täubel
Richard Taubert
Kojiro Taura
Jan Tauwaldt
Ludgero Tavares
Alessandro Tavelli
Wei Xuan Tay
Yuh Ling Amy Tay
John Tayek
Ally Taylor
Guy Taylor
Simon Taylor-Robinson

Nchimunya Nelisa Tebeka	Anna Thomas	Nikolaj Torp
Craig Teerlink	Lutz Thomas	Miguel Torralba
Gebeyehu Teferi	Sherin Sarah Thomas	Manuel Torralba
Sofia Teixeira	Sherin Thomas	Xavier Torras
Joana Teixeira Magalhães	Rachel Thomas	Aldo Torre
Javier Tejedor-Tejada	Alexander Thompson	Pietro Torre
Tufan Teker	Laura Thompson	Maria Torrens
Luis Téllez	Clare Thompson	Jason Torres
Érica Téllez	Hayley Thompson	Ferran Torres
Frederik Temmerman	Alexander Thompson	Joana Torres
Marit ten Hove	Helen Thompson-Jones	Gloria Torres
Wei Teng	Karen Louise Thomsen	Barbara Torres Guerola
Aina Teniente	Douglas Thorburn	Lilian Torres Made
Laura Tenorio	Marianna Thordardottir	Raffaella Tortora
Roxani Tenta	Anders Thorell	Annalisa Tortora
Stefan Tenzer	Katrine Thorhauge	Raffaella Tortora
Ada, Ee Der Teo	James Thorne	Guido Torzilli
François Teoule	Claire Thorne	Giulia Tosetti
Namouni Teresa	Karla Thornton	Christian Toso
Tammo Lambert Tergast	Zak Thornton	Yann Touchefeu
Mike Terkelsen	Karla Thornton	Issam Tout
Debora Raquel Terrabuo	Georgia Threadgold	Dana Toy
Daniela Terracciano	Paul J. Thuluvath	Hidenori Toyoda
Luigi Terracciano	Christine Thumann	Nurdan Tozun
Luigi Maria Terracciano	Prem Harichander Thurairajah	Giulia Tozzi
Norah Terrault	Mark Thursz	Despina Trafali
Natalia Terreni	Anja Tiede	Samuel Trammell
maria terrin	Matthieu Tihy	David Trampert
Benoit Terris	Patrick Tilleul	Henri Tran
Leon Terstappen	Dina Tiniakos	Sarah Tran
Benedetta Terziroli Beretta-Piccoli	Lesley Tinker	Steven Trasino
Giuliano Testa	Tom Tipton	Julia Traub
Barbara Testoni	Claudio Tiribelli	Janina Trauth
Elisabetta Teti	Kattleya Tirona	Christian Trautwein
Brent Tetri	Esther Titos	James traylor
Marcus Tetzlaff	Thais Tittanegro@gmail.com	Timothy Tree
Andreas Teufel	Sarah Tizzard	Sombat Treeprasertsuk
Alexander Teumer	Douglas Tjandra	Nirupma Trehanpati
Harshvardhan Tevethia	E.T.T.L. Tjwa	Valentina Tremaroli
Siva Tez PV	Bryce Tkachuk	Giada Tria
Dominique Thabut	Deirdre Tobias	Evangelos Triantafyllou
Leroy Thacker	Tsuyoshi Todo	Adam Trickey
Panarat Thaimai	Daniel Todt	Anca Trifan
Collette Thain	Manana Todua	Pascale Trimoulet
Niharika Thakur	Karin Toet	Gaurav Tripathi
gerhard thallinger	Flemming Tofteng	Dhiraj Tripathi
Nwe Ni Than	Yaman Tokat	Gaurav Tripathi
Gaya Thanabalasingham	Katsushi Tokunaga	Dinesh Mani Tripathi
Kessarín Thanapirom	Dagmar Tolenaars	Harshita Tripathi
Veera Raghavan Thangapandi	Marieta Toma	Kartikeya Tripathi
Priya Thanneeru	Lidia Tomasello	Armando Tripodi
Shalini Thapar	Melissa Tomasi	Martin Trippler
The Trainee Collaborative for Research and Audit in Hepatology UK	Krzysztof Tomasiewicz	Parth Trivedi
Alice Thebaut	Giovanni Tomassoli	Palak Trivedi
Thierry Thévenot	Santiago Tomé	Roberto Ivan Troisi
Jens Theysohn	Lukas Tometten	Jacopo Troisi
Damy Thibaud	Sabine Tomez	Giancarlo Troncone
Vincent Thibault	Jeremy Tomlinson	Matthias Trost
Tristan Thibault-Sogorb	James Tonascia	James F. Trotter
Morgane Thibaut	Steven YC Tong	Francesca Maria Trovato
Ho Thien Anh	Maria Manuela Tonini	Francesca Trovato
Robert Thimme	Pierluigi Toniutto	Ming Chao Tsai
Mira Thing	Marta Tonon	Yung-Ping Tsai
Mame Aisse Thioubou	Matilde Topa	Pei-Chien Tsai
Anaïs Thiriard	Mark Topazian	Yo-Yu Tsao
Kayleigh Thirlwell	Emilie Toresson Grip	Philip Tsao
Robert Thomas	Andreas Törnell	Keren Tsaraf
	Luis Toro	Yee-Kit Tse

Disclosures

Edmund Tse
Yee-Kit Tse
Eirini Tseligka
Kuo-Chih Tseng
Yuan Tsung Tseng
Maia Tsereteli
Tengiz Tsertsvadze
Dimitra Tsiagka
Alexandros-Pantelis Tsigas
Efrossini Tsirogianni
Irina Tskhomelidze
Emmanuel Tsochatzis
Nandintsetseg Tsoggerel
Sofia tsouka
Maia Tsreteli
Atsunori Tsuchiya
Keiji Tsuji
Xin Tu
Qingli Tu
Christelle Tual
Jo Tucker
Diana Tudor
Shannan Tuijios
Taru Tukiainen
Ina Tulaeva
Adele Tulone
Hein Tun
Ilker Turan
Laura Turco
Alexander Turdziladze
Ran Tur-Kaspa
Maud Turkenburg
Kamuran Turker
Kate Turner
Frances Turner
Fanny Turon
Lance Turtle
Maarten Tushuizen
Anna Tutusaus
Anne T Tveter
Shakun Tyagi
Anne Tybjaerg Hansen
Olaf Tyc
Thorarinn Tyrfingsson
Luke D. Tyson
Enver Ucbilek
Sara Colonia Uceda Renteria
Akira Uchiyama
Shinji Uemoto
Yusuke Uemoto
Rosa Maria Ufano Lopez
Mathias Uhlen
Natalie Uhlenbusch
Holm Uhlig
Rainer Ulrich
Burge Ulukan
Sezgin Ulukaya
Soon Ho Um
Ilaria Umbro
Juan Pablo Unfried
Kristian Unger
Emily Ungermann
Esther Unitt
Gulten Unlu
Hidemi Unozawa
Yasemin Unsal
Karolina Uranowska
Sabine K. Urban

Luca Urbani
Toni Urbanik
Markus Urheu
Iker Uriarte
Juan Isidro Uriz Otano
Jesus M Urman
Juan José Urquijo
Juan Jose Urquijo Ponce
Fichtner Urs
José Ursic Bedoya
Carla Usai
Frank Uschner
Elaine Utomo
Kirsten Utpatel
Daisuke Utsunomiya
Yigit Uysalli
Michele Vacca
Marco Vaccaro
Mariapia Vairetti
Manas Vaishnav
Tanja Vajen
Shantha Valainathan
Zina Valaydon
Pilar Valdecantos
Malou Valencia
David Valenti
Jose Valera
Heather Valerio
Rocio Valero
Patricia Valery
África Vales Aranguren
Laura Valestrand
Martina Valgiusti
Yasaman Vali
Tommaso Valigi
Clarissa Valle
Anais Vallet Pichard
Talal Valliani
Julia Vallverdú
Arun Valsan
Maria Grazie Valsecchi
Eric Van Cutsem
Aad van den Berg
Wijnand Van Den Boom
Floris van den Brand
Floris F van den Brand
Natalie Van den Ende
Anita M. van den Hoek
Annemiek Van der Eijk
Sandra van der Kooij
Luc J.W. van der Laan
Adriaan Van der Meer
Schalk van der Merwe
Koen van der Ploeg
Wendy L. van der Woerd
Egbert-Jan van der Wouden
Catherine Van Dongen
Wim van duyvenvoorde
Karel J. van Erpecum
Reyn van Ewijk
Annelies Van Eyck
Luc Van Gaal
Matthias Van Haele
Annelies Van Hecke
Stijn Van Hees
Lien Van Hoecke
Maria van Hooff
Griet Van Imschoot

Laurens van Kleef
Cees van Kooten
Arianne van Koppen
Hannah Van Malenstein
Lukas Van Melkebeke
Kim van Munster
Jos van Pelt
Martin van Royen
Minou Van Seyen
Christophe Van Steenkiste
Gilles van Tienderen
Nikki van Trigt
Hans Van Vlierberghe
Sandra Van Vlierberghe
Jeroen van Vugt
Michel van Weeghel
Elien Van Wouterghem
Vincent Vandecaveye
Elisabeth Vandekerckhove
Ann Vandeleur
Tom Vanden Berghe
Roosmarijn Vandenbroucke
Sofie Vandendriessche
Martin Vandeputte
Shauna Vander Well
Quentin Vanderbecq
Bart Vanderborght
Demontant Vanessa
Banz Vanessa
Ana Vankova
Aude Vanlander
Peter Vanlangenhove
Claire Vanlemmens
Benedict Vanlerberghe
Lisa VanWagner
Jose Pedro Vaqué
Javier Vaquero
Giulio Vara
Diana Vardanyan
Jesus Varela
Marta Varela-Rey
Hugo E. Vargas
Elena Vargas Accarino
Cruz Vargas-De-León
Adrian Varon
Nachiket Vartak
Emilia Vartiainen
Themistoklis Vasileiadis
Larisa Vasilieva
Daphne Vassiliou
Sezgin Vatansever
Maria Linda Vatteroni
Karl Vaz
Martín Uriel Vázquez Medina
Lucía Vázquez-Sirvent
Sarah Vecchio
Mara Vecchio
Rhea Veelken
José Luis Vega Sáenz
Maria Vehreschild
Janne Vehreschild
Mark Veitch
Victor Vela
Jose Antonio Velarde-Ruiz Velasco
Martín del Castillo Velasco-Herrera
Hector Velasquez
Antonio Vella
Louis Velthuis

Wilfried Veltzke-Schlieker
 Fabienne Venet
 Ramana Mallela Venkata
 Suresh Vasan Venkatachalapathy
 Paolo Ventura
 Meritxell Ventura Cots
 Esther Veramendi
 Jef Verbeek
 Robert Verdonk
 Diego Vergani
 Mercedes Vergara Gómez
 Nikhil Vergis
 Marc A.M.T. Verhagen
 Joanne Verheij
 Xavier Verhelst
 Arthur Verhoeven
 Manisha Verma
 Nipun Verma
 Marion Vermeulen
 Eugenia Vernole
 Eloi Verrier
 An Verrijken
 Lars Verschuren
 Gontran Verset
 Chris Verslype
 H.W. Verspaget
 Monique M.A. Verstegen
 Gabriella Verucchi
 Claire Verzeroli
 Umberto Vespasiani Gentilucci
 Johan Vessby
 Mette Vesterhus
 Amanda Vestito
 Marcel Vetter
 Morozov Viacheslav
 Eric Vibert
 Álvaro Vicario
 Peter Vickerman
 Judit Vico-Romero
 Silvia Vidal
 Adela Vidal
 Antonio Vidal-Puig
 Anna Vidovszky
 Paul Vigneron
 Terhi Vihervaara
 Janusa Vijayathurai
 Marta Vila
 Filipe Vilas-Boas
 Àngels Vilella
 Tatjana Vilibic-Cavlek
 Erica Villa
 Jennifer Villa
 Gerda Elisabeth Villadsen
 Ares Villagrasa
 Alejandro Villalón
 Kevin Villa-Malagon
 Maria Alejandra Gracia Villamil
 Cándid Villanueva
 Augusto Villanueva
 Carolina Villarroel
 Cristiane Villela-Nogueira
 Francois Villeret
 Marcela Villota-Rivas
 Hendrik Vilstrup
 Carmen Vinaixa
 Adriana Vince
 Leroy Vincent
 Jeanne Perpétue Vincent

Bruno Vincenzi
 Laura Vincenzi
 Michael Vinikoor
 Emily Vintour-Cesar
 L. Vinuela
 Danae Vio
 Paola Violi
 Julien Vionnet
 Agostino Virdis
 Alessia Virzi
 Alessia Visintin
 Kumar Visvanathan
 Libor Vitek
 Carole Vitellius
 Mathew Vithayathil
 Adriana Vitiello
 Anusha Vittal
 Marie Viuff
 Maria Vivanco
 André Viveiros
 Ioannis Vlachogiannakos
 Euthimia Vlahaki
 Janka Vnencakova
 Erwan Vo Quang
 Thierry Voet
 Arndt Vogel
 Serge Vogelaar
 Esther Vogels
 Sara Vogrin
 Annabelle Vogt
 Benjamin Voight
 Andrei Voiosu
 Jørn-Henrik Vold
 Kristoffer Voldum-Clausen
 Ines Volkert
 Astrid Voll-Glaninger
 Felix Volmer
 Tassilo Volz
 Johann von Felden
 Maria von Karpowitz
 Luisa Vonghia
 Trang VoPham
 Aidan Vosooghi
 Mihael Vucur
 Nicolas Vuilleumier
 Marijana Vujkovic
 Raj Vuppalachchi
 Ashish Kumar Vyas
 Mogens Vyberg
 Ross Vyhmeister
 Jan W Eriksson
 Ingrid W. Zhang
 James Wade
 Johan Waern
 Josef Wagner
 Martin Wagner
 Phyto Wah Wah
 Clare Wai
 Oliver Waidmann
 Ari Waisman
 Arata Wakimoto
 Jesper Waldenström
 Muhammad Furqan Waleed
 Bernd Walkenfort
 Andreas Walker
 Josephine Walker
 Victoria Walker
 Lorraine Wall

Marie Wallays
 Göran Walldius
 Kathryn Waller
 Martine Walmsley
 Renae Walsh
 Juliane S. Walz
 JingHong Wan
 Shang Wan
 Gilles Wandeler
 Alkwin Wanders
 Wen-Lung Wang
 Jie Wang
 Yu-Lin Wang
 Jinhai Wang
 Jianye Wang
 Yijin Wang
 Junxiao Wang
 Jian Wang
 Fu-Sheng Wang
 Bingduo Wang
 Yinghong Wang
 Yongtao Wang
 Shike Wang
 Zhe Wang
 Ling Wang
 Xiaodong Wang
 Zeyu Wang
 Chengyan Wang
 Yan Wang
 Chunyan Wang
 Jie Wang
 Bo Wang
 Bin Wang
 Zhengtao Wang
 Zhengyu Wang
 Ran Wang
 Zhengyu Wang
 Jian Wang
 Huali Wang
 Zilong Wang
 Xiaoxiao Wang
 Jian Wang
 Tongyu Wang
 Huay-Min Wang
 Vivian Wang
 Li-Yu Wang
 Yinghong Wang
 Qiuhe Wang
 Zhengyu Wang
 Jian Wang
 chun-yi Wang
 Chia-Chi Wang
 Sih-Ren Wang
 Sai Wang
 Shanshan Wang
 Zhenglin Wang
 Chun Hsiang Wang
 Surui Wang
 Qingbi Wang
 Xiao-jun Wang
 Zhili Wang
 Yuting Wang
 Sarah Wang
 Qi Wang
 Xun Wang
 Guobao Wang
 Wenjuan Wang
 Jitao Wang

Disclosures

Jinhua Wang
Ming Wang
Kirk Wangenstein
IanR Wanless
Timothy Wanninger
Caroline Ward
Stephen Warrillow
Ayumi Watanabe
Takehisa Watanabe
Martin Waterfall
Kimberly A. Watson
Robyn Watson
Adam Watson
Makayla Watt
Gerald Watts
Muriel Webb
Henry Emanuel Webel
Susanne N Weber
Achim Weber
Susanne N Weber
Achim weber
Ian Webzell
Aileen Wee
Anthony Weeks
Rinse Weersma
Olivia Wegrzyniak
Malte Wehmeyer
Jia Wei
Lai Wei
Qin Wei
Liou Wei Lun
Gerhard Weidinger
Sören Weidmann
Jochen Weigt
Clara Weil
Ola Weiland
Sofia Weiler
Marek Weiler
Christina Weiler-Normann
Sindee Weinbaum
Ethan Weinberg
Patrick Weinberger
Arndt Weinmann
David Weinstein
Marta Weinstock
Cleo-Aron Weis
Ralf Weiskirchen
Tobias Weismüller
Thomas Weiss
Felicitas Weiss
Emmanuel Weiss
Lena Weiß
Natan Weissman
Michelle Weitz
Salisa Wejnaruemarn
Rune Wejstål
Nicole Welch
Stella Wellhöner
Rebecca Wells
Christoph Welsch
Jan-Philipp Weltzsch
Julia Wendon
Honglei Weng
Tobias Wengenmayer
Christoph Wenisch
Jürgen Wenzel
Mikkel Werge
Lukas Weseslindtner

Joe West
Axel Wester
Carolyn Wester
Gunilla Westergren-Thorsson
Jukka Westermarck
Marit Westerterp
Johan Westin
Max Westphal
Aaron Wetten
Alexandre Wetzel
Nils Wetzstein
Alex Weymouth-Wilson
James White
James Whiteford
Gavin Whitehouse
Bradley Whitton
Ewa Wiberg-Itzel
Marc Wichert
Johannes Wiegand
Christiane Wiegard
Signe Wiese
Alan Wigg
Percival Wiid
Vishva Wijesekera
Katharina Wild
Anne Wilkens Knudsen
Daniel Wilkey
Alex Wilkinson
Christopher Willars
Kai Wille
Jorke Willemse
José Willemse
Martin Willheim
Claudia Willheim
Felicity Williams
Evangelia Williams
Roger Williams
Felicity Williams
Suzanne Williams
Mark R. Wills
Katharina Willuweit
Caroline Wilson
David Wilson
Phillip Wilson
Thomas Wilson
Philipp Wimmer
Ralf Wimmer
Aziza Win
Jeffrey Winick
Marc Winkler
Frances Winkler
Johnathan Winter
Hannah Wintersteller
Matilde Winther-Jensen
Theresa Hildegard Wirtz
Jan-Erik Wissmann
Elizabeth Witherden
David Withers
Linda Wittig
Linda Wittkop
Melanie Wittner
Arnon Wiznitzer
Marcus-Alexander Woerns
Dirk Wohlleber
Marius Maximilian Woitok
Lisa Wolff
Annika Wolfsberger
Annika Wolski

Jennifer Wolstenholme
Frank Wolters
Florence Wong
Randi Wong
Florncce Wong
Stanley Wong
Jason Wong
Philip Wong
Kuan Yau Wong
Rochelle Wong
Angus Wong
Hyun Young Woo
Katharina Wöran
Nicole Worms
Marcus-Alexander Wörns
Natasja Von Wowern
Małgorzata Woźniak
Thomas Wrba
Alexander Wree
Mark Wright
Gail Wright
Qipeng Wu
Jia-Feng Wu
Jian Wu
Gregory Wu
Min Wu
Gang Wu
Shusheng Wu
Chijung Wu
Juan Wu
Xinle Wu
Jianguo Wu
Cichun Wu
Chao Wu
Chia-Ying Wu
Qingyan Wu
Tong Wu
Wen-Chih Wu
Jia-Feng Wu
Guohui Wu
Maximilian Wübbolding
Lone Wulff Madsen
Ewa Wunsch
Dominik Wupperfeld
Brooke Wyatt
Sofia Xavier
Eleni Xenofontos
Tian Xia
Dongdong Xia
Jielai Xia
Huanyu Xiang
Hongyan Xiang
Dejuan Xiang
Huijuan Xiao
Huanming Xiao
Xiao-he Xiao
Jing Xiao
Shuang Xiao
Nanping Xiao
Hui Xie
Chan Xie
Dongying Xie
Yandi Xie
Qing Xie
Yandi Xie
Qing Xie
Zhe Xie
Yongning Xin

Jiaojiao Xin	Pamela Yaquich	Young Kyoung You
Huichun Xing	David Yardeni	Sara Young
Guang-Hua Xu	Satoshi Yasuda	Neil Youngson
Jiang-Hai Xu	Yutaka Yasui	Elena Younossi
Tingfeng Xu	Katherine Yates	Issah Younossi
Liang Xu	Yutaka Yatomi	Youssef Younossi
Xiaoyuan Xu	Magdalena Ydreborg	Jenna Yousif
Zhongyuan Xu	Qing Ye	Hassaan Yousuf
Cheng-Jian Xu	Lei Ye	Henriette Ytting
Jia Xu	Liangtao Ye	Ming-Lung Yu
Flora Xu	Feng Ye	QW Yu
Cheng-Jian Xu	Michael Yee	Zu-Jiang Yu
Xiao Xu	Jatin Yegurla	Amanda Yu
Pan Xu	Chau-Ting Yeh	Philip Yu
Li Xuefeng	Yen-Po Yeh	Su Jong Yu
Aikaterini Xydaki	Ming-Lun Yeh	Ming-Lung Yu
Manisha Yadav	Adi Yehezkel	Amanda Yu
Ashish Yadav	Anuroop Yekula	Jie Yuan
Hanieh Yaghootkar	Malcolm Guan Hin Yeo	Xiaojian Yuan
Reiko Yaginuma	Ee Jin Yeo	Lunzhi Yuan
Dayana Yaish	Andrew Yeoman	Yulin Yuan
Ryoko Yamada	Yubin Yeon	Lilly Yuen
Tomomi Yamada	Hing-Yuen Yeung	Merve Yuksel
Hiroyuki Yamada	Alan Yeung	Sae Yumita
Nobutake Yamamichi	Nam-Joon Yi	Marjorie Yumol
Gen Yamamoto	Ioanna Yiasemi	Diana Yung
Omer Yaman	Buket Yigit	Rossitta Yung
Hisami Yamanaka-Okumura	Mustafa Yildirim	Cihan Yurdaydin
Kazumi Yamasaki	Abdullah Emre Yildirim	Bakhodir Yusupaliev
Shunhei Yamashina	Ilknur Esen Yildiz	Harry D Zacharias
Taro Yamashita	Sezai Yilmaz	Katerina Zacharis
Tansu Yamazhan	Yusuf Yilmaz	Kalliopi Zachou
Jacinth Yan	Utku Tonguç Yılmaz	Szabolcs Zahoran
Tao Yan	Yusuf Yilmaz	Khatuna Zakhshvili
Jacinth Yan	Hyung Joon Yim	Paola Zaldera
Sien-Sing Yang	Colina Yim	Mohammadreza Zali
Longbao Yang	Hyung Joon Yim	Javier Zamora
Kun Yang	Sun Young Yim	Matteo Zampini
Hyun Yang	Zhanxin Yin	Paola Zanaga
Yao Yang	Wenwei Yin	Laura Zanatto
Ruifeng Yang	Vincent Yip	Stephan Zandanell
Yongfeng Yang	Hannele Yki-Järvinen	Alberto Zanetto
Jiahong Yang	Tomoaki Yoh	Luca Zanieri
Ying Yang	Masato Yoneda	Martina Zaninotto
Aruhan Yang	Juhwan Yoo	Giovanna Zanon
Na Yang	Jeong-Ju Yoo	Ilaria Zanon
Ke Yang	Eileen Yoon	Valentina Zanus
Fengjuan Yang	Jun Sik Yoon	Marko Žarak
Xinye Yang	Eileen Yoon	Lisa Zarantonello
Yongfeng Yang	Bo Hyung Yoon	Dorota Zarębska-Michaluk
Sheng-Shun Yang	Eileen Yoon	Amira Zaroui
Chi-Chieh Yang	Ki Tae Yoon	Daria Zatorina
Chi-Chao Yang	Kyung Chul Yoon	Michalina Zatorska
Xu Yang	Seung Kew Yoon	Christian Zauner
Linjian Yang	Eileen Yoon	Gil Zeevi
Hui Yang	Bo Hyung Yoon	Anja Zeigerer
Shengshun Yang	Eileen Yoon	Kamal Zekrini
Chi-Chieh Yang	Peter Yoon	Shira Zelber-Sagi
Yao-Hsu Yang	Eileen Yoon	Katharina Zeller
Su-Jau Yang	Yeup Yoon	Yoh Zen
Hui Yang	Bo Hyung Yoon	Qing-Lei Zeng
Xinxiang YANG	Gulsen Yoruk	Yan-Li Zeng
Shiying Yang	Atsushi Yoshida	Yi-lan Zeng
Bo Yang	Kyoko Yoshida	Qing-Lei Zeng
Ping Yang	Eric Yoshida	Zheng Zeng
Julia Yang Payne	Kenji Yoshino	Nicola Zeni
Frederick Yao	Atsushi Yoshizawa	Robin Zenlander
Suna Yapali	Hong You	Sebastian Zenovia

Disclosures

Marc Zentar
Jasmin Zessner-Spitzenberg
Mujdat Zeybel
Murat Zeytunlu
Haoran Zhang
Luyong Zhang
Peng Zhang
Jiayuan Zhang
Xinlian Zhang
Yuwei Zhang
Guoqiang Zhang
Hongxu Zhang
Guofan Zhang
Ji-Yuan Zhang
Lihua Zhang
Saisai Zhang
Dengwei Zhang
Rui Zhang
Zhijun Zhang
Hong Zhang
Qin Zhang
Wen-hua Zhang
Bo Zhang
Huai Zhang
Shi-Jin Zhang
Shuwen Zhang
Xinrong Zhang
Hong Zhang
Lei Zhang
Ingrid Wei Zhang
Yong Zhang
Mingxin Zhang
Haoran Zhang
Luyong Zhang
RanRan Zhang
Ingrid Wei Zhang
Siyi Zhang
Wei Zhang
Yan Zhang
Wenjun Zhang
Wenhong Zhang
Jiming Zhang
Yingzhi Zhang
Linzhi Zhang
Gaoli Zhang
Jiaxuan Zhang
Lukan Zhang
Xinrong Zhang
Xi Zhang
Lukan Zhang
Liting Zhang
Xian-Man Zhang
Dazhi Zhang
Shuang Zhang

Zhenfeng Zhang
Stephanie Zhang
Qingge Zhang
Liting Zhang
Guo Zhang
Shuangxia Zhang
Shujie Zhang
Xuehong Zhang
Bigeng Zhao
Wei-Guo Zhao
Xun Zhao
Lili Zhao
Qianwen Zhao
Derrick Zhao
Wenjuan Zhao
Xin Zhao
Jieling Zhao
Xiaoling Zhao
Longgang Zhao
Sergei Zhavoronok
Ming-Hua Zheng
Tian-lei Zheng
sujun Zheng
Huanwei Zheng
Tian-lei Zheng
sujun Zheng
Ming-Hua Zheng
Xin Zheng
Haoyang Zheng
Freeman Zheng
Qiuxian Zheng
Ming-Hua Zheng
Iris Zhorov
Jian Zhou
Yu-Jie Zhou
Huiping Zhou
Taotao Zhou
Xue Zhou
Xingping Zhou
Dan Zhou
Xingping Zhou
Haoming Zhou
Shi-Yi Zhou
Xiqiao Zhou
Yi Zhou
Hongwei Zhou
Xin Zhou
Hongwei Zhou
Shijia Zhu
Xiaoxue Zhu
Yanfang Peipei Zhu
Yong-Fen Zhu
Shijia Zhu
Xiaoxue Zhu

Rui Zhu
Pei-Wu Zhu
Chuanwu Zhu
Li Zhu
Dedong Zhu
Chenqian Zhu
Dedong Zhu
Chenqian Zhu
Ping Zhu
Yunxia Zhu
Xiaodong Zhuang
Ekaterina Zhuravleva
Bogna Ziarkiewicz-Wróblewska
Mariam Ziayee
Krzysztof Zieniewicz
Yuan Zihang
Michal Žilinčan
Christine Zimmer
Sebastian Zimny
Gudula Zimper
Marianne Zioli
Alexander Zipprich
Hans Zischka
Konstantinos Zisimopoulos
Giovanni Zito
Milorad Zjalic
Maria Assunta Zocco
Katharina Zoldan
Caroline Zöllner
Dominik Zölzer
Elina Zorde-Khavlevsky
Antonio Zorzano
Guizhou Zou
Haixia Zou
Honore Zougmore
Ana Zubiaga
Jessica Zucman-Rossi
María A. Zulet
Deltersaikhon Zulkhuu
Paola Zuluaga
Javier Zulueta
Dariusz Zurawek
Coral Zurera
Karen Zwaenepoel
Denise Zwanziger
Aeilko Zwinderman
Isabelle Leclercq
Dessy Chantal
Sebastian Bott
Laurent Dumas
Evangelos-Panagiotis Daskalopoulos
Hrag Esfahani

Disclosures: commercial relationships

The following abstract submitters have indicated that they have relationships with commercial entities that might be perceived as having a connection with their presentation:

Charles Aardema	Aftab Ala	Filipa Aragão
Marta Abadia	David Al-Adra	Manuela Arbune
Dalia Abdelhasseb	Kishore Alagere Krishnamurthy	Vijay Are
Manal F. Abdelmalek	Antoine Alam	Vic Arendt
Dzhamal Abdurakhmanov	Matthew Albert	Andre Arizpe
Fredrik Åberg	Dafne Alberti	Matthew Armstrong
Armand Abergel	Agustin Albillos	Enara Arretxe
Kushala Abeysekera	Wolfgang Albrecht	Yasuhiro Asahina
Abhishek. Abhishek	Thomas Albrecht	Mertixell Ascanio
Jean Louis Abitbol	Estefania Alcaraz	Amir Ashique
Katie Abraham	Soo Aleman	Fred Askari
Juan G Abrales	Leigh Alexander	Patricia Aspichueta
Frida Abramov	Sarah Ali	Tarik Asselah
Naim Abu-Freha	Naim Alkhouri	Alice Assinger
Oliver Ackaert	Manon Allaire	Christophe Aubé
Christin Ackermann	Alina Allen	Salvador Augustin
Emily Acter	Samantha Allen	Daren Austin
Vera Adamkova	Michael Allison	Francisco Averhoff
Timo Adams	Laura Almale del Barrio	Emma Avitabile
Nathalie Adda	Cristina Alonso	Mads Axelsen
Femi Adekunle	Marta Alonso-Peña	Turgay Ayer
Olayinka Adisa	Laurent Alric	Oyekoya Ayonrinde
Timon Adolph	Gema Alvarez Nieto	Walid S Ayoub
MaryVic Adona	Carmen Álvarez-Navascués	Sarah Ayton
Lannes Adrien	Domenico Alvaro	Farooq Azam
Jeroen Aerssens	Carlos Alventosa Mateu	Amy Azania
Thomas Aeschbacher	Yuichiro Amano	Karim Azer
Kosh Agarwal	Adam Amaral	James B Lorens
Abhishek Aggarwal	Philip Ambery	Henrik B. Hansen
Alessio Aghemo	Naseem Amin	Bert Baak
Germaine D. Agollah	Javier Ampuero	Fredrik Backhed
Vatche Agopian	Igor Anastasiy	Ho S Bae
Gifone Aguiar Rocha	Malena Anders	Si Hyun Bae
Victoria Aguilera Sancho	Birgitte Andersen	Adrian Baez-Ortega
Chukwuemeka Agwuocha	Jesper Andersen	Ru Bai
Arnon Aharon	Mark Anderson	Jasmohan S Bajaj
Gustaf Ahlén	Anneli Andersson	Anna Bakardjiev
Håkan Ahlström	Anne-Christine Andréasson	Barbara Bakker
Alaa Ahmad	Fausto Andreola	Anu Balaji
Mahmoud Ahmed	Pietro Andreone	Anand Balakrishnan
Nabeel Ahmed Maqbool	Massimo Andreoni	Sripriya Balasubramanian
Sang Hoon Ahn	Konstantina Andresaki	Alejandro Balbin
Sojin Ahn	Carmen Andreu-Oller	Kemal Balic
Vijay Ahuja	Paolo Angeli	Scott Balsitis
Elmar Aigner	Yesseinia Anglero-Rodriguez	David Baltimore
Melanie Aikebuse	Piekarska Anna	Jesus Maria Banales
Menachem Ailenberg	Quentin Anstee	Rafael Bañares
Guruprasad Aithal	Maja Antolić	Rajarshi Banerjee
Muhammad-Mujtaba Akanmu	Deana Antonello	Marina Barcena-Varela
Peter Akerblad	Masood Anwar	Stephen Barclay
Fatih Akisik	Myriam Aouadi	Edouard Bardou-Jacquet
Norio Akuta	Katsumi Aoyagi	Malene Barfod O'Connell
Tamer Al Eraki	Douglas Applegate	Romain Barnault

Disclosures

Eleanor Barnes
Tamara Barnett
Ana Barreira
Thijs Barten
Sofia Bartlett
Mustafa Bashir
Ahmed Ba-Ssalamah
Melanie Bathon
Pier Maria Battezzati
Sara Battistella
David JM Bauer
Ulrich Baumann
Thomas Baumert
Vipul Baxi
Michel Bazinet
Andrew Beck
Svea Becker
Mark Becker
Sonja Beckmann
Philippe Bedard
Pierre Bedossa
Alex Befeler
Danny Bega
Elke Behaeghel
Cynthia Behling
Leonid Beigelman
Claudia Beisel
Pierre Bel Lassen
Mehdi Belkhodja
Mattia Bellan
Francesco Bellanti
Najib Ben Khaled
Elias Benabadji
Leda Bencheva
Flemming Bendtsen
Bonnie Bengtsson
Adel Benlahrech
Merav Ben-Yehoyada
Christian Benzing
Rudolf Beran
Michael D. Bereket
Marina Berenguer
Thomas Berg
Christoph Berg
Ellen Berg
Irina Bergamin
Mattias Bergentall
Annika Bergquist
Tatiana Bering Bering
William Bernal
Mauro Bernardi
Barbara Bernardo
Antonio Bertoletti
Juliette Besombes
Dominik Bettinger
Maria Beumont-Mauviel
Cayden Beyer
Simon Beyer
Jorge Bezerra
Abhi Bhagat
Shripad Bhagwat
Bal Raj Bhandari
Punam Bharania
Ilaria Biancacci
Vadim Bichko
Charles Biddle-Snead
Manuela Bieri
Michael Biermer

Joanna Bilak
Griffiths Bill
Andrew Billin
Marc Bilodeau
Julien Bissonnette
Niklas Björkström
Sarah Blach
Jean-Frédéric Blanc
Charlotte Blanc
Antje Blank
Lawrence Blatt
Bruce Blazar
Alfonso Blázquez-Moreno
Rob Blissett
Magnus Blø
Sami Blom
Patricia Bloom
David Blue, Jr
Qingyan Bo
Hans Bock
Ravan Boddu
Jaysal Bodhani
Caroline Boeke
Klaus Boeker
Alina Bogdanov
Carri Boiselle
Jörg Bojunga
Selin Bolca
Galina Boldina
Jacques Bollekens
Ralf Bollhagen
James Bolognese
Maurizio Bonacini
Machaon Bonafede
Ferruccio Bonino
Herbert L Bonkovsky
Britta Bonn
Odile Bonnin
Andre Boonstra
Brian Borg
Sergio Borgia
Salvador Borrós
Trijnie Bos
Jaime Bosch
Martina Bosnar
Mohamed Bouattour
Sihem Boudina
Stéphane Bouée
Sherif Boulos
Thomas Bouqin
Stefan Bourgeois
Marc Bourliere
Jerome Boursier
Karim Bouzakri
Christopher Bowlus
Adam Boyd
Kelli Boyd
Kaan Boztug
Chiara Braconi
John Michael Brady
J Michael Brady
Emer Brady
Sylvia Brakenhoff
Clifford Brass
Marius Braun
David Breckinridge
Dominique Brees
Birgit Bremer

Natalia Breyner
Francois Briand
Paul Brinkman
Christian Brixko
Jens Brodbeck
Jan Christian Brønd
Jean-Pierre Bronowicki
Craig Brooks-Rooney
Pierre Broqua
M. Julia Brosnan
Kenneth Brown
Joanne Brown
Robert Brown
Elizabeth Brown
Sarah Browne
Jonathan Frederik Brozat
Jordi Bruix
Helmut Brunar
Maurizia Brunetto
Tony Bruns
Ksenia Brusilovskaya
Hrvoje Brzica
Arno Bucker
Grant Budas
Peter Buggisch
Elisabetta Bugianesi
Sherry Bullens
Stuart Bunting
Xabier Buque
Vinod Burade
Dara Burdette
Christophe Bureau
Lukas Burghart
Michela Emma Burlone
Rani Burm
Patrizia Burra
Sue Burrell
Maria Buti
Bryony Butler
Marcus Butler
Isabel Butrymowicz
Giuseppe Cabibbo
Edward Cable
Valle Cadahía-Rodrigo
Jean-François David Cadranel
Dachuan Cai
Stephen Caldwell
Paul Cales
Carlemi Calitz
Roberto Calle
José Luis Calleja Panero
Alberto Calleri
Vincenza Calvaruso
Calogero Camma
Francesca Campanale
Fiona Campbell
Stephanie Campbell
Eda Canales
Harriet Cant
Helena Cantero
Shengtian Cao
Maria Domenica Cappellini
Paolo Caraceni
Valentina Carapella
Lorena Carballo-Folgoso
Marco Carbone
Michael Carleton
Michal Carmiel

Pietro Carotenuto
 Sara Carpi
 Fabrice Carrat
 Fernando Carreño
 Laura Carrión
 Alba Carrodegua
 Kara Carter
 Marta Casado
 Miguel Ángel Casado
 Francesco Paolo Casale
 Robert Casper
 Markus Casper
 David Cassiman
 Andrés Castano-Garcia
 helene castel
 Andrea Cathcart
 Cyrielle Caussey
 Gail Cawkwell
 Sophie Cazanave
 Nora Cazzagon
 Anna Cederborg
 Matea Cedilak
 Jeffrey Cehelsky
 Miriam Celada-Sendino
 Ciro Celsa
 Jenny C Censin
 Jung Hoon Cha
 Naga Chalasani
 Benjamin Challis
 Naichaya Chamroonkul
 Henry LY Chan
 Sing Chan
 Wah-Kheong Chan
 Stephen L. Chan
 Calvin Chan
 Wah-Kheong Chan
 Sushmita Chanda
 Abhishek Shankar Chandramouli
 Silvia Chang
 Sandra Chang
 Jung-Chin Chang
 William Chang
 Ting Chang
 Julius Chapiro
 Edgar Charles
 Will Charlton
 Mary Chau
 Sachin Chaudhari
 Olivier Chazouillères
 Rob Cheetham
 Li Chen
 Shuhui Chen
 Shikui Chen
 Zhaobin Chen
 Xin-Yue Chen
 Jacki Chen
 Alfred Chen
 Chi-Yi Chen
 Jinjun Chen
 Ping Chen
 Yan Chen
 Meng Chen
 Yi Chen
 Fuwang Chen
 Chien-Hung Chen
 Yi-Cheng Chen
 Chien-Jen Chen
 Harry Chen

Ethan Chen
 Wei Chen
 Xin Chen
 Joseph Chen
 Yu Chen
 Charles Chen
 Deying Chen
 Pin-Nan Cheng
 Tong Cheng
 Maksym Chernyakhovskyy
 Ramsey C. Cheung
 Stéphane Chevaliez
 Jagpreet Chhatwal
 Chen-Tse Chiang
 Elaine Chien
 Rong-Nan Chien
 Michael Child
 Elaine Chng
 Jin Yong Choi
 Sang Hyun Choi
 Yun-Jung Choi
 Jong Young Choi
 Anand Chokkalingam
 Jia Ling Chong
 Ingrid Choong
 Gourab Choudhury
 Morten Christensen
 Peer Christensen
 Lee Christensen
 David Chromy
 Jay Chuang
 Wan-Long Chuang
 Vladimir Chulanov
 Diana Chung
 Raymond Chung
 Chuhan Chung
 Brian K. Chung
 Alessia Ciano
 Fiona Cilli
 Umberto Cillo
 Ernesto Claar
 Marco Claasen
 Wouter Claeys
 Thierry Claudel
 Jesper Clausen
 Karine Clément
 Gavin Cloherty
 Daniel Cloutier
 Jeremy Cobbold
 Marie Coessens
 Carla Coffin
 Taylor Cohen
 Chari Cohen
 Jon Collins
 Michelle Collins
 Massimo Colombo
 Craig Comisar
 Annie Conery
 Matteo Conti
 Brian Conway
 Galen Cook-Wiens
 Michael Cooreman
 Sabine Cordi
 Kathleen Corey
 Markus Cornberg
 Daniel Corsilli
 Alessio Cortellini
 Karina Cortez

Helena Cortez-Pinto
 Greg Cosgrove
 Montserrat Costa
 Yesenia Covarrubias
 Thomas Cowling
 Antonio Craxi
 Kate Townsend Creasy
 Jennifer Cremer
 Javier Crespo
 Laura Cristofori
 Daria Crittenden
 Hayley Cabbage
 Zhiyi Cui
 Emma Culver
 Guilherme Cunha
 Morven Cunningham
 Michael Curry
 Tristan Curteis
 Kenneth Cusi
 Daniel Cuthbertson
 Snježana Čužić
 Anissa Cyhaniuk
 Anna Czlonkowska
 Karim Dabbagh
 Stephane Daffis
 Simon Dagenais
 Kirsten Dahl
 Liting Dai
 Chia-Yen Dai
 Valérie Daix
 Marion Dajon
 Christine Dalais
 George Dalekos
 Antonio D'Alessio
 Ann K Daly
 Roberta D'Ambrosio
 Maura Dandri
 Jules Daniel
 Samuel Daniels
 Mark Danta
 Lorenzo D'Antiga
 Josep Darba
 Raphaël Dartel
 Sugato Das
 Abhishek Dattani
 Peter Davidsen
 Jane Davies
 Anne Davis
 Joshua Saul Davis
 Paul Dawson
 Cristina De Alvaro
 An De Creus
 Bo De Fooz
 Raffaele De Francesco
 Robert De Knecht
 Guy De La Rosa
 Ana de las Heras
 Victor de Lédinghen
 Marcel de Leeuw
 Robert De Man
 Sara De Martin
 Sandra De Meyer
 Sofie De Meyer
 Claudia De Oliveira
 Catalina De Schrevel
 Brittany de Temple
 Enrico de Toni
 Simon Debaecker

Disclosures

Getachew Debas Belew
Jose Debes
Martin Decaris
Elisabetta Degasperi
Oliver Degerstedt
Luca Degli Esposti
Clayton Dehn
Arnaud Del Bello
Jared Delahaye
William Delaney
Philippe Delataille
Olivier Dellis
Jonas Demant
Münevver Demir
Guohong Deng
Douglas Denham
Gerald Denk
Andrea Dennis
Alex DePaoli
Laura D'Erasmus
Supriya Desai
Todd Z. DeSantis
Marc Deschenes
Katja Deterding
Sylvie Deuffic-Burban
krishnadas devadas
Jerome Deval
Carole Devaux
Sebastien Dharancy
Tony Dhillon
Romano Di Fabio
Tommaso Di Maira
Vito Di Marco
Francesca Di Stasi
Moises Diago
Álvaro Díaz-González
Francisco Diaz-Mitoma
Amy Dickey
Christopher Dickman
Michel Didier
Lauri Diehl
Douglas T Dieterich
John Dillon
Dessislava Dimitrova
Amreen Dinani
Dora Ding
Yanhua Ding
Luciana Dini
Luciana Diniz Silva
Vanessa Ditt
Bharat Dixit
Emmanuel Dauda Dixon
Son Do
Stephen Dodge
Sowjanya Dokku
Leona Dold
Lourdes Dominguez
Raquel Domínguez-Hernández
Gregory Donadio
Hélène Donnadiou-Rigole
Claire Donoghue
Gregory Dore
Lucy Dorrell
Kate Dorrington
Michael Doukas
Joseph Doyle
Michael Drage
vera dreizin

J.P.H. Drenth
Sandra Droese
Shunda Du
Shuyan Du
Andres Duarte Rojo
Ravi Dugyala
Jacques Dumas
Aurore Dumond
Jérôme Dumortier
James Duncan
Julien Dupin
David Durantel
Geoffrey Dusheiko
Lea Duwe
Athena Dworakowski
Doug Dylla
Jessica Dyson
Lucile Dzen
Richard E Pratley
Matthias Ebert
Julien Edeline
Elazer Edelman
Hannah Edenbaum
Lindsey A Edwards
Erika Egal
Richard L. Ehman
Ursula Ehmer
Beate Eichelberger
Nicole Eichert
Petros Elliadis
Mona El Awady
Ioannis Elefsiniotis
Timothy Eley
Magdy Elkhshab
Laure Elkrief
Emad El-Omar
Ahmed Elsharkawy
Robert Elston
Birol Emir
Grupo del Registro Col-Hai Enfermedades
Autoinmunes y colestásicas
Bastian Engel
Aron Engel
Hans-Peter Erasmus
Lauren Erdman
Trépo Eric
Olof Eriksson
Megan Ermler
Hannah Esser
Whitney Essex
Rafael Esteban
Roger Esteban-Fabro
Chris Estes
Ohad Etzion
Tom Evans
Kimberley Evason
Greg Everson
Ondrej Fabian
Stefano FAGIUOLI
Christine Falk
Kitt Falk Petersen
Jonathan Fallowfield
Kristi Fan
Daiming Fan
Fabrizio Fanelli
Marie C. Fanget
Hooman Farhang Zangneh
Martti Färkkilä

Ronald Farquhar
Brian Feagan
Molly Feder
Denise Federico
Becket Feierbach
Michael Feigh
Leighland Feinman
Jeanette Feizi
Jordan Feld
Vicente Felipo
Shibao Feng
Daphna Fenyves
Beatrice Bois De Fer
Peter Ferenci
Guillermo Fernández Varo
Isabel Fernández-Lizaranzu
Giovanna Ferraioli
Pasquel Ferraro
Carlos Ferreira
Sofia Ferreira-Gonzalez
Philip Ferstl
James Fettiplace
Friedrich Feuerhake
Bart Fevery
Katia Fiaschetti
Marco Fidaleo
Isaac Finberg
Peter Findeisen
Fabian Finkelmeier
Sarah Finnegan
Jesse Fishman
Megan Fitzgerald
John F. Flaherty
Simon Fletcher
Robert Flisiak
Annarosa Floreani
Friedrich Foerster
Pelagia Foka
Erica Fong
Sylvia Fong
Helene Fontaine
Marianna Fontana
Corinne Foo-Atkins
Stuart Forbes
Alejandro Forner
Xavier Fornis
Aino Forstén
Robert Foster
Erin Foster
Robert Foster
Graham Foster
John Foster
Robert Foster
Fayssol Fouad
Slim Fourati
Céline Fournier
Claire Fournier
Céline Fournier
Kathryn Fowler
Miguel Fraile
Sven Francque
Sona Frankova
Chris Fraser
R. Todd Frederick
Peder Frederiksen
Alice Freer
Bradley Freilich
Lars Frelin

Luca Frenguelli
 Olivier Frey
 Juan P Frias
 Ragnheidur H. Fridriksdottir
 Michael Fried
 Scott Friedman
 Martin Friedrichsen
 John Fry
 Mårten Fryknäs
 Xinxiang Fu
 Claudia Fuchs
 Yan Yue James Fung
 Scott K Fung
 Karen Fusaro
 Andrew G. Cole
 Steven G. Kultgen
 Daniela Gabbia
 Adrian Gadano
 Anuj Gaggar
 Vincent Gaillard
 Simon Johannes Gairing
 Nicole Galicia
 Jonathan Gall
 Peter Galle
 Rocío Gallego-Durán
 Andrea Galli
 Nicholas Galwey
 Martina Gambato
 Ivane Gamkrelidze
 Kohilan Gananandan
 Sharie C Ganchua
 Yves Gandon
 Edward J Gane
 Abdul-Azeez Ganiyu
 Lila Gannoun
 Rasmus Hvidbjerg Gantzel
 Jin Gao
 Yanhang Gao
 Pablo Garcia de Frutos
 Federico Garcia Garcia
 Antonio Garcia Herola
 Juan Carlos Garcia Pagan
 María Ángeles García-Criado
 María del Rosario García-Lozano
 Adolfo Garcia-Ocana
 Montserrat Garcia-Retortillo
 Kelsey Garlick
 Will Garner
 Antonio Gasbarrini
 Ashwani Gaur
 Gro Gausdal
 Eline Geervliet
 Andreas Geier
 Takuya Genda
 Lei Geng
 Jacob George
 Urania Georgopoulou
 Albert Gerding
 Spiro Getsios
 Tom Gevers
 Reem Ghalib
 Mahmoud Ghazi-Khansari
 Sourav Ghorai
 Malavika Ghosh
 Gianluigi Giannelli
 Jeanne-Marie Giard
 Carl Gibbons
 Vera Gielen

Elia Gigante
 Mélina Gilbert
 Anika Gilbert-Marceau
 Antonio Gil-Gomez
 Yossi Gilgun-Sherki
 Per-Goran Gillberg
 Hunault Gilles
 Sarah Gilmore
 Pere Ginès
 Nigel Girgrah
 Sandhya Girish
 Lisann Girolstein
 Robert G. Gish
 Maria Elena Giusepponi
 Bruce Given
 Jeffrey Glenn
 Ines Glojnaric
 Esteban Gnass
 Michael Goedken
 Heidi Goenaga-Infante
 Benjamin Goeppert
 Nele Goeyvaerts
 Vikrant Gohil
 Hinrich Göhlmann
 S. Nahum Goldberg
 Guro L Goll
 Emilio Gomez-Gonzalez
 Lan Gong
 Emmanuel Gonzalès
 Maria Luisa Gonzalez Dieguez
 Maria Angeles Gonzalez-Carmona
 Irene González-Recio
 Ricardo Gonzalo
 Francois Gonzalvez
 Richard Goodheart
 Zachary Goodman
 Bryan Goodwin
 Emmanuel Gordien
 Gregory Gores
 Olivia Gorostiza
 Brian Gosink
 Joseph Gosnell
 Davide Gottardi
 Magnús Gottfredsson
 Ioannis Goulis
 Liesbeth Govaerts
 Paul Gow
 Felix Grabherr
 Katharina Grabmeier-Pfistershammer
 Gernot Grabner
 Lucy Gracen
 Hiba Graham
 Eva-Marie Gram-Kampmann
 Tassos Grammatikopoulos
 Christoph Grander
 Estelle Grasset
 Jordi Gratacós-Gines
 Isabel Graupera
 Annabel Gravely
 Jonas Graversen
 Ingrid Graves
 Christen Gray
 Kevin Gray
 Ivo Graziadei
 Peter Greasley
 Jason Grebely
 Raanan Greenman
 Robin Greinert

Tim Greizer
 Thomas Gremmel
 Sue Grepper
 Simon Griffin
 Antonella Grigoletto
 Katharine Grimmer
 Enrico Gringeri
 Sturla M. Groendal
 Mark Gromski
 Henning Grønbaek
 Bas Groot Koerkamp
 Julia Grottenthaler
 Ayelet Grupper
 Michael Gschwantler
 Wenyi Gu
 Giovanni Guaraldi
 Kellie Guarasci
 Mehtap Guendogdu
 Antonio Guerrero
 Neil Guha
 Alice Guida
 Maria Guido
 Luca Guidotti
 Encarna Guillén-Navarro
 Adrien Guillot
 Carine Guinard-Azadian
 Aliya Gulamhusein
 Chris Gulka
 Gaurav Gulsin
 Murat Gunal
 Nadege Gunn
 Ping Guo
 Kusum Gupta
 Sneha V. Gupta
 Kusum Gupta
 Ruchi Gupta
 Neil Gupta
 Denis Gusev
 David Gustein
 Thierry Gustot
 Cynthia Guy
 Chad Gwaltney
 Malte H. Nielsen
 Matthias Hackl
 Lacey Haddon
 May Hagiwara
 Hannes Hagström
 Sihoun Hahn
 Magdalena Hahn
 Annemette Hald
 Emina Halilbasic
 Tracey Hall
 Juha Halonen
 Tami Halperin
 Michael Hamill
 James Hamilton
 Julian Hamilton-Shield
 Seddik Hammad
 Niklas Hammar
 Dong Han
 Bin Han
 Steven-Huy B Han
 Guohong Han
 Nemany A. N. Hanafy
 Britta Handyside
 Remy Hanf
 Hie-Won L Hann
 Jakob Schiøler Hansen

Disclosures

Bettina Hansen
Scott Hansen
Christina Hanson
Shaorui Hao
Olaf Hardt
M. Scott Harris
Stephen Harrison
Lukas Hartl
Tarek Hassanein
Ziad Hassoun
Kelly Haston
Angelos Hatzakis
Anna Hauptmann
Liat Hayardeny
Jennifer Hayden
Peter Hayes
Kelly Hayward
Haiying He
Brendan Healy
Christy Hebner
Christina Heeke
Gavin Heffernan
Johannes Kolja Hegel
Brian Heglar
Zeev Heimanson
Femke Heindryckx
Margaret Hellard
Steve Helmke
Louise Henderson
Julie Henderson
Michael Heneghan
Mark Henkemeyer
Jim Hennan
Roland Henrar
Eugenia Henry
Jeong Heo
German Hepatitis C-Registry
Julian Hercun
Pernille Hermann
Heike Hermanns
Candido Hernández
Manuel Hernández Guerra
Virginia Hernandez-Gea
Kerstin Heurling
Helen Heymann
Matthew Hickman
Lindsey Hiebert
Hayato Hikita
Karl Hillebrandt
Jan Hinrichs
Andreas Hintz
Gideon Hirschfield
Sara Toftegaard Hjuler
Gideon Ho
Erwin Ho
Khanh Hoang
Todd Hobbs
Paul Hockings
Linn Hodneland
Lisa Hoelting
Christoph Hoener zu Siederdisen
Benedikt Hofer
Sara Hoffman
Charlotte Hoffmann
Alexander Hofmann
Sarah Hofmann
Wolf Peter Hofmann
Malcolm Hogan

Kurt Højlund
Meghan Holdorf
Adriaan G. Holleboom
David Hollenback
Julius Hollnberger
Dan Holmberg
Ben Holmes
Curtis Holt
Taus Holtug
Jin Hong
Kristian Honnens de Lichtenberg
Adelina Horhat
Patrick Horn
Maria Hörnberg
Patrick Horne
Stephen Horrigan
Raquel Horrillo
Nigel Horscroft
Thomas Horvatis
Yujin Hoshida
Mojgan Hosseini
Jinlin HOU
Inbal Hour
Michael House
Anne Hout
Johannes R. Hov
Rob Howard
Laura Howe
Yao-Chun Hsu
Heather Hsu
J-X Huang
Yan Huang
Daniel Huang
Chung-Feng Huang
Yi-Hsiang Huang
Chung-Feng Huang
Jee-Fu Huang
Genevieve Huard
Jaroslav A. Hubacek
Yvonne Huber
Samuel Huber
Sanne Hulsphas
Dean Hum
Phillip Hunt
Philippe Huot-Marchand
Dietrich Hüppe
Ryan Huss
Tanweer Hussain
Sharon Hutchinson
Simon Hutter
Carey Hwang
Seong Gyu Hwang
Anastasia Hyrina
Marco Iafolla
Matteo Iannaccone
P Ibrahim
Adam Igloi-Nagy
Arfan Ikram
Kamran Ikram
Hasan Imam
Giuseppe Indolfi
Patrick Ingiliz
Takako Inoue
Jun Inoue
Pietro Invernizzi
Christina Iott
Shahed Iqbal
Marta Iruarizaga-Lejarreta

William Irving
Gemma Iserte
Yuji Ishida
Mohamed Ismail
Robert Israel
Yoshito Itoh
Timo Itzel
Tommy Ivanics
Elena Ivanova
Sowmya Iyengar
Janani Iyer
Namiki Izumi
Alan Jaap
Mathias Jachs
Akil Jackson
Ira M Jacobson
Emmanuel Jacquemin
Vasant Jadhav
Jørgen Jahnsen
Vipul Jairath
Ruchika Jaisinghani
Rajiv Jalan
Reza Jalili
Joyce James
Khurram Jamil
Ewa Janczewska
Arun Jandor
Mariajoão Janeiro
Se Young Jang
Naveed Janjua
Giulia Jannone
Harry Janssen
Harry LA Janssen
Ronald Janzen
Maximilian Jara
Jerzy Jaroszewicz
Arjun Jayaswal
Farahnaz Jazaeri
Makuza Jean Damascene
Andreas Jekle
Robert Jenders
Rachel Wen-Juei Jeng
Craig Jenne
Dahn Jeong
Nakcheol Jeong
Mirjana Jerkic
Lutz Jermutus
John Jerzowski
Arun Jesudian
Kartik Jhaveri
Fanpu Ji
Linong Ji
Ji-Dong Jia
Li Jian
Jing Jiang
Li Jiang
Lijuan Jiang
Li Jie
Wladimiro Jiménez
Elena Jimenez Mutiloa
Maria Jimenez Ramos
Feng Jin
Milan Jirsa
Quinian Johanson
Lars Johansson
Edvin Johansson
Katharina John
Binu John

Christopher Jones
David Jones
Catherine Jones
Andrew Jones
Heidi Jones
Kelsey Jordan
William Jordan
Kristin Jorgensen
Juan Jose Perez Ruixo
Zhang Juan
Alina Jucov
Pernille Juhl
Gillmore Julian
Tomi Jun
Birgit Jung
Eun Sun Jung
Jean-Louis Junien
Marzena Jurek
Meriam Kabbaj
Kajetan Kabut
Nandita Kachru
Mohammad Kadivar
Shaul Kadosh
Apichat Kaewdech
Thomas Kakuda
George Kalamitsis
Nina Kallin
Ronald Kalmeijer
Jibrin Kama
Severin Donald Kamdem
C.Omar Kamlin
Tania Kamphaus
Atsushi Kaneko
Shuichi Kaneko
Don Kang
Ramesh Kangarajan
Aimo Kannt
Tatsuya Kanto
Jia-Horng Kao
David Kaplan
Leonard Kaps
Theofanis Karaletsos
Eirini Karamichali
Chitra Karki
Saul J. Karpen
Morten Karsdal
Nikolaos Kartalis
Nino Katchiuri
Lorn Kategaya
Naoya Kato
Sarah Kattakuzhy
Goutham Reddy Katukuri
Helena Katzman
Stefan Günther Kauschke
Ankita Kaushik
Maryam Kavousi
Norifumi Kawada
Matt Kelly
Deirdre Kelly
Scott Kelly
George Kemble
Bradley Kendall
Tim Kendall
Stuart Kendrick
Patrick Kennedy
Carla Kettler
Cassandra Key
Shameer Khader

Jaafar Khaled
Faisal Khan
Tanweer Khan
Tipu Khan
Ambreen Khan
Saifuddin Kharawala
Aditya Khosla
Kamlesh Khunti
Steven Kiddle
Alexander Killer
Alastair Kilpatrick
Jae Heon Kim
Hyun Jung Kim
Meej Kim
Yoon Jun Kim
Won Kim
W. Ray Kim
Benjamin Kim
Kyung Mo Kim
Jung-Hee Kim
Ryoon Ho Kim
Chang Min Kim
Yele King
Kathryn M Kitrinos
Ligia Akemi Kiyuna
Mette Kjaer
Maria Kjærgaard
Lise Kjems
Hartwig Klinker
Markus Klinkicht
Kevin Klucher
Heinz-Josef Klümpen
Maximilian Knapp
Cornelis Knetsch
Percy A. Knolle
Steven J Knox
Andreas Dehlbæk Knudsen
Hin Hln Ko
Jossy George Kochuparampil
Takahiro Kodama
Jan Köhler
Anita Kohli
Daphne Koller
Loreta Kondili
Philipp Königshofer
Dennis Koob
Maria Kopsida
Miroslaw Kornek
Konstantin Koro
Ioannis-Georgios Koskinas
Radina Kostadinova
Cory Kostrub
Kris Kowdley
Kris V. Kowdley
Kris Kowdley
Aleksander Krag
Filip Krag Knop
Johanne Kragh Hansen
Mel Krajden
Niels Krarup
Marcin Krawczyk
Wolfgang Maximilian Kremer
Andreas E Kremer
Felix Krenzien
Vyjayanthi Krishnan
Konstantin Kroeniger
Carlot Kruse
Simon Krzysztof

Iwona Ksiazek
Reinhard Kubale
Masatoshi Kudo
Patrizia Kuenzler
Mary Kuhns
Folkert Kuipers
Santosh Kulkarni
Anand Kulkarni
Joel Kullberg
Parag Kumar
Ravi Kumar
Sonal Kumar
Yong-Fang Kuo
Masayuki Kurosaki
Tatyana Kushner
David Kuter
Manik Kuvalekar
Martin Kveton
Paul Yien Kwo
Christian Labenz
Eternity Labio
Florence Lacaille
Alain Lachaux
Olivier Lada
Hermann Laferl
Juan Lafuente-Barquero
Felix Lai
Jennifer Lai
Gerond Lake-Bakaar
Wim Laleman
Jacob P Lalezari
Angela M Lam
Angela Lamarca
Tom Lambrecht
Twan Lammers
Frank Lammert
Pietro Lampertico
Tian Lan
Tina Landsvig Berentzen
Marcia Lange
Christian M. Lange
Miriam Langelaar
Taro Langner
Dominique Larrey
Guillaume Lassailly
Audrey H. Lau
Daryl Lau
Chi Lau
Stefan Laufer
Caroline Laurendeau
Volker Lauschke
Juliette Lavaux
Matthew Law
Adebayo Lawal
Eric Lawitz
Jeffrey Lazarus
Patrice Lazure
Kha Le
Quang Le
Bertrand Lebouche
David Lebowhl
Chee Seng Lee
Lois Lee
Yun Bin Lee
Jeong-Hoon Lee
Yeonju Lee
Samuel Lee
Soon Kyu Lee

Disclosures

Dong Ho Lee	Yang Liu	Mark Ma
Misun Lee	Tian Liu	Shenglin Ma
Justin Lee	Yan Liu	Benjamin Maasoumy
Gil Won Lee	Boya Liu	Leigh MacConell
Sanghyeok Lee	Jing Liu	Graeme Macdonald
Jina Lee	Cheng Liu	Kelli MacDonald
Alicia Lee	Yen-Chun Liu	Guilherme Macedo
Diana Leeming	Wenhui Liu	Rocio IR Macias
Ann Leen	Yunpeng Liu	Cara L. Mack
Eric Lefebvre	Su Liu	Donald Mackenzie
Sander Lefere	Yang Liu	Alison MacKinnon
Vanessa Legry	Yen-Chun Liu	Iain Macpherson
Rory Leisegang	Neus Llarch	Kairat Madin
Martin Leivers	Jose Luis Lledó	David Madoff
Frédéric Lemaigre	Ana Lleo	Andreas Nygaard Madsen
Maud Lemoine	Josep M. Llovet	Mindy Magee
Florian Lempp	Andrew Lloyd	Anna Mageras
Hans Lennernas	Emily Lloyd	Sanjiv Mahadeva
Sabela Lens	Andrew Lloyd	Sangeetha Mahadevan
Oliver Lenz	Jonathan Lloyd	Anadi Mahajan
Alvin Leong	Stephen Locarnini	Tobias Maharaj
Stefano Leporatti	Khalida Ann Lockman	Chinthaka Mahesh Udamulle Gedara
Jack Leslie	Mark Lockwood	Hassan Mahmood
Paul Lessenich	Juergen Loeffler	Nadim Mahmud
Will Lester	Alessandro Loglio	Jiajia Mai
Cynthia Levy	David Lomas	Mala Maini
Itzhak Levy	Stephen Lombardelli	Michael Maitland
Sharon Levy	Sara Lonardi	Ozren Majstorović
Jing Li	Maria Carlota Londoño	Sara Malcus
Ruidong Li	Edward Long	Elizabeth Malecha
Li Li	Jiang Long	Harmeet Malhi
Yizhao Li	Thomas Longerich	Deepa Malhotra
Hai Li	Louise Longworth	Katharina Malinowsky
Ming Li	Isabelle Lonjon-Domanec	Maryse Malysiak
Hai Li	Ida Lønsmann Lønsmann	Kwan Man
Wei Li	Rohit Loomba	Prasad Mancham
Jun Li	Kathleen M. Loomes	Mattias Mandorfer
Hongming Li	David Lopez	Alessandra Mangia
Qian Li	Domniki Loukaki- Gkountara	Kamal Kant Mangla
Tan Li	Veronique Loustaud-Ratti	Savrina Manhas
Lewyn Li	Wei Lu	Nagraj Mani
Tao Liang	Xiaomin Lu	Derek A Mann
Xi Liang	Xiangyu Lu	Jelena Mann
Yun-Fan Liaw	Henry Lu	Derek A Mann
Stephanie Liebig	Sheng-Nan Lu	Michael P. Manns
Hsiao Lieu	Yingyan Lu	Spilios Manolakopoulos
Young-Suk Lim	Mark Lubberink	Hank Mansbach
Seng Gee Lim	Tom Lüdde	Dmitry Manuilov
Young-Suk Lim	Arran Ludlow-Rhodes	Antonio Manzur
Joseph Lim	Jonas Ludvigsson	John Mao
Tse-I Lin	Folu Lufadeju	Panagiota Maravelia
Jaw-Town Lin	Amaia Lujambio	Julian Marchesi
Chuan-Hao Lin	Veronika Lukacs-Kornek	John Marcinak
MingDe Lin	Tamara Lukic	Christelle Marcou
Katherine E. Lindblad	Jennifer Lund	Maya Margalit
Anna Lindblom	Karen Lundgren	Silke Marhenke
Kajsa Linde	Fridtjof Lund-Johansen	Montserrat Marí
Daniel Linden	Elin Lundström	Rui Marinho
Björn Lindkvist	Ed Luo	Zoe Mariño
Erik Lindström	Yoav Lurie	Ed G. Marins
Lei Ling	Michael Lutz	Jonathon Marioneaux
Mattias Lissing	Jiayu Lv	Jessica Markby
Yang Liu	Yong Lv	denis marleau
Shangbin Liu	Mang M	Tonya Marmon
Weijian Liu	Christopher Ma	Xavier Marniquet
Jieming Liu	Xiaoli Ma	Christine Marotta
Yang Liu	Julie Ma	Laura Marquez Perez
Peidi Liu	Lily Ma	Fabio Marra

Thomas Marron
 Hanns-Ulrich Marschall
 Miljen Martić
 Ross Martin
 Natasha Martin
 Lily Martin
 Marian Martin
 Inigo Martincorena
 Anthony Martinez
 Ibon Martínez-Arranz
 María Luz Martínez-Chantar
 Luis Alfonso Martínez-Cruz
 Silvia Martini
 Eduardo Martins
 Elisa Martró
 Marco Marziani
 Andrew L. Mason
 Johannes Masseli
 Benedetta Massetto
 Davide Mastrocinque
 Roberto Mateo
 Philippe Mathurin
 Ana M Matilla
 Ana Matilla
 José M. Mato
 Philippa Matthews
 Gail Matthews
 Aras Mattis
 Jan Mattsson
 Stefan Mauss
 Oliver Mauthner
 Marija Mavar-Haramija
 Lindsey May
 Petra May
 Jan-Niklas May
 Douglas Maya
 Sofia Mayans
 Cristina Mayer
 Cristiana Mayer
 Douglas Mayers
 Lauren Maynard
 Tracy Mayne
 Rebeca Mayo
 Patrick Mayo
 Samra Mazhar
 Giuseppe Mazza
 Gerry McCann
 Matt McClure
 Matthew McClure
 Matt McClure
 Stefanie McFarlane
 John McGonigle
 Iain B. McInnes
 Andrew McKibben
 Patrick McKiernan
 Megan McLaughlin
 Michael McRae
 Charles McWherter
 Diogo Medina
 Mireia Medrano-Bosch
 Elina Medvedeva
 Patrick Mehlen
 Sania Mehreen
 Rashmi Mehta
 Frank Meiss
 Pedro Melgar-Lesmes
 Brian Meltzer
 Marinela Mendez

Marinela Mendez Pertuz
 Zhong-ji Meng
 Arianna Menghini
 Stephen Meninger
 Francesco Mennini
 Francesco Saverio Mennini
 Denise Menti
 Jorge Mera
 Teresa Mercade Macarulla
 Uta Merle
 Philippe Merle
 Uta Merle
 Peter Mesenbrink
 Anna Mestre
 Philip Meuleman
 Lucy Meunier
 Bernhard Meyer
 Elias Laurin Meyer
 Maurice Michel
 Peter Michielsen
 Michael Middleton
 Igor Mikaelian
 Zoka Milan
 Andrzej Milkowski
 Annabelle Milla
 Keith Miller
 Scott Milligan
 Ross Mills
 Andrew Milner
 Patrice Mimche
 Konstantinos Mimidis
 Seohyun Min
 Itziar Mincholé
 Anna-Elisabeth Minder
 Beatriz Minguez
 Anne Minnich
 Wesley Minto
 Miguel Miranda
 Marc Miravittles
 Louise Missen
 Pratik Mistry
 Nina Mitchell
 Veronika Mlitz
 Hongmei Mo
 Tudor Mocan
 Satoshi Mochida
 Søren Kragh Moestrup
 Lucile Moga
 Douglas Mogul
 Tamer Mohamed
 Hozeifa Mohamed Hassan
 Naqvi Mohammed
 Shivabrata Dhal Mohapatra
 Isabelle Mohr
 Emily Mongale
 Susana Monroy
 Michael Montalto
 Noé Axel Montanari
 Aldo J Montano-Loza
 Julie Montegut
 Emily Montosa Nunes
 Raj Mookerjee
 Andrew Moon
 Christina Moon
 Andrew Moon
 Ellen Mooneyhan
 Adi Mor
 Albert Morales

Francesca Morandini
 Kate Moraras
 Lea Mørch Harder
 Alazne Moreno-Lanceta
 Julien Moretti
 Timothy Morgan
 Cecilia Morgantini
 Ramón Morillo Verdugo
 Julie Morisset
 Wolfgang Moritz
 Scott Moseley
 Miha Moskon
 Andrea Mospan
 Alastair Moss
 Sofia Mouchti
 Victoria Mountain
 Sam Moussa
 Miha Mraz
 Linus Mrozek
 Sucheta Mukherjee
 Benjamin H. Mullish
 Theresa Müllner-Bucsics
 Petra Munda
 Breda Munoz
 Rocio Munoz Hernandez
 Sergio Muñoz Martinez
 Patricia Munoz-Garrido
 Rashmi Munshi
 Daniela Munteanu
 Carla Fiorella Murillo Perez
 Ryan Murphy
 Donald Murphy
 Suzanne Murray
 Bernard Murray
 Lucija Mušak
 Anatoly Myaskovsky
 Rob Myers
 Robert Myers
 Lindsay Myles
 Ahmed Nader
 Nejc Nadižar
 Laura Nagy
 Ronald G Nahass
 Pierre Nahon
 Mustapha Najimi
 Atsushi Nakajima
 Mitesh Nakum
 Danielle Nance
 Nikolai Naoumov
 Ruben Napolitano
 Nicole Narayan
 Yvonne Narthey
 Basil Nasir
 Patrik Nasr
 Isabelle Nassar
 Jean Charles Nault
 Nelson Ndegwa
 Guy Neff
 Cara H. Nelson
 Magdalena Neroldova
 Erik Ness
 John Nestor
 Nadia Neto
 Hans Netter
 Christoph Neumann-Haefelin
 Frederik Nevens
 Gregory Neveu
 Riccardo Nevola

Disclosures

Anat Nevo-Shor
Carolyn Newberry
Christopher Newgard
Philip N Newsome
Katina Ngo
Eric Ngonga Kemadjou
Tuan T Nguyen
Khiem Nguyen
Dan Nguyen
Mindie Nguyen
Anh-Hoa Nguyen
Mindie Nguyen
Tan Nguyen
Bich Ngoc Nguyen
Quan hong Ni
Yi Ni
Qamar Niaz
Mette Juul Nielsen
Susanne Dam Nielsen
Mette Juul Nielsen
Paola Nieri
Julia Nilsson
Massih Ningarhari
Louise Nitze
Arianna Nitzel
Junqi Niu
Julia Noack
Blanca Norero
Mazen Noureddin
Nikolai Novikov
Ioanna Ntalla
Vanessa Nunez
Onyeka Nwobi
Melanie Nyuydzefe
Colm O'Rourke
Troy O. Harasym
Fiona Oakley
Frédéric Oberti
Alastair O'Brien
Nancy Obuchowski
Pamela Odorizzi
Marie O'Farrell
Tetsuro Ogawa
Eiichi Ogawa
Lauren Ogilvie
Valerie Ohlendorf
Sigurdur Olafsson
Anouk Oldenburger
Stephanie Oldham
Peter Olinga
Pol Olivas
Isabelle Ollivier-Hourmand
Joss O'Loan
Ye Htun Oo
Jart Oosterhaven
Dorenda Oosterhui@rug.nl
Maaike Oosterveer
Yat Sun Or
Denise Oró
Michael Ortiz
Pablo Ortiz
Anu Osinusi
Carla Osiowy
Peter Ott
Ronald Oude Elferink
Denis Ouzan
Caroline Ovadia
Anne Øvrehus

Ben Owen
A. Burak Ozbay
Seyma Ozturk
Arinc Ozturk
Glenn Pacheco
Daniela Pacurar
Nagaraja Rao Padaki
Melanie Paff
Georges-Philippe Pageaux
Odelya Pagovich
Rish Pai
Agnieszka Pajak
Bo-Yeong Pak
Runa Pal
Laura J Pallett
Adriana Palom
Reddy Pamulapati
David Pan
Wei-Jian Pan
Mei-Hung Pan
Joe Panarese
Sanjay Pandya
Dimple Pandya
Wenjie Pang
Elisa Panzarini
Georgia Papadopolou
George Papatheodoridis
Neven Papic
Chris Pappas
Dimitrios Paraskevis
Bhavna Paratala
Albert Pares
Neehar D. Parikh
Jun Yong Park
Erica Park
James S Park
Jin Young Park
Richard Parker
Victoria Parker
Jacob Parsons
Anna Pasetto
K. John Pasi
Giulia Pasqual
Ana Maria Passos-Castilho
Luisa Pasulo
Gianfranco Pasut
Vishal C Patel
Sanjaykanumar Patel
Keyur Patel
Vishal C Patel
Madhukar Patel
Anita Pathil-Warth
Rashmee Patil
Carrieri Patrizia
Michael Pavlides
Jean-Michel Pawlotsky
Małgorzata Pawłowska
Jacques Payne
Markus Peck-Radosavljevic
Michela Pecoraro
Michael Lynge Pedersen
Alisa Pedrana
Marcos Pedrosa
Kai-Henrik Peiffer
Judit Peix
Vasily Pekurovsky
Amnon Peled
Sophie Pélouquin

Ryan Peltó
Cheng-Yuan Peng
Chien-Wei Peng
Gustavo Pereira
Martina Perez
Jim Perfield
Juan Manuel Pericàs
Pasquale Perillo
Marcello Persico
Nicola Personeni
Simon Peter
Mathieu Petitjean
Louis Petitjean
Oleksandr Petrenko
Aviva Petrie
Diana Petrova
Sandra Petrus-Reurer
Salvatore Petta
Daniel Pettersen
Nikolaus Pfisterer
Larissa Pfisterer
Tuan Pham
Stoffers Philipp
Alexandra Phillips
Jonathan Phillips
Salvatore Piano
Cindy Piao
Gaston Picchio
Glenn Pierce
Theodore Pierce
Lorenzo Piermatteo
Alice Pik-Shan Kong
Björn Pilebro
Dominic Pimenta
David J. Pinato
Iris Pinheiro
Jean-Louis Pinquier
Matthias Pinter
Roser Pinyol
Massimo Pinzani
Marta Piqué-Gili
Teerha Piratvisuth
Mario Pirisi
Fabio Piscaglia
Sven Pischke
Kari Pitkänen
Veronika Pitova
Robert Plesniak
John Plevris
Ondrej Podlaha
Carsten Poggel
Charles Poirier
Stanislas Pol
Wojciech Polak
Kishore Polireddy
Maurizio Pompili
Mariano Ponz-Sarvisé
Corneliu Petru Popescu
Vlad Popovic
Branko Popovic
Laura Popp
Olivia Portolese
Sam Possemiers
Aurelia Poujois
Peppi Prasit
Johann Pratschke
Tiziana Pressiani
Ulrike Protzer

K. Tao Pun
 Massimo Puoti
 Lisa A. Purcell
 Antonella Putignano
 Nikolaos T. Pyrsopoulos
 Yuquan Qian
 Lei Qin
 Hisham Qosa
 Xiujuan Qu
 Dongmei Quan
 Geoff Quinn
 Jorge G. Quintero
 Erin Quirk
 Huma Qureshi
 Zuzana Rabekova
 Pascaline Rabiega
 Liane Rabinowich
 Pierre Raboisson
 Daniel Rader
 Andrew Radley
 Pompilia Radu
 David Rafei-Shamsabadi
 Shaimaa Ragab
 Syedia Rahman
 Maruthi Raja
 Ravi Rajagopalan
 Vivek Rajwanshi
 Prakash Ramachandran
 Rakesh Raman
 Ricardo Ramirez
 Alnoor Ramji
 Savita Rangarajan
 Navpreet Ranu
 Joanna Raszeja-Wyszomirska
 Vlad Ratziu
 Monika Rau
 Pierre-Emmanuel Rautou
 Micol Rava
 Natarajan Ravendhran
 Avijit Ray
 Homie Razavi
 Devin Razavi-Shearer
 Kathryn Razavi-Shearer
 Christopher Recknor
 Nageshwar Reddy
 Gili Regev
 Helene Regnault
 Thomas Reiberger
 María Reig
 Dag Henrik Reikvam
 Tanja Reineke-Plaaß
 Florian P Reiter
 Kristina Rekstyte-Matiene
 André-Jean Remy
 Kaili Ren
 keke ren
 Hong Ren
 Yayun Ren
 Murray Resnick
 Peter Revill
 Archie C. Reyes
 Tadeja Rezen
 Christopher Rhodes
 Carlota Riba
 Andrea Ribeiro
 Rasmus Ribel-Madsen
 Anna Richards
 Holly Richardson

Armin Rieger
 Elena Riester
 Cristina Rigamonti
 Lorenza Rimassa
 Jordi Rimola
 Anthony Rinaldi
 Mercedes Rincón
 Mary Rinella
 Cristina Ripoll
 Jen Rito
 Timothy Ritter
 Mar Riveiro Barciela
 Giuliano Rizzardini
 Scot Roberts
 Lewis Roberts
 John Robertson
 Darren Robertson
 Adriana Roca-Fernandez
 Michael Roden
 Christoph Roderburg
 Kyle Rodney
 Christophe Rodriguez
 Manuel Rodríguez
 Miguel Ángel Rodríguez Sagrado
 Tamara Rodriguez-Castaneda
 Manuel Rodríguez-Perálvarez
 Sergio Rodriguez-Tajes
 Angela Rojas Alvarez-Ossorio
 Benjamin Rolland
 Tim Rolph
 Renato Romagnoli
 Krista Rombouts
 Manuel Romero Gomez
 Martin Rønn Madsen
 Maxime Ronot
 James Roper
 Manuel Roqueta-Rivera
 Silvia Rosati
 Valerio Rosato
 Jenny Rosenquist
 Elana Rosenthal
 Philip Rosenthal
 Trenton Ross
 Jean-Francois Rossignol
 Celine Rossignol
 Françoise Roudot-Thoraval
 Dominique Roulot
 Mackenzie Rowe
 Ian Rowe
 Nichola Royal
 Damjana Rozman
 Peter Ruane
 Aileen Rubio
 Luong Ruiz
 Isaac Ruiz
 Maria Grazia Rumi
 Valgerdur Runarsdottir
 Jana Rupp
 Matthew Russell
 Chris Russell
 Francesco Paolo Russo
 Vinod Rustgi
 Erica Rutherford
 Guy Rutter
 Pablo Ryan
 John Ryan
 Anna Saborowski
 Jonah Sacha

Hesham Sadek
 Shakhlo Sadirova
 Kourosh Saeb-Parsy
 Diego Saenz de Urturi
 Olga Sagalova
 Brad Saget
 Ebada Said
 Andreas Sailer
 Ryotaro Sakamori
 Magdalena Salcedo
 Matti Sällberg
 Romina Salpini
 Ayan Samanta
 Anthony Samir
 Demetrious N. Samonakis
 Sumeyye Samur
 Javier San Martin
 Jose Sanchez
 Katarzyna Sanchez
 Rubén Sánchez-Aldehuelo
 Lisa Sandmann
 Louis Sandra
 Marco Sanduzzi Zamparelli
 Bruno Sangro
 Jessica Santana
 Armando Santoro
 Sandra Santos
 Alvaro Santos-Laso
 Arun Sanyal
 Gonzalo Sapisochin
 Margherita Saracco
 Samantha Sarcognato
 Souvik Sarkar
 Christoph Sarrazin
 Janeli Sarv
 Santhosh Satapati
 Romil Saxena
 Katia Sayaf
 Pietro Scalfaro
 Ute Schaeper
 Martina Scharitzer
 Hubert Scharnagl
 Jörn Schattenberg
 Johanna Schaub
 Bernhard Scheiner
 Stacey Scherbakovsky
 Eugene R. Schiff
 Michael Schilsky
 Franklin Schlerman
 Thomas Schluep
 Moritz Schmelzle
 Michael A. Schmid
 Ingo G. Schmidt-Wolf
 Bernd Schnabl
 Stephan M Schneeweiß
 Carolin Victoria Schneider
 Kai Markus Schneider
 Guenther Schneider
 David Schoeler
 Katrin Schöneweis
 Jeoffrey Schouten
 Philipp Schuetz
 Martin Schulz
 Julian Schulze zur Wiesch
 Detlef Schuppan
 Andrew Schwab
 Christian Schwabe
 Philipp Schwabl

Disclosures

Birgit Schwacha-Eipper
Caroline Schwarz
Michael Schwarz
Kathleen Schwarz
Julian Schwärzler
Sofia Schweiger
Antonio Sciambra
Eleonora Scorletti
Jadine Scragg
Giada Sebastiani
Daniel Seehofer
Michal Segal-Salto
Martha Seif
Jessica Seitzer
Marion Selfridge
Roland Selig
Bret Sellman
David Semela
Dimitri Semizarov
Georg Semmler
Marco Senzolo
Laura Sepp-Lorenzino
Manuel Serrano
Wai-Kay Seto
Lillian Seu
Thomas Seufferlein
Heather Sevinsky
Stephen Shafran
Abdel-Aziz Shaheen
Sudha Shankar
Li Shao
Ron Shapiro
David Shapiro
Madiha Sharaf
Rohini Sharma
Shawn Sharma
Mithun Sharma
Ashish Sharma
Varun Sharma
Eilon Sharon
Debbie L. Shawcross
Anna Shcherbina
Kristen Shea
Aasim Sheikh
Ling Shen
Michael Shen
Swapna Shenvi
Andrea Shepard
Alex Shephard
Cal Shephard
Sarah Sherlock
Shishir Shetty
Annabella Shewarega
Junping Shi
Yu Shi
Dongyan Shi
Mitchell Shiffman
Sonjelle Shilton
Yusuke Shimakawa
Ronit Shiri-Sverdllov
Megan Showalter
Reshma Shringarpure
Maria Shubina
Umesh Shukla
Gerald I. Shulman
Elizabeth Shumbayawonda
Si Nafa Si Ahmed
Daniela Sia

Antoni Sicras-Mainar
Choong-Ryoul Sihn
Milessa Silva Afonso
Heewoo Sim
Benedikt Simbrunner
Irene Simeone
Jorge Simón
Jorge Simón Espinosa
Karen Sims
Marie Sinclair
Ashwani Singal
Amit Singal
Shivendra Singh
Nitesh Singh
Renu Singh
Jennifer Singh
Rohit Sinha
Claude Sirlin
Lillian Siu
Sannia Sjöstedt
Susanna Skalicky
Lubomir Skladany
Cene Skubic
Rob Slack
Leen Slaets
Janka Slatinska
David Smith
Nate Smith
Helen Smith
Alexander Smith
Delvin So
Rodolphe Sobesky
Piotr Socha
Michael J. Sofia
Etienne Sokal
Rushil Solanki
Sunil Suhas Solomon
Lorenzo Somaini
Yanna Song
Jiangao Song
Milan Sonneveld
German Soriano
Iris Soto
Geneviève Soucy
Cameron Soulette
David Southern
Johanna Spaans
Zeno Sparchez
Jan Sperl
Julius Spicak
Lynsey Spillman
Christoph Spinner
Katrin Splith
Ioan Sporea
Anna Spreafico
Martin Sprinzl
Kathrin Sprinzl
Francis Sprouse
Katherine Squires
Siddharth Sridhar
Subash Srinivasan
Pimsiri Sripongpun
Natalie Sroda
Tim St Pierre
Duncan Stacey
Bart Staels
Lawrence Staib
Luisa M Stamm

Jenny Stanton
Ingemar Starke
Peter Stärkel
Patrick Starlinger
Albert Stättermayer
Thérèse Staub
Rudolf E. Stauber
Katharina Stauffer
Jeffrey Stebbins
Kim Steel
Staci Steele
Daniel Steinacher
Alexandra Steinberg
Hans-Jürgen Stellbrink
Richard Sterling
Christiane Stern
Sarah Stevens
Kim Stever
Tatjana Stojakovic
Mark Stooze
Antitsa Stoycheva
Ellen Strängberg
Christian Strassburg
Simone Strasser
Mario Strazzabosco
Pavel Strnad
Simon Ströbel
Mark Stroh
Ekkehard Sturm
Wei-Wen Su
Tung-Hung Su
Chien-Yu Su
Angela Suárez-Noya
Goki Suda
Lydia Sulaiman
Mark Sulkowski
Mark Sulkowski
Thierry Sulpice
Binta Sultan
Suwan Sun
Mads Sundby Palte
Pil Soo Sung
Vithika Suri
Rob Suriano
Rowena Suriben
Silpa Suthram
Anvar Suyundikov
Nils Svängård
Evguenia S Svarovskaia
Valentina Svicher
Mark G Swain
Marianne T Sweetser
Eugene Swenson
Brandon Swift
Julian Symons
Vana Sypsa
Huybrecht T'jollyn
Frank Tacke
Waleed Tahir
Dean Tai
Paul Tait
Hirokazu Takahashi
Taro Takami
Takanori Takebe
Tetsuo Takehara
Bart Takkenberg
Edward Tam
Vincent Tam

Edward Tam
 Dietmar Tamandl
 Susanna Tan
 Yasuhito Tanaka
 Alexandre Pissewewoe Tanang
 Sunny Tang
 Lydia Tang
 Yanan Tang
 Fady Tanios
 Elliot Tapper
 Muhammad Tariq
 Jens M Tarp
 Chise Tateno
 Rebecca Taub
 Jörg Täubel
 Oliver Tavabie
 James Taylor
 Jeffrey Teckman
 Rosangela Teixeira
 Laura Telep
 Alison Telford
 Richard ten Broek
 Andrea Tenca
 Xiao Teng
 Bernardetta Anna Tenuzzo
 Shuji Terai
 Norah Terrault
 Andreas Teufel
 Dominique Thabut
 Mae Thamer
 Vaidehi Thanawala
 Manish Thapar
 Rajamannar Thennati
 Dickens Theodore
 George Therapondos
 Emily P. Thi
 Maja Thiele
 Robert Thimme
 Eva Thoma
 Helena Thomaidis-Brears
 James Thomas
 Richard J. Thompson
 Alexander Thompson
 Douglas Thorburn
 Thierry Thordjmann
 Bernard Thorens
 Aaron Thrift
 Theresa Thuener
 Hua Tian
 Herbert Tilg
 Erik Tillman
 Jörg Timm
 Dina Tiniakos
 Giridhar Tiruchera
 Myreen Tomas
 Krzysztof Tomasiewicz
 Haley Tong
 Miguel Torres-Martín
 David Tougeron
 Maria Isabel Toulson Davidson Correia
 Fayçal Touti
 Faycal Touti
 Francesco Tovoli
 Hidenori Toyoda
 Tram Tran
 Michael Trauner
 Christian Trautwein
 Jonel Trebicka

Will Treem
 Carla Treloar
 Daniel Trepanier
 Eric Trepo
 James Trevasakis
 Franco Trevisani
 Christos Triantos
 Huy Trinh
 Palak Trivedi
 Miriam Triyatni
 Jörg Trojan
 Phil Troke
 Torsten Trowe
 Emily Truong
 David Truong
 Wen-Wei Tsai
 Cheng-Hao Tseng
 Leo Tseng
 Cheng-Hao Tseng
 Emmanuel Tsochatzis
 Kaoru Tsuchiya
 Marianne Tuefferd
 Manuel Tufoni
 Scott Turner
 Juan Turnes
 Theresa Tuthill
 Olaf Tyc
 Yoshiyuki Ueno
 Tim Umland
 Nuruddin Unchwaniwala
 Stephan Urban
 Daren Ure
 José Ursic-Bedoya
 Frank Uschner
 Ivana Uzelac
 John T. Vaage
 Michele Vacca
 Andrew Vaillant
 Mark Valasek
 Velichka Valcheva
 Jorge Valencia
 Rudolf Valenta
 Luca Valenti
 Vaia Valiakou
 Juan Valle
 Ludovic Vallier
 Florian van Bömmel
 Nicholas Van Buuren
 Pierre Van Damme
 Stan van de Graaf
 Tim Van De Parre
 Celine Van den Broeke
 Luc J.W. van der Laan
 Adriaan Van der Meer
 Jannet van der Veen
 Leen-Jan van Doorn
 Karen Van Eunen
 Ellen Van Gulck
 Bart Van Hoek
 Freya Van Houtte
 Laurens van Kleef
 Sjoerd van Marle
 Pieter Van Remoortere
 Gilles van Tienderen
 Joris J Vandenbossche
 Axelle Vanderlinden
 Kim Vanstraelen
 Thomas Vanwolleghe

Maria Varela
 Hugo E. Vargas
 Bhavesh Variya
 Spyridoula Vasileiou
 Yovana Velazquez
 Wulphert Venderink
 Meenakshi Venkatraman
 Thierry Verbinnen
 Helena Verdaguer
 Francisco Verdeguer
 Nikhil Vergis
 Lieven Verhoye
 Henkjan J. Verkade
 Wim Verlinden
 Chris Verslype
 Monique M.A. Verstegen
 Timo Vesikari
 Florian Veyre
 Elisabet Viayna
 Elena Vicentini
 Peter Vickerman
 Jordi Vidal
 Gianpaolo Vidili
 Pamela Vig
 Ondrej Viklicky
 Tatiana Vilchez
 Jean-Pierre Villeneuve
 Ida Villesen
 Tina Vilsbøll
 Adriana Vince
 Catherine Vincent
 Alessandro Vitale
 Jennifer M. Vittorio
 Francesco Vizzutti
 Arndt Vogel
 Christian Voitenleitner
 Valery Volk
 Stephan vom Dahl
 Robyn von Maltzahn
 Erik von Seth
 Jacky Vonderscher
 Miriam Vos
 Marijana Vujkovic
 Raj Vuppalach
 Katy Wack
 Tom Waddell
 Sam Wadsworth
 Alisha Wahl
 Staffan Wahlin
 Sam Waksal
 Andrew Walakira
 Kate Walker
 Ruth Walker
 Josephine Walker
 David Wallace
 Jean-Philippe Wallach
 Jeffrey Wallin
 Liron Walsh
 Xueshuai Wan
 Guiqiang Wang
 Hongyuan Wang
 Su Wang
 Grace Wang
 Xian-bo Wang
 Pu Wang
 Yan Wang
 Xiaojun Wang
 Stanley Wang

Disclosures

Xiaohong Wang
xiaohao Wang
Bing Wang
Hee Jung Wang
Guoqiang Wang
Bin Wang
Ilan Wapinski
John Ward
Suzan Warner
Matthew Warr
Elaine Watkins
Tim Watkins
Hugh Watson
Michiel Weber
Sabine Weber
Heiner Wedemeyer
Yishuang Wei
Frank Weilert
Nina Weis
Ilan Weisberg
Karl Heinz Weiss
Markus Weissbach
Karin Weissenborn
Lisa Weissfeld
Bo Wen
Charlotte Wernberg
Christopher Westland
Jochen Wettengel
Victoria Wharton
Kristen Wheeden
Darren Wheeler
Nicole White
Thomas Wiersma
Signe Wiese
Philippe Wiesel
Bernard Willems
Philippe Willems
Jorke Willemse
Caroline Williams
Catherine Williamson
Todd Willis
Arnulf Willms
Wendy Winckler
Karin Wisskirchen
Magdalena Witschi
Jennifer Witt
Melanie Wittner
Owens Wiwa
Maciej Wójcicki
Armin Wolf
Danny Ka-Ho Wong
C Wong
Robert Wong
Steven Wong
Simon Wong
Robert Wong
Vincent Wai-Sun Wong
Grace Lai-Hung Wong
Danny Ka-Ho Wong
Alexander Wong
Robert Wong
Yu Jun Wong
David Wong
Darren Wong
Grace Wong
Wing Yen Wong
Kristy Wood
Jinny Woolgar

Xavier Woot de Trixhe
Thomas Worland
David Wraith
Min Wu
Wenqiang Wu
Jinzi Wu
Xiaoqin Wu
Tongfei Wu
Wei Wu
Tiffany Wu
Tianzhou Wu
Jamie Wu
Torsten Wuestefeld
Jay Wustner
Verhelst Xavier
Ningshao Xia
Tian Xiao
Yao Xie
Qing Xie
Lin Xie
Jiaojiao Xin
Shaojie Xin
Cheng-Jian Xu
Simin Xu
Jianfeng Xu
Simin Xu
Yuanxin Xu
Jun Xu
Qingqing Xu
Deming Xu
Zenghui Xue
Kitty Yale
Leo Yamamoto
Ran Yan
Yuemei Yan
Wenhao Yan
Ju Dong Yang
Qiang Yang
Yongping Yang
Xinye Yang
Hwai-I Yang
Yuan Yang
Genren Yang
Junlin Yang
Heng Yao
David Yardeni
Hiroaki Yashiro
Bridget Yates
Hiroshi Yatsuhashi
Tahmineh Yazdi
Lei Ye
Leland Yee
Alon Yehoshua
Yee Hui Yeo
Jian Yeo
Min Yi
Hyung Joon Yim
Terry Cheuk-Fung Yip
Masato Yoneda
Zhao Yongliang
Jeongin Yoo
Jung-Hwan Yoon
Hitoshi Yoshiji
Shaoli You
Shihyun You
Ramy Younes
Ziad H. Younes
Ramy Younes

Liam Young
Vincent B. Young
Zobair Younossi
Amir Youssef
W Yu
Zhou Yu
Qifeng Yu
Meng Yu
Ming-Lung Yu
Yun Suk Yu
Yuan Yuan
Zheng Yubao
Man-Fung Yuen
Carla Yunis
Cihan Yurdaydin
Aziz Zaanani
Giacomo Zaccherini
Syeda Zahida Sarwar
Ane Zamalloa
Florian Zanderigo
Alberto Zanetto
Alexandra Zanin-Zhorov
Ilaria Zanutto
Dorota Zarębska-Michaluk
Anna Zehnder
Lars Zender
Ni Zeng
Alitheia Zetter
Fredrick Zetterberg
Stefan Zeuzem
Jiping Zha
Guofang Zhang
Yong-Yuan Zhang
Bai-Hua Zhang
Yi Zhang
Dong Zhang
Qingling Zhang
Ningning Zhang
Xiaodong Zhang
Jiliang Zhang
Mengnan Zhang
Yingjun Zhang
Haiting Zhang
Linwen Zhang
Ke Zhang
Wen Zhang
Yuchen Zhang
Hong Zhang
Dong Zhang
George Zhang
Yanhua Zhang
Qingling Zhang
Yibo Zhang
Jun Zhang
Lening Zhang
Huafeng Zhang
Xuchen Zhang
Shu Zhang
Caroline Zhao
Jiang Zhigan
Jingye Zhou
Yuanping Zhou
Linghua Zhou
Kali Zhou
Yuhong Zhou
Qian Zhou
Julie Zhu
Qianru Zhu

Julie Zhu
Robert Zimmermann
Kerstin Zinober
Alexander Zipprich
Eugen Zizer
Heinz Zoller
Katie Zomorodi
Zhixin Zong

Guangyong Zou
Xiantong Zou
Fabien Zoulim
Massimo Giovanni Zuin
Tara Robinson
Jonathan Day
Hua Yu
Kelly Lau

Kathryn Patton
Greg de Hart
Josh Henshaw
Suresh Agarwal
Christian Vettermann
Soumi Gupta
Brian Long

Reviewers list

We express our deepest appreciation to the following people, who have given us generous and invaluable help as abstract reviewers for the ILC 2022.

Abdelmalek Manal	Gonzales Emmanuel	Postic Catherine
Adams Leon	Graupera Isabel	Raggi Chiara
Alazawi William	Grebely Jason	Ramachnadran Prakash
Aleman Soo	Gual Philippe	Ratzu Vlad
Alisi Anna	Gustot Thierry	Reiberger Thomas
Andersson Emma	Hagstrom Hannes	Reverter Enric
Armstrong Matthew	Hernández-Gea Virginia	Rimassa Lorenza
Asselah Tarik	Hoener zu Siederdisen Christoph	Rinella Mary
Bansal Ruchi	Hofmann Maike	Ripoll Cristina
Behrendt Patrick	Huch Meri	Rodríguez-Peralvarez L. Manuel
Berg Thomas	Hydes Theresa	Romeo Stefano
Bernal William	Iavarone Massimo	Romero Gomez Manuel
Beuers Ulrich	Jack Kate	Rowe Ian
Björnsson Einar	Komuta Mina	Sällberg Chen Margaret
Boni Carolina	Kondili Loreta	Sarobe Pablo
Böttler Tobias	Krag Aleksander	Schulze-zur Wiesch Julian
Buti Maria	Kuenzler-Huele Patrizia	Schwabl Philipp
Cabibbo Giuseppe	Lachenmayer Anja	Scorletti Eleonora
Calderaro Julien	Lemoine Maud	Scott Charlotte
Castera Laurent	Lemoine Sara	Semmler Georg
Cazzagon Nora	Lleo Ana	Serfaty Lawrence
Childs Kate	Loan Dao Thi Viet	Shiri Sverdlov Ronit
China Louise	Long Michelle	Spaan Michelle
Ciesek Sandra	Longerich Thomas	Spee Bart
Coll Mar	Lotersztajn Sophie	Stal Per
Conti Filomena	Louvet Alexandre	Steinmann Eike
Corey Kathleen	Luukkonen Panu	Stickel Felix
Corpechot Christophe	Makara Michael	Strick-Marchand Helene
Culver Emma	Manolakopoulos Spilios	Strnad Pavel
D'Ambrosio Roberta	Mantovani Alessandro	Tacke Frank
Dalekos George	Martin Natasha	Taubert Richard
de Lédinghen Victor	Marzoni Marco	Thompson Karen
De Martin Eleonora	Mas Valeria	Toniutto Pierluigi
Degasperi Elisabetta	Maticic Mojca	Trebicka Jonel
Deuffic-Burban Sylvie	Mauss Stefan	Trepo Eric
Dietz Julia	McPhail Mark	Triantos Christos
Durand François	Merle Uta	Tsochatzis Manolis
Elkrief Laure	Meuleman Philip	Ulrich Marschall Hans
Fabrellas Nuria	Minguez Beatriz	Vacca Michele
Faivre Sandrine	Moreau Richard	Valenti Luca
Ferraioli Giovanna	Moschetta Antonio	van de Graaf Stan
Flisiak Robert	Nault Jean-Charles	van Mil Saskia
Forner Alejandro	Negro Francesco	Vesterhus Mette
Forrest Ewan	Newsome Philip	Vonghia Luisa
Fraga Christinet Montserrat	Oude Elferink Ronald	Wagner Martin
Frances Ruben	Pais Raluca	Waidmann Oliver
Francoz Claire	Papatheodoridis George	Webb Glynn
Fraquelli Mirella	Papp Maria	Wen-Juei Jeng Rachel
Galle Peter	Pérez-del-Pulgar Sofía	Westbrook Rachel
Ganne Carrie Nathalie	Petta Salvatore	Williams Felicity
Gastaldelli Amalia	Piano Salvatore	Wong Vincent
Gastaminza Pablo	Pietrangelo Antonello	Yasuko Iwakiri
Gerbes Alexander	Pinzani Massimo	Yki-Järvinen Hannele
Gilgenkrantz Helene	Pons Monica	
Gill Upkar	Ponziani Francesca	